TRANSACTIONS

OF THE

AMERICAN INSTITUTE

OF

ELECTRICAL ENGINEERS

VOLUME 65

1946

PUBLISHED BY THE

AMERICAN INSTITUTE OF ELECTRICAL ENGINEERS

33 WEST 39TH STREET

NEW YORK 18, N. Y., U. S. A.

U OF I

LIBRARY

COPYRIGHT 1946
BY THE
AMERICAN INSTITUTE OF ELECTRICAL ENGINEERS

Printed in the United States of America by
The Mack Printing Company, Easton, Pa.

Preface

This 65th volume of the TRANSACTIONS of the American Institute of Electrical Engineers contains all approved technical program papers and related discussions presented at national conventions and District meetings during the calendar year, in accordance with the improved publication policy adopted in August 1940. Pages 1–482 and 521–860 comprise the papers published in the Transactions sections of the monthly issues of ELECTRICAL ENGINEERING, and pages 483–520 and 861–1196 contain papers and discussions that appeared in advance in the June and December 1946 "Supplements to Electrical Engineering—Transactions Section," respectively.

The technical papers and discussions in the volume were presented at these meetings:

1. 1946 winter convention, New York, N. Y., January 21–25, 1946.
2. South West District meeting, San Antonio, Tex., April 16–18, 1946.
3. North Eastern District meeting, Buffalo, N. Y., April 24–26, 1946.
4. Southern District meeting, Asheville, N. C., May 14–16, 1946.
5. Summer convention, Detroit, Mich., June 24–28, 1946.
6. Pacific Coast convention, Seattle, Wash., August 26–30, 1946.
7. Great Lakes District meeting, Indianapolis, Ind., October 9–11, 1946.

In addition this volume contains:

1. 1946 annual report of the board of directors.
2. A complete listing of AIEE officers and committees for 1946–47.

Full correlation of all material in this volume has been accomplished by means of the multientry index beginning on page 1223. Reference to any of the several subject entries for a technical paper will lead directly to the paper and to any published discussion on that paper.

Statements and opinions given in papers and discussions published in TRANSACTIONS are the expressions of contributors for which the American Institute of Electrical Engineers assumes no responsibility.

Errata

1. Page 179, Figure 6. The numeral 2^{-7} should be 2.

2. Page 179, column 3, line 18. The symbol α should be δ

3. Page 182. The first term of the second equation of the appendix should read B_{avg}.

4. Page 270, column 2, line 14. 440-ampere tests should be 550-ampere tests.

5. Page 403, column 1. The fourth line from the bottom should read "within a limited range of temperature."

6. Page 404. Equation 3 should be Log $W = A - B/T$.

7. Page 458, equation 2. The second term should read $I_{0GF}\frac{Z_{0GH}-Z_{1GH}}{Z_{1GH}}$.

All-Electric Gun Charging

WILLIAM C. ROHN
NONMEMBER AIEE

GUN-CHARGING DEVICES are used to actuate the mechanism of automatic machine guns and cannon. This is required initially in order to prepare the weapon for automatic operation, or when misfire, misfeed, or any such malfunction renders the gun inoperative. It should be noted that automatic guns depend upon the force of recoil, gas pressure generated by the exploding cartridge, or both, to perform the task of extracting and ejecting the spent cartridge and delivering a live round into the chamber. The operation of charging consists of retracting the breech block for a stroke of from seven to ten inches, depending upon the caliber of gun, and then releasing it to return unimpeded to battery* under the force of the block-driving spring. Extraction, ejection, feeding, and cocking occur by means of cams, pawls, and levers actuated by movement of the breech block as in normal firing.

When guns on pursuit airplanes were mounted in the fuselage or in manually operated turrets, it was possible for the pilot or gunner to charge them by hand. As more guns were added, they were often mounted in remote positions in the wings. This and the advent of the remote-controlled turret made manual chargers impractical.

Various types of automatic, semiautomatic, and manually controlled power chargers have been introduced. These devices are hydraulically, pneumatically, or electrically powered and either manually or electrically controlled.

Both the hydraulic and pneumatic types of chargers are piston devices. A cylinder is placed parallel to the motion of the breech block, and a projection on the piston engages the block and actuates the mechanism of the gun. The driving force in the case of the hydraulic charger is oil pressure, tapped usually from the hydraulic system on the aircraft but occasionally from individual electrically driven units. The pneumatic charger almost without exception requires a separate source of compressed air, as few fighter craft have pneumatic systems. Cylinders of compressed air or carbon dioxide are the usual provision, either with one tank supplying all of the chargers or with individual containers for each gun. Separate electrically driven compressor units have also been introduced.

Either a hydraulic or pneumatic system necessitates piping and valving which are both bulky and vulnerable. Leakage of the fluid, especially at the charging cylinder or at rotating glands in turret installation, has always been a serious problem. It was only natural then that thought was directed toward the development of an all-electric charger.

When the charger to be described was first contemplated, the following points were considered prerequisites of a good design that would overcome most of the known difficulties of electric chargers in existence.

1. Adjustment should not be critical, and any charger should be readily transferable to any gun of similar type and model without readjustment.

2. The unit should be adaptable to more than one type of gun with only minor changes.

3. As much of the working parts of the charger should be detached from the gun as possible in order that these parts are not subjected to the high-acceleration loads that are normal to automatic weapons at a high rate of fire.

4. Any attachments on the gun should project as little as possible into the area immediately around the gun, as this space is often limited in wing and turret installations.

5. A means should be provided to apply repeated charging efforts to a gun which does not respond to the initial force exerted on the breech block.

6. Means should be incorporated in the charger to "safety" the gun. This requires holding the breech block out of battery, which is a positive assurance that the weapon cannot fire. The principal uses of this feature are to stop a gun which has become

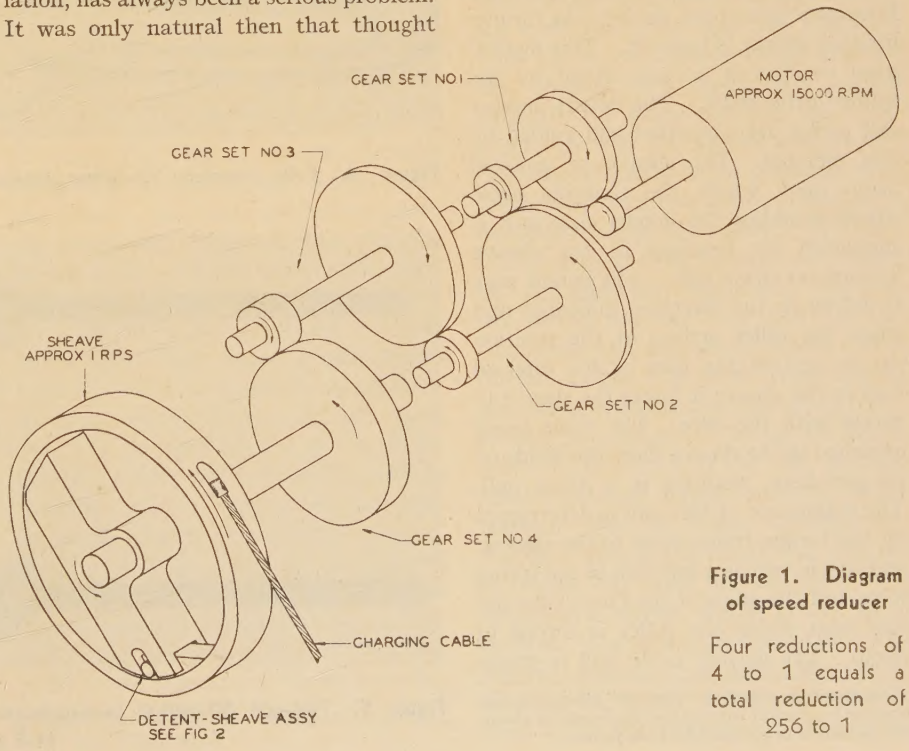

Figure 1. Diagram of speed reducer

Four reductions of 4 to 1 equals a total reduction of 256 to 1

Paper 46-1, recommended by the AIEE committee on air transportation for presentation at the AIEE winter convention, New York, N. Y., January 21–25, 1946. Manuscript submitted June 11, 1945; made available for printing October 9, 1945.

WILLIAM C. ROHN was project engineer, aircraft armament department, Bendix Products Division, South Bend, Ind., at the time this manuscript was prepared. He is at present assistant chief engineer, Allied Control Valve Company, Inc., South Norwalk, Conn.

The author acknowledges the assistance of G. A. Goepfrich and J. M. Boshka.

*A gun is in "battery" when the breech is closed and in firing position.

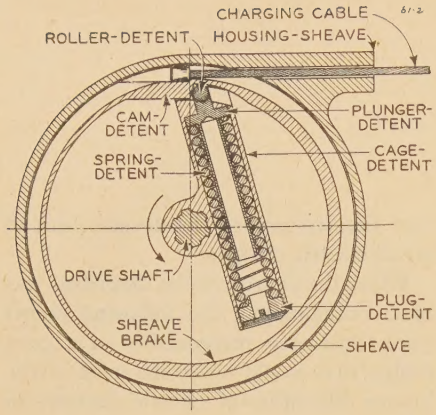

Figure 2. Diagram of detent and sheave assembly

overheated and is "cooking-off"† ammunition out of control and also to prevent accidental discharge due to the impact of carrier landings.

The resulting design consists of three basic units:

1. An electric-motor-driven speed reducer coupled to a torque-limiting detent.

2. An attachment to the body of the gun consisting of a sliding member which engages the breech block, and a guide for this member. Also two switches, one actuated by the sliding member of the charger and the other by the breech block of the gun.

3. A control box, mounted for convenience on the motor.

The motor is series wound, 24 volts direct current, developing approximately one-third horsepower at 15,000 rpm. This drives a four-stage spur-gear train (Figure 1) having a total reduction of 256 to 1. The last stage of the speed reducer is coupled by a spline shaft to the torque-limiting detent (Figure 2). This mechanism consists of a cage driven by the splined drive shaft. The detent plunger and spring are supported and guided by this member. The sheave or grooved drum upon which the charging cable winds straddles the detent cage and is supported by bearings in the sheave housing on either side. The detent cage is driven in the direction indicated and when the roller arrives at the position shown against the face of the internal cam in the sheave it forces the sheave to rotate with the cage. The cable being attached to the sheave therefore winds on its periphery, resulting in a linear pull. The magnitude of this pull is determined by the torque transmitted to the sheave, and this in turn is a function of the spring force and the angle of the face of the detent cam which the roller is forced to climb. The desired cable pull is translated in terms of torque, and the detent mechanism is adjusted to this figure. In operation then the roller engages the cam and rotates the sheave drawing in the cable. The other end of the cable is fixed to the sliding member of the attachment on the gun which engages the breech block (see Figure 3). The breech block is thereby forced rearward until its entire stroke is consumed and further movement is impossible. At this point, the torque transmitted to the sheave increases until it exceeds the setting of the detent mechanism and the roller is forced over the cam. The sheave is now free to rotate in the opposite direction urged by both the breech-block-driving spring and charger-return spring acting through the charger cable. The motor is stopped by dynamic braking, and the ratio of the charging stroke to the circumference of the sheave is arranged so that the cam comes to rest in a relationship to the detent roller convenient for the successive charging operation. The roller is in contact with the sheave brake surface during a portion of the return stroke to absorb the kinetic energy stored in the sheave mass.

The flexible cable transmitting the charging force from the power unit to the sliding member of the attachment on the gun passes through a sheath that is flexible, but rigid in compression.

The compressive load necessary to balance the tension in the cable is taken through this sheath and thereby allows practically universal position relationship between the gun and the charger power unit (Figures 4 and 5). In order to increase further the versatility of positioning, the sheave housing mounts symmetrically on the speed-reducer housing to provide eight directions of cable orientation (Figures 6 and 7).

† Ammunition is said to "cook off" when it is discharged by contact with an overheated firing chamber instead of being ignited by the primer.

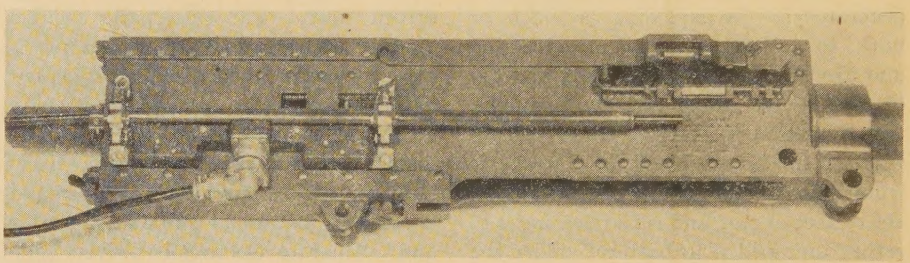

Figure 3. Attachment to gun, including guide, slide, gun switch, and charger switch

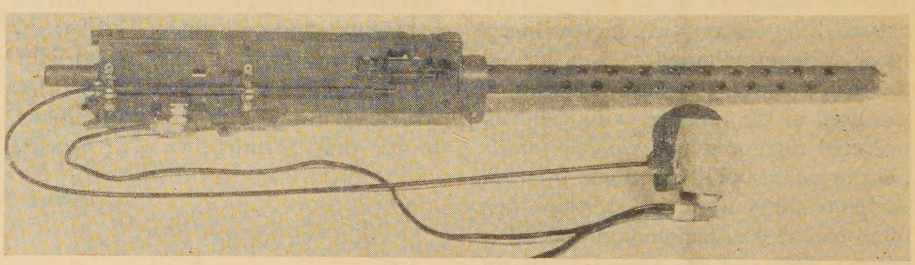

Figure 4. Fully automatic 50-caliber electric charger installation; total weight, nine pounds

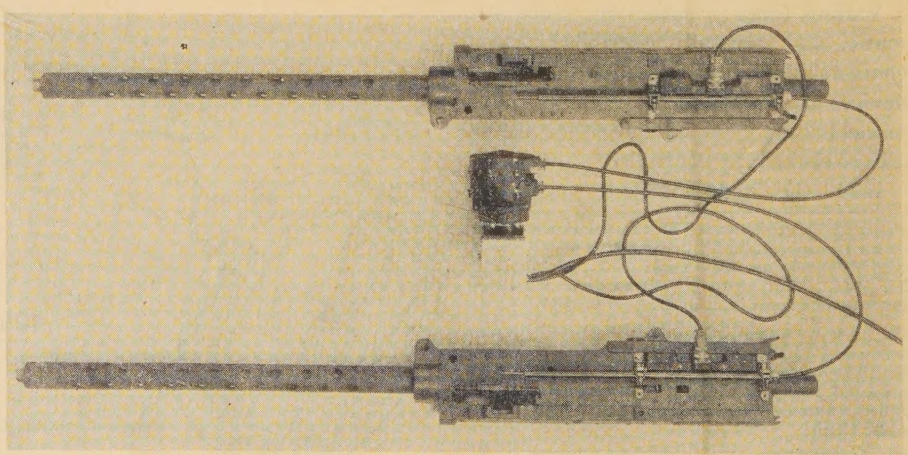

Figure 5. Two-gun 50-caliber semiautomatic electric charger installation; total weight, 11.5 pounds

The attachment on the gun consists of a bracket which supports the tube, serving as a guide for the member that engages the breech—block stud, and acts as a housing for the charging switch and the gun switch. The slide is also of steel tube construction (Figure 3), and is indexed by a slot in the guide tube so that the projecting lug will engage the breech-block charging stud. The interior of the slide houses and pilots the charger-return spring. The switching arrangement is best seen in the diagram, Figure 8. The charging switch is actuated by the lug on the slide only, and the gun switch on the other hand is actuated by the charging stud of the breech block. The charging switch normally is closed, but is held open by the charger lug in its normal position under the influence of the charger-return spring. The gun switch is normally open and is closed by the breech-block stud at its extreme rear position which occurs during a normal firing or a charging cycle.

The entire control apparatus is housed in a sheet-metal box supported on the motor. It may be mounted either above as shown or on the under side, depending upon the space characteristics of the installation. Three relays, a capacitor, and a thermal circuit breaker constitute the control elements for a single-gun fully automatic installation.

A brief description of the sequence of events in a fully automatic charging operation is as follows:

Refer to diagram, Figure 6, and consider first a normal charging cycle. With the control switch in the battery position and the circuit breaker closed, depress the trigger. This energizes the initiating relay, opens its normally closed contacts and removes from the capacitor and the time-delay relay one of the sources of positive potential. Continued firing of the gun now will maintain the other source intermittently through the gun

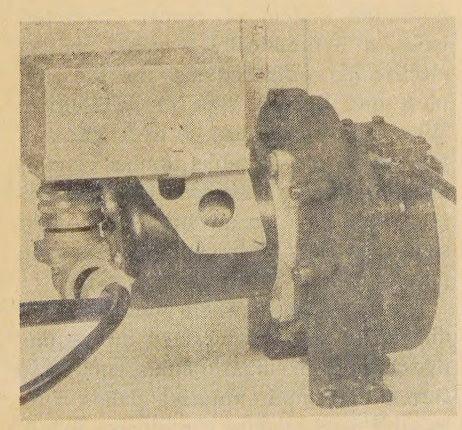

Figure 6. Speed reducer, motor, and control-box assembly

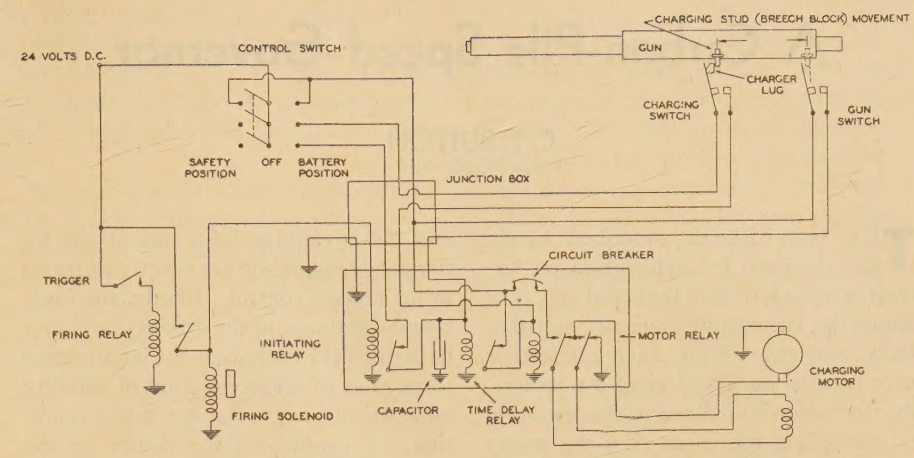

Figure 8. Schematic electric circuit, fully automatic charger

switch actuated by the breech-block charging stud. Should the gun jam‡ or fail to fire, the gun switch will remain open, thus allowing the voltage across the capacitor and time-delay relay to fall as the capacitor slowly discharges through the relay. In about one third of a second this voltage will be low enough to cause

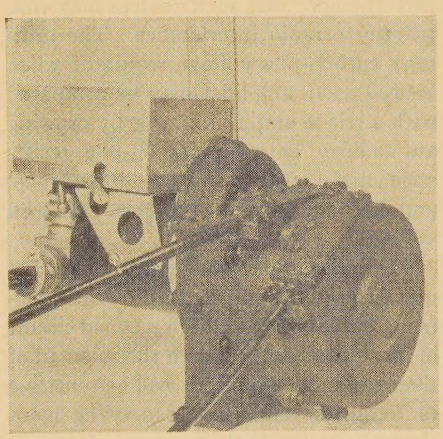

Figure 7. Speed reducer, motor, and control-box assembly for two-gun installation

the time-delay relay to close its contacts energizing the motor relay which starts the motor. The motor now will run until the breech-block stud actuates the gun switch which energizes the time-delay relay, opening the circuit to the motor relay. At this point the motor will stop unless some other means is provided to keep the motor relay energized until the charging cycle has been completed. Such means is provided by the action of the charging switch which closes a circuit to the motor relay as soon as the motor has drawn the charging lug slightly rearward. At the end of the charging cycle, the lug has returned to its forward position, opening the charging switch contacts and de-energizing the motor relay. The normally closed contacts of the motor relay

‡ A gun "jam" includes any malfunction which prevents normal operation.

provide a circuit for dynamically braking the charging mechanism to eliminate overtravel and position the detent properly for the next charging cycle. It can readily be seen that, if the rearward movement of the breech block is impeded at any point by malfunction of the gun, the torque-limiting detent will trip as in normal charging. This returns the slide and lug to the forward position, and another charge will ensue. Thus, repeated impacts will be delivered to the breech block, assuring a maximum possibility of correcting the malfunction and restoring proper operation of the weapon. The thermal circuit breaker is set to allow between six and ten charges before tripping and disconnecting the unit.

In order to "safety" (design item 6) the gun, it is only necessary to initiate a charging cycle and then stop the operation when the breech-block stud actuates the gun switch. By placing the control switch in the safety position, this is accomplished by the following sequence: Opening the circuit to the initiating relay contacts allows the capacitor to discharge, releasing the time-delay relay. This initiates a charging cycle the same as the normal one previously described. The control switch, however, also opens the circuit to the charging switch which allows the motor relay to drop out as soon as the gun switch energizes the time-delay relay, opening its contacts. The control switch may now be moved to the "off" position and the gun and charger left in the safety position with all power disconnected. The gear train is prevented from running in reverse with this imposed load by a spring-type ratchet clutch in the speed reducer. Returning the control switch to battery position completes the circuit through the closed charging-switch contacts to the motor-relay coil. The motor

A Carbon-Pile Speed Governor

C. T. BUTTON
ASSOCIATE AIEE

THE GOVERNOR described herein was designed for application on aircraft inverters, to hold the speed and, consequently, the output frequency substantially constant. While such a governor may be used on a variety of d-c motors, the discussion is confined to the operation of controlling the speed of a d-c motor which drives an a-c generator.

Comparison With Carbon-Pile Voltage Regulator

The problem of governing the speed of a d-c motor is not unlike that of controlling the voltage of an a-c generator—both involve sensitive variation of excitation of a d-c field in response to variation of the controlled quantity. By sensitive variation is meant a rapid or large change in excitation coincident with a small change in the controlled quantity. For example a two-per-cent change in either voltage or frequency of the generator output should produce perhaps 50-per-cent change in excitation of generator or motor field, respectively. Such a device may be regarded broadly as a rate-of-change amplifier with a high amplification ratio around the control point.

A contact-making regulator is the simplest form of such a device and has been used widely for both voltage and speed regulation. The limitations of a contact-making regulator are well known; and the advantages of a carbon pile for frequency regulation are exactly the same as for voltage control. Briefly, the functional advantage of the carbon pile is that it varies field excitation by infinitesimal steps so as to achieve a point of stability on a smooth curve for any given condition. A contact-making device on the other hand causes a more or less rapid fluctuation of field current by finite steps and thereby creates a modulation in output voltage. In the case of a speed governor this modulation is minimized not only by field inductance but also by rotor inertia; yet this modulation still exists in some degree. Practical disadvantages of the contact-making devices are that contact-point deterioration may affect performance; and such devices may contribute to radio interference. The ordinary carbon-pile voltage regulator when viewed as an amplifier may be compared with a triode amplifying tube by drawing an analogy between carbon-pile resistance and cathode-to-plate impedance; and between solenoid voltage and grid voltage.

The carbon-pile voltage regulator easily may be used to control speed by introducing either an inductance or a tuned circuit in series combination with the solenoid of the carbon pile so that it will be sensitive to frequency change. It may be mentioned incidentally that carbon-pile operation for a voltage regulator is opposite to that of a speed regulator in that increasing voltage requires a drop in generator field excitation, whereas increasing frequency requires an increase in motor field current.

While there are many ways of producing varying pressure on a carbon pile in response to change in frequency or speed, it may be stated without the burden of argument that probably the most direct and efficient way is to utilize thrust resulting from centrifugal force on rotating weights supported by springs. In this arrangement the spring is the basic reference for control just as it is in the voltage regulator. Incidentally it is interesting to note that centrifugal force varies as the square of the speed; and the force acting on the armature of a voltage regulator for a constant gap varies as the square of the solenoid voltage.

In the case of an armature moving in response to magnetic pull from a solenoid, ordinary simple construction results in this pull varying as a square function of the armature position. However, when weights move as a result of centrifugal force, the force varies only directly as the radius. Hence it is not necessary to provide special spring forms to prevent instability in the speed regulator.

Relatively large values of thrust are obtained easily with small weights at the speeds characteristic of aircraft inverters. No expenditure of energy is involved ex-

Paper 46-4, recommended by the AIEE committee on air transportation for presentation at the AIEE winter convention, New York, N. Y., January 21–25, 1946. Manuscript submitted September 10, 1945; made available for printing October 16, 1945.

C. T. BUTTON is sales manager, aircraft and electrical controls division, The Master Electric Company, Dayton, Ohio.

---

then will run until the return of the charging lug opens the charging switch, de-energizing the motor relay.

Several units may be linked to the same trigger and control switch. It is only necessary to connect corresponding leads in parallel at a suitable junction box in such times.

Variations of this circuit adapt the charger to different automatic weapons having approximately the same breech-block stroke. Another modification is the semiautomatic system which requires the charging operation be initiated by the gunner pressing a button and is then carried to completion automatically. With this system two guns may be charged simultaneously by one power unit containing two detent assemblies, provided the force required to retract the breech block does not exceed 250 pounds per gun (Figure 7).

The charging cycle, when operating a 50-caliber machine gun, is approximately one second, and the current drain is eight to nine amperes. Two 50-caliber guns require approximately 15 amperes and charge in about $1^1/_2$ seconds. These figures pertain to room-temperature operation. The unit, however, will operate satisfactorily at 65 degrees Fahrenheit, at approximately twice the normal charging time. The unit will handle one weapon of 50-caliber or 20-millimeter size with fully automatic operation at a total apparatus weight of nine pounds. Two weapons of either size may be served semiautomatically at a total weight of $11^1/_2$ pounds.

Weight and dependability are the most important considerations in selecting the type of gun charger to use in an installation. If, for instance, an airplane has a hydraulic system of proper characteristics, a hydraulically powered charger electrically controlled may be the simplest and lightest type of installation. When an airplane has no hydraulic system and a considerable number of guns are to be used, a pneumatic charging system could have an advantage in weight since the weight of the compressor per gun may be comparatively small.

In an installation where guns are few or difficulties are encountered in sealing hydraulic or pneumatic fluids, such as in turrets that require rotating glands or releasable package-gun containers, an all-electric gun charging system has definite advantages.

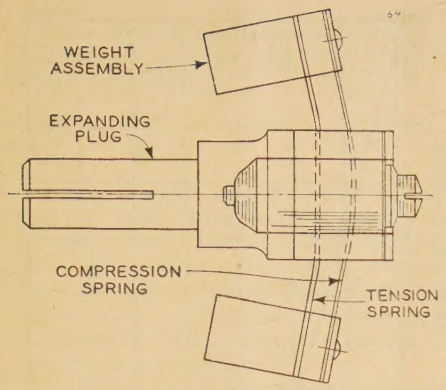

Figure 1. Rotating unit, side view of weight and spring assembly

cept a minute amount of windage and friction in transmitting a light force from the rotating assembly to the carbon pile.

While the centrifugal force varies as the square of the speed, the pressure on the carbon pile varies at a much higher rate. Just as in the case of the voltage regulator, the primary force is resisted by a spring, and the pressure on the carbon pile is a differential and may be referred to as a secondary force. Thus we may have a 10-pound thrust created by centrifugal force resisted by 9 pounds and 15 ounces from the spring and one ounce from the carbon pile. If the speed is increased one per cent, then the primary force becomes nearly 10 pounds $3^1/_4$ ounces. If constant spring tension is assumed, this means that the force applied to the carbon pile increases from 1 ounce to $4^1/_4$ ounces for a one-per-cent speed change.

For an inverter designed to operate at 8,000 rpm, for example, the governor carbon pile preferably should be subjected to not more than a light constant pressure to prevent sparking between disks until the speed is around 7,500 rpm. The pressure on the pile, as stated previously, should have its maximum rate of change at very close to the desired operating speed. In order to provide some shunt field for starting and accelerating, the carbon pile may have a light initial pressure provided by a spring, or have a fixed resistor connected in parallel with it, or both.

Description of Rotating Assembly

The physical construction of the governor may be explained in orderly manner by starting with the part which attaches to the motor shaft and proceeding outward. At the left in Figure 1 is seen a split expanding plug which is placed in a hole in the motor shaft. There is a screw which enters a tapered thread in the plug for tightening. In order to make this screw accessible, the rotating yoke separates from the plug by removing two screws. When in place, the yoke is held in concentric position by a pilot which enters a counterbore in the head of the plug.

The yoke carries a flat tension spring which lies substantially in a plane perpendicular to the axis. This spring carries a weight at each end in the position shown by Figure 1. The weights are riveted not only to the tension spring but also to the ends of a compression or arch spring. The latter is parallel to the tension spring and spaced from it by small separator blocks through which the weight rivets pass. The centers of gravity of the weights are on the inboard or plug side of the tension spring. The centrifugal force created by the rotating weights combines with a centripetal force in the tension spring to form a couple. This couple is balanced by a radial force in the arch spring acting as a column plus an additional component of force in the tension

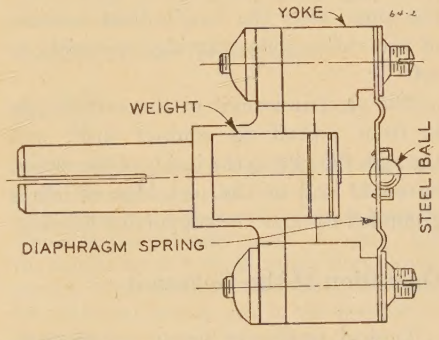

Figure 2. Rotating unit, rotated 90 degrees from view of Figure 1

spring. This simple balancing of radial forces is approximate only, as it is complicated by bending of the tension spring and the additional couples developed by the bending of the restrained ends of the arch spring.

As the centrifugal force increases, the compressive force on the arch spring becomes larger, so that the latter buckles and its center moves outward. The centrifugal force actually increases more rapidly than the square of the speed, since the centers of gravity of the weights are at an increasing radius. The force which a column will support is not linear with respect to displacement of its ends. As a matter of fact it is disclosed in the appendix that after a flat spring acting as a column starts to buckle, the force is substantially constant over a wide range of deflection. Also lateral displacement of the center of a column is not linear with respect to displacement of its ends. The net result is that the curve of displacement of the center of the arch spring plotted against speed with the latter on the horizontal axis is concave upward for a considerable distance. (dy/dS increases rapidly with S where y and S are the two quantities just mentioned.) As speed continues to increase, the arch spring comes in contact with the steel ball, which in turn presses against the stationary carbon-pile assembly. Thus there is a more or less abrupt stop to the change in configuration of the rotating weight and spring assembly resulting from increasing speed.

Also mounted on the rotating yoke is a third thin spring in a plane parallel to the tension spring but with its length at right angles to it (Figure 2). For convenience this may be called a diaphragm spring. It is attached rigidly to the yoke at its ends by eyelet rivets.

This diaphragm spring has two transverse corrugations near its ends so that it can stretch in length. Its center is required to move only a few thousandths of an inch, and it is made to be as flexible as possible consistent with maintaining concentricity of the small hardened steel ball which it carries in its center. This ball is held in a hole in the diaphragm which is cut after the diaphragm spring is assembled on the yoke and while the latter is rotating. This procedure provides the maximum assurance that the hole for the ball will be on the center line of rotation.

Figure 3 is a view of the rotating unit from the end having the steel ball.

The final operation in manufacturing the rotating unit is to drill a small hole in each weight as needed, more or less like a balancing operation, to insure that the arch spring will make contact with the ball at a speed just slightly below the operating point. The steel ball rotates without slip and transmits axial thrust from the arch spring to the contact button

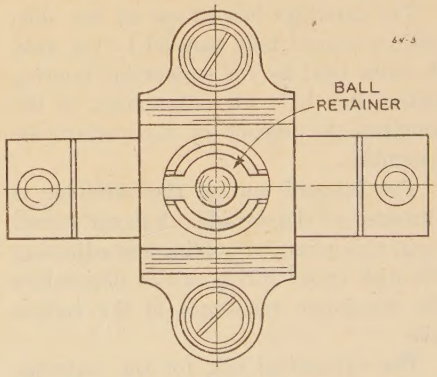

Figure 3. Rotating unit, view from outboard end

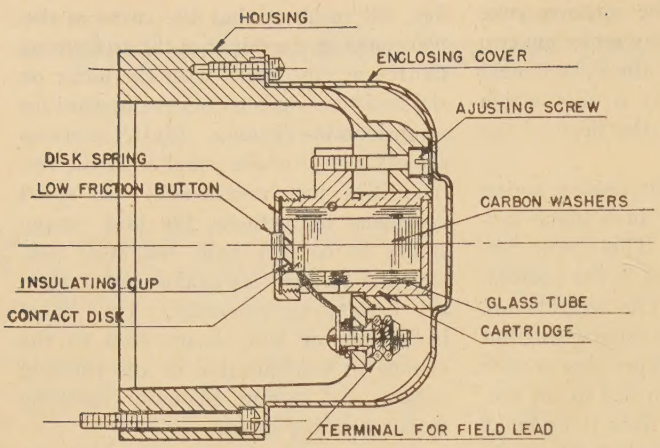

Figure 4. Stationary unit assembly, in section

of the carbon pile. This construction makes it possible to preset the governor quite closely by bringing the stationary unit up to a point where it is just touching the ball.

Description of Stationary Assembly

Proceeding from the inboard end outwardly as before, there is a small button of low-friction self-lubricating material (Figure 4) with which the rotating ball makes contact. The contact surface initially is flat and perpendicular to the axis so that no particular care in alignment is necessary. This low-friction contact button is not of hard material, and a small dimple appears from operation, since point contact is not possible in transmitting thrust.

The contact button is held by a cup made of insulating material capable of withstanding high temperature. Back of this cup is a contact disk to which is fastened a flexible pigtail attaching to a terminal for connection of the motor field lead.

The contact disk is held lightly against the pile of carbon washers by a small radial fingered disk spring, bearing against the insulating cup. A stack of carbon washers approximately one inch long is held in place by a glass tube placed inside a metal cartridge.

The cartridge has an ear on one side, with a tapped hole parallel to the axis. A screw held by the supporting housing enters this hole for adjustment of the longitudinal position of the carbon-pile assembly.

The inboard end of the cartridge is threaded on the outside. A flange screws on at this point, for holding and adjusting the disk finger spring, which determines the maximum resistance of the carbon pile.

The cylindrical hole for the cartridge in the supporting housing has a radial slot or split with transverse screw for

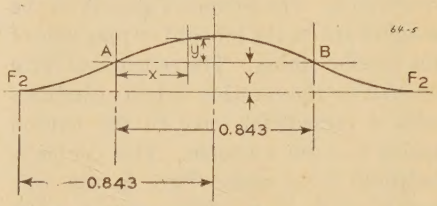

Figure 5. Curve assumed by arch spring in compression

clamping, after the longitudinal position of the carbon-pile cartridge assembly is set.

The electric circuit of the carbon pile is from pigtail to contact disk, and through the pile to the inside of the closed outboard end of the cartridge which is grounded through the supporting housing.

Operation of the Governor

Typical resistance versus speed characteristic is shown by the curve of Figure 6. In normal operation the resistance range is from one to 30 ohms.

The permissible voltage across the pile is about 20 volts maximum.

Maximum watt dissipation is of the order of 25 watts, but this figure is subject to modification, depending upon the individual application requirements, ambient conditions, and ventilation provided. Limiting ratings have not been definitely fixed at this time inasmuch as life-test data under a variety of conditions have not been accumulated.

Appendix. Calculations for the Rotating Weight–Spring Assembly

Centrifugal force is given by

$$F_1 = M(2\pi N)^2 R$$

where

M = weight in pounds divided by 32.16
N = revolutions per second
R = radius in feet

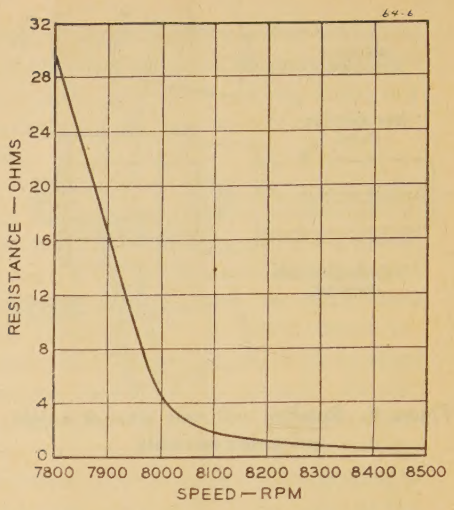

Figure 6. Typical curve of governor characteristic showing resistance versus speed, for one adjustment and a particular set of carbon rings

The total weight at each end of the spring assembly is 0.0356 pound. The center of gravity is at a radius of 0.843 inch from the center of rotation. At 7,500 rpm where the arch spring just starts to push the steel ball, the centrifugal force will be

$$F_1 = \frac{0.0356}{32.16}\left(2\pi\frac{7{,}500}{60}\right)^2\frac{0.843}{12} = 48 \text{ pounds}$$

The center of gravity of the weight assembly is at a distance of 0.162 inch from the center line of the tension spring. Thus the couple about the latter due to centifugal force is

$48 \times 0.162 = 7.75$ pound-inches

This is balanced by the couple due to compressive force in the arch spring F_2 with a lever arm of 0.137 inch (center-to-center distance between the two springs) plus the couple due to the bending at the ends of the arch spring.

In order to determine the bending moment in the arch spring, the curve of Figure 5 is referred to. A and B are points of counterflexure, with zero bending moment. The moment at the ends and the middle is $F_2 Y$ where $2Y$ is total deflection.

$F_2 Y + 0.137 F_2 = 7.75$ pound-inches

whence

$$F_2 = \frac{7.75}{Y + 0.137} \qquad (1)$$

The curve from A to B is a sine curve, and is the same as that of a column with ends free to turn, having length AB and supporting the load F_2. Incidentally, each half of the total curve is symmetrical so that the part from A to the center if rotated 180 degrees about A would coincide with the part from A to the left end.

Euler's formula for a column of length L and with free ends indicates that the column will fail if the load is

$$F_2 = \frac{\pi^2 EI}{L^2} \qquad (2)$$

For a steel spring having dimensions of 0.010 by 0.5 by 0.843 inch, the moment of inertia I would be

$$\frac{0.5}{12}0.01^3=\frac{10^{-6}}{24}$$

If E is 30×10^6, then EI would be 1.25, and the limiting load would be about $17^1/_2$ pounds. Actual test on a steel spring of these dimensions resulted in a measured force of 21 pounds maximum, which was substantially constant over a wide range of deflection and up to the point where the spring took a permanent set.

In Euler's derivation of maximum loading for a column the shape of the curve formed by a column with free ends is given as

$$y=C_1 \sin x\sqrt{\frac{F_2}{EI}} \tag{3}$$

where x and y are co-ordinates of the curve with x measured along the length of the column.

From equation 2, this is found to be equivalent to

$$y=C_1 \sin \frac{x}{L}\pi \tag{4}$$

The constant C_1 is the maximum deflection Y; and, as indicated, this is indeterminate inasmuch as the force F_2 is practically constant for a wide range of deflection.

It is interesting to note in passing that an oil-burner pump has been developed and patented utilizing the "Euler-column" spring acting on a piston. The oil pressure resulting is substantially constant for a considerable piston travel, eliminating the need for a by-pass pressure regulator.

An approximation of column deflection may be obtained by using the formula for maximum deflection of a simple beam supported at the two ends and with load in the center.

$$Y=\frac{WL^3}{48\,EI} \tag{5}$$

It will be assumed that the beam has the same dimensions as the column, and that the bending moment at the center of each is the same.

The bending moment at the center of the arch spring is F_2Y. The bending moment at the center of a beam with center load W, length L, and with supports at the free ends, is $1/4\ WL$. Equating these two moments, the beam load is found to be

$$W=\frac{4F_2Y}{L} \tag{6}$$

If L is 0.843 inch, this results in

$$W=4.75F_2Y \tag{7}$$

From equations 5 and 7,

$$Y=\frac{4.75F_2Y\ 0.843^3}{48\,EI} \tag{8}$$

Formula 8 reveals two things:

1. Since the deflection of a simple beam is directly proportional to the load W, which in turn was assumed proportional to the existing bending moment and a direct function of the deflection, F_2 is again shown to be a constant.

2. This formula indicates F_2 to be about 21 pounds, which checks the experimental result more closely than does Euler.

Formula 8 can be rewritten as

$$F_2=\frac{12EI}{L^2} \tag{9}$$

This gives a larger value for F_2 than the Euler formula by the ratio of 12 to π^2. Thus there is the choice of the Euler formula which is theoretically more accurate, and the simple beam formula which more closely checks experimental observation, at least for the actual spring used in the governor in question.

If F_2 is taken as 21 pounds, and substituted in formula 1, the total deflection $2Y$ is seen to be 0.466 inch, at 7,500 rpm. This is more than permitted by the physical construction of the rotating unit before the arch spring touches the steel ball. In production, the weights are drilled until the desired deflection is obtained. In other words, the initial construction provides for overtravel, so that the units can be adjusted individually by removing weight.

In operation, the resisting pressure from the carbon pile acting through the contact button and the steel ball limits the deflection of the arch spring after contact is made. Thus the compression-spring column action is effective at low speeds, but, as speed increases above the point where contact is made with the carbon pile, the further deflection of the arch spring is a matter of a few thousandths of an inch. It may be assumed that at operating speeds differentials in centrifugal force will be reflected solely in change in carbon-pile pressure as all other forces or moments are substantially constant.

Recapitulation of Symbols Used

F_1 = centrifugal force
F_2 = compressive force on arch spring
M = mass of weight assembly on one side of rotating unit, in pounds divided by 32.16
N = revolutions per second
S = revolutions per minute
R = radius from center of rotation to center of gravity of weight assembly
x = distance measured along arch spring, from point A to point B, Figure 5
y = deflection of arch spring at any point x
Y = maximum deflection, measured from center of line AB
E = modulus of elasticity
I = moment of inertia
L = length of column, in this case = AB
W = load in center of beam, in pounds

The Measurement of Large Varying Currents

A. C. JOHNSON
ASSOCIATE AIEE

IN OSCILLOGRAPHIC STUDIES where it is necessary to measure current in the range of from 5 to 100 kiloamperes, one must often resort to the use of shunts, because

1. Addition of a current transformer may materially change the impedance of the circuit.
2. Current transformers for large currents are unwieldy.
3. The current may be pulsating direct current which would saturate a current transformer and render it useless.

It is extremely important that the shunts used be carefully designed and so connected into the circuit that the measuring-circuit current is proportional to and in phase with the shunt current. There follows an analysis and a basis for the design of shunts for measuring these currents, so that there will be no voltage induced in the measuring circuit for any of the frequencies or harmonic components normally encountered in the measuring of currents of these magnitudes. Consequently, the measuring-circuit current will be a function only of a shunt current and the ratio of the resistance of the shunt to that of the measuring circuit.

Physical Arrangement

The shunts discussed herein are cylindrical in shape because of the resultant simplification of the mathematical analysis and the relative ease of fabrication which that geometry affords. It is generally desirable that the shunt be hollow so that the wall thickness can be made less than the skin depth at the rates of change of currents involved. Since it may be desirable to water-cool the shunts, there is an additional advantage in using a hollow cylinder.

The current which flows in the measuring circuit is a function, not only of the points of connection to the shunt, but also of the geometry of the leads from the point of connection to the indicating or recording instrument.

There are four limiting geometries of measuring-circuit leads which are possible. These are shown in Figure 1. For the purpose of calculation in this paper, the shunt is assumed to consist of part of a long straight conductor, and the return conductor is assumed to be sufficiently far away as not to affect the field of the shunt current. Thus, the current produces a symmetrical field about the shunt. If this is not the case, the actual flux distribution and the voltage induced in the leads can be calculated, but the process will be somewhat laborious. With the best arrangement (this will be shown later to be that illustrated in Figure 1D), the error resulting from the false assumption that the shunt is part of an infinitely long straight conductor is negligible. If the leads are connected as in Figure 1A, that is, parallel to each other and perpendicular to the axis of the shunt for sufficient distance so as to be effectively out of its field, the voltage across the measuring circuit will be the actual voltage between the planes perpendicular to the axis of the shunt at the points of connection of the measuring circuit.

Figure 1B is another case of Figure 1A where the distance s is considerably smaller (in practice this would be as small as physical limitations would permit). For both of these arrangements, the measuring-circuit current is shown in the appendix to be

$$i_m = i_s \frac{R_s}{R_m} - \frac{3.19l}{2\pi R_m 10^8} \frac{di_s}{dt}\left[\frac{1-3b^2}{4(1-b^2)} + \frac{b^4}{(1-b^2)^2} \ln\frac{1}{b} + \ln\frac{1}{c}\right] \quad (1)$$

where

i_m = the measuring circuit current in amperes
i_s = shunt current in amperes
l = effective length of shunt between potential connections in inches
R_s = effective resistance of shunt in ohms
R_m = resistance of measuring circuit in ohms
$c = s/r_1$
s = distance from the axis of the shunt to the point where measuring-circuit wire is parallel to the axis of the shunt
r_1 = outside radius of the shunt
r_0 = inside radius of the shunt
$b = r_0/r_1$

If we let

$$q\phi = \frac{1-3b^2}{4(1-b^2)} + \frac{b^4}{(1-b^2)^2} \ln\frac{1}{b} + \ln\frac{1}{c} \quad (2)$$

$q\phi$ is a function only of ratios s/r_1 and r_0/r_1 and has been plotted as a function of these ratios in Figure 2.

The measuring-circuit current then becomes

$$i_m = i_s \frac{R_s}{R_m} - \frac{3.19l}{2\pi 10^8 R_m} \frac{di_s}{dt} q\phi \quad (3)$$

If measuring-circuit leads are connected as in Figure 1C, the net voltage induced in the measuring circuit is the difference between the voltage induced in a wire in the center of the shunt and the voltage induced in the shunt itself.

The current in the measuring circuit is shown in the appendix to be

$$i_m = i_s \frac{R_s}{R_m} + \frac{3.19l}{2\pi 10^8 R_m} \frac{di_s}{dt}\left[\frac{1}{2} - \frac{b^2}{1-b^2} \ln\frac{1}{b} - \frac{1-3b^2}{4(1-b^2)} - \frac{b^4}{(1-b^2)^2} \ln\frac{1}{b}\right] \quad (4)$$

or

$$i_m = i_s \frac{R_s}{R_m} + \frac{3.19}{2\pi R_m 10^8} \frac{di_s}{dt} q\phi \quad (5)$$

where

$$q\phi = \left[\frac{1}{2} - \frac{b^2}{1-b^2} \ln\frac{1}{b} - \frac{1-3b^2}{4(1-b^2)} - \frac{b^4}{(1-b^2)^2} \ln\frac{1}{b}\right] \quad (6)$$

$q\phi$ is a function only of b and is also plotted in Figure 2.

Figure 3 is an oscillographic illustration of an exaggerated case of type of shunt connection in Figures 1A, B, and C. The measurements were made using a hollow copper pipe as a shunt and the shunt measurement compared to the current as measured by a current transformer. It is obvious that, with the geometry of the measuring circuit as in Figures 1A and B, the measuring-circuit current lags behind the main current. If the shunt connection in Figure 1C is used, the measuring-circuit current leads the main current. This is also apparent from equations 1 and 4. It is evident that by using some intermediate geometry the number of flux linkages can be so controlled as to result in no net induced voltage in the whole measuring circuit (including the shunt as part of the measuring circuit). Consequently, the only voltage is that due to

Paper 46-2, recommended by the AIEE committee on instruments and measurements for presentation at the AIEE winter convention, New York, N. Y., January 21–25, 1946. Manuscript submitted September 7, 1945; made available for printing October 9, 1945.

A. C. JOHNSON is electrical engineer with the Edward G. Budd Manufacturing Company, Philadelphia, Pa.

The author expresses his appreciation for the guidance and co-operation given by C. A. Adams, the assistance of H. D. VanSciver, and the sponsorship of the E. G. Budd Manufacturing Company.

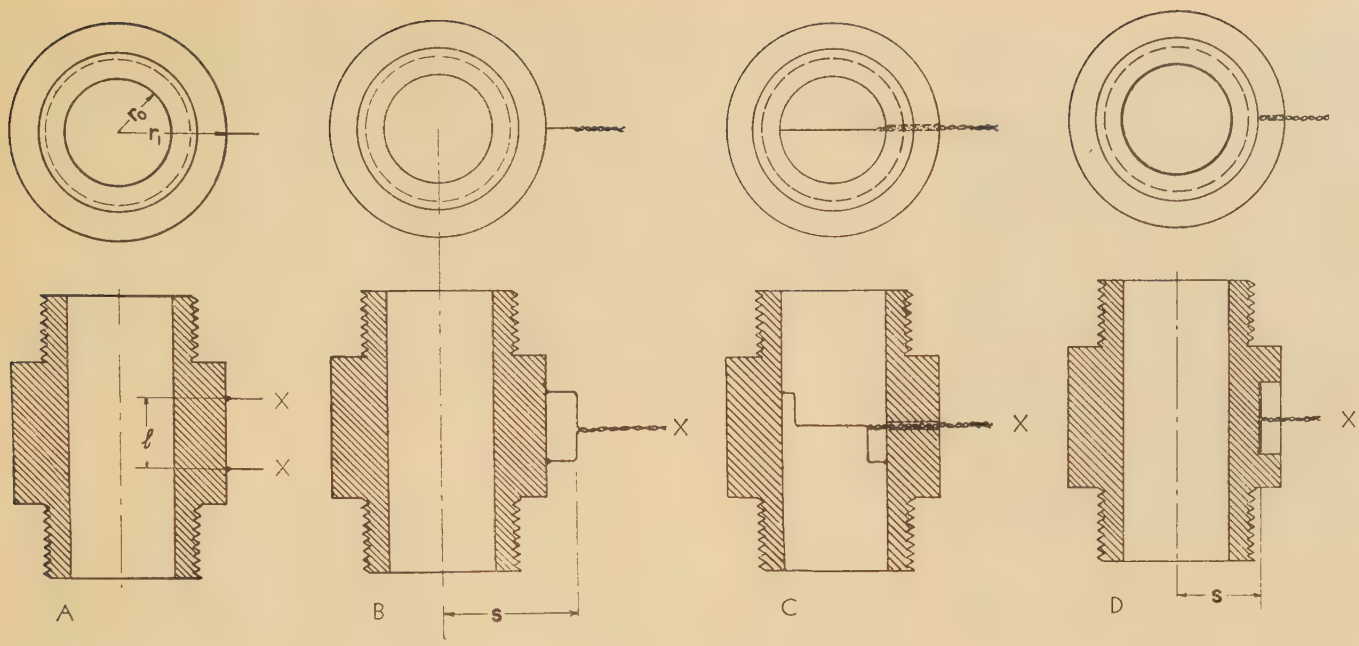

Figure 1. Various arrangements of measuring-circuit leads

By properly locating the leads the measuring-circuit current can be made to be proportional to the shunt resistance voltage at every instant

X—To measuring circuit

the IR drop in the shunt. The measuring-circuit current will therefore be proportional to the shunt current at every instant, for all rates of change of current for which the current density can be assumed to be approximately uniform.

If the measuring circuit is arranged as in Figure 1D, the measuring circuit current is

$$i_m = i_s \frac{R_s}{R_m} - \frac{3.19l\,di_s}{2\pi 10^8 R_m\,dt}\left[\frac{1-3b^2}{4(1-b^2)} + \frac{b^4}{(1-b^2)^2}\ln\frac{1}{b} - \frac{a^2-b^2}{2a^2(1-b^2)} + \frac{b^2}{1-b^2}\ln\frac{a}{b}\right] \quad (7)$$

By setting equal to zero that part of equation 7 which emanates from induced voltage, it is possible to obtain a geometry in terms of the ratios r_0/r_1 and s/r_1 which will result in a balance of flux linkages so that the induced voltages are canceled. The relationships between the ratios a, b, and c and the magnitude of the permeance factors are shown in Figure 4. The values of these ratios necessary to make the permeance factors and hence the induced voltages equal to zero are given in Figures 5 and 6.

For these geometries for which there is no net induced voltage, the measuring-circuit current obviously will be proportional to the shunt current. It is well to keep in mind that these equations are based on the assumption of a uniform current density across the section of the shunt. This assumption is valid only if the wall thickness is less than the skin depth at the greatest rate of change to be encountered. For rates of change for which this is not true, the tendency will be for more of the flux to link with the measuring-circuit wire embedded in the shunt, and the shunt will approach the condition of Figure 1C. This arrangement itself is reasonably good and produces an almost negligible error insofar as induced voltage is concerned, as is shown by the oscillograms in Figure 7. Under these conditions, the effective resistance of the shunt will not be constant. It is advisable, however, to locate the measuring-circuit wires as near as possible to the ideal position, since this will result in the most accurate shunt and also does not require that the measuring wires enter the hollow center of the shunt with the consequential difficulty of getting the wires out and keeping the water in.

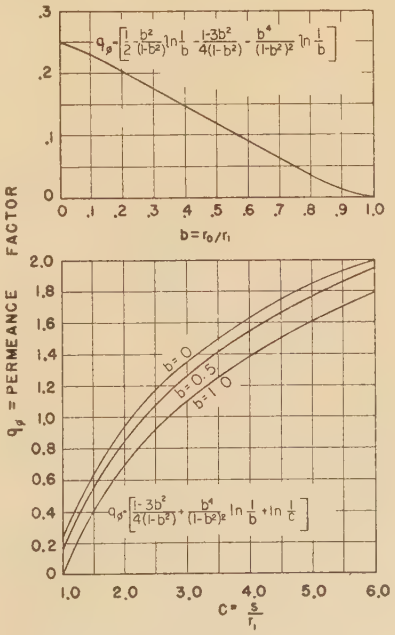

Figure 2. Permeance factors for shunts A and B

See equations 1 and 6

Thermal Considerations

It is generally advisable to water-cool shunts of the type described herein. Such shunts are usually used on low-voltage circuits, and the only precaution necessary is that rubber hose be used for the water connections to the shunt. The heat generated in the shunt is $60I^2R/1{,}055$ Btu per minute where R is not the effective resistance of the shunt between potential connections, but the entire terminal to terminal resistance. The heat removed will be 8.35 Btu per gallon per degree Fahrenheit water temperature rise. The dissipation to air and to the connected conductors can be neglected. If the shunt is to be used for the measurements of impulses, as for example for the measurement of spot-welding currents, it may not be necessary to water-cool it, unless it is part of a production set up. If t is the duration of the impulse (seconds), the heat generated will be $I^2Rt/1{,}055$ Btu. If we assume that no heat is dissipated, the temperature rise will be

$$\Delta\theta = \frac{I^2Rt}{1{,}055wc} \quad (8)$$

where

w = weight of the shunt in pounds

c = thermal capacity of shunt material in British thermal units per pound per degree Fahrenheit

If the shunt is to be air cooled and used continuously, the rate of heat dissipation to the surrounding air can be safely assumed to be approximately 0.005 watt per OC per square inch of exposed surface.

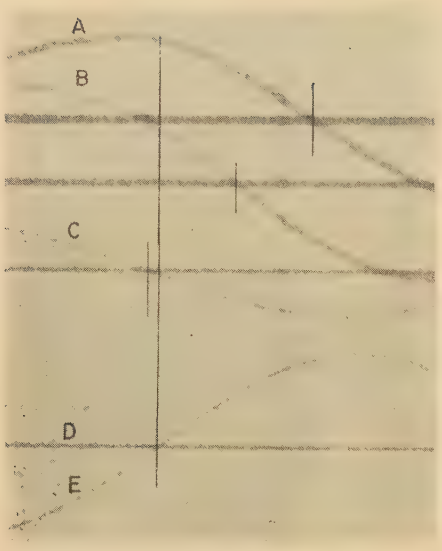

Figure 3. Oscillogram of measuring-circuit currents for different arrangements of potential leads

Traces *D* and *E* are current-transformer secondary currents. Trace *C* corresponds to shunt type *C* and leads the shunt current. Traces *A* and *B* correspond to shunt type *A* and *B* and lag the shunt current

Figure 5. Geometries for which permeance factor in equation 7 is zero

For the geometries corresponding to these ratios the measuring-circuit current is proportional to the shunt current at each instant

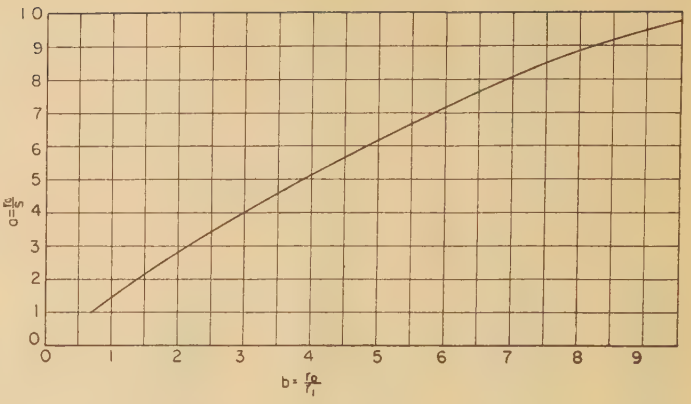

Figure 6. Geometries for which permeance factor in equation 7 is zero

For the geometries corresponding to these ratios the measuring-circuit current is proportional to the shunt current at each instant

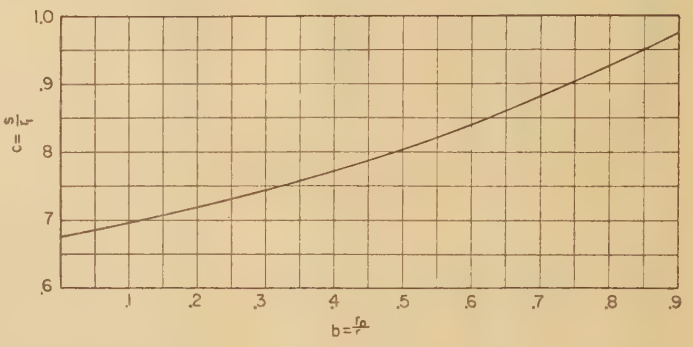

Conclusions

It is theoretically and practically possible to construct shunts for the measurement of large varying currents, so that measuring-circuit current is proportional to the shunt current at each instant. The author has successfully used such shunts for measurement where rates of change of the order of 2×10^8 amperes per second were involved.

The simplest form for these shunts is that of a hollow cylinder which may or may not be water cooled depending upon the type of service to which it is to be put.

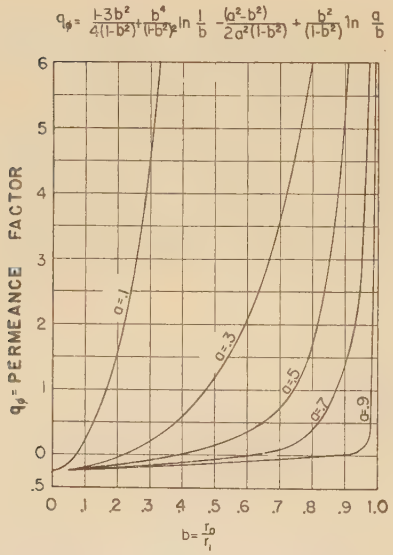

Figure 4. Permeance factor for equation 7 as a function of the ratios a, b, and c, corresponding to shunt *D*

Appendix

Calculation of Measuring-Circuit Current for Shunts A and B

The shunt is assumed to be part of a long straight conductor. The total voltage induced in the shunt per inch length is (see Figure 1B)

$$e_s'' = -L_1''\frac{di_s}{dt} - L_2''\frac{di_s}{dt} - L_3''\frac{di_s}{dt} - L_4''\frac{di_s}{dt} \tag{9}$$

where

L_1'' = that part of the inductance of the shunt due to the linkage of flux within the radius r_1, with the shunt current i_s

L_2'' = that part of the inductance due to the linkage of flux between $r=r$, and $r=s$, with the shunt current

L_3'' = that part of the inductance due to the linkage of flux outside of $r=s$

L_4'' = that part of the inductance due to the linkage of flux produced by the current I_s in the return conductor, with the current in the shunt

The voltage $L_3''(di_s/dt)$ is induced in both the shunt and the measuring-circuit wire, and cancels when voltages are added around the measuring circuit.

If d is large, the voltage $L_4''(di_s/dt)$ also is induced in the shunt and measuring-circuit wire, and hence also cancels.

$L_1'' = \psi''/10^8$ where ψ'' is the flux linkage per ampere-inch.

The flux $d\phi_1$ in an increment, dr in thickness, at a radius r inside the radius r_1 is

$$d\phi'' = \frac{3.19}{2\pi} i_s \int_{r_0}^{r_1} i_1 \frac{dr}{r} \tag{10}$$

where i_1 is the ratio of the current inside the radius r, to the total current i_s, the flux per ampere is

$$\frac{d\phi''}{i_s} = \frac{3.19}{2\pi}\int^{r_1} i_1\frac{dr}{r} \tag{11}$$

and the flux linkage per ampere is

$$i_1\frac{d\phi''}{i_s} = d\psi'' = \frac{3.19}{2\pi}\int i_1^2\frac{dr}{r} \tag{12}$$

If we assume that the current density is uniform throughout the conductor cross section,

$$i_1 = \frac{r^2 - r_0^2}{r_1^2 - r_0^2}$$

then

$$\psi'' = \frac{3.19}{2\pi}\left[\frac{1-3b^2}{4(1-b)^2} + \frac{b^4}{(1-b^2)^2}\ln\frac{1}{b}\right] \tag{13}$$

where

$b = r_0/r_1$

since

$$L_1'' = \frac{\psi_1''}{10^8}$$

therefore

$$L_1'' = \frac{3.19}{2\pi 10^8}\left[\frac{1-3b^2}{4(1-b^2)} + \frac{b^4}{(1-b^2)^2}\ln\frac{1}{b}\right] \text{henrys} \tag{14}$$

The same analysis will yield L_2. Since all of the current produces and is linked by the flux, $i_2 = 1$, hence

$$\psi_2'' = \frac{3.19}{2\pi}\int_{r_1}^{s}\frac{dr}{r} = \frac{3.19}{2\pi}\ln\frac{s}{r_1} \tag{15}$$

and

$$L_2'' = \frac{3.19}{2\pi 10^8}\ln c \tag{16}$$

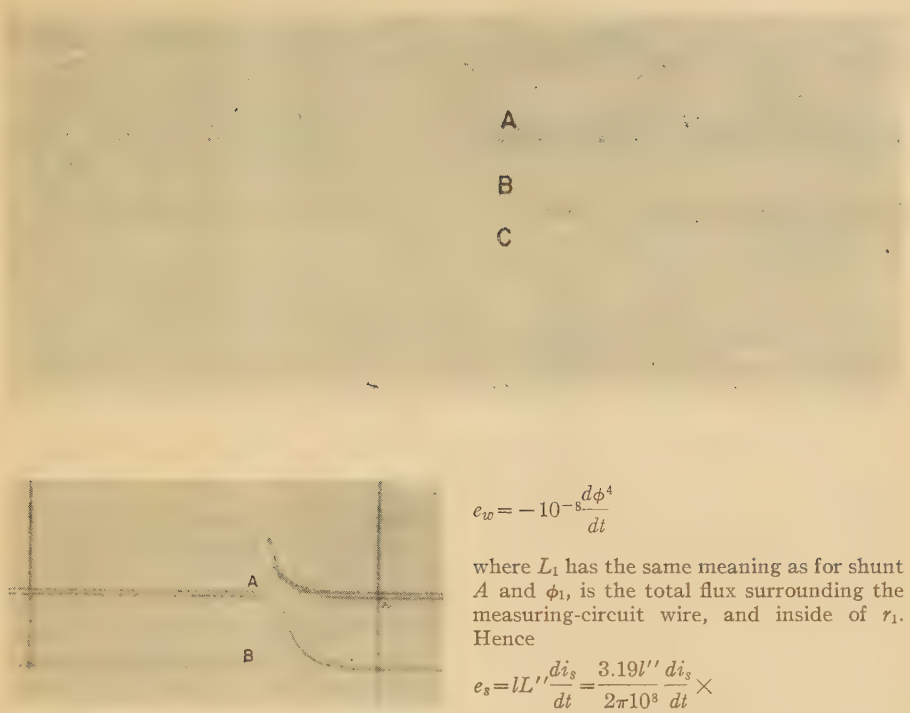

Figure 7. Oscillograms of the same current

Traces *A* show currents in measuring circuit of shunt *B*. Traces *B* show currents in measuring circuit of shunt *D*. Trace *C* is current-transformer secondary current. The capacitor discharge current reached a peak value of 40,000 amperes in 0.002 second

where

$$c = s/r_1$$

The voltage induced in the measuring-circuit wire per inch length is

$$e_w'' = -L_3'' \frac{di_s}{dt} - L_4'' \frac{di_s}{dt} \qquad (17)$$

if the field of the measuring-circuit current is neglected. The sum of the voltage drops in the measuring circuit is

$$-i_s R_s - e_s + e_w + i_m R_m = 0$$

$$i_m = i_s \frac{R_s}{R_m} + \frac{e_s - e_w}{R_m} = i_s \frac{R_s}{R_m}\left[L_1 \frac{di_s}{dt} + L_2 \frac{di_s}{dt}\right]$$

$$i_m = i_s \frac{R_s}{R_m} - \frac{3.19l}{2\pi R_m 10^8} \frac{di_s}{dt} \times \left[\frac{1-3b^2}{4(1-b^2)} + \frac{b^4}{(1-b^2)^2} \ln \frac{1}{b} + \ln \frac{1}{c}\right] \qquad (18)$$

Calculation of Measuring-Circuit Current for Shunt C

In this case, all of the flux outside of r_1 links with the shunt and with the measuring-circuit wire. The voltages thus induced by this flux cancel when voltages are added around the measuring circuit. If those terms which ultimately cancel are omitted

$$e_s'' = -L_1'' \frac{di_s}{dt} \qquad (19)$$

and

$$e_w = -10^{-8} \frac{d\phi^4}{dt}$$

where L_1 has the same meaning as for shunt A and ϕ_1, is the total flux surrounding the measuring-circuit wire, and inside of r_1. Hence

$$e_s = lL'' \frac{di_s}{dt} = \frac{3.19l''}{2\pi 10^8} \frac{di_s}{dt} \times \left[\frac{1-3b^2}{4(1-b^2)} + \frac{b^4}{(1-b^2)^2} \ln \frac{1}{b}\right]$$

$$\phi_1'' = \frac{3.19}{2\pi} i_s \int_{r_0}^{r_1} i_1 \frac{dr}{r} = \frac{3.19}{2\pi} i_s \int_{r_0}^{r_1} \frac{r^2 - r_0^2}{r_1^2 - r_0^2} \frac{dr}{r}$$

$$= 3.19 i_s \left[\frac{1}{2} - \frac{r_0^2}{r_1^2 - r_0^2} \ln \frac{r_1}{r_0}\right] = \frac{3.19}{2\pi} i_s \times \left[\frac{1}{2} - \frac{b^2}{1-b^2} \ln \frac{1}{b}\right]$$

$$e_w'' = -\frac{1}{10^8} \frac{d\phi''}{dt} = -\frac{3.19}{2\pi 10^8} \frac{di_s}{dt}\left[\frac{1}{2} - \frac{b^2}{1-b^2} \ln \frac{1}{b}\right] \qquad (20)$$

If the voltage drops are added around the measuring circuit,

$$i_s R_s + i_m R_m - e_s + e_w = 0$$

$$i_m = i_s \frac{R_s}{R_m} + \frac{3.19l}{2\pi 10^8 R_m} \frac{di_s}{dt} \times \left[\frac{1}{2} - \frac{b^2}{1-b^2} \ln \frac{1}{b} - \frac{1-3b^2}{4(1-b^2)} - \frac{b^4}{(1-b^2)^2} \ln \frac{1}{b}\right] \qquad (21)$$

Calculation of Measuring-Circuit Current for Shunt D

The correction factors for induced voltage in the final equations for i_m for shunts A, B, and C have been arranged so that the absolute value of the correction is positive. Since these correction factors appear in the two equations with opposite signs, it is reasonable to expect that for some intermediate geometry the correction factor will be zero. Hence, if the measuring-circuit wire is placed in a slot in the wall of the shunt, the depth of the slot can be determined by finding the equation for the measuring-circuit current, and setting the correction factor equal to zero. As before, if we omit those terms which produce canceling voltages:

$$e_s'' = -\frac{3.19}{2\pi R_m 10^8} \frac{di_s}{dt}\left[\frac{1-3b^2}{4(1-b^2)} + \frac{b^4}{(1-b^2)^2} \ln \frac{1}{b}\right]$$

The voltage e_w induced in the measuring-circuit wire is due to the flux between s and r_1.

The flux $d\phi_2$ in the increment r is produced by all of the current inside radius s plus that current between s and r: that is, by all of the current inside radius r. This currentis $i_s i_1$ where $i_1 = (r^2 - r_0^2)(r_1^2 - r_0^2)$

$$\phi'' = \frac{3.19}{2\pi} i_s \int_s^{r_1} i_1 \frac{dr}{r}$$

$$= \frac{3.19}{2\pi} i_s \int_s^{r_1} \frac{r^2 - s_0^2}{r_1^2 - r_0^2} \frac{dr}{r}$$

$$= \frac{3.19}{2\pi} i_s \left[\left(\frac{r_1^2 - s^2}{r_1^2 - r_0^2}\right)\frac{1}{2} - \frac{r_0^2}{r_1^2 - r_0^2} \ln \frac{r_1}{s}\right] \qquad (22)$$

If we let $r_0/r_1 = b$ and $r_0/s = a$,

$$\phi'' = \frac{3.19}{2\pi} i_s \left[\frac{1}{2}\left(\frac{a^2 - b^2}{1-b^2}\right)\frac{1}{a^2} - \frac{b^2}{1-b^2} \ln \frac{a}{b}\right]$$

$$e_w' = -\frac{1}{10^8} \frac{d\phi}{dt} = -\frac{3.19l}{2\pi 10^8} \frac{di_s}{dt} \times \left[\frac{a^2 - b^2}{2a^2(1-b^2)} - \frac{b^2}{1-b^2} \ln \frac{a}{b}\right]$$

$$i_m = i_s \frac{R_s}{R_m} - \frac{3.19l}{2\pi 10^8} \frac{di_s}{dt} \times \left[\frac{1-3b^2}{4(1-b^2)} + \frac{b^4}{(1-b^2)^2} \ln \frac{1}{b} - \frac{a^2 - b^2}{2a^2(1-b^2)} + \frac{b^2}{1-b^2} \ln \frac{a}{b}\right] \qquad (23)$$

In order to find the correct position of the measuring-circuit wire, set

$$\left[\frac{1-3b^2}{4(1-b^2)} + \frac{b^4}{(1-b^2)} \ln \frac{1}{b} - \frac{a^2 - b^2}{2a^2(1-b^2)} + \frac{b^2}{1-b^2} \ln \frac{a}{b}\right] = 0 \qquad (24)$$

Since this equation is not analytically soluble the permeance factor

$$\left[\frac{1-3b^2}{4(1-b^2)} + \frac{b^4}{(1-b^2)} \ln \frac{1}{b} - \frac{a^2 - b^2}{2a^2(1-b^2)} + \frac{b^2}{1-b^2} \ln \frac{a}{b}\right] \qquad (25)$$

has been plotted in Figure 4 against b for different values of a. As expected, there is a value of b for each value of a which makes the expression and hence the induced voltage equal to zero. The values of a or c which will result in zero correction are plotted in Figures 5 and 6 against b.

Hence, for ratios as determined from these two curves,

$$i_m = i_s \frac{R_s}{R_m} \qquad (26)$$

which is the desired relationship for any shunt. This relationship is independent of frequency so long as the wall thickness is less than the skin depth. As the frequency is increased, this shunt will approach that shown in Figure 1C. Even this latter type has been used without appreciable error for measurements involving rates of change of currents of 1.8×10^8 amperes per second.

Basic Design Principles for A-C Electric-Power Systems in Large Military Aircraft

C. K. CHAPPUIS
MEMBER AIEE

LEONARD M. OLMSTED
MEMBER AIEE

THE ELECTRIC LOADS of early aircraft were small and the electric systems resembled those commonly used in automobiles. As the design of aircraft progressed, however, additional demands upon the electric system exceeded the capacity of the 14-volt d-c system, and a 28-volt d-c system was developed. Continued increases in electrical demands were met by increased generator ratings and parallel operation of generators at 28 volts direct current. As loads and aircraft sizes increased, the 28-volt d-c system became increasingly heavy to the point where it was obvious that a more economical generating and distributing system would be required.

Two methods of attaining increased electrical capacity were selected as having promise. The 115-volt d-c system was proposed and incorporated into a large cargo airplane. Owing to the limited development personnel available, there has not been sufficient work on this system to obtain complete information on its potentialities. However, it would appear that the anticipated difficulties of commutation and switching of higher direct voltages at high altitudes may not be so serious as anticipated and that switching may actually be somewhat improved. The second method was based on the fact that a similar distribution problem had been solved many years ago by the utilities with the 115/200-volt three-phase system and it seemed reasonable to consider a similar system for several large aircraft.[1,2]

The commercial frequency of 60 cycles proved undesirable, because it limited three-phase motor speeds to 3,600 rpm and required excessive weight in the rotating equipment. Motor speeds up to 10,000 rpm already had proved desirable and analyses indicated the optimum frequency for motor designs to be at least 250 cycles. Similar analyses of electronic equipment indicated an optimum frequency of approximately 800 cycles. The selection of 400 cycles for aircraft is a compromise between these considerations, giving a choice of 6,000, 8,000, 12,000, and 24,000 rpm for motor speeds and falling between the optimum values for motor design and electronic-equipment design.

The use of single-phase and three-phase variable-frequency alternating current has been proposed for power supply to certain electronic equipment, and some installations have been made. Frequency varying over the range involved in main-engine-driven alternators cannot be considered satisfactory for motor operation, however, unless accompanied by a compensating change in voltage which cannot be tolerated by the constant-voltage electronic equipment. Likewise, it does not satisfy the requirement of certain navigation and servo devices for fixed frequency. The principle reason for considering variable-frequency alternating current has been the difficulties in developing satisfactory constant-speed drives at minimum weight.

Certain radio, navigation, radar, radar countermeasure, and similar equipment already in service operates on 115-volt single-phase 400-cycle power supply. This power is supplied on present d-c aircraft by use of inverters, which are heavy and extremely inefficient with over-all weight of 50 to 60 pounds per kilovolt-ampere of 400-cycle output. The proposed 115/200-volt system permits this type of load to be supplied single phase, from the three-phase system, without conversion, or such equipment can be redesigned to operate three phase, within certain limitations, at lesser weights or increased performance.

A review of the electric systems in use or proposed for military aircraft includes the following:

1. 14-volt direct current.
2. 28-volt direct current.
3. 115-volt direct current.
4. 115/200-volt three-phase 400-cycle alternating current.
5. 115/200-volt three-phase variable-frequency alternating current.
6. 115-volt single-phase variable-frequency alternating current.
7. 115-volt single-phase 400-cycle alternating current.

Certain of these systems are not complete in themselves but must be used in combination with others. This paper applies specifically to the design of 115/200-volt three-phase 400-cycle systems for large aircraft, although some portions may be applicable to several of the other systems.

Basic A-C System Design Requirements

The electric system must provide the utmost possible reliability in order that the aircraft may retain maximum effectiveness on its missions as well as the ability to return to its base in spite of damage. The reliability for the conditions of aircraft operation must compare favorably with the reliability of public power systems, with the exception that the expected life for aircraft equipment is 500 to 1,000 hours, instead of 15 to 25 years as in utility requirements. All of this must be accomplished with a minimum of weight. The generating and distribution system must retain its ability to supply satisfactory power to the using equipment as long as that equipment is capable of operation. From this it is apparent that such equipment as motors must remain on the line until the motor has reached a temperature beyond which immediate and permanent damage will occur. In order to supply power to all equipment until this point is reached, it is necessary to insure that the distribution and circuit protection system shall not fail earlier. This requires temperature-actuated protective devices built into the using equipment and system protection co-ordinated to avoid cutting off power to any load still in operating condition.

It is considered necessary to have at least one alternator and preferably two, as stand-by power. This is due not only to possible failure of an alternator but also to expected incidence of engine failures on long flights. The most effective use of the system requires parallel operation for best voltage and frequency regulation, which also makes available the maximum stand-by power with the least attention from the flight personnel. Since the equipment developed for three-phase 400-cycle aircraft electric systems is untried and had to be designed, built, and tested in a comparatively short period

Paper 46-3, recommended by the AIEE committee on air transportation for presentation at the AIEE winter convention, New York, N. Y., January 21–25, 1946. Manuscript submitted August 27, 1945; made available for printing October 16, 1945.

C. K. CHAPPUIS is a major with the Matériel Division, Office of Assistant Chief of Air Staff, United States Army Air Forces, Washington, D. C. LEONARD M. OLMSTED is special consultant, Air Technical Service Command, Wright Field, Dayton, Ohio.

The authors acknowledge the assistance of officers and personnel of the Army Air Force, Air Technical Service Command Engineering Division, equipment laboratory, in securing factual data, and the co-operation of aircraft and electric-equipment manufacturers in determining operating characteristics of equipment.

of time, it is felt that parallel operation cannot be guaranteed. Certainly during combat conditions it is impossible to insure that battle damage will not prevent parallel operation of alternators. Therefore, the system must be so designed that isolated operation is feasible even though not the desired operating condition. The main-power panel is somewhat complicated by this requirement, as circuit breakers are necessary to sectionalize the ring bus and load-transfer switches may be required to balance the loads for satisfactory isolated operation.

Good voltage control is essential, as many of the load devices require substantially normal voltage for satisfactory operation and life. Voltage control is accomplished at present by use of a conventional aircraft carbon-pile regulator actuated by rectified a-c system voltage and controlling the exciter field. The alternator is rated 120/208 volts and with the regulator is capable of regulation within ±2 per cent at its terminals. The excitation of the alternator will go from no load to ceiling current in approximately 0.1 second including regulator time. The system is normally considered as a 115/200-volt system inasmuch as this is approximately the normal full-load voltage at the main-power panel; the motors are designed for this voltage ±10 per cent. Design calculations indicate that with 75 per cent of the transmission capacity available and with the largest motor in locked-rotor condition, the voltage will not drop below 115/200 volts on the main-power panel and 90 per cent of this value at the most distant load bus. Thus it is apparent that the system regulation is satisfactory for motor operation. Electronic equipment, which includes radio and radar, is in a different classification as to voltage regulation requirements. Most radio equipment within the medium-, high-, and very high-frequency bands will operate satisfactorily with ±5 per cent voltage regulation. However, present radar equipment requires ±2 per cent regulation for satisfactory operation, and this problem is now being thoroughly investigated so that the characteristics of radar requirements and power supply can be reconciled.

It was necessary to develop new meters[14] inasmuch as no aircraft systems of this type were in use and consequently no suitable meters were available which were sufficiently light in weight and sufficiently reliable for the conditions of temperature and altitude encountered in aircraft operation. Wattmeters presented a design problem, but this has been solved satisfactorily, and the same meter is used to measure vars by means of a selector switch. Hermetically sealed meters would be a great improvement.

The distribution system serving this equipment likewise required extensive design effort in order that it might meet the difficult requirements of reliability, light weight, and voltage regulation. Commercial 120/208-volt systems are largely of the network type, with numerous feeding transformers located adjacent to the more concentrated loads to convert from the high-voltage primary system to utilization voltage. This type of system definitely requires parallel operation of power sources with strong ties to control the sharing of the load. It was obvious that such a system could not be used until successful parallel operation of alternators had been accomplished; attention was directed to developing an alternative type of system which would retain as many of the advantages as possible and still permit sectionalized operation from power sources out of parallel.

Operation of the system must require a minimum of attention by the flight crew. Many functions may be made automatic or partially so, and these portions of the system which are installed in multiple can be arranged to protect themselves. Every effort must be exercised to provide a system which will require the least possible specialized training for crew personnel.

Maintenance requirements must be simple enough to be handled with a minimum of special equipment and without excessive specialized training of personnel. Replacements must be convenient and require the smallest possible number of new stock items.

Power Source

Two common means are available for generating the a-c power, namely:

1. Auxiliary power plant.
2. Main-engine-driven alternators.

The first method involves electrical problems generally similar to central-station practice in that the electric system determines the size and speed of the prime mover and has sufficient capacity to assist in maintaining synchronism among several such auxiliary power units operating in parallel. The second method, while complicated by the fact that the size and speed of the prime movers are regulated by aircraft propulsion requirements, had definite advantages in savings of weight and useful space, over-all fuel economy, and availability of full-power output at all altitudes from the supercharged main engines. The main engines have been selected as the preferable power source, requiring that a power take-off be provided which converts engine speeds of 700 to 3,000 rpm to a constant speed for the alternator shaft drive. Since 400-cycle alternating current will be required to start the main engines, however, an auxiliary power unit must be provided either as a ground power source or as a supplement to the aircraft electric system.

The alternators[3] are designed for high speed and forced-air cooling to secure maximum output with minimum weight. Exciters are built into the alternator frames and directly connected to the alternator field, thereby assuring excitation to the alternator, regardless of disturbances on the a-c system. Adequate

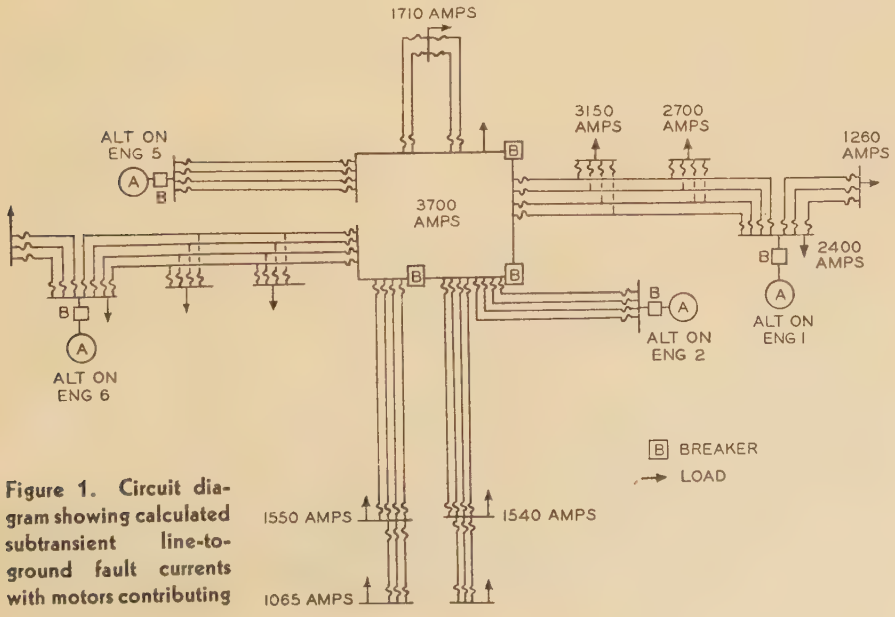

Figure 1. Circuit diagram showing calculated subtransient line-to-ground fault currents with motors contributing

capacity is provided for short overloads up to 200 per cent of rated output for five seconds without appreciable drop in terminal voltage, to facilitate the starting of large motors and the clearing of system faults. Typical characteristics of such an alternator are as follows:

Rating: 40 kva at 75-per-cent power factor, 120/208 volts, three phase
Speed: 6,000 rpm
Weight with exciter: Approximately 80 pounds

Substransient reactance $X_d'' = 0.136$ per unit
Transient reactance $X_d' = 0.191$ per unit
Synchronous reactance $X_d = 1.350$ per unit
Negative-sequence reactance $X_2 = 0.136$ per unit
Zero-sequence reactance $X_0 = 0.087$ per unit
Armature resistance (25 C) $r_a = 0.0215$ per unit
Field resistance (25 C) $r_f = 0.328$ ohm
Short-circuit time constant $T_d' = 0.01$ second
Substransient time constant $T_d'' = 0.0022$ second
D-c-component time constant $T_a = 0.002$ second
No-load rated voltage excitation = 17.6 amperes
No-load air-gap excitation = 15.6 amperes
Rated load, rated voltage excitation = 41.0 amperes
150-per-cent load, rated voltage excitation = 55.0 amperes
200-per-cent load, 203 volts excitation = 68.0 amperes
$R_1 = R_2 = R_0 = R_a$

Voltage is regulated by means of a solenoid-actuated carbon pile in the shunt field circuit of the exciter. The solenoid is connected to the 120/208-volt alternator terminals through transformers and rectifiers to measure the average of the three-phase voltages. The regulator circuit includes temperature compensation, back feed from the exciter terminals to provide antihunting features, and a connection to bias the solenoid current with reactive current.

Frequency is controlled by means of a governor in the constant-speed-drive system. This governor is actuated by alternator drive-shaft speed, biased by the electric-power output of the alternator to give a slight droop in speed at full load.[4] This characteristic permits a heavily loaded alternator momentarily to drop frequency slightly, thereby assuming an electrical angle somewhat behind other alternators carrying less load.

Parallel operation of alternators[5] requires identical shaft speeds with proper sharing of power output and reactive current. The governor itself holds reasonably uniform shaft speed, and the kilowatt sensing function of the governor control circuit tends to correct small differences in speed by introducing a slight droop in speed as load is applied to the alternator. Kilowatt division and shaft speed thus are controlled by the governor and constant-speed drive. Reactive-current division between alternators operating in parallel is controlled by the excitation; an overexcited alternator tends to supply excessive reactive current with but slight increase in system voltage, whereas an underexcited alternator shirks reactive current. Differentially connected current transformers on the alternator leads isolate the differences in distribution of reactive current, which are used to bias the voltage regulators and thereby to shift the excitation as required to correct the distribution of reactive current.

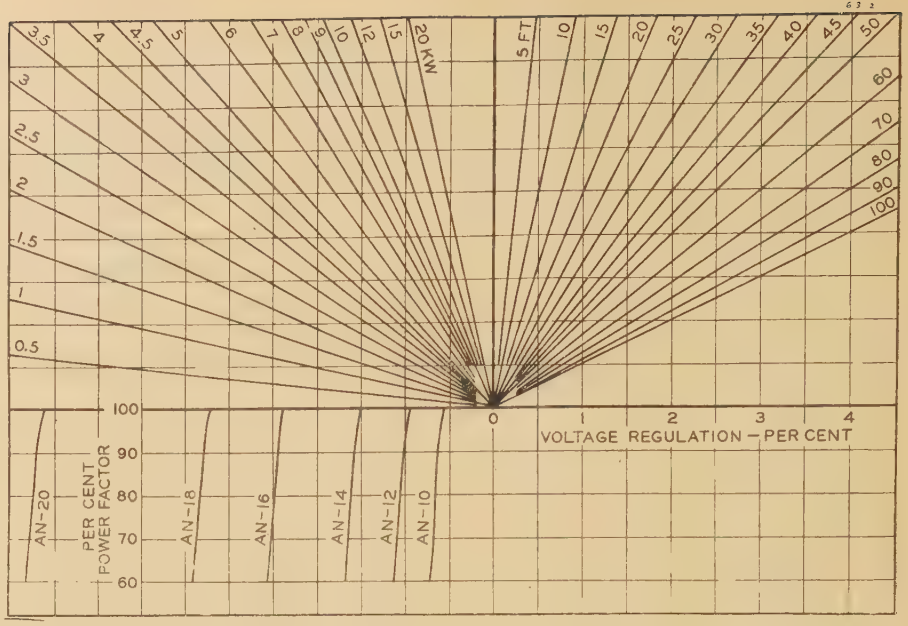

Figure 2. Voltage regulation chart—120/208 volts, 400 cycles, three phase, wires tied in close configuration

Protection in the power source is designed to isolate the power source and cut off its excitation for any of three abnormal conditions, namely:

1. Excitation at ceiling current for more than five seconds.
2. Frequency below 360 cycles.
3. Faults in the alternator armature winding or connections.

The first protects the exciter and alternator field against overheating but serves indirectly as protection for the power source against sustained heavy overload or failure to clear a fault on the system. The second protects magnetic devices on the system against excessive magnetizing currents permitted by low frequency at normal voltage. The third removes a damaged alternator from the system before the distribution system is impaired by fuse operations. This protection is accomplished by means of a ceiling-field relay actuated by the exciter field current, a frequency relay actuated by the alternator terminal voltage, and a differential relay actuated by unbalanced current in the alternator phase leads. All three relays energize the trip coil of the alternator circuit breaker which has an auxiliary contact to open the exciter field circuit. Tripping power is supplied from either rectified a-c terminal voltage or exciter armature voltage, one or the other of which can be expected to provide sufficient voltage under all normal and abnormal conditions.

Power-Distribution System

Although d-c power systems have been used on aircraft for many years, few if any data from these systems have value in a-c system design. D-c networks proposed for certain very heavy bombers have been analyzed on calculating boards, but the difference in characteristics due to the d-c generators and storage batteries makes these data inapplicable. A conference of engineers, called to discuss design requirements of the 115/200-volt three-phase 400-cycle a-c system, agreed upon the following design objectives:

1. Provide multiple power paths to all important loads as a means of protection against faulted conductors.
2. Design a system which will clear at least one fault in any section of a feeder without interruption of power to any load, unless the fault is on a load bus. The fuses adjacent to the fault shall clear the faulted section in such time that no other fuses shall lose their

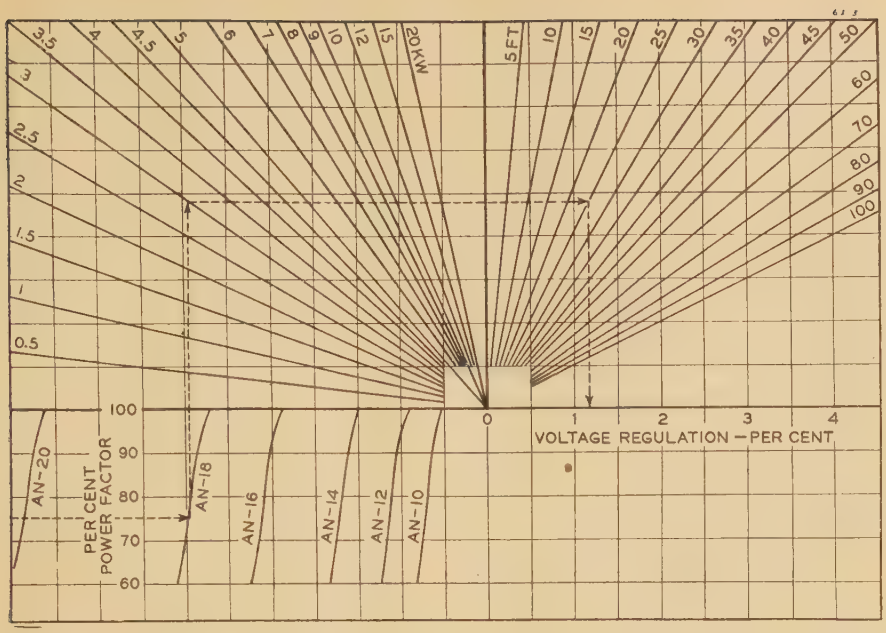

Figure 3. Voltage regulation chart—120/208 volts, 400 cycles, three phase, wires at 0.5 inch flat spacing

original ability to carry current or fail to co-ordinate in accordance with their design characteristics.

3. Be able to clear a second feeder fault in any designated load area without loss of power to the load. Damage to adjacent fuses in this case is undesirable but may be tolerated; co-ordination is essential.

4. Faults on load busses should be recognized as a secondary possibility, owing to the small area of conductor involved. Load lost should be limited to the load on the faulted bus.

5. The system should be designed to provide rapid clearing (maximum 0.1 second) to prevent motor stalling during faults with two or more alternators in parallel. Such clearing time is desirable, of course, with isolated operation but may be unattainable.

6. Any circuit must carry locked-rotor current for at least 30 seconds without damage to fuses, after the first fault has been cleared in any feeder. An exception may be necessary for motor-generator sets and hydro-pump motors.

7. Motors shall be able to start after a second fault in any feeder has been cleared.

8. Faults on the alternator terminals or the main bus should be recognized as a secondary possibility, and some means found to limit the portion of the circuit affected. Design of busses should provide mechanical features to minimize damage by gunfire.

9. The total number of fuses and range of sizes of fuses should be held as low as possible, consistent with good design.

10. The current distribution in each section, for load or fault conditions, must be balanced.

11. The system should be designed to operate in parallel or isolated. However, if the system operates isolated, the requirements of fast clearing must be somewhat relaxed.

The argument as to whether single or multiple circuits should be used depends for an answer upon the following: degree of reliability required, decrease in weight due to better cooling of smaller conductors, type of protection to be used and its weight, and characteristics of load. In general, it is found that more current can be carried in four wires than in one wire of similar weight without exceeding the maximum allowable operating temperature. Since maximum reliability is one of the prime requirements, it is necessary to provide alternate paths, so that remaining parallel circuits will operate at full efficiency after damage which isolates any one. In public power systems such reliability is obtained by a combination of loops, networks, complicated switching and protective devices, and continuous maintenance. The use of alternate paths for aircraft is feasible, provided a reliable lightweight method of insuring the continued operation of these circuits is available. It is obvious that complicated switching and protective systems, requiring balanced current, pilot wire, directional current, and similar methods of relaying which are very satisfactory for transmission lines, are in general too heavy and too complicated for aircraft. Such equipment probably would increase the vulnerability of the aircraft electric system. The use of properly balanced multiple circuits allows one of two methods to be used to clear faults. The first method is to take advantage of the small wires, allowing them to burn off and thus clear the fault. Much argument has been encountered on this method, but it appears to be rather uncertain, particularly where clearing time and co-ordination are important. The alternative is to use an accurate lightweight overcurrent device on each circuit at each bus to remove that portion of the circuit which is faulted. The most logical device of this type appears to be a small accurate high-speed fuse using a high-temperature fusing element.[6]

Radial, network, and loop circuits were examined for their applicability to large aircraft. It was found that none of these provided the most reliable, lowest weight, and best operating system. The final type of design, as shown in Figure 1, is a multiple-circuit radial system with alternators feeding to the main-power panel and also feeding loads located in the vicinity of the alternator. Thus the alternator leads to the main-power panel also serve as load feeders, and the alternator busses also serve as load busses. The output of the alternators is utilized in such a way that isolated operation is satisfactory whenever such operation is necessary. It is essential that all multiple paths between busses be equal in length, as otherwise the currents become unbalanced and make fuse co-ordination extremely difficult. One of the unbalanced loop conditions which was examined had an unbalanced current, under some fault conditions, of approximately 200 per cent which was reflected in the fuse co-ordination as an effect of 400 per cent in clearing time, owing to the I^2R effect on the fuse link. The use of combination load circuits and feeders made it mandatory to keep each alternator bus in service even though the alternator failed. The solution of this problem depends upon differential protection and high-speed breakers to remove a faulted alternator from the bus.

Three wire configurations were considered: three wires laced together, flat with one-half-inch spacing between centers, and flat with two-inch spacing between centers. The impedance of these three types was discussed by the authors in "Impedance of 400-Cycle Three-Phase Power Circuits on Large Aircraft and Its Application to Fault Current Calculations."[7] In general the impedance decreases with the decrease in separation. The ease of installation probably is increased when three wires can be placed together, but the vulnerability to gunfire and the difficulty of clearing trouble are greater. Where the wiring is easily accessible, the flat arrangement is the most satisfactory with use of one-half-inch spacing to keep the reactance low. The final decision as to wire configuration must depend upon the space available for

the installation. Voltage regulation charts are shown in Figures 2, 3, and 4.

Conductor sizes are determined by the allowable current-carrying capacities under specification *AN-J-C*-48 for a maximum ambient temperature of 160 degrees Fahrenheit. Under temperature and pressures encountered at higher altitudes, it is anticipated that wire temperatures will not exceed 100 degrees centigrade when operating at full load on the circuit and with one of the multiple paths out of service. The maximum wire size used on multiple circuits will usually be number 12 or smaller in present systems. The smallest sizes used will not be less than number 18 or number 20, owing to the mechanical weakness of smaller size.

Protection of this electric system depends upon the following: fuses, breakers, armor, and material protection. The ideal fuse characteristic for these circuits appears to be as shown by Figure 5. This is a high-speed fuse using a high-temperature link such as silver or copper to minimize the effect of differences in temperature. Owing to close co-ordination requirements the fuse must be extremely accurate, and it must also be explosion-proof with very short arcing time. The differential relays and circuit breakers used to remove any faulted alternator from the system must be extremely fast, clearing the maximum alternator bus fault in 0.02 second or less, to leave the fuses at the alternator bus intact for operation of the load circuits. In addition to this the breaker must be able to interrupt fault currents up to 4,000 rms amperes and perform all normal switching operations, up to 120 amperes, incident to operation of the aircraft. All of these operations must be performed under temperatures and altitudes required by Army Air Force specifications. Inasmuch as the requirements over wide ranges of altitude and temperature are so exacting, it is possible that development of sealed breakers may prove necessary.

Protection of the fuses, breakers, and busses can be accomplished only by mechanical means. The inherent protection of engines and heavy structural parts of the airplane can be used for part of the protection, and armor strips placed to protect vulnerable angles. The busses are so located that much natural protection is available and can be so designed structurally to minimize the possibility of battle damage by use of hollow sections of high-strength material for bus conductors.

The co-ordination of fuses and breakers is determined by the maximum fault currents, and the maximum clearing time is determined by the minimum fault current. Much research and many calculations were required to secure information on zero-sequence impedance for use in calculating line-to-ground fault currents.[7] The maximum fault currents occur from line to ground with the four alternators in parallel, and the minimum fault currents occur with three-phase faults and isolated operation. The requirement of parallel normal operation but emergency isolated operation greatly complicates the protection problem by causing a tremendous spread between maximum and minimum fault currents. The circuit arrangement and fault currents on one of these systems are shown in Figure 1. Under minimum fault-current conditions the maximum clearing time must be sufficiently small so that the rotating equipment will not stop or slow down to a point which will cause excessive reaccelerating current. The wide range of fault currents, with rigid requirements for co-ordination and fault clearing, made it necessary to design a new fuse for system protection.[6]

The alternator circuit breakers are required to co-ordinate with fuses only for failure of the alternator winding or leads; under this condition, however, co-ordination requires extremely fast differential-relay and breaker operation in order that the alternator bus fuses may remain undamaged to carry the electric load connected to that bus.[9] The same breaker, arranged for remote or manual operation, is suitable for the tie breakers on the main power bus.

The main power-panel bus is arranged as a ring bus of four sections tied with the same type of breaker as used for the alternators. By proper distribution of the load on the bus sections, it is possible to provide satisfactory load distribution for isolated operation with four alternators. By the use of two or three transfer switches, it is possible to provide acceptable load distribution for isolated operation with three alternators. Operation with two alternators whether isolated or parallel requires disconnection of some of the combat load. The load busses are so designed that the protective system can remove them from the system, in case of bus faults, without disturbance to the system. Loss of the main bus must be considered vital but sections can be lost without loss of the entire system.

Selection of the 115/200-volt three-phase 400-cycle a-c system for large aircraft permitted the use of three-phase induction motors.[10-12] Brushes and commutator problems thus were eliminated, and the motors became substantially constant-speed devices capable of reliable operation through a wide range of conditions. Momentary high torque loads can be handled by methods already established in commercial design practice. Such motors are contemplated in sizes ranging from one-eighth to 16 horsepower and speeds of 6,000 to 12,000 rpm. The few drives requiring variable speed are equipped with d-c motors supplied through motor generator sets or transformer–rectifiers. All motors are star-connected to permit emergency operation with reduced torque output after power supply to any one phase has failed, and the protective equipment must permit such operation.

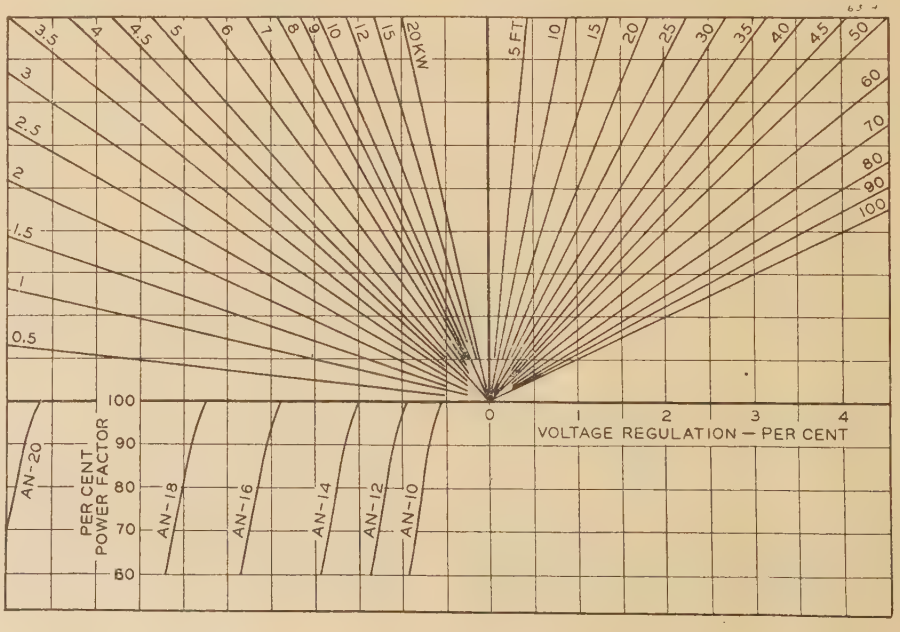

Figure 4. Voltage regulation chart—120/208 volts, 400 cycles, three phase, wires at 2.0 inches equivalent delta spacing

Provision for D-C Loads

While the major portion of the electric devices is suited to operation by a-c motors or transformers, a number of smaller devices, such as contactors and relays, solenoids, and certain instruments, still require d-c power. The connected load of these d-c devices is approximately 20 per cent of the total connected electric load of the aircraft, but many of the devices operate extremely infrequently with such diversity that their combined load probably is less than ten per cent of the total diversified load of the a-c power system. The need for this small amount of direct current adds complication to the a-c system, and there has been continuous effort to replace d-c devices with alternating current, with the ultimate objective of complete elimination of direct current from the aircraft. Under these conditions, it is expedient to install conversion equipment at the d-c load center and supply this load from the a-c system.

Both motor generator sets and transformer–rectifier sets have been built to convert the 115/200-volt three-phase alternating current to 28-volt direct current. The transformer–rectifier is quiet in operation, lighter, and somewhat more efficient than the motor generator. It has the further advantage, particularly in small ratings, of supplying acceptable voltage to relatively steady loads without the use of a voltage regulator, and thereby becomes attractive as a means of supplying the d-c load at several isolated small load centers rather than the center of the combined load.

Storage batteries appear to have little value on an electric system of this type and size. It is not practical to provide sufficient battery and conversion equipment to serve as reserve capacity for the a-c system supplying the major loads, and there is little advantage in backing up only the d-c system serving secondary loads.

Very few of the d-c loads draw enough power to require multiple circuits for carrying capacity or voltage regulation. The method is still applicable, however, to those circuits where vulnerability to damage because of length or exposure indicates the need for more than a single circuit to serve any particular device.

Future Trends

There is a continuous trend to larger electrical requirements on aircraft, and the trend is most pronounced in combat aircraft. Hydraulic lines are particularly susceptible to battle damage, inasmuch as damage to almost any part of the system may cause loss of pressure on the entire hydraulic system. Electric power for cabin supercharging would reduce air-duct requirements and weight and simplify installation of equipment. The use of electricity for propeller deicing and electric blowers to distribute heated air through small ducts at high velocities for wing and cabin deicing would reduce weight and simplify installations as well as provide positive air flow as required. Aircraft armament is increasing in size of guns and number of turrets; as flying speeds are increased, the demand for higher turret speeds and accurate split-second remote fire control is becoming more insistent; all of these add to the power requirements. With greater flying ranges and more complex tactical operations, the demand for additional communication equipment also is becoming greater. Radar and allied equipment are essential if aircraft operations are to be consistently effective in all weather conditions. Ten to 15 kva of electric power are required for radar and countermeasures equipment for special installations and are anticipated for future aircraft. Static dischargers requiring electric power are under development. The use of television to transmit information to the pilot is a distinct possibility. The all-electric airplane using electric motors to drive the propellers is within the realm of possibility. All of the "Buck Rogers" items for aircraft, control of aircraft, or against which aircraft must be defended require electric power.

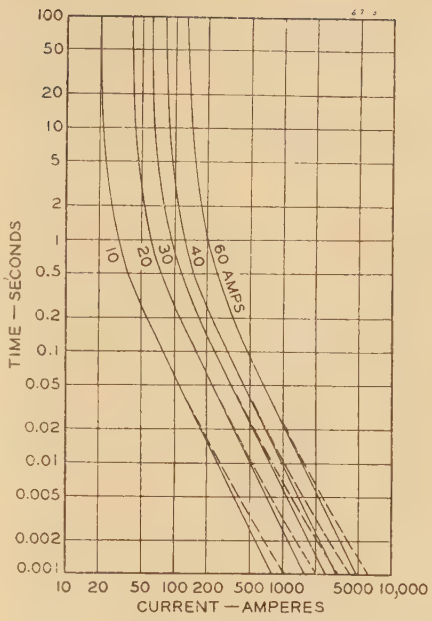

Figure 5. Time–current curve for 400-cycle 120/208-volt aircraft fuses

Solid lines—Average melting
Dashed lines—Average clearing

Any attempt to restrict the amount of electric power available to combat aircraft for these uses places the designers at a severe disadvantage. This is particularly true of electronic equipment, much of which is comparatively new. The demand for radar and countermeasure equipment is often so insistent and immediate that engineers do not have time to design it for best performance with small amounts of power. Several aircraft now under design have 120 kw of generating capacity. This capacity may be compared with public power systems, where 120 kw normally would be adequate for 100 to 125 miles of rural distribution line.

References

1. Why Tomorrow's Planes Will Have A-C Electrical Systems, **T. B. Holliday.** *Electrical Manufacturing*, July 1943, page 88.

2. Basic Considerations in Selection of Electric Systems for Large Aircraft, **W. K. Boice, L. G. Levoy, Jr.** AIEE Transactions, volume 63, 1944, June section, pages 279–87.

3. A 40-Kva 400-Cycle Aircraft Alternator, **H. E. Keneipp, C. G. Veinott.** AIEE Transactions, volume 63, 1944, November section, pages 816–21.

4. Governor Requirements for Aircraft Alternator Drives, **W. K. Boice, L. G. Levoy, Jr.** AIEE Transactions, volume 64, 1945, July section, pages 534–40.

5. Parallel Operation of Airplane Alternators, **D. W. Exner.** AIEE Transactions, volume 62, 1943, December section, pages 755–60.

6. A Current-Limiting Fuse for Aircraft Applications, **A. H. Powell.** AIEE Transactions, volume 64, 1945, July section, pages 541–5.

7. Impedance of 400-Cycle Three-Phase Power Circuits on Large Aircraft and Its Application to Fault-Current Calculations, **C. K. Chappuis, L. M. Olmsted.** AIEE Transactions, volume 63, 1944, pages 1213–20.

8. Army–Navy Aeronautical Specification—Cable; Electric, Low-Tension, Aircraft.

9. A 208/120-Volt 120-Ampere Three-Pole 400-Cycle Electrically-Operated Aircraft Circuit Breaker, **C. H. Titus, P. J. Reifschneider.** AIEE Transactions, volume 64, 1945, August section, pages 551–5.

10. Design Characteristics of 400-Cycle Aircraft Motors, **M. B. Sawyer, Sr.** AIEE Transactions, volume 63, 1944, December section, pages 877–9.

11. 400-Cycle Aircraft Motor, **G. O. Schwandt.** AIEE Transactions, volume 64, 1945, July section, pages 508–12.

12. Some Aspects of the Application of Induction Motors to Aircraft, **H. J. Braun.** AIEE Transactions, volume 63, 1944, October section, pages 769–72.

13. Alternating-Current Electrical System for Large Aircraft, Westinghouse engineers. Pamphlet *R*-1064, October 1943, Westinghouse Electric Corporation, East Pittsburgh, Pa.

14. Instrumentation of 400-Cycle Aircraft Electric Systems, **A. J. Corson, A. G. Stimson, W. A. Soley.** AIEE Transactions, volume 63, 1944, November section, pages 830–5.

Temperature Rise of Water-Cooled Power Transformers

J. R. MEADOR
MEMBER AIEE

Synopsis: This paper contains an analysis of the oil temperature rise of water-cooled power transformers. It is shown that by factoring the effect of viscosity oil temperatures can be calculated more accurately for a variety of conditions. Equations and curves are given with supporting test data for determining the temperature rise for different loads, ingoing water temperatures, and rates of water flow. The variations in temperature rise with load, water rate, and water temperature are appreciably different from published data on the subject. A discussion of winding hot-spot temperature is included, although no new test data are given.

WATER-COOLED transformers have cooling coils located in the upper portion of the tank usually adjacent to the tank wall. Water flow through these coils carries away the heat generated in the core and windings. The top-oil temperature depends on the amount of cooling coil, the transformer losses, the water rate, and the ingoing water temperature.

As the flow of oil through the windings of a water-cooled transformer is very similar to that in a self-cooled transformer having external cooling radiators, the same general equations for winding rise over oil can be used.

The purpose of this paper is to show how the transformer-top-oil temperature varies when the load, water rate, and ingoing water temperature are changed and to give curves for estimating the effect on the winding hot-spot temperature.

General Conclusions

1. Oil temperature rise over ingoing water is not a simple function of the loss dissipated. However, oil rise varies approximately as $(\text{loss})^{0.65}$ (see Figures 4 and 5).

2. When the water rate is changed, the oil temperature rise varies 40 per cent as much as the change in water temperature rise (see Figure 5).

3. When the water temperature is lowered, the oil temperature rise over ingoing water increases 0.75 per cent for each degree the ingoing water temperature is below 25 degrees centigrade (see Figure 4).

4. In a typical transformer the load can be increased 0.8 per cent for each degree the ingoing water temperature is below 25 degrees centigrade (see Figure 8).

In these general conclusions it is assumed that the radiation and convection losses from the tank surface are negligible. In a specific case the tank loss can be properly evaluated.

Components of Oil Temperature Rise

The heat generated in the windings and core of a water-cooled transformer is dissipated to the oil by free convection. The heated oil becomes less dense and flows upward to the top of the tank. The cooling coils in the upper portion of the tank receive heat from the oil by free convection. As the oil is cooled, it becomes more dense and flows downward and into the windings again. (A small percentage, usually 10 per cent to 20 per cent of the heat is dissipated from the tank surface.) The water flowing through the cooling coils removes the heat by forced convection and, in the process, the temperature of the water is raised. If the water temperature rise is measured carefully and the rate of flow is known, the watts loss carried away by the water can be calculated from the equation:

Watts loss = 264 × water rise, degrees centigrade × gallons per minute.

This thermal circuit is the basis for an equation of the following general form:

Top-oil temperature = ingoing water temperature
+ 1/2 water temperature rise
+ water-film drop (water to tube)
+ oil-film drop (tube to oil)
+ top-oil increment **(1)**

Each of these components is known or can be determined by test.

The top-oil increment is the difference in temperature between the top oil and the average oil surrounding the cooling coils (which is also approximately the average oil temperature in the windings). Experience has shown that in most water-cooled power transformers the top-oil increment is approximately two degrees centigrade over a wide range of conditions.

The oil-film drop, which is the local temperature difference between the cooling-tube wall and the adjacent oil, can be expressed with good accuracy by an equation of the following form:

$$\text{Oil-film drop, degrees centigrade} = K W_s^x \mu_f^y$$

where

W_s = watts per square inch outside surface of cooling coil.

μ_f = viscosity of oil, in centipoise, at average temperature of oil film. (Average film temperature is tube temperature plus one half of oil-film drop)

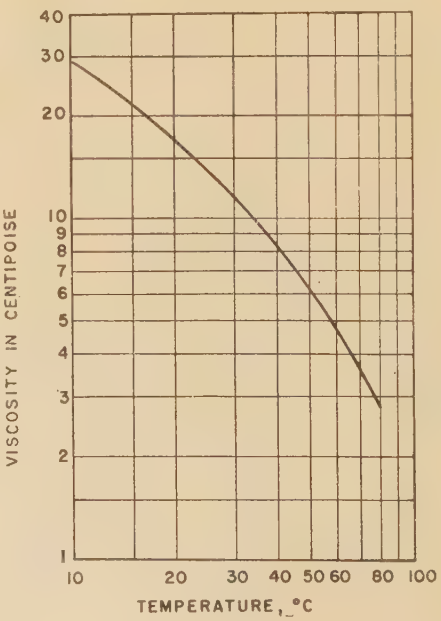

Figure 1. Viscosity of oil in test transformer

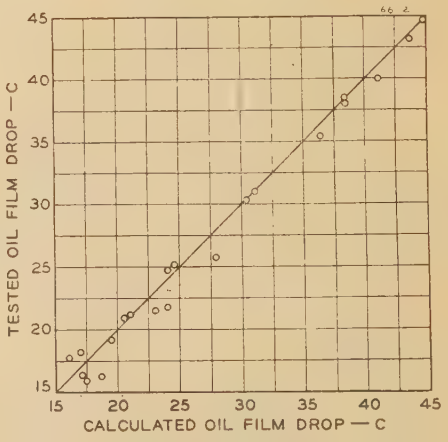

Figure 2. Comparison between calculated and tested oil-film drop

Paper 46-6, recommended by the AIEE committee on electric machinery for presentation at the AIEE winter convention, New York, N. Y., January 21–25, 1946. Manuscript submitted September 26, 1945; made available for printing October 30, 1945.

J. R. MEADOR is research engineer in the power transformer engineering division of the General Electric Company, Pittsfield, Mass.

The author acknowledges the assistance of L. Wetherill and Miss J. E. Shipton, both of the Pittsfield works of the General Electric Company in the preparation of this paper.

K = a constant
x, y = exponents to be determined

The water-film drop is the local temperature difference between the cooling-tube wall and the adjacent water flowing through the cooling coil and can be expressed with sufficient accuracy by the following equation:

$$\text{Water-film drop, degrees centigrade} = \frac{K_1 W_i^{1.0}}{V^{0.8}}$$

where

W_i = watts per square inch inside surface of cooling coil
V = water velocity in feet per second
K_1 = a constant

The water-film drop is comparatively small and can be expressed simply by $(0.37W_s^{1.0})$ in a normal power transformer.

The water temperature change enters into the equation for oil rise as water temperature rise/2. Though this is not theoretically exact, it is sufficiently accurate when the water rise is appreciably less than the oil rise. The error becomes appreciable at small loads and very low water rates.

Thus equation 1 can be written:

$$\text{Top oil temperature degrees centigrade} = \text{ingoing water temperature degrees centigrade} + {}^1/_2 \text{ water temperature rise, degrees centigrade} + 0.37W_s^{1.0} + KW_s^x\mu_f^y + 2 \text{ degrees centigrade} \quad (2)$$

The only unknowns in equation 2 are K, x, and y. These are determined from the tests given below.

Test Data

Table I contains heat-run results on a 6,000-kva water-cooled transformer with $1^3/_8$-inch-outside-diameter copper-cooling coils. The tabulated net watts loss dissipated by the cooling coils is the total loss held minus the estimated tank dissipation. This loss was varied from 21,740 watts to 75,600 watts, the water rate from four gallons per minute to 35.3 gallons per minute and the ingoing water temperature from 6.6 degrees centigrade to 40.5 degrees centigrade.

All tests were run until the top-oil rise over ingoing water was constant.

Commercial test facilities were used throughout for these heat runs with no special precautions taken to obtain laboratory accuracy.

Table I shows the calculated as well as the tested water temperature rises. The agreement is fair, usually within two degrees centigrade. In analyzing the data

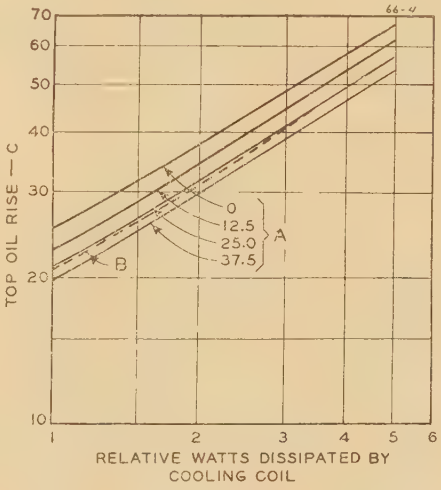

Figure 4. Effect of changing ingoing water temperature, holding ten degrees water rise

A—Ingoing water temperature, degrees centigrade
B—Design curve used since 1938 for 25-degree-centigrade ingoing water and ten-degree-centigrade water rise

averages of the calculated and tested values were used.

Analysis of Test Data

By substituting these heat-run results into equation 2, a value of oil-film drop (tube to oil) is found for each test. By analyzing these tests the unknowns K, x, and y in the oil-film-drop equation are determined. The oil in this transformer has a viscosity–temperature relationship as shown in Figure 1. Its thermal properties are essentially the same as other transformer oils used throughout the industry.

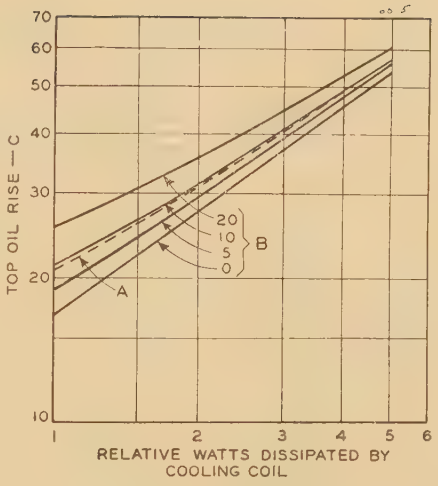

Figure 5. Effect of changing water temperature rise, holding 25 degrees ingoing water

A—Design curve used since 1938 for 25-degree-centigrade ingoing water and ten-degree-centigrade water rise
B—Water rise, degrees centigrade

$$\text{Oil film drop, degrees centigrade} = 7.4W_s^{0.88}\mu_f^{0.28} \quad (3)$$

To show that these determinations are accurate, the test values are compared with those calculated from equation 3 in Figure 2. Equation 3 is in good agreement with published data[1] on free convection in the range used in this paper.

With this factor determined the final equation for oil temperature becomes:

$$\text{Top-oil temperature, degrees centigrade} = \text{ingoing water temperature degrees centigrade} + {}^1/_2 \text{ water temperature rise, degrees centigrade} + 0.37W_s^{1.0} + 7.4W_s^{0.88}\mu_f^{0.28} + 2 \text{ degrees centigrade} \quad (4)$$

The heat-run results in Table I are

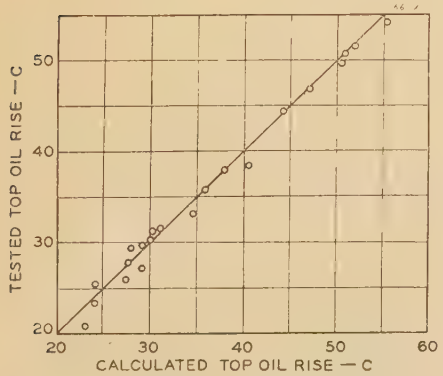

Figure 3. Comparison between calculated and tested top-oil rise over ingoing water

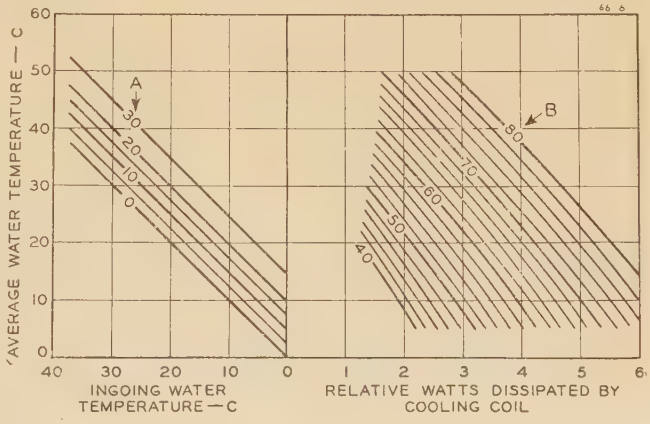

Figure 6. Effect of changing ingoing water temperature and water temperature rise on top-oil temperature

A—Water rise, degrees centigrade
B—Top-oil temperature, degrees centigrade
Water rise, degrees centigrade = watts ÷ (264 × gallons per minute)

Table I. Heat Runs on 6,000-Kva Water-Cooled Transformer

Test	Watts Dissipated by Cooling Coil	Ingoing Water Temperature, Degrees Centigrade	Water Rate, Gallons per Minute	Top-Oil Temperature, Degrees Centigrade	Water Rise, Degrees Centigrade	
					Test	Calculated*
1	59,800	24.4	35	68.7	6.5	6.5
2	61,000	24.3	20.0	71.0	10.7	11.6
3	59,800	24.8	10.0	74.4	19.5	22.6
4	62,000	6.6	35.3	57.3	6.0	6.6
5	62,000	7.5	22.5	59.0	8.8	10.4
6	60,700	7.8	10.5	61.9	19.0	21.9
7	38,000	8.1	30	43.8	3.8	4.8
8	37,900	8.1	15	46.0	9.0	9.6
9	36,200	9.6	7	48.0	17.0	19.6
10	34,500	37.0	30.0	62.9	3.9	4.4
11	31,600	37.5	15.0	65.3	8.4	8.0
12	32,100	37.7	7.5	69.2	14.0	16.1
13	30,900	40.5	7.5	70.8	14.7	15.6
14	34,000	25.0	30	54.7	4.3	4.3
15	33,300	25.5	15	56.7	6.9	8.4
16	33,500	25.0	7	58.1	14.5	18.1
17	20,300	12.0	30	32.8	0.5	2.6
18	18,800	10.8	8	34.1	8.1	8.8
19	18,900	11.1	8	36.5	8.7	8.9
20	20,100	10.8	4	37.9	14.3	19.0
21	18,800	11.6	4	40.9	16.8	17.6

*Calculated water rise = watts/(264 × gallons per minute).
The air temperature ranged from 17 degrees centigrade to 27 degrees centigrade during these tests.

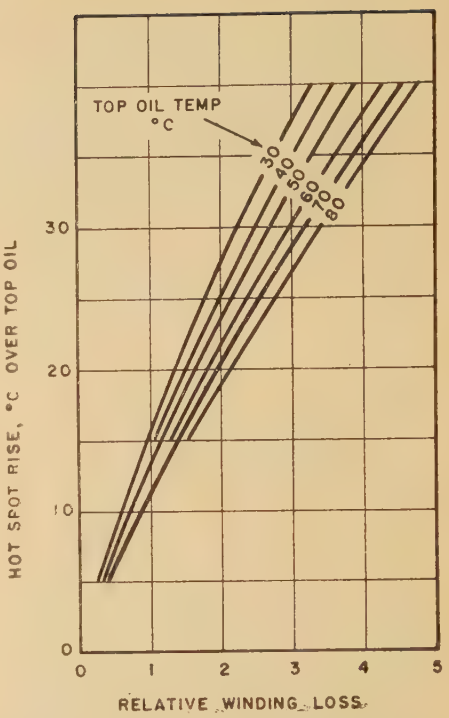

Figure 7. Winding hot-spot temperature rise over top oil as a function of winding loss and oil temperature

compared with calculations using equation 4 in Figure 3.

Curves for Top-Oil Temperature Rise

From equation 4 curves of top-oil temperature rise versus loss are plotted in Figure 4 for ingoing water temperatures from 0 degrees centigrade to 37.5 degrees centigrade, holding a constant water temperature rise of 10 degrees centigrade.

On Figure 5 similar curves are shown for water temperature rises from 0 degrees centigrade to 20 degrees centigrade, holding a constant ingoing water temperature of 25 degrees centigrade.

On both Figure 4 and Figure 5, a dotted line for 25 degrees centigrade ingoing water temperature and 10 degrees centigrade water temperature rise is plotted. This curve was derived by the author in 1938 for design use, and acceptance heat runs on dozens of transformers have shown it to be quite accurate.

In order to make these heating curves more usable by the transformer operator, the double family of curves on Figure 6 has been prepared. With these curves, if the transformer-oil temperature rise is known for any one condition of loss, water rate, and ingoing water temperature, then the temperature can be determined for any other set of conditions. As an example, for any known load and water temperature, the water rate can be predetermined to hold a specified oil temperature.

If a high degree of accuracy is required, the tank dissipation should be estimated. For each square foot of tank surface allow one watt for each degree centigrade the oil temperature is above the air temperature. For example, if the tank surface is 500 square feet and the expected oil temperature is 30 degrees centigrade above the air, the tank dissipation will be 15,000 watts. In a normal water-cooled power transformer the error in this simple calculation will affect temperature-rise calculations by less than one degree centigrade.

Winding Hot-Spot Temperature

This paper contains no new test data on winding hot-spot temperatures. It appears, however, that published information on self-cooled transformers can be used to estimate the hot-spot temperature in water-cooled transformers.

There is a wealth of information on hot-spot temperatures in self-cooled transformers in reference paper.[2] The data have to be analyzed in a somewhat different manner, however, to be used in this paper.

Reference paper 2 states that when the top-oil increment is relatively small, the winding hot-spot temperature rise over top oil varies as $(\text{loss})^{0.8}$. An examination of the tests shows this to be true if the increases in load are accompanied by an increase in oil temperature. In making normal short-time overload calculations, this relation between hot-spot rise and loss is reasonably accurate, because an increase in loss increases the oil temperature. To use these data for other conditions of top-oil temperature variation, the hot-spot temperature rise must be given a viscosity correction. Since the hot-spot rise over top oil is largely an oil-film drop, such a correction should be legitimate.

After analyzing the test data in reference paper 2 and other data on oil-film drop, the writer has come to the conclusion that hot-spot rise over top oil can be

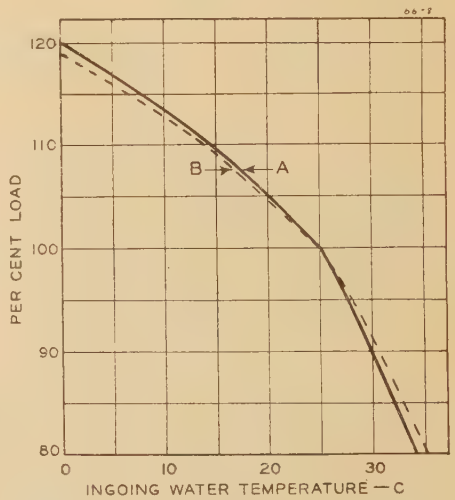

Figure 8. Effect of ingoing water temperature on permissible load, keeping constant hot-spot temperature

At 100 per cent load:
Water temperature = 25 degrees centigrade
Water rise = 10 degrees centigrade
Top-oil temperature = 69 degrees centigrade
Hot-spot temperature = 90 degrees centigrade
Loss ratio = 2:1

A—For constant water rise
B—For constant water rate

expressed approximately by the following equation:

$$\text{Hot spot over top oil, degrees centigrade} = K_2 L^{0.9} \mu_f^{0.3} \quad (5)$$

where

K_2 = a constant depending on the winding dimensions
L = winding loss in watts
μ_f = oil viscosity at film temperature in centipoise

The data supporting this conclusion are as follows.

1. The oil-film drop on the water-cooling coil was found to vary as $(\text{loss})^{0.88}$ and $(\text{viscosity})^{0.28}$.

2. Plate-to-oil tests shown in reference paper 3 can be correlated accurately by assuming the oil-film drop to vary as $(\text{loss})^{0.9}$ and $(\text{viscosity})^{0.4}$.

3. The hot-spot data from the three transformers tested in reference paper 2 can be correlated in a similar fashion. Taking only those conditions having a relatively low top-oil increment and assuming the hot-spot rise to be an oil film drop gives the following relations:

Transformer	Oil-Film-Drop Correlation
H-60-2,000 kva	$(L)^{0.9}(\mu_f)^{0.12}$
H-60-2,500 kva	$(L)^{0.9}(\mu_f)^{0.46}$
OAP-60-3,125 kva	$(L)^{0.9}(\mu_f)^{0.25}$

When all of the foregoing was taken into consideration, the use of $(\text{loss})^{0.9}$ and $(\text{viscosity})^{0.3}$ seemed to be the best average to use until more reliable data are available. From study of other unpublished data the author believes the use of these exponents for overload calculations will give conservative results.

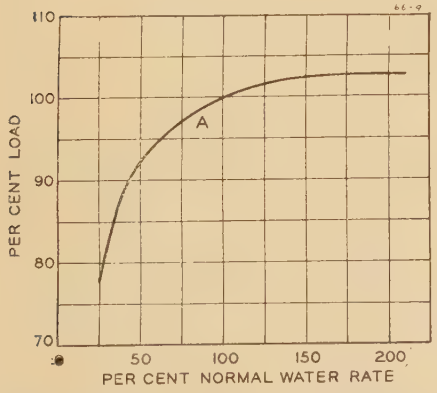

Figure 9. Effect of water rate on permissible load, keeping constant hot-spot temperature

At 100 per cent load:
Water temperature = 25 degrees centigrade
Water rise = 10 degrees centigrade
Top-oil temperature = 69 degrees centigrade
Hot-spot temperature = 90 degrees centigrade
Loss ratio = 2:1
A—For 25-degree-centigrade ingoing water temperature

This viscosity effect is particularly important for calculating permissible continuous overloads at reduced ambient temperatures. Under this condition as the load goes up the oil temperature comes down. Thus, on overloads the oil viscosity is higher than at normal load in standard ambient. The effect is to increase the hot-spot over top oil as approximately $(\text{loss})^{1.0}$. This is fortunate since turn insulation and other solid insulation temperature drops also increase as $(\text{loss})^{1.0}$.

To facilitate calculation, a family of curves has been plotted on Figure 7 showing hot-spot variation with winding loss and oil temperature as plotted from equation 5.

Permissible Loading When Water Temperature and Water Rate Are Changed

By the use of the curves in this paper, the effect of changing the water rate and the ingoing water temperature on a typical water-cooled transformer can be calculated. Assume that a transformer has the following characteristics at 100 per cent load:

Ingoing water temperature = 25 degrees centigrade
Water temperature rise = 10 degrees centigrade
Hot-spot temperature = 90 degrees centigrade
Top-oil temperature = 69 degrees centigrade
Loss ratio = 2:1

By using Figure 6 and Figure 7 the permissible loads that can be carried by this transformer with other ingoing water temperatures are shown on Figure 8. One curve is for a constant water rate, and the other applies if the water rate is changed with load to maintain ten degrees centigrade water rise at all times. It is interesting to note that very little is gained by increasing the water rate at the higher loads. For either condition the load can be increased approximately 0.8 per cent for each degree centigrade the water temperature is under 25 degrees centigrade and should be reduced approximately two per cent for each degree centigrade the water temperature is above 25 degrees centigrade.

Similarly, Figure 9 shows how the load can be varied, if the water rate is changed, holding constant ingoing water temperatures.

Figures 8 and 9 are drawn on the basis of maintaining a constant winding hot-spot temperature except for loads less than 100 per cent, where the top oil temperature is kept constant on account of the core temperature being the limiting factor.

Discussion

Incrustations in the cooling coil will increase the temperature difference between the water and the cooling coil by adding a scale temperature drop and consequently will increase the oil temperature.

It is apparent from the foregoing that the viscosity of the oil is a very important factor in water-cooled transformer calculations. If the oil in a transformer does not have a viscosity–temperature relation similar to that shown in Figure 1, the curves given in this paper will not apply. In general, however, an appreciable difference will be noted only when the ingoing water temperature is low.

Additional test data must be obtained to permit a more precise calculation of winding hot-spot temperatures in water-cooled transformers. However, with the small difference in temperature between top oil and average oil that exists in most water-cooled transformers, hot-spot temperatures are usually not a problem to the designer. This is in contrast to some self-cooled transformers that have top-oil increments of as much as ten degrees centigrade, or even more where the average winding rise must be reduced to meet the hot-spot limit.

Even in a water-cooled transformer, where the oil encounters very little friction in its path of flow, the top-oil increment may be five degrees centigrade or six degrees centigrade instead of two degrees centigrade, if the oil level is only a small distance above the core and coils or if the cooling coil extends down too far along the core and coils. For these cases the curves in this paper still can be used with little error to estimate the effect of changing load, water temperature, and water rate. (The designer must know how much the oil temperature will increase to be sure that the hot-spot-temperature limit is not exceeded.)

References

1. The Basic Laws and Data of Heat Transmission, W. J. King. *Mechanical Engineering*, March–August 1932.

2. Emergency Overloading of Air-Cooled Oil-Immersed Power Transformers by Hot-Spot Temperatures, V. M. Montsinger, P. M. Ketchum. AIEE Transactions, volume 61, 1942, pages 906–16.

3. Transformer Engineering (book), L. F. Blume, A. Boyajian, G. Camilli, and V. M. Montsinger. John Wiley and Sons, Inc., New York, N. Y., 1938. Page 314.

Formulas for Conductor Size According to Cost of Resistance Loss

HERBERT B. DWIGHT
FELLOW AIEE

IN DESIGNING an electric-power line the choice of conductor depends on several factors such as mechanical strength, corona loss, reactance, and resistance. In the early years of electric-power transmission and distribution, a size of conductor was chosen which was considered the best in view of all the requirements. At present so many different types of line conductors are available that each feature can be provided for almost independently. Thus, a core of steel or bronze may be specified to provide the required mechanical strength; a hollow conductor may be chosen to avoid corona and to reduce the reactance; and the resistance, that is the current density, may be chosen according to the cost of resistance loss or according to temperature rise.

In this paper are described formulas by which the conductor size, usually expressed by the number of circular mils, can be computed conveniently according to the cost of resistance losses.

The effect of the cost of resistance loss is such that in most cases where one is choosing a conductor for a power circuit that is to be built there is a certain current density at peak load that should not be exceeded.

The cases are divided into two classes which are markedly different. Where the conductors are owned by the company which generates the power, conditions at peak load are predominant. On the other hand, where the losses in the conductor are paid for by the kilowatt-hour, a careful determination must be made of the ratio of the yearly average resistance loss to the maximum. This ratio may be very low on some branch circuits which may go practically unused for extended periods. In spite of the difference between the two classes, the same formulas may be used for both.

Where the conductors are owned by the power company, the problem depends almost entirely on conditions at peak load, and the work of choosing a conductor size becomes comparatively simple. After the maximum advisable current density has been determined for a given location, it can be applied quickly for almost any case that might arise, and the length of line, voltage, and so forth, need not affect directly the choice of conductor cross section. After the maximum current density for uninsulated conductors has been determined, it is a simple rule to state that in specifying new conductors of that type at any voltage, this current density should not be exceeded unless there is an exceptional case.

The simplest case will be taken up first, and details arising from various items will be added later.

Let

C = circular mils of a bare overhead copper conductor

Cubic inches of copper per 1,000 feet $= \frac{\pi}{4} C \times 10^{-6} \times 12{,}000$

Cost of copper at v dollars per pound, installed, and 0.321 pound per cubic inch is

$$0.321 \times \frac{\pi}{4} 10^{-6} \times 12{,}000 Cv = 0.00303 Cv \text{ dollars per 1,000 feet}$$

Annual fixed charge at m_1 per cent $= 0.0000303 Cvm_1$ per year

Resistance at 0.692×10^{-6} ohm per inch cube at 25 degrees centigrade $= 0.692 \times 10^{-6} \times 12{,}000 \times \frac{4}{\pi C} \times 10^6 = \frac{10{,}600}{C}$ ohms per 1,000 feet

Resistance loss at I amperes $= 10.6 \frac{I^2}{C}$ kilowatts per 1,000 feet (1)

The numerical coefficients would be different for aluminum conductors as shown by equations 13 and 14.

Let power be supplied by a water-power station and an intervening power circuit whose first cost is s dollars per kilowatt and whose annual fixed charge is m_2 per cent. Let the station be enlarged enough to supply the resistance loss. Let I be the current in the conductor at the time of peak load on the station. The fixed charge for this enlargement of the station for 1,000 feet of conductor is

$$0.106 \frac{I^2 s m_2}{C} \text{ dollars per year}$$

Total annual charge for the copper and its resistance loss is

$$M = 0.0000303\ Cvm_1 + 0.106 \frac{I^2 s m_2}{C} \text{ dollars per 1,000 feet of conductor} \quad (2)$$

The rate of change of M for a given current I, as C varies, is

$$\frac{dM}{dC} = 0.0000303\ vm_1 - 0.106 \frac{I^2 s m_2}{C^2} \quad (3)$$

As long as this is negative, it pays to increase C. The most economical size is when $dM/dC = 0$. Then

$$\frac{C^2}{I^2} = \frac{0.106}{0.0000303} \frac{sm_2}{vm_1}$$

$$\frac{C}{I} = 59 \sqrt{\frac{sm_2}{vm_1}} \text{ circular mils per ampere} \quad (4)$$

Section of conductor is

$$A = \frac{\pi}{4} C 10^{-6} \text{ square inch}$$

Most economical current density is

$$\frac{I}{A} = \frac{4 \times 10^6}{59\pi} \sqrt{\frac{vm_1}{sm_2}} = 21{,}500 \sqrt{\frac{vm_1}{sm_2}} \text{ amperes per square inch} \quad (5)$$

Thus, let

$v = 0.25$ dollar per pound, installed
$s = 150$ dollars per kilowatt
$m_1 = m_2 = 12$ per cent
temperature of conductor = 25 degrees centigrade

$$\frac{sm_2}{vm_1} = \frac{150}{0.25} = 600$$

Circular mils per ampere $= 59 \sqrt{600} = 1{,}450$ by equation 4.

Fuel Cost

Let the ratio of average resistance loss to its value at the time of peak load on the generating station be b. This is less than the load factor.

The kilowatt-hours of resistance loss per 1,000 feet of conductor per year are

$$8{,}760 \times 10.6 \frac{bI^2}{C} = 93{,}000 \frac{bI^2}{C}$$

Let the fuel cost per kilowatt-hour be g dollars.

$$\text{Annual fuel cost} = 93{,}000 \frac{bgI^2}{C}$$

Annual fixed charge on a portion of the generating station to supply the line losses $= 0.106 \frac{I^2 s m_2}{C}$ where s and m_2 have the meanings already described.

Paper 46-8, recommended by the AIEE committee on power transmission and distribution for presentation at the AIEE winter convention, New York, N. Y., January 21–25, 1946. Manuscript submitted September 15, 1945; made available for printing November 1, 1945.

HERBERT B. DWIGHT is professor of electrical machinery, Massachusetts Institute of Technology, Cambridge, Mass.

Annual charge for the conductor and its loss is

$$M = 0.0000303 Cvm_1 + \frac{I^2}{C}(0.106 sm_2 + 93{,}000 bg) \quad (6)$$

$$\frac{dM}{dC} = 0.0000303 vm_1 - \frac{I^2}{C^2}(0.106 sm_2 + 93{,}000\, bg)$$

For the most economical current density, including fuel cost,

$$\frac{C^2}{I^2} = \frac{0.106 sm_2 + 93{,}000 bg}{0.0000303 vm_1}$$

$$\frac{C}{I} = 182\sqrt{\frac{0.106 sm_2 + 93{,}000 bg}{vm_1}} \quad (7)$$

at 25 degrees centigrade.

The cost of copper, v dollars per pound, should include the cost per pound for installation and also the cost of any part of the supports whose cost varies directly with the weight of copper.

If the energy is purchased at a certain amount per kilowatt-hour, this amount is to be taken as the value of g, and in such a case s is to be taken as zero unless there is a further charge proportional to the peak or demand. In computing the saving from reduced resistance losses where a step rate is used, the lowest step should be taken as the value of g. In case of payment by the kilowatt-hour, I is to be the peak current in the conductor, and b is to be computed for peak load on the conductor instead of on the generating system.

Varying Cost Per Pound of Insulated Copper

When the cost per 1,000 feet of a given type of insulated conductor is plotted, it is found that the conductor cost does not increase so fast as the weight of copper. The insulation tends to be a rather constant part of the complete conductor.

Let the rate of increase of conductor cost be h times the rate of increase of copper. An average value of h may be about 0.75, but it may be much less for small wire sizes. It usually may be taken as one for bare transmission-line conductors.

In order to find the value of h, the cost of various sizes of insulated conductor in dollars per 1,000 feet may be plotted against the number of circular mils of copper and a smooth curve drawn through the points. This curve usually is fairly straight. Suppose, for example, that two points which give the slope of the curve at a desired part of the range are \$150 per 1,000 feet for 100,000 circular mils and \$210 per 1,000 feet for 150,000 circular mils. The percentage increase in cost is $60/150 \times 100 = 40$ per cent, and the percentage increase in the copper is 50 per cent. Then $h = 40/50 = 0.8$ for this example.

Since equation 3 gives the rate of increase in cost with change of copper section, the factor h applies to the first term of equation 3 but not to the second. Thus equation 4 becomes

$$\frac{C}{I} = 59\sqrt{\frac{sm_2}{hvm_1}} \quad (8)$$

and equation 5 becomes

$$\frac{I}{A} = 21{,}500\sqrt{\frac{hvm_1}{sm_2}} \quad (9)$$

for water-power systems.

Similarly, for insulated copper conductors, equation 7 becomes

$$\frac{C}{I} = 182\sqrt{\frac{0.106 sm_2 + 93{,}000 bg}{hvm_1}}$$

circular mils per ampere (10)

The current density is given by

$$\frac{I}{A} = 7{,}000\sqrt{\frac{hvm_1}{0.106 sm_2 + 93{,}000 bg}}$$

amperes per square inch (11)

Formulas 6, 10, and 11 are the only ones that need to be put on record for copper conductors, as with bare conductors h may be put equal to one and in appropriate cases g, the fuel cost, may be put equal to zero. Where energy is purchased by the kilowatt-hour the quantity s may be put equal to zero.

The change in resistance due to temperature or other cause is easily taken into account. For instance, where the temperature of the conductor at peak load is to be taken as 75 degrees centigrade instead of 25 degrees centigrade, the resistance will be 19 per cent higher. An inspection of the derivation shows that the numbers 0.106 and 93,000 are proportional to the resistance and will be 19 per cent higher for 75 degrees centigrade. The most economical value of C^2/I^2 will be 19 per cent larger, and that of C/I will be 9 per cent larger than given by the formulas. Similarly, if the conductors are hard drawn, the resistance will be about 2 per cent higher, and the most economical value of C/I will be 1 per cent larger.

Formulas for Aluminum Conductors

If the derivation of equation 1 is repeated for aluminum instead of for copper, the cost of aluminum at v dollars per pound installed and 0.098 pound per cubic inch is

$$0.098(\pi/4)10^{-6} \times 12{,}000\, Cv = 0.00092\, Cv$$

Cv dollars per 1,000 feet

Resistance at 1.135×10^{-6} ohm per inch cube at 25 degrees centigrade is

$$\frac{17{,}300}{C} \text{ ohms per 1,000 feet}$$

Resistance loss at I amperes $= 17.3(I^2/C)$ kilowatts per 1,000 feet

The kilowatt-hours of resistance loss per year are

$$8{,}760 \times 17.3\frac{bI^2}{C} = 152{,}000\frac{bI^2}{C}$$

The annual charge for the aluminum conductor and its resistance loss is

$$M_{(a)} = 0.0000092 Cvm_1 + \frac{I^2}{C}(0.173 sm_2 + 152{,}000 bg) \quad (12)$$

For the most economical current density

$$\frac{C^2}{I^2} = \frac{0.173 sm_2 + 152{,}000 bg}{0.0000092\, hvm_1}$$

$$\frac{C}{I} = 330\sqrt{\frac{0.173\, sm_2 + 152{,}000\, bg}{hvm_1}}$$

circular mils per ampere (13)

and

$$\frac{I}{A} = 3{,}900\sqrt{\frac{hvm_1}{0.173\, sm_2 + 152{,}000\, bg}}$$

amperes per square inch (14)

for aluminum conductors.

The steel core scarcely needs to be considered, as it may be taken to be similar to an equal weight of insulation, so far as this computation is concerned.

In cases where the generating system is not fully loaded and has no prospect of being so for some years (the ownership of the conductors being the same as that of the generating system), then the equations described in this paper should not be used, but the smallest possible conductors should be specified.

The question of how heavily a conductor should be loaded with current after it has been installed is not discussed in this paper. It is an entirely different question from that of choosing the size of a conductor that is not yet installed. After a line is built, it may be advisable to load it to a higher current density than the value for greatest economy used in an original design.

The determination of conductor size according to cost of resistance loss is particularly appropriate for overhead conductors, as the heating limit is seldom approached and there is a considerable range of resistances that can be chosen without much effect on the reactance or mechanical strength. The calculation of the most economical conductor size is simple and definite, especially where it

depends mainly on the peak value of current rather than on the kilowatt-hours of resistance loss.

List of Symbols

A = area of conductor section in square inches
b = ratio of average resistance loss to its value at the time of peak load
C = area of conductor section in circular mils
g = fuel cost in dollars per kilowatt-hour
h = ratio of increase in conductor cost to increase in conductor section
I = current in the conductor at time of peak load
M = total annual charge for a copper conductor and its resistance loss
M_a = total annual charge for an aluminum conductor and its resistance loss
m_1 = per cent, annual fixed charge on conductor
m_2 = per cent, annual fixed charge on generating system
s = first cost of generating system, dollars per kilowatt
v = cost, dollars per pound of copper or aluminum

Example 1

An example that shows clearly how losses in conductors can be balanced directly against a proportionate part of the cost of the entire generating system is that of the leads from the terminals of a water-wheel generator whose rating in amperes is 1,800 amperes. Take the following values (see list of symbols):

$I = 1{,}800$ amperes — $m_1 = m_2 = 15$
$g = o$ — $s = \$160$ per kilowatt
$h = 1$ — $v = 0.20$ dollar per pound

temperature of the annealed copper = 40 degrees centigrade at rated load current

$$hvm_1 = 0.20 \times 15 = 3.0$$

$$\frac{R_{40}}{R_{25}} = \frac{235+40}{235+25} = 1.058$$

$$1.058 \times 0.106\, sm_2 = 1.058 \times 0.106 \times 160 \times 15 = 269$$

By formula 11

$$\frac{I}{A} = 7{,}000\sqrt{\frac{3.0}{269}} = \frac{7{,}000}{\sqrt{89.7}} = \frac{7{,}000}{9.5}$$

$= 740$ amperes per square inch

$A = \frac{1{,}800}{740} = 2.43$ square inch, that is, a section of 0.4 by 6 inches may be used.

It is seen that in this example one kilowatt of extra loss in the leads, whether they are long or short, would mean a reduction by one kilowatt in the rated output of the generator and of the complete water-power plant. It is worth \$160 to eliminate one kilowatt of loss in the generator leads. Even if the leads are only 20 feet long, it is right that they should have, at least, a cross section of $A = 2.43$ square inches.

A comparison is of interest with the design that might commonly be used based on current-carrying capacity and temperature-rise limit.

A single copper strap, one-fourth by six inches, has a current-carrying capacity of 1,800 amperes at about 35 degrees centigrade rise. This is 63 per cent as much copper as the 0.4-by-6-inch size.

The annual charge per 1,000 feet of conductor is given by equation 6.

The circular mils of conductor of 2.43 square inch section are

$$C = 2.43 \times \frac{4}{\pi} \times 10^6 = 3{,}090{,}000 \text{ circular mils}$$

$$M = 0.0000303 \times 3{,}090{,}000 \times 0.20 \times 15 + \frac{1{,}800^2}{3{,}090{,}000} \times 1.058 \times 0.106 \times 160 \times 15$$

$= 281 + 281 = \$562$ per year

Note that the two terms are equal, for minimum annual charge, when $h = 1$.

The circular mils of 1/4 by 6-inch conductor are

$$\frac{1}{4} \times 6 \times \frac{4}{\pi} \times 10^6 = 1{,}910{,}000 \text{ circular mils}$$

$$M = 0.0000303 \times 1{,}910{,}000 \times 0.20 \times 15 + \frac{1{,}800^2}{1{,}910{,}000} \times 1.058 \times 0.106 \times 160 \times 15$$

$= 174 + 456 = \$630$ per year

This is 12 per cent greater than the minimum, \$562. Besides saving 12 per cent in annual charges, the heavy size of copper has the advantages of lower temperature and less reactance.

As in other cases of this application of Kelvin's law, to specify heavier conductors at improved economy does not necessarily mean a larger investment by power companies which have plant extensions in prospect. The matter is a choice in engineering design, whether a certain fraction of the investment be made in conductors or in generator-station capacity. See reference 1.

Example 2

A 70,000-kva hydroelectric station and a 35-mile 115-kv transmission line with 350,000-circular-mil copper conductors were designed and built at the same time. The line carries the output of the station to a city, where the voltage is regulated by synchronous condensers. The cost data are taken to be the same as in example 1.

The transmission line of 350,000-circular-mil conductors has 3.1-per-cent resistance drop and 14-per-cent reactance drop. The circular mils per ampere are 1,000, rated current being 350 amperes.

By equation 10 the most economical value of circular mils per ampere is

$$\frac{C}{I} = 182\sqrt{\frac{269}{3.0}} = 1{,}730 \text{ circular mils per ampere}$$

$$C = 1{,}730 \times 350 = 600{,}000 \text{ circular mils}$$

By equation 6 the annual charges for 1,000 feet of 600,000-circular-mil conductor are

$$M = 0.0000303 \times 600{,}000 \times 0.20 \times 15 + \frac{350^2}{600{,}000} \times 1.058 \times 0.106 \times 160 \times 15$$

$= 55 + 55 = \$110$ per year

The annual charges for 1,000 feet of 350,000-circular-mil conductor are

$$M = 32 + 94 = \$126$$

which is 15-per cent greater than the minimum value, \$110.

Note that with usual types of conductors, to change from 350,000 circular mils to 400,000 circular mils reduces the resistance by 12 per cent, but the 60-cycle reactance at ten-feet effective spacing is reduced only one per cent. With hollow conductors the change might be made by keeping the same diameter and increasing the thickness, in which case the reactance would be changed practically not at all.

Example 3

Although the formulas in this paper are chiefly applicable to bare overhead conductors, occasionally a case occurs in which the current density in an insulated wire or cable at its maximum permissible temperature is greater than the most economical current density, and so it pays to specify a larger conductor than one ordinarily would.

A conductor insulated with asbestos and varnished cambric is used in wiring in a long run in a dry location in free air, the temperature of the copper being 75 degrees centigrade. The peak current is 600 amperes. The conductor is owned by the same company that owns the steam station supplying the power. Take

$b = 0.25$
$g = 0.002$ dollar per kilowatt-hour
$h = 0.7$
$m_1 = m_2 = 15$
$s = \$110$ per kilowatt
$v = 0.55$ dollar per pound of copper at 700,000 circular mils

$0.106\, sm_2 = 0.106 \times 110 \times 15 = 175$
$93{,}000\, bg = 93{,}000 \times 0.25 \times 0.002 = 46$
Total 221

$hvm_1 = 0.7 \times 0.55 \times 15 = 5.78$

By equation 10, with the correction factor 1.193 inserted for 75 degrees centigrade, the most economical value of circular mils is

$$600\times182\times\sqrt{\frac{1.193\times221}{5.78}}=737{,}000 \text{ circular mils}$$

for which 700,000 circular mils might be chosen. The code size for 600 amperes for the conditions described is 350,000 circular mils.

To show the effect of the factor b, let the computation be repeated with $b=0.15$

$93{,}000\ bg=93{,}000\times0.15\times0.002=28$
$28+175=203$

The most economical value of circular mils is

$$600\times182\sqrt{\frac{1.193\times203}{5.78}}=706{,}000 \text{ circular mils}$$

for which the size 700,000 again would be chosen. The difference in the two computed results is four per cent.

Again, putting $b=0$, the most economical value is

$$600\times182\sqrt{\frac{1.193\times175}{5.78}}=650{,}000 \text{ circular mils}$$

Though this is a slightly smaller size than 700,000 circular mils, it is much larger than the size given by heating considerations alone. Although the factor b for a conductor which is being specified is not always easy to estimate, the precise value of b is not of very great importance in cases where the conductor is owned by the power company, as in the case of most transmission and distribution lines.

The percentage increase in size from 350,000 to 700,000 circular mils is 100 per cent. Then the ratio in the cost per 1,000 feet of the two sizes is

$1+1.00\times0.7=1.7$

For 350,000 circular mils, the cost per pound of copper is

$$0.55\times\frac{2.0}{1.7}=0.65 \text{ dollar}$$

The annual charge for 1,000 feet of the 700,000-circular-mil conductor is by equation 6, taking $b=0.25$,

$$M=0.0000303\times700{,}000\times0.55\times15+\frac{600^2}{700{,}000}\times221=175+114=\$289$$

For 1,000 feet of 350,000-circular-mil conductor,

$$M=0.0000303\times350{,}000\times0.65\times15+\frac{600^2}{350{,}000}\times221=103+227=\$330$$

which is 14 per cent greater than $289, the minimum value.

In this example, even if the load factor were almost zero, a heavy conductor could be specified at a saving in annual cost, with the additional advantages of lower temperature, longer insulation life, less voltage drop from reactance, and greater overload capacity.

Example 4

The corridors of an apartment building are wired with number-10 wire in iron conduit. The main electrical load is the lighting fixtures which are turned on for an average of 15 hours a day throughout the year. The current in the wires of the lighting circuits is 22 amperes, diminishing uniformly toward the end of the branch circuits, plus three amperes taken for short times from the outlets. This gives a maximum current in the wire of 25 amperes, for which the code size of wire is number 10.

Because of the current's tapering off uniformly along the wire, its resistance loss is one-third of what it would be with full current in all parts. Then

$$b=\frac{1}{3}\times\frac{15}{24}=0.208$$

Take $g=0.016$ dollar per kilowatt-hour, in lieu of fuel cost, $h=0.65$, $m_1=14$, $s=0$, $v=\$2$ per pound of copper installed, including cost of conduit and insulation, for number-8 wire.

$93{,}000\ bg=93{,}000\times0.208\times0.016=310$
$hvm_1=0.65\times2.00\times14=18.2$

$$\frac{C}{I}=182\sqrt{\frac{310}{18.2}}=750$$

where $I=22$ amperes, the current which flows 15 hours each day.

The most economical section of wire is

$C=750\times22=16{,}500$ circular mils

that is, number-8 wire.

The percentage increase in size from 10,400 circular mils to 16,500 circular mils is 59 per cent. Then the ratio in the cost per 1,000 feet of the two sizes is

$1+0.59\times0.65=1.38$

For number-10 wire, the cost per pound of copper is

$2.00\times(1.59/1.38)=\$2.30$

The annual charge for 1,000 feet of number-8 wire is, by equation 6,

$$M=0.0000303\times16{,}500\times2.00\times14+\frac{22^2}{16{,}500}\times93{,}000\times0.208\times0.016$$
$$=14.0+9.1=\$23.1$$

For 1,000 feet of number-10 wire,

$$M=0.0000303\times10{,}400\times2.30\times14+\frac{22^2}{10{,}400}\times93{,}000\times0.208\times0.016$$
$$=10.1+14.4=\$24.5$$

which is six per cent greater than 23.1, the minimum value.

Example 5

Groups of lighting fixtures are supplied by number-10 wire, the conditions being the same as in example 4, except that the wiring is owned by the company which owns the steam station.

$g=0.002$ dollar per kilowatt-hour
$m_2=14$
$s=125$ dollars per kilowatt
$0.106\ sm_2=0.106\times125\times14=186$
$93{,}000\ bg=93{,}000\times0.208\times0.002=39$
Total 225
$hvm_1=0.65\times2.00\times14=18.2$

By equation 10

$$\frac{C}{I}=182\sqrt{\frac{225}{18.2}}=640$$

where $I=22$ amperes, the current which flows 15 hours per day.

If one wire size is to be chosen for this entire part of the wiring, the most economical section is

$C=640\times22=14{,}000$ circular mils

For the wires leading to the groups of fixtures, the current has full value and

$$b=\frac{15}{24}=0.625$$

$93{,}000\ bg=93{,}000\times0.625\times0.002=116$
$186+116=302$

$$\frac{C}{I}=182\sqrt{\frac{302}{18.2}}=740$$

$C=740\times22=16{,}300$ circular mils, or number-8 size

Thus, if the current density is watched for each part of the wiring, larger than code sizes may be specified free of extra cost for the more heavily loaded parts. If the slight complication of changing wire sizes is considered worth while, the advantages of reduction in voltage drop, longer insulation life, and greater overload capacity may be obtained. This applies to the same extent to example 4.

Reference

1. Resistance Loss and Conductor Size Herbert B. Dwight. *General Electric Review*, November 1938.

Measurement and Effect of Contact Resistance in Spot Welding

ROBERT A. WYANT
NONMEMBER AIEE

SPOT WELDING consists essentially of clamping two pieces of sheet metal between two copper electrodes and passing through the pieces an electric current of sufficient strength to fuse them together at the spot where the current is most concentrated. Spot welding is the simplest of the electric resistance-welding processes which depend upon the Joule effect, $H=I^2RT$, for the generation of heat. The total resistance, R, in spot welding consists of the body resistance of the metal between the electrodes plus the sum of the sheet-to-sheet and electrode-to-sheet contact resistances. The purpose of this paper is to report to the electrical-engineering profession on recent investigations of the electrical resistance of these contacts and the importance of these resistances in the spot-welding process.

Contact resistance is believed to be extremely important in the spot welding of all metals. Knowledge of the subject, however, is very limited in spite of extensive use of the spot-welding process. Doctor F. J. Studer at Union College and Doctor W. B. Kouwenhoven at Johns Hopkins University have made a good start in studying contact resistance from the point of view of spot welding, but much remains to be done.[1,2] In England R. F. Tylecote has done much to advance knowledge of the subject.[3] During the past few years much has been learned about contact resistance and the spot welding of aluminum alloys.[4] This has been largely the result of the aircraft spot-welding research program at the welding laboratory of the Rensselaer Polytechnic Institute. The work was sponsored by the National Advisory Committee for Aeronautics, the Army Air Forces, and the Navy Bureau of Aeronautics. Prior to the latter work some observations of contact resistance were made at the same laboratory in connection with research on the spot welding of steels.[5] This work was sponsored by the Welding Research Council of the Engineering Foundation, of which the AIEE is a cosponsor with the American Welding Society.

Methods of Measuring Contact Resistance

The contacts in spot welding do not have constant values of resistance. Before the welding current starts to flow the resistance of the contacts depends primarily upon the surface condition of the contacting metals. Factors of less importance are the kinds of metal in contact, the electrode force, and the size and shape of the electrode tips. As soon as the welding current starts to flow, the resistance of each contact quickly decreases as more intimate contact is made between the two metals. In studying these contacts two types of resistance measurements are necessary: a measurement under static conditions to determine the initial contact resistance and an oscillographic measurement to follow the change in resistance while the weld is forming. The latter measurement necessarily must be made with the specimens clamped between the electrodes of an actual spot-welding machine. The initial contact resistance may be measured with the specimens clamped between the electrodes of either a spot-welding machine or a small press built especially for the purpose. The small press usually is employed when contact resistance measurements are used to evaluate the surface condition of the metals to be welded.

Attention must be called to the fact that the resistances measured in this work are not simple contact resistances. The sheet-to-sheet resistance includes the contact resistance plus the resistance of one sheet of material. Likewise, the electrode-to-sheet resistance includes the contact resistance plus the resistance of one-half sheet of material. This point is illustrated by Figure 1. At the start of the weld the body resistance of the material is usually negligible in comparison with the contact resistance. As the formation of the weld progresses, the body resistance of the material accounts for an increasingly greater part of the measured resistance.

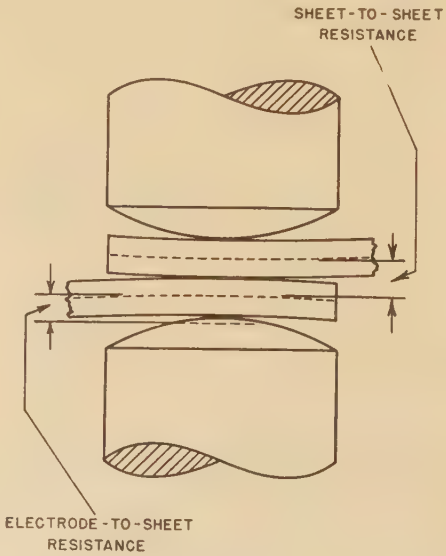

Figure 1. Diagram showing planes between which sheet-to-sheet and electrode-to-sheet resistances are measured

Static Measurements

Though there are several different methods of measuring contact resistance, they all require a small press for clamping a pair of specimens in contact with each other. A typical press is shown in Figure 2. The essential features of this press are the copper electrodes and the hydraulic jack and calibrated spring for applying a force of known magnitude to the electrodes.

The electrodes are made of one of the copper alloys which are commonly used for spot-welding electrodes. In fact the press should be designed to take a pair of standard electrode tips. One electrode has to be insulated electrically from the press in order to direct the current through the specimens. The contour of the electrode faces should be spherical with a radius of curvature of three or four

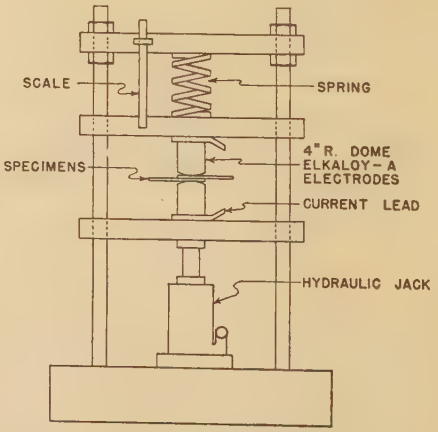

Figure 2. Press for the measurement of contact resistance

Paper 46-9, recommended by the AIEE committee on electric welding for presentation at the AIEE winter convention, New York, N. Y., January 21–25, 1946. Manuscript submitted October 2, 1945; made available for printing November 5, 1945.

ROBERT A. WYANT is assistant professor, department of metallurgical engineering, Rensselaer Polytechnic Institute, Troy, N. Y.

inches. This is an important point, because erratic measurements may result from using electrodes with flat faces. It is difficult to keep flat faces parallel, and as a result the distribution of pressure over the contact area may be inconsistent. When the electrode contour is spherical, the specimens tend to adjust themselves to that contour, as indicated by Figure 1 in which the effect is greatly exaggerated. This naturally tends to produce a more consistent area of contact and distribution of pressure over that area. Another factor, which may affect the consistency of the results, is play or freedom of movement of the electrodes with respect to their intended axis of alignment. The construction of the press must be such as to keep the electrodes rigidly in alignment and yet to permit their easy movement along the alignment axis. An electrode force of 1,000 pounds is employed with electrodes having a contour four inches in radius. Satisfactory results also may be obtained by using an electrode force of 500 pounds with electrodes having a contour three inches in radius.

At least three different circuits have been successfully employed for measuring contact resistance. At this laboratory a modified Kelvin double-bridge circuit is used, as shown in Figure 3. The current through the contact is limited to within 20–100 amperes by means of R_b. Within this range the actual magnitude of the current has no appreciable effect on the resistance of the contact, but it must be high enough to make the circuit sufficiently sensitive. In this circuit R_s is a standard resistance of 100 microhms. Each of the R_1 and R_3 resistance arms consists of two decade units in series (10 and 100 ohm steps). Each of the R_2 and R_4 resistance arms consists of a fixed resistor of the plug-in type (10, 100, or 1,000 ohms). Thus by changing R_2 and R_4 three ranges of R_x can be covered: 100 to 10,000, 10 to 1,000, and 1 to 100, all in microhms. In operating the bridge, R_1 is always kept equal to R_3, and R_2 is kept equal to R_4. The circuit is direct reading in the sense that, when it is balanced, the value of R_x in microhms is obtained simply by multiplying the reading of R_1 by a multiple of ten. Although the precision of the circuit is not great, it is ample for the requirements of this work. For more details on this circuit the reader is referred to previous papers.[6,7]

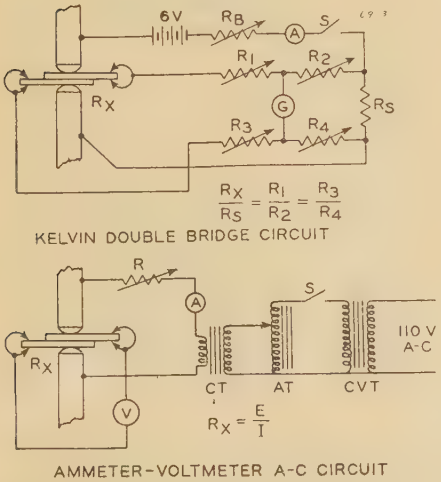

Figure 3. Circuits for measuring contact resistance

Contact-resistance measurements at some laboratories are made by the voltmeter–ammeter method using alternating current, as shown in Figure 3.[8] This circuit requires the use of a sensitive vacuum-tube voltmeter for measuring the voltage drop across the contact. Current and voltage readings have to be taken simultaneously, and, therefore, to avoid errors due to fluctuations in line voltage, a constant-voltage transformer usually is employed. The magnitude of the current in this circuit also is limited to a range from about 20 to 100 amperes. This circuit is somewhat faster in operation than the bridge circuit just described.

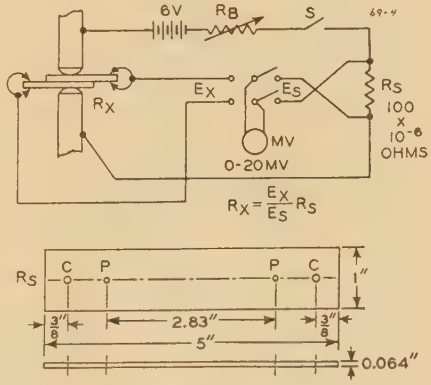

Figure 4. Circuit and standard resistance for measuring contact resistance by means of millivoltmeter

Material for R_s—Bare 24S-T aluminum alloy
C—Points for current connections
P—Points for potential connections

The circuit shown in Figure 4 is recommended for plants where there is a lack of electric equipment and where contact-resistance measurements are to be made at a minimum of expense. In this circuit the unknown contact resistance is compared with a standard resistance, R_s, of 100 microhms. The most important element in the circuit is the millivoltmeter, which should have a range of from 0 to 20 millivolts for measuring resistances below 1,000 microhms. The resistance, R_b, is used to keep the current within a range from 20 to 100 amperes. The actual magnitude of the current is not important, but it should not vary while the voltage drops across the contact and the standard resistances are being measured. A standard resistance of 100 microhms and of sufficient accuracy for this work can be easily made from a piece of 24S-T aluminum-alloy sheet as shown in Figure 4. The precision of this circuit depends upon the accuracy of the millivoltmeter and the standard resistance. Therefore, it is recommended that the resistance of the standard be checked by some means and adjusted to within at least plus or minus five per cent of its intended value. The resistance of such a standard does not change appreciably, because of the heating effect of the current while measurements are being made. The alignment chart, shown in Figure 5, is provided for obtaining the resistance of the contact from the millivoltmeter readings without making calculations.

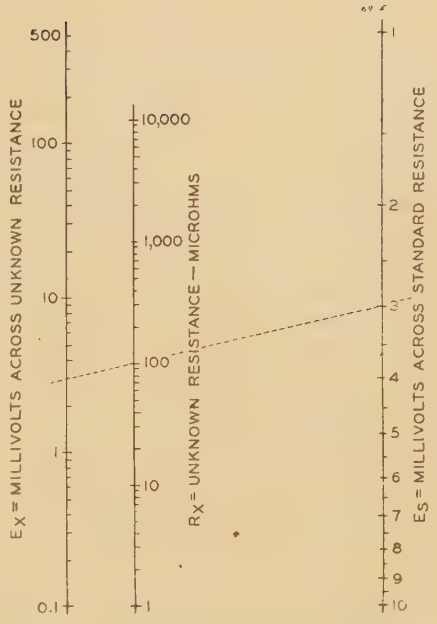

Figure 5. Alignment chart for evaluating measurements made with circuit shown in Figure 4

$$R_x = \frac{E_x}{E_s} R_s$$

$R_s = 100$ microhms

Dynamic Measurements

Contact resistance is measured during welding by means of an electromagnetic oscillograph, as shown in Figure 6. A shunt, consisting of a piece of manganin (R_s), is installed in the lower electrode holder for the purpose of obtaining a voltage drop which is an accurate measure of the welding current. Suitable potential connections are made to the shunt,

electrode tips, and specimens. The leads for these connections have to be twisted carefully and arranged to avoid inductive effects. With this arrangement a complete record of the four important voltage drops is obtained when a weld is made. The oscillograph circuits are calibrated in terms of volts per inch deflection, and the desired values of resistance are obtained by measuring the oscillograms and making the necessary calculations. This is done for each contact, and the results are plotted as a function of time. It is usually desirable to superimpose a plot of the welding current on the resistance curves.

Contact Resistance and the Spot Welding of Aluminum Alloys

The surfaces of aluminum alloys are characterized by the presence of an oxide film which must be removed or otherwise operated upon before these alloys can be satisfactorily spot-welded. The surfaces of these alloys can be prepared for spot welding by either mechanical or chemical methods. By the mechanical methods the original oxide film is removed from the surface of the metal by means of a wire brush, steel wool, or abrasive cloth. The chemical methods consist of immersing the metal in a chemical solution which removes the original oxide film or transforms it in such a way as to make the surface suitable for spot welding. Chemical methods have many advantages over mechanical methods, and during the past few years the trend in industry has been toward chemical methods.

Original Experiment

An experiment was devised in which a pair of specimens could be clamped between the electrodes of a spot-welding machine, and the contact resistance measured both before and during welding.[4] The circuit by which this was accomplished is shown in Figure 7. In the experiment specimens of Alclad 24S-*T* sheet were treated in a solution of hydrofluoric acid, which was recommended for the purpose at that time (1941). After treatment each pair of specimens was clamped between the electrodes and the initial contact resistance measured by means of the Kelvin double-bridge circuit shown in Figure 7. Without disturbing the specimens in any way the welding current next was passed, and the change in contact resistance was followed oscillographically by means of the connections that are also shown in Figure 7. The results of the initial bridge measurements are plotted in Figure 8. It will be noted that the contact resistance was a critical

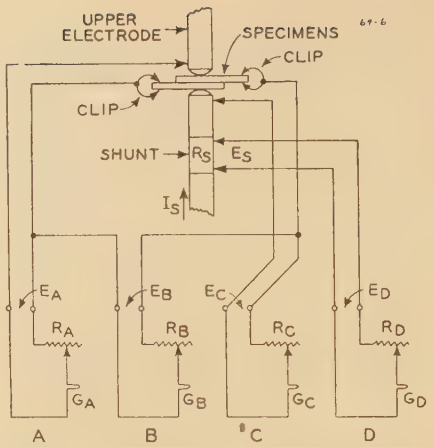

Figure 6. Oscillograph connections for measurement of voltage drops in secondary circuit of spot welder

A—Upper electrode to sheet
B—Sheet to sheet
C—Lower electrode to sheet
D—Secondary current

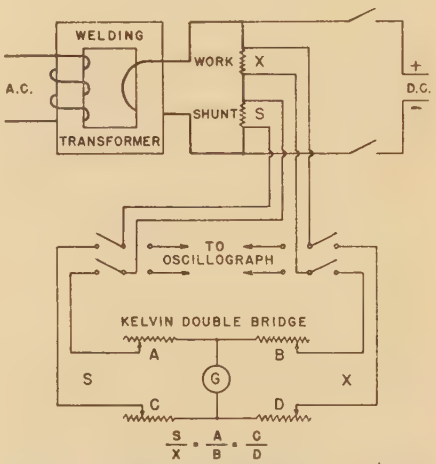

Figure 7. Circuit for measurement of resistances in original investigation of the surface preparation of aluminum alloys for spot welding

function of the time of immersion in the hydrofluoric acid. The contact resistance fell from an average of 608 microhms at zero time to 226 microhms at five seconds, and it reached a minimum of 20 microhms at ten seconds. As the treating time was increased, the contact resistance increased to 49 microhms at 15 seconds, and it reached a value of 586 microhms at 30 seconds. The welds which were made immediately following these measurements were carefully examined. It was found that the best welds, with respect to uniform shape of the fused zone, were obtained at treating times of 10 and 15 seconds where the contact resistance was low. Photomicrographs of typical sections through the welds are also shown in Figure 8. These welds indicated that, when the contact resistance was low, the welding current was distributed uniformly over the contact area, and therefore the fusion occurred uniformly across the weld zone in all directions. When the contact resistance was high, the welding current tended to concentrate at the points of least resistance on the contact area, and therefore the distribution of heat was not uniform throughout the weld zone. This was the origin of the concept that a low contact resistance is desirable for spot welding the aluminum alloys. Some typical results of the oscillographic measurements are shown in Figure 9. The values of contact resistance at zero time were the result of the initial bridge measurements, and the values at the other intervals after the start of the weld were obtained by analysis of the oscillograms. The correlation between the initial and oscillographic measurements indicated that the contact resistance measured under static conditions was essentially the same as the prevailing contact resistance at the instant when the welding current started to flow. Following this experience, the static method of measuring contact resistance in a small press was adopted to facilitate further research on the surface preparation of aluminum alloys for spot welding.

Untreated and Mechanically Prepared Sheet

Contact resistance measurements were applied to untreated and wire-brushed specimens at an early date.[4] The resistance between untreated specimens is consistently high and usually greater than

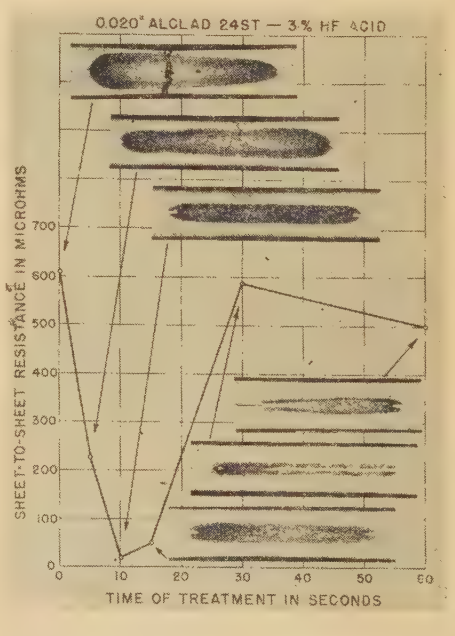

Figure 8. Surface-treating characteristic and photomicrographs showing relation between sheet-to-sheet resistance and distribution of fusion in weld zone

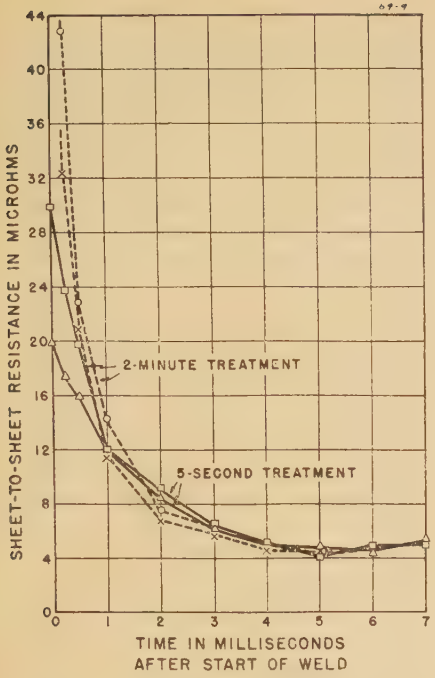

Figure 9. Sheet-to-sheet resistance during formation of spot weld in an aluminum alloy

Six per cent hydrofluoric acid, 0.040-inch Alclad 24*S*-*T*, four-inch dome tips
Electrode pressure—1,000 pounds
At $T=0$, $R_0=221$, $R_x=244$

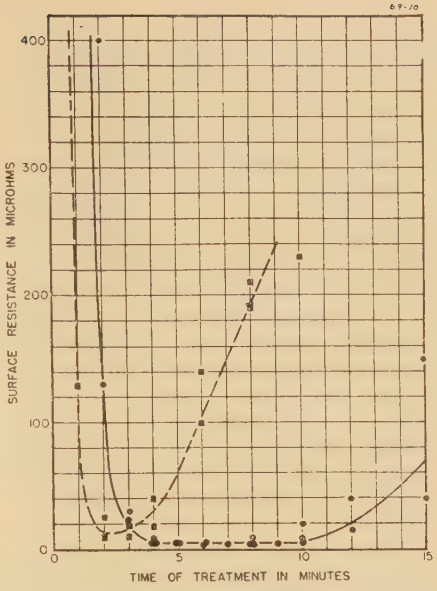

Figure 10. Surface-treating characteristics for the aluminum alloy, Alclad 24*S*-*T*, in hydrofluosilicic-acid solution at 75 degrees Fahrenheit

Three-per-cent H_2SiF_6 solution, 0.020-inch alloy
—●—Nitrate heat treated
—■—Air heat treated

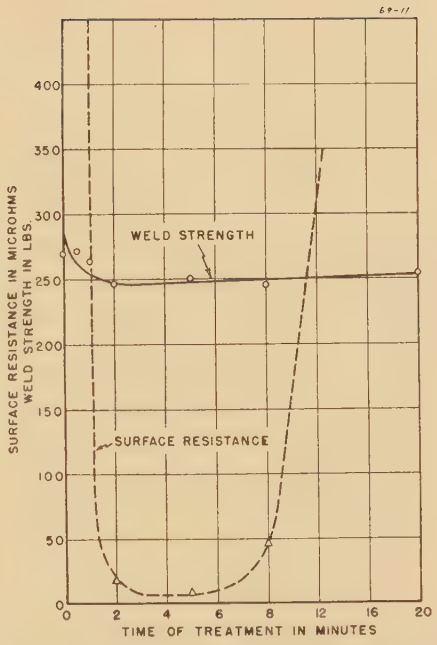

Figure 11. Graphs showing relationship between initial sheet-to-sheet resistance and weld shear strength

Three-per-cent H_2SiF_6 solution, 75 degrees Fahrenheit, 0.020-inch Alclad 24*S*-*T*, nitrate heat treated, capacitor-discharge welder, rapidly rising current, 25,000-ampere peak

1,000 microhms. Between wire-brushed specimens the resistance is consistently low and of the order of 5 to 25 microhms, provided that the surface preparation has been thorough. Untreated sheet cannot, of course, be satisfactorily spot-welded. Very good welds can be made in wire-brushed material, but this method of surface preparation has been largely displaced by chemical methods.

Development of Chemical Methods of Surface Treatment

At the time of the original experiment with hydrofluoric acid, proprietary solutions were just beginning to appear on the market for the surface treatment of aluminum alloys for spot welding. No time was lost in applying contact-resistance measurements in an investigation of those proprietary solutions and a number of purely experimental solutions.[6] All of the effective solutions gave characteristics similar to that shown in Figure 8 for hydrofluoric acid, except for the fact that they were all less critical with respect to time. Furthermore, very good welds always were obtained when the contact resistance was low, regardless of what treating solution was used. The fact soon became well established that the contact resistance between chemically prepared specimens is primarily a function of the time of immersion in the treating solution. Other factors which may affect the resistance are the initial surface condition and composition of the alloy being treated, and the composition, strength, and temperature of the treating solution. For any chemical solution that is effective for treating a given alloy, there is usually a range in immersion time over which the contact resistance is consistently low and frequently of the order of five to ten microhms. Outside this range the resistance is usually much higher.

A typical characteristic is shown in Figure 10 for the chemical surface treatment of Alclad 24*S*-*T* sheet in one of the newer solutions which has proved to be very satisfactory and economical, both in the laboratory and in production. This solution is a result of a research program in which contact-resistance measurements were employed extensively at this laboratory.[7] It consists of three per cent by volume of 28 per cent hydrofluosilicic acid, H_2SiF_6, plus 0.1 per cent by weight of the wetting agent, Nacconol NR, in water. This solution has many desirable characteristics. For example, no heating units are required as it operates at room temperature. The solution is very simple in composition. The time of treatment is not critical, there being an ample range of treating time with little danger of overtreatment. The acid is available in ample quantities and at low cost. There is no health hazard in the use of this solution, as there are practically no vapors evolved, and the solution is not ordinarily irritating to the skin. A bright smooth finish is obtained on Alclad material. The strength of the solution may be determined by a simple titration. This is an outstanding advantage of the solution, since it permits rapid and precise control. The solution is effective for treating nearly all of the aluminum-alloy sheet materials with the possible exception of the bare 24*S* and 61*S* alloys.

Many other laboratories have adopted contact-resistance measurements to facilitate the investigation, development, and control of surface-treating solutions since the original work was reported. Many improved solutions now are in use as a result. Contact-resistance measurements are employed at many aircraft plants to control the surface-treating operations in production. Furthermore, the latest Navy spot-welding specification calls for contact-resistance measurements.

Effects of Contact Resistance

In spot-welding aluminum alloys the relationships between contact resistance and the following factors are of considerable interest:

1. Size and strength of spot welds.
2. Consistency with respect to strength.
3. Uniformity with respect to shape.
4. Electrode-tip life.

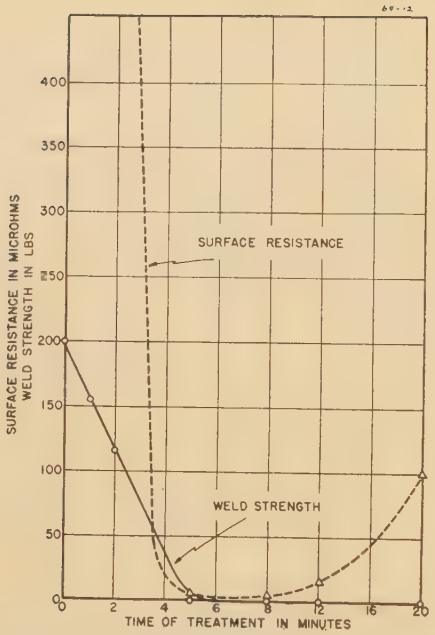

Figure 12. Graphs showing relationship between initial sheet-to-sheet resistance and weld shear strength

0.020-inch Alclad 24S-*T*, nitrate heat treated, capacitor-discharge welder, rapidly rising current, 25,000-ampere peak

The relationship between spot-weld strength and contact resistance frequently is misunderstood. The evidence at the Rensselaer laboratory indicates that there is no general relationship. This is shown by the typical curves in Figure 11 which were obtained by keeping all welding conditions constant except treating time. At short treating times, which are not long enough to obtain the minimum contact resistance, the weld strength tends to be proportional to the contact resistance. At longer treating times the weld strength tends to be constant and independent of contact resistance. In other words there does not seem to be a sound basis for the common idea that the magnitude of the welding current can be adjusted to compensate for changes in contact resistance. In Figure 11 the welding conditions were selected so as to obtain a 250-pound weld at the minimum value of contact resistance. Similar curves are shown in Figure 12 for conditions which produced a 200-pound weld between untreated specimens and a dud weld at the minimum value of contact resistance. Comparison of the latter two figures suggests that at the short treating times the effect of contact resistance on weld strength depends upon the average size of the welds produced.

The effect of contact resistance on the consistency of spot-weld strength cannot be discussed fully without reference to a characteristic of weld strength as a function of the welding current. A typical characteristic is shown in Figure 13 for the 52*S*-1/2*H* aluminum alloy. The best consistency is obtained at points toward the upper end of the curve. This is primarily caused by the fact that at low values of current the curve is steep, and small variations in current produce large changes in weld strength. It is also at the lower values of current where variations in contact resistance are most likely to affect the weld strength. The symbols used for plotting the curve in Figure 13 indicate that consistent and sound welds were obtained between 35 and 40 kiloamperes. Below 33 kiloamperes the welds were very inconsistent. Above 42 kiloamperes the welds were consistent, but expulsion of molten metal and excessive sheet separation were observed. It may be said, therefore, that the point of operation on the strength–current characteristic is a much more important factor than contact resistance in determining the consistency of spot welds with respect to strength. Surprisingly good consistency can be obtained by welding specimens with untreated faying surfaces, provided that this principle is observed

The effect of contact resistance on the shape of the spot welds was the only effect observed in the original experiment described. This effect has been confirmed many times in later work. The welds are always round and uniform in shape when the contact resistance is near its minimum value. The welds become very irregular in shape when the contact resistance is high as a result of too short a treating time. The effect of a high contact resistance as a result of too long a treating time depends upon the nature of the treating solution. There is a tendency for the welds to become irregular in shape with all solutions under this condition, but the effect is much more pronounced with some solutions than with others. This effect is illustrated by the spot-weld fractures shown in Figure 14. For another example the reader is referred back to Figure 8 and the discussion

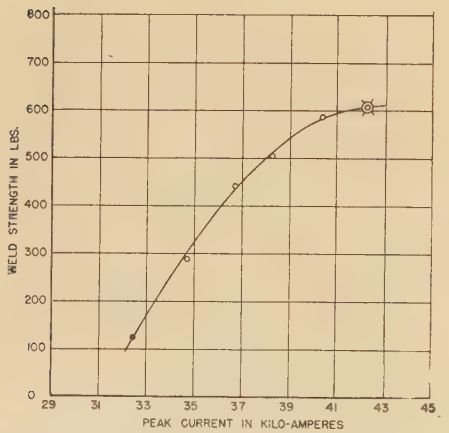

Figure 13. Typical strength-current characteristic for spot welds in the aluminum alloy, 52S-1/2H

0.040-inch alloy
Electrode tips—Four-inch *R* domes
Electrode force—1,200 pounds (weld), 2,400 pounds forge
Forge timing—34 milliseconds
Average rate of current rise—3,300 amperes per millisecond

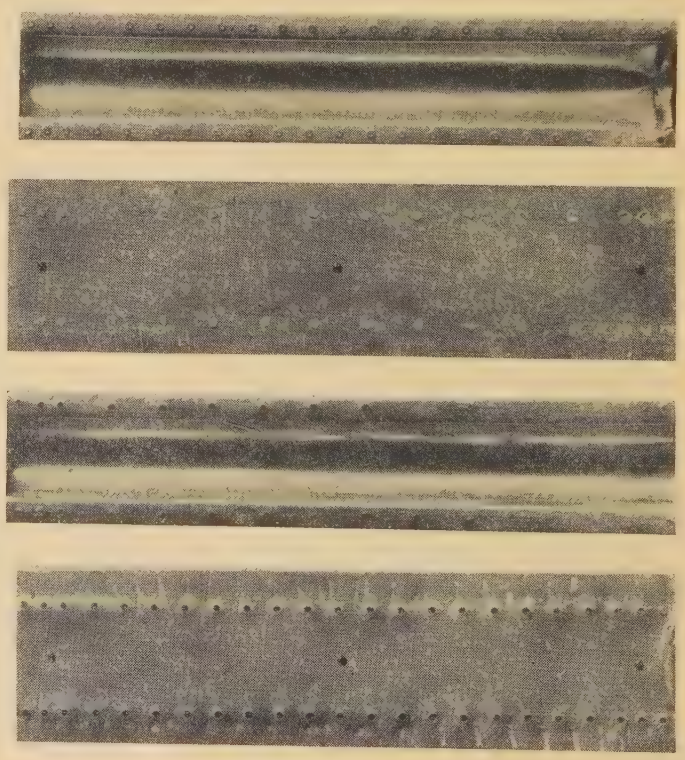

Figure 14A. Irregularities in weld shape when sheet-to-sheet resistance is high and inconsistent

Figure 14B. Uniformity of weld shape when sheet-to-sheet resistance is consistently low

thereof. It should be pointed out that the actual shape of spot welds in aluminum alloys may have little effect on their shear strength and their consistency with respect to shear strength. It is only when variations in surface condition influence the size of the weld that the shear strength is affected.

The spot welding of aluminum alloys is characterized by comparatively rapid fouling of the electrode tips with aluminum and the necessity for frequent cleaning of the tips. Perhaps the most important effect of contact resistance is on electrode-tip life or the number of welds which can be made per cleaning. It is difficult to obtain conclusive and quantitative data on this relationship, because there are so many variables which affect tip life. However, there are many indications that the best tip life is obtained when the contact resistance is near the minimum value for the material being welded. The effect of any variable on tip life is best observed under actual production conditions. Unfortunately, it is under such conditions that the effect of the variable under observation may be obscured by the effects of other variables which may not be controlled adequately or even recognized.

Contact Resistance Between Electrodes and Sheet

The emphasis in the work at the Rensselaer laboratory has been on the sheet-to-sheet resistance. This has been a result of the fact that in the original work the sheet-to-sheet resistance was found to be more sensitive than the electrode-to-sheet resistance with respect to changes in surface condition of the specimens. The electrode-to-sheet resistance deserves further study. A British investigator has gone so far as to say that the electrode-to-sheet resistance must not exceed a specified value if rapid fouling of the electrode tips is to be avoided.[9]

Measurements of Instantaneous Power

The oscillograms which are used for determining the dynamic resistance characteristics also may be analyzed in terms of instantaneous power at the sheet-to-sheet and electrode-to-sheet contacts. A plot of the resistance, power, and current characteristics of two spot welds in Alclad 24*S*-*T* is shown in Figure 15. The oscillograms for these two particular welds were chosen for complete analysis, because one weld exhibited a shear strength of 505 pounds, whereas the other weld, made under identical conditions, exhibited a strength of only 140 pounds. It will be noted that the resistance characteristics and current wave forms for the two welds were practically identical. The only difference is in the peak power at the sheet-to-sheet contact. Whether this was responsible for the extreme difference in strength is questionable. A similar plot is shown in Figure 16 for two welds which started with different values of sheet-to-sheet resistance and ended up by exhibiting a marked difference in shear strength. It should be noted that the weld which started with the higher initial sheet-to-sheet resistance produced the lower strength, in spite of the fact that the welding current and other recognized conditions were identical for the two welds. This is contrary to what might have been predicted and is further evidence that there is no sound basis for adjusting the magnitude of the current to compensate for differences in initial contact resistance. The phase relation of the power curves for the sheet-to-sheet contact should be noted in Figure 16. This difference in phase is believed to have been a result of the difference in initial contact resistance and to have been responsible for the difference in weld strengths. These cases are presented to illustrate the complex nature of the relationship between contact resistance and weld strength in working with the aluminum alloys.

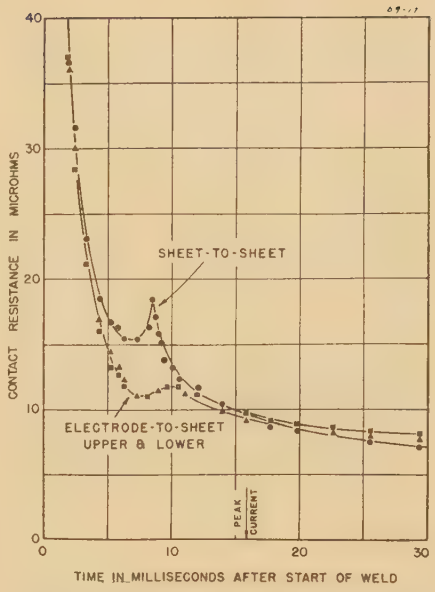

Figure 17. Dynamic resistance characteristics illustrating effect of method of drying chemically treated specimens of the aluminum alloy, *R*-301-*T* (compare with Figure 18)

0.064-inch alloy, three-per-cent H_2SiF_6 solution, wiped dry

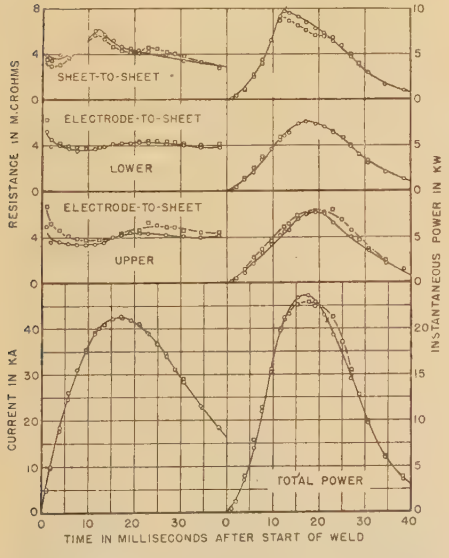

Figure 15. Dynamic resistance and instantaneous power characteristics of two spot welds made under identical conditions but exhibiting widely different shear strengths

0.040-inch Alclad 24*S*-*T*
–O– *S* = 505 pounds, R_o = five microhms
–□– *S* = 140 pounds, R_o = four microhms

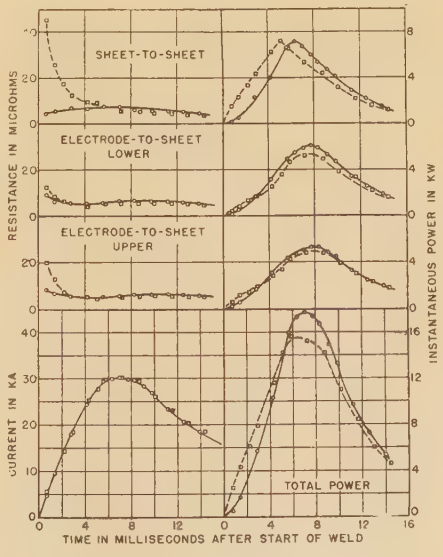

Figure 16. Dynamic resistance and instantaneous power characteristics of two spot welds illustrating an inverse relationship between initial sheet-to-sheet resistance and weld shear strength

0.020-inch Alclad 24*S*-*T*
–O– Nitrate treated, *S* = 240 pounds, R_o = 6
–□– Air treated, *S* = 160 pounds, R_o = 90

Unusual Contact Phenomena

Several very interesting contact phenomena have been observed in this work. For example, the method of drying aluminum-alloy specimens following their chemical surface preparation affects the sheet-to-sheet resistance. This was first observed in spot-welding the new aluminum alloy, *R*-301-*T*. A typical dynamic resistance characteristic is shown in Figure 17 for specimens which were dried by

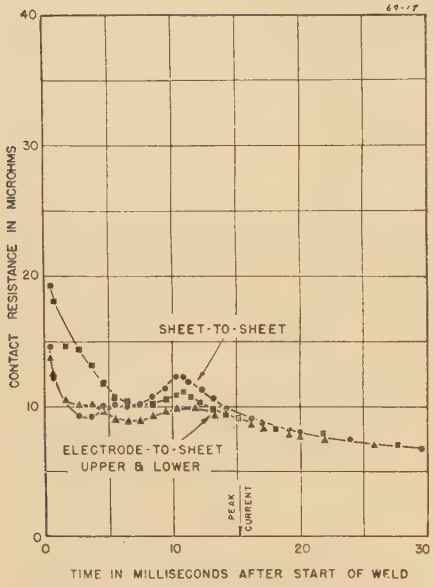

Figure 18. Dynamic resistance characteristics illustrating effect of method of drying chemically treated specimens of the aluminum alloy, *R*-301-*T* (compare with Figure 17)

0.064-inch alloy, three-per-cent H_2SiF_6 solution, air dried

wiping with a clean cloth. The irregularity in the sheet-to-sheet resistance curve should be noted. When the specimens were allowed to dry in clean air, the corresponding characteristics assumed quite a different shape, as shown in Figure 18. It should be noted also that the initial resistance was considerably lower when the specimens were dried in air. The effect of method of drying on the contact resistance of Alclad 24*S*-*T* sheet was next investigated. The results are illustrated by the surface-treating characteristics shown in Figure 19. Wiping raised the general level of the treating characteristic, and it tended to make the measurements erratic. This effect is not too important in production, because at most plants air drying is employed. The phenomenon is mentioned here, because it illustrates the great importance of details in the technique of preparing specimens for contact-resistance measurements.

Another interesting phenomenon is that of the effect of direction of current flow in determining which electrode will tend to become fouled with aluminum. In some spot welders of the condenser-discharge type the welding current always passes in the same direction. In these machines there is a definite tendency for aluminum to adhere to the electrode which is positive with respect to the work, provided that the welding conditions are all reasonably good. The same tendency has also been observed in a-c spot welding with equipment in which the first half cycle of current always passes in the same direction. In this case the aluminum tends to adhere to the electrode, which is positive during the first half cycle. It was thought that the cause of this might be revealed by comparing dynamic resistance characteristics for the positive electrode-to-sheet contact with similar characteristics for the negative electrode-to-sheet contact. However, nothing has been apparent in the experimental results to date, as shown by the resistance curves in Figures 15 and 16. The effect is much more pronounced in spot-welding the magnesium alloys, as will be shown later.

Contact Resistance and the Spot Welding of Other Metals

Magnesium Alloys

The magnesium alloys are very similar to the aluminum alloys with respect to their surface preparation for spot welding. Up to recent times no chemical methods were available for the surface treatment of magnesium alloys for this purpose. Contact-resistance measurements have played an extremely important part in the recent development of chemical solutions for this purpose. In several respects contact resistance is even more important in spot-welding the magnesium alloys than in spot-welding the aluminum alloys. For example, there is much more positive evidence that fouling of the electrode tips with magnesium is accelerated greatly when the contact resistance is high. This fact has been confirmed recently by several investigators.[10,11,12] The effect of the direction of current flow on the fouling of the electrodes is also much more pronounced. Furthermore, it is evident in the dynamic resistance characteristics for the electrode-to-sheet contacts. A set of typical characteristics is shown in Figure 20. The irregularity in the curve for the positive or upper electrode-to-sheet contact should be noted. The effect of this irregularity in terms of power is shown in Figure 21. It is evident that much more heat is developed at the positive electrode-to-sheet contact than at the negative contact. This is responsible for the rapid fouling of the positive electrode and the displacement of the weld in the sheets toward that electrode. When the flow of welding current is reversed, the same irregularity occurs in the characteristic for the positive or lower electrode-to-sheet contact.

Steel

In spot-welding steel it is usually taken for granted that the metal must be clean and free from oxide scale if high quality welds are to be obtained. This is essentially a matter of contact resistance, but it has seldom been treated as such. Steel was the chief material used in the first investigations of contact resistance in spot

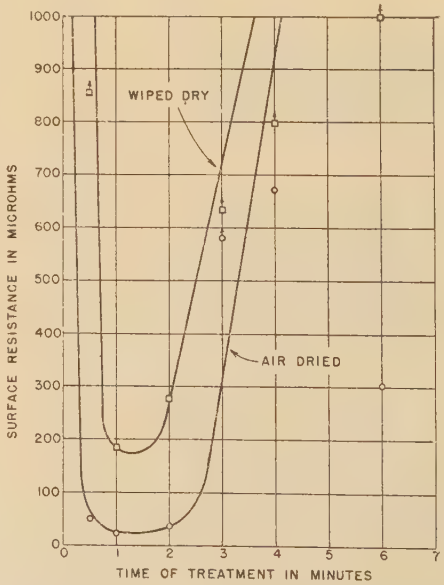

Figure 19. Surface-treating characteristics illustrating effect of method of drying chemically treated specimens of the aluminum alloy, Alclad 24*S*-*T*

0.020-inch alloy, air heat treated, three-per-cent H_2SiF_6 solution at 70 degrees Fahrenheit

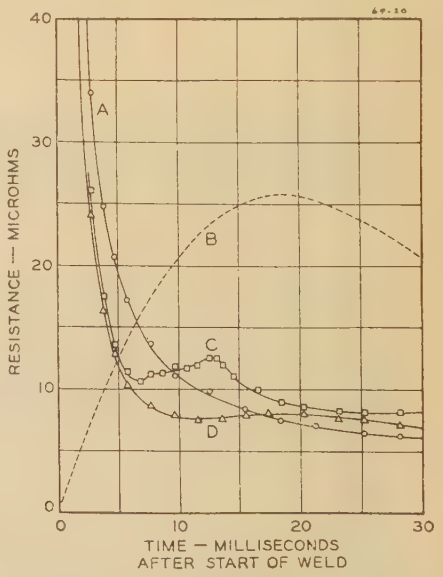

Figure 20. Dynamic resistance characteristics illustrating effect of direction of current flow in spot-welding the magnesium alloy, AM35-O

0.040-inch alloy, chemically cleaned, tip condition clean

A—Sheet to sheet
B—Current
C—Upper electrode to sheet (positive)
D—Lower electrode to sheet (negative)

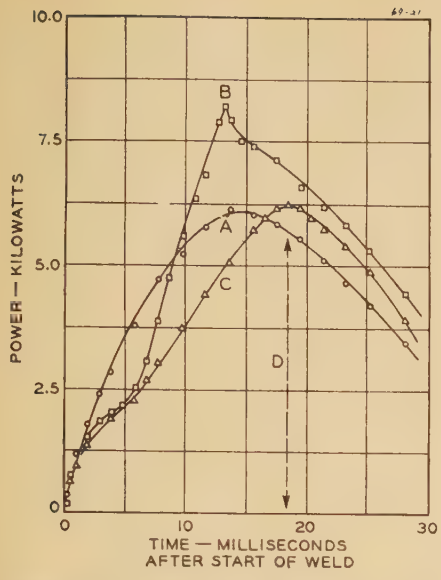

Figure 21. Instantaneous power characteristics illustrating effect of direction of current flow in spot-welding the magnesium alloy, AM3S-O

0.040-inch alloy, chemically cleaned, tip condition clean

A—Sheet to sheet
B—Upper electrode to sheet (positive)
C—Lower electrode to sheet (negative)
D—Time to peak current

welding. A good start was made in those investigations, but even yet very little is known about the fundamental importance of contact resistance in the formation of the weld. It is evident, however, that the body resistance of the metal is a more important factor in the spot welding of steel than in the spot welding of the light metals. In a number of instances trouble has been experienced in spot-welding certain steels which have been identical in composition and structure to other steels which have been easily spot-welded. The trouble is believed to have arisen from a difference in surface condition which could have been detected by contact-resistance measurements.

Copper Alloys

Practically nothing is known about contact resistance and the spot welding of the copper alloys. However, much trouble has been experienced due to contact phenomena in spot-welding a brass with a high zinc content. The zinc tends to migrate rapidly from the work into the copper electrodes. As a result the resistivity of the electrodes is increased, and the amount of heat generated at the electrode-to-sheet contacts increases with each successive weld. These phenomena may or may not be related to the surface condition of the sheet. The effect would certainly be aggravated by a surface condition that is characterized by a high contact resistance. Thus, it appears desirable to apply contact-resistance measurements in any future investigations of the spot welding of the copper alloys.

Nickel Alloys

Nickel-alloy sheet can be obtained with a surface condition that is very well suited to spot welding. However, there are instances where trouble is experienced because of the migration of nickel into the copper electrodes. Contact-resistance measurements might show that this effect is related to a surface condition that might be improved. Such measurements should not be overlooked whenever there is any evidence that surface condition is causing trouble in spot-welding these alloys.

Research Problems

There are many opportunities for further research in this field. For example, the fundamental relationship between contact resistance and the surface condition of the metals in contact should be investigated. Electron-diffraction studies should be employed to determine the presence and identification of surface films. Surface profilometers should be employed to evaluate the degree of surface roughness. Surface hardness should be determined by suitable instruments. The ultimate objective of the work would be to learn how contact resistance is affected by these three factors: surface films, surface profile, and surface hardness. Contacts between both similar and dissimilar metals should be studied.

In spot-welding a number of alloys there is a strong tendency for the electrodes to pick up or become fouled with metal from the work. A fundamental investigation is needed of the transfer of metal across contacts between dissimilar metals under the conditions imposed by spot welding. The objective of the work would be to learn how the transfer of metal is affected by such factors as composition and structure of the copper-alloy electrodes, surface condition of the metals in contact, current density, electrode force, and temperature at the contact. The contact problem in spot welding differs from other electric contact problems with respect to current density, nature of metals in contact, and the fact that the circuit is always dead when the contact is made or broken. The current density may easily reach a value of the order of 5,000,000 amperes per square inch. The contact combinations include copper to aluminum, copper to magnesium, copper to zinc, and sometimes copper to nickel. The contact never is required to conduct current unless the pressure density is within the range from about 5,000 to 50,000 pounds per square inch.

Knowledge of the fundamental part that contact resistance plays in the formation of a spot weld in any material, still is too limited. The investigations of this subject, which were interrupted by the war, should be revived as soon as circumstances permit. Contact-resistance measurements have proved to be of great value in investigations of the spot welding of the light metals. The use of such measurements should be extended to investigations of the spot welding of steels, copper alloys, and nickel alloys.

References

1. Contact Resistance in Spot Welding, **F. J. Studer.** *Welding Journal* (Research Supplement), volume 18, October 1939, pages 374-s–80-s.

2. Measurement of Contact Resistance, **W. B. Kouwenhoven, J. Tampico.** *Welding Journal* (Research Supplement), volume 19, October 1940, pages 408-s–13-s.

3. The Function of Contact Resistance in Spot Welding, **R. F. Tylecote.** *Transactions* (London, England), Institute of Welding, volume 4, July 1941, pages 154–65.

4. An Investigation of the Surface Treatment of Alclad 24S-T in Preparation for Spot Welding, **W. F. Hess, R. A. Wyant, B. L. Averbach.** *Welding Journal* (Research Supplement), volume 21, June 1942, pages 257-s–65-s.

5. Further Studies of The Spot Welding of Low Carbon and Stainless Steels, **W. F. Hess, R. A. Wyant.** *Welding Journal* (Research Supplement), volume 18, October 1939, pages 348-s–54-s.

6. The Surface Treatment of Alclad 24S-T Prior to Spot Welding, **W. F. Hess, R. A. Wyant, B. L. Averbach.** *Welding Journal* (Research Supplement), volume 23, August 1944, pages 402-s–13-s.

7. The Surface Treatment at Room Temperature of Aluminum Alloys for Spot Welding, **W. F. Hess, R. A. Wyant, B. L. Averbach.** *Welding Journal* (Research Supplement), volume 23, September 1944, pages 417-s–35-s.

8. Contact Resistance Measurements as Control for Preweld Cleaning of Aluminum Alloys, **G. W. Scott, Jr., E. B. Charles.** *Welding Journal* (Research Supplement), volume 23, January 1944, pages 1-s–7-s.

9. Spot Welding of Light Alloys—Trends in Recent Progress, **R. F. Tylecote.** *Welding*, volume 12, March 1944, pages 142–4.

10. Cleaning of Magnesium Surfaces for Satisfactory Spot Welds, **F. Linville, M. Disotell.** *Product Engineering*, volume 15, December 1944, pages 811–12.

11. Cleaning of Magnesium Alloy Sheet for Spot Welding, **K. E. Dorcas, N. H. Simpson.** *Aero Digest*, volume 48, January 15, 1945, pages 107, 212.

12. Spot Welding of Magnesium Alloys, **K. E. Dorcas, N. H. Simpson.** *Iron Age*, volume 155, April 5, 1945, pages 50–3, April 12, 1945, pages 68–73.

13. The Use of Statistical Control in Corrosion and Contact Resistance Studies, **W. E. Campbell.** *Transactions*, Electrochemical Society, volume 81, 1942, pages 377–90.

14. Die Technische Physik der Elektrischen Kontakte, **R. Holm.** Springer, Berlin, Germany, 1941; Edwards Brothers, Ann Arbor, Mich., 1944.

15. Factory Preweld Cleaning of 24S-T Alclad and 61S-W Aluminum Alloys With Hydrofluosilicic Acid Solution, **G. W. Scott, Jr., R. V. Ingram, A. A. Burr.** *Welding Journal*

Electronic Regeneration of Teleprinter Signals

H. F. WILDER
MEMBER AIEE

Synopsis: On asynchronous or start–stop telegraph circuits of extended length it frequently becomes necessary to insert at repeater points signal regenerative devices to reduce the cumulative effects of fortuitous distortion. Regeneration is a process of signal scanning by a succession of accurately timed impulses whose phase is as nearly as possible independent of the phase variations of the signal impulses. In one form of a mechanical regenerator, reception of a start signal transition permits the engagement of a brush arm with a continuously rotating constant-speed shaft. The signal polarity then is determined at the instant of contact of the brush with commutator segments that are short in comparison with the signal period. Following retransmission of the signal the brush arm is disengaged from the shaft and held on a stop to await the arrival of the start transition of a second character. Mechanical regenerators have been developed to a high level of performance, accompanied by some complexity and the need for skillful maintenance. This paper describes an electric signal regenerator utilizing the time of delay of a recurrent filter network to generate the scanning impulses, which together with the electrical equivalents of the start and stop functions provide a regenerative repeater without mechanism. The composition of an illustrative teleprinter signal character and its peculiar susceptibility to interfering line currents is discussed. The development and the electric characteristics of the delay network are described, and an explanation of the regeneration of the signal character by the device is given.

AN UNDERSTANDING of the operation of the electronic signal regenerator will be facilitated by a review of the principles of start–stop signaling and of one electromechanical device now used to decrease the fortuitous distortion on long circuits. Start–stop signals are semisynchronous; sufficiently good exactness of phase between the sending and receiving machines is maintained only for the time of duration of a single character after which a rest period must be provided to permit the entire system to come to a stop in preparation for the next character. Teleprinter signaling is thus differentiated from the synchronous systems, such as the multiplex, where each signal transition contributes to the continuous maintenance of exact phase.

The code containing the intelligence to be transmitted is common to both systems and consists of the various combinations of five unit length impulses of either spacing or marking polarity of the sending battery. In a synchronous system these arrive without interruption and are separated into groups of five units by a synchronized commutator. In an asynchronous system it is insufficient to transmit the five unit groups in isolated bursts followed by a rest period, for in some characters the first intelligence impulse is of the same polarity as the rest interval. The additional impulse required to initiate operation of the receiving device is created by a signal transition from the rest condition potential to the opposite pole and precedes the five intelligence impulses. Neither the rest nor this start impulse can be made shorter than unit length, if transmission on long lines is not to be impaired.

Though the start or synchronizing transition of the polar teleprinter signal is not inherently susceptible to the influence of random interfering line currents, phase shift of this transition is doubly damaging on a teleprinter circuit, as the selecting mechanism of the receiving printer is set in motion by the start signal and not by the phase of the average signal as in the synchronous systems. A transient disturbing current that advances the start-signal transition in time may well have its counterpart appear in the intelligence group and there delay a signal impulse by an equal amount to cause selection to be made close to the edge of the impulse. Therefore, when the interference level is the limiting factor in circuit operation, the teleprinter system requires just as careful engineering attention as a synchronous system of twice the transmission speed.

If fortuitous distortion is present in each of the separate lines of a long teleprinter circuit, the effects are accumulative when the lines are coupled by simple relays. Before the shifting in time of the signal transitions becomes sufficient to impair accuracy of service, signal regenerators are inserted at one or more of the repeater points. The basis of regeneration is a process of signal scanning by accurately timed impulses that are independent of the variations in arrival time of the signal impulses. From these observations made in the vicinity of the center of each impulse a new signal is created and retransmitted free of fortuitous distortion.

Mechanical Regeneration

The theory of a mechanical start–stop signal regenerator is shown in Figure 1. The system is at rest having completed the regeneration of the letter *F*. When released by their latches, the brush arms are rotated by the friction drives *CC* on the continuously rotating constant-speed shafts. Upon reception of a start-signal transition, the receiving-relay armature moves to the spacing contact *S*, energizing the start magnet *SM*-1 through the outer pair of brushes and releasing the brush arm on the receiving commutator shaft. As this arm moves counterclockwise, the signal polarity appearing on the tongue of the receiving relay is set up periodically on the selecting relay through connection to the shorter pickup segments. Immediately following signal selection the longer segments successively connect the selecting relay armature to the coils of the five storing relays. These relays firmly bank in the selected position. Only the intelligence impulses are scanned. If the speed of rotation of the brush arm is approximately that of the distant trans-

Paper 46-7, recommended by the AIEE committees on communications and electronics for presentation at the AIEE winter convention, New York, N. Y., January 21–25, 1946. Manuscript submitted August 9, 1945; made available for printing November 1, 1945.

H. F. WILDER is with the Western Union Telegraph Company, New York, N. Y.

(Research Supplement), volume 23, September 1944, pages 443-s–54-s.

16. SPOT WELDING—PART III—CONTACT RESISTANCE, R. F. Tylecote. *Welding Journal* (Research Supplement), volume 20, December 1941, pages 591-s–602-s.

17. THE PICKLING OF ALCLAD D.T.D. 390 AND B.S.S. 5L3 PRIOR TO SPOT WELDING, R. F. Tylecote. Institute of Welding, *Transactions* (London, England), volume 7, November 1944, pages 129–36.

18. ELECTRICAL CONTACTS, G. Windred. Macmillan and Company, London, England, 1940.

19. ELECTRIC CONTACT RESISTANCE, G. Windred. *Journal* of the Franklin Institute, number 231 June 1941, pages 547–85.

20. INVESTIGATION OF THE FINAL RINSING OPERATION IN THE CHEMICAL SURFACE PREPARATION OF ALCLAD 24S-T FOR SPOT WELDING, R. A. Wyant, D. J. Ashcraft, T. B. Cameron. *Welding Journal* (Research Supplement), volume 24, July 1945, pages 361-s–9-s.

mitter, the receiving relay will be on its marking contact, corresponding to the rest polarity, when the arm reaches the latch at the end of one revolution, and it will again come to rest.

At some time before the brush arm completes its revolution, a second pair of brushes is arranged to complete the energizing circuit of the unlatching magnet *SM*-2 to release the sending commutator brush arm. The latter continues to send the rest polarity momentarily until it passes over the segment *S* permanently connected to spacing telegraph battery to inject the start-signal impulse that must always precede the intelligence group. Further rotation of the arm connects the storing relays to the outgoing line in correct sequence and time of duration and entirely removed from the influence of the receiving relay. In circuit regulating a teleprinter is connected to the output of the sending commutator while a prearranged test signal is being received and the receiving commutator oriented until limits on the range scale are found within which the retransmitted signals are correct. The center of this angle or range is the center of the average of all the intelligence impulses; correct signal selection is most probable with this angular position of the scanning segments. This adjustment also compensates for the time interval required to accelerate the brush to shaft speed and for any change in clutch operation that may have previously occurred.

Figure 1. Theory of the mechanical teleprinter signal regenerator

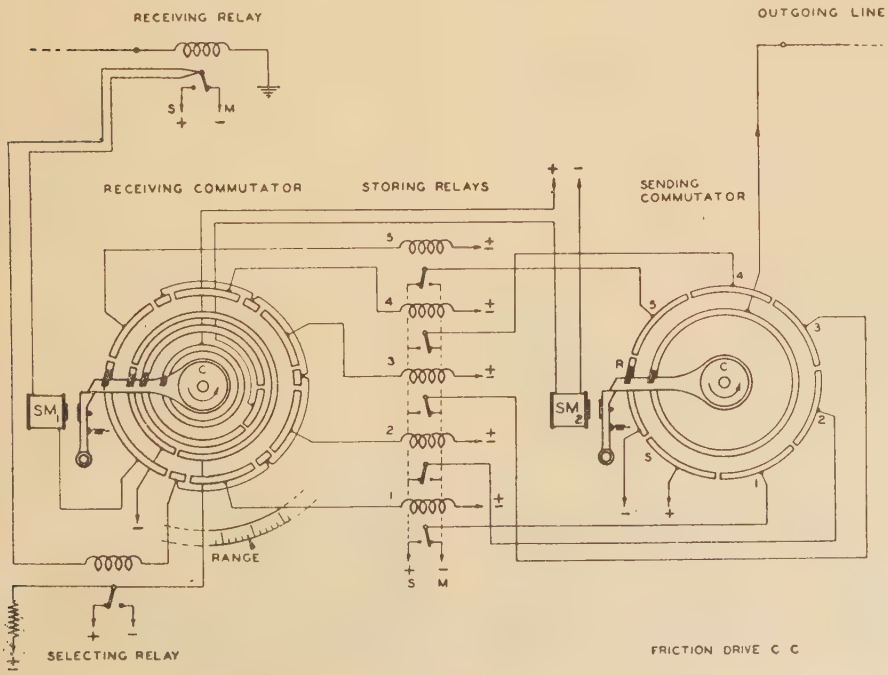

The Timing Network

Perhaps the most interesting problem in the development of the electronic regenerator was the choice of a scanning-impulse generator. Two rather incompatible requirements are presented. To insure good signal quality it is desirable that the timing of these impulses be of such an order that the last scanning impulse in any train shall not deviate from a standard time taken with the start-signal transition as the origin by more than one half of one per cent. Following the production of a single train of impulses, the generator must come to rest immediately if a retardation in the generation of a second train is not to result. And, being part of a start–stop system, the generator always must come up to speed, as it were, regardless of the time that it may have been at rest. Simple oscillators of the specified frequency stability do not lend themselves to this purpose because of the transients which cushion the change from rest to steady state and vice versa. However, the resonance phenomena that give the oscillator frequency stability may be retained in certain reactive filter networks, and in particular the uniform recurrent ladder structure, without the troublesome transient effects. With correct configuration these structures will provide time of delay between the mesh junctions dependent upon the choice of the network parameters, and, if a connection is effected between the junctions and electronic relays arranged to scan the received signal impulses, the rate of transmission of the regenerated signal will be a function of these time intervals.

For this application the network should not exhibit frequency discrimination. It should pass all frequency components in the driving force with a constant time of delay. Then the arrival curve will possess infinite slope (zero time of build up), and the triggering of the vacuum-tube relays connected to the network junctions will occur precisely at times determined only by the reactive components of the network and independent of the regulation of the power-supply voltage.

In general the attenuation and time of delay of reactive networks are not invariant with frequency. The mid-shunt or pi section of the familiar low-pass filter composed of a series inductance and shunt capacities will discriminate somewhat against frequencies even below cutoff, and the phase characteristic is so concave that frequencies near the cutoff are delayed considerably more than components approaching zero. Either frequency or delay distortion in the filter will act to decrease the slope of the transient response or arrival curve, and experiment soon confirmed the necessity for correcting the natural behavior of the network. Equalization with additional network components was objectionable because of the increased cost and space requirements, so attention was given to improving the inherent frequency characteristics of the delay-network sections. The steps leading to a section having a satisfactory transient response are shown in Figure 2.

The actual coils had ferromagnetic cores and a Q of 20 at 45 cycles per second. With this Q the effects of dissipation are not excessive, and the output voltage at the terminating resistance is more than half that of the driving force. For comparison the total inductance and total capacity in each of the four cases calculated were held constant. The loci of the short- and open-circuit reactances were first computed and the square root of their product, the characteristic impedance Z_o plotted immediately below. In the determination of the frequency response only one section of each type was considered. The section was assumed to be driven by a harmonic generator having an internal resistance equal in ohms to the nominal value of the characteristic impedance of the network and to be similarly terminated. This is the situation in the regenerator, except that several sections are in cascade. The frequency response Y is the locus of the IR drop across the terminating resistance versus frequency and is an admittance function. The time of delay has been plotted directly below the transfer admittance, and at the origin this time in seconds is the

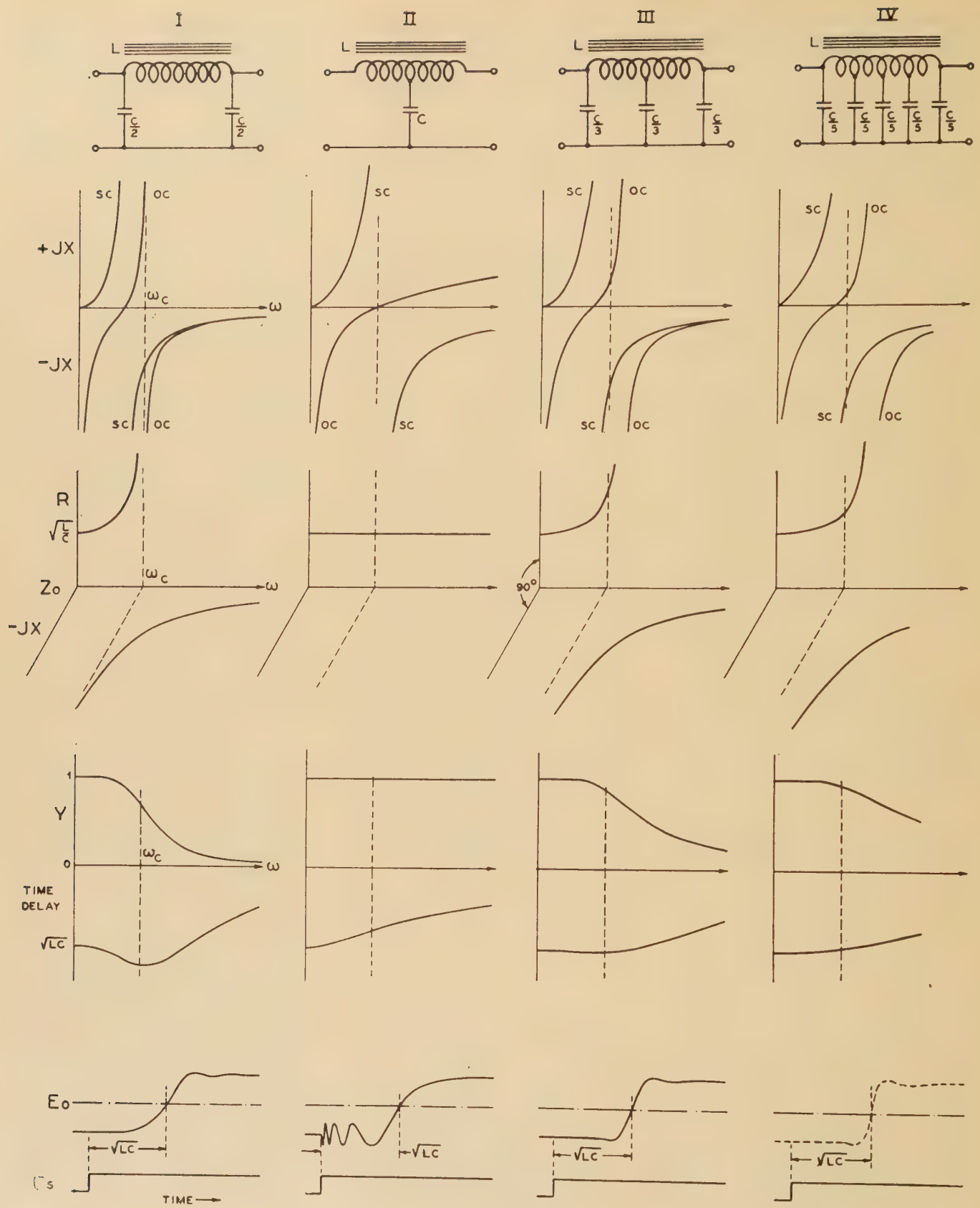

Figure 2. Frequency characteristics of delay network sections

square root of the oscillation constant, LC. With each increase in frequency the delay was obtained as the quotient of the angle of current lag in radians and the angular frequency ω. In all the loci having the angular frequency as abscissas the ordinate ω_c, the theoretical cutoff frequency of section I has been drawn in for reference.

The transient response at the resistive termination of a cascade of six sections is shown at the bottom of Figure 2. These are reproductions of oscillograms. The rectangular driving voltage is E_s. There has been no opportunity to confirm experimentally the transient response of section IV, and the dotted curve is only a prediction of its form.

Returning to the first filter studied, section I, an inspection shows that as long as the short- and open-circuit reactances are of opposite sign, the characteristic impedance, the impedance that would be seen looking into an infinite number of such sections in cascade, is a pure real quantity and has the appearance of a rapidly increasing resistance with frequency up to the cutoff point. In this range the network will absorb power from the generator and transfer this power to the resistance termination. Beyond the cutoff frequency the reactances are of like sign, the impedance becomes an imaginary quantity decreasing with frequency, and the power transmitted by the filter falls off rapidly. In the transmission range between zero and the cutoff frequency where the attenuation is low, the delay distortion is of particular interest, for in this region it has the major effect on the transient response. As the frequency of the driving force is increased, the delay is not constant but increases to a maximum at the cutoff frequency. In a section having a nominal time of delay of 22 milliseconds, for example, the cutoff frequency is 14.3 cycles, and components in this vicinity will be so delayed as to arrive nearly 180 degrees out of phase with respect to the components of the wave near zero. Beyond the cutoff frequency the delay time is of less interest, for the components beyond this point are so attenuated as to contribute very little to the slope of the arrival curve anyway. Because of this variation in transmission time the slope of the transient response continuously changes, being initially low as the low-frequency groups arrive first and only attaining maximum steepness after crossing the zero axis as the frequencies in the vicinity of cutoff finally make their appearance. This form of response is not ideal for the operation of devices responsive to the magnitude of the driving voltage, and it was recognized as similar to the arrival curve of a loaded submarine telegraph cable. Here in the receiving network a mid-series or T section with mutual coupling between the coil arms is used as a distortion equalizer, and so similar sections as in section II at first were alternated with the pi sections with considerable success.

Because the characteristic impedance of section II is real and constant, the filter transmits power without discrimination at all frequencies from zero to infinity. Its phase characteristic, however, is convex and opposite to the concave characteristic of its alternate, the pi section. The slope of the phase characteristic, the delay time, is a decreasing function of frequency. A network composed of these sections alone is just as unsatisfactory as the mid-shunt section, because now the low frequencies are the last to contribute to the arrival curve, and the higher frequencies arrive early, with those approaching infinity having no delay at all. Alternation of the two types doubled the number of coils in the complete delay network.

If a center tap on the coil of the pi section is connected to a portion of the total shunt capacity, the new filter, section III, will be found to have a response equivalent to the alternate arrangement of sections I and II. From an inspection of the characteristics we find that the pole of the characteristic impedance has moved to a somewhat higher frequency and that the impedance locus is more nearly constant over a wider range of frequencies prior to the cutoff frequency. Consequently there is less loss in the transmission range because of increased coincidence with the terminating resistances. Of equal importance is the less rapid decline in the transfer admittance beyond the cutoff frequency of the pi section. The improvement in the locus of time delay is most prominent. Up to the new critical frequency the delay is constant, as the opposite characteristics of the combined filters mutually compensate, and the ultimate decrease is at a lower rate than either alone. This region beyond the cutoff is now of real importance, as the less attenuated higher frequencies are present in the transient response in more nearly correct phase with the lows and can contribute to its steepness. The transient response is the result of the synthesis of a wider band of frequencies of nearly simultaneous arrival time, so that its time of build up is a minimum, and it is symmetrically located about the zero-voltage axis. This is the configuration used in the timing network of the electronic regenerator.

The network contains a minimum number of coils, and the timing of the individual sections may be adjusted easily in a step-by-step refinement of the nominal capacity values without disturbing the timing of the preceding sections. With trigger tubes that will operate on a voltage swing one third that available at the terminating resistance, the variation in their operating time is well within the prescribed limits for a ten-per-cent change in the power-supply voltage and the ambient-temperature range ordinarily encountered. The precision of operation is comparable to that of a well-machined commutator with a synchronous motor-driven brush arm. The actual network consisted of six sections, each having a coil of 72 henrys and a total shunt capacity of 6.7 microfarads, preceded by a seventh section of half the delay. The time of delay of each larger section is 22 milliseconds; very closely the time length of a single teleprinter signal impulse. As measured at the terminating resistance, the time of build up was 40 milliseconds, which becomes less at junctions nearer the input terminals. The network occupies a space of approximately one cubic foot.

One might theorize as to the response of a section similar to III in which the total shunt capacity is still further subdivided into a not impractical number of paths. Improvement would be evidenced by an increase in the steepness of the transient response. To confirm this speculation the frequency characteristics of such a filter, section IV, in Figure 2, were calculated. In the locus of the characteristic impedance Z_o the critical frequency has moved still farther to the right, and the real part of the impedance is more flat for a wider range of frequencies. Consequently both frequency characteristics are improved. Although the time of delay is somewhat more constant than that of section III the greater improvement appears in the frequency response, Y, which is noticeably more constant.

In this paper the time of build up of the transient response has been assumed to be the time interval between the intersection of the timing wave with a prolongation of the steady-state levels before and after its occurrence. In filter sections having nearly constant time of delay, so that all components arrive in correct phase, the time of build up will be inversely proportional to the band width. Neither section III, nor particularly section IV, can be said to have definite frequencies of cutoff limiting the band width. However, when it is recalled that after all the low frequencies furnish the bulk of the wave, it is interesting to establish arbitrarily such a limit for the three sections at a frequency 2.5 times the cutoff frequency of section I and to then compare the relation between the areas under the admittance loci and the times of build up. The inverse ratio of the areas of section III and section I is 0.74, a rather close agreement with the experimentally determined times of build up of 40 and 55 milliseconds respectively for timing net works composed of such sections alone. In like manner the inverse ratio of the areas under the Y loci of sections IV and III is 0.85, so that the predicted time of build up for section IV becomes 85 per cent of 40, or 34 milliseconds.

It seems, therefore, that continued subdivision of the shunt capacity will not increase the steepness of the timing wave reversal sufficiently to justify more numerous coil taps and capacitors. For timing purposes section IV is an adequate approach to the ideal section of constant attenuation and constant time of delay.

The Electronic Regenerator

The theory of the electronic teleprinter signal regenerator with a timing network of type-III delay sections is shown in Figure 3. The relays and regenerative circuits are in the rest condition. A series of voltages occurring in the system for the regeneration of the letter *F* is shown in the lower part of the figure. While the times t_0, t_1, and so on, represent instants of signal transition in the absence of distortion, the existence of extraneous line currents has been assumed, and the signal transitions have been delayed or advanced to an extent not greatly different from that actually encountered in operation. In any event the theoretical limit is one fourth the period of a single impulse.

In the regenerator twin-triode vacuum tubes are arranged in symmetrical push–pull circuits to eliminate polarity distortion. Pair 2 and their external plate resistors form a bridge circuit the diagonal of which is the impedance presented by the input terminals of the timing network. The plate circuits of the other low-power tube, pair 4, are the differentially wound coils of the sending relay. Telegraph battery potential is connected to the contacts of this relay, and from its armature the regenerated signal is applied to the apex of the duplexed east line. The remaining tubes are characterized by relatively low transfer conductance and high amplification factor. The pickup and latch tubes are simply electronic switches. Dependent upon the polarity of the control-grid voltage, these tubes present either an extremely high plate–cathode resistance or a resistance comparable to the impedance of the circuits to which they are transformer coupled. The remaining nine tube pairs are connected in a balanced Eccles–Jordan trigger or flip-flop circuit. This circuit displays negative resistance between plate elements over a portion of the characteristic between the stable states, and, if a momentary displacement of the grid voltage occurs, the potential from plate to plate will instantly reverse. This relay characteristic will convert any general input wave form in the grid circuit above a definite minimum to a rectangular output wave of constant amplitude.

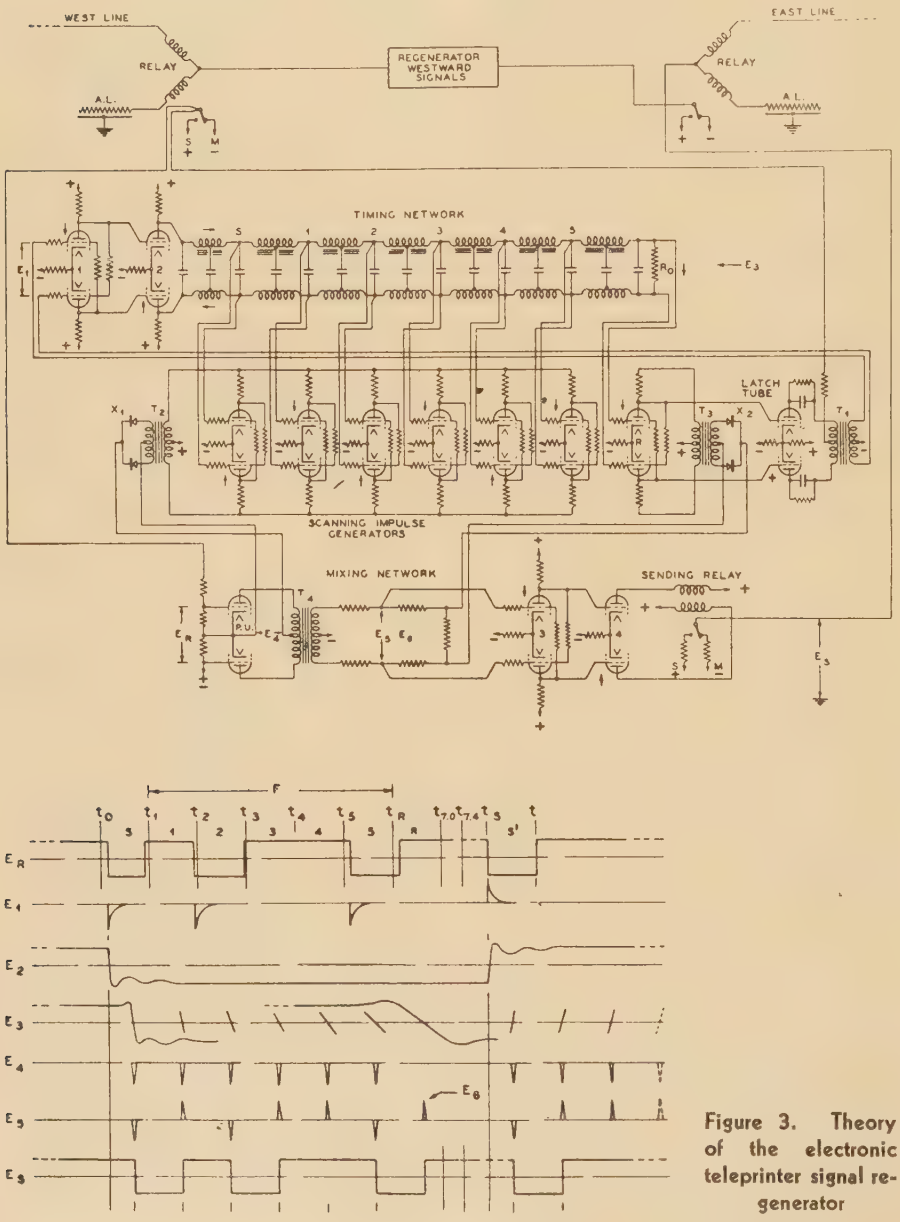

Figure 3. Theory of the electronic teleprinter signal regenerator

The nominal characteristic impedance of the timing network is equal to the resistance looking back into the bridge circuit of tube 2. Except for the first section of the network, which has half the delay of any one of the following six, each section has a time delay ($t_d = \sqrt{LC}$) equal to the time of duration of an undistorted signal impulse, or 21.98 milliseconds. Each inductor consists of two identical windings on a single silicon steel core so disposed that the cathode returns of the six scanning-impulse generators and the rest-interpolating tube are equipotential with a horizontal plane bisecting the network. A reversal of the network input potential appears across the junction *S* eleven milliseconds later and at the termination R_0 in a total elapsed time of 143 milliseconds.

Regeneration is begun by movement of the receiving-relay armature to the relay-spacing contact in response to the start impulse of a teleprinter character. As directed by the latch tube, a single reversal of potential is applied to the timing network by its driving tubes. With progression of the timing wave from junction to junction a series of six pickup impulses are generated successively activating the pickup tube scanning the incoming signal. The observed polarity of each signal impulse is at once transferred to the sending-relay drive tubes through the mixing network. Twenty-two milliseconds after the selection of the fifth intelligence impulse the timing-wave reversal appears across the resistance termination and triggers the *R* tube to interpolate an impulse

of the rest polarity in the mixing network and simultaneously to make the latch tube again receptive to any future start signal.

A more detailed description must begin with an examination of the circuit conditions with the regenerator at rest. Now the receiving-relay armature is held on its negative contact by the marking line current received, and negative battery is applied to the center tap of the transformer T-1. A second circuit from the receiving-relay armature develops the incoming-signal voltage E_r in the grid circuit of the deenergized pickup tubes. As indicated by the small arrows adjacent to the tube elements, all trigger tubes are banked in the direction last operated; a condition that will be reversed after the regeneration of a complete character.

A constant current from positive battery flows through the external plate resistor associated with the upper tube of the driving pair to the right and along the upper windings of the inductors to the terminating resistance R_0. This current returns to negative battery through the lower windings and the lower and conducting drive tube. By reversing every other pair of wires connecting the scanning-impulse generators to the network junctions, these tubes are banked in alternate directions, and the sum of their plate currents entering the center tap of the primary of T-2 is divided equally between the winding halves. Consequently as the scanning-impulse generators are triggered successively, the differential primary current never exceeds unit amplitude, and hysteresis effects in the core material are minimized.

Just as a similarity will be recognized in the function of the latch tube and the brush-arm release mechanism of the mechanical distributor, so are the R-tube functions equivalent to the R segment on the sending commutator and the two paired segments on the outer rings of the receiving commutator which permit the start magnet circuit to be energized only after a complete revolution of the brush arm. If the upper R tube is conductive, the plate of the nonconducting lower tube will be at a very high positive potential and will by direct connection correspondingly elevate the grid of the lower latch tube. Upon reception of a teleprinter signal the center tap of T-1 is at once made positive as the receiving-relay armature contacts its spacing stop. Under the conditions established, however, a charging current to only the lower-resistance shunted condenser flows in the lower half of the primary winding of T-1. The transient secondary voltage is E_1. In the course of reception of the incoming signals negative potential is at times applied to the center of T-1, and in these intervals the condenser charge is dissipated in the shunting resistance. If correctly poled the transient E_1 causes tube 1 to trigger, reversing tube 2 and the potential across the timing network. Subsequent impulses of like polarity in E_1 may occur in the reception, two more are present in the letter F, but the initial impulse alone is of importance.

Although the continuity of the description perhaps is interrupted, an interesting operating condition now may be described. This occurs when either the west line is opened or, if in circuit, regulating, the west transmitter sends steady spacing battery. In either case the marking battery applied to the apex of the west duplex line at the regenerator station causes a current to flow in the artificial line winding of the receiving relay, which holds the armature on the spacing contact and so applies positive battery to the midpoint of T-1. Now upon the arrival of the first timing wave at R_0 the conductivity of the latch tubes is interchanged while their plate circuits are energized positively and a starting impulse of local origin is created in E_1. A second timing wave is set up, and the process becomes continuous. A characteristic recurrent signal of six-unit length impulses of spacing polarity followed by a half-unit length marking impulse is transmitted to the east line; a signal that is easily interpreted by the distant east receiver as an open line west of a regenerative repeater.

Returning to the description, the R tube is also the circuit element that restores the sending relay to its marking contact after the transmission of the intelligence impulses. A reversal of the R tube in either direction produces a transient voltage in the secondary of T-3. These are introduced at the right of the mixing network after being made unidirectional by the rectifier X_2. The solid triangular impulse E_6 in the time diagram is of this origin. Consequently the regenerator cannot fail to send a rest signal.

The wave form of the timing-wave reversal across the network input terminals is shown in E_2. Until this reversal has reached the termination R_0 and operated the R tube, another reversal cannot occur, and then only with reception of a second character of which S' is the start impulse. Although a gradual decrease in slope of the wave is apparent as successive meshes attenuate the higher-frequency components, symmetry is retained as depicted in E_3. The scanning-impulse generators are triggered at intervals of at first 11, and then 22 milliseconds. The sum of their plate currents in the differentially connected primary windings of T-2 is either zero or unit amplitude, depending upon whether an even or odd number of impulse generators are at any instant banked in like electrical position, and a change in net primary current occurs six times with the passage of a single timing wave. The resultant series of six alternately poled derived impulses of extremely short duration in the transformer secondary is rectified by X-1 and introduced, as E_4, between the cathode and plates of the pickup tubes.

Any one of these scanning impulses can produce current flow only in that half of the primary of T-4 associated with a pickup tube whose grid is positively displaced with respect to the common cathode connection. The polarity of the transformer secondary voltage is therefore dependent upon the polarity of the incoming signal E_r at the instant of scanning. A proportion of the polarized pickup voltage appears as E_5 at the midpoints of the mixing network to position the sending-relay drive tubes and the sending relay. E_s is a plot of the telegraph battery potential transmitted by the sending relay to the east line. It is a reproduction of the perfect signal originally transmitted, being composed of unit length impulses as determined by the timing network and independent of variation in received-signal transition time.

If signals are transmitted from a slowly operated keyboard, the rest impulse is considerably longer than unit length. Frequently, however, intelligence groups contained in a perforated tape are passed through a transmitter that automatically inserts a rest-and-start impulse between groups. In this case the rest impulse may be considerably shortened, if, under the most adverse effect of signal distortion, the preceding start impulse suffered delay in arrival and the start transition of the following character is advanced in time. Then the rest signal is not regenerated but must absorb the total phase shift of the two start impulses. In some systems a 42-per-cent extension in length of all rest impulses is made to absorb these phase shifts, but a reduction in the number of letters per minute transmitted must be accepted if the same maximum line frequency is retained.

Performance

To measure the telegraphic efficiency of the regenerator a chemically recording transmission testing machine was used. Transmission was continuous from a pre-

pared tape, unless to simulate keyboard sending the transmitter was sporadically autostopped. To permit the time relation between any regenerated signal impulse of a character and its start impulse to be observed, the sending ring could be rotated through increments of one segment.

With this arrangement the timing of the network sections was adjusted successively until the maximum departure from normal of any regenerated impulse was less than two per cent. By moving the segment sending the start impulse with respect to the segments sending the intelligence group, the minimum time of duration of an impulse required to insure correct selection by the pickup tubes was found to be 0.5 millisecond. The response of the latch tubes to the start signal was instantaneous, irrespective of how long the regenerator had been at rest.

Physical Aspects

The electronic regenerator has been developed as an adjunct to direct-point repeaters. Any one of a group of rack-mounted unidirectional units may be inserted quickly in a teleprinter circuit at a repeater station. Experience has shown that the regenerator will operate continuously for six months without attention.

A New Submersible Network Protector of Higher Rating

G. G. GRISSINGER
MEMBER AIEE

F. D. JOHNSON
ASSOCIATE AIEE

DURING THE DEVELOPMENT of the original low-voltage a-c-network distribution system, preliminary studies indicated that the use of a relatively large number of medium-sized distribution transformers would provide the most flexible and most economical arrangement. Furthermore, very satisfactory operating experience with network systems of this type gave considerable justification for their use.

Obviously the network protectors required were also of relatively small size, since the continuous ampere rating and the interrupting rating were influenced by the size of the distribution transformers used. This meant that the majority of the protectors had continuous ampere ratings of 250 and 500 amperes at 60 cycles and interrupting ratings of 15,000 to 20,000 amperes at 220 volts.

However, the rapid growth of the a-c low-voltage-network distribution system, together with its adoption in many different types of application, soon developed the need for network protectors of considerably higher ampere ratings. The first expansion extended the continuous ampere ratings to 800 and 1,200 amperes. Subsequently the range was increased further to include 1,600- and 2,000-ampere ratings.

During this period the interrupting ratings remained at 20,000 amperes. But operating experience with systems having greater power concentrations, together with calculations of possible short-circuit currents, eventually led to the development of network protectors having interrupting ratings up to and including 40,000 amperes.

The need for the higher interrupting ratings also resulted from the use of spot networks requiring large concentrations of power and involving a number of large distribution transformers. In addition to having high interrupting ratings the network protectors for these applications required continuous ampere ratings as high as 3,000 amperes 60 cycles.

Most of the original network protectors were located in building or basement vaults not subject to flood conditions. This meant that the protectors could be mounted in the open air or in ventilated enclosures. Heat losses generated in the protectors therefore were dissipated readily, and it was not a difficult matter to provide reasonably compact units for any of the required ampere ratings.

Extension of the secondary network distribution system soon showed the desirability of installing network units in subway vaults either under the street or under the sidewalk. Installations of this type were of course subject to flood conditions, and both transformers and network protectors had to be made submersion proof. In the case of the network protectors, which were essentially automatic air circuit breakers, the enclosures had to be watertight, in fact airtight. Dissipation of heat from an airtight enclosure, with air inside the enclosure as the transfer medium, could occur only by straight conduction, convection, and radiation, with very little benefit from air flow.

This problem obviously becomes more difficult as the continuous ampere rating increases due to the greater heat losses developed. It is believed therefore that the problems involved and the methods used to produce a 3,000-ampere a-c submersible network protector of reasonable dimensions will be of interest.

General Description

The 3,000-ampere submersible network protector for 120–208-volt three-phase 60-cycle service is the latest development for application to secondary networks having highly concentrated load areas. The interrupting rating of this protector is 40,000 amperes. The accepted practice for network protectors requires that the circuit breaker withstand an initial instantaneous peak of $2^1/_4$ times the rms current which is to be interrupted, in this case a peak of 90,000 amperes, and requires that it carry the short-circuit current for 60 cycles before the current is interrupted.

The submersible network protector, as the term implies, is enclosed in a heavy steel housing suitably constructed to withstand submersion in water up to a depth of at least 15 feet and is in addition so constructed as to be readily accessible for maintenance. Figure 1 shows such a network protector completely closed as it is in service. The only electrical connections are those to the main circuit by means of the solid copper studs through porcelain bushings. The cover of the housing is a separate fabrication which is hinged, gasketed, and clamped to the tank body in such manner as to be readily

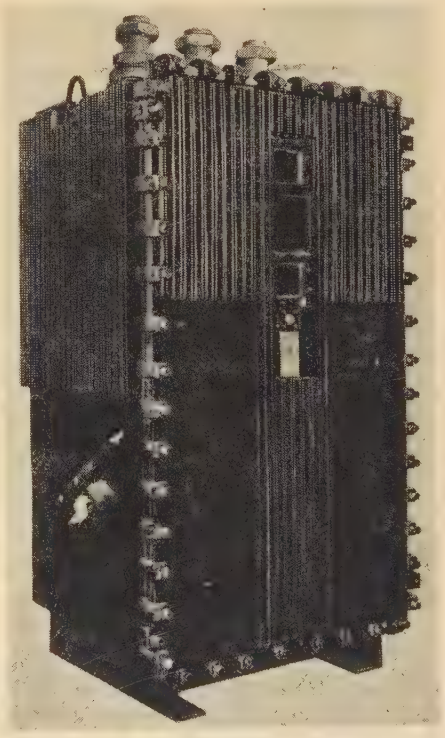

Figure 1. Submersible-type 3,000-ampere network protector for transformer mounting showing exterior cooling fins

Paper 46-11, recommended by the AIEE committee on protective devices for presentation at the AIEE winter convention, New York, N. Y., January 21–25, 1946. Manuscript submitted October 3, 1945; made available for printing November 14, 1945.

G. G. GRISSINGER and F. D. JOHNSON are in the switchgear control engineering department, Westinghouse Electric Corporation, East Pittsburgh, Pa.

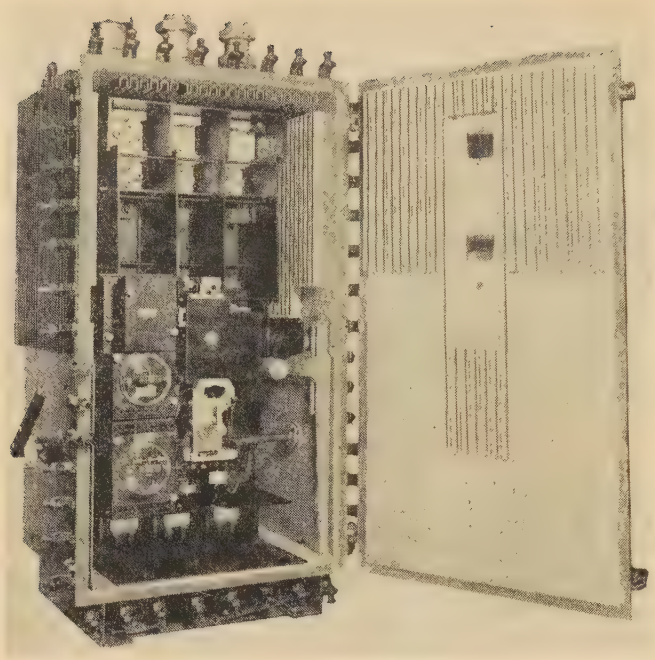

Figure 2. Submersible-type 3,000-ampere network protector for transformer mounting showing interior cooling fins

opened for access. The protector proper is a unit assembly which can be disconnected readily at top and bottom from the power circuit and rolled forward on collapsible tracks mounted within the housing. Briefly described, this protector unit consists of a three-pole motor-operated circuit breaker, three fuses, a master network relay, a phasing relay, and a desensitizing relay. See Figure 2.

Reduction of Copper and Iron Losses

It is well known that for solid copper conductors of a size suitable for carrying 3,000 amperes at 60 cycles there is considerable "skin effect" and also that there is considerable power loss in magnetic members in proximity to such conductors. Both of these factors are comparable to an increase in resistance of the conductor, and, as such, it is evident that the power loss within the protector varies directly as the square of the current carried. This is roughly a measure of the difficulty encountered in increasing the current-carrying capacity of the network protector without at the same time drastically increasing its operating temperature. It is impractical to increase the carrying capacity without some increase in total losses, and the dissipation of these additional losses through the housing to the outside air further complicates the heat problem. A network protector, like most electric equipment, must be made as compact as is consistent with good design; this mechanical requirement is in direct opposition to the tendency of higher currents to result in larger conductor sizes, higher magnetic forces on contacts, and, hence, larger mechanisms. It was the judicious balancing of these factors with certain improved arrangements which made the present development possible.

The phenomenon of skin effect is well known, and in general its effect is quite readily calculated.[1] However, in the case of a compact multiple-pole circuit breaker with its irregular current paths, proximity of adjacent phases, and proximity of magnetic materials the problem is complicated by proximity effect,[2,3] by iron losses, and by contact losses. Because of the indeterminate nature of the combined losses it was decided early to study the losses experimentally by measuring the actual a-c resistance of the circuit breaker and its parts. The loss in relay potential and current coils is a small part of the total, and hence the problem is entirely one of current losses, except for consideration of the temperature rise of the coils themselves. A search of the literature on the subject did not disclose a previously available method of readily and directly measuring the 60-cycle resistance of such heavy copper circuits. The method employed is described in the appendix.

Conductors of a size to carry 3,000 amperes at 60 cycles are most efficient when made in a tubular form, preferably of circular section, with a wall thickness of approximately 0.5 inch but specifically related to the actual diameter.[3] Because of practical considerations in arranging contacts and connections in limited space a hollow conductor of square section has been used for current-carrying parts wherever practical. Since these hollow conductors are open at each end and since they are mounted vertically, natural convection is effective for cooling inside as well as outside surfaces. (For a comparison of some typical conductors, see Table I.)

The movable contact or bridging member of the circuit breaker cannot readily take the form of a hollow conductor, especially in the limited space available in a network protector, and hence an alternate type of conductor had to be used here. The conductor used takes the form of six copper blades per pole in parallel, these being hinged at their lower end similar to the blade of a knife switch, and engaging stationary jaws at their upper end. The copper blades are arranged in pairs with three such pairs making up a bridging member for each pole. In each pair the blades are placed with the flat faces of one parallel to those of the other. The next pair is in a similar position but spaced approximately one inch away. This configuration of six flat bars in parallel if extended in length would have a current distribution over its cross section no better than would a solid conductor of the same outside dimensions. However, in this case each of the six conductors is only several inches in length and at each end there is a contact, the resistance of which is appreciable compared with that of each bar itself. The effect of these contacts is to equalize the current flowing through the six bars, and therefore the current distribution over the cross section

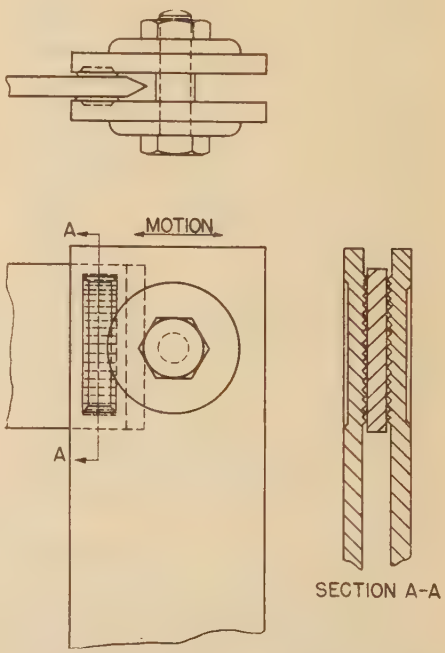

Figure 3. A view showing detail construction of the multiple silver-plated line contact at the break end of the bridging- or moving-contact members

of each bar is comparable with that which would flow in a single isolated bar, and all six bars carry current effectively.

At the hinge joint of each pair of bars the contact is a hard silver plate of substantial thickness on both the moving bars and on the stationary jaw which is placed between them. Pressure is applied to these contacts by means of a through bolt and cup-washer springs.

At the break end of the bridging members the stationary jaw is similarly silver plated and is tapered at its engaging edge to facilitate engagement with the moving bars. The bars, however, engage this jaw only for a portion of their width in order to conserve travel. The portion of a bar which engages the jaw at this point is silver-plated and then by high pressure dies is embossed into a series of parallel, raised, and hardened silver lines each with its axis in the direction of the sliding action of the contact. Figure 3 shows the arrangement of the embossed-silver multiple-line contact. Pressure on the break contact just described is secured in the same manner as at the hinge joint, that is, by means of a transverse bolt through the two bars and a cup-washer spring on either side. Figure 4 shows the construction of the circuit breaker.

Each pole of the protector is fitted with a fuse, usually on the network side, to serve as standby protection in case of apparatus failure or to open the circuit in case of a bad nonclearing fault on the network side close to the protector. These fuses are designed to operate at an unusually low temperature in order not to add unduly to the heat problems of the protector. Low operating temperature is obtained by constructing the fuse with a fusing member from a small section of low-melting-point eutectic alloy; the balance of the fuse body is heavy copper.

Network protectors commonly are enclosed in steel housings, and, because they are made as compact as practical, it is obvious that at some point the conductors will approach this steel enclosure or actually pass through it, resulting in hysteresis and eddy-current losses in the steel. These losses actually may equal or exceed the copper losses, unless preventive measures are taken. The method of measuring a-c losses which is described in the appendix was especially useful in tracing and eliminating these iron losses. It was found necessary to make the top plates where the main bushings pass through, and the rear plate of nonmagnetic steel. Also, mechanism brackets, levers and frames, and circuit breaker mechanical parts had to be nonmagnetic.

Heat Dissipation

When the circuit breaker has been developed to generate the minimum practical amount of copper and iron loss there still remains the problem of dissipating this heat through the steel housing or enclosure at the relatively small temperature differential which is available. The usual air circuit breaker has only copper loss to be dissipated and dissipates this by conduction, radiation, and convection directly to the surroundings; the usual oil circuit breaker by conduction to the oil and then by conduction, radiation, and convection to surroundings. The temperature differential available for the dissipation of heat is 85 degrees centigrade for class-*B* insulation.

The radiation of copper losses takes place in the network protector in three stages, namely, in one temperature drop from the copper to its barriers and immediate surroundings, in a second temperature drop from these surroundings to the inside of the enclosing housing, and in a third temperature drop from the housing exterior to surrounding objects. Similarly, in the dissipation of copper losses by convection it is found that there are three temperature drops in series, namely, first from the copper to the surrounding air, second from this heated air to the housing structure, and third from the housing to the exterior air. By conduction some heat is transmitted directly to immediate surroundings of the conductor and from there is taken by radiation and convection to the housing and to the outside; but the amount of copper loss which may be conducted directly to the housing structure is very small. Conduction through air to the housing walls accounts for a very small portion of the heat loss. Fortunately the iron losses which are allowed to remain are generated directly in the housing itself.

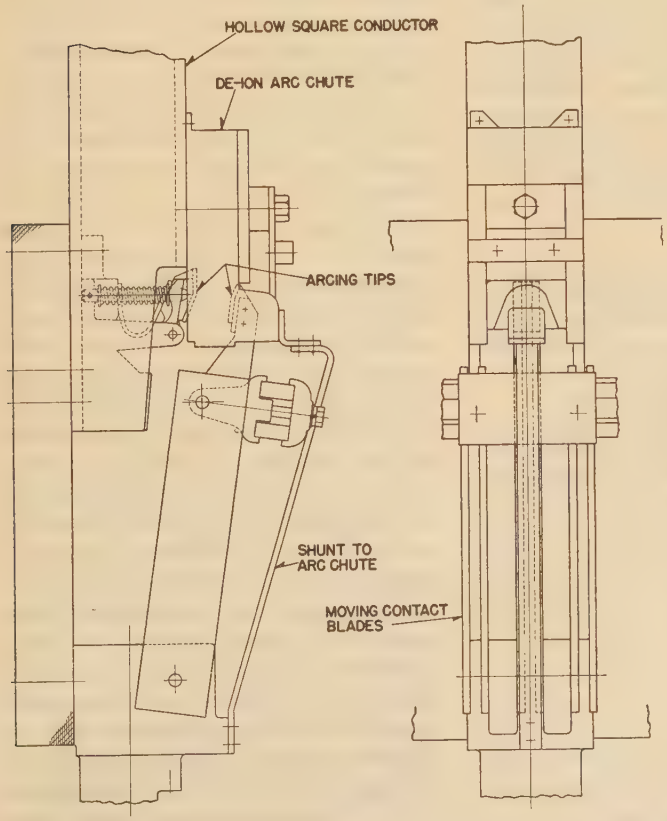

Figure 4 (left). A view showing the arrangement of circuit-breaker contacts and deion arc chute

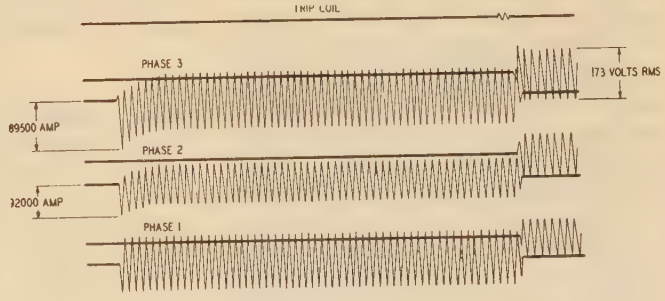

Figure 5. Oscillogram of a short circuit of 40,000 amperes at 300 volts, 60 cycles

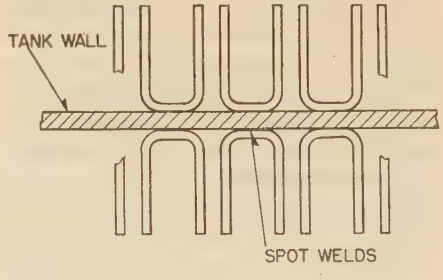

Figure 6 (right). Cross section showing arrangement of cooling fins

As radiation and convection are the chief factors in the dissipation of the copper losses, it is proper that all possible factors should be introduced into the design favoring the dissipation of the heat by these means.

The dissipation of heat by radiation is given by the Stefan–Boltzman law:

$$Q = 5.7 \times 10^{-12}(T_1^4 - T_2^4)e$$

where

Q = energy radiated, in watts per square centimeter
T_1 = absolute temperature of radiating body in degrees Kelvin
T_2 = absolute temperature of surrounding surfaces in degrees Kelvin
e = total emissivity of surfaces

Since this quantity is proportional to the difference of the fourth power of the two absolute temperatures, it is evident that dissipation by radiation can be very useful even for small temperature differentials, provided the values of e are as high as are practically obtainable. To this end the copper conductors are given an oxidized copper finish the emissivity of which is 56.8 per cent[5] as compared with unoxidized or unfinished metal surfaces which have an emissivity of four per cent or less. The housing surfaces, both interior and exterior, are finished with pigmented paints having even greater values of emissivity.

The convection factor for the removal of heat from the conductors is enhanced by taking advantage of the chimney effect of the vertical hollow conductors and by the bridging member of the circuit breaker being a number of thin conductors in parallel. The return bus bars at the rear of transformer-mounted network protectors are mounted on insulating members to the rear plate of the housing, which plate is nonmagnetic steel, with nonmagnetic steel cooling fins extending from the plate forward between the bus bar members and at each side of them. These fins, in this interleaving manner, both by radiation and by convection, extract heat from the bus bar members for their full length.

It is just as necessary to favor the heat transmission through the housing as it is to favor getting it out of the conductors. The housing is painted inside and out, giving these surfaces an emissivity of around 89 per cent, so that for radiated heat the walls are a good transmission means. However, by conduction the conductors heat the air within the housing, and it immediately rises to the upper portion of the housing, where it tends to stagnate. The conductors occupy the full height of the housing and generate

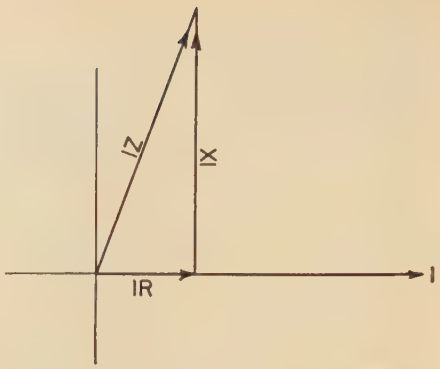

Figure 7. Diagram showing balancing of voltage components in the bridge circuit

I = test current
IR = inphase test voltage
IX = 90-degree test voltage
IZ = voltage drop of test specimen

heat for their entire length, so that the heated air tends to circulate upward past the conductors, and they get the benefit of true convection cooling. However, the heated air moving upward stagnates in the top of the housing and is cooled mainly by conduction through the housing walls. To cool this air and establish a full circulating system it is necessary to add greatly to the exposed surface of the housing, both internally and externally, in the hot region. This is done by adding cooling fins to both the inside and the outside surfaces as shown in detail in Figure 6, this being necessary only for approximately the upper one half of the housing. For each one square inch of base or radiating area, either inside or outside, there is an exposed area including fins of 5.1 square inches. The fin arrangement shown is a practical means of construction devised to get the necessary heat through the available wall area without increasing housing dimensions prohibitively; it is not theoretically correct in proportions, either in efficiency of a given amount of base surface or in the amount of metal used. Radiation alone is not sufficient to cool the conductors and housing, and it is not practical to load the conductors with cooling fins; therefore, it has been necessary to allow a relatively large temperature differential from the conductors to the air in the housing and to work toward smaller temperature drops from this air to the housing wall and from the wall to the outside air by heavily loading the housing walls with fins.[4,6,7]

Table I. Comparison of Typical Copper Conductors at 60 Cycles

	Gross Section, Square Inches	Surface, Square Inches Per Inch	A-C Resistance, Microhms Per Inch	$\frac{R_{a-c}}{R_{d-c}}$
1 1/4x4	5.00	10.5	0.327	2.07
Solid bus[4]				
4-inch hollow square 3/8-inch wall	5.24	27.3	0.193	1.22
3-inch hollow square 1/2-inch wall	4.57	17.4	0.245	1.35
3-inch outside diameter of tube 1/2-inch wall	3.93	15.7	0.224	1.30
4-inch outside diameter of tube 1/2-inch wall	5.50	22.0	0.162	1.31

Mechanical Features

Working in opposition to the requirements for low loss and low temperature rise, as well as the requirements for high interrupting ability and high short-time current rating, is the ever present need for minimum physical size. The methods used to accomplish the required temperature results have been described. The mechanical features whereby the stresses of interruption and of high currents are held under control now will be discussed.

The current values encountered in short-circuit interruption by network protectors are high and must be held under control until interruption is accomplished. The 3,000-ampere network protector is required to interrupt a short circuit, the initial crest of which reaches an instantaneous value of 90,000 amperes or more, followed by a decreasing current for 60 cycles, at which time the circuit breaker opens and interruption is accomplished at 40,000 amperes or more rms. During this time it is necessary that the large magnetic forces do not blow any of the contacts open, with the resulting burning of contacts.

The magnetic forces of short-circuit currents act in three ways, all tending to force open the contacts or bridging member of the circuit breaker. The design is such as to minimize or nullify all three of these factors. First, there is the largest of the three magnetic forces, that due to the return-current path in the bus bar to the rear of the circuit breaker. Its effect is minimized by one end of the bridging member being hinged (see Figure 4), so that 50 per cent of this force is expended at the hinge pin. The 50 per cent of the force at the contact or break end is expended, not against springs, but rather against the rigid members of the mechanism. The second component of magnetic force which is commonly encountered on bridging members of circuit breakers of this general configuration is that caused by the bridging member not forming one

straight conductor with the upper and lower conductors.[8,9] This component is minimized and controlled in the same manner as the first component and also is minimized further by the bridging member being closely in line with its terminal conductors. The third component of magnetic force tending to blow the contacts open is that due to the current converging to a small cross section and high density at points of contact. At any given point of contact this force will vary as the square of the current. This factor in the present circuit breaker arrangement is minimized by the current being divided into six contact paths (one for each of the six blades) and further into the multiplicity of line contacts at each embossed contact; the force at each detail contact will vary as the square of the current through it, but the sum of the squares of the individual currents is a value less than the square of the sum of the currents, which would be the case if the total current passed through a single contact. The effect is minimized further by the fact that the forces are in a direction 90 degrees to the main motion of the bridging member and further are more than counteracted by the cup-washer springs and by the magnetic forces of the parallel currents in each pair of blades tending to pull the blades together.

When the circuit breaker opens, the two side pairs of blades open first and transfer all of the current of one pole to the center pair which opens slightly later and in turn transfers the total current to be interrupted to the butt type of arcing contacts with tungsten-alloy arcing tips. The hinging of and flexible connection to this arcing contact are arranged so that the nonuniform magnetic field resulting holds these tips in contact until the motion of the circuit breaker and mechanism opens the contact. When the contact does open, the current is transferred to the deion arc chute for interruption. Once transferred the current is carried to the deion chute through a separate conductor for the purpose and no longer is carried by any of the circuit-breaker contacts. The general arrangement of the circuit-breaker and arc chute is shown in Figure 4.[10] Figure 5 is a typical oscillogram of an interruption.[10]

From the foregoing it is noted that the mechanism need only be large enough to close the circuit breaker against frictional forces and the forces of opening or accelerating springs. It is not required to deflect contact springs which (as commonly used in circuit breakers) are sufficiently strong to withstand directly the magnetic forces of short-circuit currents.

Appendix. Measurement of A-C Resistances at Low Frequencies in Heavy Conductors

In the case of commercial power frequencies the a-c resistance of heavy-current conductors, or the wattage of power resulting therefrom, normally is arrived at by calculation rather than by measurement. When the conductor is irregular in size and arrangement, or when return phases by proximity become factors, or when there is magnetic steel in the vicinity, calculations become tedious and often questionable. Frequently the conductors are so short that the voltage drop in their length is a matter of millivolts, even with several thousand amperes flowing, and normally the power factor through the conductor is very low. With these circumstances the problem does not lend itself to the use of the conventional wattmeter. Further complications arise from induced voltages in the potential circuits by reason of the proximity of the heavy-current circuits.

The method of measuring wattage loss developed in conjunction with high-current network protectors is based on the use of a bridge circuit wherein the voltage drop across the test specimen is balanced by a voltage made up of two components, both variable in magnitude, one component known to be inphase with the test current and the other known to be 90 degrees out of phase with the test current. See Figure 7. By calibration of the source of the inphase component the effective resistance of the specimen is determined.

The test circuit is shown in Figure 8 in diagram form. The source of test energy is a transformer of the required frequency capable of circulating several hundred amperes through the test specimen; the current value is not critical, nor is it necessary that it be constant. The test current from terminals *A–A* is circulated through a current transformer *C*, through the test specimen *B–B*, and through a section of concentric conductor *D* (shown in section), the latter being heavily shielded magnetically. All test circuits other than the source of heavy current are of the concentric shielded type. The secondary of the current transformer is connected to a potentiometer type of resistor having a double-contact type of slide *SH* and designed to have very low reactance and very low skin effect at the frequency used.[11] This potentiometer is the source of a voltage, adjustable in magnitude, which is closely inphase with the current in the primary of the current transformer, and hence is closely inphase with the *IR* component of the voltage drop through the test specimen. The position of the double-contact slide is calibrated in terms of the d-c resistance of the section of conductor which is included between the two contacts. When a balance is established (described later), the a-c resistance of the test specimen is known to be the d-c resistance of the potentiometer at the particular setting divided by the ratio of the current transformer. From the foregoing it is evident that

1. The potentiometer must have no appreciable skin effect.
2. The current transformer must have very little phase-angle error.
3. The ratio of the current transformer under load must be accurately known.

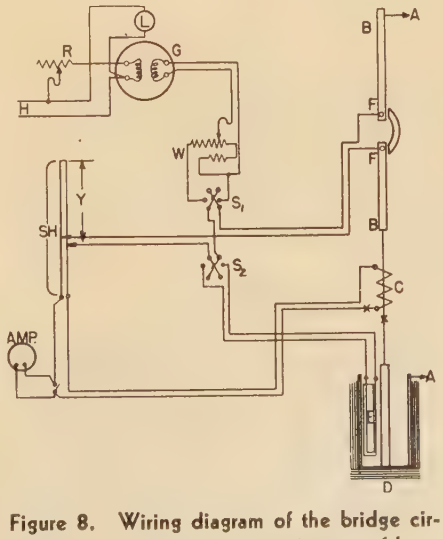

Figure 8. Wiring diagram of the bridge circuit used for measuring a-c resistance of large copper conductors

In order completely to balance the voltage drop appearing at *FF* across the test specimen it is necessary to obtain a voltage which is variable in magnitude and which is known to be accurately 90 degrees inphase position relative to the test current. This is obtained by induction from coil *E* which is mounted pivotally in the annular space between the inner and the outer conductors of the concentric conductor *D*. The 90-degree relation is known to obtain, because the magnetic flux in the annular space is of necessity inphase with the current in the central conductor, and the voltage induced in coil *E* leads this flux by 90 degrees. These phase-angle relations hold accurately for conditions of balance, for then there is no current flow in the galvanometer circuit which could upset the angular relations. The coil *E* is wound upon an entirely nonmetallic structure and is wound of very fine wire in order not to distort the phase-angle relation of voltage induced with respect to test current. The magnitude of voltage to secure a balance is obtained by adjusting the plane of coil *E* with respect to a plane described by a radius of the concentric conductor and the axis of the same conductor.

By means of shielded cable, voltages from *SH* and from *E* are connected in the same circuit with the voltage from test specimen *FF* and with vibration galvanometer *G*. Double-throw switches *S*1 and *S*2 permit of reversal of test connections and thereby eliminate some minute effects of stray fields upon the test specimen. Rheostat *W* controls the sensitivity of the vibration galvanometer. The galvanometer is tuned to the test frequency by means of the field rheostat *R*. The vibration type of galvanometer is preferred as an indicator of balance because of its fine sensitivity and because of its freedom from the effects of harmonics in the test current. *H* is the d-c source of field excitation for the galvanometer, and *W* is the lamp used for mirror and light-beam registration. The galvanometer is magnetically shielded.

The Solution of Transmission-Line Problems in the Case of Attenuating Transmission Line

GEORGE GLINSKI
ASSOCIATE AIEE

COAXIAL LINES with solid dielectric often are used as feeders. Such lines have appreciable attenuation (of the order of 1.5 decibels per 100 feet at 100 megacycles per second). Application of standing-wave method of finding the receiving-end impedance, as based on the assumption of lossless transmission line, would introduce an appreciable error, increasing with the length of the line used. The purpose of this paper is to show how by the application of the standard transmission-line theory the standing-wave method of measuring impedance can be extended to the case of transmission lines with attenuation, if the appropriate corrections are introduced. As seen from this point of view, the paper brings together and somewhat systematizes information available in the existing technical literature.[1,2]

Voltage Distribution Along the Line

The total complex voltage $\boldsymbol{V}$ at any given point of the transmission line is the sum of the incident complex voltage $\boldsymbol{V}_i$ and the reflected complex voltage $\boldsymbol{V}_r$. As we go along the attenuating transmission line from its receiving toward its sending end, the amplitude of the incident vector voltage increases. This is taken into account by the multiplication of the reference magnitude V_i by $e^{\alpha x}$. Hence, at the point x from the receiving end the incident voltage has the magnitude $V_i e^{\alpha x}$ (Figure 1). The factor α is called the attenuation constant of the line.

Also, if we go along the attenuating transmission line from the receiving toward the transmitting end, the phase of the incident complex voltage changes. This is again taken into account by the multiplication of the reference magnitude by $e^{j\beta x}$. Hence, at the point x from the receiving end the incident complex voltage is $V_i e^{\alpha x} e^{j\beta x}$ (Figure 2).

The factor β is called the phase constant of the line. As we see, the simultaneous attenuation and phase shift can be taken into account by multiplying the reference magnitude V_i by $e^{\gamma x}$ (Figure 3) where $\gamma = \alpha + j\beta$. The factor γ is called the propagation constant of the line. Hence the general expression of the incident voltage at point x from the receiving end of the line is $V_i e^{\gamma x}$.

Similarly the reflected complex voltage at the point x from the receiving end of the line can be represented by $V_r e^{-\gamma x + j\psi_0}$, where V_r is the magnitude of reflected voltage at the receiving end of the line and ψ_0 its phase difference in relation to the incident voltage at the receiving end (Figure 4).

Hence the total complex voltage at the point x from the receiving end of the line is

$$\boldsymbol{V} = \boldsymbol{V}_i + \boldsymbol{V}_r = V_i e^{\gamma x} + V_r e^{-\gamma x + j\psi_0} \quad (1)$$

The ratio of the reflected complex voltage at the receiving end to the incident complex voltage at the same point is called the voltage complex reflection coefficient $\boldsymbol{K}_R$:

$$\boldsymbol{K}_R = K_R e^{j\psi_0} = \frac{V_r}{V_i} e^{j\psi_0} \quad (2)$$

Introducing this into equation 1 we obtain

$$\boldsymbol{V} = V_i(e^{\gamma x} + \boldsymbol{K}_R e^{-\gamma x}) = V_i e^{\gamma x}(1 + K_R e^{j\psi_0} e^{-2\gamma x}) \quad (3)$$

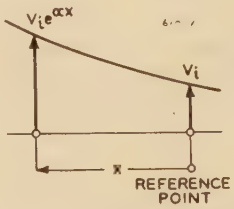

Figure 1 (left). Effect of attenuation

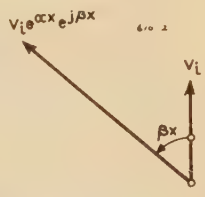

Figure 2 (right). Effect of phase shift

Voltage Distribution Near the Receiving End

Let us assume, as a first approximation, that, although the line is attenuating, the

Paper 46-10, recommended by the AIEE committee on communication for presentation at the AIEE winter convention, New York, N. Y., January 21–25, 1946. Manuscript submitted May 2, 1945; made available for printing November 9, 1945.

GEORGE GLINSKI is special studies engineer in the electronics division of the Northern Electric Company, Montreal, Quebec, Canada.

In the use of this test circuit the current is adjusted to any suitable value at the desired frequency, and balance is obtained by adjustment of *SH* and *E* until zero response is obtained on galvanometer *G*. Rough balance is made first with *W* large and then the sensitivity gradually increased as closer and closer balance is achieved. When balance is reached the a-c resistance of the test specimen is the d-c resistance of section *Y* of the potentiometer divided by the ratio of the current transformer.

Although the test arrangement described was used on appreciably heavier conductors, actual comparison with values calculated for a ten-inch length of seven-eighths-diameter copper bar was made as follows:

D-c resistance of ten-inch length, ohms	1.315×10^{-5}
Ratio of a-c–d-c resistance	1.0668
Calculated a-c resistance, ohms	1.40×10^{-5}
Measured a-c resistance, ohms	1.45×10^{-5}

With a galvanometer having an impedance better matched to the problem at hand even greater sensitivities should be obtainable.

References

1. SKIN EFFECT OF A RETURN CIRCUIT OF TWO ADJACENT STRAP CONDUCTORS, **H. B. Dwight.** *The Electric Journal*, volume 13, 1916, page 157.

2. SKIN EFFECT IN TUBULAR AND FLAT CONDUCTORS, **H. B. Dwight.** AIEE TRANSACTIONS, volume 37, 1918, part 2, pages 1379–1400.

3. SKIN EFFECT AND PROXIMITY EFFECT IN TUBULAR CONDUCTORS, **H. B. Dwight.** AIEE TRANSACTIONS, volume 41, 1922, pages 189–98.

4. FREE CONVECTION OF HEAT IN GASES AND LIQUIDS—II, **Chester W. Rice.** AIEE TRANSACTIONS, volume 43, 1924, page 131.

5. INTERNATIONAL CRITICAL TABLES, volume 5. Page 242.

6. HEAT TRANSMISSION, **Wm. H. McAdams** McGraw-Hill Book Company, Inc., 1933.

7. TEMPERATURE RISE OF ELECTRICAL APPARATUS AS AFFECTED BY RADIATION, **G. W. Penney.** AIEE TRANSACTIONS, volume 59, 1940, page 338.

8. CALCULATION OF MAGNETIC FORCE ON DISCONNECTING SWITCHES, **H. B. Dwight.** AIEE TRANSACTIONS, volume 39, 1920, part 2, pages 1337–50.

9. ELECTROMAGNETIC INDUCTION, **W. F. Dunton.** *The Electrician* (London, England), volume 105, November 28, 1930, page 681.

10. EXTINCTION OF AN A-C ARC, **J. Slepian.** AIEE TRANSACTIONS, volume 47, 1928, page 1398. THEORY OF THE DEION CIRCUIT BREAKER, **J. Slepian.** AIEE TRANSACTIONS, volume 48, 1929, page 523.

11. RESEARCH PAPER 133, United States Bureau of Standards.

attenuation of the line of a length of about $\lambda/2$ is negligible. Let us find the voltage distribution along the first half wave length of line from the receiving end. According to our assumption for this length $e^{\alpha x} \longrightarrow 1$ and from equation 3 we obtain

$$\boldsymbol{V} = V_i e^{j\beta x}(1 + K_R e^{j\psi_0} e^{-j2\beta x}) \qquad (4)$$

This is a well-known[3] equation of the voltage distribution along the lossless line. The expression in the brackets on the right side of the last equation is the vector sum of the unit vector $\boldsymbol{OA}$ (Figure 5a) drawn along the real axis and the vector $\boldsymbol{AB} = K_R e^{j(\psi_0 - 2\beta x)}$ drawn from the point (1.0) as shown on the same figure. The vector $\boldsymbol{K}_R e^{j(\psi_0 - 2\beta x)}$ rotates, with increasing x, in the clockwise direction and completes one revolution when $x = \lambda/2$ (since the phase constant $\beta = 2\pi/\lambda$).

To find the magnitude of this vector sum in the brackets for a given length of line x, we must rotate the vector $\boldsymbol{K}_R$ through the angle $2\beta x$ from its original position and in the clockwise direction. Let us assume that x is such that the vector takes the position $\boldsymbol{AB}$ in Figure 5a Then the segment OB gives us the magnitude of the vector sum. Moreover, this magnitude is proportional to the magnitude V of total complex voltage at the point x, of the line, since the factor $e^{j\beta x}$ before the brackets changes only the phase angle.

In Figure 5b the magnitude of the vector sum in the brackets versus the length x of the line is plotted. According to what has just been said, this also gives the distribution of the magnitudes of the total voltage along the line.

Voltage Distribution Far From the Receiving End

Let us suppose that the line under consideration is terminated in such a load that the receiving-end-voltage reflection coefficient and voltage distribution are as shown in Figures 5a and b.

Let us find the voltage distribution on the line starting at some distance $x_2 = n(\lambda/2)$ where $n \gg 1$. Since, according to our previous assumption, the attenuation though existing is constant along the considered $\lambda/2$ section of the line, the equation 3 yields

$$\boldsymbol{V} = V_i e^{\alpha x_2 + j\beta x}(1 + K_R e^{j\psi_0} e^{-2\alpha x_2} e^{-j2\beta x}) \qquad (5)$$

We shall use again the graphical construction. On the real axis (Figure 6a) we shall plot the unit vector $\boldsymbol{OA}$. Then, using point A as a center, we shall draw the circle of the radius $K_R e^{-2\alpha x_2}$. The

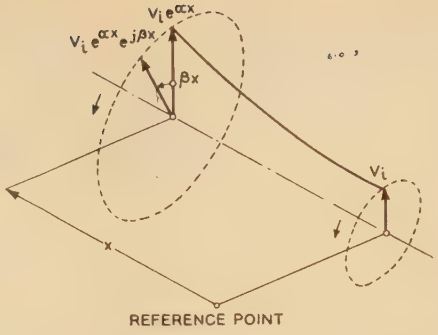

Figure 3. Effect of attenuation and phase shift

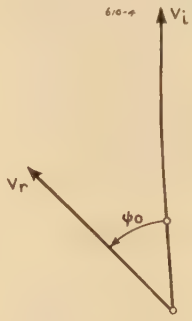

Figure 4. Incident and reflected voltages at the receiving end of the line

vector $\boldsymbol{AC}$ will be equal to $K_R e^{-2\alpha x_2} e^{j\psi_0}$ The magnitude of the vector $\boldsymbol{OC}$ is proportional to the magnitude of the total voltage at the point x_2 of the line. By rotating the vector $\boldsymbol{AC}$ in the clockwise direction and in the way just explained, we obtain again the voltage distribution on the section of line considered. This voltage distribution is plotted in Figure 6b

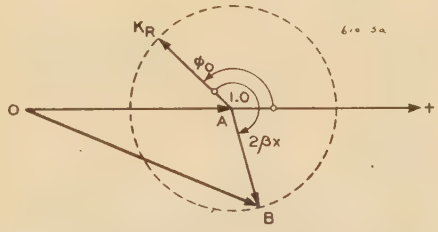

Figure 5a. Graphical construction for voltage distribution near receiving end

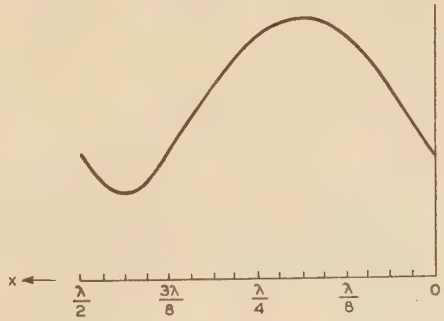

Figure 5b. Voltage distribution near receiving end

versus the distance along the line. Comparing the Figures 5b and 6b (when plotted to the same scale), we see that the voltage distribution farther from the receiving end of the line differs from that at the receiving end in two respects:

1. Farther from the receiving end the standing-wave ratio q, that is, the ratio of maximum to minimum voltage, decreases. In other words the attenuation of the line decreases the standing-wave ratio q.

2. The space average magnitude of the voltage is higher farther from the receiving end.

Attenuating Line as an Impedance-Measuring Device

For the voltage distribution starting at the point x_2 of the line (far from the receiving end), the maximum magnitude is

$$V_{max} = V_i e^{\alpha x_2}(1 + K_R e^{-2\alpha x_2}) \qquad (6)$$

and the minimum magnitude is

$$V_{min} = V_i e^{\alpha x_2}(1 - K_R e^{-2\alpha x_2}) \qquad (7)$$

Hence the standing-wave ratio in the vicinity of the point x_2 is

$$q_2 = \frac{V_{max}}{V_{min}} = \frac{1 + K_R e^{-2\alpha x_2}}{1 - K_R e^{-2\alpha x_2}} \qquad (8)$$

Solving the foregoing for K_R yields

$$K_R = e^{2\alpha x_2} \frac{q_2 - 1}{q_2 + 1} \qquad (9)$$

The last equation gives us the magnitude K_R of the receiving-end-voltage reflection coefficient. This can be used now to find from the known formula[3] the standing-wave ratio q_R near the receiving end of the line:

$$q_R = \frac{1 + K_R}{1 - K_R} \qquad (10)$$

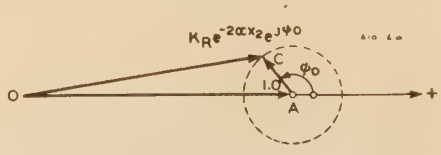

Figure 6a. Graphical construction for voltage distribution far from receiving end

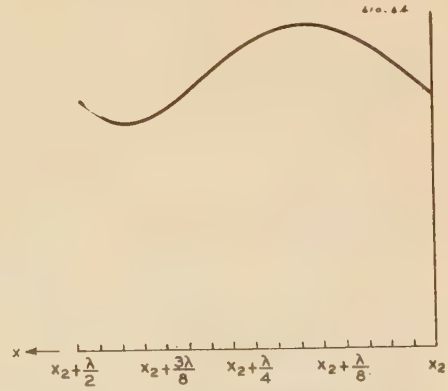

Figure 6b. Voltage distribution far from receiving end

This standing-wave ratio, together with relative shift of the voltage minimum in relation to the point x_2, can be used in the standard way[1] to find Z_R/Z_o from the appropriate chart (Z_R equals the receiving-end (load) impedance; Z_o equals the characteristic impedance of the line).

If we prefer the graphical construction, we can proceed as follows: Suppose that the vector ***OB*** in Figure 7a is proportional to the first minimum voltage encountered along the line when going from the point x_2 toward the sending end, whereas the vector ***OD*** is proportional to the maximum voltage. The circle with center A midway between the points B and D and going through these points is the locus of the reflected voltage near the point x_2 of the line. If the first minimum of the voltage is shifted a distance x_3 from the point x_2 (Figure 7b), then the corresponding angle is $2\beta x_3$. We shall rotate the vector ***AB*** counterclockwise through this angle $2\beta x_3$; this yields the vector $\boldsymbol{K}_R e^{-2\alpha x_2} \times e^{j\psi_0}$ proportional to the reflected voltage at the point x_2 of the line. Its magnitude is given by $K_R e^{-2\alpha x_2}$. Let us suppose that the attenuation constant α and the distance x_2 are known, then the factor $e^{2\alpha x_2}$ can be calculated. The multiplication of the magnitude $K_R e^{-2\alpha x_2}$ by the factor $e^{2\alpha x_2}$ gives obviously K_R.

Let us draw the circle of the radius K_R with a point A as a center. Then the vector ***AF*** gives us the reflection coefficient at

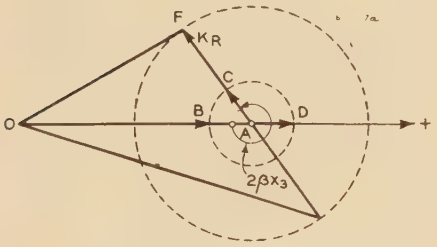

Figure 7a. Graphical construction for finding Z_R/Z_o from the voltage distribution curve far from receiving end

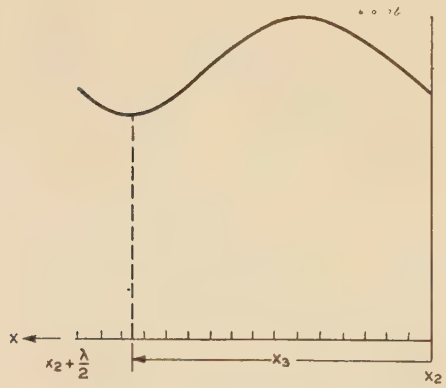

Figure 7b. Voltage distribution far from receiving end

Figure 8. Short-circuit and load voltage distributions

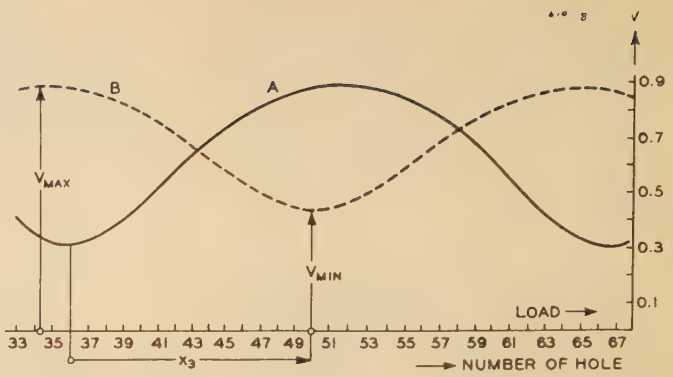

the receiving end of the line. As it is known, the ratio of segments OF and OG (the point G being diametrically opposite to the point F) gives us the magnitude of Z_R/Z_o. The phase of Z_R/Z_o is given by the angle GOF. This phase is positive (Z_R inductive), if ***OF*** leads ***OG***; it is negative (Z_R capacitive), if ***OF*** lags ***OG***.

Determination of Transmission-Line Attenuation

From the previous discussion it follows that the measurement of the receiving-end impedance Z_R requires among other things a knowledge of the attenuation constant α of the line.

The constant α can be determined readily from the measurement of the voltage distribution on the line when short-circuited at the receiving end. In this case, as we know, the magnitude K_R of the voltage reflection coefficient is equal to one and equation 9 yields

$$e^{2\alpha x_2} = \frac{q_{sh.c}+1}{q_{sh.c}-1} \qquad (11)$$

Note that $q_{sh.c}$ is measured in the vicinity of the point x_2 of the line, that is far from the receiving end.

Example

Let us assume that the coaxial measuring section of transmission line is connected through a long coaxial line to the unknown receiving-end impedance Z_R. When the line is short-circuited at the receiving end the measured voltage distribution is as shown by curve A in Figure 8. Curve B on the same figure represents the voltage distribution with the receiving-end impedance Z_R connected. The frequency of applied signal is 96.3 megacycles per second.

The total attenuation of the line can be found from the formula 11. The standing-wave ratio in the case of the short circuit is

$$q_{sh.c} = \frac{0.905}{0.32} = 2.83$$

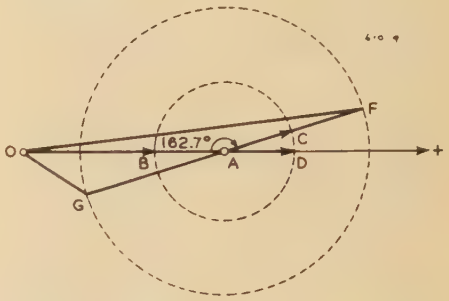

Figure 9. Graphical construction for finding Z_R/Z_o

Hence

$$e^{2\alpha x_2} = \frac{2.83+1}{2.83-1} = 2.1$$

That is, the total attenuation $\alpha x_2 = 0.37$ *nep* or 3.2 decibels.

In the case of the load connected the measured standing wave ratio is

$$q_2 = \frac{0.90}{0.445} = 2.02$$

The standing-wave ratio at the receiving end can be found from the known formula [1] using formula 9 as

$$q_R = \frac{1+2.1\,\dfrac{2.02-1}{2.02+1}}{1-2.1\,\dfrac{2.02-1}{2.02+1}} = 5.9$$

This example was chosen intentionally to show how important the correction of standing-wave ratio for the attenuation on the line between the measuring section and the receiving end can be.

The shift of the minimum when the line is loaded as referred to the minimum when the same line is short-circuited is $x_3 = 14$ holes, Figure 8, (Coaxial measuring section is provided with equidistant holes for the purpose of measuring voltage distribution. These holes are numbered and distances along the measuring section are measured conveniently in number of holes), or 0.226λ (since $\lambda = 64$ holes, as can be found from the curve B on Figure 8) toward the load. Hence the load is inductive.

Electrical Measurements on Aircraft-Engine Ignition Circuits

WM. E. BERKEY
MEMBER AIEE

Synopsis: A method of measuring ignition voltages with a cathode-ray oscillograph is described. Magneto and spark-plug voltage oscillograms covering several consecutive firing pulses were taken on a complete aircraft magneto ignition system under several engine operating conditions. Oscillograms taken with spark plugs firing in air show differences when compared with engine tests. An improved electronic oscillograph has been developed which is well adapted for ignition measurements.

THE spark ignition system is recognized as the greatest single source of trouble in an aircraft engine.[1] New ignition problems have been created, and old ignition troubles intensified in modern engine developments. The ignition system on the high-power engines of today must function under higher output per cylinder, higher temperatures, greater numbers of firing sparks per second, higher altitude operation, and more stringent radio-interference requirements. The fact that large numbers of high-power aircraft engines are in operation today reflects great credit to the ignition engineers who have succeeded in solving their major problems.

A magneto ignition system generates and distributes a series of timed transient electric discharges. The magneto output voltage is created by a sudden disturbance in two coupled circuits each simply oscillatory, and, therefore, may be regarded as the resultant of two normal modes of different amplitudes, frequencies, and damping. A distributor alternately connects the different length spark-plug circuits with the magneto through a short air gap. The current which flows in the circuit then is complicated by the magneto characteristics, the variable circuit parameters, and the spark-dis-

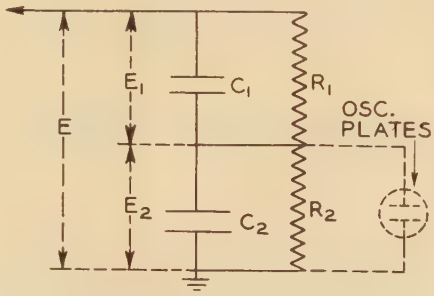

A—Simple resistor-capacitor divider

$$\frac{E_1}{E_2}=\frac{R_1}{R_2}=\frac{\frac{1}{\omega C_1}}{\frac{1}{\omega C_2}}=\frac{C_2}{C_1}$$

$$R_1C_1=R_2C_2$$

$$\frac{E}{E_2}=\frac{E_1+E_2}{E_2}=\frac{R_1+R_2}{R_2}=\frac{\frac{1}{C}+\frac{1}{C_2}}{\frac{1}{C_2}}=\frac{C_1+C_2}{C_1}$$

C_2 includes capacitance in plate circuit

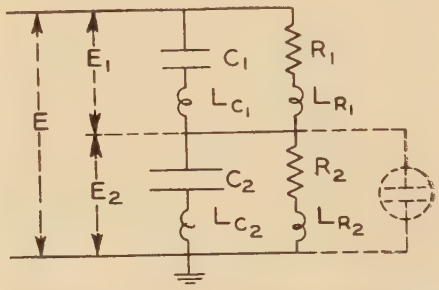

B—Resistor-capacitor compensated divider

$$\frac{L_{R_1}}{R_1}=\frac{L_{R_2}}{R_2}$$

$$C_1L_{C_1}=C_2L_{C_2}$$

$$\frac{L_{C_1}}{R_1}=\frac{L_{C_2}}{R_2}$$

$$R_1C_1=R_2C_2$$

Figure 1. Parallel capacitor-resistor type voltage divider

Paper 46-14, recommended by the AIEE committee on air transportation for presentation at the AIEE winter convention, New York, N. Y., January 21–25, 1946. Manuscript submitted June 15, 1944; made available for printing November 21, 1945.

WM. E. BERKEY is research engineer in the research laboratories of the Westinghouse Electric Corporation, East Pittsburgh, Pa.

The engine tests described in this paper were made at the Pratt and Whitney Aircraft Division, United Aircraft Corporation plant, East Hartford, Conn. The co-operation of Val Cronstedt, executive engineer, E. K. von Mertens, project engineer, and the entire ignition group is gratefully acknowledged.

Using the transmission-line calculator,[4] we shall find that the resistive component R_R and reactive component X_R of the receiving end impedance Z_R are $R_R/Z_o=3.3$, $X_R/Z_o=2.9$.

The graphical construction for this case is shown in Figure 9. It consists of the following steps:

1. Draw OB proportional to $V_{\min}$ from Figure 8, curve B.
2. Draw OD proportional to $V_{\max}$ from Figure 8, curve B.
3. Draw the circle on BD as a diameter (point A is its center).
4. Translate the shift of the minimum x_3 into the angle $2\beta x_3$. In the case considered, since x_3 is shifted toward the load, the vector BA should be rotated clockwise. The angle of rotation is equal to $4\pi x_3/\lambda$. In the case considered it is 2.84 radians or 162.7 degrees.
5. The vector $\boldsymbol{AC}$ is proportional to $K_R e^{-2\alpha x_2} e^{j\psi_o}$.
6. Find $e^{2\alpha x_2}$ from formula 11.
7. Multiply the magnitude of vector AC by $e^{2\alpha x_2}$ and draw the circle of the radius K_R with point A as a center. The vector $\boldsymbol{AF}$ is proportional to the reflection coefficient $\boldsymbol{K}_R$ at the receiving end of the line.
8. The ratio of the segments OF/OG gives us the magnitude of Z_R/Z_o.
9. The angle GOF gives us phase of Z_R/Z_o

$$\frac{Z_R}{Z_o}=4.36$$

$$\left/\frac{Z_R}{Z_o}\right.=42 \text{ degrees}$$

or

$$\frac{R_R}{Z_o}=3.22$$

$$\frac{X_R}{Z_o}=2.92$$

As we see, these figures agree fairly well with those obtained when using the transmission-line calculator.

Conclusion

As it is seen, the existence of attenuation in the transmission line does not change the method of determining the load impedance; with appropriate connection the same method can be used.

References

1. GRAPHICAL SOLUTION OF VOLTAGE AND CURRENT DISTRIBUTION AND IMPEDANCE OF TRANSMISSION LINES, **R. C. Paine.** *Proceedings* of the Institute of Radio Engineers, volume 32, 1944 number 11, pages 686–95.

2. AN ANALYSIS OF R-F TRANSMISSION LINES, **G. B. Hoadley.** *Communications*, volume 23, 1943, number 2, pages 22, 24–6, 28, 50, 52.

3. THE CONDUCTION OF HIGH-FREQUENCY OSCILLATORY ENERGY, **H. O. Roosenstein.** *Proceedings* of the Institute of Radio Engineers, volume 16, 1931, number 10, pages 1849–83.

4. TRANSMISSION-LINE CALCULATOR, **P. H. Smith.** *Electronics*, volume 12, January 1939, page 29.

Figure 2. Pratt and Whitney aircraft ignition test assembly

M—Magneto; *D*—Distributor; *P*—Plug mount

charge characteristics in both the distributor and spark plug. Calculation of an ignition circuit is thus at present not possible. Measurements of voltage and current in an ignition system are not easy, because high voltages, high frequencies, and low total energies are involved. Ignition voltages of 15 kv commonly are encountered at the magneto. Ignition currents from frequency of firing to hundreds of megacycles are detected by wave meters. A magneto ignition spark may release only 50 millijoules in the spark gap.[2]

The object of this paper is to describe some recent measurements made on a modern aircraft-engine ignition system with the hope that further investigation will be stimulated.

Figure 3. Magneto-ignition circuit constants

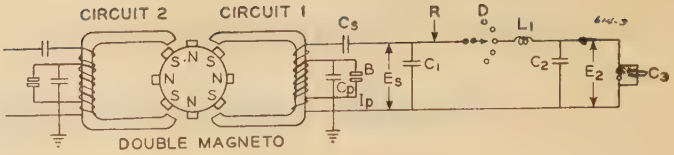

C_S = 2,000-micromicrofarad series capacitor
C_P = 0.35-microfarad primary capacitor
C_1 = 150-micromicrofarad capacitance of secondary to ground at distributor
C_2 = 100- to 300-micromicrofarad capacitance in harness and plug lead
C_3 = 35-micromicrofarad capacitance of spark plug
E_S = 25,000 volts maximum secondary open circuit volts
E_P = 85 volts maximum primary volts
L_P = 2.65 to 4.3 × 10^{-3} henrys primary inductance in coil
L_S = 30 to 42 henrys secondary inductance in coil
L_1 = 0.004 microhenry per centimeter in concentric cable (calculated)
I_P = six amperes crest
F_S = 2,000 approximate natural frequency with *D* open and *B* open
F_P = 6,000 approximate natural frequency with *D* open and *B* closed
F_1 = 10^7 cycles per second approximate frequency of $C_1L_1C_2$ (calculated)
R_S = 6,800 ohms
R_P = 0.25 ohms

Combined Capacitance-Resistance Voltage Divider

In an oscillographic study of ignition-circuit voltages it is necessary to reduce the ignition voltage to values suitable for the oscillograph deflection plates. The construction of a divider, which will not change the ignition voltage being measured and will reproduce faithfully the ignition wave on the film, constitutes a major problem. A noninductive resistance divider of ten megohms total resistance gave frequency distortion due to the oscillograph plate capacitance of 25 micromicrofarads. Capacitance dividers were found to be unsatisfactory for low-frequency measurements due to unequal leakage around the capacitors. In ignition circuits both high- and low-frequency voltages are known to be present; therefore, a combined capacitance-resistance divider was built.

The simple capacitance-resistance divider is sketched in Figure 1A. When the time constants for each divider step are made equal, the frequency of the voltage being measured has no effect upon the ratio of the divider if the lead inductance is neglected. The effect of lead

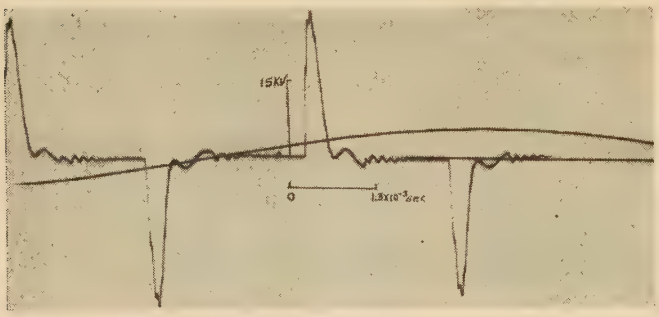

Figure 4. Open-circuit magneto voltages

A (left)—Open-circuit secondary voltage
B—Open-circuit secondary voltage with primary-circuit open

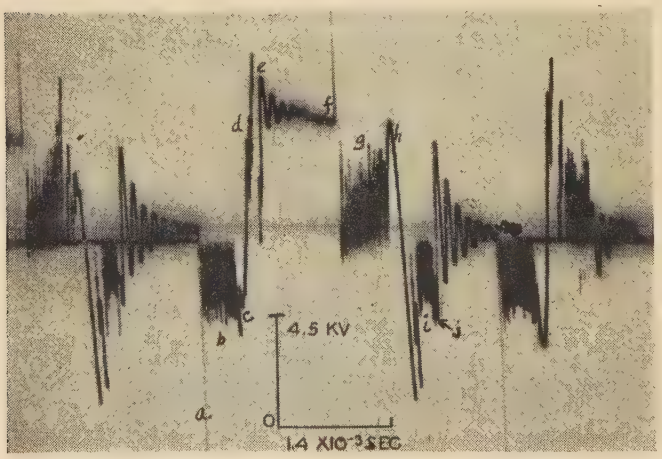

Figure 5. Distributor and plug voltage characteristics

A (left)—Distributor voltage to ground
B—Spark-plug voltage to ground

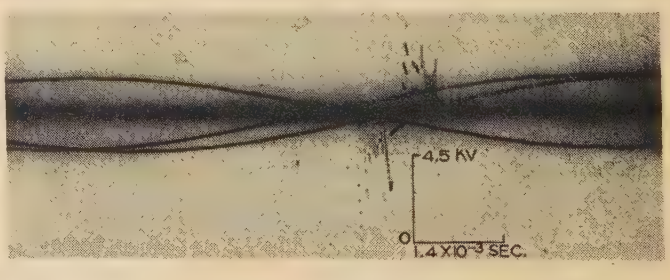

inductance is considered in the compensated divider of Figure 1B. With complete compensation it is possible to make a divider with constant ratio for direct current and high frequency.[3]

In the experimental investigation, the simple capacitance-resistance divider was found satisfactory. The constants of one divider were

$R_1 = 11.2 \times 10^6$ ohms $\quad C_1 = 25 \times 10^{-12} F$
$R_2 = 0.8 \times 10^6$ ohms $\quad C_2 = 350 \times 10^{-12} F$

It is necessary to keep the stray ground capacitance of R_1C_1 step low and to locate the divider as closely as possible to the point of voltage measurement.

Ignition Assembly Tests

The ignition system investigated was that used on the Pratt and Whitney *R*-2800 18-cylinder engine. It consists of a double magneto, which generates simultaneous ignition pulses for two circuits of 18 plugs each through the two separated distributors. Initial tests were made with this ignition system mounted upon an engine nose section with plugs firing in air as shown in Figure 2. The standard magneto and distributor gears were driven by an electric motor mounted in the rear. The magneto was an eight-pole rotating-magnet type with two coils and breaker structures. The magneto rotor was geared to rotate at $1^1/_8$ times crankshaft speed. The breaker cam had 18 lobes ground for compensated timing and rotated at one-half crankshaft speed. A series capacitor of 2,000 micromicrofarads in the coil secondary, located in the magneto housing, enables the magneto to deliver more than 1,350 rpm×18= 24,300 firing discharges per minute through each circuit. The voltage divider was attached to a spare high-voltage terminal provided in the magneto housing. A schematic circuit of this ignition system is drawn in Figure 3. The circuit constants measured and calculated for this circuit are listed below the circuit diagram.

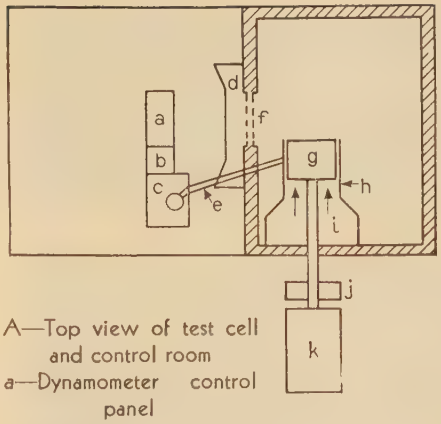

A—Top view of test cell and control room
a—Dynamometer control panel
b—High-voltage d-c rectifier
c—Oscillograph and control panel
d—Engine-control panel
e—Transmission line
f—Double window
g—Test engine
h—Shroud
i—Air blower
j—Water brake
k—Dynamometer

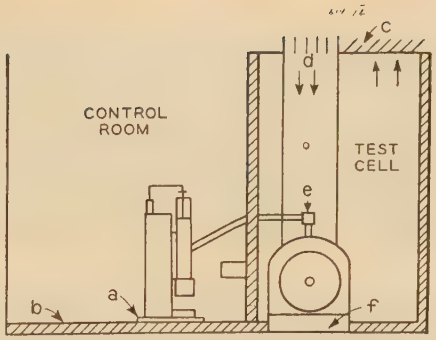

B—Side view of test cell and control room
a—Shock mount
b—Concrete floor
c—Roof vents
d—Air
e—Potentiometer
f—Bed plates

Figure 7. General layout for engine test

The rotating-film cathode-ray oscillograph[4] recorded the magneto and spark-plug voltage transients. The low-voltage side of the divider led directly to the deflection plates. The time scale was provided by rotation of the film. An exposure was made by unblocking the beam relay for a predetermined time with a voltage applied and removed by mechanical contactors.

The open-circuit voltage obtained on the magneto with the divider connected directly to the high-voltage side of the coil secondary is shown in Figure 4A. The open-circuit voltage rises to 28-kv crest with an initial rate of rise of about 400 volts per microsecond. The two frequency components of 2,000 and 6,000 cycles are visible in this oscillogram. Figure 4B shows the open-circuit voltage record obtained with the circuit breaker blocked open and the divider connected directly to the magneto.

The distributor voltage to ground obtained with the complete ignition circuit, but with the spark plugs firing in air, is shown in Figure 5A. The voltage rise at point *a* occurs when the primary circuit breakers open and the value of this crest voltage is determined by the breakdown voltage of the distributor gaps. The electric charge stored in the magneto secondary circuit up to the distributor then is shared with the spark-plug circuit on a high-frequency transient. The resultant voltage is usually high enough to break down the spark plug and discharge the secondary on a high-frequency damped-current oscillation. The air gaps then partially recover some dielectric strength, and the secondary circuit rises again, but now the voltage required to break down the distributor gaps is less than the initial breakdown, probably due to residual ionization in the gap. This action is repeated many times at *b* until finally at *c* the generated secondary voltage is no longer able to break down the gaps. The voltage reverses as a result of the buildup of reverse flux through the magneto coil, and at *d* several breakdowns occur. At *e* the primary circuit breaker closes, and the distributor spark goes out, leaving the high-voltage lead with a trapped charge because of the secondary series capacitor.

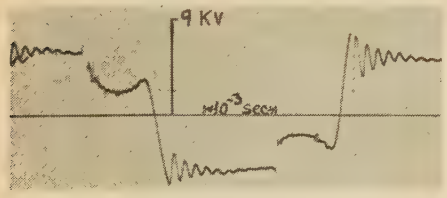

A—Type-*A* discharge voltage

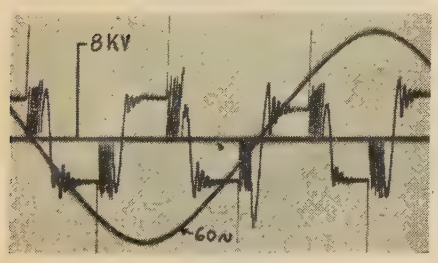

B—Type-*B* discharge voltage

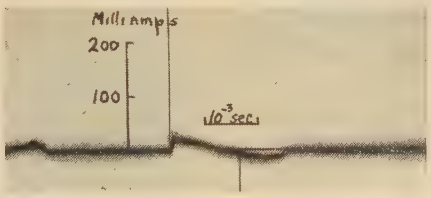

C—Type-*A* discharge current at plug; restrike on flux reversal

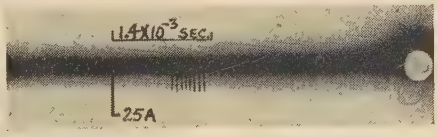

D—Type-*B* discharge current at plug

Figure 6. Voltage and current oscillograms of two types of ignition discharges

U OF I
LIBRARY

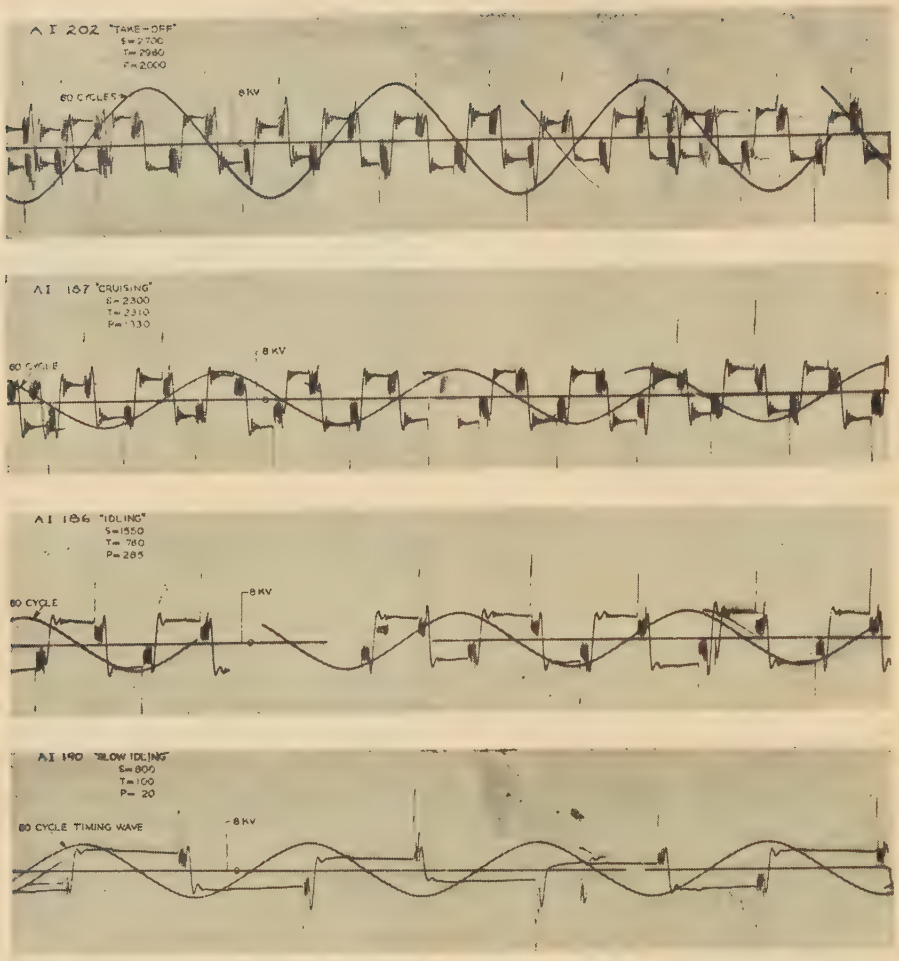

Figure 8. Magneto voltage with different engine-operation conditions

S—Speed, rpm
T—Indicated torque
P—Brake horsepower

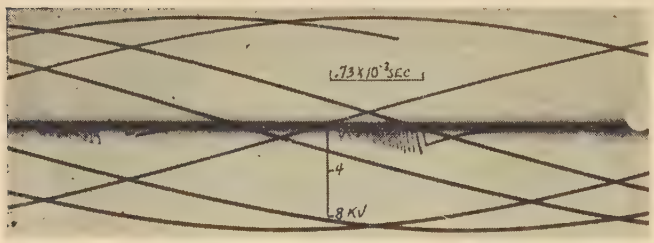

A (above)—Typical oscillogram
AI–217 number-1 front plug
S—1,500 rpm idling

B—Effect of 15,000-ohm resistor in high-voltage lead at distributor
AI–268, number 1 rear plug take-off
S—2,700, *T*—2,900, *P*—2,000
R_S = 15,000 ohms at distributor

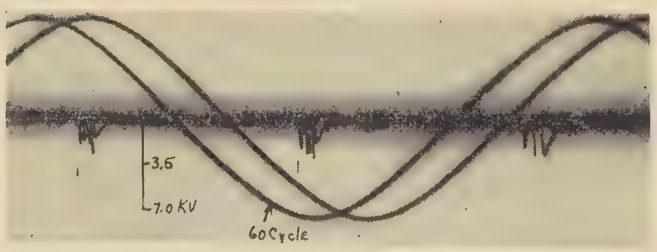

Figure 9. Spark-plug voltage records obtained during engine tests

Secondary voltage oscillations attributed to primary-current short-circuit transients are superimposed upon the residual direct voltage of this line section. At *f* the next pulse occurs on opposite polarity with the rotating distributor finger now adjacent to the next spark-plug circuit terminal. Repeated voltage rises and breakdown occur at *g*, the secondary magneto voltage reverses at *h*, and a second breakdown period is found at *i*, followed by the primary circuit breaker closing at *j*. This time the magneto–distributor lead was left at almost zero direct potential, although the a-c oscillations are relatively large.

An oscillogram of the spark-plug voltage is shown in Figure 5B. Two ignition discharges of opposite polarity taken on the same plug are recorded. Repeated charging- and breakdown-voltage varia-

Figure 10 (below). Westinghouse electronic oscillograph

A—Cathode housing, 50 kv, d-c maximum
B—Sweep and timing circuits
C—Focusing and bias control
D—Vacuum pumps
E—Calibrating and film-drum exposure control
F—Main control panel
G—Stationary film
H—Rotating film

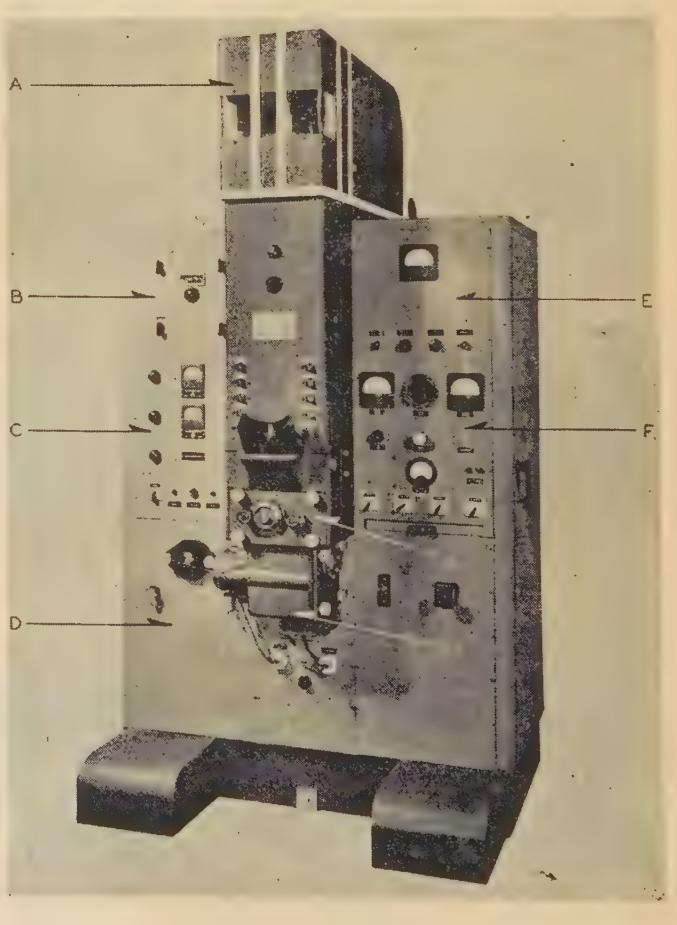

tions are observed on the film. Also complicated reflection and extinction effects are indicated in this oscillogram.

Two types of magneto firing-voltage records were recorded on the assembled ignition system with spark plugs firing in air. Figures 6A and C illustrate typical voltage–time and current–time oscillograms associated with the steady type-A discharges. Figures 6B and D show oscillograms of voltage and current associated with the intermittent type-B discharges. Other investigators[5,6] have called these discharge types "inductive" and "capacitive" sparks. The steady sparks appear reddish and diffuse, whereas the intermittent sparks appear bright bluish and concentrated.

Ignition Tests on Engine

The layout of the test cell and control room is sketched in Figure 7. The test engine was loaded with a dynamometer and a water-wheel brake. A cathode-ray oscillograph was set up in the control room with a two-wire transmission line connecting the deflection plates to the voltage divider located over the engine. The length of the line was 12 feet. The test engine was operated under several fixed conditions, and records made of the magneto firing voltage and the spark-plug voltage to ground. In Figure 8 typical records of the magneto high-voltage lead voltage to ground are shown. A 60-cycle voltage was recorded to provide calibration of each oscillogram. An external mechanical relay used in these tests to trigger the beam frequently bounced to cause apparently unconnected short portions of the trace.

The intermittent-type discharge-voltage characteristic was found in all oscillograms taken with the ignition system firing the engine. The magneto firing-voltage records obtained do not differ greatly for different engine test conditions. No significant differences in the breakdown voltages are observed in Figure 8. The restriking voltages which follow the breakdown are observed to be higher at higher speeds and greater engine power output.

A spark-plug voltage record is reproduced in Figure 9A. In this record the initial breakdown is not visible due to the extremely fast rise and fall. When a 15,000-ohm carbon resistor was installed in the high-voltage lead at the distributor, the breakdown voltage was observed as shown in Figure 9B. In this record the initial breakdown of the spark plug is clearly visible. The resistor serves to decrease the rate of rise of voltage on the spark plug.

Electronic Oscillograph

Oscillograms described in this report were obtained with an oscillograph of older design. A newly designed cathode-ray oscillograph[7] with complete operating accessories is pictured in Figure 10. New features which make it particularly valuable for ignition studies are

1. Provision for either stationary or rotating film recording.

2. Photoelectric means for exposing the rotating film for exactly one revolution, independent of speed of film rotation.

3. Enclosed and shielded electric circuits in removable panels with safety features.

4. Sweep circuit selector switches which enable a quick setting of sweeps from one microsecond to 20,000 microseconds.

The different operating circuits are built into the cabinet on removable panel assemblies. The high d-c beam voltage is supplied by a transformer and rectifier tubes with capacitor filter all built into the main cabinet. The combination of high writing speed with either short- or long-time recording makes this a useful instrument for studying ignition circuits.

Conclusions

Ignition currents and voltages are measured with a cathode-ray oscillograph. Typical oscillograms are shown which explain the operation of an ignition system used on a high-power aircraft engine. The importance of complete radio shielding and adequate electrical insulation becomes apparent with increased knowledge of ignition voltages and currents. Future ignition studies will be facilitated with a newly developed high-voltage cathode-ray oscillograph.

References

1. Shortcomings of Mica Insulation for Aviation Spark Plugs, **Val Cronstedt.** Society of Automotive Engineers *Journal*, volume 46, 1940, page 223.

2. Method of Measuring Heat Energy of Ignition Sparks, **F. B. Silsbee, L. B. Loeb, E. I. Fonseca.** National Advisory Committee on Aeronautics Technical Report 56, page 175.

3. Frequenzunabhaengige Kapazitiv-Ohmsche Spannungsteiler für Messzwecke, **O. Zinke.** Elektrotechnische Zeitschrift (Berlin, Germany), volume 60, August 1939, pages 927–31.

4. Arc-Extinction Phenomena in High-Voltage Circuit Breakers Studied With a Cathode-Ray Oscillograph, **R. C. Van Sickle, W. E. Berkey.** AIEE Transactions, volume 52, 1933, pages 850–7.

5. Principles of Ignition (book), **J. D. Morgan.** Pitman and Sons, Ltd., London, England, 1942. Pages 1–2.

6. Some Factors Controlling the Development of Electrical Ignition of Aero Engines, **G. E. Bairsto.** Royal Aeronautical Society *Journal* (London, England), volume 44, number 350, 1940, pages 119–62.

7. Electronic Oscillograph—Time Microscope, **O. Ackermann, E. Beck.** *Westinghouse Engineer*, volume 4, November 1944, page 169.

Capacitor Stabilization of Arc-Welding Transformers

J. H. BLANKENBUEHLER
MEMBER AIEE

R. V. LESTER
NONMEMBER AIEE

SINCE THE PROCESS of metallic arc welding was discovered, some of this welding has been done with alternating current. The fact that a transformer, with no moving parts and its resultant simplicity, could be used always has made the use of alternating current for welding desirable. When only bare welding electrodes were available, it was necessary to have a welding transformer with the secondary voltage so high as to be dangerous to the operator. Even with this high open-circuit voltage, the arc with the bare electrode was so unstable that it was very difficult to maintain. Consequently, the transformer was never popular as a power source for welding until the bare welding electrodes had been replaced by the modern coated electrode.

Seven or eight years ago, the standard secondary voltage for welding transformers was approximately 110 volts. Improvements in the coatings of the electrodes used for a-c welding since have enabled us to reduce the standard open-circuit voltage of these welding transformers to between 70 and 80 volts. Some transformers which are expected to be used with a limited variety of electrodes have secondary voltages as low as 50 volts.

During this period of growth, the users of the a-c equipment for welding naturally have become aware of its advantages as a power source in comparison with the rotating machinery generally used as the d-c power source, but always have been somewhat dubious about the relative safety of the two systems. Experts in both types of welding can argue at great length on this subject, but experience seems to bear out the fact that lower open-circuit voltages must be used with the a-c systems if they are to have safety equivalent to the d-c system.

During these last few years, most of the companies manufacturing a-c welding transformers have supplied as an optional feature a no-load voltage-reducing apparatus consisting of the necessary contactors and relays to change the voltage at the electrode holder from the usual no-load value of 70 to 80 volts to a lower value of 25 to 35 volts. Of course there are those who properly might contend that even these voltages are not safe, and probably one must agree that the only safe voltage is zero.

One method of arriving at a desirable voltage for the a-c welding system would be to assume that the present-day d-c welding systems are safe, because very few accidents are reported on these d-c operations. Many of these d-c welding sets have maximum no-load voltages of 90 to 100 volts. It might be reasonable, therefore, to assume that any a-c system which had a peak voltage on the a-c sine wave no higher than the voltage of the d-c welding system would be equally safe. Using this reasoning, we can assume that a transformer with a secondary voltage of 70 volts is equivalent in safety to a d-c welder with a no-load voltage of 99 volts, and a transformer with 65 volts corresponds in safety to a d-c welder of 92 volts. This logic is not easily proved to be correct, and the writers do not contend that it is; but on the basis of this logic an attempt was made to develop a transformer for general purpose welding with a secondary voltage of 65 volts which would perform satisfactorily with all makes and varieties of a-c welding electrodes.

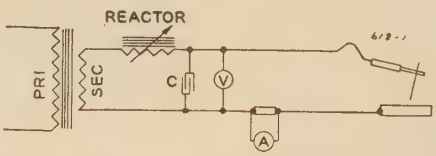

Figure 1. Circuit diagram

Investigation of the a-c welding arc with the magnetic and cathode-ray oscillograph indicated that capacitance in parallel with the arc produced a stabilizing effect because of the possible higher restriking voltages at current zero and because of the extra energy delivered to the arc immediately after restriking. Practical welding tests with capacitors connected as shown in Figure 1 bore out the results indicated by the oscillograph tests. It was then necessary to develop some means of determining the actual value of a particular amount of capacitance in reducing the required no-load voltage of the transformer. Our electrode development engineer, E. H. Turnock, suggested that welding tests with different transformer no-load voltages would indicate the degree of arc stability by the number of times the arc extinguished itself per electrode used. Tests therefore were conducted in which a number of electrodes were used at each of a number of transformer no-load voltages. The number of arc outages per electrode was recorded. These tests gave a reasonably smooth curve, indicating a definite relationship between the number of the arc outages and the transformer voltage. By extending these curves to the zero axis of the arc outage scale, one can assume that with this particular kind of electrode and welding setup, the voltage indicated by the curve to give no arc outages will be the minimum stable open-circuit voltage.

By running a series of such curves with various types and sizes of electrodes, one could determine the minimum open-circuit voltage which could be used for that variety of electrode. Similar curves also were taken with various values of capacitance connected across the transformer output terminals as shown in

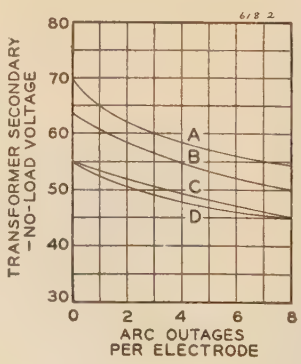

Figure 2(left). Stability curves for $^3/_{16}$-by-18-inch class 6020 electrode

60 cycles, 180 amperes

Figure 3(right). Stability curves for $^1/_8$-by-14-inch class 6011 electrode

60 cycles, 105 ampere

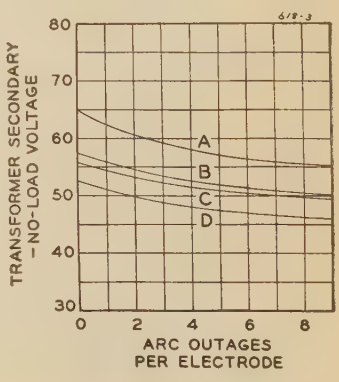

Figures 2 and 3: *A*—No capacitor, *B*—60 microfarad, *C*—120 mircofarad, *D*—180 microfarad

Paper 46-18, recommended by the AIEE committee on electric welding for presentation at the AIEE winter convention, New York, N. Y., January 21–25, 1946. Manuscript submitted November 13, 1945; made available for printing November 27, 1945.

J. H. BLANKENBUEHLER and R. V. LESTER are with the Westinghouse Electric Corporation, East Pittsburgh, Pa.

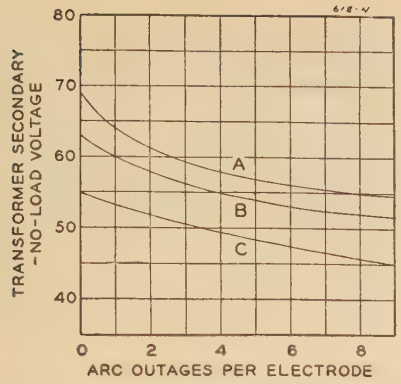

Figure 4. Stability curves showing effect of high lead reactance

$^3/_{16}$-by-18-inch class 6020 electrode, 60 cycles, 180 amperes

A—No capacitor
B—120-microfarad long leads
C—120-microfarad short leads

Figure 1. Figure 2 shows that for a given electrode, the addition of a 60-microfarad capacitor reduced the required secondary voltage from 70 volts to 63 volts, and a 120-microfarad capacitor allowed a reduction of the transformer secondary voltage to 55 volts. Figure 3 shows the results of similar tests on a different type of welding electrode.

It was expected that the long leads sometimes used for welding would introduce a considerable reactance in the welding circuit between the arc and the capacitor and reduce the effectiveness of the capacitor as a stabilizer. In order properly to determine the effect of such leads, tests were conducted with the same transformer and capacitor arrangement with 200 feet of single conductor welding cable from each terminal to the welding position. These 200-foot leads were in one test laid out on a steel floor and, in another test, were arranged in coils on a steel floor. The latter arrangement proved to have twice as much reactance as the former, and the center curve in Figure 4 indicates the result of such a lead arrangement in reducing the stabilizing effect of the capacitor. This combination of 200-foot leads in coils gave a higher lead reactance than ever has been reported in actual practice, and this is considered to be an extreme condition.

In planning a line of welding transformers using this method of stabilization, the designer must compare the additional cost of the capacitor and its mounting with the reduced size of the transformer itself as well as the more abstract, but nevertheless desirable, improvement in safety. He also must allow sufficient margin in the use of the curves obtained by such tests to care for a reasonable length of welding leads and for a low primary voltage. The amount of margin included to care for these points is empirical and must be based on the designer's experience with these factors. One could assume, however, that a 120-microfarad capacitor and 65-volt transformer would give a reasonable margin of stability as indicated by the afore-mentioned curves.

Figure 5 shows a typical oscillograph record of the welding current and arc voltage with such a transformer–capacitor combination. Figure 6 shows a similar record without the capacitor. Visual observation of the cathode-ray oscillograph screen during welding with this capacitor stabilization indicated that the capacitor gave energy to the arc not only at the current zero point, but also occasionally within the half cycle of current flow when some arc disturbance seemed to require such energy.

The capacitor during any half cycle is charged with a certain amount of energy. When the voltage drops to zero, the capacitor tends to discharge. Figure 1 indicates that there are two possible paths for discharge of this stored energy. One of these paths is through the secondary winding of the welding transformer in series with the adjustable reactor. This combination offers a very high impedance in the form of reactance to the discharge of the capacitor energy. The other possible path is through the welding arc which is presumably an air gap at the time of current zero and therefore also offers high impedance in the form of resistance to the discharge of the capacitor. This causes the potential of the capacitor to build up very rapidly until it reaches a value that will break down the air gap. This reestablishes the welding arc at a lower transformer secondary voltage than would be the case without the high initial potential of the capacitor discharge. As current flows across the arc, the capacitor discharges. If the arc opens, the capacitor potential rises again, and the arc is reignited. Figure 5 shows that the discharge of the capacitor is oscillatory and shows that this discharge may occur at other times than the zero current point.

The net result is that a stable welding arc can be maintained at a lower transformer secondary open-circuit voltage with a capacitor across the arc than without the capacitor. It is the authors' opinion that capacitor stabilization can be used economically to improve simultaneously the performance and safety of welding transformers.

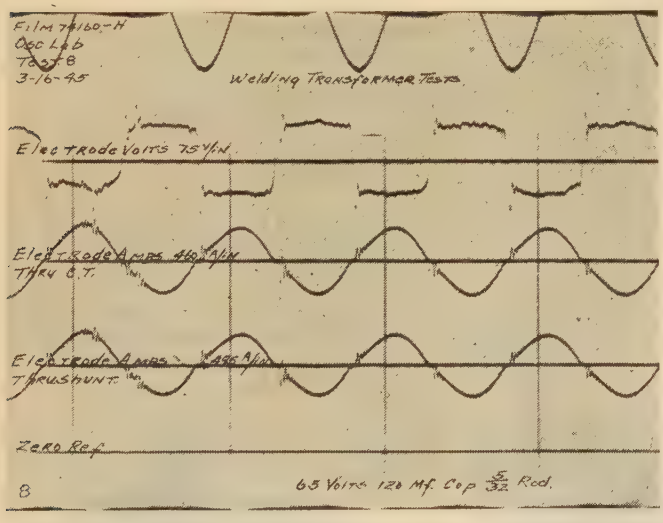

Figure 5 (left). Oscillogram of welding current and arc voltage with capacitor stabilization

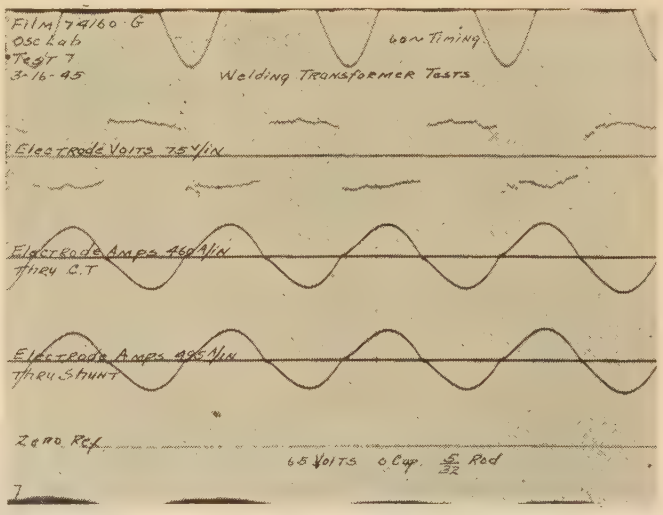

Figure 6. Oscillogram of welding current and arc voltage without capacitor stabilization

Shutdown Versus Hot-Spot Temperatures in Polyphase Induction Motors

C. P. POTTER
FELLOW AIEE

A. E. FROHARDT
ASSOCIATE AIEE

THE "Test Code for Polyphase Induction Machines," AIEE Standard 500, paragraphs 50 to 58 inclusive, contains complete instructions for making temperature tests and reads in part as follows:

"The temperatures indicated by the thermometers placed on the motor at the start of the test usually rise when the motor is stopped: These values . . . . must be recorded. . . . . The highest temperature . . . . recorded will be taken as the actual temperature attained during the test."

The test code, therefore, requires that the temperature rise of a motor taken either while running, or at any time after shutdown, must not exceed the value stamped on the nameplate.

Readings are taken after shutdown in order to disclose abnormal temperatures which may not be detected by thermometers on the windings or core or by the resistance method. There seems to be no doubt that shutdown readings are desirable and necessary, but there may be some doubt whether the shutdown temperatures always should be restricted to the same values as the running temperatures. It is the writers' purpose to report the results of certain tests which were made to investigate this point and to recommend desirable changes in the test code and in ASA Standards.

Paper 46-58, recommended by the AIEE committee on electric machinery for presentation at the AIEE winter convention, New York, N. Y., January 21–25, 1946. Manuscript submitted October 15, 1945; made available for printing December 4, 1945.

C. P. Potter and A. E. Frohardt are with the Wagner Electric Corporation, St. Louis, Mo.

Scope of Tests

Temperature tests were made at various loads and frequencies on a motor having a protected frame; with openings cut in the frame to make it of the open type; and with very large openings giving practically unrestricted ventilation. Tests also were made with most of the openings closed to imitate a totally enclosed machine. Several rotors were tested having different resistances and load losses. The temperature rise of the stator windings was measured by three methods:

1. Surface thermocouples on the hottest accessible part of the winding.
2. Resistance.
3. Embedded thermocouples (using enough to locate the hot spot).

Description of Motor Tested

The motor tested was a 50-horsepower 405-frame 1,750-rpm 3-phase 60-cycle 440-volt machine having a semienclosed slot stator wound with heavy formvar covered round wire. The windings were of the double-layer diamond type, and the free ends were completely taped. The assembled windings were given two dipped and baked coats of varnish. There were no ventilating ducts in either the stator or rotor, and the various rotors tested all were of cast aluminum construction. Figure 1 shows the motor as originally built; Figure 2 as altered to make it of the open type; Figure 3 as altered to have practically unrestricted ventilation.

Location of Temperature Indicators

Sixteen thermocouples were located inside of the windings as shown in Figure 4. Thermocouples 17, 18, 19, and 20 were silk taped inside the loops of the coils just inside the tape which covered the free ends. Thermocouples 6, 8, 10, 12, 14, and 16 were silk taped to the coils inside the slot next to the 0.025-inch insulation separating the winding from the wooden wedge. Thermocouples 5, 7, 9, 11, 13, and 15 were silk taped to coil sides which lie in the bottom of the slot, just below the 0.060-inch insulation separating the coil sides. Thermocouples 1, 2, 3, 4, 21, and 22 were on the outside of the tape on the free ends, embedded in crevices in the windings, and covered with a small amount of sealing compound. Thermocouples 0, 23, and 24 were located on the outside surface of the stator core and were covered with a small amount of sealing compound.

Test Procedure

Several temperature tests were made with various conditions of load, distribution of losses, types of enclosure, and so forth, and each run was continued until the temperatures became constant. Readings of all thermocouples were taken while

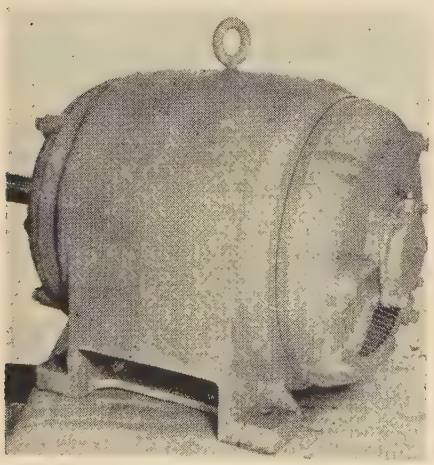

Figure 1. Protected type squirrel-cage motor

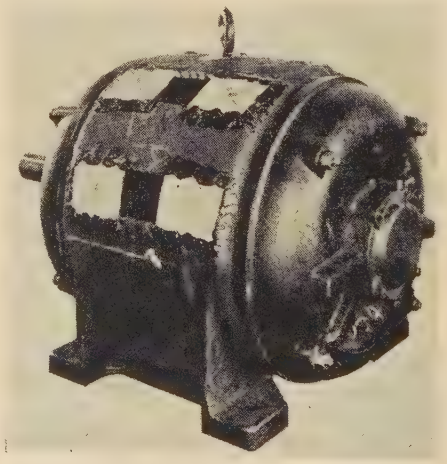

Figure 2. Normal open type squirrel-cage motor

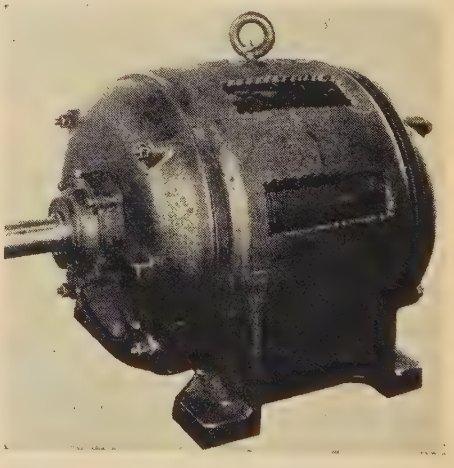

Figure 3. Exaggerated open type squirrel-cage motor

the motor was running. Readings of all thermocouples, resistance, and rotor temperatures were taken at frequent intervals after the motor was shut down to determine how the heat was redistributed. These readings were continued until well after all of them had reached their maximum.

Results

Fifteen sets of observations were made to determine the behavior of the temperatures of various parts after shutdown, and five of them are plotted in Figures 5, 6, 7, 8, and 9. The conditions of test are given in Table I.

These graphs show the behavior of the temperatures after shutdown at the hottest part of the core and the copper available to surface thermocouples, the hot spot as located by embedded thermocouple, and the rotor. The temperature rise by resistance also is plotted.

Table I. Test Conditions

Figure	Frame	Rotor
5	Totally enclosed	Low resistance
6	Protected	High resistance
7	Protected	Low resistance
8	Normal open	Low resistance
9	Exaggerated open	Low resistance

Table II. Hot-Spot and Maximum Shutdown Temperatures

Figure	Frame	Temperature Rise		Shutdown in Per Cent of Hot-Spot Temperature Rise*
		Shutdown	Hot Spot	
5	Totally enclosed	50	50.6	98.8
6	Protected	61.9	69.7	88.8
7	Protected	47.5	54.5	87.2
8	Normal open	39.0	46.4	84.0
9	Exaggerated open	38.5	48.6	79.2

* The shutdown figures are the maximum values taken by thermocouples located on the hottest part of the windings or core accessible to thermocouples.

Table III. Temperature Data for Open-Type A-C Motors

Horsepower	Table	Number of Tests	Shutdown in Per Cent of Hot-Spot Temperature Rise*
Integral	II	5	88 to 91
		1	77
Integral	IV	4	91.1 to 95.5
Fractional	I	2	92 to 95
Fractional	II	10	86.5 to 95.3
Fractional	IV	8	89 to 98
Fractional	VI	6	94 to 97
Fractional	VII	16	92 to 102

* The shutdown figures are the maximum values taken by thermocouples located on the hottest part of the windings or core accessible to thermocouples.

The hot-spot temperatures and maximum shutdown temperatures taken from these graphs are given in Table II.

Two papers published in 1945[1,2] contain data taken from temperature tests made by ten different observers, and the

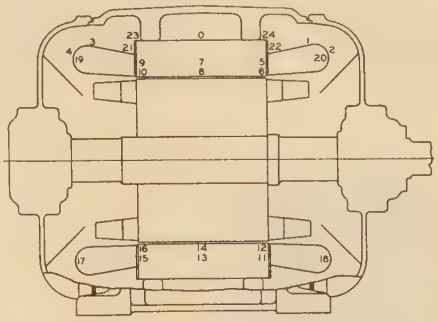

Figure 4. Location of thermocouples

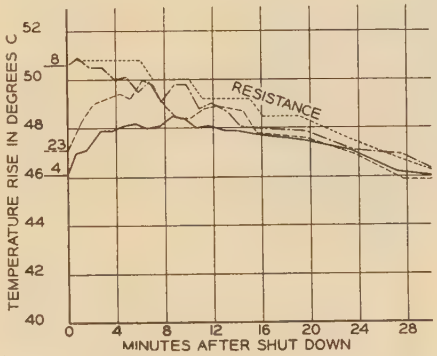

Figure 5. Behavior of temperatures, totally enclosed squirrel-cage motor

Line 8—Hot spot
Line 23—Core
Line 4—Winding surface

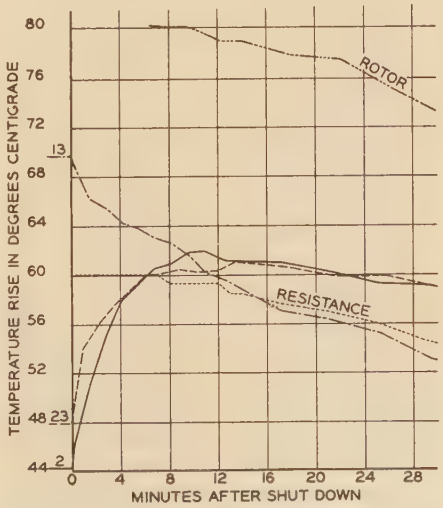

Figure 6. Behavior of temperatures, protected type squirrel-cage motor

Line 13—Hot spot
Line 23—Core
Line 2—Winding surface

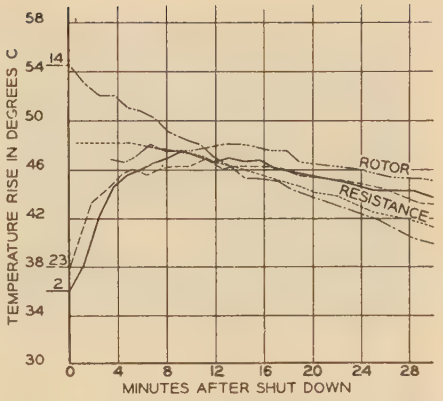

Figure 7. Behavior of temperatures, protected type squirrel-cage motor

Line 14—Hot spot
Line 23—Core
Line 2—Winding surface

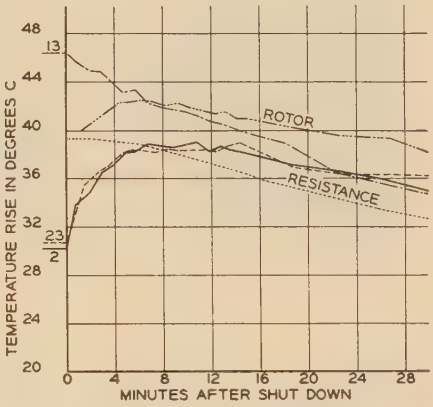

Figure 8. Behavior of temperatures, normal open type squirrel-cage motor

Line 13—Hot spot
Line 23—Core
Line 2—Winding surface

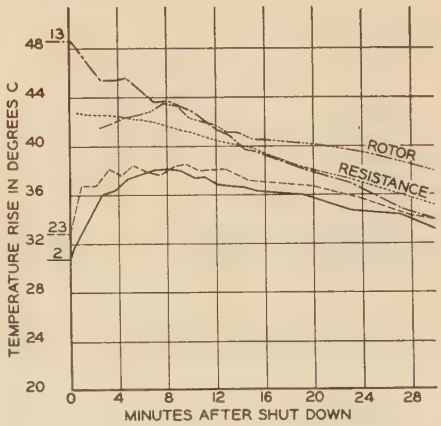

Figure 9. Behavior of temperatures, exaggerated open type squirrel-cage motor

Line 13—Hot spot
Line 23—Core
Line 2—Winding surface

Pressure-Arc-Interruption Circuit Breakers for 400-Cycle Aircraft Electric-Power System

B. O. AUSTIN
MEMBER AIEE

A THOROUGHLY TESTED lightweight circuit breaker for the 208Y–120-volt 3-phase 400-cycle a-c system for large aircraft is now a reality. The circuit breaker is electrically operated, remotely controlled, with latched-in main contacts. The design is suitable for paralleling generators and busses, circuit interruption, manual or automatic synchronization, and interlocks are provided for use in various control circuits. Operating solenoids are designed for low current requirements and for wide ranges of voltages and ambient temperatures. Size and weight have been kept to a minimum.

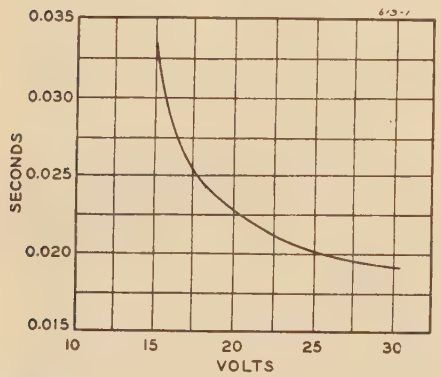

Figure 1. Curve showing closing time of 400-cycle 208–120-volt 120-ampere aircraft circuit breaker at various applied voltages

General Considerations

The Army Air Forces has become very much interested in a high-voltage high-frequency 3-phase a-c system for large aircraft. Reasons for the use of such a system in very large aircraft are many and varied and have been covered thoroughly elsewhere. ("Why Tomorrow's Planes Will Have A-C Systems," T. B. Holliday. *Electrical Manufacturing*, volume 32, July 1943, page 88.)

Paper 46-13, recommended by the AIEE committee on air transportation for presentation at the AIEE winter convention, New York, N. Y., January 21–25, 1946. Manuscript submitted November 8, 1945; made available for printing November 27, 1945.

B. O. AUSTIN is section engineer, aviation control, Westinghouse Electric Corporation, Lima, Ohio.

Circuit breakers for this system must perform under extreme variations in environment. Satisfactory performance has been proved in altitude chambers up to and including 55,000 feet, the limitations being in test equipment and not in the circuit breaker. It operates satisfactorily from −70 degrees centigrade to +60 degrees centigrade. The circuit breaker continues to function properly after being subjected to a relative humidity of 95 to 100 per cent at a temperature of approximately +40 degrees centigrade for a period of 30 days. Vibration encountered in aircraft does not affect the operation of the circuit breaker. One vibration test passed by this circuit breaker consisted of subjection to vibration for a period of more than three hours in each of the three planes of operation; the vibration consists of a simple harmonic motion having a total excursion of 1/16 inch and a frequency varied uniformly between 10 and 55 cycles per second. The circuit breaker

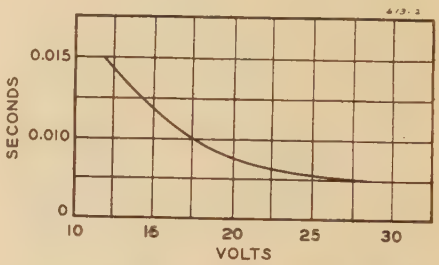

Figure 2. Curve showing opening time of 400-cycle 208–120-volt 120-ampere aircraft circuit breaker at various applied voltages

Table IV. Temperature Data on Plain Enclosed Type A-C Motors

Horsepower	Table	Number of Tests	Shutdown in Per Cent of Hot-Spot Temperature Rise*
Integral	I	2	93 to 95
Integral	II	3	95 to 98
Integral	IV	5	92.3 to 95.9
Fractional	I	2	92 to 98.5
Fractional	III	8	91.2 to 98.2
Fractional	IV	8	95 to 100
Fractional	VI	6	95 to 98
Fractional	VII	8	96 to 101

* The shutdown figures are the maximum values taken by thermocouples located on the hottest part of the windings or core accessible to thermocouples.

tests on the a-c motors may be summarized as in Tables III and IV.

Conclusions

From these tests it may be concluded that the relation between hot-spot temperature rise and the temperature rise after shutdown (taken by thermocouples which are located on the hottest part of the windings or core accessible to thermocouples) is a function of the motor ventilation. In the case of a totally enclosed motor the hot-spot temperature rise and the temperature rise after shutdown are almost equal. In the case of a motor which has a minimum amount of enclosure the ratio between the temperature rise after shutdown and the hot spot is 0.792, or when the hot-spot temperature rise is 50 degrees centigrade, the temperature rise after shutdown is 39.6 degrees centigrade. The "Test Code for Polyphase Induction Machines" was written prior to 1934 and probably was based on experience with motors having a minimum amount of enclosure and unrestricted ventilation. Squirrel-cage motors as built today are fairly well protected, and it would seem perfectly fair to conclude that the shutdown temperature rise in these motors is about 90 per cent of the hot-spot temperature rise, which would allow a shutdown temperature rise of 45 degrees centigrade instead of the 40 degrees centigrade figure now required.

Recommendations

In view of the fact that the trend is toward protected motors, it is recommended that the "Test Code for Polyphase Induction Machines AIEE 500" and the "American Standard Rotating Electrical Machinery C-50" be modified to allow a temperature rise after shutdown of 45 degrees centigrade on protected type motors having a nameplate temperature rating of 40 degrees centigrade.

References

1. INVESTIGATION OF HOT-SPOT TEMPERATURES IN INTEGRAL-HORSEPOWER MOTORS, L. E. Hildebrand, B. M. Cain, F. D. Phillips, W. R. Hough, J. G. Rosswog, C. P. Potter. AIEE TRANSACTIONS, volume 64, 1945, March section, pages 124–8.

2. INVESTIGATION OF HOT-SPOT TEMPERATURES IN FRACTIONAL-HORSEPOWER MOTORS, L. H. Hirsch, R. F. Munier, M. L. Schmidt, L. W. Wightman, F. S. Himebrook, T. C. Lloyd, O. G. Coffman, C. P. Potter. AIEE TRANSACTIONS, volume 64, 1945, March section, pages 128–36.

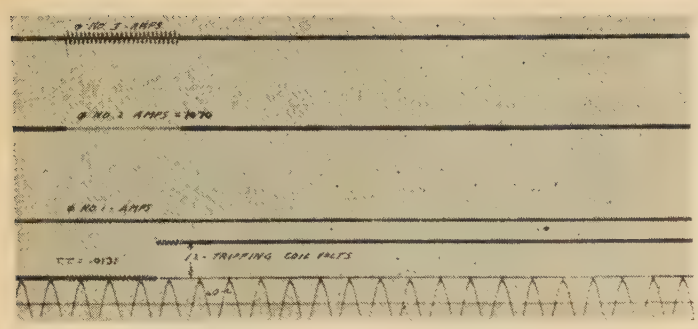

Figure 3. Oscillogram of a short circuit to neutral of a 3-phase system showing interrupting test phase number 2 at 400 cycles, 208 volts, pressure and temperature equivalent to 55,000-feet altitude (—40 degrees centigrade)

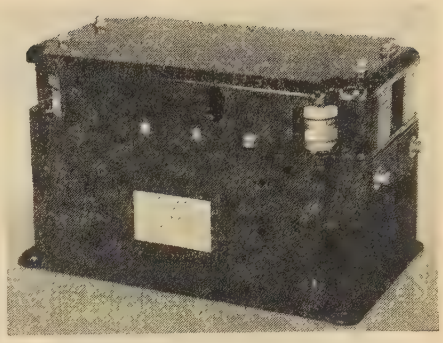

withstood a sand-laden air stream test for a period of five hours.

Obviously the most important single function a circuit breaker must perform is satisfactory interruption of current under all conditions of operation. High voltages at high altitudes are more difficult to handle when arc rupturing is involved. This is due to the decreased atmospheric pressure surrounding the arc when it is established. An effective method of controlling this difficulty is to design arc interrupters which are not subject to altitude conditions.

Figure 4 (upperright) View of complete 208Y–120-volt 120-ampere 3-phase 400-cycle remote electrically operated aircraft a-c circuit breaker

Figure 5. View of circuit breaker showing terminal cover removed

Note straps for changing interlock combinations at the control terminals; also note that the main leads enter at one end and leave at the opposite end

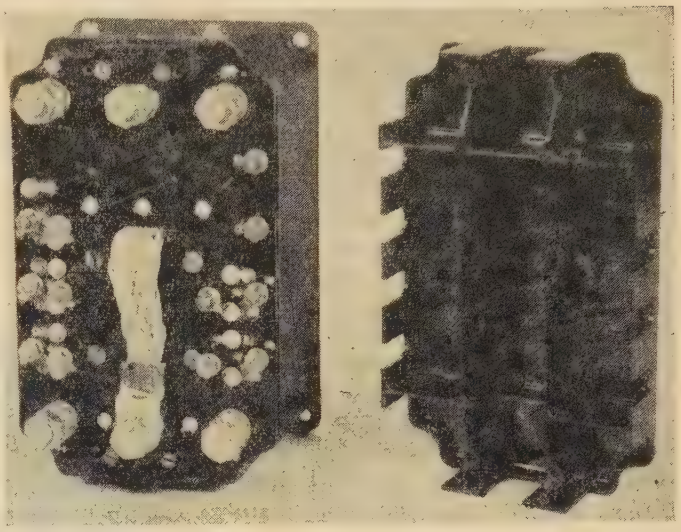

Pressurized Arc Interruption

The basic design problem in producing such a circuit breaker was the devising of a suitable structure which would deionize effectively the arc gases and thus interrupt high current and high voltages at altitude without damage. Several well-known means commonly are employed to cool and deionize the gases of the arc column, thereby producing an instability of the arc which results in its disappearance. They are

1. Lengthening of the arc column.
2. Air or gas blasts.
3. Surface deionization.
4. High gas pressure or vacuum.
5. Fluid action.
6. Multiple arc gaps.

One or more of these principles is employed in all circuit breakers.

This circuit breaker uses high gas pressure, surface deionization, and multiple arc gaps. The design is such that the circuit breaker has several operating advantages. With a self-pressurized arcing chamber the circuit breaker is independent of altitude conditions. Confinement of the arc to the self-pressurized chambers eliminates exposed flame which may contribute to fire. The simplicity of the arc-rupturing mechanism and the chambers makes possible a compact and light structure. Each of the 3-phase circuits are opened and closed by actuating the contact bridges located in the arc chambers. Each bridge bar is equipped with contacts which engage or disengage two stationary contacts. In this manner double or multiple air gaps are provided. Pressurizing the arc to extinguish it quickly also makes possible having the contact mechanism operate through a short distance, thereby making possible higher magnetic forces in a small lightweight closing magnet and high opening speed.

Arcing compartments of the circuit breaker are designed with a minimum of volumetric space. In other words the mass of the moving and stationary contacts occupies more than 50 per cent of the volume of arcing compartments. The side walls and contact parts also cool the arc, aiding in its disappearance. The circuit is broken rapidly as shown in Figure 3. Pressure which is built up in the semi-sealed-off compartments is generated by the arc, and this pressure is adequate to extinguish the arc at 55,000 feet or higher. It has not been found necessary to seal hermetically the arc compartment, and the pressure disappears fairly rapidly.

Construction

The contact mechanism is of the simple bridge type having two breaks per phase. Contact design is similar to that used on thousands of d-c contactors and has been tested thoroughly in aircraft service. Contact materials used are of the sintered type, using a mixture of silver and cadmium oxide which resist high vaporization thus limiting support to the continuity of the arc. Contact life exceeds 5,000 cycles of operation under rated load at 75 per cent power factor.

The latched mechanism used to hold the circuit breaker closed has the advantage of keeping the circuit energized, even though there is a temporary or permanent failure of the direct current which is used to control the circuit breaker. Springs with forces powerful in proportion to the masses to be accelerated are used to obtain high-speed contact separation. This reduces total operating time, reduces heating time, and, therefore, minimizes arcing and wear of contacts. Closing of the circuit breaker is accomplished by the use of a powerful solenoid which produces very high forces in proportion to the weight of masses to be accelerated. Manual operation is not provided. The small travel incident to use of pressurization permits a small magnet to develop the necessary high forces.

Six snap-action interlocks, vibration tested, are provided for use in the manual or automatic synchronizing control circuits, or in other control circuits where

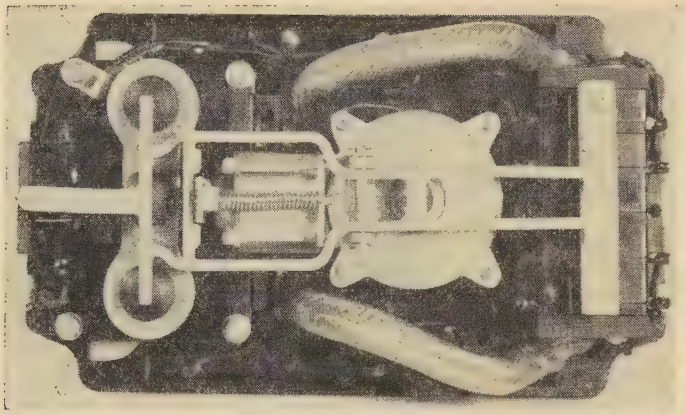

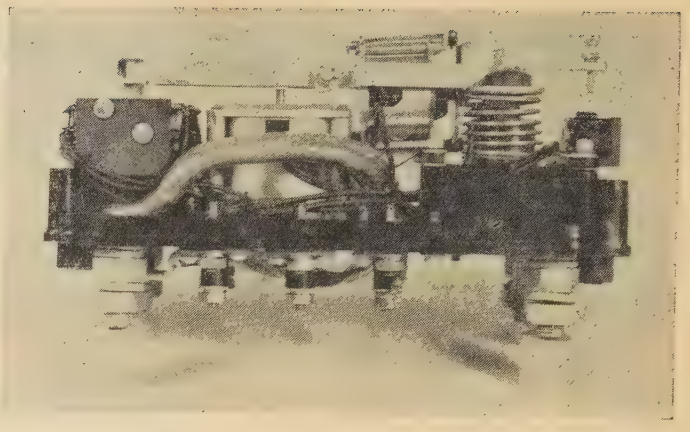

Figure 6. Plan view of circuit breaker showing closing tripping-magnet assemblies, also interlock and main contact operating lever

Figure 7 (above right). Elevation view of circuit breaker showing arrangement of internal parts

their use is necessary for the proper functioning of the controls. Individual interlocks can be made, either normally open or normally closed, simply by changing the position of the external links, thus providing the ultimate in flexibility.

One interlock operated by the main circuit breaker mechanism is in series with the operating coil and interrupts the closing coil circuit as soon as the circuit breaker is latched closed. Thus the coil is excited only during operation, and it is possible to make the solenoid assembly smaller than it would be if continuously rated. The latch mechanism is released by means of a d-c-operated solenoid.

The circuit breaker mechanism is enclosed with a seal which is sufficient to exclude dirt, water, or other foreign materials to a degree insuring operation under the most unfavorable conditions likely to be encountered.

Four mounting holes are provided, and the circuit breaker mechanism may be removed readily without disturbing the mounting or enclosure. Three main leads enter one end of this circuit breaker and leave the opposite end of the circuit breaker providing straight-through wiring. The control circuits enter from each side of the circuit breaker and at the same level as the main leads. Main and control terminals both are protected against accidental contact.

Operating Results

Speed of closing the main contacts of the circuit breaker from the time voltage is applied until the circuit is closed is very rapid. Figure 1 shows a voltage–time curve which gives actual operating speeds on closing as measured by oscillograph. The tripping or opening speed of the circuit breaker is shown in Figure 2. Operating speeds are well within the specifications of the Army Air Forces and assure proper functioning of the system under normal and fault operating conditions.

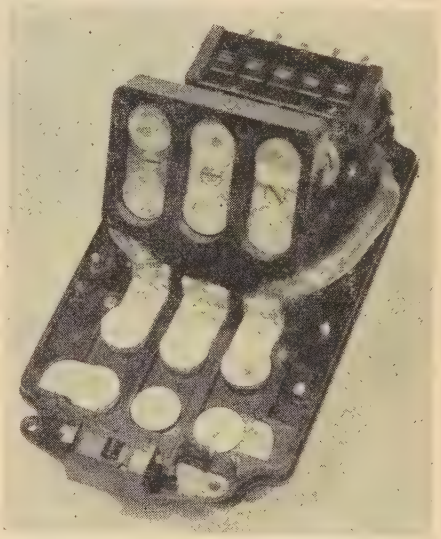

Figure 8. Exploded view of arc rupturing compartments showing contact assemblies

Closing coil and tripping coil are operated from the 28-volt d-c system which also is provided on the a-c-powered airplane, so that undesired operation will not occur during momentary faults.

Conclusions

This circuit breaker functions much the same as circuit breakers for industrial systems but weighs only a very small percentage of what a comparable industrial circuit breaker would.

Pressurized arc interruption is well adapted to circuit breaker performance under altitude conditions.

Effective sealing of the arc reduces the fire hazard present with open arcs.

Unusual high speed action during the closing and tripping periods has been obtained.

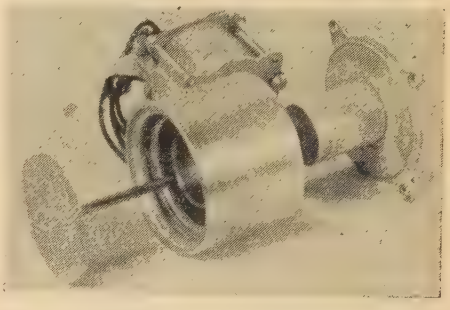

Figure 9. Exploded view of closing magnet assembly showing the component parts

Figure 10. View of moving-contact assembly showing springs and contact chambers

That operation is satisfactory under conditions of humidity, sand, dust, vibration, altitude, and acceleration normal to aircraft has been thoroughly proved.

It is handy for installation because the main lead arrangement is straight through and the control leads also are straight through at right angles to the main leads.

Lead terminals, both control and main, are shielded against accidental contact when this device is mounted in position.

Space requirements are small, and the device weighs only five pounds.

Design and test experience with this type of circuit breaker indicate that the same fundamental principles can be used for breakers having much higher ratings.

Transients in A-C Motors and Generators

GEORGE S. SMITH
MEMBER AIEE

IN THE PAST, few electrical-engineering curricula have offered the undergraduate student more than the rudiments in the study of electric transients. Even today many engineering schools offer such courses only as graduate work. The result is that most engineering graduates confronted with such problems in connection with their work must acquire such information by self study and experience.

Many engineers in charge of the design, maintenance, or operation of large power systems of today are confronted with such problems as the choice, settings, or proper operation of such apparatus as circuit breakers, relays, and other protective equipment. Such equipment must operate adequately to protect the apparatus effectively and yet not cause undue interruption of service. Many such problems involve the conditions occurring during the transient period. Thus a clear conception of the nature of the changes during such periods is of great importance.

A great amount of valuable research work has been done in such studies, and a great deal of information is available.[1-8] Some of this material is in the nature of explanation or suggested methods of procedure, while some is in usable mathematical form, but most of the literature on such studies involves a great amount of detail and too often is written for those who already have a clear conception of the principles involved.

This paper proposes no mathematical study but does attempt to give a simple and clear conception of the variations that take place in the electric and magnetic circuits of a-c motors and generators and reactions between the armature and field, as well as reflected reactions between them during changes in operation. The analysis will be based upon well-known fundamental principles, and in some cases the results will be compared with mathematically derived results found in other papers as well as with actual oscillograms. This method of arriving at a physical conception of such transient conditions has been used quite successfully in introducing undergraduate students to the more advanced information available.

Paper 46-5, recommended by the AIEE committee on electric machinery for presentation at the AIEE winter convention, New York, N. Y., January 21–25, 1946. Manuscript submitted June 21, 1945; made available for printing October 25, 1945.

GEORGE S. SMITH is a professor in the department of electrical engineering, University of Washington, Seattle, Wash.

Method of Analysis

In order to acquaint the reader with the method used in this analysis and also present a very brief review of a few rudiments of the study of electric transients for those who have not recently pursued such studies, a couple of simple transient cases will be analyzed.

First consider the sudden application of a direct voltage, E, to a simple series circuit consisting of a resistance, R, and inductance, L. Using Kirchhoff's voltage law, the algebraic summation of all the voltages involved in the closed loop must be equal to zero, which may be expressed thus:

$$Ri+Ldi/dt=E \qquad (1)$$

Solving this differential equation for the current flowing at any time after closing the switch, gives the result,

$$i=E/R-(E/R)\epsilon^{-Rt/L} \qquad (2)$$

In Figure 1, the oscillograph trace i shows this value at any time after the application of the voltage. If a horizontal line, I, is constructed at a distance above the zero line, equal to a current value of E/R to the same scale as the current i, it will be tangent to the oscillograph trace at a time when i attains its final steady-state value. Also let another curve, i', be constructed equal to $-(E/R)\epsilon^{-Rt/L}$ for the various values of t after closing the switch. The dashed decrement curve below the zero line will result. The sum of the ordinates of the two constructed curves at any time, t, always will give the ordinate of the oscillograph curve, i, for that time. This agrees with equation 2 which states that the actual current flowing in the circuit at any time after closing the switch is the sum of the final steady-state current and a hypothetical transient value.

Next consider that an alternating voltage of $E \sin(\omega t+\gamma)$ is applied to the same series circuit of resistance and inductance instead of the direct voltage E. Now the differential equation is

$$Ri+Ldi/dt=E \sin(\omega t+\gamma) \qquad (3)$$

and the solution for the instantaneous current, i, at any time, t, is

$$i=(E/Z)\sin(\omega t+\gamma-\theta)-(E/Z)\epsilon^{-Rt/L}\sin(\gamma-\theta) \qquad (4)$$

In Figure 2 the oscillograph trace, i, shows the actual current flowing at each instant. The constructed current wave, I, is equal to $E/Z \sin(\omega t+\gamma-\theta)$ or the current which would have been flowing in the circuit during the interval shown, had the switch been closed many cycles earlier. This coincides with i after steady-state conditions in the circuit are attained. The decrement curve, i', is a plot of $-(E/Z)\epsilon^{-Rt/L}\sin(\gamma-\theta)$. Here again equation 4, as well as the summation of the ordinates of the constructed curves, show that the actual current can be considered the final steady-state value plus the transient value.

The decaying transient value in each of these circuits varies as the logarithmic function of ϵ^{-x} where x in the cases mentioned was a function of time t. In Figure 3 a plot of ϵ^{-x} for varying values of x is shown and appears as a decimal factor, the value of which is unity at $x=0$ and drops to zero when x reaches infinity. It might be termed one of nature's laws of change which, in simple terms, says that the amount of decrease taking place at any time is always proportional to the magnitude at that time of the quantity changing. If the amount of change were at each instant added to the quantity changing, as in continually compounded interest, the logarithmic factor would be ϵ^{x} and

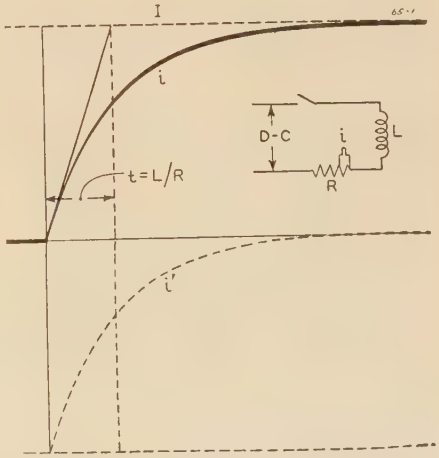

Figure 1. Building up a direct current in a circuit of resistance and inductance in series

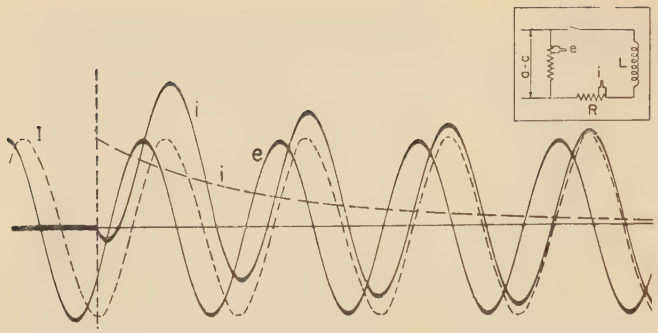

Figure 2. Building up an alternating current in a circuit of resistance and inductance in series

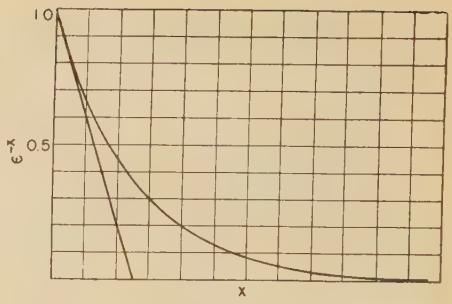

Figure 3. Decaying transient decrement curve

would start at unity when x is equal to zero and approach infinity as x approaches infinity. Other intermediate types of change factors might be such as $(\epsilon^{x}+\epsilon^{-x})\div 2$ or cosh x, or $(\epsilon^{jx}-\epsilon^{-jx})\div 2j$, or sin x, and so on.

The method of adding known components, illustrated by the two oscillograms, often proves to be a rather simple and fairly accurate method of arriving at the desired results and has been used quite extensively by Kurtz and Corcoran in their text on transient studies as one method of analyzing the transient conditions considered.

In the cases of the illustrations given, the circuit parameters were assumed constant. However, in electric machinery where magnetic materials are involved and in some circuits where the resistance or capacitance might vary for some possible reason, a mathematical determination of the components or the results in any other way is not easy. Such components or results sometimes can be determined by mathematical means, provided the law of the change involved is known; they may sometimes be determined by a series of very small but finite increments using relations known from experimental information; or they may be isolated from experimental determinations by the elimination of known components.

A final word of explanation in the use of vectors in this analysis seems also desirable. In the study of the effects of armature reaction in electric machinery, especially motors and generators, the final value and distribution of the magnetic flux is given by the resultant of all of the magnetomotive forces acting on the reluctance of the magnetic-flux path. Such magnetomotive-force components wound on the circular peripheries of the machine cannot be combined by assuming each to be a vector quantity, except as a very rough approximation. However, the resulting magnetic field-intensity along a given path resulting from each magnetomotive force can be considered more correctly a vector value. The magnetic flux caused by such a field intensity vector also can be considered a vector in the same direction, though not always proportional to the field intensity unless the permeability of the magnetic path remains constant.

Since the simplicity of this analysis depends to a large extent upon the use of vectors and since the method is not intended to be mathematically correct, the magnetomotive forces will be assumed to produce vector field intensities, and these in turn will be assumed to produce corresponding magnetic-flux vectors, which vectors will be combined in the usual manner. Where a change of permeability of importance must be taken into consideration, a gradual change in the length of the vector, according to the known law of change, will be assumed. Such assumptions will be pointed out at the time they are used.

Building Up the Rotating Magnetic Field of a Three-Phase Induction Motor

A three-phase induction motor stator (for simplicity assume a two-pole winding) connected to a suitable three-phase voltage supply has, after steady-state conditions have been attained, a single nonvarying rotating magnetic field produced by the varying combinations of magnetomotive forces of the three phases carrying the respective phase currents. In Figure 4a the three-phase windings $A_S\,A_F$, $B_S\,B_F$, $C_S\,C_F$, each is represented by a single turn in the proper angular position with respect to the polarity of the voltage applied or the direction of the current flowing in the coil at some definite instant of time. The subscript S indicates start and F finish of coil. Assume the phase currents shown in Figure 4b are flowing in the respective coils. The directions of the currents in the coils at a time indicated by the ordinate at t = zero time are identified by the usual plus and dot signs in the conductors. The resulting magnetomotive force of each phase will produce vector values of field intensities (not indicated) which would combine to produce the resultant field intensity $\boldsymbol{H}_R$. For any time later $\boldsymbol{H}_R$ can be proved to remain constant in value but to rotate counterclockwise in synchronism with the supply. This vector will be called the final steady-state field intensity and will produce the final steady-state magnetic field $\boldsymbol{\phi}_R$ shown in Figure 5a. This field flux also rotates at synchronous speed in the same direction.

Thus far the assumption has been made that the voltage had been applied at some earlier time. Now assume that the switch is closed at the time indicated by the ordinate t = zero. Since the circuit is inductive, all currents must start at zero, and similar to the case in Figure 2, the starting current in each phase will be the sum of the steady-state current in that phase plus a unidirectional decaying transient current. Both components are indicated in Figure 4b while the actual starting currents would appear

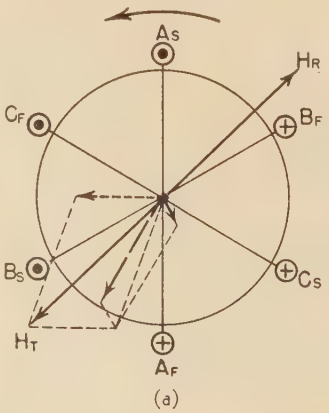

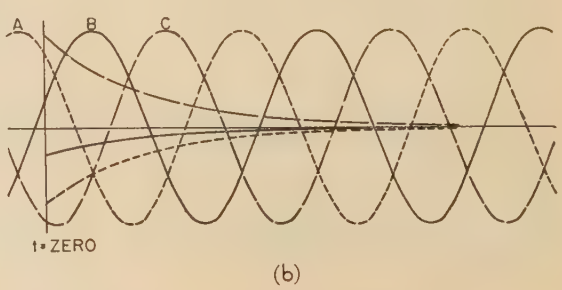

Figure 4(a) and (b). Components of field intensities and the three-phase steady and transient currents producing them

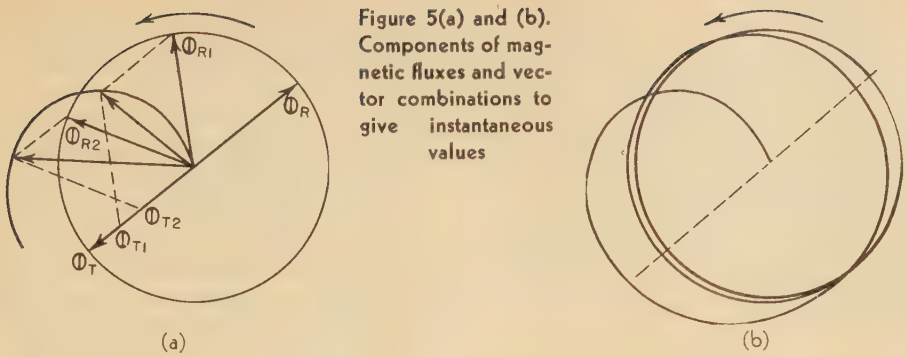

Figure 5(a) and (b). Components of magnetic fluxes and vector combinations to give instantaneous values

similar to the starting currents shown in Figure 7.

Likewise the magnetic field must start from zero and also can be assumed to be made up of the steady-state value ϕ_R, already explained, plus a component due to the combination of the magnetomotive forces set up by the transient currents in their respective coils.

In Figure 4a the corresponding instantaneous vector intensity for each of these transient currents at t=zero is shown in its proper directions and magnitudes, and their vector sum is H_T, which is equal in magnitude but reversed in direction to the rotating vector H_R. In Figure 5a the corresponding vector ϕ_T is indicated. The sum of ϕ_T and ϕ_R is zero at time t=zero, as it should be. Unlike the vectors H_R and ϕ_R which rotate, the transient vector H_T and corresponding flux ϕ_T remain stationary in space, since they are produced by unidirectional currents flowing in stationary coils. However, they decrease toward zero as time goes on in accordance with the decrement currents which cause them.

At any time after t=zero the actual magnetic field ϕ can be found by adding ϕ_R, which is in a new angular position, to the remaining value of ϕ_T. Such vector additions are shown in Figure 5a for angular positions of ϕ_R at 45 degrees and 90 degrees from the starting position.

By carrying out such vector additions at small angular increments for a few cycles of the alternating current, the value of ϕ becomes alternately greater and less than the final steady-state value but rapidly approaches a steady value as time goes on. The envelope thus derived is shown in Figure 5b, and the same values of ϕ plotted against time are shown in rectangular co-ordinates in Figure 6.

Figure 7 is an oscillogram of the actual currents flowing in the three phases of the induction-motor stator when first excited. These should correspond quite closely to curves obtained by adding the steady-state and transient values for each phase current in Figure 4b. However, in Figure 7 the permeability changes in the iron probably have introduced some distortions not assumed in Figure 4a, and the resulting magnetic-field variations also would be slightly altered from those shown in Figure 5b and Figure 6.

Three-Phase Alternator or Synchronous-Motor Load Changes

Closely related to the changes just described for the three-phase induction motor are those occurring when some sudden alteration in load takes place in the operation of a three-phase alternator or synchronous motor. Such an alteration may be from no load or part load to a much greater load or even short circuit, or it may be the reverse from a high load to a lower one or to no load. Were the machine an alternator the type of load might be resistive, inductive, or capacitive. In all cases the inductive nature of the machine's internal impedance always must be present.

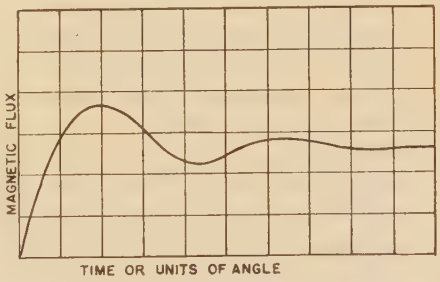

Figure 6. Variation in magnitude of magnetic field in rectangular co-ordinates

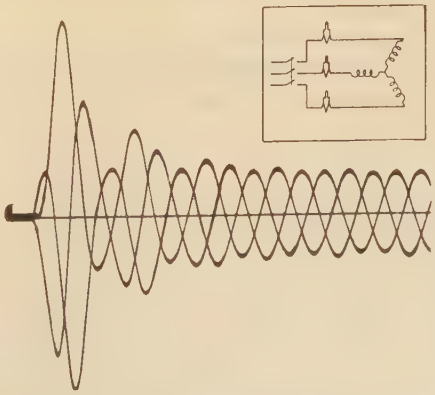

Figure 7. Initial three-phase currents in an induction-motor stator

To illustrate the method of analysis, an alternator operating at no load suddenly will have a near short-circuit load applied to its terminals. For a clear conception of all the changes occurring the reader must rely on his knowledge of armature reaction in alternators, of the effects of the load power factor, and the effects of changes in the permeability in the magnetic circuit.

A two-pole three-phase alternator stator shown in Figure 8a, identical to the one used in discussing the induction motor, will be assumed. The only addition will be a two-pole d-c-excited rotor operating at some given speed. Again the three-phase steady-state currents are shown in Figure 8b. If the load switch had been closed at the time indicated as t=0, the transient component shown for each phase is also necessary. At this point, however, a radical difference from the previous case occurs. The alternator, rotating at a constant speed and with its d-c-excited field, is generating a rather high no-load voltage, while the final sustained current shown is caused by a greatly reduced voltage in comparison, since armature reaction and permeability changes have greatly reduced the magnetic flux of the field. Thus the so-called steady-state component of current flowing in each phase at the instant of closing the switch is somewhat greater than the final sustained value, and these components would be more in the order of those shown only as tips of waves in Figure 8b. As armature reaction reduces the field flux, these currents also will drop off to the final steady-state current values.

In each phase the final sustained value of current is assumed as one component, as was done in the case of the induction motor. A second is the usual unidirectional decaying current with an initial value equal to the value of the sustained current at the instant the switch was closed but reversed in sign. The decay of this must depend upon the resistance and inductance of the armature circuit. Since the sum of these two will not account for the unusually high values at the time the switch was closed, a third component must be present. Evidently this must be the difference between the final sustained current and the so-called steady-state value indicated by only the wave tips. This component will be a full-frequency oscillating current, decaying with time and with a decay factor depending upon the rate of change in the field flux, thus is controlled by the re-

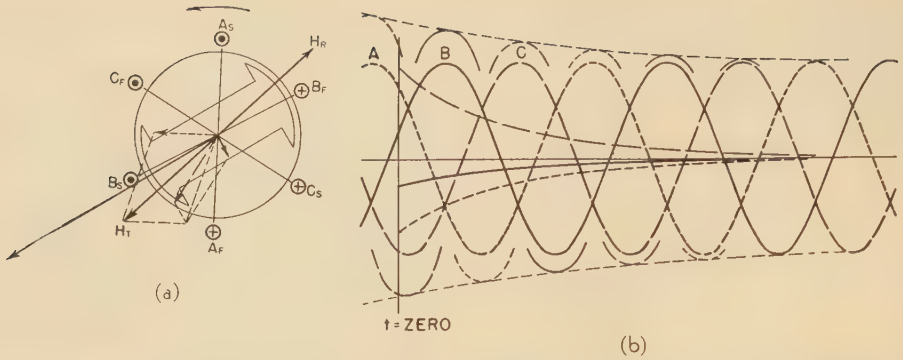

Figure 8(a) and (b). Components of field intensities and the three-phase steady and transient currents producing them

sistance and inductance of the field circuit. This has not been shown as an isolated component in the drawing.

The field-intensity components are shown in Figure 8a. The d-c field current at no load produces a field intensity of H_o. The final rotating field intensity, H_R, is the armature reaction arising from the sustained currents in the three phases. The transient intensity, H_T is due to the unidirectional currents of the three phases. As there is still another component in each phase of the armature which must have an armature reaction effect upon the field, it will rotate with the field similar to H_R but will decay to zero as the sustained armature currents are approached. This component will be accounted for by a decrease in the value of the flux generated primarily by the d-c field current.

Figure 9 is a typical equivalent single-phase vector diagram for the alternator showing the armature current and all the various voltages and voltage loss components, as well as the no-load field flux ϕ_o proportional to H_o, ϕ_R proportional to H_R, and ϕ_T proportional to H_T. The no-load voltage E_o is generated by ϕ_o. As explained in the discussion on the field-intensity components, a portion of the ϕ_0 is lost because of the high initial armature currents and the resulting excess armature reaction. Reducing ϕ_o by the amount of this loss leaves ϕ_F the final steady-state flux due to the d-c excitation. This combines with the armature reaction flux ϕ_R to leave ϕ_G as the remaining flux to generate the internal generated voltage E_g, a part of which is lost in the winding impedance to leave E_T at the terminals. The final steady-state current is I which must be in phase with ϕ_R and the near short-circuit power-factor angle is θ.

To explain further the lost component of field flux, refer to the typical partial hysteresis loop, Figure 10, showing both increasing and decreasing field-excitation values. Assume the no-load condition to be at the maximum point with H_0 excitation due to the d-c field resulting in ϕ_o as the total flux. The initial armature current reduces the excitation by the amount of H_1 with the flux following the upper saturation curve. As the armature current drops in magnitude to its final steady-state value, the armature reaction reduces to H_R, and the flux value increases on the dashed curve to the final value of ϕ_G. Had this reversal not occurred, the saturation would have remained on the upper curve and would have been greater by the component of ϕ_L. Thus the flux ϕ_L equal to $\phi_o - \phi_F$ was lost due to the changes in permeability.

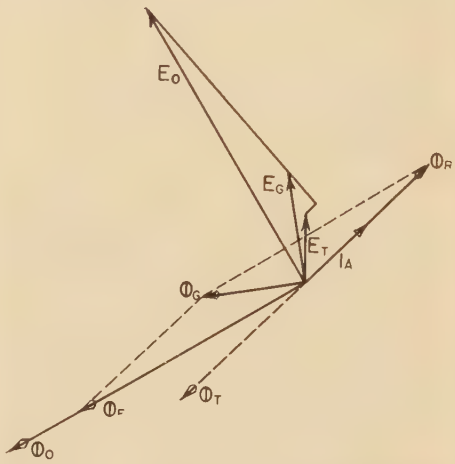

Figure 9. Equivalent single-phase alternator vector diagram

In Figure 11a the flux due to the no-load d-c excitation is shown as ϕ_o, the steady-state armature reaction at the instant of t=zero is shown as ϕ_{R0}, and the transient of the armature reaction values as ϕ_T. The vector sum of these three is evidently ϕ_o, as it should be. After ϕ_R has rotated through 45 degrees to ϕ_{R1}, the d-c excited field has rotated to ϕ_1. Notice that ϕ_1 is less than ϕ_o by a fraction of ϕ_L indicated on the field decrement curve of Figure 12 for the time angle of 45 degrees. Also ϕ_T, though stationary, has decreased to T_1 by an amount indicated on the armature decrement curve of Figure 12 for the same time angle. The sum of these three vectors gives the actual flux value ϕ_{S1} at that instant. A second step is shown after 90-degrees rotation, giving the sum of ϕ_{R2}, ϕ_2, and T_2 as the instantaneous value of flux ϕ_{S2}.

By carrying out such vector summations for small increments over a few cycles, the polar diagram envelope of the flux variations is shown in Figure 11b. The flux value starts to decrease rapidly but pulsates for a short interval, finally reducing to a steady rotating value of ϕ_G.

This varying flux is replotted in rectangular components in the graph A of Figure 13. In the graph B the various voltages acting in the d-c field coils are shown. Before the load is thrown on the alternator the direct voltage alone causes field current to flow. Just after throwing the load on, armature reaction causes a rapid decrease in the field flux ϕ_o, which change in flux induces a considerable voltage in the field coil. Because the flux value alternates, the induced voltage also alternates. The voltage is maximum when the flux is changing most rapidly and is zero when the flux is at a high or low point and not changing. The inductive nature of the field circuit will not allow the field current to change instantly, thus a transient component of voltage also must be present. This must have an initial value equal to the initial induced voltage but of the reverse polarity. The decrement factor of this transient voltage will depend upon the d-c field coil inductance and resistance.

When the ordinates of all of the components of voltage at each instant of time are added, the resulting curve is the actual voltage acting in the field circuit to cause current to flow. Thus the field

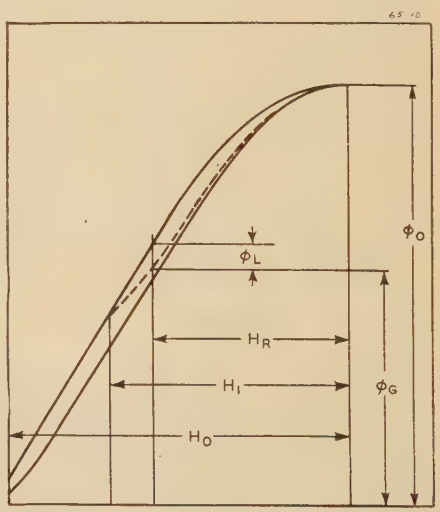

Figure 10. Typical partial hysteresis loop for alternator

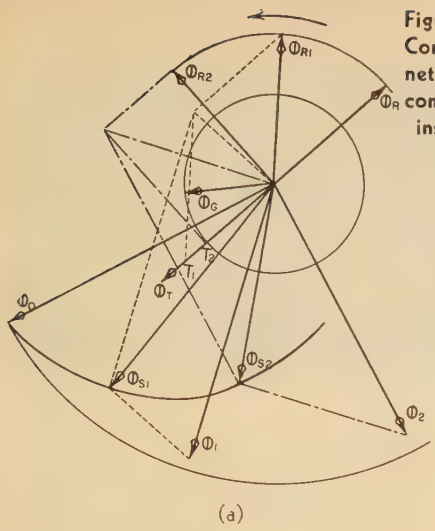

(a)

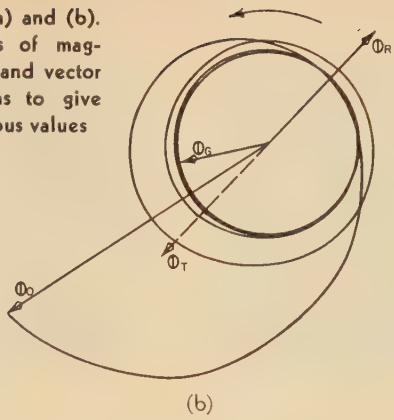

(b)

Figure 11(a) and (b). Components of magnetic fluxes and vector combinations to give instantaneous values

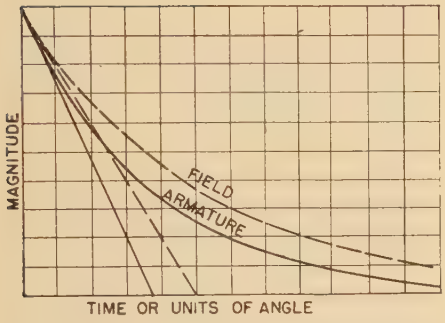

Figure 12. Armature and field decrement curves

current would be a similar curve, but lagging the voltage by some amount. A comparison of this constructed field-voltage curve with the field-current waves of oscillograms shown in Figures 14 and 15 shows the same characteristics.

The oscillogram in Figure 14 shows the voltage across one phase, the three-phase currents, the d-c field current, and the air-gap flux on a rotating-field type of alternator. Figure 15 shows the same values taken on a machine with stationary field poles and a rotating armature. This machine has a rather strong 11th harmonic due to armature slots.

The lower trace in all alternator oscillograms shows the actual value of the air-gap magnetic flux recorded by means of a bismuth-bridge type of magnetic-flux meter.[14–15] Using this with a stationary-pole type of alternator as in Figure 15 shows the rapid decrease of the flux due to armature reaction at the center of the pole face. On the leading tip the decrease is even more rapid, while on the trailing tip the flux often rises above the no-load value before it decreases, indicating flux distortion. In Figure 14 the increase in flux just after load is thrown on is caused by the position of the probe under a trailing pole tip at that instant.

Many attempts have been made to express mathematically the armature and field currents during such transient periods. Doherty and Nickle[6] give the following equations for the armature currents in phases A, B, and C:

$$i_A = \frac{e_o}{x_d}\cos(\omega t-\alpha)+e_o\frac{x_d-x_d'}{x_d\,x_d'}\times \epsilon^{-\sigma_f t}\cos(\omega t-\alpha)-e_o\frac{x_d'+x_q}{2x_d'\,x_q}\epsilon^{-\sigma_a t}\times \cos\alpha+e_o\frac{x_d'-x_q}{2x'_d\,x_q}\epsilon^{-\sigma_a' t}\cos(2\omega t-\alpha) \quad (5)$$

i_B = same as phase A except for the use of $(\alpha+2\pi/3)$ instead of α (6)

i_C = same as phase A except for the use of $(\alpha+4\pi/3)$ instead of α (7)

Each phase current is made up of the algebraic sum of the four components shown. The first is the sustained value of current and corresponds to the sustained value of current in Figure 8b. The second is a full-frequency decaying current caused largely by the high no-load voltage, and decays as the armature reaction reduces the field flux to its final steady-state value. The coefficient of its decay factor σ_f depends upon the field-circuit constants. This component was accounted for by the loss of flux ϕ_L. The third factor is the unidirectional decrement corresponding to the decrement curves in Figure 8b. Its initial magnitude is equal to, but of the opposite polarity to, the instantaneous value of the sustained current corresponding to the point on the voltage wave at which the load switch was closed. The coefficient of its decay factor σ_a depends upon the circuit constants of the armature circuit. The fourth factor, which is usually not very large and is absent or nearly so in some types of generators is a double-frequency component, the decay of which depends upon the armature constants. No attempt was made to indicate this in Figure 8b. This component often appears in salient-pole types of machines which have no damper windings. There are possible sources for many small-scale variations other than those mentioned, as changes produced in the field by armature reaction will in turn cause altered generated voltages and currents in the armature. These in turn will further alter the field. There is no limit to the reflected effects back and forth between armature and field, but fortunately each succeeding reflection rapidly decreases toward zero.

The same authors give the field-current equations as

$$i_f = e_o+e_o\frac{x_d-x_d'}{x_d'}\epsilon^{-\sigma_f t}-e_o\frac{x_d-x_d'}{x_d'}\epsilon^{-\sigma_a t}\cos\omega t \quad (8)$$

This equation might be altered thus

$$i_f = I_o+KI_o\epsilon^{-\sigma_f t}-KI_o\epsilon^{-\sigma_a t}\cos\omega t \quad (9)$$

where K is a constant depending upon the reactances involved. Here the three components are shown similar to the three components of voltage in Figure 13. The first is the current due to the direct voltage, the second is the unidirectional decaying component, the decay of which depends upon the field-circuit constants,

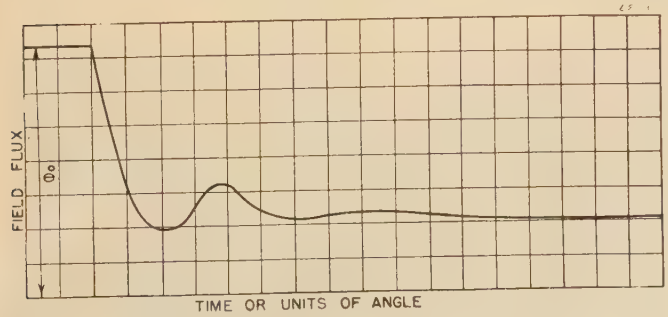

A

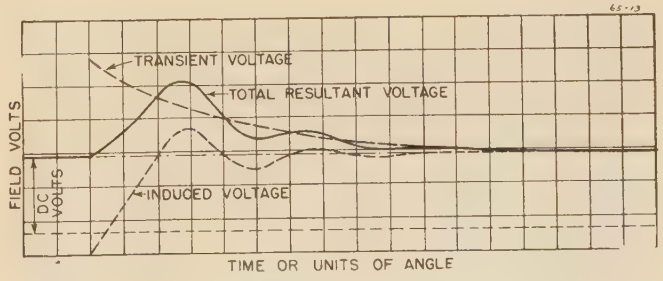

B

Figure 13. Magnetic-field variations and voltage components in field winding

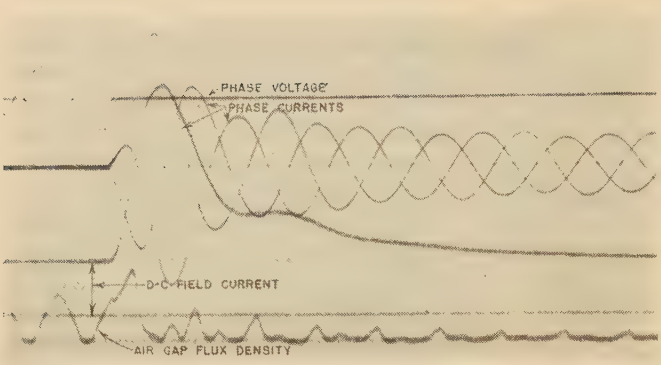

Figure 14 (left). Oscillogram of transients in an alternator with rotating field poles

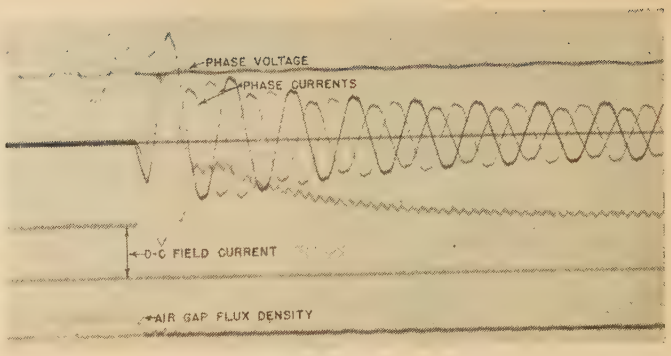

Figure 15. Oscillogram of transients in an alternator with stationary field poles

the third is the component due to the full-frequency alternating induced voltage, the decay of which depends upon the armature circuit constants.

Doherty and Nickle express all initial current components in terms of the no-load voltage e_o, assuming no saturation, and a percentage factor derived from the reactance acting, as the resistance of an alternator is usually so low its effect may be neglected in such factors. Thus the final steady-state current is the ideal no-load voltage e_o divided by the direct-axis component of synchronous reactance x_d.

A brief comment on the various reactances used in such mathematical studies might be of value here. In any circuit the current for a given voltage is limited by the impedance of the circuit. Each component of the impedance will absorb a proportional component of the total voltage, and the countervoltage of each reactance through which the current flows will just balance a corresponding component of the voltage applied. The reactance is then the ratio of that component of voltage to the current.

Referring to the armature current tracings in oscillograms such as Figures 7, 15, or 16, the impedance, or reactance if resistance is neglected, must continually vary from instant the switch is closed to the time when final steady-state conditions prevail, if the generated voltage is to be assumed constant. Since constant values of reactances are desired, certain limiting values are used. Further subdivisions of the reactances also are used. For example, synchronous reactance is a function of the armature current magnetomotive force, largely acting as armature reaction. At any given power factor of the load the armature magnetomotive force, which has been assumed to produce flux ϕ_R in Figure 9, might be considered as the resultant of two components, one acting on the axis of the main field, producing a demagnetizing action, the equivalent reactance of which is termed direct-axis synchronous reactance x_d, and the other acting at right angles to the main field, causing flux distortion of the main field, the equivalent reactance of which is termed quadrature-axis synchronous reactance x_q.

Thus the direct-axis synchronous reactance x_d for the balanced steady-state conditions might be defined as the ratio of the fundamental component of the reactive armature voltage, due to the fundamental direct-axis component of armature current, to this component of armature current, at rated frequency. The quadrature-axis synchronous reactance is defined in a very similar manner.

The reactance during the first several cycles after short circuit must be lower than the steady-state value, as the current is higher, which gives rise to the term transient reactance x'. This might be defined as the ratio of the fundamental component of reactive armature voltage due to the fundamental component of the armature current to this initial component of current at the time short circuit occurs, providing such current follows the normal decrement curve of the decreasing current. This initial value of current must be obtained by projecting the normal current transient back to the time of closing the switch. For most machines, and especially for those having damper windings on the rotor, the first two or three cycles do not follow the normal decrement curve but are abnormally high, though they decay rapidly down to the normal decrement values. For this portion of operation the reactance is still less and is accounted for by a subtransient reactance x''. This is the ratio of the generated voltage to the highest initial value of current which was produced at the instant of closing the switch. Such initial values are only the average of all three phases.

In practice both of these again are divided into the direct, x_d' and x_d'', and quadrature, x_q' and x_q'', values. All of these terms are defined in the AIEE "Standard Definitions of Electrical Terms" and may be determined by tests

Figure 16 (left). Oscillogram of transients in an alternator suddenly loaded with three-phase inductive load

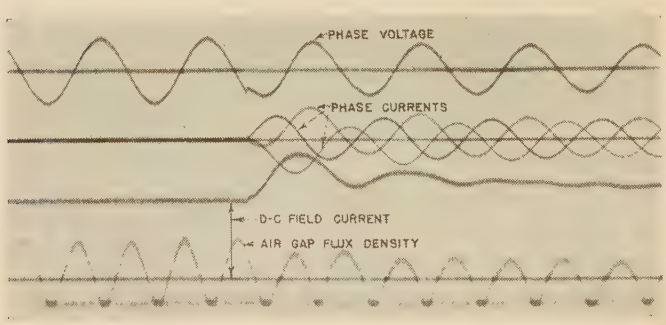

Figure 17. Oscillogram of transients in alternator suddenly loaded with a three-phase capacitive load

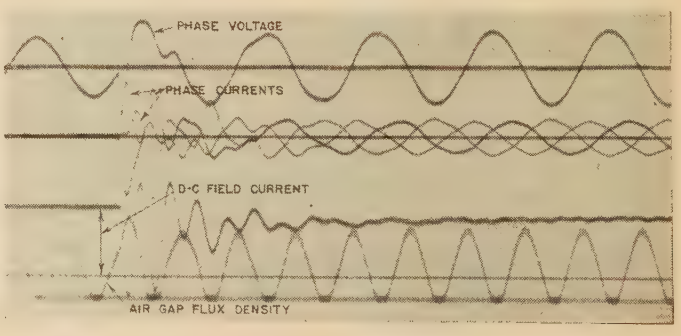

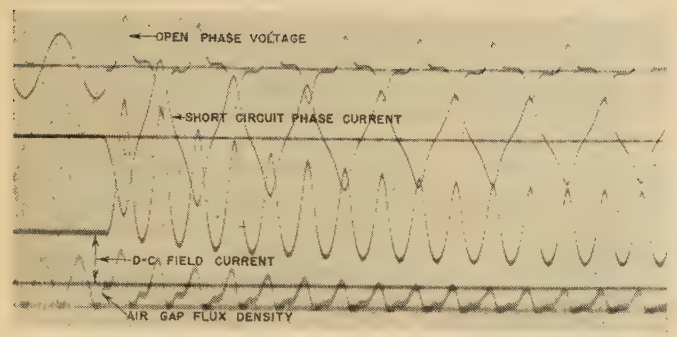

Figure 18. Single-phase short circuit on a three-phase alternator with rotating field poles, symmetrical type

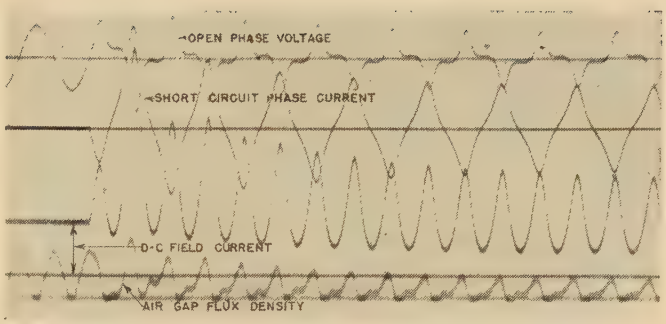

Figure 20. Single-phase short circuit on a three-phase alternator with rotating field poles asymmetrical type

or calculation, as proposed by various authors.[9–12]

Closely related to the reactance values in their importance during the transient period, are the decrement factors or their reciprocals, termed time constants T. In equation 2 the decrement factor is R/L, while the time constant is L/R and is a factor which gives an indication of the time required for the decreasing term to approach zero. In modern a-c machinery the reactance x which is a function of the inductance L purposely is made large either in the design of the machine or by introducing reactance in some part of the circuit, in order to limit the currents under short-circuit conditions. This can be done since the voltage regulator will maintain a constant voltage under steady conditions. The resulting large time constant causes the transient condition to persist for a considerable period after such changes, up to several seconds. The persistence of such high currents often may require higher settings on protective equipment than otherwise would be desired.

Many other transient conditions in alternators or synchronous motors might be analyzed in a similar manner. Two other oscillograms of such conditions are shown. Figure 16 shows the voltage, armature currents, field, and air-gap flux for the same alternator used for Figure 14, except that it is suddenly loaded with a highly inductive air-core inductance load. Here the inductance requires energy from the generator for a portion of the cycle and returns the energy the next half cycle. The resulting armature reaction in reducing the field, both during the transient period and after, is less than for the near short circuit. Figure 17 again is the same machine suddenly loaded with a capacity load. Here the capacity causes the current to lead the voltage, which gives a decided increase in the air-gap flux due to armature reaction.

Load Changes in a Single-Phase Alternator

The single-phase alternator proves quite interesting as a study of interrelated electric and magnetic fields, both under transient conditions as well as steady-state conditions. The theory is also important since faults often result in single-phase operation for their duration. The usual distortions in the voltage and current waves when using one phase of a three-phase alternator for careful tests may introduce considerable error in the results. The same is true for any single-phase alternator, unless it is specially designed to give a fair sine wave at all loads.

Such an alternator has the usual d-c excited field but has only one armature winding which usually does not use the whole periphery of the armature core. As the field rotates 180 electrical degrees for each half cycle, the armature reaction on the field always acts in the same direction, causing a continuous double-frequency pulsation in the field flux. When the load on such an alternator suddenly is changed or the alternator is short-circuited, two possible types of transient relations are possible. In the first, or symmetrical case, fairly perfect examples of which are shown by the oscillograms in Figures 18 and 19, the load switch was closed at a point on the voltage cycle at which, under steady-state conditions, the current value would have been zero, and the second, of which Figure 20 is a typical example, where the switch was thrown at a point on the voltage cycle where the steady-state current would not have been zero. This will be termed the asymmetrical case.

In making an analysis of these single-phase cases, certain assumptions again will be made which would alter the final general results only slightly. First the current waves will be assumed to be sine wave in shape, and second the effects of iron saturation will only be approximated.

Symmetrical Case

If the switch of a series resistance and inductance circuit is closed at a point on the voltage cycle when, under steady-state conditions, the current would have been zero, the usual inductive type of transient as in Figure 2 will not be present; the current will start at zero and continue at its final steady-state value. However, in the case of the single-phase alternator, as in the three-phase case, the no-load field flux and generated voltage are much higher than after the armature reaction has been able to reduce the strength of the field. Because the voltage is high at this first instant, the current also will be high but will drop as the armature reaction becomes effective in reducing the field. There then will be a decay of the armature current value but an equivalent decay will occur on both the positive and negative halves of the wave, and the resulting current will be symmetrical with respect to the zero.

Such a decaying alternating current in

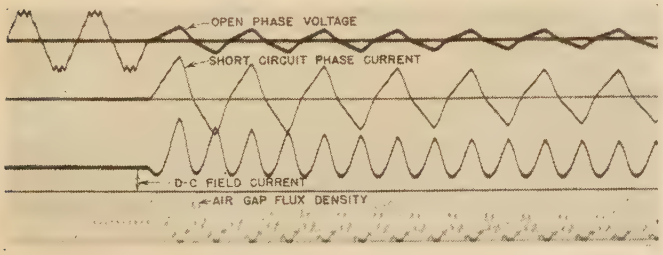

Figure 19. Single-phase short circuit on a three-phase alternator with stationary field poles, symmetrical type

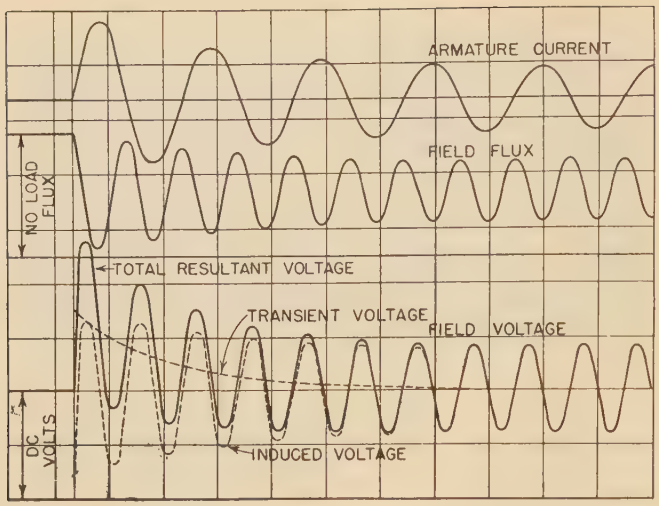

Figure 21. Armature and field components and their phase relations in a symmetrical single-phase alternator short circuit

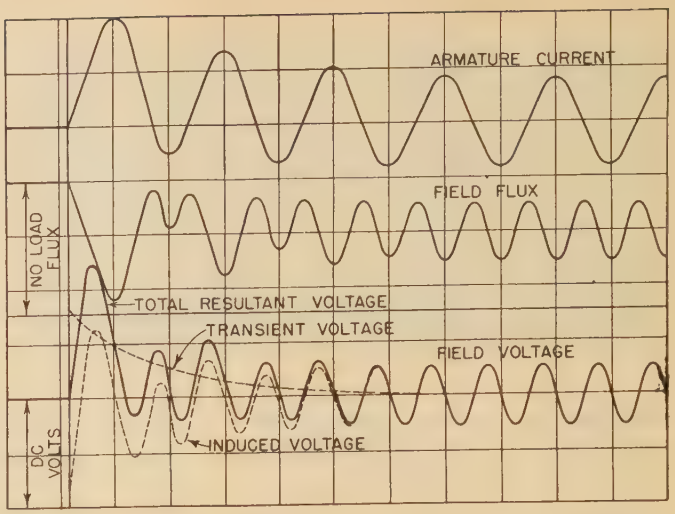

Figure 22. Armature and field components and their phase relations in an asymmetrical single-phase alternator short circuit

a single-phase alternator is shown as the top constructed curve in Figure 21. Since the d-c excited field, because of its rotation is always in a position to receive the same armature reaction effect for both polarities of the armature current, the magnitude of the flux will have two pulsations per cycle. If the usual short-circuit conditions are assumed the reaction will be to cause the flux to decrease most when the current is maximum, and the resulting field flux curve construction will be as shown by the second curve.

The variations in the field flux will generate a voltage in the d-c field winding of the same frequency and of a corresponding magnitude. This pulsating voltage is indicated as a dash curve in the lower set of curves. Since the field current and thus the field voltage must start at the no-load value and cannot jump instantly, the usual unidirectional decrement voltage, shown as a dash line, also must be present. The sum of the d-c, the pulsating, and unidirectional decrement components of voltage will give the actual voltage acting on the field circuit as shown by the full-line oscillation. This corresponds very well with the actual field current in oscillograms, Figures 18 and 19.

Asymmetrical Case

If the load switch is closed at a point on the voltage wave when, under steady-state conditions the current would not have been zero, then the type of transient shown in Figure 2 will be present. However, the effect of the high no-load voltage will amplify the magnitude of the current peaks, both positive and negative, just after closing the switch, but this excess current will die away to the final steady-state current after armature reaction has reduced the field flux to its final steady pulsating value. The upper curve in Figure 22 shows such an armature current curve. The second constructed curve is that of the resulting field flux because of armature reaction. In the lower set of field-circuit voltage curves, the pulsating induced voltage component due to the field-flux pulsations, and also the unidirectional decrement component, are shown in dash lines. Again the sum of these components, together with the direct voltage, gives the full-line curve as the actual voltage acting in the field circuit which corresponds well with the field current in oscillogram, Figure 20.

The induced voltage in the field circuit, as well as the current component resulting from this voltage, could have been further subdivided into a sustained pulsation at double-frequency component and a full armature-frequency pulsating component which decays with a decrement factor, depending upon the armature circuit constants.

Again Doherty and Nickle[5] have worked out quite complete and reasonably accurate equations for the armature field currents, as well as for the open-circuit voltage where a three-phase generator is supplying a single-phase load. For the armature current in the symmetrical case they give

$$i = 2ke_o \frac{K}{J} \sin \omega t + 2ke_o \frac{P}{J} \epsilon^{-\sigma_f t} \sin \omega t \qquad (10)$$

and for the asymmetrical case

$$i = 2ke_o \frac{1}{H} \epsilon^{-\sigma_a t} \cos \alpha - 2ke_o \frac{K}{H} \times \cos (\omega t + \alpha) - 2ke_o \frac{P}{H} \epsilon^{-\sigma_f t} \cos (\omega t + \alpha) \qquad (11)$$

In the symmetrical case, equation 10, the current is made up of the alternating sustained value plus an alternating value at the same frequency but decaying with a decrement factor depending upon the field-circuit constants. This second component is due to the high no-load field causing a high armature voltage and current at the instant of closing the load switch but dies away as armature reaction reduces the field. In the asymmetrical case, equation 11, the last two terms are components similar to those of equation 10. The additional first term is a unidirectional decaying component with a decrement factor depending upon the armature-circuit constants, with the initial magnitude depending upon the point on the voltage wave at which the load switch was closed. These components correspond very closely to the components necessary to give the armature currents assumed in Figures 21 and 22 respectively.

For the symmetrical case they give the field current as

$$i_f = e_o \frac{CK}{J} + e_o \frac{FP}{J} \epsilon^{-\sigma_f t} - e_o \frac{FK}{J} \times \cos 2\omega t - e_o \frac{FP}{J} \epsilon^{-\sigma_f t} \cos 2\omega t \qquad (12)$$

and for the asymmetrical case

$$i_f = e_o \frac{CK}{H} + e_o \frac{CP}{H} \epsilon^{-\sigma_f t} + e_o \frac{FK}{H} \times \cos (2\omega t + 2\alpha) + e_o \frac{FP}{H} \epsilon^{-\sigma_f t} \cos (2\omega t + 2\alpha) - e_o \frac{G}{H} \epsilon^{-\sigma_a t} \cos (\omega t + \alpha) \cos \alpha \qquad (13)$$

Thus the actual field current of equation 12, similar to the field voltage shown in Figure 21, is made up of a steady d-c component, plus the usual decrement

component, where a change in direct current takes place, plus a sustained double-armature-frequency pulsating component caused by armature reaction of the sustained armature current, plus a similar double-frequency component which decays with a decrement factor depending upon the field circuit constants. This component is the result of the decreasing armature current as it reduces to the final sustained value.

The field current of equation 13 similar to the field voltage of Figure 22 consists of four similar components plus a fifth decaying component, the decay of which depends upon the point on the voltage wave at which the load switch was closed. Notice that this is the full-frequency component before mentioned. All of the components in the equation are not shown as definitely separate components in Figures 21 and 22.

The constants in equations 10 to 13 are all rather involved factors made up of the various reactances of the machine and can be found in the original article; thus they will not be given here.

One additional observation might be mentioned. The voltage across the open-circuit phase in Figures 18, 19, and 20 are very distorted, and the phase current likewise is distorted. This is characteristic of single-phase loads on alternators not specially designed. The generated voltage is a function of the magnitude of the field flux and speed of rotation. If the magnetic flux is constant, the constant speed will generate a good sine wave shape of voltage. However, when the field flux is pulsating because of the single-phase armature reaction, at one instant the rate at which armature conductors are cutting flux is increased above that due to rotation by the increase in flux value and will generate a high peak of voltage, while at the next quarter cycle the flux is decreasing, which tends to decrease the total flux cutting action with the result that little or no voltage is generated at this time Rather high voltage peaks may be the result, especially at the instant just after the load switch was closed.

Conclusion

No claim is made in offering more than a very approximate method of arriving at definite values in transient conditions of this nature. Other workers have covered quite adequately the more accurate mathematical phases. However, the analysis does attempt to offer a simple means of visualizing what to expect in such cases and of comparing the component parts thus visualized to the mathematical components derived by others. In short, the author has attempted first to offer a reasonably simple means of interpreting and visualizing the changes which result in such cases for the station operator or engineer who has little interest in knowing the magnitude of results and, second, to help acquaint the engineer who must deal with such magnitudes with the aid at his disposal, as well as to offer him a simple means of visualizing the components and reasons for components involved.

Nomenclature

R = total series resistance of the circuit in ohms
L = total inductance in circuit in henrys
e_o = no-load voltage generated by the alternator, assuming no saturation
x_d = three-phase line-to-neutral synchronous reactance on the direct axis
x_d' = three-phase line-to-neutral transient reactance on the direct axis
x_q = three-phase line-to-neutral synchronous reactance on the quadrature axis
x_q' = three-phase line-to-neutral transient reactance on the quadrature axis
$\omega = 2\pi f$, where f is normal frequency
ωt = angle in radians at time t
α = displacement angle between armature winding axis and axis of field pole at time of closing the switch
γ = angle between time of zero voltage and time of closing switch
θ = phase angle between current and voltage
i_A = current in phase A of alternator
i_B = current in phase B of alternator
i_C = current in phase C of alternator
i_f = current in d-c excited field winding of alternator
σ_a = decrement factor of armature circuit, a function of armature resistance and inductance
σ_f = decrement factor of field circuit, a function of field resistance and inductance

Other constants are explained in text.

References

1. Transient Electric Phenomena and Oscillations, **C. P. Steinmetz.** McGraw-Hill Book Company, Inc., New York, N. Y. Chapter 14.

2. A Simplified Method of Analyzing Short-Circuit Problems, **R. E. Doherty.** AIEE Transactions, volume 42, 1923, pages 841–9.

3. Transient Conditions in Electric Machinery, **W. V. Lyon.** AIEE Transactions, volume 42, 1923, pages 157–79.

4. Synchronous Machines, **R. E. Doherty, C. A, Nickle.** Part I. An Extension of Blondel's Two-Reaction Theory. Part II. Steady-State Power-Angle Characteristics. AIEE Transactions, volume 45, 1926, pages 912–47. Part III. Torque-Angle Characteristics Under Power Conditions. AIEE Transactions, volume 46, 1927, pages 1–18.

5. Synchronous Machines—Part IV. Single-Phase Alternator Operation. AIEE Transactions, volume 47, 1928, pages 457–92.

6. Synchronous Machines—Part V. Three-Phase Short-Circuit Synchronous Machines. AIEE Transactions, volume 49, 1930, pages 700–14.

7. Transient Analysis of A-C Machinery **Ho H. Ku.** AIEE Transactions, volume 48, 1929, pages 707–15.

8. Two-Reaction Theory of Synchronous Machines, **R. H. Park.** AIEE Transactions, volume 48, 1929, pages 716–30.

9. The Reactances of Synchronous Machines, **R. H. Park, B. L. Robertson.** AIEE Transactions, volume 47, 1928, pages 514–36.

10. Calculation of the Armature Reactance of Synchronous Machines, **P. L. Alger.** AIEE Transactions, volume 47, 1928, pages 493–513.

11. Determination of Synchronous-Machine Constants by Test Reactances, Resistances, and Time Constants, **Sherwin Wright.** AIEE Transactions, volume 50, 1931, pages 1331–50.

12. Measurement of the Subtransient Impedances of Synchronous Machines, **Gordon F. Tracy, W. F. Tice.** AIEE Transactions, volume 64, 1945, February section, pages 70–5.

13. Test Code for Synchronous Machines. Preliminary Report. AIEE Standards, January 1937.

14. A New Magnetic-Flux Meter, **G. S. Smith.** AIEE Transactions, volume 56, 1937, April section, pages 441–5.

15. Use of Bismuth-Bridge Magnetic-Flux Meter for A-C Fields, **G. S. Smith.** AIEE Transactions, volume 58, 1939, February section, pages 52–5.

Lightning Performance of 220-Kv Transmission Lines—II

AN AIEE COMMITTEE REPORT

THE LIGHTNING performance of high-voltage transmission lines in the nominal 220-kv class was presented in a paper[1] before the Institute in 1935. That report presented data on the construction of these lines as well as their operating performance from a lightning viewpoint. There were then only ten companies operating transmission lines in the 220-kv class, and the significant data on all these companies' lines were reported.

The collection of data at one time and presentation in one place on the performance of these lines were of such interest and value in the transmission field that the committee recently was requested to bring the record up to date. Complying with this request, the committee is presenting this present paper. To obtain the data on which the present record is based, questionnaires were sent to 13 companies which were known to have lines built for operation in the 220-kv range, and replies were received from all 13 companies. The questionnaire, which was set up carefully by the lightning and insulator working group, comprised a total of 36 questions dealing with line construction, lightning outages, features used to improve lightning performance, and other features of the lines believed significant in studying and evaluating the lightning performance of the lines.

Purpose and Scope

The purpose of this report is, as just mentioned, to bring up to date the record of the lightning performance of lines in the 220-kv class. In presenting the data the lightning outage record, which was given on transmission lines reported in the previous paper,[1] has been continued to 1944 inclusive, and in one or two cases the major part of the record for 1945 is included. The record includes data from all companies in the United States and Canada known to be operating lines in the 220-kv class.

The plan of this paper is to present most of the data which are considered pertinent to the lightning record of the line and to comment on and compare in some cases the relative benefits of various factors which are known from experience and believed by theory to be conducive to better performing lines.

Another feature of value which it was expected would appear in replies to the questionnaire was any unusual means taken to improve lightning line performance and the benefits actually obtained. In addition to giving the outage record of the lines involved, the discussion presented herein gives the committee's evaluation of the effectiveness of different features of line construction. However, it is recognized that with so many variables influencing the lightning performance of lines of this type, opinion may differ as to the relative merits of different remedial measures which have been taken in actual line construction. Therefore, practically all of the data received from the contributors have been presented, so that anyone who chooses may study and analyze them in his own way.

Presentation of Data

Practically all the data which are considered pertinent to the subject at hand are included in Table I. In all cases the data are presented practically as submitted by the separate companies involved but may differ in minor features where the questions asked or the replies received were not wholly clear. Although the lines in this table are referred to as nominal 220-kv class, it should be pointed out that one (reference 2) operates at 190 kv and two (references 14 and 15) at 287.5 kv.

Paper 46-16, recommended by the AIEE committee on power transmission and distribution for presentation at the AIEE winter convention, New York, N. Y., January 21–25, 1946. Manuscript submitted November 16, 1945; made available for printing November 21, 1945.

This report was prepared by the lightning and insulator working group of the AIEE committee on power transmission and distribution. The personnel of the working group comprised: I. W. Gross, American Gas and Electric Service Corporation, New York, N. Y., *chairman;* H. A. Frey, Locke Insulator Corporation, Baltimore, Md.; W. W. Lewis, General Electric Company, Schenectady, N. Y.; J. T. Lusignan, Jr., Ohio Brass Company, Mansfield, Ohio; G. D. McCann, Westinghouse Electric Corporation, East Pittsburgh, Pa.; F. W. Packer, Pennsylvania Power and Light Company, Allentown, Pa.; Philip Sporn American Gas and Electric Service Corporation, New York, N. Y.; S. K. Waldorf, Pennsylvania Water and Power Company, Baltimore, Md.; E. R. Whitehead, Duquesne Light Company, Pittsburgh, Pa.

The committee expresses its appreciation to all 13 electric power companies for their prompt cooperation in supplying the records on which this paper is based, and also to G. D. Lippert for his efforts in compiling the data for analysis.

The extent of the 220-kv systems covered is shown in Table II, wherein it is shown that 13 companies are operating 35 lines totaling approximately 3,988 miles of line (right of way) and 6,601 miles of 3-phase circuit.

Discussion of Data

A brief summary and discussion of the outstanding features of line construction and line performance are presented. For convenience of analysis, however, some of the various factors which influence lightning performance have been segregated and discussed separately. It is realized that the effect of any one of these factors is so interlaced with that of the others, that it is not possible to evaluate definitely its influence from the insufficient data available.

Structural and Related Features

Location of Lines

The lines reported on are located in lightning territory which ranges from very light to heavy, the isokeraunic levels ranging from 5 in California to 45 in Illinois, but none being in the 70 to 90 range of the extreme southeastern section of the country. The isokeraunic levels shown in column 25 of Table I were taken from the United States Weather Bureau isokeraunic map.[3] The lightning severity, reported by each company is in column 24.

The average elevation of each line above sea level is given in column 21. These values range from 68 feet in California to 3,020 feet also in California. These figures are not considered particularly significant: first, because elevation above sea level in this range is not believed to have any appreciable influence on lightning frequency and severity; and secondly, because lines shown located in low average terrain may, and in some cases do, have part of their length in high-elevation country.

The types of country traversed by the lines (column 22) range from flat to rolling, hilly, and even mountainous. Most of the lines are in rolling to hilly country.

The average height of top conductor above ground (column 37) varies from 37 feet to 122 feet, the higher figure being on a 2-circuit line where right-of-way difficulties controlled. The more general range of top conductor elevation is from about 55 to 85 feet.

Towers, Conductors, and Overhead Ground Wires

Towers. The towers may be classified in three general types, as illustrated

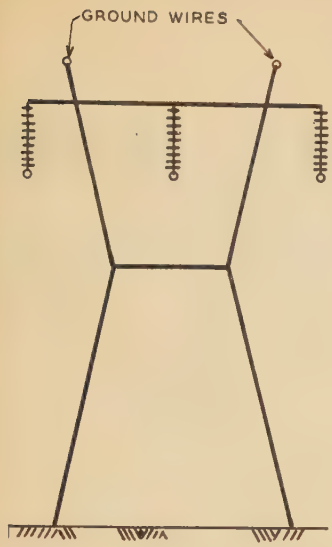

Figure 1 (left). Typical 220-kv single-circuit tower

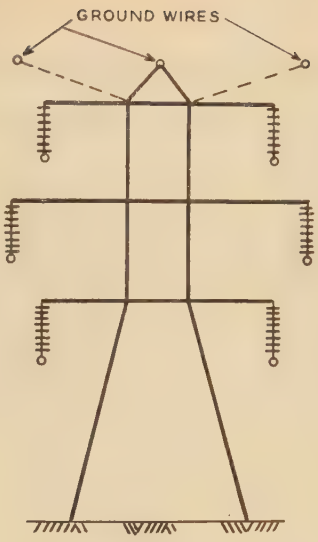

Figure 2. Typical 220-kv double-circuit tower

in Figures 1, 2, and 3. Figure 1 is a single-circuit line with conductors horizontally arranged. About 73 per cent of all the lines reported have this arrangement. Figure 2 is a double circuit structure with conductors vertically arranged. About 26 per cent of the lines have this arrangement. A part of only one line was arranged as in Figure 3, or about 1 per cent of the lines reported.

Line Conductors. The line conductors vary from 500,000 circular mils to 1,034,000 circular mils, with one line 1.4 inch in diameter. About 85 per cent of the lines have aluminum conductor steel reinforced conductors, and 15 per cent copper.

Overhead Ground Wires. About 14 per cent of the lines reported have no overhead ground wires, except that two lines have wires extending out one mile from the terminals. About 19 per cent have one overhead ground wire, and about 67 per cent have two overhead ground wires. The material is steel, aluminum conductor steel reinforced, Copperweld, and copper in the proportion of about 63 per cent, 16 per cent, 11 per cent, and 10 per cent respectively of the lines with overhead ground wires. The sizes vary for the steel wires from 3/8- to 3/4-inch diameter, for the aluminum conductor steel reinforced from 184,000 to 203,000 circular mils, for the Copperweld from 3/8- to 1/2-inch diameter, and for the copper from 2/0 to 4/0.

Insulation

Insulator Strings. In columns 12 and 13 of Table I are given the number of insulator disks and spacings between disks. The spacings vary from $4^3/_4$ to $6^1/_2$ inches. In order to place these on a comparable basis, so that published flashover data may be used, the suspension strings are reduced to equivalent number of units spaced $5^3/_4$ inches apart (column 59). It will be noted that these vary through a wide range, from approximately 10.6 to 18.4 units for lines operated at 220 to 240 kv, 8.4 to 12.3 units for lines operated at 190 to 200 kv, and 21 units for the 287-kv lines.

The critical flashover values of the insulator string[2] based on the 1.5x40 positive impulse wave are given in column 60.

Clearance to Structure. In column 57 is given the clearance to the tower with the conductor swung from the vertical to the angle given in column 58. These angles are 30 degrees, except in one case in which the angle is given as 45 degrees.

In column 61 are given the critical flashover values based on the 1.5x40 positive wave, assuming that the conductors are swung to the angle given in column 58. The rod gap values[2] are used to obtain the flashover values.

It is believed that under the wind and loading conditions prevailing in the lightning months, a 30-degree swing is ample to cover practically all cases.

Average Span

Average span lengths range from 590 feet to 1,320 feet or 9 to 4 towers per mile. The general average for all lines reported is in the order of 1,000 to 1,100 feet, or about 5 towers per mile.

Grading and Arcing Devices

The practice varies in the use of devices to grade the voltage on the insulator string or to take the arc on flashover. Some companies report using grading rings (column 26) or rings and horns, and others report horns only. In the light lightning severity territory of California, horns, or rings and horns, are used even for the early lines built between the years 1914 and 1923.

A number of companies report not using any grading or arcing devices, particularly where lines have been built in the last 15 years or so. It is suggested that the reason for the omission of these devices may be the high immunity from insulator and conductor damage experienced in service. This in turn possibly may be the result of faster clearing of faults over the insulator strings by high-speed circuit breakers or shortened relay time. It seems from the record that the use of grading shields and arcing devices on the newer lines generally is being abandoned.

Analysis of Lightning Performance

The three most important features of line construction that correlate most closely with actual lightning performance, although not necessarily in their order of importance, are thought to be:

1. Use and location of overhead ground wires.
2. Insulation.
3. Tower footing resistance.

Line Outages

The actual line outages are shown in column 54 for all lines. These have been reduced to a 100-mile-per-year basis in column 55 and to an isokeraunic level of 50 in column 56. On the 100-mile-per-year basis, actual outages vary from a high of 11.5 to a low of 0, with an average of about 2.30. The high figure of 11.5, references 7 and 7A, comprises the record of a line which initially was built and operated without ground wires and was located in a heavy lightning territory. It is interesting to note that this line, since protective features such as ground wires, counterpoises, and so forth, were installed, has a record for the past four years of 1.2 outages per 100 miles of line per year.

In case of 2-circuit lines, the single-line outages only usually are considerably

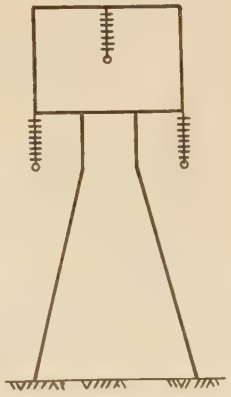

Figure 3. Special 220-kv single-circuit tower

Table I. Lightning Performance and Design Features of 220-Kv Lines

REF	NAME OF CO REPORTING	LINE DESIGNATION	DATE FIRST IN SERVICE	LENGTH OF LINE IN MILES OF W	NO OF CIRCUITS	CIRCUITS PER STRUCTURE	OPERATING KV PHASE TO PHASE	TOWERS: NO PER LINE	TOWERS: TYPE (FIG. NO.)	TOWERS: AVG. SPAN (FEET)	INSULATORS: NO. PER STRING SUSP/D.E.	INSULATORS: SPACING (2) (INCHES	CONDUCTORS: LINE: SIZE (M.C.M)	CONDUCTORS: LINE: MATERIAL	CONDUCTORS: GR.WIRE: NUMBER	CONDUCTORS: GR.WIRE: SIZE (IN. OR MCM)	CONDUCTORS: GR.WIRE: MATERIAL	WIRE SAG: GW. ON AVG. SPAN (FEET)	WIRE SAG: COND. ON AVG. SPAN (FEET)	AVG. ELEV. ABOVE SEA LEVEL (FT.)	TYPE OF COUNTRY	NATURE OF SOIL	LIGHTNING SEVERITY	ISOCERAUNIC LEVEL	INSUL. ARCING DEVICES: TYPE	INSUL. ARCING DEVICES: ARC. DIST. (INCHES)
1	2	3	4	5	6	7	8	9	10	11	12	13	14	15	16	17	18	19	20	21	22	23	24	25	26	27
1	NEW ENGLAND PWR SERV CO	FIFTEEN MILE FALLS - TEWKSBURY	9/30/30	126 4	2	1	231	1127	1	590	15/17	5 3/4	795	ACSR	2	1/2"	S	12	16	800	MOUNTAINS AND HILLS	ROCK CLAY SAND	—	24	RINGS	79 5
2	SHAWINIGAN WATER AND POWER CO.	NO 25-26	8/6/27	135 3	2	2	190	796	2	910	10/12 (1)	4 3/4 / 5 3/4	397	ACSR	2	7/16"	S	17	20	1000	HILLS ROLLING	GRAVEL	MODERATE	15	HORNS (3)	47 5 (4)
3	"	NO 31	1/ /38	108 1	1	1	240	538	1	1060	16/16	5 / 5 3/4	795	ACSR	2	7/16"	S	24	29	600	HILLS ROLLING FLAT	ROCK SAND	MODERATE	15	NONE	—
4	"	NO 35	11/-/40	74 3	1	1	200	388	1	1010	14/16	5 / 5 3/4	605	ACSR	2	7/16"	S	25	25	200	ROLLING FLAT	ROCK CLAY SAND	MODERATE	15	NONE	—
5	PHILADELPHIA ELECTRIC CO	CONOWINGO - PLYMOUTH-MEETING.	3/5/28	57 7	2	1	220	261	1	1170	16/18	5 3/4	795	ACSR	2	184	ACSR	29 2	34 8	360	ROLLING	ROCK CLAY	MODERATE	35	RINGS	83 3
6	"	PLYMOUTH MEETING - SIEGFRIED	2/18/28	99	1	1	220	57	1	916	16/18	5 3/4	795	ACSR	2	184	ACSR	18.4	21.9	300	ROLLING FLAT	ROCK CLAY	MODERATE	35	NONE	—
6A	PENNSYLVANIA PWR & LIGHT CO	"	2/18/28	38 8	1	1	220	186	1	1100	16/18	5 3/4	795	ACSR	2	184	ACSR	29 0	43 0	500	ROLLING	ROCK CLAY	SEVERE MODERATE	35	RINGS	82 3
7	"	SIEGFRIED - WALLENPAUPACK TAP ROSELAND	4/11/26	66 2	1	1	220	317	1	1100	14-16/16	5 3/4	795	ACSR	(21) 2	184 7/16"	ACSR C W	18 5	31 5	1000	MOUNTAINS ROLLING	ROCK CLAY SAND	SEVERE	35	RINGS & HORNS	72 0
7A	PUBLIC SERV ELEC & GAS CO	SIEGFRIED - ROSELAND.	4/8/32	45 8	1	1	220	211	1	1150	16-18/18-20	5 3/4	795	ACSR	2	203	ACSR	32 9	35 8	700	MOUNTAINS HILLS	ROCK CLAY	MODERATE	35	RINGS	83 3
8	"	PLYMOUTH MEETING - ROSELAND	8/31/30	46 2	1	1	220	235	1	1040	16/18	6	795	ACSR	2	203	ACSR	27 0	29 4	205	ROLLING FLAT	CLAY SAND	MODERATE	33	RINGS	85 3
8A	PHILADELPHIA ELECTRIC CO	"	8/31/30	29 6	1	1	220	145	1	1080	16/18	5 3/4	795	ACSR	2	203	ACSR	26 0	29 4	335	ROLLING	ROCK GRADE CLAY	MODERATE	35	SHIELD	83 3
9	PENNSYLVANIA WATER & PWR CO	SAFE HARBOR - RIVERSIDE.	11/11/37	50 0	1	1	220	281	1	940	20/20	5 1/4 / 5 3/4	795	ACSR	2	3/8"	CW	17.1	26 5	330	ROLLING	ROCK CLAY SAND	SEVERE	36	NONE	—
10	"	SAFE HARBOR - TAKOMA TAP - WESTPORT.	12/6/31	92 0	1	1	220	477	1	1020	20/20	5 1/4 / 5 3/4	795	ACSR	2	203	ACSR	21 5	26 5	475	ROLLING	ROCK CLAY SAND	SEVERE	36	NONE	—
11	COMMONWEALTH EDISON CO	POWERTON - CHICAGO	9/28/40	147 0	2	1 & 2	240	761 (6)	1 & 2	1020	18/20	5 3/4	900	ACSR	2	1/2"	CW	92 (1BN) / 268	166 (1PA) / 386	650	ROLLING FLAT	MOSTLY LOAM	—	45	NONE	—
12	BONNEVILLE PWR ADMINISTRATION	COVINGTON - COULEE NO 1	7/16/42	183 0	1	1	230	850	1	1140	16/18 (8)	5 3/4	795	ACSR	(7)	—	—	—	34	2500	MOUNTAINS TO FLAT	ROCK CLAY SAND	MODERATE	8	—	—
13	"	COULEE - SPOKANE 3 & 4.	3/15/43	82 8	2	2	230	422	2	1035	16/18	5 3/4	795	ACSR	(7)	—	—	33 5	51 5	2800	HILLY TO FLAT	ROCK CLAY SAND	MODERATE	8	(9)	60
14	CITY OF LOS ANGELES	BOULDER DAM - LOS ANGELES 1 & 2	10/-/36	263 5	2	1 & 2 (10)	287 5	2693	1 & 2	790/970	24/22	5/6	1.4"	CU	2	7/16"	CW	378/158	458/236	2400	MOUNTAINS TO FLAT	ROCK CLAY SAND	MODERATE LIGHT	15	HORNS	110
15	"	BOULDER DAM - LOS ANGELES 3.	5/-/40	263 5	1	1	287 5	1428	1	970	24/22	5/6	1.4"	CU	2	1/2"	S	378	458	2400	MOUNTAINS TO FLAT	ROCK CLAY SAND	MODERATE LIGHT	15	HORNS	110
16	PACIFIC GAS & ELECTRIC CO	PITT LINES NO. 1 & 2 HORIZ CONFIG SECT (11)	1923	83	2	1	230	-	1	720 (13)	13/12	5	518	ACSR	0	—	—	—	17	2000	HILLS	VARIOUS	LIGHT	5	HORNS	71
16A	"	PITT LINES NO 1 & 2 VERT CONFIG SECT (12)	11/-/23	214	2 (14)	2 (14)	230	-	2	-	13/12	5/5 1/2	500	CU	0	-	-	-	24	200	ROLLING TO FLAT	CLAY	LIGHT	5	HORN OR SHIELD	71
17	"	TIGER CREEK - NEWARK HORIZ CONFIG SECT	6/-/31	16	2	1	230	-	1	790 (13)	13/13	5 1/2	518	ACSR	0	—	—	-	17	2500	MOUNTAINS	VARIOUS	LIGHT	.5	DISC SHIELD	71 5
17A	"	TIGER CREEK - NEWARK VERT CONFIG SECT	6/-/31	93	2	2	230	-	2	-	13/13	5 1/2	500	CU	0	-	-	-	24	500	HILLS TO FLAT	ROCK CLAY	LIGHT	5	DISC SHIELD	71 5
18	"	BUCKSCREEK BELLOTA (23) BUCKSCREEK - OROVILLE SECT	1926	33	1	1	230	-	3	-	14/16	5 3/4	795	ACSR	0	-	-	-	17 5	1000	MOUNTAINS	ROCK VARIOUS	LIGHT	5	DISC SHIELD	80 5
18A		BUCKSCREEK - BELLOTA OROVILLE - BELLOTA SECT	11/44	110	1	1	230	-	2	-	14/16	5 3/4 / 5 1/2	795	ACSR	0	-	-	-	24	150	ROLLING TO FLAT	VARIOUS	LIGHT	5	DISC SHIELD	77
18B		BUCKSCREEK - BELLOTA BELLOTA HERNDON 1 & 2	6/-/31	102	2	2	230	-	2	-	14/16	5 3/4 / 5 1/2	500 CU 795	ACSR	0	-	-	-	24	150	ROLLING TO FLAT	VARIOUS	LIGHT	5	DISC SHIELD	77
19	METROPOLITAN WATER DIST OF SO CAL	BOULDER	11/1/38	2 5 1	1	1	230	945	1	1320	13/15	5 3/4	795	ACSR	(20) 2	1/2"	S	24	35	2000	HILLS TO FLAT	MOSTLY CLAY	MODERATE	15	NONE	—
20	HYDRO-ELECTRIC PWR COMMISSION OF ONTARIO	PAUGAN - CHATS FALLS - LEASIDE HASTINGS - LEASIDE SECT	10/1/28	110 7	3	1	220	1666	1	1050	18/18	5 / 5 3/4	795	ACSR	2	3/8"	S	32	36	600	HILLS	ROCK CLAY SAND	—	25	NONE	-
20A	"	PAUGAN - CHATS FALLS - LEASIDE - PAUGAN - CHATS FALLS HASTINGS SECT.	10/15/31	117 3	(24) 28 3	1	220	1631	1	1050	18/18	5 / 5 3/4	795	ACSR	2	3/8"	S	32	36	800	HILLS	ROCK CLAY SAND	—	25	NONE	-
21	"	BEAUHARNOIS - MASSON - CHATS FALLS	7/1/33	128 2	1	1	220	516	1	1310	18/18	5 / 5 3/4	795	ACSR	2	3/4"	S	32	36 5	250	FLAT	MOSTLY CLAY	—	25	NONE	—
22	"	LEASIDE - BURLINGTON	8/-/41	44 8	2	2	220	273	2	870	18/18	5 / 5 3/4	500	CU	1	3/8"	S	25.3	34	550	ROLLING	CLAY	—	25	NONE	—
23	"	BEAUHARNOIS - LEASIDE	4/9/41	300 5	1	1	220	1404	1	1125	18/18	5 / 5 3/4	795	ACSR	2	3/8"	S	32	36	250	HILLS ROLLING FLAT	—	—	25	NONE	—
24	SO CAL EDISON CO LTD	NORTH & SOUTH LIGHTHIPE - LAFRESA	2/27/30	9.7	2	2	220	57	2	900	13/15	—	667	ACSR	1	2/0	CU	12	13	—	FLAT	SAND	—	5	RING & HORN	-
25	"	BIG CREEK 2 - 2A - 3	7/15/28	5.9	1	1	220	29	1	1080	13/15	6 1/4	667	ACSR	2	3/0	CU	31	39	2950	MOUNTAINS	ROCK	LIGHT	5	RING & HORN	—
26		EAST & WEST EAGLE - BELL	1923	268	2	1	220	(32 (27) / 128	1	1090	13/15	5 3/4 / 6 1/2	667	ACSR	1 & 2	1/2"	S	19	23	1490	MOUNTAINS TO FLAT	ROCK CLAY SAND	LIGHT	5	RING & HORN	-
27	"	BIG CREEK 3 MAGUNDEN	1/24/28	128	1	1	220	457	1	1480	13/15	6 1/2	1034	ACSR	2	1/2" / 9/16"	S	33	34	2630	MOUNTAINS TO FLAT	ROCK CLAY SAND	LIGHT	5	RING & HORN	-
28	"	MAGUNDEN - EAGLE ROCK	11/14/26	102 6	1	1	220	470	1	1150	13/15	6 1/4	1034	ACSR	2 (2B)	1/2" / 9/16"	S	30	31	3020	MOUNTAINS TO FLAT	ROCK CLAY SAND	SEVERE	5	RING & HORN	-
29	"	CHINO - BARRE	9/20/39	26	2	(29) 1 & 2	220	116	1 & 2	1190	15/16	5 3/4	605	ACSR	(30) 1 & 2	1/2"	S	21	28	905	HILLS TO FLAT	CLAY SAND	—	5	HORNS	-
30	"	CHINO LAGUNA BELL	1/29/42	33 4	1	1	220	32	1	1340	15/15	5 3/4 (31) / 6 1/2	605	ACSR	1 & 2	1/2"	S	17	23	830	HILLS TO FLAT	CLAY SAND	—	5	RING & HORN	—
31	"	EAST & WEST LIGHTHIPE LAGUNA BELL	10/10/27	70	2	1	220	68	1	1090	14/15	6 1/4	1034	ACSR	1	1/2"	S	14	16	80	FLAT	SAND	—	5	RING & HORN	—
32	"	BARRE - LIGHTHIPE	8/10/41	15 8	1	1	220	91	2	920	14/15	6 1/2	605	ACSR	1	1/2"	S	12 5	15	68	FLAT	SAND	LIGHT	5	HORNS	—
33	"	EAST & WEST BIG CREEK	4/14/14	243 7	2	1	(32) 220	3448	1	700	11/13	5 3/4	667	ACSR	2	1/2"	S	8	11	2870	MOUNTAINS TO FLAT	ROCK CLAY SAND	LIGHT	5	RING & HORN	-
34	"	EAST & WEST LONG BEACH - LIGHTHIPE	6/16/28	9 8	2	2	220	55	2	345	15/15	6 1/2	650	CU	1	4/0	CU	27	24	—	FLAT	SAND	—	5	—	—
35	"	NORTH & SOUTH BOULDER - CHINO	(33) 11/15/41	233 7	2	1	220	1652	1	730	15/16	5 3/4	605	ACSR	2	1/2"	S	18	31	2870	MOUNTAINS TO FLAT	ROCK CLAY SAND	LIGHT	15	HORNS	—

1. Suspension assemblies: 12 units after 1943–44.
2. First value suspension; second value dead end.
3. Armor rods on 25 per cent of line.
4. 57 inches after 1943–44.
4A. 4.8 after 1943–44.
5. 10.5 after 1943–44.
6. 637 towers: 1 circuit per tower. 124 towers: 2 circuits per tower.
7. 1 mile of ground wire at terminals only.
8. 20 per cent porcelain, 80 per cent glass.
8A. Apparently now being added.
9. Experimental devices on 25 per cent of line (not described).
10. 222.65 miles: 1 circuit per tower. 40.85 miles: 2 circuits per tower.
11. 60 miles in 1923, 9 miles added in 1925, 14 miles added in January 1944.
12. 142 miles: 2 circuits in 1923. 43 miles: 1 circuit added in March 1944. 29 miles: 2 circuits added in April 1944.
13. Data from 1935: 220-kv paper.
14. Except 43 miles of single circuit.
15. See note 23.
16. Estimated.
17. To August 1, 1945.

Table I. Lightning Performance and Design Feature of 220-Kv Lines (Continued)

TOWER FOOTING RES. (OHMS) BEFORE AUX. GROUNDING MAX	MIN	AVG	AFTER AUX. GROUNDING MAX	MIN	AVG	AUXILIARY GROUNDING	LIGHTNING PROT. OTHER THAN G.W. AND LOW GR. RES.	LTN. IMPROVE. BEING CONSIDERED	TOP COND. ABOVE GROUND (FT.)	WIRE SPACING AT TOWER (FEET-MIN) COND. HORIZ	COND. VERT	GR. WIRE HORIZ	GR. WIRE VERT.	LIGHTNING OUTAGES ONE CIRCUIT / TWO CIRCUIT 1934	1935	1936	1937	1938	1939	1940	1941	1942	1943	1944	1945	AVG PER YEAR	AVG. PER 100 MI. PER YEAR ACTUAL	50(26) LEVEL	LINE CLEARANCE TO STRUCTURE FT.	AT COND. SWING OF (DEG.)	MIN NO INSUL. EQUIV. 5¾ IN. UNITS	1½X40 μSEC CRITICAL POS. IMPULSE KV. INSULATORS	AIR CLEARANCE AT 30° SWING	MAX SHIELDING ANGLE (DEGREES) (25)	REF
28	29	30	31	32	33	34	35	36	37	38	39	40	41	42	43	44	45	46	47	48	49	50	51	52	53	54	55	56	57	58	59	60	61	62	63
—	—	—	-	-	-	NO	NO	NO	44.2	23.5	—	25.0	14.8	3	1	10	9	10	4	9	4	6	8	11	—	6.8	5.4	11.3	72	45	15	1345	(AT 45°) 1340	37/40	1
—	—	150		—	LOW	2 CONT CP	NO	NO	73.5	23.5 33.5	12	33.5	98(5)	11/11	1/3	0/3	3/5	1/7	4/0	0/3	0/2	0/2	0/2	1/0	—	19/35	14/2.6	47/8.7	(44) 4	30	8.43	820	780	27	2
700	10	150	45	—	—	CP & GR (8A)	NO	YES ADD 2 CP	63.3	25.3	—	26.5	12.8	—	—	-	—	5	2	0	2	1	1	1	—	1.7	1.6	5.3	65	30	14.48	1310	1220	43/46	3
800	5	50	—	—	—	2 CONT CP+CP	NO	NO	62.2	26.5	—	37.0	22.5	—	—	—	—	—	—	—	0	0	0	0	—	0	0	0	55	30	12.30	11.30	10.40	20/39	4
-	—	—	—	—	242	MISC CP	NO	NO	62.0	25.5	—	25.5	16.1	0	1	2	3	1	0	2	4	1	1	0	—	1.4	2.4	3.4	60	30	16	1425	1125	38	5
—	—	—	—	—	—	ONE 600'CP	NO	NO	62.0	25.5	—	25.5	16.1	0	0	2	2	1	1	0	2	0	0	0		0.83	1.7	2.4	80	30	16	1425	1475	38	6
61	47	15	—	—	—	NO	NO	NO	65.9	26.3	—	23.8	13.6	0	0	2	2	1	1	0	0	0	0	0	2(11)				78	30	16	1425	1445	47/41	6A
330	5	75	40	1	5	CP	NO	NO	66.0	22.5	—	23.1	10.1	12	14	28	29	18	18	16	1(20)	0	1	2	3(17)	12.9	11.5	17.0	70	30	14	1265	1300	47	7
300	1	64	27	1	18	CP	NO	NO	62.5	28.5	—	28.5	14.8	0	1	1	1	0	0	(18)	(18)	(18)	(18)	(18)	—				76	30	16	1425	1405	44	7A
105	0	6	-	—	—	NO	NO	NO	62.5	28.5	—	28.5	14.8	0	1	0	0	1	1	(18)	(18)	(18)	(18)	(18)	—	0.73	0.96	1.45	76	30	16.65	1480	1405	44	8
28	1.8	10	—	—	—	ONE 650'CP	NO	NO	62.7	25.5	—	43.0	16.2	0	1	0	0	1	1	1	2	0	0	2	—				73	30	16	1425	1360	14/53	8A
450	1	67	19	1	10	CP	NO	NO	58.3	28.3	-	42.3	25.7	—	—	-	—	0	0	0	1	1	1	0		0.43	0.86	1.20	90	30	18.35	1615	1655	15/39	9
430	1	74	32	1	12	CP & GR	NO	NO	58.3	28.3	-	42.3	25.7	0	0	0	0	0	0	0	0	1	0	—		0.091	0.099	0.137	90	30	18.35	1615	1655	15/39	10
—	—	—	5	-	18	CP & GR.	NO	NO	100 (18A) 65.2	48 (18A) 33.3	20.6	48 (18A) 46.3	23.5 (18A) 29	-	-	—	—	—	—	0	0	0	0	0	—	0	0	0	93	30	18	1585	1710	19/39	11
—	—	—	850	13	—	GR.	(9)	(9)	37	27	—	37 (7)	23 (7)	—	—	-	—	—	—	—	—	5	1	8	—	47	2.6	16.2	50	30	16	1425	945	—	12
—	—	—	350	12	—	GR	(9)	(9)	376	38/31	20.3	—	22.4 (7)	—	—	—	—	—	—	—	—	-	7/1	6/2	(19) 3/1	53/13	64/16	40/10	50	30	16	1425	945	—	13
150	-	1	76	0.4	0.8	2-CP	NO	NO	112 77.1	40.5 32.5	24.5 —	40.1 50	32	-		0/0	0/0	0/0	1/0	0/0	0/0	0/0	1/0	0/0	- (19)	0.22/0	0.08/0	0.7/0	90	30	21	1825	1655	13/38	14
150	-	1	76	0.4	0.8	2-CP	NO	NO	77.1	32.5	-	50	32	-	-	-	-	-	-										90	30	21	1825	1655	13/38	15
	-	-	500 (16)	2 (16)	3 (16)	2' SQ PLATE	NO	YES GW.	44.1	19.5	—	-	—	2	1	3	2	1	2	2	0	2	0	2	- (19)	1.5	1.9	1.9.0	45	30	10.57	1000	865	—	16
—	—	—	11 (16)	0.8 (16)	4 (16)	2' SQ PLATE	NO	YES GW.	84.9	24	15	—	—	4/0	8/0	1/0	0/0	4/0	10/0	1/0	1/0	5/0	1/0	1/0	10/0	38/0	25/0	25/0	5	30	11.05	1030	945	—	16A
—	—	—	100 (16)	2 (16)	15 (16)	GR	NO	NO	46.7	20	—	—	—	0/1	0/0	0/0	0/0	0/0	0/0	0/0	0/0	0/0	0/0	0/0	-	0/0.09	0/0.56	0/5.6	45	30	12.46	1145	865	-	17
—	—	—	100 (16)	2 (16)	15 (16)	GR	NO	NO	85.3	28	15	—	—	0/0	2/0	3/0	4/0	0/0	7/0	0/0	4/1	1/0	1/0	0/2	(19) 1/0	19/0.25	2.0/0.22	20/2.7	43	30	12.46	1145	825	—	17A
(16) 100	(16) 2	(16) 15	-	—	—	NO	NO	NO	—	27	—	—	—	—	—	—	—	—	—	—	—	—	—	0	(19) 3	15	45	45	55	30	14	1265	1040	—	18
(16) 100	(16) 2	(16) 15	-	—	—	NO	NO	NO	87	27.3	16	—	—	0/0	1/0	0/0	0/0	1/0	1/0	3/0	2/0	1/0	1/0	1/1	(19) 7/0	15/0.08	0.71/0.08	7.1/0.8	57	30	14	1265	1080	-	18A
(16) 100	(16) 2	(16) 15	-	—	—	NO	NO	NO	87	27.3	16	—	—																57	30	14	1265	1080	-	18B
81	1	11.5	-	—	—	NO	NO	NO	70.5	22.3	—	31.9	16.5	—	—	—	—	—	37	22	26	33	1(20)	0	-	19.8	8.4	28	51	30	13	1185	960	21/44	19
300	3	25	-	—	—	NO	NO	NO	54.7	25.3	—	26.8	13.3	1	2	1	4	3	0	0	2	2	2	2	-	1.7	1.55	2.10	8	30	15.78	1415	1475	41/45	20
1550	2	250	1550	2	250	CP (22)	NO	NO	54.7	25.3	-	26.8	13.3	10	4	6	4	9	12	4	17	6	18	16	-	9.64	8.24	16.48	8	30	15.78	1415	1475	41/45	20A
300	2	25	—	—	—	NO	NO	NO	54.7	25.3	—	26.8	13.3	1	2	1	0	0	2	0	1	0	1	1	-	0.82	0.64	1.28	8	30	15.78	1415	1475	41/45	21
14	1	3.7	-	-	-	NO	NO	NO	-	34/54	20	—	—	—	—	—	—	—	—	—	—	1	3	0	-	1.3	2.97	5.94	8	30	15.78	1415	1475	—	22
600	1	47	25	1	65	CP	NO	NO	54.7	25.3	—	21.3	26.9	—	—	—	—	—	—	—	3	0	4	1		2.0	0.67	1.34	8	30	15.78	1415	1475	29/32	23
-	—	—	-	—	—	NO	NO	NO	121.1	31.0	20.0	-	17.6	-	-	-	-	-	-	-	-	-	-	-	-	-	-	-	-	-	-	-	-	41	24
-	—	—	—	-	—	NO	NO	NO	51.9	22.2	—	24.0	12.7	0	0	0	0	0	0	0	0	0	0	0	—	0	0	0	-	—	14.05	1270	-	39/44	25
-	—	—	—	-	—	NO	NO	NO	52.5	22.2	-	24.0	12.5	0	0	0	1	0	0	0	2	0	1	1	-	0.46	1.72	1.72	-	-	13	1.85	-	39/44	26
-	-	-		-	—	NO	NO	NO	55.3	22.2	-	24.0	12.7	0	0	0	0	0	2	0	1	0	0	2		0.45	0.35	3.5	6	30	14.05	1270	1.25	39/44	27
—	—	—	—	—	—	NO	NO	NO	55.3	22.2	—	24.0	12.7	1	3	1	0	12	7	3	4	1	4	3	-	(18) 3.54	3.45	34.5	6	30	14.05	1270	1125	39/44	28
-	—	—	—	—	—	NO	NO	NO	22.7 / 69.8 (18A)	16.5 (18A) / 23	20.7 — (18A)	— / (18A) 24	16 / (18A) 11.7	—	—	—	—	—	0	0	0	0	0	0		0	0	0	45	30	15	1345	865	43/46	29
-	—	—	—	—	—	NO	NO	NO	70.6	23.0	-	24.0	11.7	—	-	-	-				-	0	0	0		0	0	0	45	30	15	1345	865	43/46	30
-	—	—	—	—	—	NO	NO	NO	51.4	22.2	-	-	13.2	-					-		-	-	-				-		-	-	15.15	1360	-	59/0	31
-	—	—	—	—	—	NO	NO	NO	122.7	33.0	20	—	16	—	—	—	—	—	—	—	0	0	0	0	—	0	0	0	-	—	15.68	1405	—	46	32
-	—	—	—	—	—	NO	NO	NO	35.7	17.2	—	18	10.8	1/0	0/0	0/0	1/0	2/0	4/0	2/0	1/0	0/0	1/0	2/0	-	1.27/0	0.52/0	5.2/0	-	—	11	1025	—	37/40	33
-	—	—	—	—	—	NO	NO	NO	110	33	20	-	17	—	-	-	-	-	-	-	-	-	-	-	-	-	-	-	-	—	16.85	1510	-	44	34
300	0.5	-	70	0.5	18	TOWER CP	NO	NO	70.6	23	-	24	11.7	-	-		-		0	3	0	1/0	1/0	0/0	-	0.83/0	0.36/0	1.2/0	45	30	15	1345	865	43/46	35

18. Data not reported.

18A. First value for 2-circuit towers. Second value for 1-circuit towers.

19. To September 1, 1945.

20. Ground wire installed 1943.

21. Line completely equipped with ground wire 1941.

22. Counterpoise as required to reduce resistance to 25 ohms. First 10 miles from Chats Falls only.

23. Operating at 165 kv to January 1944.

24. 88.5 miles is 3 circuit. 28.8 miles is 2 circuit

25. First number for outer conductor. Second number for middle conductor.

26. On basis of 50 isokeraunic level.

27. First figure for east line. Second figure for west line.

28. No ground wire for 64 miles of line due to severe sleet loading.

29. 17 miles: 1-circuit towers. 9 miles: 2-circuit towers.

30. 17 miles: 2-ground wires. 9 miles: 1-ground wire.

31. Also some 12 and 14 units of fog type in suspension.

32. Originally designed for 150 kv.

33. North line June 22, 1939.

Table II. Extent of 220-Kv[1] Lines

13 Companies, 35 Lines

		Approximate Miles
Single circuit	Right of way	1,838
Two circuit on single towers	Right of way	717
Two circuit on separate towers	Right of way	970
Three circuit on separate towers	Right of way	463
Total miles	Right of way	3,988[2]
Total circuit miles of 3-phase line		6,601[2]

1. 135.3 miles of right of way operated at 190 kv and 263.5 miles operated at 287 kv.

2. Not including 550 miles of right of way for company references 12 and 13 (Table I) which were mentioned but not reported on.

Table III. Average Lightning Outages[1] on 220-Kv Lines

	Right of Way, Miles	Outages Per Year Actual	Outages Per 100 Miles of Line Per Year on Basis of 50 Storms Per Year
All lines	3,988.5	92.83	9.97
Lines without ground wires	916.8	21.92	19.30
Lines with ground wires	3,071.7	70.91	7.19
With ground wires[2]	349.0	32.70	24.20
With 1 ground wire	87.1	1.3	4.3
With 2 ground wires	2,446.8	32.91	3.8
With 1 and 2 ground wires[2]	86.2	0.46	0.53
With ground wire on part of line only	102.6	3.54	34.5

1. Based on actual outages and actual miles (not average of columns 55 and 56, Table I).

2. Lines having ground wire added during period of outage record 1934–45.

3. Lines having 1 ground wire on part of line, balance 2 ground wires.

higher than 2-line outages, as would be expected. The one exception is the case of line reference 2, where the single-circuit outages on a 100-mile-per-year basis is 1.4, and double-circuit outages 2.6, or nearly double.

The outage record seems to indicate clearly that, even with the highest insulation used in 220-kv lines, the insulation alone does not render the line lightning-proof without the aid of other remedial measures, such as ground wires and low tower-footing resistances.

Overhead Ground Wires

Benefit of Use. A summary of lightning outages for all lines and for lines with and without ground wires is given in Table III. Of the nearly 4,000 miles of line (right of way) covered by this report, the outages on a 100-miles-of-line-per-year basis at a 50 isokeraunic level is 9.97. Twenty-three per cent of the line mileage does not have ground wire, and its outage record is 19.3 per 100 miles of line per year. Of the line mileage 63.5 per cent has either one or two ground wires over the entire line, and its outage record is 3.8 to 4.3 outages on the above basis, the lower figure being for two-ground-wire lines, and the higher for the single-ground-wire groups.

In Figure 4 a further breakdown of the outage data on nonground-wire and ground wire lines where tower footing resistances were reported is shown. Based on a 50 isokeraunic level, the average outages per 100 miles of line per year is 27.5 for lines without ground wires, and 4.5 for ground wire lines. Ground wire lines of over 25 ohms average footing resistance have 15.4 outages, and lines with 25 ohms or less 1.94 outages.

The foregoing record clearly demonstrates the value of overhead ground wires and low footing resistance in reducing lightning outages.

Height and Spacing. Column 40 gives the horizontal spacing between the overhead ground wires where there are two ground wires. These spacings vary from 21 to 48 feet for the lines in the 190- to 240-kv class and from 40 to 50 feet for the 287-kv lines. The height of the ground wire plane above the plane of the conductors at the towers is given in column 41. This varies from approximately 10 to 29 feet for the 190- to 240-kv class lines and is 32 feet for the 287-kv lines. In Figure 5 is plotted the height of ground wires above conductors from column 40 against outages per 100 miles per year at isokeraunic level 50 from column 56. In cases where two ground-wire heights are given in the length of the line, the average height is plotted.

There does not appear to be any consistent relation between height of ground wires and outages experienced. A number of lines with heights ranging from 22.5 to 32 feet show outages from zero to 1.34 per 100 miles per year (column 56), but other lines with heights from 11.7 to 16.2 feet show outages in the same range. For example, two lines, 21 and 23, with the same impulse insulation level, 1,415 kv, show practically the same outage performance (1.28 and 1.34 per 100 miles per year,, although one has the ground wires 13.3 feet and the other 26.9 feet above the conductors.

Shielding Angle. In column 62 is given the angle between a vertical line through the ground wire and the slanting line between the ground wire and line conductor, or the so-called shielding angle. This angle varies widely, from a minimum of 13 degrees to a maximum of 47 degrees for the outside conductors of horizontally arranged lines and for the top conductor of vertically arranged lines. For the middle conductors of horizontal lines the angle is in one case as much as 53 degrees. In Figure 6 are plotted shielding angles from column 62 against tripouts per 100 miles per year at isokeraunic level 50 from column 56. Where the angle for middle conductor is different from the angle for outside conductor, the angle for the outside conductor is used.

The relationship between shielding angle and outages does not follow a consistent pattern. There is a zone of low outages with shielding angles ranging from 13 to 44 degrees (zero to 1.5 outages per 100 miles per year). Low footing resistance seems to be more important than small shielding angle.

Insulation Values

The flashover strength of the line is the lower of the values given in columns 60 or 61, that is, the insulator string flashover or the flashover from conductor to tower when the conductor is in the swung position.

In Figure 4 are plotted the impulse flashover strengths of the various lines (taking the value from column 60 or 61, whichever is lower), against the number of outages reduced to a common isokeraunic level of 50. The points are pretty well scattered, as a result of the masking effect of ground wires and tower footing resistance already discussed.

It will be noted, on comparing columns 60 and 61, that in many cases the flashover strength in column 61 is less than the insulator flashover in column 60. That is, the clearance from conductor to tower is not sufficient to develop the full strength of the insulator strings.

Mid-Span Flashovers

The possibility of getting mid-span flashovers long has been an unanswered question. If such occur to any extent, they are always difficult to detect, as the evidence, such as burned conductor at mid-span, is almost impossible to locate with certainty in the field.

A study of this feature from the data of Table I shows that mid-span clearances between ground wires and conductors have been increased by all companies. The vertical separation between ground wire and top conductor varies from 9.8

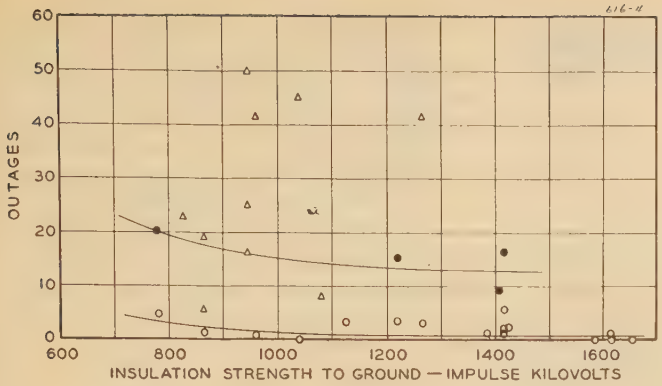

Figure 4. Insulation strength to ground versus outages per 100 miles of line per year at isokeraunic level of 50

△—No overhead ground wire
•—Over - 25 - ohms footing resistance
○—25-ohms footing resistance

to 32 feet at the tower (column 41) with an increase of minus 3 feet to 18 feet at mid-span (columns 19 and 20) with a general range of 10 to 15 feet increase on the lines of newer design where this feature apparently was given consideration. Whether this increase in ground-wire-to-conductor spacing was predicated on lightning performance only or, in some cases, on sleet considerations, the records at hand do not show.

Taking the rough average height of ground wire above conductor at the tower as 15 feet, the increase in mid-span as 15 feet, and an average shielding angle of 30 degrees, there results an average ground-wire-to-line-wire separation of about 35 feet. At 180 kv per foot sparkover in air, this spacing would have a 1.5x40-microsecond positive wave critical flashover of about 6,300 kv and, of course, much higher on a steep-front short-tail lightning voltage wave. Comparing these values with the insulation flashover at the tower, which range from about 800 to 1,600 kv, there does not seem much likelihood of mid-span flashover in general, even with waves of extremely rapid rate of rise.

Tower Footing Resistance

The data given on tower-footing resistance are rather meager in many instances (columns 28 to 33 inclusive) but do indicate extremely wide variations between maximum and minimum on particular lines, for example, 2 to 1,550 ohms on line 20*A*.

In some cases a marked decrease may be noted after counterpoises or ground rods have been used. As an example, the maximum footing resistance of line 3 came down from 700 to 45 ohms.

Means for Reducing Footing Resistances. In about 68 per cent of the lines reported, means have been taken to reduce the tower footing resistances. These means consist of various arrangements of counterpoises, driven rods, and buried plates, the percentages of the cases where

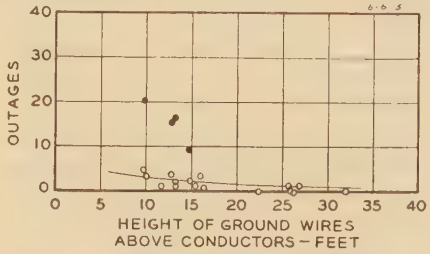

Figure 5. Height of overhead ground wires versus outages per 100 miles of line per year at isokeraunic level of 50

•—Over 25-ohms footing resistance
○—25-ohms-or less footing resistance

improvements have been made being about 62, 28, and 10 per cent respectively.

Effect on Outages. In Figures 4, 5, and 6 are plotted line outages against insulation strength, height of ground wire, and shielding angle, for two different ranges of footing resistance, that is, over 25 ohms and 25 ohms or less. In some instances a change was made in the shielding or in the footing resistance during the period covered, and these data were prorated for the figures. The benefit of low footing resistance is apparent from these figures.

Line Damage

Although a definite attempt was made by specific questions in the questionnaire to obtain information on line damage including damage to insulators, broken strings, and damaged conductors, replies

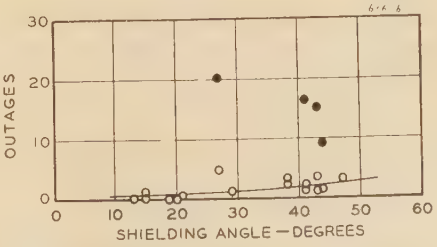

Figure 6. Shielding angle of ground wire versus outages per 100 miles of line per year at isokeraunic level of 50

○—25-ohms-or-less footing resistance

indicated that these are so extremely rare as not to present a real problem. Only two companies reported damage of any kind to hardware or conductors. One reported two cases where an insulator string was severed, and the other reported shattered insulators.

Likewise, duration of line tripouts of lines in this voltage class does not appear, from the replies received, to be of great concern. In one of the cases mentioned the line was out for ten hours. The second company reported merely "long outages" without giving the time involved.

Improved Lightning Performance Being Considered

Only three companies report that they are giving any consideration to making further changes in their line construction to improve its lightning performance. One (reference 3) is adding two counterpoises. The second company (references 12 and 13) is experimenting with devices not described in an attempt to better the line performance. Still a third company (references 16 and 16*A*) reports that it is considering installing ground wires because of the increase in lightning outages reported during the past year. This improvement apparently is being considered on only one line of the company. It should be noted in this connection that this line is in an area where the isokeraunic level is indicated as 5.

Summary and Conclusions

The lightning outage records of 35 transmission lines in the 220-kv class (operating at 190 to 287 kv) have been presented and discussed. Data also are given on some of the design features of these lines which are believed to be factors in their lightning performance.

If equal lightning intensities are assumed, theory and experience have shown that certain factors have a predominating influence on flashovers and outages, namely:

1. Overhead ground wires.
2. Insulation strength.
3. Tower footing resistance.

In the data disclosed by the present survey, it is difficult to separate definitely these influences and to place relative values upon them. However, the following conclusions seem to be justified:

1. The beneficial effects of overhead ground wires clearly is indicated in reducing lightning outages. Nonground-wire lines have a yearly outage record per 100 miles of line per year of 19.3 against 7.19 for lines now

Combined Light and Power Systems for Industrial Plants

D. L. BEEMAN
MEMBER AIEE

THE upward trend in illumination levels in industrial plants has resulted in an increased power demand of the lighting load. Illumination levels of 50 foot-candles are in general considered good practice at the present time, with some thinking of illumination levels as high as 100 foot-candles. The lighting load is a sizable portion of the total plant load. In many average manufacturing plants the lighting load will represent 2 to 4 volt-amperes per square foot, and the power load 8 to 10 volt-amperes per square foot. The same technique that has been applied in distributing power to machine tools and other power loads will pay dividends in distributing power to the lighting load.

For incandescent lamps 120-volt systems have been used almost universally. Higher-voltage incandescent lamps are fragile and generally not satisfactory.

With the introduction of fluorescent lamps the 120-volt restriction no longer applies. All fluorescent lamps have ballasts in series with them. By combining a slight transformer action with the ballast, the fluorescent lamp ballast can be supplied at any voltage from 120 to 260 volts. The industry, however, has standardized on the following ballast ratings: 118, 208, 230, and 260 volts. The introduction of higher-voltage fluorescent lamp ballasts has opened new avenues for using higher-voltage lighting circuits, thereby reducing the cost of the power system which supplies the lighting load. The trend toward load center power distribution systems also has enabled the use of combined light and power systems for industrial plants. This paper outlines the economy of combined light and power systems and higher-voltage lighting circuits.

Paper 46-52, recommended by the AIEE committee on industrial power applications for presentation at the AIEE winter convention, New York, N. Y., January 21–25, 1946. Manuscript submitted November 23, 1945; made available for printing December 4, 1945.

D. L. BEEMAN is in the industrial engineering divisions, General Electric Company, Schenectady, N. Y.

Conclusions

1. Combined light and power systems are less expensive than systems using separate substations for light and power.

2. High-voltage lighting circuits are generally most economical when using 260-volt 2-lamp 100-watt fluorescent lamp ballasts, so that the lighting load may be operated directly off the 480–277-volt substation

Table I. Cost Per Kilovolt-Ampere of Transformers, Panel Boards, and Wiring as a Function of Ballast Voltage

Line	Ballast Voltage	Transformer Rating	*Transformer Cost, Installed	**Panel Board Cost, Installed	Branch Wiring Cost (See Figure 8)	Total Cost
1	118	3 phase, 480–208Y–120 volt	12.50	5.60	6.40	$24.50
2	208	3 phase, 480–208Y–120 volt	12.50	5.60	3.80	21.90
3	120	1 phase, 480–240–120 volt	11.50	5.60	6.40	23.50
4	230	1 phase, 480–240–120 volt	11.50	5.25	3.00	19.75
5	260	1 phase, 480–265–132.5 volt	11.50	4.85	2.50	18.85

* Installation included at $2.50 per kilovolt-ampere.

** Installation included at $1.85 per kilovolt-ampere.

having ground wires (Table III). For lines having ground wires throughout the ten years covered by this report, the corresponding outage figures are 4.3 for one-ground-wire lines and 3.8 for two-ground-wire lines. One outstanding case of the benefits of ground wires is shown on line reference 7, where the observed outages averaged 19.2 for 7 years before the line had ground wires and 1 per year for 4 years after 2 ground wires were installed.

2. The sag of ground wires ranges from 11 to 45 feet, averaging 25 to 30 feet. Vertical separations between ground wire and line wire at mid-span are greater than at the tower by a range from minus 3 to 18 feet, with a general average of about 15 feet.

3. The shielding angles of ground wires vary from 13 to 59 degrees with a trend indicated that the smaller shielding angles reduce line outages.

4. Regarding overhead ground-wire location, in general these are placed from 9.8 to 32 feet above the horizontal plane of the top conductors at the towers. The general average of elevation of the ground wire, however, is about 15 feet above the top conductor.

5. Insulation supplied by a practical length of insulator string, or by a similar air clearance from conductor to tower, is not sufficient in the 220-kv class to prevent lightning flashover of the line. Flashovers have been experienced on the lines reported with impulse strengths as high as 1,600 kv.

6. Where reduction of tower footing resistances has been made, the final average values range in the general order of 1 to 20 ohms. The data submitted show definite benefits derived from the lowering of ground resistance. Reduction of ground resistances to 10 ohms or less reduces outage rates to the order of 1 per 100 miles of line per year, assuming shielding of the type reported herein, and an isokeraunic level of 50.

7. The reduction of tower footing resistances has been accomplished largely by ground rods and counterpoises, with the use of counterpoises predominant.

8. Average span lengths range from 590 to 1,480 feet with the majority of lines having a span of approximately 1,100 feet. There are insufficient data to indicate the effect of these practical span lengths on the lightning outage record of the lines.

9. Arcing devices on insulator strings, which were prevalent in the earlier designed lines, are being omitted on later built lines, with no adverse operating experience reported.

10. Damage to lines, caused by lightning, appears in general to be very infrequent and of minor concern to the service performance of the lines. Only two companies report prolonged outages; these involved shattered or broken insulators. Both cases were on lines not equipped with ground wires.

References

1. LIGHTNING PERFORMANCE OF 220-KV LINES, AIEE Lightning and Insulator Subcommittee. AIEE TRANSACTIONS, volume 53, 1934, November section, pages 1443–7; AIEE Lightning Reference Book, pages 1272–6. Discussion, AIEE TRANSACTIONS, volume 54, 1935, July section, pages 780–1.

2. FLASHOVER CHARACTERISTICS OF ROD GAPS AND INSULATORS, Edison Electric Institute-National Electrical Manufacturers Association Subcommittee on Correlation of Laboratory Data. AIEE TRANSACTIONS, volume 56, 1937, June section, pages 712–14.

3. THE DISTRIBUTION OF THUNDERSTORMS IN THE UNITED STATES, W. H. Alexander. *Monthly Weather Review*, July 1924.

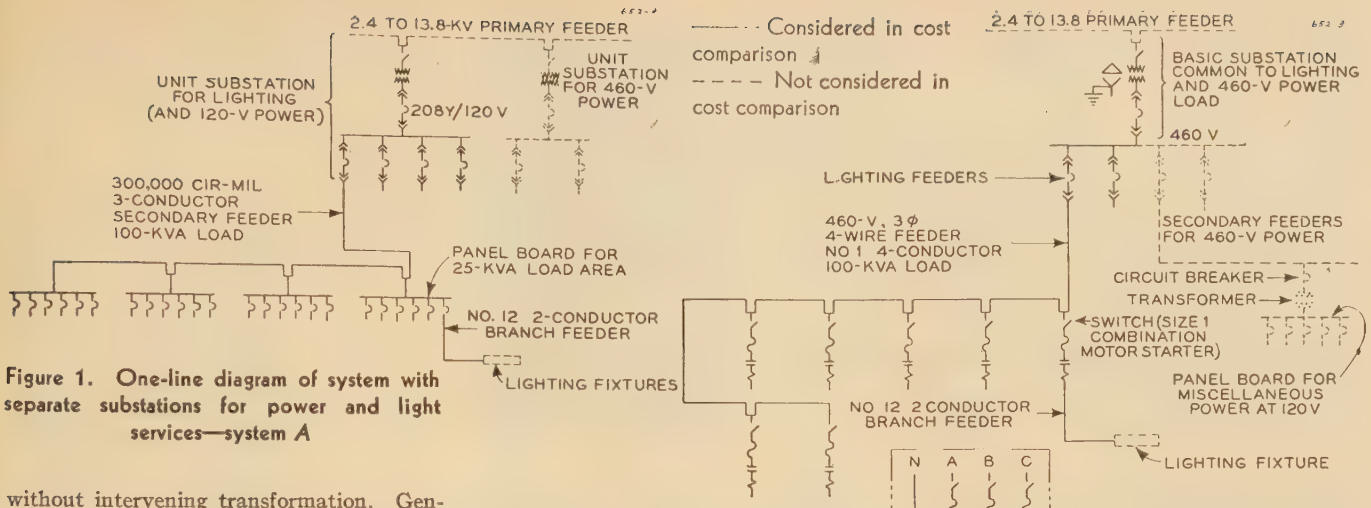

Figure 1. One-line diagram of system with separate substations for power and light services—system *A*

Figure 3. One-line diagram of system with one substation for power and light services

260-volt fluorescent lights supplied from 460-volt feeders—system C

without intervening transformation. Generally 120 volts are most economical overall for 40-watt fluorescent lamp installations.

3. With the modern load center power system, the objectionable flicker from welders practically can be eliminated by using separate transformers for resistance welders or by serving the lights from one transformer and the resistance welders from another in a secondary selective system, Figure 17.

Combinations Studied

Three basic combinations of power supply for lighting systems are considered in this paper. These are:

1. A 208Y–120-volt 3-phase 4-wire power system for lighting load, with separate substations for 460-volt power for motors, and the like, Figure 1.

2. Combined substations for power and light, that is, one 480-volt substation serving motors directly and the lighting load through step-down dry-type transformers located at strategic points through the factory, Figure 2.

3. A 460Y–265-volt combined power and lighting system in which the motors are operated at 3 phase, 460 volts and fluorescent lights from phase to neutral at 265 volts, from the same substation, Figure 3.

Figure 2. One-line diagram of system with one substation for power and light services

Lights supplied from 460-volt feeders through small dry type transformers—system *B*
——— Considered in cost comparison
– – – – Not considered in cost comparison

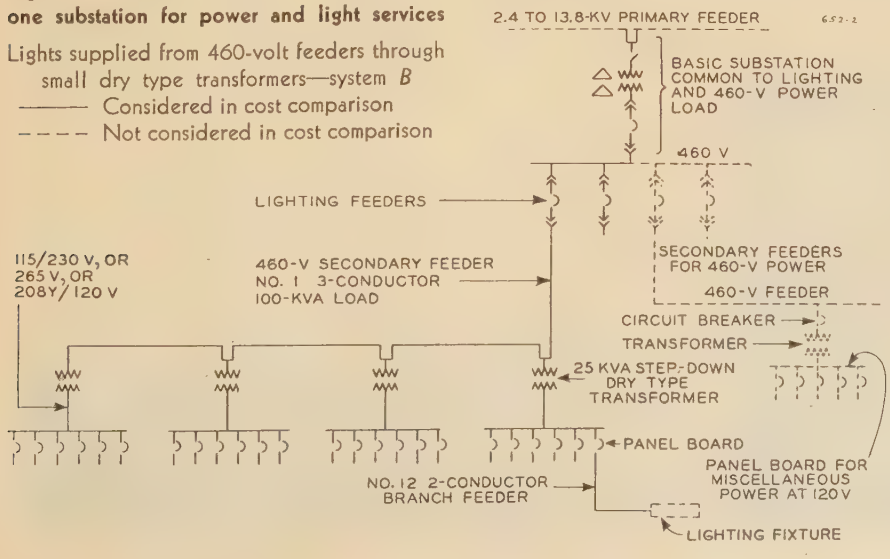

Items Included in Study

It is assumed that the primary feeder system is the same, regardless of which of the three afore-mentioned systems are selected. Therefore, the items considered are the step-down substations, secondary feeder circuit breakers, secondary feeders, dry-type transformers, panel boards, and branch wiring, as illustrated by the solid lines in Figures 1, 2, and 3.

The type of unit substation considered throughout this study is shown in Figure 4. To allow for diversity it is assumed that 1 kva of transformer capacity in the substation would have 1.25 kva of lighting load connected to it. Hence, the secondary feeder circuit breakers and cable have a capacity of 1.25 times the transformer kilovolt-ampere rating of the unit substation.

Installation cost of the substations is considered at 20 per cent of the substation price. These values—that is, 20 per cent for installation and 1.25 allowance for diversity—will be used throughout this study. The cost of substations as a function of kilovolt-ampere capacity is shown in Figure 6.

All secondary feeders are assumed to be varnished-cambric-insulated interlocked-armor cable, Figure 5.

The branch wiring from the panel board or control switch to the trough of the fluorescent lighting fixtures is included, but the wiring within the fixtures is not. The branch circuits have been limited to number 12 BX wire, with a current carrying capacity of 20 amperes, because it is believed that a 20-ampere fuse or circuit breaker is the largest which will give reasonable short-circuit protection to the ballasts. In most cases the load current per circuit is about 16 or 17 amperes. Branch circuit wiring costs are assumed to be 25 cents per foot of 2-conductor number 12 BX. To approximate the amount of branch circuit wiring for the various voltages, typical layouts were made—Figure 8.

System A—Separate Substations for Light and Power, Figure 1

This type of system may operate at either 208Y–120 volts, 3 phase, 4 wire, or 230–115 volts, single phase, 3 wire. In line with modern practice the 208Y–120-volt system will be used in the comparison.

A 208Y–120-volt system will care for the general area fluorescent lights, as well

Table II. Summary of System Comparisons

Type of System	First Cost, Per Kilovolt-Ampere	Safety: Voltage to Ground	Safety: Voltage on Fluorescent Lamps and Starters	Safety: Short-Circuit Current	Flicker Caused by 460-Volt Power Load	Ground on Power System	Where Most Adaptable
A—Separate lighting and power substations, Figure 1, 208Y–120 volt	$45	Less than 150	Same for all systems	High (more than 5,000 amperes)	None	Not required	Where all 460-volt busses have too great fluctuations in voltage, due to resistance welders; and where the total 120-volt load is over 50 per cent of the total load at 600 volts or less
B—Combined power and lighting substations, step-down lighting transformers, Figure 2	39.95	Less than 150	Same for all systems	Low (less than 5,000 amperes)	Possible (due to resistance welders)	Not required	Plants now having 460- or 575-volt delta systems. Where total lighting and miscellaneous load is less than about 50 per cent of the total load at 600 volts or less. Adaptable for incandescent, fluorescent, or any other kind of lighting
C—Combined power and lighting substations, 3 phase, 4 wire, 480Y–277 volt, Figure 3	22.95	265	Same for all systems	*Low (less than 3,000 amperes)	Possible (due to resistance welders)	Yes	In new factories, or in old factories where new 460-volt power systems are installed. Adaptable only for fluorescent or mercury-vapor lighting. Not adaptable to 575-volt power systems

* Using size 1 fused combination motor starters for controlling lighting circuits.

as the miscellaneous 120-volt power and lights. The system is laid out on the basis of $4^1/_2$ volt-amperes load per square foot to evaluate that part of the substation and secondary feeder cost which must be charged to the general area lighting system.

The minimum installed cost of the 208Y–120-volt substation and secondary feeders is $28.75 per kilovolt-ampere of substation rating when using 500-kva substations, the most economical size—top curve, Figure 6. A deviation from this size will increase the cost per kilovolt-ampere as shown by the curves.

The load per secondary feeder has been assumed to be 100 kva. The 4-conductor 300,000 - circular - mil secondary - feeder cable has an installed cost of $2 per foot. Each feeder will supply four circuit breaker panel boards of the type shown in Figure 7, with 25 kva of lighting load per panel board. The total cost of panel boards is estimated at $5.60 per kilovolt-ampere installed and wired (installation $1.85 per kilovolt-ampere).

It is realized that the circuit breakers in these panel boards do not have sufficient interrupting rating (only 5,000 amperes) for this service. However, there are no available devices which meet the space requirements for this service and which have adequate interrupting rating for the short-circuit current duty imposed on them.

The total cost of system *A* is

$28.75...Substations and secondary feeders
5.60...Panel boards
6.40...Branch wiring at 120 volts

$40.75

per kilovolt-ampere of lighting demand.

In general lighting substations as large as 500 kva (the most economical size from Figure 6) are not used. The substations often are laid out with a larger power and a smaller lighting substation at the same location. Where these small lighting units, that is, 150 kva, are used, the cost of the substation is increased. Using the cost from the top curve on Figure 6 for 150-kva substations, the total cost of system *A* is increased to

$33.00...Substation and secondary feeders
5.60...Panel boards
6.40...Branch wiring at 120 volts

$45.00

per kilovolt-ampere of lighting demand.

The cost may be increased even further if a primary protective device is required on the small lighting substation transformer. Hence, the cost of system *A* may go as high as $75 per kilovolt-ampere of lighting demand. Therefore, it is believed that $45 per kilovolt-ampere is a fair average to use in the general comparison with other systems.

System A With 208-Volt Ballast

The figures of $40.75 and $45 per kilovolt-ampere mentioned will be reduced to $38.15 and $42.40 per kilovolt-ampere, if 208-volt ballasts are used for the general area fluorescent lamps instead of 118-volt

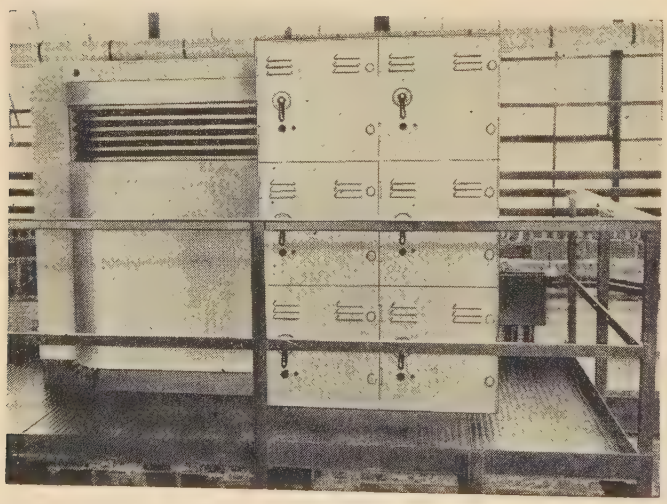

Figure 4 (left). Typical unit substation considered in cost analysis

Figure 5. Interlocked-armor type of secondary feeder cable considered in cost comparison

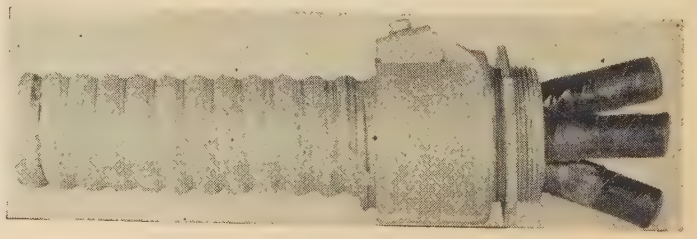

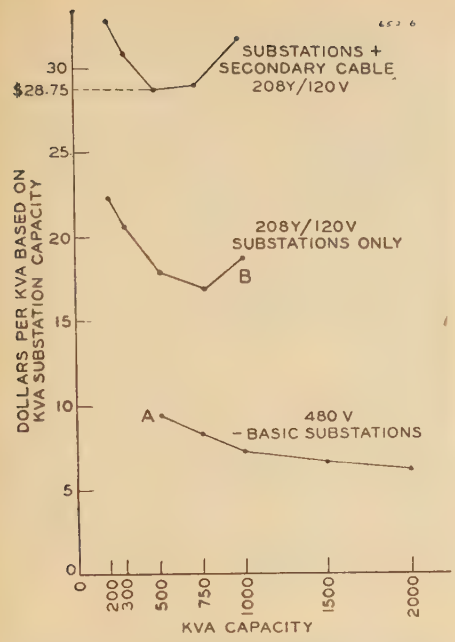

Figure 6. Cost of unit substations and secondary feeders as a function of unit substation size

20 per cent for installation
Feeder capacity is 125 per cent of substation capacity

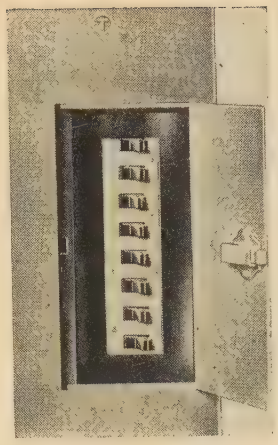

Figure 7 (left). Typical circuit breaker panel board for branch feeder protection

Figure 8. Diagrams used for determining branch circuit length

All branch circuits are number 12 2-conductor BX wire. 25-kva of lighting demand per load area

A—120-volt 1-phase branch circuits; total length 510 feet, including 240 feet for vertical runs

B—208-volt 1-phase branch circuits; total length 7/8 of 510 feet to adjust for 7 circuits; length of 7 circuits 300 feet, including 140 feet for vertical runs

C—230-volt 1-phase branch circuits; total length 240 feet, including 120 feet vertical runs

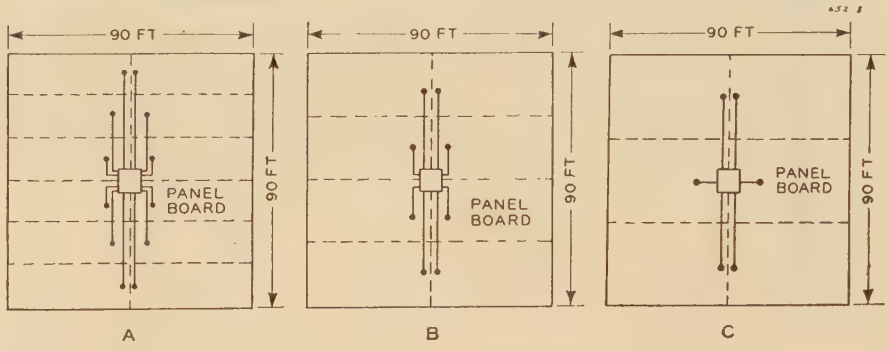

ballasts considered in the foregoing tabulations. The saving is made in branch circuit wiring only because the system is 3 phase, 208Y–120 volt up to that point. Since detail circuit arrangements may alter materially the branch circuit wiring costs, it is felt that the saving from using 208-volt ballasts rather than 118-volt ballasts may not be as great as shown. For the sake of uniformity of ballasts throughout a plant, many operators would use 118-volt rating for all ballasts if they elected to use system *A*.

System B—Combined Light and Power Substation, Figure 2

It is assumed that the same 480-volt substation will supply power to the 460-volt power feeders and to the 460-volt feeders which supply step-down transformers for the lighting load. The only portion of the step-down substation common to both the lighting and the power system is the primary switch, transformer, and main secondary circuit breaker. This is referred to as the basic substation, the installed cost of which is shown in curve *A*, Figure 6. Since other studies have shown the most economical size substation to be 750 to 1,000 kva, an average figure of $7.50 per kilovolt-ampere has been selected from curve *A* to represent the basic substation cost for the combined light and power system.

The 460-volt secondary feeder circuit breakers for the lighting system have been chosen with 25,000-ampere interrupting rating (large enough for 1,500-kva 480-volt 5.5 per cent impedance transformers). The load per feeder is maintained at 100 kva. On this basis the assumed installed cost of the secondary feeder circuit breakers is $5.40 per kilovolt-ampere.

The secondary feeder layout of Figure 9 is used to determine the length of cable for a 100-kva circuit. The 3-conductor number 1 interlocked-armor cable has an assumed installed cost of 90 cents per foot or $3.55 per kilovolt-ampere. Each secondary feeder connects directly to four step-down dry type transformers.

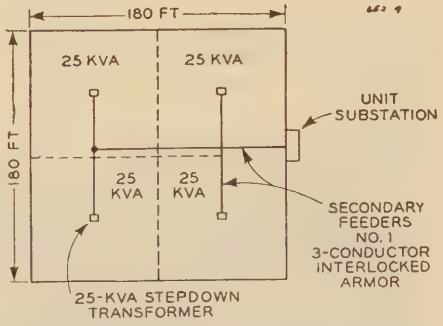

Figure 9. Diagram for determining length of secondary feeder serving 425-kva load areas—system *B*

Total length of secondary feeder cable approximately 315 feet

Use of Small Dry Type Transformers

Because they are the largest single-phase 480–240-120-volt transformer of standard design which can be used and the secondary short-circuit currents kept within 5,000 amperes, the interrupting rating of the circuit breakers in the panel boards, 25-kva transformers were chosen. Taps may be used in the 480-volt winding of these transformers to compensate for transformer voltage drop when necessary.

Separate 460-volt feeders are assumed to be used for serving lighting load only. There are many more outages on power feeders than on lighting feeders because of the greater number of changes made in power feeders. Furthermore, the power feeders may have more voltage drop due to fluctuating loads. Hence, separate lighting feeders often are used for greater reliability and to reduce voltage drop.

A typical outline of an installation of a dry type transformer and a panel board is shown in Figure 10. The installation view in Figure 11 shows two small dry type transformers and panel boards, one for the general area lights and one for miscellaneous 120-volt power.

Switches or circuit breakers are not used ahead of the dry type transformers on the lighting feeder, because the secondary feeder circuit breaker at the unit substation will provide adequate short-circuit

protection for these transformers. Since the lighting load is constant, it is assumed that overload protection is not required. However, should these transformers be connected to heavy power feeders, individual air circuit breakers should be used ahead of each transformer for protecting the transformer under short-circuit conditions and due to overload. The main circuit breaker at the unit substation will afford practically no protection for a small dry type transformer connected to a heavy power feeder.

There is a negligible difference in the cost of dry type step-down transformers and panel boards for various single-phase and 3-phase combinations of transformers and various ballast voltages—that is, 118, 208 volts, and so forth. Therefore, the selection between single-phase and 3-phase banks of small dry type step-down transformers is dependent upon local conditions.

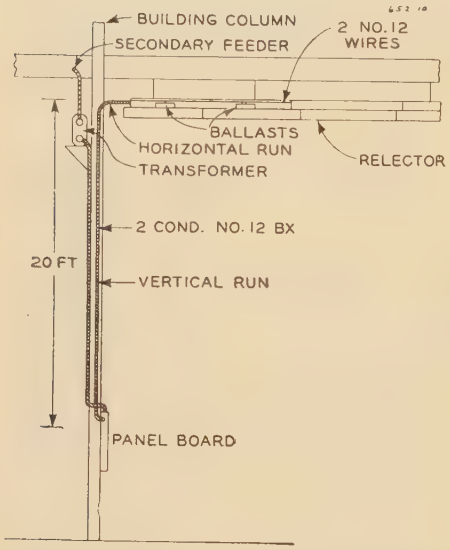

Figure 10. Arrangement of branch feeder panel board and small dry type transformer installations

Selection of Ballast Voltage for System B

The elements of system *B* considered thus far have the same cost regardless of ballast voltage. There are several different ballast voltages which may be selected—namely, 118, 208, 230, or 260 volts. To simplify the selection of ballast voltage, the cost of the items which are affected by ballast voltage are summarized in Table I. There is a slight saving in branch wiring for the higher voltages, but, as pointed out previously, the saving may largely disappear, depending upon local conditions. Hence, to have uniform ballast rating throughout the plant when using system *B*, many operators will use 120 volts, even though there is slightly higher branch circuit wiring cost for that voltage. However, the cost of branch wiring should be studied on each particular job to see if there is any substantial economic benefit to be gained from ballast voltages higher than 118 volts.

The total cost of system *B* is

$ 7.50... Basic substation
5.40... Secondary circuit breakers
3.55... Secondary cable
23.50... Step-down transformers, panel boards, branch circuit wiring, line 3, Table I

$39.95

per kilovolt-ampere of lighting demand.

Using 230-volt ballast instead of 118-volt ballast would, according to the figures of Table I, reduce the cost of system *B* to

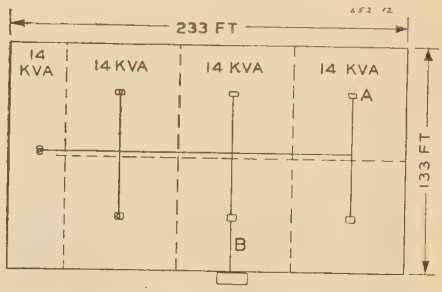

Figure 12 (above). Diagram for determining length of second feeders to serve 7 14-kva load areas, 260-volt fluorescent lamp ballasts —system C

Total length of secondary feeder cable approximately 417 feet
A — Motor starter used as switch for lighting circuit
B—Secondary feeder number 1 3-conductor and neutral interlocked armor cable

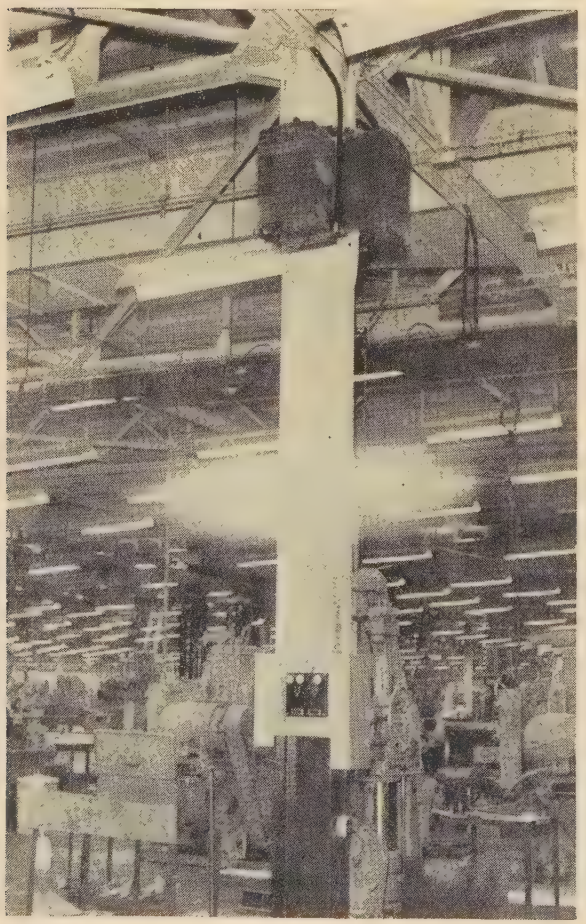

Figure 11 (left). Installation view of two panel boards and two small dry type transformers on a building column

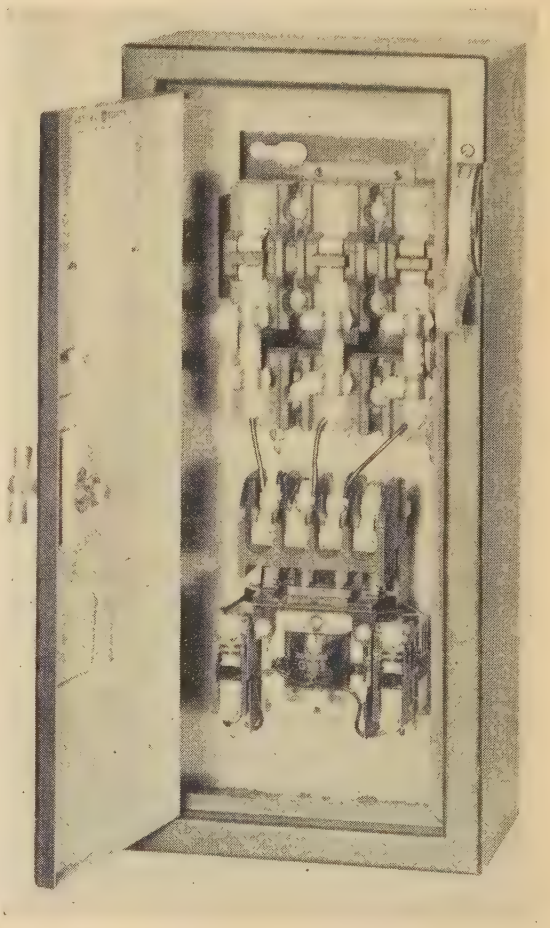

Figure 13. Typical fused combination motor starter used for switching 265-volt fluorescent light circuits—system C

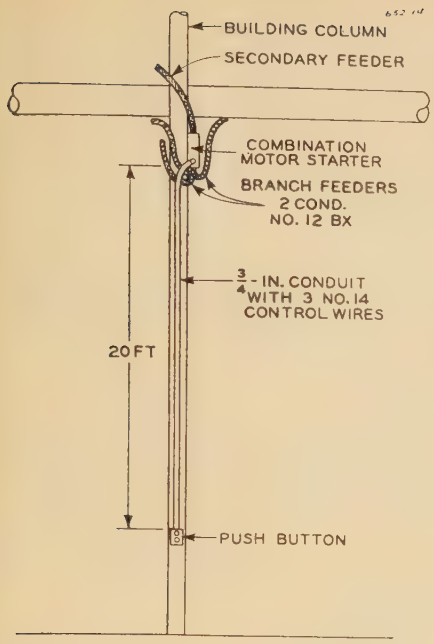

Figure 14. Typical mounting arrangement of fused combination motor starter for switching 265-volt fluorescent light circuits—system C

$36.20 per kilovolt-ampere of lighting demand.

System C—Combined Light and Power Substation, Figure 3

This system is similar to system *B*, Figure 2, except that the fluorescent lamp ballasts are rated 260 volt, and the power system substation is rated 480Y–277 volt, 3 phase with grounded neutral. Several large aircraft assembly plants built at the start of the war used this system for supplying fluorescent lighting loads for general area illumination. It also has been used in many other types of plants since that time. The reason for using this system in the aircraft plants was to save material and not to save money. However, the economic considerations now are more important than material considerations; hence, that system is being reevaluated on the basis of economics.

The substation and secondary feeder circuit breaker costs are the same as for the system *B*, that is, $7.50 and $5.40 per kilovolt-ampere, respectively.

The secondary feeder cost is higher than for system *B*, because a greater length is required to reach the smaller load areas, Figure 12, and because 4-conductor cable is used for the lighting feeders (3-conductor cable for the power feeders). The secondary cable cost is assumed at $1 per foot or $5.20 per kilovolt-ampere.

The branch circuits for the lighting load may be controlled by a 3-pole size 1 fused combination motor starter (for application on circuits with 50,000-ampere available short-circuit current) with three thermal overload elements, Figure 13. Three branch circuits at 265 volts phase to neutral are taken from each motor starter. Since these circuits are limited to about 20 amperes, the lighting load per motor starter is limited to about 14 kva. A typical method of installing a motor starter for this service is shown in Figure 14, where the motor starter is mounted up on the column at the same level as the lights, so that the branch circuits do not have to be run up and down the column. The push button may be located at any convenient spot. The motor starters and push buttons are assumed to cost $3.85 per kilovolt-ampere installed and wired (installation $1 per kilovolt-ampere).

The branch circuit wiring cost, Figure 15, is assumed at $1 per kilovolt-ampere.

The total cost of system *C* as described is

$ 7.50	Basic substation
5.40	Secondary feeder circuit breaker
5.20	Secondary feeder cable
3.85	Controller
1.00	Branch wiring
$22.95	

per kilovolt-ampere of lighting demand.

In some plants now using 260-volt fluorescent ballasts panel boards have been used instead of combination fused motor starters for switching lighting circuits. That substitution reduces the secondary feeder cable required and increases the expense for panel boards and branch wiring. If panel boards with 25 kva of load per board are used, the cost of system *C* is

$ 7.50	Basic substation
5.40	Secondary feeder circuit breakers
3.95	Secondary cable
4.85	Panel boards
2.50	Branch wiring
$24.20	

per kilovolt-ampere of lighting demand.

Short-Circuit Currents

Some operators have objected to system *C* at first glance because of the high short-circuit currents of the power system being available on the lighting circuits. The short-circuit currents on the lighting system are actually very low when the fused combination motor starter is used for controlling the light circuits. The fuses in the motor starter are decidedly current limiting in their action. The three thermal overload elements have a very high impedance and limit the current to even lower values than the fuses would without the thermal elements. The combined effect is to allow not more than about 3,000-ampere peak short-circuit current to flow for a fault in the lighting system, even though the available short-circuit current on the 460-volt power system may be as high as 50,000 rms amperes. To get proper performance of the fused combination motor starter, it is necessary to use not larger than 20-ampere fuses and to have the three thermal overload elements in place in the starter.

The panel board circuit breakers have no current-limiting action; therefore, they allow larger short-circuit currents to appear on the lighting system. However, the application of panel board circuit breakers may allow no higher short-circuit currents to flow in this system than in system *A*, which also is supplied directly from larger transformers. Panel board circuit breakers have the same limitations for application in system *C* as application in system *A* relative to their short-circuit rating.

Other Than General Area Lighting

In systems *A* and *B* 120 volts are available for general area lighting, as well as for miscellaneous 120-volt power and lighting. Therefore, all load other than the 460-volt load can be taken off the same circuits in those two systems.

With system *C* 260-volt ballasts should be used only in fixtures for general factory area lighting. These fixtures must be more than 8 feet from the floor and must not have individual switches mounted in the fixtures. The National Electric Code requires that all lighting for offices, individual benches, machines, and so forth should be operated at 120 volts. Since there is always some load of this nature around any plant, it is necessary to obtain the power for that load from the 460-

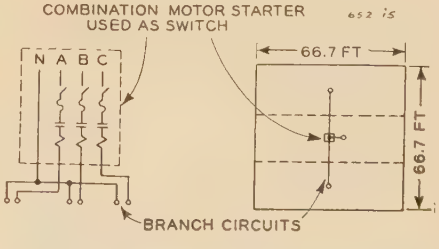

Figure 15. Diagram for determining length of branch circuits for 14-kva load area for system C

Branch circuits are number 12 2-conductor BX wire
Total length of branch circuit 45 feet

Figure 16. A fluorescent lighting installation for general area illumination

volt feeders of system *C*. This can be obtained just as in the case of system *B* with small step-down, dry type transformers as shown to the right of Figure 3. If these transformers are connected to heavy 480-volt feeders, the same precautions should be used in protecting the small transformers as outlined under system *B*.

It is believed that no sacrifice in safety is made with the higher-voltage fluorescent ballasts for the general area fluorescent lighting system, because the lamps and starter voltages are essentially the same, regardless of the voltage rating of the ballast. When the ballasts are changed, the circuit to which the ballasts are connected should be de-energized regardless of the circuit voltage.

Summary of Economic Comparison

Representative first costs of systems *A*, *B*, and *C* are

A..Separate light and power substation, 208Y–120 volt—Figure 1	$45 per kilovolt-ampere
B..Combined substations (step-down lighting transformers)—Figure 2	39.95 per kilovolt-ampere
C..Combined substations (460Y–265 volt)—Figure 3	22.95 per kilovolt-ampere

On the basis of system *A* being 100 per cent, system *B* costs only 89 per cent as much, and system *C* only 51 per cent as much. The savings of the combined light and power system will justify the selection of this system where the total 120-volt load is as high as 50 per cent of the total load at 600 volts or less.

This general comparison also will hold true where incandescent lamps are used throughout, or where other types of gaseous discharge lamps are employed. The ballast for certain types of mercury vapor lamps may be operated from 460-volt circuits.

Although cost comparisons of fluorescent lighting systems are beyond the scope of this paper, it is well to point out that the afore-mentioned figures must be considered in relation to the specific fluorescent lamp layout. The first cost of the power system is small compared with the first cost of the lighting fixtures. The carrying charges on the capital investment of the power system is small compared with the operating cost of the lighting system. Taking all those factors into account, some general guides as to over-all costs of power systems and the lighting fixture system are given in Table III.

Table III shows that even in over-all system cost, combined power and light systems are less expensive than system *A* using separate substations. System *A* does not appear once in the tabulation.

The choice between system *B* and system *C* depends, if one looks at the over-all picture, upon the type of fluorescent lighting fixture used.

For general illumination of very large areas, such as the general working area of a factory, many operators prefer the 100-watt lamp, because it takes fewer lamps and fewer fixtures to light a given area. When this combination is used, system *C*, using 260-volt ballasts, is the least expensive, either from the power system standpoint or from the over-all cost picture. In other cases the 3–40-watt lamp type of fixture is used for general area lighting, and in these cases system *B*, using 208-volt or 118-volt lamp ballast, is the least expensive when the over-all operating costs are considered.

These figures refer only to general area lighting systems, Figure 16, for, as pointed out previously, all fixtures less than 8 feet from the floor in factory areas, or all fixtures in offices or other places readily accessible to factory personnel should be operated from 120-volt systems.

Grounding of 460-Volt Power Systems

The 460Y–265-volt system must have the neutral grounded to accommodate 260-volt lighting fixtures. While some operators who have not had experience with 460-volt grounded Y systems may object to grounding, there are many advantages to having the system neutral grounded, even though 260-volt lighting fixtures may not be used. The biggest single advantage of grounding any power system is immediate isolation of a ground fault before it develops into a double line to ground fault, tripping out a considerable portion of the load.

Grounding of the 460-volt system neutral does not necessitate three thermal overload elements (1940 National Electric Code) in the motor starter for motor circuits. The thermal overload elements are for protection of the motor against overloading and not for short-circuit protection. It does require that all three

Table III

Type of Fixture	*Ballast Voltage	**Type of System With Lowest Cost: First Cost	Operating Cost	Annual Cost
3–40 watt	208	*B*	*B*	*B*
3–40 watt	118	*B*	*B*	*B*
3–40 watt	260	*C*	*C*	*C*
2–40 watt	260	*C*	*C*	*C*
2–40 watt	208	*B*	*B*	*B*
2–40 watt	118	*B*	*B*	*B*
2–100 watt	260	*C*	*C*	*C*
2–100 watt	118	*B*	*B*	*B*
2–100 watt	208	*B*	*B*	*B*

* Voltages are in order of cost, the top representing the least expensive combination and the bottom the most expensive combination for each particular type fixture.

** Includes capital investment in power system, lighting fixtures, cleaning and maintenance, energy cost, and so forth.

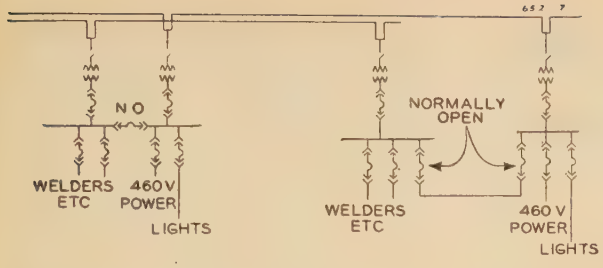

Figure 17. Secondary selective arrangement of load center power distribution system with resistance welders on one 460-volt bus and lights on the companion 460-volt bus

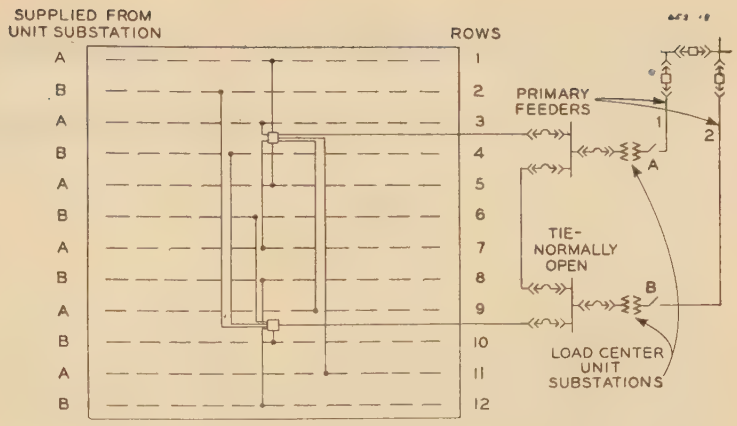

Figure 18. Secondary selective arrangement of load center power distribution system with overlapping areas of lights supplied for different substation busses to prevent complete loss of light should one bus be de-energized

phase branch circuit breakers have three overcurrent elements or three fuses.

Voltage Flicker of Combined Light and Power System

Voltage flicker due to fluctuating power loads will not cause objectionable light flicker in the average factory. Large resistance welders, or large motors which start frequently, should not be connected to the 460-volt bus that serves the plant lighting. Resistance welders are being used in increasing quantities in manufacturing plants, particularly in those that fabricate metal products. In many larger plants employing load center power distribution systems, the welders are connected to a separate transformer which supplies nothing but welding load. In these plants there is no problem of lamp flicker due to resistance welders, unless the plant is supplied by a very weak primary system, in which case the flicker problem will be essentially the same whether or not combined light and power systems are used.

In manufacturing plants where the total resistance welder load is not sufficient to justify separate welding transformers or where there are no exceptionally large welders, the secondary selective arrangement of the load center distribution system may be used, with one of the two substations (Figure 17) for general power load and resistance welders and the other for combined light and power. During normal operation the two substation busses are not in parallel, and the flicker on the bus to which the welders are connected will not affect the lights connected to the other bus. When during an emergency one of the primary feeders or one of the transformers is out of service, the busses may be paralleled, and during that emergency period the flicker may be noticeable. In general there has been no difficulty with combined light and power systems where the principles mentioned have been followed.

Increased Reliability of Lighting Circuits

With any of the systems discussed in this paper, consideration should be given to overlapping the area fed by one substation, so that an outage on that substation will not cause complete outage of lamps in any one area. One method of accomplishing increased reliability economically with the secondary selective load center power system is shown in Figure 18.

Small plants with demands of 500 to 1,500 kva usually require only one substation. It has been common practice to install a power transformer bank and a lighting transformer bank. The welders and power load are connected to the larger bank, and the lights to the smaller one. By using the arrangement shown in Figure 18 with two transformers equivalent in total kilovolt-amperes to the lighting plus the power demand, considerable increase in service reliability can be obtained without incurring objectionable flicker from the welders. With two transformers of equal size, both stepping down to 460 volts, the plant may be kept in at least partial operation with lights and major power apparatus in service with one transformer de-energized. Where separate lighting and power banks are used, this cannot be done. Increased service reliability for the same reason can be obtained in larger plants by using the secondary selective system with substations in pairs, both stepping down to 460 volts, instead of individual light and power substations scattered through the working area.

Effect of Altitude on Ventilation and Rating of Aircraft Electric Machines

CYRIL G. VEINOTT
MEMBER AIEE

Synopsis: Fundamental problems involved in the cooling and rating of aircraft electric machinery at medium and high altitudes are discussed in this paper, primarily to assist users in the application of such equipment, and to assist builders in designing equipment to meet the requirements. In addition flight tests are reported which confirm in part the blast-tube theory developed in a previous paper. For blast-cooled generators, an equation has been developed to show the maximum permissible output in terms of entering-air temperature and density, ramming-head pressure, and winding temperature. For motors curves of total winding temperature at rated load have been plotted as a function of altitude; these curves were plotted for selected values of sea-level temperature rise. Specific conclusions are drawn as to:

1. Permissible generator output as a function of altitude and sea-level rise.
2. Limiting sea-level temperature rises for motors on the basis of constant or reduced life at altitude.

This paper presents a qualitative method of analysis rather than a definitive solution of the problems involved.

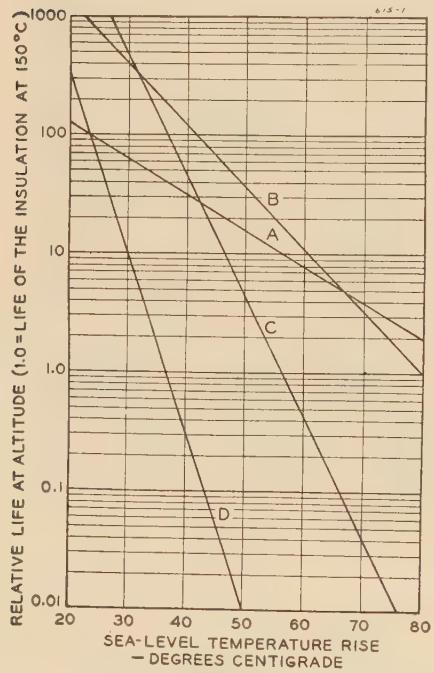

Figure 1. Effect of sea-level temperature rise of fan-cooled motors, open or enclosed, upon the insulation life at different altitudes (derived from Figure 8)

A—At sea level +60 degrees centigrade ambient temperature
B—At 20,000 feet +10 degrees centigrade ambient temperature
C—At 40,000 feet −40 degrees centigrade ambient temperature
D—At 50,000 feet −40 degrees centigrade ambient temperature

ONE of the first steps to be taken when applying a blast-cooled generator to any given airplane is to determine the amount of pressure head available for each significant flight condition. By comparing this head with the pressure on which the machine's rating is based, the application engineer can determine approximately what output can be obtained without danger of overheating the generator. One object of this paper is to demonstrate a method for readily determining the available pressure head without as many flight tests as now commonly taken. A knowledge of this pressure head under more conditions makes it possible to apply generators more accurately and to obtain more representative altitude-chamber data.

Altitude rating of generators is approached from the standpoint of determining the load required at all altitudes to give the same total winding temperature. This approach leads to the permissible output of the generator for constant insulation life at all altitudes.

Altitude rating of motors has been approached from a somewhat different angle. Load and speed are assumed constant, and relationships are established between sea-level rise and total winding temperature at altitude. By assuming that insulation life halves with each 10-degree-centigrade increase in temperature, the effect of sea-level temperature rise on the altitude life of insulation was determined and plotted in Figure 1, which was derived from Figure 8.

It must be emphasized, however, that generator outputs above full load well may be limited by commutation or by excitation power. This paper is concerned only with the influence of temperature on rating and starts with a study of blast-cooling phenomena.

Summary and Conclusions

A. A theory of blast-tube cooling has been developed and confirmed in part by actual flight tests.

B. Application of this theory appears to offer the following advantages:

1. Reduction in number of flight tests required.
2. More accurate information on ram-head pressures available for specific generators in specific airplanes.
3. More accurate information in applying generators.
4. More accurate information for altitude-chamber tests.

C. Salient features of this blast-tube theory are:

1. Air flow is measured in terms of velocity head.
2. Blast-tube characteristics can be represented by two factors:

(*a*). Closed-end pressure, analogous to open-circuit voltage of a battery.

(*b*). Air-flow resistance, analogous to internal resistance of a battery.

3. A generator without a fan has air-flow resistance only.
4. A generator with internal fan has air-flow resistance plus internal pressure.
5. Calculations of air flow (in terms of velocity head) are analogous to, and as simple as, the application of Ohm's law.
6. Closed-end pressure of a blast tube is independent of altitude, but for any given airplane is approximately proportional to the square of the indicated air speed.
7. Air-flow resistance of the blast tube, or generator, is independent of altitude, and independent of the indicated air speed.
8. Total pressure head on a blast-cooled generator, at any given indicated air speed, is substantially independent of altitude, unless the generator has an internal fan.

D. Generally speaking, the permissible output of a blast-cooled generator varies with the ramming-head pressure: above full load, the output tends to vary as the fourth root of the pressure; below full load, the output tends to vary as the square root of the pressure.

E. Altitude adversely affects the rating of the following classes of machines in the order given:

1. Fan-cooled machines (open or enclosed)—most affected.
2. Blast-cooled machines.
3. Totally-enclosed machines (not fan-cooled)—least affected.

F. Increase in altitude has its greatest effect on the rating of all classes of electric equipment in the isothermal stratosphere which begins, according to Army maximum standards, at 40,000 feet.

G. As a rule the higher the sea-level temperature rise, the more the output is affected adversely by increase in altitude. Conversely, the higher the specified maximum altitude, the lower must be the sea-level rise.

H. Since apparatus with a high sea-level temperature rise is affected more adversely by altitude than apparatus with a low sea-

Paper 46-15, recommended by the AIEE committee on air transportation for presentation at the AIEE winter convention, New York, N. Y., January 21–25, 1946. Manuscript submitted June 12, 1945; made available for printing November 23, 1945.

CYRIL G. VEINOTT is section engineer with the Westinghouse Electric Corporation, Lima, Ohio.

This paper is based on a talk made before the AIEE Dayton Section in January 1945.

The author acknowledges the assistance of Captains W. M. Green and C. A. Maple of the United States Army Air Forces and J. B. Crockford of the Westinghouse Electric Corporation in obtaining flight-test data. He also thanks H. J. Braun for permission to use Figures 8 and 10, G. G. Setterlund for permission to use Figure 7, and D. S. Pearson and J. C. Cunningham for assistance.

level rise, it follows that the use of high-temperature insulation offers less promise of weight reduction as the specified maximum altitude is raised.

I. Blast-cooled generators with class *A* insulation should be able to deliver full output up to 49,000 feet, provided the entering-air temperature does not exceed the Army maximum specification. If class *B* insulation is used, and if the sea-level rise is increased accordingly, full output should be expected only up to 40,000 feet.

J. Fan-cooled generators generally are not practicable for altitudes above 20,000 feet.

K. Fan-cooled motors which are expected to deliver full rated output with full life expectancy at 40,000 feet should have a sea-level temperature rise not exceeding:

1. 50 degrees centigrade if class *A* insulation is used.
2. 56 degrees centigrade if class *B* insulation is used.

These figures are based on an ambient temperature per Army maximum specification and full life expectancy at altitude. Considerable reduction in life expectancy at altitude does not increase the permissible sea-level rise so much as might be supposed. See Figure 1.

L. Fan-cooled motors which are expected to deliver full rated output with full life expectancy at 50,000 feet should have a sea-level temperature rise not exceeding:

1. 33 degrees centigrade if class *A* insulation is used.
2. 37 degrees centigrade if class *B* insulation is used.

These figures are likewise based on an ambient temperature per Army maximum specification and full life at altitude. Reduction of altitude life for changes in sea-level rise is shown in Figure 1.

M. Fan-cooled motors designed for a maximum altitude of 50,000 feet may be as much as 20 per cent heavier than comparable motors designed for 40,000 feet, unless the life at top altitude is considerably reduced.

N. Enclosed motors, and static apparatus cooled by radiation and free convection, can be permitted a sea-level rise of 70 degrees centigrade for class *A* insulation, or 90 degrees centigrade for class *B* insulation; such apparatus should be satisfactory for all altitudes up to 50,000 feet, provided the ambient temperature does not exceed the Army maximum value.

Air-Flow Mechanics of Blast-Tube Cooling

Heretofore the only method available for determining the total pressure head available for a particular blast-cooled generator has been by an actual flight test. This method has the advantage of being simple and direct. But it has the important disadvantage of requiring a flight test for every generator–airplane combination to be studied. Because this procedure would require too many flight tests, there is an unfortunate tendency to take a mere guess at the pressure. A

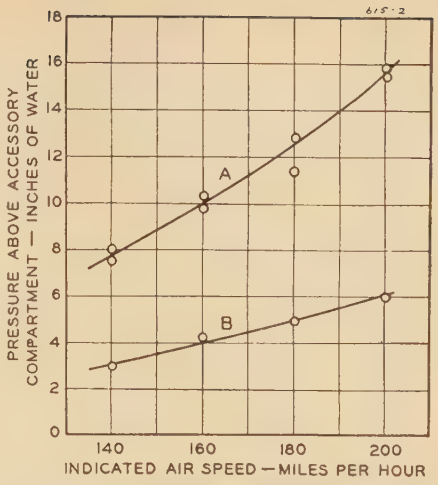

Figure 2. Flight-test measurements of the total pressure head available at the generator end of the blast tube with no generator

Four-engine bomber, number 2 nacelle
A—Closed-end readings
B—Open-end readings
Altitude: 5,000 feet

somewhat different approach to this problem was presented to AIEE in 1944.[1] Since then some flight tests have been made which tend to confirm the practicability of this approach. The method therein presented is summarized in the following paragraphs, together with flight-test data.

The underlying philosophy of this method is to measure, by means of a flight test, the pressure-flow curve of the blast tube itself; that is, a curve of total pressure head available versus the quantity of air taken from the tube. Similarly, by means of a laboratory test the pressure-flow curve of the generator under consideration is determined by measuring the pressure required to force different amounts of air through the generator. When these two pressure-flow curves are plotted on the same curve sheet, the point of intersection automatically gives the pressure across the generator as well as the amount of air flow. Likewise, the pressure-flow curve for any other generator then can be determined and plotted in order to determine the pressure and amount of air available for that particular generator *without an additional flight test.* But the pressure and amount of air can be computed even more easily by making use of the equations of Figure 4 which have been arranged in the form of simple electric-circuit equations; use of these equations is explained more fully later.

Extremely significant to this method is the factor selected as an indication of "quantity of air," namely, velocity head. Because of its importance the significance

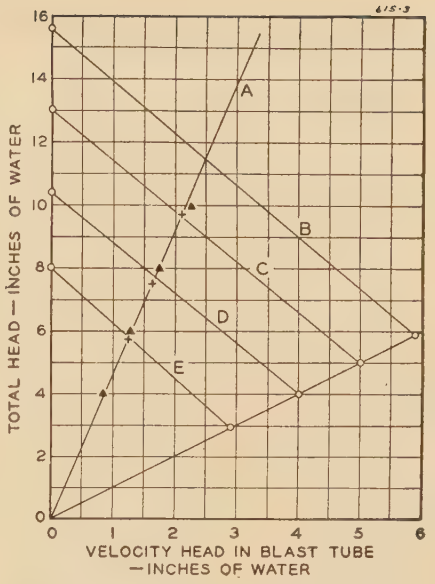

Figure 3. Pressure-flow curves of blast tubes and aircraft generators

Two-inch-diameter blast tube
O Blast-tube pressure-flow curves determined by flight tests without generators
Δ Generator pressure-flow curve determined by laboratory tests
\+ Generator pressures measured on flight test
A—Pressure-flow curve of a representative generator
B—Blast-tube pressure-flow curves at 200-miles-per-hour indicated air speed
C—At 180-miles-per-hour indicated air speed
D—At 160-miles-per-hour indicated air speed
E—At 140-miles-per-hour indicated air speed

No Fan in the Generator

Closed-end head $= h_c$
Blast-tube resistance $= R_t$
Velocity head of flow $= h_v$
Generator resistance $= R_g$

E_c = open-circuit volts
R_t = line resistance
I = current
R_g = load resistance

$$h_v = \frac{h_c}{R_t + R_g} \qquad I = \frac{E_c}{R_t + R_g}$$

$$h_g = h_v R_g = \frac{R_g h_c}{R_t + R_g} \qquad E_g = IR_g = \frac{R_g E_c}{R_t + R_g}$$

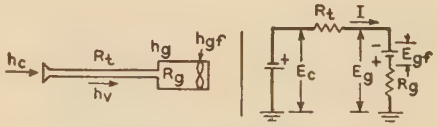

With Internal Fan in the Generator

$$h_v = \frac{h_c + h_{gf}}{R_t + R_g} \qquad I = \frac{E_c + E_{of}}{R_t + R_g}$$

$$h_g = h_v R_g - h_{gf} = \frac{R_g h_c - R_t h_{gf}}{R_t + R_g} \qquad E_g = IR_g - E_{gf} = \frac{R_g E_c - R_t E_{gf}}{R_g + R_t}$$

Note: If h_g is −, generator fan helps overcome R_t as well as R_g, and more air would flow through generator if blast tube were removed from generator.

Note: If E_g is −, E_{gf} helps overcome R_t as well as R_g, and more current would flow if terminals E_g were short-circuited.

Figure 4. Electric circuit analogue

of the use of velocity head as an indication of flow merits some discussion.

Velocity Head as an Indication of Air Flow

Air flow through the blast-tube might be measured in any number of ways: cubic feet per minute, pounds per minute, linear velocity, or velocity head. Of these, velocity head is by far the most useful for a number of important reasons. One reason is that, when flow is expressed in terms of velocity head, the pressure-flow curve of the blast tube, as well as the pressure-flow curve of the generator, *is substantially independant of air density and, therefore, substantially independent of altitude.* A second, and very important advantage of the use of velocity head, is that the pressure-flow curves of both blast tubes and generators alike become straight lines. Now, since the pressure-flow curve of a blast tube is a straight line, it is necessary to measure only two points on it. (For a generator pressure-flow curve, only a single point is needed.) These two points can be determined most conveniently by measuring the open-end and closed-end pressures, as pointed out in a previous paper.[1]

Flight Tests to Check Basic Theory of Blast-Tube Cooling

Flight tests were made at Vandalia, Ohio, with the co-operation of the Army Air Forces, for the purpose of verifying the principle and for obtaining specific data on at least one particular airplane. For purposes of these tests, a 4-engine bomber was selected. The generator was removed from number 2 nacelle, and in its place a 24-inch length of straight tubing 2 inches in inside diameter was used. Near the end of this straight tube a conventional pitot tube was installed. For the first flight test the end was capped and the airplane flown at various indicated air speeds at various altitudes. Total pressures at the end of the blast tube above accessory compartment were measured and recorded. A second flight test was made with the end of the blast tube open and with the tube discharging freely into the accessory compartment. It was found, as expected, that the total pressure above the accessory compartment, whether the end was closed or open, depended upon the indicated air speed but was substantially independent of the altitude. The open- and closed-end readings which were taken at an altitude of 5,000 feet have been plotted in Figure 2. Two additional similar curves were taken flying at altitudes of 10,000 and 15,000 feet, respectively; the resulting data

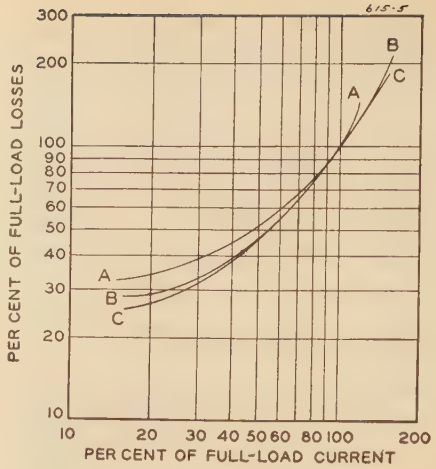

Figure 5. Variation of total losses of an aircraft generator as a function of output amperes and rpm

A—At 4,000 rpm
B—At 6,000 rpm
C—At 8,000 rpm

Generator rating: 9 kw, 30 volts, 300 amperes, 4,400–8,000 rpm

were nearly identical with those of Figure 2.

From the open- and closed-end readings taken on the flight tests, pressure-flow curves of the blast tube were plotted for different indicated air speeds; these curves are given in Figure 3. (In Figure 3 each point is the average of several readings taken at three different altitudes.) Next the generator was set up in the laboratory, and total pressure heads of 4, 6, 8, and 10 inches, respectively, were impressed on the generator. Temperature of the entering air was held at various values from −5 degrees centigrade to +20 degrees centigrade, and the pressure altitude of the incoming air was varied from 5,000 to 15,000 feet. Velocity heads of the entering air were measured and averaged for each different applied pressure. In Figure 3 velocity head in the blast tube has been plotted against total pressure head applied, obtaining the pressure-flow curve of this particular generator. (Ordinarily it is sufficient to measure the flow for a given pressure at ground-level conditions; entering-air temperature and atmospheric pressure have relatively little effect in this measurement, because velocity head is used as the measure of flow.)

Points of intersection of the pressure-flow curve of the generator with the respective pressure-flow curves of the blast tube give the pressures to be expected upon that generator in flight; these intersection points also give the velocity heads of air flowing through the blast tube and generator. As a check, this generator was installed and flight tested; observed values of generator head are indicated by crosses on the curve. The agreement is remarkable and demonstrates that the theory is workable.

Electric-Circuit Analogue an Aid to Blast-Tube Calculations

Instead of actually plotting pressure-flow curves and determining the point of intersection, it is much simpler to calculate the point of intersection. For this purpose one concept needs to be introduced—that of air-flow resistance—which is defined as the ratio of the lost head to the velocity head. This concept makes air-flow resistance comparable to ohmic resistance in an electric circuit, which is the ratio of the voltage drop to the current. In a blast tube, however, a note of caution must be given: in any given blast-tube system, all velocity heads must be referred to the same diameter of tube. Air-flow resistance of the blast tube is

$$R_t = \frac{h_c - h_o}{h_o} \qquad (1)$$

Air-flow resistance of a generator without a fan is

$$R_g = \frac{h_g}{h_{vg}} \qquad (2)$$

A tube resistance, R_t, of 4.0 means that the head loss in the tube is equal to 4.0 velocity heads. Thus, air-flow resistance, as defined and used herein, does have a definite physical significance.

Just as the characteristics of a battery can be expressed in terms of open-circuit voltage and internal resistance, so can the pressure-flow curve of a blast tube be ex-

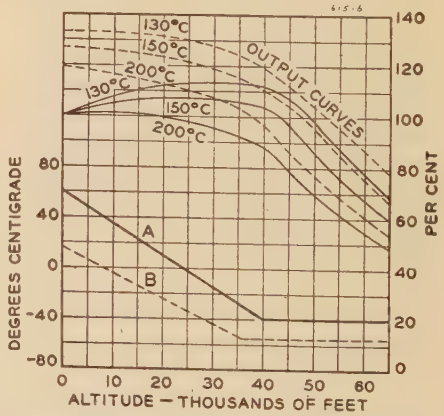

Figure 6. Influence of altitude on the permissible continuous outputs of blast-cooled generators

Calculations are based on the constant winding temperatures shown on the respective curves
—— Output based on Army maximum ambient temperatures
– – Output based on NACA ambient temperatures

A—Army maximum ambient temperature
B—NACA ambient temperature

pressed in terms of closed-end pressure and tube resistance. The blast-tube pressure-flow curves of Figure 3 are represented in Table I. It will be noted that the open-end pressures are given; these were used in calculating the tube resistance. It is particularly gratifying to note that the tube resistance does not vary with altitude, nor does it vary to any significant extent with indicated air speed. There is no particular reason why it should vary with altitude or with air speed, and the slight discrepancies noted may be due to test errors.

Equations for calculating the pressure head available for any generator of known air-flow resistance are given in Figure 4, where they are compared with exactly analogous equations for a simple d-c series circuit. The analogy is of great assistance in remembering the equations. Extension of this theory to include generators with an internal fan was a natural development of the electric-circuit analogue.

Generators With Internal Fan

Internal fans alone usually do not provide enough ventilation to make generators satisfactory above 20,000 feet. However, use of an internal fan does provide some ground power capacity and, when used in conjunction with blast cooling, has the general effect of increasing the air flow. Let the pressure of the internal fan be denoted by h_{gf}. This pressure is proportional to the square of the speed and to the first power of the air density; it can be represented by the equation

$$h_{gf}=F_p\times\left(\frac{N}{1{,}000}\right)^2\times\frac{\rho_A}{\rho_o} \qquad (3)$$

where F_p is an empirical constant. Physically, F_p is the pressure developed by the fan at sea-level air density at 1,000 revolutions per minute. This constant F_p might be measured by blocking either the inlet or the outlet and measuring the pressure at the blocked end of the generator; readings should be taken at different speeds and the constant F_p determined from equation 3.

Air-flow resistance of a fan-cooled generator can be determined by applying a known pressure head h_g and measuring the velocity head h_{vg} of the entering air. The air-flow resistance is then

$$R_g=\frac{h_g+h_{gf}}{h_{vg}} \qquad (4)$$

Velocity head of the air flowing into a fan-cooled generator and pressure head across it can be computed by using the equations of Figure 4. It is to be noted that the same constants of the blast tube apply whether the generator has an internal fan or not. However, since the pressure of the generator fan does vary with altitude, the pressure drop across the generator also will vary with altitude. If there is no internal fan in the generator, the pressure across the generator will not vary with altitude. If there is an internal fan, the general effect of altitude will be to reduce the velocity-head flow and to increase the pressure across the generator.

Of interest is the case of the blast-cooled generator with internal fan operating on the ground with no ram-head pressure applied. From the equations of Figure 4, the air flow through the generator and blast-tube combination and the pressure across the generator (necessarily negative) readily can be computed. The cooling effect, of course, is determined by the weight of air flowing, rather than by the pressure head.

Table I. Blast-Tube Characteristics Obtained From Flight Tests

Indicated Air Speed	Open-End Pressure, h_o	Closed-End Pressure, h_c	Tube Resistance, R_t
140	2.9	8.0	1.76
160	4.0	10.4	1.60
180	5.0	13.0	1.60
200	5.9	15.6	1.64

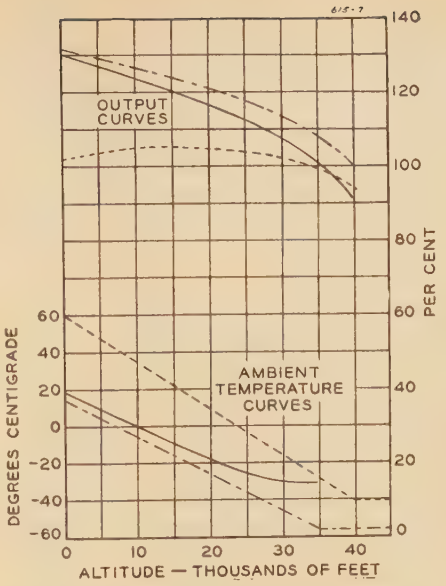

Figure 7. Influence of ambient temperatures on the permissible continuous output of a blast-cooled generator at various altitudes

Generator rating: 9 kw, 300 amperes, 30 volts

Winding temperature: 150 degrees centigrade

- - - NACA temperature

——— Actual ambient temperatures used in laboratory tests

----- Army maximum temperatures

Factors That Determine the Permissible Output of a Generator

In a blast-cooled generator the total watts taken away by the cooling air can be assumed to be approximately proportional to the total weight flow of the cooling air and also to the temperature rise of the windings above the entering-air temperature. In other words

$$P_l \propto W(T_s-T_a) \qquad (5)^*$$

but, for the general case,

$$W \propto \sqrt{\rho h_g} \qquad (6)$$

for blast-cooled generators with no internal fan

$$h_v \propto h_g$$

so that we may assume

$$W \propto \sqrt{\rho h_g} \qquad (6a)$$

therefore,

$$P_l = C_l\sqrt{\rho h_g}(T_s-T_a) \qquad (7)$$

Equation 7 is of inestimable value in evaluating altitude performance. It shows how the heat-dissipating capacity of the cooling air depends upon:

1. Air density.
2. Pressure head across the generator.
3. Winding temperature.
4. Ambient temperature.

Of even greater interest to the user of generators, however, is a knowledge of how the permissible output, rather than permissible loss, depends upon these same factors. For this purpose, it is necessary to know how the total losses in the machine vary with the output.

There is no single fixed relationship between output and losses which holds for all aircraft electric machines. Generally speaking the losses may be divided into two broad classes:

1. Constant losses.
2. Variable losses which generally vary as the square of the current.

Maximum efficiency of the generator is obtained when the constant losses are equal to the variable losses, and, at this point, the efficiency curve is usually quite flat. An efficiency curve flat over a range means that the losses are directly proportional to the output over the same range. Below the maximum-efficiency point they decrease more slowly than the output. How these total losses vary with the current has been plotted in Figure 5 for a typical 9-kw d-c aircraft generator.

* More accurately, W should have an exponent slightly less than 1.0, but for the purposes of this paper the gain in accuracy in using a decimal exponent here is hardly justifiable.

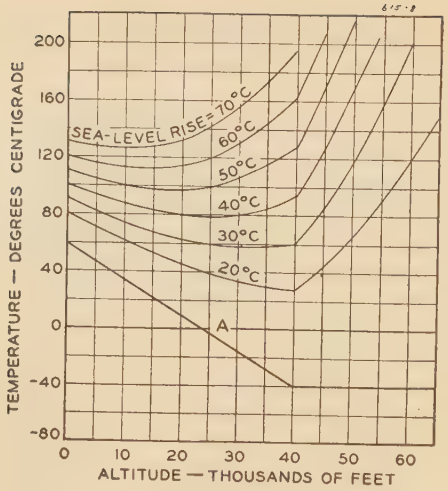

Figure 8. Fan-cooled motors, open or enclosed, effect of altitude on the winding temperature for different values of sea-level rise

Output, losses, and rpm assumed constant
A—Ambient temperature (Army maximum)

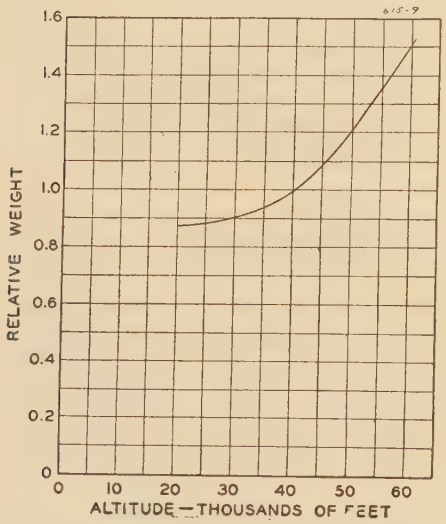

Figure 9. Curve showing approximately how the weight of an open fan-cooled motor is affected by the maximum altitude for which it is designed

Based on Army maximum ambient temperature curve and a motor designed for 40,000-foot altitude as unit weight

It will be noted that the variation of losses with current also is affected by the generator's operating speed, which changes the distribution between the constant and variable losses. It will be observed on this curve that, the higher the load, the faster the losses increase with increase in current. It would be convenient if we could express the losses as a simple function of the load current, such as

$$P_1 = C_2 I^{\beta} \tag{8}$$

Unfortunately the value of β, which is the slope of the curve, is not constant throughout the load range. However, it is sufficiently accurate and generally safe to take β equal to 2.0 for outputs above full load and to assume it equal to 1.0 for loads from full load down to half load.

Variation of the output with the ram-head pressure, h_g, on the generator now can be expressed. Equation 7 can be rewritten, first, in terms of permissible loss, as follows:

$$\frac{P_{1A}}{P_{1o}} = \sqrt{\left(\frac{\rho_A}{\rho_o}\right)\left(\frac{h_{gA}}{h_{go}}\right)}\left(\frac{T_{SA}-T_{aA}}{T_{So}-T_{ao}}\right) \tag{9}$$

Subscript A denotes any altitude, and subscript o denotes sea level. This equation shows how the losses that can be dissipated vary with altitude conditions, and with ramming-head pressure. It will be noted that the permissible watts vary as the square root of this ramming-head pressure. This relationship then can be interpreted in terms of current output as follows:

$$\frac{I_A}{I_o} = \left[\sqrt{\left(\frac{\rho_A}{\rho_o}\right)\left(\frac{h_{gA}}{h_{go}}\right)}\left(\frac{T_{SA}-T_{aA}}{T_{So}-T_{ao}}\right)\right]^{1/\beta} \tag{10}$$

When the expression in brackets is greater than unity, β may be taken equal to 2.0. When the expression in brackets is less than unity, β may be taken equal to 1.0. In other words, if the pressure available is less than the rated pressure, the generator should be derated proportionally to the square root of the applied pressure; if the pressure is more than the specified value, the generator could be uprated, so far as overheating is concerned, as the fourth root of the pressure. However, it must be borne in mind that commutation, field excitation, or some limit other than temperature rise may limit the uprating of the generator.

Equation 10 was developed for the most common case of a generator without a fan. To take into account the effect of an internal fan, equation 10 can be written as follows:

$$\frac{I_A}{I_o} = \left[\sqrt{\left(\frac{\rho_A}{\rho_o}\right)\left(\frac{h_{vA}}{h_{vo}}\right)}\left(\frac{T_{SA}-T_{aA}}{T_{So}-T_{ao}}\right)\right]^{1/\beta} \tag{10a}$$

In this equation, h_{vo} represents the velocity head of the air entering the generator at sea level with rated pressure applied. Theoretically, this equation should be applicable when no ram head is applied; practically, the equation is of rather doubtful value when extended so far because:

1. The β exponent does not hold so well for low values of load, for instance, below 30 per cent.

2. The effect of the rotation of the armature, which is more important under these conditions, is not fully taken into account.

Effect of High Altitude on Output of Blast-Cooled Generators

Factors affecting the rating of a generator at altitude, from the standpoint of winding temperature, are:

1. Density of the cooling air. (See Table II.)

2. Ram-head pressure or h_g; for a blast-cooled generator, this does not vary with altitude.

3. Ambient temperature. In the following analysis this generally was assumed to be as specified by the Army maximum curve (see Figure 6, and Table II), but this may not always be so. Test data are needed on entering-air temperatures of blast-cooled generators.

4. Permissible or assumed temperature of the windings.

5. β, that is, how much the losses vary with the current output.

A general relationship between the foregoing factors is shown in equation 10. In Figure 6 are plotted some curves calculated from this equation. In all of these curves the total winding temperature has been assumed constant at all altitudes. These curves show the influence of altitude on the permissible continuous output of blast-cooled generators. Three different machines were taken for this analysis, having assumed winding temperatures of 130 degrees centigrade, 150 degrees centigrade, and 200 degrees centigrade respectively. This would correspond approximately to class *A* insulation, class *B* insulation, and special high-temperature insulation. It further was assumed that the temperature of the entering air was at Army maximum value, as shown in Figure 6 and Table II, and that the machine had rated temperature rise at sea level. Also, the permis-

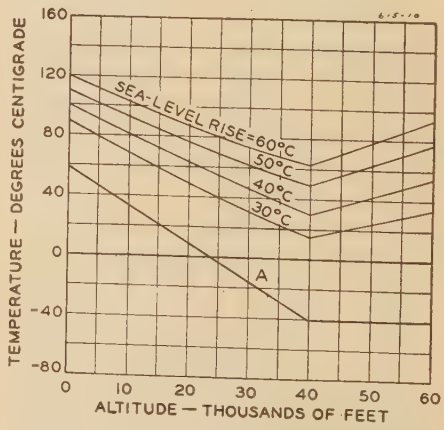

Figure 10. Enclosed motors, effect of altitude on the frame temperature for different values of sea-level rise

Output and losses assumed constant
A—Ambient temperature (Army maximum)

sible outputs of these same machines were computed on the basis of entering-air temperatures equal to National Advisory Committee on Aeronautics ambient temperatures; these temperatures are also shown in Figure 6 and Table II. Some interesting conclusions are deducible from the curves in Figure 6.

If the sea-level temperature rise is not over 70 degrees centigrade, full output rating can be obtained up to 49,000 feet. However, if the machine is designed for a higher sea-level temperature rise, such as 90 degrees centigrade, full rated output can be maintained only up to 42,000 feet. If extra-high-temperature insulation is used that permits the machine to have a sea-level rise of 140 degrees centigrade, full rating can be maintained only up to 20,000 feet. Any given machine can develop more output without overheating in an NACA standard atmosphere than in an Army maximum standard atmosphere, because the former has lower temperatures. This effect is shown in Figure 6 for the three hypothetical machines by plotting the permissible output for both ambient-temperature curves. The difference in output decreases with altitude, especially above 40,000 feet.

Curves shown in Figure 6 should be fairly representative of blast-cooled generators. For purposes of comparison, similar curves, except that they are based on actual tests on a typical aircraft generator, are given in Figure 7. These curves are based on altitude-chamber tests on a 9-kw d-c generator. Actual temperature rises were measured at different altitudes in the chamber, and the three output curves at the top of the sheet were corrected by calculation to correspond to the three different ambient temperature curves shown at the bottom. In making these corrections, it was assumed that temperature rise was directly proportional to watts loss. Permissible watts loss was converted to current output by making use of Figure 5, which applies to the particular generator that was altitude-tested. In general these curves agree with the 150 degrees centigrade curve of Figure 6 with a reasonable degree of accuracy. However, they tend to show that there is some loss in permissible output above 34,000 feet, whereas the theoretical curve of Figure 6 shows full output being maintained up to 42,000 feet.

Effect of Altitude on Aircraft Motors

Permissible loss in an aircraft motor varies with speed as well as with permissible temperature rise and air density. Hence, it is difficult to express the output as a function of altitude because of the variation in speed, particularly in the case of a series motor. Furthermore, for many applications the load imposed on the motor does not vary with altitude, so that the motor has to carry the same load at all altitudes. Therefore a new and somewhat different approach has been used. This approach involves investigating the actual temperatures encountered by the windings at different altitudes, assuming a constant load and a constant speed. However, in some applications, notably fan, the load falls off at altitude, and the speed will increase if a series motor is being used. For the present, however, the following discussion is confined to motors operating at a constant load and a constant speed.

There are two types of motors to be considered: fan-cooled, open or enclosed; and enclosed.

Fan-Cooled Motors (Open or Enclosed)

Temperature-rise tests taken in an altitude chamber on a number of aircraft motors under different conditions showed that the temperature rise was approximately inversely proportional to the density raised to the 0.9 power. By use of this empirical fact, the winding temperature of open fan-cooled aircraft motors has been calculated and plotted in Figure 8 as a function of altitude with sea-level rise as parameter. From these curves a number of interesting conclusions can be deduced:

1. Winding temperatures start to increase sharply above 40,000 feet. For satisfactory performance at high altitude, a comparatively low sea-level temperature rise is essential.

2. Use of high-temperature insulation is not particularly helpful, either in increasing the maximum altitude rating or in reducing the weight by increasing the permissible sea-level rise.

3. For a maximum altitude rating of 40,000 feet, at a maximum ambient temperature of −40 degrees centigrade, the maximum permissible sea-level rise is: for class *A* insulation, 50 degrees centigrade; for class *B* insulation, 56 degrees centigrade.

4. For a maximum altitude rating of 50,000 feet, at a maximum ambient temperature of −40 degrees centigrade, the maximum sea-level rise would be: for class *A* insulation, 33 degrees centigrade; for class *B* insulation, 37 degrees centigrade. Use of a high-temperature insulation which would permit a temperature rise of 140 degrees centigrade (total temperature of 200 degrees centigrade) still would require the motor to have a sea-level rise as low as 46 degrees centigrade.

These conclusions are somewhat pessimistic for motors smaller than 4 inches in diameter, and optimistic for motors larger than this.

Weight is always a matter of primary concern, and it would be interesting to know how the weight of a motor is affected by the maximum altitude at which the motor is intended to operate. Curves in Figure 8 show what the sea-level rise has to be in order not to exceed safe temperatures at any given altitude, but it is not so easy to determine how the weight of the motor is affected by the sea-level temperature rise for which it is designed. However, since it frequently is assumed that weight is proportional to the square root of the output, it seems fairly reasonable to assume that the weight would vary inversely as the square root of the specified sea-level temperature rise. On this assumption, Figure 9 was plotted to show how the weight of an open fan-cooled aircraft motor is affected by the maximum altitude for which the motor is designed. This curve shows that a motor actually designed for 50,000 feet

Table II. Standard Temperatures and Densities of Air for Both National Advisory Committee on Aeronautics and Army Maximum Standards

Altitude, Feet	NACA Standard Conditions: Pressure, Inches, H_g	NACA Standard Conditions: Pressure, Centimeters, H_g	NACA Standard Conditions: Temperature, Degrees Centigrade	NACA Standard Conditions: Pounds Per Foot, ρ	NACA Standard Conditions: ρ / 0.07651	NACA Standard Conditions: $\sqrt{\rho / 0.07651}$	Army Maximum Conditions: Temperature, Degrees Centigrade	Army Maximum Conditions: Pounds Per Foot, ρ	Army Maximum Conditions: ρ / 0.06617	Army Maximum Conditions: $\sqrt{\rho / 0.06617}$
0	29.921	76.00	15	0.07651	1.0000	1.0000	60	0.06617	1.0000	1.0000
5,000	24.89	63.23	5.1	0.06591	0.8615	0.9282	47.5	0.05719	0.8643	0.9297
10,000	20.58	52.26	− 4.8	0.05651	0.7386	0.8594	35.0	0.04921	0.7437	0.8624
15,000	16.88	42.88	−14.7	0.04813	0.6291	0.7932	22.5	0.04207	0.6358	0.7974
20,000	13.75	34.91	−24.6	0.04076	0.5327	0.7299	10.0	0.03578	0.5407	0.7353
25,000	11.10	28.19	−34.5	0.03427	0.4479	0.6693	− 2.5	0.03022	0.4567	0.6758
30,000	8.880	22.56	−44.4	0.02861	0.3739	0.6115	−15.0	0.02535	0.3831	0.6190
35,000	7.036	17.87	−54.3	0.02369	0.3096	0.5564	−37.5	0.02200	0.3325	0.5766
40,000	5.541	14.07	−55.0	0.01872	0.2447	0.4947	−40.0	0.017513	0.2647	0.5144
45,000	4.364	11.08	−55.0	0.01474	0.1927	0.4390	−40.0	0.013793	0.2084	0.4565
50,000	3.436	8.730	−55.0	0.011607	0.15171	0.3895	−40.0	0.01086	0.16412	0.4051
55,000	2.707	6.876	−55.0	0.009143	0.11950	0.3457	−40.0	0.008556	0.1293	0.3596
60,000	2.132	5.415	−55.0	0.007201	0.09412	0.3068	−40.0	0.006738	0.10182	0.3191
65,000	1.679	4.265	−55.0	0.005671	0.07412	0.2723	−40.0	0.005307	0.08020	0.2832

might be as much as 20 per cent heavier than similar motors designed for a maximum altitude of but 40,000 feet.

Enclosed Motors (Not Fan Cooled)

The dissipating capacity of an enclosed motor does not fall off with increase in altitude so fast as that of a fan-cooled motor, primarily because:

1. Watts loss dissipated by radiation is independent of the air density.

2. Watts loss dissipated by natural convection is proportional to the square root of the density. (With forced convection, as in blast-cooled or fan-cooled machines, the watts dissipated are proportional to the first power of density.)

Using a combination of empirical and theoretical data, the frame temperature of a totally enclosed motor has been calculated as a function of altitude, with sea-level temperature rise of the frame as parameter. These curves are given in Figure 10. (It must be borne in mind that the temperature of the winding will be somewhat higher than the frame temperature.) Comparing these curves with those of Figure 8, it readily is concluded that the rating of enclosed motors is not reduced so much at altitude as those of fan-cooled motors. In fact, if a totally enclosed motor is designed for a sea-level rise of 70 degrees centigrade, it should give satisfactory performance at all altitudes from sea level up to well above 60,000 feet. It also appears likely that a motor designed for class *B* insulation with a 90-degree-centigrade temperature rise at sea level would be satisfactory at all altitudes from sea-level up to 50,000 or 60,000 feet.

Summary of Effect of Altitude on Heat Transfer

Generally speaking, the heat generated in an aircraft electric machine may be dissipated in a number of different ways. How altitude conditions affect the amount of heat lost by each of the different components of heat transfer are summarized in the following equations.

Forced convection, blast cooling, without internal fan:*

$$\frac{P_{1A}}{P_{1o}} = \sqrt{\left(\frac{\rho_A}{\rho_o}\right)\left(\frac{h_{gA}}{h_{go}}\right)}\left(\frac{T_{SA}-T_{aA}}{T_{So}-T_{ao}}\right) \qquad (11)$$

Forced convection, fan cooling:

$$\frac{P_{1A}}{P_{1o}} = \frac{\rho_A}{\rho_o} \times \frac{RPM_A}{RPM_o} \times \frac{T_{SA}-T_{aA}}{T_{So}-T_{ao}} \qquad (12)$$

Free convection:

$$\frac{P_{1A}}{P_{1o}} = \sqrt{\left(\frac{\rho_A}{\rho_o}\right)}\left(\frac{T_{SA}-T_{aA}}{T_{So}-T_{ao}}\right)^{1.25} \qquad (13)$$

Radiation:

$$\frac{P_{1A}}{P_{1o}} = \frac{(T_{SA}+273)^4-(T_{aA}+273)^4}{(T_{So}+273)^4-(T_{ao}+273)^4} \qquad (14)$$

Symbols

A = subscript A denotes "at altitude." May be added to any of the following symbols

o = subscript o denotes "at sea level." May be added to any of the following symbols

h_c = closed-end pressure of a blast tube above accessory compartment, inches of water

h_o = open-end pressure of a blast tube above accessory compartment, inches of water

h_g = total head across the generator, inches of water

h_v = velocity head of air flowing through blast tube, inches of water

h_{vg} = velocity head of air entering generator, inches of water (equation 4)

h_{gf} = pressure head developed by an internal fan, inches of water

F_p = pressure developed by an internal fan at 1,000 rpm at sea-level air density

N = revolutions per minute

T_o = temperature of exit air, degrees centigrade

T_s = temperature of stator windings, degrees centigrade

T_a = temperature of ambient air or of air entering generator

P_1 = total watts loss carried away by cooling air

W = weight flow of cooling air, pounds per minute

ρ = specific weight of air, pounds per cubic foot

$C_1, C_2, \ldots$ = proportionality constants

β = exponent in equation 8

I_o = current rating of generator at sea-level, amperes

I_A = permissible current output (thermal basis only) at altitude, amperes

* If an internal fan is used, substitute h_{vA} and h_{vo} for h_{gA} and h_{go}, respectively.

References

1. Blast-Tube Cooling for Aircraft Generators, Cyril G. Veinott. AIEE Transactions, volume 63, 1944, July section, pages 520–5.

2. Altitude Rating of Electric Apparatus, Paul Lebenbaum, Jr. AIEE Transactions, volume 63, 1944, December section, pages 955–60.

Electrical Analogy Methods Applied to Servomechanism Problems

G. D. McCANN
MEMBER AIEE

S. W. HERWALD
NONMEMBER AIEE

H. S. KIRSCHBAUM
ASSOCIATE AIEE

Synopsis: This paper describes the application of the transient analyzer to the solution of servomechanism problems by the electrical-mechanical analogy method. The analogies for angular position servomechanisms are developed in detail together with the fundamental concepts by which the systems can be defined in terms of dimensionless parameters. This permits the results to be given in dimensionless form suitable for general application. Typical solutions of representative systems are given in the form of transient response curves. These show the response characteristics for suddenly applied constant velocity and sinusoidal motion. Also shown are the effects of varying the controlling parameters of the system including the stiffness constant, one, two, and three time delays, and methods of producing system stability including negative *RC* feedback and anticipatory control. A method is developed for setting up the analogy for a specific system on the transient analyzer by a suitable change in time and impedance bases.

WITH THE RAPID INCREASE in the use of accurate servomechanisms it has become desirable to provide a practical means of quickly and accurately analyzing in detail their performance under various operating conditions. The complexity of most servo systems makes it impractical to calculate transient response in any detail by conventional mathematical methods. Although it is usually possible to determine natural frequencies and damping rates, sufficient calculations to determine actual response for an optimum design is quite laborious and time consuming. The method of electrical analogy now has been applied to this type of system. Additional facilities in the form of special amplifier circuits have been developed to be used in conjunction with the mechanical-transients analyzer[1,2] for setting up the electrical analogue of many of the basic types of servo systems. With this equipment an analogous electric circuit is set up; the desired transient or steady-state condition to which the servo system must regulate is generated as an electrical excitation function; and the complete solution for its response is viewed or recorded on the screen of a cathode-ray oscilloscope. This paper treats the application of the transient analyzer to angular position servomechanisms, a fundamental analysis of which is given in reference 3.

Paper 46-17, recommended by the AIEE committee on instruments and measurements for presentation at the AIEE winter convention, New York, N. Y., January 21–25, 1946. Manuscript submitted November 8, 1945; made available for printing November 27, 1945.

G. D. McCann, S. W. Herwald, and H. S. Kirschbaum all are with the Westinghouse Electric Corporation, East Pittsburgh, Pa.

Electrical Analogies for Angular Position Servomechanisms

For most systems involving mechanical motion there are several practical electrical analogies.[2] Thus several completely electric circuits can be used to represent an electromechanical system. The one used here for angular position servomechanisms is illustrated in Figures 1 and 3. Figure 1 shows the case of a simple error-control system with no electric time delays. A single differential equation (equation 1) can be formed expressing the mechanical motion of the system in terms of both mechanical and electrical parameters. The inertia is represented by an inductance and the motor-generator armature circuit losses by a resistor. The analogue for the error measurer is the capacitor C_0 of Figure 1. The voltage across it is proportional to the charge that is analogous to angular displacement $\theta_1 - \theta_0$ when the circuit for simulating the motion θ_1 to be followed by the servo system is connected as shown. A wide variation in the character of the motion θ_1 can be simulated with the excitation circuits of the mechanical-transients analyzer.[2] With these a voltage is produced proportional to the assumed velocity of the device to be followed. This feeds current into C_o through a relatively high resistor, so that the voltage across C_o is negligible during the period in which the solution is obtained. The capacitor voltage (which is the error voltage) also must be very small compared to the voltages across L and R of the servo analogy so as not to distort its motion. This requires a fairly large value of capacitance for C_o. The amplifier of Figure 1 completes the analogous circuit. Its output voltage E_o is analogous to the controller torque M_c, giving the simple relationship of equation 2 (Figure 1) for the stiffness constant K.

General solutions[3] of this simple system can be expressed readily in dimensionless form as shown in Figure 2. This is of considerable value, as it greatly increases the usefulness of the solutions. As will be shown later, solutions for the more com-

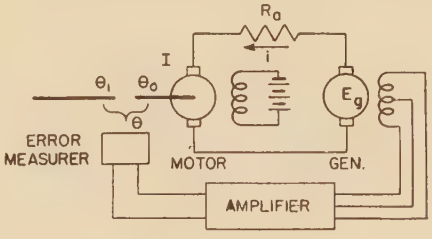

A—Mechanical system
Equation for armature circuit:

$$E_g = R_a i + g\frac{d\theta_0}{dt}$$

Equation for motor torque:

$$bi = I\frac{d^2\theta_0}{dt^2}$$

Combining in a single torque equation:

$$\frac{bE_g}{R_a} = I\frac{d^2\theta_0}{dt^2} + \frac{bg}{R_a}\frac{d\theta_0}{dt} = M_c = K(\theta_i - \theta_0) \qquad (1)$$

Figure 1. Electrical analogy used for simple error-control servomechanisms with no electric time delays

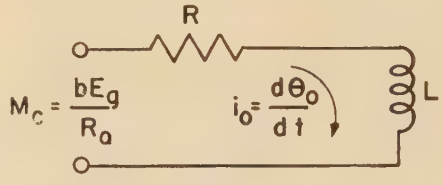

B—Analogous circuit for torque equation

$$R \equiv c = \frac{bg}{R_a}$$

$$L \equiv I$$

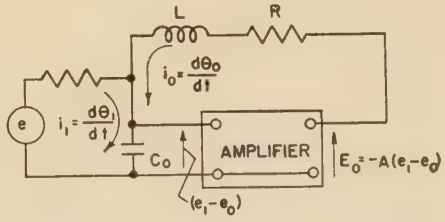

C—Complete analogous circuit

$$M_c = K(\theta_i - \theta_0) \equiv A(e_i - e_o)$$

$$(e_i - e_o) \equiv \frac{\theta_i - \theta_0}{C_0}$$

$$K = \frac{A}{C_0} \qquad (2)$$

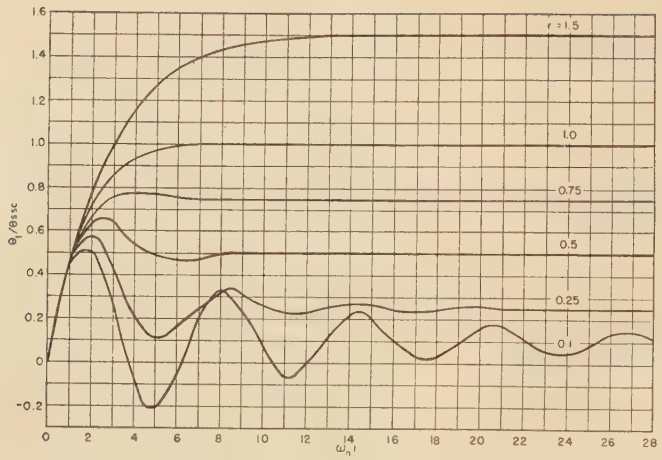

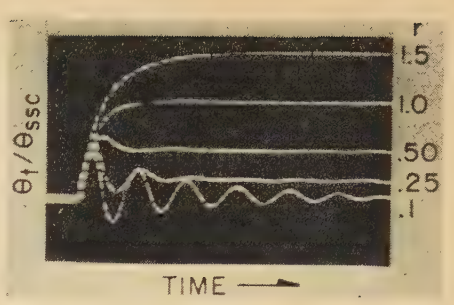

Figure 2 (left and right). Response curves of simple error servomechanisms to constant velocity

$\theta(t)$ = error angle as function of time
θ_{ssc} = steady-state error angle for critically damped systems

$$\theta_{ssc} = 2\frac{\omega_1}{\omega_n}$$

ω_1 = magnitude of applied constant velocity

$\omega_n = \sqrt{\frac{K}{I}}$ = undamped natural frequency

K = stiffness constant
I = total system inertia

$r = \frac{c}{2\sqrt{IK}}$ = ratio of actual to critical damping

c = actual damping

plex practical servomechanisms also can be put in this same dimensionless form. It is this characteristic that allows the use of a calculating board device (with a limited range of variation in its circuit constants) for the general solution of such problems. Thus for convenience in setting up a given system on the analyzer the time base and the impedance base can be changed arbitrarily to form a new system from which either the actual numerical solution for the given system or a dimensionless solution readily can be obtained. The conversion formulas for making these changes are given in Table I. These are understood readily from consideration of the equations at the bottom of the table. Since the ratios of the angular motion θ to the system torques are reduced by the factor a in the simulated system, its stiffness constant K'' must be greater than the actual stiffness K by the same ratio. The application of this table to the solution of an actual problem will be illustrated later.

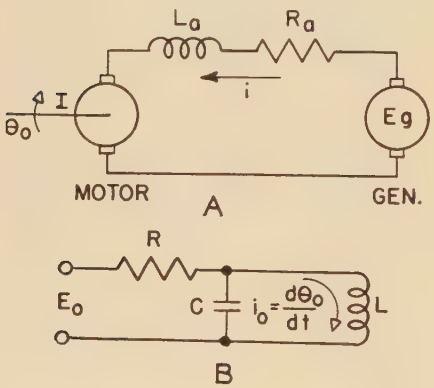

a. Representation of armature circuit inductance

A—Mechanical system
B—Analogous all-electric circuit

$$E_g = R_a i + L_a\frac{di}{dt} + g\frac{d\theta_0}{dt}$$

$$bi = I\frac{d^2\theta_0}{dt^2}$$

giving

$$M_c = \frac{bE_g}{Ra} = \frac{L_a I}{Ra}\frac{d^3\theta_0}{dt^3} + I\frac{d^2\theta_0}{dt^2} + \frac{bg}{Ra}\frac{d\theta_0}{dt}$$

Electric circuit equation:

$$E_0 = RCL\frac{d^2 i_0}{dt^2} + L\frac{di_0}{dt} + Ri_0$$

where, $R \equiv \frac{bg}{Ra}$, $L \equiv I$, $C \equiv \frac{La}{bg} \equiv \frac{T_1}{R}$

Effect of Additional Time Delays

The analogous circuit for cases where the motor generator armature circuit inductance is taken into account is developed in Figure 3a. This inductance has its analogy in a capacitance C_1, resulting in an RC time delay T_1. Other time delays, such as that in the generator field, can be represented by RC circuits placed between stages of the amplifier as shown in Figure 3b. It is necessary, however, that each delay circuit be isolated by a stage of amplification. Such time constants must be changed, when the time base is changed, as shown in Table I. When defining them for a general solution in dimensionless form they must be multiplied by ω_n.

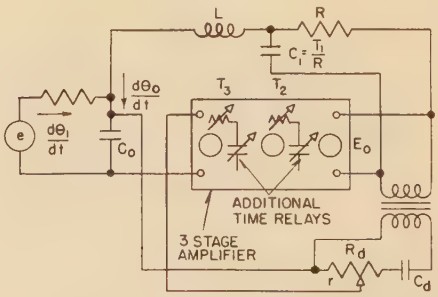

b. Analogous circuits for time delays and negative RC feedback

Equation for feedback voltage:

$$e_d = \frac{-rC_d p}{(1+pt_1)}(E_0 \equiv M_c)$$

$$p = \frac{d}{dt},\ t_1 = R_d C_d,\ n = \frac{r}{R_d}$$

$$e_d = \frac{-npt_1}{(1+pt_1)}(E_0 \equiv M_c)$$

Figure 3. Electrical analogies used for various elements of angular position servomechanisms

Stabilization With RC Feedback

For servomechanisms of this type system stability frequently is obtained by

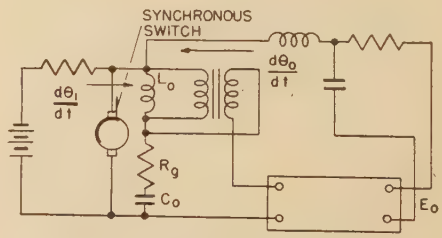

c. Analogous circuit for error-plus-error rates control

For actual system:

$$M_c = K(\theta_1 - \theta_0) + KT_a p(\theta_1 - \theta_0) + K(T_L)^2 p^2(\theta_1 - \theta_0)$$

In analogous circuit:

$$E_0 \propto M_c$$

$$E_0 = \frac{A}{C_0}(\theta_1 - \theta_0) + AR_g p(\theta_1 - \theta_0) + AL_0 p^2(\theta_1 - \theta_0)$$

$$K = \frac{A}{C_0},\ T_a = \frac{AR_g}{K},\ (T_L)^2 = \frac{AL_0}{K}$$

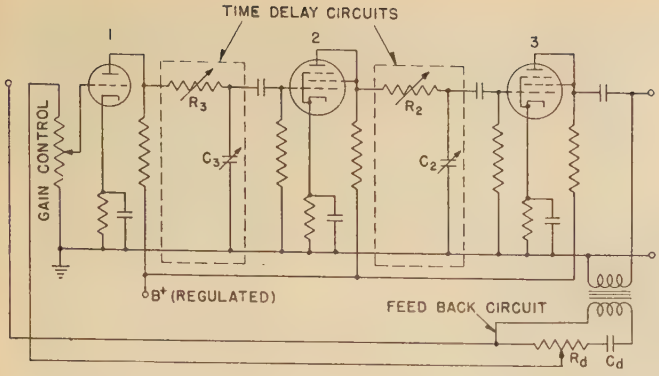

Figure 4. Circuit elements of amplifier used for servomechanism analogies

using a resistance-capacitor network connected across some voltage that is proportional to the controller torque M_c. The equation for the feed-back voltage from this type of circuit is shown in Figure 3b. It is put in general form by expressing it in terms of a dimensionless ratio n and a time constant t_1. For dimensionless solutions t_1 must be multiplied by ω_n.

Error-Plus-Error Rates Control

Other forms of system stability consist of providing an additional control torque term proportional to the first derivative of the error angle $\theta_1-\theta_0$ and possibly a negative term proportional to the second derivative of the error angle. The forms for these control functions together with their electrical analogy are given in Figure 3c. These functions are expressed in terms of the stiffness constant K and time constants, so that they can be defined readily in dimensionless form. In actual systems the control term proportional to the rate of change of the error angle (commonly called anticipatory control) usually must be produced by a mechanism having its own time delays. This is sometimes a gyroscopic mechanism. The method of representing these additional terms is shown in an example to be discussed later (see Figure 11).

Description of the Servomechanism Analyzer

Suitable amplifiers and associated circuits have been developed to be used in conjunction with the mechanical-transients analyzer to provide facilities for the rapid analysis of such servomechanisms as have been described above. The amplifier, typical elements of which are illustrated in Figure 4, is of the conventional resistance coupled type, designed to have a frequency response that is flat down to 10 cycles per second, that being the frequency at which the transient forcing functions usually are repeated on the analyzer.[1,2] This response is achieved by using large coupling and by-pass capacitors and by using a regulated power supply which prevents regeneration at low frequencies. Although the amplifiers must be linear, the added complication involved in using push-pull resistance coupled amplifiers was not justified, and single-ended triode amplifiers were found to be satisfactory. The maximum harmonic distortion in the last stage is about 5 per cent; the distortion in the previous stages is entirely negligible. Power amplifiers are used for all but the first stage, so that various damping and time delay circuits connected to the outputs of the various stages do not affect the amplification.

Time delay, such as that arising from the field of an exciter, is represented by a circuit such as R_2, C_2 of Figure 4. The voltage developed at the grid of the third tube will lag behind the plate voltage of the second tube in exactly the same way that an exciter armature voltage will lag behind the voltage applied to its field terminals. The time constant which describes this delay is R_2C_2 in seconds. Additional time delays can be introduced as shown at the input to the second stage. Resistance-capacitance feed-back damping voltages from the amplifier output are fed back to the input by using an isolating transformer. This transformer has very good frequency response down to 10 cycles per second, thus reproducing accurately the voltage which appears at the output of the amplifier. These transformers also may be used as damping transformers when simulating voltage regulating systems.[4] Flexibility in the general application of the amplifier is obtained by making the amplifier stages, the time delay circuits, the isolating transformers, and the RC feed-back circuit each a separate entity.

Figure 5 shows the laboratory equipment. To the right are the synchronous switches which repeat the transient 10 times per second. Next to the switches is the central control desk from which the operator can measure on the oscilloscopes any voltage across or any current flowing in the various circuit elements. This desk also contains generators for producing various types of arbitrary forcing functions. To the left is the servomechanism analyzer cabinet, which contains the amplifiers and associated circuits described in the accompanying paragraph. Low-loss inductances and capacitors for representing mechanical systems are contained in the cabinets arranged behind the control desk and servomechanism analyzer cabinet.

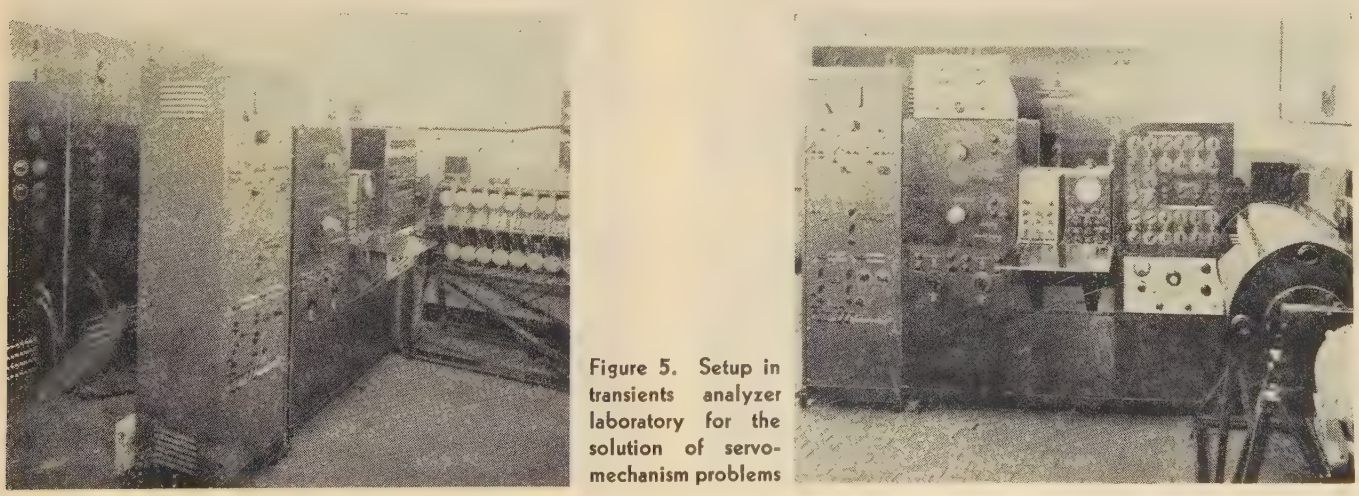

Figure 5. Setup in transients analyzer laboratory for the solution of servomechanism problems

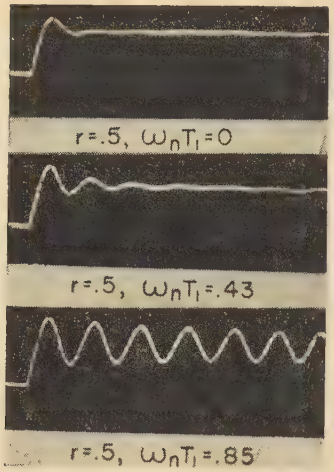

Figure 6. Response curves of error servomechanism, with one time delay, to constant velocity

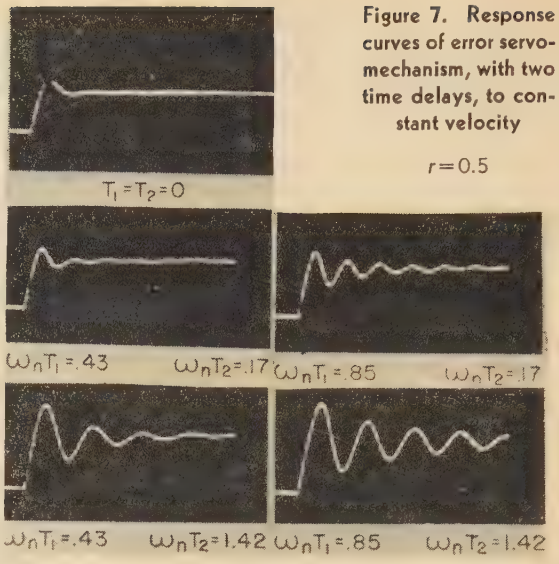

Figure 7. Response curves of error servomechanism, with two time delays, to constant velocity

$r=0.5$

Typical Solutions

In Figure 2 oscillograms are shown of general solutions for the response of the simple error control system to a constant velocity for comparison with calculated curves. The value of this method of analogy can be appreciated when it is considered that such a set of oscillograms can be obtained in a matter of minutes. Figures 6, 7, and 8 show the effect of time delays on the response of the typical angular position servomechanism to a suddenly applied constant velocity. Figure 6 shows the effect of varying the magnitude of a single time delay. The magnitudes of the time delays are given in the dimensionless form, $\omega_n T$, so that the results have general application. The results with $\omega_n T_1$ constant and a second time delay, $\omega_n T_2$, varied are given in Figure 7. Similarly, Figure 8 shows the effect of varying $\omega_n T_3$ with $\omega_n T_1$ and $\omega_n T_2$ constant. In a practical case the three time delays could represent armature, generator field, and exciter field time delays, respectively. The range of parameters used represents practical control systems.

Obtaining system stability by negative *RC* feedback is probably the most common method in use today. Figure 9 shows two cases of stability obtained by negative *RC* feedback. The time constant of the *RC* circuit, $\omega_n t_1$, as well as the system damping and time delays, all are given in dimensionless form. The large initial overshoot and the considerable reduction in system frequency which is always characteristic of negative *RC* feedback is quite apparent in each of the two examples shown in Figure 9. The *RC* time constants are large, when compared with the system time delays, and are in the optimum range for best results.

The response of any servomechanism to a sinusoidal forcing function is usually of great interest in design. Figure 10 shows the response of an angular position servomechanism to a suddenly applied sinusoidal motion of varying frequency, ω_1.

Figure 8. Response curves of error servomechanism with three time delays, to constant velocity

$r=0.5$

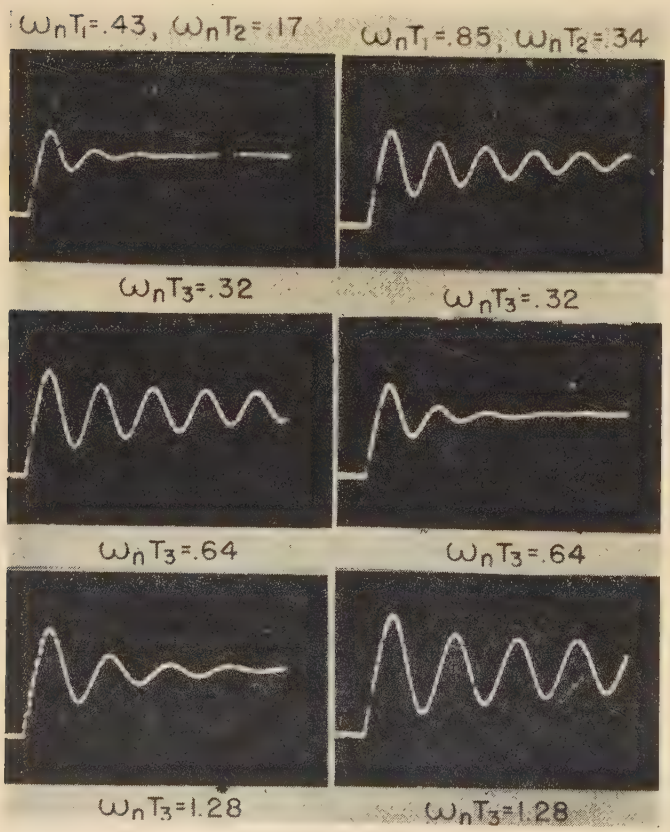

Figure 9. Response curves of error plus negative *RC* feedback servomechanism with two time delays to constant velocity

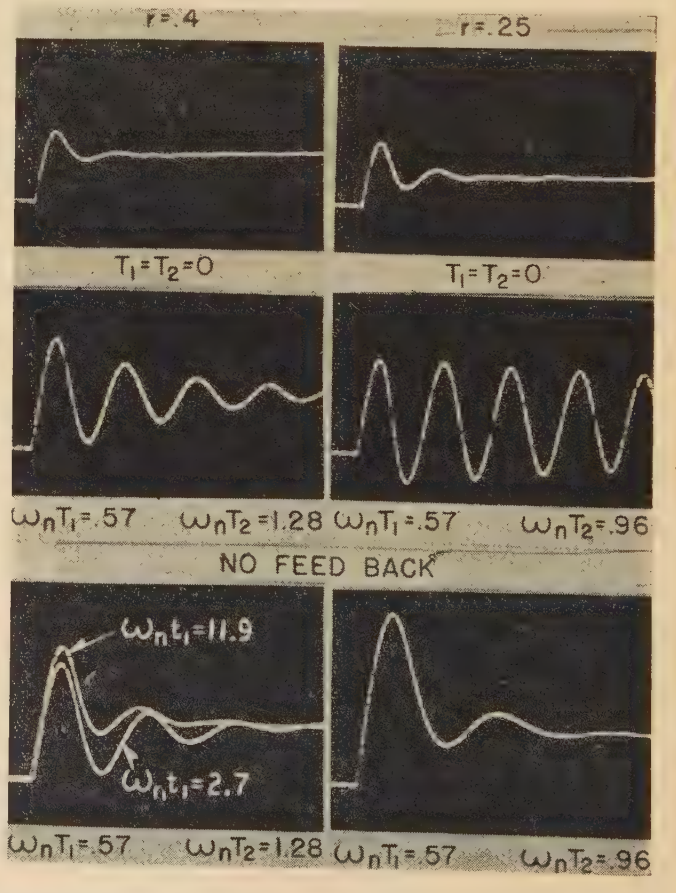

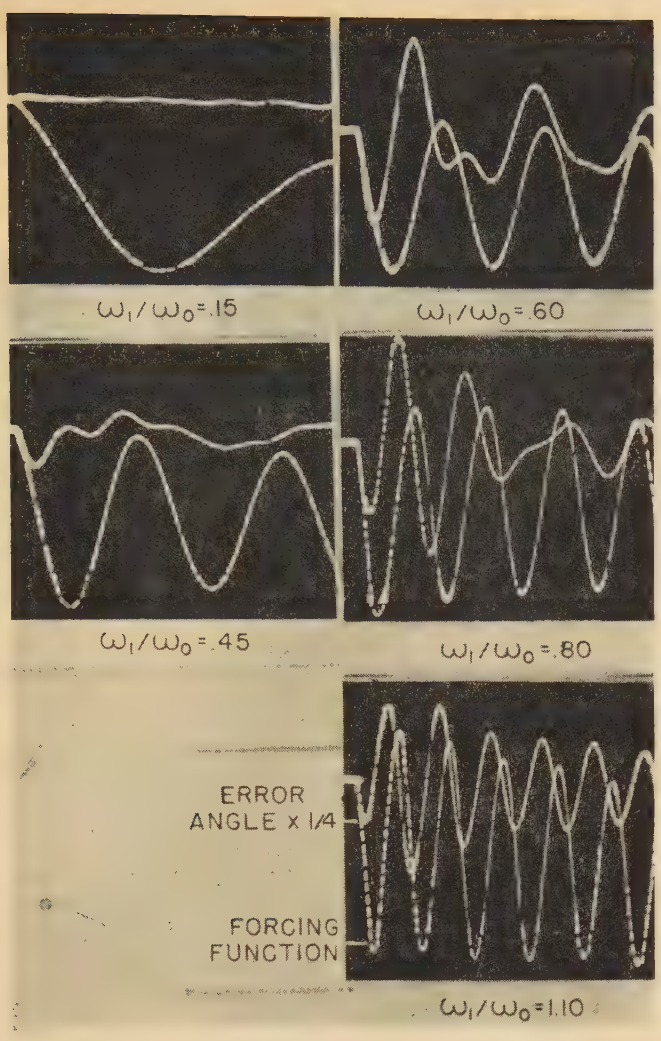

Figure 10. Response curves of error servomechanism to sinusoidal motion

r=0.17

The response at frequencies well below the system frequency, ω_0 is quite good with hardly any error appearing. However, as the frequency is increased, the response becomes poorer with large following errors. When ω_1 is very close to ω_0, such as the case $\omega_1/\omega_0 = 1.10$, the error actually becomes larger than the applied disturbance θ_1. The steady-state response to sinusoidal motion also can be obtained quite easily when an oscillator is used as the excitation function for θ_1.

Tank Turret Traverse Servo System

The following example serves to further illustrate the application of the electrical analogies and the conversion formula of Table I to the solution of a specific system. This problem is that of an electric drive that had been designed for the traverse movement of a tank turret.[5] The schematic of the mechanical system, its equation of motion, the analogous electric circuit, and the units for both the actual system and the electrical analogy are given in Figure 11a. The gyroscope in the actual system serves as the means for obtaining system stability. If the gyroscope is rotated proportional to $\theta = (\theta_1 - \theta_0)$ and is also capable of restrained rotation about an axis 90 degrees from the θ axis; any point of the gyroscope not on either axis has a motion proportional to $\theta + p\theta$. This motion is used to operate a silverstat in the generator field circuit. This is anticipating control and is a phase advance that tends to compensate for the system time delays. The rate component of gyroscope movement is caused by the gyroscope torque, exerted about the 90-degree axis, that is proportional to the speed of rotation about the θ axis. There is spring restraint, inertia, and critical damping about the 90-degree axis, so that instead of a rotation instantaneously proportional to $p\theta$ (as shown in Figure 3b) it is delayed and appears as the term

$$\frac{KT_a p(\theta_1 - \theta_0)}{(1+t_1 p)^2}$$

of the mechanical system equation shown in Figure 11a. T_a is the ratio of torque per unit velocity error, $p\theta$, to torque per unit displacement error, θ.

With the constants shown in Figure 11a, the calculated turret frequency was 1.4 cycles per second and the damping decay 78.1 per cent per cycle.[5] The oscilloscope record of Figure 11b with delayed anticipation represents the same calculation and checks to within 5 per cent or better. The remaining oscillographs of Figure 11b show the system as it would hunt without any means of obtaining system stability; what could be done with negative RC feedback, with undelayed anticipation, and what could be done by a combination of negative RC feedback and delayed anticipation. The two disadvantages of negative RC feedback compared with anticipating control are quite apparent in Figure 11b. The initial overshoot is much greater, and the system frequency has been considerably reduced. The combination of anticipation and some RC feedback gives the best response for this particular example. It is to be noted, however, that the improvement over anticipation alone is not too

Table I. Conversion Formula for Changing Time and Impedance Bases in Setting Up Analogy for Servomechanisms

Actual System	Time Base Changed to $t' = t/n$	Impedances Multiplied by Constant a
L (henrys) $= I$ (pounds-inch-seconds^2)	$L' = L/n^2$	$L'' = aL/n$
R (ohms) $= c = \frac{bg}{R_a}$ (inch-pounds/radians per second)	$R' = R/n$	$R'' = aR/n$
E_0 (volts) M_c (inch-pounds)	$E_0' = E_0$	$E_0'' = E_0$
i_1, i_0 (amperes) $\alpha \frac{d}{dt}(\theta_1, \theta_0)$ radians per second	$\theta' = \theta$	$\theta'' = \theta/a$
$\omega_n = 2\pi \times$ undamped natural frequency	$\omega_n' = n\omega_n$	$\omega_n'' = n\omega_n$
$K = \omega_n^2 I$	$K' = K$	$K'' = aK''$
$K = M_c/(\theta_1 - \theta_0)$	in analogous electric circuit	$K'' = A/C_0$
Time delays T (seconds)	$T' = T/n$	$T'' = T/n$

Equation for simple error servomechanism: $M_c = K(\theta_1 - \theta_0) = \frac{bEg}{R_a} = L\frac{d^2\theta_0}{dt^2} + R\frac{d\theta_0}{dt}$

Transformation to time base $t' = t/n$: $Mc' = L/n^2 \frac{d^2\theta_0'}{dt'^2} + \frac{R}{n}\frac{d\theta_0'}{dt'}$

Multiplying impedances by a: $Mc'' = \frac{aL}{n^2}\frac{d^2\theta_0''}{dt''^2} + \frac{aR}{n}\frac{d\theta_0''}{dt''}$

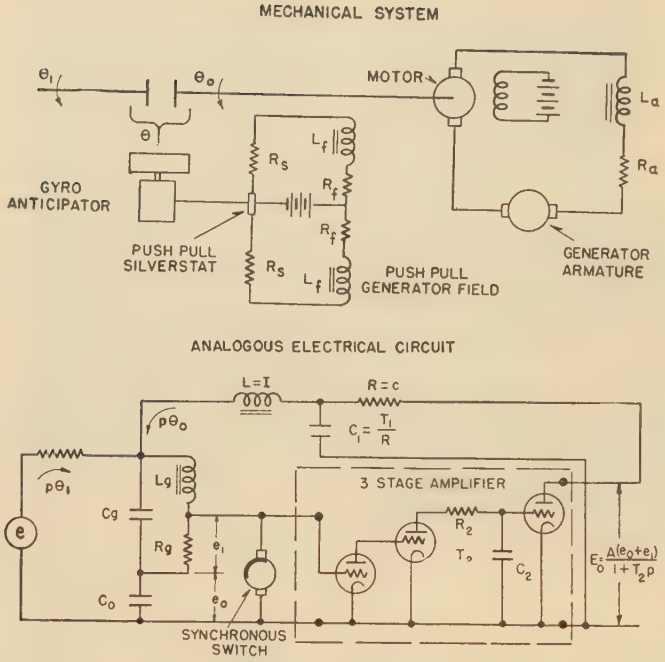

11a. Analogous circuit and system constants

Equation for mechanical system:

$$Ip^2\theta_0+\frac{cp\theta_0}{1+T_1p}=\frac{K\left(1+\frac{T_ap}{(1+t_1p)^2}\right)\theta}{(1+T_1p)(1+T_2p)}$$

Units

Actual mechanical system:

$I=7.78\times10^{-2}$ pound-inch seconds^2
$c=0.33$ inch-pound per radian per second
$T_1=0.02$ second
$T_2=0.1$ second
$K=4$ inch-pounds per radian
$T_a=0.15$ second
$t_1=0.01$ second

Converted electric system with $n=200$ and $a=3.1\times10^6$

$$L''=\frac{aI}{n^2}=6.02 \text{ henrys}$$

$$R''=\frac{ac}{n}=5{,}130 \text{ ohms}$$

$$T_1''=\frac{T_1}{n}=10^{-4} \text{ seconds}$$

$$T_2''=\frac{T_2}{n}=5\times10^{-4} \text{ seconds}$$

$$K''=aK=12.2\times10^6$$
$$C_0''=14\times10^{-6} \text{ farads}$$
$$A''=K''C_0=171$$

$$T_a''=T_a/n=7.5\times10^{-1}$$

$$R_1''=\frac{K''T_a''}{A''}=54 \text{ ohms}$$

$$t_1''=t_1/n=5\times10^{-5} \text{ seconds}$$

$$C_1''=\frac{2t_1''}{R}=1.86\times10^{-6} \text{ farads}$$

$$L_1''=\frac{R_1''t_1''}{2}=1.35\times10^{-3} \text{ henrys}$$

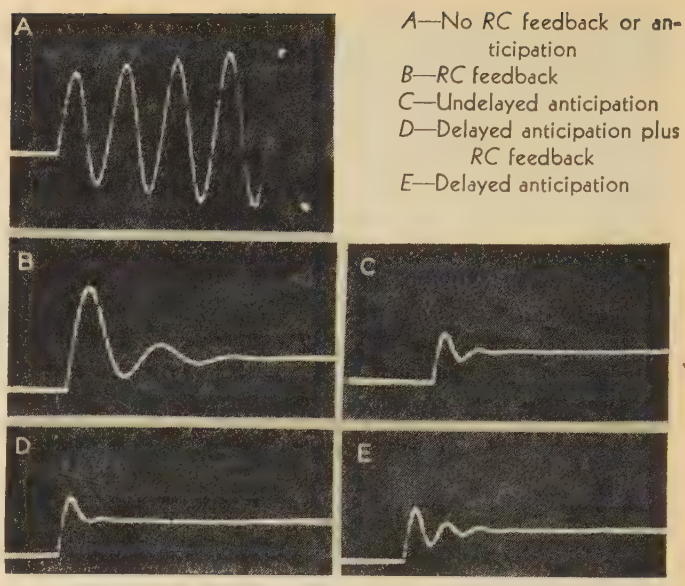

A—No *RC* feedback or anticipation
B—*RC* feedback
C—Undelayed anticipation
D—Delayed anticipation plus *RC* feedback
E—Delayed anticipation

11b. Response curves to constant velocity

Figure 11 (left and above). Tank turret traverse servomechanism

great and would not warrant the use of much extra equipment.

Conclusions

From the examples shown it can be seen that the transients analyzer offers an excellent method for solving fundamental servomechanism problems. The ease with which the response of systems involving high order differential equations can be obtained points the way toward many useful solutions not only of particular systems but also in dimensionless form for general application. The accuracy of the method has been demonstrated by close checks with previously calculated cases. It therefore provides a reliable and practical method for the general analysis of certain basic types of servomechanisms and of specific systems too complex for adequate study by conventional mathematics.

References

1. System Recovery Voltage Determination by Analytical and A-C Calculating Board Methods, **R. D. Evans, A. C. Monteith.** AIEE Transactions, volume 56, 1937, June section, pages 695–705.

2. A New Device for the Solution of Transient Vibration Problems by the Method of Electrical-Mechanical Analogy, **H. E. Criner, G. D. McCann, C. E. Warren.** *Journal of Applied Mechanics*, September 1945, volume 12, number 3, page 135.

3. Considerations in Servomechanism Design, **S. W. Herwald.** AIEE Transactions, volume 63, 1944, December section, pages 871–6.

4. Recent Developments in Generator Voltage Regulation, **C. R. Hanna, K. A. Oplinger, C. E. Valentine.** AIEE Transactions, volume 59, 1940, pages 692–700.

5. Electric Turret Traversing Mechanism for the M-4 Tank, **S. J. Mikina, Jr.** *Applied Mechanics*, December 1945, page 334.

Investigation of Arc Starting Characteristics of D-C Welders With Reference to Electrode Freezing

JOSEPH M. TYRNER
ASSOCIATE AIEE

Synopsis: A method for investigating the starting characteristics of an arc in d-c arc welding was developed and equipment was designed and built to simulate the behavior of an operator in starting such an arc. This testing equipment was used to compare the arc striking ability and the arc freezing tendency of an electrode when used with various types of welding generators. It was found that the determining factor is the electrode contact duration, that is, the time during which the operator leaves electrode and work in contact when he attempts to start an arc. Generators, to be satisfactory, should permit at least 40 milliseconds contact duration. Where the permissible contact duration between work and electrode is less than 40 milliseconds, only experienced welders are able to start an arc. Less trained men freeze the electrode to the work piece in a large percentage of their attempts. Five generators of different design were tested with the apparatus. Oscillograms of the current surge during the contact period were taken and the freezing point marked on the curves. It was found that the location of the freezing point depends on the shape of the current surge. Characteristics of a welding generator as developed in these tests which yield good striking and nonfreezing results are not contradictory to good general welding characteristics.

SUCCESS IN STARTING an arc using power from a d-c welding generator does not depend on the electric circuit alone, but also to a great extent on the skill of the operator. An experienced man has fewer failures than an untrained one. If we want to design an apparatus with something like "adjustable operator skill" we have to analyze the skill of a welder. We find that operators when striking an arc may differ in the contact pressure they exert, and also in the time they leave the electrode in contact with the work.

As far as the contact pressure is concerned, it is reasonable to assume that every operator tries to keep the contact pressure as low as possible in order to avoid freezing.

On the other hand, the aptitude of the man determines the duration of the contact between electrode and work piece. Therefore, it seems justified to accept this contact duration as the predominant characteristic of his skill.

With the foregoing in view, an apparatus was built which makes contact between the electrode and work for an adjustable and measurable duration. Figures 1 to 3 show various views of the apparatus. Figure 4 is a diagrammatic picture of it.

The apparatus consists of three parts as shown in Figure 4 numbered 1, 2, and 3. These three parts may move independently around the common axis *A–A*. Part 1 is a pendulum, on the upper extension of which an adjustable bracket (5) together with a chuck (6) is provided. The test electrode (7) is clamped in this chuck (6). The pendulum is kept in a raised position as long as the electromagnet (8) is excited to hold the armature (9). If the circuit of the coil (10) is opened, the magnet (8) releases the armature and the pendulum is free to swing.

Part 2 is the support of the work piece (11), which is used for the freezing test with the electrode (7). The weight (12) on part 2 tends to turn it counterclockwise, but part 2 is held in approximately horizontal position by the bracket (13), which rests on part 3.

The position of part 3 may be adjusted by the stop (15), against which it is held by the weight (14). In this way, the stop (15) establishes not only the position of part 3, but by means of the bracket (13), the position of part 2 as well.

When the pendulum (1) swings in a clockwise direction, the electrode (7) eventually reaches the test piece (11) and makes contact. The impact of the electrode (7), striking against the test piece (11), moves part 2 clockwise, lifting the bracket (13) from part 2. Electrode and test piece stay in contact until, on the return swing, the bracket (13) touches part 3 again. This stops part 2 and electrode and test piece become separated. In this way, the position of part 3, adjusted by the stop (15), determines the length of the contact duration. If the electrode (7) freezes to the test piece (11), the support (2) must follow, even after the bracket (13) reaches part 3. In this case, part 3 is pushed from the stop (15) and the weight (14) is lifted.

It is obvious that one weight (12) controls the contact pressure of electrode and test piece while the force which tends to separate electrode and test piece is determined by the other weight (14).

Contact pressure and breakaway force were not varied during the experiments. They were adjusted to conditions comparable to actual welding as performed by an experienced operator.

The contact duration is measured by the cycle counter (16). If the switch is in its "up" position, an a-c circuit through the cycle counter is closed as long as electrode and test piece are in contact. Swings of the pendulum with the switch in its upper position are used to adjust the contact time by setting the stop (15). The operator is protected from electric shock by the limit switch (18), which keeps the alternating voltage from the electrode-test piece gap, as long as the pendulum is held by the electromagnet (8).

The actual freezing test is made by putting one switch (17) into its down position. This removes the alternating voltage from the electrode-test piece gap and applies it to the holding coil (19) of contactor (20), which connects the genera-

Paper 46-12, recommended by the AIEE committee on electric welding for presentation at the AIEE winter convention, New York, N. Y., January 21–25, 1946. Manuscript submitted September 13, 1945; made available for printing December 11, 1945.

JOSEPH M. TYRNER is in the apparatus research department, Air Reduction Sales Company, New York, N. Y.

The author acknowledges and appreciates the cooperation given by J. J. Crowe, assistant vice-president, and E. E. Tisza of the apparatus research department, and the assistance of E. H. Cushman who built the apparatus and ran the tests covered by this paper. Acknowledgment is made also of the encouragement given to the investigation by C. I. MacGuffie, R. F. Wyer, and R. C. Freeman.

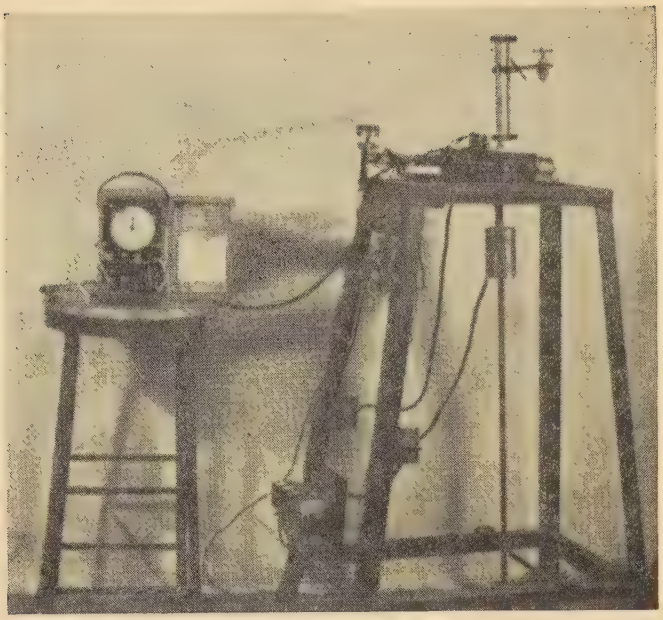

Figure 1. Apparatus with cycle counter

tor being investigated to the apparatus. Another switch (18), in this case, prevents energization of the coil as long as the pendulum is held by the solenoid. Thus, the operator is protected against an accidental flash. The circuit of the holding coil contains a second limit switch (25), which is opened by the movement of part 3 in case of freezing. This terminates the flow of welding current through the short circuit of electrode and test piece. If the electrode does not freeze, the lengthening of the arc drawn by the electrode breaks the circuit automatically and no switch is necessary.

Tests are initiated with the push button (24) which breaks the circuit of the coil (10) of the electromagnet (8).

The coil (10) of the electromagnet (8) is energized by direct current from the welding generator. It was found that the slight vibrations caused by an a-c magnet at that place falsify the test results.

The contact duration during the freezing test can be checked by taking an oscillogram as shown in Figure 5.

Procedure of Test

The operator clamps an electrode in the chuck (6) and provides a proper test piece (11). He adjusts the electrode roughly by moving the sleeve of the bracket (5) on the pendulum. The switch (17) is put into its "up" position. The button (24) is pressed and the pendulum released. The contact time is observed on the cycle counter. Then the stop (15) is adjusted to bring the contact time nearer to the desired value and the test repeated. After several trials, the apparatus is ready for test. To increase accuracy three timing swings are made without resetting the counter to zero. The reading thus becomes the sum of three contact times and one third of this value is considered to be the average contact time for the actual striking test. After the apparatus is adjusted to the desired contact time, switch (17) is put into its "down" position for the application of welding power. The next swing produces either a flash or the electrode freezes to the test piece.

A series of tests for different contact durations is run with a fairly large number of tests for each setting. For each setting, a number of freezings and a number of flashes are obtained. The frequency of freezings is calculated and plotted as a function of the contact duration. A curve thus is obtained which moves from a low percentage of freezings, at short durations, to a high percentage at long durations. The change from the low percentage to the high percentage is sudden. The contact duration yielding an equal number of freezings and flashes is called arbitrarily the "freezing time" of the generator.

Influence of Circuit Setting, Electrode Size, and Electrode Coating

It can be shown theoretically that the curve of the surge does not change much with different current settings. Therefore, the freezing time also does not change. The electrode size has no influence because the contact in the testing apparatus is a point contact only, and it

Figure 2. Front view of apparatus

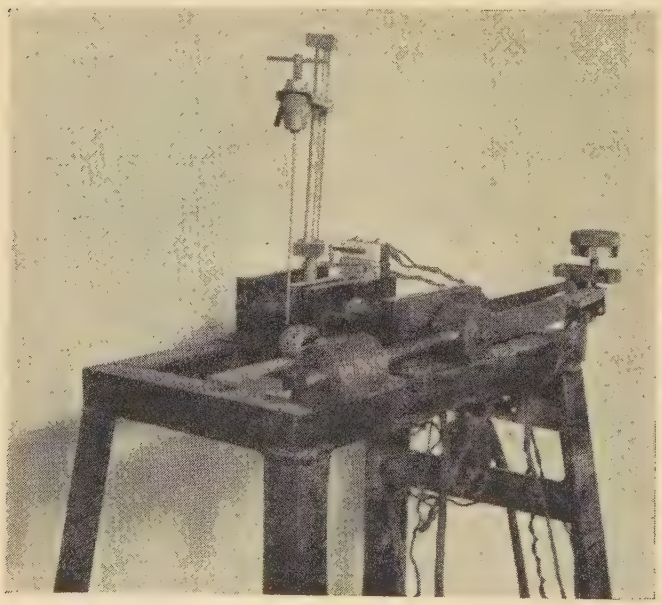

Figure 3. Rear view of apparatus

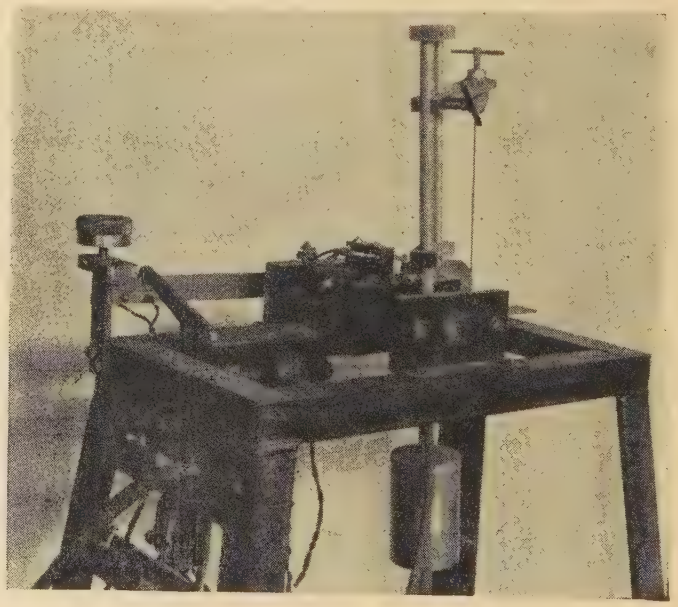

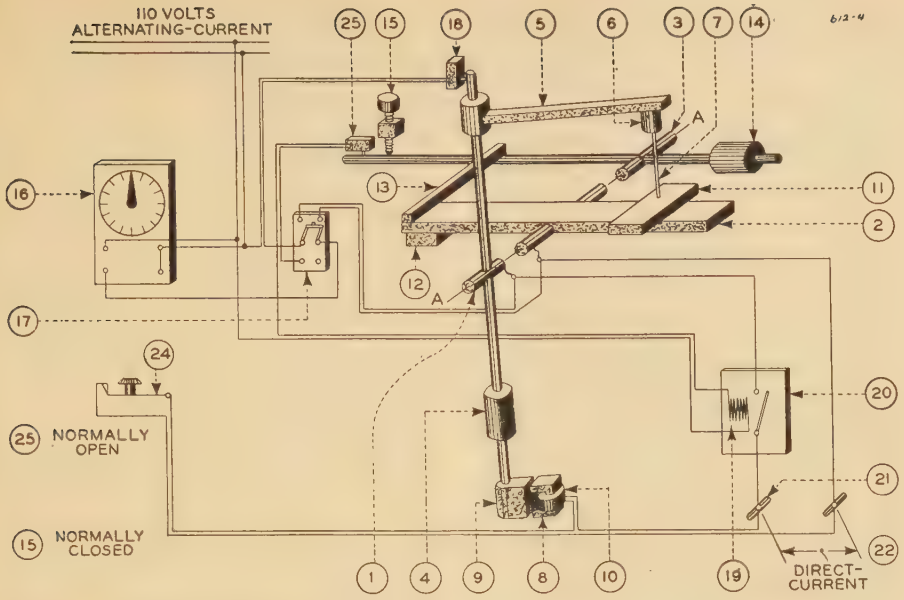

Figure 4. Diagrammatic picture of apparatus

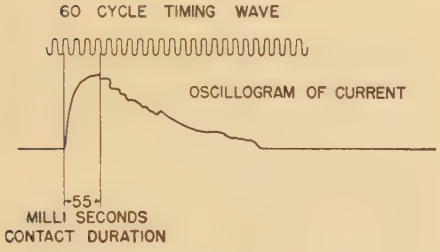

Figure 5. Oscillogram of current

does not matter whether the contact-making point is on a 1/16-inch diameter or on a 1/8-inch diameter electrode.

The coating has no influence provided the coating is kept away from the point of contact.

Consequently, it was decided to make all tests with bare electrodes of 3/32-inch diameter with generator settings of about 70 amperes welding current.

A few tests were made with other settings and with electrodes of other sizes and with different coatings. They confirmed these conclusions.

In order to eliminate the influence of scale, electrodes were ground square and test pieces cleaned thoroughly.

Generator Tests

Four commercial and one experimental generator with different circuits, but all of the same rating, were tested. All generators were set for the same welding output. The test results are shown in Table I.

Table I

Generator Tested	Critical Contact Time in Milliseconds
A	70
B	40
C (Generator *B* without external reactor)	25
D	50
E (Experimental)	1,000

In order to correlate these tests with the properties of the different electric circuits, open circuit short circuit transients of the five generators were determined by taking oscillograms. The freezing times are marked on the current curves shown in Figure 6. These curves show that freezing occurs some time after the highest point of the surge. The explanation may be that, during the decline of the surge, not enough heat is furnished to keep in a molten state the metal which melted at the height of the surge. The conclusion would be that the generator should reach its maximum current as late as possible. This is corroborated by the curve of generator *E* which approaches the maximum short circuit extremely slowly. Tests show that this generator practically never freezes.

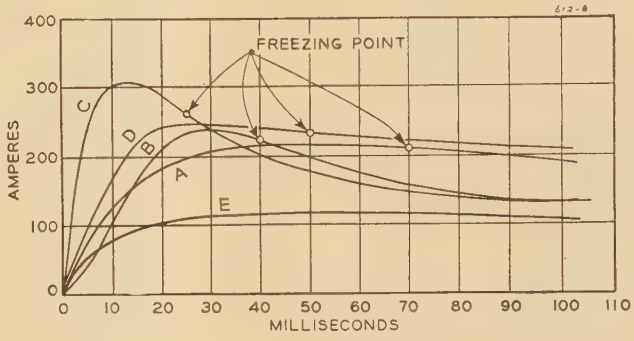

Figure 6. Threshold values of contact time

Freezing of electrodes

Operator Requirements

The requirements of the operator were determined by watching the reaction of different men to the generators which had been tested.

It was found that the average operator is satisfied with a generator which does not freeze during the first 40 milliseconds. Generators with contact times as long as 70 milliseconds are very good. Everything beyond that is excellent.

Simplified Tests

An apparatus of the kind described here usually is not available and it would be advantageous to be able to use standard equipment to judge a generator for its starting properties. Fortunately, an oscillogram of an open circuit short circuit test yields sufficient information. The curves of Figure 6 show that the critical time is approximately twice the time the generator needs to reach the crest of the surge. If we accept this without trying to find any reason for it, we may say that a generator should take at least 20 milliseconds to reach the crest of the surge. If it takes less, the generator is difficult to handle. On the other hand, a longer time indicates a generator with improved starting properties.

Stress Measurement by Electrical Means

ROBERT E. KERN
ASSOCIATE AIEE

SIDNEY B. WILLIAMS
ASSOCIATE AIEE

THE ADVENT of electric strain gauges[1] suitable for the measurement of mechanical performance on a strength basis not only has widened the field of the electrical engineer with regard to equipment and techniques but gradually has imposed upon him a responsibility to the aeronautical or mechanical engineer in his role as interpreter. For if the designer turns to electric strain gauges (and by this is meant herein the bonded wire gauge,[2] unless otherwise stated) for verification of his work, it is only natural for him eventually to leave the whole problem of gauge operation and data analysis to the electrical engineer. It is essential that both the man who measures and the man to whom the measurements are reported clearly understand the scope of their separate responsibilities. Otherwise there may exist a gap which will destroy the accuracy necessary to the honest affirmation or negation of the design. Accordingly, the authors here endeavor to present the strength evaluation problem broadly enough for one working in a relatively narrow element of it to appreciate the requirements of the whole, while emphasizing the electrical aspects primarily and keeping always in sharp focus the prime requisite, accuracy.

The Mechanical Problem

Design

As Sir Charles Darwin explained in his illuminating James Forrest lecture[3] entitled "The Extreme Properties of Matter" there is more opportunity for improvement in the strength of materials than in the refinement of almost any other property of materials. The theoretical ultimate shear strength of steel as given by Darwin is the shear modulus of elasticity divided by 2π. Depending on the grade of steel, this represents a possible improvement of 10 to 50 times, which values well might be assumed to be applicable to steel strength in general. These are figures to conjure with, but their ultimate realization probably will stand for years as the goal of physicists and metallurgists. A more realizable goal is the safe reduction of safety factors—or ignorance factors—relating the actual strength to the necessary strength. These are smaller in magnitude than the figures just quoted, lying perhaps in the range of 2 to 20, but represent possible weight and dimension savings in every industry large enough to guarantee a broad and lasting activity in strength analysis and strength measurement.

This, then, is the beginning of the problem. The optimum design stems from an accurate knowledge of the loads to be imposed. The quiescent and dynamic loads, their interrelation, the expected life and the relative importance of an occasional failure, make this problem complex. And it is complicated many-fold by that imponderable, the proper theory of failure.[4] Suffice it to say that there exist at least five theories of failure, but most test data have been reported and analyzed in terms of stress, rather than strain, energy, or other parameters. As most loading in combined stress studies appears to have been performed in terms of stress, it is reasonable to evaluate strength in terms of stress. The available literature tends to indicate that there is not enough evidence to substantiate any one general theory of failure, although certain theories appear to be more applicable than others depending upon the particular materials and loading encountered. The designer's problems, then, are the first source of error, and it is the designer's responsibility to the measurer to acquaint the latter with enough of the theory so that the proper measurements can be made. This may be as simple as a statement to the effect that the results are to be reported in terms of stress, or of strain. The nature of the available types of measurement is such that it often is not possible to correct data from one type to another after the gauge installation has been made.

Stress–Strain Relations for Plane Stress

The relations existing between the three mutually orthogonal stresses σ_x, σ_y and σ_z in the x, y, and z directions respectively and the three corresponding strains ϵ_x, ϵ_y, and ϵ_z may be found in many texts.[5] For any work involving surface measurements, however, σ_z (the stress normal to the surface) is zero, whereupon the plane stress equations on the surface may be reduced[6] to

$$\left(\sigma_x-\frac{\sigma_p+\sigma_q}{2}\right)^2+\tau_{xy}^2=\left(\frac{\sigma_p-\sigma_q}{2}\right)^2 \qquad (1)$$

where

σ_x = normal stress on x plane (in x direction)
σ_y = normal stress on y plane (in y direction) (this does not occur in the foregoing equation but represents a normal stress acting perpendicularly to σ_x)
σ_p = maximum principal stress
σ_q = minimum principal stress
τ_{xy} = shearing stress on x plane (in y direction)

Correspondingly, the strain equations for plane stress may be used to derive a similar equation:

$$\left(\epsilon_x-\frac{\epsilon_p+\epsilon_q}{2}\right)^2+\left(\frac{\gamma_{xy}}{2}\right)^2=\left(\frac{\epsilon_p-\epsilon_q}{2}\right)^2 \qquad (2)$$

where

ϵ_x = normal strain on x plane (in x direction)
ϵ_y = normal strain on y plane (in y direction) This bears the same relation to ϵ_x as σ_y does to σ_x. See equation 1
ϵ_p = maximum principal strain
ϵ_q = minimum principal strain
γ_{xy} = shearing strain on x plane (in y direction)

It will be appreciated that equation 1 and equation 2 both define circles, and it will be observed that each circle equation is of the form

$$(x-h)^2+y^2=r^2 \qquad (3)$$

where h represents the circle center and r the circle radius. Constructing these two circles, known as the Mohr circles of stress and of strain respectively, will show why individual stress measurements cannot be converted directly to strain measurements, unless enough data (three stress or three strain vector measurements at a point) are taken to draw the circles of stress and of strain. This is understood better when it is appreciated that any given measurement represents the projection on an axis of some point on the circle circumference. Normal stresses and strains are projected as points on the N axis while shear stresses and strains appear as points on the S axis. These two circles may be drawn concentrically,[6] as shown in Figure 1, provided that the scales are chosen so that the ratio of stress units to strain units is as $E_Y/(1-\mu)$ where E_Y is the modulus of elasticity in tension or compression, and μ is Poisson's ratio. When the circles are drawn in this manner it will be found that the stress circle radius is smaller than the strain

Paper 46-60, recommended by the AIEE committee on instruments and measurements for presentation at the AIEE winter convention, New York, N. Y., January 21–25, 1946. Manuscript submitted July 14, 1945; made available for printing December 11, 1945.

Robert E. Kern and Sidney B. Williams, assistant project engineer, are both in the propeller division, Curtiss-Wright Corporation, Caldwell, N. J.

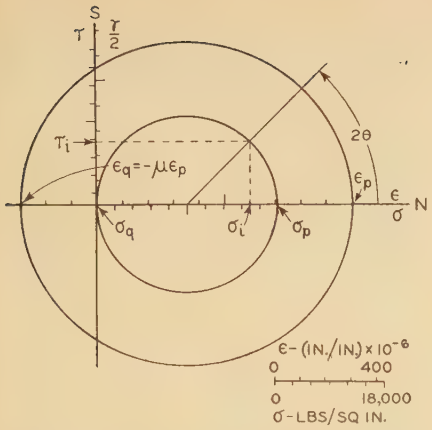

Figure 1. The Mohr circles of stress and strain for a simple axial stress of +30,000 pounds per square inch

Young's modulus is taken to be 30×10^6 pounds per square inch and Poisson's ratio to be 0.3

circle radius in the ratio of $(1 - \mu)/(1 + \mu)$ and the angular position of the point (σ, τ) on the Mohr diagram is twice that of the physical direction of measurement, so that if a measurement be made in the direction θ (with respect to the direction of principal stress) the corresponding direction on the circle diagram makes an angle of 2θ with the N axis. This is reasonable because a complete revolution around the Mohr circle must represent a 180-degree rotation of the measuring device. The concept of the two Mohr circles is not appreciated by many workers in the field, and it is perhaps for this reason that difficulty with the stress–strain relation is prevalent. It is because of the Poisson or lateral contraction exhibited by a stressed member that the ratio of stress to strain is not constant even while operating in the elastic state. For example, the ratio of stress to strain in the direction of the load (σ_p/ϵ_p) for a simple tension test is by definition equal to the modulus of elasticity, E_γ, but the ratio of stress to strain in a direction perpendicular to the load is zero. The load has no component in this direction $(\sigma_q = 0)$ but the lateral strain $(\epsilon_q = -\mu\epsilon_p)$ is finite and opposite in sign. Further examination of Figure 1 will show that the simple tension case is represented with σ_p (+30,000 pounds per square inch) positive and σ_q zero. It can be seen that $\epsilon_q = -\mu\epsilon_p$ and particularly that the ratio $\sigma_\theta/\epsilon_\theta$ is not constant as the radius is rotated, and were the center of the circles displaced somewhat $(\sigma_q \neq 0)$ even the ratio $\sigma_p/\epsilon_p = E_Y$ would not hold.

Thus far, only *normal* stresses and strains have been discussed. *Shear* stresses and strains cannot be detected as a change in length, but can be calculated from two stress or strain measurements, the difference between two mutually orthogonal normal stresses or strains being proportional to the shear stress measured on the plane whose direction bisects that of the two orthogonal measurements. In fact, this leads to the solution of the Mohr circle diagrams from three normal strains separated in direction by increments of 45 degrees:

As the first and third strains are orthogonal they must lie on extremities of some diameter of the circle, and consequently their arithmetic mean must coincide with the circle center. Now, the difference of the first and third (orthogonal) normal strains is equal to the shearing strain associated with the second normal strain, since the direction of the latter bisects that of the first and third strains. As dictated by the second term of equation 2, half of this value is plotted as an ordinate at the abscissa corresponding to the second strain, thus locating the point $(\epsilon_2,\gamma_2/2)$ on the circumference, and the radius drawn from the center to this point just found must be perpendicular to the diameter determining the points corresponding to the first and third measurements as the 45-degree increments on the specimen must exist as right angles on the strain circle diagram. The solution is completed by constructing the stress circle with its smaller radius, $(1-\mu)/(1+\mu)$ as large as the strain circle radius, whereupon the various points (σ_i, τ_i) can be obtained, although the most pertinent information usually consists of the extremes of the circle dimensions and the angle 2θ (measured counterclockwise from the direction of the first strain to the N or normal axis). The method is checked by projecting the three solution points located on the strain (or stress) circle circumference to the N axis; if the construction has been made correctly the projections will coincide with the three measured strains (or stresses). The word "stresses" is used advisedly because, with the proper gauges, stresses can be measured directly.

Electrical Measurements: The Bonded Wire Gauge

Strength measurements can be obtained from numerous types of gauges[7] but the principles controlling the use of the bonded wire resistance gauge will apply generally to other methods, except that the resistance-type units are characterized by lower mechanical inertia and lower voltage output than most. The bonded wire gauge, commonly referred to as the wire strain gauge, has for its principle of operation the variation in resistance of a fine metallic filament bonded to the surface whose deformations are to be measured. In order to make its installation practical the filament first is cemented to a paper "carrier" which, in turn, is cemented to the specimen. This carrier is in no way necessary to the operation of the gauge. In fact its elimination

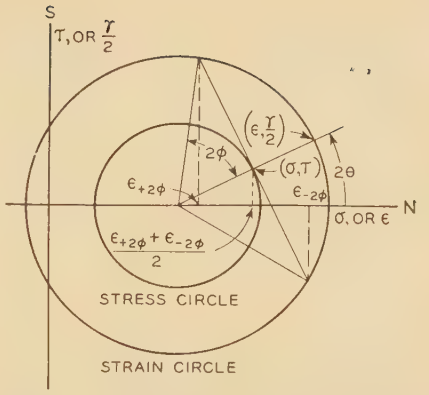

Figure 2. The Mohr circles of stress and of strain on which is shown graphically the manner whereby the Vee type of gauge can be made to yield a result proportional to the stress in the direction of its axis

would be desirable so that the filament might be closer to the specimen, while also allaying the danger of improper transfer of the "mechanical signal" to the active element of fine wire. Actually, the wire first is wound in the form of a grid to which wire leads are joined, after which the grid and leads are placed against the paper carrier for cementing. After the gauge (filament plus cement plus carrier) is cemented to the specimen the assembly acts as if it were part of the specimen in that it accepts uniformly the dimensional changes, both positive and negative, of the deformed surface, while offering negligible restraint in so doing because of its small mass and low effective moduli of elasticity. This action is possible because the dimensions of the wire filament are defined by the matrix of cement in which it is embedded, and it is essential that in the design of such a gauge the wire diameter be small enough so that this effect is achieved. Otherwise compressive strains might result in buckling of the wire with resultant destruction of the bond. This situation is somewhat comparable to the reinforcing rods in a concrete beam, wherein the concrete transmits the tension to the rods, and prevents the rods from buckling in compression (assuming that compressive loads might be placed on such a part of the beam). This transmission of the mechanical signal to the wire results in a permissible amplitude, with linear resistance-versus-strain response, in excess of the proportional limit of the filament material. This amplitude is represented by the manufacturer to approximate one per cent with negligible change in unstrained resistance, and to attain values of two to three per cent for linear operation without complete zero return. The gauge change of resistance is linear and consistent, but not explainable in terms

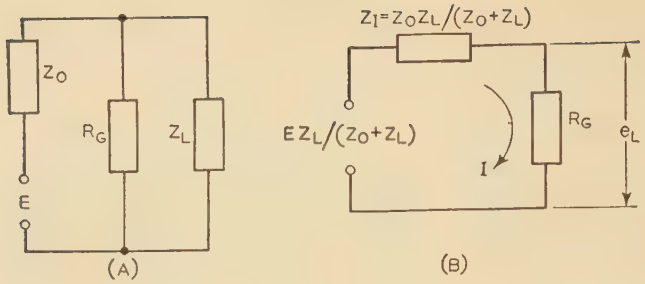

Figure 3. Fundamental gauge circuit (*A*) and its equivalent (*B*)

of the known properties of the filament material in larger sizes. Were the volume resistivity of the wire to be constant with respect to elastic strains it would be reasonable to expect the unit relative change in resistance (dR/R) for unit relative change in length (unit strain, ϵ) to be $(1 + 2\mu)$, where μ = Poisson's ratio. This ratio $dR/R\epsilon$ is defined as S, the gauge sensitivity, and because Poisson's ratio has a theoretical maximum of 0.5, the sensitivity should not exceed 2.0. Actually, certain gauges (made of "Advance" alloy) have such a sensitivity but many gauges are made with sensitivities lying in the range of -5 to $+3.5$, a fact which either contradicts the 0.5 maximum for Poisson's ratio or sheds some interesting light on the volume resistivity of fine wire materials as a function of stress. To date this anomaly is unsolved but may yield to electron microscopy (for use in determining Poisson's ratio for the strained filament). As a matter of interest the operating current density in the usual gauge wire is of the order of 25,000–50,000 amperes per square inch.

Bonded wire gauges are manufactured to meet a demand which requires both thermal stability and sensitivity. Currently these are conflicting requirements because the most sensitive materials (of which the invar, "Iso-elastic," an alloy originally developed for constant modulus of elasticity versus temperature, is representative) are very sensitive to temperature changes. Thermal stability implies that the sum of the effect of differential coefficient of expansion between the filament and the strained surface and the effect of filament temperature coefficient of resistance approaches zero, obviously a function dependent upon the characteristics of the material upon which the gauge is mounted. It is not surprising, therefore, that Advance wire gauges are thermally quite stable on steel, not as stable on aluminum, and not at all stable when suspended in air and subject to the erratic behavior of the unmounted paper carrier, the latter condition representing an academic case. Currently available are the thermally stable Advance gauges with a sensitivity of approximately 2.0 and suitable for all types of deformation measurement, and the Iso-elastic gauges with a sensitivity of 3.5 but suitable only for dynamic work. The latter type are inherently of a higher resistance, permitting generally a higher voltage drop, which condition may be interpreted as a further increase in sensitivity when the load is effectively an open circuit, such as a vacuum tube.

Gauges are available in a wide variety of dimensions and resistances ranging from units 1/16 inch square with 60 ohms resistance to others six inches long (300 ohms) and again some approximately 1/2 inch square with a resistance of 2,000 ohms. Still others, termed rosettes, are arranged in groups of two, three, or four units mounted close together, but oriented in different directions, for the measurement of the complete state of stress by means of the Mohr circle diagram.

The Stress Gauge

In a biaxial stress field the measurement of stress can be simplified greatly by the use of a gauge which responds both to strains parallel and strains perpendicular to the gauge axis[6]. Provided that the gauge specific transverse sensitivity (the ratio of the lateral to the axial response of the gauge) is equal to Poisson's ratio, the gauge output is continuously proportional to the stress in the direction of the gauge axis. This is in accordance[5] with equation 4:

$$\sigma_x = \frac{E_Y}{1-\mu^2}(\epsilon_x + \mu\epsilon_y) \qquad (4)$$

The proof of the stress response characteristic of the gauge is shown conveniently for a particular geometric pattern actually used in commercial gauges. This pattern has the wire arranged in a V, the angle between the wires being selected so that the average of the strains from each arm of the V yields an output proportional to the stress.

The measurement of stress in the direction θ with respect to the direction of the principal axis, requires that the projection of the point (σ, τ) in Figure 2 be determined. A tangent to the stress circle drawn at the point (σ, τ), will intersect the strain circle at points whose projections on the N axis have an average value proportional to the desired quantity. Thus to measure the stress in the θ direction, the gauge V arms will have directions of $(\theta + \phi)$ and $(\theta - \phi)$ respectively.

The general output expression for a gauge of this type when written as a function of the included angle 2ϕ becomes

$$\tfrac{1}{2}(\epsilon_{+2\phi} + \epsilon_{-2\phi}) = (\cos^2\phi)(\epsilon_x + \epsilon_y \tan^2\phi) \qquad (5)$$

where ϵ_x is oriented in the θ direction. The included angle of the gauge V, 2ϕ, is chosen so that $\tan^2\phi$ equals Poisson's ratio for the tested material. Then the right-hand member of equation 5 reduces to $\sigma_x/[E_Y/(1-\mu)]$. Steel, for example, with a Poisson's ratio of 0.28, requires an angle of about 55 degrees, the exact angle being determined by methods of manufacture. This type of stress gauge is used extensively in the testing of hollow steel aircraft propeller blades.

For the stress gauge, the expression which relates the relative change in gauge resistance to the stress producing it is

$$dR_G/R_G = F\epsilon' \qquad (6)$$

where R_G is the gauge resistance and ϵ' is the ratio of stress along the gauge axis to Young's modulus for the material upon which the gauge is mounted. The stress gauge factor F has the following relationship with S, the strain gauge factor:

$$F = (1-\mu)S \qquad (7)$$

It can be shown from equation 5 that the ratio of the output of a stress gauge to the output of a strain gauge of equivalent wire length and resistance and under uniaxial stress is $(1 - \mu)$.

The use of stress gauges can reduce materially the effort required to determine stresses. The direct indication of stress is of particular importance when complex vibratory stresses are measured; under such conditions two strain records separately recorded would have to be converted to stress through a point-by-point conversion if the instantaneous stresses could not be indicated directly.

Errors of Location and Installation

Before proceeding to a discussion of the electric circuits of resistance wire gauges it is appropriate to discuss the theoretical and mechanical considerations which may contribute to inaccuracy in the final conclusions. These may be called the errors of location and installation. That is, the output of the gauges must be indicative of the most critical stress in the part, the stress at the points where failure will occur

if it is to occur. Presumably this will be on the surface at the geometrical center of one of the gauges, though many failures do not start at the surface. On a test specimen such as a hollow steel propeller blade an error of a fraction of an inch in location can produce a change in output of 100 per cent or more, and since any one gauge will cover less than one-tenth per cent of the total area, the location of a few dozen gauges or less over the whole propeller must be chosen with great care. Moreover, if only one gauge is to be located at any one point, the gauge axis orientation is also important, as can be judged by Mohr circle theory. Fortunately, some knowledge of critical areas and stress direction is often available from photoeleastic[5,8] and brittle lacquer[9] ("Stresscoat") studies, discussions of which are beyond the scope of this article. The former method is not convenient for vibratory work and both tend to be laboratory procedures so that it is not always possible to simulate field loadings. Having chosen the proper location it will not always be possible to place gauges where desired due either to inaccessibility or to the physical size of the gauge, which may be so large as to cause an error by integrating the stress or strain over the gauge length when the stress gradient is such as to be masked by the use of too large a gauge length. The availability of shorter gauges has improved this latter situation but sometimes the minimum size of gauge is dictated by electric circuit background noise, the higher resistance gauges being required to produce sufficient signal to result in an acceptable signal-to-noise ratio. This difficulty is probably peculiar to tests on rotating objects such as aircraft propellers, which exhibit accessibility problems also, since flight measurements commonly are made inside the hollow blades, even near the tip, and some work has been done within the hub itself. (Flight stress measurements are made on nearly every propeller–engine–aircraft combination before final acceptance of the design by the customer.) One of the most common sources of gauge error lies in the neutral-axis correction, which is applicable to any survey involving bending stresses. The classical bending-beam theory shows that the stress is proportional to the distance from the beam neutral axis (plane of zero stress); in consequence, bending-stress measurements made at any distance from the neutral axis but that of the surface will be incorrect in direct proportion to this distance. Since the gauge acts as a part of the tested material, accurate bending-stress measurements must correct for the effective gauge elevation above the surface. The diameter of the wire filament is about 0.001 inch and its centerline is perhaps 0.003 inch above the tested surface due primarily to the thickness of the paper carrier. That this is not negligible may be appreciated from a consideration of measurements on a 0.060-inch plate in bending, where the 0.003-inch elevation will cause an exaggeration of ten per cent if the neutral axis is in the central plane of the plate (pure bending). When bending is combined with tension or compression neutral axis error sometimes can be avoided by mounting identical gauges on opposite faces of the plate; their sum eliminates the bending component to yield the tension or compression while their difference eliminates the tension or compression and thermal components, though the resultant bending measurement still is subject to neutral axis error. Returning to the problem of installation, or mounting, it hardly should be necessary to state that the proper bonding of the gauge to the tested surface is of extreme importance to a successful technique. Conservative instructions are supplied by the manufacturer, and occasionally the time allowed for curing or drying of the adhesive may be shortened, but in all cases care should be taken to insure proper preparation of the tested surface (preferably roughening with fine sandpaper plus cleaning with acetone) and adequate application of the adhesive. In the interest of quick drying there is a tendency to apply the adhesive sparingly, which may result in an incomplete bond. Poor surface preparation sometimes is evidenced by the flaking off of a gauge after the test has been completed and the tested parts are no longer available for retest. Where practical the installed gauges may be checked by a calibration with a known load, or another type of gauge, such as the Tuckerman optical strain gauge, may be placed over the installed gauge and the specimen loaded to produce a given strain. The Tuckerman gauge is relatively small and light, and often may be applied with no more force than its own weight, but it is distinctly a laboratory instrument (more often used as a standard).

Other sources of error contributing uncertainty and which pertain more directly to the tested material itself include "locked-in" or residual stresses, the deviation of the remainder of the "universe" from the sample tested, the elastic modulus (if stresses are to be computed), and "creep."[10] Unless the material is in a "dead-soft" or perfectly annealed condition there usually will be certain unrelieved or locked-in stresses remaining. Residual stresses will not affect greatly the readings obtained but will determine somewhat the interpretation read from the data by the designer, as they contribute to or inhibit failure. The actual measurement of locked-in stresses by bonded wire gauges is not possible unless the gauge can be installed prior to the manufacturing operation producing such stresses, or as now is being done to an increasing extent,[11] the gauge is installed while the residual stress is present, after which most of the restraining material is removed carefully and the local stress under the gauge relieved. The indicated stress pattern is then a "negative" of the locked-in pattern.

Young's modulus, E_Y, occurs in the equation relating stress and strain. For the two-dimensional (biaxial) case this is in accordance with equation 4. But the stress–strain relationship for many engineering materials is distinctly nonlinear (aside from the fact that E_Y at zero load is subject to a degree of uncertainty) so that an indicated vibration stress of $\pm 10{,}000$ pounds per square inch, when no steady load existed, might differ from the indicated value when a steady load of 50,000 pounds per square inch was applied simultaneously. Such considerations might be affected differently for steady locked-in or surface stress than for uniformly-distributed steady stress. Modulus correction of this nature is not known to the authors but would have to be considered in evaluating closely the probable error. Creep is the phenomenon of gradual continued deformation at constant load and is ordinarily negligible in steel at low temperatures (below 200 degrees Fahrenheit) but may be appreciable in some other materials such as lead, plastics, and gauge bonding agents when large deformations are involved. It may prevent a return to a zero-stress reading, even when the gauge itself is operating properly. It may be obscured by or confused with drift due to poor temperature compensation or the chang-

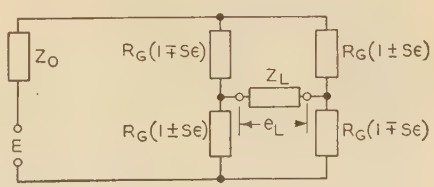

Figure 4. Equiarm strain gauge bridge circuit

Parenthetical term of R_G indicates direction and magnitude of resistance change in each gauge as a function of gauge factor and applied strain

ing leakage characteristics of the electrical insulation, as will be discussed later.

The Electrical Problem

Gauge Circuits

Two general circuits which may be used for the conversion of strain to electrical signal are shown in Figures 3*A* and 4. The simpler circuit of Figure 3*A* often may be used when a knowledge of only transient or vibratory stress or strain is desired, while the bridge circuit of Figure 4 is employed when the steady component with or without the vibratory component is to be determined or when protection from excitation circuit disturbances (as in slip-ring installations) is required.

When vibratory shear, or the difference in strain between two gauges at right angles, must be measured, the "matching" resistor, Z_O, in Figure 3*A* becomes one gauge while the active gauge, R_G, becomes the second of the two required orthogonal strain-sensitive elements. The bridge circuit can be arranged suitably to enable the measurement of total shear, since differential measurements are applicable for shear, torsion, and many bending problems.

Network theorems[12,13] are used conveniently to calculate the voltage which appears when the active circuit elements are strained. Thus the Thévenin equivalent of Figure 3*A*, shown in Figure 3*B*, yields current in the gauge of

$$I=\frac{EZ_L/(Z_O+Z_L)}{R_G+Z_OZ_L/(Z_O+Z_L)}=\frac{EZ_L}{Z_OZ_L+R_G(Z_O+Z_L)} \quad (8)$$

The change in load voltage dE_L due to a change dR_G associated with the strain ϵ is

$$dE_L=e_L=d(IR_G)=IdR_G+R_GdI \quad (9)$$

Evaluating dI (by means of the compensation theorem) and collecting terms,

$$e_L=I\left(\frac{dR_G}{R_G}\right)\frac{R_GZ_OZ_L/(Z_O+Z_L)}{R_G+Z_OZ_L/(Z_O+Z_L)} \quad (10)$$

The sensitivity S of a strain gauge has been defined previously as $dR/R = S\epsilon$. Using this relation together with the fact that the coefficient of $I(dR_G/R_G)$ is the parallel combination of R_G and Z_I, equation 10 is simply

$$e_L=ZIS\epsilon \quad (11a)$$

where $Z = R_GZ_I/(R_G + Z_I)$ evaluated at the strain frequency and I is evaluated from equation 8 at excitation frequency. For practical applications the impedances are entirely resistive, with the load impedance Z_L (usually amplifier input impedance) much greater than the gauge resistance, R_G. The greatest output voltage for a given value of E occurs when the product of ZI (or more commonly RI) is a maximum, that is, when Z_O equals R_G. When it is possible to measure two or four strains which are exactly equal but occur in conjugate pairs as shown in Figure 4, the bridge circuit increases the no-load voltage output above that of Figure 3*A* by two and four times respectively.

The voltage output equation for four active equal bridge arms is developed in a manner similar to that of equation 11a and is

$$e_L=ZIS\epsilon \quad (11b)$$

where Z, just as in equation 11a, is the impedance (at the strain frequency) measured across the terminals of the load impedance Z_L, when other voltage sources in the circuit are not generating but are replaced with their equivalent internal impedances. Expressed explicitly this impedance, Z, is $R_GZ_L/(R_G + Z_L)$. Note that when the load impedance Z_L is large with respect to the gauge resistance, the output voltage e_L is given by the expression $E\epsilon S$, and further, that I is the current of excitation frequency supplied the gauges, or $E/(R_G + Z_O)$.

The quantity $S\epsilon$ may be regarded as an average value determined by the number and characteristics of the gauges acting. If the output from a gauge (due either to its location in the bridge circuit or because of the sign of strain) tends to cancel the effects from another, the algebraic signs of the two quantities $S\epsilon$, associated with the respective gauges, may be regarded as opposite. Thus a bridge with only two active gauges (but these connected in one side of the bridge and subject to equal and opposite strains) will exhibit an output voltage of $e_L = (1/2)ZIS\epsilon$, since two of the four gauges have zero as their effective value of $S\epsilon$.

Output voltage equations 11a and 11b may be examined to ascertain the errors which may result from variation in the controllable parameters. It is immediately evident that errors in E, the excitation voltage, and errors in gauge sensitivity, S, contribute in direct proportion to the error in gauge output voltage. Excitation voltage may be monitored or controlled by the operator; the gauge sensitivity factor is supplied with commercial gauges and usually is guaranteed to plus or minus one per cent.

Since the nominal value of gauge resistance may be subject to as much as a two or three per cent manufacturing tolerance, particularly in those gauges supplied for dynamic work, it is necessary to examine the ZI term in equation 11a to evaluate the effect of changing the gauge resistance. Assuming that the impedances are essentially constant and resistive in the operating portion of the spectrum (a condition necessary for good amplitude-frequency response) and that Z_L is large with respect to Z_O, the relative change in output voltage is

$$de_L/e_L=d(ZIS\epsilon)/ZIS\epsilon=d(ZI)/ZI$$
$$=-(dR_G/R_G)(R_G-Z_I)/(R_G+Z_I) \quad (12)$$

where Z_I is $Z_LZ_O/(Z_L + Z_O)$ and dR_G/R_G is the relative change in the nominal resistance and not $S\epsilon$, which here is considered constant. The condition R_G equal to Z_I suffices for zero error in calculated output voltage as a function of tolerance in gauge nominal resistance; moreover since Z_L is large in comparison to Z_O, it is possible to have the zero error condition coincide with the maximum output condition by setting Z_O equal to R_G.

As stated previously, measurements of steady strain require that gauge resistance be a function of strain only and be unaffected by temperature or variation in electrical leakage. Temperature effects are eliminated most nearly by using a compensating gauge mounted on material equivalent to the test specimen and subject to the same ambient temperature variations. The compensating gauge may be active or passive but is connected in the bridge arm adjacent to the compensated unit.

Using an unstrained specimen equipped with two nitrocellulose bonded gauges wound with Advance wire, temperature compensation to within two microinches per inch over a range from 70 to 170 degrees Fahrenheit has been attained in the laboratory. However, general practice indicates that two microinches per inch per degree Fahrenheit is a more practical estimate of realizable temperature compensation.

The measurement of vibratory stresses up to a temperature of about 180–200 degrees Fahrenheit is possible with nitrocellulose bonded gauges. A specific case for ±400 microinches per inch of strain showed at 230 degrees Fahrenheit a drop of 30 per cent from the value of apparent gauge factor at 200 degrees Fahrenheit, the difference due to softening of the cement. For elevated temperature operation up to 300 degrees Fahrenheit, resin-bonded gauges are used.

In order to prevent "zero" instability due to absorption of moisture by the gauge or associated leads, it is necessary to weatherproof the installation by first driving off all moisture and then coating or impregnating with a nonhygroscopic

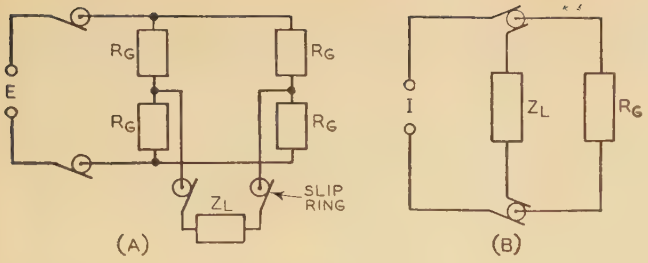

Figure 5. Location of slip rings and related components in a constant-voltage gauge circuit (*A*), and in a constant-current circuit (*B*)

material such as a hydrocarbon wax. A typical gauge, having a resistance of 120 ohms and a sensitivity of 2.0, will change in resistance by only 0.008 ohm when subjected to a stress of 1,000 pounds per square inch in steel (33 microinches per inch). This change also may be produced by a shunt resistance across the gauge of 1.8 megohms (very nearly $R_G/S\epsilon$) thus making evident the necessity for thorough moistureproofing. A value of 1,000 megohms is recommended by the gauge manufacturer. When many gauges are in a circuit possessing one or more common leads, it is often convenient to make provision for measuring the leakage to ground. Such an indication cannot be interpreted explicitly but serves as a warning of changing insulation conditions.

The nitrocellulose, and to a lesser extent the resin base, bonding agents both are subject to creep under prolonged strain and also exhibit slight apparent hysteresis over a stress–strain cycle. Proper application and curing helps reduce creep to a minimum and several preliminary loading cycles usually suffice to make hysteresis effects negligible. The possibility of errors from this source should not be overlooked if readings having a tolerance of five to ten microinches per inch must be obtained. Moreover it is only reasonable to assume that creep difficulties will increase with stress level and temperature.

Special Circuits

When the information as to the state of stress on a rotating member is to be obtained with the aid of sliding contacts, it usually will be necessary to minimize contact resistance effects by arranging a balanced bridge on the rotating element as in Figure 5*A*. Results free from slip-ring interference, especially at high surface speeds, are impossible of achievement if the slip rings are connected directly to make up part of the gauge resistance. Inspection of the current term in equation 11b shows why the bridge circuit of Figure 5*A* is relatively free from effects resulting from variation in resistance of the slip rings supplying the exciting current, and inspection of the impedance term will show how Z_L may be chosen to make the effect of output-circuit slip-ring resistance variation negligible. It is also essential that the slip rings located in the leads which supply the load do not introduce thermal electromotive forces. An alloy consisting of 97 per cent silver and 3 per cent platinum, the latter for hardness, used in conjunction with silver-graphite brushes, has proved very satisfactory under brush pressures of 40 pounds per square inch and surface speeds of about 4,000 feet per minute. Improvement in the strain signal-to-slip-ring noise ratio may be obtained by the use of a bridge-output transformer mounted on the rotating object, provided that the resultant phase and amplitude distortion versus frequency of the signal is negligible. Such a system is suited especially for use with carrier-current excitation.

Constant-current excitation sometimes is employed in slip-ring circuits to overcome the resistance variation in the transfer system. With this method, the output voltage is equal to IdR_G as the component $R_G dI$ no longer is present. The gauge output voltage for constant-current excitation is twice that obtained from constant voltage excitation when the average currents in both cases are equal. Referring to Figure 5*B*, it will be seen that the voltage drop across the slip-ring contact resistance need not be measured as two brushes, one for the excitation current and another for the signal voltage, may be used. It is still possible, however, for thermopotentials arising at the signal brush to mask out the strain voltage unless the proper materials, such as those described in the foregoing, are employed.

To find the stress in a material subject to biaxial stress, it is necessary to take the proper proportions of two orthogonal strains as explained in the discussion of the stress gauge. But if it is desired to measure two orthogonal stresses at a point the purpose perhaps can be served best by using a pair of orthogonal strain gauges with their electric circuits arranged so as to crosstalk mutually the correct lateral or transverse component each into the other (refer to equation 4) to produce the effect of two stress gauges. This arrangement requires a double installation compared to a single stress gauge but yields two stress measurements, which can be taken separately or simultaneously, just as if the strain gauge filaments had been arranged in the path of stress gauge grids and the mutual impedance removed. Both sections of such a

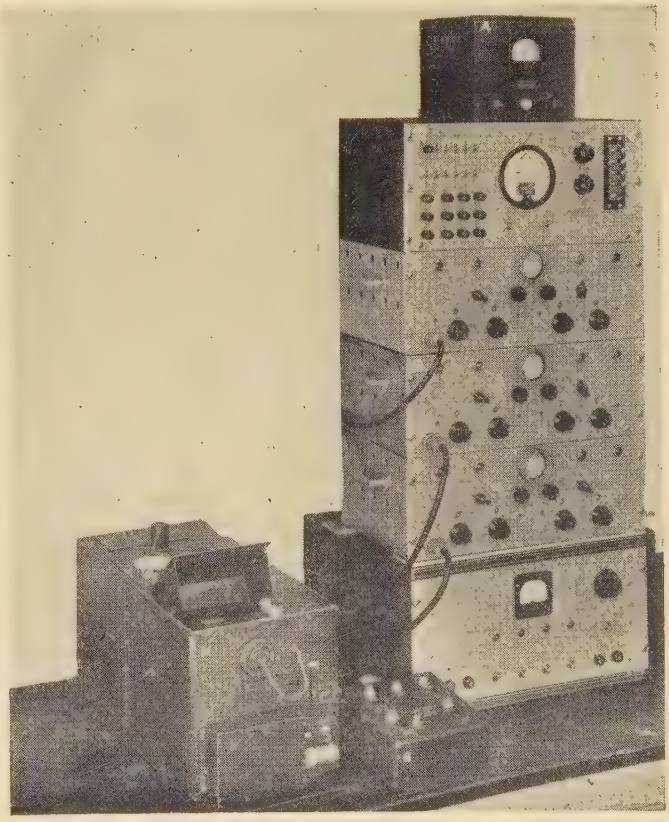

Figure 6. Twelve-channel amplifier-oscillograph equipment showing oscillograph, power supply, three banks of amplifiers, switching panel, and calibrator

circuit must be furnished excitation current, however, even if recorded at separate times. One such arrangement consists of connecting together two gauges, whose directions have the required rectangular relationship, with a common impedance Z_C joining the output or load terminals. If the two gauge circuits (composed entirely of resistive elements) have like components it can be shown that when Z_C is set equal to $R_I(1 + \beta)(1 - \mu)/(\mu - \beta)$ where R_I is $R_G R_O/(R_O + R_G)$, μ is Poisson's ratio and β is the gauge specific transverse sensitivity, then each gauge will have an output voltage proportional to the stress in the direction corresponding to the particular gauge orientation. When the gauge and matching resistor have values of 500 ohms each, Z_C becomes approximately equal to 700 ohms for representative conditions of μ and β equal to 0.28 and 0.02 respectively.

Instruments and Their Selection

As the signal is measured in terms of microinches per inch it will be readily apparent that the voltages available from low resistance gauge circuits must be small, usually less than 100 millivolts. A structure may be stressed at zero frequency, (static loading), or may be a resonant member vibrating at frequencies of several thousand cycles per second, or be subject to shock loading. Sensitive measuring equipment consequently must be selected, keeping in mind the frequencies to be encountered. Vacuum tube equipment usually is required although static and slowly varying strains are measured successfully with d-c microammeters and light-beam galvanometers. Generally, in a stress survey, a number of points must be examined and correlated with one another with respect to time or other variables. Multichannel amplifier recording oscillograph combinations prove most useful in obtaining and preserving this data for later analysis. Figure 6 shows a typical 12-channel oscillograph with 12 channels of amplifiers (three banks of four), a-c power supply, switching panel, and calibrator. For flight work the a-c power supply is replaced with a battery-powered unit.

The instruments can be chosen properly only by an honest evaluation of the response required. This implies the determination of the minimum acceptable gain and the choice of f_{min} and f_{max}, the extreme values of signal frequency which must be transmitted and between which the amplitude-frequency response must be "flat" within, say, $\pm p$ per cent. In general there will be other frequencies, f_1 and f_2, between which the phase distortion must not deviate from a linear function of frequency within some prescribed limit. Then there will be the decision upon indicating or recording instruments, and if recording, whether automatic or attended. If accuracy is very important, some null-balancing arrangement usually is indicated, though such equipment ordinarily will have but a very poor amplitude-frequency response, particularly if manual balancing is used. Generally it will be found that phase response can be improved at the expense of amplitude response and conversely. For instance, a galvanometer element with about 0.6 critical damping will exhibit a flat amplitude response to a higher frequency than it will for any other value of damping, but the phase-frequency characteristic will deviate from linearity at a lower frequency than when the damping is lower than 0.6 critical. This is a difficult choice, for phase relations in the complex stress wave are important if peak values are not to be distorted beyond the specified p per cent. To demand perfect phase and amplitude response (good square-wave characteristic) may mean using quite a different instrument. Once the response characteristics have been fixed—the least requirements for acceptable results—the size, weight, and cost of the equipment can be estimated. A very rough indication of the type of instrument required may be obtained by dividing the instruments into six classes, each one decade apart in the frequency spectrum, as shown in Table I.

Table I. Instruments Classed by Frequency Response

Nominal Frequency Spectrum (Cycles per Second)	Instruments
0–0.2	Indicating instruments and manually balanced null devices (manual recording)
0–2.0	Automatic null-balance recorders
0–20	Direct-coupled galvanometers (no amplification)
2–200	Amplifier-galvanometer combinations (magnetic damping of galvanometers, or piezo-crystal galvanometers)
2–2,000	Amplifier-galvanometer combinations (oil-damped galvanometers)
2–20,000	Amplifier-oscilloscope (cathode-ray) combinations

Static and dynamic strains may be recorded simultaneously by using carrier current excitation or d-c excitation to the bridge circuits and associated recording equipment. The former method is more complex in that it requires a high-frequency source and freedom from variational reactive components in the bridge (which in turn requires phase balancing and probably a phase-sensitive demodulator-filter arrangement). Excitation from a d-c source requires that those components of signal frequency not passed by the amplifier be recorded by some other means. A very satisfactory method which may be used with conventional amplifier-oscillograph equipment has been termed the "insertion" system,[14] whereby the signal is short-circuited cyclically. If the wave form and frequency of the switching action are chosen properly the recorder passes the zero signal pulses, thereby establishing the axis of zero signal on the recording medium. The pulse height is exactly equal to the instantaneous value of the signal, which fact sometimes is used in the exact reduction of the data. Such a system has been in use for over a year in the measurement of steady and transient strains in aircraft propellers.

The choice of instruments will be influenced by the required accuracy, particularly with respect to ambient conditions of temperature, pressure, humidity, mechanical vibration and noise, and power supply variation. Ordinarily, characteristics of the equipment may be specified so that these variables will be of little consequence but oftentimes it becomes desirable to use an instrument under conditions for which it was not intended. Variations in temperature affect the operation of oil and electrolytic capacitors, the response of oil-damped galvanometers, and the lubrication of moving parts in oscillographic equipment. Pressure and humidity affect the operation of slip ring brush combinations in oscillograph motors and transfer equipment (such as is required for aircraft propeller testing). Amplifiers often are subject to disturbance from noise or vibration or both. It even has been the experience of the authors that the severe vibration present on aircraft engine nose sections is sufficient to produce a signal comparable in wave form and amplitude to that of a stress signal, merely due to piezoelectric or electrostrictive effects on certain laminated plastic insulating materials used in the slip-ring assembly and brush rigging. This first was discovered during a check run with the excitation battery disconnected; it subsequently was eliminated by discontinuing the use of these laminated plastics as structural members in the transfer equipment and by other design changes.

When the records are analyzed there remain a few more sources of error and uncertainties. In a complex vibratory

Linear Couplers, Field Tests and Experience at York and Middletown, Pa.

E. L. HARDER
MEMBER AIEE

E. H. KLEMMER
ASSOCIATE AIEE

R. E. NEIDIG
ASSOCIATE AIEE

THE system of bus protection using linear couplers, or air-core mutual reactors, in place of current transformers was described before the Institute in January 1942.[1] By special design the mutual reactors were made astatic or insensitive to outside fields. Through the use of air core the troublesome problem of saturation of iron by the d-c transient component of short-circuit current was eliminated. At the same time adequate energy was derived for decisive relay operation. The coupler secondaries were connected in a series loop including the relay to form a bus protective system.

Several applications of this system have been made now, and it is the purpose of this paper to describe the field tests and subsequent performance of the pioneer applications at the York and Middletown Pa., stations of the Metropolitan Edison Company. Following an analysis of the field tests, which more firmly establish the operating limits of the system, the proposed field of application will be defined in relation to other bus protective systems.

The advantages of bus protection in clearing faults rapidly from a system are well recognized by the industry, and the provision of relay protection for major station busses has been standard practice for a number of years. The problems involved in such protection also are quite well known. One of the principal ones is the saturation of current transformers by the d-c transient component of the short-circuit current. In severe cases the d-c transient component may require 100 times as much flux capacity in the current transformer as is required by the a-c component to prevent saturation completely. The theory of this problem was presented before the Institute by Langguth and Marshall in 1929.[2]

Solutions

There were a number of successful solutions to the problem and it will be necessary to mention a few of these to illustrate the proper field of application of the linear coupler system in relation thereto.

First was the use of large current transformers which would not be saturated by the d-c component. These were used with low resistance leads to minimize the current transformer requirements in this respect. A formula was advanced specifying the requirement of iron cross-section, turns, and lead resistance for nonsaturation, as a function of the fault current and the d-c transient time constant. This was a "bull-by-the-horns" solution and its size, weight, and cost could be afforded only in the most important installations. However, it provided the possibility of instantaneous tripping without any time delay.

A method[3] was developed for calculating, with reasonable engineering accuracy, the time to saturate with off-set currents, and the time and current settings required to prevent misoperation with time-delay overcurrent relays and usual current transformers. However, the time delays required were frequently so long as to point the need of a better solution.

Relays[4] also were developed which would not operate falsely even when used with normal sized current transformers which saturated due to the d-c component. These are multirestraint relays; however, their success is due also to exploitation of variable percentage

Paper 46-36, recommended by the AIEE committee on protective devices, power transmission and distribution for presentation at the AIEE winter convention, New York, N. Y., January 21–25, 1946. Manuscript submitted November 19, 1945; made available for printing December 17, 1945.

E. L. HARDER is central station engineer and E. H. KLEMMER is switchgear engineer, Westinghouse Electric Corporation, East Pittsburgh, Pa. R. E. NEIDIG is electrical engineer, Metropolitan Edison Company, Reading, Pa.

---

stress wave it should be proper to consider only those stress reversals which occur often enough to be considered dangerous in the life of the tested part, but this is a matter on which it is impossible to be exact.

Conclusions

The quantity and complexity of electrical stress measurements have grown to such an extent that a relatively small part of the whole stress problem may require the full time of one or more individuals. This trend toward specialization naturally reduces the possibility of any one person appreciating the problem as a whole, with the result that one or two aspects may be emphasized while another of equal importance may be neglected. This situation, as discussed in the paper, is exemplified by a precise electrical measurement of a stress which may be subject to appreciable uncertainty in itself (due, say, to neutral axis error) or may be unrepresentative (gauge location in error), so that the responsibility for the procurement of results which depend upon many variables is evident. Although it has been possible to touch but lightly on most of these phases of the measurement problem, it is hoped that the broader consideration of stress determination, as herein presented, will prove helpful to those presently engaged in or who will enter this field.

References

1. THE DEVELOPMENT OF ELECTRICAL STRAIN GAGES, **A. V. deForest, H. Leaderman.** National Advisory Committee for Aeronautics Technical Note 744, January 1940.

2. United States Patent 2,292,549, MATERIALS TESTING APPARATUS, **Edward E. Simmons.** August 11, 1942.

3. THE EXTREME PROPERTIES OF MATTER, **Sir Charles Darwin.** *Engineering*, volume 155, February 5, 12, 19, 1943, pages 105, 106, 136, 137, and 144.

4. MECHANICAL PROPERTIES OF MATERIALS AND DESIGN (book), **Joseph Marin.** McGraw-Hill Book Company, New York, N. Y., 1942. Chapters 1–4.

5. PHOTOELASTICITY (book), **M. M. Frocht.** John Wiley and Sons, Inc., New York, N. Y., 1941. Volume 1, chapter 1.

6. THE DYADIC GAGE, **Sidney B. Williams.** *Proceedings* of the Society for Experimental Stress Analysis, volume 1, number 2, 1944, pages 43–55.

7. ELECTRIC GAGING METHODS, **H. C. Roberts.** *Instruments*, volume 17, number 6, through volume 18, number 10, 1944–1945.

8. TREATISE ON PHOTOELASTICITY (book), **E. G. Coker, L. N. G. Filon.** Cambridge Press, 1930.

9. PRACTICAL STRAIN ANALYSIS BY USE OF BRITTLE COATINGS, **Greer Ellis.** *Proceedings* of the Society for Experimental Stress Analysis, volume 1, number 1, 1943, pages 46–53.

10. Reference 4, chapter 6.

11. Papers presented at Society for Experimental Stress Analysis symposium (May 1944) on residual stresses, **C. S. Barrett** and others. *Proceedings* of the Society for Experimental Stress Analysis, volume 2, number 1, 1944, pages 147–225.

12. ELECTROMECHANICAL TRANSDUCERS AND WAVE FILTERS (book), **Warren P. Mason.** D. Van Nostrand, New York, N. Y., 1942. Pages 13–20.

13. RADIO ENGINEER'S HANDBOOK (book), **F. E. Terman.** McGraw-Hill Book Company, New York, N. Y., 1945. Page 198.

14. MEASUREMENT OF STEADY AND VIBRATORY STRESSES IN AIRCRAFT PROPELLERS, **E. F. Shelley.** Institute of the Aeronautical Sciences, New York, N. Y., 1946.

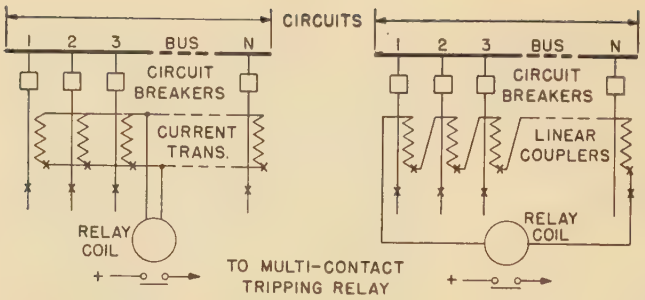

Figure 1. Schematic diagram of differential protection systems

characteristics and the tendency of the d-c component to brake, rather than drive, the induction disk. No small part of this development was the reduction of its operating limits to a few simple rules which insure safe application. This relay provides operation generally in from three to six cycles.

The linear coupler system combines the advantages of high speed and simplicity of the "bull-by-the-horns" method described first, with moderate size and weight of the multirestraint system, and some important advantages of its own. In principle it is the simplest possible system as will be noted (Figure 1b). It is the only system which can be tested at low currents to ascertain for a certainty what its performance will be at high current values. The coupling devices are no larger and often lighter than normal-sized current transformers. They can be mounted in the usual bushing current transformer compartments of circuit breakers. A single relay per phase is required irrespective of the number of circuits involved on the bus, a ground relay being used in addition if ground fault currents are relatively small. Figure 2 illustrates a typical coupler and relay.

The theory of the linear coupler system has been outlined in previous papers.[1,5] Consequently, only a sufficient résumé will be given here to show the significant factors which should be investigated in the field tests.

Résumé of Theory of Linear Couplers

As shown in Figure 1 linear couplers are connected normally in series whereas current transformers are connected in parallel to form a differential protection circuit. The current transformer is designed to produce in its secondary a current proportional to the primary current. As long as there is no bus fault the vector summation of currents in all circuits connected to the bus is equal to zero. Hence the summation of secondary currents, obtained by the parallel connection is likewise zero. In event of a bus fault the current in the relay is proportional to the fault current.

The linear coupler is a mutual reactor and consequently produces in its secondary a *voltage* proportional to the current in its primary. Usually this proportionality is 5 volts secondary per 1,000 amperes primary. If there is no fault on the bus the summation of primary currents is zero and consequently the summation of secondary voltages, obtained by the series connection, is likewise zero. If there is a bus fault the net voltage induced in the coupler-relay loop is proportional to the fault current, that is, 5 volts per 1,000 amperes of fault current in the usual design.

York and Middletown Installations

The first installations of the linear coupler scheme for bus differential protection were made on the Metropolitan Edison Company's system in the new 114-kv, outdoor substations at Middletown and York, each authorized for construction in 1942. Load growth in the York area necessitated conversion to 114 kv of the two 66-kv lines from Middletown to York. The Middletown station provides the interconnection between these two lines and the existing 114-kv circuit to Reading, as well as a principal outlet for the Middletown generation into the general transmission system. The York substation serves as the terminal for the 114-kv lines and the main source of supply into the York area, stepping down through 67,500 kva of transformers.

The Middletown substation is shown in Figure 3. Both substations are identical in basic design, utilizing a compact steel structure, protected by four overhead static wires spaced on 44-foot centers, "back-to-back" circuit bays, and main and transfer strain busses. Each circuit is provided with an oil circuit breaker having 1,500,000 kva interrupting capacity. Three coupling capacitor potential devices are connected to the main bus for relay and synchronizing potential. All secondary cables for control, current (including linear coupler secondaries), potential, power, andl ighting, as well as carrier current concentric cables, are buried directly in the earth in a common trench, between the control room and their respective terminal locations at the outdoor structure. The control and relay panels at Middletown are located about 350 feet distant from the nearest circuit breaker, whereas at York this distance is 200 feet.

A one-line diagram of the six-circuit station at Middletown is shown in Figure 4. An identical 114-kv bus diagram applies for the York station, excepting that there are five circuits instead of six.

The decision to install bus differential protection at these two important substations was made only after long deliberation, including careful analysis of the use of all known differential schemes. The calculated maximum and minimum

Figure 2

(a). Linear coupler
(b). LC-2 linear coupler relay

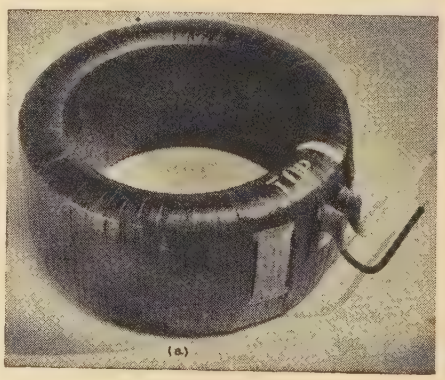

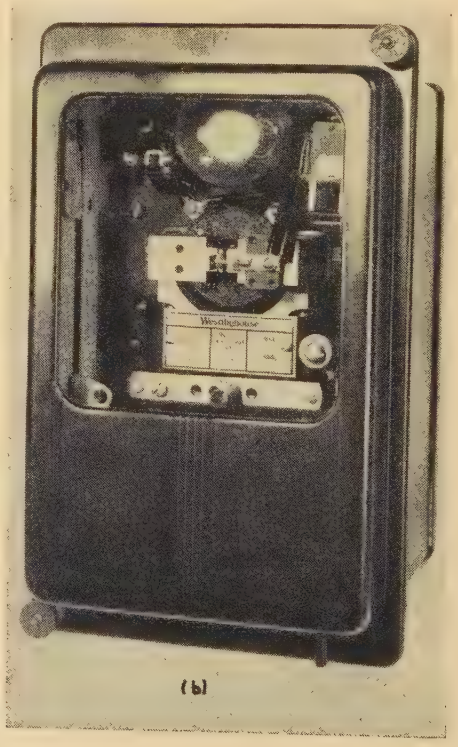

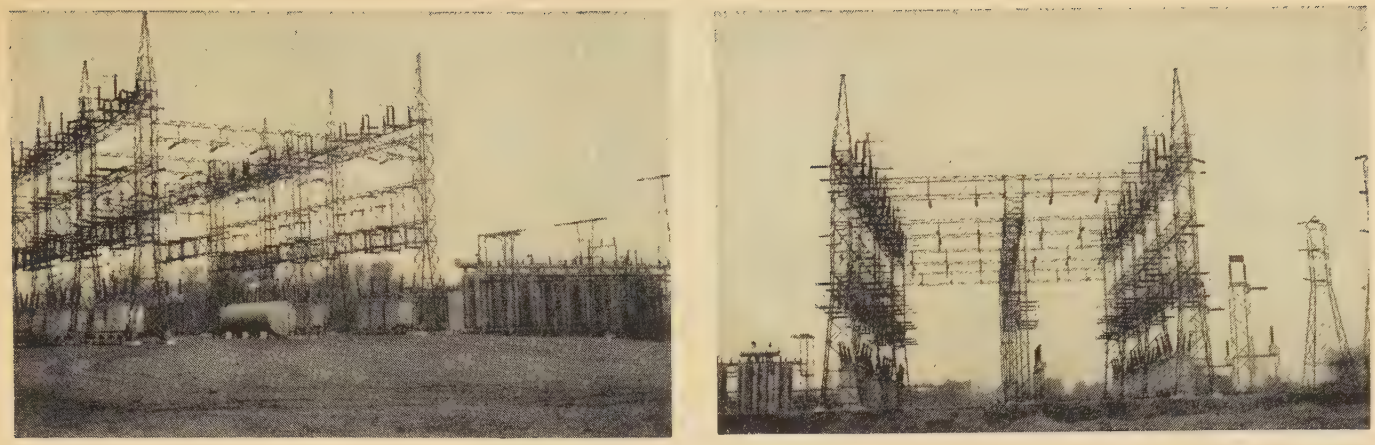

Figure 3. Views of Middletown substation

114-kv bus fault currents for which the relay systems must function were 6,250 and 1,400 amperes respectively at Middletown, and 4,500 and 1,050 amperes respectively at York. All 114-kv transformer banks on this system are wye connected with solidly grounded neutrals, resulting in bus interphase and ground fault currents of approximately equal magnitude. The calculated d-c time constant at Middletown was 0.12 second, and at York 0.06 second.

Conventional Methods Analyzed

Conventional methods, using standard bushing type current transformers in the 115-kv circuit breakers, with paralleled secondary connections, were given first consideration. The "bull-by-the-horns" method was, of course, economically impractical. The method using time delay overcurrent relays appeared unfavorable, as high-speed operation was necessarily sacrificed through provision of sufficient time delay to overcome the effects of d-c saturation in the current transformer. Calculations indicated that the intentional time delay required to permit offset transient recovery would result in relay times ranging from 7 to 60 cycles, under maximum to minimum fault currents, respectively. In addition to extending damage such times would adversely affect the co-ordination with transmission line protection.

The "multi-restraint relay" type of bus protection[4] was found applicable, and under the fault conditions previously stated would result in relay times ranging from 3 to 5 cycles. The number of circuits involved, however, required that two relays per phase be installed at each station. The current transformer connections and relay wiring would be arranged so as to maintain restraint on at least one relay per phase under all through-fault conditions. Since in general two relays per phase provide protection for up to seven source circuits per bus, the addition of main circuits at Middletown might have presented a problem.

A safe application of either of the foregoing systems requires consideration of maximum and minimum fault currents and their distribution, relay and lead burden, ratios and iron cross sections of current transformers, number of generating sources, and d-c time constant, together with other pertinent operating conditions. Since the total burden on the current transformers is an important factor in the successful application of the previously described methods, it follows that the size of conductor used in the secondary cable from the current transformer to the relay may have to be increased as the distance between them is increased.

Linear Couplers Selected

Laboratory tests of the linear coupler scheme previously described offered conclusive evidence that a simple, high-speed bus differential relay system had been developed which was free from all of the inherent problems associated with conventional current-transformer methods. While the linear coupler relay is of necessity a low energy device, any fear that unwanted operations might occur from induced potentials in the secondary cable was believed groundless. Calculations had indicated that such potentials would be very small compared with operating voltages if a continuous secondary loop circuit was provided for each phase, with the outgoing and incoming conductors in a common spiraled cable throughout. Thus, any tendency for induced potentials to appear in the coupler loop would be cancelled. This was proved in field tests at York, to be described later.

Linear coupler bus protection was therefore installed at Middletown and York substations for the following reasons:

1. Simplicity. No calculations were required other than maximum and minimum bus fault curredts and the relay setting for the desired pick-up. Sound fundamental theory of operation had been substantiated by the manufacturer with exhaustive laboratory tests.

2. Linear characteristics of couplers for all values and types of fault current meant freedom from fear of saturation effects caused by offset transients.

3. Faster relay operation (1 to 2 cycles) would be obtained through complete range of fault currents, with only one comparatively simple relay per phase, regardless of the number of circuits connected to the bus. Thus, no complex relay and current transformer secondary connections, and less switchboard space would be required.

4. A complete system required only one secondary cable consisting of six, number 10 copper conductors, running from the relay panel to the first circuit breaker, thence to the second, third, and so on until the loop is completed in the last breaker (Figure 4). Actually, a smaller size conductor can be used, depending entirely upon the desired mechanical factor of safety. A considerable reduction in secondary cable was realized with the linear coupler scheme. For example, at Middletown a total of 2,800 feet of 4-conductor cable would have been required with the multi-restraint relay scheme. For the linear coupler installation a total of 775 feet of 6-conductor cable was installed. Therefore, for the installations under discussion, the latter scheme required approximately 41 per cent of the conductor-feet, that would have been required by the former.

5. If a cable duct system is used the amount of main duct run space saved with the linear coupler scheme is the total number of circuits involved, minus one. This also applies for future circuit additions, in which case the new circuit breaker is connected into the coupler loop by simply extending a 6-conductor cable from the nearest existing breaker, plus a few feet of wire on the relay panel to connect the added breaker

trip circuit to the multicontact tripping relay.

6. With the linear coupler scheme an open circuited secondary or relay coil renders that phase inoperative, whereas such conditions occurring with the conventional current transformer schemes may cause undesirable operation sooner or later. Either manual or automatic equipment is available to check the continuity of the relay-coupler loop if desired.

7. Cost of linear couplers and relays (not including savings in secondary cables) was competitive on new installations with the multirestraint scheme using bushing type current transformers.

It is of interest to note that the 6-conductor secondary cables for both installations were installed in the same trench with all other control and secondary cables leaving the relay panel, being buried directly in the earth over the greater part of the distance to the circuit breakers. Standard 600-volt, nonleaded, unshielded "mummy finish" spiral cable was used.

Field Tests

For a successful linear coupler system which will always trip when desired for internal faults and never trip when undesired as for external faults, the following requirement must be met.

The mutual reactance, or proportionality between secondary voltage and primary current must be the same for all couplers on a bus within certain limits. If the couplers on the circuits where current entered the bus produced voltages 1.5 per cent high and those where current left the bus produced voltages 1.5 per cent low, a through-fault current would produce 3 per cent as much voltage as an internal fault of the same magnitude. Thus a through fault of 33 times the relay setting would be just enough to cause faulty tripping. The tolerance can be reduced to any desired amount but the cost is increased in proportion because of the refinements required in manufacture and testing.

Analysis and measurement of samples had indicated that a tolerance of ±1.5 per cent could be held quite readily. This tolerance includes several sources of variation which will be discussed briefly.

Linear couplers are wound in the form of a toroid similar to a bushing current transformer with a uniformly distributed winding. The core is of course nonmagnetic. This form of coil has theoretically zero mutual reactance to any conductor not linking the toroid and a constant mutual to any conductor which does link it irrespective of its position within the opening. Also its mutual theoretically is unaffected by any external magnetic fields. There are, of course, minor variations due to irregularities of winding so that the mutual is slightly affected by positions of the center and return conductor, and the presence of neighboring iron. Further variations occur due to finite steps of adjustment of individual couplers to the standard coupler. These effects have been exhaustively studied and reported previously[1] and are all included in the ±1.5 per cent over-all tolerance.

In the case of the York and Middletown installations most of the couplers were supplied separate from the circuit breakers, and were mounted in the usual bushing current transformer housings of the breakers in the field. Polarities were checked by impulsing with a flashlight battery as for current transformers. However, the field tests provided an overall check of the tolerance as described above including position effects within the circuit breaker, effect of the iron cases, leads, and coupling with other phases if any. Provision of adequate energy for operation at the proposed relay setting had been demonstrated in the prior laboratory tests of the scheme and therefore merely was confirmed by the field tests.

Tests for accuracy and performance of a linear coupler differential are extremely simple because the d-c component in a

Figure 4 (below). One-line diagram of Middletown substation

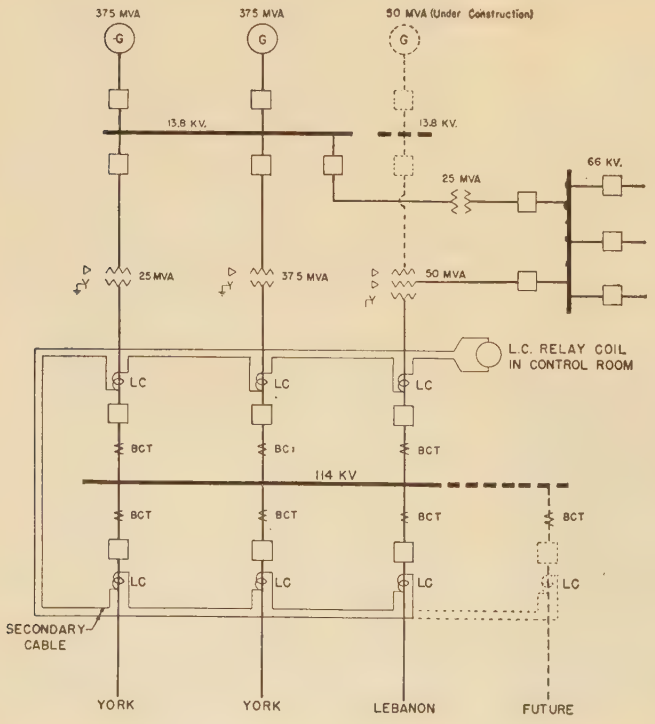

Figure 5 (right). Current–voltage relations in relay-coupler loop

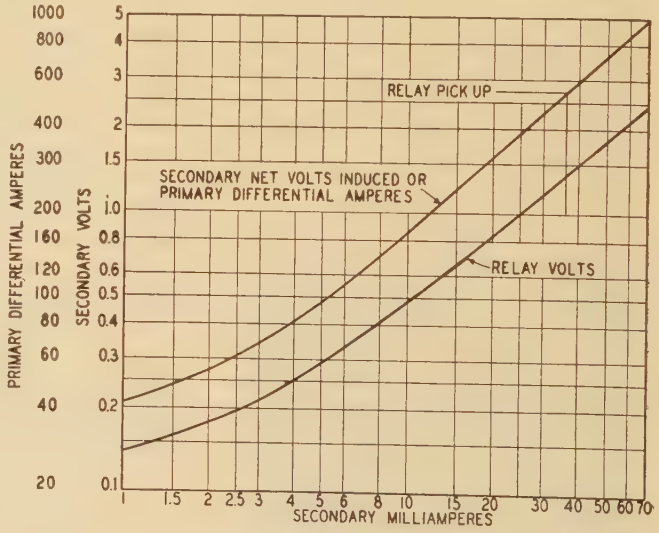

Figure 6 (lower right). Diagram of test connections

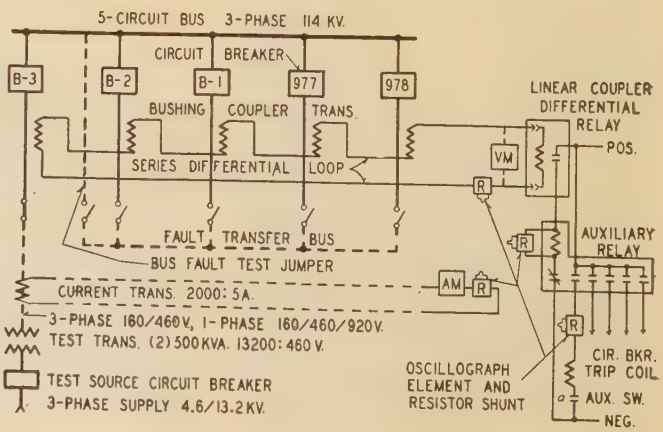

fault current has a negligible effect, and the secondary induced voltage is strictly linear with respect to the primary a-c component magnitude. Hence measurements may be made with primary currents just sufficient to give accurate readings on a secondary circuit voltmeter. An electronic voltmeter is ideally suited for reading these low voltages as it has very high impedance so as not to disturb the current flow in the differential circuit.

Methods of Measuring Differential Error

Measurements of differential error are made most directly by opening the series differential loop and measuring the net induced voltage for a through primary current passing into and from the bus. The per cent differential error is then 100 times the net induced volts divided by the secondary voltage of five volts per thousand amperes of through-fault current. Differential error also may be determined with the secondary circuit closed so as to permit normal relay operation by measuring either the voltage across the relay or the secondary current. Either of these measurements are readily translated to net induced volts by a curve (Figure 5). This curve is obtained by applying a voltage in the coupler-relay loop while all primary circuits are open, and reading total volts, relay volts, and secondary current. The operating point of the relay should be definitely noted and indicated on this curve. Tests of this type were made at both Middletown and York. In addition some oscillograms were taken at York for record purposes.

Test Facilities at York and Middletown

Test arrangements at York are shown schematically in Figure 6 and, those at Middletown were similar except that the bus has six circuits and only one 500-kva transformer was available as a test supply. The two test transformers at York permitted tests for all types of faults and a wider range of fault currents. For 3-phase faults the transformers were connected open delta. For heavy-current single-phase faults, phase-to-phase or phase-to-ground, the transformer primaries were connected in parallel and their secondaries in series. The regular high-voltage disconnect switches and transfer bus facilitated selection of the primary circuits to be used during a test. One high voltage circuit was considered the incoming circuit and each of the other circuits in turn were used as outgoing circuits to determine their percentage differential error and to check proper phasing and polarity.

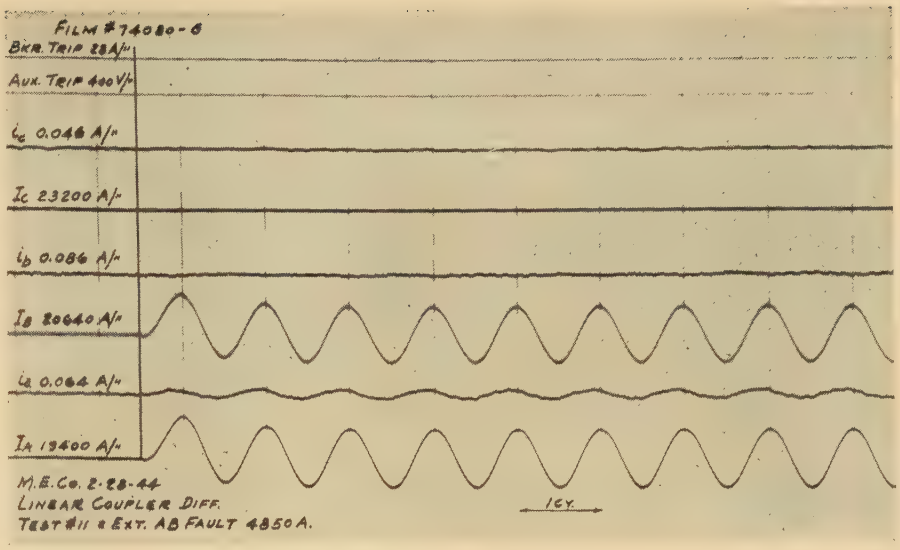

Figure 7. Oscillogram of an external phase-to-phase *AB* fault of 4,850 amperes using relay setting of 550 amperes

Reading from the bottom up the traces are:
I_A —Phase *A* primary current. It shows 4,850 amperes a-c component and a large rapidly decaying d-c transient
i_a —Phase *A* secondary differential error current. It shows 2.5 milliamperes representing 1.3 per cent error
I_B —Phase *B* primary current. It shows same as for phase *A*
i_b —Phase *B* secondary differential error current. It shows negligible error
I_C —Phase *C* primary current. It shows zero current
i_c —Phase *C* secondary differential error current. It shows no induction from the fault current
Aux. trip—Voltage across auxiliary tripping relay coil. It shows that the differential relays did not close their contacts
Bkr. trip—Current through *B*-3 circuit breaker trip coil. It shows that it was not tripped

Results of Tests

The highest differential error measured between any two couplers was found to be 2.1 per cent at York and 2.6 per cent at Middletown. The average of such differential errors was about 0.75 per cent. As maximum capacity through faults involve more than one incoming circuit and may involve more than one outgoing circuit, the actual differential error depends upon the fault current distribution through the various couplers and their individual errors. This would be less than the highest per cent differential error between any two couplers, but by assuming it to be the same an additional factor of safety is included against operation for through faults.

External Fault Oscillogram

Figure 7 shows an oscillogram for an external *AB* phase-to-phase fault of 4,850 amperes fed through circuit breakers *B*-3 and 977. The relays were set to pick up for a 550 ampere bus fault, or 11.3 per cent of this through fault current, and did not operate as the differential error was less than the relay setting. The oscillogram shows the fault currents I_A and I_B initially offset, negligible i_b differential current in the *B* phase loop, and 2.5 milliamperes i_a differential in the *A* phase loop. From Figure 5 this 2.5 milliamperes indicates 0.318 volt net was induced in the loop and this in turn represents 1.31 per cent differential error. During this test the *A* phase relay voltage was read as 0.15 volt indicating 1.27 per cent differential error, and the *B* phase relay voltage was read as 0.05 volt indicating 0.203 per cent differential error. A further check of these differential errors was obtained more precisely in a steady-state test for an external 3-phase fault of 1,075 amperes by reading the net induced voltages directly with the differential loops open; and it gave differential errors of 1.30 per cent for phase *A*, 0.208 per cent for phase *B*, and 0.524 per cent for phase *C*. With 1.3 per cent differential error and a relay set to pick up for a 550 ampere bus fault, a through fault current of over 42,000 amperes would be required to cause undesired tripping.

Internal Fault Oscillogram

Figure 8 shows an oscillogram for a 3-phase bus fault of 1,157 amperes repre-

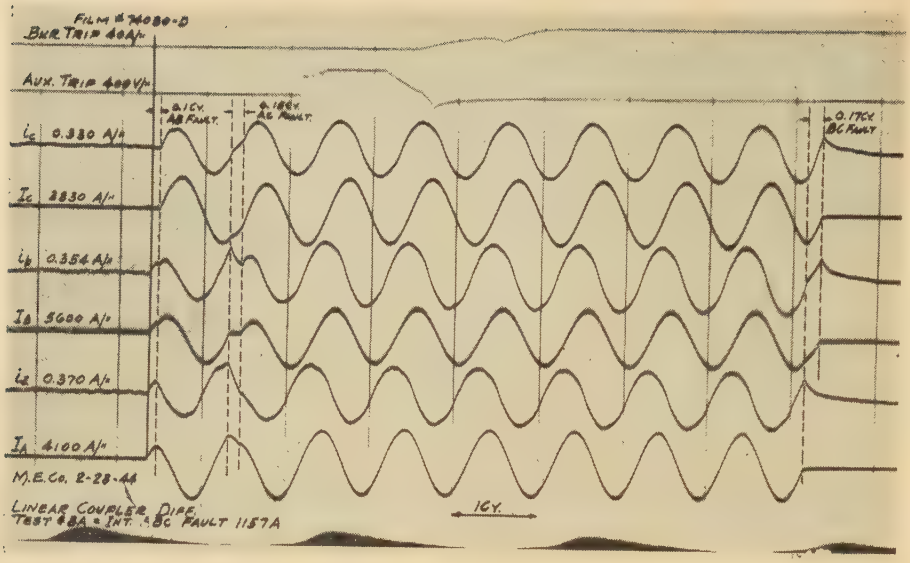

Figure 8. Oscillogram of an internal 3-phase fault of 1,157 amperes (average of 3 phases) using relay settings of 550 primary amperes, 36 milliamperes secondary current

Reading from the bottom up the traces are:

I_A—Phase *A* primary current. It shows 1,120 amperes

i_a—Phase *A* secondary differential current. It shows 87 milliamperes

I_B—Phase *B* primary current. It shows 1,310 amperes

i_b—Phase *B* secondary differential current. It shows 95 milliamperes

I_C—Phase *C* primary current. It shows 1,040 amperes

i_c—Phase *C* secondary differential current. It shows 76 milliamperes

Aux. Trip—Voltage across auxiliary tripping relay coil. It shows that the differential relays closed their contacts in 1.75 cycles

Bkr. Trip—Current through *B*-3 circuit breaker trip coil. It shows it was energized 3.13 cycles after inception of fault

senting 2.1 times the 550 ampere pick-up of the relays. It shows that the linear coupler relays energized the auxiliary trip relay in 1.75 cycles, the auxiliary trip relay energized the breaker trip coil at 3.13 cycles, and the fault was cleared at 8 cycles. This 3-phase fault was unusual in that it changed to different types of interphase faults because the test source voltage of 160 volts was not sufficient to establish or maintain arcs under oil with minute separation of the breaker contacts. The fault was successively an *AB* fault for 0.10 cycle, an *ABC* fault for about a cycle, an *AC* fault for 0.15 cycle, an *ABC* fault until the breaker started to interrupt and ended as a *BC* fault for the final 0.17 cycle. These fault transients did not interfere with operation of the relays as each showed a target, indicating all three relays closed their contacts within a 1/4 cycle period, required for the first trip circuit to be sealed. This test was a repeat of the previous test made without oscillograph and with the relay trip circuit disconnected so that the fault could be held long enough to read the three primary currents and the three relay voltages. These readings verified each other and the subsequent oscillographic record.

Summary of York Tests

These two oscillograms and their explanations are representative of the series of 19 fault tests made on the 114-kv circuits at York. They included 3-phase, phase-to-phase, and phase-to-ground faults both external and internal. The phase-to-ground faults were made through the structural steel and its multiple paths lowered the impedance to give fault currents up to 6,500 amperes. This current for a bus fault reduced the relay time to 1.33 cycles. The ground fault tests showed a neglible induction effect in the unfaulted phase loop circuits. In addition to the fault tests made on the 114-kv circuits, a ground fault was applied to a lighting circuit installed in the same trench as the bus differential leads to the structure and it was found that the 250 amperes that flowed out on the lighting circuit to return by way of ground induced quite negligible voltages, 0.012 volt, in the bus differential loops. This is less than half of one per cent of that necessary to operate the relays with the settings used.

Middletown Tests

The Middletown tests were similar but were made without oscillograph and with only one single-phase test transformer, which was able to deliver up to 4,800 amperes for a through fault. So as to demonstrate better the reliability of the linear coupler differential, the relay setting was deliberately lowered from the contemplated 700 ampere setting to 150 amperes, representing 3.1 per cent of the 4,800 ampere maximum through fault test. A complete round of 32 tests were made with this sensitive setting. The relays operated for all bus faults and did not operate for any external faults, even though differential errors up to 2.6 per cent were measured. After this the relays were returned to their normal 700 ampere pickup setting and then their complete tripping operation was demonstrated with bus faults of about 1,100 amperes.

Operating Experience

Field experience must be depended upon to show up any factors which may have been overlooked, and constancy of performance over a period of time, and to bring out any problems of maintenance or adjustment that may be involved.

Based on minimum fault current of 1,400 amperes and 1,050 amperes at Middletown and York, respectively, the linear coupler relays were set at a pick-up value of 700 amperes and 550 amperes, respectively. They have been in service approximately two years, and although during this period there have been no bus faults at either location to require operation, there have been a total of 8 faults on the Middletown-York circuits and 35 faults on the Middletown-Lebanon circuit, none of which caused incorrect operation.

A 66-kv ground fault on the 50,000 kva transformer bus structure at Middletown likewise did not cause operation of the linear coupler relays although the linear coupler secondary cable is buried in the earth in close proximity to the fault location.

Conclusions

In addition to providing assurance that the York and Middletown bus protection systems are in first class operating conditons, the tests have established the following facts of importance in general application of the system.

1. Linear couplers can be factory tested separately from the circuit breakers and then mounted in the breakers in the field, without any special adjustments.

2. The factory tolerances being maintained on the coupler mutual reactance results in over-all variations after mounting not over ±1.5 per cent.

3. With normal precautions of keeping the wires of the coupler-relay loop in a common

spiraled cable, induction from other circuits in the control ducts is negligible.

4. Field tests confirm that significant tests can be made at reduced primary currents. The system is linear and the percentage errors so determined apply equally well at higher currents. This facility is not enjoyed by any other system.

In many applications the choice lies between the multirestraint relay with current transformers and the linear-coupler system. If the current transformers already exist and are usable as they are or with rewinding, there may be an economic factor in favor of the multirestraint relay. However, this must be balanced against the lower cost of secondary cable installation with the linear couplers. Also, if partial differential feeder-backup protection is to be applied using the same current transformers, the corresponding equipment has not yet been developed for application with the couplers. The 3- to 6-cycle operating time of the multirestraint relay system has usually proved adequate from a stability standpoint.

On new installations or revamping projects where either current transformers or couplers will need to be procured, the linear coupler system offers instantaneous tripping in a very simple system which can be readily applied and tested. Its cost is competitive with the multirestraint relay system.

The multirestraint relay is applicable when the current range from maximum through fault to relay setting is up to 100 to 1. One relay per phase suffices with up to three major sources (generators, transformers, bus-ties) per bus sections; two per phase for up to seven major sources.

With the linear coupler system but one relay per phase is used irrespective of the number of circuits connected to the bus. However, energy requirements fix the lower limit of relay setting for positive action at approximately 300 amperes with six circuits per bus, plus 25 amperes per additional circuit. The range of currents from maximum through fault to relay setting has been limited purposely to 17 to 1. As demonstrated by these tests this limit is quite conservative in the case of the installations described. This range usually covers the required range for phase currents and also for ground currents on solidly grounded systems. Where ground currents are limited as by grounding resistors, making the over-all current range more than 17 to 1, a separate ground relay is required in the linear coupler system and is prevented from operating for other than single-line-to-ground faults by a ground detector relay described by Sonnemann.[6] The ground current setting cannot be below the 300 amperes for a 6-circuit bus plus 25 amperes per additional circuit.

Summarizing, local conditions will frequently dictate the proper application. Where high speed, simplicity and reliability are important, the linear coupler system should receive prime consideration.

References

1. Linear Couplers for Bus Protection, E. L. Harder, E. H. Klemmer, W. K. Sonnemann, and E. C. Wentz. AIEE Transactions, volume 61, 1942, May section, pages 241–8.

2. Current Transformer Excitation Under Transient Conditions, D. E. Marshall, P. O. Langguth. AIEE Transactions, volume 48, 1929, pages 1464–74.

3. Current Transformers and Relays for High Speed Differential Protection, With Particular Reference to Offset Transient Currents, E. C. Wentz, W. K. Sonnemann. AIEE Transactions, volume 59, 1940, August section, pages 481–8; discussion pages 1144–8.

4. Considerations in Applying Ratio Differential Relays for Bus Protection, R. M. Smith, W. K. Sonnemann, G. B. Dodds. AIEE Transactions, volume 58, 1939, June section, pages 243–52.

5. Air Core Couplers Simplify Bus Protection, E. L. Harder. *Westinghouse Engineer*, May 1942, page 43.

6. A New Single-Phase-to-Ground Fault-Detecting Relay, W. K. Sonnemann. AIEE Transactions, volume 61, 1942, September section, pages 677–80; discussion pages 995–6.

Long 60-Cycle Arcs in Air

A. P. STROM
MEMBER AIEE

Synopsis: Volt-ampere characteristics of 60-cycle arcs in still air with lengths and currents such as occur in power systems have been investigated under laboratory conditions. The arcs varied in peak current from 68 to 21,750 amperes and in length from 1/8 to 48 inches. Typical oscillograms and volt-ampere curves of these tests are presented. The voltage gradient in the arc is affected very little by current magnitude. Throughout the entire range all gradients remained between 21.5 and 50 volts per inch, with 35 per cent of all values in a 5 volt per inch interval having an average value of 34 volts per inch. The increase in apparent gradient due to voltage drop at the electrodes was found to be negligible where the arc length exceeds several feet. The decrease in short-circuit current of a power system through a series arc as compared with that for the same system with a metallic short circuit has been investigated. Data are presented showing the actual reductions observed for various conditions of circuit voltage and impedance.

SHORT CIRCUITS on transmission lines and at terminals of high voltage power apparatus practically always take place through long arcs in air. It is important, therefore, to know to what extent these arcs limit the short-circuit current and make it less than would occur with a metallic short circuit. The drop across the arc also affects the phase angle between voltage and current in directional types of relays. The data in the form presented here also can be used to indicate the current limiting effect of arcs on low voltage circuits. Although considerable data from field studies of transmission line flashovers are available,[1,2] the uncontrolled conditions do not permit any accurate determination of the arc characteristics of the arcs in the flashovers.

This investigation, therefore, has been carried out under laboratory conditions where better control of the variable factors is possible.

Testing Procedure and Apparatus

In order to cover a wide range of current values the 27,000-kva single-phase transformers in the Westinghouse high voltage laboratory at Trafford, Pa., were used to supply power for these tests. The current was limited by the impedance of the transformers and reactors connected in series.

Arcs varying in length from 1/8 to 48 inches and in peak current from 68 to 21,750 amperes were investigated. Most of these tests were made with brass electrodes at 48 inches separation. This large electrode separation was chosen so that the voltage drop adjacent to the electrodes would be negligibly small. However, owing to the limited capacity of the transformer bank, for currents in excess of 10,000 amperes the transformers had to be reconnected for smaller voltage. This voltage was insufficient to maintain the current in the 48-inch arc. For this reason these tests were made at 24-inch and 12-inch contact separations.

The arcs, which were initiated by means of fuse wires, were drawn in a vertical

Paper 46-22, recommended by the AIEE committee on protective devices and presented at the AIEE winter convention, New York, N. Y., January 21–25, 1946. Manuscript submitted November 20, 1945; made available for preprinting December 13, 1945.

A. P. Strom is with the research laboratories, Westinghouse Electric Corporation, East Pittsburgh, Pa.

Table I. Arc Volts Per Inch at Peak Current on Long 60-Cycle Arcs in Air

Test	Arc Length, Inches	Peak Arc Currents Each Half Cycle							Arc Volts Per Inch on Each Half Cycle						
		1	2	3	4	5	6	7	1	2	3	4	5	6	7
A	.48	140	145	134	136	135	137	125	25	27	31	40	35	38	27
B	.48	68.5	130	109					27	21.5	21.5				
C	.48	260	238	236	192				25	30	30	30			
D	.48	544	445	500	435	405			32	29	32	32	31		
E	.48	396	322	337	330	300			26	31	38	40	36		
F	.48	1,460	1,340	1,385	1,290	1,385	1,380	1,240	38	35	31.5	44	32	27	30
G	.48	2,500	2,680	2,630	2,680	2,630	2,480	2,525	35.5	30	30	26	28	28	27
H	.48	1,010	1,675	1,820	1,920	1,780	1,410		35	27	30	26	29	29	
I	.48	708	870	1,535	2,060	3,780			35	37	33	31	30		
J	.48	735	2,360	3,540	3,730	3,380			43	30	31	29	30		
K	.48	1,135	812						41	36					
L	.48	2,100	4,040	6,780	10,000	10,000			43	34	35	30	30		
M	.48	8,230							35						
N	.48	3,550							35						
O	.48	7,750							35						
P	.48	6,450	3,225	5,330	6,450	10,150	10,150		40	46	42	43	30	28	
Q	.48	2,580	2,420	7,750	9,500	8,550	7,600		40	38	32	34	33	36	
R	.48	5,200	7,150	6,660	7,070	6,750	6,660		35	36	36	35	30	28	
S	.48	4,370	5,440	5,150	5,100	5,150	4,800		36	31	31	31	31	31	
T	.48	4,370	5,400	5,150	5,250	5,250	4,910		34	31	31	27	27	26	
U	.48	4,270	5,490	5,000	5,250	4,910			40	34	39	31	34		
V	.48	5,400	5,150	5,250	5,250	5,150	4,910		54**	35	31	27	31	32	
W	.24	10,000	14,200	11,900	12,250	11,900			35	34	40	38	50		†
X	.24	2,010							48						†
Y	.24	7,640							47						†
Z	.12	6,840	20,500	17,500	18,500	17,700				54	59	59	56		†
AA	.12	12,450	19,100	17,500	19,100	14,900			46.3	50.5	59	56	55		*
AB	.12	11,700	21,750	21,150	20,000				45	41	41	40			‡
AC	.12	10,900	15,100	14,500	14,000	12,500			45	43	39	41	39		‡
AD	.12	6,900	8,670	7,950	8,070	7,370			41	34	36.5	40	39		‡
AE	.12	7,330	8,200	8,320	7,720				52	47	36.5	42			‡
AF	.12	6,990	8,125	7,800	7,650				37	39	38	38			‡
AG	.12	7,150	7,970	7,650	7,650	7,550			42	42	43	44	50		‡
AH	.12	6,570	8,125	7,800	7,650	7,230			38	43	38	39	43		‡
AI	.12	4,770	5,680	5,180	5,180				37	37	37	43			‡
AJ	.12	8,550	15,750	14,500	14,500				34	41	41	38			‡
AK	.12	10,450	17,700	19,700	19,700				43	43	43	43			‡
AL	0.125	15,750	15,250	15,750	14,900	14,000			(34.8)	(42.6)	(45.2)	(45.2)	(44)		‡, #
AM	0.125	22,100	26,000	25,000	23,200				(42.6)	(64.5)	(86.5)	(90.4)			‡, #
AN	.12	12,850	20,900	16,700	21,500	14,000			43	41	46	41	40		‡
AO	.12	9,970	15,250	13,300	13,500	11,200			46	47	42	45	45		‡

† Probable bowing of arc.
* Photograph indicates bowing of arc to approximately 1.5 gap length.
‡ Leads to test rearranged. Photograph shows no bowing of arc on *AB*.
# Figures give total arc volts on the 1/8-inch gap.
** Abnormally high voltage undoubtedly due to its occurrence immediately after fusing of large size fuse wire.

plane to prevent arc elongation by convection. To eliminate as far as possible any looping of the arc, the current leads to the terminals were placed along the longitudinal axis for a distance of 2 to 4 feet. Observations made through dark glasses and also by photography indicate that the arc is reasonably straight between the electrodes when these precautions are taken.

Magnetic oscillograms were taken of all tests, and measurements of current and arc voltage data were made from these records.

Variation of Voltage Gradient in the Arc With Current

Table I summarizes the data for all the arcing tests, giving the peak current and corresponding voltage gradient in the arc for each half cycle of arcing. No correction has been made for potential drop at the electrodes in this table.

Figure 1 shows graphically the variation of voltage gradient in the arc with current, using the data from Table I. A correction of 3 volts per inch was made for electrode drop in plotting the data for the 12-inch long arcs, as this is approximately the proper value indicated by tests which will be discussed further in a later paragraph. Tests *W* to *AA* inclusive were omitted from this curve, as it is believed that there was some arc elongation on these tests due to magnetic fields from the current supply leads.

This curve shows that practically all of the arc voltage gradients found in these tests fall between 25 and 50 volts per inch. The average of the gradients appears to remain constant at 31 to 33 volts per inch for all currents up to 5,000 amperes, rises slowly to 38 volts per inch at 10,000 amperes, and remains constant up to over 20,000 amperes.

The fact that the arc voltage gradients cover a rather wide band has not been entirely explained. It is believed, however, that at least a part of this variation can be accounted for by the effects of magnetic forces moving the arc about. If the

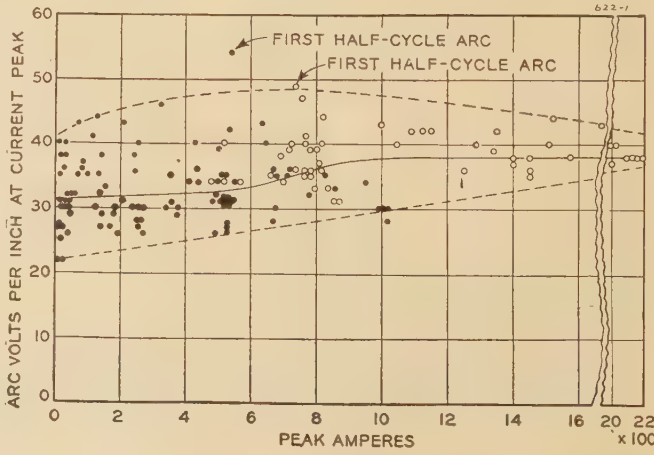

Figure 1. Voltage gradients at peak current on 60-cycle power arcs in air

● 48-inch arcs
○ 12-inch arcs

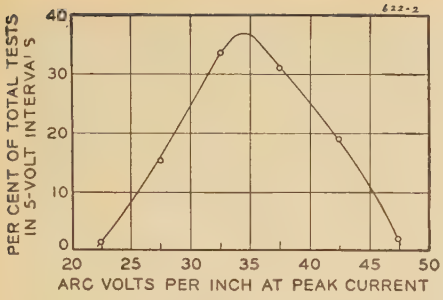

Figure 2. Distribution of voltage gradients at peak current on 153 half cycles of arcing

Peak current range from 68 to 21,750 amperes

arc terminals strike unsymmetrically, or if the axis of the arc moves away from the axis of the electrodes, magnetic forces act to accelerate such motion. This results in slight variations in arc path and relative motion of the arc and surrounding air. The effect of convection air currents and turbulence conditions at the arc boundary change and cause a more rapid loss of heat and ionization requiring higher arc voltage to maintain the current. The 3.7-ampere arc in Figure 11 shows variations in arc path of a substantially

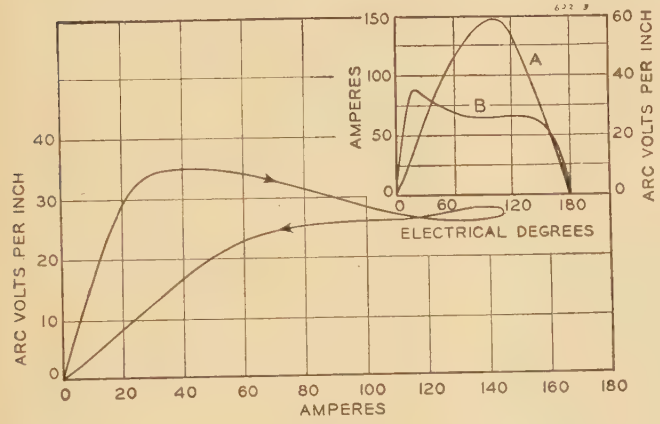

Figure 3. Volt-ampere characteristic for a 100 rms ampere arc

Test *A* of Table I.
Arc length 48 inches
A—Amperes
B—Volts

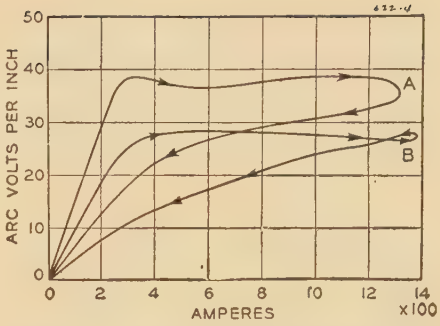

Figure 4. Volt-ampere characteristics of a 1,000 rms ampere arc

Second and sixth half cycles of test *F*, Table I.
Arc length 48 inches
A—Second half cycle
B—Sixth half cycle

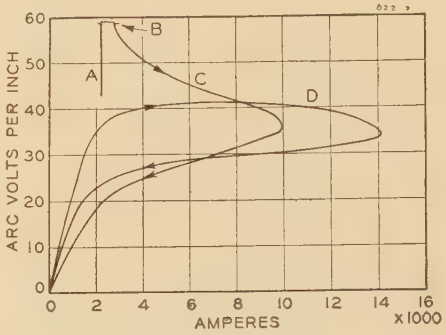

Figure 5. Volt-ampere characteristics of a 10,000 rms ampere arc

First and second half cycles of test *W*, Table I
Arc length 24 inches
A—Fusing current, 2,260 amperes
B—Arc volts at fusing, 178 volts per inch
C—First half cycle
D—Second half cycle

Table II. Current Limiting Effect of Series Arcs on Short-Circuit Currents

Test	No-Arc Short-Circuit Peak Current	Arc Length, Inches	Circuit Volts, Rms	First Half Cycle Arc Current, Per Cent of No-Arc Short-Circuit Current	Maximum Arc Current, Per Cent of No-Arc Short-Circuit Current
A	144	48	5,750	97	100
B	142	48	2,300	47.5	77
C	382	48	2,300	68	68
D	735	48	2,300	74	74
E	360	48	4,600	100	100
F	1,420	48	4,600	100	100
G	2,830	48	4,600	88	95
H	2,830	48	2,300	35	68
I	2,830	48	2,300	25	97
J	5,660	48	2,300	13	66
K	9,900	48	2,300	11.5	11.5*
L	16,600	48	2,300	12.7	60
M	16,600	48	2,300	50	50*
N	16,600	48	2,300	21.5	21.5*
O	16,600	48	2,300	48	48*
P	16,600	48	2,300	39	61
Q	16,600	48	2,300	15.6	57
R	8,150	48	4,600	64	88
S	5,630	48	6,900	77	97
T	5,500	48	6,900	80	98
U	5,450	48	6,900	78	100
V	5,450	48	6,900	99	99
W	16,300	24	2,300	61	87
X	27,300	24	1,150	7.4	7.4*
Y	27,300	24	1,150	28	28*
Z	33,400	12	1,150	20	61
AA	27,300	12	1,150	45	70
AB	27,300	12	1,150	43	80
AC	16,300	12	2,300	67	93
AD	8,100	12	4,600	85	100
AE	8,100	12	4,600	90	100
AF	8,100	12	4,600	86	100
AG	8,100	12	4,600	88	98
AH	8,100	12	4,600	81	100
AI	5,450	12	6,900	88	100
AJ	16,300	12	2,300	52	96
AK	27,300	12	1,150	38	72
AL	16,300	0.125	2,300	97	97
AM	27,300	0.125	1,150	80	95
AN	27,300	12	1,150	47	78
AO	16,300	12	2,300	61	93

* Arc extinguished itself in 1 or 2 half cycles.

Two tests in Table I, *AL* and *AM*, were made on 1/8-inch long gaps in order to determine the approximate additional voltage due to drops at the electrodes. The maximum currents on the first half cycles of these tests were respectively 15,750 and 22,100 amperes, and the corresponding arc voltages 34.8 and 42.6 volts. Although a small part of this voltage can be attributed to positive column drop in the 1/8-inch long arc, the results indicate that approximately 30–40 volts can be attributed to drop at the electrodes. The positive column gradient expressed in volts per inch is, therefore, approximately, $(e_a - 35) \div l$, where e_a is total arc volts, and l is arc length in inches. This indicates that drop at the electrodes has a negligible effect on the apparent gradient if the arc length exceeds several feet.

The distribution of voltage gradient values for the entire series of tests from

68 to 21,750 peak amperes in 5 volt per inch intervals is shown graphically in Figure 2. This curve indicates that over 35 per cent of the gradients fall in a 5 volt per inch range having an average value of 34 volts per inch.

Volt-Ampere Characteristics

Figures 3, 4, 5, and 6 show volt-ampere characteristics of arcs varying in peak current from 145 to 21,750 amperes. The volt-ampere curves are similar for both high and low currents, but there is considerable variation from one half cycle to another. This is illustrated by the curves of Figure 4 showing two half cycles of a 1,000 rms ampere arc. Here the sixth half cycle is considerably lower in arc voltage than the second. This might suggest that arc voltage decreases as arcing progresses from one half cycle to another, but examination of the test data fails to show any definite trend in this direction.

Current Limiting Effect of Arcs

The current limiting effect of the arc at short-circuit currents was studied for a considerable number of the tests recorded in Table I, by first drawing an arc between a pair of electrodes and then taking the short-circuit current under the same conditions, except with the arc gap short-circuited with a heavy copper conductor.

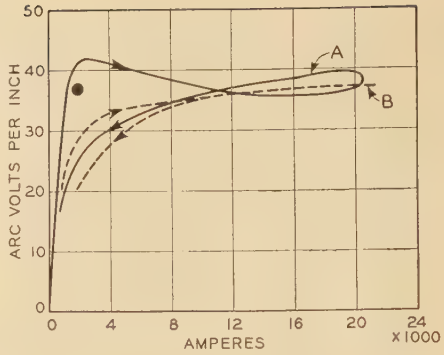

Figure 6. Volt-ampere characteristics of a 15,000 rms ampere arc

Second and fourth half cycles of test *AN*, Table I. Arc length 12 inches. Gradients corrected for drops at electrodes

A—Second half cycle

B—Fourth half cycle

In Table II the values of short-circuit current without a series arc for each test condition of Table I are given together with the percentage reduction in current observed when the same circuit is short-circuited through a series arc. Nominal values of the no-arc short-circuit currents are given for the tests in which these values were not experimentally observed.

Typical oscillograms are shown in Figures 7 and 8, illustrating the reduction in short-circuit current due to series arcs. These oscillograms show that a 48 inch long arc reduces the current very appreciably on a 4,000-ampere 2,300-volt circuit, but has much less effect at 6,900 volts with approximately the same current. This may be expected, as the arc voltage in the latter case is a much smaller part of the applied circuit volts. As a rough estimate the arc may be treated as a series resistance having a value equal to arc volts divided by normal rms short-circuit amperes. The approximate reduced value of current with a series arc then may be estimated as the quotient of rms volts and the impedance, in which the arc resistance is added vectorially to the normal circuit impedance.

Since the arc voltage, e_a, is nearly constant in value, a better estimate may be made by directly integrating the differential equation of the circuit but remembering that e_a changes sign when the current reverses. This requires a redetermination of the constant of integration at each current zero.

For example, to determine the steady state current for a circuit which consists of a pure inductance and a series arc, we may start with the equation,

$$A \cos wt + B \sin \omega t - L\frac{di}{dt} - e_a = 0 \qquad (1)$$

where

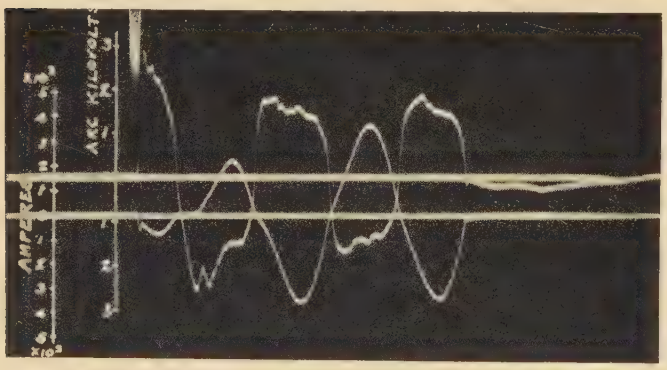

Figure 7 (above). Effect of a series arc in reducing short-circuit current in a 4,000 rms ampere 2,300 rms volt system

A. Current and arc voltage with a 48-inch series arc. Test *J*, Table I. Maximum peak current 3,730 amperes

B. Current in the same circuit without a series arc. Maximum peak current 5,660 amperes

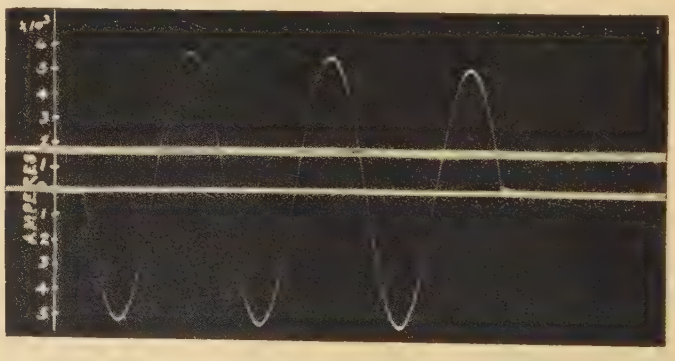

Figure 8 (below). Effect of a series arc in reducing short-circuit current on a 4,000 rms ampere 6,900-volt system

A. Current and arc voltage with a 48-inch series arc. Test *S*, Table I. Maximum peak current 5,440 amperes

B. Current in the same circuit without a series arc. Maximum peak current 5,630 amperes

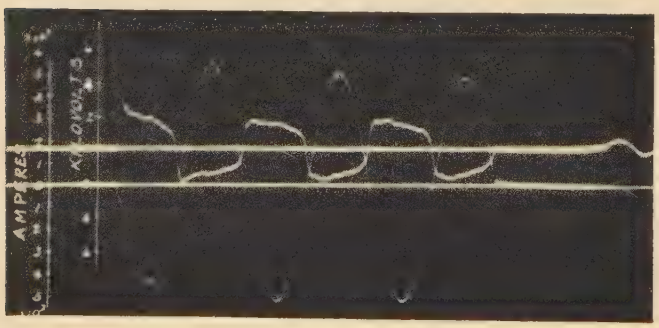

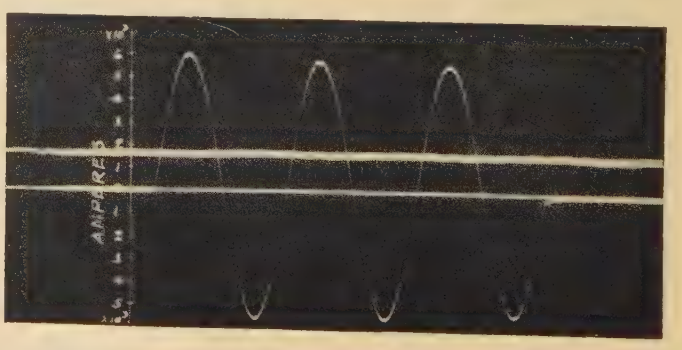

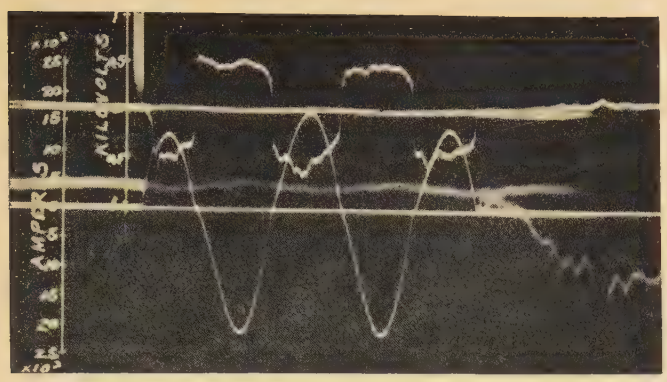

Figure 9 (above). Oscillogram of a short-circuit test on a 20,000 rms ampere, 1,150 rms volt circuit, with a 12-inch series arc

Test *AN*, Table I. Maximum peak current 21,500 amperes

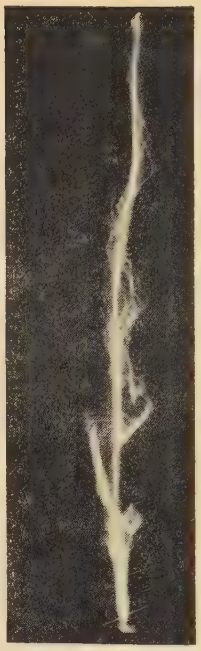

Figure 11 (right). Photograph of a 48-inch 3.7 rms ampere arc showing variations in arc path of a substantially straight arc

$A \cos \omega t + B \sin \omega t$ = sinusoidal impressed voltage

$\sqrt{A^2+B^2} = E_m$ = maximum value of impressed voltage

L = inductance in henrys

e_a = arc voltage (assumed of constant value)

Integrating equation 1 gives

$$i = \frac{A}{\omega L} \sin \omega t - \frac{B}{\omega L} \cos \omega t - \frac{e_a}{L} t + K \qquad (2)$$

Figure 10. Photographs of 12-inch high current arcs showing the effect of the magnetic field due to the supply leads on the shape of the arc

A (below, left). Substantially straight arc when current supply leads are brought in along the axis of the arc. Test *AK*, Table I. Maximum peak current 19,700 amperes

B (below, right). Bowing of the arc when the supply leads are not located along the axis of the arc. Test *AA*, Table I. Maximum peak current 19,100 amperes

The supply leads have been retouched to show their locations more clearly

as long as the current and with it e_a does not change sign.

We now assume that i is initially zero when t is zero and passes through zero again at uniform half cycle intervals. Then the constants K, B, and A may be evaluated as follows:

When $t=0$, $i=0$; substituting these values in equation 2 gives

$$K = \frac{B}{L\omega}$$

When $t = 1/2$ cycle or π/ω, $i=0$; substituting these values in equation 2 gives

$$B = \frac{e_a \pi}{2}$$

$$A = \sqrt{E_m^2 - B^2} = \sqrt{E_m^2 - \left(\frac{e_a \pi}{2}\right)^2}$$

Using these values for A, B, and K in equation 2 gives the solution for the current in terms of known constants as follows:

$$i = \frac{\sqrt{E_m^2 - \left(\frac{e_a \pi}{2}\right)^2}}{\omega L} \sin \omega t - \frac{e_a \pi}{2 \omega L} \times \cos \omega t - \frac{e_a}{L} t + \frac{e_a \pi}{2 \omega L} \qquad (3)$$

The ratio of this current at peak value to that without the series arc is very nearly

$$\frac{\sqrt{E_m^2 - \left(\frac{e_a \pi}{2}\right)^2}}{E_m} = \sqrt{1 - \left(\frac{e_a \pi}{2 E_m}\right)^2}$$

It also may be shown from equation 1 that the current lags the voltage by an angle,

$$\theta = \cos^{-1} \frac{B}{\sqrt{A^2+B^2}} = \cos^{-1} \frac{e_a \pi}{2 E_m}$$

In actual faults the arc length usually increases by bowing or looping, and the arc voltage gradient also may rise slightly as a result of air currents. Estimates of current reduction in which the values for arc voltage gradient presented in this paper are used, therefore, should give conservative, that is slightly too high, current values.

Conclusions

1. The average voltage gradients at current peak for 60-cycle arcs in air lie between 31 and 38 volts per inch for currents over the entire range from less than 100 to over 20,000 peak amperes.

2. The arc voltage varies considerably from one half cycle to another. The extreme range of this variation was from 21.5 to 50 volts per inch. Arc voltages on low currents vary over a wider range than on high currents.

3. While the variability of arc voltage has not been explained satisfactorily, it is believed that it is due at least in part to the magnetic forces acting on the arc which tend to shift the arc core into new arc paths that are less highly ionized and require higher arc voltage to maintain the current.

4. The average arc voltage gradient at current peak appears to rise from about 31 volts per inch at currents below 5,000 peak amperes to 38 volts per inch in the 10,000 to 20,000 ampere range.

5. For the complete range of currents from 68.5 to 21,750 peak amperes, 35 per cent of all the arc voltages fall within a 5 volt per inch interval having an average value of 34 volts per inch.

6. The current limiting action of arcs on short-circuit currents depends on the relative value of the total arc voltage to the circuit voltage. Approximations by calculation or graphical means of current reduction resulting from a series arc should be possible

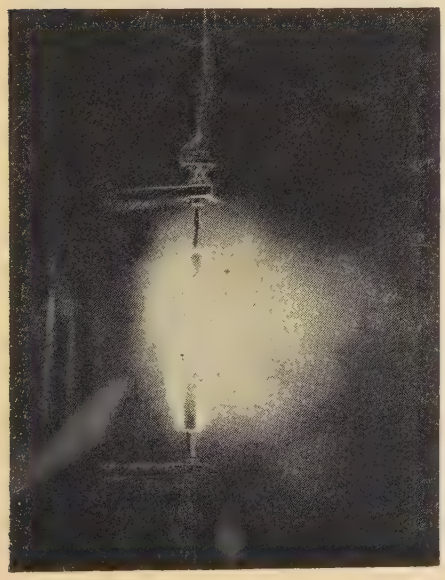

Industrial Application of Rototrol Regulators

W. R. HARRIS
MEMBER AIEE

Synopsis: The Rototrol has been applied in considerable numbers to a wide variety of industrial applications. It has met adequately the need for a simple and reliable regulator which is capable of withstanding the rigors of general industrial usage and which is sufficiently elemental in operation that it can be understood by nontechnical maintenance personnel. It has been accepted enthusiastically by industry, and applications in both existing and new fields are increasing rapidly. This paper discusses the fundamental theory of the Rototrol, the application of the circuits most commonly used, and cites operating results for typical installations.

THE Rototrol is nothing more than a d-c generator similar in design and theory of operation to the standard d-c generator, but with a number of field windings which are designed and connected in various ways, depending on the regulating problem. The Rototrol functions entirely through the interaction of these fields, and has no moving parts or circuits which require delicate adjustment for proper operation or to compensate for wear. After initial adjustment during installation no further attention is required other than the routine maintenance associated with a d-c machine of similar size. The Rototrol is driven at constant speed either by a small squirrel-cage induction motor or as a part of the motor generator set or exciter set of the adjustable voltage drive which it serves.

The Rototrol, as shown in the functional diagram, Figure 1, is one of the most simple regulators yet devised. The principal elements are a self-energizing field (either in series or in parallel with the armature) and the separately excited control fields (usually two in number). One of the control fields commonly is referred to as the pattern field and is excited from a constant potential source. The other control field measures the quantity to be regulated and is referred to as the pilot field. The pattern and pilot fields usually are connected with their ampere turns in opposition, so that the pilot field measures the quantity to be regulated and compares it with the pattern field. Any net difference in these fields will cause the Rototrol to exert corrective forces to reduce the difference, so that the pattern and pilot fields balance out when the quantity under regulation is at the proper value.

Assume for the moment that the self-energizing field is short-circuited. Under this condition the ampere turns required to generate output voltage necessarily must come from the difference in excitation of the pattern and pilot fields. Precise regulation would be impossible, as a change in operating conditions would necessitate a greater or less difference in ampere turns, and the quantity under regulation would vary. From this it is concluded that for high accuracy the pattern and pilot fields must control the Rototrol output without supplying the ampere turns required to generate output voltage. The self-energizing field must perform this function so that the control fields are free for their regulating and forcing functions.

The self-energizing field is designed and tuned by a simple resistor adjustment, so that its resistance line is coincident with the air gap line of the no-load saturation curve. For instance, if 1 ampere in the self-energizing field generates 50 volts across the brushes, and the resistance of the self-energizing field circuit including the Rototrol armature, the self-energizing field, the field of equipment under control, and the tuning resistor is 50 ohms, 50 volts will cause 1 ampere to flow through the circuit. Following this further, if 2 amperes flow in the self-energizing field, 100 volts will be generated which will cause 2 amperes to flow through the tuned or self-energized circuit. With the self-energizing field so designed and adjusted, it is possible for the Rototrol to operate over the straight portion of its saturation curve without the control fields supplying the magnetomotive force necessary to generate voltage. Such a device then may be used as a simple and accurate regulator.

In order for the saturation curve to approximate closely the self-energizing field circuit resistance line, it is necessary to minimize hysteresis effects. By the use of special steels, or by special treatment of standard steels, hysteresis or residual magnetism can be reduced to the point where its effect is negligible. For example, a recent Rototrol on the basis of normal saturation for a d-c generator tested 0.4 per cent residual voltage. A comparable value for the usual d-c machine is 5.0 per cent.

Although the foregoing discussion describes a Rototrol with two control fields, it is possible to supply additional control fields to receive main or supplementary regulating intelligence. For instance, in certain speed control problems, it is desirable to limit the armature current which flows in the main machines to a definite value. An additional Rototrol control field is added and its circuit designed so that it takes control should the current exceed a definite value for either motoring or regenerative conditions. This field acts to hold the current within definite limits during acceleration or retardation and is particularly advantageous where the inertia of the mechanical

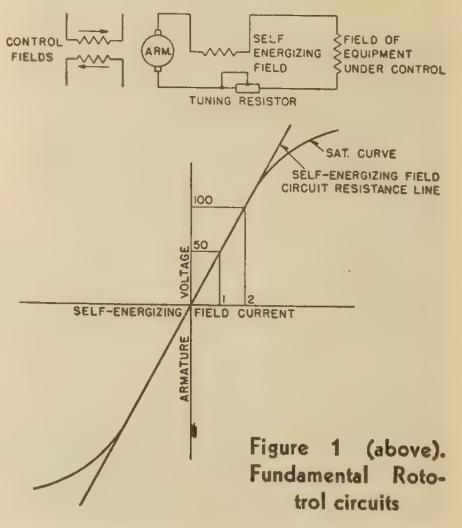

Figure 1 (above). Fundamental Rototrol circuits

Paper 46-57, recommended by the AIEE committee on industrial power applications and presented at the AIEE winter convention, New York, N. Y., January 21–25, 1946. Manuscript submitted November 23, 1945; made available for printing December 6, 1945.

W. R. HARRIS is in the industry engineering department, Westinghouse Electric Corporation, East Pittsburgh, Pa.

when arc voltages and circuit conditions are known.

References

1. A STUDY OF TRANSMISSION LINE POWER ARCS, Paul Ackerman. *Engineering Journal*, volume 11, May 1941, pages 309–23; 504

2. FREE BURNING HIGH CURRENT ARCS AT 100 KILOVOLTS A-C VOLTAGE, E. Gross. *Schweizer Archiv* (Solothurn, Switzerland), volume 7, July 1941, pages 196–201.

3. ELEKTRISCHE SCHALTVORGANGE (book), Reinhold Rüdenberg. Pages 204–15.

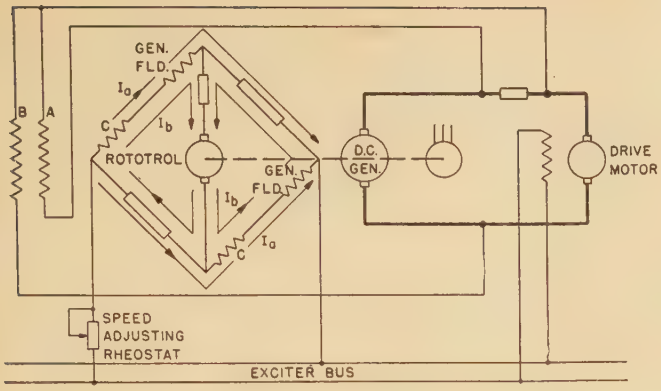

Figure 2. Elementary circuits of counterelectromotive force type speed regulator

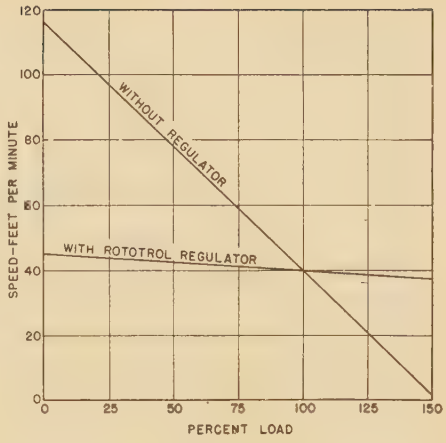

Figure 4 (right). Plot of test results at 1/30 speed for 150 horsepower supercalender drive with and without Rototrol counter electromotive force type regulator

system is large and a considerable period of time is required to accelerate from one speed to another.

The Rototrol is particularly well suited for application in closed cycle control systems. The criterion for a closed cycle system is that the deviation from the ideal performance be used to modify the flow of power to reduce the deviation. In such systems stability of operation must be carefully considered. A complete analysis of stability is beyond the scope of this paper, but a review of the factors that affect it is in order. The most important factors are the level of ampere turns in the control fields, the speed of response of the Rototrol system as determined by the time constants and mutual linkages of the various fields, series or parallel connection of the self-energizing field, and the electrical and mechanical inertias of the machines or system of machines under control. By proper evaluation of these various factors and care in the design of the system it has been possible to apply most Rototrols without the use of external stabilizing means. This makes the device well suited for industrial applications where simplicity of circuits and functions are desirable, both from the standpoint of operation and maintenance and of initial cost.

A few of the Rototrol circuits most commonly used with typical applications and operating results are described in the following paragraphs. These applications are chosen as indicative of the wide variety of functions which the device will perform.

Counterelectromotive Force Type Speed Regulator

The Rototrol counterelectromotive force type of speed regulator circuit is perhaps the most widely applied. Representative applications are feed drives for machine tools, adjustable voltage planer drives, high speed adjustable voltage elevator drives, skip hoist drives, and supercalender drives. It is applied where wide speed ranges are required with good speed regulation at all speeds, particularly at the minimum speeds. The circuit does not require a pilot generator to measure the motor speed, which results in a space saving about the machine and in a simplification of the electric equipment and circuits.

Figure 2 shows the elementary circuits of the Rototrol counterelectromotive force type of speed regulator. The speed of a d-c motor is given by the well-known formula,

$$S = \frac{V - (IaRa)}{K\phi}$$

in which S is the motor speed, Va, Ia, and Ra are armature circuit voltage, current, and resistance respectively, ϕ is the flux, and K is a constant depending on the motor design. If the motor is excited separately at constant potential, the flux may be assumed constant with small error. The motor speed is then proportional to the counterelectromotive force, which is the voltage across its armature minus the resistance drop in its armature circuit. Rototrol pilot field B measures the voltage across the armature, and pilot field A measures the armature current which is directly proportional to resistance drop. Field A is connected in opposition to field B, so that the net result of these two fields measures the motor counterelectromotive force, which is directly proportional to motor speed.

Rototrol fields C are connected in a bridge circuit with the generator field and perform the double duty of both pattern and self-energizing functions. All legs of the bridge are of the same resistance. The component of current Ia flowing from the exciter bus serves as pattern

Figure 3. High speed supercalender equipped with Rototrol counterelectromotive force speed regulator

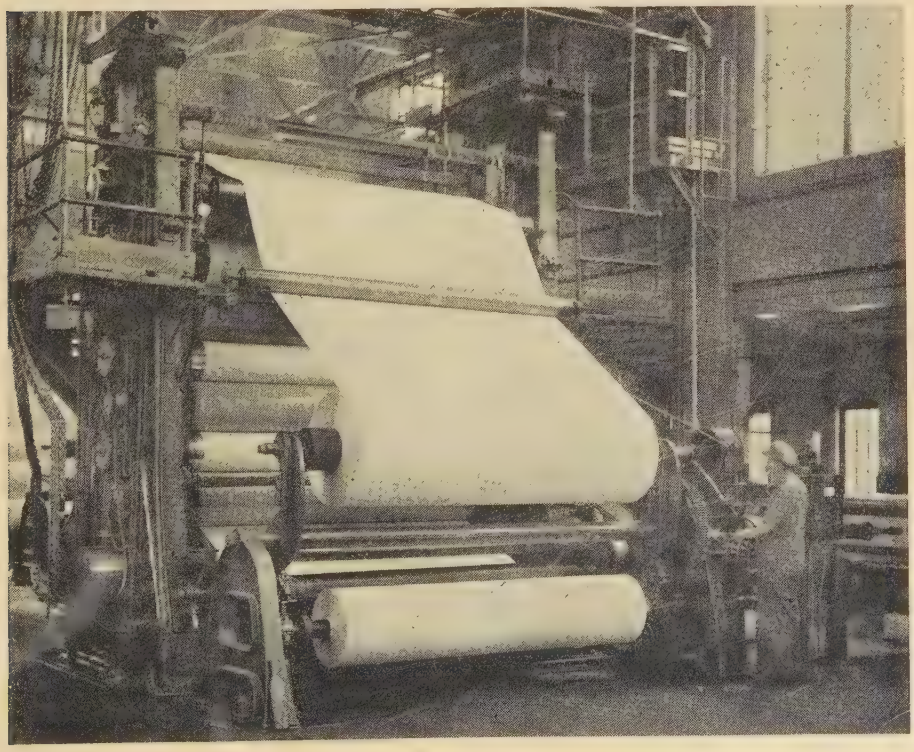

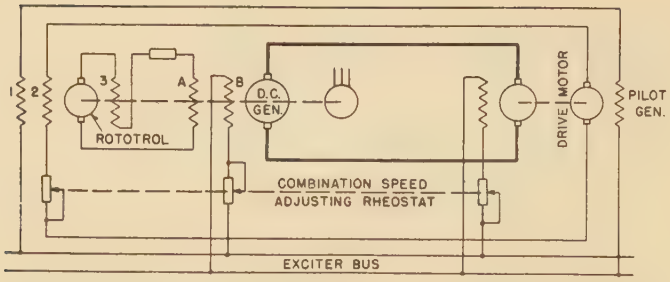

Figure 5. Elementary circuits of precision type speed regulator with pilot generator for measuring motor speed

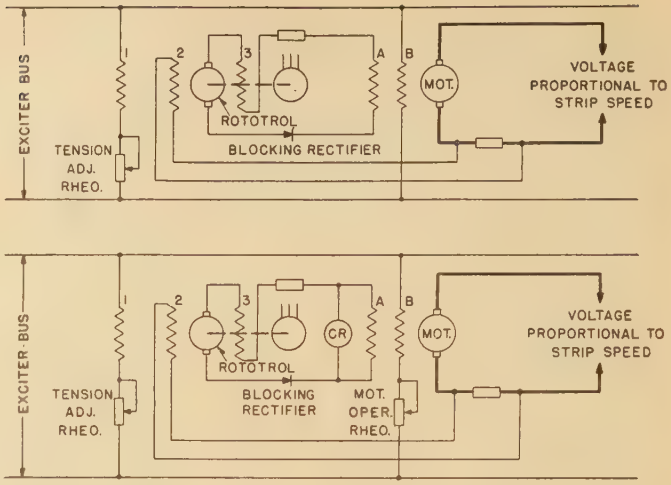

Figure 7 (right). Elementary circuits of tension control system for core type reels

a. Without speed limit feature
b. With speed limit feature

field current and in such a bridge will not cause a voltage drop across the Rototrol armature circuit. The component of current *Ib* flowing from the Rototrol armature through the bridge serves as the self-energizing component and conversely does not cause a drop across the terminals connected to the exciter bus. The circuits are arranged so that the pattern component of current through fields *C* is in opposition to the net effect of pilot fields *A* and *B*. Thus the pilot fields measure the motor speed and compare it with the pattern field component of current through fields *C*. If a difference exists, the Rototrol will compensate the generator field excitation and thus the motor speed until these fields again balance out.

A typical application of this circuit is to high speed adjustable voltage supercalender drives used in the paper industry. On supercalenders production speeds of from 1,200 to 2,000 feet per minute are becoming common, and the calender must be threaded at approximately 50 feet per minute, which results in an extremely wide speed range. Furthermore, the threading speed must be held constant for ease in threading and for safety to the operator. This requirement is complicated, because at threading speed the generator is operated near residual voltage, and a small change in residual voltage or in operating load means a relatively large speed change. Also as a result of threading the paper through the stack and the application of weighting, the load may vary 2 to 1 or more, which results in considerable speed variation with an unregulated drive.

In the past several methods of obtaining stable threading speed have been used. One method was to obtain part of the speed range by motor shunt field control which only partially eliminated the difficulty and was expensive because of the large frame size of the driving motor. Another method made use of a separate motor geared to drive the calender at threading speed to an overrunning clutch. This method gave stable threading speed but resulted in a complicated mechanical layout. The use of a Rototrol speed regulator obviates these disadvantages and is simple, as it requires only a small Rototrol set and a minor modification of the control circuits.

Figure 3 shows a view of a high speed supercalender driven by an adjustable voltage drive designed for a maximum speed of 1,200 feet per minute and a threading speed of 40 feet per minute. The entire range of 30 to 1 is obtained by armature voltage control. Figure 4 is a plot of test results at threading speed with and without the Rototrol regulator. Excellent regulation of threading speed is obtained as well as ample torque to break away the high static friction torques on the sleeve bearing stack.

Figure 6. Graphic speed charts taken on a 250-horsepower drive illustrating performance with (left) and without (right) Rototrol precision type regulator

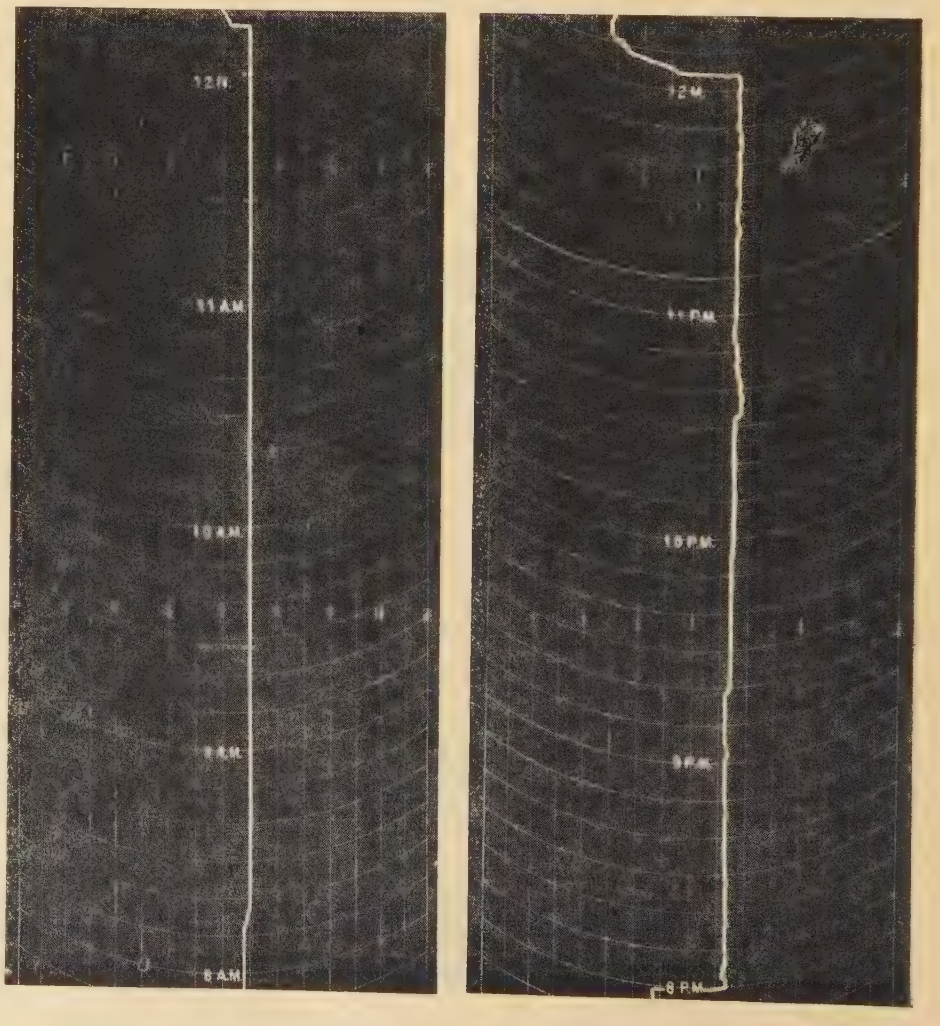

Precision Type Speed Regulator

On applications where it is desirable to hold the speed of the driving motor within very close limits, a pilot generator for measuring motor speed directly is used in conjunction with the Rototrol. Typical applications of this type of speed regulator include drives for paper machines, wind tunnel propellers, and dynamometers.

The schematic diagram of a Rototrol regulator for precise speed regulation is shown in Figure 5. A pilot generator is used to measure the drive motor speed and excites the Rototrol pattern field 2. Pattern field 1 is excited from the exciter bus as is the pilot generator field. These fields are connected in series to minimize the effect of changes in exciter bus voltage and changes due to unequal field heating. The Rototrol excites generator field *A* and supplies only the regulating field power. Generator field *B* supplies the base excitation of the generator for any speed setting. To assure high sensitivity at all speeds, the speed adjusting rheostat is located in Rototrol field 2 which is served from the pilot generator so that a constant level of forcing excitation is obtained over the complete speed range.

When the drive motor speed is at the correct value, the control fields 1 and 2 balance out. If the motor speed departs from its correct value, the speed change is detected by the pilot generator and transmitted to the Rototrol pilot field 2. A difference then will exist between the pilot and the pattern fields, which causes the Rototrol to compensate the generator excitation to bring the motor speed back to the correct value.

Operating results with this type of Rototrol speed regulator have been excellent. Typical performance is shown by the graphic charts of Figure 6 showing speed regulation before and after application of the Rototrol regulator. The charts were taken on a 250-horsepower single-motor paper machine drive which was modernized by addition of the Rototrol speed regulator. The performance was obtained without the use and complication of supplementary amplifiers and demonstrates the high amplification and speed of response of the Rototrol.

Tension Regulator for Core Type Reels

In the steel, textile, paper, and rubber industries there are a large number of windup and unwind operations utilizing core type reels. A drive for such a reel must maintain constant tension in the strip and must change its speed continually and smoothly as the roll builds up from a small core to a full roll. A number of Rototrol controlled drives for this service have been applied. The Rototrol is used in conjunction with an adjustable-speed d-c motor which has a speed range by shunt field control equivalent to the ratio of the full roll diameter to the empty core diameter.

Figures 7a and 7b show schematically the circuits for a constant tension reel drive. The reel motor is supplied with a voltage proportional to strip speed, either from the adjustable voltage generator serving the main drive or from an auxiliary generator driven at machine speed. The Rototrol modifies the shunt field excitation of the motor to compensate for changes in roll diameter and to maintain uniform strip tension. This is accomplished by maintaining the motor armature current constant, and, as the supply voltage is uniform at any particular strip speed, the power output of the motor and the tension in the strip will be substantially constant.

In Figure 7a Rototrol pilot field 2 measures the motor armature current and compares it with pattern field 1. Any net difference of these two fields will cause the Rototrol to change the excitation of motor field A to hold the armature current constant. Field *B* is the speed limit field and is adjusted to give a motor speed proportional to empty core diameter. The blocking rectifier situated in motor field *A* prevents reversal of this field in the event of a break or end of the material being reeled. Under these conditions the power formerly taken by sheet tension acts to accelerate the motor toward higher speed, and the Rototrol gradually will weaken field *A* until it is at zero excitation, at which time the blocking rectifier prevents reversal. With this scheme the equipment will accelerate to empty core speed when a break or end occurs. This is desirable when a new roll is to be started but is undesirable when rethreading is necessary.

Figure 7b shows the equipment modified to obtain a speed limit feature on strip breaks. Motor field *B* is the main field and is adjusted by a motor-operated rheostat. Field *A* receives its excitation from the Rototrol. As the roll builds up, field *A* is strengthened gradually, and the voltage across relay *CR* increases until the relay picks up. The relay contacts energize the motor-operated rheostat in such a direction as to strengthen field *B*. Simultaneously the Rototrol will decrease the excitation of field *A* in accordance with the regulator requirement of constant current in the motor armature circuit. This action progresses until relay *CR* drops out and stops the motor-oper-

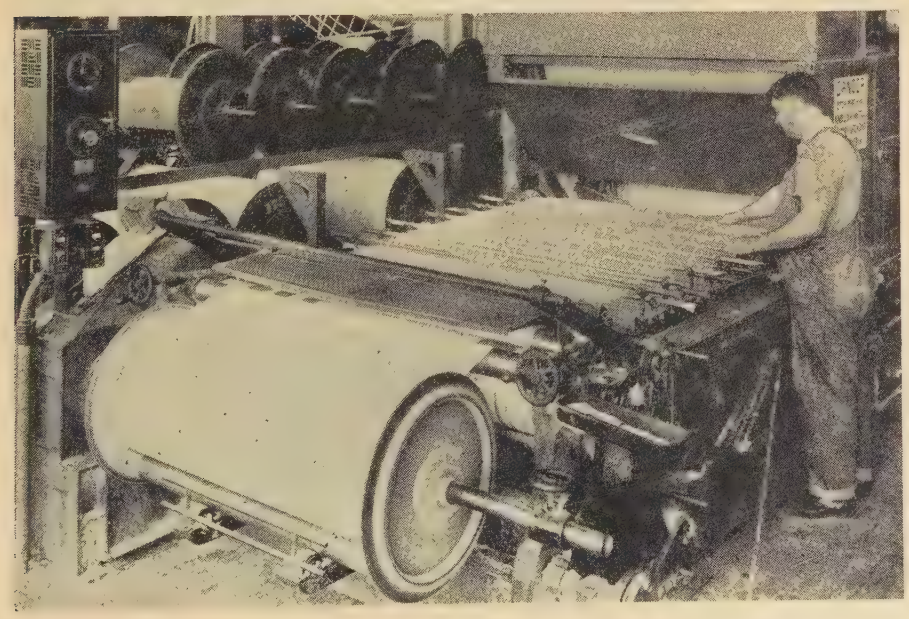

Figure 8. Core driven beam of a slasher in the textile industry using Rototrol control for speed and tension

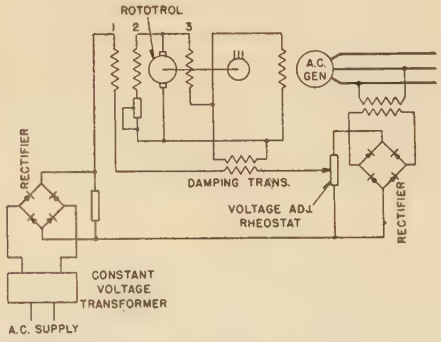

Figure 9. Schematic diagram of Rototrol voltage regulator applied to an a-c generator

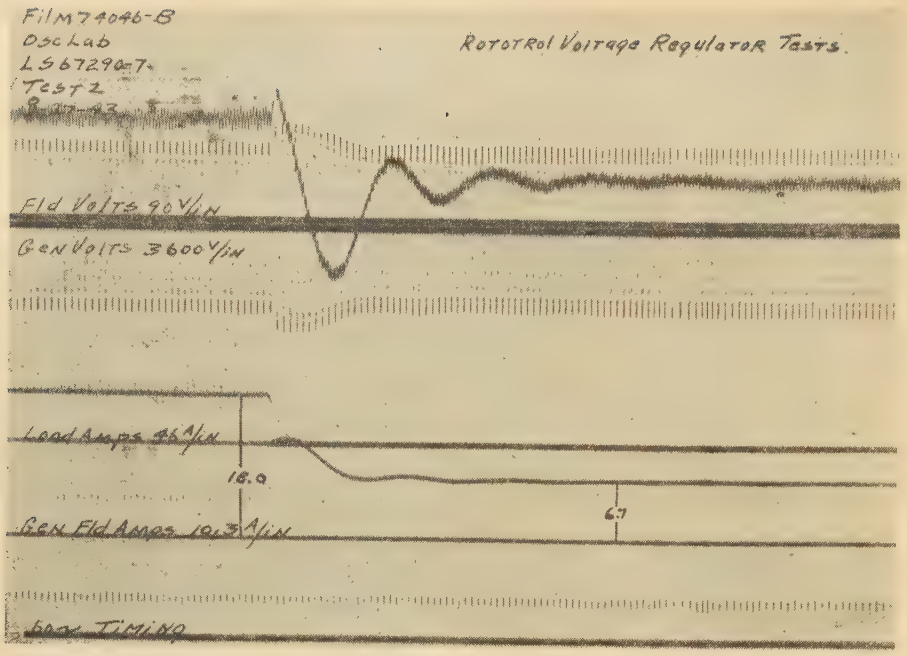

Figure 10. Oscillograph showing performance of Rototrol voltage regulator on release of 70 per cent power factor load on a-c generator

ated rheostat, and the cycle is restarted. A paper break under this condition will only speed the equipment up until field *A* is at zero excitation, as it cannot reverse because of the blocking rectifier. By proper relay selection this speed-up can be limited to between 10 and 20 per cent. Thus the roll is essentially at the proper speed, and rethreading is easily accomplished.

The strip tension is adjustable by means of a small manually operated rheostat located on the operator's panel. These adjustments may be observed readily on the motor ammeter which serves as a relative indication of tension and permits duplication of results to obtain the most satisfactory roll for any given weight and grade of material.

Essentially the same type of circuits are applied to unwind stands wherein the operation is reversed and the regenerative power fed back into the system.

Figure 8 illustrates the application of Rototrol tension control to the core driven beam of a slasher in the textile industry. Constant tension on the thread comprising the beam results in uniform beam diameter, a reduction in yarn breakage, and fewer stops for changes and adjustments, since more yardage can be wound on the beam. The more important advantages are increased efficiency in the subsequent weaving operation and improved quality of the finished cloth.

Voltage Regulation

A number of Rototrol exciters have been built for voltage regulation of a-c or d-c generators. Figure 9 illustrates the essential circuits of the regulator as applied to an a-c generator. The generator voltage is measured through a transformer and dry type rectifier and bucked against the rectified voltage of the constant voltage transformer. The difference controls the Rototrol excitation through field 1 to restore normal generator voltage. To obtain a high degree of stability, a damping transformer is used in the control field circuit. Where use of an a-c supply for the constant voltage transformer is not advisable, static "intersecting impedance" networks have been applied.[1]

To obtain high rates of response both parallel and series self-energizing fields are used. The circuit is tuned by adjustment of the resistor in field 2, so that fields 2 and 3 sustain the Rototrol output at any point on the straight portion of the saturation curve. This arrangement takes advantage of the almost instantaneous transient change in generator field current and provides extremely fast response of the Rototrol exciter.

Typical performance is shown by the oscillograph of Figure 10 which was taken during the sudden release of full load at 70 per cent power factor on a 150-kva 3-phase 60-cycle 2,400-volt generator controlled by a Rototrol voltage regulator. The voltage was returned to normal in 1/4 of a second with very little overswing. The oscillograph demonstrates excellent stability as well as very high speed of response of the Rototrol exciter.

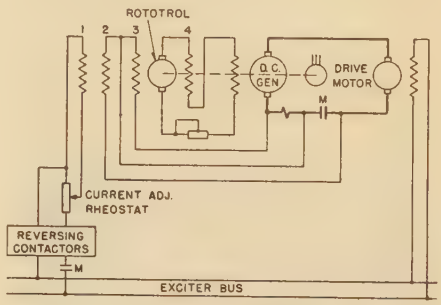

Figure 11 (above). Elementary diagram of Rototrol current regulator applied to a large tire testing machine

Figure 12. Tire testing machine using Rototrol acceleration control

Acceleration of High Inertia Loads

The Rototrol has been applied to many problems concerning acceleration and retardation of high inertia loads. For such problems it is desirable to accelerate at uniform torque from minimum to maximum speed, to reduce the current peaks and mechanical shock experienced with step type controllers, and to eliminate many of the relays and contactors associated with conventional magnetic control. The Rototrol is able to perform these various requirements with a surprising simplicity of the control circuits. Typical applications are bomb spinners, centrifugal casting machines, balancing machines, tire testing machines, and large mine hoists.

Figure 11 shows schematically the circuits of a Rototrol exciter as applied to a large tire testing machine drive. The machine consists of a flywheel which is accelerated to various speeds and then stopped by bringing the tire into contact with it. The huge flywheel has a WR^2 of 10,000,000 pound feet squared and requires an accelerating torque equivalent to 400 horsepower at 350 rpm to reach maximum speed in 30 minutes. The Rototrol is arranged to control the armature current and thus the torque of the separately excited drive motor. As the system gradually speeds up, the Rototrol increases the generator voltage to maintain uniform accelerating torque. The control is arranged to provide regenerative braking to standstill by simply reversing the pattern field 1 when such operation is necessary.

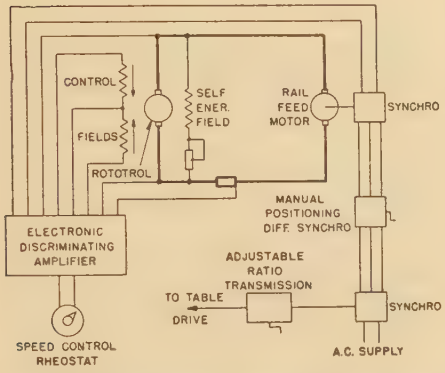

Figure 13. Simplified diagram of feed drive for large boring mill using a Rototrol in combination with an electronic discriminating amplifier

After the system is up to speed and the motor and generator disconnected, the generator voltage is matched automatically to the motor counterelectromotive force. This is desirable so that the circuits may be reclosed at any time for retardation or further acceleration. This function is accomplished by connecting Rototrol field 3 across the main circuit contactor M and de-energizing pattern field 1 when M is open. Any voltage difference will cause current to flow in field 3, which modifies the Rototrol and generator voltages to reduce the difference.

Helper Drive Torque Control

The circuit of Figure 11 with omission of field 3 has been used rather widely as a driving effort or torque regulator for helper drives operated in conjunction with a main drive. The system is applicable to either mechanically or electrically driven machines. Typical applications are the various auxiliary drives for the wet ends of paper machines and top roll drives for press rolls which are used in many industries. This arrangement assures constant helper motor torque over a wide speed range, regardless of speed variation of the main drive or changes in effective roll diameter due to change in nip pressure on soft rolls. Often a number of motors are served by a common generator. Here the total driving effort of the motors is determined by the Rototrol with the division of load secured by individual motor shunt field rheostats.

Speed Matching

Electronics often is used in combination with the Rototrol to solve difficult drive problems. An interesting application is the feed drive for a large vertical boring mill. The Rototrol is used with an electronic discriminating amplifier, and the circuits are arranged to provide either speed matching of the feed motion to the main table drive or straight speed control of the feed.

The elementary circuits are shown in Figure 14. For matching the speed of the feed screw motor to the speed of the table, small synchro units are driven from the feed screw motor and from the table drive. Angular displacement between the synchros will cause an error voltage which is fed into the electronic discriminating amplifier. The amplifier senses the direction of the error and changes the current through the Rototrol control fields to modify feed screw motor speed to reduce this angular difference. The system accurately matches the relative speeds of the feed and table over the complete range of table speed. Adjustment of relative speeds is obtained by the adjustable ratio transmission between the table and the synchro unit.

It is also desirable to operate the feed motor on straight speed control capable of adjustment over a wide range and with good speed regulation at all speeds. The discriminating amplifier is designed for this function and provided with a transfer switch to effect changeover. The motor counterelectromotive force is measured by means of armature current and voltage and balanced against a standard voltage in the discriminating amplifier. The difference controls the Rototrol excitation to maintain the proper motor speed.

This type of drive simplifies the mechanical parts of the machine by eliminating the many gear changes and the mechanical connection from the table to the feed screw on the rail. The large number of feed speeds, readily available, facilitates machine adjustment and results in increased production.

Conclusion

The large number of Rototrol applications have proved it to be an excellent and versatile regulator for industrial service. Operating experience has shown that it can be understood by nontechnical maintenance personnel, that its inherent reliability and stability assure trouble free operation with relatively little maintenance, and that it combines the necessary degrees of amplification and speed of response to meet the requirements of industrial problems. Existing applications cover a wide field, and the future holds considerable promise of broader utilization.

Reference

1. Static Voltage Regulator for Rototrol Exciter, **E. L. Harder, C. E. Valentine.** AIEE Transactions, volume 64, 1945, August section, pages 601–06.

Thermal-Demand-Meter Testing Techniques

E. E. LYNCH
MEMBER AIEE

M. E. DOUGLASS
NONMEMBER AIEE

THIS PAPER is written to encourage thinking and development on the subject of thermal-demand-meter testing procedures with specific reference to the development of shorter testing techniques. Conventional test methods in the past have involved relatively long periods of load holding to bring the meters under test to thermal equilibrium for the calibration check and adjustment. With the increasing use of thermal meters it is desirable to use some testing method which more nearly resembles tests on watt-hour meters. This paper outlines three general methods for shortening the test time and leaves to the reader the choice of the method, or modification of it, best suited to his requirements.

The principal problem in thermal-demand-meter testing is to determine the ultimate or final indication of the meter on constant load at thermal equilibrium. The response characteristic of the particular meter being tested will influence the available techniques for obtaining this information in short periods of time. This discussion is limited to meters having a simple logarithmic response, such as the meter shown in Figure 1, the characteristics of which have been covered in a previous article.[1] Appendix A gives an arbitrary definition and a mathematical description of this characteristic, and Appendix B demonstrates its importance in facilitating the establishment of a simple and sound short test method.

At the present time it is customary to return thermal demand meters to the laboratory for checking and calibration. The following or a similar step-by-step procedure usually is followed:

1. Connect meters in gangs, and apply potential to each for 2 to 24 hours.
2. Check the zero reading, and adjust if necessary.
3. Apply load to be checked, and hold constant for 45 minutes.
4. Check the meter indication against the load held, and adjust if necessary.

Paper 46-69, recommended by the AIEE committee on instruments and measurements and presented at the AIEE winter convention, New York, N. Y., January 21–25, 1946. Manuscript submitted November 23, 1945; made available for printing December 14, 1945.

E. E. Lynch and M. E. Douglass are with the General Electric Company, Lynn, Mass.

A short test method for checking thermal meters should be a distinct advantage to electric power companies, particularly as a means of checking the accuracy of these meters on the customers' premises in relatively short periods of time.

For a meter possessing the simple logarithmic response characteristic, mentioned previously, three general types of short test methods have been suggested and evaluated. Though other methods and modifications may be developed, particularly for meters having other than a simple logarithmic response, the three general types described herein provide an opportunity for large reductions in the testing time or man-hours for meters having this characteristic. The following terms have been coined to identify these three methods:

(*a*). "Two point method."
(*b*). "Double load method."
(*c*). "Thermal standard method."

The two point method is adaptable to testing on customers' premises. A graph or tabulation can be used to simplify the procedure. The double load method in one form is best adapted to testing single meters, whereas another form is more suitable for gang testing in the laboratory. The thermal standard method is usable on either gang or individual testing and is useful in its man-hour saving, although the elapsed time of test may not be shortened materially.

The Two Point Method

As the name denotes, the two point method involves obtaining sufficient readings of the meter indication at known intervals of time to predict the ultimate indication. The method is based on the solution of simultaneous equations, derived from equation 2 in Appendix A.

$$D = W(1 - e^{-kt})$$

where

D = instantaneous deflection
W = ultimate deflection
t = time
k = a constant
e = 2.72

An examination of this equation shows that there are two unknown quantities, namely k and W, when the quantities D and t are determined by simultaneous readings of the meter indicating pointer and a stop watch. Since there are two unknowns in the equation, two sets of values D and t must be determined to give two equations from which W and k can be found. To substitute the readings into the equation and perform the solution would be needlessly laborious for the meter tester, as the solution can be set up in the form of a graph. Two variations of the test are possible. In one, the pointer readings at two given times after constant test load application are used to indicate the ultimate reading. In the other, the time intervals that are required after constant load application for the meter to indicate two different scale points are used to compute the ultimate meter reading. Each of the two point methods is adapted to checking only one meter at a time, and is suitable for checking the calibration only, since at the end of the test period the meter reading still is increasing, and an adjustment under these conditions would be difficult at best. The methods have the advantage that the maximum demand pointer rather than the indicating pointer can be used for the check.

To describe briefly a step-by-step procedure to check a meter according to the first variation of the two point method, the following list is given:

1. Reverse potential with a load applied until indicating pointer reads zero.
2. Start stop watch and simultaneously apply a known load and hold constant.
3. At 3 minutes (or any other suitable time depending on the charts set up) after the load is applied, read the meter indication. Continue holding load.

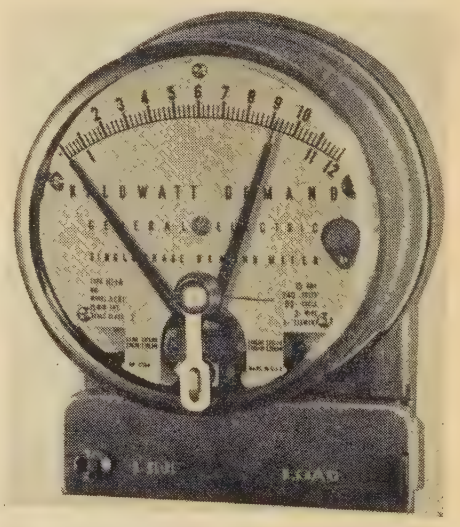

Figure 1. Thermal watt demand meter having a simple logarithmic response characteristic

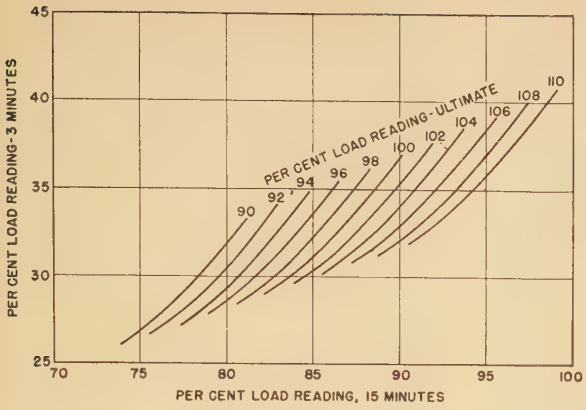

Figure 2. Chart to determine ultimate deflection when indication is read after a given time

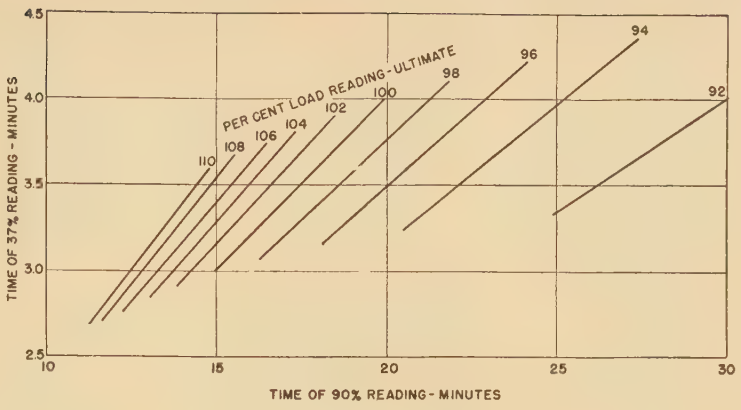

Figure 3. Chart to determine ultimate deflection when time is read for a given indication

4. At 15 minutes (or any other suitable time depending on the charts set up) after load is applied, read the meter indication.

5. Check the charts (Figure 2) to find the ultimate indication of the meter—compare this with what the ultimate indication should be from the load held.

The step-by-step procedure for using the second variation of the two point method is similar to the first, except that two stop watches are started simultaneously with the application of load in step 2, and one is stopped as the pointer reaches a predetermined point (37 per cent of the load applied); the other is stopped when the pointer reaches another predetermined point (90 per cent of the load applied). From the stop watch readings the ultimate deflection is determined from a chart (see Figure 3).

The Double Load Method

The double load method, as the name indicates, requires the application of double load to the meter under test for an interval of time, followed by a short period of holding the test load. Two variations in the general method are apparent: first, the double load may be held for a specified length of time; or second, the double load may be held until a definite indication on the meter is attained. An outline of step-by-step procedure for the first follows:

1. Reverse potential until meter reads zero indication. (Gang test meters will read zero at end of potential preheat.)

2. Apply double load for a specified time.

3. Cut load to test load, and hold constant for a specified time.

4. Read meter and compare it with the load value being held.

5. Make any adjustment necessary in the meter.

This procedure is adapted to gang testing of meters if desired, and the meter may be adjusted at the end of the test. The indicating pointer must be used during the test rather than the maximum demand pointer, as the indication at the end of the test may be lower than at the end of the double load period.

A step-by-step procedure for the second double load variation follows the first, except that the meter need not necessarily read zero at the start of the double load period, and the load should be reduced to the test load as soon as the meter reads the test load. Obviously this procedure is suitable for testing only one meter at a time. It does allow adjustment of the meter at the completion of the check.

The Thermal Standard Method

The thermal standard method requires the use of an accurately calibrated thermal meter of approximately the same response characteristics as the meter under test. Two variations of this method suggest themselves. The first is actually a combination of the double load and test standard methods. The second, which does not involve applying double load, conserves man-hours but does not reduce testing time appreciably.

Both variations of the thermal standard method are suitable for either single-meter or gang testing. Adjustments can be made on the meters at the conclusion of the test, since the test meters are at thermal equilibrium. The indicating pointer must be used rather than the maximum demand pointer, since load variation may cause a downward pointer movement during the test. The use of the accurately calibrated thermal meter as a standard eliminates the necessity for precise load holding, although reasonable limits must be maintained, so that differences in the response time of the test meter and the standard do not introduce errors.

The sequence of operations for the procedure using double load is as follows:

1. Reverse potential on test meter, and bring reading to zero.

2. Connect standard and test meter to same load.

3. Apply double load to both meters until the standard one indicates the value of the test load.

4. Drop to the test load and hold approximately correct load for a specified time.

5. Compare the reading of the standard meter under test.

The second procedure is simply to connect the accurate, standard meter and the meter under test to the same load and leave them for three or more demand intervals,[2] for example, 45 minutes for a meter used on 15-minute demand interval service. At the end of that time the deviation of the reading of the meter under test from the standard meter indicates the error of the meter under test.

In the descriptions of the various methods given, only a single point check of the meter has been considered. If the zero position of the indicating pointer is not correctly set on the scale zero, errors at points other than the one checked will be present. With a meter that does not overshoot on transient load, the following step-by-step procedure is suggested for checking the zero when desired:

1. Reverse potential, and apply load until indicating pointer reads zero.

2. Remove load, and reconnect potential.

3. With potential applied wait for one demand interval, and note the indication of the pointer. If no appreciable change has taken place, the meter is very close to correct zero. Any change that has taken place represents 90 per cent of the total deviation from zero at thermal equilibrium, and an adjustment can be made on this basis.

In connection with this brief description of some possible methods of shortening the test time a comparison of the accuracy of the various methods is given in Table I. The three test methods are listed across the top of the table, and the

Table I. Estimated Errors When Using Short Test Methods

Factors Influencing Errors	Two Point Method		Double Load Method		Thermal Standard Method	
	Indication at Given Time	Time for Given Indication	Held for a Definite Time	Held to a Definite Indication	Combined With Double Load	Thermal Standard Alone
1. Zero adjustment	No effect	No effect	No effect	No effect	No effect	No effect
2. Initial calibration	No effect	No effect	No effect	±5 per cent calibration error causes about ±0.5 per cent error in the ultimate indicated reading at end of one meter period	No effect	No effect
3. Time of response deviation	No effect	No effect	±1 minute deviation of response time from value for which test is devised gives about ±0.5 per cent ultimate indication error at end of one meter period	Insignificant effect	±1 minute deviation of response time from thermal standard causes about ∓0.5 per cent error in the ultimate indicated reading at end of one meter period	No effect if meter response times match*
4. Test timing	±seconds on 3-minute point gives about ∓2 per cent; ±5 seconds on 15-minute point gives about ±1/4 per cent	±5 seconds on 37 per cent point gives about ∓1 per cent; ±5 seconds on 90 per cent point gives about ±1/4 per cent (depends on calibration of meter)†	±20 seconds in time at which load is reduced to single value causes about ±0.2 per cent error	No reasonable variation in time of ultimate reading (±several minutes) will have any appreciable effect	No reasonable variation in time of ultimate reading (±several minutes) has any appreciable effect	No effect
5. Load holding accuracy	±1 per cent load error gives ±1 per cent error	±1 per cent load error gives ±1 per cent error	±1 per cent error in double load causes ±0.1 per cent error; ±1 per cent error in test load causes ±1 per cent error	Error in double load has no effect; ±1 per cent error in test load causes ±1 per cent error	No effect*	No effect*
6. Reading accuracy	±1 per cent on zero reading gives ±1 per cent error; ±1 per cent on 3-minute reading gives about ∓2 per cent error; ±1 per cent in 15-minute reading gives about ±2 per cent error	±1 per cent on the zero reading gives about ±1 per cent error; ±1 per cent on 37 per cent point gives about ∓1 per cent error; ±1 per cent on the 90 per cent point gives about ±1 1/2 per cent error	±1 per cent in reading zero causes ±0.1 per per cent error; ±1 per cent in reading ultimate causes ±1 per cent error	Error in reading zero does not produce any error; ±1 per cent in reading ultimate indication causes a ±1 per cent error	±1 per cent in reading zero causes about a ±0.1 per cent error or less. Reading error at the ultimate reading produces a corresponding error	Reading accuracies and calibration error of thermal standard are only errors of any appreciable magnitude in this method
7. Over-all accuracy (estimated)	±3 per cent	±2.5 per cent	±2 per cent	±2 per cent	±2 per cent	±2 per cent

* In the thermal standard methods load variation during the test will not produce any error in the ultimate deviation of test meter from thermal standard, provided that the response time of the two meters match. If response times are different on the test meter and the stan dard, load variations will cause indication differences. For reasonable load variations (±5 per cent) and reasonable response time differences (2 minutes) the errors in general from this source should be within ±1/2 per cent to ±1 per cent. †See Figure 3.

factors that contribute to errors are listed down the page on the left-hand side. At the bottom of the table are statistical estimates of the probable accuracies of each method of test. These are based on a combination of measured and estimated frequency distribution curves of the individual sources of errors involved and therefore represent only the order of magnitude of errors to be expected from these methods.

In the foregoing discussion of short test methods it has been assumed that the voltage has been applied to the meters for a sufficient length of time to produce complete change in the zero indication of the meter due to potential alone. In the case of periodic accuracy checks on customers' premises this undoubtedly would be the fact. In the case of gang testing in the shop time must be allowed for this item. In the methods where ultimate indication practically is reached, such as the double load or thermal standard methods, this potential preheating time may be overlapped with the time required to obtain final indication.

Conclusion

The purpose of this paper is to stimulate thought and experiment on short test methods and to indicate that such methods are possible. The procedures outlined are intended to show only the general steps in the various methods and are not to be considered detailed instructions for testing meters. Quite probably methods other than those suggested can be devised, and modifications and combinations of the methods discussed may be developed. Although it is possible that test methods can be found that will shorten materially the testing time of indirectly heated meters, nevertheless, this discussion has been limited entirely to testing meters with a simple logarithmic response characteristic that will not overshoot on transient load. This characteristic is realized on some thermal meters using direct (or internally) heated bimetallic spirals. Although actual test data are limited, nevertheless it indicates that short test methods are practicable when the greatest accuracy is not required.

Appendix A. The Meaning of a Simple Logarithmic Average

The simple logarithmic average is mentioned a number of times in the main portion of the paper. In this appendix an arbitrary definition of it will be given, and it will be expressed in mathematical symbols.

An understanding of the simple logarith-

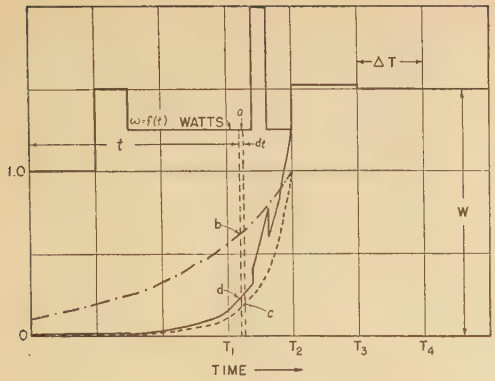

Figure 4 (left). Curve used to illustrate a definition of logarithmic average

Figure 5 (right). Curves showing overshooting and dipping characteristics of typical thermal meters

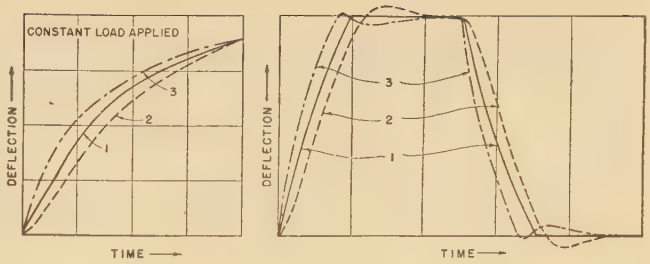

mic average is obtained best by comparing it with the arithmetic average. In demand metering both averages are used, and each has been found satisfactory for assisting in obtaining information necessary for billing. In considering an average of watts such as curve a in Figure 4, the arithmetic average at time T_2 can be expressed by $1/(T_2-T_1)\times\left(\int_{T_1}^{T_2} w\,dt\right)$ where $w=f(t)$ and represents the watts and where T_1 and T_2 are the beginning and end of the time interval concerned. If the time interval is extremely short, T_2 nearly equals T_1, and the arithmetic average approximates the instantaneous value. If the time interval is extremely long, all past watt values are given equal importance. Because in many cases neither of these arithmetic averages gives exactly what is wanted for demand purposes, the average over a given period of time, such as 15 minutes, often is used. Most mechanical demand meters indicating this sort of average do not do so continuously but do their integrating continually over definite intervals, so that changed readings are available only at the end of definite time intervals. Thermal meters indicating a logarithmic average are expected to do so continuously.

The simple logarithmic average of the watts curve will be considered as the area under a weighted curve (d in Figure 4), which is made up of the product of all points a (on the watts curve) multiplied by corresponding points on a weighting curve c. The weighting curve follows the simple logarithmic form $e^{-k(T_2-t)}$ where T_2 is the time at which the average is expressed and t is the time at which the watts were a. Mathematically it is expressed:

The simple logarithmic average,

$$D=K_1\int_{-\infty}^{T_2}[f(t)]_t e^{-k(T_2-t)}]dt$$

The proportionality factor K_1 is chosen such that for any constant load W the logarithmic average is numerically equal to the load W. It is therefore equal to the arithmetic average which is also W. That is,

$$D_{(\text{For constant load})}=K_1\int_{-\infty}^{T_2}We^{-k(T_2-t)}\times dt=W$$

This equation is satisfied only if $K_1=k$. Therefore

$$D=k\int_{-\infty}^{T_2}[f(t)][e^{-k(T_2-t)}]dt \qquad (1)$$

For constant load applied from zero indication this reduces to:

$$D_o=W(1-e^{-kt}) \qquad (2)$$

The choice of weighting curve determines the response characteristic of the meter, and for simple logarithmic weighting curves the value of k in the expression $e^{-k(T_2-t)}$ controls the relative effect of recent and remote loads. Figure 4 shows two weighting curves, curve c has k equal to 0.1535 corresponding to a 15-minute meter interval, while curve b has k equal to 0.0384 corresponding to a 60-minute meter interval.

The simple logarithmic average then is simply a value proportional to the arithmetic average of the weighted curve that is obtained when the watts curve is multiplied by a simple logarithmic weighting curve.

It has been shown previously[1] that, although the theoretical weighting curve of thermal watt demand meters is of the nature of a simple exponential curve, nevertheless the characteristics of many commercial meters differ appreciably from this ideal. However, it also has been shown that an internally heated bimetal type of meter as built does have this form of response, and it will be shown in Appendix B that such a meter will neither overshoot nor undershoot, nor will it have an indication dipping characteristic.

Appendix B. Why Simple Logarithmic Average Thermal Demand Meters Will Not Overshoot

In this paper it is disclosed that meters with certain response characteristics are well adapted to short testing methods. Meters having these characteristics measure a simple logarithmic average and, since they respond in this manner, they will neither overshoot nor dip. The proof of this will follow, but first it is necessary to understand what is meant by overshoot and dip.

Overshoot and Dip

If the pointer of a thermal meter is moving upscale owing to a relatively high load, and the load is reduced suddenly to a value close to the indication of the meter, a temporary dipping of the pointer below the instantaneous load is called dipping. If it continues temporarily to increase above the instantaneous load, it is said to overshoot. Neither condition is especially desirable when testing meters by a short method, but each characteristic can and does occur in some commercial thermal meters.

Proof That Simple Logarithmic Meters Will Not Overshoot

In order to prove that some meters cannot overshoot, a time will be taken (T_3 in Figure 4) at which the indication is a given value W. It then will be shown that, if a constant load W is held from this time on for some definite time interval (ΔT), the indication of the meter will not be changed. Since ΔT is chosen arbitrarily, it may be as long or as short as desired and even may be an an infinitesimally short time dt. Since the indication of the meter does not change for any of these conditions, it will have been proved that there is no tendency to overshoot, undershoot, or dip. The meter involved is assumed to measure a simple logarithmic average demand.

At the time T_3 the indication has arrived at a value W by any means whatever in its past history.

$$\text{Indication at } T_3=k\int_{-\infty}^{T_3}[f(t)]\times[e^{-k(T_3-t)}]dt=W \qquad (3)$$

At some later time (T_4) the indication is by definition:

$$\text{Indication at } T_4=k\int_{-\infty}^{T_4}[f(t)]\times[e^{-k(T_4-t)}]dt \qquad (4)$$

This indication (at T_4) can be separated into the integrals $\int_{-\infty}^{T_3}+\int_{T_3}^{T_4}$ as follows, since the load is constant from T_3 to T_4.

$$\text{Indication at } T_4=k\int_{-\infty}^{T_3}[f(t)]\times[e^{-k(T_3+\Delta T-t)}]dt+k\int_{T_3}^{T_4}We^{-k(T_4-t)}dt \qquad (5)$$

Since $e^{-k\Delta T}$ is a constant for a particular value of (ΔT) and since e^{-kT_4} is a constant for a particular value of T_4, they can be taken outside the first and second integrals respectively.

$$\text{Indication at } T_4=[e^{-k\Delta T}]\times\left[k\int_{-\infty}^{T_3}f(t)e^{-k(T_3-t)}dt\right]+[kWe^{-kT_4}]\left[\int_{T_3}^{T_4}e^{kt}dt\right] \qquad (6)$$

From equation 3 and a solution of the

Co-ordinated Electric Drive for a Rubber Calender Train

K. W. JOHN
MEMBER AIEE

G. W. KNAPP
ASSOCIATE AIEE

W. A. MOSTELLER
NONMEMBER AIEE

Synopsis: The continuous process of coating fabrics with rubber, such as is used in tire manufacturing, involves several individual machines that present operating problems not met successfully by mechanical drives. A new co-ordinated electric drive has been developed which does meet these requirements using amplidyne, and also electronic, control. It is expected that quality and production will be improved by this equipment. The means employed may be applied successfully to other industries.

IN THE MANUFACTURE of many rubber goods, textile fabrics are coated on both sides with rubber in a machine called a calender. Associated with the calender are auxiliary devices for handling the fabric before and after coating, making up a processing train.

Tire fabrics are one of the most important examples of this process in the rubber industry[1] and their production in a calender train, using a newly developed electric drive, will be discussed in this paper. The complete equipment now is installed in the Detroit, Mich., plant of the United States Rubber Company and parts of it are shown in Figures 1 and 2.

The calender itself, the train auxiliaries, and all of the electric equipment were manufactured from designs which were co-ordinated closely by the operating company, the machinery builders, and the electrical manufacturer. The importance of this procedure will be appreciated readily from the operating requirements.

Description of Process

A schematic diagram showing the mechanical arrangement of the processing train is shown in Figure 3.

Rolls of fabric are started at one of the entry letoffs. A maximum diameter of 42 inches can be accommodated. The fabric widths vary up to 60 inches.

The entry festoon forms a storage reserve of 80 feet of fabric so that the letoff can be stopped for changing rolls without shutting down the calender. The alternate letoff positions are provided to save time during this operation.

After drying, the fabric enters the calender rolls as shown. These rolls are 32 inches in diameter and 70 inches wide. Rubber from the top bank coats the upper side of the fabric, while that from the lower bank coats the under side.

The thickness or "gauge" of the rubber coating on either side of the fabric is determined by the opening between the rolls and also, to some extent, by the roll speed. Gauge is very important because a coating which is undersized produces an inferior tire and therefore must be rejected. On the other hand, if it is oversized, expensive rubber compound is being wasted.

While constant roll speed would have some favorable influence on gauge, there is another consideration for it which is even more important. To obtain maximum production, the calender rolls should run continuously at the maximum speed which certain processing limitations allow. This speed depends on the type of compound and fabric, and usually is established by considerations of plastic flow. If no means are provided for holding the calender speed at that maximum value, the average speed at the end of a day may be somewhat less. Even if this is only a small amount, a surprising amount of production can be lost.

The delivery festoon provides 64 feet of space for storing fabric when changing rolls at the windup. Finished rolls are wound on one of the fabric windups. The maximum diameter, as in the case of the letoff roll, is 42 inches. Alternate windup positions also are provided here. To keep layers of stock from sticking together, a separator or "liner" also is wound on the roll. This is supplied from a separate liner letoff for each fabric windup. Sometimes coated fabrics are run through the calender train a second time. For this purpose, liner windups also are provided at the entry letoffs.

Operating Requirements

The operating speed range of the train is from 7 to 70 yards per minute. A sepa-

Paper 46-56, recommended by the AIEE committee on industrial power applications for presentation at the AIEE winter convention, New York, N. Y., January 21–25, 1946. Manuscript submitted November 16, 1945; made available for printing December 5, 1945.

K. W. JOHN is an electrical engineer, United States Rubber Company, Detroit, Mich. G. W. KNAPP is in the industrial engineering division, General Electric Company, Schenectady, N. Y. W. A. MOSTELLER is in the engineering division, General Electric Company, Detroit.

---

second integral with respect to t:

$$\text{Indication at } T_4$$
$$= [e^{-k\Delta T}][W] + [kWe^{-kT_4}] \times \left[\frac{1}{k}\, e^{kt}\right]_{T_4}^{T_3}$$
$$= [e^{-k\Delta T}][W] + [We^{-kT_4}] \times [e^{kT_4} - e^{kT_3}]^{T_4}$$
$$= [e^{-k\Delta T}][W] + [W][1 - e^{-k(T_4 - T_3)}]$$
$$= We^{-k\Delta T} + W - We^{-k\Delta T} \quad (\text{since } T_4 - T_3 = \Delta T)$$
$$= W \qquad (7)$$

Thus the indication at T_4 is the same as that at T_3 (no matter what the time interval between T_3 and T_4), and therefore there has been no tendency to overshoot, undershoot, or dip.

Since the foregoing is based only on the indication of a meter whose response meets this definition of a simple logarithmic average, it is to be expected that some meters whose response differs from this average can overshoot or undershoot, or may have a tendency to dip. That this is true is shown in Figure 5, where A shows the response of three designs of commercial meters with different response characteristics when subjected to a constant load, starting from zero.

Figure 5B shows the response of these same meters when double load is applied until the pointers reach a given indication and then the load is changed to a constant load which ultimately will give this same indication. The loads are changed on the 3 meters at different times, since they arrive at the given indication at different times. All meters are correctly calibrated. The potential is reversed, and the meters run to zero. As each meter reaches zero its potential is returned to normal and its current reduced to zero. It can be seen that both meters 2 and 3 overshoot or undershoot considerably or have the characteristic of indication dipping.

When, therefore, it is desirable to eliminate overshooting or undershooting indication in order to save time during short tests or for any other reason, a meter whose response follows the simple logarithmic average should be chosen. It will neither overshoot nor undershoot, nor will it have the indication dipping characteristic.

References

1. THEORETICAL POSSIBILITIES IN AN INTERNALLY HEATED BIMETAL TYPE OF THERMAL WATT-DEMAND METER, E. E. Lynch. AIEE TRANSACTIONS, volume 61, 1942, October section, pages 764–70.

2. CODE FOR ELECTRICITY METERS. Edison Electric Institute.

rate threading speed of 7 yards per minute also is provided for running-in the fabric initially.

The calender itself should be able to operate over the speed range, independent of its train auxiliaries, for "warming up" operations when first starting. It also should be capable of reversing, with and without the central auxiliaries.

Jogging operation, forward or reverse, is required for all of the windups and let-offs. This is used either when starting or finishing up a roll that is not in train operation.

Emergency stopping is provided for the complete train from a number of control positions located throughout its length. This is an important requirement for the safety of operating personnel. There is a national code which specifies certain stopping performance that must be met.

In addition to the foregoing operating requirements, it is very desirable to maintain the tensions in the fabric, on either side of the calender, at constant values. These tensions are such that those before the calender exert a drag on it, while those after the calender are in the pull direction. The calender rolls, then, driven at constant speed, provide the necessary reactions for these tensions as a reference point. The benefits of constant tension to each part of the train have been tabulated at the bottom of Figure 3.

Past Practice, Mechanical Drive

In the past, calender trains have been driven by a single motor connected to the calender through a gear reducer. At some spot on the calender a mechanical takeoff was provided to drive a line shaft through gearing. The line shaft usually extended the length of the train and the auxiliaries were driven from it through right-angle gears, chain drives, and so forth.

Naturally, the electric drive with proper control equipment could be made to fulfill the operating requirements for the calender itself, but mechanically driven auxiliaries fall short of the mark.

To adjust tension, friction clutches and adjustable speed transmissions have been employed. These devices are not self-regulating and the operators must readjust them frequently. This is not practicable and, as a result, optimum adjustments seldom are obtained and production may suffer.

Furthermore, if good adjustments of tension have been made, there is no means for holding them there, nor can they be measured for future reproduction on other runs. There is another disadvantage in that maintenance is quite high on the friction clutches and the other mechanical component parts.

Electric Sectionalized Drive

With the electric drive, the entire train is sectionalized so that each auxiliary which ordinarily would have a mechanical drive is provided with its own motor. Co-ordinated control takes the place of the line shaft tie and, in addition, provides the proper tensions and speeds. Furthermore, once optimum adjustments have been established, the control holds them there. Electric instruments make it possible to take measurements and record the adjustments. Thus, if that same run is to be repeated in the future, the best operating conditions can be obtained very quickly.

The various pushbuttons and rheostat dials which are used for the adjustments are located remotely from the driven auxiliaries, in convenient groups. Each group consists of several interdependent and related adjustments, thus providing maximum convenience to the operator and also a more favorable opportunity to make correlated adjustments correctly.

Circuits

Power Circuits

The general arrangement of the power circuits for the various drives is shown in Figure 3.

The main drive for the calender is of the adjustable voltage (Ward-Leonard) type, providing ten to one speed range, of which five to one is by armature voltage control and two to one by motor field control.

The adjustable voltage scheme was selected because of the wide operating speed range and the advantage of being able to control the speed of the motor by adjusting its armature voltage. Furthermore, as has been pointed out by Cassidy and Mosteller,[1] the first cost is less.

The motor field range is used because at low operating speeds (below basic speed), substantially more than constant torque may be required by the calender.

The group of drives which is called the "central auxiliaries" always operates at the speed of the calender. They are not supplied, however, from the calender generator. This is done primarily for reasons of simplicity. For example, the auxiliary motors themselves are much smaller than the calender motor so that their IR drops are considerably higher. Thus, at one-tenth speed the terminal voltage that they require would be sub-

Figure 1. Calender and driving motor

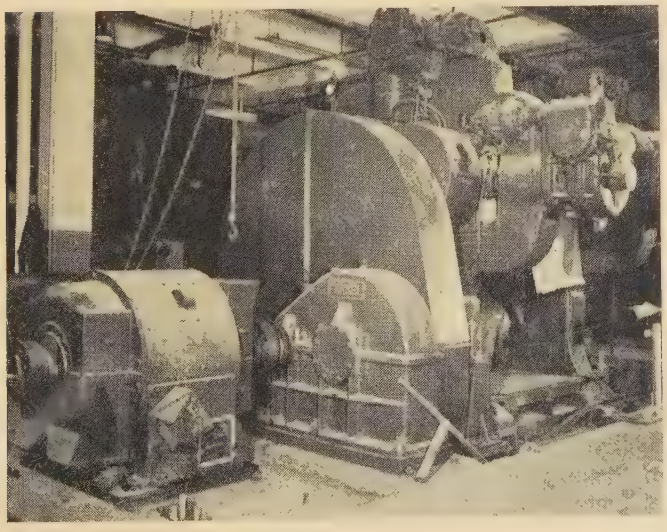

Figure 2. Calender motor-generator set and d-c control panels

One of the auxiliary motor-generator sets is in the background

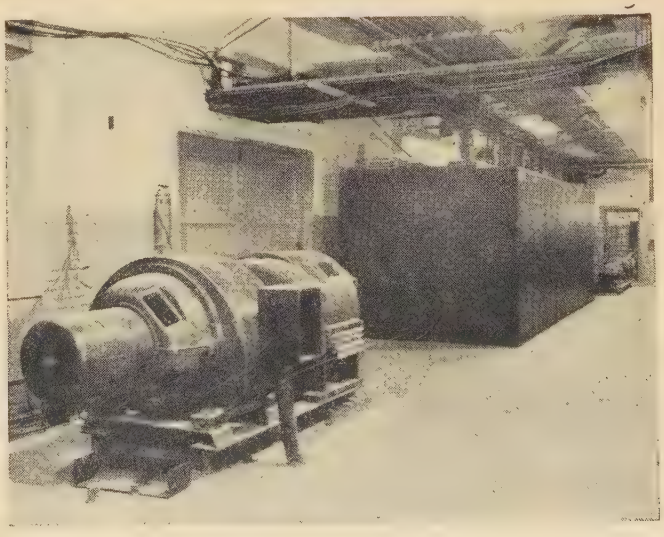

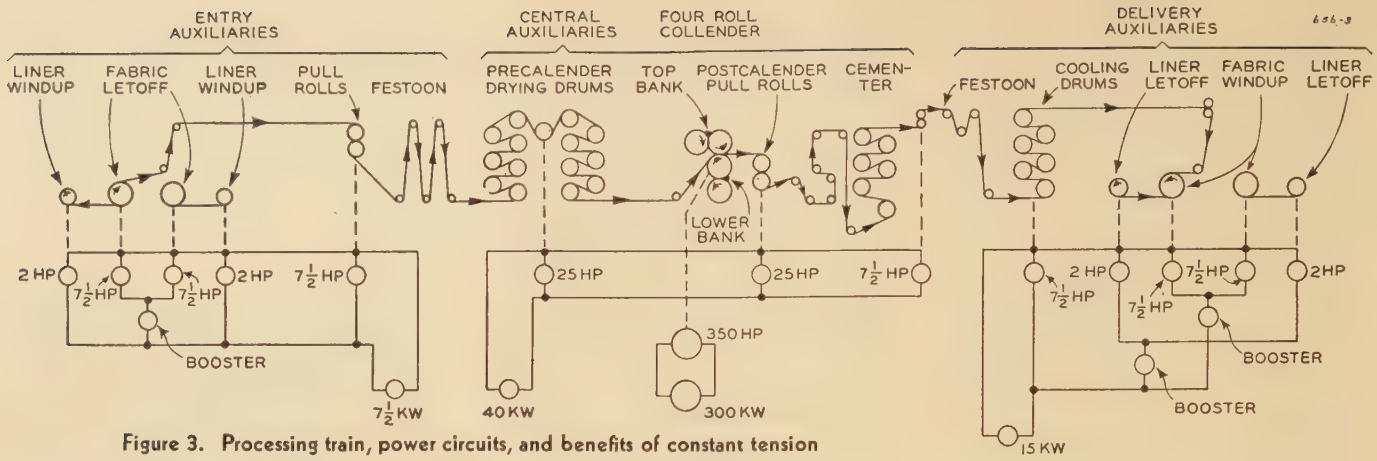

Figure 3. Processing train, power circuits, and benefits of constant tension

The Benefits of Constant Tension

Letoff	Drying Drums	Postcalender Pull Rolls	Cementer Pull Rolls	Windup
1. Compensation for elliptic or eccentric fabric rolls which produce tension variations that stretch fabric severely	1. Compensation for shrinkage or stretch 2. Elimination of loose wrinkles which would be cut by calender rolls	1. Compensation for shrinkage or stretch 2. Favorable influence on maintaining gauge	1. Compensation for shrinkage or stretch 2. Favorable influence on even distribution of cement	1. Elimination of loosely wound rolls which deform in storage 2. Elimination of tightly wound rolls where fabric sticks to liner in later operations

stantially more than what would be available from the main generator and a booster would have to be used to overcome this.

The power circuits for both the entry auxiliaries and the delivery auxiliaries are treated in the same manner. In either group the individual drives always operate together. They must be separated from the central auxiliaries and the calender because of the roll-changing requirements. They are stopped for roll changes while the calender is running, restarted, and then temporarily overspeeded to restore the amount of stock in the festoons to normal.

Calender Control

A simplified schematic diagram of the calender control circuit is shown in Figure 4. The electronic preamplifier makes use of vacuum tubes to provide excitation to the amplidyne that controls the generator field. This combination provides very accurate control of speed, preset speed, and what may be termed "timed acceleration."

So-called "timed acceleration" is simply a means for obtaining the kind of operation a motor-operated generator field rheostat furnishes but with more flexibility. It consists of a resistor–capacitor circuit in the electronic preamplifier arranged so that as the capacitor charges, the speed of the calender motor accelerates with it and as the capacitor discharges, the calender motor decelerates. The range of time provided is from 15 to 100 seconds and is readily adjustable by changing the amount of resistance. These time values represent total time from zero speed to the top speed of 70 yards per minute, or from the top speed down to zero speed. For speed changes of smaller value, such as threading speed to top speed, the time is proportionally less.

The timed acceleration circuit represents a very important operating feature in calender control as too rapid acceleration is quite undesirable. The auxiliaries associated with the calender train must follow whatever speed changes occur on

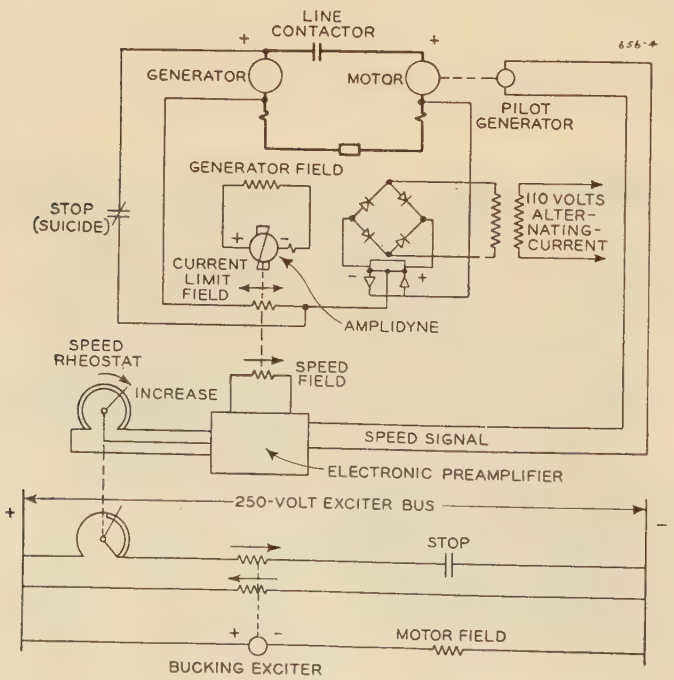

Figure 4 (left). Calender control circuit

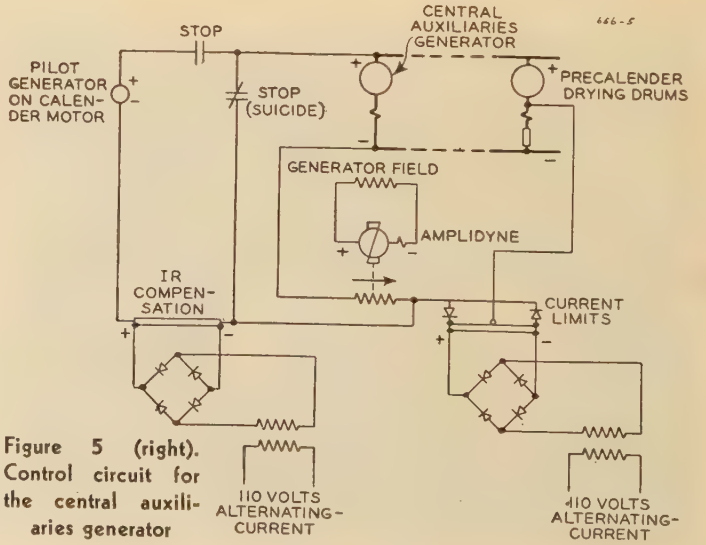

Figure 5 (right). Control circuit for the central auxiliaries generator

the calender itself. If these changes are rapid, excessive changes in tension are produced. Furthermore, the calender operators have no opportunity to adjust the calender roll screwdowns with rapid changes of speed to hold gauge.

In effect, this circuit provides an infinite number of speed points so that acceleration and deceleration are both very smooth.

The control also furnishes means for limiting both motoring and regenerative currents to values required either from the standpoint of performance or commutation. Under conditions of acceleration or normal deceleration, current limit is not necessary because of the timing circuit. It is provided only as a safety means. However, to meet the requirements of fast emergency stopping, regenerative current limit is an extremely important function.

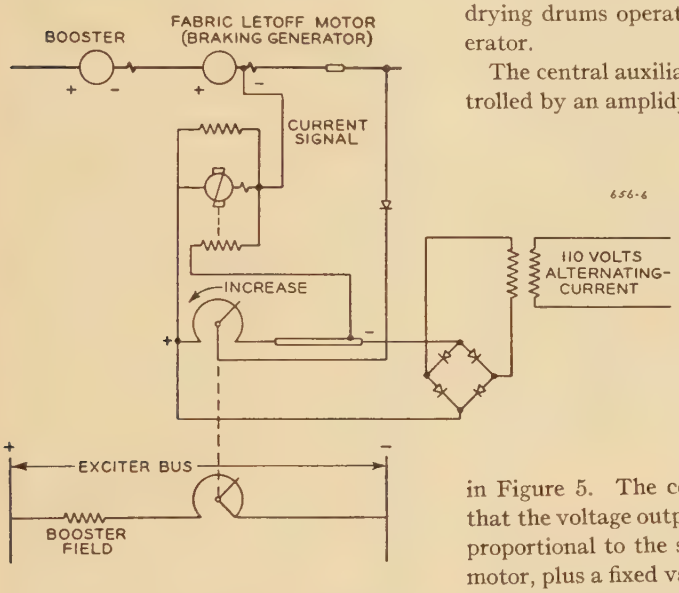

Figure 6. Control circuit for the fabric letoff motor and booster

When the stop button is pushed, the amplidyne exciting the generator is connected in a "suicide" circuit so that the generator voltage collapses rapidly. As the regenerative current from the motor to the generator reaches a value of approximately 200 per cent, the current limit circuit prevents the generator voltage from decaying at a rate faster than the decrease of the motor internal voltage with deceleration.

The regenerative current is held at the 200 per cent limit until the internal voltage of the motor, at about 5 per cent speed, no longer is able to overcome the *IR* drop of the armature loop circuit.

When stopping, full field is established in the motor as rapidly as possible. This is done to obtain maximum torque per ampere and a high rate of deceleration. The inductive lag of the motor field, which resists this change, is reduced materially by reversing the output of the bucking exciter and applying approximately twice normal voltage across the motor field.

Stopping performance is considerably better than that obtained by dynamic braking in conventional equipment operating from a constant potential d-c source. In contrast to a braking current of 200 per cent obtained by the amplidyne control with regenerative braking, the average current using dynamic braking is usually 30 or 40 per cent, with an initial peak of 200 per cent.

Control for Central Auxiliaries

In this group of auxiliaries, the motors on the post-tension rolls and the cementer pull rolls operate conventionally as motors, but the motor on the precalender drying drums operates as a braking generator.

The central auxiliaries generator is controlled by an amplidyne exciter, as shown in Figure 5. The control is arranged so that the voltage output of the generator is proportional to the speed of the calender motor, plus a fixed value for what we may call *IR* compensation. The speed-voltage component is established by taking a signal from the pilot generator on the calender motor. The motors on both the post-tension rolls and the cementer have substantially the same *IR* drop and the fixed voltage introduced for *IR* compensation is made equal to it. Hence, at any speed of the calender itself, the voltage available for these two motors will be very nearly equal to what they require for counterelectromotive force and full load current.

Each of the three motors has an amplidyne exciter. For the two machines which actually are motoring, the amplidyne control is arranged to hold constant armature current. Hence, at the voltage established by the speed of the fabric, constant current is equivalent to constant horsepower input to the motors. Neglecting their internal losses, this is substantially constant horsepower output, or constant torque at any given speed. As the friction torque required by these auxiliaries is low and does not change much, most of the motor output goes into tension, and this will be substantially constant.

As the speed of the fabric is changed, the voltage level is readjusted proportionately. The horsepower input to the motors therefore is changed accordingly, and with armature current unchanged, constant tension is maintained over the speed range.

The amplidyne control for the drying drums motor operates in a somewhat different manner. Since it is regenerating, its internal voltage not only must be sufficient to overcome its internal *IR* drop, but also the *IR* compensation voltage, which is a component of the generator voltage. This is done easily at top speeds where a very small increase in flux provides a large increase in internal voltage. However, at one-tenth speed, the flux must be increased substantially. The flux variation from top speed to bottom speed is about two to one.

For constant tension, it is necessary to hold a constant torque output from this machine at any speed within the operating range. Thus, as the flux is increased, the regenerative current must be reduced. The amplidyne control is arranged to do just that. At any particular speed, it maintains the current output constant. If the speed is increased, the current also is increased to compensate for the decrease of flux. The converse is true when the speed is decreased. At one-tenth speed, where the flux is twice the value at top speed, the control holds a current equal to only one-half the value established at top speed.

When the "stop" button is pushed, the amplidyne control of the generator is reconnected in a "suicide" circuit. Current limit control is provided, using a signal proportional to the armature current of the drying drums motor.

When stopping, there is no control over the regenerative currents from either the post-tension rolls motor or the cementer pull rolls motor, as they have lower inertias than the drying drums motor and can decelerate with it without difficulty.

Control for Entry Auxiliaries

The fabric letoff operates as a braking generator, with an amplidyne exciter holding constant current to obtain substantially constant drag tension on the fabric (Figure 6). The pull rolls motor provides the necessary reaction to overcome this tension and determines the speed at which the fabric is taken from the letoff. It is controlled by regulating the generator voltage in accordance with

the position of the bottom rolls of the festoon. The rolls adjust the air gap of a solenoid, which controls an amplidyne used to excite the generator. If the rolls drop from their normal position, the pull rolls motor is slowed down, and if they raise, the motor is speeded up.

The motor on the liner windup operates as a motor and is under constant tension control, with an amplidyne exciter regulating its armature current.

The influence of *IR* drop, particularly at the lower speeds, has a material influence on the circuit designs. If the fabric tension is increased by strengthening the regenerative current from the fabric letoff motor, the voltage level on all motors is increased because the tension reaction must come from the pull rolls machine. This makes it more difficult for the letoff motor to regenerate.

To overcome this, a booster generator is used in series with the armature of the letoff motor. The voltage from the booster is of such a magnitude and direction that it not only compensates for the internal *IR* drop of the letoff motor, but also the rise in generator voltage, when the stock tension is increased.

As the pull rolls motor and the liner windup motor both are supplied from the same generator, a booster on the windup motor is unnecessary. However, these machines must be designed so that their internal *IR* drops are the same.

Current limit control for acceleration and deceleration is employed, using a current signal from the armature circuit of the pull rolls motor.

When speed is changed in either direction, the tension being used between the letoff and pull rolls is sufficiently high so that only small changes occur. However, this is not the case for the liner windup and a circuit is used for inertia compensation. When accelerating, it increases the regulated value of current to supply an accelerating component, and conversely, decreases it under deceleration.

To replace the festoon storage after a shutdown to change rolls, the entry auxiliaries are overspeeded by a maximum of 20 per cent with respect to the speed at which the fabric is being taken away from the festoon. This is accomplished automatically by the solenoid control.

When a stop is to be made, the generator amplidyne is reconnected in a "suicide" circuit with current limit control from the pull rolls motor.

Instead of using regenerative braking, dynamic braking is used on both the fabric letoff and the liner windup. These motors have wide field control ranges. Thus, their inertias are determined by their base speed, or frame size. When operating at weak field speed, however, the torque is considerably less than full field would provide. Accordingly, if regenerative braking were used, at weak field, insufficient torque would be available.

In view of this, dynamic braking is employed. The circuit is arranged so that constant armature current is held over the field control range. Thus, when operating at weak field, as deceleration occurs and the motor slows down, the field is strengthened so that the internal voltage of the motor is kept at a constant value. Once base speed is attained, the dynamic braking current, of course, decays with speed.

Both the liner windup motor and the stock letoff motor are extremely difficult to stop and several times normal current must be used in the dynamic braking circuit.

Figure 7. Control board for the a-c accessory drives

Control for Delivery Auxiliaries

The delivery auxiliaries group is quite similar to the entry auxiliaries. The fabric windup, in this case, operates as a motor, with amplidyne control maintaining constant winding tension. The motor on the cooling drums provides the reaction to this winding tension and determines the speed at which fabric is taken from the festoon. As in the previous case, its speed is controlled by the position of the bottom rolls in the delivery festoon, using the same solenoid control scheme for generator voltage. If the rolls drop from their normal position, the cooling drums motor is speeded up; if the rolls raise, the motor is slowed down.

The motor on the liner letoff operates as a braking generator to hold a constant drag tension on the liner and is under amplidyne control.

For the delivery auxiliaries as well, the influence of *IR* drop affects the circuit design materially. As the fabric tension is increased, the voltage level is reduced to lower the torque output of the dry cans motor. As a matter of fact, at very high values of fabric tension, this machine actually must regenerate as there is insufficient festoon weight and friction load in the cooling drums to provide the tension.

The decrease in voltage level, however, makes it more difficult for the stock windup motor to obtain motoring current. A booster is used, therefore, with this machine. The voltage from the booster consists of a component to overcome the internal *IR* drop of the windup motor, and also an additional voltage equivalent to the reduction in generator voltage with increases in tension.

The liner letoff motor, which operates as a braking generator, is provided also with a booster which compensates for the *IR* drop of the letoff motor and changes in the voltage level.

For current limit control, when accelerating or decelerating, a signal is taken from the armature circuit of the dry cans motor. This control operates as it did for the entry auxiliaries, adjusting the gener-

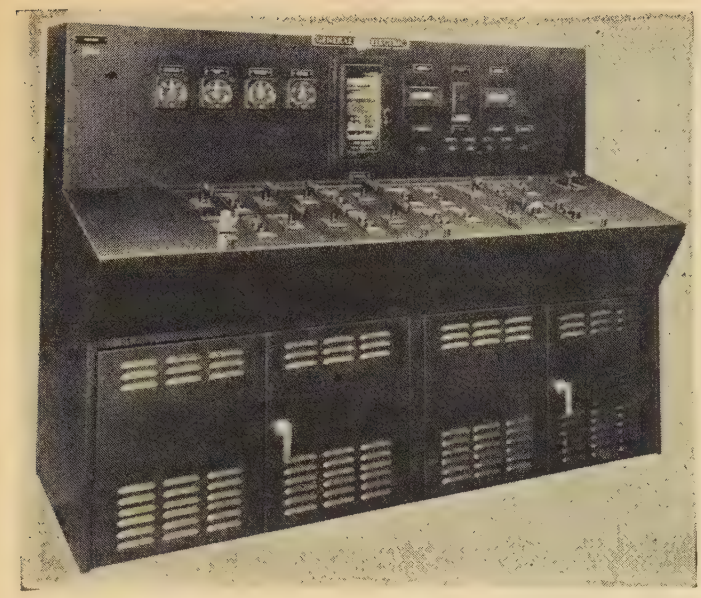

Figure 8. Main calender desk

ator voltage to hold either accelerating or decelerating current constant, as the case may be.

The fabric and liner tensions remain substantially constant when speed changes are made. However, in the case of the fabric windup, inertia compensation must be used, as explained previously for the liner windup on the entry auxiliaries.

Following the shutdown of the delivery auxiliaries for a roll change, the storage of fabric in the festoon must be removed. To do this, 20 per cent overspeed with respect to the speed at which fabric is being delivered to the festoon is available. The solenoid control does this automatically.

When a stop is to be made, the generator amplidyne is "suicided" and the current limit control from the cooling drums motor determines the rate of deceleration. Dynamic braking is used on both the fabric windup and the liner letoff for the same reasons that it was chosen for their counterparts in the entry group. Several times normal current must be used to stop these auxiliaries.

Co-ordination of A-C Accessory Drives

The driving motor of the large motor-generator set is a 450-horsepower unity power factor synchronous machine, supplied from a 2,300-volt source. A switchgear-type controller is furnished for this motor, suitably interlocked with the d-c control equipment in case of a loss of voltage, or an overcurrent indication.

There are also about 24 low voltage devices such as motors, solenoids, or valves, which operate from a 440-volt supply. These are controlled and interlocked with the d-c equipment. A load center type of control board, shown in Figure 7, is used.

The motors involved include those for ventilating fans in the cementer, cement pumps, calender lubricating pumps, water pumps for the cooling drums, feed conveyors for the rubber banks in the calender, and also the driving motors of the small motor-generator sets used for the train drive. Interlocking between these units and the d-c control is very important. For example, in case of a loss of lubrication, the calender must be shut down promptly. If ventilation is lost in the cementer, this also must be done.

Operation

To satisfy the operating requirements previously described, a substantial number of selector switches and pushbuttons is required. However, these are conveniently grouped in a main desk (Figure 8) located at the calender, an entry letoff desk, and a delivery windup desk. In addition, there is a small operator's panel located right next to the letoff and another at the windup. These contain the switches which are of immediate use to the operators when changing rolls. A considerable amount of precautionary interlocking is employed to avoid misoperation and mistakes on the part of the operators.

For normal running, once the calender train has been threaded, operation is actually simpler than with a conventional type of mechanical drive. The calender running speed, acceleration rate, and tensions are preadjusted, so that the operator only has to push a "Run" button and the entire train accelerates to the predetermined speed. This may be done only from one central point, the main desk.

On this desk also are located a recording and indicating tachometer calibrated in yards per minute, instruments for thickness gauge, and yardage counters which indicate the total yardage into and out of the train at the end of a day's operation. The master speed adjusting rheostat is also on this desk, but a speed limit rheostat which determines the maximum speed for any particular run is placed on the main control board so that it is accessible only to supervisors. Adjustment and indication of the current in both the drying drums motor and post-tension rolls motor are provided on the desk, so that the operator can control the precalender and postcalender tensions. Selector switches and pushbuttons for the roll screwdown motors and the necessary threading and jogging buttons are there as well.

The letoff and windup desks have the adjustments and instruments for the motors associated with them, as well as certain jogging and bypass buttons.

The entire train can be stopped from a number of places including several rope-operated safety switches. All stops are treated as emergency stops in order to bring the train down quickly, and give a constant check on stopping performance.

Changing Rolls at the Windup

When the operator observes from a yardage indicator on the windup desk that the fabric roll is nearly full, he places an operating switch in the "Change Rolls" position. This slows down all of the auxiliary drives associated with the delivery festoon to half speed. When the desired maximum roll diameter actually is reached, he moves the operating switch to the "Stop" position which quickly stops all of the delivery festoon auxiliaries. The calender in the meantime continues to run, filling the empty festoon.

As the delivery auxiliaries stop, a clamp roll, immediately above the windups, is set so that it holds the stock in place against the festoon weight when the operator cuts it. The cutting operation is done automatically by a "fly knife" which travels transversely across the stock.

After the cut has been made, the operator places a selector switch in position for the alternate windup. This windup previously had been operated by jogging so that a few turns of liner are wrapped around it from the liner letoff associated with it.

The operator then returns his operating switch to the "Change Rolls" position so that the alternate windup with the other delivery auxiliaries starts up. An air valve control device then actuates a small conveyor which transfers the leading end of the cut fabric from the first

windup to the one that now will be used. It puts it in such a position that it is caught automatically in the "bite" formed by the liner as it wraps around the roll.

After the stock has made several wraps around the roll with the liner, the operator puts his operating switch in the "Slack Takeup" position which automatically removes slack and establishes tension, with the delivery auxiliaries still operating at half speed. He then moves the operating switch to the "Normal" position and the delivery auxiliaries accelerate to a speed somewhat higher than that of the calender, depending upon how much storage must be removed from the festoon.

Changing Rolls at the Letoff

This operation is quite similar to that at the windup. The operating switch has the same positions. In the "Change Rolls" position the entry auxiliaries operate at half speed. In the "Stop" position a mechanical brake is set to hold the fabric against the weights of the festoon rolls when the fabric letoff no longer provides the necessary tension.

When the operator has spliced the trailing end of the stock going to the festoon to the leading end of the fabric from a new letoff roll, the "Slack Takeup" position automatically reverses the letoff and its associated liner windup to take up slack. This is very important because the splice is not strong and if slack were not eliminated, the resulting jerk at starting the entry auxiliaries might break the splice.

In the "Normal" position, the entry auxiliaries accelerate to some speed higher than that of the calender so that normal storage of fabric can be returned to the festoon.

Conclusion

It is expected that the automatic control, made possible by the use of individual electric drives, will result in a substantial improvement in the quality of the product. Regulated tensions should eliminate fabric that is stretched too much, or so slack that it wrinkles. This will reduce rejections and increase production.

The rubber industry deserves praise for pioneering this type of equipment and discarding the conventional. Processing techniques may benefit, not only in this industry but also in others, such as textiles, plastics, and photographic film where similar problems exist.

Reference

1. Continuous Processing for Automobile Tire Fabrics, G. E. Cassidy, W. A. Mosteller. AIEE Transactions, volume 58, 1939, May section, pages 218–23.

A New Crystal Channel Filter for Broad Band Carrier Systems

E. S. WILLIS
ASSOCIATE AIEE

Synopsis: A new crystal channel filter for use in broad band carrier telephone systems is described. It requires less than two-thirds as much mounting space as the earlier design and savings in materials and manufacturing effort are realized. These savings were made possible by assembling the four crystal units in one lattice-type filter section rather than two, resulting in a reduction in the number of component coils and capacitors.

CRYSTAL filters first were used commercially as channel selecting filters in a carrier system developed for use on cables.[1] Their use in that system permitted the placing of a large number of telephone channels close together in the frequency spectrum. The terminal equipment of the system was designed to provide a bank of 12 channels in a frequency band 48 kilocycles wide, suitable for any transmitting medium capable of providing this band width. Subsequent to its use on cable circuits, this 12-channel bank was applied to other new broad band carrier systems for use on open wire lines and on coaxial cables. The crystal filters used in this original bank were those described by C. E. Lane in 1938.[2]

As the demand for broad band carrier systems increased, a need developed for a channel filter which could be produced in relatively large quantities more economically than the original design. The type of design which seemed most promising was one which used a more compact configuration for the filter, thereby reducing the number of coils and capacitors required. However, this type of filter is critical of adjustment and the desired performance is realized only if the electrical characteristics of the component elements are maintained close to their theoretical values. This requires that the crystal units be adjusted precisely and that they retain their electrical characteristics accurately for variations in time and temperature.[3] As a step in this direction, the stability of performance of crystal units was improved by the development of the wire-supported mountings in place of the earlier clamp-type mountings, and the provision of hermetically sealed containers.[4] The use of this new type of crystal unit construction made it practical to provide the new filter design described in this paper. The four coils used in the old filter were replaced by two less expensive coils, and four of the capacitors were omitted in the new design. These changes and the resulting reduction in size made possible the saving of large quantities of materials and greatly reduced the required manufacturing effort.

A comparison of the size and internal appearance of this new filter (type 219) and the old filter (type 75) is shown in Figure 1. The new filter weighs less than half the old one and requires less than two-thirds as much mounting space. In order to utilize efficiently the size reduction of the filters they are assembled in a new design of terminal equipment. Figure 2 shows a typical office installation in which old and new type terminal equipments are mounted in adjacent bays. The 219-type filters appear in the equipment in the two bays on the right, whereas the 75-type are shown in the equipment on the left.

All 12 of these channel filters transmit the lower sidebands derived from the modulation of speech signals and carrier frequencies located 4 kilocycles apart in the range from 64 to 108 kilocycles. An insertion-loss frequency characteristic which applies to each of these filters is shown in Figure 3. This performance curve is very similar to that of the earlier channel filter, but the loss in the pass band is lower and the filter has sharper cutoffs than the earlier design.

Crystal filters usually are designed as lattice-type rather than ladder-type structures because of the greater flexibility afforded by the lattice design. For a lattice-type structure the functions for the propagation factor and characteristic impedance may be chosen independently as they involve only the quotient and product of the impedances or admittances of the series and diagonal branches.[5] The

Paper 46-26, recommended by the AIEE committee on communication for presentation at the AIEE winter convention, New York, N. Y., January 21–25, 1946. Manuscript submitted November 21, 1945; made available for printing December 1945.

E. S. Willis is with Bell Telephone Laboratories, Inc., New York, N. Y.

complexity of the branches of the lattice structure is dictated by the sharpness of the cutoff and the width of the pass band desired. The schematic circuit of the 219-type filter is shown in Figure 4. By relocating the shunt capacitances and series inductances as part of each lattice branch and replacing each crystal element by its equivalent network, an inductance and capacitance in series shunted by a second capacitance, the schematic of Figure 5 is obtained. The theoretical values of the elements shown in this schematic are derived from the following assumptions:

1. The location of the two cutoff frequencies.

2. The location of five frequencies of infinite attenuation.

3. The value of the impedance constant.

4. The coincidence between zeros and poles of the series and diagonal branches at the four critical frequencies occurring within the filter pass band.

Figure 6 shows the elements that comprise the filter. At the two ends are located the two air-core coils mounted in drawn copper cylinders. This coil is a duolateral type having a Q, that is, the ratio of reactance to effective resistance, of approximately 150 at the operating frequency. The same coil is used in each of the 12 filters. Because of the high coil impedance called for by the filter design, care is taken to make the parasitic capacitances between the windings and between the windings and the case as low as practicable. This is accomplished by winding the coil in four sections as shown in Figure 7. Such reduction in capacitances also results in improved stability of the coil and filter characteristics under service conditions.

Four resistances, two at each end of the filter, regulate the loss level in the pass band so that the band loss of each of the 12 filters is approximately the same. Fixed molded silvered mica and fixed and adjustable air capacitors are the remaining elements mounted on the upper side of the panel. The silvered mica capacitors and the two end adjustable air capacitors provide the shunt capacitances at the input and output of the lattice. The center adjustable capacitor is a differential air capacitor which, along with the two small fixed air capacitors, provides small capacitances across each of the four lattice branches. The four crystal plates, mounted in glass envelopes and assembled as a unit, form the basic structure of the lattice. Figure 8 shows one such group of four plates and illustrates how the 16 wires from the crystal units are connected to the terminals forming the four corners of the lattice. The main differences among the 12 channel filters are the differences in the dimensions of the crystal plates. The crystals are -18.5 degree X-cut longitudinal plates supported by fine wires located along their nodal lines. The mounting and fabrication of these crystal units has been covered very thoroughly in a recent paper by R. M. C. Greenidge.[6]

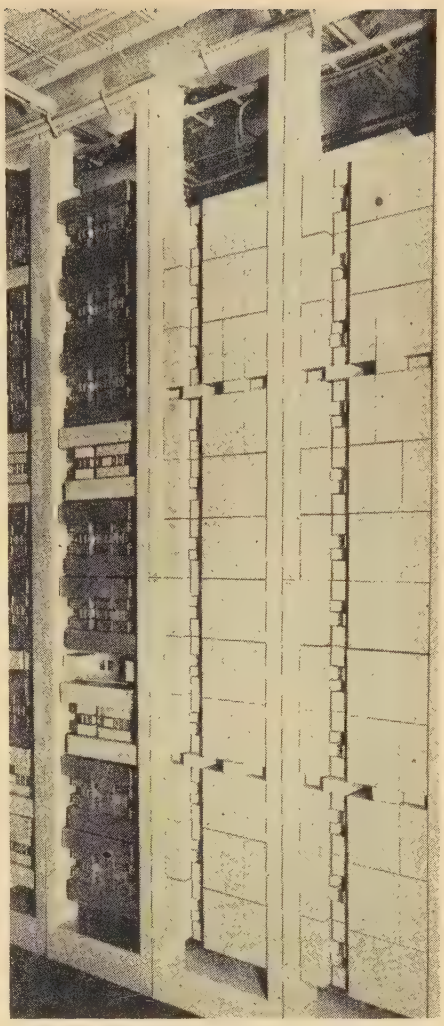

Figure 2. The 219-type filters form a part of the 12-channel banks on the right, whereas the 75-type filters are utilized in those on the left

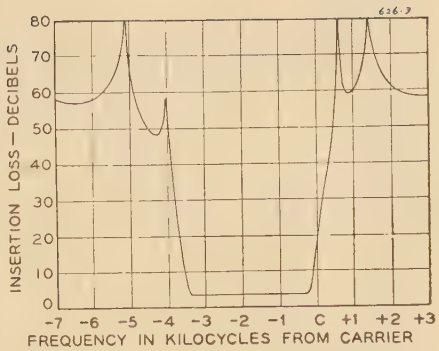

Figure 3. The insertion-loss frequency characteristics of the 12 filters are the same when plotted in cycles removed from the carrier frequencies

The length of a -18.5-degree plate in a quartz crystal unit is determined almost entirely by the frequency of resonance desired. The width and thickness are controlled mainly by the inductance. In addition to obtaining the desired resonant frequency and inductance it is essential that the strong secondary resonant frequency (this is an objectionable response) of each crystal unit be confined to a region that is not being used for the transmission of speech. There are such regions, each approximately 700 cycles wide, between the adjacent channel bands. The length, width, and thickness of the crystal plates then are determined discretely by the desired resonant frequency, inductance, and location of secondary response.

The equivalent inductances of the crystal units used in these 12 filters range in value from 38 henrys to 576 henrys. Even the four crystal units assembled in one filter cover a relatively wide range of inductance values. The ratio of the inductances of the two crystal units connected in parallel in the series branches o the lattice is five-to-one and in the diagonal branch crystal units is four-to-one. The crystal plates range in length from 1.66 inches for the lowest frequency unit

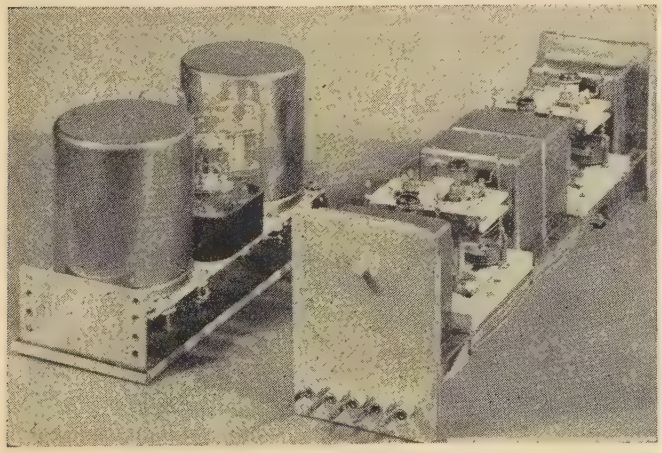

Figure 1. The 219-type filter requires less than two thirds of the mounting space and weighs less than half the 75-type filter

to 0.94 inch for the highest. The extremes in thickness are 0.019 and 0.085 inch. The ratios of the widths of the crystals to their lengths range from about one tenth to slightly less than one half. These crystal plates are narrower than the plates used in the earlier channel filters resulting in a saving in the amount of raw quartz required per system terminal.

The resonant frequency of the crystal unit is adjusted in an electric circuit to within seven to ten cycles of the desired frequency by grinding down the length of the plate. The inductance of the crystal unit is held to within three per cent of its nominal value by manufacturing tolerances on the fabrication of the plate. However, as shown later in the paper, this rather broad range of inductance values would permit a wide divergence in filter performance. In order to limit this range of performance the four crystal units used in any one filter are selected so as to have approximately equal departures in inductance from the nominal values. The magnitudes of their respective variations from a common percentage departure from nominal are plus or minus one half per cent for the two low inductance units and plus or minus one per cent for the two high inductance units.

In order to meet this close requirement on inductance grouping with the limited number of crystal units available, the inductances of a large percentage of the plates are adjusted in the manufacturing process. The inductances of all units are made to fall within one of two groups, each meeting the foregoing limits, one centered about the nominal value and the other two per cent above nominal. The inductance of a coated crystal plate may

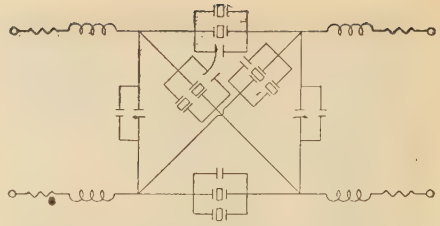

Figure 4. The schematic circuits of the 12 channel filters are the same

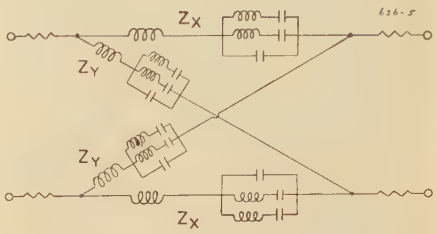

Figure 5. The schematic for design purposes has all of the elements within the lattice excepting the resistances which form a portion of the terminating impedances

be increased by isolating or effectively removing from the electric circuit a portion of the metallic coating. The procedure followed in the manufacture of the units is to divide the metallic coating on one surface of the plate by a transverse line located near one end of the plate thereby reducing the effective plated area by a small percentage. In manufacture this operation is done just prior to the assembly of the crystal plate in its cage.

These filters provide 50 to 60 decibels loss to all frequencies more than about 700 cycles from the edges of the pass band. To maintain this high loss in one lattice-type filter section necessitates a close impedance balance between the branches of the lattice. A plot of the reactance-frequency characteristics of the two branches of the lattice, Figure 9, helps to explain the transmission properties of the filter. Where the reactances Z_x and Z_y of the two branches are of opposite signs the filter is transmitting but where they are of like signs the filter attenuates. Figure 10 shows on an expanded scale the percentage difference between these two reactance curves in the attenuating region of the filter Where this difference is zero the attenuation is infinite, or, in other words, a peak of attenuation is located at this frequency. There are four peaks of attenuation located at finite frequencies as shown by the points at which this difference curve crosses zero and also a peak of attenuation located at infinite frequency where the two reactance curves meet.

To obtain discrimination of approximately 60 decibels and maintain it over the anticipated life of the filter requires precise adjustment of the filter elements and the stable performance of these elements in service. Certain elements have greater effect on filter performance than others and hence greater precision of adjustment and more stable performance is required of them. An examination of the function of each of the various elements in shaping the two reactance curves Z_x and Z_y will reveal the elements in which the greatest precision of adjustment is required. Any small change in an element which causes similar changes in the two reactance curves without changing their relation to each other will have very little effect on the attenuation curve. But, any change in an element which changes one reactance curve with respect to the other will alter the filter performance greatly. Thus changes in the elements which appear in the series branches and not in the diagonal branches or which appear in the diagonal branches and not in the series are the ones that cause relative movement of the two reactance

Figure 6. The elements are assembled on a panel in much the same position as they are shown in the filter schematic

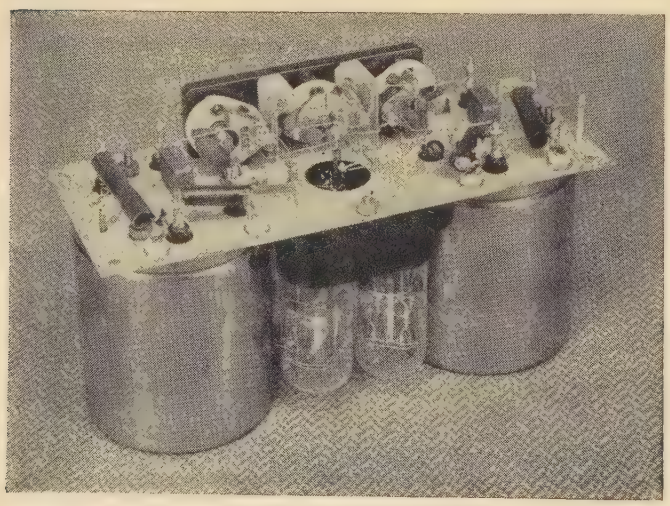

Figure 7. The coil winding is sectionalized to reduce the parasitic capacitances

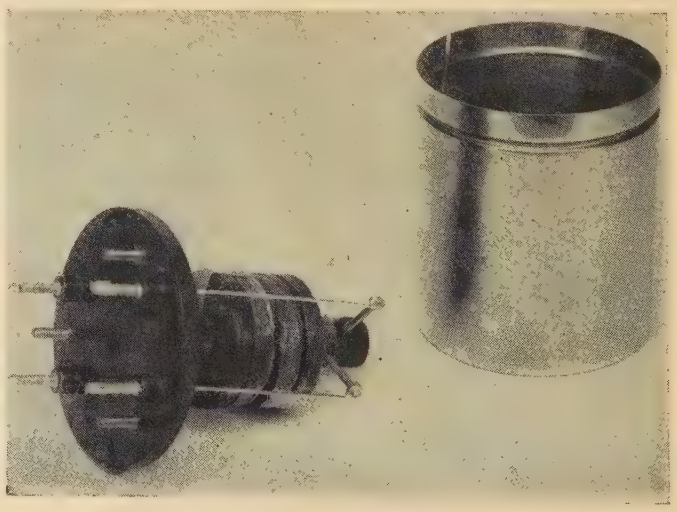

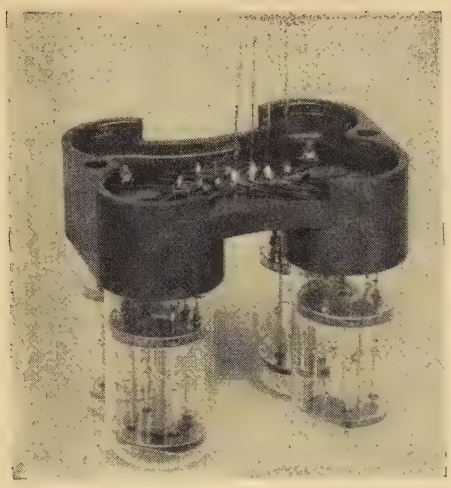

Figure 8. This crystal unit is a four-terminal lattice network comprised of four divided quartz plates and electrically providing two crystal elements in parallel in each branch of the lattice

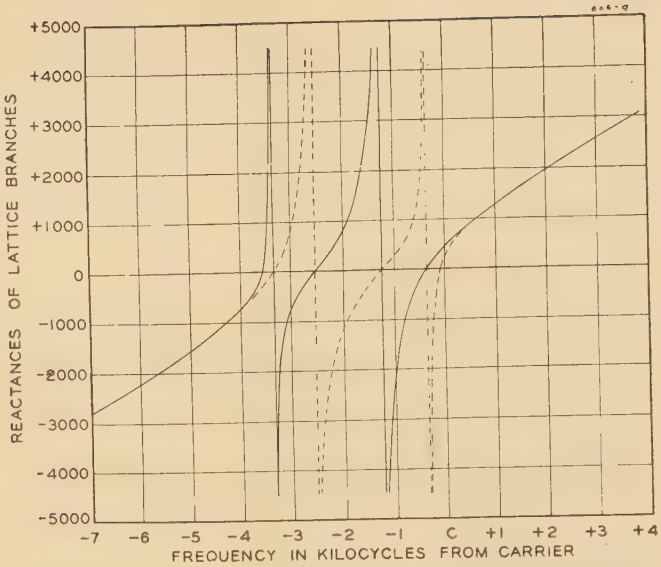

Figure 9. Where the reactances of the two branches of the lattice are of opposite signs the filter transmits and where they are of like signs the filter attenuates

curves. Hence it is the elements which appear within the lattice structure, that is, the four crystal units and the lattice of capacitances consisting of the differential air and fixed air capacitors, that require precise adjustment and stable performance.

In order to obtain uniform performance in the filters it is necessary to hold the resonant frequency and inductance of the crystal units within very narrow limits. For example, the solid curve of Figure 11 illustrates a normal transmission loss characteristic in which the elements are all at their nominal values. The two dotted curves illustrate the characteristics that result when the inductance values of the crystal units in either the series or diagonal branches depart from their nominal value by about one per cent. A negative departure in one pair of branches results in about the same effect in performance as a positive departure in the other pair. The two curves shown assume positive and negative departures for the inductances of one pair of branches. The selection and grouping of crystal units assembled in any one filter in relation to their inductance departures from nominal, as discussed earlier in this paper, restricts the variations in filter performance.

Departures of about ten cycles per second in the resonant frequencies of the crystal units of either series or diagonal branches will produce variations in discrimination of about the same type and magnitude as those illustrated in Figure 11 for departures in inductance. However, if all crystal units exhibit equal frequency departures, the entire transmission characteristic will be shifted by the frequency departure of the crystal units, and there will be little change in discrimination. For a 20-degree Fahrenheit change in temperature this frequency shift is approximately 0.03 per cent of the operating frequency.

The lattice of capacitances is balanced in the final adjustment of the filter by the tuning of the differential air capacitor. This adjustment moves one reactance curve with respect to the other to locate one of their crossings, and thus one peak frequency, at 600 cycles above the carrier frequency.

In the foregoing discussion the effect of dissipation in the elements forming the filter has been neglected. As there is some dissipation associated with each coil, capacitor, and crystal unit, the effect of each in turn will be considered. The dissipation associated with the coils may be considered as part of the terminating impedances and variation in this dissipation raises or lowers the loss level in the band of the filter without affecting the discrimination. Dissipation in the shunt capacitors at the input and output of the lattice produces similar effects on the filter. When these effects become too large, causing the loss in the pass band to fall outside the specified limit, the resistances at either end of the filter are changed in value to compensate for the change in dissipation.

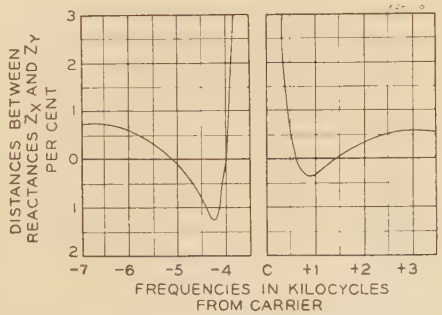

Figure 10. The two reactance curves cross at four frequencies which determine the location of the four attenuation peaks

The elements forming the branches of the lattice, that is, the crystal units and the capacitor lattice introduce very little dissipation. However, since unbalances in the dissipation associated with the lattice branches of the filter will degrade the filter performance to the same extent as reactance unbalances in these branches, extreme care must be exercised to keep the dissipation among these branches balanced. Instead of referring to the reactances of the branches of the lattice, Z_x and Z_y, it is more convenient in the following discussion to refer to their reciprocals, the susceptances B_x and B_y. Dissipation associated with these susceptances is expressed in terms of the conductances, G_x and G_y. To obtain a peak of attenuation in a lattice-type filter it is necessary to have a conductance balance as well as a susceptance balance of the series and diagonal branches of the lattice. Equal conductances across the series and diagonal branches of the lattice have the same effect as equal conductances across the input and output of the lattice. That is, they have the effect of raising the loss in the pass band of the filter slightly. However, an unbalance between the conductances of the series and diagonal branches of the lattice upsets the bridge balance at the filter peak frequencies. The effect of a slight unbalance is a reduction in the magnitude of the peak losses of the filter. As this unbalance is increased the filter peaks may disappear entirely even though there is a susceptance balance at the peak frequencies. This is illustrated by the curves in Figure 12. The solid line represents a normal transmission-loss characteristic of the 219AM filter, with carrier fre-

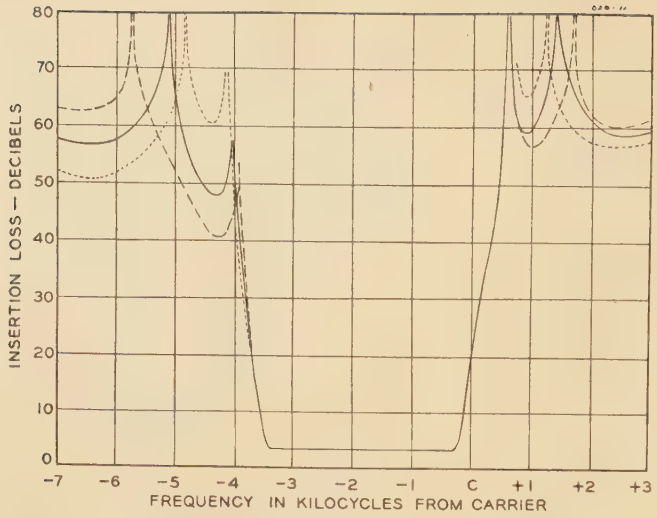

Figure 11. Precise cutting and adjustment of crystal units are required to obtain uniform filter performance

The foregoing effects were produced by inductance departures of one per cent from nominal of crystal units in either pair of lattice branches

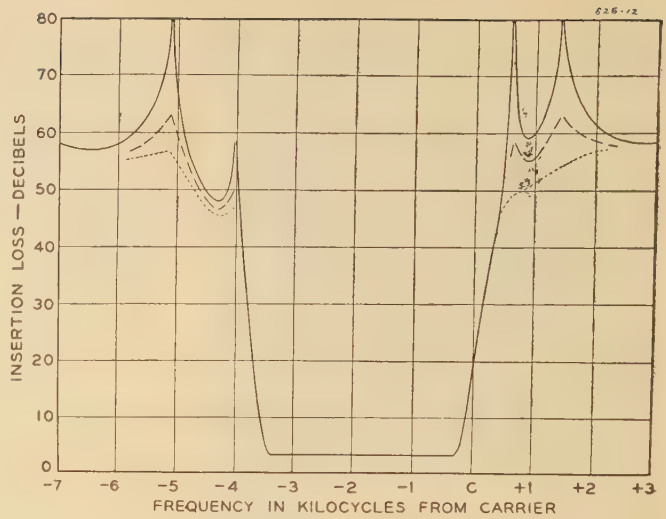

Figure 12. To obtain high peak loss in a lattice-type filter the conductances and susceptances of the series and diagonal branches must be equal

The effects of differences of 0.010 and 0.030 micromho conductance in these branches are shown, respectively, by the dashed and dotted curves

quency at 108 kilocycles, in which there is a perfect balance of both the conductance and susceptance at the peak frequencies. The dashed and dotted lines show the effect of 0.010 and 0.030 micromho conductance unbalance, respectively. Greater amounts of conductance unbalance are required to produce these same effects in the lower frequency filters in inverse ratio to the square of the operating frequencies.

Even though the crystal plates are surrounded by dry air and enclosed in sealed glass containers it is still necessary to protect the filter against atmospheric conditions of high relative humidity. The dashed curve of Figure 12 shows the effect of 0.010 micromho conductance unbalance of the lattice. This unbalance is equivalent to 100 megohms insulation resistance. With clean parts and a relatively dry atmosphere insulation resistance many times as high as this can be maintained across the branches of the lattice. However, a trace of salt or other contamination across the terminals in the molded base of the crystal unit or across the ceramic in the air capacitors will make the insulation resistance highly sensitive to the moisture in the adjacent air. To guard against this condition of low insulation resistance, the following precautions are taken:

1. Where insulating materials are required within the lattice structure only homogeneous low-loss materials are used.

2. The insulating parts assembled in the filters are kept clean.

3. The filters are adjusted, tested, and sealed hermetically when surrounded by an atmosphere in which the relative humidity is not greater than 40 per cent.

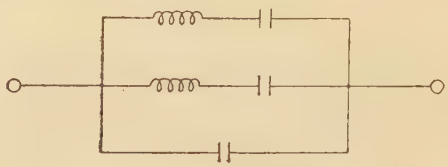

Figure 13. This two-terminal network is connected across the paralleled end of the filters to improve the transmission over the two end channels of the group of 12

In the construction of the filter the elements are mounted on the panel and wired as shown in Figure 6. This panel assembly with cover and end brackets attached is inserted in an adjusting shield through which the three capacitor adjustments are made. The resonant frequencies looking in either end of the filter are located where they should occur theoretically, by the adjustment of the two end air capacitors. The other adjustable air capacitor is used to locate a peak of attenuation at 600 cycles above the carrier frequency.

The function of the channel filters in service is to select the modulated electrical impulses from 12 subscribers' sets and combine them for transmission over the line, and at the receiving terminal to separate the various electrical impulses for transmission to the 12 subscribers' sets. Thus, in operation the 12 filters are paralleled on one end. Over the pass band frequencies of any one of the 12 filters the impedance paralleling this filter should be high so that by far the greater portion of the energy in this frequency range passes through the filter and is not dissipated in the paralleling filters. With the 12 filters connected in parallel this condition is satisfied over all channel bands excepting the two end channels. Good transmission is obtained over all channels by connecting a two terminal network, the schematic of which is shown in Figure 13, across the paralleled end of the filters.

The 219-type "Crystal Channel Filter" is the first commercial application of lattice-type filter circuits in which more than one crystal unit is used in each branch of the lattice. The use of this circuit reduces the number of component elements required in each filter and results in a saving in mounting space required. As these filters constitute a large portion of the broad band carrier terminal equipment this development has contributed to a considerable saving in office space. The labor required for producing these filters has been reduced by a third in comparison with that required for the earlier design. Also, substantial savings in the use of tin, nickel, molybdenum, brass, and raw quartz are realized.

References

1. Cable Carrier Telephone Terminals, R. W. Chestnut, L. M. Ilgenfritz, A. Kenner. AIEE Transactions, volume 57, 1938, May section, pages 237–44.

2. Crystal Channel Filters for the Cable Carrier System, C. E. Lane. AIEE Transactions, volume 57, 1938, May section, pages 245–9.

3. Effects of Manufacturing Deviations on Crystal Units for Filters, A. R. D'heedene. *Bell System Technical Journal*, volume 23, July 1944, page 260.

4. The Mounting and Fabrication of Plated Quartz Crystal Units, R. M. C. Greenidge. *Bell System Technical Journal*, volume 23, July 1944, page 234.

5. Electromechanical Transducers and Wave Filters (book), W. P. Mason. D. Van Nostrand Company, New York, N. Y., 1942.

6. See reference 4.

Die Cast Rotor Testing by Test Stator Method

P. H. TRICKEY
MEMBER AIEE

FOR some years now, it has been a common practice to die cast the squirrel cages of induction motor rotors. The die cast rotor has many advantages of simplicity, ruggedness, and durability as well as low cost. One feature of die castings is the tendency for all castings to have a perfect outside surface even though the interior may contain voids, blow holes, or porosity. This feature is an advantage when the appearance of the die cast article is of primary importance. However, in an electric rotor, it is a disadvantage as no visual inspection methods will disclose a faulty interior which may affect the electrical performance.

Since the conductivity of the best electrical materials such as copper and aluminum are affected by small amounts of impurities, there is always the possibility of low conductivity being introduced at some stage between ingot and final cast rotor. This defect also cannot be detected by visual inspection.

It is necessary, therefore, to have some means other than inspection for testing die cast rotors. Of course, one way of testing such rotors is to build them into complete motors and make thorough tests on the motors. Obviously, this has the great disadvantage of performing many expensive and time consuming operations before it is known that a rotor is defective. Sometimes also other variations in the completed motor make it very difficult to lay positively the cause of poor performance to the die cast rotor.

There are, of course, an infinite number of ways in which a rotor can be defective such as wrong laminations, core stack, skew, and shaft hole, but in general, if the resistance is correct, all other defects can be caught by inspection and gauging. Once in a great while open bars may get by a resistance test but except for rare cases a measurement of the average rotor resistance can be used to select the satisfactory rotors.

There are two common methods of measuring the effective secondary or rotor resistance of a squirrel-cage motor. One method obtains the rotor resistance from readings of slip and secondary copper loss. This has certain definite usefulness for polyphase motors, but has the disadvantage of requiring the rotor to be finished completely and tested in a motor with bearings. The other method involves a measurement of the impedance of the motor with rotor held stationary. From this impedance, the rotor resistance is separated by calculation from the stator resistance and reactance. By taking full advantage of the locked impedance method which requires no rotation, bearings, or line up variations, a very satisfactory method of testing die cast rotors may be devised.

Paper 46-64, recommended by the AIEE committee on electric machinery and technical program for presentation at the AIEE winter convention, New York, N. Y., January 21–25, 1946. Manuscript submitted August 25, 1945; made available for printing December 11, 1945.

P. H. TRICKEY is chief engineer, Diehl Manufacturing Company, Finderne, N. J.

Test Stator for Testing Die Cast Rotors

It would be possible to use a normal stator and, without end covers or bearings, make an impedance test for rotor resistance of a die cast rotor. Special care would have to be taken in testing, as the stator being designed for normal operation at full speed would draw heavy currents and get very hot with rotor standing still. The rotor also would get hot. Correction of resistance measurements for temperature would be subject to error as the temperature not only would be high, but also changing rapidly.

To overcome these and other difficulties, stators for testing die cast rotors are made of special construction and proportions.

1. The stator slots are made much larger than normal, to give 8 to 10 times the normal winding area. This in itself reduces the stator temperature and the amount of primary resistance to be subtracted from the total resistance. It gives a stator much larger in diameter than normal, but the additional size and cost do no harm for a test device.

2. The number of effective turns are usually much greater than the normal stator to give about half the normal flux densities. This keeps the iron loss of the large stator down, and reduces the effect of saturation.

3. Since under locked impedance conditions the phases operate independently, only one phase is necessary for the stator winding.

4. The inside diameter usually is made slightly larger than normal, just big enough to admit rotor cores as they come from die casting before the outside diameter is turned to final size. If the stator has open or partially open slots and the mould allows aluminum to flow over the unfinished surface, it may be necessary to remove this excess aluminum to obtain accurate readings. If it is desired to test soldered or brazed copper or brass rotors in such a stator, it may be necessary to trim off the excess solder or brazing material in order to get the rotor into the stator. Otherwise, the air gap may have to be increased too much and errors are introduced.

5. In general, the width or stack of the test stator is made as narrow as the shortest rotor likely to be tested in quantity, and used for all rotors of that diameter. There is very little error introduced when the rotor is longer than the stator, but if the rotor is shorter, new calibration curves may have to be made because of the change in air gap area.

6. Stators usually are mounted vertically and the windings given thick protective coatings to minimize the damage of rotors continually striking against the stators during insertion. In spite of all precautions, the windings ultimately become short circuited or the laminations badly worn and hammered together at the air gap. If production testing is to be continuous and shutdowns for repair avoided, it is well to have spare stators available for immediate replacement. If it is expected that the windings of individual stators will vary in resistance, it may be desirable to add a rheostat to the circuit which may be adjusted as each new stator is installed thus keeping the same value of total resistance in the primary circuit and eliminating the necessity of new calibration curves for each new stator.

7. In general a single phase concentric winding is used with the turns distributed sinusoidally. A typical core lamination is shown in Figure 7.

Testing Circuit

The equivalent circuit of each phase of an induction motor under locked rotor condition is as shown in Figure 1. For

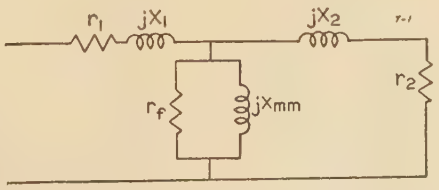

Figure 1. Equivalent circuit of induction motor with rotor locked

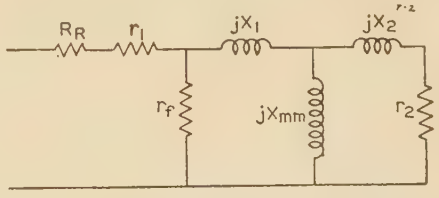

Figure 2. Equivalent circuit used in analyzing tests of die cast rotors

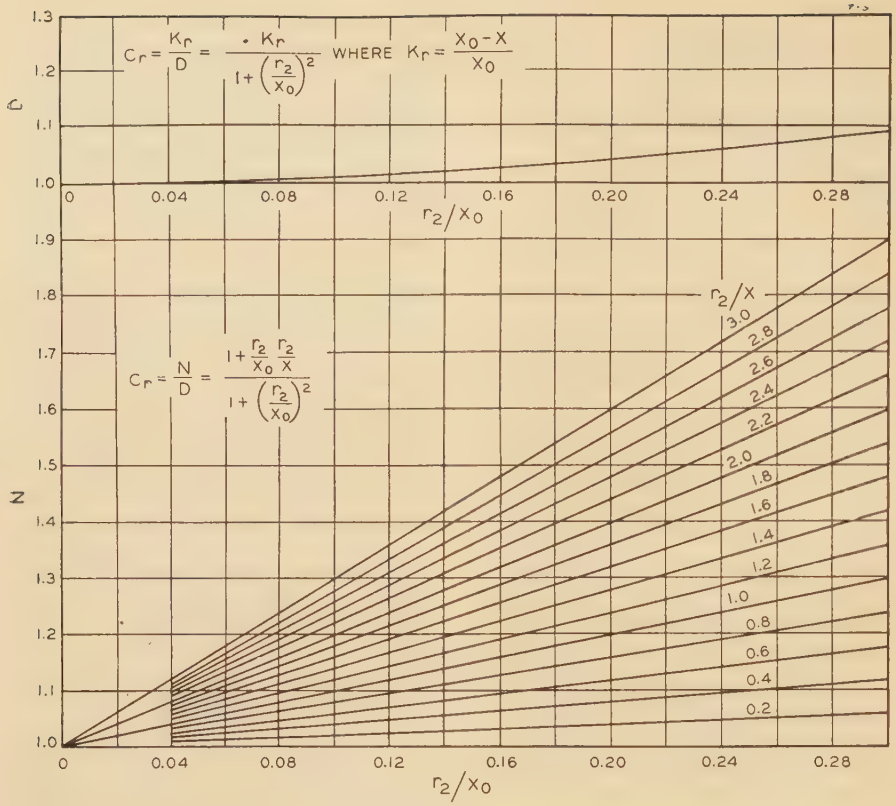

Figure 3 (left). Locked rotor impedance

Single-phase and polyphase induction motors

the purpose of rotor testing, it is satisfactory to assume the iron loss branch to be in shunt across the input as shown in Figure 2. The impedance of the network beyond the iron loss branch has been shown by C. G. Veinott to be:

$$Z_L = R_L + jX_L = (r_1 + r_2 C_r) + jXC_R$$

where

X = ideal short-circuit reactance

$$= x_1 + x_2 \frac{X_{mm}}{x_2 + X_{mm}}$$

$$C_r = \frac{X_{mm}^2}{(x_2 + X_{mm})^2 + r_2^2}$$

$$C_R = \frac{1 + \{(x_1 + X_{mm})/X\}\{r_2/(x_2 + X_{mm})\}^2}{1 + \{r_2/(x_2 + X_{mm})\}^2}$$

r_1 = primary resistance
r_2 = secondary resistance referred to primary
x_1 = primary leakage reactance
x_2 = secondary leakage reactance referred to primary
X_{mm} = mutual or magnetizing reactance

For the purpose of rotor testing, it is satisfactory to assume primary and secondary leakage reactances to be equal. With this assumption the correction factors become

$$C_r = \frac{K_r}{1 + (r_2/X_o)^2}$$

and

$$C_R = \frac{1 + (r_2/X)(r_2/X_o)}{1 + (r_2/X_o)^2}$$

I	2.5	2.5
r_2	10	50
r_2/X_0	0.0388	0.194
r_2/X	0.252	1.26
D (FIG. 3)	1.001	1.04
N (FIG. 3)	1.013	1.245
$C_R = N/D$	1.011	1.197
$X_L = X C_R$	40.2	47.5
$C_r = K_r/D$	0.845	0.815
$r_2 C_r$	8.45	40.7
r_1	2.10	2.10
R_R	0.10	0.10
$R_L = r_1 + R_R + r_2 C_r$	10.65	42.9
$Z_L = \sqrt{R_L^2 + X_L^2}$	41.5	64
$E = I Z_L$	103.9	160
IRON LOSS	7.1	16.9
$I^2 R_L$	66.5	268
WATTS INPUT = IRON LOSS + $I^2 R_L$	73.6	284.9

Figure 4. Calculation sheet for die cast rotor calibration curves

where

$X_o = X_{mm} + x_1 = X_{mm} + x_2$ = ideal short-circuit reactance

$$K_r = \left\{\frac{X_{mm}}{X_{mm} + x_1}\right\}^2 = \left\{\frac{X_{mm}}{X_{mm} + x_2}\right\}^2 = \left\{\frac{X_{mm}}{X_o}\right\}^2 = \frac{X_o - X}{X_o}$$

Figure 3 is sometimes a convenient aid in using these formulas.

Referring to Figure 2, if it is assumed that the current in the iron branch has negligible effect on the magnitude of the total line current, the following expressions may be used:

$E = IZ_L$ where $Z_L = \sqrt{R_L^2 + X_L^2}$, $X_L = XC_R$

and

$R_L = R_R + r_1 + r_2 C_r$ (R_R = rheostat resistance)
Watts input = $I^2 R_L$ + iron loss

A convenient calculation form is shown in Figure 4. It is customary to calculate a complete curve of watts versus r_2 and to use this curve in setting test limits for production test. Such a curve is shown in Figure 5.

Determination of Circuit Constants

In order to use the form shown in Figure 4, it is necessary to know the circuit constants r_1, X, X_o, and the iron loss.

r_1 can be measured easily by resistance bridge.

X can be obtained from a locked rotor reading using a typical rotor, preferably of low resistance. It is usually necessary to have tests with finished and unfinished rotors so that rotors can be tested later under either condition. Usually the same values of test constants can be used re-

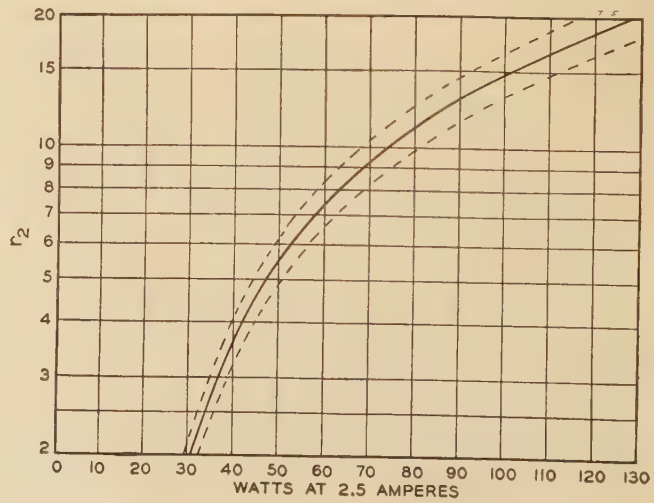

Figure 5. Typical calibration curve for test stator

Dotted curves indicate upper and lower watt limits

		T-6
1	NO LOAD (DUMMY ROTOR) VOLTS	84
2	NO LOAD (DUMMY ROTOR) AMPS I_0	0.469
3	NO LOAD (DUMMY ROTOR) WATTS	5.458
4	PRIMARY RESISTANCE AFTER NO LOAD READING	2.08
5	$I_0^2 r_1 = (2)^2 (4)$	0.458
6	IRON LOSS = (3) − (5)	5.00
7	$X_0 = Z_0 = E/I_0 = (1)/(2)$	179
8	LOCKED ROTOR VOLTS	84
9	LOCKED ROTOR AMPERES	2.5
10	LOCKED ROTOR WATTS	63.5
11	IRON LOSS	5.0
12	NET WATTS	58.5
13	R = TOTAL EFFECTIVE RESISTANCE = $(12)/(9)^2$	9.35
14	PRIMARY RESISTANCE AFTER LOCKED READING	2.10
15	P = (13) − (14)	7.25
16	$Z_L = (8)/(9)$	33.6
17	$Q = \sqrt{(16)^2 - (13)^2}$	32.2
18	$X_0 - Q = (7) - (17)$	146.8
19	r_1 = PRIMARY RESISTANCE COLD (@ 25°C)	2.08
20	$r_2 = (15)\ (7)/(18)$	8.76
21	$r_2/X_0 = (20)/(7)$	0.049
22	$1 + (r_2/X_0)^2 = 1 + (21)^2$	1.024
23	$Q\left[1 + (r_2/X_0)^2\right] = (17) \times (22)$	32.3
24	$r_2\ r_2/X_0 = (20) \times (21)$	0.43
25	X = (23) − (24)	31.9

Figure 6. Calculation sheet used for determining circuit constants

gardless of core stack, but it is well to try different stacks just to be sure. For the purpose of analyzing the locked rotor tests, we can assume the equivalent circuit of Figure 2. The locked impedance of the network beyond the iron loss branch has been shown to be

$$Z_L = [r_1 + P] + jQ$$

where $P = r_2 C_r$ and $Q = X C_R$

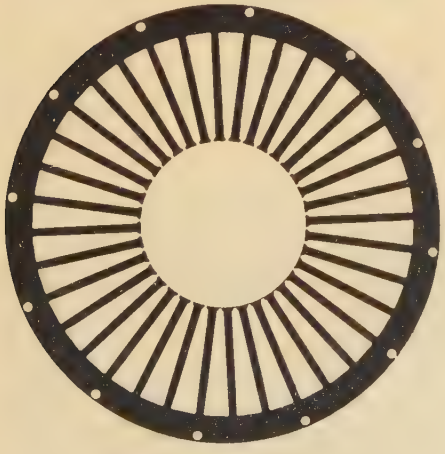

Figure 7. Typical test stator lamination for die cast rotor test

Figure 9. Test bench for die cast rotor testing

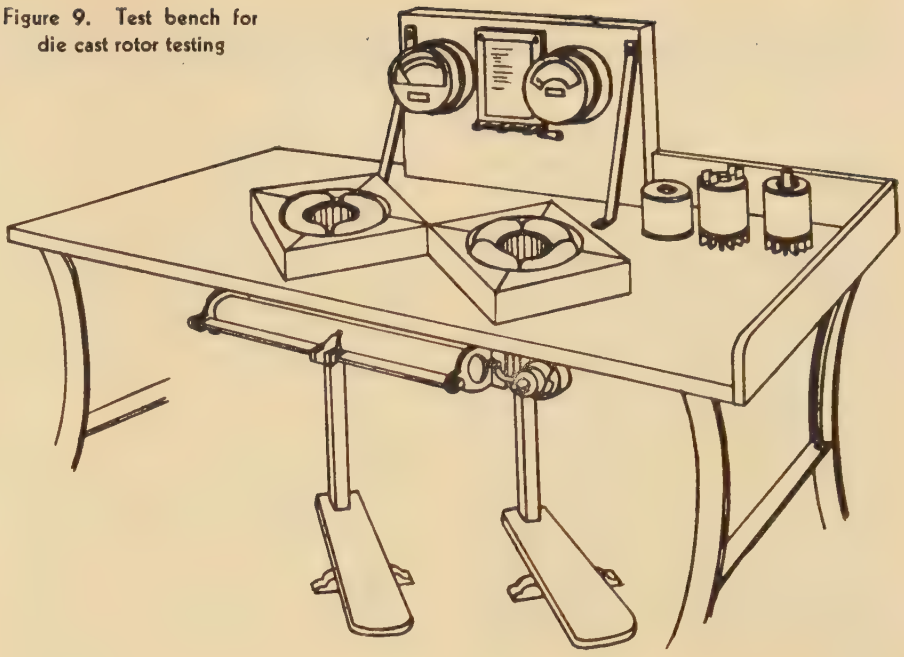

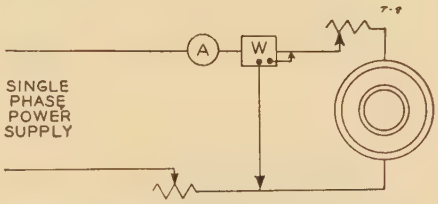

Figure 8. Wiring diagram for die cast rotor test circuit

Assuming that the current in the iron loss branch has a negligible effect on the magnitude of the total line current, we find

$$Z_L = E/I_L,\ R_L = [\text{watts input} - \text{iron loss}]/I_L^2$$

$$P = R_L - r_1 \text{ and } Q = \sqrt{Z_L^2 - R_L^2}$$

Mr. Veinott has shown that

$$r_2 = \frac{P X_o}{X_o - Q}$$

where

$X_o = X_{mm} + x_1 =$ ideal open circuit reactance

He also has shown that

$$Q = X C_R = X \frac{1 + (r_2/X)(r_2/X_o)}{1 + (r_2/X_o)^2}$$

Transposing and solving for X

$$X[1 + (r_2/X)(r_2/X_o)] = Q[1 + (r_2/X_o)^2]$$
$$X + r_2(r_2/X_o) = Q[1 + (r_2/X_o)^2]$$
$$X = Q[1 + (r_2/X_o)^2] - r_2(r_2/X_o)$$

X_o and the iron loss for this type of test stator can be obtained from input readings using a rotor similar to a typical rotor except with no squirrel cage at all.

Under this condition, it can be assumed that

$$X_o = Z_o = E/I_o$$

and that the

Iron loss = input − copper loss

In this case also, it is usually desirable to have tests with both finished and unfinished rotor diameters. It is desirable to take the dummy rotor tests over a fairly wide range of voltages to be sure to cover any case of high or low rotor resistance in later tests. A convenient form for analyzing these tests is shown in Figure 6.

References

1. Segregation of Losses in Single-Phase Induction Motors, **C. G. Veinott.** AIEE Transactions, volume 54, 1935, pages 1032–6.

2. Discussion by **P. H. Trickey** and author's closure of Segregation of Losses in Single-Phase Induction Motors, **C. G. Veinott.**

3. Single-Phase Induction Motors, **W. J. Branson.** AIEE Transactions, volume 21, 1912, pages 1749–87.

4. Starting Windings for Single-Phase Induction Motors, **C. G. Veinott.** AIEE Transactions, volume 63, 1944, pages 288–94.

5. Induction Motor Resistance Ring Width, **P. H. Trickey.** AIEE Transactions, volume 55, 1936, pages 144–50.

New Series Capacitor Protective Device

R. E. MARBURY
MEMBER AIEE

J. B. OWENS
ASSOCIATE AIEE

Synopsis: A series capacitor is best protected from overvoltage during fault by a gap having low arc drop with no tendency to cut off. In this manner the capacitor is not subjected to repetitive voltage peaks during fault, and high current oscillations in the circuit formed by the capacitor and gap are minimized. A special design of graphite gap with self-centering arc characteristics is described. A new type of by-pass switch is also described for automatically by-passing the gap and series capacitor and removing the by-pass after the fault has cleared. The switch shown provides an inherent time delay on closing thus allowing time for the capacitor to discharge through the gap and avoid damage to the switch contacts. The switch also provides time delay on reopening thus eliminating the necessity for a holding means which has been a problem always with magnetic contactors in this application. The motive power for closing the switch is derived from a sealed bellows using high resistance metal and containing a volatile liquid. The passage of current through the bellows changes the vapor pressure and furnishes the forces required to operate the switch. A device of this type is not subject to damage by steep wave front surges associated with the discharge of the capacitor through the protective gap, nor is it damaged by intermittent line faults. The combination of this gap and switch has many advantages over a conventional gap and magnetic contactor and should permit a more general application of series capacitors to distribution circuits.

Paper 46-45, recommended by the AIEE committee on protective devices for presentation at the AIEE winter convention, New York, N. Y., January 21–25, 1946. Manuscript submitted October 29, 1945; made available for printing December 13, 1945.

R. E. Marbury and J. B. Owens, Westinghouse Electric Corporation, East Pittsburgh, Pa.

A CAPACITOR connected in series with an electric circuit improves its voltage regulation by inserting a negative reactance which in effect cancels all or part of the inductive reactance of the circuit. Such a capacitor is called a "series capacitor." A series capacitor installation consists of a bank of capacitors connected in series with each phase of a transmission or distribution line, each bank having the reactance necessary to cancel the desired portion of the phase reactance and designed to handle the maximum continuous and momentary line currents.

Capacitors may be subjected for brief periods to twice their rated voltage without damage to the dielectric; therefore, series capacitors may be allowed to handle momentary currents which are twice their continuous current rating. However, in most circuits to which series capacitors are applied the currents which flow during fault conditions are considerably more than twice the maximum working current. For this reason it is necessary either to use capacitors with a continuous current rating equal to one half the maximum current which may flow during a fault or to use a voltage limiting device.

For a given reactance the cost of capacitors increases approximately as the square of the rated voltage so that usually it is much more economical to use capacitors whose rating is based on the working current and limit the voltage which can appear across their terminals by means of auxiliary apparatus.

Protective Gaps

The device used to protect a series capacitor during fault conditions must not allow the capacitor voltage to rise above twice the rated value even for a short time. Thus, it must function to by-pass the capacitor during the first half cycle of fault current. A gap is the only device which meets this requirement effectively.

The fundamental protected series capacitor circuit consists of a series capacitor shunted with a gap. If, however, this is a metallic gap which has a high arc volt

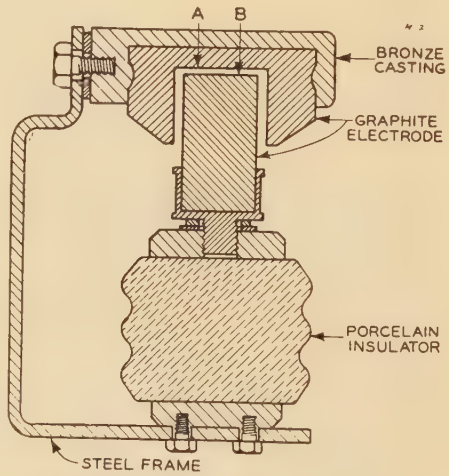

Figure 2. Cross section of new gap

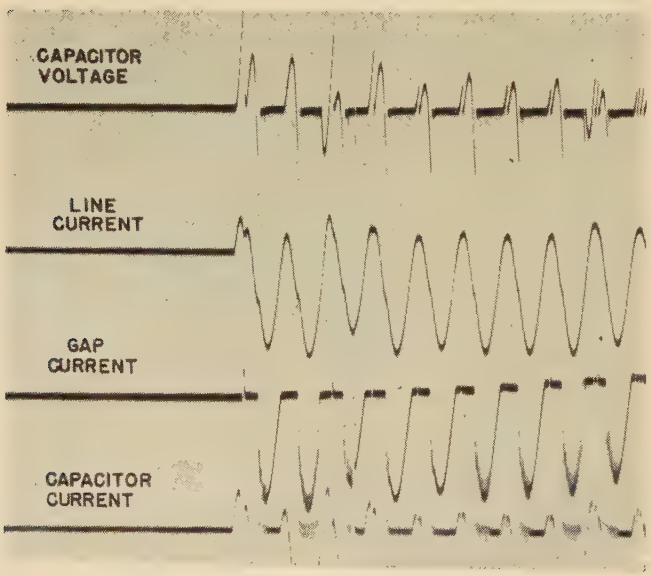

Figure 1. Oscillogram showing operation of a conventional gap protecting a 33-ohm, 60-cycle, 1,410-volt series capacitor on a 100-ampere fault

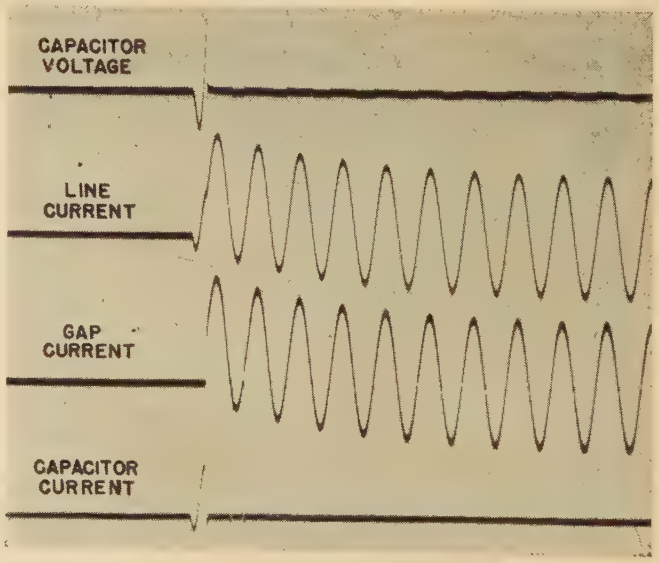

Figure 3. Oscillogram showing operation of new gap protecting a 33-ohm 60-cycle 1,410-volt series capacitor on a 100-ampere fault

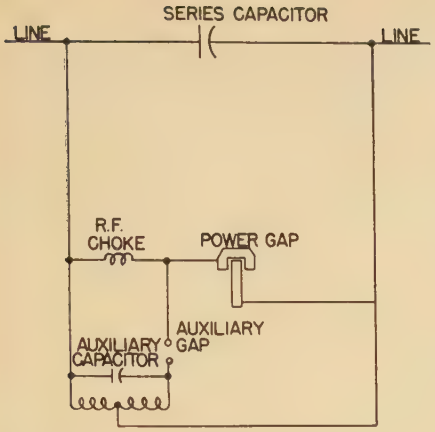

Figure 4. Series capacitor protective device for low voltage capacitors

age and a restriking arc, the series capacitor will be subjected to high currents while the arc exists in the gap. Figure 1 shows an oscillogram made of the current in a 33-ohm, 60-cycle series capacitor with a shunt gap set to break down at 3,000 volts. The gap electrodes were made of brass. The normal current of 43 amperes was increased to 100 amperes. The oscillogram shows the presence of high currents in the capacitor after the gap breakdown occurred. Such high currents cause heating of the capacitor and may cause serious damage.

The use of a gap having special graphite electrodes gives a low arc voltage and limits the current flowing in the series capacitor leads to a low value. Even with graphite electrodes, however, the arc will be moved out of the space between the electrodes by magnetic forces, thermal air currents, and random air currents unless special precautions are taken in the gap design.

Figure 2 shows the cross section of a special type of gap the authors have developed to insure a stable arc with a low arc voltage. The arc occurs between the surfaces *A* and *B* and is shielded from air currents by the upper electrode. Magnetic forces produced by the current traveling radially through the upper electrode are in such a direction as to keep the arc in the gap. Gaps of this design have been tested at currents up to 5,000 amperes for one second and sustained no damage. The arc remained between the gap faces at all currents, and there was no tendency for the arc to wander down the sides of the lower electrode. Figure 3 shows the results of a test using this new gap on the same circuit as that used for Figure 1.

As the spacing of a gap is decreased, the variation in breakdown voltage on successive operations becomes greater. For dependable operation a gap should be adjusted to break down at not less than 3,000 volts. Since the gap must function dependably at no more than twice the rated capacitor voltage, it cannot be used to protect a capacitor rated at less than 1,500 volts unless an auxiliary means is provided to ionize the gap when the capacitor voltage reaches twice the rated value.

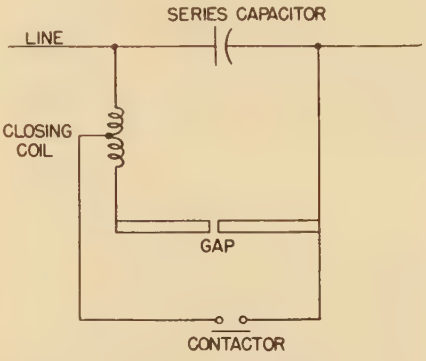

Figure 5. Series capacitor protective device with magnetic contactor to extinguish arc in the gap

Figure 4 shows a diagram of a gap-protected capacitor with a continuous voltage rating of less than 1,500 volts. A step-up autotransformer is used to increase a voltage obtained across the series capacitor to a level such that the auxiliary gap will break down when the voltage on the series capacitor is twice the rated value. The breakdown of the auxiliary gap allows the small auxiliary capacitor to discharge into a radio frequency choke which is in series with the main power gap. This discharge causes a high frequency voltage to appear across the choke. Since the series capacitor has a low impedance at this frequency, the voltage appears across the power gap causing it to break down and pass power current.

A simple gap-protected series capacitor is a satisfactory installation provided no fault is of sufficient duration that the heat generated by the arc will damage the gap, and provided the arc in the gap will go out when the line current drops to normal. Such conditions may exist on low voltage circuits. Usually, however, some special means must be employed to extinguish the arc in the gap.

Magnetic Contactors for By-Passing

Series capacitor protective devices made in the past have utilized gap current

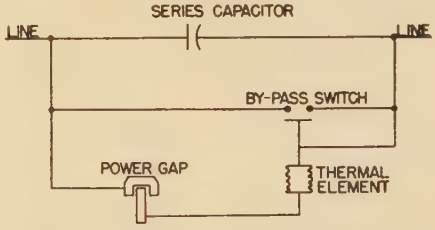

Figure 7. Series capacitor protective device using thermal switch

Figure 6 (below). Bellows operated toggle switch

Figure 8 (right). Operation of series capacitor protector using bellows operated switch

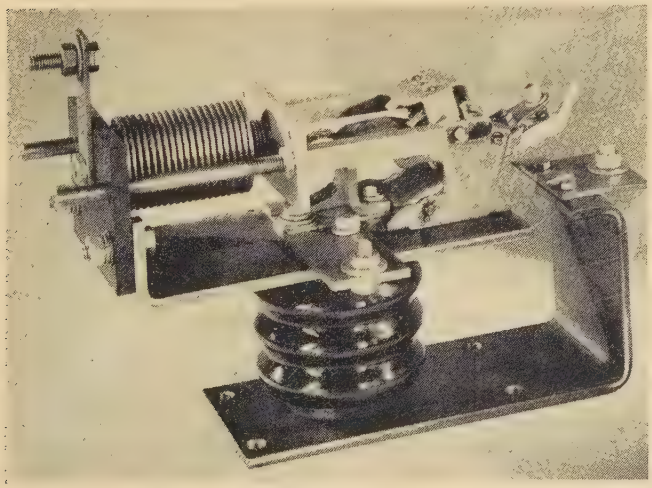

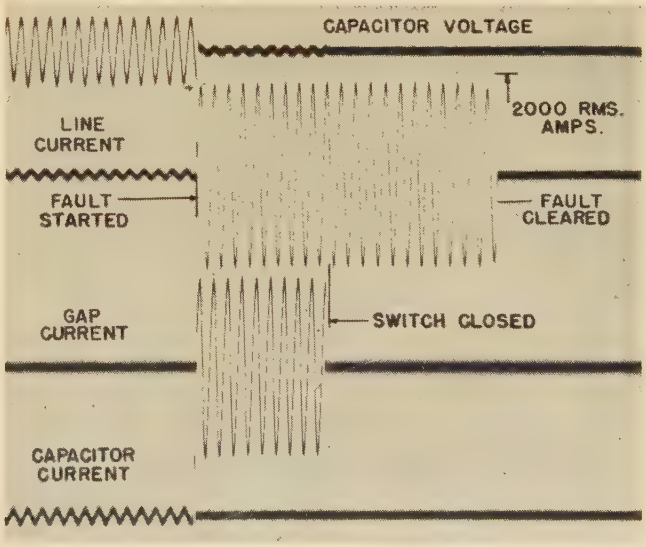

to initiate the closing of a magnetic contactor which by-passes the capacitor and gap to extinguish the arc. Such an arrangement is shown in Figure 5. The capacitor closing coil is placed in series with the gap so that when the gap breaks down the current flowing through the gap will cause the contactor to close. The contacts are connected to shunt the gap and all but a small portion of the closing coil. The number of turns remaining in the circuit is sufficient to cause the contacts to remain closed until the current in the line drops to normal. Thus, the arc exists in the gap only for the time required for the contactor to close, and the contactor shunts the capacitor for the duration of the fault.

The magnetic contactor provides adequate protection of the gap in a gap-protected series capacitor; however, a special and expensive contactor must be designed and built for each application. The size of the operating coil must be adjusted for each equipment so that the contactor will pick up at twice the rated capacitor current and drop out when the current drops to the rated value. The coil must be designed to withstand the steep wave front surge imposed upon it when the gap breaks down and the stored energy of the capacitor is discharged into the coil. In addition to stressing the coil, this surge also causes the contactor to accelerate very rapidly so that its contacts are closed while the capacitor discharge current is still high. This imposes severe duty on the contacts, and they must be carefully designed to prevent welding or excessive burning.

New By-Passing Switch

To overcome the difficulties encountered in the use of magnetic contactors, the authors set about to design a new type of by-pass switch to meet the following requirements:

1. It must close rapidly enough to protect the gap from overheating during any fault up to 2,500 amperes.
2. It should have sufficient time delay on closing in order that any capacitor bank up to 180 kva at 230 to 2,400 volts would be substantially discharged through the gap before the contacts engaged.
3. The motor element must not be damaged by the maximum combined fault current and capacitor discharge current.
4. It must have sufficient time delay on opening to allow a fault to be cleared by the line breakers so that no holding arrangement is required.

The switch shown in Figure 6 was developed for this purpose. It is a thermally actuated toggle switch which has quick-make and quick-break action and is connected as shown in Figure 7. The bellows is evacuated and charged with a small quantity of a liquid having a low vapor pressure at any ambient temperature which may be encountered in service. At such temperature the bellows remains collapsed because of external atmospheric pressure. When mounted in the switch, it is stretched to the normal length and exerts a pull more than sufficient to open the switch mechanism. When gap current passes through the walls of the bellows, heating occurs which changes the vapor pressure of the enclosed liquid. Continued heating causes the vapor to exert a pressure sufficient to actuate the toggle mechanism causing the switch to close. Figure 8 is an oscillogram showing the gap and switch operation in protecting a 16-ohm, 60-cycle series capacitor during a 2,000 ampere fault.

The closing of the switch by-passes the entire series capacitor and thus terminates the flow of gap current and allows the bellows to start cooling. Cooling causes the vapor to recondense, and the resulting differential pressure reopens the switch and restores the series capacitor to service

The gap may be allowed to reach a temperature of 250 degrees centigrade with no risk of damage. Figure 9 shows the time-current characteristics of the gap shown in Figure 2 based on an attained temperature of 250 degrees centigrade on the top casting and shows also the time required for the switch to close for the same currents. From this it is seen that the switch meets the first requirement of protecting the gap for all currents in the operating range. The tests from which these data were procured were made at an ambient of 25 degrees centigrade; however, the gap and switch combination is temperature compensating, and adequate protection is obtained throughout the operating temperature range. At high ambient temperatures the gap reaches the maximum permissible temperature in a shorter time, but the switch closes more rapidly. At low ambients the switch operates more slowly, but the gap requires longer to reach the temperature limit. Temperatures below the freezing point of the enclosed liquid do not damage the bellows because of its flexible nature and because the quantity of liquid is very

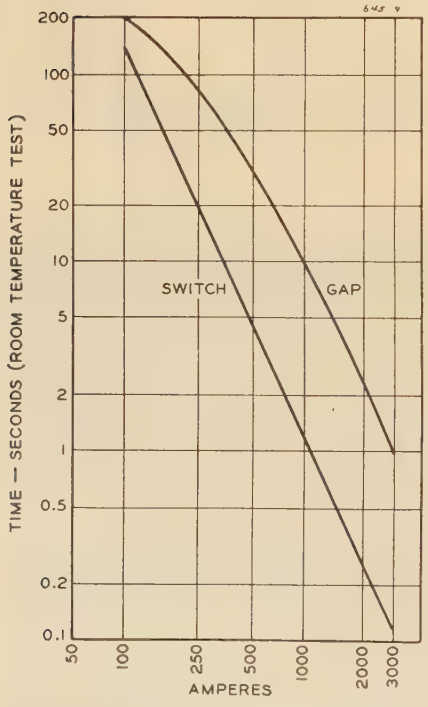

Figure 9. Time-current characteristic of gap and switch

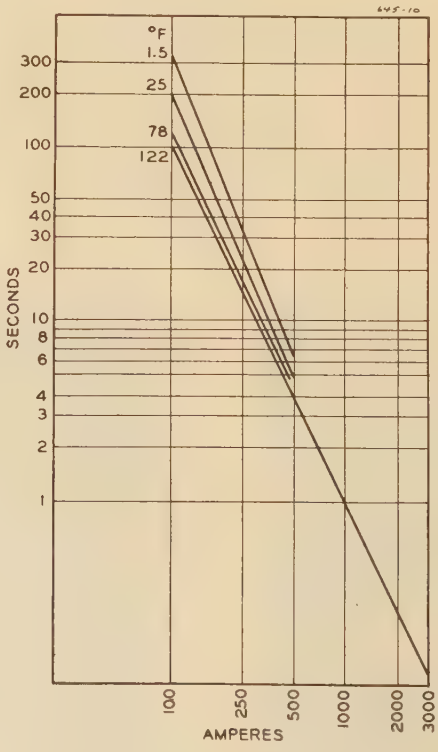

Figure 10. Variation in closing time of bellows operated switch with variations in ambient temperature

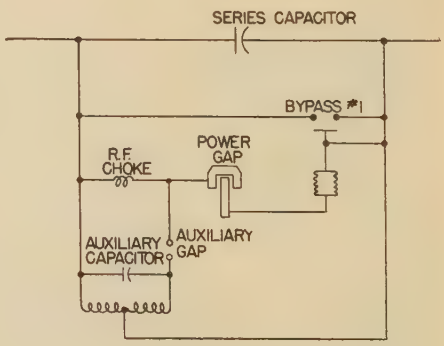

Figure 11. Low voltage series capacitor protective device

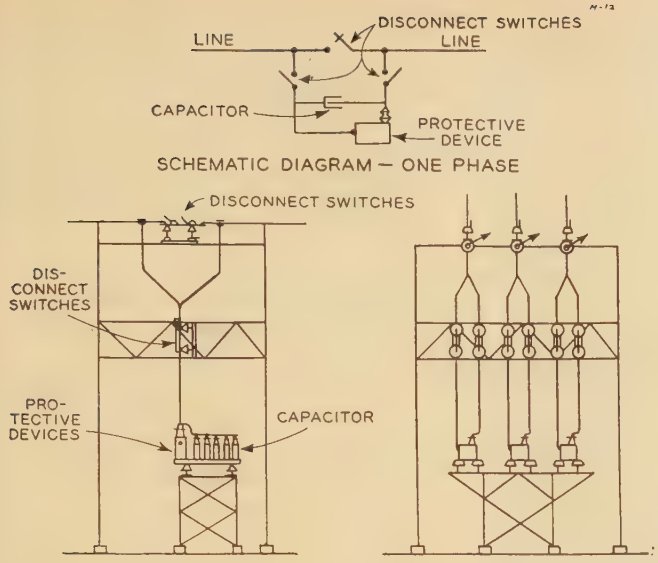

Figure 12 (left). Typical series capacitor installation

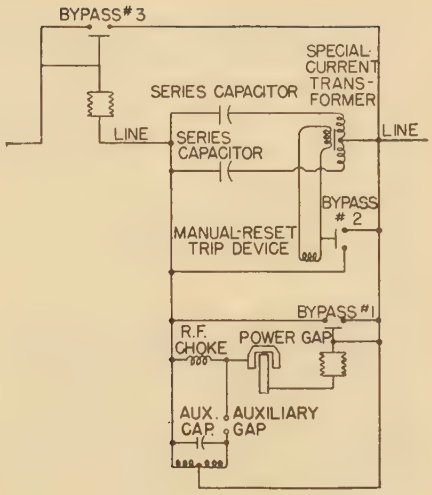

Figure 13 (right). Series capacitor with short circuit, overload, and dielectric failure protection

small. Operations at ambients below freezing do not take appreciably longer than those above freezing since the heat of fusion of the liquid is small compared to the total heat input required to raise the bellows to the operating temperature. The operating time of the switch for various ambients is shown in Figure 10.

The motor element in the new switch is essentially self-protecting since the switch operates to stop the current flow in the bellows when it reaches a certain temperature. High currents simply cause the switch to operate more quickly. The switch shown has been tested with fault currents of 2,500 amperes and capacitor discharge currents of 100,000 amperes and sustained no damage.

The opening time of the switch varies from two to five minutes over the ambient temperature range of −20 degrees centigrade to +50 degrees centigrade. Thus, any fault will be cleared by the line breaker before the switch opens to restore the capacitor to service. An arcing ground on the system cannot cause operation of the switch more often than once every two minutes so that heating in the capacitor caused by discharge through the gap cannot be cumulative and cause damage.

Method of Installation

Figure 7 is the diagram of a high voltage (above 1,500 volts) series capacitor with short circuit protection. Figure 11 shows the low voltage equipment. In either case the complete assembly of equipment for each phase is mounted on a platform which is insulated from ground for the line-to-ground voltage as shown in Figure 12. Outdoor type capacitor units are used, and the protective equipment is housed in a weatherproof steel housing with one entrance bushing. A stud on the housing serves as the other terminal. Disconnect switches are provided to bypass and isolate the capacitor for inspection and maintenance.

Operating Limits

During momentary overloads, such as might be caused by motor starting or the operation of a resistance-welding machine, the series capacitor rated current may be exceeded, and it is not intended that the short circuit protective device should operate at such times. The breakdown voltage of the protective gap is subject to variation with temperature, humidity, condition of electrode surfaces, and rate of rise of the applied voltage. To allow for these variations, the gap is set positively to break down at 200 per cent of the rated voltages and never to break down at 150 per cent of the rated voltage. Therefore, it is important that the momentary current peaks never exceed 150 per cent of the continuous current rating of the capacitor. In some cases the current peaks will exceed considerably the normal sustained current. In these cases it is necessary to use a capacitor with a sufficiently high current rating that it will never be exceeded by more than 50 per cent, even though the capacitor will run most of the time with less than rated current.

Other Types of Protection

A series capacitor will be damaged by continuous operation at more than 110 per cent of its rated current. The short-circuit protective device may not function at less than 200 per cent of rated current; therefore, it is sometimes desirable to provide overload as well as short-circuit protection. The overload protective device should have an inverse time-current characteristic which can be coordinated with that of the capacitor to allow momentary but not continuous overloads. The bellows operated switch is ideal for this purpose. It is necessary only to connect a bellows of the proper current rating in series with the capacitor and to connect the switch to shunt the capacitor and bellows.

Still another type of protection that is sometimes used for series capacitors is dielectric failure protection. This is a means of detecting a failure in the working insulation of a capacitor unit in a capacitor assembly. In an unfused capacitor bank a short-circuited capacitor unit may sustain an internal arc which will cause gas to be generated in the unit. Continued operation will cause the pressure to reach a value which will rupture the case and possibly cause damage to other units and equipment. If the units are equipped with individual fuses, a fuse operation to remove a faulty unit increases the reactance of the bank and continued operation at the rated current of the original bank will subject the remaining units to overvoltage. The by-pass switch used in a protective device for dielectric failure protection is spring biased to the closed position and latched in the open position. A magnetic device is used to trip the latch when the currents become unequal in two equal branches of the capacitor bank. Each phase of the series capacitor bank is divided into two equal branches and connected so that the two branch currents pass in opposite directions through one winding of a special current transformer. No voltage is induced in the secondary winding until the two currents become unequal as a result of a short circuit in one of the capacitor units or a removal of one or more units by operation of individual fuses.

Figure 13 shows the diagram of a series

A B–H Curve Tracer for Magnetic-Recording Wire

T. H. LONG
MEMBER AIEE

G. D. McMULLEN
NONMEMBER AIEE

Synopsis: The equipment described is able to show on the screen of an oscilloscope the cyclic hysteresis loop of a sample of magnetic-recording wire a little over one inch long and 0.004 inch in diameter. Results obtained with the equipment in studying recording wires are given. A discussion is included of the operation of the equipment, and of possible modifications.

IN EXPERIMENTAL study of the performance of any particular type of recording or playback head in relation to magnetic-wire recording it becomes evident that there are at least two variables. One of these, and frequently the most serious, is the condition of the head as influenced by accumulations of dirt. The dirt that accumulates in such a head is usually magnetic, but it is probable that any kind of dirt is almost equally bad on account of the separation it causes between the wire and the pole pieces. Magnetic dirt has the additional disadvantage of causing a shunting effect on the gap. The second variable is the magnetic character of the wire itself.

It is a matter of experience that with suitable recording and playback heads the performance of a wire recording system is stable to within about 0.5 decibel for short lengths of wire. For frequencies above 2,500 cycles the performance may be subject to variations as great as 15 decibels in playing through a 1 hour spool of wire at 2 feet per second. Performance at lower frequencies may be subject to roughly one-third as much change. These figures apply to 0.004-inch diameter stainless steel wire available early in 1945.

It is known further that a normal change in the condition of the head will account for only a small part of the change in low frequency performance but that it may account for all of the change observed at high frequencies. This situation makes it important to be able to separate the variables of head condition and wire magnetic characteristic in order to find out what actually is happening. This requires special equipment for expediently measuring the magnetic characteristics of the recording wire.

The characteristics obviously of interest in a recording wire that is to be used as a permanent magnet are retentivity and coercive force. Other magnetic characteristics that may be of interest are the shape of the normal magnetization curve, the erase noise level, and the so-called d-c saturation noise level. These last two items usually are studied on a record-and-playback setup and will not be discussed further here.

Paper 46-30, recommended by the AIEE committee on communication for presentation at the AIEE winter convention, New York, N. Y., January 21–25, 1946. Manuscript submitted November 8, 1945; made available for printing December 26, 1945.

T. H. LONG is senior research engineer and G. D. McMULLEN is research engineer with C. G. Conn, Ltd., Elkhart, Ind.

Requirements for Equipment for Magnetic Measurements

Perhaps the most important requirement for magnetic measurements is that they should be made at a sufficiently intense magnetization to insure saturation of the wire. Measurement at any arbitrarily selected lower level may not be proportional to saturated measurements and in extreme cases will give little idea of the actual magnetic property of the wire. It originally was estimated that 1,500 ampere turns per inch would be necessary for the saturation of any wire. Subsequent experience has indicated that this is satisfactory for any wire suitable for magnetic recording with present head designs but that wire can be produced that requires more than 2,500 ampere turns per inch for saturation.

A requirement of almost equal importance is that the equipment should be able to operate continuously and indicate continuously the magnetic retentivity and coercive force of the wire as it runs through the equipment at a speed comparable to recording speed. The resolving power of the equipment should correspond to something on the order of 0.1 second playing time. There seem to be no variations in performance of an undesirable nature or magnitude that are of shorter duration than perhaps one-half second. If there were shorter transients, they could be studied best by oscillographic methods on a record-and-playback system which has a resolving power of a few thousandths of one inch.

Considerations of magnetizing coil design suggest the desirability of operating at a low audio frequency, perhaps several hundred cycles. A secondary consideration pointing in the same direction is the possibility of winding the detector coil on a stainless steel (nonmagnetic) tube.

It occasionally may be desirable to make rather accurate measurements at very low inductions, such as 100 lines per square inch. In order to avoid compromising the design as far as more normal use at much higher flux densities is concerned, it may be desirable to provide for measurement in such cases on a small bundle of wires. An example of this use would be the getting of that part of the

capacitor having short circuit, overload, and dielectric failure protection. Actually, overload and dielectric failure protection are seldom needed on distribution circuit series capacitors. These capacitors are usually selected on the basis of the maximum expected line currents, and these currents are not likely to be continuously exceeded because other equipment such as transformers would be damaged. When the units are applied in this manner and are properly protected against damage from short circuits, they seldom fail in service.

Conclusions

A graphite gap designed to hold the arc in a relatively fixed position provides the most effective protection for a series capacitor because it does not permit recurring rises in voltage on the capacitor during a fault. It can be designed to handle the fault current without being damaged and without serious changes in the breakdown characteristics.

A thermally operated by-pass switch of the type described provides an economical and effective means of extinguishing the arc in a series capacitor protective gap. The bellows operating element has a negligible inductance and is not damaged by the steep wave front surge of the capacitor discharge. The time delay on closing relieves the contacts of handling capacitor discharge current. The time delay on opening eliminates the need for a holding mechanism.

The thermal switch has an inverse time-current characteristic which makes it ideal for overload protection of series capacitors.

normal magnetization curve that is near the origin.

Calibration should be simple and precise with independent adjustments for coercive force and retentivity and should be relatively stable. A permissible drift might be as much as 5 per cent per hour. An absolute calibration would be desirable.

The equipment should be adjustable to obtain full scale retentivity readings at several convenient values between 10,000 and 100,000 lines per square inch. Adjustment also should be provided for full scale ampere turns per inch from perhaps 100 to 3,000.

Theoretical Considerations

The practicability of the use of the oscilloscope in obtaining hysteresis loop information on small punched washers of magnetic material has been demonstrated by Adler.[1] It would seem that something of the same technique should be applicable to the present problem. It hardly would be practicable to form the recorder wire into a loop to apply Adler's technique directly. Such a loop would require several turns to minimize end effect; and very high magnetizing currents would be required since the recording wire is actually a very efficient permanent magnet material.

An alternative is to run a straight wire through a magnetizing coil. The magnetizing force near the axis of a magnetizing coil of practical proportions will not be constant but will increase toward the center of the coil. Most of the change will be near the ends, and, if only the central one-third of the magnetizing coil is occupied by the detector and balance coils, the variation actually encountered will amount to only a few per cent, and an average value may be satisfactorily used; this is subject to limitations imposed by end effect. If the end effect is spread out over a length of the order of 100 times the wire diameter, it should not affect the results appreciably, and this expectation has been realized.

It is clear that, since operation is required on the flux contained in one piece of 0.004-inch diameter wire, a great many turns will be required in the detector coil through which the wire will run. It is further evident that a very substantial part of the flux through this coil will be flux outside of the wire and in air. For instance, if the inside diameter of the winding is 0.312 inch and the radial thickness of the winding is neglected, the ratio of the areas of air and iron included by the coil will be about 6,000. It will be necessary to exclude the influence of this air flux from the measurements, since it would mask completely the flux being measured. This is reasonably simple to do with a balance coil having a product of turns times area slightly greater than the detector coil and located along side of the detector coil within the magnetizing coil. A potentiometer adjustment can be used for the adjusement of the final balance as one of the steps in calibrating the equipment.

A definite limitation is imposed on the equipment by the requirement of handling wire for which the maximum induction is as great as 100,000 lines per square inch, since the voltage from the balance and detector coil combination must not overload the amplifiers that precede the integrating circuit.

This voltage prior to the integrating circuit is a very peaked wave, so that a fairly wide range of frequency must be handled without appreciable distortion, and what is perhaps more important, without appreciable relative phase shift between the various harmonic components at any point in the circuit. This will require the use of unusually large capacitors on the screen grids, and the elimination of cathode by-pass capacitors with a corresponding material loss in amplifier gain.

An interesting theoretical question is an appropriate design for an air core magnetizing coil to provide 1,500 ampere turns per inch continuously at say a maximum frequency of 500 cycles. It is known[2] that for a coil wound from round or square wire, and having proportions suited to the present problem, if the eddy current loss increases the effective resistance by more than about 50 per cent, the total loss will be reduced by winding with smaller wire to the same total turns and axial coil length. This makes it ap-

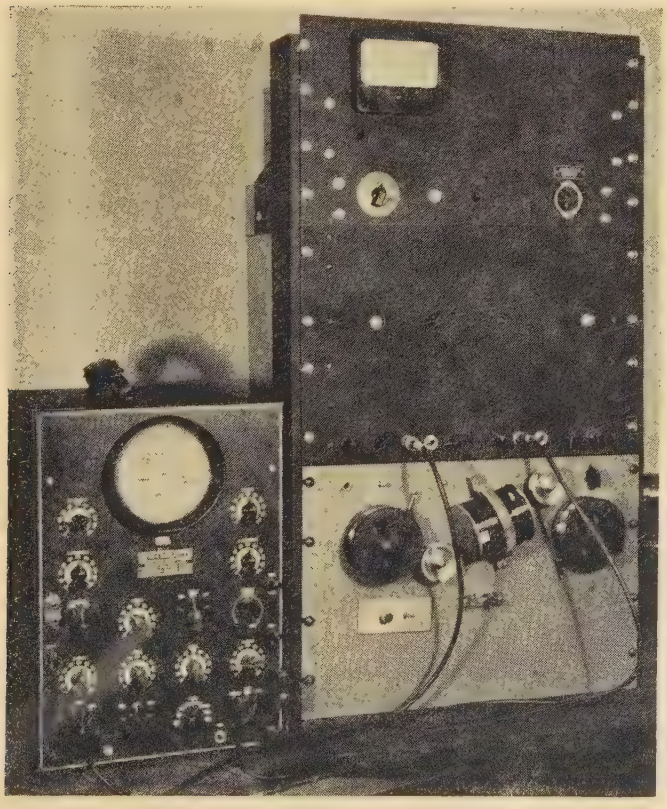

Figure 1 (left). Equipment for continuous magnetic measurements on magnetic-recorder wire

Figure 2 (below). Simplified schematic diagram of B–H curve tracer

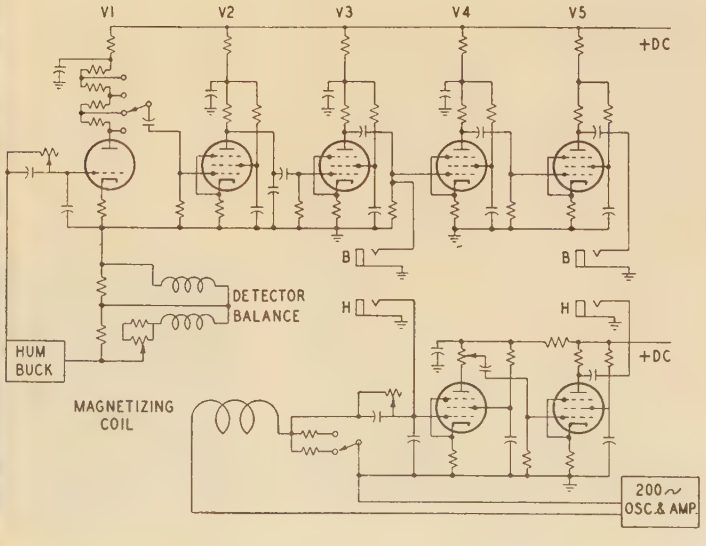

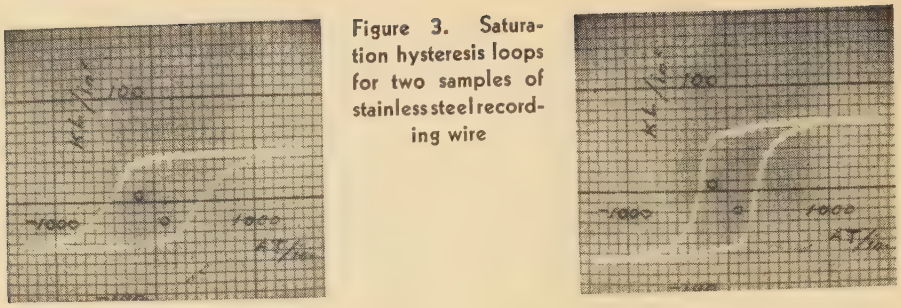

Figure 3. Saturation hysteresis loops for two samples of stainless steel recording wire

pear that for a radial winding depth of 1.25 inches the maximum practicable round wire size will be about 0.040 inch. The maximum practicable wire size will be roughly proportional to the reciprocal of the radial depth of the winding.

B–H Curve Tracer

The equipment as finally developed for the continuous measurement of retentivity and coercive force of moving or stationary samples of magnetic recording wire is shown in Figure 1. The lower section is occupied by the wire handling equipment and the magnetizing coil. Behind this unit on the relay rack is the power supply for the power amplifier that energizes the magnetizing coil at the finally selected frequency of 200 cycles. This power amplifier is at the top of the rack. In between there is a 200-cycle oscillator, an integrating circuit for the induction channel and associated amplifier, an amplifier for the magnetization channel, and the controls associated with these items. The equipment is self contained except for the oscilloscope and includes sufficient amplification for 20-volt output signals in both channels.

Figure 2 is a simplified schematic diagram in which certain standard items are designated simply by blocks. The resistance coupled amplifiers are modified from strictly conventional circuits to meet the special requirements of the present problem as just indicated. The omission of the cathode by-pass capacitors results in a reduction in the maximum practicable gain per stage to about one half of normal, or around 50 for a pentode stage. The required minimizing of phase distortion requires unusually large coupling capacitors. This results in an amplifier that has a very high gain even at a frequency of a few cycles. Transients in the 60-cycle supply come through a conventional filter sufficiently to cause substantial instability in the oscilloscope image, so a rather elaborate filter is necessary. This filter is a combination of two inductance–capacitance stages and four resistance–capacitance stages. The hum bucking circuit provides for the variation in phase and magnitude of a small inserted 60-cycle voltage and uses a capacitance–resistance phase split for the phase variation.

The afore-mentioned difficulties are increased by the necessity of using an integrating circuit in the induction channel of the amplifier, identified as B at the output jacks. This integrating circuit is, in effect, a resistance and capacitance in series that are so proportioned as to have a time constant on the order of 100 times the length of a half cycle. The resistance involved is the load resistance of amplifier $V2$ in parallel with the plate resistance of that amplifier, and the capacitance is connected from amplifier plate to ground.

In spite of the various steps taken to minimize phase distortion, a prohibitive amount remains, and this has been corrected to a tolerable value by the use of the resistance–capacitance network shown at the input to each of the channels. The adjustment of the phase correction network in the induction channel varies the position of the nearly vertical lines of the hysteresis loop, and in the proper operating range of this adjustment there is no other pronounced change in the hysteresis loop seen on the screen of the oscilloscope. This fact seems to preclude the expedient arriving at what might be called an absolute calibration of the system. Calibration against standard samples that have been measured by a point by point method is an easy way out after the standard samples have been measured. In making point by point measurements on standard samples of stainless steel recording wire it is necessary to calculate the cross section of the bundle of wire used and the cross section of the detector coil and then correct for the air flux. This correction amounts to about 10 per cent of the coercive force, when measurements are made on a ring sample.

Results Obtained With the B–H Curve Tracer

The advantages of being able to arrive quickly at the magnetic characteristics of short samples are too obvious to require further comment. The fact that these measurements are subject to an absolute error that may be as large as 10 per cent is not a serious handicap. The relative error is substantially less and depends only on the accuracy to which the image on the oscilloscope screen can be measured, on the accuracy with which the wire diameter can be measured (this influences retentivity only), and on the linearity of the oscilloscope. Figure 3 shows saturation hysteresis loops for two different samples of stainless steel wire, and Figure 4 shows two hysteresis loops taken on a single sample of wire about a foot apart; the difference may be due to the second loop's being in a part of the wire that had been welded at an earlier stage in the drawing. The change between these two loops was fairly gradual, and several half-pound spools were run through to find such a case.

When this project was started it was believed that the most important use of the equipment would be continuous measurements to determine the uniformity of the magnetic characteristics of a recording wire from one end of the spool to the other. This indeed has been important, and Figure 5 shows the retentivity and coercive force plotted against winding time for a constant spool speed that gave a nominal wire speed of 5 feet per second. The variations are of sufficient magnitude to account for several decibels of variation in the low frequency playback, but they are definitely not sufficient to account for the magnitude of frequently encountered variations in high frequency performance. The variations shown seem to be typical of current production of stainless steel wire (as of November 1945).

In the earliest use of this equipment for continuous measurements on running

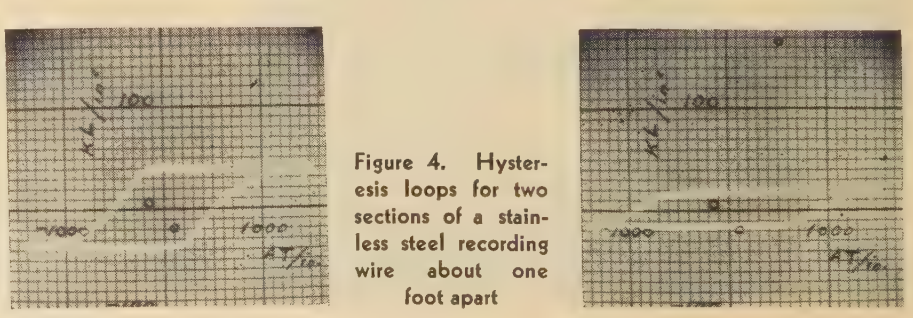

Figure 4. Hysteresis loops for two sections of a stainless steel recording wire about one foot apart

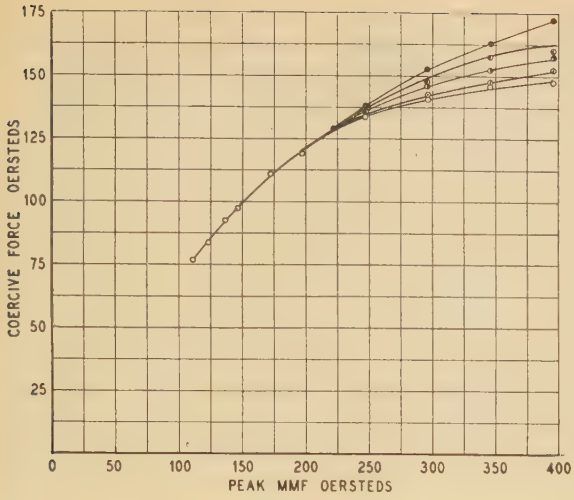

Figure 6A (left). Coercive force versus magnetization for several values of tension

Figure 6B (right). Retentivity versus magnetization for several values of tension

Both parts are for stainless steel wire of 0.004-inch diameter. Tension varied from 0 to 2 pounds in half-pound steps, maximum tension at top

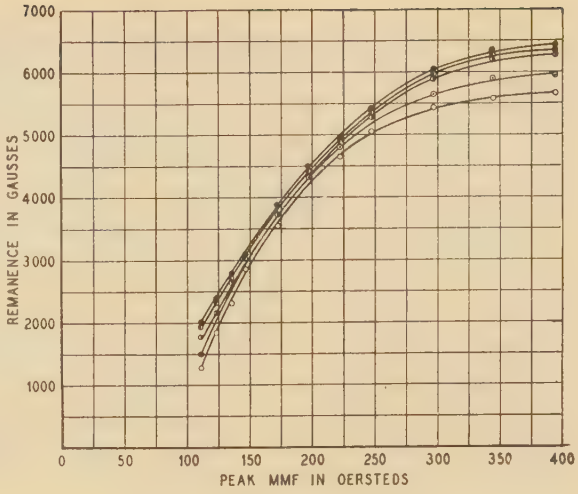

wire, a small pulsation of the hysteresis loop on the oscilloscope screen was observed. This amounted to only a few per cent of the intercepts on the B and H axes but seemed to be associated with the motion of the wire. It was found that this was caused by something analogous to magnetostriction. Small variations in tension that accompany the motion of the wire influence the magnetic properties of the wire to an appreciable extent.

A study of this effect was made in various wires to find out what the magnitude might be and how it varied between samples. Figures 6A and 6B show characteristic results in which coercive force and retentivity are plotted against peak magnetizing force for various values of tension. In general an increase in tension always is accompanied by an increase of coercive force, and may be accompanied by either an increase or decrease in retentivity. The magnitude of the affect for a change in tension from zero to two pounds varies from 0 to 12 per cent for coercive force, and from 0 to 50 per cent for retentivity.

These stated values apply to the working range of magnetizations, and some wires do not exhibit either effect appreciably in this range, although it is evident above this range.

The B–H curve tracer, which might be more conveniently called a magnetoscope, also is useful in determining normal magnetization curves of recording wire. It seems necessary in this case to use a point by point procedure, and, to get good detail at the bottom of the curve where the induction is very low, it is expedient to use several wires (perhaps as many as 10), but such curves can be obtained in about 5 or 10 minutes after the equipment has been calibrated. It usually will be expedient to measure the magnetizing force on a voltmeter connected across a resistance in series with the magnetizing coil and to read the induction on the screen of the oscilloscope. Figure 8 is a sample of normal induction curves obtained in this manner.

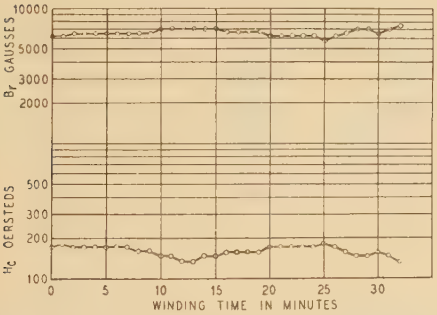

Figure 5. Retentivity and coercive force plotted against running time for a one-half pound spool of 0.004-inch diameter wire

Nominal running speed was 5 feet per second

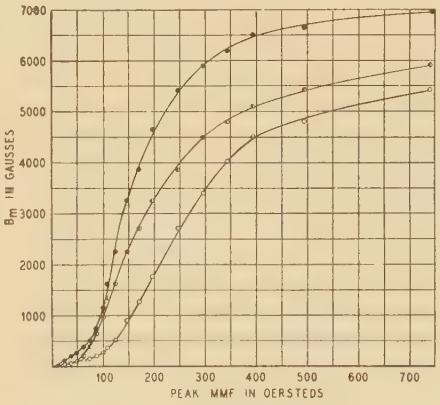

Figure 7. Normal induction curves for three samples of stainless steel wire

●—H_c 150, B_r 5,900
◐—H_c 185, B_r 5,400
O—H_c 250, B_r 4,800

Conclusions

The necessity and adequacy of the magnetoscope as a development tool in experimental work on wire recording have been demonstrated. It would seem that the magnetoscope would be equally useful in control work, if the advantages of stainless steel wire are to be fully realized.

The utility of the magnetoscope is by no means limited to the field that has been explored in some detail in this paper. For instance it might be possible to use the magnetostrictive characteristic of a magnetic material to get a direct and almost instantaneous measure of the tension in the material.

The account that has been given has been limited to a measuring device in which the end effect (or return magnetic circuit) could be safely neglected. This is not a limitation inherent in the device. In the present form of the equipment the detector coil is somewhat sensitive to magnetic material closely adjacent to the magnetizing coil. This is associated with the energy loss so caused and the consequent lag between flux and current. It is probable that an external magnetic return circuit can be employed in spite of this by energizing the magnetization channel from a search coil and integrating circuit. This would make it possible to use such equipment in measuring the magnetic characteristics of a single strip of transformer grade alloy. In such applications a detector coil of only a few turns would be required, and the balance coil would be unnecessary.

References

1. B–H Curve Tracer for Lamination Samples, Robert Adler. *Electronics*, November 1943, pages 128–31, 314, 316–17.

2. Eddy-Current Resistance of Multilayer Coils, T. H. Long. AIEE Transactions, 1945, volume 64, October section, pages 712–18.

An Automatic Oscillograph With a Memory

A. M. ZAREM
ASSOCIATE AIEE

Synopsis: The memory oscillograph described in this paper is used for obtaining photographic records of randomly occurring electric transients. This instrument differs from other oscillographs of the memory type[1,2] in that its operation is completely automatic. Forty sets of oscillograms can be recorded without the aid of an operator. Because of this feature, such an oscillograph may be used for monitoring electrical systems in which sporadic circuit disturbances are to be studied. The unit consists essentially of three cathode-ray tubes with associated power supply, a saw-tooth oscillator to provide the horizontal time axis, amplifiers for the vertical deflection circuits, a beam blanking circuit, and an automatic camera. When the memory oscillograph is in operation, the cathode ray tubes are continuously excited. The vertical deflection circuits of the tubes are connected to the voltages to be investigated, and each tube screen carries a cathode-ray pattern characteristic of the voltage applied to its vertical deflection plates. Upon the occurrence of a transient pulse, the camera shutter is released and the electronic beams of the cathode ray tubes are interrupted. The camera then records the persistence of fluorescence, which is characteristic of the material used on the tube screens. In this way a record is obtained of electric events that occurred previous to the opening of the shutter. To insure successful operation, the component parts of the automatic memory oscillograph must be electrically co-ordinated and controlled. The sequence of functions performed by a control circuit for this purpose is described. Photographic records of transients which may arise during the operation of a mercury-arc polyphase inverter are included.

IN CONNECTION WITH research and development work on mercury-arc power converters, it is frequently necessary to study electric transients which occur at irregular intervals. Particular attention has been directed to the investigation of factors which encourage faulty operation. Not all of these factors are known and those that are known are not understood entirely. It is not a simple matter to obtain information concerning the initiation of transients. The random character of backfire phenomena in rectifiers, for example, makes it difficult to study electrical conditions in rectifier circuits immediately preceding backfire. Yet such a study is of prime importance if we are to learn more about the manner in which such faults occur.

The cathode ray memory oscillograph is an ideal instrument for this purpose. It can be made to provide a record of electric conditions previous to the occurrence of a transient as well as of the transient itself. The heart of this instrument is the cathode ray tube.

The Cathode-Ray-Tube Screen

A very useful characteristic of the fluorescent materials used for coating cathode ray tubes is the persistence of their luminescence after the exciting cathode ray beam is extinguished. All other conditions being the same, the rate of decay of the afterglow depends upon the kind of fluorescent material used.

Generally speaking, these coatings fall into three classes, and the tubes in which they are used consequently are referred to as short, medium, or long persistence cathode ray tubes.

Figure 1 illustrates in a general way the relative brightness retained for three different types of cathode ray tubes as a function of time. Curve *A* is characteristic of the short-persistence type P5 tube. The screen material used for this tube is an efficient emitter of light, and fluoresces in the blue range. The relative brightness falls to ten per cent in approximately 10^{-8} second. This rapid decay of brightness limits the use of these tubes in a memory oscillograph. Screens of this type find an important application when moving film recording is to be done. Due to the very short persistence, fogging of the film is kept to a minimum.

The medium-persistence P1 tube has a screen characteristic like that given by curve *B*. The relative brightness of such a screen falls to ten per cent in about 20 milliseconds. Most of the radiant energy of the P1 screen occurs in the yellow-green region.

The long-persistence P2 screen has a brightness-time curve similar to curve *C*. At voltages below 5 kv, the photographic efficiency for this tube is much lower than that of the P5 or P1 tubes.[3]

After careful consideration of tube characteristics and the requirements imposed by the intended application, the type P1 medium-persistence tube generally will be preferred for ordinary memory oscillograph studies. With an accelerating anode potential of 3,750 volts, the P1 screen provides sufficient after glow to allow a memory time of approximately 100 milliseconds, or 6 cycles of a 60 cycle a-c wave. By increasing the anode potential to 4,500 volts the memory time may be elevated substantially. However, because the use of beams of very high intensity has a markedly adverse effect on screen life, and since a cathode ray pattern of one type or another is on the tube screen continually, it is a matter of economics to avoid the use of very high intensities when they really are not required. For this reason an anode accelerating potential of 3,750 volts is desirable for normal operation. In anticipation of occasions when greater memory time may be required, provision may be made to allow the use of a tube voltage of 4,500 volts. As a further aid to lengthening screen life, the horizontal sweep oscillator can be allowed to remain unsynchronized so that the cathode ray pattern drifts slowly across each screen. With these precautions taken, the instrument can be operated

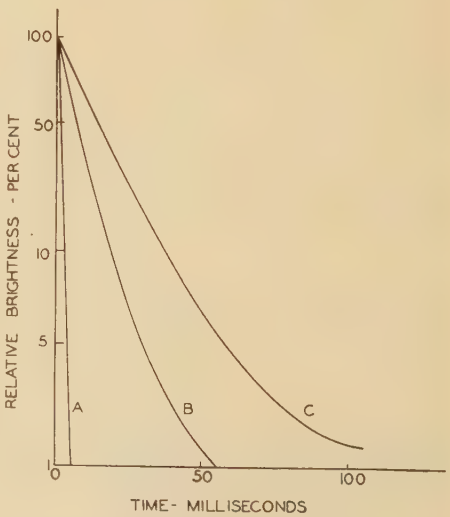

Figure 1. Curves illustrating typical variations in relative brightness as a function of time for three types of cathode-ray-tube screens

A—Short persistence
B—Medium persistence
C—Long persistence

Paper 46-67, recommended by the AIEE committee on instruments and measurements for presentation at the AIEE winter convention, New York, N. Y., January 21–25, 1946. Manuscript submitted October 29, 1945; made available for printing December 17, 1945.

A. M. Zarem is on the research staff of California Institute of Technology, Pasadena, Calif., while on leave of absence from the Allis-Chalmers Manufacturing Company, Milwaukee, Wis.

The author acknowledges the assistance of W. Richter and his associates at the Allis-Chalmers Manufacturing Company in the design of the instrument described here.

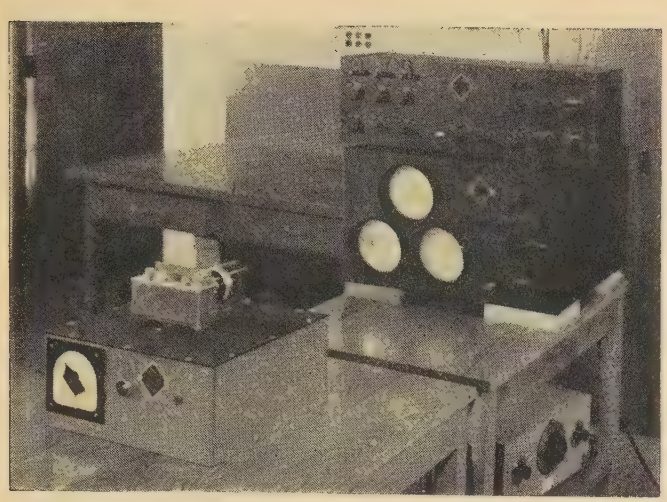

Figure 2. The automatic memory oscillograph

The automatic camera, the cathode-ray-tube unit, and the horizontal and vertical deflection control unit are shown

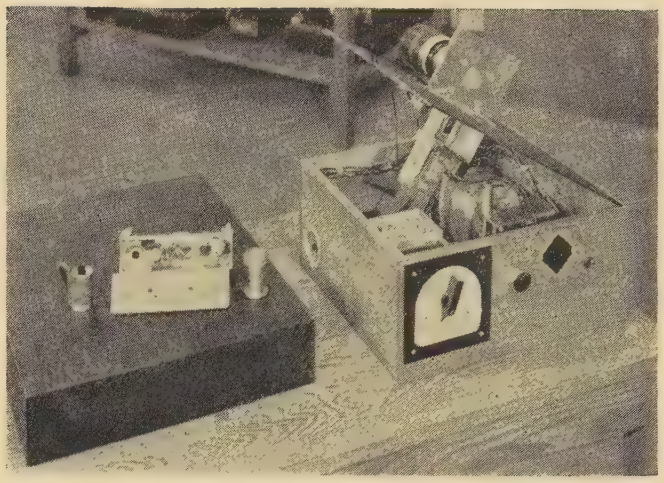

Figure 3. The automatic camera unit open to view

The camera and film loading cartridge are shown at the left

continuously 24 hours a day, with tube replacements required about once every five months. Tubes removed from the memory oscillograph, of course, will still be usable for ordinary cathode ray work.

Description of the Oscillograph Unit

Figure 2 is a picture of the automatic memory oscillograph. In normal operation a light-tight shield is placed between the camera lens and the cathode ray tubes. The lower tube unit shown in Figure 2 houses 3 5-inch cathode ray tubes with the necessary power supply and beam blanking equipment. Adjustments for focus, intensity, and accelerating potential are made by means of knobs on the front panel. Three values of accelerating tube voltage are available: 3,000 volts, 3,750 volts, and 4,500 volts.

Beam blanking may be accomplished in a variety of ways. If a trigger circuit[4] of the Eccles-Jordan[5] type is used, the output of this circuit is arranged so that the control grids of the cathode ray tubes will suddenly be made negative with respect to their cathodes when the circuit is tripped. Tripping may be accomplished by a voltage pulse of either positive or negative polarity. The pulse required is supplied by a control circuit which is actuated by the transient to be studied. Provision for adjusting the time delay between the opening of the shutter and the operation of the beam blanking circuit is contained in the control circuit. With such an arrangement, if the duration of the transient is not too great, it is possible to obtain a picture of the electrical conditions before, during, and after the occurrence of the transient. Information concerning conditions existing after the occurrence of a transient will be obtained at the expense of "memory time." However, situations may arise where such knowledge is desired.

The upper unit shown in Figure 2 contains the sweep oscillator for the horizontal timing wave and three sets of amplifiers for the vertical deflection plates of the cathode ray tubes. Each tube has its own 2-stage resistance-coupled amplifier. These amplifiers have a frequency response which is essentially flat up to 30,000 cycles per second.

The saw-tooth oscillator which provides the timing axis is common for all three cathode ray tubes. Simultaneous events therefore appear at the same relative location on all three tubes. Should the occasion demand it, the tubes may be operated with separate timing axes. This is done by means of convenient connections located on the rear panel of the tube unit. To aid in aligning electric events occurring at the same time, arrangement is made for simultaneously marking the traces on all three screens.

The usual means are provided for the adjustment of the vertical and horizontal gain as well as the vertical and horizontal positioning of the pattern for each tube. The saw-tooth oscillator may be interlocked with the frequency of the circuit being investigated, with a 60-cycle voltage, or with any outside alternating voltage.

The camera unit is shown in Figure 3. In addition to a lens and shutter, it contains a motor for automatically winding the photographic film and for closing the shutter after a picture has been taken. A step-type relay is included for the purpose of keeping count of the number of exposures made. By adjusting the knob of the relay, the unit may be preset to take a given number of pictures and then turn itself off. A maximum of 40 photographs can be taken with one loading of film. This number may be increased by changing the film loading cartridge and the step relay.

The shutter is of the focal plane type. It is kept in position against spring tension by a small movable latch placed

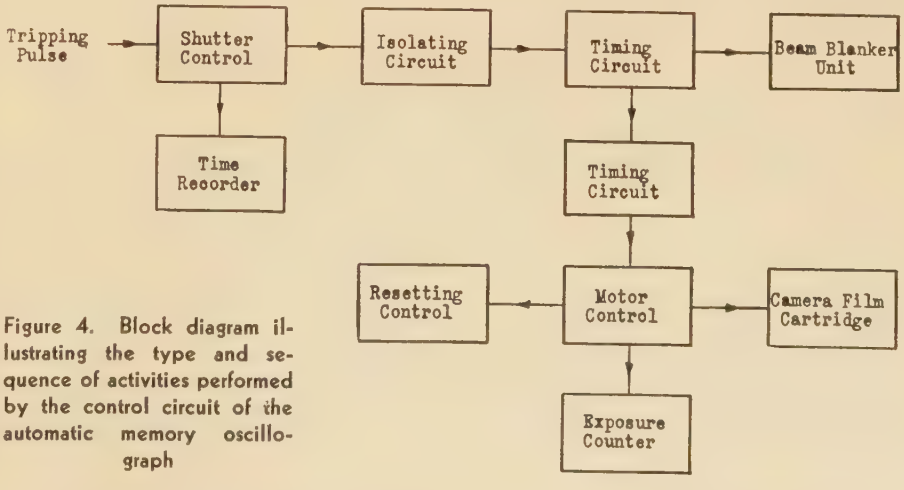

Figure 4. Block diagram illustrating the type and sequence of activities performed by the control circuit of the automatic memory oscillograph

close to the poles of an electromagnet. Release of the shutter is accomplished by exciting the current coil of the magnet.

The camera uses 35-millimeter film. Loading is accomplished by means of standard film cartridges. For photographing the green P1 medium-persistence screen, panchromatic-xx film gives excellent results. The lens has an opening of f1.5 and a focal length of three inches.

Control Circuit

Figure 4 is a block diagram illustrating the sequence of functions performed by the automatic memory oscillograph control circuit. The control is initiated by a voltage pulse applied to the grid of an electron tube. This pulse may be supplied by the transient voltage itself—or some other voltage pulse which occurs simultaneously with the transient to

Figure 7. Photographic record of oscillogram obtained with the automatic memory oscillograph connected as in Figure 6

The camera shutter coil received its impulse at *A*. The cathode ray beam was blanked at *B*. The time at which the transient occurred is given by the clock *C*. Memory time preset at 50 milliseconds

e_{a-c}—Anode to cathode voltage for one anode of the inverter

e_{d-c}—Main direct voltage of the inverter

e_{g-c}—Grid to cathode voltage

Figure 6. The automatic memory oscillograph for use in the investigation of transients in an inverter

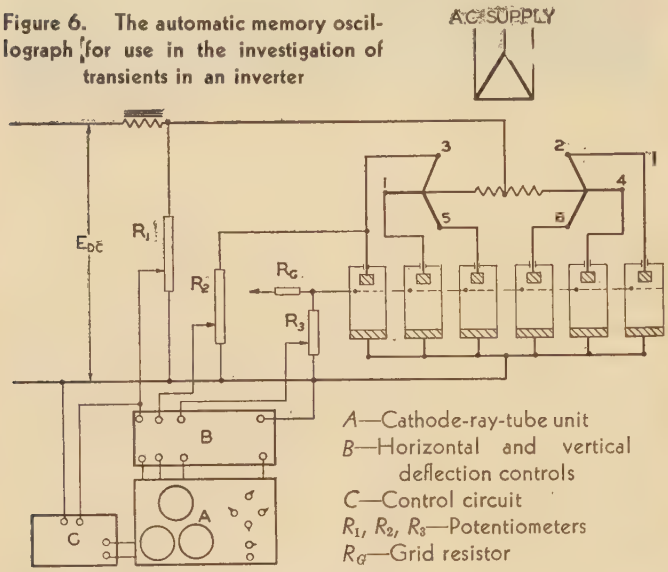

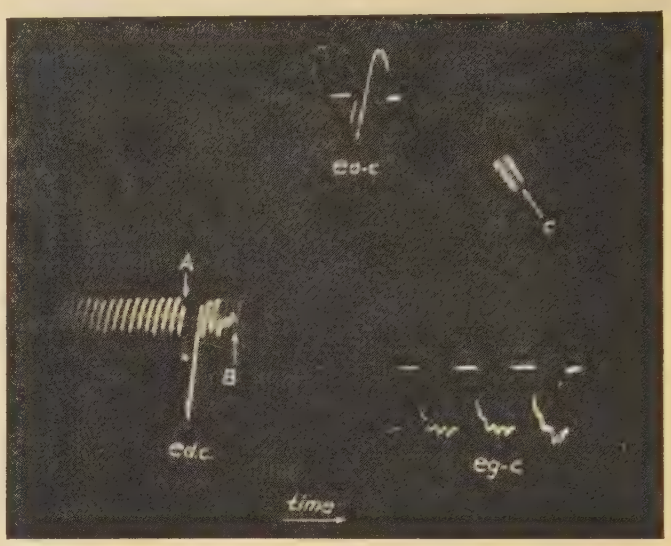

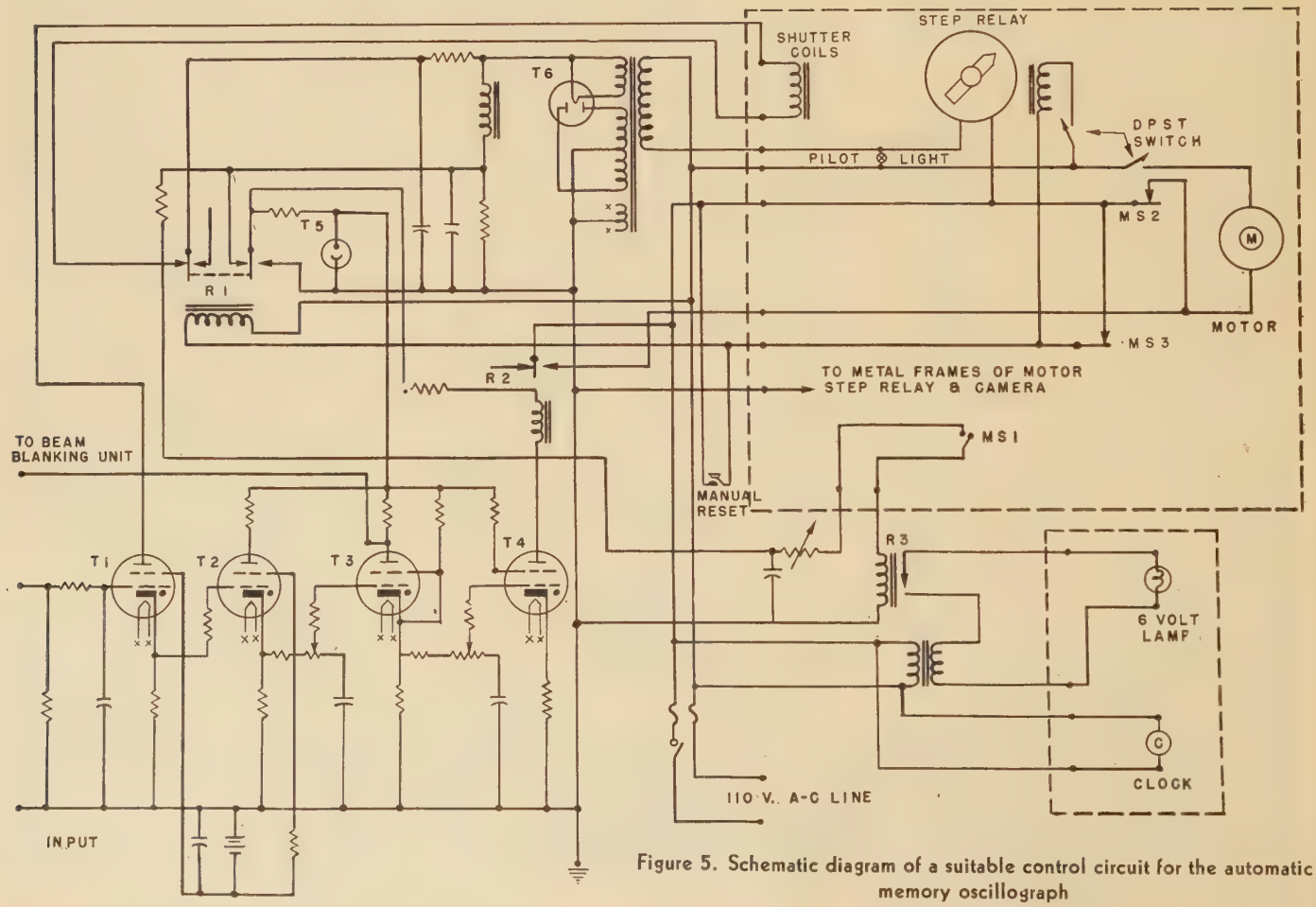

Figure 5. Schematic diagram of a suitable control circuit for the automatic memory oscillograph

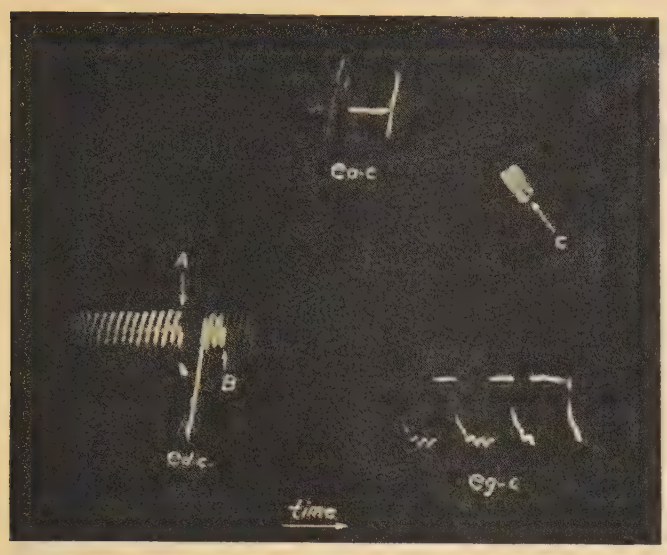

Figure 8. Record of an oscillogram obtained with the automatic memory oscillograph when the anode being monitored suffers preignition

The ability of the oscillograph to record electrical conditions preceding, during, and after the occurrence of a transient is clearly indicated. Memory time preset at 50 milliseconds

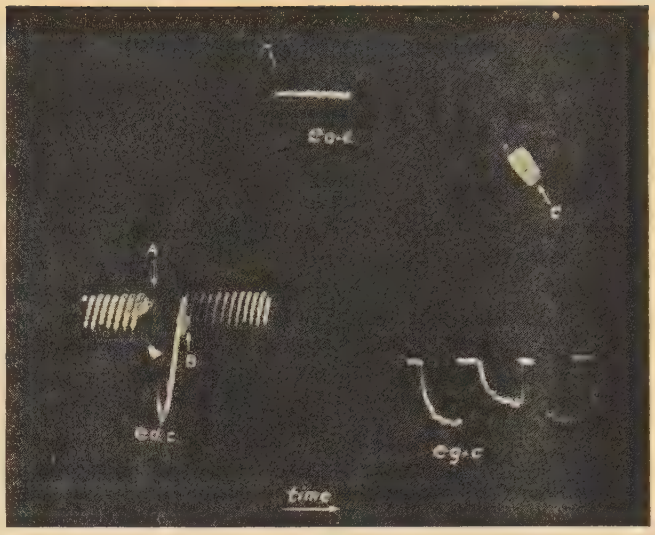

Figure 9. Photographic record of an oscillogram illustrating a backfire followed by an arc-through on a polyphase mercury arc rectifier

Memory time approximately 50 milliseconds

be studied. As the input impedance of the control circuit is quite high, very little current is required for its operation.

The first operation is a multiple one. The shutter is opened, a clock dial is momentarily illuminated, and an electric pulse is released to an isolating circuit. An adjustable time thereafter the beam blanking unit receives its impulse, and a second timing circuit is actuated. The latter operates the motor control unit which in turn resets the camera, excites the coil of the step-relay exposure counter, and places the entire control circuit in readiness for the next transient to be recorded. The timing circuits are included in order to allow the adjustment of both memory time and exposure time. The clock mechanism insures that every oscillogram record contains the time at which the initiating transient occurred.

Figure 5 is a schematic diagram of a control unit, which may be used successfully to perform the sequence of operations illustrated in the block diagram of Figure 4. $T1$, $T2$, $T3$, and $T4$ are gas-filled control tubes. $T6$ is a rectifier tube for the power supply of the unit, and $T5$ is a voltage regulator tube. $MS1$, $MS2$, and $MS3$ are microswitches.

When the circuit is ready for operation, the relay contacts, $R1$, $R2$, and $R3$ are in the positions shown and tubes $T1$, $T2$, $T3$, and $T4$ are in a nonconducting state. Tube $T1$ controls the opening of the camera shutter and applies a positive voltage pulse to the grid of $T2$ which serves as an isolating tube. A variable resistor determines the time interval between the firing of tubes $T2$ and $T3$. The voltage pulse for operating the beam blanking circuit[4] is taken from the plate of $T3$. Tube $T4$ which will become conducting an adjustable time after $T3$ is fired, controls the operation of the motor that resets the camera and places the entire control circuit in readiness for the next transient pulse. The amount of motor travel is determined by two microswitches $MS2$ and $MS3$ operated by a cam on the motor shaft. An additional microswitch $MS1$ is actuated by the shutter when it reaches the bottom of its travel. Operation of $MS1$ causes the momentary illumination of a synchronous clock mechanism located in the light-tight shield placed between the oscillograph unit and the camera.

A bell may be placed across the terminals of the motor to attract attention when a transient is recorded.

Performance of the Unit

During operation, the cathode ray tubes are continuously energized. The vertical deflection inputs are connected to the voltage sources being investigated. Screen patterns of the desired sizes and positions are obtained by adjustment of the control for the horizontal and vertical deflection plates of the various tubes. The cathode-ray-tube accelerating potential and beam intensity are set to meet the memory time requirements, and the camera is loaded with sufficient film for the number of exposures desired. The stepping relay is set for the number of photographs to be taken. After arrangement is made for the transient pulse to operate the control circuit, the equipment is ready for operation.

Upon the occurrence of a transient, the camera shutter, normally closed, immediately is triggered open and the clock dial in the light shield is illuminated momentarily. Depending upon a preset delay time, the cathode ray beams are then extinguished. The fluorescent material on the cathode ray tubes retains the images on the cathode ray screens for a time sufficiently long so that successful photographic recording is accomplished. After a fixed delay the camera motor operates, closing the shutter, winding the film to the next frame, and resetting the control circuit. This places the memory oscillograph in readiness to record the next transient disturbance.

The accuracy of reproduction and the excellent frequency response of the oscillograph amplifiers make this cathode ray instrument suitable for the study of switching transients and other disturbances of short duration. In many instances the transient voltages being investigated are of such magnitude that no amplifiers are required. For successfully recording transients of extremely high speed, cathode-ray-tube voltages higher than those used here must be employed.[3]

Results

The automatic memory oscillograph described here may be put to use in the study of randomly occurring transients in mercury arc converters. Figure 6 is an illustration showing the instrument connected for recording faults in a mercury arc polyphase converter. The con-

Design and Measurements of Capacitor Discharge Welding Transformers

T. W. DIETZ
NONMEMBER AIEE

G. M. STEIN
MEMBER AIEE

Synopsis: A method is presented to calculate the size of core and windings of a capacitor discharge welding transformer required to supply a given welding current. It is further shown how the resistance and inductance of a certain welder can be determined from oscillograms of the current and voltage. The mathematical derivation of the formulas used is included.

FOR THE SPOT WELDING processes, where high instantaneous or closely controlled welding currents are required, an energy storage system will be of advantage. For this purpose, the capacitor discharge system has been developed. One typical application for this type of welding is the light metals, like aluminum and magnesium alloys, which require a high instantaneous and also closely controlled welding current. Another example is found in stainless steel whose welding current has to be of very short duration if carbide precipitation is to be avoided.

A capacitor discharge welder fundamentally consists of a series *RLC* circuit, with the energy originally stored in the capacitor and then discharged through the *RL* portion of the circuit by means of some switching device.

The resistance and inductance of a typical aluminum welder are in the order of 50 microhms and 1 microhenry respectively. To quote a specific weld schedule for 0.102-inch 24 ST "alclad" aluminum, this impedance must be matched with 2,520 microfarads to give peak current 0.029 second after the start of the current wave. It is the function of the welding transformer to effect this impedance match.

A classical analysis of the circuit which has been worked out and expanded for the oscillating condition is included in the appendix.

Let us first study the design of the transformer. For this purpose we investigate a welder which has been built to make a given weld. The resistance and inductance of this welder can be obtained from 60-cycle measurements. The inductance so obtained will remain relatively constant over a wide variation of current wave lengths, so this value can be used without appreciable error, but the resistance may vary by 100 per cent or more due to skin effect as the wave length deviates from one-half of a 60-cycle wave. The curves in Figure 1 show the ratio of 60-cycle resistance to actual resistance under capacitor discharge conditions for various wave lengths of a standard "Hi-Wave" welder.

For determining the size of a transformer core of a new welder, the desired time T_m to the first peak current, the value I_{2a} of the first secondary peak current necessary to do the welding job in question must be known from previous welding experience, for they are the fundamental requirements to which the welder shall be designed.

Then, as shown in the appendix,

$$\phi_T = \frac{1}{N_2} I_{2a} L_2 \times 10^8 \lambda(\tau_0) \qquad (35)$$

Paper 46-41, recommended by the AIEE committee on electric welding for presentation at the AIEE winter convention, New York, N. Y., January 21–25, 1946. Manuscript submitted October 5, 1945; made available for printing December 7, 1945.

T. W. DIETZ is research engineer, The Taylor-Winfield Corporation, Warren, Ohio, and G. M. STEIN is transformer design engineer, Westinghouse Electric Corporation, Sharon, Pa.

trol impulse is taken from a potentiometer placed across the direct voltage. Faulty anode firing will cause changes in the direct voltage and these changes initiate the operation of the oscillograph.

Simultaneous oscillograms of the main direct potential $e_{d\text{-}c}$, the anode to cathode voltage $e_{a\text{-}c}$ and the grid to cathode voltage $e_{g\text{-}c}$ are obtained with a circuit similar to that shown in Figure 6. Figure 7 is an illustration of a photographic record of faults occurring in an inverter. The memory time for this oscillogram has a preset value of about 50 milliseconds. The reproduction does not show all of the "memory" present in the original film. The camera shutter coil received its impulse at *A*, and cathode ray beam blanking occurred at *B*. Time proceeds from left to right.

The anode to cathode potential in Figure 7 shows that the disturbance recorded is due to the preignition of one of the inverter anodes. The regularity of the grid to cathode voltage indicates that the grid of the specific anode under observation suffers no ill effect due to this transient. A study of the wave shapes shown reveals the phase in which the fault occurs and the moment of initiation. The time at which the oscillogram is taken is shown by the counter dial *C* in the figure.

Figure 8 is an example of loss of grid control on the anode being monitored, and Figure 9 is an illustration of a case in which a "backfire" and a subsequent "shoot-through" occur.

Concluding Remarks

The automatic memory oscillograph can serve successfully in studying transients of a random character. Oscillograms may be obtained which are of value in the investigation of faults in the operation of apparatus such as mercury arc converters. It is possible to obtain information concerning the type of fault, the moment of its occurrence, its duration, and its severity. These data are of value in stimulating research and development work on all types of electrical equipment. As a laboratory tool, the automatic memory oscillograph may far surpass the ordinary oscillograph in utility. Its application to the study of physical phenomena in all branches of engineering where random transients must be investigated is only a matter of time. The study of mechanical transients by converting them into electric pulses suggests itself. The advantages possessed by virtue of the fact that the operation of this oscillograph is completely automatic, are obvious.

References

1. A NEW HIGH-SPEED CATHODE-RAY OSCILLOGRAPH, **H. P. Kuehni, S. Ramo.** AIEE TRANSACTIONS, volume 56, 1937, June section, pages 721–8.

2. A MEMORY ATTACHMENT FOR OSCILLOSCOPES, **W. E. Pakala.** AIEE TRANSACTIONS, volume 57, 1938, December section, pages 682–4.

3. PHOTOGRAPHIC PATTERNS ON CATHODE RAY TUBES, **Rudolph Feldt.** *Electronics*, volume 17, February, 1944, pages 130–7.

4. A BEAM BLANKING CIRCUIT FOR OSCILLOSCOPES, **Walther Richter.** *Electronics*, volume 17, September, 1944, pages 128–30.

5. THEORY AND OPERATION OF ELECTRON TUBES (book), **H. J. Reich.** McGraw-Hill Book Company, New York, N. Y., page 206.

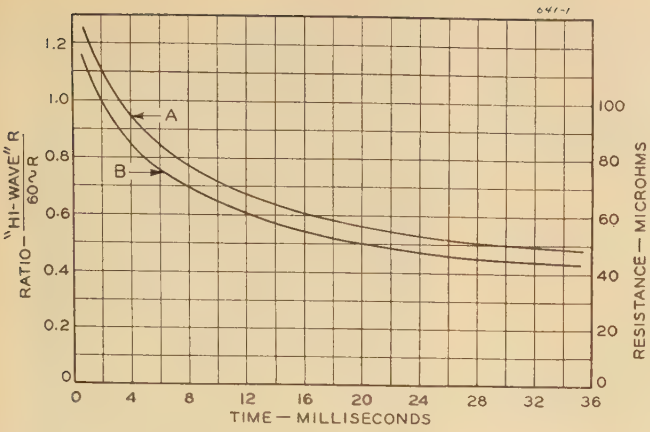

Figure 1. Variation of welder resistance as a function of wave shape

A—Ratio of actual resistance under capacitor discharge welding conditions, to 60∼ resistance, as a function of time to peak current

B—Total welder resistance referred to the secondary winding plotted against time to peak current

where

ϕ_T = maximum flux change
N_2 = secondary turns
R_2 = total resistance referred to secondary (ohms)
L_2 = total inductance referred to the secondary (henrys)
$\lambda(\tau_0)$ = a function of τ_0 (see Figure 2)
$\tau_0 = \dfrac{T_0}{\pi}\dfrac{R_2}{2L_2}$
T_0 = time to zero current (seconds)

The desired wave to make a given weld usually is expressed in terms of maximum current, and time to maximum current T_m; but T_0 is required to solve equation 35. Equation 28 shows the relationship of T_m and T_0, and can be solved for T_0 in the following way

Determine

$$g(\tau_0) = \frac{R_2}{2L_2} T_m$$

Obtain τ_0 from the curve $g(\tau_0)$ in Figure 2, and calculate $T_0 = \dfrac{2L_2}{R_2}\pi\tau_0$

Having evaluated τ_0, the amount of $\lambda(\tau_0)$ can be taken from the curve in Figure 2. The size of flux ϕ_T so obtained will be the total flux change. The first weld will leave the core magnetized with a residual flux which will vary with the type of core construction and the type of transformer steel used, but, in any case, it will be high enough to require a core of very large cross section unless it is compensated for. There are three ways to take care of this condition.

1. An air gap in the core for small transformers.

2. A magnetic flux bias by means of a direct current between welds.

3. Alternate reversal of the direction of the discharge through the welding transformer.

The third method will allow a simple economical design and therefore will be described in detail.

The residual flux for standard Hi-Wave transformers, when worked to maximum permissible flux density, is 42,000* lines per square inch and the core, which is made of special transformer steel, may be magnetized to 111,000 lines per square inch without measurable difference between primary and secondary ampere turns of the load current. This gives a maximum permissible flux density change per weld of 42,000 + 111,000 lines per square inch so that the net core area is total flux, as calculated by equation 35, divided by 153,000. Heating due to core loss need not be considered as even the highest welding speed possible at present would amount to only a very few cycles per second.

As can be seen from the problems just discussed, the accurate design of the core of a capacitor discharge welding transformer requires considerable experience, and measurements of similar setups, since most of the quantities which must be considered as known, vary with changing conditions of design, wave shape, and method of manufacture.

The next point for consideration is the copper.

Determination of effective current for the general circuit, that is for all combinations of L, R, and C, from the overdamped wave to a violently oscillating wave, is rather cumbersome from a mathematical approach.

A very large percentage of the total energy stored in the capacitor is lost in the welder and transformer so that we may assume, for design purposes, that the circuit must dissipate the total stored energy which may be expressed as

$J = {}^1/_2 CE^2$

joules per weld where

$$C = L_2\left[\frac{I_{2a}}{E}h(\tau_0)\right]^2 10^6 \text{ microfarad} \qquad (29)$$

C represents the capacity of the capacitor (microfarad). $h(\tau_0)$ can be taken from the curves in Figure 2.

The rate of energy dissipation or power will become

$$P = {}^1/_2 CE^2\frac{S}{60} \qquad (1)$$

Where J = energy in joules and S = average welding speed in spots per minute.

The power dissipated in the transformer will bear the same relation to the total power as its resistance referred to the secondary winding will bear to the total circuit resistance. It remains only to pick a desired efficiency η and, with welder resistance R_w known, to determine the corresponding total transformer resistance R_t referred to the secondary winding by the relationship $R_t = R_w\left(\dfrac{1}{\eta} - 1\right)$. With the resistance R_t determined, the copper sections can be calculated.

We now have iron cross section and copper cross section which furnish the physical size of the welding transformer. Having the loss and physical size, the temperature rise can be determined ac-

* The method of determining the residual flux will be presented later in this article.

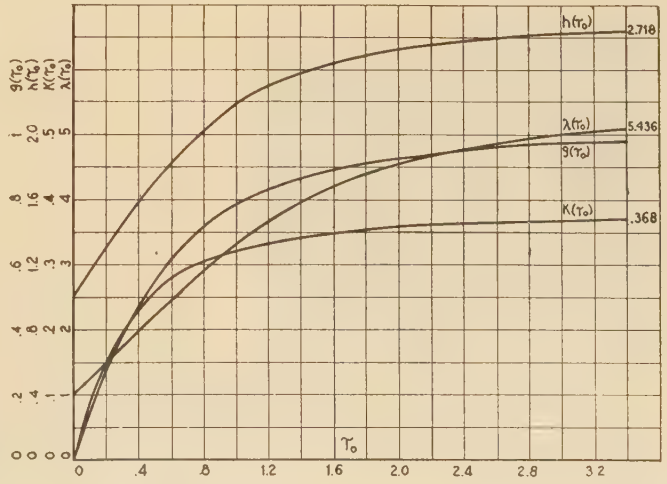

Figure 2. Characteristic functions of a capacitor discharge welding circuit

cording to standard transformer design practice which is outside the scope of this paper. The temperature rise may dictate water cooling which can be applied to the usually one turn secondary winding (see Figures 5 and 6), or it may require an increased copper section, or both.

The turns ratio remains to be fixed, and may be calculated from the expression

$$\frac{N_1}{N_2}=\frac{2Ek(\tau_o)}{I_{2a}R_2} \tag{30}$$

$K(\tau_o)$ can be taken from curves in Figure 2.

Measurements

The accuracy of a design, such as we just have considered, will depend largely on the experience of the designer and can be relied upon only when a suitable safety factor is applied which would be the correct procedure for one-of-a-kind design. When the design is to be used for a standard-line, a pilot unit should be built and accurate measurements made in order that some of the original assumptions may become definitely known quantities.

As has been stated before, all the characteristics which are considered more or less constant in the average electric circuit vary as the turns ratio and capacity are varied. It is, therefore, necessary to make measurements under the desired conditions, or over a range of capacity and turns ratio so that curves can be drawn.

Oscillograms are to be made of the primary current, of the capacitor voltage, and of a timing wave, usually 1,000 cycles. (See Figure 3.) From this we can measure all characteristics of the wave necessary for determining primary resistance and inductance of the welder and transformer circuit.

Figure 3. Oscillogram taken in the primary circuit of a capacitor discharge welder

A—Magnetizing watts
B—Magnetizing current
C—Primary current
D—Induced voltage
E—Capacitor voltage

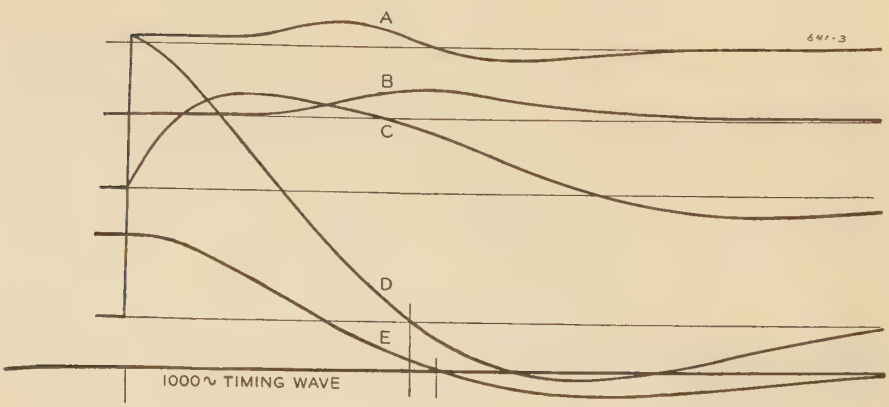

The inductance L_1 referred to the primary winding can be calculated according to equations 27 to 30, by substituting valves for g, h, and k, as

$$L_1=\frac{T_o^2\tan^2\pi\dfrac{T_m}{T_o}}{\pi^2C\left(1+\tan^2\pi\dfrac{T_m}{T_o}\right)}$$

The inductance L_2 referred to the secondary winding may be found from the relationship

$$L_2=\frac{L_1}{a^2}$$

where a = turns ratio.

The next step is the determination of the resistance of the circuit. From equation 31 we find

$$\frac{I_{1b}}{I_{1a}}=\epsilon^{-\pi\tau_o} \tag{31}$$

Where I_{1a} and I_{1b} are peak values of the primary current for the first and second half cycles respectively of the oscillating wave.

From equation 31 we find

$$\tau_o=\frac{T_o}{\pi}\frac{R_1}{2L_1}=\frac{1}{\pi}\log_\epsilon\frac{I_{1a}}{I_{1b}}$$

and determine

$$R_1=\frac{4.61L_1}{T_o}\log_{10}\frac{I_{1a}}{I_{1b}} \tag{2}$$

Having obtained actual values of R, L, T_m, T_o, and I, it is possible to make a more accurate determination of total flux change, equation 35. In addition to this we will have to find the magnitude of the actual core flux. Furthermore, the entire mathematical analysis presupposes that applied voltage is equal to induced voltage, which is not strictly true, due to IR and IX drops in the transformer primary winding. The flux change, therefore, must be determined from induced voltage oscillograms.

Figure 4. Residual and total flux in the welding transformer

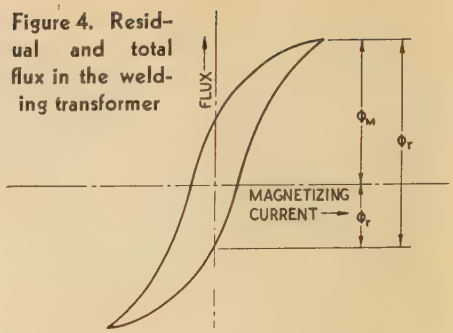

If the total flux change to produce a weld is ϕ_T, the residual flux is ϕ_r, and the maximum flux to which the iron actually is magnetized is ϕ_m (see Figure 4) then we may write

$$\phi_T=\phi_r+\phi_m \tag{3}$$

The unsymmetry of the hysteresis loop describing the reversal of the flux shall be neglected. Since we can test directly only ϕ_T, we must find a method to determine one of the other two quantities, ϕ_r or ϕ_m, in order to apply equation 3.

It was decided to measure the flux ϕ_m. As there are no pole manifestations on a transformer core, this could be done only by comparing the magnetizing current of a typical transformer with a d-c magnetization curve of the same transformer which had been prepared from 60-cycle oscillograms. To obtain the magnetizing current, it was necessary to connect the transformer primary winding in parallel with another identical transformer which had been installed in a welding machine in the normal manner. Both transformers had the same residual ϕ_r. The voltage wave form of the transformer under test was identical with that of the transformer which actually was welding, and as the test transformer's secondary winding was open, its primary winding carried only magnetizing current. After several previous discharges with the same energy, an oscillogram of the magnetizing current was taken, and its peak value was compared with the d-c magnetization curve to determine the flux ϕ_m. This value of ϕ_m is subject to the same error as that caused by considering capacitor voltage to be the same as transformer induced voltage, because the primary winding of the test transformer carries only magnetizing current, and hence the difference between induced voltage and applied voltage will be negligible. This means that the test transformer's induced voltage will be equal to the welding transformer's applied voltage. A correction factor for any one setting of capacity, voltage, and turns ratio can be established. If the total flux change is calcu-

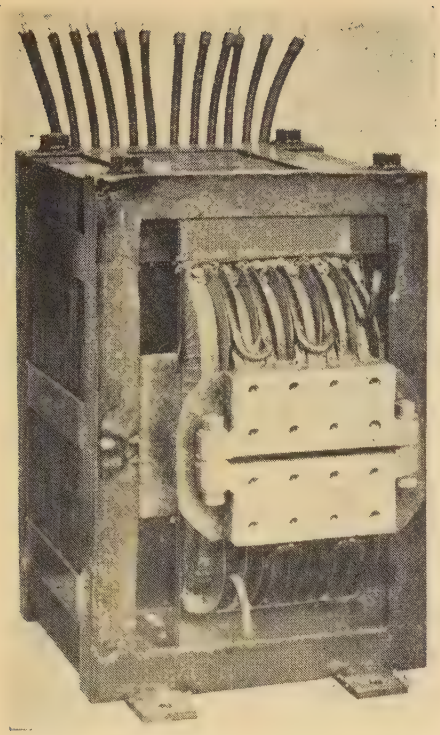

Figure 5. Standard "Hi-Wave" welding transformer

lated on the basis of capacitor voltage and called ϕ_{TC} and again is calculated on the basis of induced voltage and called ϕ_{TE}, then the actual flux to which the iron is excited may be stated as

$$\phi_m = \frac{\phi_{TE}}{\phi_{TC}} \phi_m \text{ (test)} \qquad (4)$$

if we assume the ratio of the corresponding residual fluxes ϕ_r is the same as that of the main fluxes ϕ_m and ϕ_m (test). It now remains to determine the total flux change accurately.

The fundamental voltage equation is

$$e = N\frac{d\phi}{dt} \times 10^{-8} \qquad (5)$$

where

N = number of turns
e = instantaneous voltage

From this we can write

$$\phi = \frac{10^8}{N} \int_{t_1}^{t_2} e\,dt \qquad (6)$$

where t_1 represents the time at the beginning of discharge and t_2 any time thereafter. Then $\int_{t_1}^{t_2} e\,dt$ represents the area under the voltage curve which equals

te (average) (7)

so that we may write total flux change

$$\phi_T = \frac{10^8 t}{N} e \text{ (average)} \qquad (8)$$

Inspection shows that this expression holds completely only for an oscillating condition where T_o is finite, since in a case where T_o is infinite, e will approach o and the expression becomes indeterminate. Equation 8 can be evaluated, however, for any portion of the wave so that we may evaluate from $t = o$ to a value of t where e (instantaneous) is practically equal to zero.

The value te (average) may be obtained from the area under the oscillogram of the voltage e by some graphical method.

In this way ϕ_{TC} can be determined from an oscillogram of the capacitor voltage. An induced voltage oscillogram will give the actual total flux change ϕ_{TE}.

The induced voltage can be measured by placing a search coil of several turns evenly distributed on the center core leg next to the iron.

To summarize:

1. Total flux change ϕ_{TE} can be determined by applying equation 8 to an induced voltage wave.

2. Maximum flux to which the core is excited is according to equations 4 and 8.

$$\phi_m = \frac{te \text{ (average) from induced voltage}}{te \text{ (average) from capacitor voltage}} \times \phi_m \text{ (test)} \qquad (9)$$

where ϕ_m (test) is read from a magnetization curve of the transformer in question, having measured its magnetizing current as described previously.

This method of determining maximum flux and flux change was developed to measure accurately the flux conditions of a previously designed line of transformers with a view of possible refinement of the design. Its usefulness lies in the fact that any piece of equipment whose induced voltage can be recorded on an oscillogram may be investigated, regardless of the complexity of the induced voltage wave.

Pictures of the assembly and of the secondary winding of a standard Hi-Wave CC1T capacitor discharge welding transformer are shown in Figures 5 and 6.

Appendix. Mathematical Analysis

Figure 7 shows a simplified capacitor discharge welding circuit for which we will use the following symbols:

e = voltage across capacitor (volts)
E = maximum or initial value of e (volts)
C = capacitance of capacitor (farads)
R_t; L_t = total resistance (ohms) and leakage inductance (henrys) of the welding transformer referred to the secondary side
R_w; L_w = total resistance (ohms) and inductance (henrys) of the external secondary welding circuit
R_C; L_C = total resistance (ohms) and inductance (henrys) of the external primary capacitor circuit
R_1; L_1 = resultant resistance (ohms) and inductance (henrys) referred to the primary side
R_2; L_2 = resultant resistance (ohms) and inductance (henrys) referred to the secondary side
N_1; N_2 = primary and secondary number of turns
$a = \frac{N_1}{N_2}$ = turns ratio
i_1; i_2 = primary and secondary currents (amperes)
I_1; I_2 = maximum values of i_1 and i_2 (amperes)
I_{1a}; I_{1b}; I_{2a}; I_{2b} = first and second maximum values of i_1 and i_2 for oscillating discharge (amperes)
kva_C = power rating of capacitor referred to 60-cycle excitation (kilovolt-amperes)
ϕ_T = maximum flux change of magnetic core flux of welding transformer (maxwells)
T = time (seconds) to any current peak $i_1 = I_1$ or $i_2 = I_2$
T_m = time (seconds) to first current peak
T_o = time (seconds) of half cycle of i_1 and i_2
T_C = time (seconds) to first zero e
n = number of current peaks up to time T

[Since R_c and L_c of the capacitor circuit may be neglected, we may write $R_2 = R_t + R_w$; $L_2 = L_t + L_w$]

The general circuit equations are

$$L_1\frac{d^2 i_1}{dt^2} + R_1\frac{di_1}{dt} + \frac{i_1}{C} = 0$$

$$i_1 = -C\frac{de}{dt}$$

Introducing

$$Z = \sqrt{\left(\frac{R_1}{2}\right)^2 - \frac{L_1}{C}} \qquad (10)$$

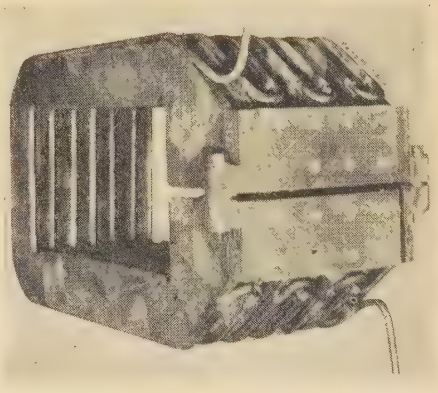

Figure 6. Standard "Hi-Wave" welding transformer secondary winding

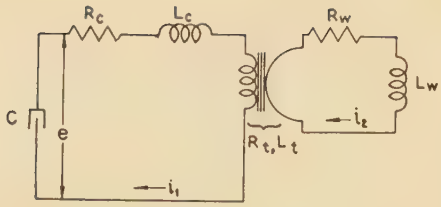

Figure 7. Simplified capacitor discharge welding circuit

The complete solution is

$$i_1 = A\epsilon^{-\frac{1}{L_1}\left(\frac{R_1}{2}-z\right)t} + B\epsilon^{-\frac{1}{L_1}\left(\frac{R_1}{2}+z\right)t}$$

$$e = A\left(\frac{L_1}{C}\right)\left(\frac{\epsilon^{-\frac{1}{L_1}\left(\frac{R_1}{2}-z\right)t}}{\frac{R_1}{2}-Z}\right)+B\left(\frac{L_1}{c}\right)\times\left(\frac{\epsilon^{-\frac{1}{L_1}\left(\frac{R_1}{2}+z\right)t}}{\frac{R_1}{2}+Z}\right)$$

where A and B are constants of integration. A and B are determined from the boundary conditions $t=O$; $i=O$; $e=E$ so that we obtain

$$i_1 = \frac{E}{Z}\epsilon^{-\frac{R_1}{2L_1}t}\sinh\frac{Z}{L_1}t \tag{11}$$

$$e = E\epsilon^{-\frac{R_1}{2L_1}t}\left[\frac{R_1}{2Z}\sinh\frac{Z}{L_1}t+\cosh\frac{Z}{L_1}t\right] \tag{12}$$

to get the maximum value I_1 of i_1 determine $\frac{di_1}{dt}$ from equation 11, equate to zero, solve for i_1, introduce $i_2=ai_1$; $a^2R_2=R_1$; $a^2L_2=L_1$, and obtain

$$T = \frac{L_1}{Z}\tanh^{-1}\frac{2Z}{R_1} \tag{13}$$

$$I_1 = E\sqrt{\frac{C}{L_1}}\epsilon^{-\frac{R_1}{2L_1}T};\quad I_2 = E\sqrt{\frac{C}{L_2}}\epsilon^{-\frac{R_2}{2L_2}T} \tag{14}$$

The foregoing solutions are general. For a numerical application the following three special cases should be considered.

Case 1. Aperiodic Discharge

$\left(\frac{R_1}{2}\right)^2 > \frac{L_1}{C}$; Z of equation 10 is real so that we may apply equations 10 to 14 directly. Since there is only one maximum $I_1=I_{1a}$ or $I_2=I_{2a}$ of the currents i_1 and i_2, we may write $T=T_m$ and obtain for

$$\text{kva}_C = \frac{1}{2}(2\pi 60)\frac{CE^2}{1{,}000}$$

the expression

$$\text{kva}_C = 0.1885 I_{2a}^2 L_2 \epsilon^{\frac{R_2}{L_2}T_m} \tag{15}$$

or

$$\text{kva}_C = > 1.4 I_{2a}^2 L_2$$

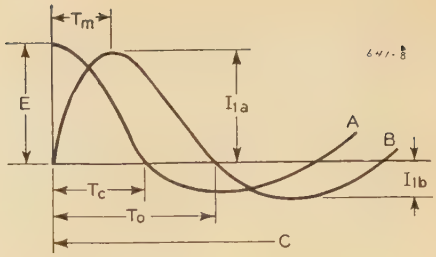

Figure 8. System of current and voltage oscillations of the primary capacitor circuit

A—Capacitor voltage e
B—Primary current i_1
C—Time t

Case 2. Periodic Discharge

$\left(\frac{R_1}{2}\right)^2 < \frac{L_1}{C}$; Z of equation 10 is imaginary so that we transform

$$\sqrt{\left(\frac{R_1}{2}\right)^2-\frac{L_1}{C}} = j\sqrt{\frac{L_1}{C}-\left(\frac{R_1}{2}\right)^2}$$

By using a real

$$Z = \sqrt{\frac{L_1}{C}-\left(\frac{R_1}{2}\right)^2} \tag{16}$$

we may write instead of equations 11 to 14

$$i_1 = \frac{E\epsilon^{-\frac{R_1}{2L_1}t}}{Z}\sin\frac{Z}{L_1}t \tag{17}$$

$$e = E\epsilon^{-\frac{R_1}{2L_1}t}\left[\frac{R_1}{2Z}\sin\frac{Z}{L_1}t+\cos\frac{Z}{L_1}t\right] \tag{18}$$

$$T_m = \frac{L_1}{Z}\tan^{-1}\frac{2Z}{R_1};\quad T = T_m+(n-1)\pi\frac{L_1}{Z} \tag{19}$$

The expressions for I_1 and I_2 remain the same as in equation 14 while I_{1a} and I_{2a} are represented by

$$I_{1a} = E\sqrt{\frac{C}{L_1}}\epsilon^{-\frac{R_1}{2L_1}T_m};\quad I_{2a} = E\sqrt{\frac{C}{2L}}\epsilon^{-\frac{R_2}{2L_2}T_m} \tag{20}$$

Kva_c is given by equation 15 and lies between the limits

$$0.1885 I_{2a}^2 L_2 < \text{kva}_C < 1.4 I_{2a}^2 L_2.$$

Case 3. Limit of Aperiodic Discharge

$\left(\frac{R_1}{2}\right)^2 = \frac{L_1}{C}$; Z becomes zero. In substituting $Z=0$ in equations 17 to 19 we have to evaluate the expressions

$$\lim_{Z\to 0}\left(\frac{\sin\frac{Z}{L_1}t}{z}\right) = \frac{t}{L_1};\quad \lim_{Z\to 0}\left(\frac{\tan^{-1}\frac{2Z}{R_1}}{Z/L_1}\right) = \frac{2L_1}{R_1}$$

and obtain, instead of equations 15 and 17 to 19

$$i_1 = \frac{E}{L_1}t\epsilon^{-\frac{R_1 t}{2L_1}} \tag{21}$$

$$e = E\left(\frac{R_1}{2L_1}t+1\right)\epsilon^{-\frac{R_1}{2L_1}t} \tag{22}$$

$$T = T_m = \frac{2L_1}{R_1} \tag{23}$$

$$I_2 = 0.368\sqrt{\frac{C}{L_2}}E \tag{24}$$

$$\text{kva}_C = 1.4 I_{2a}^2 L_2 \tag{25}$$

In spite of the fact that equations 11, 17, and 21, for example, are of greatly different form, it can be seen from the reasoning in developing equation 21 from 17, and a similar process could be applied to develop equation 21 from equation 11, that for $\left(\frac{R_1}{2}\right)^2 \backsimeq \frac{L_1}{C}$ the equations 21 to 25 could be used, without great error for either case 1 or 2.

For the purpose of machine design, equations 15 to 20 for the periodic discharge case 2 shall be transformed so that the desired machine constants may be determined for any specific wave form. In this analysis R_2 and L_2 are fixed with the selection of the size and form of the welding throat as well as of the efficiency and per cent impedance of the welding transformer. I_2 and T_m are determined by the desired welding effect, and E may be fixed if we standardize on a certain value of capacitor voltage.

If instead of T_m the time T_o of the first half current cycle is introduced, it will be possible to determine explicitly, all other values, like $a=\frac{N_1}{N_2}$; I_{1a}; E; ϕ_T; L_1 and R_1 as functions of the given circuit constants. T_o is obtained from equation 17 for $i=o$ by

$$\frac{Z}{L_1}T_o = \pi$$

or

$$T_o = \frac{L_1\pi}{Z};\quad Z = \sqrt{\frac{L_1}{C}-\left(\frac{R_1}{2}\right)^2} \tag{26}$$

This value of T_o is introduced into equations 15 to 20 by combining the functions

$$\tau_o = \frac{T_o}{\pi}\frac{R_2}{2L_2}$$

$$g(\tau_o) = \tau_o\tan^{-1}\frac{1}{\tau_o}$$

$$h(\tau_o) = \epsilon^{g(\tau_o)} \tag{27}$$

$$k(\tau_o) = \frac{\tau_o}{\sqrt{1+\tau_o^2}}\frac{1}{h(\tau_o)}$$

$$\lambda(\tau_o) = \frac{\tau_o}{\sqrt{1+\tau_o^2}}h(\tau_o)\left[\frac{-\pi\tau_o}{k(\tau_o)}+2\right]$$

$g(\tau_o)$; $h(\tau_o)$; $k(\tau_o)$; $\lambda(\tau_o)$ are plotted against τ_o in Figure 2. Using the values taken from these curves, we may write instead of equations 15 to 20

$$T_m = \frac{2L_2}{R_2}g(\tau_o);\quad T = T_m+(n-1)T_o;\quad T_C = T_o - T_m \tag{28}$$

Phonograph Reproducer Design

W. S. BACHMAN
NONMEMBER AIEE

PHONOGRAPH reproducers, which convert the mechanical motion of the stylus to a corresponding electric voltage, have been in commercial use for the past two decades. They have employed a wide variety of voltage generators such as carbon microphone buttons, variable reluctance magnetic circuits, moving coils in magnetic fields, and Rochelle salt crystals. Although excellent performance has been obtained with many of these types, there has been a continued effort to reduce the mass of the moving system and to simplify the mechanical construction, even to the extent of sacrificing output voltage.

While the carbon button type of reproducer was one of the first to appear, it was soon outmoded by subsequent types. The variable resistance principle, however, again is employed in one of the reproducers to be described in this paper. An important difference between it and the carbon button type is that the variable resistance element is a fine metallic wire the resistance of which changes in response to strain. These wires may be of the same material as is used in strain gauges, but in this case there is no need to determine the absolute value of the strain, since only the voltage resulting from the change in strain is utilized. This imposes the requirement of linearity, if distortion is to be avoided, which easily is met by most of the commonly used strain sensitive wires. Measurements have shown that the ratio of change of resistance to change of length is constant through and even beyond the elastic limit of the wire.[1]

One of the first successful designs employing a wire resistance strain element is shown in Figure 1. The stylus is carried in a small cantilever beam 9, and the strain element 14 is attached to it at a point about 1/3 of its length from the fixed end. The strain wire is held in tension sufficient to stress it about halfway to its elastic limit by the piano wire springs 15, and the Textolite pins 16 serve as snubbers to prevent the tension springs from following the motion of the cantilever. The circuit employed to polarize this reproducer is shown in Figure 2.

Since the voltage derived from the strain is proportional to the displacement, the output of this reproducer is proportional to the displacement of the stylus by the record. This makes it easy to check the frequency characteristic without knowing the actual displacements which are pressed on a frequency, or constant tone record. If the same band is driven at various speeds, the amplitude of the reproduced wave should be the same. This was found to be true from 10,000 cycles down to the low frequency resonance except for a wave form distortion at about 6,500 cycles, which was found later to be caused by the second mode of vibration of the cantilever which occurred at 13,000 cycles. This could be damped readily by placing a small block of a material such as Pyralin approximately at the loop of the second mode of vibration, at which point a negligible amount of loading would be reflected to the stylus tip for the fundamental mode of vibration. These modes of vibration are shown in Figure 3.

Although the output voltage was low, about −65 decibels below 6 milliwatts with a displacement of 0.0003 inch (Columbia WT-1, frequency record, 1,000 cycle band), the performance was very nearly ideal. In order to avoid variations in tension the design shown in Figure 4 was evolved. The strain wires were soldered to 1/16 inch diameter rods which were free to move axially in holes provided in the Textolite mounting block. The tension, as previously, was applied by means of piano wire springs, but instead of the snubbers the rods were lubricated with a viscous liquid which readily permitted them to move slowly in an axial direction to equalize variations in tension in the strain wire, but offered a high impedance to the motion resulting from the rapid strain variations due to the useful stimulation of the cantilever. In other words the strain wires were resistance terminated.

Another solution of the termination problem is shown in Figure 5. In this model use is made of the fact that an increase in strain on one side is accompanied by a decrease on the other. If both ends were terminated at the same point, the two forces would balance out. The tiny bell cranks 35 at the root of the cantilever serve to change the direction of the strain by approximately 90 degrees, and the ends of the strain element both are attached to the yoke 36, which applies the desired tension to them.

All of these designs require the use of the strain elements under tension, restricting their operating range to about half of their potential range. In order to make use of the compression as well as the tension range, the design in Figure 6 was developed. Although not shown in the

Paper 46-32, recommended by the AIEE committee on communication for presentation at the AIEE winter convention, New York, N. Y., January 21–25, 1946. Manuscript submitted November 19, 1945; made available for printing December 17, 1945.

W. S. BACHMAN is with the General Electric Company, Bridgeport, Conn.

$$C = L_2\left[\frac{I_{2a}}{E}h(\tau_0)\right]^2 10^6 \text{ microhms} \quad (29)$$

or

$$E = \sqrt{\frac{L_2}{C}}\, I_{2a} h(\tau_0) 10^3$$

$$\frac{N_1}{N_2} = \frac{E}{I_{2a}}\,\frac{2k(\tau_0)}{R_2} \quad (30)$$

or

$$I_{2a} = \frac{N_2}{N_1}\,\frac{2k(\tau_0)}{R_2}\,E$$

$$\frac{I_{2b}}{I_{2a}} = \frac{I_{1b}}{I_{1a}} = -\epsilon^{-\pi\tau_0} \quad (31)$$

$$\frac{i_2}{I_{2a}} = \frac{\tau_0}{k(\tau_0)}\,\epsilon^{-\tau_0\pi\frac{t}{T_0}} \sin \pi\frac{t}{T_0} \quad (32)$$

$$\frac{e}{E} = \epsilon^{-\tau_0\pi\frac{t}{T_0}}\left[\tau_0 \sin \pi\frac{t}{T_0} + \cos \pi\frac{t}{T_0}\right] \quad (33)$$

$$\text{kva}_C = 0.1885 L_2 [I_{2a} h(\tau_0)]^2 \quad (34)$$

Calculate also

$$\phi_T = \int_0^{T_0} \frac{e10^8}{N_1}\,dt$$

and obtain

$$\phi_T = \frac{1}{N_2} I_{2a} L_2 10^8 \lambda(\tau_0) \quad (35)$$

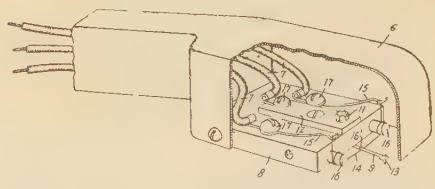

Figure 1. Early form of strained wire resistance reproducer

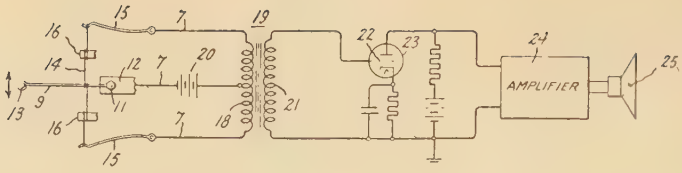

Figure 2. Circuit for polarizing variable resistance reproducer

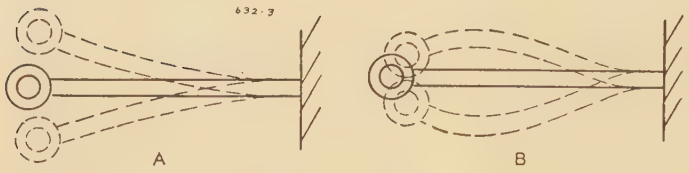

Figure 3
A—Normal mode of vibration of cantilever stylus support
B—Second mode of vibration

figure, the back end of the cantilever 55 is fastened to a stud which mounts rigidly to the tone arm. In it the strain wires were cemented to the cantilever itself to measure the strains in the outer fibers of the beam. Being attached in repose, they are subjected to both tension and compression. Although a strain element need be applied to only one side of the cantilever, it actually was applied to both, principally to permit balancing of the direct current in the primary winding of the input transformer. In this form the resistance reproducer lends itself readily to the application of a new technique for the damping of the resonance between the supporting arm mass and the suspension compliance.

It is usual, in most pickup designs to obtain damping of this resonance by introducing some dissipation in the pivots or bearings, such as by the use of rubber sleeves or blocks on the axis of oscillation. This imposes an additional load upon the record, as may be seen from a study of the electrical equivalent of the mechanical system, as shown in Figure 7.

Inspection of the equivalent electric circuit of such a reproducer, Figure 7B, shows that the presence of R is desirable to limit the impedance rise at the resonance frequency. In the useful audible range above the resonance the proper operation of the pickup depends upon the motion of M being negligible in response to signal stimulation. This requires that practically all of the applied motion be suffered by R and C (practically all of the current must travel through the path R, C). If R were omitted, the needle point impedance would decrease with frequency, but in the equivalent circuit it readily is seen that it can never drop below R as the frequency increases.

To give a quantitative illustration of the importance of this problem, consider a pickup and tone arm assembly having an effective arm mass (referred to the needle point) of 30 grams and a suspension compliance of 10^{-6} centimeter per dyne. For critical damping of the arm resonance it would require

$$R^2=\frac{4M}{C}=\frac{4\times30}{10^{-6}}=120\times10^6$$

$$R=10.9\times10^3\ \frac{\text{dyne seconds}}{\text{centimeters}}$$

Under stimulation of 15 centimeters per second, a quite usual value of velocity, a lateral force of

$$F=RV-10.9\times10^3\times15=165\times10^3 \text{ dynes or } 167 \text{ grams}$$

would be developed. Assuming 45-degree inclined groove walls, a bearing weight of 5.9 ounces would be necessary to keep the needle in contact with the groove.

Of course it is not necessary to provide critical damping of the tone arm resonance, but, if the damping is not sufficient, the reproducer will be very unstable when shock excited and even may tend to jump out of the grooves of a warped or uneven record. In many designs the bearing upon the record is made large for this reason alone.

Because of the extremely small size of the generator unit shown in Figure 6 and the fact that the output voltage is obtained as a result of the bending of the cantilever only, it became possible to apply a new arm resonance damping technique. The mechanical schematic of the system is shown in Figure 8A. The electrical equivalent of the system is shown in 8B. It is obvious in the circuit of 8B that the resonance may be damped critically without any increase in the mechanical impedance above resonance. Such a system is not mechanically stable, however, as is evident from inspection of Figure 8A. In this mechanical system there is no restoring force available to keep the needle point and the arm from wandering away from each other as energy is dissipated in R. In other words the resistor must be restricted from any except oscillatory motion. This is done by the system shown in 8C and 8D. If C_2 is made very large, the circuit of 8B approaches the performance of 8C, except that a new resonance, which would be damped only very lightly, appears at the frequency where the reactance of C_1 and C_2 in parallel is equal to the reactance of m. By proper choice of C_1 and C_2, R may be made effective for both resonance frequencies, as may be seen from the curve of mechanical impedance at the needle point versus frequency shown in Figure 9.

Figure 10 shows a design of the resistance pickup employing this new type of arm resonance damping. Corresponding to the element R in Figure 8 are the rubber sleeves bearings 72, and the Pyralin disc 74; all are in torsion. The compliance C_2 is that of the spring 80. This reproducer with only 15 grams of bearing weight on the record would not leave the groove even with quite violent shocks ap-

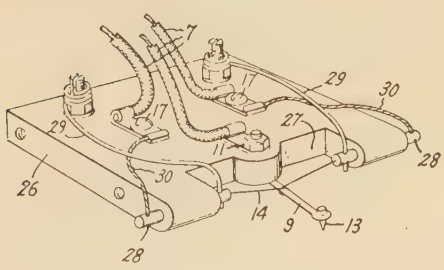

Figure 4. Strained wire resistance reproducer with means for maintaining uniform tension in resistance wire

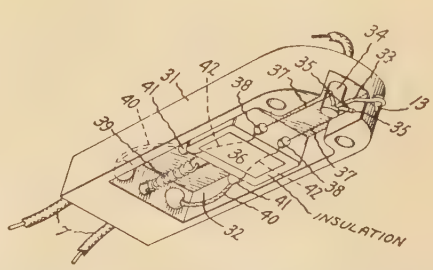

Figure 5. Alternate form of strained wire resistance reproducer in which opposing strains are balanced against each other

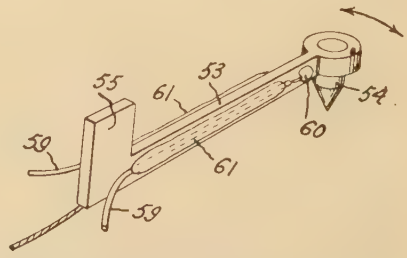

Figure 6. Strained wire resistance reproducer element having strain wires applied directly to the cantilever to measure strain in its outer fibers

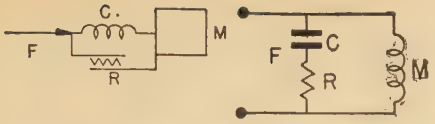

Figure 7A (above, left). Mechanical schematic diagram of a reproducer having damping material at its pivots

F = force exerted by needle upon record
C = compliance of suspension
R = mechanical resistance represented by the damping material
M = mass of cartridge and arm
Mass of needle is neglected being insignificant at low frequency

Figure 7B (above, right). Electrical equivalent of mechanical system shown in Figure 7A (motions of the mechanical elements are represented as currents in the electric network)

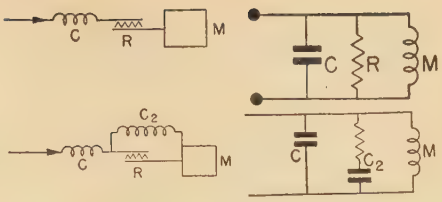

Figure 8A (above, upper left). Mechanical schematic diagram of a reproducer having a preferred form of low frequency resonance damping

Figure 8B (above, upper right). Electrical equivalent of system shown in Figure 8A

Figure 8C (above, lower left). Practical mechanical system retaining advantages of idealized system shown in Figure 8A

Figure 8D (above, lower right). Electrical equivalent of system shown in Figure 8C

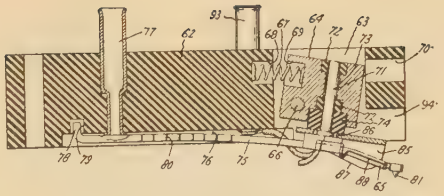

Figure 10. Design of strained wire resistance reproducer utilizing element of Figure 6 and having damping applied as shown schematically in Figure 8C

plied to the motor board and turntable. The effect of this damping system was observed by watching the displacement output of the reproducer on an oscilloscope while a tone band of a frequency record was allowed to coast down from rated speed to zero. The observed amplitude remained uniform until the resonant frequency, approximately 25 cycles, was nearly reached, below which the amplitude dropped smoothly. No rise before cutoff occurred.

While the strained wire resistance reproducer provides nearly ideal performance, the techniques acquired during its development are by no means limited to its type of generator element. The following is a description of a variable reluctance or magnetic type of reproducer embodying similar mechanical design considerations.

The fact that even a simple cantilever carrying the stylus at its free end required some damping to restrain its second mode of vibration, as mentioned in reference to Figure 3, made it very evident that no more complicated system could be relied upon to transmit the motion of the stylus tip to an armature or reed without introducing a frequency characteristic describing their relative motions. Accordingly a design was worked out in which the armature is right at the stylus, so that the motion of the armature is inseparably that of the stylus. Obviously this design could have no frequency characteristic as long as the stylus properly traces the groove, the output voltage being proportional to the stylus velocity.

The armature is a steel ribbon having a cross section of 0.010 inch by 0.030 inch. As may be seen from Figure 11, it has a 90 degree twist near the fixed end, which makes possible nearly as much compliance in the vertical direction as is provided laterally. This is desirable to permit the stylus to recede within the guard, provided by the two pole faces, when subjected to excessive downward forces such as in dropping. The small block of Pyralin just forward of the twist provides sufficient damping to restrain the second mode of vibration of the cantilever, which has already been discussed. At the free end the width of the armature is increased to receive the stylus. The dynamic mass of this stylus armature assembly is in the order of 8 milligrams. This mass is suspended on the spring, represented by the cantilever, the mechanical schematic of which is shown in Figure 12A. The electrical equivalent, Figure 12B, is a simple series circuit which expresses the mechanical impedance at the stylus tip. At low frequencies the system is stiffness controlled, and the impedance therefore decreases linearly with frequency until the resonance of M_1 and C is reached. The impedance at this resonance becomes very nearly zero, since very little mechanical resistance is reflected to the stylus tip from the Pyralin damping block attached near the fixed end of the cantilever. This, then, is the frequency at which practically no force is required to move the stylus, and with the values of

Figure 9. Low frequency needle point impedance and response of magnetic phonograph reproducer

⊙ Measured values

$\text{Response} = \frac{B_c}{Y}$

$C = 0.875 \times 10^{-6}$ centimeter per dyne
$C_2 = 3.54 \times 10^{-6}$ centimeters per dyne
$R = 6{,}000$ dyne seconds per centimeter

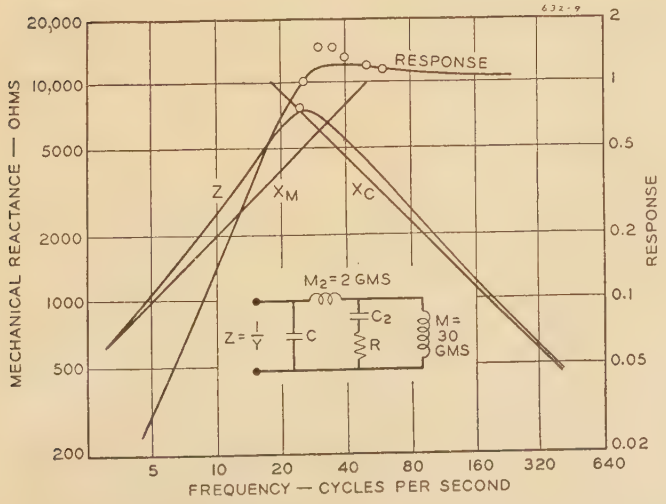

Figure 11. Magnetic or variable reluctance reproducer

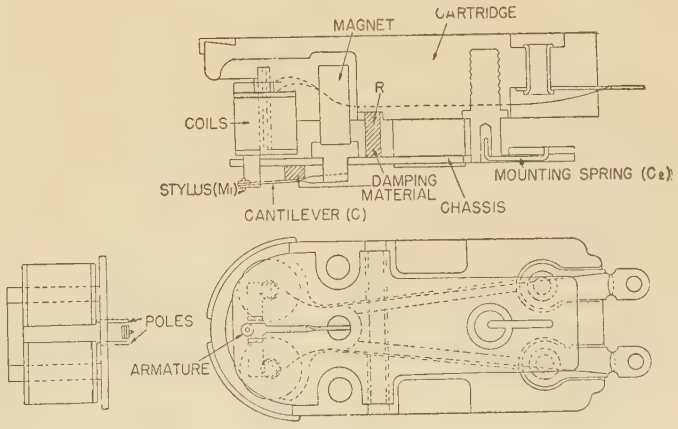

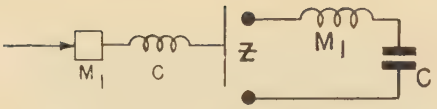

Figure 12A (left). Mechanical schematic of the stylus cantilever assembly. The fixed end of the cantilever is assumed to be rigid, which is very nearly so at high frequencies

M_1 is the dynamic mass of the stylus assembly
C is the compliance of the suspension

Figure 12B (above, right). Electrical equivalent of system shown in Figure 12A

Figure 13A. Mechanical schematic of magnetic pickup

M_1 is the dynamic mass of the stylus assembly
C is the suspension compliance
M_2 is the mass of the coils, poles, and magnet assembly
R is the arm resonance damping
C_2 is the compliance which provides the operating point for R
M is the cartridge and arm mass

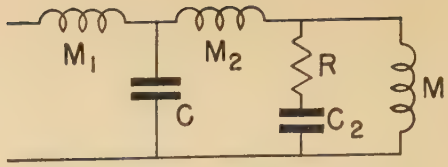

Figure 13B. Electrical equivalent of system of Figure 13A

dynamic mass and suspension compliance noted previously it occurs at approximately 2,300 cycles per second.

Above this resonance the system is mass controlled, the impedance rising linearly with frequency. Because the mass is so small, this system will remain in contact with both side walls of a 45 degree inclined side wall groove under acceleration of 2,000 g with a bearing weight upon the record of only 16 grams.

The mechanical system shown in Figure 12 accurately represents the needle point impedance except at the low frequency end of the range, where the dynamic mass of the arm and cartridge resonates with the compliance C. This condition was discussed with reference to Figure 8, and the same treatment for the control of this resonance is applied to this magnetic design. Again referring to Figure 11, the poles, coils, magnet, and armature all are mounted upon a chassis which is spring-mounted to the cartridge and arm assembly. Between the chassis and cartridge another block of Pyralin is inserted which provides the mechanical damping resistance, R. The mechanical system of the magnetic reproducer is shown in Figure 13A. It differs from that of Figure 8C in the presence of M_2. If this mass is too large, the resonance of M_2 with C and C_2 in series may be low enough so that R is not very effective, giving another frequency at which high impedance appears at the needle point. If M_2 is small enough to avoid this condition, it may be neglected. In this particular design the total weight of the magnet, coil, poles, and chassis assembly is approximately two grams. Figure 9 shows the calculated mechanical impedance, Z, of the magnetic reproducer, taking M_2 into account. The two asymptotes which the curve approaches correspond to the reactances of the suspension compliance C, and the total mass, M_1 and M. It is seen that the resonant rise is very slight.

The frequency response characteristic of this reproducer may be calculated by finding the ratio of the admittance of the path through C, referring to Figure 9, to the total admittance of the circuit. This is the same as the ratio of the motion of the cantilever to the motion imparted to the stylus tip, the open circuit voltage output of the reproducer being proportional to the velocity of motion of the cantilever. The network may be considered to be fed from a constant current source, the record groove being a stiff or high impedance source.

Also plotted in Figure 9 are measured values of response which were obtained by first measuring the output of the cartridge supported in an arm, and repeating the run with the cartridge clamped in a vise, the ratio of these values indicating the low frequency response. The source for these measurements was a crystal cutter head the exact mechanical impedance of which was not determined but which, because of the head's very evident stiffness, was regarded to be high. The agreement with the calculated response is reasonable considering this and also that the damping material is not a pure mechanical resistance. Similar technique was employed as mentioned previously in the case of the resistance pick-up for determining the response in the range above arm resonance, with the important difference that the electric output was integrated before being fed to an oscilloscope. Under these conditions no change in amplitude of the trace was observed, regardless of the rotational speed, below 78 rpm at which any tone band from 10,000 cycles down was driven. This indicates the absence of any frequency characteristic from 10,000 cycles down to the region in which the arm resonance occurs.

Reference

1. Characteristics and Aircraft Applications of Wire Resistance Strain Gauges, A. V. deForest. *Instruments*, volume 15, April 1942.

Technique of Electrical and Hydraulic Testing of Hydroelectric Units

G. D. FLOYD
MEMBER AIEE

J. J. TRAILL
NONMEMBER AIEE

Synopsis: The application of the AIEE Test Code for Synchronous Machines in field testing of hydroelectric generators is discussed, and the preferred method of making certain tests is indicated, together with reasons for its selection. Methods of making acceptance tests on turbines are outlined in sufficient detail to establish the fundamental theory, and the electrical measurements on the generator required to establish the generator input for the hydraulic test, are listed, with brief reference to the accuracy required, and to means of obtaining it. Rating and other hydraulic tests on hydroelectric units are also described.

ALTHOUGH commercial or acceptance testing of hydroelectric units has been the rule rather than the exception, very little has been written of the technique, especially of matters peculiar to field testing. The Test Code for Prime Movers of the American Society of Mechanical Engineers,[1] has been available for some years, and the AIEE Test Code for Synchronous Machines[2] was approved recently. The latter "provides in convenient reference form the more generally applicable and accepted methods of conducting and reporting tests of a commercial nature, which apply to the fulfillment of performance guarantees and to acceptance tests." This code serves a very useful purpose, permitting manufacturer and purchaser to agree on methods of conducting tests, and avoiding the necessity of specifying in detail how performance guarantees may be determined. It is the purpose of this paper to discuss:

1. The application of the Test Code for Synchronous Machines to field testing of hydroelectric generators, noting especially which methods given in the code can be used, and why alternative methods are unsuitable.

2. Certain aspects of field testing of hydraulic prime movers.

3. The frequent necessity for making electrical measurements on the generator when the primary test is on its associated turbine, and the method of measurement and accuracy required.

It is not the purpose of the paper to record methods of making either electrical or hydraulic tests where the technique is routine and straightforward, and presents no difficulties other than those usually present when tests are made on any generator or its prime mover.

Paper 46-70, recommended by the AIEE committee on power generation for presentation at the AIEE winter convention, technical meeting, New York, N. Y., January 21–25, 1946. Manuscript submitted November 26, 1945; made available for printing December 13, 1945.

G. D. Floyd is electrical consultant, electrical engineering department, Hydro-Electric Power Commission of Ontario, Toronto, Ontario, Canada; J. J. Traill is with the same company.

Electrical Tests

General

In the great majority of cases, hydroelectric generators are erected on the site. The stator iron and complete stator winding in the larger units are often assembled in the field, and field poles mounted on the rotor spider or rim. Even when the above operations can be performed in the factory the assembly of the unit is of necessity a field job, and any tests on the completed generator must be performed at the site, after erection is completed. This situation produces the first peculiarity in testing under field conditions, in that the facilities for testing may be, and usually are, restricted greatly, compared to those usually available in the factory. Restrictions may be imposed by units already in routine operation in the plant, by construction, and because the generator is permanently connected to its bus, and in fact, may have been in commercial operation before certain of its acceptance tests are made. The site may be many miles from the factory, and from the utility's laboratory. It is, therefore, essential, before proceeding to the site to make the required tests, that the specification be carefully examined, the tests to be made listed, and the methods of making them discussed. It is of the utmost importance to list all portable instruments likely to be required, of such ranges as will accommodate the potential and current transformers associated with the generator. It is very seldom necessary to provide special potential or current transformers for routine acceptance tests. Where tests of a special nature are included, it may be necessary to devise special equipment to obtain the desired measurements. All this work should be done, if possible, before the tests are started; otherwise a great deal of time may be lost, or one or more tests may have to be abandoned for lack of the proper equipment for making them.

Resistance Measurements*

Hydroelectric generators, except for units of low kilovolt-ampere rating, have very low armature and field winding resistances. Special artifices are often necessary to obtain an accurate measurement of resistance. The voltammeter method is usually employed, as use of the Kelvin bridge is not practicable for field measurements. Battery voltage and low range voltmeter have been found to be satisfactory, with the usual precautions. If the armature winding is two, three, or four circuit, as is frequently the case, each circuit can be measured separately, or all windings in one phase may be connected in series and the voltage drop across each measured. Temperature detectors almost always are specified for the hydroelectric generator, and are used to measure the winding temperature. Care must be taken to have the generator in thermal equilibrium at the time resistance measurements are made. The test current must not be so great that the winding temperature is affected by the copper loss due to the current.

The field resistance at a known temperature is required for the following reasons:

1. To determine accurately the field I^2R loss.

2. To determine the temperature rise of the field.

3. To calibrate the field temperature indicator if such is provided.

The voltammeter method should be used to make this measurement, as the "hot" resistance, of necessity, must be determined by this method. The measurement of temperature of a winding by its change in resistance requires that every source of error be minimized. The cold and hot resistances should be measured with the same instruments, and with deflections on the instruments of the same order of magnitude.

Telephone Interference Factor

Although hydroelectric generators of modern design have a telephone interference factor low enough to prevent disturbance in telephone circuits, it is possible that disturbing harmonics inadvertently may be present in the voltage wave. Conditions at some remote point, where a power and communication circuit are in-

* The sequence of these notes has been made generally the same as in the Test Code for Synchronous Machines.

volved in a parallel may be magnified by the presence of these harmonics. Measurement of the telephone interference factor is recommended where equipment is available to determine this factor, especially if the design of the generator winding is limited in freedom of choice to the point where it becomes difficult to eliminate undesirable harmonics.

Phase Characteristic Curves (V Curves)

These curves offer the best method of determining the excitation values at all loads and power factors. As discussed later under load excitation, the zero power factor saturation curve used with the open circuit saturation curve to obtain the excitation characteristics is always difficult and often impossible to obtain. It is not usually possible to set the voltage, load, and power factor at exactly the value desired when the unit is operating on the system. Small deviations from the desired values, especially in power factor, cause relatively large changes in field current. The phase characteristic curve permits greater accuracy in the determination of excitation under any condition of load, provided the voltage can be held close to normal value.

Line Charging Capacity

This characteristic may be important in the case of hydroelectric generators because the units are usually associated with a transmission network of high-voltage lines. Voltage must be built up on a line for line testing, and the generator should have sufficient line charging capacity to permit this without becoming self-exciting. Self-excitation is an unstable condition, leading to high and uncontrolled voltage on the generator and system being tested. Excitation can be reduced to zero on a hydroelectric generator with safety, and even made slightly negative, with the generator under test connected to the system. Provided the kilovars taken by the generator are not large enough to disturb system conditions, the ability of the generator to supply line charging kilovars thus can be determined exactly.

Load Excitation

It is frequently difficult or impossible to obtain a saturation curve at zero power factor and rated amperes on a hydroelectric generator. The difficulty arises because it is impossible to circulate full load current between one generator and another of equal size, even if both can be synchronized on the same low-voltage bus. It is sometimes possible to synchronize the generator with the system, and obtain one or perhaps two points on the curve at or near normal voltage. A third point is available at zero voltage from the short-circuit impedance curve. Such meager data are insufficient to plot an accurate zero-power-factor saturation curve.

As stated earlier in this paper, the use of the phase characteristic or *V* curves, which can be determined readily, is recommended.

Sudden Short-Circuit Tests and Synchronous Machine Quantities

The 3-phase sudden short-circuit test at rated voltage should not be omitted on a large machine of new design, as mechanical failures due to inadequate bracing of the stator winding are known to occur. If oscillograms are taken, the transient and subtransient reactances and their time constants can be determined. The determination of these reactances and time constants by test gives valuable information to both designer and user.

Very little information is available on the suitability of the test methods for determining other synchronous machine quantities. Those that have been tried in the field have given only fair results. There is need for an exchange of information among those interested covering the technique to be used. The instructions in the test code appear to be insufficient, and need to be proved in the field. Such tests are in a comparatively new field in testing of hydroelectric generators, although the value of a knowledge of these quantities in estimating the performance of a generator has been appreciated.

Losses

Several methods for measuring generator losses are listed in the Test Code (page 13 and those that follow). Only the retardation method has been found uniformly successful for hydroelectric units. The separate driving motor, calorimeter, cooler method, and input-output method are either impractical or require special facilities and time for execution. The electrical input method has been used, not because it was satisfactory, but because the retardation method had not been developed to the present degree of accuracy. This method requires special low-ratio current transformers, which are often difficult to mount in the leads from the generator, especially if these leads are of cable, brought out to a metal-clad bus structure. It is impossible to prevent hunting between driving and driven units, and great care is necessary to obtain a consistent set of readings. Harmonics are usually present in the current wave, and may increase the error already present from other causes. There is great danger of the units falling out of step if the voltage is lowered to a point where synchronizing power is insufficient. If this condition should develop, a heavy overload is placed on the metering current transformers, and these may burn out before they can be protected by closing their short-circuiting disconnects. The measurement of stray loss by this method is involved, and the accuracy doubtful. One major source of error arises in the use of high-ratio current transformers and low-power-factor current, giving current transformer errors and errors due to small deflections on the wattmeter used. The latter error may be decreased by using a low-power-factor wattmeter. The use of the electrical input method, at least for medium or large units, is not recommended, unless no other method can be used.

The retardation method depends for its accuracy on careful determination of the Wk^2 of the generator, and of the speed-time curve, both of which are essential for the calculation of the loss under any given condition.

A very close approximation of Wk^2 of the generator can be made for the rotor of a water-wheel generator. The weight of each salient pole is known accurately,

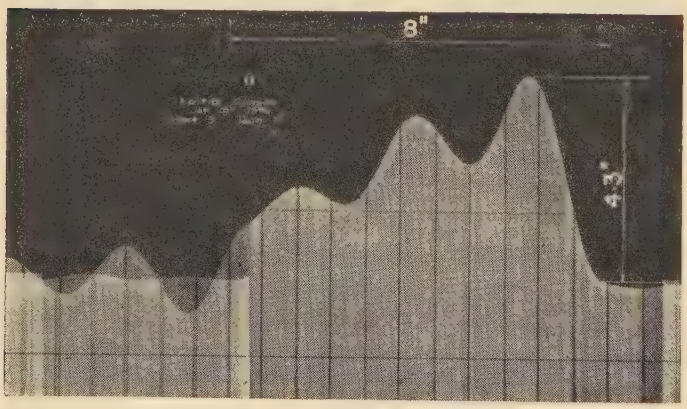

Figure 1. Gibson diagram from differential test of 66,000-horsepower unit

and the weight of the rim is also capable of accurate calculation from drawings. These calculations can be checked by test, using one or more of the methods outlined in the test code.

Use of the d-c generator separately excited, with biased output voltage (see test code, pages 18–19) has proved most successful for measurement of speed. The measurement must be made carefully, and frequent checks made during the progress of the test to prove the constancy of the calibration. This method of speed measurement is given in detail in the test code, and need not be repeated here.

The calorimeter method of determining losses[3] is applicable only to totally enclosed hydroelectric generators. Unless the temperature of the ambient air can be closely controlled, as in the case of the totally enclosed generator, it is extremely difficult to relate the temperature rise of the air to the loss or losses causing it, due to the thermal capacity of the generator. The increase in number of this type of generating unit permits use of this alternative method of loss measurement. Its chief disadvantage is the time required for a complete set of tests. A crosscheck can be obtained on the total losses, by operating the generator at rated load and measuring the temperature rise of the cooling air. The individual losses also can be measured, and windage separated from friction loss.

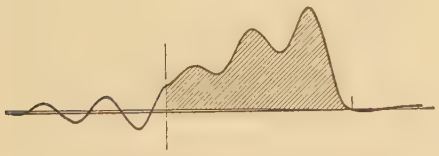

Figure 2. Delineation of area on Gibson diagram measuring impulse

Actual length of hatched area 7.75 inches or 10.6 seconds

Maximum height 4.4 inches, equivalent to 4.80 feet of water

Average height equivalent to 2.65 feet of water

The segregated generator losses are used to establish the generator efficiency, and also are used to determine generator input on the acceptance test of the prime mover. Their use in this latter respect is discussed in some detail later in this paper.

Hydraulic Tests

This section of the paper deals chiefly with the acceptance tests of the prime mover and the rating test of the hydroelectric generating unit. The acceptance test is that having as its objective the determination of whether or not the unit and its component parts satisfy the guarantees of capacity, efficiency, and reliability made by the manufacturers. The rating test determines the efficiency of the unit as a whole, and the variation in efficiency, in order that the most effective use may be made of it along with other units in the same power plant and with other plants in the same system.

The acceptance test of necessity considers the component parts of the unit separately, that is to say the generator and turbine independently of each other. The discussion will not extend to other parts such as the governing system, and water passages except incidentally. The rating test on the other hand considers the unit as a whole including not only the turbine and generator but conduits and other water passages serving that unit and no other.

For tests of both kinds, three primary quantities must be measured, namely, the power, the flow, and the head. The flow is the same whether one is considering the acceptance or the rating test, but power and head are not. In the acceptance test of the turbine the output power is the same as the input to the generator shaft and therefore includes the generator output and all generator losses while in the rating test the power is the net output of the generator. The head in the acceptance test is determined from measurements made as close to the turbine as practicable. In the rating test the head considered is the difference of elevation of forebay or headpond and tailwater.

Accuracy

At this point the authors would like to comment on certain features of the precision required in test equipment and observations. Insofar as the acceptance test is concerned, test codes of various associations and technical societies define in greater or less detail the method in which various quantities shall be measured and the acceptable degree of precision. No such criteria exist, however, to govern accuracy in rating tests. The responsibility of securing the results required at a cost no greater than is warranted by their value rests with the engineer in charge of the tests. It is the authors' considered opinion that as great accuracy is necessary in the rating tests as in the acceptance test where the representative of the manufacturer carefully scans the details of all arrangements for the test and all observations in order that the final result for efficiency may not fall so much as a tenth of one per cent below the maximum that can be shown honestly.

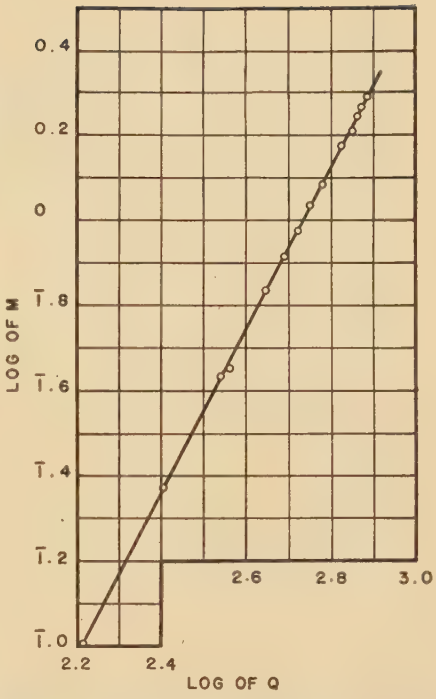

Figure 3. Relation of discharge to pressure differential between piezometers in penstock and scroll case of turbine

M = differential pressure, feet of mercury
Q = discharge, cubic feet per second

Because of their ready availability, there is a tendency to substitute switchboard meters, gauges, or instruments of low grade for test instruments of high precision and accuracy, and to use observers unskilled in tests and investigations of this type. In consequence of this, unreliable or misleading results may be secured and incorrect conclusions reached. The authors call to mind certain specific incidents that justify this criticism.

The acceptance test of the turbine and the rating test of the unit frequently are made at the same time. It is convenient therefore to give a single description of measurements and procedure applying to both. This description will be divided into three parts, each part dealing with one of the three primary quantities to be measured.

Measurement of Power

For the rating test the quantity to be measured is the output of the generator. The authors have been associated in many tests and have used instruments of various types. In general the instrument preferred is a calibrated polyphase wattmeter. Exception may be taken to this instrument and in fact many test codes require that single-phase meters be used. The objection to the use of the polyphase

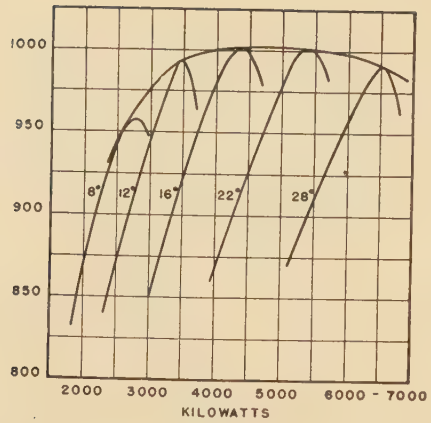

Figure 4. Power efficiency relation from an index test

The variation of efficiency with load and blade angle is found although the absolute value of the efficiency is not known

meter is based in some instances on the type of generator connection and grounding. The objection does not apply in the case of the plants operated by the organization with which the writers are connected and the advantages of using a single instrument are so evident that it is to be preferred wherever it is properly applicable.

In the acceptance test of the turbine, its power output is required. Where the turbine and generator are mounted on the same shaft, the turbine output is the generator output plus the generator losses. The accuracy required makes the method of dividing the generator output by generator efficiency unsatisfactory, although the authors have found it necessary on occasion to do this, on generating units of small size, where insufficient data were available to enable generator losses to be computed.

If generator losses have been measured on the unit under test, readings of generator voltage, stator current and temperature, field current, and exciter outputs, on each test run, will permit an accurate computation of individual losses. These can be added to the measured generator output. The precision of measurement of the losses is very high, compared to the measurement of generator output, so that it is possible to use losses as measured on a duplicate generator, or even to use the generator designer's estimate of losses, without introducing an error large enough to have any noticeable effect on the overall result.

Calibrated portable instruments of high standard should be used for the electrical measurements. The instrument transformers associated with them should have a known ratio of transformation. Otherwise they should be calibrated. In at least one instance a calibration of the instrument transformers requested by the representative of the turbine manufacturer disclosed errors that were quite unsuspected until the calibration had been made.

The importance of this test on occasion may justify duplicate measurement of power by independent observers, using separate instrument transformers and wattmeters calibrated against different laboratory standards.

Measurement of Flow

The accurate measurement of the quantity of water flowing through the turbine is one of great difficulty. Various methods of measurement are available, the choice of method depending on the particular situation in hand. Four of these methods will be described briefly. Complete descriptions of all of these considered herein are available elsewhere; hence descriptions are carried only so far as to make clear the comments on their fields of application and reliability.

The Gibson Method[4]

The Gibson time-pressure method of measurement of flow is an invention of Doctor Norman R. Gibson, and an outcome of his extensive studies of pressure-rise in hydraulic pipe lines. The method, simple in principle and fundamentally sound, is an application of the second law of motion, expressed briefly as

$$Pt = m(v_1 - v_2)$$

When a column of water flowing in the penstock of a hydroelectric unit is brought to rest by closing the turbine gates, a force is impressed on the water column in bringing it to rest. Assuming that the mass of water has its velocity changed to zero during gate closure, the change in momentum effected is the product of the mass of the water in the penstock and the original velocity. This change in momentum is equal to the impulse causing it, that is to say, the mean value of the force acting upon it to bring it to rest multiplied by the time during which it acts. Of these four quantities, force, time, mass and velocity, three can be measured and the fourth, the velocity, computed, it being the only unknown in the equation.

Equipment was devised by Gibson to measure the force or pressure acting on the water column by a mercury U-tube, and to record the pressure variations on a moving film. The equipment, with minor changes, has been used by nearly all, if not all, investigators on this continent. German scientists working mainly with Doctor D. Thoma at Munich built instruments in which pressure changes deflected a mirror through the movement of a spring-controlled piston. A beam of light of high intensity focused in the mirror is reflected through lenses to a photographic paper moving past a narrow slot. Comments on both of these types of equipment will be made later.

The Gibson instrument consists of a camera at the front of which one leg of a mercury U-tube is clamped at a definite distance from the lens. The U-tube is connected to the penstock, and the level of the mercury in it is a measure of the pressure in the penstock. At the rear of the camera is a photographic film on a cylinder which is rotated at a speed suited to the rate of closure of the turbine gate. Between the U-tube and the lens, a pendulum is arranged to cut off the light passing through the U-tube once every second. Illumination for exposure of the film is provided by a bank of photoflood lamps. The instrument is so constructed that no light can reach the film except that passing through the U-tube. As the pressure varies in the penstock corresponding movements take place in the mercury column in the U-tube and these movements are recorded on the film at the rear of the camera.

The procedure, in making a measurement of flow in a penstock, is as follows: The unit under test is loaded to the point at which it is desired to measure the discharge and sufficient time allowed for operating conditions to become satisfactorily steady. On signal from the operator at the Gibson instrument, the turbine gates are closed at a uniform, predetermined rate, during which time, and for a few seconds before and after, the moving film in the camera is exposed recording the rise and fall of the mercury column in the U-tube, and therefore the changes in pressure. From an analysis of the exposed film an area is delineated which measures the impulse bringing the mass of water in the penstock to rest. The measurements are repeated for a series of similar runs covering the whole range of capacity and flow for the turbine.

Originally it was the practice to have a connection to the penstock from one leg only of the U-tube, the other leg being carried to a sufficient height to balance the penstock pressure. The mercury column was often of great height, 20 feet or more in some tests conducted by the authors, which introduced certain difficulties in conducting the tests. It made it necessary also to secure, in synchronism with the Gibson diagram, a graphic record of the variations in headwater level.

It is the practice now, whenever possible, to connect both legs of the U-tube to the penstock at sections so far apart as to secure a diagram of satisfactory area on the film. The test made with a single connection is known as a simple test, that with two connections to the penstock as a differential test.

In Figure 1, a diagram from a differential test is submitted. The dimensions of the original are marked on the figure to give a better idea of the scale. In Figure 2 is shown a copy of this diagram with the area representing the product of pressure and time crosshatched. It is not intended to discuss here the method of determining the lower and left hand limits of the area, but this explanation should be made:

The regular waves following the end of the diagram result from the fact that the mercury column swings up and down in the tube until friction brings it to rest at its final static level. They are not due to pressure variations in the penstock. These after waves enable the end point of the diagram to be determined in most cases. The author has found it necessary for tests of plants with very short supply pipes to have a contact, closed by the servomotor piston at the end of its stroke, complete a circuit which gives an indication in the film of the completion of closure of the turbine gates.

The instruments made by Volkhardt and Deckel and used at Munich, Eitting, and Heidenheim, are much more complicated than the instrument by Gibson. One of the advantages sought in their design is the elimination of effects due to the inertia of the mercury column. This inertia, however, has certain compensating advantages, Thoma points out, enabling a more precise determination of the end point of the diagram, in certain instances, than the instruments with spring controlled pistons. Special provision is made to overcome the effect of friction. Calibration is difficult and liable to change. However, they are instruments of great precision.

Deckel submitted the results of tests by his instrument made at Munich in 1930 in which the average difference from the measurement by a calibrated weir was 0.41 per cent, only 2 runs out of 14 showing errors exceeding one per cent. Deckel's comments on the method are interesting in that other methods of measurement have found greater favor generally in the institution in which his work was done:

"The Gibson measurement process in many cases offers considerable advantages as compared with other measurement methods. These advantages are based on the practical simplicity and good theoretic foundation for the process. It must be provided, of course, that its grade of accuracy is not below that of other processes, that is, the possible error should not exceed one per cent when compared with the highly developed stage of present measuring processes . . . The tests which were carried out will confirm this."

Allen Salt-Velocity Method[5]

Professor C. M. Allen of Worcester, Mass., has, by his research, brought to a high degree of precision the measurement of flow by observations of the time for a charge of brine to pass from one section to another in a penstock. In this method the charge of brine is injected through one or more special valves suitably disposed on the cross section of the penstock and the time for it to move from the point of injection to a cross section further downstream is measured. At the lower cross section a series of electrodes is set up in the penstock and the time of passage from the point of injection to the electrodes is determined by a graphic measurement of the change in conductivity of the water, the time being accurately measured on the chart as well as conductivity. The method is adaptable to situations where the cross-sectional area of the penstock is irregular or where velocities are extremely low and other cases where the Gibson method is not readily applicable. Its disadvantages are that the disposal of the injection valves and the electrodes on the cross sections require considerable experience with this type of test. A more or less prolonged shutdown of the unit is necessary also to install the equipment.

The necessity for experience in the design of the equipment and its disposal on the cross section will be realized when it is remembered that the charge of salt coming through a valve at the center of the penstock moves downstream at a greater velocity than a charge injected at the side of the penstock. It is therefore necessary to design the equipment so that the average time of passage from one cross section to the other will be recorded correctly. The authors have attempted to use the method on one occasion and from the difficulties experienced in securing satisfactory results in that instance have some appreciation of the vast amount of effort that has been put into the perfection of the method by Professor Allen.

The Current Meter[6]

The third method to which reference will be made and one that has been used perhaps more frequently than any other, is the current meter method. The method has been brought to a high degree of accuracy for measurement of discharge of power houses through the work of a large number of investigators in North America commencing with the work of Groat and Nagler in 1912. The method has been preferred above all others for measurements in Europe and a great deal of work on the development of suitable instruments has been carried out there.

The method is simple enough in principle. It consists of the measurement of velocity at a large number of points on a cross section at the intake of the unit and the computations of the discharge by multiplying the average measured velocity by the area of the cross section. The necessity for refinement comes about because the velocities at any section are not at right angles to the cross section. In areas of disturbed flow certain meters have a tendency to over-register, that is to say, they measure a velocity greater than the resolved part of the velocity normal to the measured cross section. Other meters under-register, some to a greater degree than others. By using groups of meters of different types in a test and comparing the results, each with the other, the correct normal velocity may be determined.

The method is readily adaptable to cases where a very short supply pipe leads to the turbine, therefore making it difficult to apply the Gibson or Allen methods. As just indicated the common European practice applies the current meter method in nearly all instances, in fact it has been used frequently in Europe to measure the velocity on the cross section of a penstock

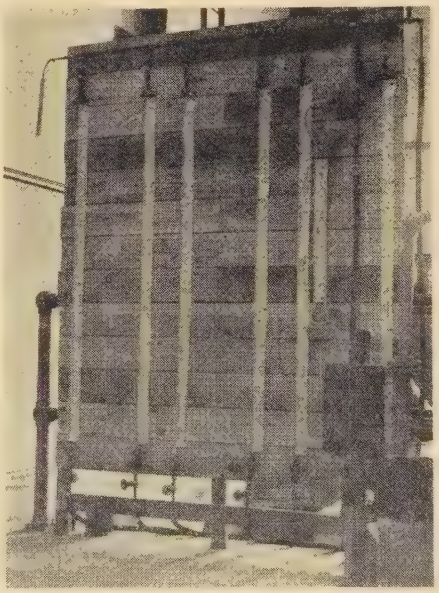

Figure 5. Bank of gauges used for index test

These are simple water columns under compressed air to depress them to the range of the scales

where in North America one of the other methods would be applied.

The Weir

In some instances it is possible to install a weir in the tailrace of the plant. Measurement of discharge by a weir is only possible in cases where the discharge is moderate, that is to say, not more than two or three hundred cubic feet per second and where the reduction in head resulting from the installation of the weir is only a small percentage of the total head.

Measurement of Head

The third of the primary quantities to be measured is the head acting on the turbine or on the plant. There is, of course, a distinction between these, sometimes of considerable magnitude, for example, in the case of a plant having a long penstock. For low-head plants the difference is not so marked. For the purpose of tests, the simpler the equipment, the more satisfactory it is for measurement of water level. In the forebay or tailrace of a plant, simple float gauges are preferred installed in float boxes connecting with the body of water, the surface elevation of which is to be measured, by a small opening in the float box which dampens surges. The usual practice in the rating test of a generating unit is to install at least two of these in the forebay and two in the tailrace, usually in the stop log checks.

In the acceptance test of the turbine unit, however, the head must be measured at the entrance to the turbine casing, and in a plant having a long penstock the head measured at this point will be appreciably different from that measured in the forebay. Bourdon gauges are unsatisfactory for this purpose and a mercury manometer is preferable even though this may be of great height, requiring two observers to read it. A case in point is a plant on which a test was made recently where the operating head was 340 feet and the mercury manometer about 24 feet in height.

In the case of the acceptance test, as indicated previously, the pressure head is measured at the entrance to the turbine casing. To the pressure head, plus elevation head at that point, there must be added the velocity head in the penstock. The net head acting on the turbine is the head at entrance to the casing, expressed as an elevation, minus the sum of tailwater elevation and the velocity head at the section at which the tailwater level is measured. In some instances, however, the velocity head in the tailrace is neglected. In the case of the rating tests of the plant the gross head only is to be considered, that is to say, the difference of level in the water in the forebay and in the tailrace.

Frequently gauges measuring these water levels are installed to give an indication in the control room of the levels, and it is most desirable to check these gauges during the tests, not only for correctness in their indications, but also for the correctness of indication by them of the true forebay or tailrace level. The location of the actuating element of the gauge is frequently such that it is affected by local disturbances and by variation in load on the particular unit near which it is installed. It is the authors' practice to observe the operations of such gauges carefully during the test in addition to making observations on special gauges installed for the test itself.

In addition to the primary measurements dealt with in the three preceding sections, a number of other quantities are observed such as gate opening of the turbine and information that will enable segregation of the hydraulic losses in the water conduits to be made.

Analysis of Data

Having computed the three primary quantities, power, head, and discharge, for each run, these are tabulated and corrected for departure of the test head from the rated head of the unit. In the case of the acceptance test, capacity and efficiency of the turbine will be given by the turbine builder for some specific head. In the tests the actual head will differ from this slightly, and power and discharge for each of the runs will be corrected to that which would have been realized had the test been made at rated head. This correction can be made without impairing the accuracy of the results provided that the test head does not differ by more than three or four per cent from the rated head. The results are then plotted in the form of a power-discharge curve. Two additional curves are plotted also, namely, the power on a base of gate opening, and discharge on a base of gate opening. The three curves are then compared and adjusted until all three are in agreement. From this point on practically all of the results secured regarding capacity and efficiency will be based on the three curves, particularly the power-discharge curve. It is customary to compute the efficiency of the unit from the adjusted power-discharge curve and not from the individual test runs.

A similar set of three curves will also be drawn based on the gross head of the plant and the generator output, these forming the basis of a report on the rating test of the plant.

Rating Discharge Against Differential Pressures

It will be appreciated from the description of the various methods of measuring the quantity of water flowing that this part of the test is difficult and expensive and may involve serious interruptions to operation of the unit. It is desirable therefore to secure records that can later be used to measure the discharge with less inconvenience and expense. The author used such a method some 23 years ago at the Queenston plant on the Niagara River by observing the reduction in head from forebay to a point at the entrance to the casing of the turbine, using a mercury manometer for the purpose. The reduction in pressure head was largely due to the great increase in velocity head at the lower measuring point and was a function of the magnitude of the flow of water in the penstock. The ratings so made in the original tests by the Gibson method were later used in tests which involved simply a measurement of the difference in the pressure head at forebay and scroll case, to determine the flow. It is common practice now to install piezometer connections at suitable points in the penstock and scroll case and to determine, at the time of the original tests when the flow is measured by one of the methods described above, the relation of the discharge to the differential pressure between two of these piezometers.

The results of such a measurement in a turbine test made recently are as shown in Figure 3. The flow was measured by the Gibson method and the differential pressure was read on a differential manometer connected to a piezometer in the speed ring and a ring of four piezometers around the downstream end of the penstock. It is only necessary at any future time to measure the differential pressure to determine discharge from the data submitted in the graph. The relation is unaffected by head, the condition of the turbine runner or other changes beyond the piezometers.

Index Tests

When, for physical or economic reasons, it is unadvisable to make discharge measurements, it is still possible in many instances to secure records of variation of efficiency of a turbine unit by measuring quantities, the variation of which with the discharge is known, approximately, if not exactly. Tests in which such quantity is measured instead of the discharge are known as index tests. From them, the power and head being measured, it is possible to derive efficiency curves which show the variation of efficiency with load but not the absolute value of the efficiency.

To illustrate: In order that the governing mechanism of a Kaplan turbine may be so designed as to secure the highest efficiency at all loads, information must be available as to the variation of efficiency with gate opening, or load, and blade angle. The quantity related to the discharge, which is measured is a pressure differential between two piezometers suitably disposed. The discharge varies approximately with the square root of the differential pressure and the efficiency therefore with the kilowatts divided by the square root of the differential pressure. In Figure 4 such a series of curves derived from a test of a Kaplan runner is shown, each curve being for a specific blade angle.

The envelope of these curves provides the information for the design of the cam which properly correlates gate opening and blade angle. Forty or more separate measurements of discharge would be required to develop the five efficiency curves shown in Figure 4. The gauge, or series of gauges set up for the test, is shown in Figure 5. Readings in this case were taken on water columns depressed by compressed air to a reading range. The various gauge columns are connected to piezometers in penstock and scroll case.

Conclusion

In conclusion, it may be stated that a definite policy of making tests on both generator and prime mover, even if considerable expense and effort is involved, undoubtedly will pay dividends. These tests make quantitative data available, the value of which may not be apparent at the time the tests were made. However, it later may make possible an engineering solution to some difficult problem of operation, or point the way to improvement in performance in the unit tested, or succeeding ones in the same or other stations.

References

1. Test Code for Hydraulic Prime Movers. American Society of Mechanical Engineers, June 1938.

2. AIEE Test Code for Synchronous Machines. Number 503, June 1945.

3. Calorimeter Measurement of Stray Load Losses of 55,000-Kva Generator Having Enclosed System of Ventilation, **G. D. Floyd, J. R. Dunbar.** AIEE Transactions, volume 51, 1932, pages 12–18.

4. The Gibson Method and Apparatus for Measuring the Flow of Water in Closed Conduits, **Norman R. Gibson.** American Society of Mechanical Engineers *Transactions*, volume 45, 1923, page 343.

5. The Salt Velocity of Water Measurement, **Charles M. Allen, Edwin A. Taylor.** American Society of Mechanical Engineers *Transactions*, volume 45, 1923, page 285.

6. Water Gauging for Low Head Units of High Capacity, **J. M. Mousson.** American Society of Mechanical Engineers *Transactions*, volume 57, 1935, page 303.

Dielectric Recovery by an A-C Arc in an Air Blast

T. E. BROWNE, JR.
MEMBER AIEE

SINCE the extinction of the arc drawn upon opening an a-c switch depends upon a rapid transition of the arc near a normal current zero from a conducting to an insulating state, much study has been given by switch designers to this transition, often referred to as dielectric recovery. However, the published experimental data with regard to the mechanism of this dielectric recovery still are meager and there is no generally agreed upon theory, even for the simpler cases. One simple case, of growing importance in this country, is that of the arc in an air-blast circuit breaker. Perhaps the simplest arrangement is found in the nozzle type of air-blast breaker variously described as radial blast or axial blast. Figure 1 is illustrative of such nozzles, somewhat reduced from practical forms.

Of particular value for the understanding of the arc extinction processes are curves showing the rise of the arcs reignition voltage, or dielectric strength, with time during the first few hundred microseconds following arc failure near a normal current zero. There have been several attempts to predict the course of such curves for the air-blast breaker, of which that by Kesselring and Koppelmann[1] is noteworthy for its completeness. Some direct experimental results defining a single curve and indicating another have been presented by Prince, Henley, and Rankin[2] for a cross-blast or splitter type of breaker at greatly reduced air pressure and unstated current. Also presented by Prince were some very interesting high-speed moving pictures of the arc in a splitter type breaker, but these, like earlier ones presented by Biermanns[3] for the nozzle type breaker, are somewhat inconclusive. These photographs and the theoretical picture of arc interruption in an air blast have been further discussed by Slepian.[4] In the theory of Kesselring and Koppelmann and others a physical cutting and progressive displacement of the permanent arc core is presumed. Slepian, in agreement with earlier discussions by Mayr,[5] has preferred to ascribe the dielectric recovery of the arc space to cooling and ion diffusion, and has pointed out the decisive importance of turbulence of the gas motion in enhancing the diffusive effects.

In the course of an extended experimental study by the writer of the factors influencing arc extinction in models of air-blast orifices like those of Figure 1, a considerable mass of data has been obtained, including 16 more or less complete curves of dielectric recovery with time by the arc space under widely varying conditions. Some of these results will be presented and briefly discussed in the light of existing theories.

Experiments

The nozzle and contact arrangement shown in section in Figure 1A is typical of the earlier forms studied. This sketch shows the location of arc resisting inserts of copper-tungsten and soapstone as generally used, these being omitted in the other sketches for simplicity. In all of the work to be described the orifice diameter was 0.765 inch and the arc was drawn by rapid downward motion of the lower (upstream) contact through the orifice to the open position shown. Compressed air from a storage tank was introduced into the annular space between the supporting fiber plates through a poppet valve, piping, and entrance orifices which reduced the steady-state gauge pressure at the interrupting orifice entrance to between 0.7 and 0.8 of the initially adjusted tank pressure. Beyond the arc space the discharged air passed through openings having $3^1/_3$ times the area of the main orifice, resulting in a pressure elevation on the discharge side of the orifice roughly 1/10 the entrance-side gauge pressure without arcing and up to two or three times this in the presence of a one or two thousand-ampere arc.

Of all the orifice arrangements tried, that of Figure 1B proved to be the most efficient in terms of required air pressure for interruption of low power factor currents up to 2,200 amperes at 13,800 volts

Paper 46-21, recommended by the AIEE committee on protective devices for presentation at the AIEE winter convention, New York, N. Y., January 21–25, 1946. Manuscript submitted November 9, 1945; made available for printing December 13, 1945.

T. E. Browne, Jr., is research engineer in the high-voltage laboratory, Westinghouse Electric Corporation, Trafford, Pa.

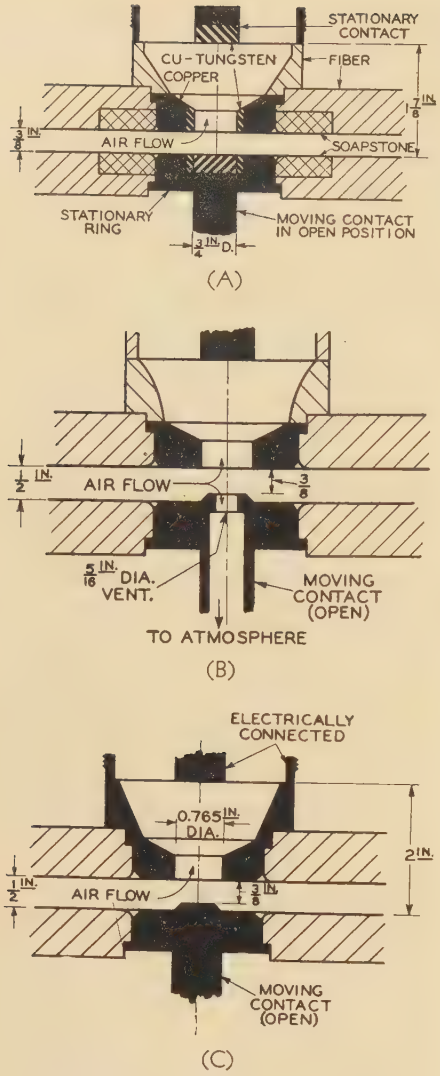

Figure 1. Experimental air-blast orifices

and 4,200 amperes at 6,900 volts, the maximum values available for these tests. Interrupting test results with this orifice are plotted in Figure 2A. The upper broken line is drawn through points representing tests at the maximum gauge pressure in the tank at which a failure to interrupt occurred and the lower line through points of minimum gauge pressure in the tank for a successful interruption. Interruptions were considered successful if not more than one cycle of arcing (at 60 cycles per second) occurred after passage of the electrode tip through the orifice. These limits were always checked by obtaining at least four tests just outside the limits all of which were either successful or unsuccessful. Thus, the region between the lines is one of uncertainty separating regions of high and of low probability of interruption. Figure 2B is a similar plot for the orifice of Figure 1C, which was a much less efficient interrupter, especially at the lower currents. The favorable features combined in the Figure 1B orifice were indicated step by step in a long series of tests leading up to it. They are principally:

1. Rounding of the edges of the orifice and contact rings to minimize electric stress concentration.
2. Proper spacing of the contacts relative to the orifice.
3. A slight crowning, or beveling of the upstream contact face.
4. Insulation of the metal orifice ring from the downstream contact.
5. Venting to atmosphere of the center of the upstream contact face through a smaller auxiliary orifice.

These features are in close correspondence with those of an orifice-type high-voltage compressed-air circuit interrupting element developed by Ludwig and Baker.[6] The orifice of Figure 1C, lacking only features 4 and 5 of the preceding list, was chosen for an extended study of dielectric recovery with time because its inferior performance permitted it to be tested adequately over a much wider range of pressures and currents than would have been possible with the Figure 1B orifice. Also, the Figure 1C orifice is itself of practical interest, since its simpler construction permits its use in simpler and more compact circuit breakers, especially those for the lower voltages.

Figure 3 shows some of the information leading up to the Figure 1B type of orifice. These data were replotted from families of curves like those of Figure 2, using points from the upper limit curves only. These maximum failure pressures are plotted in Figure 3A as a function of the spacing of the downstream contact, in this case a copper-tungsten tipped 1/4-inch rod, above the open position of the upstream contact face. For convenience in interpretation, the orifice and electrode sections are dotted in to the scale of the spacing co-ordinate with the plane of the upstream contact face at the origin. Smooth curves are drawn through the somewhat scattered points for each of the three currents, 175, 1,100, and 2,000 amperes, all of these tests being at 13,800 volts. It may be deduced from the slopes of these curves that the region near the flow constriction, or "vena contracta," is of most importance at all currents but was practically the only effective interrupting region at the higher currents. At 175 amperes, the axial region beyond the orifice was of lesser but still of considerable importance. Figure 3B is a similar plot of results of tests in which the projection into the orifice region of a 1/4-inch stud from the center of the upstream contact face was the varying parameter. These curves similarly show a more sharply restricted interrupting region for the higher currents. The minimum near 3/16-inch projection for the 175-ampere curve probably also points to the advantage of a somewhat pointed or crowned shape for the upstream contact face.

In all of the work just described the testing circuit was used without modification of its normal transient characteristics, the natural frequencies and decrements of the recovery voltage oscillation components varying with the particular circuit adjustments, particularly with the short-circuit current settings.

Figure 2. Interrupting pressure range as a function of current

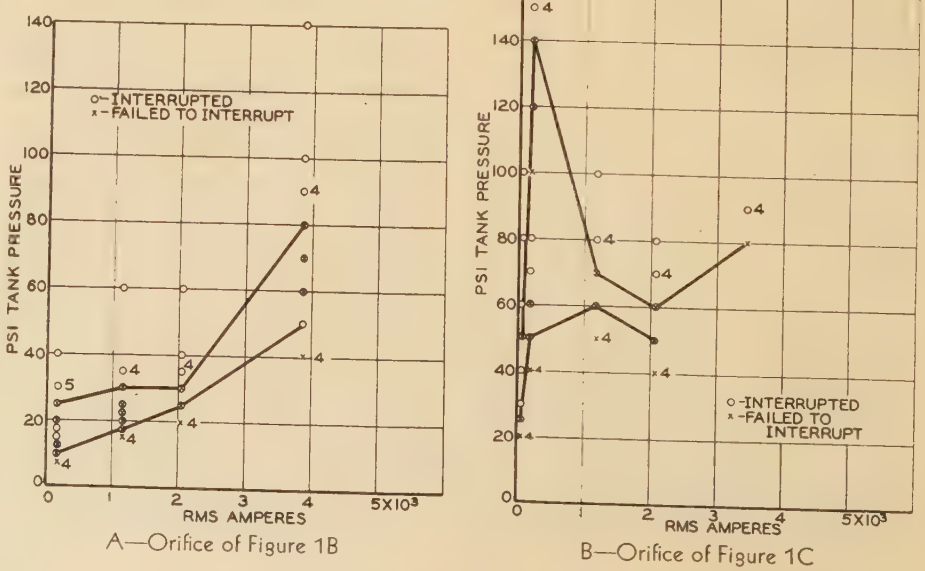

To get direct information about the course of the dielectric recovery in the arc space with time, the natural frequency of the circuit, or its rate of rise of voltage, was controlled by capacitor shunts in parallel with the arc, and the reignition voltages appearing across the arc terminals were measured from cathode-ray oscillograms. Figure 4 shows four samples of such oscillograms, taken by photographing the screen of an RCA 904 cathode-ray tube with a miniature camera. The beam was oscillated magnetically at power frequency with such phase and amplitude that it passed across the screen only during each recurrence of a small time interval embracing each current zero moment. At this time the rate of change of the deflecting magnetic field and so the speed of the beam was nearly constant. Voltage calibration was provided by superimposing the horizontal lines resulting from application of open circuit voltage (these being the positive and negative peaks of the voltage waves), and time calibration by further superimposing a small amplitude trace produced by a calibrated oscillator.

The oscillograms in Figure 4 of tests 12,417 and 12,440 show, successively, the effect on the reignition transients of a 175-ampere arc with 20 pounds per square inch air tank pressure of adding a small (0.035 microfarad) shunting capacitor. Wide variations in reignition voltage and time at successive current zeros are well illustrated by the three reignition traces in test 12,440. The smallest value (of negative polarity) probably occurred before the contacts were fully open. The oscillograms of tests 13,110 and 12,848 each show two arc reignition transients followed by an extinction transient, the currents interrupted being 1,070 amperes and 2,260 amperes, respectively. In test 13,110 the circuit, containing an air-core reactor, was unshunted and in test 12,848 a delaying shunt of 0.102-microfarad capacitance was added.

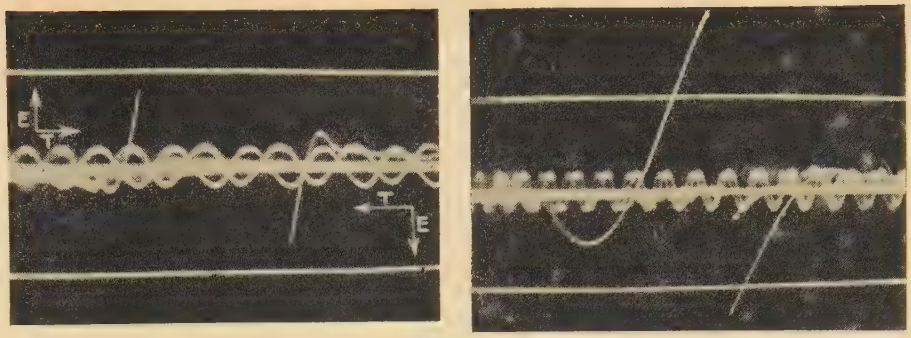

A—175 amperes at 13.8 kv, no shunt, 20 pounds per square inch in the tank, 20-kilocycle timing frequency

B—175 amperes at 13.8 kv, 0.035-microfarad shunt, 20 pounds per square inch in the tank, 20-kilocycle timing frequency

C—1,070 amperes at 13.8 kv, no shunt, 80 pounds per square inch in the tank, 20-kilocycle timing frequency

D—2,260 amperes at 9.2 kv, 0.102-microfarad shunt, 5 pounds per square inch in the tank, 33-kilocycle timing frequency

Figure 4. Cathode-ray oscillograms of arc reignition and extinction voltages

The results of a long series of such oscillographic measurements of tests with the Figure 1C type orifice were plotted and are shown in Figure 5. In addition to the reignition voltage points marked with open circles, in many cases the peaks of recovery voltage transients which did not cause reignition (extinction voltages) were also plotted and marked with solid circles. Where possible, envelopes were drawn enclosing the estimated regions of uncertainty within which most of the breakdowns occurred. Low breakdown points near or outside the envelopes, when indicated by adjacent question marks, were judged probably to indicate breakdowns at less than maximum contact separation. The dotted lines through the origin are lines of a theoretically calculated dielectric recovery to be explained later.

Figure 3. Effect of electrode position on maximum failure pressures at 13.8 kv and various currents for an orifice similar to that of Figure 1A

A—(left) Downstream electrode position varied

B—(right) Upstream electrode position varied

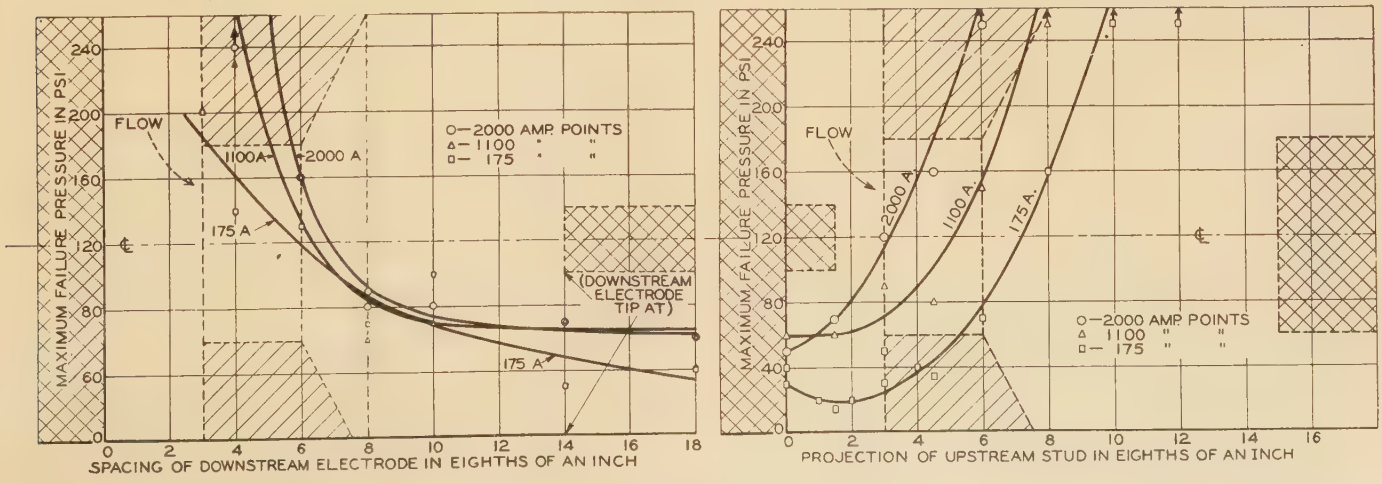

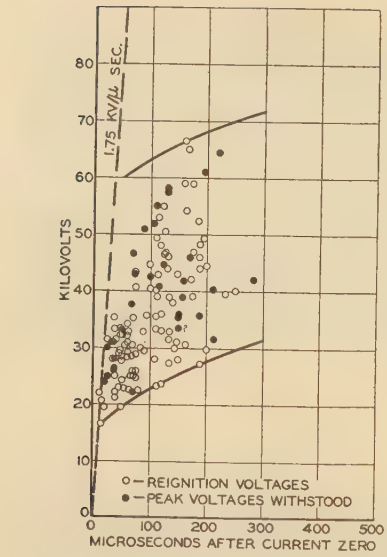

A—50 amperes at 40 pounds per square inch

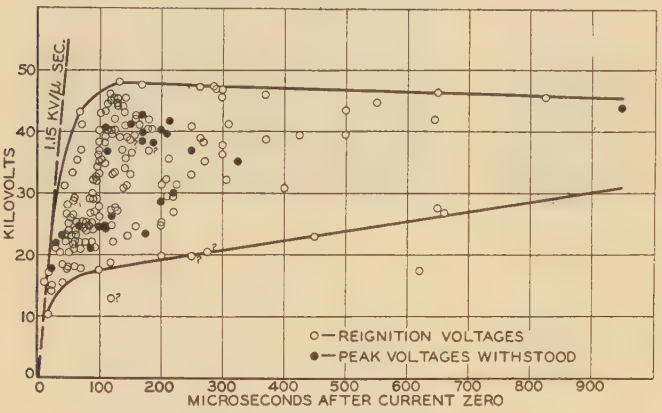

B—50 amperes at 20 pounds per square inch

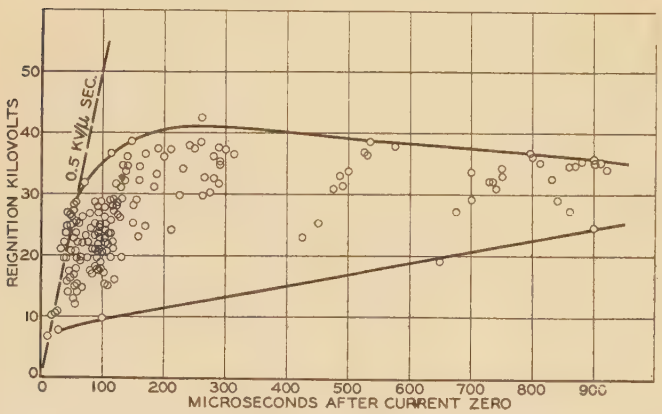

C—50 amperes at 5 pounds per square inch

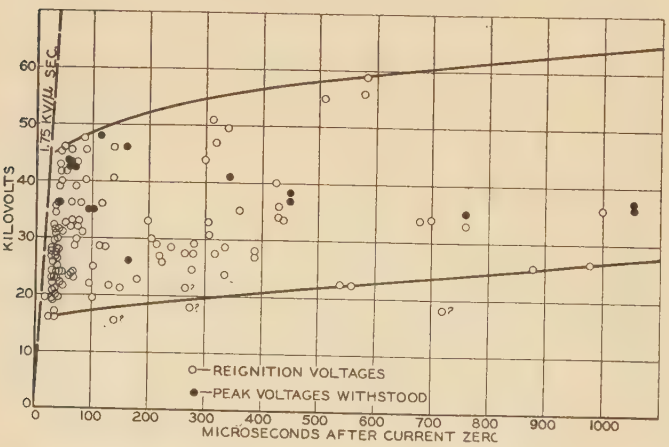

Orifice of Figure 1C

D—175 amperes at 40 pounds per square inch

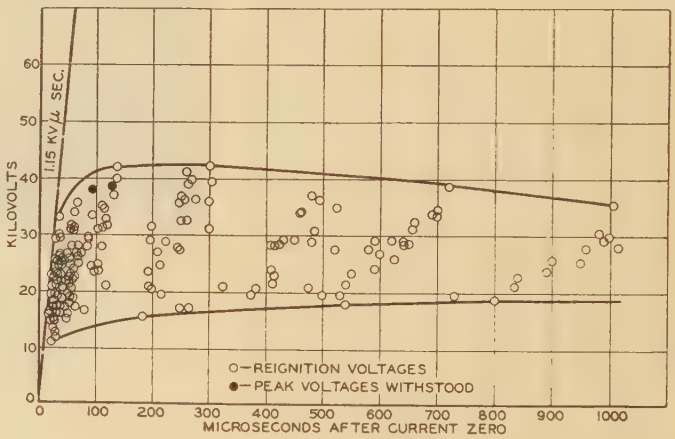

E—175 amperes at 20 pounds per square inch

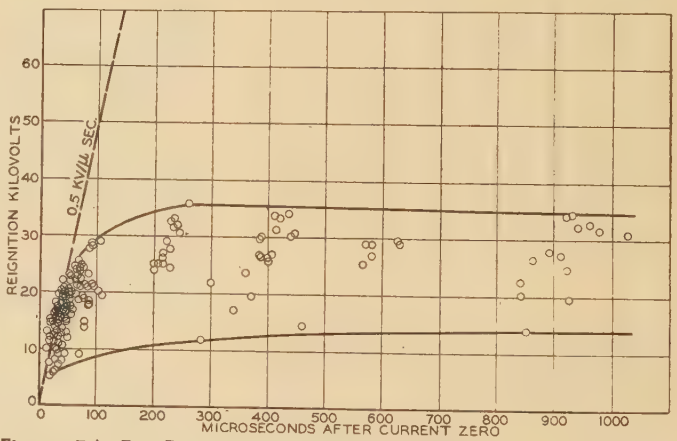

F—175 amperes at 5 pounds per square inch

Figure 5A–F. Dielectric recovery following apparent arc failure at current zero by 60-cycle arcs of various currents in a 0.765-inch solidly connected metal orifice with air flow from the tank at various gauge pressures

The method of voltage measurement from the oscillograms and of the measurement of the longer times probably involved errors of not more than 10 per cent, but random errors of as much as 50 per cent may easily be present in the measurement of recovery times of the order of 10 or 20 microseconds because of skewing of the oscilloscope axis and uncertainty in locating the often poorly defined arc "current zero" moment. This moment was taken as that at which the course of the arc terminal voltage began to be determined mainly by the circuit rather than by the arc. At low rms currents, this point on the arc terminal voltage record is generally clearly marked by a sudden radical change in slope followed by a smooth oscillation and is believed to be accompanied by a sudden virtual cessation of the arc current, or by an "arc failure." At the higher currents, however, such a transition point becomes much less clear on the oscillograms and also undoubtedly less clear in physical meaning, measurable arc conductivity often persisting up to and beyond the voltage reversal point, which is the only point at which the arc current is certainly known to be zero. It should be kept in mind, therefore, that "time after current zero" plotted in the figures actually means time after apparent arc failure.

An outstanding feature of all experiments with a-c arcs in general and arcs in an air blast in particular is the very wide and apparently random variation in dielectric recovery, not only between tests but also between successive current zero moments. These are well illustrated by all of the curves in Figures 5 and 6, as well as by the oscillograms of Figure 4. The especially great variability characterizing the reignition of low-current arcs (Figure 5, A–F) probably is due in part to the variability in the currents just preceding arc failure. Similar variations in arc failure current

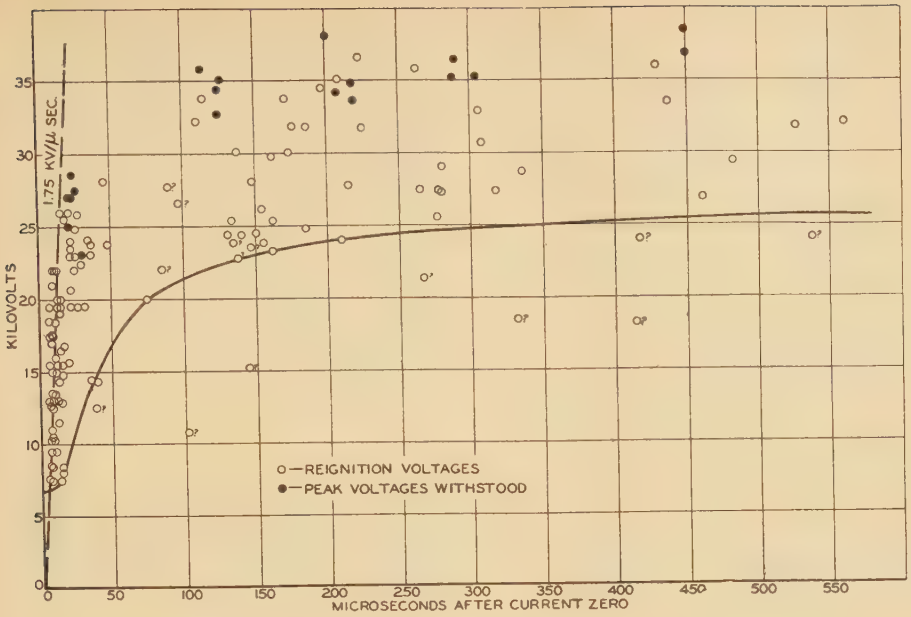

G—1,200 amperes at 40 pounds per square inch

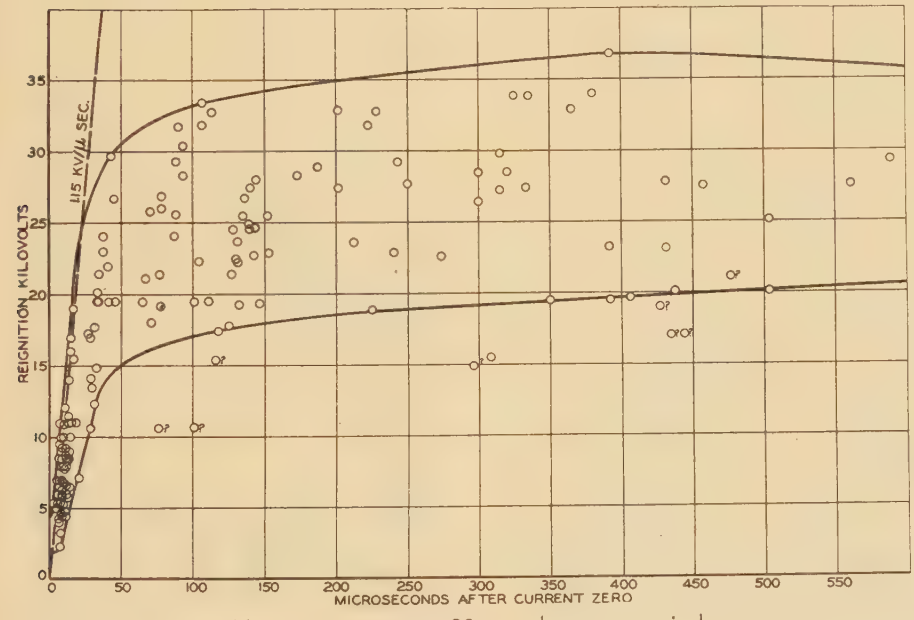

H—1,200 amperes at 20 pounds per square inch

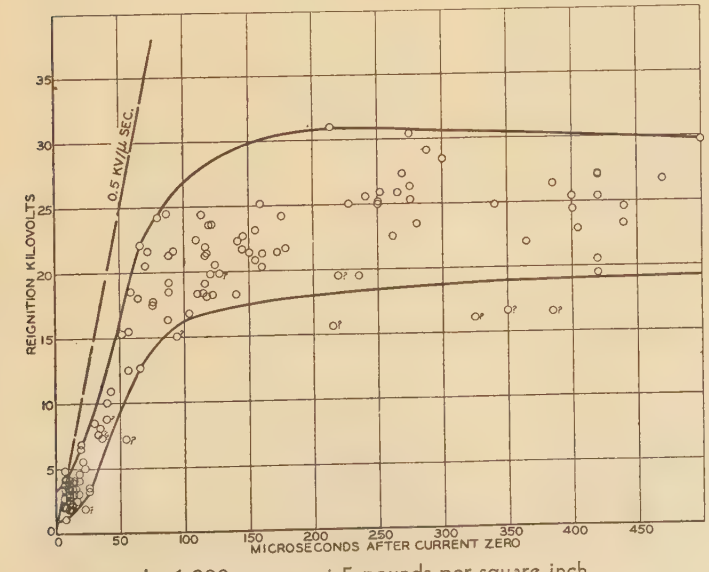

I—1,200 amperes at 5 pounds per square inch

Figure 5G–I. Dielectric recovery following apparent arc failure at current zero by 60-cycle arcs of various currents in a 0.765-inch solidly connected metal orifice with air flow from the tank at various gauge pressures

Orifice of Figure 1C

were first observed and pointed out by Attwood, Dow, and Krausnick,[7] who also measured and plotted dielectric recovery envelopes similar to those presented here except that they were for low current arcs in still air and in comparatively low voltage circuits.

A general survey of the whole array of recovery envelopes and partial envelopes of Figure 5, covering the ranges of currents and pressures: 50, 175, 1,100, 2,200, and 4,200 amperes at 40, 20, and 5 pounds per square inch air tank pressure, reveals certain basic characteristics more or less common to them all. These characteristics are most clearly shown in Figures such as 5I and 5L where a combination of high current and low air pressure resulted in a slower and so more easily followed recovery than in many of the other figures. These envelopes exhibit three separate regions or successive stages of recovery. At very short times (up to 10 or 20 microseconds in these figures) reignition voltages are only moderately higher than the last arc voltages in the preceding half cycle, indicating relatively slight dielectric recovery. After this pause, however, the reignition voltages show a rapid rise with time along loci roughly parallel to the linear rate of rise values indicated by the dotted lines through the origin. This region of rapid recovery at a nearly constant rate is ended, with this orifice, when a rather broad and nearly horizontal breakdown region is reached where the dielectric strength becomes almost independent of time on this few-hundred-microsecond scale. Although showing wide variations and not always so clearly defined, this same pattern seems to characterize the dielectric recovery under all the conditions of current and air pressure covered by these tests. At currents as low as 50 and 175 amperes, the greater natural period of the higher-inductance circuits did not permit exploration of the very short times in which the initial pause might be expected to be evident and so the results are inconclusive with regard to the existence of a delay period at such low currents. Even the rapid-rise portions of the recovery envelopes were largely missed at these currents, especially at the higher pressures. The reignitions at 40 pounds per square inch, for example (Figures 5A and 5D), apparently occurred entirely in the nearly time-independent region. At 1,200 amperes (Figure 5, G–I) most of the early reignitions fell within the rapidly rising recovery region following a possible initial pause. At 2,200 amperes (Figure 5, J–L) and more especially at 4,200

amperes (Figure 5, M–O) reignitions within an initial pause region began to be apparent. At the higher currents and air pressures the upper limits of dielectric strength in the "plateau" regions (see Figures 5G, 5J, and 5K) were above the reach of the transient voltages which the testing circuits could produce and so these limits could not be determined. At 4,200 amperes, the reignition voltages available from the 6,900-volt source were insufficient even to reach the plateau regions.

Figure 6 is a plot of a few dielectric

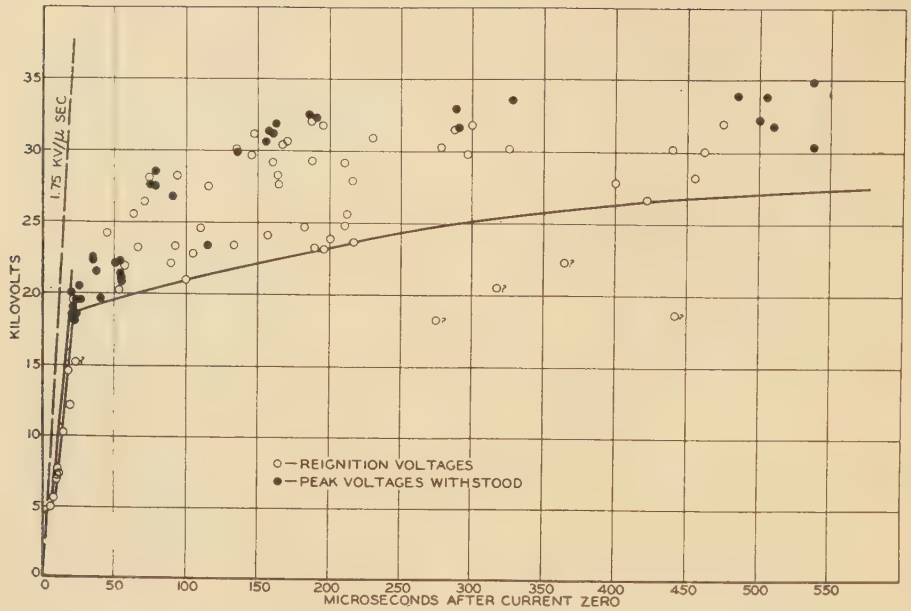

J—2,200 amperes at 40 pounds per square inch

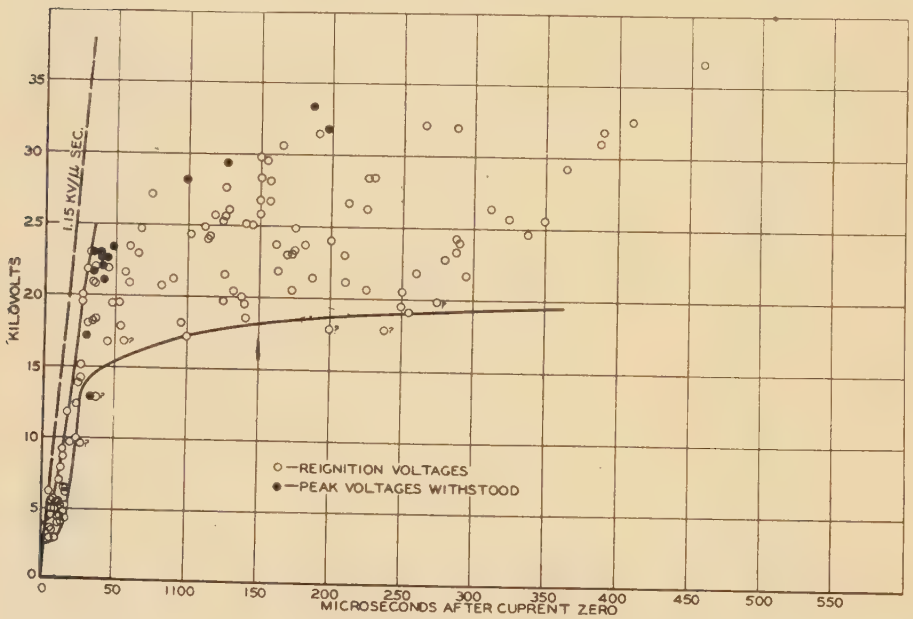

K—2,200 amperes at 20 pounds per square inch

Figure 5J–O. Dielectric recovery following apparent arc failure at current zero by 60-cycle arcs of various currents in a 0.765-inch solidly connected metal orifice with air flow from the tank at various gauge pressures

Orifice of Figure 1C

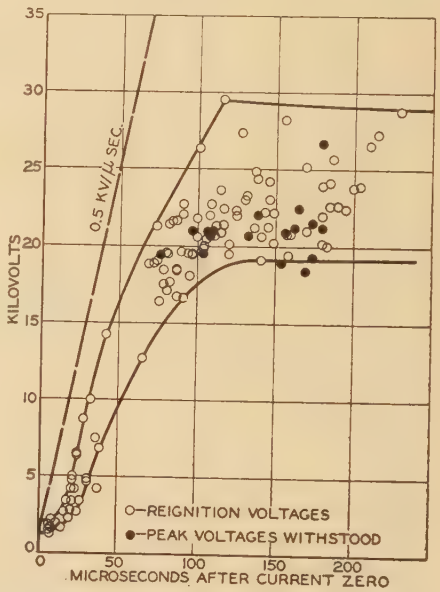

L—2,200 amperes at 5 pounds per square inch

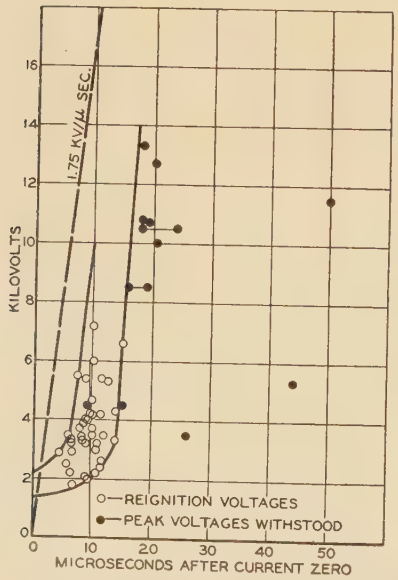

M—4,200 amperes at 40 pounds per square inch

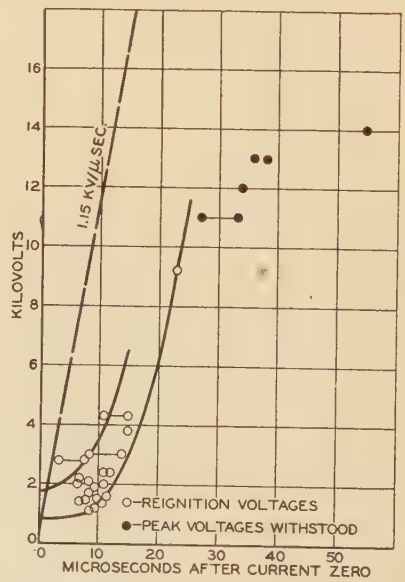

N—4,200 amperes at 20 pounds per square inch

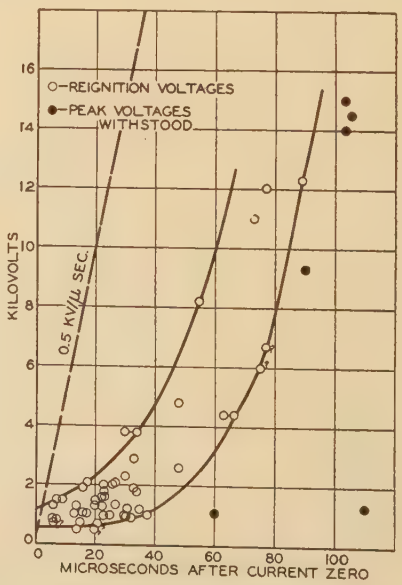

O—4,200 amperes at 5 pounds per square inch

recovery tests with the more efficient insulated and vented orifice arrangement of Figure 1B at the same current and air pressure as the results of Figure 5I for the Figure 1C orifice. The superiority of the Figure 1B orifice is evident in its slightly shorter initial pause, its somewhat more rapid subsequent recovery, and in its much higher plateau voltage limit. This latter is in agreement with the interruption data of Figure 2 where the greatest difference in performance appears at low currents where reignitions occurred only in or near the plateau region.

In conjunction with the dielectric recovery envelopes, the results of Figure 3 now help to locate in space along the orifice axis the different time regions of dielectric recovery. Since the reignitions of the 175-ampere arc in the unshunted test circuit occurred generally in the third, or plateau, time region only, the plateau dielectric strength appears, in Figure 3A, to be fairly well distributed along the flow axis. The early dielectric recovery determining the extinction or reignition of the 1,100- and 2,000-ampere arcs, however, is shown to be quite closely confined to a short portion of the arc channel near the minimum flow section. Figure 3B seems to show that this critical arc length for early dielectric recovery lies nearer to the orifice entrance for the 2,000-ampere arc (faster circuit) than for the 1,100-ampere arc (slower circuit), suggesting that effective dielectric strength makes its first appearance near the entrance and then progresses along the axis in the direction of the flow.

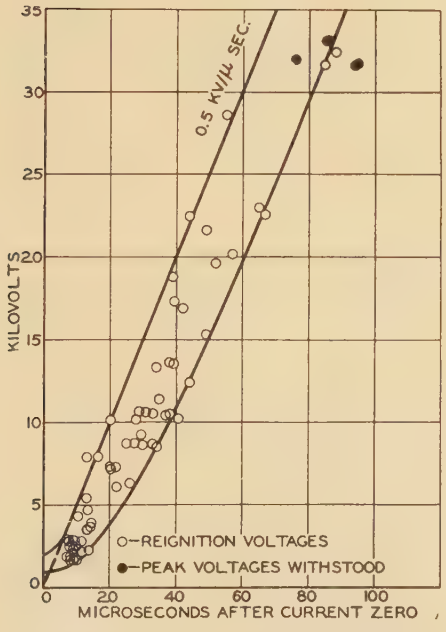

Figure 6. Dielectric recovery following current zero by a 1,100-ampere 60-cycle arc in the Figure 1B insulated metal orifice, lower contact vented, with air flow from the tank at 5 pounds per square inch gauge pressure

Discussion of Results in Terms of Theory

Space limitations do not permit an extended treatment of the various dielectric recovery theories in this paper, but a few possible theoretical interpretations of the foregoing results will be indicated briefly. There still remains so much of vagueness and uncertainty in the physical picture of the rapidly changing a-c arc space near a current zero that precise calculations on the basis of any theory are impossible. Only very broad limits, at best, can be calculated, often so broad as to be valueless in distinguishing between theories.

The apparent initial mean time delays before the beginning of rapid dielectric recovery have been estimated roughly from Figure 5, G–O, and presented in Table I as functions of pressure and rms arc current.

It is possible that these delays, observable only at the higher currents, are, or should be thought of as, mere transition periods of rapidly decreasing but still finite arc conductivity preceding actual arc extinction,[8] which extinction may coincide with the observed upturn in dielectric strength. If, on the other hand, this delay can be thought of as a period when the arc is already essentially out (having negligible conductivity) the delay may be explained in various ways. By analogy with the cooling of an initially uniformly heated solid cylinder, the diffusion theory would predict just such an initial delay preceding a rapid fall of temperature and ion density along the arc axis. Quantitative agreement with the observed time values can also be shown for a one-millimeter arc channel by using Slepian's[4] assumption of a hundred fold or so increase in diffusion rate due to turbulence. If the cooling, and deionization of the last arc filament should be much faster than this, a time delay of the same order can also be calculated to result from the finite rate of acceleration of the surrounding cold and comparatively dense air as it closes in on the low density and so electrically weak arc channel after its temperature and hence its pressure have dropped to a low value. With very rapid cooling, such a momentary associated pressure drop along the arc axis might at least be contributory to the delay in dielectric recovery.

Table I. Time Delays

Pressure		Initial Time Delay in μ sec at Various Currents		
Psi Gauge in the Tank	Abs Atm at Orifice Entrance	1,200 A	2,200 A	4,200 A
5	1.24	13	18	40
20	2.12	6	9	10
40	3.25	5	7	9

The subsequent rapid dielectric recovery also follows from the turbulence enhanced diffusion theory, both qualitatively and quantitatively. After the initial appearance of appreciable dielectric strength, probably at some most favorable point along the arc axis, it may be expected to increase rapidly also by lengthening of the affected region by axial progression of the cooling and recompression process and further by the stretching action of the nonuniform-air velocity near the flow constriction. That such a process may be tied loosely to and so tend to vary with the product of mean air velocity and air pressure (or density) is not surprising. This correspondence is evident in the rather marked agreement (discrepancy two to one or less) between the steep slopes of most of the well defined dielectric recovery envelopes and the slopes of the dotted lines drawn through the origins. These lines were drawn in accordance with the simple displacement theory of Prince[2] on the assumption of a dielectric barrier of sound air formed at "current zero" at the "vena contracta" and growing with the air velocity existing at this point. At first glance, this agreement appears to support the displacement theory, at least in part, but Slepian has shown[4] that the formation of such an assumed sound fluid barrier by simple displacement is physically impossible and the foregoing consideration of the probable diffusion process shows that the agreement can be explained on a basis other than that of simple displacement.

An interesting feature of the plateau dielectric strength values is their relative insensitivity to pressure, especially at the higher currents. The upper and lower limit values at 300 microseconds (well within the plateau region in all cases) have been plotted as a function of the air pressures at the orifice entrance in Figure 7 for different arc current values. The loci of the envelope limits are compared with a dot-and-dash line through the origin representing a linear extrapolation of the observed 60-cycle breakdown voltage at atmospheric pressure with neither air flow nor preliminary arcing. The growing departure with increasing arc current of the plateau breakdown

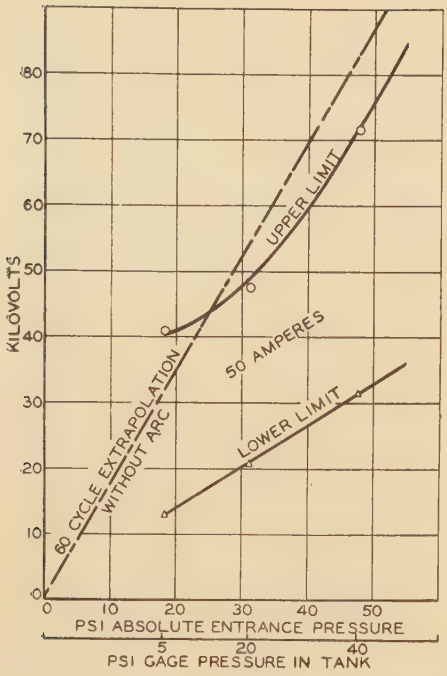

A—50 amperes

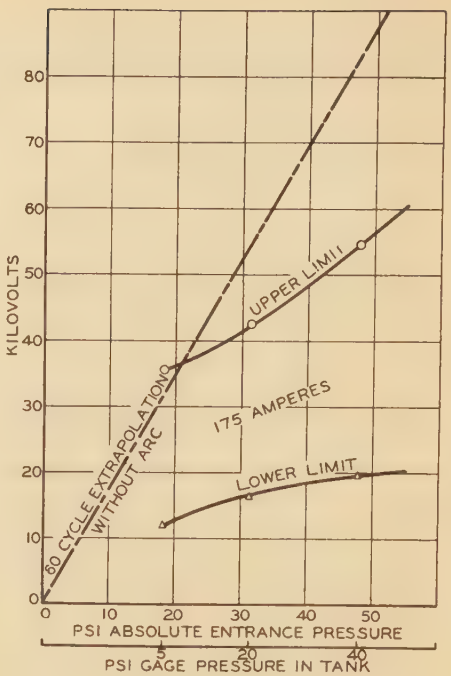

B—175 amperes

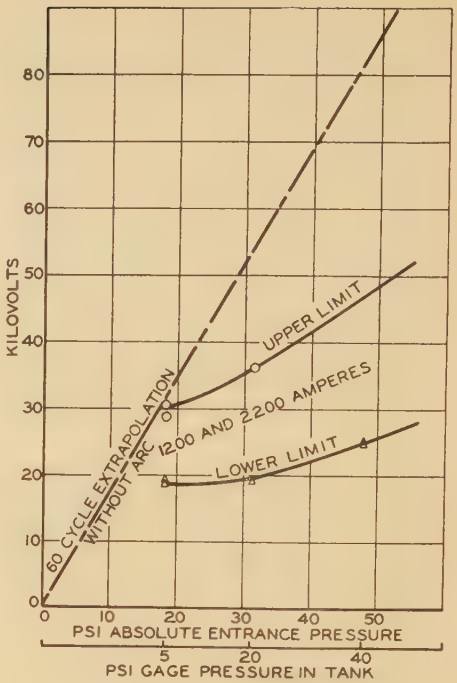

C—1,200 and 2,200 amperes

Figure 7. Effect of pressure on dielectric strength recovered 300 microseconds after extinction of arcs of various currents in the Figure 1C orifice

limits from such a no-arc line is particularly hard to explain on the basis of simple displacement of the arc channel by the air flow. It definitely seems to suggest the continuing presence of a still somewhat heated and perhaps partially ionized path along the arc channel after the initially very rapid diffusion has become comparatively slow. The presence in this orifice of a "dead space" of high pressure and low velocity gas at the tip of the upstream contact may be expected to contribute to the slow disappearance of this residual contaminated arc path. The shape of these curves and some incomplete recovery data at higher pressures suggest that these breakdown voltages all increase more rapidly with pressure in the higher pressure range used in practical circuit breakers than they do at the lower pressures covered by these figures.

References

1. Das Schaltproblem der Hochspannungstechnik, III, **F. Kesselring, F. Koppelmann.** *Archiv. fuer Elektrotechnik*, volume 30, 1936, pages 71–108.

2. The Cross-Air-Blast Circuit Breaker, **D. C. Prince, J. A. Henley, W. K. Rankin.** AIEE Transactions, volume 59, 1940, September section, pages 510–17.

3. **J. Biermanns,** Association Suisse des Electriciens *Bulletin*, volume 23, 1932, page 588.

4. Displacement and Diffusion in Fluid-Flow Arc Extinction, **J. Slepian.** AIEE Transactions, volume 60, 1941, April section, pages 162–7.

5. **O. Mayr,** *Elektrotechnische Zeitschrift*, volume 53, 1932, pages 75–81, and Association Suisse des Electriciens *Bulletin*, volume 23, 1932, pages 605–10.

6. A Vertical-Flow Outdoor Compressed-Air Breaker, **L. R. Ludwig, B. P. Baker.** AIEE Transactions, volume 60, 1941, May section, pages 217–22.

7. Reignition of Metallic A-C Arcs in Air, **S. S. Attwood, W. C. Dow, W. Krausnick.** AIEE Transactions, volume 50, 1931, pages 854–68.

8. The Electric Arc in Circuit Interrupters, **J. Slepian.** Franklin Institute *Journal*, volume 214, 1932, pages 413–42.

Applications of Thin Permalloy Tape in Wide-Band Telephone and Pulse Transformers

A. G. GANZ
MEMBER AIEE

THE development of thin permalloy tape and its use in cores have resulted from the increasing need for efficient magnetic structures at high frequencies. For some time for example, the trend in the telephone plant has been to the use of higher frequencies in the longer distance toll circuits. The reason is that these permit the simultaneous transmission of a larger number of telephone conversations over a single conducting circuit. The coaxial transmission system developed before the outbreak of the war, operates over the range of about 64 to 3,200 kilocycles and required transformers for repeater amplifiers and terminals capable of passing this wide band efficiently. Eddy current effects at these frequencies preclude the use in such transformers of magnetic material in conventional thicknesses.

With the advent of radar pulse transformers were needed urgently to transmit high power pulses. The latter are in the order of a microsecond in length and square-shaped with very steep sides. Fourier analysis of the pulses reveals large components of energy at high frequencies. Consequently, here also cores with low eddy current losses are required for the transformers, not only to assure the faithful transmission of the pulse shape, but also to reduce heating to permissible values.

The use of magnetic powder might suggest itself for these high frequency purposes. However, this involves a three dimensional subdivision of the material. The effect of the particle separations in the direction of the flux is equivalent to a large series air gap in the core, and the net permeability, even with the best alloys, is much too low. With punched laminations, as they are made thinner to reduce eddy currents, the number required for a given stack-up increases. Then fabricating, handling, and insulating the thin laminations to form cores become a problem.

There is thus an area of high intrinsic permeability and low eddy current losses which is satisfied neither by powder cores nor, at the other extreme, by practical punched lamination structures. It is here that permalloy cores of tape 2 mils and less in thickness find their field of use. The tape may be insulated and formed into cores in a continuous operation as will be described. The magnetic circuit is essentially closed. For the wide-band application small toroidal cores of one mil tape accordingly were used. For the pulse transformer applications one and two mil permalloy tape in the form of larger rectangular cores found immediate successful use. The excellence of the results obtained in these designs is largely attributable to these materials.

Fabrication

The permalloys are well adapted to use in thin tape cores. They can be rolled to one mil and less with relative ease compared, for example, with silicon iron. Nor are their magnetic properties materially impaired in the process. Of the two permalloys that mainly have been used for such purposes molybdenum permalloy has the higher permeability. It consists of 4 per cent molybdenum, 79 per cent nickel, and the remainder iron. However, 45 permalloy has a higher saturation value. It consists of 45 per cent nickel and 55 per cent iron. Both these alloys are melted in an arc furnace, and, after hot rolling of the thicker sections, the strip is cold rolled to finished size. For the thinnest tapes the final reductions are carried on in a multibacked rolling mill with small work rolls. For some applications the tape is used at 1/4 mil and 1/8 mil thicknesses. The latter is obtained by plating an equal thickness of copper onto the tape and rolling the combination down to 1/4 mil. The copper then is removed by an acid bath, leaving the desired 1/8 mil tape. Cross sections of thin tape are illustrated in Figure 1.

The method of insulation that has been found best is by cataphoresis, that is, the electrodeposition of fine colloidal particles. In this process the tape is passed through a suspension of silicic acid in acetone. The tape is kept at a positive potential of from 5 to 45 volts with reference to the container. The charged particles of the acid powder are attracted to the tape and form a very uniform coating, the thickness of which is under the control of the operator. The tape is dried by means of hot air jets as it leaves the bath and is wound under tension on a mandrel to form the core. The coating so applied is quite adherent. The apparatus that has been developed for this process is illustrated in Figure 2. The insulated core is heat treated in an atmosphere of hydrogen, and when rectangular

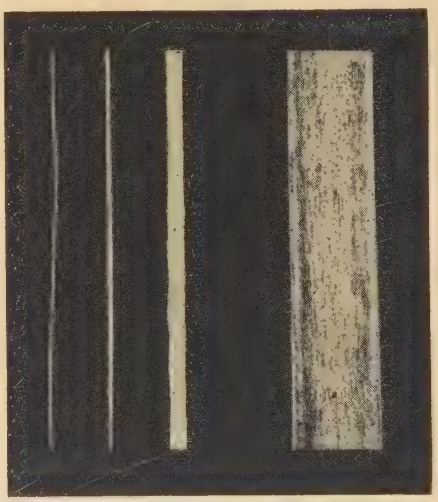

Figure 1. Molybdenum permalloy tape of 1/8 mil, 1/4 mil, and one mil thickness

Thicknesses compared with that of human hair shown at right. Magnification 100×

Paper 46-27, recommended by the AIEE committee on communication and presented at the AIEE winter convention, New York, N. Y., January 21–25, 1946. Manuscript submitted November 23, 1945; made available for printing December 12, 1946.

A. G. Ganz is with Bell Telephone Laboratories, Inc., New York, N. Y.

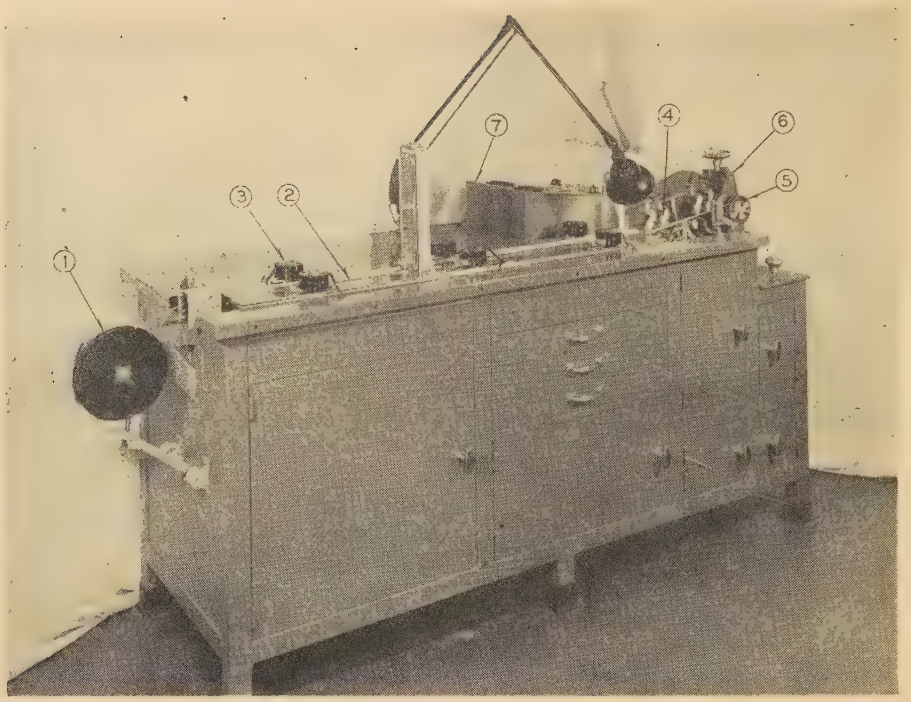

Figure 2. Cataphoresis insulating equipment

1—Tape supply spool and Prony brake
2—Cover for insulating bath
3—Motors for agitating suspension
4—Hot air jets
5—Mandrel on which core is wound
6—Take-up mechanism which winds tape under tension
7—Control panel

shaped it is held in clamps to maintain close dimensional tolerances. At the high temperatures the silicic acid dehydrates to silicon dioxide which provides the final interlaminar insulation. It also prevents welding of adjacent layers of tape during treatment. This process results in a fully adequate insulation and a typical packing factor of 80 per cent for one mil tape.

The cores so made are sufficiently rigid to require no strengthening by impregnation. Windings are applied to the closed cores by winding machines with circular shuttles. For some uses, a very small air gap is advantageous as will be described. The core is cut into halves using a wet rubber-bonded cutoff wheel. The windings are applied directly to the core halves. These are reassembled and the butting surfaces held together under pressure.

Application to Wide Band Transformers

In the design of wide band transformers* for carrier telephone circuits, the problem is to obtain a sufficiently wide transmission band with low attenuation. Leakage inductance is a major factor in limiting this band. Reducing the leakage by closer coupling of the windings usually increases the winding capacitances which also restrict the range. Lower leakage therefore must come from the use of better cores which permit fewer turns without increasing the shunt attenuation. It is for such reasons that magnetic materials having higher permeabilities at frequencies above 50 kilocycles are needed.

Transformers in telephone circuits operate at low alternating voltages, and the flux densities in the cores are correspondingly low, less than 20 gausses. Molybdenum permalloy is characterized by very high permeability at low densities and also by very low hysteresis effects. This latter feature is valuable, since magnetic modulation might otherwise cause objectionable interchannel cross talk and noise. Figure 3 gives the effective permeability and Q of molybdenum permalloy tapes in the form of cores. A curve for 14 mil material also is given for purposes of comparison. As pointed out previously, the windings are applied to these cores with shuttle type winding machines. This permits a continuous magnetic circuit to be used and the high permeability of the tape to be fully retained in the core. The fact that the permeability of thin tape holds up at high frequencies is noteworthy and accounts for the low attenuation of the transformers. Figure 4 shows a typical core of one mil tape together with a transformer in which it is used.

Application in Low Voltage Pulse Transformers

Radar indicator circuits employ transformers passing low amplitude pulses of short duration. The high frequency components of the pulses correspond roughly to those of the wide band transformers and the design considerations requiring a high effective permeability core apply here also. However, the core material then is operated over a different portion of its magnetic characteristics from that for alternating current.

Figure 3. Effective permeability and Q of three thicknesses of 4-79 molybdenum permalloy as a function of frequency

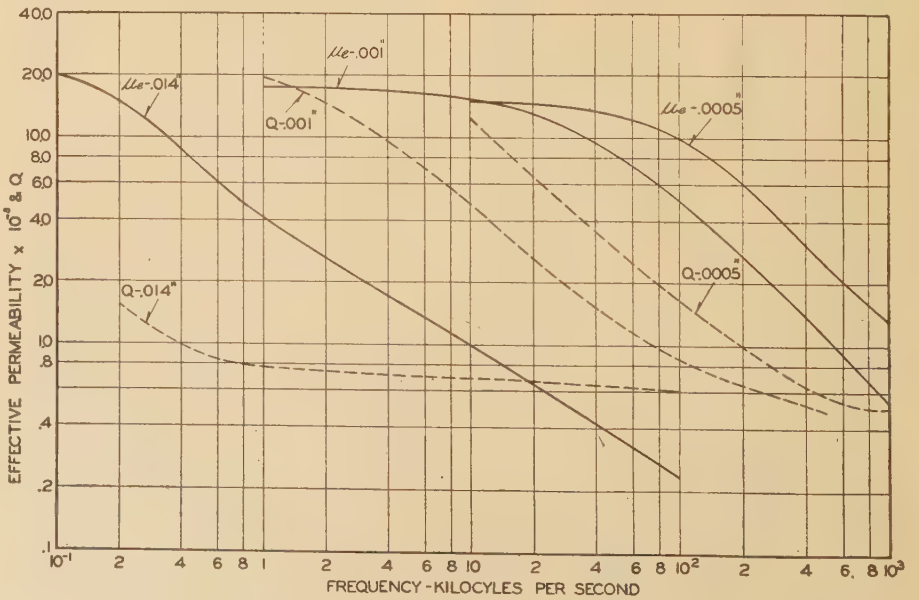

* The design of the amplifiers in which these are used impose many other requirements, the discussion of which is beyond the scope of this paper.

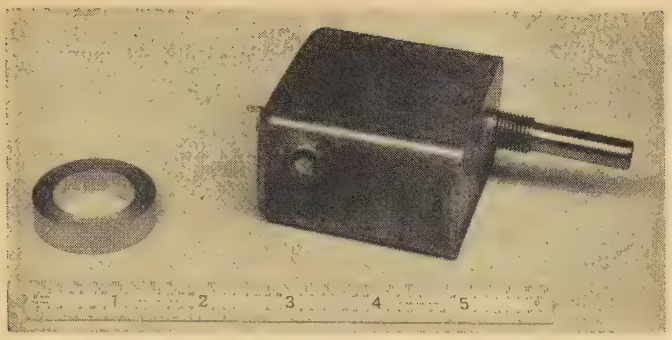

Figure 4. One mil 4-79 molybdenum permalloy core and transformer in which it is used

Operating range 64–3,200 kilocycles

Each unidirectional pulse conditions the material for the succeeding pulse. From the basic relation $e = -K_1NA \times (dB) \div (dt)$ each pulse demands a flux density change $\Delta B = (K_2Et) \div (NA)$, where E is constant during the pulse. For virgin material the initial flux density swing, $O-P_1-B_1$ leaves the material magnetized to the value B_1, as shown in Figure 5, the falling portions of the loop P_1-B_1 representing the decay occurring between pulses. The next cycle leaves the material magnetized to the value B_2, and so on. The steady state condition $B_n-P_n-B_n$ is reached when the falling portion of the loop is equal to the flux density change required by the pulse. The permeability that applies is then the ratio of the change in B to that in H for this cycle. For larger flux changes the loop becomes $B_r-P_r-B_r$ where B_r is near the retentivity of the material. This permeability value is always substantially less than the initial permeability and for molybdenum permalloy is in the order of 4,000 for a 1,000 gausses change. Reverse magnetization between pulses alters the phenomena, and this will be described under high power pulse transformers where it is more likely to occur.

The permeability values as described are of course reduced by eddy currents owing to the rapid change of flux during the pulse. For low density operation the characteristic of the material may be regarded as linear for analytical purposes. The equations for flux distribution, effective permeability, and losses for the linear case are given in the appendix. Ranges of values are given in the graphs of Figures 6 and 7.

These graphs illustrate the extreme variation of flux density which may be caused by eddy currents and the corresponding low permeability which may obtain with pulses of short duration, that is, small values of t. They also illustrate that this loss of permeability may be recovered to any desired extent by using thinner magnetic material, that is, smaller values of α. These considerations have led to the use of thin tape in low voltage as well as in high voltage pulse transformers. In a typical case one mil molybdenum permalloy was required. The core was toroidal and very similar to that illustrated in Figure 4. By this means it was possible in the transformer to transmit one microsecond square pulses with 0.05 microsecond sides without appreciable distortion.

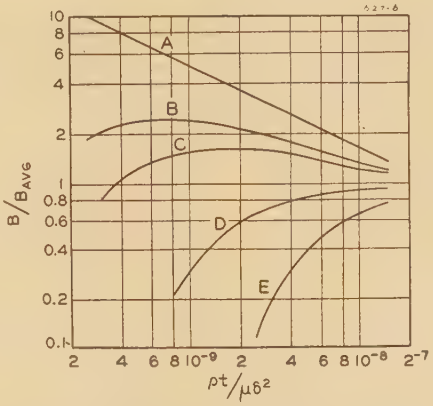

Figure 6. Relative flux density distribution in tape with square pulse voltage excitation

The average flux density B_{av} increases linearly with time

A—$y = \frac{\delta}{2}$ (surface)

B—$y = \frac{5}{12}\delta$

C—$y = \frac{3}{8}\delta$

D—$y = \frac{\delta}{4}$

E—$y = 0$

ρ = resistivity of tape in ohm-centimeters
δ = thickness of tape in inches
t = time in seconds
μ = d-c permeability
y = distance from mid-plane of tape in inches

Application in High Power Pulse Transformers

These transformers are used in the modulator circuits of radar transmitters to impress pulses on magnetrons. Power ranging from 100 to 1,000 kw is carried by these transformers for the duration of each square pulse. The high winding voltages range from 10 to 30 kv. Most uses demand small size and weight in apparatus, especially air-borne equipment. It is thus necessary that transformers for these powers insulated for the high voltages be designed on small core structures; for example, 2 pounds for 300-kw pulses. Further, the magnetrons to which the transformers are connected are voltage

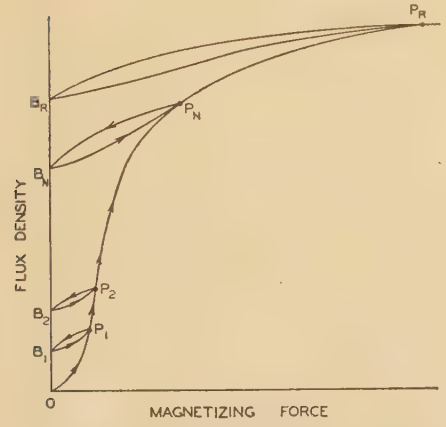

Figure 5. Sequence of flux-density changes with repeated unidirectional pulses, namely, $O-P_1-B_1$, $B_1-P_2-B_2$, $\cdots B_n-P_n-B_n$; larger changes result in $B_r-P_r-B_r$

Figure 7. Curves for computing the effective permeability and the eddy current loss in tape with square pulse voltage excitation

When t is taken as the pulse length, J is the total loss during and after the pulse, assuming that the voltage is zero after the end of the pulse

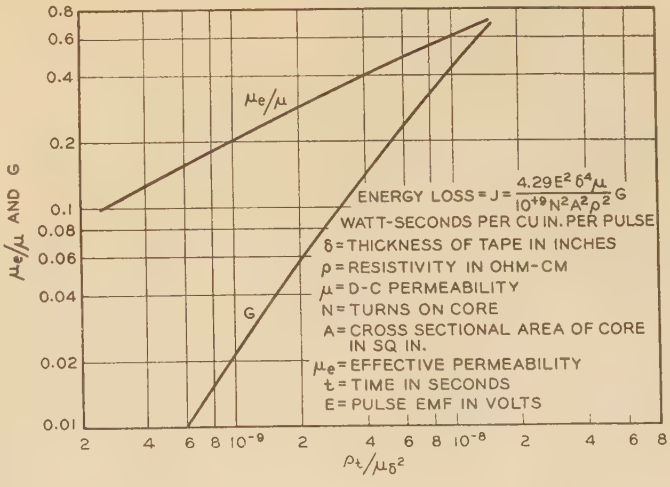

sensitive in their operation. Appreciable magnetizing current being drawn through the source impedance is objectionable as it tends to reduce the voltage applied. All these factors impose severe demands on the core material requiring thin tape of the high quality obtainable in the permalloys.*

Range of Flux Density

The power capability of the transformers obviously is governed by the flux density range in the core material. Where there is simply decay of the flux between pulses, the minor $B-H$ loops traversed are like those shown in Figure 5. The useful flux density range is limited by the difference between saturation and retentivity. Generally speaking, as the magnetic quality of materials is improved and the permeabilities increase, the loops become more nearly square. This is illustrated for the two permalloys in Figures 8 and 9. Consequently, the difference between saturation and retentivity becomes less.

The available flux range can be increased substantially by the addition of an appropriate air gap. This is illustrated by the dotted hysteresis loop of Figure 8 for molybdenum permalloy with a 0.02 per cent air gap. The loop is sheared compared with the normal loop, and the apparent retentivity has been reduced to about 400. The flux density range now is increased to B_s-B_r', approximately 8,100 for the proportions shown in the figure. The maximum permeability, however, has been reduced, which represents some sacrifice in efficiency to obtain the flux range. The principle of adding an air gap for this purpose has found general use where reversal between pulses, as will be described, was not effective.

Reverse Magnetization

If, during the long interval between pulses, the material is magnetized in a reverse direction, an even wider flux range can be obtained. Referring to Figure 9 the peak reverse current between pulses provides a reverse magnetizing force of H_r. This causes the material to traverse the $P-B_r-A-B_n$ section of the loop. The rate is slow enough not to be affected by eddy currents. When the next pulse is applied, the flux can swing from B_n to P.

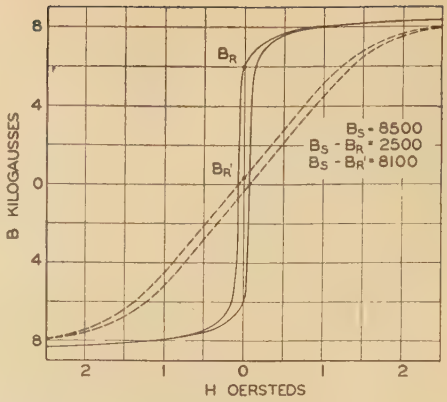

Figure 8. Hysteresis loop of one mil 4-79 molybdenum permalloy obtained on completed core, showing effect of 0.02 per cent air gap

Packing factor 0.8

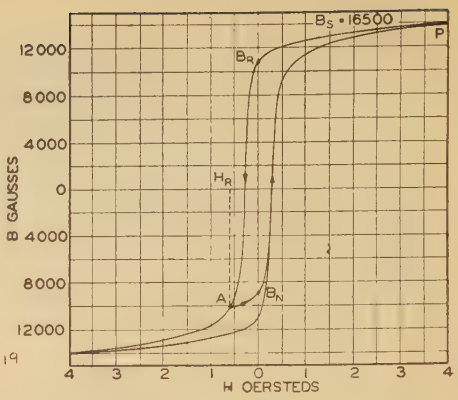

Figure 9. Hysteresis loop of 2 mil 45 permalloy obtained on completed core, showing flux density cycle with reverse magnetizing force

Packing factor 0.9

The material then is being used over the steepest part of the loop where the permeability is upwards of 50,000 over a large part of it (see Figure 9). It is possible with high enough peak reverse current to make available the limiting range from the retentivity below the axis to saturation above, that is, 10,000 + 16,500, or a total swing of 26,500 gausses for 45 permalloy. It is clear from the illustration that the reverse magnetizing force to be very effective must be at least greater than the coercive force of the material. It is also clear from comparing the solid with the dotted loops of Figure 8 that much better results can be obtained with a closed magnetic circuit than with an air gap. A reverse direct current fed to the winding has been used experimentally, raising the limiting flux swing to twice saturation. This has not been found of sufficient advantage in the pulse transformer cases considered to warrant the attendant circuit complications.

Reverse magnetization between pulses has been used very successfully in practice to obtain wide flux swings. The permalloys are especially well adapted to take advantage of this feature by virtue of their low coercive forces, which are 0.05 and 0.3 oersted as illustrated in Figures 8 and 9. These values permit reversal to be effected with minimum magnetizing forces.

High Density Pulse Magnetization

With high power operation the effect of the eddy currents on short pulses is usually to saturate the surface of the tape. This follows from the large differences in flux density within the tape as illustrated in Figure 6. Under these conditions the characteristics of the material are not at all linear, and the equations previously referred to do not directly apply. Unfortunately, the rigorous analysis of the nonlinear case is, at the least, laborious.

The high density behavior may be analyzed readily by making simplifying assumptions appropriate to the high permeability alloys. It will be observed from Figures 8 and 9 that the d-c permeability over most of the range is exceedingly high with a rapid transition to saturation. Accordingly, let infinite d-c permeability but finite saturation be assumed. At the start of the pulse the flux is confined to the surfaces of the tape which saturate. The saturated regions propagate toward the center of the tape until the pulse ends or until the entire lamination is saturated. Equations for permeability and loss for this case are derived in the appendix.

The behavior of actual tape of the best magnetic materials approximates that described. For example, for 1.1-mil tape the computed value of 5,050 for a 2.1-microsecond pulse using these equations is approached by the measured value of 4,000 (see Figure 11). The previous equations for the linear case are also of some use for high densities if a proper averaged value of d-c permeability is assumed. Together the two sets of equations provide a check on empirical data and serve as a guide in design.

Pulse Loops

Magnetic materials and cores are evaluated experimentally by pulse loops. The measuring circuit operates on the same principle as the familiar hysteresograph often used for obtaining 60-cycle loops. A schematic of the pulse circuit

* 4-43 Permalloy, a new alloy, also has been used, to a limited extent. It consists of 4 per cent molybdenum, 43 per cent nickel, and the remainder iron. It is characterized by high resistivity and the core losses are accordingly at least 30 per cent lower than other materials.

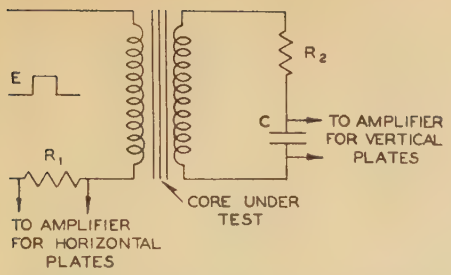

Figure 10. Simplified circuit schematic for presentation of pulse loop on oscilloscope screen

for oscilloscope presentation is shown in Figure 10. The lower portion of the loops obtained defines the material, the return trace varying with circuit conditions. Calorimetric methods are relied upon for accurate loss determinations. Figure 11 shows the pulse loop of one-mil molybdenum permalloy tape in a core with 0.3 oersted reverse bias. The effective permeability is seen to be 4,000 with a flux swing of 14,000 gausses. The loop was taken with a reverse d-c bias instead of peak reversal between pulses, since the measuring circuit is better adapted to the former procedure. Peak reversal yields somewhat less flux swing, in this instance about 12,500 gausses. Figure 12 shows how different reversals affect the pulse permeability of a 45 permalloy core. The data were obtained from pulse loops with varying average flux densities. Figure 13 gives data on the pulse permeability of two thicknesses of molybdenum permalloy with small air gaps.

Figure 14 shows a pulse transformer which has found wide use in air-borne radar equipments. The core shown with it is the one on which the pulse loop of Figure 11 was taken. Figure 15 shows a large pulse transformer with a 45 permalloy core. In contrast there is shown one of the smallest transformers of this type. These illustrate the range of application of the superior magnetic properties of thin permalloy tape.

Application to Nonlinear Coils

It is characteristic of molybdenum permalloy mentioned here that the magnetization curve is very steep, that it has a relatively sharp transition to the saturated condition, and that the permeability there is very low. Valuable use has been made of these features in the generation of groups of harmonics. The basic circuit is shown schematically in Figure 16. The generator provides current of the fundamental frequency to which the series coil and capacitor are resonant. During that part of the cycle where the nonlinear coil has a high inductance, the capacitor C_2 is charged. As the coil begins to saturate its inductance falls and the capacitor discharges through it. This carries the material farther into the saturated region where the permeability is very low. The coil thus acts as a magnetic switch by which a sharply peaked current pulse rich in harmonics is generated. These harmonics pass through appropriate equalizers and filters to supply the carrier currents to multichannel coaxial and other carrier systems. Coils of this type are attractive as modulating devices, as they are stable and have an indefinitely long life compared to vacuum tubes.

The efficiency of the device requires that the inductance during the nonsatu-

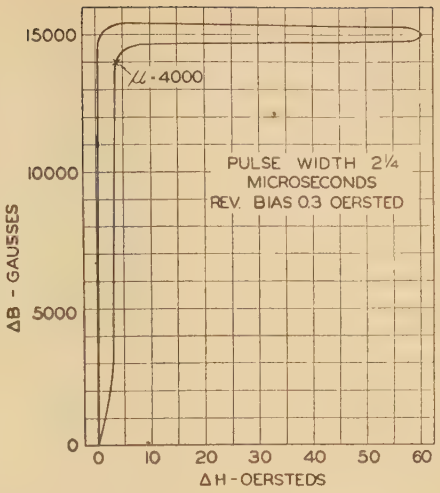

Figure 11. Pulse loop of 1 mil 4-79 molybdenum permalloy with reverse bias obtained on completed core without air gap

Packing factor 0.8

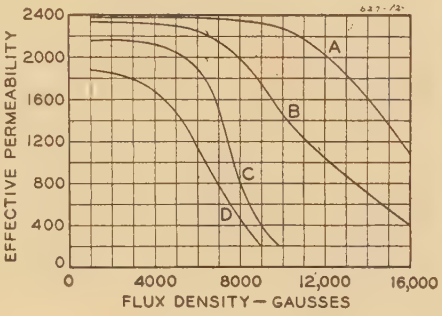

Figure 12. Effective permeability with 5 microsecond pulses obtained in completed core of 2 mil 45 permalloy without air gap

Packing factor 0.9

A—Reverse d-c bias, 0.52 oersted
B—0.28 oersted
C—0.078 oersted
D—No bias

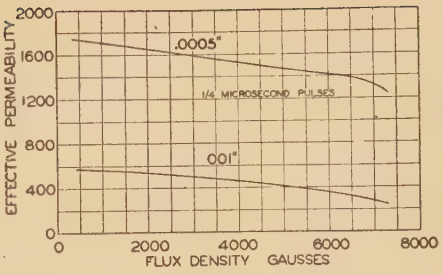

Figure 13. Effective permeability characteristics of 4-79 molybdenum permalloy obtained in completed cores with small air gaps

Packing factor 0.7 for 1/2 mil tape and 0.8 for 1 mil tape

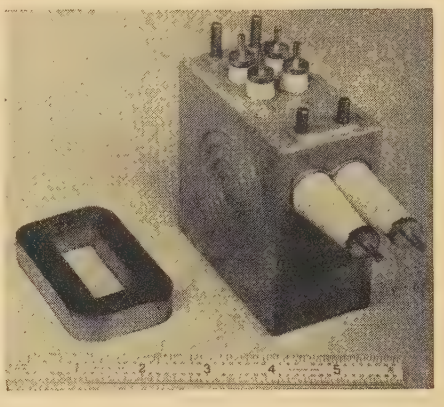

Figure 14. Rectangular core of 1 mil 4-79 molybdenum permalloy and pulse transformer in which it is used

Pulse power 100 kw

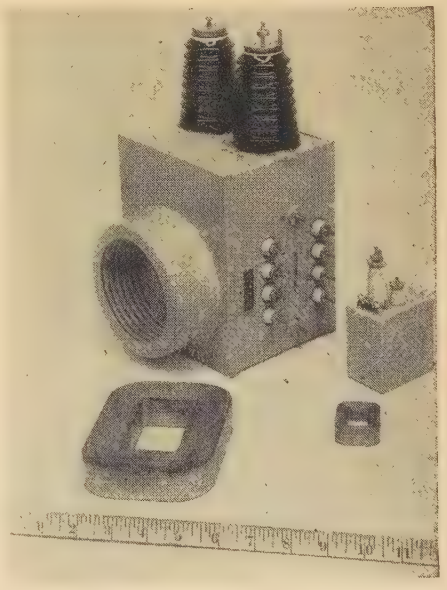

Figure 15. Rectangular core of 2 mil 45 permalloy weighing 3 pounds and 1/4 pound core of one mil 4-79 molybdenum permalloy with the pulse transformers in which they are used

rated interval be very high compared to the saturated interval. For a fundamental of 120 kilocycles the flux swing from negative saturation to positive takes place in less than 4 microseconds. The approach to saturation takes place in tenths of a microsecond. If eddy currents are not minimized, much larger power input is needed to avoid broadening the peaked pulse and so reducing the output of high frequency harmonics. These considerations again dictate a core of very thin molybdenum permalloy tape, in this instance 1/4 mil. This core in a specific case has differential permeability, with eddy currents, over the steep part of the curve of more than 10,000. This is in striking contrast to the value of 3 at the flat portion of the curve, where it is driven by the peak magnetizing force of 20 oersteds. Similar coils have found military uses. In tank communication circuits they provide means for frequency modulation of a desired harmonic of the carrier input. The fundamental frequency there is 400 kilocycles requiring 1/8 mil tape. In order to operate effectively at this frequency and with small power, the cores were designed with a diameter of 0.3 centimeter and weigh only 20 milligrams. Figure 17 illustrates coils of this type.

Nonlinear coils have found further important use as magnetic switches in the generation of high power pulses. These are accompanied by heavy currents up to 100 amperes. Nonlinear coils readily can be designed to carry heavy currents in the saturated condition. They therefore can function as high current switches with the feature that they do not deteriorate with use. Cores of one mil molybdenum permalloy tape for this purpose weigh from 2 to 30 pounds and are illustrated in Figure 18. They are used in radar equipments.

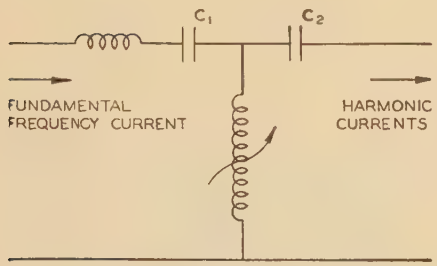

Figure 16. Elementary circuit for harmonic generation by nonlinear coil

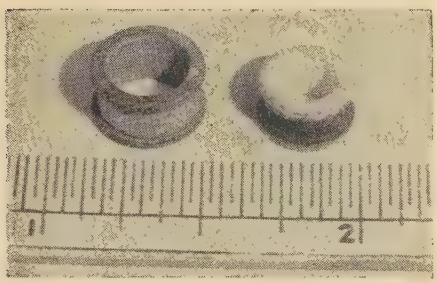

Figure 17. Cores of 1/4 mil and 1/8 mil 4-79 molybdenum permalloy used in harmonic generator coils

Tape is wound on ceramic forms for mechanical support. Weights of metal 60 and 20 milligrams, respectively

Figure 18. Cores of one mil 4-79 molybdenum permalloy tape and partially assembled nonlinear coils in which they are used

Weights of core stacks and pulse powers are as follows: 30 pounds, 1,000 kw; 2 pounds, 100 kw; 1 pound, 50 kw

Appendix

Voltage Pulse Magnetization—Linear Case

The applied voltage is taken as constant for the duration of the pulse which is the usual condition for pulse transformer operation. If a homogeneous material with constant permeability and not saturable is assumed, the following expressions are derived* from Maxwell's equations by straightforward methods. The flux distribution during the pulse after an interval of time t is given by

$$\frac{B}{B_{avg}}=\frac{2.025\mu\delta^2\times10^{-8}}{\rho t}\left[\frac{2y^2}{\delta^2}-\frac{1}{6}+\frac{49.3\rho t}{\mu\delta^2 10^{-6}}-\frac{2}{\pi^2}\sum_{n=1}^{\infty}\frac{(-1)^n}{n^2}\cos\frac{2n\pi y}{\delta}\exp\frac{-487n^2\rho t}{\mu\delta^2 10^{-6}}\right] \quad (1)$$

where the average flux density in the tape is

$$B_{avg}=\frac{15.5Et}{NA}10^{+6}$$

gauss.

The effective permeability, defined for pulses as the ratio of the average flux density in the tape to the magnetomotive force at the surface, at time t during pulse is given by

$$\mu_e=\frac{49.3\rho t}{\delta^2}\times10^{+6}\left[\frac{1}{3}+\frac{49.3\rho t}{\mu\delta^2 10^{-6}}-\frac{2}{\pi^2}\sum_{n=1}^{\infty}n^{-2}\exp\frac{-487n^2\rho t}{\mu\delta^2 10^{-6}}\right]^{-1} \quad (2)$$

The total energy loss due to eddy currents during and after the pulse, assuming that the voltage after the pulse is zero for infinite time, is given by

$$J=\frac{4.29E^2\mu\delta^4}{10^9N^2A^2\rho^2}\left[\frac{49.3\rho T}{\mu\delta^2 10^{-6}}-\frac{1}{15}+\frac{6}{\pi^4}\sum_{n=1}^{\infty}n^{-4}\exp\frac{-487n^2\rho T}{\mu\delta^2 10^{-6}}\right]$$

watt-seconds per cubic inch per pulse (3)

This equation is plotted in Figure 7. The conditions assumed apply to a well-designed pulse transformer in the usual circuit. There the voltage in the relatively long interval between pulses is small, and the total flux decays so slowly that the eddy current losses from this source can be neglected. On the other hand, eddy current losses accompany the rapid transition from a nonuniform to a uniform distribution of the flux within the tape after the pulse, and these losses are included in the foregoing expression.

If the voltage after the pulse is not small, no general expression can be given as the loss then depends on the particular conditions. However, the loss during the pulse itself, which is the major part, is determined and is given by

$$J_T=\frac{2.54E^2\delta^2}{N^2A^2\rho}\left[\frac{T}{12}-\frac{20.8\mu\delta^2}{10^{11}\rho}\sum_{n=1}^{\infty}\times\frac{1-\epsilon^{-\frac{487n^2T\rho}{10^{-6}\mu\delta^2}}}{n^4}+\frac{5.20\mu\delta^2}{10^{11}\rho}\sum_{n=1}^{\infty}\frac{1-\epsilon^{-\frac{974n^2T\rho}{10^{-6}\mu\delta^2}}}{n^4}\right]$$

watt-seconds per cubic inch per pulse (4)

where

* By Doctor L. A. MacColl, Bell Telephone Laboratories, Inc.

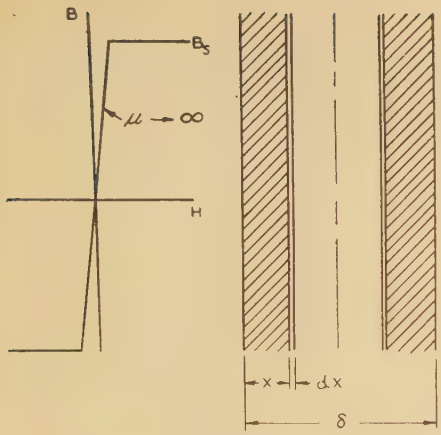

Figure 19

μ = the permeability relative to free space without eddy currents
δ = the thickness of the tape in inches
y = the distance from the mid-section of the tape in inches
ρ = the resistivity in ohm-centimeters
t = the time in seconds
T = pulse length in seconds
A = the cross section of the core in square inches
N = the number of turns in the winding
E = the electromotive force applied to the winding, in volts

Current Pulse Magnetization—Linear Case

The corresponding equations for the current pulse are given for completeness:

$$B = \frac{\mu NI}{2.02l}\left[1 - \frac{4}{\pi}\sum_{n=1}^{\infty} n^{-1} \times \left(\sin\frac{n\pi}{2}\right)^2 \sin\frac{n\pi y}{\delta} \exp\frac{-122n^2\rho t}{\mu\delta^2 10^{-6}}\right] \text{ gausses} \quad (5)$$

$$\mu_e = \mu\left[1 - \frac{8}{\pi^2}\sum_{n=1}^{\infty} n^{-2} \times \left(\sin\frac{n\pi}{2}\right)^4 \exp\frac{-122n^2\rho t}{\mu\delta^2 10^{-6}}\right] \quad (6)$$

$$J = \frac{2.58N^2I^2\mu}{10^8 l^2}\sum_{n=1}^{\infty} n^{-2}\left(\sin\frac{n\pi}{2}\right)^4 \times \left(1 - \exp\frac{-122n^2\rho T}{\mu\delta^2 10^{-6}}\right)$$

watt-seconds per cubic inch per pulse (7)

where l is the length of magnetic circuit in inches, and I is the current in amperes, constant during pulse and zero thereafter. J includes the losses during and after the pulse.

Voltage Pulse Magnetization—Nonlinear Case With Saturation

For this case an idealized magnetization curve as shown in Figure 19 is assumed. With infinite permeability the tape is divided at any instant into surface sections which are saturated and a central section devoid of flux as shown in the figure.

For a section of tape of thickness δ and unit length and width, the eddy current

$$i_e = 2\Delta B_s K_1 \frac{dx}{dt}\cdot\frac{2.54x}{2\rho} \text{ amperes}$$

where ΔB_s is change in flux density from the initial value to saturation. $\Delta B_s = B_s$ when the material originally is unmagnetized. Since the permeability is infinite, the magnetomotive force at the surface is only that required to maintain the eddy current. Whence, $H = 0.495 i_e$ oersted. The change in average flux density, $\Delta B_{avg} = (2x\,\Delta B_s) \div \delta$. Whence the effective permeability

$$\mu_e = \frac{\Delta B_{avg}}{H} = \frac{1.59\rho}{K_1\delta\dfrac{dx}{dt}}$$

For the winding

$$E = 2\Delta B_s K_1 \frac{dx}{dt}\frac{NA}{\delta}$$

By substitution

$$\mu_e = \frac{3.18\rho NA\,\Delta B_s}{\delta^2 E} \quad (8)$$

Since the change in average flux density is linear with time, this also may be written

$$\mu_e = \frac{0.493\rho T_0 10^{+8}}{\delta^2}, \text{ where } T_0 = \frac{\Delta B_s}{\Delta B_{avg}} T \quad (9)$$

where T_0 is time in seconds to saturate tape without eddy currents. It is also the time required to saturate the entire cross-section of the tape under the assumed conditions. As before, μ_e is relative to free space, ρ is the resistivity in ohm-centimeters, A is the core area in square inches, δ is the tape thickness in inches, B_s is in gauss, E is in volts, N turns, and T is pulse length in seconds.

Since the effective permeability is constant during the pulse, the loss is proportional to the square of the flux density and may be written

$$\text{loss} = \frac{6.52\,VF\Delta B_{avg}{}^2 10^{-8}}{\mu_e} \text{ watts} \quad (10)$$

where V is net core volume in inches cubed, F is in pulses per second, ΔB_{avg} is the change in average flux density to end of pulse. Since magnetic energy is proportional to $\int HdB$, there is no storage of energy at any time under the assumed condition of infinite permeability.

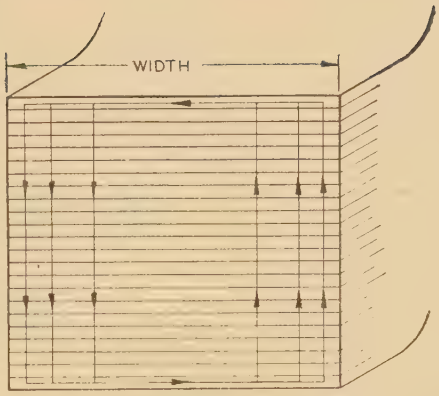

Figure 20. Distribution of intersheet eddy currents in cross section of core

Resistivity across stack ≫ than resistivity of tape. The dimension for the width shown is to be used for the thickness, δ, in the equations when these are applied to the core

Intersheet Eddy Currents

It is worth noting that all the foregoing equations for tape may be employed in dealing with intersheet effects in a core. The resistivity across the stack is ordinarily very high compared to that of the tape The eddy currents then run essentially perpendicular to the tape, and the current loops are completed in the end tapes as illustrated in Figure 20. The distribution of flux and currents in the cross section is then the same as that in a strip having resistivity equal to that across the stack, thickness equal to the stack width, and of indefinite extent in the remaining directions. It is only necessary to substitute the width w for δ in the expressions and graphs. Evidently, when the stack resistivity equals $(\rho w^2) \div \delta^2$, the stack losses are equal to those contributed by the tape.

References

1. Permalloy, H. D. Arnold, G. W. Elmen. *Journal* of the Franklin Institute, volume 195, May 1923.

2. Magnetic Alloys of Iron, Nickel, and Cobalt, G. W. Elmen. *Journal* of the Franklin Institute, volume 207, May 1929, pages 583–617.

3. Improvements in Communication Transformers, A. G. Ganz, A. G. Laird. AIEE Transactions, volume 54, 1935, December section, page 1367–73.

4. Magnetic Generation of a Group of Harmonics, E. Peterson, J. W. Manley, L. R. Wrathall. AIEE Transactions, volume 56, 1937, August section, pages 995–1001.

5. Survey of Magnetic Materials and Applications in the Telephone System, V. E. Legg. *Bell System Technical Journal*, volume 18, July 1939, pages 438–64.

Laboratory Method for Objective Testing of Bone Receivers and Throat Microphones

E. H. GREIBACH
MEMBER AIEE

THE development and testing of inertia-type transducers require equipment similar to the artificial ear used in the testing of air conduction receivers.

The problem of building a reliable artificial ear is relatively simple compared to that of constructing an artificial mastoid for testing bone conduction receivers, or an artificial throat for testing throat microphones. The artificial ear employs an air cavity, which simulates the cavity of the ear and couples the receiver under test to a condenser microphone, in order to measure the pressure produced in the cavity by the receiver. In the case of the bone conduction receiver, the role of the air cavity is played by a layer of skin, coupling the bone conduction receiver to the mastoid bone. A similar situation is encountered in the case of throat microphones, where the larynx is coupled to the throat microphone through an interposed layer of skin. The properties of the layer of skin vary over a very wide range, making it difficult to determine what is the average impedance looking into the human head or throat. There is also a controversy as to whether one should measure the pressure or the velocity transmitted through the layer of skin.

An artificial throat suitable for testing throat microphones must have a vibrating platform capable of imparting a velocity to a throat microphone through a filter simulating the layer of skin. The platform must be large enough to make the microphone response independent of small changes in orientation or locating of the microphone on its surface. The velocity of this platform should have some simple law of distribution over the desired frequency spectrum (preferably a uniform distribution) of approximately 50 to 10,000 cycles. At the same time, the platform must have a sufficiently high mechanical impedance in order for its motion not to be affected by the high impedance of the tested throat microphone at its points of resonance. In the selection of a proper system, consideration was given to a design of platform which would be controlled by one of the three possible parameters, namely: resistance, stiffness, or mass. Resistance control has the advantage of uniform velocity distribution over the frequency range, but it was very difficult to find a physical embodiment of a stable mechanical resistance. Stiffness control is difficult to realize, since in a physical stiffness element there must be some mass present.

A mass controlled platform on the other hand is relatively easy to construct. A platform having a mass of approximately 4,000 grams can be driven with a relatively small expenditure of wattless power. For example, in order to impart an amplitude A of 10^{-7} centimeters at 10,000 cycles (which amplitude is far in excess of the amplitude of vibration actually encountered) to a mass M of 4,000 grams, a wattless power of $\omega^3 MA^2 \times 10^{-7}$ or 0.001 watt, is required.

In an early model of the artificial throat, one end surface of a brass cylinder, approximately $3\frac{1}{4}$ inches in diameter and $3\frac{1}{2}$ inches in length, was used as the driving platform. The opposite end of the cylinder was designed to support a driving "voice" coil. This voice coil moves in the field provided by the cylindrical air gap of a 50 watt loud-speaker structure (Jensen, PM type) (5 in Figure 1).

In order to insure mass-controlled operation, the cylinder is supported and guided by a system of extremely flexible springs, resulting in a natural resonant frequency for the mass and stiffness combination of approximately 1 cycle per second. The power which has to be supplied to the driving coil can be estimated approximately as follows.

The total impedance of the driving coil of N turns and a diameter (D), moving in a magnetic field of intensity H, can be shown to be:

$$Z_t = Z_e + \frac{\pi^2 (NHD)^2 10^{-9}}{Z_m} = Z_e + Z_d$$

In this equation Z_e is the electrical blocked impedance of the magnetic coil, while the second term, which we may call Z_d, is the motional impedance of the coil in the magnetic field. The mechanical impedance, Z_m, in this case is essentially $j\omega M$, since the resonance frequency here is far below the frequency of forced vibrations at which the mass is driven. The motional impedance Z_d is the part of the total impedance which is responsible for the energy transfer from the coil into the mass of the cylinder. We can, therefore, state that the efficiency of the driving system is approximately proportional to $\left| \frac{Z_d}{(Z_e + Z_d)} \right|$, or, since Z_d is in this case negligible in comparison with Z_e, the efficiency is equal to $\left| \frac{Z_d}{Z_e} \right|$. Z_d is approximately equal to 0.025 ohm for actual values of $N = 250$, $D = 2\frac{1}{2}$ inches, and $H = 15{,}000$. Thus, with Z_e equal to approximately 250 ohms at 10,000 cycles, we have an energy transfer efficiency at 10,000 cycles equal to 10^{-4}. Therefore in order to impart to this mass an amplitude of 10^{-7} centimeters at 10,000 cycles, the necessary power input to the coil is 10 watts. The actual amplifier used to drive the artificial throat with a power output capacity of 50 watts was found sufficient to satisfy all requirements encountered in development work and testing.

Figure 1 shows the cross section of the artificial throat described above. The cylinder (1) is supported by four springs (2 and 3), illustrated in Figure 2. These springs serve to guide the cylinder in the axial direction. They are extremely flexible in a direction perpendicular to their plane, while they are very rigid in a radial direction. Two such springs, displaced angularly by 90 degrees to each other, are used near each end of the cylinder. These springs were punched out of thin phosphor bronze sheet, in order to keep the resonant frequencies of their free spring portion S, connecting the inner and outer rings of the springs, considerably below 50 cycles. This is important in order to prevent these springs from reacting upon the motion of the cylinder in the useful frequency range. The weight of the cylinder is supported by four very compliant helical springs

Paper 46-25, recommended by the AIEE committee on communication and technical program for presentation at the AIEE winter convention, New York, N. Y. January 21–25, 1946. Manuscript submitted November 19, 1945; made available for printing December 13, 1945.

E. H. GREIBACH, director of research, Sonotone Corporation, Elmsford, N. Y.

The author acknowledges the co-operation of the Sonotone Corporation in sponsoring the development work on the apparatus described. He desires also to express his appreciation to F. P. Greenwood, M. E. Zaret, and Jack Sobol for their co-operation in the development of the testing equipment and to H. A. Pearson for many valuable discussions during the progress of the work.

(6), which are permitted to be sufficiently extended to support the weight of the cylinder. The position of the helical springs can be adjusted by means of levers mounted in the cylinder (7), thus providing for proper centering of the voice coil (4) in the air gap. The throat microphone under test is shielded both magnetically and electrically by the series of disks shown in Figure 1.

The system of compliant springs maintains the mass of the cylinder effectively floating in air and does not affect its pure mass impedance character. This behavior of the cylinder is, however, disturbed at the frequency at which the cylinder ceases to be a rigid mass and becomes a half wave length transmission line with distributed parameters. This change occurs for a brass cylinder of the dimensions used at a frequency of approximately 17,500 cycles. Therefore, at frequencies whose second and third harmonics are equal to 17,500 cycles, marked resonance effects were observed. This resonance was shifted to a higher frequency by substituting stainless steel for brass, since the velocity of sound in stainless steel is considerably higher than in brass. By using stainless steel cylinders of a shape slightly different from the one shown in Figure 1, it was possible to move this half wave resonant frequency up to 27,000 cycles. In this way, the first resonant effect obtained was in the neighborhood of 9,000 cycles.

In order to obtain a uniform velocity of the platform in the frequency range required, it is necessary to energize the driving coil with a current increasing linearly with frequency. This was accomplished by providing the input of the linear 50-watt amplifier with a simple dividing network, consisting of condensers and resistors. Figure 3 shows the velocity distribution of an artificial throat containing the brass cylinder. Two peaks, one at 5,800 and one at 8,700 cycles are seen in this figure. They are due to a very small amount of second and third harmonics present in the output of the driving amplifier. The peaks are sharp on account of the very high Q of the brass cylinder. In the final design, using a stainless steel cylinder, the velocity distribution turned out to be uniform within ± 2 decibels in the range from 50 to 10,000 cycles.

The velocity calibration was obtained by means of the experimental setup shown in Figure 4. It consists of a second voice coil attached to the moving platform of the artificial throat under test. This coil moves inside a stationary magnetic field provided by a permanent magnet loud speaker field structure m. The magnet is suspended from a substantially vibration-proof mounting shown in the figure. This mounting consists of two heavy cylinders connected to each other by means of three very flexible springs and a large oil dash pot to provide damping. The upper of the two cylinders is suspended from the ceiling by means of a set of three chains

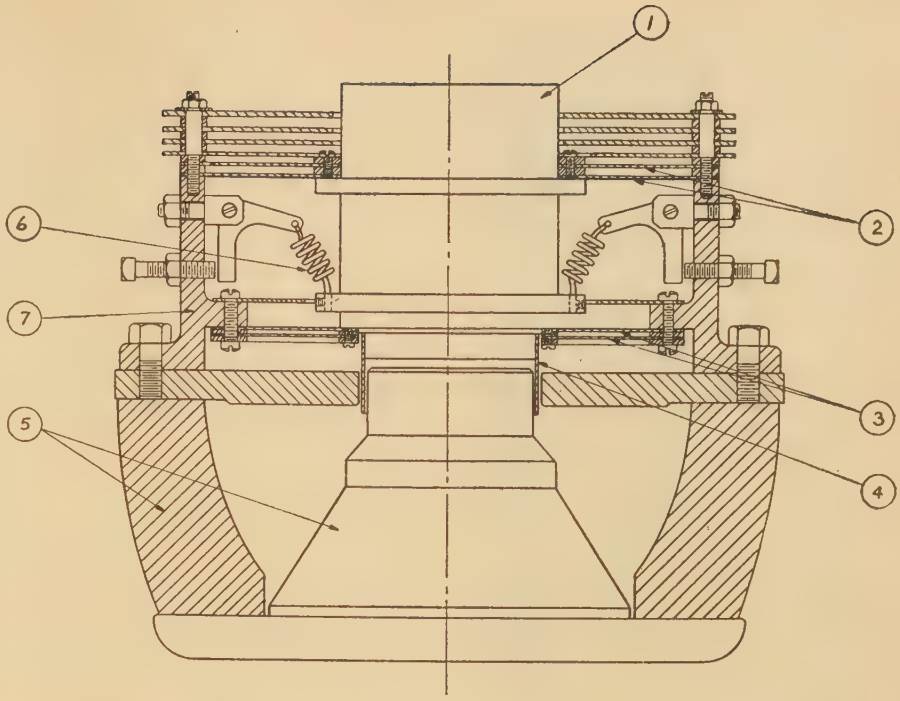

Figure 1. Cross-sectional view of artificial throat

1—Driving mass
2 and 3—Guide springs
4—Driving coil (voice coil)
5—Permanent magnet loudspeaker structure
6—Supporting springs
7—Supporting structure for driving mass

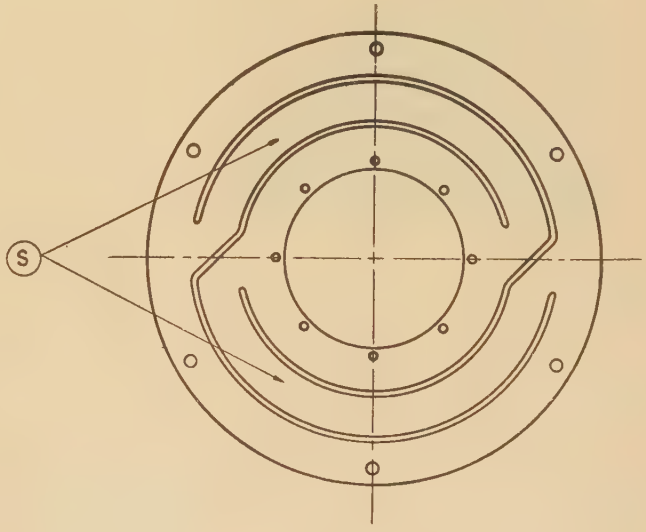

Figure 2. Support springs of artificial throat (2 and 3 in Figure 1)

S—Free spring portion

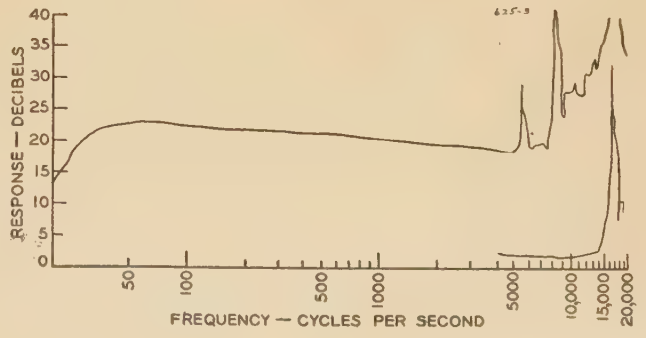

Figure 3. Frequency response curves for 50-watt artificial throat with solid brass driving mass

Upper curve is typical frequency response of artificial throat. Lower curve is 15 decibels lower than upper for location of frequency of upper peak

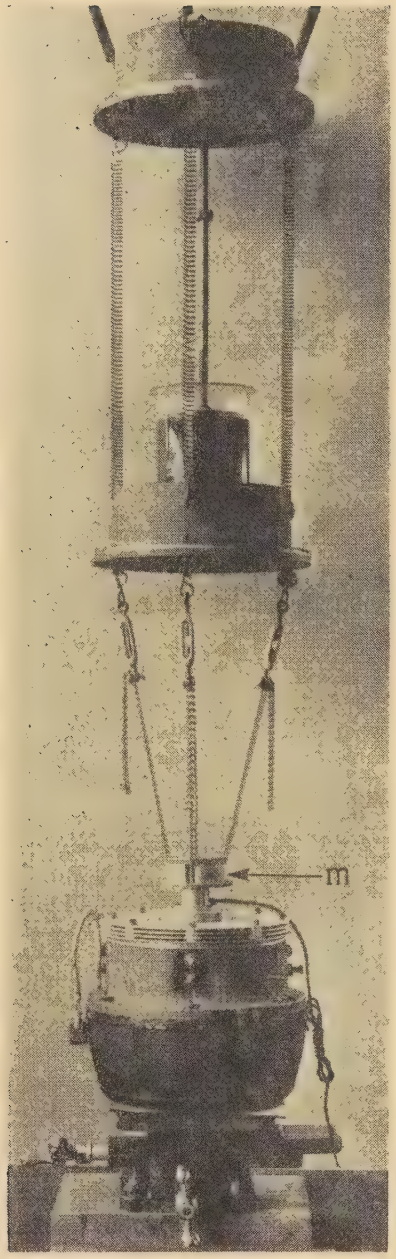

Figure 4. Artificial throat set up for operation. The system of masses, springs, and dashpot serve to keep magnet *m* stationary for calibration of the equipment

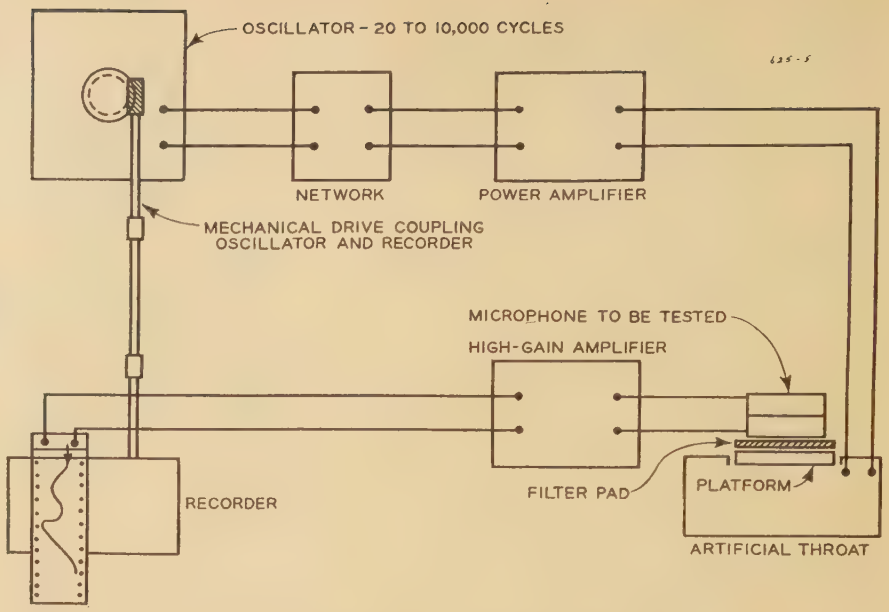

Figure 5. Experimental setup for automatically recording frequency response of throat microphone driven by artificial throat

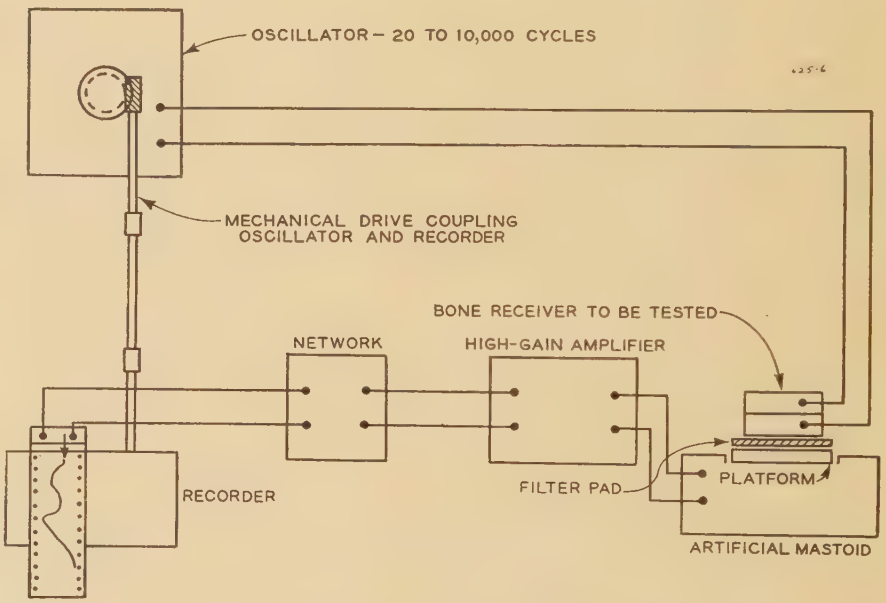

Figure 6. Experimental setup for automatically recording frequency response of bone receiver driving an artificial mastoid

and springs. The artificial throat, as seen in Figure 4, rests on a heavy table. Centering of the calibrating coil in the field of a small suspended magnet is accomplished as seen in the picture by means of an ordinary machine shop cross-feed device. Employing this set-up, it was possible to measure the velocity of the platform with good accuracy and freedom from external influence.

The block diagram of an experimental set-up for automatic recording of frequency responses of throat microphones is shown in Figure 5.[2] A beat frequency oscillator, driven by the motor of the recorder, supplies a voltage to the attenuating network mentioned above, which in turn excites a power amplifier with a voltage increasing linearly with frequency. The output of the power amplifier is fed to the artificial throat which drives a throat microphone (fastened to its platform by means of a compliant elastic band) through an interposed filter pad. The output of the throat microphone is then fed through a linear high gain amplifier to the recorder. The position of the microphone on the platform is not critical and identical response curves are obtained when the microphone is shifted on the platform.

The choice of a proper filter pad is the most difficult part of the problem. A filter pad should simulate the impedance looking into the human throat through the skin (or, in case of bone receivers, into the human head). This impedance has mainly stiffness and loss components. It was found possible to simulate either of the components by means of properly chosen pads. However, to date, serious difficulties have been encountered in constructing a pad that would give faithful reproduction of both parameters and thereby obtaining curves which are a true picture of the sensations received by the

Inertia Throat Microphones

E. H. GREIBACH
MEMBER AIEE

L. G. PACENT
FELLOW AIEE

Synopsis: This paper deals with the theory and design of magnetic inertia throat microphones. Especial attention is given to the treatment of sound power and high articulation throat microphones. The sound power microphones described contain a double frequency, undamped vibrating system, while the high articulation microphones have damping introduced, which reduces the low frequency peak with resultant increase in articulation. Wide range frequency response is obtained from the neighborhood of 100 cycles, extending up to 3,000, 4,000, or 5,000 cycles, as may be desired. These microphones have a band pass filter character with a sharp high frequency cutoff. This cutoff is desirable in order to cut out high frequency noises.

IT IS frequently necessary to send messages from noisy surroundings, such as machine shops, airplanes, and battlefields. For example, although the noise levels found in industrial plants or aircraft are often of the order of 100 or more decibels, communication must be maintained at all times. This creates the need for a discriminating microphone, that is, a microphone which will attenuate substantially the undesired sounds to favor the particular desired message. The throat microphone is such a discriminating microphone, as it is highly sensitive to vibrations transmitted to it by bodily contact with the sound-producing throat while it is quite insensitive to sound waves transmitted by air.

A throat microphone also has the advantage that it produces less discomfort than any other style, is less subject to shifting out of position or getting knocked off because of movements of its wearer. Another advantage is that it permits normal conversation to be carried on unrestricted to a degree not approached by any other form of microphone.

Throat microphones can be built on different principles, according to the method used for the conversion of acoustic into electric energy, such as carbon chambers, crystal microphones, and electromagnetic systems. Of these three kinds of elements, as will be shown, the electromagnetic system is especially well suited to provide a high articulation throat microphone.

Throat microphones reproduce speech by picking up the vibrations of the larynx rather than the sound waves generated in the air by the speaker. High frequency vibrations picked up from the larynx are subject to considerably greater attenuation than low frequency vibrations, since these high speech frequencies generally are produced in the forward portion of the mouth and have to pass over a long path of soft flesh to reach the larynx. In addition, the larynx is covered with a sheath of compliant skin, which attenuates the higher frequencies still further. The throat microphone therefore should be designed to differentiate strongly in favor of the higher frequencies of the vibrations of the larynx.

Because throat microphones operate while pressed against the throat or other portion of the human body, it is necessary to enclose the working mechanism entirely within a rigid housing in order to prevent external forces from affecting the air gap. For the same reason, it also becomes desirable to use the inertia principle in the design of such microphones.*

In short, an electromagnetic throat microphone should favor the higher speech frequencies and be enclosed in a rigid housing, which latter calls for the use of the inertia principle.

The inertia unit consists of an electromagnet L_1 supported by a spring C_1, as represented in Figure 1. The electromagnet L_1 consists of two small Alnico magnets, a central core with a coil wound around it, and a yoke and pole plate. C_1 is an S-shaped spring, supporting the electromagnet and forming the working air gap between its central portion and pole surfaces. This electromagnet struc-

Paper 46-24, recommended by the AIEE committee on communication for presentation at the AIEE winter convention, New York, N. Y., January 21–25, 1946. Manuscript submitted November 19, 1945; made available for printing December 13, 1945.

E. H. GREIBACH is director of research, Sonotone Corporation, Elmsford, N. Y. L. G. PACENT is president, Pacent Engineering Corporation, New York, N. Y.

The authors thank the management of the Sonotone Corporation for its approval of this project. They also are indebted to Mr. H. A. Pearson for many constructive discussions during the development program and to Mr. F. P. Greenwood and Mr. J. A. Kucher for carrying out the experimental work.

* E. H. Greibach, United States patents 2,255,249 and 2,255,250.

head in the case of bone conduction, or a true output of the human throat as it affects a throat microphone. While perforated rubber pads were found suitable to simulate the stiffness component of the skin and while pads of damping material, like "Viscoloid," have given a fair approach to the loss component of the skin, it was difficult to find a pad or combination of pads to simulate both stiffness and resistance together and in proper proportion.

It is readily seen that the artificial throat described above can also be used as an artificial mastoid. In the case of the artificial mastoid, the floating cylinder is driven by a bone conduction receiver through a filter pad simulating the skin over the mastoid bone, and the output of the coil mounted on the lower portion of the cylinder (driving coil for the throat) is then amplified and fed into a recorder. When it is desired to obtain response curves representing the force transmitted through the filter pad into the floating cylinder, it is necessary to use a dividing network (similar to the network used with the artificial throat) in the output of the linear high gain amplifier. This network will then deliver a voltage increasing linearly with frequency for a constant input voltage. On the other hand, response curves, representing the velocity transmitted through the filter pad, are obtained by using the linear high gain amplifier without an additional dividing network. Figure 6 shows how the equipment pictured in Figure 5 is rearranged to take frequency response characteristics of inertia bone receivers.

The above described equipment, in spite of some limitations, has proved to be a useful and powerful laboratory tool. The setups shown in Figures 5 and 6 permit the rapid taking of consistently reproducible response curves.

References

1. APPLIED ACOUSTICS (second edition). Olsen Massa. Page 286.

2. INERTIA THROAT MICROPHONES. E. H. Greibach, L. G. Pacent. AIEE TRANSACTIONS, volume 65, 1946, April section, pages 187–91.

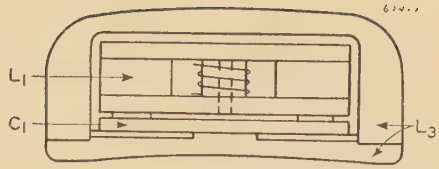

Figure 1. Construction of inertia unit

L_1—electromagnet structure
C_1—spring
L_3—housing

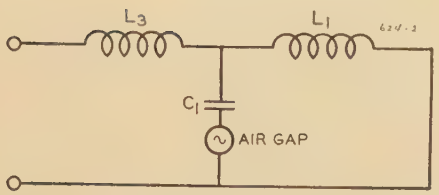

Figure 2. Equivalent electric circuit for structure shown in Figure 1

ture is surrounded by a housing, indicated schematically in Figure 1 as L_3. The equivalent electric circuit is represented in Figure 2, where the same symbols are used as in Figure 1 to designate the respective equivalent components.

The voltage produced across the magnet coil is proportional to the air gap velocity. It can be shown that the velocity I_1 of the air gap bears the following relationship to the velocity, I, imparted to the housing L_3 by external forces:

$$I_1 = Ix \frac{(f/f_o)^2}{1-(f/f_o)^2} \qquad (1)$$

where f_o is the resonant frequency of the vibrating system formed by the spring C_1 and electromagnet L_1, while f is the frequency of the force applied to the housing. For frequencies below resonance where f/f_o is small, the formula then can be written:

$$I_1 = Ix\ (f/f_o)^2 \qquad (2)$$

Equation 2 shows the air gap velocity to be proportional to the square of the applied frequency at frequencies below resonance. Therefore, magnetic or dynamic microphones will have a frequency discrimination of 12 decibels per octave in this range. In contrast, crystal or carbon microphones, in which voltage is proportional to the displacement, will have a frequency discrimination of only 6 decibels per octave. This result illustrates the advantage of the inertia magnetic throat microphone over the other types on account of its greater ability to discriminate against low frequencies.

It thus is seen that the rapidly rising response characteristic of the magnetic inertia throat microphone, below the resonant frequency, effectively compensates for the frequency distortion generated in the throat. In order to obtain satisfactory intelligibility, it is desirable to set the resonant frequency of the microphone at a relatively high value, in the neighborhood of 3,000 to 4,000 cycles. On the other hand, though such high frequency inertia throat microphones give a very good intelligibility when used with standard flat-response amplifiers, their output is low. The output can be increased substantially by lowering the resonant frequency to about 1,000 cycles, but this is accomplished at the expense of intelligibility.

Despite this difficulty, there are many applications which require that the two conflicting requirements of high sensitivity and high intelligibility be satisfied simultaneously, for example, in the case of sound powered communication systems. Through the addition of a second resonant frequency to a low frequency microphone system (approximately 1,000 cycles) a substantial extension of the sensitivity of the throat microphone can be obtained without loss of intelligibility. This second frequency is obtained by incorporating in its mechanical system a second mass and compliance system, having its resonant frequency somewhere in the range between 2,500 and 4,000 cycles. Such double resonant microphones have then a substantial output over the entire range from 1,000 to 3,000 or 4,000 cycles.

Figure 3 shows a schematic layout of a

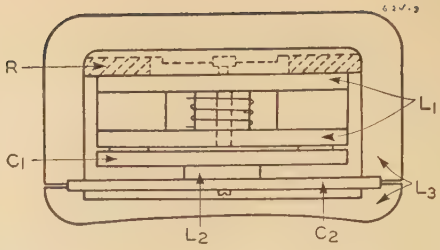

Figure 3. Construction of double resonant inertia unit

L_1—electromagnet structure
L_2—coupler
L_3—housing
C_1—spring of single resonant unit
C_2—spring for second resonance

double resonant electromagnetic inertia system. Here L_1 is the mass of the electromagnet, supported by the spring C_1 in the same fashion as shown in Figure 1. Springs C_1, C_2, and coupler of mass L_2 form the second resonant system. C_2 is connected to the spring C_1 through L_2. All parts shown in Figure 3 also are shown in the exploded Figure 4 and are designated by the same symbols. The spring C_2 is held inside a frame structure, which is necessary to facilitate the mounting of the spring inside the housing. Use of the frame structure also reduces the losses in C_2 and provides means for easy duplication of spring properties in production. Figure 5 represents the equivalent electric circuit and uses the same symbols as in Figures 3 and 4 to designate the respective equivalent components. The electromagnet L_1 is connected to the housing L_3 through a mechanical transmission system, consisting of the springs C_1 and C_2, and the interposed mass L_2. This transmission system transmits the imparted velocity to the air gap formed between L_1 and C_1 with an efficiency which increases with frequency, thus permitting emphasis on the high frequencies at the expense of the low.

Of the two resonant frequencies incorporated in this system, one is represented approximately by the system consisting of the mass L_1 and the spring C_1. The second resonance, that of the system consisting of the two springs C_1 and C_2 and the mass L_2, is considerably higher than the first one. At frequencies above the second resonance most of the velocity imparted into the housing is absorbed by the spring C_1, and only a small fraction of it can be transmitted to the air gap. This results in a relatively sharp cutoff at

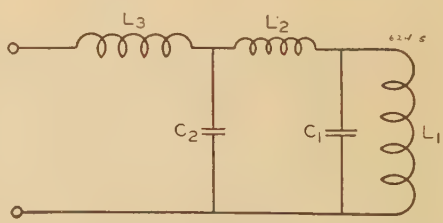

Figure 5. Equivalent electric circuit for structure shown in Figures 3 and 4

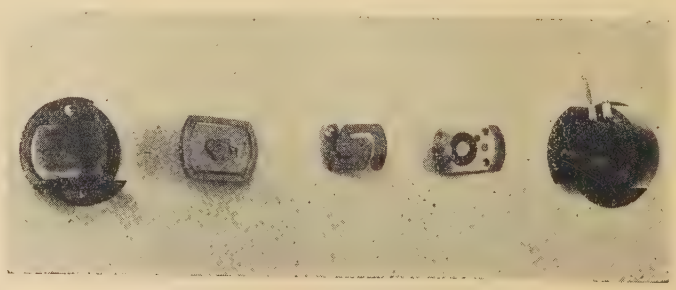

Figure 4. Exploded view of parts comprising a double resonant unit

higher frequencies and a band pass character for this type of throat microphone. The sharp cutting off of frequencies outside the range required for intelligibility is desirable, as it prevents transmission of high frequency noises and static and thus contributes to the improvement of intelligibility.

The values of the two resonant frequencies are obtained by solving the characteristic determinant of the equivalent circuit of Figure 5. Equation 3 is the solution for the two resonant frequencies with $\omega = 2\pi f$.

$$\omega^2 = \frac{1}{2}\frac{1}{L_1C_1}\left(\frac{L_1C_1}{L_3C_2}+\frac{L_1C_1}{L_2C_2}+1+\frac{L_1}{L_2}\right) \pm \frac{1}{L_1C_1}\left[\left(\frac{L_1C_1}{L_2C_2}+\frac{L_1C_1}{L_3C_2}-1+\frac{L_1}{L_2}\right)^2 + 4\frac{L_1^2}{L_2^2}\frac{C_1}{C_2}\right]^{1/2} \quad (3)$$

By expanding the square root expression and retaining the first two terms only, the following simplified approximate equations are obtained:

$$\omega_1^2 = \frac{1}{C_1}\left(\frac{1}{L_1}+\frac{1}{L_2}\right) - \delta = \omega_{10}^2 - \delta \quad (4)$$

$$\omega_2^2 = \frac{1}{C_2}\left(\frac{1}{L_2}+\frac{1}{L_3}\right) + \delta = \omega_{20}^2 + \delta \quad (5)$$

where

$$\delta = \frac{1}{L_2^2C_1C_2(\omega_{20}^2-\omega_{10}^2)}$$

The foregoing expansion is valid only when the difference $\omega_{20}^2-\omega_{10}^2$ is large, so that the correction term δ is small compared with both ω_{10}^2 and ω_{20}^2. ω_{10} and ω_{20} correspond roughly to the two resonance frequencies of the system.

For experimental purposes, as well as for different applications, it is desirable to build models having different spreads between the two resonant frequencies. This can be accomplished by changing some or all of the parameters in equations 4 and 5. On the other hand, the values of certain components remain more or less fixed on account of limitations in size, as well as the need to obtain optimum efficiency within a given volume. Among the fixed values are L_1 and C_1, which form the electromagnetic system, as well as the value of L_3, which is the mass of the housing.

Equations 4 and 5 demonstrate that, even if the values L_1, C_1, and L_3 are kept fixed, it is still possible to obtain wide variations in the value of the frequency f_2 by simply changing L_2 and C_2. It is further seen by inspecting equation 3 that the frequencies f_1 and f_2 are functions of

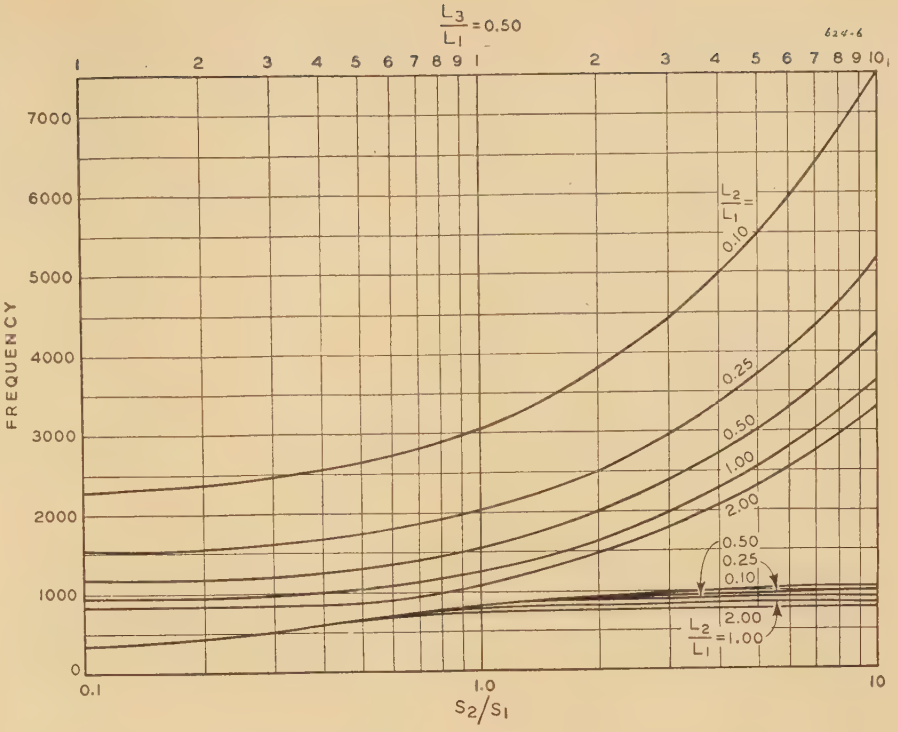

Figure 6. Curves showing relation of frequencies f_1 and f_2 as functions of the ratio $S_2 \div S_1$ plotted for various values of $L_2 \div L_1$

Curves computed for $L_3 \div L_1 = 0.50$

the two ratios: $L_2 \div L_1$ and $C_1 \div C_2$.

It is therefore possible to plot families of curves for the two frequencies as functions, for example, of the ratio C_1/C_2, the different curves corresponding to different values of L_2/L_1. Such curves, as calculated from equation 3, are shown in Figure 6. In this figure the values for f_1 form the lower family of curves, which fall closely together, as is to be expected from equation 4, where L_1 and C_1 remain fixed. On the other hand the values for f_2 show a wide spread, since as shown in equation 5 both C_2 and L_2 are variables. The curves in Figure 6 therefore can be used to construct throat microphones with different properties. The curves were computed for: $L_3 \div L_1 = 0.50$.

It is desirable sometimes to build electromagnetic transducers having an extremely narrow band of response. For example, in bridge circuits the null position must be determined very sharply for the frequency of the power source to which such a bridge is connected and for the elimination of the disturbing effect of harmonics present in the source due to unavoidable distortion. In this case it is important to have a detector which will be sensitive only to the frequency of the fundamental component of the current wave. Here equations 4 and 5 become invalid, as the difference $\omega_{20}^2-\omega_{10}^2$ becomes very small, hence δ very large.

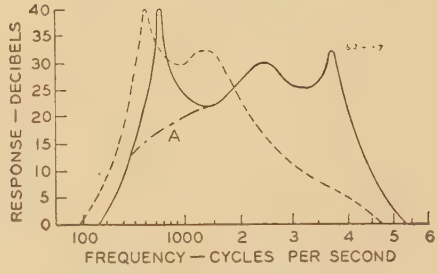

Figure 7. Comparative response curves for single and double resonant units

------ Single resonance unit
——— Double resonance unit
— — — Effect of damping on double resonant unit (high articulation)
A—High articulation unit

The complete equation 3 consequently must be used. For example, by using the values $L_2 \div L_1 = 1$ and $C_1 \div C_2 = 1$, response in the narrow band from approximately 800 to 1,250 cycles is obtained (Figure 6). Such a unit, when used as a detector (receiver), will permit very sharp balancing of a 1,000-cycle bridge.

Throat microphones built with components as illustrated in Figure 4 and having response in the band between 1,000 and 4,000 cycles have given high intelligibility scores when used as a sound powered microphone in conjunction with sound powered receivers.

In Figure 7 comparative response curves of single and double resonant units are shown. The light curve represents the response of a single resonant unit, and the heavy curve represents that of a

double resonant unit, the two units having identical electromagnets. These curves of the throat microphones were obtained by driving the microphones with an artificial throat. The artificial throat used in the preparation of these curves has a platform moving with substantially constant velocity in the frequency range from 50 to 10,000 cycles. A compliant pad, simulating the skin layer over the larynx, was interposed between the platform and the throat microphone under test. The effect of the interposed pad is to introduce an attenuation increasing with frequency and also an additional peak. The extra peak in each case is due to the compliance of the interposed pad coupling the housing to the platform.

The heavy curve in Figure 7 has an appreciable peak on the low frequency end at about 800 cycles. It is desirable for many applications, especially when throat microphones are used with flat response

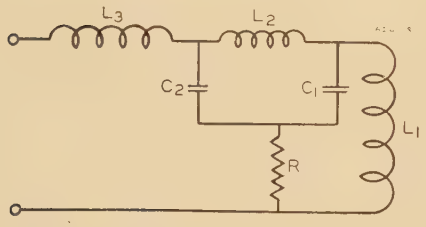

Figure 8. Equivalent electric circuit for damped double resonant unit

amplifying systems, to reduce or eliminate this peak in order to improve still further the intelligibility of such communication systems. This is done by introducing a damping member between the electromagnet L_1 and the housing L_3, as indicated schematically by the dotted lines in Figure 3. The equivalent electric circuit is shown in Figure 8. Placing the resistor R in the position shown in Figure 8 permits a very effective damping of the low frequency peak without affecting essentially the performance of such throat microphones in the neighborhood of the high frequency resonance. This is true since the damping resistance R effectively can suppress oscillations set up in the mesh, consisting of L_1, C_1, and R. On the other hand, high frequency oscillations set up in the mesh L_2, C_1, and C_2 are affected only a little by the energy absorbing resistance R, since any transfer of energy from this mesh must take place through the high impedance path L_1 in order to reach R. The dotted line in Figure 7 represents the response of a damped double resonance throat microphone. The articulation of these microphones is

Figure 9. Completely assembled typical throat microphone of electromagnetic type described in the paper

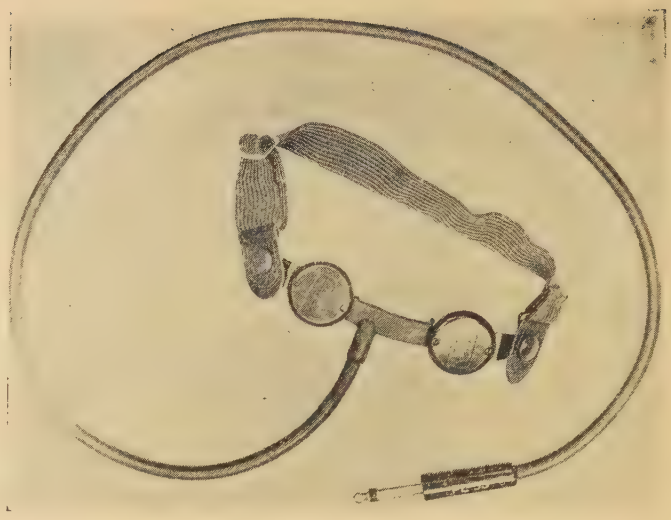

better than that of undamped throat microphones when used in conjunction with amplifying systems. The suppression of this low peak for sound power application is not important, since sound powered receivers can be built to have a somewhat attenuated response in the range corresponding to the low frequency peak of the throat microphone. The loss of sensitivity caused by the introduction of damping is not serious, as these microphones are used with amplifying systems. Damping can be obtained by using different damping materials introduced into the mechanical system, in the manner indicated in Figure 3. Best results were obtained by using a damping cup containing oil. Oil damping cups have the advantage of containing little stiffness as compared with the amount of resistance they introduce. The introduction of damping reduces to some extent the sharp cutoff characteristic of the undamped unit. The average output of a sound power throat microphone wound for 100-ohm internal impedance is approximately 15 millivolts, whereas the output of a similar high articulation throat microphone is on the average of 2 millivolts.

It is obvious that other parts of the head, such as cheeks, jaw, temple, vibrate under the influence of sounds produced in the mouth cavity and can be used to actuate such contact microphones. Especially good results are obtained when placing the throat microphone on the lips.

Figure 9 is a photograph of a typical throat microphone. This instrument consists of two units, disposed symmetrically on both sides of the throat. They are

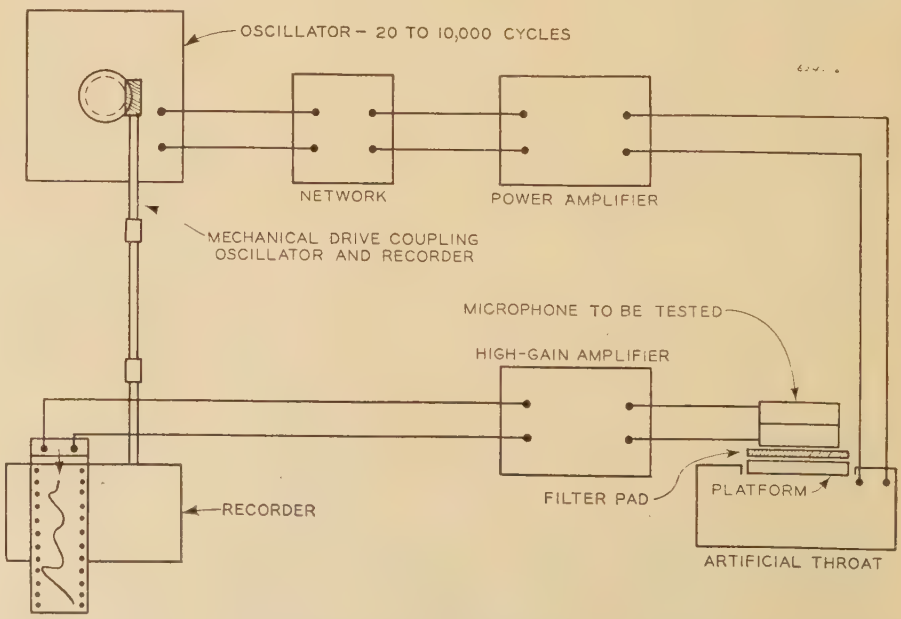

Figure 10. Experimental setup for automatically recording frequency response of throat microphone driven by artificial throat

Performance Calculations on Polyphase Reluctance Motors (Synchronous Motors Without Field Excitation)

P. H. TRICKEY
MEMBER AIEE

IN 1926, Messrs. Doherty and Nickle presented their classic paper on "Synchronous Machines" giving a complete and thorough analysis. Since many fractional horsepower engineers have occasion to design small reluctance motors (synchronous motors without field excitation) and these engineers in general have no need of becoming thoroughly familiar with the great and extensive field of synchronous motor theory, it has seemed advisable to simplify the equations from this famous paper by eliminating the terms having to do with field current and to arrange them in the form of a simple calculation sheet. It also has been found possible by the use of calculated curves to arrange a simple method of calculating the synchronous pull-out torque.

As in the case of induction motors, it is customary also in synchronous motor engineering to divide the work of designing a unit into three parts, first, choosing trial dimensions and windings, second, calculating the motor "constants" such as resistances, reactances, and iron loss and third, calculating the performance of the trial design. If the performance is not satisfactory further trial designs are made and the same procedure followed.

In the case of the first step, the experienced designer can often make the first trial very close to the correct design either from his experience or from making ratios from similar designs. If the designer is inexperienced or if the required design is radically different from any previous machine, sometimes a number of trials may be necessary.

Many papers have been written on the second step, the calculation of motor constants. Reference to some of these papers is given in the bibliography. It is not the purpose of this paper to discuss step one and two, but step three, the calculation of performance from calculated or tested constants.

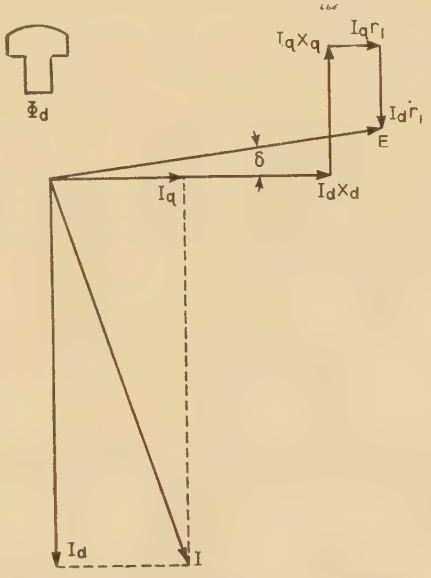

Figure 1. Vector diagram of reluctance motor

In the usual calculations of induction motors, the calculation forms are arranged so that performance is a function of slip, and trials of slip are made until the desired output is obtained. In this case, also, a trial and error method is used. This time the displacement angle is the variable and trials are made until proper output is obtained. On large machines, it is fairly easy to check the torque angle by test. With small motors below one horsepower it often is difficult to obtain the zero angle positon as a reference point. This is not greatly disadvantageous, however, as the performance versus output torque is much more important, and calculated displacement angles are usually sufficient.

Performance Equations

Rearranging Figure 20, page 925 of the reference paper,[1] to omit field excitation, we arrive at the diagram shown in Figure 1 and the equation below.

$$E = I_d X_d + I_q r_1 + j(I_q X_q - I_d r_1)$$

Solving for I_d and I_q,

$$I_d = \frac{E}{X_d} \frac{1}{1+(r_1/X_q)(r_1/X_d)} \times \left(\cos\delta - \frac{r_1}{X_q}\sin\delta\right)$$

$$I_q = \frac{E}{X_d} \frac{1}{1+(r_1/X_q)(r_1/X_d)} \times \left(\frac{1}{X_q/X_d}\sin\delta + \frac{r_1}{X_q}\cos\delta\right)$$

Line current

$$I = \sqrt{I_q^2 + I_d^2}$$

Power input

$$P = ph\,E\,(I_q\cos\delta - I_d\sin\delta)$$

Output

$$\text{Output} = \text{input} - (\text{Iron loss} + \text{friction} + \text{windage} + ph\,I^2 r_1)$$

Torque

$$T = \frac{112.7}{Syn}\ \text{output (in ounce feet)}$$

held on the throat by means of an elastic band, which is adjustable to control the pressure on the throat. As seen in the illustration, the instrument is provided with a standard cord and plug.

Figure 10 is a schematic diagram of the setup used in testing throat microphones. It consists of an oscillator mechanically coupled to a sound level recorder. The oscillator feeds a signal with continuously variable frequency through a network into a linear power amplifier. The power amplifier in turn drives an artificial throat whose platform vibrates with an essentially constant velocity in the frequency range of 50 cycles to 10,000 cycles. The throat microphone is placed on the vibrating platform with a filter pad interposed between the microphone and the platform. The purpose of the filter pad is to simulate as far as possible the layer of skin covering the larynx of an average speaker. The output of the throat microphone is amplified by a high gain amplifier and fed into the sound level recorder. Thus an automatic record is obtained of the variation of the output as a function of the frequency applied to the microphone.

Paper 46-65, recommended by the AIEE committee on electric machinery and technical program for presentation at the AIEE winter convention technical meeting, New York, N. Y., January 21–25, 1946. Manuscript submitted April 12, 1945; made available for printing December 26, 1945.

P. H. TRICKEY is chief engineer, Diehl Manufacturing Company, Somerville, N. J.

Synchronous Pull-Out Torque

The maximum torque that the motor will develop while in synchronism, known as "pull-out" torque, may be obtained as follows:

$T = (112.7/Syn)$ output $= (112.7/Syn)$ (input $-$ losses)
$T = (112.7/Syn)$ [(input $-$ copper loss) $-$ $(Fe+F+W)$]
$T = (112.7/Syn)$ $[P_1 - (Fe+F+W)]$

Since iron loss, friction, and windage are essentially constant at synchronous speed, the maximum synchronous torque will occur when P_1 is at its maximum value. By substituting the current values given above in the equations for input and copper loss, it can be shown that

$$P_1 = ph\frac{E^2}{X_d}\frac{1}{1+(r_1/X_q)(r_1/X_d)}A$$

Where A is a rather cumbersome group of terms containing r_1, X_q, X_d, and δ.

Values of A maximum have been calculated and plotted in Figure 2, so that we find it fairly easy to calculate the synchronous pull-out torque.

$$T_{PO} = \frac{112.7}{Syn}[ph\,E\,M_1\,A_m - (Fe+F+W)]$$

(ounce-feet)

Where $M_1 = \frac{E}{X_d}\frac{1}{1+(r_1/X_q)(r_1/X_d)}$

It can easily be seen from Figure 2 how important it is to keep r_1/X_q and r_1/X_d as small as possible.

Figure 3 shows a form which has been arranged to make these calculations as simple as possible. The displacement angle δ is assumed and the performance values calculated. Items 23 to 27 are only in calculating the pull-out torque.

Since reluctance motors are usually less than one horsepower, Figure 3 has been arranged in terms of actual values of volts, amperes, and ohms, instead of "per unit" values which are seldom used by fractional horsepower motor engineers.

List of Symbols

E = volts per phase
$F+W$ = friction plus windage
Fe = iron loss
I = current per phase
I_d = current in direct axis
I_q = current in quadrature axis
ph = number of phases
P = power input in watts
r_1 = primary resistance per phase
Syn = synchronous rpm
T = torque in ounce-feet
T_{PI} = synchronous pull-in torque
T_{PO} = synchronous pull-out torque

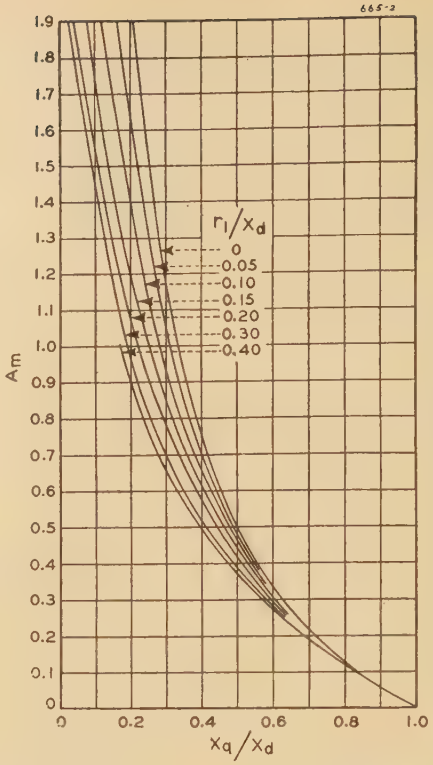

Figure 2. Constant A_m used in calculating pull-out torque

X_d = total direct axis reactance per phase
X_q = total quadrature axis reactance per phase
δ = displacement angle in electrical degrees

Appendix I. Performance Equations

Rearranging Figure 20, page 925 of the reference paper[1] to omit field excitation, we arrive at the diagram shown in Figure 1.

$E = I_dX_d + I_qr_1 + j(I_qX_q - I_dr_1)$

$E\cos\delta = I_dX_d + I_qr_1$ and $E\sin\delta = I_qX_q - I_dr_1$

Solving for I_d

$EX_q\cos\delta = I_dX_dX_q + I_qX_qr_1$ and
$Er_1\sin\delta = -I_dr_1^2 + I_qX_qr_1$
$E(X_q\cos\delta - r_1\sin\delta) = I_d(X_qX_d + r_1^2)$

$$I_d = E\frac{1}{r_1^2+X_qX_d}(X_q\cos\delta - r_1\sin\delta) = \frac{E}{X_d}\frac{1}{1+(r_1/X_q)(r_1/X_d)}\left(\cos\delta - \frac{r_1}{X_q}\sin\delta\right)$$

Solving for I_q

$Er_1\cos\delta = I_dX_dr_1 + I_qr_1^2$, and
$EX_d\sin\delta = -I_dX_dr_1 + I_qX_qX_d$
$E(X_d\sin\delta + r_1\cos\delta) = I_q(r_1^2 + X_qX_d)$

$$I_q = E\frac{1}{r_1^2+X_qX_d}X_d\sin\delta + r_1\cos\delta = \frac{E}{X_d}\frac{1}{1+(r_1/X_q)(r_1/X_d)}\left(\frac{\sin\delta}{X_q/X_d} + \frac{r_1}{X_q}\cos\delta\right)$$

Line current $I = \sqrt{I_q^2 + I_d^2}$

	E	127		
	X_d	179		
	X_q	51.8		
	r_1	6.76		
	r_1/X_d	0.0378		
	r_1/X_q	0.1306		
	X_q/X_d	0.290		
	$(r_1/X_d)(r_1/X_q)$	0.00494		
	$1+(r_1/X_d)(r_1/X_q)$	1.005		
	$M_1 = \frac{E}{X_d}\frac{1}{1+(r_1/X_d)(r_1/X_q)}$	0.705		
1	δ (IN ELEC. DEG.)	5	15	
2	COS δ	0.996	0.966	
3	(r_1/X_q) SIN δ	0.0114	0.0338	
4	(2) - (3)	0.985	0.932	
5	$I_d - M_1 \times (4)$	0.695	0.657	
6	$[1/(X_q/X_d)]$ SIN δ	0.300	0.893	
7	(r_1/X_q) COS δ	0.130	0.126	
8	(6) + (7)	0.430	1.019	
9	$I_q = M_1 \times (8)$	0.303	0.718	
10	$I = \sqrt{I_d^2 + I_q^2}$	0.758	0.973	
11	I_q COS δ	0.302	0.694	
12	I_d SIN δ	0.061	0.170	
13	(11) - (12)	0.241	0.524	
14	INPUT = ph E (13)	92.0	199	
15	$I^2 r_1$ ph	11.6	19.2	
16	Fe LOSS	21.7	21.7	
17	F + W	5.8	5.8	
18	LOSSES = (15) + (16) + (17)	39.1	46.7	
19	OUTPUT = (14) - (18)	52.9	152.3	
20	TORQUE = $\frac{112.7}{SYN}$ (19)	3.31	9.5	
21	EFF = (19)/(14)	57.5	76.6	
22	P.F. = (13)/(10)	31.8	53.9	
23	HORSEPOWER	0.0708	0.203	
24	Am (FROM FIG. 2)			1.130
25	$P_{I\,MAX}$ = ph E M_1 Am			303
26	Fe + F + W = (16) + (17)			28
27	(25) - (26)			275
28	$T_{PO} = \frac{112.7}{SYN}$ (27)			17.2

Figure 3. Calculation sheet for reluctance motors

Power input $P = ph\,E\,I_q\cos\delta - ph\,EI_d\sin\delta$
$P = ph\,E\,(I_q\cos\delta - I_d\sin\delta)$
Total losses $L = Fe + F + W + ph\,I^2r_1$
Output = input $-$ losses
Torque = $(112.7/Syn)$ output (in ounce-feet)
Efficiency = Output/input
Power factor = Input/$ph\,E\,I$

Appendix II. Pull-Out Torque or Maximum Synchronous Torque

$T = (112.7/Syn)$ output $= (112.7/Syn)$ (input $-$ losses)
$T = (112.7/Syn)$ [(input $-$ copper loss) $-$ $(Fe+F+W)$]
$T = (112.7/Syn)$ $[P_1 - (Fe+F+W)]$

Since the iron loss, friction, and windage are essentially constant at synchronous speed, the maximum synchronous torque will occur when P_1 is at its maximum value. Power input in terms of δ power input

$P = ph\,E\,(I_q\cos\delta - I_d\sin\delta)$

$$P = ph\,E\left\{\frac{E}{X_d}\frac{1}{1+(r_1/X_q)(r_1/X_d)}\left(\sin\delta\cos\delta+\frac{r_1}{X_q}\frac{X_q}{X_d}\cos^2\delta\right)-\frac{E}{X_d}\frac{1}{1+(r_1/X_q)(r_1/X_d)}\times\left(\frac{X_q}{X_d}\sin\delta\cos\delta-\frac{r_1}{X_q}\frac{X_q}{X_d}\sin^2\delta\right)\right\}\frac{1}{X_q/X_d}$$

$$\text{Input } P = ph\frac{E^2}{X_d}\frac{1}{1+(r_1/X_q)(r_1/X_d)}\times\left\{\left(1-\frac{X_q}{X_d}\right)\sin\delta\cos\delta+\frac{r_1}{X_q}\frac{X_q}{X_d}\right\}\frac{1}{X_q/X_d}$$

Copper loss in terms of δ

Copper loss $= ph\,I^2 r_1, \quad I^2 = I_d^2 + I_q^2$

Thus,

$$\text{Copper loss} = ph\,r_1(I_d^2+I_q^2)$$

$$\text{Copper loss} = ph\,r_1\left(\frac{E}{X_q}\frac{1}{1+(r_1/X_q)(r_1/X_d)}\right)^2\left\{\left(\frac{X_q}{X_d}\cos\delta-\frac{r_1}{X_q}\frac{X_q}{X_d}\sin\delta\right)^2+\left(\sin\delta+\frac{r'}{X_q}\frac{X_q}{X_d}\cos\delta\right)^2\right\}$$

$$\text{Copper loss} = \frac{ph\,E^2}{X_q}\frac{1}{1+(r_1/X_q)(r_1/X_d)}\times\left(\frac{r_1}{X_q}\frac{1}{1+(r_1/X_q)(r_1/X_d)}\right)\left\{\left(\frac{X_q}{X_d}\cos\delta-\frac{r_1 X_q}{X_q X_d}\times\sin\delta\right)^2+\left(\sin\delta+\frac{r_1}{X_q}\frac{X_q}{X_d}\cos\delta\right)^2\right\}$$

$$\text{Copper loss} = \frac{ph\,E^2}{X_q}\frac{1}{1+(r_1/X_q)(r_1/X_d)}\times\left(\frac{r_1}{X_q}\frac{1}{1+(r_1/X_q)(r_1/X_d)}\right)\times\left\{\left(\frac{X_q}{X_d}\right)^2\cos^2\delta-2\frac{r_1}{X_q}\left(\frac{X_q}{X_d}\right)^2\sin\delta\cos\delta+\left(\frac{r_1}{X_q}\right)^2\left(\frac{X_q}{X_d}\right)^2\sin^2\delta+\sin^2\delta+2\times\frac{r_1}{X_q}\frac{X_q}{X_d}\sin\delta\cos\delta+\left(\frac{r_1}{X_q}\frac{X_q}{X_d}\right)^2\cos^2\delta\right\}$$

$$\text{Copper loss} = \frac{ph\,E^2}{X_d}\frac{1}{1+(r_1/X_q)(r_1/X_d)}\times\left(\frac{r_1}{X_q}\frac{1}{1+(r_1/X_q)(r_1/X_d)}\right)\times\left\{\sin^2\delta+\left(\frac{X_q}{X_d}\right)^2\cos^2\delta+\left(\frac{r_1}{X_q}\right)^2\left(\frac{X_q}{X_d}\right)^2+2\frac{r_1}{X_q}\frac{X_q}{X_d}\left(1-\frac{X_q}{X_d}\right)\sin\delta\cos\delta\right\}\frac{1}{X_q/X_d}$$

Power input − copper loss $= P_1$

$$P_1 = \frac{ph\,E^2}{X_d}\frac{1}{1+(r_1/X_q)(r_1/X_d)}\times\left\{\left(1-\frac{X_q}{X_d}\right)\sin\delta\cos\delta+\frac{r_1}{X_q}\frac{X_q}{X_d}-\frac{r_1}{X_q}\frac{1}{1+(r_1/X_q)(r_1/X_d)}\left[\sin^2\delta-\left(\frac{X_q}{X_d}\right)^2\cos^2\delta+\left(\frac{r_1}{X_q}\frac{X_q}{X_d}\right)^2+2\frac{r_1}{X_q}\frac{X_q}{X_d}\left(1-\frac{X}{X_d}\right)\sin\delta\cos\delta\right]\right\}\frac{1}{X_q/X_d}$$

$$P_1 = ph\frac{E^2}{X_d}\frac{1}{1+(r_1/X_q)(r_1/X_d)}A$$

Output = (power input − copper loss) − $(Fe+F+W)$

Output $= P_1 - (Fe+F+W)$

Torque $= (112.7/Syn)\,[P_1-(Fe+F+W)]$

Maximum or pull-out torque will occur when P_1 is maximum. $P_{1\max}$ will occur when A is maximum. Thus

$$T_{PO} = (112.7/Syn)\,[P_{1\max}-(Fe+F+W)]$$

$$P_{1\max} = \frac{ph\,E^2}{X_d}\frac{1}{1+(r_1/X_q)(r_1/X_d)}A_m$$

$$P_{1\max} = ph\,E\,M_1 A_m$$

Where

$$A = \left\{\left(1-\frac{X_q}{X_d}\right)\sin\delta\cos\delta\left[1-\frac{r_1}{X_q}\times\frac{1}{1+(r_1/X_q)(r_1/X_d)}2\frac{r_1}{X_q}\frac{X_q}{X_d}\right]+\frac{r_1}{X_q}\frac{X_q}{X_d}\left[1-\frac{r_1}{X_q}\frac{1}{1+(r_1/X_q)(r_1/X_d)}\frac{r_1}{X_q}\frac{X_q}{X_d}\right]-\frac{r_1}{X_q}\frac{1}{1+(r_1/X_q)(r_1/X_d)}\sin^2\delta-\frac{r_1}{X_q}\frac{1}{1+(r_1/X_q)(r_1/X_d)}\left(\frac{X_q}{X_d}\right)^2\cos^2\delta\right\}\frac{1}{X_q/X_d}$$

or

$$A = \left\{\left(1-\frac{X_q}{X_d}\right)\sin\delta\cos\delta\left[1-2\left(\frac{r_1}{X_d}\right)^2\times\frac{1}{X_q/X_d}\frac{1}{1+(r_1/X_d)^2 1/(X_q/X_d)}\right]+\frac{r_1}{X_d}\left[1-\left(\frac{r_1}{X_d}\right)^2\frac{1}{X_q/X_d}\times\frac{1}{1+(r_1/X_d)^2 1/(X_q/X_d)}\right]-\frac{r_1}{X_d}\frac{1}{X_q/X_d}\times\frac{1}{1+(r_1/X_d)^2 1/(X_q/X_d)}\sin^2\delta-\frac{r_1}{X_d}\frac{X_q}{X_d}\frac{1}{1+(r_1/X_d)^2 1/(X_q/X_d)}\cos^2\delta\right\}\frac{1}{X_q/X_d}$$

Let

$$B = \frac{r_1}{X_d}\frac{1}{X_q/X_d}\frac{1}{1+(r_1/X_d)^2 1/(X_q/X_d)}$$

then

$$A = \left\{\left(1-\frac{X_q}{X_d}\right)\sin\delta\cos\delta\left[1-2\frac{r_1}{X_d}B\right]+\frac{r_1}{X_d}\left[1-\frac{r_1}{X_d}B\right]-B\sin^2\delta-B\left(\frac{X_q}{X_d}\right)^2\cos^2\delta\right\}\frac{1}{X_q/X_d}$$

$$A = \left(1-2\frac{r_1}{X_d}B\right)\frac{1}{X_q/X_d}\times\left(1-\frac{X_q}{X_d}\right)\sin\delta\cos^2\delta-B\left(\frac{1}{X_q/X_d}\sin^2\delta+\frac{X_q}{X_d}\cos^2\delta-1\right)$$

The maximum value of A against δ as the variable has been plotted in Figure 2 for different values of X_q/X_d and r_1/X_d.

References

1. Synchronous Machines, **R. E. Doherty C. A. Nickle.** AIEE Transactions, volume 45 1926, pages 912–47.

2. The Nonexcited Synchronous Motor, **P. H. Trickey.** *Electric Journal*, April 1933.

3. Calculation of Synchronous Machine Constants, **L. A. Kilgore.** AIEE Transactions, volume 50, 1931, pages 1201–14.

4. Determination of Synchronous Machine Constants by Test, **S. H. Wright.** AIEE Transactions, volume 50, 1931, pages 1331–51.

5. Calculation of Armature Reactance of Synchronous Machines, **P. L. Alger.** AIEE Transactions, volume 47, 1928, pages 493–513.

6. Graphical Determination of Magnetic Fields, **R. W. Wieseman.** AIEE Transactions, volume 46, 1927, pages 141–54.

7. End Connection Reactance of Synchronous Machines, **Alfred Still.** AIEE Journal, volume 49, 1930, pages 535–8.

8. Graphical Flux Mapping, **Calvert, Harrison.** *Electric Journal*, 1928.

9. Reactances of Synchronous Machines, **R. H. Park, B. L. Robertson.** AIEE Transactions volume 47, 1928, pages 514–36.

10. No Load Induction Motor Core Losses, **Spooner, Kincaid.** AIEE Transactions, volume 48, 1929, pages 645–55.

Governor for Variable-Ratio Transmission Used in Developmental 400-Cycle Electric System for Large Aircraft

P. F. DESCH NONMEMBER AIEE
D. E. GARR MEMBER AIEE
J. G. HUTTON NONMEMBER AIEE

Synopsis: A prerequisite for the successful parallel operation of main engine driven a-c generators is a suitable infinitely variable-ratio transmission and high speed governor to control it. This paper describes the development of such a governor and its successful operation on a developmental two-generator 400-cycle a-c system.

THE TREND of certain types of military and civil aircraft toward larger airplanes requiring large amounts of electric power, demanded equally revolutionary thinking in the field of aircraft electrical engineering. Much thought and discussion[1,2] in recent years has been given to an a-c system which would have the generators driven by the main engines and operating in parallel, which with proper controls makes possible improved continuity of service.[3] Flight conditions may demand more than a 3 to 1 speed range of the main engines, and all engines would not necessarily operate at the same speed throughout one flight. With such conditions it is essential that some form of variable ratio transmission be coupled between each prime mover and generator, so that a parallel system at substantially constant frequency is practical. Variation in the ratio of each transmission would have to be automatic, to maintain each generator speed within the range required in spite of high acceleration and wide speed differences of the prime movers. An electric governor which maintained successful parallel operation of the generators and equality of load division under various conditions of acceleration and loading was developed. Design data and performance characteristics of this governor are presented in the following.

Conclusions

Approximately 200 hours of operating experience have been gained on the developmental 400-cycle a-c two-generator system, and governor operation has been satisfactory throughout. Under both steady state and transient conditions the governor and its attendant load-frequency droop circuit have performed their required functions well. Although load division with values of no-load to full-load linear droop of less than 5 per cent was generally satisfactory, the system performance was at times erratic. A linear frequency droop from no-load to full-load of 5 per cent was found to be eminently satisfactory, and this value was adopted for all remaining tests on the two generator system.

The speed of response of the governor was good. With the generators operating in parallel, and one prime mover accelerated or decelerated, the governor responded to begin to restore initial conditions before the end of the acceleration or deceleration period.

In general, movement of the governor servomechanism began 0.008 second after inception by the control coil of the signal demanding governor response. On the equivalent of an unloaded system the effective gear ratio of the variable-ratio transmission was changed from 2:1 to 1.3:1 in 0.18 second and vice versa. Since the speed changes were brought about by a unit function change in signal voltage, the simulated acceleration approached an infinite value.

Tests on a four-generator system have not yet been made, but it is hoped to begin these, together with preliminary flight tests, in the near future.

The weight of the governor pilot valve and solenoid assembly is approximately 8 pounds; the weight of the junction box containing the control and droop circuits is approximately 5 pounds; in an aircraft installation the piston assembly is part of the variable-ratio transmission.

The governor, together with the variable-ratio transmission which it controls, and attendant electric apparatus have combined to make an a-c system with parallel operated generators practical for use on large aircraft of the future. Operation of a developmental two-generator system over a period of several months and under varying conditions has been very satisfactory. It is hoped that in the near future planned flight tests will prove further the value of a-c systems for aircraft auxiliary apparatus.

Paper 46-79, recommended by the AIEE committee on air transportation and presented at the AIEE winter convention, New York, N. Y., January 21-25, 1946. Manuscript submitted November 23, 1945; made available for printing December 13, 1945.

P. F. Desch, D. E. Garr, and J. G. Hutton all are with the general engineering and consulting laboratory, General Electric Company, Schenectady, N. Y.

Governor Requirements

The governor design and performance requirements were set up to meet the most extreme operating conditions thought possible on airplanes which require a-c accessory power. Calculations based upon the application of rated engine torque to the propeller inertia of the engine–propeller combination indicated a possible acceleration at the engine drive pad of 2,150 rpm per second. Though in practice accelerations will probably be less than this, the governor was designed to maintain parallel operation with one engine accelerated at this rate while the speed of the others remained constant. Some of the essential features of the performance requirements are that the governor be designed to operate from sea level to 40,000 feet with ambient temperature variations from −55 degrees centigrade to +60 degrees centigrade, under humid or dusty conditions with specified linear and torsional vibrations. More particularly, requirements affecting the operational design of the governor are set out as in Table I. With these conditions arising from the design of the variable ratio transmission, the governor was required

Table I. Performance Requirements of Governor

Item	Characteristic	Governor Requirement
1.	Input speed range to variable-ratio transmission	2,100–9,000 rpm
2.	Output speed of generator	6,000 rpm
3.	Speed of governor tachometer shaft for generator speed of 6,000 rpm	3,000 rpm
4.	Maximum overdrive ratio of variable-ratio transmission	2.85
5.	Maximum underdrive ratio of variable-ratio transmission	0.67
6.	Total stroke of governor tie rod	1.25 inches
7.	Oil pressure available for governor	250 pounds per square inch
8.	Force on governor tie rod	See Figure 1
9.	Tie rod speed at maximum acceleration (2,150 rpm per second at engine). Maximum overdrive	3.5 inches per second
10.	Tie rod speed at maximum acceleration (2,150 rpm per second at engine). Maximum underdrive	0.5 inch per second
11.	Maximum time for tie rod to reach required velocity	0.03 second

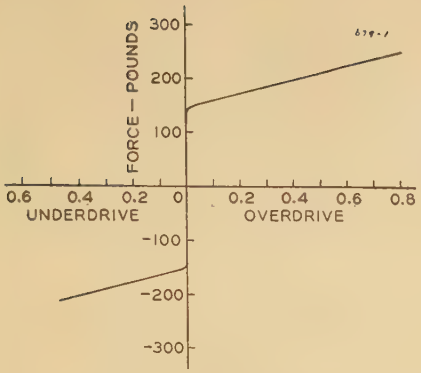

Figure 1. Curve of force on tie rod of governor servomechanism

to permit satisfactory parallel operation of the alternators under specified operating conditions with possible engine accelerations of 2,150 rpm per second. To assist in obtaining successful parallel operation of the generators an electric circuit was required which would admit of a decrease in generator speed with increasing load. Thus over the expected engine speed range of 700 rpm to 3,000 rpm, which with the step-up gear becomes 2,100 rpm to 9,000 rpm at the variable-ratio transmission, the governor was required to hold speed as follows:

Alternator Load, Kw	Speed, Rpm	Tolerance, Per Cent
0	6,300 (105 per cent)	±1
30 (100 per cent)	6,000 (100 per cent)	±1
45 (150 per cent)	5,850 (97.5 per cent)	±1
60 (200 per cent)	5,700 (95 per cent)	±1

In accordance with general aircraft practice the governor and its control circuits were required to be of minimum weight and to occupy a minimum of space in meeting all requirements.

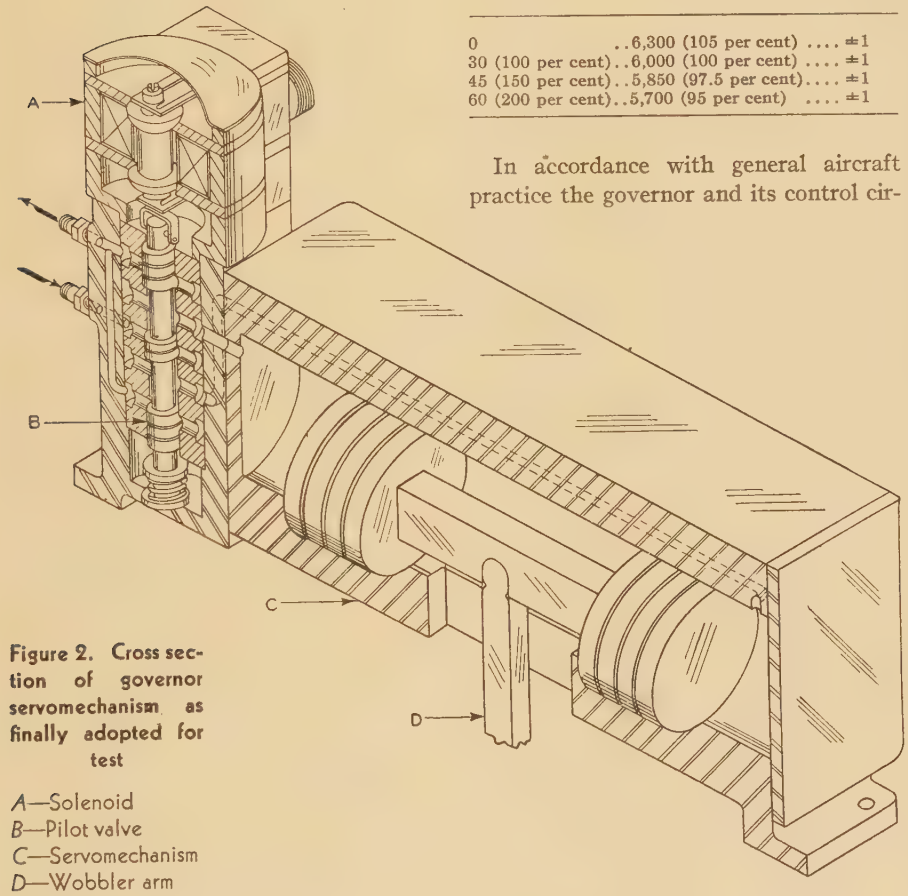

Figure 2. Cross section of governor servomechanism as finally adopted for test

A—Solenoid
B—Pilot valve
C—Servomechanism
D—Wobbler arm

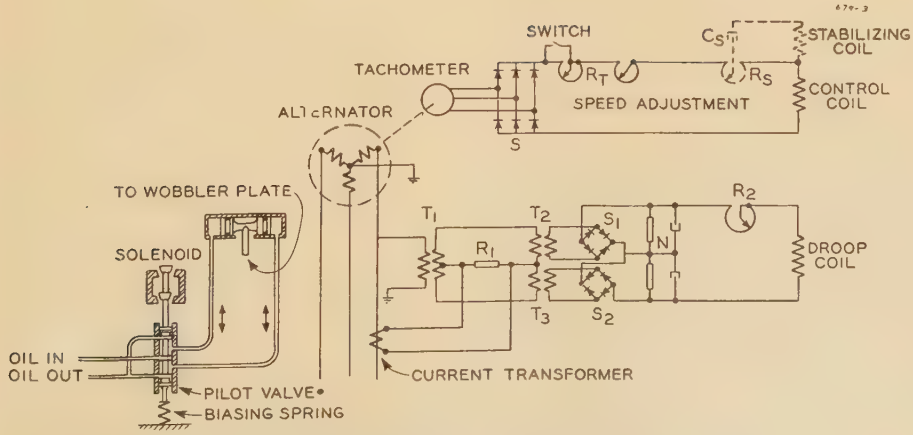

Figure 3. Schematic diagram of governor and control circuits

Design Data for Solenoid and Pilot-Valve Assembly

The governor is essentially a constant speed device. To provide suitable load division among the generators a characteristic is added to each governor which produces a 5 per cent decrease in system frequency when the generators are delivering full load. This droop circuit is independent of the actual governing circuits and therefore need not be considered in the design of the solenoid and pilot-valve assembly.

An isometric view of the governor assembly, as finally adopted for test, is shown in Figure 2 and a schematic diagram in Figure 3. Under steady state conditions the pilot valve is balanced in its mid-position against the force of a solenoid magnet by means of a biasing spring. A momentary change in current to the solenoid (because of a momentary change in output speed of the transmission) results in temporary unbalance, and oil is allowed to flow to the servomechanism until the condition is corrected. This correction must be very rapid to provide reasonably good load division among generators during engine speed transients. The pilot valve therefore must move with small changes of current through the solenoid coil. By use of a magnet with a tapered air gap, force-deflection characteristics such as those shown in Figure 4A are obtained, the various curves being plotted for different numbers of ampere turns X, Y, and Z. However, since the characteristics of the biasing spring are linear (line R^1T^1), the magnet is constrained to move linearly, resulting in an operating characteristic as represented by line RST, Figure 4A. By extrapolating from the line RST, and the curves for different ampere turns, a curve such as LMN in Figure 4B is obtained. In the working range of the governor only small ampere-turn changes are necessary for satisfactory governor operation and therefore only the portion L^1MN^1 of Figure 4B, need be considered: L^1MN^1 is essentially a straight line.

Since the magnet must be responsive to small changes in solenoid current, the required pilot valve travel also must be small. In the governor under consideration the total travel of the pilot valve is 0.1 inch, whereas under normal working conditions a movement of only ±0.010 inch is required for a tie-rod velocity great enough to ensure correct parallel performance. A solenoid force of $1^1/_2$–2

pounds is sufficient to do this, while an oil pressure of 250 pounds per square inch on a piston area of approximately 1.2 square inch is ample for movement of the servomechanism.

Other characteristics of the governor are as follows:

Control coil current	0.4 ampere
Turns on control coil	1,000
Resistance of control coil	16 ohms
Diameter of pilot valve	3/8 inch

Figure 5 shows a view of the completed governor assembly. The accumulator shown mounted on top was found from test to be unnecessary and was not used thereafter.

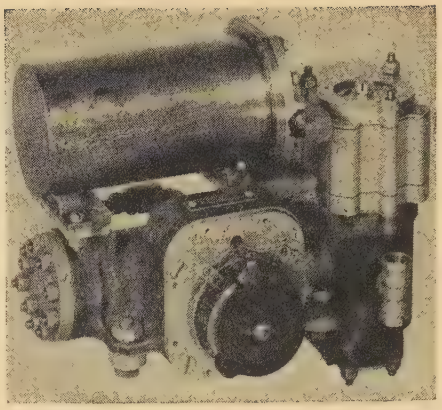

Figure 5. Oblique rear view of an experimental electric governor

Control Circuit

A schematic electrical diagram of the governor control circuit used for test is shown in Figure 3. The output voltage of a small 3-phase a-c tachometer with a permanent magnet field driven at a speed proportional to the output speed of the variable-ratio transmission is rectified by means of the 3-phase full-wave rectifier, S, shown. The output terminals of the rectifier are connected through a variable resistance to the governor control coil.

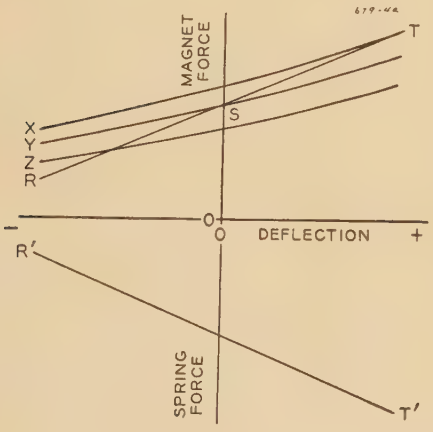

A. Force versus deflection

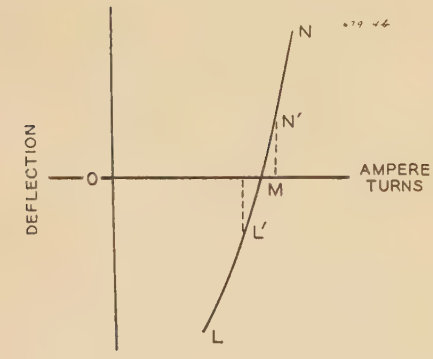

B. Deflection versus ampere turns

Figure 4. Curves of governor solenoid design characteristics

This control coil operates on a solenoid coupled mechanically to a three-land valve and biasing spring shown also in Figure 2. Under steady state conditions the force of the solenoid is balanced by the spring, and the valve floats in its neutral position. Any change in output speed of the variable-ratio transmission, either because of load variation or input speed changes, results in a momentary increase or decrease in current to the control coil. Balance of the pilot-valve assembly thus is lost temporarily, and oil is allowed to flow to and from the servomechanism controlling the transmission. The force on the servo pistons is such that the effective gear ratio of the drive is changed to restore original speed conditions. As soon as these are obtained, the pilot valve is returned to its neutral position. Steady state speed adjustments may be made by means of the trimming rheostat R_T. On an aircraft installation a rheostat may be mounted on the flight engineer's panel and connected in parallel with R_T to provide remote control of each generator speed. For parallel operated generators this is also an adjustment for load division, should the governor setting deviate during a flight.

Stabilizing of the governor may be obtained by means of the circuit shown in broken lines above the control coil in Figure 3. The rheostat R_s is geared to a rack on the servo pistons, and therefore movement of the latter will result in a change in the amount of the resistance R_s in the stabilizing circuit. Since the governor control current is essentially constant, movement of R_s results in a change in voltage to the capacitor and stabilizing coil. The capacitor therefore will either charge or discharge, depending on whether the voltage decreases or increases. In either case a current will flow through the stabilizing coil, producing ampere turns in opposition to the change in ampere turns in the control coil. A stabilizing action therefore is produced.

For successful parallel operation the alternators should be controlled, so that their speed decreases with increasing load. In Figure 6A is shown the speed–load characteristics of four alternators without controls to give speed regulation. Prior to synchronizing, the speeds of the machines probably are slightly different one from the other due to inherent instrument and human error. On synchronizing, the machine with the highest initial speed will assume all subsequent load, thus giving a very undesirable condition. In Figure 6B is shown in the same order the speed-load characteristics of the same four alternators, but in this case they have controls to give speed regulation. The same initial speed errors are shown, but, on synchronizing, subsequent load is divided among the machines in proportion to their initial speed errors. The drawing is not to scale, the percentage droop being exaggerated for the purposes of illustration.

The control circuit (load-frequency droop control) giving this desired speed regulation is part of the governing system and is shown in Figure 3. One line to neutral voltage of the alternator is supplied to the primary winding of transformer T_1. The secondary winding of this transformer is midtapped and con-

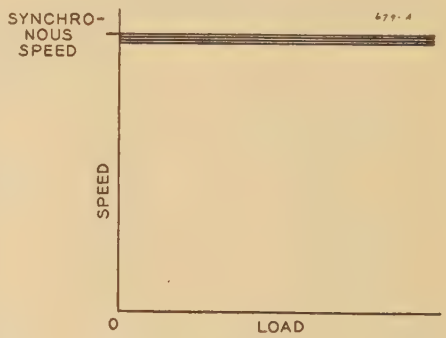

A. Without droop

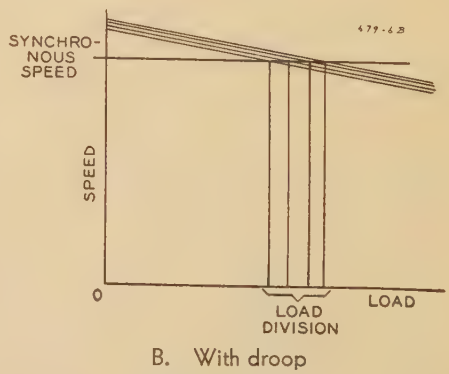

B. With droop

Figure 6. Diagram showing how load-frequency droop provides for real power division

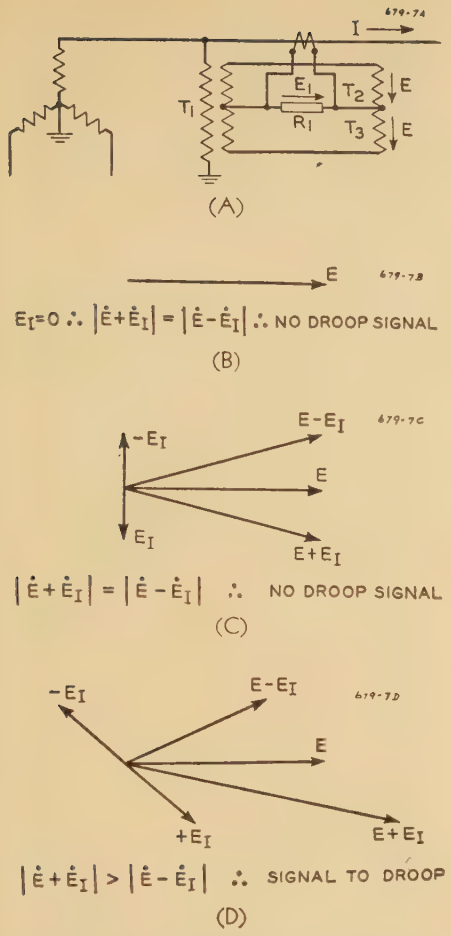

Figure 7. A. Schematic electrical diagram of a-c portion droop circuit
B, C, D. Vector relations in the primary windings of transformers T_2 and T_3 for different load and power factor conditions

B—No load
C—Zero power factor load
D—0.75 power factor load

nected through a resistance, R_1, to the primary windings of the identical transformers T_2 and T_3. The output of each of these transformers is rectified by means of selenium rectifiers S_1 and S_2. By connecting the rectifier outputs subtractive, the difference in d-c signals can be placed on the droop circuit coil connected as shown. On no load the alternator line to neutral voltage produces equal signals in the rectifiers. The resulting two d-c signals being subtractive, there is no signal to the droop circuit coil. The secondary winding of the current transformer, CT, is connected across the resistance R_1. On load, a signal proportional to alternator output current therefore is added vectorially to and subtracted from the voltage signal, thus producing unbalance in the outputs of rectifiers S_1 and S_2. This unbalance results in current flow, smoothed out by means of the capacitor-resistance network, N, shown, through the droop circuit coil. The control and droop coils are wound concentrically, the latter being connected so that on load, the flux produced is in the same direction as that of the control coil. This has the same effect as an increase in output speed of the variable-ratio transmission, and the governor acts accordingly. By means of the variable resistance, R_2, the percentage speed regulation of the alternator can be adjusted to its most effective value. On an actual aircraft installation it is expected that the value of R_2 will be fixed.

Vector relations involved in the load-frequency droop circuit are shown in Figures 7A, B, C, and D.

It is sufficient to consider the absolute magnitudes of the resultant voltages applied to the primary windings of transformers T_2 and T_3, in determining the droop coil signal voltage, since the output of each rectifier is proportional to the respective magnitude of the voltage in the transformer to which it is connected. The rectifiers are connected subtractive, and therefore the net signal to the droop coil is zero whenever the voltages applied to the primary windings of T_2 and T_3 are equal in magnitude.

In Figure 7A is shown the skeleton droop circuit and the voltages contributing to its operation. Since transformers T_2 and T_3 are identical, the voltage components, E, applied to the windings by virtue of the alternator phase to neutral voltage, are equal. Similarly a voltage component, E_I, is applied to transformers T_2 and T_3 by virtue of the drop in the resistor R_1, caused by the flow of load current through the current transformer. The voltages E and E_I therefore will be vectorially additive in one transformer and vectorially subtractive in the other transformer.

In Figure 7B, with no load on the system, the voltage E_I is zero, and consequently there is no signal to the droop coil.

In Figure 7C with zero power factor load the absolute value of the vector sum, $|\boldsymbol{E}+\boldsymbol{E}_I|$, is equal to the absolute value of the vector difference $|\boldsymbol{E}-\boldsymbol{E}_I|$. Again the signal to the droop coil is zero.

In Figure 7D with a load power factor of 75 per cent the absolute value of the vector sum, $|\boldsymbol{E}+\boldsymbol{E}_I|$, is greater than the absolute value of the vector difference, $|\boldsymbol{E}-\boldsymbol{E}_I|$. Consequently, a voltage proportional to the difference between the absolute values is applied to the droop coil circuit, actuating the governor in such a way as to tend to restore load balance. It is clear from the vector relations shown in Figures 7C and 7D, that the droop coil signal is sensitive to real power current and insensitive to reactive power current.

Performance Data

General

Performance data obtained at the time of writing the paper have been confined to a developmental two-generator system. Each prime mover of the system was a 450-horsepower 9-cylinder gasoline engine, coupled through a step-up gear in order to obtain input speeds to the variable-ratio transmission comparable with those expected on an aircraft installation. The gear output shaft was connected through a double universal coupling to the input flange of the variable-ratio transmission. A 3-phase a-c tachometer with a permanent magnet field was driven through a gear at half output speed and provided power for the governor control circuit.

A freewheeling device located between the variable-ratio drive and the alternator allows the alternator to be driven but does not permit it to attempt to drive the prime mover. Loading of the alternators was provided by water-cooled calrod units and air-core reactors, the continuous rating of the alternator being 30 kw, 40 kva, at 400 cycles per second and 208Y–120 volts.

The presence of the freewheeling unit between the drive and alternator made synchronizing of the alternators a simple matter. Successful parallel operation

Figure 8. Oscillogram showing transient division of real power between generators by governor action during acceleration of one engine

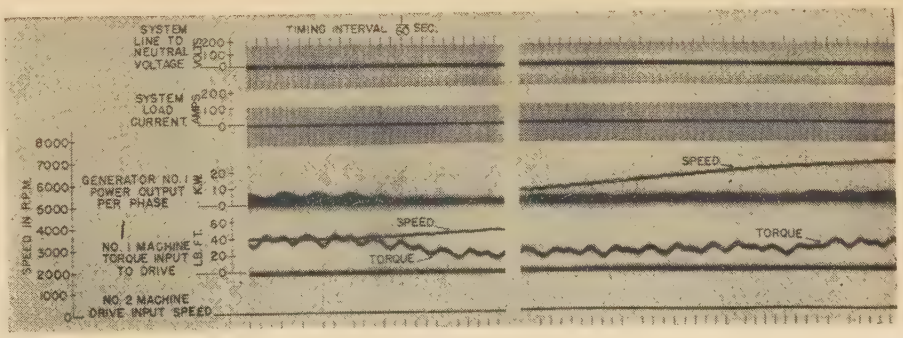

was achieved, the generators staying in step during various types of disturbances and dividing load equally under steady state conditions and reasonably well during transient disturbances (see Figure 8). The general performance of the governors was very satisfactory throughout a series of system tests which followed successful parallel operation.

Stabilizing Circuit

A considerable amount of previous development work on governors for gasoline engines used in tanks greatly expedited the development of the governor to control the variable-ratio transmission. Because of the rates of response and the values of inertia involved in controlling the tank engines, stabilizing circuits were required in governors built for this purpose. A variable resistance, R_s, and capacitance, C_s, connected, as shown dotted in Figure 3, to a second solenoid coil enabled this stabilizing to be achieved. In the case of the governor for use on aircraft where a variable-ratio transmission is to be controlled, the slip is relatively small and the speed of response high. Consequently the afore-mentioned type of stabilizing is unnecessary. Tests showed, however, that if an application should occur where stabilizing is required, this could be accomplished readily.

Droop Circuit

The value of the resistance R_2 in the droop circuit (Figure 3) was set arbitrarily to give a 5 per cent frequency decrease linearly from no load to full load on the alternator. Load division under steady state conditions was excellent, each generator taking an equal share of the load. By varying the value of R_2 the percentage droop was decreased. For values less than 4 per cent the load division became less satisfactory and erratic. The value of R_2 therefore was fixed to give a linear frequency droop of 5 per cent with full load on the alternator. With no load frequency of 420 cycles per second, a full load frequency of 400 cycles per second thus was obtained.

Part of the load on a military airplane using the a-c system for electric power may be thyratron controlled gun turrets. When in operation, these control circuits will produce a d-c component of current in the a-c system. This will tend to saturate any current transformers which may be used there. Since a current transformer was an essential part of the droop circuit, tests were performed with a thyratron controlled gun turret load to determine its effect on the operation of the droop circuit. It was found that load division was satisfactory, the saturation of the current transformers used having no noticeable effect on governor action.

Speed of Response

The general speed of response of the governor is illustrated in Figure 8 which shows two sections of an oscillogram taken with the machines operating in parallel and one engine being accelerated. The portion between the two sections of the oscillogram represents a time interval of 0.9 second. The average rate of acceleration at the input shaft to the drive for the total interval is approximately 2,000 rpm per second, the machines staying in step throughout. The left-hand section of Figure 8 shows conditions prior to accelerating. The system is carrying approximately 30 kw of load. The machine being accelerated assumes more load while the other machine takes less load as indicated in the oscillogram. However, before the acceleration is completed the governors have begun to restore conditions, so that the machine not being accelerated begins to assume its share of the load again. This is illustrated in the right-hand section of Figure 8. Other oscillograms were taken showing the effects of acceleration and deceleration when the system was supplying lagging power factor loads. Performance of the system was equally satisfactory under these conditions. However, Figure 8, which depicts the effect of acceleration with a unity power factor load on the system, is presented here, since real power changes are more readily observable in oscillograph power traces when unity power factor loads are used.

In order to determine accurately the speed of response of the governor, it was necessary to resort to somewhat artificial means. A switch SW, Figure 3, was connected across the trimming rheostat, R_T. The value of the resistance was adjusted so that by closing SW, the output speed dropped from 6,000 rpm to approximately 4,000 rpm. A battery connected appropriately to R_s, the rheostat formerly used in the stabilizing circuit, enabled movement of the servomechanism to be determined after receipt of the unit function signal by the governor control coil. The tests were performed on one governor, and variable-ratio transmission coupled to a generator but supplying no load.

Figure 9A shows a plot of movement of the governor servomechanism in terms of time after receipt by the control coil of the unit function signal. The output speed of the variable-ratio transmission was reduced from 6,000 rpm to approximately 4,000 rpm. With an input speed of 3,000 rpm this gave a change in drive ratio from 2:1 to 1.3:1.

Figure 9B shows a similar curve obtained by opening the switch S (Figure 3) and thus increasing the output speed from 4,000 rpm to 6,000 rpm. Here there is an overshoot of approximately 2 per cent. This is due to the inherent delay of the moving parts and the oil pressure of the hydraulic system, reaching steady state conditions after completion of the unit function change in electric signal.

The successful operation of the governor over a period of 200 hours under severe conditions brought about by many stops and starts with heavy loads often applied and removed suddenly indicates that a suitable automatic control has been developed for the variable-ratio transmission so necessary in the parallel operation of main engine driven aircraft alternators.

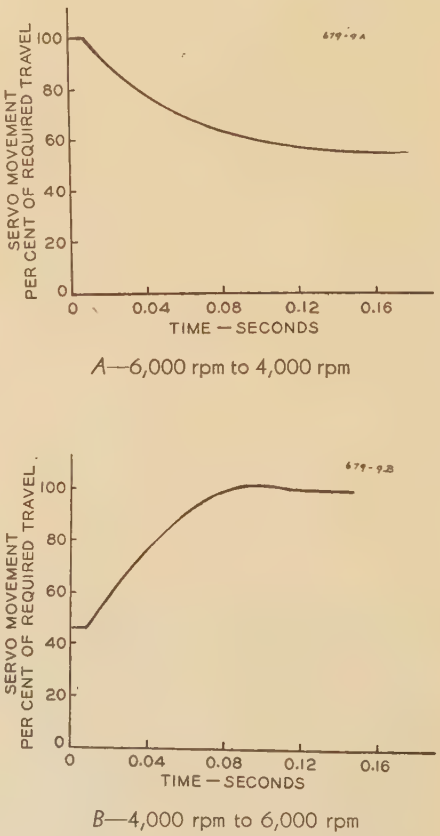

Figure 9. Curves of movement of governor servomechanism after change in electric signal

References

1. Why To-morrow's Planes Will Have A-C Electrical Systems, T. B. Holliday. *Electrical Manufacturing*, July 1943.

2. Governor Requirements for Aircraft Alternator Drives, W. K. Boice, L. G. Levoy, Jr. AIEE Transactions, volume 64, 1945, July section, pages 534–40.

3. Basic Consideration in the Selection of Electric Systems for Large Aircraft, W. K. Boice, L. G. Levoy, Jr. AIEE Transactions, volume 63, 1944, June section, pages 279–87.

Field Tests of Interrupting Capacity of 138-Kv Oil Circuit Breakers

W. B. BUCHANAN
MEMBER AIEE

G. D. FLOYD
MEMBER AIEE

Synopsis: The preliminary planning necessary to estimate the amount of current to be interrupted on a large network for staged tests under short-circuit conditions is outlined, also the precautions necessary to keep the applied fault from developing into a total system interruption. The circuit breakers under test are identified, various quantities required for record, and the means of obtaining the same are discussed. The results of a number of tests are given as well as a general discussion as to the conditions of the tests and of results obtained.

THE 25-CYCLE high-voltage network of the Hydro-Electric Power Commission of Ontario extends from the Quebec border to Windsor, with generating sources on the Ottawa, Gatineau, Lievre, and St. Lawrence Rivers in the east and on the Niagara River.[1] Primary transmission from the east is at 230 kv, while the loads located from Toronto to Windsor are supplied from a 115-kv network covering the afore-mentioned area.

The total generating capacity normally interconnected and supplying this network is in the order of 1,750,000 kva. The short circuit kilovolt-amperes on the 115-kv network has increased with system growth, with the result that, although circuit breakers had been provided at many points with the highest interrupting capacity available from time to time, the increase in short-circuit kilovolt-amperes always had to be considered in regrouping lines or paralleling busses. In some cases it has been necessary to sectionalize busses to reduce short-circuit currents, where best operating practice indicated parallel operation. The necessity of operating all generating sources to their capacity during the war also has tended to increase the short-circuit kilovolt-amperes.

When considering the point to which it would be reasonably safe to interconnect the network without inviting failure of the circuit breakers to interrupt faults, the Commission's engineers were required to answer the question, what modifying factor, if any, should be applied to the interrupting capacity of the circuit breaker at 60 cycles, as demonstrated by laboratory and field tests, when this circuit breaker was required to interrupt 25-cycle current. There appeared to be no clear-cut answer to this question. After discussion with manufacturer's engineers, it was decided to make the tests described in this paper on a modern oil circuit breaker, by having this circuit breaker interrupt actual system fault currents up to its rated interrupting capacity and observing the results.

A 138-kv single tank circuit breaker equipped with type BH deion grid, located at Burlington transformer station, having rated interrupting current of 7,950 amperes at 110 kv, was selected, the manufacturer being asked to place this circuit breaker in "factory condition" prior to the test. It also was decided to make a test on a second circuit breaker of the same interrupting capacity by installing in it temporarily an improved interrupting device, known as the type MF grid. This assembly was to be tested at not over 13,200 amperes at 110 kv.

Preliminary Work

Certain preliminary studies are required before tests of this nature can be made. Important studies include:

1. Determination of system required, including departures from normal network and generating capacity.
2. Careful scrutiny of the system and its relay protection, to determine the possibility of loss of tie lines, busses not involved in the fault, frequency changer ties, synchronous loads, and generating capacity and, where it could be done, to prevent their occurrence.
3. Listing of quantities to be measured and providing of equipment for measuring these quantities.

The circuit breaker to be tested also must be conditioned, if the tests on it are to be considered a fair demonstration of its performance.

System Required

The American Standards Association "Standard for Oil Circuit Breakers, C37-4" defines rated interrupting current as the *total* rms current at the time the contacts part. It was agreed that these standards were to apply. One problem in the preliminary work became that of determining the system setup required to produce a short-circuit current, as defined by the ASA Standard, as nearly equal to, but no greater than, the rated interrupting current given by the manufacturer.

The system upon which the fault was to be placed is shown in Figure 1. Burlington transformer substation is located at the heart of the 115-kv network. Although the only sources of short-circuit current close to the point of fault are the two 40,000-kva synchronous condensers at Burlington, there are points of infeed from eastern sources over the 230-kv network and from Niagara River plants over 115-kv lines. Generators in the latter plants, which are on busses separate from the 115-kv subsystem on which the fault was placed, also supply current to the fault by back-feeding through 230-kv transformers at Burlington to the common 230-kv bus.

It had been decided that two preliminary tests would be made, one at approximately 1/4 and one at 1/2 rated interrupting current before the final test on the lower rated circuit breaker, and one preliminary test at not over 7,900 amperes on the higher rated contact assembly. To determine the initial values of symmetrical current, and the system rearrangement required to produce them, the system shown in Figure 1 was placed on the network calculator.

System generation and loads for a normal Saturday were used with the impedance of generating sources represented by their subtransient reactance.

After a number of trials on the calculator one grouping of lines was found such that with the fault located at the distant end of the line whose line circuit breaker would be under test, approximately 1/4 rated current would flow initially, and the same network with fault located at the near end of the same line would produce approximately 1/2 rated current. It should be noted that rather severe restrictions were placed on modifying the system to develop the required values of short-circuit current. Sufficient generation had to be retained to supply the system load, and circuits could not be opened to the point where service security would be threatened seriously.

The system required to give a 3-phase

Paper 46-19, recommended by the AIEE committee on protective devices for presentation at the AIEE winter convention, New York, N. Y., January 21–25, 1946. Manuscript submitted November 19, 1945; made available for printing December 18, 1945.

W. B. Buchanan is assistant laboratory engineer and G. D. Floyd is electrical consultant with the Hydro-Electric Power Commission of Ontario, Toronto, Ontario, Canada.

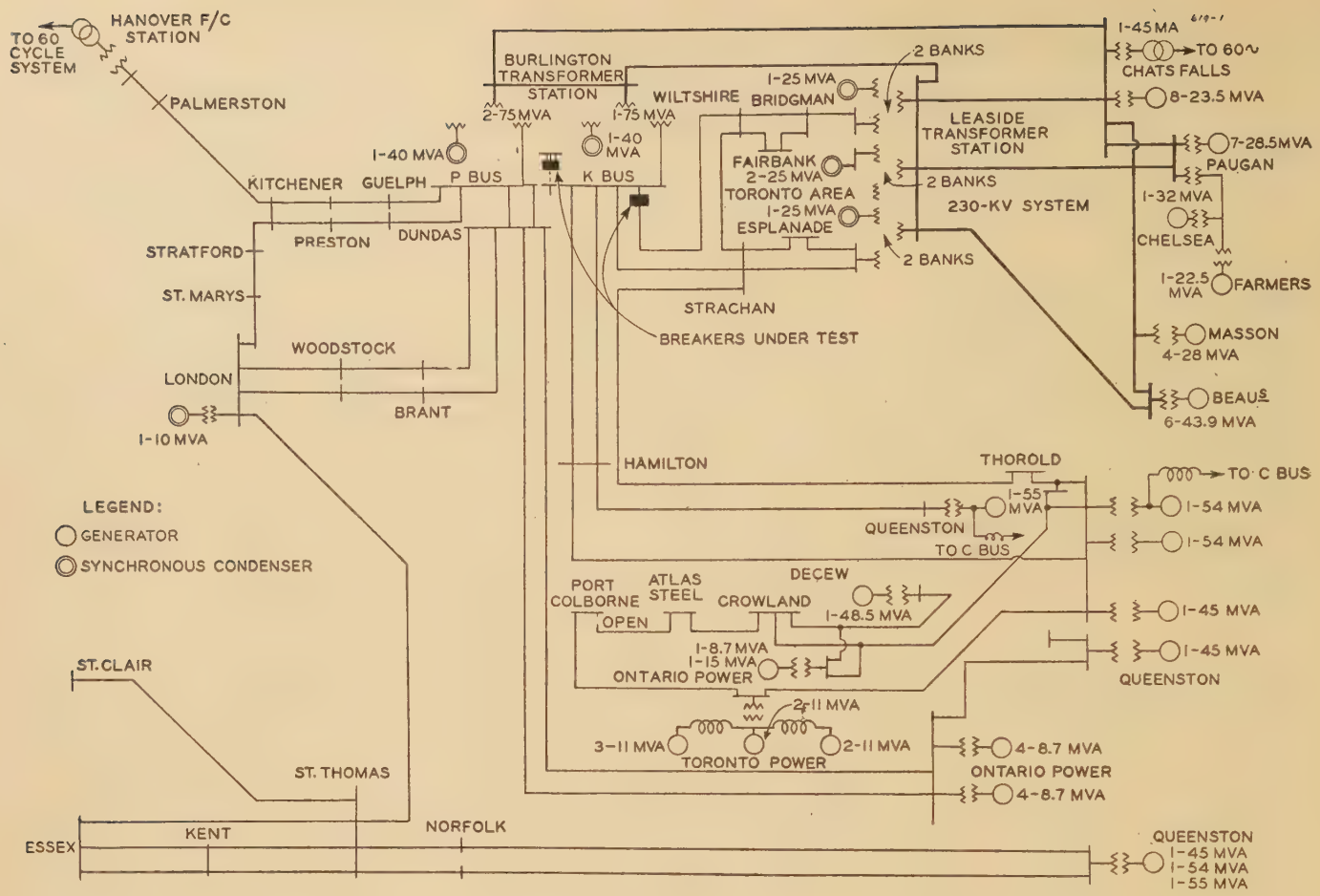

Figure 1. Niagara division transmission network of the Hydro-Electric Power Commission of Ontario

short circuit of 7,900 amperes and that required to produce approximately 13,000 amperes likewise were determined. For the latter the two 115-kv busses at Burlington would be parallelled and both synchronous condensers operating. These condensers could be used to advantage to obtain vernier calibration of the current, as the amount of infeed from each was known from the calculator readings.

Calculator readings give only *the initial symmetrical* current, so that the relation between this current and the *total* current at the time the contacts separated remained to be determined.

The d-c component of total current decreases exponentially according to the formula $i = I_0\epsilon^{-Rt/L}$. The ratio R/L is the ratio of resistance to inductance of the system looking into the system from point of fault. This ratio was determined from measurements on the calculator and found to be 33, giving a time constant of 0.03 second for the d-c component. It, therefore, was concluded that at 3 to 4 cycles (0.12 second to 0.16 second) after beginning of the fault, the d-c component would have disappeared, or at least it would be so small as to have negligible effect on the value of total current.

Standard decrement curves[2] indicated that, when corrected for frequency, the a-c component of total current at 3 to 4 cycles was practically the same as the initial a-c component.

As a result of the foregoing conclusions, the decision was made to use the system setup determined on the calculator, including as nearly as possible the same system generation without modification.

Provision for Service Security

It was of utmost importance that impairment to service should be avoided. The expected behavior of the system and its associated relay protections under severe 3-phase faults were studied to determine points of weakness. As a result of this study it was decided all frequency changer ties would be opened and certain relays on tie lines blocked for the brief test period. Backup protection for the circuit breakers under test was provided, and tested, and arrangements were made to place observers at widely separated key points to block those relays considered necessary and to be available if unforeseen trouble developed. Some loss of synchronous load appeared to be unavoidable and was accepted.

Study of Quantities to Be Measured

The quantities having direct bearing on the behavior of the circuit breaker itself and methods developed and used to obtain them are described later in the paper. Advantage was taken of every opportunity afforded by tests of this nature to obtain information on system and relay behavior. As a result observations quite foreign to those required for the test itself were included in the program, and useful data were obtained. To avoid confusion these data are not included in this paper.

Description of Circuit Breakers and Contacts

The two circuit breakers tested are 138-kv type BQOB oil circuit breakers manufactured by the Canadian Westinghouse Company. The 3 poles are mounted in a single floor-mounted tank. The spacing at the top of the bushings is the same as the minimum spacing for bushings of 3-phase transformers of the same voltage class.

The bushings are standard oil-filled condenser type, with deion grid contacts,

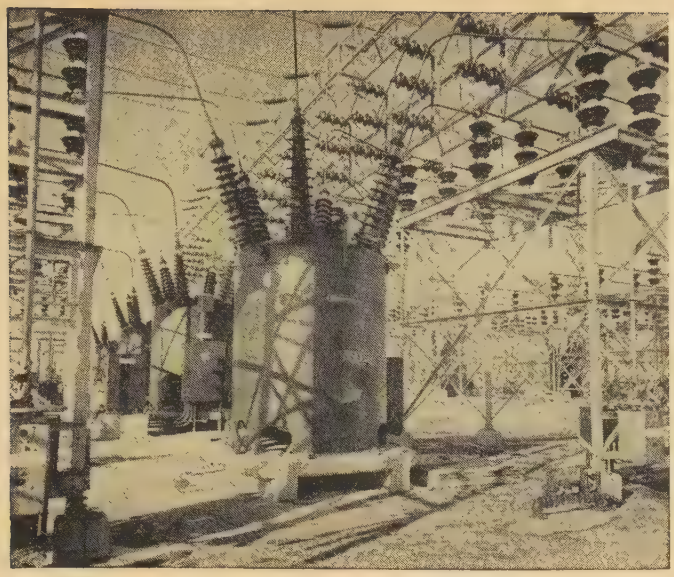

Figure 2. Type BQOB 138-kv oil circuit breakers at Burlington transformer station

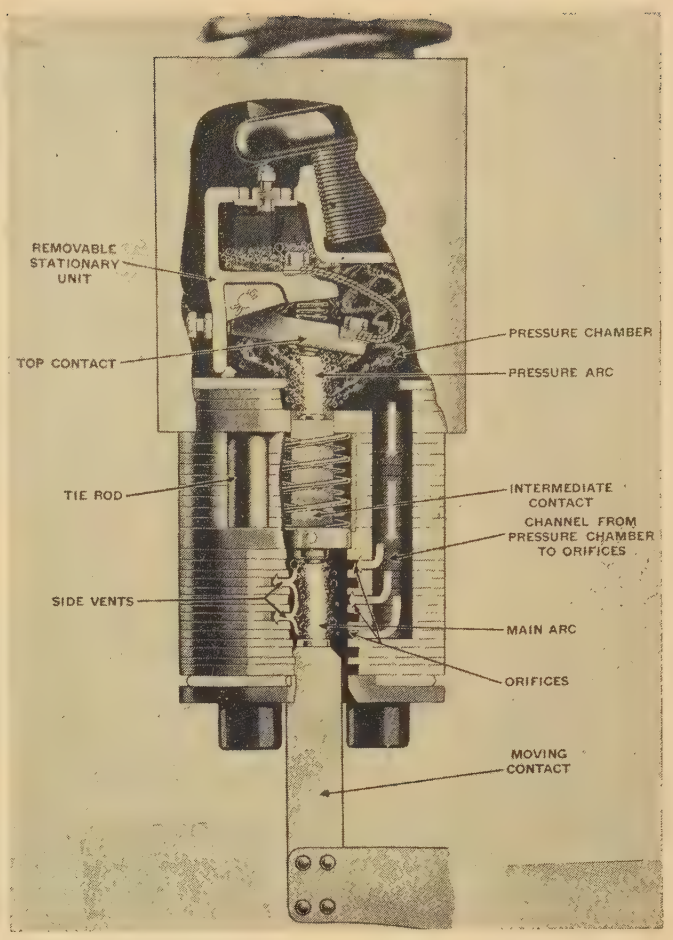

Figure 3 (right). Section through 138-kv type MF contact multiflow 5-cycle Deion grid, $2^1/_2$ million kva

type BH for the 8-cycle 1,500,000-kva rating, and type MF for the 5-cycle circuit breaker rated at 2,500,000 kva. Each grid is surrounded by a heavy circular insulating tube, which acts as a barrier between phases. Entry to the tank is through a manhole at the side of the tank. Ample space is available between the contacts and the tank for inspection and maintenance.

Figure 2 shows a row of these circuit breakers at Burlington transformer station. Figure 3 shows a section through the type MF contact.

Measuring Equipment

Past experience indicated that high internal pressures could be developed and oil ejected when circuit breakers opened on heavy fault currents. A pressure gauge therefore was installed giving an output suitable for oscillographic records. This gauge consisted of a Crosby steam gauge, in which a slide wire potentiometer had been substituted for the oscillating cylinder and fitted with a 60-pound spring. The gauge was connected to a 1-inch bushing, the latter welded to the tank about 27 inches above the concrete base. The pressures that might occur were quite conjectural, but the choice proved satisfactory for these tests.

Circuit breaker tanks also had been known to shift on their bases, and a detailed study of motions and stresses was suggested. Zenith vibration recorders were mounted, one on each of the four lifting lugs at the top of the tank. These units contain circular clock-driven charts and are very sensitive to vertical displacements that occur at high accelerations.

Other stress indicating devices, such as scratch extensometers and electric units of the strain-resistance type, were attached at the base of the tank and to the holding-down bolts.

A special travel indicator was designed, attached to the indicator arm, and a calibration curve of the relative motion between the vertical lift rod and the indicator arm was obtained. To obtain a continuous accurate record, two slide wires with independent sliding contacts were used in parallel as a potentiometer.

Line to ground voltages were obtained from the secondary windings of three potential transformers, the primary windings of which were connected line to ground on the 115-kv bus.

Currents were measured by inserting Weston multiratio current transformers in the secondary windings of the regular bushing-type current transformers, to provide a further stepdown of current to the oscillograph shunts. An over-all calibration of the oscillograph element circuits was made by circulating alternating current in the primary winding of the Weston current transformers.

The entire group of measurements required the use of 18 and occasionally 20, oscillograph elements plus some mechanical records.

Procedure on Test

Immediately before each test, duly accredited representatives of the manufacturer and of the engineering and operating departments of the Commission were consulted as to final readiness and consent obtained to proceed with the test.

Arrangements previously had been made covering the system required for each test. A request was made through the load supervisor to have this system arrangement established, and at the same time the relay section of the operating department was conferred with for any special checking or blocking of relays to maintain protection without interfering in any way with the test proposed.

Finally, the instrument operators were checked for readiness. The last group of items checked consisted of oscillographs and mechanical recorders, which were automatic in operation.

A public address system is installed in various buildings and in the yard in Burlington transformer station. The oper-

ator in charge announced to all present the test was to take place; communication was established also with operators at Niagara, Dundas, Toronto, London, and other stations, over the private telephone system. A 2-minute warning was given, then at the proper time, 10 seconds, 9, 8, and so on, and on the stroke of zero the circuit breaker was closed on the short circuit.

With one exception the actual time during which the current was maintained was about 1/8 second. In the exceptional case the short circuit was cleared in about 30 cycles by the opening of seven circuit breakers without any major interruption on the system. Data obtained from this test gave more complete information on system transients, permitting analysis of the decrement of short-circuit current.

Results of Tests

A standard operating duty cycle consists of closing the circuit breaker on a short circuit and allowing it to open automatically, then after 15 seconds delay repeating the closing and automatic opening operation. This is designated a CO-15-CO operation. In the tabulated list of results each test as listed indicates a single close–open operation.

Figures 4 and 5 are typical records of

1. The red-phase line-to-ground voltage.
2. The three 115-kv line currents.
3. The trip-coil current.
4. The record of the travel indicator.

The data shown on Table I were obtained from the oscillograms. The current listed for each test is the maximum measured on any one of the 3 phases. Duplicate records taken on another oscillograph provided a satisfactory check on the current values as listed.

The current, arcing time, and total duration of fault current were obtained by the method outlined in the American Standard for "Alternating-Current Power Circuit Breakers 37.4 to 37.9," inclusive.

The results of the electrical tests require very little comment. Close inspection of the oscillograms indicate, in some cases, an erratic variation in resistance of the arc while it was being quenched.

Vertical motion to a maximum of 0.4 inch was recorded by the Zenith recorders at the top of the tank. The precision of the figures does not warrant drawing any elaborate conclusions, but some points are of more than passing interest. Table II shows the record obtained from these instruments.

The mechanical shocks registered on the first three tests seem to be independent of current, as greater motion (approximately twice as much) was recorded on test 2, with current at 4,720 amperes as occurred on test 3-2, when 7,720 amperes were interrupted.

This suggests that the acceleration and deceleration of parts played an important part in the over-all motion of the tank. It may be noted that the vertical motion of the top of the tank of the circuit breaker equipped with the MF grids was substantially less than on that with the BH grids, though the current interrupted was very much greater.

No quantitative results have been obtained from the records of stresses at the base of the tank because of various difficulties in anticipating their performance. It is conclusive, however, that, if stresses of objectionable magnitude had occurred, they would have been detected on the records.

The hydrostatic pressures set up in the tank appeared in the form of waves of decreasing amplitude. The maximum positive pressure was greater on the circuit breaker equipped with BH grids but did not exceed approximately 25 pounds per square inch as recorded. Even this was not a sustained pressure but a pressure-wave reflected back and forth with decreasing amplitude. By dividing the time interval between pulses, the actual time of the event in the circuit breaker contacts which causes the pulse may be estimated and identified.

The pressure gauge records from tests 2, 3, and 5 have been transferred to a single chart (Figure 6) for better comparison. A timing wave for test 2 was not available on the same film, but the action is sufficiently like test 3 for identification.

The small impulse registered first in each case seems to occur at the closing of the contacts; the heavier pressure waves continued for three surge-cycles after the arc was extinguished.

This device would not record negative pressures, so it is not possible to continue the analysis of the pressure waves further, though it is an interesting and unexpected aspect of the problem.

Samples of the insulating oil were taken after each test on the circuit breakers, and later tested for dielectric strength. No deterioration could be detected from the breakdown values, though the oil had become somewhat darker in color.

Comparison of Test Results With Calculator Values of Current

A comparison of values of current obtained on test with network calculator values has been made, to establish the accuracy of the latter in determining circuit breaker interrupting capacity.

The preliminary tests at 1/4 and 1/2 rated current were found to be about 15 per cent higher than given by the calculator, but this was due in part at least to increased and different distribution of generation from that used on the calculator. There was also a slightly different system arrangement. These variations were unavoidable but indicate that the system must be set up as accurately as possible, if close estimates of fault currents are required.

Table I. Tests on 138-Kv Circuit Breakers on 3-Phase Short Circuit

Test	Maximum Current at Parting of Contacts, Amps, Rms	Phase	Type of Grid	Arcing Time, Cycles	Duration of Fault Current, Cycles	Voltage Recovery, Per Cent	Capacity Interrupted, Millions of Kva
1-1	2,730	Blue	BH	1.4	3.4	93.5	0.54
1-2	2,730	Blue	BH	1.7	4.0	92.5	0.54
2	4,720	White	BH	1.7	3.5	85.5	0.91
3-1	7,490	Blue	BH	1.4	3.5	91.0	1.46
3-2	7,720	Blue	BH	1.6	3.4	92.5	1.48
4A	7,250	White	MF	1.0	3.0	91.5	1.37
5-1	13,100	Red	MF	1.2	2.9	88.0	2.58
5-2	13,000	White	MF	1.2	3.0	83.5	2.57

Table II. Record of Zenith Recorders at Top of the Circuit Breaker in Inches

Test	Type of Grid	Recorder 1	2	3	4
1	BH	Up 0.06	0	0	Up 0.16
2	BH	Up 0.33	Up 0.4	Up 0.3	Up 0.2
		Down 0.33	Down 0.4	Down 0.33	
3-1	BH	Up 0.16	Up 0.2	Up 0.33	Up 0.1
3-2	BH	Up 0.13	Up 0.2	0	Up 0.13
		Down 0.13			Down 0.13
4A	MF	0	0	0	0
5	MF	0.2	Up 0.06	Up 0.1	Down 0.06

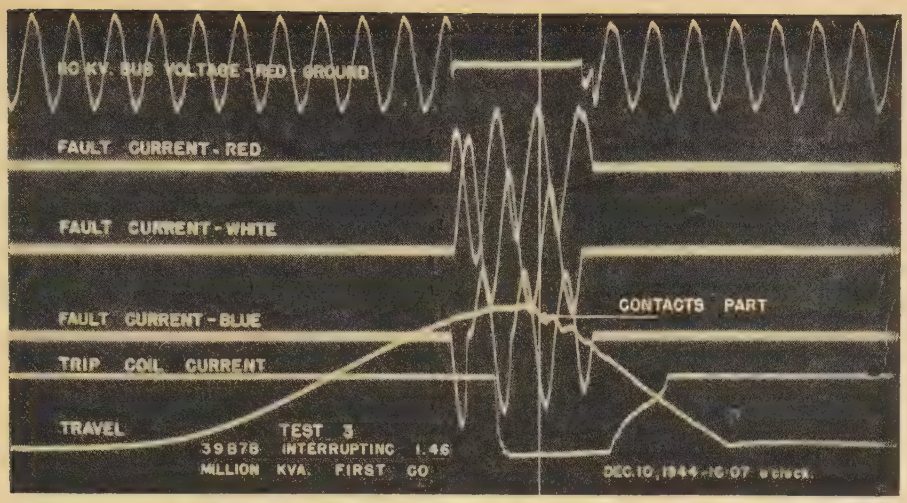

Figure 4. Oscillograph record of current interruption with BH grid

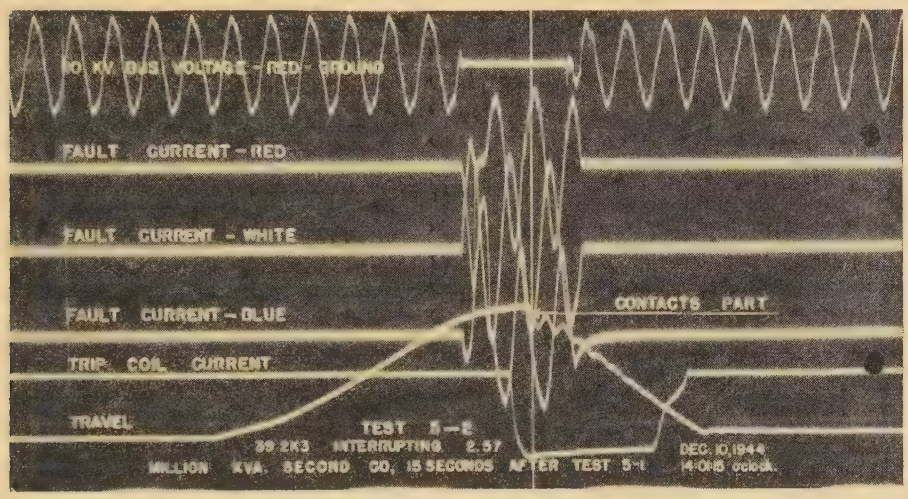

Figure 5. Oscillograph record of current interruption with MF grid

There was 5 per cent variation in fault current as measured on two field tests made with identical system arrangement, including the same generation.

On all tests it was found that the d-c component, although still measurable, added only one or two per cent to the total current. The largest value of this component on any test as measured, was approximately 15 per cent of the total.

On all but one test the duration of fault current was so short that no accurate estimate of decrement could be made. The agreement between calculated and test values of current, the former being initial values of rms symmetrical current, was an indication that for the time periods of interruption obtained on these tests it is safe to assume that no decrease in current occurred. Any error due to this assumption is in favor of the circuit breaker from the point of view of circuit breaker application, as it gives higher currents than the actual currents interrupted.

On one test the current through the circuit breaker existed for 30 cycles, until the fault was cleared by backup relays and system voltage restored to normal. This test, although it was a failure as a test on the circuit breaker, gave very useful data on the behavior of this system under 3-phase short circuit.

The currents recorded have been analyzed with the following results: The d-c component had an average short-circuit time constant of 0.06 second, compared with the 0.03 second obtained from calculator readings.

A comparison of test current (average of three phases) as measured and total current obtained from standard decrement curves, the latter corrected for a 25-cycle system by assuming an average open circuit time constant for this system of 10 seconds indicated close agreement (Figure 7). The decrement curves give values of total current, assuming a totally displaced wave. As no one of the test currents was totally displaced, it was possible to compare only the a-c components.

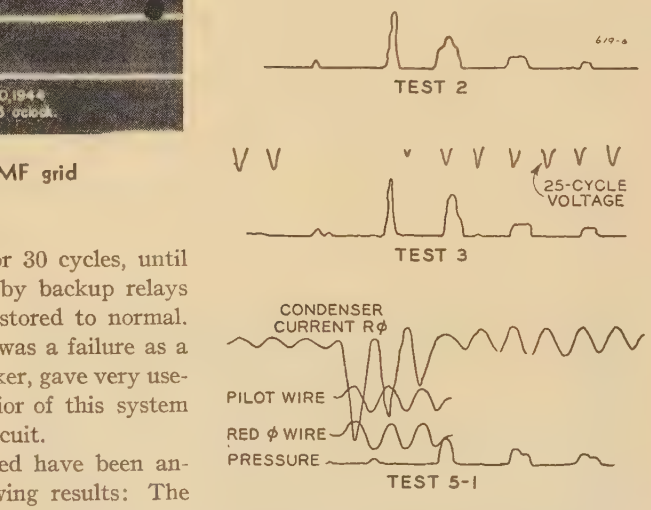

Figure 6. Record of pressures developed in circuit breaker tank on selected tests

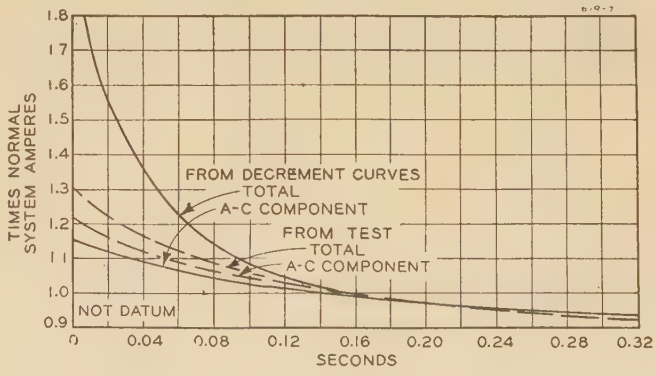

Figure 7. Comparison of test current with that from standard decrement curves

Condition of Circuit Breakers Following Tests

Circuit Breaker Having BH Grids

The circuit breaker in which the type BH grids were installed was rated at 7,950 amperes and was tested at 2,700 amperes, 4,700 amperes, and 7,700 amperes approximately with inspection following each test. Following the initial test there was only slight discoloration of oil. After the second test inspection showed discoloration of oil and slight pitting on the edge of the moving contacts. After the third test there was con-

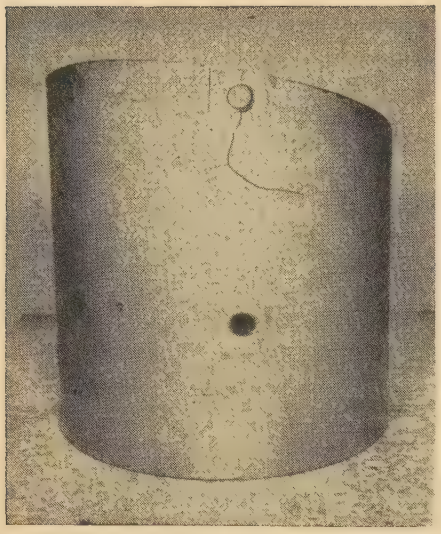

Figure 8. Micarta shield from type BH grid assembly after test at 7,500 amperes, showing crack at bolt hole

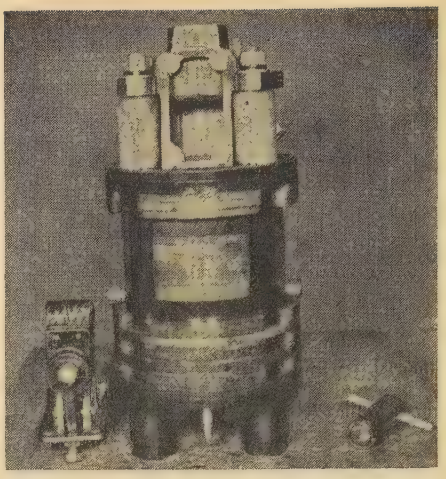

Figure 10. Type MF contact assembly and contacts after test at 13,100 amperes

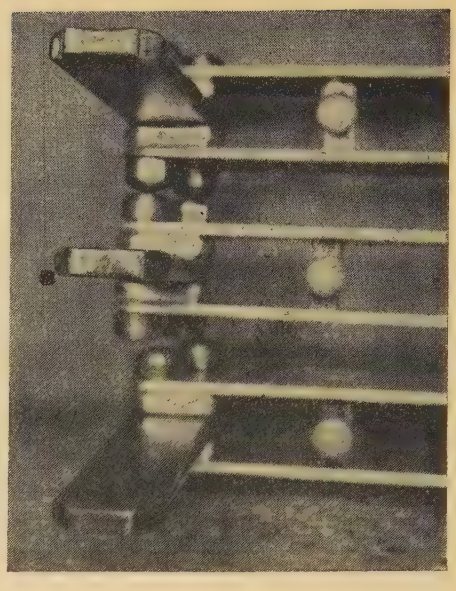

Figure 11. Moving contact assembly type MF after test at 13,100 amperes

siderable discoloration of oil but no decrease in its dielectric strength. The moving contacts were burned slightly on the outside edges. The Micarta shield on one bushing was cracked at a bolt hole (Figure 8). The alignment of lift rods, moving contacts, and grids had not changed.

The Deion grids were removed and disassembled. No permanent damage was discovered, the only evidence of the interruption being a black substance blown through a number of the stacks (Figure 9).

Circuit Breaker Equipped With Type MF Grid

This circuit breaker interrupted 13,100 amperes with very little movement of the tank. The condition of the contact mechanism is shown on Figures 10 and 11. In our opinion the contact mechanism could have interrupted an undetermined further number of short circuits at 2,500,000 kva without overhaul becoming necessary. It therefore fulfills the requirements of the American Standard C37.4 in this regard.

Conclusions

1. It is quite feasible to test circuit breakers by staged tests on a large system, provided suitable precautions are taken, and the necessary preliminary work is done to establish the generation and line arrangement required to produce the specified value of short circuit current. On a large system use of the d-c or a-c calculator to determine the system required is essential.

2. Three-phase short-circuit current values at 25 cycles obtained on the calculator agree with actual system values, at least to the same accuracy as obtained on successive tests (5 per cent), using subtransient values of generator reactance and no decrement, if the circuit breaker time is 3 cycles.

3. The standard decrement curves modified for 25-cycle conditions, agree with actual system behavior within the accuracy of the test itself.

4. The circuit breaker with rated interrupting capacity of 1,500,000 kva is capable of interrupting 7,950 amperes at 110 kv and 25 cycles, within the meaning of the American Standard C37.4.

5. The contact assembly or type MF grid is capable of interrupting 13,100 amperes at 110 kv and 25 cycles, within the meaning of the American Standard C37.4.

6. Comparison of results from this test with those made previously in the high current test laboratory at 60 cycles indicates that the margin between rated and maximum interrupting capacity appears to be reduced for 25-cycle faults.

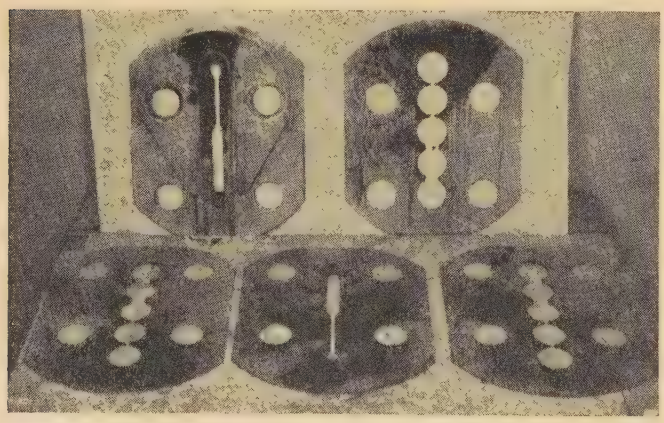

Figure 9. Plates from type BH grid stack after test at 7,500 amperes, showing material blown between plates by the arc

References

1. The 220,000-Volt System of the Hydro-Electric Power Commission of Ontario II, **A. H. Frampton, E. M. Wood.** AIEE Transactions, volume 60, 1941, pages 1215–21.

2. Standard Decrement Curves, **W. C. Hahn, C. F. Wagner.** AIEE Transactions, volume 51, 1932, pages 353–61.

Electronically Balanced Recorder for Flight Testing and Spectroscopy

A. J. WILLIAMS, JR. MEMBER AIEE
W. R. CLARK MEMBER AIEE
R. E. TARPLEY ASSOCIATE AIEE

Synopsis: A multiple-point potentiometer recorder for thermocouples is described having a slidewire driven to balance by a small induction motor powered from a 6L6 electron tube. The preamplifier gain is sufficient that the conventional input transformer (voltage step-up type) is not required, and thus a high impedance input circuit is made available. This permits the use of small capacitance values in the *RC* circuits for signal filtering and motor damping. The relation of this to the short balancing time (1.5 seconds) is discussed.

Spectroscopy supplied the incentive for the development of two additional but similar recorders. The first of these is a curve-drawing multiple-range microampere recorder with the smallest range 0.5 microampere, and with a balancing time of less than 1.0 second. The second is a multiple-range current-ratio recorder requiring only about 10 microamperes for the reference current.

IN A PREVIOUS PAPER[1] there was described the application of this recorder in potentiometer form to the measurement of 140 thermocouple temperatures during flight tests of planes. The switching of the thermocouples was described and the need for the short balancing time in the recorder was explained, but a description of the recorder itself was beyond the particular purpose of that paper. Interest in the recorder for other uses, such as wind tunnel testing, turbine checking at sea, and, in modified forms for spectroscopy is the reason for the present paper on the recorder itself.

Potentiometer Recorder

Figure 1 of the multiple-point potentiometer recorder shows the scales, the pointer, a section of the 21-point print wheel (under the pointer), and the perforated strip chart. The print wheel is pressed onto the paper once every 1.63 seconds by mechanical linkage from the same synchronous motor that drives the chart at constant speed. There is a violin string and pulley connection between the print wheel carriage and the slidewire potentiometer. All this is conventional.

Figure 2 shows the basic potentiometer circuit which is used. In operation, if the thermocouple gets hotter, its electromotive force increases above that of the potentiometer. The detector notes the unbalanced voltage and, through the balancing system *A–A*, moves the contact to balance and with it the print wheel and pointer. The current through the potentiometer is standardized by manually moving the battery rheostat, with the switch in the standardizing position, until the potentiometer contact comes within a limited region, as indicated by the pointer coming within a marked region of the scale.

Reference Junction Compensation

The circuit of Figure 3 is used for reference junction compensation. It is unconventional, as the reference junctions are remote from the recorder with plug connectors *X* of uncertain contact resistance in the leads 1, 2, 3, and 4. To minimize the effects of contact resistance and still have the reference junctions remote from the recorder, a complete bridge containing the compensating coils is located at the switch box with large end coil resistors R_A and R_B so the bridge can be supplied from the full 1.2 volts. 1.2 volts is the "end point" voltage for the dry battery with this circuit.

Mechanical Construction

In Figure 4 the door and the chart table are hinged away showing the slidewire, in large pan shaped enclosure, its vertical shaft and its direct gearing to the balancing motor. In the rear of the case, between the motor and slidewire shaft, can be seen one of the tubes in the amplifier, the chassis of which is hidden.

The amplifier and motor make up the balancing system shown as the detector and dotted line *A–A* of Figures 2 and 3.

Amplifier

The amplifier handles the unbalance as a 60 cycles per second a-c signal obtained by conversion from the d-c unbalance. The conversion is accomplished by a vibrator driven synchronously at line frequency as shown in Figure 5A. A blocking capacitor *C* prevents direct current from flowing from the thermocouple circuit to the tube or conversely. Four stages of triode voltage amplifiers are used together with one beam power output stage (6L6) with transformer coupling to one phase of the motor. The other phase of the motor is connected directly to the line. The quadrature phase relation required between the two motor windings is met by a fixed amount of phase shift in the vibrator drive-coil circuit. The mechanical drive from the motor to the slidewire completes the feedback loop. By using direct current on the heaters of the triodes, and by using rubber shock mounting on the low-level tube (first two stages), the total noise is held to less than seven microvolts referred to the first grid.

Filter Circuits

External circuits may produce alternating voltages in the thermocouple circuit as a result of capacitive or inductive coupling. If these voltages reach the detector input circuit, some interfering voltage will appear at the first grid. The vibrator suppresses the fundamental component but, like all modulators, adds components at new frequencies. The 60 cycles per second component is the only one which produces torque in the motor, but the other frequencies are almost as bad because they overload the amplifier. When overloaded at an odd frequency, the amplifier cannot handle the regular 60 cycles per second signal as it should.

All this points to the need for filtering out alternating voltages "picked up" by the thermocouple or its leads. Figure 5A shows the four-section resistance capacitance (*RC*) filter that is used. Inductances were not used for the series elements because of their inherent characteristic of "picking up" voltage from stray fluctuating magnetic flux. To shield such inductances magnetically introduces complications, size, and expense. The *RC* filter never can be built to have the sharp frequency cutoff of the *LC* filter, but it was found that it could be built sufficiently sharp to meet the requirements. The requirements are:

1. Attenuation of 60 cycles per second (and higher frequencies) by a factor of 500 or more (loss of 54 decibels or more).

Paper 46-62, recommended by the AIEE committees on instruments and measurements and electronics and presented at the AIEE winter convention, New York, N. Y., January 21–25, 1946. Manuscript submitted November 23, 1945; made available for printing December 12, 1945.

A. J. Williams, Jr., is chief, electrical division, and W. R. Clark and R. E. Tarpley are supervisory research technologists, all of the research department, Leeds and Northrup Company, Philadelphia, Pa.

The authors are grateful to Mrs. A. H. Springman for calculations on the reference junction compensation, to P. A. Towle for the slidewire on the ratio recorder, to E. W. Yetter and V. J. Porter for building and testing the ratio recorder, and to I. Melville Stein for his encouragement at times when it was most needed.

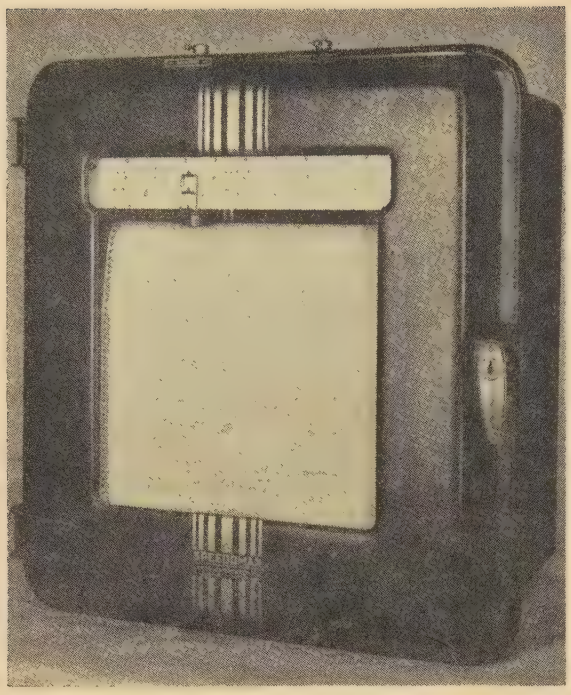

Figure 1. Multiple-point potentiometer recorder

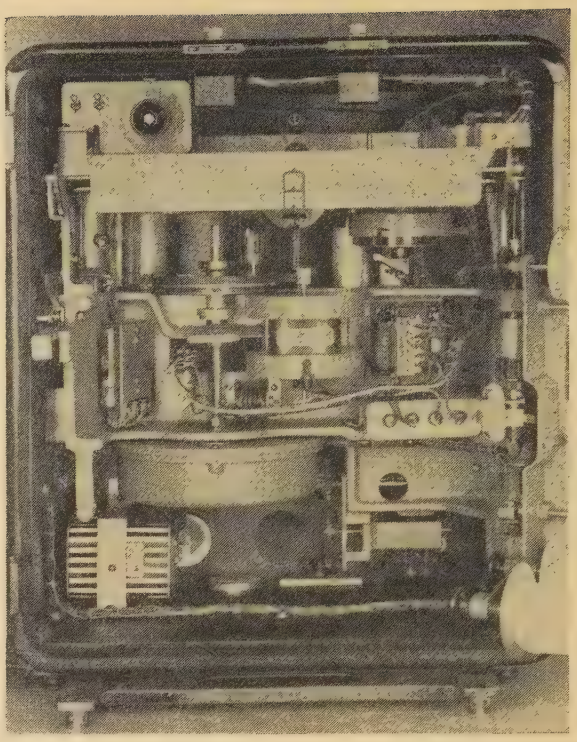

Figure 4. Internal view of recorder

2. Transmission of low frequencies of about one cycle per second and lower to 0.998 or better (loss of 0.016 decibel or less).

Requirement 2 could be stated as follows: After switching from a cold couple (reading at low end) to a hot couple (reading at the high end) the voltage at C_4 shall assume the voltage of the hot couple to within 0.2 per cent in 1.5 seconds or less.

Theoretically, the use of multiple sections in the filter is adequate to meet these conflicting requirements. Experimentally it was found that this was not sufficient. If electrolytic capacitors were used, requirement 2 would not be met. Many samples of electrolytic capacitors of many types and ratings have been tried. A typical result is shown on Figure 6A, which is a recorder response curve made with the chart driven at high speed. A satisfactory result with paper capacitors of the same 60 cycles per second capacitance is shown on curve B of the same figure. The reason for the excessive delaying action of the electrolytic capacitors was not investigated further. It may be the result of interfacial polarization inherent in the complex electrolytic film.

The impedance looking into this filter from the detector side at low frequencies (and direct current) is 20,000 ohms. The impedance of the detector is greater than this so it receives the greater part of any change in thermocouple voltage. Therefore the combination of high impedance detector and multisection RC filter using paper capacitors insures that the detector will receive changes in the thermocouple voltage without serious delay or attenuation.

Damping

Because of the inertia of the balancing motor, there is a tendency for it to overshoot the balance point. This is avoided by reversing the torque shortly before the balance point is reached. The torque is reversed by reversing the input to the detector, and this is done by introducing a voltage proportional to the motor velocity.[2] As the slidewire and motor are geared together, the slidewire velocity is proportional to the motor velocity. Figure 5B shows a simple circuit for which the output voltage E_2 is proportional to the rate of change of the input voltage, dE_1/dt, provided only that dE_1/dt has been constant long enough for the transient to have expired. If the circuit of Figure 5B were inserted into Figure 5A at B–B, there would be delivered to the detector mesh a voltage proportional to velocity as required. Of course, no voltage proportional to slidewire position would be delivered; however, if the circuit of Figure 5C is used, the voltage E_2 delivered to the detector mesh is exactly one-half the voltage E_1 of the slidewire when the slidewire comes to rest, and the transient has expired. When the slidewire is moving there is a component in E_2 proportional to the velocity. The time constant of the transient is the parallel resistance from

Figure 3. Circuit used for reference junction compensation

Figure 2. Basic potentiometer circuit

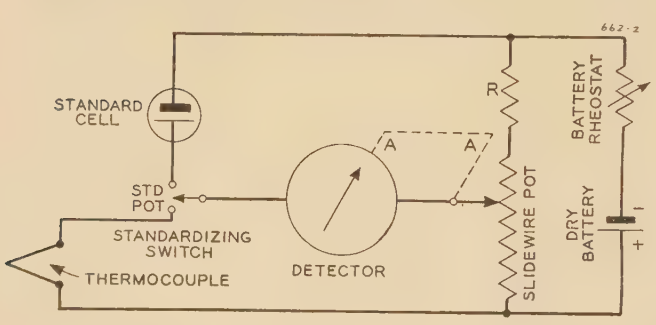

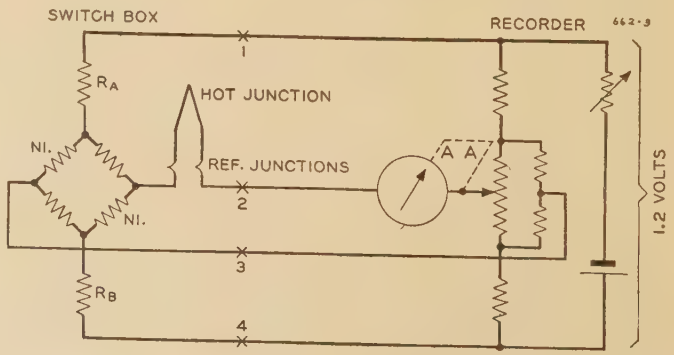

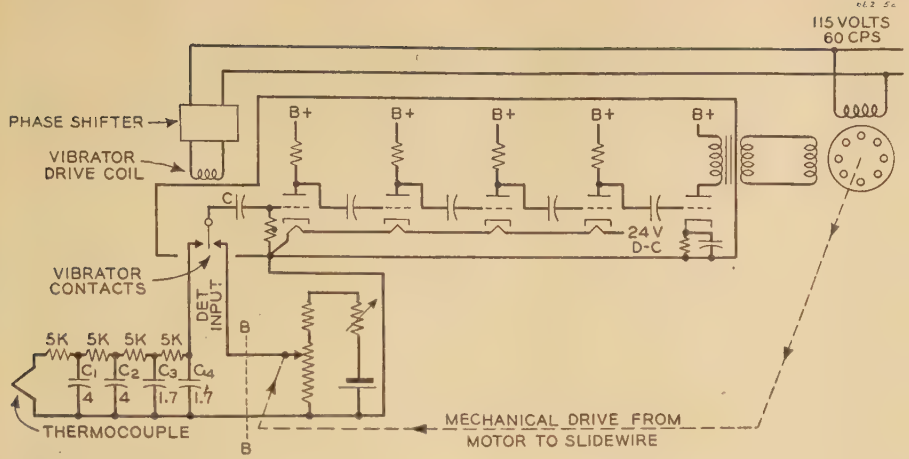

Figure 5. Circuits for balancing, filtering, and damping

A—Circuit without damping network
B—Explanatory network
C—Damping network

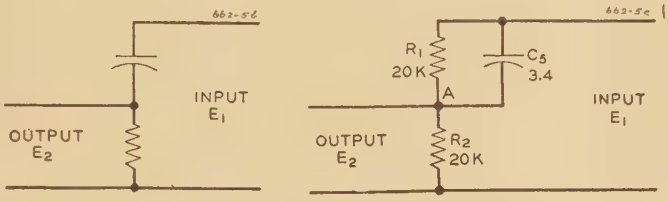

Resistor values are given in ohms and capacitor values in microfarads

point A times capacitance $= \frac{R_1 R_2}{R_1 + R_2} C_5 =$ $10{,}000 \times 3.4 \times 10^{-6} = 0.034$ second. This is so small as to have only a secondary effect, and the main object is accomplished, that is, to introduce a voltage proportional to velocity for the purpose of damping. The damping is sufficiently good to permit switching, completing a full scale balance and printing in 1.63 seconds.

It will be noticed that with this circuit some current is drawn from the slidewire even at balance. Quantitatively, however, it would require 40 ohms resistance in the slidewire, and its contact, to introduce an error of 0.1 per cent, and no such resistances ever have been found.

With the filter circuits and damping circuits described in the foregoing, and with the high impedance detector, two things are accomplished:

1. Large unbalances are completed in a minimum time without overshoot.
2. The voltage level at the detector is kept as high as possible, and therefore has the greatest possible margin above stray thermal electromotive forces.

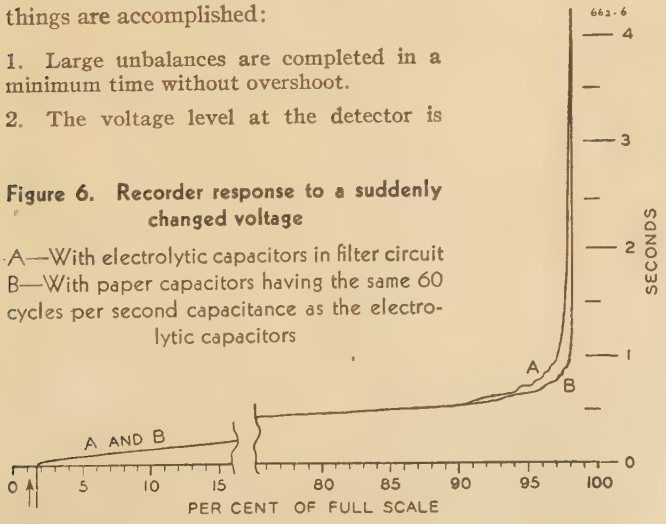

Figure 6. Recorder response to a suddenly changed voltage

A—With electrolytic capacitors in filter circuit
B—With paper capacitors having the same 60 cycles per second capacitance as the electrolytic capacitors

Microampere Recorder

For the recording of thermocouple temperatures, a potentiometer recorder is required because it is the open circuit (zero current) voltage that is the function of the temperature. For the recording of light or other radiation on a barrier layer* photoelectric cell, a current recorder is required because it is the short circuit (zero voltage) current that is the function of the radiation.

Figure 7A shows, in simplified form, how the slidewire type of null recorder can be arranged to present zero voltage to the photoelectric cell at balance. When any appreciable voltage does appear across the photoelectric cell, and hence across the detector, it operates through A–A to move the slidewire and so changes the current through the calibrated resistor until that current equals the current from the photoelectric cell, thus returning to zero the current through the detector and the voltage across the detector and photoelectric cell.

Figure 7B shows how filtering and damping are added. It will be noted that resistance is inserted between the photoelectric cell and detector for the purpose of filtering yet this resistance does not prevent the photoelectric cell and the detector reaching zero voltage at balance, as no direct current flows through this resistance at balance. As the slidewire has a low impedance, all three capacitors contribute to the filtering of alternating current from the photoelectric cell circuit away from the detector.

The damping is provided by capacitor C_3 which gives a component of voltage across the detector proportional to slidewire velocity. Figure 8 shows balancing curves with the chart speeded up in order to show detail. The balance time is approximately 0.8 second extrapolated for a full scale change. Most of the time the motor is running at top speed which is near to synchronous speed. The time lost in getting up to speed is 0.06 second or four cycles, and the time lost in stopping is 0.08 second or five cycles. Good damping is indicated by the fact that the time lost in stopping is nearly as small as the time lost in starting.

In addition to the null current range of 0.5 microampere, there have been added for convenience other current ranges and several voltage ranges by

* With an emission-type photoelectric cell it is the combination of the cell and its voltage supply which should look into a short circuit (zero voltage).

Figure 7. Circuits for microampere (null current) recorder

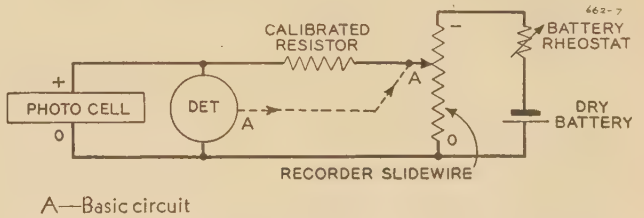

A—Basic circuit

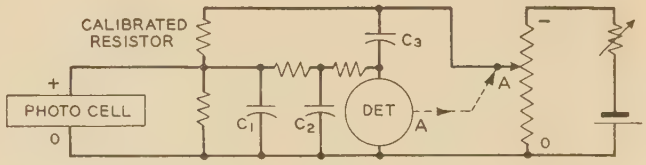

B—Circuit with filtering and damping components added

means of shunts and multipliers, respectively.

A microampere recorder of this general type has been found by Dieke to work well with photomultiplier tubes for the direct intensity measurement of spectrum lines.[3] On the lower current ranges of the recorder the dark current of the photomultipliers shows up and should be balanced out or subtracted from the readings, if the use of these low ranges is to be justified.

Ratio Recorder

The microampere recorder is suited well to the study of the intensity of spectrum lines and their variations arising from all causes. For spectrographic analysis, it is desired to measure the variation resulting from change of composition of the specimen being sparked and to suppress variations from all other causes. A big step in this direction is to measure the ratio of the intensity of two spectrum lines.

Figure 9A shows in simplified form how a slidewire type of recorder can be adapted to measuring ratio. If the fixed resistor equals the slidewire, then the ratio I_x/I_s is read directly as the fractional position of the slidewire.

Several experimental recorders have been built using this basic circuit, together with a detector and balancing system about the same as that already described.

Figure 9B shows a more detailed circuit including the photomultipliers. The slidewire resistance is 5,000 ohms so that small currents from S (ten microamperes) yield adequate slidewire voltage and hence good sensitivity. The drop coil R is 25,000 ohms so that the fundamental full scale ratio I_x/I_s is 0.2. Other ratios can be read by switching the "Ayrton" shunt ratio multipliers.

The high valued resistor R_H balances the recorder slightly on scale for $I_x = 0$, which is of value when looking for small amounts of dark current. Conventional methods of doing this were not applicable because of the common terminal at battery + for I_x and I_s.

Filtering for the signal I_x is done as already described. In order that the recorder shall plot a steady ratio for fluctuating currents (of constant ratio I_x/I_s) it is necessary to filter I_s also. Furthermore, it is necessary that the two filters shall have carefully matched frequency responses.

Figure 10A, shows the record given with currents I_x and I_s of constant ratio, but with a reduction of both to one-half value, and then a return to the initial value. Figure 10B, is a record with the same recorder, made after the chart had been rolled back and rerun. The recorder is used here as a straight microammeter on I_x by supplying the slidewire from a battery. The reduction of I_x and its return to its initial value is shown. The effectiveness of the ratio method in ironing out the effect of change in absolute magnitude of the two currents is apparent.

Figure 8. Response curve of the microampere recorder to a suddenly changed current

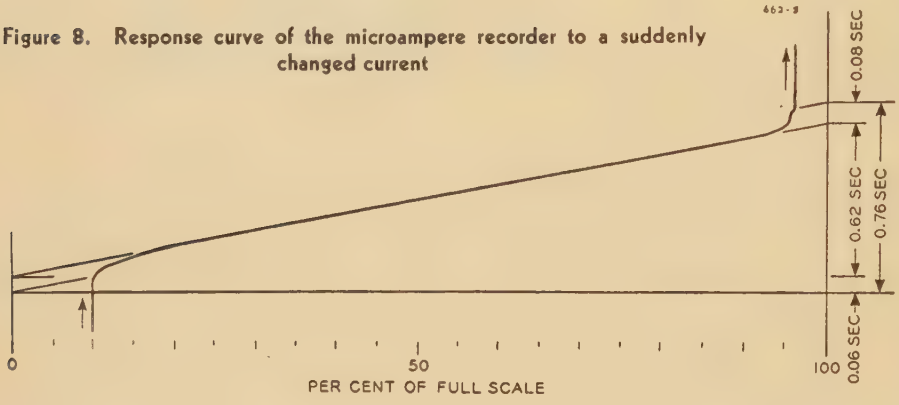

References

1. High Speed Multiple-Point Potentiometer Recorder for Measuring Thermocouple Temperatures During Test Plane Flights, **I. M. Stein, A. J. Williams, Jr., W. R. Clark.** *Transactions* of the American Society of Mechanical Engineers, volume 66, number 4, 1944, pages 271–5.

2. Combined Thyratron and Tachometer Speed Control of Small Motors, **A. J. Williams, Jr.** AIEE Transactions, volume 57, 1938, October section, pages 565–8.

3. Direct Intensity Measurements of Spectrum Lines With Photomultiplier Tubes, **G. H. Dieke, H. M. Crosswhite.** *Journal* of the Optical Society of America, volume 35, number 7, July 1945, pages 471–80.

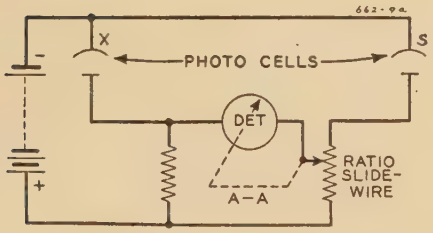

Figure 9. Circuits for the ratio recorder

A—Basic circuit
B—Circuit with filtering and damping components added

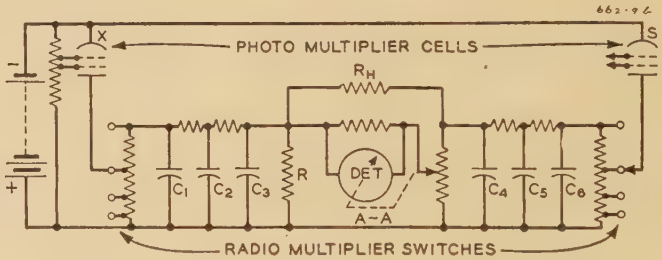

Figure 10. Response curves of the ratio recorder

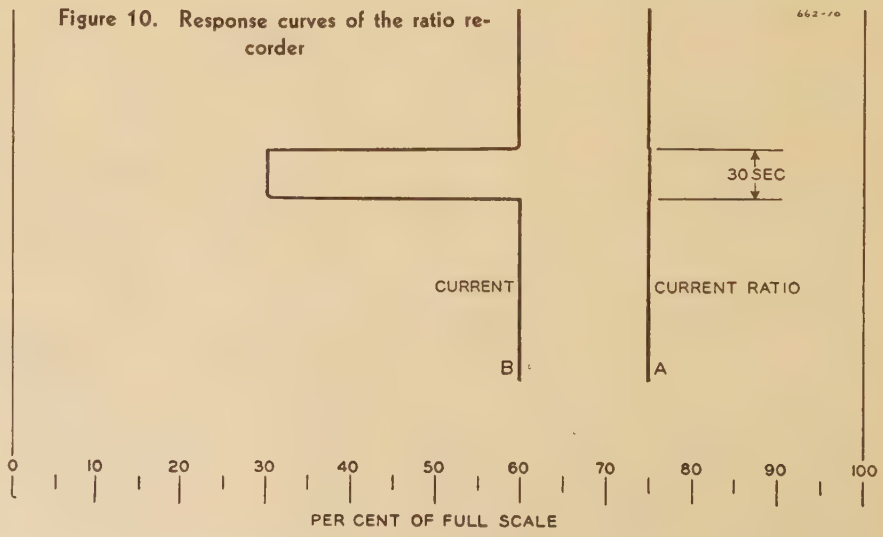

Radar Systems Considerations

D. A. QUARLES
FELLOW AIEE

IN the comparatively brief history of its development, the radar art has passed quickly through the general practitioner stage into the stage of many specialists. Today there are a dozen or more highly developed fields of specialization, all essential to the development of a new radar system. Each of these fields has its own basic science foundations and its engineering technology, and as soon as security conditions permit, each will have its own literature. To tie these several fields together calls for systems engineering and planning. The over-all characteristics and performance of a radar system are dependent both on the excellence of the component parts and the nicety with which they are fitted together to perform the desired function. It is the purpose of the present paper to discuss some of these systems engineering considerations, with examples of practical solutions that have been found, leaving to the specialists in the several fields the more detailed and exact exposition of their respective arts.

There have been many technical workers in this broad field, and both in England and this country they have enjoyed full interchange of technical information so that each could use the building blocks of the other as well as those of his own design. This makes it exceedingly difficult to recognize and give credit to the sources of specific contributions, and the present paper will not attempt to do so. Most of the illustrative solutions shown are the product of Bell Telephone Laboratories, but it is freely admitted that many of the basic ideas entering into these designs may have originated elsewhere. In particular, the Bell Laboratories worked very closely in this field first with Army and Navy laboratories and later with the Radiation Laboratory of the Massachusetts Institute of Technology, and in all cases there was the freest interchange of technical material. It is therefore a pleasure for us to recognize and acclaim the splendid research and development work that was done at these laboratories, even though specific recognition of their contributions seems impracticable at this time.

Antenna

The alpha and omega of a radar system are its antenna. This is true in a literal radiation sense. It is also true in the sense that the antenna was usually the first part of the system to be blocked out in plan and the last part to be completely frozen in design. This antenna problem is familiar to radio engineers, but in modern radar where the same antenna is used both to transmit and receive, its characteristics have an even more profound influence on the performance of the system. The simplest radar antenna resembles a searchlight in that it consists of a suitably shaped reflector illuminated by one or more sources of electromagnetic energy. If the reflector is a paraboloid of revolution with the source at its focus, the radiation is of the single lobe or beam variety in which the angular width of the beam is inversely proportional to the diameter of the reflector and directly proportional to the wave length of the radiation. While such a beam antenna has been extensively used, many of the more recent radar systems have demanded more specialized radiation patterns. For example, in airborne search and bombing radars, a fan-shaped beam has come to be considered optimum. At any one position, such an antenna illuminates a narrow wedge of the terrain below, extending, ideally, from the point of the terrain vertically beneath the plane out radially to the maximum effective range of the system. The design objective here is to produce as narrow a beam as possible with a vertical pattern such that substantially equal signals are received at all ground ranges. This requires that the effective voltage be approximately proportional to the square of the cosecant of the vertical angle measured downward from the horizon. A more recent and as yet unpublished study of this problem has indicated that some modification of this cosecant squared

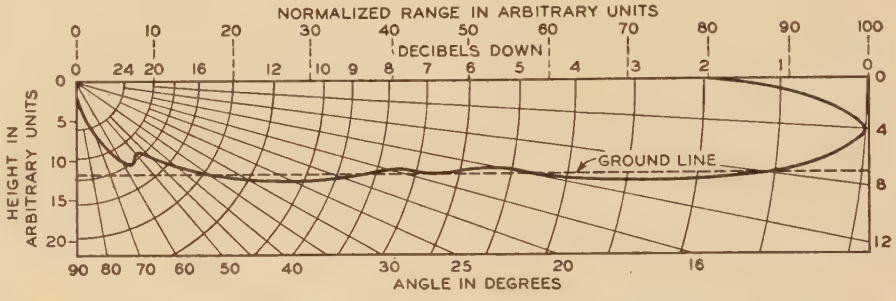

Figure 1 (above). Vertical antenna pattern (airborne radar system)

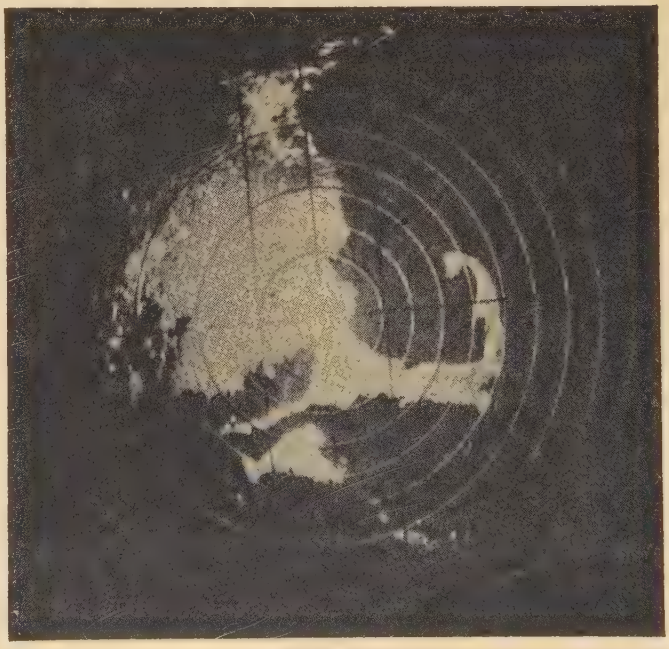

Figure 2. Oscilloscope picture of Cape Cod from 19,000 feet (range circles are spaced at five miles)

Paper 46-46, recommended by the AIEE committee on communication for presentation at the AIEE winter convention, New York, N. Y., January 21–25, 1946. Manuscript submitted December 14, 1945; made available for printing December 27, 1945.

D. A. QUARLES is with Bell Telephone Laboratories, Inc., New York, N. Y.

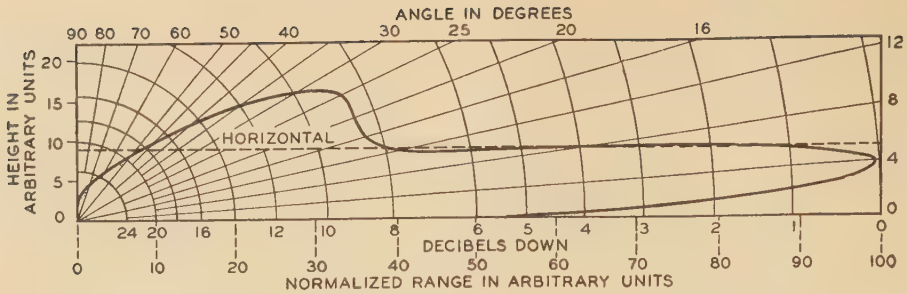

Figure 3. Vertical antenna pattern in free space (land-based search radar system)

formula may be advisable. In any event, the fair approximations to the ideal that it has been possible to achieve in actual design give satisfactorily uniform ground illumination. For example, the vertical pattern of the final stage of antenna evolution of a radar set used for search and bombing purposes in B-29 planes is shown as Figure 1. Figure 2 shows that quite satisfactory uniformity of ground illumination was achieved by this vertical pattern.

Other variations on antenna pattern include beams very much sharper in azimuth than in elevation for airplane search purposes and the reverse for height-finding purposes. One of the latest refinements here is illustrated by a typical vertical antenna pattern of a recent land-based air search antenna, as shown in Figure 3. In this case, in order to get high angle coverage, something approaching the cosecant squared pattern is achieved, the vertical angle being measured upward rather than downward from the horizon.

In general, land- and ship-mounted radar sets used to search the horizon for either ships or planes must take account of the fact that the intervening land or water surfaces reflect that part of the radiation directed below the horizon. Combination of the direct and the reflected waves produces a characteristic interference pattern in the vertical plane, greatly extending the range of the radar system at certain elevation angles and correspondingly reducing it at intermediate angles. A typical vertical performance or coverage chart of a light early-warning system is shown as Figure 4. In this case the beam in free space is fan-shaped with a horizontal width of about 3.5 degrees. The horizontal pattern is not greatly affected by the surface reflection, while the vertical pattern shows the very sharp lobes resulting from direct and reflected wave interference.

Frequency

Since the whole trend of radio development in the past two or three decades has been toward shorter wave length and higher frequency, it is not surprising that the same trend should have characterized radar development. In the case of radar, however, there were considerations over and above those applying to radio, which put a large premium on higher frequency and shorter wave length. This is because radar is essentially a seeing and measuring art, and fineness of vision and precision of measurement are related directly to fineness or shortness of wave. This, of course, comes about from the fact that with an antenna of given physical dimensions, the spread of the beam is proportional to the wave length, other things being equal, so that as the beam sweeps through an angle, its ability to discriminate between two nearby reflecting objects is an inverse function of the beam width. The above assumes that the two objects are at equal range. If, on the other hand, they are on a line with the radar antenna but at unequal range, the ability of the radar set to discriminate between them is an inverse function of the pulse length. It follows from the above broad reasoning that each radar set will be characterized by a figure of confusion in space, the cross-section of which is directly related to the beam height and width and the depth of which is directly related to pulse length. Within this figure, multiple reflectors will appear as one. Reflectors that cannot be encompassed within such a figure of confusion, on the other hand, would be resolved. Actually, certain characteristics must be met in other parts of the radar system, notably in the intermediate-frequency (hereafter referred to as i-f) and video amplification and in the cathode ray tube properties, in order to realize the theoretically possible discrimination provided by the radiation system. It is quite practicable, however, and in fact common practice, to design the rest of the system so that the discrimination of the radiation system is limiting. Since, with fixed antenna size, beam width is directly pro-

Figure 4. Vertical coverage chart (land-based radar system at a low site overlooking water)

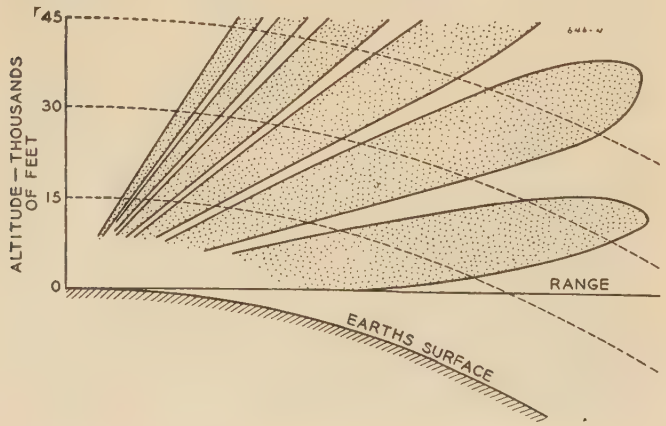

Figure 5. Effect of wave length on attenuation caused by rain

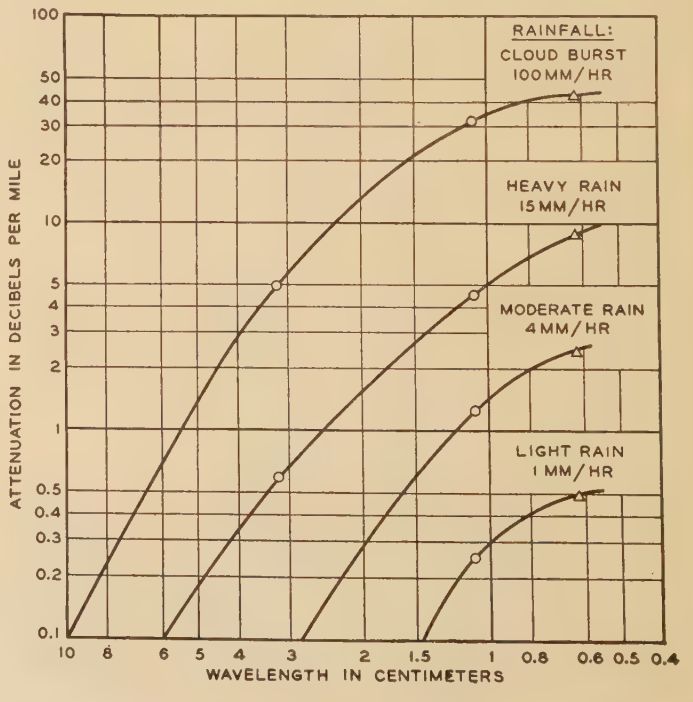

portional to wave length, it follows that to achieve high resolution or high discrimination, radar had a very special reason for seeking higher frequencies and the same reason for preferring shorter pulse lengths even though the latter, in general, meant a sacrifice in range. Actually, early radar sets made the best use of prewar technology and employed wave lengths down to about one meter. In four fairly discrete steps, this wave length was reduced successively to bands in the neighborhood of 40, 10, 3, and 1 centimeter. This change was accompanied by the use of shorter and shorter pulses so that the over-all effect of the development was to decrease the volume of the figure of confusion by about five orders of magnitude, two each for height and width and one for depth. As in so many other trends of this kind, these advantages were not gained without penalties. In fact, in the case of the shortest wave length mentioned, atmospheric absorption and raindrop interference get to be such serious limitations as to appear to restrict this and shorter wave lengths to only very special uses. Figure 5 shows the relation of attenuation to precipitation at different wave lengths, and Figure 6 shows the effect of energy absorption by gaseous components of the atmosphere. If this restriction proves real and permanent, it appears that the useful free space spectrum has now been explored and, in fact, is rapidly being conquered and settled.

Transmitter

The two principal elements of the transmitting system are the radio-frequency oscillating tube and the source of high-voltage pulses, variously called a keyer, modulator, or pulser. It is the function of the latter to deliver to the oscillator tube square-topped spurts or pulses of very high voltage of the order of a microsecond in length and spaced of the order of a millisecond apart, these specific values varying over considerable ranges according to the specific purposes of the radar equipment.

Two basic methods have been used to form the microsecond pulses:

1. Short-circuiting or open-circuiting a charged artificial transmission line, often called a pulse network.
2. Creating large-voltage surges by driving a magnetic circuit into the region of saturation.

In connection with 1, the switches used to open- or short-circuit the charged pulse network have been

1. High-voltage vacuum tubes.
2. A spark-gap discharge either of the open air or enclosed type.
3. The hydrogen filled thyratron.

Since these several forms of modulators will be described in detail by others, suffice it to say here that all of them were applied extensively in operating systems, with recent design tending toward a preference for the hydrogen thyratron.

During the brief interval of the pulse, powers ranging up to the order of a megawatt may be delivered by the pulser. Since the particular combination of current and voltage put out by the pulser may not be that required by the oscillator, it is common to interpose a pulse transformer, the function of which is to step the voltage up or down to the desired level. In some radar systems, a transmission line is required between the pulser and its associated transmitter, in which case pulse transformers may be required at each end of the line. A typical oscillogram of the magnetron input current as a function of time, delivered by a hard tube modulator used extensively in airborne

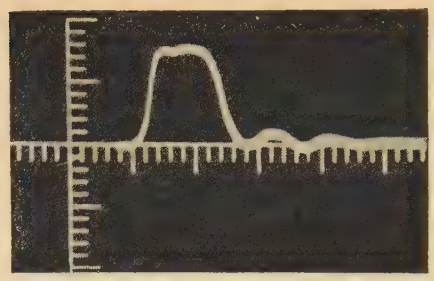

Figure 7. Magnetron input current delivered by hard tube modulator

$^3/_8$ μsec, 800 pulses per second
Magnetron current = 4.5 ma average
= 14 amp peak
Rise time = 0.03 μsec
Pulse width = 0.42 μsec
Pulse scale = 0.07 μsec per division

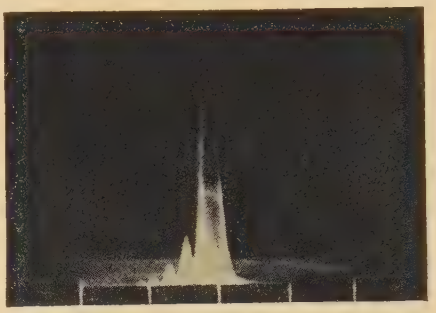

Figure 8. Magnetron frequency spectrum (scale = 10 megacycles per division)

Figure 6. Effect of wave length on attenuation caused by gases in atmosphere

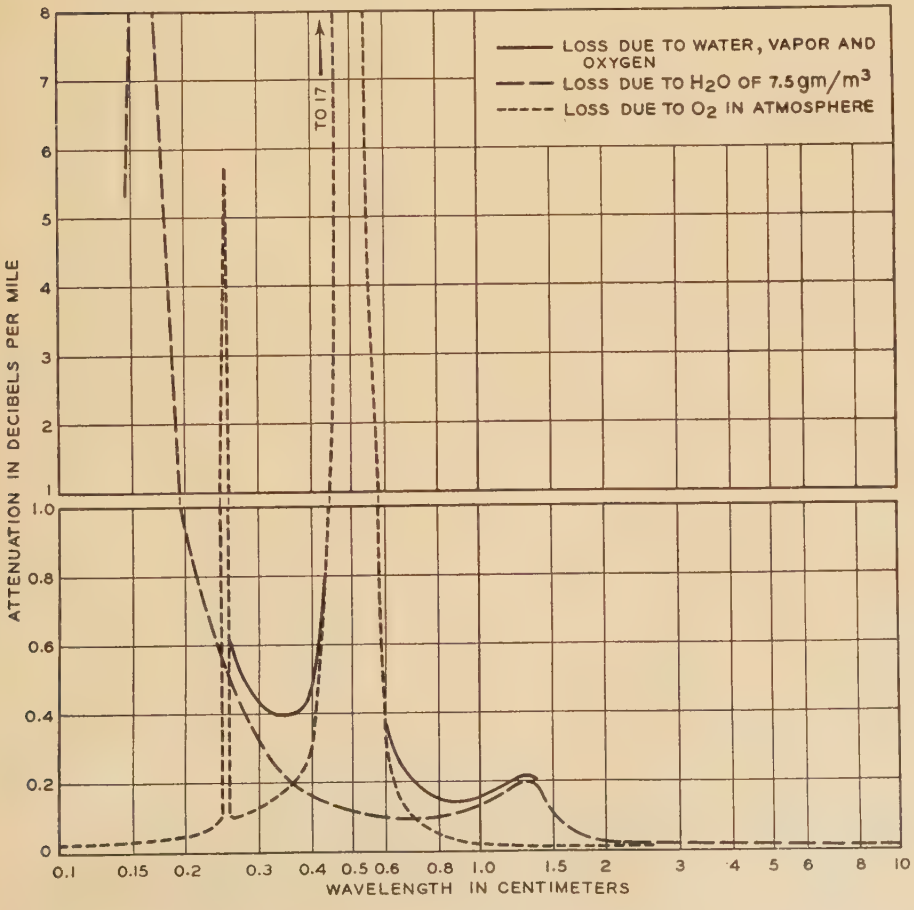

systems, is shown in Figure 7. The frequency spectrum produced by this pulse is shown on Figure 8.

Various forms of more or less conventional triodes found application as transmitting oscillators in the earlier longer wave radar sets. In this class of tube, time of flight of electron from cathode to plate must be short compared with the signal period—an increasingly serious limitation as the art moved into the microwave range. Velocity modulation tubes avoid this limitation in a sense by making use of the electron stream in flight. A particular form of velocity modulation tube, the cavity magnetron, has virtually monopolized the transmitting oscillator role in the more modern systems. In fact, its adaptation to very high power, very short pulse operation, and its very high frequency stability make it ideally suited to this purpose. In earlier forms, the magnetron was a fixed frequency device, but more recently external means of tuning over a moderate range have been devised and applied in practical design. While the frequency of the cavity magnetron is largely controlled by its built-in cavity construction, it is, of course, necessary to couple the oscillations in the internal cavities with the output line, and the reaction on the magnetron of this coupling imposes some neat problems of system design. As the antenna scans, the impedance facing the magnetron varies on account of varying reflections from discontinuities such as rotary joints in the output line to the antenna. These effective impedance changes, reflected back into the magnetron through its output coupling, tend to modulate or pull the frequency of the magnetron. Maximum power output calls for tight coupling between the magnetron and its antenna system, but such tight coupling in turn accentuates this pulling effect. In addition, there is a "long line" effect which causes an impedance irregularity to be more serious the longer the transmission path between it and the magnetron. Practical system design makes it necessary to take all of these factors into account and to tailor the characteristics of the magnetron to the degree of smoothness and excellence it is practicable to achieve in the radio frequency transmission system.

Duplexer

One of the most important practical contributions to radar design was the development of duplexer methods making it possible to use the same antenna for both transmitting and receiving purposes. Since the outgoing radar pulse occupies a very small fraction of the time, characteristically about one-tenth of one per cent, a switch which would associate the transmitter with the antenna during this brief interval and then disconnect the transmitter and connect the receiver during the relatively long silent interval, was called for. Since the total cycle, however, was only of the order of a millisecond, a very fast switch was required. In practical design, a gas-filled "TR" tube was almost universally used for this purpose. It is obvious that the requirements that this tube protect the receiver during the very high power transmitting interval and that it recover rapidly enough to admit echoes from nearby targets and thus achieve the desired minimum range for the system made it a very important element. Figure 9 shows the transmission characteristics of a typical "TR" tube assembly as measured in the transmit and receive paths over one complete pulse cycle.

Receiver

From our present point of view, the most significant elements of the radar receiver in order in the circuit are the beating oscillator, the detector, the i-f amplifier, followed by a second detector and video amplifier, and finally the display system. While each one of these elements has its own peculiar art, there are certain broad systems considerations. For the early long wave length radar sets, beating oscillators were of the more or less conventional triode construction. In fact, one very special triode, the so-called lighthouse tube, has been used as a beating oscillator up into the microwave range. As in the case of transmitting oscillators, velocity modulation has been the key to the design of most of the receiving or beating oscillators used in microwave systems, and for the most part, these have been of the single-cavity built-in type. The earlier forms had fixed or manually tuned cavities and beyond this, were tunable within a fairly narrow range by adjustment of the voltage of the repeller electrode. Not only was this voltage adjustment used for narrow range manual tuning of the receiver to its transmitter output, but automatic frequency-control circuits employing an intermediate frequency-discriminator circuit were devised which regulated the repeller voltage at the proper value for reception of echoes of the transmitted pulse. These automatic frequency-control circuits were not without their difficulties, but various improvements were introduced so that those embodied in most recent systems were quite stable and satisfactory. A typical

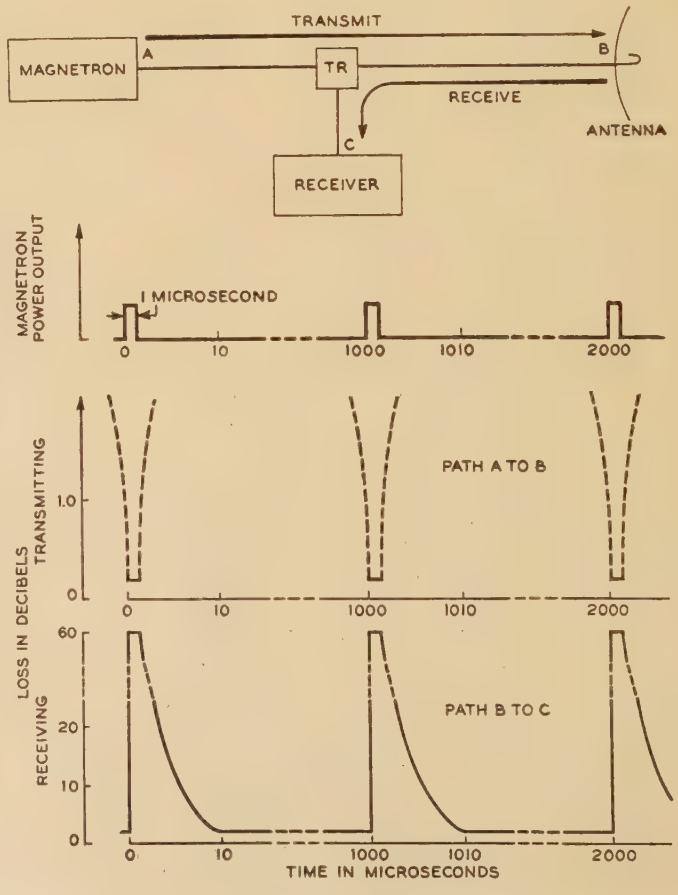

Figure 9. Transmission characteristics of "TR" tube assembly

Figure 10. Typical velocity-modulated beating oscillator

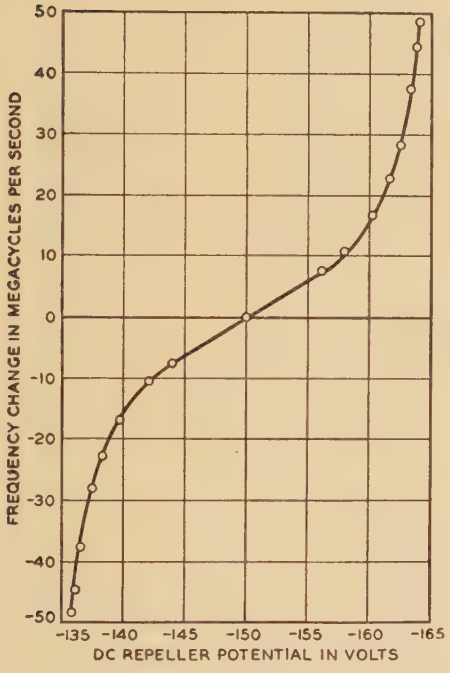

Figure 11. Beating oscillator electronic tuning

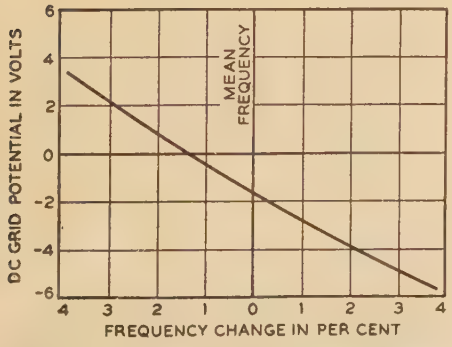

Figure 12. Beating oscillator thermal tuning

velocity-modulated beating oscillator with built-in cavity is shown as Figure 10, and the relationship between frequency and repeller voltage is shown as Figure 11.

More recently, thermal means of controlling oscillator cavity size have been devised, the heating effect being regulated by a control voltage. A typical relationship between this thermal control voltage and oscillator frequency is shown in Figure 12. Where thermal control of this type is available, automatic frequency control may be built around it rather than resorting to repeller voltage control as in the earlier systems.

First Detector (Converter)

In a radar system, the selection of frequency is based among other things on the noise figure available in the receiver. The input circuit of the receiver is the low-signal level point of the system, and the problem here has been to achieve the greatest possible freedom from noise. The longer wave radar receivers employ a combination of vacuum tube pre-amplifier and detector to achieve the best noise figure. In general, however, crystal detectors of the fixed cat's-whisker-on-silicon type have been almost universally used at wave lengths of about 30 centimeters and less. Figure 13 shows a comparison between the noise values of the lighthouse tube as an amplifier or detector, and the crystal-type detector. A great amount of development work has been done on these crystals, with the result that a uniform product has been achieved within a few decibels of the theoretical resistance noise limit. While the crystal is not strictly frequency-sensitive, optimum design calls for different crystal units for the different frequency bands. Means must be provided in the system to protect the crystal from high-voltage overload which would destroy its sensitivity.

Figure 13. Effect of wave length on receiver noise

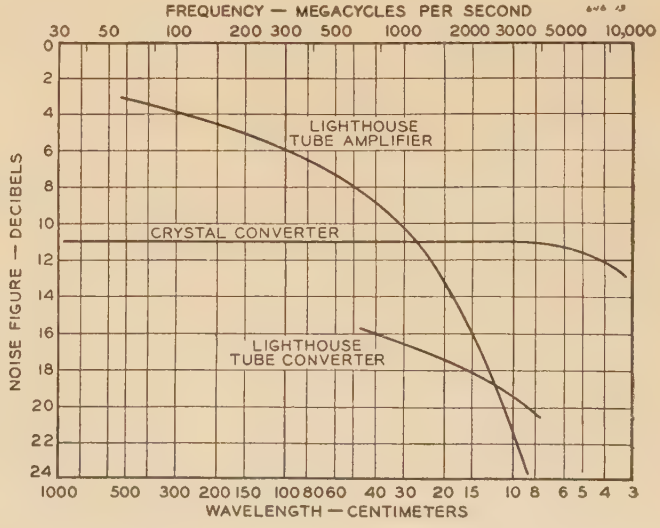

Intermediate Frequency

Choice of intermediate frequency rests on a number of factors, including signal-to-noise ratio and band width. About 90 decibels of i-f gain is required with a band width of from one to ten or more megacycles. Since resistance noise (power) is proportional to band width, the early tendency was to make i-f amplifiers as narrow as possible consistent with the pulse length to be accommodated. In more recent systems, there has been a trend toward wider band receivers as a means of sharpening up the picture. While, for example, a one-megacycle i-f system followed up by a one-half-megacycle video system would be expected to give approximately the optimum signal-to-noise ratio for a radar set employing a pulse of about one microsecond, it has been found in certain types of display that considerable advantage can be had by widening the band by a factor of as much as five. In such cases the increased noise is more than offset by the greater sharpness of the signal and by the finer grain structure of the noise.

Actually, most of the i-f amplifiers have been designed around a frequency of either 30 or 60 megacycles, but it would go beyond the scope of the present paper to discuss the relative uses and advantages of these two intermediate frequencies. Great progress has been made in achieving very low noise amplification and in producing the desired gain and gain frequency characteristic with a minimum of tubes and other components. The development of the 6*AK*5 high figure of merit miniature pentode was a great boon to i-f amplifier designers. Figure 14

attached shows an i-f strip employing six 6AK5 tubes and giving a gain of 65 decibels at a band width of 13.5 megacycles, centered at 60 megacycles. The design of the second detector and video amplification circuits is closely related to the television art and perhaps deserves no further comment in this paper.

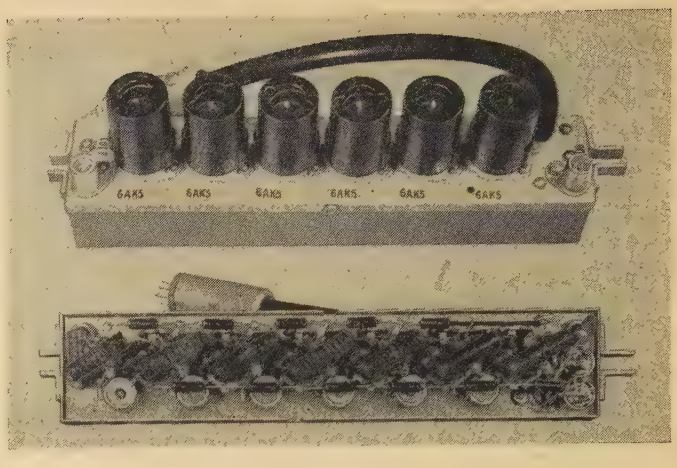

Figure 14. Typical i-f amplifier assembly

Display Circuits

The cathode ray tube has been substantially without a competitor for radar display purposes. A variety of display techniques has been developed, and a variety of cathode ray tubes of several sizes and of several different phosphors has been developed to meet the needs of radar systems. Rather than trying to tabulate these several varieties and their uses, the systems problem will perhaps be best illustrated by taking one of the most important combinations and examining its characteristics in relation to over-all performance. For this purpose, we choose a high-persistence so-called cascade phosphor and operate the tube as a plan-positon indicator in which each sweep is radial from the center to the outer edge and the direction of the sweep rotates like the spoke of a wagon wheel, at any instant the direction corresponding to the direction in space of the scanning antenna. The beam is intensity-modulated by the video signal, and the radial sweep is timed to correspond to the outward sweep in space of the radar pulse. In such a display, therefore, signals are shown on the face of the tube in their plan position relationship in space, the center of the tube normally corresponding to the position in space of the radar set. Here, again, the problem is not unlike that of a television receiver scope except that in the plan-position indicator type of display, a different scanning system is employed. In most recent systems, a permanent magnet focusing mechanism has been employed, the principal advantage being stability of adjustment and economy in the use of rectified power as compared with the earlier electromagnetic focusing scheme. To produce a wagon-spoke rotating beam needed to follow an all-around-looking antenna, best results have been achieved by placing an electromagnetic sweep coil around the neck of the tube and rotating the coil in synchronism with the scanning antenna. Gain, intensity, and focus controls parallel closely those found in television practice. It should be noted here, however, that special features such as facilities for expanding desired portions of the picture or stabilizing the picture against motions of the mother plane or ship have been devised and afford very important improvements in certain display systems. Methods also have been devised for discriminating between fixed and moving targets. These methods are of great importance in search systems where echoes from distant planes tend to be masked by permanent echoes from mountains or other features of the terrain.

Fire Control Radar

The above discussion deals primarily with radar as a search device. Many of its most important military applications, however, go beyond this search or seeing function to the more precise measuring function of fire control. In general, a radar fire control system must perform the following functions:

1. Precise three-co-ordinate location and tracking of the present position of the target.
2. Prediction of the location of the target at some future time, for example, the time at which a projectile would cross its path.
3. Generation of control orders, such as signals, to train and elevate the gun, set the fuse, and, in general, control the fire.
4. Servo systems for carrying out these orders.

When the fire control system is located on a plane or a ship, these problems are greatly complicated by the motions of the mother vehicle, calling in turn for stabilized reference systems and much other gear.

Automatic tracking is achieved by one or another form of lobe switching in which the antenna beam is rapidly switched back and forth between two angular positions and the target is centered between these positions by making the two received echoes equal. In fact, a servo system having as its input the echoes received from the two lobes can then be made to drive the antenna to a position where the two echoes are equal, and thus continuously adjust the antenna to such a position as the source of the echo moves. A variation on lobe switching in which the antenna conically scans, makes it possible to center the antenna in both azimuth and elevation and similarly uses two servo systems to track automatically in both dimensions. Automatic tracking in range involves a different technique. For this purpose, it is necessary to build into the radar a range unit producing a variable range pip or marker which may be compared with the range of the incoming signal. Here again it has been possible to make this range tracking automatic by employing a servo system which drives the range unit up or down under control of a voltage representing the deviation of the indicated range from the actual range. The same servo drive can be used to drive a shaft or potentiometer to give an output angle or voltage proportional to range. By resorting to precision methods, radar sets have been devised which not only track automatically in all three dimensions but which deliver present position information continuously to a computing system to accuracies of a few mils in angle and a few yards in range, this without the target ever being visible and, in fact, without human assistance once the radar equipment is locked on the desired target. The art, based fundamentally on feedback amplifier theory, of producing servo systems that are tight enough to give the desired speed and accuracy of response and at the same time stable over the operating range has been adequately treated elsewhere.

Computers

As it is the purpose of this paper to deal primarily with radar systems, any detailed discussion of computers would be

Figure 15. Computer used with airborne bombing radar

beyond its scope. It is pertinent to point out, however, that association with computers in a fire control system has a profound effect on the requirements to be imposed on the radar system proper. A more detailed consideration of one particular combination of radar and computer would illustrate this point. In a radar bombing system, fire control becomes bombing plane and bomb control. The computer, as before, has as inputs present-position information about the target. It must predict the future position of the target, the time interval being that required for the bomb to fall from the plane to the ground. The fire control orders in this case are directions to the pilot or to the automatic flight control equipment as to the proper course for the bombing plane and directions to the bomb release mechanism as to the instant in the plane's flight at which the bomb should be released. Such a computing mechanism must also be given as inputs the altitude of the plane and the ballistic characteristics of the particular bomb to be dropped. These are either previously known or separately determined and set into the computing mechanism in advance. Here again a great amount of development work has been done to improve the practicability and accuracy of the system and to make the best use of the not too adequate radar data available. The complexity of the problem and of the equipment required to solve it is perhaps best indicated by the photograph, Figure 15, of a bomb sight computer developed and introduced in radar bombing shortly before the termination of hostilities. Without attempting to explain the mechanism, suffice it to say that this computer performs the following operations: In association with a radar system displaying before the bombing operator a plan-position indicator type of "map" of the target terrain, the operator tracks by centering electronic range and azimuth markers on the "target." This tracking process not only feeds present position into the computer but at the same time enables the computer to determine the essential forward and transverse rates of the plane. Into the computer will previously have been set the ballistic constants of the bombs to be dropped. The height of the plane above the terrain will have been determined by a prior range tracking on the nearest ground return which would come from that vertically beneath the plane. Using these input data, the computer will predict the future position of the plane at an interval equal to the time-of-fall of the bomb; it will set up steering orders, either to the pilot or through the automatic flight control equipment, to move the plane into the correct position and heading; and it will give a bomb release order or control signal to operate the release mechanism at the correct instant. In the particular equipment shown, the computations assume level, steady flight, a limitation which it would require considerable additional gear to remove. This computer does, however, afford one very important additional facility, namely that of offset bombing. Because of the coarseness of radar data, information about the terrain is at best not too good. Certain landmarks do stand out sharply, and the geographical relation of these to strategic targets may be known or determined by reconnaissance. The ability to track a radar landmark and bomb a target of known range and azimuth offset from the tracking point greatly increases the flexibility of the equipment. The computer shown provides this feature, so that, having set in known offset co-ordinates, the operator proceeds as though to bomb the aiming point, the computer making the corrections and actually directing the attack against the target.

Radar bombing systems cover a wide range of weight and complexity and require nice judgment to reach a fair balance between such factors as operating facility and precision on the one hand and equipment bulk, reliability, and other "price" factors on the other. Enough progress has already been made to assure that highly flexible and precise radar bombing systems will become available at a "price" that is in reasonable balance with other factors.

Any discussion of radar systems would be incomplete if it failed to touch on the all-important question of testing and test equipment. Actually, the practical success of radar in the field was largely dependent on the provision of adequate specialized test gear. This was an art in itself, the treatment of which is reserved for a companion paper.

This paper will have served its purpose if it gives a technical background for the more detailed exposition of the many-sided art that is modern radar. Security will probably continue to limit workers in this field in the telling of their story, but it will be possible to tell enough to indicate clearly the truly wonderful advances in electronic and related arts that have brought radar to its present stage of development.

A New Wire Recorder Head Design

T. H. LONG
MEMBER AIEE

Synopsis: Certain defects inherent in the usual design of wire recorder heads are pointed out. Some defects are of a practical nature and one is based on theoretical considerations. An improved design is proposed on which a limited amount of experience has been obtained. A natural modification of this design permits level-winding across the record-playback head, thus distributing the wear and resulting in a head that is virtually self cleaning.

WORK with wire recording during the past few years seems to have been confined to two general types of heads for recording, playback, and erase purposes.[5] These are illustrated to a somewhat enlarged scale in Figures 1 and 2. Figure 1 shows two variations of the so-called open type of head in which the recording wire runs over a grooved pole piece, and Figure 2 shows a closed type of head in which the relation between the recording wire and the pole piece is substantially the same as in Figure 1, but in which the exciting coil surrounds both the pole piece and the wire.

Certain combination heads have been developed which combine the functions of record and erase in one structure. These always use separate gaps for the erase and the record operations. Playback is over the record gap. The structural modifications seem obvious and are not shown. The principal difference between a record or playback head and an erase head is that the latter ordinarily uses a gap of about 0.010 inch, and the playback gap for a wire speed of two feet per second is preferably about 0.0015 inch.

Figure 3 shows the relative record-and-playback characteristics for the open and closed type heads. A qualitative analysis of the situation that causes this difference between open and closed type heads has been given by Holmes and Clark.[1] According to this analysis, the so-called stray field is responsible for the irregularities, since the phase relation between the stray field and the main field depends on the frequency and the wire speed. It should be pointed out that a closed head greatly reduces the effect of stray fields, since the leakage flux has to go through the coil to contribute any adverse effect (on playback).

Figure 4 is a photograph of an equipment that has been set up to study experimentally the characteristics of various types of heads. This is arranged so that it can be operated on a continuous loop of wire about 20 or 30 feet long, or so that it can be operated from spool to spool. Provision is included for various speeds from 1.25 to 5 feet per second. The playback head is located a few feet along the wire from the record head so that in listening tests it is possible to get a quick comparison between a few bars of music as recorded and as played back. This almost instantaneous playback is very useful in collecting data, especially when working from spool to spool.

The first heads used on this equipment were of the closed type but in which the operating gap was adjustable. An optical system was used that made it possible to project on the wall of the room a 150-diameter enlargement of the operating gap and the wire traveling through it.

One of the first things discovered with this equipment was that the gummy residue that accumulates on the heads is a magnetic mud that has a shunting effect on the working gap. This seems to be of little consequence at low frequencies, but the effect at 5,000 cycles may be as great as 15 decibels or more, for a two-foot-per-second wire speed.

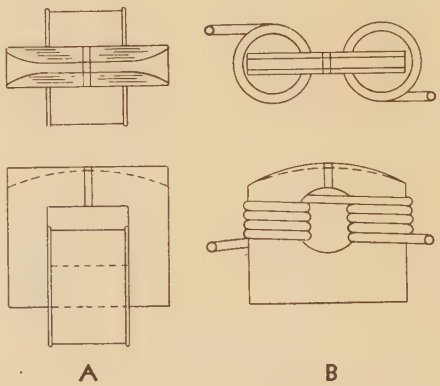

Figure 1. Open type record–playback head

A—High impedance head with laminated magnetic structure

B—Low impedance single lamination head, used with step-up transformer on playback

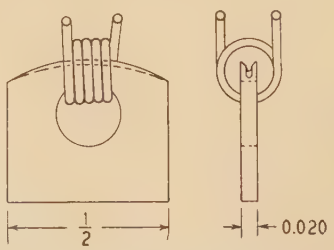

Figure 2. Closed type single lamination record–playback head

Lamination thickness is exaggerated

It was found that by frequent cleaning with carbon tetrachloride, quite consistent results were possible, even at high frequencies. It seemed apparent that in more conventional head designs there would be little trouble from this accumulation of magnetic mud, since the operating gap is filled with solder. The actual event however was contrary to this wishful thinking.

By lifting the wire a little as it moved through the gap and observing the enlarged image on the wall, it was determined that at low frequencies it made no difference where the wire was in the gap until the wire started to leave the region between the sides of the groove. At high frequencies (5,000 cycles), however, the smallest motion perceptible in the enlarged image on the wall, corresponding to about 0.0002 inch at the gap, made a difference in playback of about three decibels. These tests were made at the playback head, since there was no time lag there between cause and effect. Subsequent experiments show that for high frequencies the effect at the record head may be even more pronounced.

It is an unfortunate fact that this magnetic mud frequently will build up underneath the recording wire, even with substantial tension in the wire and working over a small radius such as one-fourth inch. This causes the actual performance of such a system to be rather uncertain above about 2,500 cycles, at least for wire speeds on the order of two feet per second.

By the simple expedient of using sufficient carbon tetrachloride and using it often enough, it is possible to keep the grooved type of heads fairly clean. But this has caused another sort of trouble, since with no lubricant whatever the wire may abrade the head sufficiently to cause a 6- or 7-decibel increase in the noise level. This noise level evidently is due to microphonic action of the head. In such cases a drop of oil on the head will bring the erase noise level down about three decibels in the first minute, and another three

Paper 46-29, recommended by the AIEE committee on communication for presentation at the AIEE winter convention, New York, N. Y., January 21–25, 1946. Manuscript submitted November 8, 1945; made available for printing December 26, 1945.

T. H. LONG is senior research engineer, C. G. Conn, Ltd., Elkhart, Ind.

or four decibels in a few more minutes.

Another minor disaster that may happen with the grooved type of head is that after running for quite a while on wire that is 0.004 inch in diameter some wire may come along that is 0.0042 inch in diameter. The least that will happen is that the wire will bind in the head. This may cause repeated breakage of the wire, and certainly will introduce a pronounced kinkyness on account of cold working one side of the wire

This also may cause a substantial change in the magnetic quality of the wire and the partial loss of any recording then on it. Unless the wire is run with an unusual amount of tension the curliness alone caused by such an accident will preclude further use of that particular section of wire. It is true that such things do not happen often but they are vastly annoying when they do happen.

This raises a question as to the practicability for home or school use of any head that depends for its performance on running the wire at the bottom of a groove, unless some means can be devised to insure intimate contact between the wire and the pole pieces. A suitable method should preclude the possibility of the binding action just described. The tendency of mud to accumulate under the wire is a factor that must be overcome by eliminating the mud or redesigning the head so it will be easy to clean.

Figure 3. Playback characteristic taken with closed type record head

O—Open type playback head
●—Closed type playback head

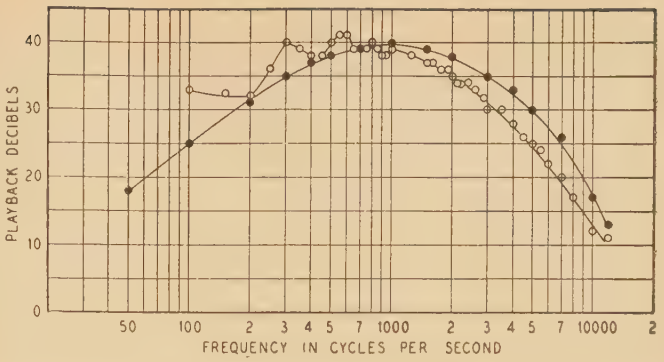

Figure 4. Experimental equipment for record and playback studies

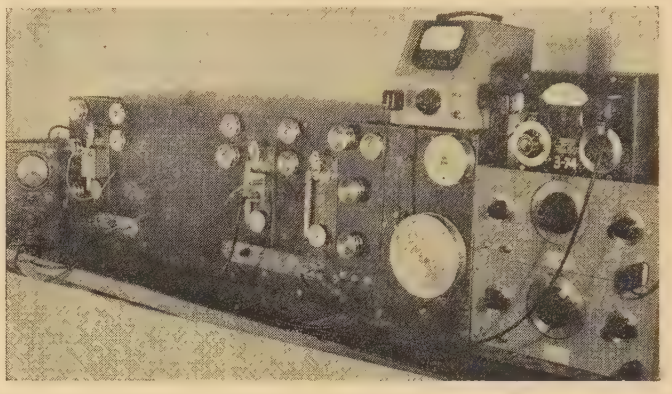

Figure 5. Record–playback characteristic versus high frequency bias voltage, using closed type playback head

A—For closed type record head
B—For new type open record head
O = 500 cycles
◐ = 2,000 cycles
● = 5,000 cycles

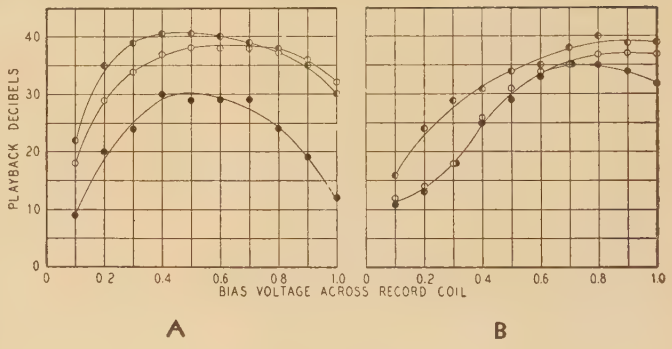

Magnetic Considerations

It can be shown (see appendix) that for small values of lamination thickness or cylinder diameter, the flux penetration is less in the lamination. By an extension of the idea that the flux penetration is a function of the curvature of the surface penetrated, it follows that the penetration will be even less into a concave surface than into a plane surface, and this decrease of penetration will be marked particularly when the concave surface has a small radius, such as 0.0025 inch.

These considerations make it appear that the conventional head design in which the recording wire runs at the bottom of a narrow groove is not a good design magnetically, unless the laminations are so thin that skin effect is not appreciable.

Since satisfactory operation requires a biasing magnetomotive force in the record gap having a frequency as high as 20 to 40 kilocycles, the required laminations would be around 0.005 thick if of conventional high permeability alloy, and a design that would be satisfactory from mechanical considerations becomes difficult. An alternative solution would be to use a low permeability alloy or even powdered iron. However, such a step would reduce the playback efficiency somewhat, and it is not clear that there would be any net gain, even if the bottom of the groove could be kept clean.

It is reasonably clear that the magnetic requirements for a good record head are somewhat opposed to those for a good playback head, since in the latter case skin effect in the magnetic structure is of no importance and a material of maximum permeability would be most desirable. In the record head any reduction in permeability without reducing the saturation flux density reduces the skin effect and therefore reduces saturation effects.

There is clear evidence of saturation in the record head at levels below that at which saturation occurs in the wire. This is shown by Figure 5A, which is a plot of the playback response versus record bias at several record frequencies, and on a conventional closed type head. The fact that the bias for maximum response decreases as the frequency increases is a clear indication of saturation in the record head. Without saturation in the record head all record frequencies would show maximum playback at the same value of bias.

Minimum third harmonic distortion is obtained at that bias that gives maximum low-frequency response, and in other frequency response curves given here, the bias has always been set at the lowest value consistent with maximum response at 500 cycles.

New Head Design

As a result of these considerations it seemed worth while to try a head design on the order of that shown in Figure 6.

We were forced to that conclusion while experimenting with a record head of the same general type but with a groove for the wire to run in and a closed type winding. The playback head in this experiment was the conventional type of Figure 2. The results seemed quite erratic, and in running down the cause it was found that at high frequencies the playback response was eight decibels higher when the wire was out of the groove and running across the top of the lamination than when the wire was bottomed properly in the groove. The single lamination used was about 0.060 inch thick, the groove about 0.030 deep including a shallow V at the top, and in operating on a continuous loop the wire frequently would not return to the groove after the knot went past.

It was found by using a head of the type shown in Figure 6 for record purposes, that with either an open or a closed type of winding it substantially duplicated the performance of the conventional closed type head of Figure 2 when used with stainless steel wire of moderate coercive force (around 175 oersteds) and usual retentivity. With this type of head (of Figure 6) there is virtually no difference between the performance with a closed type winding and with an open type winding. The reason for this is evidently the fact that the wire leaves the record head in a direction in which the magnetomotive force gradient is negligible so that it experiences negligible demagnetization except that which necessarily occurs immediately after passing the record gap. When used as a playback head it seems that the so-called stray field is quite negligible since the recording wire is running substantially tangent to a cylinder. See Figure 7A for playback response on closed type head for closed type and new open type record heads compared on the same loop of wire.

In recording with the same head on a wire that had a coercive force of about 250 oersteds, it was found that in the high frequency range the playback response was up to 10 decibels higher than with the head of Figure 2. In fact, it was so good that if the frequency range of interest is limited to 7,000 cycles[3] at the upper end, there is no point in doing much high frequency equalizing. Figure 7B shows the same sort of comparison as Figure 7A, but for wire having a coercive force of 250 oersteds.

It perhaps should be pointed out that this improvement in high frequency response depends on the production of a high coercive force wire. Without this there is no appreciable gain at high frequency except in reliability, and there

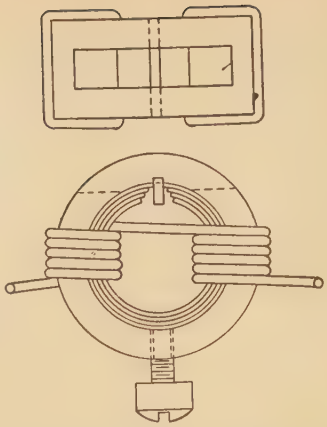

Figure 6. New design of open type head that is easily cleaned and magnetically efficient

may be a net loss of one or two decibels at frequencies on the order of 100 cycles.

The same construction is applicable to erase heads, but in this case it becomes important to use a bakelite receptacle rather than the brass ring shown. The high frequency erase current is sufficient to generate substantial heat in the brass ring.

Practical Considerations

Experience with this new type of head so far has been most instructive. When the record gap is filled with soft copper there is a pronounced tendency for metal to drag across the gap from the pole pieces, and eventually to shunt the gap. There seems also to be a tendency to undercut the copper. These two factors explain the short life occasionally experienced with the grooved type of head in which the working gap is filled with solder as a usual practice.

It would seem desirable to fill the gap with something that would wear away more slowly than the pole pieces, and hardened beryllium copper has been used for this purpose, with satisfactory results to date.

The most significant advance involved in this new type of head is that it is a very simple head to clean and keep clean. Our experience indicates that there is no way to obtain reliable performance at desirable wire speeds without virtually eliminating dirt from the record and playback heads. Eliminating dirt from the erase head is also desirable but not so critical on account of the wider gap (about 0.010 inch).

With a head design in which the operating part of the head is an element of a cylinder the possibility of level-winding across the head naturally suggests itself. This would result in playing the recording wire back and forth along the length of the working gap (the wire crosses the gap at right angles) and this would distribute the wear and at the same time help keep the working surface clean. Figure 8 shows an experimental design of such a

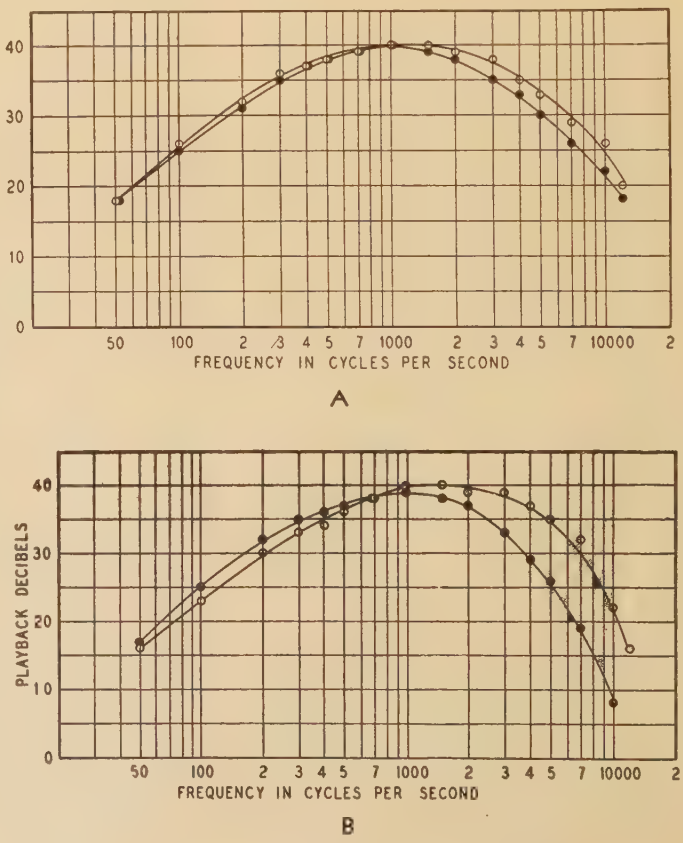

Figure 7. Comparison of closed type and new open type record heads

Playback head was closed type. Wire speed two feet per second

O—New open type head

●—Closed type head

Wire characteristics: A—H_c, 180; B_r, 5,900 Centimeter-gram-second units; B—H_c, 250; B_r, 4,650

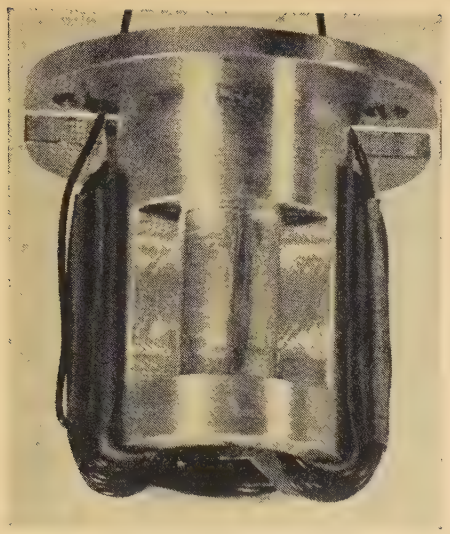

Figure 8. Experimental model of level-wind head with open type winding

This has been modified from the design of Figure 6 by lengthening the record gap along the axis of the cylinder

head in which the wire plays back and forth one half inch as the level-wind travels in and out.

Experimental results to date on this level-wind type of head have been completely satisfactory. Response data indicate the same performance as for the head illustrated in Figure 6.

Conclusions

Certain defects of a practical nature have been found in heads of conventional design. These defects seem to be inherent in the design of these heads and the nature of the problem.

Improved designs have been tried experimentally and their performance verified as far as electromagnetic characteristics are concerned.

There has not been time enough for the experience that is required to establish their practical merit beyond any question, but the nature of the change makes their practical merit seem very likely.

On the experimental equipment shown in Figure 4, a maximum range between saturation and erase noise level of 45 decibels is obtained regularly. This corresponds to a usable dynamic range of about 40 decibels. The quality is comparable to vertically cut vinylite records.

It has been shown quite clearly that the new design reduces magnetic saturation effects at the record head. It should therefore reduce cross modulation effects.

In those cases in which the level-wind feature can be sacrificed, the possibility is presented of accomplishing tone control in a very simple manner. It would be necessary only to taper the playback gap from say 0.0015 to 0.003 inch and shift the recording wire to the wider part of the gap to eliminate the higher frequencies in the playback.

Appendix

Practical units and inch dimensions are used in the work that follows, except that ρ is given in microhms per centimeter cube corresponding to usage in tables. Let

r = radius in inches to cylindrical element of radial thickness dr or distance in inches from center plane to plane element of thickness dr

r_1 = outside radius in inches of magnetic cylinder or half thickness in inches of magnetic lamination

μ = relative permeability

f = frequency in cycles per second

ρ = resistivity in microhms per centimeter cube

$\boldsymbol{B}$ = flux density at dr in lines per square inch

$\boldsymbol{B}_1$ = flux density at r_1 in lines per square inch

ϕ = integrated flux from unit length of periphery to center line or plane

$m = 0.505(\mu f/\rho)^{1/2}$

K = effective flux penetration in inches/$1.4(e/\mu f)^{1/2}$

$x = mr$

$y = mr\sqrt{2}$

$z = 2mr$

It can be shown that the differential equation of alternating magnetic flux distribution into a cylinder is[4]

$$\frac{d^2\boldsymbol{B}}{dr^2}+\frac{1}{r}\frac{d\boldsymbol{B}}{dr}-2jm^2\boldsymbol{B}=0 \qquad (1)$$

if the direction of the magnetic flux is parallel to the axis of the cylinder. The same equation obtains for the penetration into a lamination of flux parallel to the lamination, except that in this case the coefficient $1/r$ of the first order term is zero.

For the solid cylinder the solution is

$$\boldsymbol{B}=\boldsymbol{B}_1(\text{ber } y+j\,\text{bei } y)/(\text{ber } y_1+j\,\text{bei } y_1) \qquad (2)$$

For the lamination the solution is

$$\boldsymbol{B}=\boldsymbol{B}_1\frac{(\cosh x\cos x+j\sinh x\sin x)}{\cosh x_1\cos x_1+j\sinh x_1\sin x_1} \qquad (3)$$

The corresponding equations for the integrated flux from unit length of periphery to the center line of the cylinder or to the center plane of the lamination are

$$\phi=\frac{\boldsymbol{B}_1}{2m}\frac{[\sinh z_1+\sin z_1-j(\sinh z_1-\sin z_1)]}{\cosh z_1+\cos z_1} \qquad (4)$$

$$\phi=\frac{\boldsymbol{B}_1}{\sqrt{2}m}\frac{[\text{ber } y_1\,\text{bei}'\,y_1-\text{bei } y_1\,\text{ber}'\,y_1-j(\text{ber } y_1\,\text{ber}'\,y_1+\text{bei } y_1\,\text{bei}'\,y_1)]}{\text{ber}^2\,y_1+\text{bei}^2\,y_1} \qquad (5)$$

The equation in Bessel's functions applies of course to the cylinder.

The corresponding average flux densities are

$$\boldsymbol{B}_{ave}=\frac{\boldsymbol{B}_1}{z_1}\frac{[\sinh z_1+\sin z_1-j(\sinh z_1-\sin z_1)]}{\cosh z_1+\cos z_1} \qquad (6)$$

$$\boldsymbol{B}_{ave}=\frac{2\boldsymbol{B}_1}{y_1}\frac{[\text{ber } y_1\,\text{bei}'\,y_1-\text{bei } y_1\,\text{ber}'\,y_1-j(\text{ber } y_1\,\text{ber}'\,y_1+\text{bei } y_1\,\text{bei}'\,y_1)]}{\text{ber}^2\,y_1+\text{bei}^2\,y_1} \qquad (7)$$

Equations 6 and 7 may be divided by $\boldsymbol{B}_1$. Then the absolute value of the right hand sides will be the effective flux penetration as a fraction of half the lamination thickness, or as a fraction of the cylinder area which can be reduced to a radial depth.

Then the right hand side of the equation derived from equation 6 can be multiplied by r_1 to give the effective flux penetration in inches, and this may be divided by 1.4 $(\rho/\mu f)^{1/2}$ to get a factor K which gives the penetration in dimensionless terms. This value used for effective flux penetration in inches into a thick lamination, $1.4(\rho/\mu f)^{1/2}$ is equivalent to the formula for penetration in centimeters, $3.57(\rho/\mu f)^{1/2}$, given by Steinmetz.[2] The net effect of the operations described is to divide the absolute value of the term in hyperbolic and circular functions by $\sqrt{2}$.

By somewhat analogous steps the effective flux penetration into a solid cylinder may be compared to the Steinmetz formula and these comparisons are shown plotted together in Figure 9. For values of $z_1<2$ the skin effect is of little consequence, since penetration is limited by the size of the piece. For $z_1>2$ the penetration into the cylinder is substantially greater than into the lamination.

This difference is due solely to the curvature of the convex cylindrical surface and by an extension of the same idea the penetration into a concave surface would be substantially less than into the plane surface of a lamination.

This reasoning is entirely valid, but it is more satisfactory to approximate the con-

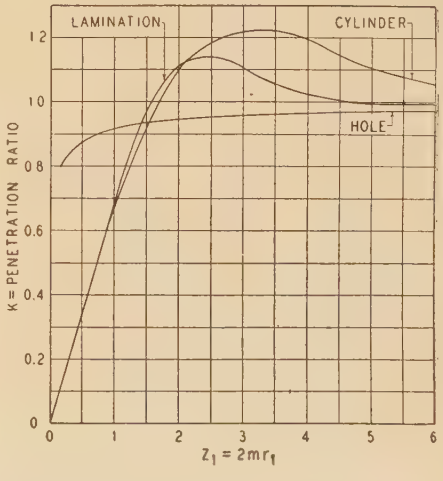

Figure 9. Actual flux penetration into a cylinder or lamination, or radially outward from a round hole in an infinite mass, divided by the Steinmetz formula value and plotted against $z_1(=2mr_1)$. Comparison is based on cylinder diameter = hole diameter = lamination thickness

Size Reduction and Rating Extension of Magnetic Air Circuit Breakers up to 500,000 Kva, 15 Kv

R. C. DICKINSON
MEMBER AIEE

RUSSELL FRINK
ASSOCIATE AIEE

AIR CIRCUIT BREAKERS rapidly are becoming the standard of the industry for voltages up to 15,000 volts and for kilovolt-ampere ratings of 50,000 to 500,000 kva. Their general desirability as compared to oil-type switchgear is now recognized by most users.

As has been previously pointed out before the Institute, the present trend of air circuit breaker development was started by the introduction in 1929 of a 500,000-kva 15,000-volt circuit breaker based on the multiple cold-cathode principle of Slepian.[1, 2] It may be noted that this rating is today, 16 years later, the highest standard rating for self-contained air circuit breakers. The original development was followed by successively producing ratings down to 100,000 kva at 2.5 and 5 kv.

Although large numbers of these multiple cold-cathode-type breakers are still giving excellent service, this principle was found to have certain limitations. Therefore, the magnetic deion principle[3] was developed, and it permitted ratings up to 250,000 kva at 5 kv.

These ratings of magnetic air breakers were smaller and simpler than the previous types of air breakers and created a demand for 7.5- and 15-kv breakers of more compact construction.

The next step in the development of the magnetic air breaker, however, was not a rush to enlarge the interrupters to cover the 7.5- and 15-kv ratings, since these were already covered by other forms of self-contained air breakers. It was instead an earnest attempt through research and development to improve further the interrupting principles so that a breaker of more compact construction and improved characteristics could be offered. These aims have now been fulfilled, and the magnetic air breakers are now available in all ratings up to 15 kv 500,000 kva. The 15-kv 500,000-kva unit, while containing the fundamental features of the original magnetic air breaker as presented to the Institute by Ludwig, Grissinger, and Nau in 1939,[3, 4] has been developed and refined until the interrupting capacity available in a given space has been more than tripled.

Paper 46-55, recommended by the AIEE committee on protective devices for presentation at the AIEE winter convention, New York, N. Y., January 21–25, 1946. Manuscript submitted November 23, 1945; made available for printing December 19, 1945.

R. C. DICKINSON is section engineer, air circuit breaker section, and RUSSELL FRINK is a member of the protective devices engineering department, Westinghouse Electric Corporation, East Pittsburgh, Pa.

The New Interrupter

It is reasonable to say that if a certain arc chute will interrupt a given voltage, then by doubling the length it will interrupt twice as much voltage. This is generally true on account of momentary current leakage following current zero, giving the effect of a potential divider to equalize voltage over the length of the arc chute. However, consideration shows that increased voltage rating obtained in this way is not economical in floor space. To keep the space requirement within desirable limits, the desirable course of action was to increase the interrupting capacity within a given space.

It was believed that by making a systematic study of all the known factors influencing arc interruption in air, each factor could be emphasized and co-ordinated into an optimum over-all design for a given rating.

From previous experience with the magnetic construction, it was decided that the general idea of multiple arc-resisting plates having V-shaped or tapered slots into which the arc is moved showed the greatest promise of success. The plate type of construction, in general, permits practical manufacture with high grade refractory ceramic material. As is well known, materials of this general class are

---

dition at the bottom of the groove by studying the radially outward penetration of magnetic flux from a hole in an infinite mass. It is assumed that a helical magnetizing coil extends through the hole. The solution of equation 1 is then

$$\boldsymbol{B}=\boldsymbol{B}_1(\ker y+j\,\mathrm{kei}\,y)/(\ker y_1+j\,\mathrm{kei}\,y_1) \quad (8)$$

Since[6]

$$\int_0^y y\ker y\,dy=y\,\mathrm{kei}'\,y \quad \text{and}$$

$$\int_0^y y\,\mathrm{kei}\,y\,dy=-y\ker' y$$

$$\phi=\boldsymbol{B}_1(-\mathrm{kei}'\,y_1+j\ker' y_1)/\sqrt{2}m\times(\ker y_1+j\,\mathrm{kei}\,y_1) \quad (9)$$

If we take the absolute values

$$\phi=\frac{\boldsymbol{B}_1}{\sqrt{2}m}\sqrt{\frac{\mathrm{kei}'^2\,y_1+\ker'^2\,y_1}{\ker^2 y_1+\mathrm{kei}^2\,y_1}}=\frac{\boldsymbol{B}_1}{\sqrt{2}m}\,Q \quad (10)$$

If p=depth of penetration in inches, the integrated flux $2\pi r_1\phi$ can be expressed in terms of p and r_1, or in terms of Q and m, so that

$$[(r_1+p)^2-r_1^2]\pi B_1=2\pi r_1 B_1 Q/\sqrt{2}m \quad (11)$$

$$p=r_1(-1\mp\sqrt{1+2Q/y_1}) \quad (12)$$

Let p_s=flux penetration in inches according to Steinmetz formula $=1/\sqrt{2}m$; then

$$K=p/p_s=y_1(-1\mp\sqrt{1+2Q/y_1}) \quad (13)$$

The values of K from this equation have been added to Figure 9 to complete the comparison. Values of the ker and kei functions and their first derivatives have been taken from Savidge's[7] table, which seems to be about the only one in existence. The tabular interval of 0.1 makes possible reasonably precise detail for values of y_1 greater than 0.1, corresponding to z_1 greater than 0.14.

It should be understood, of course, that for large values of mr_1, the actual flux penetration in any case approaches that stated by the Steinmetz formula.

References

1. SUPERSONIC BIAS FOR MAGNETIC RECORDING, **Holmes, Clark.** *Electronics*, July 1945, pages 126–136.

2. TRANSIENT ELECTRIC PHENOMENA (book), **C. P. Steinmetz.** McGraw-Hill Book Company, New York, N. Y. Page 371.

3. TONAL RANGE AND SOUND-INTENSITY PREFERENCES OF BROADCAST LISTENERS, **Chinn, Eisenberg.** IRE *Proceedings*, September 1945, pages 571–81.

4. CALCULATIONS FOR CORELESS INDUCTION FURNACE, **Dwight, Bagai.** AIEE TRANSACTIONS, 1935, pages 312–15.

5. United States patents 2,351,003, 2,351,004, 2,351,006, 2,351,007, **Marvin Camras** and others.

6. TREATISE ON BESSEL FUNCTIONS (second edition), **Gray, Mathews.** Macmillan and Company, New York, N. Y. Page 27.

7. TABLES OF KER, KEI, KER′, KEI′, **H. G. Savidge.** British Association Report, 1915. Pages 36–38.

non-gas forming and are chemically stable even when exposed to arc temperatures. They do not take on appreciable moisture from the atmosphere and are high in dielectric strength. By proper choice of composition, high resistance to thermal shock also can be obtained.

The theory of magnetic deionization has been described before the Institute.[4] Briefly, it consists of moving the arc toward the closed tops of slots in insulating arc-resisting plates. At this position the presence of a strong magnetic field imparts to the electrons an upward velocity. They in turn bombard gas particles and produce an actual blast of gas perpendicular to the arc, which action requires the arc continually to ionize fresh gas in considerable quantities. When current zero is reached, this action continues in a sufficient degree effectively to deionize the plurality of short lengths of arc near the edges of the slots.

This theory would indicate that increased interrupting capacity can be obtained by increased strength of the magnetic field. While this is a factor, it was found that blindly increasing the field strength might be detrimental rather than helpful. Slot shape, plate spacing, and magnetic field strength are interdependent and must be co-ordinated for optimum results. The design of the interrupting unit is most easily approached by blending the proper plate structure with a strong magnetic field.

The theory of magnetic deionization points out that interruption depends upon the rate of deionization at the instant of current zero. If some way could be found to control the field so that it would have appreciable strength at current zero, the interrupting capacity apparently should be increased. In other words, if the field flux was made to lag behind the arc current, it would have some magnitude at arc current zero. On the other hand, an in-phase flux is zero when the arc current is zero and positive driving forces are, therefore, momentarily absent. Tests proved that if the field flux lagged the arc current by the proper phase angle, the voltage limit of a well-designed interrupter was increased considerably.

A phase shift between the magnet flux and arc current may be accomplished by shunting the magnet coil with a resistor. It was not possible to predict mathematically the advantage to be gained by a particular phase shift. Therefore, it was necessary to make numerous tests to find the best value. However, the resistor seemed to be an undesirable appendage, and theory indicated that the same result could be accomplished with a shading coil. Such a coil was calculated to supply the same effect as the previously determined best value of resistance, and confirming tests demonstrated that this shading coil gave a correct phase shift. In the final design, the shading coil consists of a single turn around the magnet yoke adjacent to the magnet coil so that in operation it encloses the total flux.

Slot shape and plate spacing also are important factors in the performance of the interrupter, inasmuch as they control the motion of the arc through fluid friction and restriction. Mathematical analysis is helpful in determining the designs, but it is necessary to rely on empirical data on account of unpredictable factors such as gas temperatures, velocities, etc.

The fundamental theory of the magnetic Deion breaker states that interruption is accomplished by the blast of gas perpendicular to an arc held stationary at the ends of slots. This blast deionizes the arc and establishes dielectric strength. In the development of the new interrupter, it was determined that advantage could be taken of the better field and its phase relationship by elongating the arc exposed to this blast. Therefore, the full value of these factors was utilized by offsetting the ends of the slots in the plates.

Referring to Figure 1, one terminal of the magnet coil is connected to the upper stud. The other terminal is connected to the panel-end horn. The coil is introduced into the circuit by the impingement of the arc on the panel-end horn and the interruption of the short length of arc between the horn and the upper stud. The extra field strength which has been introduced to produce a more efficient interrupter gives rise to a new problem. All the flux across the interrupting space must thread the magnet coil. This means that when short-circuit current is introduced into the coil, a reactance voltage of several hundred volts appears across the terminals of the coil. To introduce the short-circuit current into the coil quickly and positively against this reactance voltage requires that an auxiliary or transfer interrupter be built into the arc chute. This interrupter, although very compact, must perform a duty comparable to that of a high-capacity low-voltage breaker.

Figure 1 is an illustration of an arc chute for a 15-kv 500,000-kva circuit breaker based on the above considerations. The magnetic structure for this unit consists of one coil and one magnet. With this type of construction, the magnet shoes form a support for the arc chute which makes possible the quick and easy removal of the relatively light arc chute for inspection while the heavy magnet remains on the breaker. However, more important is the simplification of insulation problems and the energizing of the field simultaneously over the entire interrupting structure so as to obtain fast uniform arc motion.

The contacts are of conventional design. In an opening operation, the current is transferred from the main current-carrying contacts to secondary contacts and then to the arcing contacts, which are protected by inlays of silver-tungsten alloy. When the arcing contacts part, the current loop in the contact structure causes the arc to expand into the arcing chamber. Suitably placed iron draws the arc into the transfer stack, which interrupts the section of arc between the stationary arcing contact and the panel-end arc horn. The current path is now from the top bushing stud through the magnet coil, into the adjacent arc horn, through the arc in the main interrupting stack, and into the opposite arc horn which is connected to the opposite side of the cir-

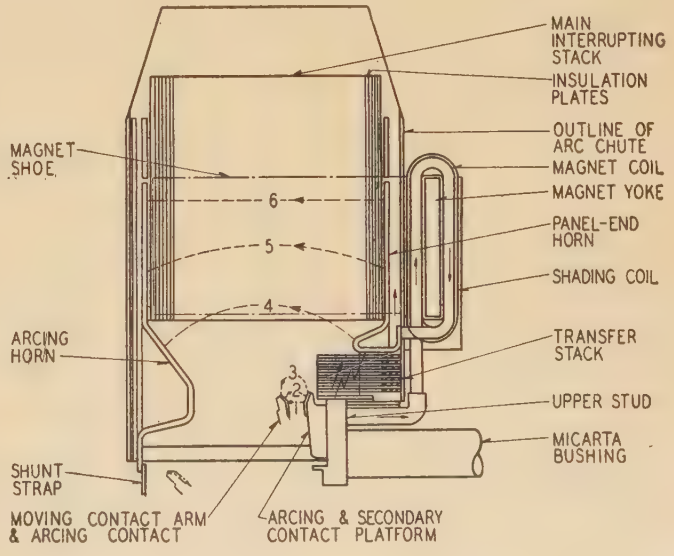

Figure 1. Schematic illustration of a 500,000 kva 15-kv magnetic interrupter

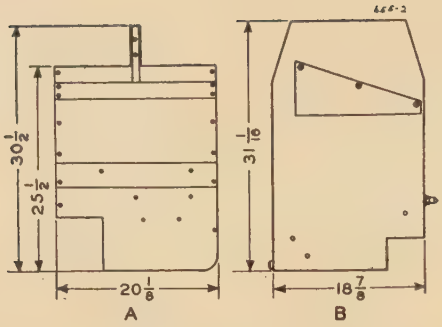

Figure 2. Progress in magnetic interrupter design

A—A 100,000-kva 5-kv arc chute of early design

B—The new 500,000-kva 15-kv arc chute

Both have ceramic interrupting plates of the same width

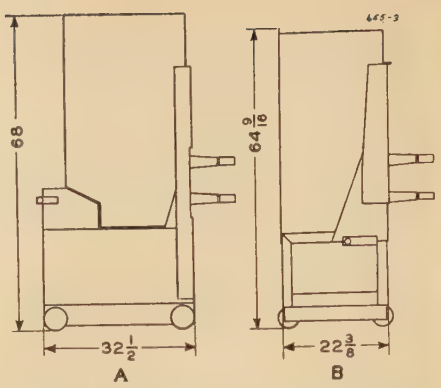

Figure 3. Progress in magnetic air breaker design

A—An early 5-kv 150,000-kva unit

B—The current design

Note smaller depthwise dimensions of the later design. Both units are for 26-inch metal-clad cell width

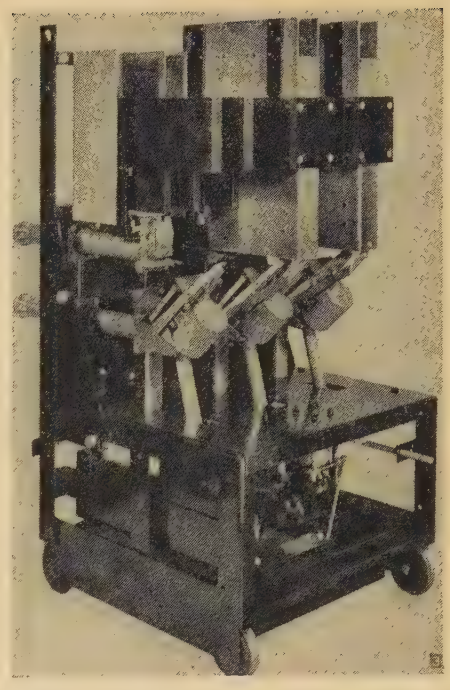

Figure 5. General view of the new 15-kv 500,000-kva magnetic air breaker for metal-clad horizontal drawout switchgear

cuit. The field is now energized, and interruption takes place at the next current zero.

The proper amount of phase shift between the current and the field is obtained by using a carefully designed shading coil placed around the magnet core adjacent to the coil. This shading coil also eases the duty on the transfer stack by slowing the rate of rise of restored voltage across it when the transfer arc is extinguished.

Figures 2, 3, and 4 illustrate some of the results accomplished by this development. Figure 2 is an outline comparing the 5-kv 100,000-kva arc chute of an earlier design with the new 15-kv 500,000-kva arc chute. Both use ceramic plates of the same width. Figure 3A shows the outline dimensions of the original magnetic air breaker for 5 kv and 150,000 kva, while 3B shows the current design for the same rating, which is also applicable at 2,300 volts. It will be noted that the later design saves considerable depth of floor space. Figures 4A, B, and C show the relative size of the original 5-kv 150,000-kva rating, the 7.5-kv 250,000-kva rating, and the latest developed design, the 15-kv 500,000-kva rating.

Figure 5 shows a general view of a new 15-kv breaker. In line with the present general trend, this unit is designed particularly for metal-clad switchgear and as shown constitutes the complete removable element. In this view it will be noted that the horizontal drawout construction results in an inherently transportable removable unit with self-contained secondary and ground contacts. This permits quick movement to the test position and quick reconnection of control circuits for testing within the cell. It also permits quick interchange of breakers in a cell. The location of the main barrier, arc chute, and contacts also permits easy removal and inspection of those parts.

The arc chute is placed above the contacts, which is the most natural position for it because this position permits the arc to be drawn horizontally and moved vertically upward. With this construction, thermal convection assists in moving low current arcs into the interrupters. An auxiliary air piston may be added to speed up interruption of low currents, but the breaker can interrupt them without its help.

The component parts of the breaker are arranged so that the arc chute compartment can be vented directly to the outside atmosphere, thus completely isolating this compartment from the bus structure. The 19-inch-long arc chute for a 15-kv 500,000-kva breaker is admirably suited for this drawout construction and adds further to its inherent advantages in the economy of floor space required.

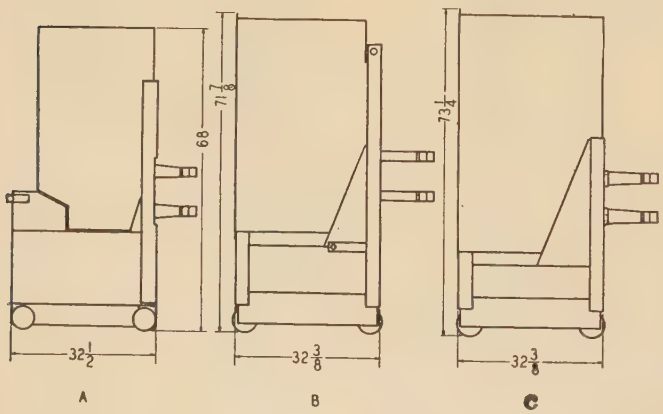

Figure 4. Progress to 15-kv magnetic air breaker

A—The 5-kv 150,000-kva breaker of early design

B—A 7.5-kv 250,000-kva breaker

C—The new 15-kv 500,000-kva magnetic breaker

Tests on the Breakers

In line with present practice, it is almost needless to say that many full power interrupting tests were made in developing the new ratings. These tests again have demonstrated the ability of the ceramic arc chute to withstand repeated interruptions with low deterioration.

The breaker was connected across the terminals of a 60,000-kva star-connected high power laboratory generator, and the short circuit was formed by a copper bar bolted across the load side of the breaker. The generator neutral was grounded through a 7-ohm resistance, while the short-circuiting bar was ungrounded, which is equivalent to a grounded fault on an ungrounded system. Currents were limited by air core reactors.

Typical oscillograms are shown in Figures 6 to 9. Figure 6 shows a 3-phase interruption at 505,000 kva and 13.2 kv. Figure 7 shows an interruption at 163,000 kva and 13.2 kv. Figure 8 is of interest in that it shows a single phase interrup-

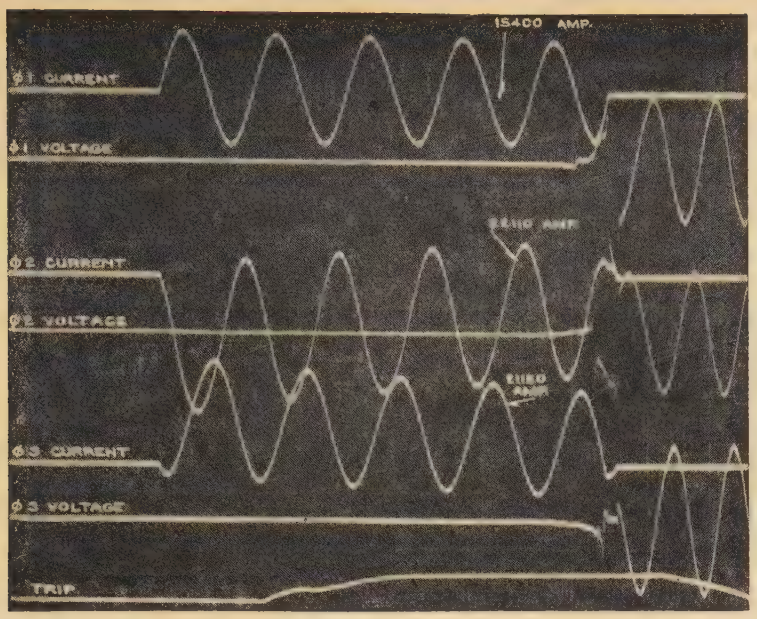

Figure 6. Oscillogram of 3-phase ungrounded short-circuit interrupting test on 15-kv 500,000-kva magnetic air breaker shown in Figure 5

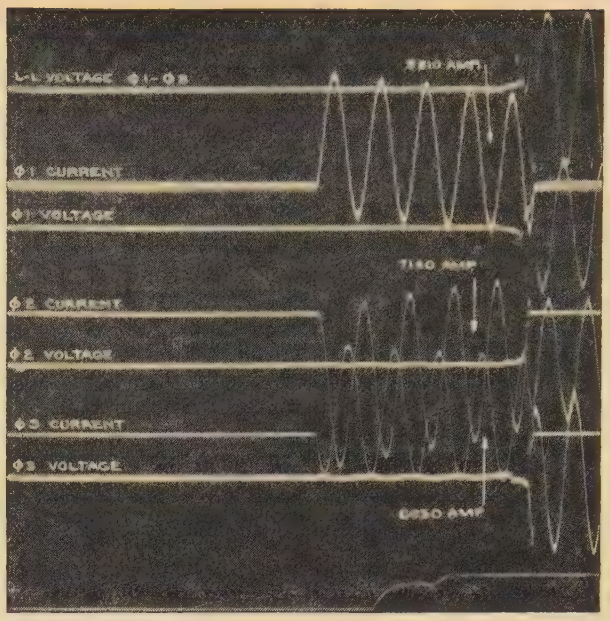

Figure 7. Oscillogram of 3-phase ungrounded fault at 163,000 kva on the 500,000-kva breaker

tion of 7,300 amperes at 13.2 kv across a single pole.

Figure 9 illustrates, by single phase oscillograms, an interesting characteristic of the new types of magnetic interrupters. On all tests except those at very low currents, when the field is energized 30 degrees or more ahead of a current zero, the breaker will interrupt on that zero. On the other hand, the current is not likely to transfer to the coil on the rising part of the current wave, and the arc will remain in the comparatively wide arc box at low arc voltage until the current has gone through its peak value. Coil transfer is then completed, and the strong field drives the arc up to the ends of the slots at extremely high velocity. At the ends of the slots, deionization and interruption is accomplished. As shown in Figure 9A, this type of interruption, with high arc energy released during only a small portion of the half cycle, is characteristic of an interrupter of this type. This produces a minimum of heating and deterioration in the arc chute. As shown in Figure 9B, another type of interruption is possible, and that is where the field is energized fewer than 30 degrees before current zero. On a probability basis, this type of interruption should occur in one out of six interruptions. Insufficient time is available to drive the arc to the top of the slots before current zero, and the arc must remain there for another half cycle. However, the high degree of restriction and the loss of ions from the arc stream on account of the field keep the arc resistance so high that the current reaches only a small magnitude. The arc energy released is not much greater than in the previously described type of interruption. Throughout all the tests made in this development, it was impossible to find any difference in interrupting capacity between the two types of interruptions.

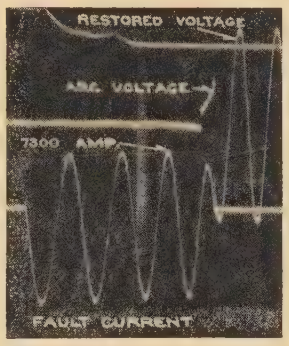

Figure 8. Oscillogram of single-phase interruption at 13.2-kv on single pole of the 15-kv magnetic breaker

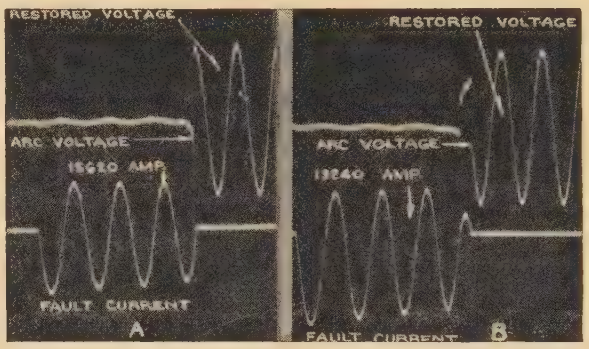

Figure 9. Oscillograms illustrating two types of interruption on the new magnetic breaker for 15 kv (see text)

The tests described and the oscillograms shown apply to the 500,000-kva 15-kv breaker. The same principle of interruption has been applied to breakers of other ratings, namely, 150,000 kva and 250,000 kva at 15 kv, and similar test results have been obtained. The same principle of interruption has been found to work equally as well on the currents encountered at 7,500 volts, including 500,000 kva at 6,600 volts and 25 cycles.

Conclusion

The principle of magnetic deionization has been extended to air circuit breakers of the 15-kv class with interrupting ratings up to 500,000 kva. The interrupter has been so refined and improved that the increase in kilovolt-amperes rating of up to 500 per cent has not resulted in undue increase in space requirements. The short arc chute, 19 inches long for a 500,000 kva 15 kv unit, has made possible compact horizontal drawout construction with all its inherent advantages.

References

1. Extinction of an A-C Arc, J. Slepian. AIEE Transactions, volume 47, 1928, pages 1398–1408.

2. Theory of the Deion Circuit-Breaker, J. Slepian. AIEE Transactions, volume 48, 1929, pages 523–527.

3. A New High-Capacity Air Breaker, L. R. Ludwig, G. G. Grissinger. AIEE Transactions, volume 58, 1939, August section, pages 414–20.

4. Magnetic "De-ion" Air Breaker for 2,500–5,000 Volts, L. R. Ludwig, R. H. Nau. AIEE Transactions, volume 59, 1940, September section, pages 518–22.

A New Line of High-Voltage Outdoor Tank-Type Oil Circuit Breakers

W. F. SKEATS
FELLOW AIEE

E. B. RIETZ
ASSOCIATE AIEE

THE TREND of the past few years and studies of future trends indicate an oncoming demand for higher interrupting capacities and decreased interrupting and reclosing times. Today there may be relatively few applications which justify these more severe requirements, but there is every indication that as time passes they will become more and more universal.

A year ago there was described before the Institute[1] a development in tank-type breakers which made possible interruption of short-circuits up to 3,500 megavolt-amperes within three cycles in the voltage range from 115 kv to 161 kv with 20-cycle reclosing. Field tests were also reported[2] substantiating this performance. The present paper describes further developments in these breakers, resulting in reduced over-all dimensions and increased convenience in handling, while maintaining or improving the desirable performance characteristics. These characteristics have also been realized in an interrupter and breaker suitable for operation at 230 kv.

Figure 1 shows the 138-kv breaker.

From both structural and functional standpoints, a discussion of these breakers divides itself naturally into four major parts:

1. The interrupter.
2. The bushing.
3. The tank and top frame.
4. The operating mechanism.

In order to meet the exacting performance requirements of high interrupting capacity, fast interruption, and rapid reclosure, and at the same time to reduce maintenance to a minimum and readily make accessible those parts which require inspection and maintenance, each one of these parts must receive careful attention from the designer. This development has involved significant improvements in all of them. These changes will be discussed under the four corresponding headings.

The Interrupter

As the interrupter is the part primarily responsible for the performance of the distinctive function of the circuit breaker, it is natural that this should receive first consideration.

A cross-sectional view of the interrupter of the earlier breaker is shown in Figure 2, and a similar view of the new interrupter is shown in Figure 3. Figure 4 shows the new interrupter with separate views of the moving system and the resistor. Figure 5 shows two interrupters mounted on bushings with blade, lift rod, and guide in place as when assembled in the tank.

The same general principle of interruption is used in both designs. Interruption is performed by a number of 2-break units, each of which consists of one break whose primary purpose is to generate pressure and a second break so located that the arc drawn there is placed in the path of a blast of oil forced out through properly located ports by the pressure generated by the first arc. For application at voltages from 115 kv to 161 kv, two such units are used in each interrupter. Thus, starting at the lower end, current enters the interrupter on the lower stationary contact, passes through the elkonite contact tips to the bridging contact, and flows from the other end of the bridging contact to the lower end of the intermediate stationary contact. This cycle is repeated in passing from the upper end of the intermediate stationary contact to the upper stationary contact. This path includes four breaks, of which those at the lower stationary contact and the upper end of the intermediate contact are located away from ports and serve principally the function of pressure generation. The other two breaks are immediately adjacent to ports, and the arc there is interrupted by the blast of oil flowing out through the ports.

An appreciable reduction in the arcing time of the new interrupter has been achieved by strengthening the opening springs on the interrupter to increase the speed of its moving parts. The tendency to increased pressure associated with this change in speed was more than counterbalanced by lengthening the arcing plates and by using the pressure control ports shown in Figure 3.

The arcing plates function by shortening the pressure generating arc.

The pressure control ports are located near the pressure-generating arc, but far enough away to be reached by the gas bubble only when interrupting high currents. Their use was suggested by the observation that in operations in which a gas bubble might be expected to be present in the interrupter, as in the second interruption of a reclosing operation, the pressures experienced were found to be much lower than when such a bubble was not present. Thus it appeared desirable to provide the cushioning effect of such a bubble for all conditions, and as the high pressures appeared only towards the end of the arcing period, the most convenient way to accomplish this was to allow the lighter pressure in the early part of the arcing period to force oil out through these ports and thus create additional expansion space for the bubbles already present at the contacts.

The effectiveness of this combination in achieving both short arc lengths and low pressures is evident from Figures 6 and 7, in which arc duration and interrupter pressure, respectively, are plotted against current interrupted for both the

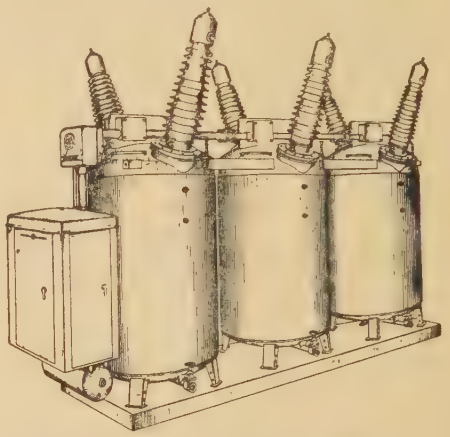

Figure 1. The new 138-kv oil-blast circuit breaker, 3,500-megavolt-ampere interrupting rating, 3-cycle interrupting time rating and 20-cycle reclosing time rating

Paper 46-20, recommended by the AIEE committee on protective devices for presentation at the AIEE winter convention, New York, N. Y., January 21–25, 1946. Manuscript submitted November 26, 1945; made available for printing December 21, 1945.

W. F. Skeats and E. B. Rietz are with the power circuit breaker division, General Electric Company, Philadelphia, Pa.

The authors wish to express their indebtedness to many of their associates who materially assisted in the development of these breakers. In particular, T. R. Coggeshall and J. M. Milne have contributed ideas for the solution of the many problems involved and have been untiring in following the innumerable details which are an indispensable part of such a program.

new and the superseded interrupter. It will be noted readily that the circled points, representing the new interrupter, show a substantial improvement in both respects, with satisfactory performance at currents well beyond that corresponding to the 3,500-megavolt-ampere standard rating.

The simplification of the present design is obvious from a comparison of Figures 2 and 3. The principal changes are as follows:

1. The ends of the interrupters are secured to the cylindrical herkolite walls by means of metal studs. This has been found to be quite as strong as the earlier construction and results in a very appreciable reduction in the diameter of conducting material. There is also a substantial reduction in weight, which is accentuated by the use of a light alloy for the end pieces.

2. The moving contact assembly has been simplified greatly by placing all of the contact springing immediately below the bridging contacts themselves, thus eliminating the necessity for any additional cushioning springs at the bottom of the interrupter. This has made possible the use of a simple textolite cylinder, which makes an excellent guide bearing, at the point where the moving part passes through the bottom plate of the interrupter. A strong opening spring and a buffer spring are placed around this cylinder, the one insuring that the moving parts of the interrupter move with the breaker crosshead to the limit of the interrupter stroke and the other controlling overtravel of the contacts on the closing stroke.

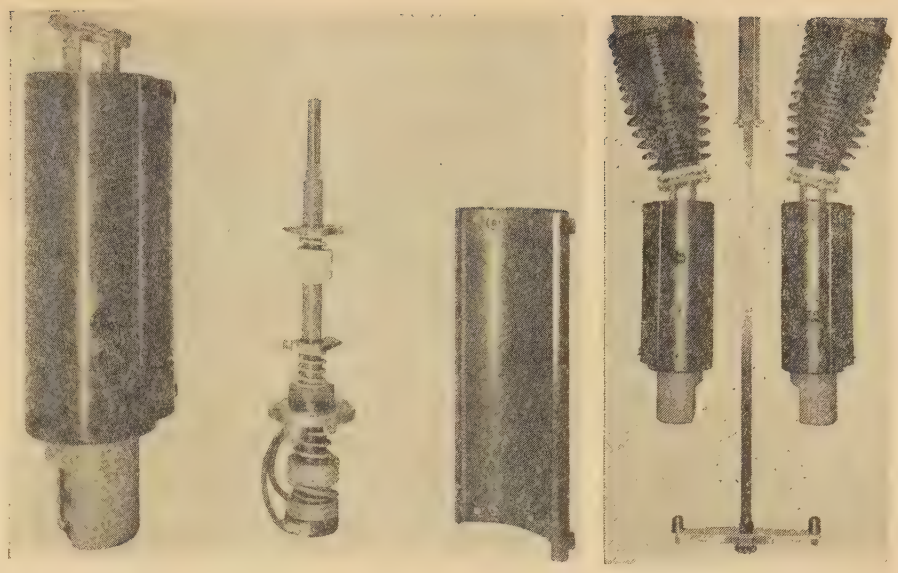

Figure 4. The 115-kv–161-kv interrupter with additional views of the moving part assembly and the resistor

Figure 5. Pole unit assembly of interrupters for the 138-kv breaker

3. Both the new and the superseded interrupter use a parallel resistor for positive control of overvoltages in connection with the interruption of line-charging currents.[3] The new resistor is shown at the right-hand side of Figure 4. It consists of a helix of nichrome wire which is wound on a grooved board that has its short dimension molded into the shape of a circle arc. Protective covers are secured to the board. The resulting assembly conforms to the outside of the interrupting cylinder and thus requires less space than the older resistor.

4. Additional items that will be helpful in facilitating inspection and maintenance are the smaller electrostatic shield at the bottom of the interrupter and the elimination of the upper insulating shield, both made possible by removal of the clamping metal outside the interrupting cylinder.

The interrupter of Figures 3 and 4 is used at voltages from 115 kv to 161 kv. For application at 230 kv, the interrupter shown in Figure 8 is used. This is quite similar in principle to the lower-voltage interrupter but has three pairs of internal

Figure 2. Cutaway view of 115-kv–161-kv interrupter of the superseded design

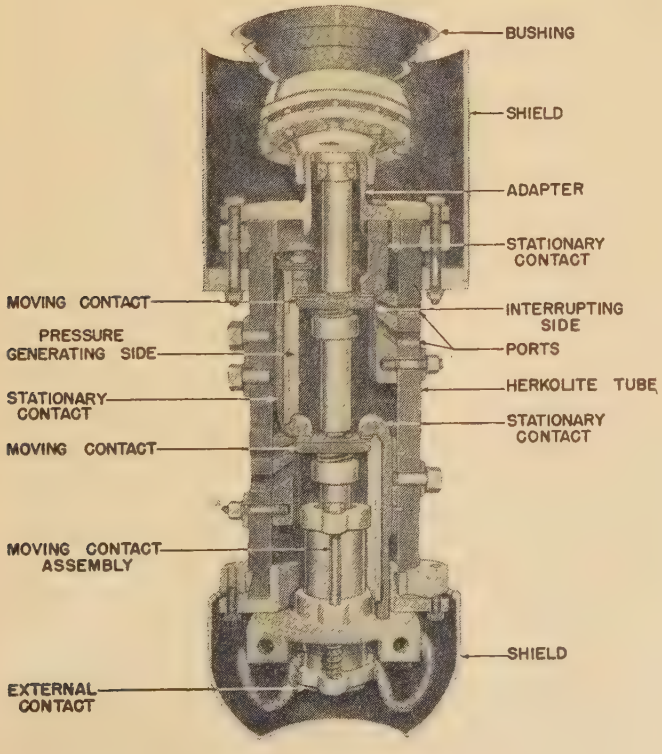

Figure 3. Cutaway view of 115-kv–161-kv interrupter of the new design

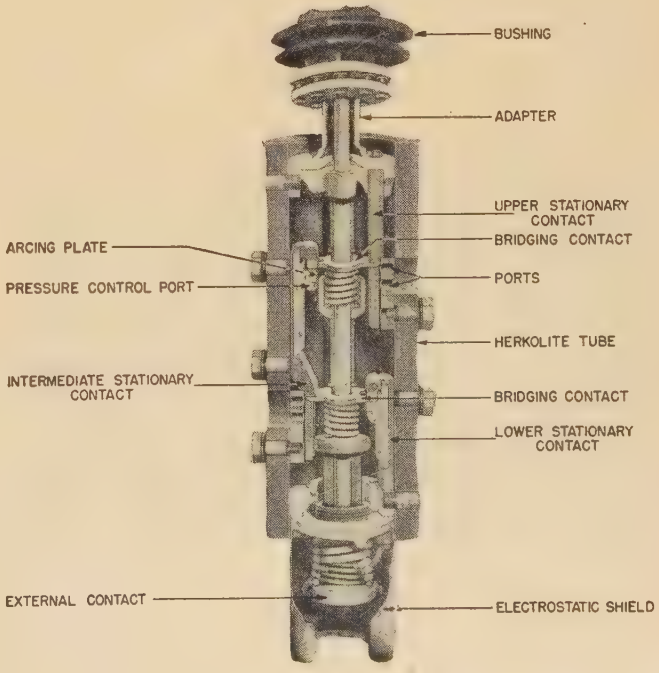

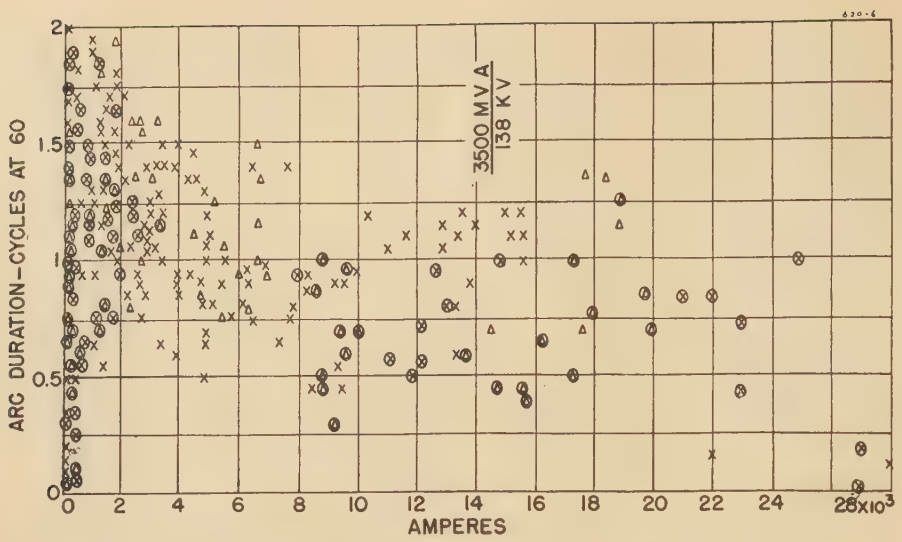

Figure 6. Arc duration as a function of current for 115-kv–161-kv interrupters

×—Superseded interrupter, initial opening operation

△—Superseded interrupter, second opening operation on reclosing duty cycle

The same symbols enclosed in circles represent the new interrupter under the same conditions

Tests made on a pole unit at voltages from 14.5 kv to 132 kv

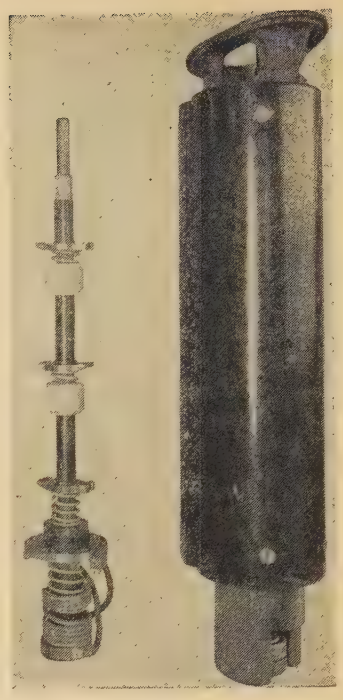

Figure 8. The 230-kv interrupter

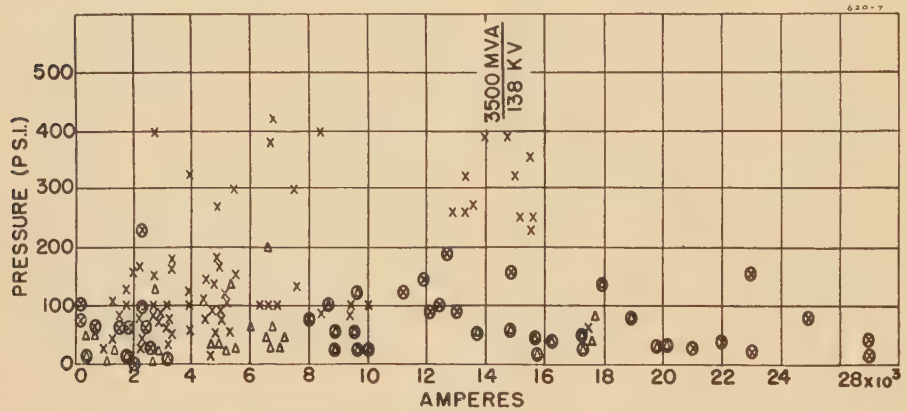

Figure 7. Interrupter pressure as a function of current for 115-kv–161-kv interrupters

×—Superseded interrupter, initial opening operation

△—Superseded interrupter, second opening operation on reclosing duty cycle

The same symbols enclosed in circles represent the new interrupter under the same conditions

Tests made on pole unit at voltages from 14.5 kv to 132 kv

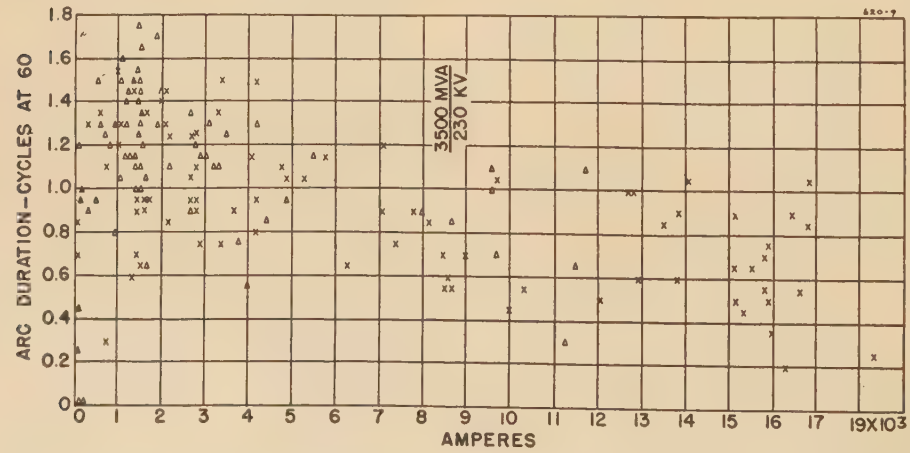

Figure 9. Arc duration as a function of current for the 230-kv interrupter

×—Initial opening operation

△—Second opening operation on reclosing duty cycle

Tests made at voltages of from 8.4 kv per interrupter to 132 kv per interrupter

breaks instead of two. Also, the resistor has somewhat more thermal capacity as required at the higher voltage. The interrupting performance of this interrupter is shown in Figure 9. It will be noted that the arcing time varies from less than 1/2 cycle to $1^1/_2$ cycles at currents above 25 per cent of rating. With a contact-parting time of $1^1/_2$ cycles, this gives a breaker-interrupting time of from two to three cycles, or with the conventional tripping arrangement, a 5-cycle interrupting time is easily realized.

The interrupting performance on line-charging currents is indicated in Table I for the 115-kv–161-kv interrupter and in Table II for the 230-kv interrupter. In each case the tests were made on a single interrupter or half a pole unit, using static capacitors. Since the resistors effectively divide the voltage between the two interrupters of a pole unit, the normal voltage for such a test is half leg voltage or 46 kv for 161-kv application and 66 kv for 230-kv application. In both cases, tests were made at approximately these voltages and also at a voltage from 20 per cent to 33 per cent higher to insure adequate margin to take care of surges introduced by any mutual effect between phases. Performance was entirely satisfactory in all tests, the voltage being limited to twice the crest value before interruption. An oscillogram of one of these tests is shown in Figure 10.

A comment is in order with respect to short-circuit interrupting tests. Under uncontrolled conditions of interruption,

there are two elements subject to rather wide variation. These are:

1. The point on the voltage wave at which the short circuit is initiated.

2. The point on the current wave at which the breaker is tripped.

With the reduction in arcing time that has taken place in recent years, the influence of these variations becomes accentuated to the point where they may be responsible for the difference between four-tenths of a cycle and a complete cycle in arc duration, with a very pronounced difference in interrupter pressure, jar, contact burning, and any other manifestation of severity of duty. To be sure of covering the worst conditions at any voltage and reactance tap, therefore, either a large number of tests must be taken or some control must be exercised over the timing. For over ten years now, the authors and their associates have made extensive use of a special fast-closing breaker with synchronous control to make possible the selection of the point on the voltage wave at which the circuit is closed, and more recently the same type of control has been applied to the tripping of the test breaker. Thus it is now possible to control both the displacement of the short-circuit current wave and the point on the wave at which the contacts separate. It has been the practice first to make exploratory tests over the complete range of variation of these controls and then to concentrate for a number of tests on that condition which appears to be worst. Thus any other random phenomena will have an opportunity to show up at their worst also, and in a reasonably small number of laboratory tests, conditions may be explored which would not appear in many times the corresponding number of field operations or uncontrolled laboratory tests.

Table I. Performance of 115–161-Kv Interrupter on Line-Charging Currents
Tests on One Interrupter

Test No.	Voltage, Kv	Equivalent Miles of Line	Current, Amperes	Arc Duration, Cycles
1	44	190	110	0.3
2	44	190	110	0.3
3	44	190	110	0.0
4	44	190	110	0.1
5	44	190	110	0.1
6	55	190	140	0.1
7	55	190	140	1.6
8	55	190	140	1.6
9	55	190	140	0.0
10	55	190	140	1.4

Table II. Performance of 230-Kv Interrupter on Line-Charging Currents
Tests on One Interrupter

Test No.	Voltage, Kv	Equivalent Miles of Line	Current, Amperes	Arc Duration, Cycles
1	66	190	140	0.7
2	66	190	140	0.2
3	66	190	140	0.7
4	66	190	140	1.0
5	66	190	140	0.9
6	88	110	110	0.9
7	88	110	110	1.2
8	88	110	110	1.1
9	88	110	110	0.9
10	88	110	110	0.6

Bushings

Oil filled bushings for high-voltage oil circuit breakers have an enviable record of performance. While the electrical and mechanical performance of these bushings has been generally satisfactory, numerous improvements have been made for the purpose of reducing maintenance. The sump washer-drain, bell-mouthed breather, amber gauge glass, and thermal seal are the most noteworthy. In recent years it has become obvious that the next step is complete sealing of the bushing against the atmosphere so as to eliminate completely any source of contamination of the filler oil. Numerous designs of sealed bushings have been developed, with the moderate voltage type *L* bushing as one of the first. The experience with over 80,000 of these bushings and varied special applications of sealed oil-filled bushings gave the proper background for developing the completely sealed bushings for the 115–161-kv ratings.

The completely sealed bushing, Figures 11 and 12, uses a general arrangement of insulation similar to that of the original oil-filled bushings, although a number of structural improvements were found desirable. The insulated conductor is surrounded by concentric insulating cylinders of treated paper of high dielectric strength spaced apart so as to give alternate layers of solid insulation and oil. These cylinders are between the live conductor and the grounded support sleeve. Electrostatic shielding is incorporated internally in these cylinders by coating a part of the paper with conducting resin as it is wound. This imbedding of the conducting shield within the cylinder is a distinct improvement over the older method of winding conducting foil on the outside of the cylinders.

Center clamping is used to clamp the bushing parts firmly together. This makes use of the center conductor as a means of clamping the lower porcelain, ground sleeve, upper porcelain, and expansion chamber into an integral unit. Adequate clamping pressure is maintained on the four gasketed joints even with slight differences caused by thermal expansion, by means of short heavy compression springs between the terminal cap fastened to the conductor and the top of the expansion chamber.

Synthetic rubber gaskets impervious to both oil and water are used at all joints. These are confined in appropriate recesses in the metal parts.

Standard circuit breaker or transformer oil is used as a filling liquid. Expansion space for this medium is present in the metal expansion chamber at the top of the bushing. The oil level is registered by a magnetic-type oil gauge incorporated in the expansion chamber and easily visible from the ground, as shown in Figure 13.

The use of center clamping results in a reduction in diameter dimensions because of the omission of the cemented-on clamping rings. This is particularly advantageous at the lower end because it permits smaller current transformers and sim-

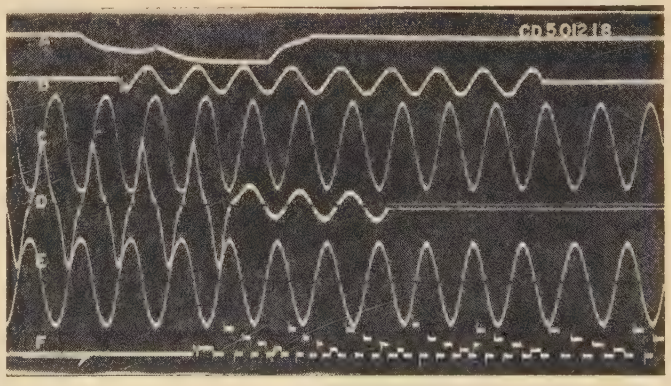

Figure 10. Oscillogram of line-charging current interruption on 115-kv–161-kv interrupter, interrupting 140 amperes at 55 kv across a single interrupter

A—Trip coil current
B—Cathode ray oscillograph control
C—Supply voltage at breaker
D—Current through breaker, showing initial capacitance current, resistor current, and final interruption
E—Alternator voltage
F—Breaker travel: one-half inch per impulse

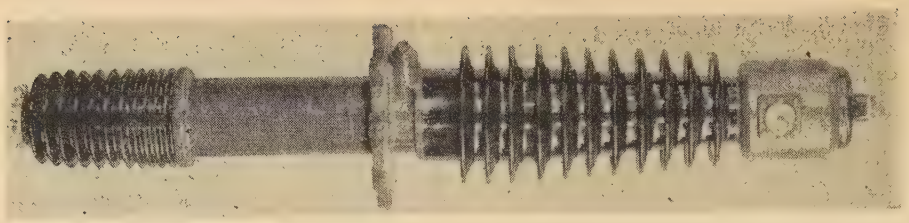

Figure 11. 115-kv sealed oil-filled circuit breaker bushing with capacitance tap having smaller dimensions resulting from center clamping and removal of cemented-on clamping rings

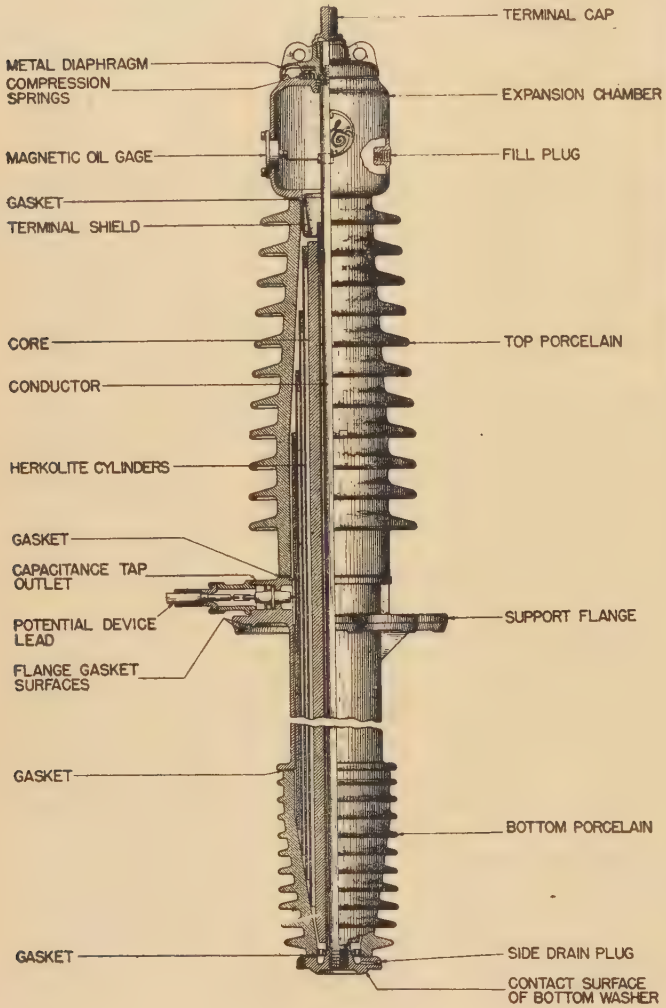

Figure12(left). 115-kv sealed oil-filled circuit breaker bushing in cutaway semisection showing arrangement of porcelains and gaskets

Figure 13 (above). Top of sealed oil-filled circuit breaker bushing showing expansion chamber and magnetic type oil level indicator

Table III. Comparison of New and Old Designs Illustrating the Substantial Reduction in Oil Requirements and Loading on Foundations

Breaker Rating	Type New	Type Old
115 Kv		
Tank diam., in.	54	54
Weight, lb	36,600	39,400
Oil, gal	2,300	2,420
138 Kv		
Tank diam, In.	54	60
Weight, lb	38,500	47,800
Oil, gal	2,400	2,970
161 Kv		
Tank diam., in.	60	72
Weight, lb	44,800	64,300
Oil, gal	2,950	4,700
230—196 Kv		
Tank diam, in.	78	108
Weight, lb	85,000	168,500
Oil, gal	7,250	14,000
230 Kv		
Tank diam, in.	84	108
Weight, lb	110,000	180,000
Oil, gal	8,800	15,400

Tank and Top Frame

The pole units of the new breakers have a number of design features resulting from changes in the essential component parts (Figure 14). The smaller-sized interrupters made a reduction in tank dimensions possible. The new sealed bushings with smaller lower end dimensions permitted smaller bushing current transformers and a simplified arrangement of the transformer housing. The increasing demand for more 3-cycle breakers made it advisable to design the pole unit linkage with this objective in mind. Many of the accessories were simplified and relocated to facilitate maintenance.

The smaller size and smooth contours of the new interrupters have permitted substantial reductions in the sizes of the 138-, 161-, and 230-kv breakers and at the same time have improved their overvoltage performance. Table III shows a comparison of the new practice and the old.

The changes in the bushing current transformer housings resulting from the smaller bushings are quite striking as compared with superseded designs. As shown in Figures 1 and 14, the smaller housing fits within the dome outline so that space is available for two current transformers per bushing without a special design. The conduit connections are large enough for the leads of two current transformers so that a second set can be easily installed in the field. The new arrangement also makes it possible to remove the current transformers over the lower end of the bushings. Thus changes can be made without the laborious pro-

plifications in the breaker top frame construction.

Exhaustive tests have been made, not only under static conditions but also under operating conditions such as the loadings that bushings are subjected to during the interruption of heavy short circuits. Every attempt has been made to find failure points under both of these conditions. The interrupting tests unquestionably subjected the bushing to the most severe mechanical loadings. On all tests the bushings gave a remarkably satisfactory performance. Many readers will be interested in a performance comparison between the new and the superseded designs. The new design has turned out to be both electrically and mechanically stronger than the older oil-filled type.

An additional feature of the new bushing is the interchangeability with the old design. A long background of interchangeable breaker bushings dictated that from a user's standpoint, the new bushing fall into the same pattern. Therefore, the mounting bolts and flange gasket locations are identical with those of the older bushings. The elimination of the lower clamping ring has permitted shortening of the bushings by about three inches. For replacements, however, a suitable spacer can be provided to compensate for this shortening, and the new bushing is available as a replacement unit for any oil-filled bushing on older oil circuit breakers.

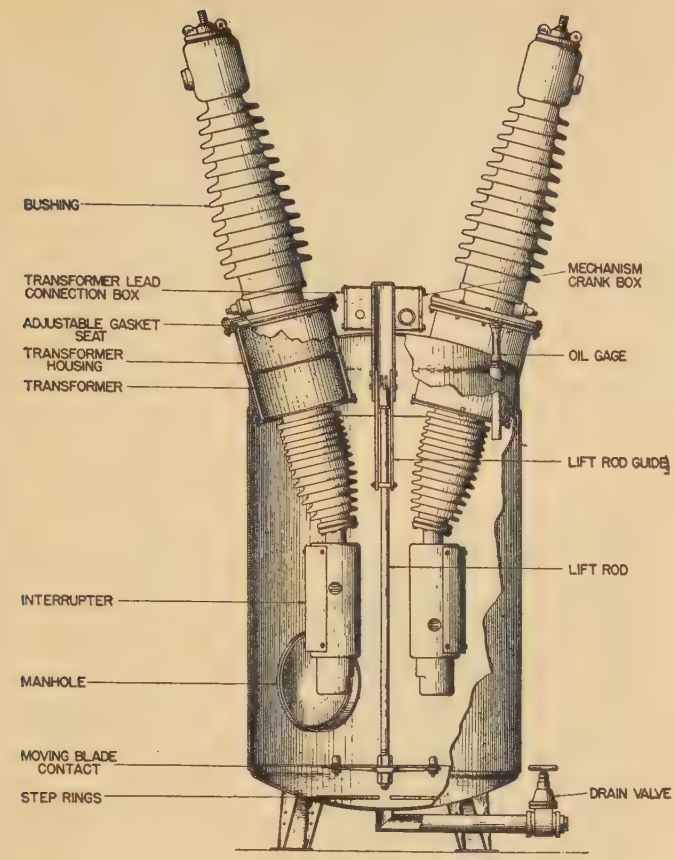

Figure 14. Cross-section of pole unit showing relationship of component parts: interrupters, bushings, tank structure, and bushing current transformers

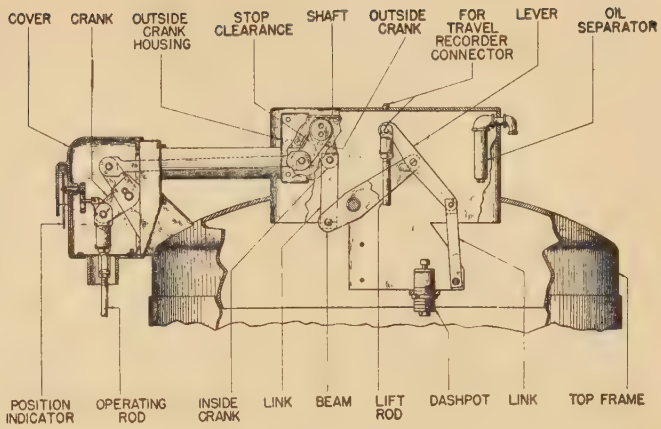

Figure 15. Pole unit breaker mechanism showing straight line linkage and crank housing above operating mechanism

cedure of removing the bushings. The new current transformers have all of the characteristics prescribed by various breaker standards. The current transformers are treated to provide a positive protection against water absorption. The tops of the transformer housings which support the bushings have a special gasket arrangement to permit tilting of the bushing to obtain proper contact alignment.

The increasing demand for 3-cycle breakers has indicated that the mechanical design should be basically suited to such performance. After several arrangements had been reviewed, it was decided to adhere in general to the straight line linkage which has been used successfully in breakers of this type for the past 20 years. But as shown in Figure 15, its size was greatly reduced by taking advantage of the relatively short breaker operating strokes which have resulted from a proper analysis of the clearing distances needed. A feature of this design is the use of low friction bearings which are particularly helpful where high-speed tripping is required. Gas- and oil-tight seals are provided on the main operating shafts by means of close-fitting bearings with splined shafts and cranks for ready assembly. An external indication is provided in the side crank box housing for determining the proper closed position of the linkage. Self-contained oil-filled dashpots absorb the energy of the moving parts at the end of the opening stroke, and their adjustment has been greatly facilitated by providing a threaded assembly with a suitable locking arrangement.

Operating springs are kept to a minimum. Lightweight moving contacts and pneumatic operation make it unnecessary to provide balancing springs for closing to offset the dead weight of the moving members. Buffer springs to limit overtravel are not required, since this function is incorporated in the interrupter contact springs. Opening springs on the rear pole unit keep the interphase connecting pipes in tension for both closing and opening and can be adjusted readily from outside of the breaker to obtain the proper opening speed characteristics.

Tank supports are used to hold the pole unit tanks above the foundation, so that complete drainage can be obtained without any enclosure which would restrict inspection and maintenance of the underside of the tank, as shown in Figure 16. This arrangement permits a reduction of the size of foundation pads. Side manhole openings as shown in Figure 17 give convenient accessibility, and parts for installation in the tanks are easily transferred. The heavy steel manhole covers are supported by hinged joints. Step rings on the outside of the top frame and on the inside of the tank bottom give a firm footing in spite of adverse weather conditions or the presence of an oil film. The oil level is shown by a float-type gauge whose sight glass is easily visible from the ground. Each pole unit has an emergency vent (Figure 18) built into the top frame for protection against permanent damage to the unit when through some unusual circumstances, excessive tank pressure is present. This has a flat copper diaphragm which is designed to rupture at a pressure much less than the tank strength. A semaphore indicator at the front end of the breaker shows the position of the moving contacts at all times. The front crank box cover can be removed for making adjustments at the upper end of the operating rod. The bottom of each pole unit tank is marked to

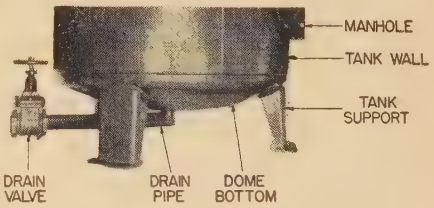

Figure 16. View showing tank supports which give maximum accessibility for maintenance under tank bottom

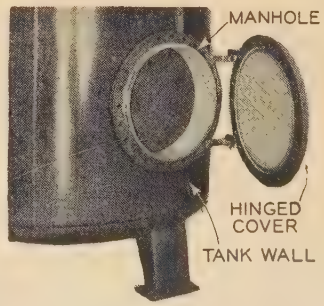

Figure 17. Maintenance manhole in side of tank provides easy access

indicate quadrant positions so that location on the foundation is facilitated. Likewise, plumb bob reference points can be used for leveling.

Operating Mechanism

The modern high-voltage oil circuit breaker requires for its operation a large amount of power delivered for a relatively short time. The pneumatic type of operation is well suited to this requirement. A self-contained unit on each breaker with its own individual air compressor equipment lends itself readily to application on various ratings of breakers whether they are new or in the process of modernization. The breaker pole unit tank is provided with mounting brackets for the support of the housing and its equipment as shown in Figure 19. Electrical connections are no different from those of other types of electrically operated mechanism. Power requirements are very light, and standard control cables will meet all requirements.

Reclosing times are constantly becoming shorter, and the basic design of the pneumatic operation should be adapted to this requirement. The pneumatically trip-free mechanism is so adapted. It is not handicapped by the relatching time of mechanically trip-free designs or any complicated arrangement to avoid it. With the pneumatically trip-free mechanism, the reclosing time is a matter of the size of the power unit and the operating pressure. It is relatively simple to provide for the minimum reclosing times without special designs.

One of the elements involved in the interrupting time of a breaker is the time required to part contacts. A goodly portion of this is dependent on the unlatching of the mechanism after the trip impulse is received. A 5-cycle breaker requires only a conventional trip coil to obtain the unlatching time commensurate with this breaker rating. A 3-cycle breaker, on the other hand, requires a very short unlatching time, and a special design of high-speed trip is necessary. In other respects, the two operating mechanisms have the same characteristics and are built with common parts.

The power unit is similar to those previously described in references 1 and 4 and is shown in Figure 20. It consists of the mechanism frame with closing and tripping linkage actuated by an air piston. The admission of air to the cylinder is controlled by an electrically operated valve as explained in reference 4. Associated with the power unit is a small compressor unit which maintains pressure in the air receiver located underneath the housing. Electrical and pneumatic controls are assembled on a common panel which is accessible through a hinged side door.

The 5-cycle breaker mechanism uses a conventional trip solenoid, as shown in Figure 21. The 3-cycle breaker mechanism uses a high-speed flux-shifting type trip similar to that described in Reference 1 and shown in Figure 22. An auxiliary air control valve admitting air above the piston also is required to obtain the equivalent time on a trip-free operation. This

Figure 19. A pneumatic operating mechanism for a 3-cycle, 20 - cycle - reclosing 115–161-kv breaker

The complete unit is mounted on the first pole unit tank

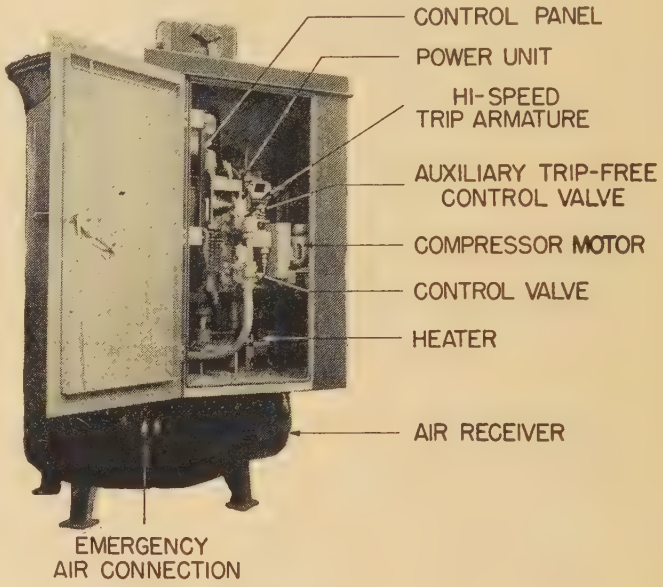

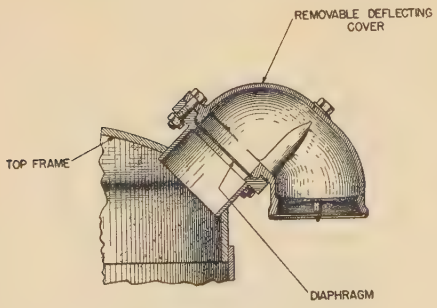

Figure 18. Assembly of emergency vent showing diaphragm which ruptures under excessive pressure and cover to direct discharge to ground

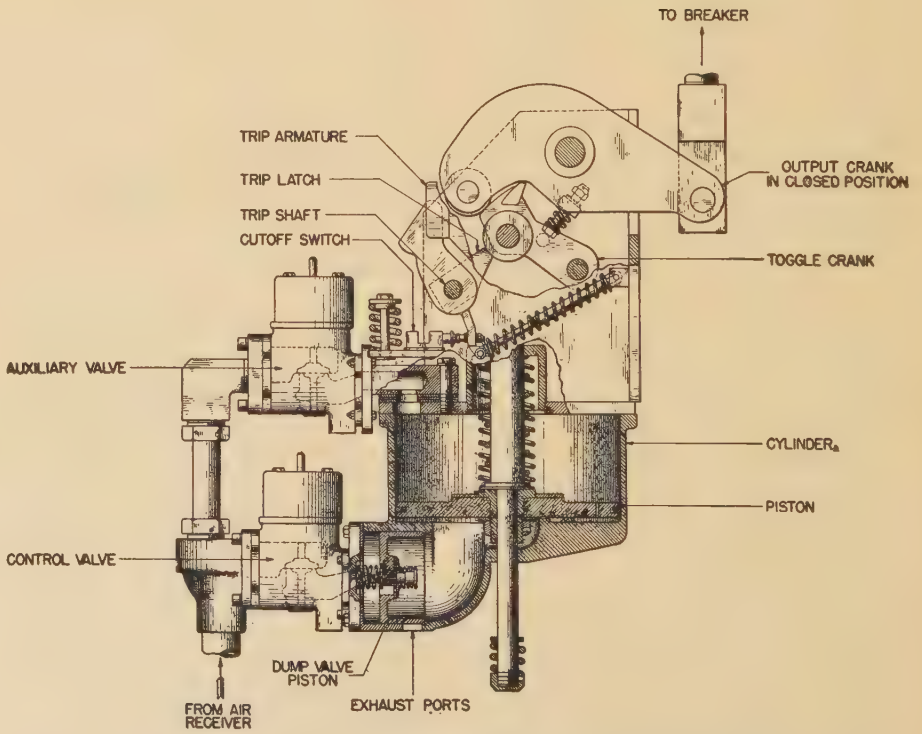

Figure 20. Cross-section of a 3-cycle pneumatic operating mechanism showing the power unit with air control valve and closing and tripping linkages

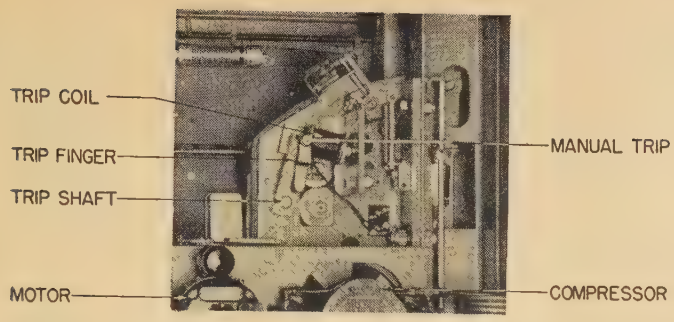

Figure 21. Trip arrangement for a 5-cycle breaker showing parts on frame for adapting high-speed 3-cycle trip

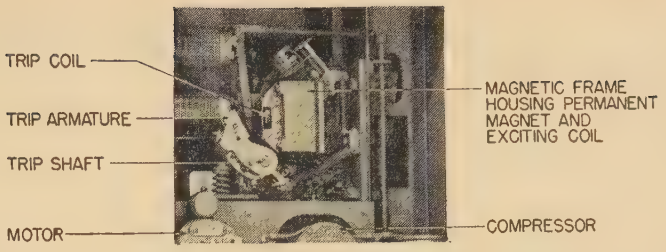

Figure 22. Trip ararrangement for a 3-cycle breaker showing flux-shifting trip for high-speed operation

is assembled directly above the main control valve.

Rating Standards

A careful examination and analysis of the breakers described in this paper indicates that there is very little about them that reasonably can be changed in order to produce a breaker with lower interrupting capacity and lower cost but otherwise meeting the high standard of performance of the breaker as described. This suggests the use of only one breaker design and one rating for each voltage. This would reduce the number of ratings listed in the present American Standards Association standards for 115- to 230-kv breakers from 13 to 4. The resulting simplifications eventually would be of benefit to both user and manufacturer.

Conclusions

This paper has described a line of outdoor tank type oil circuit breakers with voltage ratings from 115 kv to 230 kv and capable of handling all standard interrupting ratings at these voltages with liberal margins on a 20-cycle reclosing basis. The breakers can be adapted to either 3-cycle or 5-cycle operation.

These breakers incorporate improved performance, smaller dimensions, and lower weight both of the breaker as a whole and of many of the parts which require handling in inspection and maintenance.

The authors recommend consideration of the reduction of the number of standard breaker ratings in the 115-kv–230-kv voltage range to one rating for each voltage.

References

1. A High-Capacity High-Voltage Three-Cycle Oil Circuit Breaker, **H. L. Byrd, E. B. Rietz.** AIEE Transactions, volume 64, 1945, April section, pages 160–3.

2. Field Tests and Performance of Heavy-Duty High-Speed 138-Kv Circuit Breakers—Oil and Air-Blast, **Philip Sporn, Harry P. St. Clair.** AIEE Transactions, volume 64, 1945, pages 401–10.

3. Switching Overvoltage Hazard Eliminated in High-Voltage Oil Circuit Breakers, **L. F. Hunt, E. W. Boehne, H. A. Peterson.** AIEE Transactions, volume 62, 1943, February section, pages 98–106.

4. A Pneumatic Mechanism for Outdoor Oil Circuit Breakers, **L. J. Linde, E. B. Rietz.** AIEE Transactions, volume 63, 1944, July section, pages 543–6.

Shoran Precision Radar

STUART WILLIAM SEELEY
NONMEMBER AIEE

Synopsis: Shoran navigational radar is generally credited with being the most precise system of its type devised by man. The history of the conception and development of the principles employed, as well as a description of the physical make-up of the equipment, are of interest. Recent military declassification permits the exposition of both as set forth in this paper.

SHORAN is the common name for Army radar sets AN/APN-3 and AN/CPN-2. The equipment is used for high-precision position-finding in aerial navigation, principally for blind bombing and aerial mapping, although several other practical applications have been suggested. The term Shoran is a contraction of the two words short and range. What might at first appear to be a slightly derogatory title—in view of satisfactory performance out to 250 miles—has a logical explanation in the sequence of events prior to adoption of Shoran as the semiofficial designation. The history of the conception and development of the equipment pre-dates that of Loran, the widely used and now well-known long range navigational system. Development work on the latter was also carried on in RCA Laboratories under contract to the Office of Scientific Research and Development after its original inception by the Radiation Laboratory of the National Defense Research Committee. The Loran range of operation was approximately three times that of Shoran. Thus, while work progressed simultaneously on both in the same laboratory after April of 1942, Loran was the first to be adopted, named, and put into general use by the armed services, and the term Shoran for the shorter-range, higher-precision device followed almost automatically. Actually the two are completely dissimilar in equipment and operation. The only common aspect lies in the fact that each is used for aerial navigation.

History of the Shoran Development

The history of the development of Shoran is the story of a search for extreme accuracy of propagation time measurement coupled with ruggedness and reliability of equipment and simplicity of operation. It can truthfully be said that all of those aims were accomplished without compromising any one of them for another.

So much has transpired since the start of war developments that it is difficult to transport one's thoughts back seven years to the fall of 1938. At that time, war in Europe seemed a possibility but was still a year away. The concept of pulsed transmitters of radiant energy for the purpose of propagation time and distance determinations was not widespread. The term radar was nonexistent, and the only generally conceived applications of radio to war needs were for communication purposes or possible remote control of guided missiles of one sort or another.

At that time, work on television transmission and reception equipment was proceeding in many laboratories throughout the world. One of the knotty problems which vexed every television receiver engineer was that of multipath or "ghost" images which so often marred his otherwise creditable results. The television pictures in the industry service division of RCA Laboratories were no exception. The signals received at 711 Fifth Avenue in New York, N. Y., from the Empire State Building often showed as many as five separate and distinct ghost images when inside (or poorly exposed outside) antennas were used. Analysis of the picture content with particular reference to the horizontal displacement of a particular ghost image and the ratio of that displacement to the length of a complete scanning line gave a good indication of the increased path length of the reflected signal which caused the ghost.

At that time the Radio Manufacturers Association television standards specified a 441-line television picture, of which approximately 400 lines were visible, the other ten per cent being used for the vertical synchronizing action.

The aspect ratio of the pictures was four horizontal to three vertical. Thus, there were approximately 530 picture elements along each line. The time required for the scan of the visible portion of each line was 64 microseconds, and since a ghost image displaced by two picture elements was plainly discernible, it was evident that a reflected signal which arrived as much as one fourth microsecond later than the direct signal was detectable. Such a ghost would be displaced approximately 1/32 of an inch on a 12-inch tube picture, and reference to the velocity of propagation indicated that it had traveled about 250 feet farther than the direct wave. The position of multipath images displaced by as much as one fourth inch or more could often be measured to the nearest 1/64 of an inch, and thus the extra distance traveled could be determined to within ±125 feet.

These findings gave rise to the belief that specially designed equipment built primarily for the purpose of path length determination could give an accuracy of ±50 feet or better, and the considerable thought given to that possibility in the fall of 1938 resulted in the early concept of Shoran as it is today.

Actually it was not known, at first, to what uses a system for accurate transmission path length measurement could be put, but it seemed logical one use might be for blind navigation, particularly of aircraft. Blind bombing suggested itself automatically because of the apparent imminence of war in Europe.

However, if delay times equivalent to tens or even hundreds of miles instead of tens or hundreds of feet were to be measured, it was apparent that two requirements would immediately present themselves. First, a round-trip signal between the two points of distance determination would have to be used. This would call for either an extremely efficient reflector at one end of the path or for retransmission of the original signal at the path terminal. Second, some type of vernier or decimal indication would be necessary in order that the radio "yardstick" could be read to, say, ±100 feet even though the round-trip or total distance was of the order of 2,000,000 feet or 400 miles.

Many experiments were performed in the fall of 1938 and the spring of 1939 to confirm the belief that relatively long distances could be measured with even higher absolute accuracy, and thus perhaps a thousand-fold greater proportional accuracy, than the original television multipath determinations.

One interesting experiment consisted of retransmitting the television pictures from the Empire State Building between

Paper 46-49, recommended by the AIEE committee on communication for presentation at the AIEE winter convention, New York, N. Y., January 21–25, 1946. Manuscript submitted December 19, 1945; made available for printing January 2, 1946.

STUART WILLIAM SEELEY is associated with the Industry Service Division, RCA Laboratories, Radio Corporation of America, New York, N. Y.

two points on Long Island separated in such manner that the relayed picture arrived at a receiver almost exactly one line later than the direct signal. The raster on the cathode ray tube face was synchronized continuously with the direct signal from National Broadcasting Company while the video content was commutated between the direct and relayed pictures. When the relayed signal path length corresponded exactly to one line, the commutation process produced no horizontal jitter of the television image. The signal was, of course, delayed in the relay terminal equipment by the electric inertia of tuned circuits, video amplifiers, and connecting cables. These time intervals had to be taken into account, and those which could not be accurately calculated were measured by a determination of the phase shift characteristics of the modulation components of an r-f signal passing through the equipment. It is interesting to note that the total time elapsed in the relay receiver and transmitter corresponded to a path length of nearly 2,000 feet. But since it could be accurately measured to within 0.01 microsecond by the slope of the phase versus modulation frequency characteristic, errors from that source were not more than ± 10 feet. It was necessary to call on the U. S. Coast and Geodetic Survey for accurate ground distance information.

The results of that experiment and others were convincing proof that a radio "yardstick" could be constructed for first-order determination of distances out to the limits of propagation of the radio frequencies used. The latter had to be relatively high to accommodate the rapid modulation necessary for sharp time indications. Amplitude or frequency changes in the radiated wave would have to occur in the order of 1/10 microsecond if measurements with an accuracy of that order were to be possible. This called for a transmission frequency whose fundamental period was not more than 1/50 microsecond or a minimum 50 megacycles.

The transmission of what could be termed single picture elements, one at a time, with the transmitter completely quiescent between those pulses, was chosen as the most practical mode of operation. Such a system would allow relatively high power radiations with relatively low average power consumption. This principle, decided upon in October of 1938 for the original Shoran development work, has been used almost universally in all radar equipments whose function requires operational ranges greater than one or two miles.

It is not meant to imply that this date marked the first concept of pulse type operation. However, the choice of pulse type operation at that early stage of the Shoran work marked the final equipment for success. Attempts to derive the same end results by other systems have proved the wisdom of that choice.

During 1939 many types of possible vernier time measurement devices were conceived, built, tested, and discarded. Since it seemed certain that on occasion multiple pulses, due to reflected waves traveling devious paths, would arrive at the receivers at each terminal of the transmission path, and since, obviously, the first pulse to arrive would be the only one to give an indication of the direct path distance, it seemed clear that a cathode-ray-tube type of data presentation would offer the simplest means of discrimination between the desired or first-arriving information and subsequent indications. It was conceivable that circuit arrangements could be effected whereby the elapsed time could be indicated on meters or transposed to data transmission systems. However, the most straightforward procedure appeared to lie in the use of linear determinations of the position of an alteration in either the intensity or deflection of a cathode ray tube trace.

Here again this early choice of the cathode ray tube as the indicating element has certainly been vindicated by subsequent developments. Much later in the history of Shoran, circuits were developed for transferring the derived information to a data transmission system. This made it available at positions remote from the equipment; but those circuits, which will be described later, are of only secondary importance, and the cathode ray tube remains the prime indicator.

Two further principles, each of which contributed markedly to the success of Shoran, were also adopted early in its history. First, the repetition rate of the transmitted pulses, which could be controlled by quartz crystal oscillators to an accuracy of one part in 1,000,000 if necessary, was selected as the fundamental unit of measurement. Second, an old principle familiar to precision instrument makers in many fields and known as the set-back type of operation was adopted. This principle is exemplified in precision aneroid barometers wherein movement of the bellows caused by varying air pressure is counteracted either by adjustable weights or by adjustable spring tension sufficient to return the bellows distortion to a fixed zero. The weights or the spring adjustment necessary to perform that function then give an indication of the air pressure. While this type of operation seems cumbersome compared to the simpler method of causing the bellows to move a pointer around a calibrated scale, actually the increased precision is well worth the complexity.

As applied to Shoran, this system eliminates the need for the maintenance of exact linearity of the cathode-ray-tube sweep speeds in the presence of varying power line voltages, varying vacuum tube characteristics, and varying circuit parameters. So far as is known to the author, Shoran is the only radar system which adopted the continuous set-back principle. However, the advantages which accrue from its use are not as necessary in equipments which seek less inherent accuracy.

By the summer of 1939, enough experimental and developmental work had been done to indicate the probable practicability of a blind bombing navigational device founded upon the principles enumerated above. Operation would call for an equipment in an airplane which could simultaneously measure its exact distance from two separated and accurately known ground locations in friendly territory while the plane flew over enemy targets. Investigation revealed that all of Europe, together with all of the North American continent, had been sufficiently well mapped so that the distance between any two points within 250 miles of each other in those parts of the earth could be calculated with a probable error of 50 feet or less.

Armed with this information, and fortified with the confidence of many months of satisfying experimental endeavor, the project was presented by Radio Corporation of America to the United States Army Air Forces with the proposal that funds be allocated for the development of operating models of the necessary equipment to test its feasibility. That was in the summer of 1940.

It is an interesting commentary on the thinking of those times that the author felt constrained to write into the specifications of the proposal the suggestion that the probable accuracy of distance measurements would be of the order of ± 500 feet. These predictions, definitely pessimistic in view of the favorable experimental results in the laboratory, were made pessimistic principally because it appeared utterly fantastic at those times to presume to achieve even that goal. To have suggested more would have branded

the project as completely unrealistic.

Even with those moderate claims, the apparent unreality of the proposed program hindered the progress and retarded the growth of Shoran up to the very day the first Shoran bombs dropped to destroy a 30-foot-wide enemy-held bridge in northern Italy.

War in Europe had been declared at the time of these first proposals. The pace of preparedness in the United States quickened after the fateful September 1, 1939. More money was allocated to the armed services for development of new devices, and even some of the projects which were felt to be a bit on the fantastic side were given the green light.

Accordingly, a contract was awarded to RCA Laboratories in February of 1941, about nine months before Pearl Harbor. This called for completion by February 1942 of two ground station equipments and one airborne equipment to give simultaneous and continuous distance determinations from each of the ground stations to a plane, out to optical line of sight, with an accuracy not poorer than −500 feet at 100 miles or 0.1 per cent of the distance beyond that point.

The 2 1/2 years of experimental work before the awarding of the contract had allowed the plans for the model to be so well formulated that just four months later the plane equipment and one ground station were completed and ready to operate. With one complete operating chain, many previously unanswered questions could be resolved. One determination which had not been made concerned the possible variations in the propagation velocity of a radio wave at tangency with the earth's surface. It appeared that vegetation and partially conducting soil with a high dielectric constant could well have a marked effect on that all-important characteristic. Also the probable variation caused by changes in the humidity of the air was a possible source of difficulty which could only be crudely calculated. Accordingly, it was decided to place the plane equipment in the tower of the Empire State Building, put the ground station out beyond the optical horizon at Rocky Point, Long Island, and make day-to-day measurements of the distance between the two points. This was done after flight tests from Wings Field near Philadelphia, Pa., to the Rocky Point location had confirmed adequately the predicted range of operation.

Measurements between the Empire State tower and Rocky Point were continued for a period of three months during the summer of 1941. Hundreds of readings were taken and the equipment operated by many different observers. During that time the temperature varied more than 40 degrees Fahrenheit and the humidity ranged from a low of 30 per cent to a high of 100 per cent. An average of all readings indicated a distance of 56.126 miles with a total spread of 0.013 mile. There was no apparent correlation between climatic conditions and the readings. Later the United States Coast and Geodetic Survey gave the measured distance as 56.127 miles, or five feet more than the average of the Shoran readings. Obviously the transmission path to the Rocky Point location, which was 400 feet below optical line of sight, through scrub pines and over sand, was not affecting the velocity of propagation to any marked extent over and above the variations caused by normal sea level air pressure. The latter had been calculated beforehand and introduced into the equipment as a correction to the frequency of the crystal-controlled pulse repetition rate. The agreement between the Shoran and geodetic distance measurements was actually too close for comfort. Had they differed by 200 feet or so, they could have been given to the Aircraft Radio Laboratory as evidence of the potentialities of the system. Under the circumstances, it was decided that it would be best to say nothing about that particular series of measurements and let the contracting agency make its own accuracy determinations.

At the time of Pearl Harbor, the Aircraft Radio Laboratory took delivery of two specially constructed all-metal trailers which they had ordered built to specification to house the Shoran ground stations. Each of these had its own 5-kw gasoline-driven a-c generator in a glass-enclosed gas-tight compartment. These were in turn delivered to the RCA Communications Laboratory at Rocky Point and the Shoran gear installed. Further tests followed with the ground stations operating as complete self-contained mobile units. Then shortly before the contract expiration date, the entire equipment was sent to Wright Field for acceptance tests.

It is well to bear in mind the particular conditions which existed at that time. The United States had been at war for just 2 1/2 months. The mad rush to prepare for the titanic struggle which was already upon us called for emphasis on the most necessary fundamentals first. Communication radio and liaison equipment for a rapidly expanding air force were requisites of prime importance. The Aircraft Radio Laboratory at Wright Field was so completely occupied with the specification and procurement of these necessities that they had neither time nor facilities for acceptance tests of such apparently obtuse devices as Shoran. It was not until six months later, in August of 1942, that the original plane equipment was mounted in a B-17 Flying Fortress and taken to Eglin Field, Fla., for bomb-dropping tests. The mobile ground stations were set up at Montgomery, Ala., and at Tallahassee, Fla. In order to save time, the distances from each ground station to the 30-foot square-base pyramid target in the bay near Eglin Field were determined by flying over the target with a Norden bombsight set to vertical and reading the Shoran distances. This process was repeated several times, but the pitch and roll of the plane, together with the inability of the automatic pilot to do a precise job of following the bomb sight lead, resulted in considerable discrepancy between successive readings. Admittedly the bomb-dropping trials were to be handicapped, not only by the possible Shoran errors but by those of the Norden bombsight and automatic pilot as well. The distances finally determined were 108.297 miles to Tallahassee and 125.431 miles to Montgomery.

Of the first 12 100-pound sand-filled practice bombs dropped from 14,000 feet, the average dispersal from the target was 220 feet. Two of the bombs hit the 30-foot-square wooden target. The results were on a par with those to be expected from a mission dropping the same number of that type of bomb by visual means. The ballistics of sand filled practice bombs are erratic in comparison with those of heavier missiles. Additional tests were made from 20,000 feet and the results were relatively the same. It appeared that Shoran had proved its capabilities as a blind bombing device even before its precision for distance measurements had been evaluated.

The procedures developed for determination of the release point of the bomb on those early test runs are interesting. It would be beside the point to go into all the ramifications of the calculations of bomb trajectories and release points in this paper. Suffice it to say that the vector winds through which the plane was passing were determined by comparing the indicated air speed of the plane with the rate of change of Shoran distances for a given plane heading. Manual release at the proper point was effected by the simple process of pressing a button connected electrically to the bomb rack intervalometer. Human reaction time was not considered a factor because of the

anticipatory knowledge constantly supplied by the Shoran indications. Later production models were equipped with devices which automatically measured the plane speed as well as the vector wind, made the required corrections in the ground path of the plane, and automatically released the bomb at the corrected point on that path. That portion of the equipment was developed primarily by F. J. Hooven in co-operation with engineers of the Harris Seybold Potter Company under contract to the Armament Laboratory of the Air Technical Service Command. It is a marvel of ingenuity and precision, but at this writing, information regarding the details of that device is still restricted.

After the Eglin Field tests, it seemed certain that an immediate request for product designs and production schedules would be forthcoming. Much to the personal disappointment of those who had nurtured the development from its conception, such was not to be the case. Interest in blind bombing devices was at fever heat, but the new microwave techniques were coming on the scene and their freedom from any tie to fixed locations on the ground seemed to offer the only complete answer. Actually it was not until after the close of war in Europe that it was determined that 80 per cent of all strategic missions and almost 100 per cent of all tactical missions flown in that theater were within the Shoran range of operation.

A further deterrent to Shoran progress lay in the fact that by then the British had started development of a somewhat similar system and it was felt inadvisable to carry on two separate product design and procurement programs without coordination. Accordingly, a small group of military personnel headed by Lieutenant Colonel R. R. Brunner, together with two Radio Corporation of America engineers, left for England on December 1, 1942, to exchange information and to resolve the degree to which the two programs could be integrated. However, the work carried on at Telecommunications Radio Establishments under the Air Ministry was based on entirely different principles than those of the Shoran development and there appeared to be no common basis upon which the two programs could be combined.

On the return trip from England, the party split into separate groups. The group consisting of Colonel Brunner and some British military personnel coming to the United States to get a better picture of the Shoran project was lost in flying the South Atlantic Ocean. Viewed in retrospect, it seems certain that this loss was a major factor in keeping Shoran progressing at a snail's pace toward its ultimate conclusion.

Finally in March of 1943 a product design contract was given to RCA and work progressed again at full steam. The contract stated that the ultimate equipment should have an accuracy of distance measurement at least equal to that of the original model which, by then, carried the army designation SCR297-T2. It was realized by all concerned that the ± 500 feet specification was so pessimistic as to be meaningless, so no figures were mentioned. Several of the automatic features referred to previously were specified as essential to fulfillment of that contract.

That work was completed in January of 1944. It is a credit to all concerned to say that the faith of the Air Technical Service Command Aircraft Radio Laboratory in the ultimate outcome of that program was such that they recommended, and Radio Corporation of America received, large procurement orders well in advance of its completion. Thus the Shoran radar program acquired the unique distinction of having been conceived, developed, product-designed, and manufactured entirely within one company. This, of course, neglects the auxiliary equipment mentioned above.

After the completion of the design work, and while waiting for production quantities to become available, a six-month program of rigorous flight and field tests was inaugurated at Boca Ratan, Fla., under the auspices of the Aircraft Radio Laboratory. For the first time, a true indication of the accuracy of distance measurements from a plane to a fixed point on the ground was available. This was derived by the use of so-called Zenith cameras located at known control points approximately 100 miles from the Shoran ground stations. The plane was equipped with a gas-filled flash lamp on the under side of the fuselage. As the plane passed over the Zenith camera, the lamp was flashed and the Shoran distance readings recorded. Many nights of such flights with many passages back and forth across each new Zenith camera location gave sufficient data to indicate the probable error of distance measurement as being somewhat less than 50 feet out to the limit of its range. Hundreds of bombs were dropped and many different operators acted as Shoran bombardiers. As a matter of fact, no single individual ever dropped enough bombs to become really proficient in the use of the equipment, but the design was such that it was relatively simple to operate. Thus, human errors, particularly when the operator had had training on a Norden bombsight, were at a minimum.

The extreme accuracy of distance determination attracted the attention of the Army geodetic and mapping groups. As a result of their interest, the equipment is being used today for establishing control points with first-order survey accuracy at very great distances. For this work a ground station is established at each point to be located and a plane flown back and forth across the line between any two such points. The average minimum sum of the distances between the plane and each ground station, as indicated by a photographic recorder for each line crossing, gives the true distance between the points. The comparative simplicity of surveying a line from, say, Chicago to Kansas City to Amarillo, Texas, in only two jumps can be imagined. For a survey of that route, three ground stations would be used, one at each of the three cities, and 10 or 20 flights back and forth across the approximate center of each line would be all that would be required. Except for one consideration, it would be unnecessary for any individual to set foot upon the intervening terrain. Subsequent to the early tests between the Empire State Building and Rocky Point, the true effect of climatic conditions on propagation velocity and on the refraction of the radio waves between plane and ground had been determined. As a result, sounding balloon or other types of atmospheric determinations along the path are considered necessary when the equipment is used for first-order survey work. Nevertheless, the simplicity and rapidity with which unmapped portions of the surface of the earth can be brought into survey control with equipment of this type is little short of amazing.

At the completion of the Boca Ratan tests, the remarkable results achieved became known to the commanders in the fields of operation and requests for equipment began to pour in. In September of 1944, it was decided to test the equipment in actual operation against the enemy. Several personnel from the Aircraft Radio Laboratory and the Armament Laboratory (also at Wright Field) were accompanied to Corsica by three Radio Corporation of America engineers to aid in setting up the equipment and to train ground and air crews in its use over northern Italy. There were many disappointing delays in the arrival of the equipment. Boxes supposed to contain transmitter tubes were found to contain toilet necessities and flashlight batteries.

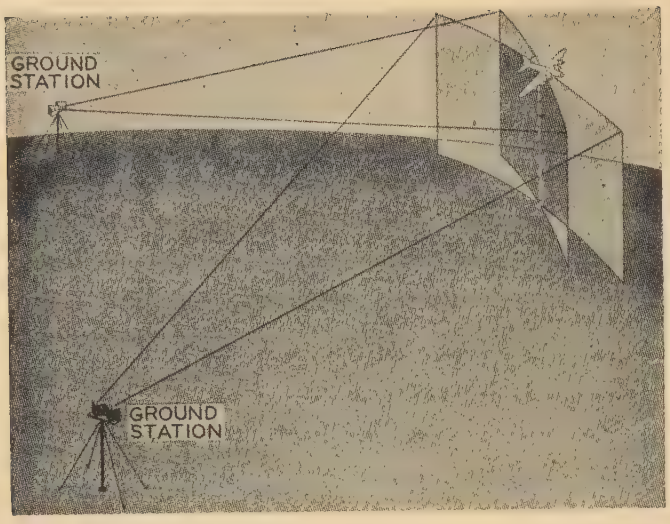

Figure 1. The Principle of Shoran

The Shoran set indicates plane's distance from two ground stations, thus "fixing" it at intersection of the corresponding circular arcs swung around the two stations

More weeks followed during which crews were training and practice bombing. Finally on December 11, 1944, the first Shoran bombs were dropped. From that time on, events moved with rapidity. Operational results were phenomenal. Bridges that had withstood many close misses by visual missions were destroyed on the first Shoran run. Weather was no hindrance to tactical air support with Shoran. By the time the war ended in Europe, the amount of tactical bombing being done in any area was predicated almost entirely upon the availability of Shoran equipment. By the time the war with Japan was brought to a close, the plans of the Army and Navy for the use of Shoran in the Pacific were astounding even to those who knew its potentialities.

The Shoran System

Figure 1 shows the 2-distance "fix" method used by Shoran to locate a position in flight. The airplane equipment transmits a series of short pulses of radio frequency energy to each of a pair of ground stations. These in turn immediately retransmit the received signals to the plane where the round-trip transmission time is measured in terms of distance. In bombing operations the plane flies in either direction on an arc about one of the ground stations. The radius of the arc is equal to the station-to-target distance. Since either ground station may be used as the center of the flight path, four different approach headings are possible when bombing a given target. With normal station-to-target distances, the curvature of the bomb run path is relatively slight. A refined type of pilot direction indicator meter, deriving its information automatically from the equipment, is in front of the pilot. During a bomb run, with the aid of this instrument, it is not difficult to keep the plane on its arc path with deviations less than the span of the plane wings.

It should be noted that no information is passed along the path joining the ground stations. If the geographic locations of those stations, as well as those of all possible targets, are accurately known, as was the case in the European use of Shoran, the geodetic problems connected with Shoran operations are relatively simple of solution. When they are not known, Shoran reconnaissance photography of possible targets will reveal their co-ordinates.

It is highly desirable that a pair of ground stations be able to serve a large number of planes bombing widely separated targets simultaneously. This is possible with Shoran installations, and the means by which it is accomplished without interference will be described later in this article.

Planning of a Shoran mission, with all the geographic distances known, is not as simple as it might at first appear. The great circle path of a plane several thousand feet in the air differs from the great circle path on the earth's surface, often by as much as one tenth mile. Contrary to a widely held belief, radio waves do not travel in a straight line over any appreciable distance, but tend to be refracted into a vertical arc. Radiant energy travels faster at bomber plane altitudes than it does through sea level air pressures. Fortunately, all of these effects are predictable accurately, and all are taken into account in determining Shoran co-ordinates for a given bombing mission. The calculations involved are completed before take-off. In bombing operations, possible corrections indicated by variations in climatic conditions are usually of insufficient magnitude to be significant.

The ruggedness and relative simplicity of operation of the components of a Shoran system, together with the freedom from equipment failures which it provided in combat use, are all remarkable in view of the extreme precision of the results obtained. Details of the individual portions of the equipment are given herewith.

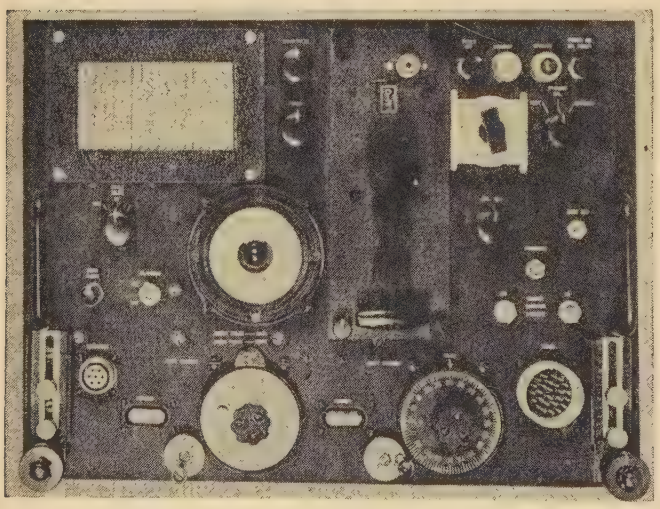

Figure 2. Panel of timing and indicating unit of Shoran plane equipment

Figure 3. The airplane transmitter

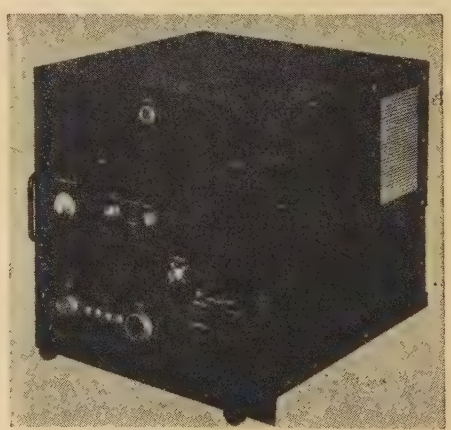

The Plane Equipment

The principal units of a Shoran plane equipment are shown in Figures 2 and 3. Figure 2 shows the timing and indicating device which is the most vital part of the Shoran system. This unit permits regulation of the timing of the transmitted pulses in such manner that the signal returned by retransmission from the ground arrives back at the plane receiver and makes its appearance on the screen of the cathode ray tube coincidentally with the fixed, or so-called T_0 marker indication. The adjustment necessary to effect this coincidence is calibrated in miles and decimal portions of a mile. Thus the mileage indications are read from the dial settings rather than from the face of the cathode ray tube, in accordance with the set-back principle referred to previously.

The pulse timing function is duplicated in the indicator unit to allow for simultaneous distance measurements from two ground stations. Reference to Figure 2 will show the two large 100-mile dials at the bottom of the panel. At the left of each dial is a Veeder-type counter, the three digits of which indicate miles, tenths of a mile, and hundredths of a mile. Estimation to the nearest 1/1,000 of a mile is possible. Adjustment of each of the two sets of distance indicators is made by rotation of the small hand wheels to the left and slightly below the large dials. In the case of a plane in motion, continuous rotation, achieved by variable speed motor drive, can be imparted to the shafts carrying the hand wheels, thus keeping the indicated data up to date. It can be readily understood that the rate of rotation necessary to maintain coincidence between the received signal and the T_0 marker is of value in determining the plane's ground speed and in the calculation of bomb release points. Beyond 100 miles the readings are repeated. Thus the readings would be the same for distances of 57, 157, and 257 miles.

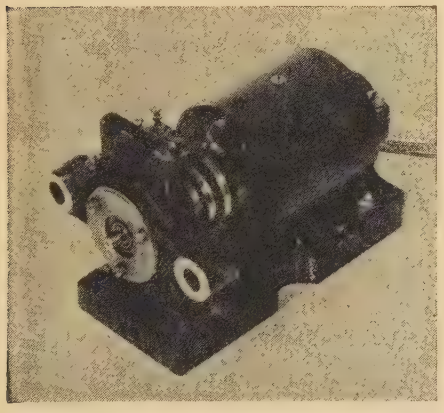

Figure 4. The goniometer which determines Shoran timing

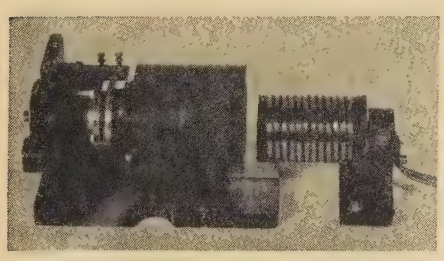

Figure 5. Goniometer with rotor withdrawn

The Faraday screen of copper ribbon covers the crossed windings of the stator

Figure 6. Bottom view of timing and indicating unit

Each goniometer is mechanically connected through reduction gears to the others in the chain

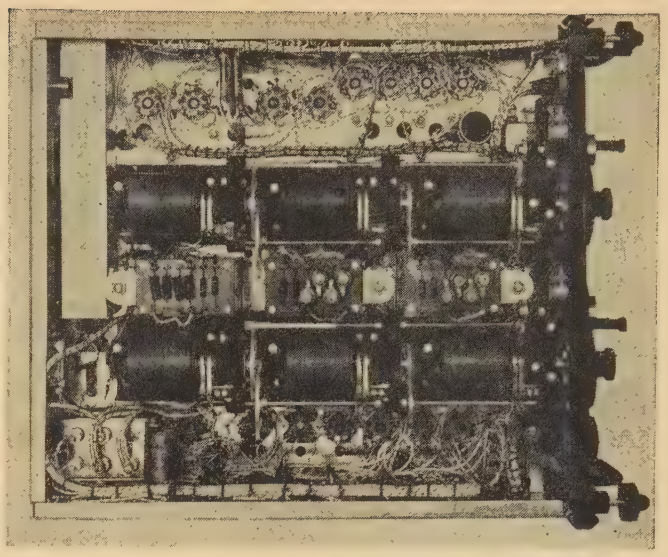

The most interesting portions of the timing and indicating circuits are those which control the timing of the transmitted pulses. The accuracy of that function depends upon the stability of a quartz crystal oscillator operating at 93,109 cycles per second. It should be noted that this figure is exactly one-half of 186,218, which is the number of miles traveled each second by a radio wave passing through sea level air pressure. Thus the period of one cycle of the oscillator is equivalent to the time required for a radiated signal to travel a *round-trip* distance of one mile.

The voltage output from the oscillator is distorted in vacuum tube circuits by clipping and differentiation processes to form a very short pulse, accurately located at a fixed phase of the cycle. This is passed to the cathode ray tube and becomes the T_0 marker on the screen. The output of the 93-kilocycle oscillator is also split into two accurately spaced quadrature components and delivered to the crossed windings of the stator of a goniometer. Pictures of this unit are shown in Figures 4 and 5. The rotor of the goniometer can be turned throughout 360 degrees, and the output potentials, derived by way of the slip rings, have a phase corresponding to the position of the rotor. This potential is likewise clipped and differentiated and produces a pip which then can be timed accurately to any point midway between two marker pips. One degree of rotation of the goniometer corresponds to a round-trip path length of 15 feet. If these adjustable pips were all used to actuate the transmitter, there would be several hundred transmitted impulses stretched out over the round-trip path between the plane and a ground station, and confusion would result. Therefore, it is necessary to select *one* pulse out of each 100 that are developed and discard the others. Accordingly, the 93-kilocycle wave is passed to a 10:1 phase degenerated frequency divider and the new frequency split into quadrature components for a second goniometer. This unit is mechanically connected to the first goniometer through 10:1 reduction gears. The resultant output is used as a gate to select one out of each ten of the developed pips. Again the process is repeated with another 10:1 divider, and a third goniometer is driven by the second through another 10:1 reduction gear. The final output voltage at 931.09 cycles selects one of the ten previously selected pips and thus discards all but one of the original 100 which were developed. The second and third goniometers have no effect on over-all accuracy if the output phase of each is correct within the selection limits of ± 15 degrees. Greater discrepancies would produce errors of exact multiples of one mile or ten miles, depending upon which of the two units was at fault. The circuits which deliver the

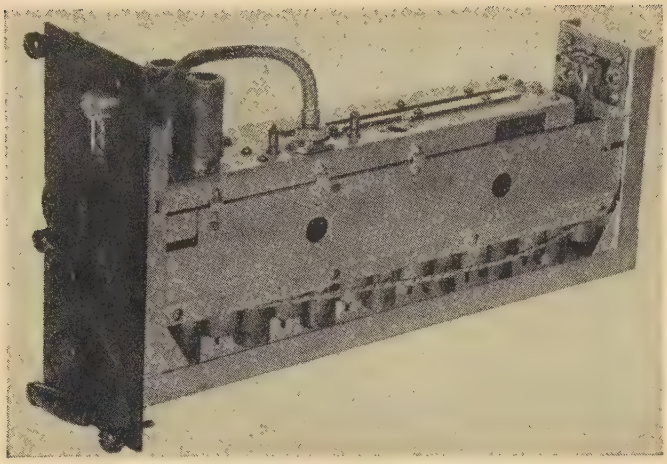

Figure 7. The Shoran receiver used in both plane and ground stations

quadrature currents to the goniometers are unique in one important characteristic. Large changes in the power factor of the stator windings produce no phase variations of the currents which flow through them. Thus temperature compensation is unnecessary, and ambient temperature variations from −70 degrees Fahrenheit to +140 degrees Fahrenheit make no readable change in indications. The complete chain of goniometers, mechanically coupled through reduction gears and supplied with the proper energy from the associated circuits, permits accurate placement of the transmitter pulse to within 1/100 of one degree of any position throughout the 100-mile repetition rate cycle. This is accomplished without excessively close tolerance specifications on any parts of the equipment. The twin rows of goniometers can be seen in the bottom view of the timing and indicating unit chassis in Figure 6.

The two timing devices are completely independent of each other, and the transmitter control is commutated between them approximately ten times per second. During the commutation cycle, the frequency of the transmitter is altered so that all pulses sent out in accordance with timing derived from the left-hand control are on one wave length, while those from the right-hand control are on another. Thus each of the two ground station receivers can pick up and retransmit the signals meant for it and discriminate against those intended for the other. The commutation process also switches the gain control function of the plane receiver alternately between two potentiometers, each of which can be adjusted separately. This allows for wide differences between the strengths of signals received at the plane from the two ground transmitters, as is the case when operating close to one but remote from the other.

One other function of importance is performed during the commutation cycle. In order to operate many planes in the air at once and have them all use the same pair of ground stations, it is necessary that transmission from a ground station to one plane not interfere with the proper operation of Shoran equipment in another. Since the repetition rate of Shoran pulses is the precise yardstick in terms of which the distances are measured, all planes utilizing a pair of ground stations simultaneously will be using that same yardstick. Thus it would be possible for the accurately synchronized indications from a ground station, meant for one plane, to be picked up by another and give the second plane crew an erroneous indication of their position. This possibility is obviated by an action of the commutator during a third portion of the one-tenth-second period of its cycle during which *no* transmissions occur. During this time, the repetition rate circuits of the timer are momentarily blocked off and then immediately allowed to resume operation precisely at the previous rate. The result is that no two plane equipments interrogating a common ground station can stay synchronized for more than a small fraction of a second, in spite of the fact that their interrogation rates are precisely the same.

The trace on the cathode ray tube is circular. There were two reasons for this choice. A 3-inch tube will accommodate a $7\frac{1}{2}$-inch circular trace compared to a $2\frac{1}{2}$-inch linear sweep. Also a circular sweep is continuous without breaks in its continuity while the spot returns to its starting position. A throw of a switch changes the deflection rate of the circular pattern from a 1- to a 10- to a 100-mile scale. For navigational purposes, out to the initial point of a bomb run, the 100-mile scale is adequate. The use of this scale allows the operator to effect coincidence of the received and marker pulses to well within the ±5-mile interval over which they are visible on the ten-mile scale. He can then repeat the process and switch to the one-mile scale. Thereafter, if the data are kept up-to-date, he need not return to the 10- or 100-mile scales, since the complete information is constantly available on the mileage dials. All traces on the oscilloscope are blanked out when using the 1- or 10-mile scales except for the particular 1- or 10-mile interval containing the T_0 time. Actually, the T_0 marker is traced on the screen for the 1- and 10-mile scales during an unused portion of the 100-mile repetition rate. Thus, the received pulses, which are outward for the left-hand mileage controls and inward for the right-hand dials, appear to be superimposed upon the marker deflection rather than to mingle with it and thus cause confusion. Matching is correct when the left-hand (leading) edges of all pulses are coincident.

The plane receiver controls are on the separate oblong panel extending upward

Figure 8. Units and cabling of ground station

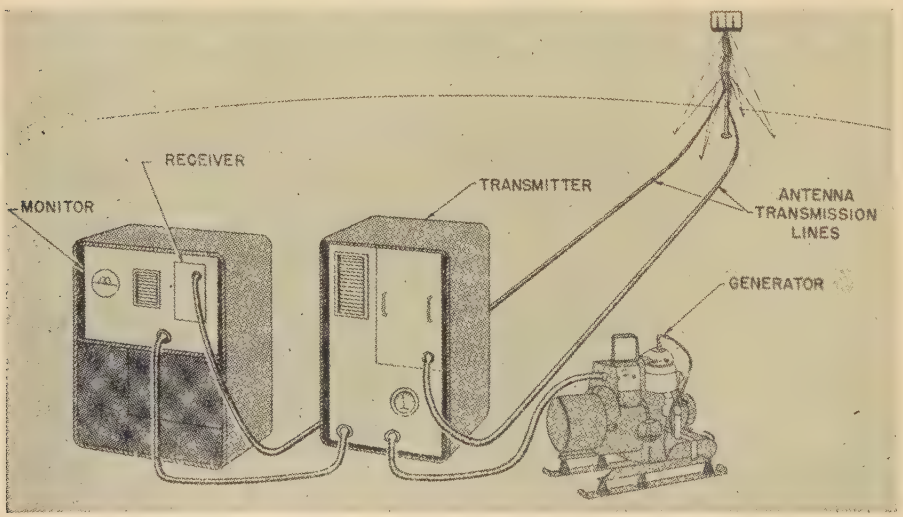

slightly to the right of center in Figure 2. The receiver can be withdrawn and replaced in a matter of only a few seconds in case of defective operation. All connections, with the exception of the antenna, are made through sliding contacts and are thus automatically broken and reestablished when the unit is removed and replaced. One of the filters for the forced air cooling system can be seen in the upper left-hand corner. Figure 7 shows a receiver withdrawn from its compartment.

Figure 3 shows the plane transmitter which generates the signals radiated under control of the timing and indicating unit. It is usually mounted in some out-of-the-way position in the airplane, since it has no adjustments that need attention while in flight. "Start," "stop," and "standby" operation are remotely controlled by relays actuated in

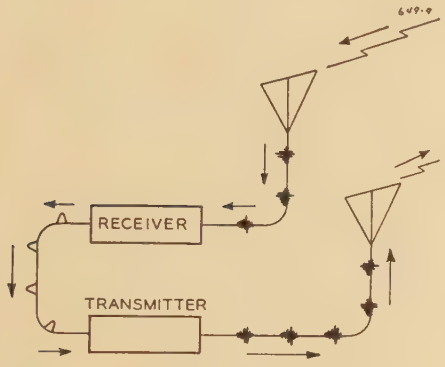

Figure 9. The function of the ground station

Pulses received from the airborne transmitter are amplified and retransmitted to the plane

conjunction with those of the timing and indicating unit.

The peak power input to the transmitter tubes is approximately 50,000 watts, and a plate circuit efficiency of about 30 per cent is realized. The low operating duty cycle results in an average plate power consumption during operating periods of only 30 watts. Positive plate, or B voltages, are not used on the two push-pull self-oscillating transmitter tubes which derived their plate energy entirely from the 5,000-volt positive swing of the secondary of the pulse modulation transformer. The two transmitter frequencies, which are commutated during operation, are adjustable in the region of 220 to 260 megacycles. Usually they are separated by from five to ten megacycles, but they must correspond to the respective ground station receiver frequencies. Commutation of the radiated wave length is made possible by the action of a solenoid-operated vacuum-contact short-circuiting bar on the resonant grid line of the oscillators. The adjustment of the position of that bar and of all other grid and cathode line connections is controlled by screw driver adjustment through the front panel. The plates of the oscillators are at radio frequency ground potential.

The antenna for radiating the transmitter power is of the stub type and is mounted vertically either above or below the fuselage. An attempt is made to produce as nearly an omnidirectional pattern of vertically polarized radiation as possible. The antenna proper is somewhat unconventional. It consists of a center rod extending approximately 1/8 wave length beyond a 1/8-wave grounded concentric sleeve. The entire assembly is about 12 inches in length. In operation the antenna has relatively broad band characteristics and produces a low order of standing wave ratios on the 50-ohm transmission feed line throughout the transmitter frequency range.

The plane receiving antenna is of the same type of construction but is somewhat shorter in over-all length, since it receives signals from ground stations which transmit on approximately 310 megacycles.

Lengths of interconnecting cables between units and between the transmitter and receiver and their respective antennas have an effect on the total time spent by pulse energy in traversing all of the plane equipment circuits. Therefore, each plane installation must be compensated by a process which involves the sending of test signals around the complete loop and making the necessary corrections in the position of the marker pulse. Actually, the adjustment is not made to zero but to a standard negative value of distance which compensates for all of the fixed delays in the ground station as well as for those in the plane. Thus, if the intervening path between the plane antennas and those of the ground station were of zero length, a pulse initiated in a timer chain reading zero would pass through the plane transmitter, all the ground equipment, and finally arrive back at the plane receiver in time to appear on the cathode ray tube exactly superimposed upon the T_0 marker. The point which bisects an imaginary line drawn between the plane transmitting and receiving antennas is that from which all measured distances are indicated.

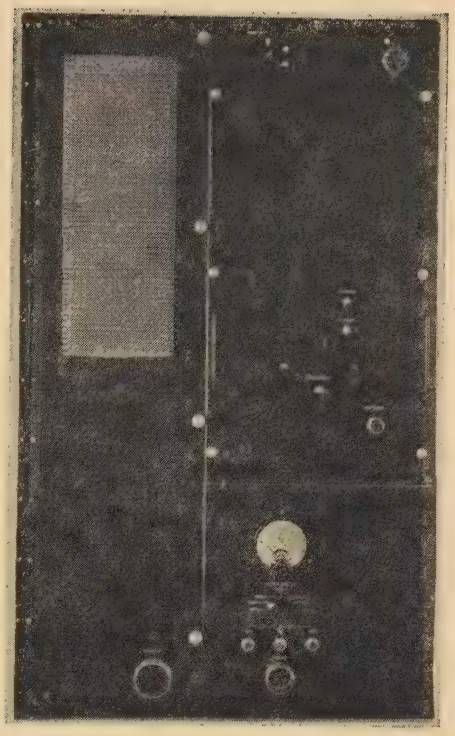

Figure 11. Panel of ground station transmitter

The Ground Station Equipment

A ground installation consists essentially of four principal units. These are the receiver-monitor, the transmitter,

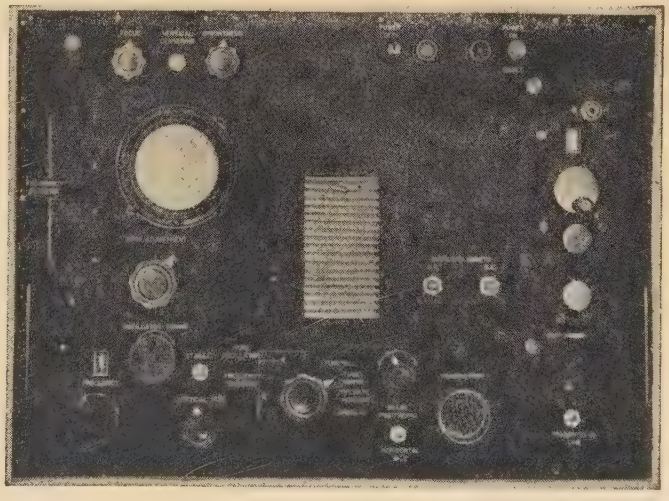

Figure 10. Panel of ground station monitor-receiver

the antenna arrays, and the gasoline-driven power supply. See Figure 8. The complete equipment is air-transportable and can be flown to a known location and put into operation within 90 minutes after arrival.

The primary function of the ground equipment is to receive, reshape, and retransmit all pulses arriving at the location on the particular wave length to which the receiver is tuned. See Figure 9. The elapsed time between the arrival of a signal at the receiving antenna and the radiation of the resultant pulse from the transmitting antenna must be accurately adjusted to a fixed standard time interval. That adjustment, as well as others necessary for proper operation of the installation, is performed with the aid of the monitor portion of the monitor-receiver unit. This is shown in Figure 10.

The oscilloscope in this piece of the equipment facilitates adjustment of frequency dividers which regulate the timing of standard repetition rate radiations independently of any received signals. These are under the control of an extremely accurate 93, 109-cycle temperature-controlled crystal and allow a plane equipment operator to make a slight adjustment in the frequency of his crystal if temperature or other conditions have caused excessive drift. Continuous radiation of standard pulses from the ground also enables the plane operator to tell whether or not he has sufficient altitude to be within range of that station even before he starts transmitting.

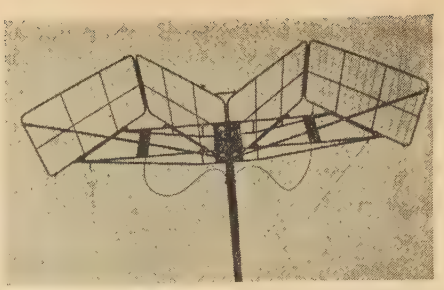

Figure 12. Ground station antenna assembly

The adjustment of the total delay interval to the standard value is made by varying the number of delay line sections in the circuit until the loop-delayed pulse matches another which is passed only through a standard delay network.

The receiver, shown on the right-hand side in Figure 10, is identical to, and interchangeable with, the receiver in a plane equipment. It has a continuously adjustable tuning range between 210 and 320 megacycles.

The transmitter, shown in Figure 11, is very similar to that used in a plane. However, it has a much higher duty cycle, when serving a large number of planes, and the modulator circuits are, therefore, made heavier to handle that load. Whereas the average plate power in a plane transmitter is 30 watts during operation, the ground transmitter may be developing as much as 400 watts. Each develops a peak input power of about 50 kw.

The transmitting and receiving antennas are shown in Figure 12. The reflectors give power gain of approximately eight to one in the forward direction with a horizontal coverage angle of about 70 degrees to the half-power points. The whole assembly is supported on a 50-foot sectionalized plywood mast.

The gasoline-driven generator delivers about 1,500 watts at 115 volts, 400 cycles, and approximately 400 watts at 28 volts direct current.

Operational Results

The use of blind Shoran bombing over the battle fields of Europe showed that it was capable of equalling visual bombing in accuracy under normal conditions and surpassing it when the latter suffered from target identification difficulties. On occasion, rolling barrages of fragmentation bombs were laid only a few hundred feet ahead of our own advancing troops. The demoralizing influence of such a barrage, from planes completely hidden in a clouded sky, was tremendous. Such operations with equipment of less precision than Shoran would have been foolhardy.

Application of the Betatron to Practical Radiography

J. P. GIRARD
ASSOCIATE AIEE

G. D. ADAMS
NONMEMBER AIEE

Synopsis: The development of the betatron, which accelerates electrons by magnetic induction making possible the production of higher energy X rays than is practical by the direct application of the accelerating potential, has extended the range of X rays indefinitely, the only limit being the size of the machine. Tests with the betatron have shown that the best energy for medical and radiographic use is 20 mev (million electron volts). The development of this machine from a physics laboratory instrument to an industrial machine is described, as well as the radiographic properties of the X rays produced.

THE FIRST successful type of betatron, invented by Doctor D. W. Kerst at the University of Illinois, is an induction electron accelerator which means that electrons are accelerated by magnetic induction instead of by direct application of high potential. The result is that the voltage insulation is not the limiting factor in the acceleration of the electrons, and they can be given energies not previously obtainable by any other man-made means.

In the betatron an alternating magnetic field holds the electrons in a stable circular orbit within an evacuated annular chamber called a "donut," and the increasing field produces a force on the electrons which accelerates them to high velocities. A special field contour is necessary to hold the electron in its orbit as its mass changes relativistically with increasing velocity.

Development of the Theory

The idea of acceleration of electrons by magnetic induction was the subject of experiments conducted by many scientists. J. Slepian stated the general principle in his patent[1] issued in 1927, but he apparently did not develop his calculations to the point of producing a satisfactorily workable machine. Wideroe[2] was the first to show that the necessary field condition for a stable equilibrium orbit is $\phi_0 = 2\pi r_0^2 H_0$ where

r_0 = radius of equilibrium orbit
ϕ_0 = flux within orbit
H_0 = field at the orbit

This was verified by Walton[3] and later referred to by Steenbeck[4] as the 1:2 relation as the flux within the orbit is twice as much as would be obtained if the magnetic field were uniform in space. Steenbeck stated that the field in the region of the orbit should be $H \propto 1/r^n$, where $0 < n < 1$. Kerst and Serber[5] verified the calculations of Wideroe and Walton and also developed the equations for transient phenomena in the magnetic field. Kerst[6] was the first to place an injector in the magnetic field for supplying electrons at a substantial initial velocity to the orbit. Several of the earlier investigators had tried to inject electrons from outside the magnetic field tangentially to the orbit but had not been successful. Steenbeck placed a heated filament in the magnetic field, but provided no means of directing the electrons emitted or of giving them an initial velocity. The injector as developed from the one used by Kerst is shown in Figure 1, and consists of a heated filament, grid, and surrounding plate so that the stream of electrons is ejected by a negative pulse applied to the filament (the plate is grounded to prevent its disturbing the orbit by its electrostatic field). The grid is a solid piece of metal used to minimize the electron bombardment of the plate and is connected to one side of the filament.

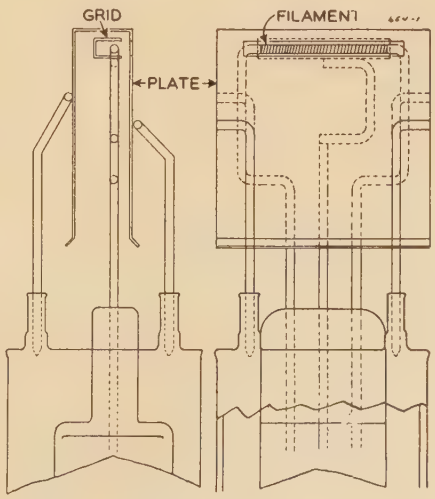

Figure 1. Injector

On the basis of the calculations made by Kerst and Serber, Kerst[6,7,8] was able to construct the first betatron to operate successfully in a practical manner.

Kerst and Serber also calculated the paths of electrons which would oscillate about the equilibrium orbit while the focusing forces are damping the oscillation. From their calculations they could predict the best value for n so that the most electrons would miss the injector on the later revolutions and be focused to the orbit.

The Kerst type of betatron is essentially a three-legged transformer with the accelerating field formed in an air gap by

Paper 46-54, recommended by the AIEE committees on electronics and industrial power applications for presentation at the AIEE winter convention, New York, N. Y., January 21–25, 1946. Manuscript submitted November 21, 1945; made available for printing December 31, 1945.

J. P. GIRARD is application engineer, transformer sales division, Allis-Chalmers Manufacturing Company, Milwaukee, Wis. G. D. ADAMS is assistant professor, department of physics, University of Illinois, Urbana, Ill.

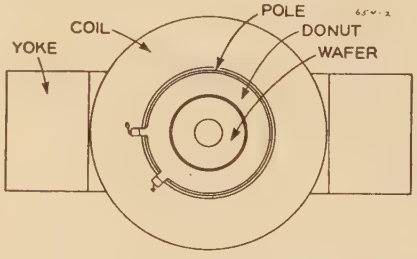

SECTIONAL VIEW SHOWING DONUT IN PLACE

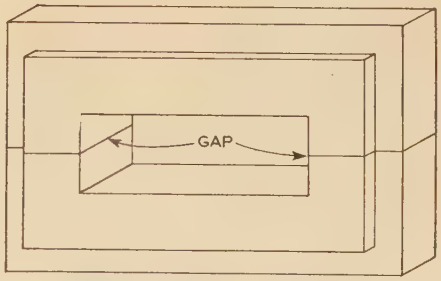

PERSPECTIVE VIEW OF YOKE

Figure 2. Betatron magnet

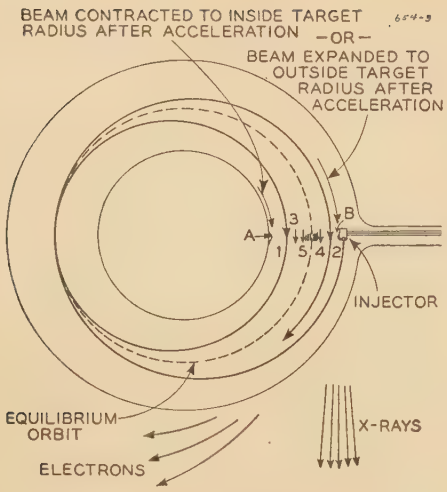

Figure 3. Sectional view of donut showing positions of injector and targets as well as electron paths

radially symmetrical poles in the center leg as shown in Figure 2. Coils shown provide the necessary flux when a voltage is applied to them. In practice a sinusoidal voltage is applied as this is the simplest means of providing the time-increasing field, although only one quarter of each cycle is utilized in the acceleration of the electrons. The donut and injector are shown in position in Figure 3 which also illustrates the various electron paths during focusing, injection, and expansion.

In operation, electrons are injected when the flux wave is at point A as shown in Figure 4. They are accelerated as the flux increases until point B is reached where they are caused to deviate from the equilibrium orbit by either of the two following means: (1) the center of the pole is allowed to saturate with the result that $2H_0$ increases faster than $\phi/\pi r_0^2$ so that r_0 becomes smaller and the electrons spiral in until they strike a target, such as A in Figure 3; or (2) a pulse of current is sent through a turn of wire on each pole face in such a direction that the flux caused so upsets the equilibrium condition

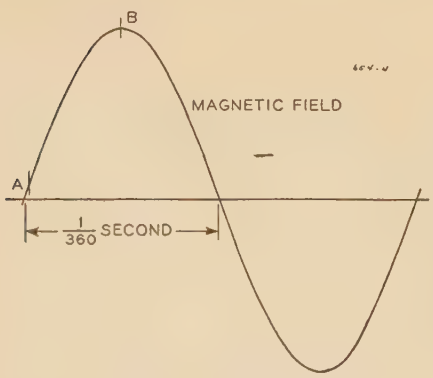

Figure 4. Flux wave

that r_0 becomes larger causing the electrons to spiral out and strike a target (B in Figure 3) mounted on the back of the injector. Kerst, in his original machine, used the first method as it is simpler and does not require a carefully timed electronic tube circuit as does the beam expansion method.

The Production of X Rays

When the high energy electrons strike the target, X rays are produced, the greatest intensity of which emerge from the donut in a narrow cone in the direction which the electrons are traveling at that time. As the conversion of the kinetic energy of the electrons to X rays is higher for high energies than low (theoretically 65 per cent of the electron energy is converted to X rays at 20 million electron volts as compared to a few per cent at 1 million electron volts) very little of the energy is absorbed by the target, so that the target remains relatively cold and does not deteriorate with use.

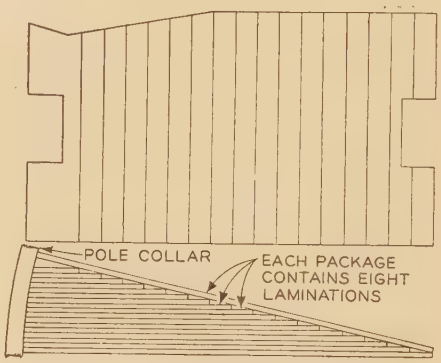

Figure 5. Details of pole laminations

Development

After successfully operating his first betatron which had a maximum energy of 2.3 million electron volts, Kerst was granted a leave of absence from the University of Illinois to supervise the construction of a 20-million-electron-volt betatron.[9] This betatron was loaned permanently to the University of Illinois for use under his direction. This and subsequent 20-million-electron-volt betatrons used expansion coils to cause the orbit to spiral out as this method results in higher maximum energy and higher X-ray output.

In order to determine whether or not the X radiation produced by the betatron was suitable for industrial use in thick section radiography, the Office of Scientific Research and Development appointed Kerst as official investigator and allotted funds for the work. When the investigation showed that the 20-million-electron-volt betatron could be used to great advantage in thick section radiography, OSRD authorized and financed the further work necessary to develop the betatron for industrial use, including the building of one machine. Kerst and his staff from the University of Illinois then obtained the co-operation of the Allis-Chalmers Manufacturing Company in this development in order to make the betatron available to war projects. The general details, such as size of pole and dimensions of yoke, are practically the same as described by Kerst with the major improvement being made in the mechanical construction of the betatron, and in the development of the donut.

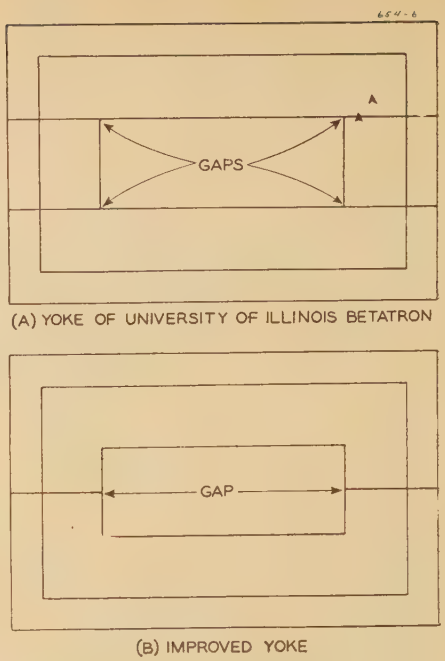

Figure 6. Betatron yoke

One of the major improvements made in this development was in the improved construction of the pole. The simplest way to construct a radially symmetrical pole is by making pie-shaped sectors of various lengths as shown in Figure 5 with several sectors making a complete pole. In the first 20-million-electron-volt betatron, these laminations were held together by a thermal setting resin which proved in operation that it was not strong enough to hold against the magnetic forces present, and gradually the pole developed short circuits until the beam was disrupted and the X-ray yield materially decreased. By careful welding and insulating, a very rigid pole was constructed. One set of these poles has been installed on the University of Illinois machine for over a year, and has been operated as many hours as

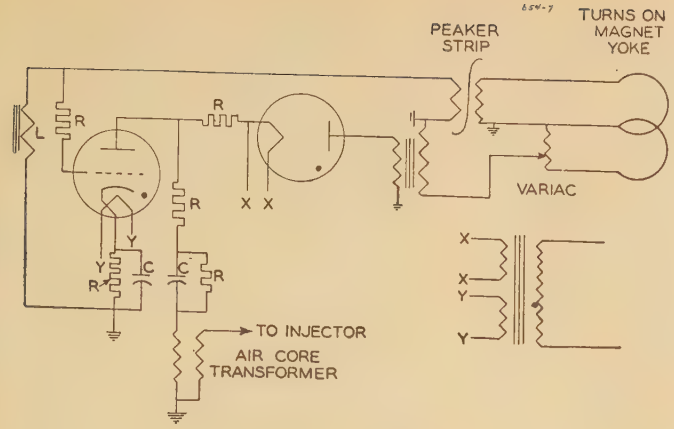

Figure 7. Injector circuit

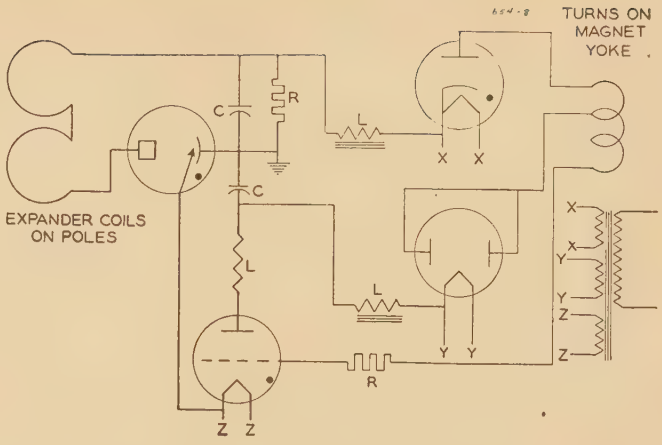

Figure 8. Expander circuit

the original set, but shows no signs of going bad. In fact, the yield is now higher than ever was obtained with the original machine. Also, the pole laminations were cut on a die which assured a very smooth and radially symmetrical pole.

The coils on the commercial machine are held very rigidly in place and air ducts provided to aid in cooling. Because of the high leakage flux caused by the air gap for the accelerating field, the turns must be stranded with each strand insulated from all others by Formvar varnish and all layers wound in the same direction in order to keep induced voltages and eddy currents at a minimum.

The yoke on the University of Illinois machine was made in four pieces as shown in Figure 6A with only the weight of the steel holding them in place. By assembling in two halves as shown in Figure 6B, a much better construction was possible, and by the use of guide rods, the alignment of the poles could be made at the time of assembly with the assurance that the poles could be separated for installation of a donut and the alignment would always be the same. Then, by installing lifting jacks operated by a gear motor with chain and sprocket system the top half of the betatron could be lifted without the use of an auxiliary hoist. The construction of the yoke in two halves also will simplify the clamping necessary to make possible the mounting of the betatron for rotation of the beam should it be desired.

One of the most interesting developments made was in the manufacture of donuts. The first donuts made for the University of Illinois 20-million-electron-volt machine consisted of two short glass cylinders forming the outer and inner wall with two glass washers forming the top and bottom. These glass parts were waxed together with tubes waxed on to hold the injector and for the pump stem. The sections of glass forming the inner surface of the donut had to be sand blasted so that a suitable conducting coating could be applied. The coating was necessary so that the stray electrons not captured by the beam and striking the donut walls would be drained off and would not be allowed to build up static charges which would disturb the beam; and, at the same time, the coat must be of high enough resistance that the eddy currents induced would not disturb the beam or heat the donut too much. The main trouble with the waxed donut was that the tube could not be evacuated and then sealed off, necessitating a pumping system. Also, owing to the heat generated by the injector filament, it was necessary to blow air on the wax close to the injector stem to prevent softening of the wax with resulting leaks.

To solve the donut problems, the Ceramic Engineering Department at the University of Illinois, under a contract with OSRD, was able to develop a porcelain which was capable of having glass sealed to it and was vacuum tight. Moreover, this porcelain donut could be made by coreless casting which resulted in a fairly inexpensive product. Some development was necessary in order to coat the inside of this tube and make the glass seals, but the difficulties were overcome and donuts were produced, evacuated, and sealed-off which have been giving very satisfactory service. This resulted in the elimination of a high-vacuum pumping system on the betatron which would have been the cause of much trouble in the successful operation of betatrons in industrial radiography.

A study was made of the injector and the design and structure were improved

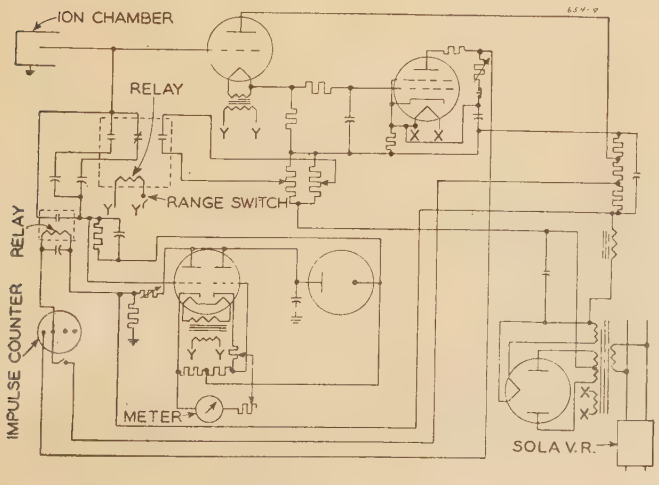

Figure 9. Exposure control circuit

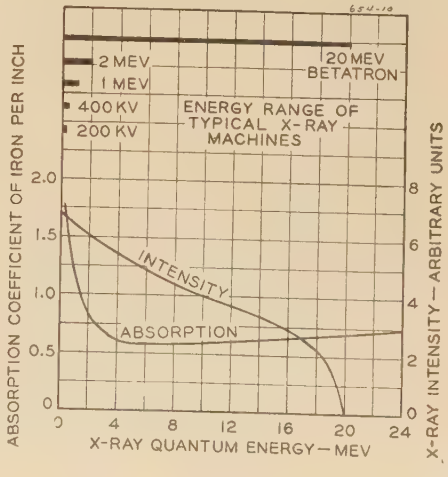

Figure 10 (right). Absorption curve for steel and theoretical X-ray spectrum at 20 million electron volts

so that an increased yield was realized. The injector, which is an electron gun, should not have too large a distance between the filament and the part of the injector closest to the orbit so that as many electrons as possible will miss the injector on successive revolutions, and be captured by the orbit. In addition, the injector must be sufficiently rigid so the vibration caused by the alternating magnetic field will not shake it apart.

The target developed made possible a focal spot of the order of 0.010 inch high. This small focal spot is one of the outstanding features of the successful betatron. If the electrons hit the back of the injector with no special target, the focal spot will be of the order of 0.050 inch high. The width in both cases is so small as not to be measurable. Calculations have been made which show that the difference in successive revolutions of the electrons as they spiral out is of the order of 10^{-4} centimeter so the width of the focal spot should be of the same order.

The circuits of producing the injection and expansion pulses described in Kerst's paper[9] were improved with the idea of providing a more satisfactory unit for industrial use. For example, all batteries were eliminated and tubes were replaced by others having more reliable operating characteristics to reduce to a minimum the variables for obtaining maximum yield. The present injector and expander circuits are shown in Figures 7 and 8, respectively. A very convenient additional circuit is the exposure control circuit (Figure 9) whereby the exposure in Roentgen units can be set on an impulse counter and the betatron will be shut off when it has produced the required amount of X rays.

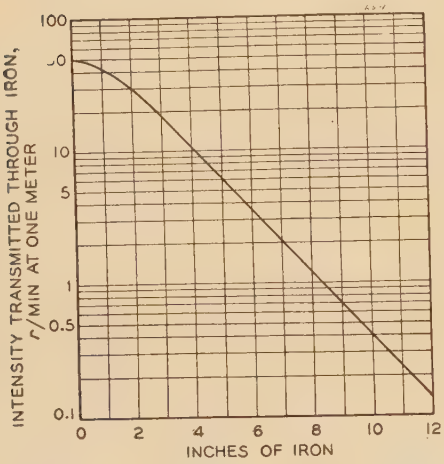

Figure 11. Transmission curve for steel at 20 million electron volts

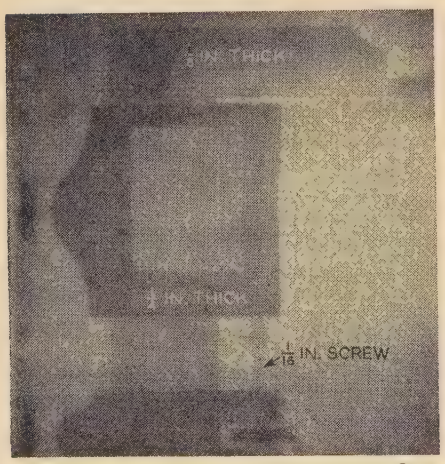

Figure 12. Radiograph of vernier caliper between two one-inch slabs of steel with jaws open 0.010 inch

Enlargement on negative was 3.3

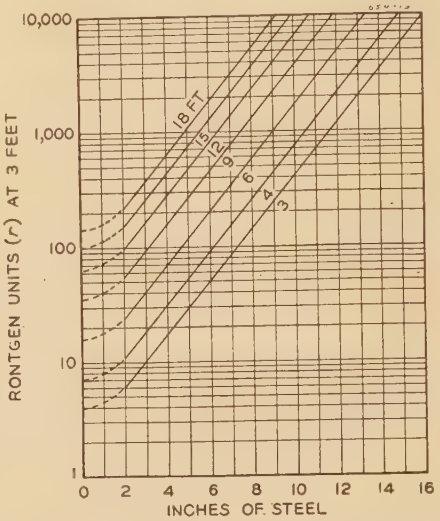

Figure 13. Exposure chart for 20-million-electron-volt X rays with Eastman industrial film, type A, 0.040-inch front lead screen, density of 2

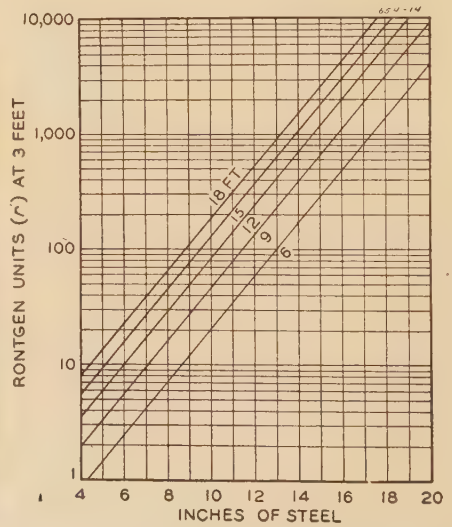

Figure 14. Exposure chart for 20-million-electron-volt X rays with Eastman industrial film, type F, 0.030-inch front lead and special intensifying screens, density of 2

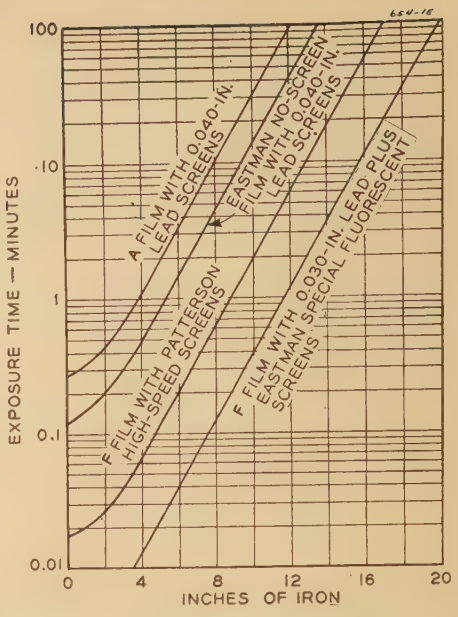

Figure 15. Chart showing comparison of different films and screens

Radiography

The betatron makes possible the radiography of thick section steel, bronze, and other heavy metals. In Figure 10 the absorption coefficient curve for iron is shown together with the theoretical intensity distribution spectrum of X rays produced by the 20-million-electron-volt betatron. From these two curves, one can see that most of the X rays produced are in the region of low absorption of steel (the absorption curves for other heavy metals are similar). In other words, the X rays in the approximate range of from 3 to 20 million electron volts are the most penetrating, and the absorption curve is nearly constant over this range which is the region of most of the X rays produced by the 20-million-electron-volt betatron. This explains the straight line transmission curve shown in Figure 11 after one or two inches of steel.

Another factor influencing the selection of 20 million electron volts as the best energy for thick-section radiography was that by going to higher energies the secondary X rays produced as a result of the absorption of the primary rays would be more penetrating than the primary rays and tend to result in a diffused image. This fact can be explained by an analysis of X-ray absorption. Unfortunately, the absorption of X rays above one million electron volt generally results in the production of electron pairs with each electron of the pair produced having on the

Figure 16. Section of radiograph of Ford model T motor. Note the damaged valve stem

average nearly one half the energy of the primary ray. These high-energy electrons lose their energy with the accompanying production of X rays which, because of the lower energy, may be more penetrating than the primary rays. The secondary rays travel in the general direction of the primary, but there is some divergence which affects the definition on the film. The 20-million-electron-volt betatron tests show that a comparatively small part of the density on the film is caused by secondary rays. With higher energy betatrons, tertiary, and higher order X rays would be produced which would be more divergent and penetrating than the secondary rays and, therefore, would produce a more diffuse image on the film.

The choice of a lower energy betatron was eliminated as the intensity for different energies at the same frequency goes as nearly the fourth power of the energy. At 10 million electron volts and 180 cycles the intensity would be 1/15 that at 20. This would necessitate a much higher frequency which would mean increased heating and higher power requirements. The heating would necessitate liquid cooling and the advantage of a lower weight machine at lower energies partially would be lost. At a lower energy output a smaller percentage of the X rays would be in the region of low absorption so that the exposure would be much longer for the same intensity. Tests at 10 million electron volts show that the fraction of density on the film contributed by the secondary rays is considerably larger than that at 20 million electron volts.

Another advantage of 20-million-electron-volt X rays is that an absolute sensitivity is obtained. This means that the size of minimum detectable flaw is the same regardless of the thickness of steel being radiographed. A 1/32-inch flaw was displayed with equal clarity through various thicknesses of steel from 2 to 12 inches on Eastman type *A* film.

In 20-million-electron-volt radiography, no blocking is necessary for variations in thickness of the specimen or around the outline. In fact, outlines may be less well defined when blocking is used.

Because the large angle of back-scattered radiation is detrimental to the image, no lead is placed behind the film. A thickness of 0.040 inch is used in front of the film for the best results. Thicknesses of from 0.010 to 0.020 inch will result in about 50 per cent more density for a given exposure, but the detail will be less clear so that it is not recommended.

The great penetration of 20-million-electron-volt X rays makes possible the study of great variations of thickness on the same radiograph. Radiographs have been taken on which differences of thickness of over six inches of steel were examined. The penetration of these X rays implies that it is difficult to detect small flaws in specimens of low density or small atomic number.

The small focal spot inherent with the betatron and not with other X-ray machines is nearly the ideal point source. The natural focal spot is 0.050 inch high and less than 0.005 inch wide. By using a special target which was developed, the height is reduced to 0.010 inch. This focal spot makes possible the enlargement of the specimen on the radiograph by increasing the specimen-to-film distance. Figure 12 shows a radiograph of a vernier caliper between two 1-inch slabs of steel with the jaws open to 0.010 inch. With a magnification of 3.3 this opening could be seen.

Figures 13 and 14 show exposure charts based on different films and screens. The exposure is given in Roentgen units *r* and on the basis that the industrial units built have given about 75 *r* per minute, the exposure times can be calculated. Figure 15 gives a comparison between different films and screens.

With the pronounced beaming of the X rays (characteristic of high energy radiation) for full utilization of the film, a good rule in the taking of radiographs is to have the target to film distance at least five times the major dimension of the film.

To show the latitude and detail of 20-million-electron-volt radiographs, Figure 16 is a radiograph of a section of a model T Ford engine. Figure 17 is a radiograph of a steel forging which showed defects that could not be determined otherwise except by very long exposures or machining and testing.

The betatron has increased to at least

Figure 17. Section of radiograph of steel forging revealing a flaw

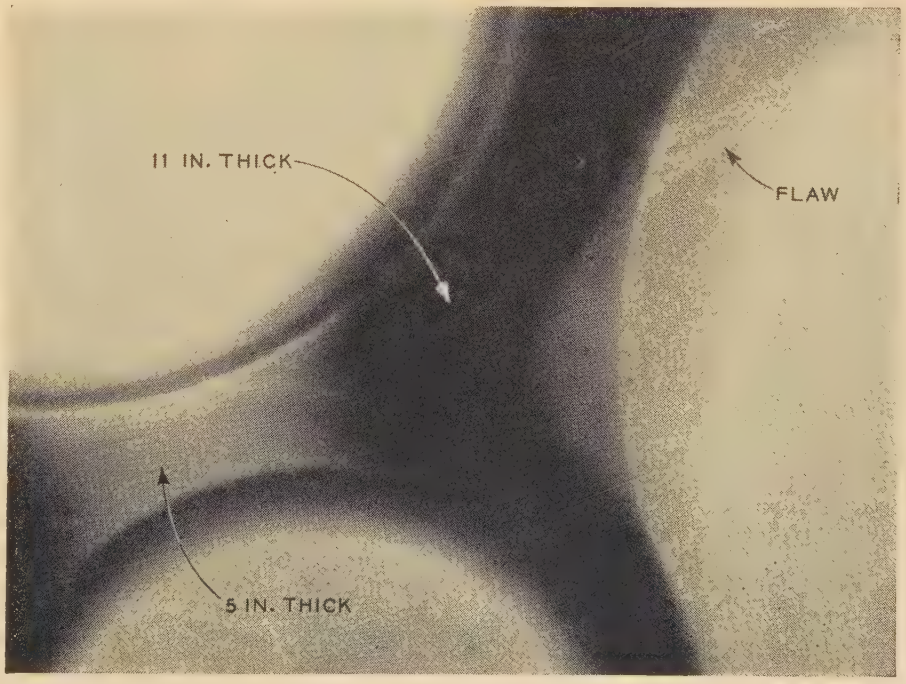

Application and Performance of Electronic Exciters for Large A-C Generators

H. A. P. LANGSTAFF
FELLOW AIEE

H. R. VAUGHAN
MEMBER AIEE

R. F. LAWRENCE
ASSOCIATE AIEE

Synopsis: Power rectifiers have proved themselves as efficient and reliable converters of a-c to d-c power for many industrial applications. They also have been used to a limited extent as exciters for synchronous motors and condensers. This paper discusses the requirements of rectifiers when used to excite large a-c generators and presents the results of tests made to determine performance under various operating conditions. The results cover preliminary tests that were made on a laboratory model in addition to extensive and more complete tests on an electronic exciter now installed in the Springdale generating station of the West Penn Power Company. The electronic exciter was designed to serve eventually as the main exciter for an 81,250-kva 3,600-rpm turbine generator just installed, but it is now supplying excitation to a 47,100-kva 1,800-rpm turbine generator. Switching arrangements are provided for exciting either unit from the electronic exciter or from an existing motor-driven exciter.

SINCE the introduction of the metal-tank type of power rectifier, particularly the single-anode type,[1] the application of rectifiers in the field of power conversion has expanded to include practically every type of industry that requires d-c power.[2] Years of experience with many thousands of kilowatts of installed capacity testify to their reliability and efficient performance. With this background of usage, power rectifiers naturally have received consideration as exciters for rotating machines. A limited number have been used to excite synchronous motors, synchronous condensers, and one or two small generators. However, there has been a hesitancy in applying them as exciters for large a-c generators because of a natural reluctance to risk anything that might jeopardize the reliability or performance of a machine as important as a large a-c generator.

Rotating exciters have been used with success for many years, whereas the ability of a power rectifier to meet the exacting requirements of a power station generator has not been demonstrated by operating experience. It is the purpose of this paper, therefore, to discuss the application of electronic exciters to large a-c generators, to present the results of comprehensive tests that were made to demonstrate the performance of an electronic exciter under severe operating conditions, and to describe an actual installation.

Paper 46-74, recommended by the AIEE committee on power generation for presentation at the AIEE winter convention, New York, N. Y., January 21–25, 1946. Manuscript submitted November 21, 1945; made available for printing December 11, 1945.

H. A. P. LANGSTAFF is with West Penn Power Company, Pittsburgh, Pa.; H. R. VAUGHAN and R. F. LAWRENCE are central station engineers with Westinghouse Electric Corporation, East Pittsburgh, Pa.

Requirements

Large generators for power systems are capable of operating and are expected to operate months at a time without shutdown. They must maintain constant supply voltage under varying load conditions and must recover rapidly from disturbances caused by severe load fluctuations or system faults. The degree to which the generator meets these conditions depends in a large measure on the performance of its exciter, which must fulfill the following requirements:

1. It must be dependable and capable of operating without shutdown over long periods of time.
2. It should lend itself to ease of maintenance so that wearing parts can be maintained, tested, or replaced without shutting down the unit.
3. It must be capable of providing the required excitation during system disturbances when the generator may be called upon to supply a high reactive current output.
4. It must be capable of operating over a broad range of d-c voltage, from generator no-load to maximum output. Momentary values of field current considerably greater than full-load magnitude may be required.
5. It must respond rapidly to high excita-

---

20 inches, the thickness of steel and other heavy materials which can be radiographed satisfactorily, the maximum thickness depending on the minimum flaw to be detected or the detail desired.

Other Possible Uses

Any new X-ray machine is considered for its possible application to medical therapy. As the main development has been in producing a machine for industrial radiography, little time has been devoted to studying possible therapeutical application. However, one paper[10] has been published demonstrating the advantages of 20-million-electron-volt X rays and theory indicates that if the electron beam can be brought out of the donut, it would be more useful than the X rays. Both the 20-million-electron-volt X rays and electrons may be powerful weapons for the therapy of deep seated cancer.

From present indication, higher energy betatrons apparently would have no advantages in industrial radiography and their main use would probably be in connection with nuclear research. At the present time, Doctor Kerst is planning the construction of a betatron capable of producing at least 250-million-electron-volt X rays. Such a machine would enable physicists to produce radiation of cosmic ray energies in the laboratory.

References

1. United States patent 1,645,304, **J. Slepian.** October 11, 1927.

2. **R. Wideroe,** *Archiv für Elektrotechnik*, volume 21, 1928, page 387.

3. **E. T. S. Walton,** *Proceedings* of the Cambridge Philosophical Society, volume 25, 1929, page 469.

4. United States patent 2,103,303, **M. Steenbeck.** December 28, 1937.

5. ELECTRON ORBITS IN INDUCTION ACCELERATOR, **D. W. Kerst, R. Serber.** *Physical Review*, volume 60, July 1, 1941, pages 53–8.

6. ACCELERATION OF ELECTRONS BY MAGNETIC INDUCTION, **D. W. Kerst.** *Physical Review*, volume 58, 1940, page 841.

7. **D. W. Kerst.** *Physical Review*, volume 59, 1941, page 110.

8. ACCELERATION OF ELECTRONS BY MAGNETIC INDUCTION, **D. W. Kerst.** *Physical Review*, volume 60, July 1, 1941, pages 47–53.

9. 20 MEV BETATRON OR INDUCTION ACCELERATOR, **D. W. Kerst.** *Review of Scientific Instruments*, volume 13, 1942, pages 387–94.

10. EXPERIMENTAL DEPTH DOSE FOR 5, 10, 15 AND 20-MILLION-VOLT X-RAYS, **H. W. Koch, D. W. Kerst, P. Morrison.** *Radiology*, volume 40, February 1943, pages 120–6.

tion requirements, particularly where system stability is to be reckoned with.

6. It must be simple in structure and operation so that it does not complicate the over-all operation of the generating unit.

7. The cost, if higher, must be justified by advantages over other available methods of excitation.

Application Problems

An electronic exciter consists essentially of a power rectifier fed from an a-c source of power and provided with the necessary control, protective, and regulating equipment. The co-ordination of these component parts presents certain problems which must be dealt with in meeting the excitation requirements of large a-c generators.

A-C Power Supply

The rectifier may be self-excited, that is, its source of a-c power taken from the terminals of the a-c generator to which it is supplying excitation, or it may be excited separately, with its a-c power supplied from a separate source. Self-excitation makes possible unit operation with no dependence on a separate source of power for excitation. At the same time, it requires no rotating machine. However, it differs from a direct-connected rotating exciter in performance in that its output is affected by voltage dips at the generator caused by disturbances on the a-c system. The d-c ceiling voltage of the electronic exciter would decrease in proportion to the a-c voltage at a time when overexcitation is actually required by the generator. This may be compensated for in two ways. One way is to provide the rectifier with an abnormally high d-c ceiling voltage with full a-c voltage applied so that when the a-c voltage drops, the necessary d-c ceiling voltage still is obtainable. During normal operation, the d-c voltage would be reduced to normal by firing delay in the rectifier. It means a rectifier transformer somewhat larger than normal and a higher angle of firing delay during normal operation of the rectifier.

The second way to compensate for drops in a-c voltage is to provide series compensators to maintain a-c voltage on the rectifier transformer during momentary system disturbances. The primary of each of the compensators would be connected in series with one phase of the generator armature. The secondaries would be connected in series with the leads to the rectifier transformer so as to boost the a-c voltage supplied to the rectifier transformer in proportion to the reactive current fed from the generator. Either method of compensation is practical.

Separate excitation of the electronic exciter requires a reliable source of a-c power such as a separate station auxiliary generator or an auxiliary generator mechanically connected to the shaft of the main generator.

If used to supply power to the electronic exciter only, the shaft generator could be designed to feed the rectifier directly without an interposing rectifier transformer. This scheme would be comparable to a direct-connected exciter from the standpoint of being independent of system disturbances.

If the electronic exciter is self-excited, a means of supplying partial excitation during the starting-up period must be provided to get the machine up to voltage. Tests have shown that a d-c voltage of approximately 15 per cent of rated field voltage at full load applied to the field of the main generator, will start firing of the rectifier and cause it to build up voltage. This primer d-c voltage may be supplied from a small motor-generator set or from a battery connected to the generator field in parallel with the rectifier during the starting period. The motor-generator set or battery may be switched off automatically when the rectifier starts firing, by means of a reverse-current d-c relay set to detect feedback into the motor-generator set or battery.

Co-ordination of Protective Devices

The usual complement of rectifier protective devices should be included with an electronic exciter to protect against arc-back, misfiring, loss of cooling water, and so forth. Anode circuit breakers should be provided to clear an arc back on one or two phases without interrupting the d-c output of the rectifier and also to permit isolating one or more of the anodes for maintenance without interfering with the operation of the others. Three 2-pole anode breakers, one for each pair of diametrically opposite phases of a 6-phase rectifier, normally would fulfill these requirements. The cathode breaker should not have overload protection.

The rectifier transformer normally would be connected to its a-c power source through a circuit breaker or through fuses to protect against an internal short circuit. Whichever device is used must be selected so that it will not operate on heavy exciter overloads or clear ahead of the anode breakers on arc-back.

Regulation

The output voltage of an ignitron can be varied over a broad range by controlling the point on the a-c voltage wave at which firing occurs. This control can be

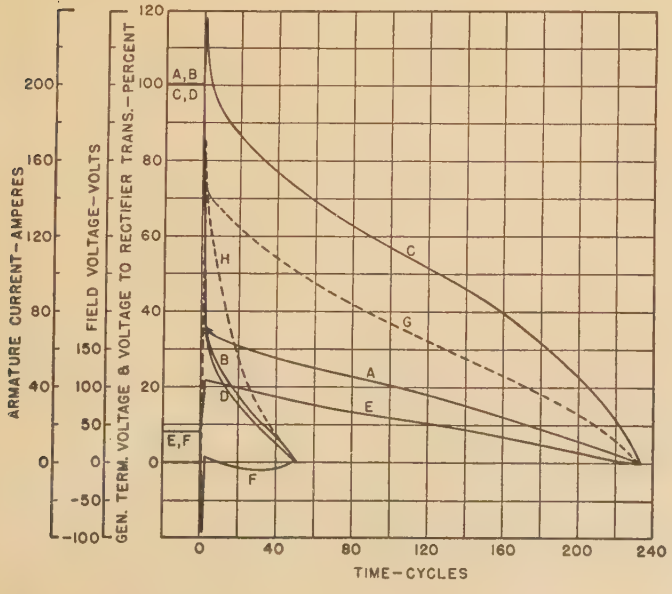

Figure 1. Three-phase fault applied on 100-kva generator through 12 per cent external reactance with generator self-excited

A, B—Terminal voltage, with and without compensator
C, D—Voltage to the rectifier transformer, with and without compensator
E, F—Field voltage, with and without compensator
G, H—Armature current, with and without compensator

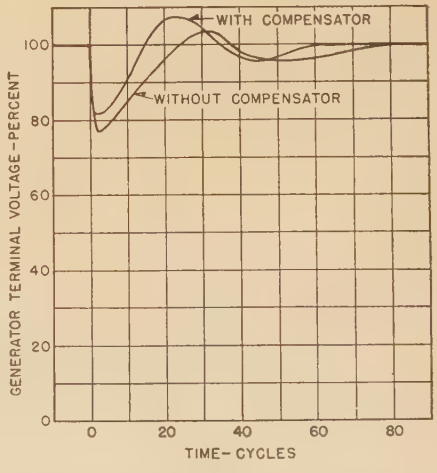

Figure 2. Application of 100 per cent reactive load on 100-kva generator, self-excited, with and without compensator

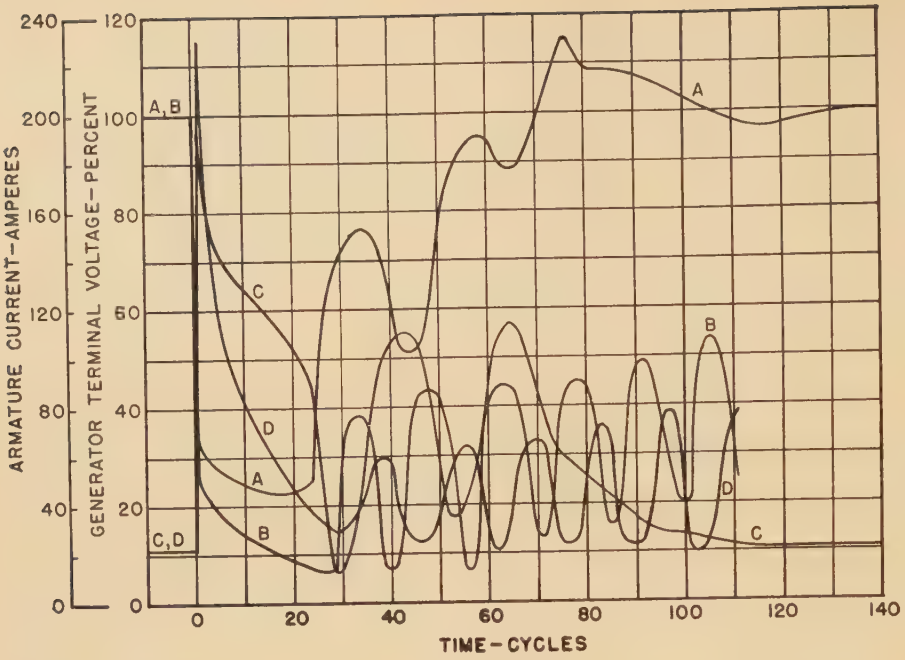

Figure 3. Three-phase fault applied one-third of electrical distance from 100-kva generator to motor, with generator supplying 40 kw at unity power factor through 22.7 reactance between generator and motor

A, B—Terminal voltage, with and without compensator

C, D—Armature current, with and without compensator

made broad enough to cover the full operating range of the generator without the necessity of a generator field rheostat. It can be accomplished automatically with a voltage regulator responsive to the terminal voltage of the a-c generator. Since the regulator controls only the firing circuit, it can be a low-energy device. No large rheostats or resistors are necessary.

The ability of an electronic exciter to build up to its ceiling voltage practically instantaneously makes it well suited where high speed of response excitation is necessary. However, this high rate of response is conducive to regulator hunting, which must be given particular attention in the design of the regulator.

Effect on Fault Current and System Relaying

The effect of an electronic exciter on the short-circuit current of an a-c generator depends on the duration of the fault, the impedance to the point of fault, and on how the electronic exciter is excited. The fault current during the subtransient period, about the first three cycles, is the same regardless of the type of exciter that is used. If the electronic exciter is excited separately, the transient fault current and the sustained current are the same as with a rotating exciter for operation without a voltage regulator. For operation with a voltage regulator, the transient current is somewhat higher with the electronic exciter on account of its faster response. The sustained currents would be proportional to the ceiling voltages of the two exciters.

A self-excited electronic exciter with a series compensator designed to maintain a-c voltage on the rectifier during the transient period would result in about the same transient current as a separately excited electronic exciter with or without regulator operation. However, the sustained current would be proportional to the generator terminal voltage and would drop to zero if the fault were close by so that the terminal voltage dropped too low to sustain firing of the rectifier.

A self-excited electronic exciter without a series compensator and without regulator operation would cause the fault current to drop rapidly to zero if the fault impedance were low. With regulator operation and with the exciter provided with a high ceiling voltage to compensate for drop in a-c voltage, the transient current would be essentially the same as with a separately excited electronic exciter or a rotating exciter. The sustained current still would collapse to zero if the fault impedance were low.

From the above, it can be reasoned that an electronic exciter would have little or no effect on modern high-speed relays that operate in the first few cycles following a fault. The decay of fault current for low impedance faults of long duration with a self-excited electronic exciter should be taken into consideration in its effect on relay operation. It is, in general, desirable to boost or at least maintain excitation during a system fault to prevent generator instability and to hasten recovery to normal voltage after the fault is cleared. However, prolonged high excitation is undesirable where the fault is of low impedance and in a location that cannot be cleared, such as an unprotected bus. A self-excited electronic exciter would cause the fault current to collapse following the transient period and thereby make the generator self-protecting. If desired, the generator voltage could be restored after the fault was cleared by automatically applying the primer voltage to the field to start firing of the rectifier.

Figure 4. West Penn Power Company's Springdale Power Station exciter system and auxiliary power sources

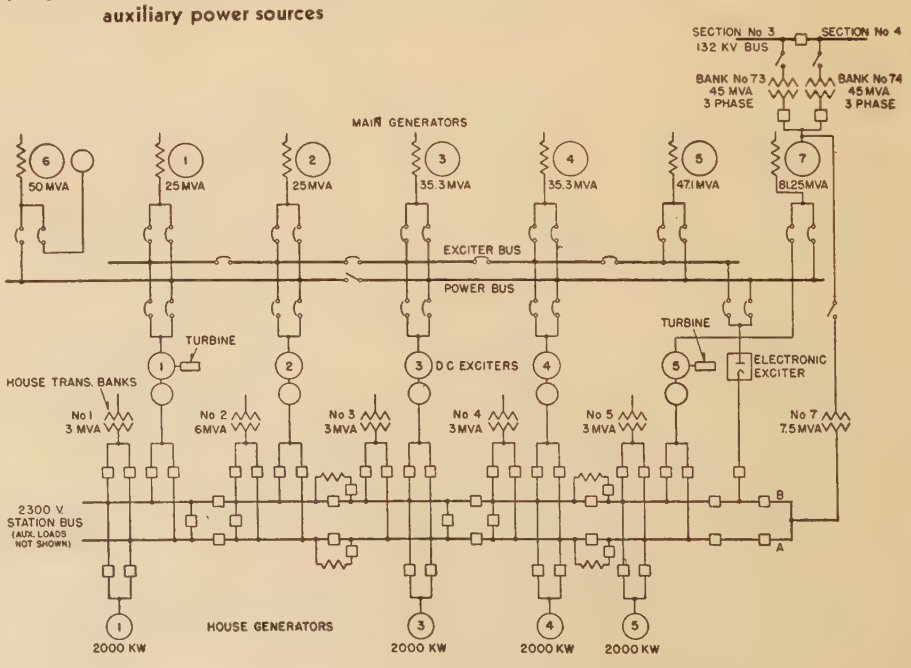

Tests on Laboratory Model

A laboratory model of an electronic exciter was built and tested in order to obtain fundamental data which would be a guide in the basic design of a large exciter and also to determine the effectiveness of a series compensator. This exciter consisted essentially of a rectifier transformer, six thyratron tubes, a grid transformer, and a direct-acting voltage regulator. It supplied excitation to a 100-kva 1,150-volt 1,200-rpm 3-phase synchronous generator. An auxiliary transformer was provided to transform the generator voltage to 230 volts for the rectifier transformer, the grid transformer, and the d-c grid bias circuit. The voltage regulator was used to regulate the generator terminal voltage by controlling the d-c grid bias voltage and consequently the firing of the thyratron tubes. This method of voltage control is the same as that used on the large electronic exciter discussed later.

Series compensators were provided, each consisting of three current transformers connected in series per phase with a reactor across the three secondary windings. The primaries of the compensators were connected in series with the generator armature leads; the secondaries were connected in series with the leads to the auxiliary transformer. The compensators were connected to boost the voltage to the auxiliary transformer with lagging reactive current flow from the generator. They were designed to give 100 per cent voltage compensation with 200 amperes in the primary.

Description of Tests

The tests consisted essentially of load changes, application of faults, steady state and transient stability, transfer of excitation, and build-up of generator terminal voltage. All references to "per cent applied load" mean that the load is zero power factor lagging and is expressed as a percentage of full-load kilovolt-ampere rating of the generator. A total of 28 tests was run with oscillograms taken for each test. The generator field current and voltage, armature current, terminal voltage, the voltage to the rectifier transformer, and the d-c grid bias voltage were recorded. Reactive loads ranging from 25 to 200 per cent were applied and dropped. Three-phase and line-to-line faults were applied through approximately 12 per cent reactance on a 100-kva base. Steady-state stability tests were run with the generator connected directly to a synchronous motor load. For transient stability tests, the generator and motor were connected together through 22.7 per cent reactance on a 100-kva base, and 3-phase and line-to-line faults were applied for about one-half second at a point one-third of the electrical distance between the generator and the load. The generator was carrying 40 kw at unity power factor. All of the tests were made with and without the compensator.

Test Results

Meter readings recorded under steady-state conditions show that the compensator boosted the voltage to the rectifier. With no compensator, the voltage to the rectifier transformer was constant for a change in generator load (80 per cent power factor) from zero to 100 per cent; with the compensator in, this voltage was about 87 per cent at no load because of the drop through the compensator. However, with an increase in load, it increased because of the boost from the compensator. At approximately 75 per cent load on the generator, it was 100 per cent and at full load was 106 per cent. At no load the angle of firing delay without the compensator was higher than with the compensator because more voltage was available to the rectifier transformer; at full load the angle of delay without the compensator was lower than with the compensator because less voltage was available to the rectifier transformer. In other words, for a change from no load to full load at a given power factor, the compensator has a regulating effect on the generator voltage with the angle of delay tending to remain more nearly constant than without the compensator.

With the generator self-excited, severe faults of long duration caused the terminal voltage and consequently the excitation to decay to zero. The faults were intentionally not cleared until after the terminal voltage had decayed to zero. As shown in Figure 1, the compensator maintains the terminal voltage approximately five times as long as without it. The compensator boosted the voltage to the rectifier transformer to approximately 113 per cent for a 3-phase fault. With an initial current of 150 amperes at two cycles, the voltage to the rectifier was boosted 77 per cent. This is equivalent to a 103-per-cent boost at 200 amperes. The decay of the armature current during the subtransient period is the same with or without the compensator. From three cycles on, the decay is much more rapid without the compensator.

Figure 2 shows terminal voltage versus time for the application of 100 per cent reactive load with and without the compensator. With the compensator the maximum voltage drop is decreased 4.5 per cent, and the generator terminal voltage is returned to 100 per cent on the first

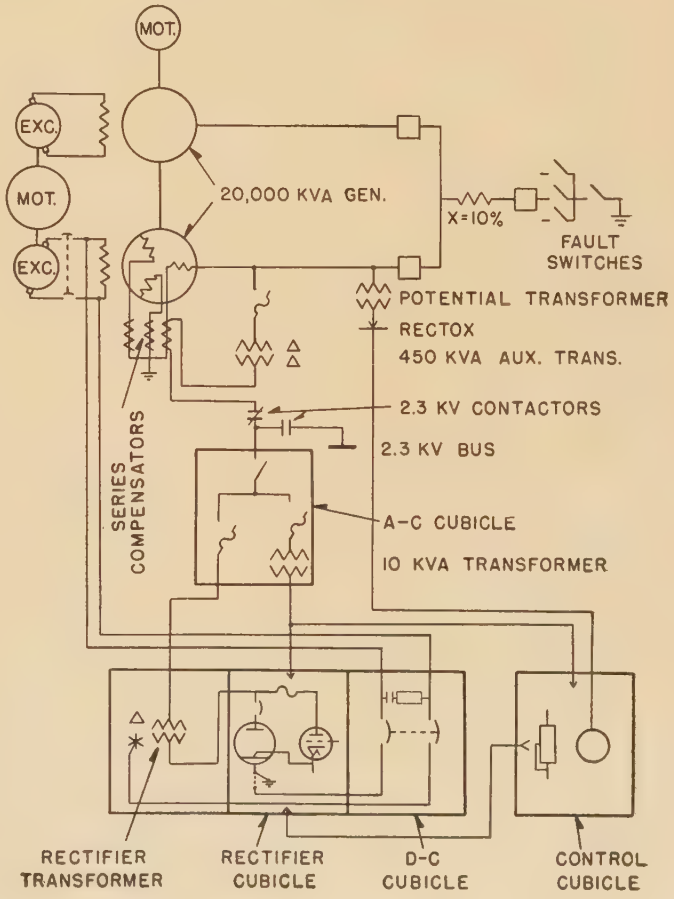

Figure 5. Schematic diagram of electronic exciter test setup in one of the a-c high-power laboratories

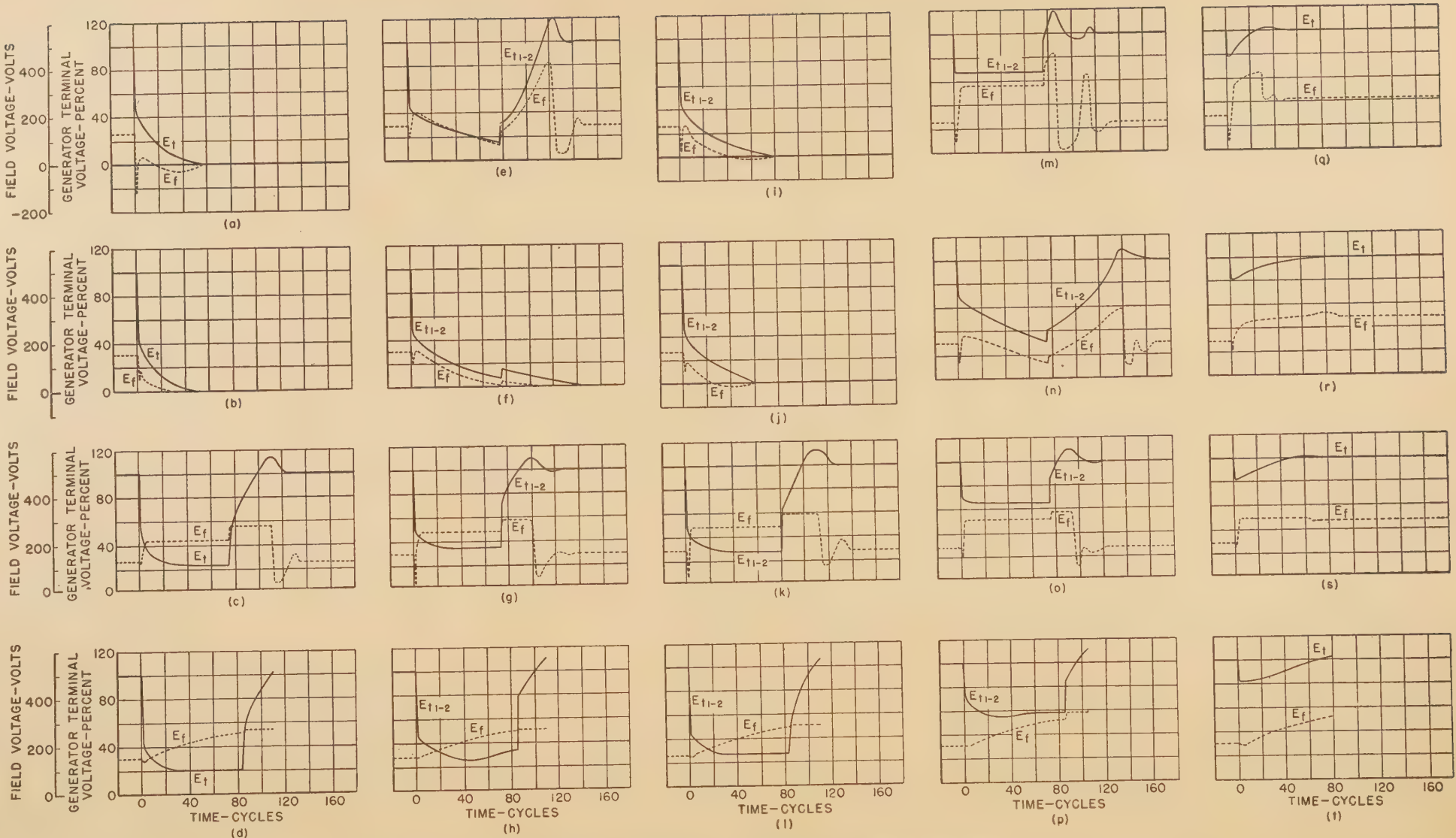

Figure 6. Curves of terminal and field voltage for application of faults through approximately ten per cent external reactance and load changes on 20,000-kva generator

a, b, c, d—Three-phase faults for conditions 1, 2, 3, and 5, respectively
e, f, g, h—Line-to-line faults on phases 1 and 2 for conditions 1, 2, 3, and 5, respectively
i, j, k, l—Double line-to-ground faults on phases 1 and 2 for conditions 1, 2, 3, and 5, respectively
m, n, o, p—Single line-to-ground faults on phase 1 for conditions 1, 2, 3, and 5, respectively
q, r, s, t—Application of 60 per cent reactive load for conditions 1, 2, 3, and 5, respectively

overshoot, ten cycles sooner than without the compensator. The terminal voltage ultimately is returned to normal in about 65 cycles with the compensator, compared with 80 cycles without the compensator.

A comparison of the transient stability characteristics of the generator with and without a series compensator is shown in Figure 3. Without the compensator the generator pulled out of step and did not regain synchronism. However, with the compensator, synchronism was not lost and the terminal voltage returned to a constant value in 111 cycles after the fault was cleared.

Application to West Penn Power Company System

The Springdale generating station includes five 1,800-rpm turbine generators excited from motor and dual-driven exciters with switching for exciting any generator from any exciter through excitation busses. There is one 3,600-rpm 50,000-kva high pressure unit with a direct-connected exciter.

The new number 7 unit, rated 81,250 kva 3,600 rpm, is practically a separate station electrically, with no paralleling of circuits other than at 132 kv. Only a few of the auxiliaries for this unit are supplied from the existing 2,300-volt auxiliary bus. A shutdown would therefore be very costly.

In order to eliminate shutdown because of the possibility of exciter trouble which might require mechanical disconnection from the shaft of the main unit, a separate exciter source was decided upon, and an electronic type was selected. Initially, this exciter supplies excitation to one of the existing generators. The number 5 dual-driven exciter, supplied from either one of the existing 2,300-volt station auxiliary busses, supplies excitation to the number 7 unit. A pilot exciter was added to the shaft of this dual set. This was considered a reliable source of excitation because there has been no outage to these busses or to the dual set over a period of years. After sufficient operating experience is obtained with the electronic exciter on one of the older units, it will serve as the main exciter for the number 7 unit for which it originally was designed. Any one of the older generators can be excited from the electronic exciter or any of the station exciters as shown in Figure 4.

Table I. Characteristics of Generators

	Laboratory Test Generator	Springdale Station No. 7 Generator
Generator rating	20,000 kva	81,250 kva
Normal rated voltage	6,600 volts	11,500 volts
Synchronous reactance, per unit	0.853	1.20
Transient reactance, $X_{d'\ sat}$, per unit	0.10	0.117
Negative-sequence reactance, X_2, per unit	0.10	0.073
Zero-sequence reactance, X_0, per unit	0.025	0.067
Open-circuit transient time constant T'_{d0}	3.2 sec	7.56 sec
Field resistance at 75° C.	0.145 ohm	0.234 ohm
No load field current	830 amp	400 amp
Full load 80% power factor field current	1,340 amp	800 amp

When the electronic exciter is used to excite the number 7 unit, it operates essentially self-excited, subject to drop in the terminal voltage of the generator. A 3-phase fault at the high-voltage terminals of the step-up transformers with the 132-kv bus tie breaker closed would cause the generator terminal voltage to drop instantly to approximately 50 per cent. Faults at other locations on the high-voltage system would result in less voltage drop.

The rectifier transformer was designed to give approximately 400 volts d-c ceiling with full a-c voltage applied, so as to assure excitation during fault periods. It also is provided with an extension to the high-voltage winding to give a ceiling d-c voltage of approximately 300 volts, which would correspond to a normal design to be operated either separately excited without a compensator or self-excited with a compensator. Both schemes of compensation were used in making the laboratory tests to be described later. The series compensators used in the tests proved inadequate for the compensation desired, so the exciter was installed to operate on the high-voltage taps without series compensators. Space is available for future installation of compensation and their connections if proved desirable.

Laboratory Tests on West Penn Power Company Exciter

Laboratory tests on the model proved the feasibility of an electronic exciter for excitation of a synchronous generator. They also showed that a series compensator could be designed which would be effective in maintaining voltage to the rectifier transformer during the transient period under fault conditions. In order to obtain complete performance data on the electronic exciter for the West Penn Power Company for operating conditions which might occur in service but which could not readily be staged on the actual installation, extensive tests were made on this exciter at the factory.

Table II. Estimated Maximum Fault Clearing Time to Permit Recovery of Generator Voltage

Type of Fault	Time in Cycles Condition 1	Condition 2	Condition 4
Three-phase	32	27	28
Line-to-line	78*	56	59
Double line-to-ground	47	34	38
Single line-to-ground	78**	75*	74*
Line-to-line fault with one anode breaker open	78*	49	57

*Fault was cleared at this time.

**Maximum fault clearing time is infinite.

The tests were made in one of the a-c high-power laboratories. A schematic diagram of the electronic exciter and the associated test apparatus is shown in Figure 5. The laboratory consists of a 3,300-horsepower motor driving two 20,000-kva generators which are synchronized mechanically so that their respective voltages are in phase A motor-driven dual exciter set is provided to furnish excitation to each generator. Switching arrangements are such that the two generators can be paralleled or one can be used alone. Facilities are available for applying any type of fault through an external reactance from zero to five ohms. Reactive load can be applied on either generator by paralleling it with the other underexcited.

The electronic exciter consists essentially of an a-c cubicle, an air-cooled rectifier transformer, a rectifier cubicle, a d-c cubicle, and a control cubicle, all shown schematically in Figure 5.

The voltage regulator and firing control circuits of this exciter and the model are the same. The thyratron tubes fire the ignitron tubes, whereas on the model they were used actually to supply power to the field circuit.

A 450-kva transformer bank transformed the generator terminal voltage to 2,300 volts to supply the rectifier transformer. Mechanically and electrically interlocked 2,300-volt contactors were provided so that power for the electronic exciter could be supplied from either the generator terminals or a separate source.

The series compensators, shown in Figure 5, were selected with the idea of boosting the a-c voltage applied to the rectifier transformer 50 per cent (625 volts per phase) with 25,000 amperes through a single-turn primary. This is the value of generator transient current that would result for a 3-phase fault on the high-voltage terminals of the transformers connected to the number 7 unit at Springdale. With the test generator connected

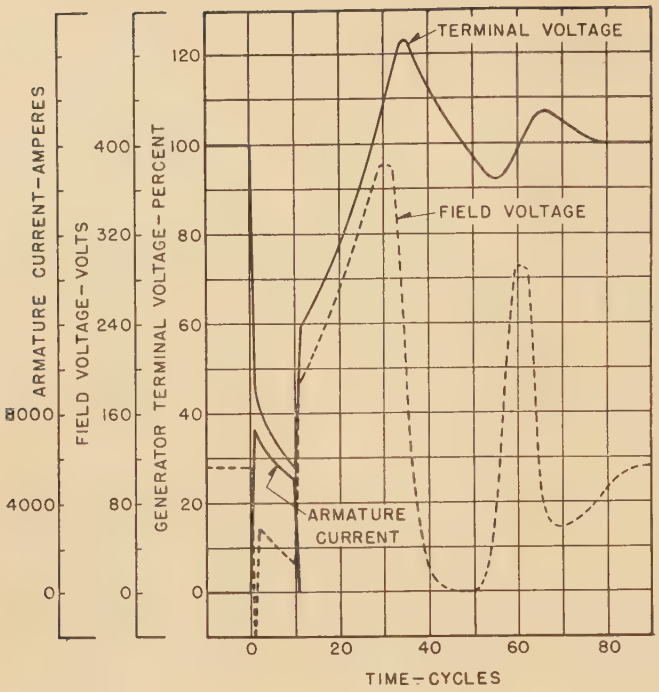

Figure 7. Three-phase 10-cycle fault applied on 20,000-kva generator through ten per cent external reactance. Generator was self-excited and rectifier transformer was on high-voltage tap

for 6,600 volts, line-to-line, the transient current for a 3-phase fault with 10 per cent (20,000-kva base) external reactance between the generator and fault is approximately 8,750 amperes. Therefore, one compensator was connected in the neutral leg of each phase of the generator with three loops through the primary to obtain the equivalent ampere turns of the actual installation. The generator neutral was grounded solidly to permit the application of ground faults.

The electrical characteristics of the test generator and the number 7 generator are compared in Table I. The full-load field voltage of the test generator during tests was about 15 per cent greater than the full-load field voltage on the number 7 generator at normal operating temperature. The full-load field current of the test generator is 1.67 times that of the number 7 generator. This, together with the smaller auxiliary transformer (450 kva compared with 7,500 kva), resulted in a higher d-c voltage regulation of the rectifier in the laboratory tests than in the actual installation. The shorter time constants of the test generator resulted in faster decay of voltages and currents during faults.

Description of Tests

The tests consisted essentially of the application of all types of faults, application and dropping of reactive load, changeover from self-excitation to separate excitation, simulated arc-backs and sympathetic arc-backs, and build-up of generator terminal voltage.

The tests were made under the five following conditions of excitation:

1. The rectifier transformer was connected on the high-voltage tap (approximately 400 volts d-c, no-load ceiling) and the compensators were not connected in the circuit. The generator was self-excited, that is, the supply to the rectifier transformer was taken from the generator terminals.

2. The rectifier transformer was connected on the low-voltage tap (approximately 300 volts d-c, no-load ceiling) and the compensators were not connected in the circuit. The generator was self-excited.

3. The rectifier transformer was connected on the low-voltage tap and the compensators were not connected in the circuit. The generator was excited separately, that is, the supply to the rectifier transformer was taken from a separate a-c source.

4. The rectifier transformer was connected on the low-voltage tap and the compensators were connected. The generator was self-excited.

5. The rotating exciter was used to excite the generator field. A high-speed contactor short-circuited the exciter field resistance to assimilate the high-speed field-forcing contactor in a rheostatic type voltage regulator. The output ceiling voltage of the rotating exciter is 270 volts and the response ratio is 0.5.

For each of these conditions, 60 per cent reactive load was applied and dropped, and a 3-phase, a line-to-line, a double line-to-ground, and a single line-to-ground fault was applied. To assimilate faults on the 132-kv bus on the actual installation, all faults were applied through ten per cent external reactance on a 20,000-kva base. Under this condition the initial generator terminal voltage drop was approximately 50 per cent. With the exception of condition 5, a line-to-line fault was applied with each of the anode breakers open. This assimilates a line-to-ground fault on the 132-kv West Penn Power Company system during operation with one rectifier cubicle (two ignitron tubes) out of service for maintenance. The duration of the faults was approximately 1.25 seconds. This was longer than would be expected in normal operation but was desirable in order to determine the performance of the electronic exciter for disturbances of long duration.

For electronic exciter tests on which oscillograms were taken, 24 quantities were recorded simultaneously on three 9-element oscillographs as follows:

3—generator line-to-line terminal voltages
3—generator line currents
1—generator field voltage
1—generator field current
1—thyratron tube d-c grid bias voltage

Figure 8. Severe long-duration fault on 20,000-kva generator with primer voltage applied to return terminal voltage to normal after fault was cleared

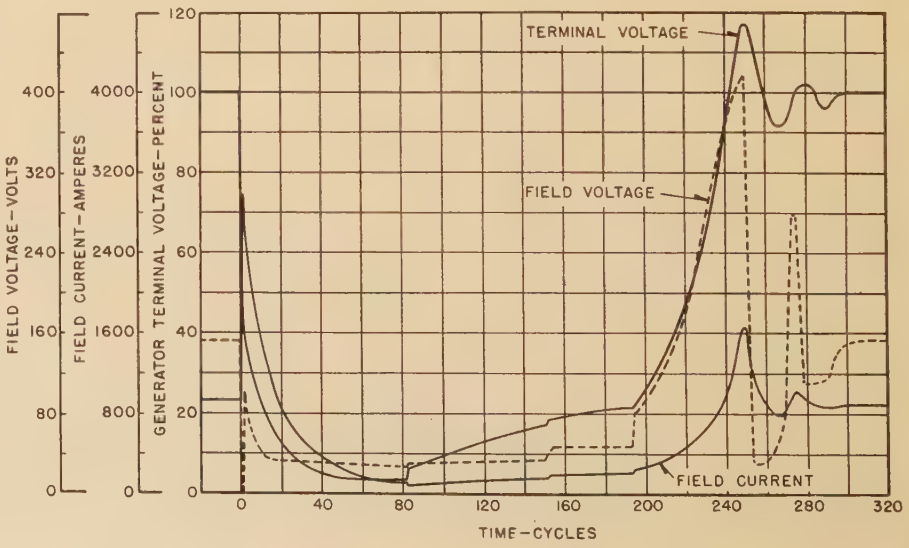

3—line-to-line voltage applied to the rectifier transformer
6—anode to cathode voltages
6—anode currents

Only the first eight quantities were recorded for tests involving the rotating exciter.

Test Results

Figure 6 shows curves plotted from oscillograms of generator terminal voltage and field voltage versus time for a 3-phase fault, a line-to-line fault, a double line-to-ground fault, a single line-to-ground fault, and application of 60 per cent reactive load. The results of the tests made under conditions 1, 2, 3, and 5 are shown. Condition 4 is not included because the results were about the same with the compensators as without them. This was primarily because of the high-voltage regulation in the a-c supply circuit to the rectifier, which resulted from the high field current requirements of the test generator. In those cases where the field voltage becomes a negative value, the induced voltage in the field resulting from fault current in the armature is higher than the rectifier output voltage.

Faults of short duration similar to those normally experienced with modern high-speed relays and breakers were also applied. Curves plotted from an oscillogram of a 3-phase 10-cycle fault are shown in Figure 7. The rectifier transformer was connected on the high-voltage tap and the generator was self-excited.

The tests showed that with the generator self-excited and the rectifier transformer on the high-voltage tap, a 3-phase fault must be cleared in approximately 30 cycles to permit the generator terminal voltage to return to normal. The maximum fault clearing times to permit recovery of generator voltage for other types of faults were estimated from the oscillogram and are shown in Table II.

Figure 8 shows how the generator terminal voltage was returned to normal following a long duration 3-phase fault which caused the rectifier to stop firing because of the decay of terminal voltage to zero. About 40 cycles after application of the fault, a 32-volt d-c source was automatically connected to the generator field. This is the lowest voltage which will cause the ignitron tubes to fire and consequently build up the generator voltage. The fault was cleared in 82 cycles and the ignitron tubes started to fire at 152 cycles. At 194 cycles the rectifier voltage was high enough to cause reverse current to flow into the 32-volt d-c supply, which was tripped off by means of a reverse current relay. From 194 cycles to 300 cycles, the curves show the action of the voltage regulator and the build-up of the terminal voltage, which becomes a constant value of 100 per cent at 300 cycles.

During the tests, one arc-back and one sympathetic arc-back occurred which caused the associated anode breaker to open. Both occurred with cold tubes and with the rectifier supplying no load excitation to the generator with operation of the tubes at a high firing delay. Such conditions are known to increase the probability of arc-back and sympathetic arc-back.[3] No oscillograms were obtained because they occurred at a time when no records were being made. Arc-backs were simulated by short-circuiting a rectifier tube. The tests were run with the rectifier transformer separately excited with no load on the rectifier and with the tubes firing at zero degrees delay. Under these conditions the arc-back currents were maximum. Sympathetic arc-backs were simulated by short-circuiting two ignitron tubes connected to adjacent phases of the rectifier transformer. Power to the rectifier was supplied from the generator terminals and the voltage regulator was in service. The anode breakers opened in $2\frac{1}{2}$ cycles and the rectifier functioned with four tubes out of service. As shown in an oscillogram of one of the tests, Figure 9, there was no disturbance to the generator terminal voltage.

A total of 43 fault, 7 load change, 14 arc-back, 22 sympathetic arc-back, 1 transfer of excitation, and 3 generator voltage build-up tests was recorded on oscillograms. In addition, a number of tests were made without taking oscillographic records. It is believed that the results of these tests provide valuable information that could not be obtained in actual service even over many years.

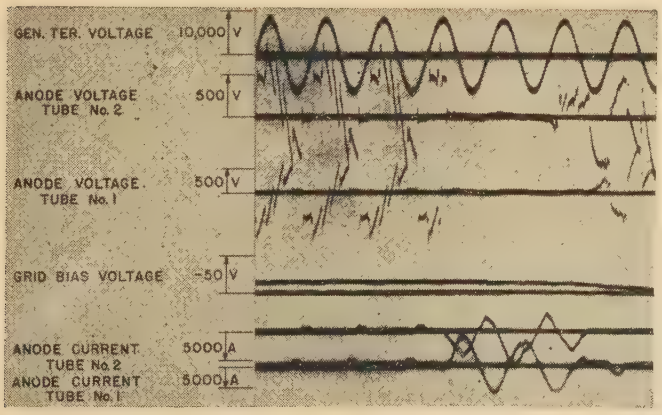

Figure 9. Oscillogram of sympathetic arc-back on ignitron tubes 1 and 2, simulated by short-circuiting each tube simultaneously

Conclusions

1. Extensive laboratory tests based on pessimistic conditions that are unlikely to be matched in service have demonstrated that an electronic exciter can be depended on as a reliable source of excitation for large a-c generators.

2. The type of a-c power supply to the rectifier best suited to the application is dependent on the particular conditions.

3. If self-excited, the electronic exciter should have either a high ceiling voltage or should be provided with series compensators to compensate for drop in a-c voltage during system disturbances. Either method is practical.

4. An electronic exciter may be installed at any desired location in the generating station, it is easy to maintain, it has an inherent high speed of response, and it is adapted easily to generator voltage regulation. Its cost is higher than that of a rotating machine.

5. Modern high-speed relaying would not be affected by using electronic exciters instead of the rotating type. Relays with long time settings, in excess of one second, might be affected if the electronic exciter operates self-excited because of faster decay of short-circuit current.

6. An a-c generator self-excited with an electronic exciter can be operated as an independent unit in an isolated station. A primer excitation for starting can be obtained from a battery or small motor-generator set.

7. The decay of short-circuit current for long-duration low-impedance faults with a self-excited electronic exciter would prevent excessive fault damage. If desired, generator voltage can be restored by automatically applying a primer voltage to the field to start firing of the rectifier.

References

1. A New Method for Initiating the Cathode of an Arc, J. Slepian, L. R. Ludwig. AIEE Transactions, volume 52, 1933, June section, page 693–8.

2. Ignitron Rectifiers in Industry, J. H. Cox, G. F. Jones. AIEE Transactions, volume 61, 1942, October section, pages 713–18.

3. Arc-Backs in Rectifier Circuits Artificial Arc-Back Tests, R. D. Evans, A. J. Maslin. AIEE Transactions, volume 64, 1945, June section, page 303–11.

Peak Voltages Induced by Accelerated Flux Reversal in Reactor Cores Operating Above Saturation Density

THEODORE SPECHT
ASSOCIATE AIEE

E. C. WENTZ
MEMBER AIEE

Synopsis: The existence of peak voltages in the windings of many sorts of series transformers and reactors, when abnormal conditions force the flux density above saturation, has been understood in a qualitative manner for many years. This paper will derive means for calculating these voltages for the various combinations of magnetizing force and rate of variation. The close agreement between test and calculation over a wide range of magnetizing forces indicates the accuracy and general applicability of the method.

THE magnetic flux in a-c apparatus usually varies nearly sinusoidally over a range of flux densities well below the saturation value. However, in certain types of apparatus, notably series apparatus, abnormal conditions will produce magnetizing forces as high as hundreds of times normal, and the flux density will not only reach saturation, but the flux variation will no longer be sinusoidal. The variation of the flux through zero is usually accelerated and induces relatively enormous peak voltages.

Examples of such apparatus are:

1. Current transformers under overcurrent, high burden (or a combination), or open circuit.
2. Preventive autotransformers when a tap change coincides with a line fault.
3. Series transformers for street lighting when a lamp burns out.

The existence of these voltages is well known, but only very approximate methods,[1] limited in application, have been derived for calculation of their values. With recent increases in capacities of systems, the possible voltages are higher and more dangerous than ever. One-ampere secondary current transformers are being used more frequently, and their voltages are five times as high as standard. Hence it has become more necessary to have more generally applicable, more exact, means of calculation of voltage.

Paper 46-68, recommended by the AIEE committee on instruments and measurements for presentation at the AIEE winter convention, New York, N. Y., January 21–25, 1946. Manuscript submitted November 8, 1945; made available for printing December 11, 1945.

THEODORE SPECHT, an electrical design engineer, and E. C. WENTZ, a transformer design engineer, are both with Westinghouse Electric Corporation, Sharon, Pa.

Peak Voltage Phenomenon and Methods of Analysis

The conventional description of the phenomenon is illustrated in Figure 1A. Starting at point *A* on the current wave, the reactor is saturated, and as the current decreases, the flux changes very little and the voltage is nearly zero. As the current decreases to the saturation value near *B*, the flux starts to decrease, and the flux change is accelerated through current zero at *C*, inducing a high-voltage peak.

The high-voltage peak, induced by the high inductance of the saturating reactor near current zero, resists the change in the primary current, the high inductance tending to maintain the current and thus to make the peak voltage itself less than it would be otherwise if the current wave maintained its sinusoidal shape. Analysis of the circuit to determine the effect of the peak voltage on the wave shape of the current and the determination of the resulting peak voltage is the first part of the problem.

The high rate of flux change induces eddy currents in the lamination which are very effective toward maintaining the flux, delaying its change. Analysis of these eddy currents is the second part of the problem.

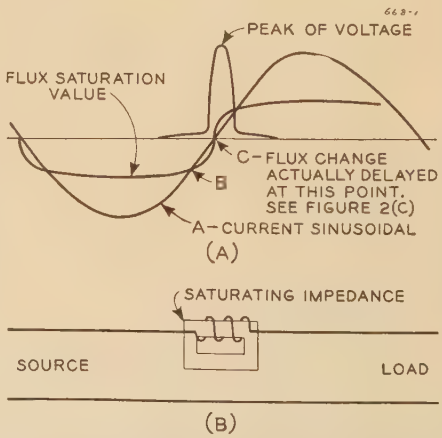

Figure 1. Illustration of the problem with conventional description of mode of flux variation

Compare with Figure 2 and Figure 11

Two methods of analysis of the whole problem have been developed. Method *A* gives a satisfactory solution of the first part of the problem (variation of voltages and currents in the circuit) based on an assumption as to the solution of the second part. Method *B* gives the solution of the second part of the problem (eddy currents and their effect on the flux distribution and voltage) based on an assumption as to the solution of the first part. The use of two methods can be justified by the fact that although neither method gives exactly the correct result, they do give the approximate upper and lower limits of possible peak voltage.

The advantage of method *A*, analysis by the assumption of uniform flux density in the lamination, is that it permits representing the actual reactor by an equivalent perfect reactor in parallel with a resistor, according to Figure 2. This enables the mathematical analysis of the circuit which will be given later.

The classic analysis of eddy currents is based on the assumption of uniform flux density. The loss then is proportional to the square of the rate of flux change or, instantaneously, to the square of the voltage induced in the reactor. Clearly, a resistor shunted across the reactor has a loss varying in the same way, and a resistor *R* in parallel with a perfect reactor *L*, as in Figure 2, will represent the actual reactor.

By method *B* determination of flux distribution in the lamination, the variation of flux is analyzed on the basis that a sine wave of current is maintained through the reactor, and the effect of the eddy currents in forcing the flux to redistribute itself toward the surface of the lamination is determined.

Method *B*, which takes account of the effect of the eddy currents in forcing the flux change to occur first at the surface of the lamination, can be expected to give lower voltages. The analyses to be given show that it gives a voltage about half as great, and the tests show that the actual values are between the two.

Mathematical Analysis

The equivalent reactor (or primary of the series transformer) in method *A* (see Figure 2B) is not a constant quantity; as the flux in the core increases toward saturation, the permeability and effective inductance decrease to a value only a small

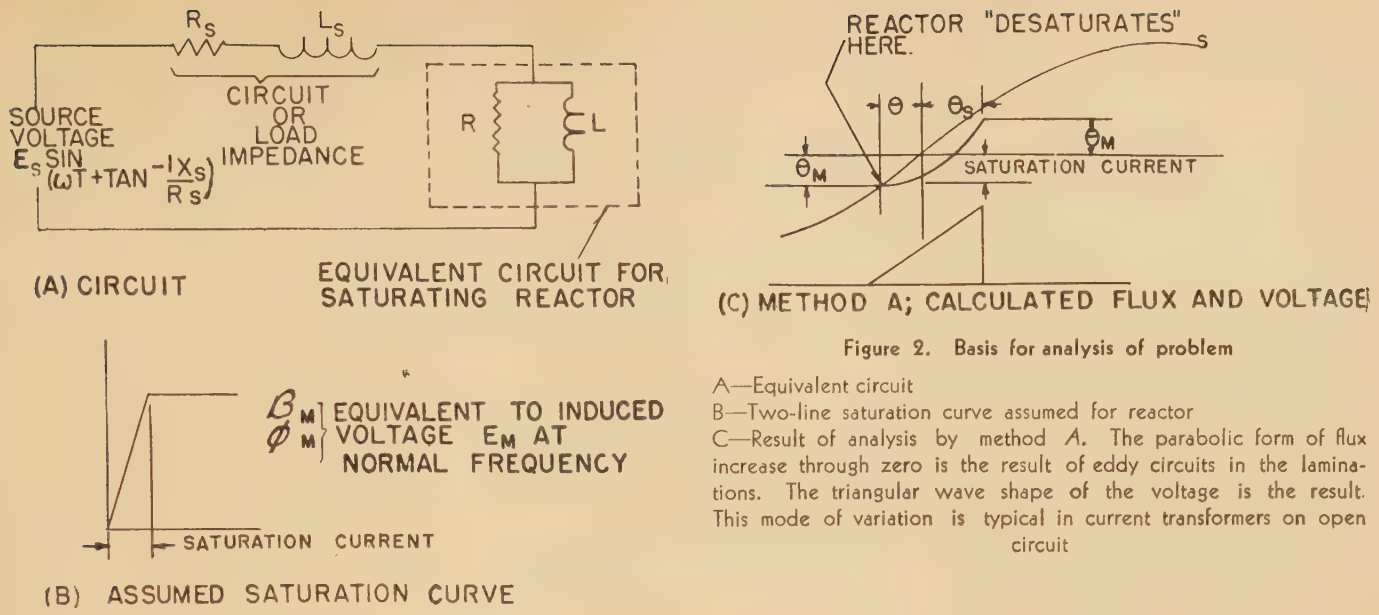

Figure 2. Basis for analysis of problem

A—Equivalent circuit
B—Two-line saturation curve assumed for reactor
C—Result of analysis by method *A*. The parabolic form of flux increase through zero is the result of eddy circuits in the laminations. The triangular wave shape of the voltage is the result. This mode of variation is typical in current transformers on open circuit

fraction of the initial value, and in a complicated manner that cannot be represented by any simple formula. Therefore some simplifying assumptions will have to be made. An obvious device which has been used in similar problems is to assume that the saturation curve is composed of two straight lines, as shown in Figure 2B. The voltage induced by B_m at normal frequency will be E_m; the method of determining E_m from the AC saturation curve of the reactor is given in Appendix I.

The hysteresis loop, by this assumption, is assumed to have zero area. As it will appear later that the permeability of the iron is not too important in determining the peak voltage, the variation of permeability during the hysteresis loop reasonably may be neglected.

Method *A*

Method *A*, as has been shown, is based on analysis of the circuit of Figure 2A. For this circuit we may write the equations

$$\sqrt{2}E_s \sin\left(\omega t + \tan^{-1}\frac{X_s}{R_s}\right) - i_s R_s - L_s\frac{di_s}{dt} - L\frac{di_L}{dt} = 0 \quad (1)$$

The reason for writing in $\tan^{-1} X_s/R_s$ is that the resulting equations are simplified. The current i_s, which would flow in the circuit if the series reactor were not present, is $i_s = (E_s/Z_s)\sin\omega t$. Time = 0 is thus when the current would be zero if the reactor were not in the circuit.

$$L\frac{di_L}{dt} = i_R R = e \quad (2)$$

$$i_s = i_L + i_R \quad (3)$$

A further limitation, inherent in the nature of the reactor, is that $L=0$ if i_L exceeds the saturation value. If we suppose the current to exceed this value initially (at point A, Figure 2C) and to be decreasing sinusoidally toward zero, it all will be flowing in the L branch, none in the R branch, of the equivalent reactor because $L=0$ while the current exceeds the saturation value. At some time $-t_d$ or time angle $-\theta_d$, the current decreases to the value at which the reactor "desaturates" and suddenly regains its inductance L. The flux must remain momentarily at the same value, so that the current in the reactor (i_L) must have an initial value at time angle $-\theta_d$ equal to the saturation value, with zero current in the resistor R and zero voltage across the reactor. The value of $-\theta_d$ is derived in Appendix II.

As the flux in the reactor reverses, the current in the reactor branch L finally reaches the saturation value again at some time t_s (angle θ_s), at which time the inductance L becomes zero, all the current transfers to the L branch, and the circuit carries on until the next half-cycle.

Equations 1, 2, and 3 are obviously very difficult to solve for i_L or i_R.* Some assumptions or simplifications must be made. The solution can be worked out by either of two assumptions.

Solution by Assumption Number 1. Neglect $R_s\{[(\sqrt{2}E_s\omega t)/Z_s] - i_s\}$. The demonstration that the solution is valid for low-power-factor circuits follows.

If we write equation 1 in the form

$$L_s\frac{di_s}{dt} + L\frac{di_L}{dt} = \sqrt{2}E_s \sin \times \left(\omega t + \tan^{-1}\frac{X_s}{R_s}\right) - R_s i_s$$

* This equation can be solved for e because the differential equation

$$\frac{d^2 i_L}{dt^2} + \left(\frac{R_s}{L_s} + \frac{R}{L_s} + \frac{R}{L}\right)\frac{di_L}{dt} + \frac{RR_s}{LL_s} i_L = \frac{Re_s}{LL_s}$$

can be derived from it (e_s = source voltage). The solution is of the form $i_L = K_1\epsilon^{\lambda_1 t} + K_2\epsilon^{\lambda_2 t} +$ steady state current. The initial and final conditions are the same. λ_1 and λ_2 come out to be rather complicated functions of R, R_s, X, X_s, while K_1 and K_2 are still more complicated functions of λ_1, λ_2 and the other variables. The final solution is difficult to work with, and as the more simple solutions give results sufficiently accurate for the purpose (especially in light of the fact that the basic assumption of a constant R introduces some error), only the simple solutions are given in complete form and the calculations will be based on these simple solutions. The values of λ_1, λ_2, K_1, and K_2 are given in Appendix V.

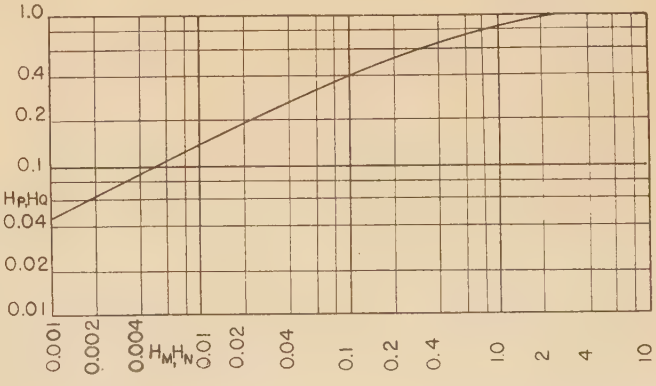

Figure 3. Curve of H_p as a function of H_m (or H_q as a function of H_n)

and if we consider the current reversal to take place in such a short time that $\sin \omega t = \omega t$,

$$L_s\frac{di_s}{dt}+L\frac{di_L}{dt}=\sqrt{2}\frac{E_sX_s}{Z_s}+R_s\left(\sqrt{2}\frac{E_st\omega}{Z_s}-i_s\right) \quad (4)$$

Now this equation can be solved if we can neglect the last term. But if the current variation is sinusoidal so that $i_s=\sqrt{2}(E_s/Z_s)\sin\omega t=\sqrt{2}(E_s/Z_s)t\omega$ the last factor will be zero. If L_s is very large compared with L, the variation will be substantially sinusoidal, the last term will be zero, and the equation can be solved. Of course, if $R_s=0$, the last term will be zero and the calculation will be exact, even if the current wave is not sinusoidal. We can determine the relative magnitude of error by solving the equation for i_s, and determining the relative magnitude of the i_sR part of the last term which has been neglected. This will indicate the approximate amount of error. The ratio of this error to the other term $\sqrt{2}(E_sX_s/Z_s)$ will come out equal to

$$\frac{R_s}{X_s}\left[\frac{X}{X+X_s}\omega(t+t_d)+\left(\frac{X}{X+X_s}\right)^2\times\frac{X_s}{R}\left(1-\epsilon^{-\frac{R(X+X_s)}{XX_s}(t+td)}\right)\right]$$

Examples worked out for different circuit constants indicate that the maximum usual error will not exceed 20 per cent. Tests to be given indicate good agreement.

Then we can write for Equation 4

$$\sqrt{2}\,\frac{E_sX_s}{Z_s}=L_s\frac{di_s}{dt}+L\frac{di_L}{dt} \quad (4a)$$

Eliminating i_s and i_L by Equations 2 and 3,

$$\frac{de}{dt}+\frac{R(L+L_s)}{LL_s}e=\frac{\sqrt{2}E_sR\omega}{Z_s} \quad (5)$$

Solving this equation, using the initial condition that $e=0$ at $\omega t=-\theta_d$,

$$e=\frac{\sqrt{2}E_sXX_s}{Z_s(X+X_s)}\left(1-\epsilon^{-\frac{R(X+X_s)}{XX_s}(\theta+\theta d)}\right) \quad (6)$$

For small values of the exponent,

$$e=\frac{\sqrt{2}E_sR}{Z_s}(\theta+\theta_d) \quad (7)$$

To find the angle of saturation, θ_s, use the relation that $e=N(d\phi/dt)10^{-8}$

$$\int_{-\theta_d}^{\theta_s}ed\theta=\int_{-\phi m}^{\phi m}\omega N\frac{d\phi}{dt}10^{-8}dt=2\omega N\phi_m10^{-8}$$

But

$$E_m=\frac{\omega N\phi_m10^{-8}}{\sqrt{2}} \quad \text{(see Figure 2B)}$$

So that

$$\int_{-\theta_d}^{\theta_s}ed\theta=2\sqrt{2}E_m \text{ volts} \quad (8)$$

Integrating equation 6 from $-\theta_d$ to θ_s, equating to $2\sqrt{2}E_m$, and rearranging terms,

$$\frac{2E_mZ_sR}{E_s}\left(\frac{X+X_s}{XX_s}\right)^2=\frac{R(X+X_s)(\theta_s+\theta_d)}{XX_s}+\epsilon^{-\frac{R(X+X_s)(\theta_s+\theta d)}{XXs}}-1=H_m \quad (9)$$

From equation 6 it is apparent that the peak voltage occurs at θ_s. Introducing an experience factor k, which will be discussed further under test results, the peak voltage is

$$e_p=k\frac{\sqrt{2}E_sXX_s}{Z_s(X+X_s)}\left(1-\epsilon^{-\frac{R(X+X_s)(\theta_s+\theta d)}{XXs}}\right) \quad (10)$$

Let

$$H_p=1-\epsilon^{-\frac{R(X+X_s)(\theta_s+\theta d)}{XXs}} \quad (11)$$

Then

$$e_p=k\frac{\sqrt{2}E_sXX_s}{Z_s(X+X_s)}H_p \quad (12)$$

It can be seen from equations 9 and 11 that H_m and H_p are functions of the same parameter. It is then possible to plot H_p directly as a function of H_m. This curve is shown in Figure 3. H_m can be calculated from the first part of equation 9, H_p read from Figure 3, and e_p calculated by equation 12. If the angle $\theta_s+\theta_d$ is desired, it can be found from equation 11 as follows:

$$\theta_s+\theta_d=\frac{1}{k}\frac{XX_s}{R(X+X_s)}\times\log_\epsilon\frac{1}{1-H_p}\text{ radians} \quad (13)$$

Here the angle is divided by the experience factor k; for whatever the peak voltage is reduced by, the angle will be increased by, as is apparent from equation 8. For accurate results this angle should be less than one-half radian.

Solution by Assumption Number 2. Neglect $L_s[(\sqrt{2}\omega E_s/Z_s)-(di_s/dt)]$. The demonstration that the solution is valid for high-power-factor circuits follows.

We may also write equation 1 in the form

$$I_sR_s+L\frac{di_L}{dt}=\sqrt{2}E_s\sin\left(\omega t+\tan^{-1}\frac{X_s}{R_s}\right)-L_s\frac{di_s}{dt} \quad (14)$$

or, as before, letting $\sin\omega t=\omega t$

$$i_sR_s+L\frac{di_L}{dt}=\sqrt{2}\frac{E_s}{Z_s}R_s\omega t+L_s\left(\sqrt{2}\,\frac{E_s}{Z_s}\,\omega-\frac{di_s}{dt}\right) \quad (15)$$

Again it appears that the equation can be solved if we neglect the last term. Again, if $i_s=\sqrt{2}(E_s/Z_s)\omega t$ so that $di_s/dt=\sqrt{2}(E_s/Z_s)\omega$, the last factor is zero, so that this equation is also valid if the series impedance is so high as to maintain sinusoidal current. And obviously it is valid for $L_s=0$, but not for $R_s=0$, so that the solution will be valid for high-power-factor circuits.

Then we may write equation 15 with-

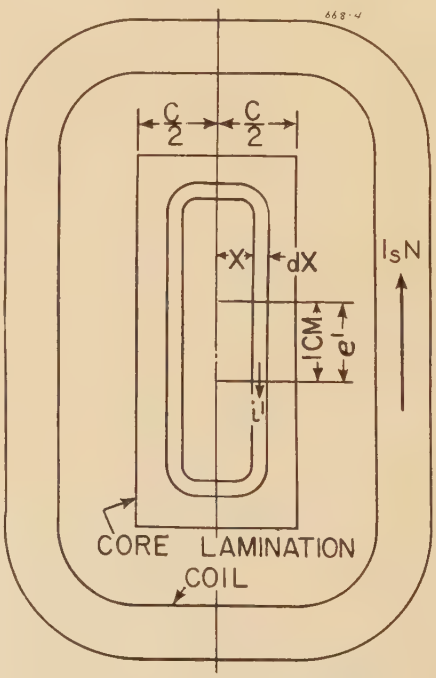

Figure 4. Cross section of a core lamination magnetized by a primary coil

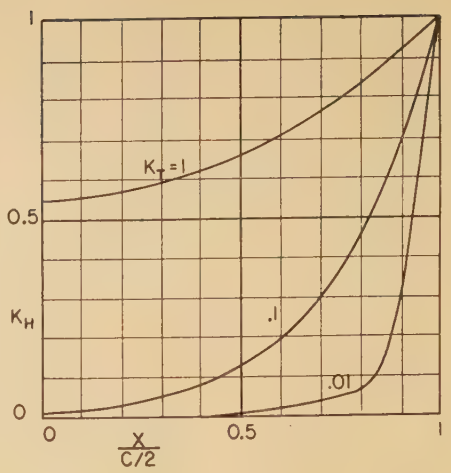

Figure 5. Distribution of flux in a lamination as a function of the distance from the center of the lamination for three values of time

See equation 46

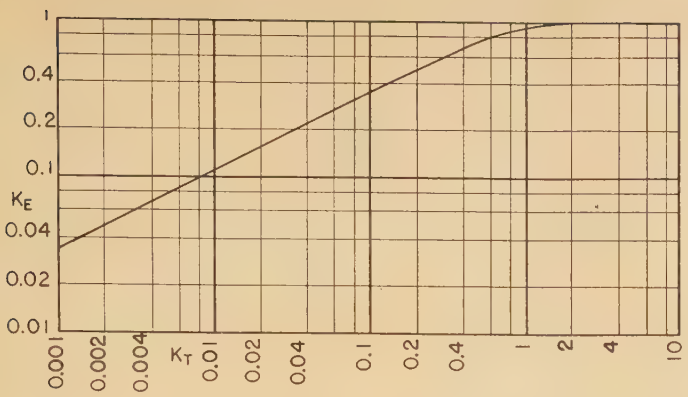

Figure 6. Curve of K_e as a function of K_t

See equation 48

out the last term, and again eliminating i_s and i_L by use of equations 2 and 3, we get

$$\frac{de}{dt}+\frac{RR_s}{(R_s+R)L}e=\frac{\sqrt{2}E_sR_sR\omega}{Z_s(R_s+R)} \quad (16)$$

At $\omega t=-\theta_d$, $e=0$,

$$e=\frac{\sqrt{2}E_sX}{Z_s}\left(1-\epsilon^{-\frac{RR_s(\theta+\theta_d)}{(R_s+R)X}}\right) \quad (17)$$

For small values of the exponent,

$$e=\frac{\sqrt{2}E_sRR_s}{Z_s(R_s+R)}(\theta+\theta_d) \quad (18)$$

Comparing with equation 7, it is seen that the two methods result in the same voltage if R_s is large compared to R. Integrating equation 17 from $-\theta_d$ to θ_s as in equation 8,

$$\frac{2E_mZ_sRR_s}{(R_s+R)X^2E_s}=\frac{RR_s(\theta_s+\theta_d)}{(R_s+R)X}+\epsilon^{-\frac{RR_s(\theta_s+\theta_d)}{(R_s+R)X}}-1=H_n \quad (19)$$

and

$$H_q=1-\epsilon^{-\frac{RR_s(\theta_s+\theta_d)}{(R_s+R)X}} \quad (20)$$

H_n and H_q are of the same form as in equations 9 and 11 but are functions of a different parameter. Introducing the experience factor k, equation 17 becomes

$$e_p=k\frac{\sqrt{2}E_sX}{Z_s}H_q \quad (21)$$

It is evident that Figure 3 also may be used to evaluate H_n and H_q. Method 1 above is exact for R_s equal to zero and method 2 is exact for X_s equal to zero. The calculated voltages for intermediate power factors will be too low by either formula unless the series impedance is high enough to keep the source current sinusoidal. If the peak voltage is calculated by both methods, the larger of the two answers should be correct within a reasonable degree of accuracy.

From Figure 3 it is evident that the straight line relationship

$$H_p=\sqrt{2H_m}\ (\text{or } H_q=\sqrt{2H_n}) \quad (22)$$

is entirely adequate if H_m or H_n is less than one-tenth. That equation 22 is the exact relation for low values of the variables can be demonstrated by expanding the expressions for H_p and H_m from equations 11 and 9 in infinite series, retaining only the lowest-powered term in each, and then eliminating the parameter between the two equations. Substituting the value of H_m from equation 9 into equation 22, and this value of H_p into equation 12, gives

$$e_p=k\left(\frac{8E_sE_mR}{Z_s}\right)^{1/2} \quad (23)$$

It can be shown that this same equation holds for method 2 for a high-power-factor circuit if R_s is large compared with R. From equations 7 or 18, it is evident that the voltage wave shape is essentially triangular.*

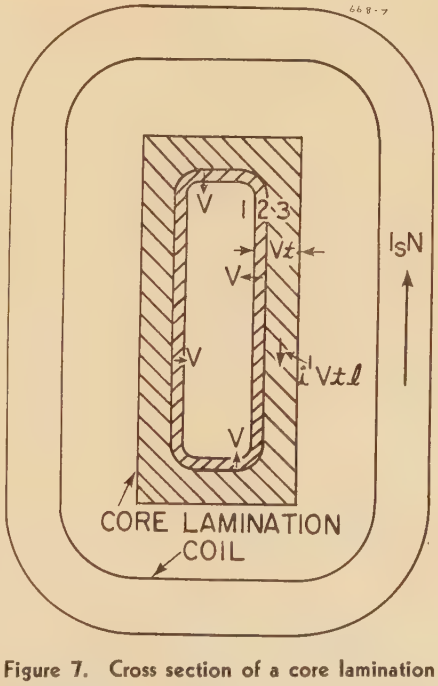

Figure 7. Cross section of a core lamination subjected to very large magnetomotive forces

The flux travels as a wave from the surface to the center. There has been little flux change in the area 1; in the relatively narrow strip 2, the flux is changing; and in the area 3, the iron is completely saturated

To get the root mean square voltage, we can write

$$\int_{-\theta_d}^{\theta_s}e\,d\theta=\frac{1}{2}\left[k\left(\frac{8E_sE_mR}{Z_s}\right)^{1/2}\right]\times(\theta_s+\theta_d)=2\sqrt{2}E_m \quad (24)$$

$$\theta_s+\theta_d=\frac{2}{k}\left(\frac{E_mZ_s}{E_sR}\right)^{1/2}\text{ radians} \quad (25)$$

The expression for the voltage e can be rewritten as follows, where e_p is the peak value as given by equation 23:

$$e=e_p\frac{\theta+\theta_d}{\theta_s+\theta_d} \quad (26)$$

To find the root mean square value of this voltage, the value of e is substituted in the following formula and evaluated.

$$e_{rms}=\left(\frac{1}{\pi}\int_{-\theta_d}^{\theta_s}e^2d\theta\right)^{1/2} \quad (27)$$

$$=e_p\left(\frac{\theta_s+\theta_d}{3\pi}\right)^{1/2}\text{ volts} \quad (28)$$

The values from equations 23 and 25 can be substituted in equation 28.

$$e_{rms}=\sqrt{k}\frac{4}{\sqrt{3\pi}}\left(\frac{E_sR}{Z_s}\right)^{1/4}E_m^{3/4}\text{ volts} \quad (29)$$

The watts loss in the core would be

$$W=\frac{e_{rms}^2}{R}=k\frac{16}{3\pi}\left(\frac{E_s}{Z_sR}\right)^{1/2}E_m^{3/2}\text{ watts} \quad (30)$$

It is possible to express these equations directly in terms of the material constants. Using the values for E_m and R developed in equations 69 and 74, Appendix I, equations 23, 25, 29, and 30 may be written as follows:

$$\frac{e_p}{NA}=k\,8.25\frac{(\omega B_m\rho)^{1/2}}{c}\left(\frac{NE_s}{lZ_s}\right)^{1/2}\times 10^{-4}\text{ v per turn per sq cm} \quad (31)$$

$$\theta_s+\theta_d=\frac{0.485c\left(\frac{\omega B_m}{\rho}\right)^{1/2}10^{-4}}{k\left(\frac{NE_s}{lZ_s}\right)^{1/2}}\text{ radians} \quad (32)$$

$$\frac{e_{rms}}{NA}=\sqrt{k}1.87\frac{\rho^{1/4}(\omega B_m)^{3/4}}{c^{1/2}}\left(\frac{NE_s}{lZ_s}\right)^{1/4}\times 10^{-6}\text{ v per turn per sq cm} \quad (33)$$

$$\frac{W}{G}=k0.29\frac{(\omega B_m)^{3/2}c}{\rho^{1/2}\delta}\left(\frac{NE_s}{lZ_s}\right)^{1/2}\times 10^{-12}\text{ w per gram} \quad (34)$$

* It is interesting to note that X does not appear in equation 23. This is a consequence of neglecting the additional terms of the form $1/n![(R/X)(\theta_s+\theta_d)]^n$ in the expansion by series to get equation 22. If X were very small, this could not be done. In effect, X has been assumed to be infinite with respect to $R(\theta_s+\theta_d)$, and in many problems this will be true. Therefore the voltage does not depend on X. This means that the change of flux in the core is limited entirely by the eddy currents, the permeability of the iron having a negligible effect.

METHOD *B*

As was mentioned earlier in this paper, high rates of change of flux in the core cause eddy currents which materially distort the flux distribution in the lamination. It is possible to write exact equations for the flux distribution in the lamination, assuming constant permeability. The condition is actually much different and vastly more complicated by the gradual yet enormous change in permeability. However, this solution will be used if the permeability value is chosen with this limitation in mind. In so doing, the mathematical analysis will be simplified if the flux density throughout the lamination is considered initially to be zero, instead of minus ϕ_m, and to rise from zero to twice its saturation value.

It would be expected that the peak voltage would occur when the surface of the lamination was just saturating. Figure 4 shows a single lamination of steel of thickness c and mean length of flux path l. It is assumed that the laminations are insulated from each other adequately and that the width of each lamination is large compared with its thickness. What occurs in this one lamination occurs in all of the others. This lamination is linked by a primary coil of N turns carrying an effective alternating current of I_s amperes. It is assumed that the transient will occur in a sufficiently short time that the slope of the current wave may be assumed constant and equal to its value at current zero. The equation for the primary coil magnetomotive force will be

$$\frac{0.4\pi\sqrt{2}I_sN\omega t}{l} \text{ oersted} \tag{35}$$

To agree with the change of flux from zero to twice maximum, this magnetomotive force will be assumed to be applied to the core at zero time. Let x be the distance out, measured from the center of the lamination; let H_o be the magnetomotive force at the center of the lamination; and let i' be the eddy current density at any point in the lamination. The magnetomotive force at x is

$$h=H_o+0.4\pi\int_0^{xi'}dx \text{ oersteds} \tag{36}$$

$$\frac{\partial^2 h}{\partial x^2}=0.4\pi\frac{\partial i'}{\partial x} \tag{37}$$

The induced voltage gradient in the lamination at any point x is

$$e'=10^{-8}\int_0^x\frac{\partial B}{\partial t}\,dx \tag{38}$$

$$B=\mu h \tag{39}$$

$$i'=\frac{e'}{\rho}=\frac{10^{-8}\mu}{\rho}\int_0^x\frac{\partial h}{\partial t}\,dx \tag{40}$$

$$\frac{\partial i'}{\partial x}=\frac{10^{-8}\mu}{\rho}\frac{\partial h}{\partial t} \tag{41}$$

Substituting equation 41 in equation 37,

$$\frac{\partial^2 h}{\partial x^2}=\frac{0.4\pi\mu 10^{-8}}{\rho}\frac{\partial h}{\partial t} \tag{42}$$

Since at the surface of the steel there will be no eddy currents to prevent the flow of flux, the magnetomotive force at the surface will be equal directly to that of the coil as given by equation 35. The

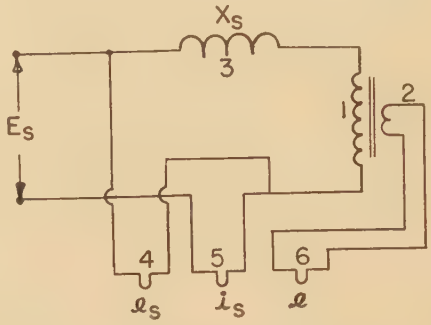

Figure 8. Test circuit for measuring peak voltages

The saturating reactor is 1, on which is wound a search coil, 2. The air-core loading reactor is 3, and 4, 5, and 6 are oscillograph elements

solution of equation 42 for these conditions (see Appendix III) is

$$h=\frac{0.4\pi\sqrt{2}I_sN\omega}{l}\left\{t+\sum_{s=1}^{s=\infty}(-1)^s\times\right.$$
$$\frac{16}{(2s-1)^3\pi^3}\frac{0.4\pi\mu 10^{-8}}{\rho}\left(\frac{c}{2}\right)^2\left(\cos\frac{2s-1}{2}\cdot\frac{\pi x}{\frac{c}{2}}\right)\times$$
$$\left.\left(1-\epsilon^{-\frac{(2s-1)^2\pi^2}{4}\frac{\rho}{0.4\pi\mu\ 10^{-8}}\frac{t}{(c/2)^2}}\right)\right\} \tag{43}$$

Let

$$K_h=\frac{hl}{0.4\pi\sqrt{2}I_sN\omega t} \tag{44}$$

$$K_t=\frac{\rho}{0.4\pi\mu 10^{-8}}\frac{t}{\left(\frac{c}{2}\right)^2} \tag{45}$$

Rewriting equation 43 using these values,

$$K_h=1+\sum_{s=1}^{s=\infty}(-1)^s\frac{16}{(2s-1)^3\pi^3}\times$$
$$\frac{\cos\frac{(2s-1)}{2}\frac{\pi x}{c/2}}{K_t}\left(1-\epsilon^{-\frac{(2s-1)^2\pi^2}{4}K_t}\right) \tag{46}$$

Figure 5 is a plot of equation 46 for various values of K_t. The total voltage induced in the coil would be

$$e=\frac{AN10^{-8}\mu}{\frac{c}{2}}\int_0^{c/2}\frac{\partial h}{\partial t}\,dx \tag{47}$$

Substituting the value of h from equation 43 and simplifying by substituting X and K_t for their equivalents,

$$K_e=\frac{e}{\sqrt{2}I_sX}=1-\sum_{s=1}^{s=\infty}\frac{8}{(2s-1)^2\pi^2}\times$$
$$\epsilon^{-\frac{(2s-1)^2\pi^2}{4}K_t} \tag{48}$$

Figure 6 is a curve of K_e as a function of K_t. It can be seen that for large values of K_t, $Ke=1$;

$$e=\sqrt{2}I_sX \tag{49}$$

In Appendix IV it is shown and from Figure 6 it can be seen that for small values of the variables,

$$K_e=\frac{2}{\sqrt{\pi}}\sqrt{K_t} \tag{50}$$

If the values for ρ and μ from equations 75 and 72 of Appendix I are substituted in equation 45 and this value of K_t substituted in equation 50,

$$e=I_s\left(\frac{8RX\theta}{3\pi}\right)^{1/2} \tag{51}$$

Comparing this equation with equation 7, this equation is seen to vary as the square root of time whereas equation 7, using the equivalent circuit, varies directly with time.

To find the angle at which the surface saturates, it is evident that the magnetomotive force at the surface is equal to that of the primary coil. From equation 37 then,

$$\mu\frac{0.4\pi\sqrt{2}I_sN\omega t_s}{l}=2B_m \tag{52}$$

Substituting the value of μ and B_m from equations 72 and 70 of Appendix I in equation 52,

$$\theta_s=\frac{2E_m}{I_sX} \tag{53}$$

Substituting this value of θ_s in equation 51,

$$e_p=\left(\frac{16I_sRE_m}{3\pi}\right)^{1/2} \tag{54}$$

Comparing this equation with equation 23 for the equivalent circuit analysis, the form is seen to be identical, except the coefficient, which is only 46 per cent as large.

Equation 54 is valid as long as the value of K_t at the time the surface saturates, or K_{ts}, is less than three-tenths.

the value of t_s from equation 52 is substituted into equation 45,

$$K_{ts}=\frac{5.06\rho B_m 10^{+8}}{\omega(\mu c)^2(NI_s/l)} \tag{55}$$

All the factors in equation 55 are constant except the permeability μ. This varies over quite a range over the region of operation. K_{ts} is evaluated for the following example, which represents an average low-voltage current transformer, using a relatively low value for the permeability.

$\omega=377$	$\rho=60$ microhms per cm cube
$\mu=1{,}000$	
$B_m=12{,}000$ gauss	$NI_s=1{,}200$ ampere turns
$c=0.033$ cm	
$l=51$ cm	$K_{ts}=37.8$

Solving equation 44 for h, the flux density becomes

$$B=\mu h=\mu.4\pi\sqrt{2}I_sN\omega t\,\frac{K_h}{l}$$

Referring to Figure 5, if K_t exceeds one, the value of K_h will be between 0.55 and 1.0 so that the flux at every point will be at least 55 per cent of the maximum value. Considering that μ usually is not known within a factor of two, B might be considered to be uniform for all practical purposes. Since method A is based on uniform distribution of flux, we can say that when K_t exceeds unity, the flux distribution is sufficiently uniform that method A applies. In the example given, K_t will exceed unity after a very small fraction of the transient time has elapsed, and thus method A will be applicable.

The permeability is, of course, higher than 1,000 over part of the transient; however, it has been found that up to 1,000 ampere turns (rms) per inch, 29-gauge laminations, 60 cycles, the effect of nonuniform distribution of flux is slight and that method A with the 0.85 correction factor is satisfactory. Above this value the correction factor decreases to a minimum of six-tenths at very high ampere turns.

Not included in this paper is the effect of capacity in the windings, which also begins to take effect when the peak of voltage is very short.

Penetration of Flux Into the Lamination. After the surface of the lamination is saturated, the reversal must spread into the center of the lamination in some manner. Figure 5 is a curve drawn to show the flux distribution for various rates of change of flux. It is apparent that the more rapidly the flux changes, the less the penetration of the flux into the center of the lamination. Also, the

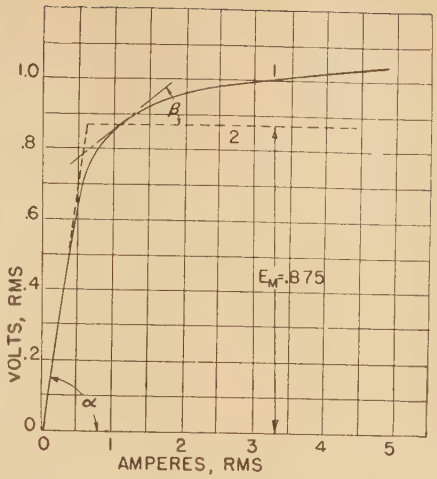

Figure 9. Iron-core reactor excitation curve

The actual curve is 1 and the assumed theoretical curve is 2. For a reactor with no air gaps, E_m is approximately the point of tangency of a line drawn tangent to the knee of the curve such that tan β=(tan α)/10

width of the zone in which the flux is changing becomes smaller the more rapidly the change is made, and as a limit the wave front is almost vertical. As soon as the surface is saturated, the flux wave will start to penetrate the steel.

During this period the material can be divided into three zones: the center where there is little flux, the wave-front zone where the flux is changing, and the outer

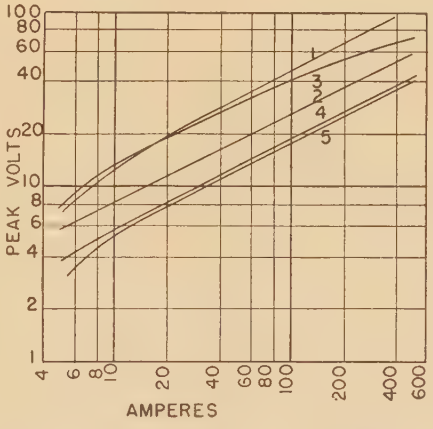

Figure 10. Peak voltage of a saturating reactor

1—Calculated curve for reactor only, using equation 12

2—Calculated curve for reactor only, assuming forcing of flux to surface of lamination, using equation 56

3—Test curve of reactor only which follows calculated curve 1 up to high values of current where it begins to bend over and approach curve 2

4—Calculated curve of reactor shunted by a 0.9-ohm resistor using equations 12 and 68

5—Test curve of reactor shunted by a 0.9-ohm resistor which follows the calculated curve 4 quite well

zone where the iron is saturated. The wave-front zone must travel in from the surface to the center. However, it must travel in with such a speed that it will induce enough voltage in the saturated zone behind it to circulate enough current to nearly balance the ampere turns of the primary coil. Enough ampere turns must be left over, though, to provide the magnetomotive force necessary for the wave-front zone. In the usual case, this will be small, and the generalization can be made that the eddy currents in the saturated zone must balance the primary ampere turns. If the flux travels in with a velocity of v centimeters per second, referring to Figure 7, the flux in the saturated zone in a strip one centimeter wide would be

$$\phi_s=2B_mvt \tag{56}$$

The voltage gradient in the saturated zone would be

$$e'=(d\phi_s/dt)10^{-8}=2B_mv10^{-8}\text{ volts} \tag{57}$$

The current density in the saturated zone is

$$i'=e'/\rho\text{ amperes per sq cm} \tag{58}$$

The total current in the saturated zone is

$$i'vtl=\frac{2B_mv10^{-8}vtl}{\rho} \tag{59}$$

This is equal to the primary ampere turns

$$\frac{2B_mv^210^{-8}tl}{\rho}=\sqrt{2}I_s\omega tN \tag{60}$$

$$v=\left(\frac{I_s\omega N\rho 10^8}{\sqrt{2}B_ml}\right)^{1/2}\text{centimeters per second} \tag{61}$$

The total voltage induced in the primary coil will be

$$e=Ne'\frac{A}{c/2} \tag{62}$$

If the value of v from equation 61 is substituted in equation 57, and this value of e' from equation 57 substituted in equation 62, and if the values of ρ and B_m from equations 75 and 70 of Appendix I are substituted in this equation for e, the peak voltage becomes

$$e_p=\left(\frac{4I_sE_mR}{3}\right)^{1/2}\text{volts} \tag{63}$$

This is seen to be a value 12 per cent lower than that given by equation 54.

The voltage given by equation 63 is a flat-topped voltage. It is to be expected then that if a direct-current voltage were applied to a reactor, the current drawn would increase linearly with time,

$$i=\sqrt{2}\omega I_st \tag{64}$$

Substituting the value of I_s from equation 63,

$$i=\frac{1.06e_p^2\omega t}{E_mR} \text{ amperes} \quad (65)$$

Shunting of Reactor With a Resistor. The open-circuit voltage of a current transformer can be controlled by connecting a resistor to the secondary terminals. The value of the resistor can be very high relative to any normal burden so that its normal shunting effect is negligible, and yet considerable reduction in voltage may be obtained. Short-circuited bands of resistance metal sometimes used for phase-angle correction have exactly the same effect. The effect can be calculated by considering this resistor to be in parallel with R (see Figure 2). The effective resistance of the burden resistance and the core resistance in parallel is

$$\frac{R_bR}{R_b+R}=\frac{R}{1+\frac{R}{R_b}} \quad (66)$$

From equation 66 it is seen that the new effective resistance is the core resistance divided by $1+(R/R_b)$.

From equation 23 it is seen that the peak voltage with a shunt resistor is equal to the peak voltage without, divided by the square root of $1+(R/R_b)$.

From equation 29 it is seen that the root mean square voltage with a shunt resistor is equal to the value without a shunt resistor divided by the fourth root of $1+(R/R_b)$.

These formulas are applicable only to method A where the core resistance can be separated out. If a resistor of any size shunts the reactor, it usually will make the formulas of method A even more applicable, as the eddy currents and flux are definitely separated.

Test Data

Tests were made on a small ring-type iron-core reactor on alternating current to determine the peak voltages developed at various values of current. Tests also were made with the reactor shunted by a resistance to determine the effect of the resistor in reducing the peak voltages.

The circuit used is that shown in Figure 8. The series inductance for loading the circuit was an air-core reactor to make certain that it would have linear characteristics. A search coil was wound on the iron-core reactor and connected to an oscillograph element. The resistance of the oscillograph circuit was kept high so that its shunting effect on the peak voltages would be negligible. The line current and voltage also were connected to oscillograph elements. Tests were made on the reactor, measuring the currents and the peak voltages developed. These tests were rerun with a resistance shunted across the test reactor.

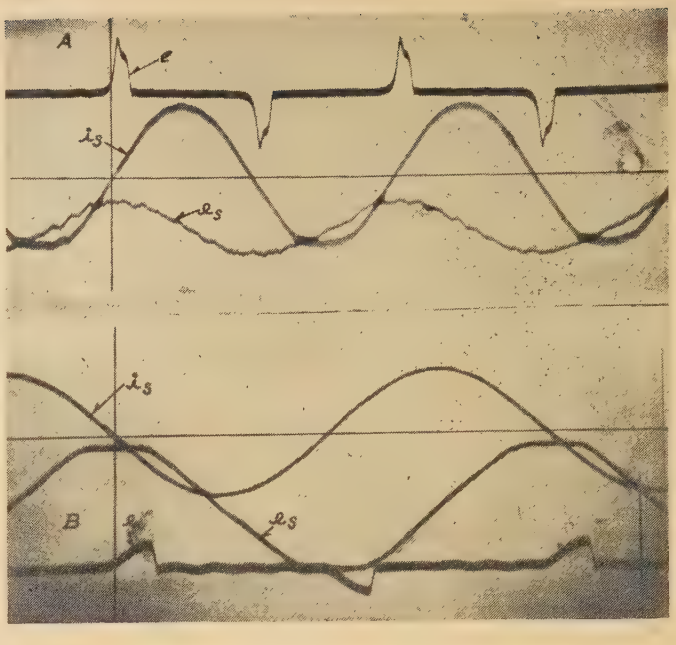

Figure 11. Oscillograms of peak voltage of a saturated reactor

Part *A* is for a reactor only; $I_s=5.8$ amperes root mean square, 60 cycles; and the peak voltage is 9.1 volts

Part *B* is for the reactor shunted by a 0.9-ohm resistor; $I_s=11.75$ amperes root mean square, 60 cycles; and the peak voltage is 5.9 volts. Part *A* shows flattening of the peaks of voltage from initial saturation of the surface and gradual penetration of the flux reversal. The minor peaks of voltage are caused by overtravel in the oscillograph. Part *B* corresponds to Figure 2C

Data for the circuit are as follows:

Power supply: 60 cycles alternating current, 0.2-ohm reactance

Air-core series reactor: 5.5 ohms

Test reactor:

Turns, $N=16$

Losses at 0.483 volts

$VA=0.159$ volt-ampere
W (total) $=0.129$ watt
W (eddy) $=0.049$ watt
$VAR=0.0925$ volt-ampere reactive

Excitation curve per Figure 9

Shunt resistor: 0.9 ohm

The results are given in curve form in Figure 10. Typical oscillograms are shown in Figure 11. It was found that the best correlation was secured between calculated and test data if a factor of 0.85 was used for k.

Calculations

Test reactor constants:

$$R=\frac{E^2}{w_e}=(0.483)^2/0.049=4.77 \text{ ohms}$$

$$X=\frac{E^2}{VAR}=(0.483)^2/0.0925=2.53 \text{ ohms}$$

From Figure 9, $E_m=0.875$ volt

Calculations by sinusoidal voltage, method *A:*

1. $I_s=5.8$ amperes, no shunt resistor

$$H_m=\frac{2E_mZ_sR}{E_s}\left(\frac{X+X_s}{XX_s}\right)^2$$
$$=\frac{2\times0.875\times4.77}{5.8}\left(\frac{2.53+5.7}{2.53\times5.7}\right)^2=0.47$$

From Figure 3, $H_p=0.68$, and using equation 12 for e_p,

$$e_p=k\frac{\sqrt{2}E_sXX_s}{Z_s(X+X_s)}H_p$$

$$e_p=0.85\frac{\sqrt{2}\times5.8\times2.53\times5.7}{2.53+5.7}\,0.68=8.3 \text{ volts}$$

2. $I_s=11.75$ amperes with 0.9-ohm shunt resistor

$$R'=\frac{RR_b}{R+R_b}=4.77\times0.9/(4.77+0.9)$$
$$=0.755 \text{ ohm}$$

$H_m=0.0366$, $H_p=0.25$

$$e_p=0.85\,\frac{\sqrt{2}\times11.75\times2.53\times5.7}{2.53+5.7}\times 0.25=6.2 \text{ volts}$$

Calculations by simplified equation 23:

1. No shunt resistor:

$$e_p=k\sqrt{8I_sE_mR}=0.85\sqrt{8I_s\times0.875\times4.77}$$
$$=4.9\sqrt{I_s} \text{ volts}$$

2. With 0.9-ohm shunt resistor:

$$e_p=\frac{4.9\sqrt{I_s}}{\left(1+\frac{R}{R_b}\right)^{1/2}}=\frac{4.9\sqrt{I_s}}{\left(1+\frac{4.77}{0.9}\right)^{1/2}}$$
$$=1.95\sqrt{I_s} \text{ volts}$$

Calculations by flux distribution, method *B;*

$$e_p=\left(\frac{16I_sE_mR}{3\pi}\right)^{1/2}=2.66\sqrt{I_s}$$

Table I. Peak Secondary Open-Circuit Voltage Developed by Typical Current Transformers With 100 Per Cent Primary Current, Maintained Sinusoidal, 60 Cycles

Type	Voltage Class	Current Ratio	Accuracy Rating	Peak Voltage
WE	600	200/5	0.5-B-0.1, 0.2	175
KO	5,000	5/5–600/5	1.2-B-0.1, 0.5	475
CT-5	5,000	5/5–600/5	0.3-B-0.1, 0.5, 2	1,800
H-5	5,000	2,500/5	0.3-B-0.1, 0.5, 2	11,000
*Ring	46,000	1,200/5	2.5-L-400	6,700
OPC-33	34,500	5/5–800/5	0.3-B-0.1, 0.5, 2	7,300
OPC-66	69,000	5/5–800/5	0.3-B-0.1, 0.5, 2	8,300

* Multiratio bushing type for use on 46-kv bushing.

These calculated curves also are placed on Figure 10.

Conclusions

The curves of Figure 10 which were calculated from method A (assumed uniform flux density in the lamination) show good agreement with the tests except at the higher values of current. At the higher values, the effect of crowding the flux to the surface becomes more noticeable. Presumably, at still higher currents the minimum value which would be calculated by method B, 46 per cent of that given by method A (when $K=1$), would be approached. The oscillograms all indicate a flattening of the top of the wave at higher currents, confirming the fact of a nearly uniform rate of flux change as the reversal travels in from the surface.

When the reactor is shunted by a resistor, accurate calculations are possible. The voltage peaks are nearly true triangles.

The method for fairly exact calculation of peak voltage will permit design of apparatus for minimum values of voltage, as far as possible, and design of proper protection against these voltages. One of the useful results of the method is that the energy available in the voltage peaks can be determined.

Table I lists the maximum open-circuit voltage that can be developed at rated current in certain typical current transformers. The voltage varies approximately as the square root of the current.

Symbols

A = net core area, sq cm
B = instantaneous flux density, gauss
B_m = maximum flux density, gauss (Figure 2)
c = core lamination thickness, cm
e = instantaneous voltage of reactor, volts
e_p = peak induced voltage of reactor, volts
e_{rms} = root mean square value of reactor peak voltage, volts
e' = eddy voltage gradient in lamination, volts/centimeter
E_s = system root mean square voltage, volts
E_m = root mean square voltage reactor will induce, volts, at B_m normal frequency
G = core weight, grams
h = instantaneous magnetomotive force in lamination, oersteds
H_m, H_n = see equation 9 and equation 19, respectively
H_o = instantaneous magnetomotive force at center of lamination, oersteds
H_p, H_q = see equation 11 and equation 20, respectively
i_r = instantaneous current through equivalent R of reactor, amperes
i_L = instantaneous current through equivalent L of reactor, amperes
i_s = instantaneous system current, amperes
i' = eddy current density in lamination, amperes per square centimeters
I_s = system root mean square current, amperes
k = experience factor for peak voltage, about 0.85
K_e = see equation 48
K_h = see equation 44
K_t = see equation 45
K_{ts} = see equation 55
l = mean length of flux path, centimeters
L = equivalent inductance for reactor, henries
L_s = system inductance, henries
N = reactor turns
R = equivalent resistance for reactor, ohms
R_b = resistance of shunt resistor, ohms
R_s = system resistance, ohms
t = time, seconds
v = velocity of flux wave, centimeters per second
W = core loss, watts
W_e = eddy component of core loss, watts
x = distance as measured from center of lamination, centimeters
X = equivalent reactance for reactor, ohms
X_s = system reactance, ohms
Z_s = system impedance, ohms
δ = core density, grams per cubic centimeter
$\theta = \omega t$, radians
θ_d = angle before current zero at which core desaturates, radians
θ_s = angle after current zero at which core saturates, radians
μ = core permeability
ρ = core resistivity, ohms per centimeter cube
ϕ = total flux in core, lines
ϕ_m = maximum total flux in core, lines
$\omega = 2\pi$ frequency, radians per second

Appendix I. Reactor Constants

At low frequencies, the equivalent circuit for the reactor is as shown in Figure 2, with an inductance and resistance in parallel. The primary definition of E_m, the maximum alternating voltage at system frequency that the reactor will induce, will be taken as equation 8. Using this as the definition has the advantage that if any correction must be applied to the theoretical values of the peak voltage, the duration of the pulse will be known to change in the opposite direction approximately the same percentage. This follows from equation 8, for the area under the voltage curve is a constant, regardless of the shape of the voltage curve. It usually will not be convenient to determine E_m in this manner, but from the sample tests it was found that the construction shown in Figure 9 gave a value of E_m that agreed with the oscillograms. Referring to Figure 9, a curve is drawn with the alternating-current voltage as a function of the alternating-current exciting current on rectangular-co-ordinate paper for a core with no air gaps. A line then is drawn tangent to the knee of the curve with a slope one-tenth the slope of the initial straight part of the curve. The point of tangency then gave E_m approximately.

The equivalent reactance X and the eddy-loss resistance, R, of the reactor can be determined from values of I, E, W (total watts loss), and W_e (watts eddy-loss) corresponding to some convenient point on the initial straight part of the excitation curve.

$$X = \frac{1}{\left[\left(\frac{I}{E}\right)^2 - \left(\frac{W}{E^2}\right)^2\right]^{1/2}} \text{ ohms} \qquad (67)$$

$$R = \frac{E^2}{W_e} \text{ ohms} \qquad (68)$$

The values of E_m, X, and R can be calculated from material constants, or the material constants can be calculated from test results by the following formulas:

$$E_m = \frac{\omega N B_m A 10^{-8}}{\sqrt{2}} \text{ volts} \qquad (69)$$

$$B_m = \sqrt{2} E_m / \omega N A \ 10^{-8} \text{ gauss} \qquad (70)$$

$$X = \omega 0.4\pi N^2 \mu A \ 10^{-8}/l \text{ ohms} \qquad (71)$$

$$\mu = Xl/(\omega 0.4\pi N^2 A \ 10^{-8}) \qquad (72)$$

$$W_e = \frac{E^2}{R} = \frac{(\omega N B A \ 10^{-8})^2}{2R}$$

$$= (\delta l A)\left[\frac{\omega^2 B^2 c^2 \ 10^{-16}}{24\delta\rho}\right] \text{ watts} \qquad (73)$$

$$R = 12N^2 A\rho/(lc^2) \text{ ohms} \qquad (74)$$

$$\rho = Rlc^2/(12N^2 A) \text{ ohms per centimeter cube} \qquad (75)$$

Appendix II. Calculation of θ_d

To calculate the angle at which the core starts to desaturate,

$$B_m = 0.4\pi N i \mu / l \qquad (76)$$

For time near current zero, the equation for the line current is approximately

$$i_s = \sqrt{2}\omega I_s t \tag{77}$$

$$\omega t = \theta_d = \frac{B_m l}{0.4\pi N \mu \sqrt{2} I_s} \tag{78}$$

Substituting the values of B_m and μ from equations 70 and 72,

$$\theta_d = \frac{E_m}{I_s X} \text{ radians} \tag{79}$$

Appendix III. Solution of Equation 43

Referring to "Mathematics of Modern Engineering," by Doherty and Keller,[5] page 282, the partial differential equation of a cable with distributed constants of series R and shunt C per unit of length is

$$\frac{\partial^2 e}{\partial x^2} = RC \frac{\partial e}{\partial t} \tag{80}$$

Comparing with equation 42, these are seen to be identical if

$$RC = \frac{0.4\pi\mu\ 10^{-8}}{\rho} \tag{81}$$

Since the terminal conditions are the same, the solution for voltage on a cable may be used for the solution of magnetomotive force for iron if the above substitution for RC is made.

The foregoing reference gives the solution on pages 285–7 for a unit function voltage applied to a cable of finite length with the receiving end open-circuited. The solution desired is that with a voltage which increases uniformly with time. This can be found very simply from the preceding solution by the following method. On page 286, equation 339 is given for the operational solution for voltage:

$$e = \frac{E \cosh nx}{\cosh nl} 1 \tag{82}$$

The solution desired for a voltage that increases linearly with time would be of the form

$$e = \frac{E' t \cosh nx}{\cosh nl} 1 \tag{83}$$

The operational form for t is $1/p$, though

$$e = \frac{E' \cosh nx}{p \cosh nl} 1 \tag{84}$$

The solution of equation 84 is

$$e = E' \int_0^t \left(\frac{\cosh nx}{\cosh nl} 1 \right) dt \tag{85}$$

Hence if the solution on page 287 is integrated from zero to t, it will be the solution for a voltage that increases linearly with time. This leads directly to equation 43.

Appendix IV. Solution of Equation 50

It is not at all evident from an inspection of equation 48 that it does approach equation 50 for low values of t. Letting $z^2 = K_t$ in equation 48,

$$\frac{dK_e}{dz} = \frac{8}{\pi^2} \sum_{s=1}^{s=\infty} \frac{\pi^2 2z}{4} \epsilon^{-\frac{(2s-1)^2 \pi^2 z^2}{4}} \tag{86}$$

If z approaches zero, this can be replaced by the integral

$$\frac{dK_e}{dz} = 4z \int_{s=0}^{s=\infty} \epsilon^{-\frac{(2s+1)^2 \pi^2 z^2}{4}} ds = \frac{4z}{\pi z} \frac{\sqrt{\pi}}{2} \tag{87}$$

$$\frac{dK_e}{dz} = \frac{2}{\sqrt{\pi}} \tag{88}$$

And for values of z near zero,

$$K_e = c_1 + \frac{2z}{\sqrt{\pi}} = c_1 + 2\frac{\sqrt{K_t}}{\sqrt{\pi}} \tag{89}$$

To show that c_1 is equal to zero, substitute in a point on the straight part of the curve of Figure 6.

Appendix V. Complete Solution for i_L

If $e_s = \sqrt{2} E_s \sin(\omega t + \psi)$, and if it is assumed that the line current has returned to its sinusoidal value after the peak during the previous half-cycle, the current through the equivalent inductance L is

$$i_L = K_1 \epsilon^{\lambda_1 t} + K_2 \epsilon^{\lambda_2 t} + \frac{\sqrt{2} E_s}{Z_t} \sin(\omega t + \psi - \beta) \tag{90}$$

$$\psi = \tan^{-1}(X_s/R_s) \tag{91}$$

$$\beta = \tan^{-1} \frac{\frac{R}{X_s} + \frac{R}{X} + \frac{R_s}{X_s}}{\frac{R}{X} \cdot \frac{R_s}{X_s} - 1} \tag{92}$$

$$Z_t = \frac{X X_s}{R} \left[\left(\frac{R}{X_s} + \frac{R}{X} + \frac{R_s}{X_s} \right)^2 + \left(\frac{R}{X} \cdot \frac{R_s}{X_s} - 1 \right)^2 \right]^{1/2} \tag{93}$$

$$\frac{2\lambda_1}{\omega} = -\left(\frac{R}{X_s} + \frac{R}{X} + \frac{R_s}{X_s} \right) - \left[\left(\frac{R}{X_s} + \frac{R}{X} + \frac{R_s}{X_s} \right)^2 - 4\left(\frac{R}{X} \cdot \frac{R_s}{X_s} \right) \right]^{1/2} \tag{94}$$

$$\frac{2\lambda_2}{\omega} = -\left(\frac{R}{X_s} + \frac{R}{X} + \frac{R_s}{X_s} \right) + \left[\left(\frac{R}{X_s} + \frac{R}{X} + \frac{R_s}{X_s} \right)^2 - 4\left(\frac{R}{X} \cdot \frac{R_s}{X_s} \right) \right]^{1/2} \tag{95}$$

$$K_1 = \frac{\sqrt{2} E_s \omega}{\lambda_2 - \lambda_1} \epsilon^{\frac{\lambda_1 \theta_d}{\omega}} \times \left[\frac{\cos(-\theta_d + \psi - \beta)}{Z_t} - \frac{\lambda_2 \sin \theta_d}{\omega Z_s} - \frac{\lambda_2 \sin(-\theta_d + \psi - \beta)}{\omega Z_t} \right] \tag{96}$$

$$K_2 = \frac{\sqrt{2} E_s \omega}{\lambda_1 - \lambda_2} \epsilon^{\frac{\lambda_2 \theta_d}{\omega}} \times \left[\frac{\cos(-\theta_d + \psi - \beta)}{Z_t} - \frac{\lambda_1 \sin \theta_d}{\omega Z_s} - \frac{\lambda_1 \sin(-\theta_d + \psi - \beta)}{\omega Z_t} \right] \tag{97}$$

$$Z_s = (R^2_s + X^2_s)^{1/2} \tag{98}$$

θ_d is found from equation 79. To use equation 90, the time of saturation, t_s, is found by setting I_L equal to $+\sqrt{2}\, I_s \sin \theta_d$ and solving for t_s. The peak voltage is the value of $L(di_L/dt)$ at t_s. There appears to be no simple manner in which to secure t_s, and the nature of the problem does not warrant the labor as compared with the approximate methods developed in the paper.

References

1. Peak Voltages Across Saturating Reactances, H. Fahnoe, A. J. Maslin. *Electric Journal*, March 1932, page 120.

2. Peak Voltages on Saturating Reactances in Three-Phase Circuits, E. L. Harder. *Electric Journal*, March 1932, pages 124–9.

3. Overvoltage Protection of Current Transformer Secondary Windings and Associated Circuits, R. H. Kaufmann, G. Camilli. AIEE Transactions, volume 62, 1943, July section, pages 467–72.

4. Evolution of Standard Lines of Current Transformers for High Overcurrent Capacity, E. C. Wentz. AIEE Transactions, volume 63, 1944, September section, pages 658–62.

5. Mathematics of Modern Engineering, volume I (book), R. E. Doherty, E. G. Keller. John Wiley and Sons, New York, N. Y., 1936. Pages 282–7.

6. Characteristics of Current Transformers on Open Circuit, W. R. Woodward. *Electric Journal*, February 1918, pages 48–50.

A Tunable Rejection Filter

R. C. TAYLOR
ASSOCIATE AIEE

Synopsis: The theory and design of a tunable bridge-type narrow-band rejection filter are given for the general case, considering elements with dissipation. Range of adjustment and effect of manufacturing variations are discussed with the help of impedance circle diagrams. Approximate attenuation formulas for various levels of attenuation are derived, and a convenient graphical method of studying performance is suggested. A formula for the effective width of a special arrangement of two filters in tandem is derived.

IN COMMUNICATION and allied branches of electrical engineering, it is frequently necessary to use a filter with a narrow stop band to reject a single interfering frequency. It is the purpose of this paper to describe the theory of operation and methods for design and reduction to practice of such a device which has proved to be valuable at frequencies from 1,000 to 20,000 cycles per second. The principles of the device are equally applicable at much lower[1] and at much higher frequencies.

The familiar bridge circuit of Figure 1, frequently employed as a delay circuit, is the basic arrangement for the narrow band rejection filter. An elementary explanation of the device[2] sets forth that each of the bridge arms is resonant at the reject frequency and the inevitable dissipation is such that the four arms become equal resistances at the reject frequency, and the bridge is therefore balanced and the undesired frequency rejected. The impedance circle diagram of Figure 2 illustrates this concept. In the practical case, resistances are functions of frequency, and although the line and circle loci are distorted, the distortion is not enough to destroy the usefulness of the concept, since most of the distortion is in those parts of the loci far from resonance. The circle applies to the parallel resonant arms and the vertical line to the series resonant arms. The familiar half-energy points of the resonance curve are found at the intersections of the 45-degree lines with these loci, which Kennelly has called the quadrantal points.[3] Both loci contain arrowheads to indicate the direction in which the tip of the impedance vector moves as the frequency increases. The narrowness of the stop region near the balance point b is a function of the velocity with which these vector loci are traced as the frequency is varied. Since they are traced most rapidly near resonance, which occurs at b, and particularly since they are traced in opposite directions near the balance point, a very narrow stop band is realized, the width of which is found to vary inversely as the circuit Q. A device of this kind rejecting 1,100 cycles per second has been inserted in a telephone circuit with negligible loss of intelligibility.

The construction of such a device with the line exactly tangent to the circle and the resonance of all arms of the bridge occurring at the same frequency is difficult and unnecessary, since closely similar performance can be realized with the balance condition illustrated in Figure 3. In Figure 3, the balance point does not occur at resonance, and the series and parallel circuits have different resonant points shown at r_1 and r_2. There are two possible balance conditions indicated by the intersection points b_1 and b_2, and either can be obtained by adjusting the resonant frequencies. The impedances of all four bridge arms at balance are equal both in magnitude and angle. This procedure requires much less accurate control of the resistance, which is often less predictable than the reactance, and assures a balance, since a balance is always possible if the line and the circle intersect. If the tangent condition is attempted, any increase in dissipation results in the separation of the two loci, and no balance is possible, although some attenuation can be obtained where the loci are nearest together.

Range of Adjustment

A considerable range of reject frequencies is obtainable with any given set of coils. Consider, for example, a coil that has no dissipation other than d-c resistance. The position of the straight line locus then is independent of frequency. The diameter of the circle locus is proportional to the square of the resonant frequency according to the equation,

$$\text{Resonant resistance} = \omega^2 L^2 / R_{DC}$$

If a rejection filter of this type, operating as shown in Figure 3, is tuned to successively lower frequencies, the circle locus will decrease in size until the tangent condition of Figure 2 is reached. With any further decrease in frequency, the loci will separate and no balance will be possible. If the frequency is increased above that corresponding to Figure 3, the diameter of the circle will increase as the square of the frequency, and the balance points b_1 and b_2 will become farther and farther separated from the resonance r_2. Balance is still possible, since the loci intersect, but it is not usually desirable to use this condition, since it produces an

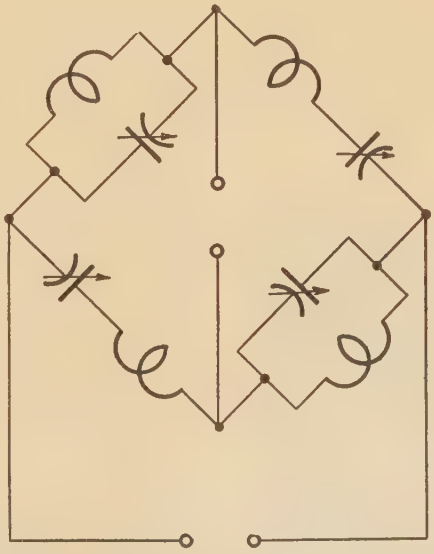

Figure 1. Basic circuit of the rejection filter

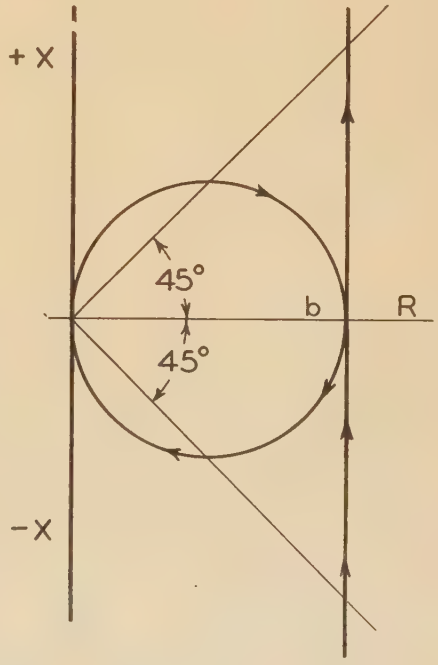

Figure 2. Impedance diagram, limiting case

Paper 46-23, recommended by the AIEE committee on communication for presentation at the AIEE winter convention, New York, N. Y., January 21–25, 1946. Manuscript submitted November 8, 1945; made available for printing December 12, 1945.

R. C. TAYLOR is with the engineering department, Western Union Telegraph Company, New York, N. Y.

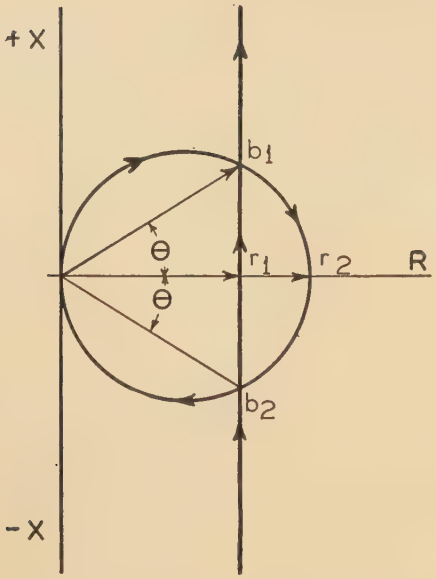

Figure 3. Impedance diagram, general case

effect very similar to reducing the Q. If an arbitrary standard were set up requiring the parallel resonant resistance to be not more than twice the series resonant resistance (line passing through center of circle), then the frequency range of adjustment in this case would be limited to $\sqrt{2}$ to 1. However, as bad a condition as this is seldom met in practice, and a range of adjustment approaching two to one is practicable in most cases. The range realized depends on the variation of dissipation with frequency and on the need for maximum narrowness of stop band.

Theoretically, infinite range of adjustment is obtained when the product of the series resonant and shunt resonant Q's is constant. As an illustration, let the dissipation of the series resonant circuit be a series resistance independent of frequency and the dissipation of the parallel resonant circuit be a shunt resistance independent of frequency and, of course, slightly larger than the series resistance. This results in constant product of the Q's and is also the condition for no distortion of the loci, and resonant resistance independent of frequency. Such a combination could be tuned to reject any frequency with equally good results. Practically, such a combination of properties is seldom available without loss of stability or circuit Q, and one is likely to find the resonant resistance of desirable components varying with the frequency, introducing some distortion of the loci and limiting the range of adjustment to about two to one.

Practical Circuit Arrangement

In practice it is usually preferable to modify the circuit of Figure 1 to that of Figure 5, where inductances with the same letter designations are on the same core. Imperfect coupling between windings is not often serious, the principal effect being the inclusion of a series inductance in the parallel resonant branches. Since at frequencies much greater than balance frequency, the useful frequencies flow to the receiver through the parallel resonant arms of the bridge, the series inductance will limit the high frequency response. In practice this limitation is not severe, since the parallel resonant inductance is a small one if the Q is ten or greater; leakage inductance can easily be made a small fraction of the total; and consequently a wide pass band above the reject frequency will exist. It has been found convenient to select transformation ratios that make the three capacitors marked C of equal capacity.

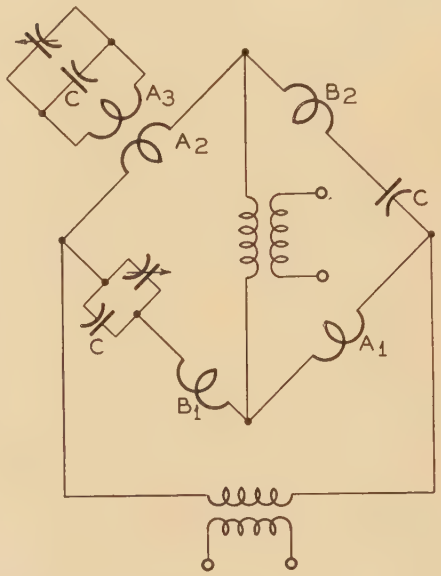

Figure 5. Practical circuit of the rejection filter

Since the stop band is very narrow, it is usually desirable to use trimmer capacitors which permit about one per cent adjustment of capacity (Figures 4 and 5). Larger air capacitors with precision mechanical drives are convenient for greater range. Figure 5 shows input and output coupling transformers to match impedance levels.

Attenuation Formulas and Graphs

The attenuation of all such reject filters is shown as a function of frequency in Figures 6 and 7. These curves can be represented for attenuations greater than ten decibels by the following equation derived in the appendix:

$$\alpha = 20 \log_{10} (K/W) \qquad (1)$$

These curves are universal curves, since the constant K has the same dimensions as the variable W, the width of the stop band on the frequency scale at attentuation α. In other words, the frequency scale may be thought of as plotted in K units as indicated in Figure 7.

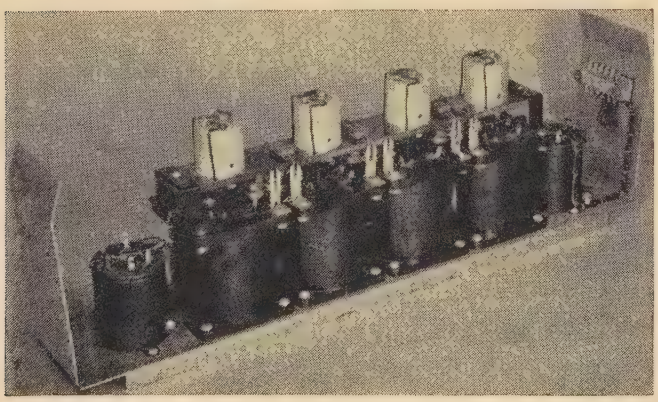

Figure 4 (left). Tandem filter showing trimmer capacitors

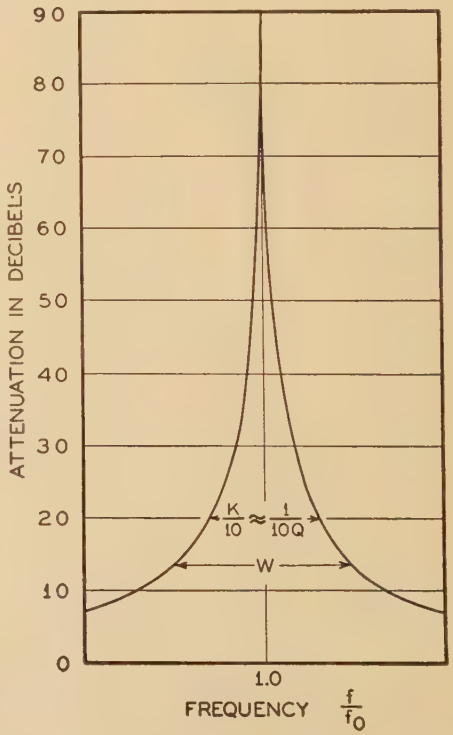

Figure 6 (right). Attenuation of single rejection filter

In Figure 7 the dotted curve at A indicates either an imperfect balance or noise present in the test equipment, and the dotted extension at B indicates a graphical method of determining K. If the data are plotted with width in cycles per second as abscissa instead of K units as abscissa, the intersection of the straight line with the axis gives the actual value of K in cycles per second.

A slightly more complicated empirical equation useful down to three decibels is

$$\alpha = 20 \log_{10} [K/W + 1/(1+K/W)] \qquad (2)$$

K can be determined graphically from the curves, as indicated, or computed by formula 25. As shown in the appendix, a better approximation for attenuations between one-tenth decibel and three decibels is given by

$$\alpha = 20 \log_{10} [1 + (1/2)(K/W)^2] \qquad (3)$$

The attenuation curve is rather difficult to measure at large attenuations, since either or both low frequency noise and harmonics of the reject frequency tend to reduce the apparent attenuation. Another difficulty is the requirement of very small frequency steps near the reject frequency. A cycles increment dial on a beat frequency oscillator is a convenience for these tests.

Figure 7 suggests the use of two crossed rejection filters as a discriminator in frequency modulation receivers, provided some ten decibels of minimum loss can be tolerated.

Two Reject Filters in Tandem

If a rejection band wider than that provided by one section of this type of filter is required to secure sufficient band width to reject a narrow band of frequencies rather than a single frequency, it may be desirable to widen the stop band by using two or more filters in tandem, each filter rejecting a slightly different frequency. In some cases this arrangement may be found advantageous to preserve the required attenuation if the circuit elements are not sufficiently stable. Two sections result in a characteristic of the type shown in Figure 8. Using equation 1, it can be shown (see appendix) that

$$W_0/W_s = \sqrt{2 \text{ antilog}_{10} (\alpha_0/20)} \qquad (4)$$

where W_s is the width of one filter at the attenuation α_0. The increase in width is shown by Table I, which shows a very large relative increase at high attenuations.

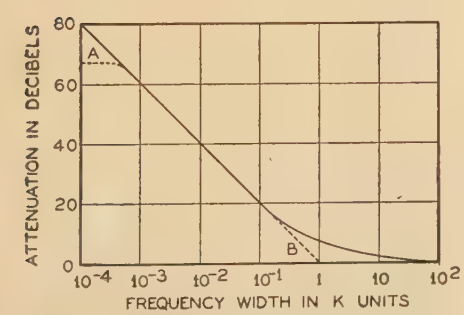

Figure 7. Graphical method of determining K

Stability Measurements

In the construction of these filters, it is essential that all components, including the resistances of the circuit, have good stability with respect to temperature, humidity, and voltage. Silvered-mica capacitors with air trimmers and powdered-iron cores made of Carbonyl E iron have been found to be of satisfactory stability. The final stability coefficient of the rejection frequency and attenuation is a complex function of the separate coefficients of the filter components and also of whichever of the two possible balance points is selected. One model designed to be tunable from 3,000 to 4,800 cycles per second was adjusted to 70 decibels attenuation at 3,600 cycles per second, and subjected to temperatures from 55 to 100 degrees Fahrenheit. The peak attenuation decreased about five decibels and the frequency at which the peak occurred changed less than two cycles per second. In any individual case, the various temperature coefficients can be made to counteract each other if components of both positive and negative coefficients are available.

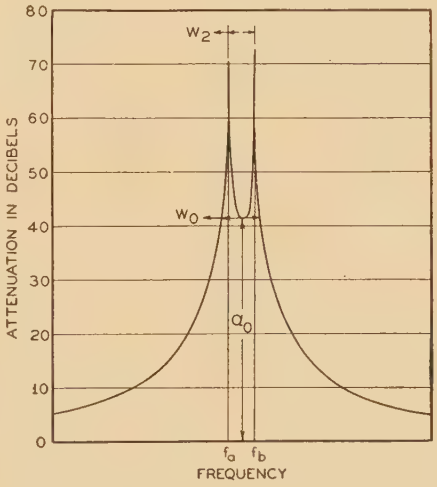

Figure 8. Attenuation characteristic of tandem rejection filters

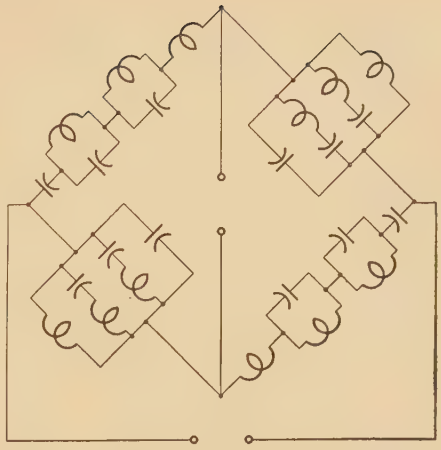

Figure 9. Multiple frequency rejection filter

Relation to Filter Theory

While it is obviously appropriate to call this device a filter, since it has pass and stop frequency regions, the attenuation in the stop band is explained only by the resistances present, while conventional filter theory excludes resistance and deals with reactances. The device illustrated in Figure 1 is an all-pass network with no attenuation at any frequency when considered as a conventional filter. It is only when resistance is considered as in Figures 2 and 3 that the attenuation region appears. If the resonant frequencies of the series tuned and shunt tuned arms are slightly separated, then an attenuation band is predicted by filter theory; but only small attenuations will be realized when reactances of the size given by the design equations are used.

The extension of these principles to multiple reject frequencies in a single section is illustrated in Figure 9. Such a device results in an economy of elements but requires variable inductors as well as capacitors, and the adjustments of various reject frequencies are not independent, so that a more practical solution may be the use of simpler sections in tandem. The bridge arms in Figure 9 are shown in a canonic form.[4]

Coil Design

Since the Q of the circuit determines the narrowness of the rejection band and

Table I. K Units

Db	W_s	W_0	W_0/W_s
20	0.1	0.447	4.47
34	0.02	0.20	10.
40	0.01	0.141	14.1
60	0.001	0.0447	44.7
74	0.0002	0.02	100.

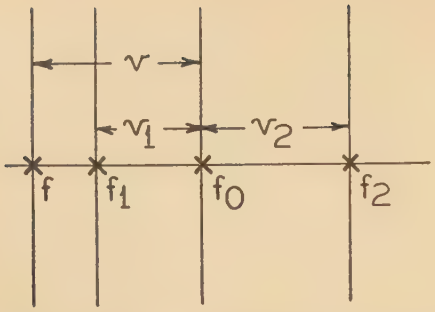

Figure 10. Relation of resonant and balance frequencies

the capacitors are responsible for little of the loss in the circuit, the design of coils with a specified high Q is fundamental. Another important factor results from the large ratio between the inductances of the parallel and series tuned branches. Equation 32 shows this ratio to be approximately Q^2 and therefore may be as high as 100,000 or more. This indirectly determines the impedance level of the bridge, since the series-tuned inductances should not be so large as to lose Q from distributed capacity and leakage effects, and the parallel-tuned inductance should not be so small as to require too small a number of turns, since it is impossible to get close coupling to the tuned winding with less than one turn, and the change of one turn in a small number results in a limited choice of inductance.

Typical windings are illustrated in Figure 11. Notice that in Figure 11A most of the space is allotted to the tuned winding to get maximum Q and consequently minimum width of the reject band.

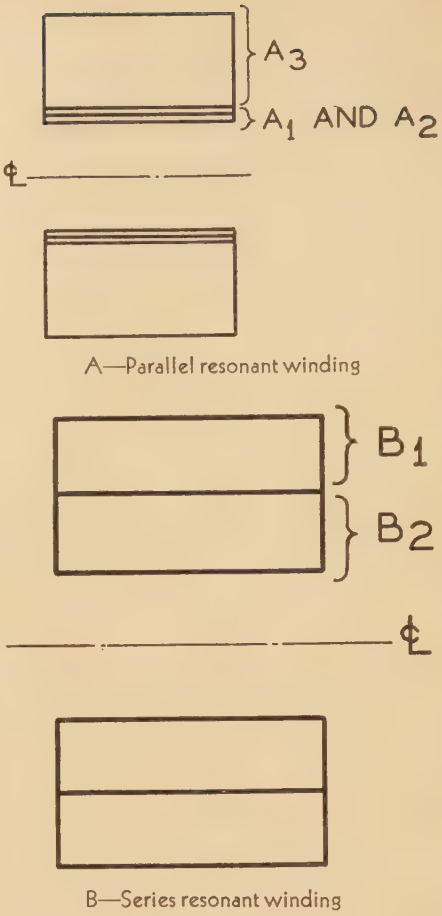

A—Parallel resonant winding

B—Series resonant winding

Figure 11

Appendix

Attenuation Formulas

The propagation constant of a bridge or lattice network is given by[4]

$$\alpha = 20 \log_{10} [(\sqrt{ZY}+1)/(\sqrt{ZY}-1)] \quad (5)$$

and balance of the bridge is obtained when $ZY=1+j0$. Two approximate forms of the equation for the propagation constant are of interest in this application. The first is applicable when

$$ZY=1+jT \qquad T \ll 1$$

and results in

$$\alpha = 20 \log_{10} (4/T) \quad (6)$$

The other is applicable when

$$ZY=-S+jT \qquad T \ll S$$

and results in

$$\alpha = 20 \log_{10} (1+T/S^{3/2}) \approx 17.37 T/S^{3/2} \quad (7)$$

The impedance of the series resonant arm is given by

$$Z_1 = -jX_1[(f_1/f)-(f/f_1)+jR/X_1] \quad (8)$$

where

$$X_1 = 2\pi f_1 L_1$$

and the admittance of the parallel resonant arm is given by

$$Y_2 = -jB_2[(f_2/f)-(f/f_2)+jG/B_2] \quad (9)$$

where

$$B_2 = 2\pi f_2 C_2$$

and R, X, G, B, Z, and Y have their usual Ohm's law meaning, and f_1 and f_2 are the resonant frequencies of Z_1 and Y_2 respectively. The appearance of the expressions may be simplified by writing them as

$$Z_1 = -jX_1(m_1+j1/Q_1) \quad (8a)$$

$$Y_2 = -jB_2(m_2+j1/Q_2) \quad (9a)$$

Using equations 8a and 9a,

$$Z_1 Y_2 = -X_1 B_2[m_1 m_2 - 1/Q_1 Q_2 + j(m_1/Q_2+m_2/Q_1)] \quad (10)$$

where

$$X_1 B_2 = 4\pi^2 f_1 f_2 L_1 C_2 = f_1 L_1 / f_2 L_2 \quad (11)$$

At balance

$$\sqrt{ZY} = 1+j0 \quad (12)$$

Consequently balance conditions are

$$m_1/Q_2 = m_2/Q_1 = 0 \quad (13)$$

and

$$1/X_1 B_2 = 1/(Q_1 Q_2) - (m_1 m_2) = 1/Q_a^2 \quad (14)$$

Calculation of m_1 and m_2 near balance may be made easier if f/f_1 is written (see Figure 10) as

$$f/f_1 = 1-(v-v_1)/f_1 = 1-a \quad (15)$$

and similarly

$$f/f_2 = 1-(v-v_2)/f_2 = 1-b \quad (16)$$

Then

$$m_1 = 1/(1-a)-(1-a) = 2a+a^2+a^3+\ldots. \quad (17)$$

$$m_2 = 1/(1-b)-(1-b) = 2b+b^2+b^3+\ldots. \quad (18)$$

and

$$m_1 m_2 = 4ab+2a^2b+2ab^2+2a^3b+a^2b^2+2ab^3+\ldots. \quad (19)$$

Near balance,

$$m_1 m_2 - 1/Q_1 Q_2 \approx -1/Q_a^2 \quad (20)$$

Since Q_1 and Q_2 vary slowly and $m_1 m_2 \ll 1/Q_1 Q_2$

$$Z_1 Y_2 \approx 1 - jQ_a^2(m_1/Q_2+m_2/Q_1) \quad (21)$$

Equation 6 is applicable, giving

$$\alpha = 20 \log_{10} [4/Q_a^2(m_1/Q_2+m_2/Q_1)] \quad (22)$$

Farther from balance, $m_1 m_2 \gg 1/Q_1 Q_2$ and

$$Z_1 Y_2 \approx -Q_a^2 m_1 m_2 - jQ_a^2(m_1/Q_2+m_2/Q_1) \quad (23)$$

Equation 7 is applicable, giving

$$\alpha = 20 \log_{10}\left[1+\frac{Q_a^2(m_1/Q_2+m_2/Q_1)}{(Q_a^2\, m_1 m_2)^{3/2}}\right] \quad (24)$$

The simplified formulas 1 and 3 can be obtained from 22 and 24 by letting $Q_1=Q_2$, which allows v_1 to be taken equal to v_2. Letting the definition of K be

$$K = 2f_0 Q/Q_a^2 \quad (25)$$

Equation 22 becomes

$$\alpha = 20 \log_{10} (4f_0/WQ_a^2) = 20 \log_{10} (K/W) \quad (22a)$$

and equation 24 becomes

$$\alpha = 20 \log_{10} [1+(1/2)(Q_a/Q)^2(K/W)^2] \quad (24a)$$

which is identical with equation 3 when $Q_a=Q$.

Stop Band for Two Filters in Tandem

If a filter rejecting frequency f_a is connected in tandem with a similar one rejecting f_b where $f_b-f_a=W_2$ (Figure 8), the sum of the attenuations will have a minimum α_0 midway between f_a and f_b. If the component attenuations are large enough for formula 1 to apply, we can determine the width W_0 of the reject band having attenuation α_0 by the following process. Let the width at frequency f (less than f_a) of the filter rejecting f_a be called W. Then the

filter rejecting f_0 has width $W+2W_2$ at frequency f.

At the central minimum

$$\alpha_0 = 20 \log_{10} (K/W_2)^2 \quad (26)$$

Let $f=f_1$ and $W=W_1$ at the edge of the stop band having attenuation α_0. Then

$$\alpha_0 = 20 \log_{10} (K/W_1)[K/(W_1+2W_2)] \quad (27)$$

For a single section with attenuation α_0.

$$\alpha_0 = 20 \log_{10} (K/W_s) \quad (28)$$

Consequently, from equations 26, 27, and 28,

$$W_1(W_1+2W_2) = W_2^2 = KW_s \quad (29)$$

and since

$$W_1 = W_0 - W_2 \quad (30)$$

equation 29 can be rewritten to give

$$W_0/W_s = \sqrt{2K/W_s} = \sqrt{2 \text{ antilog}_{10} (\alpha_0/20)} \quad (31)$$

and

$$W_0/W_2 = \sqrt{2} \quad (31a)$$

Design Equations

Combining equations 11 and 14,

$$L_1/L_2 = f_2 Q_a^2/f_1 \quad (32)$$

The second equation to permit solving for L_1 and L_2 is obtained by setting the quotient of equations 8 and 9 equal to R_0^2, where R_0 is the resistance of generator and load. This results at pass band frequencies in

$$L_1 L_2 = R_0^2/4\pi^2 f_1 f_2 \quad (33)$$

Combining equations 32 and 33, we get

$$L_1 = Q_a R_0/2\pi f_1 \quad (34)$$

and

$$L_2 = R_0/2\pi f_2 Q_a \quad (35)$$

L_1 and L_2 are the inductances actually effective in the bridge arms. If the coupled arrangement of Figure 5 is used, the coupling coefficients increase the inductances as follows:

$$L_1 = (Q_a R_0/2\pi f_1)2/(1+k_1) \quad (34a)$$

and

$$L_2 = R_0/2\pi f_2 Q_a k_2^2 \quad (35a)$$

where k_1 is the coupling coefficient between windings B in Figure 5 and k_2 is the coupling coefficient between the tuned winding A and either of the A windings included in the bridge arms.

References

1. Control of Inductive Interference to Telegraph Systems, J. W. Milnor. AIEE Transactions, volume 59, 1940, August section, pages 469–74.

2. United States Patent 2,173,722.

3. Electrical Vibration Instruments (book), A. E. Kennelly. Macmillan Company, New York, N. Y., 1923.

4. Electrical Networks, volume II, E. A. Guillemin. John Wiley and Sons, Inc., New York, N. Y., 1935.

Protection of Pilot Wires From Induced Potentials

R. B. KILLEN
ASSOCIATE AIEE

G. G. LAW
ASSOCIATE AIEE

Synopsis: The use of pilot-wire relays for protection of power transmission circuits usually requires a reliable pilot channel which is free of any induced potentials which may cause transient voltages to appear between wires even though they may be of relatively low magnitude. This is particularly true in the case of pilot relays using a sequence network in which a single-phase alternating voltage is applied to the pilot wires. Conventional methods of protection, such as those used on telephone circuits, are not suitable. As a result it frequently has been necessary to install special pilot circuits which are insulated for voltages far in excess of their normal operating voltage to insure reliable operation. This paper describes a method of protection which provides reliable and satisfactory operation of a-c pilot channels through low-voltage telephone-type cable even though the cable may be subject to induced potentials high enough to operate discharge gaps.

PILOT WIRES used for relay protection of 66-kv transmission lines on the system of The Dayton Power and Light Company in several cases parallel 12-kv distribution feeders. Lead-sheathed telephone cable is used. In overhead sections it is installed on the same poles with the 12-kv lines and in underground sections occupies adjacent ducts to 12-kv underground feeders.

Figure 1 is a map of the protected 66-kv circuits and the routes of the pilot wires and their paralleling 12-kv 4-wire feeders. Figures 2 and 3 show typical configurations of the exposures. All cable sheaths, including the pilot-wire cable sheaths, are bonded at every manhole. Power cable sheaths serve as neutral conductors and are grounded at the substation and at all terminals or risers. The pilot-wire cable sheaths are grounded at each terminal, at the dispatcher's office, and at every riser. In overhead sections the power system neutral is multigrounded but not bonded to the telephone cable sheath, except at risers. The 12-kv system neutral is solidly grounded at substations.

A schematic diagram of the pilot relay circuits, as originally installed, is shown in Figure 4. During fault conditions, single-phase alternating potentials are applied to the pilot wires by the positive- and zero-sequence networks in the pilot relays. When unequal currents flow in and out of the line section, unequal voltages are produced by the relay networks and the resultant difference in current flows through the operating coils. During faults external to the protected section, the potentials produced by the relay networks at opposite terminals act in series, circulating current through the restraint coils and pilot wires to prevent tripping.

The condition thus is established that when the voltage between pilot wires is built up to a critical value by reason of unequal currents flowing in and out of the line section, tripping occurs. It is also true that if this critical voltage is exceeded by reason of some extraneous voltage impressed between pilot wires, tripping will occur.

The maximum current and voltage impressed on the pilot wires by the relays is approximately 100 milliamperes and 60 volts. The minimum alternating potential required between pilot wires to cause the relay contacts to close is approximately 15 volts.

Incorrect Operations

Early experience in the operation of the relays disclosed the following types of incorrect operations:

1. Potentials induced by ground faults on 12-kv circuits paralleling the pilot wires caused incorrect tripping of 66-kv breakers. An example of this type of incorrect operation occurred during a 12-kv line-to-ground fault at industrial plant A (see Figure 1). Induced potentials appeared on the paralleling pilot wires, causing operation of the carbon block protectors. The discharge through these protectors, being unequal, resulted in a potential appearing between pilot wires, which caused tripping of all 66-kv circuits supplying Webster substation.

Paper 46-35, recommended by the AIEE committees on protective devices and power transmission and distribution for presentation at the AIEE winter convention, New York, N. Y., January 21–25, 1946. Manuscript submitted October 29, 1945; made available for printing December 18, 1945.

R. B. Killen is planning engineer and G. G. Law is supervisor, testing department, The Dayton Power and Light Company, Dayton, Ohio.

The authors wish to acknowledge the assistance of representatives of the American Telephone and Telegraph Company, General Electric Company, and Westinghouse Electric Corporation.

2. Normal load currents in paralleling 12-kv 4-wire feeders caused induced potentials in the pilot wires which circulated current through the alarm relays and gave incorrect alarms. Potentials of 20 to 30 volts between pilot wires and ground frequently were encountered. This potential caused current to flow through the distributed capacitance of the pilot wires to ground, some of which returned through the grounded mid-point of the supervisory relay transformer. The capacitors connected between mid-points of the insulating transformer and the ground served to by-pass some of this current. However, this did not entirely correct the difficulty.

3. Normal load currents in paralleling 12-kv 4-wire feeders caused induced potentials in the pilot wires, which incorrectly tripped 66-kv breakers if one pilot wire accidentally became grounded. Grounding of one pilot wire causes any induced potential to appear between pilot wires. If the potential exceeds 15 volts, tripping results. Several operations of this type occurred when workmen accidently grounded one of the pilot wires while working on other circuits in the cable.

As a result of these difficulties, a series of investigations was conducted to determine the magnitude of the extraneous potentials appearing on the pilot wires and to devise a suitable means of correcting these troubles.

Field Tests

Field tests were carried out on the underground exposure from Webster to industrial plant *A* and on the overhead exposure from Hoover to industrial plant *B*. These tests were designed to determine the magnitude of the longitudinal voltages with which a protective scheme would have to deal. With the power circuits disconnected from their normal busses, a 230-volt test voltage was applied to cause ground fault current to flow in the exposures. From these tests, mutual impedance values were found as shown in Table I. Applying these factors to calculated values of fault current, the maximum longitudinal pilot-wire voltage was found to be 1,650 volts. With this information, the problem was resolved into designing a protective scheme meeting certain requirements for satisfactory operation of the relays.

Pilot-Wire Protective Scheme

The fundamental requirements of the protective scheme are as follows:

1. The protective scheme should function to discharge properly any extraneous potentials imposed in the pilot wires without resulting in any appreciable potential difference appearing between pilot wires. Any such potential between wires should not exceed 15 volts.

2. The voltage from a pilot wire to ground (or other wires in the cable) must be limited to 700 volts crest value during any system disturbance to avoid exceeding the voltage rating of the cable.

3. The protective scheme should permit normal operation of the pilot relays during periods in which the protective equipment is functioning. This is necessary to insure correct relay operation in case of faults involving both 66-kv and 12-kv circuits simultaneously.

4. The proper functioning of the pilot-wire supervisory relays, which indicate to the operators the presence of open- or short-circuit conditions in the pilot wires, must be maintained.

5. The protective equipment used must automatically restore the circuits to normal after its operation.

With these requirements in mind, it appeared that a solution could be found

Table I. Pilot-Wire Voltages to Ground Resulting From Faults on Paralleling 12-Kv Feeders

	*Underground Exposure	Overhead Exposure
Mutual impedance in ohms per mile (ratio of pilot-wire voltage per mile of exposure to ground fault current in power circuits)	0.096–0.100	0.262–0.265

* Fault current in either or both power cables to industrial plant *A*.

Table II. Laboratory Measurements of Pilot-Wire Currents and Voltages

Current in ground lead of arresters, amp	18.4
Applied longitudinal pilot-wire voltage, v rms	1,500
Voltage from pilot wire to ground at terminals of insulating transformer, v rms	293
Voltage between pilot wires at terminals of insulating transformer, v rms	2.6

Table III. Zero-Phase-Sequence Constants of Underground Cables From Webster to Industrial Plant *A*

	One Cable	Two Cables
Voltage impressed between paralleled phase conductors and ground, v	210	197
Total current, amp	332.8	552
Power input, kw	49	89.6
Length of cable, miles	1.87	1.87
Z_0 in ohms per phase per mile	0.710+*j*0.722	0.472+*j*0.324

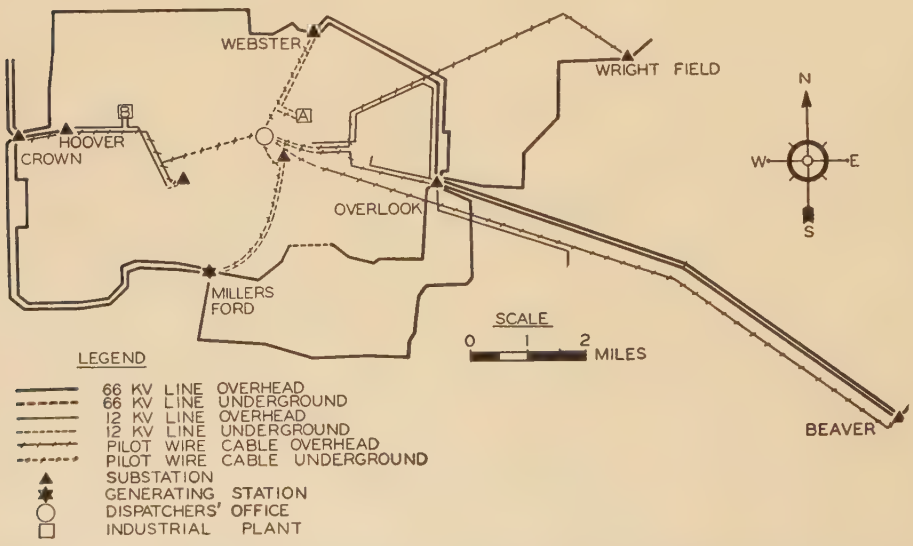

Figure 1. Map of 66-kv lines protected by pilot-wire relaying showing routes of pilot-wire cables and inductive exposures to 12-kv power feeders

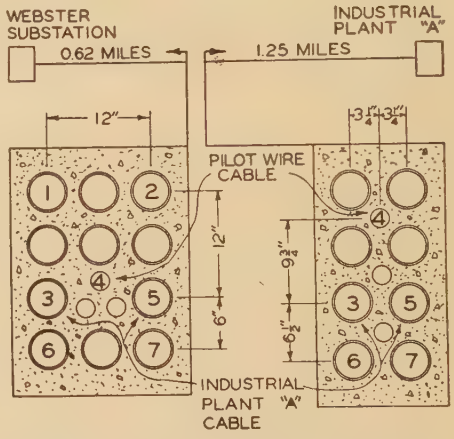

Figure 2. Details of underground ducts between Webster substation and industrial plant *A*

Cables 1, 2, 3, 5, 6, and 7 are 3-conductor 500,000-cir-mil shielded sector-type, with 13/64-inch conductor insulation and 8/64-inch lead sheath. Cable 4 is 51-pair number 19 0.075-inch-lead 0.95-inch-outside-diameter pilot-wire cable

Table IV. Phase Angle of Pilot-Wire Voltages to Ground Resulting From Faults on Paralleling 12-Kv Feeders

	Underground Exposure	Overhead Exposure
Approximate angle the pilot-wire voltage leads the power conductor current, deg	0	31

Table V. Rise in Substation Ground Potential During 12-Kv Faults to Ground

	Webster Substation	Hoover Substation
Type of 12-kv feeder faulted	Underground	Overhead
Rise in substation ground potential in volts per ampere of fault current	0.0064	0.0578
Maximum calculated rise in ground potential for faults near substation, v	130	600

Table VI. Pilot-Wire Voltages to Ground and Rise in Substation Ground Potential for 66-Kv Faults to Ground

	Webster Substation	Crown Substation
Fault current to substation ground bus, amp	1,788	1,460
Pilot-wire voltage to substation ground with opposite end grounded, v	13	174
Rise in substation ground potential, v	130	234

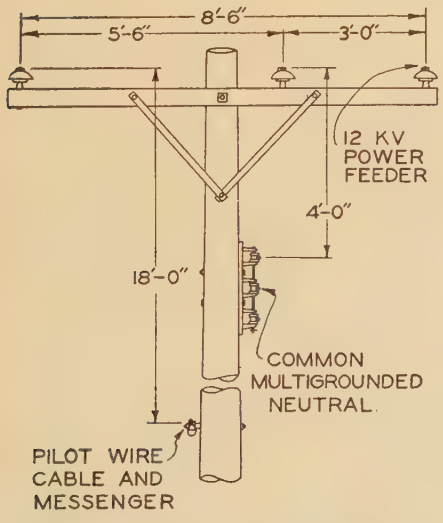

Figure 3. Typical pole top detail showing 12-kv power feeder, secondary, and 51-pair number 19 0.075-inch-lead 0.95-inch-outside-diameter pilot-wire cable, supported by 5/16-inch high-strength galvanized steel messenger

in the application of the principle used in the American Telephone and Telegraph Company's number 223-A retardation coil, used for the reduction of metallic voltages on open-wire carrier lines. It consists simply of modified drainage coils with middle connections isolated from ground by gaps. When the gaps discharge the assembly functions as a drainage coil.

Preliminary laboratory tests were made using coils of various excitation characteristics and several types of discharge gaps.

The connection diagram adopted from these tests is shown in Figure 5. It will be noted that the mutual reactors at the substations are connected to the mid-terminals of the relay insulating transformers instead of across the pilot wires. This connection was adopted in order to cause a minimum change in pilot-wire shunt impedance during discharge. However, if circumstances required connection across the pilot wires or additional protectors between terminals, the shunt impedance could be made high enough to cause only slight decrease in the sensitivity of the pilot relays.

A mutual reactor was selected, each winding of which has an exciting impedance of approximately 11,500 ohms at 200 volts. This value of impedance was considered sufficiently high to result in a negligible change in the sensitivity of the pilot relays during gap discharge. This value of impedance also was considered sufficiently high to insure satisfactory operation of the protector tubes without causing excessive excitation currents in the reactors.

A gas-filled protector tube was selected which had the following characteristics:

A-c rms breakdown voltage, v	300–500
Maximum discharge current for two seconds, amp	50
Average arc drop, v, d-c	20–30

The tube is capable of repeated discharges without material change in characteristics.

Final Laboratory Tests

Equipment was connected in the laboratory as shown in Figure 5. Resistors were used to simulate pilot-wire resistance.

Test Number 1

With protector tubes removed at points *B* and *C* and terminals 2 and 3 connected at *B*, test potential was applied between the mid-point of the mutual reactor at *B* and ground. Oscillograph elements were connected to measure quantities as shown in Table II. This test indicated that with maximum longitudinal voltage induced on the pilot wires, the potential between wires was sufficiently low to prevent incorrect relay operation. Also the voltage between pilot wire and ground was well within its insulation rating.

Test Number 2

This test was made to determine the effect of protector discharges on the sensitivity of the pilot relays.

1. With all protector tubes short-circuited, no appreciable change in the sensitivity of the pilot relays was detected.

2. A similar test was performed with current flowing in the pilot wires and protective equipment simulating discharge currents. This was accomplished by short-circuiting the protector tube at *A* and applying test potential between the mid-point of the mutual reactor at *B* and ground, with terminals 2 and 3 connected. The results of this test indicated no appreciable change in pilot relay sensitivity with currents in each pilot wire up to three amperes.

Field Application

On the basis of the laboratory tests, the 66-kv pilot-relay circuits were equipped

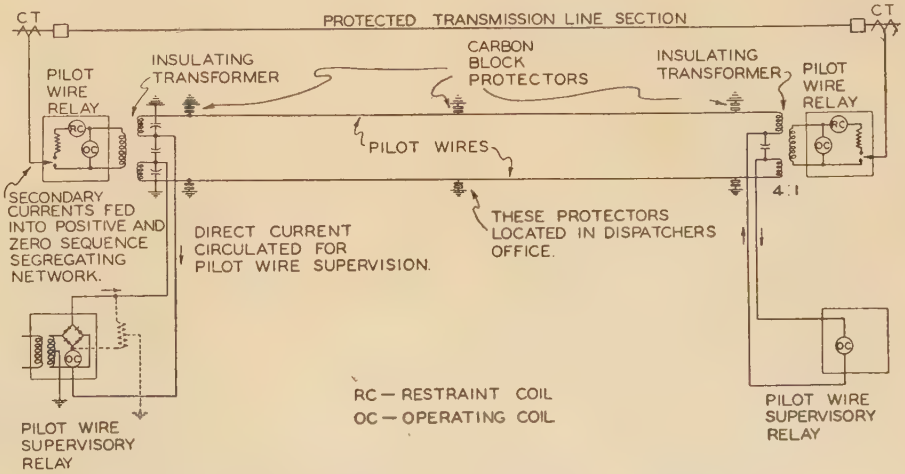

Figure 4. Schematic diagram of pilot-wire relaying as originally installed

Table VII. Substation Ground Resistance

	Webster Substation	Crown Substation	Hoover Substation
Substation ground resistance, ohms	0.14	0.87	0.36

with the new protective devices. The laboratory tests described indicated that this equipment satisfactorily would eliminate incorrect relay operations caused by ground faults on paralleling 12-kv 4-wire feeders.

The second-mentioned difficulty, involving improper operation of the alarm relays, was corrected by the relay manufacturer. A grounding resistor is used with a grounded center tap connected across the output of the rectifier in the alarm relay, instead of grounding the center tap of the transformer supplying the rectifier unit, as shown in Figure 4. This measure prevented induced potentials from causing current to flow through the rectifier and operating coil of the alarm relay.

The foregoing modifications did not eliminate completely potential between pilot wires resulting from normal load currents in paralleling 12-kv 4-wire feeders. This potential appears when a pilot wire becomes accidentally grounded. However, the voltage was reduced below the 15-volt operating level of the relays by the use of the grounding resistor on the alarm relay and the removal of the capacitors connected between the mid-points of the insulating transformer and ground. This resulted in a considerable increase in the impedance between the pilot wires and ground at this point, thereby reducing the potential between pilot wires when one wire becomes grounded. The net result of this change, as determined from field measurements, is a reduction in the potential between pilot wires of approximately 50 per cent for equivalent values of induced potential.

Final Field Tests

The operation of the protective devices was tested by staged ground faults on the 12-kv circuit at the end of the overhead exposure between Hoover substation and industrial plant *B*. Oscillograph measurements were made of the voltage between pilot wires and from pilot wire to ground, and of the fault current. With a fault current of 2,400 amperes, the voltage between pilot wires at Hoover substation was less than two volts, and from pilot wire to ground was 320 volts rms. The calculated longitudinal voltage induced for this value of fault current is approximately 1,000 volts. During the tests, protector tubes discharged, but no pilot-wire relay operations occurred.

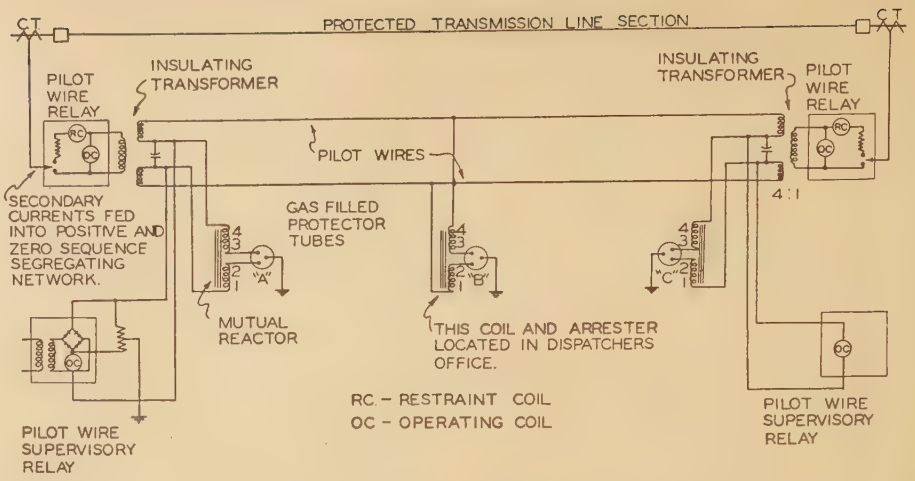

Figure 5. Schematic diagram of pilot-wire relaying equipped with new protective devices

Conclusions

The coils and protector tubes described were obtained from a limited selection of available material, and the laboratory tests were intended to indicate their suitability rather than to determine the most satisfactory design.

Field tests were not conducted on simultaneous 12-kv and 66-kv faults. However, on the basis of the laboratory tests, it is believed that such faults will be relayed correctly.

Since the installation of the protective equipment, several faults have occurred on 12-kv circuits at locations which had formerly caused incorrect operations of the pilot relays. All of these faults were cleared satisfactorily without operation of the 66-kv pilot relays. During this same period, several 66-kv faults occurred, all of which were cleared properly by the pilot relays.

Appendix

During field tests it was convenient to make certain other measurements which did not bear directly on the problem at hand Some of these data are included in the hope that they may add to the knowledge on these subjects.

Table III shows the results of measurements made to determine the zero-phase-sequence impedance of the underground cables from Webster to industrial plant *A*, illustrated in Figure 2. The duct line is removed fairly well from pipe lines or other known underground structures.

Table IV shows the results of measurements made to determine the phase position of the induced potential with reference to the current in the power conductor. These measurements were made by a voltage triangulation method using a high resistance voltmeter. A reference voltage in phase with the power conductor current was obtained by connecting a noninductive resistor to the secondary of the current transformer in the power circuit.

Table V shows the results of measurements made to determine the rise in substation ground potential caused by 12-kv faults to ground. The measurements were made between the substation ground bus and reference grounds driven approximately 1,000 feet from the substation at 90 degrees to the faulted feeder.

Table VI shows the results of measurements made to determine the pilot-wire voltage and the rise in substation ground potential during ground faults on the 66-kv system. Ground faults were applied at Webster and Crown substations to the substation ground bus. The rise in substation ground potential was measured with reference to a remote driven ground located approximately 1,000 feet from the substation and as near 90 degrees to the 66-kv lines as possible.

Table VII shows the results of ground resistance measurements of substation ground busses made with a ground resistance tester using two remote reference grounds.

Marine Radar for Peacetime Use

L. H. LYNN
NONMEMBER AIEE

O. H. WINN
ASSOCIATE AIEE

MILITARY RADAR systems by the score have been developed for such varied purposes as surface search, aircraft detection, height finding, gunfire control, range finding, and other wartime uses not as yet released from the classified categories.

In most of these systems, the prime function was connected in some way with locating the enemy accurately, judging his course, speed, and strength, and getting this knowledge quickly enough to take appropriate counteraction. The sooner such data were accumulated and evaluated, the stronger offensive (or defensive) measures were possible. For this reason, design parameters that affected cost, complexity, or operator skill were less important than those which governed range, accuracy, resistance to gunfire shock, etc.

The relative importance of these factors was reflected necessarily into the space and power requirements of the military equipment, and the very design elements that permitted excellent military radar are often those which make for an unsuitable peacetime radar.

Let us forget, for the moment, the spectacular achievements of radar during the past few years and look ahead to its function as a safety device for civilian use. Among the many jobs that have been envisioned for this branch of electronics, there is perhaps none as important as that of marine radar. From the economic viewpoint alone, the intrinsic value of ships, cargo, and time lost because of poor visibility mounts to enormous proportions. This waste, plus the attendant loss of life, can be reduced to a very small amount by the use of radar equipment properly designed for the job.

Paper 46-47, recommended by the AIEE committee on communication for presentation at the AIEE winter convention, New York, N. Y., January 21-25, 1946. Manuscript submitted December 12, 1945; made available for printing January 1, 1946.

L. H. LYNN and O. H. WINN are with General Electric Company, Schenectady, N. Y.

Design Requirements for Peacetime Radar

The design variables which are controllable include at least the following: reliability, simplicity, accuracy of range and bearing, cost, ease of maintenance, resolving power (on adjacent objects) maximum range, minimum range, appearance, accessibility of components, and size.

In either case, military or civilian, reliability comes first. Cost is a minor point in military designs, a major one in civilian designs. Simplicity of installation and operation is not too important on a battleship where dozens of technically trained men are available. A cargo ship, however, operating in a highly competitive field, must consider any extra personnel from the accountant's viewpoint and use a radar capable of operation by the regular complement of officers.

Maximum ranges of military equipments frequently exceed 100 miles and require appropriate high power for such a range. A passenger ship is concerned much more with an obstacle which may be only several miles away; hence a large equipment is neither justified nor desirable.

The minimum range of a destroyer's radar may well be a mile or two, on the theory that an enemy must be discovered long before he can approach that close. The minimum range of a radar for a cargo ship is required to be less than a ship length—the shorter the better, in order that navigation may be accomplished safely in congested harbors.

And so, all through the whole list of design factors, there must be a new philosophy of design to create suitable radar equipment for our commercial uses. Our peacetime designers must not say, "Who is shooting at my ship from over the horizon?" but rather, "Can this device permit my present complement of personnel to avoid collisions and to obtain fixes from charted landmarks?"

One Design of Commercial Radar

Early in 1943, experiments were conducted on a Great Lakes ore boat, using a modification of a military ship-borne "search radar." From six months' operating data, two outstanding facts stand out:

1. Despite some inherent weaknesses, common to all radar systems, the installation proved to be a highly useful navigational tool.

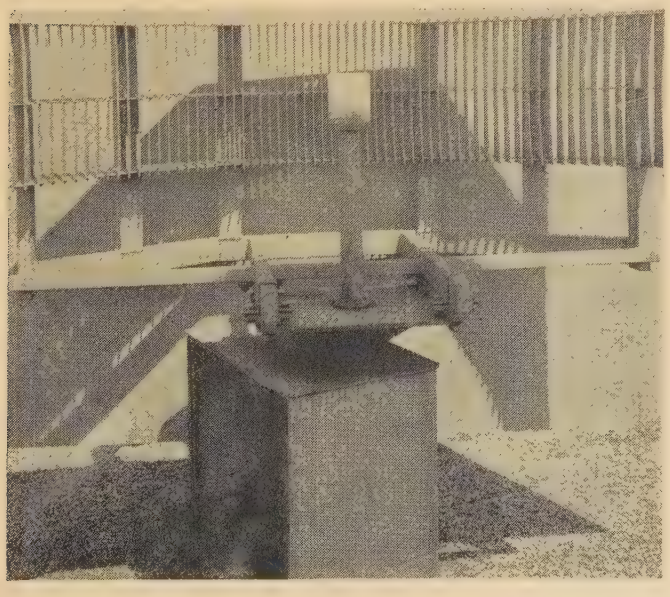

Figure 1 (left). Rotating antenna assembly

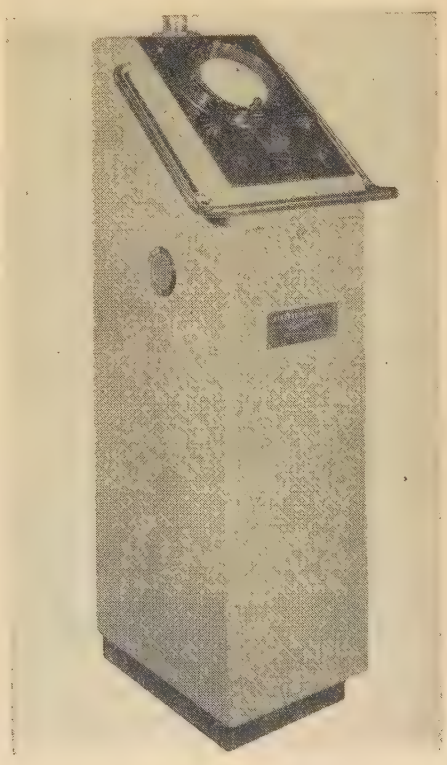

Figure 2 (right). Electronic navigator console

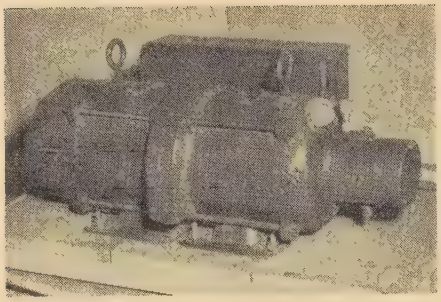

Figure 3 (left). Speed-regulated motor-alternator

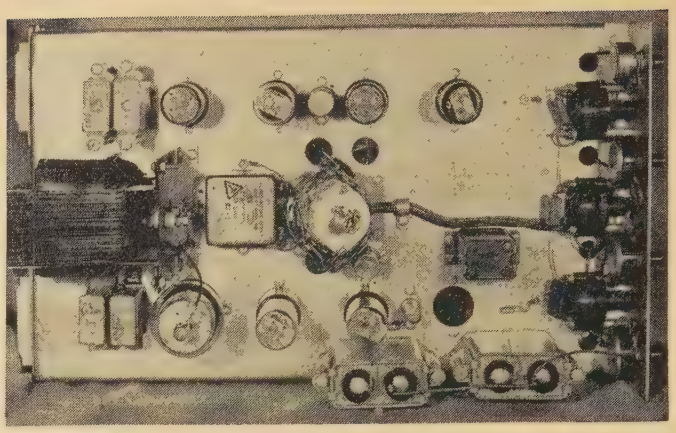

Figure 6 (right). Typical removable chassis of electronic navigator console

Figure 4. Typical beam pattern in horizontal plane, showing five degrees width at half-power points

2. It was too complex for nontechnical personnel to operate.

From these early experiences, plus a study of several hundred service reports from military installations, the present electronic navigator was evolved. Figures 1, 2, and 3 show the three units of the complete equipment: the antenna system, console, and motor-alternator, respectively.

The antenna system is driven by a gear-motor located in the antenna base, or "pedestal," and the slatted reflector rotates continuously at 10 rpm. The surface of this reflector is a truncated paraboloid of revolution and is proportioned to project a beam 5 degrees wide and 15 degrees high. (A fully parabolic reflector of the same width would project a conical beam 5 degrees wide, with the resultant danger of lost targets when the ship rolled.) Note that these figures do not imply that there is zero radiation outside the angles mentioned; the accepted method of measuring beam width is at the half-power points, as shown in Figure 4.

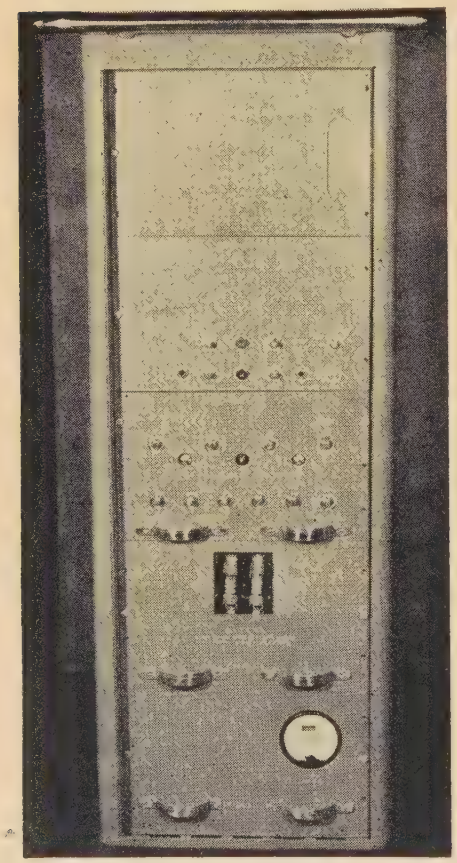

Figure 5. Electronic navigator console with front cover removed, showing removable chassis

The console, Figure 2, contains the transmitter, receiver, cathode ray tube, sweep circuits, pulsing circuits, rotating field mechanism, appropriate power supplies, and controls. During normal operation, seven controls are available to the operator. Having adjusted the instrument and selected the desired range scale (2, 6, or 30 miles) no further manipulation is required unless it is desired to take a bearing on some specific object. In this case a knob is provided to control a radial bearing line which can be caused to bisect the object in question and thus read its azimuth on a scale around the circumference of the cathode ray tube.

All other controls which are required for initial adjustment during installation are accessible to recognized service personnel only and are covered by a locked panel. Figure 5 shows these controls and also the test jacks and the panels of the various removable chassis. In case of trouble with any chassis, it is possible for the service engineer to substitute an entire chassis in a minute and repair the original one at leisure. Figure 6 illustrates a typical chassis removed from the console.

Figure 7 is a block diagram of the radar circuits and emphasizes the relative simplicity as compared with usual military designs. The pulse generator of Figure 8 is a blocking oscillator whose recurrence rate is determined by a network Z and resistors R_1 and R_2. (Most blocking oscillators employ only a capacitor in place of a network.) The function of the lumped-constant line Z is to provide a delay in the discharge time so that the tube may be allowed to conduct its full saturation current for a definite time interval, as shown in the pulse shape of Figure 9, which depicts the voltage across the primary of transformer T_1. This transformer

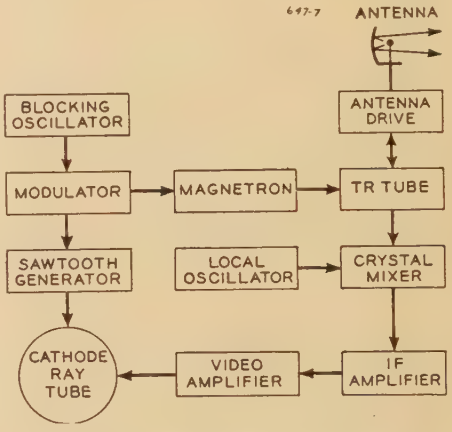

Figure 7. Block diagram of circuits

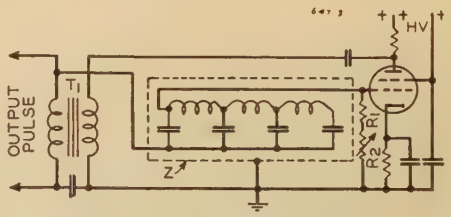

Figure 8. Pulse-forming circuit

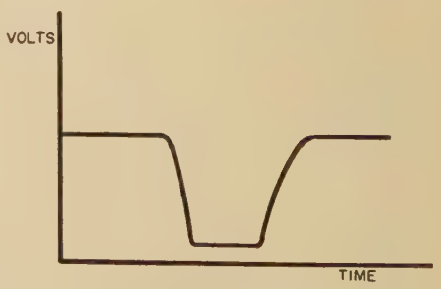

Figure 9. Pulse shape

is so connected as to provide regenerative feedback for the oscillator, and thus the cycle is repetitive and at a rate controlled by variable resistor R_2. The simplicity and reliability of this circuit makes it particularly suitable, for this application. The pulses formed by the blocking oscillator are amplified by a suitable pentode and used to drive the magnetron oscillator which operates in the 10-centimeter region. See Figure 10. The modulation transformer (T_2) permits the magnetron filament to be operated 5,000 volts above ground, for this is the order of magnitude of the amplified pulse voltage. A tap on the modulation transformer allows the modulator tube to be properly loaded.

The pulse is considerably less than one microsecond in length and repeats at about 1,000 cycles per second. Thus the peak power delivered to the magnetron is of the order of kilowatts, though the average power is but a few watts.

Referring again to Figure 7, the output of the magnetron is delivered to the antenna through the transmit-receive (T-R) tube, the function of which is to protect the receiver during transmitter pulses and to close off the path to the magnetron during the receiving time, between pulses.

The returning echo from the "target" is collected by the parabolic reflector, focused on the antenna dipole, and carried through the transmit-receive tube to the receiver circuits. In the crystal mixer the returning signal is caused to beat with the output of a klystron local oscillator, the resultant frequency being about 30 megacycles. This is amplified by a wide-band intermediate-frequency amplifier, detected and further amplified by the video amplifier, and thence applied to the control grid of the cathode ray tube.

In the meantime the antenna assembly has been rotating continuously, and its

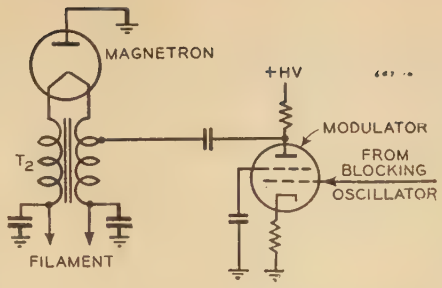

Figure 10. Modulator and magnetron circuits

motion has been transmitted by a very compact and simple Selsyn system to the rotating magnetic deflection coil located around the neck of the cathode ray tube. Impressed across this rotating coil is the sawtooth sweep voltage which provides a linear radial time axis. Time, too, is synchronized with the transmitter, and as both the outgoing pulse and the returning echo travel at the speed of light, this time axis is really a distance measure.

The over-all result is that as the radial time (that is, distance) axis rotates, any returning echo will intensify a portion of this axis as the rotating antenna "beams" on the target. With an ordinary cathode ray screen, the bright flashes of light would indicate the presence of reflecting objects, but the operator would have to remember where the flashes occurred, obviously an undesirable disadvantage.

Hence, a long-persistence screen is used, in which the cathode ray first excites a short-persistence phosphor, which in turn causes a second long-persistence phosphor to glow. This glow persists for a long enough time to "remember" a scene until rekindled by the next rotation of the radial sweep.

Since the resultant illumination is in the form of a plan view of the surrounding area, with one's own ship at the center, the system is commonly termed "plan presentation indicator," or simply "P.P.I."

Figure 11 illustrates such a picture, showing land masses, open water, buoys, and ships in the vicinity of Matinicock Point in Long Island Sound. For comparison, the actual chart of that area is printed beside the radar chart.

There are simpler presentation systems, but they require more skill in interpretation. It was felt that the plan presentation indicator picture "spoke the language" of the navigator better, since it shows him the data in familiar chart form. This has been borne out in actual experience, both with skilled navigators and students in training.

Practical Results

The particular design described above has completed an 8-months' test installation on the United States Maritime training ship, AMERICAN MARINER. During that time, several hundred persons have operated the equipment. This group has included military personnel highly trained in radar principles, captains of cargo ships, shipowners, shipyard executives, tugboat captains, river pilots, navigators, trainees, and even deckhands.

From their varied reactions, it has been possible to create a design well suited for the job, unhampered by excessive gadgeting, and capable of operation by nontechnical personnel. Further, it has been possible to spread the idea that radar is not a cure-all scheduled to usurp the functions of existing instruments; rather it is a very powerful aid to those instruments, performing new duties previously left to guess work or chance.

Figure 11. Comparison of radar picture and actual navigation chart

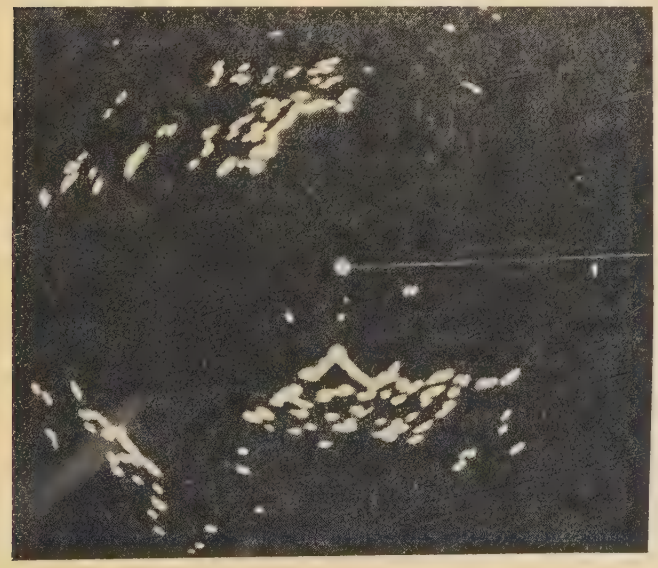

Techniques and Facilities for Microwave Radar Testing

E. I. GREEN
FELLOW AIEE

H. J. FISHER
ASSOCIATE AIEE

J. G. FERGUSON
MEMBER AIEE

Synopsis: Methods and devices are described for testing microwave radar equipment in the radio frequency range from about 500 megacycles to 25,000 megacycles and at associated video frequencies. In general, the same instruments and techniques are applicable also in testing microwave communication systems.

THAT RADAR equipments are marvels of ingenuity has long since become common knowledge. This ingenuity is reflected, however, in complexity of circuits. A rough index of this complexity is found in the number of vacuum tubes, which for a single radar set may range from 50 to 250. Notwithstanding the most careful design, it is easy for the radar performance to become impaired under operating conditions.

Not only is radar complex, but its performance criteria are less tangible than those of conventional communication systems. Ordinary radio is to some extent self-testing in that reception of intelligible speech or signals frequently constitutes a sufficient check of satisfactory performance. With radar, the greater the range coverage and the more accurate the data, the more valuable the information is likely to be. However, the working range may fall to a fraction of the possible maximum, or some other degradation or malfunctioning may occur, with nothing in the operation of the radar equipment to tell that this has happened. Since lack of maximum performance may have serious military results, measurement of performance assumes the utmost importance in radar work.

The new techniques and new frequency ranges employed for radar necessitated the wartime development of a wide variety of new types of test equipment. A large part of this development work was concentrated at Bell Telephone Laboratories and at the National Defense Research Council's Radiation Laboratory at Massachusetts Institute of Technology, working in close co-ordination with one another and with the technical services of the Army and the Navy. In the manufacture of radar test equipment, Western Electric took a major part. This article discusses the techniques of radar testing and describes the types of test gear developed by Bell Laboratories and manufactured by Western Electric. These cover the radio frequency range from about 500 megacycles to 25,000 megacycles, together with associated video frequencies.

Because of its importance during the war, emphasis has been placed on the testing of microwave radar equipment. However, similar methods and instruments also have been employed in the testing of microwave communication systems, and such applications can be expected to increase. In this situation the developers and users of microwave communication systems are fortunate in that almost all of the techniques and devices developed for radar testing are equally applicable to communication systems. This is even true of the video units, which are useful in connection with pulse-modulated telephone systems and amplitude-modulated or frequency-modulated television systems.

So many persons, both within and outside Bell Laboratories, have contributed to the developments described that the authors have reluctantly reached the conclusion that the assignment of individual credit should not be attempted.

Requirements

Subsequent discussion may be simplified by first reviewing briefly the operation of a typical radar set, as shown in Figure 1. Under the control of d-c or so-called video pulses from the modulator, short pulses of radio frequency energy are delivered by the magnetron transmitter to a highly directive antenna, ordinarily arranged to scan a section of space. Energy reflected from an object or "target" in the path of the beam is intercepted by the same antenna. The received pulses or echoes are converted to an intermediate frequency by heterodyning against a local oscillator, the frequency of which may be automatically controlled.

To enable the same antenna to serve for both transmitting and receiving, a transmit-receive tube or transmit-receive switch is usually provided. This consists of a partially evacuated resonant cavity containing a spark gap which breaks down during the transmitted pulse, thus preventing the transmitted power from injuring the sensitive receiver. A receive-transmit (RT) tube, consisting of a similar resonant cavity and spark gap, may be provided to prevent absorption of the received signal by the transmitter. After amplification and detection of the received signal, the resultant video pulses are applied to an indicator which may present information in any of several different ways. Customarily, the direction of the target (determined by antenna orientation) and its range (determined by reflection interval, 10.7 microseconds per mile) are shown. The system may be used merely for searching, or for fire control, bomb direction, or other functions, with additional equipment as required.

Types of Tests and Test Sets

Figure 2 shows an early assemblage of radar test equipment for the 10-centimeter range, initially produced in 1942, which has seen wide usage.

The more important types of tests required in radar work, either at radar operating locations or at centralized service points, are:

1. Over-all performance (range capability).
2. Transmitter power.
3. Receiver sensitivity.
4. Transmitter frequency.
5. Transmitter spectrum.
6. Standing wave ratio.
7. Radio-frequency (RF) envelope.
8. Receiver recovery.
9. Automatic frequency control (AFC) tracking.
10. Intermediate-frequency (IF) alignment.
11. Video wave shapes.
12. Range calibration.
13. Computer calibration.

The principal types of test sets required for carrying out the above are:

1. Signal generators.
2. Echo boxes.
3. Frequency and power meters (separate or combined).
4. Standing wavemeters.

Paper 46-40, recommended by the AIEE committee on communication for presentation at the AIEE winter convention, New York, N. Y., January 21–25, 1946. Manuscript submitted December 19, 1945; made available for printing December 28, 1945.

E. I. Green is test engineer, transmission development department; H. J. Fisher and J. G. Ferguson are members of the technical staff, Bell Telephone Laboratories, Inc., New York, N. Y.

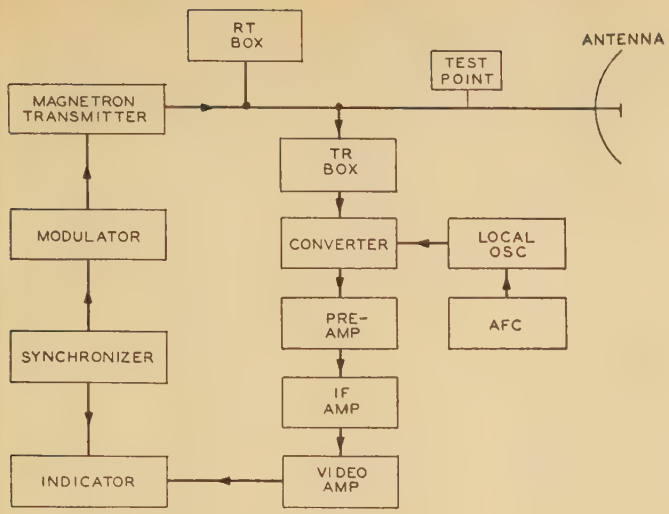

Figure 1. Diagram of typical radar equipment

5. RF loads.
6. Oscilloscopes.
7. Video dividers and loads.
8. Range calibrators.
9. Computer test sets.
10. Spectrum analyzers.

Various auxiliary testing instruments also are employed, including vacuum tube testers, intermediate-frequency signal generators, audio oscillators, flux meters, and so forth. Before discussing the above tests and devices individually, some of the requirements for radar test equipment, especially those requirements resulting from military usage, will be summarized.

Generality of Application

Radar sets perform a great variety of functions, including search and surveillance, gun laying and fire control, bomb direction, and navigation. They are used in the air, on shipboard, and on the ground; in attack and in defense; in combat zones and in rear areas. To realize the advantages of different parts of the frequency spectrum, avoid interference, and keep ahead of enemy countermeasures, it has been necessary for radar to exploit many different frequency bands and sub-bands. These diversities have bred a multiplicity of types of radar, with a corresponding variety of testing problems and requirements.

Maintenance and testing of radar equipment must be performed at many different locations. In the Army these locations, known as echelons, include

1. The operating unit.
2. Central service points, either fixed or mobile, for a number of operating units.
3. Large depots either in the military theaters or in the United States.

Navy maintenance and testing are carried out aboard the fighting ships or auxiliaries and at advance and overhaul bases.

In developing test equipment, an offhand approach might have been to provide specialized equipment for testing each radar set under specific conditions. Since this would have made the total burden of development, manufacture, and field maintenance well-nigh intolerable, a co-ordinated plan was followed whereby (with minor exceptions) each test set was made capable of widespread application in testing as many radar equipments under as varied conditions as possible.

Broadbanding

Generality of application required the designing of test equipment for broad frequency bands, bands as a rule much wider than those of the radar sets themselves. It was necessary, therefore, not only to develop new microwave testing techniques, but to advance the art still further to render the testing components as far as possible insensitive to frequency.

Precision

A radar set itself is an instrument of considerable precision. The test equipment used for checking the radar performance in the field has to have still higher accuracy. It is noteworthy that the measuring accuracy realized throughout the microwave range is comparable with that obtainable at lower frequencies where many years of background exist.

Packaging—Size and Weight

Light weight and compactness are of paramount importance where a test set

Figure 2. Early radar test set for 3,000-megacycle range

It includes signal generator, oscilloscope, power meter, test antenna, and auxiliary units

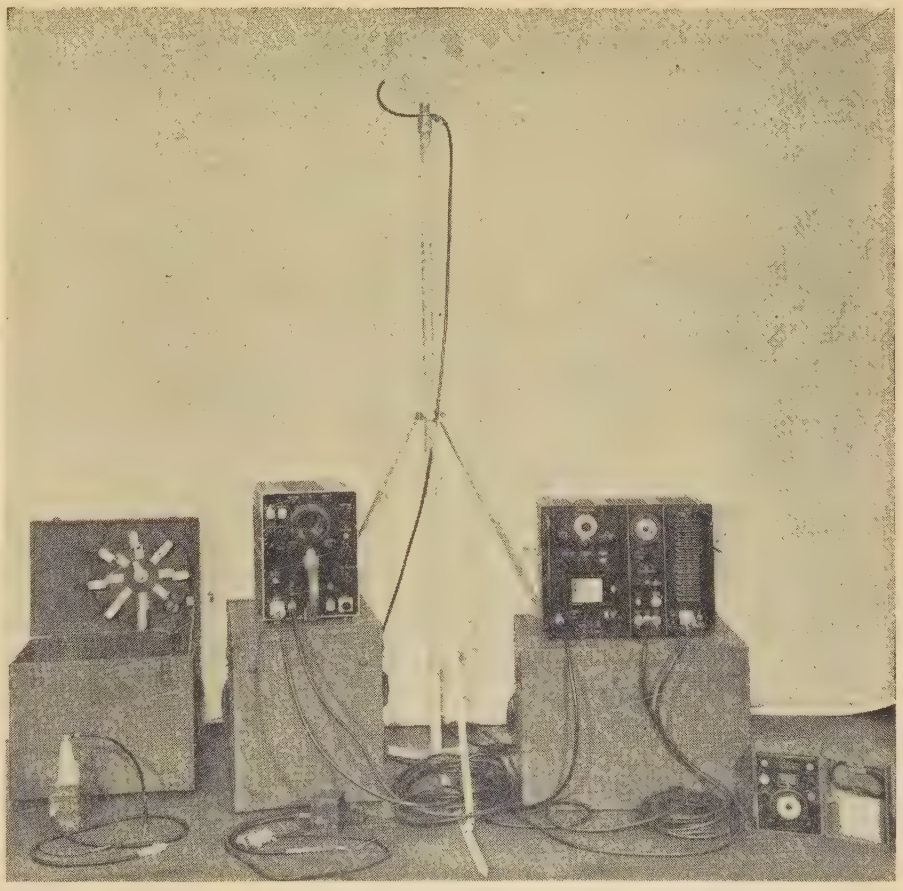

has to be carried any distance by the maintenance man; where it is used in cramped quarters in a plane, truck, or submarine; or where it has to be taken up ship ladders or through small hatchways. To permit portable use under such conditions, the design objective was established of a weight not exceeding about 30 pounds (exclusive of transit case), combined with a ruggedness adequate for all conditions of use. Through rigorous attention to both mechanical and electrical design, this objective has been real-

Figure 3. Portable units used in checking air-borne radar sets at Boca Raton, Fla.

ized (in many cases with considerable margin) except for a few sets intended primarily for bench use. Figure 3 illustrates the use of lightweight test equipment in maintaining air-borne radar equipment.

Environmental Influences

Military usage requires that the test equipment be capable of efficient operation at any ambient temperature between a minimun of the order of −40 degrees to −55 degees centigrade and a maximum of the order of +65 degrees to +70 degrees centigrade, as well as at any relative humidity up to 95 per cent. In addition, the set must withstand continued exposure to driving rain, dust storms, and all other conditions encountered in tropical, desert, or arctic climates. Often the test set in its transit case must be capable of submergence under water without ill effects. Fungus-proofing with a fungicidal lacquer is a standard requirement.

Simplicity, Reliability, Accessibility

Not only must the functioning of the test set be reliable, stable, and trouble-free, but the set must make minimum demands for special skill or technique on the part of the maintenance man. Access for maintenance purposes, while important in radar test sets, is not as controlling as in the radar equipments themselves and sometimes has to be sacrificed in part for compactness.

Ruggedness

For general application, the test equipment must be capable of withstanding airplane vibration, the shock of heavy guns, depth charges and near misses, and the combinations of shock and vibration connoted by the requirement of "transportation over all types of terrain in any Army vehicle." Test and experience have made it possible to translate these general requirements into two specific requirements, namely, the ability to withstand

1. Vibration at frequencies from 10 to 33 cycles per second, with 1/16 inch excursion for 30 minutes in each of three axes.

2. The shock produced by a 400-pound hammer falling through distances of one, two, and three feet in each of three axes and striking an anvil to which the set is attached.

These requirements have been met without using shock and vibration mounts, which are undesirable in test sets because they increase size and weight.

Range Capability

The range capability of a radar set, like that of any radio system, depends upon three things:

1. The transmitted power.

2. The loss in the medium.

3. The minimum perceptible received signal.

Two of these can be combined by taking the ratio of the radiated signal to the minimum perceptible received signal. This ratio, ordinarily expressed as a level difference in decibels, is variously termed the "system performance," "over-all performance," or merely the "level difference." It may be determined by separate measurement of transmitter power and receiver sensitivity, or by a single over-all measurement. With the powers and sensitivities commonly employed in radar, the level difference is of the order of 150 to 180 decibels.

The actual range that can be spanned for a given performance ratio varies considerably. For a given transmitted power, the echo power received by a radar set theoretically varies inversely as the fourth power of the range. The reason for this is simple. In free space the power intercepted by a target which is small in comparison with the area of the radar beam in its vicinity will vary according to the inverse square of the distance from the radar. Similarly, that fraction of the energy reflected from the target which is intercepted by the receiving antenna will vary as the inverse square law. Since the received power involves the product of these two factors, the relation becomes

$$P_r = K\frac{P_t}{R^4} \text{ or } R = \left(K\frac{P_t}{P_r}\right)^{1/4} \qquad (1)$$

where P_t and P_r represent, respectively, the transmitted and received power; R, the range; and K, a constant determined by antenna design, character of target, and so forth.

Under operating conditions, considerable departure from the above relationship may be experienced, because of such factors as

1. The curvature of the earth.

2. Interference between the direct beam and single or multiple reflections.

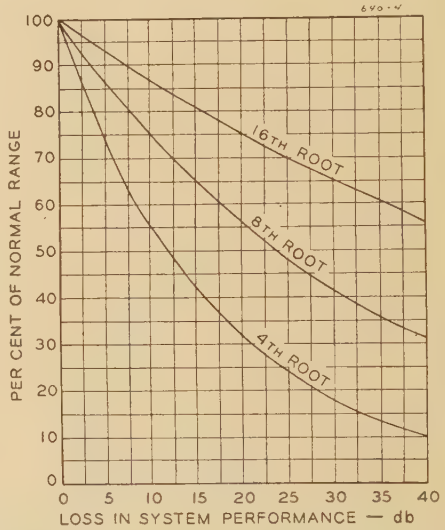

Figure 4. Effect of reduction in system performance on radar range

3. Attenuation caused by atmospheric absorption.

Except under conditions of severe attenuation such as may occur at the very short wave lengths, the received power commonly varies somewhere between the inverse fourth power and the inverse sixteenth power of distance. To state it another way, the change in effective range is somewhere between the fourth and the sixteenth root of the change in system performance. The former condition might hold for high-angle plane-to-ship search in

clear weather, the latter for ship-to-ship search in fog. The loss of range resulting from a given degradation of system performance is shown for fourth, eighth, and sixteenth root laws by the curves of Figure 4. Whatever the propagation law, reduction in performance always means loss of range.

Field surveys have shown that when test equipment is not available or not used, radar sets in the field are likely to give no more than one half to one fourth of the maximum range of which they are capable. Hence it is necessary to know with good accuracy the over-all performance. Known or so-called standard targets have often been used in the field for checking performance. Because of wide variations in transmission caused by many factors, results obtained from such targets are frequently misleading.

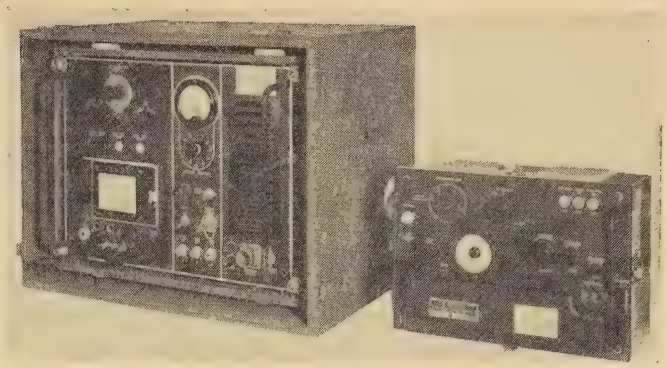

Figure 6. 1942-model signal generator (left) compared with one produced in 1945

Signal Generators

Signal generators for radar work deliver one or more different types of test signals, which may serve a variety of functions. More important among these functions are

1. Tuning or alignment of the radar components (TR and RT boxes, converter, beat oscillator, automatic frequency control, and so forth).
2. Measurement of receiver sensitivity.
3. Check of TR and receiver recovery.
4. Measurement of loss.
5. Detection of frequency pulling.
6. Check of automatic frequency control following.
7. Measurement of intermediate-frequency band width.
8. Check of automatic range tracking.
9. Measurement of standing wave ratio.
10. Check of video "gating" circuits.

Many signal generators include means for measuring the power and frequency of the test signal and also of an incoming signal.

Types of Signals

The test signals delivered by a signal generator may be continuous wave, pulsed, or frequency-modulated. Occasionally, square wave or sine wave modulation is provided.

Pulsed signal generators deliver a succession of single RF pulses or pulse trains, either of these generally synchronous with the pulses of the radar equipment under test. Multivibrator or trigger techniques are used to generate the pulses for modulating the microwave generator. The trigger pulse for synchronizing the pulsing circuits is commonly produced by rectifying RF pulses from the radar transmitter, thus avoiding a separate video connection to the radar. To avoid possible difficulties in video response, the RF test pulses should be of a width comparable with those of the radar set under test. For observing the test signals, either the radar indicator or an auxiliary oscilloscope may be used. With the single pulse method, provision is usually made for varying the delay of the test pulse with respect to the radar pulse. The width of the test pulse may also be adjustable or variable.

If the frequency of the signal generator is swept over a sufficiently wide frequency band, the IF output of the radar set traces the curve of IF selectivity, thus producing a kind of pulse. With a suitable rate of frequency sweep, this pulse becomes comparable in width with the transmitter pulse, and when synchronized with the radar set it can be used for test purposes. Since the pulse is produced in the radar equipment, comparison of the shapes of receiver input and output pulses is not possible. The nominal duration of the pulse in the IF output is

$$T = B/\gamma \qquad (2)$$

where B is the width of the IF band in cycles per second (for this purpose conveniently measured between six decibel points) and γ is the speed of frequency sweep in cycles per second per second. For best results this nominal width should be similar to the width of the transmitter pulse for which the IF and video circuits are designed. This means that the scanning speed should be in the neighborhood of $B^2/_2$.

A continuous-wave input of the same frequency as the transmitter produces in the output of the IF detector merely a direct current to which the video amplifier and radar indicator do not respond. However, continuous-wave test signals may be utilized by observing on a d-c meter (built into the radar set or separate) the change produced in detector current or converter current.

Figure 5. Block diagram of *TS-35A/AP* signal generator

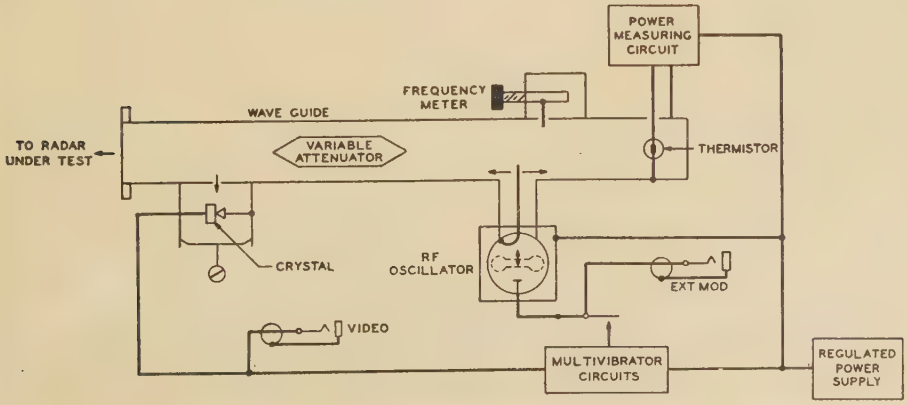

Receiver Sensitivity

Just as in radio, the sensitivity of a radar receiver is defined as the minimum received signal that is perceptible in the presence of set noise.* At microwave frequencies, atmospheric disturbances are usually negligible, so that unless accidental or deliberate interfering signals are present, the operating sensitivity is the same as the intrinsic sensitivity of the receiver.

Receiver sensitivity is commonly stated as the minimum perceptible signal power in decibels referred to a milliwatt (abbreviated as dbm). In practice, the receiver

*The term noise is commonly used even though the disturbances are observed on a cathode-ray screen.

sensitivity depends upon the noise figure of the converter, the conversion loss, and the noise figure of the IF amplifier. If a RF amplifier is used, as is the practice at lower microwave frequencies, its noise figure is likely to be controlling. By noise figure in each case is meant the noise power in comparison with the thermal noise. The thermal noise in watts delivered to a load is kTB, where k is Boltzmann's constant, T is absolute temperature in degrees K, and B is the frequency band width. Thus for a 4-megacycle band at 25 degrees centigrade, the thermal noise is -108 decibel-milliwatts. With good design the over-all receiver noise is of the order of 10 to 15 decibels higher than thermal noise. The minimum detectable signal is usually not equal to the receiver noise but depends on the type of indicator, particularly on whether the presence of an echo is indicated by spot deflection or spot modulation.

With a continuous-wave signal generator, receiver sensitivity is measured by determining the minimum input power necessary to produce a perceptible change in meter reading. This affords a satisfactory relative measure of receiver performance, but since the radar indicator usually permits better visual discrimination against noise, the minimum input as read with the meter ordinarily differs from the minimum pulse input for barely discernible indicator response.

Radio-Frequency Oscillators

Beat oscillator tubes for radar sets deliver (with sufficient decoupling or isolation to prevent undue frequency pulling) a power of the order of milliwatts. This power being adequate for most test purposes, such tubes are well adapted for use as signal generators.

Throughout the greater part of the microwave range, reflex velocity-modulated tubes,[2] both the type with built-in cavity (Pierce-Shepherd) tuned mechanically or thermally, and that with external cavity (McNally) tuned by plugs, vanes, or adjustment of dimensions, have been used. The former is more convenient for general use, but the latter usually permits wider frequency coverage. Oscillation occurs when the repeller voltage is adjusted so that the round trip transit time corresponds to an odd number of quarter wave lengths. Ordinarily there are several different ranges of repeller voltage,

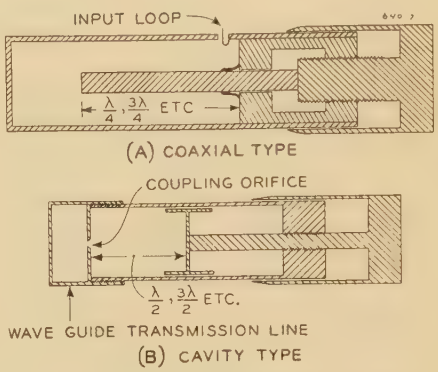

Figure 7. Types of frequency meters

corresponding to different numbers of quarter waves, each of which supports oscillation over a range of frequencies called a mode of oscillation. Pulsing or frequency modulation is accomplished by applying a pulse or sawtooth wave to the repeller.

At the longer microwaves, a triode with closely spaced electrodes, or so-called "lighthouse" tube,[3] has been employed in a tuned-plate tuned-grid oscillator of the positive grid type. Two coaxial lines, conveniently placed one inside the other, provide the tuning, with the feedback through interelectrode capacitances supplemented by loop coupling. The inner cavity (between plate and grid) controls the frequency of oscillation, while the outer cavity (between grid and cathode) provides a suitably high grid impedance. Mechanical arrangements are provided for tracking the tuning of the two cavities over a wide frequency range.

Some Design Principles

Standard signal generators which have been employed in the past for measuring the sensitivity of radio receivers usually deliver a known voltage across a low impedance. This voltage is applied in series with a dummy antenna to the receiver under test. In the microwave range, this technique is inconvenient, and signal generators are designed to deliver test power on a matched impedance basis. Receiver sensitivity is stated in terms of power (decibel-milliwatts) instead of volts.

The components of a signal generator or other test unit are commonly arranged along a microwave transmission line. The wave guide type of line possesses certain advantages over a coaxial line in affording a lower loss, facilitating attenuator design as discussed in a subsequent section, and so forth. Hence the wave guide type of line is used in test equipment for those frequencies where its size is not excessive, that is, from about 4,000 megacycles upwards, and coaxial line for lower frequencies.

A major problem in the design of microwave signal generators is the provision of shielding adequate to reduce leakage signals, caused by unwanted couplings or stray fields, well below the minimum signal required for receiver testing. This minimum level may be as low as -70 or

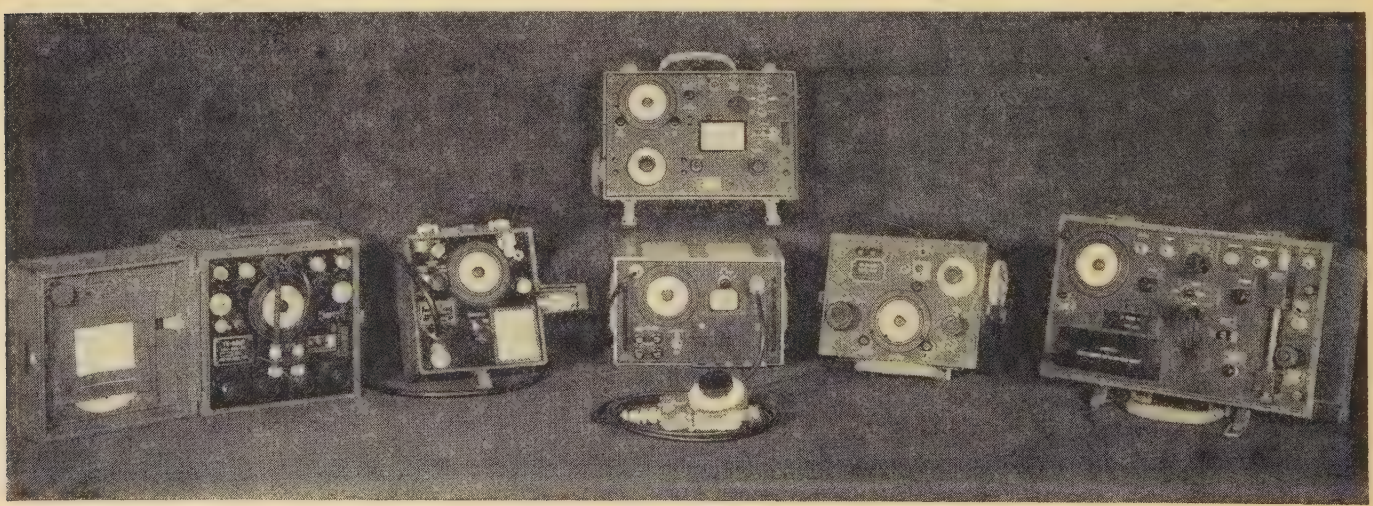

Figure 8. A group of frequency and power meters designed for various bands in the frequency range from 500 to 25,000 megacycles

−80 decibel-milliwatts depending on the coupling loss in the test connection.

Pulsed and Frequency-Modulated Signal Generator

To illustrate the functioning of a signal generator, there is shown in Figure 5 a block schematic of a design (Army-Navy type *TS-35A/AP*) which covers a 12% frequency band in the vicinity of 9,000 megacycles. An RF connection to the radar equipment is established with a wave guide flange coupling. The frequency and power of the radar transmitter are measured by means of a coaxial-type frequency meter and thermistor power-measuring circuit as described in subsequent sections. The attenuator and pad are adjusted to reduce the incoming average power to about one milliwatt, which gives a suitable deflection on the indicating meter. The

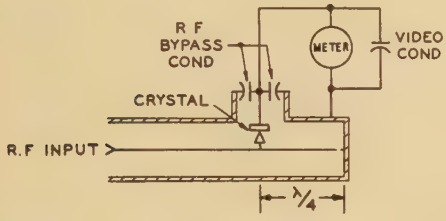

Figure 9. Crystal detector for pulsed RF signals

thermistor is mounted across the wave guide.

An RF pulse train is employed in many tests. To produce this, the RF oscillator output is modulated by a multivibrator which pulses continuously except when being synchronized. Synchronizing pulses are derived by crystal rectification of the RF pulses from the radar transmitter. The result is an initial RF pulse of seven microseconds, followed by an off period of about ten microseconds, followed by a train of RF pulses each two microseconds wide and recurring every eight microseconds until resynchronization occurs at the next radar pulse.

Using the pulse train, the radar system components can be tuned for maximum sensitivity by maximizing the signal on the indicator. To check receiver sensitivity, the continuous-wave power is first adjusted so that a power of one milliwatt is delivered to the pad and attenuator. Then with the set in the pulsed condition, the amplitude of the test signal is adjusted by means of the attenuator and pad until the signal on the radar indicator is barely discernible. It is necessary for this test that the frequency of the test signal be equal to the magnetron frequency. The frequency meter is provided as part of the signal generator for this purpose.

The receiver recovery, that is, the time required by the receiver to recover after disablement by the transmitter pulse, determines the minimum range at which a radar can be used. With this test set, the receiver recovery characteristic is indicated by the amplitude of the test pulses in the interval immediately following the transmitter pulse.

The set also is adapted to serve as a frequency-modulated signal generator. A sawtooth wave applied to the repeller gives a succession of frequency sweeps, each about 20 megacycles wide, and lasting about six microseconds. With this frequency-modulated signal, the width of receiver response may be observed on a class A oscilloscope, that is, one showing signal amplitude versus time. However, with nonadjustable intermediate-frequency strips, such measurement is seldom required. Failure of the radar automatic frequency control to follow frequency changes caused by antenna scanning or other causes is indicated by a change in the indicator presentation. Pulling of the magnetron frequency because of changes in load impedance can be detected by turning off the automatic frequency control.

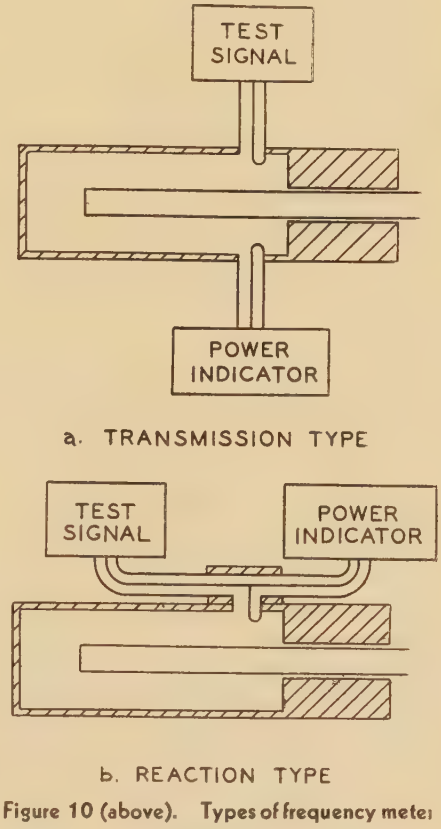

Figure 10 (above). Types of frequency meter circuits

Signal Generator Designs

Designs of signal generators developed for the military arms during the war are interesting as landmarks of progress. The signal generator of the *IE30* test set, deliveries of which began in May 1942, delivered pulsed RF signals in the ten-centimeter range, using sine wave synchronization. Following only three months later was the signal generator of the Army *IE57A* and the Navy *LZ* test sets (Figure 6), which covered a then very broad frequency band of 20 per cent in the vicinity of ten centimeters and was designed to be triggered by the incoming RF pulse from the radar set instead of by a separate synchronizing connection. This set and a redesigned version of it have seen wide usage in testing Army, Navy, and Marine Corps radar equipment.

Delivery of a test set for the three-centimeter range, designated *TS-35/AP*, started in the fall of 1943. This set furnished both a train of pulses and a train of frequency-modulated signals, both of which features have proved valuable. It covered a nine per cent frequency band with no tuning adjustment except for the oscillator. An improved design known as *TS-35A* (see Figure 6) covered a 12 per cent band.

Progress in reducing the size and weight of the test units is indicated by the fact that the *IE30* signal generator weighed 121 pounds and *IE57* weighed 74 pounds, whereas *TS-35* and *TS-35A* weigh approximately 30 pounds.

Figure 11 (below). Radar test with echo box

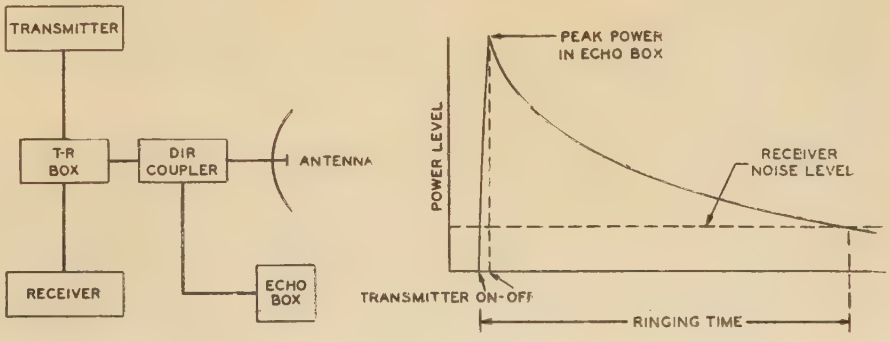

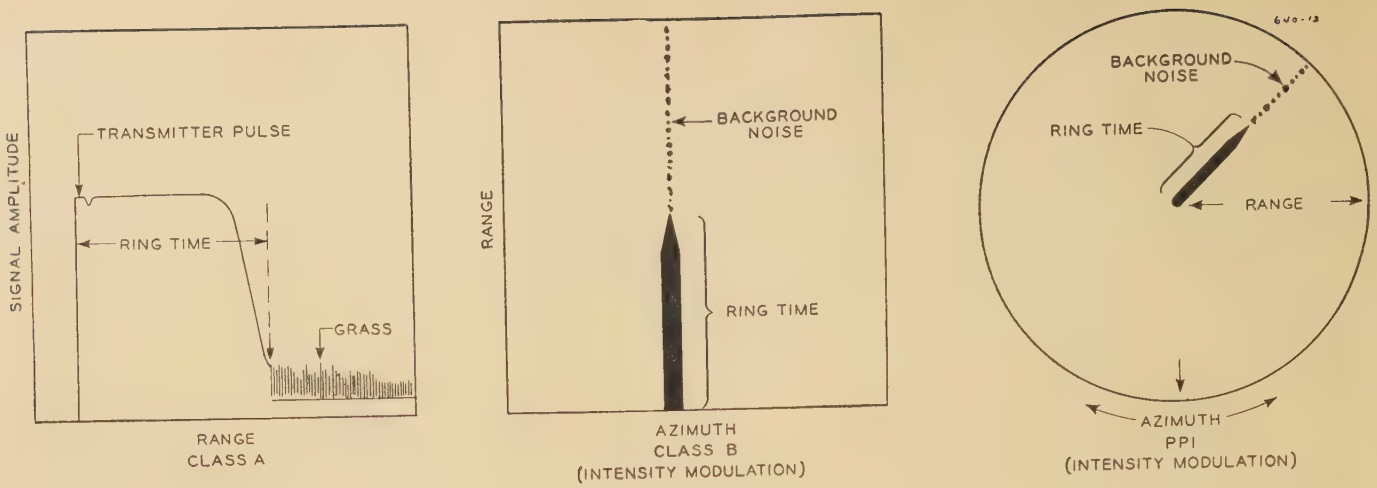

Figure 12. Typical ringtime patterns on radar indicators

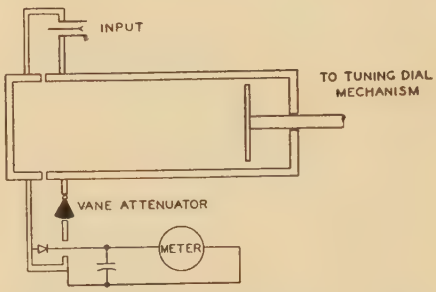

Figure 13. Functional schematic of tuned echo box

Frequency Measurement

Usually a radar set need not operate at a precise frequency. Accurate measurements are required in the field, however, to keep the operating frequency within limits, to set the local oscillator, to check the measuring frequency, and so forth. In the laboratory, accurate frequency measurement is fundamental.

Frequency measurement in the microwave range is ordinarily accomplished by

1. A resonant coaxial line or
2. A resonant cavity, generally cylindrical.

These types are illustrated in Figure 7. Sometimes a combination of the two, referred to as a hybrid or transition type resonator, is employed. The measurement is actually one of wave length, with the scale calibrated in frequency or a conversion chart provided. Some specific designs of frequency meters are shown in Figure 8.

Coaxial Wavemeters

A coaxial wavemeter is formed of a section of coaxial transmission line of small enough diameter so that only the coaxial mode (in wave guide notation, $TM_{0,0,n}$) can exist. Usually the line is short-circuited at one end and open at the other, in which case resonance occurs at the odd quarter wave lengths ($\lambda/4$, $3\lambda/4$, and so forth). The open circuit is obtained merely by terminating the inner coaxial conductor, the continuing outer conductor acting as a wave guide below cutoff. Sometimes the line is short-circuited at both ends, giving resonance at the even quarter wave lengths ($\lambda/2$, λ, and so forth).

Cylindrical Cavity Wavemeters

A cylindrical cavity wavemeter is merely a section of cylindrical wave guide transmission line[4] whose length is varied. In order to avoid confusion with other modes, it is preferable to use the dominant mode (described in wave guide notation, $TE_{1,1,n}$*), that is, the mode with the lowest cutoff frequency. The cutoff wave length (λ_c) of this mode is $1.706D$, where D is the diameter in meters. For a higher Q it may be necessary to use the circular electric mode $TE_{0,1,n}$. The cutoff wave length for this mode is $0.82D$. No useful purpose is served by using modes with l and m subscripts above unity. TM modes are often used for fixed frequency cavities, but for variable cavities TE modes are preferable since these have zero current at the inner wall of the cylinder and thus obviate moving-contact difficulty. If any mode higher than the dominant one is used, suppression of unwanted modes may be required.

The Value of Q

The accuracy of a wavemeter is dependent on its resolving power. This in turn depends upon Q, which is an index of the decrement of the resonant circuit and is equal to $f/\Delta f$, where Δf is the distance between three decibel points on the resonance curve.

In a coaxial wavemeter, maximum Q for a given inner diameter is obtained with a diameter ratio of about 3.6.[5] The basic Q of a coaxial wavemeter, assuming copper of standard conductivity, is roughly[6]

$$Q_o = 0.042D\sqrt{f} \qquad (3)$$

This expression neglects end effects and hence gives somewhat too high a value of Q.

The basic Q's for $TE_{1,1,n}$ and $TE_{0,1,n}$ cylindrical cavity resonators employing copper of standard conductivity are, respectively,

$$Q_o = 0.0937\times10^{10}\frac{A^3}{\sqrt{f}}\times\frac{1}{1+B^2\left(0.826\frac{B}{n}+0.295\right)} \qquad (4)$$

$$Q_o = 0.2762\times10^{10}\frac{A^3}{\sqrt{f}}\times\frac{1}{1+B^2\left(2.439\frac{B}{n}\right)} \qquad (5)$$

where $A = \lambda_c/\lambda$, $B^2 = A^2 - 1$, and f is in cycles per second.

The value of Q which determines accuracy is not the basic Q, but the loaded or working Q, herein designated Q_L.

The resolving power of a wavemeter used for measuring a single frequency can be made considerably better than f/Q_L. With a sensitive meter it is readily possible to detect differences less than one decibel, which corresponds to a frequency interval of $f/2Q_L$.

The required accuracy in a wavemeter is generally absolute rather than a percentage. Hence increasingly large values

*TE and TM represent, respectively, transverse electric and transverse magnetic. The subscripts l, m, n denote, respectively, the number of wave lengths around any concentric circle in the cross section, the number of wave lengths across a diameter, and the number of half wave lengths along the length of the cylinder.

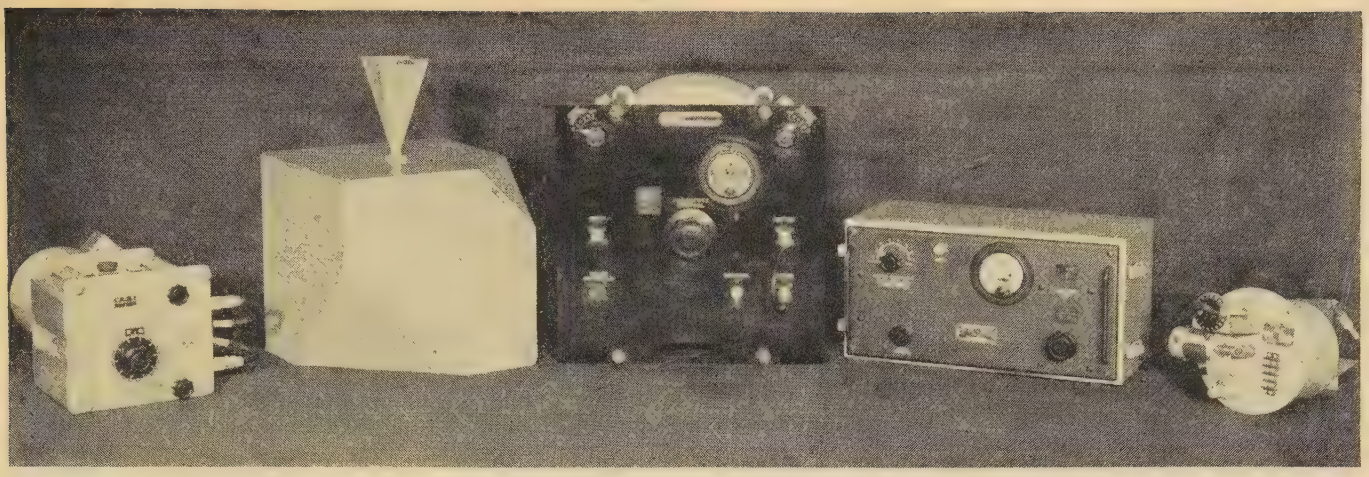

Figure 14. A group of echo boxes of various types

of Q_L are required at the higher frequencies. Thus for a resolution of one megacycle, assuming one decibel discrimination, the values of Q_L required for different frequencies are:

Frequency	Q_L	Frequency	Q_L
1,000 mc.....	500	10,000 mc.....	5,000
3,000 mc.....	1,500	25,000 mc.....	12,500

An unnecessarily high value of Q_L has the disadvantage of making it more difficult to find the desired frequency.

Linearity

The displacement of the coaxial plunger of a coaxial-type wavemeter for resonance is substantially a direct linear function of free space wave length, and if an ordinary centimeter micrometer drive is used, it is possible to read wave length differentials directly. Over band widths less than 20 per cent, displacement versus frequency is also quite linear, which is of considerable advantage for some uses.

For the cavity-type wavemeter, the displacement is a variable function of free space wave length and becomes very nonlinear as the cutoff frequency of the guide or cavity is approached. This is evident from the relation between wave length in the guide, λ_g, wave length in free space, λ, and cutoff wave length, λ_c:

$$\lambda_g = \frac{\lambda}{\sqrt{1-\frac{\lambda^2}{\lambda_c^2}}} \qquad (6)$$

A cam or mechanical linkage may be employed to obtain a linear scale.

Frequency Coverage

Increasing the length of a wavemeter is desirable because this gives a larger mechanical displacement for a given frequency interval. The permissible increase is limited, however, by ambiguity with the next lower mode in going toward the upper end of the frequency scale and with the next higher mode in going toward the lower end. This means that if ambiguity is to be avoided, the ratio of top to bottom frequency cannot exceed $(n + 2)/n$ for a coaxial line of n quarter-waves. For a cylindrical cavity resonator, the ratio for the 0, 1, n mode must be less than $(n + 1)/n$, the exact limit depending on proximity to cutoff.

Guideposts

The following guideposts are suggested for choosing the type of wavemeter in the microwave range. Where limitations of size and Q permit, the coaxial quarter-wave type should be used because of its greater linearity. If this type is inapplicable, the cavity type with $TE_{1,1,n}$ should be used unless its Q is inadequate, in which case $TE_{0,1,n}$ should be employed.

Couplings

A loop, orifice, or probe may be used for coupling to a wavemeter. Coupling to a coaxial wavemeter is generally effected by a loop placed near a short-circuited end so as to be in the maximum magnetic field. For coupling to a cylindrical cavity wavemeter, an orifice in or near the base of the cavity is usually employed. The coupling to the wavemeter is kept small enough to avoid serious reduction of loaded Q.

Types of Detectors

Various types of detectors may be associated with a wavemeter, the most commonly used being (1) a crystal rectifier and microammeter and (2) a thermistor bolometer. When a crystal rectifier is employed with a cavity or coaxial wavemeter, a circuit similar to that shown in Figure 9 is used. Important items in such a circuit are the RF by-pass capacitor, and the video capacitor. The latter, by providing a low impedance path to the video signals, improves rectification efficiency when the input signal is pulsed. The quarter-wave stub shown in the figure is used when the input or coupling circuit does not provide d-c and video paths. When the signal is pulsed at a low-duty cycle, high peak currents through the crystal are obtained even though the average current through the meter is small, and it is possible to impair or burn out the crystal unless extreme care is taken. The use of a thermistor, which is self-protecting for large overloads, avoids this danger. Another expedient is to limit the crystal current to a small value and employ a video amplifier and oscilloscope.

Methods of Use

A wavemeter may be used as either a transmission or a reaction instrument. In the former case (Figure 10A), it is inserted directly in the transmission path, so that substantially no through transmission occurs except at resonance. In the latter case (Figure 10B), the wavemeter is coupled to the transmission path or a branch circuit. When the meter is tuned off resonance, it presents such a high impedance to the main path that its effect is negligible. At resonance, however, it offers a lower impedance which reflects energy in the main line so that less power reaches the detector and a dip in the reading occurs. For most applications the reaction arrangement is preferable, since the power transmitted when the wavemeter is off tune may serve various purposes. For analysis of frequency spectrum the transmission method is necessary. This method requires two couplings to the wavemeter, which lowers the Q as compared with the reaction type.

Drive and Scale

A direct drive with a precision lead screw of the micrometer type is frequently used. Accuracy of reading is insured by spring loading to minimize backlash and by specifying close tolerances for threads and for concentricity of plunger and cavity. The scale on a wavemeter must be fine enough to permit utilization of the resolving power. The conventional micrometer type of scale sometimes makes accurate reading difficult in a small compact meter. Scale mechanisms which have been used include counter types, clock face, or expanded drum types with gearing between vernier and coarse scales, and a single direct reading scale with divisions arranged in a spiral for compactness.

Effect of Temperature and Humidity

To minimize the effects of temperature on the accuracy of readings, invar has been employed for elements whose dimensions affect the wave length. For accurate work, the scale reading must be corrected for temperature. A rough approximation is that the scale reading varies in accordance with the coefficient of expansion of the metal.

Water vapor included in the air dielectric of a wavemeter has an appreciable effect on the dielectric constant and hence on the resonant frequency.[7] Thus, for example, in going at sea level from 25 degrees centigrade and 60 per cent humidity to 50 degrees centigrade and 90 per cent humidity, the scale reading should be reduced by 0.03 per cent. Correction can be made by means of a chart, a convenient form of which has been prepared by Radiation Laboratory.

Calibration

Frequency meters are calibrated against sub-standards which in turn are calibrated against a multiplier from lower frequencies for which a high order of accuracy can be obtained. Such multipliers have been made available at Radiation Laboratory and the National Bureau of Standards. The accuracy obtained at interpolation frequencies is of course less than at exact multiples of the base frequency. In the microwave range, the accuracy is believed to be of the order of one part in 100,000.

Power Measurement

There are two needs for power measurement in radar maintenance, namely, in evaluating transmitter performance and in standardizing test signals. Power output is, of course, only one factor in transmitter performance, others being (a) frequency and (b) spectral distribution or shape of RF envelope. Ability to measure absolute power is desirable to permit interchangeable use of sets in the field.

Measurement of Pulse Power

The transmitter power as used in formula 1 is the average power during the pulse. The relationship of pulse to (long) average power is

$$\frac{P_t \text{ avg}}{P_t \text{ pulse}} = Tf_r \qquad (7)$$

T is the pulse duration in seconds and f_r is the pulse recurrence frequency (P.R.F.) in cycles per second. The product Tf_r is the duty cycle. (Sometimes the reciprocal of this number is referred to as the duty cycle. The magnitude is usually such that no ambiguity arises.)

During the early days of radar, it was the practice to measure pulse power. The test equipment was coupled to the radar set by a path of known loss. The RF envelope was derived by means of a crystal rectifier and applied to an oscilloscope. With the aid of an RF attenuator, the level applied to the crystal rectifier and oscilloscope was held constant. Calibration was obtained by using a signal generator whose output was standardized, prior to pulsing, with an averaging type of power meter. The procedure was rather involved, with several sources of possible error. Since it is much simpler to measure average power, field measurement of pulse power soon was abandoned. Though the pulse power can be computed from average power if the pulse width, pulse shape, and repetition rate are known, it soon became the practice to specify field performance requirements in terms of average power.

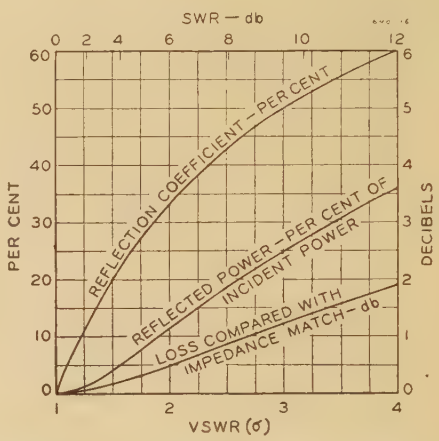

Figure 16. Relations in mismatched transmission lines

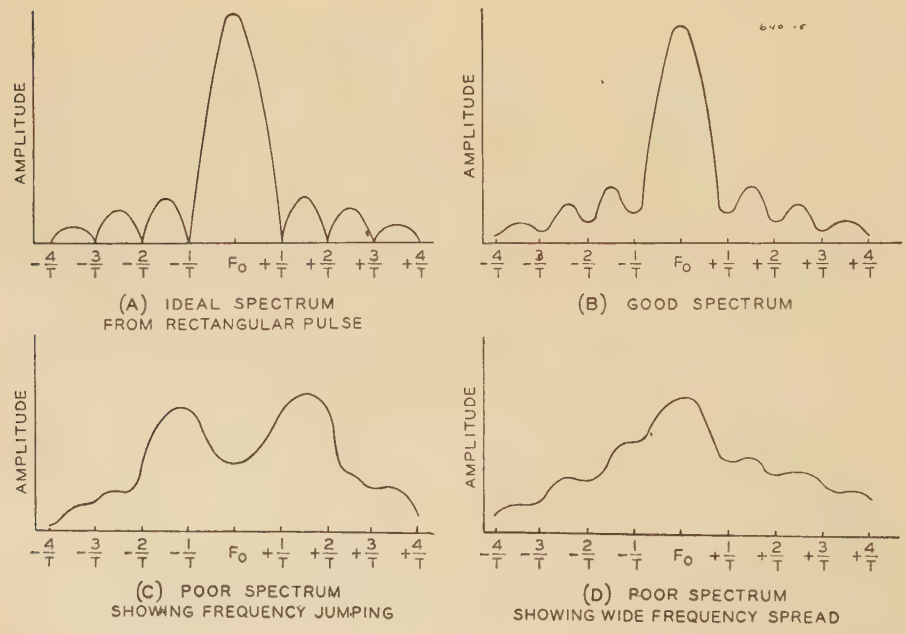

Figure 15. Radar spectrum analysis with echo box

Thermistor Power Meters

A number of devices have been used for measuring average power in the microwave range. Those suitable for handling the small amounts of power normally involved in field tests include thermistors, platinum wires, and thermocouples. In each case the RF power to be measured is absorbed in the measuring element. The measurement consists in observing the resistance change in the thermistor or platinum wire, or the thermoelectric voltage from the thermocouple. By analogy with devices used for measuring minute quantities of radiant heat, either a therm-

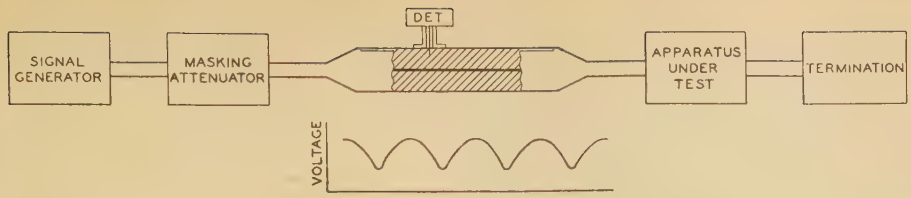

Figure 17. Standing wave measurement

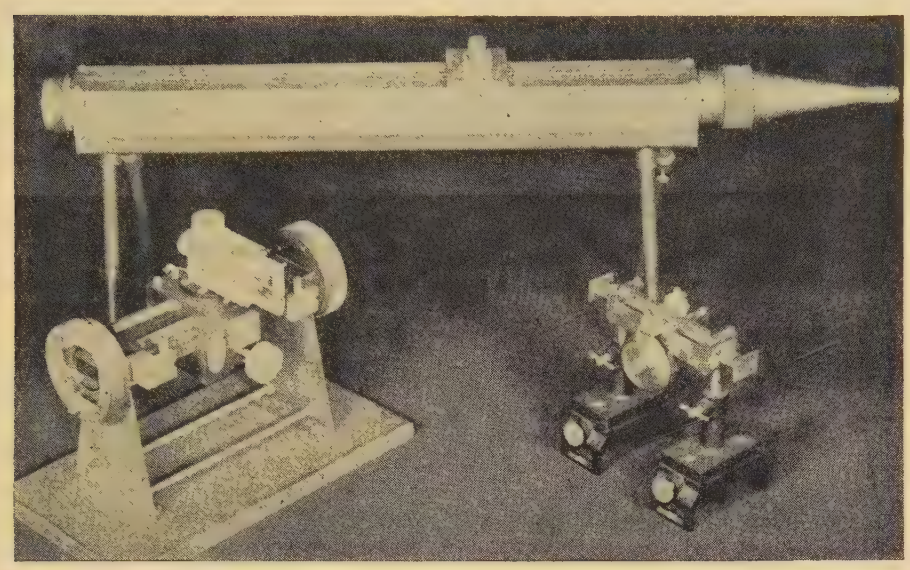

Figure 18. Standing wave detectors used on coaxial and wave guide transmission lines

istor or a platinum wire instrument is sometimes referred to as a bolometer. The platinum wire device has also been termed a barretter.

A thermistor for microwave power measurement is a tiny bead (about five mils in diameter) composed of a mixture of oxides of manganese, cobalt, nickel, and copper, constituting a resistor with a very high negative temperature coefficient.[8]

The thermistor has a number of advantages for microwave work, namely:

1. Resistance is highly sensitive to change of heating power, which obviates any need for amplification or a super-sensitive meter and makes it possible to use a rugged d-c meter.

2. Reactance is low compared with RF resistance, which makes it possible to incorporate the thermistor in a power-absorbing termination which matches the impedance of a microwave transmission line over a wide band.

3. Resistance change is the same function of electrical heating power at any frequency, which permits direct comparison of the unknown microwave power with easily measurable d-c power.

4. Sensitivity to damage and burn-out is inherently low, and added protection results from impedance mismatch during overload.

Because of these characteristics, thermistors have been far more widely used than other detectors for microwave power measurement. Broadband thermistor mounts have been designed to match both wave guide and coaxial transmission lines, the latter not only in the microwave range but also down to low frequencies. Some of the test sets specifically intended for power measurement or for combined power and frequency measurement are shown in Figure 8.

The change in the thermistor resistance caused by radio-frequency heating current is determined by placing the thermistor in one arm of a d-c bridge. By noting the d-c power necessary to balance the bridge with and without RF power in the thermistor, the magnitude of the RF power may be determined. For most purposes, however, a direct-reading power meter is preferable. This can be obtained over a moderate range of power levels by employing an unbalanced bridge. The bridge is balanced for direct current only, and the measurement consists in noting the meter deflection when radio-frequency power is added.

The resistance of a thermistor is a highly sensitive function not only of electrical heating power but also of ambient temperature. For convenient field measurement, the effect of ambient temperature must be cancelled out in the indicator circuit so that the indication depends only on RF power.

Water Loads

A method which has been used in the laboratory and the factory for measuring high level microwave power consists in terminating the RF transmission line in a water load arranged as a continuous flow calorimeter. This method can be made quite accurate but is cumbersome. More recent practice is to terminate the RF line in a solid load of a type described later in this article and to couple a thermistor power meter to the line by means of a directional coupler (described below) of known loss. Very close correlations have been obtained between the two methods over the entire microwave band.

Echo Boxes

A device unique to radar testing is a high Q resonant cavity, known as an echo box or ring box. The cavity is coupled to the radar transmission line or antenna as indicated in Figure 11. During the transmitted pulse, microwave energy is stored in the cavity. In the period immediately thereafter, energy is returned to the radar over the same path, producing a signal on the radar indicator. The energy in the cavity builds up exponentially to an amplitude dependent on the radar power. At the end of the pulse, the returned energy decays exponentially, disappearing into the noise at a point determined by receiver sensitivity. The time interval between the end of the transmitted pulse and the point where the signal on the radar indicator disappears into the background noise, called the ringtime, therefore measures the over-all performance of the radar set.

An echo box is a particularly useful instrument for radar testing because

1. It measures over-all performance directly

2. It permits a rapid tune-up.

3. It utilizes the radar transmitter as its only source of power and therefore can be made extremely portable.

Figure 12 shows typical ringtime patterns on different types of indicators. In actual practice the ringtime is read in miles on the radar range scale and hence is measured from the beginning of the transmitted pulse rather than the end. The difference is unimportant, however, since standard and limiting values of ringtime are established for operating conditions. It will be noted that the echo box does not return a true echo to the radar, so that the name "echo box" is not entirely appropriate.

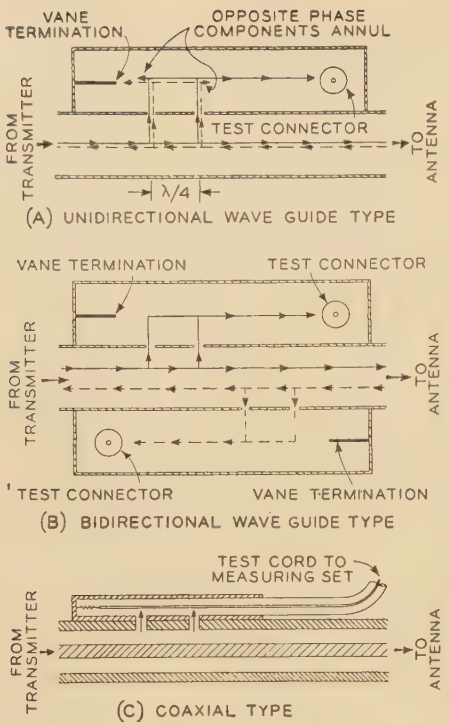

Figure 19. Directional coupler arrangement

Types and Uses

Echo boxes are of two general types, tuned and untuned. A tuned echo box is designed to resonate in a single mode adjustable over the operating frequency range. An untuned echo box is a fixed cavity of a size sufficient to support a very large number of modes within the working range. Tuned echo boxes are more versatile and more widely used than untuned boxes.

The most common type of tuned echo box is designed for hand tuning. While other shapes are possible, the most convenient one is a right cylinder whose length is adjusted by a movable piston. The $TE_{0,1,n}$ mode gives maximum Q for a given volume and minimizes the number of unwanted modes present within the desired band. The value of n is determined by the desired value of Q (see formula 5). Unwanted modes can be partially avoided by choice of design parameters. However, for high values of Q, and especially for broad frequency bands, the suppression of unwanted modes involves design problems of the highest order.

As indicated in Figure 13, a tuned echo box cavity is usually provided with two couplings. One of these is to the radar pick-up; the other is to an attenuating device, crystal rectifier, and meter, which serve for tuning the cavity and for other purposes. With such an instrument, not only can the radar be tuned up and its over-all performance determined, but many other tests can be made, to wit:

1. The setting of the plunger at resonance indicates the transmitter frequency or wave length.

2. Calibration of the crystal affords a rough measure of output power.

3. Since the Q required for adequate ringtime is so high that the cavity selects only a narrow segment of the transmitter spectrum, a spectrum analysis can be made by plotting frequency versus crystal current reading.

4. Slow recovery of TR box and receiver after the transmitted pulse can be detected by noting the behavior of the ringtime pattern at short ranges as the echo box is detuned.

5. Inability of the receiver to recover promptly after a strong signal (the result of imperfect d-c reinsertion in the video amplifier or of overloading of the IF amplifier) is indicated by a blank following the end of the ring.

6. Improper pulsing (for example, double moding or misfiring) can be determined with a class A oscilloscope.

7. The frequency and power of the local oscillator can be measured.

In tuned echo boxes, requirements for extreme fineness of tuning control and precise resettability have given rise to interesting problems in the design of the mechanical drive and indicating mechanism.

In another type of echo box, hand tuning is supplemented by motor-driven tuning or so-called "wobbling" over a frequency range wide enough to embrace expected variations in transmitter frequency. Operation is controlled by a single push-button which energizes the motor and actuates the cavity coupling. Such an instrument may be permanently installed in a plane and used to check the radar during flight.

For an untuned or multiresonant echo box, rectangular shape is convenient. The box should be large enough to make it highly probable that over the operating band, one or more modes will be present within any frequency interval of width equal to the main concentration of the transmitter spectrum. For a given rectangular volume, a cube gives the largest number of modes. The total number of modes up to a frequency of wave length λ_0 is

$$N_M = 8.38 V/\lambda_0^3 \qquad (8)$$

where V is the volume. However, because of the cubical shape, many different modes tend to coincide in wave length, a condition referred to as degeneracy. To spread out the modes, the box is made slightly off cube and one or more corners sliced off. At the longer microwaves, the size of box is determined by the number of modes, and the size becomes quite awkward. For the shorter microwaves, the size is determined by the required value of Q. Hence the use of untuned echo boxes has been limited to the frequency range from about 9,000 megacycles upwards, with sizes of the order of from 12 to 24 inches on a side. Even with an extraordinarily high probability of finding modes within the radar band, substantial differences in response are found for relatively small changes in frequency. Accordingly, untuned echo boxes are more useful for rough tune-up than for precise measurement.

A number of specific designs of echo boxes for different microwave bands are shown in Figure 14.

Q and Ringtime

For satisfactory measurement the ringtime must extend beyond nearby echoes which would obscure the test signal. For most radars a ringtime of 20 to 30 microseconds (about two to three miles) has been found satisfactory, although considerably higher values have sometimes been provided. Even apart from echoes, a long ringtime is desirable since this gives a lower decay rate and a more sensitive measurement.

Computation will show that an extremely high value of Q is necessary to obtain the desired ringtime. For maximum ringtime the cavity coupling should be such as to make the working Q (Q_L) about 90 per cent of the nonloaded Q. Values of working Q which have been provided in different frequency ranges are approximately as follows:

Frequency	Q_L	Frequency	Q_L
1,000 mc	70,000*	10,000 mc	100,000
3,000 mc	40,000	24,000 mc	200,000

*In this case a higher Q was needed for a long range ground search system.

The difference in performance corresponding to a given change in ringtime can be determined from the decay rate, which is

$$d = 27.3 f/Q_L \text{ decibels per microsecond} \qquad (9)$$

For a given frequency, the ringtime is directly proportional, and the decay rate inversely proportional, to Q. For a given ringtime, the required Q is directly proportional to frequency.

Accurate measurement of extremely high Q's is essential in echo box work. A decrement method, in which a pulsed radio-frequency oscillator and oscillo-

scope are used to determine the loss corresponding to a known time interval, has proved most satisfactory.

Spectrum Analysis

The frequency components of a non-repetitive rectangular d-c pulse may be determined by well-known methods using Fourier integral analysis. The envelope of amplitudes is of the form $(\sin x)/x$, where $x = \pi fT$. This envelope is shown by the right-hand side of the curve of Figure 15a, f_0 being assumed to represent zero frequency. The first zero occurs at the frequency $f = 1/T$.

Similarly, the envelope of the spectrum of a rectangular a-c pulse is given by the complete curve of Figure 15A, f_0 in this case being the carrier frequency. For a non-repetitive pulse, all frequencies are present in amplitude as shown by the envelope. When a stable carrier frequency is pulsed at uniform intervals and in precise phase relation, only harmonics of the repetition frequency are present under the envelope. In radar practice, conditions are, as a rule, not sufficiently stable for this to occur.

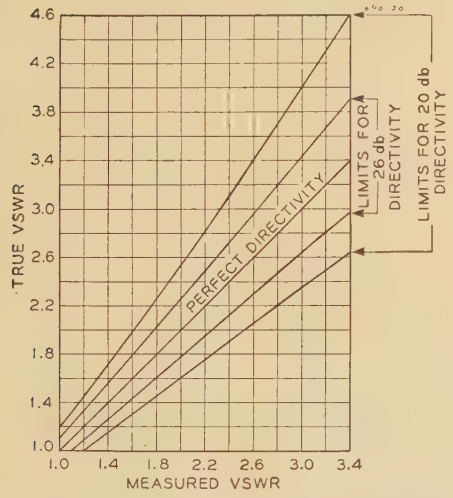

Figure 20. Error in standing wave measurements caused by directivity of directional coupler

Because of its band width, an echo box cannot reproduce the ideal spectrum envelope of Figure 15A. Instead, the curve for a good spectrum may resemble that of Figure 15B, while spectrum irregularities detrimental to radar performance may be revealed by curves such as those of Figure 15C and 15D. Broadening of the spectrum is undesirable because less energy falls within the receiver band. Energy removed from the main concentration may result from double moding

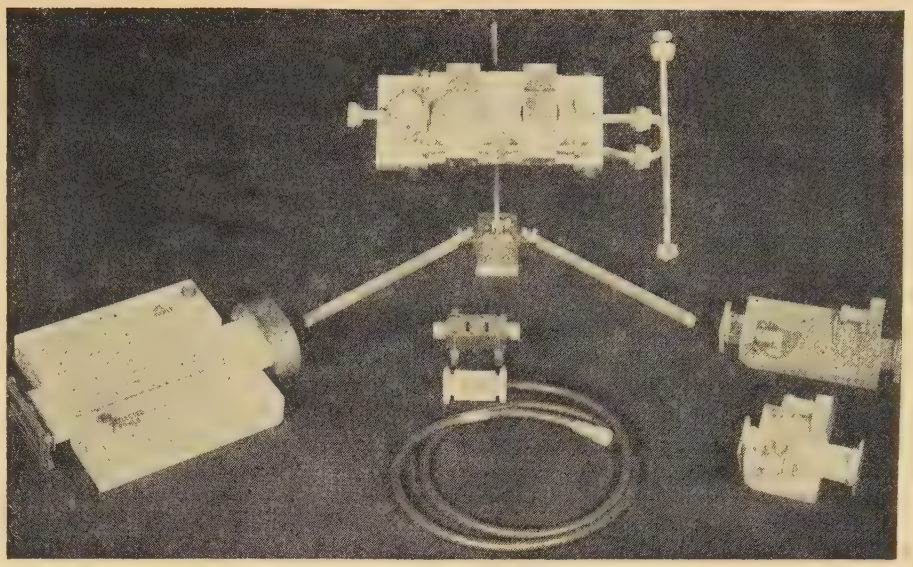

Figure 21. A group of microwave directional couplers together with a directional coupler test set

or from the occurrence of a different frequency during the rise or fall of the pulse. Frequency modulation caused by a sloping or spiked input pulse produces a non-symmetrical spectrum, not infrequently characterized by a high side lobe. Frequency jump in the middle of the pulse, resulting from line reflection, may produce two distinct maxima.

Standing Wave Measurements

The expression for the distribution of current or voltage along a misterminated line of appreciable electrical length yields two terms which may be considered as representing two waves transmitted in opposite directions, one (the incident wave) from the generator toward the load, the other (the reflected wave) from the load toward the generator. The summation is a standing wave pattern. The standing wave ratio (SWR) is defined as the ratio of the wave amplitude at a maximum point (anti-node) to that at a minimum point (node). If the standing wave ratio is stated as a numeric, it is necessary to specify whether it applies to voltage (VSWR) or power (PSWR). Possibility of ambiguity is avoided by stating the ratio in decibels.

The ratio of the reflected current to the incident current is the reflection coefficient, here designated as ρ. The value of the reflection coefficient is given both in magnitude and phase by

$$\rho = \frac{Z_0 - Z}{Z_0 + Z} \qquad (10)$$

where Z_0 is the characteristic impedance of the line and Z is the load impedance. The reflection coefficient is related to the standing wave ratio as follows:

$$\text{VSWR} = \sigma = \frac{1+\rho}{1-\rho}, \text{ or, } \rho = \frac{\sigma - 1}{\sigma + 1} \qquad (11)$$

Plots of the relationships are shown in Figure 16.

The reduction of radiated power because of reflection losses in a radar transmission line, while important, is usually less serious than other effects of impedance irregularities. Since the load impedance reacts on the oscillator circuit, the frequency and the output of most transmitter tubes are quite sensitive to load impedance. If the line is electrically long, so that its impedance varies rapidly with frequency, marked instability of oscillator frequency may occur, a condition referred to as "long line effect."

Since radar transmission lines contain many potential sources of impedance discontinuity, including not only the antenna but a variety of couplings, bends, wobble joints, rotating joints, switches, and so forth, measurements of standing wave ratio are frequently required. The need for such measurements depends in part on whether the line is "preplumbed" or is provided with field adjustments.

Devices

Standing waves may be detected and measured by several different types of devices, including

1. A slotted line.
2. A squeeze section.
3. A directional coupler.
4. A hybrid T.

All of these furnish information on the magnitude of the standing wave ratio. In some cases, phase information may be obtained also, which information permits determination of impedance,[9] but this

knowledge, while useful in the laboratory, seldom is required in field work.

A block diagram of an arrangement employing a slotted line for measuring standing waves is shown in Figure 17. The oscillator source is commonly followed by a pad or attenuator to prevent frequency pulling. The slotted section may be either a coaxial or a wave guide line employing a mode which is not disturbed by the presence of the slot (for example, normal coaxial mode, $TE_{1,0}$ in rectangular wave guide, $TM_{0,1}$ in round wave guide). A traveling pick-up probe or loop projects through the slot and couples energy from the line into a detector which delivers direct current or audio frequency to the indicator. The probe is moved longitudinally to find points of maximum and minimum field strength. To avoid distortion of the field within the line, the probe should be small and should project only a short distance inside the slot. For accurate results, extreme care must be exercised in design and construction to avoid variation in depth of immersion as the probe is moved. Several slotted lines employed for standing wave measurements are shown in Figure 18.

A squeeze section consists of a section of rectangular guide with slots milled in the center of both broad faces so that the width of the guide can be varied by external deforming means. This changes the wave length in the guide, so that maximum and minimum values may be determined by a fixed probe and indicator.

The use of a directional coupler for standing wave measurement is discussed in the following section.

Another useful device for standing wave measurement is the hybrid T or magic T. This is a sort of microwave bridge, consisting of a main wave guide to which an E plane branch and an H plane branch are joined in the same physical plane. With matched terminations of the two ends of the main guide, the two branches are conjugate. Terminating one end of the main guide in the unknown impedance and the other in a matched termination, the degree of impedance mismatch of the unknown is indicated by the magnitude of the reflected wave which appears in one branch when energy is fed into the other.

Directional Couplers

Accurate measurement of transmitter power and receiver sensitivity requires a coupling path of known loss between the radar set and the test set. The first method employed for this was to place a portable test antenna (see Figure 2) in the field of the radar antenna. Depending on the frequency range, this test antenna took the form of a dipole,[10] with or without a small reflector, or an electromagnetic horn.[11] With this method, it was necessary to calibrate the loss of the space coupling path between the two antennas. Since it proved difficult to locate the test antenna at exactly the same point and to be sure that the main antenna pattern remained the same, a separate calibration of the coupling loss was usually required whenever a measurement was made.

An alternative method was to place a single probe in the radar transmission line. This introduced another sort of difficulty. Accuracy of measurement was vitiated by the presence of standing waves which rendered the probe pick-up a function of frequency and of location with respect to the irregularities. A highly satisfactory answer to the entire problem was found in a device which is called a directional coupler because it couples only to the wave propagated in one direction. In its simplest form, a directional coupler consists of two couplings to the main transmission line, which add for one direction of transmission and cancel for the other. Thus, for example, Figure 10A shows a form of directional coupler for wave guide which is placed in the radar transmission line at the point indicated schematically in Figure 1. An auxiliary wave guide is coupled to the main guide through two identical orifices spaced $\lambda g/4$ between centers (or more generally $n\lambda g/4$, where n is an odd integer). Assuming the incident and reflected waves in the main guide to be directed as shown and the auxiliary guide to be terminated on one end, a test circuit connected to the other end will be coupled to the incident wave, while theoretically the two couplings to the reflected wave will differ by $\lambda/2$ and therefore cancel one another.

With such a device, measurements may be made of the characteristics of the incident wave independently of reflections.

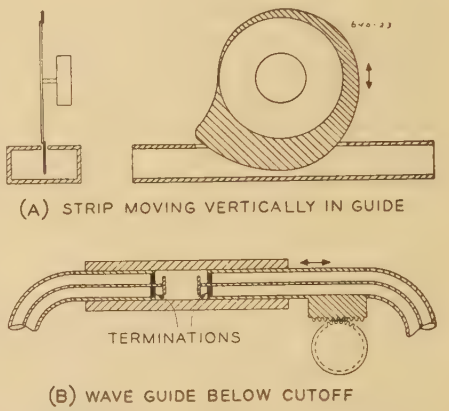

Figure 23. Microwave attenuators

If the coupling to the main line is not too close, there is no appreciable effect on the incident wave, and continuous monitoring can be had. Conversely, test signals applied through the directional coupler will travel in the main guide in the proper direction for testing the radar receiver.

If the locations of the termination and the test connection point in Figure 19A are reversed, the couplings to the main transmission line also are reversed. Such an arrangement therefore permits measurement of the reflected power, which in turn makes it possible to adjust for minimum reflected power and hence for minimum standing wave ratio. Comparison of the reflected power with the direct power determines the standing wave ratio. For convenience in measurement, two directional couplers pointed in opposite directions are frequently used, the combination being referred to as a bidirectional coupler (Figure 19B). One advantage of this arrangement is that the ability to measure the reflected power from the antenna and that part of trans-

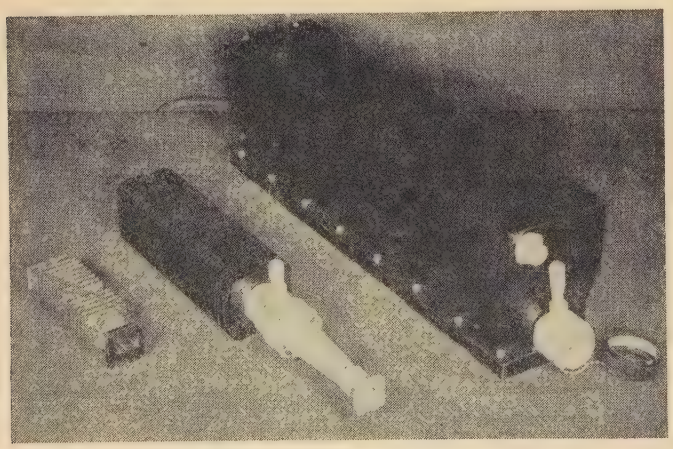

Figure 22. RF loads for different bands in the microwave frequency range

mission line beyond the coupler provides means for detecting trouble in that part of the system. Directional couplers may be applied to any type of transmission line. Figure 19C shows a simple form of directional coupler for a coaxial line.

One characteristic of importance in a directional coupler is the coupling loss. A small value of coupling loss affords increased sensitivity of measurement, while a sizable value is desirable to minimize reaction on the main transmission line, as well as for other reasons. A loss of around 20 decibels has usually been found a good compromise. It is now the practice to incorporate a directional coupler in every radar set to obtain a test connection point.

Because of unavoidable imperfections, a directional coupler never gives complete cancellation for the undesired direction of transmission. The departure from ideality is indicated by the directivity (also referred to as front-to-back ratio), which is defined as the scalar ratio of the two powers measured at the test connection point when the same amount of power is applied to the main guide, first in one direction and then in the other. For measurements of the direct wave and of receiver characteristics, a moderate directivity, of the order of 15 decibels or better is sufficient. In measuring reflected power, however, the directivity determines the amount of direct power which appears at the point of measurement, and therefore controls accuracy. The chart of Figure 20 will facilitate determination of the maximum error that may occur in measuring different values of the standing wave ratio with various assumed directivities.

With a simple two-hole coupler, the directivity deteriorates rapidly as the frequency departs from that corresponding to quarter-wave spacing. By providing additional couplings suitably spaced, the residuals from different sets of couplings also can be cancelled against one another and the directivity versus frequency characteristic can be broadened materially. With multiple hole couplings, a minimum directivity of 26 to 30 decibels over a frequency band of 10 to 20 per cent is readily practicable in quantity production, and much better values are obtained in the laboratory. Some of the numerous designs of directional couplers developed for association with operating radar equipment are shown in Figure 21.

Because they are more convenient than slotted lines and can be made more accurate, directional couplers have been extensively used for standing wave ratio measurement in the laboratory. A number of special arrangements have been devised to improve both accuracy and convenience. A directional coupler arrangement which has been provided for field measurement of standing wave ratio in the vicinity of 25,000 megacycles also is illustrated in Figure 21. In this the direct power is brought to equality with the reflected power by an attenuator whose dial is calibrated directly in standing wave ratio. A wave-guide switch facilitates the power comparison.

Auxiliaries and Components

An RF load (or dummy antenna) which will absorb the radar power in an impedance which matches the transmission line is very useful in radar work. Such a device permits testing the radar set in operating condition without actual radiation which might give information to the enemy or interfere with other radar equipment. It also makes it possible to test the radar set in locations where reflections from the ground or nearby objects otherwise would hamper or prevent a test. RF loads for microwave work usually consist of a section of transmission line (either coaxial or wave guide, depending on wave length) containing a high-loss dielectric. The impedance of such a load is necessarily low and must be matched to the radar line by tapering the dielectric over a distance of several wave lengths.[10] Moreover, if the line is to handle high power, tapering over a considerable length is necessary to distribute the heat.

A coaxial load preferably is tapered from outer conductor to inner conductor, since this both reduces the voltage gradient and facilitates heat dissipation. A dielectric consisting of a mixture of bakelite, silica, and graphite, molded in place, has been found satisfactory. For wave guides, a ceramic containing carbon may be preformed, with taper in one or two dimensions, and cemented in place.

Figure 22 shows a number of RF loads developed for different frequency bands. One of these, *TS-235/UP*, provides an excellent impedance match over the frequency range from 500 megacycles to above 3,000 megacycles. When equipped with a blower designed for uniform transverse ventilation, it will handle a peak power of the order of 750 kw with a duty cycle of about 0.001.

Microwave Attenuators and Pads

RF attenuators and pads are cornerstones of microwave testing. Attenuators are used to adjust unknown signals to levels suitable for measurement and to obtain the minute test signals required for measuring receiver characteristics. Pads serve to change levels and to prevent interaction between testing components. Microwave attenuators and pads are of two general types:

1. Those which employ dissipative elements to absorb power.
2. Nondissipative devices which introduce propagation or coupling loss.

For the shorter microwaves, the most convenient form of attenuator is of the dissipative type, employing a strip or vane of dielectric coated with a resistance material, as for example, carbon-coated bakelite. This is placed in rectangular wave guide with its plane paralleling the side of the guide. The attenuation is varied by varying the depth to which the vane is inserted in the guide (Figure 23A) or by changing its position in the guide. A valuable feature of such attenuators is that the minimum loss can be made substantially zero. For good impedance match, the strip must be tapered. By using two strips, the over-all length of the attenuator can be reduced. Extremely satisfactory attenuators of this type covering a frequency range of 8 to 12 per cent, with loss variable from 0 to 35 or 40 decibels, have been obtained in the frequency range 4,000 to 24,000 megacycles.

For the longer microwaves, where wave guides are inconveniently large, attenuators of the wave guide-below-cutoff type are very useful. These consist of a

Figure 24. Radar pulse envelopes

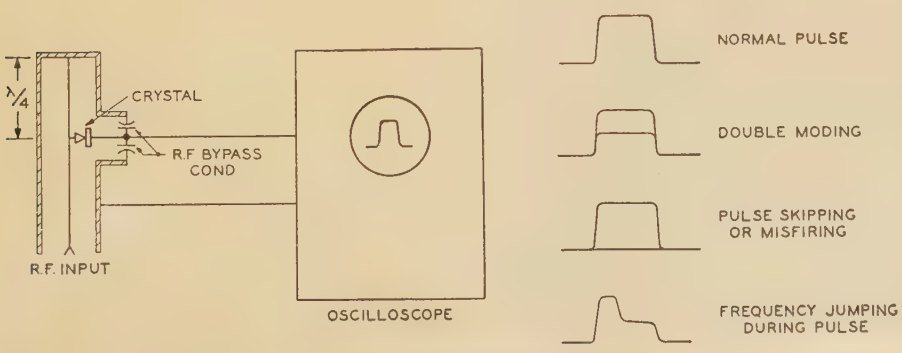

section of round wave guide the diameter of which is small compared with wave length and whose length is adjusted by telescoping. (See Figure 23B.) The $TM_{0,1}$ mode has been found very satisfactory, and $TE_{1,1}$ has also been used. Connection is made to the attenuator by a coaxial circuit at each end, with disk excitation for the $TM_{0,1}$ mode and loop coupling for $TE_{1,1}$. The attenuation formulas are[12]

$$TM_{0,1}. \quad A = \frac{41.8}{D}\sqrt{1-\left(\frac{1.31D}{\lambda}\right)^2} \text{ decibels per meter} \quad (12)$$

$$TE_{1,1}. \quad A = \frac{32.0}{D}\sqrt{1-\left(\frac{1.71D}{\lambda}\right)^2} \text{ decibels per meter} \quad (13)$$

where D = diameter of wave guide in meters. Because of the effect of other modes when the coupling is close, a minimum loss of 20 to 30 decibels is required before the attenuation becomes linear with displacement. The attenuation differentials are substantially independent of frequency. Attenuators of this type present a large impedance mismatch at either end, the effect of which may be alleviated by padding or by a termination.

Types of pads employed in microwave work include the following:

1. Flexible coaxial cable, usually with high resistance inner conductor.
2. Coaxial π with carbon-coated rod and disks.
3. Coaxial with carbon-coated rod as inner conductor.
4. Resistance strip in wave guide.
5. Directional coupler.

In calibrating microwave attenuators and pads, comparison with an accurately calibrated IF attenuator, using a heterodyne test set, has been found to give excellent results.

RF Cables and Connectors

Flexible radio-frequency cables for connecting test equipment to equipment under test are an important adjunct of field testing. At frequencies of 10,000 megacycles and below, flexible coaxial cables of about 0.4-inch over-all diameter with solid or stranded inner conductor, solid low loss dielectric (polyethylene) and braided outer conductor have been used satisfactorily, although in the upper part of this range special measures have been necessary to prevent attenuation change caused by flexure and aging. Over most of this range, coaxial jack and plug connections have been found satisfactory, but wave guide connectors are preferable at the upper end. In the range above 10,000 megacycles, coaxial cables of requisite stability have not yet been obtained, and rubber-covered wave guide with soldered articulated joints is the best form of flexible cable now available.

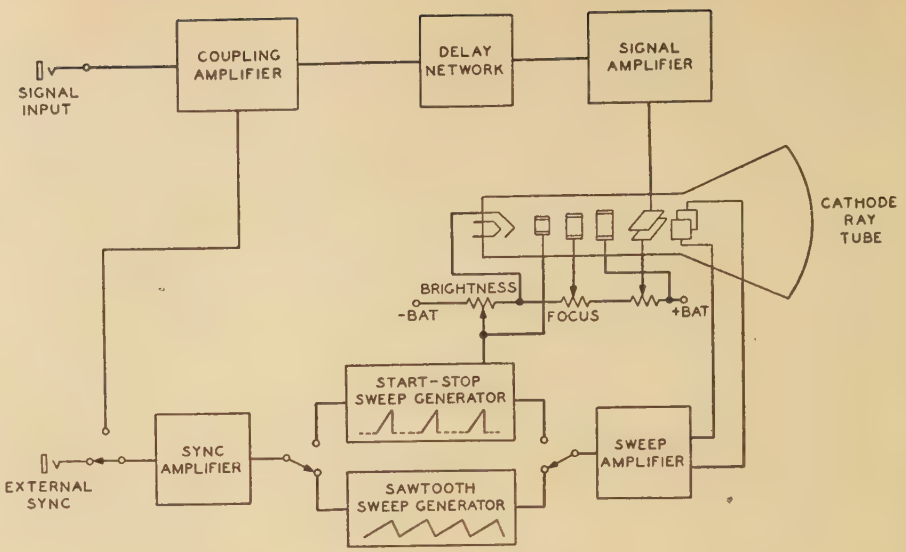

Figure 26. Block diagram of *TS-34/AP* and *TS-34A/AP* oscilloscopes

Oscilloscopes

Oscilloscopes are used extensively in radar maintenance for examination of video waves and for viewing RF envelopes. Satisfactory radar performance depends on a variety of video wave shapes, which may include trapezoidal or triangular pulses, sawtooth waves, square waves, or combinations of these. Observation of these wave shapes, supplemented if necessary by measurements of amplitude and duration, helps in diagnosing many troubles.

Examination of the envelope of the RF pulse is a convenient but less informative alternative to spectrum analysis. The envelope should be a clean, single trace of good shape. Figure 24 shows traces sometimes experienced. Double modding, that is, oscillating at different frequencies on different pulses, is shown by a double trace. Frequency-jumping during a pulse is shown by a break in the envelope. Misfiring gives a base line under the envelope. Other abnormalities in the RF envelope may result from incorrect video wave shape. Observation of the RF envelope requires a rectifier, usually a crystal, together with a suitable video amplifier. Since limitation of the oscilloscope to video functions permits general application to radar sets of all frequencies, the rectifier generally is provided externally.

The oscilloscopes available before the war did not meet the requirements of radar. Fast sweeps were necessary to permit viewing of pulses ranging from several microseconds to a fraction of a microsecond. Amplifiers were required for such pulses with low phase and amplitude distortion over a broad frequency band. Existing methods of synchronizing and phasing sweeps were also inadequate. The progress of the oscilloscope

Figure 25. Test oscilloscopes for viewing wave forms in radar equipments

Left to right: *BC-910-A* (1942), *TS-34A/AP* (1944), and *TS-239/UP* (1945)

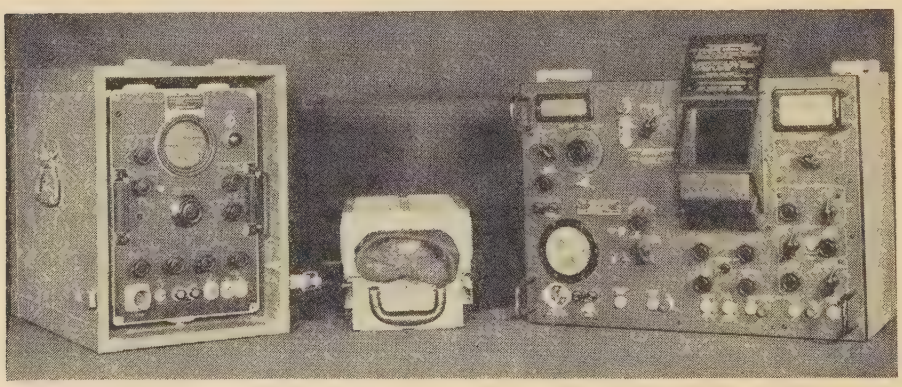

art during the war is illustrated in the successive designs of field test oscilloscopes shown in Figure 25.

The *BC*910*A* oscilloscope, gotten out as a stop gap not long after the attack on Pearl Harbor, incorporates fast sweeps and broad-band amplification. Following close upon this was the *BC*1087*A* (Navy code *CW*60*AAY*), which replaced sine-wave synchronization by a start-stop sweep triggered by the incoming pulses. This feature made it possible to superpose the erratic pulses produced by spark wheel and similar pulsers and at the same time avoided external synchronizing connections. A valuable feature conjoined with the start-stop sweep was a delay network in the main transmission path which gave the sweep time to start before the pulse reached the cathode-ray tube. This oscilloscope in original and modified form has seen wide service in all theaters. However, its weight of more than 60 pounds was a handicap for many uses.

Further advances in oscilloscope circuitry and in weight limitation resulted in *TS*-34/*AP*, weighing only 25 pounds. This combined the short-pulse features of the previous design with those of the conventional oscilloscope for viewing slower waves. A schematic diagram is shown in Figure 26. A redesign, coded as *TS*-34*A*/*AP*, incorporated variable start-stop sweeps and improved mechanical design. These two oscilloscopes, *TS*-34 and *TS*-34*A*, were produced to a total of some 12,000 and were used universally by all branches of the service for both radar and radio testing. Toward the end of the war the trend toward shorter pulses, coupled with the need for precise measurement of wave amplitude and duration, led to a new design, *TS*-239/*UP*, which embodied wide advances over *TS*-34*A* in performance and versatility but with an increase in weight.

In association with different oscilloscopes, other video devices have been employed. The amplitude of pulse applied to the magnetron is thousands of volts. To derive a voltage suitable for application to the oscilloscope, a voltage divider of the capacitor type is used (*TS*-89/*AP*). Suitable video terminations, dividers, and loads, sometimes of high voltage and power capacity, are required to obtain proper test conditions and provide convenient test points (*TS*-98/*AP*, *TS*-390/-*TPM*-4, *TS*-90/*AP*, *TS*-234/*UP*). Originally a high impedance connection to the oscilloscope was effected by a single-stage amplifier unit (*BC*1167*A*), but a simple divider-type of probe was later found more satisfactory for this purpose.

Range Calibration

Types of timing circuits used for radar range determination include multivibrators, coil and capacitor oscillators (generally without but sometimes with temperature control), and occasionally quartz crystal oscillators. The first two depend for their accuracy on capacitors, resistances, coils and other elements which are subject to error due to aging, temperature, humidity, mechanical damage, and the like. Nor is the quartz crystal oscillator wholly immune to error. Consequently, portable range calibrators are required for field maintenance.

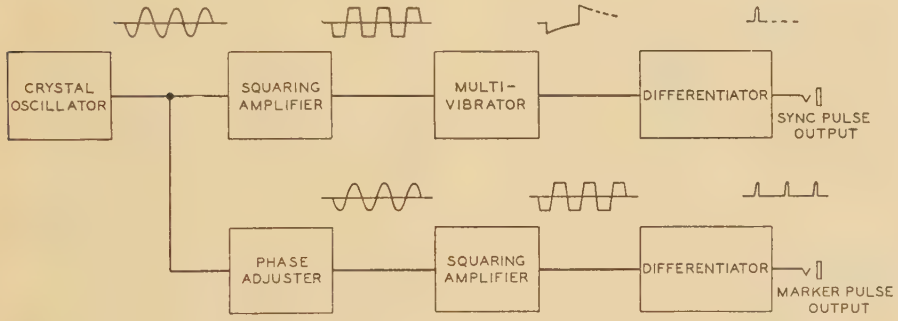

Figure 27. Block diagram of *TS*-102/*AP* and *TS*-102*A*/*AP* range calibrators

TS-102*A*/*AP* (Figure 27) and its predecessors, *TS*-102 and *TS*-19, are precision calibrators which have been extensively used for checking a large number of different air-borne bombing and gun-laying radar equipments, and ship-borne fire control and search radar equipments. These sets deliver accurately spaced marker pulses, derived from a quartz crystal oscillator, for checking the radar range pulses. A trigger pulse derived from a multivibrator synchronized with the quartz oscillator is also provided for actuating the radar timing circuits. With certain radars the calibration procedure requires an oscilloscope as well. Extreme stability of marker pulses, better than ± 0.02 microsecond, is obtained. A stop watch is included in these sets for checking rate of change in range.

Less precision is required in range calibration of search radar sets. For this purpose the *TS*-5/*AP* calibrator provides marker pulses of one-quarter, one, five, or ten nautical or statute miles, derived from a coil and capacitor oscillator with closely controlled temperature coefficients. This calibrator is designed to be triggered by the radar or some other external source.

Computer Test Sets

A number of radar sets are equipped with computers which receive the data on location of target and its direction and rate of change, together with essential related information on such factors as wind velocity, ground speed, altitude, and so forth, and deliver the solution of the ballistic problem in the form of a voltage which releases bombs, points the guns, or serves other purposes. Means for checking the accuracy of these computing devices are generally required. The type of test set needed depends upon the computer design, which has taken different forms according to the nature of the problem and the state of the art.

Two types of computer test sets are

Figure 28. Two test sets for checking the computers used in bombsight and fire control radar sets

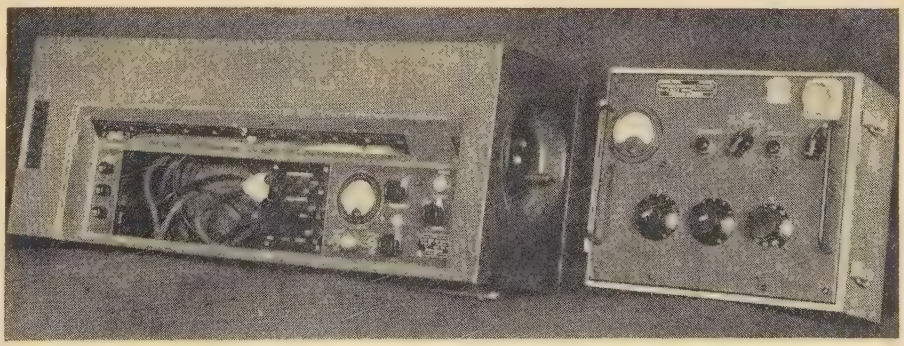

shown in Figure 28. *TS*-158/*AP*, designed for use with certain air-borne bombing radars, furnishes to the computer a signal representing a target approaching at known speed and checks the accuracy of bomb release. *TS*-434/*UP*, designed for several air-borne and ground radars is an accurate instrument for determining the voltage ratios at various points in a computer and thus checking its performance.

Conclusion

More than 200 different designs of test sets were developed during the war by Bell Laboratories to meet the exacting requirements of radar field maintenance. These differed radically from previous art. Outstanding features were portability, precision, and generality of application. The large number of designs are caused partly by the varied functions of radar and the varied conditions of use. Largely, however, it results from the fact that the frequency band that can be handled in any one set is limited, whereas many frequency ranges and subranges had to be covered in all.

Altogether, more than 75,000 radar test sets were manufactured by Western Electric Company, and these were used in all theaters of war by the United Nations forces. The production rate at the end of the war exceeded 5,000 test sets a month. In numerous cases, moreover, small preproduction quantities of test equipment were built on a "crash" basis for special missions and for training purposes. The test equipment produced for the field had to be more precise than the radar sets, and the equipment used in the factory and the laboratory to test the field test equipment had to be still more precise.

Trends of development at war's end were toward

1. Further broadbanding, simplification, and precising.
2. Coverage of new frequency ranges.

References

1. Ultra-High Frequency Techniques (book), J. G. Brainard, G. Koehler, H. J. Reich, L. F. Woodruff. D. Van Nostrand Company, Inc., New York, N. Y., 1942.

2. Reflex Oscillators, J. R. Pierce. *Proceedings of the Institute of Radio Engineers*, volume 33, February 1945, page 112.

3. The Lighthouse Tube, E. D. McArthur, E. F. Peterson. *Proceedings of National Electronics Conference*, volume I, 1944, page 38.

4. Electromagnetic Waves (book), S. A. Schelkunoff. D. Van Nostrand Company, Inc., New York, N. Y., 1943.

5. The Proportioning of Shielded Circuits, E. I. Green, F. A. Leibe, H. E. Curtis. *Bell System Technical Journal*, volume 15, April 1936, page 248.

6. Resonant Lines in Radio Circuits, F. E. Terman. AIEE Transactions, volume 53, July 1934, pages 1046–53.

7. Ultra-Short-Wave Transmission Phenomena, C. R. Englund, H. T. Crawford, W. W. Mumford. *Bell System Technical Journal*, volume 14, July 1935, page 369.

8. Thermistors in Electronic Circuits, R. R. Batcher. *Electronic Industries*, volume 4, January 1945, page 76.

9. An Impedance Transmission Line Calculator, P. H. Smith. *Electronics*, January 1944.

10. Microwave Transmission (book), J. C. Slater. McGraw-Hill Book Company, New York, N. Y., 1942.

11. Theory of the Electromagnetic Horn, W. L. Barrow, L. J. Chu. *Proceedings of the Institute of Radio Engineers*, volume 27, January 1939, page 51.

12. Attenuation of Electromagnetic Fields in Pipes Smaller Than Critical Size, E. G. Lindner. *Proceedings of the Institute of Radio Engineers*, volume 30, December 1942, page 554.

Motor-Driven Exciters for Turbine Alternators

R. B. BODINE
MEMBER AIEE

S. B. CRARY
FELLOW AIEE

A. W. RANKIN
MEMBER AIEE

THIS PAPER presents a study of the performance of a motor-driven excitation set designed for large turbine alternators connected to modern power systems. This excitation set has been so designed that its performance, both steady state and transient, is essentially comparable with the usual direct-connected (shaft-driven) exciter even when the driving motor is receiving its voltage from the alternator to which the generator is supplying excitation.

A significant trend to the unit type of generating station,[1,2] with each generator connected by its high-voltage transformer to the transmission system, has been evolving during the last 20 years. This trend has been the result of the ability to operate largeinter-connected systems with a high degree of reliability. Important factors in this evolution have been the development of high-speed high-interrupting-capacity circuit breakers, the application of quick relaying, and the experience to analyze and design systems for both normal and abnormal operating conditions. In this type of system, each generating element is a small part of the total capacity, and complete reliance on its operation is not so essential as is the reliable performance of the major transmission system. Transmission line links are required to carry blocks of power of greater magnitude than the output of individual generating units. The system is accordingly able to withstand the loss of any single unit of generation more easily than the loss of important line capacity. An element of generation may be quickly disconnected as a unit because of out-of-step operation or any other trouble. In this way the disturbance is localized and more easily cleared. Serious system disturbances, resulting in load interruptions, usually involve more than one generating element or station and are the result of failure to localize the initial trouble.

For the type of station and system where the loss of an individual generating unit is important to the system reliability, the essential auxiliaries may be driven from a separate supply such as a house alternator. Such an arrangement does not place severe requirements on the motor-driven exciter, if used, and therefore is not considered in this paper. The necessity for this type of station design will decrease in the future for even the larger capacity generating units.

With this trend in station and system design, it is natural that the essential auxiliaries of a generating element should more and more obtain their power from an auxiliary bus connected by a transformer to the alternator terminals. This practice has found considerable favor, with the possible exception of the exciter of the main generating unit. The exciter is one of the most important essential auxiliaries, and since its output is usually increased several times at the time of a system disturbance or low system voltage, it is understandable that direct-connected exciters should continue to be used in-

Paper 46-77, recommended by the AIEE committee on power generation for presentation at the AIEE winter convention, New York, N. Y., January 21–25, 1946. Manuscript submitted November 7, 1945; made available for printing December 17, 1945.

R. B. Bodine and S. B. Crary are with central station engineering division, and A. W. Rankin with turbine engineering division, General Electric Company, Schenectady, N. Y.

The authors wish to acknowledge the suggestions and co-operation of the engineers of the Dayton Power and Light Company and of L. W. Thompson, E. H. Bancker, and J. B. McClure, of General Electric Company.

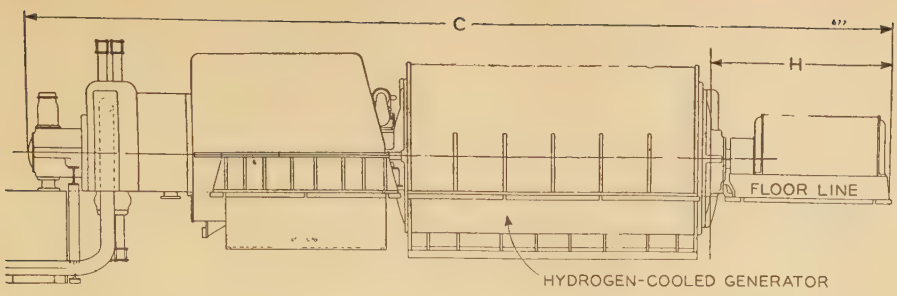

Figure 1. Outline of typical 30,000-kw 3,600-rpm turbine alternator showing comparative over-all dimensions for three types of excitation systems

Excitation system:	C	H
Direct drive, 3,600 rpm	50 ft 4 1/4 in	9 ft 4 in
Gear drive, 1,776 rpm	52 ft 11 7/8 in	11 ft 11 5/8 in
Motor drive	44 ft 2 1/4 in	3 ft 2 in*

Dimensions of motor-driven exciter set:
Length—10 ft 11 in
Width—3 ft 10 1/4 in
Height—4 ft 3/4 in
* Length to end of alternator shaft.

stead of the more flexible separately driven exciters. However, with these modern systems it is now possible, as will be shown in this paper, to design a motor-driven exciter set which will have a reliability comparable with that of the other essential auxiliary drives.

Motor-driven exciters for turbine-alternators have the following, rather self-evident, advantages over the conventional high-speed exciters which are direct-driven from the shaft of the main alternator:

1. A motor-driven excitation set can be of unit construction, and it can be installed in locations less expensive than those required by a direct-driven exciter.

2. The motor-driven exciter can be designed without gearing for a lower and more satisfactory speed for a d-c generator of its rating.

3. The design and construction of the main alternator unit is simplified.[3,4]

In Figure 1 is shown an outline drawing of a typical 30,000-kw turbine-alternator set, and on this are given the over-all lengths when each of the three major types of excitation systems is used: direct-drive, gear-drive, and motor-drive. Note that the over-all length of the turbine-alternator set using the motor-driven exciter is almost nine feet less than the over-all length of the turbine-alternator set using the gear-driven exciter. The principal dimensions of a special motor-driven 1,200-rpm exciter of co-ordinated design for a typical 30,000-kw turbine-alternator are shown in Figure 2.

Reasons for the former poor reputation of motor-driven exciters, and the modern developments which have tended to minimize the importance of these reasons, may be summarized as follows:

1. Before the use of modern switches and relays, the motor-driven exciter connected to the main system was not capable of maintaining the alternator excitation at the high values demanded during loss of synchronism and resulting periods of prolonged low voltage. This requirement, however, largely has been eliminated by better system design and modern apparatus.

2. During a period of low system frequency and consequently low motor speed, motor-driven exciters, when operated under manual control of excitation, are likely to reduce the excitation to a point where generator instability can result. This tendency was increased at such periods by the speed governor's trying to increase the kilowatt load of the alternator. With the use of modern voltage regulators, however, the desirability or necessity for operating under manual control has been eliminated. Also, the frequency change during a system emergency is now generally less as a result of the increased inter-connected system capacity.

Because of the developments outlined in the foregoing, it becomes desirable to re-evaluate the field of application for the motor-driven exciter. To fulfill the requirements of a reliable excitation source, a motor-driven exciter must be designed to meet the following performance specifications. These specifications should be met even with the driving motor receiving its voltage from the alternator to which the generator is supplying excitation so as to conform with the trend toward the simplified unit type of generator station design:

1. Maintain and develop excitation equal to that of a direct-connected exciter for alternator terminal voltages down to 70 per cent of normal for sustained periods.

2. Provide excitation equal to that of a direct-connected exciter through the most severe fault that the alternator itself can withstand without losing synchronism when operating at full rated steam flow.

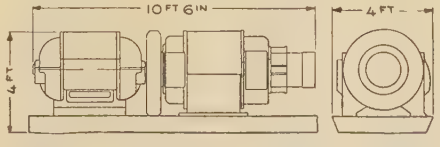

Figure 2. Outline of motor-driven excitation set of co-ordinated design for 30,000-kw turbine alternator

The above requirements, as will be demonstrated, can be obtained by the following three design features:

1. Co-ordinated design of turbine alternator, exciter, and voltage regulator.

2. Induction motor designed with sufficient torque margin to meet the condition of ceiling excitation voltage with 70 per cent alternator terminal voltage (requirement 1 preceding).

3. Sufficient additional flywheel effect for the exciter set so that reasonably rapid excitation can be applied for fault duration and severity which are not quite sufficient to cause loss of synchronism of the turbine alternator at full output (requirement 2 preceding).

Determination of Characteristics

The following is a discussion of the basis for the selection and design of a motor-driven exciter to meet the two previously defined performance requirements, that is, prolonged low system voltage and severe system faults. A motor-driven exciter set for a 30,000-kw turbine alternator built to these general system requirements was furnished the Dayton Power and Light Company. See Figures 3 and 4.

Low System Voltage Requirement

System disturbances may occur in which the system voltage may become comparatively low for relatively prolonged periods of time. A lower system design limit for this condition may be taken as 70 per cent voltage existing for a period of about three minutes.

For a system voltage of this magnitude and duration, difficulty will begin to be experienced with the other essential auxiliaries of the station; the system loads may begin to show a cumulative increase in reactive current requirement because of stalling of induction motors; and the heavily loaded system ties will tend to open because of loss of synchronism. This value of voltage and duration, therefore, seems reasonable as a design value for a motor-driven exciter. Up to these limits the turbine alternator should be capable of making a full contribution to the restoration of normal system conditions in order to prevent and reduce the possibility of such a cumulative breakdown of system interconnection and interruption of system loads. Dif-

ferent limits may, in some cases, be deemed necessary to meet a particular system condition. Operating experience and oscillographic records may indicate that more or less severe limits may be needed as the design values for the set. The important point is that the characteristics of the motor-driven exciter need not be haphazardly selected but can be designed to meet the requirements of the system.

In determining the pullout or maximum torque for which the motor should be designed, the low-voltage condition is the determining factor rather than any of the requirements for transient stability of the alternator. With the motor size determined by the low-voltage condition, a study of the duration and magnitude of this voltage, together with the probable alternator and exciter temperatures at which this condition occurs, must be made in order to obtain an excitation system with the best compromise among size, cost, losses, and pullout power. For instance, an induction motor which must furnish ceiling excitation with 60 per cent voltage at its terminals and with the alternator in the cold (25 degrees centigrade) condition will be about three times as large as one for which it is felt adequate to design for 80 per cent voltage in the hot (125 degrees centigrade) condition, and is about 1.7 times as large as a motor designed for 70 per cent voltage with the alternator and exciter temperatures midway between the hot and cold conditions.

The motor-driven excitation set for the Dayton Power and Light Company was designed for 60 per cent voltage at the motor terminals with the alternator and exciter at 75 degrees centigrade; the thermal capacity of the motor is sufficient to carry this load for isolated intervals of three minutes duration each.

Figure 3. 30,000-kw 3,600-rpm turbine alternator of Dayton Power and Light Company, designed for use with motor-driven exciter of Figure 4

Fault Requirement

The second requirement of being able to supply an excitation equal to that of a standard direct-connected exciter through the most severe fault with a duration corresponding to that which is critical for the turbine generator at full output, requires a consideration of the transient performance of the main unit and of the motor-driven exciter.

In Figure 5 is given the hypothetical system on which transient stability calculations were made to determine the operating performance of an alternator with a motor-driven excitation set. The alternator is connected to an infinite system through a step-up transformer of 10 per cent reactance and a tie-line of 25 per cent reactance. A 3-phase fault through zero impedance is assumed to occur on a stub feeder located immediately on the high side of the alternator transformer. Based on constant flux linkages, the critical switching time for this system is 0.27 second; for the calculations of Appendix I, which include the effect of flux decay, a switching time of 0.25 second is assumed. The induction motor driving the excitation set is supplied through a transformer whose high side is connected directly to the generator terminals.

This time of 0.25 second or 15 cycles for a severe 3-phase fault will be recognized as typical for the critical time of a 3-phase fault for turbine generators. Most modern systems have fault clearing times at least as low as this at and near their important generating stations, particularly when it is important for the maintenance of stability of the generating capacity.

Based on these considerations, the motor-driven exciter designed for the Dayton Power and Light Company was built having the following characteristics:

1. Exciter: 4.0* per unit ceiling exciter voltage at motor synchronous speed; 2.0 per unit (American Standards Association definition) response at motor synchronous speed.

2. Motor: Maximum shaft power with normal voltage equal to 34 per unit.** Slip at maximum power equal to nine per cent.

3. Inertia: Motor, exciter, and flywheel; $H=32$*** ($H\cong 5.0$ based on exciter nameplate kilowatt rating).

A comparison of the performance of this exciter with one of less inertia and pullout power and also with a direct-driven exciter is summarized by Figure 6,

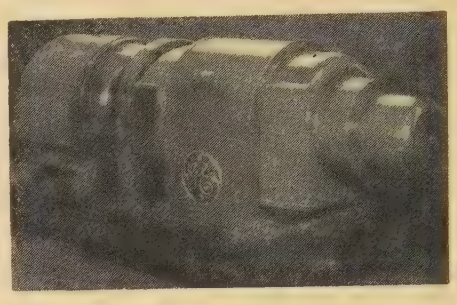

Figure 4. Motor-driven exciter for 30,000-kw turbine alternator of Dayton Power and Light Company of Figure 3

which shows the variation in alternator terminal voltage following the application and clearing of a 3-phase fault. A more complete explanation of the basis for these results, with a more detailed comparison, is given in Appendix I. It will be noted that for the case of a 3-phase high-voltage fault lasting for 0.25 second, a motor-driven exciter of proper design can be as effective as a direct-driven exciter in returning the voltage to normal and preventing loss of alternator synchronism. On the other hand, a motor-driven exciter without adequate motor power or inertia may result in loss of synchronism and, in general, in poorer performance than the conventional direct-driven exciter. This shows the importance of co-ordinating the motor and exciter design with the alternator and system characteristics.

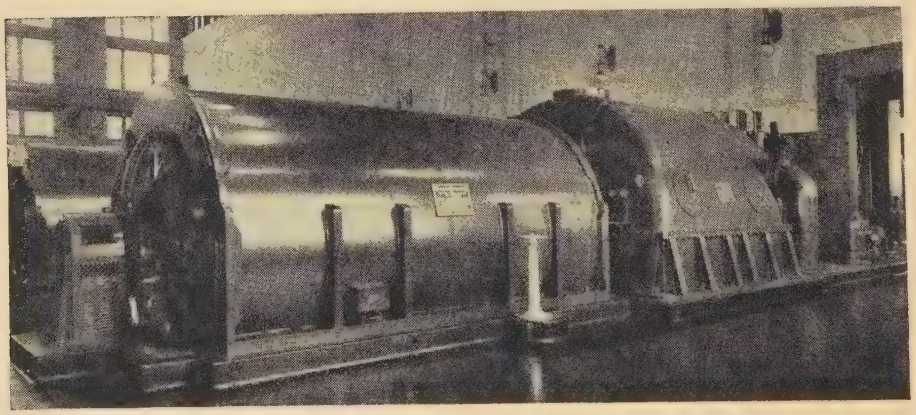

General Design Principles

In order to insure that adequate inertia, pullout, and over-all reliability are built

* Unit exciter voltage is the exciter voltage necessary to provide normal no-load alternator voltage on the air gap line with the alternator field at 75 degrees centigrade.

** Unit field power is the power supplied to the alternator field (75 degrees centigrade) with the alternator at no-load, normal voltage on the air gap line; unit field power is approximately one-sixth of the exciter nameplate rating.

*** The inertia constant, H, is based upon unit power as defined directly above and the total inertia of the entire excitation set.

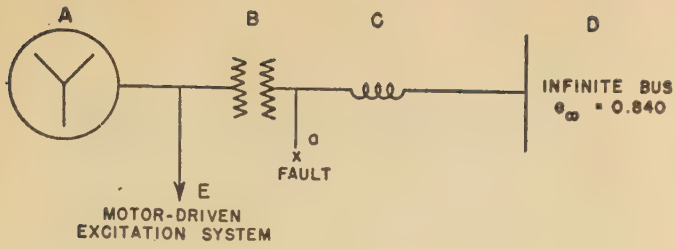

Figure 5A (above). Assumed typical system

A—Alternator
B—Line transformer
C—Line reactance
D—Infinite bus
E—Supply to motor-driven excitation system
a—Stub feed on which fault occurs

Alternator: $x_d=1.25$; $x_q=1.19$; $x'_d=0.13$; $T'_{do}=5.25$ seconds; $H=5.40$ (turbine and generator)
Line transformer: $x=0.10$
Line: $x=0.25$
Fault: 3-phase fault on stub-feeder at *a*; fault cleared in 0.25 seconds

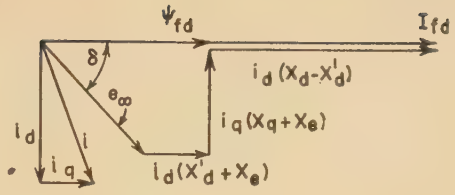

Figure 5B (right). Vector diagram of assumed system. Line and transformer are grouped together in the above diagram as x_e; saturation and resistance are neglected

into the motor-driven excitation set, the following design principles must be taken into consideration:

1. During severe faults, the induced alternator field currents cause the maximum exciter power to reach values of the order of 3.5 times the exciter nameplate rating. Subsequent to the clearing of the fault, the alternator swings coupled with the action of the voltage regulator will cause exciter loads of the order of three times the exciter nameplate rating.

2. The loads discussed in the preceding paragraph must not in any way cause collapse of the exciter voltage, since the primary duty of an exciter during system disturbances is to furnish sufficient excitation voltage to arrest and reverse, as quickly as possible, the flux decay in the alternator caused by the high induced field currents.

3. The exciter must be capable of handling, without failure, the large field currents which are induced during alternator terminal faults. These currents may reach values of the order of 5 times the exciter nameplate rating.

4. During any prolonged low-voltage period, the exciter will go to its ceiling excitation and remain there for the duration of the low voltage. During this period the alternator field current will be determined approximately by the alternator field resistance and the exciter voltage, as the induced field currents will not have a major effect.

5. During low-voltage periods of the type described in the preceding paragraph, the maximum exciter load will occur with the alternator and exciter in the cold (25 degrees centigrade) condition. If the exciter ceiling voltage with a cold exciter is ten per cent greater than the ceiling with a hot exciter, the exciter load with both alternator and exciter in the cold condition is 170 per cent of the exciter load when the alternator (125 degrees centigrade) and exciter are in the hot condition.

6. Transformers and other apparatus between the motor terminals and the alternator lines will cause the motor voltage to be lower than the alternator voltage during system disturbances.

7. During high-voltage transmission system faults for a unit type of generating station, a practical lower limit of the motor voltage will be about 30 per cent. Sufficient inertia must be built into the excitation set to carry it through this fault period without its speed decreasing to values so low as to cause collapse of the exciter voltage.

8. The main exciter and pilot exciter themselves must be designed so that the main exciter voltage will not collapse when the speed drops to the maximum slip for which the excitation set was designed.

9. The motor pullout must be high enough to prevent exciter voltage collapse during any prolonged low-voltage condition. In particular, the motor must be capable of maintaining excitation during low-voltage periods even with the alternator and exciter in the cold condition.

10. The exciter ceiling voltage must be high enough so that even with the maximum motor slip the ceiling voltage is equal to that of a conventional direct-driven exciter. An upper design limit, however, must be placed on the maximum ceiling voltage which occurs with the exciter in the cold condition, since too high a ceiling voltage at this point may produce pullout of the induction motor.

11. In order to provide the maximum reliability of operation, it is necessary to have the alternator under automatic voltage regulator control; otherwise a system disturbance results in reduction of alternator field excitation. Greater reliance can be placed on the voltage regulator when it is provided with a lower limit of excitation which is varied with valve position or steam flow. This was accomplished in the Dayton Power and Light Company's installation by using a new type of direct-acting voltage regulator with a simple type of variable lower limit. See Figure 7 for a schematic diagram of the excitation system and Figure 8 for a photograph of the regulator.

Voltage Regulator

The automatic voltage regulator used in the Dayton Power and Light Company's installation is a sturdy mechanical device consisting essentially of a torque motor and a simple spring-mounted contact system connected to taps on the regulating resistor. The design of the device is as simple mechanically as is consistent with the desired accuracy of regulation. The arrangement of parts is apparent from Figure 8.

The torque-motor, excited from the alternator terminal voltage through suitable transformers, resistors, and rectifiers, operates silver contacts by means of the lever, varying resistance in the exciter field circuit to maintain alternator terminal voltage at the desired value. An equalizing reactor in combination with a current transformer is provided to assure proper division of reactive kilovolt-amperes where two or more similar equipments are used on machines in parallel. A lower limit on excitation which varies with steam flow is obtained by a rheostat attached to the control valve cam shaft. The rheostat, connected in parallel with the regulating resistance of the voltage regulator as shown in Figure 7, determines as a function of steam flow the maximum resistance which can be inserted in the main exciter field circuit. This lower limit is effective for either manual or automatic control of excitation.

This direct-acting voltage regulator provides, in a simple mechanical device:

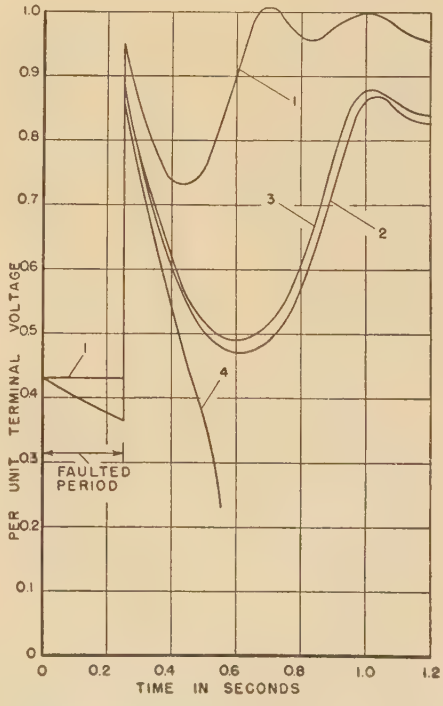

Figure 6. Alternator terminal voltage (see Appendix II)

1—Constant alternator field flux linkages
2—Conventional direct-driven exciter
3—Adequate motor-driven exciter
4—Inadequate motor-driven exciter

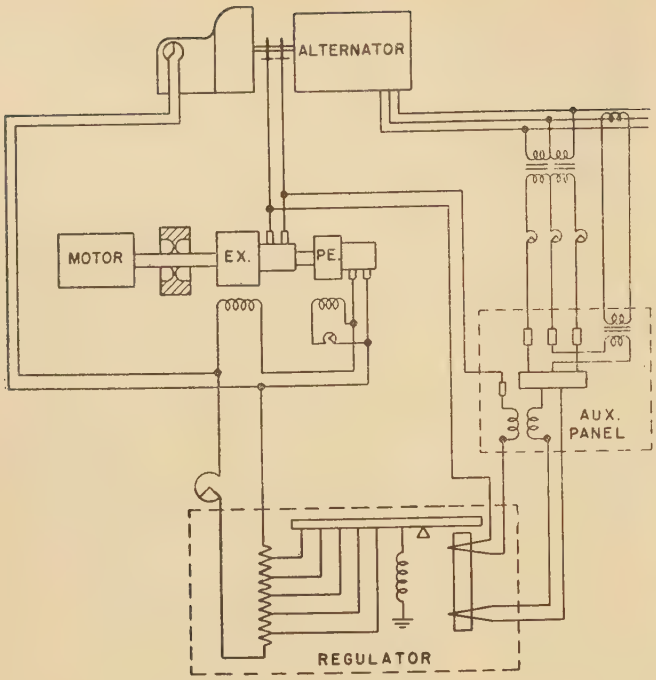

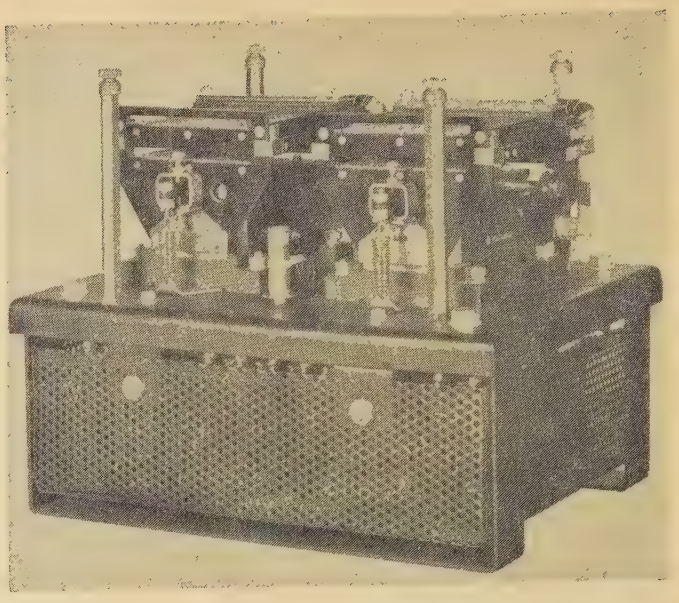

Figure 7 (left). Schematic diagram of connections for motor-driven exciter set and voltage regulator

Figure 8 (above). Direct acting voltage regulator for 30,000-kw turbine alternator of Dayton Power and Light Company

1. A smooth fast-acting accurate voltage control.

2. A lower limit on excitation which is varied with load on the turbine.

3. Proper division of reactive kilovolt-amperes between generators operating in parallel.

Losses

The losses of the competing excitation systems are not of major importance, since their magnitudes are each less than one tenth of one per cent of the total generation, with the motor-driven set being only 0.01 of one per cent of the total generation greater than the direct-driven exciter.

Conclusions

The following conclusions are drawn from the results of the study:

1. A motor-driven exciter of co-ordinated design which meets the reliability requirements of modern systems is entirely competitive and offers several advantages over the direct-connected exciter for the majority of steam stations.

2. This greater field of application results largely from the following developments:

(*a*). Quicker system fault clearing times.

(*b*). High voltage transmission line interconnections.

(*c*). Use of unit type of station arrangement.

(*d*). Development of new and improved automatic voltage regulators with variable lower limits controlled by steam flow.

(*e*). Ability to predict and analyze system requirements during emergency conditions.

3. Systems using modern equipment and design practices can readily take advantage of the possibility of using motor-driven exciters.

4. Because of the inherent advantages of the motor-driven exciter, it is expected more and more to replace direct-connected exciters in the future, particularly for the larger 3,600-rpm units.

References

1. Power Systems for Auxiliary Drives in Steam Electric Stations, J. B. McClure, S. J. Whittlesey. AIEE Transactions, volume 64, 1945, December section, pages 844–51.

2. Electric Drives for Steam-Electric Generating-Station Auxiliaries, W. R. Brownlee, S. A. Elzi. AIEE Transactions, volume 64, 1945, November section, pages 741–5.

3. Progress in Power Apparatus Development, A. C. Monteith. *Edison Electric Institute Bulletin*, June 1945, pages 169–72.

4. Standardization and Design of A-C Turbo-Type Generators, G. A. Juhlin. *The Journal of the Institute of Electrical Engineers*, volume 92, part II, April 1945, pages 147–64.

5. Two-Reaction Theory of Synchronous Machines—Part I, R. H. Park. AIEE Transactions volume 48, 1929, July section, pages 716–27.

Appendix I. Analysis of System Stability

The stability analysis of this paper is based on the representative system shown in Figure 5. Step-by-step calculations on this system were used to determine the comparative transient stability of an alternator excited by a motor-driven exciter.

Saturation effects and resistances (except the alternator field resistance) were not included in this analysis, but the alternator saliency effects were included. Step-by-step calculations were necessary in order to include the effects of alternator swings, field decrements, exciter response, and deceleration of the motor-driven excitation set.

The critical switching time for the system of Figure 5 is 0.27 second when based on constant flux linkages, and for this paper a switching time of 0.25 second was assumed. The assumed switching time is so close to the critical switching time that the flux decrement has a very pronounced effect. A diminution of alternator flux causes the synchronizing torque to decrease considerably and produces an appreciable lengthening of the alternator swings, which in turn imposes a severe load on the exciter for a relatively prolonged period.

Shorter switching times, or a stiffer tie with the infinite bus, or a partial fault instead of the assumed 3-phase fault, will all result in less severe duty on the excitation set. In addition, the resistance present in any actual system will decrease the alternator swings during the fault period, and the saturation present in any actual machine will retard the alternator flux decrement; both of these effects will therefore lessen the duty on the excitation set. It is evident from these considerations that the results given in this paper will err on the conservative side.

Constants

Alternator: $x_d=1.25$, $x_q=1.19$, $x'_d=0.13$, $T'_{do}=5.25$ seconds, $R_{fd}=0.513$ ohm at 125 degrees centigrade. The inertia constant (turbine+generator) $=H=5.40$. With 1.0 voltage, 1.0 current, 1.0 kva, 0.80 power factor at the alternator terminals, the initial angle between the alternator excitation axis and the infinite bus is 48.4 degrees.

Tie line: Line $x=0.25$, transformer $x=0.10$, voltage of infinite bus $=0.84$.

Exciter: Ceiling voltage $=4.00$ (400 volts) at 1,200 rpm, response $=2.0$ at 1,200 rpm. The main exciter is separately excited from the compound-wound pilot exciter; the main exciter voltage is assumed to vary as the cube of the exciter speed down to 85 per cent of the synchronous (1,200 rpm) speed,

and is assumed then to collapse completely. (The exciter for the direct-driven set is assumed to have a 3.0 ceiling voltage and a 1.0 response.)

Induction motor: The power-slip curve of the induction motor has a maximum power of 34 per unit at nine per cent slip, with a transformer reactance of three per cent (on a 200-kva base) between the motor and the alternator terminals. Unit motor power is defined as the power supplied to the field of the alternator with the latter at open circuit, normal voltage, on the air gap line. The H constant for the entire excitation set (motor, exciter, and flywheel) is 32 based on unit power to the alternator field.

Fault: The 3-phase fault on the stub feeder is located on the line side of the generator transformer. The fault is cleared in 0.25 second.

Critical switching time: The critical switching time, based on constant flux linkage, for a 3-phase fault as given above is 0.27 second.

Method

The vector diagram of Figure 5B can be obtained for the system of Figure 5A by using the infinite-bus voltage as a reference, and by grouping together the line, transformer, and alternator reactances.

Using the nonreciprocal unit system of Park,[5] the d-axis equations are as follows:

$$\psi_d = I_{fd} - x_d i_d$$
$$\psi_{fd} = I_{fd} - (x_d - x'_d) i_d$$
$$E_{fd} = I_{fd} + T'_{do} p \psi_{fd}$$

From Figure 5B the following are self-evident:

$$\psi'_d = e_\infty \cos\delta + i_d(x'_d + x_e) = \psi_{fd}$$
$$0 = e_\infty \sin\delta - i_q(x_q + x_e)$$
$$P = i_d e_\infty \sin\delta + i_q e_\infty \cos\delta$$

Therefore

$$P = \frac{\psi_d e_\infty \sin\delta}{(x'_q + x_e)} - \frac{(x_q - x'_d)\, e_\infty{}^2 \sin 2\delta}{2\,(x_q + x_e)(x'_d + x_e)}$$

The above expression for power is also the expression for torque, since alternator speed variations are assumed negligible.

Alternator field current I_{fd}, and alternator terminal voltage e_t, are obtained as follows:

$$\psi_{fd} = \psi_{fd} + (x_d - x'_d) i_d$$

or

$$I_{fd} = e_\infty \cos\delta + (x_d + x_e) i_d$$
$$e_{td} = I_{fd} - 1.25 i_d$$
$$e_{tq} = 1.19 i_q$$

($1.25 = x_d$ of alternator; $1.19 = x_q$ of alternator; $0.35 = x_e$ of external system: transformer plus tie line.)

$$e_t = \sqrt{e_{td}{}^2 + e_{tq}{}^2}$$

The decrement of $\psi_d'(=\psi_{fd})$ is obtained from the machine equations:

$$E_{fd} = I_{fd} + T'_{do} p \psi_{fd}$$

$$\Delta\psi_{fd} = \frac{E_{fd} - I_{fd}}{T'_{do}}\, \Delta t = \Delta\psi'_d$$

The above is the decrement in the alternator field linkages during the interval Δt. The field flux at any time t_n can be obtained by subtracting from the initial value of ψ_{fd} the sum of all the decrements $\Delta\psi_{fd}$ prior to the time t_n.

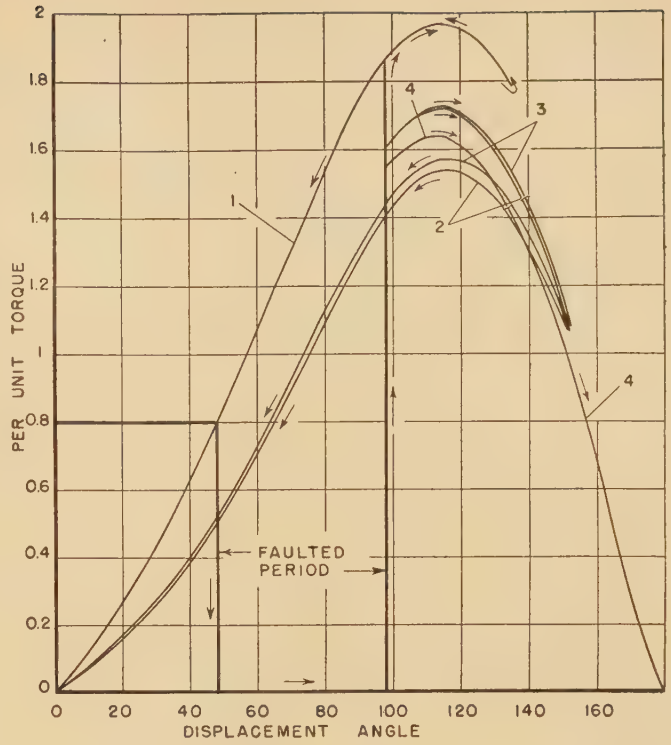

Figure 9. Torque angle curves

1—Constant alternator field flux linkages
2—Conventional direct-driven exciter
3—Adequate motor-driven exciter
4—Inadequate motor-driven exciter

Results

Based upon the analysis given above, the step-by-step calculations in Appendixes III and IV were organized. The transient performance of both the alternator and motor-driven excitation set can be obtained from these tables. The curves given in Figure 6 and Figures 9 to 14, inclusive, show the results obtained for a specific motor-driven excitation set designed for a typical 30,000-kw alternator, as well as for the other cases defined in Appendix II.

Case 1 is the ideal case usually assumed in swing curve calculations and assumes that the exciter response is sufficiently rapid to prevent any flux decrement. For the present study, this assumption is too ideal, and case 1 is of interest only in furnishing a basis for the study of the other cases.

Cases 2 and 3 are direct comparisons of the alternator performance with well-designed direct-driven and motor-driven exciters respectively. As mentioned above, the motor-driven exciter has been designed with a faster response than that of the direct-driven exciter. Figure 9 shows the alternator torque-angle curves—the alternator torque with the motor-driven exciter is always greater than the alternator torque with the direct-driven exciter. Figure 10, which shows the alternator displacement angle, shows that the alternator with the motor-driven exciter swings less than the alternator with the direct-driven exciter. Figure 11 shows that the flux linkages in the alternator excited from the motor-driven exciter are always greater than in the alternator excited from the conventional direct-driven exciter. Figure 12 shows the slip-time curves of the driving motor and shows how adequate inertia will prevent the motor slip from exceeding the slip (15 per cent) at which the exciter voltage will collapse. Figure 6 gives alternator terminal voltage versus time and shows that the

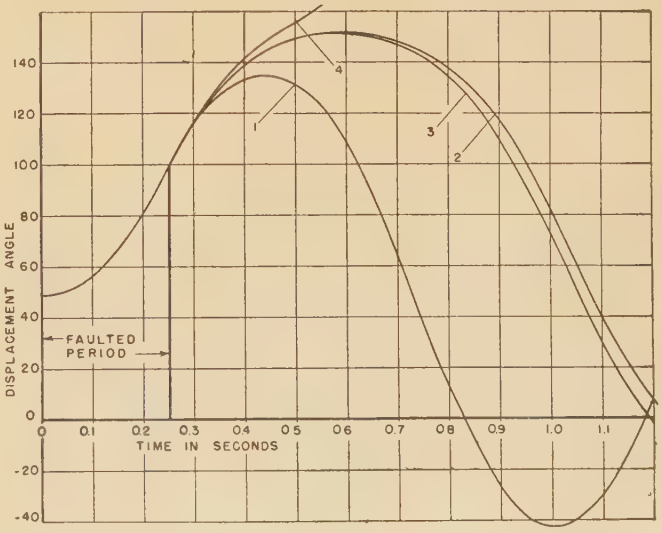

Figure 10. Alternator displacement angle

1—Constant alternator field flux linkages
2—Conventional direct-driven exciter
3—Adequate motor-driven exciter
4—Inadequate motor-driven exciter

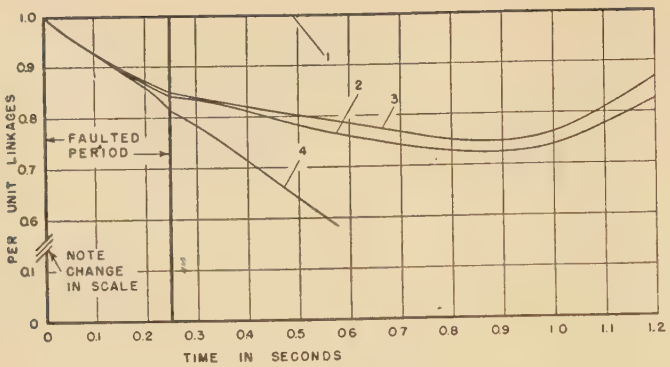

Figure 11. Alternator field flux linkages

1—Constant alternator field flux linkages
2—Conventional direct-driven exciter
3—Adequate motor-driven exciter
4—Inadequate motor-driven exciter

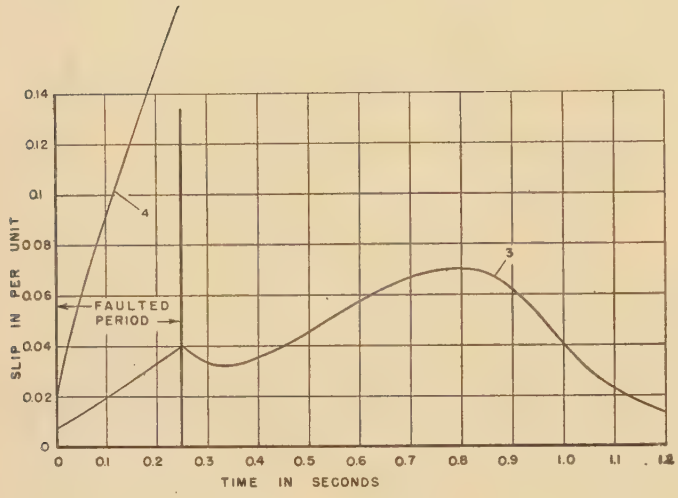

Figure 12. Slip curves

1—Constant alternator field flux linkages
2—Conventional direct-driven exciter
3—Adequate motor-driven exciter
4—Inadequate motor-driven exciter

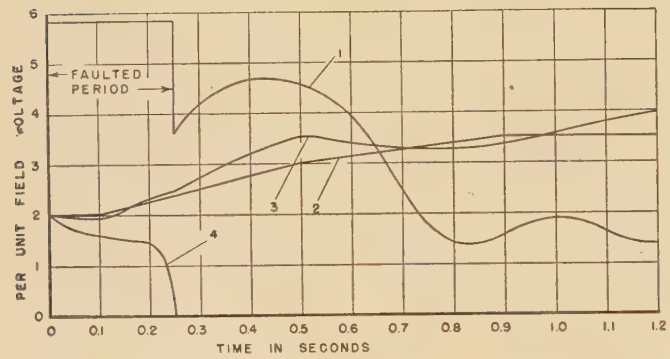

Figure 13. Alternator field voltage

1—Constant alternator field flux linkages
2—Conventional direct-driven exciter
3—Adequate motor-driven exciter
4—Inadequate motor-driven exciter

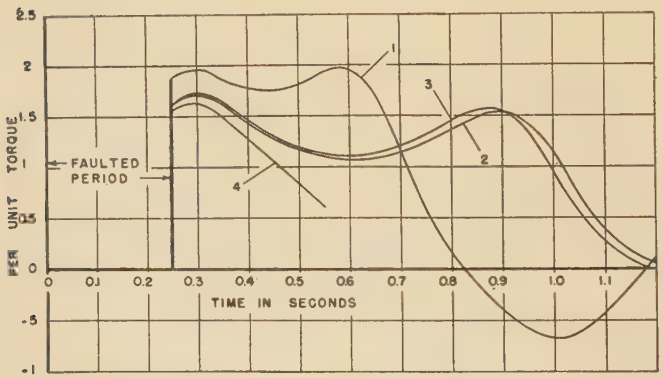

Figure 14. Alternator torque

1—Constant alternator field flux linkages
2—Conventional direct-driven exciter
3—Adequate motor-driven exciter
4—Inadequate motor-driven exciter

motor-driven exciter maintains higher alternator voltage than the direct-driven exciter for the conditions of this comparison. . On Figure 13 are shown the exciter voltage curves, and the motor-driven exciter voltage is higher than the direct-driven exciter voltage for almost the entire period. On Figure 14 are shown the alternator torque curves; the motor-driven exciter maintains a higher alternator torque than the direct-driven exciter except around one second when the torque of case 3 becomes lower than that of case 2 because the alternator is swinging back past the initial angle, and the swing with the motor-driven exciter is less than the swing with the direct-driven exciter, thereby indicating a greater stability margin with the motor-driven exciter.

Case 4 is of particular practical interest as it shows the alternator instability which may develop if the motor-driven excitation set is not designed with sufficient inertia and pullout. Figure 10 shows how the alternator displacement angle increases without limit. Figure 12 shows how the driving motor begins to stall, and Figure 6 shows how the alternator voltage decreases toward zero.

These results show that with the quick switching times of modern systems, it is possible to build motor-driven exciters whose performance is comparable with that of the direct-driven exciter.

Appendix II. Comparative Characteristics of Excitation Systems

The comparative transient performance of a turbine-generator excited by various excitation systems is given by the following figures. (Details pertaining to the calculation of the curves of these figures are given in Appendix I.)

Figure 6—Terminal voltage versus time.
Figure 9—Torque-angle curves.
Figure 10—Displacement angle versus time.
Figure 11—Field flux linkages versus time.
Figure 12—Motor slip versus time.
Figure 13—Field voltages versus time.
Figure 14—Torque versus time.

The numbers on the curves of the above figures refer to the various excitation systems and are defined as follows:

1. Constant alternator field flux linkages.

2. Conventional direct-driven exciter (direct-driven from shaft of turbine-generator); 3.0 ceiling; 1.0 response.

3. Motor-driven exciter with adequate inertia and motor power. Exciter: 4.0 ceiling at motor synchronous speed; 2.0 response at motor synchronous speed. Motor: maximum shaft power $(1.0e) = 34$ per unit;* slip at maximum power = 9 per cent; inertia: motor, exciter, and flywheel; $H = 32$.**

4. Motor-driven exciter with inadequate inertia and motor power. Exciter: 3.0 ceiling at motor synchronous speed; 1.0 response at motor synchronous speed. Motor: maximum shaft power $(1.0e) = 12$ per unit;* slip at maximum power = 10 per cent. Inertia: motor and exciter (no flywheel); $H = 6$.**

* Unit field power is the power supplied to the alternator field with the alternator at no-load, normal voltage on the air-gap line; unit field power is approximately one-sixth of the exciter nameplate rating.

** The inertia constant H is based upon unit power as defined directly above, and the total inertia of the entire excitation set.

Appendix III. Alternator Calculation

1.	Time in seconds at center of interval	t	n
2.	Displacement angle from swing sheet	δ	n
3.	d-axis field-winding flux	ψ_{fd}	n
4.	$e_\infty \cos \delta$	$e_\infty \cos \delta$	n
5.	$(x'_d+x_e)i_d=\psi_{fd}-e_\infty \cos \delta$ (3–4)	$(x'_d+x_e)i_d$	n
6.	i_d	i_d	n
7.	$(x_q+x_e)i_q=e_\infty \sin \delta$	$e_\infty \sin \delta$	n
8.	i_q	i_q	n
9.	$i_d e_\infty \sin \delta$ (6×7)	$i_d e_\infty \sin \delta$	n
10.	$i_q e_\infty \cos \delta$ (8×4)	$i_d e_\infty \cos \delta$	n
11.	$i_d e_\infty \sin \delta+i_q e_\infty \cos \delta=T$	T	n
12.	$(x_d+x_e)i_d$	$(x_d+x_e)i_d$	n
13.	$e_\infty \cos \delta$	$e_\infty \cos \delta$	n
14.	$I_{fd}=(x_d+x_e)i_d+e_\infty \cos \delta$(12+13)	I_{fd}	n
15.	E_{fd} from g of Appendix IV	E_{fd}	n
16.	$T'_{do}p\psi_{fd}=E_{fd}-I_{fd}$(15–14)	$E_{fd}-I_{fd}$	n
17.	$\frac{E_{fd}-I_{fd}}{T'_{do}}=\frac{\Delta\psi_{fd}}{\Delta t}$	$\frac{\Delta\psi_{fd}}{\Delta t}$	n
18.	$\frac{\Delta\psi_{fd}}{\Delta t}\times\Delta t$ with $\Delta t=0.05$ second. ($\Delta t=0.025$ second for discontinuous points)	$\Delta\psi_{fd}$	n
19.	ψ_{fd} of preceding interval and $\Delta\psi_{fd}$	ψ_{fd}	$n+1/2$
20.	Time at end of interval	t	$n+1/2$
21a.	I_{fd} (14)	I_{fd}	n
21b.	$x_d i_d$	$x_d i_d$	n
21c.	$e_{td}=I_{fd}-x_d i_d$ (21a–21b)	e_{td}	n
22.	$e_{tq}=x_q i_q$	e_{tq}	n
23.	$e_t=\sqrt{e^2_{td}+e^2_{tq}}$	e_t	n

Appendix IV. Induction Motor Calculation

(a).	Time in seconds at center of interval	t	n
(b).	e_t from 23 of Appendix III	e_t	n
(c).	Slip at time t	s	n
(d).	kw_m=input to induction motor=Pe_t^2. (P at slip s is obtained from power slip curve)	kw_m	n
(e).	Exciter response for zero slip	$\Delta E_{fd}(s=0)$	n
(f).	Exciter voltage for zero slip $E_{fd}(s=0)$ of preceding interval plus $\Delta E_{fd}(s=0)$	$E_{fd}(s=0)$	n
(g).	Actual exciter voltage=$(1-s)^3 E_{fd}(s=0)$	E_{fd}	n
(h).	I_{fd} from 14 of Appendix III	I_{fd}	n
(i).	Kilowatts delivered to alternator field=$E_{fd}\times I_{fd}$	kw_g	n
(j).	$kw_m-kw_g(d-i)$	Δkw	n
(k).	Δkw of $j\times\Delta t$ with $\Delta t=0.05$ second ($\Delta t=0.025$ second for discontinuous points)	Δkw seconds	n
(l).	kw seconds of preceding interval plus Δkw seconds	kw seconds	$n+1/2$
(m).	$\sqrt{\frac{kw \text{ sec of } 1}{H \text{ of excitation system}}}$=speed	δ	$n+1/2$
(n).	Slip at end of interval=$1-s$	s	$n+1/2$
(o).	Time at end of interval	t	$n+1/2$

Arcing Ground Tests on a Normally Ungrounded 13-Kv 3-Phase Bus

J. E. ALLEN
MEMBER AIEE

S. K. WALDORF
MEMBER AIEE

THE BUSSES and connected equipment in electric power stations sometimes are operated ungrounded. When a single insulation fault to ground occurs on a system of this type, the fault current is relatively small, the arc damage usually slight, and the faulted equipment in nearly all cases can be removed from service without relay action or service disturbance of any kind. However, in April 1942, faults developed simultaneously at two points 300 feet apart on the ungrounded 60-cycle 13.2-kv bus in the Holtwood station of the Pennsylvania Water and Power Company. This trouble resulted in severe arcing and damage to the bus structure before the faults were isolated.

It is unlikely that two insulators at a distance from each other would fail simultaneously without some electrical disturbance initiated by the failure of one causing the failure of the other. Numerous studies of ungrounded electric systems have been published which show that overvoltages as high as six to eight times normal theoretically can occur when a ground fault produces an arc.[1,2,3,7] This paper describes an experimental determination of the magnitude of overvoltages produced by several types of arcing grounds on the Holtwood bus, and complementary tests and analyses to determine the nature of the phenomena responsible for the insulation failures and the forced outage. The investigation differed from those previously described in technical literature in that experimental work was done with actual high voltage arcs to ground on a 13-kv station bus rather than on a high-voltage transmission line or a low-voltage theoretically equivalent circuit.

Because the work reported here was done only with arcing grounds on a 13-kv normally ungrounded station bus, conclusions are limited to only this class of service and do not include high-voltage transmission line phenomena or effects of switching surges.

Scope of Investigation

The investigation involved the following steps:

1. As an introduction to arcing ground phenomena on a 3-phase bus, a study was made of the electrical vector relationships involved.

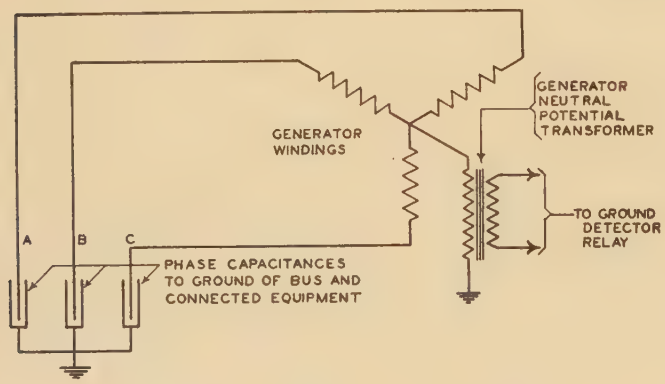

Figure 1. Simplified equivalent circuit of Holtwood 60-cycle bus

2. A study of the high-frequency characteristics of the bus and connected equipment was made to determine whether standing waves could have contributed to the generation of very high voltages on the Holtwood bus.

3. The characteristics of arcs under simulated arcing ground conditions were studied on a laboratory scale. Arc gaps were developed which had, as nearly as practicable, the characteristics theoretically required for the production of high voltages by arcing grounds.

4. Arcing grounds at high voltages were placed on the Holtwood bus under progressively more severe conditions, to determine if high overvoltages could be produced by any arcing ground condition likely to occur in service.

5. An analysis was made to determine whether the neutral voltage fault detecting method installed on the Holtwood bus can warn of impaired insulation to ground before the insulation is completely broken down. The analysis is included as an appendix to this paper. Curves were developed which can be used to determine easily the sensitivity of this type of detector to reduced insulation resistance in any similar installation.

Paper 46-44, recommended by the AIEE committees on protective devices and power transmission and distribution for presentation at the AIEE winter convention, New York, N. Y., January 21-25, 1946. Manuscript submitted November 21, 1945; made available for printing December 20, 1945.

J. E. ALLEN is chief of tests and S. K. WALDORF is senior test engineer, Pennsylvania Water and Power Company, Baltimore, Md.

The Vector Relationships on an Ungrounded 3-Phase Bus

An ungrounded bus system has distributed capacitances between each phase conductor and ground whose charges supply the current through a ground fault. When examining the vector relationships of the voltages and currents involved, the phase-to-ground capacitances can be considered as three equal lumped constants connected as shown in Figure 1.

In normal operation, the capacitances have the phase-to-neutral voltages E_{OA}, $E_O{}^b$, and E_{OC}, shown in Figure 2A, impressed upon them. The simplest type

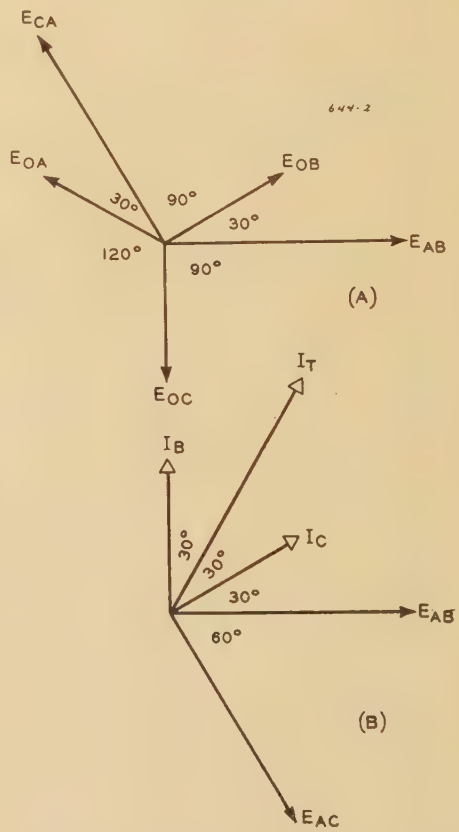

Figure 2. Vector relationships on a 3-phase bus

A—Voltage vectors

B—Voltage and charging current vectors with A-phase grounded

of ground fault to examine is a solid connection through an ammeter connected as indicated in Figure 3. With the solid ground, the phase A capacitance is short-circuited, the voltage on phase B capacitance becomes $E_A{}^b$ and that on phase C capacitance becomes E_{AC}, shown in Figure 2B. The power voltage to ground on the unfaulted phase capacitances thus becomes phase-to-phase voltage or 1.73 times the normal phase-to-neutral voltage.

When one conductor is grounded, the neutrals of Y-connected equipment on the bus are no longer at ground potential. In the case considered, the voltage between the equipment neutrals and ground becomes E_{OA}. By the connection of generator neutral potential transformers as shown in Figure 1, the appearance of a neutral voltage to ground is used at Holtwood to detect the presence of a ground fault. In the majority of cases, the operation of the ground detector relay is the only indication to the station operator that something is wrong, because the equipment continues to function otherwise in a normal manner. The characteristics of this type of fault detector are analyzed in Appendix II.

If insulation should fail on phase A, it probably will occur when E_{OA} is at or near its peak value. Phase A capacitance will be short-circuited, its charge sending a surge through the fault. The voltages on the two unfaulted phase capacitances suddenly change from the respective phase-to-neutral values to the higher phase-to-phase values. These capacitances are charged through the fault by the higher voltages. The magnitude of the surge through the fault depends upon the system operating voltage and the value of the phase capacitances. It is therefore important, when investigating arcing grounds, to know the system voltage, which can be measured directly, and the phase-to-ground capacitances or capacitive reactances. A method for measuring the latter is given in Appendix I.

Table I. Frequencies at Which Resonance Phenomena Appear on Representative 60-Cycle Units in Holtwood Station

Unit	Rating	Resonant Frequencies, Kc
No. 15 transformer	3 phase, 13.2 to 73 kv with taps, 33,750 kva	16, 18, 46, 55, 60
No. 12 transformer	3 phase, 13.2 to 73 kv with taps, 20,000 kva	15.5, 21.5, 26
No. 10 waterwheel generator	3 phase, 13.2 kv, 94.7 rpm, 15,000 kva	1.6, 10
No. 15 steam turbine generator	3 phase, 13.2 kv, 1,800 rpm, 12,500 kva	3.8, 33, 62
No. 62 frequency changer	3 phase, 60-cycle, 13.2 kv, 300 rpm, 7,140 kva	4.2, 21.2, 50

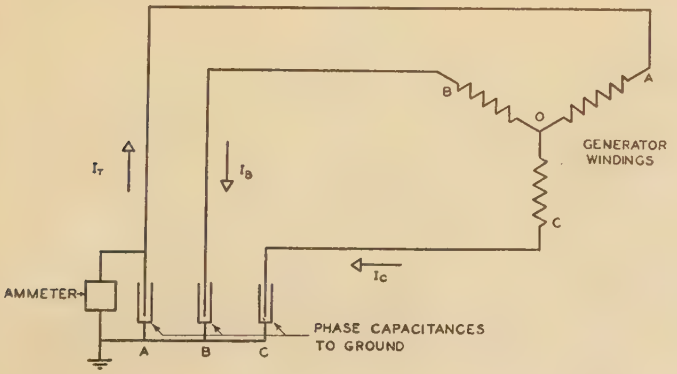

Figure 3. Circuit conditions when A-phase bus conductor is grounded through an ammeter

Figure 4. Connections for high-frequency measurements on bus

Distance between test points X and Y is about 300 circuit feet

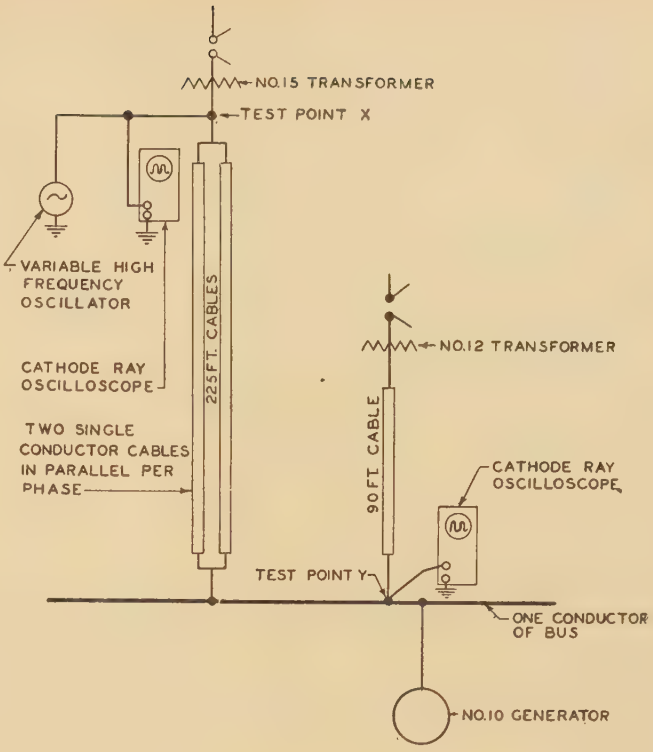

Standing Wave Characteristics of Operating Equipment

A station bus and its connected equipment do not have concentrated capacitances to ground as shown in the simplified equivalent circuit of Figure 1. Each element of bus and equipment has its inherent distributed capacitance and inductance with consequent characteristic frequencies at which resonance phenomena can occur. With the individual components of the system connected in parallel for operation, there are a number of such resonance frequencies at which oscillations might be initiated by an arcing ground. The phenomena are of interest because standing waves at the resonance frequencies can cause uneven distribution of voltage to ground along the bus system. A study of standing waves on such a system gives some insight into the way in which wave phenomena can cause overvoltages.

Standing waves on the Holtwood bus were investigated by observing changes of impedance of each type of equipment, singly and in combination, as the frequency of a voltage applied between one phase conductor and ground was varied between 100 and 100,000 cycles per second. Except for the high-frequency voltage, the equipment was not energized. The work was done expeditiously by utilizing a chart-drawing transmission line fault locator.[11] The fault locator charts were obtained quickly and on them the resonance frequencies were at once apparent.

The frequency characteristic of one unit of each type of 60-cycle equipment normally connected to the Holtwood bus was measured. The resonance frequencies and equipment ratings are indicated in Table I. The bus structure used in the tests apparently has no effect in the frequency range covered.

More directly bearing on a study of overvoltage production is the behavior of a combination of station operating units when a voltage of varying frequency is applied. The combination of equipment shown in Figure 4 was connected and energized only by the variable frequency oscillator connected in turn at test points *X* and *Y*. *X* and *Y* were chosen as test locations because it was at these points, separated by about 300 feet of lead covered cable, that the faults occurred causing the disturbance of April 1942.

The two cathode ray oscilloscopes were used as voltmeters, one at the oscillator and the other at the other test point. The ratio of the instrument indications was a measure of the voltage rise due to standing waves.

Figure 5 shows that voltage multiplication up to $2^3/_4$ times was measured with the test arrangement. The resonance frequencies for the combination were those of the connected individual units. It should be noted that the maximum voltage multiplication within the measurement range occurs at the relatively high frequencies of 50,000 and 100,000 cycles per second. These tests indicate that no voltage higher than three times normal is to be expected from standing waves at any natural frequency of the system, a point substantiated by the arcing tests described later.

Figure 5. Voltage multiplication in test circuit of preceding figure

X and *Y* are test locations indicated in Figure 4

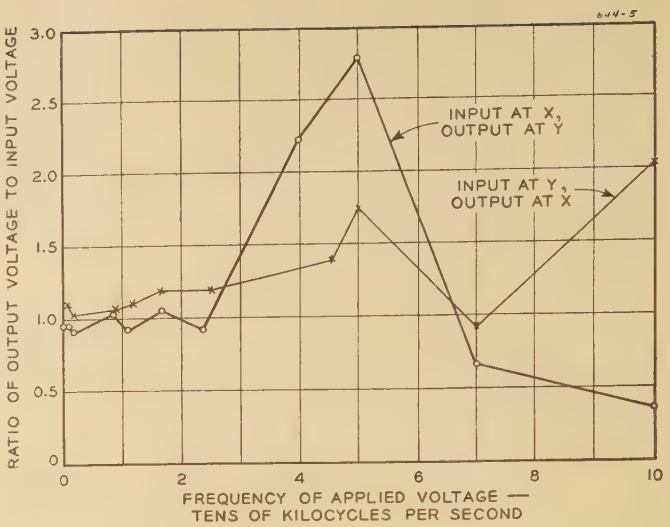

Characteristics of Arc Gaps

The ways in which overvoltages can be developed on an ungrounded system have been described in great detail in the technical literature. A few of the many papers on the subject are listed in the references of this paper. Simply stated, overvoltages can be built up by an arcing ground if the arc is made to restrike each half cycle at progressively higher voltages. If this restriking can be made to occur at the natural period of the system, the resulting voltages theoretically will be higher than if the restriking phenomenon occurs at power frequency.[1]

Before the arcing tests on the Holtwood bus were undertaken, it was necessary to study the characteristics of various types of arc gaps and to develop one having as nearly as possible the behavior which theory indicates should produce high overvoltages. While making the development, highly artificial methods were avoided such as are employed in high speed circuit breaker practice to obtain progressively higher dielectric strength in the arc gap at each restrike, because such conditions are unlikely to occur in the field.

Three-phase equipment was not available for the developmental work to supply the same arc voltage and current as would be produced in the field. However, conditions were approximated quite well with the single phase circuit shown in Figure 6. The maximum voltage that could be used was limited to 9.6 kv by the rating of the capacitors, as compared to 13.2 kv on the tested bus. The breakdown of the tested gaps during the developmental period could not exceed $^1/_2$ of 9.6 kv = 4.8 kv because of the capacitor limitation. This compares with 13.2/1.73 = 7.6 kv, the voltage initially across any fault that might develop on the actual bus.

Figure 6. Arrangement for preliminary tests of discharge gaps, oscillograph shunt, and instrument transformers used in the arcing ground tests

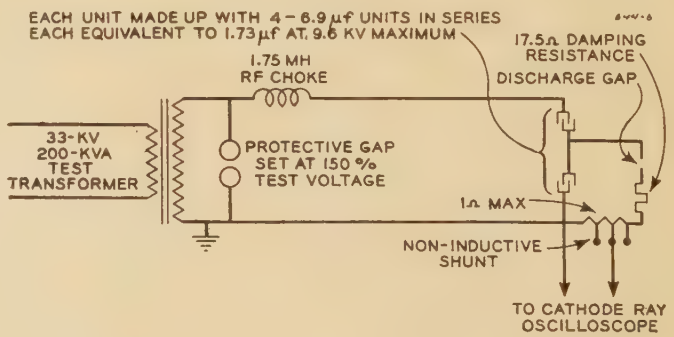

In the circuit of Figure 6, two other elements for the protection of equipment were added besides the protective gap. The 17.5-ohm resistor in series with the arc gap was included to damp out high frequency oscillations which overheated conductors in the early stages of the work. The choke coil was placed to keep stray high frequency currents from the transformer. The noninductive shunt of straight carbon rod provided the voltage drop for making the wave form of the arc current appear on the oscilloscope. Besides being used for the gap development, the circuit of Figure 6 was used to ensure that the instrument transformers used in the field tests correctly reproduced wave forms within the frequency capabilities of the oscilloscopes and oscillograph used.

The first type of gap studied was a simple air gap of the form shown in Figure 7. It was tested in the circuit of Figure 6 where it exhibited a restriking characteristic. Each half cycle the voltage on the gap rose and then dropped abruptly as the gap broke down. The wave form of the arc current also showed that the arc was out for an appreciable fraction of each half-cycle.

The initial breakdown of the gap was always at a voltage higher than subsequent breakdowns, a characteristic common to all open, fixed-length arcs in still air, and which is unfavorable for overvoltage production. A strong blast of

air blown across the gap maintained the breakdown at its high initial value and also caused several restrikes each half cycle. Since this artificial condition is not normal in the field, the air blast was not used for any bus tests.

The next type of gap tested is shown in Figure 8 and consists of a porcelain enclosed and filled gap designed to produce in a controlled way an arcing breakdown similar to that occurring when a porcelain insulator fails. The large electrodes, 1-inch diameter, were used to simulate the large metal cap and pin of an insulator which do not overheat quickly when an arc is formed. The length of this enclosed gap was set by trial to give the desired breakdown value with the gap space filled with porcelain granules. While this adjustment was being made, a high resistance was connected in series with the gap to limit the current to a small value. When the gap was placed in the test circuit of Figure 6, the arc was erratic, sometimes restriking a number of times each half-cycle. After a few cycles the porcelain granules fused and the gap practically short-circuited. The number of cycles that the arc persisted depended upon the power liberated in the arc. This gap, like the simple open gap, did not restrike at progressively higher voltages but acted more as a voltage limiter.

A third type of gap which was thought to produce more severe test conditions was constructed by converting the simple

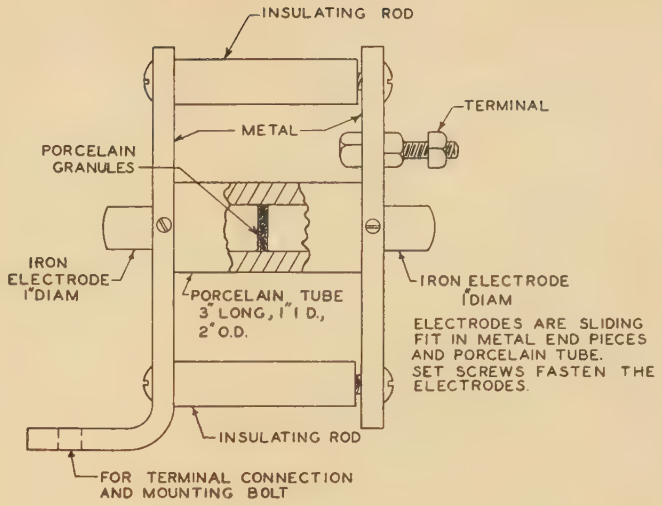

Figure 8. Porcelain enclosed and filled arc gap

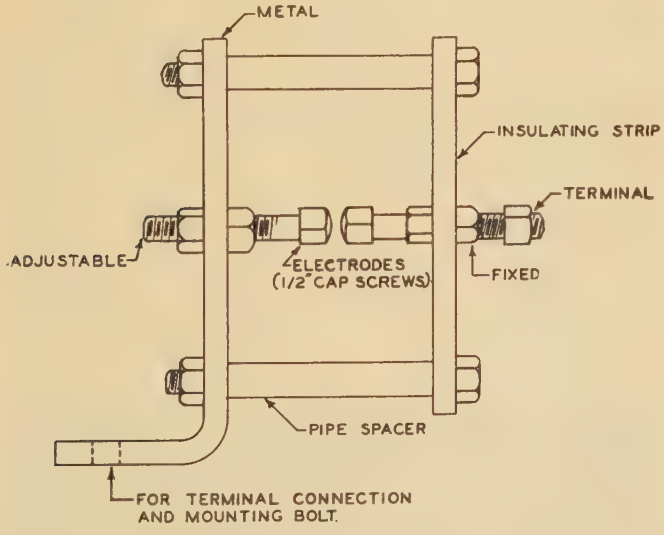

Figure 7. Open arc gap

gap of Figure 7 into a self-lengthening gap. One of the cap screw electrodes was drilled axially to hold a small fusible electrode, a number 22 gauge wire. The position of the wire was adjusted with respect to the undrilled electrode, and held fast with a set screw, to give any desired initial breakdown. After an arc formed on the self-lengthening gap, the burning of the wire during each half-cycle of power current increased the length of the arc gap, permitting the restrike voltage to rise progressively. Figure 9 shows the appearance of the self-lengthening gap, before and after a test. As described later, this type of gap produced higher voltages than the fixed length gaps when used for arcing grounds on the Holtwood bus, but still the voltages were not nearly as high as published theory indicates.

The final design of gap, which produced the most severe arcing conditions in the bus tests, was an enclosed self-lengthening gap obtained by modifying the enclosed gap of Figure 8. The porcelain tube having 1-inch inside diameter was replaced with one having 3/16-inch bore. Iron electrodes were gasket-sealed into this tube. The air gap was made self-lengthening by providing one of the iron electrodes with a projecting small copper wire to be burned away by the arc. The small sealed space occupied by the arc and the progressive arc lengthening were especially favorable to overvoltage production.

Method of Making Arcing Ground Tests on the Station Bus

The station equipment which was used for the high frequency measurements was also used for the high voltage arcing ground tests. Due to system operating conditions, number 9 generator was substituted for number 10 generator in the latter tests; the two machines are essentially duplicates. Figure 10 gives the connections for the arcing ground tests. This test arrangement produced a charging current of 2.5 amperes through a solid ground as compared to a current of about 9.1 amperes produced by the entire bus system used in normal operation. The capacitive reactance to ground of one phase conductor of the test arrangement was thus about $9.1/2.5 \times 2{,}500 = 9{,}100$ ohms as compared to 2,500 ohms for operating conditions.

The section of the bus indicated in Figure 10 was that on which occurred one of the faults of April 1942 and power transformer $T1$ was number 15 transformer where the other fault occurred. The fuse and gaps shown in the arc gap circuit of Figure 10 were included as safety precautions. Another safety measure was the insulating transformer between the oscillograph and the arc gap circuit. It was especially developed for the work, tested and modified until it had insulation adequate to protect the oscillograph operator against mishaps and it reproduced complex wave forms faithfully on the oscillograph.

The klydonograph, a photographic surge crest voltage recorder producing Lichtenberg figures, was connected to the bus through a 3-pole capacitive poten-

tiometer. The klydonograph–potentiometer combination was calibrated as a unit with 60-cycle voltage.

The test potential transformers *PT*1 and *PT*2 had a rating of 34.5 kv, $4^1/_2$ times the normal bus voltage to ground, to ensure the proper recording of any power frequency overvoltages. The klydonograph was relied upon to record any high frequency or surge overvoltages beyond the range of the magnetic oscillograph. The potential transformers *PT*3 and *PT*4, measuring the generator neutral-to-ground voltage and the phase *A*-to-phase *B* voltage, respectively, were regularly used station equipment.

Because more station equipment is normally connected to the bus than was the case during the tests, one of the tests was performed with a 3-phase Y-connected neutral-grounded bank of capacitors connected to the bus at test location *Y*. Each of the three legs of the bank had a nominal rating of 7.2 kv, 2.3 microfarads. This capacitance, with the capacitance to ground of 0.29 microfarad per phase of the station equipment, gave a phase-to-ground capacitance of around 2.6 microfarads for the test. This value is more than twice as much as the 1.06 microfarad of the equipment normally connected.

Arcing Test Procedure

Preliminary to each test, the arc gap for the test was adjusted and tested in a laboratory low-current circuit to have the desired initial breakdown value.

After the equipment was connected for a test as shown in Figure 10, the disconnecting switch in the arc gap circuit was left open and the generator voltage was then set at the chosen test value. Following this, the generator was left running at normal speed without field excitation. The disconnecting switch was then closed, connecting the arc gap circuit to the phase *A* conductor. The gap in each case was previously adjusted to 90 per cent of the preset generator phase-to-neutral voltage.

When the recording instruments were ready, the field switch of the generator was closed. This operation, in addition to exciting the generator field, also lit a small lamp, signaling the oscillograph operator to start that instrument. The generator required about 2 or 3 seconds to attain its preset voltage. When the arc gap flashed over, the voltmeter shown in Figure 10 connected to the generator neutral potential transformer, deflected. When making tests with the fixed length gaps, this was a signal to the generator operator to open the generator field breaker to extinguish the arc. When using the self-lengthening gaps, the operator delayed opening the field breaker for a few seconds after the neutral voltmeter first deflected to allow time for the arc to extinguish itself by lengthening the gap. This method of circuit control was used to ensure that any overvoltage produced during a test was due to the arcing ground alone and not due to any switching surges.

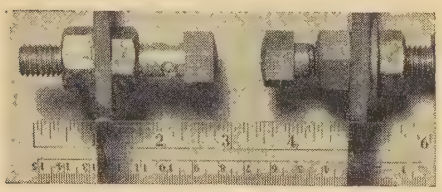

A—Before test

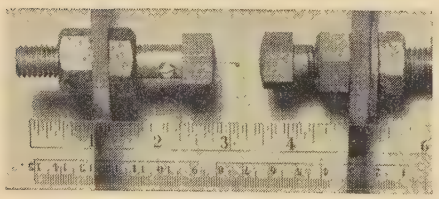

B—After test

Figure 9. High-speed self-lengthening arc gap

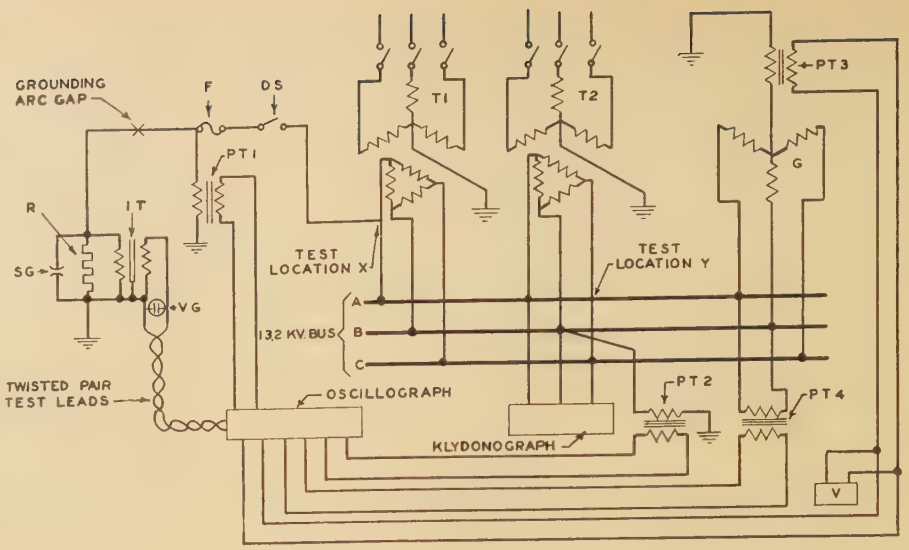

Figure 10. Connections for arcing ground tests on Holtwood 60-cycle bus

SG = 1/32-inch spill gap
R = 0.3-ohm rod resistor
IT = insulating transformer
VG = safety vacuum gap
PT1, PT2 = 34,500- to 115-volt instrument transformers
PT3, PT4 = 13,200- to 110-volt instrument transformers
F = 15,000-volt 100-ampere fuse
DS = disconnect switch
T1, T2 = power transformers
G = water wheel generator
V = generator neutral voltmeter

Results of Arcing Tests With Fixed Length Gaps

Because of the widespread belief that an arcing ground quite easily will produce dangerously high overvoltages on an ungrounded bus system, the tests on the Holtwood bus were begun with reduced bus voltage and a simple open fixed-length gap. As shown in Table II, test 1, very high voltages were not produced. The maximum did not exceed 2.3 times normal. The bus voltage was then raised in two steps to its rated value, but still the voltage to ground on the unfaulted phases was little more than can be predicted from the 3-phase power voltage relationship (Table II, tests 2, 3, and 6). The oscillogram from test 1, Table II, when the test voltage was only 50 per cent of the normal operating value, showed that the arc restruck regularly each half-cycle at almost the initial breakdown value. The oscillograms from tests 3 and 6, Table II, when the test voltage was the full operating value, showed that the arc always restruck at a voltage substantially less than the initial breakdown value. The change in the restriking phenomenon with increase of test voltage was probably due to the greater arc energy in the latter tests making the gap more difficult to deionize.

Tests 4 and 5 with the porcelain filled gap showed that an arcing ground produced by the failure of a porcelain insulator is not likely to produce high transient overvoltages. The oscillograms

Table II. Voltages Produced by Arcing Grounds With Fixed Length Gaps

Test	Generator Voltage Setting (Per Cent Normal)	Gap Type	Maximum Phase-to-Ground Voltages (Per Cent Phase-to-Neutral Voltage) From Oscillograph B Phase	From Klydonograph B Phase	From Klydonograph C Phase	Total Duration of Arcing, Sec
1	50	Open	212	226	177	1.5
2	75	Open	186	190	176	1.2
3	100	Open	183	180	150	1.43
4	75	Porcelain filled	187	156	145	0.01−
5	100	Porcelain filled	200	233	168	0.01−
6*	100	Open	192	190	190	1.42

*20 ohms on secondary of neutral potential transformer.

Arc was extinguished in these tests by opening generator field circuit.

Table III. Voltages Produced by Arcing Grounds With Self-Lengthening Gaps

Test	Generator Voltage Setting (Per Cent Normal)	Gap Type	Wire in Fusible Electrode	Maximum Phase-to-Ground Voltages (Per Cent Phase-to-Neutral Voltage) From Oscillograph B Phase	From Klydonograph B Phase	From Klydonograph C Phase	Total Duration of Arc, Sec
1	50	Open	No. 22 Nichrome	227	224	268	0.8+
2	50	Open	No. 22 copper	232	209	145	2.25
3	50	Enclosed	No. 22 copper	282	220	189	1.05
4	50	Enclosed	No. 30 copper	279	232	212	0.08
5*	40	Open	No. 22 copper	301	280	256	0.11

*2.3-microfarad capacitor added between each phase conductor and ground.

Arc extinguished itself in these tests, because of elongation of gap, before the generator field circuit was opened.

showed that the voltage across the gap was very low after the initial strike.

For each of the tests in this group, the fixed length of the gap acted as a limiter to prevent the recovery voltage across the gap from rising above the initial breakdown value. Consequently, the voltages from the unfaulted phases to ground did not much exceed 1.73 times the normal phase-to-neutral voltage in any of these tests.

Results of Arcing Tests With Self-Lengthening Gaps

After showing that high overvoltages do not accompany arcing grounds on gaps having fixed length, due to the limiting effect of the gap on the recovery voltage, further testing was done with self-lengthening gaps. The results of these latter tests are given in Table III.

Nichrome wire, size 22, was used in the first test of this group to ensure that the arc would persist long enough for overvoltage to build up, if there were any such tendency present. No very high overvoltage developed. The second test, using faster fusing copper wire, gave about the same value of overvoltage as the first test, with a total arcing time of about $2\frac{1}{4}$ seconds. Both tests were made with open gaps.

Tests 3 and 4, where the enclosed self-lengthening gap was used, showed higher overvoltages than the preceding tests, but not more than about 2.8 times normal phase-to-neutral voltage. The type of gap used for this test probably produced as severe an arcing condition as is likely to occur on the station bus under operating conditions. Most likely, an arcing ground on the bus will be formed across a gap having fixed length, where the voltage to ground will not rise much above two times normal due to the limiting action of the gap.

Figure 11 is the oscillogram obtained during test 4 of Table III for which an enclosed self-lengthening gap was used. The oscillogram shows that the arcing ground persisted for only a fraction of each cycle of power frequency, but that each strike produced a highly damped train of oscillations having a frequency of about 1,140 cycles per second. Table I shows that the lowest natural frequency for any equipment on the unenergized bus is 1,600 cycles per second, which is for the waterwheel generator with no field excitation. It is probable that the lower natural frequency obtained under arcing conditions is due to generator field excitation, which changes the inductance of the generator windings.

In test 4 the arc struck only 11 times because of the small size (number 30) of the fusible electrode used in the gap; the behavior is typical except that the arc struck more frequently during the other tests of this group.

The highest instantaneous value of

Figure 11. Oscillogram from test with enclosed self-lengthening gap

Test 4, Table III

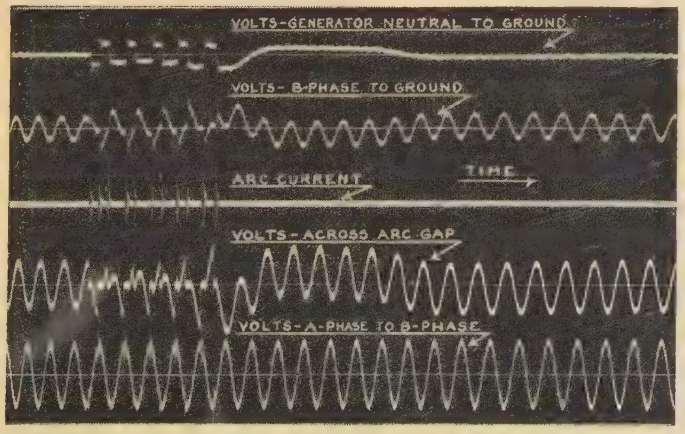

Figure 12. Test with capacitors connected to bus

Oscillogram from test 5, Table III

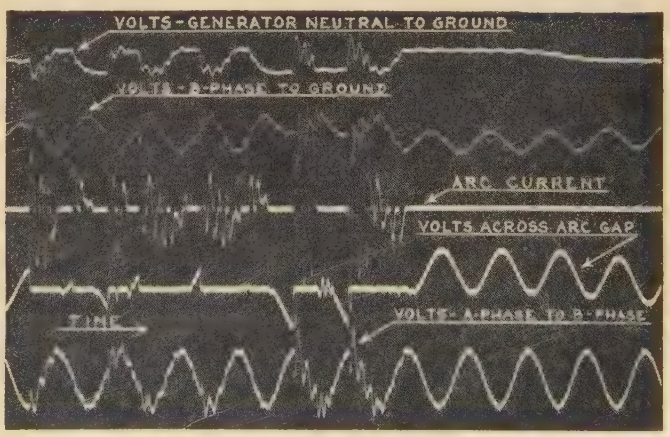

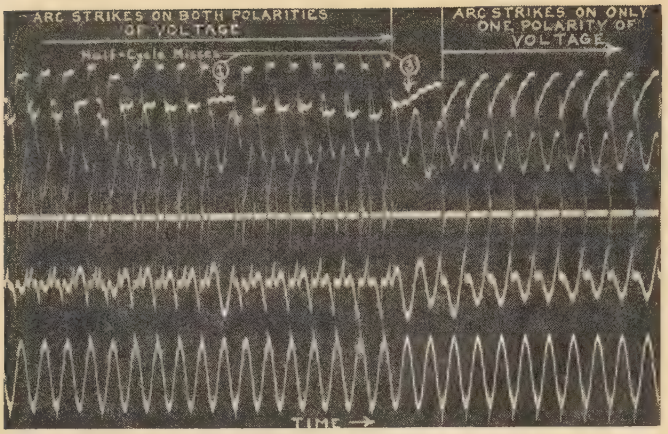

Figure 13. Arc strikes on only one polarity of voltage

Section of oscillogram from test 2, Table III

arc current recorded on the oscillogram of Figure 11 is 44 amperes, which occurred during the next to last arc strike.

The frequency of oscillations in the arc current and in the several recorded voltages was mostly between 1,080 and 1,200 cycles per second, sometimes around 1,600 cycles per second. In test 5, Table III, a capacitance of 2.3 microfarads was added between each phase conductor and ground. During this test the oscillations had four distinct frequencies, being about 460, 2,700, 4,200 and 6,780 cycles per second. Figure 12 is the oscillogram obtained during this test.

Discussion

Figure 11 shows the characteristic behavior of the 60-cycle voltages to ground after the arc remained extinguished: the almost completely displaced wave, producing a recovery voltage two times normal, and its slow return to normal. The phenomenon is caused by the relatively slow re-establishment of normal charge distribution on the three bus capacitances to ground shown in Figure 1. It is the retention of charge by these capacitances, added to the dynamic power voltages, that causes the recovery voltage wave to be two times normal by being completely displaced. Theoretically this can produce overvoltages to ground on the unfaulted phases as high as 2.73 times normal, because at the time of arc extinction, the unfaulted phase capacitances can remain charged to 1.73 times the normal phase-to-neutral voltage, to which may add the generated system phase-to-neutral voltage. By comparison, in the tests with the fixed length gaps, the recovery voltage across the arc gap was always limited to the normal crest phase-to-neutral value or less and the voltages measured on the unfaulted phases did not greatly exceed 1.73 times normal phase-to-neutral voltage.

Superimposed on the power frequency effects just described are the natural frequency transients, of which those shown in Figure 11 are typical. In addition to raising the *B* phase to ground voltage, they also raised the phase-to-phase voltage as shown in the bottom record of Figure 11. In this case the *A*-phase to *B*-phase voltage was raised a maximum of 1.56 times its normal value.

Figure 13 is a section of the oscillogram obtained during test 2 of Table III. It shows a very interesting phenomenon. The arc was quite unsteady, missing a few cycles occasionally as shown in Figure 13, then it restruck regularly on only one polarity of voltage. The single polarity arcing continued for 51 cycles, then missed a cycle and finally struck one more time. This phenomenon might have been caused by the rounded shape of one electrode of the arc gap and pointed form of the other. However, this explanation is not entirely satisfactory because none of the other tests with the self-lengthening gaps exhibited this effect even though the electrode shapes were practically the same in all tests. Repeated restriking of an arcing ground on only one polarity of voltage has not been previously reported in any of the technical literature consulted, although P. A. Jeanne[9] has reported a similar phenomenon of a few cycles of arcing at one polarity, changing to a few cycles of arcing at opposite polarity.

In the arc current record of Figure 12 there is evidence of arc extinction and restriking at the lowest natural frequency of the system, about 460 cycles per second. However, it is significant that the voltage across the arc gap did not rise appreciably prior to each restrike, apparently due to the short time available for deionization, It is doubtful if an arcing ground, either open or confined, on an actual bus will be subjected to high speed deionization, because highly artificial means, such as air or oil blast, must be employed for high speed circuit interruption. It thus appears that restriking of an arcing ground at progressively higher voltages and at resonant frequency is highly improbable on an actual bus system.

Within the frequency limitations of the electromagnetic oscillograph, that is, for voltages having a frequency less than about 3,500 cycles per second, the oscillograph is a more accurate instrument than the klydonograph. The klydonograph excels where the voltages are of high frequency or steep wave front. It will be noted in Tables II and III that the oscillograph usually indicated a higher overvoltage than did the klydonograph. This is interpreted to mean that steep-front surge voltages and voltages with a frequency above 3,500 cycles per second play no appreciable part in the production of overvoltage under the test conditions.

The klydonograph measurements in Tables II and III show that the maximum voltage to ground on the two unfaulted phases of the bus consistently are not equal when an arcing ground exists. The reason for this is indicated on the oscillogram of Figure 11, which can be taken as typical, where the arcing persists at most for only a third of a 60-cycle half wave. In this figure and also in the bottom trace of Figure 13, it will be seen that the voltage oscillations produced by the arc begin before or at the peak of *A*-phase to *B*-phase voltage. When *A* phase is grounded by an arc, the *A*-phase to *B*-phase voltage is the same as *B*-phase to ground voltage except for the arc drop, which is comparatively small. Figure 2 shows the phase relationships when *A*-phase bus conductor is grounded. With respect to the grounded conductor (*A* phase), voltage E_{AB} leads E_{AC} by 60°. Figure 14 shows the appearance of two sinusoidal half waves of power voltage having this relationship. If the arcing

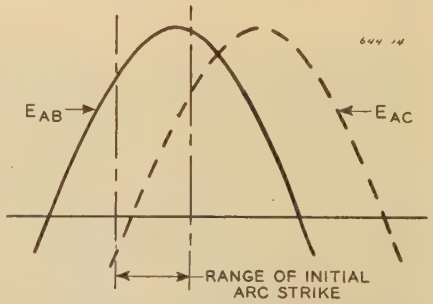

Figure 14. Period during which arcing transients begin on the phase-to-ground voltages of the unfaulted phases

Current and voltage relations when *A*-phase bus is grounded

transient occurs anywhere in the range indicated on Figure 14, it will be superimposed simultaneously on an instantaneous value of E_{AB} higher than the corresponding instantaneous value of E_{AC}. This usually makes the voltage to ground on B-phase conductor higher than that on C phase, although erratic arc strikes at other phase positions may alter this relationship. Such an unusual condition occurred in test 2 (Table III), where the highest transient voltages during the test occurred when the arc struck for voltages of only one polarity.

Summary and Conclusions

As stated previously, the following apply only to arcing grounds on normally ungrounded station busses and not to switching phenomena or effects of surges on extensive systems.

1. Arcing grounds on the tested station bus did not produce voltages to ground exceeding three times the normal crest phase-to-neutral voltage. Higher overvoltages did not materialize even though conditions in some of the tests were as severe as any likely to occur under operating conditions.

2. It has been shown in previously published literature that extremely high voltages can be produced by arcing grounds when the arcs quench and restrike at progressively higher voltages and at system natural frequency. It has been suggested that a ground fault in a pothead, cable, or other arc confining piece of equipment might provide especially favorable conditions.[12] As far as is known, build-up of voltage in excess of about three times the normal phase-to-neutral value has yet to be measured on an actual bus system operating at 13 kv or less. The study of arc gaps described in this report and operating experience published elsewhere, show that very rapid quenching of an arcing ground is not likely to be accomplished by any combination of circumstances which might occur on a station bus and associated equipment.

3. The maximum voltages to ground on the unfaulted phases of a three-phase bus are not equal under most arcing ground conditions.

4. Arcing grounds occur sometimes on only one polarity of voltage.

5. The tests revealed arcing transients which raise the phase-to-phase bus voltages as high as 1.74 times normal. The frequency of these transients was found to be as high as 6,780 cycles per second. Transients of this character may cause abnormal voltage stresses on the turn insulation of machines.

6. The faults of April 1942 on the ungrounded Holtwood bus very probably were caused by failure of defective porcelain insulators in quick succession because very careful inspection of the bus after the disturbance disclosed a number of them with minute cracks in the porcelain. It is probable that the trouble was initiated by the failure of one porcelain insulator, causing bus voltages to ground on the other phases between 1.73 and 3 times normal. This overvoltage then probably caused failure of one or more additional defective insulators. On an ungrounded bus system, it is particularly important that the insulation of the bus and of associated equipment be maintained at its initial strength and be tested periodically with the most sensitive means available for detecting defects. It is believed that many insulation breakdowns on ungrounded busses which have been attributed to voltage build-up, were probably caused by reduced insulation which might have been found by modern testing means.

7. Insulation should be provided on ungrounded busses and connected equipment capable of withstanding voltages to ground in excess of three times the normal phase-to-neutral value. Also, the turn insulation on machine windings must withstand high frequency voltages which accompany arcing grounds. How severe these latter voltages are, has not been determined. With these conditions met, advantage can be taken of the operating features which an ungrounded bus provides, and it is believed that no great concern need be felt that unlimited high voltages will be produced by an occasional ground fault.

8. A device for warning of impaired insulation on an ungrounded bus system and operated by the appearance of neutral-to-ground voltage is often inoperative until the insulation is broken down completely. In spite of this limitation, the device has proved useful in operation. A method is included in the paper for easily determining the sensitivity of a neutral voltage ground detector in any given installation.

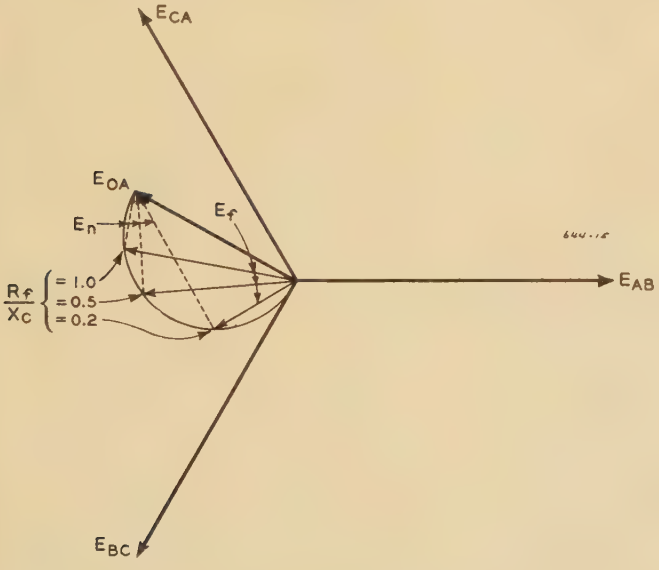

Figure 15. Vector relation between voltage across fault E_f and generator neutral voltage to ground E_n for three ratios of R_f/X_c

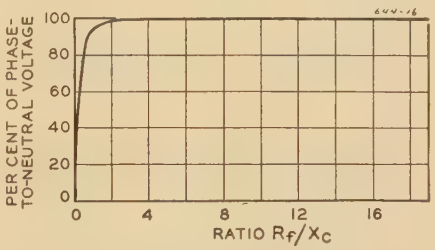

Figure 16. Variation of voltage across fault E_f for various ratios of R_f/X_c

Appendix I. Determination of Phase-to-Ground Capacitance of an Ungrounded 3-Phase Bus

The equivalent circuit of an ungrounded bus and connected apparatus is shown in Figure 1. Each item of equipment connected to the bus system, whether transformer, cable, bus, or rotating machine, contributes its share to the admittance of each phase conductor to ground. When insulation is unimpaired, the corresponding impedances are almost pure capacitive reactances which can be taken as lumped constants for purposes of analysis.

The capacitive reactances to ground of the bus system can be measured in the field by solidly grounding one phase of the system through an ammeter. When this is done, one of the bus-to-ground capacitances is short-circuited and the two ungrounded capacitances pass current through the ammeter as shown in Figure 3. With the directions of current flow as assumed in Figure 3, the vector relations of the currents are as shown in Figure 2B.

$$I_T = I_B \cos 30° + I_C \cos 30°$$

The charging currents of phase-B and phase-C bus conductors are numerically equal:

$$I_{xc} = I_B = I_C$$

Therefore

$$I_T = I_{xc} \cos 30° + I_{xc} \cos 30°$$

$$= 2I_{xc} \times 0.866 = 1.73 I_{xc}$$

or

$$I_{xc} = \frac{I_T}{1.73}$$

The capacitive reactance of one phase conductor to ground is found from the phase-

to-phase voltage E and the grounding ammeter reading I_T:

$$X_c = \frac{E}{I_{xc}} = \frac{E}{I_T/1.73} = \frac{1.73E}{I_T}$$

The capacitance can then be found by solving for C in the equation

$$X_c = \frac{1}{2\pi f C} \text{ or } C = \frac{1}{2\pi f X_c}$$

where f is the power system frequency.

Appendix II. Effect of Ground Fault Resistance on the Neutral-to-Ground Voltage of an Ungrounded 3-Phase Bus

Fault detection with a generator neutral potential transformer requires a shift in the neutral potential for its indications. An impairment of bus or equipment insulation to ground is equivalent to a shunt across the capacitance-to-ground of the phase conductor affected. A ground fault with a given resistance will have more effect on neutral potential shift if the capacitance to ground is small than if it is large. Or expressed in a more practical way, because the capacitive reactance is the quantity determined directly from a grounding ammeter test, the greater the capacitive reactance to ground of a system, the more effect a given value of fault resistance will have on neutral shift. The analysis has been made on a unit basis to

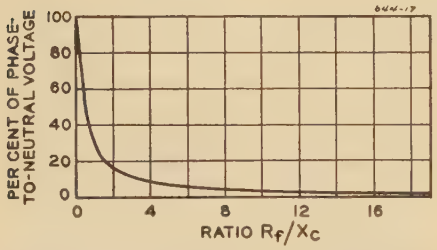

Figure 17. Variation of generator neutral voltage to ground E_n for various ratios of R_f/X_c

make the results applicable to any field condition where the capacitive reactance to ground of the bus can be measured. The steps in the analysis are as follows:

(*a*). The currents and voltages in Figures 2 and 3 are directly proportional to the system phase-to-phase voltage. In the calculations, 1,000 volts was used as the unit base for this voltage. Under these conditions, the phase-to-neutral voltage is 1,000/-1.73 = 577 volts.

(*b*). On a unit basis, the capacitive reactance to ground of each phase conductor was taken as X_c = 1,000 ohms.

(*c*). A bus insulation fault is equivalent to a resistance shunting the capacitive reactance to ground of the faulted phase conductor. Different values of fault resistance R_f were assumed in succession, ranging from one megohm to zero. This gave ratios of R_f/X_c ranging from 1,000 to zero. Each of the following steps was carried through separately for each assumed value of R_f faulting the phase-*A* bus conductor.

(*d*). The parallel circuit of the fault resistance R_f shunting the phase-to-ground capacitive reactance X_c was transformed into its equivalent series circuit, giving Z_e.

(*e*). The current through the X_c of each unfaulted phase is the corresponding phase voltage divided by $X_c + Z_e$, giving I_B and I_C, calculated separately.

(*f*). The current in the circuit composed of the faulted phase capacitance and fault resistance in parallel is $I_T = I_B + I_C$.

(*g*). The voltage across the fault is $E_f = I_T Z_e$ (Figures 15, 16).

(*h*). The generator neutral voltage to ground, E_n, is the phase-to-neutral voltage of the faulted phase minus the fault voltage or

$$E_n = E_{OA} - E_f \text{ (Figures 15, 17)}$$

(*i*). The power dissipated in the fault is

$$P_f = \frac{E_f^2}{R_f}$$

The results of the calculations are summarized in Figures 15, 16, and 17. The computations were checked in the laboratory with equivalent circuits having several values of X_c. The effect of the generator neutral potential transformers and their secondary burdens has been neglected in the computation because the impedance of each is quite high, varying from one to two megohms, depending upon the applied voltage.

Discussion

To avoid forced outages and interruption of central station electric service, it is very desirable to obtain notice of any bus insulation defect as soon as possible. At Holtwood the neutral voltage ground detector shown in Figure 1 is used. The alarm did not operate before the flashovers of April 1942 occurred. However, the relay targets were found to have operated after the trouble. Because the alarm did not give an indication until the trouble occurred, the foregoing analysis was made to determine how low the resistance of a fault must be to operate the alarm.

The capacitive reactance to ground of one phase of the Holtwood station bus is about 2,500 ohms. The relay connected to the secondary of a neutral potential transformer must be set to operate at no less than about 30 per cent of the phase-to-neutral voltage to avoid false indications during normal switching. By referring to Figure 17, it is found that about 30 per cent of phase-to-neutral voltage is obtained when the ratio of fault resistance to the phase-to-ground capacitive reactance is unity. For the Holtwood bus, this voltage is obtained when the fault resistance is 2,500 ohms. Before the fault resistance falls to 2,500 ohms, it can be seen in Figure 18 that considerable power is dissipated in the fault. The power is sufficient to cause noticeable heating of any of the usual types of incipient faults. For instance, when the fault resistance is 0.25 megohm, the power in the fault is 230 watts. The relatively large power dissipation leads to extremely rapid heating of the fault and consequent rapid lowering of fault resistance. The very rapid transition from high to low resistance in the fault explains the failure of a neutral voltage fault detector to give warning of impending insulation trouble, and also the general experience of relatively little burning of equipment when faults occur on systems with an ungrounded neutral. In the first case, when rapid heating and failure of the fault begins, the generator neutral voltage is only a few per cent of the value required to trip the fault detector; in the second case, the extremely short time required for complete breakdown of the fault limits the liberated energy to a relatively small value, even though the power level is high for a short interval.

Analysis thus reveals that a neutral voltage relay can detect impaired insulation in a large installation only when the insulation is broken down completely. Because its sensitivity to insulation resistance varies with the amount of equipment in service,

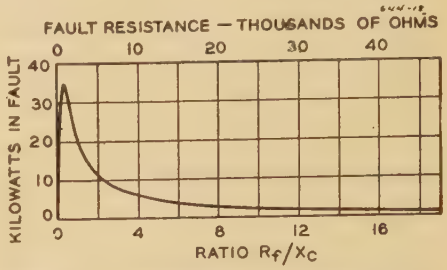

Figure 18. Variation of power dissipated in a fault with fault resistance for X_c = 2,500 ohms

the device might warn of impaired insulation prior to complete failure on a small bus system if the bus capacitance to ground and the bus voltage were sufficiently low. It must be recognized that the Holtwood fault detecting devices, even though insensitive to early stages of insulation failure, have proved valuable in service, indicating insulation failures to ground that otherwise would not have been detected promptly.

References

1. Voltages Induced by Arcing Grounds, J. F. Peters, J. Slepian. AIEE Transactions, volume 42, 1923, pages 478–89.

2. Power-System Transients Caused by Switching and Faults, R. D. Evans, A. C. Monteith, R. L. Witzke. AIEE Transactions, volume 58, 1939, August section, pages 386–94. Discussion, pages 394–7.

3. Overvoltages During Power-System Faults, E. Clarke, S. B. Crary, H. A. Peterson. AIEE Transactions, volume 58, 1939, August section, pages 377–85.

4. Critical Analysis of Rotating Machine Grounding Practice, H. A. Peterson. *General Electric Review*, April 1942, pages 215–20.

5. Merits and Methods of Generator Grounding, S. B. Griscom. *Westinghouse Engineer*, February 1943, pages 33–9.

6. How to Apply Neutral Grounding Devices, A. A. Johnson. *Westinghouse Engineer*, May 1943, pages 66–9.

7. Correlation of System Overvoltages and System-Grounding Impedance, AIEE committee on protective devices. AIEE Transactions, volume 62, 1943, January section, pages 17–24.

8. Arcing Faults in Power Systems, C. Concordia, H. A. Peterson. AIEE Transactions, volume 60, 1941, pages 340–6.

9. Discussion of reference 8, P. A. Jeanne. AIEE Transactions, volume 60, 1941, pages 614–16.

10. Overvoltages on Transmission Lines Due to Ground Faults as Affected by Neutral Impedance, Engineering Report Number 30, Joint Subcommittee on Development and Research, Edison Electric Institute and Bell Telephone System, November 15, 1934. EEI publication number D-14, 1936, pages 105–37.

11. Accurate Line Fault Location, J. E. Allen, G. J. Gross. *Electrical World*, July 20, 1935, pages 23–5.

12. Discussion by C. L. Gilkeson. AIEE Transactions, volume 58, 1939, August section, page 395.

Air-borne Radar for Navigation and Obstacle Detection

R. C. JENSEN
NONMEMBER AIEE

R. A. ARNETT
ASSOCIATE AIEE

Synopsis: The grim uses of radar in war are giving way now to a peacetime role in navigation and obstacle detection. This article discusses the results obtained with military airborne radar as a basis for understanding both the possibilities and the limitations in the application of radar to reduce aviation hazards.

RADAR has been given a great deal of publicity during recent months, and many uses for military operations have been disclosed in technical magazines and newspapers. These publications often included pictures obtained with cathode-ray tube indicators during flight over large American cities and also displayed presentations of enemy territory as viewed on bombing missions. As a result of this publicity and the predictions that have been made for the commercial use of radar, there is probably no single application that catches the public imagination as much as its possible use for navigational aid and obstacle detection in aircraft. Discussions and public expressions of opinions promoting safer navigation are stimulated by aviation accidents such as the Empire State Building disaster and others that have occurred during attempts to land under conditions of obscured vision. Possibly these accidents could have been averted by proper utilization of radar equipment designed to meet obstacle detection requirements. However, there are limitations to present radar performance in that it fails to give the pilot an ideal picture of the area being scanned in its true perspective. But in spite of these limitations, if capable technical effort is applied to the engineering problems involved and these problems are based upon realistic operating requirements and performance, there is every reason to feel that radar will contribute toward safer aircraft navigation and justify the weight of the equipment to be carried.

Paper 46-48, recommended by the AIEE committee on communication for presentation at the AIEE winter convention, New York, N. Y., January 21–25, 1946. Manuscript submitted December 17, 1945; made available for printing January 3, 1946.

R. C. JENSEN is with General Electric Company, Schenectady, N. Y., and R. A. ARNETT is with Geotechnical Corporation, Dallas, Tex.

The authors wish to express their gratitude for the courtesy extended by the National Defense Research Council Radiation Laboratory at Massachusetts Institute of Technology in permitting the use of the radar photographs appearing in this article.

Basic Radar Concepts

The simplest kind of blind navigation system has long been used by pilots of boats operating in rivers and harbors, for they have achieved some measure of success in obstacle detection by using a series of short whistle blasts and then listening for the direction and timing of the echoes.

Figure 1. Energy reflected from a smooth surface

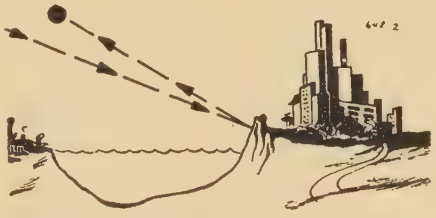

Figure 2. Energy return from a shore line

This example in the detection of reflected energy illustrates the basic principle of radar. For the benefit of the reader who is not familiar with radar, a brief outline of the fundamentals may be helpful.

The purpose of radar is to transmit radio-frequency energy in pulses of high intensity and then to measure the round trip travel time of the reflected energy with sufficient accuracy to establish the range to the obstacle. Following each pulse the transmitter is idle for a relatively long time while a receiving unit is ready to receive the echoes from the preceding pulse. Generally the same antenna is used both for transmission and reception. The finite velocity of electromagnetic waves makes it possible to measure the elapsed time from the transmitted pulse to the received echo as a direct measure of range. This elapsed time is approximately six microseconds for each 1,000 yards of range.

The measurement of range is only a part of the information obtainable with a radar system. Azimuth and elevation angles also can be determined for complete location of a target. This is accomplished by using an antenna that directs the pulsed energy in a narrow beam which may be five degrees wide or less at the half-power points. The position of the target then is determined by the direction of the antenna beam. In the cases where only the bearing angle is of importance, the pattern is narrow in the horizontal plane but broad in the vertical plane for wider angle coverage.

The received signals are displayed on a cathode-ray tube whose sweep is timed from the transmitted pulse, and targets appear as deflections of the sweep or as intensity spots. This display is not like television where an actual picture appears, but the results are interpretable to a trained operator.

To illustrate the types of echo responses from ground targets, consider a source of radio frequency energy radiated in a narrow beam from an aircraft as shown in Figures 1 through 4. If the beam is directed toward the ground at a forward angle, the reflection will be a function of the aspect of the target. The energy which strikes the smooth surface of the lake is reflected away from the source and leaves a dark region on the indicator tube. A shore line, buildings, and normal

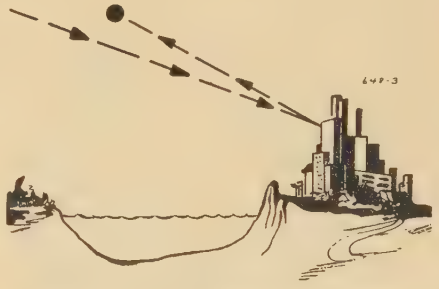

Figure 3. Energy return from structures

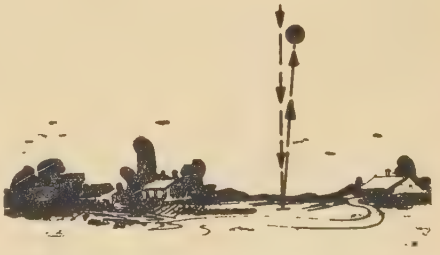

Figure 4. Altitude determination by normal incidence

incidence on the terrain directly below the plane will each provide a strong target echo. A wide beam of uniform intensity directed from the aircraft results in ground illumination and echo response as shown in Figures 5 and 6 respectively. These figures also illustrate how it is possible to correlate a radar picture with a relief map of the area.

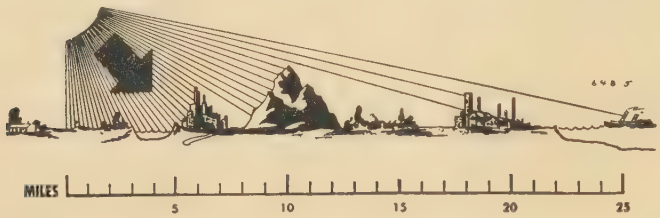

Figure 5. Illumination of generalized topography

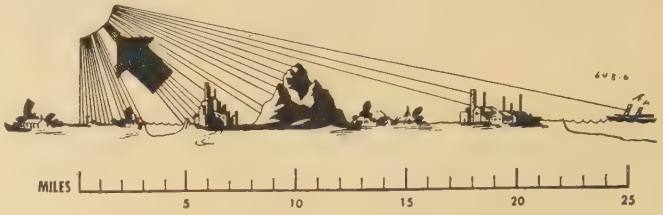

Figure 6. Energy return from ground targets

Navigation Systems

Navigation systems require that large ground areas be scanned, so antenna patterns of the shape shown in Figure 7 are used to an advantage. Note that the beam is narrow in the horizontal plane in order to obtain azimuth accuracy, while in the vertical plane the beam is broadened to sweep a large area but with a corresponding loss in elevation accuracy. The beam intensity is purposely decreased at angles below the main lobe to obtain uniform signal return at the aircraft for equivalent targets for all ranges to be covered. The shape of the beam is designed to compensate for the inverse square law decrease of the power density for both the incident and reflected energy. This type of antenna beam is known as a cosecant squared pattern because it simulates a plot of this function. One method of obtaining such a radiation pattern is to modify a conventional parabolic reflector so that part of the radiated energy is directed downward below the axis of the major lobe. In practice such patterns were obtained only after considerable experimentation with reflector shapes and types of antenna feeds. An actual plot of a cosecant squared pattern is shown in Figure 8, which indicates that with the peak of the beam tilted down 2.5 degrees and the aircraft at 6,500 feet, the radar coverage for uniform signal return extends from 2 to 20 miles.

All the material so far presented serves to show the character of ground echoes and the method of getting uniform ground illumination. If the beam is rotated or sector scanned and also synchronized with the cathode-ray tube trace of an indicator, a map of the ground relief is presented on the fluorescent screen. Rivers, lakes, shore line, valleys, and mountains will appear in relative direction and range with respect to the aircraft. This type of presentation was used to good advantage during the war on bombing missions when such targets as ships, bridges, and industrial areas were located and destroyed entirely with radar navigation. An example of this type of presentation can be observed in Figure 9, in which the coastal outline and promontories of land are spotted easily. Note how readily this picture can be correlated with the aeronautical chart of the same area shown in Figure 10. The L-shaped promontory at Plymouth is identified clearly, and the tip of Cape Cod is appearing just at the right. The circular rings are 2-mile range marks, and the inner bright ring is the start of the radial sweeps on the scope. The second bright ring is the signal return from the bay directly below and so indicates the height of the plane. If targets appear within the altitude ring, it indicates the presence of aircraft at ranges less than the height of the plane. For aircraft beyond the range of the altitude ring, the return signals are obscured fairly well by ground echoes except possibly over water, though even water may have a serious masking effect. A point of importance here is that an illumination and display which is suitable for navigation would have very little use for obstacle detection.

Figure 10 was taken with the aid of a lightweight low power radar system known as *AN/APS*-10. The essential units of this system are shown in Figure 11, and Figure 12 is a suggested arrangement for installation in a transport plane. The antenna with its parabolic reflector is mounted in a protective housing below the skin-line of the plane to permit complete vision. This housing is built of low loss materials designed for maximum transparency to microwave radio frequencies.

Higher power systems are used to get greater ranges and improved coverage as illustrated by Figures 13 and 14. In the latter figure, the circles are 100-mile marks, and the inlaid map indicates how faithfully the topography is portrayed. Note the shaded portion along the Hudson River caused by the screening hills, and the strong response from the mountainous region beyond.

The technical characteristics of radar sets vary over a wide range depending upon the application. The following tabulation has been prepared to indicate the order of magnitude of the operating characteristics employed in systems such as those used to obtain the preceding scope photographs:

Carrier frequency	3,000–10,000 megacycles
Peak power	10–1,000 kw
Pulse frequency	300–1,000 cycles per second
Pulse width	0.25–2 microseconds
Duty cycle	0.0001—0.001
Maximum range	50–200 miles
Range accuracy	40–4,000 yards
Range resolution	75–400 yards
Azimuth accuracy	0.5–1 degree
Azimuth resolution	3–6 degrees
Receiver	Superheterodyne
Intermediate frequency	30 megacycles
Intermediate-frequency band width	0.5–5 megacycles
Minimum detectable signal	1–10 micromicrowatts

Obstacle Detection

It has been stated that a cosecant-squared pattern is unsatisfactory for differentiating between aircraft and ground reflections. This difficulty arises because

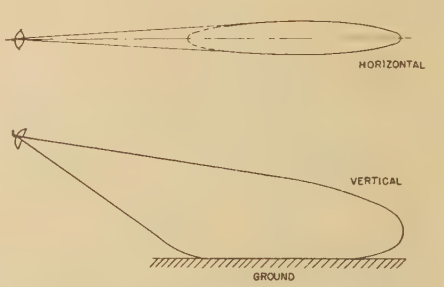

Figure 7. Conventional antenna pattern for navigation radar

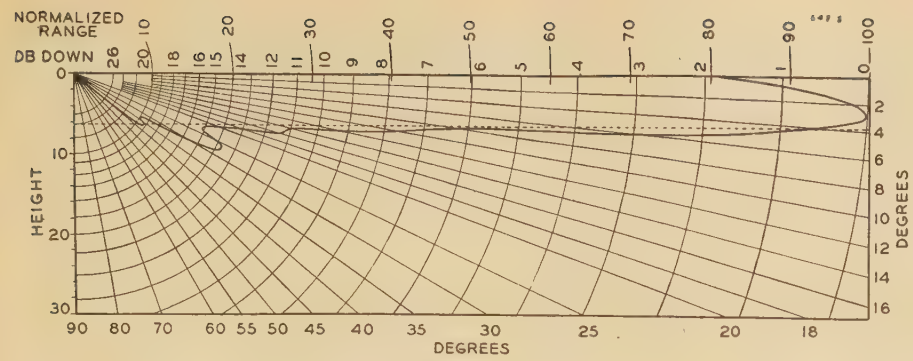

Figure 8. Actual antenna pattern for navigation radar

all targets at equivalent range and bearing appear at the same spot in the display whether at ground level or above. The display shows slant ranges from the plane, not actual ground range. Furthermore, the necessarily wide lobe in the vertical direction fails to indicate elevation even though a plane appears in the beam. There is no way for determining elevation unless the beam pattern has essentially the same configuration in the vertical plane as indicated in Figure 7 for the horizontal plane. This requirement demands considerably more performance from the antenna scanning system if the same solid angle is to be illuminated in a given interval of time. The cosecant squared antenna for a system such as *AN/APS*-10 rotates at 30 rpm, while a uniform lobe antenna must scan at many times that speed and simultaneously nod in the vertical plane in order to illuminate the same area. Such systems have been used to obtain a crude television picture of 10 or 12 lines on an indicator that presents azimuth and elevation information. As the antenna rotates, the cathode-ray tube trace sweeps horizontally and also progresses vertically in synchronism with the antenna position.

A second method for scanning a large area with a narrow beam is known as the Palmer Scan. This system employs a pattern which is narrow in both planes. The axis of the reflector is moved in a rectangular path, for example, through a horizontal angle of 75 degrees and a vertical angle of 45 degrees. During this motion the lobe is made to rotate in a rapid conical sweep such that the apex cone angle formed by the axis of the beam is as many as eight times the beam width. This results in illuminating a circular shell around a blank center region, but as the antenna system moves in its rectangular path, the entire area is filled in. A 6-degree beam which scans 21 degrees off the axis of the reflector thus can cover an area of 120 degrees by 90 degrees, while the axis of the reflector follows the borders of a rectangle 45 degrees by 75 degrees.

A third design for wide angle viewing utilizes a spiraling motion of the antenna beam. The angle of advance for the spiral is small enough so that no blank regions appear in the over-all illumination. A solid angle of coverage may be as much as 120 degrees with a lobe width of 5 degrees.

Present Limitations

These various types of antennas have been discussed briefly to indicate the problems associated with the requirement that enables the system to spot aircraft targets or tall structures and also cover a large area of scanning. They are mechanically complex and require driving mechanisms to spin or slew them at rapid rates so that the scanned area is covered in a few seconds. This is essential if the pilot is to receive scope information comparable with the speed of modern aircraft and avoid collisions. Furthermore, the complexity and fast scanning rates contribute materially toward increased weight of the equipment. In addition, it has been found that beam widths in the order of five degrees are too wide to obtain satisfactory resolution. Lobes of one and two degrees or less are necessary. This demands even faster scanning to cover a given area in a selected interval of time. The point may then be reached where the beam remains on the target for an insufficient length of time to get adequate signal return, and the object is not observed on the indicator. This limit is accepted generally as five pulses on the target during the time of one beam-width

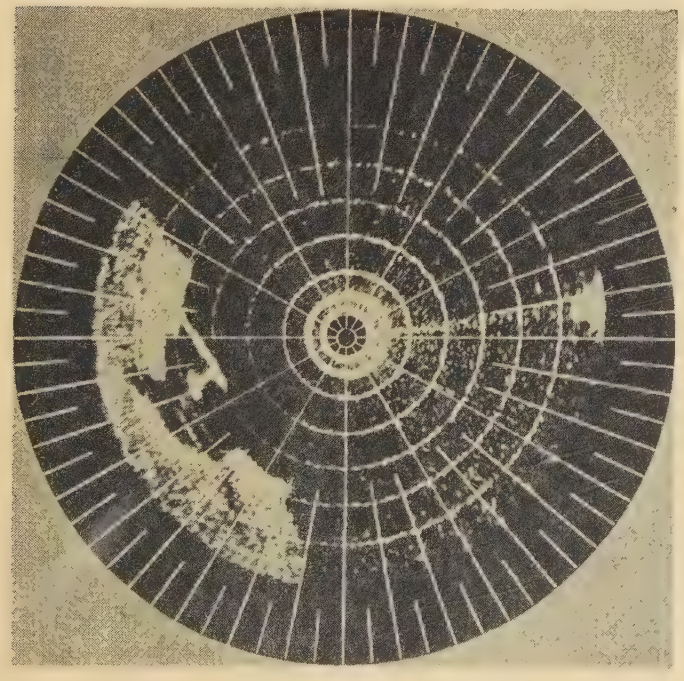

Figure 9. Radar map of Cape Cod area

Figure 10. Chart of Cape Cod area

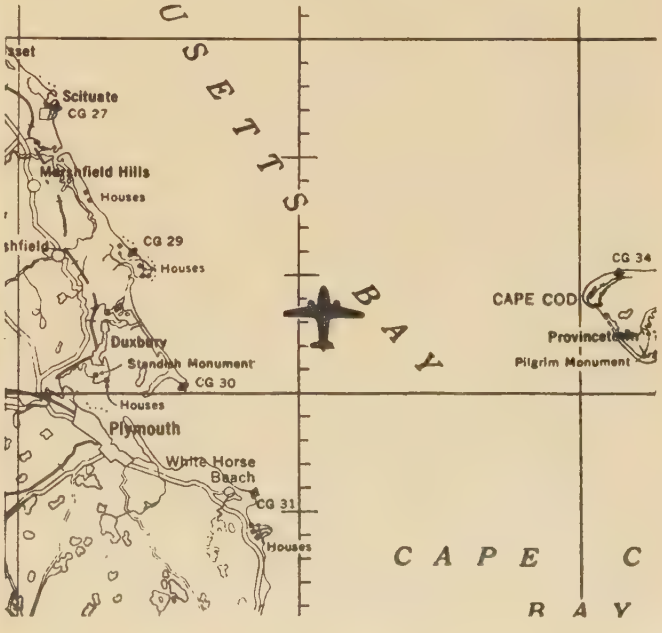

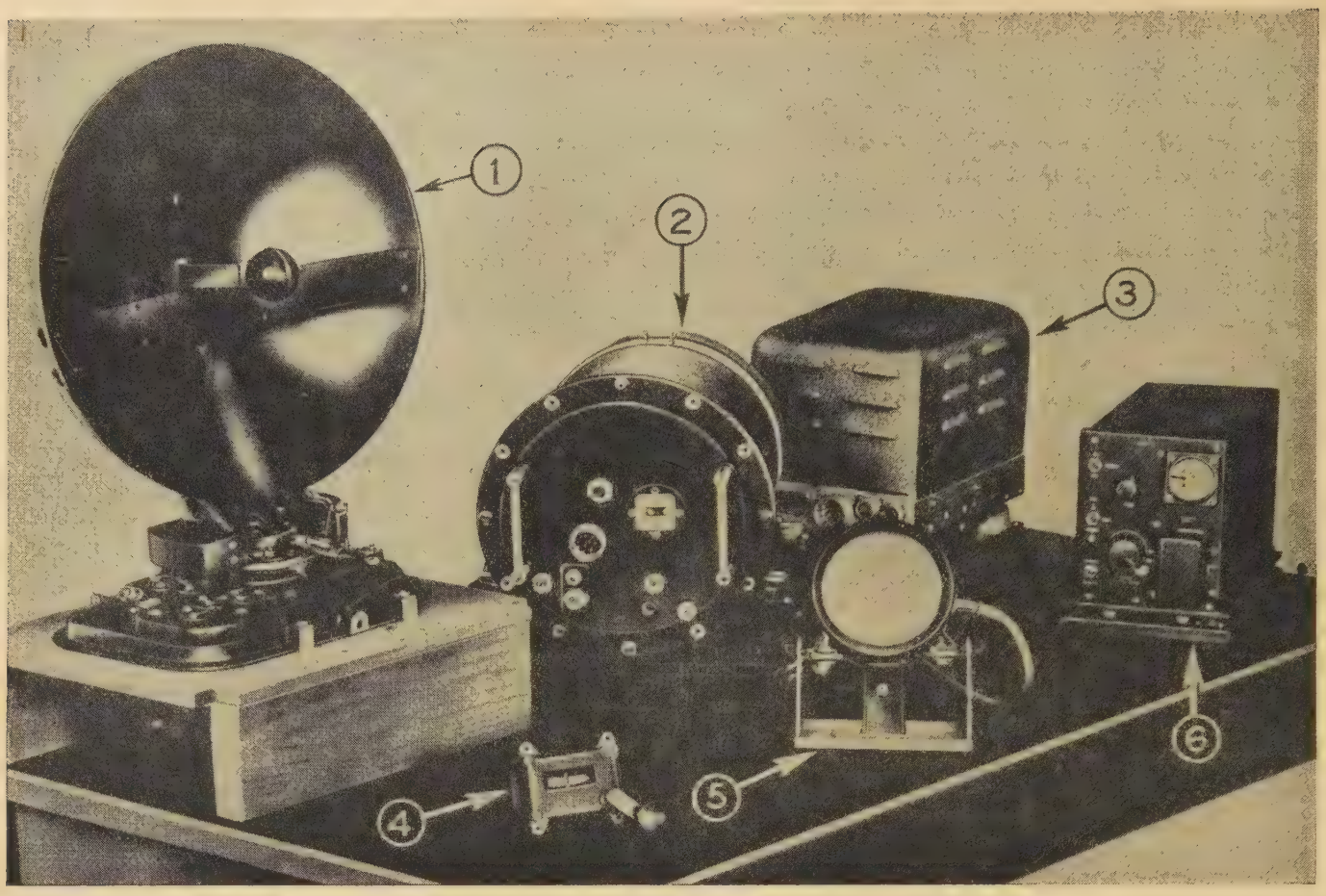

Figure 11. Air-borne radar system

1. Antenna Assembly (*AS*-154/*APS*-10). The antenna or "spinner" may be mounted in a nacelle on the belly of the plane where it revolves in operation to give 360-degree scanning. It can be tilted up and down for critical coverage

2. Transmitter-Receiver (*RT*-69/*APS*-10). This sealed can is the heart of *AN*/*APS*-10. In it are the complete self-contained transmitter and receiver. It is pressurized for operation at altitudes up to 30,000 feet

3. Rectifier Power Unit (*PP*-111/*APS*-10). This compact box is usually mounted out of the way. It converts 115 volts to six different levels of voltage for various functions. They vary from 4,000 volts down to less than 7 volts

4. Trim Control Box (*C*-226/*APS*-10). This mechanical unit is always mounted near the radar operator. As its name suggests, it is used to adjust the trim of the antenna to compensate for change in the flight altitude of the plane

5. Indicator (*ID*-99/*APS*-10). Here is where the radar information appears. The indicator (PPI) is mounted where it can be studied easily and adjusted quickly. Another one showing identical information may be mounted with the pilot or elsewhere

6. Synchronizer (*SN*-17/*APS*-10). This small box has most of the manual controls for operation of *AN*/*APS*-10. It is one of three components in the set which are always mounted within easy reach of the operator

scan. Increasing the pulse rate is the obvious solution, but the pulse repetition rate is dependent upon the maximum operating range, since the return signals should be received before the next pulse is transmitted. Otherwise there would be a confusing indication of targets on the osilloscope. There is also the important consideration of increased average power as pulse rates are accelerated because of the resultant increase in weight with greater power requirements.

The alternative requirement is to reduce the scanned area, thus confining observation to small angles for continuous rapid coverage with the option of selecting other directions for intermittent viewing. The normal operating position would be about the center line of the nose of the airplane.

Figure 12. Typical installation of air-borne radar

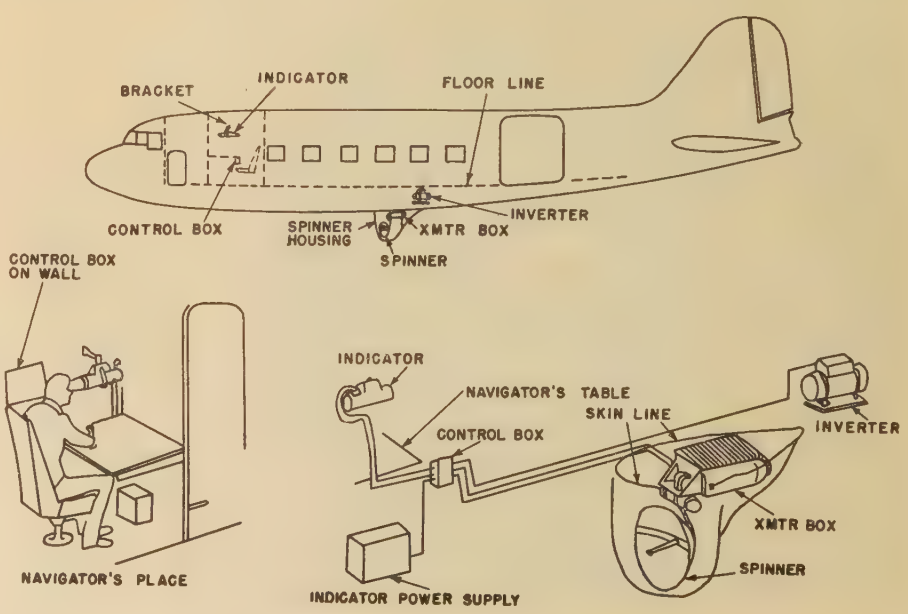

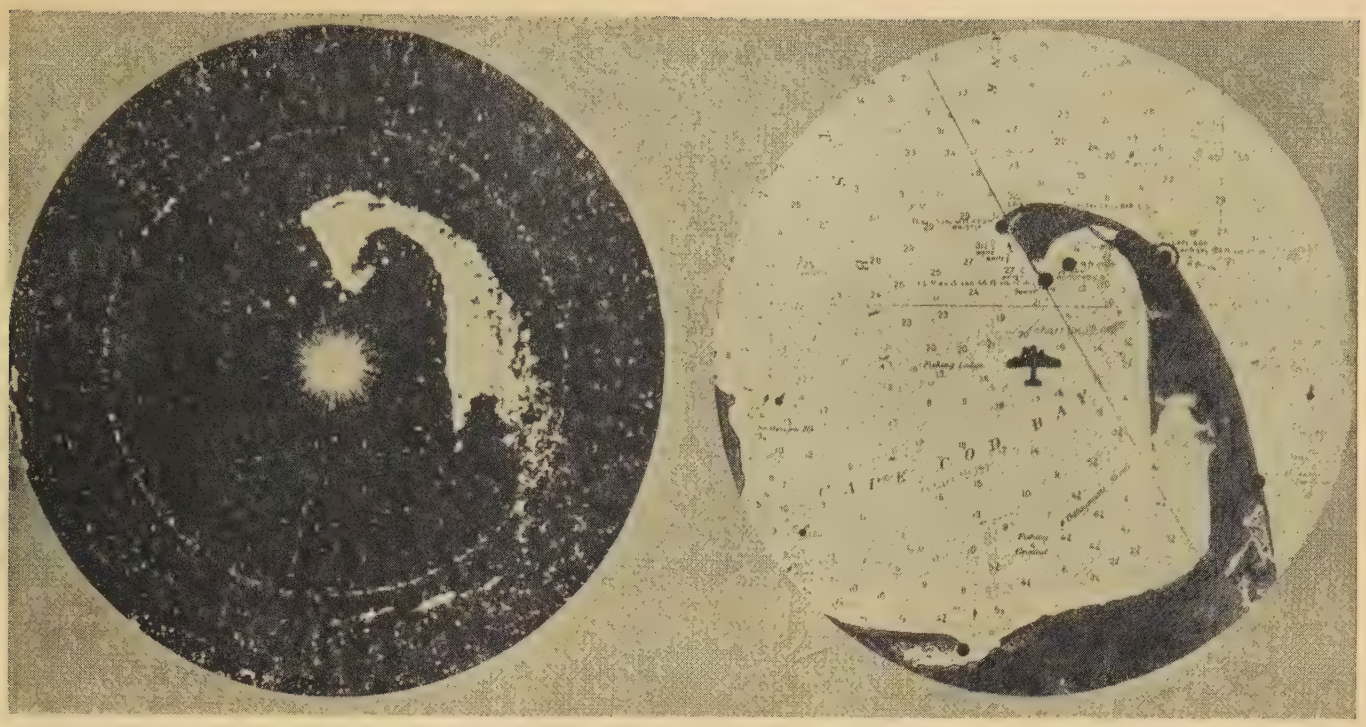

Figure 13. Correlation of radar map with chart

An example of the type of indication that is achieved with a rapid vertical scan antenna using a narrow beam is shown in Figure 15, which plots range against elevation angle. The vertical lines are 2- and 10-mile range marks, while the heavy horizontal trace is an electronic height marker which may be moved by means of a control to line up with a target to indicate elevation. This picture is not indicative of air-borne system performance because it was taken from a high power ground radar; however, it does illustrate the means of presenting target information to obtain height indications. Several aircraft are visible: two at 17 miles and 16,000 feet, very close in range, and a single plane at about 40 miles and 5,000 feet. Two more planes can be observed at about 26 miles. If the picture had been obtained from an air-borne system, the usable range would be reduced considerably because of lower power output. Instead of displaying 50 miles, possibly 20 miles might be the full-scale indication and the ground clutter undoubtedly would extend to the full range. Azimuth information must be read, of course, from a second scope that plots range and azimuth angle, or from a selsyn system that indicates the azimuth position of the antenna. The position of each target would be fixed then with respect to the aircraft.

An interesting photograph that con-

Figure 15. Radar indication of range versus elevation angle

Figure 14. Inlaid radar map of Northeastern States

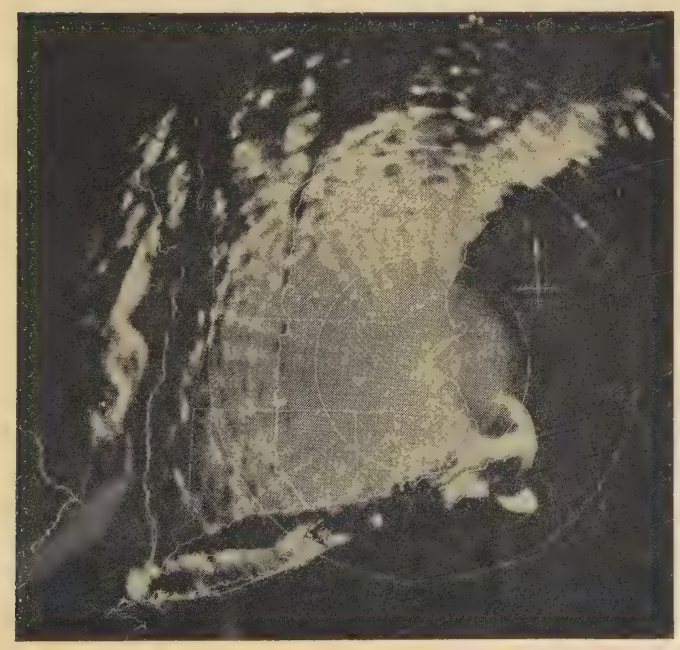

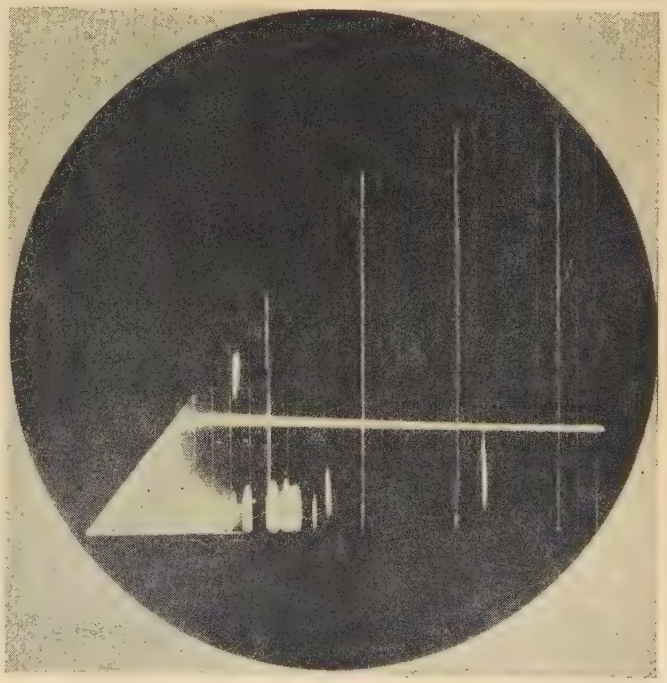

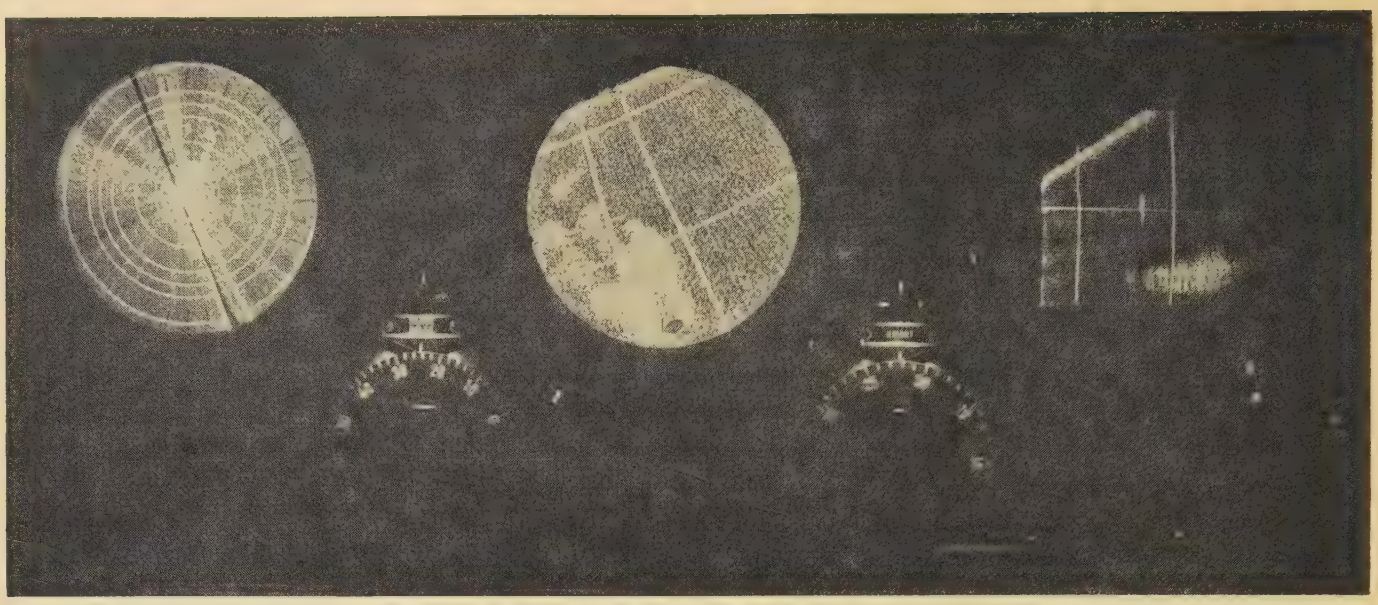

Figure 16. Radar presentation with polar plot, sector polar plot, and range elevation angle

tains both azimuth and elevation information for the same targets is shown in Figure 16. In addition to spotting aircraft, this picture demonstrates the ability of radar to give warning of storm areas. It is apparent that a storm cloud appears at the right and below the target plane in the elevation scope picture, and also can be located in the azimuth presentation.

It should be pointed out that a system which scans only a small sector in the direction of travel to avoid collisions also could obtain navigational information from supplementary land-based equipment. An example of this supplementary equipment is a radar beacon which consists of a transmitter that radiates a coded pulse when properly interrogated by an airborne system. This coded pulse appearing on the radar indicator enables range and bearing to be determined to the known location of the beacon. Such a system has a decided advantage when navigating over water where recognizable targets on a radar map are scarce. Furthermore, it aids in extending the operating range of the equipment beyond the target-response indication because of the higher power signals from the beacon. Since the high frequencies involved propagate only in straight lines, the range generally is limited to line of sight conditions.

Future Developments

The elevation scope pictures illustrate the performance that is obtainable now with ground radar equipment, and in time, equivalent resolution and satisfactory ranges will be achieved with lightweight air-borne systems. However, there are many engineering problems, both electrical and mechanical, to be overcome before an ideal design is evolved that meets the strict limitations imposed upon air-borne apparatus. Not the least of these is the problem of presenting the radar information in a manner that requires little effort on the part of the observer for quick interpretation. Azimuth and elevation data should be combined to provide the pilot with continuous infor-

Figure 17. Radar map of Greater New York

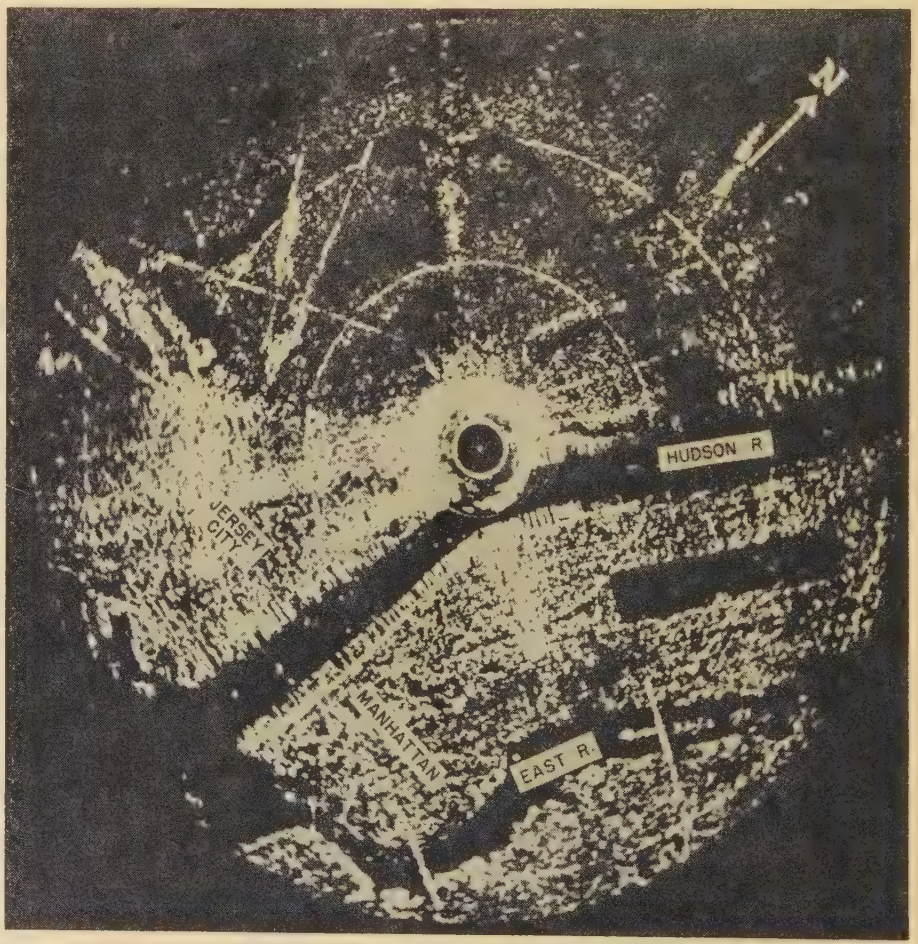

mation on all obstacles within the danger area.

The photograph in Figure 17 illustrates the definition obtainable when using a very narrow beam system. The individual docks on the Manhattan water front, the bridges across the East River, and the railroad tracks in Jersey City are clearly visible. It may well be that eventually radar will approach the equivalent of visual or television presentation in a scope picture so that a similar view of New York City and adjacent areas will enable the pilot to perceive the height of objects with the same resolution that can be observed here for range and bearing. This goal may not be achieved for some time, if ever, but in the meantime, useful radar systems can be designed which will remove many of the hazards of modern air travel.

References

1. Radar, a Report on Science at War (pamphlet), distributed by Office of War Information.

2. Aviation Communication System, **D. W. Rentzel.** Electrical Engineering, volume 64, November 1945, pages 387–91.

Differential Leakage of a Fractional-Slot Winding

M. M. LIWSCHITZ
MEMBER AIEE

IN a previous paper,[1] the differential (harmonic) leakage of an integral-slot winding and squirrel cage winding was treated. It was shown that a squirrel cage rotor reduces the harmonics and thus the differential leakage of the stator. The influence of the number of stator and rotor slots, as well as of the pitch factor of the stator winding on the damping of the stator harmonics, was discussed. Also, it was shown that skewing of the rotor reduces the damping of the stator harmonics and, therefore increases the differential leakage of the stator. The investigation was made under the following assumptions:

1. The saturation of the leakage paths is negligible.

2. The influence of slot-openings for all harmonics is the same as for the synchronous wave. That is, all harmonic fluxes are reduced by the slot-openings in the ratio of one to K_c, where K_c is the total Carter factor.

3. The magnetomotive force curve has a stepped shape.

The saturation of the leakage paths will be neglected in this paper also. The influence of slot-openings on the individual harmonics and the influence of the shape of the magnetomotive force curve on the differential leakage are treated in appendixes I and II. It follows from these appendixes that the assumptions made with respect to the slot-openings and the shape of the magnetomotive force curve are not entirely correct, but they are justified by the simplification of calculation of the differential leakage to which they lead.

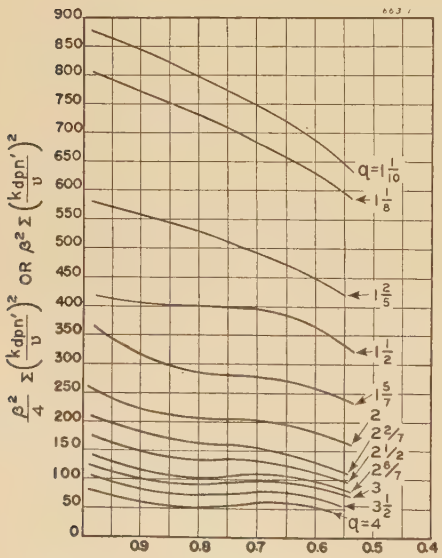

Figure 1. $\frac{\beta^2}{4}\sum_{\nu\neq\frac{\beta}{2}}\left(\frac{k_{dpn'}}{\nu}\right)^2$ and $\beta^2\sum_{\nu\neq\beta}\left(\frac{k_{dpn'}}{\nu}\right)^2$ for fractional-slot 3-phase windings

Actual Harmonics of Fractional-Slot 3-Phase Winding: Their Distribution Factors and Pitch Factors

If the number of slots per pole per phase of the fractional-slot winding is written

$$q=\frac{N}{\beta} \tag{1}$$

where N and β have no common divisor, the actual harmonics of a 3-phase winding are (for symbols see Nomenclature):

$$n'=\frac{2p}{\beta}\nu \qquad \nu=1, 2, 4, 5, 7 \ldots \tag{2}$$

when β is an even number, and

$$n'=\frac{p}{\beta}\nu \qquad \nu=1, 5, 7, 11, 13 \ldots \tag{3}$$

when β is an odd number.

For the synchronous wave, $\nu_s = \beta/2$ when β is an even number, or $\nu_s=\beta$ when β is an odd number. The number of subharmonics is equal to $(\beta-2)/2$ when β is an even number or to $(\beta-1)/2$ when β is an odd number (including those which are a multiple of three and usually do not exist in a 3-phase machine).

The absolute value of the distribution factor of the n'-th harmonic is

$$k_{dn'}=\frac{0.5}{N\sin\alpha_{n'}/2} \tag{4}$$

If P is the smallest integer which makes d an integer in the equation,

$$d=\frac{3NP+1}{\beta} \tag{5}$$

then it is true that when β is an even number

$$\alpha_{n'}=2d\alpha_m\nu+180 \tag{6}$$

and when β is an odd number

$$\alpha_{n'}=d\alpha_m\nu$$

if P is an even number and

$$\alpha_{n'}=d\alpha_m\nu+180 \tag{7}$$

if P is an odd number where

$$\alpha_m=\frac{180}{3N} \tag{8}$$

The pitch factor of the n'-th harmonic is

$$k_{pn'}=\sin\left(\frac{W}{\tau}\frac{180}{\beta}\nu\right) \tag{9a}$$

when β is an even number and

$$k_{pn'}=\sin\left(\frac{W}{\tau}\frac{180}{2\beta}\nu\right) \tag{9b}$$

when β is an odd number.

Harmonic Leakage Reactance of 3-Phase Winding

First the case will be considered where there is no damping, that is, the stator winding of a wound rotor induction motor or the stator winding of a salient pole synchronous machine without a damper winding.

The amplitude of the magnetomotive force of the wave with the length $2\beta\tau$ is

$$F_\beta=\frac{\sqrt{2}}{\pi}mNn_ck_{dp\beta}I \tag{10}$$

and therefore the amplitude of the fundamental wave with the length $2p\tau$ is

$$F_f=\frac{\sqrt{2}}{\pi}mNn_ck_{dpf}I\times\frac{p}{\beta} \tag{11}$$

The amplitude of the n'-th harmonic of the magnetomotive force is thus

$$F_{n'}=\frac{F_f}{n'}\frac{k_{dpn'}}{k_{dpf}}=\frac{\sqrt{2}}{\pi}mNn_c\frac{p}{\beta}\frac{k_{dpn'}}{n'}I \tag{12}$$

If the assumption is made that all harmonics are reduced by the slot-openings in the ratio of one to K_c, then the amplitude of the n'-th field harmonic is

$$B_{n'}=\frac{3.19}{gK_cK_s}F_{n'} \tag{13}$$

and the flux produced by the n'-th field harmonic is

$$\Phi_{n'}=\frac{2}{\pi}\tau_{n'}l_iB_{n'} \tag{14}$$

Paper 46-63, recommended by the AIEE committee on electric machinery for presentation at the AIEE winter convention, New York, N. Y., January 21-25, 1946. Manuscript submitted August 27, 1945; made available for printing December 11, 1945.

M. M. LIWSCHITZ is a consulting engineer to Westinghouse Electric Corporation and is with the Polytechnic Institute of Brooklyn, Brooklyn, N. Y.

The author is grateful to B. Limes for assistance in calculating the data contained in Table I.

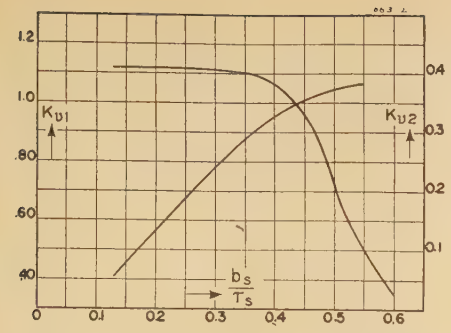

Figure 2. Factors K_{v1} and K_{v2} as functions of ratio between slot opening and slot pitch

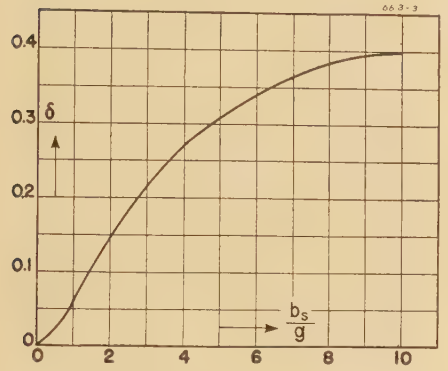

Figure 3. Factor δ as function of ratio between slot opening and air gap

The flux interlinkage caused by the flux $\Phi_{n'}$ is

$$\Psi_{n'}=\Phi_{n'}N_{ph}k_{dpn'} \tag{15}$$

Hence, the harmonic leakage reactance

$$x_h=2\pi f_1\frac{1}{\sqrt{2}I}\sum\Psi_{n'}\times10^{-8}\text{ ohms/phase}$$

$$x_h=\frac{4}{\pi^2}mf_1N_{ph}^2\frac{\tau l_t}{pgK_cK_s}10^{-7}\times\left[\frac{p}{\tau}\sum\left(\frac{\tau_{n'}}{n'}k^2_{dpn'}\right)\right]\text{ ohms/phase} \tag{16}$$

where

$$\tau_{n'}=\frac{p\tau}{n'}$$

Therefore, corresponding to equations 2 and 3,

$$\frac{p}{\tau}\sum\left(\frac{\tau_{n'}}{n'}k^2_{dpn'}\right)=\frac{\beta^2}{4}\sum_{\nu\neq\frac{\beta}{2}}\left(\frac{k_{dpn'}}{\nu}\right)^2$$

$$\nu=1,\ 2,\ 4,\ 5,\ 7\ \ldots \tag{17}$$

when β is an even number and

$$\frac{p}{\tau}\sum\left(\frac{\tau_{n'}}{n'}k^2_{dpn'}\right)=\beta^2\sum_{\nu\neq\beta}\left(\frac{k_{dpn'}}{\nu}\right)^2$$

$$\nu=1,\ 5,\ 7,\ 11\ \ldots \tag{18}$$

when β is an odd number.

The evaluation of the sums of equation 17 and equation 18 is not as simple as for an integral-slot winding. The reactance equation based upon the magnetic energy in the gap and used for the calculation of the harmonic leakage of the integral-slot winding also can be applied here, but the Goerges diagram of the magnetomotive forces of a fractional-slot winding becomes complicated, and the derivation of general formulas becomes tedious.

For this reason the direct summation of the terms $(k_{dpn'}/\nu)^2$ has been used in order to determine the sum of equations 17 and 18. As for the integral-slot windings, only a part of the harmonics of order lower than the slot harmonics of first order, and all slot harmonics, have to be taken into account.

The slot harmonics are:

$$n'_{sl}=\mp kQ+p \tag{19}$$

Thus

$$\nu_{sl}=\frac{\beta}{2}(\mp6kq+1) \tag{20}$$

when β is an even number

$$\nu_{sl}=\beta(\mp6kq+1) \tag{21}$$

when β is an odd number.

When $k>2$, the term $+1$ in the parentheses of equations 20 and 21 can be neglected. Then

$$\sum_{\nu=\nu_{sl}}\left(\frac{k_{dpn'}}{\nu}\right)^2=\frac{4}{\beta^2}k^2_{dp(n'=p)}\left[\frac{1}{(-6q+1)^2}+\frac{1}{(6q+1)^2}+\frac{1}{(-12q+1)^2}+\frac{1}{(12q+1)^2}+\frac{0.786}{(6q)^2}\right] \tag{22}$$

when β is an even number and

$$\sum_{\nu=\nu_{sl}}\left(\frac{k_{dpn'}}{\nu}\right)^2=\frac{1}{\beta^2}k^2_{dp(n'=p)}\times\left[\frac{1}{(-6q+1)^2}+\frac{1}{(6q+1)^2}+\frac{1}{(-12q+1)^2}+\frac{1}{(12q+1)^2}+\frac{0.786}{(6q)^2}\right] \tag{23}$$

when β is an odd number. Here is

$$k_{d(n'=p)}=\frac{\sin30^\circ}{N\sin\frac{30^\circ}{N}} \tag{24}$$

and

$$k_{p(n'=p)}=\sin\frac{Z}{mq}\frac{\pi}{2}=\sin\frac{Z}{q}30^\circ \tag{25}$$

Z is the coil width in slot pitches.

For the harmonics of lower order than the slot harmonics of first order, formulas 4 to 7 and also Calvert's Tables[3] have been used.

The results for the more frequently used numbers of slots per pole per phase are given in Table I. The third column does not include the subharmonics; however, the fourth column does.

It has been shown that the harmonics of lower order are damped by a squirrel cage more than the harmonics of higher order. This is especially true of the subharmonics; a squirrel cage winding in the induction motor or a damper winding in the synchronous machine damps out these harmonics practically entirely. Because of the high speed of the subharmonics, they are damped considerably by parasitic currents even when there is no squirrel cage or damper winding in the rotor. For the calculation of the harmonic leakage reactance, the subharmonics therefore can be omitted. This is also in agreement with the tests.

Figure 1 gives the sums of equations 17 and 18 without the subharmonics as function of the throw W/τ. The values for $q=2$, 3, and 4 are taken from Figure 1 of reference 1. It can be seen that the curves for fractional-slot windings have the same characteristics as those for integral-slot windings. The ratio between the sums for the same value of W/τ approximately is equal to the inverse ratio of the square of q, and so Figure 1 of reference 1 can be used in order to determine the sum for fractional-slot windings with $q>3\frac{1}{2}$.

Damping of Harmonics by Squirrel Cage Winding

The case of an induction motor with squirrel cage rotor or of a salient pole synchronous machine with damper winding will be considered now. Here the rotor harmonics which correspond to $K_2=0$ (see reference 1) damp the corresponding stator harmonics, thus reducing the leakage reactance. It has been shown there that the damping factor of the n'-th harmonic is

$$\dot{D}_{n'}=1-\frac{js_{n'}X_{mn'}}{r_{2n'}+js_{n'}X_{mn'}(1+\tau_{2n'})} \tag{26}$$

or

$$\dot{D}_{n'}=1-\dot{C}_{n'}\underline{/\theta} \tag{27}$$

where

$$C_{n'}=\frac{\sqrt{[(s_{n'}X_{mn'})^2(1+\tau_{2n'})]^2+(s_{n'}X_{mn'}r_{2n'})^2}}{r_{2n'}^2+[s_{n'}X_{mn'}(1+\tau_{2n'})]^2} \tag{28}$$

and

$$\tan\theta=\frac{r_{2n'}}{s_{n'}X_{mn'}(1+\tau_{2n'})} \tag{29}$$

The absolute value of $D_{n'}$ is

$$D_{n'}=\sqrt{(1-C_{n'}\cos\theta)^2+(C_{n'}\sin\theta)^2} \tag{30}$$

Table I

q	W/τ	$\beta^2\sum\left(\frac{k_{dnp'}}{\nu}\right)^2_{\nu\neq\frac{\beta}{2}}$ Without Subharmonics	$\beta^2\sum\left(\frac{k_{dpn'}}{\nu}\right)^2_{\nu\neq\frac{\beta}{2}}$ Including Subharmonics
1 1/2	0.890	0.0403	0.0426
	0.667	0.0397	0.0392
2 1/2	0.933	0.0153	0.0153
	0.800	0.0139	0.0139
1 3/4	0.953	0.0314	0.0488
	0.760	0.0264	0.0383
2 1/4	0.890	0.0175	0.0283
	0.740	0.0158	0.0237
2 3/4	0.969	0.0139	0.0212
	0.850	0.0114	0.0174
1 7/8	0.890	0.0263	0.0447
	0.712	0.0246	0.0366
2 3/8	0.983	0.0207	0.0253
	0.842	0.0184	0.0221
2 7/8	0.928	0.0124	0.0208
	0.812	0.0120	0.0187
1 2/5	0.954	0.0570	0.0680
	0.714	0.0495	0.0529
1 4/5	0.926	0.0297	0.0474
	0.742	0.0256	0.0372
2 1/5	0.910	0.0188	0.0308
	0.758	0.0167	0.0251
1 5/7	0.972	0.0354	0.0522
	0.778	0.0281	0.0402
2 2/7	0.874	0.0175	0.0272
	0.730	0.0164	0.0237
2 6/7	0.933	0.0119	0.0201
	0.817	0.0105	0.0172
1 7/11	0.815	0.0299	0.0369
	0.612	0.0240	0.0283
2 1/11	0.958	0.0255	0.0399
	0.798	0.0320	0.0347
2 7/11	0.885	0.0155	0.0186
	0.760	0.0138	0.0152
1 11/13	0.903	0.0271	0.0452
	0.723	0.0245	0.0371
2 4/13	0.867	0.0173	0.0260
	0.723	0.0156	0.0223
2 10/13	0.964	0.0135	0.0216
	0.842	0.0112	0.0177

A comparison between the last two columns shows that the slot leakage and the end-winding leakage cannot be neglected despite the fact that the harmonic leakage is relatively large here because of the small number of slots per pole of the rotor.

The total damping factor is

$$D_t=\frac{\frac{\beta^2}{4}\sum\left(\frac{k_{dpn'}}{\nu}\right)^2 D_{n'}}{\frac{\beta_2}{4}\sum\left(\frac{k_{dpn'}}{\nu}\right)^2} \qquad \nu\neq\frac{\beta}{2} \tag{33}$$

when β is an even number and

$$D_t=\frac{\beta^2\sum\left(\frac{k_{dpn'}}{\nu}\right)^2 D_{n'}}{\beta^2\sum\left(\frac{k_{dpn'}}{\nu}\right)^2} \qquad \nu\neq\beta \tag{34}$$

when β is an odd number. The denominators of these equations are given in Table I and Figure 1.

The evaluation of equation 34 for the example considered above gives the same value for standstill and for running with synchronous speed, namely, $D_t=0.92$. For the slot harmonics of first order, the factors $D_{n'}$, from Tables II and III have been used. For higher slot harmonics, it has been assumed that $D_{n'}$ equals one and equations 22 and 23 have been applied.

The motor in question has a throw equal to 0.788. The factor D_t has been determined for the throw 0.972 also and has been found to be practically the same as for the throw 0.788. This is in accordance with the results obtained for the integral-slot windings with $q=2$. Also, there the chording has little influence on the damping.

Influence of Slot Openings and Shape of Magnetomotive Force Curve on Harmonic Leakage

The previous considerations are based upon the assumption that the slot-openings reduce all field harmonics in the ratio of one to K_c. It is shown in Appen-

It has been shown in reference 1 that there will not be a sensible error when equation 30 is used instead of equation 26.

When $r_{2n'}$ can be neglected,

$$D_{n'}=1-\frac{1}{1+\tau_{2n'}} \tag{31}$$

and when, besides $r_{2n'}$, the slot leakage and the end-winding leakage also can be neglected comparatively with harmonic leakage,

$$D_{n'}=1-(\xi_{2n'}\eta_{2n'})^2 \tag{32}$$

where $\xi_{2n'}$ is the coupling factor of the rotor with respect to the n'-th harmonic and $\eta_{2n'}$ is the skew factor.

As an example, a 350-horsepower 60-cycle, 3-phase synchronous motor with 28 poles will be considered. $Q_1=144$, $q_1=1^5/_7$, $Q_2=5\times28=140$, $W/\tau=0.788$. The damper winding consists of five round bars per pole, three of them of copper, two of bronze with the resistivity two. The poles are not skewed. The motor will be considered at standstill ($s=s_{n'}=1$) and running with normal speed ($s=0_1$ $s_{n'}=$variable).

Table II gives the values of the rotor constants as well as of $C_{n'}$, tan θ, and $D_{n'}$ for standstill ($s_{n'}=1$). Table II gives the same values for synchronous speed ($s_{n'}$ variable). The skin-effect has been neglected and thus both tables have the same values for $r_{2n'}$ and $\tau_{(s+e)n'}$.

The examination of the tables shows that they have the same character as those for integral slot windings[1] and that the influence of the resistance is small.

Table II. Standstill

ν	n'	$s_{n'}$	$X_{mn'}$	$r_{2n'}$	$\tau_{(s+e)n'}$	$\tau_{hn'}$	$\tau_{2n'}$	tan θ	$C_{n'}$	$D_{n'}$	$D_{n'}$ for $r_{2n'}=0$	$D_{n'}$ for $r_{2n'}=0$ and $\tau_{(s+e)n'}=0$
1	+ 2	1	1,304×10⁻⁴	9.01×10⁻⁴	0.0082	0.005	0.0132	0.0068	0.988	0.0138	0.013	0.005
5	− 10	1	52.	1.66	0.0715	0.02	0.0915	0.0293	0.920	0.090	0.0837	0.0196
11	− 22	1	10.72	1.43	0.332	0.047	0.379	0.0967	0.723	0.288	0.275	0.045
13	+ 26	1	7.68	1.41	0.46	0.064	0.524	0.120	0.652	0.361	0.344	0.060
17	− 34	1	4.49	1.39	0.785	0.111	0.896	0.164	0.523	0.49	0.472	0.10
19	+ 38	1	3.6	1.39	0.975	0.156	1.131	0.181	0.468	0.556	0.531	0.135
23	− 46	1	2.46	1.38	1.43	0.196	1.626	0.214	0.377	0.635	0.619	0.164
25	+ 50	1	2.08	1.38	1.69	0.235	1.925	0.226	0.336	0.675	0.658	0.191
35	− 70	1	1.06	1.375	3.3	0.535	3.83	0.269	0.200	0.81	0.794	0.359
49	+ 98	1	0.541	1.37	6.48	1.47	7.95	0.283	0.109	0.895	0.889	0.595
65	−130	1	0.307	1.375	11.42	4.55	15.97	0.265	0.057	0.945	0.941	0.82
75	+150	1	0.208	1.38	16.92	17.86	34.78	0.187	0.0272	0.972	0.971	0.947

dix I that this assumption is not true of the slot-harmonics. Depending upon the number of slots per pole and the coil pitch, one of the slot-harmonics of first or second order may be increased by the slot-openings while the other slot-harmonic of the same pair is decreased. It is even possible that both slot-harmonics of the first or second order are increased by the slot-openings. Further, the influence of the slot-openings on the slot-harmonics of higher order than two is negligible. This shows that the division of all harmonics by the Carter factor (equation 13) leads to too small a value of the harmonic leakage, the error being larger the larger the ratio of slot-opening to slot pitch and of slot-opening to air gap, that is, the error being larger for open slots than for semiopen slots.

On the other hand, it is shown in Appendix II that the calculation with the stepped magnetomotive force curve, based upon the assumption that the ampere conductors of each slot are concentrated in the middle of the slot, leads to too large amplitudes of the slot-harmonics and, therefore, to a too large value of the harmonic leakage, the error being again larger the larger the slot-opening.

The error caused by the division of all harmonics by the Carter factor and the error caused by the assumption of the stepped shape for the magnetomotive force curve are thus of opposite sense, one decreasing the slot harmonics and the harmonic leakage, the other increasing them.

Conclusion

Experience shows that Figure 1 (as well as Figure 1 of reference 1) yields good practical results for the differential (harmonic) leakage, that is, results which agree with tests. Since these figures do not take into account the damping of the harmonics by the rotor and are based upon the assumptions that the slot-openings reduce equally all harmonics and that the magnetomotive force curve has a stepped shape, their good agreement with tests means that the error caused by the division of all harmonics by the Carter factor is approximately equal and opposite to the errors caused by the neglect of damping and the assumption of the stepped magnetomotive force curve.

Since the differential (harmonic) leakage constitutes only a part of the total leakage, the use of a simple, although not entirely exact method of calculation of this leakage, is justified.

Appendix I. Influence of the Slot Openings on the Differential Leakage

The stator of an induction motor will be considered. The results obtained apply also to the rotor.

The n'-th harmonic of the magnetomotive force curve is

$$f_{n'} = F_{n'} \sin\ (\omega t - n'\frac{\pi}{p\tau}x) \tag{35}$$

$$F_{n'} = \frac{\sqrt{2}}{\pi} m_1 N_1 \frac{k_{dpn'}}{n'} I_1 \tag{36}$$

The n'-th field harmonic has been derived from this (see equation 13) by multiplying with

$$\frac{3.19}{gK_{c1}K_{c2}K_s}$$

where the Carter factors K_{c1} and K_{c2} have to take care of the influence of the slot-openings of stator and rotor. This yields for n'-th field harmonic

$$b_{n'} = \frac{3.19}{gK_{c1}K_{c2}K_s} F_{n'} \sin\left(\omega t - n'\frac{\pi}{p\tau}x\right) \tag{37}$$

In order to determine more accurately the influence of the slot-openings, the gap permeance will be introduced[4] in accordance with the assumption that the fundamental has two poles, as

$$\left(\frac{1}{g}\right)_{eff} = \frac{1}{g}\left[1+\epsilon_1 \cos Q_1\frac{\pi}{p\tau}x+\epsilon_2 \times \cos 2Q_1\frac{\pi}{p\tau}x+\ldots.\right] \tag{38}$$

The n'-th field harmonic becomes

$$b_{n'} = \frac{3.19}{gK_s} F_{n'} \sin\left(\omega t - n'\frac{\pi}{p\tau}x\right)\times \left[1+\epsilon_1 \cos Q_1\frac{\pi}{p\tau}x+\epsilon_2 \cos 2Q_1\frac{\pi}{p\tau}x+\ldots.\right] \tag{39}$$

With the abbreviation

$$\frac{3.19}{gK_s}F_{n'} = A_{n'} \tag{40}$$

there is

$$b_{n'} = A_{n'} \sin\left(\omega t - n'\frac{\pi}{p\tau}x\right) + A_{n'}\sum_{c=1,2,3\ldots}\epsilon_c \times \cos\left(cQ_1\frac{\pi}{p\tau}x\right)\times \sin\left(\omega t - n'\frac{\pi}{p\tau}x\right)$$

or

$$b_{n'} = A_{n'} \sin\left(\omega t - n'\frac{\pi}{p\tau}x\right) + A_{n'}\sum_{c=1,2,3\ldots}\frac{\epsilon_c}{2}\times \left\{\sin\left[\omega t+(cQ_1-n')\frac{\pi}{p\tau}x\right]+ \sin\left[\omega t-(cQ_1+n')\frac{\pi}{p\tau}x\right]\right\} \tag{41}$$

Thus, because of the slot-openings of the stator, the n'-th stator harmonic produces a series of pairs of traveling waves. One wave of each pair travels in the direction of rotation, the other in opposite direction. Their respective velocities with regard to the stator are

$$\frac{p}{cQ_1+n'}\frac{\tau}{\pi}\omega \text{ and } \frac{p}{cQ_1-n'}\frac{\tau}{\pi}\omega \qquad c=1,2,3\ldots \tag{42}$$

These slot-opening waves may influence considerably those field harmonics with respect to which they are at standstill. Their influence on all other harmonics will be relatively small and can be taken care of by introducing the Carter factor, that is, by introducing in the denominator of equation 40 the factor K_{c1}.

The latter statement applies also to the influence of the rotor slot-openings on the stator harmonics, since the waves produced by them move with respect to the stator harmonics. Therefore, considering the stator

Table III. Synchronous Speed

p	n′	$s_{n'}$	$X_{mn'}$	$r_{2n'}$	$r_{(s+\epsilon)n'}$	$r_{hn'}$	$r_{2n'}$	tan θ	$C_{n'}$	$D_{n'}$	$D_{n'}$ for $r_{2n'}=0$	$D_{n'}$ for $r_{2n'}=0$ and $x_{(s+\epsilon)n'}=0$
1	+ 2	+ 0.857	$1{,}304\times10^{-4}$	9.01×10^{-4}	0.0082	0.005	0.0132	0.0079	0.986	0.016	0.0128	0.005
5	− 10	+ 1.715	52.	1.66	0.0715	0.02	0.0915	0.0171	0.915	0.085	0.0837	0.0196
11	− 22	+ 2.57	10.72	1.43	0.332	0.047	0.379	0.376	0.727	0.276	0.275	0.045
13	+ 26	− 0.86	7.68	1.41	0.46	0.064	0.524	0.14	0.654	0.354	0.344	0.060
17	− 34	+ 3.43	4.49	1.39	0.785	0.111	0.896	0.0467	0.530	0.475	0.472	0.10
19	+ 38	− 1.72	3.6	1.39	0.975	0.156	1.131	0.105	0.470	0.535	0.531	0.135
23	− 46	+ 4.29	2.46	1.38	1.43	0.196	1.626	0.0496	0.377	0.624	0.619	0.164
25	+ 50	− 2.57	2.08	1.38	1.69	0.235	1.925	0.085	0.345	0.658	0.658	0.191
35	− 70	+ 6.0	1.06	1.375	3.3	0.535	3.83	0.0448	0.207	0.794	0.794	0.359
49	+ 98	− 6.0	0.541	1.37	6.48	1.47	7.95	0.047	0.111	0.889	0.889	0.595
65	−130	+10.3	0.307	1.375	11.42	4.55	15.97	0.0257	0.059	0.941	0.941	0.82
75	+150	−10.3	0.208	1.38	16.92	17.86	34.78	0.0182	0.028	0.971	0.971	0.947

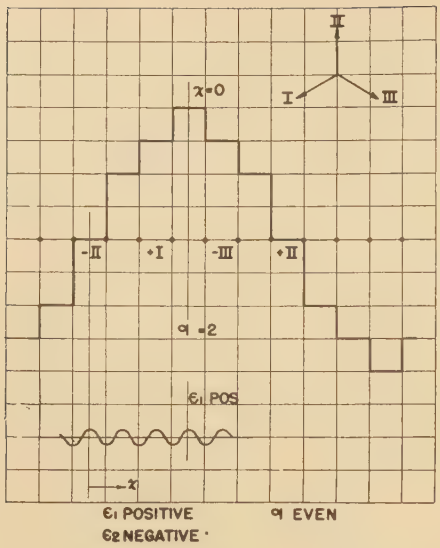

Figure 4. Determination of the signs of ϵ_1 and ϵ_2 for q = even number

harmonics, the factor K_{c2} has to be introduced in equation 40.

Now the stator field harmonics have to be determined, the velocities of which are given by equation 42. These stator field harmonics will be increased or reduced considerably by the slot-opening waves.

The n'-th stator harmonic has with respect to the stator the speed

$$v_{n'}=\frac{p}{n'}\frac{\tau}{\pi}\omega \tag{43}$$

Since the order of the stator slot-harmonics is given by the equation

$$n'_{sl}=\mp kQ_1+p \tag{44}$$

it follows that the slot-opening waves produced by the synchronous wave ($n'=p$) are at standstill with respect to the slot-harmonics and these are the only waves which are at standstill with respect to each other. It follows further from equations 42 and 44 that the slot-opening wave of the order $c=1$ is at standstill with respect to the slot-harmonic of first order ($k=1$), that the slot-opening wave of the order $c=2$ is at standstill with respect to the slot-harmonic of second order ($k=2$), and so on.

Usually only the slot-opening waves of the orders $c=1$ and $c=2$ have to be taken into account. From equation 41

$$b'_{so}=A_{(n'=p)}\frac{\epsilon_c}{2}\sin\left[\omega t-(cQ_1+p)\frac{\pi}{p\tau}x-\psi\right]\frac{I_m}{I_1} \tag{45}$$

and

$$b''_{so}=A_{(n'=p)}\frac{\epsilon_c}{2}\sin\left[\omega t+(cQ_1-p)\frac{\pi}{p\tau}x+\psi\right]\frac{I_m}{I_1} \tag{46}$$

where I_m is the magnetizing current. $A_{(n'=p)}$ is proportional to the primary current I_1. The factor I_m/I_1 takes into account the fact that the amplitude of the slot-opening waves is proportional to the resultant synchronous wave, that is, to the synchronous wave produced by the primary and secondary magnetomotive force together (I_m). The angle has to be introduced because I_m is not in phase with I_1.

The slot harmonics are

$$b'_{sl}=A_{(n'=cQ_1+p)}\sin\left[\omega t-(cQ_1+p)\frac{\pi}{p\tau}x\right] \tag{47}$$

$$b''_{sl}=A_{(n'=-cQ_1+p)}\sin\left[\omega t+(cQ_1-p)\frac{\pi}{p\tau}x\right] \tag{48}$$

The ratio between the amplitudes of the two waves which travel in the direction of rotation is

$$r'=\frac{A_{(n'=p)}}{A_{(n'=cQ_1+p)}}\frac{I_m}{I_1}\frac{\epsilon_c}{2}=\left[\frac{k_{d(n'=p)}}{k_{d(n'=cQ_1+p)}}\right]\left[\frac{k_{p(n'=p)}}{k_{p(n'=cQ_1+p)}}\right]\times\frac{cQ_1+p}{p}\frac{I_m}{I_1}\frac{\epsilon_c}{2} \tag{49}$$

and the ratio between the amplitudes of the two waves which travel opposite to the direction of rotation is

$$r''=\frac{A_{(n'=p)}}{A_{(n'=-cQ_1+p)}}\frac{I_m}{I_1}\frac{\epsilon_c}{2}=\left[\frac{k_{d(n'=p)}}{k_{d(n'=-cQ_1+p)}}\right]\left[\frac{k_{p(n'=p)}}{k_{p(n'=-cQ_1+p)}}\right]\times\frac{cQ_1-p}{p}\frac{I_m}{I_1}\frac{\epsilon_c}{2} \tag{50}$$

The ratio I_m/I_1 as well as the angle ψ depend on the speed of the machine. For the induction motor it is approximately

$$\left.\begin{aligned}\frac{I_m}{I_1}&=0.08\text{ to }0.2\\ \psi&=15^\circ\text{ to }25^\circ\end{aligned}\right\}\text{ at standstill} \tag{51}$$

$$\left.\begin{aligned}\frac{I_m}{I_1}&=0.22\text{ to }0.6\\ \psi&=78^\circ\text{ to }55^\circ\end{aligned}\right\}\text{ at high speed} \tag{52}$$

The first value refers to machines with a low number of poles, the second to machines with a high number of poles. For the synchronous motor, $I_m/I_1\backsimeq 0.35$ at standstill and $I_m/I_1\backsimeq 0.8$ to 1.1 at high speed; ψ is for both cases approximately 25 degrees.

Further, for integral-slot windings

$$\left.\begin{aligned}\frac{k_{d(n'=p)}}{k_{d(n'=\pm cQ_1+p)}}&=\begin{matrix}-1(c=1)\\ +1(c=2)\end{matrix}\\ &\text{when } q \text{ is even}\\ \frac{k_{d(n'=p)}}{k_{d(n'=\pm cQ_1+p)}}&=\begin{matrix}+1(c=1)\\ +1(c=2)\end{matrix}\\ &\text{when } q \text{ is odd}\end{aligned}\right\} \tag{53}$$

and for fractional-slot windings[2]

$$\left.\begin{aligned}\frac{k_{d(n'=p)}}{k_{d(n'=\pm cQ_1+p)}}&=\begin{matrix}+1(c=1)\\ -1(c=2)\end{matrix}\\ &\text{when } P \text{ is even}\\ \frac{k_{d(n'=p)}}{k_{d(n'=\pm cQ_1+p)}}&=\begin{matrix}+1(c=1)\\ +1(c=2)\end{matrix}\\ &\text{when } P \text{ is odd and } \beta \text{ is even}\\ \frac{k_{d(n'p=p)}}{k_{d(n'=\pm cQ_1+p)}}&=\begin{matrix}-1(c=1)\\ +1(c=2)\end{matrix}\\ &\text{when } P \text{ is odd and } \beta \text{ is odd}\end{aligned}\right\} \tag{54}$$

For the ratio of the pitch factors,

$$\frac{k_{p(n'=p)}}{k_{p(n'=\pm cQ_1+p)}}=\pm 1\text{ or }\mp 1 \tag{55}$$

that is, when one slot-harmonic has the plus sign, the other slot-harmonic of the same pair has the minus sign.

The magnitude of ϵ_1 depends upon the ratio between slot-opening and slot pitch and upon the ratio between slot-opening and gap. There is[5]

$$\epsilon=K_\nu\delta K_c \tag{56}$$

The factor K_ν takes into account the ratio between slot-opening and slot pitch; its value for $c=1$ and $c=2$ is given in Figure 2. δ takes into account the ratio between slot-opening and air gap; its value is given in Figure 3. $K_c=K_{c1}K_{c2}$ is the Carter factor. For open slots, $\epsilon_1=0.5$ to 0.7 and ϵ_2 is negligible; for semi-open slots $\epsilon_1=0.05$ to 0.25 and $\epsilon_2=0.05$ to 0.15.

In order to find the sign of ϵ_1 with respect to the synchronous wave, consider Figures 4 and 5, which relate to integral-slot windings with $q=2$ and $q=3$. It can be seen that ϵ_1 is positive for even and negative for odd values of q, while ϵ_2 is negative for even as well as odd values of q.

Because of the slot-opening waves produced by the synchronous wave ($n'=p$), one slot-harmonic of a pair may be decreased and the other increased, or both slot-harmonics of the pair may be decreased or increased. Whether the harmonic is decreased or increased depends upon the number of slots per pole and upon the coil pitch, that is, upon the sign of the pitch factor.

Equations 51 and 52 show further that the influence of the slot-openings depends upon the speed of the machine. The harmonic (differential) leakage is therefore not a constant; it changes with the speed of the machine.

As example the stator harmonics of an 800-horsepower 8-pole induction motor with open slots will be considered.

For this machine

$$\frac{b_s}{g}=\frac{0.415}{0.055}=7.49$$

$$\frac{b_s}{\tau_s}=\frac{0.415}{0.789}=0.527$$

From Figures 2 and 3,

$$K_{\nu 1}=1.06\qquad K_{\nu 2}=0.14\qquad \delta=0.37$$

The Carter factor is equal to 1.46. Therefore,

$$\frac{\epsilon_1}{2}=1.06\times 0.37\times 1.46\times 0.5=0.286$$

Further,

$$\frac{I_m}{I_1}=0.239\text{ at full speed}$$

$$\frac{I_m}{I_1}=0.06\text{ at standstill}$$

For the machine under consideration,

$$q=5\qquad \frac{W}{\tau}=0.733$$

Hence,

$$\frac{k_{d(n'=p)}}{k_{d(n'=\pm Q_1+p)}}=+1$$

and

$$\frac{k_{p(n'=p)}}{k_{p(n'=Q_1+p)}}=-1 \qquad \frac{k_{p(n'=p)}}{k_{p(n'=-Q_1+p)}}=+1$$

It follows from equations 39 and 40 for the slot harmonics of first order,

$$r'=(+1)(-1)\frac{120+4}{4}\times 0.239\times(-0.286)=$$
$$+2.12 \text{ at full speed}$$

$$r''=(+1)\,(+1)\frac{120-4}{4}\times 0.239\times(-0.286)=$$
$$-1.98 \text{ at full speed}$$

$$r'=+2.12\frac{0.06}{0.239}=+0.532 \text{ at standstill}$$

$$r''=-1.98\frac{0.06}{0.239}=-0.497 \text{ at standstill}$$

From the two waves of first order produced by the slot-openings, one, which travels with the rotation, has a sign opposite to the corresponding slot-harmonic, while the other, which travels opposite to the direction of rotation, has the same sign as the corresponding slot-harmonic. At standstill, the slot-harmonic that has the same direction of rotation as the synchronous wave is reduced by approximately 50 per cent while the other slot-harmonic is increased by approximately the same amount. The influence of the slot-openings on the slot-harmonics of second order is small here because of the open slots. It should be noted that the influence of the slot-openings on the slot-harmonics of first order is much smaller than in the considered example when the slots are semi-closed. However, in this case the slot-harmonics of second order are more influenced than in the case of open slots.

In the calculation of the harmonic (differential) leakage (equation 13), the influence of the slot-openings has been taken care of by dividing the amplitudes of the harmonics by the Carter factor, that is, by calculating with an increased gap. It follows from the results obtained above that the division by the Carter factor is correct only for the harmonics of lower order but not for the slot-harmonics.

Appendix II. Influence of the Shape of the Magnetomotive Force Curve

The foregoing considerations are based on the assumption that the magnetomotive force has the stepped shape, that is, that the magnetomotive force of a single coil is a rectangle and that the magnetomotive force changes in the center of each slot abruptly. This assumption is not correct. Flux maps indicate that it would be more correct to assume that, because of the slot-opening, the magnetomotive force of each single coil is not a rectangle but a trapezoid, as shown in Figure 6. This yields for the n'-th harmonic of an unchorded 3-phase integral-slot winding[8]

$$f_{n'}=\frac{3\sqrt{2}}{\pi}N_{ph}I\frac{k_{dn'}}{n'}\frac{\sin n'\alpha/2}{n'\alpha/2}\times$$
$$\sin\left(\omega t\mp n'\frac{\pi}{p\tau}x\right) \quad (57)$$

where

$$\alpha=\frac{b_s}{p\tau}\pi \quad (58)$$

For the rectangular shape (equations 35 and 36)

$$f_{n'}=\frac{3\sqrt{2}}{\pi}N_{ph}I\frac{k_{dn'}}{n'}\sin\left(\omega t\mp n'\frac{\pi}{p\tau}x\right) \quad (59)$$

Thus, the assumption of a trapezoidal shape introduces the factor

$$k_0=\frac{\sin n'\alpha/2}{n'\alpha/2} \quad (60)$$

Since α is a small angle, this factor will not influence the harmonics of lower order, but it will reduce the slot harmonics considerably, especially those of higher order. The harmonic (differential) leakage reactance that is built up by the sum of the leakage reactances of all harmonics, therefore, will be reduced also. The reduction caused by the trapezoid shape of the magnetomotive force will be larger the smaller the number of slots per pole per phase q, since $n'\alpha$ increases with decreasing q.

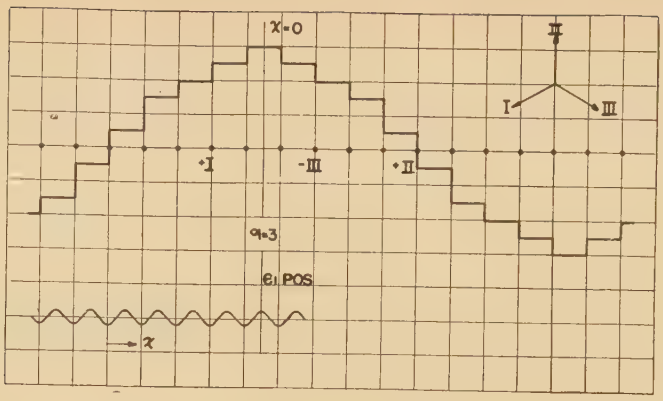

Figure 5. Determination of signs of ϵ_1 and ϵ_2 for q = odd number

ϵ_1 negative
ϵ_2 negative

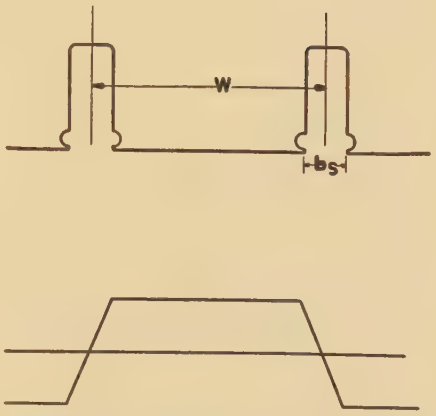

Figure 6. Shape of the magnetomotive force of a single coil in open slots

On the basis of equation 57, the harmonic leakage reactance of an unchorded 3-phase integral-slot winding becomes

$$x_h=\frac{4}{\pi^2}mN_{ph}^2pf_1l\times 10^{-7}\sum\left(\frac{k_{dn'}}{n'}\right)^2\times$$
$$\frac{\sin n'\alpha/2}{p\alpha/2}\coth\left(n'\frac{\pi g}{p\tau}\right) \quad (61)$$

For the rectangular shape of the magnetomotive force

$$x_h=\frac{4}{\pi^2}m\frac{N_{ph}^2}{p}f_1l_i\frac{\tau}{gK_cK_s}10^{-7}\sum\left(\frac{k_{dn'}}{n'}\right)^2 \quad (62)$$

While the evaluation of the sum in equation 61 is very tedious, the sum in equation 62 can be expressed by a simple formula. For this reason the calculation with the step-shaped magnetomotive force is preferred.

In the specific case of equation 61, that is, for unchorded 3-phase integral-slot windings, the following approximate formula applies:

$$x_h=4.0\frac{N_{ph}^2}{p}f_1l10^{-7}\frac{\frac{\tau}{g'}+4q}{1{,}000}\left(0.6+\frac{b_i}{\tau_s}\frac{6.5-0.6q}{q-1.2}\right) \quad (63)$$

g' is equal to the gap, g, times the Carter factor of the opposite slot.

The results obtained from equations 62 and 63 will be compared for two machines with different numbers of slots per pole per phase.

1. Six-hundred-horsepower induction motor considered in Appendix I: For this machine

$m=3$ $N_{ph}=80$ $p=4$ $f_1=60$ $\tau=11.81$
$l=11$ $l_i=10$ $\tau_s=0.789$ $b_s=0.415$
$g=0.055$ $K_{c1}=1.464$ $K_{c2}=1.047$
$K_s\backsimeq 1.05$ $q=5$ $\sum\left(\frac{k_{dn}}{n}\right)^2=0.0059$

$\left(\text{for } \frac{W}{\tau}=1\right)$

It follows from equation 62

$$x_h=\frac{4}{\pi^2}3\frac{80^2}{4}60\times 10\times$$
$$\frac{11.81}{0.055\times 1.464\times 1.047\times 1.05}\times$$
$$0.0059\times 10^{-7}=0.0873 \text{ ohm/phase}$$

and from equation 63

$$x_h = 4\frac{80^2}{4}60\times 11\frac{\dfrac{11.81}{\dfrac{0.055\times 1.047}{1{,}000}}+4\times 5}{}\times \left(0.6+\frac{0.374}{0.789}\,\frac{6.5-0.6\times 5}{5-1.2}\right)10^{-7}$$

$$= 0.098 \text{ ohm/phase}$$

2. Twelve-hundred-horsepower 26-pole induction motor with open slots: For this motor

$m=3 \quad N_{ph}=195 \quad p=13 \quad f_1=60 \quad \tau=8.12$
$l=24 \quad l_i=21 \quad \tau_s=0.901 \quad b_s=0.47 \quad g=0.065$
$K_{c1}=1.447 \quad K_{c2}=1.025 \quad K_s \backsimeq 1.05 \quad q=3$

$$\sum\left(\frac{k_{dn}}{n}\right)^2 = 0.0129\left(\text{for } \frac{W}{\tau}=1\right)$$

It follows from equation 62

$$x_h = \frac{4}{\pi^2}3\frac{150^2}{13}60\times 21\times \frac{8.12}{0.065\times 1.447\times 1.025\times 1.05}\times 0.0129\times 10^{-7} = 0.275 \text{ ohm/phase}$$

and from equation 63

$$x_h = 4\frac{150^2}{13}60\times 24\frac{\dfrac{8.12}{\dfrac{0.065\times 1.025}{1{,}000}}+4\times 3}{}\times \left(0.6+\frac{0.431}{0.901}\,\frac{6.5-0.6\times 3}{3-1.2}\right)10^{-7}$$

$$= 0.247 \text{ ohm/phase}$$

The values of the harmonic leakage obtained from equation 62, that is, on the basis of the stepped shape of the magnetomotive force curve, are about 10 to 15 per cent higher than those obtained from equation 63, that is, on the basis of the trapezoidal shape of the magnetomotive force curve. In the considered examples, q is equal to three and five, respectively. The difference between the results yielded by equations 62 and 63 becomes larger for values of q smaller than three; further, it is smaller for semi-open slots than for open slots; but in all cases the harmonic leakage obtained on the basis of the stepped shape of the magnetomotive force curve is larger than its real value.

Nomenclature

b_s = slot width at the gap
b_t = tooth width at the gap
c = order of the slot-opening wave
D = damping factor
f_1 = line frequency
f = magnetomotive force, instantaneous value
F = magnetomotive force, amplitude
g = air gap
I = current
k_d = distribution factor
k_p = pitch factor
K_c = Carter factor
K_s = saturation factor
k = order of the slot-harmonic
l_i = ideal core length
l = total core length
m = number of phases
n' = order of stator harmonics with respect to a fundamental whose wave length is equal to the circumference of the armature
$\left(n=\frac{n'}{p}\right)$ = order of the stator harmonic with respect to the synchronous wave
n'_{sl} = order of the slot harmonics
n_c = number of conductors in series per slot
N = numerator of the fraction $q=N/\beta$, that is, number of slots per phase in β poles
N_{ph} or N_1 = number of turns per phase
p = number of pole pairs
P = smallest integer which makes d in the equation $d=(3NP+1)/\beta$ an integer
Q = total number of slots
$\left(q=\frac{N}{\beta}\right)$ = number of slots per phase per pole
r_2 = resistance of the rotor per bar
s = slip of the rotor with respect to the synchronous wave
$s_{n'}$ = slip of the rotor with respect to the n'-th stator harmonic
W = coil width (in units of the pole pitch)
X_m = reactance due to the main flux
x_h = differential (harmonic) leakage reactance per phase
Z = coil width in slot pitches
β = denominator of the fraction $q=N/\beta$
ϵ = amplitude of the slot-opening wave
η = skew factor
ξ = coupling factor of the squirrel cage rotor
τ = pole pitch of the synchronous wave
$\tau_{n'}$ = pole pitch of the n'-th harmonic
τ_s = slot pitch
τ_2 = total leakage coefficient of the rotor
$\tau_{(s+e)}$ = slot and end-winding leakage coefficient of the rotor
τ_h = differential leakage coefficient of the rotor
$\omega = 2\pi f_1$

References

1. Differential Leakage With Respect to the Fundamental Wave and to the Harmonics, **M. M. Liwschitz.** AIEE Transactions, volume 63, 1944, October section, pages 1139–50. See also the bibliography to this paper containing 42 publications on the subject.

2. Distribution Factors and Pitch Factors of the Harmonics of a Fractional-Slot Winding, **M. M. Liwschitz.** AIEE Transactions, volume 62, 1943, October section, pages 664–6.

3. Amplitudes of Magnetomotive Force Harmonics for Fractional-Slot Windings of Three-Phase Machines, **J. F. Calvert.** *Iowa Engineering Experiment Station, Bulletin* 142, 1939.

4. The Theory of the Induction Motor With Squirrel Cage Rotor, **L. Dreyfus.** *Handlingar Number 34, Ingeniors Vedenskaps Akademiens* (Stockholm, Sweden), 1924.

5. Additional Losses in the Squirrel Cage Windings of Induction Motors and Synchronous Machines, **M. M. Liwschitz, H. Raymund.** *Scientific Publications of the Siemens Concern*, volume 14, 1935, page 16.

6. The Field in the Air Gap of Three-Phase Machines, **W. Putz.** *Institute of Technology*, (Berlin, Germany), 1933.

The Polyphase Commutator Regulator for Speed Control

A. G. CONRAD
MEMBER AIEE

F. E. BROOKS, JR.
ASSOCIATE AIEE

R. G. FELLERS
ASSOCIATE AIEE

Synopsis: This paper presents an explanation of the theory and explains the characteristics of an a-c adjustable-speed drive obtained by using a polyphase commutator regulator mechanically coupled to the shaft of a wound-rotor induction motor and electrically connected to its slip rings. The theoretical loci of the system current vectors with respect to the voltage vectors of the induction motor are developed in terms of the constants of the machines and the applied voltage. A method of determining the characteristics of the drive from no-load tests or from design data is presented. The characteristics predicted on these bases are in excellent agreement with those obtained experimentally.

SEVERAL methods have been employed to provide an a-c drive of large capacity with suitable adjustable-speed characteristics. The choice of the method used usually is dependent on the characteristics required by the load. One of the most satisfactory of these systems from the standpoint of speed control is obtained by supplying the primary of an induction motor from a balanced polyphase system and connecting its slip rings to a shunt-connected polyphase commutator regulator (see Figure 1).

The electrical circuit of the rotor of this regulating machine is similar to that of a d-c armature. It usually is designed for low voltage in order to obtain good commutation of the alternating currents supplied to it from the brushes. The spacing of the brushes on the commutator is determined by the number of phases on the motor rotor, that is on a 3-phase machine the angle between brushes is 120 electrical degrees. The stator or field winding of the regulator may be a normal distributed polyphase winding such as that found on a polyphase induction motor. However, for good commutation the main field windings usually are placed on salient poles between which interpoles can be provided. A compensating winding usually is placed on the stator and connected in series with the rotor or armature. The field may be designed for operation either in series or in shunt with the armature. The drive using the shunt connection is the more common and is the one which is discussed here. This connection is shown diagrammatically in Figure 1. A transformer bank normally is provided to control the voltage applied to the field winding and thereby control the speed. Excellent speed regulation can be obtained when shunt excitation of the regulator is employed. This drive is a constant horsepower device. For a given power input the torque available at the shaft is increased as the speed is adjusted to lower values.

The object of this paper is

(*a*). To develop the theory of operation of the adjustable-speed drive consisting of a wound-rotor induction motor and a shunt-connected polyphase commutator regulator.

(*b*). To obtain the expression for the primary current of the induction motor as a function of the phase voltage, the machine constants, and the slip.

(*c*). To present a method of predicting the characteristics of the drive from no-load readings taken experimentally on the machines, or from the design data of the machines employed.

Theory

When the stator, or field, winding of the polyphase commutator regulator is connected to a balanced polyphase supply, a rotating magnetic field is set up which induces a voltage in this winding which is essentially equal and opposite to the applied voltage. A voltage is induced in the conductors of the rotor also, unless it is rotating at synchronous speed in the same direction as the magnetic field. If the rotor is stationary the voltages in these conductors can be measured between brushes placed on the commutator. By proper distribution of these brushes on the commutator, these voltages can be made to form a balanced polyphase system of any desired number of phases. If the brushes are all shifted in one direction in unison, the voltages between them are unchanged in magnitude, but the time phase of these voltages with respect to the field voltage will be changed. In this way the time phase of the brush voltages may be so shifted that they directly oppose the voltages supplying the field, or the voltages normally supplied to the brushes. This is referred to as the zero

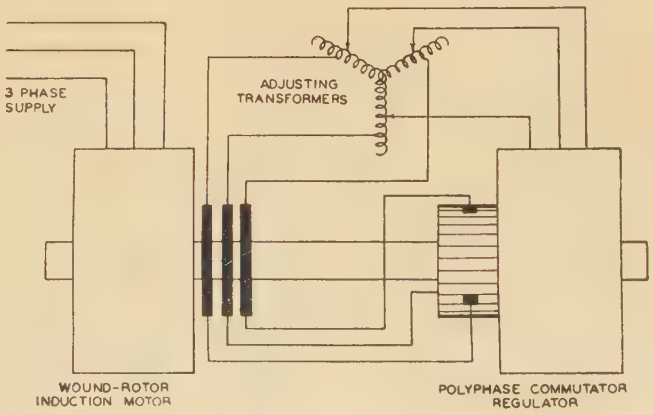

Figure 1. Complete circuit diagram of adjustable-speed drive

Paper 46-59, recommended by the AIEE committee on electric machinery for presentation at the AIEE winter convention, New York, N. Y., January 21–25, 1946. Manuscript submitted August 21, 1945; made available for printing December 4, 1945.

A. G. CONRAD is chairman, department of electrical engineering, Yale University, New Haven, Conn. F. E. BROOKS, JR., is assistant professor, department of electrical engineering, University of Texas, Austin, Tex. R. G. FELLERS is radio research engineer, Naval Research Laboratory, Washington, D. C.

brush position. If the effective turns ratio between the field and the armature is unity, that is, a given value of flux induces voltages of equal magnitude in both field and armature, and if the brushes are in the zero position, the voltage which appears at the brushes is equal and opposite to the voltage on the induction motor slip rings at standstill, which is the voltage applied to the stator winding of the commutator machine.

If the stator of the regulator is supplied with balanced alternating voltages, and the armature is rotated at some speed, N, with the brushes not connected to the line, the voltage appearing between them is still of the frequency applied to the field. The armature is divided into groups of conductors between adjacent brushes. Although at different instants different conductors may comprise these groups due to the rotation of the armature, nevertheless, the group as a unit is stationary, and the frequency which appears at the brushes is the frequency of the rotating field, regardless of the speed or direction of rotation of the armature.

This is the same as the operation of a d-c machine if an alternating voltage is applied to the shunt field. The voltage at the brushes would vary at the same frequency as the voltage applied to the field, independent of the rotation of the armature or the magnitude of the induced voltage. The magnitude of the electromotive force induced in the regulator armature is, however, proportional to the relative velocity of rotation of its synchronously revolving field and the rotor conductors. When the speed of the rotating field is N_s and the machine is rotating at a speed, N, in the same direction as the revolving field this voltage is $(N_s - N) \div N_s$ multiplied by the voltage induced in the armature at standstill. On the other hand, if the armature is rotating in the direction opposite to that of the revolving field, the voltage at the terminals is $(N_s + N)/N_s$ multiplied by the induced voltage at standstill.

In order to minimize the armature reactance of the regulating machine, a compensating winding is so placed on the stator that the magnetomotive force which it produces directly opposes that of the armature. The armature and the compensating winding carry the same current and if the effective number of turns of the two windings is the same, maximum compensation is accomplished. The only flux produced by the armature current is a leakage flux which may be interpreted as producing a reactance drop in the usual manner. It is this condition of compensation which will be considered henceforth. The magnetomotive force produced by the armature current is rotating at constant velocity, regardless of the armature speed. Likewise, the compensating winding produces a magnetomotive force which rotates in the same direction and at the same velocity as the armature magnetomotive force, but is directly opposed to it. For best compensation these two magnetomotive forces should be equal and opposite.

The compensating winding and armature are so connected that the voltages induced in them by the field flux are directly opposed. Since the two windings have the same effective number of turns, the voltages induced in them at standstill are equal and opposite. At any other speed the voltage induced in the compensating winding is the same, but that generated in the armature is changed as explained above. Let ϕ be the magnitude of the air-gap flux of the commutator machine and k be a constant involving number of turns, type of winding, and other quantities, and assume the armature to be rotating at speed N in the direction opposite to that of the rotating field. The voltage induced in the armature is then

$$\frac{N+N_s}{N_s} k\phi$$

That induced in the compensating winding is $k\phi$, and the voltage appearing at the terminals of the armature and compensating winding together is

$$E_a = \frac{N+N_s}{N_s} k\phi - k\phi = N\frac{k\phi}{N_s}$$

This shows that the electromotive force E_a appearing at the terminals of the armature and compensating winding together is directly proportional to the speed.

Since the machine is compensated, current flowing through the armature and compensating windings produces only leakage flux. Therefore the armature current induces no electromotive force in the field circuit. Then, with constant applied voltage and frequency the field current is the small, constant, exciting current, regardless of speed, load, or armature current of the machine.

The equivalent circuit of a single phase of the induction motor secondary and the regulator is illustrated in Figure 2. In this diagram and throughout this paper R_2 and X_2 represent the resistance and leakage reactance of one phase of the induction-motor secondary winding at standstill, R_a and X_a represent the corresponding quantities for the circuit comprising the armature and compensating winding of the regulating machine, and

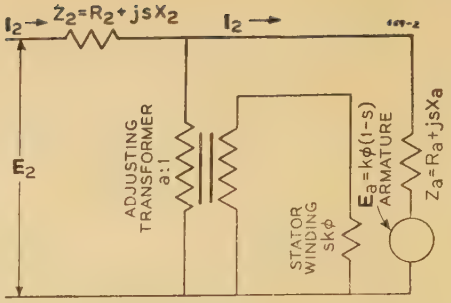

Figure 2. Equivalent circuit of a single phase of the drive

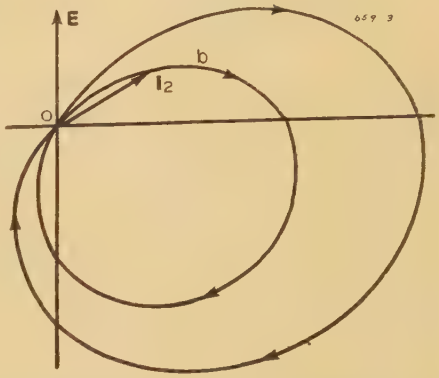

Figure 3. Locus of load component of secondary current of induction motor according to the exact theory

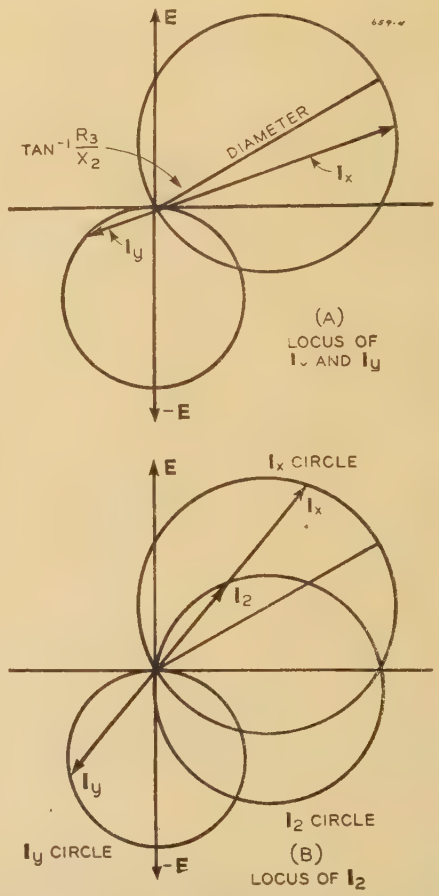

Figure 4. Loci of components of secondary current of induction motor

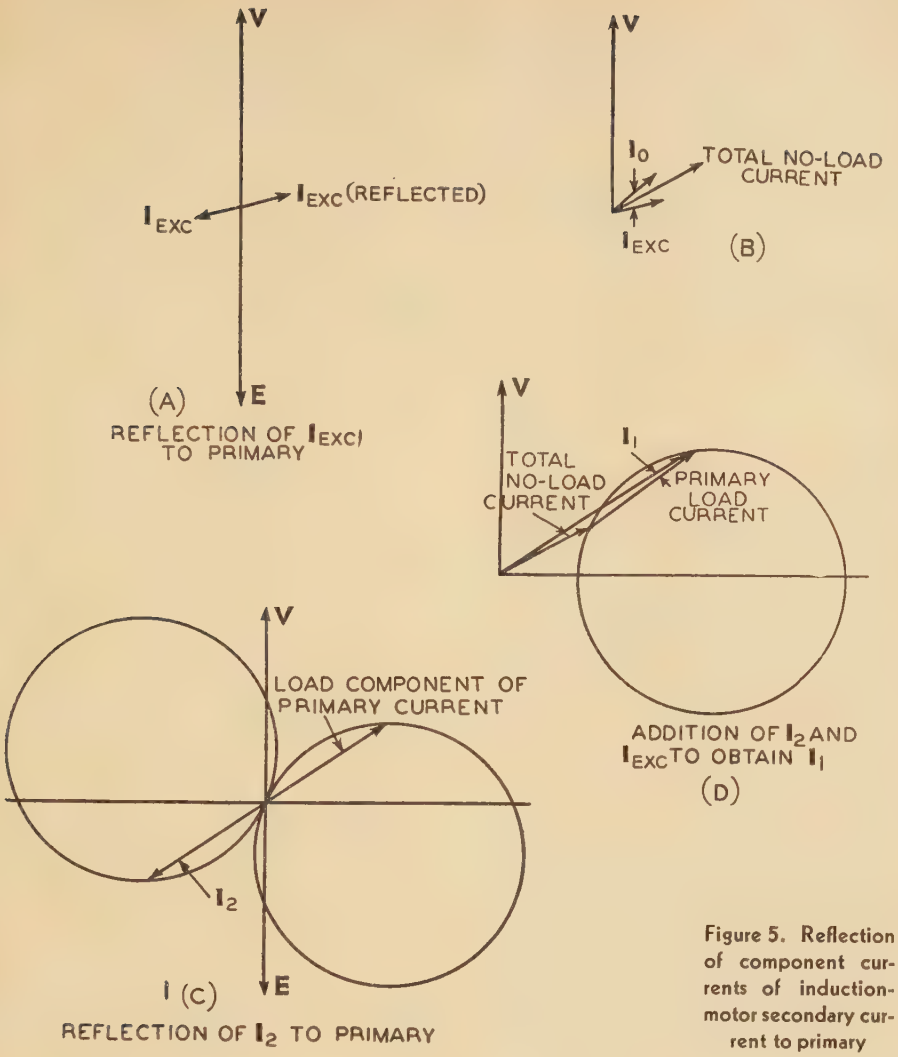

Figure 5. Reflection of component currents of induction-motor secondary current to primary

E_2 represents the voltage induced in one phase of the secondary of the induction motor. E_s is the voltage induced in one phase of the regulator field winding and it is proportional to the value of flux in the air gap and the frequency of the applied voltage. This applied voltage is of slip frequency, since it is the slip-ring voltage of the induction motor. Therefore, $E_s = k\phi s$, where s is the slip of the induction motor, ϕ is the air-gap flux of the polyphase commutator regulator, and k is a constant involving the number of turns, winding, and other factors, of the commutator regulator. The same flux generates the voltage in the armature, and if the armature is assumed to possess the same number of turns as the shunt field, the only difference between the expression for E_a, the armature circuit induced voltage, and E_s is in the manner in which slip occurs. It has been mentioned previously that the voltage appearing at the armature terminals is directly proportional to the speed of the machine, and therefore, $E_a = k\phi(1 - s)$.

By neglecting the effect of exciting current of the commutator machine flowing through the induction-motor secondary, making $Z_2 = R_2 + jsX_2$, $Z_a = R_a + jsX_a$, and letting a be the turns ratio of the transformer in the field circuit, the following circuit equations are obtained:

$$\boldsymbol{E}_2 - \boldsymbol{I}_2(Z_2 + Z_a) = (1-s)k\phi \quad (1)$$

$$\boldsymbol{E}_2 - \boldsymbol{I}_2 Z_2 = ask\phi \quad (2)$$

If the voltage induced in one phase of the induction-motor rotor at standstill is E, then E_2 is equal to sE and:

$$\boldsymbol{I}_2 = \frac{s^2(a+1)\boldsymbol{E} - s\boldsymbol{E}}{(a+1)sZ_2 - Z_2 + asZ_a} \quad (3)$$

If the load component of the secondary current of the induction motor is calculated according to equation 3 for different values of slip, the locus of the extremity of the current vector with respect to the voltage $\boldsymbol{E}$ is of the form indicated by the curve in Figure 3. The operating range as a motor is indicated by the segment *ob* of the inner loop, where *o* represents the no-load point and *b* the standstill point. Although theoretically correct, this locus possesses the disadvantage that all of the constants of both the induction motor and the commutator machine must be known in order to calculate it, and this computation must be carried out point by point as the locus is not a simple geometric figure.

If the voltage drop caused by the current flowing through the resistance of the secondary circuit of the induction motor is neglected when setting up the voltage equation for the stator circuit of the regulating machine, a circle locus defining the vector $\boldsymbol{I}_2$ may be obtained which is a very good approximation of the theoretical curve in the operating range. When this assumption is made the voltage equations for the motor secondary take the following form:

$$\boldsymbol{E}_2 - \boldsymbol{I}_2(Z_2 + Z_a) = (1-s)k\phi \quad (4)$$

$$\boldsymbol{E}_2 - j\boldsymbol{I}_2 sX_2 = ask\phi \quad (5)$$

When $s\boldsymbol{E}$ is substituted for $\boldsymbol{E}_2$ and the two equations are solved for $\boldsymbol{I}_2$, the following result is obtained:

$$\boldsymbol{I}_2 = \frac{(a+1)s\boldsymbol{E} - \boldsymbol{E}}{a(R_2+R_a) + jsa(X_2+X_a) + jsX_2 - jX_2} \quad (6)$$

For convenience, let $R_3 = a(R_2 + R_a)$ and $X_3 = a(X_2 + X_a) + X_2$. Then

$$\boldsymbol{I}_2 = \frac{s(a+1)\boldsymbol{E} - \boldsymbol{E}}{R_3 + j(sX_3 - X_2)}$$

By making use of the principle of superposition, the following component currents are obtained:

$$\boldsymbol{I}_2 = \boldsymbol{I}_x + \boldsymbol{I}_y \quad (7)$$

In which

$$\boldsymbol{I}_x = \frac{s(a+1)\boldsymbol{E}}{R_3 + j(sX_3 - X_2)}$$

and

$$\boldsymbol{I}_y = \frac{-\boldsymbol{E}}{R_3 + j(sX_3 - X_2)}$$

The currents $\boldsymbol{I}_x$ and $\boldsymbol{I}_y$ are always in time phase opposition. They may be considered as currents flowing in the impedance, $R_3 + j(sX_3 - X_2)$, caused by voltages $s(a + 1)\ \boldsymbol{E}$ and $-\boldsymbol{E}$ which are in time phase opposition. The locus of the extremity of the current vector $\boldsymbol{I}_y$ referred to the voltage $\boldsymbol{E}$ for varying slip is a circle as shown in Figure 4A. Its diameter is vertical and has a magnitude $\boldsymbol{E}/R_3$. The locus of the extremity of the current vector $\boldsymbol{I}_x$ is also a circle as indicated in Figure 4A. Its diameter is

$$\frac{(a+1)\boldsymbol{E}}{X_3} \quad \frac{\sqrt{R_3^2 + X_2^2}}{R_3}$$

at an angle $\tan^{-1}(R_3/X_2)$ with the volt-

age vector $\boldsymbol{E}$. The derivation of magnitude and position of these circles is given in Appendix I. The locus of the extremity of the vector $\boldsymbol{I}_2$ obtained from equation 7 also is found to be a circle as illustrated in Figure 4B. The proof that it has a circle locus is presented in Appendix II.

All of this analysis has been carried out neglecting the exciting current of the polyphase commutator regulator and its associated transformer, which flows in the induction-motor secondary. This exciting current is directly proportional to the voltage applied to the field winding and inversely proportional to the frequency of this voltage. As the machines slow down due to increase in load, the slip increases and the frequency of the voltage applied to the regulator field increases proportionally. The voltage across the field winding increases also, though to a lesser degree because of the voltage drop $\boldsymbol{I}_2 Z_2$ in the secondary of the induction motor. Since the speed changes only slightly with load, the voltage and frequency applied to the field of the commutator machine are essentially unchanged. The changes which do occur produce tendencies in opposite directions. Therefore, for a given setting of the regulating transformer, the exciting current of the commutator machine remains substantially constant. It is assumed to remain entirely so in the analysis presented here.

The total secondary current of the induction motor is made up of the exciting current and the current $\boldsymbol{I}_2$ just obtained. The magnitude and direction of the current in the primary winding of the induction motor resulting from these two secondary currents can be determined by reflecting them separately as vectors to the primary vector diagram. This procedure is indicated in Figure 5. The exciting current is reflected first and combined with the exciting current of the induction motor itself to give the total exciting current of the drive as shown in Figure 5B. The load component $\boldsymbol{I}_2$, of the secondary current when reflected to the primary winding produces a primary load component of current having a circle locus differing in magnitude from the secondary circle locus by the turns ratio of the motor as indicated in Figure 5C. Thus the primary current is the sum of the three components and is defined by a circle locus also. This is illustrated in Figures 5D and 6.

The characteristics of the drive may be predicted from the circle diagram of the input current.

The speed of the drive can be obtained from relations of slip to the current $\boldsymbol{I}_x$ in the following equation in which the resistance and leakage reactance of the induction motor primary are included.

$$\boldsymbol{I}_x = \frac{\boldsymbol{V}}{R_1 + \frac{R_3}{(a+1)s} + jX_1 + \frac{jX_3}{(a+1)} - \frac{jX_2}{(a+1)s}} \tag{8}$$

For the sake of convenience, let

$$\frac{R_3}{(a+1)} = R_0, \quad \frac{X_2}{(a+1)} = X_0, \text{ and}$$

$$X_1 + \frac{X_3}{(a+1)} = X_4$$

Then

$$\boldsymbol{I}_x = \frac{\boldsymbol{V}}{\frac{R_0}{s} + R_1 + jX_4 - \frac{jX_0}{s}} \tag{9}$$

The slip can now be obtained as follows. For a given current *oe*, as represented on Figure 7, the phase angle with respect to the voltage is

$$\tan^{-1}\theta = \frac{(sX_4 - X_0)}{(sR_1 + R_0)}$$

For infinite slip tan $\theta = X_4/R_1$. An arbitrary point on the vertical axis, such as *a* in Figure 7 is selected. The line *ab* is drawn at the angle γ with the horizontal such that tan $\gamma = R_1/X_4$. The $\boldsymbol{I}_x$ vector is tangent to its circle for the condition of zero slip. This line is extended to give the point *d*, and the standstill value of $\boldsymbol{I}_x$ is also extended until it intersects *ab* at *f*. The length *db* is then directly proportional to the slip. The line segment *df* is divided into 100 parts. Slip corresponding to any load current may be obtained by extending the corresponding $\boldsymbol{I}_x$ vector until it intersects this line and reading the slip directly. Proof of the validity of this procedure is found in Appendix III.

The power loss associated with the no-load current is assumed to remain constant for all values of load, just as is done in the treatment of the 2-element induction motor. This power loss is represented by the product of the in-phase component of the no-load current and the phase voltage.

Having determined the slip and the corresponding speed from the construction shown in Figure 7, the other characteristics may be determined by constructing the diagram for the motor shown in Figure 6. In this diagram (Figure 6) the load component of primary current is *ob*, and the copper loss for the current *ob* = (loss for *oc*)$(ob/oc)^2$, where *oc* is the load component of primary current for the blocked rotor condition. If the loss

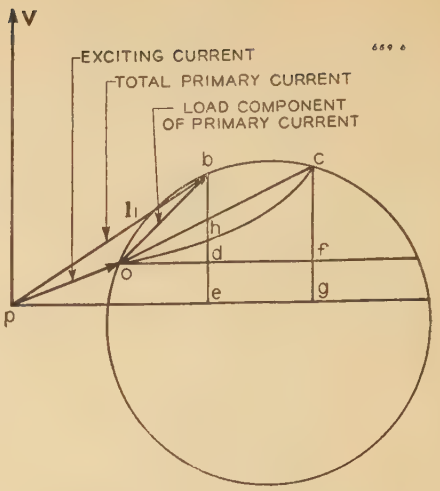

Figure 6. Locus of primary current

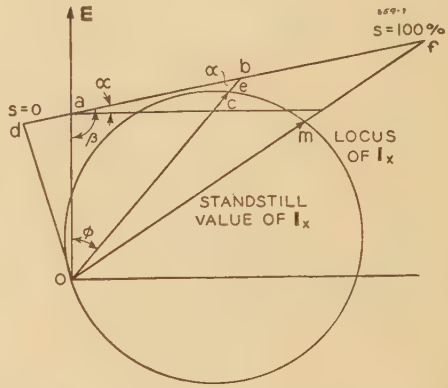

Figure 7. Determination of speed from circle diagram

for *oc* is known, the copper loss of the drive can be evaluated for all values of the load component of the current $\boldsymbol{I}_1$, and the curve *ohc* constructed such that the current *dh* when multiplied by the voltage, $\boldsymbol{V}$, gives the copper loss caused by the current *ob*. Similarly other points on the curve can be obtained for different values of input current.

The different quantities for the drive now can be obtained corresponding to any value of current $\boldsymbol{I}_1$.

1. Input = $(be)\boldsymbol{V}$ watts per phase
2. Output = $(bh)\boldsymbol{V}$ watts per phase
3. Iron loss, friction, and windage = $(de)\boldsymbol{V}$ watts per phase
4. Copper loss = $(hd)\boldsymbol{V}$ watts per phase
5. Efficiency = $\frac{(bh)}{(be)} \times 100$ per cent
6. Power factor = $\frac{(be)}{(pb)} \times 100$ per cent

All of these letters refer to Figure 6. The slip may be obtained from Figure 7.

7. Slip = $\left(\frac{db}{df}\right) \times 100$ per cent

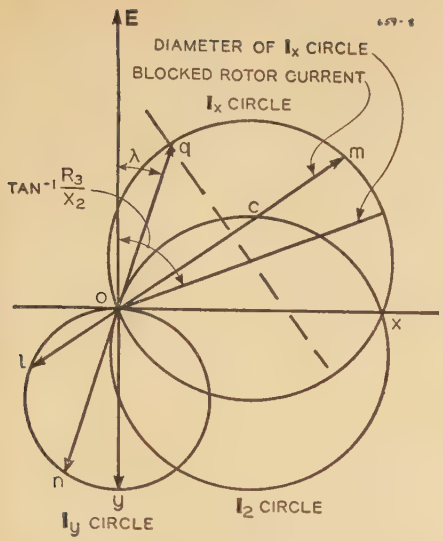

Figure 8. Construction of approximate circle current locus

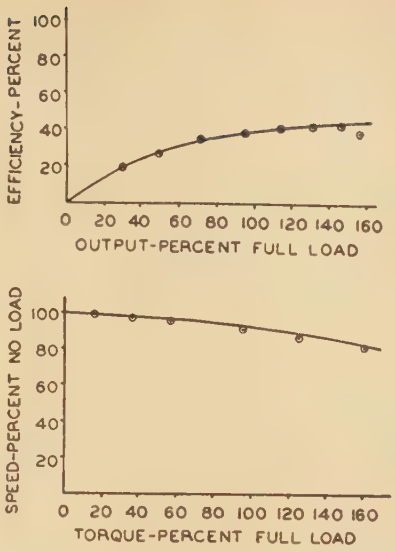

Figure 10. Operating characteristics of the adjustable-speed drive

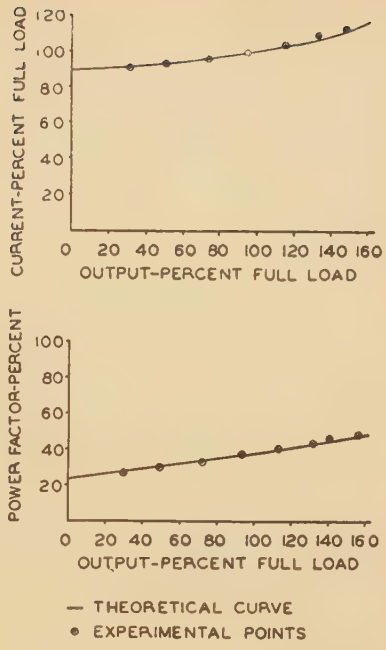

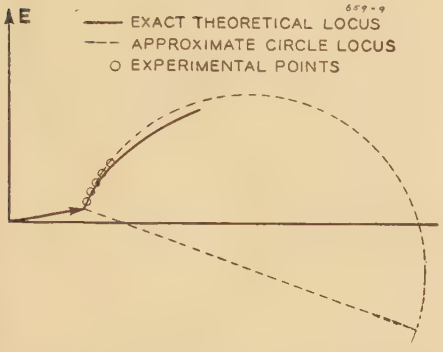

Figure 9. Input current loci of the drive according to both exact and approximate theories, and experimental points

8. Speed $= \left(1-\frac{db}{df}\right) \times$ synchronous speed

9. Torque = (horsepower output) $\times \frac{33{,}000}{2\pi N}$

On the basis of these expressions a complete set of characteristics can be predicted.

Experimental Results

In order to verify the theory thus far presented a complete set of tests was made upon a drive consisting of a 4-pole 5-horsepower wound-rotor induction motor and a polyphase commutator regulator of approximately 2-horsepower rating. The brushes of the regulator were so adjusted that the voltage appearing between them was directly opposed to the voltage applied to the primary of the adjustable transformer in its field circuit.

The method employed to obtain the locus of primary current involves a determination of (*a*) no-load voltage, current, and power input to the induction motor, (*b*) the blocked-rotor current, voltage, and input power taken both in the primary of the induction motor and in the armature circuit of the commutator machine, and (*c*) the determination of the voltage ratio *a*. Reduced voltages can be used to obtain data for determining blocked-rotor inputs at rated voltage. By making use of equation 7 for the standstill condition, and the experimentally determined value of *a*, the blocked-rotor current *om* of the I_x circle may be calculated from the blocked-rotor current *oc* of the primary current locus (see Figure 8). Likewise the blocked-rotor current *ol* of the I_y circle is determined.

The slip for which the component currents I_x and I_y are equal in magnitude can be obtained from equation 7. This value is found to be

$$s = \frac{1}{a+1}$$

Substituting this value of slip into the expression for I_x, it is then found that these two currents are equal when

$$I_x = \frac{E}{R_3 + j\left(\frac{X_3}{a+1} - X_2\right)}$$

Substituting the real value for X_3 (see list of symbols), it is found that this current has a power factor angle λ with respect to the stator voltage E such that

$$\tan \lambda = \frac{aX_a}{(a+1)R_3}$$

Since the diameter of I_y circle is determined in direction and the point *l* is now known, the I_y circle can be constructed. The diameter of this circle is E/R_3 in length. The resistance R_3 is equal to E divided by the current *oy*. The value of X_a is obtained from the blocked-rotor readings taken on the regulator. These values can be used to determine the angle λ. This angle and the I_y circle determine the direction and magnitude of the current *on* which was specified as being equal to and opposite to a current vector *oq* having its extremity on the I_x circle. The points *o*, *q*, and *m* determine the I_x circle. The intersection of the I_x circle with the horizontal axis at *x* is a point on the I_2 circle. The points *o*, *c*, and *x* determine the location of the I_2 circle.

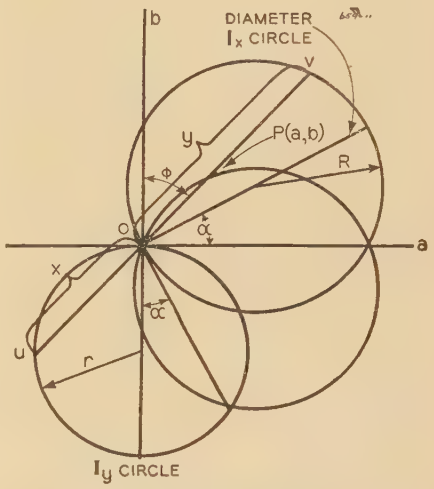

Figure 11. Proof that the terminus of the I_2 vector has a circle locus

The theoretically accurate locus, the approximate circle, and the experimental points are shown in Figure 9. Complete

characteristics were predicted on the basis of this circle, making use of the method devised in the discussion of the theory. These calculated results were in quite good agreement with the experimentally measured points. Characteristics are shown in Figure 10.

Conclusions

From the current loci it is evident that the power factor of experimental points is slightly higher than that of the theoretical locus. The explanation for this is as follows. It was assumed that the exciting current of the commutator machine was constant. Actually, it decreases with load because the frequency of the voltage impressed on the regulator field increases, thereby increasing the field reactance as the drive slows down. The field voltage, however, was found to be substantially constant with change in speed because of the effect of the voltage drop due to the impedance in the induction-motor secondary winding. This would cause the exciting current of the regulator to be slightly smaller than was originally assumed.

Reference to equations 3 and 7 shows that the impedance used in the approximate theory has a slightly higher power factor than that of the exact expression. This explains why the theoretically less accurate curve is in better agreement with experimental results than that obtained from the more exact theory.

Other errors present in the theory here presented are the statements that the loss associated with the no-load current is constant, regardless of load, and that the machine impedances are constant, independent of current. Both of these errors are inherent in normal induction motor theory.

The polyphase commutator regulator was of considerably lower power rating than the induction motor and hence possessed a higher armature resistance than was desirable. In order to load the induction motor fully, it was necessary to send currents through the armature of this machine considerably in excess of its normal current capacity. This resulted in abnormally high copper loss and the correspondingly low efficiencies observed.

It will be observed that the voltage impressed on the commutator machine is only a fraction of the voltage rating of the induction motor secondary, this fraction being the per cent slip at full load. The current capacity of the regulator, however, should be equal to that of the induction motor secondary winding, and therefore its kilovolt-ampere rating is the product of full-load slip and the rating of the induction motor. A drive designed to operate between synchronous speed and 50 per cent slip would require a commutator machine twice as large as one operating between synchronous speed and 25 per cent slip. For this reason the drive normally employed is a double-range system operating between plus 25 per cent slip and minus 25 per cent slip, rather than between synchronous speed and plus 50 per cent slip. This requires an ohmic drop exciter for passing through synchronism.

The excellent agreement of experimental results with those based on the theory presented in this paper indicates the theory to be sound. The method presented here may be used to obtain from no-load tests or design data the operating characteristics of the drive employing the polyphase commutator regulator. Results have shown the accuracy achieved to be high.

Appendix I. Derivation of Position and Magnitude of the Circle Locus of I_x for the Compensated Commutator Machine

$$I_x=\frac{s(a+1)E}{R_3+j(sX_3-X_2)}=\frac{s(a+1)E}{\sqrt{R_3^2+(sX_3-X_2)^2}}$$

This is readily recognized as the equation of a circle when it is written

$$I_x=\frac{(a+1)E}{\frac{R_3}{s}+j\left(X_3-\frac{X_2}{s}\right)}$$

The diameter of the circle is the maximum value which I_x attains. In order to obtain the value of slip for which I_x is a maximum, this expression is differentiated with respect to s and equated to zero.

$$\frac{dI_x}{ds}=\frac{\left[\sqrt{R_3^2+(sX_3-X_2)^2}(a+1)E-s(a+1)\times E[R_3^2+(sX_3-X_2)^2]^{-1/2}(sX_3-X_2)X_3\right]}{R_3^2+(sX_3-X_2)^2}$$

Multiplying through by

$$[R_3^2+(sX_3-X_2)^2]^{1/2}$$

and clearing fractions gives

$$R_3^2+(sX_3-X_2)^2-sX_3(sX_3-X_2)=0$$

Simplifying and solving for s yields

$$s=\frac{R_3^2+X_2^2}{X_3X_2}$$

Substitute this in the expression for I_x.

$$\text{Max } I_x=\frac{R_3^2+X_2^2}{X_3X_2}\cdot\frac{(a+1)E}{\sqrt{R_3^2+\left(\frac{R_3^2+X_2^2}{X_2}-X_2\right)^2}}$$

Multiply through by X_2 and simplify.

$$\text{Max } I_x=\frac{(a+1)E}{X_3}\cdot\frac{\sqrt{R_3^2+X_2^2}}{R_3}$$

The tangent of the angle which the diameter makes with the voltage is obtained from the following expression:

$$\tan\psi=\frac{sX_3-X_2}{R_3}$$

Substitute in the value of s for maximum I_x.

$$\tan\psi=\frac{\frac{R_3^2+X_2^2}{X_2}-X_2}{R_2}=\frac{R_3}{X_2}$$

Appendix II. Proof That the Combination of the I_x and I_y Circles Is Also a Circle

Employ a as the horizontal co-ordinate and b as the vertical co-ordinate in Figure 11.

Point P is obtained by extending the chord ov of the I_x circle until it intersects the I_y circle at u. The distance $uo=x$ is laid off from v along ov to obtain P. The locus of P is to be proved a circle.

α = angle which diameter of I_x circle makes with horizontal
r = radius of I_y circle
R = radius of I_x circle
d = diameter of I_y circle
D = diameter of I_x circle

From the figure for point P:

$$a=(y-x)\sin\theta$$
$$b=(y-x)\cos\theta$$
$$x=d\cos\theta$$
$$y=D(\sin\theta\cos\alpha+\cos\theta\sin\alpha)$$
$$y-x=D\sin\theta\cos\alpha+\cos\theta(D\sin\alpha-d)$$

Substitute in the expression for a and b the value of $y-x$. This yields:

$$a=D\sin^2\theta\cos\alpha+\sin\theta\cos\theta(D\sin\alpha-d) \quad (10)$$

$$b=D\sin\theta\cos\theta\cos\alpha+\cos^2\theta(D\sin\alpha-d) \quad (11)$$

Let:

$$D\sin\alpha-d=m$$

From equation 10

$$\sin\theta\cos\theta=\frac{a-D\sin^2\theta\cos\alpha}{m}$$

Substitute this into equation 11.

$$b=\frac{Da}{m}\cos\alpha-\frac{D^2}{m}\cos^2\alpha\sin^2\theta+m\cos^2\theta$$

Now

$$\cos^2\theta=1-\sin^2\theta$$

$$b=\frac{Da}{m}\cos\alpha-\left(\frac{D^2\cos^2\alpha+m^2}{m}\right)\sin^2\theta+m$$

$$\sin^2\theta=\frac{\frac{Da\cos\alpha}{m}+m-b}{\frac{D^2\cos^2\alpha}{m}+m}=n^2 \quad (12)$$

letting $n=\sin\theta$. Rewriting equation 10 gives

$$a=D\sin^2\theta\cos\alpha+m\sin\theta\sqrt{1-\sin^2\theta}$$

Substitute $n=\sin\theta$.

$$a=Dn^2\cos\alpha+nm\sqrt{1-n^2}$$

$$\sqrt{1-n^2}=\frac{a-Dn^2\cos\alpha}{mn}=\frac{a}{mn}-\frac{Dn}{m}\cos\alpha$$

Eliminate the square root.

$$0=-m^2(1-n^2)+\frac{a^2}{n^2}+D^2n^2\times\cos^2\alpha-2aD\cos\alpha$$

Substitute for n^2 from equation 12.

$$\frac{\dfrac{Da\cos\alpha}{m}+m-b}{\dfrac{D^2\cos^2\alpha}{m}+m}$$

Then

$$-m^2\frac{\dfrac{D^2\cos^2\alpha}{m}-\dfrac{Da\cos\alpha}{m}+b}{\dfrac{D^2\cos^2\alpha}{m}+m}+a^2\frac{\dfrac{D^2\cos^2\alpha}{m}+m}{\dfrac{Da\cos\alpha}{m}+m-b}+\frac{D^2\cos^2\alpha\left(\dfrac{Da\cos\alpha}{m}+m-b\right)}{\dfrac{D^2\cos^2\alpha}{m}+m}-2aD\cos\alpha=0$$

And

$$\frac{\left[\begin{matrix}-D^2m^2\cos^2\alpha+aDm^2\cos\alpha-bm^3+\\ aD^3\cos^3\alpha+D^2m^2\cos^2\alpha-bD^2m\cos^2\alpha\end{matrix}\right]}{D^2\cos^2\alpha+m^2}+\frac{a^2D^2\cos^2\alpha+a^2m^2}{aD\cos\alpha+m^2-bm}-2aD\cos\alpha=0$$

Clear fractions:

$$\begin{aligned}&a^2D^2m^2\cos^2\alpha-abDm^3\cos\alpha+a^2D^4\times\\&\cos^4\alpha-abD^3m\cos^3\alpha+aDm^4\times\\&\cos\alpha-bm^5+aD^3m^2\cos^3\alpha-bD^2m^3\times\\&\cos^2\alpha-abDm^3\cos a+b^2m^4-abD^3m\times\\&\cos^3\alpha+b^2D^2m^2\cos^2\alpha+a^2D^4\times\\&\cos^4\alpha+a^2D^2m^2\cos^2\alpha+a^2D^2m^2\times\\&\cos^2\alpha+a^2m^4-2a^2D^4\cos^4\alpha-2aD^3m^2\times\\&\cos^3\alpha+2abD^3m\cos^3\alpha-2a^2D^2m^2\times\\&\cos^2\alpha-2aDm^4\cos\alpha+2abDm^3\times\\&\cos\alpha=0\end{aligned}$$

$$\begin{aligned}&a^2(D^2m^2\cos^2\alpha+m^4)-a(D^3m^2\cos^3\alpha+Dm^4\times\\&\cos\alpha)+b^2(D^2m^2\cos^2\alpha+m^4)-b\times\\&(D^2m^3\cos^2\alpha+m^5)=0\end{aligned}$$

$$a^2-a\left[\frac{D\cos\alpha(D^2\cos^2\alpha+m^2)}{D^2\cos^2\alpha+m^2}\right]+b^2-b\left[m\frac{D^2\cos^2\alpha+m^2}{D^2\cos^2\alpha+m^2}\right]=0$$

$$\left(a^2-aD\cos\alpha+\frac{D^2}{4}\cos^2\alpha\right)+\left(b^2-bm+\frac{m^2}{4}\right)=\frac{D^2}{4}\cos^2\alpha+\frac{m^2}{4}$$

This is

$$\left(a-\frac{D}{2}\cos\alpha\right)^2+\left(b-\frac{m}{2}\right)^2=\frac{D^2\cos^2\alpha+m^2}{4}$$

This is the equation of a circle with center at $D\cos\alpha/2$, $m/2$.

Appendix III. Proof That the Line *db* of Figure 7 Is Proportional to Slip

The line ab of Figure 7 is drawn at an angle γ with the horizontal such that $\tan\gamma=R_1/X_4$. Point b is the intersection of the I_x vector with the line making the angle γ with the horizontal. Using the notation of Figure 7, the following equality may be written:

By the law of sines

$$\frac{ab}{\sin\theta}=\frac{ao}{\sin\alpha_1}$$

$\alpha_1=\sphericalangle abo$

$\beta=\sphericalangle oab$

$\alpha_1=180^\circ-(\beta+\theta)$

$\sin[180^\circ-(\beta+\theta)]=\sin(\beta+\theta)$

$$ab=\frac{ao\sin\theta}{\sin(\beta+\theta)}=\frac{ao\sin\theta}{\sin\theta\cos\beta+\cos\theta\sin\beta}$$

Divide through by $\cos\theta$

$$ab=ao\tan\theta\frac{1}{\tan\theta\cos\beta+\sin\beta}$$

Now

$$\cos\beta=-\sin\gamma,\quad \sin\beta=\cos\gamma$$

$$ab=ao\tan\theta\frac{1}{-\tan\theta\sin\gamma+\cos\gamma}$$

The functions of theta and gamma are

$$\tan\theta=\frac{X_4-\dfrac{X_0}{s}}{R_1+\dfrac{R_0}{s}}\qquad \sin\gamma=\frac{R_1}{\sqrt{R_1^2+X_4^2}}$$

$$\tan\gamma=\frac{R_1}{X_4}\qquad \cos\gamma=\frac{X_4}{\sqrt{R_1^2+X_4^2}}$$

When these values are substituted in the expression for ab, the following result is obtained:

$$ab=ao\frac{X_4-\dfrac{X_0}{s}}{R_1+\dfrac{R_0}{s}}\times\frac{1}{\dfrac{X_4-\dfrac{X_0}{s}}{R_1+\dfrac{R_0}{s}}\cdot\dfrac{(-R_1)}{\sqrt{R_1^2+X_4^2}}+\dfrac{X_4}{\sqrt{R_1^2+X_4^2}}}$$

Clearing fractions yields

$$ab=ao(sX_4-X_0)\frac{\sqrt{R_1^2+X_4^2}}{R_1X_0+X_4R_0}$$

At zero slip ob of Figure 7 is tangent to the I_x circle. Under these conditions ab is equal to ad. The magnitude of ab for zero slip is

$$ab=ad=aoX_0\frac{\sqrt{R_1^2+X_4^2}}{R_1X_0+X_4R_0}$$

Now

$$db=ab+da=ao(sX_a-X_0+X_0)\frac{\sqrt{R_1^2+X_4^2}}{R_1X_0+X_4R_0}$$

$$db=ao(sX_4)\frac{\sqrt{R_1^2+X_4^2}}{R_1X_0+X_4R_0}$$

The length db, then, is directly proportional to the slip.

Appendix IV. List of Symbols

a = ratio of number of turns in primary to number of turns in secondary of adjusting transformer in field circuit of polyphase commutator regulator

$\boldsymbol{E}$ = the voltage induced in one phase of the induction motor secondary by the mutual flux at standstill

$\boldsymbol{E}_1$ = the voltage induced in one phase of the armature winding of the compensated commutator regulator by the mutual flux

$\boldsymbol{E}_2$ = the voltage induced in one phase of the induction motor secondary by the mutual flux. It is $s\boldsymbol{E}$ where s is the slip

$\boldsymbol{E}_e$ = the effective generated voltage per phase appearing at the terminals of the armature and compensating winding together for the compensated commutator machine. It is $\boldsymbol{E}_1-\boldsymbol{E}_c=k\phi(1-s)$

$\boldsymbol{E}_c$ = the voltage induced in one phase of the compensating winding of the commutator machine by the mutual flux

$\boldsymbol{E}_s$ = the voltage induced in one phase of the stator winding of the commutator machine by the mutual flux. $\boldsymbol{E}_s=k\phi s$

$\boldsymbol{I}_1$ = total primary current of induction motor

$\boldsymbol{I}_2$ = total load component of secondary current of induction motor

$\boldsymbol{I}_a$ = armature current of polyphase commutator regulator

$\boldsymbol{I}_{exc}$ = exciting current of polyphase commutator regulator

$\boldsymbol{I}_o$ = no-load current of induction motor alone

$\boldsymbol{I}_x$ = component of $\boldsymbol{I}_2$ due to $s(a+1)\boldsymbol{E}$ for the compensated drive

$\boldsymbol{I}_y$ = component of $\boldsymbol{I}_2$ due to $-\boldsymbol{E}$ for the compensated drive

N = speed of drive in revolutions per minute

N_o = no-load speed of drive in revolutions per minute

N_s = synchronous speed of drive in revolutions per minute

Formulas for the Inductance of Coaxial Busses Comprised of Square Tubular Conductors

HENRY PETER MESSINGER
ASSOCIATE AIEE

THOMAS JAMES HIGGINS
ASSOCIATE AIEE

BY virtue of its axial symmetric geometry, the coaxial tubular bus possesses certain very desirable electrical and mechanical characteristics. Low inductance contributes to good voltage regulation. Reduced skin and proximity effects minimize line losses and average temperature rise under load. Axial-symmetric distribution of skin and proximity effects reduces current density distortion and attendant hot-spot concentrations, hence enables a greater current rating for a specified maximum copper temperature. As electromagnetic forces between conductors are eliminated largely, mechanical bracing against short-circuit forces correspondingly can be reduced. The nested conductors require less space for installation and a smaller supporting structure than they would if arranged side by side.

Yet, despite these desirable characteristics, the paucity of published descriptions of actual installations[1,2,3] indicates that few coaxial busses have been constructed to date. However, until recently factory distribution loads at frequencies greater than 60 cycles were uncommon. Again, most heavy 60-cycle loads were supplied over relatively short distances. As these conditions are such that satisfactory 60-cycle operation can be obtained with the more conventional, though less electrically effective, construction of conductors placed side by side, this limited use of coaxial busses is not surprising. Now, however, by virtue of manufacturing procedures and techniques developed during the war, the bus designer is faced with the necessity of designing heavy distribution busses which are not only long but also are to operate at frequencies of several hundred cycles and higher. But, the electrical characteristics of the coaxial bus are such that it is especially suited to satisfactory operation under either or both of these conditions. Hence it is to be expected that in the near future coaxial busses will find greater use than they have hitherto.

At present, coaxial busses are constructed of circular tubular conductor, of square tubular conductor, and of structural tubular conductor comprised of two slightly separated channels or angles placed flange to flange. To predetermine the operating characteristics of these busses requires knowledge of the a-c resistance, the a-c inductance, the copper temperature under load, and the mechanical forces exerted during short-circuit. Formulas[4] for calculating all four of these quantities are available for busses comprised of a circular tubular conductor. But for a square or structural tubular conductor, though formulas are available for calculating the a-c resistance,[5,6] the copper temperature,[6] and the short-circuit forces,[4] formulas for calculating the a-c inductance, often the determining factor in the design of the bus, are not available.

Such formulas are derived in this paper, it being assumed that the conductors are nonmagnetic, of such lengths that end effects are negligible, of uniform thickness, right-cornered, and carry currents distributed uniformly over their cross sections. Of these five conditions, the first three are satisfied in practice. The fourth, however, though essential to tractable analysis, is usually not true in practice. Square tubes, channels, and angles, drawn, rolled, bent, or otherwise formed in one piece, have rounded edges, but the error introduced by neglecting the rounded edges is small. Commonly, the result obtained, though a bit low, is yet sufficiently accurate for the work in hand. In any case, the incremental inductance associated with the rounded edges can be approximated closely by a simple semi-empirical formula derived by Dwight and Wang.[7] Finally, though skin and proximity effects render the current density over the cross sections of the conductors slightly nonuniform, the analysis in "Corrections for Rounded Edges and for Skin and Proximity Effects," later in this paper, indicates that at power frequencies the a-c inductance is practically identical with the d-c inductance.

Inasmuch as these five postulates are granted as consistent with practice, derivations of the desired formulas, though lengthy, are not difficult. The

R_1 = primary resistance per phase of induction motor

R_2 = secondary resistance per phase of induction motor

$R_3 = a(R_2 + R_a)$

$R_o = \dfrac{R_3}{(a+1)}$

s = slip measured from zero at synchronous speed

X_1 = primary leakage reactance per phase of induction motor at standstill

X_2 = secondary leakage reactance per phase of induction motor at standstill

$X_3 = a(X_2 + X_a) + X_2$

$X_4 = \dfrac{X_3}{(a+1)} + X_1$

X_a = leakage reactance per phase of armature of polyphase commutator regulator with drive at standstill

$X_o = \dfrac{X_2}{(a+1)}$

V = applied voltage per phase of induction motor

Z_2 = impedance per phase of induction motor secondary

Z_a = impedance per phase of armature of polyphase commutator regulator

α = angle which line tangent to I_x circle at origin makes with voltage vector

$\beta = \tan^{-1} - \dfrac{X_4}{R_1}$

$\gamma = \tan^{-1} \dfrac{R_1}{X_4}$

ϕ = total air-gap flux of polyphase commutator regulator

ψ = angle which the diameter of the I_x circle makes with the voltage vector = $\tan^{-1} \dfrac{R_3}{X_2}$

$\lambda = \tan^{-1} = \dfrac{aXa}{(a+1)R_3}$

Paper 46-37, recommended by the AIEE committee on basic sciences for presentation at the AIEE winter convention, New York, N. Y., January 21–25, 1946. Manuscript submitted September 18, 1945; made available for printing December 10, 1945.

HENRY PETER MESSINGER is an electrical engineer in the cyclotron laboratory, Massachusetts Institute of Technology, Cambridge, Mass. THOMAS JAMES HIGGINS is an associate professor of electrical engineering, Illinois Institute of Technology, Chicago, Ill.

This paper is based upon a thesis supervised by Professor Higgins and submitted by Mr. Messinger to the faculty of the Illinois Institute of Technology in February 1946 in partial fulfillment of the requirements for the degree of master of science in electrical engineering.

conductor cross sections can be considered in various fashions as combinations of parallel-sided square areas. By virtue of geometric mean distance theory, the inductance can be expressed in terms of the self and mutual geometric mean distances of these square areas. These geometric mean distances can be calculated from known formulas. Accordingly, determination of the inductance as a function of the parameters defining the geometry of the bus reduces, essentially, to specific determination of the geometric mean distances involved and substitution of them in the general equation for the inductance.

The general formula comprises 36 terms. A simple approximate formula similarly derived, but on the assumption that the conductors can be considered as being indefinitely thin and hence having cross sections comprised of line segments, affords values sufficiently accurate for many design purposes. As a further convenience to numerical computation, this formula is epitomized in a single curve. Conductors which are indefinitely thin are limiting cases of conductors of finite thickness, a physical consideration which indicates that the approximate formula can be considered as a limiting case of the general formula. Analytical confirmation of this deduction provides a simultaneous check of the correctness of the general and approximate formulas.

The desired formulas, having been obtained and checked, are used as illustrated by calculation of the inductance of typical busses constructed of square tubular conductors. Changes in inductance resulting from rounded corners on the conductors and from skin and proximity effects are discussed in detail. Procedures for calculating the inductance of coaxial busses, constructed of channels or angles, are advanced. Illustratively, the inductance of a bus constructed of channels is calculated and found to be in good agreement with the experimentally determined value. Finally, procedure for calculating the inductance of polyphase coaxial busses, comprised of square tubular conductors, is outlined.

General Relationships

From well-known theory,[8,9] the inductance of a bus comprised of two long parallel cylindrical nonmagnetic conductors, each of an arbitrary cross section, is

$$L = 2 \log D_{ab}^2/D_{aa}D_{bb} \text{ abhenrys per centimeter of bus length} \quad (1)$$

where D_{aa} and D_{bb} are the self geometric mean distances, and D_{ab} is the mutual geometric mean distance of the conductor cross sections.

If each of the two conductors is constructed of several subconductors connected in parallel, m composing the conductor of a cross section S_a and n that of a cross section S_b, equation 1 can be written

$$L = -(2/I^2)\sum_{i=1}^{m+n}\sum_{j=1}^{m+n} w_i w_j S_i S_j \log D_{ij} \quad (2)$$

where I is the bus current; w_i the current density in the ith subconductor of the sectional area S_i, taken positive for current flow in one direction and negative for current flow in the opposite direction; and $D_{ij} \equiv D_{ji}$ is the geometric mean distance between areas S_i and S_j.

If $S_i = RS$ and $S_j = R'S'$ are two arbitrarily located parallel-sided rectangular areas (Figure 1), the mutual geometric mean distance is

$$S_i S_j \log D_{ij} = -(25/12)S_i S_j - (1/24)\times \sum_{p=1}^{4}\sum_{q=1}^{4}(-1)^{p+q}K(A_p, B_q) \quad (3)$$

where

$$K(A_p,B_q) = (A_p^4 - 6A_p^2B_q^2 + B_q^4)\times \log (A_p^2+B_q^2)^{1/2} - 4A_pB_q^3\times \tan^{-1}(A_p/B_q) - 4A_p^3B_q \tan^{-1}(B_q/A_p) \quad (4)$$

and

$$A_1 = |D+R+R'|,\ A_2 = |D+R,|\ A_3 = |D|,\ A_4 = |D+R'| \quad (5)$$

$$B_1 = |P+S+S'|,\ B_2 = |P+S|,\ B_3 = |P|,\ B_4 = |P+S'| \quad (6)$$

Derivation of the General Formula

Consider a bus comprised of two coaxial square tubular conductors (Figure 2). Each of the conductors can be considered as constructed of two subconductors: one of a full square cross section wherein current exists in the same direction as in the tubular conductor, the other of a smaller full square cross section having current in the opposite direction. Hence $m = n = 4$, and from equation 2

$$L = -(2/I^2)\sum_{i=1}^{4}\sum_{j=1}^{4} w_i w_j S_i S_j \log D_{ij} \quad (7)$$

By definition, $D_{ij} \equiv D_{ji}$. By inspection of Figure 2, $w_1 = -w_2 = I/(a^2-b^2)$ and $w_3 = -w_4 = -I/(c^2-d^2)$. Utilizing these relationships in equation 7 yields

$$L = [-2/(a^2-b^2)^2][S_1^2 \log D_{11} + S_2^2 \log D_{22} - 2S_1S_2 \log D_{12}] + [-2/(c^2-d^2)^2]\times [S_3^2 \log D_{33} + S_4^2 \log D_{44} - 2S_3S_4\times \log D_{34}] + [4/(a^2-b^2)(c^2-d^2)]\times [S_1S_3 \log D_{13} - S_1S_4 \log D_{14} - S_2S_3\times \log D_{23} + S_2S_4 \log D_{24}] \quad (8)$$

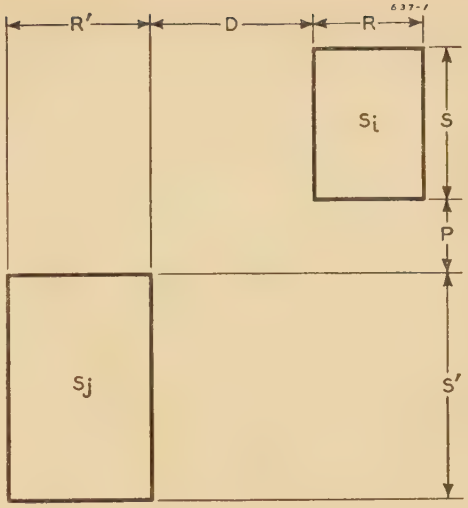

Figure 1

Determining the ten geometric mean distances in the right-hand member of equation 8 by use of equations 3 to 6, substituting appropriately in equation 8, and collecting terms (a detailed analysis appears in Appendix I) yields

$$\begin{aligned} L = {} & \{[-1/6(a^2-b^2)^2][12a^4 \log a + 12b^4\times \log b - (a-b)^4 \log (a-b) - (a+b)^4\times \log (a+b) + (a^4-6a^2b^2+b^4)\times \log (a^2+b^2) + 10(a^4+b^4) \log 2 + 8ab\times (a^2-b^2) \tan^{-1}(a-b)/(a+b) + \pi\times (a^2-b^2)(a-b)^2]\} + \{[-1/6(c^2-d^2)^2]\times [12c^4 \log c + 12d^4 \log d - (c-d)^4\times \log (c-d) - (c+d)^4 \log (c+d) + (c^4-6c^2d^2+d^4) \log (c^2+d^2) + 10(c^4+d^4) \log 2 + 8cd(c^2-d^2)\times \tan^{-1}(c-d)/(c+d) + \pi(c^2-d^2)\times (c-d)^2]\} + \{[-1/6(a^2-b^2)\times (c^2-d^2)][(a-d)^4 \log (a-d) + (a+d)^4 \log (a+d) - (a^4-6a^2d^2+d^4)\times \log (a^2+d^2) - (b-d)^4 \log (b-d) - (b+d)^4 \log (b+d) + (b^4-6b^2d^2+d^4)\times \log (b^2+d^2) - (a-c)^4 \log (a-c) - (a+c)^4 \log (a+c) + (a^4-6a^2c^2+c^4)\times \log (a^2+c^2) + (b-c)^4 \log (b-c) + (b+c)^4 \log (b+c) - (b^4-6b^2c^2+c^4)\times \log (b^2+c^2) - 8ad(a^2-d^2)\times \tan^{-1}(a-d)/(a+d) + 8bd(b^2-d^2)\times \tan^{-1}(b-d)/(b+d) + 8ac(a^2-c^2)\times \tan^{-1}(a-c)/(a+c) - 8bc(b^2-c^2)\times \tan^{-1}(b-c)/(b+c) - \pi(a^2-d^2)\times (a-d)^2 + \pi(b^2-d^2)(b-d)^2 + \pi(a^2-c^2)(a-c)^2 - \pi(b^2-c^2)(b-c)^2]\} \end{aligned} \quad (9)$$

This is the desired formula for the inductance of a single phase bus. Further, it enables calculation of the inductance of a polyphase bus as outlined in "Polyphase Coaxial Busses."

Corroboration of Equation 9

In yet another fashion, each square tubular conductor can be assumed as constructed of four subconductors, each of a rectangular cross section and having

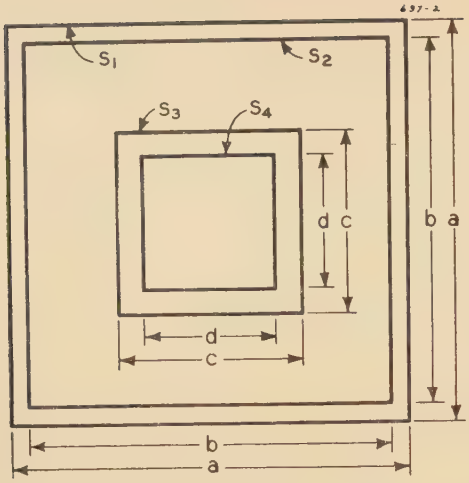

Figure 2

current in the same direction as in the tubular conductor (Figure 3). Hence $m=n=8$, and from equation 2

$$L=-(2/I^2)\sum_{i=1}^{8}\sum_{j=1}^{8}w_iw_jS_iS_j\log D_{ij} \qquad (10)$$

By definition, $D_{ij}\equiv D_{ji}$. By virtue of the geometric symmetries apparent in Figure 3, $D_{11}=D_{33}$, $D_{22}=D_{44}$, $D_{55}=D_{77}$, $D_{66}=D_{88}$, $D_{12}=D_{14}=D_{23}=D_{34}$, $D_{56}=D_{58}=D_{67}=D_{78}$, $D_{15}=D_{37}$, $D_{26}=D_{48}$, $D_{17}=D_{35}$, $D_{28}=D_{46}$, $D_{16}=D_{18}=D_{36}=D_{38}$, and $D_{25}=D_{27}=D_{45}=D_{47}$. Further, $S_1=S_3$, $S_2=S_4$, $S_5=S_7$, $S_6=S_8$; $w_1=w_2=w_3=w_4=I/-(a^2-b^2)$, and $w_5=w_6=w_7=w_8=-I/-(c^2-d^2)$. Utilizing these relationships in equation 10 yields

$$\begin{aligned}L=4\{&[-1/(a^2-b^2)^2][S_1^2(\log D_{11}+\log D_{13})+S_2^2(\log D_{22}+\log D_{24})+4S_1S_2\log D_{12}]+[-1/(c^2-d^2)^2]\times\\&[S_5^2(\log D_{55}+\log D_{57})+S_6^2(\log D_{66}+\log D_{68})+4S_5S_6\log D_{56}]+[2/(a^2-b^2)\times(c^2-d^2)][S_1S_5(\log D_{15}+\log D_{17})+S_2S_6(\log D_{26}+\log D_{28})+2S_1S_6\times\\&\log D_{16}+2S_2S_5\log D_{25}]\}\end{aligned} \qquad (11)$$

Determining the 16 geometric mean distances in the right-hand member of equation 11 as detailed in Appendix II, substituting appropriately in equation 11, and collecting terms yields, corroboratively, equation 9.

Obviously, this corroboration can be interpreted as a check of the correctness of the expressions, derived in Appendixes I and II, for the geometric mean distances indicated in equations 8 and 11.

Approximations to General Formula

The general formula for the inductance comprises 36 terms: 22 logarithmic, 6 arctangentic, and 8 algebraic. But by use of the proper tools (an electric calculating machine and the 15-place Work Projects Administration tables[10] of natural logarithms and arctangents), the computation incident to the calculation of the inductance of a given bus can be effected without difficulty. The computation, however, will be fairly lengthy. For this reason it is most desirable to have approximate formulas which enable rapid determination of values accurate enough for much (in some instances, all) of the computation incident to the final design of a bus.

A means of deriving such formulas stems from an earlier investigation[11] of the inductance of a coplanar bus comprised of rectangular tubular conductors. Therein, values of inductance calculated from the general formula were found to be in excellent agreement with values of inductance calculated from much simpler formulas derived by Dwight and Wang,[7] on the basis that the conductors are indefinitely thin. That is, they have cross sections comprised of line segments.

Consider, then, the cross section of each conductor as constructed of four line segments (Figure 4). Hence $m=n=8$, and from equation 8

$$L=-(2/I^2)\sum_{i=1}^{8}\sum_{j=1}^{8}w_iw_jS_iS_j\log D_{ij} \qquad (12)$$

By definition, $D_{ij}\equiv D_{ji}$. By virtue of the geometric symmetries apparent in Figure 4, $D_{11}=D_{22}=D_{33}=D_{44}$, $D_{55}=D_{66}=D_{77}=D_{88}$, $D_{12}=D_{14}=D_{23}=D_{34}$, $D_{56}=D_{58}=D_{67}=D_{78}$, $D_{13}=D_{24}$, $D_{57}=D_{68}$, $D_{15}=D_{26}=D_{37}=D_{48}$, $D_{17}=D_{28}=D_{35}=D_{46}$, and $D_{16}=D_{18}=D_{25}=D_{27}=D_{36}=D_{38}=D_{45}=D_{47}$. Further, $S_1=S_3$, $S_2=S_4$, $S_5=S_7$, $S_6=S_8$; $w_1=w_2=w_3=w_4=I/4a$, and $w_5=w_6=w_7=w_8=-I/4c$. Utilizing these relationships in equation 12 yields

$$\begin{aligned}L=&(-1/2)[\log D_{11}+2\log D_{12}+\log D_{13}]+(-1/2)[\log D_{55}+2\log D_{56}+\log D_{57}]+[\log D_{15}+2\log D_{16}+\log D_{17}]\end{aligned} \qquad (13)$$

Determining the nine geometric mean distances in the right-hand member of equation 13 as detailed in Appendix III, substituting appropriately in equation 13, and collecting terms yields

$$\begin{aligned}L=&[(a+c)^2/2ac]\log(a+c)-[(a-c)^2/2ac]\times\log(a-c)-\log[(ac)^2/(a^2+c^2)]-[(a^2-c^2)/ac]\tan^{-1}[(a-c)/(a+c)]+\pi(a^2-c^2)/4ac-3\log 2\end{aligned} \qquad (14)$$

Simple algebraic manipulation of the logarithmic terms of equation 14 yields alternative formulas especially convenient to numerical computation. Thus

$$\begin{aligned}L=\log&[(r^{-1}+r)(r^{-1}-r)]-1/2(r^{-1}+r)\times\log[(1-r)/(1+r)]+(r^{-1}-r)\times[\pi/4-\tan^{-1}(1-r)/(1+r)]-3\log 2\end{aligned} \qquad (15)$$

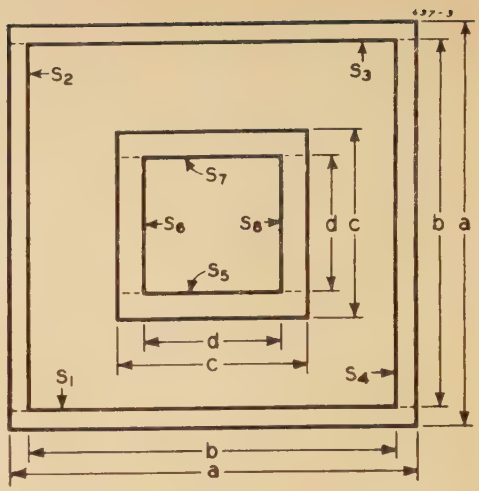

Figure 3

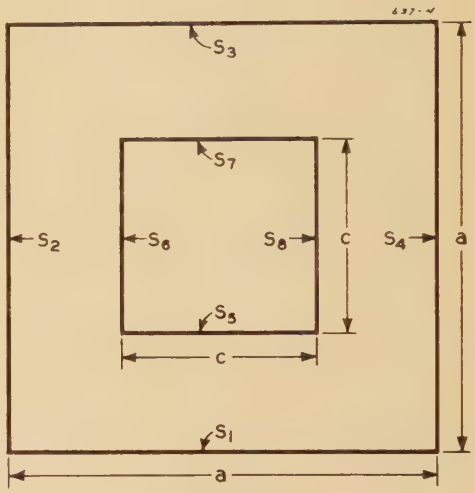

Figure 4

where $r=c/a$. Again

$$L=\log(1+A^2)-2\log(1-A^2)-(1/2r)\times(1-r)^2\log A+(r^{-1}-r)\times(\pi/4-\tan^{-1}A) \qquad (16)$$

where $A=(1-r)/(1+r)$.

For purposes of computation, these approximate formulas possess considerable advantage over the general formula. The latter comprises 36 terms, the former only a few terms. Moreover, the coefficients and arguments of these few terms are quite simple. Therefore, by virtue of the fewness and simplicity of the terms comprising the approximate formulas, they afford rapid computation. In fact, slide rule calculation is quite feasible; commonly, a 20-inch rule will afford values correct to a number of digits sufficient for most design work. But even slide rule calculation can be dispensed with in much work. The curves of Figure 5, plotted from equation 16, afford sufficiently accurate values. For actual use, of course, Figure 5 is too small, but the designer can plot his own curves from the co-ordinates tabulated in Appendix IV.

For use in "Corrections for Rounded

Edges and for Skin and Proximity Effects" in this paper, Figure 5 illustrates curves for the inductance of busses, comprised of indefinitely thin circular tubular conductor. It is interesting to note that these curves evidence the inductance of a bus comprised of thin square tubular conductors to be less than that of a bus comprised of thin circular tubular conductors having diameters equal to the sides of the corresponding square conductors.

Corroboration of the Approximate Equation

As a minor check on the correctness of equation 14, we note that if $a=c$ the conductors of Figure 4 are superimposed. As they carry equal currents in opposite directions, the bus vanishes electrically. Corroboratively, it is evident that $\lim_{a\to c}$ of the right-hand member of equation 14 is zero. A major simultaneous check on both equations 9 and 14 stems from noting that if in Figure 2 $b\to a$ and $d\to c$, we obtain a line-segment cross section as in Figure 4. Corroboratively, as detailed in Appendix V, $\lim_{d\to c}\lim_{b\to a}$ of the right-hand member of equation 9 yields the right-hand member of equation 14.

Inasmuch as the arguments and coefficients of the terms of right-hand members of equations 9, 14, 15, and 16 are without dimension, we note that in substituting in these equations, a, b, c, and d can be expressed in any like unit of length. But otherwise, the units of all quantities mentioned to this point are in the absolute system: bus dimensions in centimeters, current I in abamperes, and inductance L in abhenrys per centimeter of bus length. Multiplying abhenrys per centimeter by 3.048×10^{-5} yields millihenrys per foot of bus length; multiplying by 11.48×10^{-6} yields 60-cycle reactance in ohms per foot of bus length.

Some Illustrative Examples

To illustrate the use of the general formula and to gain knowledge of the accuracy to be expected of values calculated with the approximate formulas, we consider the following examples.

In example 1, the problem is to calculate the inductance of a coaxial bus comprised of two square tubular copper conductors: outer conductor, 6 inches square and 1/8 inch thick; inner conductor, 4 inches square and 3/16 inch thick.

Thus $a=6$, $b=23/4$, $c=4$, and $d=29/8$ inches. Substituting these values in equation 9, collecting and rearranging terms, obtaining values of the logarithmic and arctangentic terms from the Work Projects Administration tables, and effecting all calculations on a 10-row electric calculating machine yields*

$$L=0.75846_2 \text{ abhenry per centimeter of bus length} \quad (17)$$

Obviously, as by virtue of the assumptions underlying derivation of the general formula, it is unlikely that L represents the inductance of the bus to more than plus or minus several in the third decimal place, the last several digits have no physical significance. They are given to emphasize that, insofar as the numerical computation is concerned, the value of L is correct to the number of places indicated. For all logarithmic and arctangentic terms were taken to nine decimal places; values stemming from consequent arithmetic manipulations were held to the same number of decimals.

Inasmuch as the value given in the preceding equation stems from a final algebraic addition of some 32 terms, the largest of which approximates 300,000,000 and the smallest 89, it is essential that some such degree of preciseness be held. But, since the resulting value of L is significant to only two or three decimal places, it is not unlikely that a study of the number of decimal places to be held in the various stages of computation would reveal that a smaller number than actually used still would be satisfactory. However, inasmuch, as 15-place tables were employed and the calculation was performed on a 10-row electric calculating machine, the added labor is negligible, and there is no uncertainty as to the effect of cumulative errors on the accuracy of the first several digits of L.

In example 2, the problem is to calculate the inductance of a bus comprised of line-segment conductors having (1) the external, (2) the mean, and (3) the internal dimensions of the conductors of example 1:

1. $a=6.0$ inches, $c=4.0$ inches, $c/a=0.667$

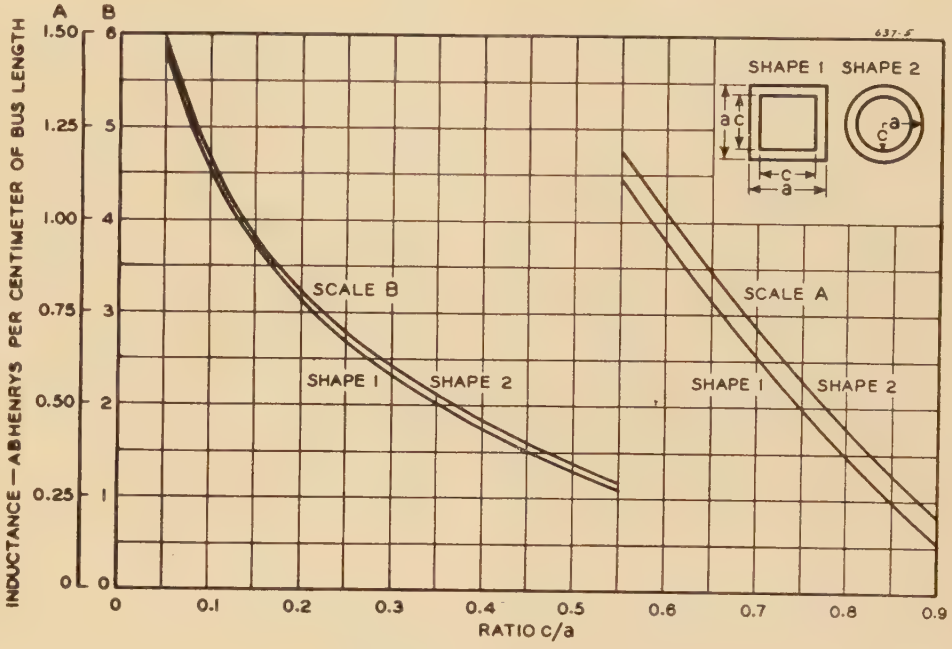

Figure 5

2. $a=47/8$ inches, $c=61/16$ inches, $c/a=0.648$

3. $a=23/4$ inches, $c=29/8$ inches, $c/a=0.631$

For these values of c/a, we obtain from Figure 5:

1. $L_e=0.74$ abhenry per centimeter of bus length.

2. $L_m=0.80$ abhenry per centimeter of bus length.

3. $L_i=0.85$ abhenry per centimeter of bus length.

We note that the value 0.74, corresponding to the use of the external dimensions, and the value 0.758, calculated in example 1 by the use of the general formula, differ by only 2.4 per cent. This close agreement indicates that for the conditions which occur in practice (small conductor thicknesses, and ratio c/a not too near one) values of inductance sufficiently accurate for most design work can be calculated from the approximate formula by use of the external dimensions of the conductors. But since the approximate formula is epitomized in the

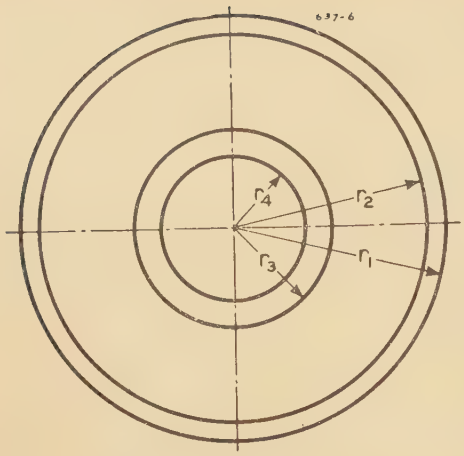

Figure 6

curves of Figure 5, from it we may obtain the inductance we need, only having to calculate the ratio c/a from the specified bus dimensions.

In consequence, considerable advantage with respect to time and labor accrues to the designer. To calculate the inductance from the curves of Figure 5 requires only several minutes, whereas several hours would be required to calculate the inductance from equation 9. Again, the values of example 2 indicate that small changes in bus dimensions result in relatively large changes in bus inductance. In that minimum inductance (hence minimum reactance and correspondingly better voltage regulation) is a desideratum of design, it behooves the designer to investigate all possible combinations of conductors (that are otherwise satisfactory) for the purpose of selecting that combination which possesses minimum inductance. But if the inductances of very many combinations had to be calculated from equation 9, the time, labor, and tedium involved would be considerable; on the other hand, the curves of Figure 5 enable evaluation in almost as many minutes as there are combinations to study.

Corrections for Rounded Edges and for Skin and Proximity Effects

Rounded Edges

To eliminate excessive edge heating caused by skin effect, square tubular conductors of commercial manufacture have rounded edges. Thus square tubular conductors of the sizes specified in example 1 have rounded edges of outer, inner, and mean radius indicated as follows:[12]

$a=6$ inches; $t=a-b=1/8$ inch; $r_o=3/4$ inch, $r_i=5/8$ inch, $r_m=11/16$ inch.

$c=4$ inches; $t'=c-d=3/16$ inch; $r_o=1/2$ inch, $r_i=5/16$ inch, $r_m=13/32$ inch.

Dwight and Wang[7] have derived, semi-empirically, that the approximate increase in inductance ΔL caused by rounding the edges of a conductor of square cross section is

$$\Delta L=2[k^2 \log k^{-1}+0.716k^2+0.5k^3+\ldots] \text{ abhenrys per centimeter of conductor length} \quad (18)$$

where $k=0.463r/s$, r is the mean radius of the rounded edge, s the mean side of the square cross section, and r is small compared with s, the accuracy increasing as $r/s \rightarrow 0$.

For the outer conductor, $s=a-t=47/8$ inches, and $r=11/16$ inch. Hence $k=0.0542$, and $\Delta L=0.022$. For the inner conductor, $s=c-t'=61/16$ inches, and $r=13/32$ inch. Hence $k=0.0494$, and $\Delta L=0.018$. Accordingly, the increase in bus inductance because of the rounded edges is 0.04 abhenry per centimeter of bus length. The corrected value, then, is 0.798 abhenry per centimeter of bus length.

The facts that rounding the corners will result in an increase of inductance and that the increase just calculated from equation 18 is of the correct order of magnitude are confirmed by the following consideration of the coaxial bus with a cross section as shown in Figure 6. As derived in Appendix VI, the d-c inductance of this bus is

$$L=\{(r_3^2-3r_4^2)/2(r_3^2-r_4^2)+[2r_4^4/(r_3^2-r_4^2)^2] \log r_3/r_4\}+\{(r_2^2-3r_1^2)/2\times(r_1^2-r_2^2)+[2r_1^4/(r_1^2-r_2^2)^2]\times \log r_1/r_2\}+[2 \log r_2/r_3] \text{ abhenrys per centimeter of bus length} \quad (19)$$

where the first and second braced terms stem, respectively, from the flux-current linkages in the regions $r_4 \leq r \leq r_3$, and $r_2 \leq r \leq r_1$ (hence they are the so-called internal inductances of the inner and outer conductors) and the third braced term stems from the flux-current linkages in the region $r_3 \leq r \leq r_2$ (hence it is the so-called intra-inductance of the conductors). Let the conductors have (1) the same thicknesses and (2) external diameters equal to the external dimensions of the corresponding conductors of example 1. Thus $r_1=3$ inches, $r_2=23/8$ inches, $r_3=2$ inches, and $r_4=29/16$ inches. Substituting these values in equation 19 and performing the indicated computation yields

$$L=0.062+0.029+0.726$$
$$=0.817 \text{ abhenry per centimeter of bus length} \quad (20)$$

Figure 7

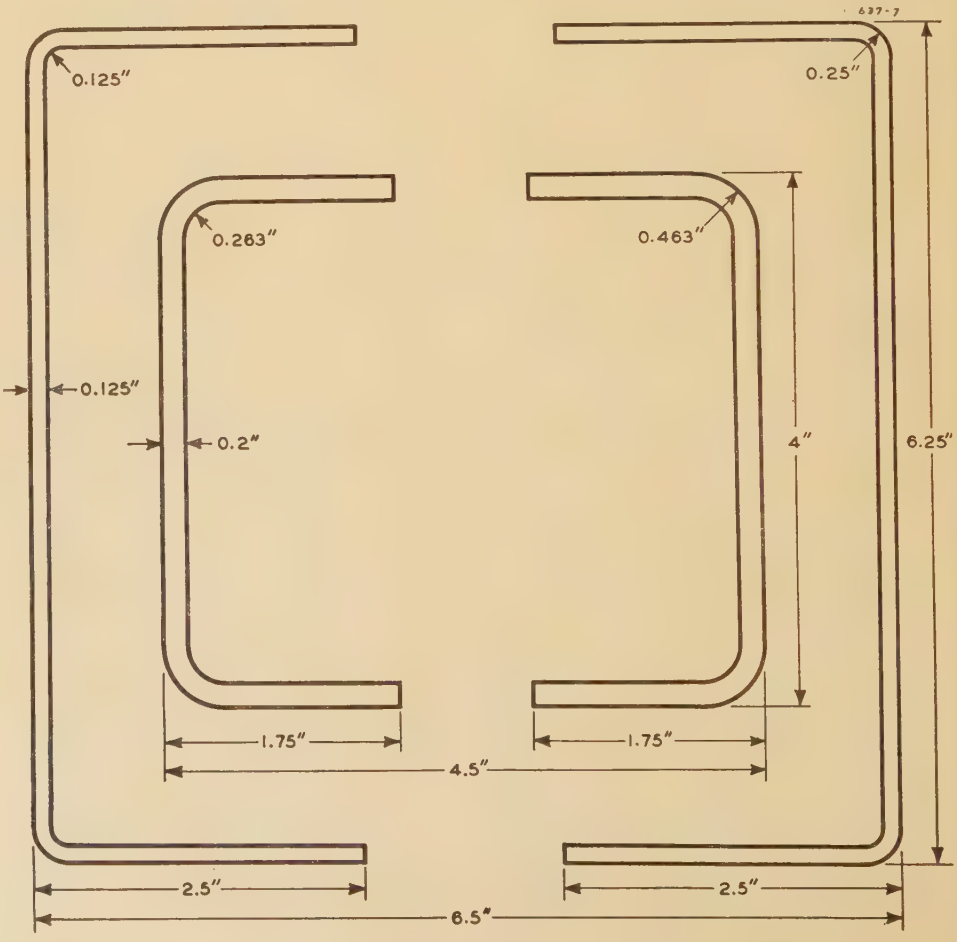

This value is a bit greater than the corrected value of 0.798 for rounded square conductors, which is to be expected. For as the radii of rounding increase, the coaxial square tubular bus approaches the coaxial circular tubular bus as a geometrical limit. Again, the magnitudes of the corrections for rounding increase with the radii of rounding. Hence it follows that the inductance of the square tubular bus approaches the inductance of the circular tubular bus as a limit and that the approach is from below.

In conclusion, it is to be noted that rounding of the edges, even if considerable, results in a relatively small increase in inductance, no matter what the sizes may be of the conductors comprising the bus. For a circular tubular conductor can be considered as the extreme case of a rounded square tubular conductor, its side being equal to the diameter of the circular conductor. Yet for all values of the independent variable of Figure 5, corresponding ordinates of the curves for the square and circular conductors differ by only a few per cent.

Skin and Proximity Effects

As the frequency increases from zero to a specified value, the currents in the inner and outer conductors of a coaxial circular tubular conductor tend to concentrate in thin surface strata on the adjacent surfaces of the two conductors. This phenomenon results in a decrease of the flux-current linkages in the regions $r_4 \leq r \leq r_3$, and $r_2 \leq r \leq r_1$. The flux-current linkages in the region $r_3 \leq r \leq r_2$ are, however, unchanged. The net result of the decrease in the internal inductances and of the constancy of the intra-inductance of the conductors is a decrease in the sum of the three, the total inductance of the bus. But, as in practical busses, the sum of the d-c internal inductances is, as evidenced in equation 20, only a few per cent of the total inductance, and as at 60-cycles the decrease in the internal inductances is only a fraction of one per cent of their d-c values, it follows that the actual change in total inductance caused by 60-cycle skin and proximity effects is negligible. Confirmatively, the authors have calculated the actual 60-cycle inductance of the circular tubular bus in a foregoing section ("Rounded Edges") and find it to be identical (to several places of decimals) with the d-c value cited in equation 20.

In view of the negligible change in the inductance of this coaxial circular tubular bus, the small two-per-cent difference between the inductance of this bus and the one of the coaxial rounded square tubular bus of example 1, and the general geometric similarity between these two busses, we conclude that in the bus of example 1, and in practical dimensioned rounded square tubular busses in general, 60-cycle skin and proximity effects are negligible insofar as the inductance of the bus is concerned. This conclusion is in accord with the results of analytic and experimental investigations of the inductance of coplanar busses comprised of square[7] tubular or rectangular[13] conductor.

Busses Comprised of Structural Tubular Conductor

A conductor comprised of two slightly separated channels or angles, placed flange to flange, usually is not of a square cross section. If, however, the cross section does not differ too greatly from a square cross section, and commonly this is the case in practice, it is to be expected that a fairly good approximation to the actual inductance of the bus can be effected by judicious use of the formulas for the square cross section. Thus for the bus dimensioned[2,3] as in Figure 7, consider an equivalent square tubular bus with conductors having the same external

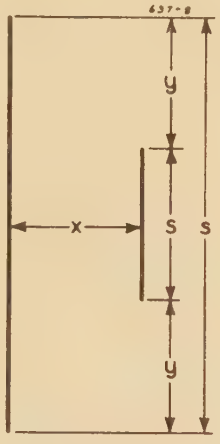

Figure 8

perimeters (rounded edges aside) as the ones in Figure 7. Then, as detailed in Appendix VII, the inductance of this equivalent bus is 0.755 abhenry per centimeter of bus length. Against this value we have the inductance, calculated (in Appendix VII) from the measured load impedance, as 0.837 abhenry per centimeter of bus length. The difference in the two values is approximately 10 per cent of the measured value. On the other hand, if we assume an equivalent bus having square conductors with sides equal to the webs of the given conductors, we obtain an inductance of 0.849 abhenry per centimeter of bus length. This value differs from the measured value by only 1.4 per cent. In general, we infer that selecting an equivalent bus on one or the other of the bases mentioned will yield an approximate value of inductance within a few per cent of the actual value, which is all that is required for most design purposes.

Polyphase Coaxial Busses

To calculate the performance of polyphase busses requires knowledge of the reactance drops on the individual conductors. The general equations for determining these reactance drops have been developed elsewhere.[8] It suffices here to mention that these equations express the reactance drops in terms of the self and mutual geometric mean distances of the cross sections of the square tubular conductors comprising the bus, and that these geometric mean distances are furnished by equation 8. For, as a comparison of equations 1 and 8 makes clear, in the right-hand member of equation 8 the first term is minus twice the logarithm

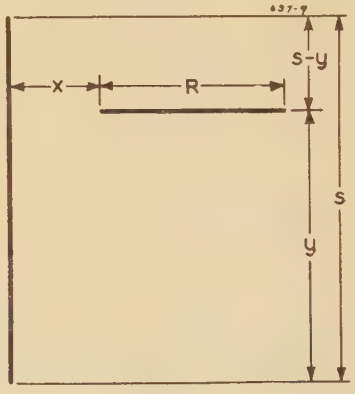

Figure 9

of the self geometric mean distance of the outer hollow square of Figure 2, the second is minus twice the logarithm of the self geometric mean distance of the inner hollow square, and the third is four times the logarithm of the mutual geometric mean distance of the two hollow squares. Hence as a, b, c, and d are arbitrary, we have general formulas for the self and mutual geometric mean distances of two concentric parallel-sided hollow rectangles of arbitrary dimensions. In essence, therefore, calculation of the reactance drops on the conductors of a specified

polyphase bus reduces to determination of the numerical values of the required geometric mean distances from the just-mentioned formulas and substitution of these values in the general equations (which are typified by equation 28 of reference 8).

Appendix I

The geometric mean distances indicated in equation 8 follow from equation 3 by substitution therein of the following values of the parameters A_p and B_q, these values being obtained from equations 5 and 6 through inspection of Figure 2:

$\log D_{11}$: $A_1=A_3=B_1=B_3=a$; $A_2=A_4=B_2=B_4=0$

$\log D_{22}$: $A_1=A_3=B_1=B_3=b$; $A_2=A_4=B_2=B_4=0$

$\log D_{33}$: $A_1=A_3=B_1=B_3=c$; $A_2=A_4=B_2=B_4=0$

$\log D_{44}$: $A_1=A_3=B_1=B_3=d$; $A_2=A_4=B_2=B_4=0$

$\log D_{12}$: $A_1=A_3=B_1=B_4=(a+b)/2$; $A_2=A_4=B_2=B_4=(a-b)/2$

$\log D_{13}$: $A_1=A_3=B_1=B_3=(a+c)/2$; $A_2=A_4=B_2=B_4=(a-c)/2$

$\log D_{13}$: $A_1=A_3=B_1=B_3=(a+d)/2$; $A_2=A_4=B_2=B_4=(a-d)/2$

$\log D_{14}$: $A_1=A_3=B_1=B_3=(b+c)/2$; $A_2=A_4=B_2=B_4=(b-c)/2$

$\log D_{24}$: $A_1=A_3=B_1=B_3=(b+d)/2$; $A_2=A_4=B_2=B_4=(b-d)/2$

$\log D_{34}$: $A_1=A_3=B_1=B_3=(c+d)/2$; $A_2=A_4=B_2=B_4=(c-d)/2$

Utilizing these parameters in equation 3 yields

$$S_1^2 \log D_{11} = -(25/12)S_1^2-(1/6)[K(a,a)+K(0,0)-2K(a,0)] \quad (21)$$

$$S_1S_2 \log D_{12} = -(25/12)S_1S_2-(1/6)\times\{K[(a+b)/2,(a+b)/2]+K[(a-b)/2,(a-b)/2]-2K[(a+b)/2,(a-b)/2]\} \quad (22)$$

and similar obvious equations are obtained for the other eight geometric mean distances.

Substituting appropriately in equation 8 and collecting corresponding terms in K yield

$$\begin{aligned}L=&[-1/3(a^2-b^2)^2]\{2K[(a+b)/2,(a+b)/2]+2K[(a-b)/2,(a-b)/2]-4K[(a+b)/2,(a-b)/2]-K(a,a)-K(b,b)+2K(a,0)+2K(b,0)\}+\\&[-1/3(c^2-d^2)^2]\{2K[(c+d)/2,(c+d)/2]+2K[(c-d)/2,(c-d)/2]-4K[(c+d)/2,(c-d)/2]-K(c,c)-K(d,d)+2K(c,0)+2K(d,0)\}+\\&[2/3(a^2-b^2)(c^2-d^2)]\{K[(a+d)/2,(a+d)/2]+K[(a-d)/2,(a-d)/2]-2K[(a+d)/2,(a-d)/2]-K[(b+d)/2,(b+d)/2]-K[(b-d)/2,(b-d)/2]+2K[(b+d)/2,(b-d)/2]-K[(a+c)/2,(a+c)/2]-K[(a-c)/2,(a-c)/2]+2K[(a+c)/2,(a-c)/2]+K[(b+c)/2,(b+c)/2]+K[(b-c)/2,(b-c)/2]-2K[(b+c)/2,(b-c)/2]\}\end{aligned} \quad (23)$$

Evaluating the various terms through the use of equation 4 yields equation 9.

As already discussed in an earlier part of this paper ("Polyphase Coaxial Busses"), the terms of the right-hand members of equation 9, and thus of equation 23, can be interpreted in terms of the self and mutual geometric mean distances of the two hollow rectangles of Figure 2.

Appendix II

The geometric mean distances indicated in equation 11 follow from equation 3 by substitution therein of the following values of the parameters A_p and B_q, these values being obtained from equations 5 and 6 through inspection of Figure 3:

$\log D_{11}$: $A_1=A_3=a$, $A_2=A_4=0$; $B_1=B_3=(a-b)/2$, $B_2=B_4=0$

$\log D_{22}$: $A_1=A_3=(a-b)/2$, $A_2=A_4=0$; $B_1=B_3=b$, $B_2=B_4=0$

$\log D_{55}$: $A_1=A_3=c$, $A_2=A_4=0$; $B_1=B_3=(c-d)/2$, $B_2=B_4=0$

$\log D_{66}$: $A_1=A_3=(c-d)/2$, $A_2=A_4=0$; $B_1=B_3=d$, $B_2=B_4=0$

$\log D_{12}$: $A_1=(a-b)/2$, $A_2=0$, $A_3=a$, $A_4=(a+b)/2$; $B_1=(a+b)/2$, $B_2=b$, $B_3=0$, $B_4=(a-b)/2$

$\log D_{13}$: $A_1=A_3=a$, $A_2=A_4=0$; $B_1=a$, $B_2=B_4=(a+b)/2$, $B_3=b$

$\log D_{15}$: $A_1=A_3=(a+c)/2$, $A_2=A_4=(a-c)/2$; $B_1=(a-d)/2$, $B_2=(b-d)/2$, $B_3=(b-c)/2$, $B_4=(a-c)/2$

$\log D_{16}$: $A_1=(a-d)/2$, $A_2=(a+d)/2$, $A_3=(a+c)/2$, $A_4=(a-c)/2$; $B_1=(a+d)/2$, $B_2=(b+d)/2$, $B_3=(b-d)/2$, $B_4=(a-d)/2$

$\log D_{17}$: $A_1=A_3=(a+c)/2$, $A_2=A_4=(a-c)/2$; $B_1=(a+c)/2$, $B_2=(b+c)/2$, $B_3=(b+d)/2$, $B_4=(a+d)/2$

$\log D_{24}$: $A_1=a$, $A_2=A_4=(a+b)/2$, $A_3=b$; $B_1=B_3=b$, $B_2=B_4=0$

$\log D_{25}$: $A_1=(a+c)/2$, $A_2=(b+c)/2$, $A_3=(b-c)/2$, $A_4=(a-c)/2$; $B_1=(b-d)/2$, $B_2=(b+d)/2$, $B_3=(b+c)/2$, $B_4=(b-c)/2$

$\log D_{26}$: $A_1=(a-d)/2$, $A_2=(b-d)/2$, $A_3=(b-c)/2$, $A_4=(a-c)/2$; $B_1=B_3=(b+d)/2$, $B_2=B_4=(b-d)/2$

$\log D_{28}$: $A_1=(a+c)/2$, $A_2=(b+c)/2$, $A_3=(b+d)/2$, $A_4=(a+d)/2$; $B_1=B_3=(b+d)/2$, $B_2=B_4=(b-d)/2$

$\log D_{56}$: $A_1=(c-d)/2$, $A_2=(c+d)/2$, $A_3=c$, $A_4=0$; $B_1=(c+d)/2$, $B_2=d$, $B_3=0$, $B_4(c-d)/2$

$\log D_{57}$: $A_1=A_3=c$, $A_2=A_4=0$; $B_1=c$, $B_2=B_4=(c+d)/2$, $B_3=d$

$\log D_{68}$: $A_1=c$, $A_2=A_4=(c+d)/2$, $A_3=d$; $B_1=B_3=d$, $B_2=B_4=0$

Substituting these parameters in equation 3 yields, in terms of K, the desired expressions for the geometric mean distances (which have been omitted here because of the space required). Substituting these expressions in equation 11 and collecting like terms yields equation 23 and hence, corroboratively, equation 9.

Appendix III

The geometric mean distance between two line segments, located as illustrated in Figure 8, is given by equation 11 of reference 9:

$$Ss \log D = (1/2)\{-[x^2-(S+y)^2]\times\log[x^2+(S+y)^2]+(x^2-y^2)\times\log(x^2+y^2)+4x(S+y)\times\tan^{-1}[(S+y)/x]-4xy\times\tan^{-1}(y/x)-3Ss\} \quad (24)$$

The geometric mean distance between two line segments, located as illustrated in Figure 9, is given by equation 15 of reference 9:

$$Rs \log D = I(R+x,s-y)-I(x,s-y)+I(R+x,y)-I(x,y)-3Rs/2 \quad (25)$$

wherein, typically,

$$I(x,y)=(1/2)[xy\log(x^2+y^2)+x^2\times\tan^{-1}(y/x)+y^2\tan^{-1}(x/y)] \quad (26)$$

The geometric mean distances indicated in equation 13 are obtained by substitution in equation 24 of the first six, and in equation 25 of the last three, of the following sets of values of the parameters x, y, R, and S, these values being obtained by inspection of Figures 4, 8, and 9:

$\log D_{11}$: $x=0$, $y=0$, $S=s=a$

$\log D_{55}$: $x=0$, $y=0$, $S=s=c$

$\log D_{13}$: $x=a$, $y=0$, $S=s=a$

$\log D_{57}$: $x=c$, $y=0$, $S=s=c$

$\log D_{15}$: $x=y=(a-c)/2$, $S=c$, $s=a$

$\log D_{17}$: $x=(a+c)/2$, $y=(a-c)/2$, $S=c$, $s=a$

$\log D_{12}$: $x=0$, $y=0$, $R=s=a$

$\log D_{66}$: $x=0$, $y=0$, $R=S=c$

$\log D_{16}$: $x=(a-c)/2$, $y=(a+c)/2$, $R=c$, $s=a$

Utilizing these parameters in equations 24 and 25 as stated yields

$$\log D_{11}=\log a-3/2$$
$$\log D_{55}=\log c-3/2$$
$$\log D_{12}=\log a+(1/2)\log 2+\pi/4-3/2$$
$$\log D_{56}=\log c+(1/2)\log 2+\pi/4-3/2$$
$$\log D_{13}=\log a+\pi/2-3/2$$
$$\log D_{57}=\log c+\pi/2-3/2$$
$$\log D_{15}=(1/2)\{\log(a^2+c^2)+[(a^2-c^2)/ac]\times\tan^{-1}[(a+c)/(a-c)]-\pi(a-c)^2/4ac-3\}$$
$$\log D_{16}=(1/4)\{[(a+c)^2/ac]\log(a+c)-[(a-c)^2/ac]\log(a-c)-2\log 2+\pi-6\}$$
$$\log D_{17}=(1/2)1\{\text{og}(a^2+c^2)-[(a^2-c^2)/ac]\times\tan^{-1}[(a-c)/(a+c)]+\pi(a+c)^2/4ac-\log 2-3\}$$

Appendix IV

The co-ordinates used for plotting the curves of Figure 5 for the square tubular conductors are obtained by substituting the indicated values of A in equation 16, obtaining the values of the logarithmic and arctangentic terms from the Work Projects Administration tables, and performing all computation on a 10-row electric calculating machine. To avoid cumulative errors all

computation was effected to eight significant figures. For actual plotting, however, the inductance need only be known to the three or four significant figures given in Table I.

Table I

A	r=c/a	L	A	r=c/a	L
0	1	0	0.6	1/4	2.693
0.1	9/11	0.354	0.7	3/17	3.389
0.2	2/3	0.744	0.8	1/9	4.315
0.3	7/13	1.164	0.9	1/19	5.809
0.4	3/7	1.617	1.0	0	∞
0.5	1/3	2.117			

The inductance of a coaxial bus comprised of indefinitely thin circular tubular conductors, dimensioned as in shape 1 of Figure 5, is $L=-2\log(c/a)$. Hence the co-ordinates of the curves of Figure 5 for shape 1 are as shown in Table II.

Table II

c/a	L	c/a	L	c/a	L
0	∞	0.4	1.833	0.8	0.373
0.1	4.605	0.5	1.386	0.9	0.193
0.2	3.219	0.6	1.022	1.0	0
0.3	2.408	0.7	0.728		

Appendix V

Equation 23 for the inductance of a bus, with a cross section as illustrated in Figure 2 is valid for conductors of arbitrary thickness. Accordingly, the inductance of a bus with a cross section comprised of line segments as shown in Figure 4 can be obtained by determining the limit of the inductance of the bus in Figure 2 as the thicknesses of the conductors comprising the bus approach zero.

To effect this determination, we require, as will be seen below, knowledge of the following derivatives: $\partial^2K(u,u)/\partial x^2$, $\partial^2K(v,v)/\partial y^2$, $\partial^2K(u,v)/\partial x\partial y$, wherein $u=(x+y)/2$, and $v=(x-y)/2$. From equation 4 we have

$$K(u,u)=-4u^4\log u-2u^4\log 2-2u^4\pi \quad (27)$$

Substituting from equation 27 into the identity

$$\frac{\partial^2K(u,u)}{\partial y\partial x}=\frac{\partial}{\partial u}\left[\frac{\partial K}{\partial u}\frac{\partial u}{\partial x}\right]\frac{\partial u}{\partial y} \quad (28)$$

and performing the indicated differentiations yield

$$\partial^2K(u,u)/\partial y\partial x=-u^2(12\log u+6\log 2+6\pi+7) \quad (29)$$

Hence

$$\partial^2K[(x+y)/2,\ (x+y)/2]/\partial y\partial x=-[(x+y)^2/4][12\log(x+y)-6\log 2+6\pi+7] \quad (30)$$

Similarly,

$$\partial^2K[(x-y)/2,\ (x-y)/2]/\partial y\partial x=[(x-y)^2/4][12\log(x-y)-6\log 2+6\pi+7] \quad (31)$$

To evaluate $\partial^2K(u,v)/\partial x\partial y$ we note that the real part of the complex function

$$W(w)\equiv W(u+iv)=U(u,v)+iV(u,v)=w^4\log w \quad (32)$$

is

$$Re(W)=U(u,v)=K(u,v)+2\pi uv^3 \quad (33)$$

This identity is easily established by separating $w^4\log w$ into its real and imaginary parts and using the identity $\tan^{-1}u/v+\tan^{-1}v/u=\pi/2$. Now

$$\frac{\partial^2U}{\partial x\partial y}=\frac{\partial^2U}{\partial u^2}\frac{\partial u}{\partial x}\frac{\partial u}{\partial y}+\frac{\partial^2U}{\partial v^2}\frac{\partial v}{\partial x}\frac{\partial v}{\partial y}+\frac{\partial^2U}{\partial u\partial v}\left[\frac{\partial v}{\partial x}\frac{\partial u}{\partial y}+\frac{\partial u}{\partial x}\frac{\partial v}{\partial y}\right]+\frac{\partial U}{\partial u}\frac{\partial^2u}{\partial x\partial y}+\frac{\partial U}{\partial v}\frac{\partial^2v}{\partial x\partial y} \quad (34)$$

Inasmuch as

$$d^2W/dw^2=\partial^2U/\partial u^2+i\partial^2V/\partial u^2=-\partial^2U/\partial v^2-i\partial^2V/\partial v^2 \quad (35)$$

we have $\partial^2U/\partial u^2=-\partial^2U/\partial v^2=Re(d^2W/dw^2)$. Accordingly, substituting appropriately in equation 34 and performing the indicated differentiations with respect to x and y gives

$$\partial^2U/\partial x\partial y=(1/4)[Re(d^2W/dw^2)+Re(d^2W/dw^2)+0+0+0]=\tfrac{1}{2}Re(d^2W/dw^2) \quad (36)$$

Substituting from equation 32 in equation 36 and performing the indicated differentiation yields

$$\partial^2U/\partial x\partial y=Re(6w^2\log w+7w^2/2)=Re[6(u^2-v^2+2iuv)\log(u+iv)+7(u^2-v^2+2iuv)/2]=3(u^2-v^2)\log(u^2+v^2)-12uv\times\tan^{-1}v/u+7(u^2-v^2)/2 \quad (37)$$

Since, from equation 33,

$$\partial^2K/\partial x\partial y=\partial^2U/\partial x\partial y-2\pi\partial^2(uv^3)/\partial x\partial y \quad (38)$$

we obtain, on substitution in equation 38 from equation 37 and expressing u and v in terms of x and y,

$$\partial^2K[(x+y)/2,\ (x-y)/2]/\partial x\partial y=3xy\times\log(x^2+y^2)-3xy\log 2-3(x^2-y^2)\times\tan^{-1}[(x-y)/(x+y)]+7xy/2+3\pi(x^2-y^2)/4 \quad (39)$$

With these identities obtained, we are prepared to consider the limiting process. For convenience, equation 9 is written in the form

$$L=(-1/3)L_1(a,b)/(a^2-b^2)^2-(1/3)L_2\times(c,d)/(c^2-d^2)^2+(2/3)L_3(a,b,c,d)\div(a^2-b^2)(c^2-d^2) \quad (40)$$

First, let $b\to a$. In the limit the outer conductor of Figure 2 is comprised of line segments. The inductance of the resulting bus is

$$\lim_{b\to a}L=(-1/3)\lim_{b\to a}L_1(a,b)/(a^2-b^2)^2-(1/3)L_2(c,d)/(c^2-d^2)^2+(2/3)\lim_{b\to a}L_3(a,b,c,d)/(a^2-b^2)\times(c^2-d^2) \quad (41)$$

Now $[L_1(a,b)/(a^2-b^2)^2]_{b=a}=0/0$; similarly $[L_3(a,b,c,d)/(a^2-b^2)(c^2-d^2)]_{b=a}=0/0$. Accordingly, the limits in the right-hand member of equation 41 are to be determined by applying L'Hospital's rule for evaluating indeterminate expressions of the form 0/0. Applying this rule to the first limit yields

$$\lim_{b\to a}L_1(a,b)/(a^2-b^2)^2=\{[\partial^2L_1(a,b)/\partial^2b]\div[\partial^2(a^2-b^2)/\partial^2b]\}_{b=a} \quad (42)$$

A second differentiation of numerator and denominator is necessary because the ratio of the first derivatives (for $b=a$) is also of the form 0/0. Performing the differentiations and substitutions indicated gives

$$(1/3)\lim_{b\to a}L_1(a,b)/(a^2-b^2)^2=2\log a+(1/2)\log 2+\pi/2+7/6 \quad (43)$$

For the second limit, L'Hospital's rule yields

$$\lim_{b\to a}L_3(a,b,c,d)/(a^2-b^2)(c^2-d^2)=\{[\partial L_3(a,b,c,d)/\partial b]/[\partial(a^2-b^2)\times(c^2-d^2)/\partial b]\}_{b=a} \quad (44)$$

Effecting the differentiations and substitutions indicated gives

$$\lim_{b\to a}L_3(a,b,c,d)/(a^2-b^2)(c^2-d^2)=L'_3(a,c,d)/(-2a)(c^2-d^2) \quad (45)$$

wherein

$$L'_3(a,c,d)=[\partial\{-K[(a+d)/2,\ (a+d)/2]-K[(a-d)/2,\ (a-d)/2]+2K[(a+d)/2,\ (a-d)/2]+K[(a+c)/2,\ (a+c)/2]+K[(a-c)/2,\ (a-c)/2]-2K[(a+c)/2,\ (a-c)/2]\}/\partial b]_{b=a} \quad (46)$$

Secondly, let $d\to c$. In the limit the inner conductor of Figure 2 is comprised of line segments, hence the cross section is now that of Figure 4. From equations 41, 43, and 45, the inductance of this line segment bus is

$$\lim_{d\to c}\lim_{a\to b}L=-[2\log a+(1/2)\log 2+\pi/2+7/6]-(1/3)\lim_{d\to c}L_2(c,d)\div(c^2-d^2)^2+(2/3)\lim_{d\to c}L'_3(a,c,d)\div(-2a)(c^2-d^2) \quad (47)$$

Except for the interchange of a and b with c and d, the second term in the right-hand member of equation 47 is identical with the first term in the right-hand member of equation 41. Hence from equation 43, we have

$$(1/3)\lim_{d\to c}L_2(c,d)/(c^2-d^2)^2=2\log c+(1/2)\log 2+\pi/2+7/6 \quad (48)$$

Now

$$[L'_3(a,c,d)/(-2a)(c^2-d^2)]_{c=a}=0/0$$

Accordingly, L'Hospital's rule yields

$$\lim_{d\to c}L'_3(a,c,d)/(-2a)(c^2-d^2)=\{[\partial L'_3(a,c,d)/\partial d]/[\partial(-2a)\times(c^2-d^2)/\partial d]\}_{d=c}=L''_3(a,c)/4ac \quad (49)$$

wherein

$$L''_3(a,c)=[\partial^2\{-K[(b+d)/2,\ (b+d)/2]-K[(b-d)/2,\ (b-d)/2]+2K[(b+d)/2,\ (b-d)/2]\}/\partial d\partial b]_{\substack{b=a\\d=c}} \quad (50)$$

Performing the differentiations by use of equations 30, 31, and 39 and substituting as indicated yields

$$(1/3)L''_3(a,c)/4ac = -(a/4c)\log[(a-c)\div(a+c)] - (c/4a)\log[(a-c)/(a+c)] + (1/2)\log[(a^2-c^2)(a^2+c^2)] - [(a^2-c^2)/2ac]\tan^{-1}[(a-c)\div(a+c)] + \pi(a^2-c^2)/8ac - \log 2 + \pi/2 + 7/6 \quad (51)$$

Finally, substituting from equations 48 and 49 in equation 47 and collecting terms yields, corroboratively, equation 14.

Appendix VI

By virtue of the fundamental definition of the inductance of a circuit, $L = W/2I^2$, wherein W is the energy in the magnetic field produced by the circuit current I, and the calculation of L reduces to the calculation of W. Because of the circular symmetry of the coaxial circular tubular bus with a cross section as illustrated in Figure 6, W easily is calculated from the well-known relation $W = 1/2$ (summation of the flux-current linkages associated with the circuit). Accordingly, $L =$ (summation of the flux-current linkages)$/I^2$.

In that a circular tubular conductor produces no field in the cylindrical space bounded by its internal surface, the flux density B, and thus the flux-current linkage, in the region $0 \geq r \geq r_4$ is zero.

In the region $r_4 \geq r \geq r_3$, we have $B = 2\mu\, I(r)/r$, wherein $I(r) = I(r^2-r_4^2)/(r_3^2-r_4^2)$ is the current in the region $r_4 \geq r \geq r$. Accordingly, the flux contained in a thin tube of unit length and of thickness dr is $[2\mu\, I(r)dr/r]$. Hence the total flux-current linkages per unit length are

$$[2\mu I^2/(r_3^2-r_4^2)^2]\int_{r_4}^{r_3}[(r^2-r_4^2)/r]dr = [2\mu I^2/(r_3^2-r_4^2)^2][(r_3^2-r_4^2)\times(r_3^2-3r_4^2)/4 + r_4^4 \log(r_3/r_4)] \quad (52)$$

In the region $r_3 \leq r \leq r_2$, the flux density is $B = 2\mu I/r$, the flux contained in a thin tube of unit length and of thickness dr is $(2\mu I/r)dr$, and the current encompassed by this flux is I. Hence the total flux-current linkages are

$$2\mu I^2 \int_{r_3}^{r_2}(1/r)dr = 2\mu I^2 \log(r_2/r_3) \quad (53)$$

In the region $r_2 \leq r \leq r_1$, we have $B = 2\mu I(r)/r$; hence the flux contained in a thin tube of unit length and of thickness dr is $2\mu I(r)/dr$. The current encompassed by this flux is $I(r) = I - I(r^2-r_2^2)/(r_1^2-r_2^2) = I(r_1^2-r^2)/(r_1^2-r_2^2)$. Thus the total flux linkages are

$$[2\mu I^2/(r_1^2-r_2^2)^2]\int_{r_2}^{r_1}[(r_1^2-r^2)/r]dr = [2\mu I^2/(r_1^2-r_2^2)^2][(r_1^2-r_2^2)\times(r_2^2-3r_1^2)/4 + r_1^4 \log(r_1/r_2)] \quad (54)$$

The total of the flux-current linkages is the sum of the right-hand members of equations 52, 53, and 54. Dividing this sum by I^2 and taking $\mu = 1$ yield the right-hand member of equation 19.

Appendix VII

The external perimeters of the cross sections of the outer and inner conductors of Figure 7 are encompassed by rectangles respectively 25.5 inches and 17 inches in perimeter. Consider equivalent conductors of square cross section, of external perimeters equal to these values, and of the same thicknesses as the given conductors. The external, mean, and internal ratios of c/a are, respectively, 0.667, 0.648, and 0.629. From Figure 5 we obtain, respectively, 0.74, 0.80, and 0.855 abhenry per centimeter of bus length. Again, $r_o = 0.1875$ and $r_i = 0.363$, thus $k_e = 0.0134$ and $k_i = 0.0415$. Hence from equation 18, we obtain respectively 0.0019 and 0.0134 abhenry per centimeter of bus length as corrections for the rounding of the edges of the outer and inner conductors. Accordingly, the total inductance of the equivalent bus, depending on the dimensions used, is

$$L_e = 0.755;\quad L_m = 0.815;\quad L_i = 0.87 \text{ abhenry per centimeter of bus length} \quad (55)$$

On the other hand, if we assume the equivalent bus to be comprised of conductors with sides of 6.25 inches and 4 inches, the dimensions of the webs of the corresponding given conductors, the corresponding ratios of c/a are 0.641, 0.621, and 0.600. From Figure 5 we obtain respectively 0.825, 0.885, and 0.938 abhenry per centimeter of bus length. Again, $k_o = 0.0142$ and $k_i = 0.0442$, hence from equation 18 we obtain respectively 0.002 and 0.015 abhenry per centimeter of bus length as corrections for the rounding of the edges of the outer and inner conductors. Accordingly, the total inductance of the equivalent bus, depending on the dimensions used, is

$$L_e = 0.842;\quad L_m = 0.902;\quad L_i = 0.950 \text{ abhenry per centimeter of bus length} \quad (56)$$

Though for comparison values of L_e, L_m, and L_i are displayed, the results in the previous section "Some Illustrative Examples" indicate that the external value would be used for actual computation. In such case, calculation of edge corrections is simplified by use of the external rather than the mean dimensions indicated in equation 18. Proceeding thus for the bus equivalent on the basis of webs yields 0.024 rather than 0.017. The difference in these two values is negligible in comparison with the total inductance. Further, as the correction increases, the calculation is on the safe side.

The a-c resistance of the actual bus is

$$R = \rho(A_o^{-1} + A_i^{-1})K_s \text{ ohms per foot of bus length} \quad (57)$$

wherein ρ is the resistivity (in ohms-circular mils per foot) of the copper at operating temperature, A_o and A_i are the areas (in circular mils) of the cross sections of the outer and inner conductors, and K_s is the skin effect factor of the conductors.

In the absence of stated experimental values, we assume conventional values of 50 degrees centigrade for the operating temperature and 98 per cent conductivity for the bus copper. Then the resistivity is $\rho = (10.37/0.98)[1 + 0.00393(50-20)] = 11.82$ ohms-circular mils per foot. The outer conductor, constructed of two rectangular strips bent into shape, is of area $A_o = 2(10.75 \times 0.125) = 2.69$ square inches, thus 3,430,000 circular mils. The inner conductor, comprised of stock channels, is of area $A = 2[2(1.75 - 0.463)0.2 + (4 - 2\times 0.463)0.2 + \pi(0.463^2 - 0.263^2)/2] = 2.72$ square inches, thus 3,460,000 circular mils. The skin-effect factor[12] for a range of square tubular conductors, which encompasses those approximating the shapes of the given conductors, is $K_s = 1.04$.

Substituting these values in equation 57 yields a resistance of 7.18 micro-ohms per foot of bus length. The measured impedance is 12 micro-ohms per foot of bus length. From this value we find the inductance to be $L = (144 - 51.3)^{1/2}/377 = 2.55$ microhenrys, or in centimeter-gram-second units, 0.837 abhenry per centimeter of bus length.

References

1. Resistance Welder Feed Has Low Resistance Drop, L. R. Bogardus. *Electrical World*, volume 110, 1938, pages 702–04.

2. Concentric Bus for Resistance Welders, W. Specht. *Electrical World*, volume 114, 1940, page 558.

3. A Concentric Channel Bus for Resistance Welders, W. Specht. *Welding Engineer*, volume 26, June 1941, pages 31–2.

4. The Design of Bus-Bar Industrial Distribution Systems: an Epitomization of Available Data, T. J. Higgins. AIEE Transactions, volume 64, 1945, pages 385–400; discussion, pages 486–8.

5. The Alternating-Current Resistance of Hollow Square Conductors, A. H. M. Arnold. *Journal*, Institution of Electrical Engineers (London, England), volume 82, 1938, pages 537–45.

6. Temperature Rise of Bus Bars, H. B. Dwight, G. W. Andrew, H. W. Tileston. *General Electric Review*, volume 43, 1940, pages 213–16.

7. Reactance of Square Tubular Bus Bars, H. B. Dwight, T. K. Wang. AIEE Transactions, volume 57, 1938, pages 762–5; discussion, pages 765–6.

8. Formulas for the Calculation of the Inductance of Linear Conductors of Structural Shape, T. J. Higgins. AIEE Transactions, volume 62, 1943, February section, pages 53–8.

9. Formulas for the Geometric Mean Distances of Rectangular Areas and of Line Segments, T. J. Higgins. *Journal of Applied Physics*, volume 14, 1943, pages 188–95.

10. Tables of Natural Logarithms (book), Work Projects Administration. Columbia University Press, New York, N. Y.

11. Tables of Arctangents (book), Work Projects Administration. Columbia University Press, New York, N. Y.

12. Formulas for the Inductance of Rectangular Tubular Conductors, T. J. Higgins. AIEE Transactions, volume 60, 1941, December section, pages 1046–50.

13. Chase Electrical Handbook (book). Chase Brass and Copper Company, Inc., Waterbury, Conn., 1941. Pages 80–1.

14. The Inductance of Linear Conductors of Rectangular Section, A. H. M. Arnold. *Journal*, Institution of Electrical Engineers (London, England), volume 70, 1931–32, pages 579–86.

Supervisory Control of 30,000-Kva Hydroelectric Plant

C. W. BOHNER
MEMBER AIEE

A. P. MANESS
ASSOCIATE AIEE

Synopsis: Ocoee 3, a 1-unit 30,000-kva supervisory-controlled generating station of the Tennessee Valley Authority, has been in operation since April 30, 1943. An underground cable was selected for the control and telemetering channel, and neutralizing transformers were installed to protect against voltage rise resulting from transmission line faults. Instrumentation, controls, and station auxiliaries were designed particularly to safeguard the unattended equipment. Maintenance includes two or three inspections per week. The cost of supervision, operation, and maintenance is as low as $0.101 per 1,000 kilowatt-hours.

THE AUTOMATIC and supervisory control features of Ocoee 3 hydroelectric plant of the Tennessee Valley Authority are of special interest because of the size and importance of the equipment controlled. The 30,000-kva generator is one of the large units in the United States operating completely unattended, and the outdoor switchyard with its 74,000-kva 161/69/13.8-kv tap-changing-under-load transformer bank serves as a switching center for the 154- and 66-kv transmission lines in the area. The entire plant is supervisory-controlled from Ocoee 2 hydroelectric plant located five miles downstream.

The geographical location and transmission line connections of Ocoee 3 plant are shown in Figure 1. The 154-kv line to Apalachia serves as a tie between the main 154-kv transmission system and the local 66-kv transmission system in the Ocoee River area. The installed generating capacities of Ocoee 2 and Blue Ridge hydroelectric plants, which are connected to the 66-kv system, are 19,900 and 20,000 kw respectively.

Ocoee 3 Dam is located 2.5 miles upstream from the powerhouse, and a connecting tunnel terminates in a surge tank at the upper end of the penstock. A butterfly valve is provided in the penstock near the surge tank. A view of the surge tank, valve house, penstock, powerhouse, and switchyard is shown in Figure 2.

A single-line diagram of the Ocoee 3 main electrical connections and the principal metering and relaying connections is shown in Figure 3. No additional generating units are to be installed in the future, but provision is made in the design for an ultimate of two 154-kv lines and four 66-kv lines.

From the system operating standpoint, it would be preferable to have Ocoee 2 plant supervisory-controlled from Ocoee 3, but this was impractical because of the unsuitability for automatic operation of the equipment in Ocoee 2 plant, which was built in 1913. It was felt that for successful remote operation without undue interruptions for minor troubles, all control features of the major equipment should be selected specially for nonattended operation, and this dictated that Ocoee 3 plant should be the controlled plant with the dispatcher's board located at Ocoee 2.

Control and Telemetering Channels

In selecting the type of channels to be used for the control and metering circuits between Ocoee 3 and Ocoee 2, three possibilities were explored: leased wire from the local telephone company, carrier current, and an overhead or underground cable between the two plants. All forms of open-wire construction were rejected as not being sufficiently reliable, and this decision eliminated the use of leased-wire facilities since only open-wire lines were available from the local telephone company. Carrier channels, while probably somewhat less expensive than an underground cable installation, were rejected because of the limited number of channels obtainable without undue complication and the feeling that at the present state of the art there would be some sacrifice in reliability and increase in maintenance with the use of carrier. The length of the channel, only six miles, was just short enough that the attractive economies of carrier channels over metallic wire channels could not be realized unless the number of channels was reduced to the absolute minimum. Overhead armored cable was considered seriously but decided against. It would have been necessary to follow the highway to avoid rough mountain terrain, and with the highway route, the hazard of malicious damage, rock slides, and traffic accidents made this scheme undesirable. Underground cable was selected finally because it was expected that it would provide practically trouble-free service with the minimum of maintenance and the maximum number of completely independent channels.

The underground cable installed consists of a 51-pair number 19-American-wire-gauge double-paper-insulated lead-covered tape-armored telephone cable with jute covering for subterranean service. The cable is similar to standard telephone cable except that the withstanding voltage from conductors to sheath is 3,500 volts, 60 cycles for 20 seconds, this being approximately double the voltage rating ordinarily used for telephone service. The cable is buried along the edge of the state highway between the plants, with manholes at each splice point spaced approximately 3,000 feet apart. The cable is gas-filled and maintained under 8-pound pressure to prevent the entrance of moisture. Pressure switches are installed in the cable at every third manhole and connected to one of the cable pairs to operate an annunciator at Ocoee 2 in the event of a break in the cable sheath and consequent loss of gas pressure. The allocation of cable pairs is shown in Table I.

Table I

No. of Pairs	Service
2	Supervisory control
23	Metering
4	Direct-wire control and pilot-wire relaying
1	Printing annunciator
8	Communication (includes TVA system communication other than for Ocoee 3)
13	Spare
51	Total

Control Cable Protection

Experience with remote-control and communication cables at a number of TVA plants had demonstrated that extraneous voltages appear on the cable conductors during phase-to-ground faults on the transmission system. With the cables enclosed in metallic sheaths and buried underground, induced voltages are avoided, but serious voltages do result from a rise of station ground potential above remote ground potential. They ap-

Paper 46-71, recommended by the AIEE committee on power generation for presentation at the AIEE winter convention, New York, N. Y., January 21-25, 1946. Manuscript submitted November 21, 1945; made available for printing December 18, 1945.

C. W. BOHNER was formerly principal electrical engineer, design department, Tennessee Valley Authority, Knoxville, Tenn., and is now with International General Electric Company, Schenectady, N. Y. A. P. MANESS is assistant production engineer, power operations department, Tennessee Valley Authority, Chattanooga, Tenn.

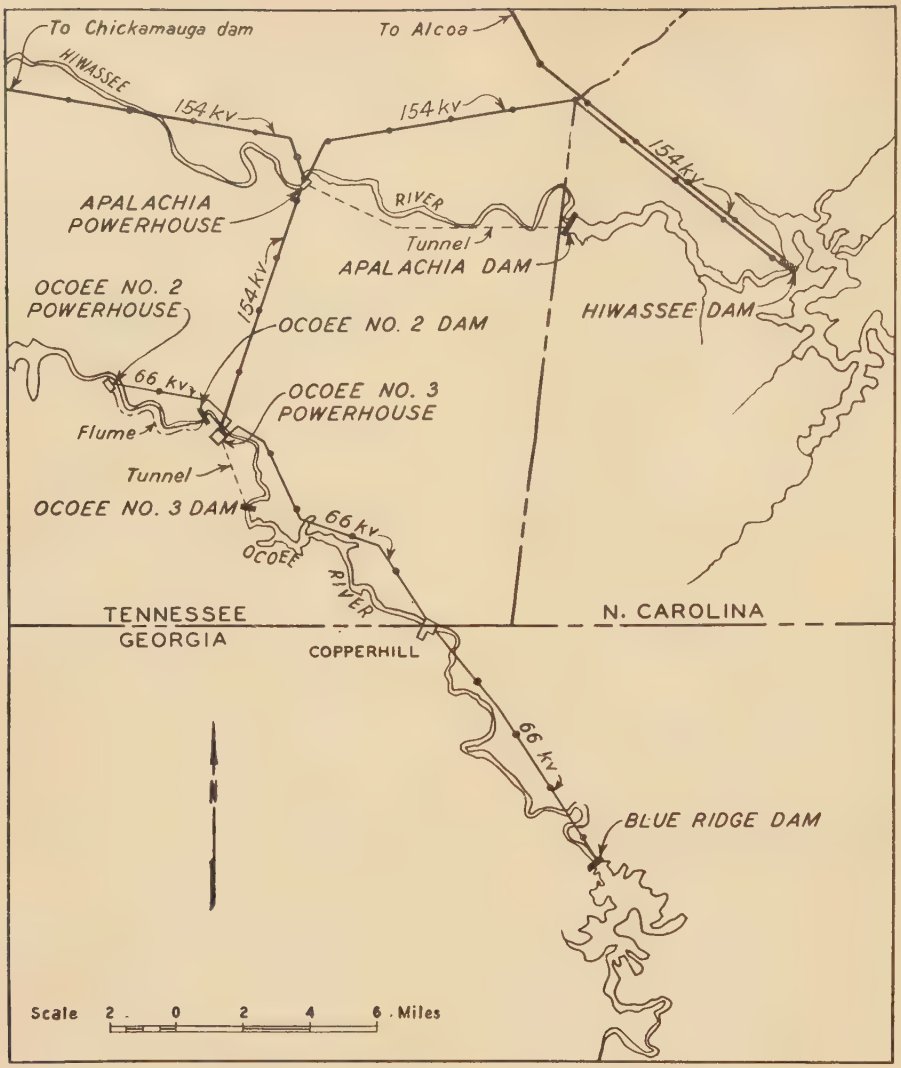

Figure 1. Location and transmission connections

pear across the cable insulation and across the protector gaps at the cable terminals. At plants where large neutral currents are allowed to flow, the extraneous voltages may become excessive and render the circuits inoperative at a time when they are most needed.

Investigation indicated that at the Ocoee plants, excessive voltages caused by the rise of station ground potential were a probability. Although one of the most effective methods of reducing the rise of station ground potential is to reduce the station ground resistance, low ground resistance was extremely difficult to obtain at the Ocoee plants because both plants are located in a mountainous region with deep rock formations underlying a comparatively thin layer of topsoil. The final tested ground resistance at Ocoee 3 was 0.5 ohm, while at Ocoee 2 the lowest value which it was practicable to obtain was 1.4 ohms. With these values of ground resistance, the calculated rise of station ground potential above remote ground for maximum ground fault current in the transformer bank neutrals was considerably in excess of the rating of the protectors. Special measures therefore had to be taken at both plants either to limit or to compensate for the rise in station ground potential.

At Ocoee 3 a 5.5-ohm grounding reactor was installed in the 66-kv neutral of the transformer bank to reduce the maximum neutral short-circuit current. The reactor is of the outdoor oil-insulated type. It reduces the maximum 66-kv neutral fault current from 4,300 to 2,600 amperes, with a corresponding reduction in the rise of the Ocoee 3 ground potential.

A similar solution could not be used at Ocoee 2 because the insulation of the old transformers at this plant is suitable for solidly grounded operation only. The protective measures adopted consisted of installing neutralizing transformers to compensate for the difference in ground potentials. The neutralizing transformers are of the 3-winding type, with the two secondaries of each transformer connected in the conductors of a cable pair and the primary connected between the cable sheath and ground. By keeping the cable sheath at remote ground potential, the difference in ground potential is impressed on the primary winding, thus introducing a compensating voltage in the conductors so that the conductors on the cable side of the neutralizing transformers are at remote ground or sheath potential while on the station side of the neutralizing transformers the conductors are at station ground potential. Obviously, it was necessary to keep the cable sheath and armor free from the influence of the Ocoee 2 station ground potential. To accomplish this, it was not considered practicable to provide an insulating covering over the sheath and armor which would not be subject to rather rapid deterioration; therefore, the cable was brought out of the ground at a point approximately 500 feet from the Ocoee 2 powerhouse and run overhead on poles to the neutralizing transformers.

The neutralizing transformers are indoor-type rated 4,000 volts and are installed in a weatherproof box mounted on a pole structure near Ocoee 2 powerhouse.

Supervisory Control Equipment

The selection of a multiconductor cable for the control channels between the plants permitted an unrestricted choice of the several types of supervisory control equipment available, since it was not necessary to keep the number of conductors required for the control channel to an absolute minimum. Had it been necessary to limit the control channel to two wires, the selection of supervisory control equipment would have been restricted to the type in which all operations are performed by coded impulsing. While this type has been successfully used in smaller installations on the TVA system, it was felt that the large amount and variety of complicated controls involved at Ocoee 3 justified utilizing any simplification which could be obtained in the supervisory control equipment itself.

Accordingly, a type of supervisory system requiring four instead of two line wires was selected. This equipment is essentially a direct-wire system of control and indication with step-type selector relays which transfer the line wires from one circuit to another. After the transfer is made, all operation of the equipment is done directly through auxiliary relays without further impulsing. Two standard 23-point units are installed, of which 30 points are used initially and the remaining

Table II

No. of Supervisory Points	Type of Service	Description
5	Control and indication	13.8-, 66-, and 154-kv oil circuit breaker control
5	Control and indication	13.8-, 66-, and 154-kv motor-operated disconnecting switch control
3	Control and indication	Automatic - manual selection for transformer tap-changing, generator voltage regulator, and generator starting and stopping
8	Control and indication	Metering selection
2	Control and indication	Generating unit automatic start-stop and penstock butterfly valve emergency close
5	Control only	Raise-lower control for gate limit adjustment, transformer tap-changing, generator voltage adjusting rheostat, and exciter field rheostat and potentiometer telemetering calibration
2	Indication only	Lock-out relay position and generator breaker tripping bus indication
16		Spare
46		Total

16 points are for future expansion. Allocation of the supervisory points is given in Table II.

Telemetering

Continuously telemetered indicators with individual transmitters and receivers are provided for all important quantities to be metered. Intermittently telemetered indicators are provided for the less important quantities, with one transmitter and receiver provided for two or more quantities, with selection by supervisory control. The telemetering provided is shown in Table III.

It was recognized that fewer telemetered indicators could be used, since if abnormal conditions should develop, there is little that the operator at Ocoee 2 could do to correct the trouble, and the automatic protective devices would have to be relied upon to shut down the faulty equipment. It was felt, however, that the additional telemeters were justified because abnormal operation of the equipment may show up on the instruments just before shutdown, and the information obtained may be of value in locating the trouble.

Torque-balance-type telemeters are used for metering amperes, kilowatts, and kilovars. Individual instruments are provided for these quantities for the generator and for transformer 154- and 69-kv amperes. A common instrument is provided for transformer 154-kv kilowatts and kilovars, transformer 69-kv kilowatts and kilovars, 69-kv line amperes, and 69-kv line kilowatts and kilovars. Selection between kilowatts and kilovars and between lines can be made by supervisory control.

Table III

No. of Transmitters and Receivers	Type	Service
3	Torque balance	Generator amperes, kilowatts, and kilovars
4	Torque balance	Transformer 154- and 66-kv amperes, kilowatts, and kilovars
2	Torque balance	66-kv line amperes, kilowatts, and kilovars
3	Potentiometer	Turbine gate position, gate limit and speed adjustment setting, and transformer tap position
2	Direct wire	Generator voltage and speed indicator
5	Direct wire	Synchroscope, incoming and receiving voltage, and frequency

Potentiometer-type telemetering is used for turbine gate position, gate limit and speed adjustment setting, and main transformer tap position. It consists of small potentiometers, mechanically connected to the device whose position is being telemetered, and milliammeter receivers with appropriate scales. The potentiometers are connected to the Ocoee 3 250-volt control battery. To provide calibration of the receivers for change in battery voltage and line wire resistance, a rheostat is provided in one of the line wires of each receiver, and a supervisory point simultaneously connects the three receivers directly to the Ocoee 3 battery supply.

Generator voltmeter and synchroscope and associated voltmeters and frequency meters are operated directly over the line wires without telemetering transmitters, as is also the turbine speed indicator which is operated from a magneto-generator geared to the main unit shaft.

A recording voltmeter with milliammeter element is operated from a rectifier current transmitter with supervisory control selection of the voltage to be recorded. A station load recorder is operated from a thermoverter. A reservoir level recorder of the impulse type is provided with float-operated transmitter located at the dam. For this latter recorder, the line wires are run overhead on poles between the dam and Ocoee 3 powerhouse and thence through the underground cable to Ocoee 2.

Main Control Switchboards

The main control switchboards at Ocoee 3 are divided into three sections: the control and instrument board section, which is installed in one of the generator room walls and faces into the generator room; the relay board section, which is installed back-to-back to the control and instrument board; and the remote control board, which faces the relay board. Figure 4 shows a floor plan layout of the generator and switchboard rooms.

A complete set of controls and instruments is provided at Ocoee 3 for local control of the plant if desired for maintenance and when the supervisory control is out of service. A view of the control and instrument board is shown in Figure 5. The local controls are similar to the manual controls provided for other TVA plants except for several additional con-

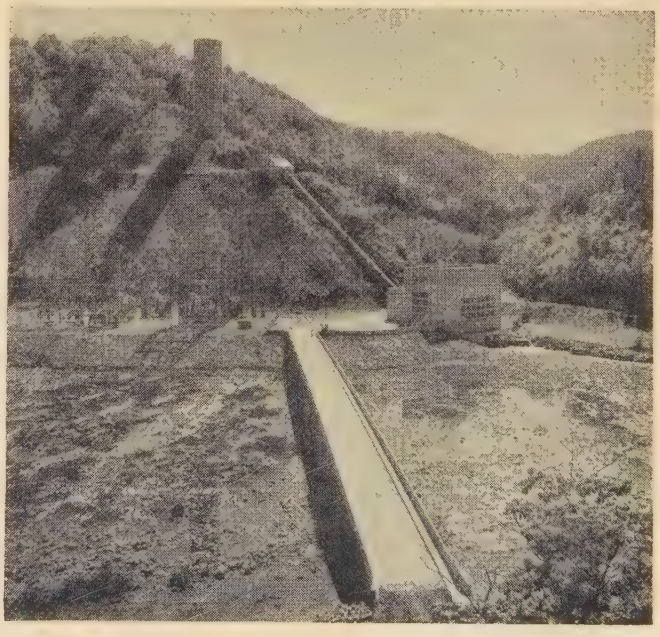

Figure 2. Surge tank, valve house, penstock, powerhouse, and switchyard

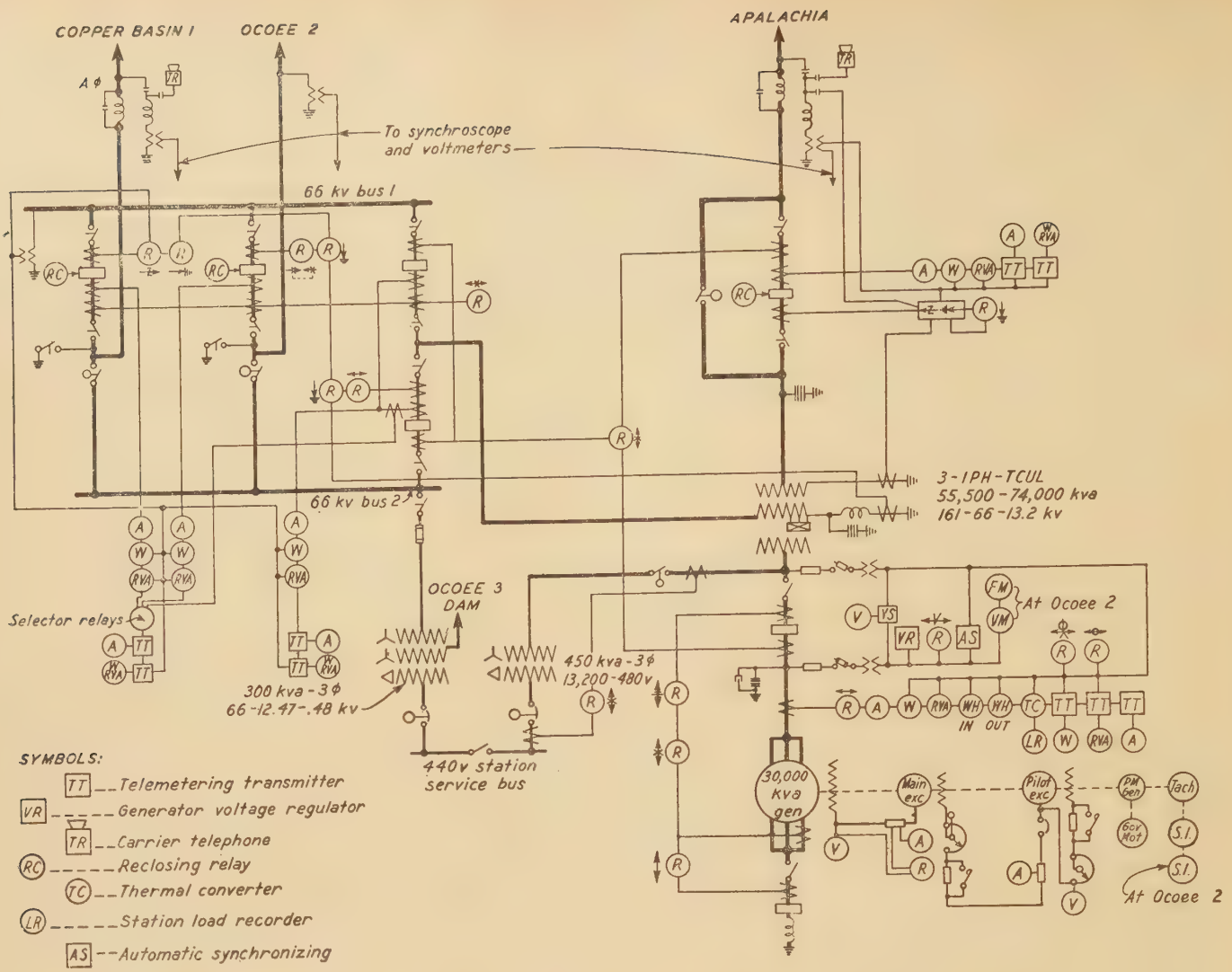

Figure 3. Single-line diagram of main connections and the principal metering and relaying

trol features required because of automatic and supervisory control operations. A switch is provided on each panel for transferring the controls on that panel to either local or supervisory control. On the generator panel a switch is provided to select either manual or automatic starting and synchronizing of the generating unit. A switch also is provided for selecting automatic synchronizing of the unit for manual starting when all auxiliaries are already in operation and it is not desired to go through the entire automatic starting sequence.

All of the main protective and automatic control relays for the generating unit, main transformer bank, and transmission lines are mounted on the relay board. Primary relays are of the withdrawal type with built-in test facilities. Differential relays are of the percentage-differential induction type. An automatic oscillograph is installed on the relay board, and facilities are provided to permit connecting the elements in the more important current and potential circuits for analysis of relay performance.

The supervisory control equipment, the telemetering transmitters, the battery charger controls, and the battery distribution equipment are located on the remote control board.

Dispatcher's Board at Ocoee 2

The dispatcher's board, consisting of a 2-panel completely enclosed cubicle, is installed at the left end of the Ocoee 2 main switchboard. A view of this board is shown in Figure 6. The recording voltmeter, generator-load recorder printing annunciator, and water-level recorder are mounted on one panel, and the indicating telemeter receivers and supervisory controls are mounted on the other panel. The supervisory controls and associated position-indicating lamps are grouped according to function, and mimic busses are provided so as to present a single-line diagram arrangement. The printing annunciator is of the impulse type and automatically prints on a paper chart all abnormal operations of the equipment at Ocoee 3 and also all opening and closing operations of the main circuit breakers.

Generating Unit and Governor

The generating unit consists of a 40,000-horsepower 200-rpm vertical-shaft Francis-type turbine direct-connected to a 30,000-kva 13.8-kv 0.9-power factor generator. The generator is totally enclosed, with Kingsbury-type thrust bearing located below the rotor and with direct-connected main and pilot exciters. The governor is of the actuator type with motor-driven governor head driven by a permanent magnet generator direct-connected to the main unit shaft.

The control and protective features of the main generating unit do not differ materially from those customarily provided for large manually operated units. The turbine guide bearing is lubricated normally by an a-c motor-driven oil pump with pressure switch control arranged to transfer on loss of pressure to an emergency battery-driven pump. An automatic control is provided for the wicket

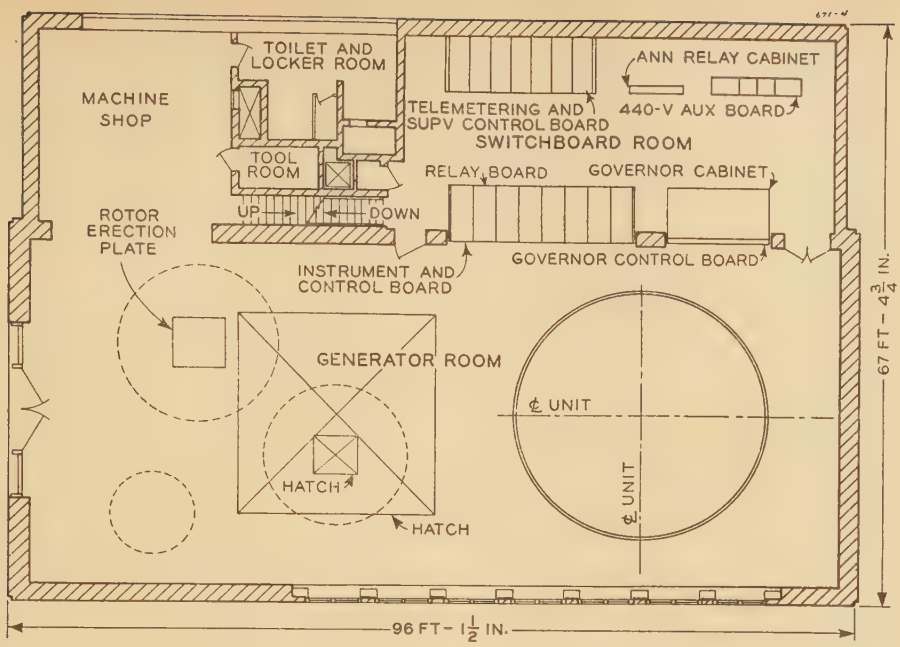

Figure 4. Main floor plan

gates to close and lock them in the closed position upon loss of governor oil pressure. The oil in the generator thrust bearing is self-circulating and no pumps are required. A float switch is provided to operate an annunciator for low thrust-bearing oil level. Temperature detectors are provided in the turbine guide bearing and generator thrust bearing for annunciation and for operation of a bearing temperature recorder mounted on the governor cabinet. An overspeed switch geared to the main shaft is arranged to energize the governor shut-down solenoid and operate an annunciator upon overspeed of the unit but does not close the butterfly valve. If the unit should run away, the operator at Ocoee 2 would be informed through the operation of the annunciator and the tachometer reading on the dispatcher's board and will close the butterfly valve by supervisory control.

The governor is of the conventional cabinet actuator type, with two motor-driven oil pumps and governing mechanism mounted on the sump tank. Both pumps are under pressure-switch control, and the control provides for the operation of one pump normally to maintain governor oil pressure. If this pump fails to maintain pressure, the second pump is started automatically. The governor manual controls, the penstock, scroll case, and cooling-water pressure gauges, the bearing "thermoverters," and the tachometer are mounted on the front of the governor cabinet.

The synchronizing and load-limit devices are motor-operated to permit operation of these devices by supervisory control and to permit automatic synchronizing by the automatic speed-matching and synchronizing relays on the main switchboard.

An automatic device is provided on the governor which, when the unit is started, allows the gates to open quickly to the speed-no-load position and then introduces a time delay to permit the governor flyballs to take control and the generator voltage to build up before the gates can be opened further for loading of the unit.

Automatically operated air brakes are provided to stop rotation of the unit after shutdown. Control is by an electrically operated pendulum timer which, after a time delay to allow the speed of the unit to drop to approximately 50 per cent of normal, applies the brakes intermittently until the unit is stopped. The control is interlocked through auxiliary switches to allow application of the brakes only if the wicket gates are completely closed and the generator breaker is open.

Generator Unit Protection

Protective equipment is provided to prevent starting of the unit if any of the following abnormal conditions exist:

1. Overspeed device contacts closed.
2. System voltage below normal.
3. Incorrect phase sequence.
4. Generator thermal relay contacts closed.
5. Exciter field rheostat not at normal voltage no-load position.
6. Main butterfly valve not fully open.
7. Generator neutral breaker not closed.
8. Main exciter field breaker not closed.
9. Lock-out relay not reset.

The following protective devices trip the generator breaker and shut down and

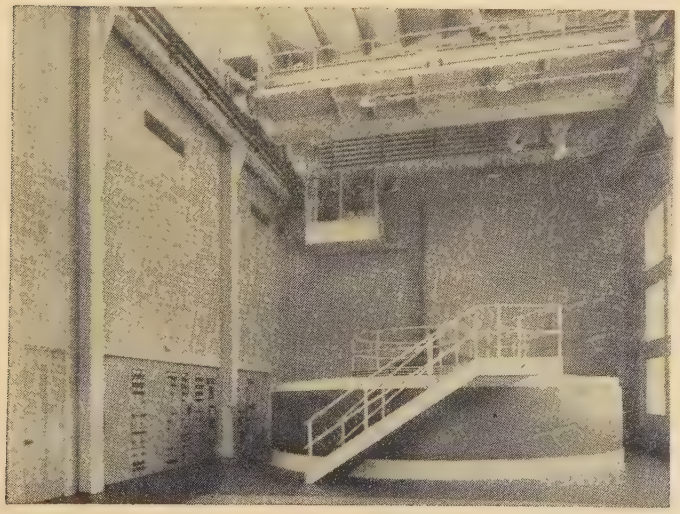

Figure 5. Generator room showing generator and main control and instrument board, with governor control board beyond

Figure 6. Dispatcher's board at left end of existing control board in Ocoee 2 plant

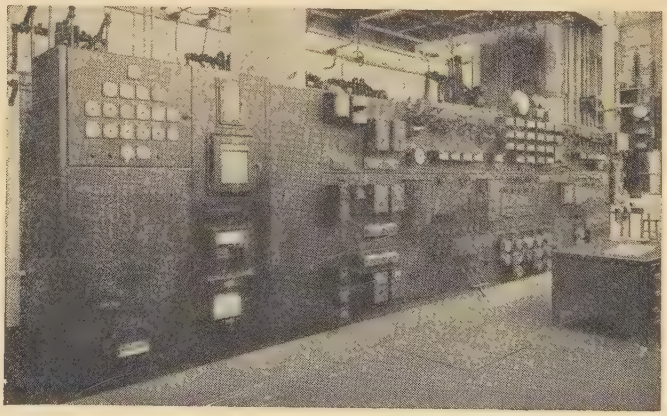

lock out the unit when abnormal conditions occur:

1. Generator differential and neutral overcurrent relays.
2. Generator thermal and phase overcurrent relays.
3. Generator a-c overvoltage relay.
4. Generator overvoltage relay for sustained overvoltage.

The following protective devices also trip and lock out the unit when abnormal conditions occur, but to prevent overspeeding, the generator breaker is not tripped until the wicket gates are closed to the no-load position.

1. Reverse-phase and unbalanced-phase current relays.
2. Field-failure relay.
3. Flow switches for low flow of turbine seal water, generator bearing water, and air cooling water.
4. Pressure switches for low governor oil pressure.
5. Float switch for low turbine-bearing oil level.
6. Temperature detectors for high turbine- and generator-bearing temperatures.
7. Incomplete starting sequence relay.

Station Service Supply

Normal auxiliary power is obtained from a 450-kva 3-phase 13.8/460-volt transformer connected to the main transformer delta bus through a motor-operated disconnecting switch. Emergency station service power is obtained from a 300-kva 3-winding 3-phase 69,000/12,450/460-volt transformer connected to the 69-kv transfer bus. The 12.45-kv winding supplies power to the dam over a 2.5-mile overhead line. Both transformers normally are kept energized, and automatic transfer control is provided to close the emergency supply 440-volt breaker if the normal supply fails.

Two 10-kw diverter-pole motor generator sets are provided for control-battery charging. One of the sets operates on floating charge at all times, and automatic transfer is provided to start the other set in the event the first set trips off for any reason. A selector switch is provided to permit selecting the set which is to operate normally.

Initial Power Operation

The operation of the reservoir for this plant is co-ordinated to provide storage in advance of floods, to fluctuate the pool elevations to aid in malaria control, and to store water on small stream flow increases for later use for power generation.

During the period from November 1942 to April 19, 1943, the sluice gates at the Ocoee 3 Dam were operated to regulate the downstream flow for power requirements at the Ocoee 1 and 2 plants and to meet the need of construction activities at the Ocoee 3 project. The gates were closed initially for the impounding of water to fill the reservoir on April 19, 1943. From this date on, the entire inflow, except that needed for the operation of the downstream Ocoee plants, was stored. The maximum reservoir elevation was reached on April 24, and the plant went into operation on April 30.

No attendants of any kind are stationed at the powerhouse or the dam. The necessary supervision and operation functions of the Ocoee 3 project are performed by the employees of the Ocoee 2 hydroelectric plant. A maintenance employee and an operating employee visit the plant two or three times a week to check batteries and lamps, test oil, inspect auxiliary equipment, clean switchboard panels, lubricate equipment, and inspect water plant. They stay from four to eight hours, depending on the work involved.

The cost of supervision, operation, and maintenance at Ocoee 3 for the first 20 months of operation is shown in Table IV.

Table IV

	First 8 Months 4/30 to 12/31 1943	Next 6 Months 1/1 to 6/30 1944	Next 6 Months 7/1 to 12/31 1944
Supervision			
Labor	$ 2,017	$ 1,410	$ 738
Material	612	384	168
Operation			
Labor	7,929	3,288	4,662
Material	2,152	612	528
Maintenance			
Labor	2,482	2,640	2,172
Material	536	804	636
Total cost	$15,728	$9,138	$8,904
Gross generation, kwhr	125,368,000	90,561,000	83,221,000
Cost per 1,000 kwhr	$0.125	$0.101	$0.107

The labor costs of supervision and operation are set up as 50 per cent of the salaries of the supervising, clerical, and operating employees. The material costs of supervision and operation and the entire cost of maintenance are charged 100 per cent to the plant.

Ocoee 3 is the first of the Tennessee Valley Authority's generating stations to be operated by supervisory control. Its excellent performance and low operation cost have encouraged an extension of this type of operation. Supervisory control is expected to be used for two other generating stations of larger capacity now under design and is being considered for a number of substations.

Signal and Noise Levels in Magnetic Tape Recording

D. E. WOOLDRIDGE
NONMEMBER AIEE

Synopsis: The primary object of the work described here was to determine what properties of the tape and associated magnetic elements are responsible for the noise and signal output levels of magnetic recordings and, if possible, to display in specific equations the pertinent relationships connecting noise and signal levels with the physical properties of the tape and polepieces. In the course of the study, methods appeared for decreasing the noise and increasing the useful signal reproduced from magnetic tape. These methods and some of the use that Bell Telephone Laboratories and Western Electric have made of them are mentioned in the discussion. While some of the work described in this paper has implications for more than one type of magnetic recording process, perpendicular recording on tape[1] is the actual subject matter dealt with. In every case discussed, the record medium was 0.050 inch wide and 0.0022 inch thick. Except where otherwise noted, a chrome-steel tape was used at a speed of 16 inches per second.

Noise Levels in Magnetic Tape Recording

Noise in Demagnetized Tape

In the experimental work on noise, the polepiece construction was as shown in Figure 1, where the active portion of each polepiece consisted of a sheet of soft magnetic material (for example permalloy) 0.0015 inch thick and 0.040 inch wide, held against the tape by a light spring tension with the narrow dimension parallel to the tape travel, the two polepieces exactly aligned with each other on opposite sides. When a piece of tape from which previous recordings have been erased by a demagnetizing process is passed between such polepieces, the signal picked up by the coils contains energy in a wide band of frequencies. This suggests that the noise may be caused by a large number of small magnetic irregularities in the tape. Therefore it is sensible to start by a quantitative consideration of the noise frequency spectrum that would be produced by such irregularities.

For concreteness, first suppose the tape is completely demagnetized except for one inclusion of magnetized material of dimensions small compared with the polepiece width (0.0015 inch). As the tape moves along, the flux passing into the polepieces must vary with time in some such way as that shown in Figure 2. The width of the flat top must be certainly less than the time required for the tape to travel one polepiece width (0.0015 inch); it may be substantially less than this. The portion of the tape that is so near the polepieces that an appreciable fraction of the flux of a magnetized inclusion gets into them will be called the region of influence of the polepieces in this paper. The curve of Figure 2 may be translated into a relative flux versus distance curve and plotted as in Figure 3; this curve $f(x)$ may be said to have the shape of the region of influence.* The course with time of the flux that links the windings is then given by

$$\Phi(t) = KMf[V(t-t_0)] \tag{1}$$

where V is tape speed, t_0 is the instant when the magnetized inclusion passes the center line of the polepieces, M is the magnetic moment of the inclusion, and K is a constant for the present considerations.

The voltage induced in the reproducing coils that surround the polepiece is

$$e(t) = KMnV \cdot 10^{-8} \frac{df}{dx} \tag{2}$$

where n is the number of turns on the coils. Figure 4 shows the shape of the voltage pulse $e(t)$ corresponding to the shape of the region of influence of Figure 3.

We are interested in the total power developed in the frequency range $\Delta\nu$ by the combined effects of N voltage pulses such as the above scattered at random throughout every time interval T. This problem is treated in Appendix I. The result is shown to be

$$P_N(\nu)d\nu = \frac{2(Kn\times 10^{-8})^2}{R} M^2 \left(\frac{N}{T}\right) S(\nu)^2 d\nu \tag{3}$$

where

$$S(\nu) = \int_{-\infty}^{+\infty} \frac{df}{dx} \sin \frac{2\pi\nu x}{V} dx \tag{4}$$

R is the impedance of the reproducing coil circuit, which is assumed to be a pure resistance independent of frequency. (Experimentally, this condition is met by connecting the reproducing coils to a high resistance.)

At this point it is possible to test whether the simple theory under investigation properly accounts for the observed shape of the noise frequency distribution. A complete test would involve computing $f(x)$ from the magnetic and geometric properties of the system and comparing the shape of the resulting $S(\nu)^2$ curve with noise measurements. It is not easy to compute $f(x)$ in more than an approximate manner. Therefore the reverse procedure has been employed. By trial and error an attempt has been made to draw an $f(x)$ curve that, employed in equation 3, leads to a noise frequency distribution that fits the observed facts. The result is shown in Figure 5, where the theoretically derived curve is superposed over the experimental noise measurements. The shape of the region of influence used in the derivation is shown in Figure 6. A study of the x-scale of this figure will show it to be reasonable for polepieces 0.0015 inch wide and tape 0.0022 inch thick.

The approximate agreement between theory and experiment that just has been established justifies some confidence in the validity of the methods and the theory under test. A somewhat more quantitative test may be obtained by comparing the noise frequency distribution and the signal frequency response characteristic. This method is developed in the following paragraphs.

In Appendix II it is shown that the power that is dissipated in the output load R when a sine wave signal of frequency ν is reproduced from the tape is

$$P_s(\nu) = \frac{1}{2} \frac{(Kn\times 10^{-8})^2}{R} (I_o ah)^2 V^2 T(\nu)^2 \tag{5}$$

where

$$T(\nu) = \int_{-\infty}^{+\infty} \frac{d}{dx}[f(x)g(x)] \sin \frac{2\pi\nu x}{V} dx \tag{6}$$

In these equations, I_o is the half-amplitude of the tape magnetization, measured when the tape is well away from the region of influence of the polepieces, while $g(x)$ is the factor by which the remanent magnetization of the free tape is enhanced

* Dependence of $f(x)$ on the depth of the inclusion in the 0.002-inch tape is taken account of only insofar as the $f(x)$ finally derived is thought of as a value averaged over the tape thickness.

Paper 46-31, recommended by the AIEE committee on communication for presentation at the AIEE winter convention, New York, N. Y., January 21–25, 1946. Manuscript submitted November 7, 1945; made available for printing December 12, 1945.

D. E. Wooldridge is with the Bell Telephone Laboratories, Inc., New York, N. Y.

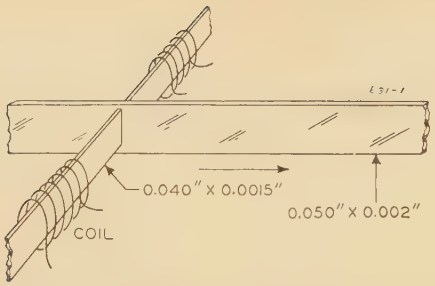

Figure 1. Dimensions of active portion of polepieces used in noise and signal level studies

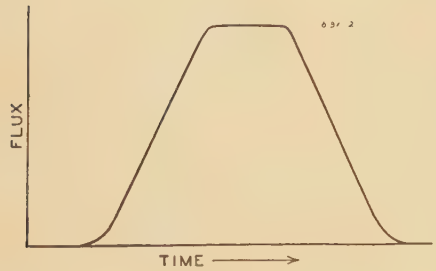

Figure 2. Time variation of flux in polepieces caused by a single small magnetized region in demagnetized tape

by the partial removal of the strong demagnetizing field brought about by the proximity of the reproducing polepieces. Letters a and h are the thickness of the tape and the polepiece height, respectively.

This expression for the reproduced power depends on frequency only through I_o^2 and $T(\nu)^2$. Moreover, I_o is practically independent of frequency if the same current is sent through the recording coils for all frequencies. For frequencies so low that the recording current remains substantially constant during the passage of an element of tape through the region of influence of the polepieces, it is obvious that this should be the case. But even for considerably higher frequencies, wherein the recording current changes appreciably while a tape element is near the polepieces, the amplitude of the recorded wave remains almost unchanged. This is because each tape element "remembers" the *highest* value of magnetizing field to which it is subjected, and not the last or even the average value. Actually, simple theory predicts a loss in I_o of two or three decibels at around 5,000 cycles, but this is opposed by a gain of roughly similar magnitude because of the decrease with decreasing wave length of the demagnetizing factor of perpendicular recording. Therefore we may take I_o to be independent of frequency and consider equation 5 to represent the over-all record-reproduce

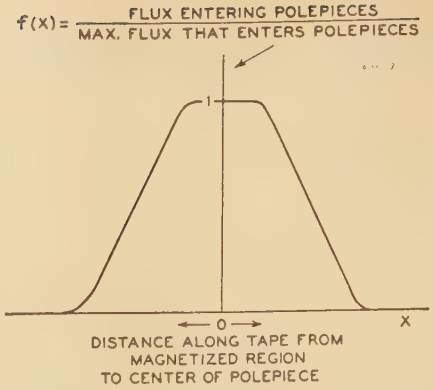

Figure 3. Qualitative shape of region of influence of polepieces

This curve is copied from one derived later and displayed in Figure 6. The sloping sides are actually curved, as indicated by the derivative curve of Figure 4. This curvature is not evident on such a small-scale figure

frequency response characteristic for constant recording current and a high impedance output circuit.

A comparison of equations 3 and 5 shows that

$$\frac{P_N(\nu)}{P_S(\nu)} = C \cdot \frac{S(\nu)^2}{T(\nu)^2} \qquad (7)$$

where C is a constant that is of no immediate interest. Moreover, $S(\nu)$ and $T(\nu)$ will be identical if $g(x)$ is a constant, that is, if the junction of the polepieces with the tape causes an inappreciable increase in the intensity of magnetization. Conversely, if the tape magnetization increases greatly because of the proximity of the polepieces, $g(x)$ will be a strongly peaked function similar to $f(x)$, and their product will be still more strongly peaked. In the first case, we should expect the noise and signal frequency characteristics to be the same; in the second case, the signal response should hold up to higher frequencies than the noise.

The conclusions of the preceding paragraph are valid only if the theory of noise on which equation 3 was derived is true, that is, that the noise is caused by many random magnetic irregularities less than 0.0015 inch in dimension. If the noise is attributable to any sort of mechanical vibration of the tape or polepieces, its frequency spectrum must be peaked at the vibration frequency or frequencies; the curve would bear little resemblance to that yielded by equation 3. If the noise is caused by many random irregularities in the tape which are *not* small in dimension compared to 0.0015 inch, the noise spectrum must be enhanced for wave lengths of the order of the irregularity dimensions. In such a case, the noise spectrum must have relatively less high frequency content than $S(\nu)$ and, therefore, less than $T(\nu)$, whether or not $g(x)$ is nearly constant.

On Figure 7 are replotted the noise measurements and the theoretical curve of Figure 5 together with signal output voltage measurements. The two sets of points have been shifted vertically along the logarithmic scale so that the low frequency 6-decibel-per-octave portions of the curves coincide. Figure 7 shows no concentration of noise at isolated frequencies, corresponding to vibration. Further, the high frequency content of the noise is definitely not lower than that of the signal response characteristic. In the light of the preceding discussions, this requires three conclusions:

1. The noise is produced by the passage between the polepieces of many randomly distributed magnetic irregularities.
2. The noise producing irregularities are smaller than 0.0015 inch in size.
3. $g(x)$ is not a strongly peaked function

While the data seem adequate to justify these conclusions, they do not explain how the noise characteristic can actually have *more* high frequency content than the response characteristic. However, the simple theory given here neglects a number of secondary effects and should not pretend to high accuracy in its predictions.

The conclusion that has been established is as important because of the noise producing mechanisms it proves negligible as for any positive contribution it may make to the theory of tape noise. For example, the noise cannot be caused by mechanical vibration of the tape or associated magnetic structures; it cannot be caused by variations in the magnetic properties of the tape because of mechanical eccentricities in the rolling mill; it cannot be caused by any kind of inclusion or grain size effect unless the dimensions of the irregularities are less than 0.0015 inch.

An obvious possible source of small magnetic irregularities in nominally demagnetized tape is found in the finite size of the magnetic domains that are believed to make up any permanent magnet. If a "demagnetized" tape is made up of many small magnetically saturated regions, oriented so as to cancel one another's field, there must be local imperfections in the cancellation process that result at any instant in the passage into the polepieces of a net flux different from zero. Statistical variations of this leakage flux along the tape must give rise to noise. In Appendix III a cal-

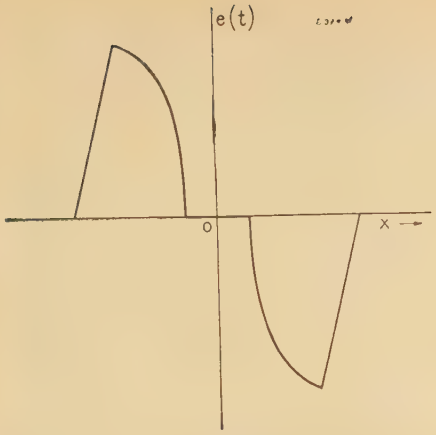

Figure 4. Voltage pulse corresponding to the region of influence shown in Figure 3

culation is carried out which leads to an expression for the open-circuit mean-square-noise voltage that should be measured if the tape consisted of saturated domains of volume v, with completely random directions of magnetization. The expression obtained is

$$E_N^2 = 3\times10^4 v \text{ volt}^2 \qquad (8)$$

Now, if the domain theory of the noise of demagnetized tape is an adequate one, equation 8 should predict a noise voltage considerably higher than that actually observed. This is because it is known that mutual interaction among the domains goes a long way toward cancelling out their resultant fields; the leakage flux must be only a fraction of that implied by random orientation, which was assumed in the derivation.

Measurements by various investigators [2,3] lead to values of v for most magnetic materials of the order of 10^{-9} to 10^{-8} centimeters.[3] For tape that is only 0.005 centimeter thick, there may be some reason to reject the higher figure, which corresponds to a linear dimension half as great as the tape thickness. Use of a value for v of 10^{-9} centimeters[3] in equation 8 leads to a noise voltage

$$E_N^2 \sim 3\times10^{-5} \text{ volt}^2$$

The experimentally measured value, for the conditions dealt with, is 2×10^{-11} volt.[2]

Obviously, the domain theory passes the first test of adequacy. From the derivation of Appendix III, it is clear that the observed noise can be accounted for even though the domains cancel all but 1/1,000th of one another's fields. It seems reasonable to conclude that the noise produced when demagnetized tape passes between the polepieces probably is caused by statistical variations in the flux leaving the tape owing to imperfect cancellation of the domain fields.

Figure 5. Comparison between observed noise spectrum of demagnetized tape and theoretical distribution based on region of influence of Figure 6

Tape speed = 16 inches per second. Polepiece width = 0.0015 inch

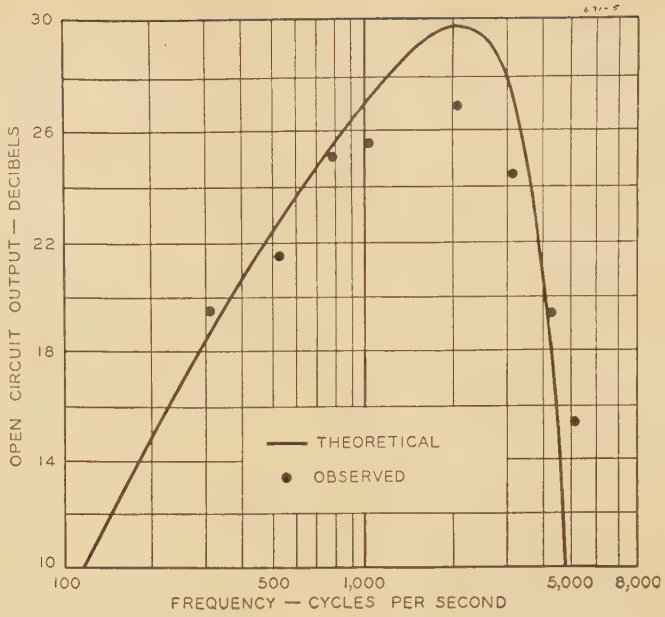

Noise in Saturated Tape

When tape from which previous signals have been erased by a saturation process is led through the polepieces, the noise produced in the output circuit is from 10 to 20 decibels higher than that of demagnetized tape, depending on the tape material, but it has the same frequency distribution. As in the case of demagnetized tape noise, this points to small magnetic irregularities as the likely source of the noise.

Since the tape is magnetized, nonmagnetic inclusions or variations in the coercive force or remanence would produce noise, where such irregularities would be ineffective in demagnetized tape. Steel tape is known to contain inclusions of carbon, whereas the coercive force and remanence, measured in the direction of tape magnetization, must vary with the orientation of the tiny crystals that make up the tape. Both these possible sources of noise have been investigated. Tape sections were etched and microphotographs made to reveal carbon particles and crystal boundaries. Measurements were made of the carbon particle sizes and numbers and of the crystal sizes. From such data, order of magnitude calculations of the resulting noise were made in a manner similar to the domain calculation of Appendix III. In both cases the predicted noise was far too low. Although there were probably some nonmagnetic inclusions in the tape that were not revealed by the etching processes used (austenite, for example), it seems unlikely that these inclusions could be numerous enough to account for the observed noise of magnetized tape.

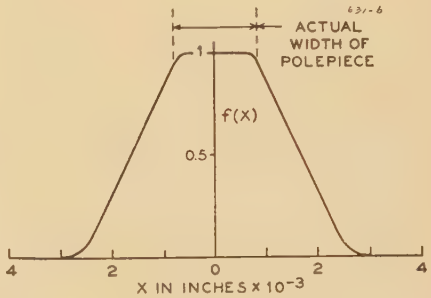

Figure 6. Shape of region of influence of polepieces assumed in deriving curve of Figure 5

As a result of these measurements and calculations, it has been concluded that the cause of noise in magnetized tape is probably rather similar to the cause of the lower noise of demagnetized tape. To account for the increased level, it is simply necessary to postulate that the process of saturating the tape and then decreasing its flux nearly to zero by its own demagnetizing field (see the section on signal levels) results in a greater degree of local disorder among the domains, whereby larger variations occur from point to point in the amount of flux leaving the tape surface.

Signal Levels in Magnetic Tape Recording

Equations 5 and 6 constitute a formal expression for the power output of a tape recording, but in greater detail than is needed for signal level considerations. For the present purposes, we may note that for an undistorted sine wave reproduction,

$$\Phi = \Phi_0 \sin 2\pi\nu t$$

where Φ is the flux linking the reproducing windings, and Φ_0 is an amplitude. The rms induced (open-circuit) voltage is therefore

$$e=\sqrt{2}\pi n\Phi_0\nu\times10^{-8}$$

It will be convenient to deal with the flux that enters the polepieces rather than the fraction of it that links the coils. Recalling (as stated in Appendix III) that the ratio of these quantities, for the magnetic structures in question, is 2 1/2 to 1, we may write

$$e=\frac{\sqrt{2}\pi}{2.5}\,n\Phi_{REP}\nu\times10^{-8}$$

where Φ_{REP} is the maximum flux that enters the polepieces during the sine wave reproduction. Substitution of n = 1,500 in this equation gives

$$e=2.6\times10^{-5}\Phi_{REP}\nu \qquad (9)$$

where e is in volts if Φ_{REP} is in maxwells and ν is in cycles per second.

The consideration given in the preceding section to the shape of the signal frequency response characteristic can be interpreted as an exploration of the dependence of Φ_{REP} on frequency and the reasons therefor. In the present section the aim will be to reconcile the observed absolute magnitude of signal output voltage with the physical constants of the tape-polepiece structure. It is both adequate and convenient to deal only with frequencies for which the wave length is so long compared with the region of influence of the polepieces that Φ_{REP} is independent of ν. Frequencies lying along the straight, 6-decibel-per-octave portion of the response curve of Figure 7 meet this requirement. Much of the data to be quoted will pertain to ν = 300 cycles, for which equation 9 becomes

$$e_{300}=8.0\times10^{-3}\Phi_{REP} \qquad (10)$$

Before it is possible to obtain from equations 9 or 10 a figure for the output voltage that should be gotten from a magnetic tape recording, it is necessary to determine the value of Φ_{REP}. The development has implied clearly that the intensity of magnetization in an element of tape when it lies between the reproducing polepieces differs from the intensity in the same element when away from the influence of the polepieces, which in turn differs from the intensity that existed in the element when it lay between the recording polepieces. It is now necessary to examine in detail the hysteresis processes to which an element of tape is subjected during the erase-record-reproduce cycle.

Hysteresis Processes in the Erase-Record-Reproduce Cycle

Two methods of recording will be discussed. The first method erases previous recordings by bringing every element of the tape to magnetic saturation (perpendicular to the tape surface), and then, in the recording process, superposes a d-c biasing field on the fields produced in the polepieces by the signals being recorded. The second method erases previous recordings by demagnetizing the tape; in the recording process an a-c biasing field is superposed on the signal fields.

Saturation Erase; D-C Bias Record. Figure 8 displays the manner in which H and I (perpendicular to the tape surface) vary throughout the erase-record-reproduce cycle. When an element of tape passes between the erasing polepieces, its resulting magnetic state is represented by the point A. As the element of tape leaves the erasing polepieces, its intensity of magnetization drops. If there were no demagnetizing effect, the intensity of magnetization would take on the value given by the intersection of the hysteresis loop with the ordinate axis, that is, the remanence of the magnetic material. However, the tape is so thin compared with its other dimensions that the presence of perpendicular magnetization gives rise to a strong demagnetizing field that tends to diminish this magnetization. For the dimensions of the tape used, the demagnetizing factor is about 95 per cent of that which would be exhibited by an infinitely thin plane. For the purposes of this discussion, it is sufficiently accurate to take the demagnetizing factor as equal to that of the thin plane: 4π. Consequently, when the element of tape under consideration passes out of the influence of the erasing polepieces, its magnetization drops along the hysteresis curve until it intersects the straight line $H=-4\pi I$. Accordingly, B represents the magnetic condition of the element of tape while it is passing from the erasing to the recording polepieces. When this element of tape comes between the recording polepieces, it is subjected to two distinct influences. Because of the junction of the polepieces with the thin tape, the demagnetizing field is diminished so that the point representing the magnetic state of the element of tape tends to move along the line BB' towards higher values of magnetization. This increase in I either is augmented or retarded by the influence of the field that is momentarily produced by the currents in the recording and biasing coils. If these currents sum to zero, the magnetization in the element of tape moves up to a value B'', where the point B'' lies on another straight line that passes through the origin but which has a

Figure 8. Magnetic history of a tape element

Saturation erase; d-c bias record

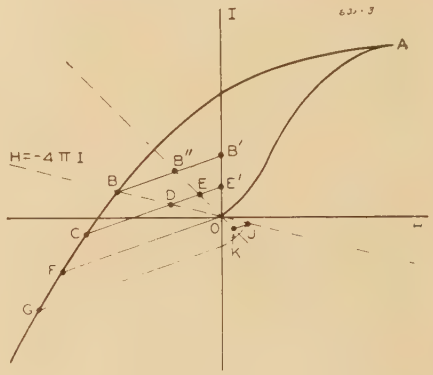

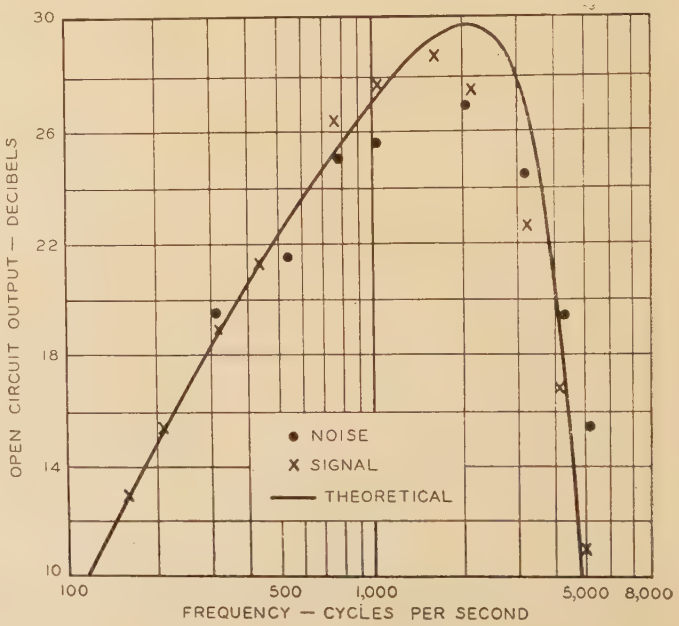

Figure 7. Comparison of noise and signal frequency characteristics

Theoretical curve and noise data copied from Figure 5

slope steeper than that of the line $H=-4\pi I$. The exact value of this slope depends upon the extent to which the demagnetizing field of the thin tape is removed by the junction of the polepieces. If the net field produced by the speech and biasing currents is positive at the instant in question, the point representing the magnetic state of the element will lie to the right of B''. If the field is negative, the representative point will lie to the left of B''. Now it is necessary to take account of an important property of most permanent magnet materials[4]; the hysteresis curve $BB''\ B'$ is nearly a straight line and is nearly reversible. This means that if the point representing the magnetic state of the element of tape while between the recording polepieces lies *anywhere* along the line BB', then the point which represents the magnetic state of that element after it leaves the recording polepieces will lie very close to B. (The representative point for an element of tape which is not in the vicinity of polepieces must always lie somewhere along the line $H=-4\pi I$.) This means that all values of recording fields that produce magnetic states in the tape represented by points lying between B and B' are nearly equivalent as far as the magnetization that they leave in the tape is concerned. It is evident, then, that when this method of recording is used, it is necessary to employ a negative biasing field so that all points representing the magnetic states of elements of tape while between the recording polepieces will lie somewhere along the hysteresis curve to the left of B. When this is done, the magnetic state of an element of tape while between the recording polepieces is represented by some such point at C. When that element of tape leaves the recording polepieces, its magnetization increases along the nearly straight line CE until the point D is reached. When the element of tape comes between the polepieces again for reproducing the magnetization moves up to the still higher value represented by the point E, as the demagnetizing field is diminished by the junction of the polepieces. Since over a limited range the curves whose intersections determine the positions of the points D and E are nearly straight, as is the hysteresis curve BC, the magnetization induced in the reproducing polepieces (at E) is linearly related to the recording current (at C).

The processes just described are shown in the curves of Figure 9, which have been plotted from tracings made on the screen of a cathode ray oscilloscope. The electrical circuit employed in these measurements was so arranged that the voltage supplied to the vertical plates of the oscilloscope was at every instant proportional to the flux density in the element of tape lying between the reproducing polepieces. (This was done by the use of low frequency sine wave recordings on the tape and an appropriate output integrating circuit); the voltage supplied to the horizontal plates was proportional to the recording current that had been used when this particular element was originally magnetized. (The fundamental of the reproduced signal, properly phase-adjusted, supplied this voltage.) In Figure 9, (a) corresponds to the case in which no biasing field was used on recording; in the case of (b), a small negative biasing field was used; in curve (c) a somewhat larger field, and so forth. The sine wave recording current was kept the same for all the curves. It is evident from these pictures that the phenomena described in the preceding paragraph have taken place. When the biasing field was small, as in (a) and (b), a large portion of the recording sine wave was nearly ineffective; when the biasing field became so large that the point representing the magnetic condition of the element of tape while between the recording polepieces always lay to the left of B (Figure 8), the reproduced signal was large and free from distortion, as in (c). When the biasing field became too great, the recording began to get into the overload region of the hysteresis curve, and as a result weak, distorted signals began to appear, as in (d) and (e). When the biasing field was positive, as in (b′) and (c′), the reproduced signals were weak and distorted, as was to be expected.

It has been seen that there is a sharp upper limit to the recording fields that can be employed, and that this limit is the field corresponding to the point B in Figure 8. There is also a lower limit. The lowest recording field which may be used without high distortion is the field corresponding to the point F. This is because the curves $BB''\ B'$, CDE, FO, and so forth begin to diverge markedly from straight lines if they are prolonged beyond the I axis. Consequently, the process GJK, which corresponds to a strong negative recording current, results in a reproduced negative intensity of magnetization I_K which is smaller than it should be if distortionless recording were to be done. This effect is shown in Figure 10. The measurements plotted on this figure were made on a rod of one of the materials from which our magnetic tape is made (vicalloy[5]), which had been heat treated so as to have approximately the same magnetic properties as the tape. (X-ray measurements on vicalloy tape show little preferred orientation of the crystals; hence the longitudinal properties of the rod and the perpendicular properties of the tape should be similar.) The rod was magnetized, demagnetized, and remagnetized in such a way as to

Figure 9. Oscillograms showing reproduced flux density as a function of recording current

Saturation erase; d-c bias record

a, b, c—Correspond to increasingly negative biasing fields

a, b′, c′—Correspond to increasingly positive biasing fields

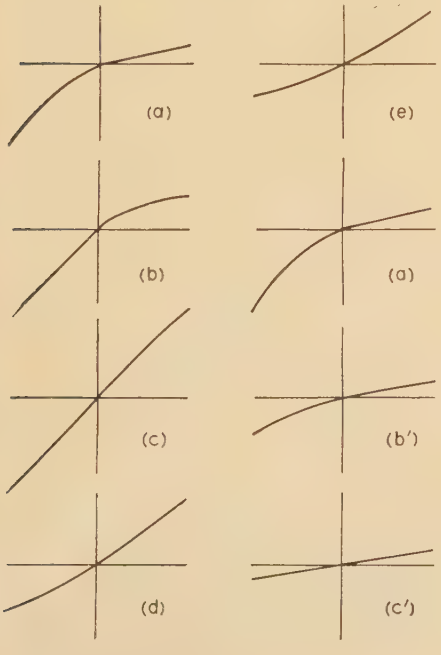

Figure 10. Plot of measurements on vicalloy rod when subjected to the hysteresis processes of the erase-record-reproduce cycle

Demagnetizing field assumed between record and reproduce $=-4\pi I$; at reproduce, $-(1/3)4\pi I$

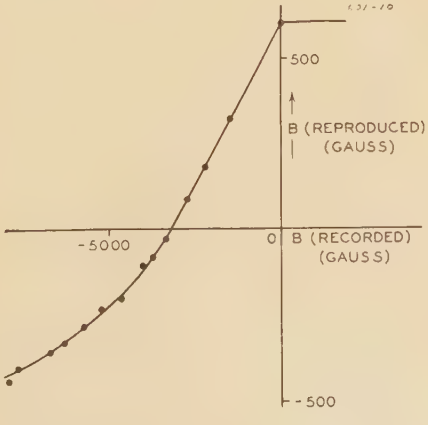

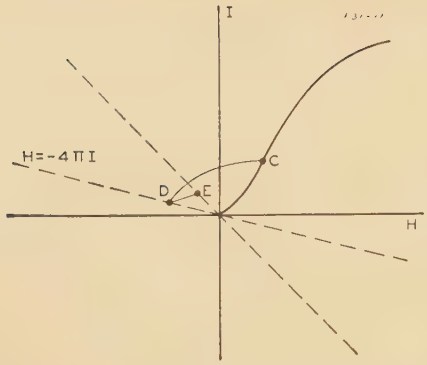

Figure 11. Magnetic history of a tape element

Demagnetization erase; no bias record

trace out curves of the type *ACDE* (Figure 8). For the relation between H and I characteristic of point E, a demagnetizing factor for the tape polepiece combination of amount $(1/3)4\pi$ was used. In later paragraphs it will be shown that a figure of $(1/2)4\pi$ might have been better, but the difference should not affect the conclusions drawn. From experimental determinations of the flux densities at various corresponding points C and E, the curve of Figure 10 was plotted, where the ordinate represents the flux density in the tape when in the reproducing position and the abscissa is proportional to the recording field which originally magnetized the tape. From Figure 10 it is evident that a linear relation between output flux and input field ceases to exist when the reproduced flux becomes negative.

Thus it is clear that this method of recording can employ only the recording currents that correspond to points on the line segment BF. The double amplitude of the maximum flux density that can be reproduced without high distortion is $B_{B''}$. This is only half the amplitude of the overload signal output. Therefore the conclusion: The maximum undistorted volume range of the magnetic tape for this type of recording is at least six decibels less than the maximum distorted range. This is an important practical result which always has been found to be true.

Demagnetization Erase; AC Bias Record. In the section on noise, it has been pointed out that demagnetized tape is 10 to 20 decibels less noisy than tape that has been saturated. Obviously it would be desirable to record on demagnetized tape. But if recording is done directly, without any biasing field, the reproduced signal is highly distorted. This is a natural consequence of the hysteresis cycle through which a tape element goes. In Figure 11, the letters C, D, and E have the same significance as in Figure 8, that is, they represent the state of the tape element while between the recording polepieces, while away from the polepieces, and while between the reproducing polepieces, respectively. Since the magnetization characteristic of a permanent magnet material is strongly curved near the origin, the reproduced intensity of magnetization at E could not be expected to have a linear relation to the magnetizing field at C. Such a linear relation can be achieved by the use of a d-c biasing field that causes recording to be done on the straight portion of the magnetization curve. However, the field required is so high that it restores the noise level practically to the value characteristic of saturated tape.

There is a method whereby the magnetization curve can be effectively straightened out and distortionless recordings thereby made on demagnetized tape. This result, which is achieved by the simple expedient of superposing on the recording fields a moderate field of supersonic frequency, is now well known in the art and will not be gone into here.* For the present purposes, it is sufficient to observe that the effects of the a-c biasing field are properly deduced if it is thought of as simply eliminating the curvature of the magnetization characteristic through the origin. Figure 12 shows the resulting hysteresis cycle through which an element of tape is taken. The curved path CD, which varies with the recorded signal strength is a feature of the hysteresis cycle that is not present in the other method of recording; it is conceivable that this might introduce nonlinearity in the relation between the reproduced magnetization and the recording flux density. In actual practice, however, this is found not to be the case; high quality recordings are produced by this method.

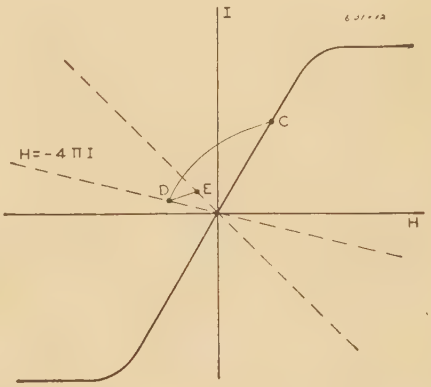

Figure 12. Magnetic history of a tape element

Demagnetization erase; a-c bias record

If the magnetization curve of Figure 12 were perfectly straight up to the saturation value of I, where it overloaded sharply, the double amplitude of the maximum distortionless reproduced flux density would be $2B_{B''}$ (see Figure 8). In such a case this method of recording would be capable of useful output levels six decibels higher than the method previously discussed. In practice the gradual nature of the overload reduces this gain to about four decibels.

Let us now return to the problem of calculating the level of the maximum useful signal that can be reproduced from the tape. Actually, let us deal with the saturation signal, from which we may deduce the maximum signal having comparatively low distortion.

We may start with equation 10, which now becomes

$$e_{\substack{800 \\ SAT}} = 8.0 \times 10^{-3} \Phi_{B''} \qquad (11)$$

The problem now is to obtain a value for $\Phi_{B''}$, the maximum flux that enters the polepieces during the reproduction of an overload sine wave signal.

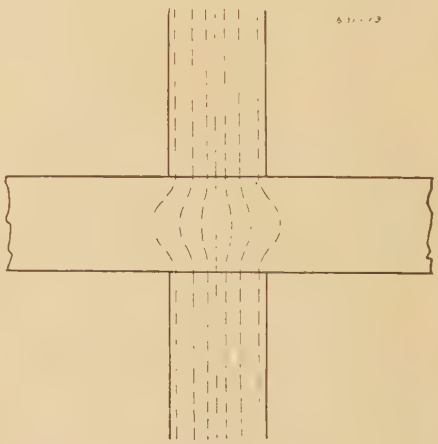

Figure 13. Configuration of lines of force during reproduction

Permeability of tape and polepieces $\gg 1$. Intimate contact between tape and polepieces

* Credit for the discovery of this recording method apparently belongs to W. L. Carlson and G. W. Carpenter, who filed a patent application on it in 1921 (United States patent 1,640,881, issued on August 30, 1927). The first commercial use of the method is believed to have been the audience-participation stereophonic recording display of the Bell System exhibit in the New York World's Fair, 1939–40. Some new techniques for handling the high frequency erasing and biasing problems are disclosed in United States patent 2,235,132, issued to D. E. Wooldridge on March 18, 1941. See also United States Patent 2,351,004, filed by Marvin Camras on December 22, 1941.

Evaluation of $\Phi_{B''}$

Figure 13 shows qualitatively the configuration of the lines of force in the vicinity of the reproducing polepieces. Although a large part of the flux leaks out of the side of a polepiece, through the air to the other polepiece, and back to the tape without linking the windings of the reproducing coils, this leakage is not shown on the drawing. Calculations of the reluctances of the leakage paths involved and search coil measurements agree in establishing that this leakage occurs well away from the pole tips, in a low reluctance portion of the magnetic circuit, and is properly taken account of by the factor of 0.4 that has been used in relating Φ_g and Φ_{REP}. All reluctances that are important in determining the amount of flux entering the polepieces are associated with the portion of the magnetic circuit shown on the figure.

The flux configuration depicted in Figure 13 is appropriate if the permeability of tape and polepieces is high and if intimate contact exists between them. In such a case, nearly all the flux enters the polepiece face, as shown.

The flux that passes into the polepieces may be determined from simple magnetic circuit considerations to be

$$\Phi = \frac{H_c a}{R} \tag{12}$$

where H_c is the value of H when $B=0$, which, for the pertinent hysteresis line $BB''B'$ (Figure 8), is simply the coercive force of the material; R is the reluctance of the complete magnetic circuit, including the tape, polepieces, and connecting yoke.

The reluctance of the circuit was measured directly. A single turn of fine wire was fitted snugly around the very tip of the polepiece lamination, and the voltage induced in it was measured when a small known 1,000-cycle current was sent through the 1,500-turn windings. A vicalloy tape that had been erased by saturation lay between the polepieces. In an obvious way the reluctance of the magnetic circuit was computed. Since there is no question that the reluctance of the circuit lies almost entirely in the pole tip tape region, both for this measurement and for the conditions during reproduction of a signal, this measurement should yield a value of reluctance approximately the same as that called for by equation 12. The measured value was 9.0 centimeter-gram-second units.

Substitution of $R=9.0$ in equation 12, together with the measured coercive force of 250 oersteds and the tape thickness of 0.0022 inch, gives $\Phi_{B'}=0.16$ maxwell. This value of $\Phi_{B''}$, when set into equation 11, predicts a 300-cycle-overload open-circuit reproduced signal of 1.3×10^{-3} volts. The value measured experimentally is 1.6×10^{-3} volts. The discrepancy lies within experimental limits.

Therefore it is possible to conclude that the reproduced signal levels are satisfactorily accounted for by the simple theory that has been given, wherein a detailed study of the hysteresis cycle through which a tape element travels has led to the conclusion that the maximum signal should be determined by the coercive force of the tape and the reluctance of the complete magnetic circuit.

If the theory is to be wholly satisfactory, it must meet the need of the analysis of the frequency characteristics of noise and signal, wherein it was pointed out that the similarity of the curves seemed to require that the magnetization of the tape element should not increase by a very large factor as it comes between the reproducing polepieces. The value of $\Phi_{B''}$ that has just been deduced, 0.16 maxwell, corresponds to a flux density of 180 gausses at the center of the polepieces, if $g(x)$ is *assumed* to be a constant and the flux therefore leaves the tape in accordance with the $f(x)$ shown in Figure 6. From the known relation between H and I, and therefore between B and I, given by the magnetic data that specify the hysteresis line $BB''B'$ of Figure 8 ($H_c=250$ oersteds, $B_{B'}=1{,}500$ gausses), this value of flux density can be computed to correspond to

$$4\pi I_{REP} = 400 \text{ gausses}^*$$

The value before the tape element comes between the polepieces is $4\pi I=250$ gausses. Therefore the assumption that $g(x)$ is constant leads to a result that is consistent with $g(x)$ varying by less than a factor of two, from $x=0$ to $x=\infty$. Replacement of the $f(x)$ used in this calculation by $f(x)\ g(x)$ for such a slowly varying $g(x)$ results in a trivial increase in the derived I_{REP} (about six per cent). It is clear that the correct figure for $4\pi I_{REP}$ at the center of the polepiece is not greatly higher than the value that has been calculated above, and that $g(x)$, as required by the frequency analysis, is such a slowly varying function that its replacement by a constant should produce only a slight change in the shape of the derived response characteristic.

The analysis of signal levels is not complete without an inquiry into the reasonableness of the value of 9.0 centimeter-gram-second units that has been measured to be the reluctance of the magnetic circuit. The reluctance of the circuit is made up of two parts, that of the polepieces and connecting yoke, and the reluctance of the tape element itself. For the structures used, the polepiece-yoke reluctance is easily computed to have a value of about 0.2 centimeter-gram-second units. Use has been made already of the fact that this is a negligible part of the total reluctance. The reluctance of the tape element cannot be accurately computed without a detailed knowledge of the flux configuration, but an upper limit can be set by assuming no bending of the flux between the polepieces. When the appropriate permeability value (obtained from measurements of $B_{B'}$ and H_c for vicalloy) and dimensions are set in the obvious equations, a maximum reluctance of 2.2 centimeter-gram-second units is predicted for the tape. Thus the computations predict a reluctance for the magnetic circuit of no more than 2.4 centimeter-gram-second units, as contrasted with the value of 9.0 which was measured, and which properly accounts for the observed signal strength!

It seems likely that the high reluctance of the circuit is caused by a region of low permeability at the tip of each polepiece. This may be thought of as introducing an effective air gap between each pole tip and the tape. The measured reluctance corresponds to a width of 0.0005 inch for each of these air gaps. The existence of an effective air gap of this order of magnitude between the surfaces of soft magnetic materials when pressed together is a common phenomenon in magnetics.[6] The effective air gap is attributed primarily to the pole tips and not to the tape because the reluctance of the circuit was found to be affected but slightly when the tape was removed and the pole tips allowed to touch one another.

Practical Applications

Up to this point the method of procedure has been simply to subject some of the principal features of perpendicular magnetic tape recording to simple analysis in order to arrive at an improved understanding of the physical processes involved. This section is devoted to a discussion of some of the practical implications of the results of the preceding two sections.

---

* Thus $\frac{-H}{4\pi I} \sim 1/2$, under the assumptions used. That is, the demagnetizing factor in the presence of the polepieces is half as great as for free tape

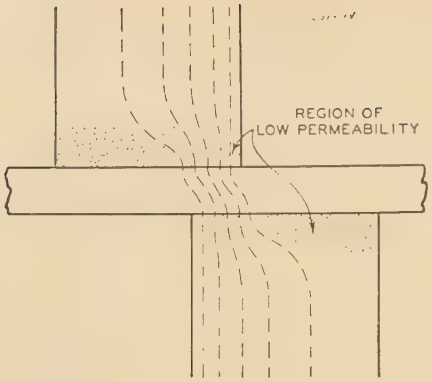

Figure 14. Action of wide offset polepieces

Reluctance of region of low permeability is decreased by increased cross section of the flux path. Region of influence is characteristic of the small overlap length and is not increased by wide polepieces

Increased Signal-to-Noise Level

If the conclusions reached in the first section are correct, a low noise level requires a tape material having a small magnetic domain size and/or a high degree of exactness in the mutual cancellation of the domain fields. The present state of magnetic domain theory does not permit the correlation of tape noise with any measurable magnetic properties. Empirical experiments on various kinds of tape have revealed no such correlation. The only useful generalization that can be drawn about tape noise is that demagnetized tape is always quieter than tape that has been saturated.

From the second section of this paper, a high signal level should be produced by a tape having a high coercive force. This principle guided Bell Telephone Laboratories in the development of vicalloy tape, which has a coercive force of 200 to 250, compared with the value of 40 or 50 characteristic of the chrome steel alloy formerly used. The signal output level is higher than that of the chrome steel tape, but the noise level is not enhanced. When recording is done on demagnetized vicalloy tape by the method that employs a supersonic field superposed on the recording field to straighten out the magnetization characteristic, a volume range (to overload) of 55 decibels is obtained. This signal-to-noise ratio is obtained in a system equalized from 100 to 8,000 cycles, at a tape speed of 16 inches per second. The equalization is done in the output circuit only. Under these circumstances the volume range is practically independent of frequency.* The useful volume range depends on the harmonic content that can be tolerated but is several decibels fewer than 55.

This combination of vicalloy tape and the superposed high frequency method of recording first was used commercially in the audience-participation stereophonic recording display of the Bell System exhibit in the New York World's Fair, 1939–40.

Simplified and Improved Polepiece Structure

When it was discovered that the output signal level was being limited largely by a region of high reluctance in the tips of the polepieces, a search was instigated for polepiece material that would exhibit lower tip reluctance than the molybdenum permalloy in use. The search succeeded in turning up a few other materials as good as the molybdenum permalloy but none better. The resultant directing of attention to other ways of decreasing this reluctance led to the idea of replacing the thin exactly aligned polepiece laminations by wide offset polepieces such as those pictured in Figure 14. The hope was that the region of influence of the polepieces would be controlled by the small overlap so that high frequency sensitivity would not be lost, but that the flux would be able to spread out in the region of low permeability, thus decreasing the reluctance and increasing the output signal level. On Figure 15 are replotted from Figure 7 the output signals obtained from the usual record-reproduce unit, in which the magnetic part of the pole faces consists of a 0.0015 inch by 0.040 inch lamination. In addition are plotted measurements on a unit in which the polepieces consist of molybdenum permalloy rod 0.041 inch by 0.040 inch, the leading edge of one polepiece being exactly opposite the following edge of the other (no overlap in Figure 14). The vertical difference between the two curves is adjusted for the measured difference in flux loss from pole tips to coils for the two units. The two curves correspond to recorded levels the same distance below saturation. Figure 15 shows a general increase in the output level that may be attributed to the expected decrease in pole tip reluctance. The shape of the high frequency portion of the curve is somewhat different for the new unit, but there is no evidence of an increase in the effective polepiece width. The upward bulge in the response of the new unit at low frequency is caused by a longitudinal component of magnetization, which, for the polepiece dimensions used, has a maximum at 200 cycles. This is all to the good, of course, since it reduces the amount of equalization needed. The position of this bulge is controlled by the width of the polepieces. This is the principal reason for the use of pieces 0.041 inch wide. The over-all signal level and moderate-to-high frequency response are just as high for 0.020-inch pieces, for example.

The wide, offset polepieces are also more efficient on recording, about eight decibels fewer ampere turns being required to saturate the tape than with the old unit. Furthermore, the 0.041-inch tip is sturdy and self-supporting. Its use permits a much simpler and cheaper record-reproduce unit design than that associated with the thin laminations, which had to be incorporated in a supporting structure of bakelite and brass and provided with a fairly complicated framework containing guides and yokes. The mechanics of the thick polepiece structure also permit a coil design that recovers practically all of the reproduced

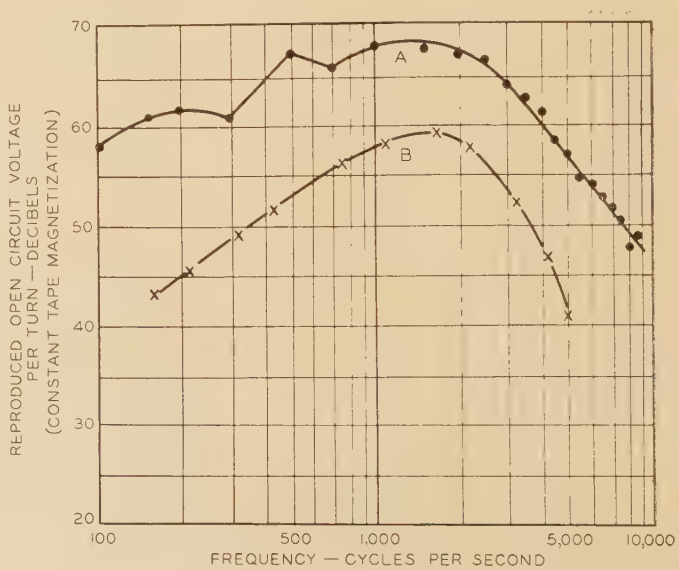

Figure 15. Comparison of output efficiencies of narrow aligned polepieces and wide offset polepieces

Curve *A*—Polepiece dimensions, 0.041 inch by 0.040 inch
Curve *B*—Polepiece dimensions, 0.0015 inch by 0.040 inch
Tape speed = 16 inches per second

* This is a consequence of the similarity between the noise and signal frequency characteristics.

flux that in the older structures leaked out of the polepieces without linking the windings. This adds another eight decibels to the relative efficiency of the new unit. As a result of all these gains, the new unit has an over-all record-reproduce transfer loss twenty-six decibels fewer than that of the old unit at 1,000 cycles. The complete comparison of the efficiencies of the two units is given in Figure 16.

Figure 17 shows the record-reproduce unit used in the Western Electric Mirrophone. The unit contains two polepiece-coil structures, one for erasing, the other for recording and reproducing.

Summary

In the first section of this paper, it was shown that the shape of the noise frequency distribution curve of both magnetized and demagnetized tape can be semi-quantitatively accounted for if it is assumed that the noise is caused by many random magnetic irregularities in the tape, of average dimension smaller than 0.0015 inch. An incidental result of the treatment was a derivation of the shape of the signal frequency response characteristic and an explanation of its similarity to the noise frequency distribution. Various possible sources of noise were examined. The only source found to be qualitatively and quantitatively acceptable consisted of statistical variations in the net flux entering the polepieces because of the finite size of the magnetic domains of the tape material.

In the section on signal levels, detailed consideration was given to the hysteresis processes through which an element of tape travels in the erase-record-reproduce cycle. Both the saturation erase d-c bias record and the demagnetization erase a-c bias record systems were considered. It was shown that the latter system not only is less noisy than the former, but also is capable of somewhat higher level high quality recordings. The magnitude of the overload signal was predicted in terms of the coercive force of the tape material and the reluctance of the magnetic circuit. The signal level prediction was shown to be in satisfactory agreement with experiment. The measured reluctance of the magnetic circuit was found to be so high that it required the existence of an effective air gap of about 0.0005 inch between each pole tip and the tape surface.

In the last section of the paper, it was shown how the search for a tape material having the characteristics that the theory indicated should give a high signal output, resulted in the development by the Bell Telephone Laboratories magnetic and metallurgical groups of a vicalloy tape having a markedly higher signal-to-noise ratio than had previously been obtainable. Attempts to diminish the pole tip reluctance that had been concluded to be a limiting factor in output signal strength were shown to have led to the development of a new type of record-reproduce unit with an improved frequency response, increased efficiency, and greatly simplified design. By a combination of vicalloy tape, the superposed high frequency method of recording, and the new unit design, high quality recordings equalized from 100 to 8,000 cycles with a useful volume range of more than 50 decibels can be made. A tape speed of only 16 inches per second is required, and the erase-record-reproduce unit combines simplicity of construction with low transfer loss.

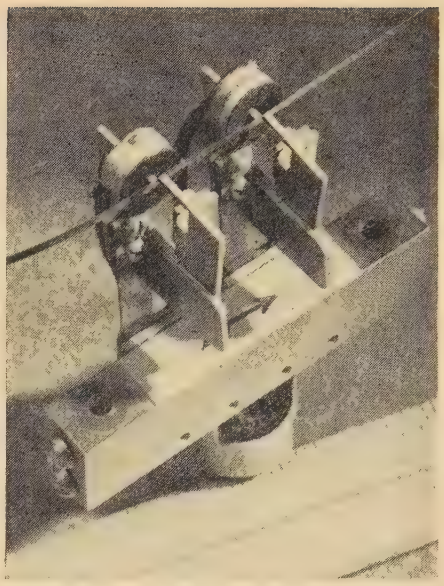

Figure 17. Illustration of erase-record-reproduce unit used in Western Electric Mirrophone

Tape guides and dust cover removed

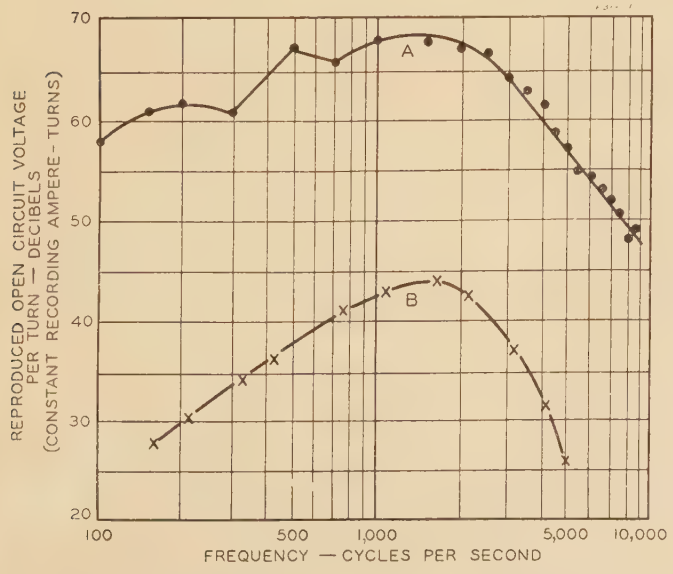

Figure 16. Comparison of over-all record-reproduce efficiencies of new (A) and old (B) units

Recording ampere turns the same for all measurements. Tape speed = 16 inches per second

Appendix I. Frequency Distribution of Noise Power Caused by Random Small-Voltage Pulses

The Fourier expansion of the $e(t)$ of equation 2 over a time interval T which includes the pulse in question is

$$e(t) = \sum_{m=1}^{\infty} B_m \sin\left(\frac{2\pi mt}{T} + \Phi_m\right) \qquad (13)$$

where

$$B_m = 2KMn \times 10^{-8}, \quad \frac{1}{T}\int_{-\infty}^{+\infty} \frac{df}{dx} \sin\frac{2\pi mx}{VT}\, dx \qquad (14)$$

In equation 13 the phase Φ_m depends on the position of the pulse in the time interval chosen for the expansion. Extension of the limits of integration to $\pm\infty$ is permissible since the integral is zero outside of the small interval occupied by the pulse.

The power developed in the frequency range $\Delta\nu$ by the combined effects of N voltage pulses, such as the above scattered at random throughout every time interval T (large compared with the pulse duration), is

$$P_n(\nu)\Delta\nu = \frac{1}{R}\sum_{m_1}^{m_2} E_m^2 \qquad (15)$$

where the reproducing coil circuit is assumed to have a resistance R for all frequencies, and the range $m_2 - m_1$ is related to $\Delta\nu$ through the equation

$$\frac{m_2 - m_1}{T} = \Delta\nu \qquad (16)$$

E_m^2 is the mean square noise voltage at frequency m/T and is

$$E_m^2 = 1/2NB_m^2 \qquad (17)$$

In equation 17 the 1/2 is caused by the usual relation between average power and voltage amplitude. NB_m^2 is the square of the amplitude of the noise voltage of frequency m/T, caused by N voltage pulses of identical size and shape scattered at random throughout the interval. (In the case of random phases of the elementary pulses, the squares of the amplitude add directly.) Combinations of equations 14, 15, 16, and 17 give, for the noise power in the range $d\nu$ at frequency ν,

$$P_n(\nu)d\nu = \frac{2(Kn\times 10^{-8})^2}{R} M^2\left(\frac{N}{T}\right) S(\nu)^2 d\nu \tag{18}$$

where

$$S(\nu) = \int_{-\infty}^{+\infty} \frac{df}{dx} \sin \frac{2\pi\nu x}{V} dx \tag{19}$$

Appendix II. Frequency Response Characteristic of Tape Recording

The problem to be considered is the following: For a given sine wave intensity of magnetization on the tape before it passes between the reproducing polepieces, how does the mean square reproduced signal power depend upon frequency?

At any instant the flux that enters the polepieces from an element of tape of length dx a distance x from the center line of the polepieces is

$$d\Phi = KdMf(x) \tag{20}$$

where dM represents the magnetic moment of the specified element of tape and the other quantities have the same meaning as in equation 1. For dM we may write

$$dM = ahI(x)dx \tag{21}$$

where a = tape thickness (0.0022 inch), h = polepiece height (0.040 inch), and $I(x)$ = intensity of magnetization of the tape a distance x from the center line of the polepieces. $I(x)$, in turn, may be expressed as

$$I(x) = g(x)I_o \sin \frac{2\pi\nu}{V}(x - Vt) \tag{22}$$

where $I_o \sin \frac{2\pi\nu}{V}(x-Vt)$ describes the variation with x and t of the magnetization that would exist if the reproducing polepieces were removed from the tape, while $g(x)$ is the factor by which the remanent magnetization of the free tape is multiplied by the partial removal of the strong demagnetizing field brought about by the proximity of the reproducing polepieces.*

* The hysteresis processes involved are discussed in the section on signal levels.

Equations 20, 21, and 22 give

$$\Phi = KahI_o \int_{-\infty}^{+\infty} f(x)g(x) \sin \frac{2\pi\nu}{V}(x - Vt)dx \tag{23}$$

Employment of the conditions $f(+x)\ g(+x) = f(-x)\ g(-x)$ and $f(\infty)g\ (\infty) = 0$ permits simplification to

$$\Phi = \frac{V}{2\pi\nu} KahI_o \sin 2\pi\nu t T(\nu) \tag{24}$$

where

$$T(\nu) = \int_{-\infty}^{+\infty} \frac{d}{dx}[f(x)g(x)] \sin \frac{2\pi\nu x}{V} dx \tag{25}$$

The reproduced signal power is

$$P_s(\nu) = \frac{1}{2} \frac{\left(10^{-8} n \frac{d\Phi}{dt}\right)^2_{\max}}{R}$$

of

$$P_s(\nu) = \frac{1}{2} \frac{(Kn\times 10^{-8})^2}{R} (I_o ah)^2 V^2 T(\nu)^2 \tag{26}$$

Appendix III. Tape Noise Caused by Saturated Domains of Random Orientation

The calculation must start with an evaluation of the constant K, of equation 18. K is the amount of flux that links the windings of the reproducing coils because of an element of unit magnetic moment lying directly between the polepieces. For the magnetic structures used in these tests, only about 40 per cent of the flux that entered the poletips succeeded in linking the windings. The exact value of the flux that enters the polepieces because of a magnetized region between them depends in a complicated way on the depth of the region in the tape and on the magnetic and geometric properties of the tape-polepiece structure. However, the correct answer can be shown to lie within a factor of three or four of $4\pi\frac{M}{a}$. This is accurate enough for the purpose at hand. Thus

$$K \sim \frac{4}{2.5} \frac{\pi}{a} \sim \frac{4}{a} \tag{27}$$

For evaluating $S(\nu)^2$, the $f(x)$ of Figure 6 may be used. A graphical integration gives

$$\int_o^{5{,}000 \text{ cycles}} S(\nu)^2 d\nu = 5{,}500 \text{ sec}^{-1} \tag{28}$$

Therefore, from equations 18, 27, and 28,

$$E_N^2 = R \int_o^{5{,}000 \text{ cycles}} P_N(\nu)d\nu$$

$$= 1.76\times 10^{-11} n^2 \frac{M^2}{a^2}\left(\frac{N}{T}\right) \tag{29}$$

where E_N^2 is the mean square open-circuit noise voltage, measured in a circuit covering the frequency range 0–5,000 cycles, and M, a, and T are in centimeter-gram-second units. For the reproducing coils used, n = 1,500 turns, whereas the tape thickness was about 0.005 centimeter. Therefore equation 29 becomes

$$E_N^2 = 1.58 M^2\left(\frac{N}{T}\right) \text{ volt}^2 \tag{30}$$

Both M and N/T depend on the domain size. If we consider it to have a volume v,

$$M = vI_{SAT}$$

where I_{SAT} is the saturation intensity of magnetization of the tape. For the materials used, $B_{SAT} \sim 15{,}000$ gausses, or $I_{SAT} \sim 1{,}000$ centimeter-gram-second units.

$$M \sim v \times 1{,}000 \tag{31}$$

For the number of domains per second that pass by the polepieces,

$$\left(\frac{N}{T}\right) = \frac{Vha}{v}$$

Substitution of the values $V = 16$ inches per second, $h = 0.040$ inch, $a = 0.002$ inch, gives

$$\left(\frac{N}{T}\right) = \frac{0.021 \text{ cm}^2 \text{ sec}^{-1}}{v} \tag{32}$$

Equations 30, 31, and 32 give

$$E_N^2 = 3.3\times 10^4 v \text{ volt}^2 \tag{33}$$

References

1. Sound Recording on Magnetic Tape, C. N. Hickman. *Bell System Technical Journal*, volume 16, April 1937, pages 165–78.

2. Barkhausen Effect II. Determination of the Average Size of the Discontinuities in Magnetization, R. M. Bozorth, J. F. Dillinger. *Physical Review*, volume 35, April 1, 1930, pages 733–52.

3. The Magnetic Structure of Iron Crystals, W. C. Elmore. *Physical Review*, volume 62, November 1942, pages 486–93.

4. Werkstoffe fur Dauermagnete, H. Neumann. *Archiv fur Technisches Messen*, number 69, March 1937, pages T38–42.

5. Vicalloy, a New Permanent Magnet Material, E. A. Nesbitt, G. A. Kelsall. *Physical Review*, volume 58, July 15, 1940, page 203.

6. Magnetic Core Materials Practice (booklet), Allegheny Steel Company, Brackenridge, Pa., 1937, page 89.

The Mho Distance Relay

R. M. HUTCHINSON
ASSOCIATE AIEE

THE NEED for more adequate discrimination by means of distance relays, between fault conditions and power swings has been heightened in recent years by the construction of longer transmission lines and by the transmission of larger amounts of energy over existing lines.

Several recent papers[1,2,3] have described the inadequacy of the impedance- and reactance-type directional distance relays to fulfill this need without the addition of auxiliary operating units. Auxiliary units always introduce additional sources of trouble, increase the need for maintenance, and make the maintenance more difficult. R. E. Cordray and A. R. van C. Warrington have described the use of a relay which measures a constant component of admittance for providing this discrimination, in addition to providing correct directional action and accurate distance measurement, all in one unit.[4] This characteristic has been named a mho characteristic.

Figure 2, which has been taken from their paper, illustrates how a relay at *A*, with a mho characteristic set to protect 90 per cent of the line to *B*, will operate over a smaller band of power swing conditions than the impedance or reactance-type relays. The line *AB* is the locus of impedance seen by the relay for metallic faults along the line. The mho distance relay operates for impedances within its circle. The impedance-type relay operates for impedances which lie within its circle of constant impedance and which are above and to the right of the straight-line characteristic of the directional element. The reactance-type relay operates for impedances which lie below its constant reactance locus and which are within the circular characteristic of the starting unit. It has been shown that a relay with the mho characteristic will provide instantaneous tripping during a power swing only if the electrical center of the system is within the section of the line protected by the relay and only if the voltages at the ends of the section become approximately 90 degrees out of phase. Such a condition usually indicates loss of synchronism, and it is usually desirable to sever the system at its electrical center.

It is the purpose of this paper to describe a 3-step distance relay operating on the mho principle. It has three independent units, each capable of providing a complete mho characteristic, thus approaching the ultimate in relaying simplicity—one contact in the trip circuit. Three mho distance relays (type GCY), with an auxiliary timing relay, provide 3-step distance phase protection to one terminal of 3-phase line. This relay also can be used as part of a distance pilot carrier-current relaying terminal.

Every high-speed distance relay has a tendency to trip on faults beyond its ohmic setting when the fault current has a large d-c offset. The induction cylinder-type mho relay has reduced this transient overreach to a few per cent, even for highly lagging transmission line circuits.

Another unique characteristic of the mho unit is its "memory action," which provides a strong polarizing flux for even a zero voltage fault. This condition causes the relay to operate fastest for nearby faults.

Arrangement

The general arrangement is shown in Figure 3, and the ohmic characteristics in Figure 4A. Each mho distance relay has three units providing 3-step directional distance protection for faults between two phases of a 3-phase line.

The first or instantaneous tripping zone is provided by the M_1 unit, which is usually set to operate for faults within the first 90 per cent of the protected section *AB*. The M_2 unit operates through contacts with a slight time delay to clear faults in the neighborhood of the next bus at *B*. The conventional third zone, providing time delay backup for faults beyond *B*, is provided by the offset mho unit, OM_3. The offset, resulting in an ohmic characteristic which encircles the origin, provides a strong steady torque for faults in the vicinity of the relay bus. As a by-product, it provides time delay backup for nearby faults in the reverse direction. It can be used with no offset if desired.

It is possible to reverse the polarity of the OM_3 unit to obtain the reversed OM_3 connection shown in Figure 4B. This provides time delay backup for faults between *A* and the bus behind it at *D*. The merits of the reversed OM_3 connection are discussed in a companion paper.[5]

One mho distance relay of drawout construction which affords ease of maintenance and testing is illustrated in Figure 1. The relay occupies approximately 6 by 20 inches of panel space.

Three mho distance relays combine with a common timing relay to give directional distance protection from one end of a 3-phase line. An elementary diagram for the relays at one terminal is shown in Figure 5. For clarity, the d-c connections to two of the mho distance relays are indicated by light lines because they parallel the connections of the third relay.

Figure 1. The mho distance relay

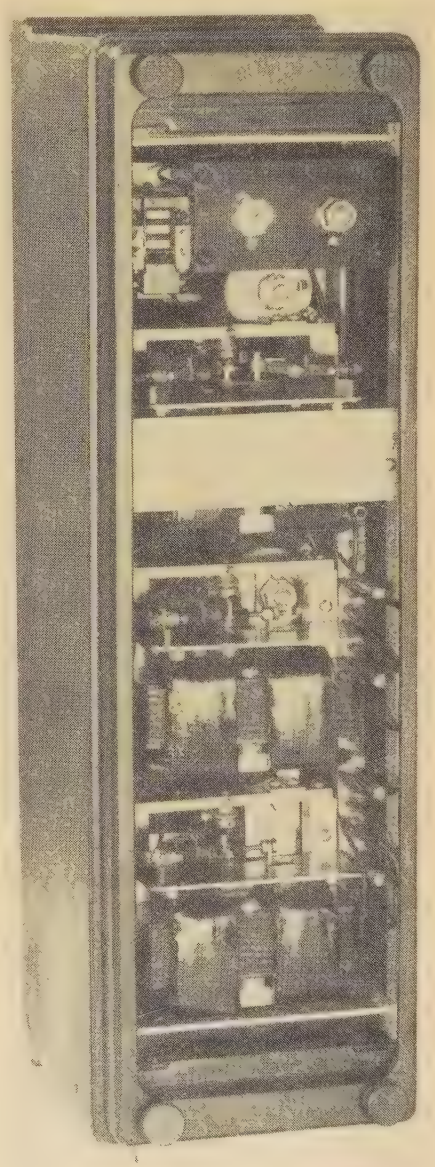

Paper 46-39, recommended by the AIEE committee on protective devices for presentation at the AIEE winter convention, New York, N. Y., January 21-25, 1946. Manuscript submitted November 23, 1945; made available for printing December 18, 1945.

R. M. HUTCHINSON is a project engineer with the Brown Instrument Company, Philadelphia, Pa.

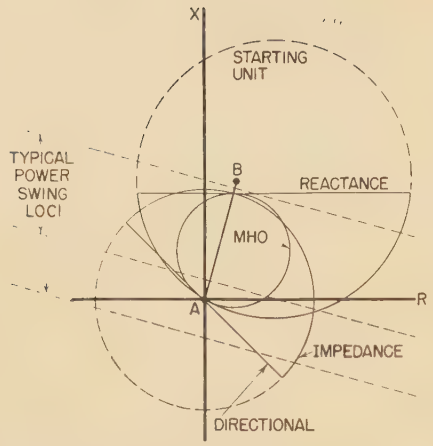

Figure 2. Impedance diagram illustrating tripping zones for impedance, reactance, and mho-type directional distance relays at *A* set to protect 90 per cent of the line *AB*

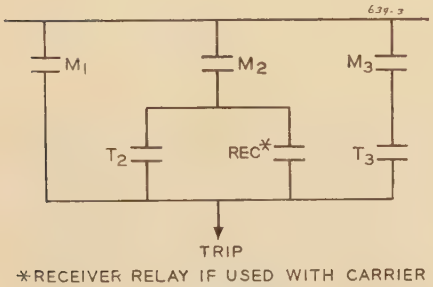

Figure 3. Fundamental trip circuit

The seal-in unit in each mho distance relay gives a target indication to show which phases are affected, while the targets mounted in the timing relay indicate which distance zone has operated.

Construction of the Mho Units

The mechanical construction of the mho unit is shown in Figure 6. Four laminated poles encircle a stationary core or inner stator with a small annular air gap between. Within the annular gap there turns an aluminum induction cylinder supporting a lightweight moving contact structure. The contacts are fine silver cylinders at right angles to provide the ideal point contact and are protected from excessive pressures by means of a clutch. This clutch is adjusted by means of a helical spring on the rotating shaft. The lead-in spiral for the contacts acts as a light control spring to give the contacts a positive position when the relay is de-energized. A lower jewel bearing with a highly polished pivot at the bottom of the shaft and a highly polished guide pin engaging a phosphor bronze bushing in the top of the shaft reduce friction to an almost imperceptible amount.

The arrangement of the coils on a unit which operates for faults between phases 1 and 2 is shown schematically in Figure 7A. The unit is polarized by the same potential that provides the restraining torque and derives its operating torque from double current windings, providing flux proportional to the difference of the currents in the two phases involved. This condition provides the same reach for 3-phase, phase-to-phase, or double phase-to-ground faults.

The two side poles carry the polarizing windings, which are tuned by the capacitor C_2 to have a slightly leading current. This condition causes the natural frequency of the polarizing circuit to be very close to 60 cycles. Therefore, when the terminal voltage drops to almost zero during bus faults, the polarizing flux continues for a period long enough to cause most rapid operation of the unit. See Figures 13, 14, and 15.

Figure 8 illustrates a cathode-ray oscilloscope screen with a recurrent sweep showing the current in the polarizing coils before and during a zero-voltage fault. The accuracy required of the M_1 unit during transient conditions makes the tuning of this circuit critical, so that the tuning reactor X_2 is used in this unit only. In the past, memory action has been incorporated into units which had a primarily directional function. For this purpose, phase resonance[6] was used and proved satisfactory, but to obtain accurate distance measurement also, it is necessary to tune to period resonance. Tuning a circuit for phase resonance produces current at unity power factor, which is the condition generally considered as resonance. Tuning for period resonance produces a circuit whose natural frequency is equal to the frequency of the applied voltage. When resistance is present, there is a difference between these two types of tuning.

Returning to Figure 7A, the restraining flux in the rear pole is supplied by two coils on the rear of the magnetic structure. The size of the ohmic characteristic is adjusted by means of taps on an autotransformer. The resistor R_1 is provided for a factory adjustment of the maximum restraint setting. The capacitor C_1 provides a certain amount of memory action to the restraining circuit of the M_1 unit to aid in preventing false operation of the unit during transient conditions at the inception of a fault, either caused by unsymmetrical currents or the result of mechanical rebound caused by spring in the lightweight rotating structure upon a sudden loss of restraining torque.

The current coils for providing operating flux to the front pole are wound on top of flux shifting windings on the two front legs of the magnetic structure.

With the accurate tuning of the polarizing circuit of the M_1 unit, no phase shift of the operating flux is necessary to obtain maximum operating torque at 75 degrees lag, because the circuit constants are such that tuning for maximum torque at 75 degrees and natural frequency at 60 cycles occur at the same point. Therefore the flux shifting coils are open-circuited for the 75-degree setting. Use is made of the flux shifting coils in order to obtain two other values of the angle of maximum torque, 60 degrees and 45 degrees. Using capacitive circuits to complete the circuit in the M_1 unit aids in reducing transient operating torques caused by d-c components in the current waves. The angle of maximum torque of the M_1 unit is selected by means of leads on a connection block.

The connections of Figure 7A for the M_2 unit are schematic in that the circuit of the flux shifting coils is completed permanently through R_2 instead of being brought out to a connection block. Ad-

Figure 4

A. Typical setting of mho distance relay for conventional 3-step protection
B. Typical setting of mho distance relay using the reversed OM_3 connection

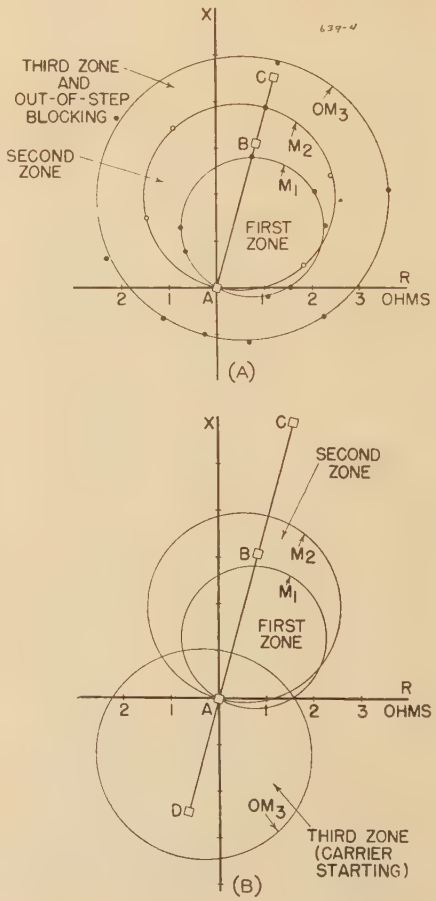

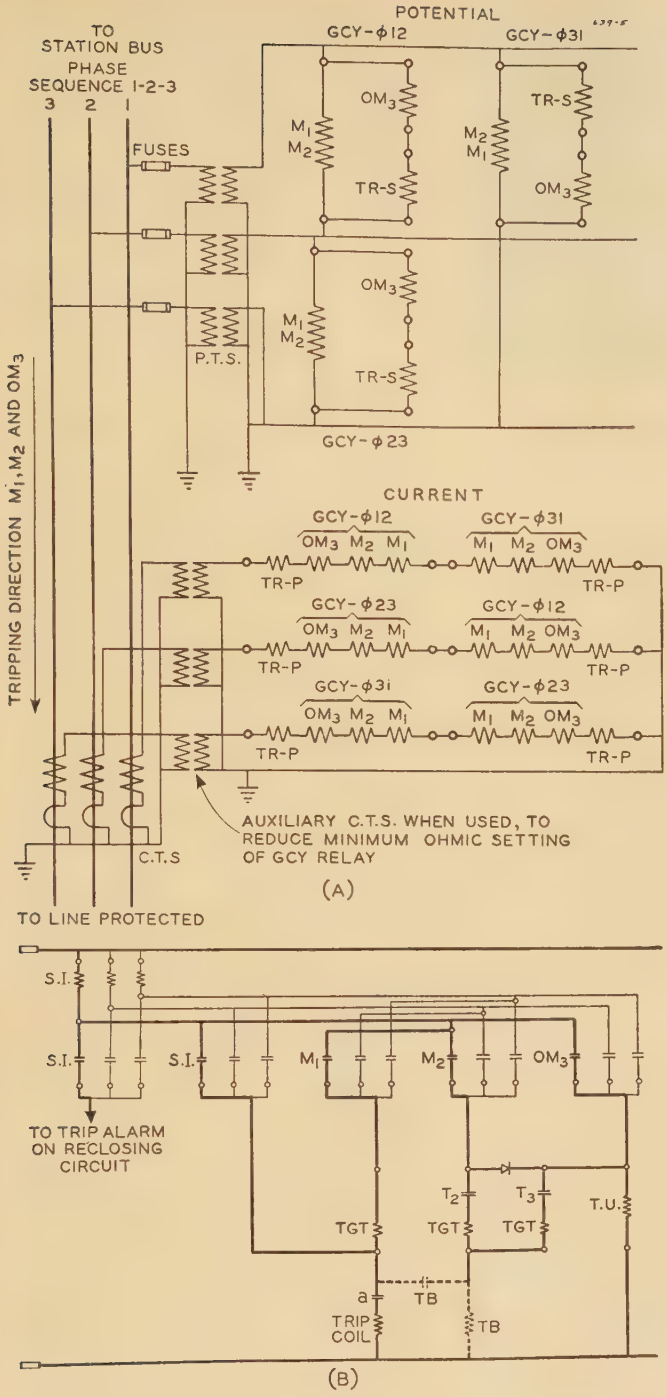

Figure 5. Elementary diagram of connections for one 3-phase terminal

A. A-c circuits
B. D-c circuits

M_1 = mho unit, first zone
M_2 = mho unit, second zone
OM_3 = offset mho unit, third zone
TR-P = transactor primary
TR-S = transactor secondary
S.I. = seal-in unit
T.U. = timing relay operating circuit
T_2 = zone 2 contact of *T.U.*
T_3 = zone 3 contact of *T.U.*
TGT = target
TB = relay for blocking instantaneous reclosing after time delay trip. Omit *TB* if this feature is not required, and connect lower terminals of all three targets
a = auxiliary switch closed when breaker is closed

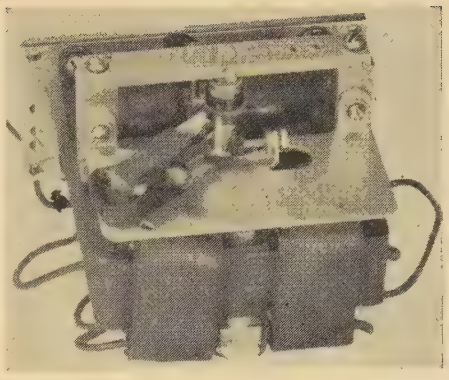

A. A single mho unit

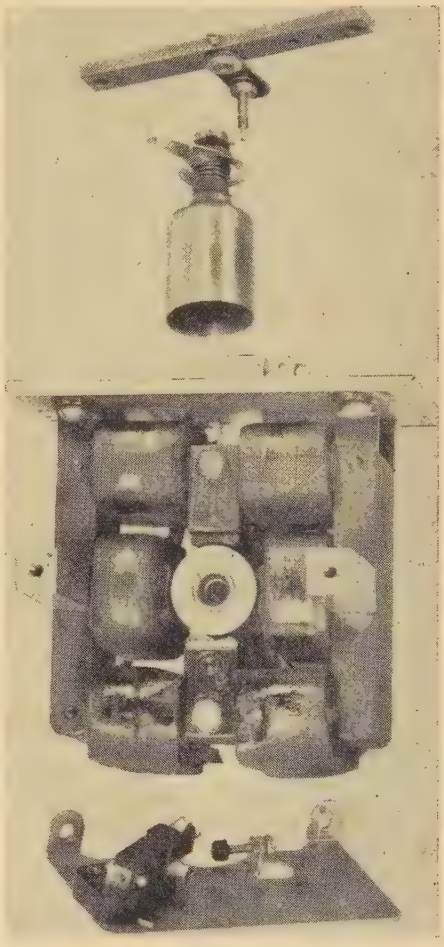

B. Exploded view of mho unit

Figure 6

justment of the R_2 will provide a continuous range from 60 degrees to 75 degrees for the angle of maximum torque.

The restraining torque of the M_1 and M_2 units is given by the expression $K_1E_{pol}E_{rest}$, where K_1 includes the sine of the angle between the two fluxes and the restraint transformer tap setting. The operating torque expression is $K_2E_{pol}I\cos(\phi-\theta)$, where θ is the phase angle of the relay characteristic, depending upon the phase angle of the polarizing circuit and the phase shift of the operating flux by the flux shifting circuit, and ϕ is the phase angle of the fault current $(I=I_1-I_2)$. Therefore the relay torques are balanced when $E_{pol}\ (I\cos(\phi-\theta)-(K_1/K_2)E_{rest})=0$. E_{pol} can be cancelled out of the preceding equation because it is not zero, even for zero voltage faults, because of memory action, leaving

$$\frac{E_{rest}}{I\cos(\phi-\theta)}=\frac{K_2}{K_1}$$

At the angle of maximum torque, $\phi=\theta$ and $E_{rest}/I=Z=K_1/K_2$.

With the closest manufacturing tolerances attainable, it is impossible to eliminate very minor mechanical, and consequently magnetic, dissymmetries from the unit. These introduce spurious torques proportional to the current squared which become strong enough under short-circuit conditions of high current and low voltage to overcome the torques produced by interaction with the polarizing flux.

These torques are reduced to negligible magnitudes by two means. The current coils are connected in parallel in order that the induced voltages in each of a pair of windings will be as nearly equal as possible, thereby producing equal fluxes. Any further adjustment that is

necessary is made by a slight shift in the position of the inner stator by means of a fine screw shown at the rear of the unit in Figure 6B.

The operating unit of OM_3 is identical with the M_2 unit. In order to produce the offset characteristic shown in Figure 4, a transactor is used as shown in Figure 7B. Transactor is the name that has been given to a reactor which has a secondary winding for a voltage several times that corresponding to the impedance drop produced in the transactor's primary winding, without increasing the burden.

The transactor in the OM_3 unit has double current winding, as does the operating unit, so that the voltage induced in its secondary winding is proportional to $I=I_1-I_2$ and leads I by 90 degrees. By connecting the proper amount of resistance R_4 across the transactor's secondary winding, the secondary voltage can be made to lead the primary current, I, by 75 degrees. The addition of this secondary voltage from the transactor in series with the potential transformer secondary

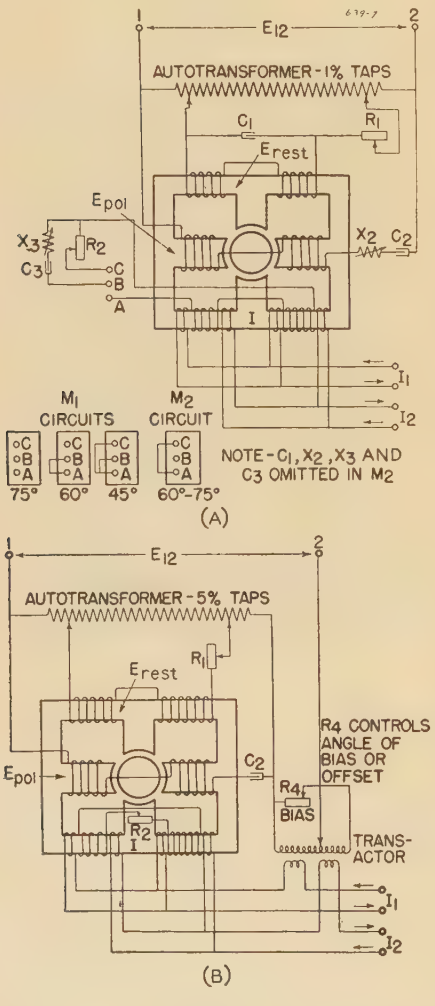

Figure 7

A. Diagrammatic wiring of M_1 and M_2 units
B. Diagrammatic wiring of OM_3 unit

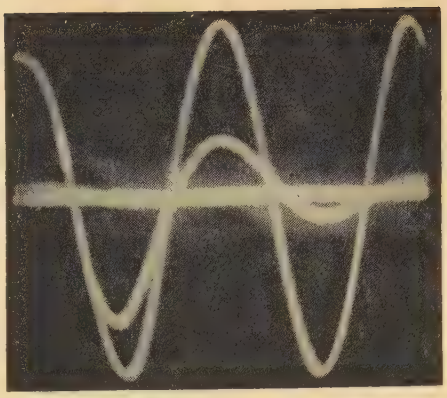

Figure 8. Current in polarizing winding of M_1 unit during zero-voltage fault

voltage, which is applied to the relay terminals, results in a shift of the unit's ohmic circle so that it no longer passes through the origin. This shift, or offset, is a distance corresponding to (transactor secondary voltage)/(I_1-I_2) ohms at a 75-degree phase angle.

Adjustment of R_4 can be made to cause the offset to be along any angle between 75 degrees and 60 degrees to match the angular setting of the operating unit. The magnitude of the offset is governed by taps on the transactor secondary winding.

Characteristics

Each unit has been designed to meet the requirements of its use in either a purely distance relaying scheme or a directional carrier current scheme.

The M_1 unit is purely a directional distance unit. It has been designed to operate for faults out to 90 per cent of the line section and for swing conditions which cause the voltages near the two ends of its protected section to be 90 degrees out of phase. It is provided with connections for setting the angle of maximum torque on 75 degrees, 60 degrees, or 45 degrees. In order to operate properly in the presence of resistance added by arcing faults (Figure 9) it is expected that the 60-degree setting will be used most frequently. This setting is discussed more fully in a companion paper.[5] The 75-degree setting is intended for longer lines, the 45-degree setting for short lines.

The plotted points shown in Figure 4A illustrate the negligible deviation of the operating characteristics of the units in a typical relay from the theoretical mho circle, when rated voltage is applied. This circular characteristic is a result of the steady torque produced in an induction cylinder unit. Units whose operating forces are pulsating throughout a cycle do not produce a true circle, thus adding difficulty to the calculation of settings for obtaining accurate relaying during power swings.

As is common with distance relays, the accuracy falls off at low values of current (and voltage). Figure 10 shows that the contacts of an M_1 or M_2 unit will close under steady state conditions for any fault in the correct direction from zero ohms up to the setting of the unit, so long as the current is greater than the vicinity of seven amperes. At two amperes the contacts will fail to remain closed under steady state conditions for faults within the first five per cent or the last five per cent of the relay's setting. That is, the ohmic circle maintains a constant center, but becomes smaller. This change occurs because the torques caused by the control spring and friction are no longer negligible with respect to the electrical torques in the unit.

The curve in Figure 10 is valid for an M_1 or an M_2 unit on its minimum distance setting. For other settings the accuracy is approximately the same for the same value of relay voltage.

Figure 10 represents accuracy under steady state conditions. With a rapid seal-in unit, the tripping area for fault conditions will be expanded by contact closure caused by transient torques. For faults at the relay bus, the memory action produces a strong torque in the correct direction for currents down to five amperes. For faults a short distance beyond the setting of the M_1 unit, its contacts may close because of a phenomenon known as transient overreach. For this reason the M_1 unit is set to cover 90 per cent of the line section under steady state conditions, allowing ten per cent for such errors. The minimum reach of the M_1 unit for faults near the end of its setting is as shown in Figure 10, but the maximum reach will be approximately ten per cent

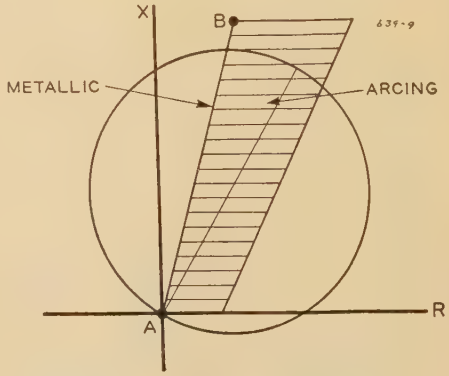

Figure 9. Effect of arcing fault

more. See "Transient Overreach" later in this paper.

The M_1 unit has correct directional discrimination for currents as low as 1.5 amperes at one volt and operates correctly for a period long enough to cause tripping when necessary for currents as low as five amperes on zero-voltage faults.

Figure 10. Steady state accuracy of M_1 and M_2 units

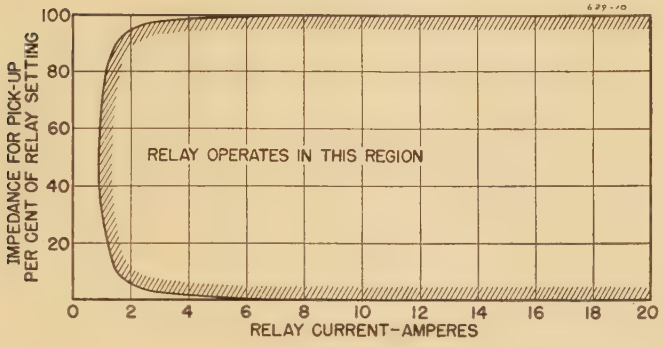

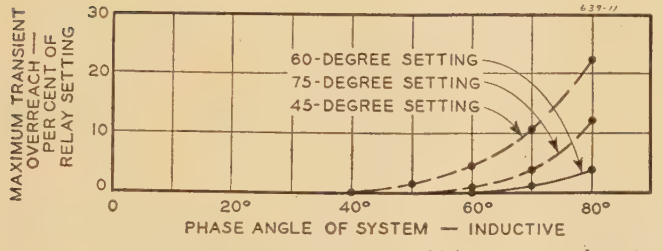

Figure 11. Maximum transient overreach of M_1 unit; normal setting is 60 degrees

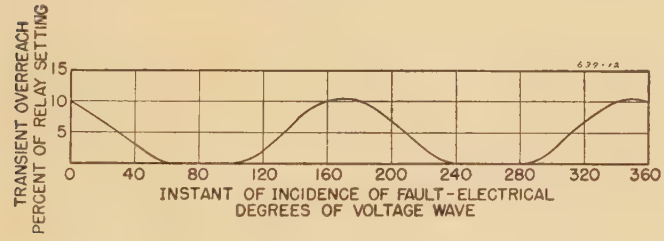

Figure 12. Variation of transient overreach in M_1 unit with instant of incidence of fault

The very small amount of transient overreach for this type of unit has been obtained at the sacrifice of some speed. Operating times of the M_1 unit are shown in Figure 13.

The M_2 unit is used with a short time delay in the timing relay to give the second zone of a distance relay setting, or it can be used as the directional relay to cause tripping in a carrier current relaying system. A large amount of transient overreach can be tolerated for either of these functions. Speed is important for the second function. Therefore the operating times have been made as short as possible (Figure 14), disregarding the transient overreach. The accuracy under steady conditions is the same as that of the M_1 unit, as well as the memory action at zero voltage.

If the OM_3 unit were used without using the transactor to obtain offset, it would operate exactly like an M_2 unit. In addition to the transactor, it has had a normally closed contact added.

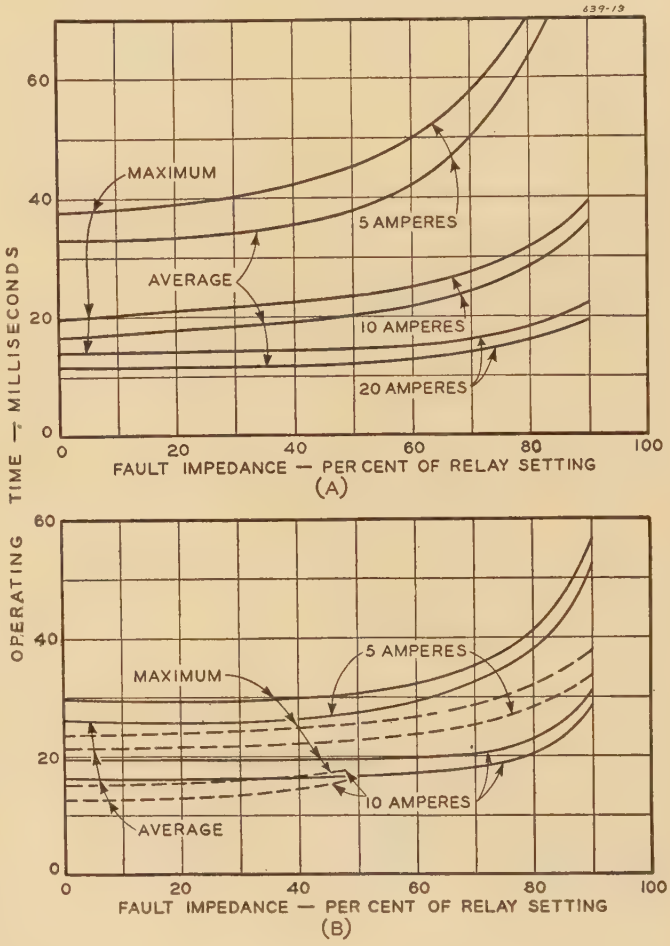

Figure 13

A. Operating times of M_1 unit with 3-ohm setting
B. Operating times of M_1 unit
Solid line—6-ohm setting
Broken line—12-ohm setting

The OM_3 unit is designed for use as a time-delay backup unit, for which accuracy is not important, and for use as a fault detector to start the carrier signal when carrier-current relaying is used. For this latter function, speed is very important. The normally closed contacts open in one-half of a cycle (60-cycle basis) for most fault conditions. In order to maintain them in their open position after the initial torque has disappeared for bus faults, it is necessary to use some offset.

Figure 15 shows typical operating times for the OM_3 unit. There are other conditions of distance setting and ohmic offset, but these same curves are approximately correct for the other conditions. Actual curves for the conditions not illustrated would show faster operating times.

The OM_3 unit's setting for the data shown in Figure 15 was three ohms with 1-ohm offset. This means that the ohmic circle has a diameter of three ohms, offset one ohm from the origin. Therefore the reach is two ohms in the unit's forward direction and one ohm in the offset direction.

The effect of the offsetting transactor is to introduce an operating torque proportional to the square of the current. In the offset direction, this I^2 torque has to overcome the torque caused by memory action, resulting in the increased operating times for faults in this direction. For this reason, it is necessary to use the reversed OM_3 connection whenever the OM_3 unit is used for starting a carrier-current signal.

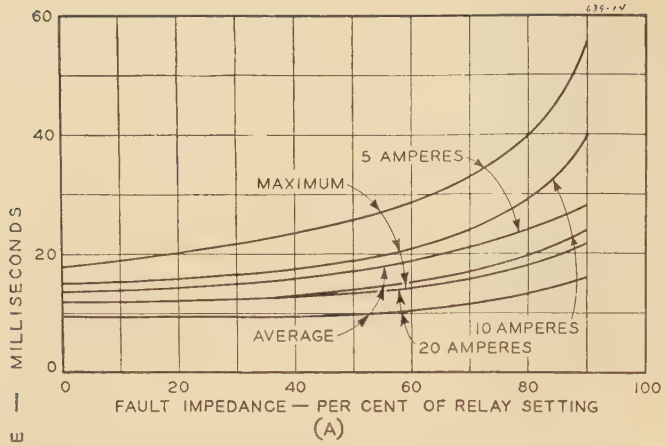

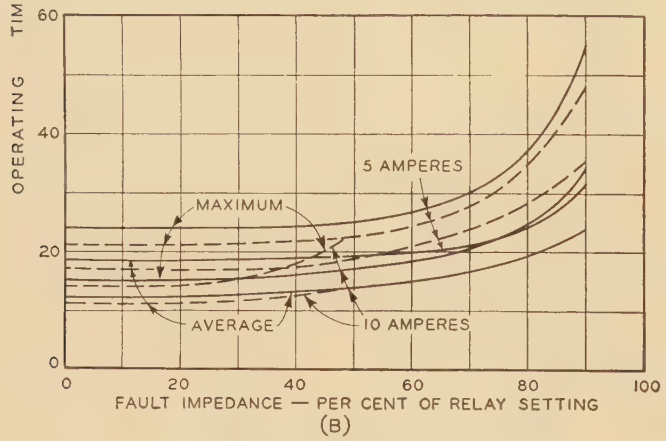

Figure 14 (above)

A. Operating times of M_2 unit with 3-ohm setting
B. Operating times of M_2 unit
Solid line—6-ohm setting
Broken line—12-ohm setting

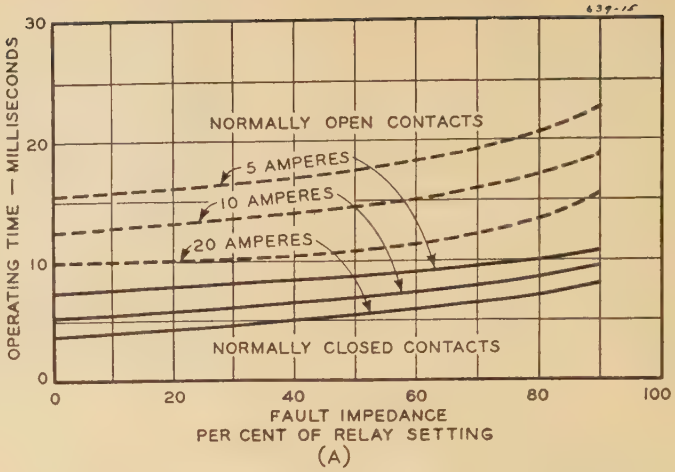

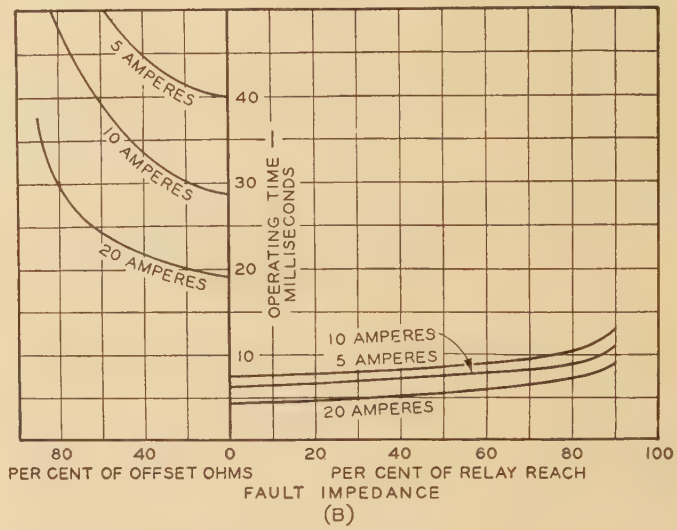

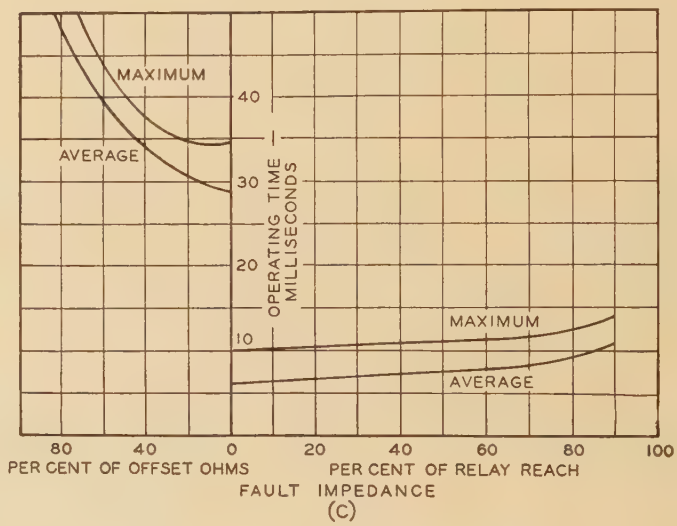

Figure 15 (right)

A. Average operating times of OM_3 unit with 3-ohm setting, zero offset
B. Average operating times of OM_3 unit with 3-ohm setting, 1-ohm offset
C. Operating times of OM_3 unit at ten amperes with 3-ohm setting, 1-ohm offset

Transient Overreach

The transient overreach of the M_1 unit mentioned under "Characteristics" is caused by transient conditions at the inception of a fault. These transient conditions may produce torque in the contact-opening direction, which will result in long operating times for faults within the setting of the unit. When the transient torque is in the contact-closing direction, the operating time is fast, and the contacts will close momentarily for faults a short distance beyond the setting of the relay.

The transients have been minimized in the potential circuits by the use of tuned circuits. The transients in the current circuit have been reduced for the 60-degree setting by the use of a capacitive flux shifting circuit. This reduction is illustrated by the small amount of overreach for the 60-degree setting in Figure 11.

Maximum transient overreach coincides with maximum d-c offset in the current wave. Thus in Figure 11, the higher the phase angle of the system, the greater the possible overreach. Figure 12 shows that for each half-cycle, faults initiated during the period which yields maximum d-c offset are most subject to overreaching.

This d-c offset can become quite large. For example, the equation for the short-circuit current of a fault occurring at the instant which produces the maximum d-c offset can be written

$$i = I(\epsilon^{-(R/\omega L)\omega t} - \cos \omega t)$$

where I is the peak value of steady state current and the shunt capacitance is

neglected. For a 60-cycle system whose ratio $R/\omega L$ produces an 80-degree phase angle, this fault must occur at an instant corresponding to ten degrees before the zero of the voltage wave, and the current becomes

$$i = I(\epsilon^{-66.5t} - \cos 377t)$$

The first current maximum occurs at 0.0081 second and has a magnitude of $1.58I$.

Good current transformers reproduce transients accurately during the first half cycle so that this maximum value is transmitted to the relay. Some types of distance relays have operating forces proportional to the square of the current, thereby multiplying the transient operating force by a factor of 2.5 without a compensating increase in the restraining force.

A d-c offset in the current wave of such magnitude can introduce additional errors when an impedance characteristic is offset into a mho characteristic by using the current to reduce the restraining force.

Ratings

The relay is rated for 115 volts and 5 amperes. In order to achieve the utmost reliability, the mho unit was designed to have the greatest possible torque. Not only was memory action employed, but the input to the relay is as high as thermal conditions will permit.

The maximum burdens for a practical setting of the mho distance relays at one terminal for 5 amperes and 115 volts are approximately 40 watts per phase at 95 per cent lagging power factor in the potential circuits, and 17 volt-amperes per phase at 60 per cent lagging power factor in the current circuits.

The basic ohmic setting of the three units, M_1, M_2, and OM_3, is 3 to 30 ohms phase to neutral at the relay terminals. Where shorter settings are required, auxiliary current transformers with a tap providing a three-to-one or a two-to-one ratio are used to obtain ranges of 1.0 to 10 or 1.5 to 15 ohms respectively. This enables the relays to be readily interchangeable and at the same time permits a high setting of restraining torque on all relays and the utilization of the maximum torque permitted by thermal limits. The connections to these auxiliary current transformers are shown in Figure 5.

The current sensitivity decreases in direct proportion to the ratio of the auxiliary current transformer. For this reason the relay is not applicable to short lines with small short-circuit currents. All characteristics have been presented for the relay without the auxiliary current transformers.

The ohmic offset of the OM_3 unit can be set for zero, one, two, three, or four ohms, phase to neutral. When the auxiliary current transformers are used, these values are reduced to 0, 0.33, 0.67, 1.0, or 1.33 for the 1.0- to 10-ohm range, or 0, 0.5, 1.0, 1.5, or 2 for the 1.5- to 15-ohm range.

Although the relay is designed principally for angular settings of 60 degrees for the M_1 unit and 75 degrees for the M_2 and OM_3 units, provisions have been made for setting the M_1 unit on 75 degrees or 45 degrees, and the M_2 and OM_3 units along with the transactor between 60 degrees and 75 degrees. Changes in the angular setting change the ohmic ranges of the units, with the minimum values as illustrated in Table I, the maximum remaining at ten times the minimum.

Application Limits

There are two limitations on the applicability of the mho distance relay. On systems where a fault near the end of the M_1 unit's setting can result in a small value of current, the unit will be slow, or possibly fail to operate and delay tripping until the time for the second zone. On very short lines, there is a possibility that the resistance added by arcing faults will place the impedance, measured by the relay for a fault which is actually in zone one, to be outside the zone-two setting of the relay. These limitations are discussed in a companion paper.[5]

In some cases, the M_1 unit can be set on 45 degrees to allow for the effect of arc resistance. If this is done on a system whose phase angle under fault conditions is greater than 70 degrees, the transient overreach of the M_1 unit requires that it be set to protect less than 90 per cent of the line section.

Setting of the GCY Relay

The angular setting of the M_1 unit is by means of leads on a connection block as illustrated in Figure 7A. If the angular settings of M_2 and OM_3 are to be changed, they must be changed by test.

The procedure for setting the diameters of the ohmic circles is the same as the one which has been in use for the well established type GCX reactance relay. The output tap settings of the two autotransformers shown in Figure 7 are chosen according to the following formula (the M_1 and M_2 units use the same transformer):

$$\text{Percentage output tap setting} = \frac{\text{unit's minimum ohms} \times 100}{\text{desired ohms}}.$$

The ohmic offset of the OM_3 unit can be adjusted by means of a lead on another connection block. The ohmic reach has to be increased by an amount equal to the ohmic offset to obtain the "desired ohms" in the formula.

Out-of-Step Blocking

As can be seen from Figure 4A, when the OM_3 unit is set to include the M_2 unit's setting, it will pick up on power swings before the M_2 unit. This characteristic can be utilized to recognize an out-of-step condition by the addition of a time delay relay such as *TB* in Figure 5. If the OM_3 unit operates at least four cycles, for example, before the M_2 unit, *TB* operates and can be used to open the tripping circuit. However, the mho unit's inherent characteristic of tripping at the electrical center of the system usually makes it advantageous to permit tripping and to use *TB* to prevent automatic reclosure after tripping caused by out-of-step conditions.

Table I. Change in Minimum Ohmic Setting at 115 Volts Versus Change in Angular Setting of Unit

Angular Setting	Minimum Ohmic Setting	
	M_1	M_2 and OM_3
75°	2.23–2.44	2.94–3.06
70°		2.82–2.97
65°		2.64–2.87
60°	2.94–3.06	2.37–2.78
45°	2.10–2.20	

Conclusions

1. A high-speed directional distance relay has been designed using a unit of the induction cylinder type so that it has an inherent directional characteristic and distance measuring accuracy, permitting one contact to protect 90 per cent of a line section.

2. A modification permitting transient overreach provides speed acceptable for use as a directional relay in carrier-current application.

3. The use of a transactor provides a quasi-impedance unit suitbale for starting a carrier signal and providing time delay backup protection.

4. A combination of the three units with a timing relay provides 3-step distance protection.

Metal-Clad Unit-Type Switchgear for 33-Kv Service

C. H. KREGER
MEMBER AIEE

Synopsis: The experience of the Public Service Company of Northern Illinois with metal-clad switchgear has been outstanding, both from the standpoint of reliability of operation and safety to personnel, two of the principal objectives sought by the engineers of the company when they pioneered this type of equipment. This equipment has been applicable not only to the voltage classes up to and including 15,000 volts, but also in the 33,000-volt class, of which the company has seven major installations which have been in service from 13 to 16 years. This report of experience with 33-kv metal-clad switchgear is offered as proof that development and use should be resumed and continued in what is undoubtedly a fertile field for the application of principles which are now generally accepted. It is not a detailed discussion of the design and construction of metal-clad equipment, but rather a factual record of progress already made and proved by 13 years of operating experience. Conclusions drawn from this report are that the main objectives sought after in the development of metal-clad type of switchgear have been obtained satisfactorily. Experience has demonstrated clearly its outstanding operating reliability as compared with the conventional open type, and its perfect safety record for operating and maintenance personnel has been made possible by the inherent safety features which are practical only in metal-clad equipment. If these and other factors which cannot be evaluated precisely are taken into consideration and if the further exploitation in the post-war period of materials and methods developed during the war is kept in mind, it would appear that there is no question about the continued development of metal-clad type of switchgear in all voltage classes. Repetitive manufacturing, standardization, and prefabrication are some of the most potent means of combating the continually rising cost of electrical station and substation installations. The electrical equipment manufacturers are applying these principles to a growing extent and are promoting their use throughout the industry. The principles, of course, are not new, the present movement being directed mainly toward a more intensive and wide-spread application. Neither the manufacturer nor the utilities can afford to neglect any application of these principles that can be justified economically.

IN the initial use of metal-clad equipment, the engineers of the Public Service Company of Northern Illinois had certain definite objectives in view. Subsequent operating experience has shown that very substantial advances had been made toward these objectives before progress was interrupted about 1931 by economic conditions. This experience indicates that development and use of this equipment should be extended to higher voltages.

The outstanding characteristics of the installations of all voltages made by the Public Service Company of Northern Illinois were complete enclosure in metal, maximum practical factory assembly, and the filling of all space in the enclosing structure with an insulating medium other than air. Various terms were applied to such equipment, the one in most general use being "metal-clad gear." The equipment of this nature now being manufactured and used is enclosed in metal and factory assembled but, with possibly a few exceptions, is not filled with an insulating medium. It also is designated by various terms, including "metal-clad." Complete enclosure and maximum factory assembly are fundamental, but the filling or nonfilling of the housing can be considered a matter of design keeping in view the objectives.

Objectives

Broadly speaking, the objectives of advantages to be obtained from metal-clad construction are Safety, Reliability, and Economy. The first two can be obtained without the third; the third cannot be obtained without the first two.

Safety of personnel is fundamental and needs no explanation.

Reliability can be considered as the quality of being available at all times for the service for which it was designed and rendering that service continually.

Economy is more involved than the other two main objectives and includes both, because no installation can be truly economical if it is not safe and reliable. Safety and reliability in themselves, however, are of sufficient importance to warrant special consideration. They do have a very real and substantial monetary worth, but it is impractical to assign a definite dollar value to it. Economy, therefore, is considered herein as the actual dollar expenditure in rendering service from a given installation. To obtain fair comparisons, economy must include the following cost factors:

1. First cost (manufacturer's cost to user).
2. Engineering, supervision, and overhead (user's).
3. Installation and transportation.
4. Maintenance and repair.
5. Operation.
6. Durability (life expectancy).
7. Space occupancy and appearance.
8. Salvage value.

History and Progress

For the purpose of determining what progress has been made in the attainment of the objectives, we can consider the history of the 33-kv installations as a group in reference to each objective.

5. The unit which causes instantaneous tripping for faults in the first zone can provide correct tripping during out-of-step conditions on most systems without auxiliary blocking relays.

References

1. PROTECTIVE RELAYING FOR LONG TRANSMISSION LINES, A. R. van C. Warrington. AIEE TRANSACTIONS, volume 62, 1943, June section, pages 261–8.

2. PERFORMANCE REQUIREMENTS FOR RELAYS ON UNUSUALLY LONG TRANSMISSION LINES, F. C. Poage, C. A. Streifus, D. M. MacGregor, E. E. George. AIEE TRANSACTIONS, volume 62, 1943, June section, pages 275–83.

3. IMPEDANCES SEEN BY RELAYS DURING POWER SWINGS WITH AND WITHOUT FAULTS, Edith Clarke. AIEE TRANSACTIONS, volume 64, 1945, pages 372–84.

4. THE MHO-CARRIER RELAYING SCHEME, R. E. Cordray, A. R. van C. Warrington. AIEE TRANSACTIONS, volume 63, 1944, May section, pages 228–35.

5. APPLICATION OF THE OHM AND MHO PRINCIPLES TO PROTECTIVE RELAYS, A. R. van C. Warrington. AIEE TRANSACTIONS, volume 65, 1946, June section, pages 378–86.

6. AMERICAN STANDARD DEFINITIONS OF ELECTRICAL TERMS, C42-1941. American Standards Association, New York, N. Y., 1941. Section 05.05.401.

Paper 46-43, recommended by the AIEE committees on protective devices and power transmission and distribution for presentation at the AIEE winter convention, New York, N. Y., January 21–25, 1946. Manuscript submitted October 29, 1945; made available for printing December 19, 1945.

C. H. KREGER is engineer, electric station and substation design, for the Public Service Company of Northern Illinois, Chicago, Ill.

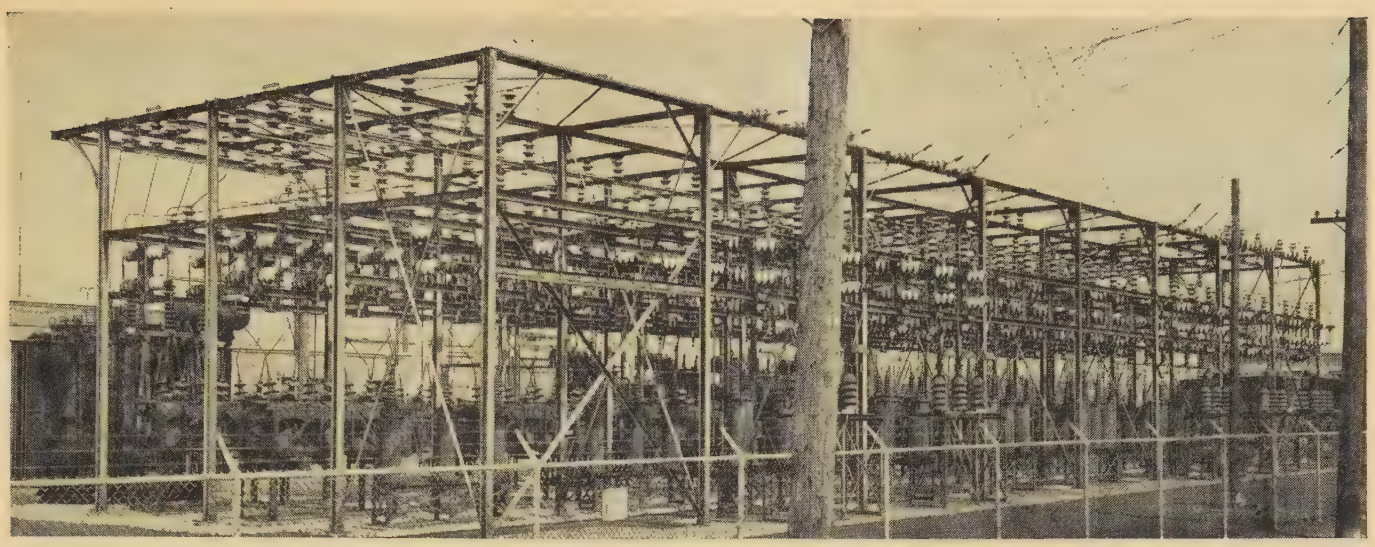

Figure 1. Typical 33-kv open-type structure
This shows installation used for cost comparison

Safety

There can be no doubt that working conditions are immeasurably safer on all of these installations than on conventional open-type installations. The safety factor is self-evident when it is considered that all current-carrying parts are enclosed in grounded metal and interlocks provided to prevent wrong operations and exposure of energized parts. Interlocking on metal-clad gear is entirely practical to an extent beyond possibility on open-type.

The prevention of inadvertent contact with energized parts can be accepted on the basis of the design. The proof, however, is negative because incidents occurring while working on metal-clad equipment, which would have caused an accident if the equipment had been open-type, are not recorded for the simple reason that there was no accident. An example of this is shown in the routine maintenance work of painting. Since 1928 there have been two accidents on 33-kv open-type structures, one resulting in a fatality and the other in an injury, definitely attributable to painting. These accidents could not have happened on metal-clad equipment. There is no record, of course, of painting in the wrong place on metal-clad because it can be painted while energized.

Since 1928, when the first 33-kv metal-clad gear was installed, to date there have been no accidents caused by inadvertent contact with energized equipment. This is also true of the lower voltage equipment, of which there are many installations on the system of the Public Service Company of Northern Illinois. Only one accident resulting in injury was recorded in this period. This accident was caused by burning oil from a ruptured box housing an oil-immersed disconnect switch. The switch blade fell into a ground clip because of the failure of an operating rod in one of the earliest installations. The failure definitely was caused by a defect in design which has been corrected.

During the same period, three fatalities and four injuries have occurred on open-type 33-kv equipment, all of which, except two of the injury cases, were caused by contact with energized conductors. One of the latter resulted from the failure of a bushing, and the other was the result of falling porcelain from an insulator which had failed mechanically.

Experience has shown that the metal-clad installations have a distinct advantage in reduction of nonelectrical accidents also, mainly by the elimination of the necessity of temporary staging and ladders or the climbing of complicated structures. When necessary, permanent ladders, platforms, and railings are provided easily.

Reliability

The same major characteristic which provides safety in metal-clad gear, that is, the enclosure of all current carrying parts, also gives it an inherent quality of reliability, since it excludes practically all foreign elements which interfere with normal operation, such as weather, animals, birds, deleterious gases, dirt, and solid objects. There is no need to cite the instances of outage or damage to open-type equipment from these causes; they are all too familiar. Two outstanding examples might be mentioned, however. One metal-clad installation is immediately adjacent to a railroad right-of-way, and, in addition to normal heavy traffic, locomotives stand for extended periods on a side track within 20 feet of the structure, which is sometimes obscured in smoke. It is doubtful if an open-type installation could be kept in service at this location. Just recently the Public Service Company of Northern Illinois was forced to remove an open-type 33-kv switching structure on account of many insulator flashovers caused by contamination of the air by an industrial plant one-fourth of a mile distant. It might be well to mention birds particularly, which are a source of trouble and expense in open steel structures. They build nests in enclosed structures also, but there they are merely an annoyance and not a hazard to service.

All of the 33-kv metal-clad installations made by the Public Service Company of Northern Illinois are still in operation and giving reliable service. There were, of course, operating difficulties at the start which are to be expected in any newly designed equipment, particularly in a radical departure such as 33-kv metal-clad was at that time.

Electrical Difficulties

The most serious of the problems arose in connection with the shell bushings which were mounted over openings in the bottom of the metal boxes or housing of the gear and served as the sockets for plugging in the oil circuit breaker. Thus, the inside surface of the shell itself was exposed to air while the outside was exposed to the oil in the box or compartment. The first 33-kv gear was installed in April 1928, and the first failure of a shell bushing occurred in March 1929 with others following. The fact that the failures usually occurred during a rising

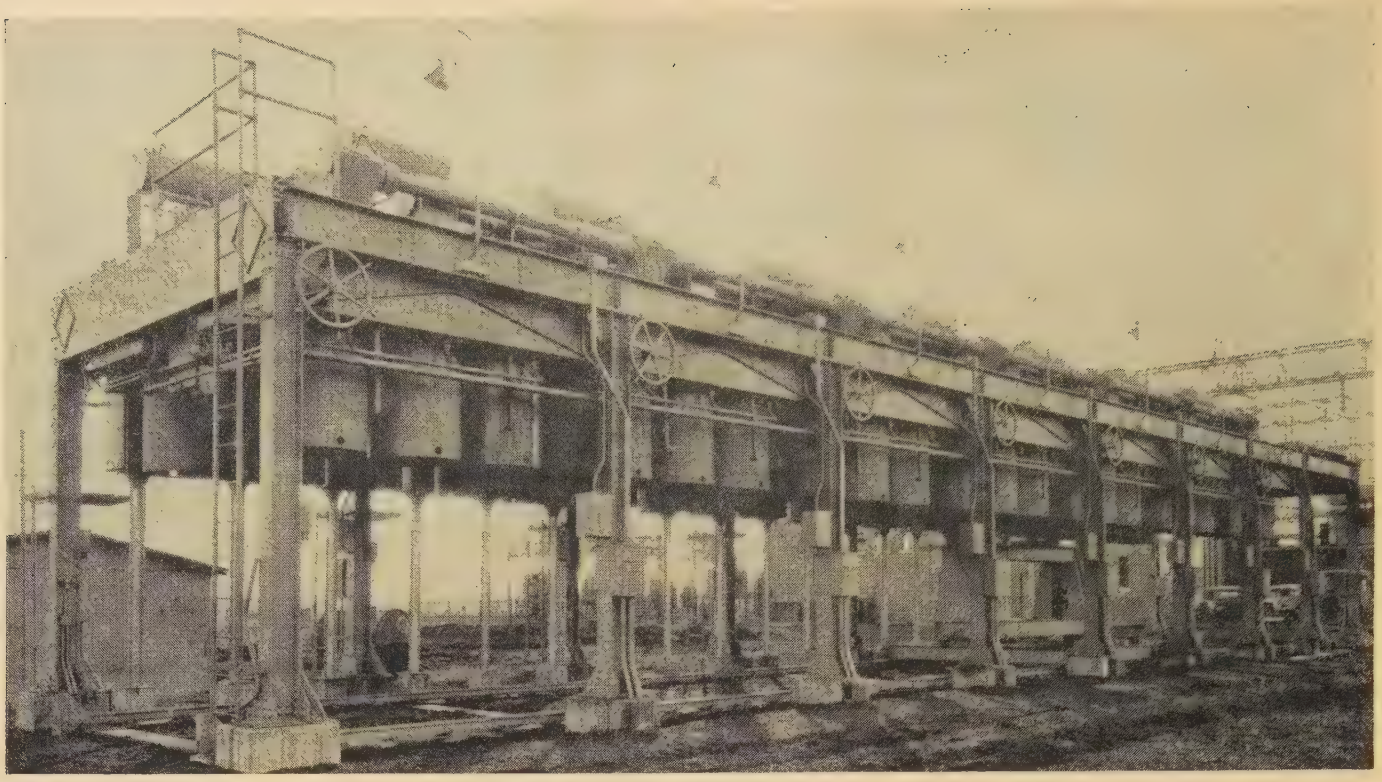

Figure 2. Metal-clad installation used for cost comparison

atmospheric temperature or high humidity indicated that condensation on the surface of the shell bushings in the circular space between the shell and the breaker bushing was a contributing factor. This condensation was pronounced because the temperature of the mass of the gear lagged behind the rising ambient temperature. In some of the installations, the lower end of the shell bushing orifice was not closed entirely when the breaker was in place. In the other installations, the orifice was closed by a soft gasket on the base of the breaker bushing when the breaker was raised to operating position. As the shells which were open at the bottom gave by far the most trouble, it was supposed at first that dirt on the surface combined with the moisture from condensation was the cause of flashover, and a cleaning program was instituted.

It soon was noted that severe corona discharges were taking place within shells previous to failure, even to the extent of being audible and visible. It also was noted that these discharges started very soon after cleaning in some cases, particularly during a rapid rise in atmospheric temperature.

Investigation and tests were continued and led to certain conclusions. The bushings, although open to the air (breathing occurred through the gaskets even in those closed at the bottom), were not exposed to the cleaning action of the elements as were ordinary outdoor bushings. This condition was conducive to corona and surface leakage from the energized metal parts at the top and the formation of nitric acid when condensation supplied the water. Conducting paths thus were established, and the process was cumulative until breakdown occurred over the surface of the porcelain. A contributing factor was metal salts from the corrosion of caps and contacts at the top of the shell. As the deposits on the porcelain did not yield readily to ordinary cleaning, special methods involving the use of carbon tetrachloride, alcohol, and certain dilute acids were tried.

Actual failure from this cause occurred at the original installation only, although corona discharge was observed at other locations. The cleaning program prevented the discharges from extending to the point of failure.

The bushing assemblies in the various makes of switchgear differed considerably in detail, and these were studied further in an attempt to eliminate or at least reduce the cleaning required.

As mentioned before, it was assumed at first that the closing of the shells at the bottom would eliminate or at least materially reduce the trouble, and this was the first step taken. The manufacturer was reluctant but later agreed, and that change was completed on the first installation about September 1930.

The closing of the bottom of the shells, of course, was a question of exclusion of deposits from the atmosphere, and leaving them open was to allow circulation of air to reduce condensation. Neither result was accomplished, however. It was impractical to seal the opening tight enough to prevent breathing; and, although actual dirt might be excluded, air usually contains certain acids such as sulphur dioxide, particularly in cities or industrial centers. The circulation of air in the bushings left open was practically nil, as the only opening was at the bottom, and this was very restricted. Some shells are still open, others closed.

This all indicated that the opening or closing of the shell opening was not the answer to the problem. Accelerated time tests in the laboratory indicated all shells were subject to the formation of nitric acid and metallic salts from the slight corrosion of the metal parts at the top. To prevent the corrosion, lead gaskets were eliminated and plating of copper parts experimented with. Chrome plating was tried but was not entirely satisfactory, owing to the difficulty of getting a perfect homogeneous coating on the odd-shaped parts. Tinning all but contact surfaces, which were silvered, finally was adopted for the installations giving the most trouble. There still remained some defective porcelain in one installation and the short leakage distance and inability to clean entirely at

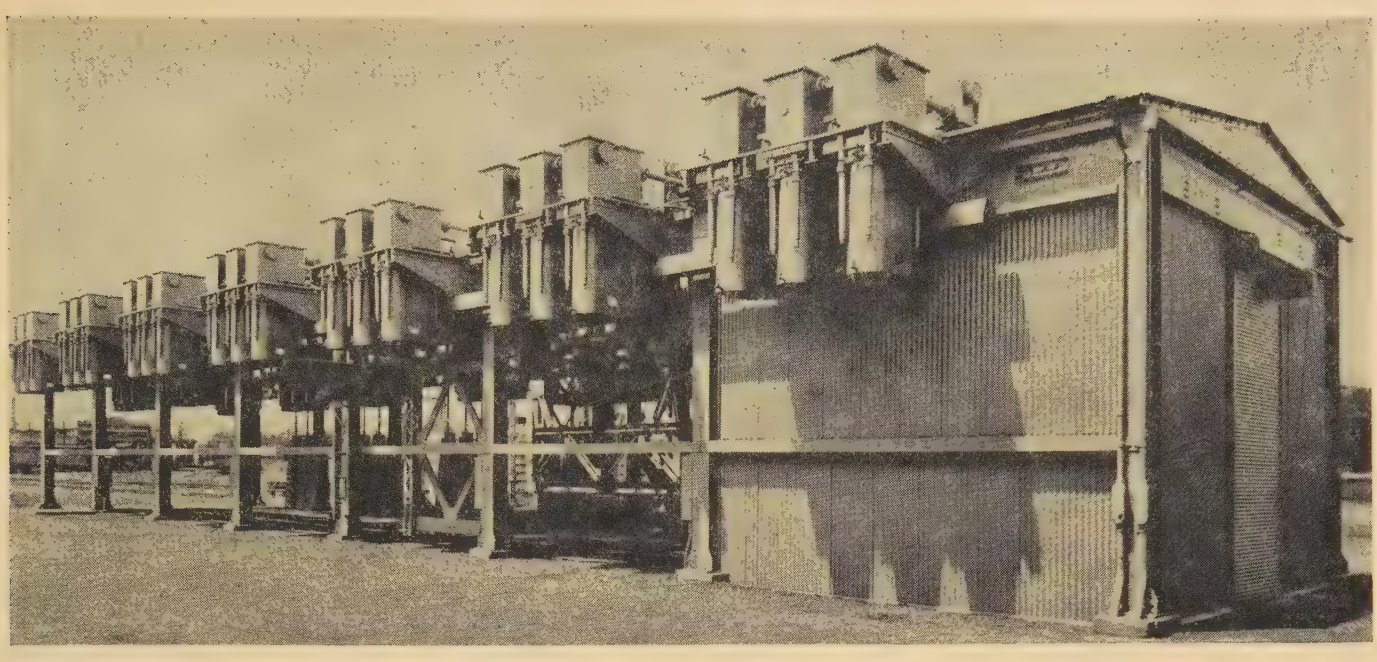

Figure 3. First installation of 33-kv metal-clad switchgear, showing overhanging removable potential transformers

another. These shells all were replaced finally with smooth instead of corrugated porcelain and redesigned contacts and corona shields.

While the changes stated have not eliminated the problem, they have provided shells with better characteristics and have lengthened the interval between cleanings. At present all 33-kv shells are cleaned each fall and spring with a weak solution of muriatic acid followed by thorough washing with a cleaning compound. This program has been followed for the past ten years with no further trouble.

Other than the shell bushings, only one electrical weakness affecting reliability developed. This also was in the first installation and resulted in two cases of bus failure to ground. The bus in all the installations is copper tubing insulated with machine-wound impregnated paper or fabric and supported at intervals centrally in an outer copper pipe by spools of insulating material. The space in the outer pipe around the conductor is filled with oil. The spools at first were turned from a laminous material of pressed paper; later spools were of porcelain or paper wound directly on the conductor insulation. The first theory was that minute drops of water from condensation had collected at the bottom of the bus pipe under the spool, concentrating the electrical stresses and forming creepage paths that resulted in final failure. The manufacturer recommended circulating the oil and heating at intervals to remove moisture, and this was done for a short period. The process was rather expensive and critical, however, as it was necessary to maintain the oil temperature within rather close limits, that is, high enough to remove moisture but not high enough to cause sludging. After the second failure, notice was taken of the fact that although the spools were in halves held around the conductor by cord, the failure was not at the junction of the halves but directly through the spool and parallel to the laminations where they were radial. As previously stated, these spools were turned from a laminated material. This indicated that creepage started between the laminations, and the spools were replaced with a non-laminated material. There have been no failures since, and circulation of oil was discontinued.

It should be noted that neither of these failures caused any damage beyond a small hole in the insulation and outer copper tube and loss of oil in one bus section. There was no fire in either case. The failure was direct to ground. The bus was protected by bus fault relays.

The only actual failure since the early ones mentioned occurred in 1939, and the indications were that it originated with the oil circuit-breaker bushing. In this respect the failure was similar to those occurring in open-type gear. As the breaker was mounted in metal-clad gear, however, the effects must be noted. The failure was in the annular space between the oil circuit-breaker bushing and the shell on the bus side of a line position. Both shell and bushing were fused and burned, severely, typical of an external flashover. The shell was cracked severely but remained in place. The cracking, however, permitted oil to flow into the annular air space between bushing and shell, where it was ignited by the arc and blown out of the shell orifice at the bottom across the top of the breaker, forming an external oil fire which continued after the arc was extinguished. Since the oil burned as it flowed down the wall of the inspection bay before it was extinguished by the gravel bed at the ground level, the fire was more spectacular than damaging. The loss was limited to the breaker bushing, the porcelain shell, the escaped oil, and scorched paint. There was no internal damage to the gear or breaker.

The weather was clear, warm, and dry, which eliminated excessive condensation as a contributing factor as in the earlier troubles.

It was difficult to determine definitely whether the failure originated across the shell or the bushing. There was some evidence of a very slight oil leak at the top of the shell through a defective gasket which formed an oil film on the surface of the shell to which air-borne particles might have adhered and gradually decreased the creepage distance to ground. On the other hand, the particular type of bushing used had been the source of trouble in open-type equipment. The pertinent question for this discussion, however, is whether the failure was the result of or indicated any inherent weakness in the basic hypothesis of the type of installation. Neither the faulty gasket nor the faulty bushing would indicate this. They were both representative of the occasional freaks encountered at

times in any type of construction. Preventive measures against recurrence are the same in this case as for conventional open-type equipment, that is, greater care in fabrication, inspection, and testing and faster relaying to limit fault duration.

It also should be noted that only features peculiar to the type of installation are considered here. For example, there were certain troubles with oil circuit breakers, but these were of the type common to both metal-clad and open-type construction.

Mechanical Difficulties

Early experience with the first installations naturally disclosed certain mechanical features which were undesirable or troublesome. None of these was an insurmountable difficulty, nor did the remedy force any basic changes in design.

Soon after the first installation was made, some shell bushings developed circumferential cracks at or close to the upper edge of the bottom metal mounting ring which was cemented to the outside of the porcelain. This had no bearing on the electrical failures and was purely a mechanical problem. The metal mounting flange and cement, of course, were on the outside (oil side) of the shell, so the ring gasket was placed under the lower edge of the porcelain. As the bolt circle was outside of this gasket, a cantilever strain was imposed on the porcelain which was enhanced by slight inequality in tightening the bolts. A very slight shock or misalignment at the top of the shell then could easily cause the crack. The condition was remedied in the new shells by making the relation between the lower edge of the porcelain and the mounting surface such that there was metal-to-metal contact between the mounting flange and the mounting surface. This equalized and limited the strain on the porcelain. This condition existed at certain installations only, as the shells in the other installations were mounted with the flange below the mounting plate.

The only mechanical failure that was at all serious in its results was the breakage of the operating rod on an oil-immersed disconnect switch mentioned previously. As stated, this was remedied by proper design.

Some difficulty was encountered at first in preventing leakage of oil. The various boxes and enclosures in the first installation were of welded steel plate with flat covers and flat cork gaskets. It was soon evident that these gaskets, if not confined, would spread and set, permitting seepage of oil. Further tightening of bolts was only a temporary cure and soon reached its limit. After trials of other gaskets, it was found that a cork gasket confined in a groove and compressed by a tongue gave satisfactory results, and gaskets in later gear were so designed. To change the original flat gaskets to the confined type, however, was impractical and further trials were made ending in the use of a cork or other soft gasket with a thin soft metal sheath. The original gear was equipped with this type several years ago, and oil leaks and seepage have ceased. There was also some oil seepage through welds on boxes and directly through the metal of cast boxes used on the later installations. Tinning of the inside of welds and the inner surface of cast boxes prevented this seepage. Improved welding and the use of different material for cast boxes made tinning unnecessary. This matter of oil leaks and seepage is largely a question of appearance, as in no case was it sufficient to reduce the amount of oil in the gear to any appreciable extent over a very considerable period.

Figure 4. Installation of 33-kv metal-clad switchgear with main and transfer bus

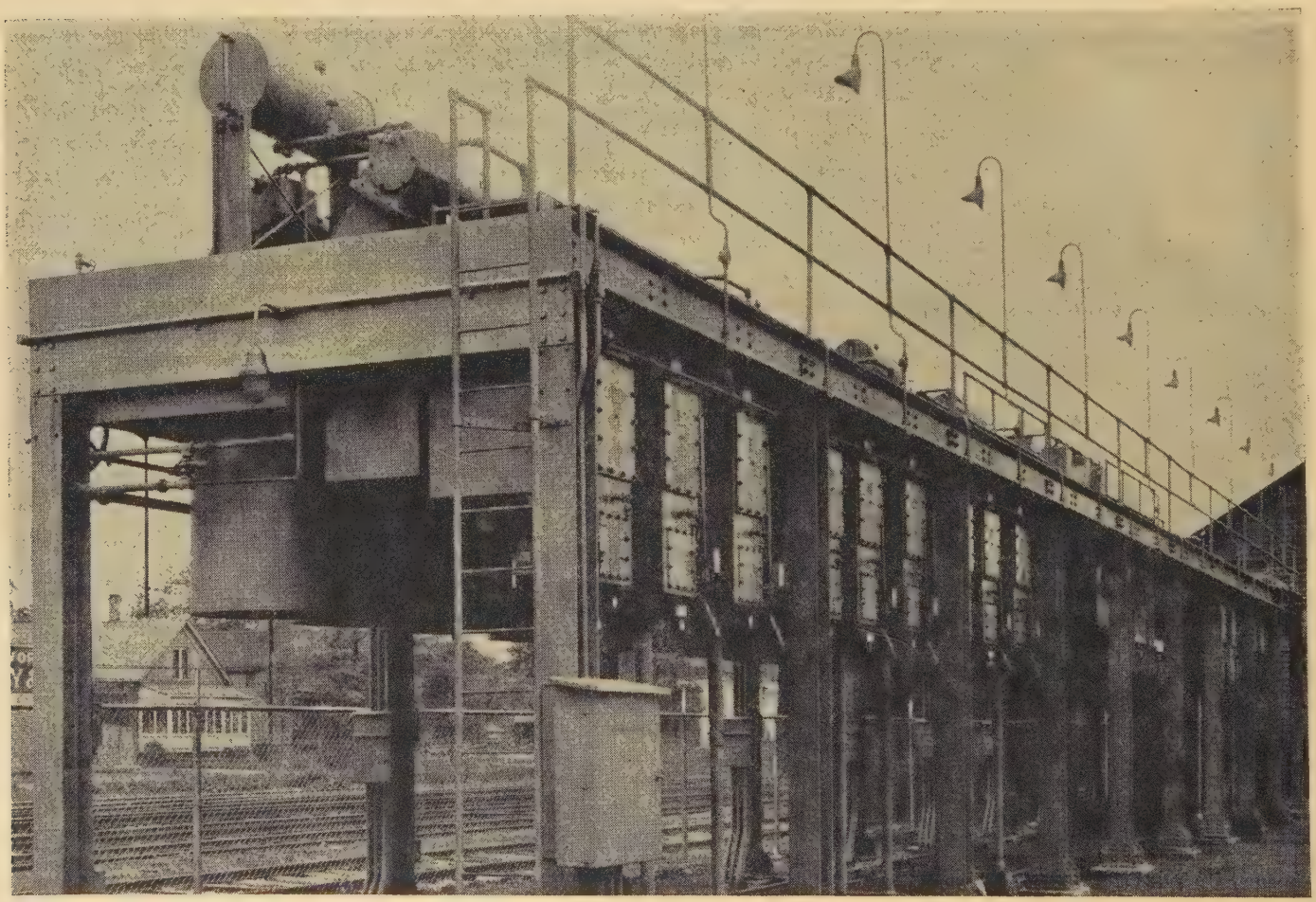

The availability factor of reliability is influenced materially by ordinary routine maintenance requirements. In open-type installations, it is necessary to take out of service major portions or even an entire structure for such work as cleaning or replacement of insulators, painting, and lubrication of moving parts. Frequently busses or lines not being worked on must be de-energized to provide proper safe working clearances. This class of maintenance, with the exception of the semiannual washing of shell bushings mentioned previously, requires no outage of metal-clad equipment. Even an outage for cleaning is reduced to only the particular line or bay directly concerned.

Economy

First Cost. First cost, of course, is a manufacturing problem involving design, fabrication, and assembly. This factory assembly is of major importance. It increases first cost of metal-clad above equipment for a comparative open-type installation but reduces field installation costs, and we are considering over-all economy, as mentioned before. The seven installations made by the Public Service Company of Northern Illinois covered a period of only about three years and were fabricated by three different manufacturers. Naturally, first cost was somewhat high because of development charges and because effort was concentrated on design for safety and reliability rather than cost of manufacture. There was considerable variation also in price among different manufacturers and among different installations by the same manufacturer because there was no background of experience on which to base manufacturing costs.

Each of the installations made was an individual development and did not approach even the first phase of being on a production basis. Two manufacturers built two installations each and one manufacturer built three, and naturally any part or feature developed for the first was used wherever possible in the second. This possibility was exceedingly limited, however, owing to changes in detail design. There were only two major changes in design made during the period which might affect first cost. One was the manner of connecting and mounting potential transformers, and the other was the use of cast boxes or compartments in place of welded plate. In the original installation, connection boxes overhung the structure and were provided with shell bushings permitting the potential transformers to be raised into place or lowered the same as the oil circuit breakers by means of a special traveling elevator on the structure. In all subsequent installations, the potential transformers were connected solidly and mounted in boxes as an integral part of the gear with an arrangement for replacing fuses. This eliminated many shells and bushings as well as an elevator. The use of cast boxes not only affected the cost of the boxes themselves but provided round cover flanges and covers into which it was cheaper to machine grooves for confined gaskets.

A major factor in the cost of any installation is the bus and switching arrangement. Two common variations are complete double bus with two oil circuit breakers per circuit and main and transfer bus with one circuit breaker per circuit. In the latter a breaker is usually provided for energizing the transfer bus from the main bus with section breakers or disconnect switches in the main bus on each side of this feed to permit taking part of the bus out of service for maintenance or keeping part in service in case of bus failure.

The first installation was a double bus arrangement, however; only one circuit breaker was provided for each of two transformer circuits. This possibility of reducing cost and still retaining the advantage of a double bus because the breakers were movable from one bus position to another, a condition which does not exist in conventional open-type construction.

The installation which followed was a main and transfer bus arrangement. There were two reasons for this: first, the available space was limited in width, and only one breaker per bay resulted in a narrower structure; second, it provided a practical trial of that particular bus and switching arrangement as applied to that type of equipment. This required the development and use of enclosed oil-immersed disconnect switches, which present certain problems. While this arrangement reduced the cost per bay, the total cost was not reduced materially because of the provision of two bus section breakers and the transfer bus feed breaker. As equivalent operating facilities at little additional cost could be provided by a double bus arrangement with only one breaker per circuit in some cases, all subsequent installations were built according to this arrangement. The moving of a breaker of any line or transformer position by means of the motor-driven elevator from one bus to the other is comparable to the operating of disconnect switches for connecting a line or

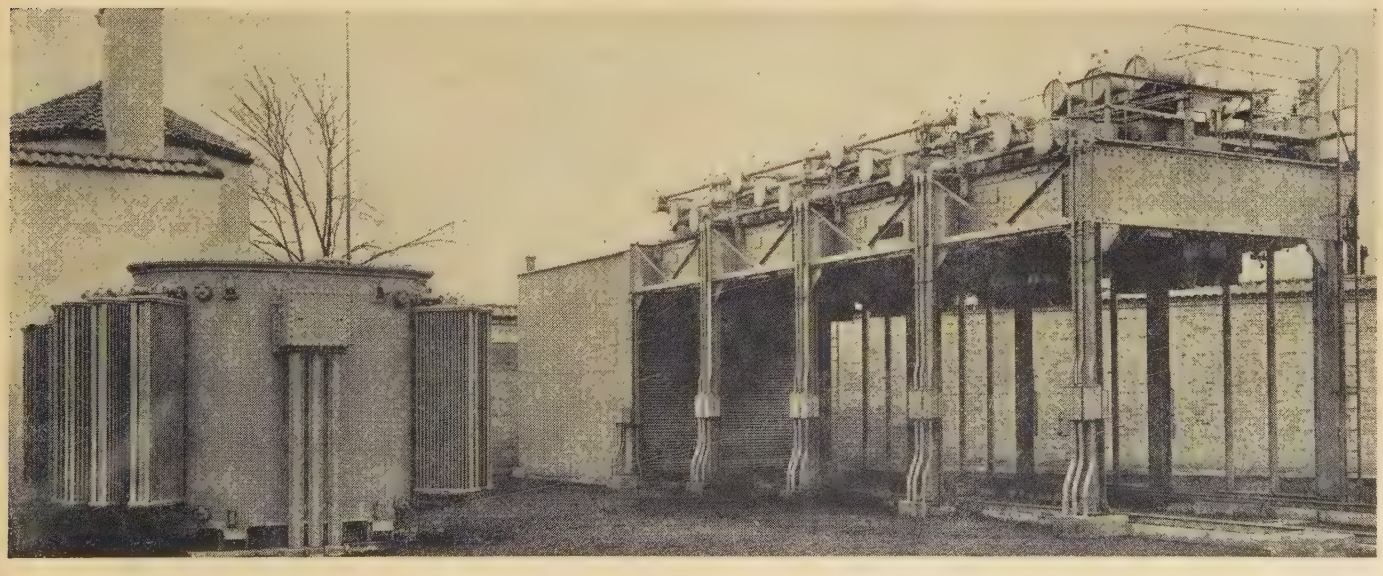

Figure 5. One of the later installations in a residential district

Ornamental brick wall enclosing property is shown

transformer to a transfer bus in open-type structures.

Engineering. The engineering ordinarily considered as preliminary, such as determination of necessity, number, capacity, and location of lines, feeders, and equipment, can be considered as equal in cost for both types of equipment if we forget for the moment an advantage of metal-clad equipment in the matter of location. What might be termed construction engineering follows. For an open-type installation, this consists of considering, specifying, counting, ordering, listing, and delivering to the job various pieces of major equipment and innumerable items for connecting and mounting. Construction specifications and many drawings must be prepared for the assembly of all these parts into a satisfactory structure. For metal-clad equipment the user need specify but one piece of equipment, and very few drawings are needed for installation, thus reducing his engineering costs materially.

It is true that much of the user's engineering cost is transferred to the manufacturer and must be included in first cost because the manufacturer must design and assemble the various parts of the unit. These costs should be considerably less, however, when this work is done by the manufacturer because he is designing and assembling many units, while the user must design each unit for himself. Factory assembly is inherently cheaper than field assembly for several reasons, freedom from weather interference being one.

This, of course, assumes a certain degree of standardization, and metal-clad equipment lends itself to this standardization to a far greater extent than open-type. Standardization in conventional design more usually is limited to component parts.

Installation. Field installation is where metal-clad equipment must show the greatest reduction in cost as compared with open-type. Again consider the innumerable small pieces of an open-type structure which must be assembled piecemeal contrasted with the very few large parts of metal-clad. Here again design plays a major role.

When the first installation was purchased, the goal of unit assembly was in the minds of those concerned. Experience had been had with lower voltage gear, and design changes had brought this to the point where even complete bus sections were shipped and installed as a unit. At that time, to assemble even one bay of a 33-kv structure into a single unit which would be within railroad clearances appeared impossible, at least to the manufacturer, and the first gear was shipped in many parts which were assembled on the job. The installation cost was the highest of any of the installations. As a result of much consultation with manufacturers, a design was worked out which enabled the next installation, which was a main and transfer bus arrangement, to be assembled at the factory and shipped in units of one bay as were all subsequent installations. The component parts as shipped from the factory were the main bay assembly (containing busses, instrument transformers, cable terminals for outgoing circuits, and all connections), the supporting columns on which the bay assembly was mounted, the circuit breakers, and the traveling elevator for raising and lowering breakers.

The next installation having a double bus was shipped assembled, and the complete cost of installation per bay was slightly under 25 per cent of the cost of the first installation.

Transportation of large pieces in carload lots from one point of shipment is more economical than many pieces from many different points for equal distances and total weight. Note also must be taken of the increased cost of following and co-ordinating the receipt of numerous items of equipment required for an open-type structure as compared with factory-assembled units.

An element of cost exists in many installations which does not appear in the cost records. This is elapsed time as distinct from man-hours. There frequently is a very definite saving in meeting a service date or a definite loss in not doing so which is distinct from the actual dollar cost of the installation. Metal-clad equipment has a definite advantage here which will be enhanced by more extensive use and standardization.

As an indication of what was done and what experience was obtained, some of the design features which made unit assembly possible should be mentioned. The unit-type principle must be in mind at all times in design. Considerable study was required so to design the various boxes and compartments comprising the main section as to permit an arrangement compact and rigid enough to make shipment by rail practical. These assemblies or units were shipped complete and filled with oil. The breakers were shipped separately, as they would be removed from their operating position in any case for test and inspection before being placed in service.

The busses presented another problem, as they, of course, extended the length of the structure to form a continuous conductor across all bays. In the first installation, the busses were received entirely separate from any other part and not even complete in themselves. The insulated tubing was in lengths which did not coincide with the width of bay. For subsequent installation, a satisfactory joint was developed for both bus conductor and enclosing tube that could be used at the junction of any bay, a development which permitted all complete busses to be mounted on each bay in the factory ready for connection to busses of an adjacent bay. These joints and other parts were so designed that all mechanical erection could be completed before any electrical work was necessary. Even control and secondary wiring was in place and brought to terminals for connection to the wiring from the control board.

Maintenance and Repair. Maintenance and repair were discussed under the preceding subjects of safety and reliability, and the same factors in metal-clad equipment which increase safety and reliability over that of open-type decrease the direct cost of maintenance and repair. Practically all ordinary routine maintenance such as painting, cleaning, and lubricating, can be performed on metal-clad without removing any part from service. This is seldom true on open-type, and for this reason much of this work is done at night or on Sundays or holidays when lighter load conditions are such that equipment can be taken out of service. This involves overtime which greatly increases the cost.

Repairs are necessary as a result of failure, deterioration, or wear. It is obvious that cost of repair decreases in proportion to increase of reliability.

Operation. If the presence of operators is required at a given substation, these costs will be equal for both types of installations. Metal-clad equipment, however, is more adaptable to control from remote points because of the absence of open disconnect switches and complete protection from interference by the elements.

Durability. The life expectancy of metal-clad equipment is much greater than open-type. The only part exposed to the weather is the enclosing metal structure. Organic insulation, if used on conductors, is not even exposed to the air. All of the 33-kv gear installed by the Public Service Company of Northern Illinois is oil-filled and equipped with

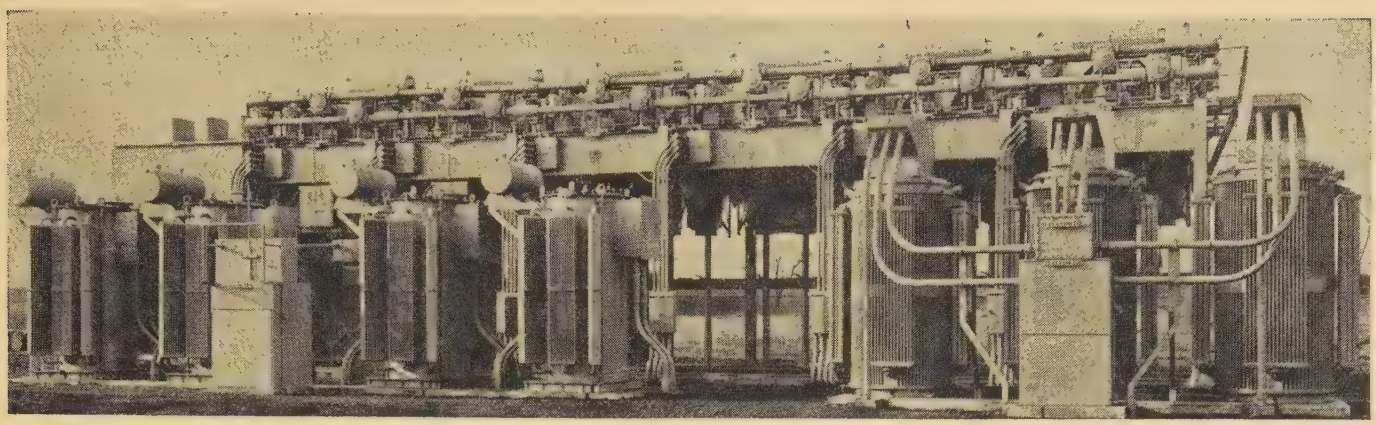

Figure 6. One of the later installations, showing method of enclosing transformer connections

conservator tanks similar to those commonly used on transformers. Experience has shown that oil deterioration is not a problem, as practically all of the original oil is still in service in the gear. There has been no filtering or treatment of any of this oil except that following the failure of the bus insulators mentioned previously, and as stated, that was unnecessary. This of course refers only to the oil used primarily as an insulating and filling medium in the various bus tubes and connection compartments. This oil is far less subject to factors causing deterioration than oil as ordinarily used in transformers or circuit breakers.

After from 13 to 16 years of service, all seven installations can be considered practically in the same condition as when new.

Space Occupancy and Appearance. Here again metal-clad has a very definite advantage, and if space is at a premium, the savings could be considerable. One of the installations, for example, could not have been made at its present location as an open-type structure. It was an old substation site very close to the center of town, bounded on one side by a steam railway and on the other by an electric railway. An open-type 33-kv structure would have required a new location at some distance, involving large costs for new property and building and also new transmission and distribution facilities.

At one location two metal-clad bays were added as an extension to an existing open-type structure and afford a striking comparison. The bays in the open structure occupy 729 square feet each, while the bays in the metal-clad structure occupy 605 square feet each, a saving of about 17 per cent. The height of the open structure is exactly 27 feet; that of the metal-clad is exactly 22 feet. This is not the entire story, however, as there are open disconnects and wiring on the outside of the open structure which require proper clearance and operating space. At one of the installations, there are six double bus bays and an inspection bay, and the structure from the center line to the center line of columns is exactly 90 feet long by 20 feet 8 inches wide. An enclosing fence placed three feet from the center line of columns would give ample space for all operation and inspection. (It could be on the columns if necessary.) Using the 3-foot space, however, gives an enclosed area of exactly 96 feet by 26 feet 8 inches, or 2,560 square feet. An open structure for controlling the same number of circuits would be exactly 108 feet long by exactly 36 feet wide based on the bay size of existing structures, and an enclosing fence should be at least ten feet from the center line of columns (usually it is more). This gives an enclosed area of 7,168 square feet, 2.8 times that required for metal-clad including the inspection bay.

Appearance has a definite economic value in public relations and also an indirect value similar to the space factor by permitting installations at locations where an open structure would be objected to by adjacent property owners. A metal-clad structure does not have the raw and unfinished appearance of an open structure, and if necessary can be camouflaged much more easily by architectural features or landscaping.

Salvage Value. Substation and equipment replacements in a great majority of cases are required by inadequate capacity because of load and system growth or changes. Retirement charges are high unless equipment for which the duty has become too great can be reused where the demand is smaller. This involves removal and reinstallation, and with an open-type structure, the same factors which cause high labor costs in installation also cause high cost of removal. An open-type structure must be dismantled completely to be relocated; and while the major items of equipment can be moved without loss, there is usually considerable retirement in connection with such items as structure, conductors, supports, control conduit, and wiring. A unit-type installation is moved in complete units as at first installed, with no retirement of material or equipment as far as the structure itself is concerned. The retirement of connecting cables and foundations would obtain in either case.

Comparison of Costs. A detailed study of the actual installed costs of one of the metal-clad installations and a comparable contemporary open-type structure gives the following percentage costs for the metal-clad, the cost of each item of conventional open-type being considered as 100 per cent:

Material cost per bay	145.4%
Labor cost per bay (including engineering)	62.6%
Foundations per bay	60.6%
Total installed cost	131.5%

This comparison is made on the actual dollar expenditure only and includes only the first three factors of over-all economy heretofore mentioned. Any reasonable evaluation of the remaining factors should more than offset the additional dollar cost of the metal-clad installation. In addition it must receive a very substantial credit for the high degree of safety and reliability in order to arrive at true over-all economy.

Future Development

In the foregoing discussion, the difficulties and faults of the present 33-kv metal-clad installations are covered in some detail in order to show that these difficulties and faults were overcome and eliminated. There is some accent on the

original installation because it was the first developed and furnished the experience for improvements in those which followed. The possibilities for further improvement, however, are by no means exhausted, particularly in the field of economy.

In future design the possibility of eliminating all shell bushings should be considered. All present installations are arranged with what might be termed removable or plug-in circuit breakers with a rather expensive motor-operated carriage elevator for raising, lowering, and moving them to an enclosed bay at the end of the structure. It is questionable if this is necessary. If the breakers are underhung as an integral part of the structure with a device for lowering tanks only, practically all maintenance and repairs could be accomplished. The gear structure would afford far more protection from the weather than is obtained for breakers in open structures unless temporary enclosures are built. If necessary, it would be a relatively small matter to provide a temporary enclosure on the sides of a metal-clad structure. If desired, this enclosure might be made permanent and enclose the entire lower part of the structure. This also will eliminate the inspection bay and reduce materially the cost of the transfer carriage.

If the breakers are in a fixed position, it will be necessary to provide means for entirely disconnecting them while they are being worked on. The first thought for this is an oil-immersed or enclosed disconnect switch, which is not difficult in itself but which presents certain problems in safety and operation. Being enclosed, the actual opening in the circuit cannot be observed and checked, and reliance must be placed on the operating mechanism or some other indicator. Indicators can be devised which are independent of the operating mechanism and in case of failure or breakage will not give a safety signal. Glass windows have been tried to provide direct view of the disconnecting device but are not always practical, particularly when looking into an oil-filled compartment. There may be a possibility in some of the new plastics in this connection. Even though the break will be visible, there is still the question of possible breakdown across the gap in a disconnect of this sort. A metal (grounded) barrier across the gap may be a solution.

The use of standard forms of cable for busses and connections should be considered as a possible means of reducing the cost and the amount of oil if oil is used.

The means for replacement of potential-transformer fuses can be studied to good advantage, as they are rather complicated and expensive. The reliability of present-day potential transformers suggests that primary fuses might be omitted, a factor which would be a major simplification.

The question of the necessity of an external terminal for testing, phase flashing, and so forth, should be considered. Such a terminal was provided on one of the installations, but in order to maintain the highest degree of safety, rather complicated interlocking on the various disconnect and grounding switches was involved. It must be remembered that as soon as exposed terminals which can be energized are introduced, the high degree of safety provided by entirely-enclosed metal-clad gear is lowered.

Recent development in the production of light metals opens up possibilities of reduction of weight and lowering of handling and installation costs.

Experience with gaskets enclosed in soft metal indicates that recessed gaskets may be eliminated.

Conclusions

From this discussion and the experience which it records, certain definite conclusions may be drawn:

1. Totally enclosed metal-clad construction provides the maximum degree of safety for personnel in the operation of electrical equipment.

2. The reliability of totally enclosed metal-clad equipment is far greater than conventional open-type.

3. While over-all economy of totally enclosed metal-clad equipment has been obtained, there are many possibilities for further advancement toward this objective.

4. Thirteen years of operating experience with seven different installations confirms the above conclusions.

5. A great advancement toward the objectives of safety and reliability in electrical equipment having been made, the research, engineering, and labor expended in making that advancement should be further exploited by continuing the development and use of totally enclosed equipment for voltages of 33 kv and above.

6. The present use of factory-assembled enclosed units indicates that the manufacturers have accepted the principles involved. The lack of development for higher voltages apparently is caused by the high first cost.

7. Metal-clad unit-type factory-assembled equipment for 33 kv is highly adaptable to standardized quantity production, and proper development will reduce first cost as well as over-all cost.

8. This development offers a definite possibility of combating the steadily rising cost of conventional construction.

9. The above possibility warrants earnest co-operation between manufacturer and user.

Induction Heating of Long Cylindrical Charges

HERBERT F. STORM
ASSOCIATE AIEE

Synopsis: With the remarkable expansion of induction heating applications during recent years, a growing number of persons is being involved in the design and operation of induction heating equipment. While the general principle of induction heating is obvious to most, the concepts of certain important peculiarities such as skin effect, including its bearing on the intensity of heat generation, are not as widely understood. One reason for this state lies in the classic approach by partial differential equations[1,2] involving operations with which many engineers interested in induction heating are not familiar. A previous paper by the author offered a new approach for the analysis of the induction heating effect by using concepts commonly applied to a-c engineering and not involving differential equations.[3] A limitation of that paper consisted in the assumption that the radius of the charge will be very large in comparison with the so-called depth of penetration. It is the object of this paper to cast off this limitation and hence provide an analysis which is valid for any size of the radius of the charge and the depth of penetration. The generated heat is expressed in terms of rapidly converging series. The analysis is applied finally to the case where the charge is subdivided into a number of cylindrical rods. It is shown that for one certain radius of the individual rods, the inductor efficiency reaches a maximum. While in the case of a single (not subdivided) charge, the inductor efficiency cannot increase over a certain limit depending on the material of the charge, the subdivision of the charge removes such limitation, and inductor efficiencies can approach asymptotically 100 per cent for any material.

THE BODY to be heated is called the charge and is exposed to an alternating magnetic flux produced by an inductor, for instance a solenoid, which is energized from an a-c generator of suitable frequency (Figure 1). The alternating magnetic flux induces voltages within the charge. As a result, currents, the so-called eddy currents, flow through the charge and produce I^2R heat. Because the heating effect is originated by voltages generated by induction, it is called heating by induction, or induction heating. Heat also may be produced by hysteresis in the case of ferromagnetic materials at temperatures below the Curie point. For a large majority of practical applications of induction heating, the hysteresis loss is negligible and will be disregarded in the following.

Viewing the calculation of the generated heat as the final objective, the first step will be to compute the intensity of the eddy currents and their distribution within the charge.

For a cylindrical charge, the direction of the induced electric field intensity is perpendicular to the radius r, hence the eddy currents follow circles, whose centers coincide with the axis of the charge (Figure 2). The circles are positioned in planes perpendicular to the axis; if the ratio of length to diameter of inductor and charge approach infinity, the magnetic field intensity produced by the current in the inductor is uniform inside the inductor, while the magnetic field intensity on the outside of the inductor is zero.[4] Voltages and eddy currents will be the same along lines parallel to the axis. It follows that a slice cut out of the charge perpendicular to its axis is representative of the state of the entire charge.

Since the voltages and the eddy currents follow concentric circles, and thus have no radial components, a subdivision of the slice into a number of sleeves all telescoped into each other will not change the state of the slice, even if the sleeves were insulated from each other. In order to obtain uniformity of induced voltage and eddy current over the cross-section of the sleeve, its radial thickness is assumed infinitely small; consequently the number of sleeves is infinitely large. The charge thus is reduced to a (infinite) number of electric circuits amenable to quantitative circuit analysis.

Because of the resulting simplification in the analysis, the ratio of length to diameter of inductor and charge will be assumed approaching infinity. A very simple relation between magnetic intensity and ampere-turns per centimeter then results. In practical cases where the ratio of length to diameter of inductor and charge is finite, the spreading of the flux at the ends of the inductor results in a weakening of the induction, hence the formulas derived for the infinite case will give too high values for the generated heat.[5,6,7] However, as the ratio of length to diameter increases, the deviation from the infinite case becomes less and approaches zero asymptotically.

The analysis utilizes two different methods of approach, depending on the ratio between the radius a of the charge and the depth of penetration p. Each method has its special usefulness in its region of application, the border line between the two cases being at a ratio of $a/p = 3$. The results obtained by these methods are identical with the power

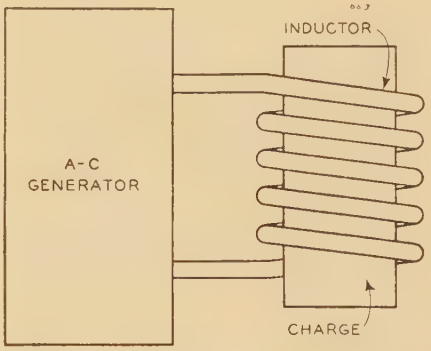

Figure 1. Arrangement of inductor and charge

series of Bessel functions, obtained as solution from an analysis based on partial differential equations.[2]

Case a/p<3

For this case the eddy currents in the charge are calculated by a method of successive approximations. As previously explained, the charge can be reduced to a number of electric circuits. Suppose the charge is now slotted radially from the surface to the axis. All circuits in the slice become open. When such a fictitious charge is inserted into an energized inductor, open circuit voltages will appear across the slots of the various sleeves; the slots, however, prevent eddy currents from circulating through the sleeves.

Suppose the slots are now closed. Eddy currents start to flow through the sleeves, and it will be assumed as a first approximation that the eddy currents are given by the open circuit voltages of the various sleeves, divided by the electrical resistance of the respective sleeves.

Paper 46-53, recommended by the AIEE committee on industrial power applications and the subcommittee on induction and dielectric heating for presentation at the AIEE winter convention, New York, N. Y., January 21–25, 1946. Manuscript submitted October 29, 1945; made available for printing December 21, 1945.

HERBERT F. STORM is with the General Electric Company, Schenectady, N. Y.

The actual eddy currents will differ from those thus obtained for two reasons:

1. According to Lenz's law, the eddy currents tend to weaken the magnetic field produced by the inductor, resulting in a reduction of the open circuit voltages.

2. Voltages of mutual reactance are induced in the various sleeves by eddy currents circulating in other sleeves.

In order to obtain a second approximation, the magnetic field distribution as determined by the first approximation is calculated. A new group of voltages is induced in the charge, which, in combination with the resistance of the sleeves, cause a new set of eddy currents to circulate through the sleeves. These voltages and eddy currents obtained by the second approximation are much smaller in magnitude than those obtained by the first approximation. The total eddy currents in the charge, thus far considered, consist of the sum of the eddy currents of first and second approximation. The actual eddy currents again will differ from those thus far obtained because the eddy currents of second approximation will weaken the previous magnetic field; moreover, voltages of mutual reactance are induced in the various sleeves by the eddy currents of second approximation, circulating in other sleeves. It will be noted, however, that the weakening of the magnetic field by the eddy currents of second approximation is of far lesser degree than previously encountered by the eddy currents of first approximation. Equally reduced in magnitude are the voltages of mutual reactance as a result of the eddy currents of second approximation, compared with the voltages of mutual reactance as a result of the eddy currents of first approximation. Further approximations can be obtained by proceeding in analogous fashion. This process leads to a power series which will be found to be rapidly convergent.

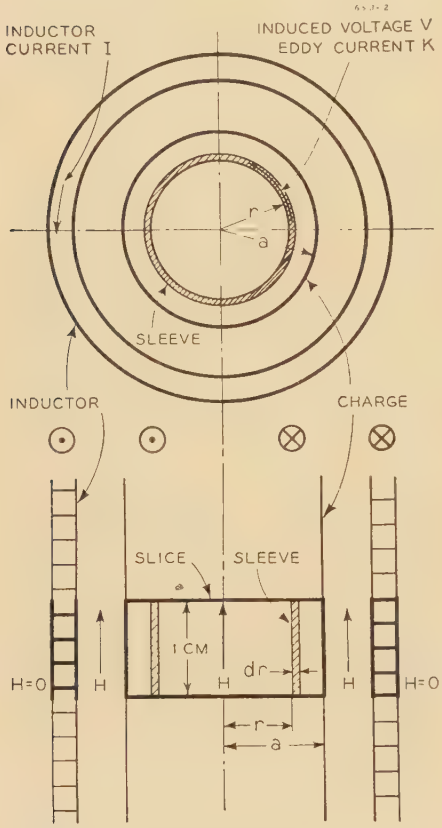

Figure 2. Sectional view of inductor and charge

Positive directions were assigned to the magnetic field intensity H and to the current I in the inductor. They are shown (Figure 2) by arrows parallel to the axis of the inductor and by the head and tail symbols, respectively, indicating a right-hand system. For alternating magnetic intensities and currents, the arrows show the direction of the instantaneous values, provided the latter appear positive in their respective vector diagrams. For a charge inserted into the inductor, the same positive directions are retained for the magnetic intensities H and currents K in the charge.

The magnetic-field intensity, henceforth abbreviated magnetic intensity, follows for an empty inductor from

$$\boldsymbol{H}_o = 0.4\pi \boldsymbol{I}_o n \tag{1}$$

A cylindrical charge is now inserted into the inductor. The induction B_o in the charge (caused by the inductor field) equals

$$\boldsymbol{B}_o = \mu \boldsymbol{H}_o \tag{2}$$

The magnetic flux Φ_o, which is surrounded by a sleeve with the radius r, equals

$$\boldsymbol{\Phi}_o = r^2 \pi \boldsymbol{B}_o \tag{3}$$

As a result of Φ_o, voltages V_o, and hence eddy currents K_o, are produced in the charge. The eddy currents, however, produce magnetomotive forces of their own, resulting in the weakening of the original flux Φ_o, and in the induction of voltages in the various sleeves by mutual inductance. These effects of the eddy currents are nullified by introducing a so-called compensating current in the inductor, which is to offset the weakening action of the eddy currents with respect to the flux Φ_o, and furthermore by introducing compensating voltages in the sleeves. The latter voltages are connected in series with each sleeve and develop a voltage equal in magnitude and opposite in sign with respect to the voltage induced in the sleeve by the eddy currents in the charge and by the compensating current in the inductor. Under these assumptions the current I_o in the inductor produces a flux Φ_o (equation 3) which in turn induces a voltage V_o in the sleeve, as expressed conventionally by

$$\boldsymbol{V}_o = -j\omega \boldsymbol{\Phi}_o 10^{-8} \tag{4}$$

where

$$\omega = 2\pi f \tag{5}$$

Utilizing equations 1 to 5, V_o follows as

$$\boldsymbol{V}_o = -j8\pi^3 10^{-9} (\mu f)(\boldsymbol{I}_o n) r^2 \tag{6}$$

It is apparent that the radial distribution of the induced voltage V_o is parabolic. The slice is shown in Figure 3, looking in the axial direction. The magnitude of V_o as a function of the radius is shown by the graph superimposed on the view of the slice.

Before analyzing the implications of equation 6, it will be well to remember that the flux Φ_o also will induce a voltage in the inductor. If the object is to determine the voltage induced in the inductor by the entire flux inside of the charge, the variable radius r in equation 6 is replaced by the outside radius a of the charge. The voltage per turn of the inductor, caused by only the flux within the charge, follows from equation 6

$$\boldsymbol{E}_o/n = -j8\pi^3 10^{-9} (\mu f)(\boldsymbol{I}_o n) a^2 \tag{7}$$

and the voltage E_o per centimeter axial length of inductor is

$$\boldsymbol{E}_o = -j8\pi^3 10^{-9} (\mu f)(\boldsymbol{I}_o n) a^2 \tag{8}$$

It should be observed that other voltages are induced additionally in the inductor. There are the voltages resulting from the magnetic field within the inductor conductor and caused by the magnetic field in the air space between inductor and charge. Furthermore, an ohmic voltage component exists because of the copper loss in the inductor. The current in the inductor, multiplied by the various voltages listed, indicates the true and reactive power spent in the various parts such as the inductor proper, the air gap between the inductor and the charge, and the charge itself. Since this discussion is concerned only with the power requirements introduced by the charge itself, voltages induced in the inductor by parts other than the charge do not require further attention.

Returning to the voltage V_o (equation 6), currents, the so-called eddy currents, will flow in the sleeves as a result. The magnitude and phase of the eddy currents

are controlled by the voltage V_o, the resistance of the individual sleeve and the voltages induced in the sleeve by self inductance and mutual inductance.

While the voltage of self inductance is zero because the infinitely small cross-section of the sleeve multiplied by a finite current density (amperes/centimeter^2) results in a current (in amperes) of zero magnitude, the effect of the voltages caused by mutual inductance has been eliminated temporarily by the inception of sources called compensating currents and voltages, as previously indicated.

Curie point, the permeability drops to unity with an attendant drop in heat generation.

A further inspection of equations 11 and 12 reveals the important facts that the density of the eddy currents K_o is zero at the center of the charge and increases as a linear function of the radius toward the surface (Figure 3). Since the rate of heat generation W_o per unit volume of the charge is proportional to the square of the current density (equation 12), it is obvious that the rate of heating W_o is also zero at the center of the charge,

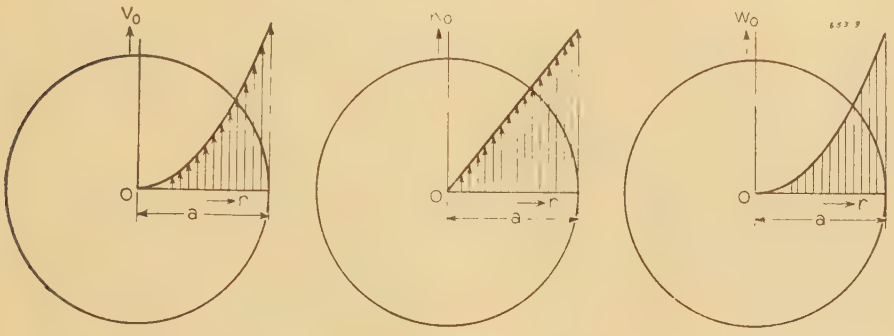

Figure 3. Radial distribution of induced voltage V_o, eddy current density K_o, and generated heat W_o

The eddy current is now solely a function of V_o and the resistance of the sleeve.

If the slice has a height of one centimeter, the resistance of a sleeve of infinitesimal thickness dr is then

$$R = 2r\pi\rho/dr \tag{9}$$

and the eddy current density K_o will equal

$$K_o = V_o/2r\pi\rho \tag{10}$$

From equations 6, 7, and 8, one obtains for K_o

$$K_o = -j4\pi^2 10^{-9}(\mu f/\rho)(I_o n)r \tag{11}$$

Finally, the I^2R heat generated by induction is, per cubic centimeter,

$$W_o = K_o^2\rho/2 = 8\pi^4 10^{-18}(\mu^2 f^2/\rho) \times (I_o n)^2 r^2 \tag{12}$$

where W_o is average value and K_o is peak value.

At this point it is worthwhile to pause for a moment in the further development and to focus our attention on the interpretation of equations 11 and 12. It will be recognized that the generated heat is controlled by the ampere-turns and frequency of the inductor current, by the electrical resistivity and magnetic permeability[8] of the charge, and furthermore by the distance from the axis. The permeability of a number of ferromagnetic materials varies with the magnetic intensity and with the temperature. When the temperature of the charge has reached the

but increases with the square of the radius toward the surface of the charge. The greatest concentration of heat generation thus occurs in the surface layer (Figure 3). This concentration of heat generation toward the surface makes induction heating suitable for surface hardening applications. Although most of the heat is generated in the surface layer, the entire body of the charge can be heated if so desired; this is done simply by continued application of power, the heat being conducted thermally to the interior.

Such, briefly sketched, are the conclusions reached from an inspection of equations 11 and 12. These equations were obtained by disregarding the effect of mutual inductance. The validity of the conclusions, therefore, has to be limited to the region in which the effect of mutual inductance remains negligible. It is the object of the following to demarcate this region and to investigate what modifications the foregoing conclusions have to undergo when the effect of mutual inductance becomes pronounced.

Eddy currents K_o flowing in the charge create a magnetic flux Φ_1, which is interlinked with the sleeves and with the inductor. The flux Φ_1 is a function of the magnetic intensity H_1 which follows from Ampere's law

$$\oint_l H_1 dl = 0.4\pi \int\int_s K_o ds \tag{13}$$

Remembering that H_1 has no radial component and equals zero at the outside of the charge, the line integral on the left hand side of equation 13 simplifies for a slice of the height of one centimeter to H_1 (Figure 4). The surface integral on the right hand side also simplifies somewhat, resulting in

$$H_1 = 0.4\pi \int_r^a K_o dr \tag{14}$$

Simplifying the expressions for K_o by introducing a new parameter p, where

$$p = \frac{1}{2\pi}\sqrt{\frac{\rho 10^9}{2\mu f}} \tag{15}$$

one obtains

$$K_o = -j(1/2p^2)(I_o n)r \tag{16}$$

Substituting equation 16 into equation 14 and integrating, one obtains finally

$$H_1 = (-ja^2/8p^2)\cdot 0.8\pi(I_o n)[1-(r/a)^2] \tag{17}$$

The radial distribution of H_1 is parabolic. The induction B_1 follows as

$$B_1 = \mu H_1 \tag{18}$$

and is shown in Figure 5.

The magnetic flux Φ_1 will be obtained from

$$\Phi_1 = \int_o^r B_1 \cdot 2r\pi \cdot dr \tag{19}$$

The following method of splitting the induction B_1 into two components $B_{1,m}$ and $B_{1,n}$ will greatly simplify the further analysis:

$$B_1 = B_{1,m} + B_{1,n} \tag{20}$$

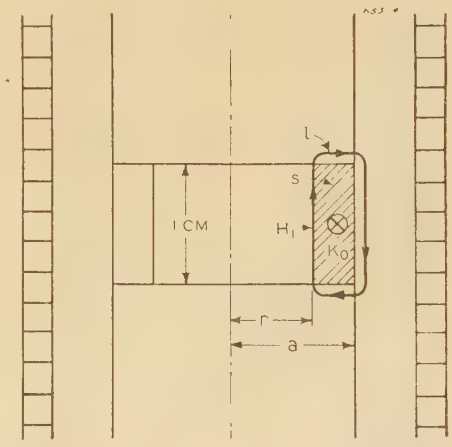

Figure 4. Sectional view of slice for illustration of Ampere's circuital law

Component $B_{1,n}$ shall have such radial distribution that the resulting flux $\Phi_{1,n}$ is not interlinked with the inductor:

$$\Phi_{1,n}\Big|_o^a = \int_o^a B_{1,n}\cdot 2r\pi\cdot dr = 0 \qquad (21)$$

Integrating equation 20 and substituting from equation 21, one obtains an integral equation for $B_{1,m}$:

$$\int_o^a B_1\cdot 2r\pi\cdot dr = \int_o^a B_{1,m}\cdot 2r\pi\cdot dr \qquad (22)$$

The simplest radial distribution which can be assigned to $B_{1,m}$ is to be constant:

$$B_{1,m} = \text{constant} \qquad (23)$$

Applying equation 23 to equation 22, we have

$$\int^a B_1\cdot 2r\pi\cdot dr = B_{1,m}\int^a 2r\pi\cdot dr \qquad (24)$$

and

$$B_{1,m} = \frac{1}{a^2\pi}\int_o^a B_1\cdot 2r\pi\cdot dr \qquad (25)$$

Utilizing equations 17 and 18, the integration of equation 25 results in

$$B_{1,m} = (-ja^2/8p^2)\cdot 0.4\pi\mu(I_o n) \qquad (26)$$

The other component $B_{1,n}$ follows from equations 17, 18, 20, and 26:

$$B_{1,n} = (-ja^2/8p^2)\cdot 0.4\pi\mu(I_o n)\times [1-2(r/a)^2] \qquad (27)$$

Both components $B_{1,m}$ and $B_{1,n}$, whose radial distributions are illustrated in Figure 5, form together the flux Φ_1. This flux therefore can be considered as consisting of two components: $\Phi_{1,m}$, which has a constant density $B_{1,m}$ throughout the charge, and $\Phi_{1,n}$, which is not interlinked with the inductor.

When considering the effect of the eddy currents K_o and hence of flux Φ_1 on the inductor, only the component $\Phi_{1,m}$ requires attention because the interlinkage of the other component $\Phi_{1,n}$ with the inductor is zero.

It was stated previously that the weakening effect of the eddy currents K_o with respect to the inductor field can be nullified by the introduction of a compensating current I_1 into the inductor, which easily can be determined now. Current I_1 has to produce an induction $B'_{1,m}$ which nullifies $B_{1,m}$.

$$B'_{1,m} = -B_{1,m} \qquad (28)$$

From equations 1, 2, and 28,

$$0.4\pi\mu(I_1 n) = B'_{1,m} = -B_{1,m} \qquad (29)$$

Applying equation 26, one obtains for the compensating current I_1 in the inductor

$$I_1 = -(-ja^2/8p^2)I_o \qquad (30)$$

If this current I_1 is added to the original inductor current I_o, as it will be assumed, the magnetic action of the eddy currents K_o, as far as flux $\Phi_{1,m}$ is concerned, is completely cancelled. After the introduction of current I_1, the flux $\Phi_{1,m}$ ceases to exist and hence does not require any further attention. The only modification of the original eddy current

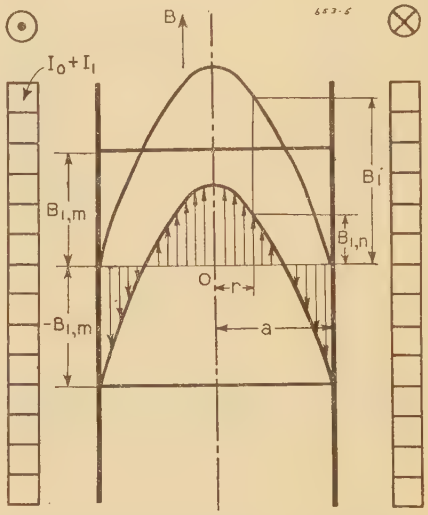

Figure 5. Longitudinal section, illustrating the distribution of induction B_1 caused by eddy currents K_o

distribution as expressed in equations 11 and 12 will be caused by induction $B_{1,n}$ (Figure 5).

In addition to cancelling part of the eddy current field, current I_1 reflects into the inductor the I^2R loss, which occurs in the charge caused by the eddy currents K_o. The current I_1 is in phase with the voltage E_o and thus expresses true power consumption by the inductor (Figure 6). It can be proved that this power P_o expressed in terms of I_1 and E_o (equations 8 and 30) equals the energy dissipated in the charge by the eddy current K_o (equations 11 and 12):

$$P_o = E_o I_1/2 = \pi(a/2p)^4\rho(I_o n)^2 \equiv \int_0^a (K_o^2\rho/2)\cdot 2r\pi\cdot dr \qquad (31)$$

Returning to induction $B_{1,n}$, the corresponding flux $\Phi_{1,n}$ follows in analogy to equation 3:

$$\Phi_{1,n} = \int_o^r B_{1,n}\cdot 2r\pi\cdot dr \qquad (32)$$

The induced voltage V_1 in the charge, caused by flux $\Phi_{1,n}$, is

$$V_1 = -j\omega\Phi_{1,n}10^{-8} \qquad (33)$$

Substituting from equations 27 and 32, one obtains

$$V_1 = [(-ja^2/p^2)\pi\rho(I_o n)r^2/a^2]\times [(-ja^2/8p^2)(1-r^2/a^2)] \qquad (34)$$

These voltages V_1 are induced in the charge by the flux $\Phi_{1,n}$ and previously have been disregarded after compensating voltages were introduced. Actually such compensating voltages do not exist and hence the voltages V_1 will be acting on the charge. Summarizing the reasoning thus far, it can be stated that the inductor carries the currents I_o and I_1, while the charge carries the eddy currents K_o. In addition, free residual voltages V_1 exist in the charge.

At this point an examination of the relative magnitudes of V_1 with respect to V_o is in order. Since the voltages V_1 will cause the flow of eddy currents K_1, just as V_o caused the flow of the eddy currents K_o, the relative magnitude of V_1 with respect to V_o will indicate whether the expression for the heat generation in the charge (equation 31) is sufficiently accurate or whether the effect of the voltages V_1 has to be taken into account.

Recasting the expression for V_o by using equations 6 and 15,

$$E_o = (-ja^2/p^2)\pi\rho(I_o n)r^2/a^2 \qquad (35)$$

The ratio V_1/V_o becomes (equations 34 and 35)

$$V_1/V_o = (-ja^2/8p^2)(1-r^2/a^2) \qquad (36)$$

For a ratio of $a/p<1$, the ratio of the voltages V_1/V_o, and consequently of the eddy currents K_1/K_o, becomes small. Since the generated heat is proportional to K_o^2, and respectively K_1^2, the heat generated by the eddy currents K_1 is then negligible with respect to the heat generated by the eddy currents K_o, and the expression for the heat generation (equation 31) applies.

The current I in the inductor is

$$I = I_o + I_1 = I_o[1+j(a^2/8p^2)] \qquad (37)$$

Solving for I_o,

$$I_o^2 = I^2/[1+j(a^2/8p^2)]^2 \qquad (38)$$

Introducing I_o^2 into equation 31 and remembering that equation 31 is valid only for $a/p<1$, I_o^2 can be approximated very closely by the inductor current I. Since the effective value of the inductor current

$$I_{\text{eff}} = I/\sqrt{2} \qquad (39)$$

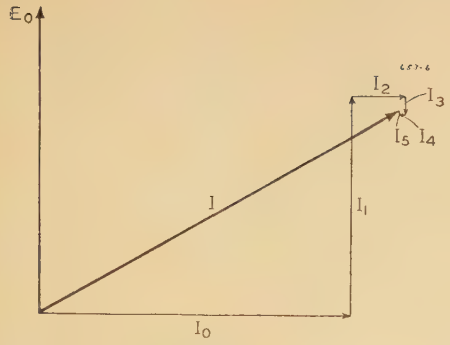

Figure 6. Vector diagram of currents in inductor

the heat generated in the charge can now be expressed as follows:

$$P_o = 2\pi(a/2p)^4 \rho (I_{eff} n)^2 \qquad (40)$$
for $a/p \leq 1$

If, however, $a/p > 1$, the effect of V_1 has to be investigated. Just as the voltage V_o produces the eddy current K_o, the voltage V_1 produces a new eddy current K_1, as fully explained in Appendix I. The effect of the eddy currents K_1 can be resolved in an additional current I_2 in the inductor (Figure 6) and free voltages V_2 as follows:

$$K_1 = \left(-j\frac{a^2}{8p^2}\right)^2 \frac{4}{a}(I_o n)\frac{r}{a}\left(1-\frac{r^2}{a^2}\right) \qquad (42)$$

$$I_2 = -\left(-j\frac{a^2}{8p^2}\right)^2 I_o \cdot \frac{1}{3} \qquad (50)$$

$$V_2 = \left(-j\frac{a^2}{8p^2}\right) V_1 \left(\frac{2}{3}-\frac{r^2}{3a^2}\right) \qquad (53)$$

Thus the current in the inductor consists of the vector sum of I_o, I_1, I_2, while the eddy currents consist of the vector sum of K_o, K_1. In addition, free residual voltages V_2 exist in the charge.

With the new eddy currents K_2 (in analogy to equation 42),

$$K_2 = \left(-j\frac{a^2}{8p^2}\right)^2 K_o \left(-\frac{2}{3}+\frac{r^2}{a^2}-\frac{r^4}{3a^4}\right) \qquad (54)$$

flowing in the charge, it can be seen that

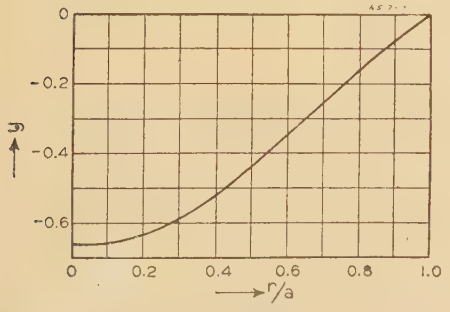

Figure 7. Function y indicates the progressive reduction of eddy current density toward the axis of charge

K_2 is in counterphase with eddy currents K_o, and hence K_2 can be algebraically subtracted from K_o in order to obtain the total nonquadrature eddy current thus far derived. The charge also carries the eddy current K_1. This current K_1 is, however, in phase quadrature with K_o, and its effect on K_o will be neglected for reasons of simplicity. Under this assumption K_2 expresses the amount by which the original intensity K_o of the eddy currents (equation 16) will be modified if the voltages V_1 and V_2 are not negligible.

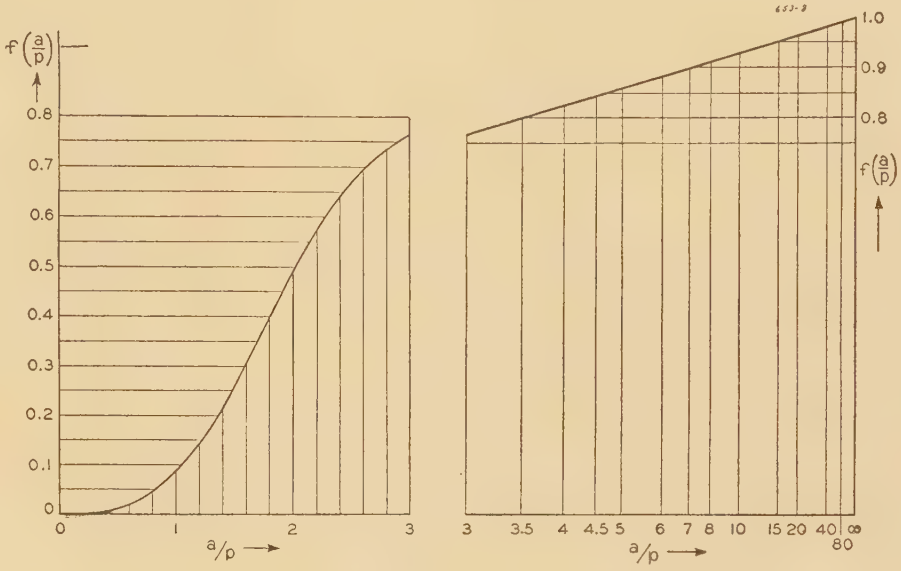

Figure 8. Graph for f(a/p) (from equations 71 and 81)

In order to compare the new eddy current K_2 with the original eddy current K_o, the first is expressed in terms of the latter as shown in equation 55:

$$K_2/K_o = \left(-j\frac{a^2}{8p^2}\right)^2 \left(-\frac{2}{3}+\frac{r^2}{a^2}-\frac{r^4}{3a^4}\right) = y \qquad (55)$$

Aside from the term $(-ja^2/8p^2)^2$, the new eddy current K_2 equals the original eddy current K_o times a function y. For better illustration, the function y is plotted in Figure 7. This figure reveals:

1. In the interior of the charge the new eddy current K_2 is opposed to the original eddy current K_o at every point, resulting in a smaller eddy current density than expressed in equation 16, and therefore resulting in less heat generation than expressed in equation 12.

2. The eddy current density, and hence heat generation, is progressively reduced toward the center of the charge.

3. The relative reduction of eddy current density and heat generation in the interior is a function of the ratio a/p.

As pointed out in the preceding paragraphs, the generated heat decreases toward the axis at a higher rate than expressed by equation 12. The result is a preponderance of heat generation in the surface layer, called the skin of the charge which effect is called skin effect. If the ratio a/p is increased, the reduction of heat generation toward the axis of the charge is intensified resulting in a still greater preponderance of heat generation in the surface layer of the charge. Besides frequency, resistivity, and permeability, the radius a of the charge is an additional controlling factor for the skin effect. The skin effect may be produced equally in the case of a higher frequency and a charge of smaller diameter, as in the case of a lower frequency and a charge of larger diameter.

After this discussion of skin effect, the attack on the main problem, namely the computation of heat generation, will be resumed. The eddy currents K_2 lead to magnetic intensities H_3 which, in turn, are resolved in a current I_3 in the inductor and free voltages V_3 in the charge. If this method is repeated, further currents I_4, I_5, I_6 are obtained for the inductor:

$$I_1 = -(-ja^2/8p^2)I_o \qquad (30)$$
$$I_2 = -(-ja^2/8p^2)^2 I_o \cdot {}^1/_3 \qquad (50)$$
$$I_3 = -(-ja^2/8p^2)^3 I_o \cdot {}^1/_6 \qquad (56)$$
$$I_4 = -(-ja^2/8p^2)^4 I_o \cdot {}^4/_{45} \qquad (57)$$
$$I_5 = -(-ja^2/8p^2)^5 I_o \cdot {}^{13}/_{270} \qquad (58)$$

The current components in Figure 6 are shown for $a/p = 2.4$. It is evident from Figure 6 that the current components converge rapidly and hence the current represented by I is a very close approximation for the actual current in the inductor. For decreasing ratios of

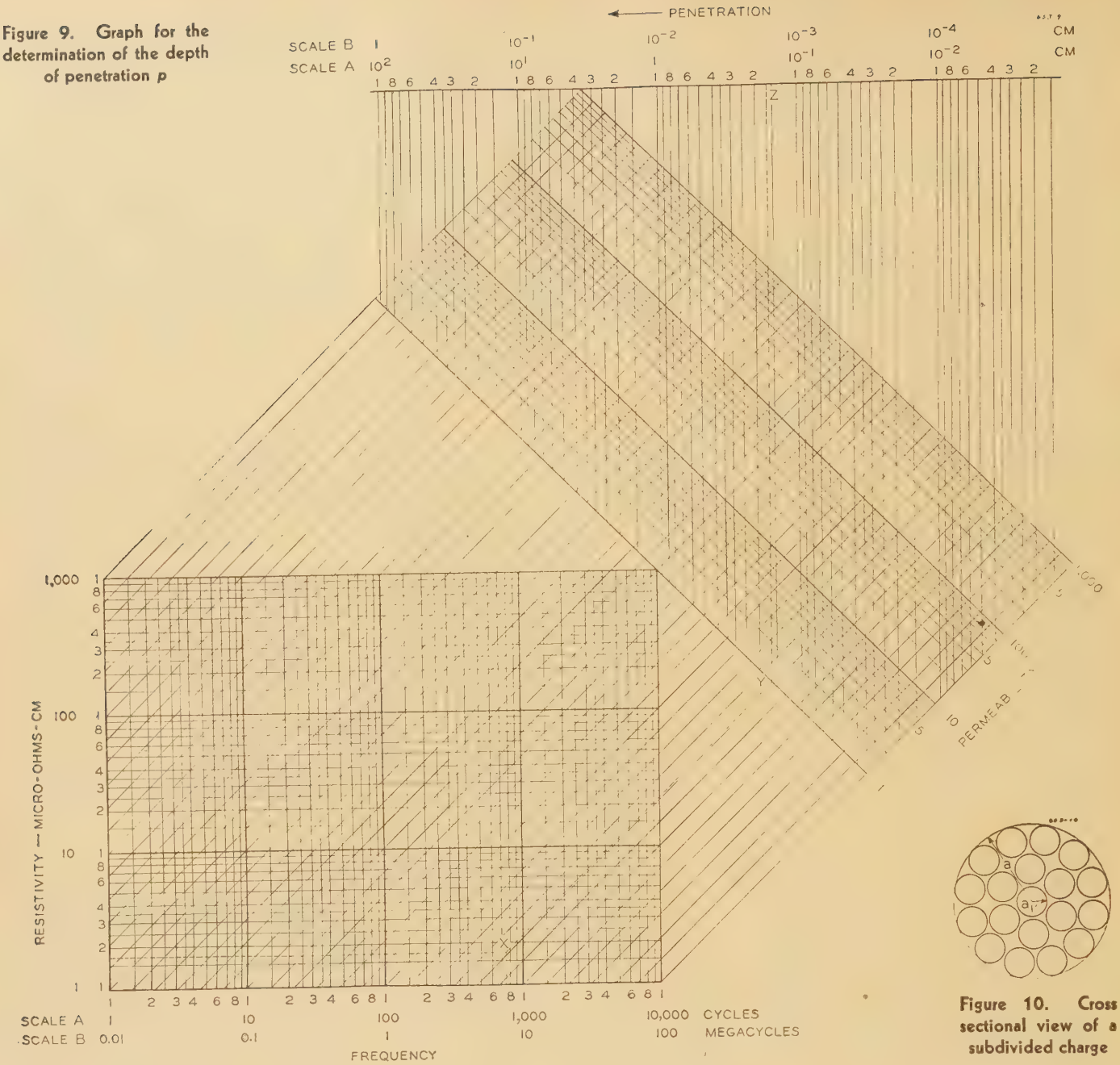

Figure 9. Graph for the determination of the depth of penetration p

Figure 10. Cross sectional view of a subdivided charge

a/p, the convergence is more rapid yet and hence the approximation is still closer.

When the true components I_1, I_3, I_5 are multiplied with the inductor voltage E_o, the true power P dissipated in the charge is obtained. This is shown in Appendix II, resulting in

$$P=2\pi\rho\frac{\frac{1}{16}\left(\frac{a}{p}\right)^4}{1+\frac{11}{384}\left(\frac{a}{p}\right)^4-\frac{77}{2{,}211{,}840}\left(\frac{a}{p}\right)^8}(I_{eff}n)^2$$

for $a/p<3$ (69)

Thus the generated heat has been determined in the form of a series, as a function of radius, resistivity, permeability of the charge, and the ampere-turns and frequency of the inductor current. For $a/p = 3$ the accuracy of the series is within 1.1 per cent. For smaller ratios of a/p the error rapidly approaches zero. The convergence of the series is so rapid that for a ratio of $a/p \leqslant 2.2$, the third term in the denominator of equation 69 can be neglected without introducing an error of more than 1.2 per cent. The remaining series is still very rapidly converging for decreasing ratios of a/p. If $a/p = 0.8$, the second term in the denominator can be neglected without causing an error of more than 1.2 per cent, which error rapidly decreases for decreasing ratios of a/p.

The formulation of generated heat by means of a sharply converging series introduces a new tool for the analytical attack of various theoretical problems. For practical rapid determination of the heat, equation 60 is split into 2 parts:

$$P=P_\infty\cdot f\left(\frac{a}{p}\right) \tag{70}$$

where

$$f\left(\frac{a}{p}\right)=\frac{\frac{\sqrt{2}}{16}\left(\frac{a}{p}\right)^3}{1+\frac{11}{384}\left(\frac{a}{p}\right)^4-\frac{77}{2{,}211{,}840}\left(\frac{a}{p}\right)^8} \tag{71}$$

for $a/p<3$

$$P_\infty=\pi\sqrt{2}\rho\frac{a}{p}(I_{eff}n)^2 \tag{72}$$

While function $f\ (a/p)$ is plotted in Figure 8, a graph shown in Figure 9, and

explained later in the text, facilitates the rapid determination of p.

Case a/p ≥ 3

It can be shown[3] that for a magnitude of p which is negligible with respect to the radius a, the heat generation W per unit volume at a radial distance d from the surface of the charge, can be expressed by

$$W=\frac{1}{2}\left(\frac{In}{p}\right)^2 \rho\epsilon^{\frac{-d\sqrt{2}}{p}} \tag{73}$$

where

$$d=a-r \tag{74}$$

The heat generated in a slice of one centimeter height is

$$P=\int_0^a W\cdot 2r\pi\cdot dr \tag{75}$$

If this integral is evaluated as shown in Appendix III, the following expression for the generated heat is obtained as follows:

$$P=\pi\sqrt{2}\rho\frac{a}{p}\left(1-\frac{1}{\frac{a\sqrt{2}}{p}}\right)(I_{eff}n)^2 \tag{80}$$

for $a/p\geq 3$

Equation 80 is accurate within 0.1 per cent for $a/p = 3$. For larger ratios of a/p, the error rapidly approaches zero.

It will be recognized that the application of equation 72 leads to

$$P=P_\infty\cdot f\left(\frac{a}{p}\right) \tag{70}$$

where

$$f\left(\frac{a}{p}\right)=1-\frac{1}{\frac{a\sqrt{2}}{p}} \tag{81}$$

for $a/p\geq 3$

and

$$P_\infty=\pi\sqrt{2}\rho\frac{a}{p}(I_{eff}n)^2 \tag{72}$$

The function $f(a/p)$ (equation 81) can be plotted very rapidly as a straight line, using a hyperbolic scale for the abscissa axis, as shown in Figure 8.

Graph for the Determination of the Depth of Penetration

Every one of the important equations in the preceding analysis contained the factor p (equation 15). For a radius of the charge which is very large compared to p, the magnetic intensity declines exponentially from the surface toward the interior of the charge.[3] At a distance of $p\sqrt{2}$ from the surface, the magnetic intensity and hence the eddy currents are $1/\epsilon$ of their respective values at the surface. The decay of the magnetic intensity as a function of its penetration into the charge can thus be expressed in terms of p, and hence p is often referred to as depth of the magnetic field penetration.

For rapid determination of p, the graph in Figure 9 is recommended. Suppose the penetration should be determined for copper at room temperature ($\rho = 1.7\cdot 10^{-6}$ ohm-centimeters, $\mu = 1$) and a frequency of 750 cycles. Erect verticals on the frequency and resistivity axes at the required points, as shown by dotted lines, and intersect at point X. Draw a line through X under 45 degrees until intersection is made with the permeability system at the desired permeability (point Y). Erect a vertical line on Y and intersect penetration axis at point Z. If scale A has been used for frequency, use scale A for penetration; if scale B has been used for frequency, use scale B for penetration. For the foregoing example the solution is 0.17 centimeter.

Subdivided Charge

Thus far the charge consisted of one cylinder with the radius a. When induction heating is applied to melting operations, the charge with which the heating process is started may consist of a multitude of solid pieces of metal, so-called scrap whose upper range of size is limited by the inside diameter of the crucible. As far as the geometry of the crucible is concerned, there is no lower limit for the size of the scrap. It has been observed, however, that the time for melting the same weight of scrap depends upon the size of the scrap, other conditions such as magnitude and frequency of the inductor current remaining the same. Under these assumptions the energy spent on copper losses in the inductor is merely a function of the time during which the current is applied. If various sizes of scrap require various amounts of time for melting, although the weight of scrap remains the same, it is obvious that the size of the scrap influences the efficiency of heating.

In order to analyze the effect of scrap size, it will be assumed that the charge consists of a number of solid, identical, round bars which fill the interior of the crucible as shown in Figure 10. Singling out one bar with the radius a_i, the generated heat can be computed, as previously shown in equation 70, substituting a_i for a. Since the charge, in this case the bar, does not create a magnetic field outside its contours, the space around the bar remains at the same magnetic intensity whether the bar is present or not. This means that the state within one bar is unaffected by the presence of other bars within the same inductor. If, however, the bars touch each other, a current can be transferred across the common surface making the bars interdependent. It will be assumed in the following that the bars do not touch each other, or that oxides are present at the surface of the bars which are sufficiently insulating to make the current transfer betwen bars negligible.

As in the preceding (equation 70), the heat generated per centimeter length of one bar equals

$$P_i=P_{\infty i}\cdot f\left(\frac{a_i}{p}\right) \tag{82}$$

where

$$P_{\infty i}=\pi\sqrt{2}\rho\frac{a_i}{p}(I_{eff}\cdot n)^2 \tag{83}$$

If the number of rods is i, the total area A of the cross sections of the rods equals

$$A=ia_i^2\pi \tag{84}$$

The total heat generated in all bars per centimeter length follows from Appendix IV:

$$P=A\cdot(\mu f 10^{-9})\cdot\varphi\left(\frac{a_i}{p}\right)\cdot(I_{eff}n)^2 \tag{90}$$

The function of $\varphi(a_i/p)$ (equations 88 and 89) has been plotted in the graph, as shown in Figure 11. The most striking feature of the function is its maximum. It means that for a certain ratio of a_i/p, the generated heat is a maximum. Since the magnitude and frequency of the current in the inductor are assumed constant, the losses in the inductor are also constant, and hence maximum heat generation means maximum efficiency. In order to find the maximum, the conventional approach of differentiating function $\varphi(a_i/p)$ (equation 88) is applied. The solution is

$$\left[\varphi\left(\frac{a_i}{p}\right)\right]_{max}=29.86 \tag{91}$$

for $a_i=2.53p$

For a given material and frequency, there is one certain radius at which maximum heat generation is achieved. It should, however, be borne in mind, that most metals increase their resistivity with increasing temperature. The penetration p at lower temperature is smaller (equation 15) than at higher temperature. If the radius $a_i = 2.53\ p$ has been determined for the low temperature, the heat generation will be at maximum at

the outset of heating. As the heating process goes on, the temperature of the charge will rise and its resistivity increases. The factor p will also increase, resulting in a decreasing (a_i/p). It is obvious from Figure 11 that a reduction of heat generation will occur. The thermal losses of the charge, however, increase with the temperature, while the generated heat decreases. It is therefore possible that a temperature equilibrium establishes itself below the desired temperature.

In order to avoid this limitation of temperature, the radius a_i of the charge has to be computed from a penetration p, which is based on a resistivity of higher value than at room temperature. If p is based on the resistivity of the metal at its highest temperature, the generated heat also will reach its maximum at the highest temperature.

The maximum heat generation follows from equations 90 and 91:

$$P_{max} = 29.86A(\mu f 10^{-9})(I_{eff}n)^2 \tag{92}$$

From the point of view of efficiency of induction heating, equation 92 is very significant. If the charge is not subdivided, and provided $a \gg p$, the generated heat P is given by equation 70. The heat generation P is proportional to the radius of the charge, and the copper losses in the inductor are in proportion to the radius of the inductor. If the radius of the charge is increased, the radius of the inductor has to be increased by a proportional amount. The result is that the ratio between heat generation and inductor loss remains constant, which in turn means that the efficiency is limited to a constant amount depending on the resistivity and permeability of the charge.

For a subdivided charge no such limitation exists. While the loss in the inductor increases linearly with its radius, the area A of the total cross-section of the bars increases approximately with the square of the radius. The result is that by increasing the radius of the inductor, the heat generation in the charge increases much faster than the losses in the inductor, hence the efficiency approaches asymptotically 100 per cent.

Appendix I

The voltage V_1 will cause the flow of new eddy currents of the density K_1. The magnitude and phase of these new eddy currents is controlled by V_1, the resistance of the sleeves, and the voltages V_2 induced in the sleeves by the eddy currents K_1 caused by mutual reactance. A compensating current I_2 is introduced in the inductor to counteract the weakening action of the eddy currents K_1. Furthermore, a compensating voltage $-V_2$ is introduced in series with each sleeve, developing a voltage equal in magnitude and opposite in sign with respect to the voltage induced in the sleeve by the eddy currents K_1 in the charge, and the compensating current I_2 in the inductor, thus nullifying the voltages of mutual reactance. The eddy current K_1 is now only a function of V_1 and the resistance of the sleeve (equation 10):

$$K_1 = E_1/2r\pi\rho \tag{41}$$

Taking V_1 from equation 34, one obtains

$$K_1 = \left(-j\frac{a^2}{8p^2}\right)^2 \frac{4}{a}(I_0 n)\frac{r}{a}\left(1-\frac{r^2}{a^2}\right) \tag{42}$$

The magnetic intensity H_2 results in analogy to equation 14:

$$H_2 = 0.4\pi \int_r^a K_1 dr \tag{43}$$

and integrating equation 42,

$$H_2 = \left(-j\frac{a^2}{8p^2}\right)^2 \cdot 0.4\pi(I_0 n)\left(1-2\frac{r^2}{a^2}+\frac{r^4}{a^4}\right) \tag{44}$$

Again, the resulting induction B_2 is split into two components similar to equation 20:

$$B_2 = B_{2,m} + B_{2,n} \tag{45}$$

Stipulating the same requirements for $B_{2,m}$ and $B_{2,n}$, as previously for $B_{1,m}$ and $B_{1,n}$, respectively,

$$B_{2m} = \left(-j\frac{a^2}{8p^2}\right)^2 \cdot 0.4\pi\mu(I_0 n)\cdot\frac{1}{3} \tag{46}$$

The other component $B_{2,n}$ follows from equations 44 and 46:

$$B_{2,n} = \left(-j\frac{a^2}{8p^2}\right)^2 \cdot 0.4\pi\mu(I_0 n)\left(\frac{2}{3}-2\frac{r^2}{a^2}+\frac{r^4}{a^4}\right) \tag{47}$$

In order to cancel the effect of $B_{2,m}$, a compensating current I_2 has to flow through the inductor which produces an induction

$$B'_{2,m} = -B_{2,m} \tag{48}$$

From equations 1, 2, and 48

$$0.4\pi\mu(I_2 n) = B'_{2,m} = -B_{2,m} \tag{49}$$

Applying equation 46 one obtains the compensating current I_2:

$$I_2 = -\left(-j\frac{a^2}{8p^2}\right)^2 I_0 \cdot \frac{1}{3} \tag{50}$$

Only the component $B_{2,n}$ can be effective in inducing voltages V_2 in the sleeves. The corresponding flux

$$\Phi_{2,n} = \int_0^r B_{2,n} \cdot 2r\pi \cdot dr \tag{51}$$

which, in turn, induces voltages V_2 in the charge

$$V_2 = -j\omega\phi_{2,n}10^{-8} \tag{52}$$

Substituting for $\Phi_{2,n}$ in equation 52 results in an expression for V_2 as follows:

$$V_2 = \left(-j\frac{a^2}{8p^2}\right) V_1\left(\frac{2}{3}-\frac{r^2}{3a^2}\right) \tag{53}$$

Appendix II

The inductor current I has two components: the resistive component I_R in phase with the voltage E_0 and the inductive component I_x lagging 90 degrees behind.

$$I = I_R + I_x \tag{59}$$

The resistive component I_R follows from

$$I_R = I_1 + I_3 + I_5 \tag{60}$$

and the inductive component I_x equals

$$I_x = I_0 + I_2 + I_4 \tag{61}$$

The resistive component I_R follows from equations 30, 56, 58, and 60:

$$I_R = jI_0\left\{\frac{a^2}{8p^2}\left[1-\frac{1}{6}\left(\frac{a^2}{8p^2}\right)^2+\frac{13}{270}\left(\frac{a^2}{8p^2}\right)^4\right]\right\} \tag{62}$$

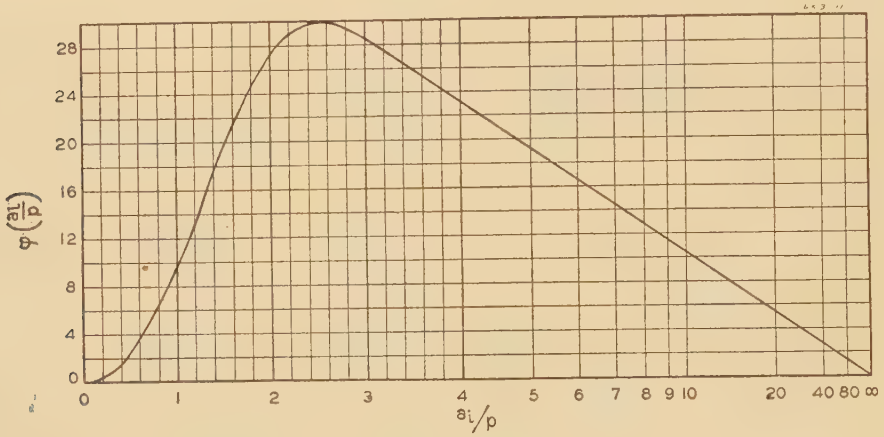

Figure 11. Graph for $\varphi(a_i/p)$ (from equations 88 and 89)

and the inductive component follows from equations 50, 57, and 61

$$I_x = I_o\left[1+\frac{1}{3}\left(\frac{a^2}{8p^2}\right)^2-\frac{4}{45}\left(\frac{a^2}{8p^2}\right)^4\right] \quad (63)$$

The absolute value of the inductor current I (equation 59) is

$$I=\sqrt{{I_R}^2+{I_x}^2} \quad (64)$$

Substituting for equations 62 and 63 in equation 64 and neglecting terms of sixth power and up, one obtains for the current I

$$I=I_o\sqrt{1+\frac{5}{3}\left(\frac{a^2}{8p^2}\right)^2-\frac{2}{5}\left(\frac{a^2}{8p^2}\right)^4+\cdots} \quad (65)$$

The heat generated by eddy currents is taken from the line in the form of the resistive component I_R of inductor current I. The average value of generated heat therefore can be expressed as

$$P=E_oI_R/2 \quad (66)$$

where E_o and I_R are peak values.

The resistive component I_R is obtained from equations 62 and 65:

$$I_R=I\left(\frac{a^2}{8p^2}\right)\cdot\frac{1-\frac{1}{6}\left(\frac{a^2}{8p^2}\right)^2+\frac{13}{270}\left(\frac{a^2}{8p^2}\right)^4}{\sqrt{1+\frac{5}{3}\left(\frac{a^2}{8p^2}\right)^2-\frac{2}{5}\left(\frac{a^2}{8p^2}\right)^4}} \quad (67)$$

This expression can be used in equation 66, and by further reference to equations 8 and 67 one obtains for the average power

$$P=4\pi\rho\left(\frac{a^2}{8p^2}\right)^2\times\frac{1-\frac{1}{6}\left(\frac{a^2}{8p^2}\right)^2+\frac{13}{270}\left(\frac{a^2}{8p^2}\right)^4}{1+\frac{5}{3}\left(\frac{a^2}{8p^2}\right)^2-\frac{2}{5}\left(\frac{a^2}{8p^2}\right)^4}(In)^2 \quad (68)$$

Dividing the denominator by the numerator and neglecting terms of sixth and higher powers, equation 68 simplifies to

$$P=2\pi\rho\,\frac{\frac{1}{16}\left(\frac{a}{p}\right)^4}{1+\frac{11}{384}\left(\frac{a}{p}\right)^4-\frac{77}{2{,}211{,}840}\left(\frac{a}{p}\right)^8}(I_{eff}n)^2 \quad (69)$$

for $a/p<3$

Appendix III

Applying the expression for W (equation 73) to equation 75 and integrating between the limits $r = 0$ and $r = a$ results in the following operations:

$$P=\frac{1}{2}\left(\frac{In}{p}\right)^2\rho 2\pi\int_o^a r\cdot\epsilon^{-\frac{(a-r)\sqrt{2}}{p}}\cdot dr$$

$$=\frac{1}{2}\left(\frac{In}{p}\right)\rho 2\pi\cdot\epsilon^{-\frac{a\sqrt{2}}{p}}\int_o^a r\cdot\epsilon^{\frac{r\sqrt{2}}{p}}\cdot dr \quad (76)$$

$$\int_o^a r\cdot\epsilon^{\frac{r\sqrt{2}}{p}}\cdot dr=\frac{p^2}{2}\left(\frac{r\sqrt{2}}{p}-1\right)\epsilon^{\frac{r\sqrt{2}}{p}}\Bigg|_o^a$$

$$=\frac{p^2}{2}\left[\left(\frac{a\sqrt{2}}{p}-1\right)\epsilon^{\frac{a\sqrt{2}}{p}}+1\right] \quad (77)$$

Using the results of equation 77 in equation 76 leads to

$$P=\frac{1}{2}\left(\frac{In}{p}\right)^2 2\pi\rho\,\frac{p^2}{2}\left(\frac{a\sqrt{2}}{p}-1+\epsilon^{-\frac{a\sqrt{2}}{p}}\right) \quad (78)$$

$$\epsilon^{-\frac{a\sqrt{2}}{p}}\ll\frac{a\sqrt{2}}{p}-1 \qquad \text{for } a/p\geq 3 \quad (79)$$

The exponential term in equation 78 thus can be neglected and the generated heat per one centimeter height of the charge is

$$P=\pi\sqrt{2}\rho\,\frac{a}{p}\left(1-\frac{1}{\frac{a\sqrt{2}}{p}}\right)(I_{eff}n)^2 \quad (80)$$

for $a/p\geq 3$

Appendix IV

From equations 70, 82, 83, and 84,

$$P=A\sqrt{2}\,\frac{1}{a_ip}\cdot\rho\cdot f\left(\frac{a_i}{p}\right)(I_{eff}n)^2 \quad (85)$$

Recasting equation 85 and substituting from equation 15 for p,

$$P=A\sqrt{2}\cdot 8\pi^2(\mu f10^{-9}/\rho)\times\left\{\left[f\left(\frac{a_i}{p}\right)\right]\Big/\left(\frac{a_i}{p}\right)\right\}(I_{eff}n)^2 \quad (86)$$

Introducing

$$\varphi\left(\frac{a_i}{p}\right)=8\pi^2\sqrt{2}\left[f\left(\frac{a_i}{p}\right)\right]\Big/\frac{a_i}{p} \quad (87)$$

for $a_i/p<3$ the function $\varphi\left(\frac{a_i}{p}\right)$ follows from equation 71:

$$\varphi\left(\frac{a_i}{p}\right)=\pi^2\,\frac{\left(\frac{a_i}{p}\right)^2}{1+\frac{11}{384}\left(\frac{a_i}{p}\right)^4-\frac{77}{2{,}211{,}840}\left(\frac{a_i}{p}\right)^8}$$

$a_i/p<3$ (88)

And for $a_i/p\geq 3$ the function $\varphi\left(\frac{a_i}{p}\right)$ follows from equation 81:

$$\varphi\left(\frac{a_i}{p}\right)=8\sqrt{2}\pi^2\left(1-\frac{1}{\frac{a_i\sqrt{2}}{p}}\right)\Big/\frac{a_i}{p} \quad (89)$$

$\frac{a_i}{p}\geq 3$

Returning to the heat generation it can be expressed as

$$P_{max}=29.86A(\mu f10^{-9})(I_{eff}n)^2 \quad (92)$$

Appendix V. Definitions of Symbols

A = total area of subdivided charge, in square centimeters
a = radius of nonsubdivided charge, centimeters
a_i = radius of bars in subdivided charge, centimeters
B = induction, peak value of sinusoid, gausses
d = distance of a point inside of charge to surface, centimeters
E = voltage, peak value of sinusoid, volts
f = frequency of inductor current, cycles per second
$f(a/p)$ = a function of (a/p)
H = magnetic intensity, peak value of sinusoid, oersteds
I = current, peak value of sinusoid, amperes
I_{eff} = current, rms value, amperes
i = number of bars in subdivided charge
$j=\sqrt{-1}$
K = current density of eddy currents, peak value of sinusoid, amperes per square centimeter
l = length of line over which integral is taken
n = number of turns of inductor per centimeter axial length
P = power, average value, watts
p = penetration, centimeters
s = surface over which integral is taken, square centimeters
t = time, seconds
V = induced voltage in charge, peak value of sinusoid, volts
W = generated heat, average value, watts per cubic centimeter
ϵ = base of natural logarithms, 2.71828
μ = permeability, unity
π = 3.14159
Φ = magnetic flux, peak value of sinusoid, maxwells
$\varphi(a_i/p)$ = a function of a_i/p
ρ = resistivity, ohm-centimeters
ω = angular velocity, radians per second

References

1. The Induction of Currents in Cores, O. Heaviside. *Electrician* (London, England), volume 12, May 3, 1884, page 5 3.

2. A Treatise on the Theory of Alternating Currents (book), A. Russell. Cambridge University Press, 1904. Volume 1, page 368.

3. Surface Heating by Induction, H. F. Storm. AIEE Transactions, volume 63, 1944, October section, pages 749–55.

4. Electric Circuits (book), Staff, Massachusetts Institute of Technology. John Wiley and Sons, Inc., New York, N. Y., 1944. Page 37.

5. Industrial Electric Heating, N. R. Stansel. *General Electric Review*, volume 39, number 9, September 1936, page 440.

6. Efficiency of Induction Heating Coils, G. H. Brown. *Electronics*, volume 17, number 8, August 1944, page 124.

7. Design of Induction-Heating Coils for Cylindrical Nonmagnetic Loads, J. T. Vaughan, J. W. Williamson. AIEE Transactions, volume 64, 1945, August section, pages 587–92.

8. Induction Heating of Moving Magnetic Strip, R. M. Baker. AIEE Transactions, volume 64, 1945, April section, pages 184–9.

Application of the Ohm and Mho Principles to Protective Relays

A. R. van C. WARRINGTON
MEMBER AIEE

THE mho relay unit was first used 15 years ago as the directional unit for an early-type reactance relay. Thus it can be said that "mho" applied to relays is a new term applied to an old principle. The mathematical justification for the term has been given in a paper[1] describing the use of the mho unit in a carrier-current relaying scheme. The mho unit in its present form is a directional impedance unit whose accuracy is comparable with that of the reactance ohm unit used in a distance relay.

The mho characteristic (Figure 1C) is suited ideally for protecting long or heavily loaded transmission lines because it is much less likely to trip on power swings than the conventional reactance or impedance relays. Another desirable feature is that a relay for phase faults should operate only on faults involving the phase pair with which the relay is associated; all other faults or system conditions should not affect it. In Figures 1A and 1B, the large tripping area of the impedance characteristics of the impedance and reactance relays shows that these relays are susceptible to power swings and faults in other phases (denoted by asterisks), whereas the snug fit of the mho circle around the fault area in Figure 1C indicates that the mho relay effectively prevents tripping for power swings and for any faults but those for which the relay is set to trip.

The fact that the mho unit combines sensitive directional action with accurate ohmic measurement means that one mho unit does what two conventional units did before. This not only eliminates the contact races that can occur between the directional element and the measuring element but obviously simplifies the circuits to which the relay is applied.

With these advantages it might appear that the mho unit should be used universally for all applications involving distance measurement. This is generally true, but there is a lower limit of impedance for which it can be set for reasons discussed later. Lines too short for the mho unit still must be protected by the reactance ohm unit.

Several new relays will be described, some of which use ohm units and mho units to perform existing relay functions more efficiently and others to perform some new functions. In order to understand the operation of these new relays, it may be helpful first to consider briefly their operation and to compare their pickup characteristics on the impedance diagram.

Relation Between Ohm and Mho Units

First of all, it should be understood that ohm units and mho units are merely refinements of the straight impedance relay. All distance relays measure the distance to a fault by comparing the current in the faulted circuit with the potential across it. In the impedance relay, this is done by opposing the torques of two electromagnets, one having a current winding and the other a potential winding (Figure 2A). The impedance measured by such a relay is not always a true measurement of distance, however. On short lines the additional potential drop in an arcing fault tends to prevent the impedance relay from operating, and on long lines, the current may be high enough under load or power swing conditions relative to the voltage to present to the relay an impedance as low as that of a fault and cause undesirable tripping.

This difficulty can be overcome largely by the use of the product-type relay whose torques are not proportional to current and voltage alone but to the products of I and E with a third quantity which, being common to both, does not affect the ratio balance E/I but provides phase-angle discrimination. This is shown schematically in Figures 2B and 2C.

The flux from the additional pair of poles (shown vertically in Figures 2B and 2C) acts in much the same way as the current or potential polarizing flux in a directional ground relay, and for want of a better name it will be referred to in the following as a polarizing flux.

The current polarizing flux in Figure 2B goes from the upper I pole through the induction cylinder and the central core iron stacking to the lower I pole and induces a current in the cylinder which flows perpendicular to the plane of the paper up and down the sides of the cup opposite the other two poles. The current opposite the operating pole I reacts with the flux from that pole to produce an I^2 torque tending to close the relay contacts, and the current in the cylinder near the E pole reacts with the flux from that pole producing an EI torque tending to keep the contact open.

In the following paragraphs, it will be shown that the provision of what we have called polarizing poles not only overcomes the above difficulties of distance measurement but provides some interesting new applications. Figure 3 shows the general construction of a high-speed product-type unit, the 4-pole induction cylinder unit.

Current Polarization (Ohm Units)

The torque is the product of the current polarizing flux times the fluxes from the opposed I and E poles. Hence the equation for the operating point, which determines the pickup characteristic, is

$$I[KI - E\cos(\phi - \theta)] = 0 \qquad (1)$$

where K is a winding constant, ϕ is the phase angle of the protected circuit, and θ is the angle of the relay characteristic.

Dividing through by I^2 and rearranging the terms, the equation becomes $Z\cos(\phi-\theta)=K$. Thus the current polarizing winding makes the relay respond to impedance only at a particular angle which is determined by the phase angle of the potential circuit of the relay. For example, a simple 4-pole induction cylinder unit with a current polarizing winding, reacting with a current operating pole and a potential restraining pole, operates on a component of impedance 20 degrees more leading than resistance. Such a relay (Figure 4) has been used as a blinder[2] for preventing other protective relays from tripping during very severe power swings. Two such ohm units, polarized in opposite directions, can be connected through auxiliary relays so as to detect an out-of-step condition after the first half swing period.

Adding a capacitor to make the potential circuit of the aforementioned unit at unity power-factor makes $\theta=90$ degrees in the pickup equation, which becomes $(E/I)\sin\phi=K$ or $X=K$. In other words, the relay operates on reactance (Figure 5).

The reactance relay is used where the

Paper 46-38, recommended by the AIEE committee on protective devices for presentation at the AIEE winter convention, New York, N. Y., January 21–25, 1946. Manuscript submitted November 26, 1945; made available for printing December 18, 1945.

A. R. van C. Warrington is in charge of application of protective relays, General Electric Company, Philadelphia, Pa.

arc resistance is likely to be comparable with the impedance of the protected section and hence likely to interfere with the operation of the impedance relay. The reactance relay ignores the arc resistance and hence is indispensable for short lines and for protecting against ground faults.

Potential Polarization (Mho Units)

With potential polarization, the torque is the product of the potential-polarizing flux times the fluxes from the opposed I and E poles. Hence the equation for pickup is

$$E[I \cos (\phi-\theta)-K'E]=0 \qquad (2)$$

or $-K'E^2+EI \cos (\phi-\theta)=0$. Dividing through by E^2 and putting the K' term on the right, we get $Y \cos (\phi-\theta)=K'$, which is a straight line on an admittance diagram and thus represents a constant component of admittance, that is, the relay will pick up at a constant value of mhos at a certain angle and therefore has been called a mho unit. This is parallel to the case of the ohm unit which picks up at a constant component of impedance, as shown in the impedance diagram of Figure 4A.

It is generally more convenient to plot distance-relay characteristics on an impedance diagram. The impedance equation of the mho unit is obtained by putting the EI term on the right side of the equation and dividing through by $K'EI$, which gives $Z=(1/K') \cos (\phi-\theta)$.

This is the equation of a circle, of diameter $1/K'$, which passes through the origin (Figure 6A). The impedance characteristic of a mho relay is therefore a circle passing through the origin.

The fact that the characteristic passes through the origin means that the unit is inherently directional. The phase angle of the relay characteristic is the angle θ between the diameter of the impedance circle and the R axis. By making θ equal to or a little less lagging than ϕ, the phase angle of the line, the circle is made to fit very closely around the fault area so that the relay is less sensitive to power swings and hence valuable for the protection of long or heavily loaded lines.

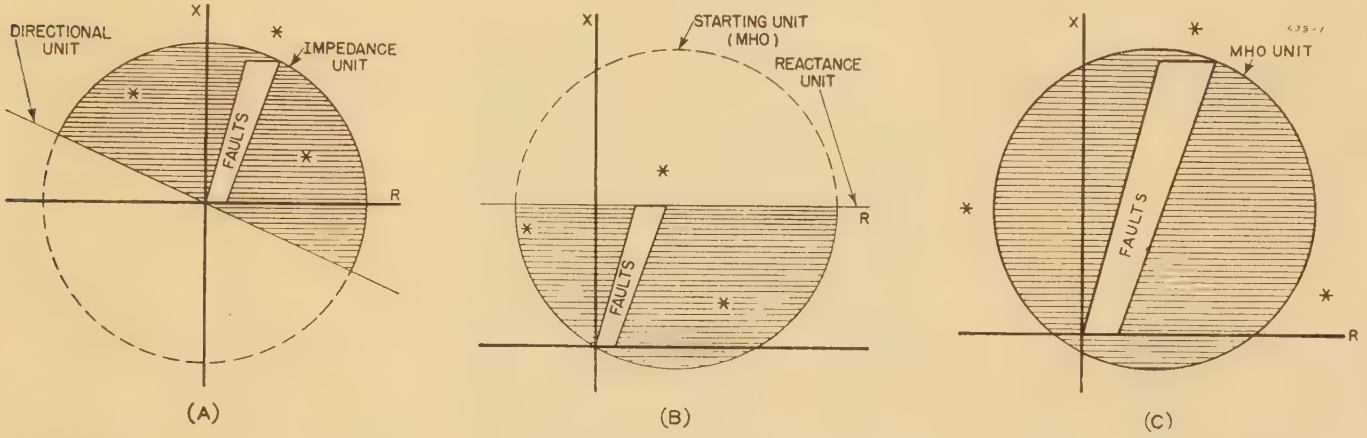

Figure 1. Tripping characteristics

A. Impedance unit
B. Reactance unit
C. Mho unit

The relays trip in the shaded area. Crosses are conditions for which tripping is undesirable

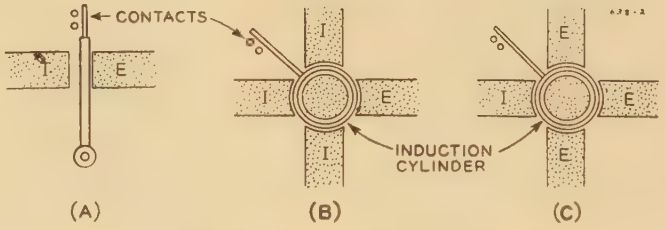

Figure 2. Schematic diagrams

A. Impedance unit
B. Ohm unit
C. Mho unit

Offset Mho Circle

Since both the terms of the equation of the mho relay contain E, it would appear that the relay has zero torque when the potential is zero, as for a bus fault. This shortcoming is avoided in an instantaneous mho relay by providing memory action in the polarizing circuit which maintains the relay polarizing voltage E_{pol} for a few cycles after the line voltage has disappeared, but does not affect the ohmic characteristic. This will be apparent from the torque equation

$$E_{pol}[I \cos (\phi-\theta)-K'E]=0 \qquad (3)$$

Memory action cannot be made to last long enough for the time-delay backup step, but the torque can be maintained in this case by adding torque caused by current alone. The functions of the third step of a distance relay are usually to start carrier blocking and to control the backup time-delay trip. Memory action is used to provide initially high torque to ensure starting carrier very promptly and the contacts are held closed after the expiry of the memory action by the current torque. The introduction of the current torque puts the KI^2 term back into the equation of the mho unit, thus making it the general equation

$$KI^2-K'E^2+EI \cos (\phi-\theta)=0$$

(See Appendix I.)

The offset is secured by adding to the

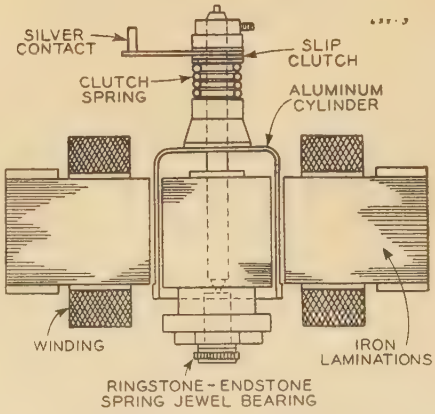

Figure 3. Schematic diagram of 4-pole induction cylinder unit

line potential a biasing potential, IZ_b, proportional to the current, which has the effect of moving the characteristic impedance circle bodily by an amount Z_b. Substituting $E+IZ_b$ for E in the equation for the mho relay, we get

$$-K'(E+IZ_b)^2+(E+IZ_b)I\cos(\phi-\theta)=0 \quad (4)$$

Dividing through by I^2, the equation becomes

$$-K'(Z+Z_b)^2+(Z+Z_b)\cos(\phi-\theta)=0$$

or

$$Z=\frac{\cos(\phi-\theta)}{K'}-Z_b \quad (5)$$

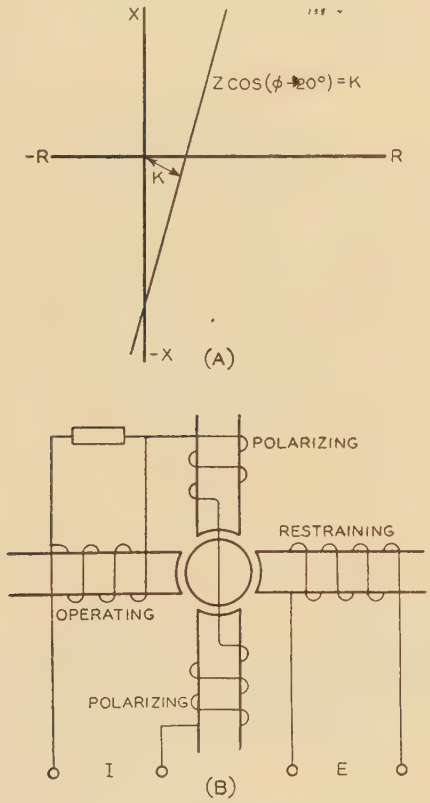

Figure 4

A. Characteristic of ohm unit (blinder)
B. Schematic connections of ohm unit

This shows that the characteristic circle is the same as before except moved through an impedance Z_b (see Figure 7A).

Figure 7B shows how the offset of the mho unit is obtained by introducing, in series with the supply potential, a biasing potential that is obtained from a reactor in the current circuit. Every point on the impedance characteristic of the unit thereby is moved through an impedance equal to that of the reactor. In order to reduce the burden imposed on the current transformers by the reactor, it is provided with two windings. The primary winding with few turns is in the current circuit, and the secondary winding with many turns is in the potential circuit. It is thus a contraction of a transformer and a reactor and is called a transactor.

This offset characteristic is particularly useful for out-of-step blocking because, with the opening of circuit breakers after a fault and hunting between two or more groups of machines, the impedance "seen by the relay" may approach the relay characteristic at almost any angle. Hence the only sure way of initiating out-of-step blocking is by a relay whose characteristic entirely surrounds the characteristic of the tripping relay as shown in Figure 8A.

Relays Using Polarized Impedance Units

A typical form of the polarized impedance unit is the 4-pole induction cylinder unit, which is illustrated in Figure 3 and has been used for ten years in the type GCX reactance relay. The front and back poles are respectively the current operating and potential restraining. The fluxes from these poles produce torque on the induction cylinder by reacting with the currents induced in the cylinder by the flux from the side poles which have the polarizing windings. Another sinusoidal torque is produced by the flux from the polarizing poles reacting with the currents in the cylinder induced by the operating and restraining poles. The second torque is equal to the first and displaced 90 degrees from it in time so that the total torque is not sinusoidal but continuous. This is one of the most valuable features of the induction cylinder and induction dise units and is an advantage not enjoyed by any other relay units. The pickup and dropout of induction cylinder units are practically the same, and their characteristic circles are very close to geometrical perfection.

These units are available in three forms: the current polarized (ohm) unit, the potential polarized (mho) unit, and the offset mho unit in which the potential is biased from the current circuit. In the following paragraphs, uses of these units will be discussed.

Applications of the Mho Unit

One-Step Distance Relay

The simplest application requires a single-step mho relay, type CEY, one per phase. The mho units trip instantaneously and are usually set to cover 90 per cent of the protected section. Backup protection for the neighborhood of the next bus can be provided by the mho type IBCV directional overcurrent relay to be described.

The instantaneous tripping zone provided by the single-step mho relay is superior to that of instantaneous overcurrent or single-step impedance protection because:

1. It is inherently directional, so that only a single contact appears between the battery and the trip coil, which is the ultimate in simplicity and reliability.

2. It is insensitive to offset waves; hence it can be set to cover more of the protected section without risk of overreaching.

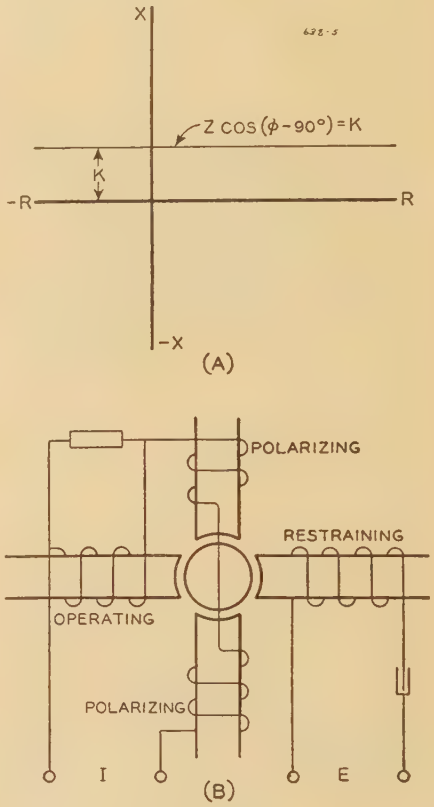

Figure 5

A. Characteristic of reactance unit
B. Schematic connections of reactance unit

3. Its distance reach is not affected by variation in generation as an overcurrent relay would be.

4. It is relatively insensitive to power swings.

Directional Time Overcurrent Relay

Conventional overcurrent relays will not clear faults during periods of minimum generation if the short-circuit current then is less than the maximum load current with maximum generation, unless the settings of the overcurrent relays are changed between maximum and minimum conditions.

The substitution of a mho unit for the conventional directional unit solves this difficulty by permitting overcurrent settings of less than normal load to be used all the time. In other words, if the directional relay has a voltage restraint, it becomes a mho unit and will not operate nor, with the usual directional control arrangement, permit the overcurrent unit to operate unless the impedance presented to the relay falls sufficiently to indicate a fault on the line.

A widely used type of directional overcurrent relay has an induction cylinder directional unit with alternate potential and current coils around the cylinder. It

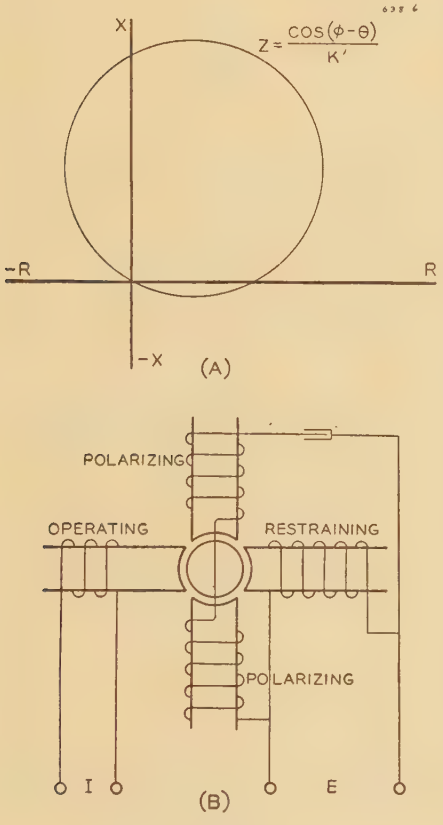

Figure 6

A. Characteristic of mho unit
B. Schematic connections of mho unit

is necessary only to replace some of the current coils with potential coils to provide an E^2 restraining torque, while the remaining coils provide the EI directional torque and thus, change the directional unit into a mho unit.

The directional overcurrent relay with this mho characteristic can be provided with current taps from $1^1/_2$ to 6 amperes on the overcurrent unit instead of the usual 4- to 16-ampere taps. The more sensitive overcurrent settings permit operation on low-current faults, and faster operation can be obtained on heavy faults.

Three-Step Distance Relay

The conventional distance relay consists of a directional unit, a timing unit, and one or more distance measuring units. An instantaneous step and two time-delay steps are usually provided, the three steps being controlled in distance reach either by three distance measuring units (reactance, impedance, or mho) or by one unit whose distance reach is increased in steps by the timing unit.

The first zone unit is used for instantaneous tripping of faults up to 10 per cent from the remote end of the protected section. The second zone unit clears faults in the neighborhood of the next bus in a delayed time, and the third zone provides backup protection for the relays and breaker in the next section beyond.

Reactance Distance Relay

A typical 3-step reactance relay, type GCX, has essentially a mho unit for the directional unit so that it provides the third step of measurement. The normal setting of the reactance unit controls the first step. If the fault is beyond the range of the first step, the timing unit changes the setting of the ohm unit after a time delay to increase its reach and provide a second step.

Mho Distance Relay

A typical 3-step mho relay, type GCY, is described in a companion paper.[3] It has three mho units per phase, M_1, M_2, and OM_3, for measuring the three zones and employs a separate timing unit. No directional unit is necessary because each mho unit is inherently directional. This factor provides more effective backup than where all the units depend upon a common directional unit; it also simplifies the circuit and reduces the number of contacts in the trip circuit. Figure 9 shows schematically the d-c tripping connections for one phase. It can be seen that the zone 1 mho unit, M_1, trips directly so that only a single relay contact is required between the battery and trip coil, which is the ultimate in simplicity and reliability.

The third-step mho unit, OM_3, of the GCY relay has a transactor which can offset its impedance characteristic so that it overlaps the origin, as shown in Figure 7. If polarized in the same direction as the first and second steps, M_1 and M_2, the OM_3 unit can be used for out-of-step detection as well as for time-delay backup protection on lines in which the electrical center of the system is located. The out-of-step condition is detected by making the OM_3 impedance characteristic concentric with the M_2 characteristic, as shown in Figure 8, and somewhat larger, so that the changing impedance seen by the relays during a power swing will always operate the OM_3 unit before the M_2 unit. The OM_3 unit then is arranged to pick up an auxiliary relay with a small time delay; blocking is prevented on faults because the M_2 unit de-energizes the auxiliary relay if the OM_3 does not operate first by the margin of the pickup time of the auxiliary relay. The auxiliary relay generally is arranged to pre-

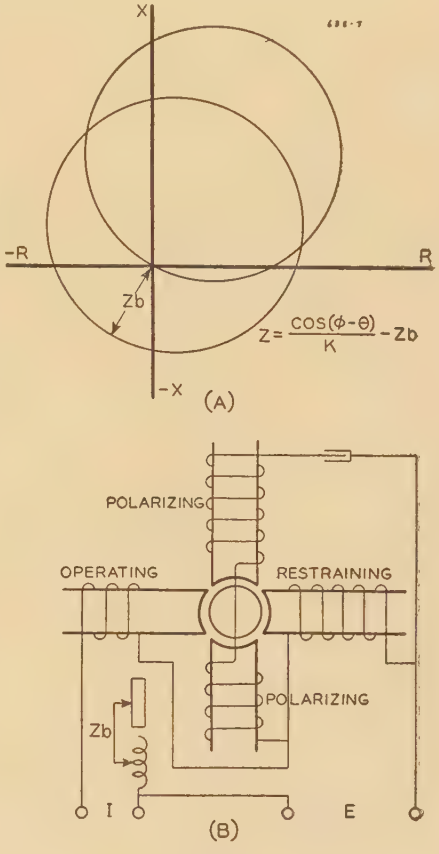

Figure 7

A. Offset mho characteristic
B. Schematic connections of offset mho unit

vent automatic reclosing after a trip on out-of-step conditions but can be used to prevent tripping. It should be remembered, however, that this is necessary only if the relay characteristic circle includes the electrical center of the system, because a mho unit will not trip on out-of-step unless its characteristic is cut by the power swing locus.

In the application of distance relays the first two zones are primarily intended to operate for faults in the protected line section only. Hence they are required to be directional and to operate only for

fault current flowing into the protected line.

The third zone of the distance relay is used for backup protection. As such, it operates only in cases of failure to isolate a fault on some other line section than the one covered by zone 1 and zone 2. Past practice has been to set the third zone element at A of the relays on line AB so that it would operate for a fault at C (see Figure 10A). This meant that the ohmic setting has to equal the line ohms from A to C plus the apparent increase in ohms caused by any fault current fed in at B. Where the line AB is long in terms of secondary ohms, this often resulted in

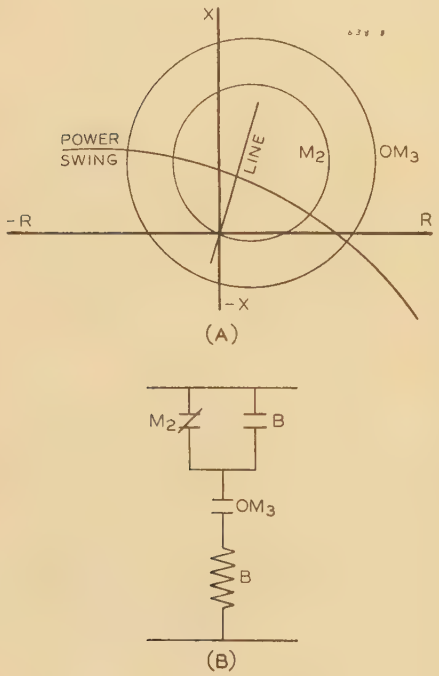

Figure 8

A. Out-of-step blocking with offset mho unit
B. D-c connections of blocking unit

an ohmic setting that would not permit emergency loads to be carried.

With mho relays, since each unit is inherently directional, the third zone tripping direction may be the same as or opposite to that of zone 1 and zone 2. Hence where a third zone setting would be too high in ohms if set in the same direction as zone 1 and zone 2, considerably better settings can be obtained by reversing zone 3. When this is done, the zone 3 element at B on line AB is set to operate for faults at C. The setting in ohms of each zone-3 element is decreased by the impedance of line AB by this reversal, while the over-all protective coverage remains the same. There is no loss of backup protection, since in either case, faults in lines BC or AD result in opening line AB if these faults last for the duration of zone 3 time. In one case, a fault near C opens the breaker at A; in the other case, the breaker at B opens.

It will be seen from Figure 10B that with backup provided by the relay nearest the fault, tap lines in the unfaulted sections will remain in service, whereas with the conventional method of backup, they are lost. On the other hand, it must be understood that failure of the d-c supply or the a-c potential supply could, if it remained undetected, prevent the backup relay from operating, but the conventional backup from the next station would not be affected by this condition. The degree of possibility of such a condition must be weighed against the advantage of improved backup operation when the d-c supply and a-c potential are available.

To summarize, with long lines, adequate backup coverage of the next section often requires such a high ohmic setting for zone 3 in the conventional direction that it may operate on power swings and emergency overload conditions. Hence it is generally advantageous to reverse the zone 3 unit for long lines, especially where some of the sections have tap lines.

Also, where the mho relay is used with carrier, the OM_3 unit must be polarized in the reverse direction from the M_1 and M_2 units because carrier blocking is required only for external faults.

In the case of no tapped lines and no carrier, a check can be made graphically to determine whether the OM_3 unit may operate on power swings and hence whether it is necessary to reverse it. This procedure is described in Appendix II. In such cases a separate offset mho unit is required for out-of-step detection.

Offset Mho Relay

The single-step mho relay can be given an offset characteristic by providing it with a transactor, as described under the heading "Offset Mho Circle." It can be used for out-of-step blocking or backup protection in the same way as has been described for the OM_3 unit of the GCY 3-step distance relay.

When line-to-line faults are not cleared promptly, a power swing may start, and until the fault is cleared, there will be an asymmetrical condition wherein the impedance presented to the relays will be different in each phase. This impedance is a combination of the single-phase impedance of the fault and the balanced 3-phase impedance of the swing. If the relay happens to be connected in the faulted pair of phases, it will measure only the impedance to the fault because the power swing components of current cancel out in the faulted phase pair because of the double current windings of the mho unit. In one of the two remaining phase pairs, the fault current adds to the power swing current and in the other it subtracts from it, so that the impedances measured will be different.

When a power swing follows a fault that has been cleared promptly, it presents a balanced 3-phase condition almost at its inception and certainly before it can operate any out-of-step blocking relays.

For these reasons only one out-of-step blocking relay is required when the system is protected by high-speed relays and breakers, and it can be connected in any phase pair. On the other hand, on systems protected by slow-speed relays and breakers, it is advisable to connect an offset mho unit in each phase so as to ensure recognition of the out-of-step condition and to initiate the blocking as early as possible.

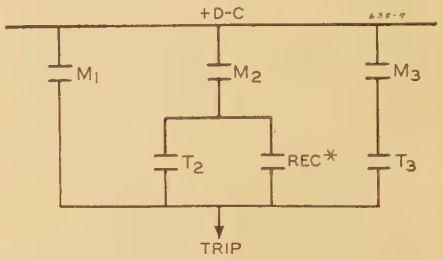

Figure 9

D-c connections of 3-step distance relay

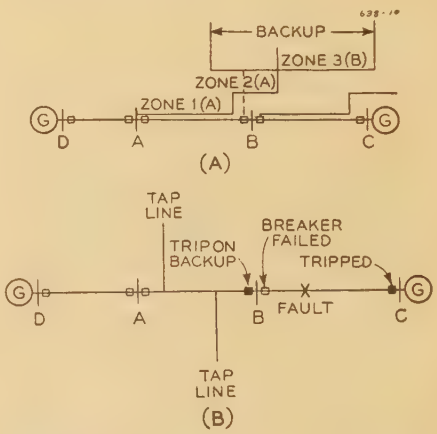

Figure 10. The reversed backup characteristic

A. The time zones
B. Tap lines saved

Applications of the Ohm Unit

Bus Protection

Where a bus section is separated from other circuits by reactors, as shown in Figure 11A, reactance ohm units have

been used to provide protection for the generators and for the bus. Each generator has a reactance ohm unit set to reach into, but not beyond, any of the bus-tie or feeder reactors. A fault in a generator will be cleared immediately because its ohm unit will measure reactance in the reversed direction. A fault on the bus will disconnect all the generators because it will be within the ohm settings of their ohm units.

The main difficulty of conventional differential bus protection is the balancing of the current transformers in all the circuits around the bus to ensure that there is no current to operate the relay during an external fault. This difficulty does not appear with the ohm units because they are connected only to the current transformers in the generator leads.

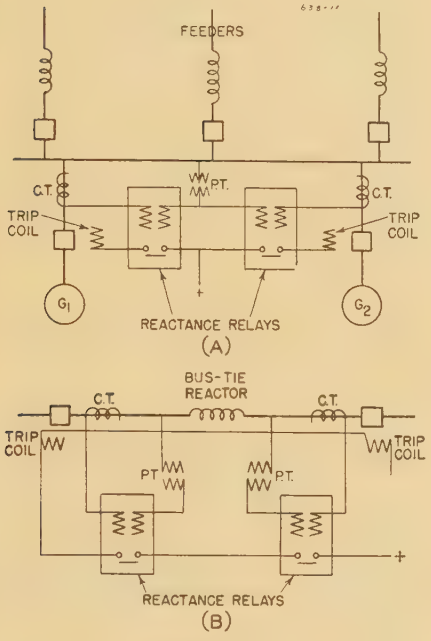

Figure 11

A. Ohm units protecting a bus and generators

B. Ohm units protecting a bus and bus-tie reactor

This form of protection also has been used for bus-tie reactors. Each reactor is protected by two reactance ohm units (Figure 11B) with their contacts in series. The ohm units are polarized away from the reactor so that a fault in the reactor is in the reverse direction for both of them and causes them both to trip and isolate the reactor. A fault on the bus also causes them both to trip and isolate the reactor. In addition, a fault on the bus causes both ohm units to operate, one because it is within its ohmic setting and the other because the fault appears to it in the reverse direction.

Blinders

One application of the ohm unit is to extremely long lines where even the mho unit is not immune to tripping on power swings because the mho circle has to be large in order to cover the long line. In such a case, the straight line characteristic of the ohm unit may be arranged parallel with the line impedance vector so as to cut off one or both sides of the tripping characteristic (Figure 12A) and confine the tripping zone to a strip wide enough to permit tripping on arc resistance.

This scheme was the first attack on the problem of relaying long or heavily loaded lines[2] and is applicable to any form of relay including overcurrent relays. In most applications only one blinder is necessary because the major flow of power generally is in one direction. It is only on interconnections where the maximum power flow is the same in either direction, that two blinders are necessary.

Out-of-Step Tripping

When synchronism is lost, the impedance measured by a relay will pass through the line impedance vector from right to left if the relay is located at the leading or fast end of the system and from left to right if at the lagging end. Two blinders are arranged to operate an auxiliary relay if the impedance crosses the characteristic of one of them before the other, in either direction. This auxiliary relay can be arranged to operate an alarm, trip a breaker, or initiate some form of control.

The advantages of this form of out-of-step relay are:

1. Its operation is not affected by variation in the location of the electrical center of the system.

2. It will not trip under any fault conditions.

3. It trips instantly after the first half cycle of system oscillation. Existing relays require the machine to slip several poles before they will operate.

4. Distinction can be made between speeding up and slowing down of the local generation.

A single-phase relay is adequate for tripping on out-of-step because the regular protective relays will trip during a fault. If the swing continues after the fault has been cleared or if the swing was caused by switching of load or generation without a fault, only a single-phase out-of-step relay is required for tripping because all three phases act similarly.

Reclosing

By means of auxiliary relays, reclosing is prevented after a time-delay trip and after a trip on loss of synchronism. The first is accomplished by an auxiliary relay whose coil is energized whenever the tripping circuit is completed through the timing unit contacts and whose contacts open the reclosing circuit; the connections of this relay are shown in Figure 5 of the companion paper.[5] The second is accomplished by an offset mho unit in a manner already explained earlier in this paper under the heading "Mho Distance Relay."

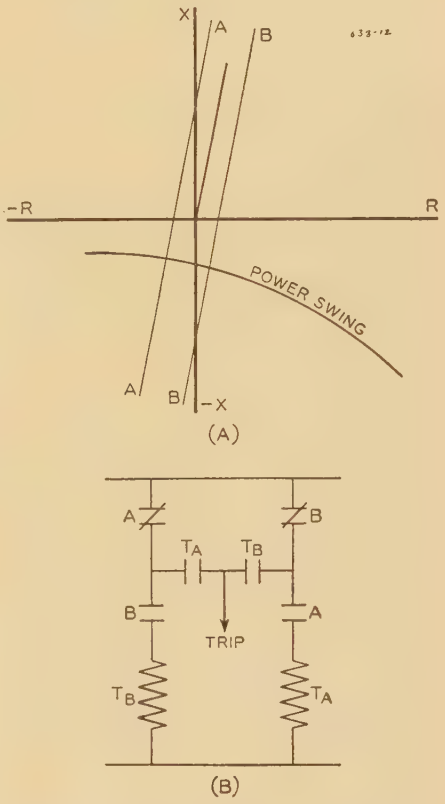

Figure 12. Characteristics of a pair of ohm units for out-of-step tripping

Carrier Relaying

The application of ohm relays to carrier has been discussed in previous papers. The use of mho relays for carrier is the same in function, but the self-contained directional and power swing blocking features of the mho unit simplify the d-c circuits very considerably (Figure 9) and minimize the possibility of sneak circuits.

Mho carrier alone was described in an earlier paper. When carrier is added to mho distance relays, it is necessary only to add two relays containing ground directional and carrier auxiliary elements. The

chief difference between the addition of carrier to mho distance relays and to impedance or reactance relays is the use of the reversed offset mho unit instead of the impedance unit for starting carrier. Figure 13 shows how the OM_3 unit of the 3-step mho distance relay can provide the necessary blocking on external faults with the minimum tendency to operate on power swings and heavy loads.

The OM_3 unit is extremely fast for an induction-type unit. Its minimum time is one-fourth cycle. The time with an average fault is about one-half cycle. This provides a considerable margin of safety between the starting of carrier by the OM_3 unit and tripping for an external fault by the M_2 unit of the relay facing the fault.

Limitations of Ohm Units and Mho Units

For distance-relay applications, the phase angle of the ohm relay is adjusted to make it measure reactance and ignore the resistance component, and, hence, make it indispensable for very short lines where the arc resistance may be comparable with the line impedance. Like the impedance relay, the reactance relay requires a directional unit; this unit is usually of the mho type and also serves as a backup for remote faults. The reactance relay is applicable to lines not subject to overload or power swing conditions which present an impedance low enough to cross the relay characteristic. Whether this will occur can be found only by calculation of the swing impedance. If the system arrangement can be simplified to a 2-machine problem, Appendix II describes a simple construction for plotting the swing impedance.

The phase angle of the mho relay can be adjusted to be approximately the same as that of the line. This ensures the smallest reach at right angles to the line impedance vector, and hence the least tendency to operate on power swings that may be expected on long lines and on heavily loaded lines of medium length. The potential polarizing winding of the mho relay limits its application to long lines because, even with memory action, the torque is likely to be low on very short lines during second zone fault, after the memory action has expired.

Arc resistance also places a limit on the shortness of a line to which the mho unit can be applied. Arc resistance increases as the current decreases and becomes more effective on shorter lines. This is in the same direction as the other limitation of minimum voltage to provide adequate

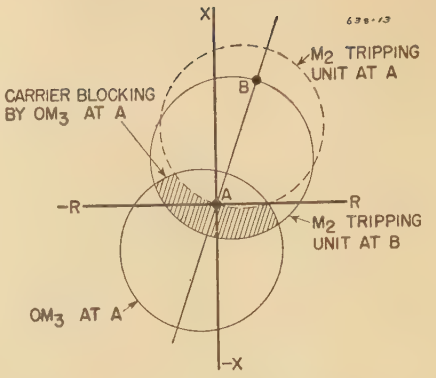

Figure 13. Carrier blocking with offset mho unit

torque. Since the arc resistance limitation is more severe, we shall consider it in detail.

Minimum Length of Line

From the ohmic characteristics in the companion paper[3] on the "Mho Distance Relay," it will be seen that the accuracy of the GCY relay is within ten per cent variation down to eight volts at the relay terminals. This means that if the instantaneous zone is set to cover 90 per cent of the protected section, it may cover only 81 per cent of the section if the section is so short or the fault current is so small that the IZ drop is only eight volts secondary. Although in many cases a greater variation may be permissible, this value will be taken for the purpose of establishing a limit. It should be realized, however that this value has no relation to the ability of the relay to operate reliably on faults within the protected zone because the actual pickup of the relay is around $1\frac{1}{2}$ volts.

Hence for accurate operation, IZ equals eight volts at the relay terminals for a fault at the ohmic setting of the M_1 unit. From this fact, we can determine the minimum line length and fault current for which the relay can be set. Changing to primary phase to neutral values, we have $IZ = 8R_p/\sqrt{3}$, where I is the minimum fault current, Z the ohmic setting of M_1, and R_p is the ratio of the potential transformers. If M_1 is set to cover 90 per cent of the protected section, which is L miles long and has an impedance of 0.9 ohm per mile, then

$$I \times 0.9 \times 0.9L = \frac{8{,}000 \text{ kv}}{115\sqrt{3}}$$

or

$$L = \frac{50 \text{ kv}}{I} \text{ miles}$$

In other words, the relay is applicable to lines down to a minimum length of 50 kv/I miles, where I is the minimum fault current, and kv is line-to-line voltage in kilovolts.

Arc Resistance

The presence of arc resistance will reduce the reach of the mho relay. A small reduction of the instantaneous zone is acceptable, but the intermediate zone always must reach beyond the next bus, that is, faults within the section must not trip in zone 3 time, or selectivity between stations will not be possible.

In Figure 14A, R is the arc resistance, Z is the impedance of the protected section, ϕ is its phase angle ($\tan^{-1} X/R$), and K is the fraction of Z by which the second zone mho unit M_2 reaches beyond the end of the section. It is assumed that the mho unit characteristic is given the same angle ϕ as the line.

The circle in Figure 14A is the characteristic of a mho unit used for the second distance step and is assumed to reach a short distance beyond the end of the protected section. It is noted that

$$a^2 + b^2 = (\text{diameter})^2$$

therefore,

$$R^2 + K^2Z^2 - 2KZR\cos\phi + R^2 + Z^2 + 2ZR\cos\phi = (Z + KZ)^2$$

$$2R^2 - 2KZ^2 + 2RZ(1-K)\cos\phi = 0$$

$$R = \frac{Z}{2}\left[\sqrt{\cos^2\phi(1-K)^2 + 4K} - (1-K)\cos\phi\right]$$

which equals maximum arc resistance to permit zone 2 time or less for all faults within the section.

If M_2 is set for 20 per cent beyond the next bus, $K = 0.2$. Assuming $\phi = 60$ degrees, then, from the formula, $R = 0.29Z$ or $Z = 3.45R$.

The initial arc resistance, assuming 16 kv per foot of insulator string and 440 volts per foot of arc,[4] is

$$R_{arc} = \frac{440}{I_{prt}} \times \frac{\text{kv}}{16\sqrt{3}} \times \frac{115\ C.T.}{1{,}000 \text{ kv}}$$

$$= \frac{1.83}{I_{sec}} \text{ ohms phase-to-neutral}$$

With a fault drawing five amperes secondary, $R_{arc} = 1.83/5 = 0.36$ ohm phase-to-neutral. Since $Z = 3.45R$, from a preceding formula, $Z = 1.24$ ohms for the minimum secondary impedance of a line section that can be protected safely with mho relays.

Where the line impedance is less than 1.24 ohms secondary, each case should be examined individually. If there is a heavy short-circuit current, the arc voltage will be less than 440 volts per foot.

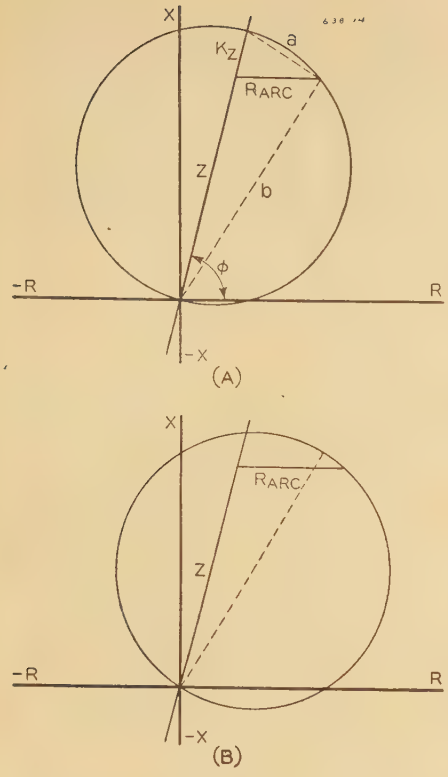

Figure 14

A. Arc resistance shortens reach of mho unit
B. Effect of arc resistance reduced by leading mho characteristic

On the other hand, if the fault occurs near the station, the number of insulators may be higher and the arc resistance proportionately increased; furthermore, at low short-circuit currents, the volts per foot may increase to 600 or 1,000 and should be checked from the formula $R_{arc} = 8{,}750L/I^{1.4}$ ohms, where L is the arc length in feet.

If the arc resistance is too high for a reasonable application, some leeway can be obtained on highly lagging lines by setting the mho relay characteristic at a less lagging phase angle than that of the line impedance. This permits more arc resistance anywhere in the section before the relay will fail to pick up (see Figure 14B) or permits the normal application down to one ohm impedance.

Conclusions

The product-type impedance unit is a very useful relay tool whose flexibility enables it to cover the entire field of transmission line protection with simpler circuits and better characteristics than heretofore.

The only limitations to the application of current and potential polarized units are those which prevent either from covering the whole range alone. The natural field for current polarized distance relays is short lines and ground fault protection; interphase faults on long or heavily loaded lines require potential polarized (mho) distance relays.

Appendix I

The characteristic of any ohmic relay on an impedance diagram is a circle. This is because the torque from any form of electromagnetic drive is proportional to the square of the flux or to the product of two fluxes, and the fluxes in turn are proportional to the currents or potentials. The torque[5] of a relay having current and potential windings must therefore be of the form

$$KI^2 - K'E^2 + EI\cos(\phi - \theta)$$

where K and K' are winding constants, ϕ is the phase angle of the protected circuit, and θ is the angle of the relay characteristic. At the balance point of the relay, the torque is zero and the equation for balance is

$$KI^2 - K'E^2 + EI\cos(\phi - \theta) = 0$$

This general equation of a relay has the two main variables E and I, which can be reduced to one by changing it to an impedance diagram.

Dividing the equation through by $K'I^2$, we get

$$\frac{K}{K'} - Z^2 + \frac{Z\cos(\phi - \theta)}{K'} = 0$$

Transferring K/K' to the right-hand side and adding $(1/2K')^2$ to both sides, this equation becomes

$$Z^2 - \frac{Z\cos(\phi - \theta)}{K'} + \left(\frac{1}{2K'}\right)^2 = \frac{1 + 4KK'}{(2K')^2}$$

This is the equation of a circle of radius $\sqrt{1+4KK'}/2K$, whose center is $1/2K'$ from the origin at an angle θ from the reference vector R (see Figure 15).

The constants K and K' are functions of the turns, and so forth, of the current and potential windings respectively. These constants can be determined from the impedance circle by solving for K and K' in the expressions for the radius and the location of the center. For instance, a 4-ohm circle at 60 degrees with one ohm offset in the direction of the origin has a radius of two and its center is one from the origin. $1/2K' = 1$, or $K' = 1/2$, and substituting this value in the expression for the radius, $\sqrt{1+4KK'}/2K'$, we get $\sqrt{1+2K} = 2$, or $K = 3/2$. Hence the equation is

$$\frac{3}{2}I^2 - E^2 + EI\cos(\phi - 60°) = 0$$

This equation is typical of the offset mho characteristic in Figure 7A.

Appendix II. Power Swing Check

A simple geometrical construction can be used to determine whether a relay will operate during a swing condition. This method assumes that the system can be simplified to an equivalent system of two machines separated by impedance. It determines the angle between the machines at which the relay will operate. Thus, it can be used to determine whether a reactance or impedance relay should be replaced by a mho relay, whether to reverse the third zone or not, or whether a blinder is needed to prevent the M_1 and M_2 units from tripping on a very severe power swing.

Referring to Figure 16, AB is the impedance of the protected section, SA is the

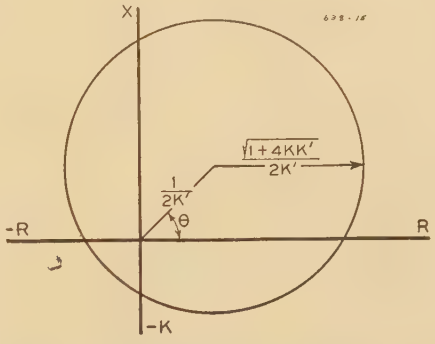

Figure 15. Impedance characteristic corresponding to general relay equation $KI^2 - K'E^2 + EI\cos(\phi - \theta) = 0$

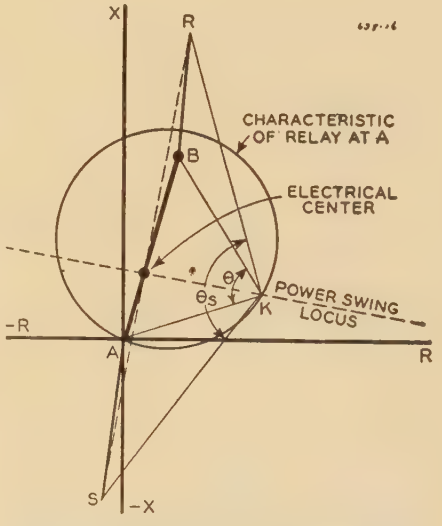

Figure 16. Construction for checking operating point of relay on a power swing

system impedance beyond terminal A, and BR is the system impedance beyond terminal B.

Draw a perpendicular through the midpoint of RS. From the point K where it cuts the relay characteristic, draw lines to R, S, A, and B. RKS is the angle θ_s between the generated electromotive forces at R and S at which the relay at RA will trip. BKA is the angle θ between the terminal voltages at A and B at which the relay at A will trip, and AK is the impedance it sees.

The power swing locus is shown as a straight line. This implies equal generated

The Development, Design, and Performance of Magnetic-Type Power Circuit Breakers

L. J. LINDE
MEMBER AIEE

B. W. WYMAN
ASSOCIATE AIEE

Synopsis: Power circuit breakers for voltage services of 2,300 volts and above use either of two basic principles to complete circuit interruption. The more familiar types, oil breakers or compressed air breakers, complete their operation by maintaining a low resistance arc until the final current zero where interruption is completed. Magnetic air circuit breakers establish a high resistance arc prior to circuit interruptions which modifies the circuit constants before recovery voltage is established. The "Magne-blast" breaker falls in this second class of breakers. The treatment of the arc in this breaker to obtain a high arc resistance is explained in some detail. Also, design practices and operating characteristics of the final magnetic type breaker are reviewed.

IN studying the various types of circuit interrupters in power circuit breakers and the principles on which they operate, it becomes apparent that these interrupters can be placed in one or the other of two classes:

1. Low-arc-resistance interrupters whose arc resistance is maintained low until current zero and then is transformed suddenly into or replaced by a high-resistance dielectric.

2. High-arc-resistance interrupters whose arc resistance is increased gradually to such a high value prior to current zero that arc re-establishment is made impossible following current zero.

Low-Arc-Resistance Interrupters

Power circuit breakers rated 2,300 volts and above generally have functioned as low-arc-resistance interrupters. They are recognized as oil blast breakers, impulse breakers, air blast breakers, and so forth. These breakers interrupt the circuit by drawing a short low-resistance arc in some type of control chamber where a blast of insulating fluid is directed at it. To complete the interruption at current zero, the low resistance of the arc gap must be replaced abruptly by a high-resistance dielectric. This type of interruption can be understood best by reference to the typical oscillograms of a short-circuit interruption shown in Figure 1. In this oscillogram the breaker contacts part at t_0 and the short-circuit current I is interrupted at t_1. During the arcing period ($t_0 - t_1$), the arc resistance remains so small that the arc-resistance voltage drop e_a at no time rises to more than a few per cent of the generated voltage (shown dotted). The introduction of this low-arc-resistance voltage drop into the circuit does not affect appreciably either the magnitude or the phase angle of the short-circuit current.*

For the circuit to be interrupted as the current passes through zero at t_1, the fluid blast suddenly must increase the low resistance across the contact gap by cooling or displacing the hot ionized arc products to prevent arc re-ignition as the system recovery voltage rises following current zero.

Immediately following current zero at t_1, the voltage across the contacts begins to rise to the system-generated voltage, which at this instant is at its crest (zero power-factor fault). Because of the energy stored in the circuit, the actual voltage appearing across the contacts will rise above the system voltage crest and oscillate about it, as can be seen on the oscillogram in Figure 1, immediately following the current interruption. Figure 2 shows this recovery voltage extended to a microsecond time scale. For the simple single frequency circuit, shown in Figure 3, this frequency is equal to

$$f = \frac{1}{2\pi\sqrt{LC}}$$

The high frequency transient recovery voltage-oscillation superimposed upon the 60-cycle crest voltage causes the total voltage appearing across the contact gap to approach two times the normal crest voltage on the first oscillation. A tangent erected to the first oscillation crest, as shown in Figure 2, determines the rate of rise of recovery voltage. On the highest frequency circuits, this rate-of-rise tangent may equal several thousand volts per microsecond.

The fluid blast in the low-arc-resistance type of interrupter must increase the insulation strength between its contacts immediately following current zero fast enough to withstand this rate of rise of recovery voltage to prevent arc re-establishment after current zero. As the actual rate of rise of recovery voltage encountered in practical applications varies between wide limits, various configurations of low-arc-resistance interrupters have been designed to insure the required fluid velocity to interrupt the highest recovery-rate circuits.

In many breakers using low-arc-resistance interrupters in which the high-velocity fluid blast bodily displaces the low resistance-arc gases, the resistance of the arc gap rises abruptly at current zero to substantially infinity immediately following current zero. These breakers are capable of withstanding rates of rise of recovery voltage higher than any which can be encountered in service and can be duplicated only in the laboratory.

In other breakers using low-arc-resistance interrupters, an auxiliary resistor is inserted into the circuit following the current zero to limit the rate of rise of recovery voltage. Such resistors, shunted into the circuit in parallel with some portion of the contact break, absorb the energy of the transient voltage-oscillations. Applications as now practiced are

*The actual instantaneous values of arc resistance r_a are proportional to the arc length and are an inverse function of arc current because the arc diameter increases and decreases with current. As the short-circuit current approaches zero, r_a will increase proportionately, but the voltage drop in the arc e_a, which equals $i_a r_a$, will remain low.

electromotive forces and no line capacitance. These assumptions simplify the construction and have negligible effect on the angles θ and θ_s at which the relay operates.

References

1. THE MHO CARRIER RELAYING SCHEME, **R. E. Cordray, A. R. van C. Warrington.** AIEE TRANSACTIONS, volume 63, 1944, May section, pages 228–35.

2. PROTECTIVE RELAYING FOR LONG TRANSMISSION LINES, **A. R. van C. Warrington.** AIEE TRANSACTIONS, volume 62, 1943, June section, pages 261–8.

3. THE MHO DISTANCE RELAY, **R. M. Hutchinson.** AIEE TRANSACTIONS, volume 65, 1946, June section, pages 353–60.

4. INTERESTING FACTS ABOUT POWER ARCS, **A. R. van C. Warrington.** *General Electric Company Relaying News*, January 1941.

5. A CONDENSATION OF THE THEORY OF RELAYS, **A. R. van C. Warrington.** *General Electric Review*, volume 43, number 9, September 1940.

Paper 46-42, recommended by the AIEE committee on protective devices for presentation at the AIEE winter convention, January 21–25, 1946. Manuscript submitted November 23, 1945; made available for printing December 27, 1945.

L. J. LINDE is with the A. B. Chance Company, Centralia, Mo.; B. W. WYMAN is with the power circuit-breaker division, General Electric Company, Philadelphia, Pa.

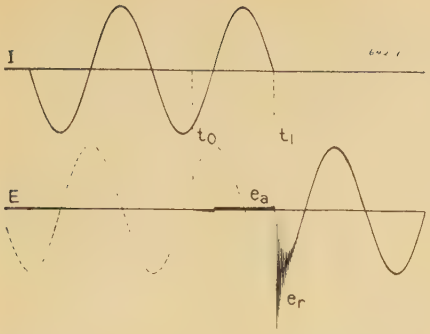

Figure 1. Typical short-circuit interruption by low-arc-resistance type of interrupter (fluid blast) showing high-frequency transient immediately following interruption

E = generator voltage
I = short-circuit current
e_a = arc voltage drop (small on account of low arc resistance)
e_r = transient recovery voltage appearing across contacts of breaker immediately following interruption
t_0 = instant of contact parting
t_1 = instant of circuit interruption

successful in holding the rate of rise of recovery voltage to moderate values, definitely limit the severity of circuit transients, and reduce the rate at which gap resistance must be built up across the contacts.

Such resistors also have proved of value when interrupting faulted circuits to stabilize the clearing of transmission lines, discharging the capacitance charge remaining on the line faster than the generated voltage reverses and thereby preventing possible restriking at the breaker contacts because of excessive overvoltage stresses.[12]

High-Arc-Resistance Interrupters

The high-arc-resistance interrupter, as contrasted with the low-arc-resistance interrupter, builds up a high arc resistance prior to current zero, thereby modifying the circuit current and achieving an early interruption by advancing the current zero to, or near, the recovery voltage zero. The rate of rise of recovery voltage also is held to very low values, a factor which permits the build-up of insulation across the electrodes at the moderate rates achieved by rapid cooling of the arc column. The more successful interrupters of this type are recognized as magnetic-type circuit breakers.

With any magnetic-type air circuit breaker, the arc magnetically is forced to loop away from the contacts and may travel out on diverging arc runners where its length is further increased many times.

As the arc is lengthened and cooled, its resistance increases rapidly so that the resultant resistance voltage drop in the arc column becomes an appreciable percentage of the total circuit voltage. This high-resistance-arc drop has a two-fold effect on the short-circuit current:

1. It reduces the magnitude of the short-circuit current to a fraction of its previous value.

2. It improves the power factor of the circuit bringing the current more nearly into phase with generated voltage, causing the current zero to occur near a voltage zero rather than its normal 90-degree lagging or crest position.

These effects can be seen best by reference to the typical interruption with a magne-blast breaker shown in Figure 4. Here the voltage drop in the arc column rises at a rate of several thousand volts per half-cycle so that the short-circuit current in the last half-cycle is reduced to approximately half its original value. Moreover, the introduction of the arc resistance into the circuit has advanced the current zero from the normal crest point on the generated voltage wave, in this case to approximately one-half crest voltage.

As the instantaneous system voltage at the point of current zero has been reduced greatly, the amplitude of the high-frequency oscillation is reduced correspondingly. This reduction in amplitude of the high-frequency oscillation will reduce the circuit rate of rise of recovery voltage in direct proportion even if the resistance of the arc column were raised to infinity immediately following current zero.

In this type of breaker, however, it has been found that the long hot gaseous post-arc stream between the arc runners immediately following current zero affords an excellent resistor further to damp out recovery voltage-oscillations. Although the resistance of this cooling column of arc gases r_a increases to infinity in a few hundred microseconds after current zero, it is a recovery-rate-limiting resistor just after current zero, fully as effective as the auxiliary resistor used with some types of low-arc-resistance interrupters. The manner in which the pre-current zero arc resistance varies during the current-zero period as plotted from a typical interruption is shown in Figure 5A.

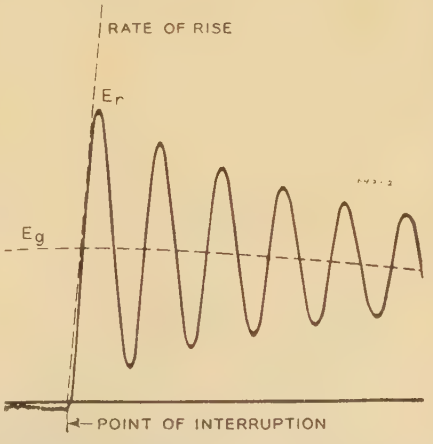

Figure 2. Transient recovery voltage across contacts of low resistance breaker following interruption.

The dotted line tangent to the first oscillation is the rate of rise of recovery voltage

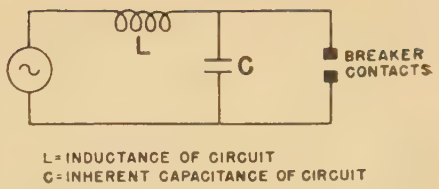

L = INDUCTANCE OF CIRCUIT
C = INHERENT CAPACITANCE OF CIRCUIT

Figure 3. Simple single-frequency test-circuit

$$\text{Oscillating frequency} = f = \frac{1}{2\pi\sqrt{LC}}$$

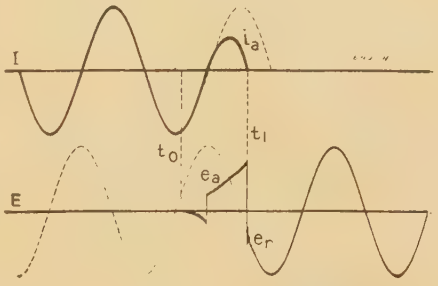

Figure 4. Typical short-circuit interruption by high-arc-resistance type of interrupter (magne-blast) showing high-arc-resistance voltage drop during arcing period which results in marked reduction in both short-circuit current and transient recovery voltage

E = generator voltage
I = short-circuit current
e_a = arc voltage drop (high on account of high arc resistance)
e_r = transient recovery voltage
t_0 = instant of contact parting
t_1 = instant of circuit interruption

The resistance r_a, of this cooling gaseous column immediately following current zero will vary with

1. The design of the arc chute, which determines the rate of cooling of the hot gases.

2. The magnitude of the current being interrupted, which determines the cross section of the hot gas column.

The initial resistance of this hot gaseous column varies inversely with the short-circuit current being interrupted. This means that the maximum rate of rise of recovery voltage which can appear across the breaker terminals will decrease as the value of short-circuit current is increased. Figure 5B shows how this resistance r_a

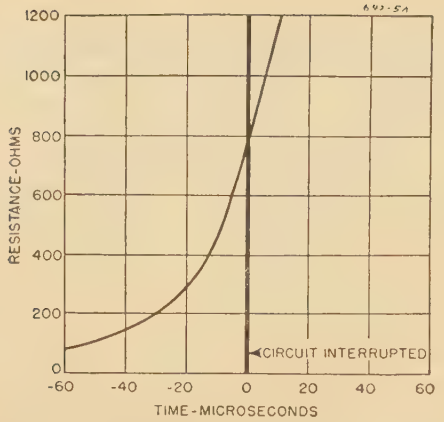

Figure 5A. Increase in resistance of arc column during instant of current zero on an actual interruption by a magne-blast breaker

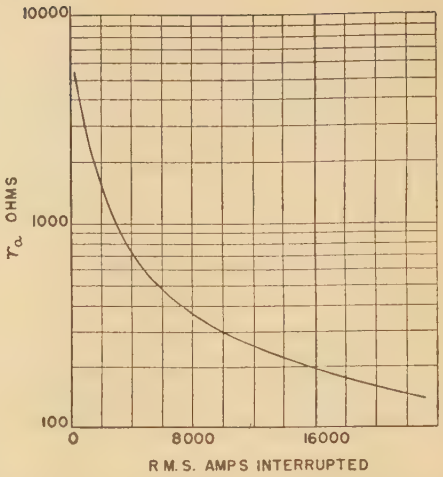

Figure 5B. Variation of arc column resistance r_a following interrupting current zero versus short-circuit current being interrupted

immediately following current zero varies in a 5-kv 100,000-kva breaker.

On circuits having very low inherent capacitance C and high natural rates of rise of recovery voltage, the resistance of this cooling arc column r_a will damp out entirely the oscillating frequency. To do this, the ohmic value of r_a must be less than the critical damping resistance of the circuit, or $r_a < 2\sqrt{L/C}$.

The total effect of the high-resistance-arc type of breaker on the rate of rise of recovery voltage appearing across its terminals may be seen by reference to Figure 6. Here is shown the rise of recovery voltage following an interruption with a magne-blast breaker extended to microsecond scale. For comparison, the dotted curve shows the recovery oscillation which occurs with a low arc resistance interrupting the same circuit at a crest voltage point and without benefit of arc resistance following current zero. Besides the radical reduction in the rate of rise of recovery voltage shown with the magnetic breaker, the first peak of transient recovery voltage-oscillation is reduced from 1.9 times normal crest to 0.35 times normal crest.

The magne-blast breaker has proved that the operation of magnetic air breakers, when properly designed, is independent entirely of natural oscillating frequency or inherent rate of rise of circuit recovery voltage.

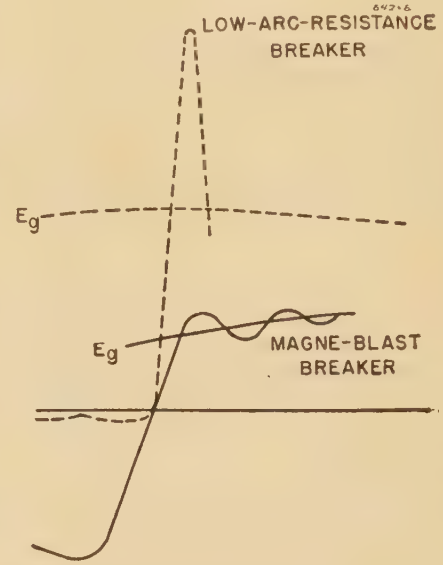

Figure 6. Transient recovery voltage obtained with high-arc-resistance breaker (magne-blast breaker) shown full as compared with transient recovery voltage of low-arc-resistance breaker (fluid blast) shown dotted

Development of High-Arc-Resistance Interrupter Designs

There have been many interesting attempts to develop pure resistance interrupters that might function with little or no arcing. Several years ago the authors made and tested a resistance interrupter designed to interrupt high values of alternating or direct current at 600 volts and to do this with no appreciable arcing. This interrupter (Figure 7) consisted of a stack of graduated wafer-like compound resistances whose composition varied from pure copper, through copper carbon mixes to carbon clays, to a final wafer of fired clay. It was to function much the same as a large rheostat being turned into the circuit. Although the tests on this device demonstrated the need for much improved commutation before arcing could be eliminated at high currents, they did confirm the value of resistance as an interrupter. In a later investigation the arc itself was used as a suitable commutating "brush" to insert a series of ceramic resistance rods into the circuit. These resistance rods were U-shaped and were so arranged that a series of arcs would travel up between them to insert their resistances into the circuit being interrupted, as shown in Figure 8. The separate series arcs were moved up these electrodes by concentrated magnetic fields. This arrangement was acceptable in its performance up to 100,000 kva at 5,000 volts. A careful analysis of its operating characteristics, however, showed that the series arcs were contributing the major portion of the resistance required for successful interruptions and that the complex ceramic resistance rods hardly were justified. This was true particularly if the arcs were controlled properly. Successful air breakers have been built using resistance arc runners, but even in these designs the arc contributed much more resistance than did the runners.

These early studies firmly established the value of a controlled and confined arc

Figure 7. Graduated resistor breaker made up of gradually increasing resistance elements

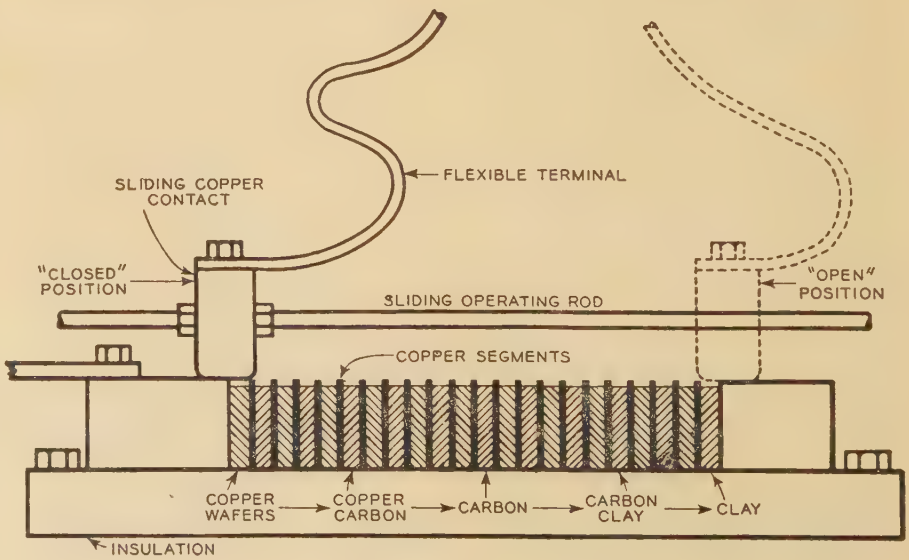

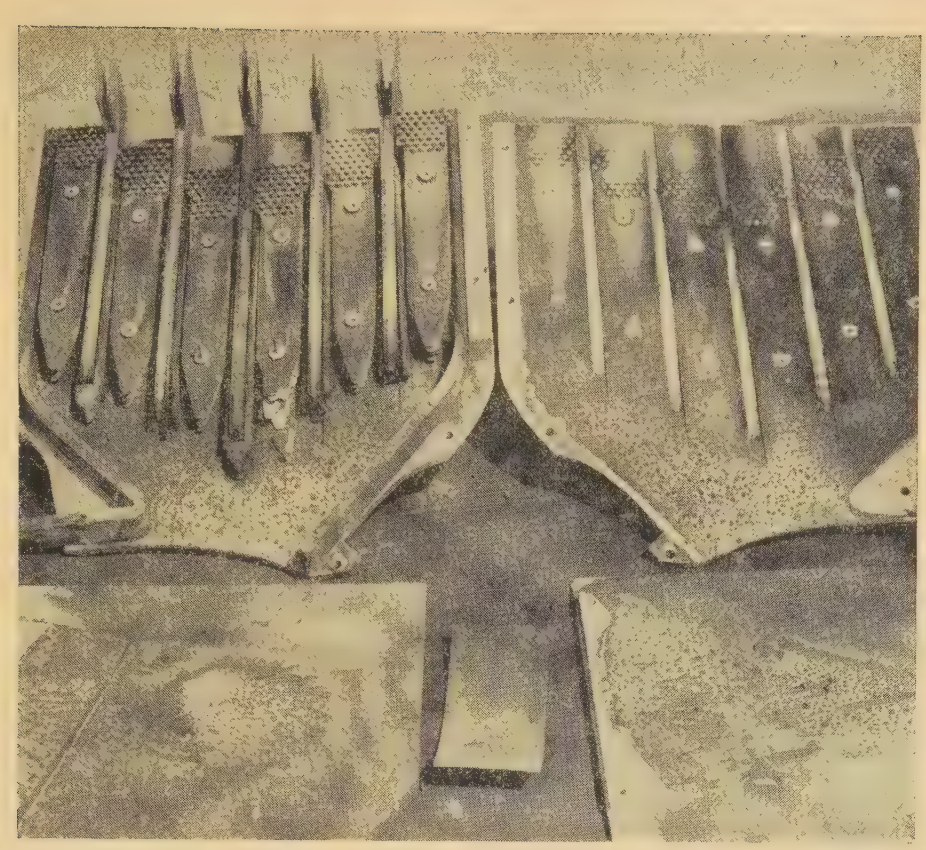

Figure 8. Disassembled arc chute of high voltage breaker using U-shaped resistor rods inserted in circuit by short arcs

The photograph was taken after high-current tests

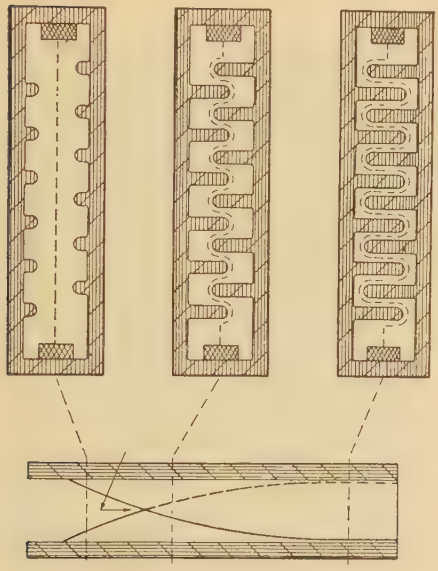

Figure 9. Interleaving fin type of arc chute obtaining arc lengthening in more than one plane by serpentine configuration

in air as a controllable resistor for the interrupters of power circuit breakers. A study then was initiated to determine the most effective way of controlling and confining the arc to establish the proper high-resistance characteristics.

There is a history of successful low-voltage air breakers (600 volts and below) that operate as high-arc-resistance interrupters. The most common arrangement is recognized as the plain break low-voltage circuit breakers where the arc is established between separating electrodes and is cooled and extinguished in open air. Although such circuit breakers are satisfactory interrupters, given sufficient space and time, they are limited in their physical applications because of the long arc in open air required to establish sufficient resistance.

More modern breakers of this low-voltage class, which can be classed as high-arc-resistance interrupters, increase the resistance of the arc per unit length by increasing the arc-cooling by either one of two methods:

1. Forcing the arc into a series of cold metallic pins or plates which cool it and break it into several shorter arcs.

2. Forcing the arc between closely spaced sidewalls of cool ceramic insulation.

When attempting to cool the arcs of a breaker for higher service voltages (2,300 to 15,000 volts) to extinction, it soon became apparent that the necessary arc length in a metallic pin or plate-type arc chute requires greater physical dimensions

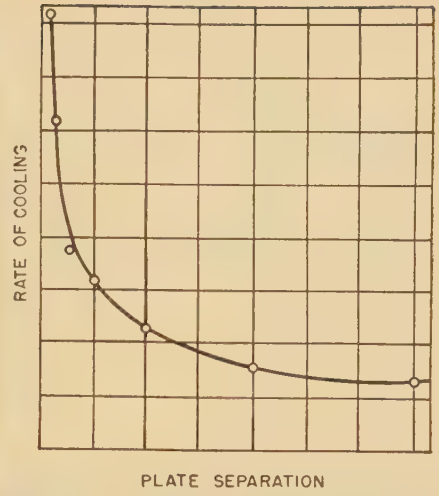

Figure 10. Variation in arc cooling with spacing between insulating plates

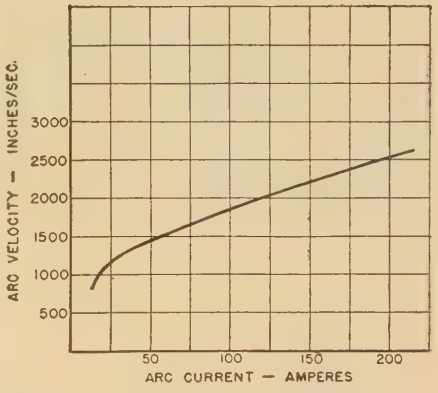

Figure 11A. Variation in arc velocity with arc current in constant transverse magnetic field of 400 gausses

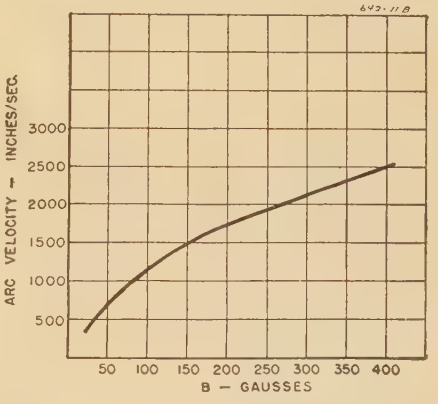

Figure 11B. Variation of arc velocity with transverse magnetic-field strength of 200-ampere arc between parallel arc runners

than the compact design of switchgear equipment for these voltages now affords. Neither can insulating-plate types of arc chutes for these voltages be accommodated to obtain sufficiently high arc resistance in the allowable spacing of modern metal-enclosed equipment if all

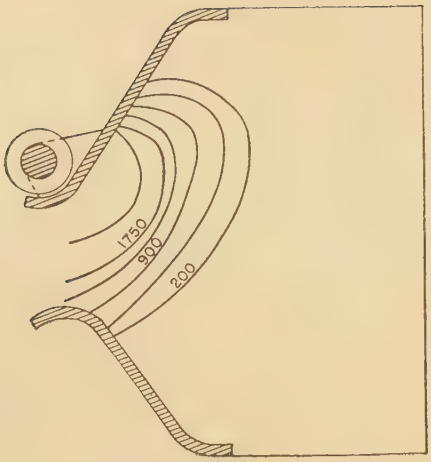

Figure 12A. Poor transverse magnetic-field distribution over area of arc chute resulting from use of single strong magnetic blowout coil

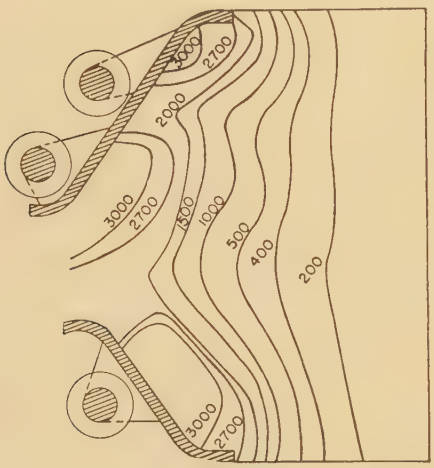

Figure 12B. Improved transverse magnetic-field distribution over area of arc chute with three magnetic blowout coils distributed along arc runners

arc lengthening is performed in one plane. When attempts were made to elongate and confine the arc between closely spaced insulating plates in more than one plane, it soon was realized that a high-arc-resistance type of interrupter could be practical for power circuit breakers. The final arrangement established an arc between electrodes at the throat of a specially constructed arc chute that would force the arc up between interleaving fins of ceramic insulation. This arc movement forced it into a closely confined serpentine pattern of considerable length.

In 1939 the first magne-blast breaker for voltages up to 5,000 volts was presented before the Institute.[2] It used a specially designed arc chute with tapered insulating fins alternately spaced from the inner sidewalls to form an interleaving path for the arc column. As the arc column is forced magnetically into this chute, it is folded back and forth between these fins to extend its length to many times the longitudinal distance between the arc runners, as is shown in Figure 9.

By this construction, an arc chute with a one-foot spacing between arc runner tips creates an arc path several feet in length, depending on the length and amount of overlapping of the interleaving ceramic fins in the chute between the runners. Besides greatly increasing the length of the arc, these closely spaced fins come into very intimate contact with the arc column, flattening it out of its naturally circular cross section. The intimate contact thus effected between the high-temperature arc column and the cool surfaces of the fins extracts heat from the boundary layers of the arc column at a rapid rate, giving a high arc-resistance per unit length. Suits has shown the rate of cooling in an arc column to increase as fins are brought closer together in accordance with the curve shown in Figure 10.

The cooling rate of the arc by the closely spaced fins determines the voltage drop per unit length e_1 in the arc column. The total voltage drop in the arc column e_a is equal to

$$e_a = e_1 l$$

where

e_a = total resistance voltage drop in arc column
e_1 = resistance voltage drop per unit length
l = total length of arc

The total arc-resistance voltage drop e_a required for circuit interruption of a given current is directly proportional to the system voltage E_m. This may be demonstrated easily by connecting two arc chutes in series and noting the double voltage which may be interrupted. If the fin spacing which determines e_1 is held constant, it is then necessary to increase the total arc length l in direct proportion to the circuit voltage. As the number of fins determines the total interleaving arc length, the number of fins required in the arc chute in the magne-blast breaker is proportional to the rated voltage of the breaker

Magne-Blast Design

The Interrupter

The material from which these fins are made is a highly heat-resistant dielectric developed specially for magnetic-breaker arc chutes. As the temperature of the arc column is several thousand degrees centigrade, it loses its heat to the fins by forming a thin molten glaze on the fin surfaces. Immediately following the passage of the arc, this glaze solidifies and its heat passes into the body of the chute. The relatively great mass of the chute provides sufficient thermal storage to accept repeated operations far beyond any service requirement. Because this phenomenon is one entirely of thermal conductance, there is no physical change in the arc chute. As the same thickness of glaze becomes molten and solidifies on each operation, no deterioration in the materials of the arc chute is apparent during the life of a circuit breaker.

Figure 13. Test setup of magne-blast breaker with small quartz rods projecting into side of arc chute to serve as windows for taking high-speed photographs

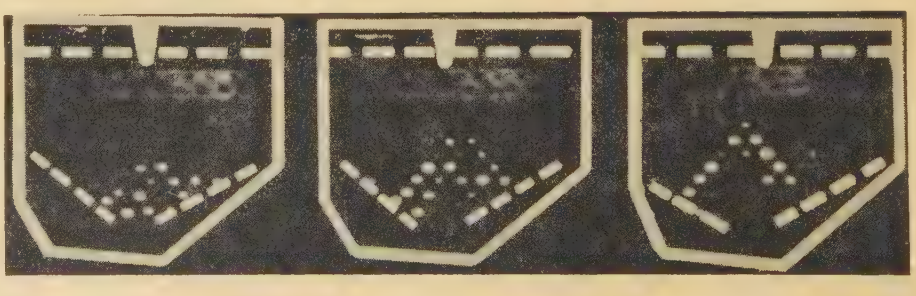

Figure 14. Actual photographs taken with Rankin high-speed camera showing arc behind windows

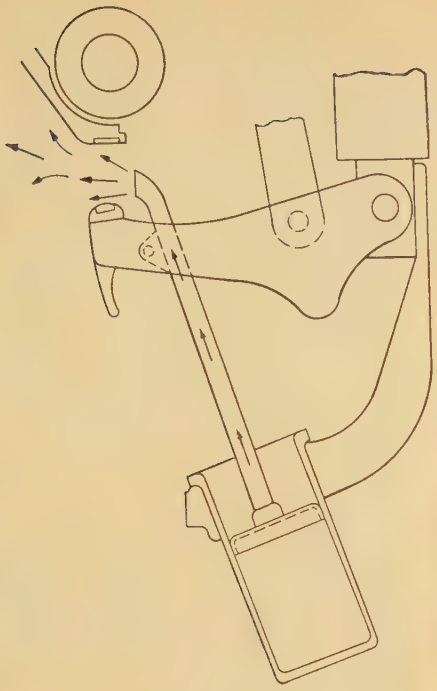

Figure 15. Cross section of piston air booster and movable contact

Figure 16. Curve of arcing time versus current of arc chute with piston booster (solid curve) as compared to arcing time without piston booster (dotted curve), showing drastic reduction in arcing time at lower values of short circuit in magnetic air breaker

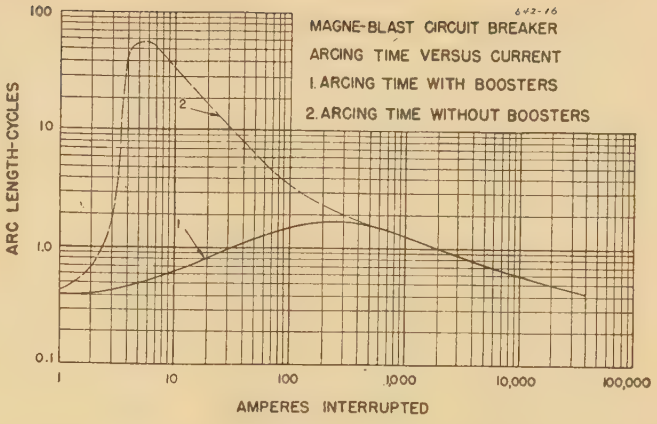

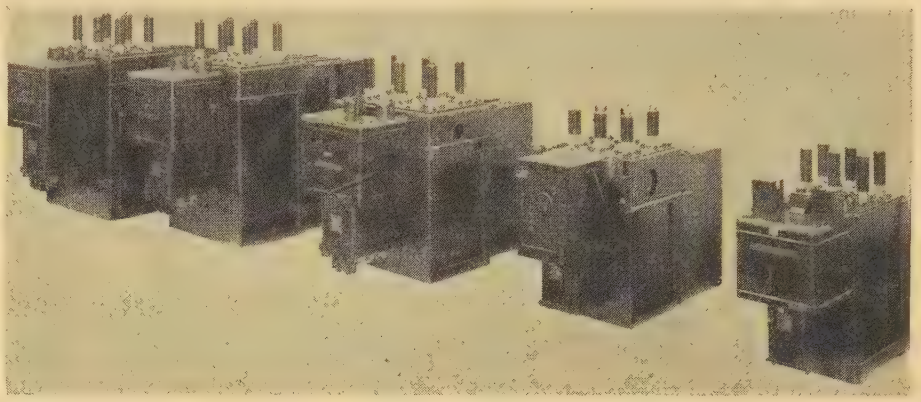

Figure 17. Complete line of magne-blast breakers rated 50,000 to 500,000 kva for use in vertical lift metal-clad switchgear

The faster the arc is moved over these fins of the arc chute, the cooler the fin surfaces will remain and the greater is its cooling effect on the arc. This arc speed is a function of both the current flowing in the arc column and the strength of the transverse magnetic field. Figure 11A shows the variation in velocity of an arc in free air when only the current is varied, while Figure 11B shows the velocity variations of an arc in free air when the transverse magnetic field is the only variable.

It is apparent that a strong uniform magnetic field must be established over the entire working area of the arc chute for maximum arc-chute efficiency. To obtain maximum field-strength uniformity in the larger arc chutes for the higher voltage breakers, it is necessary to use several blowout coils distributed along the arc runners. Several small blowout coils have proved much more effective than a single powerful coil because the magnetic field strength decreases rapidly with the distance away from the coil as a result of leakage flux. This can be seen by reference to Figure 12A which shows the poor field-strength distribution which is obtained over an 18-inch arc chute with a single strong blowout coil. The low flux density reduces materially the arc speed at the extremities of the chute. This would cause arc slowing or arc lingering near the chute extremities, resulting in high local heating and poor arc cooling. The addition of two more blowout coils, as shown in Figure 12B, improves this distribution considerably and maintains a high arc speed over the entire working area of the arc chute.

To study better the effects of localized magnetic blowout coils on arc speed, a special high-speed motion-picture camera developed by Mr. Rankin was used to photograph the movement of the arc through the chute. The extreme speed of this camera (120,000 frames per second maximum) is capable of recording the position of the arc as it passes by tiny quartz windows scattered across the chute sidewalls. Figure 13 pictures the set-up of a magne-blast circuit breaker used for this investigation. The windows are 5/16-inch-diameter quartz rods which project through the magnetic side plates, insulation, and arc-chute side and are flush with the inner ceramic surface. Actual photographs showing this recorded arc travel are shown in Figure 14.

The faster the arc moves into the arc chute, the more rapidly its resistance will increase, resulting in a more rapidly increasing arc-resistance voltage drop e_a. The more rapidly e_a rises, the greater will be the reduction of short-circuit current i_a and the shorter the arc duration $t_0 - t_1$. For very high rates of increase in arc

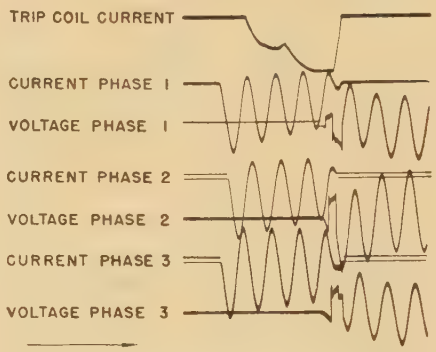

Figure 18A. Oscillogram of 3-phase short-circuit interruption at 560,000 kva, 13,000 volts, showing large reduction in last loop of short-circuit current prior to interruption

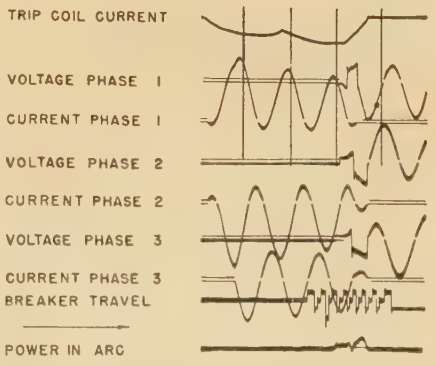

Figure 18B. Oscillogram of 3-phase short-circuit interruption at 550,000 kva, 14,500 volts

Table I. Performance Characteristics of Magne-Blast Circuit Breakers*

Type of Test	Circuit Voltage	Maximum Peak Amperes	Maximum Rms Amperes	Maximum Rms Amperes in Arc	Cycle Arc Duration	Cycles Trip to Interruption	3-Phase Kilovolt-Amperes
500,000-Kva Breaker, 15 Kv							
O	14,500	2,800	1,660	1,580	1.8	4.5	40,000
O	14,500	4,900	2,900	2,900	1.2	3.9	73,000
O	14,500	13,000	8,100	7,500	1.1	3.8	190,000
O	14,500	22,000	13,300	10,200	0.8	3.4	260,000
O	14,500	30,000	18,200	15,800	0.8	3.4	400,000
O	14,500	55,000	33,000	22,000	1.0	3.5	550,000
O	13,000	66,000	40,000	22,000	0.8	3.2	500,000
O	6,500	111,000	70,000	46,000	0.5	2.8	520,000
CO	6,500	110,000	70,000	44,000	0.5	2.8	500,000
250,000-Kva Breaker, 15 Kv							
O	14,500	5,500	3,200	3,000	1.8	4.2	75,000
O	14,500	14,500	7,000	7,000	1.1	3.5	175,000
O	14,500	22,000	13,000	11,000	0.9	3.3	280,000
O	11,000	42,000	26,000	16,200	0.8	3.2	310,000
O	6,600	46,000	27,000	22,000	0.8	3.2	260,000
CO	11,000	40,000	22,000	13,100	0.8	3.2	250,000
CO	6,600	48,000	27,000	23,000	0.8	3.2	260,000
250,000-Kva Breaker, 5 Kv							
O	5,000	5,400	3,200	2,300	1.6	3.6	20,000
O	5,000	24,000	14,400	11,600	1.0	3.0	100,000
O	5,000	47,000	28,000	23,000	0.9	2.9	200,000
O	5,000	65,000	38,000	34,000	0.6	2.6	290,000
CO	4,200	84,000	50,000	34,000	0.7	3.7	250,000
150,000-Kva Breaker, 5 Kv							
O	5,000	1,200	720	610	2.4	4.5	5,300
O	5,000	13,500	7,800	6,600	1.1	3.1	57,000
O	5,000	29,000	17,000	14,400	0.8	2.8	130,000
O	5,000	46,000	27,000	21,000	0.9	2.9	180,000
CO	5,000	63,000	37,000	20,000	1.0	3.0	170,000
CO	2,300	80,000	49,000	38,000	0.7	2.7	150,000
100,000-Kva Breaker, 5 Kv							
O	5,000	1,560	940	940	2.4	4.4	8,100
O	5,000	13,300	7,700	6,700	0.8	2.8	49,000
O	5,000	29,000	17,000	14,400	0.8	2.8	130,000
CO	5,000	28,000	16,700	15,600	0.7	2.7	110,000
CO	2,300	55,000	33,000	25,000	0.7	2.7	100,000
50,000-Kva Breaker, 5 Kv							
O	5,000	1,350	810	690	2.0	4.4	6,000
O	5,000	5,000	2,900	2,300	1.0	3.4	20,000
O	5,000	15,700	9,400	6,300	1.2	3.6	55,000
O	2,300	32,000	17,500	13,200	0.8	3.2	53,000
CO	4,200	14,600	8,800	7,200	1.0	3.4	54,000
CO	2,300	32,000	19,200	13,800	1.1	3.1	55,000

*The above table is a tabulation of actual test data on various ratings of magne-blast breakers.

voltage, as obtained in the magne-blast breaker with its strong uniform magnetic field, the total energy liberated is kept low and the over-all temperature rise of the arc chute is limited to a few degrees.

The total energy liberated in the arc chute during an interruption is equal to

$$\text{Total energy} = \int_{t_0}^{t_1} e_a i_a dt$$

where

e_a = instantaneous arc-voltage drop
i_a = instantaneous arc current
t_0 = time of arc initiation (contact parting)
t_1 = time of arc interruption

At low currents, however, the magnetic field strength from the series blowout coils is very weak, which would result in low arc speeds and long arc durations if this magnetic field were the only driving force. Magne-blast breaker contacts are equipped with simple air-piston boosters to supplement the magnetic field with a blast of air as the contacts part. On light currents the arc, therefore, is carried into the interleaving arc chute with approximately the same speed as on heavy currents. Figure 15 shows the construction of the contact-assembly piston booster on a 15-kv breaker.

The total arcing time of a typical magne-blast breaker with air booster for all values of current is shown in Figure 16. Tests have shown this arcing time to be entirely independent of the direction in which the arc chute is pointing, whether this direction is upward, downward, or in a horizontal plane. The air-piston booster therefore encourages extreme flexibility in breaker design by permitting the arc chute to exhaust either horizontally, downward, or upward, thereby simplifying the design of this breaker for modern vertical-lift metal-clad equipment. Without the air booster, the arcing time at very light currents would be considerably longer, as shown by the dotted line at the top of the figure. The shape of this dotted curve is generally characteristic of all magnetic air breakers without boosters, regardless of the direction of arc-chute exhaust.

Early studies showed that the incandescent gases exhausted from the chute when interrupting high short-circuit currents in closed metal enclosures occasionally would cause flashover if these exhaust gases were not cooled properly before being released from the chute. To cool these exhaust gases, alternate plates of fiber and corrugated metal are assembled as a muffler and successfully cool exhaust gases to a low value before releasing them to the atmosphere. By cooling these exhaust gases and reducing their volume before releasing them to the atmosphere, the audible report also is reduced to a fraction of its unmuffled value.

The Breaker

A proper combination of arc elongation, arc cooling, and arc movement has provided a circuit interrupter that satisfies all of the requirements and benefits of a high arc-resistance interrupter. Arc elongation is achieved by its movement in three planes to form a serpentine path. Arc cooling results by squeezing the arc between ceramic walls and moving it rapidly across these cooling surfaces. Arc movement is established and controlled by directing the circuit currents through multiple blowout coils designed to maintain a strong uniform magnetic-field transverse to the major plane of the arc chute. As accessories to this magnetic field, air boosters assist arc movement at light currents, and a muffler cools the exhaust gases of exceptionally high currents.

The development of an interrupter, however, does not mark the completion of a circuit-breaker design. Contacts, operating means, insulation, conductors, and accessories are all a vital part of the complete device. The magne-blast breaker, adapted for vertical lift metal-enclosed equipments, uses a heavy-duty solenoid mechanism to operate its contacts. These contacts use fine silver primaries to carry load currents with minimum loss and to carry the inrush currents of a heavy fault. As the breaker trips open the current is transferred to an intermediate contact in a parallel circuit. This intermediate contact handles the small arc that is established as the reactance of the first blowout coil is shunted into the circuit through the arc-resistant alloy arcing contacts. The final interrupting arc then is drawn when the arcing contacts part and is carried, by the moving arc contact, to the lower arc runner where a second blowout coil assists in moving the arc along the diverging arc runners and into the arc chute. As the arc travels along these runners, supplemental blowout coils are shunted into the circuit to extend the

magnetic field over the working area of the chute.

The circuit breaker is well insulated by using conventional compound bushings around the conducting studs and by enclosing each phase in a removable housing of insulation. This construction emphasizes accessibility with increased reliability. All operating parts may be exposed readily by removing these subassembled box barriers. The conventional construction of the operating mechanism, accessory devices, and general problems of application have profited by the experience of engineers responsible for the design of the many other varieties of power circuit breakers manufactured.

A complete line of these breakers rated from 50,000 kva to 500,000 kva for use in modern vertical lift metal-clad switchgear is shown in Figure 17. Figures 18A and 18B are two typical oscillograms of the 500,000-kva breaker interrupting in excess of 500,000 kva at 13,000 and 14,500 volts respectively and illustrating the marked reduction in the last loop of short-circuit current caused by the high arc resistance even at these voltages.

It is fortunate that this type of high-arc-resistance breaker conforms to the general pattern and size of correspondingly rated oil circuit breakers while it offers the advantages of no oil. Its application to the same type of metal-clad equipments which have proved their worth for oil circuit breakers is therefore comparatively simple.

References

1. Air-Break Magnetic Blowouts, **J. F. Tritle.** AIEE Transactions, volume 41, 1922, page 262.

2. Magne-Blast Air Circuit Breaker for 5,000-Volt Service, **E. W. Boehne, L. J. Linde.** AIEE Transactions, volume 59, 1940, April section, pages 202–08.

3. The Oil Blast Circuit Breaker, **D. C. Prince, W. F. Skeats.** AIEE Transactions, volume 50, 1931, pages 506–12.

4. Determination of Circuit Recovery Rates, **E. W. Boehne.** AIEE Transactions, volume 54, 1935, pages 530–9.

5. Geometry of Arc Interruption, **E. W. Boehne.** AIEE Transactions, volume 60, 1941. pages 524–32.

6. High Speed Circuit Breakers, **J. W. McNairy.** AIEE Transactions, volume 47, 1928, pages 1276–84.

7. Heat Transfer in Arc Interruption, **Dr. C. G. Suits.** *General Electric Review*, volume 42, October issue, 1939.

8. Magnetic-Type Air Circuit Breaker for 15,000-Volt Services, **L. J. Linde, B. W. Wyman.** AIEE Transactions, volume 63, 1944, March section, pages 140–4.

9. Solenoid Mechanism for Magne-Blast Breakers, **B. W. Wyman, J. H. Keagy.** AIEE Transactions, volume 64, 1945, May section, pages 268–74.

10. Arcing Phenomena of Circuit Interruption, **S. Horikosi.** *ETJ*, January 1940, pages 17–21.

11. Cross Air Blast Circuit Breaker, **D. C. Prince, J. A. Henley, W. K. Rankin.** AIEE Transactions, volume 59, 1940, September section, pages 510–17.

12. Switching Overvoltage Hazard Eliminated in High-Voltage Oil Circuit Breakers, **Lloyd F. Hunt, E. W. Boehne, H. A. Peterson.** AIEE Transactions, volume 62, 1943, February section, pages 98–106.

The Short-Circuit Characteristics of D-C Generators

G. E. FROST
ASSOCIATE AIEE

KNOWLEDGE of the short-circuit characteristics of d-c machines is an essential factor in the design of d-c electric systems having a large low-voltage machine capacity concentrated in a small area. This information is particularly important in the design of systems such as those encountered aboard ship where circuit breakers, fuses, relays, and other protective equipment must be so applied and co-ordinated as to provide a high degree of reliability and service continuity. Available information relative to d-c short-circuit currents has been limited to theoretical analyses based on formal solution of the differential equations of current flow and the machine inductance and resistance values. As a tool in the routine design of d-c systems, this information has not been adequate, particularly when estimates must be made of the effect of fault resistance, choice of machine construction, and so forth.

For some years, the design of a-c systems has been facilitated by the use of the transient and subtransient reactances and the corresponding time constants of synchronous machines. These constants, based on application of the theorem of constant flux linkages to the a-c machine, represent to practical accuracy the performance of that machine under rapidly varying conditions such as those existing during short circuits. Relatively simple tests can be made to determine the various reactance values for a particular machine and form a basis upon which machine and system design requirements may be developed. With the aid of this theory, it has been possible to conduct extensive calculations of short-circuit current flow on a-c systems under a wide variety of conditions of external resistance, external reactance, and so forth, without the formal differential equations which otherwise would be required. The availability of this theory has contributed in no small measure to the high standard of performance which has been obtained on a-c electric systems.

An analysis has been made of d-c machine characteristics with the purpose of deriving a group of machine constants similar to those now applied to a-c machines. It has been found that the effect of magnetic saturation is very large in the short-circuited d-c machine and must be taken into account if a useful analysis is to be made. However, this condition has not prevented derivation of a group of machine constants directly analogous to corresponding a-c machine constants which can be applied practically to d-c system design calculations. In addition, these constants provide a convenient method of describing the effect of series and compensating windings on d-c machine performance. It is the purpose of this paper to describe this analysis. Although the calculation and application of machine constants is illustrated for the particular case of a 60-kw 250-volt shunt wound generator, tests have shown the theory to be applicable to machines of other types and sizes.

Equations for the short-circuit current of a shunt wound d-c machine having negligible armature circuit inductance are derived from the differential equations of current flow in Appendix I. Similar equations are derived for the compound wound machine in Appendix II. The assumption of negligible armature inductance permits armature current to rise practically instantaneously, thereby making the theorem of constant flux linkages applicable. Inasmuch as this theorem is understood more readily than the differential equations and furnishes a useful physical interpretation of the machine constants, the results of the analysis will be described in terms of constant flux linkages.

Short Circuit of the Shunt Wound D-C Machine

Curves of armature and field current taken from an oscillogram of short circuit of a typical 60-kw 240-volt shunt wound d-c generator are shown in Figure 1. The construction of this machine is shown in Figure 2. The current changes following short circuit may be divided into two distinct periods: (1) a period of rapidly increasing armature and field current (*O-A*, Figure 1) and (2) a period of slowly decaying armature and field current (*A-B*, Figure 1). During the former period, total flux linkages in the shunt field winding are maintained nearly constant by current change in that winding, and the machine air-gap voltage changes only to the extent permitted by armature and field leakage flux. Current rise from zero to the peak value takes place at a rate determined by armature circuit inductance and the machine air-gap voltage. Shunt field current increases as required to maintain nearly constant the total effective shunt field flux linkages. The latter period consists of a slow current decay during which shunt field flux linkages, and consequently armature and field currents, are reduced from the value at the peak current point to the final steady short-circuit value. Current change during this period is so slow that armature circuit inductance has a negligible effect, and the rate of field and armature current decay is determined by the field circuit time constant corresponding to the peak value of field current attained.

It is evident from this discussion that the short-circuit characteristics of a d-c machine are closely analogous to those of an a-c machine. In each machine increased armature current associated with the short circuit has a demagnetizing effect on the field winding, which causes the field current to increase as required to maintain nearly constant the total effective field flux linkages. Likewise, after the peak value of armature current is reached (rms current in an a-c machine), the armature current decays to a steady state value at a rate determined by the field circuit time constant. Furthermore, the d-c machine of Figure 1 reaches a steady state short-circuit current value of

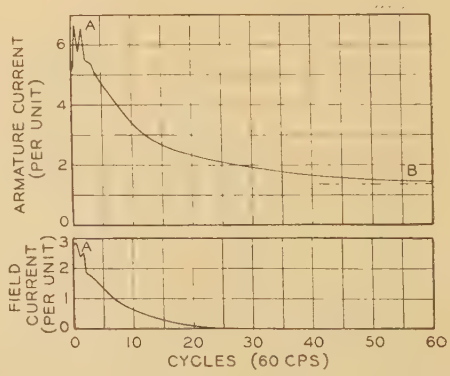

Figure 1. D-c short-circuit transient (no brush shift)

Paper 46-66, recommended by the AIEE committee on electric machinery for presentation at the AIEE winter convention, New York, N. Y., January 21–25, 1946. Manuscript submitted September 8, 1945; made available for printing December 20, 1945.

G. E. Frost is a patent attorney with the General Electric Company, Schenectady, N. Y.

The author desires to extend his appreciation to C. J. Werner, of the Delco Products Division, General Motors Corporation, for conducting tests required for this study, and to P. N. Ross, central station engineer, Westinghouse Electric Corporation, for his suggestions in the conduct of the analysis.

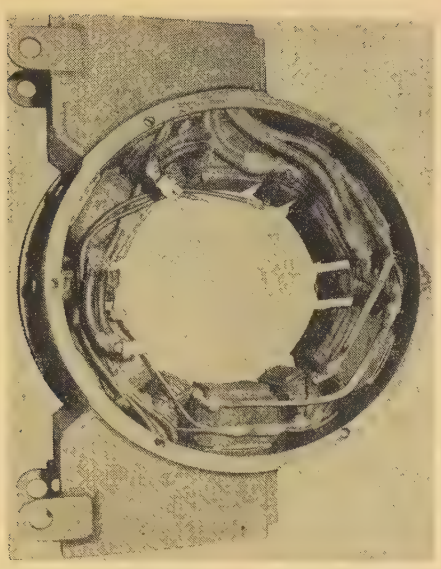

Figure 2. D-c machine typical of those tested

about 1.3 per unit, a value not greatly different from the steady state short-circuit currents encountered on a-c machines.

Magnetizing Effects

Analysis of magnetizing effects during short circuit of a d-c machine can be made most conveniently by considering the machine to have two sets of axes, as shown in Figure 3. The first set of axes, the direct and quadrature field axes, correspond to the actual field structure of the machine. Flux in the direct field axis links only the main field poles, whereas flux in the quadrature field axis links only the interpoles. Since the shunt field winding is on the direct field axis, the flux linkages maintained constant by that winding are the direct field axis flux linkages. The second set of axes, the brush axis and the quadrature brush axis, determines the actual generated voltage within the machine and the direction of armature magnetomotive force. Flux in the quadrature brush axis is effective in producing generated voltage, whereas flux in the brush axis gives no generated voltage. The magnetomotive force produced by the armature, however, is entirely along the brush axis. It is evident that when the brushes are located on the quadrature field axis (the so-called neutral axis), there is no distinction between the pole position and the brush position, and the two sets of axes coincide.

Figure 4 shows the steady state characteristics of a typical separately excited shunt wound d-c machine in terms of total field ampere turns, armature current, and quadrature-brush-axis air-gap flux. The latter quantity represents the machine flux in the quadrature brush axis, and hence the effective flux generating armature voltage. The machine terminal voltage in per unit equals the quadrature-brush-axis air-gap flux in per unit less the per unit voltage drop caused by machine resistance. In the case of a zero resistance fault, there can be no terminal voltage, and the per unit quadrature-brush-axis air-gap flux must equal the machine resistance drop in per unit. Operation therefore must be at some point along the machine *IR* drop line of Figure 4. Since armature inductance effects are negligible during the current decay period (*A-B*, Figure 1), the current changes during this period can be considered to follow the *IR* drop line of Figure 4 as a locus, the rate of motion being determined by the rate of shunt field current decay.

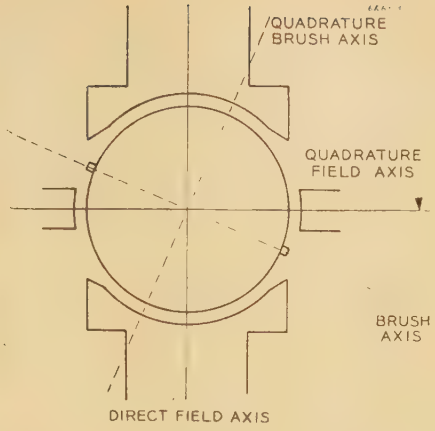

Figure 3. Magnetic structure of d-c machine

The curve of Figure 4 shows that with constant field current, quadrature-brush-axis air-gap flux decreases as armature current is increased. This change is caused by two demagnetizing components: (1) direct-field-axis armature magnetomotive force and (2) apparent direct-field-axis armature magnetomotive force associated with the quadrature-field-axis armature magnetomotive force. The first component is the result of actual direct-axis armature ampere turns and is proportional to the sine of the angle of brush displacement. The second component results from pole face and armature tooth saturation associated with cross flux from the quadrature axis armature magnetomotive force. As shown in Figure 5, the magnetomotive force added on one side of the main pole by quadrature-field-axis ampere turns is equal to that subtracted on the other side, but saturation causes the flux added to be less than the flux subtracted. Hence a lower value of average flux results. Tests show that, for the values of brush shift normally encountered in d-c machines, the effect of direct-field-axis armature ampere turns is small compared to the apparent magnetomotive force caused by the saturating effect of quadrature-field-axis armature ampere turns.

The effect of armature magnetomotive force just discussed is directly analogous to armature demagnetizing action in the a-c machine. There is one vital difference, however, for the armature demagnetizing action in an a-c machine is nearly proportional to the reactive component of armature current, whereas the armature

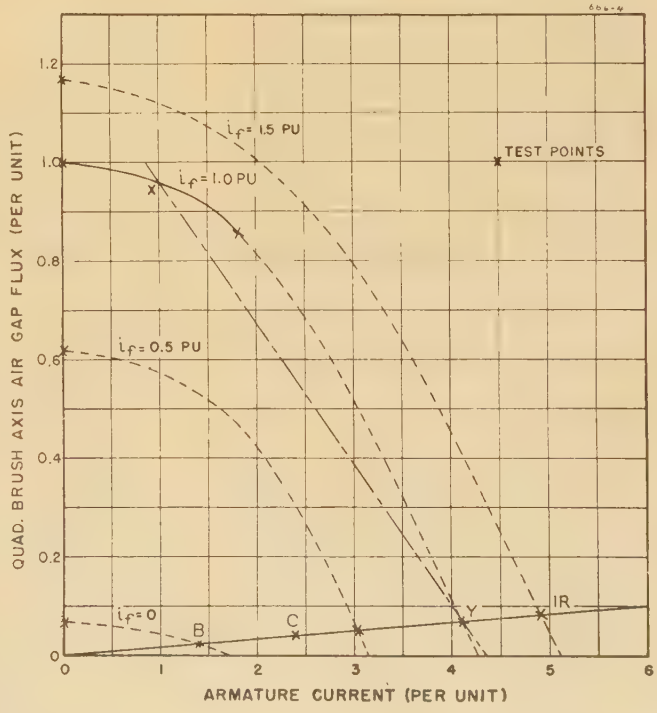

Figure 4. Steady state characteristics of a d-c machine (no brush shift)

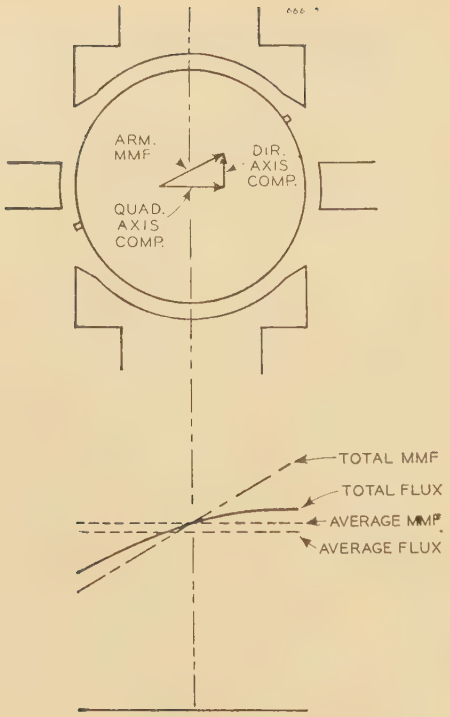

Figure 5. Armature demagnetizing effect in a d-c machine

demagnetization in a d-c machine largely results from magnetic saturation and is not directly proportional to armature current. In the a-c machine, the combined effect of reduced air-gap flux caused by demagnetization and internal voltage drop resulting from leakage reactance is lumped in the machine constant of synchronous reactance. A similar synchronous resistance may be used as a d-c machine characteristic. However, any single value of this resistance is effective only between specific values of armature current, and some error is involved even if these values are relatively close together. In the case of the machine of Figure 4, for instance, synchronous resistance based on the line X-Y may be used at armature currents in excess of one per unit. This line corresponds to one per unit generated voltage (quadrature-brush-axis flux) drop for 3.49 per unit current or an apparent resistance of 0.29 per unit. Adding 0.02 per unit ohmic resistance drop, a total synchronous resistance of 0.31 results.

Steady Current

Figure 4 shows that quadrature-brush-axis air-gap flux exists in a d-c machine even though no field current is flowing. This flux is the combination of two components: (1) residual flux in the direct field axis and (2) the quadrature-brush-axis component of interpole flux. The latter flux is determined by the angle of brush shift, being approximately proportional to the sine of that angle. In the case of a generator, brush shift against rotation results in a positive voltage from interpole flux, whereas brush shift with rotation results in a negative voltage. The residual flux in the direct field axis is the result of previous magnetization of the field poles and is relatively independent of the brush position. Figure 6 shows the variation in quadrature-brush-axis air-gap flux at no field excitation when brush position is changed. It is evident from the figure that the principal source of this flux, within the brush angles shown, is the residual direct-field-axis flux.

Peak Current

In passing from the condition of normal quadrature-brush-axis air-gap flux (Figure 4, point X) to the final short-circuit condition of 0.03 per unit quadrature-brush-axis air-gap flux (Figure 4, point B), the direct-field-axis flux is reduced substantially. In making this transition, however, there can be no instantaneous change in shunt field flux linkages as the infinite

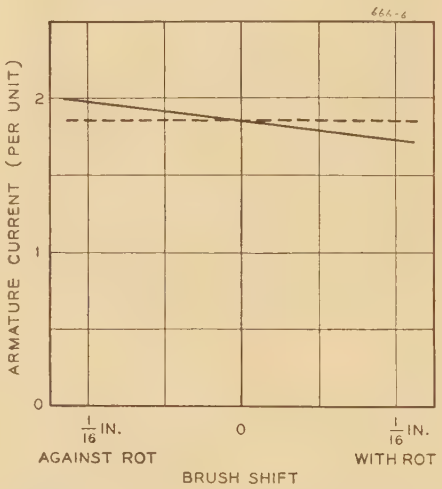

Figure 6. Effect of brush shift on steady state short-circuit current

voltages required to make such change are not available in the shunt field circuit. Accordingly, shunt field current rises to a value sufficient to give constant total flux linkages. At this point the flux linking the shunt field winding differs from the net quadrature-brush-axis air-gap flux by the field and armature leakage fluxes.

Figure 7 shows approximately the paths of armature and field flux components within a short-circuited d-c machine. Field flux consists of two components: (1) flux linking both the field and air gap, φ_{FA} (Figure 7), and (2) flux linking the field winding but not the air gap, φ_{FL}. Armature demagnetizing effects may be considered to produce two flux components, oppositely directed with respect to the main field flux. The first of these components, φ_A, links both the air-gap and the shunt field winding, whereas the second component, φ_{AL}, links only the air-gap. Since the armature leakage flux φ_{AL} does not link the field winding, it can change instantaneously. The combined effects of armature leakage flux and field leakage flux may be lumped in a total effective leakage coefficient which may be used to represent the over-all performance of the machine.

Figure 8 shows the results of a test to determine the magnitude of armature leakage flux. A short circuit was placed on the machine used in the test of Figure 1 and suddenly opened one-fifth second later. Since the shunt field flux linkages were nearly the same value after opening the short circuit as before, the value of terminal voltage following opening indicates the magnitude of armature leakage. The value of armature voltage during short circuit indicated in Figure 8 represents the actual quadrature-brush-axis flux computed from the product of arma-

Figure 7. Basic flux paths in the d-c machine

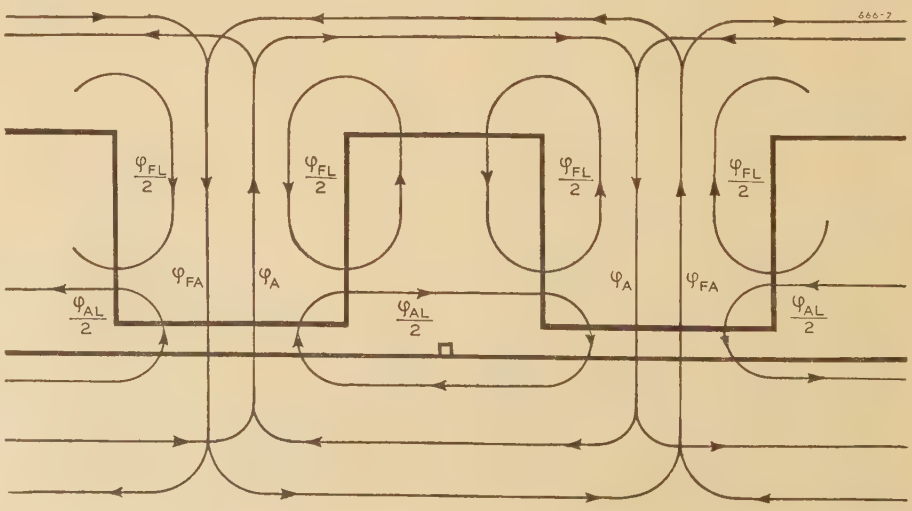

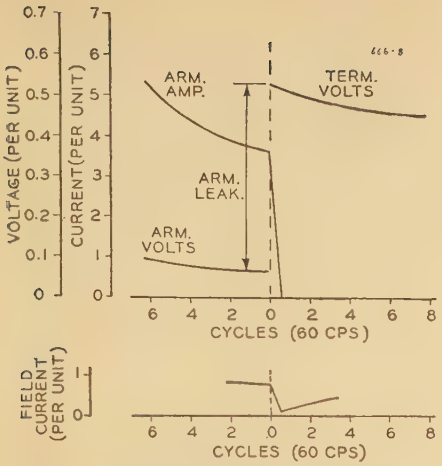

Figure 8. Interruption of a d-c short circuit

ture resistance and armature current. The field current before opening the fault was about 0.8 per unit, giving a value of φ_{FA} of 0.8 per unit (neglecting saturation). Since the net air-gap flux is equal to $\varphi_{FA}-\varphi_A-\varphi_{AL}$ (Figure 7) and is shown on the armature voltage curve to be 0.08, the sum of armature flux φ_A and armature leakage flux φ_{AL} is 0.72 per unit. The net shunt field flux is equal to $\varphi_{FA}+\varphi_{FL}-\varphi_A$ and is held constant by field current change. From the figure this value after opening the short circuit is 0.53 per unit. Assuming 0.2 per unit field leakage flux at one per unit field current, the field leakage flux component becomes 0.16 per unit at the 0.8 per unit field current prior to opening. Substituting this value of field leakage flux and field air-gap flux (0.8 per unit before the opening), the value of armature flux φ_A is 0.43 per unit. Since the sum of armature flux and armature leakage flux is 0.72 per unit, the value of armature leakage flux φ_{AL} is 0.29 and the armature leakage coefficient $[n_a=\varphi_{AL}/\varphi_A]$ is 0.67. Substituting this value of armature leakage flux and a value of 0.2 for the field leakage flux coefficient in equation 13, Appendix I, the value of apparent field leakage coefficient becomes unity.

Analysis of the cause of armature leakage flux in the d-c machine is complicated by the varying degrees of magnetic saturation existing throughout the magnetic circuit. However, a qualitative indication of the origin of this flux may be gained from consideration of Figure 9, which shows an equivalent electric circuit for the simplified magnetic structure of a 2-pole machine. In the figure batteries represent magnetomotive force values, and resistances represent reluctance. The two groups of four parallel resistance–battery combinations represent the four armature teeth assumed to be located under each main pole. In order to represent the effects of saturation, the reluctance values corresponding to the more saturated armature teeth and pole face areas are made larger than those corresponding to the less saturated portions of the magnetic circuit. From the figure it is evident that a substantial armature leakage flux exists in the circuit. If tooth and pole face saturation is neglected, this leakage flux becomes zero. Evidently this effect accounts for the high value of armature leakage flux shown in the tests.

From this analysis, it is evident that the peak armature current of a short-circuited d-c machine equals the value determined on the basis of synchronous resistance plus a current increment taking into account the increased field current required to maintain constant field flux

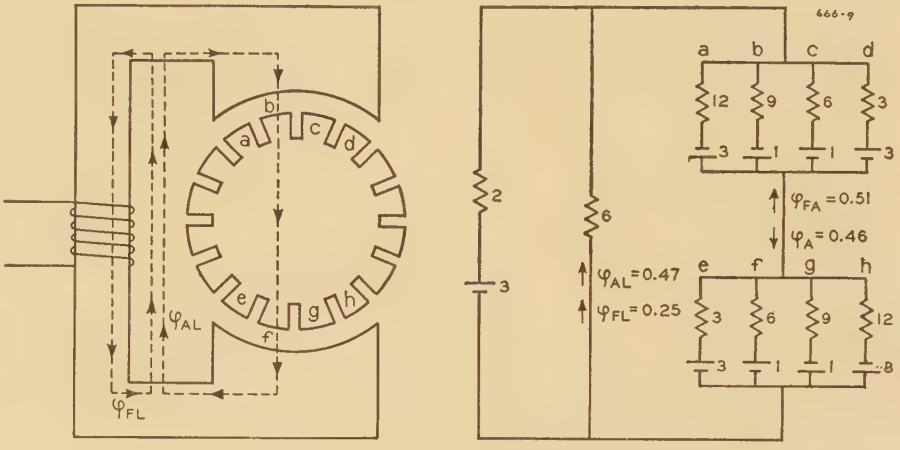

Figure 9. Equivalent magnetic circuit of a d-c machine

linkages. This current may be computed directly by regarding the d-c machine as having a transient resistance similar to direct axis transient reactance of an a-c machine. In Appendix I it is shown that the value of this transient resistance is $R_A+(n/1+n)R_e$, where R_A is the armature ohmic resistance, n is the total effective field leakage flux coefficient, and R_e is the equivalent armature resistance corresponding to the line X-Y, Figure 4. Designating transient resistance by R'_e, the peak short-circuit current from full voltage, full load is

$$i_{peak}=\frac{1+R'_e}{R_x+R'_e}\text{ per unit} \qquad (1)$$

where R_x is the fault resistance.

Equation 1 is directly analogous to the equation of peak transient short-circuit current for an a-c machine. The numerator of the equation can be considered to represent the voltage behind the transient resistance or the flux remaining constant during the short-circuit interval. In the case of the a-c machine, this flux actually exists across the air gap, whereas in the case of the d-c machine it is a purely fictitious flux since equation 1 is derived on the basis that armature demagnetizing effect does not commence until armature current reaches one per unit. The denominator of equation 1 represents the total effective circuit resistance retarding short-circuit current flow.

As shown in Figure 4, a reasonably accurate approximation of the demagnetizing effect of armature current in a d-c machine may be made by neglecting all armature demagnetizing effects for armature currents less than one per unit. Equation 1 is derived on this basis with

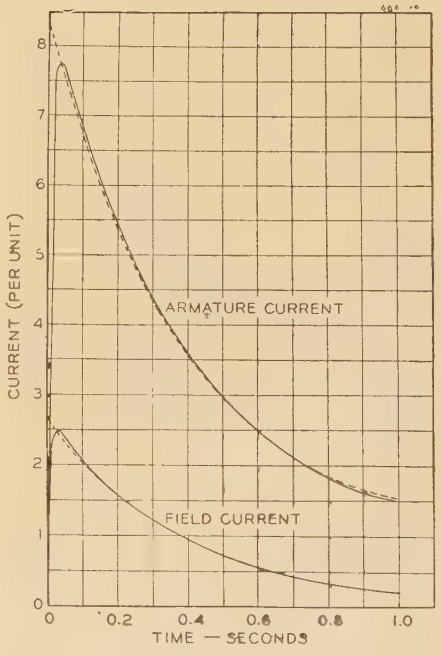

Figure 10. Effect of neglecting armature inductance

———Including armature inductance
– – – –Neglecting armature inductance

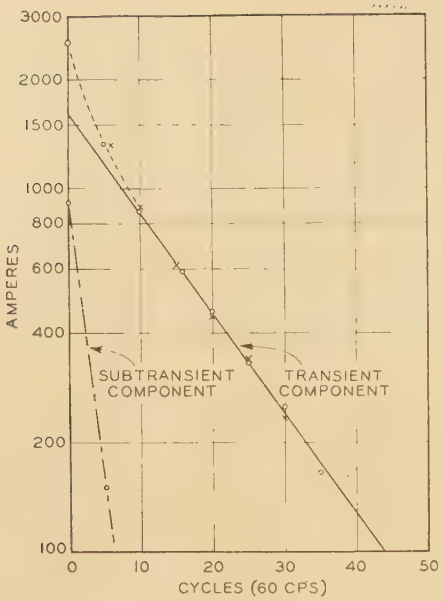

Figure 11. Current decay in d-c machine

o—One-sixteenth-inch brush shift with rotation

x—One-sixteenth-inch brush shift against rotation

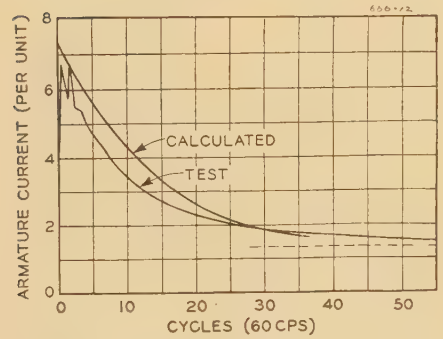

Figure 12. Calculated d-c short-circuit current

the further provision that initial armature current is one per unit. Inasmuch as the initial value of air-gap flux varies only to the extent required by armature resistance as initial armature current is changed from zero to one per unit, there is a very slight change in initial field flux linkages when armature current is changed within this range. Accordingly, equation 1 applies very nearly to all short circuits from initial armature currents between zero and one per unit.

Current Rise

Armature, interpole, and other armature circuit inductances prevent the short-circuit current of a d-c machine from instantaneously reaching the peak value determined by transient resistance. The character of this current rise is exponential if the armature demagnetizing effect behaves as a pure resistance and the armature circuit inductances do not saturate.

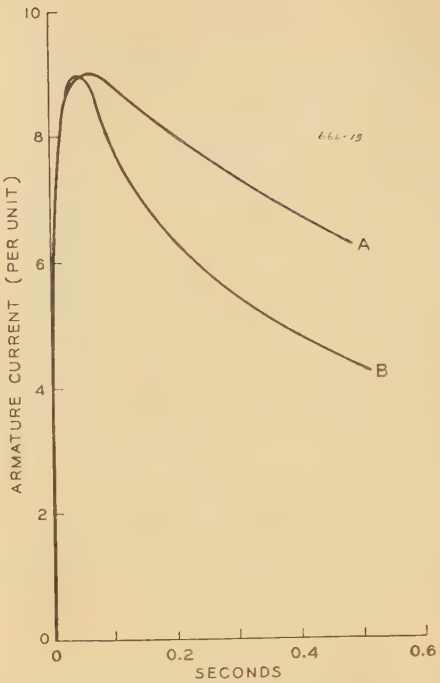

Figure 13. Effect of series field on d-c short-circuit current (300 kw machine)

A—Cumulative field

B—Differential field

Inasmuch as this does not represent the true condition, the current rise deviates from an exponential to some extent. Tests show that initial short-circuit current rise in small d-c generators (60–300-kw) is extremely rapid, varying from 500 to over 1,000 per unit per second. In fact, this current rise has been so rapid that it has been impossible to determine the exact shape of the current rise curve from test data.

Figure 10 shows the effect of the finite value of current rise on the calculated armature current following short circuit. The solid curve is the result of a computation based on the assumptions of Appendix I, but taking into account armature and interpole inductance. It was assumed in this calculation that armature circuit inductance gave an initial current rise of 800 per unit per second. From the figure it is evident that the curves correspond in all respects, except for the peak value and rate of rise of armature and field current. In the peak values, an error of eight per cent is involved, a small error in view of the approximations used in the analysis.

Current Decay

Armature current decays from the value associated with transient resistance to the final steady value at a rate dependent on the field circuit time constant of the machine. In the absence of saturation, this decay is an exponential curve which becomes a straight line when plotted on semi-log paper. Figure 11 shows a curve of this type for two short circuits of a 100-kw 1,200-rpm shunt-wound machine, one with the brushes leading and the other with the brushes lagging. With the exception of the first ten cycles, the decay is very nearly exponential, having a time constant of about 15 cycles. The effect of brush shift on current during the decay period is so small that negligible effect is shown in the figure.

It is shown in Appendix I that the time constant of decay for a zero resistance fault may be computed from

$$T=\frac{R'_e}{R_S}T_{FO} \qquad (2)$$

where T_{FO} is the field time constant at full load, full voltage and R_S the synchronous resistance. This relation is directly analogous to the equation for the transient short-circuit time constant of an a-c machine.

Subtransient Effects

Figure 11 is typical of several tests which have shown that current during the first few cycles following short circuit of a d-c machine exceeds the value based on transient resistance. This evidently is the effect of pole iron, bolts, welded sections, and so forth, in maintaining flux for a short period of time, thus giving the d-c machine a subtransient resistance analogous to the subtransient reactance of an a-c machine. From Figure 11 the approximate value of this resistance is 12 per cent and the time constant three cycles (0.05 second). These values are consistent with subtransient reactance and time constant values encountered on a-c machines of similar size.

Accuracy

To check the above theory, a calculation has been made of the transient short-circuit armature current of the machine used to obtain the data of Figures 1, 4, 8, and the equations of Appendix I. Values of synchronous resistance, effective field leakage coefficient, and open-circuit transient-time constant were taken as 0.31 per unit, 1, and 0.5 second respectively. The corresponding transient resistance is 0.16 per unit. Armature resistance was assumed to be 0.02 per unit. The results of the calculation are shown in Figure 12. It is evident that the computation checks in order of magnitude the actual short-circuit current transient obtained, all that can be expected in view of the assumptions used in deriving the equations of the appendix.

Compounding and Compensation

Figure 13 shows the short-circuit current of a d-c generator for two series field connections, one cumulative and the other differential. The peak armature current is practically the same value in each case, for the shunt field current maintained the same value of total field flux linkages nearly constant during the period of current buildup. That is the same air-gap flux, and therefore shunt field flux linkages, existed in the machine prior to each short circuit, and the same increase in total field magnetomotive force was required to maintain constant these flux linkages. Since the maximum value of total field magnetomotive force is the same in each case, the peak short-circuit currents are identical. However, the rate of current decay following the peak current value for the differential field connection is greater than for the cumulative field connection because the shunt field current required to maintain constant shunt field flux linkages in the former case is substantially greater than in the latter. This condition results because of the influence of the series field in supplying field magnetomotive force, aiding the shunt field in the cumulative wound machine, and opposing the shunt field magnetomotive force in the differential wound machine.

In addition to determining the rate of decay following peak short-circuit current, the presence of a series field alters the steady state short-circuit current value. The magnitude of this effect may be estimated from the curves shown in Figure 8 If a cumulative series field gives 0.1 per unit magnetomotive force at full load, for instance, there will be an added contribution of 0.1 per unit field magnetomotive force for every one per unit armature current. Hence for the case of Figure 4, point *B* will be moved along the line *IR* until the total field magnetomotive force in per unit corresponds to ten per cent of the armature current value, thereby placing point *B* in a position corresponding to 2.4 per unit armature current (point *C*, Figure 4).

The short-circuit curves of Figure 13 are based on two series field connections for a particular generator. If a machine is designed to give a particular value of voltage regulation, the series field winding may be used in lieu of other design changes to achieve this regulation. In particular, a large value of synchronous resistance may be used with a relatively strong cumulative series field to give the same voltage regulation as with a low synchronous resistance and no series field.

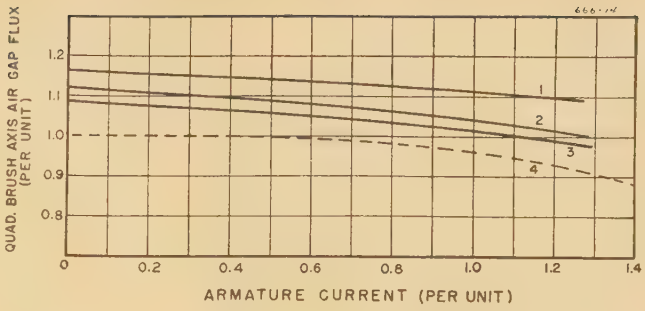

Figure 14. Steady state characteristic of compensated generators (no brush shift)

Curves 1, 2, and 3—1,100 kw 416-volt compensated generators

Curve 4—60-kw 240-volt uncompensated generator

In this case a smaller peak armature current on short circuit will be obtained than with the machine designed to achieve the same voltage regulation with only a shunt field winding. Tests show, however, that this effect is small with machines of 60 to 300 kw capacity, and that these machines have substantially the same peak short-circuit current, whether designed as shunt machines or series machines meeting the same voltage regulation requirements.

Compensating windings are provided in the pole face structure of d-c machines to reduce the magnetizing effects of armature current, thereby limiting saturation caused by quadrature axis armature magnetomotive force and decreasing the value of machine synchronous resistance. A corresponding reduction in transient resistance can be expected. If the compensation secured is perfect, the demagnetizing effects of armature current are reduced to zero and, with the brushes on the neutral axis, the short-circuit current will rise to a value limited only by armature resistance. On large machines this value may exceed 50 times normal current. Actually it does not appear that currents of this magnitude are to be expected, for actual compensation falls far short of the theoretically perfect compensating winding. This condition is evident in Figure 14 which shows a plot of the variation of quadrature-brush-axis air-gap flux with armature current for three 1,100-kw 416-volt compensated generators. By comparison with the curve of the machine of Figure 4, it appears that these particular compensated machines probably have synchronous resistance values comparable to the uncompensated machine of Figure 4.

Fault Resistance

The influence of fault resistance on peak short-circuit current of a d-c generator may be calculated from equation 1. A plot of calculated peak short-circuit current as a function of fault resistance for a particular machine is shown in Figure 15. The two test points indicate that the relation of equation 1 gives approximately correct results.

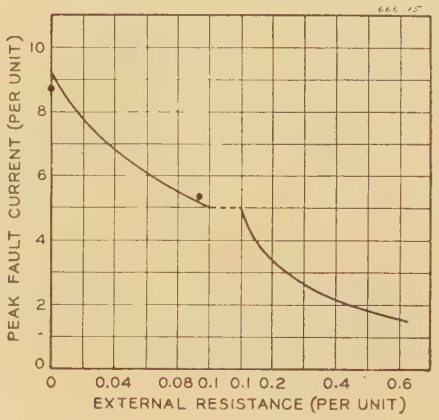

Figure 15. Effect of fault resistance on d-c short-circuit current

●—Test points

The influence of fault resistance on steady state short-circuit current may be estimated from the steady state machine short-circuit characteristics shown in Figure 4. In this case, a new *IR* drop line corresponding to the new total armature circuit resistance is constructed and the steady value of short-circuit current read from that curve.

Commutator Flashover

It generally is assumed that commutator flashover on short-circuited d-c machines can be prevented only by the use of circuit breakers having a combination of high operating speed and low trip setting which prevents buildup of armature current to the full short-circuit current value. A considerable number of tests on d-c machines of the shunt, stabilized shunt, and compound types varying from 60 to 300 kw, 240 volts, and having peak currents from 6 to 11 per unit have failed to produce a flashover. Although the tests were made under controlled conditions, they are considered to show that the probability of flashover has been exaggerated somewhat. In fact, it appears that generators in this range may be constructed economically to have a relatively low prob-

ability of flashover on short circuit, even after a period of service.

If the machine is designed to withstand short-circuit current, or the probability of flashover is considered remote, there appears little need for circuit breakers having the high operating speeds and low trip settings normally used. The entire short-circuit curve of Figure 1 then becomes available for use in establishing circuit-breaker settings, and co-ordination of circuit breakers may be obtained readily. Furthermore, if the circuit breaker is capable of withstanding the peak short-circuit current, an actual reduction in circuit-breaker duty may be achieved by intentional time delay. Inasmuch as the curve of Figure 1 is very similar to the short-circuit-current curve of an a-c machine of equivalent size, the same principles used in establishing circuit breaker settings in a-c systems may be applied to d-c systems of equivalent size, thereby simplifying the design and construction of the d-c system and taking full advantage of a-c developments.

Conclusions

Calculations of the short-circuit current of d-c machines may be conducted by the use of machine constants of synchronous resistance, transient resistance, subtransient resistance, and the corresponding time constants. These values are directly analogous to the constants which have been applied to a-c machine calculations. The principal difference between the application of these constants to a d-c machine and the application of analogous constants to an a-c machine lies in the necessarily approximate method which must be used to represent the effect of machine saturation. This approximation does not, however, prevent reaching useful results.

The value of transient resistance for d-c machines is influenced to a considerable degree by the high value of armature leakage flux. This flux, apparently caused by the saturating effect of flux in the armature teeth, has given armature leakage flux coefficients of the order of 0.7 and corresponding total apparent field leakage flux coefficients of unity. These high values, as compared with the effective field leakage flux coefficient of from 0.2 to 0.4 on a-c machines, constitute an important distinction between the performance of the two types of machines under transient conditions.

The presence of a compound field winding has no influence on the peak value of short-circuit current attained by a d-c machine. However, a winding of this type is of considerable importance in determining the rate of armature current decay from the peak to the final steady value and the value of the final steady current reached. Compensating windings, which theoretically should result in extremely high values of transient resistance, do not appear sufficiently effective to produce this result, and there is little reason to believe that the high values of short-circuit current sometimes assigned to these machines actually will be reached. Further test data on these machines, however, will be required before definite conclusions can be reached.

In the case of small d-c machines, the probability of commutator flashover under short circuit appears to be somewhat exaggerated, and it is believed possible to establish circuit-breaker settings taking advantage of the probability that flashover will not occur. In this case the effective short current transient is very similar to that of equivalent a-c machine, and the methods developed for the design of a-c systems may be applied.

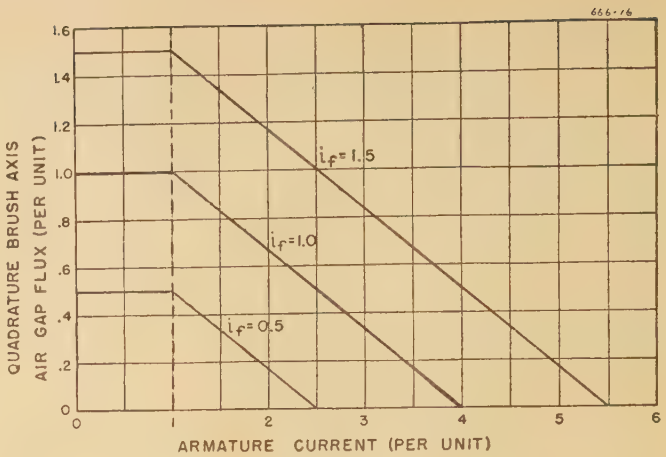

Figure 16. Assumed d-c generator characteristic

Appendix I. Short Circuit of a Shunt Machine—Mathematical Analysis

This analysis is based on the following assumptions:

1. Generated voltage (quadrature-brush-axis air-gap flux) may be represented by the following two components:

(*a*). A positive component proportional to field current, representing the magnetizing effect of field magnetomotive force.

(*b*). A negative component proportional to the excess of armature current over full load armature current, representing the demagnetizing effect of armature magnetomotive force (including saturation of the pole faces caused by quadrature axis flux).

This assumption amounts to representing the machine characteristics by the straight lines in Figure 16.

2. Field current (in amperes) is negligible as compared with armature current (in amperes).

3. The short circuit takes place from an initial condition of rated armature current and rated voltage.

4. Armature and interpole inductance is negligible. From Figure 10 it is evident that no significant error in peak current or current during the decay period results from this assumption.

Subject to these assumptions, the machine circuit equations may be written:

$$E_t = i_f - R_e(i_a - i_1) - R_a i_a \tag{3}$$

$$E_t = R_f i_f + L_f \frac{di_f}{dt} - M\frac{d}{dt}(i_a - i_1) \tag{4}$$

$$E_t = R_x i_a \tag{5}$$

where

E_t = terminal voltage in per unit

i_f = field current in per unit (based on the field current for rated armature voltage at no load)

R_a = armature ohmic resistance in per unit

i_a = armature current in per unit

R_e = equivalent armature resistance corresponding to the demagnetizing effect of armature current in per unit

i_1 = current value above which R_e is measured in per unit (one per unit this analysis)

R_f = field resistance in per unit (based on the units of i_f and E_t)

L_f = field inductance in per unit (per unit field voltage induced by one per unit field current change per second)

M = coefficient of mutual inductance representing the shunt field voltage in per unit corresponding to one per unit armature current change per second

R_x = short-circuit resistance

It is convenient to base the calculation of M on the conventional system of units. Then

$$M_A = \frac{N_f \varphi_f}{i_a} \cdot 10^{-8} \tag{6}$$

where

M_A = value of M in henries

i_A = armature current change in amperes required to produce a change in shunt field flux linkages of $N_f \varphi_f$ maxwell turns

From Figure 16 it is evident that an armature current increase (above one per unit) equal to $1/R_e$ per unit causes the quadrature-axis air-gap flux to be reduced one per unit. The corresponding change in shunt field flux linkages can be shown to be $1/1+n_a$ per unit, where n_a is the ratio φ_{AL}/φ_A (Figure 7). Inasmuch as $1/R_e$ per unit current change produces $1/1+n_a$ per unit change in shunt field flux linkages, the current change required to make a one per unit change in shunt field flux linkages is $(1+n_a)/R_e$.

It is convenient to use as a basis of substitution in equation 6 the shunt field flux linkages upon which the shunt field inductance at no load, full voltage, is based. This value of flux is one per unit plus the shunt field leakage flux. If the shunt field leakage coefficient n_f is equal to $\varphi_{FL}/\varphi_{FA}$ (Figure 6), the shunt field flux at no load, full voltage is $(1+n_f)$ per unit. Since armature current must change $(1+n_a)/R_e$ per unit to give a one per unit change in shunt field flux linkages, an armature current change of $(1+n_a)(1+n_f)/R_e$ per unit is required to give a shunt field flux linkage change corresponding to the value of shunt field flux linkages at no load, full voltage. The value of this current in amperes is

$$i_A=\frac{i_{Au}(1+n_a)(1+n_f)}{R_e} \tag{7}$$

where i_{Au} is the rated armature current in amperes.

The value of $N_f\varphi_f$ at no load, full voltage is the value upon which the open circuit field time constant is based. If $\boldsymbol{L}_f$ is the shunt field circuit inductance (in henries) corresponding to this time constant, the value of $N_f\varphi_f$ is

$$N_f\varphi_f=\boldsymbol{L}_f i_{fu}\cdot 10^8 \tag{8}$$

where i_{fu} is the shunt field current in amperes at no load, full voltage (base field current).

Then

$$M_A=\frac{\boldsymbol{L}_f R_e i_{fu}}{(1+n_a)(1+n_f)i_{au}} \tag{9}$$

The values of M_A and $\boldsymbol{L}_f$ in per unit notation are

$$M=\frac{M_A i_{Au}}{V} \tag{10}$$

$$L_f=\frac{\boldsymbol{L}_f i_{fu}}{V} \tag{11}$$

where V is rated armature voltage. Hence

$$M=\frac{L_f R_e}{(1+n_a)(1+n_f)} \tag{12}$$

It is convenient to consider the operation of the machine in terms of an equivalent shunt field leakage coefficient which combines the effects of field and armature leakage. This leakage coefficient may be defined by

$$(1+n)=(1+n_a)(1+n_f)$$

or

$$n=(1+n_a)(1+n_f)-1 \tag{13}$$

For small values of n_a and n_f, the value of n is nearly equal to n_a+n_f. Then

$$M=\frac{L_f R_e}{1+n} \tag{14}$$

Substituting equation 13 in equations 3, 4, and 5 and eliminating, it follows that

$$\left.\begin{aligned} -i_f+(R_a+R_x+R_e)i_a&=R_e i_1\\ R_f i_f+L_f\frac{di_f}{dt}-R_x i_a-\frac{L_f R_e}{1+n}\frac{di_a}{dt}&=0\end{aligned}\right\} \tag{15}$$

The Laplace transform of equation 15 is[4]

$$\left.\begin{aligned} -i_f(s)+(R_a+R_e+R_x)i_a(s)&=\frac{R_e i_1}{s}\\ (R_f+L_f s)i_f(s)-\left[R_x+\frac{L_f R_e s}{1+n}\right]i_a(s)&\\ =L_f i_{fo}-\frac{L_f R_e}{1+n}i_{ao}&\end{aligned}\right\} \tag{16}$$

where i_{fo} and i_{ao} are the initial field and armature current, respectively, and T_o is the open circuit time constant of the field circuit.

Assuming the fault to take place from an initial condition of full voltage, full load, the constants of equation 15 become

$$R_f=\frac{1}{1+R_a},\ i_{fo}=1+R_a,\ L_f=T_o,\ i_{ao}=1$$

The value of i_1 has been taken previously as one per unit and therefore

$$\left.\begin{aligned} -i_f(s)+(R_a+R_x+R_e)i_a(s)&=\frac{R_e}{s}\\ \left[\frac{1}{1+R_a}+T_o s\right]i_f(s)-\left[R_x+\frac{T_o R_e s}{1+n}\right]\times&\\ i_a(s)=T_o(1+R_a)-\frac{T_o R_e}{1+n}&\end{aligned}\right\} \tag{17}$$

Solving

$$\left.\begin{aligned} i_a(s)&=\frac{1}{sD}\left[\frac{R_e}{1+R_a}+sT_o\left(1+R_a+R_e\frac{n}{1+n}\right)\right]\\ i_f(s)&=\frac{1}{sD}\left[R_x R_e+sT_o\left((1+R_a)(R_a+R_e+R_x)-\frac{R_e}{1+n}(R_x+R_a)\right)\right]\\ D(s)&=\frac{R_a(1-R_x)+R_e}{1+R_a}+sT_o\left(R_a+R_x+R_e\frac{n}{1+n}\right)\end{aligned}\right\} \tag{18}$$

The inverse transformation of equation 17 gives

$$\left.\begin{aligned} i_a&=A+(B-A)\epsilon^{-t/T}\\ i_f&=C+(D-C)\epsilon^{-t/T}\end{aligned}\right\} \tag{19}$$

where

A = steady value of armature current
B = peak value of armature current
C = steady value of field current
D = peak value of field current
T = time constant of decay

and

$$A=\frac{R_e}{R_a(1-R_x)+R_e} \tag{20a}$$

$$B=\frac{1+R_a+R_e\frac{n}{1+n}}{R_a+R_x+R_e\frac{n}{1+n}} \tag{20b}$$

$$C=\frac{R_e R_x(1+R_a)}{[R_a(1-R_x)+R_e]} \tag{20c}$$

$$D=\frac{(R_e+R_a+R_x)(1+R_a)-(R_x+R_a)\ \frac{R_e}{1+n}}{R_a+R_x+\frac{n}{1+n}R_e} \tag{20d}$$

$$T=\frac{(R_a+R_x+\frac{n}{1+n}R_e)(1+R_a)T_o}{R_a(1-R_x)+R_e} \tag{20e}$$

The time constant equation 20e may be simplified to

$$T=T_o\frac{(R_e'+R_x)(1+R_a)}{R_s-R_a R_x} \tag{21}$$

where R_s is the synchronous resistance, and R_e' is the transient resistance. If full load field time constant $T_o(1+R_a)$ is designated T_{FO}, and fault resistance is negligible, then

$$T=T_{FO}\frac{R_e'}{R_s} \tag{22}$$

Appendix II. Short Circuit of Compound Machine

In the series machine, armature current contributes to direct axis magnetomotive force. If the ratio of series field magnetomotive force to shunt field magnetomotive force at full load is k, then equations 3, 4, and 5 become

$$E_t=(i_f+ki_a)-R_a i_a-R_e(i_a-i_1) \tag{23}$$

$$E_t=R_f i_f+L_f\frac{di_f}{dt}-M\frac{d}{dt}(i_a-i_1) \tag{24}$$

$$E_t=R_x i_a \tag{25}$$

In addition to this change, the value of M must be altered to take into account the increased mutual inductance associated with the presence of the series field. The total mutual inductance can be considered as comprising two components: (1) that resulting from R_e and (2) that resulting from the series field. From equation 14 the mutual inductance attributable to R_e is $(L_f R_e)/(1+n)$. From a similar derivation, using the series field current required to produce a change in shunt field flux linkages equal to the no load full voltage linkages, it can be shown that the series field contribution to mutual inductance is $-L_f k$ (neglecting leakage flux between the shunt and series fields). The value of M then becomes $L_f[(R_e/1+n)-k]$.

In the compound wound machine, the initial value of field current must reflect the series field magnetomotive force contribution. For full voltage, full load, the shunt field current is $(1+R_a-k)$ per unit and the corresponding field resistance $1/(1+R_a-k)$ per unit.

Substituting and solving as in the case of

shunt machine, the constants A, B, C, D, and T of equation 18 become

$$\left.\begin{aligned}
A &= \frac{R_e}{(R_a-k)(1-R_x)+R_e} \\
B &= \frac{1+R_o+R_e\dfrac{n}{1+n}}{R_x+R_a+\dfrac{n}{1+n}R_e} \\
C &= \frac{R_xR_e(1+R_a-k)}{(R_a-k)(1+R_x)+R_e} \\
D &= \frac{\left[(R_a+R_e+R_x-k)(1-R_a)-\dfrac{R_e}{1+n}(R_a+R_x+kn)\right]}{R_x+R_a+R_e\dfrac{n}{1+n}} \\
T &= \frac{\left(R_x+R_a+\dfrac{n}{1+n}R_e\right)(1+R_a-k)}{(R_a-k)(1-R_x)+R_e}T_o
\end{aligned}\right\} \quad (26)$$

The peak armature current obtained by use of the values of equation 23 is

$$\frac{1+R_a+\dfrac{n}{1+n}R_e}{R_x+R_a+R_e\dfrac{n}{1+n}}$$

or the same value as obtained from the values for the shunt machine given in equation 19.

Appendix III

The equations derived in Appendix I and Appendix II disregard effects of residual flux, saturation, and armature inductance. It is convenient to have empirical relations taking these effects into account. These relations can be obtained by using the peak current values and time constants from Appendix II and the initial rate of rise and final steady current from other data. The complete equation for armature current then becomes

$$i_a = I_s + (I_p - I_s)\epsilon^{-t/T} - I_p\epsilon^{-t/T} \quad (27)$$

where

I_s = steady current value following short circuit

I_p = peak current value following short circuit from equation 26,

$$\left[\frac{1+R_a+R_e\dfrac{n}{1+n}}{R_x+R_a+R_e\dfrac{n}{1+n}}\right]$$

T = time constant of current decay from equation 26

$$\frac{\left(R_x+R_a+\dfrac{n}{1+n}R_e\right)(1+R_a-k)}{(R_a-k)(1-R_x)+R_e}T_o$$

T' = time constant corresponding to the initial rate of current rise. If i' is the initial rate of current rise in per unit per second, then $T' = \dfrac{I_p - I_s}{i'}$

References

1. Electrical Transmission and Distribution Reference Book, Westinghouse Manufacturing Company, 1943, page 135.

2. Protection of Large D-C Machines by Means of High-Speed Circuit Breakers, **J. E. Housley, O. Jensen.** AIEE Transactions, volume 63, 1944, September section, pages 637–40.

3. Present D-C Aircraft Electric Supply Systems, **H. C. Anderson, S. B. Crary, N. R. Schultz.** AIEE Transactions, volume 63, 1944, June section, pages 265–72.

4. Transients in Linear Systems (book), **Gardner, Barnes.** J. Wiley, Inc., New York, N. Y., 1942.

5. D-C Machine Flashover and Bus Short-Circuit Protection, **T. B. Montgomery, J. F. Sellers.** AIEE Transactions, volume 60, 1941, pages 1168–73.

6. Short Circuit Current and Protection of Large Direct Current Generators, **H. Hess.** *Archiv fuer Elektrotechnik*, volume 27, 1933, page 467.

7. Transients in Arc Welding Generators, **A. R. Miller.** AIEE Transactions, volume 52, March section, 1933, pages 260–7.

8. Principles of Direct-Current Machines (book), **A. S. Langsdorf.** Mc Graw-Hill Book Company, New York, N. Y. Fourth edition, 1931. Page 214.

9. Synchronous Machines—IV, **R. E. Doherty, C. A. Nickle.** AIEE Transactions, volume 47, 1928, April section, pages 457–87.

10. Three-Phase Short Circuit Synchronous Machines—V, **R. E. Doherty, C. A. Nickle.** AIEE Transactions, volume 49, 1930, April section, pages 700–14.

The Influence of the Concentration and Mobility of Ions on Dielectric Loss of Insulating Oils

BUN PO KANG
ASSOCIATE AIEE

Synopsis: The causes of dielectric loss in insulating oils and the means to reduce it to a minimum have always been important in high voltage engineering. In this study the relationships between the amount of impurities, which furnish a source of free ions in an oil, and the viscosity, which influences the mobility of the ions, on the one hand and the dielectric loss on the other are investigated. The results present some definite relationships between them and point out that in two oils of the same "electrical purity," the one with higher viscosity will have lower dielectric loss.

SINCE DIELECTRIC LOSS is a matter of primary importance in high voltage insulation, many phases of the phenomenon have been a subject of frequent discussion among high voltage engineers. In liquid dielectrics, such as mineral oils which are used extensively for transformer and cable insulations and for many other purposes, the loss has been found to be caused largely by ionic conduction.[1,2] In a few cases, dielectric absorption caused by molecular polarization has been found to be present also.[1] However, polarization in oils resulting in an absorptive component of dielectric loss seldom appears significant.

In the study of the nature of and the mechanism that causes dielectric loss in oil, where the loss is due to ionic conduction alone, there are two important factors which merit investigation. In order to have ionic conduction, the oil must possess ions, and the ions must be free to move. If the ion content of an oil is constant, the dielectric loss should vary inversely as the viscosity. It has been found that within a limited rage of temperature, this relation holds true, and the product of the conductivity and the viscosity of the oil is approximately a constant. This product has been suggested as a measure of the free ion content, which has also been termed the "electrical purity" of the liquid.[3]

Under constant electric stress, the dielectric loss for liquids without significant dielectric absorption is proportional to the conductivity of the liquid.

$$W = \frac{\lambda A E^2}{L} \qquad (1)$$

where

A is the area of electrode in square centimeters
L is the electrode separation in centimeters
E is the applied potential in volts
λ is the conductivity in mhos per centimeter
W is the dielectric loss in watts

Since in the cases of ionic conduction the conductivity should be directly proportional to the ion content, it follows that the ion content also should be proportional to the product of the viscosity and the dielectric loss. However, this is not always borne out by experiment except within a very small range of temperature. If the range of temperature be extended, the ion content is found to increase with temperature. Apparently this is caused by thermo-agitation, which in turn causes further ionic dissociation and the generation of new ions within the oil.[4]

For the same degree of purification, the dielectric loss is invariably lower in an oil of higher viscosity. Even though the amount of impurity and the number of ions present in two different oils may be identical, the mobility of the ions is much greater in the oil of lower viscosity and consequently the conduction current is higher.

Since it is not only interesting but useful to know the relationships between the concentration and mobility of the ions of an insulating oil on the one hand and dielectric loss on the other, it is the purpose of this work to establish a correlation between them.

The Experiment

Three original oils, designated as oil sample 1, oil sample 6, and oil sample 7, were used. Samples 1 and 7 were highly refined oils furnished by well-known refineries, sample 1 being of low viscosity and sample 7 being of high viscosity. Sample 6 was an oil known to be highly susceptible to oxidation and was subjected to severe oxidation at 150 degrees centigrade under atmospheric condition for seven days. Oil samples 2 to 5 were mixtures of samples 1 and 6 (by weight) at 10, 25, 50, and 75 per cent, respectively, of oil 6. Oil samples 8 to 11 were mixtures of oils 7 and 6 in similar percentages.

For the measurements of viscosity and dielectric loss, these samples were classified into two groups. Group A, oil samples 1 to 6, consisted of the low viscosity samples, and group B, oil samples 7 to 12, consisted of the high viscosity samples. Samples 6 and 12 were the same oil.

Viscosity measurements were made with a standard Saybolt viscosimeter. The 60-cycle power factor measurements were made with an Atkinson bridge.[5] The samples were measured in a nickel cell with an electrode area of 40.742 square centimeters and a distance of separation of 1.27 millimeters at a voltage stress of 197 volts per millimeter. The values of dielectric loss given on the following figures are the total loss of each specimen under test. If the loss per centimeter cube is desired, these values

Paper 46-110, recommended by the AIEE committee on basic sciences for presentation at the AIEE summer convention, Detroit, Mich., June 24–28, 1946. Manuscript submitted June 27, 1945; made available for printing May 1, 1946.

BUN PO KANG is a research engineer with the plastics department of the E. I. du Pont de Nemours and Company and an electrical engineer on leave of absence from the Yungli Chemical Industries, Ltd., China. This paper was written when he was a post-doctoral scholar at Johns Hopkins University and concurrently an engineer with the high tension laboratories of the General Cable Corporation. He wishes to acknowledge his appreciation to Professor J. B. Whitehead and Mr. R. W. Atkinson for their interest and advice concerning this work, and the General Cable Corporation for the use of its facilities.

Table I. Viscosities of the Oil Samples at Different Temperatures

Sample	40 C	60 C	80 C	100 C	120 C	150 C
1	—	0.086	0.05	0.031	0.02	—
2	0.21	0.10	0.055	0.035	0.021	—
3	0.305	0.13	0.073	0.046	0.03	—
4	0.65	0.23	0.115	0.065	0.04	—
5	1.60	0.53	0.205	0.10	0.06	—
6	4.90	1.10	0.40	0.17	0.094	0.048
7	5.00	1.40	0.54	0.24	0.14	0.074
8	—	1.40	0.54	0.24	0.135	0.069
9	—	1.35	0.505	0.23	0.13	0.066
10	—	1.35	0.455	0.201	0.105	0.06
11	—	1.20	0.43	0.19	0.10	0.059
12	4.90	1.10	0.40	0.17	0.094	0.048

The values of viscosity given are in poises.

Table II. Power Factor and Dielectric Loss of Oil Samples in Group *A*

Sample		40 C	60 C	80 C	100 C	120 C	150 C
1	Capacitance	—	66.7	66.1	65.7	65.0	—
1	Power factor	—	0.18	0.41	0.61	1.56	—
1	Dielectric loss	—	2.9	6.3	12.6	23.9	—
2	Capacitance	67.7	67.2	66.7	66.0	65.5	—
2	Power factor	0.55	1.59	4.39	10.20	18.25	—
2	Dielectric loss	8.82	25.2	69.3	167.5	283.0	—
3	Capacitance	68.6	67.9	67.5	66.7	66.0	—
3	Power factor	0.82	2.58	7.10	17.2	33.8	—
3	Dielectric loss	13.2	41.5	113.0	272.0	530.0	—
4	Capacitance	69.4	68.8	68.5	67.6	67.2	—
4	Power factor	0.75	2.72	7.85	20.1	36.3	—
4	Dielectric loss	11.95	44.1	127.5	322.0	575.0	—
5	Capacitance	70.7	70.0	69.4	69.0	68.5	—
5	Power factor	0.36	1.85	6.52	19.7	39.9	—
5	Dielectric loss	5.97	30.2	107.0	322.0	642.0	—
6	Capacitance	71.8	71.0	70.5	69.5	68.8	68.1
6	Power factor	0.19	0.98	4.55	15.7	42.5	89.8
6	Dielectric loss	3.75	16.4	75.6	258.0	693.0	1450.0

Capacitance is given in micromicrofarads, power factor in per cents, and dielectric loss in microwatts.

must be multiplied by a factor of 0.00312, which is the ratio of L/A, where L is the distance of separation and A is the effective area. The voltage stress was kept low to utilize the linear portion of the well-known current-voltage relation curve. For group A, the low viscosity oils, readings were taken at 40, 60, 80, 100, and 120 degrees centigrade for each sample, and for group B, the high viscosity group, readings were taken at 60, 80, 100, 120, and 150 degrees centigrade.

Experimental Results

The specific gravity temperature relations of the three original oil samples are given in Figure 1. The specific gravity of each of the mixtures at various temperatures can be computed easily from these curves by the use of the following relations:

$$\rho_x = \frac{\rho_1\rho_2(W_1+W_2)}{\rho_1 W_2+\rho_2 W_1} \qquad (2)$$

where

ρ_1, ρ_2 represent the specific gravities of the components

ρ_x represents the specific gravities of their mixture

W_1, W_2 represent the weights of the components

After converting the viscosity readings at different temperatures for each sample from Saybolt seconds into poises, the results were given in Table I. To follow the more customary way of representing relationships of this kind, the logarithm of viscosity was plotted against the reciprocal of the absolute temperature in Figures 2 and 3. It is quite obvious that the relationship is essentially logarithmic. However, none of the curves is exactly a straight line but only very near to one.

The values of power factor and dielectric loss for each mixture at different temperatures are given in Table II for group A, and Table III for group B. Figure 4 gives the relations of the logarithm of dielectric loss as a function of the reciprocal of absolute temperature. Several of these curves are essentially straight lines and others are quite near to straight lines within limited range of temperatures. These relations may be expressed as

$$W = A - \frac{B}{T} \qquad (3)$$

where

W is dielectric loss in microwatts

T is temperature in degrees Kelvin

A and B are constants

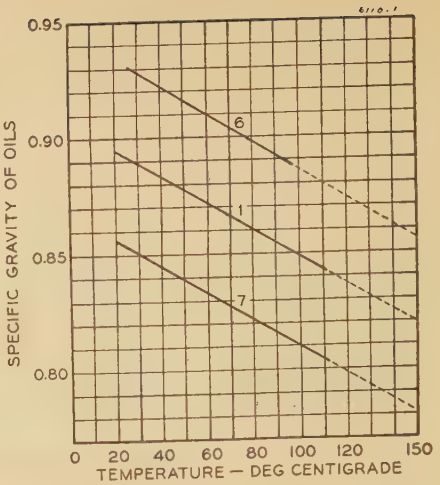

Figure 1. The variation of specific gravity with temperature of the original oil samples

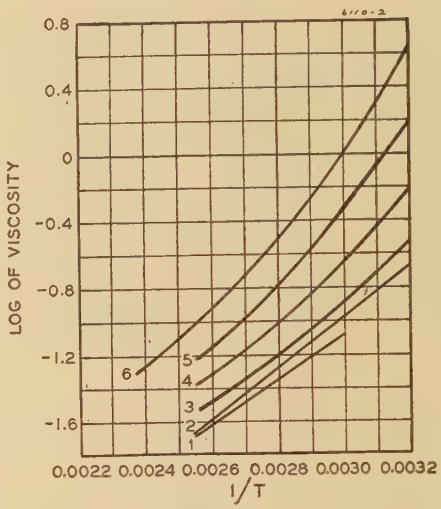

Figure 2. The viscosity–temperature characteristics of the oil samples in group *A*, η being viscosities in poises, *T* being temperatures in degrees Kelvin, and numbers designating the oil samples

which are similar to the expression used by Fuoss for the relation between conductivity and temperature.[6]

Dielectric Loss and Viscosity Relation

Based on the curves of Figures 2, 3, and 4, a relationship between viscosity and dielectric loss of each sample can be established. Figure 5 presents clear evidence that the relation is logarithmic,

$$\log W = A - B \log \eta \qquad (4)$$

The curves are approximately straight lines within reasonable allowance for experimental error, and each group of samples appears to have a constant slope of its own. These results confirm the prediction of other workers in this field.[4]

Discussion

Since the dielectric loss of sample 6 is much higher than that of samples 1 and 7 (from 6 to 30 times under similar conditions), the ions present in the various mixed samples may be assumed as coming from sample 6. If there were no other causes for further dissociation in the oil, the dielectric loss of each sample should be a linear function of the percentage of deteriorated oil added. Figure 6 shows dielectric loss as a function of percentage of deteriorated oil added at different constant temperatures. The curves of group *A* for temperatures below 100 degrees centigrade show an increase of dielectric loss with the percentage of deteriorated oil added, but only up to a certain point, and beyond this point the losses decrease again. The ascending portion of each curve is caused by the increase of ion content of the specimen by adding a larger quantity of deteriorated oil. Since the deteriorated oil, sample 6, has much higher viscosity than sample 1, upon addition of sample 6, the viscosity of the mixture increases rapidly. Even though the ion content continues to increase, the mobility of these ions is greatly reduced by the increase in viscosity. After reaching a certain point, the viscosity becomes so high that even though the ion content continues to increase, the mobility of the ions diminishes rapidly and the dielectric loss decreases again.

Based on these curves, if one assumes that the ion content N is equal to the product of viscosity η and dielectric loss W, mathematical analysis shows that in Figure 6 all curves in group *A* should pass through a maximum, but not the curves in group *B*. This is found to be true. However, because of the fact that sludges and other solid impurities might have been formed in oil 6 because of oxidation, the viscosities of the mixtures did not follow exactly the relation usually used for computing the viscosity of mixtures of nonpolar liquids.

$$\frac{1}{\eta_x}=\frac{X}{\eta_1}+\frac{1-X}{\eta_2} \tag{5}$$

where

η_1, η_2, η_x are viscosities of the components and the mixture

X is the percentage of the liquid with viscosity η_1

The theoretical values are lower in comparison with experimental data. Based on theoretical considerations, one can show that the maximums of dielectric loss occur when

$$X=\frac{\eta_1}{2(\eta_1-\eta_2)} \tag{6}$$

provided η_1 is not equal to η_2. The experimental values deviated from this prediction somewhat because of the high viscosities obtained. However, the general shapes of the curves support very well the assumption that

$$W=\frac{N}{\eta} \tag{7}$$

In group *B*, both samples 6 and 7 have approximately the same viscosity; in fact, the viscosity of sample 6 is a little lower than the viscosity of sample 7, and consequently the increase of the percentage of deteriorated oil increases both the concentration and mobility of the ions, and the conduction current and dielectric loss also are increased.

In a limited range of temperature within which new ions are not generated by thermo-agitation in the oil, the dielectric loss should be proportional to the percentage of deteriorated oil added if the viscosity of the mixture is kept constant. This is found to be true for samples of higher viscosities according to Figure 7, curves *B* and *C*. In this group the viscosities of the two components were only slightly different, and the temperature differences were small when the samples were brought to the same viscosity. Consequently, thermal effects may be considered negligible.

If the viscosities of the two components

Table III. Power Factor and Dielectric Loss of Oil Samples in Group *B*

Sample		60 C	80 C	100 C	120 C	150 C
7	Capacitance	64.0	63.2	62.8	62.4	61.1
7	Power factor	0.062	0.25	0.59	1.28	3.96
7	Dielectric loss	0.945	3.78	8.82	18.9	57.3
8	Capacitance	64.5	64.0	63.2	62.8	61.8
8	Power factor	0.25	0.58	1.51	3.05	9.0
8	Dielectric loss	3.78	8.82	22.7	45.3	132.48
9	Capacitance	65.5	65.2	64.5	63.8	63.0
9	Power factor	0.31	1.11	3.05	6.7	14.8
9	Dielectric loss	4.73	17.0	46.7	101.0	220.0
10	Capacitance	67.5	66.8	66.3	66.0	64.5
10	Power factor	0.56	1.99	6.01	13.3	25.5
10	Dielectric loss	8.82	31.5	94.5	208.0	392.0
11	Capacitance	69.3	68.6	67.9	67.2	67.1
11	Power factor	0.81	3.42	11.0	24.2	47.6
11	Dielectric loss	13.25	55.5	177.0	385.0	756.0
12	Capacitance	71.0	70.5	69.5	68.8	68.1
12	Power factor	0.98	4.55	15.7	42.5	89.8
12	Dielectric loss	16.4	75.6	258.0	693.0	1450.0

Capacitance is given in micromicrofarads, power factor in per cent, and dielectric loss in microwatts.

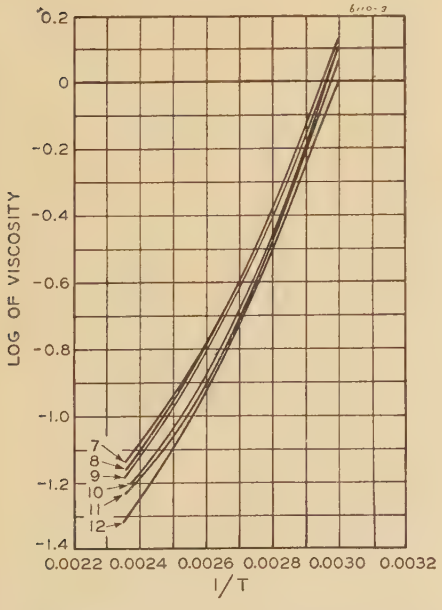

Figure 3. The viscosity–temperature characteristics of the oil samples in group *B*, η being viscosities in poises, *T* being temperatures in degrees Kelvin, and numbers designating the oil samples

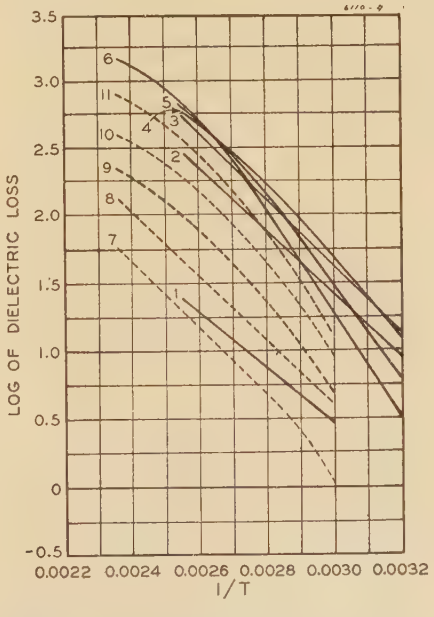

Figure 4. The variation of dielectric loss with temperature, loss being given in microwatts, temperature in degrees Kelvin, solid lines for oils in group *A*, and dotted lines for oils in group *B*

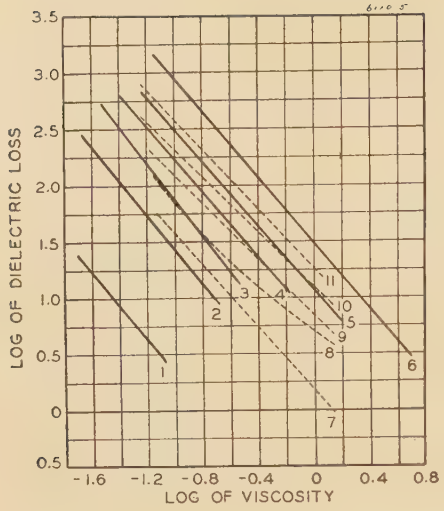

Figure 5. The variation of dielectric loss with viscosity, loss being given in microwatts and viscosity in poises

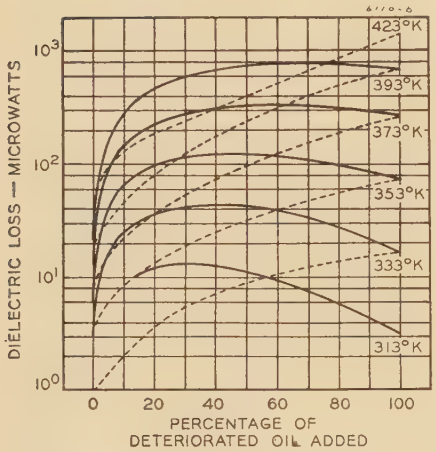

Figure 6. The variation of dielectric loss with percentage of deteriorated oil added at various temperatures, solid lines representing oils in group *A* and dotted lines, oils in group *B*

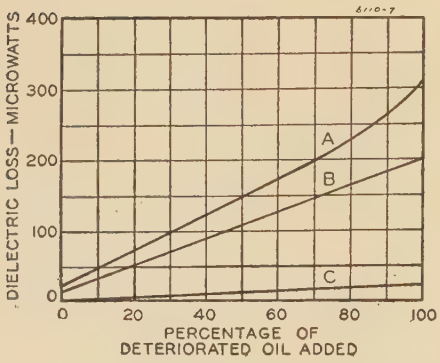

Figure 7. The influence of deteriorated oil on dielectric loss at constant viscosity for high viscosity mixtures

Curve *A* at 0.15 poise, curve *B* at 0.2 poise, and curve *C* at 1.0 poise

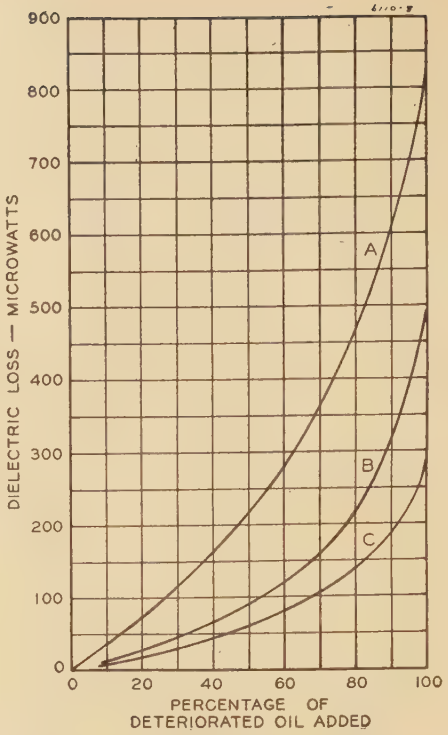

Figure 8. The influence of deteriorated oil on dielectric loss at constant viscosity for low viscosity mixtures

Curve *A* at 0.08 poise, curve *B* at 0.15 poise, and curve *C* at 0.2 poise

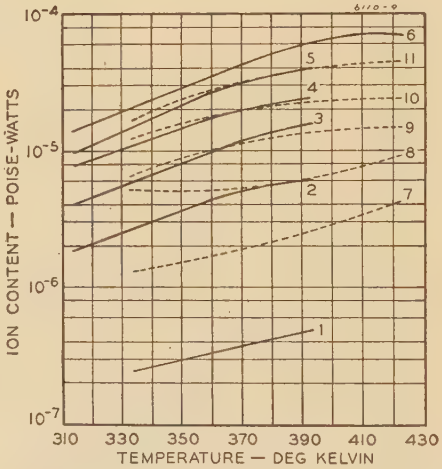

Figure 9. The variation of ion content with temperature, solid lines representing oils in group *A* and dotted lines, oils in group *B*

of the mixture are greatly different, the dielectric loss does not follow the percentage of deteriorated oil added. Figure 8 shows this relation. The increase in temperature required to bring the heavier oil to the same viscosity causes thermoagitation and results in furthur ionic dissociation in the oil, principally from the impurity content, which accounts for the unusually rapid rise of dielectric loss at the higher percentages of the added deteriorated oil.[7]

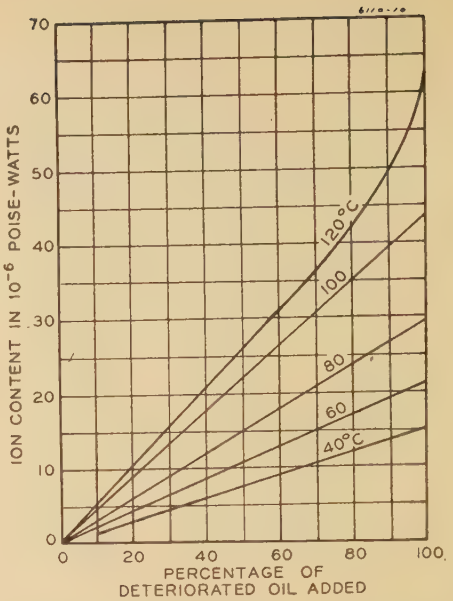

Figure 10. The influence of deteriorated oil on ion content at constant temperature for low viscosity mixtures

In order to substantiate the assumption that temperature increase will increase the concentration of ions in the oil, two sets of curves are plotted in Figure 9, using ion content as a function of temperature for each mixture. The values of ion content for different samples are taken as that which was suggested by Whitehead, namely, the product of conductivity and viscosity.[8] For want of a suitable unit to express ion content, these values are expressed in poise-watts. In these particular cases, dielectric loss is used instead of conductivity. As it has been seen in equation 1 that for a constant value of applied voltage, the dielectric loss is a linear function of conductivity. The curves will have the same slope whether dielectric loss or conductivity is used as the ordinate. If the temperature rise should have no effect on the ion content, these two sets of curves ought to be horizontal lines. In the actual cases the curves are found to rise with temperature, having almost similar constant slopes for each group. Based on the average slope of these curves, the relations may be expressed in the equation

$$\log \frac{N_2}{N_1} = 0.008T \qquad (8)$$

where

N_1 is the ion content at temperature 1
N_2 is the ion content at temperature 2
T is the difference in temperature in degrees Kelvin

In a more general form, this expression may be written as

$$N_2 = N_1 e^{cT}$$

A New Electronic Timing Relay for Reducing Outages on Power Circuits

FRANK S. DLOUHY
ASSOCIATE AIEE

Synopsis: This paper describes a new timing relay for controlling relaying time on automatically reclosed circuit breakers on which inverse-time overcurrent relays are supplemented by instantaneous overcurrent relays. This device incorporates the advantages of instantaneous circuit breaker opening on the first, and in some cases the second, tripout to clear transient faults, and inverse-time opening on subsequent tripouts to obtain co-ordination with branch or sectionalizing fuses. It was designed for universal application on feeder circuits of the Oklahoma Gas and Electric Company system. Certain features which provide for optimum service reliability were incorporated in the design.

EVEN THOUGH all possible protective measures of prevention have been taken in the design of overhead circuits, faults, the majority of which are transitory in nature, still will occur. In order to minimize damage to equipment and interruption to service, the faulted section must be isolated promptly from the rest of the system. Experience has shown that transmission and distribution circuits, on which fault duration is limited to a maximum of 0.2 second, will seldom be out of service for long periods of time as a result of damaged insulators or burned conductors at the point of fault, except in peculiar cases of rare occurrence. Thus, the speed with which protective relays and circuit breakers operate to clear abnormal conditions has a direct bearing on service reliability.

The practice of instantaneous tripping of the source breaker for a fault at any point on the circuit is, by definition, a protective measure of amputation. But, when supplemented by rapid automatic reclosing, its effect on the ultimate load entitles it to be classified as a protective measure of mitigation. It limits the occurrence of permanent faults which are initiated by transient disturbances. In addition, it restricts branch or sectionalizing fuse operation, where possible, to faults of a permanent nature, and thereby reduces long outages on branches or sections of the circuit. Consequently, the realization of the advantages of instantaneous tripping supplemented by immediate initial reclosure has furnished an incentive for designing many ingenuous relaying schemes.

Probably the most effective and certainly the most economical method of securing high-speed relaying on circuit breakers serving multibranch fused circuits is that of superimposing controlled instantaneous overcurrent relays on inverse-time overcurrent relays, and utilizing immediate initial reclosure. This applies to the ground relay as well as the phase relays on grounded neutral circuits. The instantaneous relays are set, where possible, to initiate circuit breaker clearing of faults at any point on the circuit. When these relays are utilized for the second as well as the initial tripout, inrush magnetizing current transients following the initial reclosure may place a minimum limit on the pickup setting.

The co-ordination desired from this type of protective scheme is protection to the entire circuit during the first, and in some cases the second, tripout, in order to give temporary faults, such as flashovers resulting from lightning or momentary conductor contacts, an opportunity to clear before permanent damage occurs and before a branch or section is interrupted by fuse operation. Thus, in the case of faults which are cleared on the initial tripout, a momentary service interruption is substituted for a long outage from damaged equipment or blown fuses. In effect, this momentary service interruption is no more adverse than the voltage

Paper 46-80, recommended by the AIEE committee on protective devices for presentation at the AIEE South West District meeting, San Antonio, Tex., April 16–18, 1946. Manuscript submitted January 22, 1946; made available for printing March 7, 1946.

FRANK S. DLOUHY is relay engineer, Oklahoma Gas and Electric Company, Oklahoma City, Okla.

This gives further substantiation that the ion content is a function of temperature.

Following this indication, it suggests that if temperature should be kept constant, the value of ion content would be a definite function of the percentage of deteriorated oil added. Curves plotted using ion content as a function of percentage of deteriorated oil added at each temperature are shown in Figure 10. These curves show definitely that the ion content is a linear function of the percentage of deteriorated oil added when temperature is reduced to a constant.

Conclusion

This study shows that

1. Provided there is no dipole loss, the relationship between the dielectric loss W and viscosity η of an insulating oil may be expressed as

$$\log W = A - B \log \eta$$

which points out that the mobility of ions is an important factor in dielectric loss of an insulating oil.

2. Thermo-agitation, which causes further dissociation of the oil, increases dielectric loss by increasing the number of ions present.

3. Dielectric loss is increased rapidly by the addition of deteriorated oil. This bears out that dielectric loss is a function of the concentration or content of free ions in the oil.

4. An increase in concentration of ions in an oil may result in an actual decrease in dielectric loss if the viscosity is increased to the point where the mobility of the ions is decreased relatively more than the ion concentration is increased.

5. If nonpolar oils of the same degree of "electrical purity" are used for the low frequency or 60-cycle applications where the flow of the liquid is not important, it is seen that an oil of higher viscosity is preferable from the standpoint of lower dielectric loss.

References

1. THE CONDUCTIVITY OF INSULATING OILS—II, **J. B. Whitehead.** AIEE TRANSACTIONS, volume 50, 1931, pages 692 8.

2. THE CONDUCTIVITY OF INSULATING OILS UNDER ALTERNATING CURRENT STRESS, **J. B. Whitehead, B. P. Kang.** *Journal of Applied Physics*, volume 11, September 1940, pages 596–603.

3. THE DIELECTRIC LOSSES IN IMPREGNATED PAPER, **J. B. Whitehead.** AIEE TRANSACTIONS, volume 52, 1933, pages 667–81.

4. LIQUID DIELECTRICS (book), **A. Gemant.** John Wiley and Sons, New York, N. Y. Pages 67–8.

5. HIGH TENSION BRIDGE FOR MEASUREMENT OF DIELECTRIC LOSS IN CABLES, **R. W. Atkinson.** *The Electric Journal*. February 1925, page 58.

6. ELECTRICAL PROPERTIES OF POLYVINYL CHLORIDE-DIPHENYL SYSTEM, **R. M. Fuoss.** *Journal of American Chemical Society*, volume 63, February 1944, page 382.

7. LIQUID DIELECTRICS (book), **A. Gemant.** John Wiley and Sons, New York, N. Y. Page 69.

8. IMPREGNATED PAPER INSULATION (book), John Wiley and Sons, New York, N. Y. Page 57

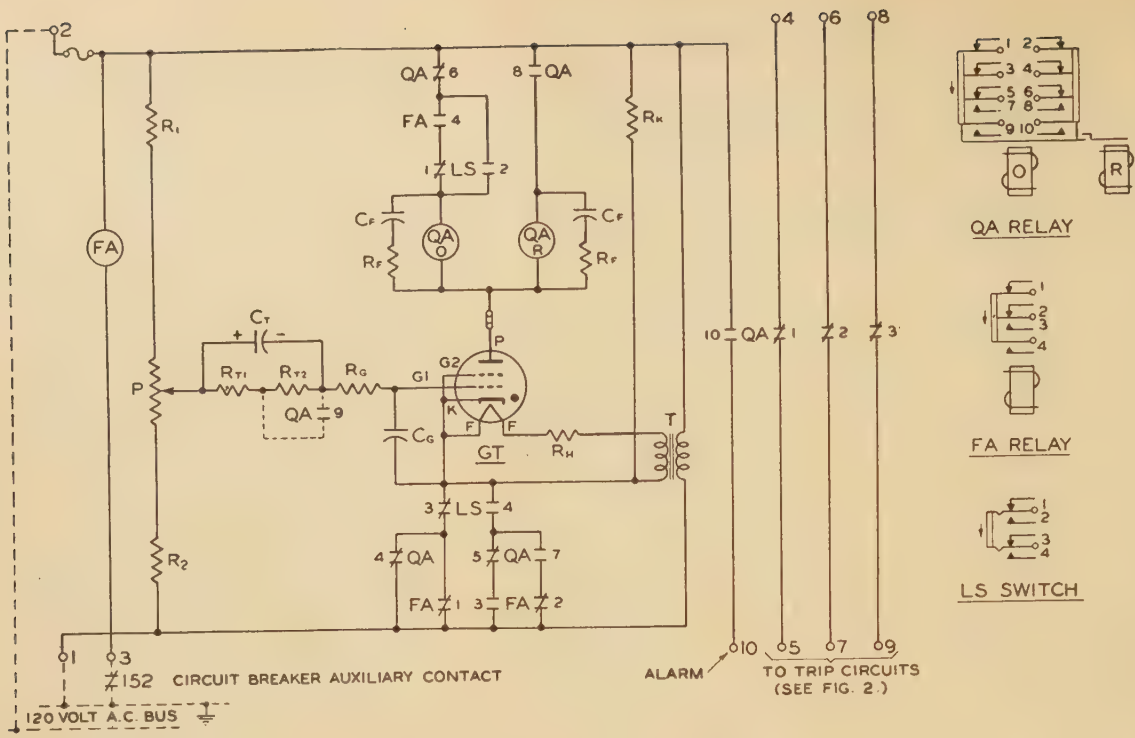

Figure 1. Schematic diagram of the electronic timing relay assembly

disturbance created by a longer clearing time of a fuse. When instantaneous relay protection is also utilized on the second tripout, the time interval between the initial and the second reclosure should be made as short as the imposed circuit breaker duty will permit in order to minimize outage time. Thus, in the case of transient faults which are not cleared initially but disappear on the second tripout, a 30- to 60-second service interruption is substituted for a probable long outage on some portion of the circuit.

To provide backup protection and selectivity between the circuit breaker and the branch or sectionalizing fuses in the event of a permanent fault, the instantaneousrelays must be removed from service prior to the initial, or in some cases the second, reclosure, and the inverse-time relays depended upon for subsequent tripping. Through time–magnitude coordination, the inverse-time relays will permit branch or sectionalizing fuses to clear the faulted section before initiating breaker operation for backup protection. Where sufficient co-ordination can be realized, these relays are seldom called upon to clear a fault.

Also, in the event of punctured insulators or lightning arresters, the prolonged arcing time secured on the inverse-time relays may produce additional damage and perhaps shatter the faulty equipment. This will permit the fault to be more easily located by patrolmen.

Once removed from service, the instantaneous relays should be held inoperative for a definite time after a reclosure as assurance that the fault was not permanent; otherwise, in the absence of selectivity a lockout of the circuit breaker will occur, resulting in a needless long outage on the entire circuit. To accomplish this, a preset time delay must be interposed between each reclosure and reestablishment of the instantaneous relays. This reset timing is as important in preventing long outages as the instantaneous relays themselves. It should be the minimum time necessary to determine a successful reclosure in order to provide instantaneous relay protection against the contingency of rapidly recurring transient faults.

It is apparent from the foregoing that an auxiliary device capable of the following functions is required:

It must remove the instantaneous relays from service prior to the initial, and in some cases the second, reclosure.

It must hold them inoperative until a successful reclosure is assured and then reinstate them to re-establish initial conditions for future disturbances.

Description of the Timing Relay

In view of the fact that a device fulfilling the foregoing requirements was not available and that existing methods of changing relaying time have certain undesirable features, an electronic timing relay was designed for universal application with relaying schemes utilizing instantaneous and inverse-time overcurrent relays. Briefly, it consists of an assembly of two telephone type relays, a thyratron timing tube, and associated electronic control components mounted in a small drawout case. Figure 1 is a schematic diagram of the assembly in which:

Thyratron *GT* is a gas tetrode, similar to type 2050, operated as a negative control tube. Its operation is discussed under "Theory of the Timing Circuit."

Relay *QA* is a telephone type electric-interlocking relay. It consists of two quick-acting relays mounted as a unit with their armatures mechanically interlocked. When lockup relay *QA-O* is energized, its armature latches and holds its contacts in the operated position until the release relay *QA-R* is energized to trip the latch. The release relay *QA-R* does not latch, but drops out when it is de-energized. Since these relays are pulse operated through their own contacts, a filter consisting of capacitor C_F in series with resistor R_F is shunted across each coil to assure positive operation.

Relay *FA* is a telephone type a-c relay operated as an equivalent circuit breaker auxiliary switch. Its unoperated position corresponds to the closed position of the circuit breaker.

Lever Switch *LS* is a double-pole double-throw selector switch which provides the selection of either one or two instantaneous relay operations.

Transformer *T* is a voltage dropping transformer for supplying the heater of the thyratron.

Other components: Resistors R_H and R_G are merely current limiting resistors. Capacitor C_G provides protection against high voltage transients. The functions of the other components are discussed with reference to Figure 3 under "Theory of the Timing Circuit."

To avoid confusion, the graphical symbols used in all the diagrams are, insofar

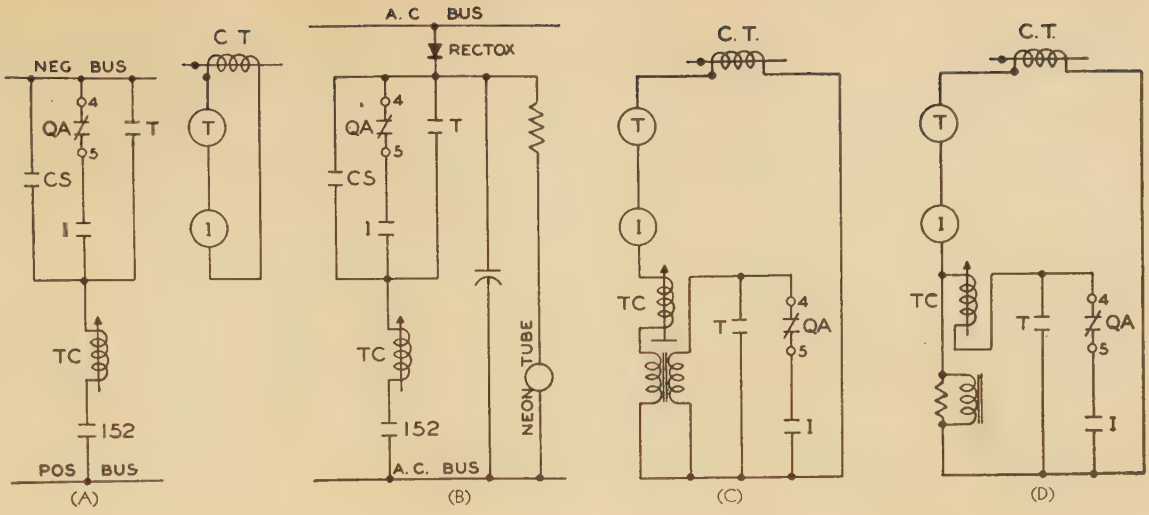

Figure 2. Location of electronic timing relay contacts in breaker tripping circuits

I—Instantaneous overcurrent relay
T—Inverse-time overcurrent relay
QA—Electronic timing relay (Figure 1)

A—D-c method
B—Capacitor method
C—Transformer method
D—Reactor method

as possible, those recommended by American Standards Association. Device contacts are shown for the de-energized or unoperated position of the device. All tube voltages are referred to the equipotential cathode. Instantaneous values of varying electrical quantities are represented by lower case letters, and their peak values by capital letters. Where possible, subscripts are chosen so as to be indicative of that portion of the circuit to which they apply.

Theory of the Timing Circuit

The basis of the timing relay design is the electronic timing circuit shown schematically in Figure 3, in which timing action is obtained by grid amplitude bias of the gas tetrode *GT*, acting as an inertialess circuit closing or opening device in series with relay *QA*.

An alternating voltage e_L of commercial frequency is impressed between *L*1 and *L*2, and the tube heater circuit is energized from a filament transformer (not shown). The fixed resistors R_1 and R_2 in series with potentiometer *P* form a voltage divider circuit for controlling the potential applied to the control grid *G*1. With switch *S*1 open and switch *S*2 closed, unidirectional pulsating electron current flows from the cathode *K* to the grid *G*1 during the half cycles in which *L*1 and the grid are positive with respect to *L*2 and the cathode. As a result of this rectification, a charge of the indicated polarity will accumulate in the timing capacitor C_T and which will be maintained as long as switch *S*1 is open. Also, with switch *S*1 open, the cathode *K* is connected through resistor R_K to line *L*2 and is approximately at the same potential as the anode *P*; consequently, no electron current flows from cathode to the anode to energize the relay even though switch *S*2 is closed.

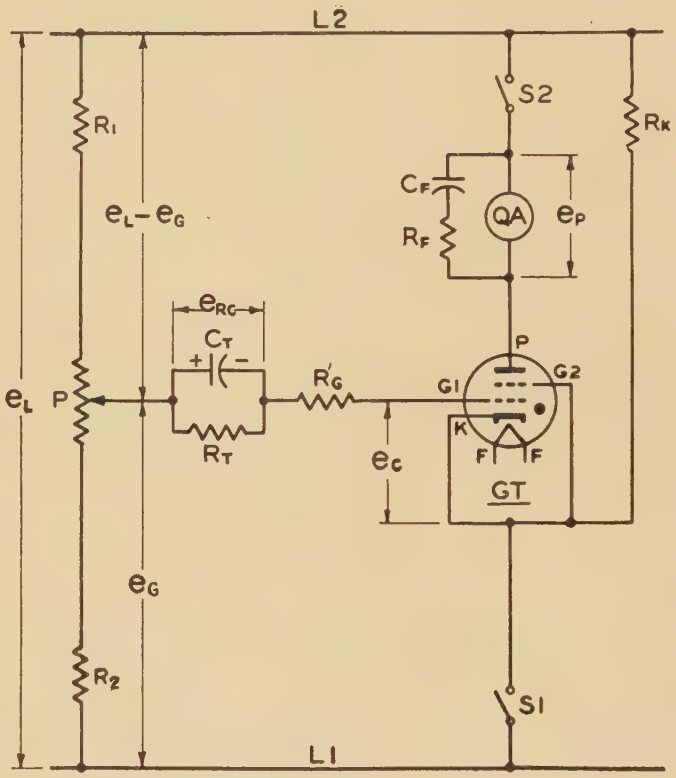

Figure 3. Schematic diagram of the electronic timing circuit

When switch *S*1 is closed, the cathode is connected directly to line *L*1 which impresses voltage e_L across the anode–cathode circuit and superimposes an alternating voltage e_G (in phase with the anode voltage) on the negative grid bias voltage E_{RC} of the timing capacitor C_T. The alternating component e_G of the grid bias voltage e_c tends to drive the grid positive at the same time the anode is positive; however, the tube does not conduct between cathode and anode until the grid bias voltage e_c is equal to or more positive than the critical ionization value determined from the tube's control characteristic.

The instantaneous relationship of the anode and control-grid voltages is shown graphically in Figure 4, in which time is reckoned from the instant switch *S*1 is closed, and the alternating voltages are zero and increasing in the positive direction. It is apparent from this graphical representation that the magnitude of the grid bias voltage is a time function of both the unidirectional component e_{RC} and the alternating component e_G and defined by the equation

$$e_C = e_{RC} + e_G \qquad (1)$$

in which

$$e_{RC} = E_{RC}\epsilon^{\frac{-t}{R_T C_T}} \qquad (2)$$

is the solution of the differential equation defining the time-voltage characteristic of

capacitor C_T discharging through resistor R_T, where

E_{RC} = potential difference across C_T at the time discharge is initiated ($t=0$) and is approximately equal to $E_L - E_G$ if $R_G + R_K$ is small in comparison with R_T

C_T = capacitance in farads

R_T = resistance in ohms

t = time in seconds from initiation of discharge

ϵ = base of natural logarithms (2.718 . . .)

Solving equation 2 for time gives

$$t = R_T C_T \log_\epsilon \frac{E_{RC}}{e_{RC}} \qquad (3)$$

from which the time required for E_{RC} to decay to a desired value of e_{RC} may be calculated.

Since the values of the timing capacitor C_T and discharging resistor R_T are fixed, the time constant is fixed and the time range is determined by the setting of the potentiometer P and the relative values of the components in the voltage divider circuit. The upper end of the potentiometer determines the minimum peak voltage to which the timing capacitor charges before initiation, the maximum peak voltage of the grid bias component after initiation, and therefore the minimum time delay between initiation and energization of relay. Conversely, the lower end of the potentiometer determines the maximum peak voltage to which the timing capacitor charges before initiation, the minimum peak voltage of the grid bias component after initiation, and thus the maximum time delay between initiation and energization of relay.

After expiration of a preset time delay, the tube "fires" and conducts current in the anode–cathode circuit during the half cycles in which the anode is positive with respect to the cathode, energizing relay QA and charging the filter capacitor C_F. The relay is held in during the nonconducting half cycles by the energy stored in the filter capacitor. Thus, the relay will remain picked up until the anode–cathode circuit is opened by switch $S1$. Opening switch $S1$ re-establishes initial time ($t=0$) conditions. By properly coordinating the circuit components, the reset time requires only a few cycles, after which the timing cycle may be repeated.

By merely reversing the sequence in which switches $S1$ and $S2$ are operated, essentially instantaneous energization of relay QA is obtained. With switch $S2$ open and switch $S1$ closed, the peak voltage to which timing capacitor C_T charges is approximately equal to the peak voltage of the alternating grid bias component, so that the grid is approximately at cathode potential during the positive peaks of the alternating grid bias component. That is, E_{RC} is approximately equal and in phase opposition to E_G; consequently, after switch $S2$ is closed, ionization will occur on or near the first positive peak of e_G.

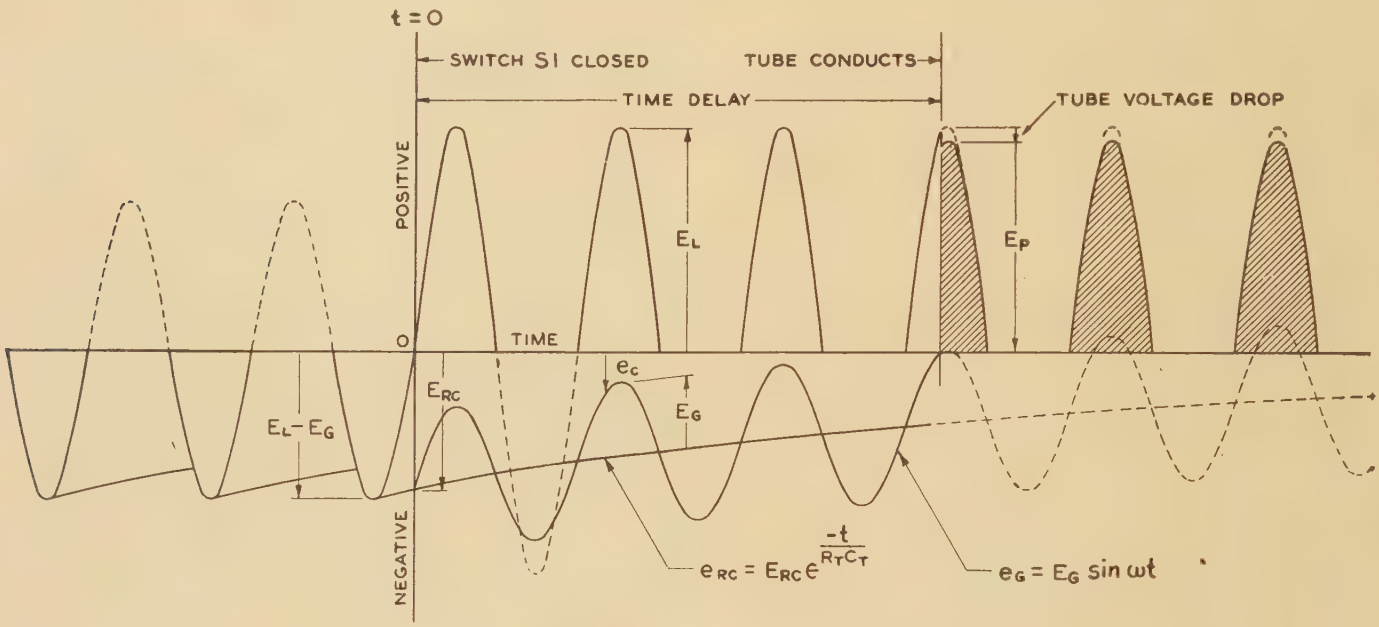

Figure 4. Instantaneous relationship of anode and control grid voltages

External Connections

The timing relay is operated from any 120-volt a-c source connected across terminals 1 and 2, and it is controlled through a contact of the circuit breaker auxiliary switch (152) connected between terminals 1 and 3. These connections are indicated on Figure 1 by the broken lines. In a majority of cases the timing relay may be controlled directly from the circuit breaker indicating light or alarm circuits since the only requirement is energization of relay FA when the circuit breaker is open.

Contacts QA_1, QA_2, and QA_3 brought out on terminal 4-5, 6-7, and 8-9 are connected into the circuit breaker tripping circuit as shown in Figure 2. Only one of these contacts is required for multiphase potential or shunt trip methods (A and B of Figure 2), since the contacts of all the instantaneous overcurrent relays are paralleled and actuate a single trip coil. But, in the case of multiphase current or series trip methods (C and D of Figure 2) a separate contact for each instantaneous overcurrent relay is required, since these actuate separate tripping elements.

Contact QA_{10} brought out on terminal 10 may be used for initiating an alarm or operation counter.

Operation for One Instantaneous Tripout

Where instantaneous relay protection on the initial tripout with inverse-time relay protection on subsequent tripouts is desired, lever switch LS is set in the unoperated "off" position as shown in Figure 1, in which position the timing relay is set up for immediate operation to open the trip circuits of the instantaneous relays prior to the immediate initial circuit breaker reclosure.

When the circuit breaker opens, auxiliary switch contact 152 closes and ener-

gizes relay *FA* which closes the anode circuit through contact FA_4, and tube conducts immediately to energize lockup relay *QA-O*. As a result: The trip circuits of the instantaneous overcurrent relays are opened by contacts QA_1, QA_2, or QA_3; lockup relay *QA-O* is de-energized (but not released) by contact QA_6; release relay *QA-R* is connected into the anode circuit by QA_8; and the cathode is opened by contact QA_4, allowing timing capacitor C_T to charge for reset timing. All of which occurs within 0.05 second after the circuit breaker trips. This operating time provides definite assurance that the instantaneous overcurrent relays are inoperative in advance of immediate circuit breaker reclosure, since the average operating time from initiation of tripping to reclosure of circuit breakers, such as employed for feeder service, ranges from about 0.5 to 1 second.

On reclosure of the circuit breaker, auxiliary switch contact 152 opens and de-energizes relay *FA*. This closes the cathode circuit through contact FA_1, and the tube conducts after a preset time-delay to energize release relay *QA-R* which releases lockup relay *QA-O*. As a consequence, the timing relay will reset to re-establish initial conditions if the circuit breaker remains closed through a timing cycle. However, in the case of faults which are not cleared on the initial tripout, the circuit breaker will be tripped by the inverse-time overcurrent relays, and the timing relay will remain in its operated position to maintain inverse-time tripping until the circuit breaker is successfully reclosed. The reset time delay should be the minimum necessary to co-ordinate with the circuit breaker clearing time on the inverse-time overcurrent relays, in order to provide instantaneous relay protection against the contingency of rapidly recurring faults.

Operation for Two Instantaneous Tripouts

Where instantaneous relay protection on the second, as well as the first, tripout is desired, lever switch *LS* is set in the "on" position, so that contacts LS_1 and LS_3 are open, and LS_2 and LS_4 are closed. In this position the timing relay is set up for time-delay operation, since when the cathode circuit is open through contacts FA_3 and QA_7, timing capacitor C_T is precharged for timing action.

When the circuit breaker opens, auxiliary switch contact 152 closes and energizes relay *FA* which closes the cathode circuit, but the tube does not conduct until after the preset time delay. If the immediate initial reclosure is successful, relay *FA* is de-energized, and initial conditions are re-established. However, if the fault is not cleared initially, this time delay allows the circuit breaker to be tripped again by the instantaneous overcurrent relays.

In the case of faults which are not cleared on the second tripout, the tube "times out" and then energizes lockup relay *QA-O*. As a result: The trip circuits of the instantaneous overcurrent relays are opened by contacts QA_1, QA_2, or QA_3; lockup relay *QA-O* is de-energized (but not released) by contact QA_6; release relay *QA-R* is connected into the anode circuit by contact QA_8; and the cathode circuit is opened by contact QA_5 which permits timing capacitor C_T to charge for reset timing. All of which occurs prior to the second reclosure, so that subsequent tripping of the circuit breaker is initiated by the inverse-time relays.

Following a successful reclosure, the timing relay will reset in a manner similar to that described under "Operation for One Instantaneous Tripout."

Since the timing adjustment (potentiometer *P*) is common to both operation and reset, it must be such that the preceding requirements are fulfilled. In some cases, it may be desirable to have less time-delay on reset than on operation, and this is accomplished by short-circuiting a section of the timing capacitor discharging resistor as shown by the dotted connection of contact QA_{10} across resistor R_{T2} in Figure 1. The reverse can be accomplished by making QA_{10} a normally closed contact.

Conclusions

The most salient features of the timing relay are:

1. Universal application regardless of circuit breaker mechanism or method of control.
2. Selection of either one or two instantaneous tripouts.
3. Independent of the control source voltage during fault conditions.
4. Reset timing independent of reclosing relay.
5. Ease of installation.

The initial installation of this equipment was made February 1945 on a breaker serving a high exposure 24-kv grounded Y circuit. As a result long time outages previously experienced on this circuit practically have been eliminated.

Sixty similar installations will be made on the Oklahoma Gas and Electric Company system during 1946.

With certain changes in the internal wiring, this device can be converted into an instantaneous or time-delay "one-shot" recloser with quick reset on a successful reclosure.

Silicone-Resin-Treated Magnet Coils

GRAHAM LEE MOSES
MEMBER AIEE

JULIUS J. TOROK
MEMBER AIEE

MAGNET COILS present somewhat different insulation problems from rotating machines. This was recognized when separate magnet coil standards[1-3] were set up by AIEE, National Electrical Manufacturers Association, and American Standards Association which permit higher maximum observable temperatures than do the rotating machine standards. AIEE Standard 1 states, "How long an insulation will last will depend not only on the class of material used but also upon the physical support of the insulation and the severity of the physical forces tending to disrupt it." Following this line of reasoning, AIEE Standards 15 and 16 permit higher observable temperatures on magnet coils as shown in Table I. Work by Erikson[4] indicates the desirability of separate consideration of magnet coils and suggests the possibility of higher operating temperatures even with organic insulation.

This distinction became more pronounced with the development of silicone insulation. Magnet coils were therefore considered as a special study of the basic work previously reported[5,6] on the general application of silicone varnishes to electric machinery. The test on coils was planned with the view of determining:

(*a*). The temperature–life relationships of the silicone varnish.

(*b*). The maximum operating temperatures of magnet coils for normal life expectancy.

(*c*). The effect of aging at various temperatures on the thermal conductivity of the assembly.

(*d*). Design advantages offered by higher temperature operation.

Test Program

Paralleling the motor test program[7] a like series of tests was planned for magnet coils. Briefly this program consisted of operating coils at different temperatures to determine the thermal life expectancy of the coils. In order that these tests might be useful and representative of standard practice, a commercial contactor and coil design were chosen. This is a conventional magnetic contactor for d-c control circuits which is widely used for industrial and railway service. The general construction is shown in Figure 1. All tests were run on this design of contactor in order that results obtained would be subject to direct comparison.

The operating temperatures from 200 to 275 degrees centigrade were chosen. The top limit was chosen because it was anticipated that at 275 degrees centigrade failures by short-circuited turns would probably occur in a few weeks. Another factor limiting the test to 275 degrees centigrade was the melting point of the solder (304 degrees centigrade) which held the coil leads to the terminals. Early estimates based on extrapolated curves for silicones indicated that 200 degrees centigrade would be the maximum operating temperature resulting in the full life expectancy of the coils. Thus the tests were started with 12 coils, three each at 200, 225, 250, and 275 degrees centigrade.

The data desired were to be obtained by day to day operating temperature readings (by resistance), mechanical stressing by thermocycling and operating the contactors, periodic measurement of cold resistances to determine wire oxidation and possible short-circuited turns (indications of failure), notation of color changes of resin on surface, and power input.

Coil Design

The coils tested were essentially a standard mechanical design to simulate normal conditions. They were wound with number 25 (0.0179 inch diameter) single glass covered copper wire (silicone varnish treated). Silicone wire enamel was not used because at that time the enamel development had not progressed far enough. All winding and insulating details were fiber glass and fiber-glass-backed mica (all bonded and treated with silicone resins). The spool was fabricated of fiber glass laminated tubes with a special resin bond (not silicone) and asbestos phenolic end washers. At the time these coils were made, thermosetting silicone moulding resins had not been developed to a usable state. The terminals were soldered with a high temperature solder (304 degrees centigrade solidifying temperature). No organic materials such as paper, cotton tape, string, glue, shellac, or varnish were used in the coil construction. The complete coil was treated by vacuum-pressure impregnation with DC-990-A silicone varnish, a product of Dow Corning Corporation, at 70 per cent solids and baked for 24 hours at 225 degrees centigrade. This was followed by a dip in 50 per cent solids DC-990-A silicone varnish and baked at 225 degrees centigrade for 16 hours.

The following design data give significant details of the coils used for this test:

Spool—$3^1/_4$ inches long by $1^5/_{32}$ inches inside diameter by 3 inches outside diameter.

Washers—1/8 inch thick.

Double insulating tube construction, each 1/16 inch thick.

Magnetic core—$1^1/_8$ inch diameter.

3,500 turns of number 25 wire having a resistance of 61 ohms (25 degrees centigrade).

Winding volume—11.6 cubic inches.

Barrel surface—25 square inches.

Test Procedure

The coils were connected to a 120-volt d-c motor generator set through variable nichrome resistors. Thus the current in each coil could be controlled without affecting the others.

The general testing procedure is detailed in Appendix I. Volt-ampere readings were taken every day, after which the coils were switched on and off ten times. Approximately once every week the cooling curves were run to check the hot volt-ampere resistance readings of each coil. The coils were then left off overnight and then cold resistance readings made the following morning, and the coils again energized.

Changes were made periodically to correct the test conditions for increases in

Table I. Comparison of Permissible Temperature Rise and Observable Temperature for Magnet Coils and for General Purposes

Class	Maximum Permissible Temperature Rise by Resistance, Deg C		Equivalent Maximum Observable Temperature,* Deg C	
	General[1]	Magnet Coils[2,3]	General[1]	Magnet Coils[2,3]
A	60	85	100	125
B	80	105	120	145

* Rise plus 40 degrees centigrade as maximum permissible ambient.

Paper 46-104, recommended by the AIEE committee on industrial control devices for presentation at the AIEE summer convention, Detroit, Mich., June 24–28, 1946. Manuscript submitted November 13, 1945, made available for printing April 11, 1946.

GRAHAM LEE MOSES is section engineer, development insulation section, transportation and generator division, Westinghouse Electric Corporation, East Pittsburgh, Pa.; JULIUS J. TOROK is in the development department, Corning Glass Works, Corning, N. Y.

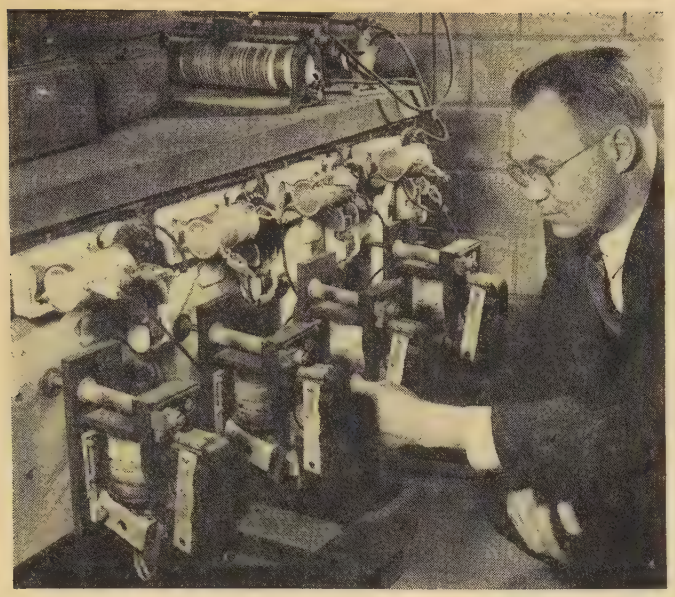

Figure 1. Laboratory test setup showing magnet coils under test being examined by Mr. Torok

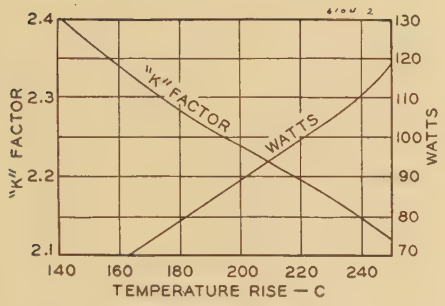

Figure 2. Effect of temperature rise on *K* factor and watts

cold resistance of the winding due to oxidation of the copper. After one year of operation without a failure, it was believed that the test could be made more severe by additional thermal cycling of the coils. The thermal cycling consisted of switching the power off the coils twice each day. The coils would be de-energized for approximately two hours in which time the coils would cool to a little above room temperature. Then power would be applied for four hours, a period more than sufficient for them to reach stabilized operating temperature. The power was then turned off for two hours and then left on overnight. Once each week the power would be off overnight and a cold temperature reading made the following morning.

Test Results

The change in heat dissipation factor *K* was used as a basis for observing insulation aging. This *K* factor is the average temperature rise divided by watts input and represents the temperature the coil must attain to dissipate the energy liberated within its body. Since average temperatures by resistance were used, the heat dissipating ability of the boundaries of the coil was only one factor involved. The heat transmission within the coil has an appreciable influence as it determines the distribution of temperature within the body of the coil. If the heat conductivity of the body is low, the internal temperature may be much higher than the surface temperature, where the heat is dissipated. Thus the average temperature being higher, the coil would have a very high *K* factor. However, if the heat conductivity within the coil were very good, the surface and internal temperature would be more nearly the same and a low *K* factor would result. Thus a change in *K* factor may represent a change in the rate of heat dissipation, but more likely the change in thermal conductivity within the body of the coil.

Aging and heat deterioration in organic and semiorganic materials generally are accompanied by weight loss, which results in dimensional changes or the formation of voids. The resinous bonds between the turns in the coil act not only as physical supports but as thermal conductors. As the impregnant ages, it shrinks or otherwise forms voids and its thermal conductivity diminishes. Resins shrink slightly as they cure and cause some voids which manifest themselves as a rise in *K* factor. Figure 2 shows the original *K* factor as a function of temperature rise above 25 degrees centigrade ambient temperature. Figure 3 shows the per cent increase in *K* factor as a function of hours aging under each temperature condition.

After the tests had been in progress, changes in cold resistance were observed. Thereafter periodic observations of cold resistance were made and the changes recorded. Figure 4 shows the per cent change in cold (25 degrees centigrade) resistance as a function of time of aging at various temperatures.

No definite coil failures occurred. Only two coils encountered trouble during the whole test and these were the result of faulty soldered joints at the terminal. They were detected by variable resistance readings.

Figure 5 shows the conditions of coils 2, 4, 5, 8, 9, 10, 11, and 12 after the conclusion of the test. All the coils except number 4 had been at temperature 12,615

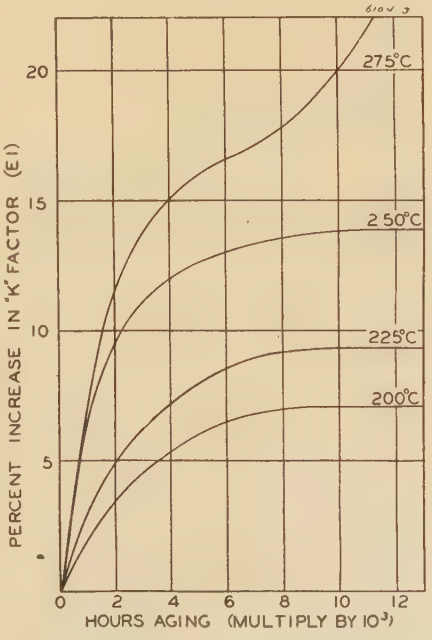

Figure 3. Effect on *K* factor of aging at elevated temperatures

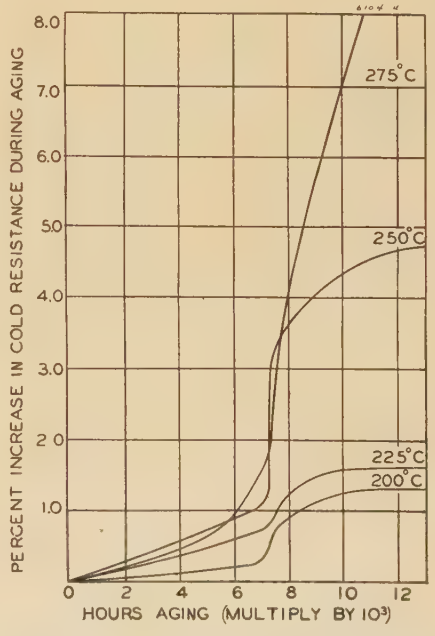

Figure 4. Effect of aging at elevated temperatures on the cold (25 degrees centigrade) resistance of magnet coils

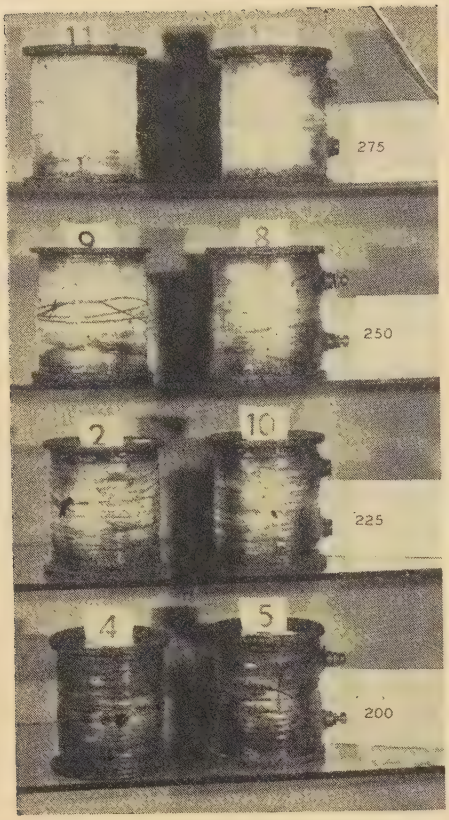

Figure 5. Coils showing external condition after 12,000 hours aging at temperatures of 200, 225, 250, and 275 degrees centigrade

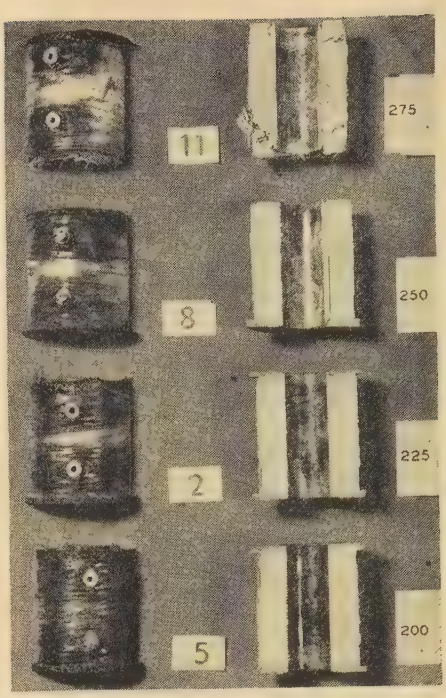

Figure 6. Coils showing internal condition after 12,000 hours aging at temperatures of 200, 225, 250, and 275 degrees centigrade

hours. Coil 4 had been at temperature 11,006 hours.

The coils shown in Figure 5 were subjected to electrical tests as follows:

(*a*). All passed the standard low-voltage short-circuit test ("E" iron balanced watt meter tester).

(*b*). All the coils except numbers 11 and 12 successfully withstood surge comparison tests[8] up to 10.6 kv (the limit of the tester available). Coils 11 and 12, which were aged 12,615 hours at 275 degrees centigrade, failed at 8 kv. These test voltages were surge peak values across two coils in series.

After electrical tests, the coils were cut open for physical examination. The condition of typical coils is shown in Figure 6. Detailed observations are given in Table II. These may be summarized in the following statements:

(*a*). Coils at 200 degrees centigrade were in excellent condition showing few if any signs of aging.

(*b*). Coils at 225 degrees centigrade were beginning to age, but were well bonded and in good condition.

(*c*). Coils at 250 degrees centigrade showed unmistakable signs of aging, but were still in fair condition, being well bonded but brittle.

(*d*). Coils at 275 degrees centigrade were still operable. However, they were in a condition which might be expected to result in failure under actual service conditions, as the bonding between wires as well as parts of the spool was near the failure point.

Thermal decomposition of silicones produces a reversal of color change from that normally encountered in organic resins. Organic resins decompose to carbon, a black conducting substance, whereas silicones decompose to silica, a white insulating substance. The aging of these coils clearly shows this color change which was an important indication. (The real significance of this color change requires further study.)

Examination of Copper Conductor

One of the coils which had operated on this test for 9,000 hours at 275 degrees centigrade was cut open for examination. The microstructure of this wire was normal for electrolytic tough-pitch copper and no hydrogen embrittlement could be detected. A black coating was present on the wire (about 0.0004 inch thick) which was found to be a mixture of cuprous and cupric oxide by X-ray diffraction analysis. The X-ray pattern for this copper was normal.

It was concluded that the test conditions had no deleterious effect on the copper wire except for slight oxidation of the surface. This surface oxidation resulted in increase in conductor resistance.

Discussion of Test Data

Over 12,000 hours ($1^1/_3$ years) operation at temperatures of as much as 275 degrees centigrade did not destroy a single coil or produce a case of serious trouble (except the two which were attributable to original workmanship in soldering).

The change in heat dissipation factor K shows an upward trend as the coils age. The rate of increase in K factor is greater at higher temperatures as shown in Figure 3. The initial rise in K factor may be considered as indicating completion of internal cure. However, the abrupt break in the curve for coils at 275 degrees centigrade (at 8,000 hours) is believed to indicate thermal degradation.

Resistance changes, though definite, were not of a serious nature even on coils at 250 degrees centigrade for the full period of the test. At 275 degrees centigrade the resistance change shown in Figure 4 is approaching a serious condition indicating that the temperature limitation may be established by copper rather than insulation. The rate of copper oxidation is known to increase as the temperature rises. Since copper oxide at low potentials is effectively an insulator, the rate and extent of oxidation can be determined by the change in resistivity of the copper wire. Periodic coil resistance readings were necessary to determine the extent of oxidation of the windings. The cold resistances remained essentially unchanged until the test had progressed to above 6,000 hours, then they started to rise and approach a constant level except at 275 degrees centigrade. At that temperature, no saturation level was observed. This level rose at an increasing rate as the temperature

Table II. Physical Condition of Magnet Coils After Thermal Aging for Approximately 12,000 Hours

Aging Temperature, Deg C	Coil Numbers	Condition of Washers	Condition of Winding	
			Color	Bond Strength
200	4–5	Well bonded	Dark	Excellent
225	2–10	Well bonded	Beginning to lighten	Good
250	8–9	Fairly well bonded	Light	Still bonded but brittle
275	11–12	Loose	Light	Poor—ready to fall apart

rose above 200 degrees centigrade. This seems to indicate that the copper oxide forms a protective film over the copper which decelerates the oxidation for a given temperature. That the oxidation did not appear until about 6,000 hours as compared to an almost immediate rise in K factor also indicates that the silicones' adhesion to copper is good and it is the last place where voids begin to form. The extent of oxidation might be greatly reduced if the bare copper wire had a protective coating, such as cadmium plating, under the insulation.

Interpretation of Data

One of the main objectives of this program was to obtain some idea of the order of magnitude of the thermal life of the silicone resins and composite silicone insulation. A recent review[11] of the aging characteristics of insulation disclosed general agreement that thermal aging of insulation is a logarithmic function of temperature. This concept was utilized in extrapolating the results of this series of tests. Extrapolation of short time tests is recognized as difficult but if predictions are to be made, it offers at least an opportunity for an "intelligent guess."

Figure 7 has been constructed as follows to extrapolate these data:

(a). The actual test hours at the various temperatures were plotted as points A, B, C, and D.

(b). A suggested life curve for silicone insulated motors was plotted for reference, with a 12 degree centigrade slope for half-life. (By coincidence this passes through point B.)

(c). From examination and tests, it was concluded that there is little likelihood of failure at the condition resulting from the 250 degrees centigrade test (point C). However, the condition resulting from the 275 degree centigrade test (point D) was interpreted to be near the end point. These points were therefore assumed to represent minimum and maximum life and were used to locate the boundaries of the "probable failure zone." Curves then were drawn through these points parallel to the suggested life curve for silicone insulation on motors.[7]

(d). A reference bench mark is drawn at 7 years and reference points are shown on this line for class B motors and class B magnet coils, at temperature limits established by AIEE Standards, as indicating probable life expectancy.

From this curve, it can be seen that the probable "minimum life" curve for magnet coils intersect the bench mark line at 225 degrees centigrade. It is of interest that this is 25 degrees centigrade above the probable motor insulation life curve which is the established difference for magnet coils over motors for class A and class B insulation (see Table I). Thus the test results indicate that the increase in temperature for comparable life is consistent between motors and magnet coils with silicone insulation when compared to the present allowed temperatures for class B motors and magnet coils.

The proposed temperature allowances[6] for silicone motor insulation corresponding to AIEE Standard 1 are 160 degrees centigrade observable by resistance. This is well below the insulation life value indicated by tests on motors.[7] It, therefore, is consistent and conservative to suggest a permissible temperature for silicone magnet coil insulation below the indicated value of 225 degrees centigrade by resistance. It is the opinion of the authors that a value of 200 degrees centigrade as observed by resistance would be satisfactory.

Effect of Operating Temperature on Design

The permissible operating temperature is an important factor in magnet coil design. Temperature rise above ambient temperature can be approximated at conventional operating temperatures for a given coil design by the following formula:

$$E=\sqrt{\frac{R\times\Delta t}{K}\left(1+\frac{\Delta t}{234.5+t_a}\right)}$$

where

E = continuous rated voltage for temperature rise of Δt

R = cold resistance of winding at temperature of t_a

Δt = temperature rise by resistance above t_a

t_a = ambient temperature (for operating or test conditions)

K = heat dissipation constant of coil design, in degrees rise per watt

This formula assumes that the temperature rise is proportional to the watts generated in the coil winding. This is reasonably accurate until the higher temperatures are reached when the K factor tends to decrease (heat dissipation is not a linear function of temperature rise).

The relation between continuous voltage rating and temperature rise is shown in Figure 8 based on the foregoing formula. This curve also shows that the ampere turns, while increasing with rated voltage, do not increase in the same ratio because of the increase in winding resistance at the higher temperature.

From Figure 8, it is clear that the present difference between class A coils at 85 degrees centigrade rise, and class B coils at 105 degrees centigrade rise (assuming the same space factor), is somewhat less than nine per cent improvement in ampere turns. This difference is not of sufficient importance to justify the use of class B magnet coils on most applications, hence they are not used generally. To obtain a significant advantage from increase in operating temperature (with a standard size of coil), it would be necessary to increase the permissible rise from 85 degrees centigrade to approximately 160 degrees centigrade (about equivalent to one standard wire size).

Figures 9 and 10 illustrate the advantage to be gained in reduced size of winding through increase in temperature rise.

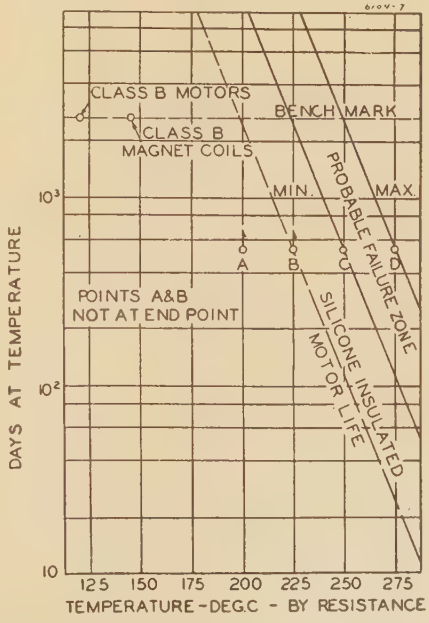

Figure 7. Thermal aging curve interpreting test results

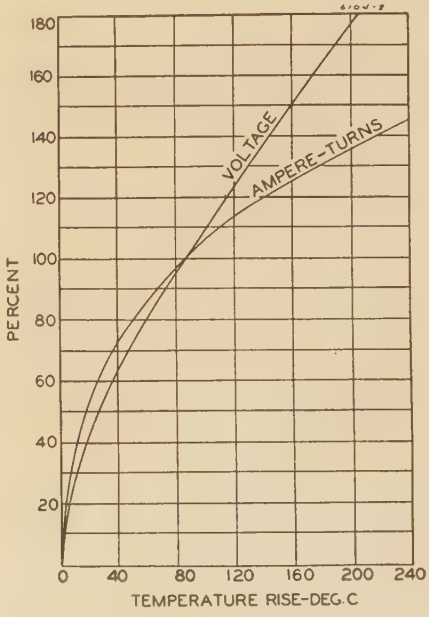

Figure 8. Effect of temperature rise on voltage and hot ampere-turns of magnet coils

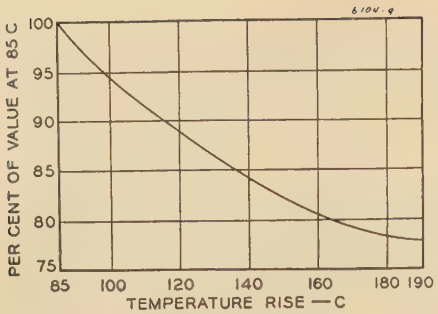

Figure 9. Effect of temperature rise on active coil length and copper weight

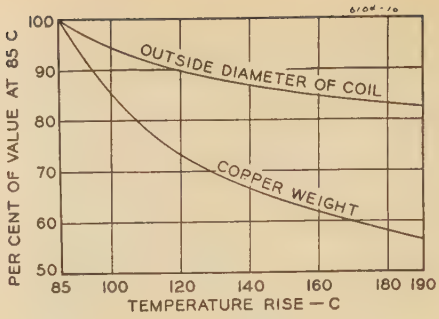

Figure 10. Effect of temperature rise on coil diameter and copper weight

These calculations are based on a constant value of minimum hot ampere turns at a specific percentage of rated voltage. The coils used as the basis for these calculations are the same size and construction as used for the tests reported herein.

Conclusions and Recommendations

One unmistakable conclusion drawn is that the combination of fiber glass and silicone resin makes an important contribution to improving the thermal life of magnet coil insulation. The end of the reliable life of such coils is believed to be determined by the failure of the silicone resins as bonds. The glass fibers provide positive turn separation and the by-products of silicone decomposition are nonconducting. Therefore, the probability of short-circuited turns is not great, even at the condition described herein as "maximum life," unless there is severe mechanical distortion of the winding.

The tests were begun about $2^1/_2$ years ago and employed DC-990-A resin which was the best silicone resin available at that time. Silicone resins have been improved (the corresponding improved resin is known as DC-993). Other short time tests indicate that similar coils with DC-993 will have even greater thermal endurance than indicated by the tests reported herein. Parallel tests employing the improved resins are in progress.

Though the experience is meager, there is considerable evidence to indicate that silicone insulated magnet coils employing fiber glass insulated wires can be rated at temperatures appreciably above the 160 degree centigrade temperature by resistance proposed for silicone insulation on rotating machinery.

Increase in permissible temperature rise will provide a real design advantage through an appreciable increase in net ampere turns. This advantage is obtained at some sacrifice in efficiency, as the watts per ampere turn are increased at elevated temperatures.

It is recommended that other investigators study this problem in order that sufficient confirming data be obtained to warrant establishing a new standard for silicone magnet coils, and particularly that they explore the elevated temperatures where designers may obtain an appreciable advantage (one standard wire size change).

It is the recommendation of the authors that an observable temperature limit of 200 degrees centigrade by resistance be considered as a future standard for silicone insulated magnet coils employing fiber glass conductor insulation. This would permit a temperature rise of 160 degrees centigrade (above 40 degrees centigrade ambient temperature) as observed by resistance.

Appendix I. Test Specification for Temperature Runs on Magnet Coils

Set up complete apparatus with coil assembled in its normal operating position. Shield apparatus from abnormal drafts where necessary but leave unrestricted room for flow of normal ventilating air.

Apply several thermocouples to coil surface. These should be distributed around the surface so as to obtain several readings for an average indication. Make sure that these are in intimate contact with coil surface and that the sensitive element is covered with a small felt pad or insulating cement.

Place a thermometer in room air adjacent to the apparatus to record ambient temperature. This should be near enough to the apparatus to indicate accurately the surrounding room air temperature but should not be in a position where the apparatus temperature will affect it.

Next accurately measure the coil resistance and record it with the coil surface temperature as well as the ambient temperature.

Only after these preliminaries should power be applied. The voltage specified for test should be held constant throughout the test. During the early part of the test, frequent readings should be taken, but in the latter part, as the coil temperature approaches a steady state, less frequent readings will suffice. Heating data should be observed and recorded as follows:

1. Time of reading with reference to cold start.
2. Volts applied to coil terminals.
3. Amperes flowing through coil.
4. Surface temperatures.
5. Room air temperature.

After all observed values reach a steady state (or the increase does not exceed the variation due to change in ambient temperature) take a set of shutdown readings. Arrangements should be made before power is shut off to change the coil connections quickly to a Wheatstone bridge. The time that power is shut off must be observed accurately and related to the cooling data taken. After power is shut off, frequent readings of coil resistance should be made until the change in coil resistance is at least half the total increase due to temperature rise. The coil resistance at the instant of shutdown is determined by plotting the values observed during the cooling period and extrapolating to the time that power was removed.

References

1. General Principles Upon Which Temperature Limits Are Based in the Rating of Electrical Machinery and Apparatus, AIEE Standard 1, June 1940.

2. American Standards for Industrial Control Apparatus, AIEE Standard 15, March 1944.

3. Standards for Electric Railway Control Apparatus, AIEE Standard 16, January 1933.

4. Insulation Temperature Standards for Industrial-Control Coils, **B. W. Erikson.** AIEE Transactions, volume 63, 1944, July section, pages 546–8.

5. Organo-Silicon Compounds for Insulating Electric Machines, **T. A. Kauppi, G. L. Moses.** AIEE Transactions, volume 64, 1945, March section, pages 90–3.

6. The Application of Silicone Resins to Insulation for Electric Machinery, **J. DeKiep, L. R. Hill, G. L. Moses.** AIEE Transactions, volume 64, 1945, March section, pages 94–8.

7. Silicone Insulation Proved by Test, **T. A. Kauppi, Geo. Grant, G. L. Moses, R. F. Horrell.** *Westinghouse Engineer*, September 1945, pages 135–40.

8. Winding-Fault Detection and Location by Surge-Comparison Testing, **G. L. Moses, Earl F. Harter.** AIEE Transactions, volume 64, 1945, July section, pages 499–503.

9. Magnet Coil Design, **G. L. Moses.** *Product Engineering*, volume 9, December 1938, pages 483–6.

10. Coils and Magnet Wire (book), **Charles Runderbill.** McGraw-Hill Book Company, Inc., New York, N. Y., 1925.

11. Synthetic Insulation and the 10-Degree Rule, **G. L. Moses.** *Westinghouse Engineer*, July 1945, page 106.

Inductive Co-ordination Aspects of Rectifier Installations

AN AIEE COMMITTEE REPORT

THIS REPORT discusses the inductive co-ordination aspects of rectifier installations from the standpoint of effects on the a-c side and presents methods of classifying proposed installations into one of the three following categories:

Category I. Very *unlikely* to cause important induction problems.

Category II. Indeterminate.

Category III. Very *likely* to cause important induction problems.

Suggested dividing lines between categories are set up in terms of estimated harmonic currents or voltages and types of power and telephone systems involved. In using these figures, it is important to keep in mind that the phenomena involved are complex and that simple estimates are necessarily approximate: a difference of less than about 25 per cent in any of the results obtained by these estimates is ordinarily not significant. It is particularly important that none of the figures be construed to be any sort of limit. (For working material, see pages 420 and 421.)

Among the advantages of classification of installations in the manner described herein are:

1. Considerable time and effort can be saved by avoiding useless detailed studies and tests in connection with installations which simple analyses would show to be relatively innocuous, that is, to be in category I. After an installation in this category is placed in service, a few tests may be made to check the indications of the rough estimates and catalogue the case for future reference.

2. It will be easy to recognize those installations in which the only way to find out definitely whether remedial measures are needed—and if so the best type—is by detailed tests of power system influence and telephone noise before and after the rectifier is put into operation, that is, installations in category II.

3. The occasional situation in which the rectifier load would cause immediate and severe problems, that is, installations in category III, can be recognized and suitable precautions taken. These precautions are, usually, to provide remedial measures in advance, or if this is not feasible, to confine the harmonics to areas where they can do little harm until tests can be made and remedial measures designed and installed.

4. It will facilitate co-operative advance planning, for example, selection of methods of power supply and number of phases, to minimize the probability of important induction problems.

5. Where tests are required, it will facilitate setting up test programs to obtain information of the maximum usefulness with minimum effort.

While this report is devoted primarily to rectifiers of the sort usually encountered in industrial, railway, and radio applications, methods are given later for treating certain of the types encountered less frequently. The following matters pertaining to harmonics associated with rectifiers are not covered, but references to other information are included as indicated:

1. Harmonics on the d-c side of rectifiers (see items 21, 32, 33, 34, 35, and 36 in References).

2. Effect of harmonics on the a-c side on heating of power equipment and on balance of rectifiers (see items 3, 16, and 31 in References).

3. Single-phase rectifiers (see item 36 in References).

More complete treatments of specific aspects of the subject are contained in the literature listed under References, which are referred to in the following text. Appendixes I and II contain, respectively, brief discussions of the fundamentals of induction and of the propagation of harmonic currents and voltages over power circuits, which may be found useful in obtaining a more comprehensive picture of the phenomena involved. Appendix III gives pertinent data on a few of the installations which have been studied.

Nature of Problem

In this section are discussed the basic factors of the inductive co-ordination problem relating to rectifier installations from the point of view of the a-c power system. An understanding of these factors will be helpful in analyzing situations involving inductive co-ordination problems and in finding remedial measures.

Factors Affecting Problem

Considering the a-c side of a rectifier installation, the only significant effect of the installation from the inductive co-ordination standpoint is the production of harmonic currents and voltages in the power system.[1, 2, 3, 8, 9, 17, 30, 31, 32, 34, 53] These harmonic currents and voltages set up magnetic and electric fields of corresponding frequencies about the power lines; they, in turn, may induce voltages of the same frequencies in paralleling telephone circuits which may cause noise in these circuits. Induction caused by power circuit currents is called magnetic; that caused by power circuit voltages is called electric (see Appendix I). Whether noise problems will occur and, if so, their severity and extent, will depend on the magnitudes of the harmonic currents and voltages at various places over the power system, the characteristics of the power system, the amount, type and location of situations of proximity between power and telephone circuits (that is, "exposures"), and the characteristics of the telephone circuits. These matters are discussed more fully in Appendix I.

Generation of Harmonics

The current taken by a rectifier unit from the a-c line has a step-type wave shape resulting from the flat top wave shape of the anode currents. Typical wave shapes of rectifier a-c line currents are shown in Figure 1.

Table I shows the orders (that is, the multiples of the fundamental frequency) of the harmonics on the a-c circuits associated with rectifiers of different numbers of phases. The magnitude of any harmonic which is present with any particular number of phases is the same as for a 6-phase rectifier if all other conditions are the same. For example, the magnitudes of the twenty-third and twenty-fifth harmonics are approximately the same whether the rectifier has 6, 12, or 24 phases.[3, 5, 8, 9, 20, 31]

The magnitudes of the harmonic currents have a definite relation to the magnitude of the total rectifier current and also depend on the order of the harmonic. The higher the order of a harmonic, the smaller is its magnitude.

Paper 46-105, recommended by the AIEE committee on electronics for presentation at the AIEE summer convention, Detroit, Mich., June 24–28, 1946. Manuscript submitted March 26, 1946; made available for printing April 17, 1946.

This report was prepared by a working group of the electronic power conversion subcommittee, AIEE committee on electronics, consisting of H. R. Huntley (M '29, *chairman*), operation and engineering department, American Telephone and Telegraph Company, New York, N. Y.; R. D. Evans (F '40), consulting transmission engineer, Westinghouse Electric Corporation, East Pittsburgh, Pa.; C. W. Frick (A '19), general engineering laboratory, General Electric Company, Schenectady, N. Y.; H. E. Kent (M '31), engineer, Edison Electric Institute, New York; H. Winograd (M '39), engineer in charge, rectifier design, electrical department, Allis-Chalmers Manufacturing Company, Milwaukee, Wis.

Effect of Power Circuit Impedance

In Figure 2 is shown a simple power supply circuit for a rectifier installation. The rectifier unit R is supplied from a power source G over a 3-phase line A. The power supply circuit has an impedance Z, which includes the impedances of the line and the power source. From the point of view of the power circuit, the rectifier unit can be considered as a generator of harmonic currents. The impedance of the power supply circuit will effect some reduction in the harmonic currents, the extent of the reduction depending on the magnitude of the impedance.

If a harmonic current I_n flows from the rectifier over the line to the power source, a voltage drop in the line will result because of the impedance Z_n of the power circuit at the harmonic frequency. This will produce at point S a harmonic voltage $E_n = I_n Z_n$. If a communication circuit should have an exposure to the power line A, experience shows that the controlling inductive effect in such a case is almost always caused by the harmonic current rather than by the harmonic voltage; the latter can, therefore, be neglected without much error for an exposure to the main supply feeder.

However, if the power line should have an extension B for supplying other loads, as shown in Figure 3, the harmonic voltage at S will cause a harmonic current to flow over that line also, although the power to the rectifier is supplied only over line A. This harmonic current in, as well as the harmonic voltage on, line B and any lines that may branch from it could cause induction in communication lines exposed to them.

The higher the value of impedance Z_n the greater will be the harmonic voltage at S and the higher the magnitude of the harmonic current flowing over line B. Actually, the harmonic currents from a rectifier can flow into any part of an a-c system to which it is connected, as determined by the impedances of the various branches of the system at the harmonic frequencies, regardless of the location of the source of power supply or the direction of power flow.[18,19] In practice, however, the circuit over which the rectifier receives its power usually has the lowest impedance and draws the greater part of the harmonic currents.

Table I. Harmonics Arising in Rectifiers

Orders of Harmonics Present With Balanced Operation*							
6-Phase Rectifier	12-Phase Rectifier	18-Phase Rectifier	24-Phase Rectifier	36-Phase Rectifier	48-Phase Rectifier	Harmonic Frequencies on 60-Cycle System, Cycles
5	.. —	.. —	.. —	.. —	.. —	... 300
7	.. —	.. —	.. —	.. —	.. —	... 420
11	.. 11	.. —	.. —	.. —	.. —	... 660
13	.. 13	.. —	.. —	.. —	.. —	... 780
17	.. —	.. 17	.. —	.. —	.. —	...1,020
19	.. —	.. 19	.. —	.. —	.. —	...1,140
23	.. 23	.. —	.. 23	.. —	.. —	...1,380
25	.. 25	.. —	.. 25	.. —	.. —	...1,500
29	.. —	.. —	.. —	.. —	.. —	...1,740
31	.. —	.. —	.. —	.. —	.. —	...1,860
35	.. 35	.. 35	.. —	.. 35	.. —	...2,100
37	.. 37	.. 37	.. —	.. 37**	—	...2,220
41	.. —	.. —	.. —	.. —	.. —	...2,460
43	.. —	.. —	.. —	.. —	.. —	...2,580
47	.. 47	.. —	.. 47	.. —	.. 47	...2,820
49	.. 49	.. —	.. 49**	.. —	.. 49**	...2,940
53	.. —	.. 53	.. —	.. —	.. —	...3,180
55	.. —	.. 55**	.. —	.. —	.. —	...3,300
59	.. 59	.. —	.. —	.. —	.. —	...3,540
61**	.. 61**	.. —	.. —	.. —	.. —	...3,660**

* Other harmonics may be present if the rectifier is unbalanced, as by differences in load or phase control between units, or by harmonics in the power supply.

** The series continues above these values.

Effect of A-C Line Voltage

For a given kilovolt-ampere input to a rectifier installation, the higher the a-c line voltage the lower is the a-c line current and the lower the magnitude of the harmonic currents, because the magnitude of the harmonic current components has a definite relation to the rms value of the rectifier current. When the harmonic currents are lower, usually the harmonic voltages produced by them are also lower. Also, there are fewer long close exposures of telephone circuits to high-voltage transmission circuits than to power distribution circuits. Thus as the voltage of the line supplying a rectifier installation is increased, the probability of interference in communication circuits in the vicinity of the rectifier installation is decreased.

Harmonic currents and voltages can be transmitted through power and distribution transformers in the a-c system and their magnitudes changed in accordance with the transformation ratios of the transformers. However, the factors controlling the propagation of harmonics over power networks are different quantitatively from those controlling the fundamental, as discussed in more detail in Appendix II.

Effects of Phase Control

Phase control is used on a rectifier for the purpose of reducing the d-c output voltage below the value obtained without phase control. It is accomplished by retarding the firing point of the anodes in the alternating-voltage cycle, through grid or firing control. When phase control is used, there is no change in the transformation ratio of the rectifier transformer, and the ratio between the rectifier d-c current and the a-c line current remains practically unchanged.

If the d-c output is maintained constant while the d-c output voltage is reduced by phase control, the kilowatt output of the rectifier unit is reduced while the magnitude of the a-c line current and the kilovolt-ampere input remain unchanged, the power factor at the a-c line terminals of the rectifier transformer being lowered thereby. The result is that the magnitude of the harmonic components in the a-c line current, per kilowatt output of the rectifier, is increased.

Phase control also produces a steeper rise and fall of the anode currents at the beginning and the end of the anode firing period, while the current is commutated between successive anodes (see Figure 4). This is reflected in a steeper change of current between successive steps of the a-c line current wave, which results in harmonic components of higher magnitude.[8,9]

These effects increase as the amount of phase control employed is increased. The use of an appreciable amount of phase control is therefore likely to increase the co-ordination problem between a power system supplying rectifiers and communication circuits. It is important, therefore, that the use of phase control in excess of actual requirements be avoided, particularly in the range of full-load and overload ratings of rectifiers.

I·T Product and Voltage TIF

In the remainder of the body of the report, the terms "I·T product" and "voltage TIF" are used freely. These terms are discussed in Appendix I. At this point it is sufficient to note that I·T prod-

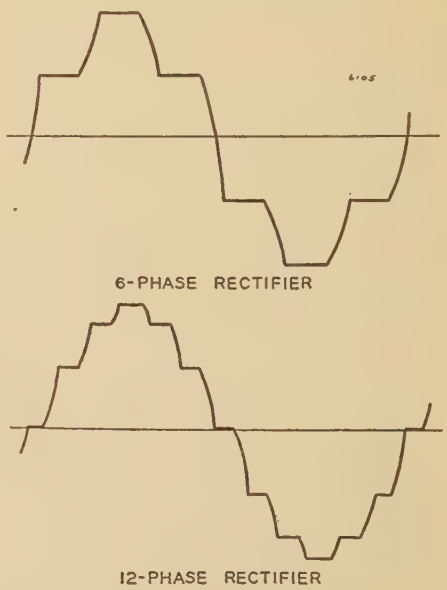

Figure 1. A-c line currents

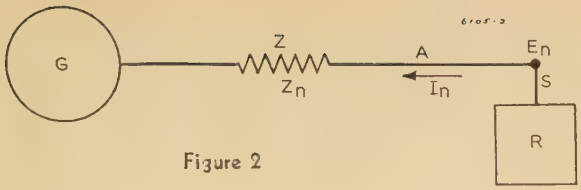

Figure 2

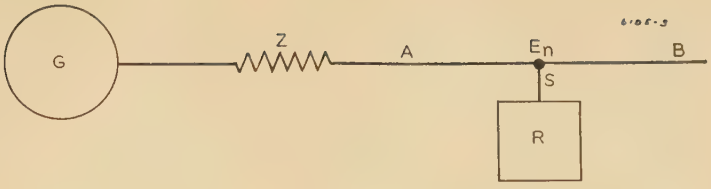

Figure 3

uct is a measure of the over-all noise influence of a current (including fundamental and harmonics); voltage TIF is a similar measure for voltage of known rms value.[27,28]

Ground Return and Balanced Harmonics

Harmonics arising in rectifiers supplied on a 3-phase basis start out as balanced, that is, the phase currents are equal and 120 degrees apart, as are also the phase-to-neutral voltages. If the power system were perfectly balanced, that is, if at harmonic frequencies the series impedances of the three phase wires were equal and also if the admittances to ground of these wires were equal, these currents and voltages would remain balanced. However, with three or more wires on a pole head, the series impedances of the different wires are usually not identical nor are the admittances to ground identical. In many cases these inequalities are accentuated by the presence of single-phase branches and single-phase loads. As a result, on distribution circuits (and to a limited extent on transmission circuits), the vector sum of the harmonic phase currents or of the phase-to-ground voltages is not zero; the vector sum is called "residual." That part of the residual harmonic current which returns in the ground is called "ground return"; it has a larger inductive effect than currents confined to the wires. Similarly, the effect of residual voltages is larger than that of balanced voltages. These matters are discussed in more detail in Appendix I.[10,11,12,23]

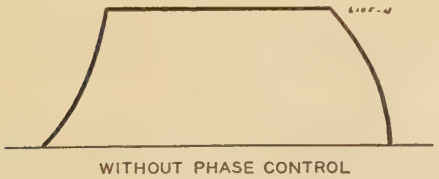

WITHOUT PHASE CONTROL

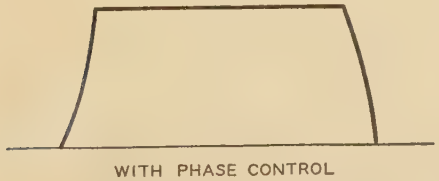

WITH PHASE CONTROL

Figure 4. Anode currents

Relations Between Harmonic Voltage and Harmonic Current

Harmonic voltages on a power system may be important from two standpoints, namely:

1. Where open wire telephone circuits are involved, the induction from these voltages may be important.

2. In many situations, the more important effect of harmonic voltages is in causing harmonic currents in parts of systems on which these voltages are impressed. For example, in Figure 3 the effect of a harmonic voltage E_n in causing a harmonic current in part B of the system is likely to be more important than the direct effect of E_n. This is particularly likely to be true if part B is unbalanced, as by single phase branches and loads, so that part of the current becomes ground return.

In connection with 1 above, the harmonic current into B at any frequency f_n is the impressed harmonic voltage of that frequency E_n divided by the impedance looking into B at that frequency. This impedance is not the series impedance of the wires of B alone; it depends not only on these series impedances but also on the impedances in shunt with the circuit, such as, for example, the impedances of loads or capacitors connected to the circuit and of the capacitances of the wires to each other and to earth. All of these impedances vary with frequency—some directly, some inversely, and some in a complex manner. Estimating the I·T on an actual circuit under these conditions would, therefore, be quite involved. For rough estimates only, it has been found useful to assume a direct relation between the voltage TIF on the circuit and ground return I·T.

Procedure in Classifying Proposed Installations

On pages 420 and 421 are shown the steps involved in the classification of a proposed rectifier installation together with essential data and equations. In the remainder of this section, these steps and data are discussed.

Step 1 (Refer to Table III, Page 420)

It is convenient to start with a schematic diagram of the power supply system. A typical diagram, shown in Figure 5A, includes the rectifier and its transformer, the supply feeder and its transformer, and associated power sources which may involve generators, a supply network, or both. In addition, the location of present or proposed telephone circuits, in relation to power circuit feeders, should be determined as illustrated by exposures to power feeders A, B, C, and N. These exposures illustrate the groupings that are convenient in classifying installations from the co-ordination standpoint. While in a detailed study it is necessary to have rather complete information on exposure conditions, it usually is sufficient for classification purposes to know their general type and extent; for example, the extent to which the power circuits are or are likely to be involved in joint use of poles with telephone cables or in joint use or roadway exposures to telephone open wire.

It is usually convenient, next, to draw an impedance diagram similar to Figure 5B. In this diagram the reactances of the various parts of the circuit through which power flows to the rectifier are indicated as percentages on the total rectifier transformer kilovolt-ampere base. If the rectifier transformer kilovolt-amperes is known, it is used directly; if it is not known, a sufficiently good approximation for the present purpose can be obtained from equation 1. The per cent commutating rectance ($\%X_{cn}$) of the rectifier transformer can be obtained from the manufacturer or can be approximated from Table II.*

* The per cent impedance given on rectifier transformer nameplates should not be used because it applies only to the case where voltage is applied to the primary, and all of the secondary terminals are short-circuited.

Table II. Approximate Per Cent Commutating Reactance of Rectifier Transformers

Voltage Class on A-C Side, Kv	Approximate Reactance, Per Cent: Rectifiers for Railway and General Industrial Service	Approximate Reactance, Per Cent: Rectifiers for Electrochemical Processes
Up to 15	5	9
34.5	6	9
69	8	9
115	10	10
161	12	12
230	14	14

Table III. Summary of Classification Procedure

Step 1. Schematic and Impedance Diagrams of Power Supply System (as Figure 5)

1. Indicate exposures
2. Classify circuits as to type (as *A*, *B*, *C*, or *N*)
3. Determine per cent reactance of circuit elements at 60 cycles on total rectifier transformer kilovolt-ampere base
   - *A.* Commutating reactance of rectifier transformer from Table II or from manufacturer
   - *B.* 60-cycle power source reactance (use name plate data or Tables VIII and IX for reactances, and equations 4 and 5 for conversion to rectifier transformer kilovolt-ampere base)
   - *C.* Rectifier feeder (see equations 2 and 3)
4. Obtain *total* per cent commutating reactance (total $\%X_c$) on total rectifier transformer kilovolt-ampere base by combining items 3A, 3B, and 3C above; or
5. If data on reactances are not available, assume total per cent commutating reactance of eight per cent for industrial and railway installations supplied from distribution circuits and the values in Table II plus two per cent for all other installations

Step 2. Direct-Feeder Exposure (Exposure A, Figure 5)

1. If phase control is not used at rectifier rated load, estimate I·T product from Figure 6
   - *A.* Interpolate between curves, using total $\%X_c$ obtained in item 4 or 5 of step 1
   - *B.* Divide ordinate by phase-to-phase voltage in kilovolts and multiply by total rectifier transformer kilovolt-amperes
2. If phase control is used at rated load, obtain I·T product as discussed under "Substantial Amounts of Phase Control" rather than from Figure 6
3. Classify exposure as in Table IV*

Step 3. Indirect Distribution Exposures (Exposure B and C of Figure 5)

1. If phase control is not used at rectifier rated load, estimate voltage TIF on bus supplying feeder *B* or *C*, from Figure 7
   - *A.* Interpolate between curves, using total commutating reactance ($\%X_c$) obtained in item 4 or 5 of step 1
   - *B.* Multiply ordinate by per cent reactance from (and including) 60-cycle power source to point of power supply to feeder *B* or *C*
2. If phase control *is* used at rated load, obtain voltage TIF as discussed under "Substantial Amounts of Phase Control" rather than from Figure 7
3. Classify exposure as in Table V*

Step 4. Exposures to Supply System Network (Exposure N, Figure 5)

1. Starting with the I·T product obtained in step 2
   - *A.* Obtain division of this I·T product between network (*N*) and generator (*G*) on basis of their inverse impedances
   - *B.* Multiply *network* I·T from (*A*) above, by line voltage of direct feeder (*A*) and divide by line voltage of the *network*
2. Classify exposures as in Table VI*

Estimates of per cent reactance of other circuit elements on total rectifier transformer kilovolt-ampere base can be obtained from equations 2, 3, 4, and 5. The following suggestions may be of help in estimating reactances to use in these equations:

1. For generators and other synchronous

* In Tables IV, V, and VI, the classification of installations into categories has the following general significance:

Category I. Very *unlikely* to cause important induction problems.

Category II. Indeterminate.

Category III. Very *likely* to cause important induction problems.

Table IV

Type of Feeder A	Type of Telephone Plant	Approximate I·T Product on Feeder A for Category I*	Category II*	Category III*
Cable	All	All	—	—
Overhead circuit, but so located that there are and will be no exposures more than a few spans long	All	All	—	—
Overhead distribution circuits with normal existing or possible future exposures	Cable†	Less than about 10,000	About 10,000 to about 100,000	More than about 100,000
	Long open wire	Less than about 5,000	About 5,000 to about 50,000	More than about 50,000
Rural,‡ with present or possible future exposures	Long open wire	—	All	—

† With or without short open-wire extensions. ‡ Feeder of low capacity with single-phase loads.

Table V

Type of Distribution Circuit Involved in B and C	Type of Telephone Plant	Approximate Voltage TIF on B or C for Category I*	Category II*	Category III*
Cable	All	All	—	—
Overhead, so located that no exposures more than a few spans can exist	All	All	—	—
Overhead, urban, with no capacitors more than a few blocks away from the rectifier	Cable†	Less than about 50	About 50 to about 150	More than about 150
Overhead, urban with a likelihood of capacitors some distance away	Cable or open wire	Less than about 40	About 40 to about 100	More than about 100
Overhead circuit supplying scattered industrial and residential loads in relatively open country and without extensive single-phase branches	Long open wire	Less than about 30	About 30 to about 75	More than about 75
Rural‡	Long open wire	Less than about 20	About 20 to about 50	More than about 50

† With or without short open-wire extensions. ‡ Feeder of low capacity with single-phase loads.

Table VI

Characteristics of Supply System	I·T Product Into the System (N) Category I*	Category II*	Category III*
Extensive cable networks of type found in large cities	All	—	—
Overhead subtransmission systems	Less than about 20,000	About 20,000 to about 100,000	Over about 100,000
Extensive high-voltage transmission systems:			
A. Rectifier with 6–24 phases	Less than about 5,000	5,000 to 25,000	Over 25,000
B. Rectifier with 30–48 phases	Less than about 10,000	10,000 to 50,000	Over 50,000
C. Rectifier with 72 or more phases	All	—	—

Table VII. Equations Used in Estimating Reactances Associated With Rectifier Installations

Nature of Reactance	Equation	Number
To estimate: A-c line kva of rectifier transformer $(\text{kva})_R$ from rectifier kw and phase control	$\text{kva}_R = 1.15\,\frac{(100+\%\text{ phase control})}{100} \times \text{rectifier kw}$ Here "% phase control" is amount of phase control at rated voltage and load	(1)
Per cent reactance ($\%X_L$) of line of length L (in miles), on rectifier transformer kva base	$\%X_L = (0.00375)(L)\,(\text{kva}_R)$ for 4-kv circuits	(2)
	$\%X_L = \frac{(0.075)(L)(\text{kva}_R)}{E_L^2}$ for 13-kv and higher-voltage circuits, where E_L is phase-to-phase voltage, in kv	(3)
To find: Per cent reactance ($\%X_{Rx}$), on rectifier transformer kva base (kva_R), of equipment having a known per cent reactance ($\%X_x$) with respect to some other kva base (kva_x)	$\%X_{Rx} = \%X_x\,\frac{\text{kva}_R}{\text{kva}_x}$	(4)
Per cent reactance ($\%X_{Rx}$), on rectifier transformer kva base (kva_R), of a reactance given in ohms (X_x) in a line of voltage E_L	$\%X_{Rx} = (X_x)\,\frac{(\text{kva}_R)}{10E_L^2}$ E_L is phase-to-phase voltage, in kv	(5)

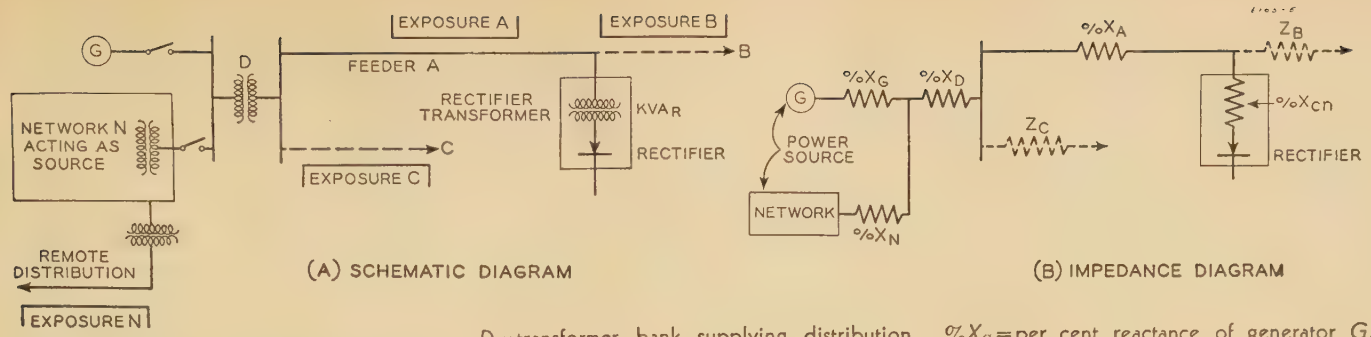

Figure 5. Typical power-supply and telephone exposure diagram for classifying rectifier co-ordination problems

A = feeder to rectifier

B = distribution system extending beyond rectifier station

C = distribution system fed from supply substation

D = transformer bank supplying distribution system

G = generator

$\%X_{cn}$ = per cent commutating reactance of rectifier transformer

$\%X_A$ = per cent reactance of feeder A, on rectifier transformer kilovolt-ampere base

$\%X_D$ = per cent reactance of transformer D, on rectifier transformer kilovolt-ampere base

$\%X_G$ = per cent reactance of generator G, on rectifier transformer kilovolt-ampere base

$\%X_N$ = per cent reactance of network N, on rectifier transformer kilovolt-ampere base

Z_B = impedance presented by distribution circuit B, to voltages of nth harmonic frequency

Z_C = impedance presented by distribution circuit C, to voltages of nth harmonic frequency

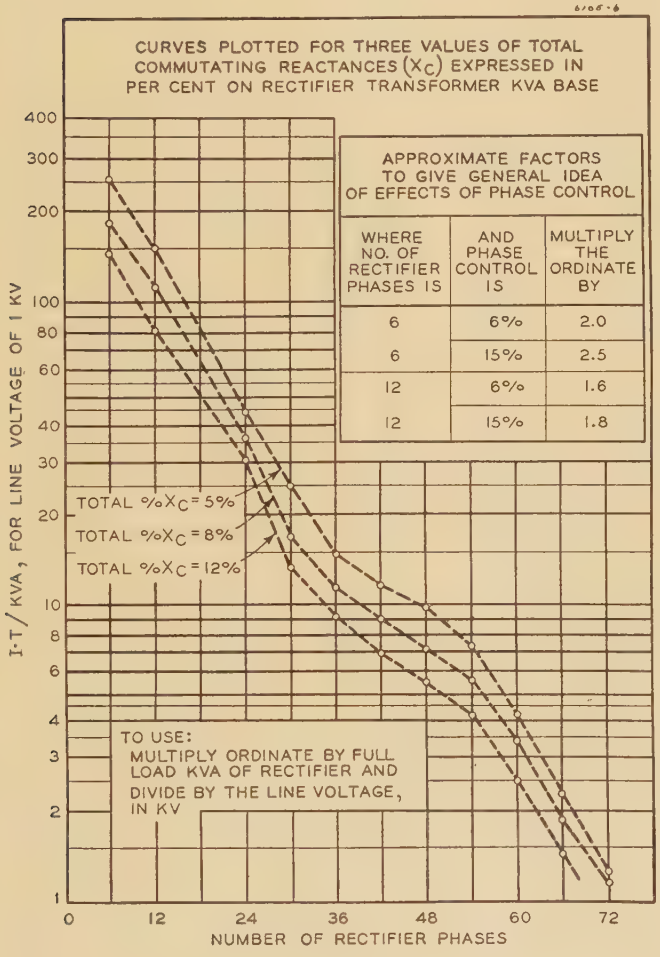

Figure 6. I·T per kilovolt-ampere of rectifier transformer capacity for 1-kv line voltage versus number of rectifier phases (60-cycle systems)

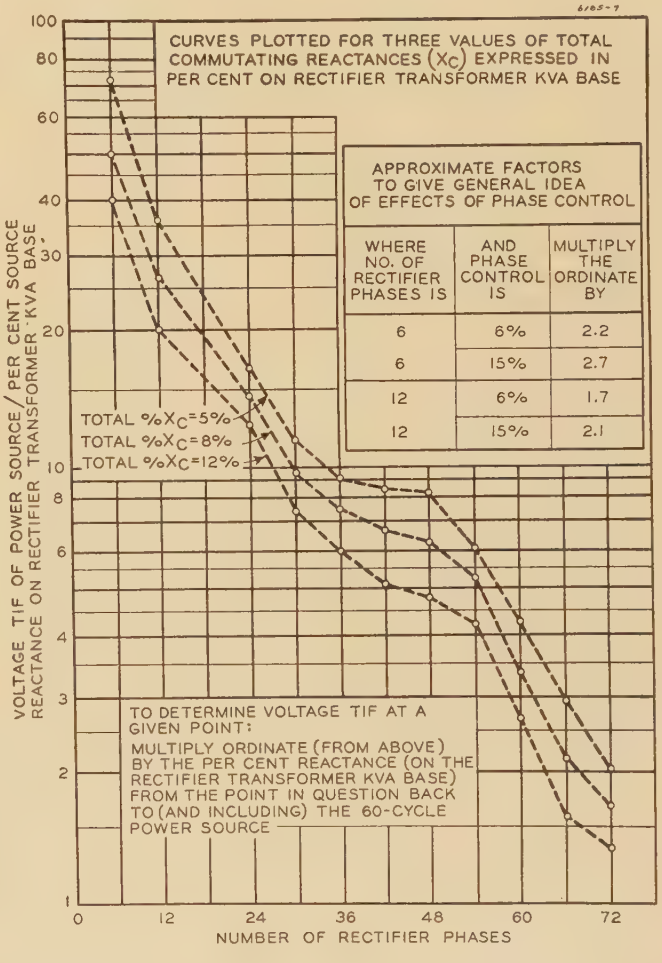

Figure 7. Source voltage TIF per per cent source reactance on rectifier transformer kilovolt-ampere base versus number of rectifier phases (60-cycle systems)

machinery, the average of the subtransient and negative sequence reactances may be used. If these reactances are not known, the approximate percentages on the machine kilovolt-ampere base, shown in Table VIII,[14,37] may be used.

2. If the reactance of a power transformer bank is not known, the approximate figures in Table IX may be used.

Table VIII. Approximate Reactances of Synchronous Machines

Type of Machine	Reactance on Own Base for Use in Equation 4, Per Cent
2-pole turbine generator	9
4-pole turbine generator	15
Salient pole generator or motor	
With dampers	24
Without dampers	45
Synchronous condenser	25

3. Where the "network acting as power source" includes a transformer bank between the lines and the bus, about the best approximation is to consider the impedance, looking into it from the bus as being equal to the reactance of the transformer bank alone. This approximation is good if the network is

Table IX. Approximate Reactances of Power Transformers

Voltage Class on High-Voltage Side of Transformer, Kilovolts	Approximate Reactance on Own Base for Use in Equation 4, Per Cent
Up to 15	5
34.5	7
69	8
115	10
161	12
230	14

a high voltage system; it gets successively poorer as the voltage of the network approaches that of the bus.

Having set down the reactances as percentages on the total rectifier transformer kilovolt-ampere base, they are combined to obtain the approximate total commutating reactance in per cent on rectifier transformer kilovolt-ampere base, that is, total $\%X_c$.* In cases where data are not available on reactances, total $\%X_c$ of eight per cent can be used for industrial and railway installations supplied from distribution systems and the values shown in Table II plus two per cent for all other installations.

Step 2. Direct Exposures to Rectifier Feeders (Exposure *A* in Figure 5)

Step 2 covers a direct distribution type feeder supplying power to a rectifier. As indicated under "Nature of Problem," experience indicates that in practically all such cases, magnetic induction is controlling, and that electric induction can be safely neglected. While the ground return I·T is the most significant measure of magnetic influence, it is difficult to estimate; however, for given power circuit conditions, the ground return I·T is about proportional to phase I·T, and the latter provides a sufficiently reliable indication for classification purposes.

It has been found for installations of ordinary rectifiers of a given number of phases operated at full load without phase control, that the quantity "I·T product per kilovolt-ampere of rectifier transformer capacity" usually lies within a fairly narrow range. In Figure 6 are plotted average values of "I·T product per kilovolt-ampere of rectifier transformer capacity" for a 60-cycle system having a phase-to-phase voltage of one kv. Three curves are shown for values of total commutating reactance (total $\%X_c$) of 5%, 8%, and 12% on the rectifier transformer kilovolt-ampere base. The total commutating reactance at rated load may be determined as explained previously and then used to interpolate between the three curves of Figure 6. The I·T per kilovolt-ampere thus obtained, when multiplied by the rectifier transformer kilovolt-amperes and divided by the a-c phase-to-phase voltage in kilovolts, will give the I·T product for feeder *A*. The data from Figure 6 also apply if phase control is used only at fractional load or if small amounts of phase control (not over a few per cent) at full load are used to balance loads among units forming a multiphase installation.** If larger amounts of phase control are used in normal operation, the methods outlined in "Installations Using Substantial Amounts of Phase Control" should be used.

With known I·T product, installations can be classified from the standpoint of exposures similar to exposure *A* as in Table III.

Step 3. Indirect Distribution Exposures (Exposures *B* and *C* of Figure 5)

From the standpoint of exposures *B* and *C* in Figure 5, the factor of primary interest usually is the ground return I·T product. This factor, however, is very difficult to estimate, and for that reason, the voltage TIF impressed on the feeders and their extent and type are usually employed. This approximation is rather poor quantitatively but is good enough for classification purposes. Where open wire telephone circuits are involved, the voltage TIF itself is of importance.

The voltage TIF on feeder *C* at the substation is produced by the voltage drops caused by the harmonic currents flowing through the reactances of transformer bank *D* and the source as explained in "Nature of Problem." The voltage TIF may be estimated with the aid of Figure 7. The value of the total commutating reactance obtained in step 1 is used to interpolate between the curves of Figure 7. The ordinate thus obtained for the particular number of rectifier phases is the voltage TIF contribution per "per cent power source reactance" on the rectifier transformer kilovolt-ampere base. This value when multiplied by the appropriate per cent power source reactance gives the voltage TIF on the feeder. "Power source reactance," as here used, is the reactance on the power source side of the point considered. In case of feeder *C*, the power source reactance includes the reactances of transformer *D* and of the power supply to it.

In thus using Figure 5, the estimated voltage TIF impressed on feeder *B* is the voltage TIF per per cent source reactance as estimated above times the power source reactance to the point where feeder *B* is supplied. The per cent source reactance to the point where feeder *B* is supplied is equal to the source reactance used for feeder *C* plus the per cent reactance of feeder *A*. The reactance of feeder *A* can be determined conveniently from equation 2 or equation 3, depending on the circuit voltage.

Having obtained estimates of voltage TIF at the points supplying power to feeders *B* and *C*, installations can be classified from the standpoint of exposures *B* and *C* as in Table V.

If no exposures exist or will be created in the future in a particular location, there is no occasion for estimating voltage TIF for that feeder location or supply bus.

Step 4. Exposures to Supply System Network (Exposure *N* in Figure 5)

The power supply system may range from a single generator *G* to many generators and may include an extensive transmission or subtransmission network. Where such a network is involved, the primary consideration from an induction standpoint is whether the harmonic current fed to it will have a significant effect on the influence of distribution systems (particularly rural) connected to it and over how large an area this will occur. The rectifier harmonics do, of course, tend to increase the influence of the high voltage circuits themselves, but as a rule problems from this cause are less widespread or important than problems associated with the effects on distribution systems supplied by these circuits. Experience has shown that the most useful factors in estimating the effect of rectifier harmonics from this standpoint are:

1. The I·T product put into the network by the rectifier.
2. The general characteristics of the network.

The I·T product on the direct feeder *A* has already been obtained in step 2. This I·T product will divide between the generator and network circuits in the inverse ratio of their impedances, from which the I·T product put into the network can be estimated. Where the network is connected to the bus through a transformer bank, the impedance looking into the

* For rectifier installations of 12 or more phases, strict theoretical accuracy would require application of correction factors to the a-c system reactances before combining them with the commutating reactance of the rectifier transformer to obtain total $\%X_c$. For the purposes of this report, this refinement was not considered essential and was omitted for the sake of simplicity.

** It has been found by experience that the minimum I·T is secured when the loads among units in a multiphase installation are well balanced even if this requires the use of small amounts of phase control in some of the units.

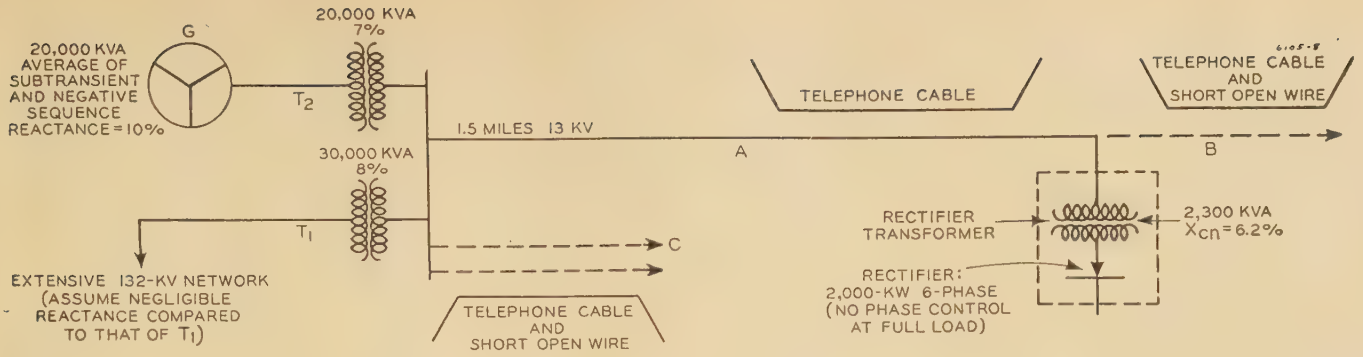

(A) SCHEMATIC DIAGRAM

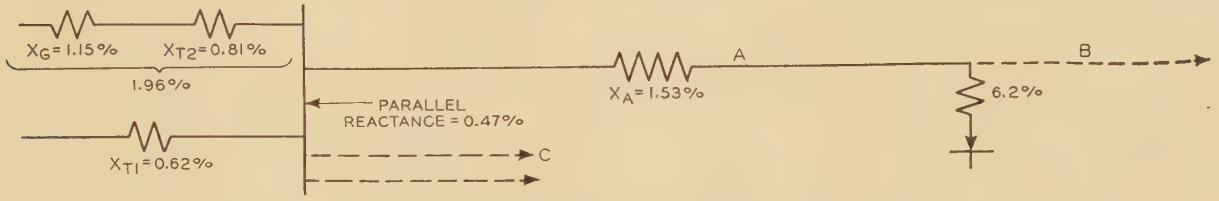

(B) IMPEDANCE DIAGRAM ON RECTIFIER TRANSFORMER KVA BASE

network can be assumed to be that of the transformer bank; where there is no transformer bank, the safest assumption is that all of the I·T goes into the network. In estimating magnitude of I·T products at various points, it is, of course, necessary to take into account the ratios of any transformers through which the currents pass.

While a wide range of supply network and exposure conditions may be encountered, the most useful and convenient classification from the co-ordination standpoint is based on the information outlined in Table VI.

Discussion

Rectifier co-ordination problems involve complex phenomena. As a consequence, a few installations which appear to be in category I cause important problems; conversely, a few installations which appear to be in category III turn out to be innocuous. Categories I and III have been set up so as to make them as definite as practicable, while category II covers a wide range of intervening conditions. The chance of a particular case's actually falling outside of its indicated range depends to a considerable extent upon its nearness to the edge of the range.

Certain additional factors may be considered qualitatively in estimating the likelihood of important induction problems for installations, particularly those in category II. Some favorable and unfavorable factors in exposures to distribution circuits (exposures *A*, *B*, and *C* of Figure 5) are:

Figure 8. Illustrative example of installation to be classified

1. Heavy industrial type feeders supplying mainly 3-phase loads provide a favorable factor. The lighter the load, the more scattered it is; and the larger the proportion of single-phase line and load, the greater will be the likelihood of a co-ordination problem, assuming normal urban exposure conditions.

2. Large banks of capacitors at or near rectifier installations of 12 or more phases are usually favorable; for 6-phase installations they may be favorable or unfavorable. The reason for the differentiation is that resonance between capacitors and urban distribution circuits is most likely to be important for frequencies of from 200 to 500 cycles, which are normally suppressed with rectifiers of 12 or more phases.

3. Capacitor banks electrically remote from rectifier installations may be unfavorable, particularly for 6-phase rectifiers.

Certain additional favorable and unfavorable factors in exposures involving the supply network (exposure *N* of Figure 5) are:

1. For urban power cable networks, the greater the lengths of cable which the harmonics must traverse before reaching overhead circuits, the less is the likelihood of a problem.

2. The larger the number of transformers through which the harmonics must pass before they reach overhead distribution circuits, particularly rural circuits, the smaller is the likelihood of a problem.

3. Supply to a rectifier direct from a generator bus is favorable; a generating station connected to a high voltage transmission system through transformers may be favorable or unfavorable; usually the effect is not large.

In a number of the cases investigated, it was found that the rectifiers were operating with unnecessarily large amounts of phase control at full load. As a result, the I·T product and voltage TIF were substantially higher than would normally be expected. In most of these cases, selection of different transformer taps and, occasionally, readjustment of the phase-control mechanism reduced the harmonics substantially.

In some installations, one or more of circuits *A*, *B*, or *C* may be missing and need not be considered in the classification procedure. For example, some installations are supplied from high voltage networks through transformer banks which supply power only to the rectifiers and the plants in which they are located; in such cases only the I·T into the high voltage network is of interest.

Illustrative Example

In order to illustrate the application of these methods, consider Figure 8.

Step 1. Figure 8A shows a schematic diagram of an assumed power system associated with a rectifier, and Figure 8B shows an impedance diagram on the rectifier transformer kilovolt-ampere base.

Assume that the exposures to *A*, *B*, and *C* are normal urban, miscellaneous joint use and roadway, and that power circuits *B* and *C* extend into residential areas.

The reactances in Figure 8B were determined as follows:

$$\%X_A = \frac{0.075 \times 1.5 \times 2{,}300}{13^2}$$

$$= 1.53\% \text{ (using equation 3)}$$

$$\%X_{T_1}=8\times\frac{2{,}300}{30{,}000}$$
$$=0.62\% \text{ (using equation 4)}$$
$$\%X_{T_2}=7\times\frac{2{,}300}{20{,}000}$$
$$=0.81\% \text{ (using equation 4)}$$
$$\%X_G=10\times\frac{2{,}300}{20{,}000}$$
$$=1.15\% \text{ (using equation 4)}$$
$$\%X_G+\%X_{T_2}=1.15+0.81=1.96\%$$

Reactance of T_1 and generator branch in parallel is

$$\frac{1}{\frac{1}{1.96}+\frac{1}{0.62}}=\frac{1}{0.51+1.61}=\frac{1}{2.12}=0.47\%$$

The total commutating reactance on rectifier transformer kilovolt-ampere base:

$$\text{Total } \%X_c=6.2+1.53+0.47=8.20\%$$

Step 2. The total I·T in feeder *A* is determined as follows:

With a total X_c of 8.2 per cent, the I·T per kilovolt-ampere on a 1-kv circuit is, from Figure 6, about 180. The total I·T in *A* is then:

$$\frac{180\times2{,}300}{13}=32{,}000$$

From Table IV, the installation would be classified in category II from the standpoint of the direct feeder *A*.

Step 3. The per cent power source reactance used to estimate the voltage TIF on feeders *C* is the reactance of the generator branch and T_1 in parallel, which is 0.47%. From Figure 7, the voltage TIF per per cent source reactance is (for a total X_c of 8.2%) about 50. The voltage TIF impressed on *C* will thus be about $50\times0.47=24$.

From Table V, the installation would be classified in category I, from the standpoint of feeders *C*.

The per cent power source reactance used to estimate the voltage TIF impressed on *B* is $0.47+X_A=0.47+1.53=2.00\%$. Again, the voltage TIF per per cent is 50; the voltage TIF on *B* will then be about $50\times2.0=100$.

From the standpoint of circuit *B*, the installation will be (from Table V) in category II. If capacitors are to be used on the power system, it will be near the upper edge of category II. If circuit *B* should be used to supply a rural system, the installation would probably be in category III from the standpoint of the rural system.

Step 4. The total I·T on a 13-kv base going into the generator and high voltage network branches in parallel is (from step 2) 32,000. That going into the generators is of no interest. That going into the transmission network is

$$32{,}000\times\frac{1.96}{1.96+0.62}=24{,}000$$

On the 132-kv high voltage network, this I·T is reduced by the ratio of transformation of transformer T_1, or it is

$$24{,}000\times\frac{13}{132}=2{,}400$$

From Table VI, it will be seen that from the standpoint of the high voltage network, the installation is in category I.

Discussion of Example

From the analysis, it can be seen that the area in which problems are most likely to occur when the rectifier is placed in operation is that supplied by feeder *B*. It is possible that there will be some problems associated with feeder *A*, but unless the exposure extends practically the whole length of the feeder, they probably will not be unduly severe. The chances of problems associated with feeder *C* or with remote distribution systems fed from the 132-kv network are small.

It would seem wise in this case to examine the situation with regard to feeder *B* in more detail before placing the rectifiers in operation; for example, ascertain whether capacitors are used at widely separated points, the general degree of circuit balance, and the amount and type of exposure (particularly between the rectifier and the capacitors). Arrangements might be made for applying telephone cable sheath shielding in advance of the start of rectifier operation and for some method of emergency operation to take care on a temporary basis of any difficulties that might develop until permanent measures could be applied if tests indicated their necessity.

It probably also would be advisable, if practicable, to make tests on feeders *A* and *B* and on some telephone circuits exposed to them before the rectifier is brought up to full load, possibly during the preliminary tests of the rectifier.

Little, if any, attention need be given to the high voltage network or to feeders *C* except possibly to make a few tests after the rectifier is in regular operation to be sure that no unforeseen conditions exist.

It is of interest to note that in this case a ten per cent voltage reduction at full load by phase control would result in more than doubling the I·T's and voltage TIF's with a consequent substantial increase in likelihood of problems; for example, it would result in putting the installation well into category III from the standpoint of *B*, in category II from the standpoint of *C*, and close to category II from the standpoint of the high voltage network. (See example under "Installations Using Substantial Amounts of Phase Control.")

On the other hand, if the installation were 12 phase without phase control at full load, the I·T's and voltage TIF's would be reduced 35 per cent to 45 per cent, with a consequent substantial reduction in the likelihood of problems.

Small Rectifiers of Three or Four Phases

For small rectifier installations, the capacity may be less than that of 6 or 12 tubes of conventional size. For these cases it may be desirable to use four or eight rectifier tubes with a transformer connected in Scott/4-phase cross, or three tubes with a transformer connected in delta/3-phase zigzag. Estimates of harmonic effects of these connections may be based on the methods of analysis and the data given for 6-phase rectifiers, and increasing the I·T product and voltage TIF factors by the multipliers given in Table X.

Table X

Phase	Relative I·T and Voltage TIF Factors*
4	1.20
3	1.33

* These multiplying factors are to be applied to estimates based on 6-phase rectifiers.

Application to System of Other Than 60 Cycles

In order to apply the methods outlined here in cases where the power system frequency is other than 60 cycles, it will be necessary to obtain voltage TIF and I·T products from other sources.[3,8,9,17] With these factors known, installations can be classified as outlined in the foregoing.

Co-ordinative Measures

The solution of problems involving rectifiers where the application of co-ordinative measures is indicated is no different from other types of inductive co-ordination problems, in that close co-operation of all interested parties is necessary. Guiding principles and general practices are given in the report on "Principles and Practices for Inductive Co-ordi-

nation," by the Edison Electric Institute and the Bell Telephone System,[30] which recognizes that characteristics of both the power and the telephone systems must be taken into account. Of the various kinds of co-ordinative measures applicable to the power or telephone system, the following are the most important in connection with rectifier problems:

1. Advance planning of the method of supplying the rectifier from the standpoint of minimizing wave shape distortion.[32]
2. Phase multiplication of rectifier installation.[3,5,6,20]
3. Frequency selective devices.[21,32]
4. Reduction of power system unbalance to ground.[10,11,12,23]
5. Co-ordinated transpositions.[24] (Transpositions in power distribution circuits are of negligible value but may in some cases be useful in transmission circuits.)
6. Reduction of telephone system unbalance to ground.[10,11,12,23,26]
7. Shielding of telephone cable circuits.[25]

Some of these already have been referred to as factors in evaluating the likelihood of a given installation's causing trouble.

It is impracticable within the scope of this report to present a sufficiently detailed discussion of these measures to provide the information required for reaching a solution of a particular situation. However, the following general discussion of these measures, with some indication of their field of use, may be helpful in a more detailed examination of the material listed in the references.

Induction problems associated with rectifiers are most likely to involve exposures between power distribution circuits and telephone exchange circuits. The difficulties of applying and maintaining co-ordinative measures on a specific exposure basis, where power and telephone distribution circuits are involved, has led in recent years to relying more and more on the maintenance of the lowest practicable susceptiveness* of telephone circuits in general and of the smallest practicable wave shape distortion on power circuits in general. This is particularly true in rural areas where changes and extensions are frequent and where the power circuit influence is very greatly affected by wave shape.

Improved balance-to-ground of the newer types of telephone subscriber and central office equipment, which reached the stage of large-scale production just prior to the war, was most helpful in this connection. Another helpful factor in the prewar years was the increase in use of carrier on telephone toll circuits, which was accompanied by much more effective telephone transposition arrangements. Of great importance from the standpoint of power system influence was the development and application of the principle of phase multiplication, particularly in view of the tremendous expansion during the war in large scale rectifier installations.

Figures 6 and 7 have illustrated the effectiveness of phase multiplication in reducing the I·T and voltage TIF. This results from a reduction in the number of harmonic orders present as indicated in Table I. Another advantage of a relatively large number of phases is that power system resonance conditions tending to magnify the effects of harmonics are much less likely to occur at frequencies above the twenty-fifth harmonic (60-cycle base). Furthermore, if induction problems do arise, remedial measures are much less expensive than for a smaller number of phases because

1. The number of harmonics to be cared for is smaller.
2. The volt-ampere capacity of devices to reduce harmonics goes down rapidly as the lowest frequency which they must handle goes up.

The number of phases in an installation is, of course, limited to the number of anodes. To secure the greatest effectiveness of phase multiplication, the d-c loads on the individual rectifiers must be well balanced. Where they are not well balanced, shifting the phase of successive rectifier units to obtain phase multiplication will be much less effective. When one of the units in a multiphase installation is out of service, as for maintenance, the effectiveness of phase multiplication is reduced, but in only a small number of cases has this presented a problem of importance.

While phase multiplication is a powerful tool in the larger capacity installations, there are still many smaller installations of limited number of anodes where it cannot be employed. The only presently available method of controlling harmonics, other than phase multiplication, is some form of frequency selective device. Most of these devices have consisted of several resonant shunts or of a series reactor and shunt capacitor, per phase. The use of series reactors increases the voltage regulation of the rectifier unit which must be taken into account in many cases. Resonant shunts involve precision tuning and, where several shunts are used per phase, may involve special mounting arrangements.

With the more extensive use of power factor correction capacitors on power systems, a somewhat different approach to the frequency selective device design problem may, in some cases, be advantageous. This approach is first to consider what capacitor installations have been made or can be justified for power reasons and next to consider whether they will, or can be made to, produce harmonic control. For example, if a fairly large block of capacitors can be justified for power reasons at or near the rectifier location, they may be adequate alone, as has been the case in several large metallurgical rectifier installations, or coils to tune the entire bank broadly or to tune parts of the bank to particular frequencies might be added. The same thing might be done with capacitors at a supply substation bus if harmonic currents in the direct feeder are not important. In any such installations—whether equipped with tuning coils or not—the chances of adverse resonance at the lower harmonic frequencies need to be considered. In general, the reduction in I·T and voltage TIF would not be expected to be as large with the broadly tuned arrangement as with several sharply tuned resonant shunts, but in view of its very low cost (assuming the capacitors would be available, anyway), it may be advantageous in some cases, particularly where large reductions are not needed.

The extent to which other measures can be substituted in place of control of the rectifier harmonics in a specific case depends on many circumstances which cannot be described in detail here. However, a few of the more general considerations can be given, namely:

1. Situations where the effect of the rectifier is confined to the feeder between the source of supply and the rectifier offer the best field for the use of measures other than harmonic control, or a combination of these measures with a moderate degree of harmonic control.
2. In cases where the effect of the rectifier spreads beyond the feeder, but only to a limited extent, the same situation exists, although the advantage of reducing the harmonics is greater because of the greater uncertainties as to conditions in the future.
3. In cases where the effects spread over wide areas and involve numerous power distribution systems, it is almost hopeless to attempt to correct induction conditions without limiting the harmonics at the rectifier.

Installations Using Substantial Amounts of Phase Control

For installations employing substantial amounts of phase control at rated load,

* See Appendix I for explanation.

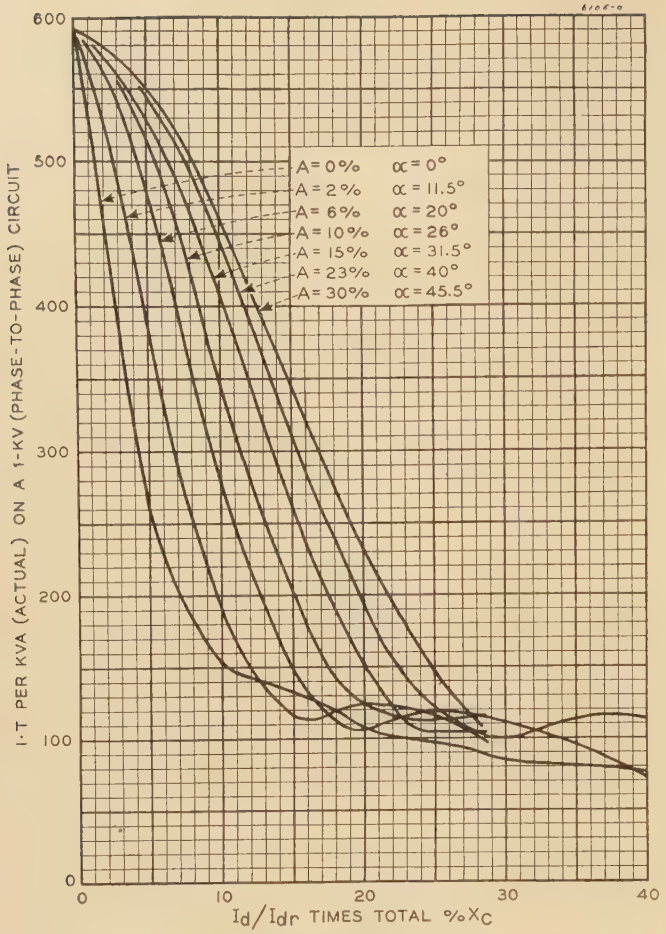

Figure 9. Six-phase rectifiers

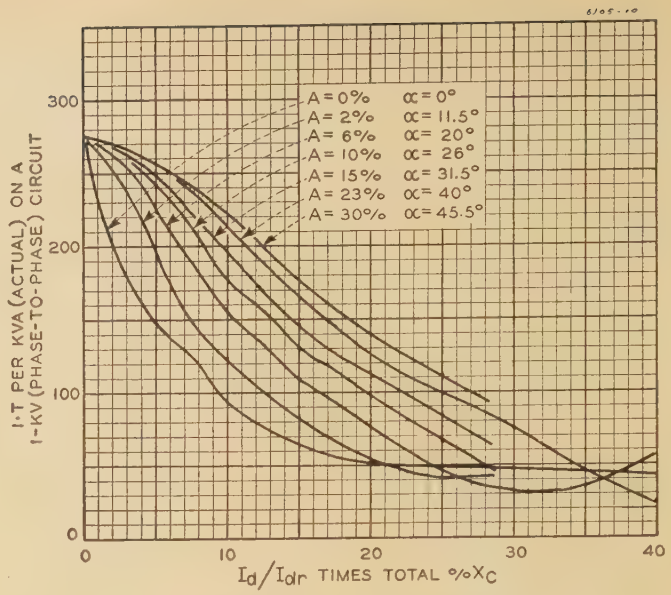

Figure 10. Twelve-phase rectifiers

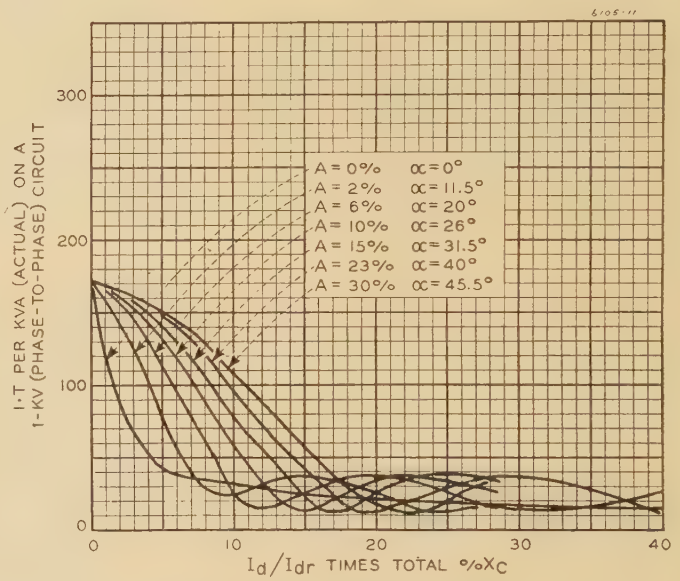

Figure 11. Twenty-four-phase rectifiers

Figures 9, 10, 11. I·T per kilovolt-ampere on 1-kv circuit for 6-, 12-, and 24-phase rectifiers with different amounts of phase control

For 60-cycle systems
I_d = actual d-c load current
I_{dr} = rated d-c load current
Total $\%X_c$ = per cent commutating reactance of rectifier transformer bank and supply system on rectifier transformer bank kilovolt-ampere base
α = phase control angle of retard
A = amount of phase control or per cent voltage reduction below output voltage with zero phase control ($A = 1 - \cos \alpha$)

To find I·T

1. Determine the value of I_d/I_{dr} times total $\%X_c$ for the particular load under consideration. Where the I·T for the rated capacity only is desired, total $\%X_c$ is used directly

2. From the curve for the appropriate number of phases and amount of phase control, determine the I·T per kilovolt-ampere

3. Multiply the I·T per kilovolt-ampere read on the curves by the *actual* kilovolt-ampere and divide by the phase-to-phase line voltage in kilovolts. This is the estimated phase I·T. Actual kilovolt-amperes can be obtained by multiplying rated kilovolt-amperes by the ratio I_d/I_{dr}

Figures 6 and 7 cannot be used to obtain I·T products and voltage TIF's. However, I·T products can be estimated from Figures 9, 10, and 11 which show I·T per rectifier kilovolt-ampere on a 1-kv line with various amounts of phase control, for 6-, 12-, and 24-phase installations, respectively, operating in a balanced manner. Voltage TIF can be estimated by using Figures 12, 13, and 14, which show voltage TIF per per cent power source reactance on rectifier transformer kilovolt-ampere base, with various amounts of phase control, for 6-, 12-, and 24-phase installations, respectively, operating in a balanced manner.

To illustrate the use of these curves, consider the example discussed under "Procedure in Classifying Proposed Installations" (see Figure 8), but assume ten per cent phase control at rated output voltage and current. The I·T product on the direct feeder A and the voltage TIF on B will be estimated:

1. The rectifier transformer kilovolt-amperes required for this rating will be (see equation 1)

$$1.15 \times \frac{(100+10)2{,}000}{100} = 2{,}530 \text{ kva}$$

2. The parallel reactance of the generator and T_1 on the rectifier transformer kilovolt-ampere base will be 0.47 (2,530/2,300) = 0.52 per cent (equation 4).

3. The line reactance (X_A) on rectifier transformer kilovolt-ampere base will be 1.53(2,530/2,300) = 1.7 per cent.

4. The total $\%X_c = 0.52 + 1.7 + 6.2 = 8.4$ per cent.

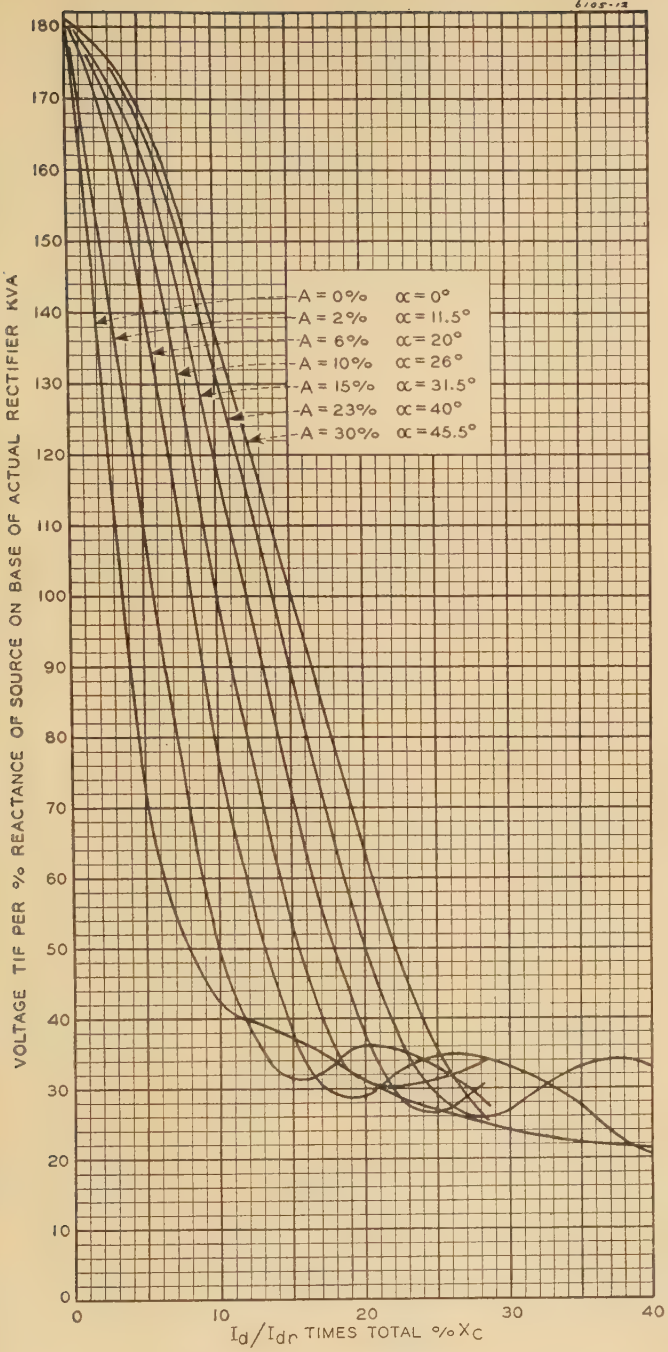

Figure 12. Six-phase rectifiers

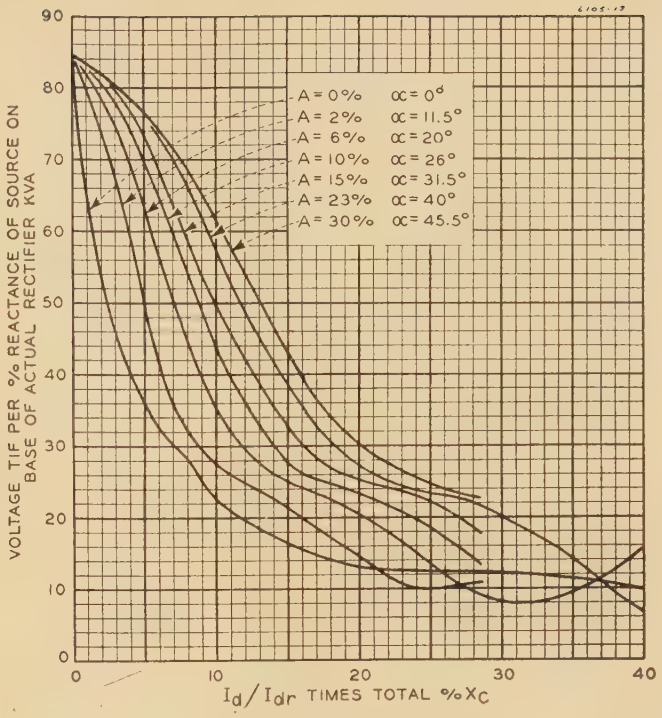

Figure 13. Twelve-phase rectifiers

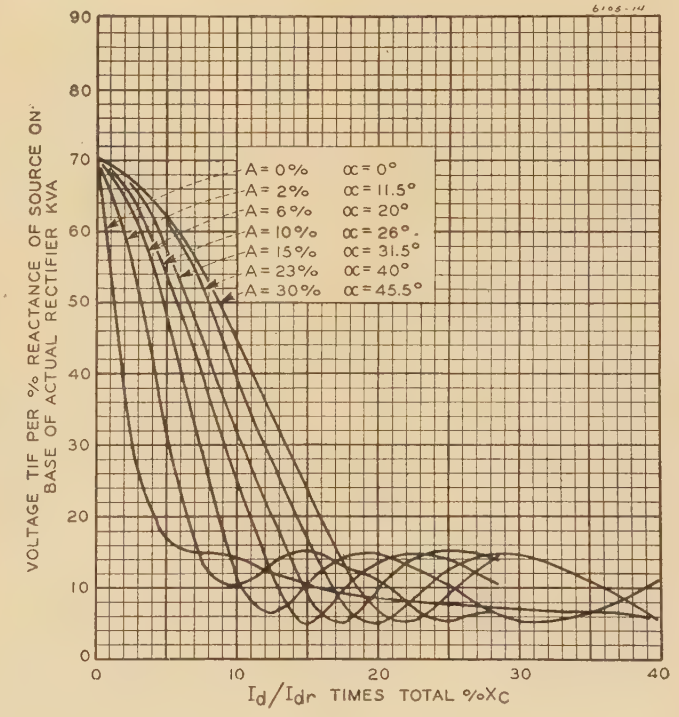

Figure 14. Twenty-four-phase rectifiers

Figures 12, 13, 14. Voltage TIF per per cent reactance of power source for 6-, 12-, and 24-phase rectifiers with different amounts of phase control

For 60-cycle systems
I_d = actual d-c load current
I_{dr} = rated d-c load current
Total $\%X_c$ = per cent commutating reactance of rectifier transformer bank and supply system on rectifier transformer rated kilovolt-ampere base
α = phase control angle of retard
A = amount of phase control or per cent voltage reduction below output voltage with zero phase control ($A = 1 - \cos \alpha$)

To find voltage TIF:

1. Determine the value of I_d/I_{dr} times total $\%X_c$ for the particular load under consideration. Where the TIF for the rated capacity only is desired, total $\%X_c$ is used directly

2. Determine the per cent power source reactance on the base of *actual* rectifier kilovolt-amperes. For partial load, this can be found by multiplying source reactance on the base of rectifier transformer rated kilovolt-amperes by the ratio I_d/I_{dr}

3. From the curve for the appropiate number of phases and amount of phase control, determine the voltage TIF per per cent source reactance

4. Multiply the value read on the curves by source reactance found in step 2. This is the estimated voltage TIF

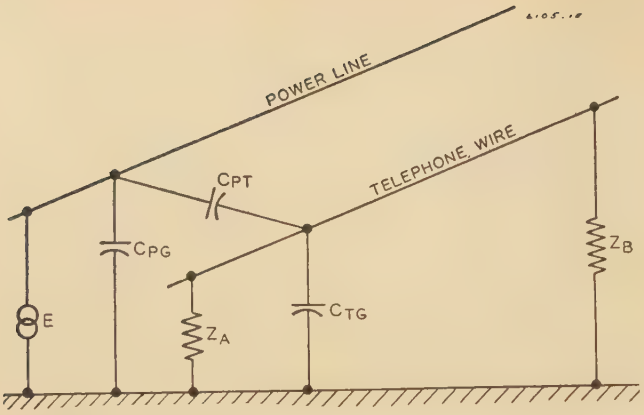

Figure 15. Nature of electric induction

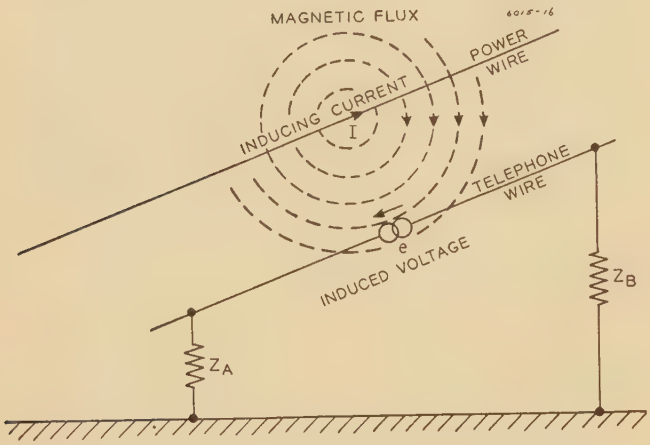

Figure 16. Nature of magnetic induction

5. From Figure 9, the I·T per kilovolt-ampere on a 1-kv circuit for total $\%X_c$ of 8.4 per cent, $\frac{I_d}{I_{dr}}$ equal to one, and phase control of ten per cent, is about 410; or on a 13-kv circuit, it is 410/13=32. The total I·T on feeder *A* is then 32×2,530=80,000.

6. From Figure 12, the voltage TIF per per cent power source reactance is about 120. The total per cent power source reactance to point *B* is 0.52+1.7=2.2 per cent. The estimated voltage TIF at point *B* is, then, 120×2.2=260.

To illustrate the method of obtaining I·T products and voltage TIF's at partial load, suppose it is desired in the example just illustrated (that is, the same as Figure 8 but with a 2,530-kilovolt-ampere rectifier transformer) to find the conditions at a *current* output of 0.6 times rated output, but with 15 per cent phase control at this load. Proceed as follows:

1. $\frac{I_d}{I_{dr}} \times \%X_c = 0.6 \times 8.4 = 5.0$ per cent.

2. I·T per kilovolt-ampere on 1-kv circuit with 15 per cent phase control is (from Figure 9) about 530. On a 13-kv circuit, it would be 530/13=41. The kilovolt-ampere input can be taken as 2,530×0.6=1,520. The total I·T on the feeder is 1,520×41=62,000.

3. The voltage TIF per per cent power source reactance is (from Figure 12) about 163. To estimate voltage TIF at point *B* in Figure 8, multiply per cent power source reactance by 0.6; that is, 0.6×2.2=1.3. Next, multiply by 163, that is, voltage TIF at *B* equals 1.3×163=212.

Figures 10, 11, 13, and 14 assume balanced operation between the 6-phase units making up the 12- and 24-phase installations; that is, it is assumed that the d-c loads are equal, that the voltages of the d-c transformer windings on all units are identical, that the differences in phase control between units are small and that the harmonic voltages on the power supply system are too small to result in unbalances. If the d-c winding voltages of the rectifier transformers differ between units (which may be caused by operation on different transformer taps) and different amounts of phase control are used, the curves no longer give accurate results, even if the d-c loads are balanced. Under such conditions, the suppression of the "normally suppressed" harmonics is likely to be impaired and partial suppression of "normally unsuppressed" harmonics may occur.

Other Forms of Conversion Equipment

Co-operative investigations have been made in connection with two installations of large frequency changers connecting 60-cycle and 25-cycle 3-phase systems.[15;39] Tests have also been made on two installations of equipment for converting from 3-phase 60 cycles to single-phase at a frequency on the order of 1,000 cycles.[38] The test results indicate that the methods outlined herein can be applied in connection with such installations without large error.

Data are not available for estimating I·T products and voltage TIF's for other forms of conversion apparatus, such as electronically controlled motors. It appears, however, that where the power supply to such devices is balanced 3-phase, estimates made along the lines discussed herein would provide at least a good starting point in studies.

The inductive effects of single-phase rectifier installations are subject to much wider variations than 3-phase installations, and the methods outlined herein cannot be applied to such installations.

Appendix I. Fundamentals of and Terms Used in Noise Frequency Co-ordination Work

In this appendix, fundamentals of and terms used in noise frequency inductive co-ordination work are discussed.

Electric and Magnetic Induction—Coupling

Voltages induced on telephone circuits by power circuit voltages are said to be caused by electric induction; voltages caused by power circuit currents are said to be the result of magnetic induction. These forms of induction exist independently and must be so treated.

The process of electric induction in its simplest form is shown in Figure 15. The power wire has on it a harmonic voltage *E* to ground.

1. Between the power wire and a nearby telephone wire, electric coupling, represented by capacitance C_{PT}, exists. The magnitude of this capacitance is directly proportional to length of exposure and increases as separation between the wires decreases. Its impedance is inversely proportional to frequency.

2. The telephone wire has finite impedances to ground, Z_A and Z_B, outside the exposure. These impedances are usually much smaller than the impedance of C_{PT}. The current to the telephone wire is therefore controlled by C_{PT}; it is directly proportional to the coupling and to frequency and magnitude of *E*. The voltage on the telephone wire is the current through C_{PT} times Z_A and Z_B in parallel; it is roughly proportional to coupling and frequency.

The magnetic induction process in its simplest form is shown in Figure 16.

1. A mutual reactance, or magnetic coupling, exists between the power wire and the nearby telephone wire by virtue of the fact that the magnetic flux associated with the power wire current links the telephone wire. The total amount of flux (per unit of power wire current) which links the telephone wire is proportional to length of exposure and increases as separation is decreased.

2. The voltage *e* induced along the telephone wire is proportional to the total flux which links it and is also proportional to frequency. The current in the telephone wire is this voltage divided by (Z_A+Z_B). The voltage to ground at one end of the exposure is this current times Z_A; at the other, times Z_B.

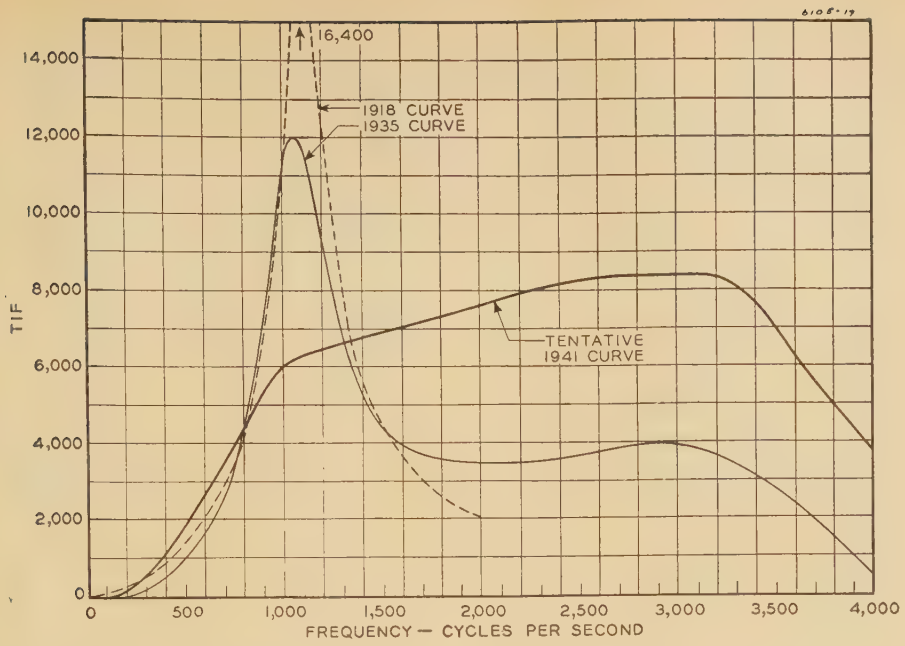

Figure 17. TIF weightings

Voltage TIF and I·T Products

The frequencies in human speech range from the order of 125 cycles to upwards of 10,000 cycles per second. A much narrower band of frequencies is sufficient to carry on a satisfactory conversation and most telephone circuits are designed to transmit such a narrower band.

Each harmonic voltage or current in a power system induces a voltage of the same frequency in a paralleling telephone circuit which, in turn, may actuate a telephone receiver and cause an audible sound. The composite of the sounds of all such frequencies present usually results in a humming sound commonly called noise. Different interfering effects[27,29] depending on the characteristics of the telephone circuits, receiver, the human ear, and other factors; relative interfering effects are called noise weightings and have been ascertained by extensive tests. The composite of the noise voltages in the circuit can be measured by means of a noise measuring set which contains networks having frequency-transmission characteristics in accordance with the noise weightings, and a meter which adds components as the square root of the sum of the squares.

Since the effects of both electric and magnetic coupling are directly proportional to frequency, the relative noise influence of voltages and currents on the power system is proportional to the product of noise weighting and frequency. For any frequency, this product (times a constant) is known as TIF (telephone influence factor) weighting. TIF weighting curves as functions of frequency are shown in Figure 17.

There are three different sets of TIF weightings which reflect changes in transmission-frequency characteristics of telephone circuits and instruments over a long period, namely:

1. The "1918" weightings. These were known as telephone interference factor weightings, and this name is still used to distinguish them from the later weightings which are called telephone influence factor weightings.

2. The "1935" weightings.[28]

3. The tentative "1941" weightings. These weightings have not been standardized yet.

The very small weightings of 60 cycles explains why, from the noise frequency induction standpoint, only the harmonics are of interest.

While much induction work is carried on on the basis of individual harmonics, it frequently is desirable to use an over-all measure of the influence of a current or a voltage in a power circuit. This over-all measure is obtained by multiplying the magnitude of each harmonic present (amperes, for current; kilovolts for voltage) by its TIF weighting, and taking the square root of the sum of the squares of these products. The result is, for current, I·T product; for voltage, KV·T product. These products can be measured directly by the use of a noise measuring set and a TIF coupler, the latter having a transmission-frequency characteristic directly proportional to frequency. So-called TIF meters also can be used.

Balanced, Residual, and Ground Return Currents and Voltages

Suppose in Figure 16 there were another power wire very close to the one shown there and that it carried a current equal and opposite to the current in the original wire; such a set of currents would be called balanced. The flux cutting the telephone wire then would be only the difference between the fluxes at that point arising from the currents in the two power wires. If the separation between the power wires were small, this difference would be small and hence the coupling would be small as compared to that for current which goes out on one or more wires and returns through the earth, that is, ground return current.

A similar analysis with respect to voltages would indicate the same conclusions.

For a power circuit of any number of phases and wires, the following terms apply:

1. Ground return current is the vector sum of the

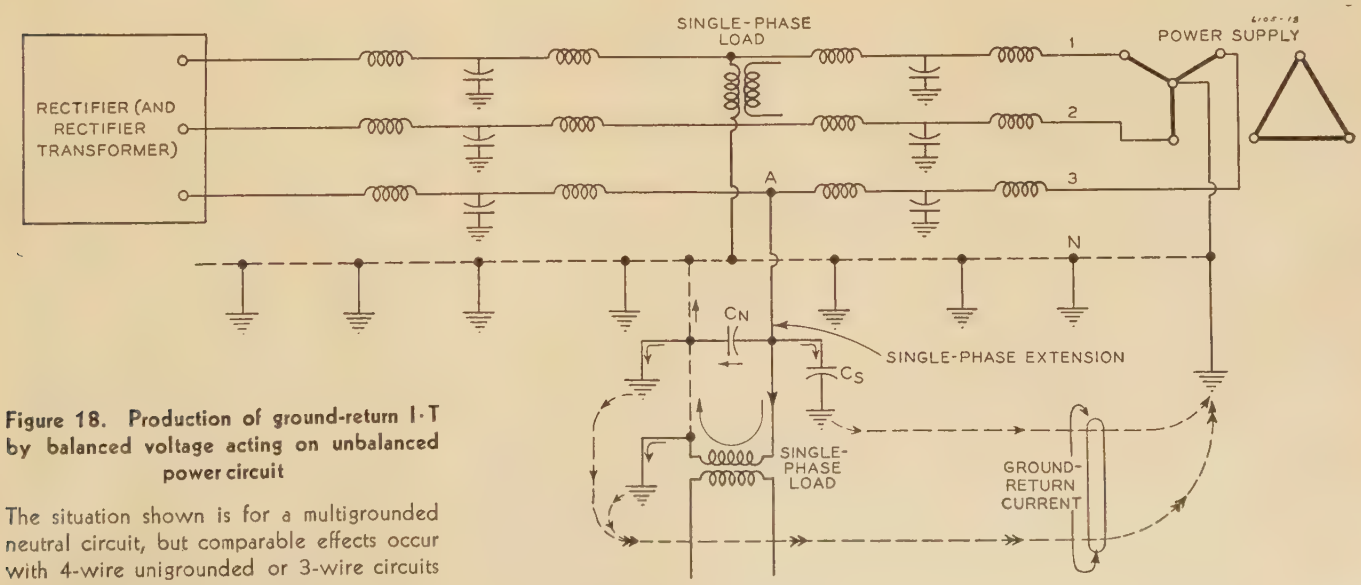

Figure 18. Production of ground-return I·T by balanced voltage acting on unbalanced power circuit

The situation shown is for a multigrounded neutral circuit, but comparable effects occur with 4-wire unigrounded or 3-wire circuits

actual currents in all the wires of the circuit.

2. Residual current is the vector sum of the actual currents in the phase wires. In a 3-phase 3-wire circuit, residual and ground return currents are the same. In a 4-wire 3-phase circuit, part of this residual current may stay in the neutral wire, and the influence of this part is about the same as if it were balanced. In a 2-wire circuit consisting of an extension of a phase wire and neutral of a 3-phase 4-wire circuit, phase and residual current are the same; part of this residual current is ground return.

3. Balanced currents are those components of the actual phase currents whose vector sum is zero.

4. Residual voltage is the vector sum of the voltages between phase wires and earth.

5. Balanced voltages are those components of the actual phase-to-ground voltages whose vector sum is zero.

The over-all influence of any one of these components is measured by its I·T or KV·T product. For distribution circuits, and in many cases for transmission circuits, over-all influence is controlled by ground return I·T, or residual KV·T. In dealing with voltages of known magnitude, voltage TIF is frequently used instead of KV·T; it is KV·T divided by voltage in kilovolts. For residual voltages on 3-phase generators, residual component voltage TIF is sometimes used; it is one third residual KV·T divided by phase-to-neutral voltage.

In a 3-phase circuit with no single-phase extensions or loads, the ground return I·T and the residual KV·T are usually small except for triple harmonics (third and odd multiples thereof). If, however, there are single-phase taps or loads, ground return harmonic currents can occur even though the harmonic voltages are impressed in a perfectly balanced manner, as by a rectifier. The conditions leading to this effect are shown in Figure 18. Here is shown a feeder from a power source to a rectifier; there is a single-phase extension. For simplicity in explanation, a multigrounded neutral circuit is shown; comparable effects may occur with unigrounded neutral or 3-wire circuits as explained later.

As explained in "Nature of Problem" in the main body of this report, the harmonic currents produced by the rectifier load flow through the phase wire reactances and produce harmonic voltages. The harmonic voltage-to-neutral thus caused at point A in Figure 18 is impressed on the single-phase tap. Capacitance exists between the phase wire in the tap and the neutral (C_N) and between the phase wire and ground (C_S). The load likewise presents a finite impedance between the phase wire and the neutral and ground in parallel. Harmonic currents flow through the capacitance and load impedances. Part of this current flows in the neutral wire (about 40 per cent in the usual case) and part in the ground (usually about 60 per cent). The ground current returns to the power circuit via the neutral ground on the supply transformer bank. Thus on the tap itself and on the portion of the 3-phase circuit between the tap and the power source, there is ground return harmonic current. Harmonic currents through single-phase loads connected directly to the 3-phase line produce ground return harmonic current in a similar fashion. In an actual circuit, there are usually numerous single-phase taps and single-phase loads; ground return current can circulate between one tap or load and other taps or loads, so that the ground return I·T is likely to be different at different places along a 3-phase circuit.

That comparable effects can occur on long unigrounded neutral or 3-wire circuits can be shown as follows:

1. Consider first a 4-wire unigrounded neutral circuit with a single-phase tap. Imagine that, in Figure 18, all grounds on the neutral are removed except the one at the power supply bank and series inductances and shunt capacitance are distributed along the neutral as well as the phase wires. Harmonic current can still flow through the capacitance between the phase wire and ground; this current is ground return. Furthermore, under some conditions, substantial voltages to ground can exist on the neutral at harmonic frequencies; they may cause harmonic currents through the neutral-to-ground capacitance, and these currents are ground return.

2. On a 3-wire circuit, the single-phase tap would be connected to two of the phase wires. Harmonic currents can flow through the capacitances to ground from both phase wires and become ground return. Even if there is no neutral-to-ground connection at the power supply bank, these ground return currents can exist; they return to the system through the capacitance to ground of the remaining phase wire in other parts of the system.

As a general rule, overhead urban distribution systems are so short that the capacitances can be neglected. Ground return current can occur in such systems only if the neutral is multigrounded. Rural systems, however, are usually long enough so that the harmonic currents through the capacitance are frequently controlling; substantial ground return I·T can occur regardless of whether or not a neutral wire is present or where or how the system is grounded.

There are three other methods by which ground return harmonic current can be caused by balanced impressed harmonic voltages or currents (as by a rectifier), namely:

1. The currents in the phase wires magnetically induce voltages along the neutral or ground wire. If the phase wires are not disposed symmetrically with respect to the neutral, the voltages induced along the neutral wire by the balanced currents in the three individual phase wires will not be equal. The vector sum can, in a multigrounded neutral circuit or a transmission circuit equipped with a ground wire, cause current to circulate between the neutral or ground wire and ground; this current is ground return. This effect usually is important only in cases where the circuit is very well balanced otherwise.

2. On a multigrounded neutral urban circuit with capacitors, small differences between the reactances of the individual phase wires can cause substantial ground return harmonic current if the capacitors and circuit are very close to resonance at one of the harmonic voltages present. This phenomenon is discussed more fully in Appendix II.

3. In some cases the minor differences in the reactances of the phase wires can cause ground return harmonic currents even in the absence of capacitors. Such ground return currents can occur only when

(*a*). The circuit is long enough to permit appreciable currents through the natural capacitances, *or*

(*b*). There are two or more transformer bank neutral-to-ground connections between which the ground return current can circulate.

Metallic and Longitudinal Telephone Voltages and Currents—Susceptiveness

Assume that in Figure 16 another telephone wire is added parallel and close to the first. The second wire will be linked by nearly the same flux as the first, and the difference in the voltages along the two wires will be a small fraction of that along either one. If these two wires are used as a metallic telephone circuit, the noise voltage acting around this circuit will be a small proportion of that which would act in a telephone circuit consisting of one wire with ground return, that is, a ground return circuit.

The same analysis could be carried through for electric induction with the same conclusions.

Thus in a metallic telephone circuit, there is longitudinal circuit induction which is the voltage along or to ground on the conductors in parallel, and direct metallic circuit induction, which is the difference between the voltages along or to ground on the two wires, the direct metallic circuit induction being much the smaller.

Direct metallic circuit induction can be reduced still further by transposing the telephone circuit, that is, interchanging the positions of the conductors periodically so that the voltages on both tend to be equal. In open wire circuits the reduction obtainable, while large, is limited by unavoidable irregularities in exposure conditions. In cable circuits the pairs are twisted so as to be continuously transposed, and direct metallic circuit induction can be neglected. In addition, the telephone cable sheath provides practically perfect shielding against electric induction if grounded at one or more points, and it provides some shielding against magnetic induction if grounded at both ends, the degree of shielding being limited by the resistance of the sheath and of the grounds.

Longitudinal circuit induction can cause noise in a metallic circuit by acting on tele-

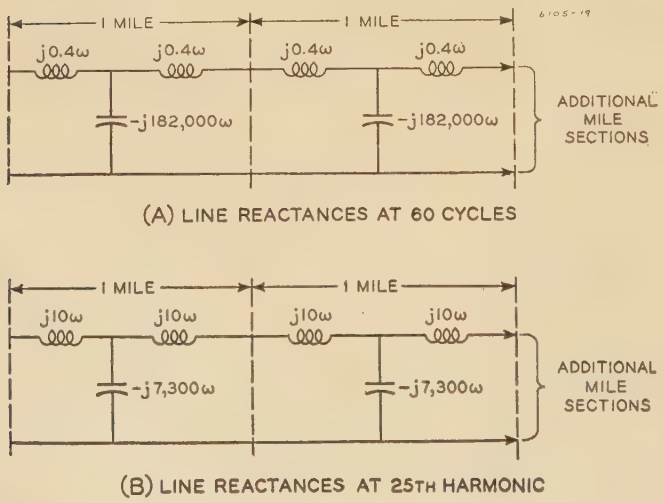

Figure 19. Phase-to-neutral inductive and capacitive reactances of typical transmission line

Figure 20. Sending-end phase-to-neutral impedance of typical transmission line with far end open and short-circuited

——— Sending-end inductive reactance $= +jX$

– – – – – Sending-end capacitive reactance $= -jX$

Impedances are for condition of no losses in circuit. For effect of losses, see text

phone circuit unbalances. These unbalances are of two types:

1. Series impedance unbalances, that is, differences in the impedances of the two wires of the circuit.

2. Shunt admittance unbalances, that is, differences in the admittances between the two wires of the circuit and ground.

Unbalances can occur in line, station, or central office equipment. Typical types of unbalances in these three locations are:

1. Lines. Series unbalances may be caused by imperfect joints or by variations in cross section or composition of the two conductors of a circuit. Shunt unbalances may be caused by such things as missing insulators, foliage touching the wires, transposition irregularities, and unbalances in capacitance to ground in cables.

2. Stations. Shunt unbalances only need to be considered. The principal unbalance is the ringer-to-ground connection used for party-line ringing. Its magnitude depends on the impedance of the ringer and the details of the subset connections.

3. Central office. Series unbalances can occur on account of unbalances in relays used for supervision, differences in capacitance of condensers used to block direct current paths, and so forth. Shunt unbalances may be caused by differences in the inductances of relay, retard or repeating coil windings connected between the wires and ground, differences in the capacitances to ground of wires, repeating coil windings, and other factors.

The degree to which a telephone circuit can be affected by given extraneous electric and magnetic fields is called its susceptiveness. Susceptiveness depends on such things as balance and adequacy of transpositions, and on the frequency response of the circuits and instruments and the level (magnitude) of the telephonic current and voltages at the point where the exposure exists.

Inductive Co-ordination

It is theoretically possible to have power circuits with practically zero influence (for example, by having no harmonics), they would not cause noise in any telephone circuit regardless of its susceptiveness. It is theoretically possible to have telephone circuits of practically zero susceptiveness (for example, by having perfect balance and transpositions); they would not be noisy regardless of the influence of nearby power circuits. Also, of course, if the power and telephone systems were separated by large distances, the coupling, and hence the noise, would be negligible. None of these methods is practicable, in general, in the present state of the art. The practical job of noise frequency inductive co-ordination consists of so controlling coupling, influence, and susceptiveness within practical limits that telephone circuit noise is controlled adequately at minimum cost and maximum satisfaction to both power and telephone customers.

Appendix II. Propagation of Harmonic Currents and Voltages

Line Characteristics

For short feeders between a source of power supply (generator or substation) and a rectifier installation, only the inductive reactances need be considered in estimating harmonic voltages and currents. But for longer circuits such as transmission or rural distribution circuits, the capacitances between the different wires and between the wires and ground must be taken into account when dealing with harmonic frequencies.

Why the capacitances associated with the wires have a greater effect at harmonic frequencies than at 60 cycles can be shown by considering the constants of a typical transmission line as illustrated in Figure 19. Here are shown the series inductive reactances and shunt capacitive reactances on a phase-to-neutral basis for such a line (Figure 19A) at 60 cycles and (Figure 19B) at the twenty-fifth harmonic. It can be seen that at 60 cycles the shunt capacitive reactances are very large compared with the series inductive reactances; a line of short or moderate length can be considered simply as consisting of $j0.8$ ohm per mile. But at the twenty-fifth harmonic, the series impedances are increased 25 to 1, and the shunt impedances are decreased 25 to 1. At the twenty-fifth harmonic, the total series impedance becomes as large as the total shunt impedance in 19.1 miles of line (that is, $19.1 \times 20 = 382 = 7{,}300/19.1$), whereas in the case of 60 cycles, this equality does not occur until the line is about 480 miles long.

To obtain an idea of how, quantitatively, this difference affects line performance, consider Figure 20, which shows the sending-end impedance of a typical transmission line with the far end open and with it short-circuited, as a function of length and frequency, neglecting losses. These curves are computed from the formulas:

Sending-end impedance with far end open $= -jZ_0 \cot \theta$

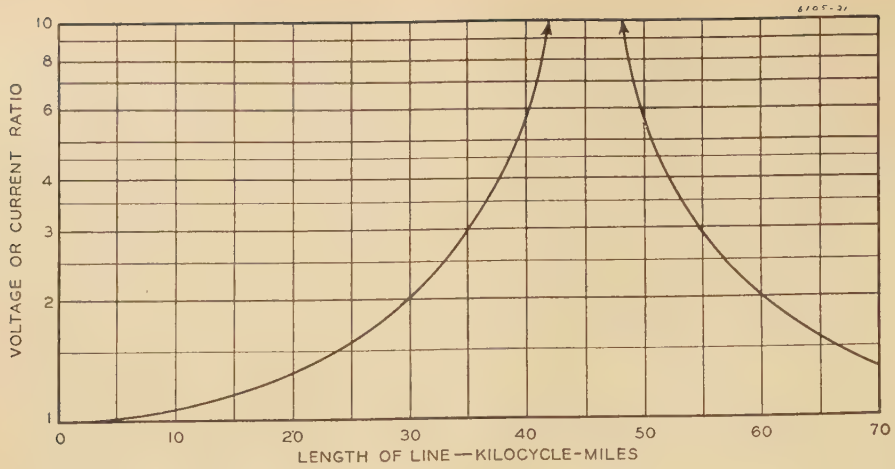

Figure 21. Ratio of current at far end to current at near end with far end short-circuited and ratio of voltage at far end to voltage at near end with far end open

Ratios are for condition of no losses in circuit. For effect of losses, see text

Sending-end impedance with far end short-circuited $= jZ_o \tan \theta$

where

Z_o = characteristic impedance to neutral (380 ohms in the example)

θ = line angle (or phase shift) in degrees = frequency times length times 360 divided by velocity of propagation

Since, in a smooth circuit without losses (a good approximation for power transmission circuits at harmonic frequencies), the velocity is independent of frequency, the curves can be plotted using length times frequency, that is, kilocycle-miles, as abscissas.* For example, a 100-mile line at 60 cycles is 0.06 kilocycle times 100 miles = 6 kilocycle-miles; a 20-mile line at 1,500 cycles is 30 kilocycle-miles, and so forth. For such lines the velocity is about 180,000 miles per second.

With a velocity of 180,000 miles per second, θ, or phase shift, is two degrees per mile per kilocycle, which can be derived as follows:

$$\text{Wave length at frequency } f = \frac{180{,}000 \text{ miles}}{f}$$

Wave length = 360 degrees

$$\text{Whence } \frac{180{,}000}{f} \text{ miles} = 360 \text{ degrees}$$

$$\text{Degrees per mile} = \frac{360\,f}{180{,}000} = 2° \times \frac{f}{1{,}000}$$

If f is in kilocycles, degrees per mile = two degrees times f (in kilocycles).

It will be noted from Figure 20 that

1. With the far end open, the impedance looking into the near end is capacitive reactance up to 45 kilocycle-miles; with the far end short-circuited, it is inductive reactance up to that length. Above 45 kilocycle-miles, the signs are reversed.

2. At 22.5 and 67.5 kilocycle-miles, the impedances with the far end open and short-circuited are the same in magnitude but opposite in sign.

3. At 45 kilocycle-miles, the impedance with the far end open is very low; with the far end short-circuited, it is very high. That is, at this length a short circuit on the far end tends to look like an open circuit at the near end; an open circuit at the far end tends to look like a short circuit at the near end. Actually, the near end impedances would go to zero or infinity except for the losses in the circuit. The significance of 45 kilocycle-miles is that it is "quarter wave length." That is, 45 × 2 degrees = 90 degrees, which is one quarter of 360 degrees. The effects at this length are sometimes referred to as "natural line resonance" because a line of this length with the far end open looks from the sending end like a series resonant circuit; with the far end short-circuited, it looks from the sending end like a parallel resonant circuit.

Another factor of importance in considering propagation is what happens to harmonic currents and voltages as they traverse the line from the sending-end to the far end. Figure 21 shows, for the same line as used in Figures 19 and 20, the ratio of voltage at the far end to that at the near end with the far end open, and the ratio of current at the far end to that at the near end with the far end short-circuited. This curve is based on the formula

$$R = \frac{1}{\cos \theta}$$

where

R = ratio of voltage at far end to that at near end with far end open, or ratio of current at far end to that at near end with far end short-circuited.

θ = line angle in degrees = two degrees times kilocycle-miles.

The abscissas are again in terms of kilocycle-miles. It is of some interest to note that these two ratios are shown by the same curve, that is, the voltage ratio with the far end open is the same as the current ratio with the far end short-circuited. The quarter wave length effect is again evident.

Here again the difference between the way a line performs at 60 cycles and at harmonic frequency may be noted. Consider a line 50 miles long with the far end open. The data for a few typical frequencies are set down in Table XI.

In most practical cases the far end of a line is not open nor short-circuited. While the treatment of the general case is beyond the scope of this appendix, it may be said that for transmission circuits the impedance at harmonic frequencies across the far end is frequently almost pure inductive or capacitive reactance. In such cases the effects shown in Figures 20 and 21 occur, but for different line lengths than shown there.

Equipment

Transformers and rotating machinery present almost pure inductive reactances; the impedance at harmonic n is very closely equal to n times the 60-cycle impedance

Table XI

Harmonic	Frequency	Kilocycle-Miles	Ratio of Far End Volts to Near End Volts (From Figure 21)	Sending-End Impedance (From Figure 20)
1	60	3	1.006	$-j3{,}650$
7	420	21	1.35	$-j425$
17	1,020	51	4.8	$+j84$
25	1,500	75	1.15*	$+j660$**

* Obtained from fact that the ratio for L kilocycle-miles is the same as the ratio for (90-L) kilocycle-miles, that is, the ratio for 75 kilocycle-miles is the same as the ratio for 15 kilocycle-miles.

** Obtained from the fact that sending-end impedance with far end open of a line L kilocycle-miles long is the same as sending-end impedance with far end short-circuited of line (L-45) kilocycle-miles long, that is, sending-end impedance with far end open of line 75 kilocycle-miles long is the same as impedance with far end short-circuited of line 30 kilocycle-miles long.

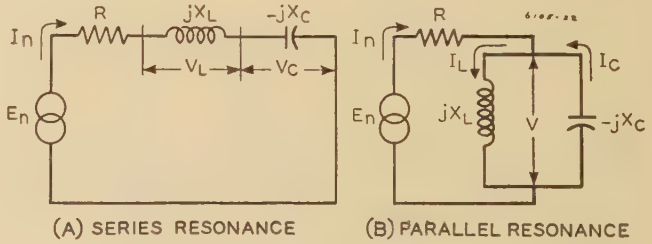

Figure 22. Series and parallel resonance

For series resonance,

$$I_n = \frac{E_n}{R + jX_L - jX_c}$$

If $X_L = X_c$, then

$I_n = E_n / R$

$V_L = I_n X_L$

and

$V_c = I_n X_c$

For parallel resonance,

$$I_n = \frac{E_n}{R + \dfrac{(jX_L)(-jX_c)}{jX_L - jX_c}}$$

If $X_L = X_c$, then

$$I_n = \frac{E_n}{R + \dfrac{X_L X_c}{0}} = 0$$

$V = E_n$

$I_L = V / jX_L = E_n / jX_L$

and

$I_c = V / -jX_c = E_n / -jX_c$

* That frequency and length can be combined is also obvious from the fact that the inductive reactance as well as the capacitive admittance (reciprocal of reactance) are directly proportional to length and frequency.

A capacitor presents practically pure capacitive reactance of a magnitude equal to its 60-cycle reactance divided by n. For generators and synchronous motors, the average of the negative sequence and subtransient 60-cycle reactances is used in estimating harmonic reactance.

Transformers step up or step down impedances by the square of the turn ratio; that is, if an impedance Z is connected to the low side of a transformer having a voltage ratio K, it appears when looking through the transformer from the high side as ZK^2. Where transformers are used, the impedances of equipment on one side can be transferred to the other either by computing them as if they were actually operated on the desired voltage base or by computing them on their own voltage base and multiplying by the square of the transformer ratio.

Resonance Between Equipment and Lines

It has been noted in Figure 20 that over comparatively wide ranges of frequency times length, the sending-end impedance of lines is capacitive reactance. Since the reactance of transformers and rotating machinery is inductive, it is not uncommon to find a frequency at which the reactances of the apparatus and the line are equal and opposite.

When equal and opposite reactances are connected together, a condition known as "resonance" occurs. Two variations of resonance can be recognized, that is, series resonance and parallel resonance, as illustrated in Figure 22. There it is shown that:

1. For series resonance, the current through and the voltages across the inductive and capacitive reactances are limited only by the resistance in the circuit. Thus, in a low loss series resonant circuit, large voltages and currents can occur even with relatively low impressed voltage.

2. For parallel resonance, the current in the reactive elements is equal to the impressed voltage divided by the reactance of the element. The voltage across the circuit does not exceed the internal voltage of the source. Consequently, large currents can occur only when the internal voltage of the source is high or the reactances of the elements are low. On the other hand, the current through and the voltage across the reactive elements are relatively unaffected by the internal resistance of the source.

In Figure 23 are shown examples of possible resonance conditions which may be set up at a harmonic frequency between the inductive reactance of equipment and the capacitive sending-end reactance of lines. It is assumed that the source is putting out a harmonic of the resonant frequency.

Rotating machinery and transformers usually have low internal resistance so that substantial increases in harmonic voltages and currents at particular frequencies can be caused by either of the types of situation illustrated. Transmission lines with harmonics put on at remote points usually also act as sources with low internal resistance when considering harmonics impressed on distribution systems. This is because

1. The impedance looking into a transmission line, to which most of the apparatus connected has inductive reactance, usually has a relatively small resistive component.

2. Further, the resistive component (as well as the reactive component) is stepped down by the square of the transformer ratio when considered on the distribution circuit voltage base.

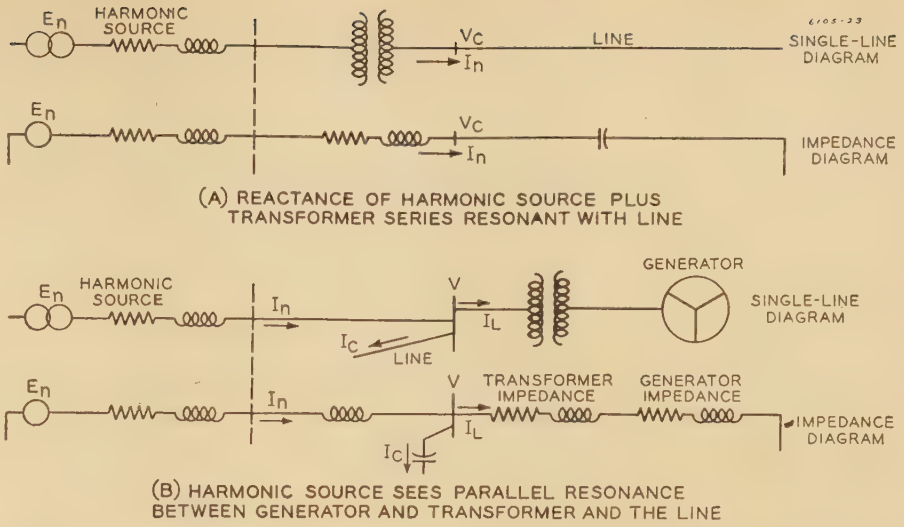

Figure 23. Examples of resonance between equipment and lines

On the other hand, the internal resistance of a rectifier, considered as a source of harmonics, is significant; the resistance is an inverse function of the load. Therefore, except for the larger rectifier installations, which are characterized by low internal resistance, large increases in harmonic currents or voltages at the sending ends of lines because of resonance are likely to occur only in cases of parallel resonance (as in Figure 23B).

Fortunately, most of the resonances encountered in practice are relatively sharp, and there is usually no harmonic present of exactly the resonant frequency. Consequently, the increases in harmonic voltage and current because of resonance are only moderate in most cases, although in rare cases these increases may be ten or more to one.

The ratios of harmonic currents and voltages at the two ends of a line (shown in Figure 21) are independent of whether the magnitudes at the sending end are affected by resonance.

Rural Distribution Circuits

Propagation of harmonics over rural distribution circuits differs from that over transmission circuits in two important respects:

1. The impedance presented by load is largely resistive in series with inductive reactance, the latter being caused by the load transformers. At night, and sometimes during the day, the load is light and the line operates essentially with the far end open.

2. A large proportion of the line mileage is likely to be single-phase, so that the ratio of ground-return harmonic current to phase harmonic current is much higher than for a transmission line. For single-phase multigrounded neutral rural lines, the ratio of ground return to phase harmonic current is on the order of 0.6; for unigrounded neutral or delta lines, the ratio is variable and it may be as high as unity.

Because of the facts that over substantial periods, rural power lines act as if they were open and that the line length is moderate, the sending-end impedance is likely to be capacitive reactance at the frequencies of the important harmonics. The sizes of transformers used to supply rural lines are frequently such that resonance occurs somewhere between the fifth and twenty-fifth harmonics. During heavier load periods, this resonance is considerably damped by the load; as a result, the noise influence of a rural power circuit usually is substantially higher at night than during the periods when the load is heavier.

In dealing with the single-phase branches of distribution circuits, it is rather common to use impedance-to-ground instead of impedance-to-neutral. Impedance-to-ground is phase-to-ground voltage divided by ground-return current or, conversely, ground-return current is phase-to-ground voltage divided by impedance-to-ground. Figures 20 and 21 can be used to obtain an idea of what happens on a single-phase rural line with the far end open or short-circuited when a harmonic voltage is impressed on it by making the following changes:

1. Before using the curves, multiply the actual kilocycle-miles by the following factors to take account of the lower velocity of propagation:

Unigrounded neutral	1.3
Multigrounded neutral	1.1

2. Multiply the ordinates in Figure 20 by about two. The ordinates in Figure 21 are unchanged.

There are many factors affecting the influence of a rural power line which cannot be discussed here. References 11, 12, and 23 discuss these matters in detail.

Urban Distribution Systems

Overhead urban distribution systems are usually so short that the effect of capacitance can be neglected except possibly for unusually long lightly loaded circuits with unusually high impressed magnitudes of the higher frequency harmonics. Consequently, in the absence of capacitors, the only path for harmonic currents is through the loads. Unlike rural distribution circuits, ground-return harmonic current can flow only where the neutral is multigrounded.

Where capacitors are used, they frequently present lower impedances at harmonic frequencies than do the loads. It not infrequently occurs that the resonant frequency of the capacitors and supply transformers and line is between the fifth and about the eleventh harmonic. In some cases this results in relatively large harmonic currents and voltages at one of these frequencies. In some cases the small differences between series reactances of the three

Table XII. Summary of Studies Made in a Few Selected Cases of Rectifier Installations

Case	Size, Kilowatts	Number of Phases	Feeder A of Figure 5	Part B of Figure 5	Part C of Figure 5	Supply Transformer D, Figure 5	Supply System N, Figure 5	I·T* In A	I·T* In N	Voltage TIF* On B	Voltage TIF* On C	Co-ordination Problems	Remarks
A	21,600 +5,400	12 6	—	—	—	—	Extensive 154 and 120 kv	—	32,000 on 120 kv	—	—	Extensive over several states	Changed to 30-phase with condition as indicated in example A[1]
A[1]	27,000	30	—	—	—	—	Extensive 154 and 120 kv	—	2,600 on 120 kv	—	—	None	—
B	41,000 +20,500	48 24	—	13-kv feeding distribution	—	75,000 kva	Extensive 115 and 230 kv	—	11,000 on 115 kv	50(E)	—	Moderately extensive without capacitors connected	Large capacitor bank for power purposes reduced effect to negligible value
C	114,800	24 36 48	—	—	—	—	Extensive 230, 69, and 115 kv	—	11,000 on 230 kv	—	—	Not very extensive because of particular layout of power system. Potentially important if power interconnections changed	Tentative plans made to change 24-phase to 48-phase. Action depends on future of plant
D	32,500	36	—	—	—	36,000 kva	110 kv	—	5,000	—	—	Severe caused primarily by quarter wave length power line at 1,020 cycles, particularly when one 6-phase rectifier unit shut down	Change in power layout and removal of minor irregularities in the rectifier phase shifting arrangements corrected condition
E	2,000	6	13-kv cable direct to generator bus	Urban distribution	—	—	Generating station, 13- and 26-kv cables feeding urban and suburban distribution	42,000	42,000	60	20**	A few	Resonance between cables and generator at 1,020 and 1,140 cycles resulted in substantial increase in influence. Change to 12-phase operation practically eliminated effect
F	1,000	12	13 kv, overhead	Urban distribution	None	None	Metropolitan cable and open-wire network	17,000	17,000	85–125 Value depends on method of feed	—	Fairly extensive to parts *A* and *B* only	Filter installed which reduced voltage TIF and I·T about 4.5 to 1 and eliminated problem
G	1,000	12	13 kv, overhead	None	None	None	Metropolitan cable and open-wire network	19,000	19,000	—	—	None	No problem because of absence of parts *B* and *C*
H	3,000	6	12-kv cable	—	—	—	Extensive urban cable network	60,000(E)	60,000(E)	—	—	No a-c problem. Filter required on d-c side	Substantial exposure of telephone cable circuits to d-c feeders and trolleys resulted in telephone noise problem
I	200	6	8 miles, 13 kv, semirural	40 miles, 13 kv, semirural	—	—	Extensive high-voltage network	2,300	Negligible	100(E)	—	Extensive because of part *B*	Filter installed; reduced voltage TIF and I·T about 5 to 1. Power factor improvement provided by filter turned out to be valuable
J	1,300	6	—	—	—	—	Fairly extensive 33 kv	—	5,000	—	—	Severe over about 600 square miles	Filter applied which eliminated problem
K	600	6	6.9 kv, industrial	6.9 kv, industrial and suburban	6.9 kv, industrial and suburban	—	25-kv heavy industrial	24,000–16,000(E)***	6,000–4,000(E)***	120–335***	20–50***	Little or none	Appears to be some likelihood of problems if power or telephone conditions change
L	400	6	6.9 kv, semirural	6.9 kv, semirural	6.9 kv, semirural	—	—	16,000(E)	—	190	—	Severe locally	Filter installed; reduced TIF and I·T about 4 to 1

* Measured except where noted by (E)—estimated.

** Voltage TIF at generator bus.

*** Range among 4 similar installations.

phase-wires (because of mutual inductance between them or between them and a multi-grounded neutral) may cause a fairly large proportion of this harmonic current to become ground return. This can be illustrated by the following (rather extreme) example:

1. Assume a 180-kva capacitor bank located two miles away on a 4-kv feeder from a 3,000-kva supply transformer bank with five per cent reactance. Assume 60-cycle phase-to-neutral impedance as follows:

Transformers	$j0.29$	ohm
Line:		
Phase 1	$j1.6$	ohms
Phase 2	$j1.65$	ohms
Phase 3	$j1.71$	ohms
Capacitors	$-j96.$	ohms

2. Assume that a seventh harmonic voltage exists in the circuit impressed with the power supply. The reactances at that frequency are:

Transformers	$j2.0$	ohms
Line:		
Phase 1	$j11.2$	ohms
Phase 2	$j11.6$	ohms
Phase 3	$j12.0$	ohms
Capacitors	$-j13.7$	ohms

Totals are:

Phase 1 $= j13.2 - j13.7 = -j0.5$ ohm
Phase 2 $= j13.6 - j13.7 = -j0.1$ ohm
Phase 3 $= j14.0 - j13.7 = \ j0.3$ ohm

3. If the harmonic voltages impressed on the three phases are equal, it can be seen that (neglecting resistances) the harmonic current in phase 2 will be about five times that in phase 1 and three times that in phase 3. Also, the current in phases 1 and 2 lead the impressed voltages; in phase 3 it lags the impressed voltage. The vector sum will be larger than the current in any of the phases; about 60 per cent of this vector sum will be ground return.

Examples From Field Experience

A few examples of situations encountered in the field which illustrate some of the foregoing principles are outlined:

1. One of the early large electrometallurgical rectifier installations was operated for a time with several 12-phase units and one 6-phase unit. The voltage TIF on the 154-kv supply at the rectifier was about 75. After traversing over 150 miles of transmission line, passing by a large generating station, and being impressed on a rural line, the voltage TIF was close to 500. The voltage TIF at numerous places within about 200 miles was higher than at the rectifier.

2. There have been cases where difficulties were encountered in the operation of rectifiers because of excessive fifth harmonic voltage either because of high impedance at that frequency looking out from the rectifier because of parallel resonance or because of stepup of fifth harmonic voltage arising in other sources because of series resonance.

3. In a number of cases, large changes have been noted at irregular times in the severity of inductive exposures (usually involving rural power circuits) without any apparent cause. In several of them, these changes were finally associated with opening or closing of circuit breakers on the transmission line network, in some cases literally hundreds of miles away. Evidently, changes in propagation conditions on the transmission system resulting from the operation of the breakers were responsible.

4. In one of the first metallurgical rectifier installations to employ a large bank of capacitors, an attempt was made to determine the effects on inductive co-ordination of operation with certain rectifier units shut down in the presence of suspected resonance between the capacitors and the power system at one of the frequencies normally suppressed by phase multiplication. The attempt was abandoned because of difficulties in rectifier operation and danger of burning out the capacitors because of large currents at the resonant frequency.

5. One of the sharpest resonance cases encountered was between a rural line and the transformer feeding it. Here a modest 1,380-cycle voltage was stepped up to about 20 per cent of the rms; the 1,380-cycle current was larger than the 60-cycle current.

6. Very large fifth harmonic currents have been observed in power factor correction capacitors on distribution systems because of resonance, and some cases of capacitor overheating have been observed, mainly in installations by power company customers and because of resonance with the supply transformers.

7. One of the highest voltage TIF's on record, about 2,500, was caused by about a four to one stepup caused by resonance between a small generator and transformer and a rural power line.

Appendix III. Examples of Types of Situations Studied

In Table XII a few of the installations which have been studied are summarized. The examples listed there were chosen to represent a number of different types of situations.

Items *A* through *D* are typical of very large installations and are included to illustrate several factors, namely:

1. The large advantage of phase multiplication, for example, compare examples *A* and *A*[1], which are for the same installation before and after phase multiplication was applied.

2. The further reduction in influence obtained through the use of large banks of capacitors installed for power operating reasons (see example *B*).

3. Example *D* illustrates the type of situation which occasionally arises where some difficulty may be experienced even with 36 phases, particularly when one unit is out of service. In this situation, during the existence of the unfavorable power layout, the removal of units for maintenance was confined as far as practicable to periods of low telephone traffic.

Items *E*, *F*, *G*, and *H* are street railway rectifier installations chosen to illustrate a range of conditions. Item *E* illustrates a rather extreme condition in that while most factors involved were favorable, there was a condition of resonance between an extensive cable network and a large generating station which accentuated the seventeenth and nineteenth harmonics. Changing to 12-phase operation greatly reduced these harmonics and practically eliminated the problem. Items *F* and *G* are two similar street railway rectifiers installed in the same city and supplied over about the same length of the same type of feeder. The only difference was that in case *F* the feeder supplying the rectifier also supplied an extensive distribution system; in case *G* the feeder ended at the rectifier. The reason for the unusually large values of I·T in these cases is imperfect suppression of the seventeenth and nineteenth harmonics in the 12-phase arrangement. This condition was rather common in earlier rectifiers; it is seldom observed in more recent installations.

Item *H* is typical of many thousands of kilowatts of street railway rectifiers which have produced no problems on the a-c side but have occasionally produced problems on the d-c side.

Items *I* and *J* are radio station rectifiers and are included primarily to illustrate how the inductive effects are likely to be increased when the rectifiers are installed away from densely developed areas. A larger proportion of radio station rectifiers have caused co-ordination problems than any other class of installation because of this fact.

Items *K* and *L* illustrate again the difference in effects of relatively small rectifiers depending on location and power system conditions. Installation *K* is one of several in a very heavy industrial area and illustrates the type of situation where harmonic control would be desirable if cheaper methods were available; the influence and noise conditions are on the ragged edge, with little margin for future changes. Installation *L* is in a much less heavily developed area.

References

AIEE Papers

1. Effects of Rectifiers on System Wave Shape, **P. W. Blye, H. E. Kent.** AIEE Transactions, volume 53, 1934, January section, pages 54–63.

2. Current and Voltage Wave Shape of Mercury Arc Rectifiers, **H. D. Brown, J. J. Smith.** AIEE Transactions, volume 52, 1933, pages 973–84.

3. Harmonics and Load Balance of Multiphase Rectifiers: Considerations in the Selection of the Number of Rectifier Phases, **R. D. Evans.** AIEE Transactions, volume 62, 1943, April section, pages 182–7.

4. A Short-Cut Method of Estimating Telephone-Influence Factor of Power Systems With Rectifier Load, **C. W. Frick.** AIEE Transactions, volume 63, 1944, March section, pages 91–6.

5. Wave Shape of 30- and 60-Phase Rectifier Groups, **O. K. Marti, T. A. Taylor.** AIEE Transactions, volume 59, 1940, April section, pages 218–24.

6. Electric Equipment for Large Electrochemical Installations, **T. R. Rhea, H. H. Zielinski.** AIEE Transactions, volume 61, 1942, October section, pages 733–41.

7. Ignitron Rectifiers in Industry, **J. H. Cox, G. F. Jones.** AIEE Transactions, volume 61, 1942, October section, pages 713–18.

8. Harmonics in the A-C Circuits of Grid-Controlled Rectifiers and Inverters, **R. D. Evans, H. N. Muller, Jr.** AIEE Transactions, volume 58, 1939, pages 861–70.

9. Analysis of Rectifier Circuits, **E. F. Christensen, C. H. Willis, C. C. Herskind.** AIEE Transactions, volume 63, 1944, pages 1048–58.

10. Inductive Co-ordination of Common-Neutral Power-Distribution Systems and Telephone Circuits, **J. O'R. Coleman, R. F. Davis.** AIEE Transactions, volume 56, 1937, January section, pages 17–26, 189.

11. Noise Co-ordination of Rural Power and Telephone Systems, **H. W. Wahlquist, T. A. Taylor.** AIEE Transactions, volume 57, 1938, November section, pages 613–20.

12. Inductive Co-ordination of REA Distribution Systems and Telephone Systems, **K. J. Plucknett, W. T. Smith, T. A. Taylor.** AIEE Transactions, volume 60, 1941, pages 586–95.

13. Measurement of Telephone Noise and Power Wave Shape, **J. M. Barstow, P. W. Blye, H. E. Kent.** AIEE Transactions, volume 54, 1935, December section, pages 1307–15.

14. First Report of Power System Stability, **AIEE Subcommittee on Interconnection and Stability Factors.** AIEE Transactions, volume 56, 1937, February section, pages 261–82.

15. The Electronic Converter for Exchange of Power, **F. W. Cramer, L. W. Morton, A. G. Darling.** AIEE Transactions, volume 63, 1944, pages 1059–69 and discussion, page 1413.

16. Operation of Nonsalient-Pole-Type Generators Supplying a Rectifier Load, **M. D. Ross, J. W. Batchelor.** AIEE Transactions, 1943, November section, pages 667–70.

Reports of Joint Subcommittee on Development and Research, Edison Electric Institute and Bell Telephone System

17. Wave-Shape Characteristics of Power Circuits Supplying Rectifiers, Engineering Report 22.

18. The Impedances of A-C Supply Systems at

Maintenance of Rectifiers on Electrochemical Installations

J. E. HOUSLEY
FELLOW AIEE

G. N. HUGHES
MEMBER AIEE

Synopsis: Operating experiences and information gained over a period of years from the operation of a large group of mercury arc rectifiers have shown that, while rectifiers provide a very economical means of converting from a-c to d-c power, they are not entirely trouble free. The principal operating difficulty has been the seemingly inherent tendency for a rectifier to arc-back. This peculiarity has challenged both the designer and operator since it has been found that both contribute toward the solution. The present paper presents the features which have been found advisable for the operator to observe and control in order to keep the occurrences of arc-back at a minimum.

LARGE INSTALLATIONS of mercury arc rectifiers in the electrochemical industries of the United States made their first appearance in 1938 when they were installed to supply direct current necessary for the production of aluminum.

With the advent of the war and the demand for the light electrochemically produced metals, large amounts of direct current were required so that the development and installation of rectifiers was carried on very rapidly.

The details of the equipment[1] and the nature of the operating problems are well known.[2] Improvement in the operating characteristics of this relatively new apparatus is of interest to operating and design engineers. Possibilities for improvement, especially in the older or multi-anode design rectifiers, are disclosed in this paper covering the operating experience at one large installation. A broader view of remedies available possibly might be presented in discussions from other operating engineers, covering experience in irregular operation somewhat different from that of the installations on which this paper is based. Experience and observations reported cover equipment operated continuously at full load, which is peculiar to the electrochemical industry.

One of the oldest and most troublesome problems encountered in rectifier operation is the arc-back. Much research has been carried out on this problem and some improvement has resulted. In the 250-volt rectifiers, arc-backs are no longer a serious problem. With higher voltages the problem still exists to some extent, and there remains much to be learned about the cause and prevention of arc-backs.

It generally is agreed that the basic cause of an arc-back is the formation of a cathode spot on the anode. This spot destroys the valve action and constitutes a short circuit which must be cleared immediately. While there are several known causes for the formation of a cathode spot on an anode, a full explanation has not been found as yet, and it is believed that there are still many unknown causes.

In the various engineering publications, there is a wealth of highly technical data and discussion on arc-backs and their causes. Such data are available to all engineers and are not within the scope of this paper.

The equipment under consideration consists of rectifiers used in the production of aluminum. Two rectifiers are served by one transformer, which steps 13,200 volts down to 560 anode volts. The rectifiers covered are of three different types:

12 anode multianode type
12 tube ignitrons
12 tube excitrons

Figure 1 shows an inside view of one station of multianode rectifiers. Figure 2 shows one of these rectifiers with the anode plate assembly removed in order to repair a single anode.

The multianode rectifiers and the excitrons are of the grid controlled type. Voltage control is obtained by applying an adjustable negative potential to the grid, which correspondingly delays the firing of the anode. The ignitrons have a grid, but it is not used for voltage control. Ignitron voltage control is obtained by delaying the impulses to the ignitor. The main connections of a transformer and its rectifiers are shown in Figure 3.

Arc-backs are random in nature and are unpredictable. Some rectifiers have operated a year and a half without an arc-back, whereas others have had over a

Paper 46-96, recommended by the AIEE committees on electronics and industrial power applications for presentation at the AIEE Southern District meeting, Asheville, N. C., May 14–16, 1946. Manuscript submitted November 23, 1945; made available for printing April 5, 1946.

J. E. HOUSLEY is district power manager with the Aluminum Company of America, Alcoa, Tenn., and G. N. HUGHES is an electrical engineer, Alcoa reduction division of the same company.

HARMONIC FREQUENCIES TO BALANCED COMPONENTS, Engineering Report 23.

19. THE IMPEDANCES OF A-C SUPPLY SYSTEMS AT HARMONIC FREQUENCIES TO RESIDUAL COMPONENTS, Engineering Report 24.

20. WAVE SHAPE OF MULTIPHASE RECTIFIERS, Engineering Report 49.

21. SELECTIVE DEVICE FOR REDUCING HARMONIC IN POWER SYSTEMS: PART 1, D-C SYSTEMS, Engineering Report 21.

22. SELECTIVE DEVICES FOR REDUCING HARMONICS IN POWER SYSTEMS: PART II, A-C SYSTEMS, Engineering Report 34.

23. INDUCTIVE CO-ORDINATION OF RURAL POWER AND TELEPHONE SYSTEMS, Engineering Report 40.

24. THE USE OF POWER AND TELEPHONE TRANSPOSITIONS WITHIN EXPOSURE SECTIONS, Engineering Report 36.

25. EFFECTS OF BONDING AERIAL TELEPHONE CABLE SHEATH TO MULTIGROUNDED POWER NEUTRALS, Engineering Report 43.

26. SUSCEPTIVENESS OF SUBSCRIBER STATION SETS, Engineering Report 46.

27. RELATIVE INTERFERING EFFECTS OF DIFFERENT SINGLE FREQUENCY NOISES IN TELEPHONE CIRCUITS, Engineering Report 32.

28. THE TELEPHONE INFLUENCE FACTOR OF SUPPLY SYSTEM VOLTAGES AND CURRENTS, Engineering Report 33.

29. FREQUENCY WEIGHTING FOR MESSAGE CIRCUIT NOISE, Engineering Report 45.

Other Publications

30. REPORTS OF JOINT GENERAL COMMITTEE OF EDISON ELECTRIC INSTITUTE AND BELL TELEPHONE SYSTEM ON PHYSICAL RELATIONS BETWEEN ELECTRICAL SUPPLY AND SIGNAL SYSTEMS, Publication M5, Edison Electric Institute, New York, N. Y., July 1945.

31. RECTIFIER CIRCUIT POWER FACTORS, HARMONICS, AND WAVE SHAPES, R. D. Evans. *Electrical World*, October 1943.

32. RECTIFIER WAVE SHAPE, Publication E1, Edison Electric Institute, New York, N. Y., April 1937.

33. MODERN DEVELOPMENTS IN RAILWAY SIGNALING. *Journal of the Institution of Electrical Engineers*, England, volume 78, page 353; volume 79, page 231.

34. PRINCIPLES OF MERCURY ARC RECTIFIERS AND THEIR CIRCUITS (book), D. C. Prince, P. B. Vogdes, McGraw-Hill Book Company, New York, N. Y., 1927.

35. MERCURY ARC POWER RECTIFIERS (book), Othmar K. Marti, Harold Winograd, McGraw-Hill Book Company, Inc., New York, N. Y., 1930.

36. MERCURY ARC CURRENT CONVERTERS (book). Rissik, Pitman, London, 1935.

37. ELECTRICAL TRANSMISSION AND DISTRIBUTION REFERENCE BOOK (book), Westinghouse Electric Corporation.

38. MERCURY ARC HEATING FREQUENCY CONVERTER, S. R. Durand, *Electronic Industries*, June 1945.

39. MERCURY ARC FREQUENCY CHANGER LIMITS ROLLING MILL DEMAND, R. W. Holman. *Electrical World*, April 13, 1946, pages 112–16.

hundred in that length of time. There are not sufficient data available to say what constitutes too many arc-backs, or how many such mechanical shocks a transformer will stand. The shock the transformer receives is proportional to the value of the arc-back current, and the use of high speed anode circuit breakers reduces this current and, consequently, the transformer shock. As to frequency, the authors have used a sort of par or standard permissible rate of one arc-back per month per rectifier. This figure was based to some extent upon the rate existing at the time it was established, but subsequent experience has indicated that this figure can be reduced materially for single-anode per tank rectifiers.

A group of multianode rectifiers showed an over-all average of 1.8 arc-backs per month per rectifier during the first six years operation. The individual performance over this same period ranged from 0.6 to 3.0 arc-backs per month average.

From an operating standpoint, arc-backs may be divided empirically into two classes, and for the want of better terms may be called normal and abnormal arc-backs. Normal arc-backs are those which occur during the normal steady state operation and for which no cause is evident. Abnormal arc-backs are those which occur during or after some interruption to normal operation, such as removal from service or abnormal temperature or vacuum.

Some rectifiers, especially the multianode type, may have a good normal arc-back rate and a bad abnormal rate. Thus a rectifier may become sensitive or reach a condition wherein it operates better than par on steady service, but if taken out of service for a few hours it may arc-back a dozen times within five or six hours after having been restored to service. Conversely, some may have a poor normal rate but not be sensitive to such removal from service.

The cause for this behavior is not understood fully, but possible causes are the presence of condensed mercury in the vicinity of the anodes or the introduction of contamination from the anode shaft seals. The latter could result from the slight expansion and contraction of the shafts from temperature changes.

Operating Conditions

The majority of abnormal arc-backs are caused by contamination or leaks. Other causes are abnormal temperature or vacuum and excessively delayed firing for voltage control. Also, there are indications that some arc-backs are caused by droplets of liquid mercury or mercury dew on the anode or other surfaces at anode potential. Such arc-backs may occur after the rectifier has been out of service a short time and has cooled down somewhat. For example, there have been instances where the rectifier arced back as soon as the anodes were energized, even though there was no excitation or any d-c back feed. Sometimes four or five arc-backs would clear the trouble, but in other cases the bad anode would have to be disconnected for a few hours, after which it would operate normally.

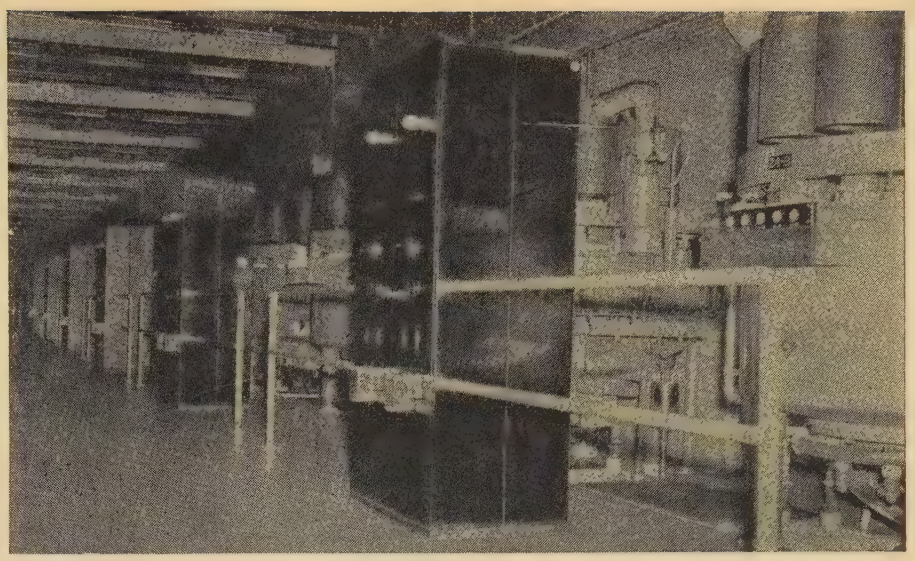

Figure 1. Interior view of one station of multianode rectifiers

High temperature of cooling water tends to cause arc-backs but does not seem to be critical, because a good rectifier will permit a considerable increase of temperature without apparent bad effects. As an experiment a rectifier, whose normal jacket water temperature was 52 degrees centigrade, was operated about 24 hours at a temperature of 95 degrees centigrade without an arc-back. This rectifier, however, was one with a good record. A so-called sensitive rectifier very likely would arc-back under such treatment.

Shortly after a number of ignitrons were placed in service, a very prolific cause of arc-backs was found to be the splashing of mercury against the grid and anode. A small pocket in the bottom of the individual tank vacuum valves eventually filled with condensed mercury and overflowed down the pipe and against the baffle, and some of course went through the holes and against the anode itself. These arc-backs frequently set off one or more additional arc-backs. The accepted explanation of this phenomenon is that the concussion precipitates the overflow of the pockets in other valves.

This trouble was corrected by installing internal baffles to prevent the mercury from reaching the anode.

Contamination

During the assembly of a rectifier, a certain amount of foreign material unavoidably is left in the tubes. Such material may consist of dust in the air, lint and dirt from workmen's clothing and wiping rags, residue from cleaning fluids, sandblasting, and possibly other cleaning methods. New parts and the mercury itself may contain some impurities.

Some materials are much worse than others. Oil and grease, for example, are particularly bad, and their presence always will result in arc-backs. On the other hand, such materials as coarse sand, steel shavings, and broken porcelain insulation do not seem to cause much trouble. Even the lint from wiping rags and clothing does not cause as much trouble as would be expected.

In general, every effort should be made to keep the internal parts of rectifiers as clean as possible. The manufacturers and those industries that use a large number of rectifiers find it advisable to have a special air-conditioned room for opening and repairing rectifiers. Such a room should be controlled as to temperature and humidity.

Cleaning fluids, such as pure grade benzene (benzol), should be tested before using. An easy test is to evaporate about a pint and note the residue. If there is enough residue to be visible, it should not be used.

Where the various seals are made of materials such as rubber or asbestos, a certain amount of contamination may

come from these seals unless they are made suitably. During the war, for instance, some rubber gaskets were replaced by synthetic rubber. Under the influence of heat and vacuum, these gaskets liberated surprising amounts of compound into the tanks, and caused so many arc-backs that overhaul was required.

There has been no trouble which could be ascribed definitely to contaminated mercury. Such impurities as it may collect tend to rise to the surface where they are easily removed. A clean bright surface usually indicates satisfactory condition. It appears to be very difficult to make any laboratory tests which are any more reliable than visual inspection. Furthermore, the presence of certain kinds of foreign materials does not seem to cause any trouble.

As an experiment, several ignitrons were contaminated purposely with copper, tin, zinc, silver, and alumina (Al_2O_3), only one material, of course, being in each tank.

These materials have been in the rectifiers for periods ranging from seven months to a year and have a total of only two arc-backs for the five tanks. The only one examined to date is the one with the copper, which operated nearly a year without a single arc-back. Most of the copper was deposited conspicuously on the cooling coil and its support. The quartz ring in the mercury was definitely copper colored and a faint copper color was evident in spots on the grid. The scum on top of the mercury showed positive traces of copper, and there was some evidence of a slight amalgamation of the copper in the mercury, although this was not certain.

Mercury, which is removed from a rectifier cathode, always is given a standard cleaning treatment. This treatment consists of washing in nitric acid and distilled water, and then a double distillation is made. Mercury, which is suspected of containing oil, is given an extra washing with either grain alcohol or chemically pure benzol. The surface of clean mercury should be absolutely clear with no specks or film visible under a strong light.

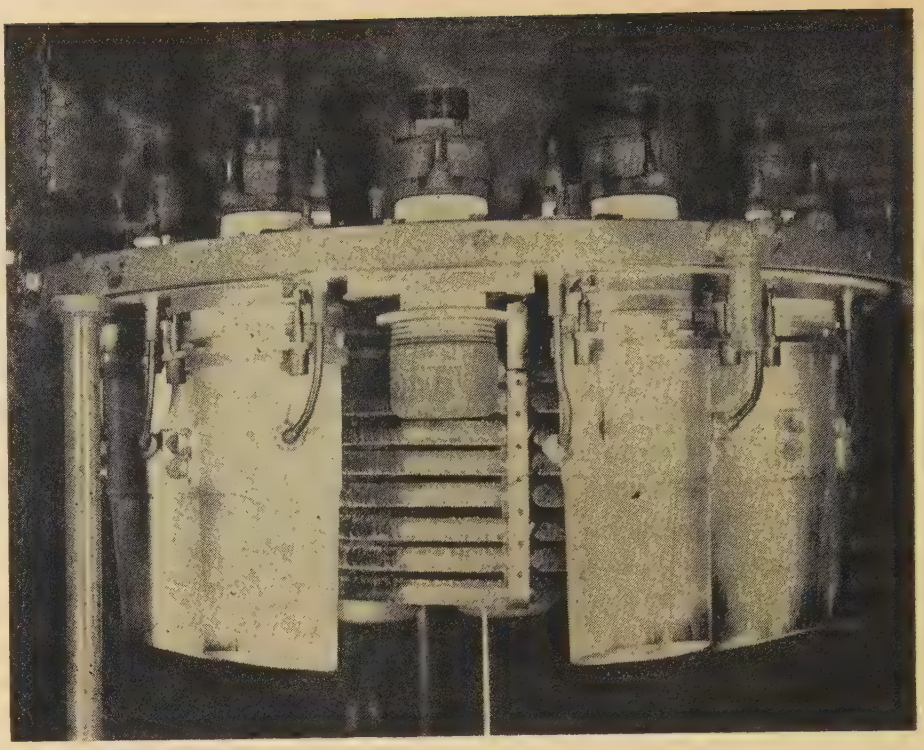

Figure 2. Assembly of cooling coil and anode plate for multianode rectifier

Tests and Repairs

When the arc-back frequency shows a sudden increase or becomes what is considered excessive, the first step is to determine which anode or anodes are responsible. There are various devices and methods for indicating this action. One method, that has proved quite satisfactory, involves the use of a standard commercial surge-crest ammeter, which consists of a meter that measures the amount and direction of the magnetism in a special small magnetic link. One of these links is placed about six inches from each anode cable. The reverse current from the arc-back magnetizes the link correspondingly, so that the identity and magnitude of the arc-back can be determined by measuring the links after an arc-back with the surge-crest ammeter.

When such tests show only one anode in trouble, this one anode is usually repaired alone. If it is a multianode type rectifier it is opened and the one anode repaired. A special effort always is made to complete the work and close the rectifier up the same day, since with a short exposure time the degassing period can be shortened to a few hours.

Many of these single anode arc-backs are caused by leaks in the vicinity of the anode. This fact is especially true on seals consisting of organic material. Other causes are found in the anode assembly, such as broken grid insulation. Where there are two anodes in parallel, a broken grid wire on one will overload one anode, thereby tending to cause arc-backs. On the ignitrons a broken or wetted ignitor will have the same effect.

When the arc-back pattern is scattered over all or several anodes, and the rectifier is not a newly repaired one, an air or water leak is suspected first. Such a leak may be in the vacuum manifold, pumps, or some location an appreciable distance from an anode, so that its effect may be distributed over the whole rectifier. The easiest and first test for leaks is a hot pressure rise test, in which the low vacuum pump is stopped and the pressure rise noted for about an hour with the rectifier on normal load. A good rectifier will operate for hours with only a few microns increase in pressure. In fact, they have been known to operate a couple of weeks with the main valve closed and both pumps down. If there is a serious leak, the pressure should rise sharply in an hour or less. This pump stop test may be supplemented or confirmed by a cold pressure rise test. In this test the rectifier is cooled first to room temperature, and then the main vacuum valve is closed for several hours and the pressure rise noted. The temperature of the rectifier should be constant of course during the check period. The permissible rise for such a test varies with the types and sizes of rectifier tanks, but a rough figure is from three to six microns in six hours. Some tubes will show as little as one micron rise in this period, while others as much as 10 or 12 and still be acceptable. Some air leaks sufficient to cause arc-backs may be within the pump capacity and, consequently, not show up on the vacuum meter. These leaks will be indicated, however, by the foregoing tests, and in some cases can be measured with a low reading gas meter.

If these tests indicate that there are no

air leaks, then contamination, water leaks, or internal trouble is suspected, and the only course is to open the rectifier.

Air and water leaks leave a certain amount of discoloration at their source. Contamination usually leaves some discoloration or spots, and in some cases a definite deposit on surfaces near the source.

The inside appearance varies considerably with different rectifiers. On some the inside of the tank and the cooling coils have a dark smoked appearance, whereas others show various temper colors of blue and straw. Air leaks usually leave a light brown rust deposit on the metal surfaces. On others a great portion of the surface is white because of the amalgamation of mercury vapor.

The inside of the tank and the cooling coils are sandblasted. Finished steel surfaces are polished with emery cloth. All cleaned surfaces then are wiped with a clean lintfree rag and a cleaning fluid such as pure benzene. Insulating parts also are sandblasted and cleaned the same way.

Great care and cleanliness must be used in the assembly. A touch by the bare skin on a finished surface will produce a small rust spot which is a possible source of contamination. Clean cotton gloves and clothing must be worn while making the assembly.

In most cases the same cathode mercury possibly could be reused by skimming off the surface, but it is advisable to use only mercury which has been renovated thoroughly, as previously described.

In old rectifiers the insulating parts which are exposed always show a certain amount of metallization. This metallization is a gradual process in which metal from the steel parts is deposited on the various insulating parts. The actual causes and details of the transfer of metal does not seem to be understood thoroughly, but one theory is that the arc stream for some reason may be diverted from its normal path and travel through some steel part, such as the cooling coil or tank wall, thereby vaporizing some of the metal. Pitted spots have been found in rectifiers which indicates that this phenomenon occurs.

Under normal operation the metallization is quite slow and may require years to become critical. At the other extreme, there are cases where it became so bad within a few weeks that the rectifier had to be reopened and cleaned. In such cases there is always a reason for this condition which may or may not be discovered. Improper degassing operation, in which the pressure is allowed to run too high, excessive tank temperature, leaks, and contamination will hasten the process of metallization.

When this metallization has progressed far enough, the insulating value of the insulating parts is impaired to a point where improper operation results. Thus the grid and anode insulation may become so low that the grid will receive its potential from the anode instead of its regular source, and, consequently, lose its voltage control ability. In the final stages of metallization, the arc-back rate increases and the rectifier must be opened and cleaned.

Degassing

When a rectifier has been exposed to air, it must be degassed in order to remove the gas which was absorbed during the exposure.

The degassing time depends to a great extent upon the length of the exposure time. Thus a rectifier, which has been opened and closed the same day with an exposure of only a few hours, can be degassed in a few hours. On these short exposures, it is possible to degas in service on line voltage at low loads, and, while this practice sometimes is followed, it has been found better to give it at least a short period on short circuit degassing.

A "green" rectifier, that is, one which has been opened for several days, requires from 60 to 120 hours of degassing.

The common practice in degassing is to short circuit the rectifier by connecting the cathode to the transformer neutral (the negative line) and apply 40 to 80 volts to the anodes. On 13-kv transformers, for example, 1,700 to 2,300 volts on the primary makes a satisfactory degassing voltage for 600-volt class rectifiers. On grid control type rectifiers, there should be some resistance in series with each anode in order to insure proper load division. This resistance is of the order of one-half to one ohm at the start and is reduced as degassing progresses. At about three-quarters of the rated full load current, the resistance may be removed if desired and the degassing finished without resistors. The short circuit current is controlled by the regular voltage control method of either grid bias or ignitor phase shift, depending upon the type of rectifier.

Ignitrons may be degassed satisfactorily without anode resistors even when "green." Some users, however, insert a low resistance of about one-fourth ohm in each anode until the current has reached

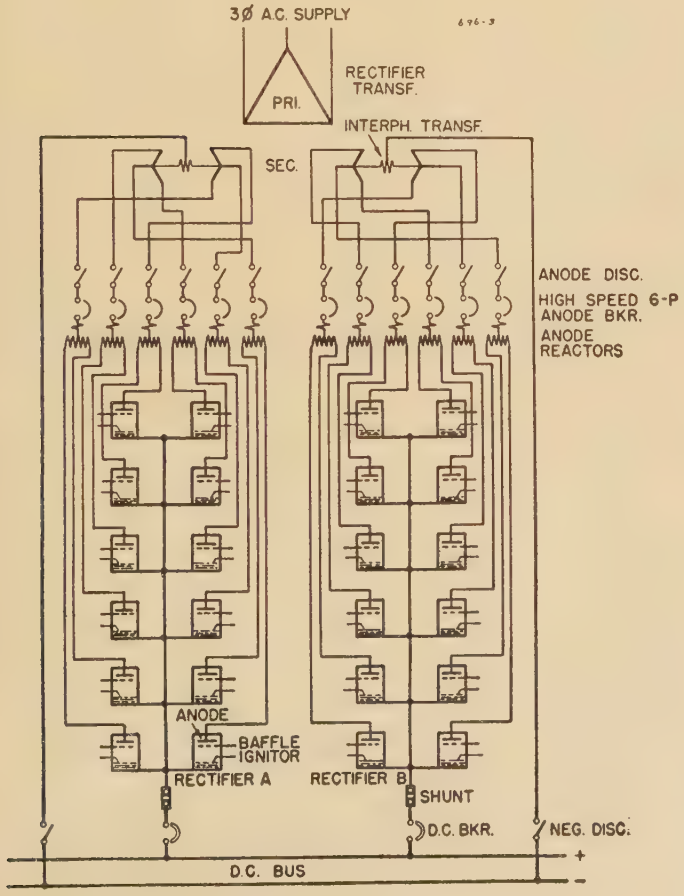

Figure 3. Unit connection diagram for ignitron rectifier

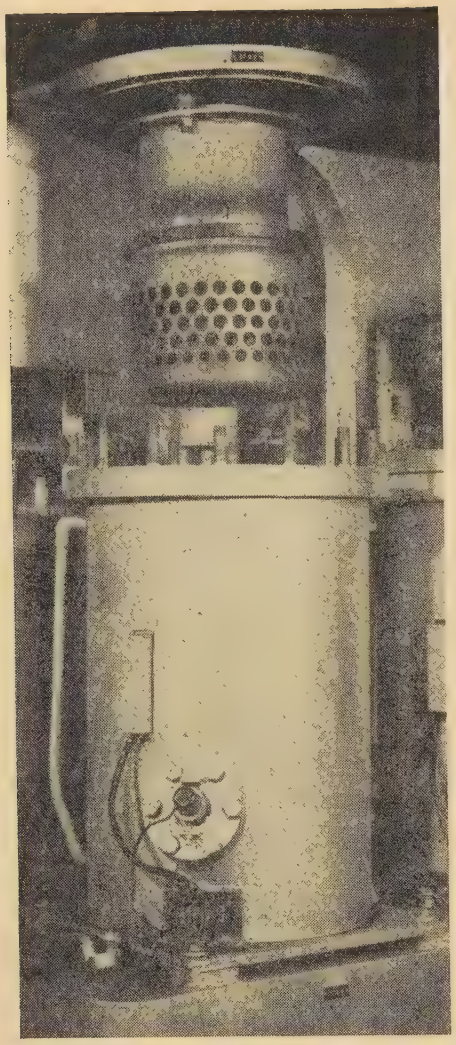

Figure 4. Anode and grid assembly of an ignitron

one-fourth to one-third rated value. This resistor balances the anode currents and results in a more uniform cathode current.

The degassing current is started at about two per cent of normal for multianode tubes and about ten per cent of normal for ignitron tubes, and increased as fast as the vacuum will permit. Before starting, the tube is pumped down to practically zero pressure on both the McLeod and electric gauges. During the degassing period, the vacuum on the multianode rectifiers is held within two microns on the McLeod gauge, and from four to ten microns on the electric gauge. The higher indication of the electric gauge during degassing is caused by the presence of condensable gases, which are not recognized by the McLeod gauge. After the rectifier has been degassed thoroughly, both gauges will settle down to approximately the same reading.

Ignitrons may be degassed with a somewhat higher pressure than the multianode type. McLeod readings of four or five microns and electric gauge readings of 12 to 15 microns are permissible on the ignitrons.

While the liberation of gas is fairly uniform during most of the degassing period, the gas occasionally will come out in sudden bursts or bubbles as though a pocket were released. When this action occurs, the degassing current must be reduced or removed to enable the vacuum pumps to restore proper vacuum. There are evidences that such pockets develop after the rectifier has been degassed and put back in service. For example, there have been several instances in which an arc-back on a recently overhauled rectifier was accompanied by sufficient increase of pressure to show on the vacuum gauge. This condition existed for only a few minutes.

After the regular degassing period, a rectifier occasionally continues to liberate a measurable amount of gas for several days, or even weeks after it is back in normal service. For electrochemical service it has been found advisable to finish a degassing operation by applying an overload current of 25 to 50 per cent for a few hours, in order to remove as much gas as possible. During the degassing period, a large rectifier will liberate from one-half to nearly one cubic foot of noncondensable gas. Figure 5 shows the time-gas volume curves obtained at Alcoa from the degassing of two "green" rectifiers selected at random.

In the degassing of "green" rectifiers, the gas is liberated most rapidly at relatively low current loads ranging from about 15 to 40 per cent of the normal operating load. Thus, in a typical degassing operation, the current is increased more or less uniformly until this critical value is reached. At the critical value, the gas is released as fast as the pumps can handle it, and the current may have to be maintained constant for several hours.

Having once passed this "hump," it progresses more rapidly as the load is increased. When a rectifier has been given a complete overhaul and placed back in service, it occasionally will arc-back several times during the first week or so, after which it settles down gradually to good performance.

It is believed that this behavior is caused by contamination left in the tube after overhaul. In order to hasten decontamination, a process called "aeration" has been tried several times at Alcoa. This process consists of cooling the rectifier and admitting clean dry air for some two or three hours. This air is admitted through a tube containing a filter and a drying agent, such as activated alumina. The air then is pumped out and the rectifier degassed on full voltage and a slowly increased load. The theory of this "aeration" is that a certain amount of the contaminants are oxidized and mixed with the air, and these products are pumped out sooner than they would be in normal operation. Engineers are not in full agreement on this theory, but favorable results have been obtained and the method should be given thorough trial.

Conclusions

It generally is agreed that the single anode type, such as the ignitron and the excitron, is superior to the multianode type. Their efficiency is higher because of the lower arc drop, and their maintenance is simpler and cheaper.

As compared to rotating equipment, modern rectifiers with their associated auxiliaries require somewhat less maintenance although this maintenance does require more care and skill, especially in supervision.

Rectifiers are capable of a certain amount of reduction from full voltage by delaying the time in the cycle at which

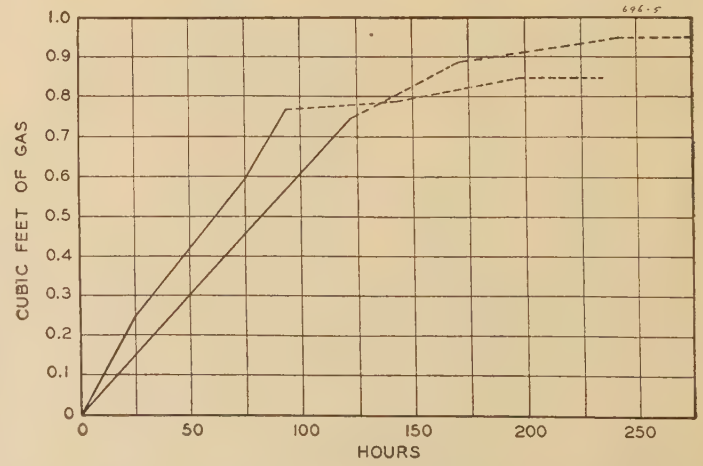

Figure 5. Time-gas volume curves obtained from the degassing of two "green" rectifiers selected at random

——— Degassing
------ On line

the anode begins passing current. Such control is obtained at the expense of an increase in arc-back frequency, a lower power factor, and a slight decrease in efficiency. The greater the reduction, the more pronounced are these undesirable effects, so that reduction in excess of some 15 or 20 per cent is of doubtful value. For this reason it is preferable to operate with the minimum firing delay compatible with operating conditions. This voltage control feature stands in need of further improvement.

Inasmuch as a cold rectifier is more likely to arc-back, means must be provided to keep them warm. For continuous service this is no great problem, but for intermittent service suitable heaters usually are provided.

One of the most vulnerable points of a rectifier is the seals. These seals have been improved much in recent years, but there is still room for further improvement. This fact is especially true where they are made of organic materials, such as rubber and fiber.

There is not yet sufficient operating experience to say definitely how long a pumped type rectifier will operate before requiring a major overhaul, but the authors' experience would indicate a period of not less than six or seven years with continuous operation and uniform load. Aside from damage or failure of parts, the long time factor that should dictate a major overhaul is the metallization of parts or possibly an excessive amount of carbon in the mercury pool. Some minor repairs, such as ignitor renewal or seal repair, should be expected during the period.

From the user's standpoint, the outstanding problem is the cause and elimination of arc-backs. They are so unpredictable and so many occur without any known cause that they are a constant challenge to engineers and operators.

Among the known causes, contamination should have a great deal more study. There is much uncertainty as to the nature and amount of contamination necessary to cause serious trouble.

Since rectifiers are still on the threshold of their development, it is expected that future developments and research will simplify operation and reduce present maintenance problems.

References

1. Alcoa Rectifier Installation, J. Elmer Housley, H. Winograd. AIEE Transactions, volume 60, 1941, pages 1266–74.

2. Aspects of the Operation of Mercury Arc Rectifier Stations, J. Elmer Housley, J. H. Studley. Transactions, Electrochemical Society, volume 86, 1944, pages 169–85.

Fault Location and Relay Performance Analysis by Automatic Oscillographs

H. P. DUPUIS
ASSOCIATE AIEE

W. E. JACOBS
ASSOCIATE AIEE

Synopsis: The purpose of this paper is to describe a method developed for determining the location of ground faults on an extensive 140-kv grounded neutral transmission system. This method applies particularly to ground faults in a network of two or more parallel lines and is based on a comparison of the magnitude of ground currents in the faulted circuit and in the unfaulted circuits. Since the relative distribution of ground fault current in a network depends only on the zero sequence impedance of the system, an analysis of ground faults by comparison is independent of generation, fault resistance, or whether one or two phases are involved to ground. The paper also describes the use of ground fault current curves in determining the critical conditions for relay selectivity and summarizes the results of five years of satisfactory experience with automatic oscillographs used in the analysis of faults and relay operations on the system.

THE SYSTEM referred to in this discussion includes nearly 1,000 miles of line widely distributed over the State of Michigan, as shown geographically in Figure 1. The first automatic oscillograph was installed in 1931, and two more were added in 1935. These were used at various points on the system to study system behavior. In 1941 an additional one was acquired, and the four instruments were located permanently to coordinate fault records on the 140-kv grounded neutral system. In the period from 1941 to 1945 inclusive, oscillographic records were obtained for approximately 250 line faults. These records showed 96 per cent of the line faults involved either one or two conductors to ground. From this, it is obvious that fault studies on this system are concerned primarily with ground currents, and the location of the oscillographs and the element connections have been selected to give maximum information on ground faults.

Location and Initiation of Oscillographs

The instruments are located at the four principal neutral grounding points on the system: Croton Station on the Muskegon River, Morrow Station east of Kalamazoo, Blackstone Station at Jackson, and Weadock Station, Bay City. Initiation of the oscillographs is by instantaneous undervoltage relays connected to 140-kv potential devices and by instantaneous overcurrent relays in the 140-kv neutrals of the grounded transformer banks. The initiating relays are set to insure operation of at least two oscillographs for all faults within the network. It is a decided advantage in ground fault analysis to have films from two instruments for comparing current values or for determining the total fault current. In the event that one instrument fails to operate, a fairly satisfactory analysis may be made from one film.

Connection of Elements

The oscillographs in service are the 6-element type using sensitized paper. Except as noted, three elements of each instrument are used to record line-to-neutral voltage, and three are connected in the current transformer neutrals of the lines to record ground current. At the Morrow Station, four elements are required for residual current in the lines, leaving only two elements available for potential indication. These are connected to record line-to-line voltage.

Calibration

Records obtained on automatic oscillographs are no more accurate than the calibration data. In determining the values to be used for current calibration, it is first necessary to calculate the maximum value of fault current that may be obtained in the various elements, and to decide on the maximum amplitude that may be permitted on each element with maximum fault current. On elements centrally located on the paper, the total amplitude must be less than the width of the paper. On elements located near the top or bottom of the paper, it is not necessary to restrict the amplitude so that both the top and the bottom of the wave is confined to the paper under fault conditions. The zero line of the element can be drawn in readily and the total amplitude determined from the half wave which remains on the paper. For calibration tests a total amplitude of 12 millimeters on potential elements and 15 to 20 millimeters on current elements has proved satisfactory. A total amplitude of 12 millimeters is taken to mean six millimeters above and below the zero line.

Adequate account should be taken of the breakdown of current transformer ratios when measuring ground current, and in converting calibration test data into terms of primary ground current, the effective current transformer ratio must be used.

Valuable information has been obtained on relay and circuit breaker operating time by using a bias or offset on the current elements. This is obtained by connecting a shunt in the d-c trip circuit of the breaker to its respective element, causing the center line to shift when the trip circuit is energized. This is shown in Figure 7.

Factors Used in Ground Fault Analysis

1. Magnitude and relative values of ground currents from each end of the faulted circuit with both ends closed.
2. Magnitude of ground current in the faulted circuit after one end opens.
3. Relative values and direction of ground currents in unfaulted circuits in parallel with the faulted circuit.

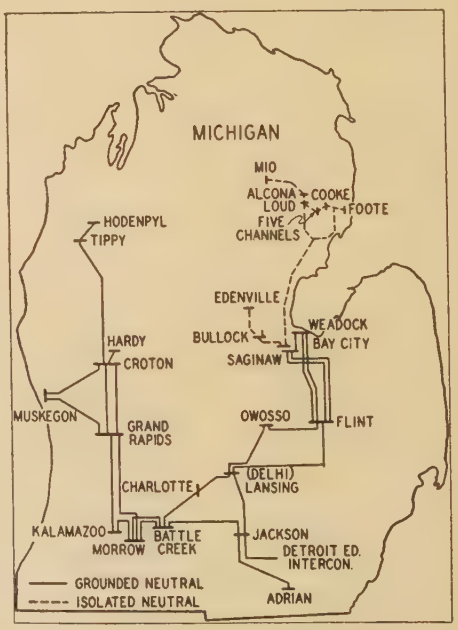

Figure 1. Consumers Power Company 140-kv system (1945)

Paper 46-109, recommended by the AIEE committee on protective devices for presentation at the AIEE summer convention, Detroit, Mich., June 24–28, 1946. Manuscript submitted March 18, 1946; made available for printing May 1, 1946.

H. P. DUPUIS is an electrical engineer, Commonwealth and Southern Corporation, Jackson, Mich. W. E. JACOBS is system dispatch supervisor, Consumers Power Company, Jackson.

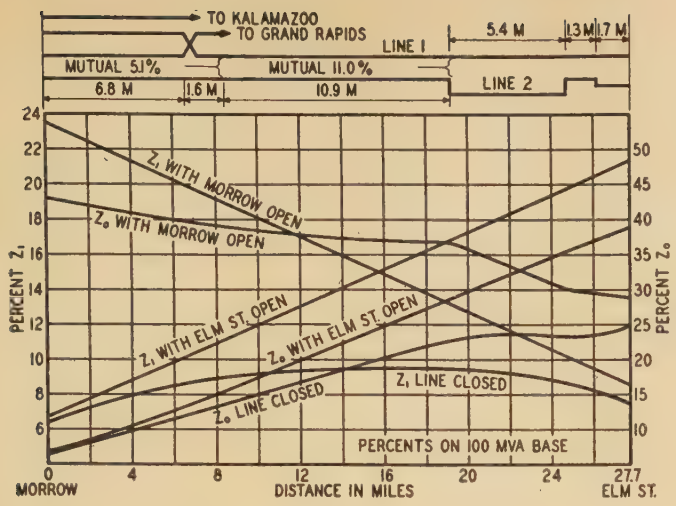

Figure 2. Curves of total fault impedance for line 1 and characteristics of line 1 and line 2 from Morrow Station to Elm Street Station, Battle Creek

(*a*). Both ends of the faulted circuits closed.

(*b*). After one end of the faulted circuit opens.

4. Magnitude and relative values of currents in contributing circuits from ground sources.

5. Recorded potential.

6. Changes in magnitude of ground fault current with changes in the nature of the fault, that is, one line to ground changing to two lines to ground.

7. Relay operation.

(*a*). Operating time of time delay relays.

(*b*). Pickup and operating range of instantaneous relays.

Calculations for Ground Fault Curves

Making up ground fault curves requires a considerable amount of work, but once completed, they provide a fast and accurate means of locating faults. A complete set of curves to utilize these factors consists of impedance curves, maximum ground fault current curves, and ratio curves.

The first step in making up data for curves is to have positive and zero sequence diagrams of the system and to calculate the positive, negative, and zero impedance for the total system at each station and at a sufficient number of points on the lines between stations to insure the drawing of accurate curves. On the average length of line, three or four points will be sufficient. Similar calculations are made for the lines open at either end. Ordinarily the positive and negative sequence impedances can be assumed to be equal. Calculations can be simplified by using linear values of impedance rather than the complex $R + jX$ form and are usually sufficiently accurate. If system generating conditions require the switching of grounded transformers which change the relative distribution of ground current, it may be necessary to make up more than one set of curves. As will be explained later, a second set of curves is not necessary for changes in generation only.

When calculating the total zero sequence impedance at each point, it is necessary to determine the distribution of ground current, not only in the faulted circuit but also in the parallel circuits and other contributing circuits. This is especially important for parallel circuits having mutual relation with the faulted circuit. For systems not involving too many mutuals, these values may be calculated by setting up mutual equivalents[1] or by simultaneous equations. It is important that fault points be taken at the ends of mutual sections, as the ground current curves change their slope at these points. On complicated systems with multicircuit mutuals, it is advisable to use an a-c calculating board.

Values of the total positive sequence impedance are more easily calculated or can be obtained on a d-c board.

Application of Curves

The two 140-kv circuits between Morrow Station and Elm Street Station, Battle Creek, designated as line 1 and line 2, have characteristics as shown at the top of Figure 2. A complete set of curves for line 1 is reproduced for illustration.

Impedance Curves

Curves shown on Figure 2 are for maximum positive and zero sequence impedances with the line closed and with the line open at either end. These data are convenient for checking a fault location when the nature of the fault changes. For example, assume a single-line-to-ground fault changes to a two-line-to-ground fault. If positive and negative

Figure 3. Maximum current curves for single-line-to-ground faults on line 1, closed at Morrow and Elm Street

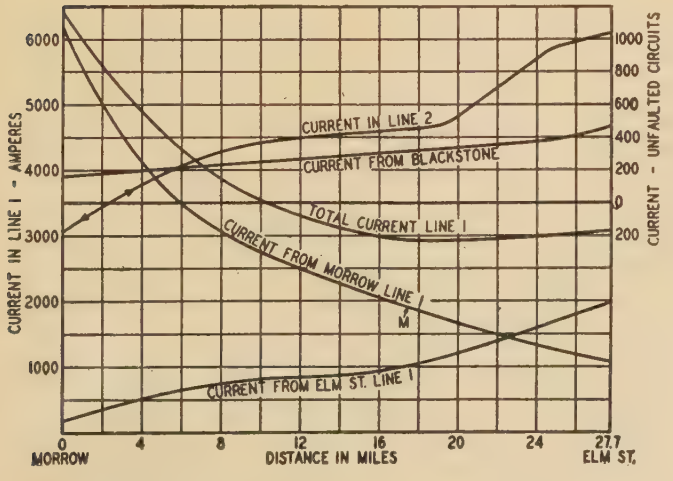

Figure 4. Ground current ratio curves for faults on line 1, closed at Morrow and Elm Street

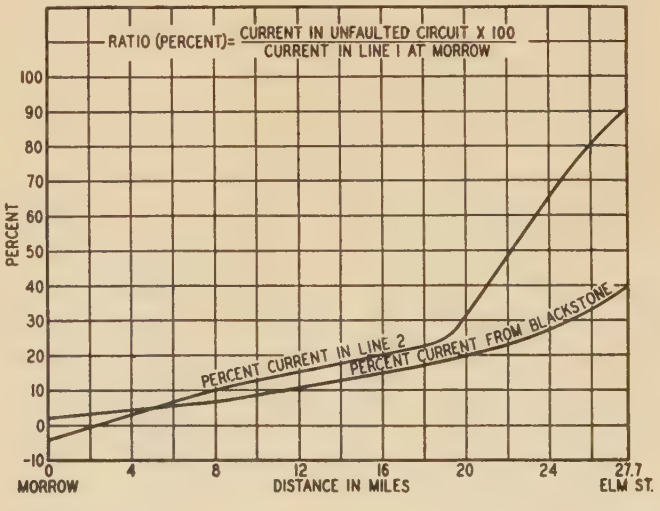

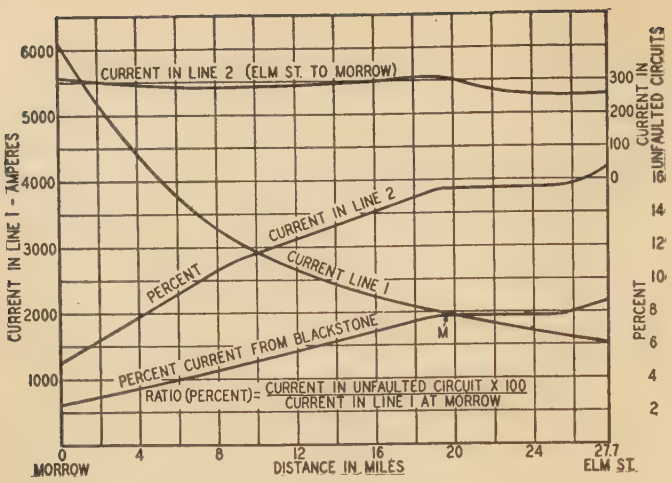

Figure 5. Maximum ground current curves and ratio curves for faults on line 1, open on Elm Street end

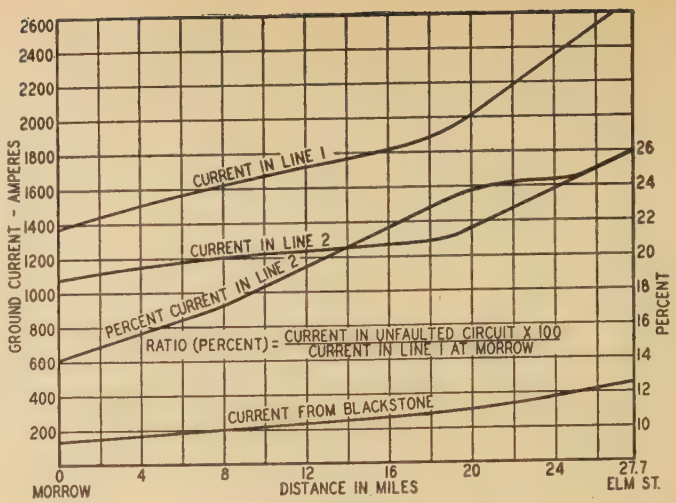

Figure 6. Maximum ground current curves and ratio curves for faults on line 1, open on the Morrow end

phase impedances are considered equal,

Single-line-to-ground current

$$= \frac{3\times 10^7}{(2Z_1+Z_0)\sqrt{3}\text{ kv}} \quad (1)$$

Two-line-to-ground current

$$= \frac{3\times 10^7}{(Z_1+2Z_0)\sqrt{3}\text{ kv}} \quad (2)$$

A value of Z_1 and Z_0 for the same location can be taken from the impedance curves which when applied in the above formulas will be equal to or proportional to the current values shown on the oscillograph film. This is usually a good indication of fault location, especially on a line section where there is a large variation in the ratio of Z_1/Z_0.

Current Curves

Current curves may be used directly in determining fault location if the fault currents are near maximum values. The curves are also very useful in determining the critical conditions for relay selectivity and for co-ordinating the magnitude and duration of fault current with observed line damage.

Maximum current curves for single-line-to-ground faults with the line closed at both ends are shown in Figure 3.

Curves for line 1 open at Elm Street and open at Morrow are shown combined with ratio curves in Figures 5 and 6, respectively. Note in Figure 3 that the current in line 2 passes through the zero line at about two miles from Morrow Station. That is, for faults within two miles of Morrow, the current in line 2 is from Elm Street to Morrow, and for faults beyond two miles, the current in line 2 flows from Morrow to Elm Street. Whether or not the current in a parallel circuit reverses after a circuit breaker opens on one end of the faulted line is often a definite indication of the fault location.

The difference in the slopes of the current curves in the 10.9-mile section and in the 5.4-mile section clearly indicates that the effect of mutual impedance cannot be neglected.

Ratio Curves

The distribution of ground fault current depends only on the zero sequence impedance of the system. The relative distribution in the faulted circuit and in parallel or contributing circuits is the same for one line-to-ground or for two line-to-ground faults. Fault resistance or changes in generation affect the magnitude of ground fault current but do not change the relative distribution. This fact can be utilized in making up a set of ratio curves independent of fault resistance and generation. Using the current in one circuit as a reference, the current in the other circuits can be plotted in per cent of the reference current.

It is apparent that fault locations can be determined more accurately if the ratio curves have a steep slope. On networks having only two currents to compare, it is not always possible to have one ratio curve that will have adequate slope over the entire length of line. However, nearly all line faults are cleared by the sequential opening of breakers at each end. This supplies data for making up three ratio curves, one of which can be used for accurate indication of fault location on a specific section of the line.

On more complicated networks where three or more currents can be compared, it may be advisable to make up two sets of ratio curves for the same condition by using different currents as reference. That is, by proper selection of reference currents, one curve may have a steep slope for a section of the line where the other curve is relatively flat.

Ratio curves apply specifically to faults with reduced values of current, but they can be applied equally well to faults with maximum current values. In some cases the ratio of currents may give a more definite indication than the individual currents.

The ratio curves of Figure 4 are obtained by plotting maximum current values, taken from Figure 3, in per cent of the current in line 1 at Morrow. Ratio curves with the line open at Elm Street and at Morrow are included in Figures 5 and 6.

Application of Oscillograph Data for Fault Location

The oscillograph films, Figure 7 and Figure 8, were obtained from Morrow Station and Blackstone Station respectively for a fault on line 1.

A preliminary inspection of the films shows the two line-to-line potentials at Morrow are approximately equal, indicating that the Z phase was involved. Reference to the Blackstone line-to-neutral potentials shows definitely that the fault was Z-phase-to-ground throughout. Further inspection of the film shows that the line opened at Elm Street in 19 cycles and at Morrow in 48 cycles. Targets were reported on the time delay ground relays at both Elm Street and Morrow. As indicated at M in Figure 5, the maximum reach of the instantaneous relays on line 1 at Morrow after the line opens at Elm Street is approximately 19

miles. Failure of this relay to operate indicates that the fault was more than 19 miles from Morrow or within nine miles of Elm Street. The bias was applied when the trip circuit at Morrow was energized. This shows that the oil circuit breaker on line 1 had five cycles clearing time.

Use of Current Curves

A detailed analysis gives measured values of fault currents in primary amperes as shown in Figures 7 and 8. The current values of the fifth and sixth elements of both films are not required in this analysis.

No film was obtained from Weadock for this fault, but previous calculations determined that for a fault at Elm Street, 51 per cent of the ground current from the eastern part of the system is contributed over the line from Blackstone, and 49 per cent over the line from Lansing. From the measured and calculated values of current, the distribution in the lines was as shown in Figure 9A for the initial fault and in Figure 9B after Elm Street opened. This gives a complete picture of the fault and indicates that the calculated total of 2,965 amperes was very nearly maximum current for a fault near Elm Street.

Applying the values shown in Figure 9A to the maximum current curves of Figure 3, the 1,400 amperes in line 1 from Morrow gives a fault location of 4.5 miles from Elm Street; 860 amperes in line 2 gives a location of four miles from Elm Street; 360 amperes from Blackstone gives a location of 5.5 miles from Elm Street; and the calculated value of 1,565 amperes in line 1 from Elm Street gives a location of 4.5 miles. This close agreement on fault location is a further indication that the fault currents were very nearly maximum value.

After the line opened at Elm Street, the values shown in Figure 9B applied to the current curves of Figure 5 give a location of five miles from Elm Street for 1,750 amperes in line 1, and 5.5 miles from Elm Street for 270 amperes in line 2. Note that the direction of current in line 2 reversed after line 1 opened at Elm Street. The curve of total amperes on Figure 3 is too flat at this point for close application, but the calculated total indicates the fault as being between four and six miles from Elm Street. All of the above determinations give the fault location as between 4 miles and 5.5 miles from Elm Street. The actual location was five miles from Elm Street, and the damage reported was three broken bells and light burns on the conductor.

Figure 7. Oscillogram from Morrow Station for a fault on line 1, Morrow to Battle Creek

Element 1. *YZ* phase potential
Element 2. *ZX* phase potential
Element 3. Ground current in line 1 to Battle Creek
Element 4. Ground current in line 2 to Battle Creek
Element 5. Ground current in Kalamazoo line
Element 6. Ground current in Grand Rapids line

Use of Ratio Curves

To illustrate the application of the ratio curves, assume that fault resistance or decreased generation had reduced the fault current to 80 per cent of the above values. Relative values then would be as shown in Figures 10A and 10B. Applying the values in Figure 10A to the current curves of Figure 3, the 1,120 amperes in line 1 from Morrow indicates the fault to be at or near Elm Street, while 690 amperes in line 2 places the fault at six miles from Elm Street, and 290 amperes from Blackstone gives the location as 14 miles from Elm Street. Similarly, the values of Figure 10B applied to the current curves of Figure 5 all indicate the fault as being at or near Elm Street. This wide discrepancy in the indicated fault location is characteristic of current values that are less than maximum and is an indication that the current curves cannot be directly applied, and the ratio curves should be used.

From the values of Figure 10A, the current in line 2 from Morrow is 61.5 per cent of the current in line 1 from Morrow, and the current from Blackstone is 26 per cent of the current in line 1. Applying these percentages to the ratio curves of Figure 4 gives fault locations of 4.5 miles and 4 miles from Elm Street as previously determined with actual fault currents. The currents in Figure 10B, after Elm Street opens, applied in the same way gives 15.5 per cent for the current in line 2 and 7.8 per cent for the current in the Blackstone line. These values fall on the flat part of the ratio curves of Figure 5 and serve only as a check.

From an inspection of the ratio curves of Figures 4, 5, and 6, it is evident that for faults within nine miles of Elm Street, the most accurate determinations can be made from the curves of Figure 4. For faults within 19 miles of Morrow, any one of the three sets of curves could be used with sufficient accuracy.

Other Applications of Oscillograph and Curve Data

Line Damage

During the past two years each fault analysis included calculations to correlate fault current and clearing time with the observed damage. In these calculations a factor has been used equal to (amperes/1,000)^2 × cycles. The currents used are taken from the oscillograph films supplemented by calculations and values from the current curves where necessary. For the actual fault discussed in this paper, the values used were 2,965 amperes for 19 cycles and 1,750 amperes for 29 cycles: $(KA)^2$ cycles = 255. While this study has not been carried on for a sufficient length of time to warrant any definite conclusions, it is indicated that the data may be

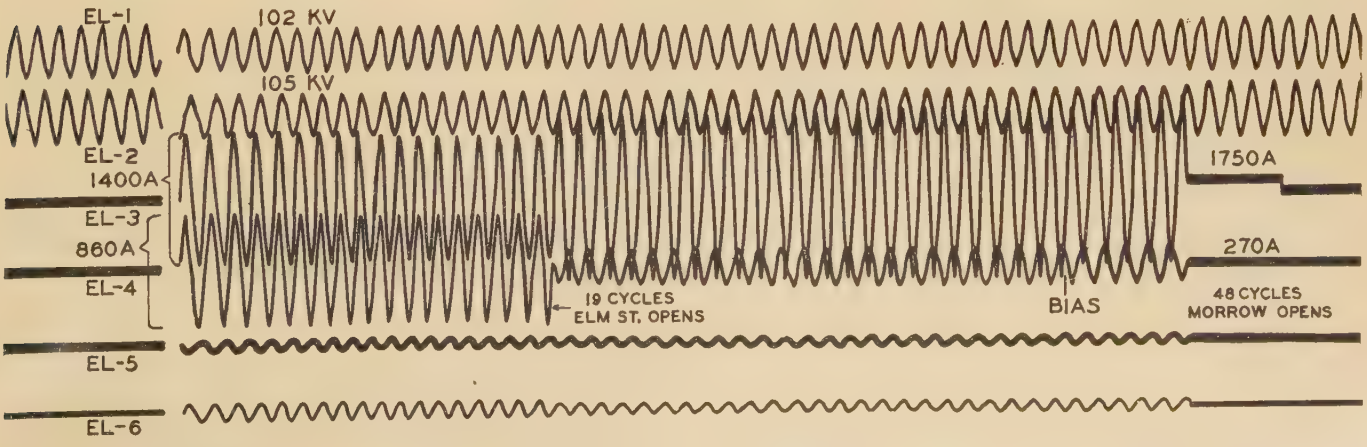

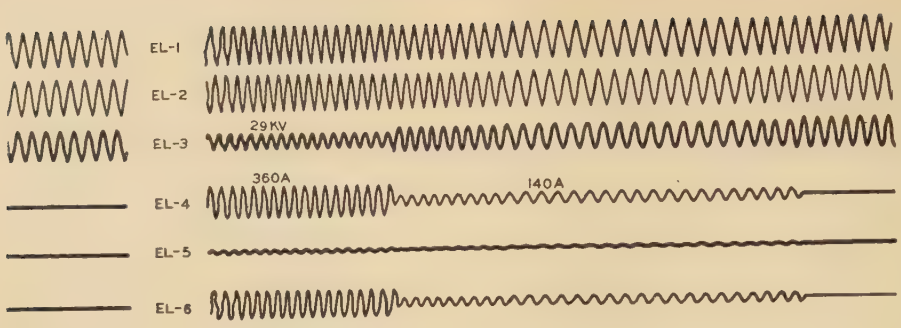

Figure 8. Oscillogram from Blackstone Station, Jackson, for a fault on line 1, Morrow to Battle Creek

Element 1. *X*-phase-to-neutral potential
Element 2. *Y*-phase-to-neutral potential
Element 3. *Z*-phase-to-neutral potential
Element 4. Ground current in line to Battle Creek
Element 5. Ground current in line to Lansing
Element 6. Ground current in interconnection

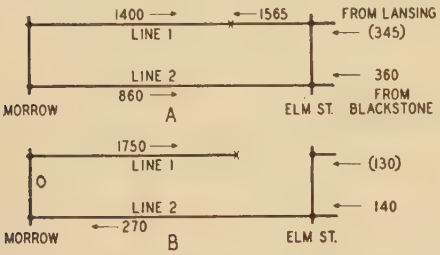

Figure 9. Distribution of maximum ground fault current

A. With line 1 closed at Morrow and Elm Street
B. After line 1 opened at Elm Street

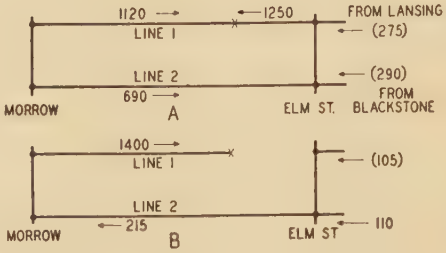

Figure 10. Distribution of ground fault current, 80 per cent of maximum

A. With line 1 closed at Morrow and Elm Street
B. After line 1 opened at Elm Street

of considerable value in determining whether or not a special patrol is necessary when no damage is found on the initial patrol.

Relay Performance

As a final step in the analysis, the operating time of each time delay ground relay is calculated for the value of ground current as measured on the films, and this calculated time is compared with the actual operating time as recorded. This furnishes a positive check on relay operation. In case of faulty films, this process can be reversed to calculate fault currents. Surprisingly accurate determinations have been made based entirely on relay operating time. Occasional faults near the end of the instantaneous relay zone supply data on the accuracy of pickup adjustment.

In the preparation of ground relay settings, the current curves are very useful in determining the critical points of selectivity. In many cases the critical point is at the end of the instantaneous relay zone where the time delay relay must be considered. This is especially true on parallel circuits with mutual couplings.

It can be seen in Figure 5 that the effect of the mutual is to maintain an almost constant value of current in line 2 for faults in the parallel section. And it is evident that faults on line 1 over 20 miles from Morrow may be critical for selectivity between the Elm Street relay on line 2 and the Morrow relay on line 1. Selectivity can be checked quickly and accurately by taking current values from the curves at any questionable point.

Summary

When making analyses of faults, it is of interest and value to prepare sheets for recording data on each fault. Tables I and II summarize the types and cause of 256 line faults analyzed over a period of five years. Exactly 50 per cent of these faults caused no visible damage and could not be located.

Table I. Types of Line Faults

Faults starting 1-line-to-ground	78%
Faults starting 2-line-to-ground	18%
Faults starting phase-to-phase	4%
Faults starting 1-line-to-ground and changing to 2-line-to-ground or to 3-phase	10%

Table II. Cause of Line Faults

Lightning	80.0%
Interference (birds, machinery, etc.)	9.0%
Wind	7.4%
Line material failure	1.2%
Unknown	2.4%

Conclusions

This method of determining ground fault location as developed by one of the authors has been in use for several years and has proved very satisfactory. For this discussion the particular line section and fault were selected to illustrate best some of the principles involved, and it should not be presumed that the same degree of accuracy can be obtained for all faults. With the present number of oscillographs on the system, the average degree of accuracy is in the order of ten per cent for faults in the network; that is, on a line 30 miles long it is expected that the faults can be located within three miles. With oscillographs at each station, it is probable that faults could be consistently located within one mile. The calculated locations of ground faults on radial lines are accurate only if tower footing and fault resistances are low.

One of the most important applications of the oscillograph is the information that is obtained when a fault is not cleared properly. In most cases these data definitely point to the cause of incorrect operation or failure to operate so that immediate steps can be taken to prevent a recurrence. By indicating the location of inconspicuous damage and potential sources of trouble, the oscillographs are becoming an increasingly important factor in transmission line maintenance. The diligent use of oscillograph data has resulted in greatly improved relay performance.

Reference

1. Equivalent Circuits, F. M. Starr. AIEE Transactions, volume 51, 1932, page 291.

Modern Diesel-Electric Drilling Rig Equipment

T. R. RHEA
ASSOCIATE AIEE

Synopsis: A modern Diesel-electric powered drilling equipment for drilling oil wells consists of several internal combustion engines driving d-c generators, which supply adjustable voltage power to the several d-c motors driving the various motions. This paper gives a description of the functions performed by the draw works, mud pumps, rotary table, and coring reel, and a typical arrangement of apparatus or elementary power diagram showing the main d-c circuits with the arrangement of drill-hoist contactors and manual transfer switches. In addition, there are related the general scheme of operation, strictly from the driller's point of view, without the details of how these functions are accomplished; the operating principles of the electrohydraulic governor that make this scheme of operation possible; as well as the various control features provided by the amplidyne excitation of the main generators. The electrohydraulic governor, a war development, is applied for the first time to Diesel-electric drilling rig equipment. This governor gives to the engines a degree of protection never before attained, by preventing the engine from being overloaded. The governor also permits running the engines at the lowest speeds consistent with the desired rig motion and not at full rated speed at all times as in the past. The electrohydraulic governor provides for engine paralleling without the driller having to pay any attention to the engine throttles. The merits of a-c versus d-c auxiliary drives are pointed out, and separate engine-driven auxiliary a-c generators are recommended instead of the usual practice of driving auxiliary d-c generators from the main engines. This gives a saving in first cost of auxiliaries conservatively estimated at 25 per cent, as well as gains in simplicity, sturdiness, and less weight.

A MODERN Diesel-electric drilling rig equipment for drilling oil wells consists of several internal combustion engines driving d-c generators. These generators supply adjustable voltage power to the several d-c motors driving the draw works, mud pumps, rotary table, and coring reel.

Most oil well drilling is done by steam engines or Diesels that mechanically drive the various motions through a system of gears and clutches. However, oil wells are being drilled deeper in search of new sands, requiring more power. As in surface transportation and propulsion, the flexibility of transmitting this power electrically is becoming more and more evident.

It is estimated that approximately 35,000 wells will be drilled in 1946. The average depth will be about 4,500 feet. However, a great deal of the exploratory drilling between 10,000 and 15,000 feet now is being done with Diesel-electric equipment where its flexibility is of particular advantage.

It is the purpose of this paper to describe a typical modern Diesel-electric powered drilling equipment and not to discuss the relative economics of Diesel-electric versus mechanical and steam rigs.

Description of Functions

A modern deep well is drilled by means of a bit attached to a drill stem (drill stem is special hollow pipe) and rotated to bite through the sand, gravel, and rock formations of the earth's crust. The diameter of the hole may be 12 inches at the top and six or eight inches near the bottom of a 10,000- or 12,000-foot hole. For clarity, the functions of the various drives are given.

Draw Works

This equipment is the hoist for lifting the drill stem in and out of the hole, and a good view of it is shown in Figure 1. Bits have to be changed every day or two and sometimes every few hours. The draw works operates like a hoist with several mechanical gear changes. To change a bit, a section or two of drill stem is lifted out of the hole, unscrewed, stacked in the side of the derrick, and the traveling block and hook is lowered to pull up the string of drill stem another couple of sections, and so on. Usually, all engines are required for this operation while the mud pumps, rotary table, and coring reel remain idle.

Rotary Table

The rotary table rotates the drill stem with the bit on bottom and drills the hole. The driller regulates the weight of pipe permitted on the bit by means of a mechanical brake on the draw works. The chips and sand are removed by circulating mud.

Mud Pumps

The principal functions of the mud pumps are to circulate the mud which lubricates the drill stem and bit, pick up the chips and sand, and bring them to the surface, suspended in the mud, in the annular space between the drill stem and the outside steel casing, as illustrated in Figure 2. Getting the mud to the right consistency to do this job is a "black" art known only to the drillers. Keeping the mud flowing is important because a 10,000-foot column of mud has a burden of chips which will settle out at the bottom and may freeze the drill stem in the hole if left to stand for a few hours.

Coring Reel

This reel is a light-duty high-speed hoist used to remove sample cores from the hole and for logging purposes. It is used when other apparatus is not in use and is, mechanically, entirely independent.

Typical Arrangement of Apparatus

A typical arrangement of apparatus for 15,000 foot drilling is shown in Figure 3. In this example, three Diesel-engine-driven generators are shown. In some cases, four, five, or even six such sets are employed. However, the minimum rating of Diesel-engine set often is dictated by the rating of the mud pump so that one engine generator set can supply its full rating. The number of such sets is dictated by the rating of the draw works.

The auxiliary motor-driven apparatus, such as miscellaneous pumps and blowers, and the power-system used to supply it will be discussed later.

General Scheme of Operation

Perhaps it will give a better understanding of the equipment operation to describe the results obtained by modern electric equipment from the driller's point of view, before describing in detail the equipment used for accomplishing the results.

Each of the motors operates at constant field strength. Speed is controlled entirely by generator voltage (that is, by generator field and engine speed).

Assume that on Monday morning all equipment is at rest. The engines are started and idled at half speed. From this part on, all control of the rig by the driller

Paper 46-81, recommended by the AIEE committee on industrial power applications for presentation at the AIEE South West District meeting, San Antonio, Texas, April 16–18, 1946. Manuscript submitted January 22, 1946; made available for printing March 4, 1946.

T. R. Rhea is an engineer with the chemical section, industrial engineering department, General Electric Company, Schenectady, N. Y.

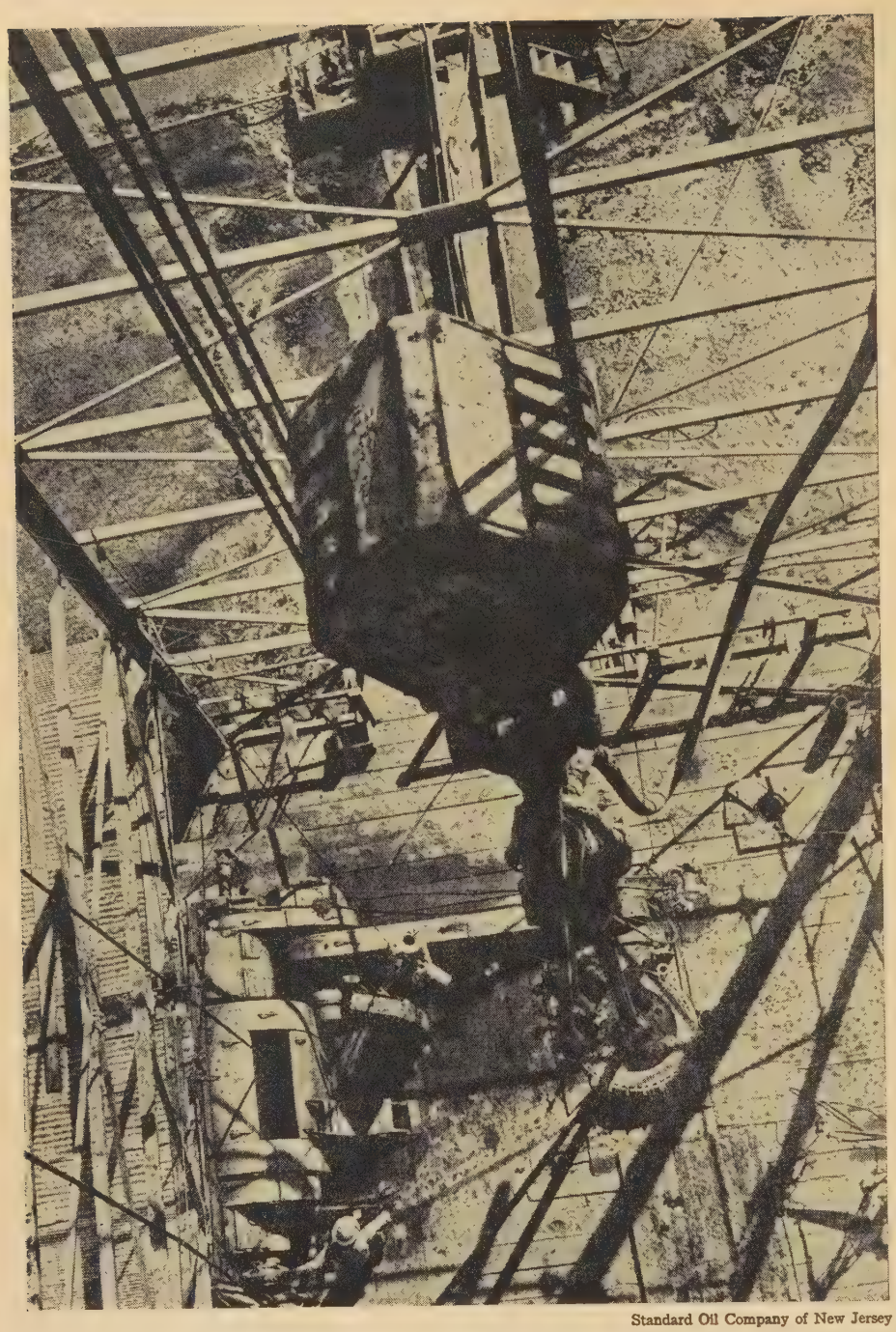

Standard Oil Company of New Jersey

Figure 1. General view showing draw works, swivel with mud-hose connections, hexagonal kelly, and rotary table

is from the four driller's speed master switches and the selector switch shown in Figure 3. To illustrate how the driller's control works, observe what the driller does to start a mud pump. An engine-generator set previously has been assigned, by means of the manual transfer switches, to supply power to this particular mud pump.

The driller moves the speed master switch handwheel from the off position which starts the mud pump. The further he moves the handwheel, the faster the mud pump runs. Up to approximately half motor speed, the engine remains at its half speed. As the driller calls for more motor speed by moving his speed master switch further, the engine automatically speeds. The driller does not have to touch the engine throttle, nor worry about overloading the engine. If the mud pump should become overloaded or even stalled, the load on the engine will be reduced so that the engine is not harmed. These functions are accomplished automatically by means of the engine governor and amplidyne control, which will be explained later.

If desired, the control equipment can be preset to limit the stalling torque on the motor from 75 to 150 per cent of normal motor torque. The engine may be operating at full speed and the mud pump suddenly stall, caused by a plugged bit at, let us say, 125 per cent of normal torque, regardless of where the driller's master switch may be. This torque limit adjustment is made at the control cabinet and not at the drillers position.

To stop the mud pump, the driller returns the master switch to the off position. The Diesel engine returns to idling, at half speed, and the mud pump motor stops.

The controls for all the other motors are the same. Reversing a particular motor merely requires the master switch to be returned to the off position, the handwheel pulled out and rotated as before. The motor reverses and accelerates in the opposite direction. Reversing is not required for mud pumps but is available.

Consider a few of the typical driller's operations.

"Spudding-in"

"Spudding-in" is a process of starting a hole and drilling it the first several hundred feet. There is not sufficient weight on the bit to make it bite at this stage. It is necessary for the driller to lift the drill stem a few feet and then drop it, thus giving the bit a fresh bite. Then it is rotated and may be done at the rate of several times per minute.

The driller has a common speed master switch for the draw works and the rotary table, as shown in Figure 3. It will operate either, but not both simultaneously. There is a "drill-hoist" selector switch which connects generators alternately to the rotary table or to the draw works, provided the speed control switch is in the off position.

The driller turns the drill-hoist selector switch to the *DW* position and turns the speed control master switch, raising the drill stem a little way. He then returns the master switch to the off position and declutches the motor from the hoist drum (the clutch is a pneumatically operated device) and lets the tool drop.

The drill-hoist selector switch is turned to the opposite position to *RT*, and the speed master is turned to rotate the table for a few revolutions. Then the process is repeated.

During this operation, one mud pump motor and engine set has been operating, probably at low speed, circulating mud. This engine set has been prevented from transferring in response to the drill-hoist selector switch by means of a selector switch on the control board.

Drilling

The "drill-hoist" selector switch is thrown to the drill position, which con-

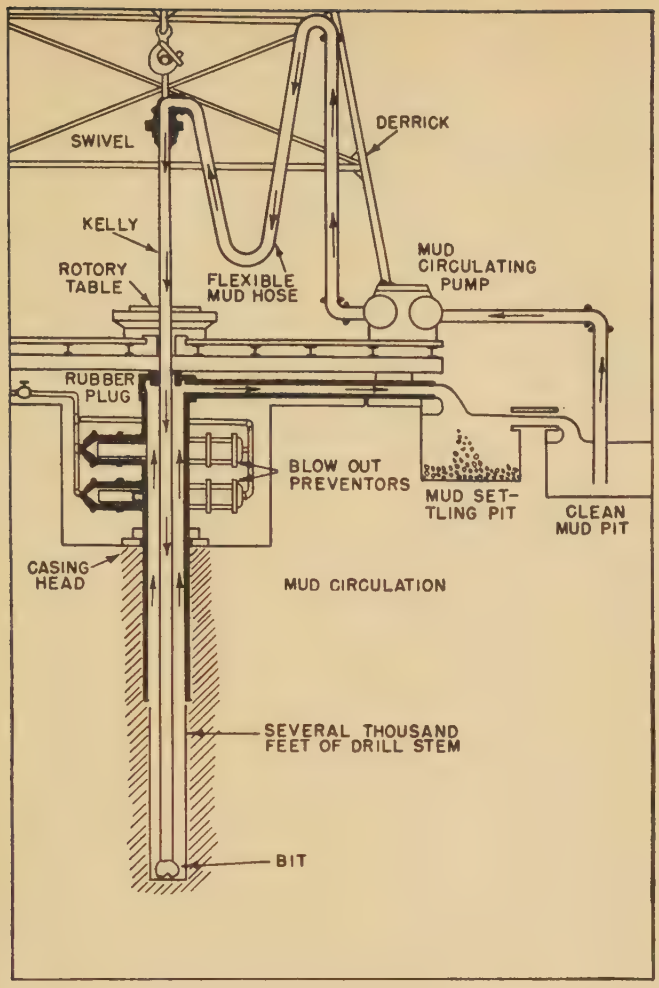

Figure 2 (left). Cross section of rig showing how mud pump circulates mud

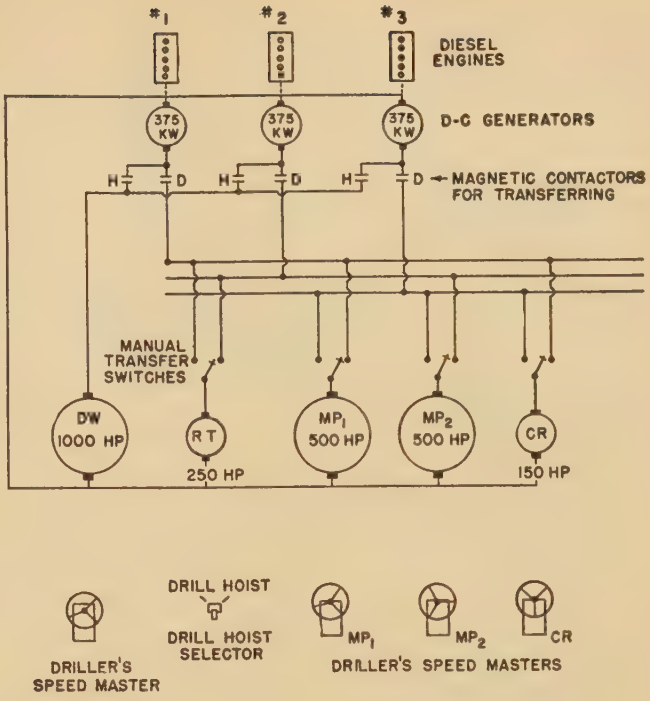

Figure 3 (above). Elementary power diagram of typical d-c drilling rig equipment

nects one engine set to the rotary table and another engine set to a mud pump. The third engine may be used on the second mud pump or it may be shut down.

The driller starts and runs the rotary table, at the desired speed with the speed master, and has no throttle control for the engines, since this is under the control of the engine governor.

Hoisting

When it becomes time to change the bit on the end of the drill stem, the mud pumps are shut down first and the flexible mud hose, swivel, and kelly assembly disconnected from the drill stem. Meanwhile, the engines are idling at half speed because all of the speed masters are in the off position.

The mud hose swivel and kelly (the square piece of drill stem that slides up and down in the square hole in the rotary table) then is dropped in the "rat hole." The "rat hole" is a spare hole that the driller thoughtfully has dug in advance for storing the kelly. It can be discerned in Figure 1.

The drill-hoist selector switch is thrown to the hoist position, which connects all of the engine-generator sets to the draw-works motor for maximum power. All of the engines are paralleled automatically and each may be loaded in accordance with its ability to carry load. The driller turns the speed master in accordance with the desired hoisting speed. If the string of drill stem is exceptionally heavy, the motor will slow down automatically to keep its input within the engine's ability, regardless of the speed-master position. If the drill stem should get stuck, the draw-works motor would stall at about 200 per cent torque or some less adjustable value without damage to the engines, generators, draw-works motor, or to the mechanical equipment, even if the speed master is in the maximum speed position. However, the driller should not let this condition persist for any period of time, since the thermal capacity of the draw-works motor does not permit it to develop 200 per cent torque continuously.

After the drill stem has been hoisted three lengths (a "thribble"), the driller returns his speed master to the off position and sets his hand brake. The drill stem remaining in the hole is wedged carefully into the rotary table. The driller then unscrews the withdrawn lengths of drill stem by holding the withdrawn portion with tongs and rotating the rotary table by power.

After the withdrawn drill stem section is stacked over in the derrick, the hook is driven down at high speed and light load to get another grip on the drill stem remaining in the hole. For this operation, the driller's speed master is pulled outward and turned as far as it will go to get maximum speed.

It may require several hours to take the drill stem out of the hole, attach a new bit, and lower it into the hole again, section by section. This process is called a "round trip."

In lowering a heavy load, however, the draw-works motor is declutched and the lowering energy is dissipated in a water-cooled brake. The Diesel engine cannot absorb very much energy and regenerative lowering has not been resorted to as yet.

In all this maneuvering, the driller needs pay no attention whatever to anything but his speed master and drill-hoist selector switch. All paralleling, speeding up, and slowing down of engines is entirely automatic. When they are paralleled, as on hoisting duty, there is no delicate adjusting of throttles to contend with or nursing of a smaller or defective engine. The automatic governors will make the engines take all the load of which they are capable, and no more, and make each engine parallel with the others.

Manually Selected Combinations

It may be necessary to shut down an engine-generator set for maintenance purposes or simply because its power is not needed. It is desirable, therefore, to give each main drive motor two choices of

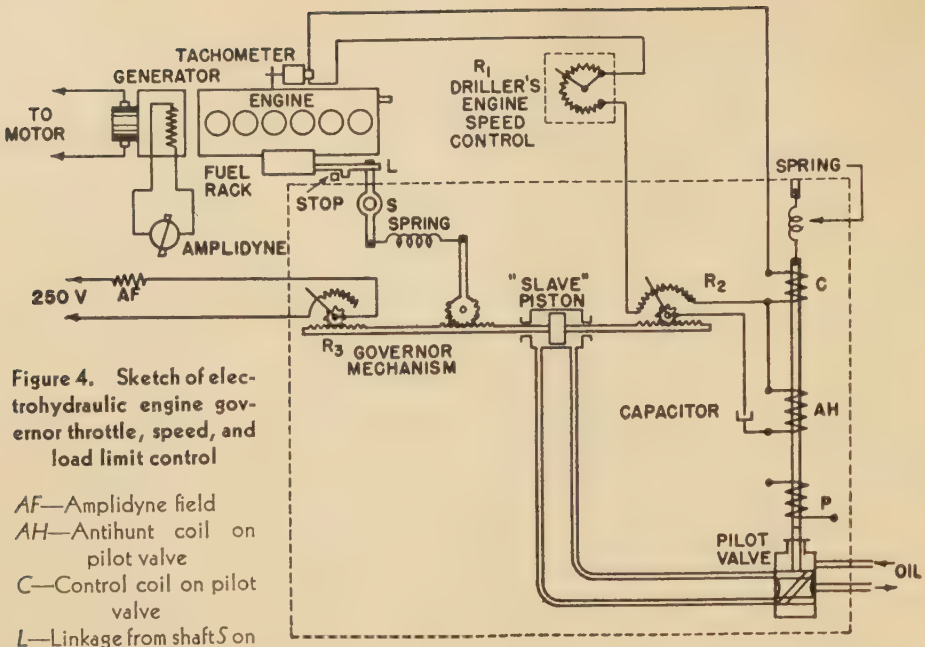

Figure 4. Sketch of electrohydraulic engine governor throttle, speed, and load limit control

AF—Amplidyne field
AH—Antihunt coil on pilot valve
C—Control coil on pilot valve
L—Linkage from shaft *S* on governor to engine fuel rack
P—Coil on pilot valve for paralleling engines
R_1—Driller's speed control rheostat
R_2—Antihunt rheostat
R_3—Rheostat load limit
S—Governor shaft for connection to fuel rack

engine-generator sets. This choice is provided by the manual transfer switches on the control panel.

A selector switch for each engine, located on the control panel, will take away control from the driller's drill-hoist selector switch so that an engine may be retained on some special duty, such as driving a mud pump for mud mixing even while hoisting.

Electrohydraulic Engine Governor

The internal combustion engine is essentially a constant-torque device over an adjustable speed range. It rapidly overheats when submitted to overloads with resultant increase in maintenance.

Since a drilling load is both intermittent and varying, it is highly desirable to run the engines only at the lowest speed consistent with the power required. This rate of speed saves both fuel and wear and tear on the engine. To appreciate this point, just imagine the maintenance and fuel consumption on an automobile engine if it is run always at top engine speed, and the car started and stopped at each traffic light with the clutch and gear shift. That procedure had been followed by the drilling industry with Diesel-electric drives up to the advent of the electrohydraulic governor.

The fuel injection system on most Diesels is such that at low speeds, full throttle opening will overheat the engines. That is, with the throttle wide open and the engine at low speed, actually more fuel per stroke is injected than at full rated engine speed. Thus a requirement of the governing system is to adjust automatically the throttle stop as a function of engine speed.

Functions of the Governor

The functions of the governor can be summarized as follows:

1. It measures engine speed and adjusts the engine throttle to maintain this speed up to permissible full throttle opening.
2. When the throttle is fully open and a further attempt is made to increase load on the engine, it automatically reduces the generator field.
3. It automatically adjusts the position of the throttle stop as a function of engine speed.

All these requirements are accomplished rather simply by the electrohydraulic governor. Refer to Figure 4.

An electric tachometer produces a d-c signal proportional to engine speed. This signal is put into a solenoid operated pilot valve. The pull of the solenoid *C* is balanced against a spring. A slight unbalance in engine speed thus permits the pilot valve to let in a little oil, under pressure, to one side or the other of a "slave" piston, which can move as far as necessary in adjusting the throttle to restore the engine speed and thus the balance between solenoid *C* and the spring.

These factors are the elements of any governing system. Since the slave piston has no restoring spring and can take up any position necessary to balance the solenoid *C* against the spring, the system is isochronous. This condition means that the system has no engine speed droop whatever as the load is applied.

The engine speed controller R_1 is a rheostat inserted between the tachometer and the solenoid *C*. The more resistance is cut in, the faster the engine has to run to establish the balance between solenoid *C* and the spring. The combination of pilot valve, "slave" piston, and throttle will see to that condition. Thus the engine will run at adjustable constant speed levels, depending on the position of rheostat R_1. It is usual to run the engines over either a 2/1 or a 3/1 ratio of speed range. The engine speed set by rheostat R_1 is entirely independent of the load the generator tries to put on the engine. R_1 is a part of the drillers speed master.

Suppose now the generator load has been increased slowly (or suddenly) until the "slave piston" has the throttle wide open and against the fuel stop. Suppose a further increment of load is imposed by the generator on the engine. The engine slows momentarily, unbalances the pilot valve and moves the "slave" piston. A spring between the "slave" piston and the fuel rack permits the former to move further.

This additional movement of the "slave" piston operates a rheostat R_3, which reduces the generator field, and therefore the load, just sufficiently to maintain engine speed.

Let us go back now to the instant where the load on the generator has just brought the throttle to full throttle position. If suddenly two cylinders cut out because of, for example, clogged fuel injectors, the engine will slow down momentarily and the "slave" piston will move. Since the fuel rack is already against the stop, the "slave" piston will simply reduce the generator field and thus keep the remaining cylinders fully loaded, but not overloaded. In this way the governor recognizes the engine's ability to take load. Refer to Figure 5 where this condition is illustrated by a generator curve.

With R_1 in the maximum engine speed position, the usual differential compound-wound generator volt-ampere characteristic for 100 per cent engine speed and 100 per cent field current is followed from no-load current up to point *X*. At this point the governor reaches the fuel stop, and the load limit rheostat R_3 shown in Figure 4 takes over and reduces the generator field. As more ampere load is put on the generator, R_3 makes the generator characteristic follow the load limit line shown in Figure 5, which is, of course, a constant kilowatt or horsepower load on the engine.

If a couple of cylinders were to cut out,

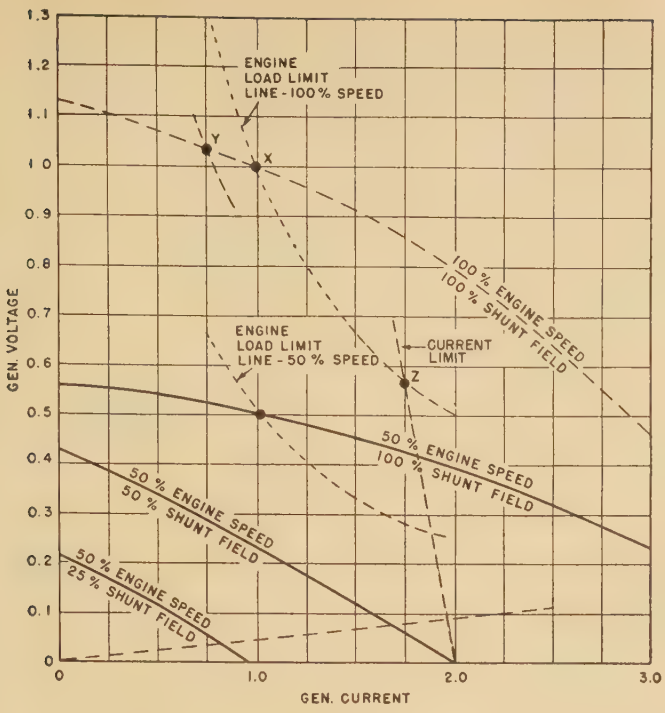

Figure 5 (left). Generator characteristics with electrohydraulic governor load limit and amplidyne current limit

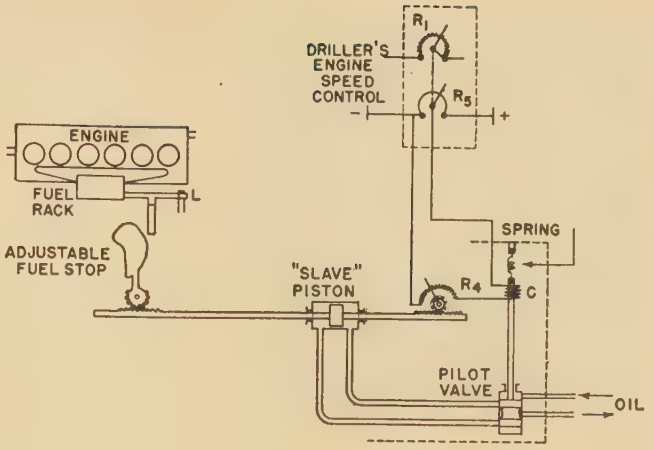

Figure 6 (above). Sketch of electrohydraulic engine governor showing mechanism for adjusting throttle stop as a function of engine speed

the fuel stop would be reached earlier at some such point as Y, and the generator volt-ampere characteristic would follow a constant kilowatt or horsepower curve below the other. Thus the governor automatically adjusts the load to suit the engine condition. This feature is very valuable as the engines get older and less able to carry the same load than when new and in good repair.

Of course, as the driller's engine speed control rheostat R_1 is moved, the whole voltage characteristic moves up and down, as shown in Figure 5.

Throttle Stop Positioning. As yet nothing has been said about adjusting the position of the throttle stop as a function of engine speed. This adjustment is done with a completely separate mechanism from that so far discussed. As shown in Figure 6, the fuel stop is adjusted by a "slave" piston and solenoid-operated pilot valve which are, mechanically, duplicates of those used for the fuel-rack control. This system simply positions the "slave" cylinder in response only to the position of the potentiometer rheostat R_5.

Rheostat R_5 is on the same shaft as the driller's engine speed control rheostat R_1, and, together, they constitute the driller's speed master.

Note that the "slave" piston drives a cam-shaped stop for the fuel rack. The shape of this cam is determined by the engine manufacturer's curve of speed versus maximum-fuel, which is not a straight line.

Any kind of servomechanism would serve as well as that shown to position the fuel-stop cam as a function of engine-speed rheostat position, but a solenoid-controlled pilot valve and "slave" valve are most convenient, since oil under pressure is already available in the governor. The parts are duplicates of those on the throttle control.

All the solenoid valves, "slave" pistons, fuel stops, oil pressure regulating valve, and rheostats R_2, R_3, and R_4 are housed in one frame and mounted on the engine, convenient to the fuel rack, as illustrated in Figure 7.

The antihunt circuit for the governor shown in Figure 4 consists of rheostat R_2, a capacitor, and an AH coil on the pilot valve. A movement of the "slave" piston transiently introduces a force in the pilot valve in the opposite sense. This stabilizing action is very effective.

Advantages of Governor

To recapitulate, the advantages of the electrohydraulic Diesel engine governor for d-c drilling rig equipments are as follows:

1. It automatically prevents overloads on the engine, thus removing one of the principal causes of engine wear and failure.

2. It provides engine speed control by the driller at a remote location by means of a very simple rheostat and electrical connections. It thus permits the driller to run the engines at the lowest speed consistent with the required drilling operation. This feature promotes both fuel economy and low maintenance.

3. Paralleling several engine-generator sets, as required by the draw-works motor, and controlling them from one driller's controller is very simply accomplished by mechanically paralleling the speed control rheostats R_1. Proper division of load among the several engine sets is provided automatically by the governors.

4. The governor provides a "wrap-around" or constant kw characteristic of the generator around the engine characteristic, as shown in Figure 5. This characteristic permits the maximum torque at the maximum speed of the drilling motors at all points within the ability of the engines, instead of only at one fixed point as with conventional 2- or 3-field generator characteristics. This feature is, in effect, an automatic gear shift providing a continuously adjustable choice of ratios between the engine and the driven load.

Amplidyne Control System

An amplidyne is used, instead of a conventional exciter, to excite and control the main generator field because the greater amplification factor of the amplidyne requires only a few watts for the amplidyne field. This factor makes possible the very small and extremely sturdy rheostats used in the governor (illustrated in Figure 7) and in the drillers speed master.

The first requirement of the control system is that the generator voltage be manually controlled and adjusted in either direction. The principles of this system are shown in Figure 8.

The driller's control rheostat R_6 is a potentiometer across a source of d-c control power. A potential V_2 from the potentiometer R_6 is compared with a potential V_1 through the main amplidyne control field F_1F_2. Note that V_1 is a potential drop across a resistor A in the

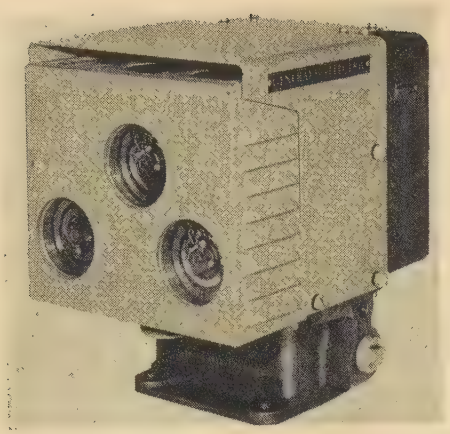

Figure 7. An electrohydraulic governor (tachometer not shown)

main generator field. Thus movement of the driller's rheostat R_6 adjusts the main generator field, and, as a result, the generator characteristics of Figure 5 for different values of generator field current are obtained. The very high amplification factor of the amplidyne makes V_1 always very nearly equal to V_2.

A set of forward and reverse contactors are actuated by pulling out the driller's master switch handle before rotating it, giving forward or reverse generator field excitation.

Instead of comparing the voltage V_2 with main generator field current, it might have been compared directly with the main generator voltage. However, if this were done, the amplidyne would try to nullify the action of the generator differential series field. Each time the main generator differential series field tried to pull the voltage down, the amplidyne would try to pull it up. Also, as has been proved by many types of installations, the stability of the system is much better if the control potential V_2 is balanced against main generator field current, leaving the differential series field to do its duty.

The engine load-limit potentiometer rheostat R_3 is inserted between the driller's control rheostat R_6 and the amplidyne control field F_1F_2, and is the same governor-actuated rheostat R_3 as shown in Figure 4.

Since several generators are to be controlled in parallel from one driller's control master switch, when hoisting, several amplidyne fields can be paralleled on one R_6 rheostat.

The potentiometer R_6, shown in Figure 8, and the engine speed control rheostat R_1 (Figure 4) are on one shaft and form the complete drillers speed master. The complete travel of the drillers speed master is about 330 degrees. The first 165 degrees of movement raises the generator field from zero to full value, but does not raise the engine speed. The next 165 degrees cut in R_1 to speed up the engine.

Current Limit

The next function to be provided is current limit so that the commutating ability of the generators and motors will not be exceeded, even if the motors stall. Likewise, it is desirable to limit the applied torque on the mechanical equipment to prevent damage. For example, the rotary-table-drive motor, when rotating a long string of drill stem, may require a definitely limited maximum torque to prevent twisting it off.

It should be understood clearly that the current limit function now under discussion is entirely separate and distinct from the engine load limit previously discussed. Current limit control is provided by a separate field on the amplidyne. This control field F_5F_6, illustrated in Figure 9, always is excited in the opposite direction from the control field F_1F_2 and must overpower it, and thus reduce main generator excitation whenever the main generator current reaches a certain value.

The current limit must be ineffective until a certain selected value of current is reached, regardless of the direction of flow of that current, and be effective when that value is reached.

In Figure 9 is shown the elementary diagram of the amplidyne connection used to accomplish this function.

A pair of rheostats R_7 are placed across a source of d-c control power. This reference voltage is compared, through a pair of blocking selenium rectifiers, to the drop across the commutating and series fields, which is proportional to generator current.

For one direction of main generator current, V_3 must be greater than V_4 before blocking rectifier BR_1 will permit current to flow in current limit field F_5F_6.

When the generator current reverses, which depends on a reversal of the control field F_1F_2, the drop V_5 is in the opposite direction. When V_5 exceeds V_6, the blocking rectifier BR_2 permits current to flow in the current limit field F_5F_6 in such a direction as to oppose control field F_1F_2.

The effect of current limit control is shown in Figure 5. The cut-off point Z can be adjusted for any desired value of current by adjusting rheostat R_7. While current limit begins to cut off at the control setting of point Z, the generator current has to rise a further 10 or 15 per cent

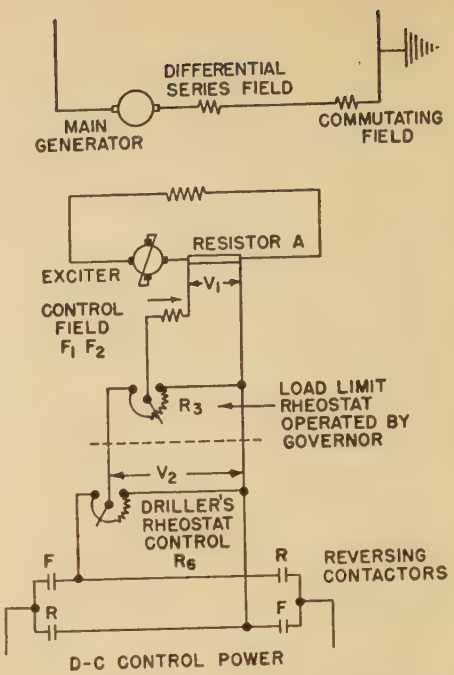

Figure 8. Elementary diagram of amplidyne field and engine load limit control

before the current limit field F_5F_6 can overcome completely the control field F_1F_2 and bring the generator voltage to zero.

Antihunt and Paralleling

An antihunt field F_7F_8 is provided on the amplidyne so that any sudden rise of amplidyne voltage causes a transient current to flow through the capacitor and control field F_7F_8, which opposes the change.

A paralleling field F_9F_{10} is connected, as shown, and connects to a similar arrangement on any additional generators connected in parallel. It tries to make the generator divide the loads and operates exactly by the same manner as a paralleling connection on regulators.

The paralleling field F_9F_{10} shown in Figure 9 is quite weak in comparison with the other fields and is mainly effective at light generator loads or for very sudden transients (for example, one generator out of several in parallel suddenly losing its field). Paralleling field F_9F_{10} is completely overcome and supplanted in function whenever the load limit feature of the governor goes into action.

Auxiliary Drives

In addition to the main drive motors, there are a number of auxiliary motors for driving ventilating blowers, pumps, air compressors, shale shakers, blowout preventer, and bug fans. The require-

ments for such motors may total 50 or 60 horsepower on a typical rig. Also, six or seven kilowatts is required for adequate lighting. Approximately 15 kilowatts of excitation power is required for the main drive motors.

On Diesel-electric rigs, it has been the practice in the past to add a constant potential d-c auxiliary generator to each engine. A typical rating is 30 kw, 125 volts d-c (125 volts has been selected in the past because of the lighting requirements).

Because the main engines are usually started by compressed air, a small battery-started gasoline engine-driven generator of five or ten kilowatts is installed to supply power to the air compressor motor, when the main engines are down, and to supply lighting power when rigging up or tearing down the rig.

This almost universal practice of supplying 125-volt d-c auxiliary power requires expensive d-c auxiliary motors and d-c control, generally with explosionproof enclosures.

Since the auxiliary drives require only constant-speed motors, a-c auxiliary power is recommended. This a-c power permits very simple sturdy control and the auxiliary motors to be squirrel-cage induction motors, explosionproof if desired.

A very careful analysis of the costs of d-c versus a-c auxiliary power reveals that the cost of auxiliary equipment for a-c power is about 25 per cent cheaper than for d-c power. In making this comparison, two full capacity engine-driven 440-volt, 3-phase 60-cycle alternators were included. One of these alternators is a complete spare to the other, since the entire rig depends on this auxiliary power being available.

The cost comparison includes the cost of two auxiliary engines, but takes credit for eliminating the small 5-kw emergency lighting engine generator and reducing the size necessary for the main engines.

The use of entirely separate engine-driven auxiliary power generators is made even more desirable by the use of adjustable speed main engines. If d-c auxiliary power generators are driven by the main engines, they have to give full output at the lowest engine speed. This condition increases the cost of such d-c auxiliary equipment, and the foregoing cost comparison was made on the basis of running the main engines over a two to one speed range. With a-c auxiliaries, the lighting circuits are standard 115 volts, stepped down from 440 volts by transformers.

The advantages of a-c versus d-c auxiliaries can be summarized as follows:

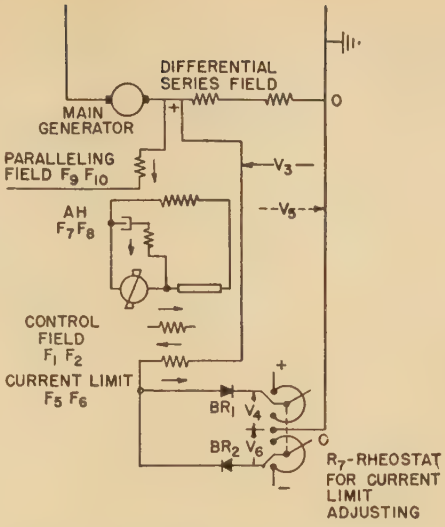

Figure 9. Elementary diagram of amplidyne control showing current limit, antihunt, and paralleling fields

1. About 25 per cent reduction in first cost.

2. The main engine-driven-generator units are simplified, lighter, easier to move and set up because of the elimination of the top-mounted belt-driven constant-voltage d-c auxiliary generators, and the consequent reduction in size of the main engine required.

3. The main control panel is reduced in size and weight because of simpler a-c instead of d-c control for auxiliaries.

4. Auxiliary a-c power at 440 volts, 3 phase, requires smaller cable to distribute power than does 125 volts d-c.

The disadvantages of having two small 100 or 125 horsepower internal combustion auxiliary engines to maintain are more than overcome by not having to run the main engines when only auxiliary power is required. Also, the 5- or 10-kw engine-driven set is eliminated.

Ventilation

The main rig motion motors are usually force-ventilated because they frequently are required to operate at very low speeds and full torque. Also, it is desirable to bring in fresh air, free from explosive gas mixtures, to eliminate the explosion hazard which would otherwise be present when the well strikes gas.

The most usual method of ventilation is to mount a small motor-driven blower on the top of each main d-c motor and run a duct away from the derrick to a safe source of fresh air.

These ducts have been made of steel in the past and are considered a nuisance to tear down and move approximately every two months. There is now a probability of obtaining flexible rubberized non-collapsible ducts which will be very easy to move.

The generators are self-ventilating and are located away from the derrick in a nonhazardous area.

On barge-mounted rigs, there is usually a central blower system, and air is piped to the various motors.

Because of the duty on the coring-reel motor, it usually can be totally enclosed and one-hour rated, thus eliminating the cumbersome duct work. However, to make this large totally-enclosed motor truly explosionproof would be very expensive, but it is a very simple matter to infiltrate a very small amount of safe air from the compressor system to keep this motor purged and under slight pressure.

Frequently, the mud pumps are located far enough away from the rig so that no duct work is necessary to bring in safe air, and their blowers take air directly from the ambient surroundings.

References

1. Electric Equipment on Rotary Drilling Rigs, **G. R. Prout.** *Petroleum Engineer*, May 1940.

2. Amplidyne; A New Tool of Many Uses, **F. Mohler.** *Iron and Steel Engineer*, September 1940.

3. Fundamental Principles of Amplidyne Applications, **F. E. Crever.** AIEE Transactions, volume 62, 1943, September section, pages 603–06.

4. Industrial Applications of Amplidyne Generators, **D. R. Shoults, M. A. Edwards, F. E. Crever.** *General Electric Review*, volume 43, 1940.

5. Steady-State Theory of the Amplidyne Generator, **T. D. Graybeal.** AIEE Transactions, volume 61, 1942, October section, pages 750–6.

6. Modern Rotary Drilling Machinery and Practices, **W. S. Crake.** *Oil and Gas Journal*, July 7 to August 18, 1945.

7. New 2,100 Horsepower Diesel-Electric Drilling Rig Is Compact and Portable, **K. Marshall Fagin.** *Petroleum Engineer*, August 1945.

8. Practical Features of Diesel-Electric Rig in Service, **J. E. Brantly.** *World Petroleum*, May 1938.

9. Deep-Well Drilling With Direct Current, **L. D. Banderob, P. L. Savage.** *Petroleum World*, September 1942.

10. Direct-Current Rigs for Deep-Drilling Operations, **R. A. J. Dawson.** *Petroleum Engineer*, August 1943.

11. Variable Voltage Equipment for Rotary-Drilling Rigs, **E. H. Lamberger.** AIEE Transactions, volume 59, 1940, April section, pages 248–56.

12. Diesel-Electric Rigs in Gulf Coast Service, **Orville Adams.** *Petroleum Engineer*, June 1941.

13. New Diesel-Electric Rig, **Arch Rowan.** *Oil Weekly*, October 7, 1935.

14. Electric Power for Drilling in Jungle or Desert, **W. G. Taylor.** *World Petroleum*, May 1936.

15. Parallel Operation of Main-Engine-Driven 400-Cycle Aircraft Generators, **L. G. Levoy, Jr.** AIEE Transactions, volume 64, 1945, December section, pages 811–16

16. Governor for Variable-Ratio Transmission Used in Developmental 400-Cycle Electrical System for Large Aircraft, **P. F. Desch, D. E. Garr, J. G. Hutton.** AIEE Transactions, volume 65, 1946, April section, pages 194–8.

Dynamic Braking Control of D-C Series Motors—Calculation of Stability Limit

G. W. HEUMANN
MEMBER AIEE

W. P. SMITH
NONMEMBER AIEE

Synopsis: This paper presents an extension of the conventional method of calculating speed-torque curves for d-c series motors used with dynamic braking controllers, which permits determination of the stability limit with overhauling loads such as occur on crane hoists. It is shown that such stability limit can be increased by the addition of series resistance.

IN laying out control equipment, the design engineer looks for methods which enable him to calculate, with a minimum of effort and with reasonable accuracy, the speed-torque curves obtained on various controller points. Direct-current series motors are widely used for heavy duty intermittent drives, such as cranes, hoists, ore and coal unloaders, and other material handling equipment. Control of such motors is obtained by inserting resistance in the various branches of the motor circuit, that is, the armature and the field.

Considering that commercial resistors may deviate as much as ten per cent from their rated resistance, that line voltage may vary by ten per cent or even more, and that it is difficult on most motor applications to predict actual load conditions within a few per cent, it does not appear necessary to forecast motor performance with a greater accuracy than a few per cent. It is of greater importance to have a method available which permits making approximate calculations quickly so that control systems can be compared and analyzed without spending an undue amount of time and effort.

A simple method of calculation which is widely used by design and application engineers has been described by A. A. Merrill.[1] The information required from the motor designer is the characteristic curves of the motor, in which speed and torque are plotted as a function of motor current, as well as armature resistance $R_{a,b}$ commutating field resistance R_c, series field resistance R_f, and equivalent brush drop resistance R_b. As the armature and field current of a series motor are normally the same, all values entering into the calculations can be expressed in terms of either field or armature current.

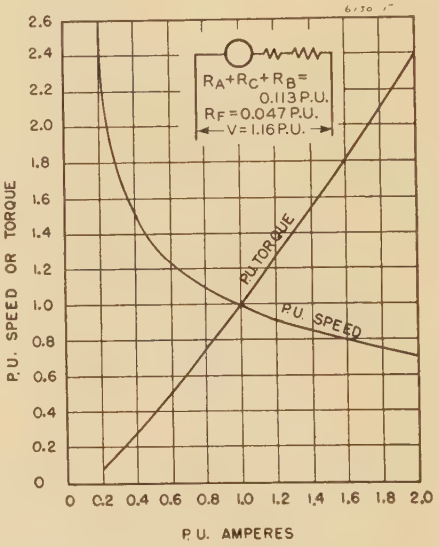

Figure 1. Per unit characteristic curves of d-c series motor

Average of line of 30-minute-rated mill motors

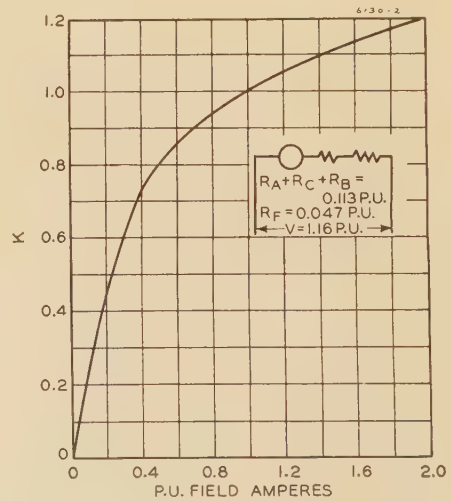

Figure 2. Factor *K*, calculated from Figure 1, as a function of field current

To obtain results which are generally applicable to motors of various sizes, it is convenient to express operating quantities in "per unit" (pu), rather than in actual numerical values. Rated or normal values are called base values, expressed as unity, and all other values are expressed as a decimal fraction of the base values. Base quantities used in this paper are defined as follows:

base current = rated full load current
base torque = rated full load torque
base speed = rated full load speed
base voltage = generated armature electromotive force at rated torque and rated speed
base resistance = base voltage divided by base current
base flux = flux per pole at rated full load speed and current

Figure 1 represents the average characteristic curves of a line of 30-minute-rated mill type d-c series motors. All values are expressed in per unit, based on rated 30-minute load. The actual load expressed by base current or base torque is higher than the same machine would be required to carry if it were rated on a continuous basis. Consequently, the magnetic and electric loadings are high, and the effects of saturation and armature reaction are more noticeable than for continuous rated machines of similar physical size, when loads are expressed in per unit, based on rated values.

Conventional speed-torque calculations are based on two fundamental equations for dynamo electric machines which state that

$$S = \frac{E}{k_s \phi} \tag{1}$$

and

$$T = k_t \phi I_a \tag{2}$$

where

E = generated voltage
T = developed torque
ϕ = magnetic flux per pole
I_a = armature current
S = speed of rotation
k_s and k_t = constants, the value of which is determined by motor design and by the units of E, R, I_a, and S

Let

$k_s \phi = K_s$ and $k_t \phi = K_t$

Then

$$S = \frac{E}{K_s} \tag{3}$$

and

$$T = K_t I_a \tag{4}$$

Paper 46-130, recommended by the AIEE committee on industrial control devices for presentation at the AIEE summer convention, Detroit, Mich., June 24–28, 1946. Manuscript submitted October 30, 1945; made available for printing April 11, 1946.

G. W. HEUMANN is with the industrial control engineering division, General Electric Company, Schenectady, N. Y. W. P. SMITH is with the d-c armored motor engineering division, General Electric Company, Erie, Pa.

The authors wish to acknowledge the assistance given them in the preparation of this paper by C. W. Lange, engineer, d-c armored motor engineering division, General Electric Company, who first called attention to the effect of series resistance on the stability limit.

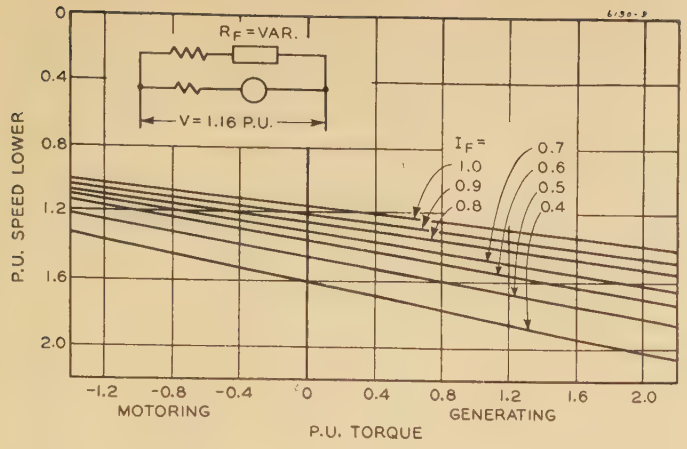

Figure 3. Speed-torque curves of a dynamic braking controller, calculated with constant K

In the per unit system, $K_{s(\text{pu})}$ and $K_{t(\text{pu})}$ have the same numerical value because they are both directly proportional to the magnitude of the flux. This may be shown as follows:

$$K_{s\,\text{base}} = \frac{E_{\text{base}}}{S_{\text{base}}} = k_s\phi_{\text{base}}$$

$$K_{s1} = k_s\phi_1$$

$$K_{s(\text{pu})} = \frac{K_{s1}}{K_{s\,\text{base}}} = \frac{k_s\phi_1}{k_s\phi_{\text{base}}} = \frac{\phi_1}{\phi_{\text{base}}}$$

$$K_{t\,\text{base}} = \frac{T_{\text{base}}}{I_{a\,\text{base}}} = k_t\phi_{\text{base}}$$

$$K_{t1} = k_t\phi_1$$

$$K_{t(\text{pu})} = \frac{K_{t1}}{K_{t\,\text{base}}} = \frac{k_t\phi_1}{k_t\phi_{\text{base}}} = \frac{\phi_1}{\phi_{\text{base}}}$$

Therefore

$$K_{s(\text{pu})} = K_{t(\text{pu})} = K \tag{5}$$

Also

$$K_{s(\text{pu})} = \frac{E_{(\text{pu})}}{S_{(\text{pu})}} \tag{6}$$

and

$$K_{t(\text{pu})} = \frac{T_{(\text{pu})}}{I_{a(\text{pu})}} \tag{7}$$

Therefore:

$$K = \frac{E_{(\text{pu})}}{S_{(\text{pu})}} \tag{8}$$

or

$$K = \frac{T_{(\text{pu})}}{I_{a(\text{pu})}} \tag{9}$$

and

$$S_{(\text{pu})} = \frac{E_{(\text{pu})}}{K} \tag{10}$$

$$T_{(\text{pu})} = KI_{a(\text{pu})} \tag{11}$$

Values of K may be calculated from Figure 1 by equation 8 or 9. When equation 8 is used, $E_{(\text{pu})}$ is obtained from the equation

$$E_{(\text{pu})} = V_{(\text{pu})} - I_{a(\text{pu})}R_{a(\text{pu})} \tag{12}$$

where

$V_{(\text{pu})}$ = per unit line voltage
$I_{a(\text{pu})}$ = per unit amperes in armature circuit
$R_{a(\text{pu})}$ = per unit ohms in armature circuit

For generator operation, $E_{(\text{pu})}$ is given by

$$E_{(\text{pu})} = V_{(\text{pu})} + I_{a(\text{pu})}R_{a(\text{pu})} \tag{13}$$

The data so calculated are then plotted against field amperes as illustrated by Figure 2. The data shown in Figure 2 are based on values and curves given in Figure 1.

Speed and torque for any given set of conditions can be calculated using Figure 2. When field current, armature current, line voltage, and motor resistance are known, generated voltage is calculated by equation 12 for motor operation, or equation 13 for generator operation. Speed is then obtained from equation 10, and developed torque from equation 11, using the value of K corresponding to the given field current. The shaft torque may be obtained by multiplying the developed torque by torque efficiency for motor operation, or dividing the developed torque by torque efficiency for generator operation. In subsequent speed-torque calculations, torque efficiency is considered to be unity.

A family of speed-torque curves for a dynamic braking controller, calculated by the method described above, is given in Figure 3. In this type of controller, the series motor is connected as a shunt machine on lowering points. Heavy loads overhaul the motor, which acts as a shunt generator and develops a dynamic braking torque restraining the load. This torque is indicated as positive in Figure 3. An empty hook or a light load is driven down by the motor, which acts as a shunt motor, deliverying a torque to accelerate the load. This torque is indicated as negative. Line voltage used for the calculation is 1.16, total internal motor resistance being 0.16.

The calculated curves of Figure 3 show that any desired no-load speed can be obtained by inserting sufficient resistance in series with the field. The straight-line curves give the impression that speed varies only slightly within the operating range between motoring and generating. This conclusion is incorrect. J. A. Jackson[2] has called attention to the fact that when operating with weakened field, the motor develops less dynamic braking torque than the curves of Figure 3 indicate. As braking torque and armature current increase, armature reaction plays an important role, reducing the effective flux. For a given overhauling torque, the speeds are higher than the calculation indicates. There is a definite limit of dynamic braking torque which the machine can develop with a given

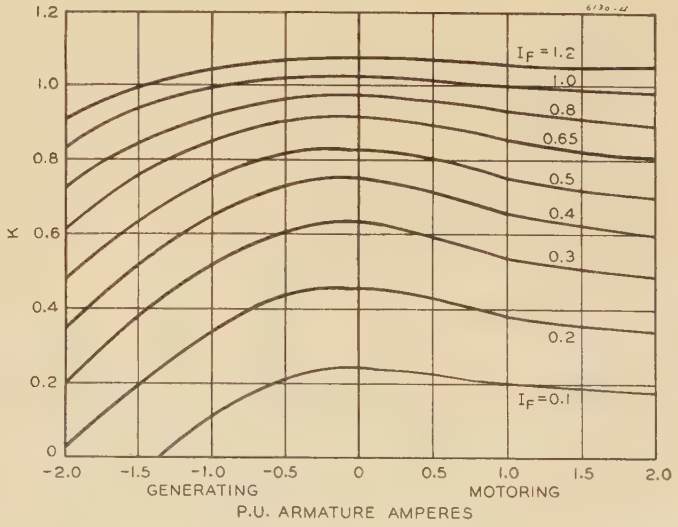

Figure 4. Factor K for d-c machine operating as motor or generator

Average of line of 30-minute-rated mill motors

amount of field current. If the load exceeds this torque, the machine becomes unstable, and a runaway condition results. To calculate the actual performance and the stability limit, it is necessary to abandon the concept that K is an independent function of field current.

Stability Limit

To obtain a true picture of the variation in the value of K with variation in armature current, it is necessary to test the motor over a range of loads both motoring and generating at several different values of field current. The average results, expressed in per unit values, of a number of such tests on a line of mill type d-c series motors are given in Figure 4. It has already been shown that the value of K is directly proportional to the magnetic flux in the motor, and it is evident from the curves of Figure 4 that the magnitude of the armature current does materially influence the amount of magnetic flux. This influence is the result of two factors:

1. Demagnetization produced by cross-magnetizing armature reaction.
2. Magnetization or demagnetization produced by currents flowing in armature coils undergoing commutation.

The theory of demagnetization produced by armature reaction may be found in any textbook on d-c machinery. In brief, the cross-magnetizing reaction produces a distortion in the flux distribution between the main poles and the armature which, because of the characteristic shape of the saturation curve, results in a net loss of flux. The effect is the same whether the machine is operating as a motor or as a generator.

The magnetizing or demagnetizing effect produced by current in the armature coils undergoing commutation would not be noticeable in a commutating pole machine if compensation could be adjusted exactly for all conditions of load. However, the magnetic loading of 30-minute-rated d-c motors is high, and this leads to saturation of the commutating pole magnetic circuit at heavy loads. When saturation occurs, the machine is operating in an undercompensated condition, and the current in the armature coils short-circuited by the brushes then has sufficient magnitude and such direction as to produce a direct magnetizing or demagnetizing effect on the main pole magnetic circuit. Analysis shows that this effect is demagnetizing for generator operation and magnetizing for motor operation.

Considering the combined effect of these two phenomena, it will be noted that they are additive and demagnetizing for generator operation. It is to be expected that the result would be an appreciable loss of flux, and the test results presented in Figure 4 confirm this expectation. For motor operation the two effects are opposing, and the loss of flux at heavy overloads is much less, particularly at very heavy and very light field currents where the effect of cross-magnetizing armature reaction is minimum.

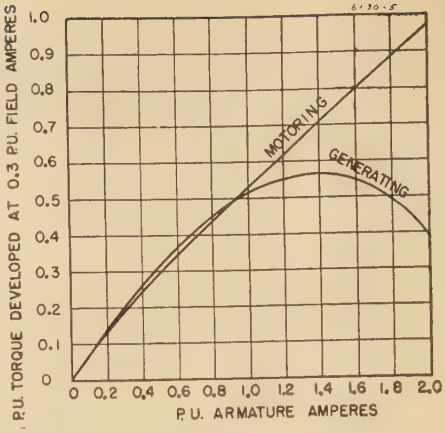

Figure 5. Developed torque, motoring and generating

The loss of flux with increasing armature current when operating as a generator results in very definite torque limitations. Equation 11 states that developed torque is equal to the product of K and armature current. Since K is an inverse function of armature current for generator operation, the product has a definite maximum value, as illustrated by Figure 5. It is the maximum value of torque which determines the limit of stable operation. When it is exceeded, even under transient conditions, dynamic braking control is lost and cannot be regained, because increase in speed corresponds to decrease in torque. With loss of braking control, the load quickly accelerates to a dangerous speed.

In order to indicate the significance of variable K to the speed-torque curves of a dynamic braking controller, Figure 6 shows the actual performance curves obtained with a series motor, connected as a shunt machine. These curves apply to the same circuit and field conditions as Figure 3, but variable K has been used from Figure 4. The no-load speeds obtained by the two methods of calculation differ only slightly. In the region of power torque the curves differ somewhat, and especially with weak field the slope of the curves with variable K is less than for the curves calculated with constant K.

Performance in the dynamic braking region shows the most significant difference between the two methods of calculation. Figure 6 indicates that, with heavy loads, considerably higher speeds are obtained than would be expected from Figure 3. Also, for each value of field current, there is a definite torque beyond which the machine is unable to retard an overhauling load, that is, beyond which the machine becomes unstable. Assuming that an average crane hoist has a mechanical efficiency of 0.85, a dynamic braking torque of $(0.85)^2$, or 0.72, would then be required to lower full rated load. This torque is dangerously close to the motor stability limit with a field current of 0.5 or less.

Speed-torque curves such as plotted in Figure 6 represent steady-state operating conditions. While switching between controller points, transient armature current peaks and corresponding torque peaks occur. Even though the steady-state stability limit may be greater than full-load torque, switching transients may cause the stability limit to be exceeded, resulting in a runaway condition. This means that the control designer is not free to select any no-load speed he can obtain by field weakening. The amount of field weakening which is permissible, and thus the no-load speed which can be realized, are definitely limited by motor stability when lowering full load.

Effect of Series Resistance

A simple method of increasing the stability limit is to insert a block of resistance in series with the parallel circuit formed by the armature and the field. Resistance between 0.10 and 0.20 has only a slight effect on no-load speed and on the slope of the curves in the motoring quadrant. In Figure 7 a set of speed-torque curves is plotted for the same circuit conditions as in Figure 6, except that series resistance of 0.15 has been added. For each curve the amount of resistance in series with the field is held constant at such a value that the indicated value of I_f would be obtained if R_s were zero. On each curve there is a point at which no current is taken from the line, and at this point the indicated value of I_f actually flows through the field, whereas under all other operating conditions field current is either somewhat smaller or larger.

Series resistance has the effect of changing the distribution of current between field and armature at any given operating point. In the range of motoring and light overhauling torques, field current is smaller than it would be without series resistance. This is of no practical conse-

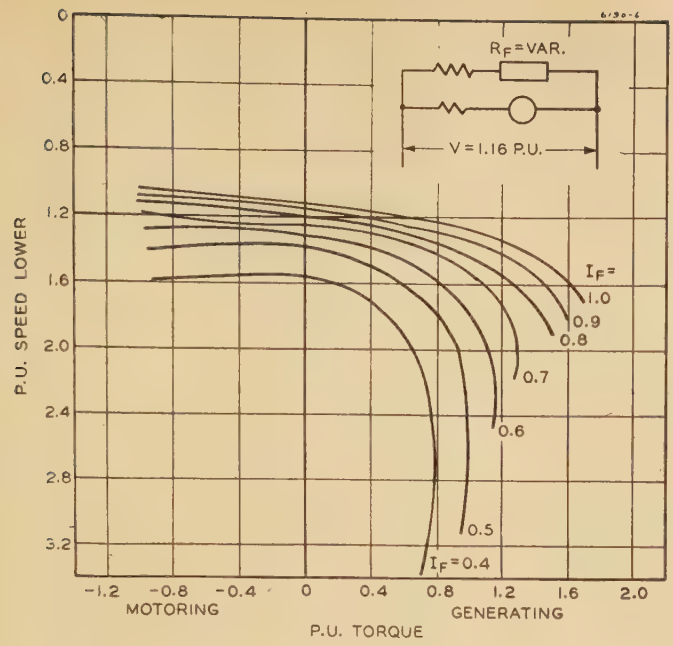

Figure 6. Speed-torque curves of a dynamic braking controller, calculated with variable *K* from Figure 4

No series resistance

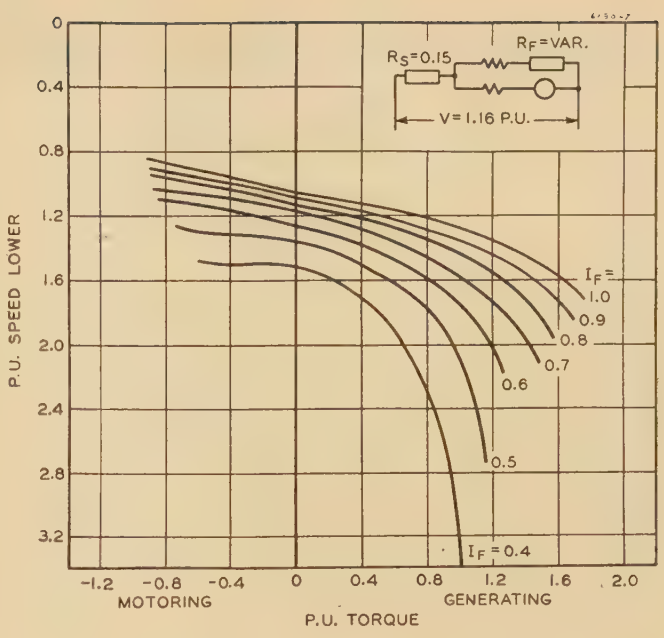

Figure 7. Speed-torque curves of a dynamic braking controller, calculated with variable *K* from Figure 4

With series resistance

Values of field current I_F indicated on curves exist only for the condition that line current is zero. Field resistance R_F for each curve is the same as in Figure 6

quence, as this is a stable motor operating range. Under high overhauling load conditions, however, the field current is greater. As factor K increases correspondingly, the motor is able to develop a higher braking torque, and the stability limit occurs at higher load. Comparing Figure 7 with Figure 6 for each value of field current, the slope of the curve is decreased in the higher torque region.

Assuming that the controller design permits transient torque peaks of twice normal when switching between controller points, the stability limit should occur at a braking torque of not less than twice the torque required to lower rated full load on the hook, that is, $2 \times 0.72 = 1.44$. Without series resistance, a field current of 0.70 would result in a runaway. With series resistance, a field current of 0.60 (at zero line current) would still be permissible.

Conclusions

The method of calculating speed-torque curves by using a variable factor K can be used for any d-c series motor for which sufficient test data are available for determining K both for motoring and generating operation. While the per unit data given in this paper permit the calculation of performance curves for the purpose of comparing various control circuit designs, actual motor test data may vary over a considerable range and must be used to determine the performance of any given motor application.

In designing dynamic braking controllers, using the motor field with suitable resistance in parallel with the armature, resistance in series with the parallel circuit formed by field and armature should be used to increase the motor stability limit.

References

1. The Speed-Torque Curves of a Series Motor, **A. A. Merrill.** *General Electric Review*, October 1933.

2. D-C Crane Equipment for Modern Steel Mill Cranes, **J. A. Jackson.** *Iron and Steel Engineer*, October 1938.

Operating Experience With Distance Ground Relays

W. A. WOLFE
MEMBER AIEE

DISTANCE RELAYS for protection against wire-to-wire, two wire-to-ground, and three phase faults on transmission lines have met with wide acceptance. However, the use of distance relays for protection against single wire-to-ground faults has been limited to relatively few installations. From the information available, it would seem that the Kansas Gas and Electric Company is one of the few companies using distance ground relays. The experience gained in the use of these relays over the past seven years has demonstrated their reliability and good operating performance.

Theory of Distance Ground Measurement

The theory of distance ground measurement was first presented in 1931.[1] In general, distance relays compare the magnitude of a voltage with that of a current, the ratio being an indication of the distance to the fault. Zero sequence current and voltage (usually associated with ground relaying) are not suitable for distance ground relaying, because a comparison of these quantities is not a measure of the distance to the fault. The zero sequence voltage at the relay is equal to the sum of the zero sequence voltage drops from the relay to the source of ground current, and not from the relay to the fault as is required in distance relaying. Instead of these quantities, distance relays for ground faults use phase-to-ground voltage with the current in the corresponding phase, thus requiring three relays for the protection of each 3-phase line. This number is in addition to the relays required for protection against phase faults. For correct distance measurement under all system conditions, reactance type relays must be used and suitable compensation must be applied. The compensation used involves the zero-sequence current in the line section being protected and in the parallel line, if any.

As already shown,[1,2] the general expression for the line-to-ground voltage at the relay during a line-to-ground fault (see Figure 1) is

$$E_{aG} = mZ_{1GH}\left(I_{aGF} + I_{0GF}\frac{Z_{0GH} - Z_{1GH}}{Z_{1GH}} + I_{0GH}\frac{M_{0GH}}{Z_{1GH}}\right) + (I_{aGF} + I_{aHF})\,R_G \quad (1)$$

where

E_{aG} = line-to-ground voltage, A phase at G
m = fraction of distance from G to H at which fault is assumed to occur
I_{aGF} = phase A fault current in faulted line at G
I_{0GF} = zero-sequence fault current in faulted line at G
Z_{1GH} = positive-sequence impedance, station G to H
Z_{0GH} = zero-sequence impedance, station G to H
M_{0GH} = zero-sequence mutual impedance between the two parallel lines from G to H
I_{0GH} = zero-sequence fault current in parallel line
I_{aHF} = phase A fault current from opposite end of faulted line
R_G = fault resistance
G = substation where relaying is considered
H = substation at opposite end of line section
F = fault location

Looking at equation 1, it will be observed that if we could obtain a single current for the relay equal to the current expressed within the first brackets, namely

$$I_{\text{relay}} = I_{aGF} + I_{0GF}\frac{Z_{0GH} + Z_{1GH}}{Z_{1GH}} + I_{0GH}\frac{M_{0GH}}{Z_{1GH}} \quad (2)$$

we obtain a very simple result, as follows:

$$Z_R = \frac{E_{aG}}{I_{\text{relay}}} = mZ_{1GH} + \left(\frac{I_{aGF} + I_{aHF}}{I_{\text{relay}}}\right)R_G \quad (3)$$

where:

Z_R = impedance indicated by the relay
I_{relay} = current through relay

The first term of this expression is directly proportional to the distance from the fault to the relay and is independent of conditions external to the section being protected. The second term is a function of fault resistance R_G and, therefore, represents a voltage in phase with the fault current. By using a reactance type relay, which is responsive only to the reactive component of the voltage, the effect of the last term is rejected. This rejection is necessary because this last term varies with changing system conditions, and also because R_G itself is likely to vary over wide limits as compared with the fault resistance experienced in wire-to-wire faults.

In practice the proper relay current is obtained by the use of an auxiliary current transformer which takes the proper proportion of the residual current of the protected line and combines it with the proper proportion of the residual current from the parallel line (if any). In one type of distance ground relay, this current is added to the phase current I_{aGF} (equation 2), and the total fed into the relay. In another type of distance ground relay, the phase current I_{aGF} is fed into one winding of the relay, and the output of the auxiliary current transformer is fed into a second winding of the relay. Both windings then operate on the same element. The net result is the same.

A vector diagram of the currents and voltages involved in distance ground relaying is shown in Figure 2. In one type of distance ground relay, instead of using the voltage 90 degrees from the faulted phase for polarizing the directional element, as shown, residual or zero phase sequence current and voltage is used in the directional element.

Figures 5 and 6 show examples of typical installations of distance phase and ground relays.

Figure 7 is a typical wiring diagram for an installation of one type of distance ground relays. The phase relays are not shown.

Reasons for Use

There are several reasons why distance ground relays were considered justified and installed on the Kansas Gas and Electric Company system instead of ordinary directional ground relays or carrier pilot relays. The reason why Peterson coils could not be used also is explained.

Distance ground relays give the same high speed protection against ground faults that distance phase relays give against phase faults. Each line section is protected selectively without cascading settings. Although, in general, it is not necessary to cascade the settings of directional ground relays to anything like

Paper 46-83, recommended by the AIEE committee on protective devices for presentation at the AIEE South West meeting, San Antonio, Tex., April 16–18, 1946. Manuscript submitted January 31, 1946; made available for printing March 7, 1946.

W. A. WOLFE is system protection engineer with the Kansas Gas and Electric Company, Wichita, Kan.

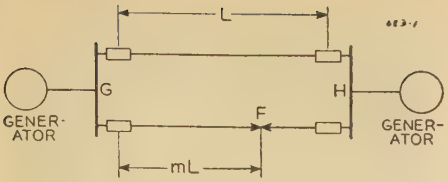

Figure 1. One-line diagram of assumed system

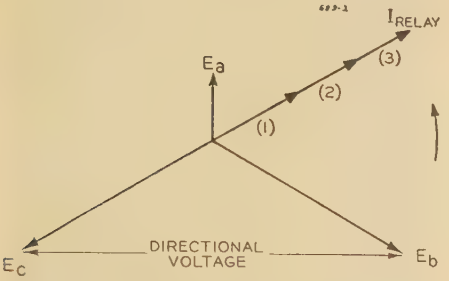

Figure 2. Vector diagram showing relation of currents and voltages for a one-wire-to-ground fault on phase A; I_{relay} = total of three components, namely:

(1). I_{aGF} = current in phase A

(2). $I_{0GF}\dfrac{Z_{0GH}-Z_{1GH}}{Z_{1GH}}$ = a percentage of the zero-sequence current in the protected line

(3). $I_{0GH}\dfrac{M_{0GH}}{Z_{1GH}}$ = a percentage of the zero-sequence current in the parallel line

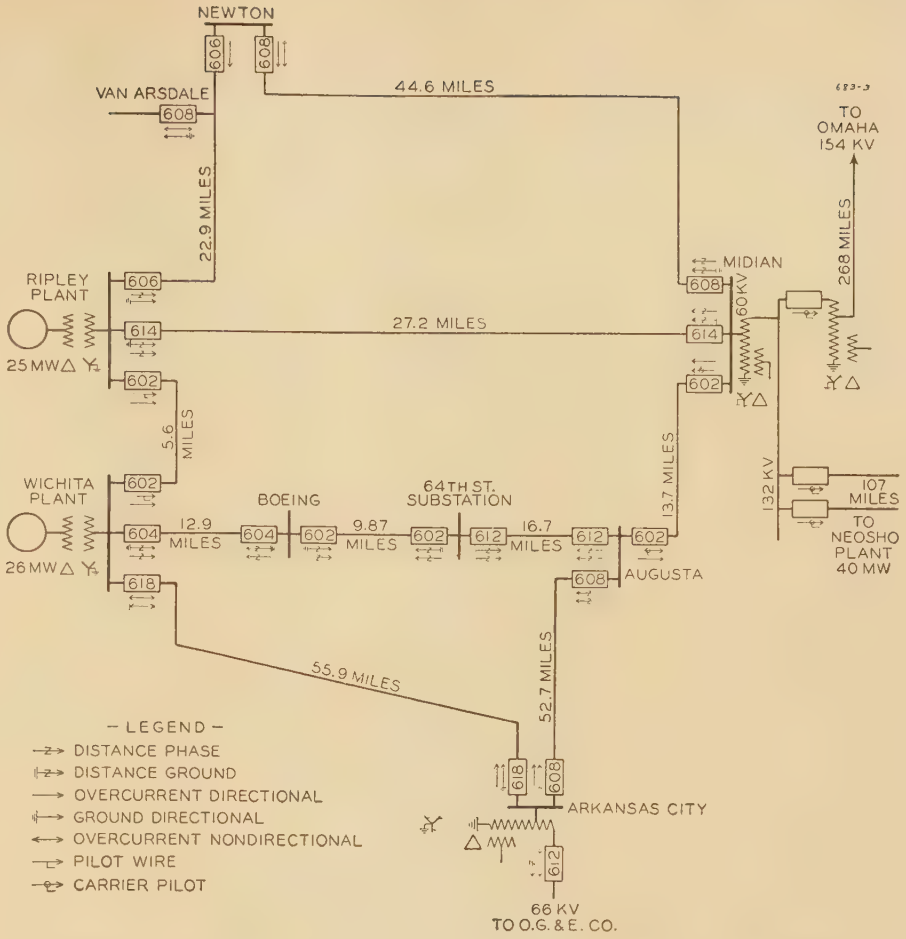

Figure 3. Central Kansas 60-kv system of the Kansas Gas and Electric Company

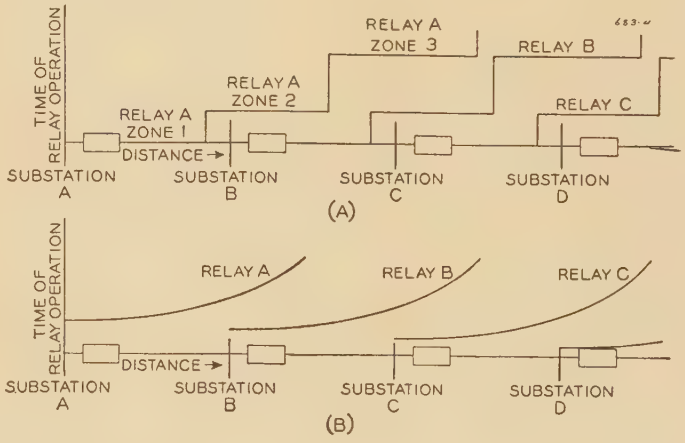

Figure 4

A—Distance relay characteristic; all but last 10 or 15 per cent of line is instantaneous trip

B—Induction relay characteristic

the extent necessary in the case of conventional overload phase relays, high speed distance ground relays do offer a very substantial saving in relaying time in most cases. This fact is especially true where there are a number of stations between grounding points, as on the loop between Wichita Plant and Midian, by way of 64th Street substation and Augusta (see Figure 3). The time saving to be gained by the use of distance relays instead of induction type ground relays is illustrated in Figure 4.

A very high percentage of all line faults on the Kansas Gas and Electric Company's 60-kv system are one wire-to-ground. For example, out of 451 "trip-outs," which have occurred on circuit breakers relayed with distance ground relays since their installation, 378 (83.8 per cent) were one wire-to-ground and 73 involved more than one wire.

Although the shock to the system is less severe for single wire-to-ground faults than for faults involving more than one wire, the large percentage of ground faults was considered justification for an expenditure for ground relaying equal to that for phase relaying.

Ground faults, when not cleared rapidly, frequently result in burned down conductors or overhead ground wires.

The cost of an installation of phase and ground distance relays is approximately half the cost of a carrier pilot relay installation. This cost makes complete distance relay protection for all types of faults very attractive in those cases where good relaying is desired, but where there exists no real necessity for going to carrier relaying.

It was not feasible to consider the use of Peterson coils on this system because of its complexity and number of grounding points. But, the main reason was that at Midian and Arkansas City (Figure 3) large autotransformers are used having graded insulation and solidly grounded neutrals which could not be isolated from ground by a Peterson coil.

Disadvantages

Distance ground relays have the disadvantage of being more complicated than distance phase relays. They require a set of auxiliary blocking relays, which block operation upon the occurrence of wire-to-wire or two wire-to-ground faults, in order to prevent overreaching into the next line section on these types of faults. As pre-

Table I. Typical Relay Operating Record

Ripley Midian Line

OCB Number	Date	Time	Relays	Cause
Ripley 614	3-15-44	11:42 a.m.	GB1	Lightning
Midian 614	3-15-44	11:42 a.m.	GB1	Lightning
Ripley 614	4-10-44	9:57 p.m.	GB1	Lightning
Midian 614	4-10-44	9:57 p.m.	GB1	Lightning
Ripley 614	4-22-44	1:46 a.m.	GB1	Lightning
Midian 614	4-22-44	1:46 a.m.	?	Lightning
Ripley 614	4-23-44	3:38 p.m.	GA1-A1	Lightning
Midian 614	4-24-44	3:38 p.m.	GA2	Lightning
Ripley 614	5- 1-44	1:02 a.m.	GB1	Lightning
Midian 614	5- 1-44	1:02 a.m.	GB1	Lightning
Ripley 614	5-29-44	4:39 p.m.	GB1	Lightning
Midian 614	5-29-44	4:39 p.m.	GB1	Lightning
Ripley 614	7- 8-44	9:17 p.m.	GB1	Lightning
Midian 614	7- 8-44	9:17 p.m.	GB1	Lightning
Ripley 614	7-10-44	3:17 p.m.	GB1	Lightning
Midian 614	7-10-44	3:17 p.m.	GB1	Lightning
Ripley 614	7-11-44	4:22 a.m.	GB1	Lightning
Midian 614	7-11-44	4:22 a.m.	GB1	Lightning
Ripley 614	7-18-44	8:42 a.m.	GB1-A1	Lightning
Midian 614	7-18-44	8:42 a.m.	GB2	Lightning
Ripley 614	7-25-44	3:03 a.m.	GB1	Lightning
Midian 614	7-25-44	3:03 a.m.	GB1	Lightning
Ripley 614	7-27-44	9:43 p.m.	GB1	Lightning
Midian 614	7-27-44	9:43 p.m.	GB1	Lightning
Ripley 614	8-13-44	5:50 p.m.	GB1-A1	Crossarm broken
Midian 614	8-13-44	5:50 p.m.	GB2	Crossarm broken
Midian 614	8-13-44	5:51 p.m.	GB2	Crossarm broken
Ripley 614	8-13-44	6:21 p.m.	GB1-A1	Crossarm broken
Ripley 614	9-10-44	4:20 a.m.	GB1	Lightning
Midian 614	9-10-44	4:20 a.m.	GB1	Lightning
Ripley 614	11- 2-44	10:37 p.m.	GB1	Lightning
Midian 614	11- 2-44	10:37 p.m.	GB1	Lightning

Table II. Typical Relay Operating Record

Augusta—64th Street Line

OCB Number	Date	Time	Relays	Cause
Augusta 612	1-27-44	12:28 a.m.	A1	Wind storm
64th Street 612	1-27-44	12:28 a.m.	A1	Wind storm
Augusta 612	4-26-44	12:37 a.m.	GC1	Lightning
64th Street 612	4-26-44	12:37 a.m.	GC1	Lightning
Augusta 612	6- 8-44	3:24 p.m.	GA1	Lightning
64th Street 612	6- 8-44	3:24 p.m.	GA1	Lightning
Augusta 612	6-18-44	7:25 p.m.	GB1	Lightning
64th Street 612	6-18-44	7:25 p.m.	GB1	Lightning shattered insulator
Augusta 612	6-18-44	7:26 p.m.	GB1	Lightning shattered insulator
Augusta 612	6-18-44	7:34 p.m.	GB1	Lightning shattered insulator
Augusta 612	7-27-44	9:53 p.m.	GC1	Lightning
64th Street 612	7-27-44	9:53 p.m.	GC1	Lightning
Augusta 612	8-24-44	7:01 a.m.	GB1	Lightning
64th Street 612	8-24-44	7:01 a.m.	GB1	Lightning

viously mentioned, they also require an auxiliary current transformer for zero-phase-sequence compensation. The experience has been that these disadvantages are not of such a nature that they should preclude the use of distance ground relays.

The relay installation for each oil circuit breaker consists of three distance phase relays and three distance ground relays, a total of six relays. It would be possible, by means of current and potential switching circuits, to reduce the number of relays required to one phase relay and one ground relay,[3,4] but with some increase in tripping time. It is believed that the scheme employing two relays has its principal application on subtransmission lines, 33 kv and lower, rather than on important 60-kv and higher voltage lines.

Relay Installations

The first installation on the Kansas Gas and Electric Company 60-kv system was completed October 6, 1938, and was followed from time to time by other installations, until at the present time ten installations of distance ground relays are in service.

A 1-line diagram of the Kansas Gas and Electric Company Central Kansas 60-kv system is shown in Figure 3. The loca-

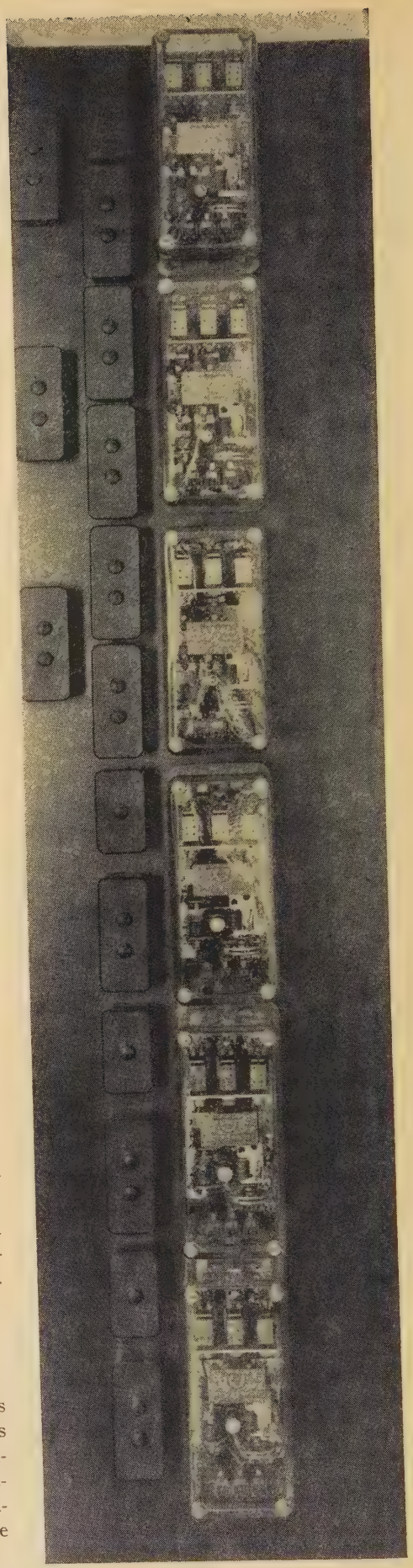

Figure 5. Installation of distance phase and distance ground relays (the three top relays are ground relays)

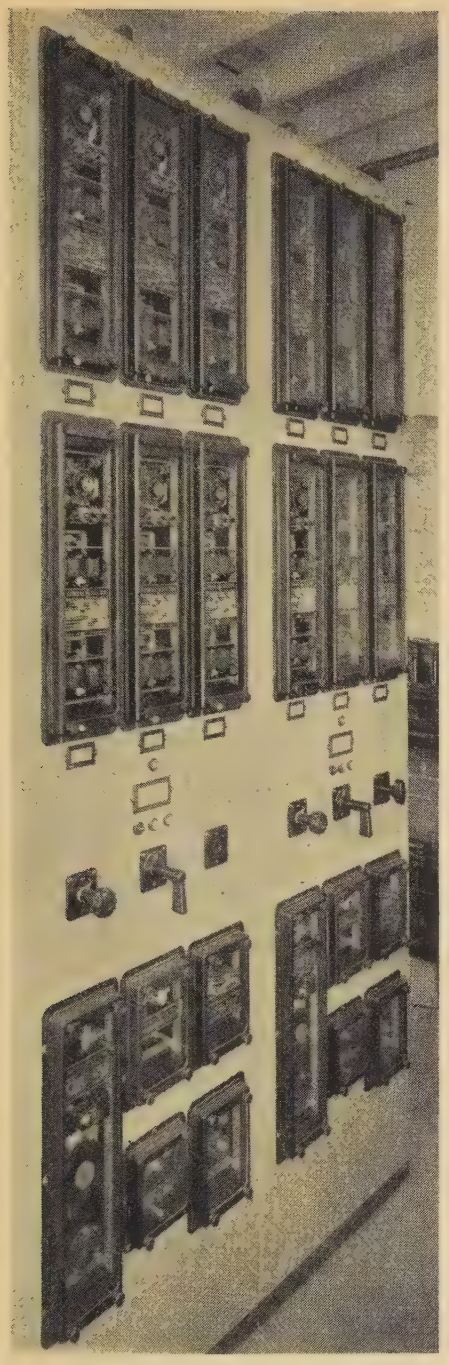

Figure 6. Installation of distance phase and distance ground relays for two 60-kv circuit breakers

The phase relays are across the top of the panel and the ground relays are across the middle. The relays in the lower section are, with the exception of the auxiliary blocking relay, associated with the ground relays for automatic reclosing and synchronous check functions

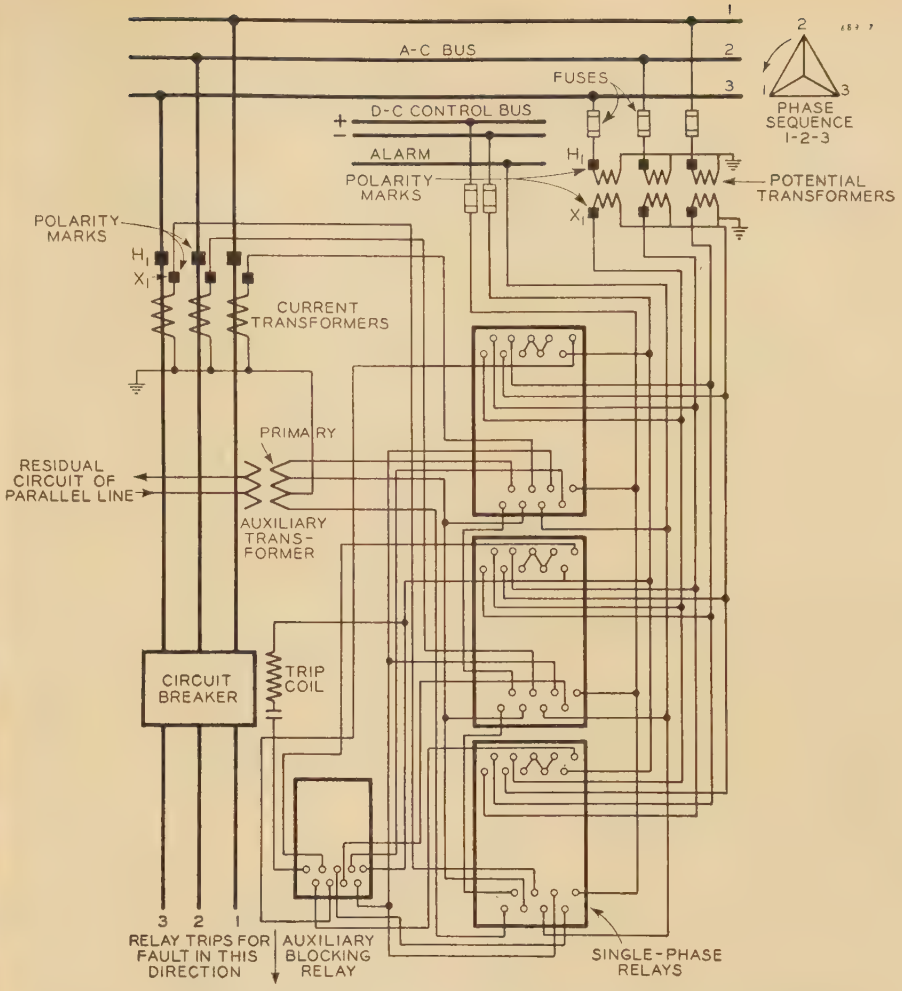

Figure 7. Typical wiring diagram for one type of distance ground relay installation

tion of distance ground relays is indicated by symbol on this diagram. The dates on which the various installations were completed are as follows:

Ripley 614	October 6, 1938
64th Street 602	April 4, 1941
64th Street 612	April 4, 1941
Augusta 612	May 9, 1941
Wichita 604	June 7, 1941
Midian 608	July 14, 1942
Midian 614	July 23, 1942
Augusta 608	August 17, 1942
Boeing 602	February 4, 1943
Boeing 604	February 4, 1943

Previous to the installation of distance relays and other modern relays on this system, induction overload and directional relays were used. Ground relays were installed on only a few of the circuit breakers. Co-ordination between the relays on the various circuit breakers was by time sequence, taking advantage of the diversity of current flow in the various circuits under fault conditions as much as possible. Instantaneous overload relays, set to cover 90 per cent of the line length under maximum generating conditions, were used on lines which were long enough to secure reasonable coverage under average generating conditions. At this stage, Boeing and 64th Street substations had not been built and the Wichita–Augusta line was one continuous line. Nor had Ripley been built, but there was a 60-kv substation not far from the plant site having three 60-kv circuit breakers, making the same system connections as the three circuit breakers at Ripley do now. Even with the help of the instantaneous relays on the longer lines, the relay time on the majority of the circuit breakers at Wichita Plant and Midian were quite long. In addition, it was found impossible to find relay settings which would fit all system conditions. Instability troubles frequently developed between Wichita and Midian because of the long relaying times involved.

Sometimes the opinion is expressed that zone type distance relays cannot be applied to a system on which they must be co-ordinated with induction overload relays. It is believed, however, that this fear has been exaggerated. No particular difficulty has been experienced in applying distance relays to the system under consideration. The distance relays were put in service, one or two installations at a time, over a period of several years, with the old induction relays continuing in service on the remaining circuit breakers. In fact the transition is still not complete since, as can be seen on Figure 3, six circuit breakers remain which have the

Table III. Standard Code for Marking Relay Targets

Kind of Protection	Function or Type	Symbol
Ground	Overload, time delay	G
Ground	Overload, instantaneous	G1
Ground	Distance; HX, GCX	GA1, GB1, GC1 (for zone 1); GA2, GB2, GC2 (for zone 2); GA3, GB3, GC3 (for zone 3)
Phase	Overload, time delay; IA, IAC, CO, CR, IB, and so forth	A, B, C
Phase	Overload, instantaneous	A1, B1, C1
Phase	Distance; HZ, GCX	A1, B1, C1 (for zone 1); A2, B2, C2 (for zone 2); A3, B3, C3 (for zone 3)

Table IV. Summary of Distance Relay Operations

Year	Ground Relays			Phase Relays		
	Correct	Questionable	Wrong	Correct	Questionable	Wrong
1938	2	0	0	0	0	0
1939	21	0	0	2	0	0
1940	9	2	1	1	0	0
1941	40	0	1	7	0	0
1942	40	0	2	21	0	0
1943	87	0	4	16	0	2
1944	108	0	3	21	0	0
1945	71	0	0	5	0	0
	378	2	11	73	0	2

old relays. On most of these circuit breakers, instantaneous overload attachments help greatly in effecting good coordination, mostly by reducing the second zone setting which otherwise would be necessary on some of the distance relays.

Operating Results

Operating experience with distance ground relays has been excellent. They are called upon to operate from three to five times more than are the phase relays, and they can be depended on to operate correctly when properly applied.

An example of the operating performance of these relays is shown in Tables I and II, which give a part of the relay operating record of the Ripley–Midian line and the 64th Street–Augusta line respectively.

For the purpose of assisting in the understanding of the relay operations indicated in Tables I and II, Table III is included, which gives a partial list of the standard method of marking and reporting relay targets used by the Kansas Gas and Electric Company.

An analysis of the distance ground relay operations from October 1938 through 1945 discloses that there have been a total of 391 operations, of which 378 were correct in every respect. During the same period, there were a total of 75 distance phase relay operations (counting only those breakers on which distance ground relays also were installed.) Of these, 73 were correct in every respect. The summary of these operations is given in Table IV. Several instances of the first zone overreaching the next substation developed in the case of two installations, but this condition was corrected easily by shortening the distance setting slightly. The experience has been that if the relays are set to reach 85 per cent of the distance to the next station, there will be no trouble from overreaching. When set for 90 per cent, as is the usual practice for phase relays, the two instances mentioned occurred.

This analysis may be summarized as follows:

Questionable Operations: Ground

1. Zone 2 fault tripped in zone 3 (or was so reported) 1
2. Two ground relay targets reported for one "tripout" (GA1 & GB1). Only one relay should operate because of blocking units 1

Total 2

Wrong Operations: Ground

1. Overreached. Tripped in zone 1 for fault beyond next substation 3
2. Bad auxiliary contact caused unnecessary "tripout" 2
3. Loss of potential (fuse blown) 6

Total 11

Wrong Operations: Phase

1. Failure to operate because of faulty contact adjustment 2

Total 2

Loss of potential was the cause of more false operations than any other one thing. It is expected that less trouble will be experienced from this cause in the future since heavier potential transformer fuses now are used, which are not likely to fail from deterioration. Instantaneous overcurrent fault detector relays can be used to prevent tripping from loss of potential. In order to keep the burden on the current transformers to a minimum, three such relays, mounted separately, should be used to supervise both the phase and ground relays rather than equip each phase and ground relay with its own fault detector.

Conclusion

There is reason to believe that distance ground relaying deserves much wider acceptance than it has received so far, since operating experience has demonstrated that distance ground relays give results which are in every way as satisfactory as those obtained with distance phase relays, the use of which is well established.

It also is believed that if more engineers would study the possibilities of distance ground relays in combination with distance phase relays and compare them with the much more expensive and complex carrier pilot relaying, they would find that distance relaying would give adequate protection in many cases where otherwise more expensive relaying would seem desirable.

References

1. Fundamental Basis for Distance Relaying, **W. A. Lewis, L. S. Tippet.** AIEE Transactions, volume 50, 1931, June section, pages 420–2.

2. A New Distance Ground Relay, **S. L. Goldsborough, R. M. Smith.** AIEE Transactions, volume 55, 1936, June section, pages 697–703; discussion, November section, pages 1255–6.

3. Control of Distance Relay Potential Connections, **A. R. van C. Warrington.** AIEE Transactions, volume 53, 1934, January section, pages 206–13; discussion March section, pages 465–6, and April section, page 617.

4. Distance Relay Protection for Subtransmission Lines Made Economical, **L. J. Audlin, A. R. van C. Warrington.** AIEE Transactions, volume 62, 1943, September section, pages 574–8; discussion pages 976–9.

High Voltage Ignitron Rectifiers and Inverters for Railroad Service

J. L. BOYER
ASSOCIATE AIEE

C. G. HAGENSICK
ASSOCIATE AIEE

Synopsis: Single-anode pumped-type mercury-arc-rectifier tubes have been established in the 300-, 600-, and 900-volt field in the past few years, and as a result they have become the most important type of equipment for large power conversion at these voltages. The ignitron was the major development which brought about the change from multianode to single anode tubes in this low voltage field.[1] Recently sealed ignitrons have been developed for very high voltages and lower currents.[2] This paper describes high voltage pumped ignitrons which have been made available for power conversion in the 3,000- to 4,000-volt range. The major application for mercury arc rectifiers in this voltage range is for railroad service. Therefore, the requirements for railroad loading have been given special consideration in the design of the high voltage ignitron. Both rectifier and inverter characteristics were desired in one unit so that a maximum of flexibility could be obtained. The characteristics of combined rectifier and inverter operation are described. Accepted fundamental rectifier and inverter relationships are presented, and curves are included to aid in determining operating characteristics. The design and tests which led to the successful development of the high voltage pumped ignitron are discussed. Pumped ignitrons are compared with sealed ignitrons for high voltage applications so that the field of each can be better defined.

THE DEVELOPMENT of the 3,000-volt ignitron rectifier was begun after the characteristics of single anode tube and multianode mercury arc rectifiers were compared. In low voltage applications, the lower arc drop of single anode tube rectifiers results in an appreciable improvement in the efficiency and is the determining factor in the selection of the type of rectifier. In the high voltage field, the arc drop is a smaller percentage of the direct voltage, and the lower arc drop improves the efficiency only slightly. However, single anode tube rectifiers have a number of minor advantages that are important when considered together.

The maintenance of single anode tube rectifiers is simplified because they consist of a number of similar tubes. This fact also makes it possible to operate at reduced capacity with some of the tubes removed. Since large numbers of tubes are required, mass production methods can be used in the manufacture.

Ignitron rectifiers have the following advantages over continuously excited mercury arc rectifiers:

1. Cathode spot excitation independent of load.
2. Angle of retard unaffected by load current or water temperature.
3. No moving parts in excitation circuit.
4. No cathode insulation required.

Single anode tube rectifiers have the disadvantage that their excitation circuits are somewhat more complicated. However, since the excitation circuits are almost independent of the kw rating, it is found that this disadvantage is outweighed by the advantages for the higher ratings.

Ratings

Typical ratings required for rectifier units for railroad loading are 2,000 kw and 3,000 kw. These ratings were used as a basis for the design of the 3,000-volt ignitrons.

Railroad loading usually requires very heavy overload ratings. Ignitron rectifiers are especially suited for suddenly applied overloads, because they show no tendency to cause arc surges at any reasonable water temperature and because their arc-back performance is less dependent on previous loading.

The proposed AIEE heavy duty rating,[3] which is used in the testing of high voltage rectifiers for railroad service, is the following:

100 per cent rated load continuously

150 per cent current for two hours, following 100 per cent load

300 per cent current for five minutes, following 100 per cent load

With low voltage high current ignitrons, it is found that the inverter rating of a given design is lower than the rectifier rating. In high voltage rectifier operation, the required design results in improved inverter performance.

Regeneration

One of the important requirements for a railroad substation in mountainous country is regeneration. This requirement can be accomplished by mercury arc rectifiers in a number of different ways:

1. A given unit may be operated first as a rectifier when power is required and then as an inverter when regeneration is required. A reversing switch to change the polarity of the power circuit and means for rapidly changing the ignition angles must be provided. This scheme has the advantage that duplicate equipment is not required, but has the disadvantage that a time delay is necessary to change from rectification to inversion and that the reversing switch has considerable duty.

2. Two or more units may be operated on the same bus, with one permanently connected with reversed polarity and excited as an inverter and the others being operated as rectifiers. This method provides a smooth changeover between rectification and inversion, but has the disadvantage that duplicate equipment is required.

3. Where heavy overloads and heavy regenerative loads are expected, a combination of the first two methods can be used. Both units can carry the overloads, and as the load drops, one unit can be switched over to inverter operation to carry normal regenerative loads. If a heavy regenerative load is required, both units can be changed to operate as inverters. This type of operation makes possible a smooth transition between rectification and inversion.

Figure 1 gives a typical rectifier and inverter circuit illustrating the second method, which is considered to be the most important. Load and regenerative voltage characteristics are shown in Figure 4 for a system having identical transformers for rectifier and inverter units. These regulation lines give the direct voltages for various load currents and for different ignition angles α of rectifier and β of inverter. The slope of these lines is determined mainly by the transformer reactance, and the values at zero current are proportional to the cosines of the ignition angles.

Circuit Characteristics

General Theory

In normal operation the action of any type of rectifier is to allow energy flow in only one direction, because a reverse current cannot be conducted through the rectifier elements. However, the flow of

Paper 46-91, recommended by the AIEE committees on electronics and land transportation for presentation at the AIEE North Eastern District meeting, Buffalo, N. Y., April 24–26, 1946. Manuscript submitted November 13, 1945; made available for printing March 11, 1946.

J. L. Boyer and C. G. Hagensick are design engineers in the rectifier section, a-c engineering department, Westinghouse Electric Corporation, East Pittsburgh, Pa.

The authors acknowledge and express appreciation for the assistance of J. H. Cox, W. E. Pakala, and M. Garbuny for their suggestions on the design, and of L. A. Casanova and other members of the rectifier laboratory for their co-operation in the testing.

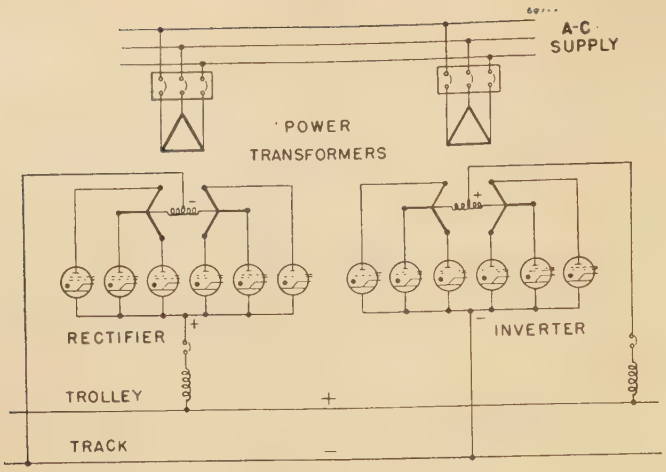

Figure 1. Delta 6-phase double-Y rectifier and inverter circuit for railroad substation

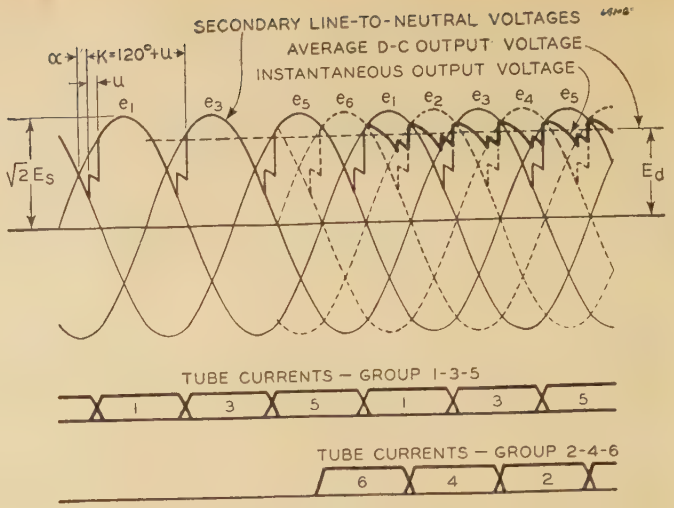

Figure 2. Operation of 6-phase double-Y rectifier

energy in any circuit element can be reversed by changing either the direction of current through the element or the polarity of the voltage across the element. In a converter in which the conducting period of the elements can be controlled, the polarity of the direct voltage can be reversed by making effective the opposite polarity of the alternating voltage. This action is the principle of operation of the inverter, which permits power to be transmitted from the d-c circuit to the a-c circuit.

With railroad service, the need for regeneration is indicated by a rise in the direct voltage. The effect of this rise on rotating equipment would be to reverse the direction of current flow, but with the rectifier the elements support the additional voltage and there can be no reverse current. A second converter with a reversed connection may be controlled so that the ignitrons can conduct during periods in which the alternating voltages of their transformer windings are opposed to the flow of current. With this type of operation, energy can be transmitted from the a-c circuit to the d-c circuit by the rectifier and from the d-c circuit to the a-c circuit by the inverter.

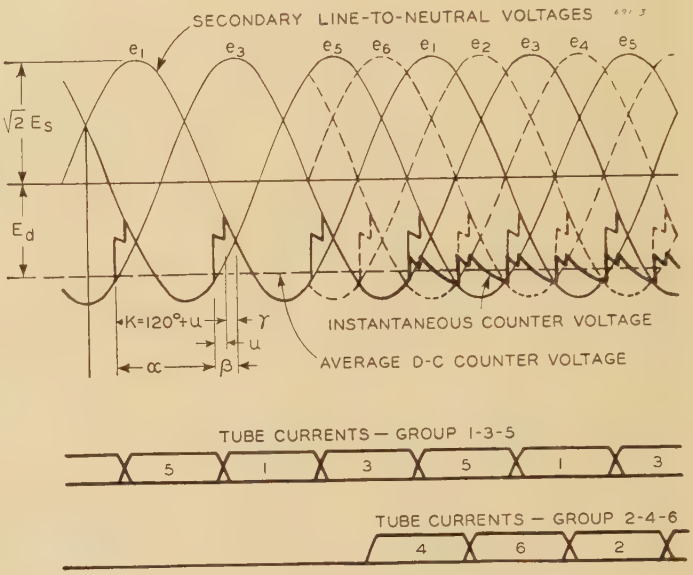

Figure 3. Operation of 6-phase double-Y inverter

Rectifier Operation

In the simplified rectifier and inverter circuit shown in Figure 1, the rectifier operates as a normal delta 6-phase double-Y rectifier, since operation is not changed greatly by the addition of the inverter. Two separate transformers may be used as shown, or one transformer with a single primary may be used. The rectifier output voltage and current wave forms are shown in Figure 2.

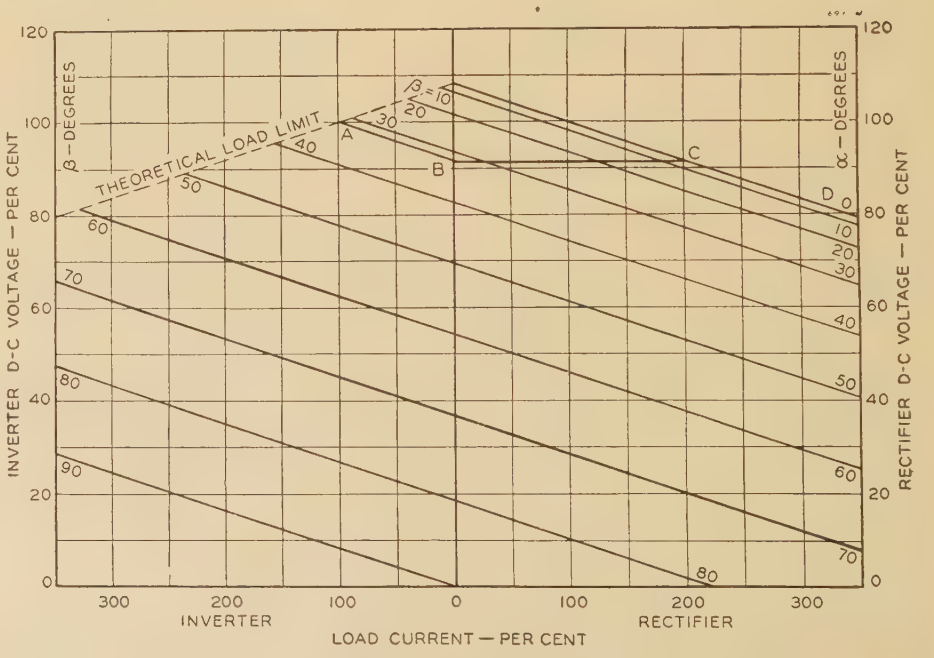

Figure 4. Regulation curves of rectifier and inverter, eight per cent regulation and same transformer secondary voltages

The average value of the d-c output voltage of a rectifier at no load with ignition delay is*

E_{dc} = theoretical average value − average arc drop

$$E_{dc} = E_{do} \cos \alpha - E_a \quad (1)$$

where

$$E_{do} = \sqrt{2} E_s \frac{p}{\pi} \sin \frac{\pi}{p}$$

The average value of the d-c output voltage of a rectifier under load is

E_d = theoretical average value − commutating reactance drop − resistance loss drop − average arc drop

$$E_d = E_{do} \cos \alpha - E_x - E_r - E_a$$
$$= \sqrt{2} E_s \frac{p}{\pi} \sin \frac{\pi}{p} \cos \alpha - \frac{p}{2\pi} I_c X_c - \frac{P_r}{I_d} - E_a \quad (2)$$

or, using other quantities,

$$E_d = E_{do} \left[\cos \alpha - \frac{\cos \alpha - \cos(\alpha + u)}{2} \right] - \frac{P_r}{I_d} - E_a \quad (3)$$

For a delta 6-phase double-Y circuit, $p = 3$ and $I_c = I_d/2$. Therefore,

$$E_d = 1.17 E_s \cos \alpha - 0.239 I_d X_c - \frac{P_r}{I_d} - E_a \quad (4)$$

For a delta 6-phase star circuit and a delta 6-phase fork circuit, $p = 6$ and $I_c = I_d$. Therefore,

$$E_d = 1.35 E_s \cos \alpha - 0.955 I_d X_c - \frac{P_r}{I_d} - E_a \quad (5)$$

Inverter Operation

Figure 3 shows the operation of a 6-phase double-Y inverter. Each anode conducts during the negative portion of the corresponding alternating voltage wave, in order to provide a d-c counter voltage opposing the flow of current.

The average value of the d-c counter voltage of an inverter at no load is

$$E'_{dc} = E'_{do} \cos \alpha' - E'_a$$

or

$$= -[E'_{do} \cos \beta' + E'_a] \quad (6)$$

where

$$E'_{do} = \sqrt{2} E'_s \frac{p'}{\pi} \sin \frac{\pi}{p'}$$

The average value of the d-c counter voltage of an inverter under load is

$$E'_d = E'_{do} \cos \alpha' - E'_x - E'_r - E'_a$$
$$= \sqrt{2}\, E'_s \frac{p'}{\pi} \sin \frac{\pi}{p'} \cos \alpha' - \frac{p'}{2\pi} I'_c X'_c - \frac{P'_r}{I'_d} - E'_a \quad (7)$$

or, using other quantities,

$$E'_d = E'_{do} \left[\cos \alpha' - \frac{\cos \alpha' - \cos(\alpha' + u')}{2} \right] - \frac{P'_r}{I'_c} - E'_a$$

$$= -\left\{ E'_{do} \left[\cos \beta' + \frac{\cos(\beta' - u') - \cos \beta'}{2} \right] + \frac{P'_r}{I'_c} + E'_a \right\} \quad (8)$$

For a delta 6-phase double-Y circuit,

$$E'_d = -\left[1.17\, E'_s \cos \beta' + 0.239\, I'_d X'_c + \frac{P'_r}{I'_d} + E'_a \right] \quad (9)$$

For a delta 6-phase star circuit and a delta 6-phase fork circuit,

$$E'_d = -\left[1.35\, E'_s \cos \beta' + 0.955 I'_d X'_c + \frac{P'_r}{I'_d} + E'_a \right] \quad (10)$$

Combined Characteristics

Under normal operating condition of a rectifier and an inverter, as shown in Figure 1, the ignition angles must be such as to have the rectifier average d-c output voltage less than or equal to the inverter average d-c counter voltage, so as to prevent circulating currents. In the 6-phase double-Y circuit, there is a light load voltage rise in the rectifier and a light load voltage dip in the inverter. These changes occur when the load current becomes less than that required for magnetizing the interphase transformer, resulting in a transition to 6-phase conduction periods. These light load voltage changes can be eliminated by adjustment of ignition angles so that a small current circulates between the rectifier and inverter when there is no load on the system.

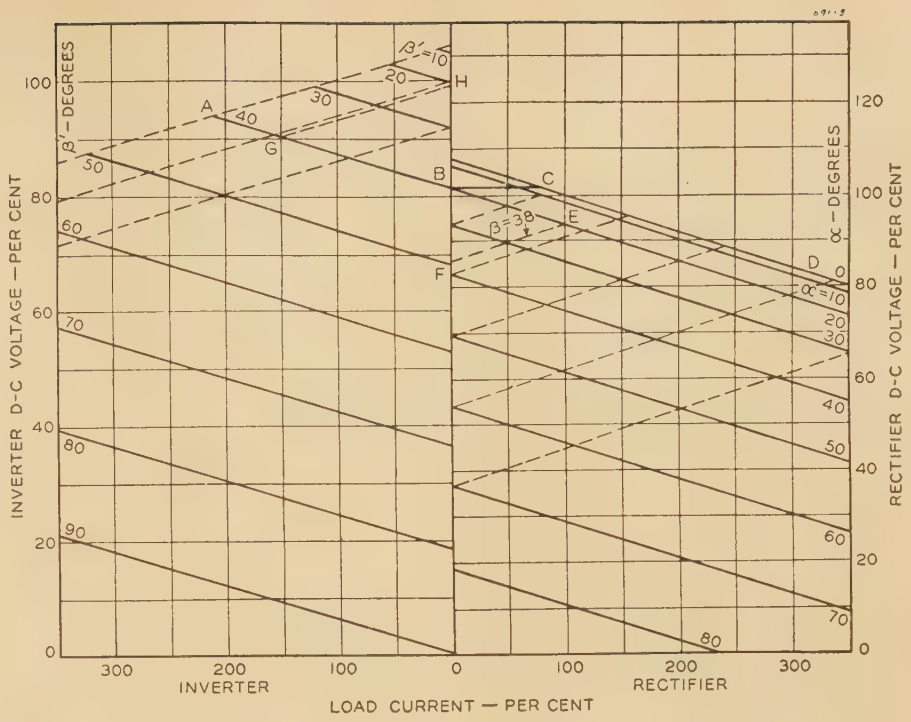

Figure 5. Regulation curves of rectifier with eight per cent regulation, and inverter with six per cent regulation and higher secondary voltage

Figure 4 shows the combined characteristics of a rectifier and inverter for various ignition angles, with eight per cent regulation neglecting losses.

The rectifier curves have dropping voltage characteristics and are to the right of the zero current axis, and the inverter curves have rising characteristics and are to the left. The inverter curves terminate at the theoretical load limit line, where the commutation angles are exactly equal to the advance angles. In actual operation it is necessary to operate below the theoretical load limit so as to provide margin angles greater than tube deionization requirements.

When the transformer secondary voltages are the same for both rectifier and inverter, it is necessary to operate at high angles of delay in the rectifier to have

* Definitions of the symbols are given at the end of this paper. Unprimed symbols are used for rectifier quantities and primed symbols are used for inverter quantities.

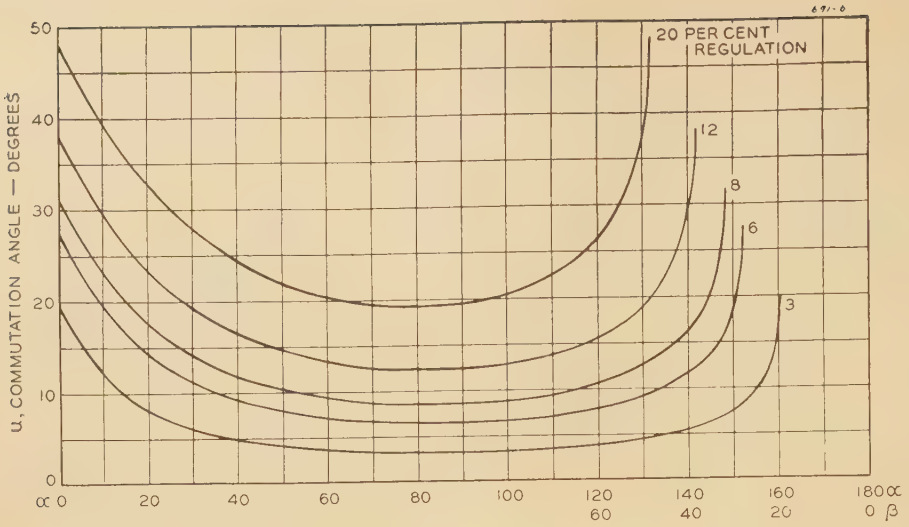

Figure 6. Commutation angles of a p-phase rectifier or inverter, neglecting losses

$$\text{Per cent regulation} = \frac{E_{do} - E_d}{E_d} 100, \; E_d \text{ at rated } I_d \text{ and } \alpha = 0$$

$$\frac{\cos \alpha - \cos (\alpha + u)}{2} = \frac{\text{regulation}}{1 + \text{regulation}}$$

α = angle of retard, degrees
β = angle of advance, degrees

sufficient advance angles in the inverter to carry the required regenerative loads. For the inverter to carry 100% current, the theoretical minimum advance angle β must be 32 degrees, shown along line AB. Actually less than 100 per cent current can be carried at this angle. The rectifier must operate at a minimum of 32 degrees delay at B to avoid circulating currents. As load is increased, the voltage may be kept constant by phase control from B to C.

Figure 5 shows a condition which is more practical. The rectifier is not required to operate at high angles of delay, by having a higher transformer secondary voltage on the inverter. The direct voltage of the rectifier is held constant between B and C by phase control as the load increases. With further increase in current, the voltage will drop along the $\alpha = 0$ line from C to D.

Regenerative loads will be carried by the inverter with a d-c counter voltage given by the line AB, for $\beta = 40$ degrees. Any desired voltage characteristic can be obtained by automatically changing the firing of the inverter as the load changes, providing care is taken to operate at a sufficient amount below the theoretical load limit line.

A method of making reasonably accurate determinations of rectifier voltage, ignition angles, and commutation angles under various load conditions is by use of imaginary inverter regulation lines superimposed on the rectifier lines. These lines are shown dotted and of equal slope as the rectifier lines, but with rising characteristics. The advance angles β of these lines are equal to the delay angles α of rectifier lines starting from the same point on the zero current axis. From the symmetry of the rectifier and inverter voltage wave forms (Figures 2 and 3), the imaginary β values correspond to α plus u values of the rectifier.

The direct voltage of the rectifier at rated current and 20 degrees delay can be found by moving down on regulation line BE for $\alpha = 20$ degrees from B to 100 per cent current at E, and reading 93 per cent rated voltage opposite E. The imaginary inverter line EF gives $\beta = 38$ degrees by interpolation between the 30- and 40-degree lines. The rectifier commutation angle u is equal to 38 minus 20, or 18 degrees.

Inverter conditions can be determined in a similar manner by using the dotted imaginary rectifier lines. For example, the inverter counter voltage for 150 per cent current at 40 degrees advance is given as 90 per cent at point G. The imaginary rectifier line GH gives $\alpha = 21$ degrees as the imaginary rectifier ignition angle; this value corresponds to the inverter margin angle γ. The inverter commutation angle u then is β minus γ, or 40 minus 21 equals 19 degrees.

Choice of Circuit

Most of the 3,000-volt mercury arc rectifiers which have been applied up to the present time have used 6-phase star or fork transformer secondaries. The important reason for this use has been to avoid the light load voltage rise of the double-Y circuit. However, in stations in which there are both rectifiers and inverters, the light load rise can be eliminated as described previously. For a given rated direct current and for equal direct voltage regulation, the 6-phase double-Y circuit has the following advantages over the star or fork connections:

1. Peak anode currents are half.
2. Rms anode currents are lower by ratio of $\sqrt{2}$.

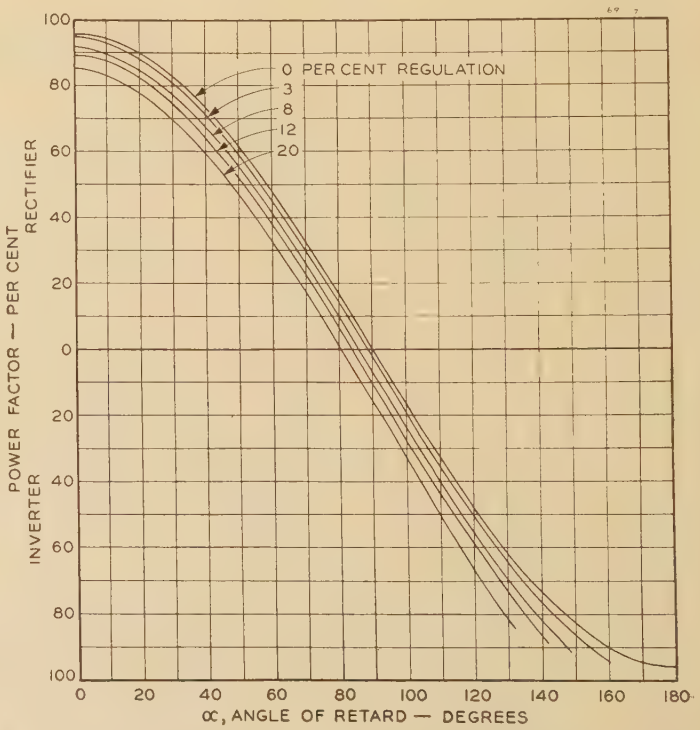

Figure 7. Power factor of 6-phase rectifier or inverter at rated current, neglecting exciting currents and losses

3. Transformer kilovolt-amperes is lower.

4. Final commutation rate of anode current is lower by the ratio of 2.

5. Short circuit and arc back currents are lower.

6. Low transformer commutating reactance is not required.

The 6-phase star or fork circuits have the following advantages:

1. Initial inverse voltage is lower by ratio of 2.

2. There is no light load voltage rise.

The circuits are the same in the following:

1. Average anode currents are equal.

2. Peak inverse voltages are equal.

3. Commutation angles are equal.

4. Power factors are equal.

Figure 6 shows the commutation angles of any type of rectifier circuit as a function of the angle of retard and the d-c regulation, neglecting losses. Figure 7 shows the theoretical power factor of the 6-phase double-Y, the star, and the fork circuits as a function of the angle of retard and voltage regulation.

Faults

The important type of electronic fault with rectifier operation is the arc-back, which is defined as the failure of the tube to hold the negative anode to cathode voltage, with the result that a current flows in the reverse direction because of the formation of a cathode spot on the anode. An arc-back on one anode produces a short circuit on both the d-c and a-c circuits and must be cleared by opening both the a-c and d-c breakers. With high voltage rectifiers, the tubes may be blocked by electronic arc suppression to prevent the flow of forward current in the unfaulted tubes. However, the d-c breaker must be opened to interrupt the flow of current from any equipment capable of sustaining a direct current through the faulted tubes.

If a rectifier is operating with voltage reduction by ignition delay, the positive anode to cathode voltage may cause breakdown of the tube before it is released. This type of fault is known as a forward-fire. If only one such fault occurs, it is self-correcting without opening any circuit breakers, but if all tubes continue to forward-fire, the output voltage will be increased and the unit may be overloaded. With ordinary water temperatures and the tight shielding used on high voltage rectifiers, faults of this type almost never occur.

Another general class of faults is the misfire, which is the failure of a tube to begin conducting at the proper time. An occasional misfire in a rectifier will not cause any serious disturbance, but a series of misfires will result in the lowering of the average output voltage.

In inverter circuits the voltages are such that an arc-back will not cause a tube to continuously carry current in the reverse direction. An inverter tube may have an arc-back caused by the negative voltage on the anode at the end of the conduction period, but the voltage on the tube reverses and stops the flow of the fault current. An arc-back usually will lead to the arc-through, which is the more serious fault of the inverter.

An arc-through is defined as the conduction of power circuit current in the forward direction through a tube during a scheduled nonconducting period of the cycle. An arc-through may be caused by one of the following:

1. Forward-fire, the failure of a tube to block the forward voltage on the anode. This tube fault may or may not produce a circuit fault.

2. Misfire, the failure of a tube to begin conducting current at the start of the scheduled conducting period, thus producing an arc-through on the preceding tube. It is a fault caused by either the excitation circuit or the tube and always produces a circuit fault for at least one cycle.

3. Recommutation, the failure of the load current to be commutated completely from one tube to another within the required angle, with the result that current is commutated back to the original tube. It is a fault caused by the power circuit.

If a rectifier and an inverter are operating on the same bus and an arc-back occurs on the rectifier, the inverter will

Figure 8. Single-grid high-voltage ignitron

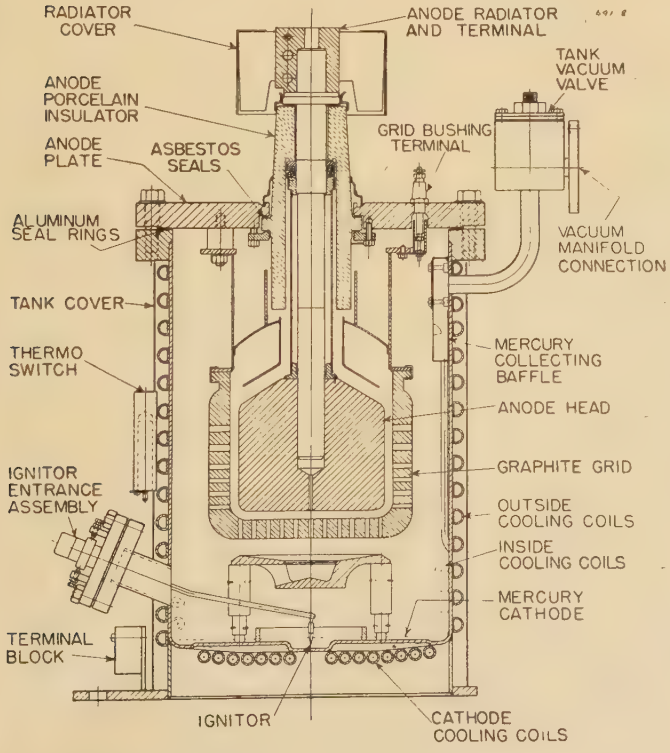

Figure 9. Double-grid high-voltage ignitron

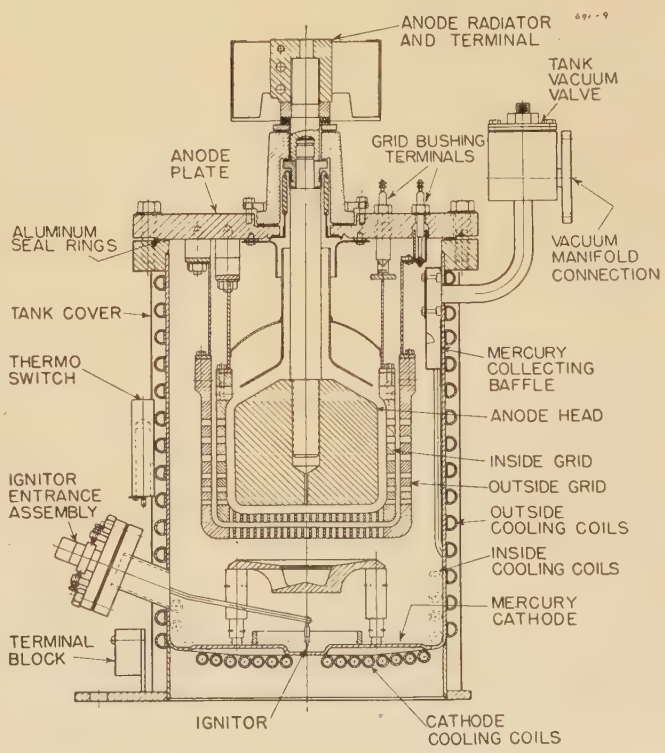

not feed current into the short circuit. However, if an arc-through occurs on the inverter, the rectifier will supply a fault current to the inverter. The other tubes in the inverter, which do not have a fault, do not supply any current to the faulted tube or tubes. If the units are identical, the peak arc-back currents are about equal to the peak arc-through currents.

Ignitron Design

In the design of the 3,000-volt pumped ignitron, attention was given to obtaining a rectifier with a low arc-back rate and high overload capacity. The operating outlet water temperature was to be 55 degrees centigrade. The same design was to be used for either the rectifier or the inverter, and the shielding of the anode was to be such that only ignitor control would be required for either type of operation.

To accomplish the above objectives, two designs of ignitrons were made at about the same time. Both of these were manufactured and placed on test. The results were compared, and the best design was selected and given additional tests.

The first design of ignitron used a single grid with a high ion attenuation and with a high deionization influence around the anode. A porcelain anode bushing with a soldered seal was used on this design. Figure 8 shows the cross section of this single grid design.

The second design used two grids having a total deionizing effect about the same as that of the single grid in the first design. The grids were mounted separately and a circuit was connected to each through insulating bushings. The original design of the double grid ignitron had a porcelain bushing with a soldered seal, and the first tests were made with this type of bushing, but later an improved type of bushing was used. This new bushing and the final design of the double grid tube are shown in Figure 9.

Tests

Single Grid Design

Power Circuit. The power circuit used in the tests of the high voltage ignitrons is shown in Figure 10. The four d-c machines were used either as a load for rectifier tests or as a d-c supply for inverter tests. This arrangement of motor-generator sets provided a continuous rating of 2,000 amperes at 3,000 volts. In order to change from rectifier testing to inverter testing, it was necessary to reverse the d-c power circuit and to reverse the polarity of the holding coil in the high speed d-c breaker.

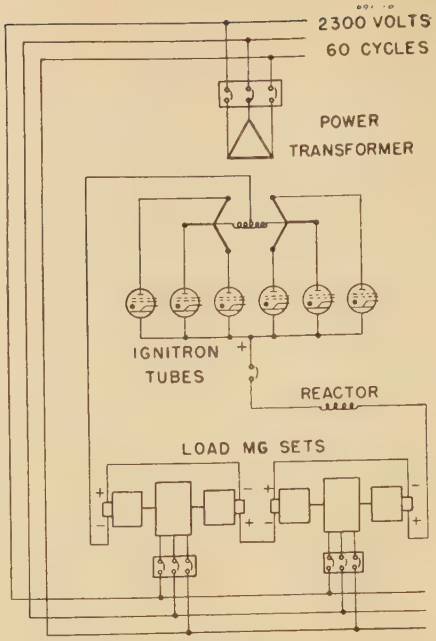

Figure 10. Circuit for laboratory tests of high voltage ignitrons

Excitation Circuits. At the start of the high voltage tests, standard firing and grid circuits were used. The grid circuit soon was found to be unsatisfactory for the 3,000-volt ignitron, as there was difficulty in the pickup of the main anode. At normal operating temperatures, the firing of the ignitors and the pickup of the grids were satisfactory, but the main anode had frequent misfires and required high minimum load current for pickup. This difficulty was corrected by increasing the grid circuit current by a considerable amount.

Power Circuit Faults. In the original 3,000-volt rectifier tests, it was found that a high arc-back rate was obtained. The faults of the single grid design and the original double grid design had about the same characteristics, and they appeared to be produced by the same causes.

With rectifier operation the arc-backs seemed to be the result of entirely different causes than are experienced in low voltage mercury arc rectifiers. The arc-backs were almost independent of load current and were found to occur even at no load. It was believed that this characteristic was caused by mercury condensed on the cold anodes. This theory was eliminated, however, when it was possible to make several tests in which the rectifier operated without arc-backs for several hours and then had a series of arc-backs in a few minutes. Operation at reduced voltage to warm the ignitrons, and then change to the high voltage did not improve the performance and indicated that mercury on the anodes was not the major cause of the arc-backs.

One of the important clues as to the cause of arc-backs was the phase angle in the inverse voltage period at which they occur.[7,8] The most accurate and complete data were obtained by the use of the memnoscope.[9] A memnoscope oscillogram of the anode to cathode voltage of three tubes is shown in Figure 11. The fault occurred near the peak inverse voltage, where the anode to cathode voltage dropped to zero. In most of the records taken of the high voltage ignitrons, the faults occurred near the peak of the inverse voltage. The breakdown characteristics of the ignitrons were investigated with no ionization in the tubes. It was found that a new tube just degassed would break down at slightly below its rated inverse voltage. However, if the testing was continued with repeated breakdowns, the voltage held between the anode and cathode could be increased to many times the rated value.

One of the first phenomenon which was investigated was the effect of mercury dew on the surface of an insulator. It was thought that enough mercury could be condensed to reduce substantially the value of the creepage distance on the insulator. A test setup was made in which a voltage stress could be placed on an insulator with a controllable temperature in mercury vapor at pressures corresponding to those in an ignitron. This test indicated that it took a large amount of mercury condensed on the surface of an insulator to reduce the creepage breakdown voltage even a slight amount. These tests were definite enough to indicate that this phenomenon was not the cause of the breakdowns in the ignitrons.

Another possibility that was investigated was the effect of mercury drops at the junction of the insulator and the conductor. It was believed that there might be a condition similar to that existing between an ignitor and the mercury pool, which would make it possible to start the cathode spot of the arc with potential gradients that appeared to be low. An investigation of the conditions at the junction of the anode stem and the insulator, and of models with similar arrangements, indicated that it was very probable that this junction was a source of the cathode spots which were producing the arc-backs. The junction was placed close to the anode plate, and it appeared that there was enough capacitance between the mercury drops and

the anode plate to produce cathode spots at the junction. Another, but less likely, explanation was that high resistance ignitor action took place at the junction, even though most of the insulator did not have mercury on it.

Since condensed mercury was the cause of the arc-backs, bushing heaters were used so that the junctions were held at a temperature at which mercury would not condense. An interesting fact was observed that at higher loads, higher bushing temperatures were required to prevent the start of a series of arc-backs. Heavy overloads frequently were found to produce arc-backs which occurred 10 or 15 minutes after the overload was completed. These arc-backs also were corrected by operating with a sufficiently high bushing temperature.

In the investigation of the probable causes of arc-backs, a high voltage ignitron was built with several windows in the tube. The conditions in the tube during the various portions of the cycle were investigated by means of a stroboscope. One observation was that large numbers of mercury drops were moving in the grid-cathode space at high speed. It was believed that if one of these mercury drops hit the hot anode during the negative portion of the cycle, there would be a high probability for an arc-back. By using a special design of grids and baffles it was possible to shield the anode from the drops. However, it is still possible that this factor may be one of the important causes of arc-backs in all mercury arc rectifiers.

Double Grid Design

Power Circuit. The power circuit used in testing the double grid design was the same as that used for the single grid design and is shown in Figure 10. For some of the rectifier tests and for most of the inverter tests, the d-c inductance was increased so that there was less ripple in the direct current.

Excitation Circuit. The use of a double grid tube greatly increased the number of types of excitation circuits which could be used. However, it was desirable to keep the excitation circuit as simple as possible. With the double grid ignitrons, there was little trouble with pickup, either of the inside grid or the anode, because the ion attenuation of each grid was not unusually high. For rectifier operation, it was found that the most desirable grid circuit was with sine wave excitation at a low voltage, and with angles of retard determined by the ignitors.

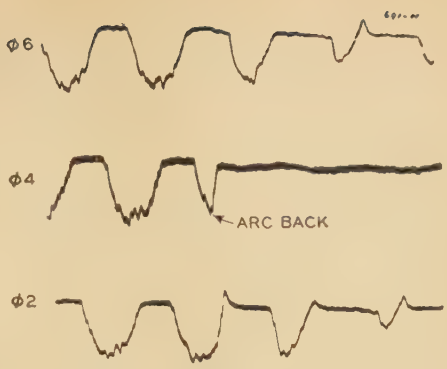

Figure 11. Oscillograms of anode-cathode voltages, showing arc-back in phase 4

For inverter operation, the problem of excitation was found to be more difficult. For inverter operation with normal overloads, the same low voltage grid circuit and ignitor control could be used as in rectifier operation. However, if unusually high overloads were required on the inverter, it was necessary to use a grid circuit in which the outer grid released the inner grid when the ignitor was fired.

Rectifier Tests. The rectifier tests with double grids and porcelain-enclosed glass kovar sealed bushings were considered very satisfactory. The new bushing was found not to be critical to the collection of mercury dew, as its permissible operating temperature was far above that at which mercury would condense in the tube. This condition made it possible to eliminate completely the bushing problem, since a high temperature could be maintained by the use of anode and bushing heaters.

The use of a double grid greatly increased the load current which could be carried with a permissible arc-back rate. By operating the grids at low voltage, forward-fires practically were eliminated, even when operating at high angles of ignition delay. The rating obtained for the rectifier was higher than the required rating.

Inverter Tests. The double grid ignitrons operated as inverters with ignitor control, making it possible to have a simple excitation circuit. The limiting rating of the inverter was less than that of the rectifier.

Most of the faults which occurred in the inverter were arc-throughs caused by forward-fires. The memnoscope oscillograms indicated that the loss of control usually occurred just after the anode became positive. Rarely, a recommutation fault was observed when there was a disturbance in the a-c line voltage caused by some other equipment on the shop bus.

Sealed Ignitron Tubes

The possibility of using sealed ignitron tubes for the 3,000-volt class should be considered for some railroad applications. Sealed ignitrons have been developed for voltages up to about 7,000 volts d-c in single way circuits, and economical designs could be obtained for 3,000 volts.

There should be no fundamental difference in the performance of pumped and sealed ignitrons. Up to the limit of size for which experience has been obtained in sealed tube construction, any electrical design used in pumped tubes also can be used in sealed tubes with an equal rating.

The decision as to whether pumped or sealed ignitrons should be used in a given application should be based on the relation between the required continuous and overload ratings and the available tube ratings. Economic considerations may be the determining factor for some current capacities.

Conclusions

High voltage pumped ignitrons of an improved design have been built and tested for the requirements of 3,000- to 4,000-volt railroad service. All of the circuit characteristics, which are available with grid controlled rectifiers and inverters, are obtained by the use of ignitor control. Rectifiers and inverters can be used in one substation to provide the desired characteristics for either load or regeneration.

The high voltage ignitrons are designed for heavy overloads of the type required for railroad service. A new design of porcelain-enclosed glass kovar sealed anode bushing, which has a temperature limit far above that obtained in normal operation, has been developed.

The selection of either pumped or sealed construction for high voltage ignitrons must be based on the rating, economic factors, and special requirements for each application.

Nomenclature: Rectifier Symbols

a_m = coefficient of sine term of Fourier expansion for the mth harmonic (crest value)

b_m = coefficient of cosine term of Fourier expansion for the mth harmonic (crest value)

c_m = coefficient of resultant of Fourier expansion for the mth harmonic (crest value)

E_a = average direct voltage drop caused by loss in the converter elements (average arc drop)

E_d = average direct voltage under load

E_{dc} = average direct voltage, no load, with phase control and with arc drop

E_{do} = theoretical direct voltage (average direct voltage at no load assuming no overlap, no phase control, and zero arc drop)

E_{il} = initial inverse anode to cathode voltage

E_L = a-c system line-to-line voltage in rms volts

E_N = a-c system line to neutral voltage in rms volts

E_{pf} = peak forward anode to cathode voltage

E_{pi} = peak inverse anode to cathode voltage

E_r = average direct voltage drop caused by resistance losses

E_s = transformer direct winding line to neutral voltage in rms volts

E_x = average direct voltage drop caused by commutating reactance

ΔE = total average direct voltage drop because of regulation

f = frequency of a-c power system

$F_x = \frac{I_c X_c}{E_s} = 2\sqrt{2} \sin \frac{\pi}{p} \frac{R_{gx}}{1+R_{gx}}$ = reactance factor

I = a-c line current (crest value)

I_a = average anode current

I_c = direct current commutated between two rectifying elements in a commutating group

I_d = average d-c load current

I_e = transformer exciting current in rms amperes

$I_H = \sqrt{I_5^2 + I_7^2 + I_{11}^2}$ = equivalent totalized harmonic component of I_L

I_L = a-c line current in rms amperes

I_1 = fundamental component of I_L

I_{1P} = watt component of I_1

I_{1Q} = reactive component of I_1

I_m = harmonic component of I_L, of the order m

I_p = transformer a-c winding current in rms amperes

I_s = transformer d-c winding current in rms amperes

L_d = inductance in the d-c reactor in henries

m = order of harmonic

p = number of phases in a simple rectifier

P_r = total copper resistance losses in watts

q = total number of rectifier phases

$\underline{R}_g$ = per-unit direct voltage regulation based on full load voltage with no phase control

$\underline{R}_{gx}$ = per-unit direct voltage regulation caused by reactance based on full load voltage, with no phase control and assuming no losses

R_p = ohmic resistance of the a-c winding

R_s = ohmic resistance of the d-c winding

u = commutation angle (angle of overlap)

X_c = commutating reactance line to neutral in ohms

X_L = ohms reactance of supply line (per line)

$\underline{X}_L$ = per-unit reactance of supply line (expressed on basis of rated volt-amperes at the line terminals of the transformer a-c winding)

$\underline{X}_T$ = per-unit reactance of transformer (expressed on basis of rated volt-amperes at the line terminals of the a-c windings)

α = angle of retard (delay angle, ignition angle; the angle by which the start of conduction lags the point where the incoming and outgoing rectifying elements have equal positive voltages)

$\cos \alpha$ = phase control ratio

β = angle of advance (the angle by which the start of conduction leads the point at which the incoming and outgoing rectifying elements have equal negative voltages)

γ = margin angle (the angle by which the end of commutation leads the point where the incoming and outgoing rectifying elements have equal negative voltages)

$\cos \phi$ = displacement component of power factor

$\cos \delta$ = distortion component of power factor

κ = conduction angle for one rectifying element

References

1. Ignitron Rectifiers in Industry, **J. H. Cox, G. F. Jones.** AIEE Transactions, volume 61, 1942, October section, pages 713–18.

2. Pentode Ignitrons for Electronic Power Converters, **H. C. Steiner, J. L. Zehner, H. E. Zuvers.** AIEE Transactions, volume 63, 1944, October section, pages 693–7.

3. Standards for Acceptance Tests for Metal Tank Mercury Arc Rectifiers. AIEE Report 6, June 1937, sections 6–153, 6–154.

4. The Mercury Arc Rectifier Traction Substations of the Electricity Supply Commission on the Natal and Reef Electrified System of the South African Railways, **K. M. Cunliff.** *Transactions*, South African Institute of Electrical Engineers (Johannesburg, South Africa), March, 1941, pages 50–114.

5. A 3,000-Kw Mobile Mutator Substation for Traction Service and Regenerative Braking Duty, **E. Kern.** *Brown Boveri Review* (Baden, Switzerland), May–June 1943, page 110.

6. Backfires in Mercury Arc Rectifiers, **J. Slepian, R. L. Ludwig.** AIEE Transactions, volume 51, 1932, March section, pages 92–104.

7. Phase Occurrence of Arc-Backs in High Current Mercury-Arc Rectifiers, **W. E. Pakala, W. B. Batten.** AIEE Transactions, volume 59, 1940, June section, pages 345–7.

8. The Phase of Arc-Back, **A. W. Hull, F. R. Elder.** *Journal of Applied Physics*, volume 13, March 1942, pages 171–8.

9. A Memory Attachment for Oscilloscopes, **W. E. Pakala.** AIEE Transactions, volume 57, 1938, December section, pages 682–5.

Modern Double-Reduction Traction Motor

LANIER GREER
MEMBER AIEE

Synopsis: Incorporated in the modern double-reduction motor and gear unit are many new design features which have made it an outstanding motor for the past five years. Oil lubrication is provided for all gearing and bearings in the oil-tight double-reduction gear unit. Special design constants, which have been developed as a result of many years of experience with high-speed motors, are used. Self-ventilation is successful on a high-speed motor and simplifies locomotive design. Specially insulated field coils provide for good heat transfer from the coils to steel and air. A small motor with a high-speed armature results in low copper loss and high efficiency at high tractive effort. A steep speed curve with a large amount of field shunting makes it possible to use all motors connected permanently in parallel. The motor is small, compact, and lightweight, which has made possible its use on a wide range of locomotives. Here is a small motor doing a big job.

AS EARLY as 1931, some thought was being given to the use of lightweight high-speed motors on gas-electric rail cars. The idea was to adapt motors which were designed for gas-electric drive on busses, for use in rail transportation. The first rail applications used a motor mounted either on the truck or body of the car. The motors were not designed sufficiently rugged to withstand the shock of operation when axle-mounted. On these applications automotive-type double-reduction or worm gearing was used, with a propeller shaft and double universal joints connecting the gearing and the motor. In 1938 a similar scheme was tried on lightweight industrial Diesel-electric switching locomotives. The 23-ton and 43-ton locomotives were the first on which this type of drive was used. These locomotives were equipped with a high-speed motor and double-reduction gearing.

The GE-733 is a lightweight double-reduction axle-mounted motor designed especially for Diesel-electric switching locomotives. The first of these was designed and built in 1940, and since that time a large number of these motors have been built and are in service all over the world. This machine was designed to cover a wide range of applications and therefore was built with many new electrical and mechanical features which have made it capable of doing the job well for the past five years. Figure 1 shows the motor complete with double-reduction gear unit.

More Tractive Effort

The primary objective in traction motor design is pulling power or tractive effort. It is the constant aim of the designer to secure more continuous tractive effort per pound of motor weight in each new design. If this can be done, the resulting small motor can be used on small-diameter wheels and on narrow gauge locomotives. Such a motor can be adapted to a wide range of locomotive sizes, simplifying their design. For example, weight saved in the traction motor may be used in the Diesel engine to make a more powerful locomotive without increasing the weight.

Figure 2 shows continuous tractive effort per pound of motor weight for various motors. Column *A* shows single-reduction motors which were being built in the period 1925 to 1930. Column *B* shows single-reduction motors which are being built today. Column *C* shows an early design of double-reduction motor which was built in 1936. Column *D* shows the GE-733 lightweight double-reduction motor as it now is being built and used on a wide variety of locomotives. The continuous tractive effort per pound of motor weight for the various motors shown on the chart in Figure 2 is based on the maximum reduction gearing which will give clearance under the gear case, as specified by the Interstate Commerce Commission, with the minimum wheels for which the motor is designed. This chart shows that steady progress has been made in the more efficient use of materials in both single-reduction and double-reduction motors. The continuous tractive effort per pound of the lightweight double-reduction motor is over $3^1/_3$ times as much as that of the 20-year old single-reduction motors and 43 per cent greater than that of the earlier design of double-reduction motor. This more efficient use of material is accomplished by using a high-speed lightweight motor and high torque multiplication in the double-reduction gear unit.

Figure 3 shows a graph of the continuous tractive effort and motor weight for the same groups of motors that are shown in Figure 2. For instance, the lightweight double-reduction motor weighs only one-third as much as a comparable present-day single-reduction motor and has 70 per cent as much continuous tractive effort rating. To judge a motor by this chart, place a straightedge along the abscissa and rotate it counterclockwise toward the ordinate, using zero as the center of rotation. The better motors, so far as continuous tractive effort is concerned, are nearer the ordinate.

How Much Horsepower?

A motor cannot be judged solely by its continuous tractive effort. Consideration also must be given to locomotive speed. If it were not necessary to consider locomotive speed as well as continuous tractive effort, triple-reduction or quadruple-reduction gearing could be used. This would give much higher

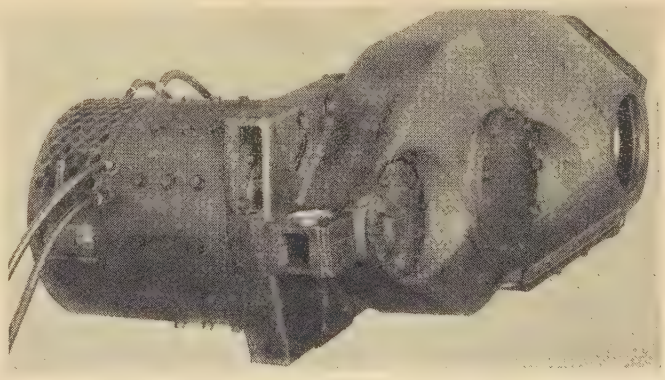

Figure 1. GE-733 d-c traction motor with double-reduction gear unit

Paper 46-90, recommended by the AIEE committee on land transportation for presentation at the AIEE North Eastern District meeting, Buffalo, N. Y., April 24–26, 1946. Manuscript submitted November 23, 1945; made available for printing March 11, 1946.

LANIER GREER is a design engineer with the transportation motor engineering division, General Electric Company, Erie, Pa.

The author wishes to thank his associates for the assistance given in the preparation of this paper.

torque multiplication and therefore a corresponding increase in tractive effort, since tractive effort is motor torque translated to the rim of the locomotive wheel. The data given in Figure 4 take into consideration locomotive speed as well as tractive effort. These factors have been combined to obtain a measure of horsepower. This has been done by the approximate formula

$$\text{Horsepower} = \frac{\text{continuous tractive effort}}{375} \times \frac{\text{maximum miles per hour}}{3}$$

The reason for the "3" in the formula is that continuous tractive effort and maximum speed never occur at the same time in a Diesel-electric locomotive. In general, the continuous tractive-effort rating comes somewhere near one-third of the maximum speed. Any motor may be used with various capacity engines, but this formula makes possible a fair comparison between motors. The chart is shown in horsepower per thousand pounds of motor weight, and is shown for both single-reduction and double-reduction motors. The nomenclature of the columns in Figure 4 is the same as that used in Figure 2. As indicated by the height of the columns, much progress has been made in the past 20 years in the design of single-reduction motors. Also, the modern double-reduction motor shows approximately 20 per cent more horsepower per thousand pounds of motor weight than the earlier double-reduction motor, and 67 per cent as much as the modern single-reduction motor. This, together with the data shown in Figures 2 and 3, indicates that there is a place for double-reduction motors in light-traction road service, as well as in industrial switching service, where maximum power and operating speeds are not too high. However, on the heavier high-speed road locomotives, the horsepower to be handled is so great that large-diameter armatures are necessary for commutation. These large diameters make it necessary to keep the revolutions per minute low on account of the centrifugal forces involved. With low revolutions per minute, there is no advantage in having double-reduction gearing, because all of the reduction needed can be built into one set of gearing.

New Double-Reduction Gear Unit

The specially designed 1-piece cast steel gear case which forms a part of the motor and gear unit is shown in Figure 5. This is a view of the axle and motor side and shows axle preparation, gear cover bolting flange, intermediate gear shaft bearing opening, bolt circle for mounting the motor, and air outlets for the motor ventilating fan. The gear cover is a separate piece and is cast of malleable iron. It is bolted to the gear case along the bolting flange. Figure 6 shows a photograph of the double-reduction gear unit with gear cover and axle caps removed. This illustration shows the gear unit completely assembled with all gearing and bearings in place. All bearings and pinions are arranged so that they can be disassembled without removing the motor and gear unit from the locomotive. Also, the complete motor can be removed and still leave the gear unit mounted in the locomotive. Thus, by using a high-speed motor, the size of the motor has been reduced to such an extent that it has become a part of the gear unit rather than the gear unit being a part of the motor, as on conventional

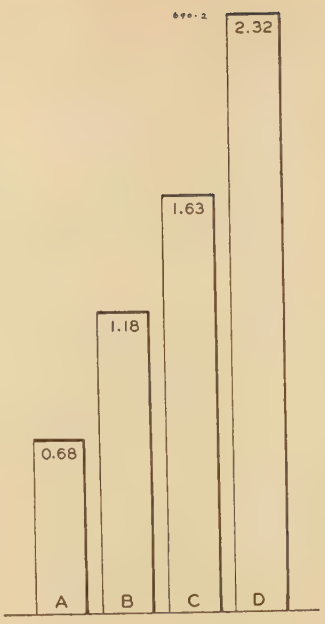

Figure 2 (left). Continuous tractive effort per pound of motor weight

Figure 4 (right). Horsepower per thousand pounds of motor weight

$$\text{Horsepower} = \frac{\text{continuous tractive effort}}{375} \times \frac{\text{max mph}}{3}$$

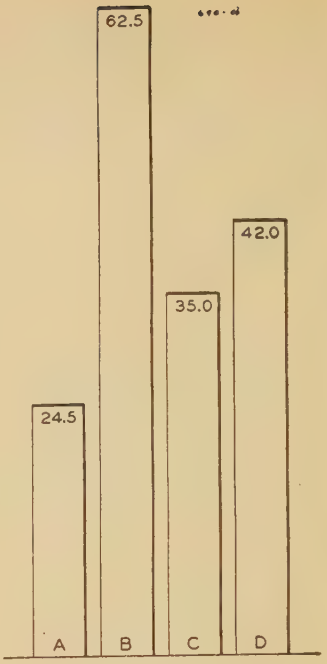

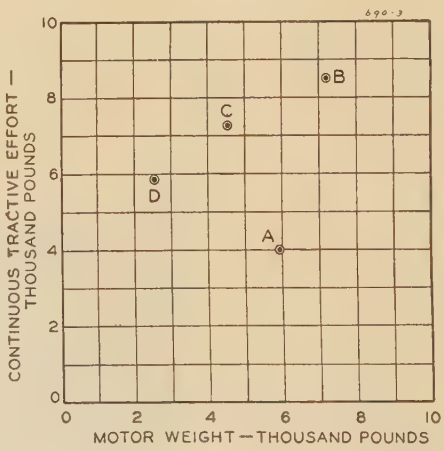

Figure 3. Continuous tractive effort and motor weight

single-reduction machines. Figure 1 shows the motor and gear unit nose support which is located so that, for either direction of motion of the locomotive, there will be no tilting to throw the gear mesh out of alignment or place a twisting load on the axle bearings under the heavy tractive efforts encountered in service. Hardened spur gearing operating in an oil-tight gear case has a long life. Both the high-speed and low-speed pinions are straddle-mounted to maintain alignment.

The flood-lubricating system in the gear unit uses oil of about the viscosity of SAE 60 for normal operating temperatures, and lighter oil for lower temperatures. This lubricates all bearings in the gear unit, the pinion end motor bearing, the sleeve axle bearings, and thrust surfaces, as well as all of the gearing.

Mechanics of a High-Speed Motor

The motor is self-ventilated, which eliminates motor blowers and thus simplifies the locomotive design. This is found to be practical in a motor which is used with double-reduction gearing, since even in slow-speed switching service motor speeds are high enough to make the motor fan effective. The fan, which is mounted on the pinion end of the armature shaft, provides for multiple ventilation of the machine. One air path is over the commutator, through the space between the field coils and over the armature surface; the other is under the commutator and through longitudinal ducts in the core and armature heads.

A tight cylindrical smooth commutator is essential to the successful operation of

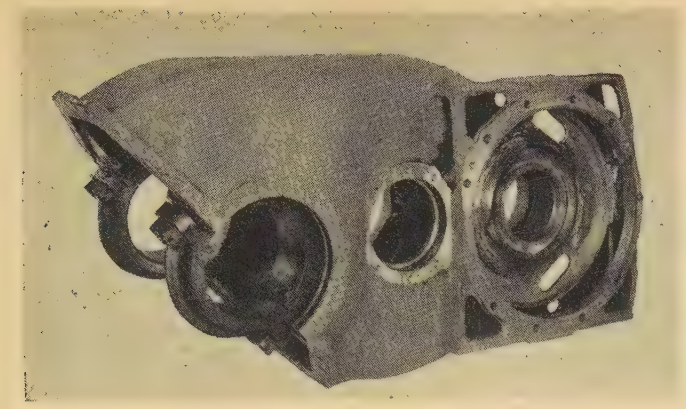

Figure 5 (above). Gear case for double-reduction gear unit

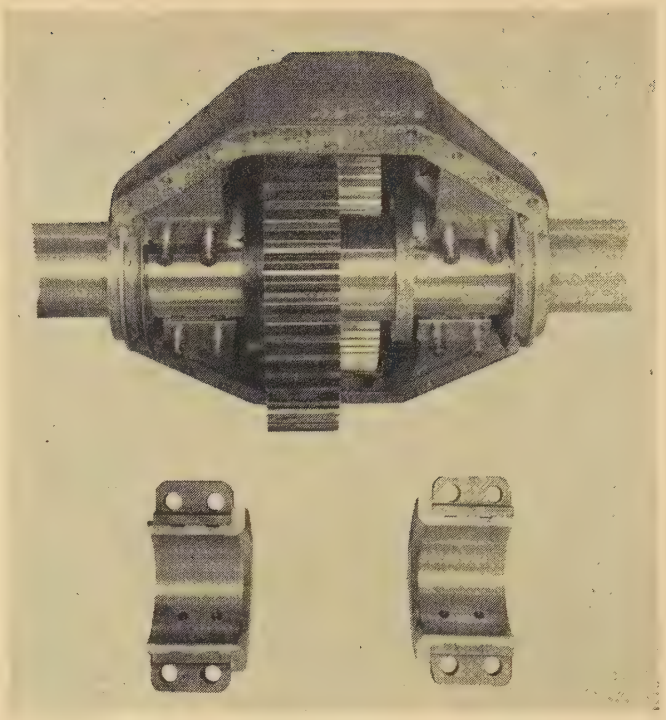

Figure 6 (right). Double-reduction gear unit with gear case and axle caps removed

any high-speed d-c machine. This is obtained by using commutator design constants, which have been developed over a period of years of experience with high-speed motors. Commutators are seasoned after the armature is completely assembled. This seasoning consists of subjecting the commutator to centrifugal forces and thermal stresses in excess of those which are encountered in service and tightening, and grinding the commutator until it operates smoothly, both hot and cold.

The armature is designed to withstand the stresses of high-speed operation that go with double-reduction gearing. The coils are held in the core slots by wedges, and the end windings are held with binding wire. The completed armature is dynamically balanced to close limits so that it operates smoothly at all speeds. It is also equipped with anti-friction bearings on both ends. The commutator end bearing housing is designed so that the armature can be removed without opening the bearing housing and exposing the bearing to dirt. This bearing also is arranged with all-metal labyrinth seals to keep grease in and to keep dirt out. The bearing on the pinion end of the motor armature is mounted outside of the motor pinion to form a straddle-mounting for the pinion. The bearing on this end is housed in the gear case and lubricated with the same oil as the gearing. The commutator end bearing is grease-lubricated.

The frame of the motor is bolted to the gear case so that the two become an integral unit and are mounted as such. Figure 1 shows a photograph of motor and gear unit.

Electrical Features

High-temperature insulating materials, such as asbestos cloth, asbestos paper, fiber-glass, and mica, are used in the modern double-reduction motor. With the aid of modern synthetic high-temperature varnishes, asbestos and mica, as well as fiber-glass and mica, have been combined to form tapes and wrappers. These materials have made it possible to use thinner insulation of a better quality and get a better-insulated machine. Thinner insulation leaves more space for copper and iron and at the same time improves the heat transfer coefficient through the insulation. Another advantage of these materials is their ability to stand high temperatures and at the same time have long life. High temperatures make it possible to get more tractive effort rating per pound of material. Inherent long life of insulating materials keeps maintenance costs low.

Proper proportioning of copper and iron in the magnetic circuit has made it possible to reduce materially the size and weight of the field structure. The field coils have been reduced in size by the use of new insulating materials and methods. Both exciting and commutating coils are edgewise wound and formed to fit the poles. They are insulated between turns with asbestos paper. A sufficient number of turns on the armature and frame sides of the coils are taped with mica and fiber-glass to provide the required insulation. Figure 7 illustrates an exciting and a commutating field coil with this type of insulation. The commutating coil is shown before the asbestos insulation has been inserted between the turns and before the coil has been dipped in high-temperature insulating varnish. The exciting field coil is shown completely insulated and ready to be mounted on the pole piece. Mica insulating collars around the pole pieces protect the field turns that are not taped. The coils are mounted on the poles and given a number of dips and bakes in high-temperature synthetic insulating varnish; thus the pole and coil become a complete unit and are assembled in the motor as such. With this type of coil, the heat transfer coefficients, both to air and iron, are much higher than for a conventional coil. After the poles and coils are assembled in the frame, the complete assembly is dipped in modern synthetic varnish and baked to fill completely and insulate all connections and joints so that they are sealed and protected from water, oil, and other foreign materials that may enter the motor.

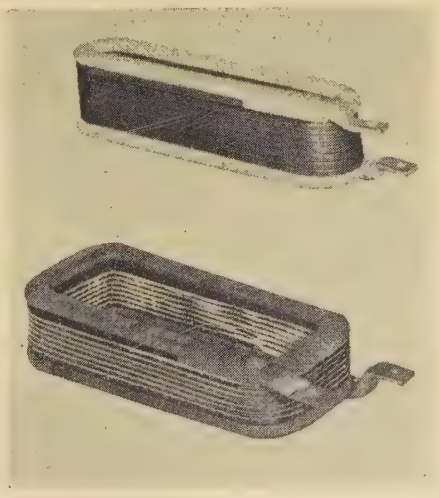

Figure 7. Exciting and commutating field coils for modern double-reduction motor

The design constants of the motor have been made to produce a steep speed curve which, with the maximum amount of field shunting, makes it possible to use the motors connected permanently in parallel. This motor connection reduces wheel slippage and gives the locomotive more pulling power. Figure 8 shows characteristic curves of the GE-733 motor on 250 volts and for two field strengths. The wide change of flux in the motor, between maximum tractive effort and maximum permissible speed, together with the engine generator characteristics, makes a locomotive with a wide range of full utilization of the available engine horsepower.

High Efficiency

The power of a Diesel-electric locomotive is limited to that which the Diesel engine can deliver. For this reason, it is necessary that the transmission efficiency be kept as high as is compatible with reasonable design. This is especially true on switching locomotives where small engines are used and where heavy loads are handled at low speeds and high

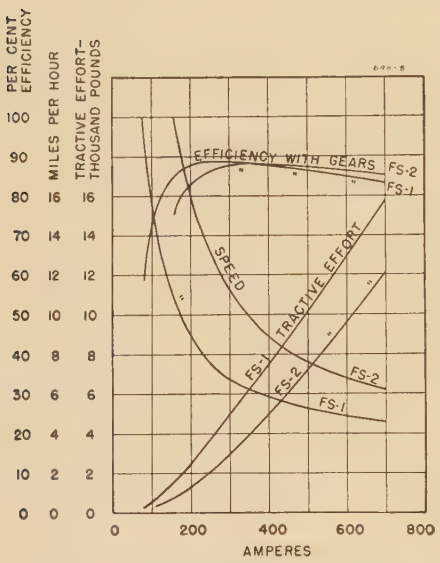

Figure 8. Characteristics of GE-733 motor on 250 volts and maximum reduction

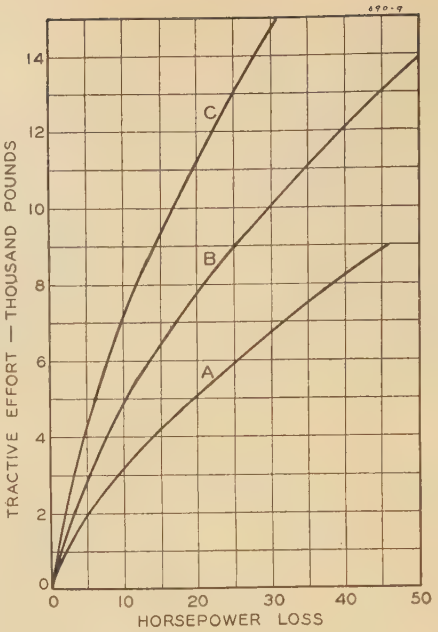

Figure 9. Comparative motor resistance loss curves of traction motors with single-reduction and double-reduction gearing

tractive efforts. Figure 9 shows comparative efficiencies of various motors based on motor resistance losses at 110 degrees centigrade copper temperature, with an assumed two volts for brush drop. Curve *A* is for the older type of single-reduction motors, such as were being built in the period 1925 to 1930. Curve *B* is for single-reduction motors as they are built today. Curve *C* is for the double-reduction motor. All three of these curves are based on the maximum reduction which can be used and still maintain clearance under the gear case as specified by the Interstate Commerce Commission. A study of these curves clearly shows the advantage of the double-reduction motor for locomotives that are required to operate at moderate or low speed and to produce high tractive effort. At the starting point of the locomotive, all of the losses are in resistance. The difference between curve *B* and curve *C* in Figure 9 shows the additional tractive effort that can be produced with the modern double-reduction motor over the modern single-reduction motor for a given horsepower loss. For example, this amounts to 47 per cent increase at 30 horsepower loss.

Universal Use

The modern double-reduction motor is used on a wide range of locomotive sizes. The motor has been applied on locomotives for all classes and types of industrial switching, and also for lightweight railway switching and road service.

A rule-of-thumb measure of the capabilities of the motor is given by these facts: with maximum reduction gearing, it can be applied on 50,000 pounds of locomotive weight per motor and will have a continuous tractive effort rating of 11.7 per cent adhesion, with a maximum permissible speed of 20 miles per hour.

Table I lists the locomotives on which the GE-733 motor is used. This tabulation also shows the number of motors used per locomotive, the maximum permissible speed, and the continuous adhesion rating of the locomotive. The largest number of these motors have been used on the 25-ton and 45-ton locomotives for industrial service and the 44-ton locomotive for railway service. A limited number of motors have been used on the 65-ton industrial and the 70-ton railway locomotives. In all of these applications, the double-reduction motors have given excellent service.

Table I. Tabulation of Locomotives Equipped With Modern Double-Reduction Traction Motors

Weight, Tons	No. of Motors	Max. Speed	Adhesion Per Cent
Industrial Diesel-electric locomotives			
25	1	20	11.7
45	2	20	11.7
65	4	30	11.5
Railway Diesel-electric locomotives			
44	4	35	14.6
70	4	25	12.5

Determination of Cable Temperatures by Means of Reduced-Scale Models

ANDREW GEMANT
NONMEMBER AIEE

JOSEPH STICHER
MEMBER AIEE

Synopsis: A method, using reduced-scale model installations, is developed for the laboratory determination of cable temperatures obtaining in the field. The theory of the method is given, followed by the description of three sets of experiments conducted to show the feasibility of the method. One set of experiments is concerned with a single-conductor cable buried directly in the soil of the model setup, and temperatures obtained are compared with computed values. Another set is concerned with a single-conductor cable in a model duct bank, and sheath and duct temperatures obtained are compared with those of field determinations in an actual field installation. The third set is concerned with a model three-conductor cable in a duct bank, and conductor-sheath temperature differentials are compared with field data. All tests show that the accuracy of the method is sufficient for practical purposes.

THE determination of cable temperatures, under both stationary and transient conditions, is essential for the evaluation of maximum permissible loads. This statement follows from a consideration of the factors that limit the loads, that is, deterioration of the paper-oil insulation and undue stretching and longitudinal movement of the sheath. All these factors are considerably dependent on temperature, so that, indeed, temperature limits the loads.

Determinations of cable (conductor and sheath) temperatures can be and sometimes are carried out in the field. If, however, a wide variety of cable combinations and loading schedules is to be investigated, field tests are time consuming and costly.

A second possibility of obtaining cable temperatures is by calculation. This method, however, is suitable only for very simple arrangements, such as a cable buried directly in the ground. For duct systems of cables, a computation on a rigorous basis cannot be carried out.

A third method of attacking the problem is the use of electrical analogies. This method has been developed by Victor Paschkis[1] and applied successfully to a number of thermal problems. For several cables in duct banks, the necessary electrical equipment would be too involved, so that at present this method cannot be used for this purpose.

The method to be described in this paper was developed for the purpose of providing a more satisfactory means than those just described. As will be seen from the following, the equipment even for involved cable problems is relatively simple and, once the installation is assembled, the time required to solve any specific cable temperature problem is relatively short.

Theory

Thermal problems in a system of cables belong, strictly speaking, to the group of 3-dimensional problems, but, if the length of the cable is at least 10 to 20 times larger than the depth of the cable below ground level (a condition that is nearly always fulfilled), the heat flow along the length can be neglected as compared with the heat flow in radial directions. Thus, cable heat-flow problems can be considered as 2-dimensional.

By examining the equations of heat flow in 2-dimensional cases,[2,3] a dimensional analysis shows that there is a possibility of a scale reduction in such problems, and that the rules according to which this reduction is to be carried out are rather simple. Thus, installations can be reduced in size and yet give the same information concerning temperature distribution as the original large installations. This, briefly, is the principle of the method developed and described in this paper.

The following is a brief presentation of the dimensional analysis mentioned. One of the basic equations[2] in 2-dimensional heat problems is the temperature distribution around an instantaneous cylindrical heat source in an infinite medium, the temperature of which becomes zero at infinity. Let H_o denote the instantaneously generated heat per unit length of the cylinder with radius a, g the thermal resistivity, D the thermal diffusivity of the medium surrounding the source, T the temperature, t the time, and r the radial distance from the axis of the cylinder. Then

$$T=\frac{H_o g}{4\pi t}\exp\left[\frac{-(r^2+a^2)}{4Dt}\right]J_0\left(\frac{ira}{2Dt}\right) \qquad (1)$$

where J_0 = Bessel function of the first kind and zero order. In this equation, the several variables occur in two combinations. One is (with l = any characteristic length of the installation)

$$x=\frac{l^2}{Dt} \qquad (2)$$

the other

$$y=\frac{T}{Hg} \qquad (3)$$

where H stands for the heat rate H_o/t and

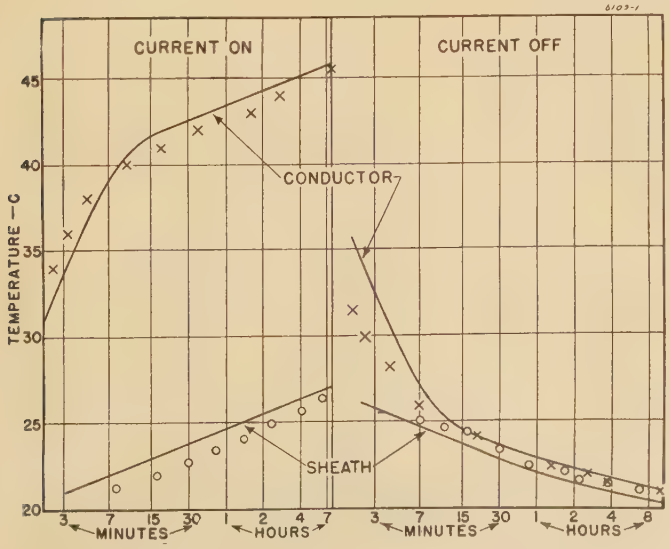

Figure 1. Temperatures of conductor and sheath of one single-conductor cable buried directly in ground of model installations

Eight-hour loading at 120 amperes and subsequent cooling (x and o are measured data; solid curves are calculated)

Paper 46-103, recommended by the AIEE committee on power transmission and distribution for presentation at the AIEE summer convention, Detroit, Mich., June 24-28, 1946. Manuscript submitted November 27, 1945; made available for printing April 11, 1946.

ANDREW GEMANT and JOSEPH STICHER are with The Detroit Edison Company, Detroit, Mich.

The authors wish to express their thanks to their colleagues in the research department of The Detroit Edison Company, Arnold Featham, T. A. H. Jeffery, and R. J. McCausey for their help in carrying out this research; also to W. D. Sanderson, of the electrical system of the same company, for having placed certain field data at the authors' disposal; and to Doctor R. J. Wiseman, of the Okonite-Callender Cable Company for having supplied the 3-conductor model cable.

has the meaning of heat generated per unit length per unit time. Both x and y are dimensionless, as is shown by the following.

D stands for $l/g\rho c$, with ρ = density and c = specific heat, and has the dimension l^2t^{-1}. Hence, x is dimensionless. Concerning equation 3, T as temperature is dimensionless, the dimension of H (heat per unit length per unit time) is mlt^{-3} (m = dimension of mass), and that of g is $m^{-1}l^{-1}t^3$; consequently, y is dimensionless. As can be seen from equations 2 and 3, equation 1 has the form

$$y=f(x) \tag{4}$$

where f stands for a function of the single argument x, containing no other parameter.

By further examining equations of 2-dimensional heat flow, it will be found that all of them can be reduced to a dimensionless form similar to equation 4. As a further example, a cylindrical space bounded by an inner cylinder of radius a, and an outer cylinder of a radius a' is considered. The inner cylinder generates heat in the amount of H per unit time per unit length; the outer cylinder is maintained at zero temperature. The thermal constants of the medium between the two cylinders are g and D, as before. The temperature of the inner cylinder T at any time t is then given[3] by

$$T=\frac{Hg}{4\pi}\sum_{n=1}^{\infty} k\left[J_0\left(\frac{\rho a}{a'}\right)\right]^2\left[1-\exp\left(-\frac{\rho^2 Dt}{(a')^2}\right)\right] \tag{5}$$

where

$$k=\frac{2}{\frac{\pi}{4+n-1}} \tag{6}$$

and, approximately,

$$\rho=2.40+(n-1)\pi \tag{7}$$

the infinite series to be extended from $n=1$ to infinity.

It can be seen that equation 5 contains all variables in the form of x and y, as before, and, in addition, z; where

$$z=\frac{l}{l'} \tag{8}$$

l and l' denoting two characteristic lengths of the installation. Hence, equation 5 can be written in the general form

$$y=f(x, z) \tag{9}$$

f standing for a function of the arguments x and z only.

From the existence of functional equations such as 4 and 9, the conclusion is drawn that any two installations for which x, y, and z are respectively the same are physically similar. A closer investigation of equations 2, 3, and 8 reveals the conditions of similarity, as follows:

1. Equation 8 shows that a scale reduction of an installation is feasible if all linear dimensions normal to the running direction of a cable or a duct system of cables are reduced in the same ratio. For instance, the ratio a/a' in a concentrical cylindrical case should be the same both in a scale model and an actual cable.

2. If the heat-conducting substances are the same in the two corresponding installations, that is, if D is the same for both, then equation 2 shows that the time t required to attain the same temperature in both cases is reduced by a factor that is equal to the square of the reduction factor of linear dimensions. This can be seen by writing $t=l^2/Dx$ and recalling that x is the same in the original and the model. This indicates the considerable gain in time that may be obtained by carrying out temperature measurements on a reduced-scale installation. It should be added that, while the method covers transient conditions, as shown, it is obviously applicable for the limiting case of $t=\infty$, the steady-state condition. Equation 5, for instance, is valid for the steady-state condition if the exponential is replaced by zero, thus making the second bracket unity. Steady-state conditions are approached, according to equation 2, faster in the reduced-scale installation than in the original.

3. Equation 3 shows the following condition. Since the same materials are used for both the actual installation and the model, g is the same. If, now, the reduced-scale system should yield the same temperatures T as does the original system, the condition that follows from equation 3 is that H, the heat dissipated per unit time and unit length, should be the same in both cases. Disregarding dielectric and sheath losses in obtaining a first approximation, H is given by

$$H=I^2R \tag{10}$$

where I = current in a conductor and R = resistance of the conductor per unit length. Because of condition 1, the cross-sectional area is reduced by the square of the linear reduction factor, and R increases in the same ratio. Thus, in order that H be the same, the current has to be reduced by the same factor as the linear dimensions.

If the reduction factor q be introduced and if quantities referring to the reduced-scale installation be designated by the index r, then condition 1 requires

$$l_r=\frac{l}{q} \tag{11}$$

condition 2 requires

$$t_r=\frac{t}{q^2} \tag{12}$$

and condition 3 requires

$$I_r=\frac{I}{q} \tag{13}$$

The last equation is approximate; since the influence of skin effect varies with the size of conductors, a small correction factor that is available from tables has to be considered. If these three conditions are fulfilled, corresponding temperatures in the model and original installations are the same.

The larger q, the smaller is the model installation. Practical considerations, however, limit its value, and for 3-conductor 24-kv cables, a value in the approximate range of from four to five has been found to be suitable.

Test Results

The theory of scale reduction, as outlined above, does not need experimental proof, as it is based on straightforward mathematics. To what extent it could be put to use could, however, be determined only by experiment, because in building the model installation, some approximation of the theoretical requirements could not be avoided. To mention a few examples: the insulation of the model cable could not be easily built of paper five times thinner than real cable paper, that is, 1 to 0.6 mil thick; the concrete in the duct bank could not be easily built of pebbles reduced five times the original size; and the soil surrounding the duct bank could not easily be maintained at exactly the same moisture content, and hence at the same insulation level, as the soil in the field.

Apart from these approximations, resulting from a compromise because of details of construction, there is another divergence between actual installations and the conditions required by the theory as developed. The latter refers to heat transfer by conduction. This condition generally is fulfilled in cable systems with the exception of the space between the cables and the ducts, in which part of the heat transfer takes place by radiation and convection and for which the scale reduction as developed is not valid. These local processes within the duct play a definite and by no means negligible part in determining the temperature distribution. By means of approximate calculations, it is possible to assess their role in a semiquantitative manner.

In the following sections, three particular tests, carried out for the purpose of checking the degree of accuracy obtainable in practical use of the theory, are described and the results discussed. One of these tests concerns one single conductor cable buried directly into the ground of the model installation. In this case a comparison of test results is made with calculated results. Such calculations are

feasible in this simple case. The second test refers to a single-conductor cable in a model duct system, and comparison is made with the results of an actual field test in a corresponding installation. The third test refers to a model 3-conductor cable in a model duct system and comparison is made with results of the same full scale field test as in the second test.

All these tests were carried out in a wooden box 15 feet long, 5 feet wide, and 4 feet high filled with soil (a yellow clay obtained from the location of the field installation just referred to). A volume of soil equal to that of the space in the box to be filled was dug in the field and placed in the box by tamping. Only about five cubic feet were left over, so the density of the soil in the box had nearly the original value obtaining in the ground. Moisture determinations revealed that the soil contained originally 17.5 to 20 per cent water. Although a certain decrease of the moisture content with time could not be prevented, lining the box with tar paper, covering it with tarpaulin, and occasional watering of the top kept the drying out of the soil within reasonable limits. For future tests, it is considered advisable to install the model in a room in which the moisture content is artificially maintained at a relatively high level, say 80 per cent.

The thermal resistivity of the soil was measured by means of a cylindrical soil-resistivity cell[4] in the field, and shortly before removal of the sample a value of 72 thermal ohms was obtained. The diffusivity D was obtained as follows. The density ρ was 2.1 grams per cubic centimeter. The clay-to-water ratio was four to one and, since the thermal capacities of clay and water are 0.22 and 1.0 respectively, the thermal capacity of the soil is 0.37. From $D=1/g\rho c$, a value of 4.2×10^{-3} square centimeters per second was obtained for the diffusivity. These values for g and D were used in the calculations.

Single Cable Buried in Ground

This arrangement was selected because the temperature distribution in and around one single conductor cable buried in the ground could be computed theoretically. A comparison between experimental and computed data would indicate the accuracy and reliability of measurements obtained from a small size model installation.

The test cable used was a single-conductor, number 6 American Wire Gauge, paper-insulated cable having an insulation thickness of 9/64 inch, lead sheath thickness of 6/64 inch, and over-all diameter of 0.65 inch. The cable was installed ten inches below the ground surface in the box. The ratio of depth of burial to length of cable being 1 to 18, the error introduced by the end-effect, according to data of S. Whitehead,[4] was between one and two per cent.

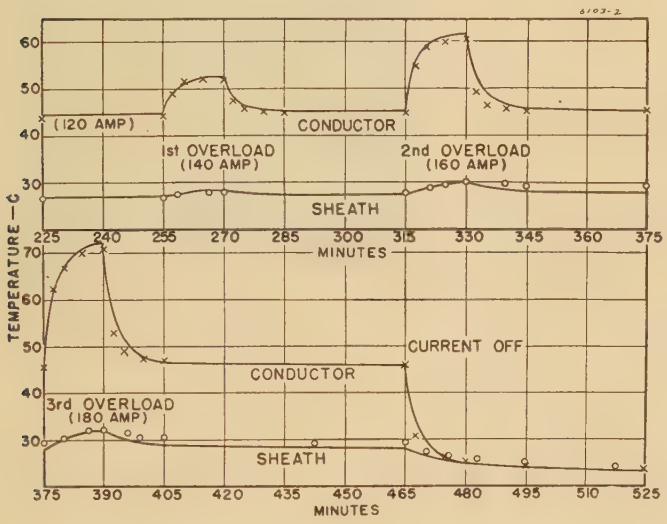

Figure 2. Temperatures of conductor and sheath of one single-conductor cable buried directly in ground of model installation

Overloads of 20, 40, and 60 amperes superimposed upon steady current of 120 amperes (x and o are measured data; solid curves are calculated)

The temperatures of both the conductor and the sheath were measured. The model method permits the copper temperature to be obtained by means of a thermocouple inside the conductor, since it is possible to pull a thermocouple into a narrow channel within the conductor. In this particular case, the central one of the seven conductor strands was pulled out before the test in order to accommodate a thermocouple; another thermocouple was soldered on the lead sheath to obtain sheath temperatures. The temperatures were continuously registered by means of a recording instrument. Thus, it is possible to maintain uninterrupted registration of copper temperatures during the whole load cycle. In contrast to this procedure, copper temperatures in field tests are obtainable only by resistance measurements, necessitating a temporary interruption of the loading.

A current transformer with the necessary control and measuring equipment was provided for the loading of the cable.

With regard to calculation of temperature in this case, equations recommended by S. Whitehead[4] were used. By considering the sheath as the source of heat flow, the basic equation 1 immediately gives the solution in the case of the buried cable. Since the ground surface is an isothermal plane, the field of an image sink above ground, added to the field of the real source, constitutes the solution of the problem. For values of $a^2/4Dt$ that are small as compared to unity, the solution for the sheath temperature T_s becomes

$$T_s=\frac{Hg_s}{4\pi}\left[-Ei\left(-\frac{a^2}{2Dt}\right)+Ei\left(-\frac{b^2}{Dt}\right)+\exp\left(-\frac{a^2}{2Dt}\right)\log 2\right] \quad (14)$$

where g_s is the thermal resistivity of the soil, Ei stands for the exponential integral,[5] and b denotes the depth of the cable below ground, the other symbols being the same as in equation 1.

The rise of the copper temperature above sheath temperature can be computed by considering both the thermal capacity C_c and the thermal resistance G_c of the cable per unit length as lumped elements, in which case the solution is an exponential. This solution, although approximate, is sufficiently accurate for the purpose at hand. The copper temperature is then given[4] by

$$T_c=HG_c\left[1-\exp\left(-\frac{2t}{C_cG_c}\right)\right]+T_s \quad (15)$$

T_s being known from equation 14. The factor 2 in the bracket is approximate: it accounts for the fact that the center of the cable is heated instantaneously, while the periphery is heated across the resistance G_c; in the average, a resistance of $G_c/2$ is operative.

The numerical values used for the two constants G_c and C_c were evaluated from the geometry of the cable and the known characteristic data of each cable constituent. G_c is given by

$$G_c=\frac{g_c}{2\pi}\log\frac{r_s}{r_c} \quad (16)$$

with g_c = thermal resistivity of insulation, r_s = inside radius of sheath, and r_c = radius of conductor. For g_c a value of 550 thermal ohms was taken. With $r_s=0.232$ inch and $r_c=0.092$ inch, the value

obtained for G_c is 81 ohms or 81×10^{-7} centimeter-gram-second units.

The thermal capacity was computed by adding the values for copper, insulation, and lead. The specific heats are respectively: 0.42×10^{7}, 1.8×10^{7}, and 0.147×10^{7} centimeter-gram-second units, resulting in thermal capacities per unit length of 0.42×10^{7}, 1.98×10^{7}, and 1.78×10^{7} centimeter-gram-second units, giving a total for $C_c=4.18\times10^{7}$ centimeter-gram-second units.

The steady-state temperatures are given by the well-known formulas:

$$T_s=\frac{Hg_s}{2\pi}\log\frac{2b}{a} \tag{17}$$

and

$$T_c=HG_c+T_s \tag{18}$$

Since the temperature of the conductor and, consequently, its resistance varies during a load cycle, in order to maintain a constant heat loss H, upon which the theoretical equations used for calculation are based, the current must be adjusted occasionally. This adjustment is possible when the copper temperature is registered continuously. The currents reported in the subsequent parts of this paper are the values applied at 20 degrees centigrade copper temperature and at which the conductor resistance was 15.4×10^{-6} ohms per centimeter.

The first test was carried out with a load of 120 amperes corresponding to $H=$ 6.8 watts per foot. Loading continued for about eight hours, after which the current was switched off. Both the heating and the cooling curves—temperature versus time—are shown on Figure 1 for the conductor as well as for the sheath. The time is plotted on a logarithmic scale. The crosses and circles indicate measured data; the solid lines were computed from equations 14 and 15, using the numerical values given.

The agreement between calculated and measured data is satisfactory, the discrepancies being generally one to two degrees centigrade, except the copper temperature within five minutes after switching off the current, where the divergence is up to four degrees centigrade. The amount of disagreement between computation and test is partly caused by the fact that the equations, although theoretical and without arbitrary constants, contain, as explained above, some unavoidable approximations. Part of the disagreement, however, is certainly caused by deficiencies of the equipment (end-effect, boundary layer between sheath and soil, drying of the soil, time lag in temperature recorder, and so forth). But

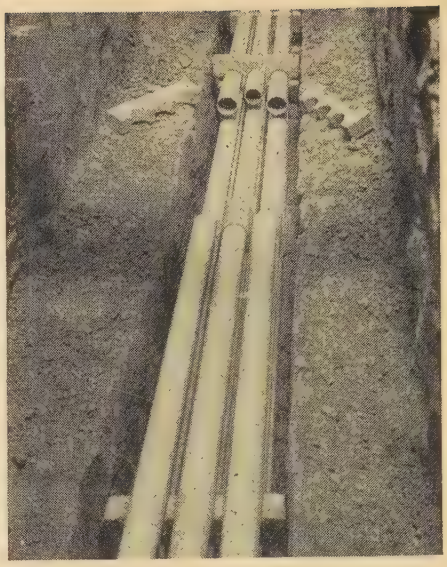

Figure 3. Details of assembly of model ducts in model trench

since a disagreement of less than two degrees centigrade is of no great practical significance, and since the cooling period is of relatively little interest to the practical cable engineer, who is not greatly concerned with the precise rate of temperature decrease after the temperature has reached its maximum, the method is considered satisfactory. For higher accuracy some of these deficiencies might be eliminated: for instance, the use, instead of moist soil, of a suitable dry and stable powdered material having the same thermal resistivity is being considered.

A second test (Figure 2) shows the temperature changes during and after short overloads. A current of 120 amperes was first maintained for about four hours (255 minutes), after which three overload cycles of 60 minutes duration, with overloads on for 15 minutes each, were applied. The total overload currents were respectively 140, 160, and 180 amperes (values reduced for 20 degrees centigrade copper temperature). The corresponding heats dissipated are 9.2, 12.0, and 15.2 watts per foot. The degree of agreement between test results and calculation is the same (deviation generally within two degrees centigrade) as in the first test. The agreement during the temperature maxima, which are of particular interest from a practical standpoint, is rather good. These findings are encouraging with regard to the practical application of a model installation (see conclusions at end of paper).

Single Conductor Cable in Duct Bank

This test was carried out in order to show whether the model was satisfactory in a case involving ducts. Since computation for such a case is not possible, a set of field tests conducted by The Detroit Edison Company was duplicated in the model setup to determine the degree of agreement between the two.

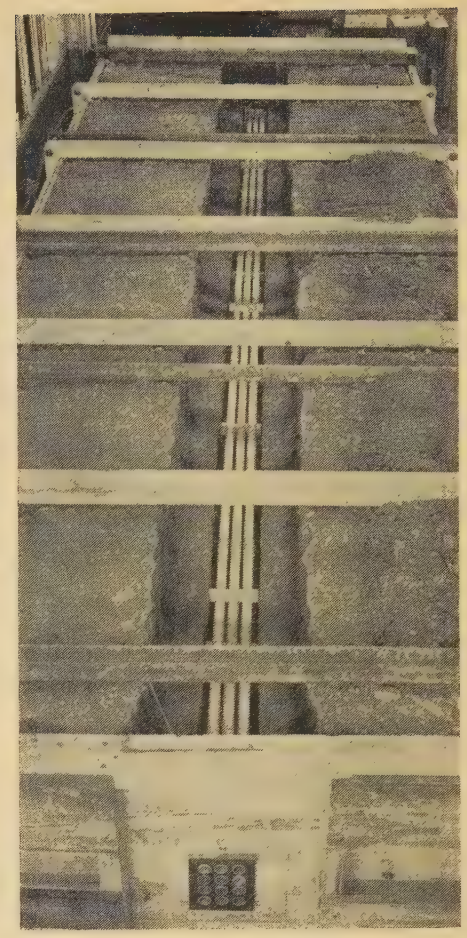

Figure 4. Completed model duct bank prior to pouring of concrete

It is planned for all tests of this type in the future to use reduced scale replicas of those cables that are involved in the actual field installations in question. At the time of carrying out the test to be described in this section, such model cable was not available, and the same single conductor cable that was used in the preceding test was installed in the model duct bank. In spite of this difference, sheath and duct temperatures, apart from the initial transients, in the model and the field should be the same. Because of the difference in the cable structures, however, copper temperatures in the field and in the model were not comparable in this particular test, and, as they are not essential in answering the specific question concerning the role of ducts in scale model tests, they are not given here.

A fiber-conduit–concrete duct bank for 12 4-inch ducts (3 wide by 4 high; $22\frac{1}{2}$ by $28\frac{1}{2}$ inches) was reproduced in a reduced size model. The linear reduction

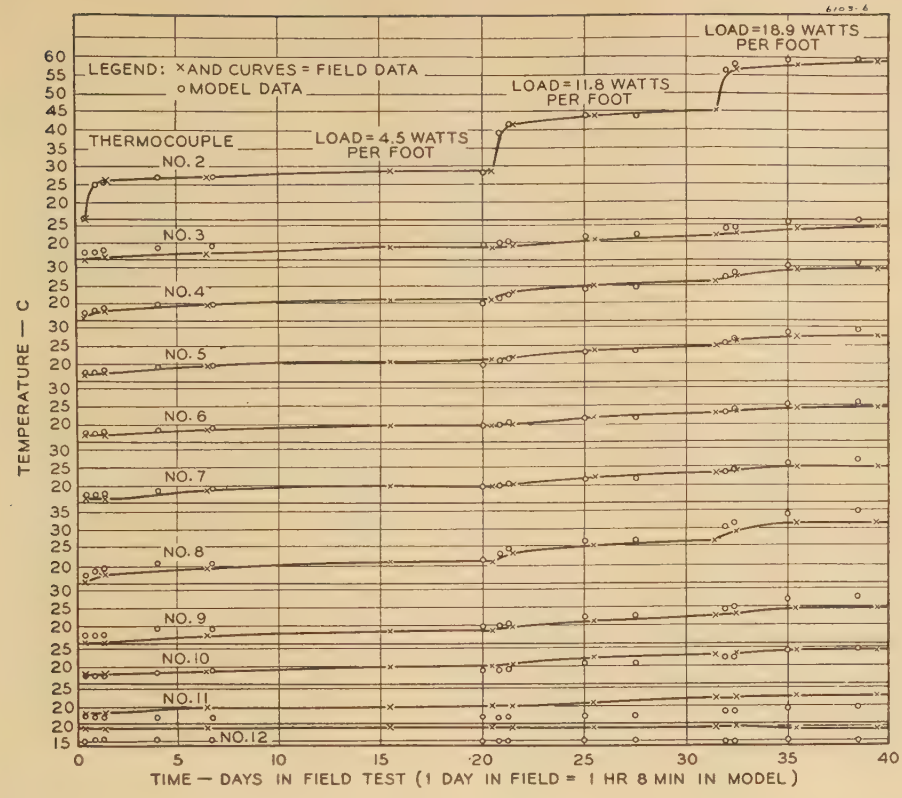

Figure 6. Temperatures of a test cable, ducts, and ground at three different indicated loads for both field and model installations

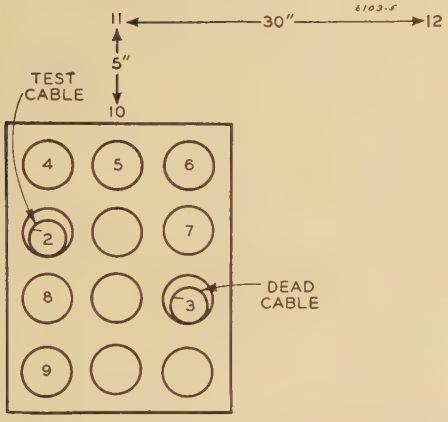

Figure 5. Diagram (not to scale) of model duct with number and location of thermocouples

factor q (see equation 11) was chosen as 4.6. This figure was selected in order to enable number 8 American Wire Gauge stranded wire to be incorporated in the model 24-kv 350-Mcm round conductor cable in the subsequent tests. The conductor diameter of the 24-kv cable is 0.68 inch, that of the number 8 wire 0.147 inch, the ratio of the two being 4.6. With $q=4.6$, the inside diameter of the model ducts was 7/8 inch, and the wall thickness was 1/16 inch. Three-foot lengths of bakelite-impregnated linen tubing, joined by short pieces of 1-inch inside diameter tubing as sleeves, were used as the conduit. The thermal resistivity of this material is comparable with that of fiber conduit as used in the field. Scale model concrete spacers between the ducts were used. A scale-model trench with a cross-sectional area of 4.9×6.2 inches was dug in the soil contained in the wooden box mentioned previously, and the duct bank was assembled in the trench. The manner in which the ducts were assembled is shown in Figure 3.

Two bakelite plates attached to the end walls of the box fixed the position of the ends of the duct bank. Pebble-free concrete containing sieved sand mixed with fly ash and having a two to one sand-to-cement ratio, was poured into the trench. The soil was tamped down on top of the duct bank, the top of the concrete being $11\frac{1}{2}$ inches below the top of the soil (corresponding to four feet four inches below ground level in the field). The completed assembly, prior to pouring the concrete and refilling the soil, is shown in Figure 4.

The ends of the bank were protected from air currents by close-fitting wooden boxes attached to the outside of the main box.

The arrangement of the cables and the location and number of thermocouples, as used in the field test and in the model, are shown in Figure 5. The length of the test cables was 17 feet. It should be noted that curve 2 (thermocouple 2) refers to the sheath of the test cable (thermocouple 1, as used in the field test was not reproduced in the model); curves 3 to 9 inclusive refer to the air temperature in the center of the various ducts; and curves 10 to 12 inclusive refer to the soil.

The results of the test are shown in Figure 6. The crosses and the curves drawn through them show the temperatures, in degrees centigrade, indicated by the 11 thermocouples used in the field tests; the circles show the data obtained with the model. The 40-day field test took 45 hours in the model setup (the time reduction factor from equation 12 is $4.6^2=21.2$).

Since it was realized that the ducts in this particular test were wet, some water was introduced in the duct containing the test cable in the model. A total of 200 cubic centimeters was introduced in order to insure a conducting path between cable and duct wall. This point is discussed in detail later.

Three different consecutive loads were applied. According to the requirements of the model theory, the heat input per unit length of cable has to be the same in the model as in the field. The three loads applied were 4.5, 11.8, and 18.9 watts per foot, respectively.

In studying Figure 6, it can be seen from curve 12 that no attempt was made to duplicate in the model setup the ambient temperatures recorded in the field; hence, the same disagreement prevails also for curve 11. The agreement for the sheath, the various ducts, and the soil just outside of the bank (shown by curve 10) is reasonably good, with a deviation of no more than about three degrees centigrade.

Additional Tests on Single-Conductor Cable in Duct Bank

While the results shown in Figure 6 answer the chief question, namely, whether the model method works in the case of ducts, it was deemed advisable to supplement the results by a few additional tests. As mentioned previously, one of the main causes of doubt with regard to the feasibility of the model test in the case of ducts is that heat is transferred not only by conduction, but also partly by radiation and convection. The scale reduction theory, however, took into consideration conduction only. If, now, the two other mechanisms play only a minor role in ducts, the error in the model test is relatively small. While the satisfactory answer of the main test (Figure 6) answers this question in a favorable sense, it was thought advisable to strengthen the confidence in the model method by additional tests directed toward showing spe-

cifically whether the errors introduced by radiation and convection in a duct are appreciable or not.

Radiation

It is useful in this connection to consider the Christiansen equation, which controls radiation from a convex body in an enclosure[6] and which, applied to the present problem, reads approximately:

$$H_r = 2\pi\sigma a \frac{(T_s^4 - T_d^4)}{\left(\frac{1}{\epsilon_s} + \frac{1}{\epsilon_d} - 1\right)} \qquad (19)$$

where H_r = heat radiated per second, σ = Stefan-Boltzmann constant = 5.7×10^{-5} absolute units, a = radius of sheath, T_s and T_d = sheath and duct temperatures, in absolute units, and ϵ_s and ϵ_d = emissivities of sheath and duct. The emissivities of a tarnished lead surface and a fiber surface are 0.56 and 0.93, respectively.

In order to assess experimentally the role of radiation in the model setup, the following procedure was adopted. From equation 19 it can be seen that ϵ_s has a marked influence on the radiation. Thus by varying the emissivity of the cable surface, all other conditions being left unchanged, it is possible to determine the magnitude of the role of the radiation in a duct. The variation of ϵ_s was carried out by coating the cable with flat black, thus producing a surface with an emissivity of 0.97. The factor

$$\frac{1}{\frac{1}{\epsilon_s} + \frac{1}{\epsilon_d} - 1}$$

is then changed from 0.54 to 0.90, that is, increased by 66 per cent.

The test described in the preceding section, "Single Conductor Cable in Duct Bank," was repeated with the black sheath, and in this manner sheath temperatures, for the same watts input, were obtained with the cable coated black as were obtained with the cable in its original condition. Results, obtained at identical loads and times for the two surface conditions, are shown in Table I. The duct was dry in these tests; hence the temperatures are higher than shown in Figure 6. It can be seen that, considering the differences in the respective starting temperatures, the increases in temperature are practically identical for the two different surfaces.

The results show that a substantial change in the radiation does not cause a measurable change of the sheath temperatures in the model setup. This conclusion, while reassuring from our particular standpoint, does not, however, prove that there is equally little change between sheath temperatures in the field and the model, in case the radiation resistance in the two is not the same. An estimate, based on equation 19, will provide this missing information for the steady-state condition.

Table I. Sheath Temperatures, Degrees Centigrade, for Different Sheath Surface Conditions

	Load = 4.5 Watts Per Foot		Load = 11.8 Watts Per Foot		Load = 18.9 Watts Per Foot	
Time, Hours	Plain Lead	Flat Black	Plain Lead	Flat Black	Plain Lead	Flat Black
0	17	20	35	37	63	62
1	33	35	59	60	84	82
2	33.5	36	60.5	61	86	85
3	34	37	60.5	62	87	85.5

Since equation 19 contains the radius a, the radiation resistance of the duct space in the model is 4.6 times that in the field, while the thermal resistance remains unchanged in a scale-reduced model. If the total heat flow is the same in both cases, the sheath temperature in the model, because of the higher radiation resistance, will be somewhat higher than in the field. It can be shown, however, that a very little increase, of the order of one to two degrees centigrade, is sufficient to satisfy the equations of heat flow in the two cases.

All data in equation 19, with the exception of T_d, are known. The latter was determined, at least approximately, by introducing a thermocouple into the duct containing the test cable and taking duct air temperatures. For a load of 11.8 watts per foot, T_d = 35 degrees centigrade (or 308 degrees Kelvin) was obtained, and it is probably correct to say that the same (or nearly the same) duct temperature exists in the field, too. With a cable diameter of three inches and T_s = 43 degrees centigrade = 316 degrees Kelvin, equation 19 yields for H_r in the field 2.2 watts per foot, which is about 20 per cent of the total heat. Neglecting convection (see the following), the balance of heat, namely 9.6 watts per foot is transferred by conduction.

The general equation for equilibrium conditions of temperature and heat flow in the duct is

$$H = A(T_s - T_d) + B(T_s^4 - T_d^4) \qquad (20)$$

where A and B are the conductances caused by heat conduction and radiation (the latter given by equation 19), and in the present case (for the field):

$$11.8 = 1.2\,(T_s - 308) + 2.2 \times 10^{-9} \times (T_s^4 - 9 \times 10^9)$$

and this equation is satisfied with T_s = 316 degrees Kelvin = 43 degrees centigrade. In the model, A remains the same, but B is reduced by a factor of 1/4.6. Hence, for the model:

$$11.8 = 1.2(T_s - 308) + 0.48 \times 10^{-9} \times (T_s^4 - 9 \times 10^9)$$

and it can be shown that a value T_s = 317.3 degrees Kelvin = 44.3 degrees centigrade satisfies this equation. This value is only 1.3 degrees centigrade higher than that in the field, and this difference is well within the reported deviation of 3 degrees centigrade. This conclusion is valid for wet ducts, which constitute the majority of existing ducts. For dry ducts the error caused by radiation is certainly larger.

Convection

A certain amount of heat is transferred across the duct space by means of free convection. There are empirical equations,[1,6] that permit approximate computations. H_c, the heat transferred per unit length by convection from a pipe to air, is given by

$$H_c = k a^{3/4} (T_s - T_d)^{5/4} \qquad (21)$$

where k = a constant depending on the ratio of cable radius to duct radius; for the present case, $k = 2.7 \times 10^3$ absolute units.

In order to check the influence of convection on the sheath temperature, the free convection normally active around the sheath was increased by forced convection. This was obtained by forcing nitrogen longitudinally through the duct. If V denotes the rate of flow of the nitrogen, ρ_N its density, c_N its specific heat, and ΔT the temperature differential along the duct, then the heat removed per unit time from the sheath by way of forced convection, H_{fc}, is given by

$$H_{fc} = V \rho_N c_N \Delta T \qquad (22)$$

V and ΔT were measured, and H_{fc} calculated from equation 22. The rate of flow, V, was adjusted so that H_{fc} equalled approximately twice the value of H_c (known from equation 21) times the length of the duct. The sheath temperatures measured before, during, and after applying the forced flow gave an indication of the influence of convection on the temperature distribution.

Table II shows the data obtained on two loads: 11.8 and 18.9 watts per foot,

Table II. Sheath Temperatures, T_s, for Different Conditions of Convection

	Load = 11.8 Watts Per Foot		Load = 18.9 Watts Per Foot	
	Free Convection Alone, 5 Watts	Forced Convection Superimposed, 8.5 Watts	Free Convection Alone, 8.5 Watts	Forced Convection Superimposed, 19 Watts
Before forced convection	59	—	84	—
During forced convection	—	59.5	—	83
After forced convection	60	—	83	—

with the duct dry. T_s for the two loads is 59 and 84 degrees centigrade; T_d is 37 and 51 degrees centigrade respectively.

It can be seen that the influence of a forced convection, amounting in terms of heat loss to about double that for free convection, is practically negligible. As before, in the case of radiation, this result refers to the model only and does not give specific information as to a divergence between field and model data caused by a possible difference in convection. This difference, however, can be estimated from equation 21.

Considering the medium load, 11.8 watts per foot, the value of H_c, the heat dissipated by way of convection, for the field and the model respectively, is 0.3 and 0.1 watt per foot, that is three and one per cent of the total. In contradistinction to radiation, which amounts to appreciable percentages of the total heat dissipated—without, however, affecting correct duplication of the field test by the model—convection amounts to only a small percentage of the total heat dissipated. The effect of this small amount, being reduced in a ratio of one to three in the model as compared with the field, has certainly no influence upon the duplication of the sheath temperatures.

Water in Ducts

As a last additional test, the question of the amount of water that is required to make a wet duct out of a dry duct was investigated. In comparing sheath temperatures shown in Table I (dry duct) with those shown for the model test in curve 2 of Figure 6 (wet duct), it can be seen that a dry duct results in sheath temperatures higher than those in a wet duct. It was important to find out how much water should be introduced in the model duct in order to approximate field conditions. From physical considerations it appeared that a certain minimum amount is required in order to establish a conducting path of water between the cable and the bottom of the duct wall and that further additions of water should have little effect. Table III gives the results of a test, referring to a load of 18.9 watts per foot, in which increasing amounts of water were added to the duct containing the test cable. It can be seen that for the model, small amounts of water (ten cubic centimeters) were sufficient to bring the temperature of the sheath from 83 degrees centigrade down to 65 degrees centigrade. It appears that ten cubic centimeters is sufficient to cause an appreciable drop in temperatures and that 50 cubic centimeters is sufficient to insure the formation of a complete conducting path along the length of the model duct and to bring the temperature level down to 60 degrees centigrade, which was the level as measured in the main test and also in the field. Further additions of water change the temperature only slightly. The equivalent amount of water present in a wet duct in the field is then at least $10 \times 21.2/15 = 14$ cubic centimeters per foot.

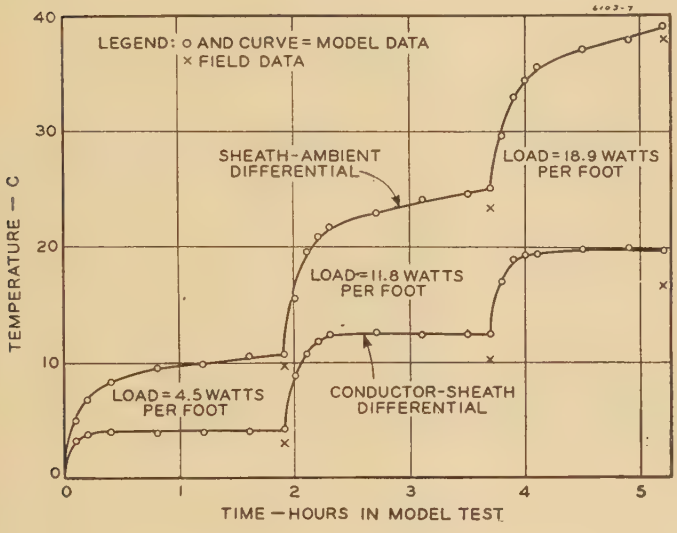

Figure 7. Temperature differentials between sheath and ambient, and conductor and sheath for a 3-conductor model cable

Installation and load schedule is the same as indicated in Figures 5 and 6. Field data for the conductor are equilibrium values

Model 3-Conductor Cable in Duct Bank

The tests described in the two preceding sections were carried out with a single-conductor cable, and accordingly conductor temperatures were not comparable with those in the field because the field tests involved 3-conductor cables. In order to fill this last gap in the research, it was necessary to have a model of the 3-conductor 350,000-circular-mil cable used in the field. Through the courtesy of Doctor R. J. Wiseman, the Okonite Callender Cable Company manufactured such a cable according to developed specifications.

The cable was constructed according to the following design. The conductor was number 8 American Wire Gauge wire having an over-all diameter of 0.147 inch, which is, as pointed out previously, 4.6 times less than the conductor of the high-voltage cable. One of the three conductors was a copper tube of an outside diameter of 0.156 inch and a wall thickness of 0.032 inch; the cross-sectional area of the tube was nearly identical with that of the stranded wire. The purpose of the tube was to accommodate the thermocouple for conductor temperature measurements. The insulation

Table III. Sheath Temperatures, Degrees Centigrade, for Increasing Amounts of Water in Duct

Load = 18.9 Watts Per Foot	
Amount of Water, Cubic Centimeters, in 15-Foot Duct Containing Test Cable	Sheath Temperature, Degrees Centigrade, of Test Cable
0	83
10	65.5
20	57 (?)
30	67
40	65.5
50	62
60	60
70	61
80	62
100	60.5
120	59
140	58
200	59.5

thickness was 0.31/4.6=0.068 in. The outermost layer was metallized paper. In order to compensate for the larger outside diameter of the tube, one layer of paper was omitted from its insulation. Fillers of suitable size and a binder tape made of 4-mil copper were used. (A copper tape of reduced thickness, say, 2-mil, is more advisable.) The lead sheath was 2/64 inch thick, and the over-all diameter obtained was 0.69 inch, which is close to the theoretically correct 0.68 inch, that is, 3.1/4.6.

The single-conductor cable used as test cable in the last test described (Figure 6) was then replaced by this model cable, and the same load cycle schedule applied, except that for the sake of simplification the duration of the cycles was not more than about two hours each. This was sufficient in this case, since the main interest of this test centered around the sheath-conductor temperature differential, and this reached its final value in about that time.

The results of this test are reproduced in Figure 7. Both sheath-to-ambient and conductor-to-sheath differentials are shown. The corresponding field data for the conductor refer to equilibrium values as obtained at the end of each load period.

While the sheath temperatures are in rather good agreement with those in the field, the discrepancy for the conductor-sheath differential is somewhat larger, up to three degrees centigrade. This difference is partly inherent, inasmuch as the insulation structure, and therefore the thermal resistivity, for a real and a model cable cannot be made strictly identical. Part of the difference, however, is caused by uncertainties and difficulties in the measurement of copper temperatures in the field (obtained from the electrical resistance of the conductor). A deviation of up to three degrees centigrade, nevertheless, is not objectionable from a practical standpoint.

In closing, a few remarks concerning end-effect are in order. Since these tests were carried out with the idea of later developing the method into a practical one, it was tried to keep it as simple as feasible; no attempt was made, therefore, to compensate for a possible end-effect. In order to ascertain whether or not an appreciable error is introduced on this account, the last test with the model cable was used also for the measurement of the magnitude of this effect. A thermocouple was inserted into the tube, about six inches inside the end walls of the box. At the end of the first load period, the end was cooler by one degree centigrade than the center; at the end of the second load, the end was warmer by two degrees centigrade than the center; and at the end of the third load, this difference increased to six degrees centigrade.

An approximate calculation shows that these differentials are not likely to lead to an appreciable error. From the dimensions of the cable and the thermal resistivity of copper, the thermal conductance of the three conductors from both ends to the center is found to be 0.0013 watt per degree centigrade. For the worst case (the third load) the heat that flows toward the center is only 0.008 watt. Even with the conservative estimate that this heat is dissipated along a length of, say, only one inch, for which the load is 1.6 watts, the error is only one-half per cent, and thus is negligible.

Conclusions

The present research shows that a reduced scale model installation can be used successfully for determining cable temperatures and hence maximum permissible loads, both normal and overload. Such an installation is meant to be used as a laboratory tool, just as any other measuring device. Its chief use probably will be found in cases of several cables in a duct bank, each cable having a different prescribed load schedule. By reproducing any desired cable and load combination in the model, a reliable answer to any specific problem can be obtained in a relatively short time.

References

1. Establishment of Cooling Curves of Welds by Means of Electrical Analogy, **Victor Paschkis.** *Welding Journal*, October 1943, page 462-s.

2. Operational Methods in Applied Mathematics (book), **H. S. Carslaw, J. C. Jaeger.** Clarendon Press, Oxford, England, 1941. Page 109.

3. Operational Methods in Applied Mathematics (book), **H. S. Carslaw, J. C. Jaeger.** Clarendon Press, Oxford, England, 1941. Page 128.

4. Current Rating of Cables for Transmission and Distribution, **S. Whitehead, E. E. Hutchings.** Institution of Electrical Engineers, London, England, volume 83, 1938, pages 551–2.

5. Tables of Functions (book), **E. Jahnke, F. Emde.** Dover Publications, New York, N. Y., 1943. Page 6.

6. Elements of Heat Transfer and Insulation (book), **Max Jakob, G. A. Hawkins.** John Wiley and Sons, Inc., New York, N. Y., 1942. Page 125.

7. Heat Transmission, **T. B. Drew, H. C. Hottel, W. H. McAdams.** *Transactions*, American Institute of Chemical Engineers, volume 32, 1936, page 271.

Shutdown Versus Hot-Spot Temperatures in Polyphase Induction Motors

Discussion of paper 46-58 by C. P. Potter and A. E. Frohardt, presented at the AIEE winter convention, New York, N. Y., January 21–25, 1946, and published in AIEE TRANSACTIONS, 1946, February section, pages 56–8.

B. M. Cain (General Electric Company, Lynn, Mass.): The authors have touched upon a very important point in connection with the relationship between observed temperatures and the temperature at the hottest spot. Others have reasoned, as did the authors, that ventilation has a marked effect on this relation, but this paper has gone much further by presenting the data to prove it.

There is another element of this problem which deserves recognition, namely, the effect of the size of the machine. I set out to study analytically the effect of machine size on the ratio of end winding temperature to hot spot temperature. To do this, I calculated the theoretical maximum temperature drop along the winding for double end ventilated induction motors from 1 to 250 horsepower, 1,800 rpm. The calculations were made by assuming that the stator copper and iron losses are dissipated uniformly along the entire length of the end windings. The calculations therefore will not apply to motors having radial ventilating ducts through the core. Figure 1 shows the calculated differences plotted versus horsepower. As might be expected, the temperature difference increases considerably with increased size of machine.

To compare the calculated results with tests, I took available data[1] and estimated average per cent temperature differences for different values of horsepower. The averages were estimated by plotting the test points versus horsepower and drawing a representative curve through the points. Three tests on motors having radial ventilating ducts were omitted since the calculated curve would not apply to this type of construction. If these observed differences bear any direct relation to the differences indicated by the calculations, the curves should have the same slope when plotted with double logarithmic scales. Figure 1 shows that the theoretical and observed curves do have nearly the same slope, thus confirming the assumption that size as well as ventilation has an important effect on the difference between the observed temperature and the hot spot temperature.

It is important to note that the temperature difference between end winding and hot spot increases with physical size and with motor speed because of the better ventilation with higher speed. However, since physical size is approximately proportional to horsepower divided by speed, the effect of speed tends to cancel so that temperature difference tends to increase directly with horsepower. For motors above about ten horsepower, this difference begins to be quite appreciable, so that if some other means of temperature measurement less sensitive to size and ventilation effects could be used, this would be very desirable.

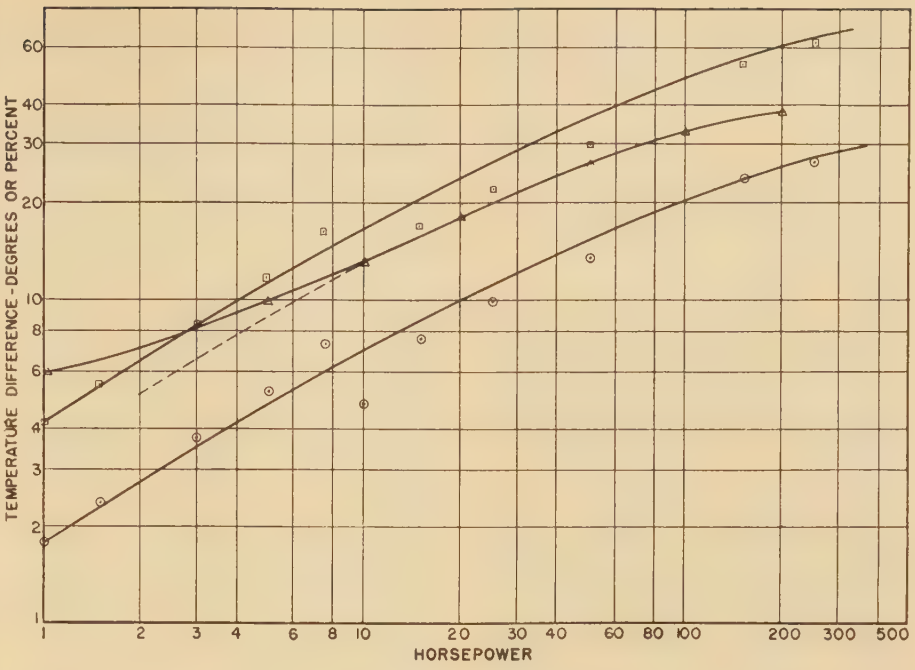

Figure 1. Temperature differences along windings plotted versus horsepower

⊡—Calculated theoretical maximum temperature difference in degrees between minimum end winding temperature and maximum hot-spot temperature

⊙—Calculated theoretical maximum temperature difference in degrees between minimum end winding temperature and average temperature of entire winding

△—Observed temperature difference in per cent between thermocouple on end winding and thermocouple at hottest spot[1,2]

With this point in mind, I have made the following comparison of rise by resistance and rise by thermocouple in per cent of hot spot for the tests which the authors have reported:

	Thermocouple (Per Cent)	Resistance* (Per Cent)
Totally enclosed	98.8%	100%
Protected	88.8%	89%
Protected	87.2%	92%
Normal open	84.0%	89%
Exaggerated open	79.2%	90%

*Rise by resistance was obtained by extrapolating the authors' curves along the same slope as the major portion of the curve.

Note that the rise by resistance is affected much less by differences in ventilation than the rise by thermocouple.

In further confirmation of the greater dependability of resistance measurement as an indication of hot spot temperature, note the following analysis of the data on open integral horsepower motors[1] covering a range from 5 to 250 horsepower:

	Number of Tests	Average Per Cent of Hot Spot	Standard Deviation
Thermocouple	17	79	10.0
Resistance	17	86	8.1

REFERENCES

1. INVESTIGATION OF HOT-SPOT TEMPERATURES IN INTEGRAL-HORSEPOWER MOTORS, L. E. Hildebrand, B. M. Cain, F. D. Phillips, W. R. Hough, J. G. Rosswog, C. P. Potter. AIEE TRANSACTIONS, volume 64, 1945, March section, pages 124–8.

2. INVESTIGATION OF HOT-SPOT TEMPERATURES IN FRACTIONAL-HORSEPOWER MOTORS, L. H. Hirsch, R. F. Munier, M. L. Schmidt, L. W. Wightman, F. S. Himebrook, T. C. Lloyd, O. G. Coffman, C. P. Potter. AIEE TRANSACTIONS, volume 64, 1945, March section, pages 128–36.

Die Cast Rotor Testing by Test Stator Method

Discussion and author's closure of paper 46-64 by P. H. Trickey, presented at the AIEE winter convention, New York, N. Y., January 21–25, 1946, and published in AIEE TRANSACTIONS, 1946, March section, pages 139–41.

L. C. Packer (Westinghouse Electric Corporation, Springfield, Mass.): I was very much interested in Trickey's paper. This method will check the rotor resistance, and thereby reject any rotors with high resistance caused by excessive porosity, variation in alloy, broken bars, and so forth. However, I would like to ask Trickey how he checks for broken bars as such. Rotors with a large number of bars would show a small increase in resistance with one or two broken bars which may be within the resistance limits. The small change in reactance may be caused by other changes and within normal limits, unless there is a large number of broken bars which may increase the resistance and reactance to values outside the limits set up. It is well known that broken bars cause noise.

P. H. Trickey: The test stator described in this paper will measure average resistance and will not pick out cores where only one

or two bars are open. If readings are taken with rotor in several different positions, bad cases of single phase in rotor, caused by cold molding, can be detected.

The Polyphase Commutator Regulator for Speed Control

Discussion of paper 46-59 by A. G. Conrad, F. E. Brooks, Jr., and R. G. Fellers, presented at the AIEE winter convention, New York, N. Y. January 21–25, 1946, and published in AIEE TRANSACTIONS, 1946, June section, pages 321–8.

Fred Baumann (General Electric Company, Schenectady, N. Y.): The analysis of the adjustable speed drive presented by the authors is both interesting and useful. The added complications sometimes involved in this form of drive, such as series and shunt power factor correcting transformers, have been eliminated to good advantage for the purpose of this analysis. The internal voltage of the wound rotor motor is assumed to be substantially constant. This condition together with a few other assumptions and the splitting of the secondary current I_2 into two components I_x and I_y have led to a very simple solution proved by tests on a small set.

While tests were taken on a small set, it usually is not economically feasible to use the polyphase commutator regulator for sets below several hundred horsepower. For smaller ratings, other forms of drives, such as Ward Leonard or the Schrage brush shifting motor have considerable advantage.

I thought that it would be interesting to comment on the Scherbius type of commutator regulator. The Scherbius machine, so-called because of its 3-phase compensation invented by Arthur Scherbius,* usually has both shunt and series interpole windings in addition to compensating windings. The compensating windings compensate for armature reaction. The series interpole windings perform their usual function of canceling the reactance voltage caused by current commutation. The shunt interpole windings produce a flux which introduces a speed voltage in the armature windings. This speed voltage cancels the transformer voltage under the brushes at one particular speed and partly cancels it at other speeds.

The transformer voltage is induced in the armature by the main field which is excited at slip frequency. The main field flux is proportional to the slip (neglecting impedance drops) and inversely proportional to the speed of the regulating machine. For a directly connected regulating machine, it therefore is evident that the shunt interpole flux necessary to cancel the transformer voltage under the brushes is approximately proportional to the square of the slip and inversely proportional to the square of the speed.

This condition necessarily limits the speed range or the size of machine which can be built economically. It has been found in practice that a slip frequency of about 20 cycles approaches the upper limit of slip. Above this slip, the necessary shunt interpoles become disproportionately large.

One of the best applications of the polyphase commutator regulator is its use in connection with large asynchronous frequency changers. The frequency changer set usually consists of a synchronous machine directly connected to a wound rotor induction machine, a polyphase commutator regulator, and an ohmic drop exciter. The secondary of the wound rotor machine is connected to the polyphase commutator regulator and the field of the regulator is connected to the ohmic drop exciter. Since the amount of frequency or speed regulation is usually small, the maximum slip frequency is low and the size of the commutator machines is small compared to the induction machine.

By means of this arrangement, a flexible tie between two power systems is obtained. The frequency of either system may vary and the active or reactive power can be fed in either direction. Frequency changers of the order of 25,000 kva using polyphase commutator regulators are in operation.

In general, the use of the polyphase commutator regulator for speed control on a-c systems should be considered particularly if the amount of power is large and the speed range is limited.

* United States patent 1,084,040, January 13, 1914.

The Short-Circuit Characteristics of D-C Generators

Discussion and author's closure of paper 46-66 by G. E. Frost, presented at the AIEE winter convention, New York, N. Y., January 21–25, 1946, and published in AIEE TRANSACTIONS, 1946, June section, pages 394–402.

A. M. Harrison and **B. Litman** (Westinghouse Electric Corporation, East Pittsburgh, Pa.): Frost has contributed some valuable information on calculation of short-circuit currents. We have compared the calculated results with test data we have obtained on both compensated and noncompensated machines and find that, with certain modifications to suit the characteristics of these machines, good agreement can be obtained.

Frost makes use of the oscillogram of Figure 8, to separate the armature and field leakage coefficients. In so doing, he assumes the field leakage coefficient to be 0.2, which yields an armature leakage coefficient of 0.67. It appears that these two coefficients should be roughly the same in magnitude, since approximately the same leakage path exists for either of these fluxes in comparison to the main field path available for these fluxes. If we assume 0.3 for the field leakage, we then obtain 0.37 for the armature leakage by using the same data from Figure 8, which gives values that are much closer together and hence more reasonable. The over-all apparent leakage coefficient then will be much smaller than the value of 1.0, which the author has assumed. It also is possible to calculate the over-all leakage coefficient from the peak field current and armature current at short circuit, based on the assumption of constant linkages in the shunt field circuit. This method gives an over-all leakage of 0.59 which, again, is much less than the author's assumed value.

In checking the author's equivalent electric circuit of Figure 9, we observe that the value of φ_{AL} is slightly larger than φ_A, which does not appear to be correct since φ_{AL} is just one of the two parallel current components into which φ_A is separated. φ_{AL} should be much smaller in comparison to φ_A, which would then give a more reasonable value for the armature leakage coefficient.

In order to obtain the proper peak short-circuit current from the formulas with this reduced value of leakage, it is necessary to assume a larger demagnetizing magnetomotive force from the armature at the short-circuit current (for example, a larger value of synchronous resistance R_e). The value of this demagnetizing magnetomotive force can be calculated from the peak field current and armature current at short circuit, and a value of 2.99 per unit is obtained.

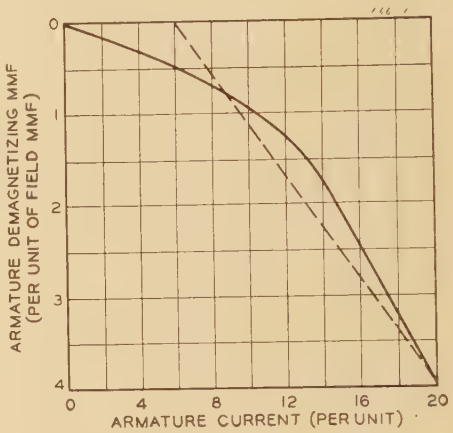

Figure 1. The reduction in main field flux versus armature current for a large compensated machine

This value is larger than would be expected by extrapolating the straight line curve of Figure 16 to the peak short-circuit current point, and indicates that, beyond the steady state short circuit point, the armature demagnetization begins to grow at a much larger rate. If we increase R_e sufficiently to make the straight line pass through this point, the formula for short-circuit current then will yield a value in agreement with test. We include an illustration of a curve (Figure 1), which is similar to the one shown in Figure 4 of the original paper, showing the reduction in main field flux versus armature current for a large compensated machine. This machine was rated 1,000 kw 1,500 volts, and the curve is carried out to 20 times full load current, which is the value of peak short-circuit current. It is apparent from this curve that armature demagnetization effects do not become important until we go well beyond full load to a point approximately six times full load. Using a straight line through this point to represent the synchronous resistance, we again can obtain good agreement with tests if we modify the formulas to use a value of

$I_1=6$, instead of $I_1=1$. Thus for peak short-circuit current, we have the formula

$$I_{a\ \text{peak}}=\frac{1+R_a+I_1R_e\dfrac{n}{1+n}}{R_a+R_x+R_e\dfrac{n}{1+n}}$$

Since this generator was compensated almost perfectly, we must look for other sources of armature demagnetization. One of the principal sources is the shifting of the neutral zone of commutation from under the center of the brushes, because of commutating pole saturation. At short circuit, we may assume that the current in the coils undergoing commutation, undergoes practically no change until the trailing edge of the brush is reached when it reverses abruptly in an arc. In fact, photographs of this machine under short circuit indicate that this arc extends beyond the trailing edge for quite some distance, and making calculations on the basis of the size of the arc, we can account for about 70 per cent of the experimentally observed demagnetizing magnetomotive force. The remainder probably is caused by such effects as commutating pole saturation, which also saturates part of the main field flux path in the frame yoke. This machine used a commutating pole of very large iron cross section so that good commutation was obtained even at currents of seven times full load. This fact explains why armature demagnetization effects do not become appreciable until we pass this load, and why such a large peak short-circuit current (20 times full load) is obtainable. The presence of these effects also would explain why, in the author's test machine, armature demagnetization began to rise more rapidly at currents beyond the steady state short-circuit value.

Thus it appears that test curves, such as shown in Figure 4, should be carried well beyond the steady state short-circuit point in order to obtain an average value of R_e, which is representative for currents as high as the peak short-circuit value.

T. M. Linville (General Electric Company, Schenectady, N. Y.): The paper is an important one, usefully defining the short-circuit performance of d-c machines in terms of simple factors. I welcome the opportunity to help evaluate the factors for practical use, particularly R_e' which determines the maximum short-circuit current.

Some additional light is thrown on the nature of R_e', as well as on the physical concept of the paper, by recognizing that experience with big machines shows that the peak current is obtained with the internal electromotive force of the machine substantially sustained. To make this clear, numerous tests (of circuit breakers), using large d-c machines for power, have shown that the typical value of peak transient field current i_f' ranges from two to three in per-unit terms, when short circuit occurs with negligible external resistance and with normal voltage on the machine. Therefore, if the internal armature voltage previous to short circuit is one per unit and the field flux linkages are $(1+n_f)$, where n_f is the leakage coefficient of the field circuit, the internal electromotive force immediately after short circuit must be at least $(1-2n_f)$. This result is apparent by equating the field linkages before short circuit $(1+n_f)$ to those after short circuit $(\rho+n_f)i_f'$, where $\rho i_f'$ is the linkages created by air gap flux. This latter term also is equal to per-unit armature electromotive force. With n_f equal to 0.10 to 0.15 by tests and calculations for these big machines, it is evident that the armature electromotive force is sustained at some 70 per cent of full voltage until the transient field current decreases appreciably. Therefore, the peak short-circuit current is expected to be 70 per cent of full voltage divided by the resistance of the armature circuit. It also is known from experience that the peak current with zero fault resistance falls far short of reaching a value equal to 70 per cent of full voltage divided by the resistance of the machine windings. Therefore, there evidently is another element of resistance on which R_e' depends in addition to those described in the paper.

This resistance is that of the brush contact, or more exactly that of the reactance voltage of the alternating current in the armature coils, which appears as a brush contact voltage. To show clearly what this resistance is and to give more understanding of the matter in general, an expression will be derived for the peak current and for R_e'.

The field linkages before short circuit are $(1+n_f)i_{fo}$, where i_{fo} is normal field current (equals one per unit). Immediately after short circuit, the field linkages are $(\rho+n_f)i_f'$, where ρ is the ratio of permeance for air gap flux after and before short circuit, respectively. Then the transient field current is

$$i_f'=\frac{1+n_f}{\rho+n_f}\ \text{per unit}$$

and the armature electromotive force is

$$e=i_f'\rho=\frac{(1+n_f)\rho}{\rho+n_f}\ \text{per unit}$$

Here it is interesting to note that in the original paper, i_f' for any sudden rise in armature current is determined by M, the coefficient of mutual inductance representing the shunt field voltage in per unit corresponding to one per-unit armature current change per second. This factor has been the stumbling block of all earlier attempts to determine short-circuit performance of d-c machines because M involves variable magnetic saturation. At normal loads there is very little magnetic coupling between the armature winding and the shunt field winding, that is, n_a is very large. On short circuit as the current rises, this coupling goes through a gyration, but under heavy overload current is low again. At least this condition is found in large machines because when short circuit occurs, while there is always a decrease in the exciting flux, there is a very large increase in cross flux and armature leakage flux, such that flux densities above the intrinsic saturation density for steel occur in the pole tips at both sides of the pole and in the armature teeth at both sides of the pole arc. Under these conditions, which hold for peak short circuit current, the permeance for the exciting flux is substantially linear again and is the fraction ρ of its value before short circuit. The coupling between the shunt field and armature windings is nearly zero, and the peak shunt field current and corresponding armature voltage are given by the foregoing equations.

If we let the resistance of the circuit be (r_w+r_b'), where r_w is the resistance of the machine windings and r_b' is the resistance of the brush contact, then the peak current on short circuit is

$$i_{sc}'=\frac{(1+n_f)\rho}{(r_w+r_b')(\rho+n_f)}\ \text{per unit}$$

Be sure to notice that for small values of n_f this current becomes nearly independent of ρ. If i_{sc}' is set equal to equation 1 of the paper, it is evident that

$$R_e'=\frac{(r_w+r_b')(\rho+n_f)}{(1+n_f)\rho-(r_w+r_b')(\rho+n_f)}$$

It is essential that the size of the factor r_b' be recognized. It is very large because the sudden rise of peak current on short circuit leaves the machine substantially without the benefit of commutating pole flux until after peak current is reached. Therefore, the reactance voltage of commutation appears as a voltage drop at the brushes of each polarity so that

$$r_b'>\frac{2E_R}{V}\ \text{per unit}$$

where

E_R = reactance voltage of an armature coil at rated full load conditions
V = rated voltage

The symbol for "greater than" is used because without benefit of commutating pole flux, commutation is delayed to occur at the trailing side of the brushes with increased rate of change of current in the commutating coils and, therefore, increased reactance voltage. If the energy at the brushes is taken to be equal to the energy of the magnetic field of the commutating coils, it can be shown that

$$r_b'=\frac{E_Rb}{V}\ \text{per unit}$$

where

b = the number of commutator bars covered by the width of the brush

Always a large factor in determining the peak current, r_b' can be evaluated by calculating the reactance voltage, and even in many cases by inspection of the machine. By the latter method, it is determined roughly by counting the turns of the armature and commutating field windings and calculating the net difference in their ampere turns, then using the following formula

$$E_R=6.38\times AT\times G\times L\times S\times 10^{-8}$$

where

AT = net ampere turns
G = measured length of the commutating pole air gap and nonmagnetic shims
L = measured length of the core
S = revolutions per second times the measured periphery of the armature

A third method, based on the relation between E_R, rated kilowatts, and armature diameter, uses the formula

$$E_R=c_r\times\text{kilowatts/armature diameter}$$

where

c_r is a reactance voltage coefficient which does not vary widely for large machines of normal design

Then

$$r_b' = \frac{E_R b}{V} = \frac{c_r \cdot \text{kilowatts} \cdot b}{Vd} = \frac{c_r I_a b}{1{,}000 d} \text{ per unit}$$

where

I_a = rated full load current
d = armature diameter

For large machines c_r averages 0.12, so that

$$r_b' = 1.2 I_a b \, 10^{-4}/d \text{ per unit}$$

In conclusion, it is possible to evaluate R_e' with useful accuracy in accordance with these comments (taking 0.25 as an average value of ρ). If a machine has a usually high field leakage coefficient n_f, an accurate value for ρ may be essential. In this way it is possible to calculate not only the peak current, but also the corresponding armature electromotive force. This fact is of the greatest importance not only for circuit breaker protection, but for determining the maximum mechanical stresses.

P. N. Ross (Westinghouse Electric Corporation, East Pittsburgh, Pa.): In contrast with the large amount of data available on the short-circuit characteristics of a-c generators and simplified methods for the calculation of short-circuit currents in a-c systems, there has been little similar information available for those concerned with the design of d-c systems. The reason is that the field of application of d-c generators has been relatively limited, and the need for such information, therefore, has not been as great. Nevertheless, in certain industrial, marine, and railway applications, when d-c systems are used, information on the short-circuit characteristics of d-c generators is often necessary. This fact is particularly true in regard to the proper application of protective devices. Frost's analysis of the problem should prove very valuable in the design of such systems. By reducing the problem to one involving the determination and use of relatively few constants directly analogous to those which are well known in connection with a-c generator short-circuit calculations, the author has made it possible to perform similar calculations on d-c systems in a practicable manner.

In connection with the analogy between d-c and a-c machine constants, such as transient resistance, transient reactance, synchronous resistance, and synchronous reactance discussed in the paper, it is worthwhile to point out the following additional manner by which these quantities are interrelated. It is well known that when an a-c generator is short circuited, the suddenly induced increment in field current is always equal to the product of $(X_d - X_d')$ and the sudden increment in armature current. Thus, for zero fault impedance, the increment in field current is $(X_d - X_d')/X_d'$ for a fault from no load. A similar constant of proportionality can be shown to exist between the increment in field current and the increment in armature current for a short circuit on a d-c generator. Referring to Appendix I of the paper, the increment in field current under short circuit can be found by subtracting the initial value of $(1+R_a)$ from the peak value given by equation 20d. The results show that the field current increases by an amount equal to $(R_s - R_e')$ times the increase in armature current. This result also checks, of course, with the relationship between the short-circuit and open-circuit transient time constants as given in the paper.

The constant of proportionality between the field and armature currents is also of value in connection with the determination of the over-all apparent field leakage coefficient defined in the paper as n. Thus it can be shown that neglecting armature resistance the apparent field leakage coefficient is equal to the reciprocal of the per unit increment in field current. By this method a value of n equal to 0.5 was derived from the test curves in Figure 1. This value differs considerably from that derived by the author from Figure 8, but agrees very closely with that which can be derived, using the author's method and assumptions, from the peak field and armature currents in Figure 1.

In view of the foregoing, it is apparent that the leakage coefficient is not actually a constant, but varies somewhat with armature and field currents caused by variations in armature tooth and pole face saturation. Similarly, R_e also must vary with armature current as well as field current, since it is dependent to some extent on the value of n. Some idea of the variation of R_e with field current can be obtained from Figure 4, where for 1.5 per unit field current, R_e is seen to be equal to 0.375 per unit, based on the assumptions used in deriving equation 3 of Appendix I, namely, no saturation in the magnetic circuit of the field. Actually, it is evident that considerable saturation exists in the field circuit at 1.5 per unit field current. Consequently, it appears probable that instead of representing the no load saturation curve by an equation of the form

$$e_t = i_f$$

this equation should be changed to the form

$$e_t = i_f - s(i_f - 0.8)$$

as a closer approximation for values of field current above 0.8 per unit, where s is a factor taking into account saturation of the field circuit.

Then, if R_e is defined by an equation of the form

$$e_t = i_f - s(i_f - 0.8) - R_e(i_a - i_1) - R_a i_a$$

the variations in the over-all leakage coefficient n with armature and field current can be avoided.

Because of the close check between the calculated and test values of the transient current for external resistance, as shown in Figure 15 of the paper, it seems reasonable to assume that the method of analysis and the nature of the phenomena taking place in the machine, as described in the paper, is substantially correct, despite the variations in R_e and n which have been noted. However, while representation of the machine by a transient resistance, which will enable the effective determination of the output current and voltage under transient conditions, is sufficient for most purposes, it is essential that the actual phenomena in the machine acting to limit the current definitely be known when calculating the short-circuit torques. The latter are determined by the actual net air gap flux and the armature current. If the short-circuit current is limited primarily by the reduction in air gap flux, as described in the paper, the torque will be much smaller than if the current is limited by other phenomena, such as brush drop, wherein the air gap flux is reduced only by the magnitude of field leakage.

G. E. Frost: The author is indebted to Linville, Ross, Harrison and Litman for generally adding valuable contributions to the analysis of the paper and to the theory of d-c short circuits.

The principal difficulty relative to the analysis of the paper appears to reside in explaining the low peak short-circuit current as compared with the peak field current. The following factors have been mentioned in explanation of this effect:

1. Apparent armature leakage flux caused by flux between the poles, which is a result of shifting of the neutral axis from coincidence with the pole structure, to some other position determined by the unsymmetrical saturation existing at the pole faces. This analysis is one way to visualize the leakage flux considered in the paper.

2. Apparent armature resistance voltage drop caused by the abnormal increase in reactance voltage (or brush contact drop) associated with saturation of the commutating poles. Linville describes this phenomenon in detail.

3. An apparently greater value of R_e because of the apparent brush shift associated with sparking at the brushes. Harrison and Litman describe this effect.

In addition, very great variations in the leakage flux coefficient, R_e, or armature resistance, as armature and field current vary, might lead to an apparent inconsistency in the values of peak armature and field current.

The analysis by Ross offers an opportunity conveniently to determine the effective values of the apparent leakage flux coefficient and R_e at the instant of peak current. Using the relation he derives for the ratio of increment in armature current to increment in field current, the following equation may be written:

$$\Delta i_f = (R_s - R_e')\,\Delta i_a = [(R_e + R_a] - \left(R_e \frac{n}{1+n} + R_a\right)) \Delta i_a R_e/(1+n) \qquad (1)$$

From equations 19 and 20, Appendix I, the following additional equation may be derived:

$$n = (1/\Delta i_a - R_a)\,\Delta i_a/\Delta i_f \qquad (2)$$

From Figure 1, the value of Δi_a is about 5.7 per unit for the machine described, and the value of Δi_f is about 1.7 per unit. From equation 2, the value of n is then 0.52 for 0.02 per unit armature resistance, and 0.42 for 0.05 per unit armature resistance (a value based on the effective machine resistance during steady state short circuit). Substituting in equation 1, the value of R_e then is 0.45 at 0.02 per unit armature resistance, and 0.42 at 0.05 per unit armature resistance.

It should be noted, however, that the values calculated above represent only the values at the instant of peak short-circuit current and do not indicate necessarily the

effective average values during the short-circuit interval. In the machine considered in the paper, for example, the value of R_e based on Figure 4 (an average value representing armature currents from one per unit to the peak value at one per unit field current) is 0.29 rather than 0.42 to 0.45, as calculated from the peak short-circuit current values. In fact, the slopes of the curves shown in Figure 4, corresponding to $i_f=1$ and $i_f=1.5$ at zero air gap flux, correspond to a value of R_e of about 0.44, a value in close agreement with the foregoing calculated values. Inasmuch as the curves of Figure 4 are based on the test points actually indicated in the figure, this accuracy may be accidental.

From the computed constants, it might appear that peak torque can be determined without reference to an exact value of effective armature resistance. It can be demonstrated that this fact is not true by computing air gap flux from equation 3, Appendix I (deleting the term $R_a i_a$ and substituting $i_1=1$) to give

$$E_{\text{air gap}}=i_f-R_e(i_a-1) \qquad (3)$$

Inasmuch as per unit torque is equal to per unit air gap flux times per unit armature current,

$$T=i_a(i_f-R_e(i_a-1)) \qquad (4)$$

Substituting the value of R_m, as determined by equations 1 and 2,

$$T=R_a i_a^2 \qquad (5)$$

Hence the value of peak torque necessarily involves a determination of effective armature resistance.

At the time the paper was written, the author did not appreciate the significance of the steady state value of armature current as an indication of the effective armature resistance. From Figure 4, it is evident that when i_f equals zero a residual flux of about 0.07 per unit exists, and the corresponding armature current flow is about 1.4 per unit. This value corresponds to an apparent resistance of 0.05 per unit, or about 2.5 times the value measured at standstill. Inasmuch as no significant sparking took place at this time (and hence commutation was on the neutral axis), this value of armature resistance substantiates Linville's analysis that the increment of armature resistance associated with brush contact drop (or reactance voltage) is substantial.

If the value of apparent armature resistance is assumed constant at the value of 0.05 per unit, and the apparent leakage flux coefficient is calculated from Figure 8 as described in the paper, the value of air gap voltage prior to opening the circuit is 0.18 per unit, and the apparent armature leakage flux coefficient is 0.42. The corresponding total leakage flux coefficient is 0.70, a value consistent with that calculated for the instant of peak short-circuit current, but sufficiently different therefrom to indicate a definite change in this coefficient with armature and field current.

In view of the preceding analysis, together with the analyses of the discussions, it is evident that the machine constants given in the paper should be revised.

On the basis of available information the following characteristics seem most probable:

	At the Instant of Peak Current	Average During Entire Short Circuit
R_e	0.4	0.3
n	0.4	0.7
R_a	0.05	0.05

The suggestion of Harrison and Litman that apparent brush shift, as a result of sparking, accounts for a substantial proportion of the armature demagnetizing effect in compensated machines requires that the statements of the paper be modified accordingly. Under such circumstances, perfect compensation would not prevent armature demagnetizing effects.

The value of φ_a (Figure 9) should be 1.38.

Linville's use of the permeance factor ρ offers an attractive alternate method of considering the performance of a d-c machine under short circuit. This method not only conforms more closely to physical realities in avoiding the purely artificial representation of armature demagnetizing effect as a magnetomotive force, but also offers an opportunity to evaluate peak current without the machine constants that have proved such a source of difficulty in connection with the analysis of the paper. It should be noted, however, that this method does not permit a direct analogy with the a-c machine and necessarily requires solution of a nonlinear differential equation to determine the complete short-circuit current curves.

Pressure-Arc-Interruption Circuit Breakers for 400-Cycle Aircraft Electric-Power System

Discussion of paper 46-13 by B. O. Austin, presented at the AIEE winter convention, New York, N. Y., January 21–25, 1946, and published in AIEE TRANSACTIONS, 1946, February section, pages 58–60.

D. W. Exner (Westinghouse Electric Corporation, Lima, Ohio): The design of a successful main circuit breaker for the 208 Y/120-volt 3-phase 400-cycle aircraft power system is an important factor in the growth of this system. Its designers are to be commended for having combined the important features of adequate rupturing capacity, high operating speed, confined arc space, and reasonable operating coil current values in a structure weighing only five pounds.

One feature which should not be overlooked is the comparatively low operating coil current required. This factor is one which is important to the user and to the designer of associated control equipment, because it reduces the demand from auxiliary control power sources and permits a reduction in size of contacts on control relays, thereby reducing the size and weight of the relays and associated wiring. Reduced maintenance of relay contacts will result.

The oscillogram shows that the arc is extinguished at the end of the first half cycle. A large number of tests at both low and high currents has shown that this performance is characteristic of the device. As a result the contact erosion is very low and maintenance is reduced.

Basic Design Principles for A-C Electric-Power Systems in Large Military Aircraft

Discussion and author's closure of paper 46-3 by C. K. Chappuis and Leonard M. Olmsted, presented at the AIEE winter convention, New York, N. Y., January 21–25, 1946, and published in AIEE TRANSACTIONS, 1946, January section, pages 12–17.

G. E. Sylvester (Consolidated Vultee Aircraft Corporation, Fort Worth, Tex.): During the past few years there has been considerable discussion among aircraft electrical engineers on the subject of the most suitable aircraft electric system, and many honest opinions exist. At the outset it must be realized that each particular airplane presents peculiar problems as to size, location, and character of loads, service ceiling, and other factors.

When operation of aircraft at high altitudes became a military necessity in1939 and 1940, aircraft electric equipment available at that time was wholly inadequate. Test flights on airplanes, such as the B-24 Liberator, had to be terminated after only a few hours flying at high altitude because of brush failures on generators. As airplanes increased in size in order to carry loads for longer distances, continued operation at high altitudes became necessary.

For extremely long range airplanes, the weight empty (total gross weight of the aircraft minus payload, fuel, oil, ammunition, and crew) becomes extremely critical. For example, the amount of fuel and oil required to carry a pound of weight empty may be as much as two pounds; that is, one pound of weight empty actually represents three pounds of gross weight.

Since structural limitations and flight conditions define a maximum gross weight of the airplane, it is necessary to give all possible consideration to obtaining the least possible weight for the entire aircraft including structure and equipment. It has been estimated that approximately 2,000 pounds could be saved by the use of a high voltage electric system on a large aircraft over what would be required if the conventional 28-volt d-c system were used. This weight is saved in all components, generators, distribution wiring, and load equipment. For example, a 16-horsepower motor geared down to an output speed of 3,600-rpm weighs 22.75 pounds.

If large aircraft are successful in operation, the maintenance troubles associated with present day d-c equipment must be reduced. By the use of squirrel cage induction motors, commutator and brush problems have been eliminated. When it is realized that there may be over 100 electric motors on a single aircraft, it is easy to see

that maintenance problems are reduced materially.

The foregoing is only a brief elaboration as viewed by the aircraft electrical engineer on the discussion presented in the first part of the excellent paper prepared by the authors. The paper covers thoroughly the design objectives that are set forth to attain as foolproof an aircraft electric system as possible. The modern large military aircraft is dependent wholly upon the proper functioning of the electric system for its operation and accomplishment of its mission. The authors have presented those factors believed necessary to achieve the objective of a lightweight serviceable foolproof aircraft electric system.

J. C. Cunningham (Westinghouse Electric Corporation, East Pittsburgh, Pa.): This record of system design criteria will be very helpful to engineers planning new aircraft power systems, and also to those who will be associated with the particular system described in the examples. In the interest of further clarification, there are several comments and questions I would like to address to the authors.

It is stated that a particular system provides a minimum of 90-per-cent nominal voltage during motor starting. This minimum should provide adequate motor starting torque. I would like to ask whether it should be considered a specific design objective, and whether this voltage is adequate for satisfactory operation of other equipment, such as fluorescent lights, radio, radar, and control devices. Under normal circumstances, a locked rotor condition would only persist for a fraction of a second; but, as the authors mention in objective 6, the system is expected to withstand this condition for 30 seconds in the event of jamming of equipment caused by ice or mechanical damage.

In the list of typical alternator characteristics, the negative sequence reactance is shown equal to the direct axis subtransient reactance. I would like to ask whether these two reactances actually were measured and found equal or merely were assumed to be equal, as is the case in most turbo-alternators or those which have connected dampers. At least one alternator design for aircraft service has nonconnected dampers, with the result that the negative sequence reactance is greater than the direct axis subtransient reactance. An inequality also will be found between the positive sequence resistance and either the negative or zero sequence resistance. In these cases the magnetic fields set up by negative- and zero-sequence currents produce losses in the damper windings and pole faces.

A net saving in weight and greater flexibility in alternator control have been achieved by the use of a latched control relay between the fault protective relays and the breaker and exciter trip circuits by comparison with direct tripping, as described in the paper.

Will the authors clarify the term "any section of a feeder" in design objective 2, as compared with "load area" in objective 3.

Note that objectives 4 and 8, though desirable, are not accomplished fully by the system illustrated in Figure 1.

Objective 10 does not appear necessary if requirements 2 and 3 are satisfied.

The observation that "there is little advantage in backing up the d-c system" should be examined for any given system, in view of the critical nature of some of the devices which may be supplied from the d-c system.

Leonard M. Olmsted: Preparation of this paper was started nearly two years ago. Even as the manuscript was being written, progress in the design of several experimental aircraft required further consideration of the principles and occasional modification of the original thoughts. The authors finally concluded that, if this paper ever were to be offered to AIEE, it would be necessary to establish a deadline and record the basic principles as of that date. Modifications have continued and the a-c electric power systems finally installed in aircraft undoubtedly will differ in some respects from the information in this paper.

Motor starting depends upon the torque characteristics of the driven device, as well as of the motor itself. Generally speaking, however, if the motor terminal voltage can be maintained within ten per cent of nominal, there is little need for concern over the ability of the motor to start and come up to speed. Present indications are that a system designed to maintain 90 per cent voltage during the starting of all frequently started motors will maintain voltage suitable for lights, radio, radar, and control devices at the more centrally located load busses which supply these devices. The few large motors, for which it may be difficult to maintain this starting voltage, operate infrequently and justify special consideration to assure starting and coming up to speed at lower voltages. Lights, radio, and radar may be affected somewhat, but it is believed that infrequent disturbances can be tolerated, particularly as they are not likely to occur during combat. The objectives presented in this paper apply to the ability of the system to protect itself against fault and retain the ability to carry load. At the time they were written, comparatively little specific information was available regarding the operating characteristics of the electric equipment. This information has become available during the development of designs following the predetermined objectives and eventually might be added to them when it becomes desirable to start a new design project.

Cunningham's comments in regard to alternator characteristics, alternator control, and d-c system storage batteries are typical of considerations requiring modification of the original objectives as actual design progresses. The paper records the information available at the time it was written, but such improvements are being incorporated in the aircraft electric systems wherever they are found applicable.

By "load area" in objective 3, the authors intended to include both a second fault in any section of a feeder and a first fault in an adjacent section. Either of the feeders running downward from the central bus shown in Figure 1 illustrates this reasoning. Assuming that the first fault occurs in and isolates one of the sections of the 4-circuit multiple portion of the feeder, without damaging any fuses except those required to isolate the faulted section as required by objective 2, then a second fault occurring subsequently in the load area, either in a second section of the 4-circuit multiple portion or in the adjoining 3-circuit multiple portion, must clear at its own fuses without isolating either of the load busses. The requirements for this second fault are relaxed to the extent that other fuses may be damaged, but not blown.

These same circuits shown in Figure 1 serve to illustrate discussions of the comment that objections 4 and 8 are not accomplished fully. While a fault on any of the busses at the extreme ends of the 3-circuit multiple portions will isolate only the faulted bus, it is true that a fault on the busses where the 3-circuit multiple portions originate can isolate both the faulted bus and the load bus at the extreme end. This condition is not too objectionable, however, as the additional load dropped by the extreme end bus either is of secondary importance or its operation depends upon a control device energized by the faulted bus. Objective 10 is covered adequately by objectives 2 and 3 for a system of the type shown in Figure 1, but was written to apply to other arrangements considered earlier in the development of the a-c system for aircraft.

Sylvester's discussion assists materially in presenting the basic reasons for the a-c electric power system. He makes it quite clear that weight economy in itself is accomplished by the use of higher voltages, either direct or alternating, but that the a-c system affords the additional advantage of eliminating such problems as brush and commuter trouble, which have necessitated frequent maintenance on present d-c equipment.

Effect of Altitude on Ventilation and Rating of Aircraft Electric Machines

Discussion and author's closure of paper 46-15 by Cyril G. Veinott, presented at the AIEE winter convention, New York, N. Y., January 21–25, 1946, and published in AIEE TRANSACTIONS, 1946, February section, pages 84–90.

H. J. Braun (Westinghouse Electric Corporation, Lima, Ohio): Figures 8 and 10, which show the effect of altitude on the temperature rise of fan-cooled and enclosed aircraft motors, were derived from tests on several motors rated at approximately one-third to three-quarters horsepower. Heat dissipation by conduction was minimized by using heat insulation material to isolate the motor from surrounding objects.

Whether or not tests on a particular motor check these curves depends on a combination of many things. For instance, how was the motor mounted, what is the ratio of heat dissipated by radiation to that dissipated by either free or forced connection, is the motor fundamentally an iron or copper motor, and how easily is heat conducted and transferred inside the motor? Any of these variables and many others may alter the final test results.

Heat conduction is not affected appreciably by altitude. If a motor is mounted to a good conducting surface whose temperature would tend to follow the ambient temperature, the heat dissipated by conduction would increase with temperature rise. Thus at altitude the over-all temperature rise would be less than that shown on the curves.

In very small fan-cooled motors, a large percentage of the heat is dissipated by radiation. Such motors would tend to have characteristics somewhere between those shown for fan-cooled motors and those shown for enclosed motors.

Fan-cooled motors having larger horsepower ratings than those from which these curves were derived would dissipate less heat by radiation and, therefore, would depart from the curves shown. The temperature rise would tend to be higher at altitude.

The temperature rise curve of any particular motor depends upon the design characteristics built into it and the particular set of conditions which surround it when it is tested.

These curves were derived as an aid to judgment. In general, they have proved satisfactory for motors of $1^1/_2$ horsepower and below. Each individual new design must be checked and its application made with consideration of the design's limitations.

D. E. Fritz (Westinghouse Electric Corporation, Lima, Ohio): In making use of the principles outlined in this and Veinott's previous paper,[1] closer co-operation between the air frame manufacturer and the electric accessory manufacturer than now exists will be necessary. In the design of an aircraft electric system, blast tube characteristics are as important as load charts, if the generator is to meet requirements at the least cost in weight.

Another factor that has not been sufficiently emphasized in specifications is the duty cycle of the machine with respect to altitude cycles. It has been general to state that for specifications for electric apparatus the machines shall operate satisfactorily at altitudes between sea level and 50,000 feet, although, as Vienott shows, unless the sea level temperature rise is relatively low, insulation life at 50,000 feet is considerably less than insulation life at 40,000 feet. In present airplanes, operation above 30,000 feet occurs infrequently, and for relatively short periods. However, this is not recognized in the specifications. If a manufacturer interprets the specifications literally, he must design a much heavier machine than would be necessary if he followed his experience as to actual requirements.

This premise is supported by the fact that in the past few years military specifications for aircraft electric apparatus have specified altitudes, first of 30,000 feet, then 40,000 feet, and now 50,000 feet, with no increase in allowable weight. Manufacturers have made great weight savings by increasing the sea level operating temperatures of the machines. Yet, each time they increased the temperature rise of the machines, they were deviating farther from the literal requirements of the specifications, and reducing the high altitude life of the machines. It has been believed generally that the development of high temperature insulations would result in aircraft machines with higher output per pound. Unless a designer is familiar with the principles outlined in Veinott's paper, machines designed to use these high temperature insulations to obtain low weight are likely to have high sea level temperature rises, so that the temperatures at altitude may exceed the safe limits of high temperature insulation, since, as Vienott shows, an increase in sea level temperature rise is multiplied when the machine operates at altitude.

It is hoped that this problem will be recognized by both manufacturers and users of aircraft electric equipment, and that eventually the constants of the blast tubes and the factors of time-altitude cycles, will be considered fully. The result will be aircraft electric apparatus that will be much more satisfactory, without unnecessary weight.

REFERENCE

1. BLAST-TUBE COOLING FOR AIRCRAFT GENERATORS, Cyril G. Veinott. AIEE TRANSACTIONS, volume 63, 1944, July section, pages 520–5.

Cyril G. Veinott: Braun's comments reflect the experience of a designer of aircraft motors. Fritz points out that the present tendency in writing specifications is to ask for more than the service actually requires, whereas electric equipment manufacturers tend to build to meet the requirements of the service, rather than meeting specifications. The author concurs with Fritz in the hope that manufacturers and users of aircraft electric equipment will follow a more realistic engineering approach in the specification, design, and application of electric machines for aircraft service.

Application of the Betatron to Practical Radiography

Discussion of paper 46-54 by J. P. Girard and G. D. Adams, presented at the AIEE winter convention, New York, N. Y., January 21–25, 1946, and published in AIEE TRANSACTIONS, 1946, May section, pages 241–6.

G. W. Dunlap (General Electric Company, Schenectady, N. Y.): The authors of this paper have done a service to the Institute by bringing to its attention the important implications of the betatron. A great amount of development work on this device was carried on during the war under security restrictions, and the results only recently have begun to appear in print. In addition to this paper and those listed in the bibliography, a description of a 100-million-volt betatron or induction accelerator recently was published,[1] and an important improvement has been suggested.[2]

The paper indicates that a 20-million-volt machine is the optimum size for two of the three present applications. This conclusion is open to question. It would appear more reasonable that the proper voltage level should be selected to fit the specific application, rather than that a compromise be effected between the requirements of two such different applications as industrial radiography and medical therapy.

For example, in the field of radiography, the requirements are maximum penetration, maximum intensity, and maximum coverage. Figure 10 of the paper shows that there is little change in penetration above 5 or 6 million volts. While intensity varies exponentially with energy as stated, there is no doubt that comparable intensities can be produced by a machine of lower voltage than 20 million volts. In a smaller machine, higher frequencies present no insurmountable problem, and even liquid cooling can be included with an over-all saving in weight.

It is on coverage, the third requirement, however, that a lower voltage machine has the greatest advantage. As the authors state, the useful X-ray beam emerges as a cone. The angle of this cone varies inversely with energy as follows:

Millions of Volts	Cone Angle in Degrees
2	90
10	22
20	9
100	2

It will be seen from this tabulation that in order to obtain the same coverage with a 20-million-volt machine as with, for example, a 10-million-volt machine, it would be necessary to place the object approximately 2.4 times as far away from the source. Since a point source of radiant energy is provided by this equipment, the well-known inverse square law holds, so that for equal coverage at a given intensity the rated intensity of the 20-million-volt machine would have to be 2.4 squared, or 5.8 times that of the 10-million volt machine. This amount, then, partially offsets the energy advantage of the 20-million-volt machine, even at a fixed frequency, and, with an increase in frequency for the smaller machine, the entire operational advantage of the 20-million-volt machine disappears.

In the field of medical therapy, the requirements are quite different. The most important consideration is the so-called depth dose relationship (reference 10 of the original paper). It is indicated that the depth dose relation is improving with increased energy as far as studies have been made. Therefore, it is quite probable that for medical therapy a machine of considerably higher energy than 20-million volts will be desirable; in fact, up to 50-million volts appears to be practical and advantageous.

The third application for betatrons, apparent at the present time, is in the field of nuclear research. Here it has been found that very important nuclear reactions can be produced in the energy range of 50 to 100 million volts, and a session of the recent American Physical Society meeting in New York was devoted to a description of some of these reactions. Some of these results have been reported,[3] which include the artificial production of mesons, as well as other very arousing reactions. It is interesting to observe that very many important studies are being made with the existing 100-million-volt betatron,[1] and there appears to be a wide field, which can be explored during the time that developments are progressing, for the production of higher energies.

In summarizing, one then might predict that the betatron will find its optimum use in at least three different sizes to meet the specific needs of the applications involved.

References

1. A 100-Million Volt Induction Electron Accelerator, W. F. Westendorp, E. E. Charlton. *Journal of Applied Physics*, volume 16, number 10, October 1945, pages 581–93.

2. The Use of Direct Current in Induction Electron Accelerators, W. F. Westendrop. *Journal of Applied Physics*, volume 16, number 11, November 1945, pages 657–60.

3. Marcel Schein, G. S. Klaiber, A. J. Hartzler, D. C. Baldwin. *Bulletin*, American Physical Society, volume 21, number 1, January 24, 1946.

A Tunable Rejection Filter

Discussion and author's closure of paper 46-23 by R. C. Taylor, presented at the AIEE winter convention, New York, N. Y., January 21–25, 1946, and published in AIEE TRANSACTIONS, 1946, May section, pages 263–7.

A. R. D'Heedene (Bell Telephone Laboratories, Inc., New York, N. Y.): The filter described by Taylor has considerable merit in its simplicity and in that it can be tuned readily to reject any particular frequency over a wide band.

A point of considerable interest is the relation of the configuration of this filter to so-called conventional filter theory. By a consideration of general filter theory, it can be shown that Taylor's configuration is a special case of one type of filter design.

The term "conventional filter theory" is subject to several definitions. It is true, as the author states, that the usual type of filter is designed to use only reactance. In this type of filter, resistance is objectionable. However, the filter designer need not be restricted to circuits using only reactances. There are, in general, two types of filters. One type provides discrimination by the reflection of energy back to the generator, while the other type provides discrimination by the absorption of energy.* The filter described in the paper is a particular case of the type that absorbs energy.

The general configuration for filters of the type described is a bridge circuit, the conjugate branches of which contain networks having inverse impedances. As an illustration consider a bridge-type circuit with high pass filters in each branch. Let these filters be terminated by matched loads at the far end. In one pair of opposite branches, the filters are to be midseries terminated, while in the other and conjugate pair of branches they are to be midshunt terminated. Since the filters are terminated by matching impedances, their input impedances will equal their image impedances. Finally, since the midseries image impedance is the inverse of the midshunt image impedance, the inverse impedance condition is satisfied.

A consideration of these impedances explains the performance of the bridge circuit. Above the cutoff frequency in the pass band of the high pass filters, both of the branches will have resistive impedances. Hence the bridge circuit will absorb frequencies in the pass band of the high pass filters. Similarly, below the cutoff, in the attenuating region of the high pass filter, the impedance of the midseries terminated filter will be a negative reactance while the impedance of the midshunt terminated filter will be a positive reactance. Hence the bridge circuit will transmit freely at frequencies attenuated by the high pass filters. The resulting bridge circuit constitutes a low pass filter in which the energy at frequencies above the cutoff is absorbed.

An interesting feature of this type of structure is that it can be designed to provide a constant resistance at all frequencies.

The circuit described by Taylor may be considered a particular case of this general structure with the arms of the bridge containing band pass filters of a single branch. The terminating loads are provided entirely by coil dissipation. The band width of such structures will be inversely proportional to Q.

* See United States patents 1,724,987 and 2,043,345.

R. C. Taylor: D'Heedene's discussion of the two general types of filters is good, and properly classifies the rejection filter described in the paper as an absorption-type, where the absorption takes place in the incidental dissipation of the coils and capacitors. It is not necessary to consider the bridge arms as inverse networks or as filter image impedances, since the sufficient condition for a rejection filter is balance of the bridge. For instance, if a variable coil or variable capacitor is substituted for the series resonant arm, a narrow rejection band can be realized although, of course, not as narrow as that obtained with inverse networks.

A New Crystal Channel Filter for Broad Band Carrier Systems

Discussion of paper 46-26 by E. S. Willis, presented at the AIEE winter convention, New York, N. Y., January 21–25, 1946, and published in AIEE TRANSACTIONS, 1946, March section, pages 134–8.

V. F. D'Agostino (Western Electric Company, Kearny, N. J.): It might prove of interest to supplement Mr. Willis' paper with a brief glimpse of the effect this new filter had on the Western Electric Company's manufacturing operations.

The mechanical design of the new filter offered a considerable number of advantages over the old type. To begin with, the fundamental structure, including the container, was used as the basis for a standardization program in which Western Electric and Bell Laboratories engineers collaborated. This program was designed to reduce the variety of structures and piece parts and to simplify operations. Recognizing the manufacturing problems associated with the production of 25,000 such filters per year, Mr. Willis effected further economies by reducing the variety of coils required on all 12 filters to a single type having one inductance value. With a view toward using power-driven nut and screw drivers, the varieties of nuts and screw heads were reduced to three types, corresponding to three different assembly positions on our production line. Moreover, all process assembly and wiring operations were consolidated, as were all process electrical adjusting and testing, enabling the use of a straightforward line of progressive assembly and testing.

The use of sealed crystal units and the change to air-core coils permitted the assembly and wiring of the new filter outside the air-conditioned room previously required. Moreover, the crystal containers gave added protection to the quartz plates during assembly and wiring operations.

While these measures afforded inestimable relief during the war effort, they are proving to be almost equal in importance now in the face of the demands for communication equipment brought on by the reconversion period.

R. W. Chestnut (Bell Telephone Laboratories, Inc., New York, N. Y.): This paper by Mr. Willis brings to us information of another very important milestone reached in the progress toward better and cheaper filters which began over 30 years ago. In the design of this filter, it seems to me that Mr. Willis for the first time has taken full advantage of the high precision and the high stability which is inherent in quartz. I am sure that his paper will be of interest to all who have to do with the design and use of quartz crystal band filters and perhaps of other types of filters also. The filter is already in extensive commercial use on important long-distance telephone communications circuits and its performance seems to be very good.

Application of the Ohm and Mho Principles to Protective Relays

Discussion and author's closure of paper 46-38 by A. R. van C. Warrington, presented at the AIEE winter convention, New York, N. Y., January 21–25, 1946, and published in AIEE TRANSACTIONS, 1946, June section, pages 378–86.

W. R. Brownlee (The Commonwealth and Southern Corporation, Jackson, Mich.): The combinations of voltage and current, which can be used on the multipole induction cylinder elements as outlined by the author, give promise of even broader coverage of the transmission line relay protection field.

Limitations of the mho units on shorter lines are readily apparent, and for these the author recommends the reactance relay, but suggests "applications to lines not subject to power swing conditions...." It is believed that this restriction well could be removed, since the shorter lines naturally result in more restricted relay zones and, therefore, less sensitivity to power swings if the starting unit of the reactance relay had a characteristic similar to the mho unit. With the polyphase starting unit used with present reactance relays, the mho characteristic is achieved only on 3-phase faults (and load current). Accordingly, the response of the relay for phase-to-phase faults and the degree to which the system voltage is collapsed varies over such a range that the relay must be made $1^1/_2$ to 2 times as sensitive

to 3-phase load current as would be necessary with mho type units. It is hoped that further developments will make it possible to take full advantage of the characteristics of reactance relays for shorter lines.

One caution is desirable in considering the use of biased circle characteristics (Figure 7 of the paper) and memory action of the first zone of the relay, both of which may cause false tripping in the presence of load current if the potential supply is removed suddenly. The principal disadvantage encountered in early distance relay applications was that of incorrect tripping caused by the corrosion of potential transformer secondary fuses, loose fuse clips, and so forth. Since these conditions produce a very low voltage (but not zero voltage) on one of the relays, false tripping is inevitable unless a valuable part of the distance relay characteristic is sacrificed. Accordingly, several companies have replaced all secondary fuses supplying distance relays with 2-pole or 3-pole air circuit breakers, which are more reliable than fuses in the first place, and which open all three phases of the potential supply at once. False tripping thus is avoided if the relays themselves will not trip when all three phases of the potential supply circuit are opened suddenly.

The use of auxiliary relays responding to the time sequence between operations of different impedance zones has its limitations in preventing incorrect operations on power swings, particularly since these are not smooth, but are influenced by oscillations between generators on the same side of a long system tie line. Where a carrier current channel is used, the line may be made practically immune to swings which do not result in actual out-of-step conditions. A number of system stability analyses have shown that slight restrictions in coverage of zone 1 of back-up distance relays will prevent false operation, but that many swing conditions would result in tripping by zone 2 of the back-up relays. Since primary dependence is placed on the carrier current tripping for internal faults (and on bus protection for bus faults), zone 2 may be made inoperative when the carrier current protection is in service, either by normally disconnecting these elements and cutting them in service with the same switch which cuts out carrier current tripping, or by a simple auxiliary relay to block zone 2 tripping in the absence of a carrier current signal.

Eric T. B. Gross (Illinois Institute of Technology, Chicago, Ill.): Looking back some 25 years, when the first impedance relays appeared on the market, it is apparent that we have made great progress in the art of designing distance relays to fit any characteristic desired—ohm or mho, impedance or reactance, and combinations of arbitrary choice. We have learned to apply the distance relays in the field of systems protection and to take care of all the faults involving more than one conductor of the 3-phase circuits. If we recall that on the average 20 per cent of all faults are of the kind mentioned (involving more than one conductor), we can say proudly that we cover 100 per cent of these faults where distance protection is in use. However, what about the remaining 80 per cent of all faults, the single line-to-ground faults?

Here, we do not seem to have been equally successful; as a matter of fact, distance relays have been applied for the protection against single line-to-ground faults in but a few systems. In other words, our high powered schemes of distance protection, though extremely efficient, only apply to the minority of faults, and we still are using the old idea of inverse time relays to protect against the faults which occur most frequently. It is somewhat puzzling that most of the money is spent for the protection involving about 20 per cent of all faults, and only a small amount to cover the remaining 80 per cent which are the single line-to-ground faults. Would it not be wise to distribute the money in a different way?

Both the types of distance relays required and the theory about their proper external connections to instrument transformers have been developed and are available. Perhaps the next 25 years will bring us the practical applications of these developments, and with them the solution to the whole problem of distance protection.

A. R. van C. Warrington: The author thanks Brownlee and Doctor Gross for their interesting discussions. Brownlee pointed out that the application of the reactance relay could be extended in the direction of longer lines if the starting unit were modified to be a pure mho unit. This is true but not necessary, however, because there is already a more than adequate overlap of the ohm and mho type distance relays (see Figure 1 of this discussion). Furthermore, the advantages of the mho unit have been shown in the paper to be such as to make it more desirable to extend the application of the mho unit to shorter lines rather than apply the (reactance) ohm unit to longer lines.

Brownlee called attention to the tendency of the mho relay to trip on load current if the secondary potential supply fails. All distance relays tend to trip if the potential supplied to the relay is reduced accidentally to a value which, in relation to the load current, represents an ohmic value within the setting of the unit. It generally is considered preferable to connect distance relay potential circuits around the fuses directly to the potential transformer circuits.

Where fuses are used, the potential with one blown fuse will be normal across one phase pair and half normal across the other two, and the mho relay will trip on a load current of four amperes if the ohmic setting is above $115/2\sqrt{3}\times 1/4 = 8.3$ ohms phase to neutral. The memory action does not affect this condition, but an offset mho unit will trip on a lower value of current or ohmic setting because of its additional torque caused by current alone. Brownlee advocates the use of circuit breakers instead of fuses. This is a very good solution if the circuit breakers have suitably interlocked contacts in the trip circuit. The only other solution known to the author is to use instantaneous overcurrent units in series with the distance relays, as has been done for many years. This practice, of course, is only possible where the fault current is always above load current.

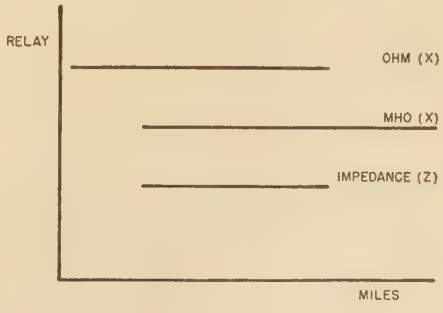

Figure 1

Where the power swing is so severe that the impedance presented to the relay enters the second zone mho circle, it is customary to use a blinder ohm unit to limit the tripping to the fault zone. Brownlee pointed out that, where carrier blocking is used, the second zone time-step can be eliminated because the carrier tripping extends to the end of the section, and this may be done by the same switch that cuts out carrier tripping. In the first zone the distance trip operates, backed up by the carrier trip. In the end zone of the section, tripping is by carrier with second zone time trip as back-up. Any tripping on external faults is done by the time delay distance steps if the breaker in the next section does not trip instantaneously.

Doctor Gross says that phase relaying has made great strides in speed and selectivity, whereas ground relaying is still in the time-overcurrent era, although most faults are ground faults. It is true that no ground relay unit corresponding to the mho unit has been developed yet, but the standard reactance distance relay can be used just as successfully for ground faults as for phase faults, and, of course, good protection against all faults can be secured by the addition of carrier. For some unknown reason, however, very few companies use distance relays for ground faults. They are used widely abroad, the same relays normally being connected for phase faults and switched to ground fault connections on single-phase ground faults only. The Kansas Gas and Electric Company is the outstanding user of complete phase and ground distance protection in the United States.

Air-borne Radar for Navigation and Obstacle Detection

Discussion of paper 46-48 by R. C. Jensen and R. A. Arnett, presented at the AIEE winter convention, New York, N. Y., January 21–25, 1946, and published in AIEE TRANSACTIONS, 1946, May section, pages 307–13.

L. V. Berkner (Carnegie Institution of Washington, Washington, D. C.): In this discussion I should like to emphasize four points to aid in assessment of the future of air-borne radar.

In the field of navigation, observation on a single fixed target or radar beacon can establish uniquely the position and movement of an aircraft in space. Other types of navigational devices do not provide this absolute information as precisely or as quickly from a single point. A radar obser-

vation on a single point is all the information needed to establish any ground track or flight path.

To utilize radar information efficiently and effectively, a computer is required. With a computer, automatic flight over any predetermined track within horizon range of the radar beacon or reference point is entirely feasible. Air-traffic control problems certainly can be simplified by radar. Problems of air spacing, stacking, and close landing order can be solved to a greater extent than heretofore with radar methods. Crowding and channelization of air traffic can be eased when ground tracks need not be confined to narrow channels as at present.

Radar differs from ordinary vision or from beaconry by providing exact range. There is a tendency to believe that a television picture would be ideal. I believe, in contrast, that carefully computed and presented desired information ultimately will prove the more important, for radar provides more than simple vision.

It is not essential that an airplane carry a high powered radar to get all possible radar information. Radar information can be relayed to an airplane equipped with a lightweight radar receiver, making available the selected output of one or more powerful radars strategically located on the ground or in other aircraft. Figure 1 demonstrates the possibilities in this regard. When receiving such a picture, simple radar beacons on the airplanes can serve to locate uniquely the plane itself or other aircraft on its map.

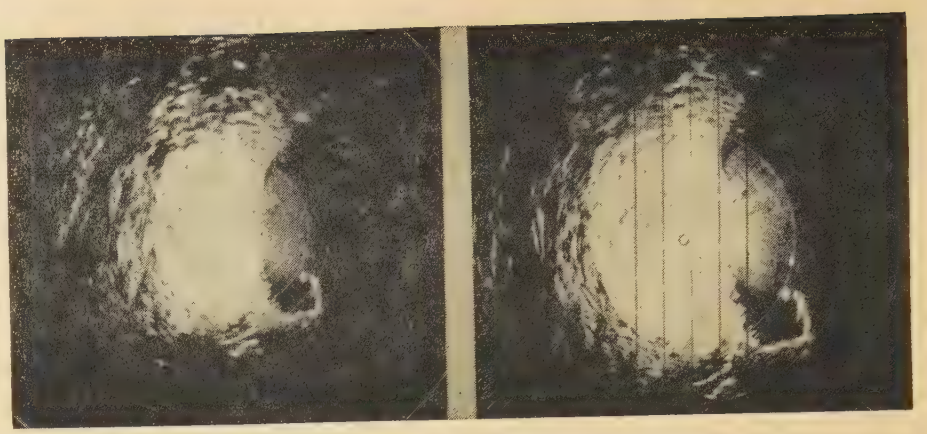

Figure 1. Simultaneous photographs of a PPI (plan-position indicator) scan before relay of radar information at 100-mile range (left) and after relay of radar information at 80-mile range (right)

Note direct comparison of shipping and other targets showing no loss in relay link transmission

Co-ordinated Electric Drive for a Rubber Calender Train

Discussion and authors' closure of paper 46-56 by K. W. John, G. W. Knapp, and W. A. Mosteller, presented at the AIEE winter convention, New York, N. Y., January 21–25, 1946, and published in AIEE TRANSACTIONS, 1946, March section, pages 128–34.

John Grotzinger (Goodyear Tire and Rubber Company, Akron, Ohio): As an electrical engineer connected with the rubber industry, I am very much gratified to see an important co-ordinated rubber mill drive made the subject of a paper, and I want to congratulate the authors for performing a very fine job. Unlike the steel and paper industries which have similar electrical problems, that are discussed freely by their engineers to the great benefit of the industries named, we in the rubber industry have worked behind closed doors too long. I hope that this paper will "break the ice" and be the forerunner of other application papers in the near future.

I readily agree that the calender train described has many advantages over one in which the auxiliaries are driven mechanically from the calender proper. The whole plan concerning the selection and grouping of drives and automatic features controlling acceleration and deceleration, the control of tension, as well as arrangement of centralized and local operator's control stations, is well chosen and entirely practical. However, these advantages only will be realized if a maintained demand for the product makes possible continuous production at high speed. Comparatively few rubber mills enjoy these favorable conditions. I do not mean to say that the train described cannot be started and stopped easily, where frequent changes of specifications make this necessary, but rather that the actual hourly or daily production will be very much lower than optimum production unless uninterrupted speed can be maintained over protracted periods.

The industry is not entirely of one opinion on the relative merits of coating the fabric simultaneously on both sides on a 4-roll calender, or coating it successively on one side and then on the other on a train of two 3-roll calenders. However, a 2-calender train, incorporating all the essential features outlined in this paper, could be arranged without serious difficulties.

I would like comments from the authors on the following points:

1. Details on the screw-down motors and control.
2. Is the control of gauge of the coated fabric manual or automatic?
3. What is the coasting distance, measured on the surface of the calender roll, when making an emergency stop with the calender running idle at a speed of 60 yards per minute?

V. O. Johnson (United States Rubber Company, New York, N. Y.): In the design of complex control equipment such as this drive, the designer always has the choice of several alternate systems. I have noted that one of these alternates is the possibility of using booster control to regulate tension in the central auxiliaries group of the calender train. The system described in the paper makes use of field control for this purpose. There are several advantages to using booster control accompanied by some increased cost. Tension in a fabric is proportional to the torque it exerts on a constant diameter roll, and hence is proportional to the product of armature current and flux in the driving motor. Constant tension thus is attained by holding constant armature current and flux. By using booster control, armature current regulation is obtained without altering the field excitation. With field control it is necessary, in one instance, to compensate for the change in flux at low speed by regulating at a different value of armature current from that at top speed. Continuously running boosters will maintain tension in the fabric for short shutdown periods. With field control, armature voltage is removed from the motors at shutdown.

Another point where an alternate design might be considered is in the entry auxiliaries. There, in place of regulating the reel motor armature current to maintain tension between the reel and the pull rolls, the pull rolls motor armature current might be regulated. Since the pull rolls have a constant diameter and the motor a constant field excitation, the regulation problem is simplified somewhat. Although the pull rolls' speed is controlled by the position of the festoon, the control of tension can be attained through automatic adjustment of the reel speed. IR drop compensation to maintain the reel motor generated electromotive force accurately proportional to the surface speed of the fabric would not be required.

These remarks are meant, if possible, to contribute some ideas to this control system which is already rich in clever applications of the latest knowledge of electric control possibilities. The authors have given a great deal of thought to the design of this control with special emphasis on its application to the needs of the rubber calender operator, his safety, and the protection of the machine. For that reason, the authors are to be congratulated on this fine paper.

K. W. John, G. W. Knapp, and W. A. Mosteller: As Grotzinger has pointed out, the benefits of this equipment can be realized to the fullest measure, only if continuous production at high speed is required. However, electric drives with comparable control are being used on calenders making all kinds of products at various speeds, with substantial improvements in the performance achieved. The flexibility of operation and ease with which new arrangements can be made, that are inherent in this type of drive, are outstanding performance features when making a multiplicity of products.

A drive of this type, consisting of an entry let-off, two 3-roll calenders in tandem, and a delivery windup, has been in operation for approximately two years. It serves many purposes in one of the smaller rubber proc-

essing plants, and it has made a fine record.

In answer to Grotzinger's specific questions, we wish to offer the following:

1. The screw-down motors may be operated individually or in pairs at the choice of the operator by push button control. When operated in pairs, the motors are tied together by a selsyn circuit.

2. Gauge control is manual, with indicating instruments provided for the operator, showing the gauge of both the top and bottom coatings on the right side and left side of the fabric.

3. When making an emergency stop with the calender running idle at a speed of 70 yards per minute, the stopping distance is calculated to be 45 inches, without the effect of friction included. In a short time, tests will be made to verify this calculation.

Boosters may be used, as pointed out by Johnson, to simplify the control for the central auxiliaries. Actually, the resulting simplification is not of material advantage, and the first cost is higher. His remarks regarding an alternative design for the entry auxiliaries are very interesting. Such a system was not considered by the authors in designing the present equipment and first consideration indicates that it might have considerable merit. In our opinion, before it should be applied, the complete electromechanical system should be studied for its stability characteristics, to make sure that there is nothing in it which would have a tendency to produce hunting.

Technique of Electrical and Hydraulic Testing of Hydroelectric Units

Discussion and authors' closure of paper 46-70 by G. D. Floyd and J. J. Traill, presented at the AIEE winter convention, New York, N. Y., January 21–25, 1946, and published in AIEE TRANSACTIONS, 1946, March section, pages 163–9.

H. R. Sills (Canadian General Electric Company, Ltd., Peterborough, Ontario, Canada): Mr. Floyd, surprisingly, has omitted from his paper an item on which he is well qualified to write, that is, temperature tests. For some reason, it is customary to take loss tests at a number of points from zero to over full load and from zero to over rated voltage, and work up the efficiency over this range even though the losses at part ratings can be approximated closely from those at rated conditions. It is also customary to take rated voltage (saturated) reactances and rated current (unsaturated) reactances. Yet, it is not customary to take zero and part load temperature tests, though these data cannot be estimated, and such tests can be made with a small increase in the total time required for the test. In the majority of cases, there is a net saving in time, for in practice, it is usually necessary to resort to considerable tap changing and system shuffling to approximate rated load conditions. This rearranging can be avoided if several runs are made at available conditions, and rated load conditions interpolated from these curves. This procedure should be an accepted method in the test code.

Figure 1 is a record of a test made at zero, three-quarter, and full load on the stator, but a considerable overload on the field as the station voltage was high. The temperatures are plotted against the square of the load as the curves are essentially straight lines on this base. Some variation in voltage at rated kilovolt-amperes does not affect the stator temperature appreciably, but does make an appreciable difference in the field temperatures. However, when the field temperatures are charted against the square of the rated excitation, it is an easy matter to pick off the temperature rise at rated load.

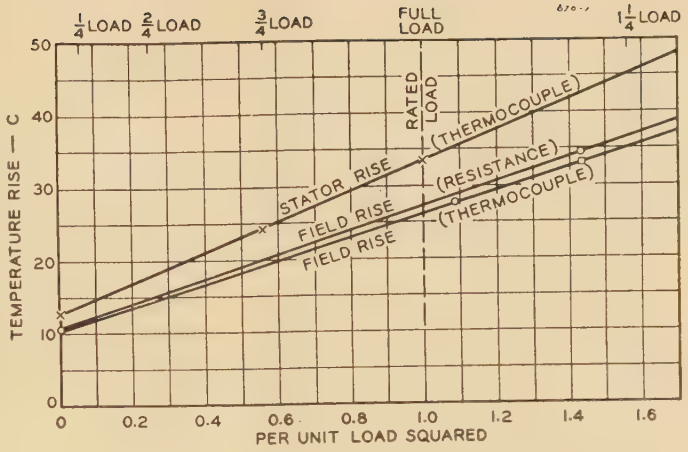

Figure 1. Sustained temperature rises of a 15,000-kva 0.9-power factor 150-rpm 12,000-volt generator at zero, three-quarter, and full load (tests made at 12,800 volts and plotted against a base of per unit rated kva squared for the stator, and per unit rated excitation for the rotor)

This curve is always of use. Any increase in temperatures caused by fouling of the machine can be followed readily at its operating load, and so provision for load adjustment or cleaning may be made in ample time.

It also is desirable to take the temperature over the whole heating period for each incremental increase in load, as this record gives the thermal time constant of the machine, which may vary from 15 minutes to an hour, depending upon the losses, mass, and ventilating characteristics of the machine. The temperature of a machine at any time after a sudden increase in load is approximately

$$T = T_2 - (T_2 - T_1)\epsilon^{-t/\tau_T}$$

where

T_2 = sustained temperature of the increased load (from Figure 1)

T_1 = sustained temperature of the initial load (from Figure 1)

τ_T = thermal time constant

t = time in same base as the time constant

$\epsilon = 2.718$

These data are often of value in calculating permissible overloads from various base loads.

Figure 2 shows the temperature rise of a machine taken during a zero, three-quarter, and full load heat run, and the method of determining the thermal time constant.

Another time factor that should be determined is the rate of temperature rise of an enclosed machine with the cooling water shut off, so that the operator may know the safe time that the machine may be operated without cooling water.

The same data should be secured on the bearings with the water shut off. These data are defined best as a rate of rise rather than a time constant, because failure occurs before a stable condition is reached.

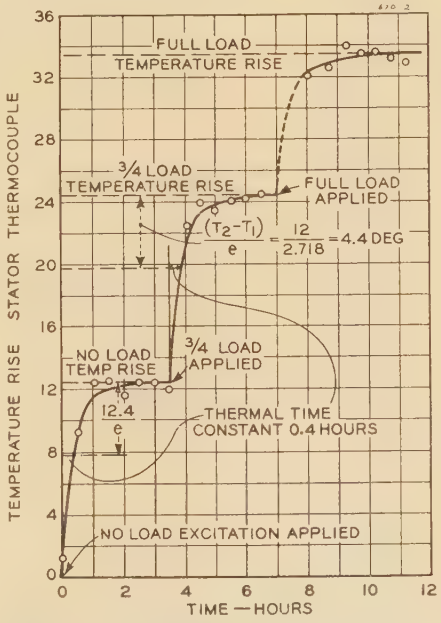

Figure 2. Test temperature rise readings of a 15,000-kva 0.9-power factor 150-rpm 12,000-volt generator at zero, three-quarter, and full load plotted against time (shows method of obtaining the thermal time constant)

G. D. Floyd and J. J. Traill: Mr. Sills has raised a point of some importance regarding the temperature test. This test is made almost universally by loading the unit under test on the system. System conditions usually must be taken as found. As a result interpolation later becomes necessary, and the interpolated data may not have a sound basis. If the actual temperature rise is approaching the guarantee, as many elements of inaccuracy as possible should be removed. Although the result obtained by the method suggested by Sills also is interpolated, it has a sound basis and should be considered when a revision of the test code is made. The method has been used on acceptance tests of two units purchased by the commission, the results from one of which have been used as an illustration in Sills' discussion. Use of this method of testing in the future will determine its suitability. It would appear to be very suitable for the enclosed water-cooled type of generator. The only objection that appears is that a test made in this manner usually would take more time than the standard test.

Amplifying the suggestion in the paper that it is desirable to widen the scope of the tests as much as possible, an example is submitted of a case where the additional information gained thereby later was found to be very valuable. In 1936, in tests of a group of 66,000-horsepower units in the Abitibi Canyon plant in Northern Ontario, as one of the units, separated electrically from the other units, was carrying a steam boiler load, the opportunity presented itself to make tests on this unit at speeds varying by ten per cent above and below normal. The information was of some use in connection with the plant at which the turbine then was installed, but later proved to be of great value. During the war, to meet an urgent need for power in the Niagara district, this particular unit was moved from the Canyon where the head is 240 feet to DeCew Falls where it is operating now under a head of 268 feet. The results of the variable speed tests proved to be very valuable in determining the operating characteristics of the unit under the higher head.

A B-H Curve Tracer for Magnetic-Recording Wire

Discussion and authors' closure of paper 46-30 by T. H. Long and G. D. McMullen, presented at the AIEE winter convention, New York, N. Y., January 21–25, 1946, and published in AIEE TRANSACTIONS, 1946, March section, pages 146–9.

H. A. Leedy (nonmember; Armour Research Foundation, Chicago, Ill.): It has been very gratifying to learn about the development of an instrument of the type described by Long for measuring the magnetic properties of recording wire. The Armour Research Foundation especially is interested in such an instrument because in recent weeks a set of specifications on recording wire has been drawn up by a committee formed from a group of industrial organizations working with the foundation on magnetic recording. Such an instrument appears to be suitable for determining whether or not a given wire meets the magnetic specifications.

We at the foundation have developed a 10-kilocycle hysteresis loop tester, but this has been found somewhat unsatisfactory because of difficulties in correlating results obtained from this test unit with those obtained with a d-c permeammeter. This lack of correlation may be caused by an uneven flux distribution in the wire resulting from 10-kilocycle eddy currents.

Long and McMullen apparently have gone to a 200-cycle hysteresis loop tester to obtain a better correlation with d-c permeammeter measurements. I would like to ask the authors whether or not they have been able to correlate their results with those obtained from a d-c permeammeter.

In addition, since a 60-cycle frequency is so much more readily available than 200 cycles, I would like to ask the authors why, in the design of their test equipment, they did not use the readily available 60-cycle source. Obviously, this usage would mean lower voltages induced in the B coil and hence require greater amplification, but perhaps the authors have their reasons for using the 200-cycle frequency in addition to the above.

T. H. Long and **G. D. McMullen:** In the development of the B-H curve tracer, our first experiments were made at 60 cycles with a rather crude setup. Our conclusion from this test was that such equipment for 60-cycle operation would either be impractical or very difficult on account of hum.

Fortunately (or unfortunately), audio frequency was almost as readily available to us for this purpose as was 60 cycles, since we had access to a 75-watt power amplifier. It looked as though the job would be at least eight times as easy at 500 cycles as at 60 cycles.

A rather scattered 500-cycle equipment was experimented with and found to operate satisfactorily, but in order to get the maximum excitation we had to go to 200 cycles, evidently on account of eddy current loss in the magnetizing coil. This equipment then was built into a single unit with a few minor changes that had been indicated by experience.

We never experienced, at any time after establishing a ring sample calibration for the equipment, lack of reasonable correlation between hysteresis loop measurements and permeammeter measurements from other laboratories. For agreement to exist between measurements at different peak magnetizations, the coercivity force of the wire must be less than about 40 per cent of the lesser peak magnetizing force. The caption of Figure 4 in the advance copies of the paper was in error on this point since the right-hand loop almost certainly is not saturated.

In Table I of this discussion *Hci* denotes the intrinsic coercivity force, that is, the magnetic field strength required to reduce a saturated total induction to zero intrinsic induction. This is inevitably the coercive force read on a B-H curve tester if the balance control is set to produce a straight horizontal line with no sample in the detector coil.

Uneven Flux Distribution at 10 Kilocycles

It hardly seems possible that the correlation difficulty encountered at 10 kilocycles could be the result of that uneven flux distribution in 0.004-inch diameter stainless steel wire, caused by eddy current in the wire itself. In equation 5 of the appendix of the companion paper,[1] it is shown that for a long magnetic cylinder magnetized axially in a sinusoidal field the ratio of magnitudes of the 90-degree lagging component to the in phase component of flux is

$$(\text{ber } y_1 \text{ ber}' y_1 + \text{bei } y_1 \text{ bei}' y_1) \div (\text{ber } y_1 \text{ bei}' y_1 - \text{bei } y_1 \text{ ber}' y_1) \qquad (1)$$

in which y_1 is the product 0.713 times the cylinder radius in inches, times the square root of the quantity (permeability times frequency in cycles per second, divided by resistivity in microhms per centimeter cube); ber and bei are the Bessel functions defined by the series

$$\text{ber } y = 1 - y^4/2^2 4^2 + y^8/2^2 4^2 6^2 8^2 - \ldots.$$
$$\text{bei } y = y^2/2^2 - y^6/2^2 4^2 6^2 + \ldots.$$

and ber′ y and bei′ y are the first derivatives of those functions.

Such an equation, of course, assumes constant permeability, and a permanent magnet material in a saturating a-c field has a permeability that is anything but constant. It would seem, however, that an estimation of the maximum possible effect of eddy currents could be obtained by taking as the permeability the maximum value of what is called the differential permeability, by measuring the maximum slope of the saturated hysteresis loop in permeability units.

So, if we take the left hand hysteresis loop of Figure 3 of the present paper as representative of the maximum differential permeability encountered in stainless steel wire of good recording quality, we find that the maximum value of the differential permeability is about 40. It might be explained that the right hand loop of that figure is not representative of good wire, and that the maximum differential permeability of wire according to the new wire specification that Doctor Leedy refers to is around 10 to 20. The resistance of such wire is around 40 times that of annealed copper wire, so that the ratio of lagging to in phase flux should be the same as for a copper wire of the same diameter.

For a wire diameter of 0.004 inch and a frequency of 10 kilocycles, the value of y_1 will be around 0.1066. For values of $y_1 < 0.2$, equation 1 can be evaluated to about four significant figures by using the first term of each of the appropriate series, so that the ratio of the 90-degree lagging component to the in phase component is $y_1^2/8$. Evaluated, this is 0.00125 and 0.005 for $y_1 = 0.1$ and 0.2 respectively.

The ratio of the in phase component at the center to the in phase component at the surface is

$$(\text{ber } 0)/(\text{ber}^2 y_1 + \text{bei}^2 y_1)^{1/2}$$

Table I. Comparison of Magnetic Measurements

Sample Number	Hysteresis Loop Measurements by B-H Curve Tester: At 500 Oersteds Hci	Br	At 750 Oersteds Hci	Br	Permeammeter Measurements From Other Labs: At 500 Oersteds Hci	Br
287	295	1,860	325	1,860	325	1,800
295	319	540	412	970	350	400
330	200	2,480	210	2,480	240	2,100
331	190	3,180	195	3,180	220	2,900
332	190	2,640	205	2,640	225	2,300
333	205	2,710	208	2,710	235	2,200
433			235	2,180	236*	2,461

* Measured at 1,000 oersteds at Armour Research Foundation. This was undoubtedly a measurement on a different piece, but from the same spool of wire.

This term can be evaluated as the foregoing to equal

$(1-y_1^4/64)/(1+y_1^4/32)=1-3y_1^4/64$, when $y_1<0.2$

It should be understood, of course, that it is possible for eddy currents in other parts of the magnetic circuit to cause the flux through the coil to lag up to 45 degrees behind the magnetizing current in the coil.

Magnetizing Coil Design for 10 Kilocycles

When this project of magnetizing coil design was undertaken, it simply did not occur to us to think about it in terms of anything less than about 1,500 ampere turns per inch peak magnetizing force on a continuous basis. It is at least theoretically possible to obtain this magnetization at ten kilocycles without water cooling the coil, but rather awkward as a little calculation will show.

For instance, equation 6[2] can be written

$$2ma \backsimeq (144\ R_e/R_{dc}N^2)^{1/4} = 2(R_e/R_{dc})^{1/4}(3/N)^{1/2} \quad (2)$$

where

a = conductor thickness in inches
D = radial depth of copper in winding in inches
N = number of layers in winding
$m = 0.505(\mu f/\rho)^{1/2}$
f = frequency in cycles per second
μ = fictitious permeability (<1) to account for end effect
ρ = conductor resistance in microhms per centimeter cube
$R_e = R_{ac} - R_{dc}$, or the increase in resistance due to eddy currents caused by the axial field

Since $N=D/a$, this substitution can be made in equation 2 so that

$$2ma \backsimeq 2(R_e/R_{dc})^{1/4}(3a/D)^{1/2} \quad (3)$$

$$a = 11.8(R_e/R_{dc})^{1/2}\rho/\mu f D \qquad N>5 \quad (4)$$

When layer thickness is the independent variable, total losses are a minimum for $R_e/R_{dc}=0.33$ approximately. Then, assuming $D=1$, $\mu=1$ (this ignores end effect), $f=10{,}000$, and $\rho=2.0$, the layer thickness is found to be 0.00136 inch. Several of our approximations have contributed to making this value too small and the layer thickness should be at least 0.0015, but certainly less than 0.002 inch for minimum loss. Taking the former value and allowing 0.0003 inch for layer insulation, the radial depth of the winding will be 1.2 inches. A 670-turn spiral winding having one turn per layer of 0.0015-inch thick copper foil is assumed at this point as a possibly practical interpretation of the mathematics. Equation 2 does not take into account the extra eddy current loss at the ends of such a coil caused by radial field, but this loss will be substantially independent of layer thickness and so does not influence the problem, although it may burn up the coil.

The voltage across such a winding for any given peak magnetizing force and frequency almost will be independent of the length of the winding, but for simplicity let the coil length be assumed to be 3 inches and the inside diameter of the winding be 0.5 inch. Neglecting end effect, the inductance will be about 0.00633 henrys, and the reactance at 10 kilocycles will be 397 ohms. A peak excitation of 1,500 ampere turns per inch will require 4.73 rms amperes (still neglecting end effect), and the voltage across the winding will be 1,880 volts.

The only possibly practicable alternative to the 670-turn spiral coil would be something on the order of 1,000 (preferably many more) $\times$ 0.002-inch Litz wire, which simply was not available.

However, a practical coil for 500 cycles can be wound from 0.040-inch round wire, and the potential across such a coil at 1,500 ampere turns per inch will be around 250 volts. This makes it quite obvious why our thinking about high frequency stopped at 500 cycles.

References

1. A New Wire Recorder Head Design, T. H. Long. AIEE Transactions, volume 65, 1946, April section, pages 216–20.

2. Eddy-Current Resistance of Multilayer Coils, T. H. Long. AIEE Transactions, volume 64, 1945, October section, pages 712–18.

Signal and Noise Levels in Magnetic Tape Recording

Discussion and author's closure of paper 46-31 by D. E. Wooldridge, presented at the AIEE winter convention, New York, N. Y., January 21–25, 1946, and published in AIEE TRANSACTIONS, 1946, June section, pages 343–52.

R. E. Zenner (nonmember; Armour Research Foundation, Chicago, Ill.): We were very interested in the paper presented by Doctor Wooldridge, and we feel that this work represents a very excellent study on signal and noise levels in magnetic tape recording.

In any study of noise frequency distribution, the shape of the resulting curve may be affected by the band width of the equipment with which the data are taken. I should like to ask the author if he would discuss the band width characteristics of the equipment used for determining the noise frequency distribution curve.

Also, I should like to ask the author if he has made any study of the effects of changes in alloy composition or processing on the resulting noise level, and if so, what the results of this investigation have been.

D. E. Wooldridge: The noise frequency distribution measurements were made with an analyzer that passed a band of 20 cycles per second width at all measuring frequencies.

We have made noise measurements on tapes of various kinds. Changes in either composition or processing, in general, were found to change the noise level, but not the shape of the frequency distribution of noise. We were unable to establish any clear correlation between noise level changes and composition or processing changes.

A New Wire Recorder Head Design

Discussion and author's closure of paper 46-29 by T. H. Long, presented at the AIEE winter convention, New York, N. Y., January 21–25, 1946, and published in AIEE TRANSACTIONS, 1946, April section, pages 216–20.

D. E. Wiegand (Armour Research Foundation, Chicago, Ill.): The type of magnetic recording and reproducing heads developed in the early stages of the rebirth of the magnetic wire recorder at Armour Research Foundation approached ideal electrical and magnetic characteristics. They provided very close coupling between the recording medium and the energizing or pickup winding, and the structure of the magnetic pole pieces provided very thorough shielding around the recording medium. This type of head, however, required threading the wire through a small hole in the head lamination. This construction required considerable care in the threading operation and did not allow the use of knotted splices in the recording wire.

The tendency in subsequent design has been away from this ideal magnetic structure, and toward mechanical simplicity and convenience of threading. First, the drilled lamination was replaced by one with a slot in the edge, and the coil window was enlarged to allow the passage of knots through the head. This compromise still required threading the recording wire through the coil window, but the operation was simplified greatly.

Next, the so-called open-type head was developed. In this design the windings were placed around one or more legs of the yoke of the head lamination. This construction greatly simplified the threading operation and allowed a wire on two spools to be placed on the machine without the necessity of unspooling one of them. This further compromise decreased coupling between the recording medium and the coil, increased leakage flux, and stray field effects caused by the greater separation of coil and recording medium.

These compromises in favor of mechanical convenience did not have as great an effect on performance as might be expected. Complete tests and operating experience on these heads have shown them to be entirely satisfactory.

There are several further compromises that seem quite serious in the head described by Long. Twisting of the wire in the spooling and respooling operations in the normal record and playback operations will allow the wire to pass over the head in the playback process in different angular orientations from those it had in the recording process. We wonder if in the author's opinion variations in response, particularly at the higher frequencies caused by this twisting action will be much greater than the variations caused by magnetic mud in a slotted head, which the new design is supposed to eliminate. We have found that if the wire is allowed to run over a head surface not in the slot, there is a serious loss in the high frequencies, apparently because of twisting of the wire between recording and playback operations. In the test setup de-

scribed by Long, there is not much chance of the wire twisting between the record and playback operations.

Has the author experienced any difficulty in getting smooth lateral motion of the wire in level winding across the head? Any slight variation in the head surface may cause the wire to pause in its lateral motion, thus wearing in an increased irregularity at this particular point. There would seem to be a cumulative effect in wearing grooves in the head surface. Each of these grooves would tend to collect magnetic mud, and the final magnetic shunt effect well could be more serious than in the case of the head design with a single slot.

There also is the question of whether the effect of different optimum biases at different signal frequencies noted by the author is a definite indication of saturation in the head. We have noticed a similar effect in record and playback systems in which the heads were solenoids linked by the recording medium, having no magnetic material in their construction. In this case, of course, there was no possibility of head saturation entering into the picture.

The difference in response at high frequencies for the two types of heads shown in Figure 7A of Long's paper is within the range of variations that might be expected among heads of the same design. Therefore, unless these curves represent average data for several heads of each type, they should not be used as a basis of comparison of the two design types.

Response curves for the closed-type head in Figures 7A and 7B show an effect which is contrary to our experience. We have found that when a head is tested first with a low coercive wire and then with a high coercive wire, the decrease in response at high frequencies is less for the high coercive wire, providing the bias current is adjusted properly in each case. However, Figure 7B shows a 7-decibel greater drop from the maximum response than Figure 7A, even though the B curve was obtained with a wire of higher coercive force. Possibly, recording conditions may not have been adjusted properly for the higher coercive wire in obtaining data for the B curve for the closed-type head.

The number and thickness of laminations is another item that confuses the comparison of the two type heads. In Figure 6, the new design is shown to have several laminations in its core structure. While present practice is to build open- or closed-type heads with a single lamination, as shown in Figures 1 and 2, they could, of course, be built with several laminations and thus show improved response at high frequencies.

Absolute value of signal level is also an important item in the comparison of different head designs. When a head is used in conjunction with a coupling transformer, it is usually possible to sacrifice signal level in order to gain on frequency response. Therefore, absolute values of signal level should be shown in order to get a fair comparison on heads of different types. Also, each of the heads should be matched to its transformer so as to give the best compromise between signal level and frequency response. This matching may require the use of a separate transformer for each head. Whether these precautions were taken and whether all the response curves have the same reference level is not clear.

We believe that the troubles with the grooved-type heads presently in use are overemphasized in Long's paper. The process of removing foreign material which may accumulate in the wire groove is a very simple one, especially with the open-type head. Even the most critical listener will need to perform this cleaning operation no more often than he would change needles in a disk phonograph, and the two operations are of about the same complexity.

Long's trouble with a slightly oversize wire jamming in the head groove is the first case of this kind that has come to our attention. The deepened portion of the groove worn in by the wire always will be slightly wider than the diameter of the wire because of the random lateral motion of the wire, and the lateral forces caused by the level wind motion, which will cause a certain amount of wear on the sides of the groove. Chances of this jamming action, therefore, seem extremely remote.

T. H. Long: I wish to thank Doctor Wiegand for his concise review of the very good developmental progress, that has consisted mainly of mechanical simplifications by Armour Research Foundation on the grooved type of head, and suggest that what may be called the cylindrical head described in the present paper is merely another step in the process of mechanical simplification.

High Frequency Localization

It has been suggested that the grooved head may be less subject to trouble from the localizing of high frequencies on the wire than is the cylindrical head, and this is true. The situation, however, is one that involves an inevitable choice between "eating this cake" and having it. If the grooved head has a groove that fits the wire quite precisely, then a high frequency signal will be recorded at least half way around the wire while the groove is clean, but there will be a region in which there is very little recording, or at least theoretically there should be. Whether or not there is such a region is unimportant since for mechanical reasons it is not practical to operate with such a precise fit between the wire and the head, and as Doctor Wiegand suggests later, it is probably not possible anyway. Even if it were mechanically possible for a little while, it inevitably would lead to binding or wedging of the wire in the groove; at least that is what our experience leads us to believe.

On the other hand, if there is, for example, 0.0005-inch clearance between the wire diameter and groove width, the recording occurs with virtually the same sort of line contact as is the case with the cylindrical head. Even so, such a head is not proof against jamming.

Quantitatively, the effect of the localization of the high frequencies in the case of either head type is quite comparable to the effect of magnetic mud in the grooved type of record head. Our experience indicates definitely that, at least for some cases, the localization of high frequency recordings makes no difference, since there is a pronounced uniformity in the angular orientation with which the wire unwinds from reel to reel. Apparently, the only things that are able to cause any substantial disturbance in the uniformity of this performance are the twists that usually are introduced into a wire when a break is spliced with a knot. Thus if several twists are introduced into a wire having music recorded on it, the playback will suffer a transient loss of quality comparable to that which occurs when someone walks between the listener and the loud speaker. There should be no perceptible difference in such cases between the cylindrical head and the grooved head.

Probably the best evidence of the uniformity of the angular orientation is the performance of the wire recorder with musical selections involving high frequencies. These recordings may be played back several dozen times (at least) with no apparent loss of quality. Visual confirmation can be obtained readily by a simple experiment. By using a small wheel with a very fine grit in a high-speed hand grinder, it is possible to mark the surface of a limited area of the circumference of the wire, without removing an appreciable amount of material as the wire runs between reels. If the grinder is held at a slight angle to the wire, it will cause vibration of the wire, so that there will be regular alternate skips and grinds about 1/32 inch long. If the arrangement is such that this wire winds up on the outside of the reel, the resulting pattern will be obvious to the eye and will persist through successive wind and rewind cycles. This indicates that any random or progressive twist is negligible.

Equipment such as that shown in Figure 4 of the paper that involves a rather long run of wire from reel to reel definitely is subject to difficulty from twist in the wire, especially when the record and playback head positions are spaced about 30 inches to make shielding unnecessary. Even when operating on a loop, it has sometimes been quite a trick to avoid a variable twist between the record and playback heads. Remarkably enough, this variable twist will go through a regular cycle corresponding to the length of the loop. The cycle is not invariable, but changes are very slow. This trouble can be avoided by getting the record and playback heads close together and shielding them carefully. Another expedient is to mount one of the heads so it can be shifted around the wire to the most favorable position.

Questions Relating to Bias

It is difficult to interpret as anything other than evidence of saturation the fact that the optimum bias decreases as the recorded frequency goes up. I would appreciate another explanation. The report of the same effect in the absence of a magnetic recording head is difficult to appraise in the absence of information as to the bias frequency and maximum differential permeability of the recording medium and other details. It is at least possible that there was appreciable skin effect in the medium. Since minimum harmonic distortion seems to be obtained at the lowest bias consistent with maximum response at 500 cycles (or any other convenient low frequency), it follows that this is the best bias to use unless the design is to be compromised in favor of high frequency.

The comment that the two curves of Figure 7A come within the range of variations that might be expected with heads of the same design is quite correct. An effort was made to use representative heads rather than take an average on a number of heads.

The apparent discrepancy between the curves of Figure 7A and B is really an excellent illustration of the point I was trying to make more directly in Figure 5. The apparent discrepancy entirely depends on the method of determining what is a proper bias. The results shown were obtained in each case at the lowest bias consistent with maximum 500-cycle response. Markedly different results can be obtained by setting the bias for maximum response at 7,000 cycles, or some other high frequency.

It is regretted that the playback reference level was not stated explicitly in the preprint of this paper. The level used throughout was that standardized by Armour Research Foundation for this work as far as playback is concerned, namely, zero decibels equals ten microvolts at the secondary of the playback transformer. The same grooved-type low-impedance playback head and transformer were used for all curves of Figure 7, and probably for all other curves except the curve for the open-type head in Figure 3. With the same exception, all curves were taken at a record current level that was independent of frequency and that corresponded to playback about ten decibels below saturation level for that frequency at which the playback was a maximum.

Miscellaneous Comments

It may be true that the deepened portion of the groove worn in by the wire always will be slightly wider than the wire, but even if this is so, it does not eliminate jamming. In one particular case, a combination type of head also was being used as the level wind. The machine operated at a wire speed of two feet per second, and the wire that was on the machine had made between 10 and 20 round trips through the head. So we had a listening test in which various recording systems were compared. When the turn came for this particular instrument, it emitted the most horrible sounds for perhaps 30 seconds, after which the difficulty substantially cleared and operation was normal. During the 30-second period, the trouble was a very pronounced flutter having (by guess) a frequency of 15 cycles per second and an amplitude in excess of one per cent. Only one-half hour before this trouble, the same wire in the same head had operated perfectly. A subsequent unreeling of the wire in which the difficulty had occurred showed that when released it curled on about a one-quarter inch diameter.

I have been censured somewhat for making an unfair comparison when I measured the performance of a cylindrical head having several thin laminations against that of a single lamination grooved head, but the fault is hard for me to see. The comparison is reasonable since one of the advantages of the cylindrical head is this simplicity of construction which makes it so readily possible to use several thin laminations. Assuming an equal precision of construction, it seems obviously possible to do as well with a grooved head assembled from several thin laminations, but the lack of evidence of anyone having done this is adequate evidence of the difficulty.

The predicted multiple grooving of the head caused by irregularities of lateral travel has been observed, but even when it happens it does not seem serious. The possible seriousness has not been evaluated, but the lateral motion of the wire definitely prohibits any appreciable accumulation of mud. Beside this condition, the irregularities of lateral travel can be avoided readily and completely. One of the first heads we made of the type illustrated in Figure 8 of the paper provided for a wire travel of 0.5 inch. This head was used for several hours in an experimental setup where it was not expedient to provide any lateral travel of the wire, and this setup resulted in two fairly pronounced grooves. These grooves caused a fairly pronounced irregularity in the motion of the wire when lateral motion again was introduced. Occasionally, this irregularity of motion would cause a barely audible sound on playback, but after several more hours of operation the grooves were gone and no irregularity of motion was perceptible, either to the ear or to the eye. The only requirements seem to be that the wire tension should be more than about one ounce and the wrap on the head less than about ten degrees.

Conclusion

The relative merits of the cylindrical and grooved types of heads can be established only by more experience than is now available. Since very satisfactory recordings can be made with either type, it would seem reasonable to assume that electromagnetic advantages either way are not particularly pronounced, especially since different advantages can be claimed for each type. I cannot agree, however, that the mechanical advantages of the cylindrical type of head were overemphasized in the paper.

Formulas for Conductor Size According to Cost of Resistance Loss

Discussion and author's closure of paper 46-8 by Herbert B. Dwight, presented at the AIEE winter convention, New York, N. Y., January 21–25, 1946, and published in AIEE TRANSACTIONS, 1946, January section, pages 22–5.

William S. Peterson (Department of Water and Power, City of Los Angeles, Calif.): In Professor Dwight's paper, the statement is made that the cost of copper, v dollars per pound, should include the cost per pound for installation and also the cost of any part of the supports whose cost varies directly with the weight of copper. The point I desire to emphasize is that the cost of the supports relative to the weight of copper carried is a rather intricate problem and is a very important part of the cost considerations involved. In connection with the economic design of the Boulder Dam transmission lines of the City of Los Angeles, we found it desirable to develop curves for the cost and weight of transmission towers which could be expressed most readily for any given crossarm length, in terms of resultant conductor tower loadings and height to the top crossarm. These data, taken in conjunction with the proper tower dimensions to meet independent selection of conductor diameter, conductor area, maximum tension, and various span lengths, gave the basis for the ultimate selection of the values for each of the four independent variables to achieve the best economy.

I believe Professor Dwight would find it very interesting to try to develop formulas that would express the foregoing relationships in terms of cost formulas for economic use of copper conductors.

G. D. Floyd (Hydro-Electric Power Commission of Ontario, Toronto, Ontario, Canada): No one can question the fact that it is possible to determine by mathematical means the desirable cross section area of the conductor in a given application when a definite value can be assigned to the cost of resistance losses. However, in practice it is extremely difficult to assign a definite figure to this value of the resistance loss.

Depending on the type of system (that is, whether steam or hydraulic supplied) and depending on the relationship between the system generating capacity and system load, the value of resistance losses may vary from virtually zero to the actual selling price of the primary power. Furthermore, as the relationship between system capacity and load varies over the years, the coincident value of losses also may vary over this same range.

For example, under given conditions it may be shown that the value of losses is the incremental cost of additional generation. This incremental cost probably would not exceed 0.5 mill per kilowatt-hour in a hydroelectric system in which excess capacity exists, or it may be an incremental generating cost of the order of 1.5 to 2.0 mills per kilowatt-hour in a steam-electric plant where excess capacity is available. On the other hand, with existing system facilities loaded to the practical limit, this incremental cost may be the cost of developing the next available power source.

Again, system conditions temporarily may be such that a saving in losses is reflected in additional saleable power at primary rates, which would be several times the incremental cost quoted above. However, this condition almost certainly would be temporary, and it would appear that such a high value of losses seldom could be justified.

In the application of the formulas proposed by Professor Dwight, there could be, therefore, as many answers as there are values assigned to the variable cost of power. However, it is not intended to infer that it is futile to apply this form of mathematical analysis to this type of problem. In the general case, at least, the results will be of material assistance in forming the final judgment as to a reasonable selection of conductor size.

Herbert B. Dwight: Referring to Peterson's discussion, the data from the cost study which he describes apparently can be used in the formulas of the paper quite directly. By plotting the total cost of conductors plus towers on a base of weight of conducting metal, and drawing a tangent to the curve at the point under consideration, the place where the tangent cuts the axis of y shows the part of the cost which is constant, and also the part which varies directly with the weight of copper, thus determining the value of v for the formula.

In other words, the cost study is not really complete until a high-resistance conductor is charged with the cost of the additional rating of generating-station capacity, which its high resistance makes necessary if the output is not to be decreased.

A cost study such as Peterson describes is applicable, of course, only to the particular type of line for which it was made.

Referring to Floyd's discussion, without implying that the cost determinations are at all times simple and definite, a large part of the uncertainties expressed seem to be caused by the effort to state all costs in mills per kilowatt-hour. An effort has been made in the paper to depart from this practice to a considerable extent.

If one is designing a generating station and a power circuit connected to it, one does not need to wait until the facilities are loaded to the practical limit in order to put enough copper in the circuit so that the losses will not be excessive from the point of view of economy. In order for the cost of resistance loss to affect the choice of conductor size, there is needed only a normal amount of confidence in the growth of the power system.

Arcing Ground Tests on a Normally Ungrounded 13-Kv 3-Phase Bus

Discussion and authors' closure of paper 46-44 by J. E. Allen and S. K. Waldorf, presented at the AIEE winter convention, New York, N. Y., January 21–25, 1946, and published in AIEE TRANSACTIONS, 1946, May section, pages 298–306.

Eric T. B. Gross (Illinois Institute of Technology, Chicago, Ill.): This paper should be of considerable interest because its conclusions can be applied not only to bus systems, but also to others with similar or larger phase-to-ground capacities at the same or higher voltages. Most of the capacity-to-ground is very likely not caused by the bus proper, but by the underground cable connections from the alternators and transformers to the bus. In an ungrounded system of 13-kv line-to-line voltage, an arcing ground will not be self-extinguishing if the charging current to ground is larger than about 5 amperes. Therefore, if the charging current-to-ground is 9.2 amperes, as mentioned in the paper, overvoltages will be produced by single-phase flashovers to ground, and flashovers on the other phases can be expected to follow.

To prevent such overvoltages, some kind of neutral grounding seems advisable. The installation of a ground fault neutralizer would prevent arcing transients and damages to the system. The application of resonant neutral grounding (tuned with an accuracy of ±25 per cent) will restore all the advantages of the operating features which an ungrounded system provides.

An early indication of impaired insulation is very desirable. The sensitivity of a neutral voltage ground detector is increased considerably if the system is resonant grounded. The impedance of the system to ground is increased largely by a ground fault neutralizer. If the ground fault neutralizer is tuned, that impedance will be the system's leakage resistance to ground, which will be in the order of at least ten times the capacitive reactance to ground. This statement is based on an analysis which is similar to the one in Appendix B of the paper.

H. A. Peterson (General Electric Company Schenectady, N. Y.): It is not often that a system is subjected to tests as complete as these appear to be. The results and conclusions, in general, further substantiate the contention that high overvoltages to ground in ungrounded systems are not produced by the arcing in the fault to ground. High overvoltages are much more likely to be obtained during the subsequent switching necessary to remove the portion of the circuit which has the ground fault on it solid or otherwise. It is extremely important that this fact be emphasized in connection with interpreting the results of the tests as reported by Allen and Waldorf.

There is another thought in the paper on which I would like to comment and that has to do with the effect of high frequency oscillations in producing excessive turn-to-turn insulation stresses. It would seem that the actual frequency of oscillations during arcing conditions, such as these reported in this paper, is of secondary importance. Of primary importance is the magnitude of voltage across the arc path just preceding a restrike. The actual restrike, then, is equivalent to injecting an extremely steep front wave of voltage into the circuit at the fault point at this instant. If this fault point is near the terminals of a rotating machine, then this restrike is equivalent to injecting a steep front surge directly into the machine, and certainly most of this abrupt voltage change will pile up across end turn insulation. If restriking takes place at low voltages, this "piling up" of voltage between end turns may be of little significance. However, as this restriking voltage increases up to values approaching two times normal line-to-neutral crest, as indicated in some of the test oscillograms (Figures 11 and 13), then the actual voltages across turn insulation for the end turns of multiturn coils may reach magnitudes which cannot be ignored.

This fact has even further significance. Suppose that the arc is on a bus, and that connecting each machine through its breaker to the bus, there is a length of cable, say of four or five hundred feet. Then at the instant of a restrike, as already mentioned, a steep front surge is injected at the point of fault, in this case on the bus. This surge is transmitted with practically no change of slope or magnitude to the cable circuits on the faulted phase and travels toward each machine. As the surge reaches a machine terminal, it is reflected and almost doubled in magnitude because the cable surge impedance is low and the machine winding surge impedance may be as high as ten times the cable surge impedance or more. Thus, the severity of such a restrike may be doubled as far as end turn-to-turn insulation is concerned, because of the cable between the restriking point and the rotating machine.

Of course, for this latter and more severe case, protective capacitors at the terminals of each machine effectively slope off the surge transmitted through the cable to the machine so that the rate of change of voltage at the machine terminals is held to safe values. Protective capacitors are just as effective in accomplishing this objective for restriking voltages as they are for lightning surges. On the other hand, for the former case, where no cable is present, or if the restriking in the fault is taking place at the machine terminal, protective capacitors can be of little, if any, assistance in reducing turn-to-turn stresses resulting from restriking of the fault arc to ground. This condition prevails because, in order for the capacitors to be effective, the wave must approach them through a surge impedance, that is, as a traveling wave.

These comments apply not only to hydroelectric stations, but also to many industrial installations where generators and possibly many motors may be involved. Not only is the arc to ground of significance, but the subsequent switching operations may be of even greater concern in this regard. Consequently, in dealing with problems concerned with adequate protection of rotating machines against overvoltage stresses, surges associated with faults and switching should not be ignored. In considering such surges, it becomes apparent that more effective grounding can be very helpful in reducing the magnitude of restrike voltages.

J. E. Allen and S. K. Waldorf: Doctor Gross states that an arcing ground on one conductor of an ungrounded system, having a charging current to ground in excess of five amperes, will produce high voltages on the other two phase conductors sufficient to cause flashovers. Test 5 of Table III in the paper was performed under conditions that produced a charging current through a solid ground on one conductor approximately equal to 2.6 microfarads/1.06 microfarads×9.1 amperes=22 amperes. This current is considerably in excess of the critical current of five amperes mentioned by Doctor Gross, and the overvoltages to ground did not exceed three times the normal phase-to-neutral voltage. If the equipment on a bus under these conditions was not deteriorated, it is doubtful that a flashover or breakdown would be produced.

Any device, which will give an early indication of impaired insulation on an ungrounded bus, will be quite useful. Doctor Gross's disclosure of an additional benefit of a ground fault neutralizer in increasing the sensitivity of a neutral voltage ground detector is quite interesting.

As Mr. Peterson brings out, it is necessary for an understanding of the behavior of ungrounded bus systems that a distinction be made between high voltages to ground produced by arcing grounds, and those produced by the switching required to isolate the fault. A careful analysis of experience with ungrounded bus systems, made perhaps by an appropriate AIEE committee, should do a good deal toward establishing the limits to which voltages rise on actual bus systems. If this analysis can be made, it then will be possible to operate an ungrounded system with some certainty of its behavior should a ground fault occur.

It should be recognized that an arcing ground fault necessarily is not followed im-

mediately by switching to isolate the fault. It is common experience that appreciable time elapses between the occurrence of an arcing ground and the switching for fault isolation. Ordinarily, after this interval of time, the fault is no longer arcing, any transient overvoltages caused by the arcing have disappeared, and the overvoltage accompanying switching is only that which occurs normally. Therefore, the possibility is quite remote that a transient overvoltage caused by switching could occur simultaneously with that of an arcing ground.

Mr. Peterson discusses the phenomenon of voltage doubling caused by reflection at the terminals of a machine, particularly under those conditions where a surge initiated by a fault travels through a length of cable. As shown in Figure 10 of the paper, the test arcs were produced at test point X. A surge originating at test point X had to travel through at least 225 feet of cable, as shown in Figure 4, to reach the terminals of the generator. In Table III it is shown that the voltage at the machine did not exceed three times normal. The connection of capacitors at the terminal of a generator for surge protective purposes increases the current in an arcing ground, increases the ionization in the arc space, and thereby reduces the restrike voltage.

Lightning Performance of 220-Kv Transmission Lines—II

Discussion and author's closure of paper 46-16 by the lightning and insulator working group of the AIEE committee on power transmission and distribution presented at the AIEE winter convention, New York, N. Y., January 21–25, 1946, and published in AIEE TRANSACTIONS, 1945, February section, pages 70–6.

M. S. Oldacre (Commonwealth Edison Company, Chicago, Ill.): The report gives exceptionally valuable information and conclusions about operation of 220-kv lines, but it seems to lead to even more important ones.

It is stated that the installation of ground wires, low ground resistance, and the line insulation are the three most important items in obtaining good performance from the high voltage transmission lines. This seems a logical conclusion, if certain other design factors, such as adequate clearance between conductors, and between conductors and grounded objects, and also proper co-ordination of mechanical and electrical characteristics in all parts of the line structure, are accepted as basic conditions for the line design.

However, a further analysis of the data in the report, particularly that for two of the lines, indicates that low ground resistance is a necessary adjunct to the use of ground wires and that ground wires with low ground resistance is the most important individual element so far as lightning is concerned.

The insulation of the line, that is, the number and spacing of the insulator units, seems more important for protection other than lightning protection. This will be discussed a little later.

There is another point of view worth thinking about for a moment. Instead of considering only the lightning performance of the high voltage lines, it is suggested that the over-all service record be studied and the cause of all outages be investigated.

The actual number of outages of a line per year is usually of more importance to the utility and its customers than the number per 100 miles per year. The latter figure is valuable in a statistical analysis, but actual outages per line are the important element of reliability if service is to remain an essential item in line design. For example, two outages on a 50-mile line will not be considered as satisfactory service as one outage on a 25-mile line, even though both have an outage record of four per 100 miles per year.

A low number of outages per line irrespective of length seems to be a matter of some importance, for the report indicates, with one exception, that where there were more than two outages of a line per year, improvements have been made or are contemplated.

The line covered by reference 11 of Table I was designed on the basis that it should be at least as reliable as the generators supplying it. This is a single circuit line and not two circuits as indicated in the report. The line originally was designed ten years before it was built, and it included the best design knowledge of that time. However, a review of the design just before the line was built resulted in an almost complete redesign, partly for lightning reasons but equally as much for good operation at all times.

Experience on other lines in the territory, as well as in other sections of the country, indicated that short circuits caused by partial removal of sleet from conductors or by "galloping" of conductors was an equal or greater hazard than lightning, assuming of course that the best information about lightning protection was utilized.

Clearances between the conductors and also from the ground wires were provided in accordance with the theories which had been developed and published by A. E. Davison. Every span was checked, and, when necessary, individual towers were modified to give the required clearances.

The record to date has been as satisfactory for sleet troubles as for lightning outages.

The report seems to indicate that lightning has been conquered as far as transmission line operation is concerned and that it is probably a small factor in total outages and maintenance costs.

It therefore is suggested that a general study of the operating record of high voltage lines, probably 132 kv and higher, would be a very valuable aid in the improvement of transmission line operation.

Some of the causes of outages to consider are as follows:

1. Sleet accumulation and sleet preventive measures.
2. "Galloping" of conductors.
3. Dirt and condensation on insulators.
4. Defects in line material and construction.
5. Defects in terminal station equipment, if they prevent use of the line.
6. Time required for maintenance.

The item of "dirt and condensation on insulators" is an old one that crops up periodically and then is forgotten until the next time. In some sections of the country, dirt and moisture are more of a problem than lightning.

The data in the report seem to indicate that as far as lightning is considered, the insulation between conductors and the supports can be varied over a wide range, provided that adequate ground wires and grounding facilities are installed. Thus insulation is primarily a low frequency problem under dirt and moisture conditions. Careful investigation and development may bring forth a new and better insulator design for use under severe conditions.

A recent article in an English technical journal stated that about 60 per cent of the outages on the English 132-kv grid were caused by lightning. It is believed that the record in this country will be entirely different, probably 10 to 15 per cent of the total number of outages and probably less than 5 per cent of the duration of the outages will be due to lightning.

Thus there seems to be a fertile field for investigating the major causes of transmission line outages to seek improvements that will reduce outages and maintenance costs economically, as well as expenditures for reserve facilities.

William S. Peterson (Department of Water and Power, City of Los Angeles, Calif.): On the 287.5-kv Boulder Dam transmission lines of the Department of Water and Power of the City of Los Angeles listed as reference 14 and 15 of Table I in the paper, the connection between the buried copper counterpoise and the towers is made through a 1/16-inch concentric insulating gap for the purpose of avoiding electrolytic action and corrosion of the tower footings. This gap also has proved to be of service in connection with counting lightning strokes that have hit the tower system and in making some rough estimate of the current flow involved. To this end an approximate calibration of such gaps was made by testing with impulse currents and a calibration determined between the area or length of burn and the current flow.

With due reference to individual storms and the seasonal characteristics of lightning, the patrolmen and engineers conduct a program of checking these gaps and reconditioning them, so that a complete record is maintained of gap burning. These field results are analyzed in the office to determine and estimate the number and severity of lightning strokes.

Although only two strokes have caused flashovers of the lines during a 10-year period of operation, a very high number of strokes actually have hit the towers. The number of these strokes per year varies from as low as 70 to as high as 218. The detail by years is as follows:

Year	Number of Strokes	Year	Number of Strokes
1936	158	1941	70
1937	91	1942	201
1938	138	1943	187
1939	218	1944	185
1940	161		

The foregoing values are for the complete line of three circuits, but, in general, more than half of the strokes are concentrated in the first one-third of the line nearest Boulder.

It is interesting to know that of the two strokes that did flash over the line insulation, the counterpoise burning was such as to indicate relatively small current flow. A very careful examination of the overhead ground wire and tower structure revealed no burning from lightning stroke termination. A small beaded burn on the tip of the upper arcing horn seemed to be the only possible point of termination of the lightning stroke, with other normal burning between the upper and lower arcing horns from the arc across the insulator string. The general conclusion is that each of these lightning strokes must have been from a cloud of relatively low potential close to the ground. This is in line with the observation made by Mr. Davison of the Hydro-Electric Power Commission of Ontario with respect to its lines.

G. D. Floyd (Hydro-Electric Power Commission of Ontario, Toronto, Ontario, Canada): This discussion covers the lightning outages listed in Table I of the paper for the line shown as reference 23. This line was placed in service in 1941, and the record shows 8 outages in 4 years, due presumably to lightning. At least one of these is very doubtful. This line is not uniform in design over its whole length. The first 30 miles from the west terminal station have the initial tower design, the next 240 miles have the new tower with elevated ground wires as indicated in reference 23. The easterly 25 miles is again the earlier designed tower with river crossing towers.

The lightning outages shown do give the performance of the line as a line. It would be wrong to conclude that the performance as shown indicates the reaction of the improved design of tower to lightning. One of the 8 outages classed as due to lightning is doubtful, at least 3 occurred on the sections of line which have the older type of tower. This reduces the total outages occurring on the new section of line to 4, making the average for the new design of tower substantially less than shown in the reference for the whole circuit.

A much better conception of the effect of factors in design for lightning is obtained for the trunk lines (references 20–23) if the line to be studied is divided roughly in half sections. The easterly sections are generally in rocky country, and the westerly sections in clay, with corresponding conditions as to tower footing resistance. For a given design, the performance is quite different in the two sections, and a more accurate analysis of performance can be made, if the line is subdivided as has been done in references 20 and 20A.

H. N. Ekvall (Philadelphia Electric Company, Philadelphia, Pa.): This very complete report on 220-kv aerial steel tower line construction and operating performance throughout the United States and Canada is not only timely but also a very valuable guide for use in postwar design work on lines in this voltage class. Of particular interest is the general conclusion that the predominating factors influencing lightning performance of these lines are

1. Overhead ground wires.
2. Insulation strength.
3. Tower footing resistance.

However, on existing well-insulated lines having overhead ground wires, lowering of tower footing resistance is the only one of these three factors which appears practical to apply. The 220-kv lines of the Philadelphia Electric Company are in this category, and, therefore, I believe it would be of interest to supplement the reported data from that company with a brief discussion of steps taken to lower tower footing resistance and to indicate the apparent benefits to line performance.

As indicated in Table I of the committee report, the four 220-kv lines of the Philadelphia Electric Company radiate from Plymouth Meeting, two going to Conowingo, one to Roseland, and one to Siegfried; the latter two tying in with adjacent systems. The two circuits to Conowingo parallel each other on separate tower lines spaced about 150 feet apart. Each of the four lines is equipped with two overhead ground wires, but has no continuous counterpoise.

Apparent tower footing resistance has been lowered by application of short sections of counterpoise along the line or with cross bonds between adjacent towers of paralleling lines. Also in two instances multiple ground rods were used.

In 1929, the year after the Conowingo lines were placed in service, 21 pairs of towers having high ground resistance were cross-bonded. In 1939 six additional pairs of towers in one section in which there appeared to be particular susceptibility to lightning flashover also were cross-bonded. At three other locations cross-bonding was applied together with auxiliary counterpoises paralleling the line. Altogether 30 pairs of towers have been cross-bonded using an average of 167 feet of wire between towers buried to an average depth of 18 inches. Since cross-bonding, only one flashover has occurred on these towers, and fears that cross-bonding might lead to simultaneous flashover on both lines, due to a major stroke to one, have not been substantiated.

Multiple ground rods were used in two locations where the hilly terrain made it difficult to obtain effective results with the counterpoise alone. At one of these, the pair of towers was located on a high resistance knob. At this location 12 driven rods were installed in marshy low land about 125 feet down the slope from the towers and connected to the towers by counterpoise. This reduced the apparent tower footing resistance from 81 ohms to 8.3 ohms. No flashovers have occurred at this location.

At the other location, which happens to be near Conowingo, occurrence of a flashover led to the discovery that the rods had been removed maliciously. Presumably the theft of the rods occurred before flashover. Also at Conowingo a counterpoise which was laid in the river bed disappeared, apparently by theft, and had to be replaced. More recently theft has been discouraged by the use of 5/16-inch black surfaced Copperweld strand instead of 2/0 American Wire Gauge stranded copper wire formerly used.

In addition to the above improvements on the Conowingo lines, counterpoises also were extended about one-half mile out from Plymouth Meeting substation on each of the four lines. These were installed as a precautionary measure to minimize chances for flashover at the substation and not because of unusually high resistance grounds or poor line performance. Thus far these sections have been free of lightning flashovers.

In conclusion, it appears that improvement of grounding conditions at about 15 per cent of the towers along the Conowingo lines and for about one-half mile out from Plymouth Meeting substation on all four lines has resulted in good operating performance without the need for installing a continuous buried counterpoise throughout.

A. E. Davison (Hydro-Electric Power Commission of Ontario, Toronto, Ontario, Canada): Grading rings are reported in column 26 of Table I of the paper. It may be of interest to designers of 220-kv lines to know that the original HEPC lines installed in 1928 and shortly after, and reported under references 20A and 21 of Table I, were among the first, if not the first lines at this voltage to omit the use of grading rings. The late E. T. J. Brandon was of the opinion that the mechanical effects upon the conductors, for instance, at the throats of clamps would be much more severe if grading rings were added to the mass of the clamps. Another feature was in mind: arcing horns had been installed on a 100-mile section of double-circuit, 110-kv line some 10 or 15 years previously. Experience was such that a decision had been made prior to 1928 to eliminate these arcing horns as opportunity arose. Since that time electrical burns on the 220-kv and other conductors and on the insulators due to arcing have not been such as to warrant the extra cost or weight of either arcing horns or grading rings. Another obvious factor, the reduction of arcing distance sometimes as much as 15 or 17 inches, is reflected in the operating records.

I. W. Gross: In presenting and discussing the record of lightning performance given in the paper, the committee recognized, as it was not so familiar with the lines under discussion as those who operate them, some features peculiar to the various systems well might be discussed and enlarged upon by the contributors. It is gratifying to find that this has been done in several cases.

From his analysis Mr. Oldacre has reached the conclusion that low ground resistance is a necessary adjunct to the use of ground wires. This, of course, is according to theory, but enough data were not available on the lines in question to draw this conclusion from the record. The purpose of the ground wire, of course, is to intercept the stroke which otherwise might terminate on the line conductor, and the value of the low ground resistance limits the voltage across the insulator string. This preassumes that adequate shielding of the conductors is obtained by a suitable location of the ground wires. As the insulation on lines of this voltage class is high, only the higher strokes have to be considered.

His comments on the number of yearly outages per line as a figure to emphasize rather than the outages per hundred miles

of line per year call for some comment. First, the intent of the analysis of the paper was to show the structural and insulation features which seem to make the line more highly lightning resistant. Whether or not one or ten outages can be tolerated on a line will depend on the importance of the line in the company plan of service continuity. If a load or load center is supplied by parallel or loop lines, the number of outages per year may not be of much concern if service is maintained over the remaining good line; in fact, double circuit transmission lines have been shown to have value in lessening the total number of lightning outages as compared with a single circuit line. Again, if the load can be held by high speed reclosing circuit breakers, the numerical outage record is not particularly important to service. In brief, the choice of method of reducing lightning outages, or eliminating them if possible, is one of application depending on service requirements. The choice of method of protection is one of economics and results required.

We are glad that Mr. Oldacre has brought to our attention that the line 11 is a single circuit and not two circuit. The confusion in reporting this line was due to the fact that some towers were indicated as two-circuit towers, but it seems from a reanalysis of the data that only one 220-kv circuit was strung on such towers.

It seems to be a fair conclusion to draw from the records that, where special pains have been taken to make a line highly lightning resistant by adequate conductor spacing, shielding, ground wire location, and low tower footing resistance, a highly resistant line is possible.

Mr. Oldacre has brought up the point of the over-all outage performance of lines, including not only those due to lightning but also those resulting from other causes such as sleet, galloping conductors, contaminated insulators, and failure of equipment. A study such as he has proposed on high voltage lines indeed would be interesting, and it is hoped it can be undertaken. The figure of some 60 per cent of outages caused by lightning on the English 132-kv grid may not be far out of line with records of some of our systems in this country. One 132-kv system, which has been analyzed over a 4-year period, showed 64.1 per cent of the outages caused by lightning, 22 per cent caused by station troubles, and 3.5 per cent caused by trouble on other circuits or foreign systems. This accounts for nearly 90 per cent of the outages. If this trend is followed by other systems, it leaves about 10 per cent resulting from miscellaneous causes such as sleet, wind, mechanical failure, kites and birds, and unknown causes.

Mr. Peterson's comments on the Boulder line are particularly significant in showing that, where great care and consideration have been given to designing the line to be highly lightning resistant, many lightning strokes can hit the line without causing flashover. The nine years' record presented shows an average of 156 strokes per year to the line with only two of sufficient magnitude to cause line flashover.

Mr. Floyd's comments on line 23 stating that approximately half the outages occurred on about 18 per cent of the line clearly indicate that the type of construction with the elevated ground wires has distinct advantages over the older design. The importance, therefore, of analyzing the line by sections is undoubtedly that it is more accurate in evaluating the different factors which contribute to improving the outage record.

Mr. Ekvall's citation of the various steps taken to reduce tower footing resistances on his system are further confirmation of the present day conception that low tower footing resistances are essential in reducing lightning outages. It is interesting to note that the reduced resistance obtained by wire connections from 125 to 167 feet long, to other grounds, have resulted in lower resistances which are quite effective. The old idea that low ground resistances no matter how obtained were effective in reducing lightning outages is now not accepted generally. For example, if a tower footing resistance can be reduced from 100 ohms to 10 ohms by installation of a wire some thousand feet long to a low resistance point, it cannot be expected that such a method of reducing the resistance will be as effective as providing a 10-ohm ground immediately adjacent to a tower.

Again, Mr. Ekvall's conclusion that improvement of grounds at about 15 per cent of the towers on the Conowingo line has produced satisfactory operating performance indicates, as mentioned by Mr. Floyd, that careful analysis of individual sections of line undoubtedly can produce the desired reduction in lightning outages by applying remedial measures to only those parts of the line which appear to be most susceptible to lightning.

Mr. Davison has pointed out that grading or arcing rings were omitted from his system some years ago apparently for mechanical reasons. The arcing device did apparently serve a most useful purpose in the early days of slow relaying of line faults where concentrated power might exist over an insulated string for a sufficiently long time to cause extensive damage. With the speeding up of relay systems and the shorter clearing times of fault currents by high speed circuit breakers, the need for these arcing devices has decreased very greatly, if indeed it has not disappeared.

Formulas for the Inductance of Coaxial Busses Comprised of Square Tubular Conductors

Discussion and authors' closure of paper 46-37 by Henry Peter Messinger and Thomas James Higgins, presented at the AIEE winter convention, New York, N. Y., January 21–25, 1946, and published in AIEE TRANSACTIONS, 1946, June section, pages 328–36.

L. P. Lanigan (Chase Brass and Copper Company, Waterbury, Conn.): After making a careful study of this paper, we believe that it presents data which have been needed for some time. Quite frequently in the past, our company has received inquiries from customers regarding low inductance busses which are to operate at the present conventional frequencies. Since there is necessity to operate at much higher frequencies in the future for certain purposes, we feel that the demand for such types of busses will be much greater, and the coaxial square tubular busses will prove very satisfactory for many of these installations. The fact that there is a relatively small number of coaxial busses at present is probably caused by, in part, the lack of readily available data such as that supplied in this paper.

Although the general formula will be very important for certain uses, the approximation to this formula, in conjunction with Figure 5 which was plotted from values derived from the latter, undoubtedly will prove to be especially valuable in commercial work where there is a limited amount of time which can be devoted to any one problem. The degree of accuracy, which is attained by resorting to Figure 5, should be sufficient for most of the commercial problems encountered in everyday practice.

The advantages of coaxial square tubular busses are many, as enumerated in this paper. Low inductance with the resulting decrease in voltage drop and the reduced skin and proximity effects are some of these advantages. One of the outstanding points in favor of square tubular busses is the high mechanical strength in all directions, but when such conductors are arranged coaxially, even much greater strength is added so as to eliminate the necessity, in many cases, of bracing to withstand short-circuit forces. The supporting structures, therefore, can be made smaller and lighter. Less space is required for the coaxial busses, which very often is a very important consideration in designs where there is a limited amount of space available.

In conclusion, we believe that this paper presents data which will assist considerably in the design of many bus installations in the future.

Henry Peter Messinger and **Thomas James Higgins:** The authors agree with Lanigan that values of inductance sufficiently accurate for most industrial work can be obtained from the curves of Figure 5. For actual use, however, the designer should follow the suggestion made under "Approximation to the General Formula," namely, to plot the curves (or parts of the curves) on a larger scale than that of Figure 5. The coordinates listed in Table I afford a more accurate plotting than the shorter list given in Appendix IV. For plotting, r must be converted to decimal values.

Table I.

A	r = c/a	L
0	1	.0
0.10	9/11	0.354
0.15	17/23	0.546
0.20	2/3	0.744
0.25	3/5	0.951
0.30	7/13	1.164
0.35	13/27	1.386
0.40	/7	1.617
0.45	11/29	1.861
0.50	1/3	2.117
0.55	9/31	2.395
0.60	1/4	2.693
0.65	7/33	3.022
0.70	3/17	3.389
0.75	1/7	3.812
0.80	1/9	4.315
0.90	1/19	5.809
1.00	0	∞

A New Line of High-Voltage Outdoor Tank-Type Oil Circuit Breakers

Discussion and authors' closure of paper 46-20 by W. F. Skeats and E. B. Rietz, presented at the AIEE winter convention, New York, N. Y., January 21–25, 1946, and published in AIEE TRANSACTIONS, 1946, April section, pages 224–31.

M. H. Hobbs (Westinghouse Electric Corporation, East Pittsburgh, Pa.): About two years ago, a new line of high voltage oil circuit breakers was introduced[1] with greatly reduced size and oil volume, and a standard interrupting time of five instead of eight cycles. At that time some comments were made regarding possible lowered factors of safety as to dielectric strength and interrupting ability. It is gratifying to have others, such as the authors of this paper, confirm the practicability of such a reduction in over-all dimensions, even for interrupting ratings as high as 3,500,000 kva.

One of the most important parts of a high voltage breaker is the bushing. As stated in the paper, the sealed oil-filled bushing has gained wide acceptance, and the use by the authors of conducting layers in a paper-wound core for limiting the voltage gradient and providing a potential tap further confirms the well-established capacitor principle for high voltage bushing design.

I believe we must take issue with the authors' proposal to standardize at this time on only one breaker design and one rating for each voltage at 115, 138, 161, and 230 kv. This setup, of course, appears attractive from our point of view as manufacturers, but it should be examined carefully as to sound economics and be certain that undue hardship is not imposed upon the operating systems which require only the lower rated breakers. The new American standards for power circuit breakers recently were published. Table 3 as indicated in a recent review of these standards[2] has been simplified and, except for the two top voltage classes, still retains several ratings for all voltages. These ratings were considered essential by the committee, based upon actual purchases of the lower rated steps.

If the maximum rupturing capacity in the high voltage class of circuit breakers were limited to 2,500,000 kva, and this rating could be obtained in the smallest tank diameter and lightest feasible construction suitable for the voltage class, perhaps a single rating at each voltage would be satisfactory. However, with 3,500,000-kva ratings already standardized and 5,000,000-kva under serious consideration, it would appear reasonable to keep at least two or three different interrupting ratings at the same voltage. Gas generation, particularly at the higher currents, tends to reduce momentarily the effective clearances between live parts in the breaker. Although the sustained pressures accompanying high power interruptions undoubtedly are reduced greatly in modern breakers as compared to those of 15 or 20 years ago, nevertheless, the momentary shock pressures, particularly when using multibreak arrangements operated at very high speed, may be even more severe than in slower breakers having fewer interrupting elements. For these reasons, differences in tank diameter and wall thickness, as well as other structural details, still may be justified economically to correspond with a range of interrupting capacity requirements and different speeds of opening.

It is evident that the demand for 3-cycle interrupting time on several transmission systems has encouraged the use of multibreak contact structures, and the authors are to be commended on the relatively simple assembly which they have achieved. Nevertheless, it may be difficult to maintain the position that it is not possible to provide an even simpler and lower cost construction with fewer contact breaks where high speed and high interrupting capacity are not required. Our studies show that 5-cycle breakers are appreciably lower in cost than 3-cycle designs.

The authors have not indicated the time required to interrupt the residual resistor current of some 50 amperes, but it does not seem likely that the circuit could be cleared completely until perhaps 5 or 6 cycles after energizing the trip coil. How may this be reconciled with a 3-cycle interrupting time rating?

As a contribution to the discussion of heavy short-circuit duty on high voltage breakers, it may be of interest to mention a series of tests at Grand Coulee Dam recently completed. A 230-kv 3-cycle oil circuit breaker containing multiflow grids,[1] with a rupturing capacity of 3,500,000 kva, was subjected to several 3-phase short circuits up to the full rating. In addition, a number of single-phase faults all were interrupted successfully, reaching a maximum current equivalent to a 3-phase short circuit of 4,300,000 kva at rated voltage. This is believed to be the highest power field test so far made, and gives increased confidence in the practicability of extending breaker ratings to 5,000,000 kva and even higher.

REFERENCES

1. HIGH-VOLTAGE OIL CIRCUIT BREAKERS FOR RAPID RECLOSING DUTY, **A. W. Hill, W. M. Leeds.** AIEE TRANSACTIONS, volume 63, 1944, March section, pages 113-18.

2. IMPORTANT NEW DATA IN STANDARDS FOR A-C POWER CIRCUIT BREAKERS, **H. R. Summerhayes, G. Sutherland.** *Industrial Standardization.* American Standards Association, October 1945, pages 221-22.

E. W. Whitmer (American Gas and Electric Service Corporation, New York, N. Y.): In describing the completely sealed line of breaker bushings, the authors certainly are to be congratulated in the emphasis they have placed on mechanical details. Surely, the past operating troubles with bushings have been largely mechanical in nature. The mechanical troubles, however, frequently lead to electrical weakness. In the new bushings it is hoped that any mechanical troubles have been eliminated so far as is possible in an assembly of porcelain and metal parts which are joined together by means of gaskets. It seems reasonable to expect, however, that in service a few bushings might develop slow leaks. We have found that some older sealed bushings operate with internal pressures which are considerably below atmospheric. This factor, presumably, is caused by the gas in the expansion space being absorbed by oil or solid materials inside the bushings, thus causing the internal pressure to approach the vapor pressure of the oil. With an internal pressure below atmospheric pressure, any leak that might develop would draw in air, water, or whatever happened to be located at the outside of the opening. I would like to ask the authors if any means has been considered for maintaining in service a positive internal pressure in the sealed bushings, so that any leaks that might develop would be outward rather than inward, thus decreasing the possibility of anything being drawn into a bushing that would weaken the insulation.

It is gratifying to note that the matter of interchangeability has been considered. The new bushings can be used to replace existing old ones. Presumably, however, there would be some difficulty in replacing a new bushing in a new breaker with one of the old style bushings on account of difference in length of the bottom end. Complete interchangeability, therefore, has not been obtained between the new and old breaker bushings. If this interchangeability had been achieved, it would have been an advantage from the operating standpoint so far as the stocking of spare replacement bushings is concerned.

Philip Sporn (American Gas and Electric Service Corporation, New York, N. Y.): Notwithstanding the rather spectacular performance of the air blast breaker which we tested up to 3,500,000 kva at the Philo plant of the Ohio Power Company in 1944, and later described,[1] the quiet and consistent performance of the conventional tank-type oil circuit breaker, tested at the same time and under the same conditions, was a convincing demonstration that the oil circuit breaker is far from being on its way out. The 60-inch diameter tank for the 138-kv 3,500,000-kva breaker tested then was a long step in size reduction from the limit of 1,500,000 kva obtainable in this size only a few years ago. It is especially gratifying, therefore, to see that the 60-inch tank, only comparatively recently used for ratings up to 2,500,000 kva, now has given way to a 54-inch tank, and that the rating again has been increased, this time to 3,500,000 kva.

In carrying out the developments which have made this result possible, the authors and their associates, in my opinion, have performed an outstanding job and are to be commended highly. As pointed out in Table III of the authors' paper, the change in tank size from 60 inches to 54 inches for the 138-kv breaker, a reduction of approximately 20 per cent, also results in about the same percentage reduction in both the over-all weight of the breaker and the quantity of oil required. This step, and possibly further reductions yet to be brought about, indicate a trend which should augur well for keeping high voltage switchgear costs under control.

The authors' suggestion of a single breaker rating for high voltage breakers of 115 kv and above is, I believe, a reiteration of a similar suggestion made approximately a year ago in discussing papers presented by Byrd and Rietz[2] and Hill and Leeds[3] dealing with the development and testing of high-capacity high-speed breakers in this voltage range. The further extension of the trend toward concentrating higher interrupting capacity in a smaller

space, as exemplified by the authors' presentation, would seem to lend considerable plausibility and logic to this proposal. As St. Clair points out in discussing this paper, the requirement of minimum dimensions for adequate clearances at these voltages would seem to preclude the possibility of any appreciable saving in material in attempting to build a lower interrupting capacity breaker. In other words, having abandoned the old criteria for capacity, such as the 72-inch tank for 2,500,000 kva and the 60-inch tank for 1,500,000 kva, both in the 138-kv class, we definitely have lost practically all of the actual difference in weights and materials required on which to base the different interrupting ratings and corresponding prices. The simplification in the schedule of standard ratings resulting from these inescapable facts also should work toward an over-all reduction in circuit breaker costs.

Referring again to the papers on high voltage circuit breakers presented last year,[1,2,3] I also should like to re-emphasize the matter of the still officially listed, but utterly outmoded, derating factors applied to these high voltage breakers when used for high speed reclosing or other repetitive duty cycles. The developments and tests described in these papers showed unmistakably the feasibility of eliminating these derating factors, and the present developments described by the authors in this paper certainly add further corroboration to the same conclusion. Is not now the time, therefore, to bring our practice in line with the engineering facts in the case?

REFERENCES

1. FIELD TESTS AND PERFORMANCE OF HEAVY-DUTY HIGH-SPEED 138-KV CIRCUIT BREAKERS—OIL AND AIR-BLAST, **Philip Sporn, Harry P. St. Clair.** AIEE TRANSACTIONS, volume 64, 1945, pages 401–10.

2. A HIGH-CAPACITY HIGH-VOLTAGE THREE-CYCLE OIL CIRCUIT BREAKER, **H. L. Byrd, E. B. Rietz.** AIEE TRANSACTIONS, volume 64, 1945, April section, pages 160–3.

3. THE NEXT STEP IN INTERRUPTING CAPACITY—5,000,000 KVA, **A. W. Hill, W. M. Leeds.** AIEE TRANSACTIONS, volume 64, 1945, June section, pages 317–23.

H. P. St. Clair (American Gas and Electric Service Corporation, New York, N. Y.): The authors have made the interesting suggestion that only one breaker rating be included in the standards for each voltage at 115 kv and above, since there is little that can be changed in the present design to reduce interrupting capacity and cost and still meet the same performance standards at reduced capacity. With dimensions already down to what would seem to be a minimum required for clearances, I am inclined to agree with the authors' suggestion. A number of users, as those of the system with which I am associated, have been on a single rating basis for some little time, following the policy of buying only the largest breakers at these higher voltages and taking care of outlying stations by transferring lower rated breakers from heavier stations, where the newer breakers then will be installed.

It will be argued, of course, that smaller systems have no need for such a high interrupting capacity and, therefore, would be penalized. The only answer seems to be the realistic fact pointed out by the authors that, for their own design at least, there is not any way to cut down the interrupting capacity and save any money. It would seem logical to expect that in the long run, the industry would gain by such a simplification and that even the smaller systems would not be penalized appreciably, particularly since in an era of continued growth which we all look forward to the smaller systems are likely to become larger ones.

These new developments also suggest a further simplification in the matter of ratings, and that is the clear-cut elimination of derating factors for high speed reclosure on these high voltage breakers. In the light of accumulated results of field tests, I have felt for some time that these derating factors were unnecessary and, as a matter of fact have paid little attention to them in applying breakers. This, of course, is a matter for consideration of the Association of Edison Illuminating Companies–Edison Electric Institute–National Electrical Manufacturers Association triple joint committee on circuit breakers, and it is understood that it is on the agenda for the next meeting. This suggestion, therefore, constitutes another plea for a realistic and clear-cut approach to this question.

W. F. Skeats and **E. B. Rietz:** In suggesting the use of only one rating per voltage class, the authors considered the points raised by Hobbs but found little to justify the continuance of the present multiplicity of ratings. While it is quite true for instance, as Hobbs suggests, that there are momentary pressure impulses in the lower part of the tank, conservative design requires that the tank thickness be great enough to withstand the pressure that would result from ignition of the gases in the air space, and this pressure is not exceeded appreciably by the momentary impulses associated with interruption. Also, while it might be possible to make some saving in the manufacture of individual breakers by the use of inferior interrupting parts for 5-cycle application, it is felt that the use of the fast interrupters is well justified by their short arcing time and the consequent reduction in oil carbonization and contact deterioration. As St. Clair points out, the simplification of the rating structure that will result from this step may be expected in the long run to benefit both large and small systems.

It is felt that the flow of resistor current for one or two cycles beyond the 3-cycle interrupting time will not be of any importance from the standpoint of damage at the point of fault, since the magnitude of this current is substantially less than even the normal load current of the breaker. From the standpoint of system stability, it is generally an advantage since it reduces the tendency of the generators to accelerate and pull out of synchronism with the load.

In reply to Whitmer's question, the bushings are filled with nitrogen at a pressure sufficient to insure that the pressure will remain above atmosphere at all anticipated temperatures.

The question of interchangeability has been discussed with a number of users and the general consensus has been that the requirements in this respect are met substantially if the new bushing can be used in old breakers. This situation is very fortunate as it permits the breaker designer to take advantage of bushing improvements in building a better breaker.

Sporn and St. Clair have raised the question of derating factors. These factors now are under review in the appropriate industry committees.

Field Tests of Interrupting Capacity of 138-Kv Oil Circuit Breakers

Discussion and authors' closure of paper 46-19 by W. B. Buchanan and G. D. Floyd, presented at the AIEE winter convention, New York, N. Y., January 21–25, 1946, and published in AIEE TRANSACTIONS, 1946, April section, pages 199–204.

A. W. Hill (Westinghouse Electric Corporation, East Pittsburgh, Pa.): While a high power laboratory is indispensable for the development of large oil circuit breakers, the verification of interrupting capacity afforded by field tests such as these is of great value both to the designer and the user. Since most laboratories have only limited short-circuit capacity at 25-cycle frequency, it is particularly gratifying to have tests on a 115-kv 25-cycle system up to 2,500,000 kva, the maximum power ever interrupted on staged tests at this voltage and frequency.

The excellent performance of both the magnetic type BH and the multiflow type MF De-ion grid contacts confirm the applicability of these interrupters to the single tank type of oil circuit breaker.

Short-circuit tests on a high voltage power system are always of value in verifying circuit breaker rupturing capacity and providing a comparison with high power laboratory performance. The tests described by Buchanan and Floyd are of particular interest because of the 25-cycle system frequency. Circuit breaker rating standards recognize differences in the continuous current capacity as a function of frequency, but there has been no suggestion that the interrupting capacity may not be the same at all frequencies.

An a-c high voltage circuit breaker extinguishes an arc by waiting for a current zero and then deionizing the arc space so as to prevent reignition. After reaching the critical contact separation, the waiting time to the next current zero will average longer at the lower frequencies. The increased arcing time, of course, will be most significant in high speed circuit breakers, which tend to interrupt at the first or second current zero. Additional effects of frequency on the arc energy and oil pressure have been noted, which vary considerably according to the type of arc extinguishing structure used.

High power laboratory tests had indicated an interrupting capacity of 1,500,000 kva for the magnetic type BH De-ion grid interrupters at 25-cycle frequency, although at 60 cycles an interrupting capacity of 2,500,000 kva has been demonstrated. The tests described in this paper give a satisfactory confirmation of the 25-cycle rating of 1,500,000 kva at 115 kv.

The phenomenon of pressure waves in an oil circuit breaker tank, persisting for some time after arc extinction, was studied in some detail a number of years ago. The sequence of events appears to be as follows:

During the arcing period, rapid gas generation builds up an initial pressure peak. Horizontal forces on the tank walls are fairly well balanced. The vertical acceleration imparted to a considerable mass of oil above the arcing contact absorbs the upward force, leaving, however, an unbalanced blow on the floor of the tank. The tank supports and foundation deflect downward, and then the entire breaker structure tends to rebound upward, this being the familiar breaker jump. As soon as the arc is extinguished, the gas bubble is cooled rapidly. Also, the inertia of the rising oil mass expands the gas further. The pressure falls sharply and may even reach a partial vacuum. Compression of air above the oil, plus friction, is sufficient to stop and reverse the motion of the moving oil. Recompression of the gas bubble produces a second pressure peak, and subsequent oscillations of the oil may result in several additional pressure impulses of progressively reduced amplitude.

The breaker used in these tests offers an interesting example of one form of construction in which De-ion grids may be used. The single tank idea evidently has considerable local appeal, although where phase spacing must be varied to meet the requirements of many different station layouts, the single tank design does not have the flexibility required for general application. The same good performance has been secured in three separate tanks of the type GM breaker, with equivalent cost and weight of oil and steel, and described here in January 1945. There is a further advantage to the design using separate tanks, in that it is a relatively simple matter to secure single pole operation, which has come into prominence during recent years. Some users prefer the added factor of safety of phase isolation.

As Chubbuck pointed out, speed of closing and opening has been secured through a combination of motor operation and clutch drive, and the performance shows that this combination is quite reliable. Where large control batteries are not desired, the pneumatic mechanism offers considerable advantage in that its closing current is as little as one per cent of the equivalent motor or solenoid. Our experience in the United States with all three (solenoid, motor, and pneumatic) has shown a marked trend toward the pneumatic as the most favored type.

A feeling of confidence must have been brought to the minds of both the user and the designer by the series of field tests described by Buchanan and Floyd, and they are to be congratulated for successfully carrying out their program at a time when war-time loads were straining both equipment and personnel.

L. B. Chubbuck (Canadian Westinghouse Company, Hamilton, Ontario, Canada): As stated by the authors, the breakers used in these tests were Canadian Westinghouse, with all three poles in one tank. This 138-kv size has been in operation for about five years. Lower voltage outdoor sizes, down to 15 kv, have been in operation up to approximately 15 years, and with over 700 in service there has been no case of voltage breakdown because of their compact construction. As compared with three tank breakers—the tank, tank lever, pullrod—conduit and waterproofing features are simpler, and only one tank is involved in maintenance. Less oil is required than for three tank breakers.

With the De-ion grids used, there is little tendency for the arc to strike across phases, but to ensure against this a concentric micarta tube barrier is mounted around each grid.

All three pole breakers are tested, shipped complete, and erected as one unit. One man inside the 138-kv breaker, and protected from the weather, can adjust contacts without signaling from tank to tank.

A compact motor operating mechanism is used for these breakers. This mechanism has ample power and speed for 5-cycle breaker operation and 20-cycle reclosure.

W. B. Buchanan and **G. D. Floyd:** The comments by Hill on the action of pressure waves are interesting. Presumably, such phenomena become more apparent with high speed interruption of current. The tests reported seem to indicate more than one series of waves present (Figure 6). This condition may have been caused by the presence of three phases in one tank, or to the impact of a direct wave followed by that of a reflected component from the bottom of the tank. The data obtained are interesting but very limited.

The need for a lower limit of capacity on a 25-cycle rating may still be debatable, but, lacking any more definite information, it seems prudent to be conservative. The tests were made on a 3-phase nongrounded short circuit directly on the load side of the switch. This condition allows the neutral to shift, and two phases of the breaker in series to complete the final interruption of the short circuit. An irregularity in the line-to-ground voltage is shown in Figures 4 and 5. It is conceivable that a single-phase short circuit to ground might have imposed a more severe duty on one phase.

Long 60-Cycle Arcs in Air

Discussion and author's closure of paper 46-22 by A. P. Strom, presented at the AIEE winter convention, New York, N. Y., January 21–25, 1946, and published in AIEE TRANSACTIONS, 1946, March section, pages 113–18.

W. R. Brownlee (Commonwealth and Southern Corporation, Jackson, Mich.): The author presents interesting laboratory data which are valuable in isolating various phases of the problems of arc resistance. The two practical uses for this information mentioned by the author are the calculation of short-circuit current reduction and the influence on the phase angles of directional relays. A more important and more serious influence of arc resistance is its effect on distance relays. The arc resistance may be small compared to the total system impedance, but large compared with the impedance of the line being protected.

The results of the tests are rather startling, both with regard to the relatively low voltages per foot obtained and to the apparent independence of this voltage on the magnitude of the current. Possibly further consideration of the two to one variation encountered, even under carefully controlled conditions, may provide an explanation.

One criterion of arc resistance, as experienced in practical systems, is the impedance allowed for it in published transmission line relaying applications. One example is found in the description of the Kansas–Nebraska interconnection relaying[1] (Figure 12), where the arc resistance is indicated as 125 ohms (phase to neutral). With short-circuit currents estimated from the system characteristics, this value corresponds to about 960 volts per foot of arc for a 60-foot arc. On top of this, an allowance has been made of some 16 per cent of the total impedance (line and arc) in determining the setting for the instantaneous element. In the Fort Peck–Rainbow transmission line application[2] (Figure 12) the allowance made for the unstretched arc resistance is 40 ohms (phase to neutral). This amount corresponds to some 900 volts per foot of arc, on top of which an over-all relay margin of 16 to 20 per cent has been allowed. In the New England Power Company tests,[3] arc voltage rose to 63 kv in one second, which corresponds to a 60 foot arc at over 1,000 volts per foot, or if it is assumed that the arc resistance was 400 volts per foot, then the arc length must have been some 160 feet.

The above allowances for arc resistance are compromises in protection between safe coverage of faults and the necessity of preventing incorrect relay operations during system swings. In my personal experience, dozens of arcing tests have been performed on 115-kv and 161-kv systems, with arcs varying from 10 feet to 50 feet in length. Oscillographic measurements showed values from 1,300 volts per foot at 100 amperes to 500 volts per foot at 500 amperes, the values of ohms per foot being inversely proportional to the 1.4 power of the current. Even the Canadian tests[4] showed a variation of arc resistance between 200 amperes and 500 amperes corresponding inversely to the 1.4 power of the current. In searching for possible explanations of these discrepancies, the author's statement dealing with slight variations in the arc path may be significant. That is, arcs on transmission lines are exposed practically always to both magnetic and wind effects to provide these slight variations in the path, even before the arcs have time to stretch appreciably. The no-load voltage used for the test is not given, but mention is made of as much as 6,900 volts. Perhaps material differences are introduced when the no-load voltage is some 138 kv.

References

1. Staged Fault Tests of Relaying and Stability on Kansas–Nebraska 270-Mile 154-Kv Interconnection, C. W. Minnard, R. B. Gow, W. A. Wolfe, E. A. Swanson. AIEE Transactions, volume 62, 1943, pages 358–67.

2. Transmission and Relaying Problems on the Fort Peck Project, Erik Floor, H. N. Muller, Jr., S. L. Goldsborough. AIEE Transactions, volume 63, 1944, May section, pages 209–14.

3. Interesting Facts About Power Arcs. General Electric *Relaying News*, January 1941, pages 1–2.

4. A Study of Transmission Line Power Arcs, Paul Ackerman. *Engineering Journal*, volume 11, May 1941, pages 309–23; 504.

J. D. Cobine (General Electric Company, Schenectady, N. Y.): A few years ago, a search of literature for long arcs revealed only the work of Grotrian of 30 years ago.[1] It was surprising that no information was published on the long heavy current arcs that so often appear, though unwanted, in practice. Grotrian's arcs were of the order of 50 centimeters (1.64 feet) long and burned in a tube with a spiral flow of gas to stabilize them. The currents were under three amperes, direct current. For these very special conditions and copper electrodes in air, he found

$$e_a = 60 + \left(12.8 + \frac{35.5}{i}\right)x$$

where

e_a = arc drop in volts
i = current in amperes
x = length in centimeters

For the currents used in the present paper, the second term in parentheses can be neglected. Converting the gradient constant (12.8) to inch units gives 32.5 volts per inch. This value is in surprisingly good agreement, considering the extreme range of currents involved, with the present value of 34 volts per inch. The constant electrode drop found by Strom (35 volts) seems a better value for general use than the 60 volts of Grotrian.

Three of the volt-ampere characteristic curves show an interesting reverse loop with a fairly rapid rise in voltage at nearly constant current. How prevalent was this effect? Is this caused by a rapid increase in length synchronized with the peak current, that is, initial dissymmetry accelerated by magnetic forces? Is there any evidence of the length of time the vapor of the fuse wire remains in the column? The presence of metallic vapor would cause some departure of the column gradient from that for air alone.

Figure 1 of the paper shows a slow but definite increase of arc gradient with increasing current, whereas theory[2] calls for a slow decrease. This increase is probably caused by the indefinite size of column, possibly parallel paths, shown in Figure 11, which result in greater ion losses than for the idealized case.

References

1. **W. Grotrian.** *Annalen der Physik* (Leipzig, Germany), volume 47, 1915, page 47.

2. **C. G. Suits, H. Poritsky.** *Physical Review*, American Institute of Physics, volume 55, 1939, page 1184.

I. B. Johnson (General Electric Company, Schenectady, N. Y.): From studies of static arcs, such as those made by W. B. Nottingham and C. G. Suits, it is known that the voltage gradients in the arc column are a function of the gas in which the arc is burning, of the electrode materials, and of the kind of metal vapor contained in the arc, if any. Thus, for example, if Nottingham's equation for arcs in air (arc length greater than 15 millimeters), e (total voltage drop) = $A+Bl+C+Dl/i^m$ is applied to an arc in which the anode material is copper, the voltage gradient for arcs 48 inches long and for arc currents of 100 and 10,000 amperes are 49 and 43 volts per inch respectively. If the anode electrode is lead, the gradients are 32.4 and 22 volts per inch for arc currents 100 and 10,000 amperes respectively. Similarly, for zinc the results are 24.5 and 16.5 volts per inch. It is an interesting coincidence to note that these results for copper and lead are within the range of gradients as measured by Strom for the long dynamic arc. Calculations for arcs 12 inches long give gradients approximately the same as those for arcs 48 inches long, the greatest difference occurring for the 10,000-ampere arc with zinc electrodes, the gradient being 15 volts per inch as compared to 16.5 volts per inch for the 48-inch arc.

In the experimental work of Doctor Suits on static arcs, arc gradient measurements for metallic electrodes in air for 10-ampere arcs show the following:

	Volts Per Inch
Copper (oxidized surface)	10.5
Copper (lathe turned surface)	28
Copper (polished)	51
Lead	23
Zinc	35
Tungsten	48.5
Silver	46

These values should be less at higher currents. Spectroscopic studies indicate that arcs between electrodes of copper (polished), tungsten, and silver are essentially metal vaporfree arcs, while the others contained metal vapor characteristic of the electrode material. The effect of metal vapor is to lower the gradient appreciably. In Doctor Suit's study, precaution was taken to hold the arc stationary.

The mechanism of the arc is considered to be one of thermal ionization, the thermal and electrical properties being related by Saha's equation

$$\log\left(\frac{n^2}{N}\right) = -\frac{5{,}040}{T}V_e + 1.5\log_{10}T + 15.38$$

where

n = electron density
T = temperature
N = molecular density
V_e = ionization potential of the arc gases

The quantity n^2/N can be related to the arc current density I and the arc voltage gradient E by $(n^2/N)\alpha(I/E)^2$. Thus, if there is random motion of the arc and consequent random cooling, the effects on T and E, it would seem, should be likewise. If the arc is a metal vaporfree arc, then no changes in V_e will result in no changes of E. However, if the arc is a metal vapor one of a nonhomogeneous sort or if in the random motion the arc changes from a metal vapor to a metal vaporfree arc, random changes in the arc gradient could be expected. For gases such as N_2 and O_2, the ionization potentials are about 15.8 and 12.5, respectively, while for metals the ionization potential runs as low as 5 volts.

From the foregoing, then, the questions that arise are the following:

1. Is the long dynamic arc studied in this paper essentially a metal vapor or a metal vaporfree arc?

2. If it is a metal vapor arc, what metals determine its characteristics?

3. Of what metal or metals was the initiating fuse wire made, to what extent did it effect the results obtained, and would different kinds of fuse wires produce different voltage gradients?

4. In long 60-cycle arcs, will different electrode materials produce wide differences in voltage gradients?

5. Is a long 60-cycle arc initiated by a high voltage impulse, a metal vapor, or a metal vaporfree arc?

J. H. Hagenguth (General Electric Company, Pittsfield, Mass.): The paper is very interesting in that it confirms measurements by other investigators of the voltage drop in arcs in air. There are a few questions which arise, however, particularly with regard to Table II. This table shows the percentage of the first current peak of the arc to the current peak for a solid short circuit, which, for the lower circuit voltages, is usually less than the solid short-circuit current. The conclusion, then, is drawn that the current-limiting action of arcs on short-circuit currents depends on the relative value of the total arc voltage to the circuit voltage. This condition, undoubtedly, is true, particularly where the arc voltage becomes a large percentage of the circuit voltage. However, the limitation of the circuit current must have other causes besides the one mentioned. For instance, in the 2,300-volt circuit for a nominal short circuit of 16,600 amperes, the first half cycle arc current is between 12 and 50 per cent of the no arc current from Table II. It seems doubtful that this wide variation is caused by arc resistance alone, because from Table I it is

Table I. Instantaneous Resistance of Arc Path

$$R_i = \frac{0.016 \times l \times 1{,}100}{I_x}$$

Test	R_i Test, Ohms	R_i Calculated, Ohms	I_x Average, Amperes	Gap Length, Inches	Circuit Volts, Rms
A	12.5	11.5	135	48	5,750
B	8.7	13	120	48	2,300
C	6.6	7	222	48	2,300
D	3.25	3.37	460	48	2,300
J	0.405	0.45	3,550	48	2,300
L	0.144	0.156	10,000	48	2,300
W	0.085	0.065	12,000	24	2,300
Z	0.039	0.022	17,900	12	1,150
AC	0.035	0.029	13,666	12	2,300
AI	0.087	0.073	5,346	12	6,900

found that the arc voltage varies only between 30 and 40, with one case at 43 volts per inch.

I wonder whether one reason for this variation is that the arc was struck at different points of the voltage wave. The oscillograms of Figure 7A seem to indicate a phase difference compared to those of Figure 8A. A further contributory factor may be the vaporization of the wire. Tests vaporizing thin wires with high current impulses[1] have shown that the resistance of the wire, because of its temperature, becomes so great that in the critical stage the spark cannot be maintained and the current goes to zero, although the spark voltage would be sufficient to maintain the spark proper. Perhaps some such phenomenon may have been involved in the tests described.

It would be useful in connection with the mathematical solution given in the paper to know the impedances involved in the power supply, including generator, transformer, and reactors.

Considering the narrow range of arc drops measured, it may be worth-while to speculate on an equation for the instantaneous arc resistance at peak current. J. W. Flowers[2] has found that the current density in a spark discharge approaches a constant value of about 1,100 amperes per square centimeter. These measurements were made under conditions such that metal vapor from the electrodes did not contribute materially to the conduction. If we assume such a value to hold for power arcs in air (values ranging between 400 to 3,000 amperes per square centimeter are mentioned by L. B. Loeb[3]), then we can write the equation for the instantaneous resistance R_i of the arc at current peak:

$$R_i = 0.0116 \times l \times \frac{1{,}100}{I_x}$$

where

l = length of the arc in centimeters
I_x = current crest through the arc in amperes

The factor 0.0116 represents the resistivity of the arc in ohms per cube centimeter, assuming an arc voltage of 30 volts per inch. Using this equation for calculating the arc resistance and comparing these values with the experimental resistances, good agreement is obtained for the 48-inch arc, as shown in Table I of this discussion.

For the shorter gap lengths, the calculated values are lower than the experimental values. The latter are based on averaging usually three fairly consistent half cycle peak values of current and arc drop.

The better check for the longest gap may indicate that the electrode vapors do not contribute greatly to the conduction in the gap, but have some effect for the shorter gap lengths.

References

1. Vorgänge Beim Schmelzen und Verdampfen von Drähten mit Sehr Hohen Stromdichten, **J. Wrana.** *Archiv für Elektrotechnik* (Berlin, Germany), volume 33, number 10, 1939, page 657.

2. The Channel of the Spark Discharge, **J. W. Flowers.** *Physical Review*, volume 64, numbers 7 and 8, October 1 and 15, 1943, pages 225–35.

3. Fundamental Processes of Electrical Discharge in Gases (book), **L. B. Loeb.** John Wiley and Sons, New York, N. Y., 1939, page 610.

A. P. Strom: The author wishes to thank the discussers of this paper for calling attention to various problems in connection with long arcs in air, as well as for raising a number of significant questions in regard to this work. Not all of these questions can be answered specifically with the information now available, and this suggests that additional studies can be made profitably to gain a more complete understanding of these phenomena. The work presented in this paper was compiled with the preliminary study of the characteristics of high current 60-cycle arcs in mind, such as are found in power systems, and does not pretend to be a complete theoretical study of the physics of such arcs. Precautions were taken, nevertheless, to keep the conditions as nearly as possible to those of typical power arcs burning in air.

In regard to the conclusion made in the paper that current limiting action of arcs depends on the relative value of arc volts to circuit voltage, Hagenguth comments that this action does not appear to hold for the first half cycle of arcing.

The arc voltage does act to reduce the current even in the first half cycle, but if transient conditions exist, they also affect the current. In making these tests, a synchronous trip was used, so that the current started very nearly at the point of maximum circuit voltage. Introducing the arc into the circuit shifts the current more nearly into phase with the circuit voltage, and, therefore, tends to reduce the time duration and magnitude of the first half cycle of arc current.

There is also the transient effect resulting from striking the arc with a small fuse wire. The current rises rapidly before the wire fuses, so that at fusing the current density is higher than in the normal arc, giving an instantaneously high arc voltage. While this high voltage disappears quickly so that at the peak current a practically normal arc voltage exists, it may reduce appreciably the first half cycle of arc current. This effect varies with the size of fuse wire and appears to be the main cause of the variation in the first half cycle of current on the 16,600 ampere tests of Table II.

The fuse wires used to initiate these arcs (tests L to Q inclusive) were respectively:

1. L—two strands of 9-mil diameter copper wire.
2. M—one 40-mil diameter copper wire.
3. N—one 45-mil nichrome wire.
4. O—one 40-mil copper wire notched at 2- or 3-inch intervals to about one-half normal section.
5. P—three lengths of 40-mil copper wire alternately in series with four lengths of 2-strand 9-mil copper wire.
6. Q—three strands of 9-mil copper wire.

Power was supplied to these tests from the lines of the Duquesne Light Company paralleled with the Westinghouse power plant at Trafford. The approximate impedance of the circuit may be calculated from the no arc short-circuit tests of Table II.

The equation developed by Hagenguth for the resistance of an arc, $R_i = 0.0116 \times l \times 1{,}100/I$, is correct (except that 0.0116 should be 0.01075) for the assumptions made, namely, 30 volts per inch gradient and 1,100 amperes per square centimeter current density. However, it should be pointed out that having assumed a potential gradient it is superfluous also to assume a current density. The resistance, regardless of current density, is potential gradient times arc length, divided by the current.

Rewriting this equation, including the derivation of the first term

$$R_i = \left(\frac{30}{2.54I} \cdot \frac{I}{1{,}100}\right) \times l \times \frac{1{,}100}{I}$$

Hence it is clear that the current densities cancel out so that

$$R_i = \frac{30 \times l}{2.54I} = \frac{30 \times L}{I}$$

where L is inches. The calculated values in the table, therefore, should differ from the observed values only as the assumed gradients differ from the observed gradients.

Johnson's calculations of arc gradients from Nottingham's equations are of interest, since it appears that the right order of magnitude of arc gradients for high current a-c arcs can be obtained by extrapolation of these data for low current d-c arcs to many hundreds of times the current at which the equations were derived. In general, however, little confidence could be placed in such extrapolations without experimental verification, and that, of course, is one of the main reasons for the present study.

As Johnson points out, studies have shown that gradients of short arcs are affected materially by metal vapors from the electrodes. While there are, undoubtedly, some metal vapors from the electrodes even in longer arcs, it is believed that the arcs used were of sufficient length so that this effect was relatively unimportant. Even in those tests where the arc length was reduced to 12 inches, no decrease in arc gradient was observed over that for the 48-inch long arcs, as would be expected if the metal vapors play an important part. Further evidence is found in the arc data from field tests where the arcs were as long as 17 feet, and where it appears very unlikely that any appreciable metal vapor could be present. These tests give gradients that agree well with those of this paper. Some of these tests will be discussed in a later paragraph.

The fuses used in these tests were for the most part fine copper wires. For the smaller currents, a 3-mil diameter wire was used. For larger currents, one to three strands of 9-mil copper wire were used generally. In the series of tests, L to Q inclusive, fuse wires of various sizes and metals were used as discussed in a previous paragraph. It was found that the fuse wire could be increased in area by from 7 to 20 times, or changed from copper to nichrome with no appreciable change in gradient.

Assuming the Saha equation for thermal ionization to hold, it would be possible to calculate the gradients in arcs, provided the arc diameters and current distribution in the arc, as well as effective ionizing potentials, arc temperatures, and electron mobilities were known accurately. For the current ranges covered by these tests, these constants are not sufficiently well known to give any confidence in results obtained from such calculations, but perhaps with more accurate determinations of constants such methods might become useful.

Doctor Cobine inquires about the rather strange phenomenon of reverse loops shown in three volt-ampere characteristic curves. The occurrence appears to be random.

The phenomenon might be explained by turbulence caused by magnetic disturbances of the arc, which would increase with the current and have a time lag so that maximum turbulence occurs slightly after the peak current.

Brownlee presents in his discussion some interesting data on arc impedances as applied to relay systems. That estimates of arc resistance in relay applications should be considerably higher than the figures given in this paper seems reasonable, since allowance must be made for some arc elongation, wind effects, and factors of safety. Obviously, the tables in this paper give only the minimum arc gradients to be expected in still air, and suitable allowances must be made where conditions are present tending to increase the arc voltage.

However, the statement is difficult to understand that the arc voltages actually measured or computed at the 100- to 200-ampere range on field tests is almost invariably two to three times as high as given in the tables of this paper. Could these results have been caused by inclusion of impedance elements other than that of the arc itself, or special conditions such as tests on low current capacitive circuits? On reviewing the field tests found in the literature, and comparing the results with the present data, fairly good agreement is found even at the 100- to 200-ampere range. For example, Figure 5 in a previously published paper,[1] shows a summary of the results of field tests by a number of experimenters, all of which agree in order of magnitude with the data of this paper. At 140 rms amperes, the data for the first cycle of arcing in the Canadian tests[3] show arc gradients of 275 to 410 rms volts per foot or 390 to 580 peak volts per foot, whereas the average found in our tests was 375 volts per foot.

A report[2] by the Joint Subcommittee on Development and Research of the Edison Electric Institute and Bell Telephone System gives additional results from transmission line field studies.

Appendix II of this report, "Experimental Studies of Power Arc Characteristics—Croton Dam Tests," presents data that also agree reasonably well with the results of this paper. While rather large random variations occur in the data recorded, the average gradient is about 300 volts per foot, and no gradient is in excess of 580 peak volts per foot in the seven tests at currents in excess of 50 amperes. Two tests on low current capacitive circuits do show peak gradients of 900, 1,000, and 1,750 volts perfoot, but this is to be expected because of the characteristic nonsinusoidal current in such circuits with high initial peaks in the arc voltage.

A typical oscillogram for a current in the 100- to 400-ampere range is shown in Figure 34 of the report. Measurements from this oscillogram show arc gradients at peak current of 350, 360, 315, and 330 volts per foot, corresponding to currents of respectively 340, 350, 160, and 120 peak amperes. These results do not appear to indicate a variation of arc gradient corresponding inversely to the 1.4 power of the current. The arc lengths varied from about 8 to 17 feet, indicating that the gradient practically is independent of the arc length or voltage on the system.

REFERENCES

1. POWER SYSTEM FAULTS TO GROUND, C. L. Gilkeson, P. A. Jeanne, J. C. Davenport, Jr. AIEE TRANSACTIONS, volume 56, 1937, April section, pages 421–33; 474.

2. CHARACTERISTICS OF POWER SYSTEM FAULTS TO GROUND, (report number 39), D. A. Pierce, H. M. Trueblood. *Engineering Reports of the Joint Subcommittee on Development and Research* (Edison Electric Institute and Bell Telephone System), volume 5, February 1937, pages 5–39.

3. A STUDY OF TRANSMISSION LINE POWER ARCS, Paul Ackerman. *Engineering Journal*, volume 11, May 1941, pages 309–23; 504.

Dielectric Recovery by an A-C Arc in an Air Blast

Discussion and author's closure of paper 46-21 by T. E. Browne, Jr., presented at the AIEE winter convention, New York, N. Y., January 21–25, 1946, and published in AIEE TRANSACTIONS, 1946, March section, pages 169–76.

B. P. Baker (Westinghouse Electric Corporation, East Pittsburgh, Pa.): The deficiency of technical literature on a-c arc extinction, the lack of total agreement between theories explaining arc extinction phenomena, and the diversity in design of arc extinguishing devices clearly indicate the need for more fundamental information such as that which Doctor Browne has presented. His excellent work deserves our commendation.

Doctor Browne's findings regarding the processes of arc extinction resulting from turbulent diffusion, cooling, and the subsequent instability of the arc, and the effect of the circuit on this instability seem to provide an adequate explanation of high power arc extinction. However, the range of his data is limited somewhat in current, voltage, and air pressure, and, therefore extrapolation to high kilovolt-ampere arc extinction must be made with caution.

There are considerable data at high current and voltage to indicate that the rate of restoration of dielectric strength in the arc gap near the apparent current zero and the circuit characteristics are interdependent and affect each other tremendously as the point of maximum instability in the arc is reached. This interdependence seems to be more marked at the higher values of current. Fortunately, the fastest circuits generally are encountered at low voltages (generator voltages) and at high currents. Under these conditions the concept of arc extinction resulting from an increase in arc resistance as a function of time seems more pertinent than the notion of dielectric growth accompanied by negligible conductivity.

Tests made on high power commercial circuit breakers have shown that the arc space at the time of current zero for a 100,000-ampere arc may have an effective resistance of about 100 ohms. This resistance will exert a large influence on the transient recovery voltage of fast circuits. To meet the requirements of instability the circuit breaker must be able to increase the effective resistance of the arc space during this period, and thereby complete the interruption. Failure to do so results in reignition. Since this balance may be so critical, extrapolation from low powers to high, or reliance on any kind of test other than one in which full current and full voltage under normal transient recovery conditions are obtained, may prove unwise.

Figure 5 shows, as pointed out by Doctor Browne, that the growth of dielectric strength following the apparent current zero is divided into three stages: A slow initial growth, in some cases involving many microseconds, a region of rapid recovery, and a high dielectric plateau obtained some time after apparent current zero. Test results as presented before the Institute,[1,2] show circuit breaker performance in which the circuit characteristics were such that high voltages were applied within 2 or 3 microseconds after current zero. This is well within the region of the pause described in Doctor Browne's paper.

Typical tests from these data indicate that the cross-blast or splitter type of interrupter operated satisfactorily at 150 pounds per square inch, 13,200 volts, 8,000 amperes on a circuit where the transient recovery rate was 13,600 volts per microsecond. Also, at 53,000 amperes, 11,000 volts the circuit transient recovery rate was 7,100 volts per microsecond, in which case 15,000 volts was reached in 2 microseconds. At 125 pounds per square inch, 13,200 volts 105,000 amperes also was interrupted satisfactorily on a 2,080-volt-per-microsecond circuit. The circuit transient in all three of these tests, if uninfluenced by the arc conductivity, would produce high voltage peaks well within the times corresponding to the dielectric pause shown in Figure 5. Even after damping the low-energy high-frequency oscillations, the restored voltage reached as high as 10,000 volts in 2 microseconds on the 53,000-ampere test, which indicates that interrupting phenomena at high currents and pressures differ materially from that shown in Figure 5.

Again I wish to congratulate Doctor Browne on his excellent paper and assure him of our interest in the continuation of this work into the range of higher currents, pressures, and voltages.

REFERENCES

1. A 2,500,000-KVA COMPRESSED-AIR POWER HOUSE BREAKER, L. R. Ludwig, H. M. Wilcox, B. P. Baker. AIEE TRANSACTIONS, volume 61, 1942, May section, pages 235–41.

2. TRANSIENT RECOVERY VOLTAGES AND CIRCUIT-BREAKER PERFORMANCE, R. C. Van Sickle. AIEE TRANSACTIONS, volume 61, 1942, November section, pages 804–13.

J. W. Beatty (nonmember; General Electric Company, Philadelphia, Pa.): The data presented in this paper are of great interest to those concerned with the manufacture and use of circuit breakers, and the author is to be commended on the use of a small model for the close study of the important time following current zero. As Doctor Browne no doubt knows, however, the model chosen for investigation is not an ideal type interrupter, and as such, the erratic results obtained must not be construed as representing the performance of a properly designed air blast interrupter. The author has plotted his reignition voltages versus time for various tank air pressures and currents and, in addition, has added a line which is said to be the rate of rise obtained by the displacement theory of interruption. In this way, the author evidently is at-

tempting to determine the validity of this theory. However, if one examines the arrangement drawing of the apparatus, it will be seen that no provision has been made for removing the hot gases and metal vapor which surely must surround the upstream electrode. The result is shown by the sketches of Figure 1. The only way for this dielectric-damaging material to be dispersed is through local cooling and being swept downstream into the interrupter. Thus, the displacement theory, which presupposes the insertion of clean dielectric at the velocity given by the design and operating conditions, is defeated by the very design of this unit. Therefore, it would be optimistic indeed to expect a verification of the displacement theory with the model used by the author. With this in mind, the writer has plotted the accompanying curves which compare the actual performance of the interrupter model, at 50 amperes, with the displacement theory recovery rate. The latter curve was constructed, in all cases, by:

1. Assuming that the arc is broken initially at the point of greatest constriction, and that subsequently the ionized gases attached to the downstream electrode are swept out in this direction with the prevailing air velocity.

2. Determining the prevailing pressure and velocity at the orifice given by adiabatic expansion from room temperature and the specified supply pressure.

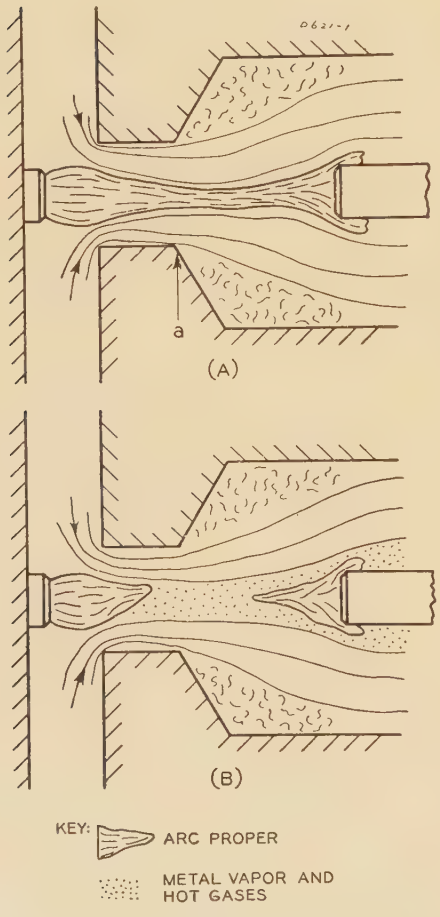

Figure 1. Schematic flow and arcing of Westinghouse test interrupter

A—Before interruption
a—Estimated location of initial break in arc
B—After interruption

3. Obtaining the breakdown strength of air between sharp electrodes for the orifice air density and for various gap lengths.

4. Determining the elapsed time, from the velocity, for obtaining a given separation of ionized materials and hence for obtaining a given dielectric strength.

The results of this procedure are agreeably surprising, especially in view of the simplicity of the theory. The curves given by theory are very close to the best test results obtained. The worst divergence, that at 40 pounds per square inch, shown by Figure 2, arises in part from oversimplification in the computation of the pressure–velocity relations under conditions of sonic flow. Had the resulting standing pressure waves been taken into account, the displacement theory curve would have been lowered.

Doctor Browne notes that the "plateau" region of dielectric recovery is particularly hard to explain on the basis of the displacement theory. However, one can point out that by the time the ionization attached to the downstream electrode has been swept out completely, only the bare electrodes are left, and hence a constant electrode separation exists. Unfortunately, a complication sets in because we still have ionized particles and metal vapors in the immediate vicinity of the upstream contact where they swirl and eddy at the will of the prevailing air stream. These particles gradually are swept downstream between the separated contacts, thus producing continuing erratic reignition voltages. That this contamination should be more pronounced the higher the current is to be expected, since the metal vapor and ionization adjoining the electrodes are increased proportionally. These results are shown by the final curves of the paper.

In conclusion, it appears unfortunate that the promising test model which was provided with means for scavenging the region adjacent the upstream contact was not tested thoroughly. Such a design would have been dictated on the basis of the displacement theory, and the tests would give very valuable design data.

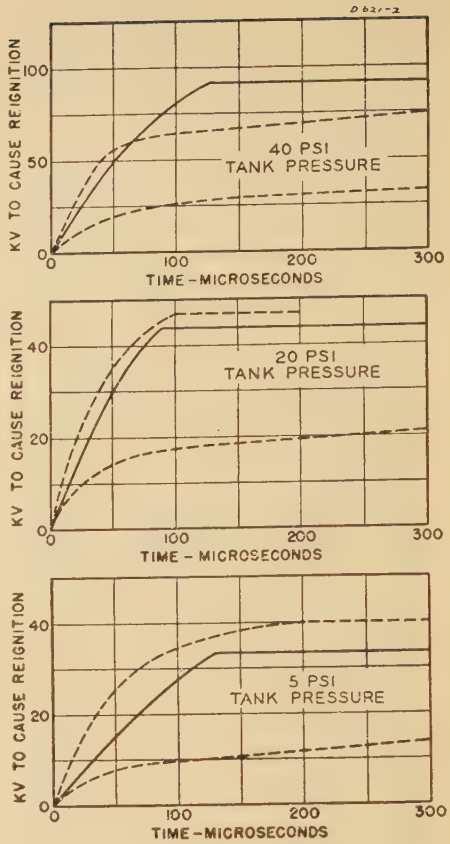

Figure 2. Reignition strength of Westinghouse test interrupter at 50 amperes

---- Envelope of test results
—— Displacement theory

T. E. Browne, Jr.: Mr. Baker's remarks help to fill in an admitted gap between this laboratory work and the field application of air-blast circuit breakers and so are appreciated. He did well to emphasize the difference between the air pressure, voltage, and current ranges covered by these tests and those at which high-power compressed-air circuit breakers generally operate. Some evidence was obtained during the tests that the course of the dielectric recovery at considerably higher air pressures, even at the lower currents, may be rather different from that observed at 40 pounds per square inch and below. The tabulated values of "initial time delay" do seem to suggest that this pause should persist at higher air pressures if the arc current magnitude is also correspondingly higher, but it is not certain how far this extrapolation can be carried. One reason for uncertainty is the breakdown of the concept of arc dielectric strength at high arc currents. In the work described in the paper, the concept of a "race" between circuit recovery voltage and recovery of dielectric strength by the arc space was held to deliberately for the sake of simplicity. However, this is an idealization which, as intimated by Mr. Baker, becomes increasingly inadequate as arc currents are increased and arc "resistances" correspondingly diminish. At the highest currents, it is undoubtedly true that the arc can be described more realistically as an electrothermal mechanism of rapidly fluctuating conductivity possessing an inherent hysteresis which may or may not permit it to pass through a current reversal without losing its stability. Unfortunately, this is a far more complex concept to work with than that of dielectric recovery, but progress is being made with it. An immediate objective of the work in our laboratory is to obtain experimental data on the reignition or extinction of high-current arcs in an air blast from this latter point of view.

Mr. Beatty in an interesting contributed discussion has attempted to support the displacement theory of dielectric recovery in the light of the data presented in the paper, following closely the concepts of Prince, Henley, and Rankin (reference 2 of the paper). As stated in the paper these and other results at first glance do seem to offer partial support for the displacement theory, and the author has himself made serious attempts to explore the extent of such support. The difficulty always arises, however, that a careful analysis of the displacement concept destroys the illusion of beautiful simplicity characterizing the original theory. This is illustrated unusually well by Mr. Beatty's sketch of the test interrupter after inter-

ruption. For instance, on what basis can a designer distinguish between the "arc proper" and the "metal vapor and hot gases" in order to establish such boundaries as those sketched and so estimate a rate of relative displacement between such boundaries? Mayr[1] has attempted such a distinction on the basis of an arbitrary temperature level during cooling, but this part of his picture does not bear any direct relation to a calculable physical displacement. With regard to the breakdown strength to be assumed for the dielectric medium, Mr. Beatty's "metal vapor and hot gases" of the sketch seems a rather far cry from the "clean dielectric" which, as he says, the displacement theory presupposes. Also, one still must agree with Doctor Suits when he says: "Many questions may be raised concerning the physics of the breakdown between 'ionized stumps' described . . . as part of the displacement process."[2] Such objections to the displacement theory have been pointed out repeatedly in discussions before the Institute by Doctor Slepian, who has shown further (reference 4 of the paper) that fluid flow alone cannot cut or displace the hot gaseous arc residue, even though metal vapor may be excluded from it by a suitable double flow arrangement.

Hence, in view of this general vagueness and of the uncertainties in the appropriate values for a displacement calculation of dielectric recovery, it does not seem particularly surprising that curves such as those plotted by Mr. Beatty can be made to fit observed data; but such a fit hardly justifies the implied claim that the performance of any flow-type interrupter can be predicted accurately in such a manner. If further illustration of the difficulties is needed, one need only compare the dielectric recovery plots of the paper for currents much larger than 50 amperes with Mr. Beatty's curves. Unfortunately, the results show that much more work will be necessary before the theoretical picture of the recovery of dielectric strength by the arc space in a gas blast can be considered to be complete or even entirely clear.

REFERENCES

1. ÜBER DIE THEORIE DES LICHTBOGENS UND SEIBER LÖSCHUNG (THEORY OF THE ARC AND ITS EXTINCTION), O. Mayr. *Elektrotechnische Zeitschrift* (Berlin, Germany), 64, 1943, page 651.

2. Discussion by C. G. Suits of THE CROSS-AIR-BLAST CIRCUIT BREAKER. AIEE TRANSACTIONS, volume 59, 1940, page 1121.

Metal-Clad Unit-Type Switchgear for 33-Kv Service

Discussion of paper 46-43 by C. H. Kreger, presented at the AIEE winter convention, New York, N. Y., January 21–25, 1946, and published in AIEE TRANSACTIONS, 1946, June section, pages 360–8.

M. H. Hobbs (Westinghouse Electric Corporation, East Pittsburgh, Pa.): The paper presents a very complete report on the experience of Kreger's company with outdoor oil-filled metal-clad switchgear for 33-kv service, starting with the first installation in 1928, and comprises an excellent record for the future reference of the industry.

It is particularly valuable because it covers not only several installations, but because it includes the product of three different manufacturers. Kreger has been quite frank in pointing out shortcomings as well as advantages of the design.

The service experience generally has been shown to be satisfactory, and particular stress is placed upon the permanence of the insulation and the fact that the equipment can be installed in industrial and railroad yard districts, where smoke and dirt would make the maintenance on open-type substations almost prohibitive or impossible.

The cost comparison, including both equipment and installation, shows a figure approximately 30 per cent higher than the open frame type, but this increase is justified on several counts. It is questionable whether the prices at which the equipment was sold were adequate for the type of construction, and this will require further study and development by the manufacturers. Oiltight construction requires very close machine work, as well as tightness of the metal itself, all of which is more expensive than unfilled structures.

Another point in question is the use of removable- or disconnecting-type breakers in structures of this class. We agree with the author that this feature appears to be unnecessary. Disconnecting switches appear preferable and more economical since the precision construction required for interchangeable removable-type breakers thus is eliminated.

One of the most important points is the use of oil for filling the bus and connection enclosing structure. Operators in the United States have been reluctant to accept oil or even compound filling, and even in England there now appears a tendency to eliminate it, where it has been the invariable rule in the past. In the United States, on two different systems, oil filling was used on the first installation in each case, and unfilled equipment on later gear. These were indoor installations, one for 26.4 kv and the other for 25 kv, both with 80-kv 60-cycle test insulation.

Some consideration is being given to indoor metal enclosed, but unfilled, switchgear with compressed air breakers, and equipment of this type for 33-kv service actually has been built. We would appreciate the author's opinion of this type of construction as compared to the oil-filled outdoor.

It is interesting to note that on the Joliet and Bellwood installations described, as well as on a similar installation at State Line in the same district, the first applications were made on a large scale of the solder seal process of attaching metal to porcelain. In spite of the severe temperature conditions, the service was excellent and the basis for the present solder seal designs of weather casings for condenser bushings on high voltage breakers and transformers, which have proved so successful.

Kreger and his associates are to be commended not only for the excellent report and service record submitted, but for their pioneering work in the metal-clad switchgear field.

B. R. Nevins (Philadelphia Electric Company, Philadelphia, Pa.): The application of metal-clad switchgear to high voltage outdoor use is a greater departure from the conventional outdoor construction than is the case with indoor metal-clad gear. It is interesting, therefore, to have presented the experiences of the Public Service Company of Northern Illinois resulting from several years of pioneering in the use of 33-kv outdoor metal-clad switchgear.

While it is significant that this company after a fair trial of seven major installations, all of which have been in service 13 years or more, is enthusiastic about 33-kv metal-clad gear to the point of advocating more general adoption, the writer cannot agree fully with the author that some of the arguments in favor of this type of equipment are substantiated by his paper.

The safety of the metal-clad equipment is undoubtedly of a very high order, and this is an important point in its favor, however, with proper safeguards and interlocking, the open-type construction can be made quite safe. The high reliability and low cost maintenance claims do not seem to have been borne out by experience. The two bus faults reported seem to indicate no greater reliability than with open-type construction. The semiannual maintenance required by the shell bushings would appear to offset the possibility of longer periods for the rest of the equipment. Maintenance of circuit breakers does not appear to be as simple as with open-type construction.

In making this criticism, the writer realizes that the switchgears in question are among the first of their type to be built, and little or no opportunity has been afforded the manufacturers to build improved designs since their installation. However, there is no definite evidence presented to prove that the difficulties encountered would be overcome easily on future installations.

Should future development of this type of equipment be undertaken it is the writer's opinion that serious consideration should be given to the elimination of oil. The hazards of oil fires and explosions seem to more than offset the hazards caused by exposure inherent in open-type construction. The development of a breaker connection which would eliminate the shell bushing difficulties would be very desirable. A dry-type bus, while open to the objection of requiring more space, might improve the shell bushing difficulty.

The writer does not condemn the principle of the outdoor high voltage metal-clad switchgear, but rather feels that the advantages realized are not sufficient to justify its development economically. The cost always would be high since the field of application is much smaller than is the case with the lower voltage equipments, and the advantages of repetitive manufacture would not be realized to as great an extent.

H. V. Nye (Allis-Chalmers Manufacturing Company, Milwaukee, Wis.): To one like myself, who was connected intimately with the design of some of the oil-filled vertical lift outdoor switchgear described in this paper, it is highly gratifying to find that the service record of this equipment has borne out so well the expectations on which these designs were predicated. Perhaps only those who were involved appreciated to what extent both the customer and manufacturer were pioneering in building such large outdoor switching units, metal-enclosed and oil-filled. The fact that all of

this equipment, from three different manufacturers, has given satisfactory service over a period of from 13 to 16 years seems to me to justify confidence in the new designs of switchgear apparatus which are being brought forth today, and back of which we do not have many years of operating experience.

I believe Mr. Kreger has done a service to the industry in presenting such a careful and impartial record of his experience with these installations. Such presentations of operating experience are the basis upon which real progress must be founded.

In regard to the future of outdoor metal-clad switchgear, it seems to me that it depends to a large extent on the value operating companies place on the advantages of this type of switchgear, and which are stated so ably in the paper itself. Without question, changes in the design can be made which will somewhat cheapen the manufacture, but it is doubtful if outdoor metal-clad switchgear in voltages of 33 kv and over can be produced economically unless there is general acceptance of the desirability of going to this construction.

I feel that we, the manufacturers, must rely on the operating companies for guidance as to the type of construction which most adequately meets their needs. Then, as manufacturers, it will be our duty to meet their requirements.

H. W. Haberl (Quebec Hydro-Electric Commission, Montreal, Canada): The author indicates that metal-clad switchgear for 33-kv service is reliable, durable, and safe. It is my opinion that his statement is correct in all respects; however, in the matter of an operating company using metal-clad switchgear to supply a large number of customers should a defect arise (and the author mentions some difficulties with certain bushings), the outage might be long and the customers certainly would complain. I agree with the author in that such an installation of metal-clad switching is a reasonably safe device from a safety standard. Also, this equipment should be used in customers' locations where an outage would result in not more than one customer shutdown, but constructing major substations in such a manner would involve long shutdown for repairs to numerous customers.

The author mentions the elimination of smoke hazards adjacent to railroad sidings and cites an installation. I would prefer to see the more conventional type of switchgear housed in a reasonably cheap cover and using air-blast circuit breakers in lieu of oil equipment. In this way the danger from fire hazards would be eliminated entirely, the cover over the equipment would eliminate weathering, and the ease of immediate repair is available in the open-type of switchgear. I will admit that safety to personnel in the open-type of switchgear is more hazardous than with the metal-clad; however, most operating companies personnel are thoroughly conversant with all electrical hazards, and the danger to the personnel is probably greater while walking on city streets than from working in substations. Again, I endorse Kreger's metal-clad switching for customers' installations where the personnel is not as conversant with the electrical hazards, and a shutdown for repairs affects only one customer.

Size Reduction and Rating Extension of Magnetic Air Circuit Breakers up to 500,000 Kva, 15 Kv

(46-55)

The Development, Design, and Performance of Magnetic-Type Power Circuit Breakers

(46-42)

Discussion and authors' closure of paper 46-55 by R. C. Dickinson and Russell Frink, and discussion of paper 46-42 by L. J. Linde and B. W. Wyman, presented at the AIEE winter convention, New York, N. Y., January 21–25, 1946, and published in AIEE TRANSACTIONS, 1946, April and June sections, pages 220–3 and 386–93.

B. W. Wyman (General Electric Company Philadelphia, Pa.): The problems encountered by Dickinson and Frink in their extension of magnetic air breakers to 15 kv are of particular interest to me because they so closely parallel my own experience several years ago in extending the Magne-blast breaker to 15 kv.[1]

It was pointed out that higher voltage interrupting performance could be attained by increasing the total length of the arc. Apparently Dickinson and Frink have reached the same conclusion, as they now state that they have offset the ends of the tapered slots in alternate ceramic plates of their arc chute, which will force the arc into a zig-zag serpentine path as it travels into the slots, the same as is formed by the interleaving fins of the Mange-blast breaker.

The arc chute which they describe then properly can be called an interleaving slot type of chute compared to the interleaving fin type of chute in the Magne-blast breaker. In comparing the performance of the interleaving slot type of chute with the interleaving fin type of chute, there is one outstanding difference. In the interleaving slot chute described by Dickinson and Frink, the arc interleaves and increases in length as the slots interleave, but the arc is halted abruptly when it hits the ends of the slots. It then must stand still while waiting for the current to pass through zero, which will result in excessive plate temperatures and melting at the ends of the slot. Interruption then must be accomplished at the ends of these extremely hot slots. It, therefore, is not surprising to find that it has been necessary to install special magnetic field structures to interrupt high currents under such adverse conditions.

However, in the interleaving fin type of arc chute used on the Magne-blast breaker, no such slot end is present. The arc is free to continue at its initial high speed ever deeper and deeper into the interleaving fins. It, therefore, arrives at current zero still traveling at the same high speed on fresh cool fin surfaces, which easily cool the hot arc gases faster than recovery voltage can be established. Besides effecting much easier interruption, this type of chute provides the additional benefit of moving the arc so fast at all times that no local excessive chute temperatures are reached, which is advantageous when applying these breakers on high speed reclosing service.

Another interesting feature in their breaker is the auxiliary low voltage interrupter required in each arc chute to aid arc transfer onto the arc runner. The authors state that this interrupter is required because of the high reactance of the blowout coil connected in series with the runner. It is not readily apparent why this complication is resorted to when the arc runner may be shunted into the circuit by the contacts themselves before any arc is drawn, as is done in the Magne-blast breaker.

In the photograph of the breaker shown in Figure 5, the contacts are equipped with auxiliary air pistons. In the text it is stated that such air pistons may be added to speed low current interruptions, but the breaker can interrupt without their help. We have had much experience with piston air boosters, having equipped all Magne-blast breakers with them. While it has been our experience that most magnetic breakers can interrupt low currents without boosters, the arcing times on low current interruptions become very long. These long arcing times on normal load currents greatly increase contact and runner erosion so that boosters are much more than justified in the decreased maintenance of the breaker.

Reference

1. A Magnetic-Type Air Circuit Breaker for 15,000-Volt Services, L. J. Linde, B. W. Wyman. AIEE Transactions, volume 63, 1944, March section, pages 140–4.

H. V. Nye (Allis-Chalmers Manufacturing Company, Milwaukee, Wis.): Since both of these papers relate to the design and performance of magnetic air circuit breakers, I wish to comment on the two papers simultaneously.

Each of these papers presents in an interesting and able manner a neat piece of development and design work which has resulted in improving the performance of the magnetic breaker, and the authors should be congratulated on the way they have handled the subject matter of their papers. I am inclined to think, however, that the authors of each paper might be criticized for the emphasis they have placed on the treatment of one factor entering into the successful operation of a magnetic breaker, to the virtual neglect of other equally vital factors.

Dickinson and Frink describe an ingenious means of using whatever blowout coil strength they have available to gain the maximum effect on the arc in the time interval during which the current is near the zero value, and the efficacy of doing this is quite apparent by the reduction in dimensions of their arc chute. From a consideration of the oscillograms given and the general design of the arc chute, I am convinced that they also try to take full value of the advantages to be gained by attenuation of the arc, and the cooling effect obtained by driving it into intimate contact with the surfaces of the heat resistant ceramic barriers. I am sure also that the authors of both papers have endeavored, by proper contact and runner

design, to facilitate the transfer and movement of the arc, independent of the other features.

The point I wish to make is that the designer who succeeds in co-ordinating all of these factors, in order to obtain the best over-all result, probably will produce the most efficient and economical design. That, I believe, is the result we are all striving for.

R. C. Dickinson and **Russell Frink**: The discussions which have been presented are appreciated. We thoroughly agree with Nye that the ideal magnetic air circuit breaker will be a balanced design in which all factors are co-ordinated properly with each other. The small size of the arc chute in the 15-kv magnetic deion circuit breaker gives clear evidence that a balanced design has been reached. However, in presenting the paper, stress was placed on the features which were considered novel, and features which have been covered in previous papers have been touched on only lightly.

Some questions have been opened by Wyman which should be dwelt on further. The statement is made that there is one outstanding difference between the interleaving slot type of chute and the interleaving fin type. In fact there are several outstanding differences. By comparison, the Magne-blast arc chute appears to be about 30 inches long in the direction in which the arc is extended, while the magnetic deion arc chute is 19 inches long in the same direction. Other dimensions of the two arc chutes seem to be about the same. A test was made to find the relative performance of fins and slots. Two arc chutes were used, identical except that in one chute the slots were terminated between the magnet shoes in the high-field region, while in the other the slots were extended two inches above the magnets so that the plate edges more nearly approached fins. It was found that the chute with the slots terminated in the high-field region had approximately 60 per cent greater interrupting ability than the chute in which the slots were lengthened. This fact indicates that the slot-type design has something that provides extra interrupting capacity, which is not found in the fin-type. This feature is the actual driving of a blast of air through the arc held stationary at the ends of the slots. When a fin-type structure is used, this action is not possible because the arc would be carried along with the blast of air and emerge at the exhaust end of the chute. It is evident that when the arc is thus free to move, little relative motion between the arc and the surrounding gas is possible, and most of the heat liberated by the arc must be absorbed by the chute. It is not surprising that Wyman, with his experience founded on such a structure, would be concerned with undue heating. With the magnetic deion breaker, the arc is subjected to a magnetically induced blast of cool air which carries away much of the heat, so that only a fraction is absorbed by the plate structure. Considerable discussion could be presented on heating, but it should suffice to state that the magnetic deion breaker has ample capacity to perform all standard reclosing duty cycles without undue heating, and to interrupt its maximum short-circuit rating repeatedly with no appreciable deterioration.

We also note Wyman's statement concerning a special magnetic field structure. According to published illustrations, the Magne-blast circuit breaker requires six separate coil and magnet assemblies for the 15-kv ratings, while the magnetic deion breaker performs similar duty with only one coil and magnet. Under the circumstances, it is difficult to reconcile the statement referring to the deion field structure as special. In construction it is simplicity itself.

Wyman has criticized the use of an auxiliary interrupter to introduce the blowout coil into the circuit. This action undoubtedly can be accomplished in other ways, but this method offers certain distinct advantages. In the first place, the auxiliary interrupter tends to interrupt the transfer arc always at approximately the same point in the current wave. This factor gives definite field timing which drives the main arc into the slots consistently at the same point in the cycle, a decided advantage in obtaining arc control. If the field were introduced by the contacts as in the Magne-blast breaker, this timing would not be present as time of contact parting is purely random. Also, when a reactance is introduced into the circuit between the sequential opening of two pairs of contacts, the arc must spend more time on the contacts than it would otherwise. By divorcing the blowout coil transfer from the contacts, we cut down the time of arcing on the contacts themselves and thus increase their life. At the same time, we eliminate the necessity of insulation between the secondary and arcing contacts.

Several differences have been pointed out between the interleaving fin type of arc chute and the magnetic deion type, but the most outstanding difference is the fact that the magnetic deion type of construction has produced an arc chute for 15-kv breakers sufficiently small to make possible compact accessible horizontal-drawout breakers, which are not practical with any other design of air breaker available today.

New Series Capacitor Protective Device

Discussion of paper 46-45 by R. E. Marbury and J. B. Owens, presented at the AIEE winter convention, New York, N. Y., January 21–25, 1946, and published in AIEE TRANSACTIONS, 1946, March section, pages 142–6.

A. A. Johnson (Westinghouse Electric Corporation, East Pittsburgh, Pa.): There are a number of series capacitors in service on distribution circuits scattered throughout the United States. Two general types of trouble have been associated with series capacitor installations:

1. Troubles associated with the protective device in parallel with the series capacitor.
2. Troubles resulting from the fact that series capacitors inserted into a distribution circuit may resonate at frequencies other than the normal system frequency.

I believe that the protective device described will cure the difficulties associated with the parallel protective device, because this new equipment is purely mechanical in its operation and therefore is free from resonant or current surge difficulties, which may be associated with the series circuit consisting of the series capacitors and the protective circuit.

The difficulties encountered with series capacitors, which are a part of a transmission or distribution circuit, usually are associated with circuit resonance at frequencies which are less than the normal system frequency. There are several conditions under which resonance may occur, but the most likely situation to develop is series excitation of an induction motor when the motor is started. When this happens, the motor fails to come up to normal operating speed, and in effect the rotor of the motor acts as a generator of a frequency at which the source circuit is resonant when looking into the circuit from the rotor. The rotor locks in at a speed substantially corresponding to this subsynchronous frequency and will not pull out as long as the circuit remains fixed.[1]

Series capacitors are ideal for improving the voltage levels on circuits supplying lagging power factor loads. In effect, they shorten the circuit by cancelling out inductive reactance. Because of possible circuit resonant difficulties, however, indiscriminate application of series capacitors, without due consideration of the type of load to be supplied, definitely should be discouraged regardless of how satisfactory the parallel protective device may be. It is believed that there are a number of places where series capacitors can be applied safely, but that advance consideration of the application may dictate special equipment be provided to make the series capacitors perform in a satisfactory manner.

Reference

1. Self-Excitation of Induction Motors, C. F. Wagner, AIEE Transactions, volume 58, 1939, February section, pages 47–51.

Investigation of Arc Starting Characteristics of D-C Welders With Reference to Electrode Freezing

Discussion and author's closure of paper 46-12 by Joseph M. Tyrner, presented at the AIEE winter convention, New York, N. Y., January 21–25, 1946, and published in AIEE TRANSACTIONS, 1946, March section, pages 97–9.

G. H. Fett (University of Illinois, Urbana, Ill.): This paper gives an objective test of a quality of a welder which has been heretofore chiefly a matter of opinion. To make the paper of greater value, some additional information should be supplied.

First, what was the force on the electrode when contact was made, and when the contact was broken? How does this compare with the average force applied by several different welders in different circumstances? How does the magnitude of the applied force affect the freezing current?

Second, the author states that the current setting of the generator theoretically should

not affect the freezing time. From experience with the welding generator set at higher currents than the 70 amperes mentioned, the likelihood of electrode freezing at higher currents is considerably higher than at low values of current. It would seem desirable to have some experimental check on the effect of greater currents.

Third, the method of determining the satisfaction of an operator with a nonfreezing contact of 0.040 second as compared with a time of 0.070 second seems difficult. How was this determined? Could the operator distinguish between these two times, both smaller than a tenth of a second?

J. M. Tyrner: First, the forces when contact was made and when the contact was broken were both approximately two pounds.

It was assumed that welders keep their contact force low, because subconsciously they want to avoid freezing. However, welders would object if they had to tear the electrodes from the work by force. Slight changes of the applied forces do not affect the freezing time.

Second, contrary to the experience of Professor Fett, we did not find an increased tendency to freeze at higher current. However it is possible that the generator used by Professor Fett had very different transient characteristics at high and low currents. We did not run tests on very much higher current than 100 amperes, because we felt that the problem of sticking is serious only with comparatively low current.

Third, the time the operator keeps electrode and work in contact is different every time he strikes an arc. Sometimes he is inadvertently slower, and the electrode freezes. If the generator permits a longer contact time, the percentage of freezings is considerably lower, and that is noticed by the operator. The operator prefers a generator with a longer critical time, because he feels he does not have to be too careful.

Design and Measurements of Capacitor Discharge Welding Transformers

Discussion of paper 46-41 by T. W. Dietz and G. M. Stein, presented at the AIEE winter convention, New York, N. Y., January 21–25, 1946, and published in AIEE TRANSACTIONS, 1946, March section, pages 154–9.

G. M. Stein (Westinghouse Electric Corporation, Sharon, Pa.): Since this paper was published, a new and improved analytical design method has been developed.

The original analysis furnishes explicit design formulas for the periodic discharge only, and expresses all values in terms of the time of one-half cycle.

The new calculation extends this analysis into the range of the aperiodic discharge, and represents all design elements as functions of the time to the first current peak. This procedure simplifies the numerical calculation, because the time to the first current peak is given directly as part of the required performance of the welder.

The new analysis is based on the fundamental formulas already developed in the original paper, and also uses the same symbols.

In addition to this, a new variable

$$\left.\begin{aligned} v &= \tanh^{-1}\frac{2Z}{R_1} \text{ for the aperiodic discharge} \\ v &= \tan^{-1}\frac{2Z}{R_1} \text{ for the periodic discharge} \end{aligned}\right\} \quad (1)$$

is introduced into the expressions for T_m and T_o, given by equations 13, 19, and 26 of the original paper.

As a result the variable v, the time T_o, and the design functions h, k, and λ can be represented in terms of the time T_m by combining

$$h = \epsilon^{\frac{R_2}{2L_2}T_m} \quad (2)$$

with

$$\left.\begin{aligned} \frac{R_2}{L_2}T_m &= 2\frac{v}{\tanh v} \\ k &= \frac{1}{h}\cosh v \\ \lambda &= 2h\cosh v \end{aligned}\right\} \quad (3)$$

for the aperiodic discharge and with

$$\left.\begin{aligned} \frac{R_2}{L_2}T_m &= 2\frac{v}{\tan v} \\ k &= \frac{1}{h}\cos v \\ \lambda &= 2h\cos v + h^{\left(2-\frac{\pi}{v}\right)} \\ T_o &= \frac{\pi}{v}T_m \end{aligned}\right\} \quad (4)$$

for the periodic discharge. The values of v, h, k, and λ are plotted in Figure 1 as functions of $(R_2/L_2)T_m$ for the range of the aperiodic and periodic discharge. For the periodic discharge, the function $(R_2/L_2)T_o$ is added to these curves. As can be seen, the periodic discharge extends between $0<(R_2/L_2)T_m<2$, while the aperiodic discharge covers all values of $(R_2/L_2)T_m>2$. The amount of $(R_2/L_2)T_m=2$ represents the limit of the aperiodic discharge.

The graph shown in Figure 1 makes the amounts of v, h, k, and λ directly available for numerical calculations. These design functions of equations 2 to 4 therefore are introduced into the expressions for i_1, e, z, and $I_2=I_{2a}$, given in equations 10, 11, 12, 14, 16, 17, 18, and 20 of the original paper.

If these latter values also are combined with

$$\left.\begin{aligned} \phi_T &= \int_0^{\infty}\frac{e10^8}{N_1}dt \text{ for the aperiodic discharge} \\ \phi_T &= \int_0^{T_c}\frac{e10^8}{N_1}dt \text{ for the periodic discharge} \end{aligned}\right\} \quad (5)$$

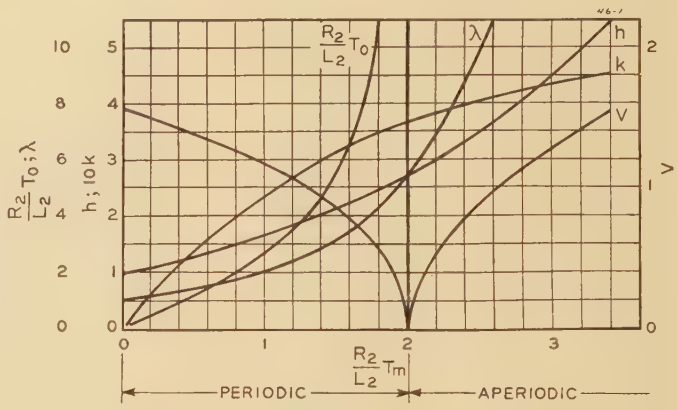

Figure 1. Design functions of capacitor discharge welding circuit

they furnish the design elements

$$\left.\begin{aligned} C &= h^2\left[L_2\left(\frac{I_{2a}}{E}\right)^2 10^6\right] \text{microfarads} \\ \frac{N_1}{N_2} &= k\left[2\frac{E}{I_{2a}R_2}\right] \\ \phi_T &= \lambda\left[\frac{I_{2a}L_2}{N_2}10^8\right] \text{maxwells} \end{aligned}\right\} \quad (6)$$

as well as the oscillograms

$$\left.\begin{aligned} \frac{i_2}{I_{2a}} &= \frac{1}{\sinh v}h^{\left(1-\frac{t}{T_m}\right)}\sinh v\frac{t}{T_m} \\ \frac{e}{E} &= h^{-\frac{t}{T_m}}\left[\frac{1}{\tanh v}\sinh v\frac{t}{T_m} + \cosh v\frac{t}{T_m}\right] \end{aligned}\right\} \quad (7)$$

for the aperiodic discharge and

$$\left.\begin{aligned} \frac{i_2}{I_{2a}} &= \frac{1}{\sin v}h^{\left(1-\frac{t}{T_m}\right)}\sin v\frac{t}{T_m} \\ \frac{e}{E} &= h^{-\frac{t}{T_m}}\left[\frac{1}{\tan v}\sin v\frac{t}{T_m} + \cos v\frac{t}{T_m}\right] \\ \frac{I_{2b}}{I_{2a}} &= -h^{-\frac{\pi}{v}} \end{aligned}\right\} \quad (8)$$

for the periodic discharge in an explicit form to the designer; because in any actual design problem, the values of R_2, L_2, I_{2a}, and T_m are given by the size of the work pieces and the type of weld to be made, and the voltage E is known as a manufacturing standard of the capacitor. Herewith, $(R_2/L_2)T_m$ is calculated, and the amounts of v, h, k, and λ are taken from the graph shown in Figure 1. If all these values are inserted into equations 6 to 8, the design elements C, N_1/N_2, and ϕ_T of the welder and its performance i_2/I_{2a}, e/E, and I_{2b}/I_{2a} can be computed for the whole range of the periodic and aperiodic discharge.

Measurement and Effect of Contact Resistance in Spot Welding

Discussion and author's closure of paper 46-9 by Robert A. Wyant, presented at the AIEE winter convention, New York, N. Y., January 21–25, 1946, and published in AIEE TRANSACTIONS, 1946, January section, pages 26–34.

C. L. Pfeiffer (Western Electric Company, Chicago, Ill.): Whenever anyone discusses the effects and methods of ascertaining the resistances of various sections of the weld zone in a spot weld, I think he is probing into the most difficult and most important problem in resistance welding. Methods of controlling and measuring the resistances, particularly the contact resistances, are not so much a laboratory matter as a real production problem. Professor Wyant's paper and his list of references cover the important investigation made in this field, all of which have been quite recent.

In connection with Figure 1, the author refers to sheet-to-sheet resistance, which "includes contact resistance plus the resistance of one sheet of material. Likewise the electrode-to-sheet resistance includes the contact resistance plus the resistance of one-half sheet of the material." Concerning the dynamic measurements made with an oscillograph, I assume that the quantities measured are voltage drops across a section of the weld zone, and a particular voltage drop divided by the total current, as measured by the shunt in series with the work, gives the contact resistance at that instant of the weld zone in question. Is that correct? Furthermore, are the resistances and reactances of the connecting leads and joints considered as negligible, or is their voltage drop added to the voltage drop across the oscillograph measuring unit?

In graphs of contact resistances, the values vary considerably during the period of current flow. Sometimes the contact resistance goes up considerably after having reached a fairly low point. I should like an expression of opinion, or even factual evidence as to whether this is caused by changes in points of contact between sheets or changes in current density at various contact points, or possibly is due to the lack of instantaneous follow-through on the part of the pressure means.

The paragraph headed "Copper Alloys," which states that "Practically nothing is known about contact resistance and the spot welding of the copper alloys," should stimulate researches along such lines.

I wish to congratulate the author on an excellent paper and particularly on his final three paragraphs titled "Research Problems."

B. L. Averbach (nonmember; Massachusetts Institute of Technology, Cambridge, Mass.): The measurement of contact resistance has provided a tool which is simple, yet accurate enough to be used for the statistical control of the spot-welding process. Since the contact resistance seems to be an important factor in the production of uniform spot welds, its measurement offers a method by which various surface preparations of the material may be evaluated quickly in the laboratory. In addition, this measurement can be taken right into the shop and used on a statistical basis to make certain that the material, when it reaches the welding machine, has a reasonably good chance of establishing a uniform contact resistance within a predetermined range under the welding electrodes.

By such a statistical control of the surface preparation the possibility of making a substandard weld is lowered, and the possibility of making a "dud" weld, barring machine failure, should be almost eliminated. It is interesting to see that even such often neglected features as rinsing and drying can have an important effect on the surface conditions, and it will be interesting to hear the results of the author's investigation of this phenomenon by electron diffraction.

The aircraft industry has been reluctant to accept spot welding on primary structures because of inadequate data on its reliability. If the spot-welding industry can demonstrate that it has sufficient control over all phases of its production, so that the aircraft designer can depend on getting a weld each time of uniformly high strength, then an important stride will have been made in the application of this inherently low cost joining method to the important structural members of the air frame.

Robert A. Wyant: Mr. Pfeiffer's assumption is correct with regard to the quantities measured and the method of calculating the contact resistance. The resistance and reactance of the potential connections are accounted for in the calibration of the oscillograph galvanometer circuits. There is little factual evidence of the specific cause of the occasional rise in measured contact resistance during the formation of a weld. It may be due to an increase in body resistance of the metal, as a result of increasing temperature. I should like to refer Mr. Pfeiffer to Figures 9 and 10 of reference 5 for better evidence of a rise in resistance for the above reason. The apparent rise in contact resistance also may be due to a decrease in conductivity of the metal at the points of contact for the same fundamental reason. I do not believe that it can be explained by a reduction in electrode force due to failure of the electrode system to follow through rapidly enough.

Mr. Averbach was associated with me throughout much of the experimental work described in my paper, and he made many important contributions to the work. Mr. Averbach refers to contact resistance measurements as a tool to be used in the statistical control of the spot-welding process. I should like to point out that the surface condition of the metal is only one of many variables which have to be brought under reasonable control before statistical methods can be applied to the control of the spot-welding process. I should like to call attention to the fact that industry has made quite an advance with respect to this application of statistical methods during recent years. I like to look upon contact resistance measurements simply as a means of evaluating surface condition and controlling surface treating processes for the preparation of metals prior to spot welding. Mr. Averbach expresses an interest in our application of electron diffraction methods to the study of the surface preparation of metals for spot welding. This is an interesting subject, and a summary of our work in this field was published in the "Research Supplement" of the *Welding Journal*, February 1946.

The Measurement of Large Varying Currents

Discussion of paper 46-2 by A. C. Johnson, presented at the AIEE winter convention New York, N. Y., January 21–25, 1946, and published in AIEE TRANSACTIONS, 1946, January section, pages 8–11.

F. B. Silsbee (National Bureau of Standards, Washington, D. C.): This paper, when viewed in connection with its background, affords an interesting example of the way in which a single problem and its various possible solutions may arise successively and be solved independently in different branches of electrical engineering. It also shows how, in spite of the best efforts of the engineering societies to stimulate the exchange of technical information, there is too much impedance to the flow of ideas.

The need for noninductive shunts seems to have been felt first in the precise testing of current transformers for ratio and phase angle. Paterson and Rayner[1] as long ago as 1909 described a noninductive shunt of tubular water-cooled construction similar to Johnson's type B, but with a tubular potential lead to render it less sensitive to stray external magnetic fields. Similar developments at the National Bureau of Standards[2,3] suggested other lead arrangements. For instance, the shunt shown at *d* in Figure 9,[2] is the same as Johnson's type C, and hence equation 45 is identical with equation 6 of the subject paper.

The next need for noninductive shunts arose in the measurement of surge currents in testing lightning arresters, and papers have been contributed on that subject.[4,5] At the National Bureau of Standards, we have found type C shunts satisfactory in the measurement of surge currents up to rates of change of 5 times 10^{10} amperes per second.

With the welding art comes still another application for the noninductive shunt, and the present clever contribution of the type D shunt with its potential leads embedded in slots in a thick-walled tube.

I feel that the term "somewhat laborious," by which the author describes the task of correcting for the effects of a nonsymmetrical return circuit, is a bit euphemistic. In all but very simple cases, such computations are exceedingly laborious, and in many cases impossible because the distribution of current is not known definitely. It seems preferable to use shunts provided with a number of pairs of potential leads symmetrically spaced around the shunt and connected in parallel. The use of only two or four such pairs of leads makes the shunt almost perfectly astatic. The limit of this process is obtained, of course, in using a tubular potential lead.[1]

In the case of thin-walled tubes when the compensation arrangement of type D is not feasible, other compensating tricks [2,3] are applicable.

References

1. Noninductive Water-Cooled Standard Resistances, **C. C. Paterson, E. H. Rayner.** *Journal*, Institution of Electrical Engineers (London, England), volume 42, 1909, page 455.

2. A Study of the Inductance of Four-Terminal Resistance Standards, **F. B. Silsbee.** *Bulletin*, United States Bureau of Standards, volume 13, 1916, page 375.

3. Notes on the Design of Four-Terminal Resistance Standards, **F. B. Silsbee.** *Journal of Research*, United States Bureau of Standards, volume 4, 1930, page 73.

4. Heavy Surge Currents—Generation and Measurement, **P. L. Bellaschi.** AIEE Transactions, volume 53, 1934, January section, pages 86–94.

5. Discussion by **Theodore Brownlee** of Heavy Surge Currents—Generation and Measurement. AIEE Transactions, volume 53, 1934, March section, pages 481–2.

An Automatic Oscillograph With a Memory

Discussion and author's closure of paper 46-67 by A. M. Zarem, presented at the AIEE winter convention, New York, N. Y., January 21–25, 1946, and published in AIEE TRANSACTIONS, 1946, March section, pages 150–4.

C. M. Foust (General Electric Company, Schenectady, N. Y.): The author has adopted what seems to be the best of several methods of recording wave shapes of random surges, particularly those of very short time duration. In general three methods have been used for this work: the time delay cable, the moving magnetic tape or links, and the after glow or memory of the fluorescent screen of a cathode-ray oscillograph. Invariably the conditions under which the recordings have to be made will determine which of these methods is most appropriate.

The first cathode-ray memory oscillograph was developed by A. W. Hull of the General Electric research laboratory, and reported to the National Academy of Sciences at its autumn meeting on November 18, 1935.[1]

Prior to this, early in 1935, Doctor Hull initiated the building of a 3-tube oscillograph, which was designed and constructed in the general engineering laboratory of the General Electric Company under the writer's supervision. This instrument was completed in 1936, and applied successfully.[2]

Possibly the most important difference between this oscillograph and the one described by Mr. Zarem is in the beam accelerating voltage. The 1936 instrument utilized a beam voltage of 15 kv, achieving therefrom an oscillograph writing speed substantially in excess of that obtainable with the author's 4,500-volt beam. Writing speeds in excess of one meter per microsecond are realized readily at 15 kv on single-sweep basis.

The successful use of this type oscillograph resulted in a second instrument being built along the same lines, so that six circuits could be studied simultaneously. This second memory oscillograph was completed in 1943.

C. C. Herskind (General Electric Company, Schenectady, N. Y.): The memory oscillograph is a very useful and valuable tool for the development and testing of mercury arc rectifiers. It has been used for a number of years for this purpose.

We have had two memory oscillographs in use for a number of years in connection with work on large mercury arc rectifiers. Each of these instruments has three cathode-ray tubes. By operating the instruments together it is possible to obtain records on all six anodes of a rectifier at one time.

The type of information which the memory oscillograph provides is illustrated by the following experience. During the years 1942–43 some of the ignitron rectifiers on the large electrochemical installations were operating with too high frequency of arcback. Extensive factory and field tests to determine the cause of these arcbacks were made without success. Finally a memory oscillograph was installed on one of the faulty units. It was connected to record the anode-to-cathode voltage. Records showed that the arcbacks were occurring throughout the inverse cycle with almost a uniform distribution. Of particular interest were records of arcback occurring so late in the inverse cycle that no circuit breakers tripped or interruptions occurred, and arcback would not have been suspected without the memory oscillograph record. The uniform pattern of arcback occurrence greatly reduced the probable causes of arcback.

The cause of arcback was found to be the flow of mercury from the exhaust pipe line into the rectifier striking the anode. The time of arcback from such a cause would be expected to be uniform in distribution throughout the cycle and, therefore, in agreement with the data obtained by the memory oscillograph. Once the cause was known, the fault was readily corrected.

The foregoing example illustrates an important application of the memory oscillograph. It undoubtedly will prove valuable in other fields where random phenomena are experienced and continuous records would be impractical.

A. M. Zarem: C. M. Foust and C. C. Herskind separately point out the previous use of oscillographs of the memory type in the study of the operation of mercury arc converters. Both men kindly have offered specific examples of the utility of such an instrument as a research tool. I should like, however, to summarize here the essential differences between the ordinary memory oscillograph and the automatic memory oscillograph. This matter is touched upon briefly in the first and last paragraphs of the paper under discussion.

The automatic camera and the electronic control unit form the heart of the automatic memory oscillograph. The combination of these two components with a beam blanking device and a cathode-ray oscillograph puts the resulting instrument in a class of its own. In addition to obtaining memory time, continuous monitoring of electric systems then becomes possible.

The advantages of automatic operation are tremendous when electrical conditions preceding randomly occurring transients are to be investigated. As the time of occurrence of these transients is unknown, the use of an operator to change films after a record has been obtained is not very practical. Under many conditions of operation, the recording equipment may not be at ground potential, making frequent film changing activity hazardous. In addition, since there is no assurance that a sporadic transient of a given type will occur twice, there are even instances where vital information may be lost during the time delay between changing of films.

Several other features serve to enhance the utility of the automatic memory oscillograph. Perhaps the most important of these is the inclusion of means for exercising accurate control in presetting the memory time desired. Other essential additions are the control of the instant of beam blanking, means for adjusting the camera exposure time, and the inclusion of a clock mechanism for identifying each transient with its time of occurrence.

The use of additional cathode-ray tubes for studying multiple phenomena is obvious. In this connection mention should be made of the new multiple beam cathode-ray tubes now commercially available. These tubes employ two sets of insulated accelerating guns and deflection plates, allowing the simultaneous appearance on one cathode-ray screen of two wave forms from sources at different potentials. Two very slow transients also can be studied with one cathode-ray tube by means of electronic switching.

It is believed that the automatic memory oscillograph is a definite advance in the development of a suitable device for recording electrical conditions preceding, during, or after the occurrence of an electric transient. It already has proved its value both as a laboratory tool and as a practical instrument for monitoring electric systems.

Thermal-Demand-Meter Testing Techniques

Discussion of paper 46-69 by E. E. Lynch and M. E. Douglass, presented at the AIEE winter convention, New York, N. Y., January 21–25, 1946, and published in AIEE TRANSACTIONS, 1946, March section, pages 124–8.

Perry A. Borden (The Bristol Company, Waterbury, Conn.): Without the late Doctor Paul Martyn Lincoln—father of the thermal watt demand meter—discussion of a paper dealing with that instrument seems almost a sacrilege. If he were here at the present time, or if he is permitted to be with us in spirit, we can appreciate his satisfaction in knowing that after 30 years of an up-hill fight the thermal meter has come into its own as a means for establishing the demand of an electric power load. Upon first reading the paper by Lynch and Douglass, I

was disposed to be critical of their policy in not making reference to the classic writings of Doctor Lincoln when he introduced the thermal watt demand meter, and as he carried it to higher stages of refinement; but, as I find the bibliography of Lynch's 1942 paper, to which he makes reference, places honor where honor is due, the omission may be excused. However, to those interested in demand determination and rate-making, but who belong to a younger generation that does not know Lincoln, I would recommend his writings and the discussions they engendered as an inspiring background against which the more modern work of the present writers may be projected brilliantly.

Electrical Analogy Methods Applied to Servomechanism Problems

Discussion and author's closure of paper 46-17 by G. D. McCann, S. W. Herwald, and H. S. Kirschbaum, presented at the AIEE winter convention, New York, N. Y., January 21–25, 1946, and published in AIEE TRANSACTIONS, 1946, February section, pages 91–6.

G. H. Fett (University of Illinois, Urbana, Ill.): In this paper the authors have developed the equivalent circuit of the motor from the mechanical viewpoint. That is, the authors have examined the motor at the mechanical terminals, the shaft, and expressed the result in terms of an electric circuit.

It is fruitful to examine the motor at the electric terminals, and express the result in terms of an electric circuit.

Consider a separately excited constant field motor with an armature resistance R_a, an armature inductance L_a, and a load on the shaft with a moment of inertia J and viscous friction coefficient F. Furthermore, assume that the armature current I_a will vary sinusoidally at an angular frequency ω. Then I_a, as well as the torque developed by the motor, and the load resisting torque all may be expressed properly in complex notation.

The voltage drop across the armature then is written as

$$\boldsymbol{V}=\boldsymbol{I}_a(R_a+j\omega L_a)+\boldsymbol{V}_g \qquad (1)$$

where

$\boldsymbol{V}_g$ = speed voltage of the armature

The speed voltage may be written as

$$\boldsymbol{V}_g=K\phi j\omega\theta_M \qquad (2)$$

where

ϕ = constant field flux
θ_M = maximum angular oscillation of the armature
K = a constant depending upon the number of poles, conductors, and armature paths

The motor torque T_M will vary sinusoidally and may be written as

$$\boldsymbol{T}_M=k\phi\boldsymbol{I}_a \qquad (3)$$

where k is another machine constant. Furthermore, the motor torque is given by the resisting load torque

$$\boldsymbol{T}_L=(-\omega^2J+j\omega F)\theta_M \qquad (4)$$

The combination of these four expressions gives for the voltage equation

$$\boldsymbol{V}=\boldsymbol{I}_a\left[R_a+j\omega L_a+j\omega\frac{Kk\phi^2}{(-\omega^2J+j\omega F)}\right] \qquad (5)$$

since

$$\theta_M=k\phi I_a/(-\omega^2J+j\omega F) \qquad (6)$$

and

$$\boldsymbol{V}_g=j\omega Kk\phi^2I_a/(-\omega^2J+j\omega F) \qquad (7)$$

The quantity in brackets in equation 5 is seen to represent a series impedance, and the last term is evidently the effect of the load on the shaft upon the electric circuit. The last term may be simplified by dividing through by $j\omega$, and, considering that it represents an impedance which has an admittance,

$$\boldsymbol{Y}=(F+j\omega J)/Kk\phi^2 \qquad (8)$$

This admittance represents a parallel electric circuit with a conductance $g=F/Kk\phi^2$, and a capacitive susceptance $b=\omega J/Kk\phi^2$.

The statement then may be made that the effect of the load is to insert an impedance in series with the armature resistance and inductance, this impedance to consist of a resistance $R_L=Kk\phi^2/F$ and a capacitance $C_L=J/Kk\phi^2$ in parallel.

If the friction is negligibly small, F is zero and the shunting resistance R_L becomes infinite or of no effect. Then the equivalent circuit has only the armature resistance, inductance, and the capacitance C_L in series.

The capacitance C_L is seen to vary directly with the moment of inertia and inversely as the flux squared. These relations have been checked numerically.[1]

In place of a parallel circuit to represent the effect of the load, a series circuit, of course, may be substituted. If the friction term F is much smaller than ωJ, which could occur at high frequencies or large moment of inertia, then the equivalent series circuit may be shown to consist of a resistance

$$R_s=Kk\phi^2F/\omega^2J$$

and a capacitance

$$C_s=J/Kk\phi^2$$

These relations are similar to those expressing a condenser with power loss in terms of a series circuit. The evident disadvantage is that the resistance depends upon the frequency used.

REFERENCE

1. NEGATIVE RESISTANCE AS A MACHINE PARAMETER, G. H. Fett. *Journal of Applied Physics*, volume 14, 1943, page 674.

G. D. McCann: Fett has presented another analogy for representing the differential equations of a motor. This is one of several other suitable analogies which could be used if desired. He has shown how to represent additional mechanical quantities, all of which can be represented readily in any of the possible analogies, including the one used by the authors.

Motor-Driven Exciters for Turbine Alternators

(46-77)

Application and Performance of Electronic Exciters for Large A-C Generators

(46-74)

Discussion and authors' closures of paper 46-77 by R. B. Bodine, S. B. Crary, and A. W. Rankin and paper 46-74 by H. A. P. Langstaff, H. R. Vaughan and R. F. Lawrence, presented at the AIEE winter convention, New York, N. Y., January 21–25, 1946, and published in AIEE TRANSACTIONS, 1946, May section, pages 290–7 and 246–53.

F. W. Gay (Public Service Electric and Gas Company, Newark, N. J.): This paper proves to the satisfaction of most engineers that motor-driven exciters will perform satisfactorily when driven from their generator terminals provided system protection devices function as hoped for. The safety factor inherent in this method of excitation is admitted to be very slim by even its promotors. The writer suggests that all engineers and managers of large utility systems not dependent to a very great extent on remote hydroelectric plants, analyze those system troubles which may be charged to generation, high voltage transmission, and subvoltage transmission. If such faults are indexed on the basis of minutes lost per customer chargeable to the various system faults, I venture to say that conditions will be found to be about as follows:

All minor troubles added together will cause total outages not greatly exceeding 20 per cent of the total. On the order of 80 per cent of the total will be chargeable to calamities. A careful study will probably show that of those 80 per cent of the total outages, little or no help would have been obtained by faster relaying or faster circuit breaker operation. The major trouble probably will be found owing to personnel failures and to a lesser extent due to equipment failures.

It would be my estimate that about 90 per cent of the literature both in the Institute and other publications is devoted to preventing faults in the class that will be found to cover the 20 per cent of the total minutes out per customer chargeable to minor faults and not more than 10 per cent will be devoted to faults that will be found to cover the 80 per cent of the outages (which may be listed as calamities). I venture to say that because of this overemphasis on the larger number of minor troubles, it will be found that the large utility companies spend 90 per cent of their money to prevent 20 per cent of the outage time and only 10 per cent of their money to avoid the 80 per cent outage time.

One characteristic is common to all electric utility calamities. That characteristic is that the voltage drops instantaneously to a very low value in the vicinity of the trouble and rises rapidly to a high value at locations remote from the fault. However, if a major fault is not removed within a half-second in almost any system, that system is on the brink of disaster. The voltage distribution at the end of one-half second (in

the system I am now discussing) still will be such that the faulty section will have the lowest voltage and can still be removed selectively. However, within a period of two seconds, the remote generator will have its voltage pulled down to such an extent that the location of the fault will be difficult or impossible to locate by voltage conditions.

It is my opinion that the most important subject to be discussed at these meetings and to be guarded against by the large metropolitan utility companies is a suitable backup method of removing from the system all those parts which have suffered sustained low voltage for about one-half second.

Let us study the excitation system proposed by the authors. We find that it appears to be perfect if the system operation is perfect, but a more or less complete collapse is imminent if low voltage persists for one-half second. I do not believe that many utility companies will install a system that will not allow the exciter to recover if low voltage persists for one-half second. This, in my opinion, is one of the most vital conditions that should be discussed in the use of this type of excitation. It has been completely ignored.

Where there are a number of such units in a station, it is entirely feasible to supply both excitation and auxiliary power normally from each unit, but in case of sustained low system voltage, all the auxiliary power can be thrown over to one of the plant units, and this unit can be disconnected from the system so as to provide auxiliary power protection in case of a major disaster.

It is important to note that in the large metropolitan utility system any major disaster which will drag down the voltage to 60 per cent of normal for one-half second or longer will result in throwing off a large amount of load (dumped load will return only gradually and the load will not build up to its normal value in much less than 15 minutes). Therefore the temporary loss of one-third of the capacity in any location following a prolonged system fault in that location should not be serious.

It is my opinion that a very much safer method of handling auxiliary power, including motor generator exciters, is to use a shaft-driven auxiliary power generator and obtain a source of power for the motor-driven exciter as well as for all other auxiliaries which is substantially independent of system faults.

J. F. Miller (General Electric Company, Schenectady, N. Y.): A great majority of the current orders for turbine generators specify shaft-driven exciters, and this would indicate that at the present time the industry prefers this type of exciter. Therefore, in this discussion I should like to point out that, while the motor-driven exciter system was being developed, considerable progress was made by the General Electric Company in the design of highly reliable shaft-driven exciters. Two types are now offered to the industry: gear-driven exciters in ratings from 125 kw to 250 kw or higher as required, and direct-driven exciters in ratings to and including 250 kw. The following discussion applies equally well to both types.

The problems affecting performance and reliability of shaft-driven exciters are varied but interrelated.

A high-speed commutating machine does not perform properly under conditions of undue vibration. In fact, vibration of a magnitude less than that considered acceptable on the main generator or turbine shaft, may prove detrimental to commutator and brush performance. Vibration may cause uneven wear of a commutator, making it out of round. Excessive wear of stationary parts also may be caused by vibration. The most direct sources of vibration are

1. Unbalance of the exciter and main generator shafts.
2. Stimuli transmitted through the foundation to the exciter.

Vibration of the new exciter is reduced to a minimum by mounting the rotor on bearings of its own and separating it from the generator by a flexible coupling of special design. Flexible mounting of the main generator stator cores has eliminated double frequency vibration from being carried to the exciter through the foundation.

The exciter stationary parts and the exciter rotor are designed in such fashion that no resonance occurs near 60 or 120 cycles, so that stimuli of these common frequencies transmitted to the exciter through the foundation will not be amplified. These features have been proved by vibration tests in the factory.

It is well known that oil or oil vapor is detrimental to commutator and brush performance. In the presence of oil, most commutators will build up a thick film which may flake off in spots and start threading of the commutator. Dry carbon dust on the exciter parts does not affect insulation resistance greatly, but carbon dust in a film of oil may cause leakage paths of low resistance and result in low megger readings and a dangerous condition under which to operate. The exciter bearings and reduction gear are sources of oil vapor, and special measures have been taken in bearing design and ventilation circuit arrangement to eliminate oil vapor from these sources.

The ventilation circuit of the exciter is related to both the oil vapor and carbon dust problems, but it also brings in a factor of its own, that of humidity of the ventilating air and its effects on commutator film and brush performance. As a result of our experience, we have standardized on the room ventilated system.

A commutator which may become loose always presents a hazard to exciter performance. A few high bars may cause severe sparking and even broken brushes. Dimensional changes of copper and insulation with changes in temperature are responsible for loose commutators. A special commutator construction has been devised which keeps it tight throughout the load cycle, and a remarkably stable commutator has resulted from this procedure.

The problem of brush types and application is broad and somewhat controversial, and it will be sufficient here to say that the new brush and brush holder which have been developed result in longer brush life and longer commutator life with less maintenance.

This exciter is tested and shipped as a complete unit. All that is necessary is to line it up and connect it to the main unit, and it is ready to deliver kilowatts.

Figure 1

Figure 1 shows one of the new 125-kw 3,600-rpm direct-driven exciters. This unit excites a 37,500-kva 3,600-rpm hydrogen-cooled turbine generator in the Bainbridge station of the New York State Electric and Gas Corporation.

The afore-mentioned problems all have been solved in the new General Electric standard shaft-driven exciters, and accessibility and ease of inspection and maintenance have been keynotes in the design of the housing and exciter parts.

Thus, to those who will continue to purchase shaft-driven exciters we can offer equipment which, by virtue of these improved features, will have adequate performance and excellent reliability and availability.

S. B. Crary (General Electric Company, Schenectady, N. Y.): This paper gives a good account of the performance characteristics of an electronic excitation system. Concise information is presented in a summary of test results given in Figure 6.

The present interest in excitation systems may be attributed primarily to the more completely interconnected power systems of improved reliability and the continued trend to larger generating elements at 3,600 rpm. The over-all system economy can now be improved to an important extent by continuous operation of the more efficient and larger generating units. This has focused a degree of critical attention on the shaft-driven rotating exciter for those units which are required to operate with high availability. The required reliability has been, as

indicated by cases of operating experience, beyond that which was obtained from some shaft-driven exciters. Recently, substantial improvements have been made in the design of higher-speed exciters, and further improvements may be expected. Even with greatly improved shaft-driven exciters, there is reason to believe that a source of excitation which can be maintained independent of the operation of the main unit will represent a worthwhile improvement for some of the larger units even if realized by additional complication in the excitation system itself.

The desirability of using a self-excited system of excitation (excitation energy obtained from the main a-c generator) has greatly increased with the decided trend to the unit type of station with each generator connected through its own transformer to the high voltage transmission system and with the auxiliary power obtained from the main a-c generator terminals. Fortunately, this unit type of station has two features which make a practical self-excited excitation system more easily realizable. These are

1. The high voltage faults are promptly cleared by quick-acting relays and switches for stability reasons.

2. The stepup transformer impedance and the low generator transient reactance inherent with turbine generators tend to sustain the terminal voltage for high voltage transmission system faults.

It seems reasonable that this type of unit station and system arrangement should be used as a basis for the development and design of competing types of self-excited excitation systems. This has been borne out by the emphasis placed on this type of system by two of the papers presented at this session. For this type of system the following conclusions seem justified:

1. Either the motor-driven or the electronic excitation system allows for omission of the shaft-driven exciter.

2. Either type can be designed to give a high standard of performance with the unit type of station design.

3. Present costs tend to favor the co-ordinated motor-driven exciter for comparable performance levels for the large generators.

From Figure 6 it would appear that for a 3-phase high voltage fault of 15-cycle duration without a compensator, the actual per unit response would be quite low, possibly negative, that is, the integrated exciter volt-seconds above the initial exciter voltage for the first half-second following a 15-cycle 3-phase system fault would be negative. In order to obtain an actual per unit response during the first half-second following such a system fault comparable to that obtainable with a standard shaft-driven exciter, we would estimate that the ceiling voltage of the electronic exciter would have to be of the order of 600 to 700 volts with normal alternating voltage applied or that the voltage regulation of the excitation system when carrying high induced field currents would have to be reduced.

M. M. Morack (General Electric Company, Schenectady, N. Y.): The authors are to be complimented on their fine paper covering the design, development, and application of an electronic exciter for large a-c generators. The requirements for the exciter and the equipment design are closely akin to those of electronic exciters for large synchronous condensers. Since several of these units have been in service a number of years, a brief history of their performance will serve to further the conclusion that the electronic exciter is a reliable and efficient source of excitation for large a-c generators.

An early installation of an electronic exciter[1] for a synchronous condenser was made in the United States in 1934 on a 15,000-kva unit located in a generating plant. The unit utilized six 75-ampere hot cathode thyratrons for the rectifying elements. These were replaced by sealed ignitrons in 1939 because of hot cathode tube life limitations.

A commercial installation of sealed ignitrons was made in November 1936 in an electronic exciter for a 30,000-kva synchronous condenser. This large a-c machine is part of the American Gas and Electric Company system and it is located at Fostoria, Ohio, at the junction of a number of transmission lines. This sealed ignitron exciter is rated 435 volts and is designed to deliver a variable d-c output, with a continuous rating of 777 amperes, and with a short time rating of 1,050 amperes for 10 minutes and 1,550 amperes for one minute. It will deliver 777 amperes direct current to the field when the a-c supply voltage has fallen to 50 per cent of normal. The equipment includes six FG-238B sealed main power ignitrons, six FG-172 thyratron igniter firing tubes, six single pole anode air circuit breakers, an electronic voltage regulator, a water-to-water heat exchanger, auxiliary control, and a main transformer bank fed from an 11,500-volt 60-cycle system.

The main losses of the rectifier are removed by means of a water-to-water heat exchanger designed in two parallel sections with valves, whereby either section can be closed off for the purpose of cleaning without necessitating a shutdown of the exciter.

Each of the sealed ignitrons is mounted in a completely metal-enclosed compartment. The doors of these compartments are so interlocked with their single pole anode circuit breakers and the rest of the apparatus, that any of the tubes may be replaced safely without requiring shutdown of the synchronous condenser. With these mechanical features, there has been no problem in keeping the equipment in operation for extended times.

The main problem of maintenance has been one of tube replacement. In the years 1936–1939 the average tube mortality was about 10 per unit per year, which is not too surprising as that was the period in which the sealed ignitron tubes were being improved and perfected. The initial silicon-carbide igniter points were satisfactory for welding service but gave short life in rectifier service. It was necessary to change the igniter material to boron-carbide, which so increased the life span that igniter point life has ceased to be a problem.

There have been approximately ten years of tube experience with sealed ignitrons in this group of electronic exciters. It is to be appreciated that the tube duty is more severe than that encountered in industrial service, in that the rectifying elements must operate at large angles of phase retard. In addition they must operate for short times in the inverting quadrant. Tubes which have been in operation for many thousand hours under this severe duty sometimes show increased arc-back frequency, resulting in anode circuit breaker operations. Examination of a tube removed because of unacceptable arc-back frequency, after approximately four years of service, indicated that the vacuum was still good, igniter points were in good condition but showed particles of loose graphite floating in the mercury pool. The method of series compensation outlined by the authors should tend to increase tube life further, because compounding reduces the phase control duty.

REFERENCE

1. THYRATRON EXCITED CONDENSERS, **Philip Sporn, G. G. Langdon.** *Electrical World*, volume 105, June 22, 1935.

C. E. Valentine (Westinghouse Electric Corporation, East Pittsburgh, Pa.): The use of the electronic type exciter aroused interest in the means used to control the exciter. With regard to the automatic means, that is, the alternating voltage regulator, there are several factors which require consideration. Among these are simplicity, reliability, maintenance, and repair or replacement costs.

Any one of several types of voltage regulators may be employed. It should be noted that the use of an electronic exciter does not necessarily require the use of an electronic type voltage regulator. As a matter of fact, the regulator should be chosen on the basis of the type best suited to the application. This choice well may take into account availability, performance record, and experience with the types under consideration.

A direct acting rheostatic regulator was applied to the West Penn Power Company's electronic exciter as being the available regulator best suited for the job. Its sensitivity of plus or minus one half of one per cent was considered adequate. Simplicity, reliability, freedom from maintenance, and long life has been demonstrated on numerous applications over a period of several years.

The length of service that a voltage regulator will give without maintenance or replacement costs is an important consideration. For turbogenerators in central station service, it is desirable to have the regulator in service at all times, although manual control can be used temporarily if necessary.

The electronic type regulator has inherently the characteristic of little or no inertia, as regards the response of its tube components. In its circuits, considered as a whole, however, there may be small time delays, or other small errors, which render it something less than a perfectly accurate and instantaneously responding device. These same remarks apply to various types of static networks, involving resistors, reactors, capacitors, and rectifiers. These considerations lead to the conclusion that an electromechanical type regulator, such as the direct acting rheostatic type possesses some advantages and no great disadvantage for applications where good regulator performance is required, and where the utmost in speed of response or the utmost in sensitivity is not needed.

In the electronic type regulator, its inherent lack of inertia, and speed of building up or building down the voltage of the exciter it controls are valuable assets, but at present its tubes have a limited life, and tube maintenance is an item which should re-

ceive due consideration. The maintenance of an electronic regulator involves checking of the tubes at regular intervals. By means of such periodic tests, any change in tube characteristics that might indicate deterioration or failure will be noted in advance. Tube replacement then may be made as required to keep the regulator performance and reliability at a maximum.

In a conventional excitation system, when a change in excitation takes place, the greatest time delay usually is found in the field of the a-c generator. Next to this in magnitude is the exciter field delay. The voltage regulator element or circuit delay is only a small part of the machine field delays. In combining the use of the direct acting type regulator and the electronic exciter, the time delay of the conventional exciter field is eliminated, and, at the same time, generator field forcing of a high order of magnitude is achieved.

F. M. Porter and **J. H. Kinghorn** (American Gas and Electric Service Corporation, New York, N. Y.): Paper 46-74 on electronic exciters mentions that rectifier applications for excitation of rotating machines have been tried only to a limited extent and primarily on synchronous machines other than generator.s These applications are mostly on the systems of the American Gas and Electric company where there are installed 9 electronic exciters and 14 electronic regulators which have been in service varying lengths of time and all of which in general have given satisfactory performance since they were placed in operation. The great amount of operating experience obtained with these applications convinces us that the excitation of alternators and synchronous condensers by means of rectifying equipment no longer is to be considered as being in the experimental stage, and therefore no serious difficulties should be encountered with the operation of this type of equipment.

In 1930, a small electronic exciter was installed at Shelby, Ohio, for supplying current to the field of a motor-driven exciter of a large synchronous condenser. In 1931, two similar exciters were installed at Glen Lyn, Va., for supplying current to the fields of the direct-connected exciters of two large turbine-driven generators at that plant. The same type of arrangement also was installed for a synchronous condenser exciter in 1936, and a similar installation was placed in service about six years ago for a hydroelectric generator.

In 1933, we placed in operation at Scranton, Pa., a 78-kw six tube electronic exciter for the 15,000-kva synchronous condenser at that location. Since then three additional exciters with capacities from 125 to 175 kw were placed in service. These were used for excitation of three synchronous condensers, ranging in capacity from 30,000 to 36,000 kva. The combined operating time for these four exciters amounts to approximately 30 years. Totaling the operating time for all the electronic exciters just mentioned, we have had approximately 77 years' performance, which for the most part has been very satisfactory.

As to regulators, all of the foregoing applications are taken care of electronically, either by a bridge type or voltage standard type of circuit. In addition, we have six amplidyne controlled excitation installations on condensers and generators, all of which are equipped with tube-type regulators, so that these regulators together with those on the afore-mentioned electronic exciters have given us combined service experience of over 88 years with this type of voltage control for large rotating machines.

Referring specifically to paper 46-74, we note the requirements stated for obtaining satisfactory performance for an electronic exciter. We believe our experience with three exciters of approximately the same size as the one discussed in the paper indicates that tube-type applications will take care of most and probably all of the items mentioned satisfactorily. However, this new installation at the Springdale station will provide a splendid opportunity for obtaining performance for exciting directly a large turbogenerator. Incidentally, if it is not already planned, we suggest that an electronic regulator might well be tried, along with this new exciter, since the reliability and desirability of such control have been demonstrated amply.

With reference to paper 46-77 on motor-driven exciters for turbine alternators the suggested specially designed motor generator set undoubtedly has merit, but we wonder how the complete installation will compare in initial and maintenance costs to a direct-driven exciter arrangement, a standard type motor-generator set and an electronic exciter. If the direct-connected exciter is not to be used, it may be preferable, if economics permit, to eliminate entirely a rotating-type exciter so long as satisfactory and excellent performance can be obtained from a tube-type arrangement. As already mentioned, we have six applications using amplidyne generators in series with fields of self-excited exciters, and these arrangements with electronic regulators also have given excellent results. This arrangement is being tried on several turbogenerators and may prove to be the preferred scheme for generator excitation when all factors are considered.

The foregoing gives only a brief outline of results obtained with electronic exciters and regulators and other excitation arrangements on the systems of the American Gas and Electric company. We hope to be able to present before the Institute in the near future descriptions of the exciter installations mentioned, as well as our detailed experiences with this equipment from both an operating and maintenance standpoint.

J. B. McClure (General Electric Company. Schenectady, N. Y.): The authors of papers 46-74 and 46-77 are to be complimented on their thorough analysis of the requirements of a properly co-ordinated motor-driven exciter set and on their report of tests on an electronic exciter for a large turbine-generator. These papers are particularly timely and should encourage a wider acceptance of other than shaft-driven exciters.

Motor-driven exciters, of course, are not new. In the past many have been standard motor-generator sets; some have had oversize motors and some have had huge flywheels on independent bearings but it is certainly safe to state that their design did not follow any definite pattern. Now, improved system performance makes it possible, as has been pointed out, to design a simple, practical, compact set which will adequately meet the requirements.

Many users have inquired recently about motor-driven exciters, and several have decided on them for their new turbine-generators now on order. These special motor-driven exciter sets will be 1,200 rpm. The motors will be of the standard dripproof construction, and of such rating as to have liberal torque ability to carry through sustained periods of low voltage at the motor. The exciters will be of the enclosed room-ventilated type and will incorporate all the improved features of the shaft-driven exciters which contribute to long life, low maintenance, and high availability. These features have been noted by J. F. Miller in his discussion. In applications where the auxiliary power is supplied by a house generator or shaft generator, the exciter sets are being supplied without flywheels, but for all other applications flywheels have been included.

At this time, therefore, it appears that a prospective purchaser of a turbine-generator set has his choice of a special motor-driven exciter set, a gear-driven exciter, or a high-speed shaft-driven exciter for essentially the same price.

Electronic exciters for large synchronous machines are not new. The company with which the writer is associated built three electronic exciters which have been in operation with synchronous condensers for a combined period of 27 years.

Based on this experience, electronic exciters can be expected to give good performance and have high availability, but at the present time their initial cost and maintenance are considerably higher than that of the rotating exciters.

R. B. Bodine, S. B. Crary, and **A. W. Rankin:** The discussers all have made valuable contributions to the general subject of excitation systems.

Mr. Gay has called attention to the reason he considers it inadvisable to obtain the excitation energy directly from the main a-c system. It may be well to re-emphasize, in view of Mr. Gay's remarks, that the motor-driven exciter normally would be driven from the same electric supply as the other auxiliaries of the main unit. Mr. Gay is, therefore, in effect making a plea for the continuance of the use of house generators as a means of avoiding serious system troubles, rather than comparing the performance of the motor-driven exciter set with the other types. An independent supply for the auxiliaries of the station well may be justified for some systems, particularly if the circuit protective equipment cannot be relied on to clear severe faults promptly, and if the system must be designed to extricate itself from severe disturbances by pulling itself back into synchronism. Such a philosophy for some types of closely coupled metropolitan systems may require the continued use of house generators.

However, as is well known, there is a continuing trend to obtain the energy for the auxiliaries from the main system. Entirely satisfactory performance has been obtained from a wide variety of installations, as has been indicated further by the other discussers. Mr. Kinghorn and Mr. Porter report the satisfactory experience of several years of operation with electronic excitation sources which derive their energy directly

from the main system. Mr. McClure reports on the continued interest and use of motor-driven exciters which will derive their energy from the main a-c supply.

Many operators feel that they can capitalize on the greatly improved performance and reliability of their main system by deriving all of the auxiliary supply, including the excitation, from the main a-c system. It is important to note further that the motor-driven exciter, when connected to the main a-c system, can be designed for even more extreme system conditions than those used as criteria for the design of the exciter-set reported in our paper. However, in our opinion, more severe criteria generally will not be justified. The point we have tried to make is that such a set can be designed to meet a wide range of system requirements.

Mr. McClure points out that the manufacturers can supply several types of reliable excitation systems. These can be selected to meet the system requirements and the basic system design philosophy.

Mr. Miller has reviewed briefly the improvements which have been made in one manufacturer's shaft-driven exciters. These important changes and refinements in design further make the choice of an excitation supply more a matter of satisfying the particular system requirements, and should encourage a more careful analysis of system operation during normal and emergency conditions.

We are looking forward with interest to Mr. Kinghorn's and Mr. Porter's more complete account of their experience with different types of excitation systems and also hope that other engineers will be encouraged to describe their experiences at this time, when it is desirable to correlate apparatus improvements with system operating experience.

H. A. P. Langstaff, H. R. Vaughan, and **R. F. Lawrence:** The experiences of the American Gas and Electric company systems with the use of electronic exciters is certainly a valuable testimony to the ability of this type of equipment to operate successfully over a period of years. This, backed up by the operating records of thousands of kilowatts of power rectifiers installed in industrial plants, proves quite conclusively that power rectifiers can be depended on for reliable service. While the experience gained with the five small electronic rectifiers and the four electronic main exciters used on synchronous condensers is indicative of the type of performance to expect, there was still considerable uncertainty as to how an electronic exciter would perform under abnormal conditions when used on a large generator. The requirements are somewhat different, and any faltering in the excitation system may prove extremely serious. It was believed that the only way to establish just how the electronic exciter would function under all types of faults and load change conditions was to stage tests where the conditions would be definitely known and all pertinent data could be recorded.

Regarding the use of an electronic regulator—extensive tests were made with such a device. Since there was no material gain in performance in using the electronic type, it was believed that there was some advantage in using a simple mechanical type regulator which has practically no moving parts and which has proved itself in many applications.

The proposed presentation before the Institute of the different types of exciters installed on the American Gas and Electric systems should be a welcome contribution to the industry. At the presentation of this paper it was hoped that some actual operating experience on the Springdale exciter could be given. This was not possible, since the installation of the exciter was incomplete. However, it is hoped that at some future meeting a report of this nature can be presented.

Mr. Morack's description and history of two electronic exciters for synchronous condensers are of interest, because they give factual information on two actual installations. Of particular interest is the high short time overload ratings which are inherent in this type of equipment and of great advantage in any excitation system. It would be interesting to know whether or not operating experience has justified six anode circuit breakers, that is one single pole circuit breaker per anode. The tests on the Springdale exciter indicated that three 2-pole circuit breakers are entirely adequate, particularly when provided with automatic reclosing. The fewer number of circuit breakers, of course, simplifies the construction and control.

The manufacturer of the Springdale exciter earlier built an electronic exciter for a 25,000-kva condenser on the American Gas and Electric company system at New Carlisle, Ind. This exciter is equipped with one anode circuit breaker per ignitron tube and has an electronic regulator. In nearly four years of continuous service it has not caused a shutdown.

Mr. Crary has presented an excellent summary of the application requirements and present thinking in regard to excitation systems. We are happy that his opinions agree with those expressed in the paper.

In comparing the motor-driven or electronic exciter with the shaft-driven type there are several fundamental characteristics that should be considered. There are two reasons why some operators might prefer to dispense with a shaft-driven exciter. One of these is to do away with a rotating type machine. The other is to make it possible to maintain completely the exciter without interfering with the operation of the main generating unit. The electronic exciter is the only one that satisfies both of these requirements. Either the electronic type or the motor-generator set type of exciter has the inherent disadvantage that its performance is affected by the alternating voltage supply. This is of particular importance where unit type of operation is required. In either case it is necessary to compensate for this disadvantage by special design characteristics which include flywheel effect and high pull-out torque with the motor-generator set, and high ceiling voltage or series compensation with the electronic type. In order to take the motor-driven exciter out of operation for maintenance without interfering with the operation of the main unit, it is necessary to have a spare exciter. The parts of the electronic exciter that may need periodic maintenance can be taken out of service individually without taking the exciter out of service. These fundamental requirements should be given consideration in comparing the over-all advantages of the different types of exciter system.

It is true that the excitation output of the electronic exciter is low during a 3-phase fault. If deemed necessary, this condition can be corrected by using an exciter with a high ceiling voltage or with a series compensator. It will be noted that the excitation output is high for other types of faults, including a double line to ground fault. Since this latter type of fault usually is considered the practical limit as a criterion for stability, it is questionable whether extra complications and cost can be justified to obtain high excitation output during a 3-phase fault.

Referring to the curves of Figure 6 of the paper which show test results for the application of load and faults for four different conditions, the actual per unit response can be negative, as for example in Figure 6a. The exciter was designed for a maximum voltage drop at the generator terminals of 25 per cent. Under this condition, with the supply to the rectifier taken from the generator terminals and with the rectifier transformer connected to give the higher d-c ceiling voltage, a no-load d-c ceiling voltage of 300 volts would be obtained. This gives a rate of response of approximately 2.2. The conditions for which the tests were run were purposely pessimistic with respect to the maximum voltage drop and the duration of the fault in order to obtain performance data under the most adverse conditions. These conditions are unlikely to be matched in actual service.

In AIEE paper 46-77 curves were plotted which show that the system is stable using either a co-ordinated design motor-driven exciter or a direct-connected exciter. Using a self-excited electronic exciter having a 4.95 per unit ceiling excitation (one per unit equals field voltage required to give normal rated voltage on the air gap line), the system would be stable for a 3-phase 15-cycle fault on the high voltage terminals of the transformer connected to the main generator. The per unit ceiling excitation of 4.95 is the same as that of the exciter for the West Penn Power Company with the rectifier transformer connected to give the higher d-c output voltage.

Mr. McClure's discussion leads one to believe that a wider acceptance of other than shaft-driven exciters should be encouraged. That was not the purpose of the paper on the electronic exciter. It is believed that the extensive background of operating experiences with shaft-driven exciters has proved conclusively that they are good in performance and have a high availability factor. More recent improvements in the design make for ease of maintenance and elimination of minor troubles that have been experienced, so that future operating records should be even better than those in the past. It is believed that either electronic exciters or motor-driven exciters should be considered as alternate means of excitation which might suit certain applications or industrial preferences better.

It is agreed that electronic exciters for synchronous machines are not new, although they are still used to a very limited extent. The number of electronic exciter installations expressed as a per cent of the total number of excitation systems in operation is practically a negligible figure. Previous applications were on condensers and generators of relatively small capacity, the maximum condenser rating being 36,000 kva and the maximum generator rating being 15,000

kva. The Springdale exciter is of major importance in that the generator for which it was designed is more than five times the capacity of any existing generator having an electronic exciter. It is believed that the experiences gained with synchronous condensers were only indicative of the performance to be expected with large generators and were not final proof that the electronic exciter system would perform adequately under all types of abnormal operating conditions.

In evaluating the over-all cost and maintenance of exciters, one should consider the entire exciter system including control, regulation, and necessary spare equipment. When all of these are considered, particularly if there is only one generating unit in the station, it is believed that the electronic exciter will not be too far out of line from the standpoint of either maintenance or initial cost. The higher initial cost of the electronic type may be justified by preventing expensive shutdowns which might result from some other type of excitation system not having as high an availability.

Mr. Valentine has given a concise comparison of the electromechanical and electronic types of regulators for electronic exciters. As pointed out previously the electronic regulator proved to have no material advantage over the electromechanical type in the extensive tests that were made. One of the outstanding advantages of the electronic type exciter is the inherent ease with which its direct voltage output can be regulated. It is believed that this inherent advantage should be retained, if at all possible, by using the simplest voltage regulator available, if this can be done without sacrificing over-all performance. The simple electromechanical type of regulator seemed to be the best solution.

Parallel Circuits in Servomechanisms

H. TYLER MARCY
ASSOCIATE AIEE

AN excellent way to describe a servomechanism is to picture it as a device which acts with power on the difference, or error, between a desired quantity and an actual quantity. It acts in such a way as,

1. To make the error approximate zero in the steady state.
2. To limit peak errors and the error-time integral when the output quantity is following a typical random input quantity.
3. To recover from sudden disturbances with adequate speed of response and degree of stability.

A block diagram of a group of components is illustrated in Figure 1 in which the foregoing interpretation is very powerful. Much has been written on the analysis and synthesis of such systems. Several recently published or released works have described powerful analytical tools used in the design of linear servomechanisms of this type.[1-4,7,8]

This paper deals in particular with a class of servomechanisms which has not received adequate treatment thus far. Many servomechanisms, as in Figure 2, can be described accurately only when a component is included in the feed-back path. At times this is desired, and compensating devices are used to aid the performance of the servomechanism. At other times, undesirable characteristics of the measuring instruments introduce delay in the transmission of signals back to a point where they are to be compared with the desired quantity. The signals then used to excite the control amplifier are no longer the error between desired and actual quantities.

In cases where there is a modification of the controlled quantity previous to comparison with the desired quantity, no place exists in the circuit where the actual error can be measured. This is most likely to be true when the servomechanism is not in steady-state operation. The ratio of output to error as a function of frequency when the input is varying sinusoidally is, in these cases, not a simple function of any one of the components or any of the components in cascade. This will be developed mathematically as a part of the linear treatment of servomechanisms of the type represented in Figure 2.

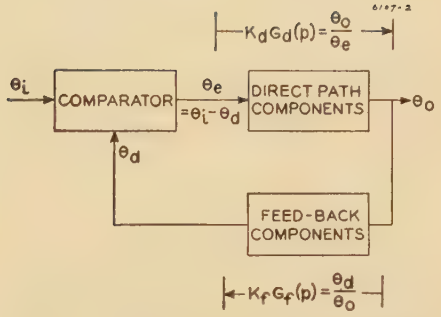

Figure 2. Block diagram of a servomechanism where the components in the direct circuit are paralleled by components in a feed-back circuit

General Analytical Techniques

A mathematical treatment of a dynamic system as complicated as a servomechanism is difficult on the basis of classical mathematics. The differential operator p is used here to represent an operator which will be replaced by $j\omega$ when the steady-state sinusoidal characteristics of the system are to be considered, or by d/dt when the differential equations are to be considered.

The general analytical techniques described here are, basically, simple extensions of previous work.[1,2] In electric network theory, the consideration of all circuits on the basis of impedance characteristics to the exclusion of admittance characteristics would be foolish. Similarly in a study of servomechanisms it is often desirable to work with component or system functions which are ratios of input to output instead of their reciprocals.

Components of servomechanisms (such as amplifiers, thermocouples, tachometers, and motors) can be considered as analogous to a four terminal network whose input and output are related by a differential equation describing its behavior. In this paper a system function will be defined as a nondimensional ratio of output to input. A component will have a system function, and a combination of components will have a system function. It is, therefore, necessary to describe carefully what a given system function includes. It is also necessary to describe the operator used in expressing the system function. If the operator is a pure imaginary frequency, then a ratio of θ_o to θ_i will be written

$$\frac{\theta_o}{\theta_i}(j\omega)$$

The more general operator p is implied by the simple expression θ_o/θ_i, instead of always writing $\theta_o(p)/\theta_i(p)$. Similarly $\theta_i(p) - \theta_o(p)$ will be written $\theta_i - \theta_o$.

A reciprocal system function will be a

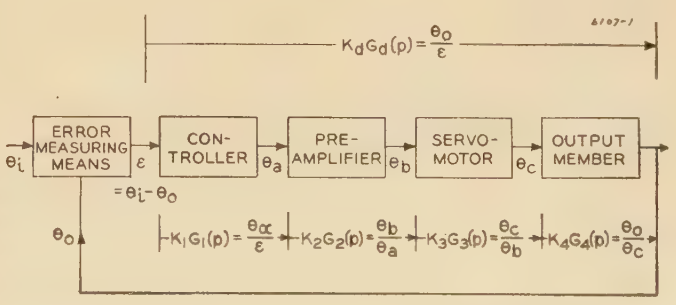

Figure 1. Block diagram of a servomechanism where the components may be considered as elements in a cascade circuit

Paper 46-107, recommended by the AIEE committee on instruments and measurements for presentation at the AIEE summer convention, Detroit, Mich., June 24-28, 1946. Manuscript submitted March 15, 1946, made available for printing April 29, 1946.

H. TYLER MARCY, who is now in the special projects department, M. W. Kellogg Company, Jersey City, N. J., formerly was research engineer in the servomechanisms laboratory, Massachusetts Institute of Technology, Cambridge, Mass.

The author appreciates the aid and encouragement of Doctors G. S. Brown and A. C. Hall and of his colleagues at Massachusetts Institute of Technology, particularly C. C. Holt and C. R. Wieser.

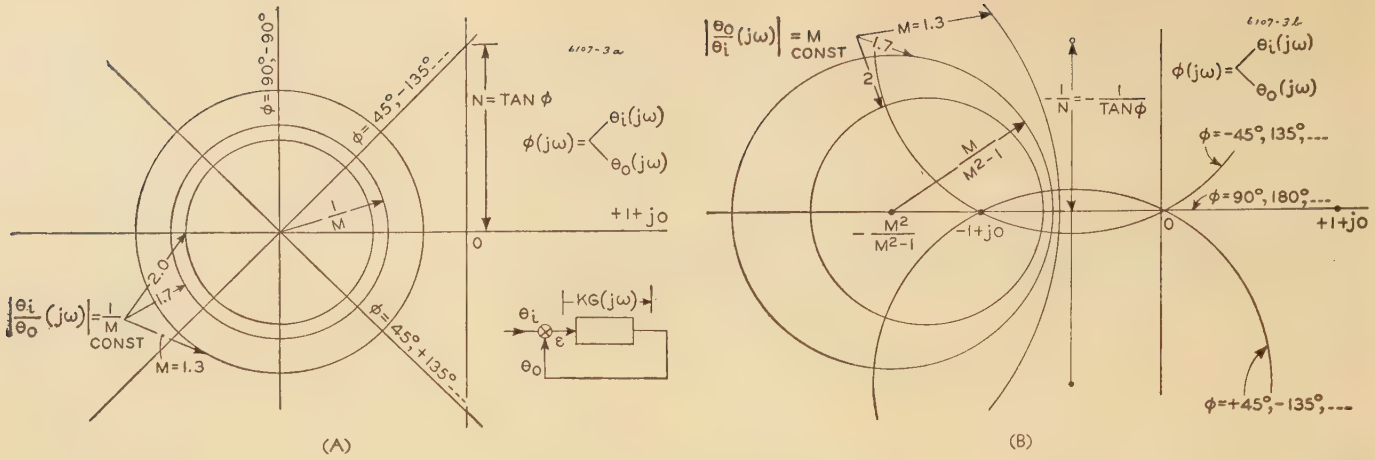

Figure 3. Loci of constant magnitude of the ratio of the output quantity to the input quantity of a servomechanism and loci of constant phase angle between the output quantity and the input quantity of a servomechanism as they appear on two complex planes

A. Plane of $1/KG(j\omega)$. A complex plane where the radius vector is the complex ratio of the error of the servomechanism to the output quantity

B. Plane of $KG(j\omega)$. A complex plane where the radius vector is the complex ratio of the output quantity to the error of the servomechanism

nondimensional ratio of input to output. A component will have a reciprocal system function, and a combination of components will have a reciprocal system function.

The use of reciprocal system functions allows a separation of the component characteristics not otherwise realizable, which leads to greater simplicity of analytical treatment. With reference to Figure 1

$$\frac{\theta_o}{\epsilon}(j\omega) = K_d G_d(j\omega) = K_1 G_1(j\omega) K_2 G_2(j\omega) \times K_3 G_3(j\omega) K_4 G_4(j\omega) \quad (1)$$

and

$$\frac{\theta_o}{\theta_i}(j\omega) = \frac{K_d G_d(j\omega)}{1 + K_d G_d(j\omega)} \quad (2)$$

Inversion of equation 1 leads to

$$\frac{\epsilon}{\theta_o}(j\omega) = \frac{1}{K_d G_d(j\omega)} \quad (3)$$

and inversion of equation 2 leads to

$$\frac{\theta_i}{\theta_o}(j\omega) = 1 + \frac{1}{K_d G_d(j\omega)} \quad (4)$$

and demonstrates that the system may be studied by a treatment of the function $K_d G_d(j\omega)$, or by a treatment of the reciprocal function

$$\frac{1}{K_d G_d(j\omega)}$$

It does not matter which technique is used, because the effect of any one component, for instance $K_1 G_1(j\omega)$, may be studied by a vector product manipulation on a polar plot.

In one important way, however, the use of reciprocal system functions simplifies the problem of synthesis of simple cascaded systems. In a complex plane, in which the vector from the origin at $\omega = \omega_1$ is

$$\frac{1}{K_d G_d(j\omega_1)}$$

loci for

$$\left|\frac{\theta_i}{\theta_o}(j\omega)\right| = \text{constant}$$

are circles, concentric about the $-1 + j0$ point with a radius equal to the magnitude. Loci of constant angle between input and output are straight lines which pass through the $-1 + j0$ point and a point on the imaginary axis equal to the tangent of the angle. These loci are shown in Figure 3, where they may be contrasted with similar loci as they appear on a plane where the vector from the origin at $\omega = \omega_1$ is $K_d G_d(j\omega_1)$.

A simple demonstration of the nature of the loci of constant

$$\left|\frac{\theta_i}{\theta_o}(j\omega)\right|$$

is to set the radius vector

$$\frac{1}{K_d G_d(j\omega)} = R + jX$$

and find the analytical geometric equation for constant

$$\left|\frac{\theta_i}{\theta_o}(j\omega)\right|$$

Substituting in equation 4

$$\frac{\theta_i}{\theta_o}(j\omega) = 1 + R + jX \quad (5)$$

from which

$$\left|\frac{\theta_i}{\theta_o}(j\omega)\right| = \sqrt{(R+1)^2 + X^2} = \frac{1}{M} \quad (6)$$

where the constant M has been defined so as to be consistent with Hall.[1,2] Equation 6 represents a circle whose center is at $-1 + jO$ and whose radius is $1/M$.

The manner in which loci of constant

$$\left|\frac{\theta_i}{\theta_o}(j\omega)\right|$$

and loci of constant angle between θ_i and θ_o appear on the complex plane of

$$\frac{1}{K_d G_d(j\omega)}$$

is important only when these loci are used as design criteria for the servomechanism. In design work the degree of resonance often is limited by specifying a maximum allowable value of M. In terms of the degree of stability of servomechanism transient response this is a rough approximation at best. This is unfortunate because specifications for the speed of response and degree of stability of servomechanisms usually are given in terms of their transient response.

The transient response is related mathematically to the frequency response by the Fourier integral.[5] A perhaps oversimplified interpretation of this relationship is used in specifications of servomechanisms. Such specifications limit the amplification, by resonance effects, of the input and demand a sizable output magnitude at high frequencies. For complicated systems, however, this gives the designer something tangible toward which to work, as well as a good approximate prediction.

The use of the complex plane of

$$\frac{1}{K_d G_d(j\omega)}$$

permits a quick determination of resonance by noting the proximity of the locus to the $-1 + j0$ point. This advantage is, of course, not fundamental. It

is apparent in the solution of numerical problems.

To return to the more complicated system represented in Figure 2: the ratio of output to input is

$$\frac{\theta_o}{\theta_i}(j\omega)=\frac{K_dG_d(j\omega)}{1+K_dG_d(j\omega)K_fG_f(j\omega)} \tag{7}$$

and the ratio of output to error (defined as $\theta_i-\theta_o$) is

$$\frac{\theta_o}{\epsilon}(j\omega)=\frac{K_dG_d(j\omega)}{1+K_dG_d(j\omega)K_fG_f(j\omega)-K_dG_d(j\omega)} \tag{8}$$

This is a hopeless tangle to unscramble when an alteration in either $K_dG_d(j\omega)$ or $K_fG_f(j\omega)$ is needed. However the inversion of equation 7 leads to

$$\frac{\theta_i}{\theta_o}(j\omega)=\frac{1}{K_dG_d(j\omega)}+K_fG_f(j\omega) \tag{9}$$

and the inversion of equation 8 leads to

$$\frac{\epsilon}{\theta_o}(j\omega)=\frac{1}{K_dG_d(j\omega)}+K_fG_f(j\omega)-1 \tag{10}$$

Both equation 9 and equation 10 make possible a separation of the frequency characteristics of the two essential components in the system. Equation 9 and equation 10 indicate a vector addition of the characteristics of the components. The result is obtained with comparative ease and leads quickly to a qualitative idea of the effect of a change in one or the other of the two parallel components.

It would seem from examination of equation 9 and equation 10 that the ratio

$$\frac{\theta_i}{\theta_o}(j\omega)$$

might be plotted instead of

$$\frac{\epsilon}{\theta_o}(j\omega)$$

since the criteria of resonance concerns

$$\frac{\theta_i}{\theta_o}(j\omega)$$

directly. If this is done then loci of constant

$$\left|\frac{\theta_i}{\theta_o}(j\omega)\right|$$

are obviously circles about the origin.

When problems are actually being solved, it often will be convenient to plot on the same sheet of paper a locus of

$$\frac{\epsilon}{\theta_o}(j\omega)$$

and a locus of

$$\frac{\theta_i}{\theta_o}(j\omega)$$

With reference to equation 9,

$$\frac{1}{K_dG_d(j\omega)}$$

may be plotted as the radius vector, and the resonance of the system may be studied by considering the locus to be

$$\frac{\epsilon}{\theta_o}(j\omega)$$

where $K_fG_f(j\omega)$ is always unity. For this purpose circles may be constructed about the $-1+j0$ point. Then, on the same sheet of paper a locus of $K_fG_f(j\omega)$ may be added vectorially to the locus of

$$\frac{1}{K_dG_d(j\omega)}$$

The resulting locus has a radius vector which is

$$\frac{\theta_i}{\theta_o}(j\omega)$$

and the resonance of the final system may be studied by constructing circles of radius

$$\left|\frac{\theta_i}{\theta_o}(j\omega)\right|$$

about the origin.

Time Delays in Measuring Output

In order to control a process with a servomechanism, it is necessary to measure the output quantity. The accuracy with which the measurement is made, both statically and dynamically, is in large part indicative of the success of the controller. Unfortunately many measurements are made, for one reason or another, with equipment that responds to a sudden input with a time delay. The response delay may be either a characteristic of the measuring instrument or a characteristic of some smoothing circuit that is used.

As an illustrative problem, to show how the effects of a time delay in error measurement may be treated, a system will be discussed where the direct circuit, including control amplifier and process, is characterized by the system function

$$K_dG_d(p)=\frac{K_d}{p(T_dp+1)} \tag{11}$$

Equation 11 is representative of a cascaded control amplifier sensitive only to the input to it (and not to the derivatives or integrals of that input) and a process characterized by a characteristic time, T_d. Such a system is described in Figure 7 where

$K_d=K_{\epsilon c}K_{co}/f$ and $T_d=J/f$

This much of the system is equivalent to the type I controller of reference 1 in which the ratio of the static stiffness K to the output damping, f, is K_d, or the velocity-error constant, and the ratio of the output inertia, J, to output damping, f, is T_d.

The output measuring device of the illustrative problem will be assumed to have a response indicated by the transfer function,

$$K_fG_f(p)=\frac{1}{T_fp+1} \tag{12}$$

If the measuring device is considered by itself and is subjected to a sudden input, X_i, then equation 12 indicates that the output, X_o, will have the form

$$X_o=X_i\left(1-e^{\frac{-t}{T_f}}\right) \tag{13}$$

Before equation 11 and equation 12 are inserted in equation 9 and equation 10 to study the characteristics of the servomechanism, it is desirable to make one change of variable. If T_dp is replaced by λ; the ratio T_f/T_d defined as A; and the product K_dT_d defined as B, then the problem can be generalized, so that the solution will apply to any numerical value of T_d. Equation 11 then may be rewritten as

$$K_dG_d(\lambda)=\frac{B}{\lambda(\lambda+1)} \tag{14}$$

and equation 12 may be rewritten as

$$K_fG_f(\lambda)=\frac{1}{A\lambda+1} \tag{15}$$

The servomechanism characteristics then are determined by a substitution in equation 9 and equation 10. A nondimensional frequency variable is introduced when the operator λ is replaced by ju

$$\frac{\theta_i}{\theta_o}(ju)=\frac{ju(ju+1)}{B}+\frac{1}{jAu+1} \tag{16}$$

$$\frac{\epsilon}{\theta_o}(ju)=\frac{ju(ju+1)}{B}+\frac{1}{jAu-1}-1 \tag{17}$$

The effect of change of gain factor B for a given ratio A is illustrated in Figure 4 by a graphical construction of the problem, based on the frequency loci. As illustrated, the functions

$$\frac{1}{K_dG_d(ju)}$$

and $K_fG_f(ju)$ are plotted separately and combined by vector addition. The degree of resonance for a particular adjustment is noted by observing the proximity of the proper locus of

$$\frac{\theta_i}{\theta_o}(ju)$$

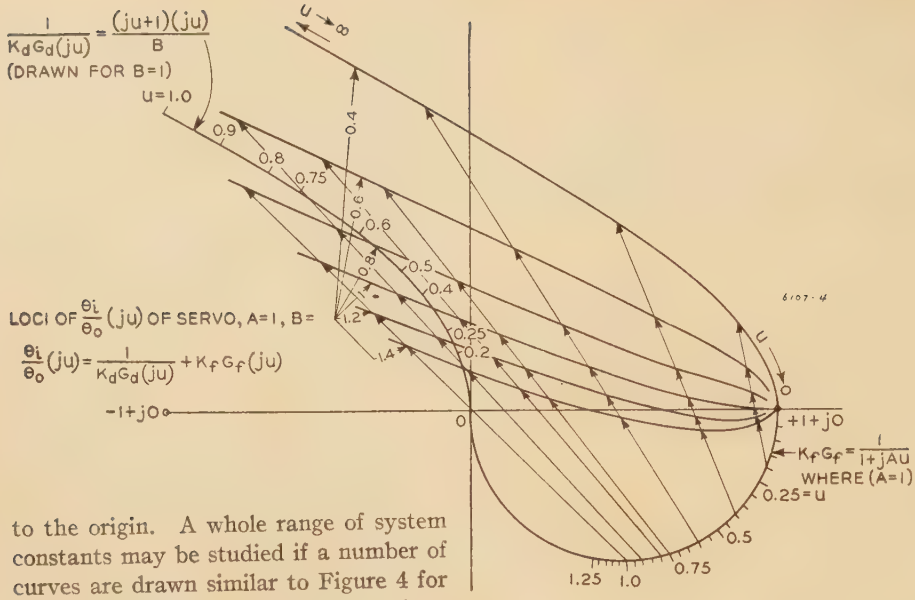

Figure 4. Loci for a proportional servomechanism with a time delay in the feed-back circuit to show the effect of change in direct circuit gain for the case of equal characteristic times in direct and feed-back circuits

to the origin. A whole range of system constants may be studied if a number of curves are drawn similar to Figure 4 for different values of A. From each of these plots a secondary group of curves may be made relating the resonant frequency and degree of resonance

$$\left(\text{minimum value of } \left|\frac{\theta_i}{\theta_o}(j\omega)\right|\right)$$

to the parameter being varied. Finally the data may be translated to the form shown in Figure 5, where lines of constant

$$\left|\frac{\theta_i}{\theta_o}(j\omega)\right|_{\text{minimum}}$$

and lines of constant resonant frequency are plotted as functions of A and B.

The process of examining the effect of change of a system parameter over a range is a laborious process. This is true to different degrees depending on the analytical technique used. Most often the analysis would not be carried so far as the one illustrated. Generally, the nature of the particular problem fixes a number of the parameters, and the problem is reduced in complexity. Quite often, too, the apparatus being considered is at hand for experimental study, and the analysis is used simply as an aid in visualizing the trend that should be observed following a change in the system.

For the problem being discussed it is practical to make a study of the transient response of the system, as well as a study of the frequency response. If the general operator λ is used instead of ju and equation 16 is combined and inverted, then

$$\frac{\theta_o(\lambda)}{\theta_i(\lambda)} = \frac{B(A\lambda+1)}{\lambda(\lambda+1)(A\lambda+1)+B} = \frac{B\left(\lambda+\frac{1}{A}\right)}{\lambda^3+\frac{A+1}{A}\lambda^2+\frac{1}{A}\lambda+\frac{B}{A}} \qquad (18)$$

The denominator of the right hand side of equation 18 is the characteristic equation of the system when set equal to zero. The roots of the characteristic equation are indicative of the transient response, as has been discussed often in articles of servomechanisms.[1]

The characteristic equation for the problem being discussed is

$$\lambda^3+\frac{A+1}{A}\lambda^2+\frac{1}{A}\lambda+\frac{B}{A}=0 \qquad (19)$$

which may be factored into the form

$$(\lambda+\alpha)(\lambda^2+2\zeta\mu_n\lambda+\mu_n^2)=0 \qquad (20)$$

for particular values of A and B. The undamped natural frequency, μ_n, and the exponential decay constant, α, have been nondimensionalized by the use of the operator λ instead of the operator p. For a particular value of T_d the exponential characteristic time is T_d/α seconds and the undamped natural frequency of the quadratic root, ω_n, is μ_n/T_d radians per second. The damping ratio ζ, defined as the ratio of actual to critical damping of the quadratic factor, is already a nondimensional factor and does not change in value with the reversion of the problem to one of particular values for the process characteristic time T_d and measuring instrument characteristic time T_f.

If a number of solutions of equation 20 are made for several values of A when B is constant, then for the same values of A when B is constant at another value, a series of curves may be drawn which represent α, ζ, and μ_n as a function of A when B is constant. Finally the solution may be redrawn as shown in Figure 6 where lines of constant α, ζ, and μ_n are plotted as a function of A and B. This figure demonstrates immediately the results that will be obtained for a particular adjustment of parameters. There is, however, an omission, in that the magnitude of the two modes of recovery are not compared, which is not serious because it is necessary to admit at the outset, that, unless every system parameter is known

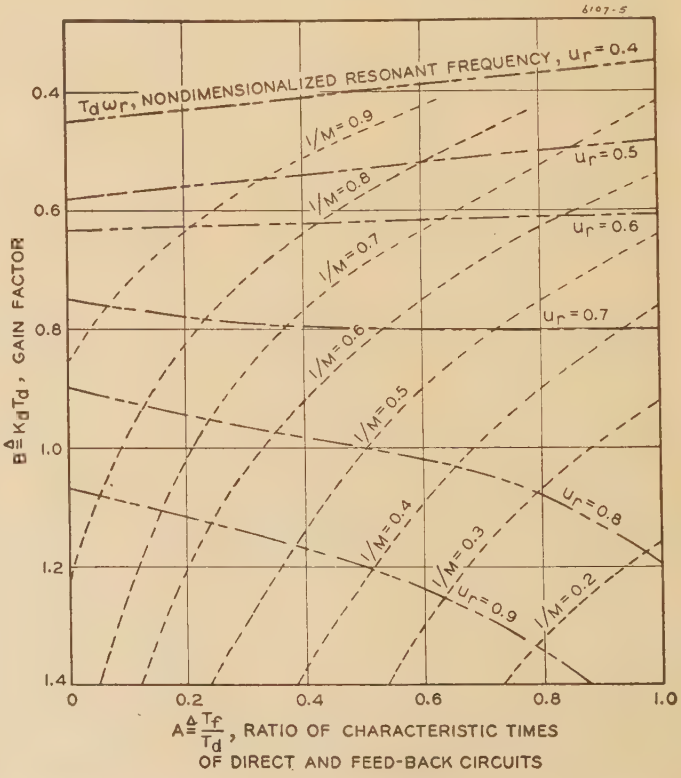

Figure 5. Resonant frequency and degree of resonance, $\left|\frac{\theta_i}{\theta_o}(j\omega)\right|_{\min} = \frac{1}{M}$, as a function of nondimensionalized system parameters of a proportional servomechanism with a time delay in the feed-back circuit

exactly and complete solutions are made for each adjustment, there will have to be a final experimental adjustment of the system. The purpose of the analysis as used in practice is to determine the approximate correct adjustment of the system and to indicate the direction implied by a proposed change of parameter values.

Because the solution to the characteristic equation of the illustrative problem can be presented fairly readily in the form of Figure 6, it is possible in this case to compare the criteria for servomechanism frequency response with criteria for transient response over a range of system adjustment by a comparison of Figures 5 and 6.

An empirical figure of merit for the design of servomechanisms by use of frequency response data has been to limit approximately the degree of resonance so that

$$M_{\max}=\left|\frac{\theta_o}{\theta_i}(j\omega)\right|_{\max}=1.5^*$$

or

$$\frac{1}{M_{\max}}=\left|\frac{\theta_i}{\theta_o}(j\omega)\right|_{\min}=0.67^{1,2}$$

For a simple system such as the one just discussed where $A=0$ and $\alpha=\infty$, there is a simple relationship between the damping ratio, ζ and the degree of resonance, $M_{\max}$. This relationship is shown graphically in Figure 7 where a value of $M_{\max}=1.5$ may be seen to correspond to a damping ratio $\zeta=0.35$. For the more complicated illustrative problem the correspondence between $M_{\max}$ and ζ can be seen to remain very similar to that for the simpler system with no delay in the feed-back circuit. This is a peculiarity of this particular problem and has been shown in unpublished work of others not to be a general case.** For more complicated systems the indications are that, when the degree of resonance is limited, the degree of stability can vary over a substantial range. A great deal still can be done to clarify the relationship between criteria for servomechanism design.

In concluding a discussion of the problem used as an illustrative example, it is desirable to point out that the characteristic equation, equation 19, is the same as any that would result from any time delay in the circuit. If, for example, the transfer function of the direct circuit were of the form

$$\frac{\theta_o}{\epsilon}=\frac{K_d}{p(T_dp+1)}\quad\frac{1}{(T_fp+1)} \tag{21}$$

where the components formerly in the feed-back circuit are moved to the direct circuit, then

$$\frac{\theta_o}{\theta_i}=\frac{K_d}{p(T_dp+1)(T_fp+1)+K_d} \tag{22}$$

or

$$\frac{\theta_o(\lambda)}{\theta_i(\lambda)}=\frac{B/A}{\lambda^3+\frac{A+1}{A}\lambda^2+\frac{1}{A}\lambda+B/A} \tag{23}$$

where λ, A, and B are as defined for equation 14 and equation 15. The denominator of equation 23 is identical to that of equation 18.

The foregoing discussion leads to a general comment on the nature of the transient response resulting from any sudden disturbance, no matter where in the closed loop of a single-loop servomechanism it is inserted; namely, that the system always will recover with the same modes of oscillation and degree of stability and/or with the same exponential decay times. The predominance of one part of the response over another, however, will change, depending on where in the closed cycle the transient disturbance is introduced. This conclusion applies in a limited degree when there are multiloop systems involved.

In a similar way, the system response at the output resulting from a sinusoidal disturbance depends on where the disturb-

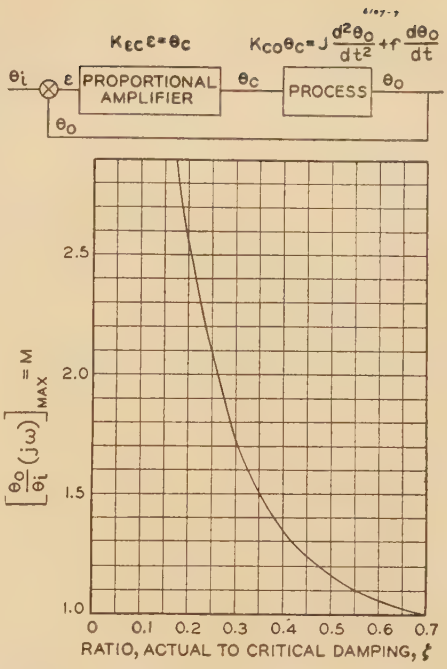

Figure 7. Correlation of degree of resonance M, with the ratio of actual to critical damping, ζ, for a proportional servomechanism

$$M=\frac{1}{2\zeta(1-\zeta^2)^{1/2}}\quad\zeta<0.707$$

$$\omega_n=\sqrt{K/J}$$

$$K=K_{ec}K_{co}$$

$$\beta=\frac{\omega}{\omega_n}$$

$$\zeta=\frac{f}{2\sqrt{KJ}}$$

Peak of frequency response occurs when

$$\beta=\sqrt{1-2\zeta^2}$$

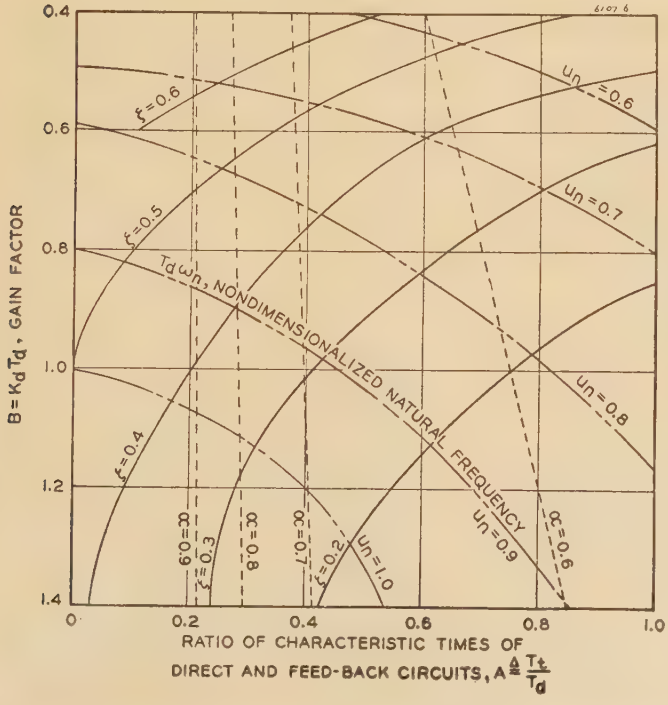

Figure 6. Presentation of the salient features of the transient response of a proportional servomechanism with a time delay in the feed-back circuit as a function of nondimensionalized system parameters

System characteristic equation

$$\lambda^3+\frac{A+1}{A}\lambda^2+\frac{1}{A}\lambda+\frac{B}{A}=(\lambda+\alpha)\times(\lambda^2+2\zeta\mu_n\lambda+\mu^2_n)$$

*The number varies considerably depending on the designer and the application.

**The manner of presentation of the roots of the characteristic equation as functions of system parameters and the comparison of these with similar data from frequency response studies is identical to that used by D. F. Tuttle of Massachusetts Institute of Technology. He compared the criteria for an integral control system.

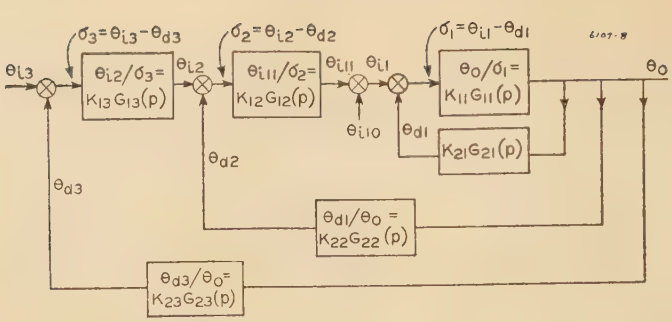

Figure 8. Diagrammatic arrangement of components in a multiloop servo system

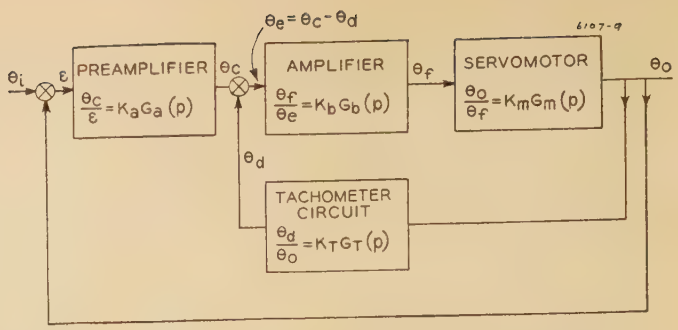

Figure 9. Diagrammatic arrangement of components for use of tachometric feedback in a positional servomechanism

ance is inserted. Any one system may have to be capable of satisfactory behavior following any of several disturbances, and there may therefore be a dual specification. The same general techniques of analysis employed in solving the illustrative problem can be used to determine response to a sinusoidal disturbance somewhere in the closed-cycle and hence be indicative of the transient response to a sudden disturbance at the same place. With reference to Figure 1, if the disturbance is $\theta_t(p)$ between the preamplifier and the servomotor then

$$\frac{\theta_t}{\theta_o}=\frac{1}{K_3G_3(p)K_4G_4(p)}+K_1G_1(p)K_2G_2(p) \quad (24)$$

General Treatment of Multiloop Systems

The technique described for the study of a servomechanism whose output quantity is not measured instantaneously is a powerful tool in dealing with much more complicated systems. It is particularly useful for studying systems where there are feed-back paths within feed-back paths, or in another way of speaking, where there are several loops.

A block diagram is drawn as Figure 8 to illustrate a multiloop system in general terms. The number of loops have been limited because the treatment of a larger number of closed loops is a logical extension of the treatment of a limited number.

The reasons for a large number of closed loops in a servomechanism system may be several. There are, however, three most likely reasons for such complicated structures:

1. A servomechanism may be required to serve in more than one capacity wherein it may be used by itself or it may be used, after a switching operation, as a part of an inclusive control system.

2. It may be possible to improve servomechanism performance by the use of compensating networks whereby additional control signals are introduced, in addition to the master input, which is a function of the output quantity or its derivatives or integrals.

3. It may be necessary to measure the output quantity with a device which cannot be considered perfect as compared with the rest of the system.

The following analytical representation of the system of Figure 8 is general, in that it does not define the purpose of the several components.

(*a*). For the inside loop with others disconnected where θ_{i1} is the independent variable

$$\frac{\theta_{i1}}{\theta_o}=\frac{1}{K_{11}G_{11}(p)}+K_{21}G_{21}(p) \; . \quad (25)$$

(*b*). For the second loop with the outside loop disconnected, where θ_{i10} is zero and θ_{i2} is the independent variable

$$\frac{\theta_{i2}}{\theta_o}=\frac{1}{K_{12}G_{12}(p)}\left[\frac{1}{K_{11}G_{11}(p)}+K_{21}G_{21}(p)\right]+K_{22}G_{22}(p) \quad (26)$$

(*c*). For the third loop where $\theta_{i10}=0$ and θ_{i3} is the independent variable

$$\frac{\theta_{i3}}{\theta_o}=\frac{1}{K_{13}G_{13}(p)}\left[\frac{1}{K_{12}G_{12}(p)}\left(\frac{1}{K_{11}G_{11}(p)}+K_{21}G_{21}(p)\right)+K_{22}G_{22}(p)\right]+K_{23}G_{23}(p) \quad (27)$$

which process can be continued to include as many closed loops as there are in the system. The final result is indicative of the characteristics of the whole system.

To consider the characteristics of the inside closed loop, the outside loops may be treated as additional feed-back paths. If an input θ_{i10} is considered as adding to the output from $K_{12}G_{12}(p)$.

(*a*). For the outside loop disconnected and θ_{12} held at zero the input to the circuit $K_{11}G_{11}(p)$ is

$$\theta_{i10}+[K_{12}G_{12}(p)K_{22}G_{22}(p)]\theta_o-[K_{21}G_{21}(p)]\theta_o \quad (28)$$

and this is reproduced at the output as

$$K_{11}G_{11}(p)[\theta_{i10}+K_{12}G_{12}(p)K_{22}G_{22}(p)\theta_o-K_{21}G_{21}(p)\theta_o]=\theta_o \quad (29)$$

or

$$\frac{\theta_{i10}}{\theta_o}=\frac{1}{K_{11}G_{11}(p)}+K_{21}G_{21}(p)-K_{12}G_{12}(p)K_{22}G_{22}(p) \quad (30)$$

which is a result which can be obtained by the addition of a new vector locus to the original one, equation 25, for the inside loop with the others disconnected.

(*b*). If the third loop as well as the second loop is connected and θ_{i3} held at zero, then the quantity σ_2 is the difference between θ_{i2} and θ_{d2}, and this is a simple addition to equation 30

$$\frac{\theta_{i10}}{\theta_o}=\frac{1}{K_{11}G_{11}(p)}+K_{21}G_{21}(p)+K_{12}G_{12}(p)\times[K_{23}G_{23}(p)K_{13}G_{13}(p)-K_{22}G_{22}(p)] \quad (31)$$

The foregoing process may be continued to include as many loops as are necessary. Even though the systems are very complicated, there is a reasonable way to consider the effect of change in any of the circuits by graphical construction of the loci of the reciprocal system function, where the operator is $(j\omega)$, and by observation of its salient characteristics.

Comments on Compensating Networks

The performance required of a given servomechanism is derived from the specifications for the operation of the whole control system. Such specifications are particular to any one application but are generally of two types

1. Those concerned with the steady state response to a typical input.

2. Those concerned with the dynamic or transient response.

In the first group, familiar specifications are concerned with: static accuracy; steady-state following error when the input is uniformly changing; steady-state sinusoidal errors when the input is moving sinusoidally at low frequencies; errors introduced by the application of load on the output. The second group of specifications is concerned primarily with the speed of response and degree of stability of the system, following suddenly applied inputs or loads. The problem for the designer of servomechanisms usually re-

solves itself into determining means for obtaining the desired steady-state response without harming the dynamic response characteristics.

In accomplishing this purpose in designing servomechanisms, the engineer usually resorts to the use of certain general techniques which are economic of equipment and which often make the control system feasible. These techniques center around

1. The close specification of the characteristics of the process, so that it is more controllable.

2. The use of special control circuits.

One widely used technique is to make the control amplifier sensitive to derivatives and integrals of the servo error as well as the error itself. The controller then is described as one which anticipates and remembers. The general purpose of the use of derivatives of error is to improve the degree of stability of the system, thereby making possible larger sensitivity. The general purpose in the use of integrals of the error is to increase the system sensitivity statically or at low frequencies without materially harming the performance of the system at frequencies where it is likely to oscillate. The techniques for the design of these compensating devices are not the main concern of this paper. They have been discussed widely (see reference list) and can be treated as cascaded elements in the system. In Figure 1, a change in the controller, represented by the operational transfer function $K_1G_1(p)$, can be treated readily since it is multiplied by the transfer functions of the remaining cascaded elements. This has been indicated previously in equation 1.

There are a number of other compensating networks which cannot be accurately described as cascade elements in the control system. Several examples of these are enumerated:

1. Feedback around a component or group of components. This often is done to improve the dynamic response of elements or to remove the dependence on open-loop instrumentation in the action of an element. Integral controllers sometimes are made by the use of feedback.

2. Output feedback. It is often possible to obtain a stabilizing device by returning signals to the controller which are functions of the derivatives of the output quantity, as well as functions of the output quantity itself. When these signals are used without subtracting them from similar functions of the input, then they are no longer cascade elements.[1,8]

3. Input feed-forward. This is a term used to describe systems which measure a function of the derivatives of the input as well as the input itself, thus supplying the control system with advance knowledge of what is going to be required of it.[8]

4. Tuned loads. These are used to impose a restraint on the output member which is frequency sensitive. They are devices that limit the ability of the output member to oscillate at the resonant frequency of the system.

All of the afore-mentioned techniques are fairly complicated in their application. It is not practicable to treat them all, and the opportunity to obtain general solutions is limited. They can, however, be studied quite satisfactorily by the use of appropriate system functions. The remainder of this paper will deal with an illustrative example wherein output feedback is used to improve the performance of the system.

Tachometric Feedback in Positional Servomechanisms

If the speed of the output of a position control is measured, and a function of this signal is fed back degeneratively into the amplifier stages, where it is added to the positional error signal, the performance of the servomechanism may be improved. This may be visualized physically by comparing this technique with that of employing the derivative of the servo error. When the servo input is stationary, the two are identical in function if the tachometric signal is not modified by some additional network. It would be concluded, therefore, that tachometric feedback has a stabilizing effect, since the good use of error derivative techniques is well known.[1,2]

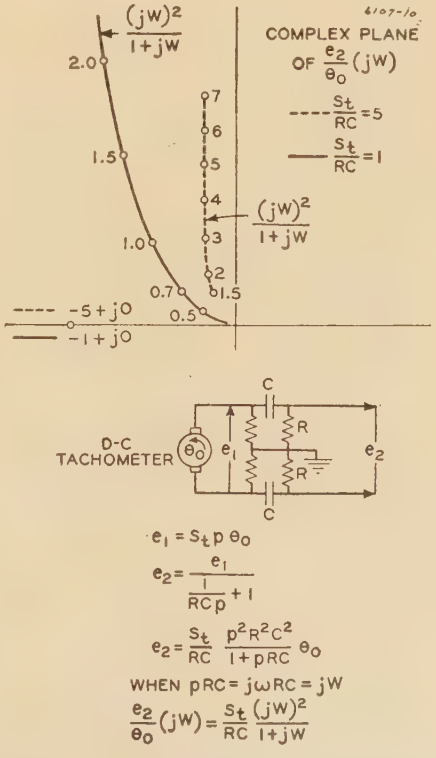

Figure 10. D-c tachometer with high-pass filter

Actually the tachometer signal usually is modified to improve the steady-state error that results when the input is moving at a constant velocity. A high-pass filter usually is used, so that no signal is sent back when the output is moving at a constant velocity or is following sinusoidal inputs of relatively low frequencies. The filter, however, allows the tachometer signal to pass freely at frequencies where the servomechanism is likely to oscillate. A simple filter is shown in a tachometer circuit as a part of Figure 10. By this technique the stabilizing effect of the tachometer is made available at frequencies where the servomechanism is likely to oscillate and does not require an even greater error signal to make the output move at a given speed.

The tachometer signal need not be added to the control system at the same place where the positional error signal is introduced. A general arrangement of components is illustrated in block diagram form in Figure 9. The preamplifier may use an integrating circuit or some other compensating circuit if the specifications for the servomechanism cannot be met without their use. For the first example to be discussed here the amplifier will be assumed to be proportional and characterized by a gain factor, K_a. Also in the first example it will be assumed that the servomotor is one in which the output damping is negligible and that the inertia of the motor and output member is the only energy storage element on the output shaft Under these conditions the transfer function $K_mG_m(p)=K_m/J_mp^2$. Without the use of some sort of compensating device this system would be unstable. To stabilize the system let the tachometer circuit of Figure 10 be used. The amplifier $K_bG_b(p)$ will be assumed to be proportional and to have no time lags. Equations for the system may be written on the basis of the foregoing simplifications:

$$\theta_e=\theta_c-\theta_d=K_a\epsilon-\frac{S_tRCp^2\theta_o}{RCp+1} \tag{32}$$

$$\theta_e=\frac{J_mp^2}{K_bK_m}\theta_o \tag{33}$$

from which

$$\frac{\epsilon}{\theta_o}=\frac{1}{K_a}\left[\frac{J_mp^2}{K_bK_m}+\frac{S_tRCp^2}{RCp+1}\right] \tag{34}$$

and since by definition, $\epsilon=\theta_i-\theta_o$

$$\frac{\theta_i}{\theta_o}=1+\frac{1}{K_a}\left[\frac{J_mp^2}{K_bK_m}+\frac{S_tRCp^2}{RCp+1}\right] \tag{35}$$

which may be written in the form

$$\frac{\theta_i}{\theta_o}=1+\frac{S_i}{K_aRC}\left[\frac{J_m}{RCK_bK_mS_i}\lambda^2+\frac{\lambda^2}{\lambda+1}\right] \quad (36)$$

where $\lambda=RCp$. If the right hand side of equation 35 is expressed in terms of a common denominator, the numerator of the resulting fraction is the characteristic equation when equated to zero.

$$J_mRCp^3+(K_bK_mS_tRC+J_m)p^2+K_aK_bK_mRCp+K_aK_bK_m=0 \quad (37)$$

The characteristic equation may be written in terms of λ instead of p and two nondimensional parameters defined

$$F=\frac{J_m}{RCK_bK_mS_t} \quad (38)$$

$$D=\frac{S_t}{K_aRC} \quad (39)$$

$$\lambda^3+\left(1+\frac{1}{F}\right)\lambda^2+\frac{1}{FD}\lambda+\frac{1}{FD}=0 \quad (40)$$

Equation 40 is in a form where it may be broken down readily into a study of the real and quadratic factor. These factors could be expressed graphically as functions of F and D in a manner similar to Figure 6.

An important deduction can be made with reference to equations 38 and 39. It can be seen that F and D may be controlled separately in magnitude by adjustment of the time constants and component sensitivities in the system. This means that mathematically any desired result may be obtained for the response of the system.

There are two practical limitations on the procedure of unlimited adjustment. The first, and most important, is that no physical system can be represented by such simple differential equations as a first order approximation when the natural and resonant frequencies for the system become very high. The second limitation is that the specifications for the performance of the servomechanism do not, as a rule, justify the expense in equipment in obtaining better performance than is required.

By using the same substitutions given in equations 37, 38, and 39 the frequency response loci may be studied in accordance with the functional relationship indicated by equation 35. Setting $\lambda=jW$

$$\frac{\theta_i}{\theta_o}(jW)=1+D\left[F(jW)^2+\frac{(jW)^2}{1+jW}\right] \quad (41)$$

Figure 11 shows an example of the construction of typical loci for one particular value of D and two values of F. In drawing these loci, it would have been as easy to construct them by adding to the locus of

$$\frac{(jW)^2}{1+jW}$$

shown in Figure 10, the locus of $F(jW)^2$ and work with the resultant locus as a reciprocal system function

$$\frac{\epsilon}{\theta_o}(jW)$$

The polar expansion of this locus is controlled by the gain factor D.

The same conclusion about the adjustment of the system may be reached from a study of the frequency loci as was reached from a study of the characteristic equation; namely, that any response desired could be obtained by appropriate selection of parameter values.

There is, however, one important failing of this technique in that there is no simple way known to the author that has yet been evolved to see the presence of predominating real roots in the transient response by simple examination of the locus. It has been suggested that the rate of change of phase near zero frequency might hold a clue, but this has not been investigated thoroughly. Even in a complicated system, however, it is not a long problem to evaluate a real root and its coefficient for particular values and for a specified disturbance. Hence, there is the desirability of always keeping in close touch with the transient specifications of a system when the major part of the study is done by frequency characteristics.

It will be desirable to conclude this discussion of tachometer feedback by studying the application to a system more exactly represented by higher order differential equations than the afore-mentioned one. In doing this, only the frequency response technique will be studied, because a study of the transient response becomes hopelessly complicated, except for final checks on the presence of undesirable real roots in the characteristic equation which are excited by typical inputs expected in the application.

A typical servomotor for a position controller will be an integrating device with an elastance storage element as well as an inertia storage element. The transfer function, K_mG_m, for such a servomotor would be of the form

$$K_mG_m(p)=\frac{S_m}{p(J_mp^2+f_mp+k_m)} \quad (42)$$

where K_m is S_m/k_m and is expressible as per unit speed output per unit input. If the numerator and denominator of equation 44 are divided by k_m, and the open-loop undamped natural frequency of this component be written as $\omega_n=k_m/J_m$, and the ratio of actual to critical damping of the open-loop characteristic be written as

$$\zeta=\frac{f_m}{2\sqrt{J_mk_m}}$$

then equation 44 may be rewritten

$$K_mG_m(p)=\frac{\frac{K_m}{\omega_n}}{\frac{1}{\omega_n}p\left(\frac{1}{\omega_n^2}p^2+\frac{2\zeta}{\omega_n}p+1\right)} \quad (43)$$

and transformed, when

$\lambda=\frac{1}{\omega_n}p$ into

$$K_mG_m(\lambda)=\frac{S_m/k_m\omega_n}{\lambda(\lambda^2+2\zeta\lambda+1)} \quad (44)$$

The amplifier used with such a power motor probably has an open-loop speed of response of the same order of magnitude as the servomotor itself. If the transfer function of the amplifier be assumed to be of the form

$$K_bG_b(p)=\frac{K_b}{\tau p+1} \quad (45)$$

where the characteristic time, τ, is arbitrarily set equal to $1/\omega_n$, which is commensurate with the foregoing statement regarding its speed of response, equation 45 then may be rewritten in terms of

$$K_bG_b(\lambda)=\frac{K_b}{\lambda+1} \quad (46)$$

The cascade of the amplier and servomotor then may be written as

$$K_mG_m(p)K_bG_b(p)=\frac{\frac{K_bK_m}{\omega_n}}{(\lambda+1)(\lambda^2+2\zeta\lambda+1)\lambda} \quad (47)$$

The preamplifier will be assumed to be characterized by a gain K_a and negligible characteristic time.

If the components are assembled in a servomechanism without tachometer feedback and the gain of the system

$$\frac{K_aK_bK_m}{\omega_n}$$

be adjusted to give the highest resonant frequency possible with a peak degree of resonance

$$\left|\frac{\theta_i}{\theta_o}\right|_{\min}$$

of 0.7, then the resulting frequency locus will be as shown in Figure 12 where $\zeta=0.3$ and $\lambda=j\mu$. The gain adjustment was such as to make

$$\frac{K_aK_bK_m}{\omega_n}=\frac{1}{2.8}$$

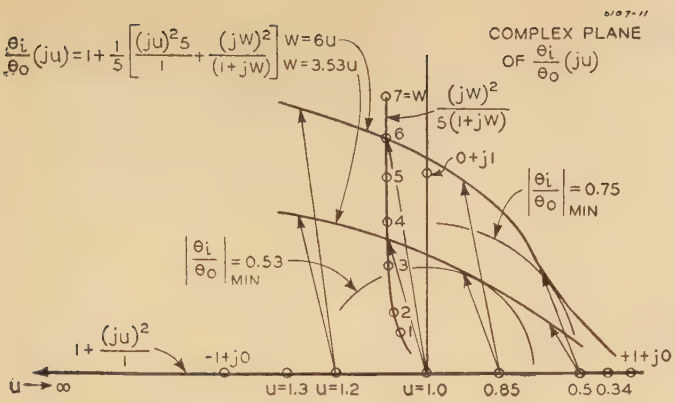

Figure 11. Loci illustrating a study of the application of tachometer feedback to a proportional servomechanism whose output member is characterized by load inertia and no damping

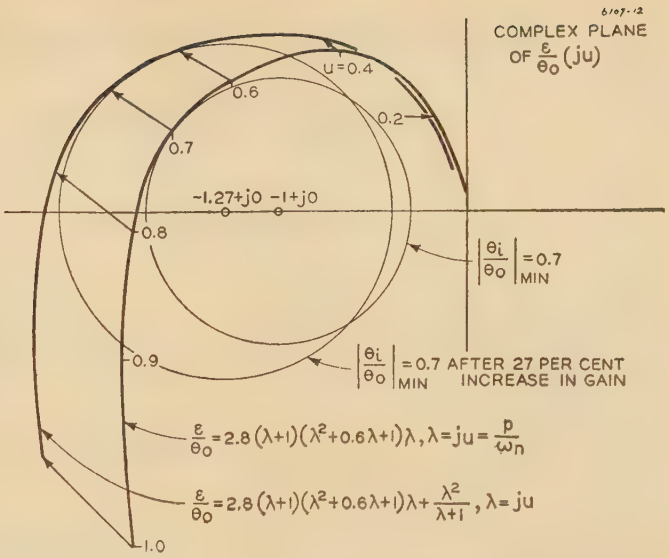

Figure 12. Loci illustrating a study of the application of tachometer feedback to a positional servomechanism with four energy storage elements

If, now, tachometer feedback is to be added to the system, the analytical combination of the system is indicated in equation 48.

$$\frac{\epsilon}{\theta_o}=\frac{1}{K_a}\frac{1}{K_m G_m(p) K_b G_b(p)}+K_t G_t(p) \qquad (48)$$

which is derived for the system block diagram of Figure 9.

The type of tachometer feedback used will be that illustrated in Figure 10, so that

$$K_t G_t(p)=-\frac{\frac{S_t}{RC}R^2C^2p^2}{RCp+1} \qquad (49)$$

A question immediately arises about the magnitude of the tachometer signal that can be made available, or in other words what is a reasonable value of K_t with respect to the sensitivity of the amplifier and servomotor in cascade. If K_t were exactly equal to $1/K_mK_b$ then, in the absence of the tachometer RC network, the amplifier K_a would have to supply just twice as much signal to make the output run at a given speed as it would in the absence of the tachometer. Calculation would show that a locus resulting from substitution in equation 50 would be altered very little by the addition of tachometer feedback with so low a tachometer sensitivity, unless the characteristic time of the RC network is made very large. Unfortunately, if the characteristic time of the RC network is made much larger than those in the remainder of the system, the speed of response of the servomechanism will be reduced by the introduction of a predominant exponential decay in the transient response. This conclusion is largely an experience deduction based on heuristic reasoning about the flow of correcting signals through the circuits. However, it has been substantiated by actual calculation in a number of instances.

In Figure 12 the original locus is shown modified by a tachometer feed-back circuit with the particular adjustment

$$RC=\frac{1}{\omega_n} \qquad (50)$$

and

$$K_t=\frac{S_t}{RC}=\frac{\omega_n}{K_aK_mK_b}=2.8 \qquad (51)$$

The addition of tachometer feedback allows an increase in the preamplifier gain of 27 per cent without increasing the degree of resonance.

The allowable increase in gain may be obtained by evaluating the polar contraction of the final locus before again becoming tangent to the $1/M=0.7$ circle. Another technique is to find by trial and error a new circle, whose radius is 0.7 times the length along the axis to the center, that will be tangent to the new locus. The amount by which the gain may be increased is read immediately from the scale on the negative real axis.

In summary it cannot be emphasized too strongly that the major value of such analytical techniques as are described here is to give a quantitatively approximate idea of the correct approach to a problem. However, when the analysis includes experimental data on the performance of the major components, then the design of the remaining circuits can be done very exactly, although always subject to check on the applicability of the criteria used for design.

References

1. Dynamic Behavior and Design of Servomechanisms, **G. S. Brown, A. C. Hall.** American Society of Mechanical Engineers preprint 45-A-20.

2. The Analysis and Synthesis of Linear Servomechanisms (book), **A. C. Hall.** Technology Press, Massachusetts Institute of Technology, Cambridge, Mass., 1943.

3. Theory of Servomechanisms (book), **L. A. MacColl.** D. Van Nostrand Company, New York, N. Y., 1945.

4. Network Analysis and Feed-back Amplifier Design (book), **H. W. Bode.** D. Van Nostrand Company, New York, N. Y., 1945.

5. Communication Networks (book), **E. A. Guillemin.** Volume II. John Wiley and Sons, Inc., New York, N. Y., 1935.

6. Solutions of the Cubic Equation and the Cubic Charts, **L. W. Evans.** Privately printed by the department of electrical engineering of Massachusetts Institute of Technology, Cambridge, Mass., 1943.

7. Considerations of Servomechanism Design, **S. W. Herwald.** AIEE Transactions, volume 63, 1944, December section, pages 871–7.

8. The Analysis and Design of Servomechanisms, **H. Harris.** Section D-2, Fire Control Committee, National Defense Research Council, 1942. Office of Scientific Research and Development publication 454.

A Fractional Termination for Ladder Networks

WILBUR REED LePAGE
MEMBER AIEE

Synopsis: When using a uniform ladder network to simulate a smooth transmission line, the possibility is considered of deriving a termination which would be intermediate between the usual mid-shunt and mid-series types and which would have advantages over the latter. It is found that a new termination is possible which gives some improvement throughout a limited frequency range. For the dissipationless case, the range corresponds to a line of less than a quarter wave length. The improvements attainable are of the order of a few per cent and become less significant the greater the number of network sections. Thus, although the formula for the new termination and the estimates of the results which it will accomplish are given for any number of sections, the new termination is of most practical value for circuits of few sections. In arriving at this termination, consideration is given to the variation of each of the elements of the pair on each end; but of these two, the end element is the only one whose variation yields an improvement. For the frequency range for which the modified circuit is an improvement, the distinction between the two original types of termination largely is lost, the modified midshunt and modified mid-series terminations being almost identical. Beyond this range there is a difference between them, and the corresponding original and new networks are nearly equivalent. A possible application of the results is suggested in which the simulation of a smooth line is not involved.

IT is well known that by taking a sufficient number of sections, a mid-shunt or mid-series terminated uniform ladder network may be made to approximate a smooth line as closely as desired over a low-pass band of frequencies the width of which increases as the number of network sections is increased. It is also true, considering the network in the 4-terminal sense, that under some conditions a mid-shunt termination gives the best results while with other terminal conditions the mid-series arrangement is superior. The question to be treated is whether an intermediate termination can be found which will give a uniformly good approximation for all conditions and, if possible, a superior performance. This is to be investigated with the understanding that the network must retain its 4-terminal identity, which implies symmetry about the line indicated in Figure 1. This rules out known nonuniform networks that offer economy of circuit elements when the line is to be represented in a 2-terminal sense only.[1]

Properties of Uniform Ladder Networks

It is considered that an analysis of the ladder network, when terminal quantities are involved, is most reasonably carried out in terms of the 4-terminal network parameters A, B, and C, which are defined by the equations

$$E_S = AE_R + Z_T B I_R \tag{1a}$$

$$I_S = Y_T C E_R + A I_R \tag{1b}$$

in the symmetrical case. The voltages and currents involved are indicated in

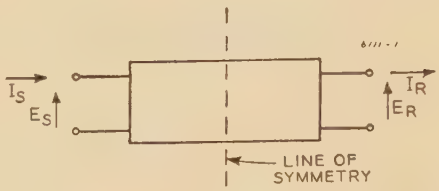

Figure 1. Notation for a 4-terminal network

Figure 1, and Z_T and Y_T are respectively the total series impedance and shunt admittance of the line. This notation is slightly different from the usual practice in that B and C are written respectively with the factors Z_T and Y_T removed. This change simplifies many of the subsequent equations. One may obtain the quantities that are necessary for expressing the circuit in other forms from equations involving A, B, and C, which may be found in standard texts on circuit analysis.[2]

Expressions for A, B, and C in power series of the variable $Z_T Y_T$ have been given in a previous paper[3] for a uniform ladder network with either type of termination. The series form is used because it affords simple comparisons with corresponding formulas for a smooth line. These formulas are repeated here for easy reference, but with primes on all quantities so that unprimed notation may be used for the derived circuits. For a network of M identical T sections connected in cascade we define

$$\alpha' = \sqrt{Z'_T Y'_T} \tag{2}$$

and have

$$A' = \sum_{\lambda=0}^{M} a'_\lambda (\alpha')^{2\lambda} \tag{3a}$$

$$B' = \sum_{\lambda=0}^{M} b'_\lambda (\alpha')^{2\lambda} \tag{3b}$$

$$C' = \sum_{\lambda=0}^{M-1} c'_\lambda (\alpha')^{2\lambda} \tag{3c}$$

in which

$$a'_\lambda = \frac{1}{(2\lambda)!} \prod_{n=0}^{\lambda-1} \left(1 - \frac{n^2}{M^2}\right) \tag{4a}$$

$$b'_\lambda = \frac{1}{(2\lambda+1)!} \left(1 + \frac{\lambda}{2M^2}\right) \prod_{n=0}^{\lambda-1} \left(1 - \frac{n^2}{M^2}\right) \tag{4b}$$

$$c'_\lambda = \frac{1}{(2\lambda+1)!} \prod_{n=0}^{\lambda} \left(1 - \frac{n^2}{M^2}\right) \tag{4c}$$

The corresponding results for M identical π sections in cascade are obtained by interchanging B' and C',[3] and the corresponding coefficients for a smooth line are obtained from equations 3 and 4 by allowing M to become infinite. The parameters and coefficients for the smooth line subsequently will be referred to as ideal values and will be written with a bar above the appropriate symbol.

Modified Terminations

The simple relationship between the B and C parameters of the T and π section constructions maintains even when all network sections are not identical, so long as the modifications of corresponding elements of the two networks are related dually.[3] That is, so long as a given change in a series element of one network is represented by an equivalent change in the corresponding shunt element of the other network, we need treat only one network. This enables us to proceed by analyzing only the T-section case.

The algebra is simplified if we assume an ordinary mid-series terminated uniform network on each end of which is connected a new series element. The new total series impedance will be designated by Z_T, and the element added to each end will be of magnitude ρZ_T. These definitions are illustrated in Figure 2A, along with Figure 2B, which shows

Paper 46-111, recommended by the AIEE committee on basic sciences for presentation at the AIEE summer convention, Detroit, Mich., June 24–28, 1946. Manuscript submitted March 25, 1946; made available for printing May 2, 1946.

WILBUR REED LEPAGE is a senior research engineer, Stromberg Carlson Company, Rochester, N. Y.

the equivalent π-section case, the results for which will be included, as explained above.

For the new circuit

$$\alpha = \sqrt{Z_T Y_T} \tag{5a}$$

$$Z'_T = (1-2\rho) Z_T \tag{5b}$$

$$Y'_T = Y_T \tag{5c}$$

$$\alpha' = \alpha\sqrt{1-2\rho} \tag{5d}$$

No adjustment is possible if the network has only a single section, so the number of sections (M) must be greater than or equal to 2. The formulas for A, B, and C, the new network parameters, are easily obtained by considering the network to be formed by the cascade connection of three elemental networks as indicated in Figure 2. This connection lends itself to the use of matrix algebra in the following way:[4]

$$\begin{pmatrix} A & BZ_T \\ CY_T & A \end{pmatrix} = \begin{pmatrix} 1 & \rho Z_T \\ 0 & 1 \end{pmatrix} \times \begin{pmatrix} A' & B'Z'_T \\ C'Y'_T & A' \end{pmatrix} \begin{pmatrix} 1 & \rho Z_T \\ 0 & 1 \end{pmatrix} = \begin{pmatrix} A'+\rho C'\alpha^2 & [2A'\rho + B'(1-2\rho) + \rho^2 C'\alpha^2] Z_T \\ C'Y_T & A'+\rho C'\alpha^2 \end{pmatrix} \tag{6}$$

The formulas for A, B, and C may be picked from the matrix on the right of the above equation. Equations 3a–3c are used for A', B', and C' with the observation that the $(\alpha')^{2\lambda}$ factors may be replaced by $\alpha^{2\lambda}(1-2\rho)^{\lambda}$. Also, noting that whenever the term α^2 appears in the final matrix of equation 6, it always carries C' as a coefficient, and that the maximum exponent in the series for C' is two less than in the series for A' or B', it follows that the maximum exponents of α in the series for A, B, and C will be the same as in equations 3a–3c. Hence

$$A = \sum_{\lambda=0}^{M} a_\lambda \alpha^{2\lambda} \tag{7a}$$

$$B = \sum_{\lambda=0}^{M} b_\lambda \alpha^{2\lambda} \tag{7b}$$

$$C = \sum_{\lambda=0}^{M-1} c_\lambda \alpha^{2\lambda} \tag{7c}$$

Formulas for a_λ, b_λ, and c_λ are obtained from the individual elements of the last matrix of equation 6, in conjunction with equations 3a–3c. The results are

$$a_\lambda = a'_\lambda (1-2\rho)^\lambda + \rho c'_{\lambda-1}(1-2\rho)^{\lambda-1} \tag{8a}$$

$$b_\lambda = 2\rho a'_\lambda (1-2\rho)^\lambda + b'_\lambda (1-2\rho)^{\lambda+1} + \rho^2 c'_{\lambda-1}(1-2\rho)^{\lambda-1} \tag{8b}$$

$$c_\lambda = c'_\lambda (1-2\rho)^\lambda \tag{8c}$$

In formula 8a, a negative subscript is understood to indicate a value of zero for that coefficient. At this point it is well

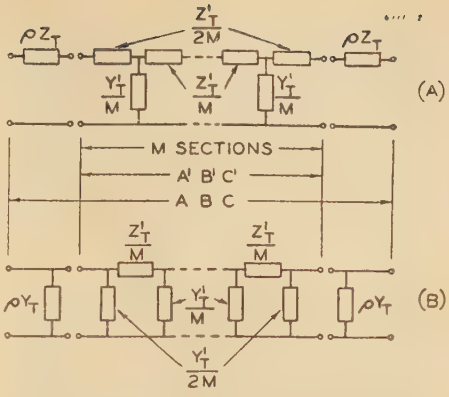

Figure 2. Single-element modification

to make the cautionary remark that if these are to be interpreted for the shunt-terminated case, it is only the formulas for b_λ and c_λ that should be interchanged. Reflection will show that b'_λ and c'_λ must not be interchanged if they are still given by equations 4a–4c. Of course, if an exchange is made there also, the change should be made in equations 8a–8c as well. In other words, if b'_λ and c'_λ are not interchanged, they retain their significance of respective coefficients of B' and C' for a uniform mid-series terminated network, while if they are interchanged, their new significance relates to a mid-shunt terminated uniform network.

The condition for the new termination has been stated as the removal of the distinction between series and shunt element termination with, if possible, an improvement in the approximation for a smooth line. The non-equivalence of the two ordinary terminations arises from the non-equality of b'_λ and c'_λ in equations 4a–4c. One therefore proceeds by first making $b_\lambda = c_\lambda$ for as many values of λ as possible, starting from $\lambda = 0$, and later checking whether they are less in error than their corresponding primed coefficients. From equations 4a–4c it is seen that a'_0, b'_0, and c'_0 each has its correct value, and from equations 8a–8c it follows that

$$a_0 = b_0 = c_0 = 1 \tag{9}$$

It also is seen from equation 8a, and the fact that $a'_1 = 1/2$ and $c'_0 = 1$, that

$$a_1 = a'_1(1-2\rho) + \rho c'_0 = {}^1/_2 \tag{10}$$

Thus, to have the first terms correct in the power series expansions of B and C and to have the first two terms correct in the expansion of A, it is only necessary to have the total series impedance and shunt admittance equivalent to those of the simulated line so α will have the correct value.

Attention logically is turned next to a_2, b_1, and c_1. It is shown in Appendix I that these are interrelated by the formula

$$a_2 = \frac{b_1 + c_1}{2} - \frac{1}{8} \tag{11}$$

so a_2 will be automatically determined when b_1 and c_1 are established. We shall proceed by putting $\lambda = 1$ in equations 8b, 8c, and so on to obtain, after substituting values for the primed coefficients from equations 4a–4c, the following:

$$b_1 = \rho(1-2\rho) + (1-2\rho)^2\left(\frac{1}{6}\right)\left(1+\frac{1}{2M^2}\right) \tag{12a}$$

$$c_1 = (1-2\rho)\left(\frac{1}{6}\right)\left(1-\frac{1}{M^2}\right) \tag{12b}$$

Formulas 12a and 12b may be equated to yield a quadratic equation in ρ the solution of which readily is found to be

$$\rho = 1 - \frac{1}{2}\sqrt{\frac{4M^2-1}{M^2-1}} \tag{13}$$

The negative sign is chosen for the radical from knowledge that $\rho = 0$ must correspond to infinite M. It is interesting to note that ρ is negative, implying a reduction of the end element. This is reasonable because it physically means a compromise between the two ordinary terminations. The substitution of this value of ρ in equation 12b gives

$$b_1 = c_1 = \frac{1}{6}\sqrt{1-\frac{1}{M^2}} \times \left(2\sqrt{1-\frac{1}{4M^2}} - \sqrt{1-\frac{1}{M^2}}\right) \tag{14}$$

It remains to be seen whether this value is less in error than b'_1 and c'_1. It should be noted parenthetically that when comparisons are to be made between the new and the old coefficients, the latter must represent a network having the same overall impedance and admittance as the new circuit. This only affects A', B', and C', through Z'_T, Y'_T, and α', and not a'_λ, b'_λ, and c'_λ. It is only the interpretation which is affected by varying Z'_T, and Y'_T. This is equivalent to saying that the primes may be removed from Z'_T, Y'_T, and α', but that they must be retained on the parameters and coefficients. It will be assumed that this is done for all the subsequent comparisons.

The error of $b_1 = c_1$, as given by equation 14, may be estimated by the process shown in Appendix II. It is found that

$$\frac{1}{24M^2} < \frac{1}{6} - c_1 = \frac{1}{6} - b_1 < \frac{3}{49M^2} \tag{15}$$

while the errors of b'_1 and c'_1 are, from equations 4a–4c,

$$b'_1 - \frac{1}{6} = \frac{1}{12M^2} \tag{16a}$$

$$\frac{1}{6}-c'_1=\frac{1}{6M^2} \tag{16b}$$

It thus is assured that the errors in b_1 and c_1 are less than those in b'_1 and c'_1.

An estimate of the error in the corresponding a_2 may be obtained from equation 11 and inequality 15. One directly obtains

$$\frac{1}{24M^2}<\frac{1}{24}-a_2<\frac{3}{49M^2} \tag{17}$$

It is also important to know how it compares with its value when $\rho=0$. An estimate of the ratio a_2/a'_2 can be found by a procedure shown in Appendix III which gives

$$\frac{(M^2-1/4)(M^2-7/4)}{(M^2-1)^2}<\frac{a_2}{a'_2}<\frac{(M^2-2/5)(M^2-8/5)}{(M^2-1)^2}<1 \tag{18}$$

This remains near, but less than, unity. The estimate is less accurate when M is small, so actual values of the ratio are tabulated in Table I along with the ratios of a'_2, a_2, b'_1, $b_1=c_1$, and c'_1 to their ideal values. One must observe that the error in a_2 is greater than the error in a'_2. This follows from equation 4a, which shows that a'_2 is less than $\bar{a}_2$, and from relation 18, which shows a_2 to be less than a'_2.

When $|\alpha|$ is sufficiently small, only the first two terms in each of the series for A', B', and C' will be important because it is known that the coefficients decrease with increasing λ. Therefore if the coefficients for the new circuit, when λ is greater than or equal to 2, are not brought into prominence by the modification, the new circuit will have less error and will be more symmetrical in B and C, for this range of $|\alpha|$. Estimates of a_λ, b_λ, and c_λ are therefore in order for $\lambda\geqq 2$. The methods used in obtaining these estimates are illustrated in Appendix III, with the results given in the following inequalities:

$$\left(\frac{M^2-2/5}{M^2-1}\right)^{\lambda-1}\left(\frac{M+1/4}{M+1}\right)<\frac{a_\lambda}{a'_\lambda}<\left(\frac{M^2-1/4}{M^2-1}\right)^{\lambda-1}\left(\frac{M^2-11/5}{M^2-1}\right) \qquad \lambda\geqq 3,\ M\geqq 3 \tag{19a}$$

$$\left(\frac{M^2-2/5}{M^2-1}\right)^{\lambda-1}\left(\frac{M-1}{M+1}\right)<\frac{b_\lambda}{b'_\lambda}<\left(\frac{M^2-1/4}{M^2-1}\right)^{\lambda-1} \qquad \lambda\geqq 2,\ M\geqq 4 \tag{19b}$$

$$\left(\frac{M^2-2/5}{M^2-1}\right)^{\lambda}<\frac{c_\lambda}{c'_\lambda}<\left(\frac{M^2-1/4}{M^2-1}\right)^{\lambda} \qquad \lambda\geqq 2,\ M\geqq 2 \tag{19c}$$

The second of these is valid only for $M\geqq 4$ for a reason which is pointed out with its derivation. The actual values of b_λ/b'_λ for the range not covered by relation 19b have been computed and are as follows: with $M=2$ and $\lambda=2$, ratio $=0.7221$; with $M=3$ and $\lambda=2$ and 3, ratios equal 0.8505 and 0.7965, respectively. A statement about the application of these estimates for the shunt terminated case is necessary to avoid confusion. In the light of the statement following equations 8a–8c, one would correctly conclude that b'_λ and c'_λ retain their positions, while b_λ and c_λ are interchanged. However, this leaves the ratios in unreasonable forms, so it is better here to interchange b'_λ and c'_λ with the understanding that they are given by formulas 4a–4c in an interchanged condition. This is in agreement with the alternative proposition contained in the statement referred to. Relations 19a–19c make it clear that none of the coefficients is greatly changed by the modification.

Before continuing with the investigation, the meaning of these results will be discussed rather fully because they have a bearing on the development to follow. It has been pointed out that the B and C coefficients for the new circuit are more nearly equal, and are nearer the ideal value, only so long as $|\alpha|$ is sufficiently small to make the first two terms predominant in the series for A, B, and C. It would be convenient to be able to specify this range definitely, but it depends on the circuit termination and on the angle of the complex number α. Something can be said about the range, however. In the following discussion the range of $|\alpha|$ over which the new circuit is an improvement will be referred to as the useful range. From equation 11, if we take Δb_1 and Δc_1 as the respective errors of b_1 and c_1, it follows that the error (Δa_2) in a_2 is

$$\Delta a_2=\frac{\Delta b_1+\Delta c_1}{2} \tag{20}$$

Considering these terms only, we see that when $|\alpha|=1$ the error in A caused by Δa_2 is as great as the averaged errors of B and C caused by Δb_1 and Δc_1. For larger $|\alpha|$ the error of A will become rapidly worse because a_2 is the coefficient of α^4, while b_1 and c_1 are coefficients of α^2. Thus it would seem that the useful range is about $|\alpha|<1$. However, when considering a_2, it must be remembered that its error is only slightly less in the original circuit. Since we are discussing improvements, although a_2 may cause more error in A than the errors of b_1 and c_1 cause in B and C, the new circuit actually still may be better so long as B and C are more accurate. This argument is reinforced by the realization that in use the B and C parameters have multiplying factors which depend on Z_T and Y_T, and on the terminal conditions. Thus A, B, and C may have different effects on the performance and, so long as B and C are less in error and the error in A is not too much greater, the new circuit may be better. An exceptional case would be one in which the original circuit errors in A and B or C were mutually compensating. In view of these ideas, it would seem logical to define the useful range as that range for which the errors in B and C remain less than in the original circuit, with the understanding that some cases may arise for which the new circuit is not better beyond $|\alpha|=1$. This still does not lead to a unique definition, but it does lead to the expectation of a range somewhat greater than $|\alpha|<1$ because b_2 and c_2 are each much less than a_2 and do not need to be considered until $|\alpha|$ is considerably greater than unity.

Some estimates of the useful range for the dissipationless case may be obtained from Figure 3. A', B', C', A, B, and C are shown as functions of $\alpha=j\omega\sqrt{LC}$ (L and C being the respective total inductance and capacitance of the line) for three values of M. From these graphs a range of $|\alpha|<1.5$ seems to be reasonable for this condition. This range is sensibly independent of M, a consequence of having improved only b_1 and c_1 in all cases. The only advantage of increasing M is to make the errors smaller. This statement refers of course only to the useful range. Increasing M reduces the errors of all circuits for larger $|\alpha|$.

The estimates given in relation 19 are applicable in judging the relative behavior of the circuits beyond the useful range. The percentage variations of the coefficients of order higher than $\lambda=1$ may be of the same order of magnitude as the percentage improvements realized in b_1 and c_1. However, the latter are significant because those coefficients are nearly correct, while for the former the errors are so large as to make the changes of

Table I

M	$a'_2/\bar{a}_2$	a_2/a_2	$a_2/\bar{a}_2$	$b'_1/\bar{b}_1$	$b_1/\bar{b}_1=c_1/\bar{c}_1$	$c'_1/\bar{c}_1$
2	0.7500	0.7082	0.9443	1.1250	0.9288	0.7500
3	0.8888	0.8813	0.9916	1.0555	0.9703	0.8889
4	0.9375	0.9353	0.9976	1.0313	0.9838	0.9375
5	0.9600	0.9590	0.9990	1.0200	0.9900	0.9600

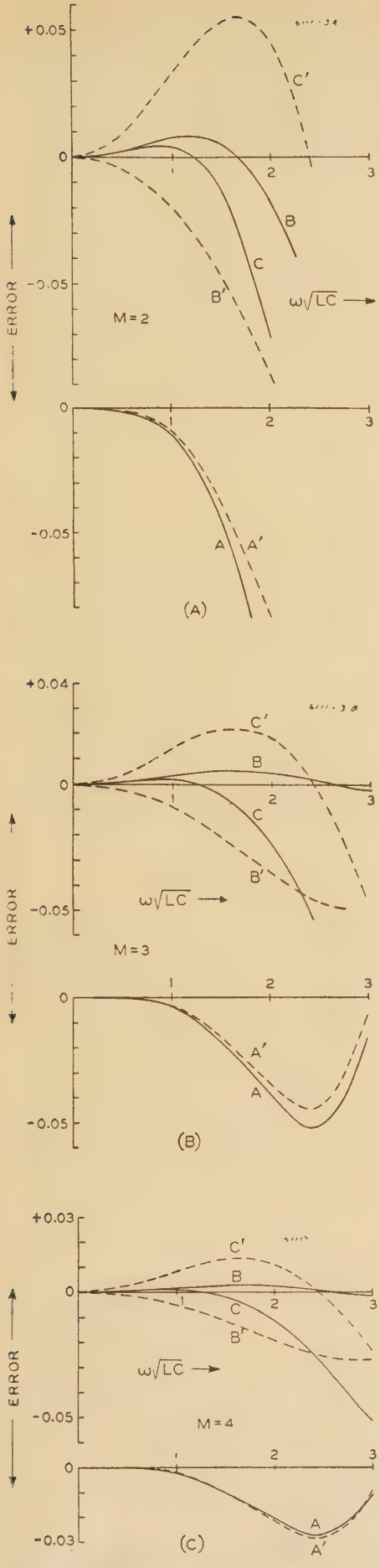

Figure 3. Performance of a dissipationless modified network

small significance. Therefore, although there will be differences, we should expect no appreciable difference between the new and old circuits when $|\alpha|$ is beyond the useful range. It is perhaps more correct to say that both circuits are equally bad in this extended range.

Other Modifications

Since the large error in a_2 may prevent the full realization of the gains made in b_1 and c_1, one may ask whether a more useful circuit might not be obtained if one could reduce the error of a_2 by allowing b_1 and c_1 to have errors of opposite algebraic sign. This question is treated in Appendix IV with results which are negative. It also is shown there that the minimum possible error in a_2 comes when the circuit is unmodified.

The above statements are with respect to variations of only the end elements. The possibility of improving a_2 by modifying the elements second from the end is considered in Appendix V. No improvement is found. The minimum possible error in a_2 still maintains when there is no modification at all. Furthermore, if b_1 and c_1 are again made equal, their minimum error comes when the shunt element has its uniform-network value and the terminal elements are modified in the manner already described (speaking of the series-element terminated case). Corresponding conclusions, of course, would follow if the shunt-element terminated case were treated. No analysis was made to determine the effects of modifying other elements of the network.

Conclusions

Within the limits afforded by the consideration of the end pair of elements, it has been shown that the best modification is that of the end elements alone. The specification for that modification is given below, in terms of the parameter $k=-2\rho$ which is introduced because ρ is negative. We have

$$\frac{Z'_T}{2M}+\rho Z_T=\frac{1-k(M-1)}{2M}\,Z_T \qquad (21a)$$

$$\frac{Y'_T}{2M}+\rho Y_T=\frac{1-k(M-1)}{2M}\,Y_T \qquad (21b)$$

for the series-element and shunt-element terminations, respectively. The other elements are chosen as if for a uniform network but with the series (or respectively shunt) elements each increased by the factor $(1+k)$.

It has been found possible to modify the terminations of a uniform ladder network to make it electrically more symmetrical in B and C (that is, the distinction between shunt-element and series-element termination is reduced) and electrically more nearly like its corresponding circuit of distributed characteristics, both effects being true only over a limited range of frequencies. Since the frequency range is independent of the number of sections and the improvements are small, the results are probably not of great practical importance. However, some improvement was found of a magnitude sufficient to make the new termination of value in an experimental application in which only a few sections are used. With many sections the need for accuracy would have to be extreme to make the new terminations useful.

In the discussion, emphasis has been placed on enhancing the similarity between the lumped network and a smooth line. Z_T and Y_T each can have any form, so any type of physical line is represented. Many forms of Z_T and Y_T, however, do not represent a realizable line at all. In such cases the electrical symmetry improvement, in the afore-mentioned sense, may be of some advantage.

In spite of the limitations on the practical value of the results, it is thought that they are worthwhile from the academic viewpoint alone. A theoretical survey is given, with definite proofs, of what can and cannot be done by varying both elements on each end of a uniform ladder network.

Appendix I

It is well known that only three of the four parameters of a 4-terminal network are independent and that when the network is symmetrical, only two are independent. The relation among them is well known[5] being, in our notation,

$$A^2-1=BC\alpha^2 \qquad (22)$$

This is true for any symmetrical 4-terminal network, so the notation is perfectly general within that limitation. Expressing each side as a series in α^2 and carrying out the indicated multiplications give

$$a_0^2-1+2a_1a_0\alpha^2+(a_1^2+2a_0a_2)\alpha^4+\ldots = b_0c_0\alpha^2+(b_1c_0+c_1b_0)\alpha^4\ldots \qquad (23)$$

Coefficients of like powers of α must be identical on the two sides so

$$a_0^2=1 \qquad (24a)$$

$$2a_1a_0=b_0c_0 \qquad (24b)$$

$$a_1^2+2a_0a_2=b_1c_0+c_1b_0 \qquad (24c)$$

from which is obtained

$$a_0=1 \qquad (25a)$$

$$a_1=\frac{b_0c_0}{2} \qquad (25b)$$

These are generalizations of previous results making them applicable to any symmetrical network. It is seen that if $b_0=c_0=1$ and equations 25a–25b are substituted in equation 24c, the desired result, equation 11, is obtained. Equation 9 gives the necessary values for b_0 and c_0 for the case under consideration.

Appendix II

From a rearrangement of equation 14, one may write

$$6b_1=2\left(1-\frac{1}{2M^2}\right)\sqrt{1-\frac{M^2}{(2M^2-1)^2}}-1+\frac{1}{M^2} \quad (26)$$

The radical obeys the inequality

$$1-\frac{M^2}{2(2M^2-1)^2}-\frac{M^4}{2(2M^2-1)^4}<\sqrt{1-\frac{M^2}{(2M^2-1)^2}}<1-\frac{M^2}{2(2M^2-1)^2} \quad (27)$$

as will now be proved. The right-hand inequality is evident since the upper bound indicated is obtained if $M^4/4(2M^2-1)^4$ is added under the radical to form a perfect square. The writing of the proof for the left-hand half will be simplified if the letter W is used for the quantity $M/(2M^2-1)$. W^4 is greater than W^6 and W^8, because W is less than unity, so the following inequality may be formed:

$$\left(1-\frac{W^2}{2}-\frac{W^4}{2}\right)^2=1-W^2-\frac{3W^4}{4}+\frac{W^6}{2}+\frac{W^8}{4}<1-W^2-\frac{3W^4}{4}+\frac{W^4}{2}+\frac{W^4}{4}=1-W^2 \quad (28)$$

which is equivalent to the left-hand half of relation 27. The combination of formulas 26 and 27 yields a form which readily reduces to

$$1-\frac{1}{2(2M^2-1)}-\frac{M^2}{2(2M^2-1)^3}<6b_1<1-\frac{1}{2(2M^2-1)} \quad (29)$$

This is still too complex to be useful as an estimate, but it may be simplified by using the relations

$$2M^2-1=2\left(M^2-\frac{1}{2}\right)\geqq 2M^2\left(1-\frac{1}{8}\right)=\frac{7M^2}{4} \quad (30a)$$

and

$$(2M^2-1)^3=2^3\left(M^2-\frac{1}{2}\right)^3\geqq 2^3\left(M^2-\frac{1}{2}\right)^2\geqq 2^3M^4\left(1-\frac{1}{8}\right)^2=\frac{49M^4}{8} \quad (30b)$$

which are true when $M\geqq 2$. Using these, and the relation $2M^2-1<2M^2$, appropriately in inequality 29 we get

$$1-\frac{4}{14M^2}-\frac{8M^2}{98M^4}<6b_1<1-\frac{1}{4M^2} \quad (31)$$

Relation 15 follows directly from this.

Appendix III

The results of Appendix II, the fact that $b_1=c_1$, and the simple form for c_1 given in equation 12b allow estimates of ρ and $1-2\rho$ to be obtained with ease. Without giving the details of the algebra, it is found that

$$\frac{M^2-18/49}{M^2-1}<1-2\rho<\frac{M^2-1/4}{M^2-1} \quad (32a)$$

and

$$\frac{31/98}{M^2-1}<-\rho<\frac{3/8}{M^2-1} \quad (32b)$$

For convenient usage in the subsequent work, these may be replaced by the inequalities

$$\frac{M^2-2/5}{M^2-1}<1-2\rho<\frac{M^2-1/4}{M^2-1} \quad (33a)$$

and

$$\frac{3/10}{M^2-1}<-\rho<\frac{3/8}{M^2-1} \quad (33b)$$

which are nearly as good.

Now consider the formula for a_λ. From equations 4a–4c it is obvious that $c'_{\lambda-1}=2\lambda a'_\lambda$, which may be used to simplify the expression for a_λ to

$$a_\lambda=a'_\lambda(1-2\rho)^{\lambda-1}[1+2\rho(\lambda-1)] \quad (34)$$

When $\lambda=2$, this reduces to $a_\lambda=a'_\lambda(1-4\rho^2)$, which reduces to relation 18 when bounds of ρ are taken from inequality 33b. A general estimate may be obtained for $\lambda\geqq 3$ by using both parts of relation 33 and whichever value of λ (3 or M) enhances the limit in question. This procedure yields inequality 19a.

Proceeding to the derivation of inequality 19b, we find complication because of the complexity of the expression for b_λ. From equations 4a–4c, it follows that $a'_\lambda=b'_\lambda\times(2\lambda+1)(2M^2)/(2M^2+\lambda)$, and $c'_{\lambda-1}=b'_\lambda\times(2\lambda)(2\lambda+1)(2M^2)/(2M^2+\lambda)$. These, when substituted in equation 8b, yield

$$b_\lambda=b'_\lambda(1-2\rho)^{\lambda-1}\left\{(1-2\rho)^2+[\rho^2(2\lambda+1)\times(2\lambda)+2\rho(1-2\rho)(2\lambda+1)]\frac{2M^2}{2M^2+\lambda}\right\} \quad (35)$$

An upper bound of b_λ will first be found. The first term in the brackets is positive and the second is negative. This necessitates the use of upper bounds for all components of the former and lower bounds for all components of the latter. Since $2M^2/(2M^2+\lambda)$ is a factor of each, it is subject to this general statement in its two roles as a multiplier. Satisfactory upper and lower bounds for $-\rho$, ρ^2, and $1-2\rho$ are given in relations 33. When $2M^2/(2M^2+\lambda)$ multiplies the first term, it may be replaced by 1, while in the other case it may be replaced by the lower bound $M/(M+1)$. Also $(2\lambda+1)(2\lambda)$ is less than $(2M+1)(2M)$, and $(2\lambda+1)\geqq 5$ if $\lambda\geqq 2$. Omitting the details of the algebra, it is found that

$$b_\lambda<b'_\lambda\frac{(M^2-1/4)^{\lambda-1}}{(M^2-1)^{\lambda+1}}\left(M^4-2M^2-\frac{15M^2}{16}+\frac{105M}{32}+\frac{1}{16}\right) \quad (36)$$

When $M\geqq 4$ the quantity represented by the three terms on the right of the above parenthesis is less than one, so if this restriction is imposed on M, the entire parentheses on the right may be replaced by $(M^2-1)^2$, which conveniently cancels against part of the denominator, leaving

$$b_\lambda<b'_\lambda\left(\frac{M^2-1/4}{M^2-1}\right)^{\lambda-1} \quad (37)$$

The upper bound is treated in a similar fashion. When $\lambda\geqq 2$, the quantity $(2\lambda+1)\times(2\lambda)$ may be replaced by the lower bound 20; in the other term $(2\lambda+1)$ may be replaced by the upper bound $(2M+1)$; and $2M^2\div(2M^2+\lambda)$ may be replaced by the upper and lower bounds 1 and 1/2 in appropriate locations. Proceeding as before, one obtains, after simplifications,

$$b_\lambda>b'_\lambda\frac{(M-2/5)^{\lambda-1}}{(M^2-1)^{\lambda+1}}\left(M^4-\frac{3M^3}{2}-\frac{31M^2}{20}+\frac{3M}{8}+\frac{499}{400}\right) \quad (38)$$

When $M\geqq 4$, the expression in the parentheses on the right is greater than $M^4-2M^3+2M-1=(M-1)^2(M^2-1)$, which if substituted cancels partially against the denominator to yield

$$b_\lambda>b'_\lambda\left(\frac{M-2/5}{M^2-1}\right)^{\lambda-1}\left(\frac{M-1}{M+1}\right) \quad (39)$$

Inequalities 37 and 39 combine to give inequality 19b.

Recalling the formula for c_λ, we see that it already is taken care of by the estimate of $1-2\rho$. Relation 19c follows directly.

Appendix IV

It is evident from the analysis leading up to equation 13 that b_1 and c_1 each cannot be equal to 1/6. However, one might suppose that b_1 and c_1 could be given errors of opposite sign to make $b_1+c_1=1/3$. Writing this out from equations 8b–8c, we obtain

$$\rho(1-2\rho)+\frac{1}{6}\left(1+\frac{1}{2M^2}\right)(1-2\rho)^2+\rho^2+\frac{1}{6}(1-2\rho)\left(1-\frac{1}{M^2}\right)=\frac{1}{3} \quad (40)$$

the solution of which is

$$\rho^2=-\frac{1}{4(M^2-1)} \quad (41)$$

The indicated imaginary value for ρ is physically impossible using passive elements because it must hold over a range of frequencies.

Let us now find the condition on ρ that will give a minimum error in a_2. At such a value the derivative of b_1+c_1 with respect to ρ will be zero. Differentiating the left side of equation 40 and setting the result equal to zero give, after reduction,

$$\frac{2\rho}{3}\left(\frac{1}{M^2}-1\right)=0 \quad (42)$$

Since $M=1$ never occurs, the solution is $\rho=0$. It is evident, since there is only one root and since the error can never be zero, that

this corresponds to a minimum and not a maximum error.

Appendix V

The analysis for the changing of two elements on each end of the network will proceed with reference to the circuit of Figure 4. This is built up by starting with the mid-shunt terminated network between lines P-P, with a subsequent double application of the modification principle already described in the text. The original network has a total impedance and admittance, respectively, of Z'_T and Y'_T. We first add a shunt element of magnitude βY_T^*, where Y_T^* will indicate the new total admittance. The transformation, in similarity with equations 5a–5d, involves the quantities

$$\alpha^* = \sqrt{Z_T^* Y_T^*} \tag{43a}$$

$$Z'_T = Z_T^* \tag{43b}$$

$$Y'_T = (1-2\beta) Y_T^* \tag{43c}$$

$$\alpha' = \alpha^* \sqrt{1-2\beta} \tag{43d}$$

As has been pointed out in the text, equations 8a–8c will give the coefficients for the new circuit if the equations for b_λ and c_λ are interchanged, due attention being given to differences in notation. Specifically, a_λ, b_λ, and c_λ become, respectively, a_λ^*, c_λ^*, and b_λ^*, while a'_λ, b'_λ, and c'_λ still are given by equations 4a–4c. The circuit between the lines Q-Q is then in a condition to receive a series element on each end, giving it the appearance of a modified mid-series terminated network. Let the added element on each end be σZ_T, and let the following additional notational changes take place:

$$\alpha = \sqrt{Z_T Y_T} \tag{44a}$$

$$Z_T^* = (1-2\sigma) Z_T \tag{44b}$$

$$Y_T^* = Y_T \tag{44c}$$

$$\alpha^* = \alpha \sqrt{1-2\sigma} \tag{44d}$$

Equations 8a–8c again may be applied, this time as they stand, with a'_λ, b'_λ, and c'_λ replaced by the corresponding starred coefficients. Thus, unprimed coefficients apply to the over-all circuit of Figure 4. For simplicity of notation, M-1 will be replaced by N until the results are achieved. It will be necessary to consider only the four coefficients b_0, b_1, c_0, and c_1, which, as derived by the foregoing plan of action, are

$$b_0 = 2\sigma a_0^* + b_0^*(1-2\sigma) = 1 \tag{45a}$$

$$b_1 = 2\sigma(1-2\sigma)a_1^* + (1-2\sigma)^2 b_1^* + \sigma^2 c_0^* = \sigma(1-2\sigma) + (1-2\sigma)^2(1-2\beta)c'_1 + \sigma^2 \tag{45b}$$

$$c_0 = c_0^* = 1 \tag{45c}$$

$$c_1 = (1-2\sigma)c_1^* = (1-2\sigma)[2\beta a'_1(1-2\beta) + b'_1(1-2\beta)^2 + c'_0\beta^2] \tag{45d}$$

The simplifications which already have been included in the writing of these equations come from the facts that $a_0^* = b_0^* = c_0^* = 1$, and $a_1^* = 1/2$, in similarity with equations 9 and 10. Since the correctness of b_0 and c_0 assures the correctness of a_1, as before, our attention may be confined to b_1 and c_1. The algebraic work may be expedited by changing the notation to

$$x = 1-2\beta \tag{46a}$$

$$y = 1-2\sigma \tag{46b}$$

The reduced formulas for b_1 and c_1 are obtained by taking a'_1, b'_1, c'_0, and c'_1 from equations 4a–4c, with M replaced by N. This gives

$$b_1 = \frac{1}{4} - \frac{y^2}{4} + \frac{1}{6}\left(1 - \frac{1}{N^2}\right)xy^2 \tag{47a}$$

$$c_1 = \left[\frac{1}{4} - \frac{1}{12}\left(1 - \frac{1}{N^2}\right)x^2\right]y \tag{47b}$$

We first will see if b_1 and c_1 each can be made equal to 1/6, or at least if their sum can be 1/3 so that a_2 will be correct. Accordingly, assume $b_1 = 1/6 + \epsilon$ and $c_1 = 1/6 - \epsilon$, which represents both conditions, since ϵ

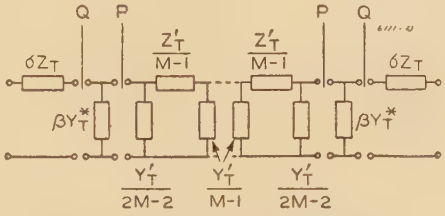

Figure 4. Two-element modification

may be zero. The result of these substitutions and the subsequent combination of equations 47a–47b is a quadratic in ϵ, as follows:

$$144G\epsilon^2 + (12F - 48G)\epsilon + (4G - F) = 0 \tag{48}$$

where

$$G = G(N, x) = 3 - 2\left(1 - \frac{1}{N^2}\right)x \tag{49a}$$

$$F = F(N, x) = 9 - 6\left(1 - \frac{1}{N^2}\right)x^2 + \left(1 - \frac{1}{N^2}\right)^2 x^4 \tag{49b}$$

The discriminant of equation 48 is easily computed to be $144F(F-4G)$. It must be positive if a real solution is possible, so we are interested in

$$F - 4G = \left(\frac{N^2-1}{N^2}\right)\left(\frac{N^2-1}{N^2}x^4 - 6x^2 + 8x - \frac{3N^2}{N^2-1}\right) = \frac{N^2-1}{N^2}H(N, x) \tag{50}$$

Before investigating the positiveness of $H(N, x)$, it should be noted that to have a physically realizable circuit it is necessary that $-1/2(N-1) < \beta < 1/2$. Outside of this range the end shunt elements either would vanish completely, thus changing the number of network sections, or would be greater than half the total admittance. The corresponding range of x is $0 < x < N/(N-1)$. If $H(N, x)$ is computed for $N = \infty$ throughout the largest possible range of x, it will be found to be everywhere nonpositive. Furthermore, as may be easily shown, $\partial H(N,x)/\partial N$ is always positive, so $H(N,x)$ is less than $H(\infty, x)$ and is therefore always negative in the pertinent range. Thus there is no real solution of equation 48, so b_1 and c_1 cannot be real and also have 1/3 as their sum.

Following a procedure similar to that used in the simpler case, we next investigate whether the error in a_2 can be made a minimum. The total differential of $b_1 + c_1$ is

$$d(b_1 + c_1) = \left(\frac{\partial b_1}{\partial x} + \frac{\partial c_1}{\partial x}\right)dx + \left(\frac{\partial b_1}{\partial y} + \frac{\partial c_1}{\partial y}\right)dy \tag{51}$$

The smallest possible error will occur when dx and dy are independent and thus when their coefficients are each zero. As may be seen easily by carrying out the necessary differentiation, equating the coefficient of dx to zero gives

$$\frac{1}{6}\left(1 - \frac{1}{N^2}\right)(y^2 - xy) = 0 \tag{52}$$

from which one obtains the condition $y = x$, since $N \neq 1$. With the substitution of x for y in the derivatives of the coefficient of dy, the setting of this equal to zero gives

$$x^2 - \frac{2N^2}{N^2-1} + \frac{N^2}{N^2-1} = \left(x - \frac{N}{N-1}\right) \times \left(x - \frac{N}{N+1}\right) = 0 \tag{53}$$

The $N/(N-1)$ solution gives a value of β which wipes out the shunt element on each end and is found to correspond to a maximum error. The other solution gives $\beta = 1/2(N+1)$. The corresponding complete end element is $Y_T[(1-2\beta)/2N + \beta] = Y_T/(N+1) = Y_T/M$. This means that all shunt elements will be the same. Also, the series element is $\sigma Z_T = \beta Z_T$, since $y = x$, which gives the value $Z_T/2M$, which is a mid-series termination. This should have been expected, since the case for uniform shunt elements has already been treated.

Now suppose we make $b_1 = c_1$. This makes y and x interdependent, so dy and dx in equation 51 are no longer independent. Also, since b_1 and c_1 are to be equal as x and y vary, it is only necessary to take the derivative of one of them. dy/dx may be obtained from the implicit function $b_1 - c_1 = 0$ as

$$\frac{dy}{dx} = -\frac{\partial(b_1 - c_1)/\partial x}{\partial(b_1 - c_1)/\partial y} \tag{54}$$

Thus

$$\frac{db_1}{dx} = \frac{\partial b_1}{\partial x} + \frac{\partial b_1}{\partial y}\frac{dy}{dx} = \frac{\frac{\partial b_1}{\partial x}\left(\frac{\partial b_1}{\partial y} - \frac{\partial c_1}{\partial y}\right) - \frac{\partial b_1}{\partial y}\left(\frac{\partial b_1}{\partial x} - \frac{\partial c_1}{\partial x}\right)}{\frac{\partial b_1}{\partial y} - \frac{\partial c_1}{\partial y}} \tag{55}$$

The denominator of equation 55 cannot be infinite, so we set the numerator equal to zero, giving, after reduction,

$$-\frac{\partial b_1}{\partial x}\frac{\partial c_1}{\partial y} + \frac{\partial b_1}{\partial y}\frac{\partial c_1}{\partial x} = 0 \tag{56}$$

The substitution of the expressions for these derivatives gives an equation from which y can be eliminated. The remaining equation in x is identical with equation 53. Thus $x = N/(N+1)$ is again the solution, but of course y is no longer equal to x. It is not necessary to compute y because it has been

Geometric Mean Distances for Rectangular Conductors

HERBERT B. DWIGHT
FELLOW AIEE

THE USE of geometric mean distance for calculating reactance of parallel conductors is increasing, so much so that the self geometric mean distance often is tabulated in catalogs of heavy conductors along with other characteristics, such as resistance, current capacity, and weight.

The logarithm of the geometric mean distance between two areas or cross sections is defined as the average of the logarithms of all possible distances from points on one area to those on the other, and the logarithm of the self geometric mean distance of an area is the average of the logarithms of all possible distances between two points on the area.[1]

The inductance, as computed by the geometric mean distance method, is the inductance at zero frequency. Metal of uniform conductivity, such as copper, is taken to have constant current density, or more generally, the current in a conductor is taken to be proportional to the conductance of that conductor, as it would be with direct current.

The self geometric mean distance of an area is sometimes called the geometric mean radius of the area, although it is not a radius nor an average of radii. It is, as the definition states, the mean distance (geometric, as distinguished from arithmetic) of all possible distances between two points on the area, and of course, most of these are not radii. It seems better to use a name which is in agreement with the facts of the case, rather than one which is practically no more convenient and which does not describe the quantity truly.

Formulas for the geometric mean distance of geometrical shapes can be obtained by a process of integration.[1] However, the formula for two rectangles, even when the problem is simplified by specifying two duplicate rectangles placed opposite each other, fills half a page. For engineering purposes, curves of reactance values for rectangular conductors can be used.[2] See also Tables I–III in a paper published in 1929 by Professor F. W. Grover.[3]

In this paper are given curves for geometric mean distance between rectangular areas which will give a somewhat more direct solution for general types of problems, such as those involving polyphase circuits or conductors in parallel.

In circuits or portions of circuits where the parallel conductors are not transposed, the reactive voltage drop in the various conductors is different. It may be computed by counting flux caused by each conductor, up to a certain large distance u. In a complete system of parallel conductors in the steady state, the sum of all the currents is zero, that is there is as much return current as going current in the group. The quantity u cancels out as it is associated with all of the conductors in turn (see equation 2). Therefore, the result is the same,

Figure 1. Geometric mean distance of rectangular areas, face-to-face position

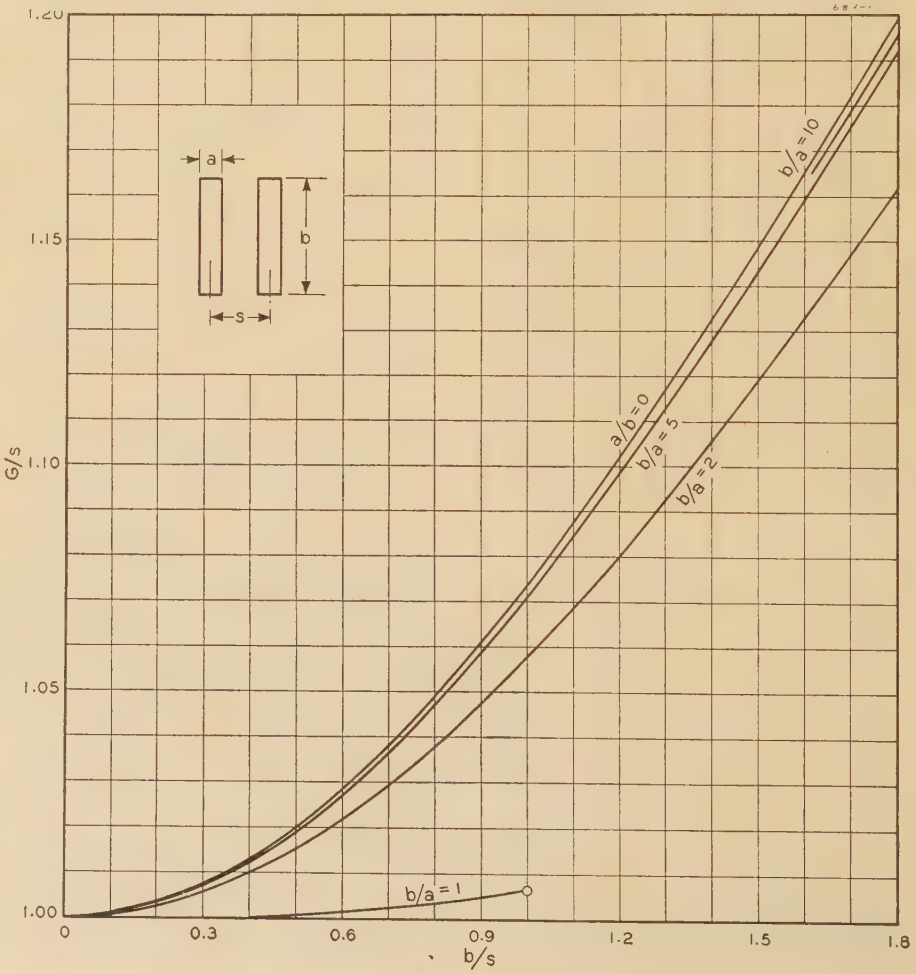

Paper 46-84, recommended by the AIEE committee on basic sciences for presentation at the AIEE North Eastern District meeting, Buffalo, N. Y., April 24–26, 1946. Manuscript submitted February 25, 1946; made available for printing March 21, 1946.

HERBERT B. DWIGHT is a professor of electrical machinery, Massachusetts Institute of Technology, Cambridge, Mass.

The author wishes to acknowledge the assistance of C. A. Uluant in preparation of parts of this paper.

shown that when x has this value the shunt elements are all uniform. This means that the determining of y is equivalent to the finding of ρ in the problem as originally treated.

References

1. SYSTEM RECOVERY VOLTAGE DETERMINATION BY ANALYTICAL AND A-C CALCULATING BOARD METHODS, **R. D. Evans, A. C. Monteith.** AIEE TRANSACTIONS, volume 56, 1937, June section, pages 695–705.

2. COMMUNICATION NETWORKS, Volume II (book), **E. A. Guillemin.** John Wiley and Sons, New York, N. Y. Page 137.

3. FORMULAS FOR THE FOUR-TERMINAL NETWORK PARAMETERS OF UNIFORM LADDER NETWORKS, **W. R. LePage.** AIEE TRANSACTIONS, volume 63, 1944, August section, pages 604–08.

4. Reference 2, page 145.

5. Reference 2, page 139.

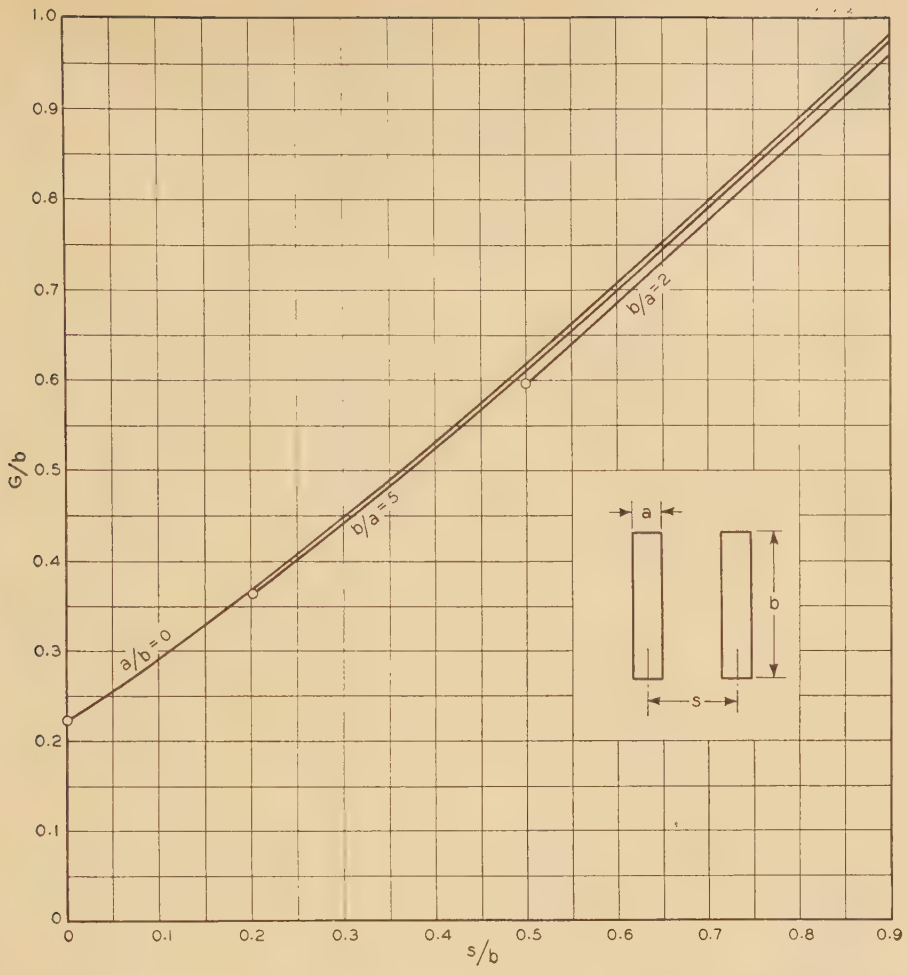

Figure 2. Geometric mean distance of rectangular areas, face-to-face position, close spacing

no matter how large u may be. The currents, as well as the conductor arrangement, may be unbalanced or balanced and are in amperes.

If R_A is the resistance per centimeter of conductor A of a group of long parallel conductors A, B, C, . . ., if G_{sA} is its self geometric mean distance, if G_{AB} is the geometric mean distance of the section of A from that of B, and so forth, the voltage drop in conductor A is

$$I_A R_A + j4\pi f \times 10^{-9}\left[I_A \log_\epsilon \frac{u}{G_{sA}} + I_2 \log_\epsilon \frac{u}{G_{AB}} + I_3 \log_\epsilon \frac{u}{G_{AC}} + \ldots\right] \text{ volts per centimeter} \quad (1)$$

where f is the frequency. Putting

$$(I_A + I_B + I_C + \ldots) \log_\epsilon u = 0 \quad (2)$$

u being a finite constant, although as large as desired, we have the reactive voltage drop in conductor A:

$$= -j4\pi f \times 2.303 \times 10^{-9}[I_A \log_{10} G_{sA} + I_B \log_{10} G_{AB} + I_C \log_{10} G_{AC} + \ldots] \text{ volts per centimeter} \quad (3)$$

or

$$= -j0.0529[I_A \log_{10} G_{sA} + I_B \log_{10} G_{AB} + I_C \log_{10} G_{AC} + \ldots] \text{ volts per 1,000 feet at 60 cycles} \quad (4)$$

Note that A, B, and C necessarily do not mean different phases, but merely different conductors.

Equations 3 and 4 are general formulas for the reactive voltage drop in any one of a group of long parallel conductors whose currents are given. The conductors may be of different phases or they may be branches in parallel.

The self geometric mean distance of a rectangular sectional area $a \times b$ is given within 0.13 per cent by the formula

$$G_s = 0.2234(a+b) \quad (5)$$

Actually, the numerical term varies from 0.2231 to 0.2237 for different ratios of a to b.[4]

The geometric mean distance between two equal rectangular areas, placed opposite each other with the sides parallel, may be read from the curves shown in Figures 1, 2, or 3, depending on the ratios of the dimensions. For the use of these curves see the examples.

The geometric mean distance between two equal rectangular areas, placed obliquely and not very close together, may be taken as the distance between their centers for a first approximation. The percentage error resulting from this procedure may be estimated by reference to Figures 1 and 3. For instance, if the distance between centers of two comparatively thin straps is 1.25 times the strap width, then from Figure 1, for the parallel plane position, $b/s = 0.8$ and G is five per cent greater than s. From Figure 3, for the edgewise position, $a/s = 0.8$ and G is six per cent less than s. Then for an oblique position, with the afore-mentioned distance between centers, the error in taking $G = s$ may be expected to be numerically less than plus or minus six per cent. However, this result does not mean six per cent error in reactance, since log G is involved.

In either equation 3 or 4, the distances G_{sA}, G_{AB}, G_{AC} . . . may be all in centimeters or all in inches (or in feet), so long as they are all in the same unit.

When there is complete transposition so that each conductor occupies all the positions in succession to an equal extent, the geometric mean distance method may be extended to give a convenient calculation for the average voltage drop. For this calculation, values of geometric mean distance of rectangles taken from Figures 1, 2, and 3 are useful, as well as in problems where equations 3 and 4 are used.

Precise values of $\log_\epsilon$ geometric mean distance are given for equal squares in many relative positions.[5] By combining these squares into rectangles of various shapes and positions, the precise value of the logarithm of the geometric mean distance was computed for a considerable number of cases of rectangles opposite each other. From these determinations and from values of G_s (equation 5), reactance values in micro-ohms per foot at 60 cycles were obtained. Formulas for infinitely thin rectangular conductors, that is for $b/a = 0$ and $a/b = 0$, are given[4] and curves of reactance values were plotted.[2]

In the present paper, instead of values of loop reactance, values of the geometric mean distances themselves are plotted. Their use has been described and is illustrated in the examples. For these curves a number of additional values have been determined.

Example 1

Find the reactive voltage drop in a single-phase ventilated bus bar circuit made up of four straps of size 1/8 by 3 inches, side by side in vertical planes. Each bus bar consists of two straps at $^1/_2$-inch centers. The distance between centers of bus bars is $2^1/_2$ inches. The cur-

rent of the circuit is 900 amperes, 60 cycles.

Let the four straps be called A, B, C, and D. Then the center-to-center distance from A to B is $^1/_2$ inch, 2 inches from B to C, and $^1/_2$ inch from C to D. A and B are connected in parallel. Neglecting circulating currents, A and B will each carry +450 amperes, and C and D each −450 amperes.

For computing the voltage drop in A by equation 4, using logarithms to base 10,

$G_s = 0.2234 \times 3\ 125 = 0.698$ inch
$\log 0.698 = \bar{1}.8439 = -0.1561$

For G_{AB},

$s/b = 0.5/3 = 0.167$, $b/a = 24$

From Figure 2,

$G_{AB} = 0.343 \times 3.0 = 1.029$
$\log 1.029 = 0.01242$

For G_{AC},

$b/s = 3/2.5 = 1.20$

From Figure 1,

$G_{AC} = 1.101 \times 2.5 = 2.752$
$\log 2.752 = 0.4396$

Alternatively, by Figure 2,

$G_{AC} = 0.917 \times 3 = 2.751$

Similarly,

$\log G_{AD} = 0.508$
$I_A \log G_s = 450 \times (-0.1561) = -\ 70$
$I_B \log G_{AB} = 450 \times 0.01242 = +6$
$I_C \log G_{AC} = -450 \times 0.439 = -198$
$I_D \log G_{AD} = -450 \times 0.508 = -228$
$-496 + 6$
$-496 + 6 = -490$

By equation 4, the reactive drop in A for 70 feet is

$j\,0.0529 \times 490 \times 0.070 = j\,1.81$ volts

In a similar way, the drop in B is found to be

$-j\,0.0529 \times 0.070(-70 + 6 - 163 - 198) = j\,1.57$ volts

The difference in these computed voltage drops in A and B may be said to result in an unbalance of current, which may be computed if desired.

The result of this problem agrees with the results of previously computed problems.[2]

Example 2

Find the reactive drop in each conductor of a 3-phase circuit consisting of three rectangular conductors (one conductor per phase) in parallel planes, the distance between centers being $1^1/_2$ inches. The conductors are 1/4×3 inches and each is 100 feet long. The current is 750 amperes, 60 cycles.

Figure 3. Geometric mean distance of rectangular areas, edgewise position

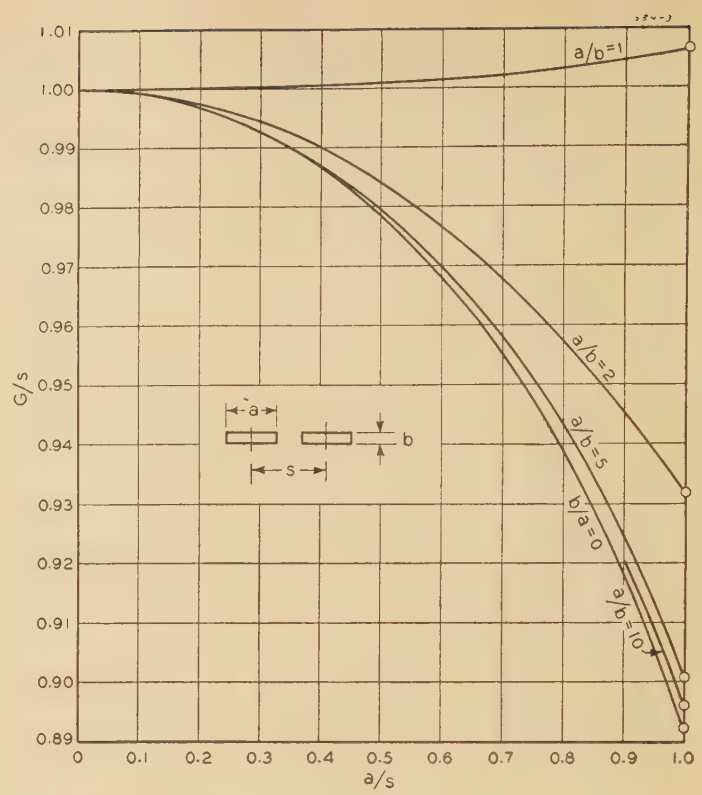

Let the three conductors be called A, B, and C, and let

$I_A = 750$ amperes
$I_B = 750(-0.5 + j\,0.866)$ amperes
$I_C = 750(-0.5 - j\,0.866)$ amperes

By equation 5,

$G_s = 0.2234\ (0.25 + 3) = 0.726$ inch
$\log 0.726 = \bar{1}.8609 = -0.1391$, omitting the subscript 10 in $\log_{10}$

For G_{AB},

$s/b = 1.5/3 = 0.5$, $b/a = 12$

From Figure 2,

$G_{AB} = 0.616 \times 3.0 = 1.848$ inches
$\log 1.848 = 0.2667$

For G_{AC},

$b/s = 3/3 = 1$, $b/a = 12$

From Figure 1,

$G_{AC} = 1.072 \times 3.0 = 3.216$ inches
$\log 3.216 = 0.5073$
$I_A \log G_s = 750(-0.1391) = -104$
$I_B \log G_{AB} = (-375 + j650) \times 0.2667 = -100 + j173$
$I_C \log G_{AC} = (-375 - j650) \times 0.5073 = -190 - j330$
$-394 - j157$

By equation 4, the reactive drop in A for 100 feet is

$-j\,0.0529 \times 0.10(-394 - j157) = -0.83 + j2.09$ volts $= 2.24$ volts

For the reactive drop in conductor B,

$I_B \log G_s = (-375 + j650) \times (-0.1391) = 52 - j\ 90$
$I_C \log G_{BC} = (-375 - j650) \times 0.2667 = -100 - j173$
$I_A \log G_{AB} = 750 \times 0.2667 = 200$
$152 - j263$

By equation 4, the reactive drop in B is

$-j\,0.0529 \times 0.10(152 - j263) = -1.40 - j\,0.81 = 1.62$ volts

The reactive drop in conductor C has the same numerical value, 2.24 volts, as in A.

The result of this problem agrees with already proved similar problems.[2]

It is a little more straightforward to use geometric mean distances and equation 4 as in this paper, than to rearrange the problem so as to use reactance values of single loops. The geometric mean distance method is applicable also to a wide range of reactance problems.

References

1. Electricity and Magnetism (book), Clerk Maxwell. Clarendon Press, Oxford, England, 1873. Paragraph 691.

2. Electrical Coils and Conductors (book), Herbert B. Dwight. McGraw-Hill Book Company, New York, N. Y., 1945, pages 139–40.

3. Calculation of the Inductance of Single-Layer Coils, F. W. Grover. *Proceedings*, Institute of Radio Engineers, volume 17, 1929, page 2056.

4. Formulas and Tables for Mutual and Self-Inductance, E. B. Rosa, F. W. Grover. Bureau of Standards *Bulletin*, Washington, D. C., volume 8, number 1, scientific paper 169, 1912, page 168.

5. On the Geometrical Mean Distances of Rectangular Areas and the Calculation of Self-Inductance, E. B. Rosa, F. W. Grover, Bureau of Standards *Bulletin*, Washington, D. C., volume 3, number 1, 1907, page 19.

The Frequency Response of Automatic Control Systems

HERBERT HARRIS, JR.
NONMEMBER AIEE

Synopsis: This paper illustrates the advantages of the frequency response approach to the analysis of automatic control systems, as contrasted to the analytic solution of transient responses. At the same time the equivalence of information available from the two approaches is demonstrated. A numerical example is given based upon a torque amplifier using a motor-generator type control.

THE purpose of this paper is to show how the concept of frequency response is being applied analytically and experimentally in the design of automatic control systems such as servomechanisms. This concept long has been used in the radio and telephone arts to express the fidelity of response of equipment, and as a result a considerable background of established mathematics and experimental procedure has been made available to instrument and automatic control engineers.

A transient analysis of the response of an automatic control to some standard type of disturbance is an accepted procedure, but with the more complex systems it becomes unwieldy, and useful design criteria become increasingly difficult to develop. A frequency analysis based on the mathematics of the Fourier series and the Fourier integral provides information equivalent to the transient analysis but with much less calculation and with more easily interpretable results. This paper will show this equivalence and the mathematical procedures involved in the design of a servomechanism.

Typical Servomechanisms

A servomechanism is a system in which some variable quantity is controlled to follow a definite function of some other varying quantity. Typical servomechanisms are

1. A self-balancing potentiometer[1] in which the controlled variable is the mechanical position of the pen and slide wire, and the desired position is proportional to the varying quantity, namely the voltage under measurement.

2. A machine tool pattern follower for which the controlled variable is the tool position, and the desired position is proportional to the varying shape of the pattern as the tool moves along.

3. A data transmission system[2] which reproduces a mechanical motion at a remote point, often with greatly increased force.

4. A highly degenerative feed-back amplifier[3] in which the output voltage faithfully reproduces a varying input voltage. The recognition of the similarity between servomechanisms and feed-back amplifiers makes available to the automatic control engineer many valuable analytical tools developed by communication engineers.

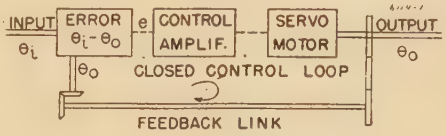

Figure 1. Torque amplifier

Figure 1 is a block schematic of the components of a torque amplifier which reproduces the motion of the input shaft and drives a heavy load, without placing any appreciable load on the input shaft. The load is driven by a motor controlled by a signal or motion from a device which measures the difference or error between the input and output shafts. This error-measuring device is the only load on the input shaft and may be made quite light. All of the examples listed are similar in that they all comprise an input, an output, an error-measuring device, an amplifier, and a power unit which drives the load to bring the error to zero.

The Transient Analysis

All systems which take the form of a closed loop as in Figure 1 have a tendency to be unstable and hunt, or at least to perform damped oscillations about their zero error position. The first problem in proper servomechanism design is to minimize these oscillations after any transient disturbance. The second problem of proper design is to minimize errors which occur under steady conditions, such as a constant velocity or acceleration motion of the input shaft, and errors caused by the loads on the output shaft. Usually the solution must be a compromise between the best solutions for these two problems.

One procedure for studying the oscillatory character of a system analytically is to assume a motion for the input and then calculate the resultant transient response of the output. A typical input is a suddenly applied constant velocity as is shown in Figure 2 along with a typical resulting output motion.

With the assumption that the system is linear over the region under investigation, any one of several classical, operational, or transform methods[4] for solving linear differential equations with constant coefficients may be used for calculating such a transient response. Whatever method is used, there are four essential steps in the solution.

1. The differential equations for the system are set up.

2. The characteristic equation of the above set is obtained. This equation has the form

$$a_n p^n + a_{n-1} p^{n-1} + \ldots a_1 p + a_0 = 0$$

in which the coefficients contain the various parameters of the system, such as amplifier gain, inertia, friction, and circuit constants.

3. The characteristic equation is solved for its roots. The roots will be real or in conjugate complex pairs. $p_n = \sigma_n \pm j\omega_n$

4. The final solution contains a term of the form $Ae^{\sigma t}\cos(\omega t + \alpha)$ for each complex root, an exponential term for each real root, and a particular solution which depends on the input motion. The coefficients A and phase angles α will depend upon the initial conditions of the system.

In this solution the rate of decay of the oscillatory terms is determined by the real parts of the complex roots, namely the σ_n's. If these are large and negative, the oscillations will damp quickly. If one is small, then the damping will be slow. If any one is positive, the system will be unstable and oscillations will increase.

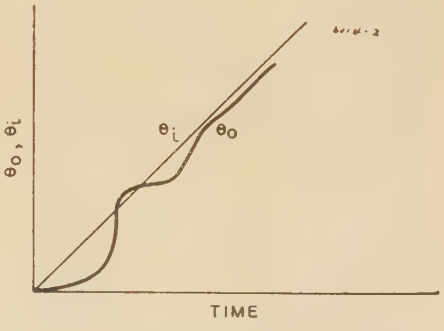

Figure 2. Transient response to an input velocity

Paper 46-114, recommended by the AIEE committee on instruments and measurements for presentation at the AIEE summer convention, Detroit, Mich., June 24-28, 1946. Manuscript submitted April 8, 1946; made available for printing May 7, 1946.

HERBERT HARRIS, JR. is with Sperry Gyroscope Company, Inc., Great Neck, N. Y.

The basic material presented in this paper is part of a National Defense Research Council report by the author dated December 1941.

The solution of the characteristic equation is the key point in all the methods of transient analysis. If the degree n is five or more, only a numerical solution may be obtained and then only by such laborious calculations that an engineer often cannot afford the necessary time. This situation is accentuated by the fact that even after a solution is found there is often no feasible way to tell what parameters must be changed to improve the system because the system parameters are so completely intermixed in the coefficients a_n. A later illustration will bring out this point.

Stability Criteria

Instead of solving the characteristic equation, a compromise often is resorted to which merely tells whether the system is stable or unstable. Hurwitz or Routh criteria[4] when applied to the coefficients a_n will tell whether there are any roots with positive real parts. This may be an unsatisfactory compromise, since many stable systems damp very slowly and the stability criteria do not show what changes are needed for improvement.

The System Transfer Function

The frequency response method of analysis eliminates the necessity for solving the characteristic equation and brings out with great clarity the effect of each parameter on the performance of the system. For this method to be valuable, it is necessary to show first that the obtainable results give information which is at least roughly equivalent to that obtained from a transient solution.

Consider the input and output motions as shown in Figure 2. The transient completely dies out after a certain period of time, and if a new similar disturbance is introduced after this time, the response will repeat. This may be repeated again and again so that the input and the response will appear as in Figure 3. As is well known, both of these periodic time functions may be analyzed into a Fourier series of sinusoidal terms of frequencies which are multiples of $1/T$. By including a sufficient number of terms in the series, the motions may be approximated arbitrarily closely.

Corresponding to each sinusoidal term which is a component of the input motion there is a term of the same frequency which is a component of the output motion. The two corresponding terms at each frequency will differ in amplitude and in phase angle between the input and the output. The ratio of the output amplitude to the input amplitude is known as the magnitude of the system transfer function, and since it is a function of frequency, it may be plotted as in Figure 4. Similarly, the difference of the input and output phase angles is called the phase of the transfer function and may be plotted also as in Figure 4.

Since all the input frequency components add together to form the input transient and all the output components add together to form the output transient, the transfer function which tells how these components are modified must contain all the information available from the system differential equation. The proper interpretation of curves such as those in Figure 4 will yield this information. This interpretation is discussed immediately following, while the calculating procedure is deferred until later.

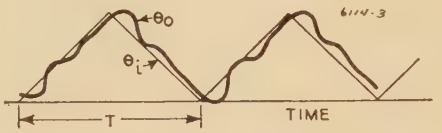

Figure 3 (above). Response to a periodic input

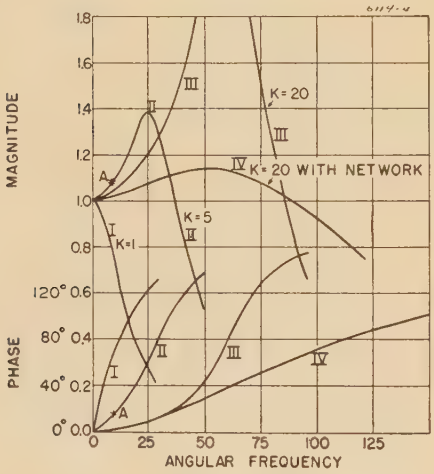

Figure 4 (left). System transfer functions

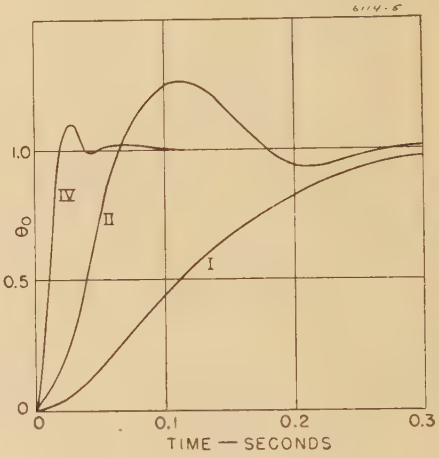

Figure 5 (right). Response to a unit step input

Interpretation of the Transfer Function

The ideal transfer function from the standpoint of perfect following of the input would be one which does not in any way change the components. This would occur with a magnitude of unity and a phase difference of zero over the whole frequency range. Actual transfer functions differ from the ideal in three important aspects.

1. Certain frequencies are accentuated or amplified as illustrated by the frequencies near $\omega = 25$ radians per second for curve II of Figure 4. This peaking of these frequencies is called resonance. A transient disturbance will result in a damped oscillation at a frequency near the resonant frequency as shown in a corresponding transient response curve, II of Figure 5. There is a correlation between the height of the resonance peak and the time required for the transient oscillation to die out, but it is not generally expressible in quantitative form.

The allowable height of a resonance peak can be specified only from experience with systems of similar application, but this is also true of any specification of desired damping for a transient response. For data transmission systems such as the one described below, a peak of about 1.2 is a good maximum value for high performance systems, but peaks as high as 1.5 are sometimes acceptable.

2. The higher frequencies always are attenuated; that is, the magnitude of the transfer function approaches zero as the frequency is increased. This results in the output being more or less sluggish and less harp than the input motion. This is illustrated by curves I and IV of Figures 4 and 5. The system which passes more of the high frequencies has the faster motion. Two systems which have exactly the same form of transfer function but with different frequency scales will have exactly the same form of transient response but with a time scale which is inverse to the frequency scale. Thus, by doubling the frequency response of a system the transient response time is halved.

Another aspect of the frequency bandwidth concept is that the usual input motions predominate in low frequencies. For example, even in the unattainable periodic square wave of position in which the input periodically jumps forward a certain amount and then back, the amplitude of the frequency components drops off as $1/\omega$. For a periodically positive and negative velocity which is less sharp, the amplitudes drop off

as $1/\omega^2$, and for a periodically positive and negative acceleration, the amplitudes are proportional to $1/\omega^3$.

Since most input motions predominate in the low frequencies, more attention should be paid to the behavior of the transfer function at low frequencies. As an example, a resonance peak at a high frequency acceptably may be somewhat greater than a peak at a low frequency, since it is less likely to be excited. Similarly, it is preferable to have a good phase function, as discussed below, at low frequencies rather than high ones if a choice must be made.

Sometimes it is desirable to use a servomechanism as a filter to remove from the output motion certain bands of frequencies which are present in the input. A common filter removes high frequency noise from the input, and this then determines the band of frequency response.

3. The phase characteristics as in Figure 4 also carry information concerning the response of a system, since the phase lag may be considered as a time delay for each component. In general, the best response is obtained with a system which has the least phase lag in the transfer function, particularly at the lower frequencies.

One important phase characteristic to recognize is the case for which the phase lag is proportional to frequency. In this case, since each component will be delayed by a time,

$$t_o = \frac{\text{phase lag in radians}}{\text{angular frequency in radians per second}}$$

all components will be delayed equally, and therefore the complete transient response will be delayed by a time t_0. A special case of this occurs when the servomechanism is following a constant velocity input at speed n; then the lag in following, after transients have died out, will be (nt_D) where t_D is the slope of the phase curve near zero frequency.

While it is often convenient to consider the phase functions in the interpretation of the transfer function, it is not absolutely necessary since there is a definite relationship between the phase and magnitude functions, as later discussion will show.

Electrical Torque Amplifier

While these criteria for good frequency response are quite qualitative in nature, they do provide a basis for the comparison of servomechanisms, and, more important, they provide a powerful aid in thinking about the various factors that can produce stability or instability in a system. This will be illustrated by an analysis of the torque amplifier of Figure 1, which is detailed in Figure 6.

The motor drive for the torque amplifier consists of a d-c motor and a controllable motor generator set. The servomotor has a constant field excitation and its armature voltage is supplied from the motor generator set. The generator is driven at constant speed, and its fields are in the output circuit of an amplifier which varies the excitation and therefore the generated voltage.

The amplifier is of the d-c type and has a push-pull output stage arranged so that the field flux is proportional to the output unbalance, which in turn is proportional to the input. Inductance in the field circuit prevents a sudden change in input voltage from producing a sudden change in field flux. This inductance and the consequent delay will have an effect on the stability of the system.

A network, often called a lead or derivative network, is included in the amplifier circuit for the purpose of stabilizing the system and improving its response, as later analysis will show.

The device for measuring the error between the input and output may, for example, be a reluctance type of bridge which provides an alternating voltage proportional to the error without placing an appreciable load on the input shaft. A direct voltage is obtained proportional to the error by means of a phase-sensitive detector, and a simple RC type filter is included to filter the detector output. The filter also will have an effect on the servo stability.

Analytical Derivation of the System Transfer Function

The most straightforward, but a tedious, procedure for the calculation of the transfer function is summarized as follows:

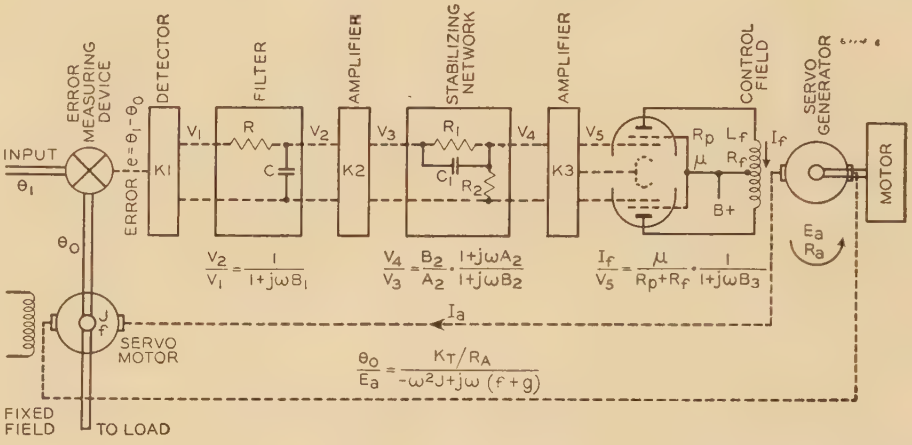

Figure 6. Torque amplifier

θ_o, θ_i = output and input positions in radians

$e=\theta_i-\theta_o$ = error or deviation in radians

V_1, V_2, V_3, V_4, V_5 = direct voltages as shown in figure

$K_1=\frac{V_1}{e}$, $K_2=\frac{V_3}{V_2}$, $K_3=\frac{V_5}{V_4}$ amplification or attenuation ratios

R, C = filter element values

$B_1=RC$ = filter time constant

R_1, R_2, C_1 = stabilizing network element values

$A_2=R_1C_1$ = stabilizing network time constant

$B_2=A_2\frac{R_2}{R_1+R_2}$ = stabilizing network delay time constant

R_p, μ = output tube plate resistance and amplification factor

L_f, R_f, ϕ_f = servo generator control field inductance, resistance, and flux

$B_3=\frac{L_f}{(R_p+R_f)}$ = servo generator control field time constant

E_a, I_a = armature circuit generated voltage and current

$T=K_T I_a$ = servomotor torque

J = servomotor plus load inertia

f = servomotor plus load viscous friction

g = effective viscous drag caused by motor back electromotive force

1. Set up the linear differential equations for the system.

2. Replace each derivative dx/dt by px and each integral $\int x dt$ by x/p just as in the transient solution and then solve the resulting set of simultaneous equations for the output-to-input ratio. For the system detailed in Figure 6 and with symbols given in the accompanying list, this expression comes out as

$$\frac{\theta_o}{\theta_i}=\frac{K(1+A_2p)}{\left\{\begin{array}{r}K+p(KA_2+f+g)+p^2[J+\\(f+g)(B_1+B_2+B_3)]+p^3[J(B_1+\\B_2+B_3)+(f+g)(B_1B_2+B_2B_3+\\B_3B_1)]+p^4[J(B_1B_2+B_2B_3+B_3B_1)+\\(f+g)(B_1B_2B_3)]+p^5(JB_1B_2B_3)\end{array}\right\}} \quad (1)$$

The denominator of this expression becomes the characteristic equation for the system. This is a fifth order equation which only can be solved numerically, and it illustrates the intricate interdependence of parameters which result from this approach. Since it is to serve only as an illustration and not for calculation, the detailed derivation is not given.

3. Substitute $p=j\omega$. This results in the equation

$$\frac{\theta_o}{\theta_i}=\frac{K(1+j\omega A_2)}{\left\{\begin{matrix}K-\omega^2[J+(f+g)(B_1+B_2+\\ B_3)]+\omega^4[J(B_1B_2+B_2B_3+\\ B_3B_1)+(f+g)(B_1B_2B_3)]\end{matrix}\right\}+ j\omega\left\{\begin{matrix}(KA_2+f+g)-\omega^2[J(B_1+\\ B_2+B_3)+(f+g)(B_1B_2+\\ B_2B_3+B_3B_1)]+\omega^4JB_1B_2B_3\end{matrix}\right\}} \quad (2)$$

This expression is known as the system response transfer function, and from it the magnitude and phase angle may be determined by the usual manipulations with complex numbers. Thus

$$\frac{\theta_o}{\theta_i}=\frac{R_N+jX_N}{R_D+jX_D} \quad (3)$$

where the R's and X's are all real functions of the angular frequency $\omega=2\pi f$.

The magnitude of θ_o/θ_i is

$$M=\frac{\sqrt{R_N{}^2+X_N{}^2}}{\sqrt{R_D{}^2+X_D{}^2}} \quad (4a)$$

The phase angle of θ_o/θ_i is

$$\phi=\tan^{-1}\left(\frac{X_N}{R_N}\right)-\tan^{-1}\left(\frac{X_D}{R_D}\right) \quad (4b)$$

M and ϕ may be calculated by equations 4a–4b for particular parameter values to obtain plots such as in Figure 4. This analysis has eliminated the necessity for the solution of the characteristic equation, but the parameters still are intermixed so completely that interpretation is difficult.

The Loop Transfer Function

A second and simpler approach to the system transfer function is through the use of an auxiliary transfer function which leaves most of the system parameters independent. The type of automatic control under discussion is based upon the use of an error signal which is the difference between the input and output motions,

$$e=\theta_i-\theta_o=\text{error} \quad (5)$$

This expression yields

$$\frac{\theta_o}{\theta_i}=\frac{\left(\frac{\theta_o}{e}\right)}{1+\left(\frac{\theta_o}{e}\right)} \quad (6)$$

Equation 6 is of basic importance, since it states that the complex system transfer function may be expressed in terms of an auxiliary complex transfer function θ_o/e, which may be called the loop transfer function. It will be shown that the loop transfer function is simpler to derive and interpret than the system function, and a geometrical evaluation of equation 6 can be used. The term "loop transfer function" is borrowed from feed-back amplifier terminology,[3] and the similarity of θ_o/e to the often quoted $\mu\beta$ characteristic is apparent.

Reference to Figure 6 indicates that between the output θ_o and the error e there is a series of separate component circuits

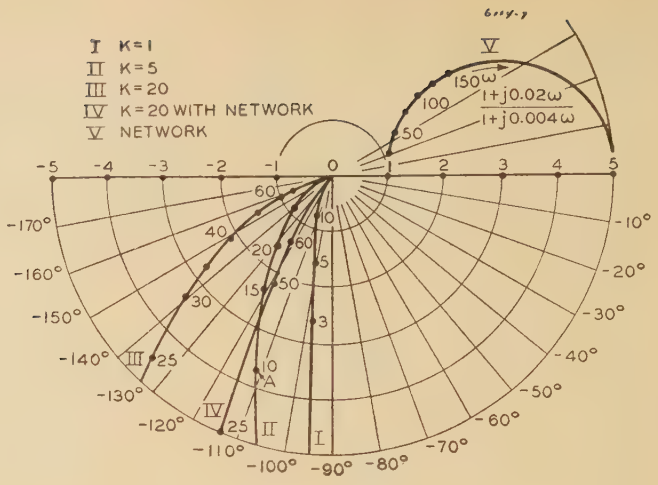

Figure 7. Loop transfer functions

each with its own transfer function. Physically it is understandable that the magnitude of the resultant transfer function θ_o/e should be equal to the product of the magnitudes of the component transfer functions. Similarly, the resultant phase angle should be the sum of the component phase angles. This method of combination is also a property of the multiplication of complex numbers, so that the following equation may be written:

$$\frac{\theta_o}{e}=\frac{V_1}{e}\cdot\frac{V_2}{V_1}\cdot\frac{V_3}{V_2}\cdot\frac{V_4}{V_3}\cdot\frac{V_5}{V_4}\cdot\frac{I_f}{V_5}\cdot\frac{\phi_f}{I_f}\cdot\frac{E_a}{\phi_f}\cdot\frac{I_a}{E_a}\cdot\frac{T}{I_a}\cdot\frac{\theta_o}{T} \quad (7)$$

in which each transfer function is a complex number.

The next step is to calculate all the individual transfer functions for substitution in equation 7. This step requires only simple electrical circuit theory. For the filter,

$$\frac{V_1}{e}\cdot\frac{V_2}{V_1}=K_1\cdot\frac{1}{1+j\omega RC}=K_1\cdot\frac{1}{1+j\omega B_1} \quad (8)$$

For the stabilizing network,

$$\frac{V_3}{V_2}\cdot\frac{V_4}{V_3}=K_2\frac{R_2}{R_1+R_2}\times\frac{1+j\omega R_1C_1}{1+j\omega R_1C_1\cdot\frac{R_2}{R_1+R_2}}=K_2\frac{B_2}{A_2}\cdot\frac{1+j\omega A_2}{1+j\omega B_2} \quad (9)$$

For the generator field current,

$$\frac{V_5}{V_4}\cdot\frac{I_f}{V_5}=K_3\cdot\frac{\mu}{R_p+R_f+j\omega L_f}=K_3\cdot\frac{\mu}{R_p+R_f}\cdot\frac{1}{1+j\omega\frac{L_f}{R_p+R_f}}=\frac{K_3\mu}{R_p+R_f}\cdot\frac{1}{1+j\omega B_3} \quad (10)$$

For the generated voltage,

$$\frac{\phi_f}{I_f}\cdot\frac{E_a}{\phi_f}=K_4 \quad (11)$$

a constant which depends upon the generator design.

The terms of equation 7 between the generated voltage and the output motion cannot be separated into a series of individual transfer functions, since there is an

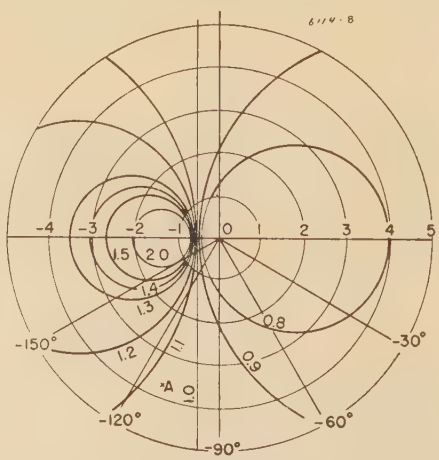

Figure 8. Loci of constant magnitude M on the θ_o/e complex plane

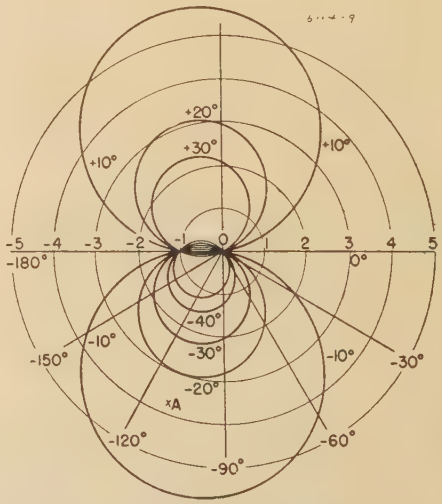

Figure 9. Loci of constant phase ϕ for θ_o/θ_i on the θ_o/e complex plane

interaction between the output motion and the armature current caused by the back electromotive force of the motor. The following three equations specify this interaction:

$$I_a R_a + K_m \frac{d\theta_o}{dt} = E_a$$

$$T = \text{torque} = K_T I_a$$

$$T = J\frac{d^2\theta_o}{dt^2} + f\frac{d\theta_o}{dt}$$

By setting $\frac{d}{dt} = j\omega$ and $\frac{d^2}{dt^2} = -\omega^2$ and combining the three equations:

$$\frac{\theta_o}{E_a} = \frac{\frac{K_T}{R_a}}{-\omega^2 J + j\omega(f+g)} \tag{12}$$

where

$$g = \frac{K_T K_M}{R_a}$$

Finally, for the loop transfer function, the combination of equations 8–12 into equation 7 yields

$$\frac{\theta_o}{e} = K \cdot \frac{1 + j\omega A_2}{\left\{\begin{array}{l}(1+j\omega B_1)\cdot(1+j\omega B_2)\times \\ (1+j\omega B_3)\cdot(-\omega^2 J + j\omega(f+g))\end{array}\right\}} \tag{13}$$

where the A's and B's all have the dimensions of time, and the K lumps together all of the gain constants in the loop

$$K = K_1 K_2 \frac{B_2}{A_2} \cdot \frac{K_3 \mu}{R_p + R_f} \cdot K_4 \cdot \frac{K_T}{R_a}$$

Relation Between the Loop and System Transfer Functions

When equation 13 is introduced into equation 6, the system transfer function of equation 2 results. For the graphical interpretation of the relationship 6 between the loop and system transfer functions, it is desirable to plot the loop transfer function in a different manner, on polar co-ordinates. At any one frequency the transfer function has a magnitude and an angle which entirely specify a point on polar co-ordinates. As the frequency varies, the point will move and the resultant locus of points is the plot of the transfer function. Several such loci are shown in Figure 7 with the frequencies shown as numbers along each curve.

On the polar co-ordinate system on which these loop transfer functions are plotted, there must be a locus of points which all result in the same magnitude of system transfer function. These loci are the circles shown in Figure 8 for several different magnitudes. If any frequency point of θ_o/e falls on one of these circles, then the magnitude of the system transfer is determined by the value of M for that curve. Similarly, there are a series of equal phase angle curves ϕ as shown in Figure 9.

The fact that these loci are circles is based upon the representation of θ_o/e as a vector from the origin and $1+(\theta_o/e)$ as a vector to the same point from -1. Then $M = |\theta_o/\theta_i|$, according to equation 6, is the ratio of these two distances, and by a geometrical theorem the loci of constant M are circles of radii $M(1-M^2)^{-1}$ at centers $M^2(1-M^2)^{-1}$. Similarly, the angle ϕ is the difference between the angles of the two vectors, and the loci of constant ϕ are circles of radii $\frac{1}{2}|\text{cosec } \phi|$ at centers $-\frac{1}{2}+j\frac{1}{2}\cot\phi$.

The similarly numbered curves of Figure 7 and those of Figures 4 and 5 correspond to the same system. As an example of this method of calculation, consider the point A at $\omega = 10$ for the loop transfer function II in Figure 7. This point falls on Figures 8 and 9 as shown and corresponds to $M = 1.08$ and $\phi = -17°$. These values then appear on Figure 4 for the same frequency. With sufficient experience with this sort of calculation, it is no longer necessary always to plot the system transfer functions, and the engineer easily can interpret the characteristics of a system directly from the loop transfer functions of Figure 7.

If the loop transfer function falls in the neighborhood of the (-1) point, the resonance of the system becomes very high. Loci near the negative imaginary axis will not have resonance peaks. Also, for all large values of θ_o/e, the magnitude of θ_o/θ_i, will be near unity and the phase angle will be near zero.

The Torque Amplifier Loop Transfer Function

To obtain an understanding of the effect of each component network on a system, it is often desirable to study first a system with only the most important components and then gradually add the less important components. For the torque amplifier system of Figure 6, all the delays and the stabilizing network may be neglected at first, and the simplified loop transfer function

$$\frac{\theta_o}{e} = \frac{K}{-\omega^2 J + j\omega(f+g)} \tag{13}$$

may be studied.

Typical parameter values for a 0.1 horsepower system are

$J = 0.005$-inch-ounces torque for one radian per second² acceleration of the motor.
$(f+g) = 0.125$-inch-ounces torque for one radian per second velocity of the motor.

The value of K is determined by the amplification of the system. Experimentally, if the motor shaft is displaced one radian from zero error, the torque required to accomplish this is numerically equal to K. Curves I, II, and III are drawn for $K = 1$, 5, and 20 inch ounces per radian respectively.

Since K is merely an amplification factor, the loop transfer functions I, II, and III of Figure 7 only are expanded or contracted versions of each other. For $K = 1$, no resonance peak occurs, since the locus does not go near the point -1, but on the other hand the response drops off at a very low frequency. $K = 5$ produces a system with a wider frequency response, but a resonance of 1.38 occurs at $\omega = 25$ radians per second. $K = 20$ has a very wide frequency response, but it also has an extremely high resonance peak.

From the standpoint of resonance, the system with $K = 1$ is best, but its actual performance is poor, since the low frequency response results in a very sluggish system. Moreover, since it requires so much error to produce a torque, any load on the motor will produce a large error. For example, in order to drive a 10-inch-ounces dry friction load, a motor error of ten radians would be required at $K = 1$-inch-ounce per radian. $K = 5$ results in faster and tighter response, but even this is usually not enough for a high performance system. $K = 20$ is much more desirable from every standpoint except that of the high resonance peak.

The design problem usually resolves into the necessity for providing some adequate means for reducing the resonance peak of the system with $K = 20$. The network shown between V_4 and V_3 of Figure 6 is a common one used for this purpose. Its transfer function is

$$\frac{R_2\cdot(1+j\omega R_1 C_1)}{(R_1+R_2)\left(1+j\omega R_1 C_1 \cdot \frac{R_2}{R_1+R_2}\right)} = \frac{B_2}{A_2}\cdot\frac{1+j\omega A_2}{1+j\omega B_2}$$

and its polar plot is shown in Figure 7 for $R_2/(R_1+R_2) = 0.2$, and $R_1 C_1 = 0.02$ second with K adjusted by changing other factors to take care of the attenuation of this circuit at $\omega = 0$ which is 0.2

When this network is inserted in the system, the two complex transfer functions of the unstabilized system and the stabilizing network are multiplied together. Thus, at each frequency the two magnitudes are multiplied and the two phase angles are added so that the network shifts the loop transfer function away from the high resonance region near the -1 point. For the above values and $K = 20$, the resulting loop transfer func-

tion is shown as IV in Figure 7, and the system transfer function is shown as IV in Figure 4.

The introduction of the stabilizing network has reduced the resonant peak to 1.14 at 50 radians per second and also has broadened the frequency response and reduced the phase lag.

An interesting question which illustrates the power of this method is the determination of the proper value for the time constant R_1C_1. The form of the locus which is a circle is independent of R_1C_1, but the position of each frequency point is determined by R_1C_1. For example, if a low time constant of say only 0.002 second had been chosen, the stabilizing network would not be able to introduce an appreciable positive phase angle until the very high frequency region after the loop transfer function already had passed through the highly resonant region. Conversely, if R_1C_1 is too large, say 0.2 second, the large positive phase angles would occur at very low frequencies and the phase would have returned to near zero at the frequencies for which the loop transfer function passes near the point -1. This relationship is shown in Figure 10 by an exaggerated sketch.

The Effect of Delays

With the addition and proper design of the stabilizing network, the torque amplifier has been given quite satisfactory characteristics, but certain delays which initially were assumed to be of secondary importance still are to be investigated. The transfer function for a single delay has been given in equation 10, and it is well known that its locus is a circle with negative phase angles, as shown by curve E of Figure 11. Since such a delay adds a negative phase angle into the loop transfer function it will shift the locus toward the (-1) point and cause an increase in the resonance peak. A delay of this sort is to be considered important or not depending upon whether or not it introduces an appreciable phase shift at the frequencies near the resonant point.

Figure 11, curve A, shows the locus of the stabilized system without delays. Curve B shows the same locus as it is shifted by a 0.004-second delay which might occur with a pentode tube driving the field circuit. In this case the shift increases the resonance to 1.5 from its previous value of 1.14. Curve C shows the effect of a single 0.02-second delay as might occur with a triode driving tube. This delay is quite appreciable and the resonance has risen to almost four.

To illustrate another feature, curve F is the locus of the transfer function for two 0.01-second delays and curve D shows their effect on the system. These two delays might occur in the filter network and in the field circuit, respectively. They have the transfer function $(1+j.01\omega)^{-2}$ and are shown to have a greater effect than that of a single 0.02-second delay.

Curve D of Figure 11 represents a system that is worse than just resonant; it is unstable, and oscillations increase in amplitude with time, rather than die out. Any locus for which the vector from the (-1) point to the locus rotates through a resultant negative angle as ω goes from zero to infinity will be unstable. Thus, curve C could represent also an unstable system if the gain were increased until the locus circled the (-1) point. For a fully rigorous statement and proof of this stability criterion, usually called the Nyquist criterion, reference should be made to the writings of Nyquist,[5] Bode,[7] and MacColl.[8]

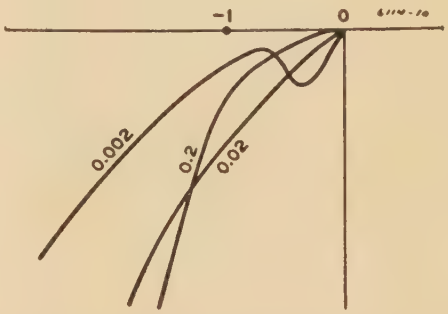

Figure 10. Effect of the stabilizing network time constant on θ_o/e

In the event that these delays are appreciable, it is necessary to reduce the loop gain or add other suitable phase correcting networks, but since this is only an illustrative example, the design will not be completed here.

Inverse Transfer Functions

Equation 6 may be placed in a form which still further simplifies the calculating procedure in many cases. The reciprocal of equation 6 is

$$\frac{\theta_i}{\theta_o}=\frac{e}{\theta_o}+1 \tag{14}$$

In this equation θ_i/θ_o and e/θ_o represent an input-to-output ratio rather than an output-to-input ratio and therefore are called the inverse system transfer function and the inverse loop transfer function, respectively. The graphical solution of equation 6 is particularly simple since, if e/θ_o is plotted on the complex plane as before, the same curve may be used for θ_i/θ_o with a new origin at the (-1) point. Loci of constant magnitude and constant phase for θ_i/θ_o are the concentric circles and intersecting lines of the polar co-ordinate system at the (-1) point. Thus $M^{-1}=|\theta_i/\theta_o|$ is the distance from the (-1) point to the locus, and $(-\phi)$ is the angle of the vector from the (-1) point to the locus.

The Calculus of Transfer Functions

When several components or complete systems are placed in cascade, their transfer functions combine as

$$Me^{j\phi}=M_1e^{j\phi_1}M_2e^{j\phi_2}=M_1M_2e^{j(\phi_1+\phi_2)} \tag{15}$$

This relation was used in equation 7.

Similarly the inverse transfer functions which have the reciprocal magnitude and the negative phase angle of the transfer functions combine as

$$M^{-1}e^{j(-\phi)}=M_1^{-1}M_2^{-1}e^{j(-\phi_1-\phi_2)} \tag{16}$$

When one component feeds back from the output of another component as shown in Figure 12, the resultant transfer function is

$$Me^{j\phi}=\frac{M_1e^{j\phi_1}}{1+M_1M_2e^{j(\phi_1+\phi_2)}} \tag{17}$$

while the inverse transfer functions combine as,

$$M^{-1}e^{j(-\phi)}=M_1^{-1}e^{j(-\phi_1)}+M_2e^{j\phi_2} \tag{18}$$

Since this is only a vector addition, its graphical construction is very simple and provides one of the advantages of the inverse transfer function approach.[6] This is particularly so in the study of regulators and process controls. Another advantage is that it places the loci near the origin for the low frequencies which are of interest.

Regulator Principles

For the torque amplifier example, only its response to an input motion has been considered, and it was desirable for the system to have a wide frequency response. If the torque load on the servomotor should vary, however, it would be desirable to have a minimum response to these variations. That is, if torque variations are considered as an input, the output θ_o should be filtered as completely from these variations as is possible. In this sense the torque amplifier is acting as a regulator, and the use of equation 18 with inverse transfer functions becomes advantageous.

If a torque T_L is applied at the load shaft with the armature circuit connected

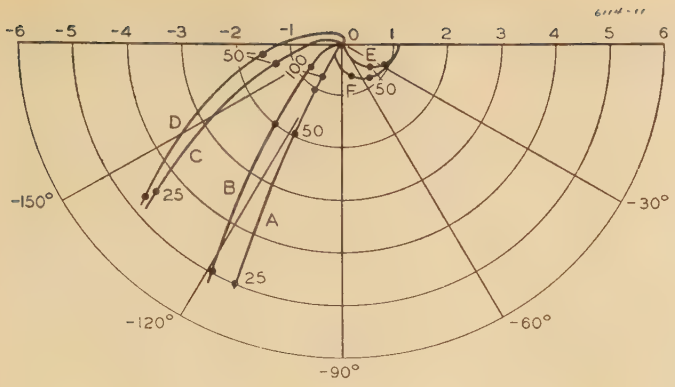

Figure 11. Loop transfer function for stabilized system with delay

A—Basic system with no delays
B—A 0.004-second delay
C—A 0.02-second delay
D—Two 0.01-second delays

but with the amplifier off, the resultant output will be calculated as

$$T_L = Jp^2\theta_o + fp\theta_o - T$$

$$T = K_T I_a = -\frac{K_T K_M}{R_a} p\theta_o = -gp\theta_o$$

$$\frac{T_L}{\theta_o} = p^2 J + p(f+g) \qquad (19)$$

T_L/θ_o is an inverse transfer function and may be identified with $M_1^{-1}e^{-j\phi_1}$ of equation 18.

The return transfer function $M_2e^{j\phi_2}$, which is the ratio of the torque produced by a motion of the output from the zero error position, is (with $B_1 = B_3 = 0$)

$$M_2e^{j\phi_2} = K \cdot \frac{1+j\omega A_2}{1+j\omega B_2} \qquad (20)$$

Combination of equations 19 and 20 into equation 18 yields

$$\frac{T_L}{\theta_o} = p^2 J + p(f+g) + K \cdot \frac{1+j\omega A_2}{1+j\omega B_2} \qquad (21)$$

for the system with the amplifier on.

T_L/θ_o of equation 19 represents the inverse transfer function for a disturbing torque with the amplifier off, and as such it is a measure of the self-regulating properties of the load. It is plotted in Figure 13, curve *A*, for the values $J = 0.005$-inch-ounce per radian per second^2 and $(f+g) = 0.125$-inch-ounce per radian per second. Thus at $\omega = 10$, T_L/θ_o is only slightly greater than one and only 1-inch-ounce torque is required to move the load with an amplitude of one radian at this frequency.

T_L/θ_o of equation 21 is the same transfer function with the control loop closed. Curve *B* in Figure 13 is the plot for this function, with $K = 20$, $A_2 = 0.02$, and $B_2 = 0.004$. T_L/θ_o is greater than 20 at all frequencies for this system, and this is a measure of how well the torque amplifier is regulated against load changes.

The equivalent condition to a high resonance peak would occur if the locus came relatively close to the origin for certain frequencies. Then disturbances at these frequencies would be regulated less well than disturbances at other frequencies.

Phase and Magnitude Relationships

In the foregoing discussion the phase and magnitude of the transfer function have been treated as more or less independent quantities. Actually since they are derived from the same function of a complex variable, there must be a relation between the two which definitely limits the variety of polar plots which are available in physical systems. Bode[7] has developed several such relations which are useful in feed-back amplifier design and consequently in automatic control design. The dependence of phase upon magnitude for these linear stable systems can be written only in an implicit integral form, but its essence may be stated simply as follows.

In physically realizable stable systems of the kind we are discussing, there is a tendency for the phase angle of a transfer function to depend upon the rate of increase or decrease of the magnitude of the function with frequency. If the magnitude decreases as $1/\omega^k$ over a region of frequency, then the phase will tend toward an angle of $-k\pi/2$ radians. The simple delay $(1+jB\omega)^{-1}$ illustrates this, since at low frequencies the magnitude is slowly varying and the phase is near 0 degrees, while at high frequencies the magnitude decreases as $1/\omega$ and the phase approaches -90 degrees. The transition between two rates of change of magnitude results in a smooth variation in phase between the two values. All the transfer functions plotted illustrate this relation ship.

Figure 12 (right). Feedback over a component or system

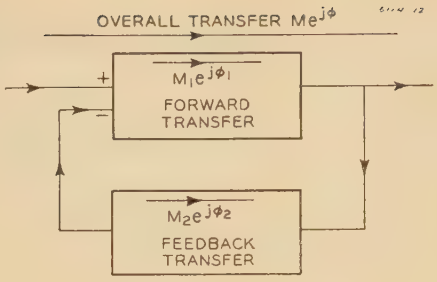

The important feature to note is that if the loop transfer function magnitude decreases as $1/\omega^2$ or faster for a region near unity, the phase angle will be near $-180°$ or more and the system will be highly resonant. A good loop transfer function should not decrease in magnitude any faster than, say, $1/\omega^{1.5}$ until the magnitude is below about 1. Then the resonance peak will be no greater than 1.3. The stabilizing network discussed in the foregoing is useful, since it has a rising gain characteristic over a region near unity for which the loop magnitude is decreasing too fast. MacColl[8] has demonstrated this approach in detail.

Experimental Techniques

Experimentally many methods for testing a whole system for frequency response or for obtaining the transfer function of individual components will suggest themselves. A sinusoidal disturbance is placed

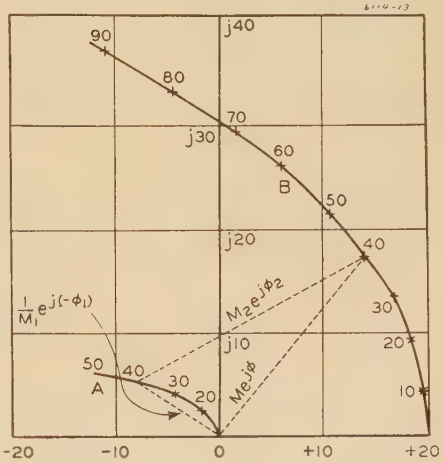

Figure 13. The open and closed loop inverse transfer functions for a disturbing torque

at the input of the component or system, and the relative phase and magnitude of the output is measured. One important advantage of this type of analysis is that the transfer function for some critical component which is difficult to analyze may be determined experimentally and

Factors Affecting the Range of Radar Sets

L. R. QUARLES
MEMBER AIEE

W. M. BREAZEALE
NONMEMBER AIEE

IT is now well known that most of the radar sets used in the past war function by transmitting a pulse and measuring the time necessary for the signal to reach the target and the echo to return. Of particular interest is the problem of finding how much power must be transmitted so that the echo will be of sufficient strength to be detected satisfactorily by the radar receiver. When dealing with microwave equipment and the consequent line-of-sight transmission paths, the problem can be solved by geometric means.

Consider a point source which is radiating energy uniformly in all directions.* The rate at which energy passes through unit area at a distance r from the source is $P_t/4\pi r^2$ where P_t is the power output of the transmitter. This must be true because the area of the sphere of radius r, through whose surface all the energy passes, is $4\pi r^2$.

A radar transmitter which radiates equally in all directions is difficult to obtain. However, a very common short wave antenna is the dipole which has a radiation pattern similar to that shown in Figure 1. This is a polar diagram of the field strength through a plane containing the dipole. The flow of energy in directions A is roughly 3/2 that of the ideal point source and hence the power gain of the dipole is said to be 3/2. Thus the energy flow through unit area at a distance r from the dipole, in the directions A, is $3P_t/8\pi r^2$.

Viewed as a receiving system, the so-called effective cross section of a dipole[1] is a function of the wave length, λ, and is approximately equal to $3\lambda^2/8\pi$. This is numerically equal to the cross section of a disk which, if placed normal to the incident radiation, will absorb an equivalent amount of energy. Thus if two similar dipoles are placed a distance r apart, the received power, P_r, in terms of the transmitted power, will be the product of the energy density at the receiving dipole and the dipole cross section,

$$P_r = \frac{3P_t}{8\pi r^2} \times \frac{3\lambda^2}{8\pi} = P_t\left(\frac{3\lambda}{8\pi r}\right)^2 \qquad (1)$$

At microwave frequencies, it is convenient to use a parabolic reflector, with the dipole at its focus to narrow the radiated energy into a beam. Figure 2 is a sketch of this arrangement showing the dipole at the focus of a paraboloid. The

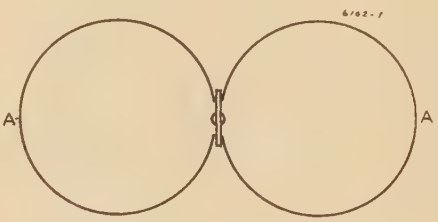

Figure 1. Field pattern of dipole

effectiveness of this reflector is expressed in terms of the energy density along the axis of the paraboloid compared with the energy density at the same point attributable to the dipole alone, or, remembering the reciprocity theorem, in terms of the increase in the magnitude of a received signal resulting from the addition of the reflector. Using the latter line of reasoning, a first approximation to the power gain, G, of the reflector can be obtained by dividing the cross section area of the paraboloid by the effective cross section of the dipole,

$$G = \frac{\frac{\pi D^2}{4}}{\frac{3\lambda^2}{8\pi}} = \frac{2}{3}\left(\frac{\pi D}{\lambda}\right)^2 \qquad (2)$$

where D is the diameter of the paraboloid and λ the operating wave length. The beam width θ between half-power points in terms of reflector size and wave length is given roughly by

$$\theta = \lambda/D \text{ radians} \qquad (3)$$

Referring to equation 1, if paraboloids are used behind each dipole, then the received power is increased by the product of the gains of these reflectors. Assuming paraboloids of equal size, the expression for the received power P_r becomes

$$P_r = P_t\left(\frac{3\lambda}{8\pi r}\right)^2 \times G^2$$

$$P_r = P_t\left(\frac{\pi D^2}{4\lambda}\right)^2 \times \frac{1}{r^2} \qquad (4)$$

As might be expected, this equation shows that the received power is inversely proportional to the square of the separation.

* This discussion is adapted in part from a series of lectures given by W. W. Hansen at the Radiation Laboratory, Massachusetts Institute of Technology, in 1940 and 1941.

Paper 46-102, recommended by the AIEE committee on communication for presentation at the AIEE Southern District meeting, Asheville, N. C., May 14–16, 1946. Manuscript submitted March 18, 1946; made available for printing April 19, 1946.

L. R. QUARLES and W. M. BREAZEALE are members of the department of electrical engineering, University of Virginia, Charlottesville, Va.

placed along with other transfer functions which are determined analytically.

In some cases it may be desirable to work with the magnitude of the transfer function alone because of difficulty in making phase measurements. Then the phase-magnitude relationship is useful.

For experimental verification of the methods discussed, it is important that the system remain linear; in particular, the applied disturbances should not be large enough to overload the amplifiers or saturate the motor. In view of this limitation, this analysis yields necessary conditions for good performance but not always sufficient conditions.

References

1. THE "SPEEDOMAX" POWER LEVEL RECORDER, W. R. Clark. AIEE TRANSACTIONS, volume 59, 1940, pages 957–64.

2. POLARIZED-LIGHT SERVO SYSTEM, T. M. Berry. AIEE TRANSACTIONS, volume 63, April 1944, pages 195–8.

3. STABILIZED FEEDBACK AMPLIFIERS, H. S. Black. *Bell System Technical Journal*, January 1934.

4. TRANSIENTS IN LINEAR SYSTEMS (book), M. F. Gardner, J. L. Barnes. John Wiley and Sons, New York, N. Y., 1942.

5. REGENERATION THEORY, H. Nyquist. *Bell System Technical Journal*, January 1932.

6. PARALLEL CIRCUITS IN SERVOMECHANISMS, H. Tyler Marcy. AIEE TRANSACTIONS, volume 65, 1946, August-September section, pages 521–9.

7. NETWORK ANALYSIS AND FEEDBACK AMPLIFIER DESIGN (book), H. W. Bode. D. Van Nostrand Company, New York, N. Y., 1945.

8. FUNDAMENTAL THEORY OF SERVOMECHANISMS (book), L. A. MacColl. D. Van Nostrand Company, New York, N. Y., 1945.

9. DYNAMIC BEHAVIOR AND DESIGN OF SERVOMECHANISMS, G. S. Brown, A. C. Hall. American Society of Mechanical Engineers *Transactions* volume 68, July 1946, pages 503–24.

It is the fundamental relation describing point-to-point operation, such as microwave radiotelephone service where a line-of-sight path is involved.

For the radar case, however, it is necessary to find the energy in the echo. If the target is an airplane, the energy scattered is a function of the size of the airplane, materials, wave length, aspect, polarization of the incident wave, and so forth. An effective cross section A_t can be defined as the area intercepting that amount of power which, if scattered equally in all directions, will give an echo equal to that from the target.

With this assumption, the energy density at a distance r from the target is

$$P_s = P_t \times \frac{A_t}{4\pi r^2} \tag{5}$$

where P_t is the incident energy density and P_s the density of the scattered energy at a distance r from the target.

In a microwave set the same antenna system is used for transmitting and receiving; hence the received energy is the product of equations 4 and 5, since equation 4 represents the energy which would be received if it were reflected without loss of any sort and equation 5 is the loss factor of the target.

$$P_r = P_t \left(\frac{\pi D^2}{4\lambda}\right)^2 \times \frac{A_t}{4\pi} \times \frac{1}{r^4} \tag{6}$$

Will this energy be sufficient to operate the receiver? While it is possible to get almost infinite gain in a receiver, the sensitivity, that is, the smallest signal that the receiver can utilize, is determined by the noise in the receiver input.

The theoretical lower limit of this noise level is fixed by the thermal-agitation-noise (Johnson noise) in the resistive component of the input.[2,3] This thermal-agitation-noise voltage is $\sqrt{4kTBR}$ volts. Remembering that the maximum power which can be drawn from a generator of electromotive force E and internal resistance R is $E^2/4R$, the maximum noise power available to the receiver is kTB watts. Here k is Boltzman's constant, 1.37×10^{-23} Joule per degree absolute, T about 290 degrees absolute; and B the effective noise band width of the receiver in cycles per second, which is roughly equal to the band width of the receiver between half-power points. For satisfactory pulse reception, the band width should be inversely proportional to the length of the pulse. For a one-microsecond pulse, this is 10^6 cycles. The ratio of the equivalent noise level at the receiver input to the thermal-agitation-noise is defined as the "noise figure," symbol F,

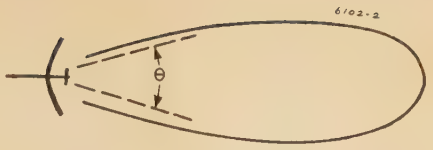

Figure 2. Field with parabolic reflector

and in a microwave receiver may be as low as four or five.

An expression for the maximum range of a radar set can now be written. If it is assumed that a received signal-to-noise ratio of one is acceptable, then the value of the equivalent noise level can be substituted for P_r in equation 6 giving

$$kTBF = P_t \left(\frac{\pi D^2}{4\lambda}\right)^2 \times \frac{A_t}{4\pi} \times \frac{1}{r^4} \tag{7}$$

Solving this for the range r gives the relation

$$r = \sqrt[4]{P_t \left(\frac{\pi D^2}{4\lambda}\right)^2 \times \frac{A_t}{4\pi} \times \frac{1}{kTBF}} \tag{8}$$

To illustrate by a numerical problem, the following is representative of a microwave search radar:

P_t, peak transmitted power, $= 100$ kw
λ, wave length, $= 10$ centimeters
Beam width $= 3$ degrees, or,
D, diameter of reflector, $= 190$ centimeters
A_t, effective cross section area of a medium bomber, $= 2 \times 10^5$ square centimeters
B, band width, $= 10^6$ cycles per second. (This permits a 1-microsecond pulse)
F, noise figure, $= 10$

The maximum range is then roughly 150 land miles. The airplane could be tracked this far (in theory) if it flew at sufficient altitude to permit a line-of-sight path between it and the radar antenna.

Several interesting conclusions can be drawn from equation 8. The effective range varies at the fourth root of the transmitted power, that is, to double the range it is necessary to increase the peak power by a factor of 16. The range also varies as the fourth root of the effective cross section area of the target. For this reason a large bomber cannot be tracked to a much greater distance than a small fighter. Again, the range appears to be inversely proportional to the square root of the wave length, but this is not the whole story. As shown in equation 3, the beam width is directly proportional to the wave length, and if one endeavors to increase the range by decreasing the wave length with the consequent decrease in beam width, the beam speedily becomes too narrow for successful searching. In other words, it is possible for the beam to pass completely over the target between pulses. Actually it is desirable for at least three or four pulses to strike the target while the beam is sweeping over that point.

The range also appears to vary directly with the diameter of the reflector. But here again one runs into the problem of decreasing size of the beam and the consequent unsuccessful scanning. If the beam width is held constant, which means that the ratio of D to λ is fixed, then the range actually falls off with decrease in wave length, because the size of the reflector must be reduced in proportion to the reduction in λ. It should be added here that a paraboloid, such as was assumed in the foregoing numerical example, is not very practical for a long range search set because the beam is too narrow in the vertical direction. One way to overcome this difficulty is to use a truncated paraboloid which has a considerably wider beam in elevation than in azimuth. The gain, of course, of such a reflector is less than the complete paraboloid.

The range is also proportional to the fourth root of the peak power of a pulse. But increasing the peak power by shortening the pulse to keep the same average power also requires that the band width be increased; hence the noise level of the receiver will increase in proportion. If the peak power is increased without shortening the pulse, which means that the average power is increased, then, of course, the range also will increase, but slowly.

Finally, it is seen that the range is inversely proportional to the fourth root of the noise figure. In fact, as far as this characteristic is concerned, decreasing the noise figure is as effective as increasing the average power. This explains why such a tremendous amount of work has been done in the direction of reducing the noise figure of radar receivers. Reducing the noise figure by three decibels may not be as sensational as increasing the peak power from one megawatt to two megawatts, but the increase in range is just as great.

The recent experiments which resulted in obtaining radar echoes from the moon have been described in a recent publication.[4] After making certain corrections for the increase in gain of the radar antenna caused by reflections from the ground and so forth, it was found that the strength of the received echo agreed closely with the value predicted by calculation. A long-wave radar set was used (110-megacycle frequency and a pulse length, of 0.02 second or more). This long pulse allowed the over-all receiver band width to be reduced to 50 cycles per second with a consequent reduction in the thermal-agitation noise. A peak trans-

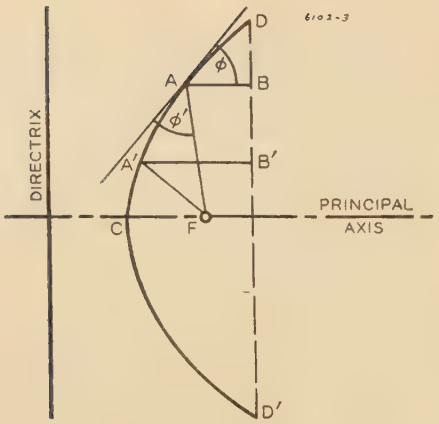

Figure 3. Parabola

mitted power of three kw gave a very adequate signal.

Earlier in this paper reference was made to a simple relation for the gain of a parabolic reflector (equation 2), and an idealized field pattern with only one lobe was shown in Figure 2. The true picture is somewhat more complicated. Because the diameter, or aperture, of the reflector is at the most a few dozen wave lengths, the field distribution is the result of diffraction of the radiation at the aperture. Hence the gain depends on other factors beside the size of the reflector and the wave length, and the field shows side lobes in addition to the main lobe.

A complete mathematical discussion of the action of the dipole and parabolic reflector is long and rather involved. However, a qualitative discussion will give a reasonably clear picture.

By definition a parabola is the locus of a point whose distance from a fixed point, the focus, is equal to its distance from a fixed line, the directrix (Figure 3). The parabola also has the property that the angle which any focal radius, such as FA, makes with a tangent to the parabola at the point of intersection is equal to the angle the tangent makes with a line through this point of intersection and parallel to the principal axis. These angles are shown as ϕ and ϕ' on the figure.

A geometric construction shows at once that the distance from the focus to any point on the parabola plus the distance from that point to a line parallel to the directrix but situated on the other side of the vertex is a constant. Referring again to Figure 3, this means that $FA+AB=FA'+AB'$, and so forth.

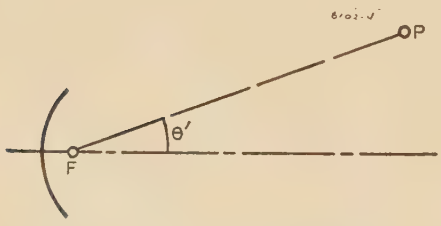

Figure 4. Location of point P

If a source of radiation is placed at F and DCD' is a parabolic reflector, all the waves reflected from it will arrive at DD' in time phase. Therefore we can consider DD' (actually the disk equal to the aperture of the parabola) as a constant phase surface radiating to the right. Next this constant phase surface can be divided into elemental areas and the contribution of all these areas to the field at the point under consideration summed. In general, the distribution of the field intensity will have the form

$$E=(\text{constant})(1+\cos\theta')\,\frac{\sin X}{X} \qquad (9)$$

where

$$X=\frac{\pi D}{\lambda}\sin\theta'$$

D = diameter of paraboloid DD'

θ' = angle between principal axis and line from focus to point under consideration (Figure 4)

Figure 5 is a plot of this function for D/λ roughly equal to ten, and Figure 6 is a polar plot of the field for a somewhat smaller reflector. The pattern of field intensity can be altered drastically by changing the focal length of the parabola, by distorting the reflector, and by varying the field intensity distribution across the aperture. The presence of direct forward radiation from the dipole feed also modifies the pattern. If the dipole is placed an odd number of quarter-wave lengths from the vertex of the parabolic reflector, then the forward radiation will reinforce the reflected wave (remembering that a wave is reflected with a 180-degree reversal in phase), and if placed an even number of quarter-wave lengths will tend to cancel it.

A typical design of a parabolic reflector calls for a ratio of focal length to diameter equal to 0.30 and also specifies that the product of the focal length and the depth shall equal one-fourth the diameter. Under these conditions, with a dipole feed, the gain is roughly that given in equation 2 and the beam width between half-power

Figure 5. $\frac{\text{Sin } X}{X}$ function

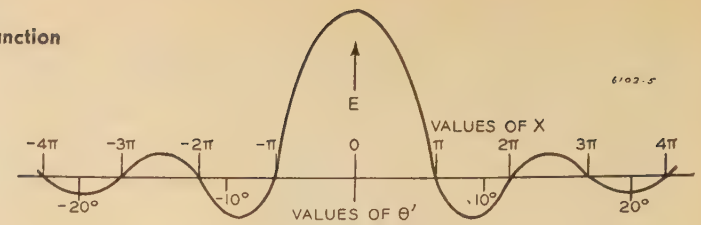

Figure 6. Typical antenna pattern showing side lobes

points 1.2 λ/D radians. With a reflector of reasonable size, the side lobes are small enough to be unobjectionable.

The relations just discussed do not take into account any of the phenomena associated with refraction or reflection from external surfaces, or the fact that very short waves are absorbed by fog and rain.[5] For wave lengths much less than one inch, the latter problem is serious. Reflection can be both an aid and a hindrance. Properly situated ground radar search sets are subject to increases in received signal strength of as much as 12 decibels caused by ground reflections. On the other hand, when the target and the radar set are near the surface of the earth, it is entirely possible for the difference in path lengths of a direct and reflected echo (that is, the ray reflected from the surface of the ocean) to be some odd multiple of a half-wave length, and in this case the resultant echo field will be very nearly zero. This phenomenon has been encountered when searching for ships with shore-based radar sets.

Further work is being done on the measurement of the absorption by the atmosphere of wave lengths less than one inch. As might be expected, there are strong absorption bands due to oxygen, water vapor, and so forth. The results will have considerable bearing on future selection of wave lengths.

References

1. A Note on Transmission Formula, **H. T. Friis.** *Proceedings*, Institute of Radio Engineers, volume 34, May 1946, page 255.

2. Noise Figures of Radio Receivers, **H. T. Friis.** *Proceedings*, Institute of Radio Engineer, volume 32, July 1944, page 419.

3. The Absolute Sensitivity of Radio Receivers, **D. O. North.** *R. C. A. Review*, volume 6, January 1942, page 332.

4. Radar Echos from The Moon, **J. Mofenson.** *Electronics*, volume 19, April 1946, pages 92–8.

5. Effect of Rain at 1- and 3-Centimeter Wave Lengths, **S. D. Robertson, A. P. King.** *Proceedings*, Institute of Radio Engineers, volume 34, April 1946, page 178.

The Preservative Treatment of Various Species for Poles and Crossarms

J. D. MacLEAN
NONMEMBER AIEE

THE heavy drain that the war has imposed on the forests of America, the backlog of pole requirements that has been built up over the war period, and the present labor shortage have made it impracticable to obtain a sufficient number of poles of the species formerly used.

Up to the present time, southern yellow pine and western red cedar have been the species most extensively used for poles. Coast Douglas fir and northern white cedar also are recognized as good pole woods, but poles of these species have not had the wide distribution nor the extensive use that southern yellow pine and western red cedar poles have had. In addition to the woods mentioned, treated lodgepole pine poles have been used to a limited extent in the Rocky Mountain region.

Cedar poles and in certain localities some of the less durable species have been used in past years without preservative treatment, but the present discussion will be confined to poles that are to be treated. Since the sapwood of all species has low resistance to decay, the economy of preservative treatment is recognized even for cedar poles that normally have a fairly thin sapwood and a naturally durable heartwood.

In order to meet some of the problems resulting from the current pole shortage, specifications have recently been prepared covering pole species to be used by the Rural Electrification Administration. The American Standards Association has prepared specifications designated as "American War Standards Specifications and Dimensions for Wood Poles." The specifications mentioned cover miscellaneous conifers that are to be given a preservative treatment and that heretofore have not been included among the recognized standard pole woods.

The proposed substitute woods have been grouped according to the allowable fiber stress in the following order:

Group I. Fiber stress 5,600 pounds per square inch
(*a*). Atlantic white cedar (*Chamaecyparis thyoides*)
(*b*). Spruce (*Picea*)—all species

Group II. Fiber stress 6,000 pounds per square inch
(*a*). Eastern white pine (*Pinus strobus*)
(*b*). Ponderosa pine (*Pinus ponderosa*)
(*c*). Sugar pine (*Pinus lambertiana*)
(*d*). Western white pine (*Pinus monticola*)

Group III. Fiber stress 6,600 pounds per square inch
(*a*). Jack pine (*Pinus banksiana*)
(*b*). Red (Norway) pine (*Pinus resinosa*)
(*c*). White fir (*Abies concolor*)

Group IV. Fiber stress 7,400 pounds per square inch
(*a*). Douglas fir other than coast type (*Pseudotsuga taxifolia*)
(*b*). Eastern hemlock (*Tsuga canadensis*)
(*c*). Western hemlock (*Tsuga heterophylla*)
(*d*). Eastern larch (Tamarack) (*Larix laricina*)
(*e*). Western larch (*Larix occidentalis*)

The foregoing fiber stresses were obtained from a study made by the Forest Products Laboratory and are based on the American Standards Association recommended stresses for lodgepole pine.

Wood Preservatives for Poles

Creosote

Prior to the war a large proportion of the poles used in the United States were treated with American Wood Preservers Association specification grade one coal tar creosote with a specified distillation residue of not over 20 to 25 per cent above 355 degrees centigrade.

The federal specification covering creosote for pole treatment limits the residue to 25 per cent. Shortages resulting from the war, however, made it difficult to obtain cresote with a low distillation residue, and it became necessary to increase the allowable residue in the federal specification to as much as 35 per cent. This wartime emergency provision has been discontinued. An important reason for specifying low residue cresote oils for pole treatment is to reduce the tendency to bleed.

Before the war a large amount of creosote was imported from Europe and Japan. Because this supply practically has been cut off and because the domestic production probably will not be able to meet the heavy postwar demands, a creosote shortage may exist for some time to come. This situation has forced pole users to consider the use of other preservatives less well known but that offer promising results. In extreme cases it even may be necessary to use treatments that are known to be less economical because of the shorter service life obtained. Such treatments may be less economical because the materials lack the preservative properties suitable for conditions under which poles are used or because of inadequate treatment. Nevertheless, there should be few cases where inferior and uneconomical treatment is necessary because of present shortages.

Chlorinated Phenols

During the past ten years, the chlorinated phenols have been receiving considerable attention as possible substitutes for creosote or as materials that can be used in mixtures with creosote.[1,2] Pentachlorophenol is the best known in this group and has been the most extensively used, but tetra-chlorophenol and 2-chlororthophenylphenol, in mixtures with pentachlorophenol, have also been given consideration. Pentachlorophenol has the advantage of a lower water solubility than the other two phenolic compounds. Tests show that these chemicals have a high degree of toxicity, and five per cent solutions (on a weight basis) are apparently suitable when solution absorptions needed to obtain the necessary penetrations are employed. A five per cent solution of penetachlorophenol (on a weight basis) commonly is recommended at present. This is for absorptions similar to those specified for pole treatment with creosote.

Both toxicity and permanence are highly important qualities of a good wood preservative, but only long-time service tests provide a satisfactory measure of permanence, and such tests are needed to determine fully the relative merits of the chlorinated phenols. The limited number of service tests that have been started during the past few years indicate that the chlorinated phenols have a promising future, but little information is available on the performance of these solutions when applied by the pressure process. Data thus far obtained apparently indicate that solutions of the chlorinated phenols made with the heavier petroleum

Paper 46-123, recommended by the AIEE committee on power transmission and distribution for presentation at the AIEE summer convention, Detroit, Mich., June 24-28, 1946. Manuscript submitted April 18, 1946; made available for printing May 8, 1946.

J. D. MacLEAN is an engineer, Forest Products Laboratory, Forest Service, United States Department of Agriculture, Madison, Wis.

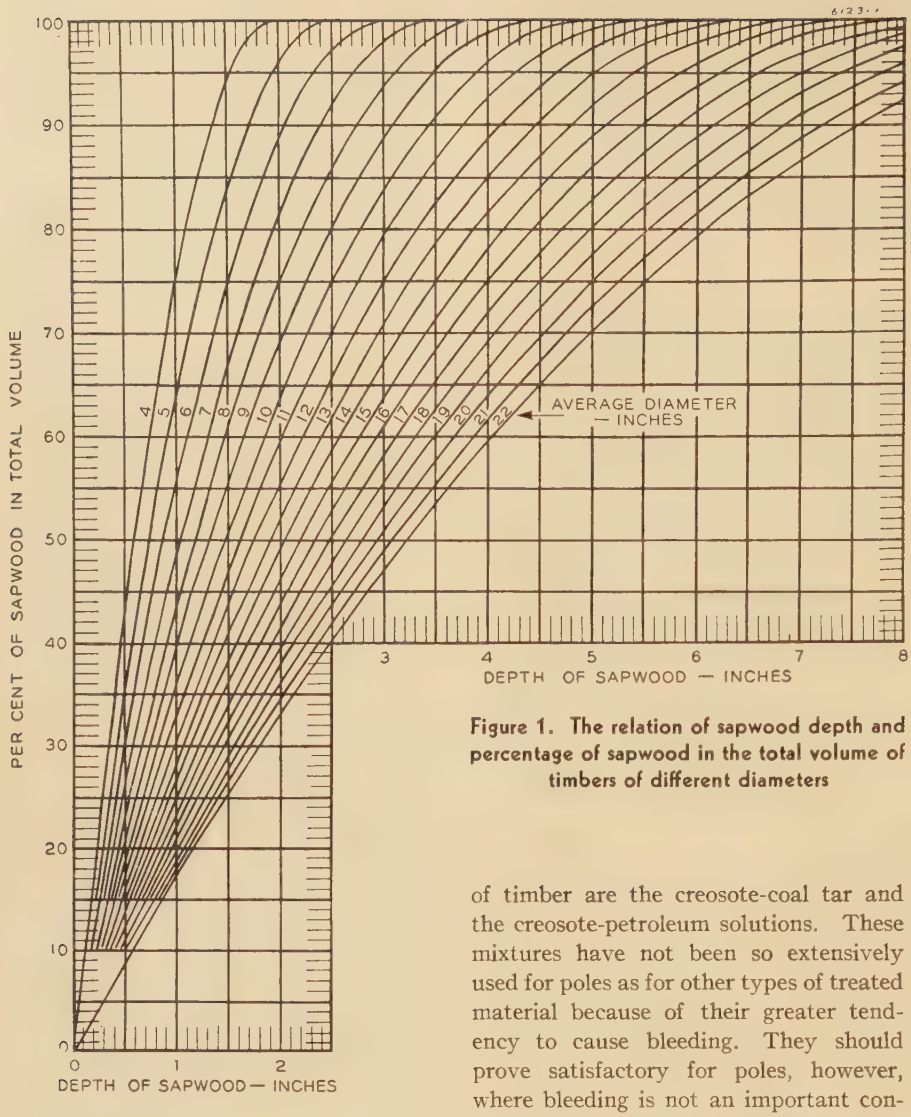

Figure 1. The relation of sapwood depth and percentage of sapwood in the total volume of timbers of different diameters

oils may give better protection than solutions in which the more volatile oils are used. On the other hand the more volatile oils penetrate the wood more readily when the solutions are applied by nonpressure methods. It has been found that some petroleum oils are more suitable than others both as solvents and from the standpoint of freedom from sludging.

The problem of sludging is also of importance in the use of creosote-petroleum mixtures. Experience has shown that petroleum oils with an asphaltic base are much less likely to give trouble than the oils with a paraffin base. Some pole users now are having poles treated with pentachlorophenol mixtures containing varying proportions of coal tar creosote. These mixtures also have an increased tendency to cause sludging unless a suitable petroleum oil is employed.

Creosote Solutions

Blended preservative oils that have been used successfully for various kinds of timber are the creosote-coal tar and the creosote-petroleum solutions. These mixtures have not been so extensively used for poles as for other types of treated material because of their greater tendency to cause bleeding. They should prove satisfactory for poles, however, where bleeding is not an important consideration.

Bleeding

The problem of bleeding is of particular interest when poles are used in urban line construction where the oily surface may cause damage to clothing and result in public complaint. Bleeding is naturally of less importance in rural lines, but in any case it is objectionable to linemen who must climb the poles when the line is installed and when repairs are required. The bleeding problem may be particularly aggravating when the poles have been treated shortly before they are placed in service. While this trouble becomes less acute after the poles have been in service for a time, in some installations bleeding may persist to a variable extent for a considerable period.

It must not be assumed that all poles treated with preservative oils bleed, but it is difficult to predict what poles, if any, will bleed and to what extent they will bleed.

Five factors that appear to have an important bearing on bleeding are

1. Type of preservative oil used.
2. Absorptions obtained.
3. Method of treatment.
4. Species.
5. Temperature conditions to which the wood is exposed.

Heavy absorptions usually cause more bleeding than light absorptions, heartwood will bleed more than sapwood, and species with the more resistant sapwoods will normally bleed more (with the same absorption) than species in which the sapwood is easily penetrated. Bleeding may occur either in summer or winter but is generally most severe in the hot summer months. Straight coal tar creosote usually gives less bleeding trouble than mixtures of coal tar creosote and petroleum, or creosote-coal tar solutions. Likewise, creosote with a high residue above 355 degrees centigrade usually causes more bleeding than low residue creosote oils.

Methods of Treatment

Pressure Treatment

The pressure process is the most effective method of treating timbers of all kinds, since it affords a means of controlling the pressure to any desired amount. By using different initial air pressures, a considerable variation in absorption can be obtained, thereby making it possible to get heavy or fairly light absorptions for a given depth of penetration. The principal objection to pressure treatment is that it requires relatively large and expensive equipment and is therefore not well adapted for the treatment of small quantities of timber nor for treating material that would require long distance transportation to the treating plant.

Nonpressure Treatment

Next to pressure treatment, the hot-and-cold bath method is the most effective. This treatment depends on atmospheric pressure utilized by first heating the wood in a heating medium and then cooling it in the preservative. When the wood is heated, the air contained within its cells is expanded, and part of that in the surface region of the timber is forced out of the lumina or air spaces. In the subsequent cooling bath, a partial vacuum is formed and more or less preservative is forced into the wood cells by atmospheric pressure, depending upon the permeability of the wood and upon the amount of air forced out by

expansion during the heating period. Very little preservative is absorbed during the hot bath, and it is obvious that the pressure forcing preservative into the wood during the cooling period cannot exceed atmospheric pressure. Generally the available pressure will be lower than atmospheric. For this reason the hot-and-cold bath treatment is more suitable for treating round timbers in which only the more easily treated sapwood needs to be penetrated. This method has been extensively used in the butt treatment of western red cedar poles and now is used to some extent in full length treatment of these poles. Lodgepole pine poles also have been butt treated by this method for use in the Rocky Mountain area.

Incising before treatment has been found very helpful when the sapwood is somewhat resistant to penetration, as in the case of cedar. When the sapwood is very resistant to penetration, as in species like the true firs and spruces, it is doubtful that even when the resistant sapwood is incised it will be possible to obtain satisfactory penetration without the use of pressure treatment.

The principal advantages of the hot-and-cold bath treatment over pressure treatment are

1. The cost of the treating equipment is small compared with the cost of pressure treating equipment.
2. Butt treatment or full length treatment can be used as desired.
3. It is more convenient to treat small quantities of timber by this method.
4. It is usually possible to make the treatments near where the timber is cut.

The principal disadvantages are

1. The pressure available for forcing the preservative into the wood is limited compared with the wide range of pressures available when the pressure process is used.
2. Considerably heavier absorptions usually are required for a given penetration than when the wood is treated by pressure methods because an initial air pressure cannot be applied as in the Rueping treatment.
3. This method of treatment is not well adapted for round timbers with unusually resistant sapwood nor for species that have a deep sapwood easily penetrated, since in species having a deep sapwood undesirably heavy retentions may be obtained or there may be incomplete sapwood penetration.
4. Evaporation of the lower boiling constituents of preservative oils used in the hot bath often causes an appreciable loss of preservative.

Absorption Specified for the Pressure Treatment of Poles

Most of the southern yellow pine and Douglas fir poles treated up to the present time have been treated by the empty-cell process with specified minimum net retentions of about eight pounds of creosote per cubic foot. Minimum absorptions specified for lodgepole pine poles have ranged from about four to eight pounds per cubic foot. The lower absorptions specified for the lodgepole pine have been possible partly because of the more shallow sapwood in this species. The sapwood of lodgepole pine commonly ranges from about one half to two inches in thickness compared with two to four inches in southern yellow pine and one to two inches in coast Douglas fir poles. Another reason for the use of lower absorptions in lodgepole pine is that poles of this species have been used mostly in the Rocky Mountain states where decay conditions are usually much less severe than those under which the southern yellow pine and coast Douglas fir poles are used.

Present American Wood Preservers Association specifications for the treatment of southern yellow pine poles permit a minimum net retention of six pounds per cubic foot provided the penetration specified for the 8-pound treatment is met and provided the poles are to be used under conditions that do not favor rapid decay. Various power companies have specified net retentions ranging from 10 to 16 pounds of either creosote or creosote-coal tar solutions in southern yellow pine poles.

The question of obsolescence is usually of more concern to telephone and telegraph companies than to power companies, and it is natural that they do not want to employ preservative treatments that may give a service life well beyond the time their pole lines would become obsolete. On the other hand, it obviously would be unwise and uneconomical to count on obsolescence and later find the service life was too short.

Sufficient service records are not yet available to show the minimum absorptions of different preservatives that can be expected to give satisfactory results for poles of different species when used under various climatic conditions. For this reason it would seem desirable to defer the extensive use of absorptions much lower than those commonly specified until the relative merits of the lower absorptions can be determined from suitable service tests. The following are some of the more important advantages of using absorptions that are known to be adequate as demonstrated by experience:

1. They furnish a better reserve against depletion by leaching and evaporation.
2. They insure better distribution and deeper penetration of the preservative.
3. When the preservative has a variable toxicity, the heavier absorptions serve as a safeguard against deficient toxicity.
4. They reduce the danger of insufficient absorption because of careless treatment.
5. They help protect against the possibility of inadequate treatment of the more resistant timbers in a charge or of those of the larger sizes when the charge contains timbers of different dimensions.
6. They reduce the danger of wide variations between the maximum and minimum penetrations obtained in the same or in different timbers.

The principal disadvantages of heavier absorptions are the somewhat higher initial cost of treatment and the possibility of objectionable bleeding when oily preservatives are used. The higher initial cost of treatment, however, does not necessarily mean that the annual charge will be higher over the period the timber is in service. Within reasonable limits the higher first cost may be much more than offset by the increased service life and consequent reduced cost of renewals.

There are a variety of factors that should be kept in mind in deciding upon the net retention that will prove most economical or most desirable because of other considerations.

The thickness of sapwood also will have a definite bearing on the absorptions that should be specified. Woods with deep sapwood, like that of ponderosa pine, red pine, and the southern pines, naturally have a greater proportion of wood that can be treated than poles of thin sapwood species, like the cedars, western larch, and mountain type Douglas fir. Figure 1 shows the proportion of sapwood in the total volume of poles of different average diameters ranging from 4 to 22 inches. These curves were computed from the relation that if t is the average depth of sapwood and D is the average diameter of the timber, the percentage of the sapwood P, based on the total volume, is given by

$$P = 100\left[\frac{4t(D-t)}{D^2}\right] \qquad (1)$$

If P_t is the percentage of sapwood in the total volume when the average sapwood thickness is t inches, and P_T is the percentage of sapwood in the total volume when the average sapwood thickness is T inches, then

$$\frac{P_t}{P_T} = \frac{t}{T}\left[\frac{D-t}{D-T}\right] \qquad (2)$$

For example, assume $D = 10$ inches, $t = 0.75$ inch, and $T = 3$ inches. Then the ratio

$$\frac{P_t}{P_T} = \frac{0.75}{3}\left[\frac{10-0.75}{10-3}\right] = 0.33$$

In other words, a 10-inch-diameter pole with a sapwood thickness of 0.75 inch would have about 33 per cent as much sapwood as a pole timber of the same diameter with a sapwood thickness of three inches. Equation 1 or Figure 1 shows that the percentage of sapwood in the total volume of a timber 10 inches in diameter with a sapwood thickness of 0.75 inch is about 27.7, while the same diameter timber with an average sapwood thickness of three inches would have about 84 per cent sapwood in the total volume. For the same concentration of preservative, it might be assumed that poles with a sapwood thickness of 0.75 inch would require only 33 per cent as much preservative as when the sapwood is three inches thick. It should be borne in mind, however, that there is a greater opportunity for more rapid loss of preservative from thin sapwood through leaching and evaporation because the preservative is concentrated closer to the surface. In the latter case, somewhat heavier absorptions would help compensate for this difference in depth of penetration.

Equation 2 will be found convenient for comparing the relative proportions of sapwood in a timber of any given diameter when different depths of sapwood are assumed.

Treating Conditions and Pressure Treatment Specifications

In addition to specifying the preservative, the average absorption and penetration required, and the method of seasoning or conditioning the poles for treatment, it is desirable to specify the maximum preservative temperatures and pressures to be used, since these have an important bearing on the success of treatment. Some species will withstand more severe treating conditions than others.

Conditioning

Green southern yellow pine poles commonly are conditioned for treatment by the steaming and vacuum process. Although the average amount of water removed is usually not more than about five to six pounds per cubic foot, the removal of this amount of water and the heating of the wood to a favorable treating temperature as a result of the steaming make this method a very satisfactory means of conditioning southern yellow pine poles. This method, nevertheless, is not well adapted for conditioning other woods commonly treated because either the other woods are injured more easily by the temperatures and heating periods required in steam conditioning or the final moisture content still may be too high for good penetration after the steaming treatment is applied.

Green coast Douglas fir poles are conditioned by the Boulton, or boiling under vacuum, process. In this process, round timbers are usually boiled under vacuum with a specified maximum preservative temperature of 220 degrees Fahrenheit. Since water is evaporated during the boiling period, the wood temperature is usually considerably lower than the temperature of the heating medium. This process also is applied in the conditioning of other species in the green condition and has the advantage that it removes water from green material under mild temperature conditions.

Air seasoning is, of course, the most widely used method of conditioning wood preparatory to treatment.

Treating Temperatures

Both laboratory experiments and subsequent studies made under commercial treating conditions have shown that treating temperatures of 190 degrees to 200 degrees Fahrenheit are much more effective in obtaining good penetrations than lower temperatures. This applies when either preservative oils or water solutions are used. Temperatures a little higher than 200 degrees Fahrenheit often can be used to advantage for some species, such as the southern pines.

Preservative Pressures

Preservative pressures should be kept low enough to prevent objectionable checking and collapse. Some species, as for example southern yellow pine and some of the hardwoods, can withstand treating pressures considerably higher than many other woods. Whenever objectionable checking or collapse occurs as a result of the temperature and pressure conditions employed, the preservative temperature should be maintained in the range of 190 degrees to 200 degrees Fahrenheit, and the treating pressure should be lowered as may be needed to prevent unnecessary checking or collapse.

Specifications

The American Wood Preservers Association for many years has had specifications covering the pressure treatment of southern yellow pine and coast Douglas fir poles, and these specifications have been revised at various times. In recent years this association has prepared specifications for the pressure treatment of western red cedar, lodgepole pine, jack pine, and red pine poles.

Treatment of Species Listed in the Various Groups

The recommendations made in the subsequent discussion are based on experiments made by the Forest Products Laboratory in a study of the treatment of the species named.

Species in Group I. Atlantic white cedar has a sapwood depth about the same as that of western red cedar (about one half to one inch for most timbers) and can be treated under the same conditions as specified for western red cedar (American Wood Preservers Association).

The spruces are resistant to penetration in both the sapwood and heartwood, and it is also difficult to distinguish the sapwood from the heartwood. Sapwood of the freshly cut timbers usually has a high moisture content in the range of 140 to 165 per cent or over. In order to avoid objectionable checking and collapse in the spruce species, it is desirable to limit the preservative pressure to about 150 pounds per square inch when the Rueping process is used and to about 120 to 130 pounds per square inch when the Lowry, or full cell treatment, is applied.[3]

Species in Group II. The sapwood of ponderosa pine usually ranges from about two to three inches in thickness, and the sapwood moisture content of the freshly cut wood is relatively high, averaging about 150 per cent. This is one of the few softwood species that are comparatively easy to treat in both the sapwood and heartwood when air seasoned.

The sapwood of the white pines commonly ranges from about one to two inches and occasionally to three inches in thickness.

In general, the treating conditions specified for the southern pines will be suitable for the pines listed in group II.

Species in Group III. Jack pine has a sapwood that commonly ranges from about $1^1/_2$ to $2^1/_2$ inches in thickness, although poles grown in some regions may have sapwood considerably less than one inch in thickness. Like lodgepole pine, this species is injured more easily by high pressures than some of the other pine species, and the maximum treating pressure should not exceed 150 pounds per square inch and in most cases should be somewhat lower. The treatment of poles of this wood is covered in the American Wood Preservers Association specification for the pressure treatment of jack pine poles.

Red (Norway) pine has a fairly deep sapwood that ranges from about two to four inches in thickness. This species has

a high average moisture content of about 135 per cent in the sapwood when the timber is freshly cut. The treatment of poles of this species is covered in the American Wood Preservers Association specification for the pressure treatment of red pine poles.

The white firs, like the spruces, are very resistant to treatment in both the sapwood and heartwood, and the sapwood is not distinguishable from the heartwood. Treating conditions previously discussed for the spruce species also will apply for the true firs, such as white fir (*Abies concolor*).

Species in Group IV. The sapwood of Douglas fir poles grown in the region between the Pacific Coast and the Cascade Mountains normally has a range in thickness of about $^3/_4$ to $2^1/_4$ inches. In most cases it will average between 1.3 and 1.4 inches. The moisture content of the sapwood in freshly cut timbers usually will average around 115 per cent. The treatment of the coast-type Douglas fir poles is covered in the American Wood Preservers Association specification for the pressure treatment of coast Douglas fir poles.

The mountain-type Douglas fir has a thinner sapwood than the coast type and is usually about one inch or less in thickness. The so-called Inland Empire or intermediate type that grows between the coast and the Rocky Mountain region has a sapwood thickness ranging from about one to two inches.

While the heartwood of the timber that grows in the Rocky Mountain region is far more resistant to treatment than the heartwood of the timber grown in the coast region, the sapwood of the mountain type can be treated satisfactorily by the pressure process. Although the mountain type wood has a lower mechanical strength than the coast wood, the timber grown in the mountain region will withstand a somewhat higher treating pressure without showing a marked increase in checking and collapse. Treating pressures as high as 140 to 150 pounds per square inch generally can be used for the Rocky Mountain wood, while it is usually desirable to use pressures 25 to 30 pounds lower for the coast material.

The sapwood of eastern hemlock is difficult to distinguish from the heartwood and, like the heartwood, is relatively resistant to treatment. The average moisture content of the sapwood of the eastern species is in the neighborhood of 120 per cent in freshly cut wood. Poles of this species should be air seasoned for treatment.

The sapwood of western hemlock is sometimes lighter in color than the heartwood and is usually not much over an inch in thickness. The average moisture content of the sapwood of the western species is considerably higher than that of the eastern species and averages around 170 per cent. Both hemlock species can be treated using pressures up to about 150 to 160 pounds per square inch.

The sapwood of both eastern and western larch is usually less than one inch in thickness; hence the sapwood thickness of these woods is similar to that of the cedars, Rocky Mountain Douglas fir, and western hemlock. The average moisture content of the sapwood of freshly cut western larch is in the neighborhood of 125 per cent.

Treating pressures as high as 175 pounds have been used in treating larch timbers. This species usually can withstand somewhat higher treating pressures than most of the softwoods grown in the western states.

The purpose of the foregoing outline discussing treating conditions and specifications is to point out some of the more important variables that should be considered in the preparation of specifications for pressure treatment. It should be borne in mind that if the best results are to be obtained, the treating conditions should be adjusted to meet the structural variability of the different woods.

Crossarms

The suitability of a given species for crossarms will depend largely on the strength properties and freedom from such defects as cross grain and knots.

Up to the present time, southern yellow pine and coast Douglas fir have been considered the standard woods for crossarm material. The southern pines usually have a larger proportion of sapwood, and since the crossarms of this species are used in large quantities in the South where service conditions are more severe, it is customary to pressure-treat them. The absorptions commonly specified range from around 8 to 12 pounds of creosote per cubic foot.

Coast Douglas fir crossarms generally are used without treatment because they normally have little sapwood and are used more widely in the northern and western states where decay conditions are less severe than in the southern states.

Conditions under which crossarms are used are generally less favorable to decay than where wood is in contact with the soil. For this reason the heavier absorptions used for timbers exposed to the more severe service conditions are not so important for crossarms. The shortage of southern yellow pine and Douglas fir arms that, as in the case of poles, has developed as a result of the war, has made it necessary to consider substitute species.

In the pole species listed under groups I to IV, the conifers that seem most promising for crossarm material include western larch, mountain or intermediate-type Douglas fir, western hemlock, and red pine.

Treatment of Crossarms

Species that have a considerable proportion of sapwood or that do not have good durability in the heartwood should be treated if good service life is to be obtained. Woods of this kind include western hemlock and the various pine species.

Crossarms made from western larch or the Rocky Mountain and intermediate-type Douglas fir would have little sapwood because of the thin sapwood in trees of these species. The heartwood of these woods is similar to the coast-type Douglas fir heartwood from the standpoint of natural durability. When heartwood crossarms are pressure-treated, it is probable that it would be difficult to keep the net retentions much below five to six pounds per cubic foot because of the large amount of surface area in proportion to the volume. Pressure treatment, however, should give deeper penetrations in heartwood material, and when there is a considerable amount of sapwood it should require somewhat lower net retentions than when the open-tank treatment is used.

One of the larger pole using companies has now revised its crossarm specifications to include open-tank-treated red pine, jack pine, lodgepole pine, and the inland or intermediate Douglas fir. Jack pine and lodgepole pine are somewhat lower in strength properties than the other species named, but it is assumed that they will provide suitable crossarms for the lighter service conditions. This company has treated several thousand arms of these woods using a hot bath of coal tar creosote and a cold bath of five per cent pentachlorophenol in an aromatic petroleum oil. These treated arms have been installed in service, and an examination of their condition is to be made at various periods.

Although the use of the pentachlorophenol solutions is still in the experimental stage, it would seem that an open-tank treatment, such as that mentioned, should give good results. The open-tank treatment of crossarms appears to be the most suitable substitute treatment where pres-

Electric Equipment for Cornell Variable Density Wind Tunnel

C. C. CLYMER
ASSOCIATE AIEE

M. A. DE FERRANTI
MEMBER AIEE

Synopsis: Spectacular advances in airplane design during the past decade have created an increasing demand for additional testing facilities with which to obtain those data essential to successful design. To answer partially this demand and to facilitate more basic aerodynamic research on the subject of compressibility effects experienced in high speed flight, several new wind tunnels were constructed during this same period. These tunnels vary widely in size and in requirements for air density and air speed in the tunnel working section. Correspondingly, the horsepower output requirements for their main fan drive motors vary widely. But in all cases close speed regulation at preselected speed values over a wide range is essential to good test results. Most modern tunnels also incorporate suitable electric equipment for the operation of powered models and for the calibration of motors used in these models. This paper describes the Cornell variable density wind tunnel from the viewpoint of electrical engineers and discusses principles governing the selection of electric equipment for wind tunnels.

THE WIND TUNNEL with details as shown by Figure 1 is the variable density high speed tunnel recently constructed by the Curtiss-Wright Corporation Research Laboratory (now Cornell Aeronautical Laboratory), Buffalo, N. Y. This project was initiated by Doctor Norton B. Moore, then of the Curtiss-Wright Corporation, and construction was started under his direction in 1942. The basic design of the tunnel was prepared by members of the staff of the California Institute of Technology under the supervision of Doctor Clark B. Millikan. This group also acted as consultants during construction of the new facility. The design was financed jointly by the Curtiss-Wright Corporation and by a group of four Southern California aircraft companies which finances and owns a basically similar facility, known as the cooperative wind tunnel, in Pasadena, Calif.

The tunnel consists of a reinforced steel duct of circular cross section, housed in a brick-faced frame building, which adjoins a laboratory and power plant building. The principal dimensions of the duct, which is built of steel plate approximately seven-eighth inch thickness, are shown in Figure 2. The duct forms a closed circuit through which air is circulated by the fan system indicated as *A* in Figure 1. With the outlet door of the tunnel closed the static pressure of the air in the tunnel may be varied between one-fourth atmosphere and four atmospheres, and then the air may be caused to circulate in this condition. Vanes built into each corner to guide the air flow are shown in Figure 2. Cooling of the air is accomplished by a bank of finned coil radiators mounted on the downstream side of the turning vanes in one corner of the tunnel. This is shown at *B* in Figure 1. Cooling water is pumped through these radiator coils and the heat is transferred to the atmosphere by means of the cooling tower shown at *C* in Figure 1. This cooling system is of adequate capacity to remove heat corresponding to the maximum continuous power input to the fan system, while limiting the air temperature inside the tunnel to 125 degrees Fahrenheit.

The airplane model shown as *D* in Figure 1 is supported in the "test section" of the tunnel within a sphere, which can be isolated from the rest of the tunnel duct by means of lock gates. This arrangement, unique to this tunnel and the similar one at the California Institute of Technology, Pasadena, allows pressure to be maintained in 90 per cent of the total tunnel volume, while the sphere is isolated decompressed, and the model serviced or changed. Considerable effort was made in the design to speed up this process, thus reducing to a minimum the time during which the tunnel is out of service.

In Figure 2, in the plan view of which the air flow is counterclockwise, the contraction leading into the "working section" and the diffuser downstream of the working section are shown. The inside diameter of the duct at the beginning of the contraction is 31 feet 6 inches, the cross-sectional dimensions of the working or experimental area are 12 feet wide by $8\frac{1}{2}$ feet high, and finally the inside diameter of the duct at the end of the diffusion area (ahead of the first corner downstream of the working section) is 17 feet 9 inches. The airplane model is mounted on supports which, when the tunnel is operating, are integral with a basic metrical (force measuring) system, to which the forces and moments produced on the model by the air stream thus are transmitted. These forces and moments are transmitted hydraulically to a "control" room for indication and recording. For servicing or changing of a model, a transfer cart, the top of which forms the floor of the working section, is raised and carries with it the model supporting struts. Raising of the transfer cart floor disengages the support system from the metrical system and provides clearance for the transfer cart to be motored out of the tunnel on steel transfer rails. Interchangeable transfer carts make it possible to set up completely and "instrument" one model in the model preparation room while a second model is in the tunnel under test.

The fan system, mentioned previously, is driven through a 30-foot hollow steel shaft by a 10,250-horsepower continuous rated 2-unit motor set. Speed adjustment of this drive over a range from 0 to 570 rpm, with close regulation at preset values between 50 and 570 rpm, is arranged for remote operation from the control room near the tunnel door. Power supply for the complete installation is taken from the 115,000-volt 3-phase 60-cycle lines and stepped down to 4,800 volts before it enters the power area building and is connected to the metal-clad switchgear. Figure 13 shows the operators' console for the Cornell variable density wind tunnel.

Paper 46-85, recommended by the AIEE North Eastern District meeting committee for presentation at the AIEE North Eastern District meeting, Buffalo, N. Y., April 24–26, 1946. Manuscript submitted March 5, 1946; made available for printing March 19, 1946.

C. C. CLYMER and M. A. DE FERRANTI both are in the industrial engineering divisions, General Electric Company, Schenectady, N. Y.

sure treatment with creosote or with solutions of creosote and pentachlorophenol is not feasible or does not seem necessary for the conditions of service to which the crossarms are exposed.

References

1. PRESERVATIVES, PRIORITIES, AND PROCESSES, G. M. Hunt, R. H. Baechler, J. O. Blew. American Wood Preservers Association *Proceedings*, 1942, pages 62–84.

2. INFORMATION ON PENTACHLOROPHENOL AS A WOOD PRESERVING CHEMICAL, Ira Hatfield. American Wood Preservers Association *Proceedings*, 1944, pages 47–65.

3. PRESERVATIVE TREATMENT OF ENGELMANN SPRUCE TIES, J. D. MacLean. American Wood Preservers Association *Proceedings*, 1930, pages 164–81.

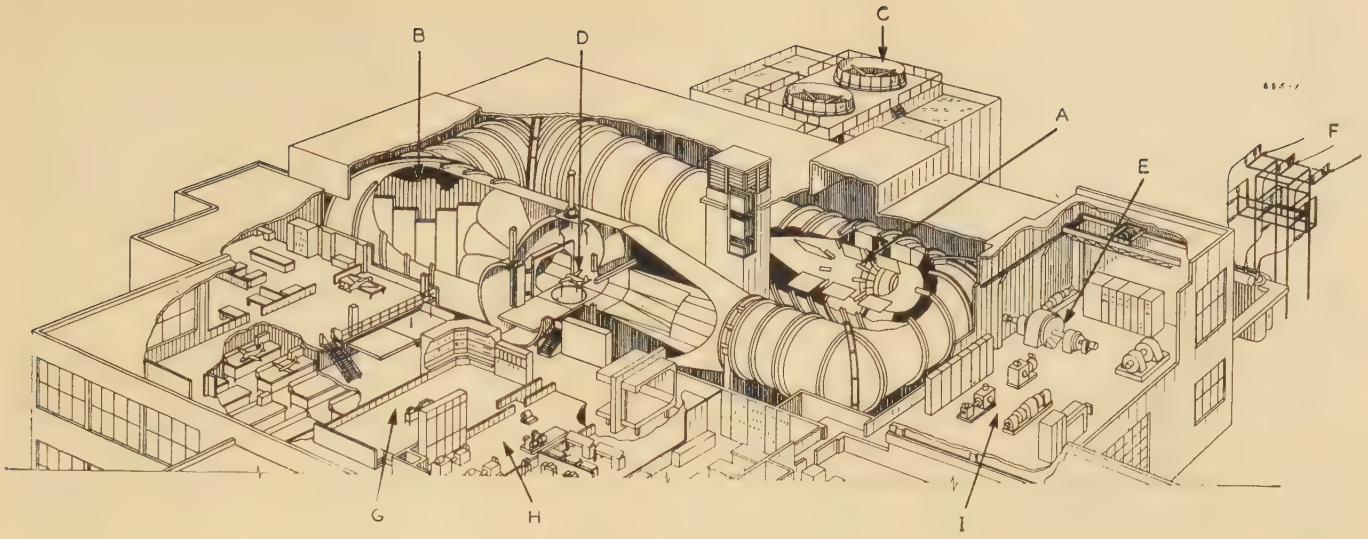

Figure 1. Cutaway view of Cornell Aeronautical Laboratory showing wind tunnel installation

A—Fan impeller
B—Heat exchanger
C—Cooling tower
D—Airplane model in test section
E—10,250-horsepower driving motor
F—115,000-volt 60-cycle power supply
G—Control room
H—Dynamometer room
I—Adjustable frequency system

For operation of powered models in the working section of the tunnel, an adjustable frequency system with frequency adjustment over a range from 60 to 450 cycles per second is arranged for remote operation from the control room. Precision metering of this variable frequency power supply is provided for indication and recording in the control room. The motors used in the powered models are calibrated on induction-type dynamometers capable of testing model motors up to speeds of 27,500 rpm, and up to maximum horsepower ratings of 200. Additional details of the electric equipment briefly mentioned in the foregoing will be given later in this paper.

Aerodynamic Principles Determining Power Requirements of Tunnel

Some knowledge of the aerodynamic principles influencing the design details of the tunnel is necessary for correct application of electric equipment on an installation of this type, although it is the intention of this paper to dwell on the electrical phase of the subject.

The primary object of all wind tunnels is to perform tests on scale models, which tests will produce data to assist the airplane designer in his design of new airplanes or in modifications of existing designs. For this purpose the wind tunnel is designed to measure accurately the reactions on the model at various altitudes and in an adjustable velocity uniform air flow. Various forms of tunnels have been designed[1] to produce effectively this adjustable uniform air flow through an experimental section in which the model is mounted, but the majority of recently designed tunnels built for testing in air velocities up to the speed of sound follow the general geometry of that shown in Figure 2. Force and moment reactions on the airplane model (and the coefficients derived from these) correspond to similar information on the full-size airplane, only if the model is geometrically similar to the full-scale design and also only if the model test is made at a Reynolds number equal to that expected on the full-size airplane in flight. Remembering that Reynolds number

$$R = \frac{Vl\rho}{\mu} \tag{1}$$

in which

V = relative velocity between body and fluid
l = a characteristic dimension of the body
ρ = mass per unit volume of the fluid
μ = coefficient of viscosity of the fluid

it can be seen that for testing in an atmospheric pressure tunnel, the Reynolds number for flight conditions can be equalled only by using a full-scale model, or alternatively testing a fractional scale model at higher velocities than flight

Figure 2. Outline of wind tunnel structure

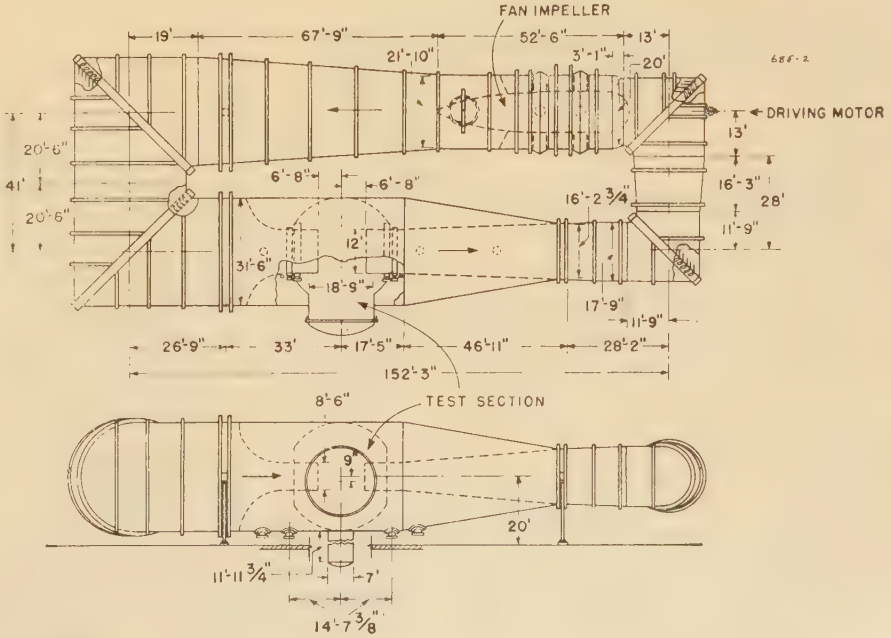

conditions. In the case of airplane testing, velocities above that of flight conditions may introduce other more serious errors because of the compressibility of the air and, consequently, the testing of a full-size model is dictated. Some wind tunnels for full-scale testing are in operation, but their initial costs and the power required for their operation are so high that, to date, they have been installed only by centralized government agencies. The majority of wind tunnel testing is done on fractional scale models at reduced Reynolds number values; full-scale conditions are extrapolated from these data.

Inspection of equation 1 indicates that change of density causes a corresponding change in the Reynolds number. The density is proportional to the air pressure, and the viscosity is approximately independent of pressure, so that Reynolds number may be changed approximately proportional to the pressure. A wind tunnel taking advantage of this feature was first built and operated by the National Advisory Committee for Aeronautics at Langley Field, when a relatively small tunnel operating with compressed air at 20 atmospheres pressure was put into operation in 1927. This feature also was incorporated in the design of the tunnels recently built by the Curtiss-Wright Corporation (now the Cornell Aeronautical Laboratory), the California Institute of Technology, and by the National Advisory Committee for Aeronautics at Ames Aeronautical Laboratory, Moffett Field, Calif.

Consider now the power requirements for wind tunnels: Corresponding to a specific air velocity through the working section (throat) of the tunnel, the kinetic energy of the air stream passing through the throat is given by the equation:

$$KE = 1/2\rho_o V_o^3 A_o \qquad (2)$$

Where

ρ_o = mass density of air in the throat
V_o = rated air velocity at throat
A_o = cross-sectional area of throat

Assuming approximately uniform velocity distribution throughout, the summation of energy loss in the various portions of the tunnel duct may be expressed in the form

$$\text{energy losses} = K_o 1/2\rho_o\ A_o\ V_o^3 \qquad (3)$$

where K_o is the basic loss coefficient. With rated velocity conditions, this is the energy which must be supplied by the fan and, taking into account fan efficiency ηf, the fan shaft power input is given by the equation

$$\text{hp} = \frac{K_o 1/2\rho_o A_o V_o^3}{\eta f \times 550} \qquad (4)$$

From equation 4 it can be seen that for a fixed throat cross section, the horsepower delivered from the main fan drive will be

$$\text{hp} = \frac{K\rho_o V^3}{\eta f} \qquad (5)$$

in which

$$K = \frac{K_o \times A_o}{2 \times 550}$$

and from which will be found an explanation for reducing tunnel static pressure (and therefore ρ_o) sufficiently to increase materially the air velocity in the throat without increasing the power input. For example, assuming that fan efficiency is maintained (by pitch change) a reduction from one atmosphere to one-fourth atmosphere in static pressure allows a velocity increase of approximately 58 per cent without increasing the horsepower input to the fan. This ability to study high velocity performance on models, without increasing fan input horsepower, prompted designers to provide for static pressure reduction in several modern wind tunnels. This equation also indicates that an increase in air pressure (and corresponding increase of Reynolds number) calls for a corresponding increase of fan shaft horsepower or, alternatively, air velocity at the throat will be reduced if horsepower input to the fan is held constant. For example, by equation 4, if the density is increased from atmospheric to that at four atmospheres pressure, the velocity at the throat will be reduced to approximately 63 percent of that at atmospheric pressure, if horsepower input is held constant.

Summarizing, the change of static pressure above and below atmospheric pressure has provided a means of increasing the Reynolds number and the air velocity, respectively, without requiring a proportionate increase of model size or fan horsepower input.

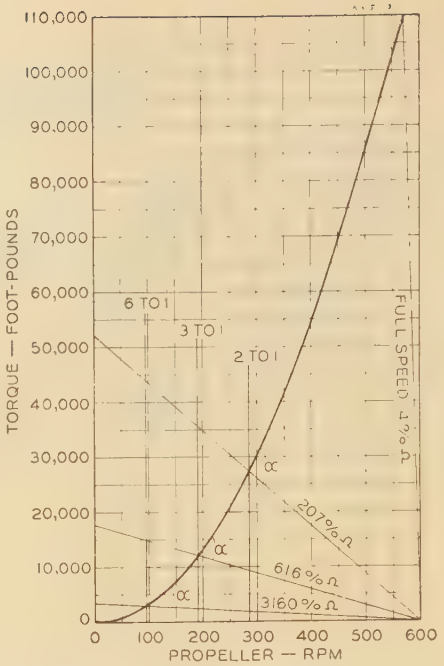

Figure 3. Speed-torque characteristics of 12,000-horsepower 570-rpm fan load

Values of secondary resistance required with a single speed slip ring motor for 2:1, 3:1, and 6:1 speed reduction also are shown

Selection of Main Drive

Wind tunnel power plants can and do take many forms, depending upon the type of tunnel to be powered, and the purchaser's preference. In this particular instance we are considering electric drive, and as the tunnel is of the two dimension or variable density type, with single rotation, the propeller drive unit will be mounted outside the tunnel proper—a construction detail which simplifies greatly the problem of the motor design. Also, power requirements are quite moderate, therefore permitting the use of any of the various types of drives.

The slip ring induction motor is perhaps the least expensive variable speed electric motor unit. This machine, with resistance in the secondary winding, has series characteristics, the speed being a function of secondary resistance and shaft torque.

The conventional propeller system has a torque characteristic which varies as the square of the speed for any established blade angle and air density. At rated speed, torque is, of course, 100 per cent, while at half speed it is 25 per cent. Usually the minimum requirement for speed range is 6 to 1, with the torque requirement at one-sixth speed equal to approximately three per cent. This is, of course, far outside the practicable operating range of a single speed slip ring motor. As a matter of fact, it taxes the performance of a two speed or pole changing motor with a two to one synchronous speed, and a horsepower range of the order of 8 to 1.

Such two speed drives have a point of discontinuity at the speed change point. They also require two slip regulators. With induction motors the speed varies

with change of applied voltage for a particular setting of secondary resistance and the propeller torque varies with changes of the model attitude, or change of model size in the test section. Corresponding to a change in load torque the induction motor speed will change, and the amount of change varies widely according to the amount of resistance in the secondary circuit. This type of motor inherently operates at low power factor, especially when lightly loaded. Because of these characteristics this combination of machines has not found complete acceptance on the part of wind tunnel operators. Economics, of course, play a major role in any large program of this nature, and the consultants for the subject project wished to retain the economies of the induction motor drive for maximum power requirements, and supplement the single speed induction motor with some different type of speed control between minimum speed and half speed.

One of the fundamental tunnel specifications was a 10 to 1 speed range which obviously could not be met through the use of the slip regulator, as will be evident from the speed torque requirements of a 12,000-horsepower 570-rpm propeller system (Figure 3). The parabola, of course, is the propeller torque curve, while the straight lines are the speed torque curves of the induction motor with various secondary resistances, with resistance values in per cent. The angle of the intersection (α) decreases rapidly below 50 per cent speed. The slip regulator, however, should function successfully between half speed and full speed.

Various systems were studied, but it was found to be most economical, for the rating involved, and yet fully reliable, mechanically, to combine the two basic adjustable speed drives, that is to combine an adjustable voltage (Ward Leonard) drive, with the slip ring motor and slip regulator to form a tandem drive. The adjustable voltage drive is operating alone over the range of 10 per cent to 45 per cent speed, while between 45 per cent and 100 per cent speed, both drives share the load: the d-c equipment providing the vernier control, so to speak, and the induction motor with its slip regulator the coarse adjustment.

The basic power requirement for the tunnel was set at 12,000 horsepower at 570 rpm for 30 minutes, the use of adjustable pitch propellers permitting this specification to fit into any tunnel pressure or air density. The power requirements of the conventional propeller vary as the cube of the speed. Thus, at half speed, or 285 rpm, the torque is reduced to 25 per cent rated, and the horsepower to 12.5 per cent or 1,500 horsepower.

The d-c part of the drive, as noted previously, provides the entire power to the propeller up to 45 per cent of rated speed, or 260 rpm. The motor rating of 1,250 horsepower (continuous) is more than ample to meet this requirement. Speeds

Figure 4. Schematic diagram of power circuits of the fan drive of the Cornell Aeronautical Laboratory

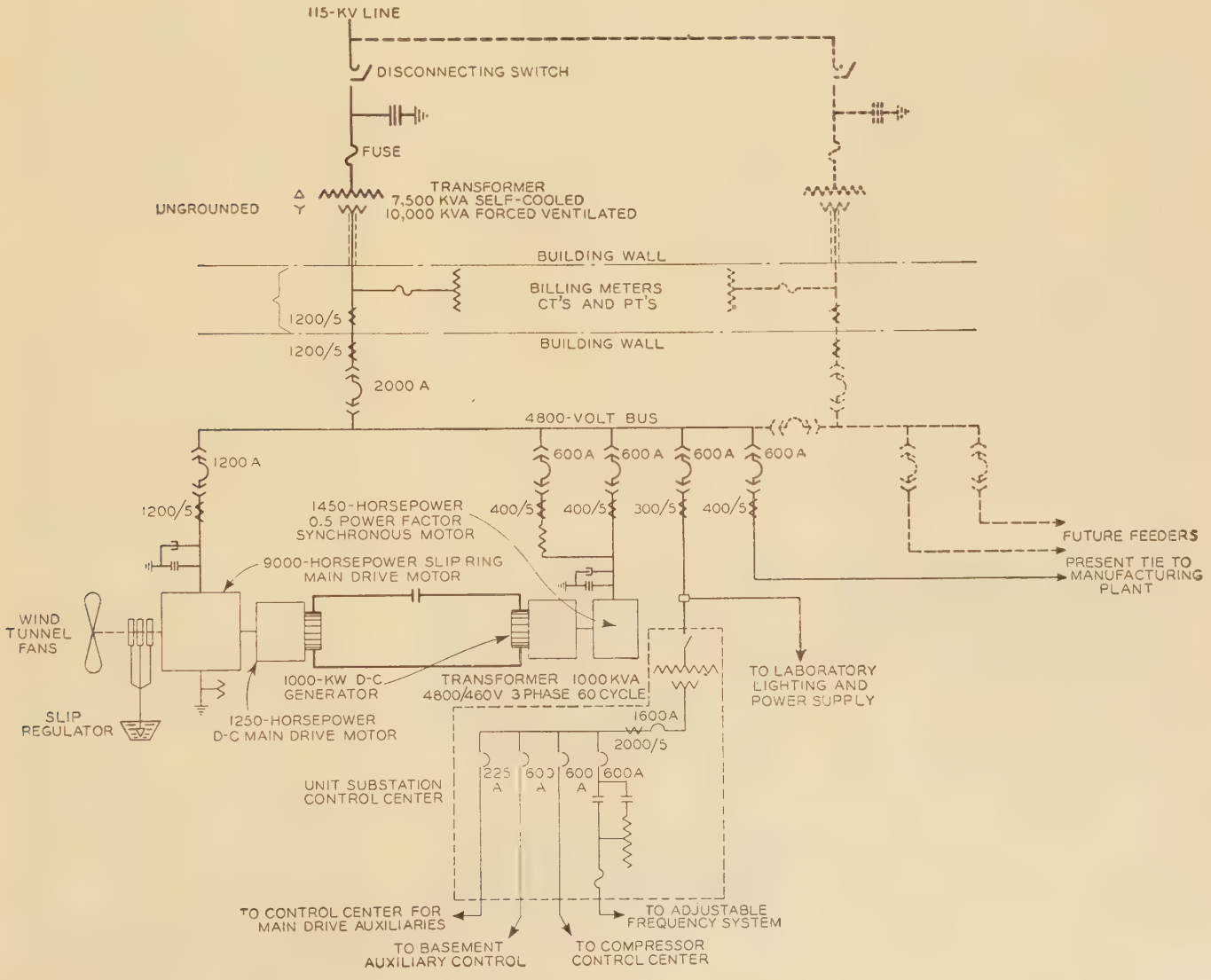

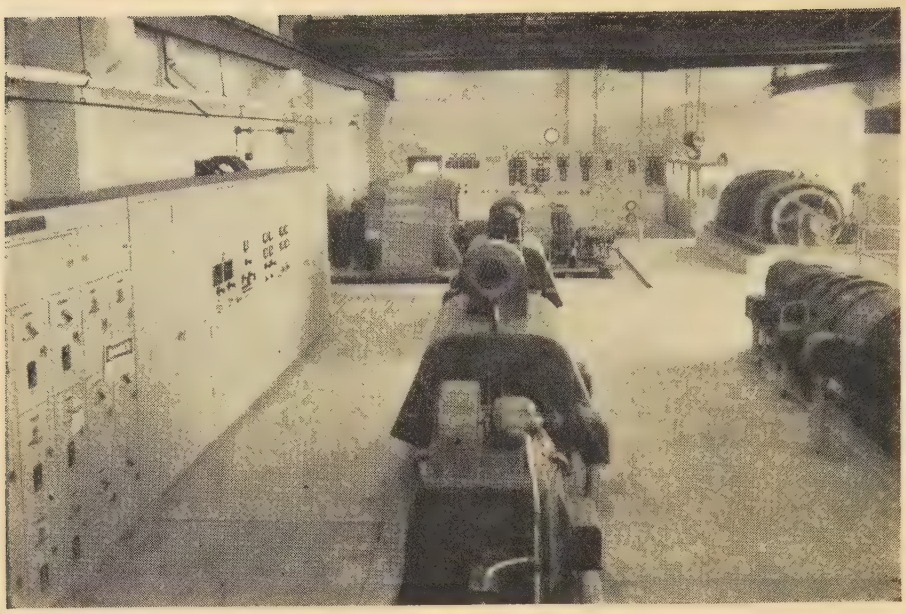

Figure 5. Motor room of Cornell variable density wind tunnel

In background is 4,800-volt metal-clad switchgear and main drive control. In center is 10,250-horsepower continuous rated tandem motor set and 1,000-kw motor-generator set. In foreground are adjustable frequency system machines and on left its control and control center for all motor room auxiliaries

higher than 260 rpm are provided by motor field weakening, at constant generator voltage; that is, constant horsepower (1,250 horsepower) is available throughout the range 260–570 rpm.

Power to this d-c motor is derived from a 1,000-kw motor generator set operating from the 4,800-volt 3-phase 60-cycle power supply. Generator voltage (Ward Leonard) control is used to obtain motor speed range 0–260 rpm. Obviously, the available horsepower then is reduced in proportion to generator voltage. The d-c motor and the motor generator are designed for continuous duty at their nameplate rating and are capable of carrying short-time loads of 200 per cent rating (that is 2,500 horsepower at full voltage).

The induction motor was rated on a continuous basis of 9,000 horsepower at 590 rpm and is capable of delivering 11,250 horsepower for 30 minutes. The tandem unit has a total capacity of 12,500 horsepower for 30 minutes, with ability to handle peak loads corresponding to a torque of 15,000 horsepower (torque) at 570 rpm. Figure 4 shows the general schematic diagram for this drive, the arrangement of the machines, and the power supply. Figure 5 shows the tandem drive unit installed.

Speed and Load Control

The d-c part of the drive serves as a means of controlling the speed and of maintaining it at the value preset by a master rheostat. The slip regulator is used for controlling the division of load between the d-c motor and the induction motor. A schematic diagram indicating the speed and load control system is shown in Figure 6.

The drive is started from rest by generator voltage control using the 1,250-horsepower d-c motor only; the induction motor remains disconnected from its power supply during this starting period. In this manner speeds up to 260 rpm are obtained. Above this speed the power requirements of the fan exceed the rating of the d-c machines, and the induction motor is connected automatically to the line with the slip regulator in its "all resistance in" position. The "load control" responsive to the direct current in the armature circuit of the 1,250-horsepower motor causes the slip regulator to change the secondary resistance of the induction motor until the latter assumes load such that the a-c motor and the d-c motor each are loaded to approximately the same percentage of their rated capacity.

The load proportioning is effected by use of an amplidyne regulator. Stated briefly, it operates in the following manner: A voltage proportional to the d-c motor armature current is compared with a voltage which varies inversely as the height of the slip regulator electrodes. The difference of these two voltage signals is applied to the field of an amplidyne generator. The armature of this amplidyne is connected to the armature of a separately excited shunt wound d-c motor driving the slip regulator electrodes up or down. This increases or decreases, respectively, the secondary resistance of the induction motor causing it to transfer load to or from the d-c motor until the two signal voltages are equalized, and the electrode motor stops.

The speed of the drive is maintained by means of an electronic-amplidyne regulator as follows: The drive is equipped with a permanent (Alnico) field tachometer generator. Its voltage is compared with a potentiometer connected across a regulated 125-volt d-c reference source. The position of this potentiometer determines the speed at which the drive operates.

The difference between the voltages of the tachometer generator, on the one hand, and the potentiometer, on the other hand, is applied to the grid of an electronic tube. Thus amplified, this voltage then is applied to the regulating field of an amplidyne exciter. The latter controls the voltage of the 1,000-kw d-c generator, and regulates speed to preset values throughout the speed range. Thus, if the tachometer voltage is lower than it should be, the drive is speeded up until the proper speed level is reached.

An amplidyne exciter also supplies the field of the 1,250-horsepower d-c motor. The field current of this motor is held constant for speeds between 0 and 260 rpm and is preset at lower values (by the master rheostat) for speeds between 260 and 570 rpm.

Power Factor Control

As will be appreciated readily, a large induction motor operating at light load would have a very poor power factor, drawing in this instance about 2,200 reactive kva. To bring this power factor up to 95 per cent minimum (lagging) for all conditions of operation, the synchronous motor on the motor generator set has a rated output at 50 per cent power factor, leading, and a power factor regulator was added to the control. Thus, when the induction motor is connected, the power factor regulator automatically comes into play, the leading kilovolt-amperes of the synchronous set counteracting the lagging kilovolt-amperes of the induction machine.

This regulator is responsive to the power factor in the incoming 4,800-volt feeder supplying both the 9,000-horsepower motor and the 1,000-kw set and controls the excitation of the 1,450-horsepower synchronous motor to maintain this power factor at the high value mentioned. Figure 6 shows schematically the

elements of this system and indicates that the 1,450-horsepower synchronous motor field actually was supplied by a conventional d-c exciter. This in turn is excited separately by an amplidyne exciter, the field of which is controlled by the power factor regulator.

Main Power Supply

The availability of an adequate power supply is an important consideration in determining the location of an installation of this type.

The power system must be selected to handle high intermittent loads corresponding to full power running of the tunnel, although total energy consumption is comparatively small. For example, the Cornell tunnel will have 20-minute peaks of approximately 10,000 kva which will occur when running the tunnel at top air speed. Such tests would consume perhaps ten per cent of the running time of the tunnel, while the majority of tunnel tests will have power demands of less than half this value. It will be remembered that the power required varies as the cube of the air speed; for example, a half speed test in the tunnel requires only one eighth the power of a full speed run.

An adequate power supply for the Cornell tunnel is provided by a short overhead stub feeder from the 115-kv 3-phase 60-cycle transmission line of the Niagara Lockport and Ontario Power Company. The laboratory end of the feeder line is terminated on an outdoor substation structure. This structure mounts 115-kv manually-operated disconnect switches, thyrite lightning arresters, and boric acid fuses, connected ahead of the transformer as shown by the schematic diagram in Figure 4. The transformer is a 3-phase oil-immersed unit rated 7,500-kva self-cooled, or 10,000-kva forced ventilated. It steps down the voltage from 115 kv to 4,800 volts. The ventilating fans are started automatically as a function of transformer temperature or whenever the tunnel fan drive is run above a predetermined speed.

The secondary winding of the transformer is throat connected through the wall of the wind tunnel motor room, at first floor ceiling height. After passing through a secondary metering room the 4,800-volt copper tube bus connection is carried up through the first floor ceiling directly into an incoming feeder unit of a metal-clad switchgear line-up. Figure 4 shows, diagramatically, the electrical layout of the 4,800-volt switchgear, the air circuit breaker ratings, and the provision for future extension of the system.

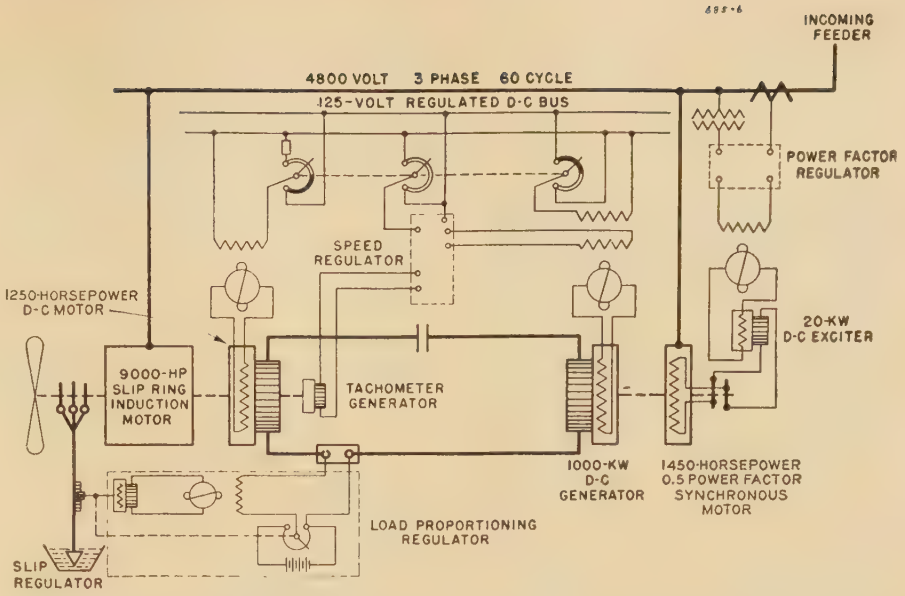

Figure 6. Elementary diagram showing speed-load, and power factor regulating features, incorporated in control of fan drive

Powered Model Testing

It has been pointed out how the force acting on a model airplane may be measured in the test section of the wind tunnel. The lift and drag, of course, are determined readily, but the behavior of the airplane under the resultant forces imposed by its power plant have not been determined. These forces may be provided by building a power plant in the model airplane. An electric motor is used in place of the gasoline engine. The model, of course, will be an exact scale model. If this model is one tenth the size of full-scale model, the propeller will be one-tenth the diameter of the actual propeller. Its speed, therefore, must be ten times the speed in order to maintain the model propeller tip speed at the same value as that of the full-scale propeller. If the rated speed of the actual propeller is 900 rpm, the model must run at 9,000 rpm, and power requirements are reduced inversely as the square of the scale.

The high frequency motors used for this purpose are quite special. Space limitations are usually quite severe. Consider, for instance, the one-tenth scale model. If the nacelle frontal diameter is 40 inches, the model can be but four inches. If the output of the full-scale engine is 1,800 horsepower, the model must be 18 horsepower. It is then no mean task to build an 18-horsepower motor with a diameter of four inches. Motors of this type are water-cooled; that is, the frame includes a water jacket. Air cooling is not practicable because the discharge of air produces a jet effect, and this would affect the accuracy of the results.

Model motors are almost without exception tailor-made. Speeds as high as 80,000 rpm at 0.1-horsepower $1^3/_4$-inch diameter have been provided, and horsepowers as high as 3,000 at 2,400 rpm at the other extreme with a diameter of 29 inches. Figure 7 shows some of these machines. A motor of 300 horsepower at 20,000 rpm also has been built, in the type of construction shown. Figure 8

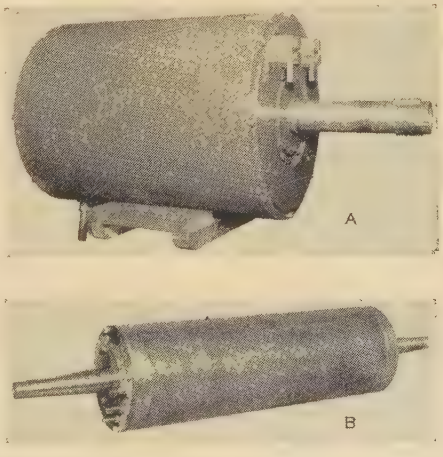

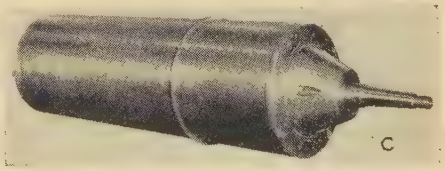

Figure 7. Water-cooled induction motors for use in airplane powered models

A. 1,000 horsepower, 2,200 rpm, 28 inches in diameter by 39 inches long

B. 200 horsepower, 5,000 rpm, 10 inches in diameter by 21 inches long

C. 250 horsepower, 10,800 rpm, 9 inches in diameter by 19 inches long

shows a counterrotation unit. This unit consists of two motors built in tandem; one has a hollow shaft. This is provided for counterrotation propeller studies.

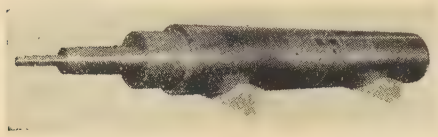

Figure 8. Contraturning water-cooled induction motor for airplane powered model

Hollow shaft unit (front) and solid shaft unit (rear) each are rated 75 horsepower at 3,000 rpm. Over-all diameter of motor is ten inches

Such speeds require a power supply at high frequency. These frequencies may be obtained with alternators, or frequency converters. Reference to Figure 9 will show, at the top, a 5-unit set driven by a 400-horsepower 1,200-rpm synchronous motor, operating from the 440-volt 60-cycle supply. The alternators *A* and *B*, each rated 156 kva, 440 volt, 60 cycle, furnish power to frequency converters *A* and *B*, respectively. The d-c generators *A* and *B*, each rated 100 kw, 250 volt, supply power to 140 horsepower 960/-1950-rpm d-c motors driving, respectively, these converters *A* and *B*. By varying the voltage of generators *A* and *B*, the speed of the converters *A* and *B* is adjusted. In this manner, the converters, receiving electric power at 60 cycles at their collector rings, change it to 60/450 cycles at their stator output. This output is used to operate the model motors at the required high speed. The voltage of this output is regulated by controlling the field of the corresponding alternator *A* or *B*.

With two independent frequency converters available, it is possible to operate them either in parallel, or separately, at different frequencies. This arrangement also readily permits studies in counterrotation of model motors and propellers. Counterrotation, as is well known, permits the use of smaller propellers, that is propellers with less sweep, and the torque on the airplane balances out. Although, in practice, contrarotating propellers have been driven, through gears, by a single power plant, the two independently adjustable power supplies described in the foregoing permit the study of counterrotation at various ratios between the two propeller speeds. The two independent power supplies also make it possible to perform a test in the tunnel at the same time as calibrating a second model motor in the dynamometer room.

The capacity of the adjustable frequency system is required to be adequate for operation of all powered models which may be tested in the tunnel. In selecting the specified capacity for each independent half of this system, the tunnel designers took into consideration the type and scale of airplane models to be tested. As will be appreciated from earlier discussion of powered models, the horsepower capacity of the model motor goes up but the frequency of its supply must come down, as the scale of the model is reduced. Also affecting the capacity of the adjustable frequency system required at various frequencies is the fact that both single propeller and multipropeller models will be tested. To satisfy these requirements the designers specified that each frequency changer should deliver 125 kw at 150 cycles and 50 kw at 450 cycles. The induction frequency converter designed to meet the first requirement has a capacity of 375 kw at 450 cycles. While each converter is inherently oversize at the high frequency, the driving motor of each frequency changer set can be selected to meet more exactly the requirements without excess capacity. The d-c driving motor of each frequency changer set is rated 140/75 horsepower 950/1,950 rpm at 250 volts. It is started from rest by generator voltage control, and operated in this manner up to 950 rpm. The frequency output of the converter which it drives varies correspondingly from 60 cycles to 250 cycles. Above this point the generator voltage is maintained at 250 volts, while the d-c motor speed is increased to 1,950 rpm by weakening its field. Frequency of the converter output varies correspondingly from 250 to 450 cycles. Under these conditions of operation the d-c motor load increases from 0 to 140 horsepower at 950 rpm, then decreases gradually from this speed to 75 horsepower at 1,950 rpm.

As pointed out in the foregoing, large model motors are required to operate at low frequency, and in order to keep the motor leads as small (and therefore as flexible) as possible it is normal to design the windings of these motors for a higher voltage per cycle than the higher speed smaller motors. On the other end of the range extremely high-speed small motors operating at, perhaps, 450 cycles, require a winding designed for low voltage per cycle in order to avoid excessively high voltages and mechanically fragile wire. Although national standards are not established, normal practice is to design model motor windings for operation at one of the following values of volts per cycle: 0.625, 1.25, or 3.75. This accepted practice imposes a further requirement, of wide voltage range, on the adjustable frequency power supply. To satisfy this requirement each frequency converter is arranged for reconnecting the stator winding to operate either as a single circuit delta or double circuit delta machine.

This power supply equipment is unique in that electronic control is used on the generator field, motor field, and the converter exciter (alternator) field. Such control is new, of course, only in this particular field, it having been applied successfully on wind tunnel main drives where very special characteristics were desired. It also has been used on many other industrial drives. This type of control saves space and lends itself readily to the extreme flexibility needed for a laboratory tool of this type.

A unique feature incorporated in this installation, and made possible by the electronic control, is a volts-per-cycle regulator of the converter output. This is of extreme value in the operation of model motors because of the need to operate nearer to the flux saturation point in this design of motor

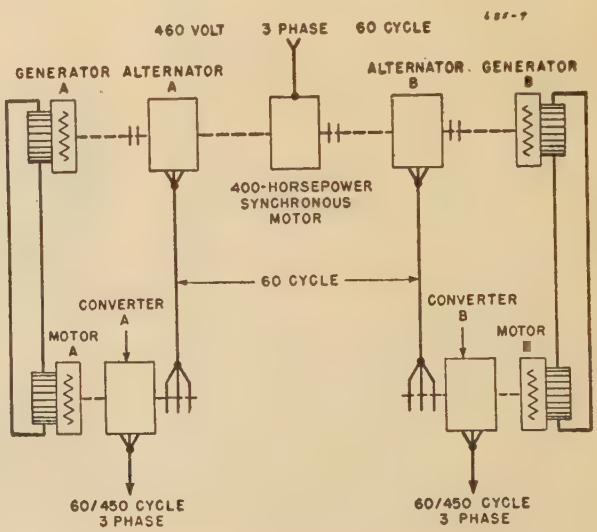

Figure 9. Schematic diagram of adjustable frequency supply system

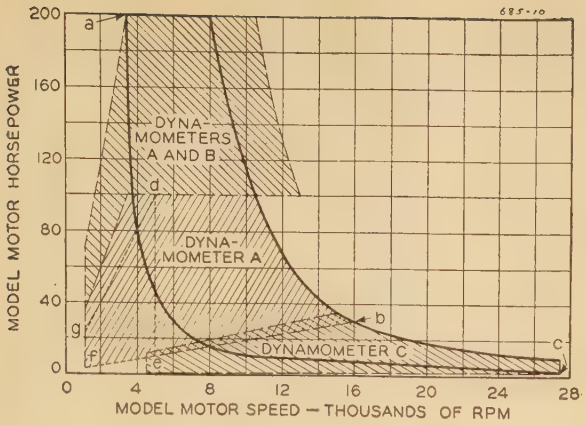

Figure 10. Horsepower-speed envelope of model motor maximum ratings to be tested on dynamometers, and coverage provided by dynamometers

than in more conventionally designed induction motors.

Model Motor Calibration

When testing a powered model in a wind tunnel it is, for aerodynamic reasons, necessary to control accurately the power delivered to the model propellers, according to the lifting force on the airplane model, as indicated by the wind tunnel balance system. The power input to the propellers may be determined either by direct torque and speed readings or by deduction from the electric power input to the model motors. The Cornell installation is equipped to use the latter method. In this method it is first necessary to calibrate the model motors for mechanical power output versus electric power input over the full range of torque and speed through which the motors can operate safely. A cradled dynamometer to perform this calibration for a specific motor presents no new problems but the selection, design, and manufacture of dynamometer equipment which will calibrate accurately all model motors to be used in one wind tunnel calls for many special features.

The selection of adequate capacity, range, and flexibility in the dynamometer installation must depend largely on the aerodynamicists' advice of what powered models can be tested in the tunnel, and his predictions of what will be tested. Based on such information, the design consultants for the Cornell tunnel defined an envelope of maximum horsepower and speed ratings of model motors to be calibrated on the dynamometer installation. This envelope is shown in solid lines in Figure 8. Specifications for calibrating equipment also required that, for any specific motor with maximum rating falling anywhere within the afore-mentioned envelope, the motor maximum torque be indicated accurately to within plus or minus one-quarter per cent. For a model propeller driving motor the maximum torque and maximum horsepower output will occur, of course, at maximum speed. For torque measurement below the maximum output it is desirable to indicate torque with an absolute error not greater than that corresponding to one-quarter per cent of the torque at maximum output of the motor on test.

It is also necessary to be able to calibrate all motors over a wide range of speed and torque. In Figure 10, a point *d* represents the maximum output of a motor for which calibration is required. The area *d, e, f, g,* indicates the full range of speeds and torques for which calibration of this motor is required.

Consideration of a few points in the envelope shown in Figure 10 gives a better conception of the total range of torques for which calibration equipment must indicate accurately. Consider the 200-horsepower 3,500-rpm model motor represented by point *a*. Its torque at maximum output is approximately 300 foot-pounds and it should be calibrated down to 30 foot-pounds torque. Then the 35-horsepower 16,000-rpm model motor is represented by point *b*. Its torque at maximum output is approximately 11.5 foot-pounds and it should be calibrated down to 1.15 foot-pounds torque. Finally the 2-horsepower 27,500-rpm motor is represented by point *c*. Its torque at this maximum rating is approximately 0.38 foot-pounds and it should be calibrated down to 0.038 foot-pound torque.

It is desirable to calibrate completely a model motor, throughout its speed and torque range, on a single dynamometer or, at most, on two dynamometers. On the other hand, the requirement of high accuracy over such a wide range of torques and speeds makes it desirable, from a design standpoint, to use several dynamometers to cover the range. In selection of machines to cover these requirements, consideration was given first to eddy current inductor-type dynamometers. In this design, mechanical power input to the dynamometer is converted into eddy current losses within the machine. These losses are removed from the machine by cooling water conducted to and from the cradled machine by flexible hoses. It is obvious that this type of machine can absorb only mechanical power and that the minimum torque which it can measure is that required to overcome friction and windage losses within the dynamometer. Although machines of this type are suitable for model motor testing from the standpoint of speed and required capacity, friction and windage are higher than desirable from the viewpoint of precision testing. Also, the necessity of cooling water hose connections is a handicap to attaining the required accuracy of torque measurement on this installation.

On the basis of using three dynamometers to cover the complete envelope of

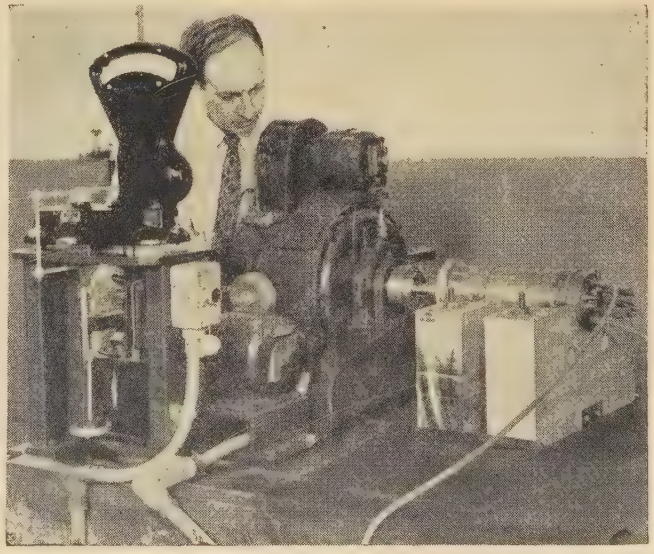

Figure 11. Water-cooled model motor being calibrated on a 35-horsepower 15,000/27,500-rpm induction-type dynamometer

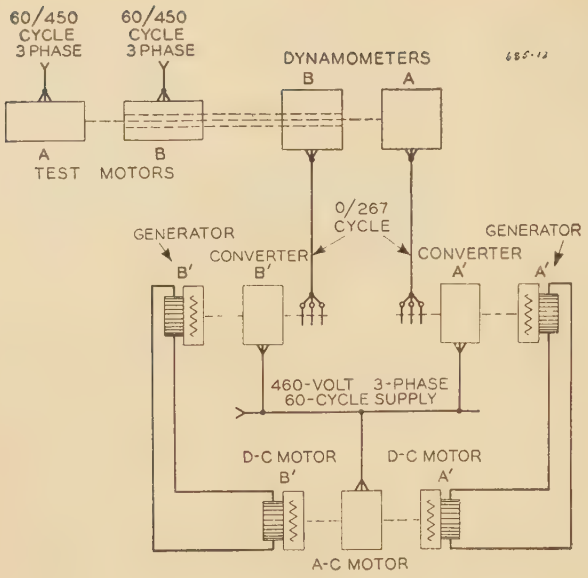

Figure 12. Schematic diagram of dynamometers and power absorption equipment connections

requirements, design studies indicated friction and windage losses to be in excess of the minimum torque values to be measured. Apart from any other considerations, this called for some means of supplying electric power to the stator of the dynamometer to compensate for the friction and windage losses. The substitution of induction-type machines in conjunction with adjustable frequency absorption equipment satisfies these requirements.

The induction-type dynamometer used consists of a squirrel cage induction motor with the stator cradled in oscillating trunnion bearings. Connections to the stator windings are made through mercury cups in order to minimize inconsistent interference which would reduce the precision of these instruments. These dynamometers act as induction generators, or in some cases (as explained later) as induction motors, and heat to be removed represents no more of a problem than in conventionally designed induction motors of equivalent rating. Ventilation is provided by constant speed blowers mounted on the cradled dynamometers, and connections are carried through mercury cups.

Reference to Figure 10 shows, by the shaded areas, the manner in which three cradled induction dynamometers were selected to cover the envelope of horsepower speed requirements for this installation.

Dynamometer A has a 100-horsepower absorption rating over a speed range of 3,500 rpm to 10,500 rpm. It is of solid shaft construction and when used, alone, will operate up to 16,000 rpm, at which speed the absorption capacity required is 30 horsepower. It also may be operated with dynamometer B either in tandem or for testing of contraturning model motor units. For either of the latter two mechanical arrangements, top speed is limited to 13,000 rpm, at which speed dynamometer A has the required capacity of 55 horsepower. Dynamometer B has a 100-horsepower absorption rating over a speed range of 3,500 rpm to 10,500 rpm. It is of hollow shaft construction, arranged for use with dynamometer A, either in tandem or for testing of contraturning model motor units. Under either of these conditions it may be operated up to a maximum speed of 13,000 rpm, at which speed it has the required capacity of 55 horsepower.

Figure 13. Operators' console in control room of Cornell variable density wind tunnel

Dynamometer C has a 35-horsepower absorption rating at 15,000 rpm and is capable of operating up to 27,500 rpm, at which speed it has more than the required capacity of 10 horsepower. It is of solid shaft construction. Figure 11 shows this dynamometer installation.

Reference to Figure 12 will show the manner in which the 100-horsepower dynamometers are connected electrically to feed energy back to the 60-cycle system. D-c motors A' and B' each are rated 60 kw (absorption), 250 volt, 1,800 rpm, and are driven by a 125-horsepower 440-volt 60-cycle squirrel cage induction motor. Induction frequency converters A' and B' each are rated 70-kw absorption and each connected to a 75-horsepower (input) 250-volt 500/1,800-rpm d-c generator. Each of the dynamometers A and B are of 2-pole construction and their synchronous speed frequencies corresponding to a speed range of 1,125 to 16,000 rpm are between 18 and 267 cycles. The converters A' and B' are designed to receive power on the slip rings over this frequency and, by varying the speed of d-c generators A' and B', deliver power from the stator to the 60-cycle system. The speed of generators $A'B'$ is changed between 0 and 500 rpm by armature voltage control. Above this value, armature voltage is maintained at 250 volts and speed is increased to 1,775 rpm by field weakening. At this point frequency on the converter slip rings is 267 cycles corresponding to 60 cycles at the stator terminals.

Consider the method of operating this system to calibrate test motor A on dynamometer A. The constant speed set, of

which motor A is a part, first is started by connecting the 125-horsepower a-c motor to the 440-volt 60-cycle line. Converter A' with stator winding connected to the 60-cycle line then is started from the d-c end in the same direction of rotation as its magnetic field. The speed of this set is raised by armature voltage control until the frequency on the slip rings of the converter is about five or ten cycles. At this point dynamometer A, with its model motor mechanically connected but electrically isolated, is connected electrically to frequency converter A'. The frequency applied to dynamometer A then is raised by first lowering the speed of the converter close to zero revolution per minute, then reversing it and raising the speed in the opposite direction. When the desired minimum test speed for the model motor is reached, its supply frequency will be matched, and the motor will be connected to its supply. Incidentally, this procedure for connecting the model motor to its supply also is followed for a model motor in the tunnel. In this case the model propeller with its motor is "windmilled" by the tunnel air stream, and the power supply must be matched to the motor speed before connecting it to the motor. In order to load the "test" motor, while its speed is held constant by its power supply, it is merely necessary to slightly lower the frequency at the terminals of dynamometer A. This is accomplished by vernier adjustment of the field of motor A.

The 35-horsepower dynamometer is operated in a similar manner by connecting it to a suitable adjustable frequency source.

Conclusion

These are some of the problems to be considered in the application of electric equipment for an installation of this magnitude. There are, of course, many others. However, this indicates to some degree their nature and complexity. More than that, it demonstrates how important is the correct selection of electric equipment.

Other laboratory facilities will have comparable problems, but electrical engineers will find that all demand the same approach. A careful analysis must be made, a practical, thorough, and detailed study of the performance expected by the scientists who are going to operate the new instrument.

Reference

1. Aerodynamic Theory (book), Durand. Volume 3, division 1.

F-3 Lead Alloy—An Improved Cable Sheathing

L. F. HICKERNELL
FELLOW AIEE

C. J. SNYDER
NONMEMBER AIEE

OPERATING EXPERIENCES have demonstrated that the attainment of good service reliability of most electric power cables has become substantially more a function of the characteristics of the sheath than of the insulation. Modern underground installations of impregnated-paper-insulated, lead-covered power cable include

1. Solid-type cable with
(*a*). Compound-filled joints without reservoirs.
(*b*). Oil-filled joints with reservoirs.

2. Oil-filled cable operated at 10- to 15-pound gauge pressure.

3. Gas-filled (or pressure) cable operated at
(*a*). Low pressure (10- to 15-pound gauge).
(*b*). Medium pressure (24- to 40-pound gauge).
(*c*). High pressure (150- to 300-pound gauge).

Aerial installations, in which the cable is suspended by rings to a messenger strung between poles, consist generally of the same basic cable designs.

Depending upon the type of cable and installation, modern requirements for lead sheath include some or all of the following properties in addition to the time-honored criteria of strength, ductility, hardness, "cleanliness," and concentricity:

1. Resistance to slow bending fatigue resulting from movement in the manholes caused by expansion and contraction during daily load cycles.

2. Resistance to creep (expansion) at low internal pressures (10- to 30-pound gauge).

3. Resistance to burst caused by high internal pressures developed at the bottom of slopes and vertical risers, in pressure-type cable systems, and in solid-type cable systems having reservoirs of oil, connected to the joints.

4. Resistance to abrasion caused by installation and movement in ducts.

5. Resistance to vibration fatigue caused by traffic on any type of installation and by wind on aerial cable.

6. Stability from age-hardening or self-annealing so that the foregoing properties are retained throughout the life of the cable and so that the cable can be withdrawn from ducts and reinstalled without cracking the sheath.

7. Workability, which facilitates melting and extruding as sheath with sound welds and uniform composition.

8. Corrosion resistance.

Some commercial grades of lead have given satisfactory service in a great many installations, especially up to about 20 years ago. The sheaths have become increasingly the limitation[1–5] on the serviceability of power cable with the advent of the following:

1. Decrease in viscosity of impregnating compound.

2. Use of oil reservoirs connected to joints.

3. Improvement in thoroughness of insulation impregnation.

4. Increase in maximum allowable temperatures for normal operation.

5. Establishment of still higher temperatures for emergency operation.

Item 5 was the last to occur, and its use has accentuated the need for an improved cable sheathing.

Numerous lead alloys have been developed to overcome these difficulties, but each, it seems, is lacking in one or more important property.

Antimony alloy (0.75 to 1.0 per cent) has poor creep resistance[6] and undergoes change in properties with age,[7] including loss in ductility.

Tin alloy (two per cent) has relatively poor creep resistance[6] and about the same or slightly better resistance to vibration fatigue than the best commercial grades of lead (refer to Figure 13).

Cadmium-antimony and cadmium-tin alloys, known as BNF alloys, offer extrusion difficulties, age-harden, and have poor creep resistance.[8]

Calcium alloys (0.025 and 0.031 per cent) are difficult to extrude (very drossy) and undergo slow and serious age hardening, which has caused troubles to develop in a few years of service because of brittleness and early cracking in the manholes.[9]

Paper 46-115, recommended by the AIEE committee on power transmission and distribution for presentation at the AIEE summer convention, Detroit, Mich., June 24–28, 1946. Manuscript submitted April 29, 1946; made available for printing May 8, 1946.

L. F. Hickernell is chief engineer, and C. J. Snyder is engineer in charge, metallurgical laboratory, Anaconda Wire and Cable Company, Hastings-on-Hudson, N. Y.

The authors are indebted to many of their engineering associates who have assisted in the test program and preparation of this paper and wish to make specific acknowledgments to A. A. Jones, Anaconda Wire and Cable Company, and G. E. Johnson, International Smelting and Refining Company.

Tellurium alloy (0.05 to 0.10 per cent) tends to segregate in the welds during extrusion and, according to unpublished data, has poor creep resistance.

An Improved Lead Alloy

To satisfy the need for a lead alloy having the desired improved properties, the Anaconda organization instituted a research program to develop a suitable alloy. The best material developed in this program is known as F-3 lead alloy.[10] It is composed of arsenical lead containing small amounts of tin and bismuth. This new material when suitably hardened by heat treatment also has physical properties which may meet the requirements set for medium-pressure gas-filled cable.[11] The sheaths are characterized by their strong tough welds, outstanding resistance to bending fatigue, excellent creep resistance, and bursting strength.

Chemical Composition

The chemical composition used for the F-3 alloy pig metal is

Arsenic (As)	0.15 per cent
Tin (Sn)	0.10 per cent
Bismuth (Bi)	0.10 per cent
Copper (Cu)	Minimum
Antimony (Sb)	Minimum
Lead (Pb)	99.65 per cent

This alloy is extruded in conventional equipment with the same technique employed in handling commercial grades of lead. It is a "clean" alloy not subject to excessive drossing associated with some other lead alloys. This feature results in strong welds and facilitates the making of wiped joints. Beginning early in 1945, a number of large orders of paper-lead cable with F-3 alloy sheath have been produced, shipped, and installed without difficulty.

Bending Resistance

The current carried by a power cable usually varies in a daily load cycle which causes a daily variation in temperature. This variation produces longitudinal expansion and contraction of the cable which accumulates in the manholes where expansion loops are provided. The accompanying daily bending of the cable in the manholes has, in some cases, broken the sheaths. Repairs have not proved very satisfactory, and in many cases replacement of lengths of perhaps 300 to 500 feet of cable has been necessary. For many installations, current-carrying capacity and life of the cable are determined more by the ability of the sheath to withstand such slow bending than by the ability of the insulation to withstand the voltage.[3,5]

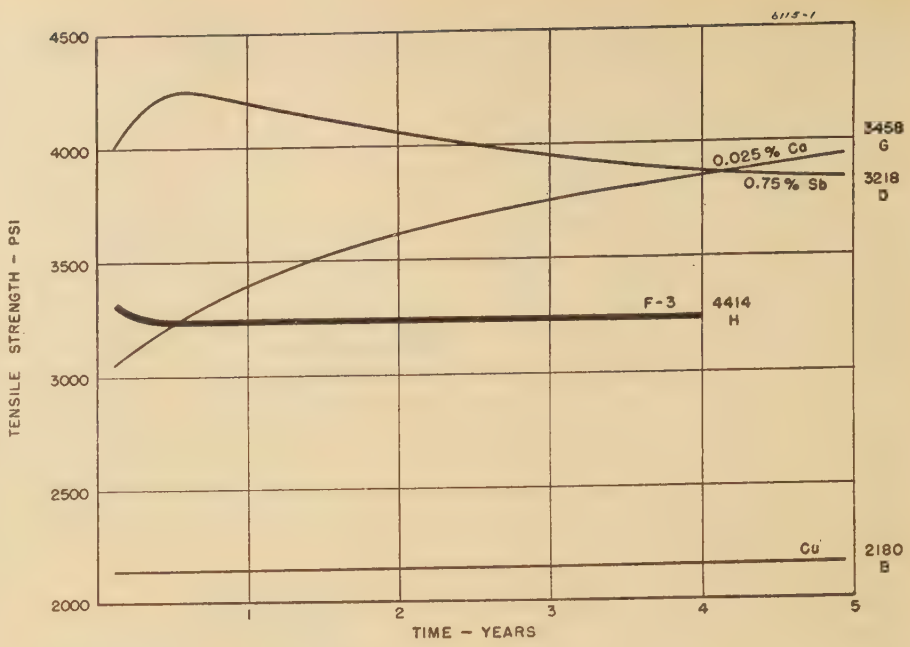

Figure 1. Age hardening
Room temperature

Tests have been conducted on the bending of various types of cable at room temperature and elevated sheath temperature. The results obtained on accelerated cyclic bending, 0.5-inch cable movement at each duct mouth, indicate that the life of F-3 sheath is between three and four times the life of copper-bearing lead sheaths on the same kind of cable.

Abrasion Resistance

A large majority of underground cables in this country are pulled into ducts. In recent years increasingly longer lengths and larger and heavier cables have been used. In some cases as much as seven tons or more of cable have been installed in one pull. Irregular ties or pebbles in the ducts cause scoring of the sheath. Also, it is subject to bruises in handling and working around it. After it is installed, expansion and contraction with daily changes in temperatures cause continual movement during the life in service.

In aerial cable, abrasion resistance is needed, not only to withstand the effects of installation and of cable movement caused by expansion and contraction, but also to minimize cutting of the sheaths at the rings which support the cable.

The most suitable indication of abrasion resistance is the hardness test, although it is recognized that some factors other than those involved in such tests are influential. The relative hardnesses of various lead and lead alloy materials are shown in Table I.

These hardness data apply to extruded material which has aged at room temperature for about three to eight months. Generally, lead alloys grow appreciably harder with age, but the hardness of F-3 alloy remains about the same.

While hardness is desirable to obtain abrasion resistance, the harder materials usually lack ductility and break under tensile stress with very small elongation. Age-hardening materials lose generally in ductility with age, becoming in some cases too brittle for use. The new F-3 alloy has both hardness and good ductility which is retained with age, as is shown later.

Long-Time Aging

The F-3 alloy does not harden with age, as calcium, antimony, and to some extent tin alloys do. Instead of an increase in tensile strength, a slight decrease occurs, as is shown in Figure 1. These data were obtained from tests of water-quenched tubes which were aged and tested at room temperature. Similar results were obtained in tests of sheath removed from cable.

Materials which harden appreciably with age lose ductility, a fact which is

Table I. Hardness of Lead and Alloys
Room Temperature

Sample Number	Material	Brinell Hardness Number
2,264	Desilverized lead—A	3.9
2,180	Copper lead	4.5
2,296	Chemical lead	4.5
3,458	0.025 per cent calcium	8.1
4,414	F-3 alloy	8.4
4,212	2 per cent tin	9.0
1,228	0.031 per cent calcium	10.4
3,218	0.75 per cent antimony	10.4

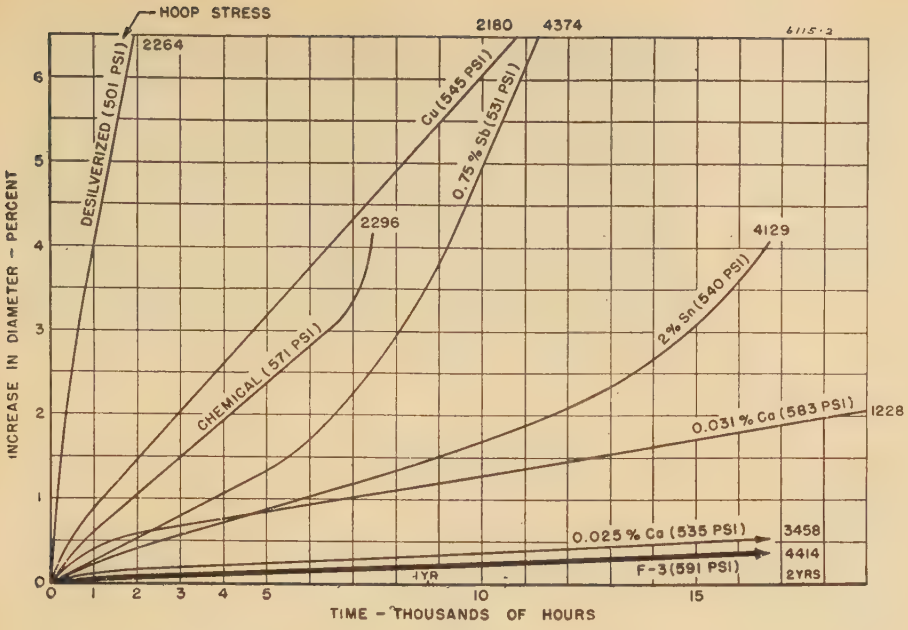

Figure 2. Creep of tubes
61-pound gauge, room temperature

shown by decreasing amounts of elongation to fracture in tensile tests of strips removed from cable sheaths. F-3 alloy has given an elongation to fracture of about 23 to 30 per cent throughout the four or five years during which tests have been made. Further information on this characteristic is given under "Fracture and Ductility."

Creep Resistance

Resistance to creep under tensile stress is especially beneficial for sheaths on oil-filled and gas-filled cables and on solid-type cable having a hydrostatic head of oil. In all of these the continuous internal pressure tends to expand the sheath. Under relatively low stress for periods of years, the safe expansion of commercially pure lead sheaths is much less than the 30 to 50 per cent obtained to fracture in short-time tensile tests. It is of the order of three to five per cent. For most of the alloys the elongation that can be expected without fracture is less than that for lead in both short-time and long-time tests.

In solid-type cable having no additional oil available, the sheath is expanded by bending during installation and by thermal expansion of the conductors and insulation within the sheath. Since lead has little elasticity, a large part of the expansion remains as permanent distension of the sheath, leaving a gap on the inside. Void spaces thus are produced which are likely to appear in the insulation. Such voids are detrimental to the electric strength of the insulation in high-voltage cables. Thus good creep resistance is beneficial in obtaining long life for both the sheath and the insulation.

Tube or sheath specimens 15 inches long and without cable inside were sealed with compression fittings and subjected to constant internal oil pressures.[12] The creep (that is, increase in tube diameter) was measured by a special type Al-SR4 strain gauge[13] over a period of from one to five years. This method was found capable of measuring changes in diameter in the order of 0.002 per cent. Test lines were operated at gauge pressures of 61, 42, and 35 pounds at room temperature and at 35 pounds at 65 degrees centigrade.

Figure 3. Creep of tubes
35-pound gauge

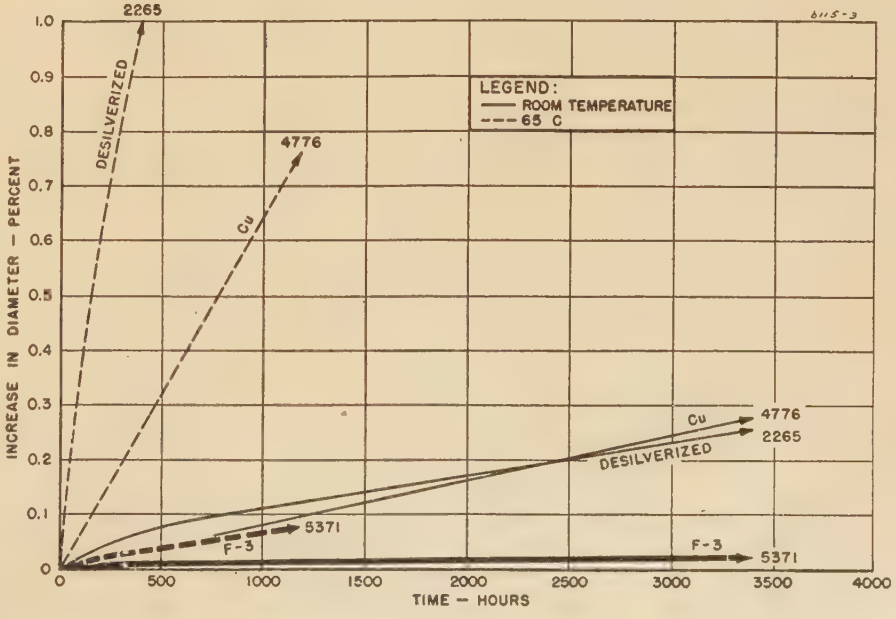

Typical data, selected from the 105 samples tested, are shown in Figures 2 and 3 in diameter with time. From Figure 4 in which the data are shown as creep rates, it is evident that F-3 alloy has a creep resistance at room temperature about 45 times that of copper-lead and 25 times that of chemical lead at a stress of about 500 to 600 pounds per square inch and at least equal to any heretofore known lead-alloy sheath material. The curves in Figure 3 for creep at 35 pounds (approximately 300 pounds per square inch hoop stress) indicate that F-3 alloy has about 30 times the creep resistance of copper-lead at room temperature and about ten times that of copper-lead at 65 degrees centigrade.

Fracture and Ductility

Bursting Strength of Tubes

Tube specimens 15 inches long were tested at various stresses and the time required for failure obtained as described by Bassett and Snyder.[12]

Figure 5 shows the data obtained for F-3 alloy and other materials. (This figure is essentially the same as Figure 7 of reference 12 with a few deletions and the addition of new data.)

Data from fracture tests of lead show customarily that at low stresses, such as 400 and 600 pounds per square inch, lead alloys do not have as much advantage over common lead and copper-lead as their tensile strengths would indicate. At higher stresses, such as 1,000 and 1,500 pounds per square inch, the alloys, of course, are better. Figure 5 shows that in these tests at room temperature, F-3 alloy has bursting characteristics different from other alloys. It seems to retain its strength ratio to copper-lead equally at all stresses.

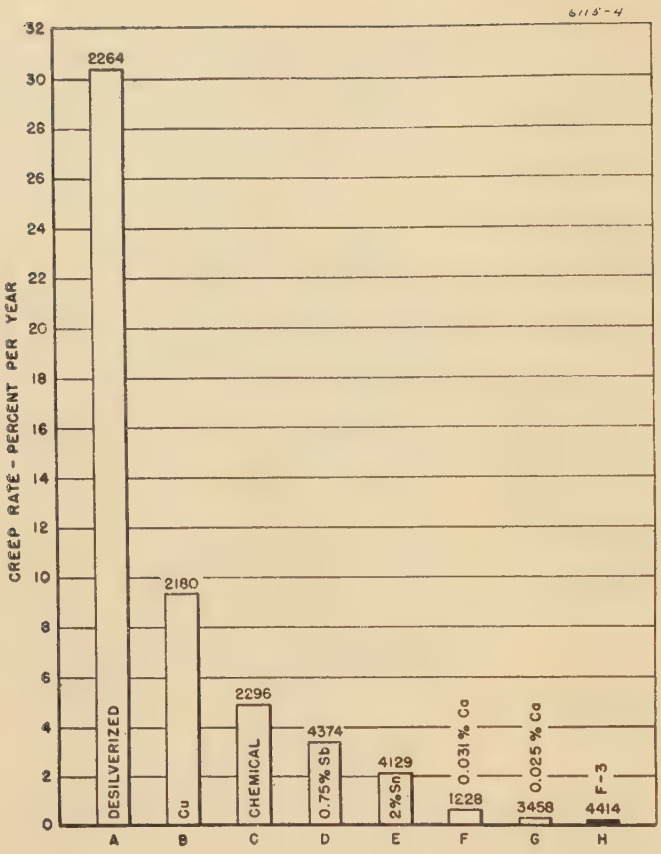

Figure 4. Creep rate of tubes

61-pound gauge, room temperature

prising the total footage from one to three complete lead press charges, were conducted to locate the weakest part of the length. These samples were sealed on the ends with compression fittings and subjected to continuous 85-pound air pressure until failure. After the initial failure, ten feet of pipe from the finish of the charge was resealed on the ends and the test continued until final failure.

Table II summarizes the data thus obtained.

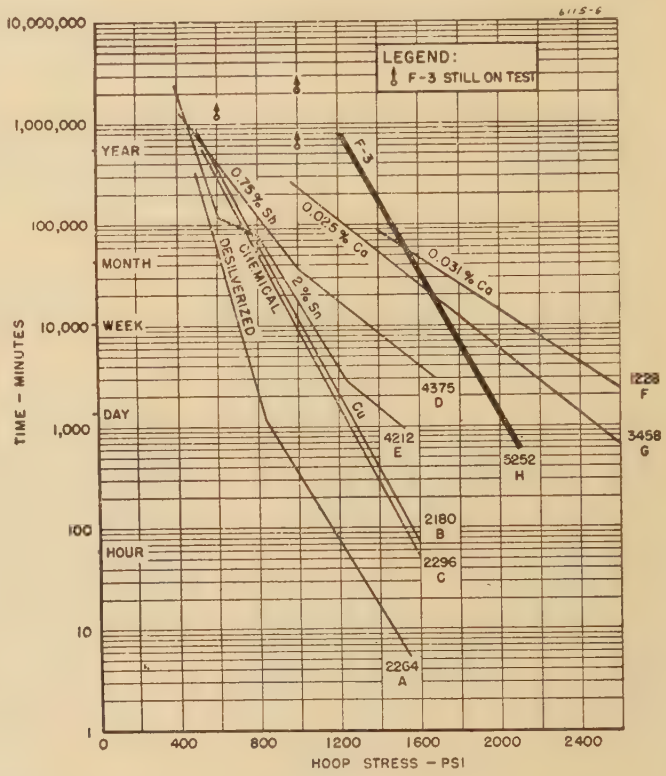

Figure 5. Bursting strength of tubes

Room temperature

This behavior leads to another point, that of the type or appearance of the failure. It has been observed that when lead fails under static long-time load at stresses up to approximately 30 per cent of ultimate strength (too low to cause appreciable plastic flow), the fractures are intercrystalline.[12,14,15] This type of failure is referred to as "stress cracking." The types of fracture produced by burst tests for commercial grades of lead and some alloys were described by Bassett and Snyder.

Figures 6, 7, and 8 show the type of failure obtained with F-3, calcium, and tin alloys. Other illustrations appear in reference 12.

No sample of F-3 alloy has failed in these bursting tests at stresses of 1,000 pounds per square inch or less, even though specimens have been on test for over four years. Specimens tested at 1,250 pounds per square inch have failed without stress cracking.

Data presented in Figure 9 indicate that F-3 alloy retains its good ductility in low-stress long-time tests as well as in short-time tests.

Bursting Strength of Long Lengths

Burst tests on long lengths (150 to 300 feet) of F-3 alloy pipe, each length com-

Table II. Bursting Strength of Full-Charge Lengths of Pipe

Approximately 850 Pounds Per Square Inch, Room Temperature

Material	Approximate Time to Failure, Months: Weakest Point of Full Length	Approximate Time to Failure, Months: Uniform 10 Feet at End of Charge	Location of Weakest Point of Full Length
Copper-lead	1	3	Charge weld
Tin alloy	1/2	3	Charge weld
Antimony alloy	1	9	Charge weld or where deformed by mechanical damage
Calcium alloy	1/2	24	Charge weld or where deformed by mechanical damage
F-3 alloy	12	No failure after four years	Adjacent to press-stop mark

Stress–Strain

Nonferrous metals including lead do not behave elastically; that is, they do not follow Hooke's law up to a certain stress point, the yield point. However, they do exhibit a certain degree of elasticity on short-duration tests. Elasticity, if present in a cable sheath, would be of some practical importance in producing some recovery in the radial expansion of the sheath after the initial high pressure developed during the start of a load cycle.

Test specimens 15 inches long like those used for burst tests were fitted with SR-4 strain gauges and subjected to repeated pressure cycles of successively increasing magnitude. The strain and recovery during each test cycle were noted and plotted in Figures 10 and 11. Each point on the curves represents about one minute elapsed time. The figures show that copper-lead undergoes rapid strain at stresses above about 500 pounds per square inch hoop

Figure 6. Burst failure of F-3 alloy

Ductile break (magnified four times), sample 5,252
1,250 pounds per square inch, 10,400 hours, 18.4 per cent expansion

stress, whereas F-3 alloy withstood about three times this stress to produce the same amount of permanent set.

Vibration Fatigue

Flattened-strip specimens were machined with reduced sections and carefully calibrated for stress calculations. These were flexed in a vibrating-reed Bell-Laboratories-type machine at 750 cycles per minute, the deflection being varied to obtain different stresses in duplicate specimens.

Figure 12 shows the data as stress versus number of cycles (S/N) curves. The resistance to vibration fatigue of F-3 alloy is much superior to that of copper-lead and also superior to that of antimony and tin alloys which have been used commonly for sheaths on overhead power cables.

Corrosion

Laboratory corrosion tests indicate that F-3 alloy has resistance to ground water and acidic fluids equivalent to that of most high-purity leads.[16] It has been observed that F-3 alloy sheaths are brighter and remain brighter in ordinary atmospheric exposure than copper-lead.

In general, it has been found that where corrosion is experienced, mitigating measures are required regardless of the chemical composition of the sheath.

Joint Sleeves

If the joints on impregnated-paper-insulated cable are completely filled with compound and sealed without any provision for thermal expansion, then internal pressures developed in the cable during load cycles will appear also in the joints. Joint sleeves are usually considerably larger in diameter than the cable sheaths, and hence for given internal pressures, the hoop

Figure 8. Burst failure of two per cent tin alloy

Intercrystalline break (magnified four times), sample 4,212
1,000 pounds per square inch, 216 hours, 1.8 per cent expansion

Figure 7 (above). Burst failure of 0.025 per cent calcium alloy

Intercrystalline break (magnified four times), sample 1,867
1,500 pounds per square inch, 292 hours, 1.7 per cent expansion

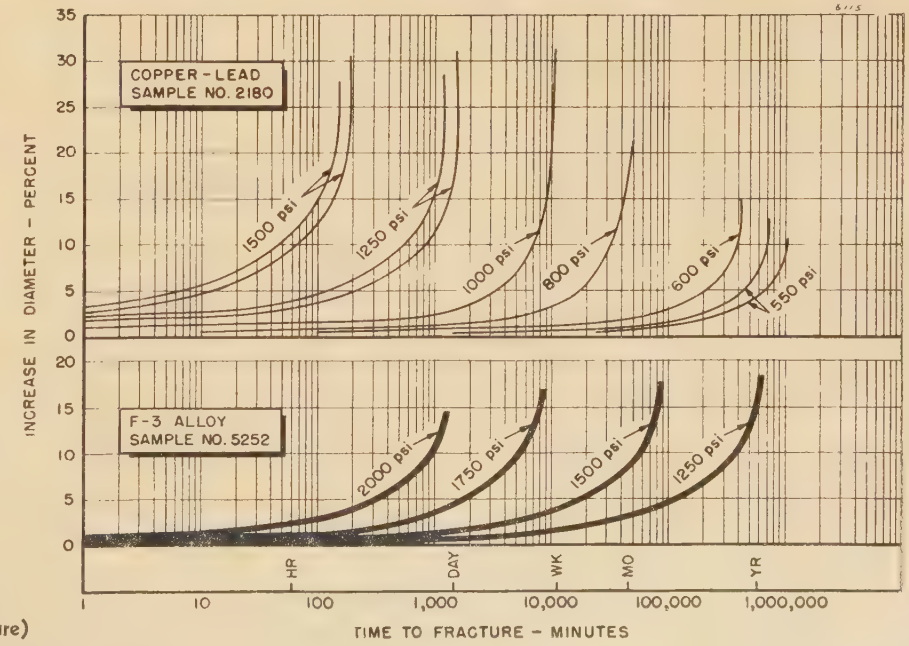

Figure 9. Ductility of tubes (room temperature)

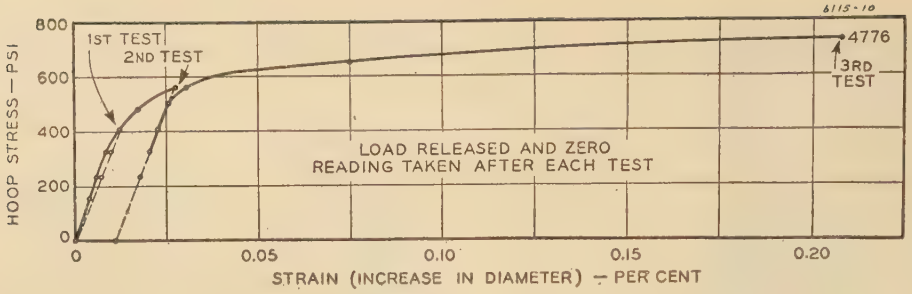

Figure 10. Stress–strain, copper-lead (tubes, room temperature)

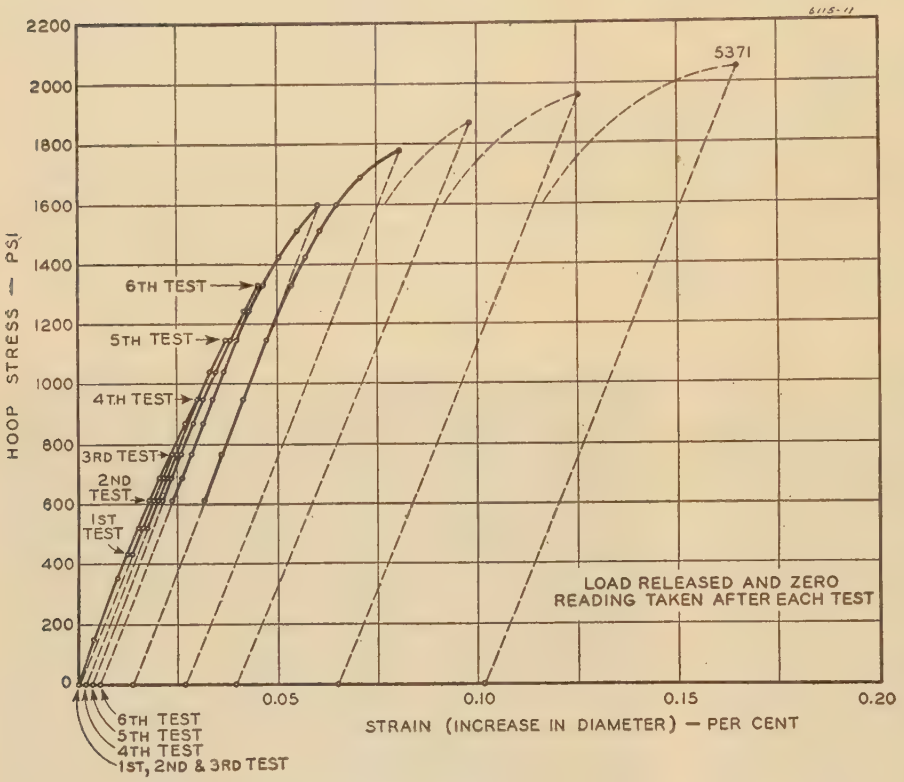

Figure 11. Stress–strain, F-3 alloy (tubes, room temperature)

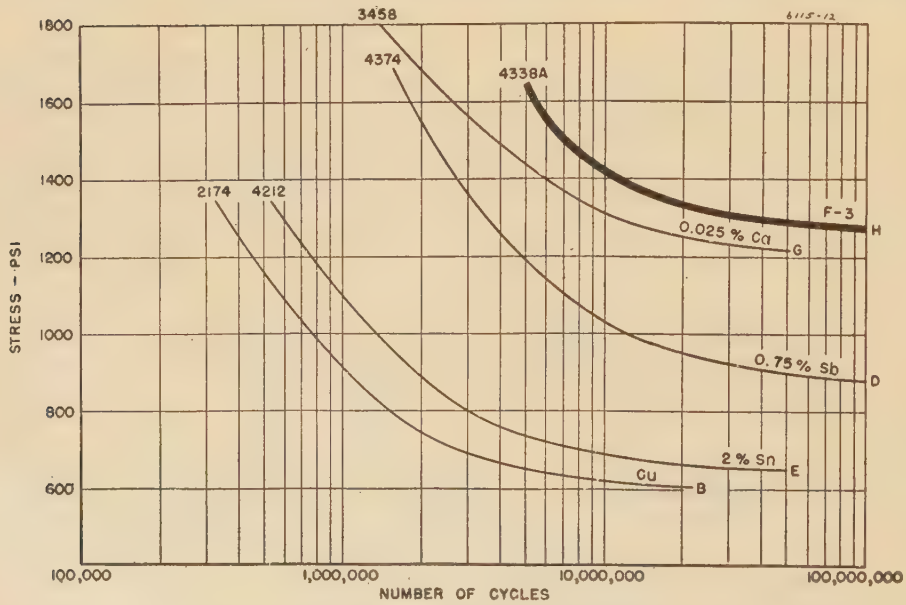

Figure 12. Vibration fatigue of flat strips

750 cycles per minute, room temperature

stresses in the sleeves are usually considerably greater than those in the sheaths unless the sleeves are made appreciably thicker.

With F-3 alloy for the cable sheath, having somewhat greater strength and considerably lower creep rate than lead sheaths, higher internal pressures can be expected in the sheaths and joint sleeves. It will become desirable, therefore, either to use material stronger than lead for the joint sleeves or to use some method of reinforcing the joint casing. Thus it may be quite desirable to have the joint sleeves made of F-3 alloy as well as the cable sheaths. Test joints have been made from extruded F-3 alloy sleeves and no difficulty was experienced in beating the ends or in wiping the joints.

Advantages of Improved Cable Sheathing

For some underground cables, the life in service is limited by the ability of the sheath to withstand repeated bending in the manholes caused by cable movement. In such cases the use of F-3 alloy will permit either higher loading for equal life of the cable or longer life with equal loading. For many installations, changes in the system or other factors make it more economical to obtain greater usage of the investment rather than to obtain much greater life.

The lower creep rate of the F-3 alloy will permit the use of higher internal pressures. This is especially beneficial on either oil-filled or gas-filled cables. A limiting hoop stress of 125 pounds per square inch has been established for design purposes for copper-bearing lead sheaths. This limitation restricts the internal pressures for oil-filled cables with standard sheath thicknesses to about 14-pound gauge for 2 $^1/_2$-inch cable or 12-pound for 3 $^1/_2$-inch cable. To withstand higher internal pressures, lead sheaths must be reenforced with layers of paper and copper tapes which require a costly double-sheath construction.

With F-3 alloy sheath, the equivalent stress for a similar creep rate is about 200 to 300 pounds per square inch based on data for tube specimens. If the limit is tentatively set at 200 pounds per square inch then with standard thicknesses the internal pressures can be increased safely to 22.5 pounds for 2 $^1/_2$-inch-thick cable or 19 pounds for 3 $^1/_2$-inch cable. By increasing the sheath thicknesses 40 or 50 mils, it becomes possible to use single sheaths on pressure-type cables with internal pressures of 25- or 30-pound gauge. This would avoid the use of double-sheath construc-

tion on, for example, some medium-pressure gas-filled cables.

Since cable sheathing must withstand the working and wear involved in installation which produce gouging and scoring of the outer surface, the thicknesses for most solid-type cables should not be reduced much from the present standard thicknesses. The sheath must be sufficiently thick to have long life in spite of such damages. The present standard thicknesses for lead have been evolved from long experience and are known to be adequate for normal conditions of use. At least until more experience is obtained in the use of F-3 alloy, the same thicknesses as for lead are recommended. For special conditions, where in the past extra-thick sheaths of ordinary lead have been required, the use of F-3 alloy will warrant a reduction.

Conclusions

1. A new cable sheath alloy of arsenical lead (F-3 alloy) has been produced. It has been successfully applied in manufacture to cable which has been installed in commercial lines.

2. F-3 alloy has been shown to have much better properties for power cable sheaths than any of the materials previously tried.

3. With this new type of sheath, the larger cables can carry higher loads without shortened life caused by cracking of the sheaths in daily bending in the manholes.

4. The limiting internal pressures will be appreciably higher than for lead sheaths, which may permit the use of single sheaths on some pressure-type cables where with lead the more costly double-sheath construction is required.

5. Since this alloy is harder than commercially pure lead, a reduction in troubles in service caused by mechanical damages can be expected.

References

1. Lead Sheath Investigations in Chicago, **Herman Halperin.** Transmission and Distribution Committee, Edison Electrical Institute, October 24, 1934, and Edison Electric Institute *Bulletin*, November, 1934 page 365.

2. Maximum Safe Operating Temperatures for 15-Kv Paper-Insulated Cables, **C. W. Franklin, E. R. Thomas.** AIEE Transactions, volume 58, 1939, October section, pages 556–62.

3. Load Ratings of Cable, **Herman Halperin.** AIEE Transactions, volume 58, 1939, October section, pages 535–53.

4. Load Ratings of Cable—II, **Herman Halperin.** AIEE Transactions, volume 61, 1942, pages 930–42.

5. Cycle Movement of Cable—Its Causes and Effects on Cable-Sheath Life, **Clement S. Schifreen.** AIEE Transactions, volume 63, 1944, pages 1121–30.

6. Investigation of Creep and Fracture of Lead and Lead Alloys for Cable Sheathing, **H. F. Moore, B. B. Betty, C. W. Dollins.** *Bulletin 306*, August 19, 1938, University of Illinois Engineering Experiment Station, Urbana, Ill.

7. Effect of Small Quantities of Third Elements on Aging of Lead-Antimony Alloys, **E. E. Schumacher, G. M. Bouton, L. Ferguson.** *Industrial and Engineering Chemistry*, volume 21, 1929, page 1042.

8. Properties of Lead and Lead Alloy Cable Sheaths, **J. C. Chaston.** *Electrical Communications*, International Standard Electric Corporation, volume 13, number 1, July 1934, page 31.

9. Age Hardening Proves Fatal to Lead-Alloy Cable Sheaths, **G. B. McCabe.** *Electrical World*, October 13, 1945, page 104.

10. U. S. Patents 2,300,788 and 2,375,755; others pending.

11. Low-, Medium-, and High-Pressure Gas-Filled Cable, **G. B. Shanklin.** AIEE Transactions, volume 61, 1942, October section, pages 719–26.

12. The Testing of Lead Cable Coverings, **W. H. Bassett, Jr., C. J. Snyder.** *ASTM Proceedings*, American Society for Testing Materials, volume 40, 1940, page 910.

13. The SR-4 Bonded Resistance Wire Strain Gage, *Sales Bulletin 179*, Baldwin Southwark Division, Baldwin Locomotive Works.

14. The Creep and Fracture of Lead and Lead Alloys, **H. F. Moore, B. B. Betty, C. W. Dollins.** *Bulletin 272*, February 5, 1935, University of Illinois, Engineering Experiment Station, Urbana, Ill.

15. Fracture and Ductility of Lead and Lead Alloys for Cable Sheathing, **H. F. Moore, C. W. Dollins.** *Bulletin 347*, October 19, 1943, University of Illinois, Engineering Experiment Station, Urbana, Ill.

16. The Corrosion of Underground Cables, **W. G. Radley, C. E. Richards.** *Journal*, Institution of Electrical Engineers, London, England, volume 85, December 1939, page 685.

Electrical Accuracy of Selsyn Generator–Control Transformer System

HAROLD CHESTNUT
ASSOCIATE AIEE

THE military requirements for high accuracy position control systems have placed emphasis on the need for a voltage signal source which can indicate electrically a mechanical shaft position. In addition this signal source must have high accuracy, marked dependability, and the capability of continuous mechanical rotation. A modification of the conventional Selsyn generator-motor system[1] has been developed and used extensively to fill this need.

This system,[2] shown schematically in Figure 1, consists of a generator in which a single phase a-c field is established with its space orientation determined by the position of the rotor, electrically connected to a control transformer in the rotor winding of which is induced a similar alternating voltage whose magnitude and polarity depend on the relative position of this rotor with respect to that of the generator. Ideally the control transformer rotor voltage versus the difference in the rotor angular position characteristic is a sinusoidal one, as is shown in Figure 2.

In effect, the presence of the single-phase magnetic field in the generator rotor induces voltages in the three stator windings of the generator. These voltages impressed on the three stator windings of the control transformer produce currents there which establish a single-phase magnetic field in the air gap of the same space position as that of the generator rotor. Depending on the actual orientation of the control transformer rotor with respect to the generator rotor, the voltage induced in the rotor winding may vary from a maximum of one polarity through zero to a maximum of the other polarity. If the control transformer rotor is positioned so as to maintain zero voltage across its terminals, it then maintains a fixed angular relationship to the generator rotor. Hence, it is possible to position the control transformer shaft properly with respect to the generator position by maintaining zero voltage on the control transformer terminals.

Although this system inherently has a high accuracy of the order of 0.3 degree, it is not completely error-free. To design Selsyn systems which are more accurate, it is necessary therefore to determine the effect of various factors which can contribute to electrical errors. The conditions under which errors are to be considered here are

1. Stationary orientation of both machines. This condition also explains the predominate error phenomenon from standstill up to speeds of three or four per cent of synchronous speed.

2. Constant velocity for both machines with a fixed angular separation between them. This condition considers the effect of "speed" voltages caused by rotation at speeds of from three or four per cent of synchronous speed on up to and above synchronous speed.

Conclusions

From calculations based on the analysis presented here, as well as other analyses, and from test measurements, the following conclusions are evident:

1. Static errors are of two general types, those which are predominately
(*a*) in time phase with the normal position error, or
(*b*) in time quadrature (out of phase) with the normal position error.

2. The in-phase errors are caused by unbalanced reactance either in the stator windings or the interconnecting lines or in the mutual reactance between rotor and stator of either machine. For this condition, zero magnitude control transformer voltage can be obtained, but not with the control transformer rotor 90 degrees from the generator rotor.

3. The out-of-phase errors are caused by unbalanced resistances in the stator windings or lines between generator and control transformer. For this condition there is no one control transformer rotor position where zero magnitude voltage is obtained.

4. Errors present at standstill are minimized by proper electrical design and care in manufacture. By judicious choice of the pitch, distribution, and skewing of windings and by properly shaping the pole face of the rotors, the fifth and seventh harmonics of mutual flux between rotor and stator of the two machines are eliminated and the in-phase errors thereby are reduced. Care in manufacturing insures that there is a minimum of phase unbalance of resistance or reactance, thus tending to eliminate the errors noted in items 2 and 3.

5. Constant velocity errors tend to be a combination of the in-phase and out-of-phase type. At low speeds the dominant effect is to shift the rotor position at which zero voltage is obtained, there still remaining a small out-of-phase component. At high speed the dominant effect is the introduction of an out-of-phase voltage, the so-called speed voltage.

6. The constant velocity errors are dependent on the ratio of the actual speed of rotation to the synchronous speed for the given excitation frequency. Hence, the use of higher excitation frequencies such as 400 cycles instead of 60 cycles would tend to minimize these effects.

Analysis

Accuracy at Standstill

The generator-control transformer system at standstill appears as three inductive coupled circuits as shown in Figure 3. The steady-state a-c equations of voltages for these circuits are

$$[r_{ag}+r_{ac}+j(X_{ag}+X_{ac})]i_a+ [r_{abg}+r_{abc}+j(X_{abg}+X_{abc})]ib+ jX_{MDag}I_D=0 \quad (1)$$

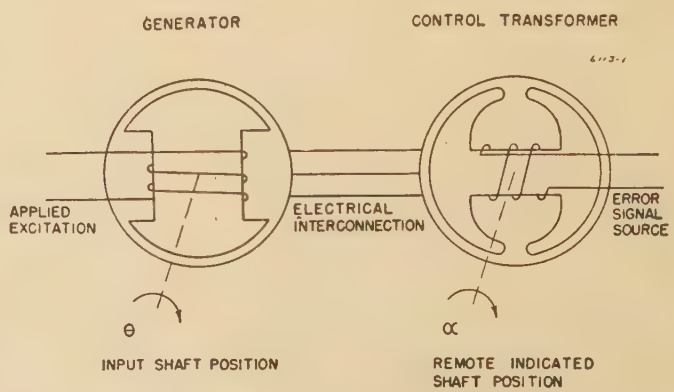

Figure 1. Schematic diagram of Selsyn generator-control transformer system

Paper 46-113, recommended by the AIEE committee on industrial control devices for presentation at the AIEE summer convention, Detroit, Mich., June 24–28, 1946. Manuscript submitted November 15, 1945; made available for printing May 6, 1946.

Harold Chestnut is with the aeronautics and marine department, General Electric Company, Schenectady, N. Y.

The author wishes to thank T. C. Johnson, who suggested this investigation and assisted in obtaining the experimental measurements. Thanks also are due Miss Jane Crawford, who is responsible for determining many of the calculated curves.

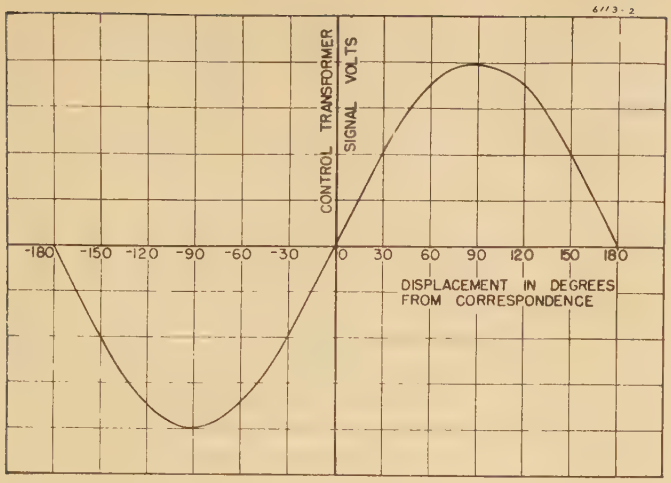

Figure 2. Ideal transformer voltage output versus angular displacement

$$[r_{abg}+r_{abc}+j(X_{abg}+X_{abc})]i_a+[r_{bg}+r_{bc}+j(X_{bg}+X_{bc})]ib+jX_{MDbg}I_D=0 \quad (2)$$

$$jX_{MDag}i_a+jX_{MDbg}i_b+(R_D+jX_{Dg})I_D=E_g \quad (3)$$

The various symbols used are defined in the nomenclature and are consistent with the synchronous machine representation of Doherty and Nickle,[3] Prentice,[4] and Park.[5] It will be noted that the nomenclature provides direct relationships between line-to-line reactances, easily obtainable from test, and the direct and quadrature reactances, which are very convenient for analytical work and are used extensively in the references cited above.

The mutal reactances X_{Mbag} and X_{MDbg} here considered include only the lower order harmonics, that is, up to the eleventh. Only odd harmonics are present because of the salient pole construction, and the third and ninth components are absent because of the 3-phase stator winding arrangement. Higher harmonics could well be included in a similar fashion. The control transformer is effectively a round-rotor machine and is represented as such.

From equations 1–3, the vector currents i_a and i_b which have a magnitude and time phase can be determined. The voltage which exists in the control transformer rotor is dependent on these currents and α, the angular position of the control transformer rotor. Thus,

$$E_c=jX_{M1c}[i_a\cos(\alpha+30)+i_b\cos(\alpha-30)] \quad (4)$$

The Selsyn control transformer indicating system depends on there being a fixed angular displacement between the generator rotor position, θ, and the control transformer position of zero voltage. This displacement is normally 90 degrees hence the position error ϵp, can be defined as

$$\epsilon p=\theta-(\alpha+90) \quad (5)$$

where θ is the independent variable used in equations 1–3 and α is calculated from the condition $E_c=0$ in equation 4.

Referring to equation 4, zero control transformer volts is obtained when

$$i_a\cos(\alpha+30)+i_b\cos(\alpha-30)=0 \quad (6)$$

Assuming that the currents i_a and i_b from equations 1–3 may not be in time phase, and taking the instant when i_a is zero as a time reference,

$$i_a=I_a\sin\omega t \quad (7)$$

$$i_b=I_b\sin(\omega t+\beta) \quad (8)$$

where I_a and I_b are the current magnitudes, and β is the phase angle between them.

Combining equation 6–8 and separating the resultant expression into sin ωt and cos ωt components,

$$\sin\omega t[I_a\cos(\alpha+30)+I_b\cos\beta\times\cos(\alpha-30)]+\cos\omega t[I_b\sin\beta\cos(\alpha-30)]=0 \quad (9)$$

For equation 9 to be equal to zero for all values of time, the coefficients of the sin ωt and cos ωt terms both must be zero. With $\beta=0$, the cost ωt coefficient goes to zero, and the coefficient of sin ωt gives the following defining condition for α at zero control transformer voltage:

$$\tan\alpha=-1.732\left(\frac{I_b+I_a}{I_b-I_a}\right) \quad (10)$$

Referring to equation 9 and noting that in the usual case the time phase difference β is small, one realizes that by positioning α in the location defined by equation 10, the sin ωt component of voltage is made zero.

Hence there remains only a cos ωt component of voltage which, since β is small, is also small.

For the case where $\beta\neq0$, the control

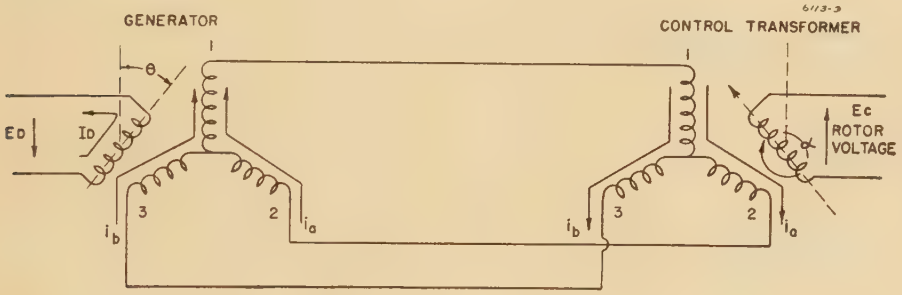

Figure 3. Elementary diagram of Selsyn generator-control system at standstill

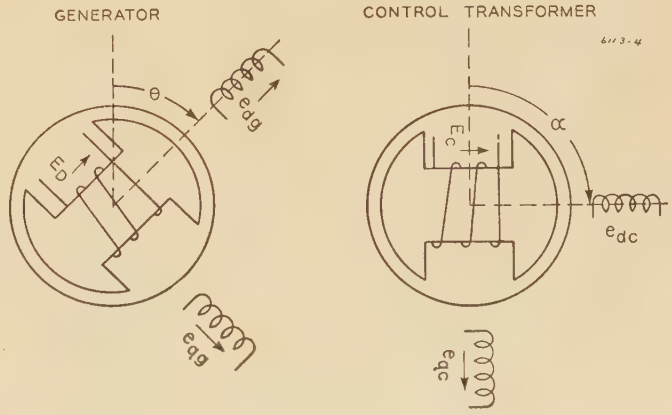

Figure 4. Two-reaction theory presentation of generator and control transformer

transformer error is then a voltage the magnitude of which is

$$\epsilon u = I_b X_{M1c} \sin \beta \cos (\alpha + 30) \quad (11)$$

The foregoing analysis indicates the significant fact that there is a 90-degree difference in time phase of the errors ϵp, where the voltages are of sin ωt time phase, and the errors ϵu, where the voltages are of cos ωt time phase.

Through use of the analytical means developed in the preceding analysis, the effects of phase unbalance in such machine parameters as reactance, resistance, and mutual coupling have been investigated.

Data for generator:

$r_{ag} = 10$ ohms	$E_g = 115$ volts
$r_{abg} = 5$ ohms	$\omega = 377$ radians per second
$r_{bg} = 10$ ohms	$X_{M3g} = 0$ except as noted on curves
$R_D = 5$ ohms	$X_{M1g} = 0$ except as noted on curves
$X_{dg} = 120.5$ ohms	
$X_{qg} = 39.5$ ohms	
$X_{Dg} = 110$ ohms	
$X_{M1g} = 95$ ohms	

Data for control transformer:

$r_{ac} = 100$ ohms	$X_{dc} = X_{qc} = 1{,}200$ ohms
$r_{abc} = 50$ ohms	$X_{M1c} = 1{,}000$ ohms
$r_{bc} = 100$ ohms	

Accuracy Under Constant Velocity Operation

In the treatment of the generator-control transformer system for this condition, it is premised that both machines have balanced windings. The effect of resistance or reactance phase unbalance is not considered, and only the fundamental component of mutual reactance between rotor and stator winding is included.

The following equations may be written for the generator machine in Figure 4, where the direct and quadrature axis voltage equations include transformer and speed voltage effects in the manner of Park.[5]

$$e_{dg} = r_{dg} i_{dg} + p\psi_{dg} - \psi_{qg} p\theta \quad (12)$$

$$e_{qg} = r_{qg} i_{qg} + p\psi_{qg} + \psi_{dg} p\theta \quad (13)$$

$$E_D = R_D I_D + p\psi_{Dg} \quad (14)$$

Where the flux linkages are related to reactances and currents by the following equations

$$\psi_{dg} = X_{dg} i_{dg} - X_{M1g} I_D \quad (15)$$

$$\psi_{qg} = X_{qg} i_{qg} \quad (16)$$

$$\psi_{Dg} = X_{Dg} I_D - X_{M1g} i_{dg} \quad (17)$$

Eliminating equation 14 and using equations 15–17, equations 12 and 13 may be written as

$$e_{dg} = (r_{dg} + pX'_{dg}) i_{dg} - pE'_D - X_{qg} i_{qg} p\theta \quad (18)$$

$$e_{qg} = (r_{qg} + pX_{qg}) i_{qg} + X'_{dg} i_{dg} p\theta - E'_D p\theta \quad (19)$$

Where the symbols X'_{dg} and E'_D are abbreviations of more complex quantities, namely,

$$X'_{dg} = X_{dg} - \frac{pX^2_{M1g}}{R_D + pX_{Dg}} \quad (20)$$

$$E'_D = \frac{X_{M1g}}{\omega}\left[\frac{E_D}{R_D + pX_{Dg}}\right] \quad (21)$$

For the control transformer, there is no rotor current, so the equations for this machine are

$$e_{dc} = (r_{dc} + pX_{dc}) i_{dc} - X_{qc} i_{qc} p\alpha \quad (22)$$

$$e_{qc} = (r_{qc} + pX_{qc}) i_{qc} + X_{dc} i_{dc} p\alpha \quad (23)$$

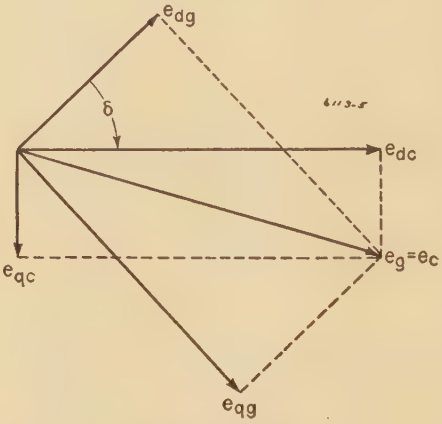

Figure 5. Relationship between d and q axes in the two machines

In terms of the actual phase voltages, the terminal conditions for generator and control transformer are the same. The phase currents for generator and control transformer, however, are opposite in sign. From these relationships, one can relate the direct and quadrature components of voltages and currents for the generator in terms of the control transformer.

$$e_{dg} = e_{dc} \cos \delta - e_{qc} \sin \delta \quad (24)$$

$$e_{qg} = e_{dc} \sin \delta + e_{qc} \cos \delta \quad (25)$$

$$i_{dg} = -i_{dc} \cos \delta + i_{qc} \sin \delta \quad (26)$$

$$i_{qg} = -i_{dc} \sin \delta - i_{qc} \cos \delta \quad (27)$$

$$\delta = \alpha - \theta \quad (28)$$

For continuous operation at a constant velocity,

$$p\theta = p\alpha = V\omega \quad (29)$$

where

$$V = \frac{\text{actual speed}}{\text{synchronous speed at frequency } \omega}$$

Under steady-state conditions with excitation frequency ω, the operator p preceding the reactance terms is replaced by j. The $p\theta$ and $p\alpha$ velocities are handled as indicated in equation 29. Finally the instantaneous voltage E_D is replaced by the corresponding vector voltage,

$$E_D = \sqrt{2} E_g \sin \omega t = E_g \underline{|0} \quad (30)$$

In vector terms, E'_D is equivalent to

$$E'_D = \frac{X_{M1g}}{\omega}\left[\frac{E_g \underline{|0}}{R_D + jX_{Dg}}\right] \quad (31)$$

Combining the preceding equations and simplifying the results yield the following two expressions:

$$Ci_{dc} + Di_{qc} = j\omega E'_D \quad (32)$$

$$Mi_{dc} + Ni_{qc} = +V\omega E'_D \quad (33)$$

where C, D, M, and N are symbols which are defined as

$$C = -[r_{dg} + r_{dc} + j(X'_{dg} + X_{dc})] \times \cos \delta + V(X_{qg} + X_{dc}) \sin \delta \quad (34)$$

$$D = [r_{dg} + r_{qc} + j(X'_{dg} + X_{qc})] \times \sin \delta + V(X_{qg} + X_{qc}) \cos \delta \quad (35)$$

$$M = [r_{qg} + r_{dc} + j(X_{qg} + X_{dc})] \times \sin \delta + V[X'_{dg} + X_{dc}] \cos \delta \quad (36)$$

$$N = [r_{qg} + r_{qc} + j(X_{qg} + X_{qc})] \times \cos \delta - V[X'_{dg} - X_{qc}] \sin \delta \quad (37)$$

From equations 32 and 33

$$i_{dc} = \frac{Nj\omega E'_D - DV\omega E'_D}{CN - DM} \quad (38)$$

and the actual control transformer output voltage is

$$E_c = -jX_{M1c} i_{dc} \quad (39)$$

Calculations were made using equations 31–39 for speeds ranging from 0 to synchronous speed, using the following data:

Generator:

$r_{dg} = r_{qg} = 29.7$ ohms $\quad X_{Dg} = 208$ ohms

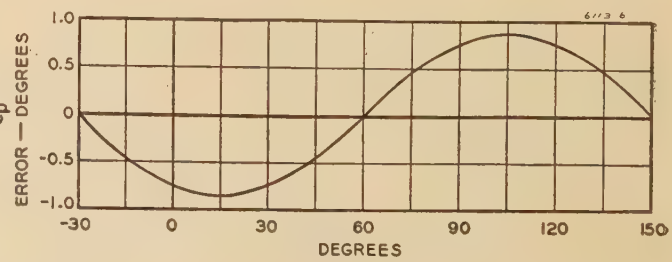

Figure 6. Control transformer error versus generator rotor position with unbalanced stator phase reactance

$$\frac{\Delta(X_{ag} + X_{ac})}{X_{ag} + X_{ac}} = 1$$

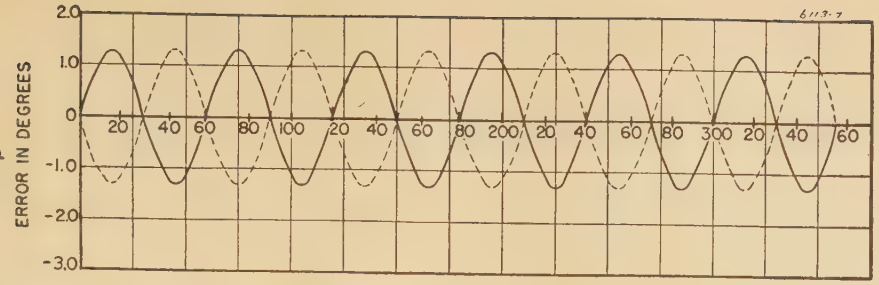

Figure 7. Control transformer error versus generator rotor position with harmonics of generator mutual reactance between rotor and stator

Solid line—$X_{MDag}=95 \cos(\theta+30)+2\cos(5\theta+30)$

Broken line—$X_{MDag}=95 \cos(\theta+30)+2\cos(7\theta+30)$

$X_{dg}=230$ ohms
$X_{M1g}=204$ ohms
$X_{qg}=62$ ohms
$R_D=12.7$ ohms
$|E_g|=115$ volts
$\omega=377$ radians per second
$V=0$–1.0

Control transformer:

$r_{dc}=r_{qc}=686$ ohms
$X_{dc}=X_{qc}=3{,}320$ ohms
$X_{M1c}=1{,}860$ ohms

Results

The qualitative nature of the results has been verified by test and calculations. The quantitative results are not applicable to all machines but do indicate a performance representative of the more common type of generator-control transformer combination. In studying the effects of resistance and reactance unbalances, the magnitude of the quantities were chosen arbitrarily and do not reflect the usual values of machine constants.

The accuracy of Selsyn systems in use at present is remarkably high. As shown in Figure 8, position errors not in excess of 0.2 degree are obtainable. Although the generators and control transformers themselves are manufactured with resistance unbalances of less than ten ohms, an out-of-phase voltage of 0.25 volt, such as shown in Figure 9, may be obtained when these machines are used in system including switches.

Although the results are discussed in two separate sections, namely static accuracy and constant velocity accuracy, it should be noted that in actual operation errors due to both unbalance and velocity exist simultaneously and may combine in a number of ways to make up the total error. Hence, comparisons with test measurements under dynamic conditions tend to be difficult to analyze.

Static Accuracy

Since the impedance of the generator and control transformer is largely reactive, it follows that an unbalance in the phase values of reactance of either machine causes the in-phase current magnitudes to be altered from the values necessary for errorless operation. This shifts the flux orientation in the control transformer and requires that the rotor be moved slightly from its position of correspondence with the generator.

Specifically, unbalance in the stator phase values of reactance produces a space error which varies with the second harmonic of the generator rotor orientation (Figure 6). The maximum value of error for values of unbalance reactance up to about ten per cent is given by the expression

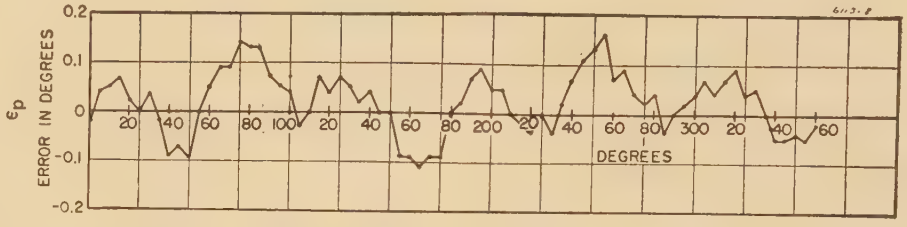

Figure 8. Typical generator-control transformer error versus generator rotor position

From test data

Figure 9. Control-transformer quadrature error voltage as a function of generator rotor angle

For various amounts of added resistance in one stator line

Points of maximum, minimum, and zero values of voltage are joined by straight lines

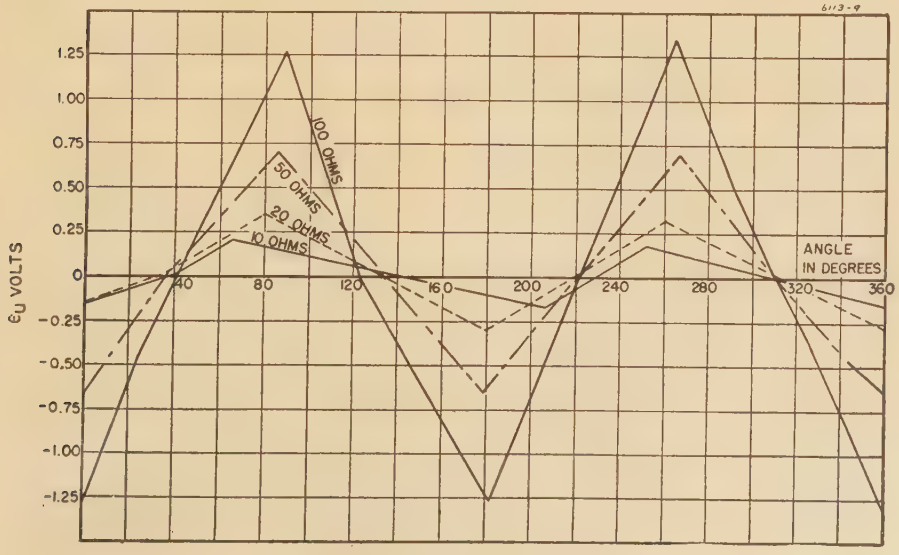

$$\epsilon p \text{ max} = 8° \frac{\Delta(X_{ag}+X_{ac})}{X_{ag}+X_{ac}}$$

This relationship applies for machine constants given in the data in the section on static accuracy.

The presence of fifth and seventh harmonics in the mutual flux between rotor and stator of either machine is evidenced by the occurrence of a space error which varies as the sixth harmonic of the generator rotor orientation. As shown in Figure 7, the direction of the error is opposite for positive values of the fifth and seventh harmonics of mutual flux so that theoretically a balance can be obtained where one compensates for the other. The magnitude of the maximum error varies about linearly with the magnitude of the harmonic flux, thus

$$\epsilon p \text{ max} = +57.3° \frac{X_{M5g}}{X_{M1g}} \text{ for + fifth harmonic}$$

$$\epsilon p \text{ max} = -57.3° \frac{X_{M7g}}{X_{M1g}} \text{ for + seventh harmonic}$$

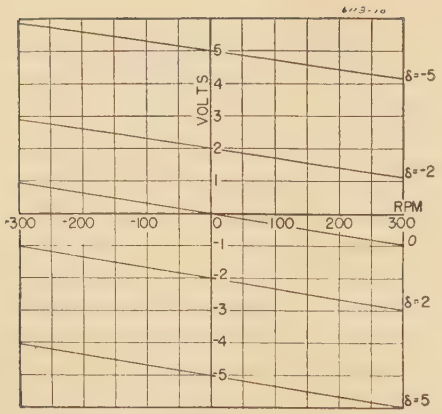

Figure 10. Calculated values of control transformer voltage (in phase component) versus speed

For generator-control transformer with fixed angular separation (δ)

Figure 7 verifies these approximate relations for the case of a machine with constants as given in the section on static accuracy.

In Figure 8 is shown a typical error curve measured on a generator-control transformer and indicating a pronounced sixth harmonic.

By modification of the generator rotor flux distribution to reduce the seventh harmonic component, the resultant error was reduced. The fifth harmonic of flux is absent from this type machine because of the stator slot winding arrangement.

The presence of unequal values of resistance in the different stator phases causes a shift in the time phase of the stator currents. The current magnitudes which are determined primarily by the phase reactances are relatively unchanged. Under this condition there is no control transformer rotor position where zero voltage exists at all instants of time. At zero ϵp error position, there exists a voltage induced in the control transformer rotor which is in time quadrature with the normal position error voltage. Turning the control transformer rotor from the zero space error position merely brings the voltage in phase with the normal signal voltage and greatly increases its magnitude. The polarity of the voltage depends on the direction in which the rotor is moved. The magnitude of the time quadrature component of voltage is about linearly proportional to the amount of unbalanced resistance as shown in Figure 9. This curve, obtained experimentally, verifies calculations which indicate a second harmonic variation of control transformer rotor minimum voltage as a function of generator rotor position.

Constant Velocity Accuracy

A generator-control transformer system which has zero error at standstill suffers a shift in the angular relationship between generator and control transformer rotor positions where zero control transformer rotor voltage is obtained when the two machines are running at the same speed. Stated conversely, if the angular relationship between the two rotors is maintained fixed and the two rotors are run at a number of constant speeds, the control transformer rotor voltage changes magnitude as a function of speed, the frequency of the output voltage being maintained constant throughout. Figure 10 shows the calculated values for the in-time-phase component of rotor voltage as a function of speed for a number of fixed values of relative rotor displacement. These curves compare fairly well with the experimentally measured curves shown on Figure 11, which show the smoothed "average" voltage-speed effect for the same type machines as were considered in the calculations. The presence of errors caused by irregularities of phase resistance or reactance introduces spurious errors which tend to obscure measurements of the speed voltage effect at these low voltages where the effect amounts to about 1 volt (=1 degree) per 320 rpm. Actually the discrepancy between calculations and test is well within the limit of experimental accuracy.

In Figure 12 is shown the in-phase and out-of-phase components of control transformer rotor voltage as a function of speed up to synchronous speed for a number of fixed values of angular separation. The applied voltage to the generator rotor is taken as the in-phase voltage reference. A time phase shift of about 15 degrees at 60 cycles per second takes place in this generator-control transformer system at standstill. In Figure 13 the control transformer output voltage at standstill is chosen as the reference for the in-phase voltage, otherwise the data are the same as on the preceding figure. From these curves it can be seen that the effect of high speed rotation is primarily to introduce an out-of-phase component of control transformer rotor voltage which becomes quite dominant as the rotation speed approaches synchronous speed. At the lower speeds the major effect is to shift the zero voltage position, thus causing the error in transmission of about one degree per 320 rpm noted previously.

It is of interest to note that the effect of rotation on error is not a function of the absolute speed but rather the relative speed of rotation ($v\omega$) compared to the synchronous speed of rotation (ω) of the

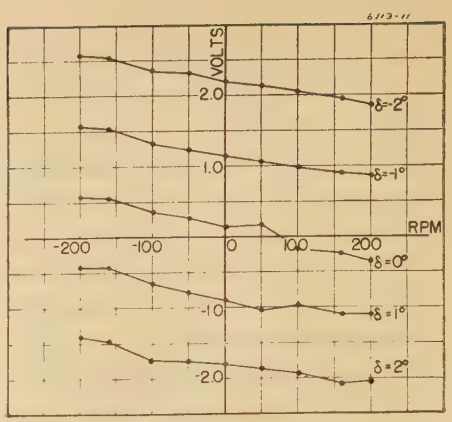

Figure 11. Averaged measured values of control transformer voltage versus speed

From test data. For generator-control transformer with fixed angular separation (δ)

excitation frequency. Thus by doubling the excitation frequency, an error of one degree would be obtained at about 640 rpm instead of 320.

Summary

The Selsyn generator-control transformer system has a high accuracy of the order of 0.3 degree. The static errors which are present because of resistance or reactance unbalance are evidenced by a second harmonic periodicity with rotor rotation. Errors caused by improper shaping of the rotor appear as higher harmonics of rotor position such as the sixth.

Even though a generator-control transformer system has no static errors, speed voltage effects produce a dynamic error which is of the order of one degree per 320 rpm for present-day 60-cycle machines.

Nomenclature

r_{ag} = line-to-line resistance in ohms of generator from terminal 1 to terminal 2

r_{bg} = line-to-line resistance in ohms of generator from terminal 1 to terminal 3

r_{abg} = resistance in ohms of phase 1 of generator

r_{ac} = line-to-line resistance in ohms of control transformer from terminal 1 to terminal 2

r_{bc} = line-to-line resistance in ohms of control transformer from terminal 1 to terminal 3

r_{abc} = resistance in ohms of phase 1 of control transformer

R_D = resistance in ohms of generator rotor

$r_{dg} = r_{qg}$ = per phase resistance in ohms of generator

$r_{dc} = r_{qc}$ = per phase resistance in ohms of control transformer

X_{ag} = line-to-line reactance in ohms of generator as seen by loop current i_a flowing from phase 2 to phase 1 with i_b not flowing. This reactance is a

second harmonic function of generator rotor position. Its numerical value may be obtained from a measurement of maximum and minimum values of the line-to-line reactance as viewed from terminals 1 and 2, with terminal 3 not connected. Expressed in terms of the per phase values of direct and quadrature axis reactances,

$X_{ag}=X_{dg}+X_{qg}-(X_{dg}-X_{qg})\times\cos(2\theta-120)$

X_{bg} = line-to-line reactance in ohms of generator as seen by loop current i_b flowing from phase 3 to phase 1. This reactance is a second harmonic function of generator rotor position, and its value may be obtained from a measurement of maximum and minimum values of line-to-line reactance as viewed from terminals 1 and 3.

$X_{bg}=X_{dg}+X_{qg}-(X_{dg}-X_{qg})\times\cos(2\theta+120)$

X_{abg} = mutual reactance in ohms of generator between circuit of loop current i_a and that of loop current i_b. Expressed in terms of the values of direct and quadrature reactances noted above,

$$X_{abg}=\frac{X_{dg}+X_{qg}}{2}-\frac{(X_{dg}-X_{qg})}{2}\times\cos[20-120]$$

X_{ac} = line-to-line reactance in ohms of control transformer as seen by loop current i_a flowing from phase 1 to phase 2 with i_b not flowing. Because of the absence of reactance variation with a change in control transformer rotor position,

$X_{ac}=X_{dc}+X_{qc}$

X_{bc} = line-to-line reactance in ohms of control transformer as seen by loop current i_b flowing from phase 1 to phase 3 with i_a not flowing

$X_{bc}=X_{ac}=X_{dc}+X_{qc}$

X_{abc} = mutual reactance in ohms of control transformer between circuit of loop current i_a and that of loop current i_b

$$X_{abc}=\frac{X_{dc}+X_{qc}}{2}$$

X_{Dg} = reactance in ohms of generator rotor

X_{MDag} = mutual reactance between generator stator windings, phases 1 and 2 and the generator rotor winding. This reactance is a function of the odd harmonics of rotor position; however, because of the 3-phase arrangement of the stator windings, those harmonics which are multiples of three are missing. Expressed in terms of the maximum values of the fundamental, X_{M1g}, fifth, X_{M5g}, and seventh, X_{M7g}, harmonics of generator mutual reactances between the rotor and the line-to-line stator windings,

$X_{MDag}=X_{M1g}\cos(\theta+30)+X_{M5g}\times\cos(5\theta-30)+X_{M7g}\cos(7\theta+30)$

X_{MDbg} = mutual reactance between generator stator windings phases 1 and 3 and the generator rotor windings. It is an odd harmonic function of generator rotor position as X_{MDag}. Expressed in terms of X_{M1g}, X_{M5g}, and X_{M7g},

$X_{MDbg}=X_{M1g}\cos(\theta-30)+X_{M5g}\times\cos(5\theta+30)+X_{M7g}\cos(7\theta-30)$

X_{M1g} = maximum value in ohms of fundamental of mutual reactance between generator rotor and stator windings, line-to-line

X_{M5g} = maximum value in ohms of fifth harmonic of mutual reactance between generator rotor and stator windings, line-to-line

X_{M7g} = maximum value in ohms of seventh harmonic of mutual reactance between generator rotor and stator windings, line-to-line

X_{M1c} = maximum value of mutual reactance in ohms of control transformer between line-to-line of stator and rotor winding

X_{dg} = per phase value of direct axis reactance in ohms of generator stator windings. In terms of the maximum value of X_{ag},

$$X_{dg}=\frac{X_{ag}}{2}\text{ (maximum)}$$

X'_{dg} = symbol used to represent the apparent reactance of the stator direct axis as modified by the presence of the current flowing in the rotor

X_{qg} = per phase value of quadrature axis reactance in ohms of generator stator windings. In terms of the minimum value of X_{ag},

$$X_{qg}=\frac{X_{ag}}{2}\text{ (minimum)}$$

X_{dc} = per phase value of direct axis reactance in ohms of control-transformer stator windings. In terms of X_{ac},

$$X_{dc}=\frac{X_{ac}}{2}$$

X_{qc} = per phase value of quadrature axis reactance in ohms of control-transformer stator windings. In terms of X_{ac},

$$X_{qc}=\frac{X_{ac}}{2}$$

$\Delta(X_{ag}+X_{ac})$ = ohms value of unbalance in

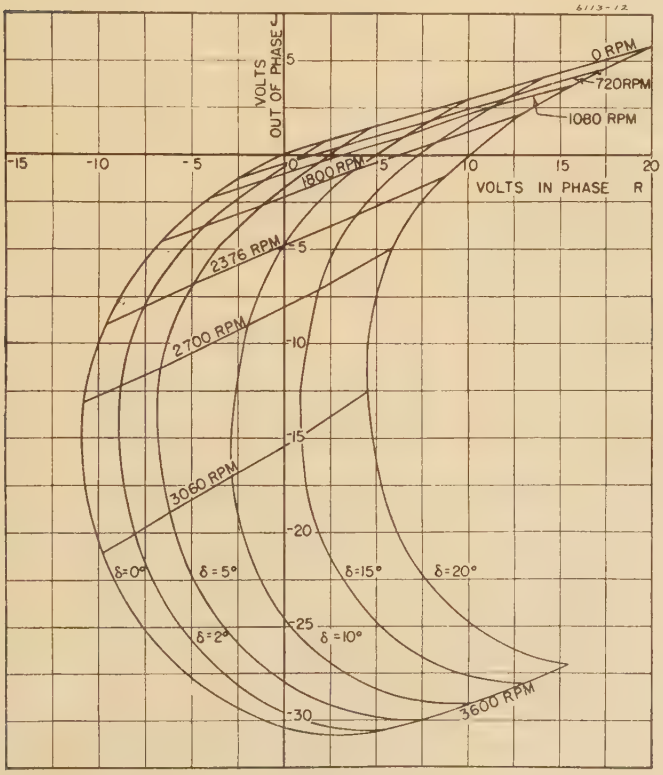

Figure 12 (left). Control transformer voltage components for constant velocity operation with fixed separation between rotors

Generator excitation voltage used as in-phase reference (R)

Figure 13 (below). Control transformer voltage components for constant velocity operation with fixed separation between rotors

Control transformer voltage at standstill is in-phase reference

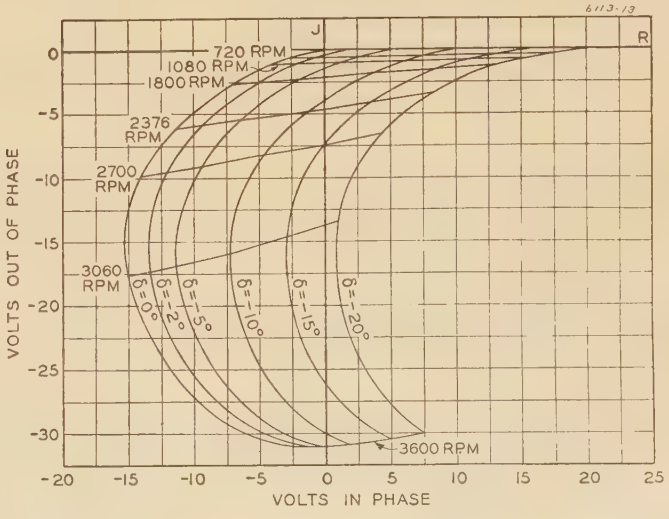

loop reactance used for specifying error voltage ϵp as a function of reactance unbalance

i_a, i_b = loop currents in amperes flowing in generator-control transformer stator circuits as shown in Figure 3

I_D = generator rotor current in amperes flowing as shown in Figure 3

I_a = rms value of the magnitude of the loop current i_a

I_b = rms value of the magnitude of the loop current i_b

i_{dg} = direct axis current in amperes flowing in generator stator circuit shown in Figure 4

i_{qg} = quadrature axis current in amperes flowing in generator stator circuit shown in Figure 4

i_{dc} = direct axis current in amperes flowing in control-transformer stator circuit shown in Figure 4

i_{qc} = quadrature axis current in amperes flowing in control-transformer stator circuit shown in Figure 4

ψ_{dg} = direct axis flux linkages in the generator stator

ψ_{qg} = quadrature axis flux linkages in the generator stator

ψ_{Dg} = direct axis flux linkages in the generator rotor

E_g = rms value of the magnitude of the excitation voltage impressed on the generator rotor

E_c = rms value of the voltage present at the rotor of the control transformer. This is the so-called control transformer signal voltage

E_D = excitation voltage applied to generator rotor

E'_D = symbol used to represent the voltage present in the stator of the generator produced by the actual excitation voltage in the generator rotor

e_{dg} = per phase value of direct axis voltage in volts for generator stator

e_{qg} = per phase value of quadrature axis voltage in volts for generator stator

e_{dc} = per phase value of direct axis voltage in volts for control transformer stator

e_{qc} = per phase value of quadrature axis voltage in volts for control transformer stator

ϵp = position error in degrees between the control-transformer rotor position for zero volts output and the position 90 degrees displaced in a lagging direction from the generator rotor. See equation 5 for sign convention employed

ϵu = rms value of the magnitude of the out-of-phase component of control transformer rotor voltage for that rotor position where ϵp is zero

θ = angular position of generator rotor. In general, the units associated with θ are degrees, but in those cases where the term $p\theta$ is used, the units of θ are radians, so $p\theta$ equals an angular velocity in radians per second

α = angular position of control-transformer rotor. The same comments in regard to units apply to α as to θ

β = phase angle in degrees between the loop currents i_a and i_b. See equations (7) and (8) for the sign convention employed

ω = angular frequency in radians per second of generator excitation voltage. In the calculations, $\omega = 377$ radians per second corresponding to 60 cycles per second

V = speed of generator and control transformer rotors expressed as a ratio to synchronous speed at excitation frequency ω

$\delta = \alpha - \theta$ = difference in angular position between generator and control

C, D, M, N = symbols used to replace the more complicated reactance expressions of equations 34–37. These are of use only in literal work and need not appear in the numerical calculations

t = time in seconds

$p = \frac{d}{dt}$ = derivative with respect to time

j = operator indicating $\sqrt{-1}$

High Voltage D-C Testing of Rubber-Insulated Wire

W. N. EDDY
FELLOW AIEE

W. D. FENN
MEMBER AIEE

AT DIFFERENT STAGES in the manufacture of insulated wire and cable, various electrical and physical tests are made to ensure the quality and serviceability of the completed cable. One of the most important of these tests is the high voltage test, a-c or d-c. It may be applied to short sections of the insulated conductor as it passes through electrodes of various types, dry or wet, or to full factory lengths of the insulated wire, dry or wet.

The scope of this paper is limited to the results of an experimental study made on the voltage limits suitable for the high voltage d-c testing of factory lengths of plain insulated wire immersed in water. In addition to many sample tests, the study included tests on more than 5,500 different factory lengths of submarine cable conductor, insulated with natural rubber, synthetic rubber, or polyethylene. Such factors as testing voltage, type of fault, and immersion time were varied over a wide range. From these data test voltage limits are suggested; the lowest test voltage that will indicate serious defects and the highest test voltage that can be used without causing damage to sound insulation, from either the d-c test voltage itself or from impulse voltages incidental to the testing.

In the following discussion all insulating compounds are of the submarine type, all wire sizes are American Wire Gauge and all voltages are given as volts per mil thickness of insulation (total voltage per mils thickness). All alternating voltages are root-mean-square. Unless otherwise indicated, all d-c tests were made with negative polarity on the conductor.

Paper 46-121, recommended by the AIEE committee on power transmission and distribution for presentation at the AIEE summer convention, Detroit, Mich., June 24–28, 1946. Manuscript submitted April 18, 1946; made available for printing May 8, 1946.

W. N. Eddy and W. D. Fenn both are in the electrical engineering laboratory, Simplex Wire and Cable Company, Cambridge, Mass.

Dielectric Strength of Rubber and Polyethylene Insulated Wire

Knowledge of the d-c and impulse dielectric strength is essential to the proper selection of a suitable d-c test voltage. In Table I are given typical values for the dielectric strength of the materials covered in this discussion. They represent many tests made over several years time. All test specimens were five feet active length tested after 24 hours immersion in room temperature water. The

References

1. Selsyn Instruments for Position Systems, T. M. Linville, J. S. Woodward. AIEE Transactions, volume 53, 1934, June section, pages 953–60.

2. Selsyn Design and Application, T. C. Johnson. AIEE Transactions, volume 64, 1945, October section, pages 703–08.

3. Synchronous Machines, Parts I and II, R. E. Doherty, C. A. Nickle. AIEE Transactions, volume 45, 1926, pages 912–42, discussion, page 946.

4. Fundamental Concepts of Synchronous Machine Reactances, B. R. Prentice. AIEE Transactions, volume 56, 1937 supplement, pages 1–21.

5. Two-Reaction Theory of Synchronous Machines: Generalized Method of Analysis—Part I, R. H. Park. AIEE Transactions, volume 48, 1929, pages 716–30.

calculated impulse wave was 1.5x40 microseconds. The d-c tests were made with a voltage increase of 700 volts per second. The alternating voltage was increased 500 volts per second. The wire size varied over a moderate range in the neighborhood of number 12 6/64 inch thickness.

Damage to Sound Insulation by Excessive Test Voltage

The tests reported in Tables II and III were made to investigate the possibility that the application of high d-c test voltage might damage sound insulation by causing a permanent decrease in the dielectric strength.

The tests in Table II were made on insulated wire samples of five feet active length after 24 to 48 hours immersion in room temperature water. All samples of the same size were cut from the same length and grouped in such a way as to minimize the effect of variation of dielectric strength along the length. After a 30-minute application of the direct voltages indicated in the table the samples were tested for a-c dielectric strength with a voltage increase of 500 volts per second. In all cases the a-c tests were made the day after the d-c tests, without removing the samples from the water.

The tests in Table III were made on number 12 solid, 6/64 inch thickness of natural rubber. A 175-foot length in water was tested at 640 volts d-c per mil for five minutes without failure and then cut into samples of 5-foot active length

Table I. Dielectric Strength of Rubber and Polyethylene Insulated Wire

Type of Insulation	Impulse Strength in Volts Per Mil	D-C Strength in Volts Per Mil	A-C Strength in Volts Per Mil
Natural rubber	1,070	1,500	350
GR-S rubber	1,030	1,400	370
Polyethylene	1,500	3,000	350

for the tests indicated in the table. The dielectric strength tests were made with a direct voltage increase of 700 volts per second and an impulse wave of 1.5x40 microseconds. There were five samples in each of the four groups. In other respects the testing conditions were similar to those of Table II.

The results in Tables II and III show no real decrease in a-c or d-c strength resulting from previous applications of direct or impulse voltage. None of the variations apparent in the tables exceeds those usually found in such a collection

Table II. Effect of High Voltage D-C Tests on Subsequent A-C Strength

Size	Previous Test	Number of Samples	60-Cycle Breakdown Voltage: Highest Volts Per Mil	Lowest Volts Per Mil	Average Volts Per Mil	Average in Per Cent of No D-C Test
Number 12 (7 strands)—6/64 inch thickness polyethylene	None	15	361	278	326	100
	800 volts per mil d-c	5	350	317	338	104
	1,600 volts per mil d-c	10	333	266	301	93
Number 6 (7 strands)—10/64 inch thickness GR-S rubber	None	15	350	293	319	100
	500 volts per mil d-c	5	363	286	313	98
	800 volts per mil d-c	10	388	300	334	105
Number 12 solid—6/64 inch thickness natural rubber	None	13	455	344	411	100
	500 volts per mil d-c	5	419	328	374	91
	800 volts per mil d-c	8	415	338	378	92
Number 6 (7 strands)—8/64 inch thickness natural rubber	None	5	445	361	422	100
	800 volts per mil d-c	5	470	378	440	104

of dielectric strength data. Therefore, the use of d-c testing voltages as high as one half of the 5-foot d-c dielectric strength in Table I should not result in any appreciable decrease in the dielectric strength of sound insulation.

Relation Between Type of Fault and Necessary Test Voltage

The object of high voltage testing is to indicate weak spots or partial faults in the insulation by applying enough voltage to cause the complete failure of such spots. Therefore, it is desirable to know something of the relation between the type of the partial faults and the test voltage necessary to develop such spots into complete failure.

In Table IV are given the results of voltage tests made on artificial faults in number 12 standard, 6/64 inch thickness natural rubber. After tying the wire to a wooden splint each fault was made by forcing a needle or revolving drill through the insulation to the conductor as indicated by completion of a buzzer circuit, then withdrawing the needle or drill. These faults were tested with high direct voltage after immersion in water for three days. The results in Table IV indicate that such faults may withstand direct voltage as high as 225 volts per mil of insulation for 40 minutes (20 minutes each polarity) without failure. Thus, a test voltage as low as this may not indicate faults that extend entirely through the insulation thickness. Open artificial faults were made in the same size wire by cutting away part of the insulation thickness at one spot. High voltage d-c tests on these faults indicated that a remaining thickness of 3/64 inch, or only one half the total thickness, is enough to withstand 500 volts d-c per mil of the total thickness without failure. A similar relation also is indicated by comparison of the test voltage with the dielectric strength values in Table I. For instance, a test voltage of 500 volts d-c per mil is only one third the d-c dielectric strength of natural rubber. Thus, a small part of the insulation at a single spot might withstand a test voltage of 500 volts per mil total thickness.

When rubber insulated wire is wound on a reel there may be considerable pressure between adjacent turns of wire. The results in Table V show the effect of such pressure on the d-c dielectric strength of artificial faults in wire, number 12, 6/64 inch thickness natural rubber. The d-c strength of needle faults in water was increased from 150 to 690 volts per mil, by applying pressure from adjacent rubber insulated wire as on a reel.

Also in Table V are the results of similar tests on a fault in the same size wire consisting of a *U*-shaped knife cut all the way to the conductor. After immersion

Table III. Effect of High Voltage D-C and Impulse Tests on Subsequent D-C Strength

Previous Test	D-C Dielectric Strength Volts Per Mil: Highest	Lowest	Average
a—None	1,450	1,290	1,360
b—640 volts per mil d-c for 30 minutes	1,500	1,120	1,340
c—640 volts per mil d-c for 5 minutes, 6 times	1,480	1,310	1,360
d—850 volts per mil impulse, 6 times	1,530	1,360	1,470

in water for 24 hours under pressure from adjacent rubber insulated wire this fault had a d-c strength of 600 volts per mil and after the first failure a voltage of 480 volts per mil was necessary to cause a second failure.

In addition to these data on artificial faults two examples of natural faults are offered:

1. Three thousand feet of number 14 solid 3/64 inch thickness of natural rubber withstood, without failure, three voltage tests

five minutes each at 340 volts d-c per mil during a 12-day water immersion. After six months' additional room temperature immersion the wire had an insulation resistance of less than 10 megohms per 1,000 feet at 500 volts d-c because of two air pockets in the insulation so large that only ten per cent of the wall remained in a sound condition.

2. Ten thousand feet of number 12 standard, 6/64 inch thickness GR-S rubber withstood, without failure, three voltage tests five minutes each at 570 volts d-c per mil during a 12-day immersion. Subsequent immersion and high voltage testing finally disclosed an iron chip so located within the insulation that only one third of the thickness was left effective.

These data on both artificial and natural faults indicate that under some circumstances it is possible for serious faults to withstand several applications of d-c testing voltage as high as 500 volts per mil without failure.

Damage to Sound Insulation by Impulse Voltages Incidental to High Voltage D-C Testing

When factory lengths of insulated wire are at the d-c test voltage, abrupt grounding of the conductor is likely to produce momentary voltages that are higher than the test voltage. If these voltages exceed the impulse strength of the insulation, failures will ensue. There are three principal ways in which the conductor may be grounded abruptly:

1. Accidental flashover during test.
2. Intentional grounding after completion of test.
3. Failure of insulation on test.

The first way can be prevented by care and the second by the use of series resistance but limitation of the test voltage is the only known method of preventing damage from the third cause.

In a total of more than 17,000 voltage tests on more than 5,500 factory lengths with an insulation thickness in the general neighborhood of 6/64 inch and with different test voltages between 300 and 620 volts per mil on rubber and between 500 and 1,000 volts per mil on polyethylene, impulse failures have been limited to test voltages of 580 volts per mil and higher on natural or synthetic rubber and to 850 volts per mil and higher on polyethylene.

Investigation of these impulse voltages with cathode-ray oscillograph at direct voltages less than 100 volts indicates that such voltages may get as high as 1.8 of the applied voltage (test voltage). Application of this ratio to the impulse strengths in Table I gives minimum test voltages of 593, 573, and 835 volt per mil for natural rubber, GR-S rubber, and polyethylene respectively, at which impulse failures might be expected. These indications admittedly are not conclusive because of the low test voltage but it is interesting to note the close agreement with the testing experience reported in the preceding paragraph.

Conclusions

High voltage d-c testing has been found of considerable value in controlling the quality of insulated wire but no implication is intended in this paper that such testing is essential to the maintenance of satisfactory quality. Comparison of high voltage d-c testing of factory lengths with other kinds of testing is outside the paper's limited scope. If high voltage d-c tests are made on factory lengths it would be well to consider the following voltage limitations that have been indicated by experimental study to date.

If the d-c test voltage used on factory lengths is too high there is a possibility of developing enough impulse voltage to cause failures in sound insulation.

As a value for the highest d-c test voltage at which there is no danger from impulses one of the following is suggested:

1. Fifty per cent of the 5-foot impulse strength.
2. Five hundred volts per mil on rubber and 750 volts per mil on polyethylene if the impulse strength is not known.

Prolonged or repeated applications of d-c test voltage as high as 50 per cent of the 5-foot d-c strength do not cause any reduction in the dielectric strength of sound insulation. This value is above the maximum limitation in test voltage imposed by the impulse strength of the insulation.

The dielectric strength of some faults is surprisingly high and may be increased further by pressure from adjacent wire. For this reason 25 per cent of the 5-foot d-c strength is suggested as the lowest voltage at which such tests should be made. The faults described and tested in the foregoing are not common in well-organized factories but it is possible for such faults to withstand tests as high as 33 per cent of the 5-foot d-c strength without failure.

Because of these voltage limitations to high voltage d-c testing it is important to increase the effectiveness of the testing as much as possible, by such means as increase of the soaking time and decrease of the pressure from adjacent wire.

Table IV. Dielectric Strength of Artificial Faults

	D-C Strength in Volts Per Mil Thickness					
Needle diameter, inch	0.025	0.025	0.025	0.050	0.057	0.042
Type of needle point	Extra fine	Fine	Medium	Medium	Blunt	*
	205	159	142	200	68	27
	225†	230	159			
	285**†					

* Hole made with 0.042-inch twist drill.

** Insulation stretched by bending wire before puncturing insulation. Wire then straightened and bound to a splint.

† No failure after 40 minutes on 20 kv (5 minutes plus, 5 minutes minus, 15 minutes plus, 15 minutes minus).

Table V. Effect of Pressure on Strength of Artificial Faults

Test Specimen	D-C Strength in Volts Per Mil After 24 Hours in Water
Needle fault with no pressure	135
Needle fault squeezed against one adjacent wire without fault by wooden clamp	170 310
Needle fault squeezed in group with three other wires without faults, by binding with cotton string	340 690
U-knife cut fault squeezed in group with 6 other wires without foregoing faults	600 then 480

Dangerous Electric Currents

CHARLES F. DALZIEL
MEMBER AIEE

Synopsis: This paper discusses lethal electric currents and their accompanying physiological effects, and interprets the data of a previous paper[4] in accordance with an original method of analysis found useful by the author in his own investigations of let-go currents. The present analysis concerns itself with threshold currents likely to produce instantaneous electrocution in one-half per cent of a large group of normal men. Although the conclusions are derived from tests made on animals, it is believed that the results may be indicative of what might be expected to occur in man. The majority of the work is based on experiments made at 60 cycles with shock durations of 0.03 to 3.0 seconds. Predictions of lethal currents for both direct current and capacitor discharges, while more speculative because of the limited data available, are included because of their importance due to the greatly increased use of direct current and electronic equipment.

PROGRESS in the development of electric equipment has brought increasing demands for additional knowledge on the effects of electric shock, particularly with regard to the maximum current that man reasonably might be expected to withstand without fatal results. Sensations, muscular contractions, and the current required to cause the victim to freeze to a circuit have been covered fairly well in recent papers on let-go currents.[1,2,3] The object of this paper is to extend the analyses and discuss effects at higher currents.

Any definition of lethal currents must consider the following factors:

1. Current pathway through the body.
2. Physical condition of the victim.
3. Magnitude of the current.
4. Shock duration.
5. Frequency.
6. Wave form.
7. The phase of the heart cycle at the instant the shock occurs.

Electric shocks produce different effects depending upon the structure through which the current passes. Currents flowing in the region of the heart may produce a condition of the heart muscle known as ventricular fibrillation. This condition usually is fatal and commonly is referred to as instantaneous electrocution. Currents passing through nerve centers controlling breathing may produce respiratory inhibition, that is, stoppage of respiration. Failure of the breathing mechanism often is temporary, the paralysis lasting from a few minutes to a few hours after interruption of the current. These victims often may be saved by prompt application of artificial respiration. Currents passed across the head from temple to temple may produce unconsciousness and muscular convulsions. Shocks of this type are used currently in electric shock treatment in certain types of insanity. If the current pathway involves lower nerve centers, the shock might produce ejaculation. Electric ejaculation and artificial insemination apparently have promise in breeding animals. If the pathway involves only an extremity, such as a hand or leg, memory of a disagreeable experience might be the only lasting result. Because of such variations in the effects of electric shock, it is customary to discuss lethal currents with respect to the most dangerous current pathway likely to be experienced in accidents. This is a pathway involving the heart, with external contacts usually assumed between the hands, or between one hand and the opposite foot.

Much attention has been given the study of fatal accidents. These studies have been very helpful in developing practical safety procedures and safety codes. From a technical point of view, results have been qualitative rather than quantitative. This is largely because of the difficulty of determining accurately the many variables involved. In addition to the factors already mentioned, it usually is possible only to make rough estimates in arriving at values of circuit impedance, body and contact resistances, and elapsed time between occurrence of the accident, rescue, and resuscitation.

Often these uncertainties have resulted in erroneous conclusions and have confused the issue. Perhaps the most serious misconception concerns the effects of voltage versus the effects of current. Current and *not* voltage is the proper criterion of shock intensity. The remainder of this paper will be devoted to a discussion of the electric shock hazards, caused by currents of various shock durations, wave shapes, and frequencies.

Sixty-cycle currents at the let-go level, that is, currents of from 10 to 20 milliamperes from hand to hand, are painful and hard to endure for even a short time. If long continued, they may lead to collapse, unconsciousness, and death. The physical condition of the victim is of prime importance in determining this hazard. The muscular contractions and accompanying sensations increase in severity as the current is increased. The muscular contractions progress up the arm to the chest until they become so severe that the victim is unable to breathe. Obviously, if the current flows for more than a few minutes, death may result from asphyxiation. However, if the circuit is interrupted in a reasonable time, breathing resumes automatically, and no serious after-effects result. Currents considerably in excess of those required to cause a stoppage of breathing by excessive muscular contraction of the chest muscles may produce a temporary paralysis of respiration by action on the nerves. It has been known for some time that respiration might be inhibited by currents passing through the respiratory nerve center located in the base of the brain. Observation of temporary muscular paralysis in human accidents has prompted Howard Miller, Southern California Edison Company, to suggest that respiratory inhibition also might be caused by currents affecting the nerve centers controlling the diaphragm. The suggestion is in agreement with W. Einthoven, who some 30 years ago demonstrated that electric currents applied directly to a nerve, insufficient to cause permanent damage, could produce complete blocking of the nerve for periods of the order of one-half hour. The respiratory paralysis may last for a considerable period after interruption of the current. In this case, resuscitation must be applied immediately to prevent asphyxial death. Often the paralysis disappears in a few minutes or in a few hours, and continued application of artificial respiration may save the victim. Mere cessation of natural breathing is not likely to produce serious aftereffects or permanent damage, as evidenced by the many persons who have been resuscitated successfully.

Much valuable information on currents producing ventricular fibrillation

Paper 46-112, recommended by the AIEE committee on safety for presentation at the AIEE summer convention, Detroit, Mich., June 24–28, 1946. Manuscript submitted November 2, 1944; made available for printing May 6, 1946.

CHARLES F. DALZIEL is associate professor of electrical engineering, College of Engineering, University of California, Berkeley, Calif.

The author wishes to acknowledge and thank Doctor H. B. Williams, professor of physiology, College of Physicians and Surgeons, Columbia University, for his many helpful suggestions and assistance in reviewing the manuscript.

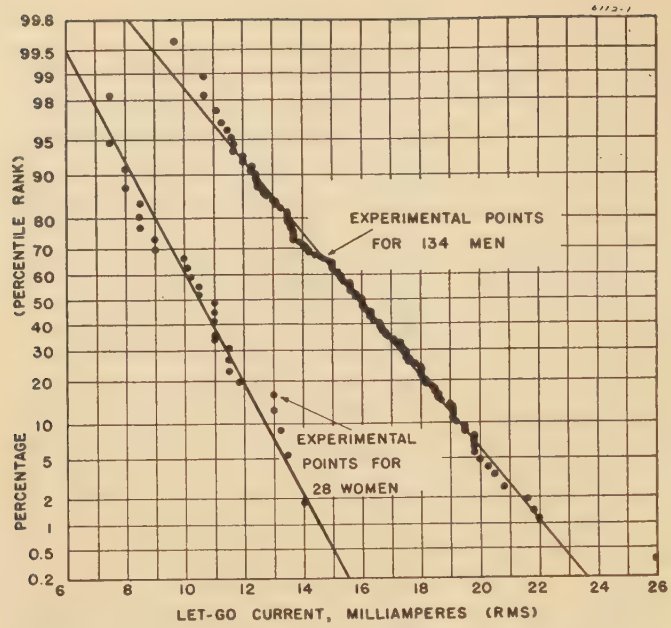

Figure 1. Sixty-cycle sine wave let-go current distribution curves for men and women

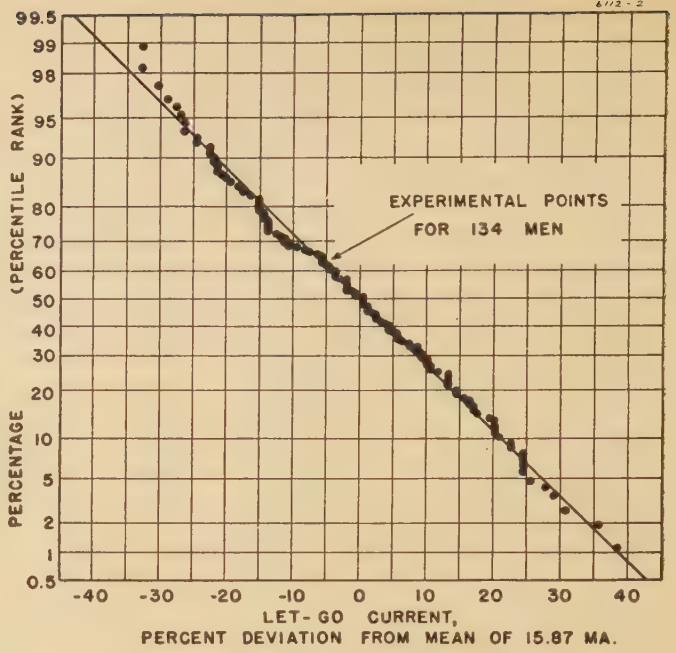

Figure 2. Sixty-cycle sine wave let-go current deviation curve for men

has been obtained from extensive experiments performed on animals at Columbia University by Ferris, King, Spence, and Williams.[4] These authorities adeptly have described the fibrillating condition as follows:

"Currents somewhat greater than those just necessary to stop respiration by action on the muscles may cause fatalities, even though the duration of such shocks is but a few seconds or less—far too short to be important from the standpoint of interruption of respiration, and obviously too short to give any opportunity for rescue before the end of the shock. Death under such conditions is brought about by ventricular fibrillation, which is a disruption of normal heart action. This condition is an uncoordinated asynchronous contraction of the ventricular muscle fibers in contrast to their normal co-ordinated and rhythmic contraction. It results from an abnormal stimulation rather than from damage to the heart. In the fibrillating condition, the heart seems to quiver rather than to beat; no heart-sounds can be heard with a stethoscope—the pumping action of the heart ceases; failure of circulation results in asphyxial death within a few minutes."

Most of the experiments were made on sheep, calves, pigs, and dogs, in which chest dimensions, body weights, heart weights, and heart rates were comparable to those of man, although several species of smaller animals, including guinea pigs, rabbits, and cats were included to establish the general trend of effects with weight and other physiological factors. Foremost of their findings from the practical point of view are:

1. The susceptibility of the heart to fibrillate depends on the phase of the heart cycle at the instant the shock is applied.

2. Repeated shocks are not cumulative in their effects on the heart, and the heart generally returns to normal in about five minutes if fibrillation does not occur.

3. The results on the whole indicated that sinusoidal currents in excess of 100 milliamperes at 60 cycles from hand to foot would be dangerous for shock durations of three seconds or more.

The statement establishing the threshold current producing ventricular fibrillation in man at 100 milliamperes for 60-cycle sine-wave shocks of three seconds or more has been accepted quite generally by the profession. Without any thought of depreciating the value of this conclusion, it is fair to say that much is to be desired yet in the way of additional information, with special regard to the variation of effects with shock duration, wave form, and frequency.

Before proceeding with the proposed analysis of fibrillating currents, it is helpful to review briefly certain conclusions found in the let-go current investigations.[2,3]

Experimental points representing let-go currents for 134 men and 28 women are shown in Figure 1, in which the ordinate gives the percentage of subjects who can release their grasp of a conductor carrying the current shown in the abscissa.[2,3] It is important to emphasize that a sufficient number of points was obtained to determine a normal distribution, as evidenced by the fact that the data closely follow a straight line when plotted on probability paper. Figure 2 shows the results for the 134 men plotted as per cent deviations from 15.87 milliamperes, the mean of the group. The straight line governed by the majority of the points of Figure 2 has been called the deviation curve. When points representing the women were plotted as per cent deviation from the mean of their group, it was found that they followed a deviation curve having the same slope. Similar results were found for composite waves consisting of a mixture of alternating current and direct current, for rectified 60-cycle sine waves, and for sine-wave alternating currents from 5 to 5,000 cycles. This finding is important because it permits improved accuracy in predicting results for large groups based on a relatively small number of experimental points.

This procedure will be used now to study 60-cycle fibrillating currents obtained by Ferris and his associates. Figure 3 shows fibrillating currents plotted as per cent deviations from the mean of each series, respectively, for eight different tests. Although the distribution of the points does not line up as well as that found for let-go currents, it does establish that a definite trend exists. This holds for the four species of animals for 3-second shocks, and for the sheep for shock durations of 0.03 to 3.0 seconds. It is possible that the same trend also might hold for shocks of various durations for the other animals and for man.

Because of the small number of points available for any test, the straight line governed by all the points was drawn to determine the deviation curve. Apparent discrepancies of a few of the points

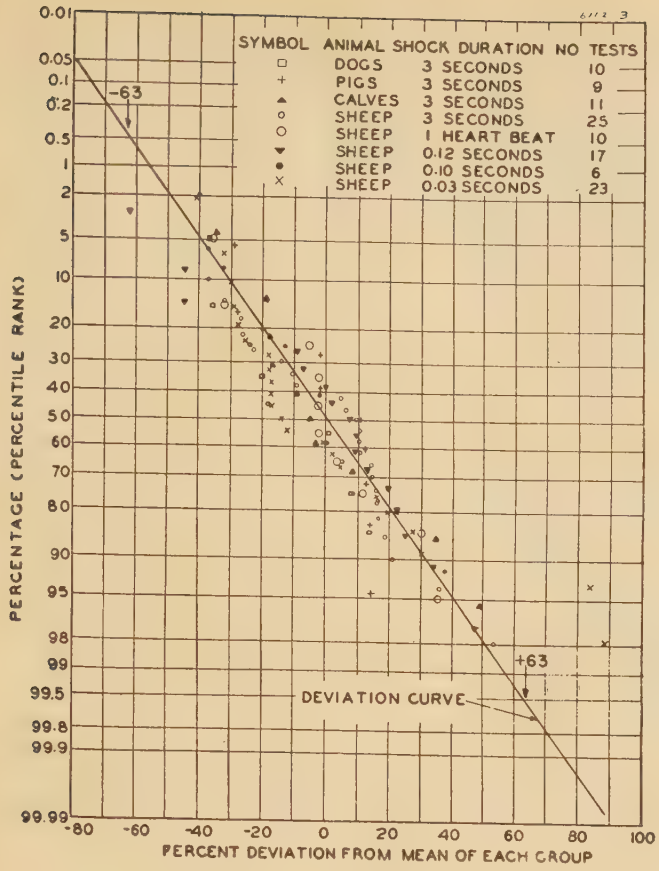

Figure 3. Sixty-cycle sine wave fibrillating current deviation curve for various animals

from the deviation curve are believed to be caused by the small number available for any single test, to experimental errors in applying the shocks at the most susceptible phase of the heart cycle, to the rather wide variation in body weights, and to other factors which properly are included in the term biological variability.

The fibrillating current for an animal was taken as 1/2 (minimum current causing fibrillation + maximum current not causing fibrillation). It is believed that the value so obtained should be reasonably close to the current just required to produce fibrillation during the most susceptible phase of the heart cycle, and the statistical method of analysis should minimize errors.

The current pathway for these experiments was between the right foreleg and the left hind leg. Experiments also were made using four other pathways, namely, across the chest, chest to foreleg, head to hind leg, and between both hind legs. For the current pathway between the two hind legs, the portion of current reaching the heart was evidently too small to produce fibrillation for currents within the operating range of the equipment. Differences in values for the other pathways did not appear great enough to be significant, and it was concluded that results obtained for the pathway between the foreleg and the hind leg should be sufficiently accurate for most engineering purposes.

Data obtained by the investigators at Columbia University[4] for 129 points were furnished the author. Of this number, 111 were used and 18 omitted in the statistical analysis. The points rejected represented two different conditions. Eight high points, designated by these investigators as mode *A*, were omitted to give conservative results. The remaining ten points were from the 0.47-second shock test made on sheep.

The following is submitted as justifying rejection of the 0.47-second test:

1. Results of the 0.47-second shock test are shown in Figure 4 in which the response follows a deviation curve of much smaller slope than that found for the other tests. Wide differences in the results of two almost identical tests suggest the possibility of error. The points representing shocks of one heartbeat (large open dots, Figure 3) are consistent with all the other tests, and fall very nicely about the deviation curve. The duration of the shocks for this test was adjusted to equal as nearly as possible the time of the individual's heartbeat and varied from 0.36 to 0.55 second, averaging 0.45 second. It is untenable that a difference of only 0.02 second in the average shock duration would be sufficient to cause the difference in response indicated by the two deviation curves.

2. The accuracy of analyses based on statistical procedures depends upon a representative number of points. It was difficult to establish deviation curves for let-go currents for less than about 25 points. The apparent inconsistency of a single test involving only 10 points therefore is not considered sufficient to invalidate the analysis.

Fibrillating currents for three-second shocks for seven species of animals versus body weight are shown in Figure 5. Points representing the larger animals total 55, and none were discarded. The smaller animals were represented by average values only, as data for these cases were not furnished the author. The 50 per cent line was drawn by inspection through the points representing the means of the various tests. The author is still in doubt as to where to draw the best line, and the analysis was carried on from here, using a broken line neglecting the points for the pigs, and a solid line in which the effect of the pigs was weighed by eye. The fact that the upper line passes very close to the points representing the averages for each of the other six tests is believed significant. It is unfortunate that only nine pigs were used.

In spite of the wide scattering of individual points, it is evident that in general the fibrillating current is proportional to body-weight. Similar variations were encountered when studying let-go currents, but all efforts to find a correlation with age, weight, strength of grip, or arm measurements, were without conclusive results; however, higher values were obtained on well-developed individuals having the appearance of good health. Other things being equal, it is believed that both let-go currents and

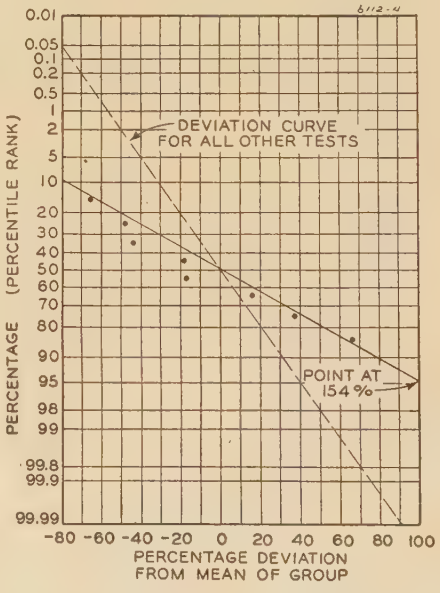

Figure 4. 60-Cycle sine wave fibrillating current deviation curve for sheep

Shock duration 0.47 second
Ten cases tested

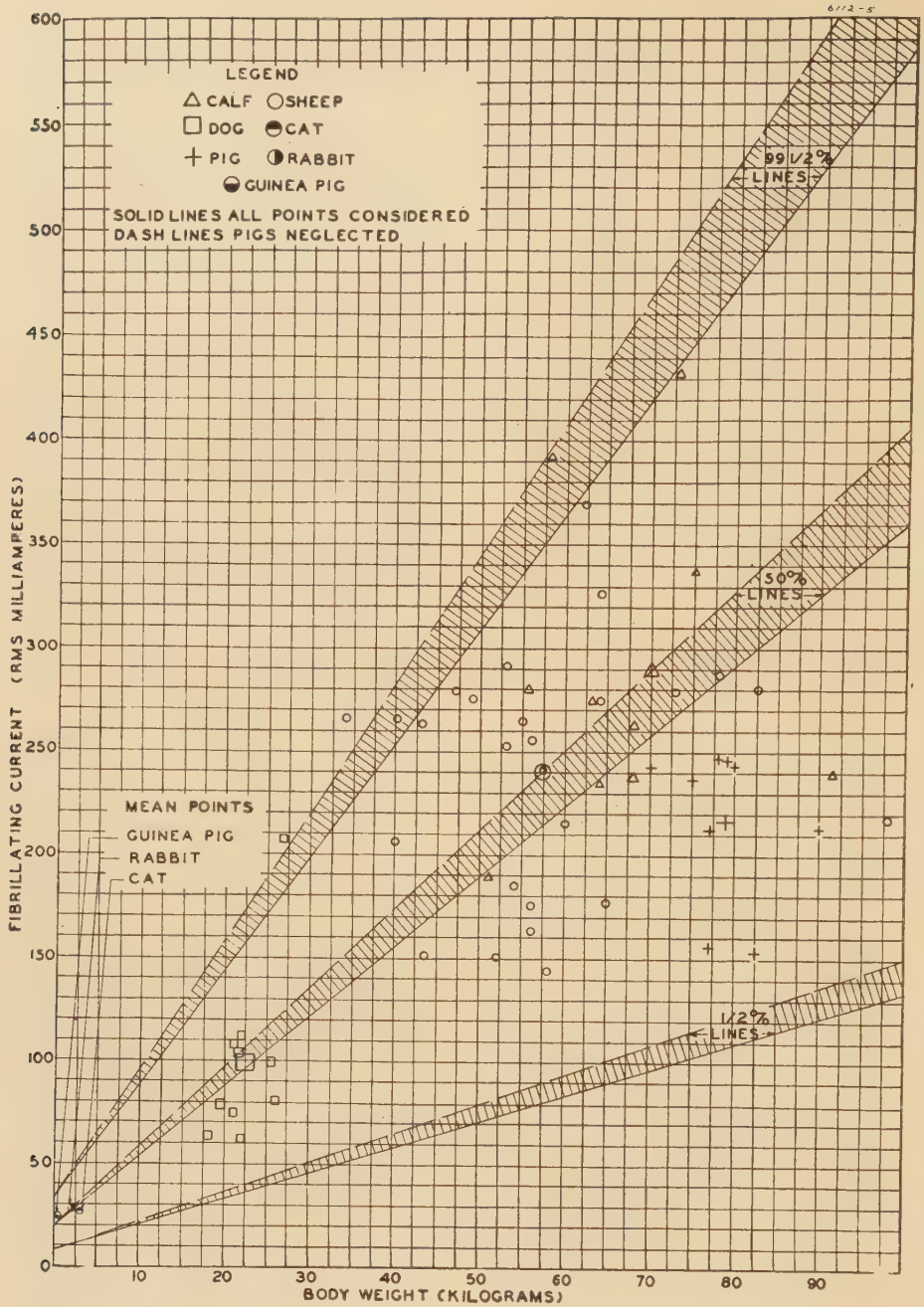

Figure 5. Relation of 60-cycle sine wave fibrillating current of various animals to body weight

Shock duration 3.0 seconds

fibrillating currents at least should be roughly proportional to size and weight.

The $99^1/_2$ and 1/2 per cent lines of Figure 5 were computed using equation 1, reference 2, and the deviation curve of Figure 3. The currents corresponding to a given percentile rank = mean of sample $\times$ (1 $\pm$ deviation from mean). The deviation from the mean for $99^1/_2$ per cent and for 1/2 per cent = ± 0.63, hence:

$$I(99^1/_2 \text{ per cent and } {}^1/_2 \text{ per cent}) = I(50 \text{ per cent})(1 \pm 0.63) \quad (1)$$

Assume that the analysis applies to man. Enter the graph at 70 kilograms which is the weight of an average man, and proceeding vertically indicates that 60-cycle sine-wave alternating currents between 95 and 107 milliamperes and three seconds duration might produce ventricular fibrillation in one half of one per cent of a large group of normal men. This is in close agreement with the generally accepted figure of 100 milliamperes proposed by Ferris, King, Spence, and Williams.[4]

The equation for the lower one half per cent line may be written:

$$I({}^1/_2 \text{ per cent}) = 1.26W + 7.4 \text{ milliamperes} \quad (2)$$

in which W denotes body weight in kilograms.

Figure 6 shows the results obtained on sheep plotted on log–log graph paper in the attempt to determine a relation between fibrillating current and shock duration. A total of 99 points is shown in this figure, including the rejected points, mode A and the 0.47-second shocks previously discussed. Because of the rather wide spread in the body-weight of the various animals, calculated points, shown as open dots on Figure 6, were corrected to 57.4 kilograms to obtain a standard reference. The 1/2 per cent and $99^1/_2$ per cent points were calculated using equations 1 and 6. The $99^1/_2$, 50, and 1/2 per cent lines were drawn with emphasis given the 0.03- and 3.0-second tests because of the greater number of animals used, and to obtain conservative results. Attention is directed to the lone point falling below the one half of one per cent line for the 0.47-second test. This exception must be given serious consideration in deciding whether or not the proposed analysis is acceptable.

If we assume a straight line may be used conservatively to represent the general trend, equations for the lines of Figure 6 may be expressed:

$$I = KT^n,$$

where

n = slope = $-^1/_2$
T = shock duration in seconds

Therefore

$$I = \frac{K}{\sqrt{T}} \qquad K = I\sqrt{T} \quad (3)$$

The equation for I(1/2 per cent) for 57.4-kilogram sheep is found as follows. From Figure 5, when T = 3 seconds, I(1/2 per cent) = 89.5 milliamperes. Substituting in equation 3,

$$\left.\begin{aligned} K &= 89.5\sqrt{3} = 155 \text{ milliamperes} \\ I({}^1/_2 \text{ per cent}) \text{ sheep} &= \frac{155}{\sqrt{T}} \text{ milliamperes} \end{aligned}\right\} \quad (4)$$

The I(1/2 per cent) equation for all 57.4-kilogram animals is found as follows. From Figure 5, I(50 per cent) sheep = 240.5 milliamperes, and W = 57.4 kilograms. The mean fibrillating current for the solid line for a weight of 57.4 kilograms = 215 milliamperes. The corresponding 1/2 percentile value is $89 \times 215/240.5 = 79.6$ milliamperes. Therefore,

$K = 79.6\sqrt{3} = 138$ from equation 3

Therefore, for all 57.4-kilogram animals tested, including sheep,

$$I({}^1/_2 \text{ per cent}) = \frac{138}{\sqrt{T}} \text{ milliamperes} \quad (5)$$

Equations for $I(1/2$ per cent), including effects of shock duration and various body-weights, are obtained as follows. Let subscripts 1 and 2 be used to represent animals 1 and 2, respectively. Equation 2 then may be written

$$\frac{I_1(^1/_2 \text{ per cent})}{I_2(^1/_2 \text{ per cent})}=\frac{1.26W_1+7.4}{1.26W_2+7.4}$$

or

$$I_1(^1/_2 \text{ per cent})=I_2(^1/_2 \text{ per cent})\times \frac{1.26W_1+7.4}{1.26W_2+7.4} \text{ milliamperes} \quad (6)$$

Substituting equation 5 in equation 6,

$$I(^1/_2 \text{ per cent})=\frac{138}{\sqrt{T}}\times \frac{1.26W+7.4}{1.26\times 57.4+7.4} \text{ milliamperes}$$

$$=\frac{2.18W+12.8}{\sqrt{T}} \text{ milliamperes}$$

Inserting $W=70$ kilograms (average weight for man),

$$I(^1/_2 \text{ per cent}) \text{ fibrillating current for man} =\frac{165}{\sqrt{T}} \text{milliamperes} \quad (7)$$

The broken line (neglecting the effect of the pigs) of Figure 6 was obtained by substituting equation 4 in equation 6 and $W=$ 70 kilograms. It is interesting to note that the uncertainty of the current versus weight-lines of Figure 5 produces an inappreciable difference in the final result, as indicated by the small width of the crosshatched area of Figure 6.

It should be repeated that this analysis is based on experiments in which the duration of the shock was varied from 0.03 to 3.0 seconds. Extrapolation for larger range of shock durations should be made with caution; possibly the relations might hold for durations from five seconds to one cycle or possibly one fourth cycle. No account is taken here of inhibition of respiration or of the cumulative effects of shocks at intervals of the order of seconds. These relations are based on the assumption that the heart recovers fully from one shock before a second shock occurs. In other words, the threshold currents are for single shocks. No data are available regarding the effects of repeated shocks such as those produced by intermittent electric fence controllers.[5,6] It must be stressed that application to man is entirely conjectural.

Relatively large currents (amperes and not milliamperes) may produce sufficient heat to destroy nerves, protoplasm, bone and cause hemorrhages resulting in immediate death. Delayed death may be due to burns or other complications.

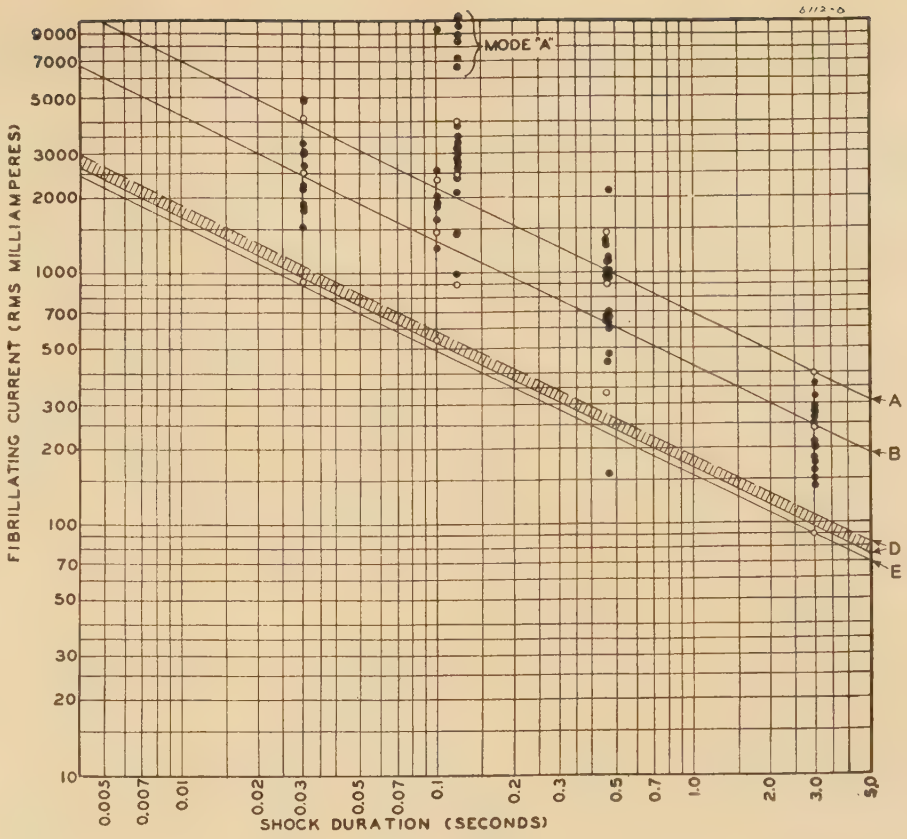

Figure 6. Relation of 60-cycle sine wave fibrillating current to shock duration

- Experimental points
- o Calculated points

A—99$^1/_2$ per cent line for 57.4-kilogram sheep
B—50 per cent line for 57.4-kilogram sheep
C—$^1/_2$ per cent line for all 70-kilogram animals including man
D—$^1/_2$ per cent line for 57.4-kilogram sheep

For 0.03-second shocks, the hearts of sheep seemed to be most susceptible to fibrillate at currents of about six amperes, and less sensitive as the current was either increased or decreased from this value. Figure 7 was taken from reference 4 to illustrate the point. The explanation of this phenomenon is that high currents cause complete contraction of the entire heart musculature, and fibrillation is prevented. If the shock is of appreciable duration, death is inevitable. However, if the shock is of short duration, when the current is interrupted, relaxation may be followed by a spontaneous resumption of normal rhythmic contractions. It is believed that the abdominal massage and accompanying stimulation of the heart caused by the application of artificial respiration may be beneficial in assisting the heart to regain its normal rhythm. This is offered in explanation of infrequent accident cases in which victims apparently withstand relatively large currents.

Ventricular fibrillation may be caused by mechanical stimulation of the heart when it is exposed during surgical proce-

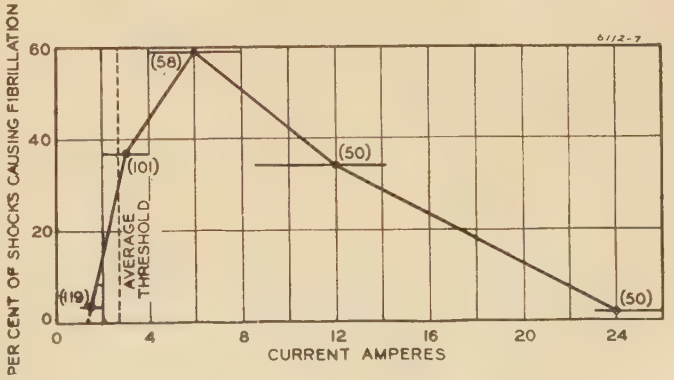

Figure 7. Effect of current on susceptibility of sheep hearts to ventricular fibrillation

Shock duration 0.03 second frequency 60 cycles. Shocks applied in partial refractory period of cardiac cycle. Number of shocks and current spread indicated for each point on curve

dures as well as by electric shock, and occasionally the heart goes into fibrillation during major operations involving the chest. Although several investigators have reported a degree of success in using counter-electric shocks to arrest fibrillation in animals, C. S. Beck[7] is the first to publish a procedure for human beings. He reports two cases in which two large electrodes were held directly against the heart and an alternating current of 1.5 amperes successfully defibrillated the ventricles and saved the patients. Procedures applicable to the surgeon's operating table are vastly different from those encountered in most accidents. The brain and nervous systems remain viable from three to five minutes after circulation ceases. This time interval is so short that once ventricular fibrillation occurs in man, little can be done to save the victim.

The hazard due to direct current is of increasing importance due to the greatly increased use of d-c welding equipment and high-voltage power supplies. The ratio of average d-c release to 60-cycle let-go currents is about 4.8 to 1. Ferris and associates determined the direct current required to produce ventricular fibrillation in 11 sheep for 3-second shocks. The ratio of average d-c to a-c fibrillating current was 5 to 1. This information, although obtained for only 11 animals, is the only quantitative data available on fibrillating direct current. It is to be expected that the fibrillating current for very short shocks would approach the 60-cycle crest value. This is a ratio of $\sqrt{2}$ to 1. If we assume that the lines of Figure 6 apply for durations as short as one fourth cycle, that is, 0.0042 second, a second value may thus be established. A series of straight lines for direct current shocks similar to those of Figure 6 could be drawn, using the factors 5 and 1.41 for shock durations of 3.0 and 0.0042 second, respectively.

The danger from capacitor discharge is of vital importance. It generally is believed that the initial current and charge are of prime importance in determining the hazard. The time constant of the circuit and the stored energy also may be important, but no data are available on this phase of the subject. An idea of threshold fibrillating currents may be obtained from Figure 6, if we assume that the 60-cycle response holds for shocks of 1/4-cycle duration. The one half of one percentile value for man corresponding to 0.0042 second is 2,600 rms milliamperes. Multiplying by $\sqrt{2}$ gives 3.7 crest amperes, which may be considered as the equivalent capacitor initial current.

Table I. Impulse Tests on Animals

No. of Animals	Age, Mos	Est. Weight, Lbs	Open Circuit Voltage	Capacitor Charge, Milli-coulombs	Animal Resistance, Ohms	Avg. No. of Shocks	Remarks
Spring lambs. Contacts—metal electrode on lips to rear feet in bucket of salt water							
10	4–6	72	1,400	18.2	550–1,750	3	
10	4–6	70	1,600	20.8	550–1,750	3	Three sheep stunned for 5–15 sec*
13	4–6	72	1,750	21.0	550–1,750	3	One sheep stunned for 5–15 sec*
6	4–6	72	1,750	22.7	550–1,750	2	One sheep stunned for 5–15 sec*
Pigs. Contacts—insulated feed trough to rear feet on wet earth							
1		180–200	1,400	4.2		4	
25		180–200	1,400	7.0		4	
1		215–225	1,000	10.0		1	
2		215–225	1,200	12.0		1	
1		215–225	1,600	16.0		1	
25		215–225	1,750	17.5		1	
1		215–225	1,400	16.8		1	
12		215–225	1,750	21.0		1	One pig stunned f 60 sec*

* Animals were stunned on third or fourth consecutive shock.

Reference 5 contains an account of studies made by the author in the attempt to determine the hazard due to impulse currents. The investigation was made to determine the hazard of capacitor-discharge electric-fence controllers and included a survey of human accidents on lightning generators. A few capacitor discharge tests were made on male volunteer subjects on voltages up to 1,750. Impulse tests using larger capacitors were made on spring lambs and pigs. Table I shows some of the data obtained from tests made on the animals. No fatalities were experienced and higher power was not used because of limitations of equipment. No attempt was made to co-ordinate the shocks with the sensitive phase of the heart-cycle. However, because of the large number of shocks applied, it is reasonable to assume that they were distributed throughout the heart-cycle, and probably many occurred during the sensitive phase. It would seem that the highest currents given the smallest animals might give some idea of reasonably safe upper limits. The average weight of the spring lambs was 72 pounds or 32.6 kilograms, maximum voltage 1,750, and maximum charge 22.7 millicoulombs. Considerable difficulty was experienced in measuring the body-resistance of the animals because of unavoidable variations in contact resistances. Best results were obtained using a d-c ohmmer, the values ranging from 550 to 1,750 ohms. Using a conservative value of 930 ohms for circuit, animal, and contact resistance, equation 6 gives an initial current of 3.7 amperes which compares with that suggested in the preceding paragraph. If we assume that equation 6 holds for both current and charge, the corresponding value for man is 45 millicoulombs.*

The criterion proposed for defining dangerous current thresholds is based on the current which might produce ventricular fibrillation in one half of one per cent of a large group of normal adult men. The choice of course is arbitrary, and any other number could be selected. There is no intention to be ruthless about the remaining one half per cent; however, one has to stop somewhere, and the 1/2 percentile was considered a reasonable stopping point. Perhaps the best justification for choosing the 1/2 percentile is that it was used in estimating reasonably safe let-go currents and provoked no adverse comment.[1,2,3] As previously mentioned, all available experimental data were analyzed carefully, and in instances which required special judgment (such as just where to draw the best line to determine the general trend of a response), an attempt was made to adopt procedures which would give a conservative final result. Several different attempts were made to correlate the data, but the method proposed is believed to be the best that can be done. It is indeed unfortunate that statistical predictions must be expressed numerically, as there is a tendency to place too much emphasis on mere numbers. Quite aside from the uncertainties of the present analysis, there remains the important uncertainty of transferring results obtained from animal experimentation to man. However, data from numerous human accidents, although meager and inconclusive, seem to

* The charge or quantity of electricity passing a given point in a circuit is given by:

$Q = 10^{-3} \int i \, dt$ millicoulomb (milliampere-seconds)

For a capacitor of C microfarads charged to E kilovolts,

$Q = CE$ millicoulomb (milliampere-seconds)

An Electronic Drive for Windup Reels

K. P. PUCHLOWSKI
ASSOCIATE AIEE

REELING OPERATIONS impose a number of special requirements on the reel drive, particularly if the latter is of the so-called core type as compared to the rather rarely used peripheral type drive.

In a core type drive the reel is driven through a center axle on which it is mounted. This type is usually preferred to the peripheral type drive which involves traction along the periphery of the reel and thus requires a direct contact and a sufficiently high tangential force exerted upon the material being wound. It is apparent that, although the peripheral drive usually will represent a much simpler electric system since it is not influenced by the change in the diameter of the reel, it is often undesirable or even impossible to transmit the driving torque directly through the material involved in the winding operation.

The core type drive, on the other hand, does not present these disadvantages, and is used most commonly, although it normally involves other problems and the resulting complications of the electric system.

Two basic quantities usually are associated with any reeling operation where a continuous strip of material such as yarn, fabric, wire, or steel, for example, is drawn by the so-called take-up reel and wound on it, so that the diameter of the reel gradually increases during the process. The first quantity is the speed, and the second, the tension of the strip. Some reel systems impose exacting requirements as to the automatic regulation and control of one or both of these quantities.

This paper presents the description of a recently developed electronic drive and control for a core type take-up reel where the speed of the strip is maintained constant automatically during the entire reeling operation. In addition, the speed of the strip can be preselected by the operator within a wide and stepless range. The problem of tension of the strip is not considered here. In many of the applications, tension of the strip is of secondary importance, and proper control of speed is a fundamental requirement. Furthermore, tension regulating devices always can be added, if so required, by proper control of the unwinding reel. The drive described in this paper has been developed for take-up reels in systems where the reel also performs the drawing of the strip and thus determines the speed of the line.

Paper 46-125, recommended by the AIEE committee on industrial control devices for presentation at the AIEE summer convention, Detroit, Mich., June 24–28, 1946. Manuscript submitted April 26, 1946; made available for printing May 9, 1946.

K. P. PUCHLOWSKI is design engineer, industrial control engineering department, Westinghouse Electric Corporation, East Pittsburgh, Pa.

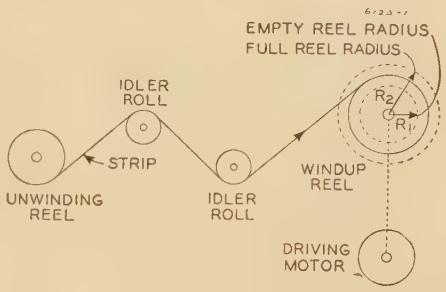

Figure 1. Outline of a windup reel system

Principles of Core Type Reeling

In Figure 1 is shown schematically a take-up reel with its minimum and maximum diameters. The radius of the reel builds up during the reeling operation from a minimum value R_1 to a maxi-

---

indicate that the proposed threshold values are conservative. It is the author's opinion that currents much in excess of the proposed threshold values must be considered very dangerous to human life. Perhaps, at some future date, sufficient time and funds may be available and a more accurate solution be obtained.

We are indebted to H. B. Williams for the following discussion of effects at high frequency. On sinusoidal high-frequency alternating currents, or on repeated current pulses of very short duration, account must be taken of the fact known to physiologists that, as the shock duration decreases, its strength must be increased in order to produce the same stimulation. As the duration becomes very small, this increase must be very great, finally becoming so great that destruction of living substances may occur before it can respond. At higher frequencies, large currents may pass without causing stimulation of muscles or nerves, and these may cause deep heating effects. Since the heat-sensitive mechanism is located in the skin, there is a possibility of damage to internal organs by high-frequency currents even though no very unpleasant sensations may be apparent. The currents necessary to produce this effect would be in the order of an ampere or more. High-frequency currents of several hundred milliamperes are used quite commonly by the medical profession for deep heating. This form of treatment is called medical diathermy.

In concluding, it should be mentioned that, because of the wide variation in the physical condition of individuals, an occasional death is to be expected from casual contact involving electric currents known as safe for most normal, healthy individuals, but these are probably not fibrillation deaths. It is gratifying indeed that victims surviving the initial shock of an electrical accident seldom suffer serious aftereffects or other permanent disability. Since it is impossible for the layman to distinguish between respiratory inhibition, ventricular fibrillation, and heart failure, he should begin artificial respiration immediately and summon medical aid as soon as possible.

References

1. ELECTRIC SHOCK, C. F. Dalziel, J. B. Lagen, J. L. Thurston. AIEE TRANSACTIONS, volume 60, 1941, December section, pages 1073–9.

2. EFFECT OF FREQUENCY ON LET-GO CURRENTS, C. F. Dalziel, E. Ogden, C. E. Abbott. AIEE TRANSACTIONS, volume 62, 1943, December section, pages 745–50.

3. EFFECT OF WAVE FORM ON LET-GO CURRENTS, C. F. Dalziel. AIEE TRANSACTIONS, volume 62, 1943, December section, pages 739–44.

4. EFFECT OF ELECTRIC SHOCK ON THE HEART, L. P. Ferris, B. G. King, P. W. Spence, H. B. Williams. AIEE TRANSACTIONS, volume 55, 1936, May section, pages 498–515.

5. THE ELECTRIC FENCE, C. F. Dalziel, J. R. Burch. *Agricultural Engineering*, volume 22, November 1941, pages 309–406.

6. ELECTROCUTION BY ELECTRIC FENCE CONTROLLER, C. F. Dalziel. *Agricultural Engineering*, volume 25, August 1944, page 308.

7. DIAGNOSIS AND TREATMENT OF CARDIOVASCULAR DISEASE (book), Volume 2. Edited by W. D. Stroud. Chapter 37, Resuscitation of Heart from Standstill and from Ventricular Fibrillation, C. S. Beck. F. A. David, 1940. Pages 1181–2.

mum value R_2. The speed of the strip may be expressed by the following equation

$$v = 2\pi nR \text{ feet per minute} \quad (1)$$

where

n = motor speed in revolutions per minute
R = instantaneous radius of the reel in feet

The torque developed by the motor

$$T = FR + T_0 \text{ pound-feet} \quad (2)$$

where

F = tension of the strip in pounds
T_0 = torque loss due to friction in the reel, gears and windage

The power developed by the motor may be expressed as

$$P = 2\pi nT$$

or, considering equation 2,

$$P = 2\pi n(FR + T_0)$$
$$P = 2\pi nRF + 2\pi nT_0 \quad (3)$$

The first term of equation 3 obviously represents the useful power required to draw the strip, and is the product of the strip speed v, and strip tension F. The second term, which is the product of the motor angular speed and the friction torque of the reeling system at the motor shaft, represents the loss of power of the reeling system. Thus, the efficiency of the reeling system

$$\eta = \frac{1}{1 + \frac{T_0}{RF}} \quad (4)$$

It is apparent from equation 1 that in order to maintain constant line speed v, the speed of the driving motor must change in inverse proportion to the diameter of the reel. On the other hand, if the friction torque T_0 is neglected, then the power required during the reeling operation

$$P = vF = 2\pi nRF = \text{constant}$$

Thus, if a constant line speed is to be maintained during the reeling from an empty reel with a radius R_1, to a full reel with radius R_2, the speed of the driving motor n corresponding to any intermediate radius R of the reel should be

$$n = n_1 \frac{R_1}{R} \quad (5)$$

where n_1 is the motor speed for an empty reel.

As was mentioned previously, the power requirement imposed on the drive during reeling remains essentially constant and, consequently, the most adequate and economical way of obtaining the required speed control is by controlling the field excitation of a d-c shunt-wound motor.

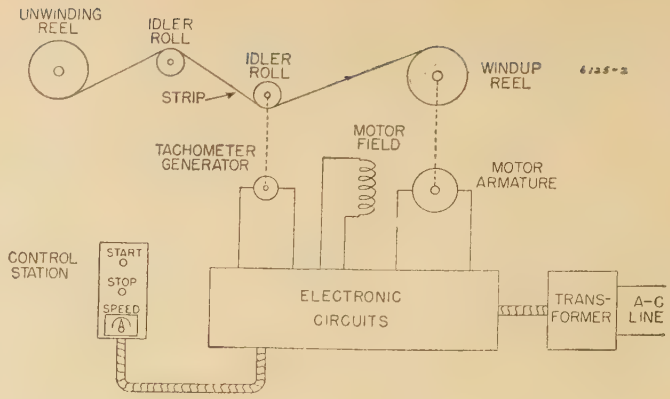

Figure 2. General scheme of the electronic drive for windup reels

Another type of speed control is necessary to provide an adjustable strip speed, and it is often required that a speed range as wide as ten to one be provided by the drive. Here, if an approximately constant tension is assumed, for any given radius of the reel, the required torque is independent of the line speed (see equation 2), and the required horsepower is directly proportional to the line speed v (if the friction torque T_0 is neglected). Consequently, the armature voltage control of a d-c shunt-wound reel motor is the most suitable means of obtaining the control of the strip speed.

A clear distinction between the two types of the reel-motor speed control should be specifically emphasized. For any given diameter of the reel, the line speed should be adjustable by armature voltage control of the driving motor, and the speed of the motor should remain constant for a given excitation and a given speed setting, even if the torque is varied within wide limits. This speed control should not respond to changes in the diameter of the reel.

The second type of speed control should respond automatically to any change in the diameter of the reel, so that with increasing diameter, the excitation of the motor should increase automatically to slow the motor down just enough to prevent the speed of the strip from being increased. The field control of the motor should not respond, generally speaking, to any change in line speed obtained through the armature voltage control.

Basic Control System

To maintain a constant strip speed with varying diameter of the reel, an electronic field regulator is incorporated into the system. The term regulator, or servomechanism means an automatic control system characterized by a closed cycle of interdependence of quantities involved, so that a slightest deviation of the regulated quantity from the predetermined value results in the appearance of the so-called restoring force, which acts in the direction to oppose any change in regulated quantity, or, if some change has already occurred, to restore the quantity to its original value. Actually, the most accurate and sensitive regulator is unable to restore the deviated quantity to exactly its original value, when a definite cause for the deviation exists. This is so because the regulator creates a restoring force or "back-to-normal" action only in response to some existing deviation, and a new balance of the system always will be established only with the existence of some deviation. However, a satisfactory regulating system will reduce the deviation to such a minimum that, depending upon the application, it may be assumed to be negligible.

Any regulator is characterized by the following four basic elements which form the links of the previously mentioned closed cycle of interdependence of quantities:

1. Indicator of the regulated quantity.
2. Standard reference quantity with which the regulated quantity is compared.
3. Amplifier which originates a sufficiently strong restoring force even for minor deviations of the regulated quantity from the prescribed value.
4. Restoring force which manifests itself in an action opposing any deviation of the regulated quantity.

In addition, a regulator may have a number of secondary elements such as damping (antihunting) and anticipatory elements which play a vital part in the stability and the time of recovery of the regulating system.

The electronic reel drive is shown schematically in Figure 2. A tachometer generator driven by the strip through an idler roll is used as the indicator of the regulated quantity, that is, of the line speed. Since this generator is required to deliver only negligible

power, its size may be small and, consequently, its WR^2 and losses equally small. The preferable tachometer generator is a d-c permanent-magnet type, as here there is no need to provide separate excitation or, as in the case of an a-c type, to amplify and then rectify the output to make it a useful indication of speed. Besides, the permanent-magnet type tachometer generators usually have an excellent voltage–speed characteristic. The output voltage of a d-c permanent-magnet tachometer generator represents a linear function of its speed, particularly when the current output is negligible. The voltage output is relatively high, of the order of 50 volts per 1,000 rpm, and for all practical intents and purposes, independent of temperature changes or any other external influences. A typical voltage–

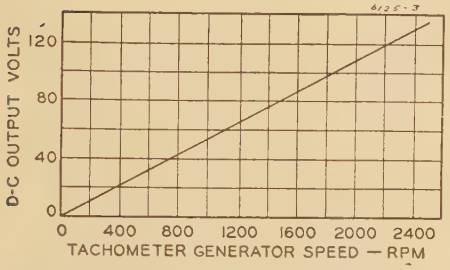

Figure 3. Typical output voltage of a d-c permanent magnet tachometer generator

speed characteristic of a permanent-magnet tachometer generator is shown in Figure 3.

The output voltage of the tachometer generator (see Figure 2) is introduced into the field control portion of the electronic drive where it is balanced or compared with a reference voltage. The difference of the two is then fed into an amplifier, and after the amplification, is used to control the output of a thyratron-exciter which supplies the field current to the reel motor. As it will be seen later, the control circuits are so designed that when the line speed tends to increase because of the increase in the diameter of the reel (see equation 1), the field of the motor is strengthened to slow the motor down in accordance with equation 5. This forms the previously mentioned closed cycle of interdependence of quantities, which is represented in Figure 4.

The armature power supply and armature control of the electronic drive is obtained by means of a controlled rectifier consisting of thyratron elements and various control circuits. These circuits provide a constant-speed characteristic so that for a given excitation of the field, the speed of the motor remains essentially constant for any variation of torque within the operating range of torque values. The armature control circuits are of the voltage regulated, *IR* drop compensated type. They provide a properly rising voltage–current characteristic and essentially constant speed–current characteristic. Current limit features also are incorporated in the armature control circuits, to take care of the starting and overload conditions of the drive.

In addition to a constant speed–torque characteristic, the armature control circuits provide means for adjustment of the motor speed by voltage control, and in that manner the strip speed can be changed. Each setting of the speed control dial corresponds to a different but strictly determined line speed, automatically regulated to stay constant and independent of the changes in the diameter of the reel. Usually, the line speed control dial is a small $1^1/_2$ inch in diameter potentiometer, assembled as a part of a separately mounted control station, which also includes other operator's controls such as start and stop push buttons and threading speed push button. The operator's control station usually is mounted remotely from the cabinet housing all the electronic controls and at a location most convenient for the operator. The armature control portion of the drive as well as the operator's control station is shown schematically in Figure 2.

Special Problems

Outside of system stability problems which are, of course, present in any regulating system and require special stabilizing means, the following two problems are of particular importance:

1. Field control during the acceleration.
2. Field regulator response to a change in line speed resulting from the readjustment of that speed by the operator.

Although these problems will be discussed in more detail later, in connection with the description of circuits, it seems appropriate to mention their nature in advance.

Referring to the acceleration problem, it should be noted that at the instant of starting the reel drive, the voltage output of the tachometer generator is zero. Furthermore, at the start of the reeling operation the reel is empty and, obviously, the driving motor and reel should accelerate to a maximum operating speed, corresponding to the lowest operating value of the motor field. Consequently, it follows that on starting of the drive, when the speed of the line is zero, the regulator, responding to a low speed signal of the tachometer, will naturally tend to decrease the field excitation of the motor to a minimum. Considering a relatively low value of starting current limited by the current limit circuit (see section on armature control) to about 200 per cent of rated armature current, it will become apparent that a very low starting torque will be developed by the reel motor so that the latter may not accelerate at all. To prevent this, a special electronic accelerating circuit is added to the field regulator. When the reel motor is not running, this field accelerating circuit maintains full field current, and when the motor is started, the field still is maintained during the initial portion of the

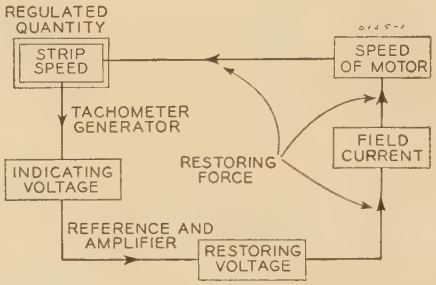

Figure 4. Cycle of interdependence of the strip speed regulator

accelerating period. Then the field current gradually is decreased exponentially with time, but, owing to a special electrical coupling between the armature and field control circuits, it never is allowed to decrease below a certain minimum value, as long as the armature current exceeds the rated value more than by about 50 per cent. As soon as the armature current drops to its normal operating value, indicating that the acceleration of the motor is completed, the action of the field accelerating circuit disappears, and the field current of the motor is controlled by the regulator through the tachometer generator which has by that time accelerated to its operating speed. From now on the regulation of the line speed proceeds as described previously.

The problem of the field regulator response to a change in tachometer generator signal, when caused by the readjustment of the line speed by the operator, deserves special attention. As pointed out before, the slightest change in the tachometer generator output voltage, indicating a change in line speed, normally

will result in the action of the regulator to properly change the motor excitation and its speed in such a way as to oppose any change in the tachometer generator signal voltage. However, if the change of the tachometer generator voltage is caused by the line speed change through armature voltage control, the regulator obviously should not respond to that change. In other words, when the change in the tachometer generator voltage is a result of the change in diameter of the reel, the regulator should respond and control the motor field, but for any given diameter of the reel, the field current of the motor should remain essentially the same for different line speeds.

This requirement is fulfilled by using two potentiometer units mounted in tandem as operator's line speed control. One of the potentiometer units is used in a regular manner as the armature speed control, the other properly changes the field regulator reference voltage. Thus, for example, when the knob of the speed control is operated to call for a higher line speed, the tachometer generator signal voltage will become higher, and this normally would cause the regulator to increase the excitation of the motor. However, the operation of the control knob in the direction to increase the line speed also will increase the reference voltage of the field regulator in such a manner that the difference between the two voltages will remain the same, and the field current will not be changed.

The voltage across the reference potentiometer of the regulator can be easily adjusted so that a change in line speed and in armature voltage is accompanied by a proper change in reference voltage of the regulator. In fact, this adjustment by no means is critical, and some small changes in the field current for different operating line speeds can be tolerated, since this will not produce any adverse effect on the operating or regulating properties of the drive.

Electronic Circuits of the Drive

A simplified schematic diagram of the electronic drive is shown in Figure 5. It includes all the elements necessary for the proper explanation of the principles of operation of the system. For the sake of simplification, details of various auxiliary d-c power supplies have been replaced by batteries. Heater circuits for all the electronic tubes have been omitted, and all the grid controlled tubes, both of the thyratron and high vacuum type, are represented as triodes. All the by-pass and filtering capacitors also have been omitted. The diagram covers the entire electric system of the reel drive and is divided distinctly into the armature control and the field control portions.

Armature Control Circuits

The armature control circuits are similar to those described and analyzed in detail in a previous paper.[1] They consist, as shown in Figure 5, of four major groups: the controlled power rectifier, master regulating and control circuits, *IR* drop compensating circuits and the current-limit circuits. The power rectifier circuit is shown as a symmetrical 2-phase rectifier (often called single-phase full-wave rectifier) although it may be also a 3-, 4-, or 6-phase unit, depending upon the horsepower rating of the drive. The rectifier consists of a center-tapped winding of the main transformer *T*1, two thyratron tubes 1 and 2, contacts *FCR* of the main contactor, fuses in the anode circuits, grid transformer *T*3, and current transformer *T*2. A phase-shift circuit consisting of a center-tapped winding of transformer *T*1, resistor *R*14, and capacitor *C*1 provides a voltage which lags the rectifier anode supply voltage by about 90 to 100 degrees. This lagging voltage is applied to the primary winding of the grid transformer *T*3. The grid control voltage of the thyratrons consists of an a-c component supplied by transformer *T*3 and a d-c component. The latter is applied between the cathodes of tubes 1 and 2, and the center tap of the grid transformer *T*3. During the control process the angle of ignition of the thyratrons is changed either automatically or manually by proper changes in the d-c component which may assume both negative and positive values so that the constant a-c component of the grid voltage, superimposed upon the variable d-c component, can be moved up or down and control the angle of ignition in a well-known manner.

Control of the d-c component of the thyratron grid voltage is obtained through the variable voltage across the load resistor *R*10 of the main control tube 5. If tubes 3, 4, and 6 are disregarded temporarily, it will be easy to notice that the armature system is an adjustable voltage regulator. Thus, the voltage across *R*2 is the indicator of the regulated quantity, being proportional to the armature voltage. The adjustable portion of the potentiometer *PA* represents the reference voltage. The *PA* voltage is negative with respect to the grid of tube 5 and the *R*2 voltage is positive. Since the voltage across the adjustable portion of *PA* always is higher by several volts than the voltage across *R*2, their difference applied to the grid of the master control tube represents a negative voltage of several volts.

The grid circuit of the thyratrons is completed from the cathodes through *R*2, *PA*, *R*12, *R*10, and *R*6 to the center tap of transformer *T*3. All the d-c components in that portion of the circuit essentially are constant except the voltage across *R*10 which changes with the plate current of tube 5, and performs the actual control of the angle of ignition of the power thyratrons. It is important to note that the direct voltage across *R*10 has a negative polarity with respect to the grids of thyratron tubes. Thus, when the plate current of tube 5 is high, the angle of ignition of the thyratrons is delayed greatly, and if the current of tube 5 still will increase, the thyratrons will be cut off altogether. Conversely, when the plate current of tube 5 is decreasing, the negative voltage component across *R*10 will decrease, and the angle of ignition of the power thyratrons will be advanced, increasing either the voltage or the current output of the armature rectifier, or both.

It is apparent that the voltage across *R*10 together with the grid control of the thyratrons represents the restoring force of the armature voltage regulating system, since any deviation of this voltage from the prescribed value will result in a response of the amplifier 5 and a change in voltage across *R*10 in the direction to oppose the deviation of the armature voltage. Furthermore, a change in the reference voltage obtained by the readjustment of *PA* will result in a change in rectifier voltage output so that a new balance of the system will be obtained at a different armature voltage, that is, a different speed of the motor. The difference between the reference and the indicating voltages, however, will not be changed appreciably because of the strong amplifying action of the regulating tube 5.

It is well known that if the armature voltage remains constant, for a constant excitation, the speed of the motor usually will drop with increasing torque, as is normally the case for shunt-wound motors. This drop is caused mainly by the *IR* drop in the armature circuit. Although this drooping speed–torque characteristic is usually not objectionable at rated motor speed, at lower speeds such as one-tenth of the base speed, a

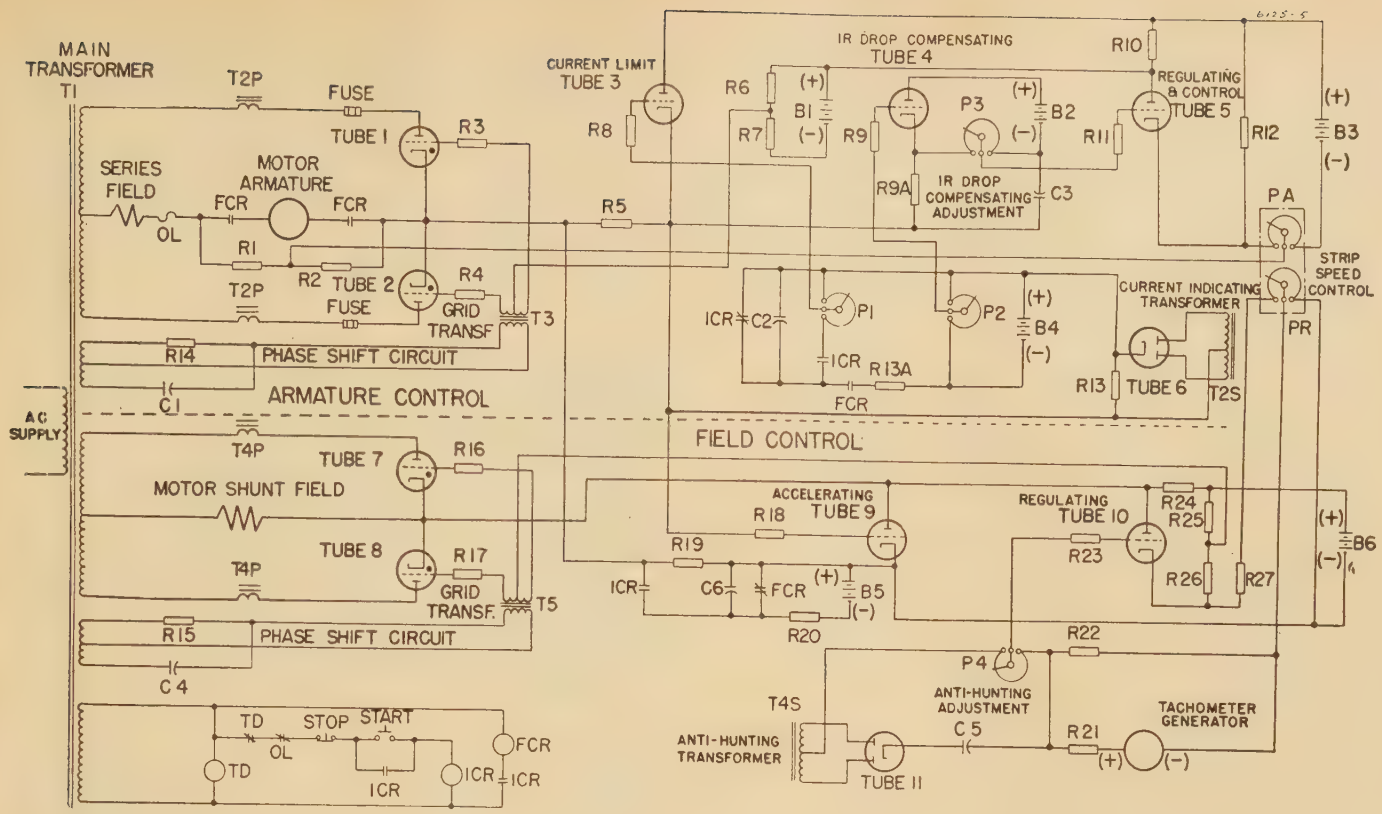

Figure 5. Schematic diagram of the electronic drive for windup reels

normally drooping characteristic of about 10 per cent will mean a very poor speed regulation and even the inability of the drive to develop full torque.

In order to correct this objectionable droop, an *IR* drop compensating circuit is provided. The main element of the compensating circuit is tube 4, which is controlled automatically by a grid voltage proportional to the armature current. The indication of the latter is obtained through a special current transformer *T2* whose two primary current windings *T2P* are connected in series with the anodes of the power thyratrons 1 and 2. Although each of the windings conducts unidirectional current pulses, connections are such that the resultant magnetic effect is the same as if an alternating current were flowing in the current windings. This prevents the saturation of the current transformer. The voltage generated in the voltage winding *T2S*, generally speaking, is proportional to the motor current. This voltage is rectified by means of tube 6 and then filtered out (the filter is not shown in Figure 5) so that the direct voltage across *R*13 may be used as an indication of the armature current.

There are two main voltage components in the grid circuit of tube 4: the negative bias voltage obtained from *P*2, necessary to determine the proper operating point of tube 4, and the positive current-indicating voltage, described in the preceding paragraph. Thus, an increase in motor torque and motor armature current will cause an increase in plate current of tube 4 and an increase in magnitude of the voltage across *P*3. It will be noted that *P*3, which represents the *IR* drop compensating adjustment, forms part of the grid circuit of the master control tube 5. The voltage across the adjustable portion of *P*3 forms an additional negative component of the grid voltage of tube 5, and with increasing load current of the motor, the grid of tube 5 becomes more negative, the plate current decreases, and the firing point of the power thyratrons is advanced just enough to compensate for increasing *IR* drop of the motor. Conversely, the opposite will occur with decreasing load of the motor.

Tube 3 acts as a current-limiting element of the armature control system. This tube, which is characterized by a sharp cut-off, is biased off by an adjustable negative voltage obtained from *P*1 and does not conduct any current for all the normal loads of the motor. However, when the load current of the motor exceeds a certain critical value, the voltage across *R*13 becomes so high that tube 3 will start to conduct. It will be noted that the load resistor of tube 3 designated as *R*5 is in the grid circuit of the master control tube 5. As soon as tube 3 starts to conduct, a voltage appears across the resistor *R*5, and the polarity of this voltage is positive with respect to the grid of tube 5. Since tube 3 itself provides a considerable amplification, a very small increase of the voltage across *R*13 beyond its critical value results in appearance of a much higher voltage across *R*5. As a result, the plate current of tube 5 is increased, the firing point of the thyratrons delayed, and the armature voltage lowered.

If the motor current continues to rise, the delay of firing point of the rectifiers will soon become so great and the armature voltage so low that the motor will stall with the armature current reaching its limit value. This limit is normally of the order of 200 per cent of the motor rated current, although it may be adjusted by means of the potentiometer *P*1. The current limit which, for a given excitation of the motor, may be called torque limit, plays an obviously important part during the acceleration and overload of the drive.

Capacitor *C*2 connected in parallel with the current limit control potentiometer *P*1, as well as contacts 1*CR* and *FCR* in series with *P*1, have an important function during the starting and stopping

of the drive. On stopping of the drive, contact 1*CR* in series with *P*1 opens first and causes an immediate disappearance of the negative bias voltage for tube 3, so that the latter will conduct its full current. This, of course, will cause the tube 5 also to conduct full current, and the thyratron tubes will be cut off, even before the *FCR* contacts will have time to open completely. As a result, no arcing across main *FCR* contacts will occur.

When the motor is stopped, capacitor *C*2 is discharged by a parallel contact of 1*CR*. On starting the motor, the thyratrons are cut off by grid control as initially there is no voltage across *P*1. After the closure of the relay 1*CR* and contactor *FCR*, the voltage across *P*1 appears gradually since it has to follow the voltage across capacitor *C*2 which is charged from the source *B*4 through the resistor *R*13*A*. Consequently, the firing angle of the thyratrons is advanced smoothly until the current limit circuit takes over the control of the acceleration. Thus, during the starting of the drive, no objectionable current surges may occur in thyratrons 1 and 2, and no sparking on the main contacts of *FCR* ever takes place.

Field Control Circuits

A general outline of the strip speed regulator operating through the field control of the motor was given in one of the previous sections of the paper. A simplified schematic diagram of the strip speed regulating system is shown in Figure 5. It must be noted that the power rectifier portion of the electronic field exciter is fundamentally the same as the power rectifier for armature control, described in the previous section. It consists of two thyratron rectifiers 7 and 8, a center-tapped transformer winding, a grid transformer *T*5, and a phase-shift circuit which provides the constant a-c component of the thyratron grid voltage. The current transformer *T*4, however, has a function different from that of transformer *T*2.

The variable d-c component of the thyratron grid voltage is developed between the cathodes of the thyratrons and the center tap of the grid transformer. It consists of two voltages: a constant negative voltage across *R*25 and a variable positive voltage across *R*24. The voltage across resistor *R*24 is changing with the plate current of either tube 10 or 9, or both.

Tube 10 is the field regulating tube and represents the amplifier of the strip speed regulator. The grid circuit of tube 10 includes the negative reference voltage across *R*27 and a portion of *PR*, and the positive strip-speed indicating voltage across *R*22 obtained from the tachometer generator. The reference voltage always is higher by several volts than the indicating voltage, and the difference of the two represents a negative voltage of several volts applied to the grid of tube 10.

It should be noted that the reference voltage in Figure 5 is obtained as part of the main voltage divider which also includes resistors *R*25 and *R*26 and is supplied from the d-c source *B*6. Although the plate current of tube 10 will flow through *R*27 and *PR* and will change the reference voltage, such a simplified arrangement is permissible if the resistance of *R*27 and *PR* is relatively low so that the voltage drop in these resistive

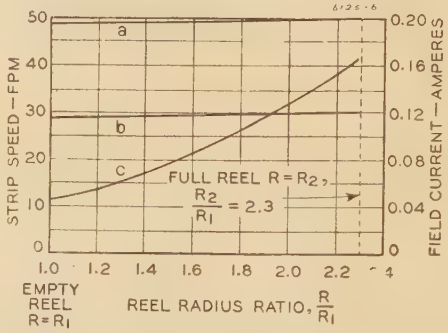

Figure 6. Typical operating characteristics of the electronic drive

elements caused by the plate current of tube 10 is small. Furthermore, one must remember that during the operation of the regulator the plate current of tube 10 changes only slightly because of the general amplification of the system, so that the actual change in reference voltage caused by the change in plate current of tube 10 is negligible.

As an example, with total reference voltage of 25 volts, the resistance of *R*27 and *PR* equal to 1,000 ohms and the change in the operating plate current of tube 10 of 0.1 milliampere for the entire reel-diameter build-up of two to one, the resulting change in reference voltage will be equal to 0.1 of one volt. Thus, the error caused by the change in the reference voltage will amount to 0.4 of one per cent.

Although the figures cited in the previous paragraph are based on actual test records, they may vary for different motors and different reel-diameter ratios, and in some cases it may be advisable to provide a separate d-c supply for the reference voltage of the regulator, particularly if extreme accuracy of the regulator is required.

The general principles of operation of the regulator were described in one of the previous sections. With reference to Figure 5, it is apparent that when the speed and the signal voltage of the tachometer generator tends to increase because of the increasing radius of the reel, a slight increase in voltage across *R*22 will cause the grid of tube 10 to become less negative, and the plate current of this tube will increase. This will cause the appearance of a restoring force which will manifest itself through an increase in voltage across *R*24, the advancement of the firing point of the thyratron tubes 7 and 8, and the resulting increase in the excitation current of the reel motor.

If the strip speed is increased by a clockwise turn of sliders of the combination unit *PA–PR*, the tachometer generator voltage as well as the voltage across *R*22 will increase in proportion with the strip speed, but if properly adjusted, the reference voltage across the active portion of *PR* will increase likewise. In that manner, the difference of the two voltages in the grid circuit of tube 10 will remain the same and the field current of the reel motor will not change.

Under normal operating conditions, during the regulating process, the accelerating tube 9 does not conduct any current being biased off by the negative grid voltage across *R*19. It will be noticed that in addition to resistor *R*19 the grid circuit of the accelerating tube 9 also includes the resistor *R*5 whose significance in the armature control circuits was described previously. This resistor, however, plays a very important part in the field control circuits as well.

Before the drive is started the relay 1*CR* is de-energized, and there is no voltage across the resistor *R*19. Consequently, the accelerating tube 9 conducts full current resulting in full voltage across *R*24 and full exciting current of the reel motor. After the start pushbutton is depressed both 1*CR* and *FCR* pick up and the negative bias of tube 9 gradually appears across the resistor *R*19. The increase of the voltage across *R*19 is gradual because of the charging of capacitor *C*6 through resistor *R*20. As a result, the plate current of tube 9 and the voltage across *R*24 will decrease slowly and so will the excitation current of the motor. In the meantime, however, the motor and the tachometer generator will continue to accelerate, so that at a

certain moment when the tachometer generator voltage becomes high enough, the regulating tube will start to conduct current and will take over the control of the motor excitation in the manner as described previously. If, however, the motor does not have enough time to accelerate to its operating speed before the capacitor $C6$ is charged completely, discharging of capacitor $C5$ will flow through $P4$. Thus, a transient voltage will appear across $P4$ and this voltage always will be of such polarity with respect to the grid of tube 10 that an action opposing a fast change in the restoring force will occur. It should be noted that this damping action will take place in response to the rate of change of the entire reeling operation. Theoretically, if a constant speed motor were used (an induction motor for example) the strip speed during the reeling would increase in proportion, that is, the speed at the end of the reeling operation would constitute 230 per cent of the speed at the start of reeling.

With the electronic drive the strip speed changed from 48.8 feet per minute for empty reel to 50.0 feet per minute for a full reel, that is, increased by 2.46 per cent. The accuracy of the regulator is related closely to the general stability of the whole system and depends upon the type of the motor, the reel-diameter ratio, the behavior of the back-tension during the reeling operation and other similar factors. For many systems of the more stable character, the accuracy of regulation can be easily improved to one or even one-half of one per cent at full strip speed. For lower strip speeds the amplification of the system will be lower, and the percentage of regulation will be increased correspondingly. Thus, for a strip speed set at 30 feet per minute (see Figure 6), the speed will change from 28.8 feet per minute to 30.0 feet per minute or by 4.16 per cent.

An important condition for a satisfactory operation of the drive is the selection of a proper operating range of the motor field current. The portion of the motor magnetic characteristic which represents the range of appreciable saturation should not be used, since over that range the overall amplification of the system is reduced considerably. It may be noticed from the field current graph in Figure 6 that the range of high saturation of the motor has been left outside the operating range of the system. In other words, if the motor is designed so that its full field current corresponds to an appreciable saturation of its magnetic characteristic, the operating full field current should be sufficiently below the rated full field current of the motor.

A typical 3-horsepower electronic drive for a windup reel is shown in Figure 7. It includes the complete electronic rectifier and control system enclosed in the cabinet, the reel motor, the tachometer generator and the operator's control stations. In addition to the parts shown in Figure 7, a complete system also includes a power transformer, not shown in the figure.

Figure 7. Main elements of a 3-horsepower drive for windup reels

the presence of the positive voltage across $R5$ will prevent both the plate current of tube 9 and the field current of the motor to decrease below a certain minimum value, so that an adequate accelerating torque will be maintained. As soon as the acceleration of the reel system is completed, the armature current will drop to a normal operating value, the voltage across $R5$ will disappear, and, if the charging of capacitor $C6$ was completed before, the plate current of tube 9 will disappear also.

The antihunting circuit of the regulator consists of transformer $T4$, tube 11, capacitor $C5$ and potentiometer $P4$. Transformer $T4$ is basically of the same type as transformer $T2$ which was described previously. The voltage obtained in winding $T4S$ of this transformer is rectified by means of tube 11, but the d-c component of the rectified voltage does not appear across $P4$, being blocked by capacitor $C5$. However, if the field current will tend to change abruptly, a transient current caused by charging or average field current and not to the change itself. Thus, if the average field current tends to increase abruptly, a high charging current of capacitor $C5$ will cause the appearance of a transient negative voltage in the grid circuit of tube 10. This voltage will tend to decrease the plate current of the regulating tube, and, consequently, oppose the previously mentioned rise of the field current.

Performance and Conclusions

Typical operating characteristics of the electronic drive are shown in Figure 6. They represent the strip speed in feet per minute as a function of the reel-radius ratio for two different strip speed settings.

The corresponding change in the field current of a 3/4-horsepower reel motor is also shown in Figure 6.

It will be noted that in the particular case represented in Figure 6 the radius of the reel increased 2.3 times during the

Reference

1. Electronic Control of D-C Motors, K. P. Puchlowski. AIEE Transactions, volume 62, 1943, pages 870–7.

Protection of Industrial Plants Against Insulation Breakdown and Consequential Damages

H. R. VAUGHAN
MEMBER AIEE

Synopsis: Experience has shown that multiple electrical failures may occur simultaneously in an industrial plant as the result of an initial breakdown of insulation causing high transient voltages. Available methods of surge protection to guard against insulation breakdown and neutral grounding to prevent high transient voltages are presented. Consideration is given to the merits and limitations of these methods when applied to industrial plants.

PROTECTION against insulation breakdown and its consequential damages long since has been considered paramount by utility engineers. Their experiences in supplying dependable power at low cost have proved that in the electrical industry there is much wisdom in the old adage, "An ounce of prevention is worth a pound of cure." As industrial plants become more and more electrified, and they are doing so rapidly, industrial engineers likewise must pay more heed to this very important problem. It is the purpose of this paper, therefore, to review some of the factors involved and to outline modern methods of protection that have proved beneficial in industrial plants.

Fundamental Considerations

Electricity under control is mankind's most submissive form of power and functions with almost magic imperceptibility. However, it is ever on the alert to escape its fetters and, once on the loose, it becomes a violently destructive force that defies submission. It is imperative, therefore, that great care be taken to keep it under control, that its path of destruction be limited in case it gets out of control, and that it be brought back under control as quickly as possible. In the language of the protection engineer, these fundamental requirements are:

1. Guard against insulation breakdown or flashover by adequate surge protection.
2. Prevent high transient voltages or severe burning as a result of insulation failure by proper neutral grounding.
3. Clear faults rapidly by fast and well-co-ordinated relaying.

It is intended that this paper deal mainly with the first two requirements.

Protection Against Insulation Breakdown

The insulation of a circuit or piece of apparatus will withstand safely the normal operating voltage for which it is intended unless it has become defective as a result of moisture, overheating, or mechanical damage. Trouble from these causes can be minimized by proper maintenance, careful handling, and periodic maintenance. However, it is not practical to build enough insulation into distribution circuits or apparatus windings to withstand surge voltages to which they may be subjected. Protection against these surges, therefore, must be provided commensurate with the severity of surges to be expected and the type of insulation involved.

Industrial plants that receive their power from distant sources usually are supplied over one or more high voltage circuits, 33 kv or higher, into transformers that step down the voltage to 13.8 kv or less for distribution in the plant. If the source is close by or within the plant, power generally is supplied directly at distribution voltage. The circuits may be underground, overhead, or a combination of the two. If they are entirely underground they are free from lightning and require no surge protection. If overhead and exposed, they are subject to lightning surges that may flash them over, break down the insulation of apparatus connected to them, or both. Where combination overhead and underground is used, it is possible for dangerous surge voltages to build up at the junction points between the overhead and underground circuits. Surge voltages also may pass on into the cable and reflect to high values at the far end. The type of circuits and methods of apparatus connection, therefore, have a direct bearing upon the overall scheme of protection which should include protection against both line flashover and breakdown of apparatus insulation.

Paper 46-122, recommended by the AIEE commitee on industrial power applications for presentation at the AIEE summer convention, Detroit, Mich., June 24–28, 1946. Manuscript submitted April 24, 1946; made available for printing May 8, 1946.

H. R. VAUGHAN is with the Westinghouse Electric Corporation, Kansas City, Mo.

Line Flashover

Overhead lines can be insulated and shielded to be practically free from lightning flashover.[1] While this commonly is done with high voltage circuits, 69 kv and above, where the insulation and clearances are inherently high, it usually is not considered practical for the lower voltages because of the extra insulation and conductor spacings required. There are exceptions, however, where shielding of low voltage lines can be justified to provide protection to important apparatus connected to the line. Such circuits often are shielded partially by near-by buildings, trees, and so forth.

Low voltage lines, 13.8 kv and below, may flashover from induced surges as well as direct strokes. If wood construction is used as it generally is, some of these flashovers do not result in trip-outs, although many do.

It is quite common practice to minimize the disturbance caused by trip-outs by

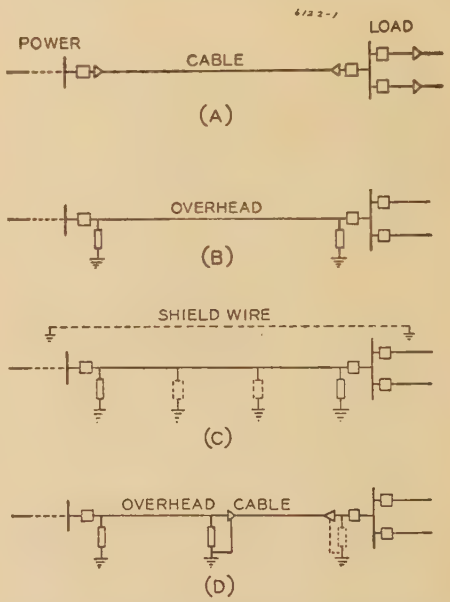

Figure 1. Surge protection of distribution circuits

A—All cable, no protection required
B—Overhead, terminal protection only
C—Overhead, lightningproof protection by either shield wire or spaced lightning arresters
D—Combination overhead, underground. Arresters not required at load end if cable length is less than 100 feet

rapid reclosing of the feeder breaker. In some cases, where trip-outs are extremely undesirable, line flashovers can be prevented by spacing line-type lightning arresters along the line at 500- to 1,000-foot intervals.

Lightning arresters should be provided at junctions between overhead and underground circuits to protect against high voltages at those points caused by reflected traveling waves. The arresters should be connected directly between the conductors and the cable sheath, and grounded. If the cable is over 100 feet in length, arresters also should be provided at the far end, particularly if the cable feeds into an exposed line or has important apparatus with low surge strength, such as rotating machines, connected to it.

The recommended methods of protecting the different types of distribution circuits that might be involved in an industrial plant are shown schematically in Figure 1.

Apparatus Protection

There are two general classes of electric apparatus that must be considered in the over-all scheme of protecting an industrial plant. One of these includes that equipment, such as oil-insulated transformers, that has surge strengths equivalent to basic insulation levels that have been established for the different voltage classifications.[2] This class of equipment can be protected adequately by standard lightning arresters of the proper voltage rating connected between the exposed line leads and ground. The arresters should be located as close as possible to the apparatus frame or tank as shown in Figure 2.

The second class includes apparatus such as air-cooled transformers and rotating machines that have impulse levels

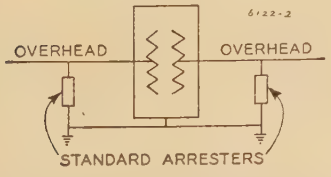

Figure 2. Surge protection of apparatus meeting basic insulation levels

lower than the basic insulation levels. A comparison of the impulse levels of oil-insulated and air-cooled transformers from 1.2 kv to 15 kv classification is given in Table I. The surge strength of rotating machines are normally somewhat less than the values shown for air-cooled transformers. Because of its lower impulse level,

Table I. Comparison of Impulse Insulation Levels

Insulation Class (Kv)	Impulse Levels $1^1/_2 \times 40$ μsec Wave Kv Crest: Oil-Insulated Transformer	Impulse Levels $1^1/_2 \times 40$ μsec Wave Kv Crest: Dry-Type Transformer (Proposed)
1.2	30	10
2.5	45	20
5.0	60	25
8.66	75	35
15.0	95	50

this second class of apparatus requires special protection, particularly when connected directly to overhead lines that are exposed to lightning surges.

Air-cooled transformers that are subject to surge voltages should be protected by special arresters, similar to those used for rotating machine protection, at the

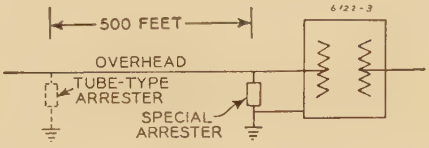

Figure 3. Surge protection of dry-type transformers

transformer terminals,[6] (Figure 3). If the transformer is connected directly to an overhead line, a set of standard arresters, either valve or tube type, also should be connected about 500 feet ahead of the transformer. Tube-type arresters are influenced somewhat less by arrester ground resistance. Liquid-filled transformers should be used in preference to air-cooled transformers where the circuit is exposed highly to severe surges.

Recommended methods of protecting rotating machines are given in a paper by by McCann, Beck, and Finzi.[5] The essential requirements are to limit the magnitude of surge voltage at the machine terminals to protect the insulation to ground, and to slope the front of the surge wave so that it will not pile up across a few turns of the machine winding and overstress the turn-to-turn insulation. The first of these requirements is accomplished by special lightning arresters having low sparkover characteristics, and the second by shunt capacitors and series inductance. These fundamental components of the protective scheme are illustrated in Figure 4*A*. Actually, the series inductance may be a section of the incoming line, 500 feet in length, immediately ahead of the machine (see Figure 4*B*). A standard line-type arrester is required ahead of the series inductance to limit the magnitude of surge voltage that can pass in to the inductance and shunt capacitor combination. This arrester preferably should be a tube type if the ground resistance is more than two or three ohms, because the discharge voltage across the tube collapses to near zero for a half cycle, thus resulting in only a small amount of surge energy being transmitted into the protective devices at the machine terminals. Where the line is exposed to severe surges, or where the arrester ground resistance is higher than about five ohms, one or more additional sets of arresters should be placed out on the line at about 500-foot spacings. The first 500-foot line section ahead of the machine should be shielded (see Figure 4*C*) if there is danger of a direct stroke of lightning in that section.

The special arresters at the machine terminals should be valve type because of its lower sparkover voltage. The best protection is provided by station-type arresters which are recommended where the kilovolt-ampere rating of the machine or machines protected exceeds 1,000. The special line type generally is considered adequate for smaller sized machines.

Where several rotating machines are connected to a common bus, adequate protection can be provided by means of a single set of special arresters and capacitors connected to the bus, if each machine

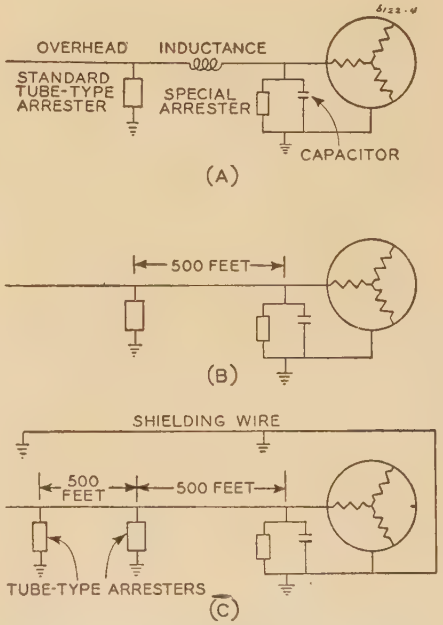

Figure 4. Surge protection of rotating machines

A—Fundamental scheme
B—Equivalent scheme
C—Protection against severe surges including line shielding and spaced lightning arresters

is connected to the bus by an unexposed circuit not over 200 feet in length. Otherwise, each machine should be provided with a set of capacitors and special arresters mounted near its terminals. If there is enough cable connected to the bus (see Table II) to provide the required shunt capacitance, no capacitors are necessary.

In some industrial plants, there may be individual motor loads, such as pump motors, tapped off a common overhead circuit at intervals along the line. For the best protection to all the motors the line should be shielded against direct strokes and special rotating machine protection provided at each motor. If shielding is not feasible, each motor should be provided with a series choke coil, special valve-type arresters and wave sloping capacitors at the motor terminals, and a standard line-type arrester ahead of the choke coil.

Rotating machines connected to the secondary windings of transformers whose primary windings are connected to overhead lines may not need rotating machine protection if the primary winding of the transformer is protected adequately. However, if large or important machines are involved, and are located close to the transformer, the risk of failure from surges passing through the transformer justifies the provision of special arresters and wave sloping capacitors at the machine terminals. Reference 5 includes a method of analyzing the need for such protection.

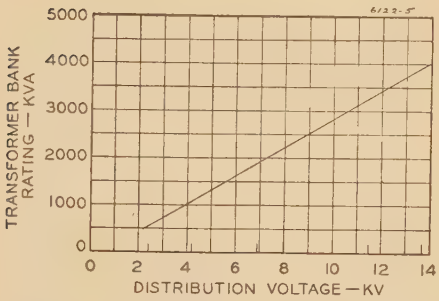

Figure 5. Approximate maximum sizes of transformer bank that can be grounded solidly without exceeding 2,500 amperes ground fault current

Protection Against Fault Damage

Even with good maintenance and surge protection there will be occasional faults, most of which will start as short circuits between one phase and ground. Such a fault may result in considerable damage by causing either severe arcing or high transient voltages, depending on whether the system neutral is grounded, and if so, how.[7–10]

Table II. Surge Capacitors or Equivalent Length of Cable Required for Rotating Machine Protection

Machine Voltage Class (Kv)	Capacitance Per Phase (Microfarad)	Cable Voltage Class (Kv)	Length of Cable (Thousands of Feet)			
			00	250,000 Cir. Mils	500,000 Cir. Mils	750,000 Cir. Mils
2.4	0.5	2–3	35	25	20	15
4.16	0.5	4–5	45	30	25	20
6.9	0.5	7–8	50	35	25	20
13.8 (grounded)	0.25	14–15	30	25	20	15
13.8 (ungrounded)	0.5	14–15	60	50	40	30

Neutral Point Available

If the neutral of the source of power to the distribution system, either generator or transformer bank, is grounded solidly, there will be no transient voltages of dangerous magnitude produced by a phase-to-ground fault. However, the ground current will be high, particularly if the grounded neutral machine is a steam-turbine-type generator supplying power directly to the distribution system. It will produce a noticeable dip in voltage and result in severe burning at the fault, unless the fault is cleared rapidly. It also may distort the windings of the grounded neutral generator which normally is designed to withstand short-circuit current no greater in magnitude than that resulting from a 3-phase short-circuit. The line-to-ground short-circuit current from a solidly grounded neutral generator usually will be greater than the 3-phase value.

If the source of distribution power is a transformer bank supplied from a high voltage line, grounding the neutral solidly will prevent dangerously high transient voltages resulting from ground faults. The magnitude of ground fault current will depend on the distribution voltage and the size of the bank. It will not cause excessive arc burning with moderate speed relaying if it does not exceed about 2,500 amperes. The approximate maximum sizes of transformer bank that can be grounded solidly without exceeding 2,500 amperes ground current are given in Figure 5. Higher ground currents are permissible if high speed relaying is provided.

If the neutral of the supply source is left ungrounded there will be no fault current when one phase becomes grounded except a few amperes of charging current through the circuit capacitance to ground. The extinction and restriking of this charging current may cause transient voltages between the unfaulted phases and ground high enough to destroy protective devices or to break down equipment insulation, thus causing one or both of the other phases to become grounded. A compromise between the high ground current and no transient voltages on the one hand and the high transient voltages and no ground current on the other hand is usually the best practical solution.

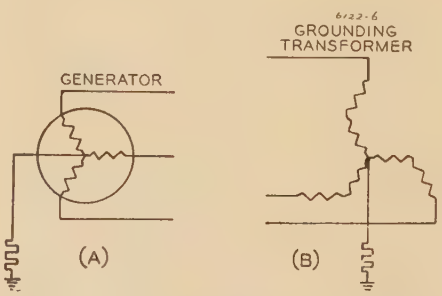

Figure 6. Low resistance neutral grounding

A—Generator neutral resistor
B—Grounding transformer with neutral resistor

Neutral Impedance

The magnitude of ground fault current can be reduced by inserting impedance in the neutral ground circuit. However, care must be exercised in fixing the make-up of this impedance. If it is resistance only, there is a wide range in the value of resistance that may be used to eliminate the high transient voltages. It may be classed as either "low" or "high" resistance grounding (Figure 6) depending on the resultant magnitude of ground fault current. The lower limit of ground fault current for "low resistance" grounding is the minimum value that will assure dependable relaying with ground relays, about rated full load current with minimum generating capacity. The upper limit is dictated by the amount of energy that can be dissipated in the resistor during fault, both from the standpoint of practical resistor size and shock to the supply generators. A reasonable value to use for the upper limit is 150 per cent of the rated load current of the minimum generating capacity, or 2,500 amperes,

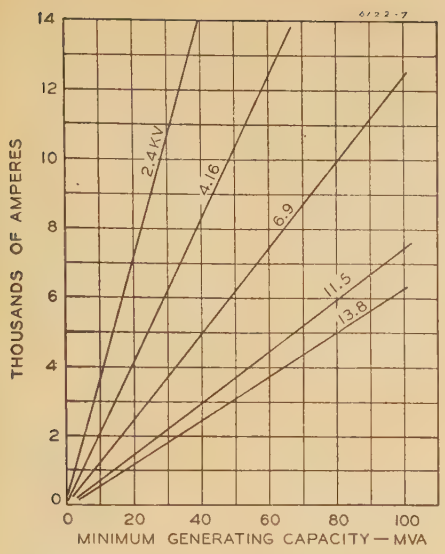

Figure 7. Approximate maximum values of ground fault current with neutral resistor grounding

whichever is the smaller. It usually will be desirable to approach this upper limit to assure prompt operation of ground relays under maximum fault resistance conditions. The curves of Figure 7 show values of ground fault current limited to 150 per cent of rated full load current for the voltages commonly used in industrial plant distribution systems. The minimum value of neutral resistance in ohms that should be used is equal to the line-to-neutral voltage divided by the value of fault current given by the curves.

From the standpoint of limiting the transient voltages, it is only necessary to use a neutral resistor of low enough resistance to dissipate energy equal in kilowatts to the charging kilovolt-amperes supplied the system at the time of a ground fault. This depends upon the maximum amount of circuit, particularly cable circuit, and the number and size of machines connected at any one time. With this value of neutral resistance, classed as "high" resistance, the current in the fault would be only about 50 per cent more than the charging current which would be but a few amperes at the most. The faulted circuit, therefore, could be left in service without danger from transient voltages or arc burning until convenient to remove it. In practice, an alarm actuated from a voltage relay connected to measure voltage between neutral and ground would be used to indicate when a grounded conductor existed. The circuit relaying, initially set up on the basis of ungrounded neutral service, would not be affected.

The effect of such a high resistance, neutral ground (Figure 8), can be provided more practically for 2,300 volts and higher by using a standard distribution transformer with a low voltage resistor connected across its secondary winding. The primary winding should have a voltage rating equal to the circuit voltage. It should be connected between the generator neutral and ground. The secondary winding may be 120, 240, or 480 volts, depending on the rating of the most applicable resistor which should be chosen to dissipate power during a line-to-ground fault equal in kilowatts to at least the maximum charging kilovolt-amperes drawn by the system during a ground fault. A voltage relay generally is connected across the resistor to serve as a fault detector.

When resistance grounding is used, the system neutral becomes displaced almost fully during a ground fault. This requires that lightning arresters connected to the system have a voltage rating not less than line-to-line voltage as is necessary with ungrounded neutral operation.

If the neutral impedance is reactance (Figure 9) there is a limit to how far the ground fault current can be reduced without causing high transient voltages. To be safe, this minimum value should not be less than about 50 per cent of the magnitude of the 3-phase fault current. The curves in Figure 10 show the minimum safe ground fault currents with reactance grounding for the different distribution voltages.

A combination reactor and resistor in parallel will permit high transient voltages unless the resistance is low compared to the reactance. Therefore, the two in parallel offer very little, if any, advantage over a resistor only.

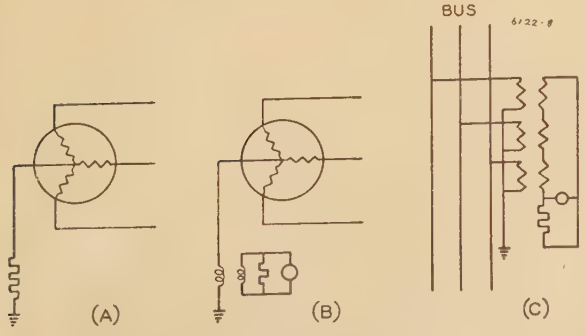

Figure 8. High resistance neutral grounding

A—Generator neutral resistor
B—Distribution transformer in generator neutral with secondary resistor
C—Bank of distribution transformers with secondary resistor

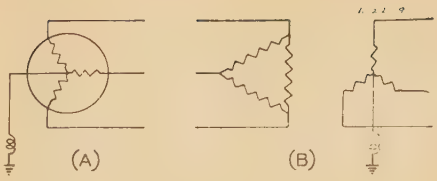

Figure 9. Reactance grounding

A—Generator neutral reactor
B—Transformer with or without neutral reactor

Any neutral ground scheme that permits enough ground fault current to cause arc damage requires ground relays. If the neutral is grounded solidly, the ground fault current would in most cases be high enough to operate phase relays. However, there may be occasional high resistance ground faults that would not draw enough current to operate phase relays in which case considerable damage from burning might result if ground relays were not provided.

Neutral Point Not Available

Many industrial plant distribution systems do not have a neutral point available for grounding, particularly those that operate at 2,300 or 6,900 volts, delta. As previously pointed out, such systems are conducive to high transient voltages during ground faults. Experience has shown that a failure of a machine winding or cable circuit to ground often results in the simultaneous failure of other machines or cables. The remedy is to supply one or more supplementary neutral grounds to assure that all feeder sources are grounded adequately at all times.

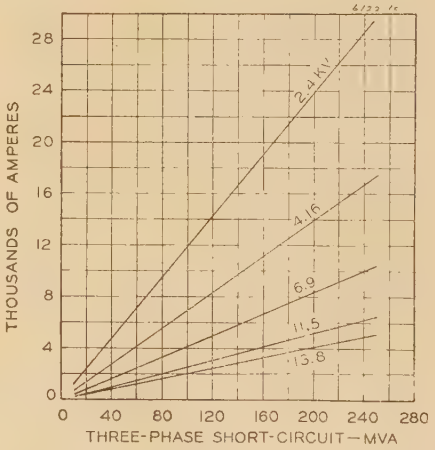

Figure 10. Approximate minimum values of ground fault current with reactance grounding

If the distribution system draws only a few amperes charging current and is relatively simple in make-up so that a grounded conductor can be located without too much difficulty, a high resistance neutral ground may be established with a small bank of distribution transformers and secondary resistor as shown in Figure 8*C*. The star-connected primary windings should be connected to the distribution bus with neutral grounded. The resistor should be connected inside the delta of the low voltage winding. The resistance should be chosen to dissipate energy equal in kilowatts to at least the charging kilovolt-amperes of the system during a ground fault. This scheme of grounding is similar to the distribution transformer–secondary resistance scheme described previously, in that it serves only to limit the transient voltages and to indicate a ground fault. The fault current is too low to cause arc burning so that ground relays are not necessary.

The other method of providing a supplemental neutral ground is to use a grounding transformer, either zig-zag or star delta connected with the neutral grounded. If grounded solidly it is classified as reactance grounding and carries the same limitation as described previously, that is, that the ground current should not be less than about 50 per cent of the 3-phase fault current. If grounded through a resistor (Figure 6*B*) the ground current can be reduced to the minimum permissible for satisfactory ground relaying. If a "low resistance" neutral resistor is used, the reactance of the grounding transformer should be such that if the transformer were grounded solidly, the ground fault current would not be less than about 50 per cent of the 3-phase value. Relays that will clear ground faults promptly are necessary to prevent excessive arc burning.

Preferred Method of Neutral Grounding

The essential requirement of a neutral ground is that it will suppress high transient voltages during ground faults. The scheme best suited to any particular industrial plant depends on a number of factors, such as the surge protection required, the magnitude of the power source, whether a neutral point is available or not, the number and complexity of circuits involved, and the type of relaying that is or can be provided. From the standpoint of surge protection, either solid neutral or reactance grounding that limits the ground fault current to not less than 60 per cent of the 3-phase fault current is preferable, because either one makes it possible to apply reduced rating (80 per cent) arresters. If the insulation is questionable, this may be the deciding factor. However, either of these types of grounding produces high ground fault currents if the distribution system is supplied at generator voltage and the generating capacity is large. When those conditions exist, resistance grounding generally will be suited better. The distribution transformer–secondary resistor scheme often works out advantageously where the distribution system is not too complex and where it is not feasible to add ground relays.

Conclusions

There are methods available for surge protecting almost any combination of circuits and apparatus that may be encountered in industrial plants. Consequential damages due to high transient voltages resulting from unavoidable ground faults can be prevented by proper neutral grounding. Experience has shown that, where these precautions are taken, trouble from electrical failures has been reduced to a minimum.

References

1. Transmission and Distribution Reference Book, chapter 13.

2. Transmission and Distribution Reference Book, chapter 14.

3. Protection of Rotating A-C Machines Against Traveling Wave Voltages Due to Lightning, **W. J. Rudge, Jr., R. W. Wieseman, W. W. Lewis.** AIEE Transactions, volume 52, 1933, pages 434–40.

4. Surge Protection of Rotating Machines, **J. F. Calvert, A. C. Monteith, E. Beck.** *Electrical Journal*, March 1933.

5. Lightning Protection for Rotating Machines, **G. D. McCann, E. Beck, L. A. Finzi.** AIEE Transactions, volume 63, 1944, pages 319–32, page 319.

6. Dielectric Strength and Protection of Modern Dry-Type Air-Cooled Transformers, **P. T. Bellaschi, E. Beck.** AIEE Transactions, volume 64, 1945, November section, pages 759–63.

7. Transmission and Distribution Reference Book, chapters 15 and 17.

8. Overvoltages During Power-System Faults, **Edith Clarke, S. B. Crary, H. A. Peterson.** AIEE Transactions, volume 58, 1939, August section, pages 377–85.

9. Merits and Methods of Generator Grounding, **S. B. Griscon.** *Westinghouse Engineer*, February 1943.

10. Grounding Principles and Practice—II, **A. A. Johnson.** Electrical Engineering, volume 64, March 1945, pages 92–9.

Fundamental Properties of the Vacuum Switch

R. KOLLER
ASSOCIATE AIEE

Synopsis: The main results of a study of the various phenomena which take place during the interruption of currents in high vacuum are given. The experimental results obtained lead to a theory of the basic mechanism affecting switching in high vacuum. With a proper design of the switch, a constant working pressure can be obtained which represents an equilibrium between gases and vapors evolving from the electrodes and a pumping action based on the sputtering of cathode material. A detailed study is made of the factors determining the loss of electrode material because of switching. The most essential design features of a vacuum switch are discussed briefly.

SWITCHING is one of the most frequently performed operations in electrical circuits. Even though switching plays a very important role, the equipment performing this operation, the switches and circuit breakers, have by no means reached the last degree of perfection.

No satisfactory d-c breaker has been developed yet for the interruption of medium or heavy loads at high voltage.

The interruption of alternating current is made much easier by the periodical occurrence of the current zero which represents a natural means of deionization. The difficulty here lies in the fact that severe requirements are made with respect to the time of interruption.

System stability studies indicate that faults on transmission lines, particularly of large interconnected systems, should be cleared in a minimum of time. This is the main reason why the increase in load of the past 15 years gradually has placed stronger requirements on the opening time of breakers. Whereas in 1930 a 10- to 15-cycle breaker was found to be satisfactory, today the tendency is to clean faults in three cycles. It is to be expected that in the near future still more severe specifications will have to be made on the interruption time.

In some cases no restrikes after the first current zero are permissible, as for example in the interruption of charging current. Restrikes would result in high overvoltages, exceeding the normal line voltage several times.[1,2] This is particularly dangerous on power lines where sections of cable are incorporated.

With the present designs of circuit breakers, it is very difficult to meet requirements of the type mentioned above. The main difficulty encountered by the present methods of arc extinction lies in the small dielectric strength of the interrupting medium. The rate of recovery of dielectric strength is small, even when large opening speeds are used.

It was recognized early that the use of high vacuum as an interrupting medium is expected to have two features which are of great importance for the rapid interruption of currents:

1. The dielectric strength of high vacuum[3,4,5] is greater by far than that of any other interrupting medium in use.

2. Once an arc has been formed in a high vacuum, a fast radial diffusion of the current carrying particles takes place and provides a most ideal means of deionization.

A great deal of research and development has been done on vacuum switches. In 1921 the first small vacuum switch was built commercially by the Swedish Birka Company.[6] From 1923 to 1926, Sorensen and Mendenhall[7] performed extensive tests with larger vacuum switches at the California Institute of Technology. Around 1932 interesting investigations were carried out by Seitz[8] and Jubitz[9] in Germany.

As a result of these efforts, excellent small current capacity vacuum switches are commercially available and are finding a steadily increasing field of application.

Today, however, the vacuum switch is not able to compete in power circuits. No explanation for this fact can be found in the literature. There is also no theory given explaining the various processes affecting the interruption in high vacuum.

The aim of the investigation described in this paper was to clarify some of the important and basic points involved in this problem.

Experimental Setup

The investigation was carried out entirely on direct current. The interruption of alternating current only would have complicated the analysis greatly without giving any new information about the basic mechanism of the interruption.

The two switches shown in Figures 1 and 2 were built for this study. The switch of Figure 1 is completely glass-sealed, allowing studies to be made at very low pressures of 10^{-6} millimeter of mercury or less. This switch is actuated magnetically by means of a nickel plunger and a trip coil. The second switch, shown in Figure 2, was developed after it had been established that pressures below 10^{-4} millimeters of mercury were not required for a successful operation. Two main improvements were incorporated in this switch. First, it provides a simple and quick way of opening and resealing. Picein was used as a sealing wax around the steel base and the ground bottom of the glass jar.

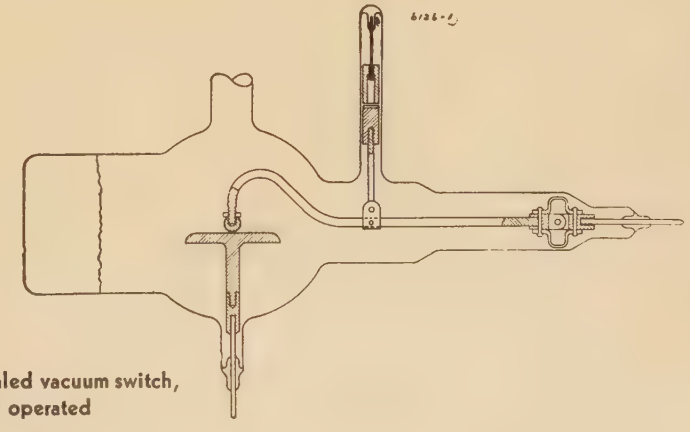

Figure 1. Glass-sealed vacuum switch, magnetically operated

Paper 46-126, recommended by the AIEE committees on electronics and industrial control devices for presentation at the AIEE summer convention, Detroit, Mich., June 24–28, 1946. Manuscript submitted April 22, 1946; made available for printing May 9, 1946.

R. KOLLER is a member of the electrical engineering department, University of California, Berkeley, Calif.

The material presented in this paper is abstracted from a dissertation presented for the degree of doctor of philosophy in electrical engineering at the University of California. Acknowledgment is made to Professor L. B. Loeb, of the University of California, for his many valuable suggestions during the course of this work. The acknowledgment is extended also to Professor W. G. Hoover, of Stanford University, for his help in the oscillographic work done at the Ryan Laboratory.

The second improvement consisted of an accurate and easily changeable speed of separation of the electrodes, which is a significant variable. A spring located in the socket of the lower electrode provided the desired contact pressure. When the switch was tripped, the lower electrode followed the parting upper electrode until a stop in the socket was reached. At this point the lower electrode was arrested and the electrodes separated.

The switch is actuated by an outside mechanism shown in Figure 3. The motion is transmitted to the switch by means of a metal bellows located at the top of the switch.

The disk D of Figure 3 is rotated at synchronous speed. The opening spring Sp is expanded by means of a pin A mounted eccentrically on the disk B. A short time before the maximum stretching of the spring is reached, the cam switch SW closes and energizes the coil and the magnet M. This locks the tripping toggle T by means of the latch L. The tripping coil TC releases the tripping toggle. This results in a rapid opening of the switch. The trip coil can be energized by closing the switch S or through the cam switch CS. This cam switch permits the automatic operation of the vacuum switch. This is important because thousands of operations are required to determine accurately the average loss of electrode material per interruption, which is very small.

The vacuum system used is illustrated by Figure 4. The vacuum is created by a forepump F and a 2-jet mercury diffusion pump J. Another forepump M was used to reduce the time required for the complete evacuation of the vessel. The use of this pump for the first part of the evacuation also helped greatly to keep the two liquid air traps clear of ice formation.

The pressure in the vessel was measured with a cold cathode ionization gauge I of the Penning[10] type. The McLeod gauge G was used for checking purposes only.

The speed of separation of the electrodes of the spring operated switch was measured with a mechanical speedograph.

Another method had to be devised for the measurement of the opening speed of the magnetically operated switch. There the force available from the magnetic plunger was too small for the use of a speedograph. An optical method illustrated in Figure 5 was used instead.

A narrow vertical beam of light is obtained by means of the condenser lens L_1 and the slit S. In the closed position of the switch, this parallel beam of light is obstructed completely by the electrodes. During the separation, a beam of light which is proportional to the width of the gap reaches the lens L_2 and is focussed on the phototube. The resulting phototube current then is amplified in order to give a satisfactory deflection on the screen of a cathode ray oscillograph.

A curve can thus be obtained on the screen, giving the separation of the electrodes as a function of time. Such curves used in conjunction with recovery voltage oscillograms allow one to determine the electrical field strengths present during interruption.

The Mechanism of Interruption

In what follows, a detailed analysis of the mechanism of interruption is given. This analysis is based on the various observations made by means of different methods, such as cathode ray oscillograms, fast movie films, microscopic studies of the electrode surface, and so forth.

At the beginning of the separation of the electrodes, the contact area is decreased rapidly. This results in a fast increase in current density, leading eventually to melting and evaporation of the electrode material. A vapor arc thus is created which rapidly blows itself out because of the rapid radial gaseous diffusion active in the evacuated space. The loss of current carriers because of this radial diffusion is large enough to disrupt quickly the self-sustaining discharge.

The average velocity of diffusion is given by[11] $C = \sqrt{4kT/m}$, where k = Boltzmann constant, T = absolute temperature, and m = mass of a gas molecule. At a temperature of a few thousand degrees Kelvin, the diffusion velocity is of the order of 10^5 centimeters per second, which is about 1,000 times greater than the speed of separation of the electrodes.

As soon as this first arc is blown out, a recovery voltage builds up across the gap, which is by now only about 10^-

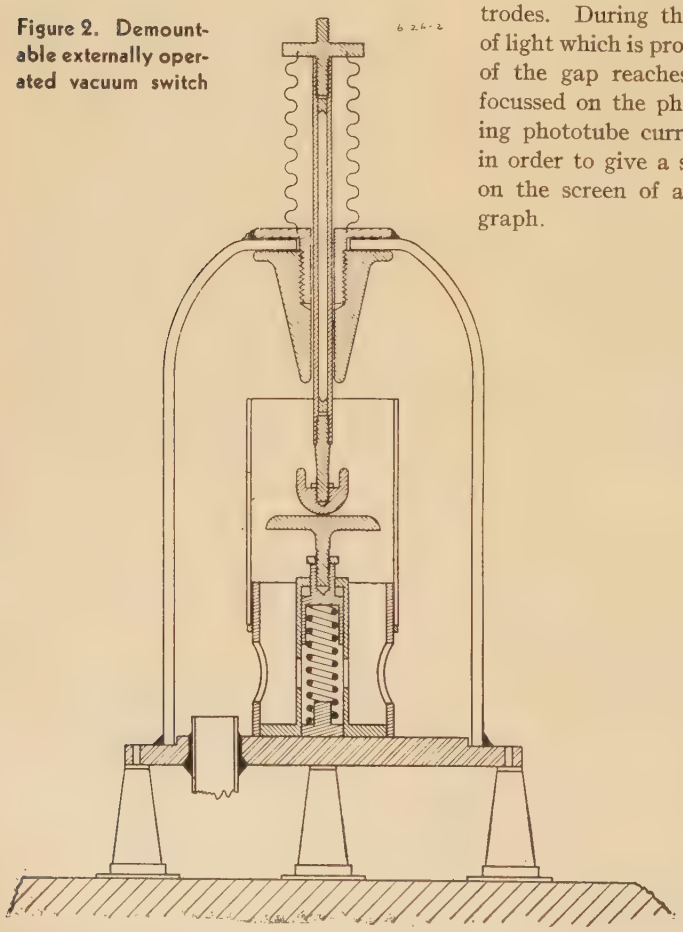

Figure 2. Demountable externally operated vacuum switch

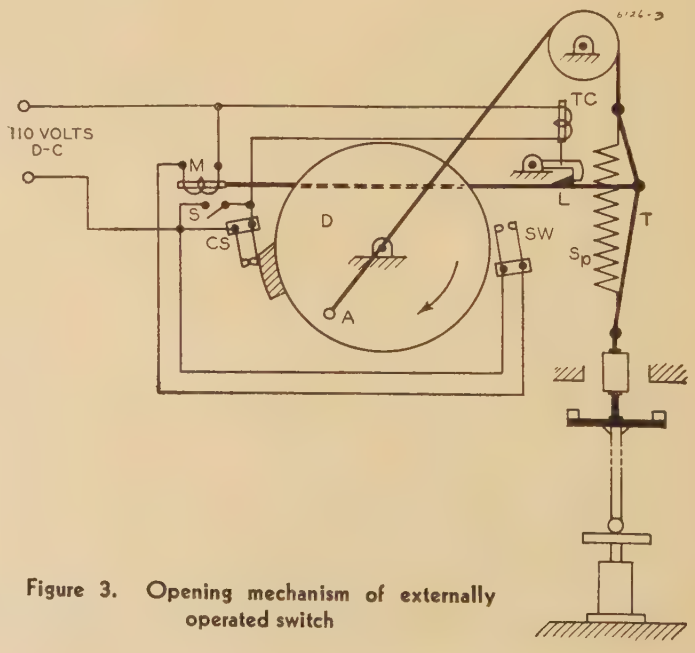

Figure 3. Opening mechanism of externally operated switch

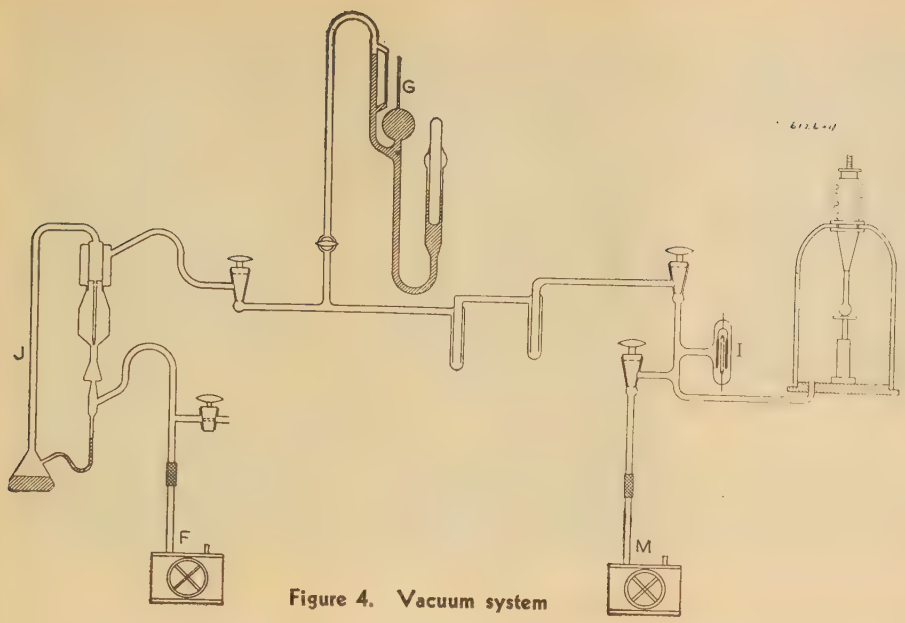

Figure 4. Vacuum system

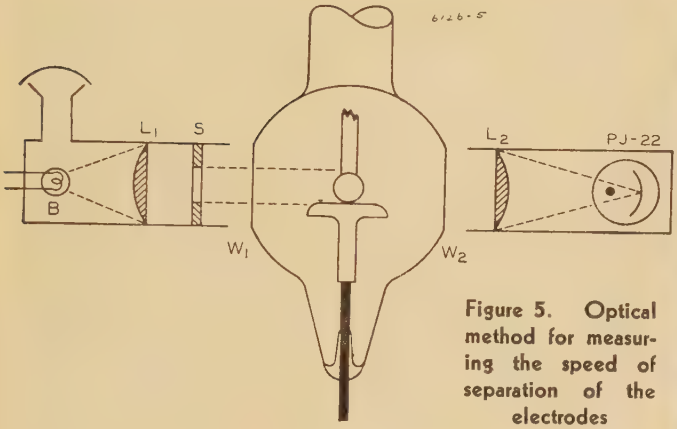

Figure 5. Optical method for measuring the speed of separation of the electrodes

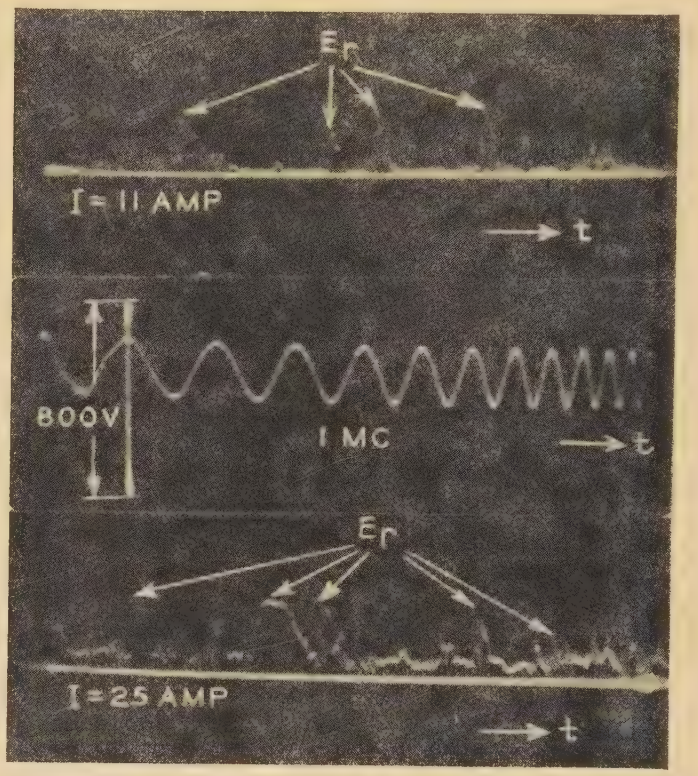

Figure 6. Voltage oscillograms with one megacycle timing wave—copper electrodes

of arc bursts of microsecond duration, interspersed with periods of extinction of even shorter duration. It is significant that the random character of this process is found by experiment not to be affected by the circuit constants.

For the case of a plate-cathode and a spherical anode, fast movie films show that the spark-arc mechanism moves away from the center of contact along a single radial line. This situation is represented schematically in Figure 7. It can be seen that the radial diffusion of the gas and vapors originated during each single arcing episode A_1, A_2, A_3... creates ring-shaped zones of greatest gas vapor and ion density. The successive breakdowns B_1, B_2, B_3...following the recovery voltages E_1, E_2, E_3...take place in the regions where the ring-shaped

centimeters wide. Under this condition a relatively small recovery voltage creates a field strength of sufficient magnitude to break down the gap in the form of a special kind of spark arc mechanism to be discussed later. The initiating spark preferably will take place along a path where a small density of gas and vapors is left, that is, about one millimeter away from the former point of contact, owing to the diffusion in the microsecond of the first arc. The arc following the initiating spark is blown out again, and another recovery voltage E_r leading to a new breakdown builds up across the gap. Recovery voltages E_r of this type are well resolved in the oscillograms of Figure 6. It can be seen that the mechanism consists of a series zones overlap, that is, along a single radial line.

In the case of large currents, spark-arc mechanisms will occur along many separate radial lines. The separate arcs occurring simultaneously at a given time all will be located on a concentric circle around the former point of contact. This form of discharge along an arc of a circle is found to take place for currents exceeding about 30 amperes.

The interruption is completed when such a series of arcing episodes ceases. This happens once the path along the greatest gas density is too long, that is,

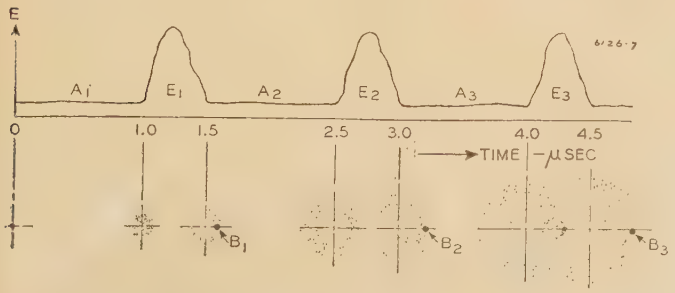

Figure 7. Schematic representation of the spreading of the discharge on a cathode plate along a single radial path

Center of the cathode plate

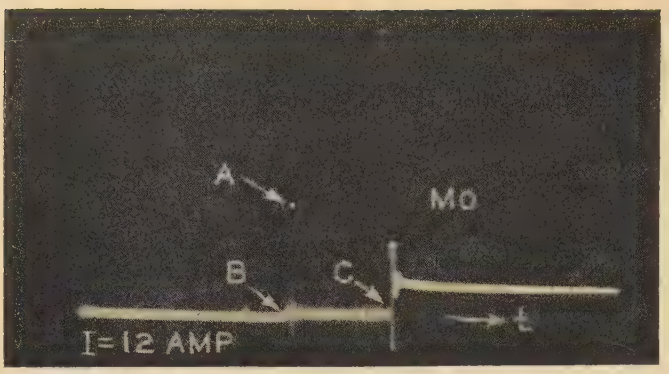

Figure 8. Voltage oscillogram—molybdenum electrodes

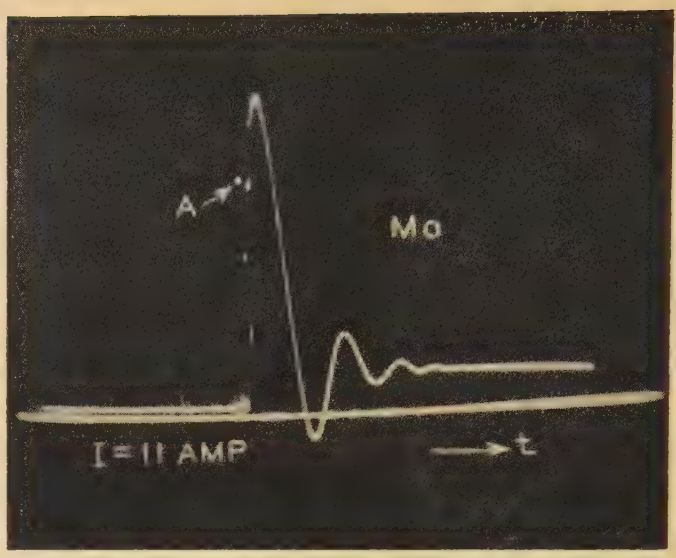

Figure 9. Voltage oscillogram—molybdenum electrodes

when its dielectric strength prevents a further breakdown. At the end of such a series of arcing episodes, the electrodes are still close together. If the circuit conditions create a high recovery voltage, the gap will break down near the center by field emission. This usually starts another succession of radial spark-arcs. Fast movie films were able to give evidence of repeated breakdowns near the center of the gap. The field strengths corresponding to such breakdowns exceed 10^6 volts per centimeter. It is therefore clear that this type of breakdown is initiated by field emission.[12]

Figure 8 shows a typical voltage oscillogram where a high recovery voltage occurred at point A, 3×10^{-5} second after the start of the interruption at point B. The total time of interruption (B to C) amounted to 3.2×10^{-4} second. The recovery voltage at point A was 552 volts, corresponding to a field strength of 2.76×10^6 volts per centimeter. The succeeding large recovery voltage which is clearly resolved occurred at point C and amounts to 1,380 volts, giving a field strength of 1.26×10^6 volts per centimeter. Large recovery voltages are always present at the end of the interruption of an inductive d-c circuit. The resulting field strengths are, however, no longer able to restrike. Figure 9 shows an interesting case where a field emission breakdown occurred at point A which was not able to reignite a new series of arcing episodes.

The fact that the mechanism of interruption is affected by field emission explains the observed great variations of the time of interruption. The determination of the statistical average time of interruption requires, therefore, the data of a large number of interruptions.

The study of electrode surfaces with the microscope revealed another interesting phase of the mechanism of interruption. Figure 10 shows the many microscopic craters of about 10^{-3} centimeter diameter which have been created on a tungsten cathode. The cathode also shows cracking and peeling of the surface which was caused by the heat resulting from the intense positive ion bombardment. The anode shows many fused spots; the rest of the surface is covered with sputtered material from the cathode. Carbon electrodes show even more distinctly the difference between cathode and anode surfaces. Figure 11 shows how the cathode surface is broken up to a great depth by the combined action of the positive ion bombardment and the explosive action of the suddenly liberated gas.

The anode has a smooth surface covered with sputtered carbon from the cathode. The microscopic craters observed on all cathodes reveal the presence of a focusing action. The conditions present during the periods of recovery voltage E_1, E_2, E_3... (see Figure 7) as well as during cold emission restrikes are leading to the conclusion that a magnetic self-focusing action of the Bennett[13] type takes place. This magnetic self-focusing concentrates the positive ion bombardment on small areas on the cathode, resulting in local fusion and evaporation. This creates microscopic craters of the type indicated by arrows in Figure 10. The self-focusing action lasts only about one microsecond. After this interval of time, the conducting streams are no longer self-focusing because the density of matter near the cathode leads to frequent collisions between current carriers and neutral atoms. The conditions for self-focusing hold, however, only as long as the energy loss caused by such collisions is negligible. As soon as the focusing action ceases, a transient arc of short duration is established. This arc is quickly deionized by the fast radial gaseous diffusion. This then is followed again by a series of arcing episodes as described earlier.

Variations of Pressure Produced by Switching

Contrary to previous statements, it has been found that the vacuum switch normally operates at a vessel-pressure of 10^{-4} millimeter of mercury or less, provided that the electrodes are well outgassed.

Throughout this investigation, stock-material was used for the electrodes. The outgassing or conditioning of such electrodes was achieved in interrupting frequently with gradually increasing currents. The heat created by radiation and particularly by the positive ion bombardment of the cathode was sufficient to free the electrodes from adsorbed gases. A satisfactory conditioning of the electrodes required about 100 operations. All interruptions have to be started at a vacuum in the vessel of 10^{-4} millimeter of mercury or better. The use of vacuum-melted material, of course, would shorten considerably the time required for the conditioning.

Once the eleotrodes are conditioned properly, it was found to be of no advantage to operate the switch at pressures below 10^{-4} millimeter of mercury. Higher pressures result in a considerably longer time of interruption, as will be shown later.

An important property of the vacuum switch is the fact that the pressure in the vessel does not necessarily increase as a result of switching. With the vessel disconnected from the pumping system, a definite constant working pressure estab-

lishes itself in the vessel as a result of frequent switching. In the course of the experiments, the vacuum switches often were disconnected from the pump for hours, performing thousands of identical operations, without resulting in a change of the vessel pressure.

The working pressure was found to vary with the vessel diameter, the current, and the electrode material. The working pressure even can become appreciably lower than the pressure which is present in the vessel before the interruptions of currents. This behavior indicates that a strong pumping action is initiated by the interruption of currents. The observed constant working pressure thus represents an equilibrium between this pumping action and the gases and vapors which necessarily evolve from the electrodes. Real and virtual leaks, of course, also will affect this equilibrium. The pumping action is based on two distinct processes, both of which result from the sputtering of the cathode material. One process acts like a diffusion pump, whereas the other is based on the getter action which some materials like molybdenum display very strongly. The mechanism of the diffusion pump like process is as follows: The sputtered cathode material diffuses at high speed to the walls. Gas molecules present between the discharge region and the walls then are caught by the diffusing metal atoms and are plastered on the walls. These gas molecules are bound firmly to the walls and can be freed only when the walls are heated above 300 degrees centigrade, as is well known from the case of glow discharge tubes. Pumping in the manner described will occur when the distance from an active spot on the cathode to the nearest section of the wall is of the order of the mean free path of the gas in that region. This mean free path is a measure for the collision probability between the gas molecules and the sputtered particles. Under the conditions of the experiment, it always was found that the mean free path corresponding to the pressure in the vessel (measured with the ionization gauge) was several times larger than the average distance S of the active spots to the wall. This can be explained by the fact that as a rule the evaporating metal atoms greatly outnumber the gas molecules in the volume exposed to the blast of sputtered material. For example, during an interruption of 25 amperes with copper electrodes, the evaporated copper atoms outnumbered the gas molecules by a factor of fifty. The fact that the mean free path is larger than the distance S means that only a fraction of the metal atoms succeed in plastering gas molecules to the walls. The actually resulting reduction of gas molecules, partially balanced by the evolution of gases from the electrodes, thus will maintain a lower gauge pressure than that corresponding to a mean free path equal to the distance S.

It was found that the working pressure p, as measured by the gauge, varies inversely with the baffle or vessel diameter d, as $p_1/p_2 = d_2/d_1$.

This relation holds well for materials like copper and aluminum which do not display a strong getter action. Thus the judicious use of baffles may be of value in the switch design.

The current does not affect greatly the working pressure since it equally affects two opposing processes: the liberation of gas from the electrodes and the amount of sputtered material. The electrode material has a similar effect on the working pressure in affecting the evolution of gas as well as the sputtering. Materials which sputter very little (molybdenum, tungsten) require larger currents in order to display a strong pumping action.

The getter action also can contribute to an appreciable reduction in pressure. The fine film of sputtered material which collects on the walls is very efficient in absorbing gas molecules. Molybdenum displays a particularly strong getter action which was observed to last with diminishing intensity for 30 minutes or longer.

The reduction in pressure resulting from the two combined pumping actions can be considerable and is in part responsible for the fact that a current can be interrupted repeatedly in vacuum.

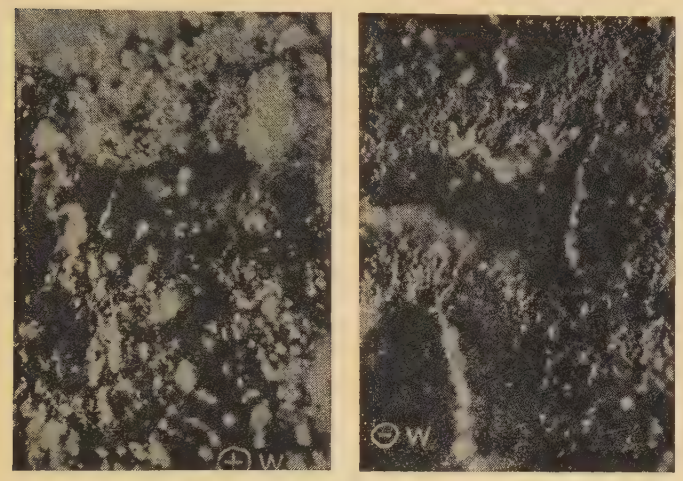

Anode Cathode

Figure 10 (above). Molybdenum electrodes (× 90)

Figure 11 (below). Carbon electrodes (× 70)

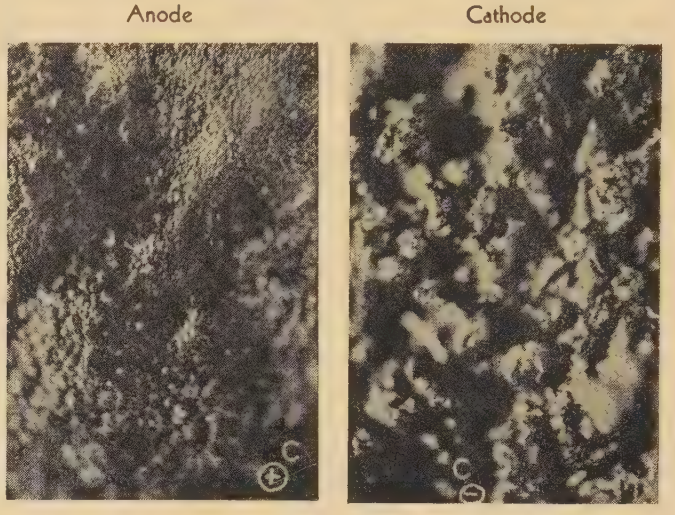

Factors Determining the Loss of Electrode Material

From the knowledge of the mechanism of interruption, it follows that the loss of electrode material caused by the interruption of currents will depend on the mass of material sputtered or evaporated at each striking of the arc and on the number of individual arcing episodes occurring during the time required for the interruption of the circuit. The mass of material sputtered at each striking of the arc is probably proportional to the energy dissipated in such an arc. The amount of mass sputtered per watt-second, however, will depend particularly on various physical constants of the electrode material and therefore will differ a great deal among various ma-

terials. For a given material the losses must thus depend on the over-all time to terminate the interruption and on the currents and potentials involved.

From the mechanism of interruption described earlier, it follows that the primary loss of material comes from the cathode. According to observations of the electrode surface, it is to be expected that the anode gains in mass by the sputtering of cathode material onto it.

Unfortunately, too little is known today about the mechanism of sputtering to enable one to make a thorough quantitative analysis of the various factors influencing the loss of electrode material. Two distinctly different types of sputtering have been observed in the course of the experiments. One is the atomic sputtering resulting from the evaporation of electrode material. The other type of sputtering is caused by occluded gases in the electrode material. The positive ion bombardment produces a fast local heating of the cathode surface which results in an explosive gas evolution and in the blasting out of chunks of material from the cathode. There has been visible evidence of such incandescent tiny chunks streaking from the arc region toward the walls and often rebounding from them. Carbon contains great amounts of absorbed gases and therefore displays with great intensity this second type of sputtering. The diffusion pump like action, described in an earlier part of this paper, is caused entirely by the atomic type of sputtering.

In what follows, the experimental results of the investigation on electrode material losses are given.

Distribution of Sputtered Material

All switching experiments resulted in a gain in mass of the anode and in a loss in mass of the cathode. The material sputtered from the cathode deposits on the anode, on the walls of the switch, and is reflected partially to the cathode. The loss of anode material which is known to occur from electron streams is overcompensated largely by the cathode material collecting on the anode surface.

The distribution of the sputtered material is determined chiefly by the design of the switch and particularly by the size and the shape of the electrodes. However, it also is affected slightly by the current, the recovery voltage, and the speed of separation of the electrodes.

Influence of the Gas Pressure

During this investigation, the pressure in the vessel was brought to a definite value before each interruption. Insignificant changes in losses were observed in interrupting at pressures ranging from 10^{-6} to 10^{-4} millimeter of mercury. At pressures above 10^{-4} millimeter of mercury, the losses increase rapidly because of a lengthening of the time of interruption.

If the pressure becomes too high, a permanent arc was able to maintain itself and switching action ceased. The lengthening of the time of interruption with increasing pressure obviously is caused by a corresponding decrease of the velocity of the radial gaseous diffusion.

Influence of the Shape of the Electrodes

The size of the anode was found to have no noticeable effect within the range investigated, that is, from 0.5 centimeter to 50 centimeters diameter. The curvature of the cathode has a pronounced effect, in increasing the loss and the time of interruption for a smaller radius of curvature. With a small radius of curvature, the radial travel of successive arcing episodes leading to extinction is no longer possible as it was in the case of a plate cathode. The restrikes, therefore, will be confined to a limited area around the former point of contact until the separation of the electrodes is too great to restrike the arc. This localization of the interruption process results in more continuous arcing episodes with a deeper localized heating of the area. This yields more gas evolution and evaporation and consequently heavier instantaneous arcing-currents result.

Influence of the Vessel Diameter

It was found that the loss of cathode material was slightly higher for smaller vessel- or baffle-diameters. The effect is very small and can be explained by the increase of the working pressure, resulting from the smaller diameter.

Figure 12. Average cathode loss versus average time of interruption of a d-c circuit

Cathode: 2-inch diameter plate
Anode: 1-inch diameter sphere
Opening speed 75 centimeters per second

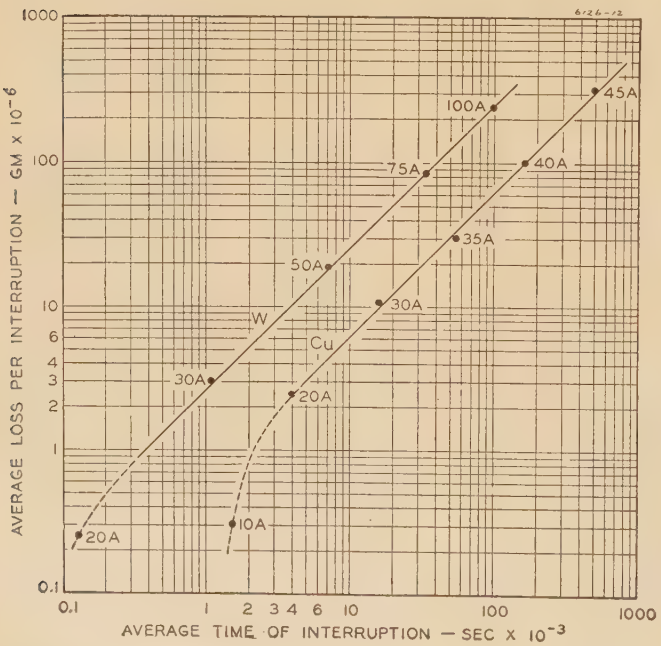

Figure 13. Average cathode loss versus line current I and I^2 of a d-c circuit

Cathode: 2-inch diameter plate
Anode: 1-inch diameter sphere
Opening speed 75 centimeters per second

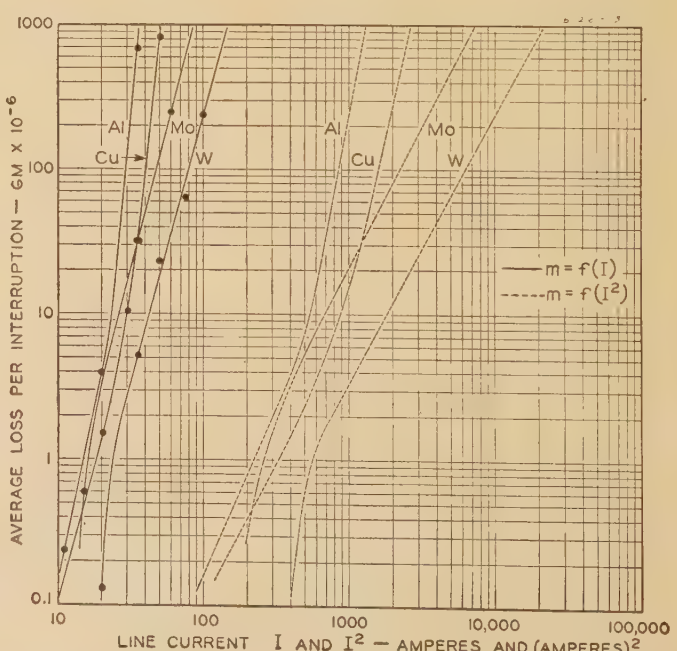

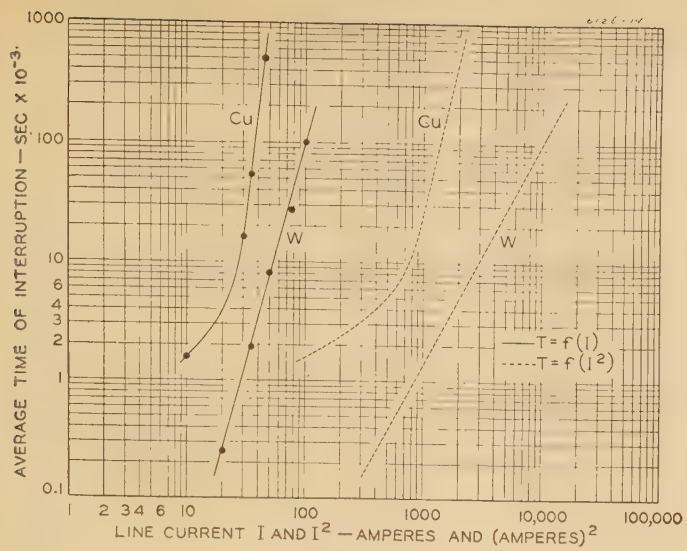

Figure 14. Average time of interruption versus line current I and I^2 of a d-c circuit

Cathode: 2-inch diameter plate
Anode: 1-inch diameter sphere
Opening speed 75 centimeters per second

Influence of the Line Voltage

The line voltage had no effect on the losses within the range investigated, that is, from 50 to 500 volts direct current. This is also in accordance with the findings of Sorensen and Jubitz. The line voltage is not of great significance in any such phenomena inasmuch as the recovery voltage is usually much higher. The recovery voltage is a much more significant variable and acts in two ways. One of these is to increase the chance of restriking and to increase the number of arcing episodes, thus lengthening the time of interruption. The other is directly to affect the sputtering. In the operation of glow discharge tubes, it is well known that sputtering increases materially once one enters the region of abnormal cathode fall, where the voltage increases with increasing current.

Influence of the Speed of Separation of the Electrodes

A few simplified considerations have to be introduced in order to understand the effect which the opening speed has on the loss of electrode material.

The energy equation[8] of a circuit having capacity C and inductance I is as follows:

$$1/2LI^2=1/2CE_r^2+A$$

where I=line current, E_r=recovery voltage, and A=loss of energy in the circuit and in the switch because of heat and radiation. The term on the left side of the equation represents the magnetic energy stored in the system at the time of interruption. It is a constant for a given current. Referring to Figure 12, it is seen that except for small currents the loss of cathode material is directly proportional to the time of interruption T. Therefore the loss of energy A in the circuit is also closely proportional to T. For a given current and a given set of electrodes, a definite separation d of the electrodes is necessary for the interruption of the circuit. Hence $d=vT$, where v is the speed of separation of the electrodes.

If d would remain constant, then T would be inversely proportional to v. The experiments, however, have shown that the mass-losses of the cathode are always less than proportional to $1/v$. The reason for this is that an increase in the opening speed v tends to reduce A in making T shorter. Since the right hand side of the above equation is constant, it follows that the recovery voltage E_r has to increase. This actually has been observed. A greater separation d_1 of the electrodes therefore is required for the interruption of the circuit.

Since d is not a constant, it follows that an increase in velocity will always result in a decrease in mass loss which is less than proportional to $1/v$.

Influence of Line Current and Electrode Material

Figure 13 shows the average cathode material loss for various electrodes and different values of current flowing in the line prior to interruption.

In the same figure the broken-line curves show the relationship between cathode losses and I^2. This is a measure of the magnetic energy $1/2LI^2$ stored in the circuit before the time of interruption. Figure 14 shows the relation between the average time of interruption T and I as well as I^2.

The electrodes used for all the data given in Figures 12, 13, and 14 consisted of a 2-inch-diameter plate cathode and of a 1-inch-diameter spherical anode. The opening speed was in each case 75 centimeters per second. Referring to Figure 13, it is seen that the refractory metals give the smallest losses in the high current region. At lesser currents the different metals behave in a different fashion, the more refractory metals indicating a greater slope and the low melting point metals a smaller slope. It appears that two mechanisms may be at work in different current ranges. The difference in losses between the higher and lower melting point metals indicate why good conducting metals like silver and copper often are used in low current capacity vacuum switches.

The line current has a two-fold effect on the losses. Considering the energy equation of the circuit, it follows that the current determines essentially the sum of $1/2CE_r^2+A$. It affects the recovery voltage E_r as well as the energy loss A. The latter term is particularly affected by the amount of evolved gases and vapors, which depend on the current magnitude and which greatly affect the time of interruption. It is obvious that well outgassed electrode materials, giving off only small amounts of gas, will result in small losses. It therefore is expected that vacuum-melted materials would give considerably smaller losses than can be expected from Figure 12 and Figure 13.

The surface conditioning as used throughout the present investigation is not sufficient for currents exceeding 150 to 200 amperes where craters are dug to a depth which is beyond the region outgassed by previous conditioning. This results in excessive gas formation, which would be dangerous, particularly for the case of sealed-off switches.

Essential Design Features

The mechanism of interruption, the behavior of the pressure, and the character of the losses of electrode material indicate that improvements can be made in the design of vacuum switches for moderate- and high-interruption duties.

The fact that a very high vacuum is not essential for the proper operation makes a practical design of a vacuum switch possible.

The vacuum vessel can be made of glass or metal, preferably stainless steel. The seals can be of the enamel type; welded, brazed, or soft soldered joints are also satisfactory. Glass-to-metal joints have to be ground and can be made vacuum-tight by means of a low-vapor-pressure wax, like picein. Greases should be avoided because they dissociate easily

under the intense radiation of the discharge.

The switch requires, for conditioning, a relatively low capacity diffusion pump backed by a medium-sized fore pump. The cooling of the traps can be achieved satisfactorily by means of a mixture of dry ice and alcohol.

It is expected that the judicious choice of seals and materials will make a permanently sealed-off vacuum switch possible. In this case it will be of even greater importance to use the correct vessel or baffle diameter by means of which full use of the pumping action can be made. Metal or glass baffles are also useful in shielding the insulating parts of the switch from sputtered material. A thorough outbaking will be required for a sealed-off switch.

The vacuum switch is ideally suited for the interruption of high voltage circuits. It is necessary, however, to reduce the evolution of gases and vapors as much as possible. Therefore, it is necessary to limit the current per contact and to choose electrode materials with small gas and vapor evolution. For larger currents, refractory metals are best suited.

The electrodes have to be conditioned in order to reduce the gas evolution. The conditioning by positive ion bombardment, as described earlier, limits the current to from 100 to 200 amperes per single contact. For larger currents, vacuum processed metals have to be used.

Exposure to air during the insertion (of new contacts, for instance) tends to contaminate the surface of such materials and therefore indicates the necessity of a short conditioning procedure preceding the operation of the switch after each shutdown period.

The interruption of higher currents and voltages also can be accomplished by multiple contacts. Such contacts will have to break with a fair degree of simultaneity.

All current carrying parts exposed to the vacuum should have large cross sections in order not to be heated appreciably by the normal line current or by short circuit currents of short duration. Too high a temperature of these elements would result in an undesirable evolution of gases from their surfaces.

The small distance of separation of the electrodes required for the interruption allows tripping the switch with great accuracy. With alternating current it is thus possible to interrupt close to current zero. In this way only small currents and recovery voltages have to be handled by the switch, resulting in a small loss of cathode material.

The loss of material and the time of interruption can be influenced further by the speed of separation of the electrodes. A speed of one meter per second or more should be used at the instant of separation.

The radius of curvature of the cathode should be large. The shape of the anode is not essential. For the interruption of alternating current the same contact arrangement as used for direct current is applicable provided the switch is always tripped at the same polarity. Both electrodes have to have a large radius of curvature and have to be symmetrical if the switch interrupts on either polarity.

By means of a magnetic field applied at right angles to the axis of the switch, the discharge can be confined to a small area. This considerably reduces the time required for the conditioning as well as reduces the necessary amount of vacuum melted material. A magnetic field of great intensity will disturb the focussing action and thus result in a faster deionization of the arc.

The use of parallel capacitors and resistors,[1,2] of course, also will improve the performance of a vacuum switch in reducing the recovery voltage.

Conclusion

It is believed that on the basis of the suggestions made here, a satisfactory working model capable of interrupting medium a-c or d-c loads can be constructed for test purposes.

References

1. Effect of Restriking on Recovery Voltage, **C. Concordia, W. F. Skeats.** AIEE Transactions, volume 58, 1939, August section, pages 371–5.

2. Switching Overvoltage Hazard Eliminated in High-Voltage Oil Circuit Breakers, **L. F. Hunt, E. W. Boehne, H. A. Peterson.** AIEE Transactions, volume 62, 1943, February section, pages 98–106.

3. Über kalte und warme Elektronenentladungen, **W. Schottky.** *Zeitschrift für Physik*, volume 14, 1923, page 71.

4. Cold Emission from Unconditioned Surfaces, **W. H. Bennett.** *Physical Review*, volume 37, 1931, pages 582–90.

5. Fundamental Processes of Electrical Discharge in Gases (book), **L. B. Loeb.** John Wiley and Sons, Inc., New York, N. Y., 1939, page 472.

6. Der Birkaregler und seine Bedeutung für die elektrische Heiztechnik, **A. Scherbius.** *Elektrotechnische Zeitschrift*, volume 47, number 1, 1926, pages 224–8.

7. Vacuum Switching Experiments at California Institute of Technology, **R. W. Sorensen, H. E. Mendenhall.** AIEE Transactions, volume 45, 1926, September section pages 1102–05.

8. Ausschaltüberspannungen bei Kleinvakuumschaltern, **E. O. Seitz.** *Elektrotechnische Zeitschrift*, volume 52, number 2, 1931, pages 1305–07.

9. Uber die bisherige Entwicklung des Protos Vakuumschalters, **W. Jubitz.** *Siemens Zeitschrift*, volume 10, 1930, pages 420–7.

10. Ein neues Manometer für niedrige Gasdrucke, insbesondere zwischen 10^{-2} und 10^{-5}, Millimeters, **F. M. Penning.** *Physica*, volume 4, number 2, 1937, pages 71–5.

11. Kinetic Theory of Gases (book), **L. B. Loeb.** McGraw-Hill Book Company, New York, N. Y., 1934, page 116.

12. Hochspannungstechnik (book), **A. Roth.** Julius Springer, Vienna, Austria, 1938, pages 586–7.

13. Magnetically Self-Focussing Streams, **W. H. Bennett.** *Physical Review*, volume 45, 1934, pages 890–7.

Semiconducting Shielding for A-C Power Cable

EDWIN J. MERRELL
ASSOCIATE AIEE

ELECTRIC SHIELDING of a-c power cable is provided primarily for the purpose of directing and confining the electric field within the insulation so as to prevent the occurrence of unduly high electric stresses in dielectrically weak directions or regions of a cable. Martin Hochstadter laid down the principles governing such shielding in 1913, with particular application to impregnated paper insulated cables for high voltages.[1]

Such cable was not used widely during the following years, although the subject of shielding had been considered by many cable engineers in the United States. An excellent summary of shielding history and practice was presented in 1938 by L. F. Hickernell to the transmission and distribution committee of the Edison Electric Institute under the auspices of the Insulated Power Cable Engineers Association.[2]

During this time, various types of shielding, including the semiconducting type, were being considered. Semiconducting shielding may be defined as the practice of "partially" confining the electric field within the insulation by means of a semiconducting covering, its most important function being prevention of corona discharge. In 1928 cable with this form of shielding was described in an article by M. J. Lowenberg.[3] This article told of the failure of cotton-braided varnished-cambric cable, because of "arcs formed between the braid and the duct in which the cable was installed." Lowenberg then proceeded to tell how this trouble was eliminated by the substitution of a conducting cotton or asbestos braid for that of ordinary saturated cotton. The shielding effect of the braid, because of its partial- or semiconductivity, made possible the success of this venture.

Semiconducting shielding has been employed in a number of a-c cable installations in recent years, but an exact theory of its use has not been published. Consequently, most characteristics of this type of shielded cable have remained obscure, and the field to which semiconducting shielding may be applied safely has been limited unnecessarily.

It is hoped that the subject matter covered by this paper will assist in coordinating knowledge on the shielding of power cable, so that more effective use may be made of this electrical property.

Paper 46-118, recommended by the AIEE committee on power transmission and distribution for presentation at the AIEE summer convention, Detroit, Mich., June 24–28, 1946. Manuscript submitted April 9, 1946; made available for printing May 8, 1946.

EDWIN J. MERRELL is research electrical engineer, Habirshaw wire and cable division, Phelps Dodge Copper Products Corporation, Yonkers, N. Y.

The author wishes to acknowledge the kind assistance of William A. Del Mar and John H. Palmer.

Theory of Semiconducting Shielding

While Lowenberg's paper dealt principally with the application of semiconducting shielding to varnished-cambric insulated station cables, probably its most important application is to rubber-insulated cables, as rubber is subjected to corona cutting from spark-generated ozone. The protective requirements of this type of installation may be met by semiconducting shielding.

Oscillographic observations of cable charging currents at ground points have verified the shielding effect of semiconducting cable coverings. Illustrative of this type of study are the oscillograms of Figure 1. They are typical of traces produced on the screen of a cathode-ray tube by the charging currents of three types of cable identical but for the electrical properties of their external coverings. Thus, the current traces of the cables having semiconducting and highly conducting shielding are smooth, and free of the high frequency components which are indicative of corona discharge. In contrast, unshielded cable under equal voltage conditions gives rise to a profusion of high frequency discharges. These oscillograms were obtained by carrying the 60-cycle charging current of the cable samples to ground through a 0.25 millihenry inductance, with the vertical plates of an oscillograph connected across the inductance.

To aid in interpreting the meaning of these observations, a theory of the electrical function performed by semiconducting cable coverings has been developed. This theory is based on an adaptation of the exact hyperbolic formulas for transmission lines to the circuit condi-

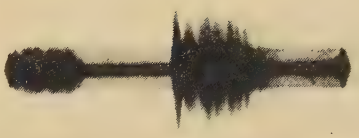

Figure 1. Charging current of shielded cable versus unshielded cable

tions present in a cable dielectric and semiconducting coverings. The simplified circuit of Figure 2 has been adopted as the electrical equivalent of cable insulation and outer coverings. The uniformly distributed capacity represents the dielectric, the conductance of which has been disregarded, its contribution to the admittance being negligible. The uniformly distributed resistance represents the semiconducting outer covering, the reactance of which also has been ignored, inasmuch as it has a comparatively minute effect on the impedance. The parallel capacity to ground likewise is neglected, as its operation reduces the current flow through the semiconducting covering by shunting a portion of the current, and, for practical purposes, this effect constitutes a factor of safety. Finally, the conductor is considered equivalent to the infinite ground in transmission calculations, inasmuch as for the cable lengths herein considered there is insignificant voltage drop along the conductor. The following formulas, expressed in co-ordinates adapted to measurement on the finished cable, were de-

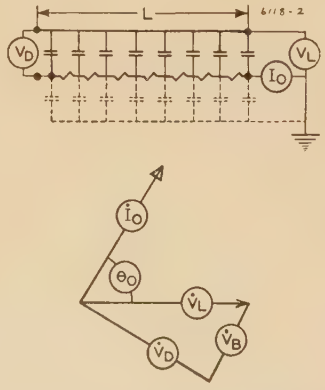

Figure 2. Equivalent circuit of cable insulation and outer semiconducting covering for single conductor cable

rived through these simplifying assumptions:[4]

$$V_B = V_L - \frac{V_L}{\cosh 0.001\sqrt{j(2\pi fcRL^2)}} \quad (1)$$

$$V_D = \frac{V_L}{\cosh 0.001\sqrt{j(2\pi fcRL^2)}} \quad (2)$$

$$I_0 = (10^{-9})(V_L)(L)\sqrt{j\left(\frac{2\pi fc}{RL^2}\right)} \times \frac{\sinh 0.001\sqrt{j(2\pi fcRL^2)}}{\cosh 0.001\sqrt{j(2\pi fcRL^2)}} \quad (3)$$

$$\theta_0 = \left[\tan^{-1}\frac{\sin 0.1146\sqrt{\pi fcRL^2}}{\sinh 0.002\sqrt{\pi fcRL^2}}\right] + 45° \quad (4)$$

where

V_L = vector line voltage to ground in volts

V_D = vector voltage drop across the insulation at a point midway between grounds

V_B = vector voltage drop lengthwise along the outer semiconducting covering, from the midpoint between two grounds to the ground points

I_0 = vector current in amperes at the ground point from the half-length of cable on one side of ground

θ_0 = power factor angle in degrees measured between the conductor and the ground point; this is the angle due to the power loss resulting from passing the charging current through the semiconducting shield to ground

f = frequency in cycles per second

c = capacity in micromicrofarads per inch length of cable

R = longitudinal resistance of the semiconducting covering in megohms per inch length of cable; this is the a-c resistance

L = one-half the distance between grounds in inches

Graphs for Use in Design of Semiconducting Shielded Cable

It will be noted that the foregoing formulas are functions of RL^2, RL^2 being a function of the a-c resistance of the semiconducting covering and the spacing between ground points. This fact has made feasible the calculation and drawing of graphs which have the common coordinate RL^2 and which encompass all probable cable constants. That this has been possible is very fortunate for, though simplified, the formulas still are comparatively unwieldy in applications to routine measurement and design; and it is quite difficult to appreciate fully the relation between the several electrical characteristics which they represent. The standard electric power frequency of 60 cycles per second has been employed in calculating the graphs, calculations being made for cables having capacities of 1, 5, 15, 30, and 50 micromicrofarads per inch length. Characteristics of cables possessing intermediate capacities may be obtained with sufficient accuracy for most practical applications by rough interpolation.

Figure 3 is a polar plot of the vector voltage relations at 60 cycles in a single conductor cable dielectric versus RL^2. Figure 4 is a semilogarithmic graph of the cable charging current versus the common abscissa, RL^2. Figure 5 likewise is a semilogarithmic graph with RL^2 as abscissa, and as ordinate the cotangent of the power factor angle, θ_0. Figure 6 is a similar graph of the maximum heat generation possible in watts in the inch of cable covering adjacent to the ground point, resulting from the passage of the charging current through the covering.

Figure 7 gives the thermal surface resistance in thermal ohms per inch length of cable for various cable diameters. These thermal resistance curves have been included because they are useful for determining the effect which semiconducting coverings may have on the thermal characteristics of a particular cable design, and because the data have been employed in checking the efficacy of the semiconducting shielding theory proposed. The curves have been derived from a paper published by S. J. Rosch.[5]

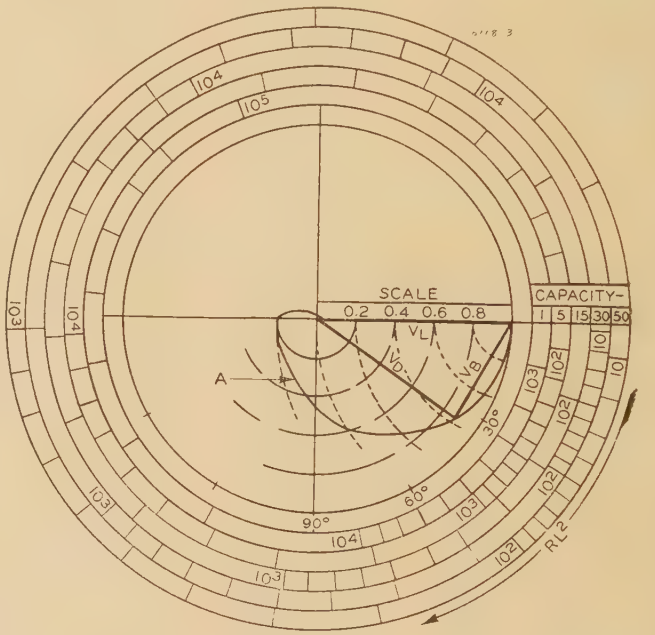

Figure 3. Dielectric vector voltages versus semiconducting shield resistance for single conductor cable

A—Locus of midpoint insulation and braid voltage vectors

Examples in Use of Graphs

To illustrate the use of these graphs in cable design, consider an aerial cable supported on metal rings 20 inches apart, rated at 10,000 volts to ground, and characterized by a capacity of 15 micromicrofarads per inch and a semiconducting shield resistance to alternating current of two megohms per inch. For this case L equals 10 and RL^2 equals 200.

According to Figure 3, V_B, the maximum voltage drop longitudinally along the braid, would be equivalent to 55 per cent of the line voltage, that is, 5,500 volts. Moreover, V_D, the voltage impressed upon the insulation at the midpoint between grounds, would be reduced to 86 per cent of the line voltage.

Figure 4 predicts a charging current of 0.5 milliampere for the half length of cable on one side of a ground ring. As the semiconducting covering has a lengthwise resistance of two megohms per inch, a maximum voltage drop of one volt per mil would be developed by the passage of this charging current, a stress much too low to cause corona discharge.

Figure 5 shows that this cable would not behave as a pure capacity; instead it would have a cotangent θ_0 of approximately 0.37, which corresponds to an operating power factor of 35 per cent. Figure 6 indicates a loss of 0.5 watt in the inch of covering adjacent to the ground point.

If this cable has an over-all diameter of two inches, and is installed so that there is a free movement of air about it, the cable will possess a thermal surface resistance of approximately 24 thermal ohms per inch of cable length, according to curve A' of Figure 7. Since the temperature difference required to liberate heat from a cable surface is equal to the product of the watts times the surface resistance in ohms, a temperature rise of 12 degrees centigrade will be produced in the semiconducting covering adjacent to the

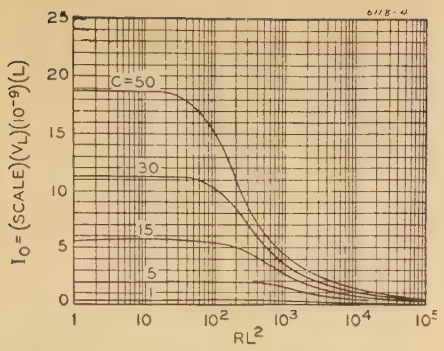

Figure 4. Charging current versus semiconducting shield resistance for single conductor cable

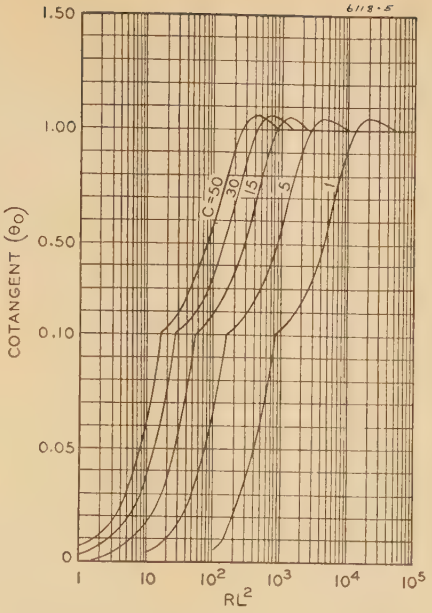

Figure 5. Power factor versus semiconducting shield resistance for single conductor cable

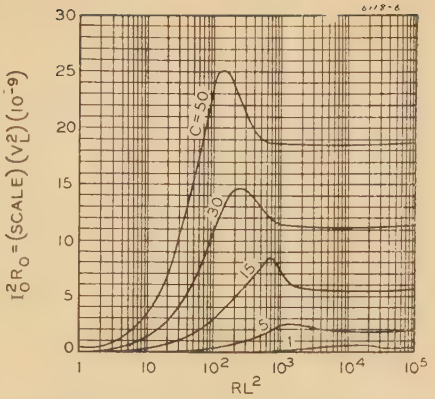

Figure 6. Watts loss versus semiconducting shield resistance for single conductor cable

ground point, because of the power loss resulting from passing the charging current through the semiconducting shield to ground.

Measuring Technique

In order to make available through the theory and graphs explained in the foregoing complete data relative to a particular sample of semiconducting shielded cable, seven constants must be measured. These are

1. The diameter over the outer coverings of the cable in inches, D.
2. The voltage applied for the measurements in volts, V_L.
3. The half-length in inches between ground loops, L.
4. The cotangent of the power factor angle of the combined semiconducting covering plus insulation, θ_2.
5. The ground point current corresponding to θ_2, I_0.
6. The cotangent of the insulation power factor angle, θ_1.
7. The capacity in micromicrofarads per inch length of cable, c.

In test procedure the first step is to measure the diameter, D, over the outer coverings. Next, the sample is prepared for the cotangent θ and ground point current measurements. The semiconducting covering is stripped from each end of the length, but is left intact on the center section. Wire loops are spaced on the active center section so as to form a number of π sections, similar to electrical models of long transmission lines or communication circuits. The number of sections and their length depend both upon the characteristics of the cable and the sensitivity of the bridge circuit employed for the measurements. Thus, in the analysis of a cable design having a low unit capacity and a high unit covering resistance, a larger number of sections of shorter length is necessary, than if the opposite be true. It is apparent that this aspect of the measurement requires an exercise of judgment and some experimenting before an efficient arrangement can be secured. In addition, the prepared sample must be placed on an insulated support, so that parallel capacity effects may be held to a minimum in accordance with the assumptions made in deriving the simplified formulas. With the sample so placed, all the wire loops except one are connected, through shielded leads, directly to the low tension side of a 60-cycle Schering bridge. The excepted loop is connected to the bridge through an a-c milliammeter or microammeter, so that the ground point current may be read. For the current measurement a ground loop adjacent to an end is preferable, because the current recorded at this point corresponds to the half-length current of the formulas and graphs. If the meter is connected to a loop in the center of the semiconducting section, twice this current is read, as it is collected from two half-lengths. The voltage now is applied and both the ground point current and cotangent of the power factor angle read. The half-length, L, corresponding to these measurements is recorded in inches, the voltage, V_L, in volts, the cotangent as that of θ_2, and the half-length current as I_0.

Two measurements remain: the unit capacity, and the insulation power factor angle. To obtain these, the remaining semiconducting covering is stripped from the center section of the cable sample, and replaced with a highly conducting metal foil wrapping. Then the cotangent of the insulating power factor angle, θ_1, is measured, as is the capacity of the length in micromicrofarads. The capacity in micromicrofarads per inch, obtained from this measurement, is the unit capacity, c, employed in the formulas and graphs described in the foregoing.

The first step in employing these measured data to make an analysis of the characteristics of the semiconducting covering is to obtain the value of cotangent θ_0. This may be done by subtracting θ_1 from θ_2, the difference angle being θ_0, this procedure is in accordance with one of the original assumptions in deriving the theory, namely, that the insulation conductance was ignored so as to aid in simplifying the formulas and calculations. Having found the value of cotangent θ_0, and knowing the capacity of the cable in micromicrofarads per inch of length, the corresponding RL^2 may be obtained from Figure 5. In turn, the unit resistance of

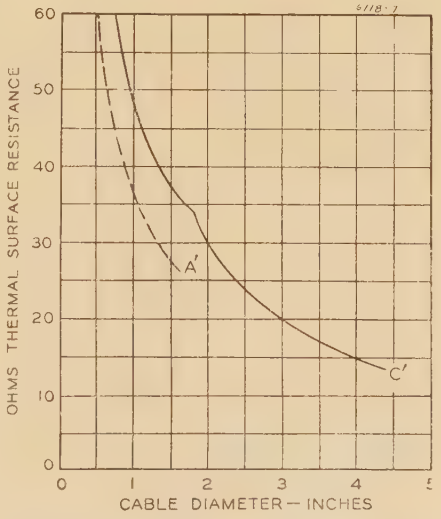

Figure 7. Surface resistance in thermal ohms per linear inch of cable for single conductor cable

A'—Braided cable in air
C'—National Electrical Manufacturers Association standard

Table I. Comparison of Calculated and Experimental Data

Sample	Cable Specification D	V_L[a]	L	R[a]	C[a]	Measured V_B	V_D	I_0[c]	T_0	Calculated V_B	V_D	I_0	T_0
A	1.62	5,000	.39	.0.01	8	120[b]		0.6×10^{-3}		125		0.63×10^{-3}	
		72,000	.39						21				19
B		5,000	.22	.0.26	5.6	115[b]		0.24×10^{-3}		750		0.24×10^{-3}	
C		111	.10	.2.5	.11.3	68[d]	100[d]			60	.99		
		10,000	5	.3.6	.11.3			0.22×10^{-3}				0.21×10^{-3}	
D		2,500	5	.4.4	.10			0.048×10^{-3}				0.045×10^{-3}	

[a] = value of constants obtained from calculations based on 60-cycle Schering bridge measurements.
[b] = measured with vacuum tube voltmeter
[c] = measured with rectifier type milliammeter
[d] = null-type measurement, Figure 8

the semiconducting covering in megohms per inch of cable length may be obtained by dividing the value of RL^2 by the square of the half-length used in the cotangent θ_2 measurements. Having established the value of R, it becomes comparatively simple to predict the performance of the cable design for any ground point spacing by calculating the particular RL^2 and applying this to Figures 3 through 7.

Experimental Confirmation of Theory

Table I contains data obtained from cable designs which were selected to test the correctness of the theory. The choice of samples represents a range of 60-cycle semiconducting covering resistance from approximately 0.01 megohm to slightly over four megohms per inch of cable length. The agreement between values calculated from the cotangent measurements and those measured directly is very good for this type of measurement and thereby certify the practical worth of the theory.

Inasmuch as some interesting problems in measuring technique presented themselves in the course of this experimental work, it has been thought worthwhile to explain them in detail for their possible application to similar measurements in the field of dielectric research. Many measurements were made which did not fit in as well as was expected with the calculated theory. This was true particularly of the readings taken of the voltage built up lengthwise along the semiconducting covering by the flow of the cable charging current. For example, the measured V_B of sample *A* agreed very well with that calculated, but that of sample *B* did not. Both these voltages were read with a vacuum tube voltmeter, which was supposed to approximate a zero energy device. This it does for most measurements to which it is applied, but in the case of sample *B*, which possessed a covering of medium high resistance, the parallel capacity to ground of the voltmeter pickup prod was sufficient to constitute a partial ground. As a result, a considerable portion of the cable charging current passed through this partial ground and therefore was not available to cause a voltage rise along the covering. This phenomenon is illustrative of the manner in which parallel capacity to ducts and conduits affects the characteristics of semiconducting shielded cable.

The vacuum tube voltmeter was still more ineffective in attempts to measure the voltage characteristics of sample *C*, which was characterized by a high-resistance "semiconducting" covering. It was necessary to employ a true zero energy measuring technique for these readings. The circuit of Figure 8 shows the method by which this was accomplished. The voltage built up on the cable covering under test was balanced at a midpoint between grounds by a voltage applied through a phase shifter. The magnitude of this applied voltage was varied by means of an autotransformer placed in the primary winding of the phase shifter, and the value of the voltage output of the phase shifter was read by a voltmeter. The phase of the voltage applied to the covering as related to the line voltage impressed on the cable conductor was indicated by connecting a cathode-ray oscillograph as shown to form Lissajous figures.[6] A Schering bridge was used to indicate balance; thus, if the braid voltage were not balanced by the voltage from the second circuit, the latter would constitute a partial ground and cotangent θ would be lowered as a result of the length between grounds in effect being shortened. If the braid voltage were overbalanced, cotangent θ would be raised; but the same cotangent would mean a null balance, that is, V equal to V.

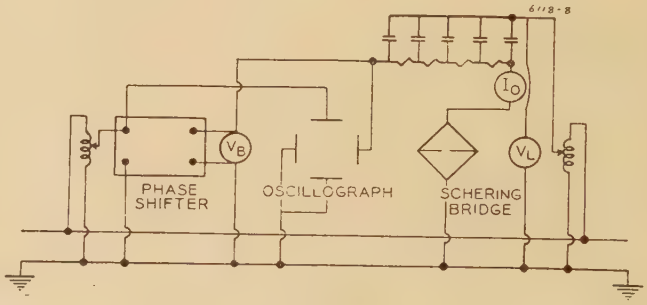

Figure 8. Null point method of measuring phase and value of voltage on the semiconducting covering of semiconducting shielded cable

Discussion

Semiconducting shielding, like high conductivity shielding, requires adequate grounding. If contact resistance or impedance is too high, arcing will occur at ground points with attendant destructive thermal and chemical effects.

Power loss in a semiconducting shield also may be, under certain conditions, sufficiently great to reduce the current carrying capacity of a cable markedly. Thus, consider a 2,000,000 circular mil cable, with a unit capacity of 15 micromicrofarads per inch, an over-all diameter of 2.7 inches, operated at 10,000 volts to ground. If RL^2 equaled 600, the power loss in the inch of semiconducting shield adjacent to the ground point would be 0.8 watt. Inasmuch as the thermal surface resistance of this cable is 23 thermal ohms per inch, a hot spot would result with a temperature rise equal to the product of watts and thermal ohms, or 18 degrees centigrade above normal. This temperature rise would result entirely from the passage of charging current, and would have to be superimposed upon that resulting from the load current.

Conclusions

A theory of semiconducting shielding has been presented which may be used as a guide in the application of this type of shield to electric power cable.

The electrical resistance required of a semiconducting shield for a particular cable installation is determined by several interrelated factors: the maximum spacing between ground points, the cable capacity per unit length, the line voltage, and the over-all diameter of the cable.

Automatic Control of Large Synchronous Condensers

M. J. BROWN
MEMBER AIEE

Synopsis: The considerations involved in the design of an automatic synchronous condenser control are discussed in this paper with an aim toward helping the designer and user of synchronous condenser equipment obtain modern and complete facilities in his design. A typical push-button-operated control for a large synchronous condenser is described and the diagrams involved are shown. The description includes a detailed résumé of starting sequence, protective device operation, and automatic control of voltage and load. Emphasis is put on the adaptability of push-button control to full automatic operation or remote operation by direct or supervisory control.

WHILE there is no clear line of demarcation between large and small synchronous condensers, it will best serve the purposes of this discussion to define large synchronous condensers as those having a rating of 5,000 kva or above. Numerically, there are about as many synchronous condensers below the 5,000-kva rating as above it, but the connected capacity of the large machines represents nine-tenths of the total capacity and the small machines only one-tenth. Hydrogen cooling appears on machines above 15,000-kva rating and at present will be found on about 12 per cent of these machines. There is reason to believe that hydrogen cooling will become more general in this class.

Paper 46-106, recommended by the AIEE committee on automatic stations for presentation at the AIEE summer convention, Detroit, Mich., June 24-28, 1946. Manuscript submitted March 18, 1946; made available for printing April 23, 1946.

M. J. BROWN is design engineer, switchboard engineering department, Westinghouse Electric Corporation, East Pittsburgh, Pa.

Automatic control for condensers in the larger sizes offers advantages that are attractive to users of these machines. The starting procedure, which begins with the acceleration of the rotor and involves field application at the time that synchronous speed is reached and ends with applying full voltage to the machine stator, is a routine sequence that involves several operations that must be properly timed. The timing of these operations as well as the checking of various mechanical and electrical conditions during the starting sequence is a duty that can be more efficiently handled automatically than manually. Besides this very practical consideration of accurate procedure, there are other reasons for adapting automatic control. The time consumed in going through the starting procedure will be a minimum, and the operating personnel can be reduced in number or skill. These two features are of interest to operating supervisors who bear the responsibility for efficient and punctual operations in the system. Automatic operation, which is manually initiated and terminated, will have as its primary element a manually operated push-button or control switch. It is not difficult to extend this control to full automatic operation wherein the machine is started by undervoltage conditions and removed when machine load drops. Remote control of starting and stopping is another alternative. Such control simply is an extension of the local manual control over a direct wire or as a point on a supervisory control system.

Apparatus Associated With Large Synchronous Condensers

There are two general methods of obtaining starting torque. One method employs an induction motor directly connected to the condenser shaft as a source of accelerating torque. The second is a self-starting method wherein the reduced voltage is applied to the stator and the rotor accelerates on torque from the damping bars. Which of these two methods is to be used is determined by system conditions.

Should the system demand minimum disturbance, the induction motor should be used. If, however, it can tolerate the power swings involved in low voltage starting, this method will be found to be more economical in both equipment and space requirements.

Low voltage starting may be effected by using an autotransformer, tapped power transformer, series reactor, or a series-parallel stator connection scheme. The autotransformer scheme is the most generally used and is the basis of the control discussed in the following pages.

Two autotransformer connection schemes are in general use. Figure 1 shows the two schemes. They differ in the location of the starting breaker. The choice between the two is based upon breaker costs and economy of installation. Satisfactory performance is obtained with either connection, and neither has any operating advantage over the other.

Excitation for the field can be obtained from either a direct-connected exciter or a separately driven exciter. The latter is employed with hydrogen-cooled machines when it is desired to keep the d-c machine and its commutator out of the hydrogen chamber. The main exciter will be equipped with a main and differential field, the latter being used for overcoming the exciter residual so that the low voltages required for lagging capacity may be obtained. The main and differential field will be under the control of the voltage regulator system whose motor-driven rheostat and field forcing resistors will alter excitation to meet changing demands for reactive power output of the condenser. A pilot exciter on the same shaft as the main exciter will furnish excitation current for the main exciter fields. A field cubicle containing the field breaker and discharge resistor completes the excitation equipment.

The larger condensers will be equipped with bearing lift pumps that must be used as a means of floating the shaft on a film of oil prior to starting. There will

To be noted particularly is the fact that all pertinent electrical characteristics are functions of the product of the shield resistance and the square of half the ground point spacing.

References

1. ELECTRICAL CONDUCTOR, **Martin Hochstadter,** United States patent number 1,119,789.

2. SHIELDING OF INSULATED POWER CABLES, **L. F. Hickernell.** Minutes of the transmission and distribution committee, Edison Electric Institute, February 1938.

3. BRAID DISCHARGE IN SINGLE CONDUCTOR CABLE IN DUCTS, **M. J. Lowenberg.** *Journal* AIEE, volume 47, July 1928, pages 534-5.

4. ELECTRICAL ENGINEERS HANDBOOK, **Pender Del Mar.** Third edition, John Wiley and Son, New York, N. Y.

5. THE CURRENT CARRYING CAPACITY OF RUBBER-INSULATED CONDUCTORS, **S. J. Rosch.** AIEE TRANSACTIONS, volume 57, 1938, March section, pages 155-67.

6. STUDY OF PHASE DISPLACEMENT IN ELECTRICAL CIRCUITS FROM LINEARLY EXPANDED LISSAJOUS FIGURES, **H. D. Brailsford.** Underwriters Laboratories *Bulletin of Research*, 1939.

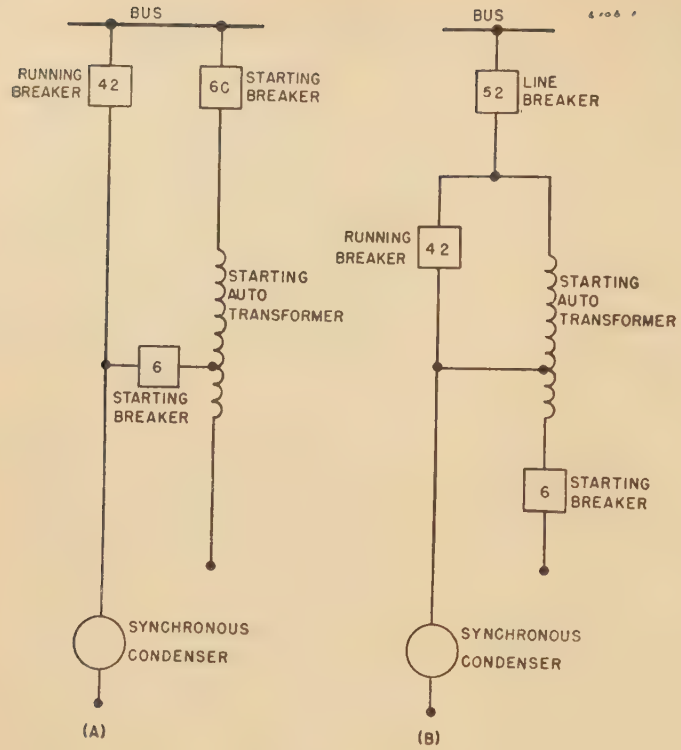

Figure 1. Synchronous condenser connections to autotransformer

be oil pumps employed in some cases for circulating lubricating oil in the bearings that must operate continuously as long as the motor is running. On other machines, oil rings provide lubricating oil circulation without the need for auxiliary oil pumps.

The instruments, relays, control switches, and associated devices will require switchboard mounting. Figures 2 and 3 show one section of a tunnel-type switchboard designed for the control of a 25,000-kva synchronous condenser. This type of construction has been adopted widely because the control switches and instruments are very accessible and constantly observable on the front panel of the switchboard, while the relays are easily attended on the back panel of the board. All wiring, terminal blocks, and fuses are concealed and protected within the tunnel housing. This area of the switchboard can be reached by entering a door at either end of the switchboard assembly. Drawout relays with built in test switches offer flexibility of handling when maintaining the relays.

Starting Characteristics of Synchronous Condensers

When a condenser is brought up to speed with a direct-connected induction motor, the problems encountered in putting it on the line are exactly the same as those experienced when a generator is put on a line. The machine must be brought to synchronous speed, its voltage matched to the line voltage and synchronized with it. At the time when these conditions exist, the running breaker may be closed. The disturbance caused by closing the running breaker will be negligible if voltage and phase are matched closely.

When self-starting on reduced voltage is employed, the least disturbance is encountered if the field is applied before full voltage is put on the stator. Figure 5 shows the "V" curves for a typical condenser. The lower curve indicates the line current to be expected for various values of field excitation when operating the machine at 22.5 per cent rated voltage. The upper curve indicates line current variation with field excitation when the machine is operating at full line voltage. The intersection of these two curves gives a value of field current which may be used during starting if the leading reactive load during starting is to be the same before and after transfer from starting to running voltage.

The sequence of events in a typical start is shown by the graph in Figure 6. This shows the variation of reactive

Figure 3 (right). Rear panel relay arrangement of switchboard shown in Figure 2

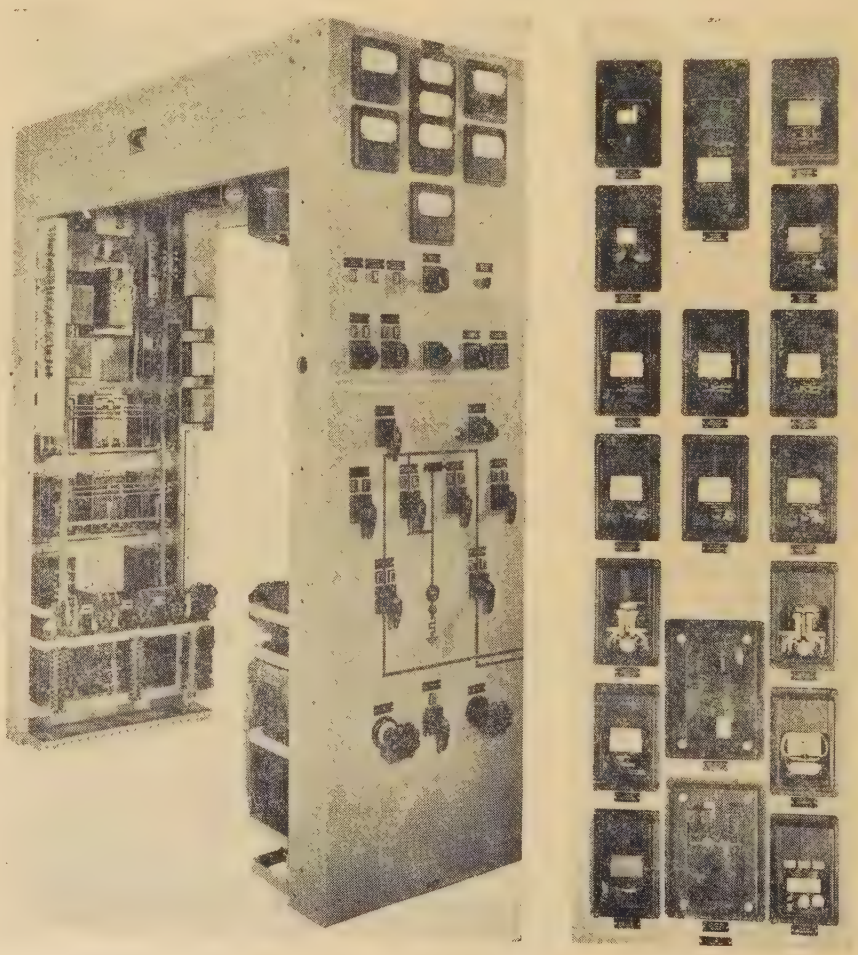

Figure 2. Tunnel-type switchboard section designed for synchronous condenser control

power, as seen by a graphic varmeter when the machine is accelerated and put on the line. The initial reactive inrush is lagging and diminishes in value as the machine accelerates. At half speed a slight drop is noted, but the decline continues smoothly until synchronous speed is approached. Hunting appears as a wavy trace in the graph and as synchronous speed is reached, the reactive power drops to a low steady value. When the field is applied, the reactive power becomes leading, building up in magnitude as the field builds up. The field eventually stabilizes and the machine is operated for a brief period under these conditions to assure that hunting has subsided. The transfer from starting to running voltage is made at this point. Although the actual transfer requires only a fraction of a second its effect is to reduce field flux to a low value. A subsequent delay is encountered in rebuilding the field. During the transfer, the field current will be dropped to nearly zero as the induced voltage in the field winding opposes the exciter voltage. The reactive power changes sharply during transfer from leading to lagging and returns slowly to leading again as field flux reappears.

The disturbance on a system caused by a synchronous condenser coming on the line is the net effect of the various reactive power swings encountered in the period extending from the time of initial inrush to final stabilized operation at full line voltage. The best operating point can be determined only by evaluating the effect of the individual disturbances during this period on the system to which the condenser is applied. The field excitation determined by the intersection of the "V" curves in Figure 5 will give satisfactory operation in many cases. A decrease in field current will increase the severity of the lagging reactive power peak encountered at the time of transfer. An increase in excitation will decrease this peak, but it also will bring the condenser on the line at a higher load, at both the starting and running voltage.

Table I. Device Table for Schematic Diagrams

1 = start-stop push button
4 = master relay (multicontact type)
6 = starting breaker
14 = locked rotor protective relay (slow release telephone type type)
  14X1 = pendulum relay (telephone type)
  14Y1 = counting chain relay (telephone type)
  14Y2 = counting chain relay (telephone type)
  14Y3 = counting chain relay (telephone type)
  14Z = pulsing relay (telephone type)
18 = acceleration relay (current operated induction disk type)
  18X = auxiliary relay (solenoid contactor)
26 = thermal relay
  26H = hydrogen temperature in machine
30 = annunciator relay
  30-1, 30-2, and so forth = individual drops
  30X = auxiliary relay (electrically operated, manually reset)
  30Y = bell alarm cutoff relay (solenoid contactor type)
38 = bearing thermal relay
40 = field failure relay (solenoid contactor type)
41 = field breaker
42 = running breaker
46 = current balance relay (induction disk type)
47 = undervoltage, single and reversed phase relay (induction disk type)
48 = incomplete sequence relay (a-c timing relay)
49 = thermal overload relay (thermal lag—thermostatic relay)
51 = inverse time overcurrent relay (induction disk type)
52 = line breaker
53 = exciter voltage relay (instantaneous solenoid type)
56 = field application relay (a-c timing relay)
  T_1 = short time contact
  T_2 = long time contact
59 = a-c overvoltage relay (induction disk type)
63 = pressure relay
  63H = hydrogen pressure in machine
  63HB = hydrogen pressure in bottles
  63QF = oil pressure in front bearing
  63QR = oil pressure in rear bearing
  63QX = auxiliary oil pressure relay (solenoid contactor type)
  63W = cooling-water pressure
  63WM = water detector relay
86 = lockout relay (electrically operated, manually reset)
87 = differential relay (induction disk type)
88 = auxiliary motor
  88E = exciter motor
  88EX = exciter motor breaker
  88W = cooling-water valve motor
  88WX = cooling-water valve motor relay
  88Q = oil lift pump motor
  88QX = oil lift pump motor relay
90 = voltage regulator
  90C = current regulator operating coil
  90CX = a-c timing relay (induction disk type)
  90CY = a-c fault detector relay (instantaneous solenoid type)
  90CHR = antihunt coil—current element—raise
  90CHL = antihunt coil—current element—lower
  90CZ = auxiliary relay (multicontact type)
AR = quick-raise contact (voltage element)
AR' = quick-raise contact (current element)
AL = quick-lower contact (voltage element)
CR = raise contact (current element)
CL = lower contact (current element)
CSR = control switch raise
CSL = control switch lower
I = contact closed in indicating position of regulator transfer switch
LC = lowering contactor
LS = limit switch
M = contact closed in manual position of regulator transfer switch
NR = normal-raise contactor
NL = normal-lower contactor
NH = antihunt coil—normal raise and lower contacts
QR = quick-raise contactor
QL = quick-lower contactor
QH = antihunt coil—quick-raise and -lower contacts
R = contact closed in regulating position of regulator transfer switch
RL = red light indicating raise required
LL = green light indicating lower required
VR = raise contact (voltage element)
VL = lower contact (voltage element)

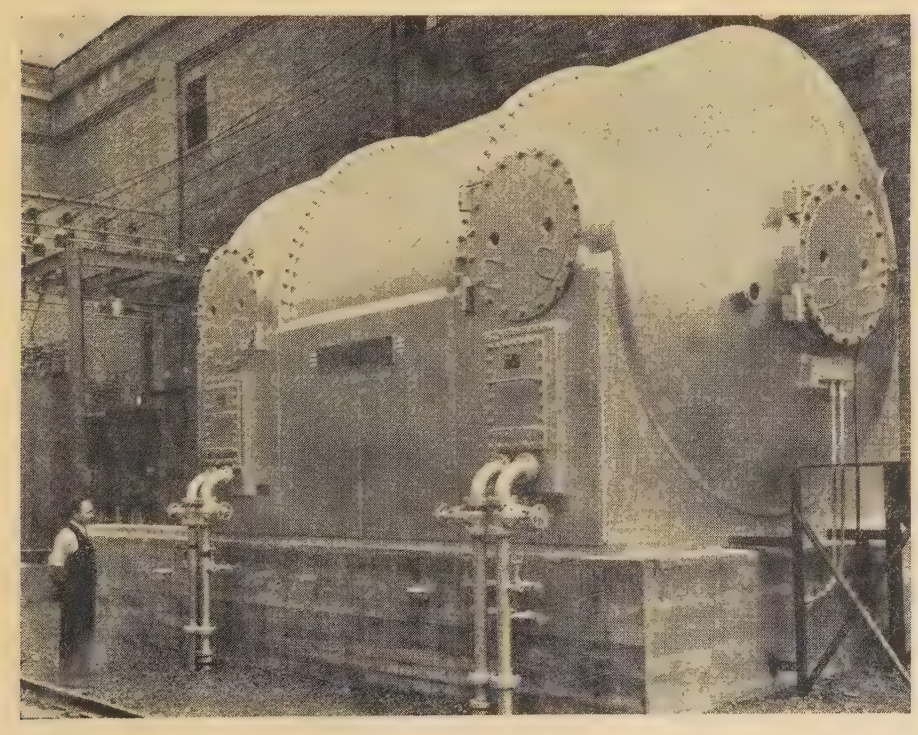

Figure 4. A 15,000-kva hydrogen-cooled outdoor synchronous condenser

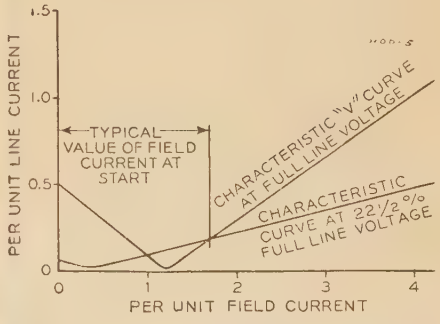

Figure 5. Characteristic curves for a typical synchronous condenser

An alternative method of starting suggests itself; that of accelerating the machine on low voltage, applying full voltage, and then applying field at the no-load value. The inrush of reactive power is far greater in this case when full voltage is applied than in the case where field is on before full voltage is applied. With this method, the phase and magnitude of the internal voltage of the condenser are less favorably matched to line voltage phase and magnitude when transfer is made than would be the case if the field were excited. Consequently, the inrush is greater with this method than with the method where field is applied before transfer is made.

Automatic Sequence for Controlling Synchronous Condenser

The following description applies to the control of a self-starting hydrogen-cooled machine operating from an auto-transformer. Figure 7 shows the single line diagram of this control and Figure 8, the control diagram. This is a typical scheme and would be altered in practice by changes in details to suit each particular application. The functional sequences are as follows:

Push-Button Starting

1. Operate push button.

2. Start incomplete sequence timing relay. Failure to complete the starting sequence in a definite length of time will cause lockout.

3. Check position of control elements.
(*a*). Check to assure that line breaker is open.
(*b*). Check to assure that starting breaker is open.
(*c*). Check to assure that running breaker is open.
(*d*). Check to assure that field breaker is open.
(*e*). Check to assure that motor-operated rheostat is in pre-set position.
(*f*). Check to assure that lockout relay has been reset.
(*g*). Check to assure that proper voltage and phase rotation exists on the a-c line.
(*h*). Check to assure that station battery voltage is at an operative value.

4. Start auxiliaries.
(*a*). Start oil lift pumps.
(*b*). Start separate exciter.
(*c*). Start flow of bearing cooling water.

5. Check operation of auxiliaries.
(*a*). Check oil lift pump pressure.
(*b*). Check exciter voltage.
(*c*). Check cooling water pressure (or flow) to hydrogen cooler and bearings.

6. Close starting breaker.

7. Check closing of starting breaker.

8. Close line breaker.

9. Check for machine rotation. Failure to rotate will cause lockout.

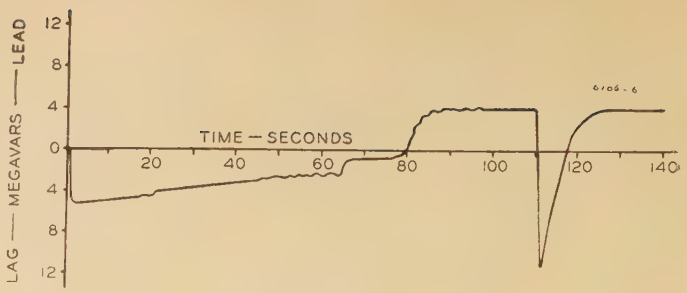

Figure 6. Graphic varmeter trace of reactive power drain by a 25,000-kva synchronous condenser during starting

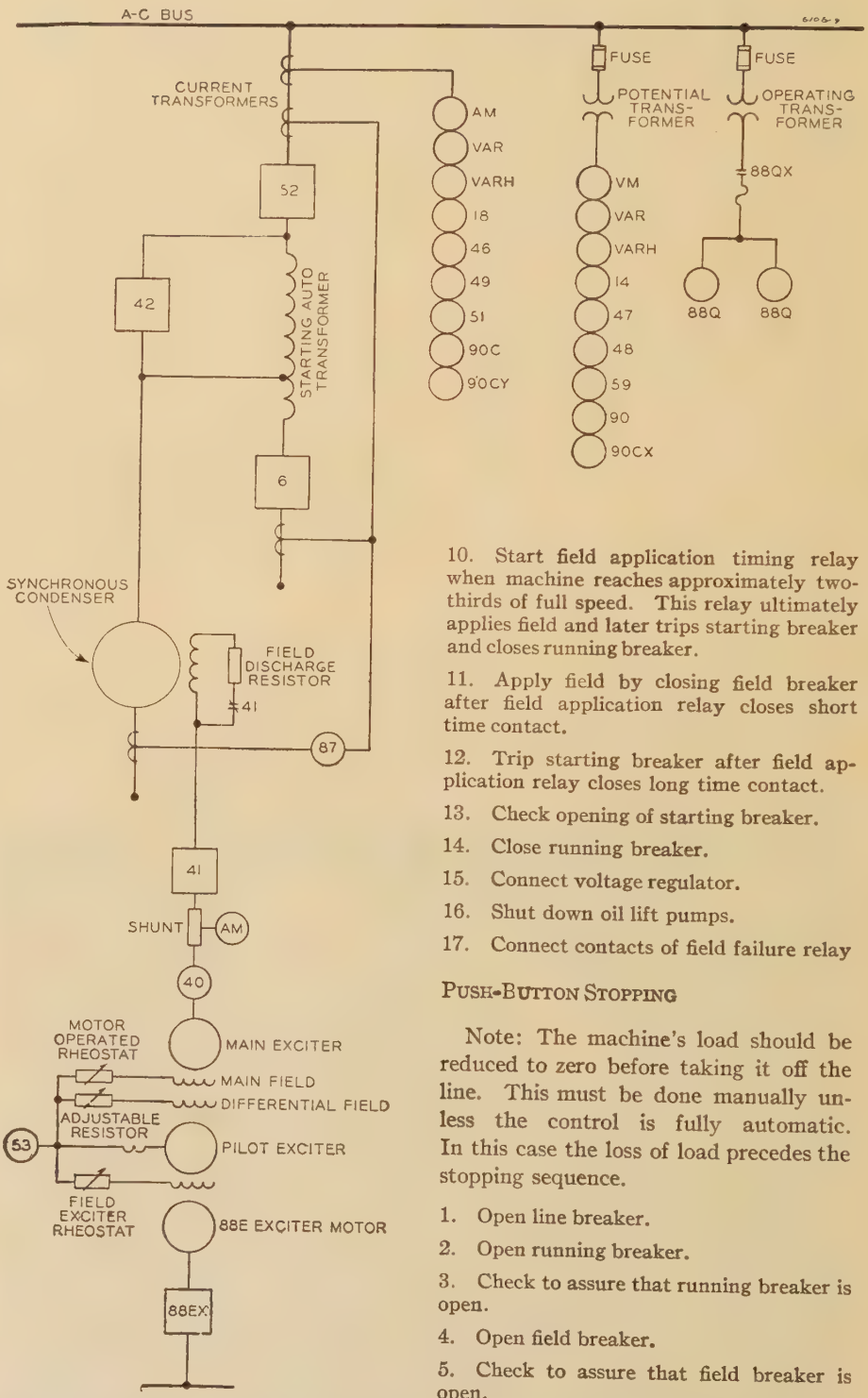

Figure 7. Single-line diagram of a typical synchronous condenser and associated equipment

10. Start field application timing relay when machine reaches approximately two-thirds of full speed. This relay ultimately applies field and later trips starting breaker and closes running breaker.

11. Apply field by closing field breaker after field application relay closes short time contact.

12. Trip starting breaker after field application relay closes long time contact.

13. Check opening of starting breaker.

14. Close running breaker.

15. Connect voltage regulator.

16. Shut down oil lift pumps.

17. Connect contacts of field failure relay

Push-Button Stopping

Note: The machine's load should be reduced to zero before taking it off the line. This must be done manually unless the control is fully automatic. In this case the loss of load precedes the stopping sequence.

1. Open line breaker.

2. Open running breaker.

3. Check to assure that running breaker is open.

4. Open field breaker.

5. Check to assure that field breaker is open.

6. Open exciter motor breaker.

7. Drive motor-operated rheostat to starting position.

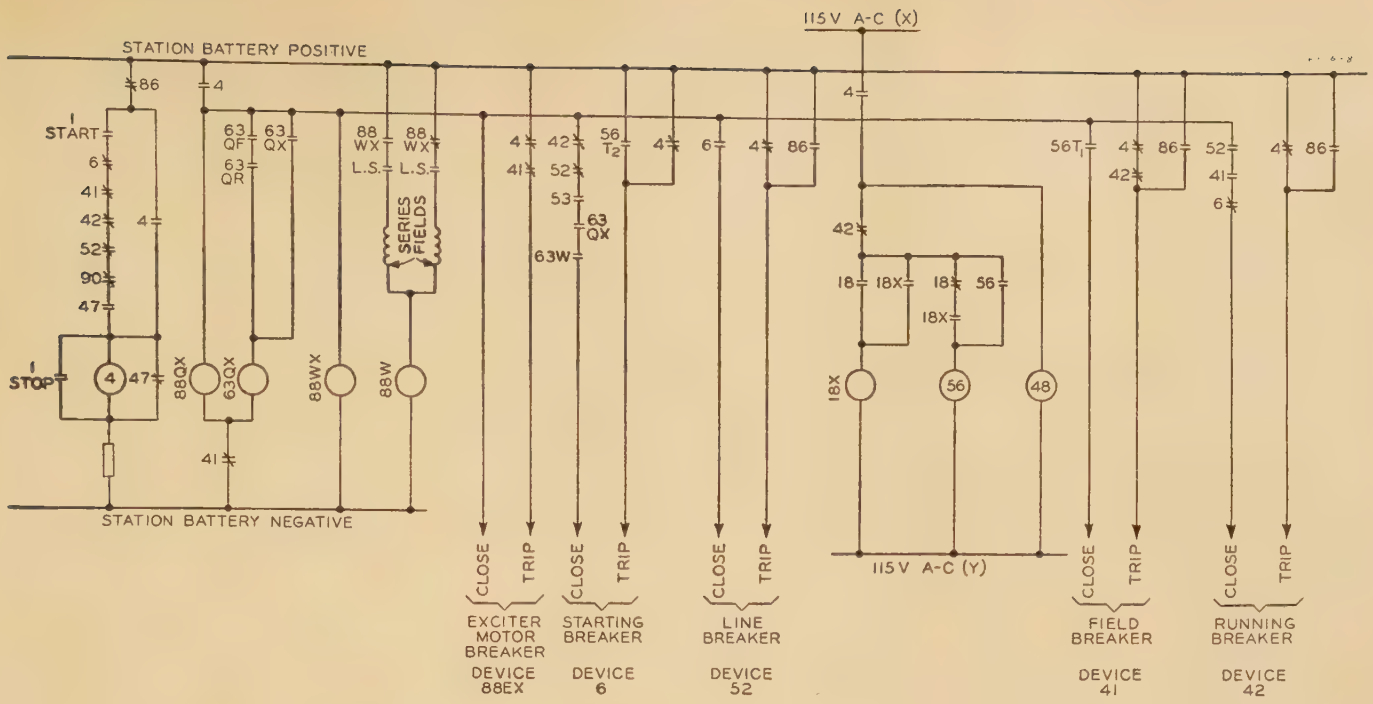

Figure 8. Control-relay diagram for automatic control of a synchronous condenser

8. Shut down accessories: Hydrogen and bearing cooling water.

EMERGENCY STOPPING

1. Open line breaker.
2. Open running breaker.
3. Open field breaker.
4. Check to assure that field breaker is open.
5. Open exciter motor breaker.
6. Drive motor operated rheostat to starting position.
7. Shutdown accessories: hydrogen and bearing cooling water.

Voltage and Current Regulator

After the machine is on the line, voltage regulation of the bus to which it is connected can be delegated to a voltage regulator. This regulator increases or decreases field current as the bus voltage tends to decrease or increase. The machine, however, is limited by its capacity in the amount that it can correct line voltage. If it cannot raise the line voltage, it will overload itself in the attempt unless something is done to limit the reactive load that it takes. For this reason, a current regulator is added to the voltage regulator scheme on condensers. If the voltage regulator tends to raise excitation to a point where the line current would exceed the maximum permissible value, then the current regulator makes the voltage regulator ineffective. If the line current exceeds this value for any reason, then the current regulator lowers the excitation to a safe value.

During fault conditions there would be a tendency for the current regulator to take immediate control and reduce excitation. Since this is a transient condition, a timing relay scheme is employed that holds the current regulator ineffective for a short time during the fault. If the fault persists, the current regulator begins to operate and reduces excitation.

The bus voltage value that the condenser maintains can be selected by adjustment of the voltage regulating rheostat in the voltage regulator circuit.

In some applications it is the purpose of the synchronous condenser to keep the power factor of a load constant even though this load may change rapidly and its power factor vary widely. Electric arc furnaces draw this type of load. In these cases it is necessary to employ a power factor regulator instead of a voltage regulator. The power factor regulator operates on load current and voltage and is sensitive to changes in the phase angle between the two. If the power factor drops below the desired value, a contact closes, causing increased condenser excitation. A raise in power factor above the regulating value decreases excitation A current-limiting element must be used with the power factor regulator. However, quick raise and quick lower devices are not necessary, nor are the devices employed with the current regulator for rendering it ineffective during faults.

Protecting Synchronous Condenser

The abnormal conditions which may develop in the synchronous condenser, its control, and auxiliaries may be segregated into two classes. The first group embraces those troubles which are dangerous because of their damaging effect on the machine, auxiliaries, or connected lines. These demand immediate protective action and in general call for a complete shutdown and lockout. The second group includes the abnormal conditions that cannot be immediately responsible for damage or disturbance but demand attention before more serious consequential conditions arise. These faults demand immediate annunciation but do not require shutdown.

In the first group are the following conditions, conveniently termed lockout faults:

1. Locked rotor. Machine fails to rotate when starting voltage is applied.
2. Bearing overtemperature.
   (*a*). Condenser.
   (*b*). Exciter.
3. Field failure.
4. Overcurrent.
   (*a*). Instantaneous.
   (*b*). Inverse time delayed.
   (*c*). Long time overload.
5. Overvoltage.
6. Internal fault in machine (differential relay operation).
7. Phase current unbalance.
8. Failure to complete starting sequence.

The second group, which may be

termed annunciating faults, are as follows:

1. Overtemperature of hydrogen.
(*a*). In main chamber of machine.
(*b*). In collector chamber of machine.

2. Underpressure in hydrogen bottles.

3. Underpressure in machine.

4. Presence of water in water collectors beneath machine.

Full Automatic Control

The start contact in Figure 8 can be replaced by a delayed make-contact of an undervoltage relay. The delay eliminates starting on passing conditions of undervoltage and assures that the condenser will be started only when voltage is low and remains low for a definite period of time.

The stop contact can be replaced by an underload contact which closes in a definite period of time after the condenser load drops to a low value.

The voltage regulator in the full automatic station controls the load on the condenser. Since the voltage-adjusting rheostat will be pre-set, the regulator will alter excitation as required to maintain the bus voltage corresponding to this setting. The bus voltage which it will tend to maintain can be altered by changing the voltage-adjusting rheostat manually.

Supervisory Control

The control of starting and stopping is only one of the functions which must be considered when applying supervisory control to the condenser station. There also must be considered the supervision of protective devices, telemetering of the electrical quantities involved, and remote operation of the voltage adjusting rheostat.

A practical operating scheme would provide continuous telemetering of kilovars. The supervisory control would assign two points to the condenser control. One point would permit starting or stopping of the condenser. Following a start operation an indicating light would show when the master relay picked up and another light would show when the running breaker closed. A third light indication would follow the stop operation. The second supervisory point would operate the voltage-ajusting rheostat. Changes in kilovar load resulting from operation of the voltage-adjusting rheostat would be observed on the kilovar telemeter by the dispatcher. The supervisory control may be operated over a metallic pair or a carrier current channel.

Detailed Description of Typical Scheme

The synchronous condenser connections of Figure 7 can be considered typical for a hydrogen-cooled machine of large size. Instrumentation is simple. Line voltage, line current, kilovars, and kilovar-hours are the a-c quantities of interest. Field current, main exciter voltage, and pilot exciter voltage are the d-c quantities of interest. A temperature indicator connected to the exploring coils in the machine, although not shown schematically here, is also desirable on the switchboard.

The main exciter motor operates from the station service 440 volts. An operating transformer supplies 230 volts a-c to the oil lift pump motors. A potential transformer on the high voltage bus supplies the instruments and relays. A double secondary current transformer on the line side of the condenser breaker is connected so that one secondary operates instruments and relays and the other secondary operates the differential relay. During starting, the current in the condenser windings will be several times the line current, and a third set of current transformers may be employed in the autotransformer neutral to balance the currents on the two sides of the differential relay during a normal start. An alternative method is to use a differential relay that is spring-restrained from operation at the values of current involved during starting. This adjustment is normally within the range of conventional differential relays.

In Figure 8 the progression of the starting sequence can be followed by moving from left to right on the diagram. If, as will be seen from the circuit to coil 4, the lockout relay is reset, the starting push-button depressed, all breakers out, and the motor-operated exciter field rheostat in the proper position for starting, normal voltage conditions existing, relay 4 will pick up and seal in around all contacts except the lockout relay contacts. It will remain picked up unless short-circuited by the stop push-button contact or the reverse phase and undervoltage relay, or de-energized by the opening of the lockout relay.

Make contacts of relay 4 set up circuits to all the devices operated in the starting sequence. Linestarter 88*QX* is operated immediately after relay 4 picks up to start operation of the oil lift pumps. Likewise, the cooling water valve motor relay 88*WX* immediately is picked up to cause opening of the cooling water valve. At the same time, the exciter motor breaker is closed to start the exciter and the incomplete sequence relay timer is started.

When lift pump oil pressure builds up, relay 63*QX* is picked up, seals itself in, and is released later when the field breaker closes. The contacts of relay 63*QX* in series with a cooling water pressure contact and an exciter voltage relay contact initiate the closing of the starting breaker, device 6. A contact of 42 is in this circuit to assure that under no circumstances can breaker 6 be closed when breaker 42 is closed.

The closing of starting breaker, device 6, initiates the closing of the line breaker, device 52. After the line breaker closes, the condenser is on the line at low voltage, and it will draw current that will tend to cause relay 18 to close its front contacts. Relay 18 is a current-operated induction disk relay, and as the machine accelerates, it drops out on the reduced current, eventually closing its back contact. When 18 closes its front contact, it picks up relay 18*X*, which seals itself in. A contact of 18*X* in series with the back contact of 18 picks up and seals in timer 56.

At the end of a definite timing period, relay 56 closes the field breaker, device 41. Further operation of timer 56 causes starting breaker, device 6, to trip. The condition that the line and field breakers are closed and breaker 6 is open sets up a circuit to close breaker 42, thereby putting the machine on the line at full voltage.

The voltage regulator shown in Figure 9 is brought into service by the closing of breaker 42, provided the control switch whose contacts are shown as *RI* is in either the regulating or indicating position. This switch has "manual," "indicating," and "regulating" positions. In the "manual" or "indicating" position, the motor-operated rheostat may be raised or lowered by hand through the contacts *CSR* and *CSL* of a control switch. In the "indicating" position, the voltage regulator performs all of its functions except that it does not move the motor-operated rheostat. In the "regulating" position, the voltage regulator is in full operation.

The d-c motor which drives the motor-operated rheostat has a split series field. Energization of the armature in series with one field will raise excitation; the other will lower. Limit switches prevent excessive travel of the mechanism. Cam switches are connected in the rheostat motor circuit to drive the rheostat to the starting position after the running

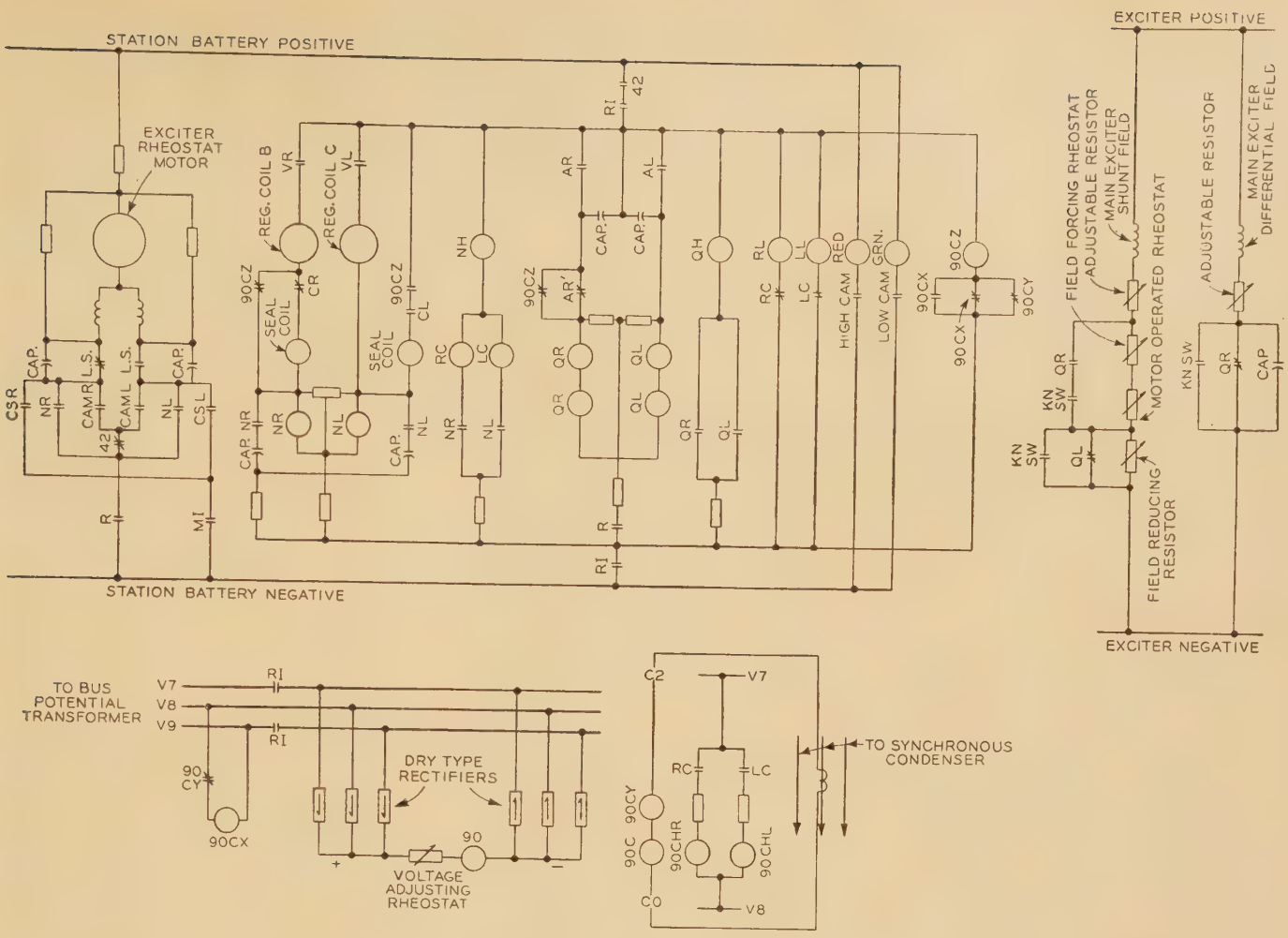

Figure 9. Voltage and current regulator connections used with synchronous condenser control

breaker closes on a shutdown. Contactors *NR* and *NL* control the rheostat under direction of the voltage regulator.

An indication comes from the voltage regulator element that a raise in excitation is necessary by the closing of contact *VR* in series with regulator coil *B*. Contactor *NR* is picked up by this action, and it not only operates the motor-operated rheostat, but picks up relay *RC* and antihunt coil *NH*. The latter functions mechanically to open contact *VR* even before any rise in voltage is felt on the bus. *VR* is permitted to close if, after a time delay, an adequate rise in bus voltage is not experienced. Relay *RC* provides back contacts to operate the indicating light *RL* and front contacts to operate the current element antihunt coil 90*CHR*. Similarly, a demand for reduction in voltage involves contact *VL*, regulator coil *C*, contactor *NL*, relay *LC*, and antihunt coil *NH*.

Sudden wide changes in voltage demand more rapid changes in excitation than normal operation through the motor-operated rheostat will provide. In this case, contacts *AR* and *AL* operate the quick-raise contactor *QR* or quick-lower contactor *QL*, as the case may be. These contactors energize the antihunt coil *QH* and also switch the field forcing or field reducing resistors into the circuit. In the event of a demand for quick raise, *QR* de-energizes the differential field also.

The current regulating coil is effective during moderate overcurrent conditions and also during fault conditions of extended duration. Normally the time delay relay 90*CX* is energized and holds the multicontact relay 90*CZ* up. This holds open the shunt around current element contact *CR* in the circuit to contactor *NR* and allows this current element contact to be effective. Likewise, a contact of 90*CZ* is held closed to make the current element lowering contact effective. The arrangement of the current element contacts is such that the demand for a raise in excitation is blocked if the current element finds that full load current is being exceeded. If current is high enough to demand reduction, the current element contact *CL* operates the motor-operated rheostat to lower the excitation.

During faults, the instantaneous overcurrent relay 90*CY* picks up, de-energizing relay 90*CX*, causing it to drop out. When 90*CX*, which is a magnetically damped induction-disk voltage relay, returns to its reset position, it closes its back contact and picks up relay 90*CZ* to put the current regulator in service again. Thus no attempt is made to regulate current or interfere with the operation of the voltage regulator during fault unless the fault remains on for an extended time.

The lockout and annunciator scheme is shown in Figure 10. The faults demanding lockout operate contacts that energize device 86. This is a manually reset relay which, when electrically tripped, closes its contacts and maintains them closed until it is reset. Its contacts drop out relay 4, energize the trip circuits of the various breakers, and set up the alarm circuit. Those conditions which require annunciation only, operate relay 30*X*, which is also a manually re-

set device. Like relay 86, it cannot be reset successfully unless the trouble contacts themselves have been reset. The contacts of 30*X* operate the bell alarm and lamp. In this circuit, the bell and the lamp will be cut off when 86 and 30*X* are reset. During the period

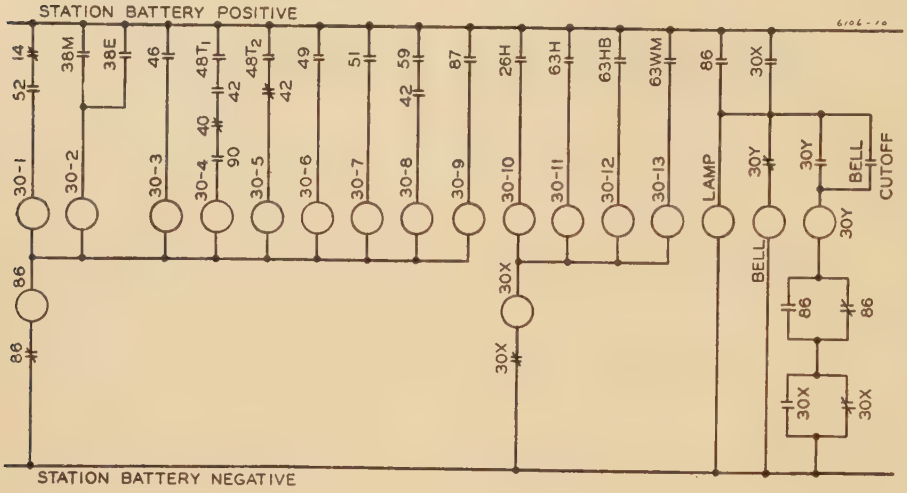

Figure 10. Annunciator schematic diagram showing alarm circuits and lockout relay

when trouble is being located, the bell alarm may be cut off by picking up relay 30*Y* with a bell cutoff push-button, leaving the lamp lighted. Subsequent resetting of 86 or 30*X* will put out the lamp and drop out 30*Y* to re-establish the bell alarm circuit. There is also the provision that the bell will ring if it has been cut off with the push-button following the

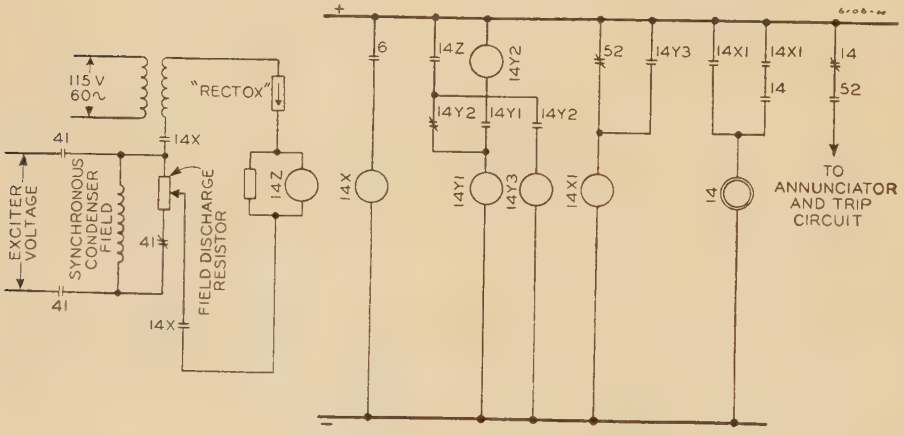

Figure 11. Locked rotor protective relay connection diagram

operation of one relay, say 86, and the other operates, in this case 30*X*. A break-contact of 30*X* in the coil circuit of relay 30*Y* is adjusted to open just as it begins to pick up, and it drops out relay 30*Y*. After relay 30*X* closes its make-contact, relay 30*Y* may be picked up again by the bell-cutoff push-button.

The circuit of the locked-rotor protective relay is shown in detail in Figure 11. The voltage appearing across the field-discharge resistor is compared with the voltage of the bus in such a way that any beat frequency between the two will operate relay 14*Z*. At standstill, a voltage is obtained from the field-discharge resistor that is equal in frequency and magnitude to the voltage received from the bus potential transformer. It may have any phase relation with this potential, however, and may or may not pick up relay 14*Z*. As the rotor begins to turn, the phase relations change and 14*Z* alternately is picked up and dropped out. This action is employed as an indication of rotation. If relay 14*Z* picks up, drops out, and picks up again, the relay chain consisting of 14*Y*1, 14*Y*2, and 14*Y*3 will energize relay 14*X*1, which in turn will hold relay 14 energized and prevent trip-out through its back contact. Initially, relay 14*X*1, which is a pendulum relay, is picked up in the period of time between the closing of the starting breaker and the line breaker, and during the period when the rotor should start rotating, it is vibrating, alternately opening and closing its contacts in the circuit to the coil of relay 14. This relay is a slow-to-drop-out relay that will remain picked up even though 14*X*1 makes only intermittent contact. Should relay 14*Y*3 fail to energize relay 14*X*1 before it drops out, relay 14 will set up the circuit to the lockout relay to shut down the starting sequence.

The stopping sequence begins with the de-energization of relay 4. Back contacts of relay 4 trip the line breaker, and if the starting sequence is incomplete, they will trip the starting breaker. When the line breaker comes out, it trips the running breaker, and the running breaker trips the field breaker. The field breaker shuts down the exciter by tripping the exciter motor breaker. The voltage regulator runs to the start position after the running breaker opens. The cooling-water valve motor runs to the close position when relay 4 drops out.

Emergency stopping does not respect sequential tripping. All breakers are tripped simultaneously by 86 and relay 4 is de-energized.

Conclusions

The operating complications involved in placing a synchronous condenser on a line demand that a certain portion of the control sequence be automatic. It is of practical advantage to design the sequence so that it is entirely automatic, allowing the user the choice of manual push-button control, remote supervisory control, or full automatic control.

Protective devices can be provided to protect against any contingency, and these devices either may sound an alarm to indicate an abnormal condition requiring attention or can lockout the machine in the presence of a dangerous condition.

Electronic Register Control for Multicolor Printing

W. D. COCKRELL
MEMBER AIEE

Synopsis: The proper register for multicolor printing, that is, the printing of as many as five colors on top of one another to the required accuracy of a few thousandths of an inch, has been successfully solved by the use of phototubes and associated electronic equipment. In the system described, the electronic portion extends all the way from the phototubes to the thyratrons which supply the required current to energize the correcting motor armature in the proper direction and at the speed for correct register. A typical installation is shown in Figure 1.

The Problem

THE NUMBER of copies of each issue of present day popular magazines runs into the millions, and the only practical way to print such a large number of copies is by means of a continuous web press. This means that the colored illustrations must be printed on large rotogravure presses in which the paper speed may be as high as 1,000 feet per minute. At this high speed each color, in turn, must be printed, then dried while in motion so that it will not smudge as the next color is printed. This wetting and drying of the paper causes shrinkage and stretching which differs with each individual roll of paper, depending on its composition and the amount of latent moisture present. The paper often moves 30 to 40 feet through the drying section before it reaches the next impression cylinder. Also if a printing cylinder is even a few thousandths of an inch over- or under-size, the tension between stands will differ greatly. A typical press and control are shown schematically in Figure 2.

A particularly critical situation occurs when a "flying paste" is made from the end of one roll to the beginning of the next. As the splice passes through each succeeding section of the press, the tension drops to a low value, and the critical tension balance necessary for correct register is completely lost. If no correction is made, as many as 300 copies might be spoiled before the correct tension balance is regained.

Before the application of electronic control, the most usual way to check register was by means of a battery of control handwheels located at the folder. At intervals the pressman would draw a cut-and-folded copy from the outcoming stream and unfold it to be scanned for evidence of misregister. He then would make the proper corrections by turning the appropriate handwheel the amount necessary as judged from long experience. Even though the pressman was continually in motion as many as 50 copies might be spoiled before the correction could be made.

Needless to say, holding register manually has never been a pleasant job, particularly if the paper has not been permitted to season, that is, to remain in a special storeroom long enough for every roll to attain the same conditions of temperature and humidity. No attempt was made to hold register through a splice, and it was usually assumed that all copies printed during acceleration or deceleration of the press would be spoiled.

Fundamentals of the Electronic System

The first fundamental requirement of the electronic control is to check each printing cylinder after the first to find if it is in the correct position to lay its impression exactly upon the previously printed one. Next, when an error has been found, means must be set in motion to correct the error. Since the accuracy of register must be within 0.003 inch to be acceptable, it will be seen that the system must respond to signals as short as 0.00001 of a second, or ten microseconds, if satisfactory operation is to be obtained. A complete electronic system is the only practical solution.

The second requirement is to apply power to the correcting motor, as indicated by the amount of error found. Although other means could be used to accomplish this function, electronic circuits using thyratrons eliminated noisy moving parts which, at the large number of operations required, would present a serious maintenance problem.

The Error Detecting Equipment

In order to detect the error, we must have a standard indication of the position of the paper at any instant and the position of the cylinder at that same instant. Along a margin of the paper where it can be trimmed off, or placed in the fold, are printed a series of register marks in the first color to be used. This is usually yellow. Typical marks are 0.020 inch in the direction of paper motion, and about one half inch across. Although a mark only one fourth inch long is needed, the extra length permits greater latitude in lining of the paper and in correcting side lay or side register. These marks are equally spaced, as seen in Figure 3, usually 16 to the cylinder circumference. While fewer marks can be used, the larger number permits greater correction speed and thus higher accuracy and more nearly perfect copies.

As this thin yellow mark arrives near the succeeding cylinders for printing of

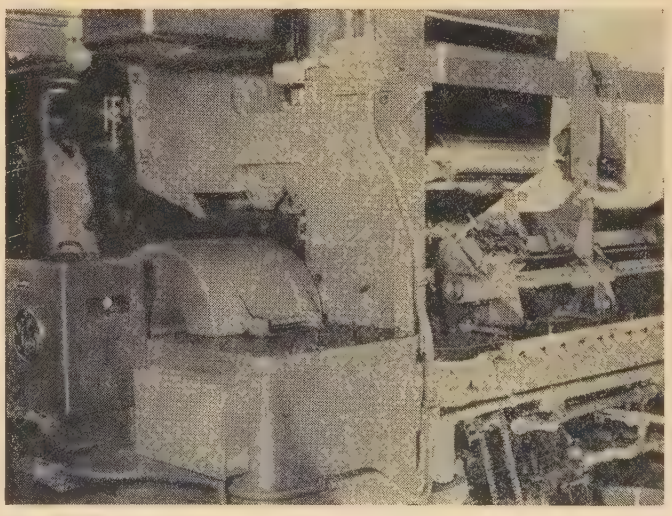

Figure 1. At each printing cylinder the web scanning head at right and the cylinder scanning head at lower left feed signals to the mixing panel at top. This determines proper operation of the correcting motor at lower right

Paper 46-132, recommended by the AIEE committees on industrial control devices and industrial power applications for presentation at the AIEE summer convention, Detroit, Mich., June 24–28, 1946. Manuscript submitted April 19, 1946; made available for printing May 13, 1946.

W. D. Cockrell is in the apparatus department, industrial engineering division, General Electric Company, Schenectady, N. Y.

the other colors, its presence is detected by a phototube in the web head through an optical system which produces the effect of a very narrow slit, only a few thousandths of an inch wide. A dark blue glass filter provides a much better contrast between the yellow mark and the white paper.

The indication of the passage of the mark in front of the phototube leaves the web head in the form of a square wave of voltage of very short duration.

Detecting the Cylinder Position

Likewise, the position of the printing cylinder must be found so it can be checked against the relative position of the web. The basic indicating element is a disk or drum which contains the same number of axial slits as there are register marks on the first printing cylinder. A typical disk is ten inches in diameter, and the slits are one fourth inch wide. They are laid out so that the trailing edges of the slits are spaced very accurately around the circumference, as seen in Figure 4. The indicating point is not the whole slit but the trailing edge. An optical system directs light through this slit to a stationary slit before a phototube. The phototube and optical system can be moved around the drum to allow for setting up and for adjustment. The signal sent from this cylinder scanning head is a square voltage wave much broader than that from the web head, but which has a very accurate and abrupt trailing edge.

The Mixing Panel

The mixing panel, mounted on the press near each cylinder, may be considered the nerve center of the register equipment. Here the signals from the web mark and the cylinder disk slits are checked against each other and the proper correction action is initiated. For correct register, the cylinder disk phototube is moved until the trailing edge voltage change splits exactly the signal received from the 0.020 inch web mark. When this occurs, the correction circuit is balanced and no corrective action takes place. However, should the edge arrive even a few microseconds earlier or later than the midpoint of the mark, the difference is detected in the mixing panel, and the proper correction action is started. This comparison is made by charging one small capacitor as a result of the presence of the mark signal before the edge arrives, and charging a second capacitor after its arrival. These two charges then are compared and the difference is stretched out in time and amplified to apply the necessary correction. This correction signal, in the form of a small current of a few milliamperes, leaves the mixing panel in one of two leads, depending on which direction the correction is to be made. Perhaps the schematic drawing of Figure 5 will assist in clarifying the mixing panel action.

Since at this point the correcting motor control signal is at a low power level and in a low impedance circuit, it provides an ideal place to insert the push button stations desired for manual control of the correcting motor during setting up.

The mixing panel also contains an indicator "magic-eye" tube to assist the operator in setting up the panel and obtaining the original register adjustment.

The Motor Power Panel

Now that the correction signal has been obtained, it remains only to amplify the power for the correction, that is, the energy for the correcting motor. These correcting motors are usually d-c shunt gear-motors of about one half horsepower rating. They may operate differentials to change the relative position of the printing cylinders or may move the usual compensating rolls up and down.

The motors are run with full field strength to obtain maximum torque and fastest correction. The motor fields usually are fed from a common rectifier using phanotron tubes. The motor armatures are fed from 60-cycle alternating current through a pair of inverse-parallel thyratrons. Since the thyratrons are controlled rectifiers, if the first thyratron conducts a pulsating direct current, current flows through the motor armature in one direction. However, if the second thyratron conducts instead, the current flows through the armature in the opposite direction and opposite rotation is obtained. An iron core reactor in series with the motor armature smooths out the current and prevents excessive armature heating.

The only thing now required is a connecting link between the correcting signal from the mixing panel and the thyratron grid. This is supplied in the form of small saturable reactors in a bridge circuit which changes the phase of the grid. These reactors, of course, are saturated by the direct current from the mixing panel to regulate the grid phase as required. Figure 6 shows a complete motor control cabinet.

The Electric Circuit

Now that we have obtained a bird's-eye view of the operation of the equipment, let us retrace our steps and see the electric circuit used to obtain these results.

Figure 2. Schematic drawing of a multicolor gravure press with photoelectric register control

1. Cylinder register scanning disk
2. Cylinder scanning head
3. Web scanning head
4. Selector switch unit
5. Impulse comparison controller with "magic eye"
6. Main controller
7. Register adjusting pilot motor
8. Push button stations for manual adjustment

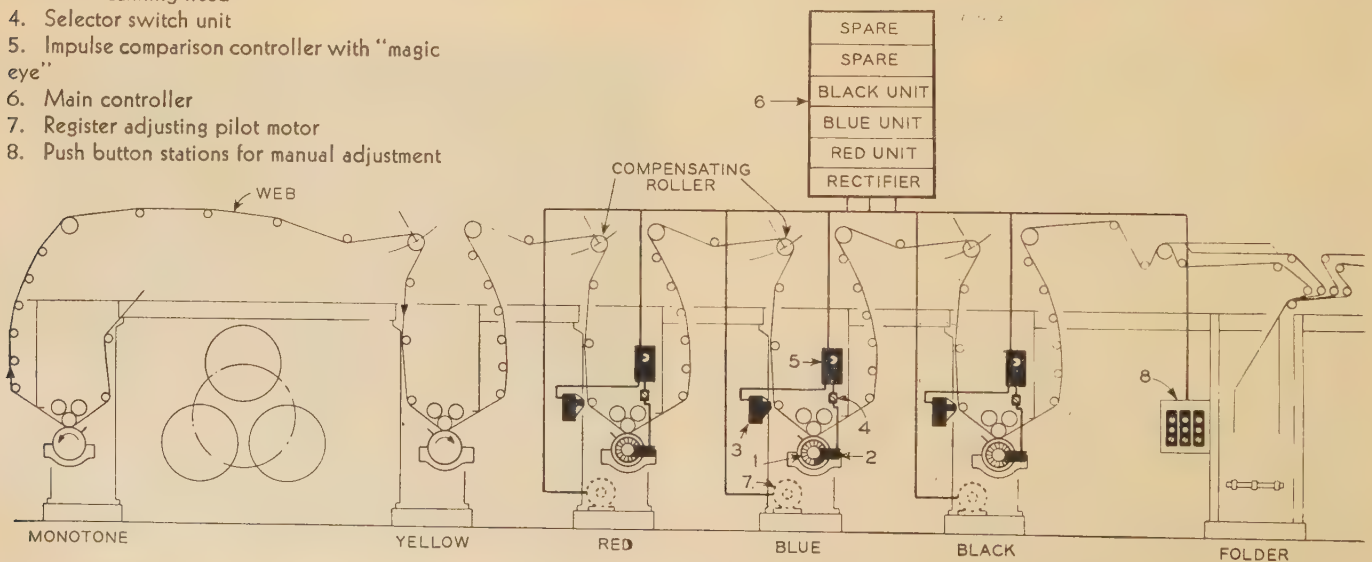

Figure 3. The register marks along the edge of the sheet usually are printed yellow and are almost invisible to the eye

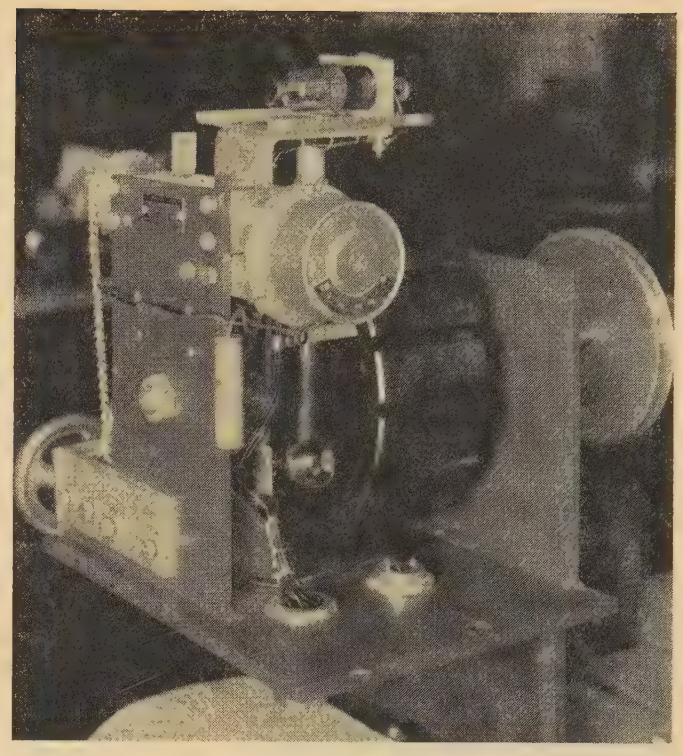

Figure 4. Cylinder scanning head showing slits in disk, lamp in center and phototube at top

Vernier adjustment motor is at upper right. (View taken during test with covers removed)

The Web Scanning Head Circuit

The web head consists of an automobile headlamp-type bulb and an optical system to flood the path of the register mark with an intense spot of light at the point where the phototubes must scan it. An optical system picks up the light from the mark and conducts it to the slit in front of the phototube, and the blue glass filter, mentioned previously, provides a more positive light change.

Because the change in light on the phototube as the mark passes is so extremely small and so rapid, it is necessary to use an extremely sensitive amplifier to provide a signal sufficiently strong to be transmitted to the mixing panel. A two-stage amplifier is used, and if the signal is to be transmitted for a considerable distance, a third tube as a cathode-follower is included. The tube chassis must be shock mounted to prevent the vibration of the press from causing bad microphonic disturbances. Figure 7 shows the chassis removed from the web head.

Although there are no arcing parts in the head, it always is made dustproof and when conditions require, explosion-proof.

Cylinder Scanning Head

Since the slits in the cylinder reference disks or drums permit operation on direct light transmission rather than by reflected light, a single stage of amplification is sufficient to provide a satisfactory signal of the passage of the slit. Here again, however, if the signal must be transmitted a long distance, the cathode-follower tube should be added.

A special feature of the cylinder scanning head is the mounting of the optical system and amplifier chassis. These are mounted on a radial arm which is pivoted at the cylinder axis so that the complete system can be swung around the disk in a limited arc. This is provided to obtain proper register in setting up the equipment and for the vernier control of register during operation. The arm is moved by a small reversible adjusting motor which is controlled by push buttons at the folder.

Although only about one half inch of each drum slit is required for operation,

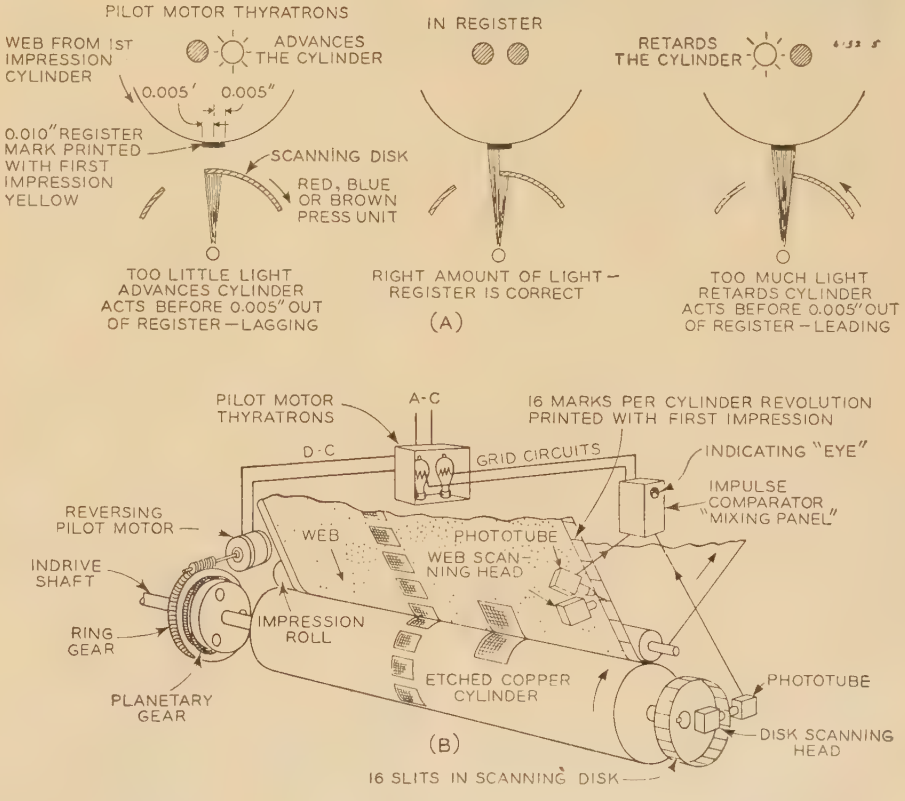

Figure 5. Schematic drawing to show the principle used to check register and to indicate the correction to be made

A. As impulse comparator evaluates the combined impulses from two phototubes
B. Photoelectric register control on four color press—one of four or more units shown

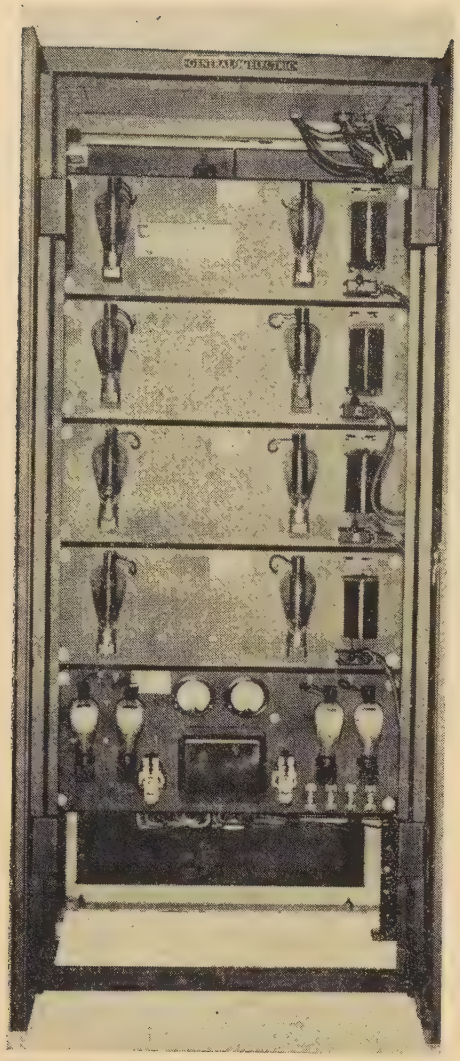

Figure 6. Motor control cabinet

There are three motor control panels at center, a spare panel at top, and the two rectifiers on the lowest panel

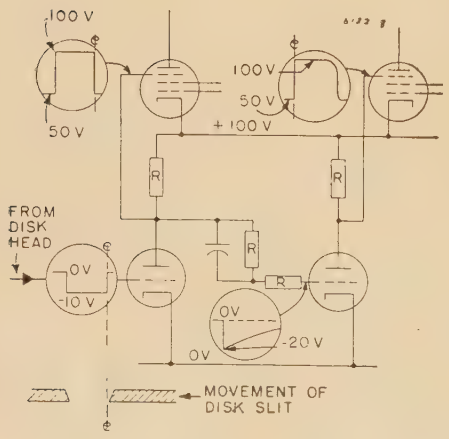

Figure 8. The action of the disk signal amplifier and phase-inverter

The wave shapes of the incoming and outgoing signals are shown also
e represents the instant that the trailing slit edge passes
Inserts are voltage wave forms

it is made much longer to permit the cylinder to be adjusted along its axis for best side-lay or register. This side register adjustment is usually a manual operation.

In some press installations a master cylinder scanning head is used rather than one at each printing cylinder. In this case the master unit is mounted on the main drive shaft, and optical systems for each color are located around it.

A single master cylinder scanning head permits a more compact installation than the separate heads, particularly when explosion-proof equipment must be furnished, but it can be used only with the compensating-roll type of correction.

Mixing Panel Circuits

The mixing panel must perform a number of functions. Let us take them up one at a time.

The incoming signal from the disk or cylinder scanning head is in the form of a square voltage wave which corresponds to the passage of the slit. In order to minimize the number of false operations due to random ink spots or paper blemishes, the region of active operation is limited to a fraction of an inch on each side of the correct register point. The signal from the slit provides a convenient live zone ahead of the correct point, while a similar active period after the slit has passed is obtained by means of a simple multivibrator circuit which uses grid rectification to charge a small capacitor during the slit passage to stop conduction in the trailing tube for a corresponding period. This twin triode also acts as a phase inverter. That is, one anode ceases to conduct during the time of the first active period, and then the second anode ceases conduction during the second active period. Figure 8 shows this circuit in simplified form.

The next step is that of comparing the disk head signal with that from the web head. This is done by means of the number one grid and number three grid of a pentode tube. Since the grids of a pentode act as valves in series, if either grid is sufficiently negative with respect to the cathode, there will be no current flow in the tube. The action is as follows: Two pentode tubes are used. The number one grid of both tubes normally is held negative, but rises to cathode potential when the marks on the web pass the phototube. But no current can flow unless the number three (suppressor) grid is also at cathode potential. These grids are controlled by the output of the two anodes from the twin-triode phase inverter, which cease conduction respectively before and after the register point. Thus,

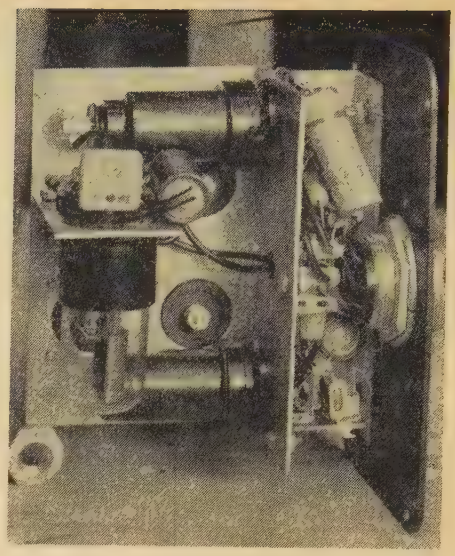

Figure 7. The web scanning head chassis

The small change in phototube current due to the passing register mark is amplified by the two pentodes at the right. The tube panel is isolated from press vibration by the three rubber mountings seen behind the tubes

one pentode conducts when the mark is passing and the slit is passing at the same time. The second pentode conducts if the mark passes for a short time after the slit has passed, as determined by the timing circuit. If the mark passes exactly in register, the first pentode will conduct while the first half of the mark is passing, and the second half passing after the slit will permit the second pentode to conduct.

If the mark does not appear, there will be no conduction in either tube and no correction made. This is important, for it means that if the mark does not print, the correcting action ceases, but there will be no false correction as in some systems.

The mixing circuit and typical wave forms are shown in Figure 9. Both the twin-triode and the pentodes are operated from cutoff to saturation and thus act as limiters to produce uniform voltage

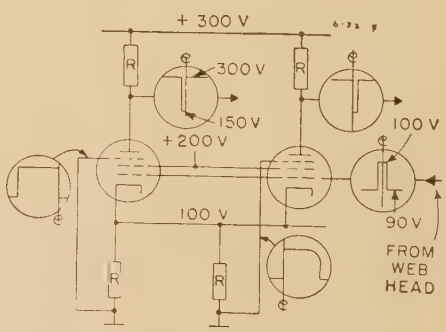

Figure 9. The circuit and wave forms of the pentode-tube mixing circuit

changes at the output. From the output of the pentode we now have signals which indicate the direction required for the correction, and by their relative duration, indicate the amount of correction needed.

The final function of the mixing panel is that of stretching out the fast microsecond pulses of the pentode output to a time sufficient for operation of the correcting motor. This is done by means of small capacitors which store the energy presented to them at each mark passage and permit it to leak off at a rate slow enough to permit motor operation to take place. This pulse-stretching circuit is shown in Figure 10.

Each time one of the two pentodes conducts, its corresponding capacitor begins to charge through the small rectifier tube. The capacitor charge next is amplified by a triode tube, and the output of this tube is passed on to the motor panel.

At this point, the action may be summarized thus. If the trailing edge of the disk slit passes at the same instant as the midpoint of the register mark, equal direct current will flow from the two triodes at the output of the mixing panel. If the register mark passes somewhat early so that there is an excess of mark before the slit edge passes, there will be a larger current in one triode, or if the register mark arrives late, there will be a larger current in the second triode output.

The "Magic-Eye" Indicator

In addition to the control circuit, the mixing panel also has an auxiliary circuit, consisting of a twin triode and a double "magic-eye" tube which permits a visual indication of whether the register is balanced or is off in either direction. This circuit also is fed from the small pulse-stretching capacitors. If the mixing panel is mounted remote from the press, the indicator tubes may be mounted at the folder.

Manual Push Button Control of Correcting Motors

On its way to the motor control panel, the output of the mixing panel passes through the push button stations used for manual control of the correcting motor. These push buttons are used principally for setting up the work at the beginning of a run. When they are operated, the circuit from the mixing panel is broken, and direct current from a separate source is fed into the motor-panel circuit to operate the motor in the desired direction.

Motor Panels

For convenience, the motor panels usually are assembled together in a large floor-mounted cabinet. This cabinet also contains the common rectifier supply for the motor field and a rectifier to supply the mixing panels. A tap also is taken off this second rectifier supply for the push button operation. Each motor panel is complete in itself with jack and plug connections for all leads. In some installations, a spare motor panel is included in which the thyratrons are kept at operating temperature so that should a tube failure occur, the spare panel may be substituted for the inoperative circuit and a minimum of time lost.

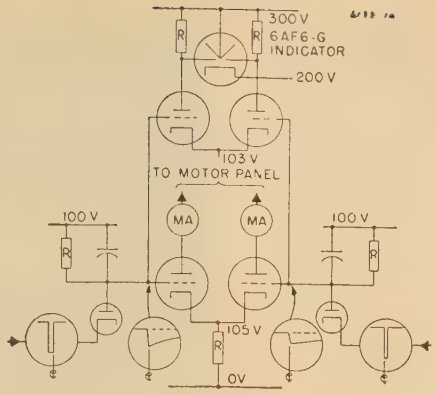

Figure 10. The correction signal pulse-stretching circuit, the output triode amplifiers, and the "magic-eye" indicator (6AF6-G) tube circuit

Assuming register mark center arrives before slit edge

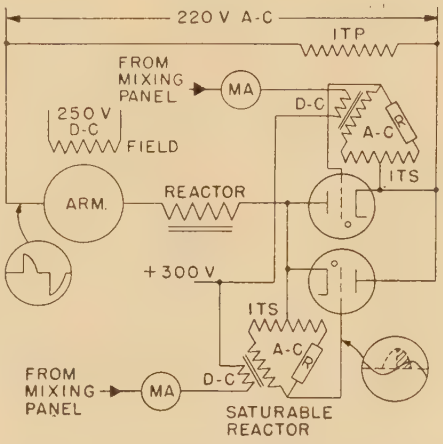

Figure 11. The power circuit and the grid control circuit for the correcting motor

The motor field is supplied from the common rectifier

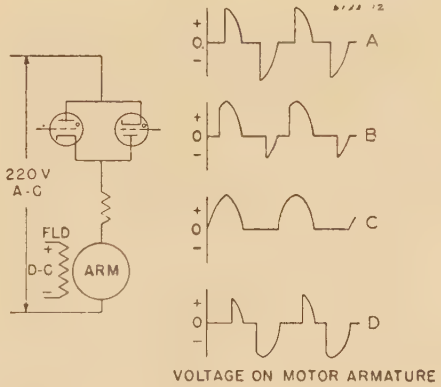

Figure 12. Representative wave forms of voltage applied to the correcting motor armature under various conditions of register error

A—Balanced, no motion
B—Forward slow
C—Forward fast
D—Reverse slow

The armature circuit consists of a reactor in series with the armature and the two inverse-parallel thyratrons which are used to produce the reversing action of the armature. Each thyratron has its own grid circuit which consists of a center-tapped transformer feeding a saturable reactor-resistor bridge, as shown in Figure 11. Since the a-c and d-c windings of the saturable reactors are electrically separate, the motor circuit is insulated from the control circuit coming from the mixing panel.

In operation, a larger current flowing in the d-c winding of the saturable reactor decreases its reactance, and the grid of the thyratron is phased forward. This permits the thyratron to conduct earlier in the cycle, and more current flows through the motor armature. The mixing panel circuit is so designed that, when register is correct, sufficient current will flow into the saturable reactors of each of the thyratron grid circuits to cause both thyratrons to conduct for approximately one-quarter cycle. The opposing currents balance in the motor armature so that it does not rotate but vibrates slightly at 60 cycles. However, when the register is out by even a few thousandths of an inch, the current to the reactors is unbalanced so that the thyratron currents are not balanced and the motor moves in the direction determined by the larger current. The shape of the voltage wave applied to the motor for various conditions is shown in Figure 12.

When the controlling current is completely unbalanced, that is, when the register marks arrive completely before or after the disk edge arrives, full correcting motor speed is obtained. This is reduced to zero as the slit edge intercept comes nearer to the center of the register mark. Antihunt circuits in the mixing panel prevent overshooting.

Aids for Maintenance and Repair

In the printing business it especially is important that production schedules be

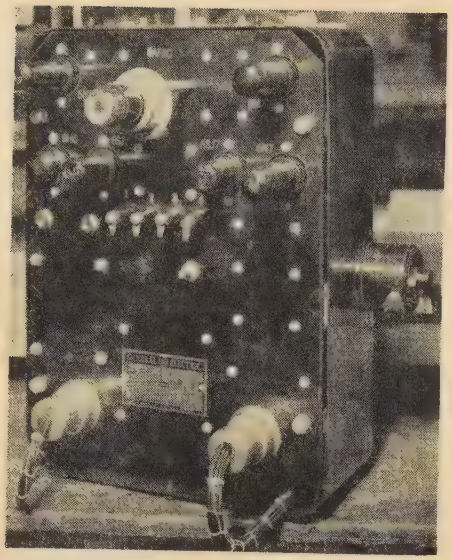

Figure 13. Mixing panel with cover removed

This shows "magic-eye" indicator tube at top, milliammeter jacks at left-center, test terminals at center, and connecting leads plugged in at bottom

Figure 14. Preventative maintenance

Checking the equipment operation with a small cathode ray oscillograph

met. Therefore, even short delays in press operation are serious. It has already been mentioned that the motor panels are provided with plug and jack connections and that sometimes a spare motor panel is added and kept warmed up for instant substitution without the delay of even the five minutes needed to preheat the thyratron cathodes. Although there are no moving or wearing parts on the web and disk scanning heads, or on the mixing panel, all of these are also provided with plug and jack connections, and a spare of each is often kept on hand for substitution whenever needed.

To assist in preventative maintenance and trouble shooting, milliammeter jacks and test terminals are located on the mixing panel, as seen in Figure 13. The milliampere readings of the output to the motor panel permit a quick checkup of the over-all mixing panel operation, while the test terminals permit key potentials to be seen on a cathode-ray oscilloscope to check the operation of the two scanning heads and the internal circuits of the mixing panel. To the experienced operator the characteristic flicker of the "magic-eye" indicator tube can convey much information about the over-all operation of the equipment.

Putting the Equipment Into Operation

In conclusion, let us follow the press operator as he puts the register equipment into operation when starting a new run on the press. The inkwells are filled, the paper is threaded, and the backing rolls are let down. The first copies coming off the folder look very little like the finished product, but if the press crew is experienced, the register will be within a fraction of an inch correct on all colors. Standing at the folder with a copy in front of him, the head pressman then presses the proper push buttons operating the one half-horsepower correcting motors to bring the cylinders into approximate register with the first color, usually yellow. First the red impression from the second cylinder comes into line, next the blue, and finally the black from the last cylinder.

The press is then run up to a moderate speed so that the normal tension in the web is obtained, and the register is again checked and corrected by the push buttons. The register may now be assumed to be good enough to be placed on the automatic operation. To do this the pressman first operates on the red cylinder disk scanning head, and moves the scanning head arm until register is obtained as indicated by the "magic-eye" operation, indicating a balance of the mixing panel output. He then throws the switch to automatic, and the red is locked in step with the yellow. He then repeats this process on the blue and on the black cylinder. Finally he returns to his normal station near the folder and checks the outcoming copies. Probably during the time he has been away the register has crept off a few thousandths. He now brings this back into accurate register by again operating the small reversible adjustment motor on the disk head optical system. Operation of the push button controlling the correcting motor at this time will have no effect because the automatic operation immediately would bring the register back to the previous setting.

After these refinements have been made, the register is locked in step in the correct position and will hold this through wide changes in press speed, through splices, and through the many differences in paper which may be found, such as tension, humidity, surface conditions, and others.

Conclusion

It was said in years gone by that only one copy in 25 was perfectly registered. With electronic register control, fewer than one in 25 will be found which are not perfectly registered. Electronics has provided a quiet, precise method for holding register. Since there is no wear of critical parts the high accuracy which can be obtained will continue throughout years of untiring service.

Design of D-C Auxiliary Controllers for Marine Service

W. SCHAELCHLIN
MEMBER AIEE

CONSIDERABLE progress has been made in recent years in the design of marine control equipment. Under the impact of the war, the performance of controllers has been improved and better equipment of lighter weight has been made available. It is the purpose of this paper to discuss some of the more important design features on which the controller performance is based.

Controller Components

The function of a motor starter is to connect the motor across the line without excessive disturbance to the motor or the power supply. The simpler the equipment used for this purpose, the more satisfactory, in general, it will be in service.

There are a great variety of motor starters, ranging from the simple manual line starter to the more complex magnetic controller. Different methods of automatic acceleration are used with the number of starting steps varying to suit the application and rating of the motor. Other design features, such as overload protection and selection of resistors have an equally important bearing on the controller performance.

Number of Starting Steps

The current surges during starting of a motor depend primarily upon the number of starting steps and the regulation of the motor. This relation can be solved mathematically but perhaps is more clearly illustrated in Figure 1 from a typical shunt motor with 10-per-cent speed regulation and a constant torque load of 100 per cent.

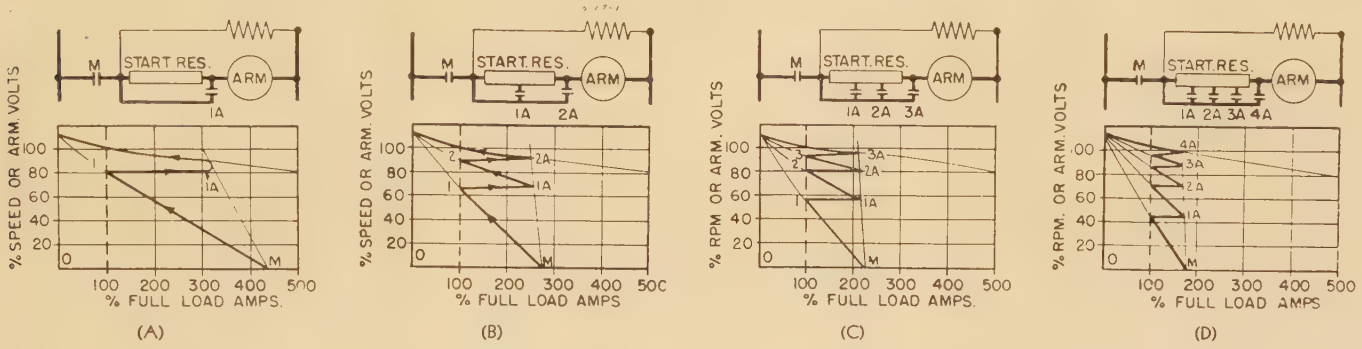

Figure 1. Schematic diagram and current surges for various numbers of starting steps

On closing the line contactor M, the armature current increases from 0 to M. As the motor accelerates, this current decreases to one, at which point the accelerating contactor $1A$ cuts out the starting resistor and connects the motor across the line. For multistep starters, this process is repeated by operating accelerators $1A$, $2A$, $3A$, $4A$, and so forth, in sequence until the starting sequence is completed.

Figure 1 illustrates clearly that the starting current surges can be reduced by increasing the number of steps. This fact is taken into consideration by providing more steps for large motors than for small motors. Table I shows standard number of starting steps and approximate maximum current surges for various motor ratings.

Further reference to Figure 1 indicates that the starting current surge is made higher for the low armature speeds than for the high armature speeds. This is done because the average motor can commutate current surges better at low speed than at high speed, a fact which is well illustrated in Figure 2.

This oscillogram shows a starting test with a standard 3-horsepower 250-volt motor connected directly across the line without a resistor step. Commutation was fairly good at low speed even though the current inrush was about 1,300 per cent. At approximately full speed, however, the motor flashed over, although the current had decreased to about 750 per cent.

Of additional interest is the fluctuation of the field current I_f during the starting of the motor. This current suddenly increased several hundred per cent, which indicates a pronounced weakening of the flux due to the armature reaction. The subsequent dip of I_f below the normal value is due to the line voltage disturbance caused by the short circuit.

Applications with high inertia loads

Table I. Number of Starting Steps and Maximum Current Surges for Various Motor Ratings

Hp at 230 V	Number of Starting Steps	Approximate Current Surge, Per Cent Full Load Amp
1/2	0	1,000
3 to 5	1	450
7 1/2 to 25	2	275
30 to 40	3	225
50 to 150	4	175

Paper 46-127, recommended by the AIEE committee on marine transportation for presentation at the AIEE summer convention, Detroit, Mich., June 24-26, 1946. Manuscript submitted October 18, 1945; made available for printing May 10, 1946.

W. SCHAELCHLIN is with the Westinghouse Electric Corporation. East Pittsburgh, Pa.

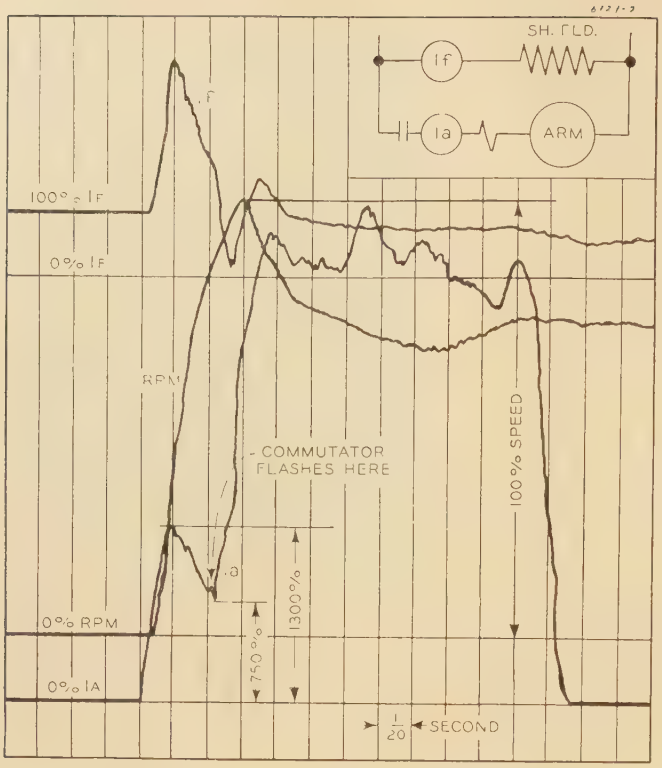

Figure 2 (left). Oscillogram showing line starting of 3-horsepower 250-volt shunt motor

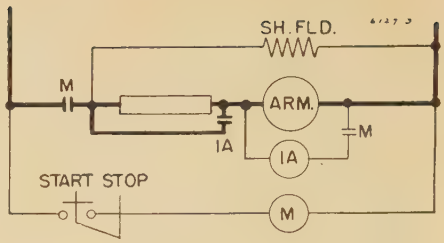

Figure 3. Starter diagram with counter-electromotive force acceleration

such as fans and oil purifiers are more critical and possibly should have more starting steps to keep down the current surges.

Methods of Starting of Motors

Various methods are available for starting of motors, namely—

(*a*). Manual starting.
(*b*). Counter-electromotive force starting.
(*c*). Current limit acceleration.
(*d*). Definite time acceleration.

Manual Starter. This type of starter undoubtedly provides the simplest means of starting a motor. It is particularly suitable for motors up to one half of one horsepower where the stalled armature current does not exceed 1,000 per cent. Sometimes it is provided with a starting step for use with motors up to five horsepower. In such cases, the operating lever may be equipped with a mechanical offset to make the operator pause on the start position before going to the run position.

In general, it is not desirable to handle large currents with manual controllers since there is no assurance of positive contact movement, which is essential for satisfactory operation.

Counter-Electromotive Force Starting. This method measures the armature voltage and cuts out the starting resistors when this voltage has reached a predetermined value. A schematic diagram, which is self-explanatory, is shown in Figure 3.

The counter-electromotive force starter is somewhat critical in its adjustment and can be used only for single-step starters. Figure 1A shows that the accelerating contactor $1A$ has to be adjusted to operate at 70–80 per cent in order to avoid an excessive current surge when it closes. With possible line voltage drops of 20 per cent this setting is rather critical, particularly if the pull-in voltage is increased due to heating of the magnet coil.

Multistep starters of the counter-electromotive force type would require even a higher setting of the last accelerating contactor as shown in Figure 1B, which makes use of the counter-electromotive force method for multistep starters impractical.

Current Limit Acceleration. This method is suitable equally for starting low and high inertia loads and will bring the motor up to speed in a minimum of time. A one-step starter of this type is shown in Figure 4.

The accelerator $1A$ is of the spring closed type and has a main winding $1A_M$ to close the magnet and a holding winding $1A_H$ measuring current. See Figure 5. Depressing the start button first will insert the starting resistor and then close the line contactor M. As the motor accelerates and the current decreases, the holding coil $1A_H$ will let go and close contact $1A$, thereby connecting the motor across the line.

The accelerators are calibrated usually to operate at about 135 per cent current so as to make sure that they function when starting heavy loads. Thus the current surges will be somewhat higher than indicated in Figure 1.

Definite Time Acceleration. Definite time starting probably is the most practical method of bringing a motor up to speed. It includes one or more accelerators adjusted to function in predetermined time intervals. A single-step starter is shown in Figure 6.

The accelerator or "timetactor" operates on the basis of the well-known and reliable flux decay principle and is shown in sizes of 100 and 300 amperes in Figure

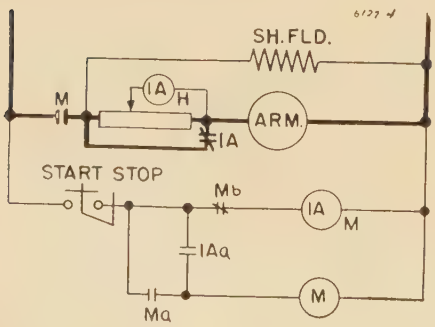

Figure 4 (left). Starter diagram with current limit acceleration

Figure 5 (right). Accelerating contactors for current limit or definite time acceleration

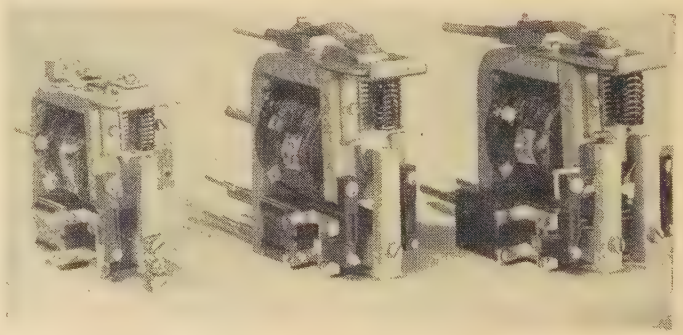

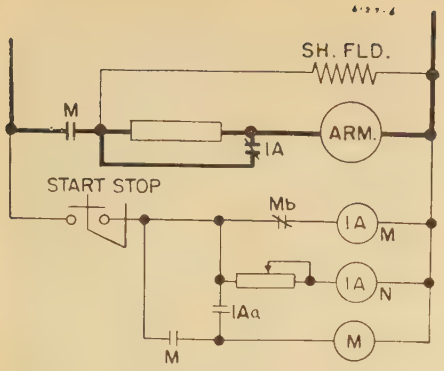

Figure 6. Starter diagram with definite time acceleration

5. In general, the time starter is identical to the controller of Figure 4 except that the accelerator is connected to obtain a fixed time instead of measuring current. Time adjustment is obtained by changing the current in the neutralizing winding $1A_M$.

There is, of course, the problem of selecting the proper time adjustment for the timetactors, so that the motor can accelerate without excessive current surges. This, however, should not be too difficult a task since starting conditions for the various ships' auxiliaries are well known and it is therefore a simple matter to adjust the accelerating time slightly longer than needed to obtain minimum current surges. Definite time starters can be tested and adjusted very readily with the motor disconnected and therefore have a decided advantage from a maintenance point of view.

Speed Control

The speed of a d-c motor may be controlled by varying the armature voltage or the strength of its field. Motors below five horsepower used for hull ventilation sometimes are provided with armature speed control in order to reduce the motor size. This gain, however, is practically offset by the increased size of the controller which has to absorb the resistor loss as shown in Figure 7.

In most cases, the motor speed is changed by varying the shunt field. Motors with speed changes of two to one or less have sufficient starting torque to permit good starting with weak field. The torque tests shown in Figure 8 were made with a 20-horsepower 230-volt motor of 600/1,800 rpm and a speed regulation of 20 per cent at the high speed. It is interesting to note that the flux weakening due to armature reaction is practically independent of the speed setting as evidenced by the bending of the three curves at 300 per cent load.

Controllers for motors with speed ranges greater than two to one are provided with a field relay in order to avoid too long an accelerating time particularly when used with fans of high inertia. The field relay is usually of the fluttering type.

Overload Protection

Each motor is provided with overload and short circuit protection. In line with well-established practice the overload relay is made part of the controller, while short-circuit protection in form of feeder breakers is located on the distribution board.

Protection of Continuously Rated Motors. Overload protection of these motors is usually obtained by means of a thermal relay set at 115 to 125 per cent of full load. Its time constant should be long enough to permit starting of the motor without tripping even though the starting time is long and the current surges are high.

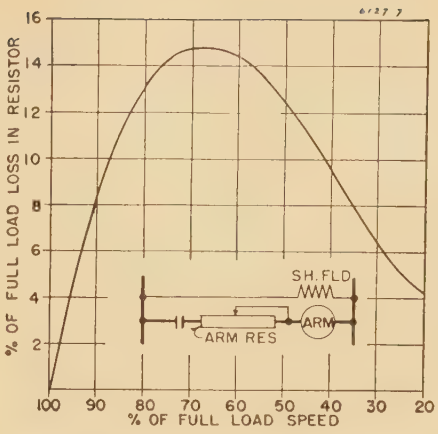

Figure 7. Resistor loss for armature speed control

In view of the high ambient temperatures encountered in engine rooms, the thermal overload relay is usually of the compensated type, that is, its calibration is made practically independent of the room temperature. Experience has shown that the noncompensated type is liable to trip under normal operation, thereby seriously interfering with the operation of the ship. A compensated overload relay is shown in Figure 9. It is provided with a special bimetal that corrects for changes in room temperature and thereby maintains the calibration practically constant.

Protection of Intermittently Rated Motors. There is a great deal of controversy as to whether overload protec-

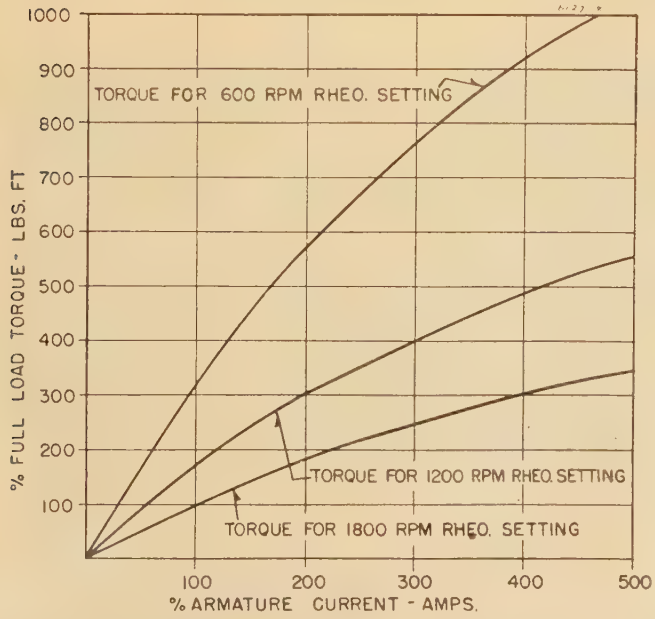

Figure 8. Starting torque of typical 20-horsepower 230-volt adjustable-speed shunt motor for different excitation and armature current

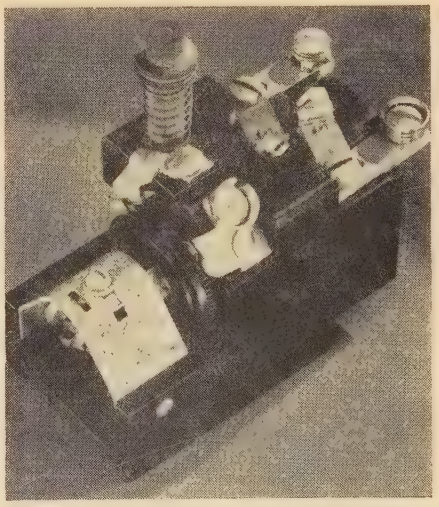

Figure 9. Compensated thermal overload relay for a-c and d-c applications

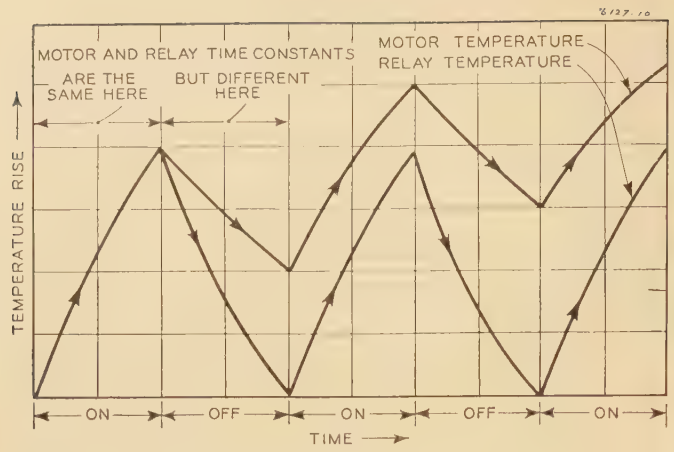

Figure 10. Heating curves showing inability of thermal overload relay to follow winding temperature of intermittently operating motor

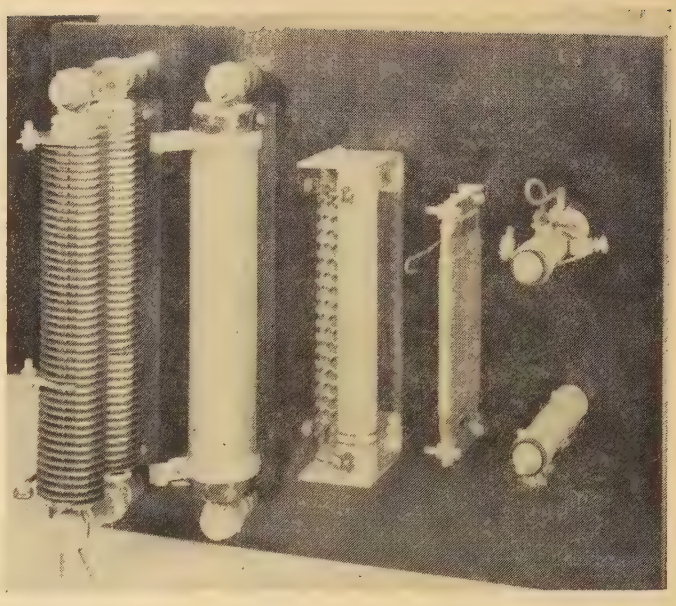

Figure 11. Various types of resistors

tion of intermittent motors by means of a thermal relay is practical. It is admitted that in order to be satisfactory such a relay should have the same time constant as the motor, that is, their temperatures should vary at the same rate when subject to various heating and cooling cycles.

This is a condition that is most difficult if not impossible to meet. Considering the fact that the time constant of motors may vary as much as three to one, depending upon their speed, ventilation, and size, it would not be feasible to design a multiplicity of relays to cover the whole range. Moreover, the co-ordinating of the time constants would be difficult since in most cases the desired information probably would not be available.

There is another important factor against matching time constants of motor and overload relay, namely, the unequal cooling of the motor while running and standing still. Tests show that with the motor standing still, the ventilation is very poor so that it will cool at a much slower rate than it heated during the running period.

Figure 10 shows that for intermittent operation the motor temperature will rise gradually above the relay temperature so that the motor is not protected even though the two time constants are matched while the motor is running.

For this reason, intermittently rated motors are protected by instantaneous overload relays set to trip at 200 to 300 per cent. They are intended to operate in case of emergency only, such as flashover of commutators or fouling of the anchor.

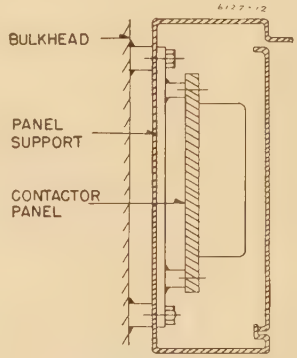

Figure 12. Typical drip-proof cabinet for bulkhead mounting

There is, however, the possibility of providing overload protection by means of thermoguards attached to the motor winding, thereby measuring motor temperature directly and stopping the motor when the temperature reaches a dangerous value.

Overload protection for capstans and windlasses is obtained with an instantane-

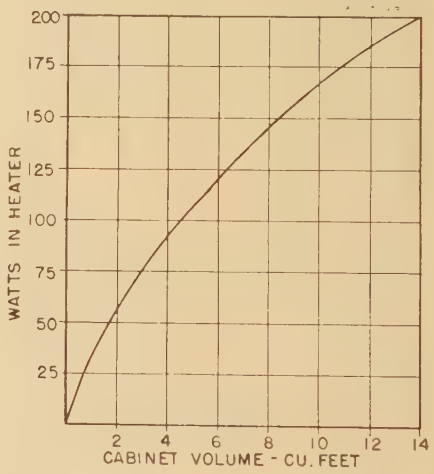

Figure 13. Heater capacity required for waterproof cabinets

Table II. Resistor Classification for Various Applications

Application	Duty	Resistor Class	Duty Cycle Sec On	Duty Cycle Sec Off
Starters below 40 hp	Starting	116	5	75
Starters above 40 hp	Starting	136	10	70
Windlass	Speed regulating	174DJ*	15	15
Capstan	Speed regulating	174J†	15	15
Cargo winch	Speed regulating	164D‡	15	30
Cable reel	Speed regulating	164	15	30
Boat hoist	Speed regulating	164	15	30

* Dynamic breaking and jamming protection with 125 per cent current for 5 minutes. Continuous running on last point lowering.

† Jamming protection with 125 per cent current for 5 minutes.

‡ Dynamic breaking in lowering direction.

The capacity of the resistors is based on good natural ventilation with not more than six tubes mounted on top of each other unless special baffles are provided.

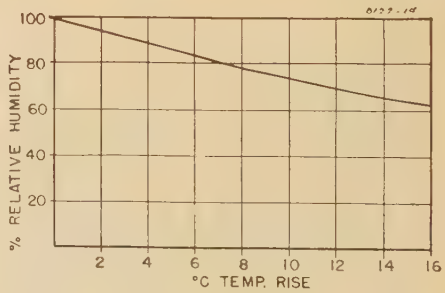

Figure 14. Relative humidity as a function of air temperature rise

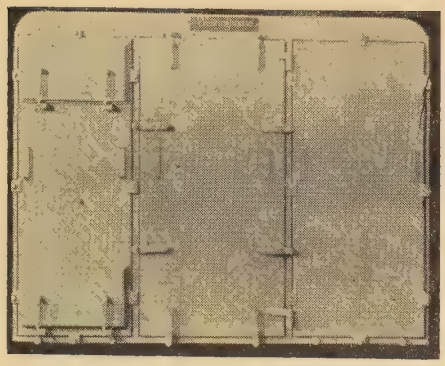

Figure 15. Typical waterproof cabinet for deck application

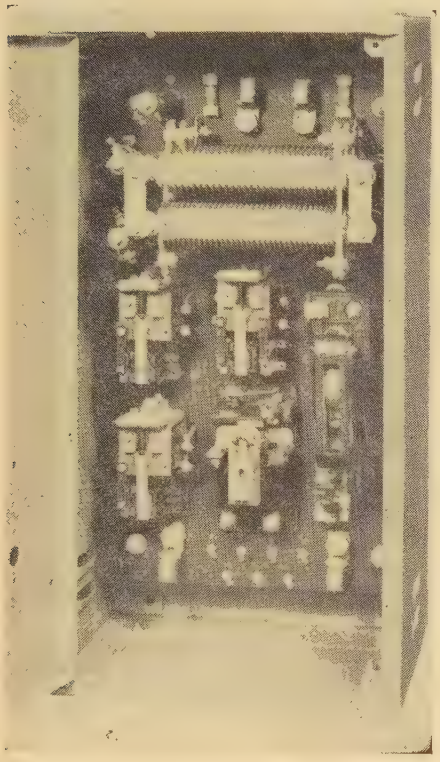

Figure 16. Typical drip-proof under-deck controller

ous jamming or step-back relay which inserts resistance in the armature circuit and reduces the stalled current to about 125 per cent rather than stopping the motor completely. This is done to maintain the tension in the anchor chain or the hawser while the ship is being warped or getting under way.

Resistors for Starting and Speed Regulating Duty

Practically without exception these resistors are of the nonbreakable and noncorrosive ribbon type using a nickel or chromium steel alloy suitable for 500–600 degrees centigrade continuous duty.

The maximum permissible temperature rise of a resistor depends a great deal on its location. When mounted in a controller cabinet, it is not desirable to exceed 365 degrees centigrade rise because it is close to apparatus with organic insulation.

However, it is satisfactory to go as high as 500 degrees centigrade rise when the resistors are mounted separately and are spaced sufficiently from other equipment to avoid undesirable heat transfer.

The tap or terminal is an important design detail of the resistors. Depending upon the design of the resistor, the terminal is either clamped, silver-soldered, or welded to the resistor ribbon. Any of these methods is satisfactory, although the welded terminal may be preferable, particularly for higher temperatures.

In order to insure a stable and permanent resistor connection, the latter must stay tight. Only in this way is it possible to keep the oxides away from the points of contact and maintain a metal-to-metal contact.

Two factors have to be considered when designing resistors for starting or regulating duty, namely, resistance and capacity. The selection of starting resistors is relatively simple since both factors are given by the number of steps and the accelerating time. Resistors for speed regulating duty, however, are more difficult to determine since the duty cycle depends a great deal on the judgment or habit of the operator.

Based on operating experience, resistor designs have been established for various applications, as shown in Table II. Special controllers with long accelerating time or heavy-duty cycle require, of course, more resistor capacity.

Controller Enclosures

Practically without exception, controller cabinets are built of structural steel in order to secure maximum strength and minimum weight at low cost. This applies to drip-proof as well as waterproof enclosures.

Designs for drip-proof cabinets are fairly well standardized. The contactor panel is mounted on rigid panel supports which, in turn, are bolted directly to the bulkhead as shown in Figure 12. This forms a strong mounting arrangement and permits a relatively light enclosure. Floor mounted drip-proof cabinets consist of the usual angle iron frame with removable sides and back to permit ready access to the apparatus. Ventilation of cabinets is usually obtained by means of louvers arranged in the side of the cabinet. This limited ventilation is sufficient for small losses such as caused by magnet coils. Larger losses, such as produced by speed regulating resistors,

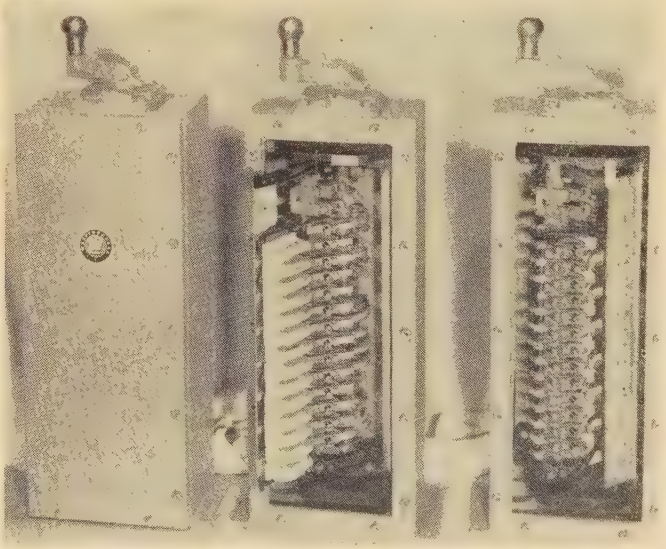

Figure 18. Waterproof manual controllers for deck auxiliaries

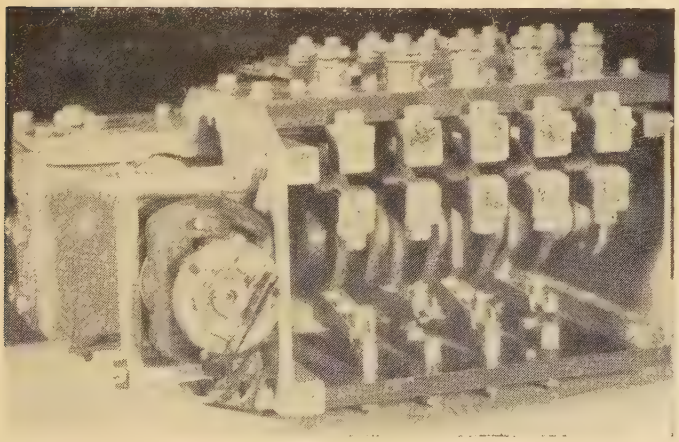

Figure 17. Accelerating drum for large motor starter with many steps

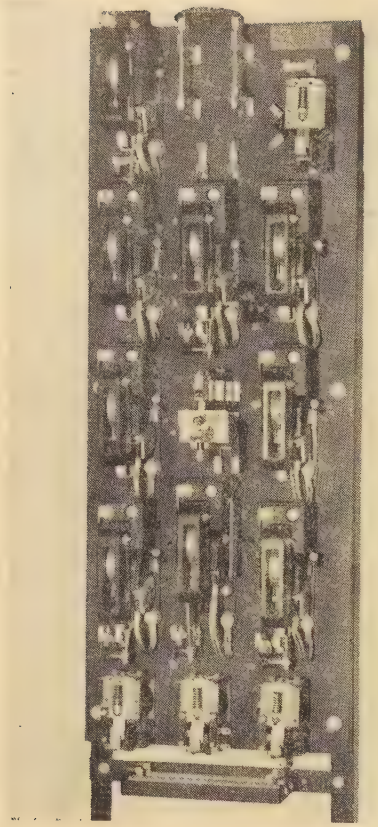

(A)

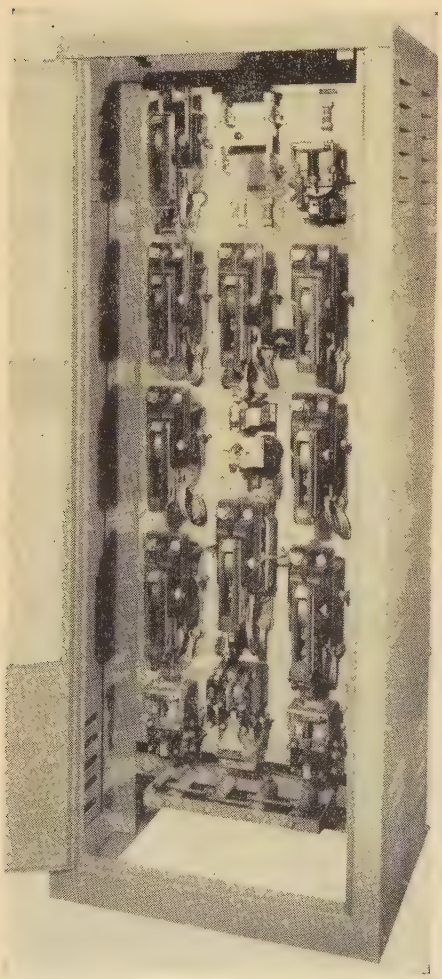

(B)

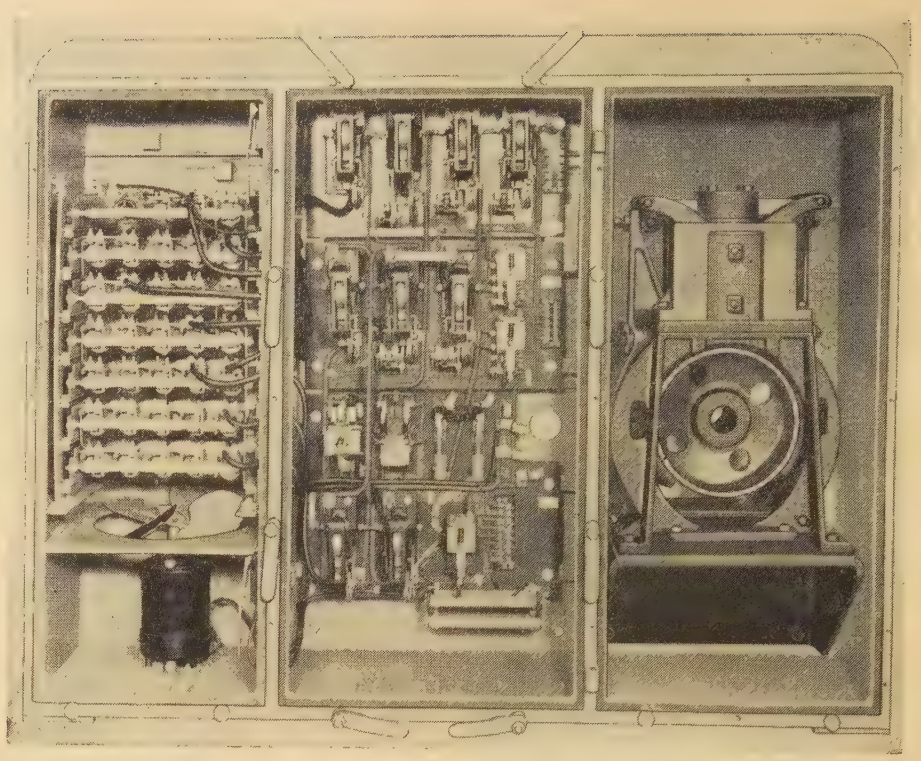

(C)

Figure 19. Magnetic controllers for deck auxiliaries

A. Open type
B. Drip-proof type
C. Waterproof type

require enclosures with raised top to permit better circulation of air.

Waterproof cabinets for deck mounting have to be made strong enough to withstand the impact of green water and to guard against corrosion eating through the walls in a relatively short time.

Corrosion of deck controllers is difficult to prevent because of condensation resulting from breathing action. The highly saturated air inside the cabinet is heated up to 50–60 degrees centigrade during a hot day and therefore, can hold considerable moisture. During the night this air is cooled off, and thus is unable to hold the water which is deposited on the inside surface, and finally collects at the bottom of the cabinet. This process is going on day after day so that under unfavorable conditions a sizable amount of water may collect in the cabinet, rendering the air so damp that even the best finish will break down after a while. There are two effective means of minimizing this corrosion. One consists in providing heaters inside the cabinet to keep the air always above the dew point. The watts required for this purpose can be determined from Figure 13. Experience has shown that a temperature rise of the air inside the cabinet of about 10 degrees centigrade is sufficient to keep the cabinet dry The reduction of relative humidity by heating the air is illustrated in Figure 14.

An additional improvement is obtained by providing a check valve at the bottom of the cabinet to drain any possible water and to provide some circulation of fresh air. Actual tests in the field have shown that a considerable improvement is obtained with surprisingly small openings.

It cannot be emphasized too much to provide substantial bolts not less than 3/8 inch diameter for mounting of doors or covers. Sizes below that will be twisted off when trying to force a corroded thread. Doors that have to be opened very readily sometimes are equipped with locking dogs as illustrated in Figure 15. They have to be made substantial enough to withstand rough handling when covered with ice.

Controller Assemblies

It is not the purpose of this paper to give a detailed description of the various applications. Rather than do this it is proposed to show some typical controllers which illustrate the lastest design trends.

Underdeck Controllers

Figure 16 shows a typical three-step starter for a 25-horsepower motor. All controller components are mounted in front of the panel to permit ready inspection and removal of parts if necessary. Studs with solderless lugs are arranged

top and bottom for external cables, the wiring of which is facilitated by detachable and standardized lead plates of ample size. Whenever possible, the push button is mounted on the starter door to obtain a unit assembly and to reduce wiring at the shipyard to a minimum.

Large starters of high-current capacity requiring many starting steps very often are provided with a motor-operated accelerating drum as per Figure 17, which combines one line contactor and all accelerators in one single and compact unit. The spring-closed cam-opened switch units are provided with silver tips and cut out the starting resistor in predetermined intervals. The speed of the pilot motor is adjustable within a one to two speed range.

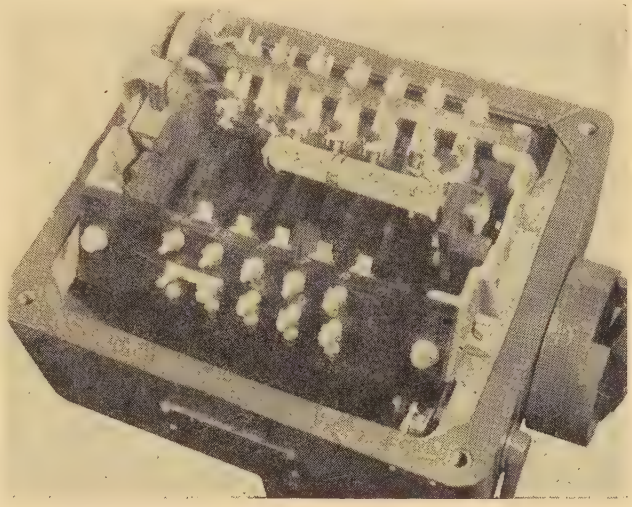

Figure 20. Two views of typical waterproof master switch for deck controller

Controllers for Deck Auxiliaries

Manual as well as magnetic controllers are provided for winches, capstans, and windlasses. Manual controllers as shown in Figure 18 are limited usually to smaller motors not exceeding 30 horsepower at 230 volts or 15 horsepower at 115 volts, because experience has shown that maintenance is excessive for current ratings above these values.

Magnetic controllers are being supplied with open, drip-proof, or waterproof unit construction as shown in Figures 19A, 19B, and 19C. There has been a great tendency in recent years to favor the unit construction, particularly for cargo winches, since it reduced the installation work on the part of the shipyard to a very minimum. Its possible weakness is maintenance at sea, particularly in bad weather, although experience so far has been very satisfactory.

Master switches are invariably of the waterproof construction, either cast or sheet steel and with an offset in the handle movement to provide a positive stop in the off position. A safe-on auxiliary switch is also provided to permit shutting down the control circuit when the equipment is not in operation. See Figure 20.

Very often it is preferred to make the master switch spring returned to obtain the so-called "dead man's feature" and to make sure that the motor cannot stay energized and accidentally burn out while the operator has "gone out for lunch." A master switch of this type is illustrated in Figure 21. Its lever is arranged so that the switch can be operated conveniently either with the stevedore standing beside the controller or sitting on it. This latter feature is desirable particularly for cargo handling where operation extends over many hours.

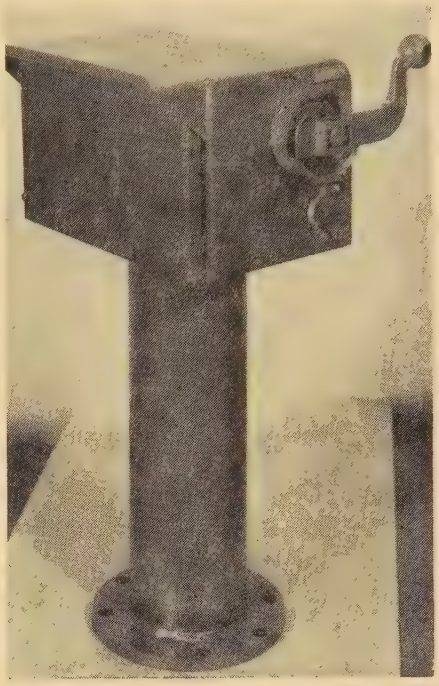

Figure 21. Waterproof master switch with spring-returned handle and seating facility for operator

Limitation of space does not permit discussion of special features required for different applications. Whatever control functions, however, are provided, emphasis should be placed on simplicity of design to obtain the desired results with a minimum amount of apparatus.

A New Approach to Probability Problems in Electrical Engineering

H. A. ADLER
ASSOCIATE AIEE

K. W. MILLER
MEMBER AIEE

THE PROBABILITY of simultaneous occurrences of events for which the individual rate of occurrence is known can be determined by the well-known binomial law. This law states that if n events have each a probability or rate of occurrence p, then the probabilities that 0, 1, 2, 3, etc., of the n events occur simultaneously, are given by the consecutive terms of the binomial function $[p + (1-p)]^n$. Therefore, the probability that r out of the n events occur simultaneously is

$$P_r = \frac{n!}{r!(n-r)!} p^r (1-p)^{n-r} \qquad (1)$$

Applied to the probable frequency of simultaneous occurrences, this expression merely says that if each of the n events occupies a fraction p of the period of time under consideration, say a fraction p of a year, then the simultaneous occurrences of r events occupy a fraction P_r of the period under consideration. However if P_r were found to be 1/52 according to the binomial law, then it would be known only that in a year the simultaneous occurrence of r out of the n events would occupy in the average a period of one week. It is not known, however, whether this simultaneous occurrence does happen once a year with a duration of one week, or once every two years with a duration of two weeks, or seven times a year with an average duration each time of one day.

It is obvious that knowledge of the duration and intervals between overlapping events can be of considerable importance in many practical cases. In problems of congestion, such as in telephone operation, not only the probability of the use of r out of n available channels is of interest, but also the average duration and frequency of such an occurrence. Similar problems arise in connection with intermittent use of electric power, such as by welding apparatus and elevators. In statistical problems of unavailability of equipment, average length and average intervals between occurrences of unavailability may be important, such as in cases of outages of lines, transformers, or generators of electric utilities.

The equations presented in the following, which apply to a variety of problems are based on an extensive analysis and on enumerations of a great variety of cases. The equations were found to be correct also for limiting or borderline cases. The methods of analysis and derivations of the equations are not presented, as they would require too much space and exceed the scope of this paper. For the same reason, discussion of some of the purely mathematical implications and extensions of these equations are omitted.

Special Case

Starting with the most simple case, assume that each of n events has a rate of occurrence $p = t/T$ so that each event occurs once in a period of T units of time and lasts each time t consecutive units of time. Further, be it assumed that the starting points of the events can change only in steps of multiples of the unit of time selected. Then the average duration, or overlap, of r simultaneous events out of n, expressed in the selected units of time is

$$t_r = \frac{T\frac{n!}{r!(n-r)!}t^r(T-t)^{n-r}}{\left\{T\frac{n!}{r!(n-r)!}t^r(T-t)^{n-r} - T\frac{n!}{r!(n-r)!}(t-1)^r[(T-t)-1]^{n-r}\right\}} \qquad (2)$$

or simplified,

$$t_r = \frac{t^r(T-t)^{n-r}}{t^r(T-t)^{n-r} - (t-1)^r[(T-t)-1]^{n-r}} \qquad (3)$$

From a standpoint of statistical mathematics, the numerator of equation 2 is the sum of all possible durations of the r-fold simultaneous events and the denominator is the sum of all repetitions of such r-fold simultaneous occurrences.

In terms analogous to the binomial law, the average overlaps may be expressed by the expansion of the function

$$\frac{[tx+(T-t)]^n}{[tx+(T-t)]^n - [(t-1)x+(T-t-1)]^n} \qquad (4)$$

(Here x is merely a "generating function" for convenient identification of terms corresponding to exponent r on x. Only the coefficients are of interest.) The overlap t_r is then the ratio of the coefficients of x^r which occur in numerator and denominator. This ratio is identical with equations 2 and 3.

As stated before, equations 2 and 3 assume that the start of the events can shift only in multiples of the unit of time chosen. Of course, these steps can be made as small as desired by choosing a small enough time unit. The restrictions of unit steps can be completely removed if we substitute pT for t in equation 3 and pass to the limit. We then obtain for the overlap duration, t_r expressed as a fraction of the entire period T under consideration.

$$\lim_{T\to\infty} \frac{t_r}{T} = \frac{(1-p)p}{r+p(n-2r)} \qquad (5)$$

With P_r from equation 1 and t_r from equation 3 or 5, we get the average interval T_r between r-fold simultaneous events by

$$T_r = t_r/P_r \qquad (6)$$

The frequency of such overlaps is

$$f_r = \frac{1}{T_r} = P_r/t_r \qquad (7)$$

Following is a practical application of these equations A single-phase 60-cycle circuit is supplying 30 welders On the average, each welder gives 25 random current impulses per minute to the circuit. Each impulse lasts on the average 5 cycles. What are the average durations and frequencies of the various possible amplitudes of impulses? Here $t = 5$ cycles, $T = 1/25$ minute or 144 cycles, and $p = 5/144$. The durations and frequencies of the impulses of various amplitudes, as calculated by equations 5 and 7, are given in Table I.

Values of currents up to six times the rating of one welder are quite frequent, indicating the possibility of serious voltage flicker. From the data in Table I, it is simple to calculate the equivalent current in the cable which produces the same heating of the conductor as the various current impulses.

More General Case

In the case discussed, all individual events had the same rate and duration of occurrence. Now consider the case where each of the n events occurs again once in

Paper 46-128, recommended by the AIEE committee on basic sciences for presentation at the AIEE summer convention, Detroit, Mich., June 24-28 1946. Manuscript submitted March 18, 1946; made available for printing May 10, 1946.

H. A. ADLER is in the engineering department staff division of the Commonwealth Edison Company, Chicago, Ill.; K. W. MILLER is chairman of the electrical engineering division of the Armour Research Foundation, Chicago, Ill.

Table I

r, Number of Welders Overlapping in Operation	t_r, Average Duration of Overlap in Cycles	f_r, Frequency of Overlap Per Minute
0	4.63	269
1	2.45	548
2	1.664	423
3	1.259	187.3
4	1.010	56.5
5	0.847	12.63
6	0.728	2.2
7	0.638	0.309
8	0.568	0.036
9	0.512	0.0035

the period T, but the duration of each event is different. The duration t has different lengths $a, b, c \ldots$ for the different events and the probabilities $p = t/T$ have consequently different values. Then, assuming first that each event can shift only in steps of multiples of the time unit, the average duration or overlaps of r-fold simultaneous occurrences, expressed in the units of time chosen, is given by the ratios of the coefficients in the numerator and denominator of the expanded function 9, that is,

$$t_r = \frac{gx^r}{hx^r} \tag{8}$$

where g and h are the coefficients of x^r in the numerator and denominator, respectively, of the expanded function

$$\frac{\Pi[tx+(T-t)]}{\Pi[tx+(T-t)]-\Pi[(t-1)x+(T-t-1)]} \tag{9}$$

Here Π signifies the products of the terms in the parentheses, with t assuming all the different values $a, b, c \ldots$. Written differently and assuming only three events with durations a, b, and c, the average duration of the various overlaps are given by the ratios of the coefficients of x^r in the numerator and denominator of the function

$$\frac{[ax+(T-a)][bx+(T-b)][cx+(T-c)]}{\{[ax+(T-a)][bx+(T-b)][cx+(T-c)]-[(a-1)x+(T-a-1)][(b-1)x+(T-b-1)][(c-1)x+(T-c-1)]\}} \tag{10}$$

Again the steps in which the events shift can be made as small as desired by choosing the unit of time suitably small. The limitation of shift in multiples of the time units can be eliminated completely by setting

$$p_a = \frac{a}{T},\quad p_b = \frac{b}{T},\quad p_c = \frac{c}{T}$$

$$q_a = 1-p_a,\quad q_b = 1-p_b,\quad q_c = 1-p_c$$

and passing to the limit $T \to \infty$. Then the overlaps of r-fold simultaneous occurrences expressed as a fraction of the period T are given by the ratios of the coefficients in the numerator and denominator of the terms x^r of the following function

$$\frac{(p_ax+q_a)(p_bx+q_b)(p_cx+q_c)}{(x+1)[(p_ax+q_a)(p_bx+q_b)+(p_ax+q_a)(p_cx+q_c)+(p_bx+q_b)(p_cx+q_c)]} \tag{11}$$

which can, of course, be generalized to any number of terms $n > 3$.

As an example, assume that a distributing station of an electric power company is supplied by three lines from different sources. According to statistical data each of the three lines can be expected to be forced out of service once a year. Due to the different nature of the lines, 48 hours are required to restore the first line to service, 24 hours are required for the second line, and 12 hours are required for the third line. Then, $a=48$, $b=24$, $c=12$, $T=8{,}760$, $p_a=48/8{,}760$, $p_b=24/8{,}760$, and $p_c=12/8{,}760$. The average duration and intervals of outages as calculated by equation 10 or 11 is given in Table II.

Table II

Number of Lines out of Service	Average Duration of Outages in Hours	Average Interval of Outages in Years
0	2920	0.344
1	27.9	0.334
2	12.2	53.14
3	6.8	37,747

Events of Different Amplitudes

The preceding equations gave information on only the number of lines out of service. If the loads which can be carried by the three lines are different, then it may be more important to obtain information on the kilovolt-amperes out of service rather than the number of lines out of service. If the three lines of the preceding example have different load-carrying capacities, L_a, L_b, and L_c, then the average duration and intervals of loss of various amounts of kilovolt-amperes can be obtained from equation 10 by substituting x_a, x_b, and x_c for x. Then the average duration of the loss of L_a kilovolt-amperes is the ratio of the coefficients for x_a in the expanded numerators and denominators, the loss of L_b+L_c kilovolt-amperes is given by the coefficients of x_bx_c, the loss of $L_a+L_b+L_c$ kilovolt-amperes is given by the coefficients of $x_ax_bx_c$, and so on.

Completely General Case

Assume that an event n occurs f_n times during the period T where f_n may be different for each event. The lengths of the f_n occurrences of the event n may be all different and so may be the intervals between occurrences. The individual lengths of these occurrences may be $t_{n\alpha}$ $(\alpha=1, 2, \ldots, f_n)$ units. The individual lengths of intervals between occurrences may be $\delta_{n\alpha}(\alpha=1, \ldots, f_n)$ units.

Table III

Number of Channels in Use	Average Length of Overlap in Seconds	Frequency of Overlap Per Second
3	1.02	0.206
2	0.88	0.501
1	0.74	0.392
0	0.62	0.097

Let

$$\sum_{\alpha=1}^{\alpha=f_n} t_{n\alpha} = \theta_n$$

and

$$\sum_{\alpha=1}^{\alpha=f_n} \delta_{n\alpha} = \Delta_n$$

In other words θ_n is the sum of the lengths of the f_n different occurrences for the event n, and Δ_n is the sum of the intervals between occurrences. Therefore,

$$\theta_n + \Delta_n = T$$

Then, assuming again that the events can shift only in multiples of the unit of time, the average duration or overlap of 0, 1, 2, . . .n, simultaneous occurrences is given by the ratios of the coefficients of the various terms x^r in the expansion of the function.

$$\frac{\prod_{n=1}^{n}[\theta_nx+\Delta_n]}{\prod_{n=1}^{n}[\theta_nx+\Delta_n]-\prod_{n=1}^{n}[(\theta_n-f_n)x+(\Delta_n-f_n)]} \tag{12}$$

It is of special interest that in the numerator as in the denominator, the individual lengths of occurrences for each event and the order of occurrences have no effect on the result, but only the sums of the lengths of occurrences and of the intervals and the frequency of occurrence, or number of repetitions are of importance. This fact, of course, simplifies the application of this general formula considerably. Finally, we can remove the restriction of shift of events in multiples of the time unit by substituting p_nT for θ_n and q_nT for Δ_n and, furthermore, setting $p_n/f_n=v_n$ and $q_n/f_n=w_n$.

When we pass to the limit $T \to \infty$ we obtain for the duration of the average

overlaps expressed as fractions of the period T,

$$\lim_{T\to\infty}\frac{t_r}{T}=\frac{\left(\prod_{v_n}^{r}\times\prod_{w_n}^{n-r}\right)}{\sum\left(\prod_{v_n}^{r-1}\times\prod_{w_n}^{n-r}\right)+\sum\left(\prod_{v_n}^{r}\times\prod_{w_n}^{n-r-1}\right)} \quad (13)$$

where the superscripts on the product symbols designate the number of terms in the product. Each double product contains each index of one to n not more than once. The summations are taken over all different combinations of n subscripts or indices in two groups of r and $(n-r)$, each in the numerator, and of $(r-1)$, and $(n-r)$, and of r, and $(n-r-1)$ each in the denominator corresponding to the double products.

If all values of v_n are identical and, consequently, all values of w_n are identical, equation 13 reduces to

$$\lim_{T\to\infty}\frac{t_r}{T}=\frac{vw}{mw+(n-m)v} \quad (14)$$

If $f=1$, then $v=p$ and $w=q=1-p$, and equation 14 reduces to equation 5.

As an example of the general case, assume that of three available channels the first is in use once in the period T of 10 seconds and the duration of use is 5 seconds. The second channel is in use twice in each period T of 10 seconds and the two durations of use, 2 and 5 seconds, occur with equal frequency. The third channel is in use three times in each period T of 10 seconds and the equally likely durations of these three uses are 1, 2, and 3 seconds, respectively. Then the average durations and frequencies of overlaps, as calculated by equation 12, are given in Table III.

This example, admittedly artificial to illustrate the general formula, is typical of problems which can occur in telephone practice and in other fields of electrical engineering. Still further generalization is possible, and has been carried out though not elaborated here, along two general lines. First, it is possible to work out a method—but not a formula—to express the duration and interval between recurrences of "r or more" simultaneous occurrences and to further extend it to "w or more" kilovolt-amperes, say, when individual events are of unequal capacity. Secondly, it is possible to determine the deviations from the mean of the durations and intervals given by the above formulas.

The methods and equations as outlined have helped considerably in solving practical problems which could not be solved by equations previously available.

Excitation, Control, and Cooling of Ignitron Tubes

C. C. HERSKIND
MEMBER AIEE

E. J. REMSCHEID
MEMBER AIEE

APPLICATION DATA for mercury pool tubes or tanks must include information covering rectifier capacity, control characteristics, excitation requirements, losses, cooling requirements, and other essential characteristics.

The factors affecting rectifier capacity, the relations between these factors, and the procedure for specifying rectifier capacity have been set forth in a companion paper. This paper presents a description of the excitation, control, and cooling characteristics of typical mercury-arc tubes of the ignitron type and outlines a procedure for specifying these characteristics, together with the limitations and operating requirements which must be considered.

Excitation

The excitation system must establish and maintain the conditions required for arc conduction. To do this it must perform three functions:

1. Start a cathode spot on the cathode pool.
2. Maintain the cathode spot.
3. Extend the ionization to the anode region.

Ignitors

In rectifiers of the ignitron type, a cathode spot is started each cycle by the ignitor. In order to perform the starting function successfully, the ignitor must be supplied with sufficient energy to assure reliable operation. The instantaneous volt-ampere requirements of the ignitor depend upon its construction, composition, and treatment. Individual ignitors vary in resistance and starting characteristics because of small differences introduced during manufacture or operation. In order to assure reliable ignitor operation, definite specifications have been set up for ignitor performance. Acceptable ignitors must fire at peak voltages and currents within the specified maximum values.

The ignitor excitation requirements are best described by a volt-ampere characteristic of the type shown in Figure 1. The "minimum" curve gives the instantaneous volt-amperes that this excitation circuit should deliver. It must be understood that an ample margin should be allowed between the "minimum" curve and the maximum volt-amperes required to fire acceptable ignitors. The "maximum" curve indicates the highest value of instantaneous volt-amperes that the firing circuit may deliver without damage to the ignitor or seal assembly.

A wide variation in the resistance of individual ignitors is permissible, and the dotted curves show typical characteristics for ignitors having resistances ranging from 2 to 100 ohms. The peak short-circuit current and open-circuit voltage indicated by the solid curves are particularly useful in specifying the excitation circuit requirements. Further limitations and requirements of the ignitors are indicated in Table I.

Auxiliary Anodes

In order to minimize the power consumed by the ignitors and also the physical size of the firing circuit components, the ignitor volt-amperes are usually sustained for only a few electrical degrees (from 10 to 25 degrees in most circuits). Auxiliary excitation or relieving anodes, therefore, are used to perform the following functions:

1. Maintain the cathode spot for the required period. Many circuits require that excitation be maintained for 90 degrees in order to assure reliable operation at light load.
2. Furnish additional energy for ionization of the arc space.
3. Reduce the duty on rectifying elements in the firing circuit by providing a shunt path.

Table I. Ignitor Limitations and Requirements

Maximum rms current allowed, amperes	15
Maximum avg current allowed, amperes	3.0
Maximum instantaneous inverse voltage allowed, volts	5

Paper 46-138, recommended by the AIEE committee on electronics for presentation at the AIEE summer convention, Detroit, Mich., June 24–28, 1946. Manuscript submitted April 26, 1946; made available for printing May 14, 1946.

C. C. Herskind and E. J. Remscheid are in the power rectifier department, General Electric Company, Schenectady, N. Y.

These auxiliary anodes may be located either in the open arc path or in a shielded space adjacent to the cathode pool. They are usually excited from a sinusoidal source. Typical wave forms are shown in Figure 2.

The inverse voltage applied to the excitation anode must be held to a low value in order to limit the positive ion bombardment and avoid arc-backs. The maximum allowable inverse voltage depends upon the amount of shielding around the excitation anode and the time of application of the inverse voltage, that is, whether the inverse voltage is applied during the main anode conduction or during the main anode inverse period. By proper phasing

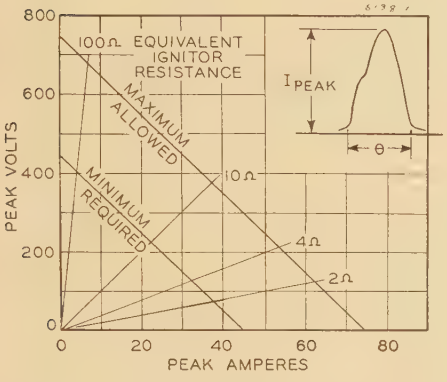

Figure 1. Ignitor instantaneous volt-ampere requirements

Pulse duration $\theta = 10$ to 15 degrees at 25 to 60 cycles

of the excitation anode voltage with respect to the ignitor firing point, the excitation anode conduction period may often be fixed so that inverse voltage is applied to the excitation anode only during the main anode inverse period. Where this is not possible, some means, such as a rectifying element), must be provided to limit the inverse voltage which may be applied. Further limitations and requirements are indicated in Table II.

Grids

While the grids are also a part of the excitation system, in that they help to establish the conditions for conduction, this is only incidental to their control action. Their characteristics are covered in the section on control.

Control

In an ignitron, control of conduction may be obtained by means of either ignitors or grids. The ignitor provides the only means of control in many small tubes which are built without grids. In

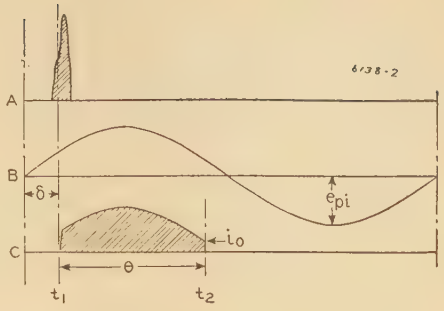

Figure 2. Excitation anode wave forms

A—Ignitor current
B—Excitation anode voltage
C—Excitation anode current

such tubes, the ignitor usually provides effective control over the full range of operation. However, most larger tubes are equipped with one or more grids.

The primary function of the grid is to control both the arc phenomena in the neighborhood of the anode and the starting of anode conduction. While the establishment of suitable arc conditions at the anode is essential to the action of the rectifier and affects the rectifier capacity directly, the control function of the grid is the more important from an application standpoint.

The grid action depends directly upon the electronic processes taking place in the rectifier throughout the cycle. These are well illustrated by the oscillographic observations shown in Figure 3. These observations were made on a pumped ignitron operating in a six-tank unit at $E_{do} = 1{,}294$ volts and $I_d = 2{,}000$ amperes load current. In order to facilitate analysis of the action, the grids were excited from a rectangular voltage wave of 125 volts peak through 500 ohm resistors.

Referring to Figure 3, main anode conduction starts at time t_0 with a positive grid current. At time t_1, before the end of conduction, the voltage applied to the grid circuit is made negative. The grid

Table II. Excitation Anode Limitations and Requirements

Maximum rms current allowed, amperes	10
Maximum avg., current allowed amperes	5
Minimum instantaneous current required to maintain cathode spot, amperes	3
Maximum peak inverse voltage allowed during conduction, volts	25
Maximum peak inverse voltage allowed during inverse, volts	150

potential remains substantially unchanged although the grid current is reversed. The positive ion current collected by the grid is limited only by the resistance of the grid circuit. Main anode conduction ends at time t_2. However, the grid current is sustained as the grid continues to collect positive ions from the residual ionization. As deionization continues, the intensity of ionization finally, at time t_3, falls below that required to sustain the full positive ion grid current, and the grid current then falls off along a

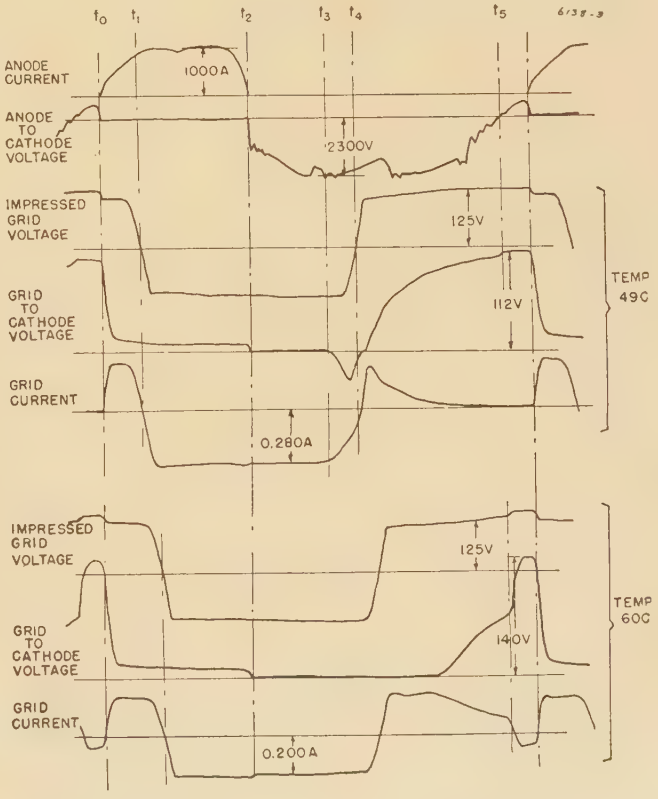

Figure 3. Grid characteristics on pumped ignitron with single grid

decrement curve as deionization progresses. At time t_4, the voltage applied to the grid circuit again becomes positive. The grid now collects electrons and since these are more mobile than the positive ions and can be drawn from the entire arc space, the grid current again reaches the limiting value fixed by resistance. However, the deionization process continues and this current also falls off on a decrement.

Late in the unverse cycle, the main anode becomes positive at time t_5. Since the rectifier is operating with phase control and the ignitor has not yet fired, conduction does not begin. However, the grid again collects ions as it is made negative with respect to the anode. This action is quite pronounced when operating at 60 degrees centigrade temperature.

Many conclusions regarding the action may be deduced from these observations. Some of these are as follows:

1. Ionization persists throughout the inverse cycle.
2. The deionization time is a function of the control temperature.
3. The action of the grid assists the decay of ionization.
4. The grid shields the anode from the ionization which persists in the arc path during the inverse cycle.

Grid Characteristics

Most ignitron tubes with a single grid have a negative grid characteristic, that is, require a negative grid potential to prevent conduction. This negative grid characteristic is obtained because the arc path is usually quite open and a high level of ionization is provided at the grid by the ignitor and auxiliary anode arc.

Typical grid-blocking characteristics for a pumped ignitron having a single grid are shown in Figure 4. These characteristics apply where the ignitor is energized and the blocking action of the grid is utilized to prevent conduct on while the rectifier is being placed in operation. The grid current which flows as a result of the ionization produced by the ignitor and excitation anode is shown in Figure 5.

The grid characteristics, when operating with phase control, are similar to those for blocking, except that the presence of the ionization from the conduction of the preceding cycle increases the negative voltage required on the grid to prevent arc-through, or loss of control. The slow deionization of a single grid tube is shown clearly in Figure 3. For this reason, a single grid does not provide effective control over a wide range of temperature and ionization. A wider range of control may often be obtained by the ignitor than by the grid in a single grid tube.

Table III gives a further list of typical grid limitations and requirements.

Where a wide range of phase control is required to obtain blocking action from no load to fault currents, full phase control at all loads, and accurate timing of firing, two or more grids are usually provided in the ignitron tube. With two grids, the outer grid shields the inner from the ionization in the arc path and permits more rapid and complete deionization of the space around the anode and the inner grid so that better control characteristics are obtained. A wide variety of firing characteristics may be obtained by such arrangements. These are generally similar to those for the single grid. However, further studies are necessary for a full treatment of their characteristics, limitations, and requirements.

Table III. Grid Limitations and Requirements

Minimum grid resistance allowed, ohms	500
Maximum grid resistance allowed, ohms	5,000
Maximum inverse voltage allowed during conduction, volts	150
Maximum inverse voltage allowed during inverse, volts	300
Minimum positive voltage required to fire, volts	50
Maximum positive voltage allowed, volts	300

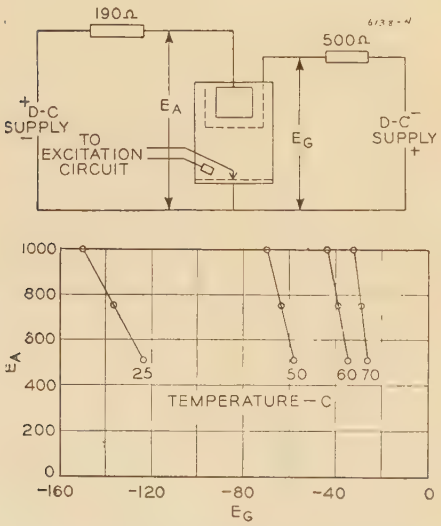

Figure 4. Grid blocking characteristic of pumped ignitron with single grid

E_g—Grid to cathode voltage at start of discharge

E_a—Anode to cathode voltage

Cooling and Temperature Control

Mercury-pool tubes must be operated within a specified temperature range in order to deliver rated power output, assure reliable operation, and prevent damage during faults. The temperature also affects the rectifier efficiency since the arc losses are a function of temperature.

The temperature regulating equipment which is provided for the purpose of establishing the desired temperature conditions must perform the following major functions:

1. Remove the heat produced by the arc losses.
2. Maintain the desired control temperature.
3. Maintain the desired temperature gradient on the anode seals.
4. Minimize corrosion.

Arc Losses

Most ignitron tubes have an arc drop ranging from 15 to 25 volts. The losses are approximately proportional to the load current although the arc drop increases somewhat with the load. The maximum cooling requirements are usually determined by the arc loss obtained when operating at the current required for the two-hour overload condition. Since the heat storage capacity of the usual tube structure is equivalent approximately to a thermal time constant of 15 to 30 minutes, overloads of short duration,

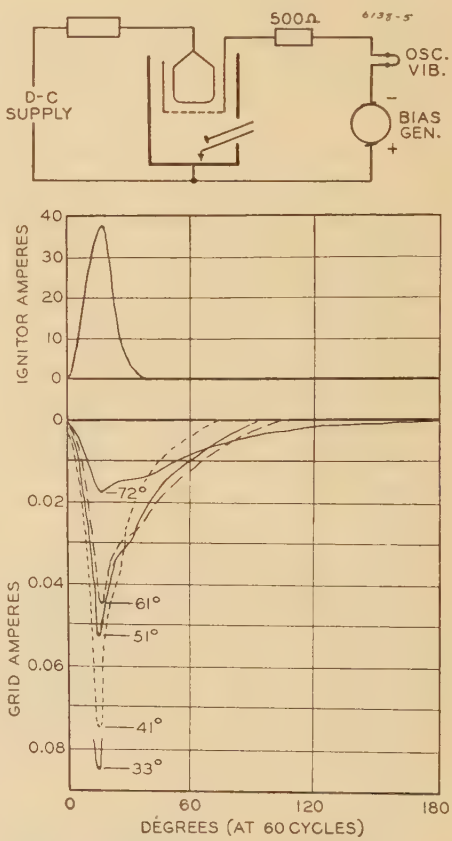

Figure 5. Grid current during blocking tests

Anode to cathode voltage = 0
Grid to cathode voltage = −300 volts
Temperature as shown

such as one minute, need not be considered in the determination of the cooling requirements.

Figure 6 shows a typical arc drop characteristic for a pumped ignitron operating in a unit of six tanks with a double-Y connection. This represents the usual mode of operation where $P = 3$, the conduction period is $(120° + u)$, and the peak tube current is three times the average tube current. An alternate connection which is sometimes used is the fork where $P = 6$, the conducting period is $(60° + u)$, and the peak tube current is six times the average tube current. The arc drop in this case will be higher because of the increased peak current and the losses, therefore, will be greater. Tests on two units show that the losses at the same load are increased approximately eight per cent over those obtained when operating double-Y. A similar correction factor, but having a different value, may be determined for other modes of operation.

Cooling

The majority of power rectifiers are cooled by water which is passed through suitable water jackets. Two general systems of water cooling may be employed. One is the direct raw water-cooling system in which water is taken from a suitable supply, passed directly over the cooling surfaces of the rectifier, and discharged. The other is the heat-exchanger cooling system in which a coolant is passed over the cooling surfaces of the rectifier, then cooled in a heat exchanger and recirculated.

Direct raw water cooling requires the least amount of equipment and, therefore, frequently is used on small units ranging from 75 kw to 300 kw. In such systems, tubes must operate over a wide temperature range with varying water flow. In order to conserve water, the tube water jackets usually are connected in series.

Heat-exchanger cooling systems are used for all the larger rectifiers where it is desired to operate the tubes at the optimum temperature and utilize their full capabilities. Pertinent information necessary in applying a heat exchanger to a rectifier unit is as follows:

1. Type and design of rectifier.
2. Water flow in gallons per minute.
3. Pressure drop through water jacket, in pounds.
4. Approximate arc losses in kilowatts.

Anode Heaters

It is necessary to maintain a temperature gradient at all times from the anode and grid seals to the tank, so as to prevent the condensation of mercury on the seal insulators. On equipment employing sealed tubes, with direct raw water cooling, usual service conditions are generally such that no heaters are required. Where sealed ignitrons operate under unusual service conditions which are unfavorable, anode heaters must be provided. Anode heaters generally are required on all pumped ignitrons. These heaters range up to 350 watts, depending upon the size of the tube and the service conditions.

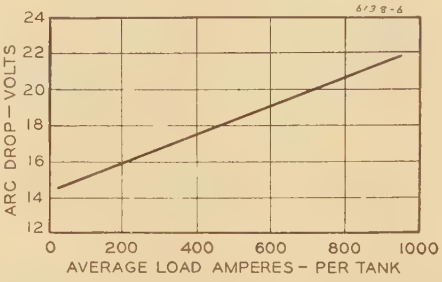

Figure 6. Typical arc-drop characteristic for pumped ignitron

Corrosion

The prevention of corrosion in rectifier cooling systems, involves two considerations, one, a proper choice of metals which come in contact with the water, and second, the control of the chemical constituents of the coolant. The sealed tubes employ stainless steel for the vacuum tank in order to insure vacuum tightness. A complete corrosion-resistant water chamber is readily obtained by providing water jackets of the same material. The stainless steel construction of sealed tubes makes them suitable for use in direct raw water cooling systems. Pumped rectifiers employ vacuum tanks made of boiler plate steel. They must be proved with copper cooling coils for use in direct raw water-cooling systems.

For heat exchanger systems, where a recirculating coolant is used, the materials in the associated piping which is connected to the rectifier should consist of malleable iron pipe and fittings. It is good practice that the recirculating water be treated with sodium chromate ($Na_2 - CrO_4$), using either distilled or an approved raw water.

Conclusions

The factors which must be considered in the application of mercury-pool tubes and the design of rectifier units have been described. Also a procedure for specifying their characteristics, limitations, and requirements has been outlined.

A full knowledge of the characteristics, limitations, and requirements of the ignitron tube is essential to the design of a successful and economical rectifier unit inasmuch as the auxiliaries required for excitation and temperature control are an important part of the unit.

References

1. Rectifier Capacity, C. C. Herskind, H. C. Steiner. AIEE Transactions, volume 65, 1946, October section, pages 667–70.

2. Ignitor Excitation Circuits and Misfire Indication Circuits, A. H. Mittag, A. Schmidt, Jr. AIEE Transactions, volume 61, 1942, August section, pages 574–7.

3. The Water-Cooled Steel-Tank Rectifier Corrosion Problem, E. J. Remscheid. AIEE Transactions, volume 60, 1941, April section, pages 173–8.

Dimensionless Analysis of Servomechanisms by Electrical Analogy

S. W. HERWALD
ASSOCIATE AIEE

G. D. McCANN
MEMBER AIEE

THE MECHANICAL transients analyzer[1,2] provides a fast and simple method of obtaining the complete solutions to the performance equations of servomechanisms under any type of operating condition. It has been found to be applicable to the detailed analysis of specific systems. Also, because of the great rapidity with which parameters of a basic system can be changed once that system is set up, the analyzer is admirably suited to generalized studies of various types of systems. This paper presents a general study that has been made of variable-voltage angular-position servomechanisms. The data give dominant system frequencies and damping rates for a two time delay system with simple error control and for a wide range of parameters. Similar data are presented for error control plus optimum anticipation time constants, together with other performance characteristics. Because of the many curves required for the same type of analysis of the several variations of resistance-capacitance-feedback and other forms of antihunt or damping devices, they will not be treated here.

The range of parameters chosen is sufficiently wide to cover all practical types of variable-voltage servo applications. The performance of a given system or the choice of parameters for optimum performance can be quickly obtained from the dimensionless data on the curves.

Paper 46-150, recommended by the AIEE committee on basic sciences for presentation at the AIEE summer convention, Detroit, Mich., June 24–28, 1946. Manuscript submitted April 24, 1946; made available for printing May 15, 1946.

S. W. HERWALD and G. D. McCANN are with the Westinghouse Electric Corporation, East Pittsburgh, Pa.

The authors wish to acknowledge the helpful assistance of H. M. Watson who made a number of check calculations.

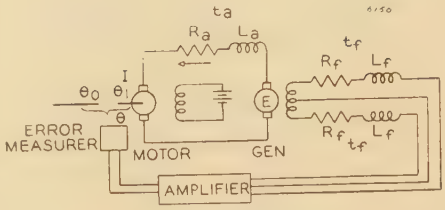

Figure 1. Schematic diagram for variable-voltage angular-position servomechanism (see appendix)

Description of System Studied

A schematic diagram of the system studied, together with the definition of all parameters and the system equations, is given in Figure 1. In this system two time delays are included. One of these, t_a, can only represent the armature circuit time delay. However, if the field time delay of the system being studied is negligible, t_f can represent any other time delay back in the system. The appendix gives the dimensionless parameters upon which the generalized study is based.[3] These include the undamped natural frequency ω_n with no time delays, the ratio, r, of actual to critical damping with no time delays, and the time constants put in dimensionless form through multiplication by ω_n. In the accompanying curves, the performance solutions plotted as functions of the above parameters are actual dominant system frequencies, dominant system damping rates, and crest values of the error angle. The first two are applicable to any form of disturbance or motion to be followed. As shown in the appendix, system frequencies are put in dimensionless form by expressing them as a fraction of ω_n. Damping is given in per cent per cycle. Since a suddenly applied constant velocity is considered to be the most basic type of disturbance function for such systems, the actual solutions were obtained for this case and the crest error angles, θ_{max}, or transient overshoots, were put in dimensionless form by expressing them as a function of the steady-state error angle, θ_{ss}, for such disturbance (see appendix).

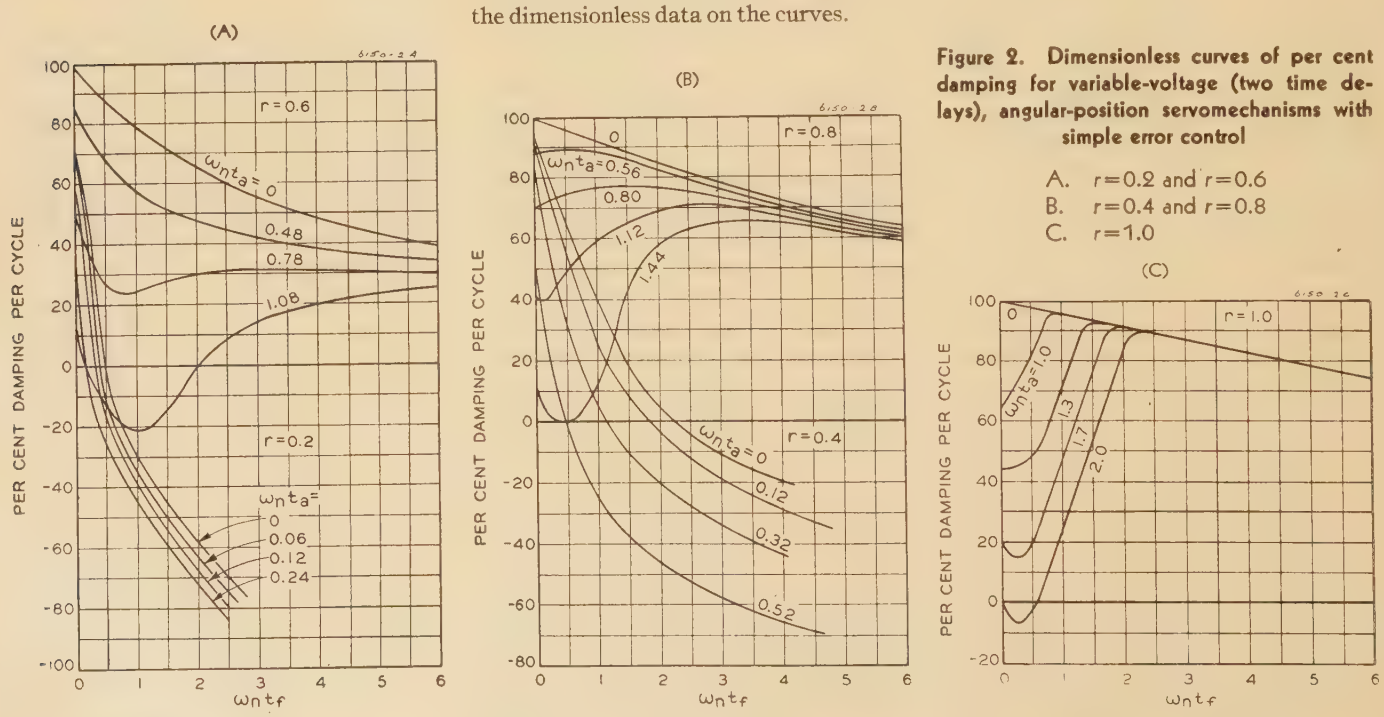

Figure 2. Dimensionless curves of per cent damping for variable-voltage (two time delays), angular-position servomechanisms with simple error control

A. r=0.2 and r=0.6
B. r=0.4 and r=0.8
C. r=1.0

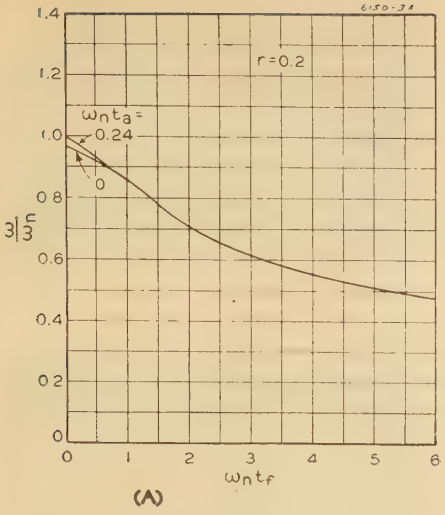

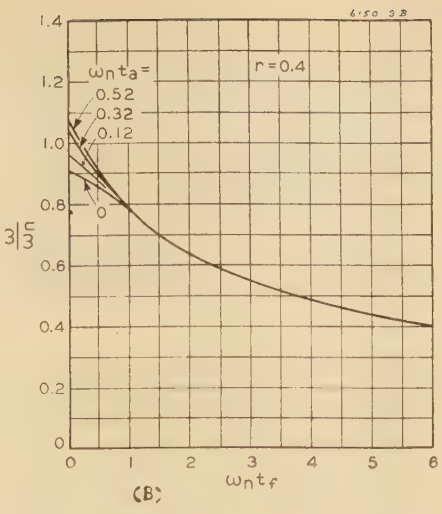

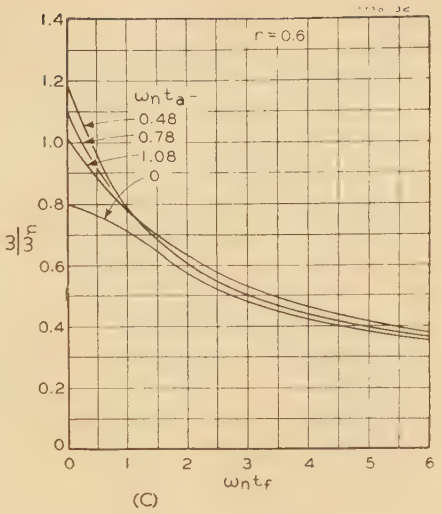

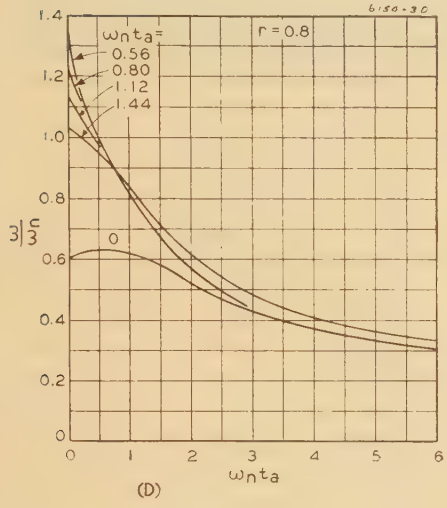

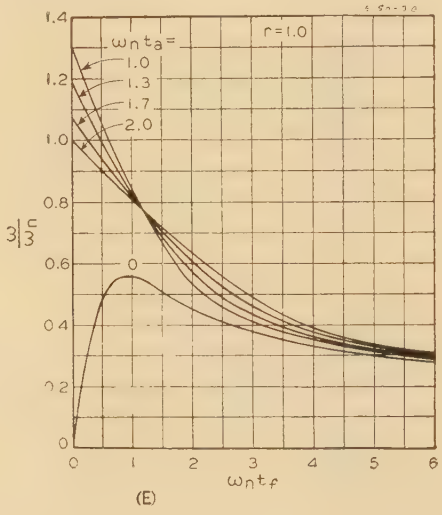

Figure 3. Dimensionless system frequencies for variable-voltage angular-position servomechanisms with simple error control

A. $r=0.2$
B. $r=0.4$
C. $r=0.6$
D. $r=0.8$
E. $r=1.0$

The method of studying such systems on the transients analyzer is discussed in detail in reference 1. The basic torque equation of Figure 1 is represented as an electric circuit with suitable circuit constants and amplifiers. The exact circuits and analogies used are given in the above reference. The complete transient solutions were observed or photographed on the screen of a cathode-ray oscilloscope. In reading and recording data either from the oscilloscope screen or the photographs, precautions were taken to obtain about five per cent accuracy. Numerous check calculations were made for the case of simple error control, all of which checked well within ten per cent. It should be pointed out that the data presented represent the equivalent of the solution of several thousand servo-equations. The greatest number of solutions would be required in obtaining the optimum anticipation which is quite simple with the analyzer.

Analysis of Data

The information presented in Figures 2, 3, and 4 is in dimensionless form. Therefore, any physical system of the type shown in Figure 1 is represented by the curves of Figures 2, 3, and 4 regardless of the actual numerical values of its parameters.

Figure 2 shows curves of per cent damping per cycle plotted as a function of $\omega_n t_n$ for different values of $\omega_n t_a$, and r equal to 0.2, 0.4, 0.6, 0.8, and 1.0. All symbols used are as defined in the appendix. In Figure 3 the ratio of actual frequency, ω, to the undamped natural frequency, ω_n, is also plotted as a function of $\omega_n t_f$ for various values of $\omega_n t_a$, and r equal to 0.2, 0.4, 0.6, 0.8, and 1.0. The data of Figure 4 were obtained by choosing an anticipation time, $\omega_n T_a$, to provide the best compromise between damping, response, and overshoot. These data give per cent damping per cycle, the ratio of maximum angular error, θ_{max}, to the steady-state angular error for a constant input velocity, θ_{ss}, the ratio of actual to undamped frequency, ω/ω_n, and the optimum value of anticipation time, $\omega_n T_a$, as a function of the two system time delays. Separate curves are given for r equal to 0.2, 0.4, 0.6, 0.8, and 1.0. Figure 5 shows photographs of some of the typical solutions obtained in deriving the curves of Figure 4. The ordinate is angular error θ, and the abscissa, time.

A study of Figures 2, 3, and 4 shows that any general conclusions drawn may have exceptions at particular points. Thus, although frequency and damping generally decrease with increase of $\omega_n t_f$, in Figure 3C, for $\omega_n t_a = 0$, frequency increases with increase of $\omega_n t_f$ up to about 1.0, and in Figure 2C, damping increases for a number of values of $\omega_n t_a$ for increase in $\omega_n t_f$ to 1.0 or better.

In order to have satisfactory performance of the simple-error type of servomechanism, it can be seen in general in Figures 2 and 3 that large values of r and small values of $\omega_n t_a$ and $\omega_n t_f$ are required. The exception to the above statement is found at values of r of 0.8 and 1.0 where it is possible to increase the damping to a satisfactory level by increasing $\omega_n t_f$, although there is a sacrifice in frequency ratio.

The use of an error rate or anticipation term in the controller usually results in a well-damped system with good frequency response when r is small and the time delays $\omega_n t_a$ and $\omega_n t_f$ are large. This is well illustrated by Figure 4 and by actual photographs of such a case, Figures 5A and B. However, for the practical range of time delays for r equal to 0.2, damping decreases for all cases of increasing time delays. Difficulty is encountered in obtain-

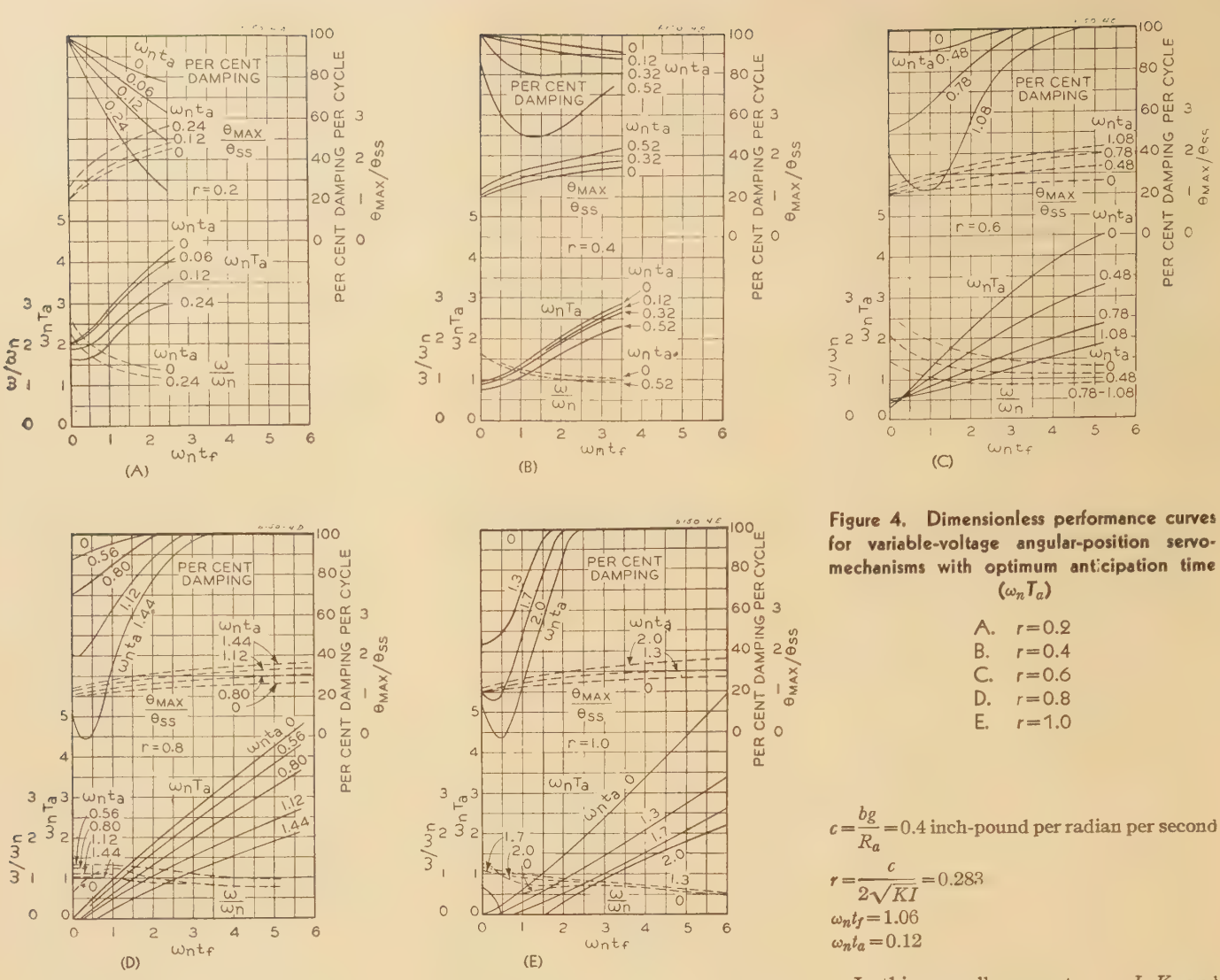

Figure 4. Dimensionless performance curves for variable-voltage angular-position servomechanisms with optimum anticipation time ($\omega_n T_a$)

A. $r=0.2$
B. $r=0.4$
C. $r=0.6$
D. $r=0.8$
E. $r=1.0$

ing sufficient damping at r equal to 0.6, 0.8, and 1.0 for large values of $\omega_n t_a$ and small values of $\omega_n t_f$. The photographic record of Figure 5C and D shows this. In Figure 5D the principal effect of anticipation is to reduce the magnitude of the oscillation with little or no increase in damping. It should be recognized immediately that this is not a common operating point, for the armature time delay is rarely even of the same order of magnitude as the field delay.

In general, the optimum anticipation time, $\omega_n T_a$, increases; the frequency ratio, ω/ω_n, decreases; and the peak ratio, θ_{max}/θ_{ss}, increases with increase in $\omega_n t_f$.

Remembering that high values of r bring correspondingly higher steady-state errors for a constant input velocity and greater power loss, the advantage of anticipatory control over the simple error control is apparent.

The curves of Figures 2, 3, and 4 have been smoothed so that some of the small kinks, caused by the large number of roots in the differential equations, have been omitted. At all points, however, the curves are well within an accuracy of ten per cent. There is no difficulty in choosing the dominant frequency in most cases. However, where a second frequency is pronounced, the ω chosen was that which corresponded to the time for the initial overshoot to first return to the steady-state angular error, θ_{ss}.

Typical Example

To clearly illustrate how easily the data in Figures 2, 3, and 4 can be used, a typical variable-voltage angular-position servomechanism problem is worked out below.

The parameter values are as follows:

$I=10^{-1}$ pound-inch-second^2
$K=5$ inch-pounds per radian
$R_a=6$ ohms
$L_a=0.10$ henry
$R_f=100$ ohms
$L_f=15$ henries
$b=4$ inch-pounds per ampere
$g=0.6$ volt per radian per second

$$\omega_n=\sqrt{\frac{K}{I}}=7.07 \text{ radians per second}$$

$$c=\frac{bg}{R_a}=0.4 \text{ inch-pound per radian per second}$$

$$r=\frac{c}{2\sqrt{KI}}=0.283$$

$\omega_n t_f=1.06$
$\omega_n t_a=0.12$

In this case all parameters as I, K, and b that are a function of shaft speed are given at the motor shaft.

Any shaft geared to the motor could easily have been used as a reference instead, as long as all the values were given at that shaft. At times this may be desirable.

Referring to Figure 4 and interpolating between Figure 4A and B for $r = 0.28$ gives the following data:

Optimum $\omega_n T_a=2.0$
Per cent damping per cycle = 83
$\omega/\omega_n=1.4$
$\theta_{max}/\theta_{ss}=1.7$

Therefore, if in the actual system T_a is made $2.0/7.07=0.283$ second, the actual system will have a frequency of $1.4\times 7.07=10$ radians per second, and a maximum angular error at the motor shaft for a suddenly applied constant velocity, ω_1, of

$$1.7\times\frac{2r\omega_1}{\omega_n}=0.137\omega_1$$

The damping per cycle of the system is 83 per cent.

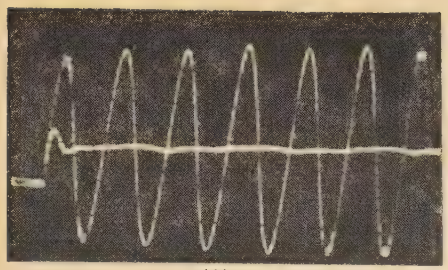

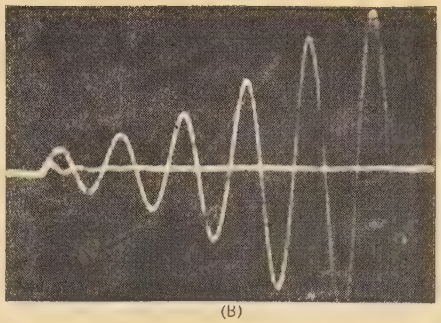

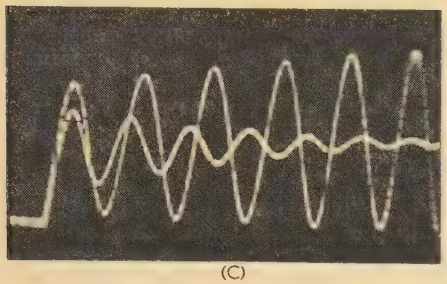

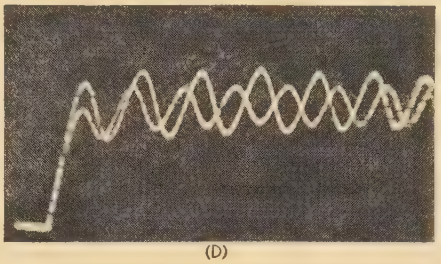

Figure 5. Typical solutions as obtained with the mechanical-transients analyzer

A. $r=0.2$, $\omega_n t_a=0$, $\omega_n t_f=0.53$, $\omega_n T_a=2.19$
B. $r=0.2$, $\omega_n t_a=0.24$, $\omega_n t_f=0.53$, $\omega_n T_a=1.64$
C. $r=0.6$, $\omega_n t_a=1.08$, $\omega_n t_f=1.06$, $\omega_n T_a=0.6$
D. $r=1.0$, $\omega_n t_a=2.0$, $\omega_n t_f=0.53$, $\omega_n T_a=0.55$

Conclusions

The data presented provides in clear form the solutions to any variable-voltage angular-position servomechanism with two time delays for either simple error control or error plus error rate (anticipatory) control. The solutions include system frequencies and per cent damping per cycle that are applicable to any system disturbance, and maximum overshoot data are provided for the case of suddenly applied constant velocity. A typical practical example of the use of the data is given.

It should be emphasized that the solutions are directly applicable only to systems that are approximately linear, although the correct order of magnitude of results will be obtained even for systems that materially depart from linearity.

Appendix

Equations for Figure 1

t_a = armature time constant
t_f = field time constant
T_a = anticipation time constant
K = stiffness constant

Equation for armature circuit:

$$E_g = R_a i + L_a p i + g p\theta_0; \quad p = \frac{d}{dt}$$

Equation for motor torque:

$$bi = Ip^2\theta_0$$

Giving the mechanical torque equation

$$M_c = \frac{bEg}{R_a} = \frac{L_a I}{R_a} p^2\theta_0 + Ip^2\theta_0 + \frac{bg}{R_a} p\theta_0$$

$$M_c = (1+t_a p) Ip^2\theta_0 + cp\theta_0$$

Controller torque M_c for simple error control:

$$M_c = \frac{K(\theta_1-\theta_0)}{(1+t_f p)}$$

Controller torque for error control plus anticipation:

$$M_c = \frac{K(1+T_a p)(\theta_1-\theta_0)}{(1+t_f p)}$$

Dimensionless parameters for generalized analysis:

$\omega_n = \sqrt{K/I}$ = undamped natural frequency with no time delays

$r = \dfrac{c}{2\sqrt{IK}}$ = ratio of actual to critical damping with no time delays

Dimensionless time constants $= \omega_n t$
Dimensionless system frequencies $= \omega/\omega_n$
ω_1 = suddenly applied constant velocity

$\theta_{ss} = \dfrac{2r\omega_1}{\omega_n}$ = steady-state error for suddenly applied constant velocity

References

1. Electrical Analogy Methods Applied to Servomechanism Problems, **G. D. McCann, S. W. Herwald, H. S. Kirschbaum.** AIEE Transactions, volume 65, 1946, February section, page 91.

2. A New Device for the Solution of Transient Vibration Problems by the Method of Electrical-Mechanical Analogy, **H. E. Criner, G. D. McCann, C. E. Warren.** *Journal of Applied Mechanics*, September 1945, volume 12, page 135.

3. Considerations in Servomechanism Design **S. W. Herwald.** AIEE Transactions, volume 63, 1944, December section, pages 871–6.

4. Dynamic Behavior and Design of Servomechanisms, **G. S. Brown, A. C. Hall.** American Society of Mechanical Engineers *Transactions* volume 68, 1946, July section, pages 503–24.

5. Theory of Servomechanisms (book), **L. A. MacColl.** D. Van Nostrand Co., New York N. Y., 1945.

6. Automatic Control Engineering (book). **E. S. Smith.** McGraw-Hill Book Company, Inc., New York, N. Y., 1944

Circuit Cushioning of Gas-Filled Grid-Controlled Rectifiers

D. V. EDWARDS
ASSOCIATE AIEE

E. K. SMITH
NONMEMBER AIEE

Synopsis: In certain common rectifier and inverter circuits, gas-filled rectifier tubes supplying highly inductive loads with firing delayed by grid control, are subjected to the application of high rates of rise of initial inverse voltage. This phenomenon results in short tube life because of the sputtering of anode material by the impact of residual ions attracted at high velocity to the negatively charged anode with consequent gas cleanup. The paper describes a method of slowing down or cushioning this rate of rise of initial inverse voltage. A small resistance and capacitance circuit connected between cathode and anode of each tube delays the voltage rise the few microseconds necessary to eliminate gas cleanup. Life test data and practical applications are cited.

GAS CLEANUP, or gradual disappearance of the gas filling of gaseous discharge tubes was noted by Plucker in 1858, and later studied more extensively.[1] The present work was undertaken to explore the phenomenon as related to hot-cathode xenon- and argon-filled grid-controlled rectifiers.

The exploration was prompted by a reported tube life of 40,000 hours without cleanup in one circuit, contrasted with a circuit which consistently caused cleanup within 250 hours.

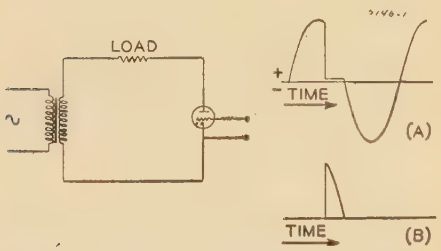

Figure 1. Circuit of test 1 with oscillograms of tube voltage and current

A—Voltage across tube
B—Current through tube

Cleanup Test Data

Life tests were initiated in 1936 under the tube operating conditions listed in Table I, using a tube type which tests on resistive load under widely varied conditions had shown to be free from gas cleanup and dependable for lives in excess of 3,000 hours.

Before this work was undertaken, it was thought that cleanup might accompany rapid ionization.

Test 1 was designed to give rapid current buildup by reason of a low impedance power supply and transformer. Tube current rose abruptly from zero to 90 amperes each cycle. As the test was at overload, the life obtained was considered normal. Tests after failure showed that cleanup did not occur. Hence rapid buildup of ionization is not cause for cleanup at least up to rates of current rise of several million amperes per second.

Test 2 applied high initial inverse voltage caused by the current carry-over forced by the inductive load, shown in the diagrammatic oscillograms of tube voltage and current in Figure 2. Here no rapid buildup of ionization occurred, but in each cycle, at the end of conduction, a high inverse voltage abruptly appeared. This initial inverse voltage is indicated on the oscillogram of the tube voltage in Figure 2. With this circuit condition rapid cleanup occurred.

In test 3 the load inductance was made larger to prohibit appreciable change of current throughout the cycle. At the end of each cycle, the inductance generated the instantaneous voltage necessary to overcome negative supply voltage, thus forcing current to flow through the conducting tube until relieved by the firing of its successor. Current flowed through each tube in square blocks, thereby maintaining full current just prior to applying the initial inverse voltage. This test caused drastic cleanup.

Table I further indicates by test 4 that lowered initial inverse voltage alleviates cleanup somewhat, whereas increased frequency in test 5 aggravated cleanup.

As a result of this and other data, and numerous installations where it was shown by test that cleanup did not occur, it was concluded that gas cleanup would not occur, provided:

1. The circuit did not apply each cycle high initial inverse voltage immediately following substantial current conduction.
2. No sizable ion current was drawn to the grid during tube conduction nor was a sizable electron current drawn to the grid during periods of high inverse voltage on the anode.
3. There were no parasitic glow discharges or tube abnormalities.

Items 2 and 3 had been found some years previously to be possible causes for cleanup. In the tests reported in Table I, suitable grid resistors were used (approximately 50,000 ohms) to eliminate cause 2. Many previous tests of this tube type on resistance loads under various conditions had demonstrated that the tubes were free of cleanup from cause 3.

Since 1937, limitation 1, as part of the tube application notes of one company, prohibited many commercial applications of gas-filled tubes. Desiring to remove this restriction, the details of the abrupt transfer from conducting current to withstanding inverse voltage were probed further.

Commutation

This transition for the circuit shown in Figure 3 is depicted with expanded time scale in Figure 4. The process of current commutation commences at instant t_0 as the tube about to enter construction 2 is fired by grid action. Its anode voltage falls precipitously and conduction current arises. However, leaving tube 1 continues conduction by reason of the inductance of the supply and transformer, shown schematically as equivalent leakage inductances L_1. Similar inductance L_2 momentarily limits the growth of current through entering tube 2. With both tubes conducting concurrently, both anodes are at the same potential and

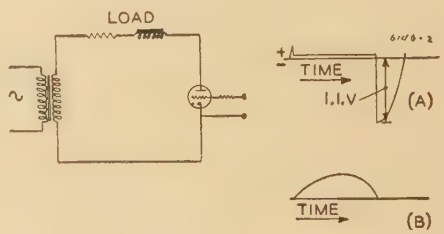

Figure 2. Circuit of test 2 with oscillograms of tube voltage and current

A—Voltage across tube
B—Current through tube

Paper 46-146, recommended by the AIEE committee on electronics for presentation at the AIEE summer convention, Detroit, Mich., June 24–28, 1946. Manuscript submitted April 22, 1946; made available for printing May 15, 1946.

D. V. EDWARDS is president of, and E. K. SMITH is engineer with, Electrons, Inc., Newark, N. J.

the transformer is temporarily short-circuited. Full voltage during this period is applied to L_1 and L_2 in a direction to increase current in L_2 and depress it in L_1. By the time t_1, current through leaving tube 1 has been brought to zero and load current transferred to entering tube 2. Rectifier action prohibits reverse current, therefore the rate of change of current through L_1 disappears and the voltage across it collapses from maximum value to zero. This applies the full negative voltage of the winding to the leaving anode. Simultaneously, load current, which cannot change rapidly because of the high load inductance, becomes the only current flowing through

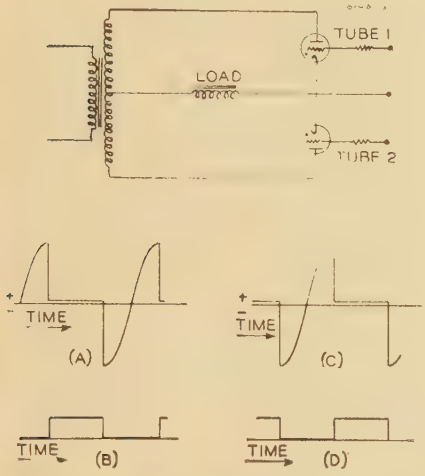

Figure 3. Circuit of tests 3, 4, 5, and 6 with oscillograms of tube voltages and currents

A—Voltage across tube 1
B—Current through tube 1
C—Voltage across tube 2
D—Current through tube 2

Figure 4. Details of commutation in circuit shown in Figure 3

Showing equivalent circuit and oscillograms of tube voltages, tube currents, and transformer output voltages during current commutation and rise of initial inverse voltage

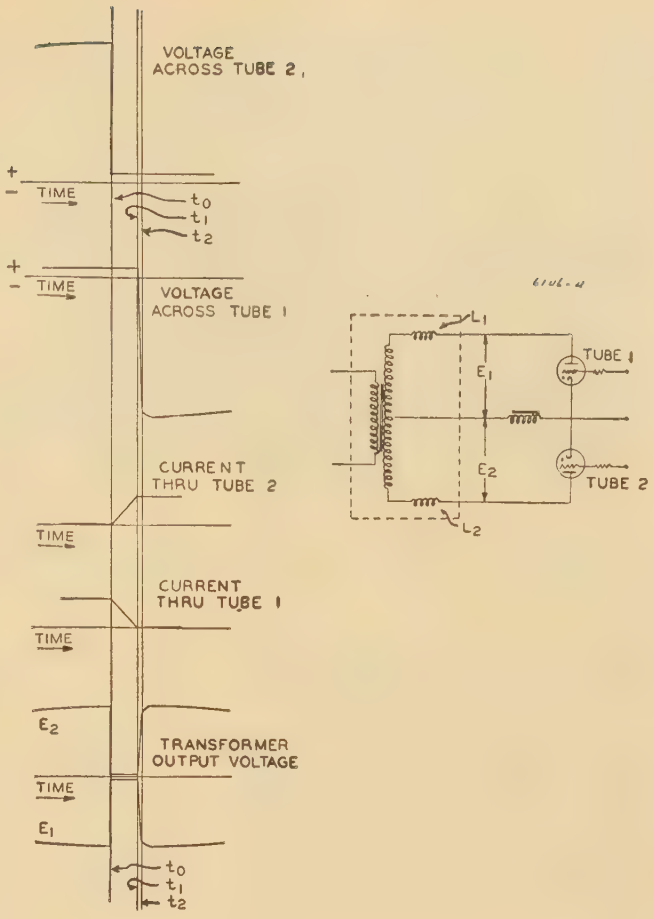

L_2, causing voltage across L_2 to disappear and further increasing the initial inverse voltage on leaving tube 1. Stray capacitances and core losses in the various inductances prevent the initial inverse voltage from appearing absolutely instantly. It is not until t_2, that full initial inverse voltage appears. However, on circuits of a few kilowatt capacity, voltage often appears at a rate of over 100,000,000 volts per second. All of the commutation events just described occur in a time so small compared to 60-cycle waves that they often go unnoticed.

Cushion Test Data

Experiments were conducted in which the rate of rise of the initial inverse voltage was modified by adding a capacitor and resistor across each tube, as shown in Figure 5. The capacitor-resistor circuits have been called cushion circuits to indicate that they cushion the fall of anode potential.

Life tests using tubes of lower current rating than those reported in Table I were run under the conditions listed in Table II.

Cleanup occurred in all tubes tested in test 6, whereas none was detectable in any tube after failure in test 7. As before, the particular tube type had been thoroughly tested on various resistive loads and found to be free from cleanup. In addition to demonstrating the effectiveness of cushioning, this test gave further evidence that initial inverse rather than build-up of ionization was responsible for cleanup, as test 7 built up conduction current slightly faster than test 6.

Operation of Cushion

The operation of the cushioned circuit of Figure 5 may be described as follows. For the half cycle prior to entry of tube 2, cushion capacitor C_1 is discharging through R_1 and tube 1. It stands discharged at the moment t_0 when entering tube 2 fires. Current commutation is instituted at t_0 as previously described. Also, entering cushion capacitor C_2 is discharged through R_2 and tube 2. Time t_1 marks the end of current com-

Table I. Life Test on Tube

Tube Rating: 750 Applied Peak Forward Volts, 5 Amperes Average Current, 60 Amperes Peak Current

Test	Circuit	Frequency	Applied Peak Forward Voltage	Applied Peak Inverse Voltage	Initial Inverse Voltage	Avg Amp	Peak Amp	Hours Life
1	Figure 1	60	155	155	0	10	90	1,955
2	Figure 2	60	15	650	650	5	14	269
3	Figure 3	60	650	650	650	5	10	25
4	Figure 3	60	310	310	310	4	8	120
5	Figure 3	500	680	680	680	5	10	3

mutation. Thereafter, the initial inverse voltage cannot appear on leaving tube 1 except as current builds up through L_1 and L_2 to cause voltage drops across R_1 and C_1. By proper choice of resistor and capacitor relative to the leakage inductances L_1 and L_2, this rise of initial inverse voltage can be delayed a few microseconds and yet have enough resistance to prevent oscillations. Rates of rise of the order of 10,000,000 volts per second are often satisfactory.

It may help to attempt to visualize the phenomenon occurring within the tube during the commutation and application periods. While conducting current, ionized atoms of xenon populate the electron stream, neutralizing electron space charge. The number of ions varies as some function of current. On a decrease of current, the ion requirements will decrease, allowing the excess to seek electrons and return to atoms. A short time, that is, the order of ten^{-5} seconds, is required for the ionization to readjust to the new conditions. Thus, at the instant that current reaches zero, there still will be present residual ionization representing current flow some microseconds earlier.

At the cessation of current, the initial inverse voltage appears on the anode at the rate established by the circuit. The negative anode attracts residual positively charged ions to it. If ions, being relatively heavy particles, fall through a high potential drop, they acquire enough momentum to sputter or evaporate anode material when they impinge.[2] Sputtering appears to trap gas atoms both in the anode and in the deposited film of sputtered material. If negative voltage is applied slowly enough to allow sweeping out the residual ions at relatively low voltage, sputtering is avoided and cleanup eliminated.

To expedite testing, sensitive pressure gauges were attached to tubes which were then operated under varying current commutation rates and initial inverse voltage application rates. Cleanup could be detected in shorter testing time by this expedient. These data are necessarily tentative, but they do disclose that the permissible rate of rise of initial inverse voltage, above which cleanup sets in, depends upon current commutation conditions. Low reactance transformers, which commutate swiftly, require a lower rate of application of initial inverse voltage, that is, larger cushion capacitors. High reactance transformers may be completely cushioned with quite small capacitances.

It might be noted that, during the course of the experiments using extremely high commutation and recovery rates, there were several cases where the inverse rating of the tube could be changed by adjusting the recovery rates. This undoubtedly has a bearing on the problem of arc-backs, particularly in view of the reported fact that many arc-backs in mercury-arc rectifiers occur just after current commutation.[3,4] This seems to merit a separate inquiry and report.

Based on the pressure gauge tests, the safe rating for the maximum rate of rise of initial inverse voltage is being specified for the present on some tubes as

$\frac{K}{A_{10}}$ = maximum safe rate of rise of intial inverse voltage in millions of volts per second

where

K is a constant for each tube type (6.6 for a typical 6.4 A tube)

A_{10} is the current flowing 10 microseconds before current zero

A_{10} can be determined from measurement of total current flowing and duration of current commutation.

This formulation assumes a linear relation between residual ionization and A_{10} which admittedly is a first approximation, but appears to cover the range of measurable voltage rates moderately well. The factor K usually is larger the smaller the rating of the tube, as might be expected from the smaller ionized volumes. This, plus the fact that fractional ampere circuits do not often have high initial inverse voltage application rates, usually makes it unnecessary to cushion low power tubes.

Table II. Life Test on Tube

Tube Rating: 450 Applied Peak Forward Volts, 1 Ampere Average, 8 Amperes Peak Current

Test	Circuit	Frequency	Applied Peak Forward Volts	Initial Inverse Voltage	Avg Amp	Peak Amp	Hours Life
6	Figure 3	60	423	423	1	2	449
7	Figure 5	60	423	423	1	2	14,200

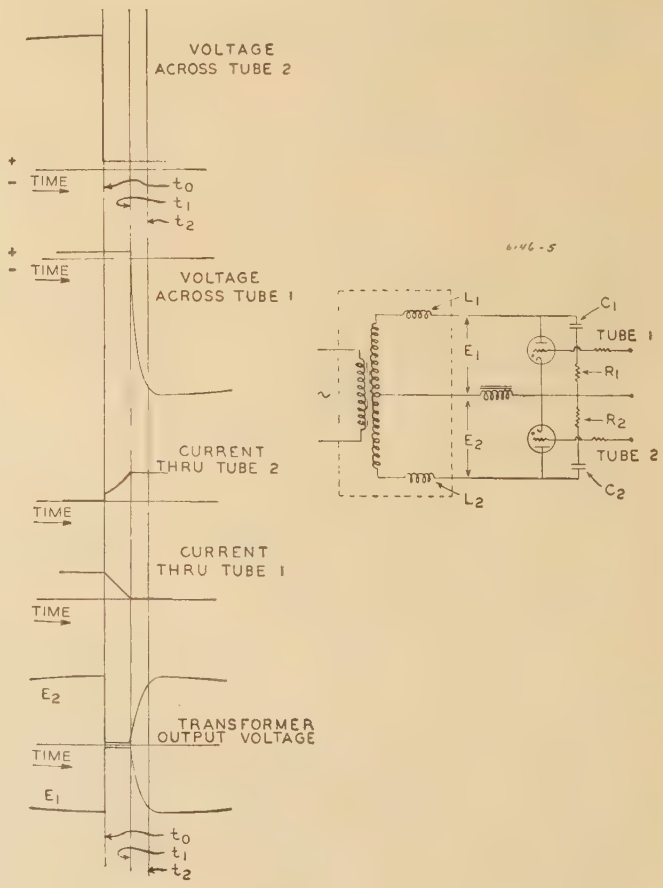

Figure 5. Details of commutation of cushioned circuit

Showing equivalent circuit and oscillograms of tube voltages, tube currents, and transformer output voltages

There is a small power loss in the cushion resistors. It is usually less than two per cent of full output and may be made considerably smaller by proper transformer design.

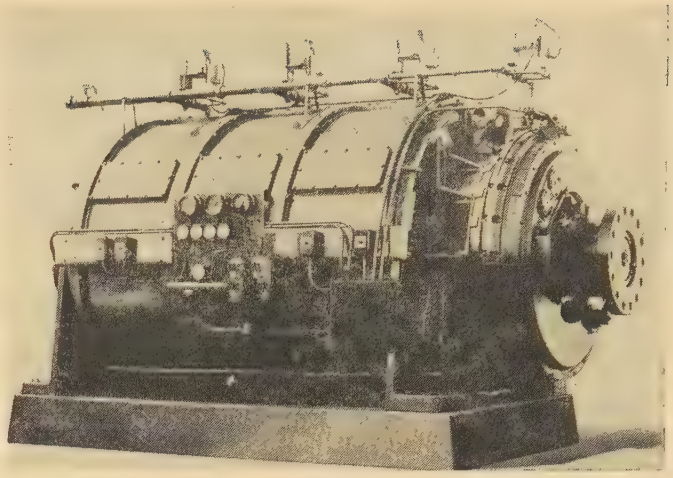

Figure 6 (right). A 12,000 horsepower speed-controlling magnetic clutch regulated by cushioned rectifier

Measurement

Commutation and cushioning occur so rapidly that they ordinarily escape detection. However, by proper cathode-ray oscilloscope technique they may be observed and measured readily. Anode-to-anode voltage properly attenuated is applied directly to the oscilloscope deflection plates. This voltage wave is viewed with an expanded sweep voltage that is a multiple of supply frequency. It is convenient to apply a synchronizing signal from a small capacitance connected to an anode. The scene thus obtained permits the time of current commutation and the rate of rise of the initial reverse voltage to be scaled off.

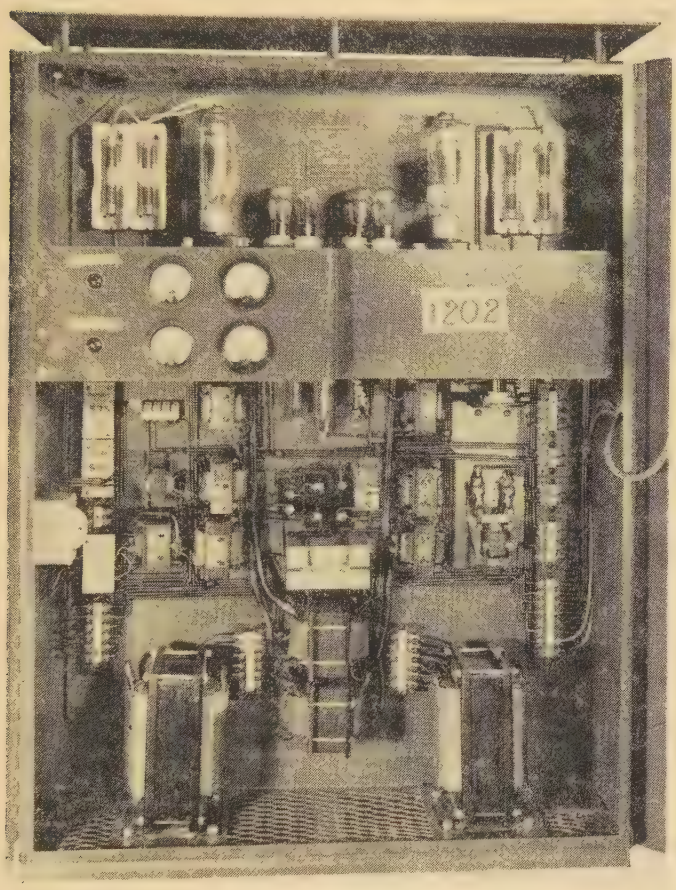

Figure 7 (left). Control rectifier unit for magnetic clutch

There are two sources of error that deserve mention. The signal attenuator must be noninductive and without capacitance errors. The stray capacitance within the oscilloscope between its power source and the oscilloscope ground lead must not be allowed to distort the reading.

Application

The following circuits apply initial inverse voltage if firing is throttled by grid action.

Cushioning is indicated to accommodate the maximum amount of throttling expected in service.

1. Full wave or polyphase rectifiers with inductive load.
2. Polyphase rectifiers with any load operating in continuous current region.
3. Parallel inverters.
4. Half wave control rectifiers with inductive load and back rectifier (only back rectifier requires cushioning).

The conclusions arrived at by life tests have been verified by a large number of actual installations ranging from small controlled rectifiers supplying motor and generator field excitation all the way up to the 12,000-horsepower adjustable speed magnetic clutch shown in Figure 6. Magnetizing power for such units is controlled precisely by a cushioned rectifier as shown in Figure 7. Cushioned control rectifiers have been used successfully over the past two years in many such applications which formerly were impractical.

Conclusions

Experiment indicates that there is a safe rate of rise of initial inverse voltage on gas-filled grid-controlled rectifiers above which gas cleanup may be expected and below which cleanup may be completely avoided.

Tests indicate that the safe rate of rise of initial inverse voltage is a function of the current commutation and of tube construction. This rate of rise may be controlled by proper cushion circuit design.

References

1. Vacuum Practice (book), L. Dunoyer. G. Bell and Sons, Ltd. (London, England), 1926.
2. Gaseous Conductors (book), J. D. Cobine. McGraw-Hill Book Company, Inc., New York N. Y., 1941.
3. New Trends in Mercury Arc Rectifier Developments, O. K. Marti. AIEE Transactions, volume 50, 1931, pages 73–9.
4. Phase Occurrence of Arc-Backs in High-Current Mercury-Arc Rectifier, W. E. Pakala, W. B. Batten. AIEE Transactions, volume 59, 1940, June section, pages 345–7.

Short-Time Current Ratings for Aircraft Wire and Cable

B. W. JONES
MEMBER AIEE

J. A. SCOTT
MEMBER AIEE

Synopsis: This paper gives the results of a series of tests on two sizes (AN-16 and AN-8) of insulated aircraft wires and cables, which were made to determine their permissible short-time current-carrying capacities. The times under consideration ranged from 0.01 to 1,000 seconds. A description is given of a very simple but adequate electrical test together with an accompanying insulation test to determine what are considered permissible transient temperatures. Tentative recommendations of short-time current-carrying capacity for aircraft cable sizes AN-22 to AN-00 are made.

WIRE SIZES for aircraft power supply and control circuits, selected on the basis of steady-state temperature rise may prove inadequate for other conditions of operation. Short circuits arising from gunfire or other causes must be anticipated and protected. A great many motors are used to drive the many devices and controls found on the modern plane.

If small wire sizes such as numbers 22 to 6 are used for supplying power to induction motors, d-c motors, and similar loads which may take six times rated current or more during the starting period, and if this branch line is protected by means of temperature overload relays, these branch lines should be capable of carrying six times motor current without exceeding a permissible temperature for a duration corresponding to the time required for the overload relay to trip. It has been recognized commonly that these smaller wire sizes generally will be deficient in their ability to carry this overload for the required period when the selection of the wire size is based entirely on its continuous rating. This deficiency generally is not present in the larger wire sizes.

The purpose of this paper is to supply needed data on aircraft wires to application engineers who sometimes have made the error of using too small a wire size on loads of this character because adequate information generally has not been available. It should also be pointed out that although these data were taken on wires which had insulation appropriate for 30-volt d-c aircraft application, some spot checks were made on a few sizes of wires insulated for 600-volt service and it was found that their short time ratings were quite close to those of the aircraft wires. The insulation on the aircraft wire is actually comparable to that on the 600-volt wire in spite of the lower voltage of the aircraft service. It is believed permissible to apply the present data on aircraft to industrial 600-volt insulated wires, or similar, until data are made available for each specific type of wire. Any difference that may be found between these two types of wires will be on the safe side.

Transient currents in excess of the normal continuous current ratings of the supply wiring and cabling of military aircraft electrical systems are caused by:

1. Starting currents of connected electrical devices when starting under normal conditions.

2. Starting currents of connected electrical devices during abnormal conditions, such as after a period of low temperature shut down during which bearing lubricating oils and greases have congealed or during which connected moving parts have iced or frozen.

3. Actual short circuits resulting from faulted conductors caused by sustained abrasion, vibration, or gunfire.

Circuit breakers or contactors controlled by temperature overload relays are the commonly used means to limit the duration of these currents to prevent the wire temperature from rising to values which would result in damage to the insulating covering of the wires.

The safe time duration depends on the following factors in addition to the current:

1. Initial wire temperature.

2. The heat storage capacity of the copper conductor itself.

3. The heat storage capacity of the wire insulation and its relation to that of the copper conductor.

4. The radiation characteristics of the wire covering.

5. The external air temperature, pressure, and the degree of cooling provided by convection and ventilating air currents.

6. The groupings of the wires in bundles or runs.

The steady-state continuous rating of the wire based on 100 degrees centigrade maximum insulation temperature is governed by radiation characteristics and external cooling factors. These are well established for sea-level conditions in still air, but further work is necessary to study altitude conditions and the special ventilation conditions that exist in a plane in flight. They will not be discussed further in this paper.

The short-circuit momentary-overload condition involves so short a time interval that its safe time duration is governed largely by the initial temperature of the wire and its heat storage capacity at the temperature which may be determined as safe for that time exposure. Values of safe times can be calculated. This paper will discuss these limitations only briefly. For the present, it is assumed that the maximum safe instantaneous copper temperature for all wire sizes is 150 degrees centigrade, for time intervals below one second. Fuse and circuit-breaker designers for many years have used so-called I^2t curves in providing overload protection to circuits. These curves are calculated on the assumption that all the energy is absorbed in heating the copper conductor. They include curves of temperature rise for various currents and times. Such a set of curves is shown on Figure 3. These curves are very satisfactory for periods of time below one second, which include most true short-circuit occurrences.

The problem, then, of selecting wire sizes resolves itself into

1. The selection of wire size for steady-state conditions generally is made on the basis of the continuous rated current capacity of the wire. These ratings are based on rules well established in the industry, though for aircraft use they are based on 100 degrees centigrade maximum operating temperature (70 degrees centigrade rise over 30 degrees centigrade ambient temperature) rather than more usual conservative values.

2. The selection of wire size for overloads of known or estimable duration below one second can be made on the basis of the previously mentioned I^2t curves. It is recommended that 150 degrees centigrade be the maximum allowable temperature to be attained by the copper.

It is recommended that the selection of wire sizes for overloads whose duration is between 1 second and 100 seconds be made on the basis of curves presented in this paper. These curves are given in Figure 4, and are derived from the present series

Paper 46-145, recommended by the AIEE committee on air transportation for presentation at the AIEE summer convention, Detroit, Mich., June 24–28, 1946. Manuscript submitted March 15, 1946; made available for printing May 15, 1946.

B. W. Jones and J. A. Scott are in the industrial control engineering department, general engineering laboratory, General Electric Company, Schenectady, N. Y.

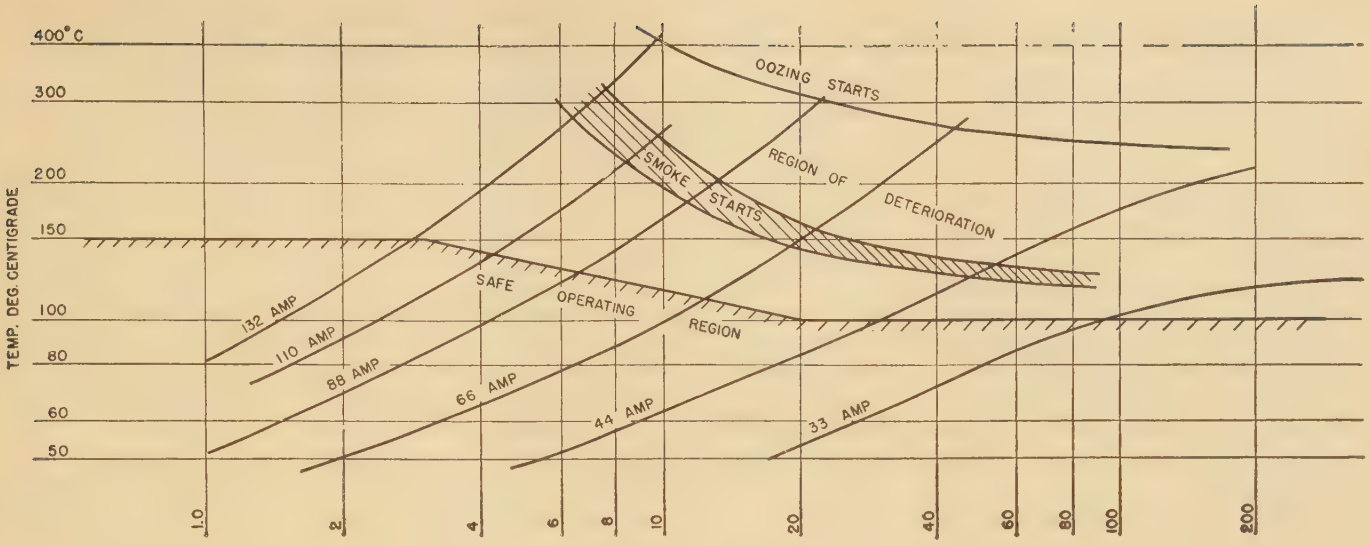

Figure 1. Current-time-temperature curves from 30 degrees centigrade ambient temperature for aircraft cable size AN-16

of tests conducted to study the damaging effects on the insulation of overload currents whose duration was between 0.1 second and several hundred seconds. The tests and the derivation of the curves are described in the following paragraphs.

Method of Test

There is no accepted standard method for determining the short-time current-rating of wires. Some engineers have measured temperature rise of wires by means of thermocouples embedded in the center of a wire or brazed to the copper strands. Others have used an oscillograph to obtain a simultaneous reading of current and voltage, while others have used the voltmeter-ammeter method. In this investigation the authors used all three methods and compared their results. Based on this work we will recommend a method which we found was the most practical and yet gave a sufficiently accurate result.

There are two important factors that must be accurately determined when making a test of this kind to ascertain the permissible short-time current-carrying capacities of various wire sizes.

The first is to be sure that the recorded temperatures are accurate, so that the insulation is actually subjected to contact with a wire of the recorded temperature. To illustrate, it was found that the thermocouples gave readings very appreciably lower than the actual wire temperatures as determined by resistance methods. Thermocouples are not suitable for determining temperatures of rapidly heated wires (there are also other limitations for the use of thermocouples).

The second factor is to judge correctly the degree of damage to the insulation that resulted from the above temperature and times. There are standardized methods for measuring the dielectric breakdown and also the cold bend test, but with these having been made there still remains a fair degree of judgment that must be used which should be seasoned with a fair degree of background on this subject. Figures 6A, B, and C, show what is to be expected of such tests. However, as it was found actually that the evolution of smoke was observed even before actual deterioration occurred, and since smoking cannot be tolerated in air-

Figure 2. Current-time-temperature curves from 30 degrees centigrade ambient temperature for aircraft cables size AN-8

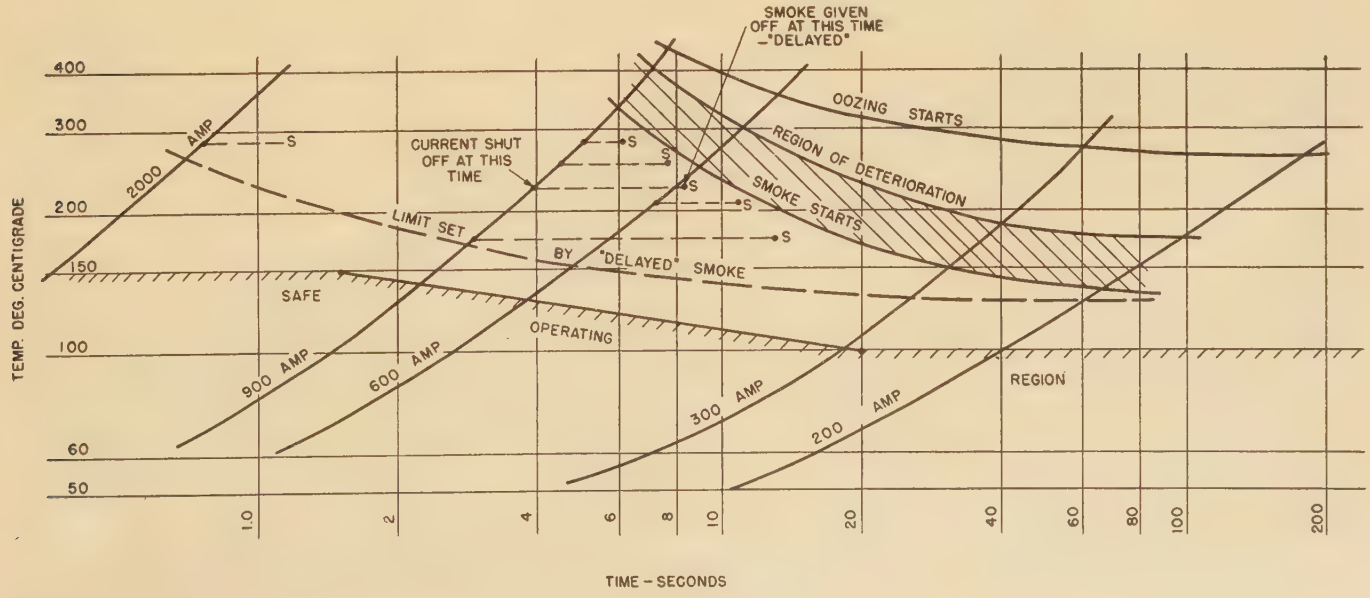

planes, its occurrence became the only necessary observation.

A 25-foot length of the wire to be tested was cut and its cold resistance was measured accurately by means of a Kelvin doublebridge in the same ambient temperature where the test was made. A ten-foot central section of this wire was measured accurately for length and marked. This wire then was mounted horizontally about five feet above the test floor and its ends connected to the power supply cables. In order to check the effect of thermoplastic flow of the insulation during the heating, a one-pound weight was suspended from the wire by a hook of one-inch radius made of 1/8-inch diameter steel wire. This weight was located three feet from one end of the wire as indicated in Figure 5. Two steel needles were forced through the insulation and the stranded wire at the two points which marked the ten-foot length. To each of these steel needles was soldered a six-inch length of ten-mil diameter nichrome wire, and this in turn, was soldered to the necessary length of copper wire which ran to the voltmeter terminal. The purpose of the nichrome wire was to minimize the amount of heat that was conducted from the test wire into the voltmeter leads. The circuit arrangement was that shown in Figure 5.

A field controlled d-c generator was the source of power. Current was applied by closing a contactor at the zero time and held constant until the voltage on the voltmeter reached a previously calculated value, corresponding to the temperature to which it was desired to heat the wire. The cold resistance of the 10-foot span was assumed to be 40 per cent of the 25-foot span which had previously been measured by the Kelvin double bridge. The ammeter and voltmeter could be read quite accurately, and the interval of time between the start and the stop also could be timed easily and accurately by stopwatch. Oscillograph records were taken simultaneously of the current, voltage, and time. These provided very accurate measure of all quantities and were in close agreement with the voltmeter-ammeter values. Therefore, since the voltmeter-ammeter method is the simpler, this should be the preferred method, except for time intervals below five seconds where the oscillograph must be used.

Samples of aircraft cable sizes AN-16 and AN-8 were subjected to a number of current values, and at each of these different values of current, wires were allowed to rise to several predetermined values of temperatures so that we could determine the value that should not be exceeded. The rate of temperature rise varied over wide limits.

The samples that were allowed to exceed the safe temperatures to a small degree, gave evidence of this by smoking, and other samples that appreciably exceeded this safe temperature demonstrated this by the sudden oozing of the compound out through the insulation surface. The time at which smoking started was observed, and similarly, when the test was continuing until oozing occurred, this time was recorded.

Current-time-temperature curves obtained as a result of these tests were plotted for both sizes of wire, see Figure 1 (size AN-16) and Figure 2 (size AN-8). These curves show temperatures plotted against time for all of the current values tested. The times at which smoke occurred for each current value are shown by the shaded area. The time at which oozing occurred is shown by the wave labeled oozing starts. In the case of the larger wire AN-8, it was observed during the tests that smoking for some values of current occurred after the current had been shut off. This is due to the great relative heat storage capacity in the larger conductor compared to that of its insulation. The smaller wire gives up its heat to its insulation with a rapid drop in temperature. This delayed smoke is shown on Figure 2 and indicated by the notes calling

Figure 3. Time–current curves of one circular mil of annealed copper

Calculated on these assumptions:

1. Radiation neglected
2. Resistance of one centimeter cube of copper at 0 degrees centigrade = 1.589 microhms
3. Temperature coefficient of copper at 0 degrees centigrade = 1/234

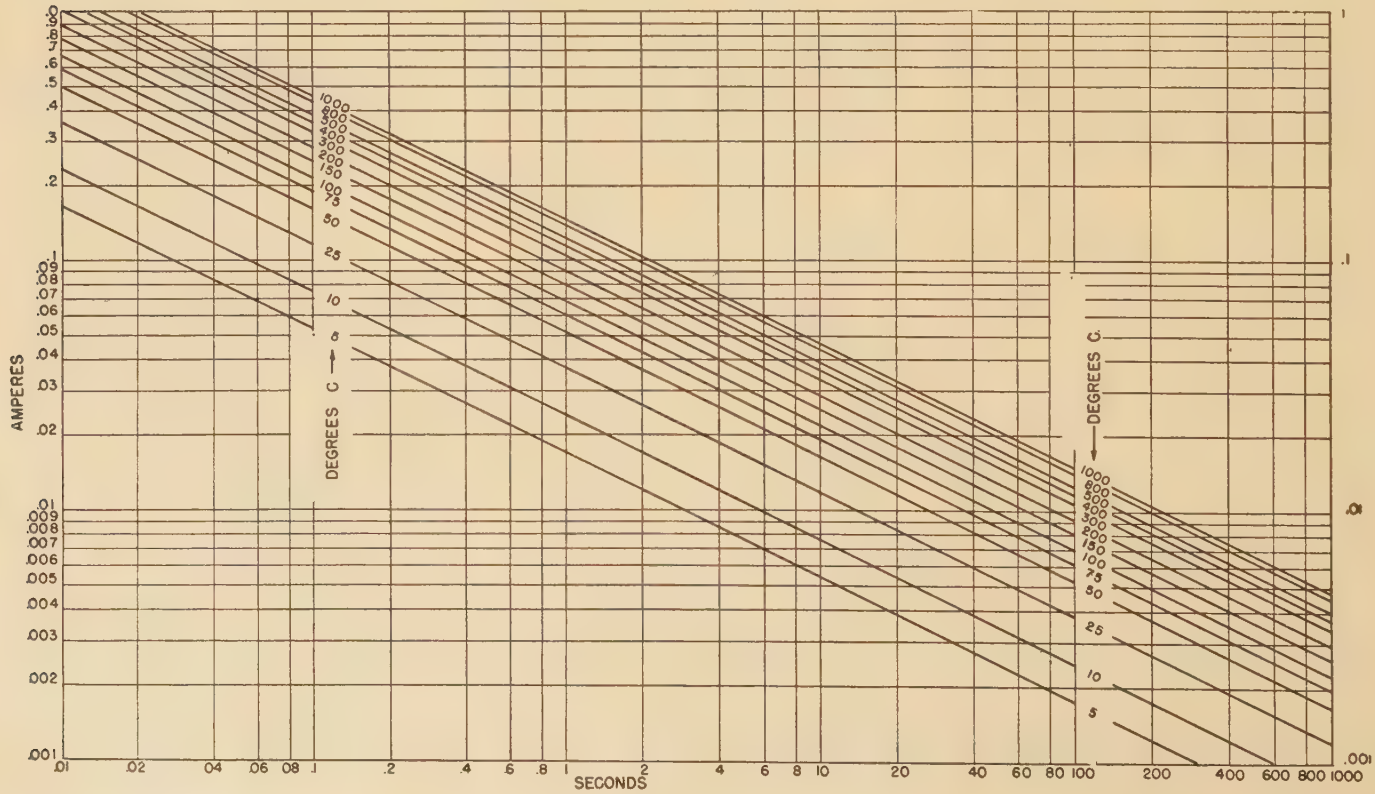

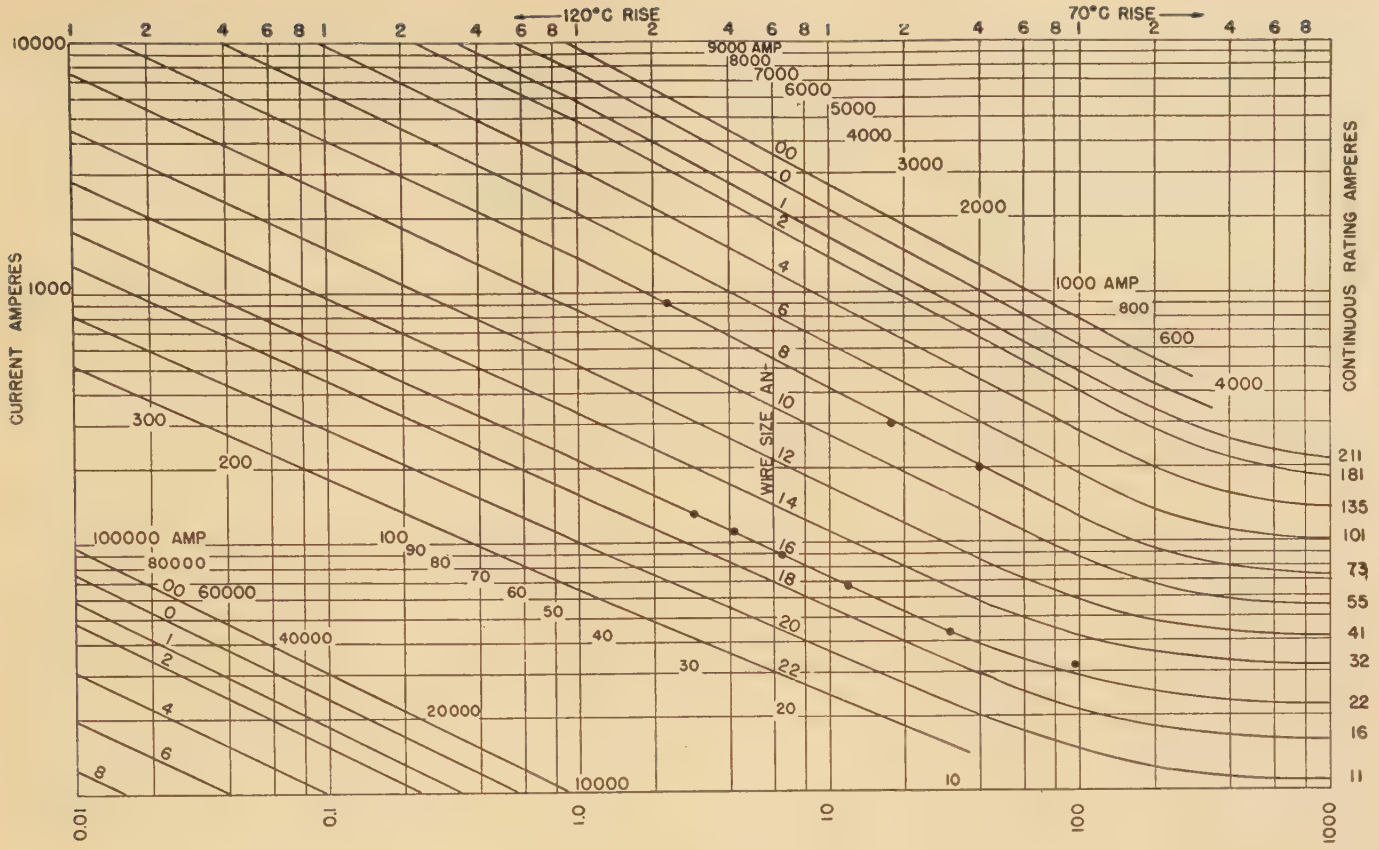

Figure 4. Suggested current–time ratings for aircraft cable AN-J-C-48a for 30 degrees centigrade ambient temperature

attention to this phenomenon. The safe operating region shown on Figures 1 and 2 is drawn at what is considered a sufficiently safe margin below the temperature time limitations imposed by smoke to represent safe operation.

After the test exposure described earlier, each sample of wire was tested for insulation condition as follows:

1. The end sections which supported the one pound weight were tested for dielectric breakdown in accordance with Army-Navy specification, AN-J-C-48a paragraph F-4b(5), entitled, Dielectric Breakdown.

2. One half of the ten foot test section was tested in accordance with Army-Navy specification, AN-J-C-48a paragraph F-4b(6), entitled, Cold Bend Test.

3. The other half of the ten foot test section was tested in accordance with Army-Navy specification, AN-J-C-48a paragraph F-4b(4)c, entitled, Water Immersion Test.

The results of these dielectric breakdown tests are presented graphically in Figures 6A, B, and C, respectively.

It should be noted that a reasonably large number of tests were made because we were endeavoring to find the short time permissible temperatures. But if the temperatures that are recommended here are accepted, any future tests can be simplified very greatly by merely finding the time required for any selected current to produce the maximum temperature shown in Figures 1 and 2.

Recommended Test Procedure

Establish by trial a current which will produce the allowable temperature rise (usually 70 degrees centigrade) in approximately 20 seconds (between 10 and 40 seconds) and determine by test the exact time required. On a sheet similar to Figure 4, locate this one point of time and current. Then from Figure 3 calculate the current required to heat (on a no-loss basis) the wire size in question to a value equal to 150 degrees centigrade minus the assumed ambient temperature in 0.01 second. This will give another point on the afore-mentioned sheet. Then draw a straight line between these two points and that will be the permissible short-time current-carrying ability of that wire size. By testing in this simple manner about four or five sizes of wire, for any one type of wire the whole range of ratings can be drawn in by proportioning the intermediate sizes in proportion to their respective cross sections.

Beyond the 100-second region this straight line can be extended so as to become asymptotic to the current line, corresponding to the continuous rating of this wire, which usually is available for the assumed ambient temperature.

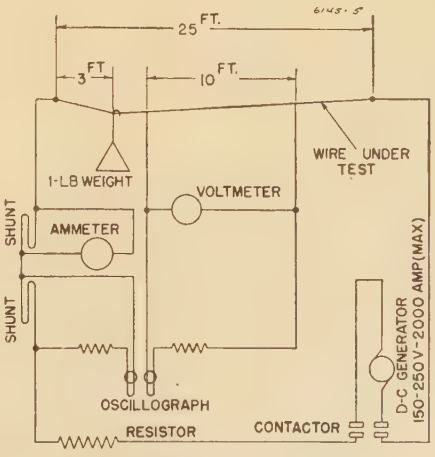

Figure 5. Test circuit for current-time-temperature rise test on aircraft cables

Discussion of Results

The smoke criterion of damage occurred before any other evidence of deterioration. On the larger wire, size AN-8, smoke often was delayed considerably after the current had been removed. This is indicated by the delayed smoke limit curve, Figure 2. This is evidence of the large energy storage in the conductor during the short circuit, and the low heat capacity and heat transfer constant of the insulation compared to that of the large conductor.

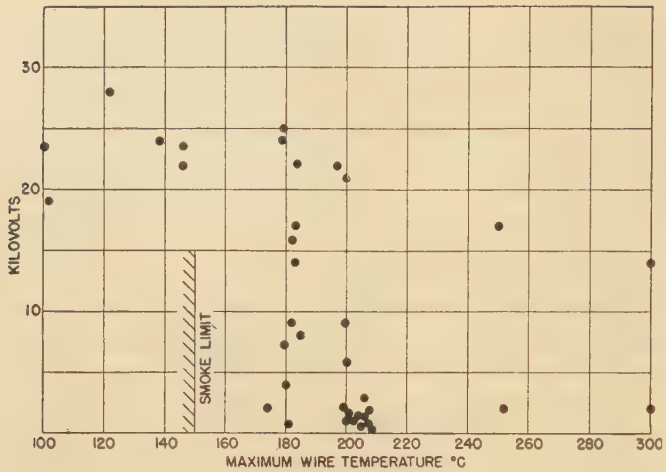

Figure 6A. Kilovolts breakdown in water at 25 degrees centigrade of samples containing point of attachment of one pound weight, one 1/8-inch diameter wire hook, AN-J-C-48a paragraph F-4b(5)

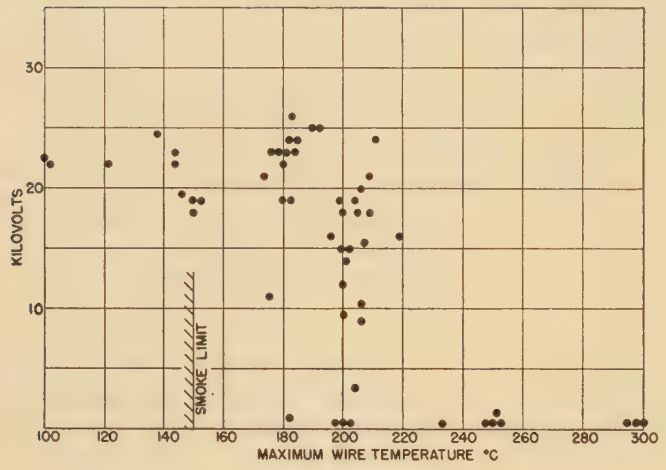

Figure 6B. Cold bend test kilovolts breakdown of samples in water after one hour at 40 degrees centigrade, AN-J-C-48a paragraph F-4b(6)

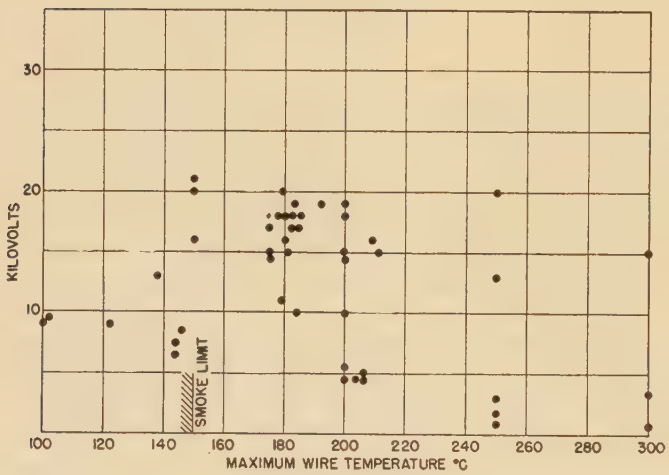

Figure 6C. Kilovolts breakdown in water at 50 degrees centigrade after immersion in water for 20 hours at 50 degrees centigrade AN-J-C-48a paragraph F-4b(4)c

The dielectric breakdown values given in Figures 6A, B, and C, gave evidence of deterioration only when the insulation had been carried to a considerably higher temperature than that at which smoke first appeared. Dielectric breakdown results vary over a large range, but do indicate definite deterioration when the wire has been exposed to temperatures of 200 degrees centigrade for the short time intervals covered by these tests.

The appearance of smoke, then, is the first indication of abnormal conditions, and if current is not removed immediately a condition of serious damage soon will result. It is also a condition which cannot be tolerated for psychological reasons in airplanes. The instinctive association of smoke with impending or possible fire is so strong, and the hazard of fire so great in an airplane, that we have adopted the slightest appearance of smoke as the limiting condition of current and time below which we must operate.

On each of Figures 1 and 2 is shown a so-called safe operation region which has been arbitrarily bounded as follows:

Wire, Size	Time, Seconds	Maximum Temperature, Deg C
AN-8	0–1.5	150
AN-8	Over 20	100
AN-8	1.5–20	From sloping line connecting these temperatures
AN-16	0–2.5	150
AN-16	Over 20	100
AN-16	2.5–20	From sloping line connecting these temperatures

Using this boundary of the safe operating region, values of times for the various test currents were obtained for these two wire sizes, in the time range 1 to 100 seconds. These are plotted on Figure 4. To extend these curves to the left to lower times, values of current to produce 150 degrees centigrade at the end of 0.01 second were obtained from Figure 3, namely, 12,300 amperes and 1,700 amperes for sizes AN-8 and AN-16, respectively. These points were plotted and connected by straight lines to the curves already drawn between 1 and 100 seconds.

To extend the curves to the right for times greater than 100 seconds, the curves were connected by smooth arcs to the steady-state values, 73 amperes and 22 amperes, respectively, which were obtained from the steady-state ratings given by the AIEE committee on aircraft wire and cable.

Curves for other wire sizes between 16 and 8 were interpolated on the basis of the theoretical spacing. Similar extrapolation was made to wire sizes 20 and 00. These curves are tentative only and subject to verification by further tests.

Conclusion and Recommendations

Current-time-temperature tests on wires, carried to the point at which smoke first appears, provide a suitable method of determining the short-time current-carrying characteristics of wires. The temperature-time measurements must be made carefully and accurately. Wire temperature should be determined by copper resistance, using a voltmeter-ammeter method for times down to five seconds and using an oscillograph method for shorter times. Thermocouple measurements are not recommended.

The suggested current time ratings for aircraft cable AN-J-C-48a presented in Figure 4 based on a 30 degrees centigrade ambient temperature is recommended for consideration.

Low-Current-Secondary Current Transformers

AN AIEE COMMITTEE REPORT

APPLICATION REQUIREMENTS for current transformers sometimes indicate the use of secondary currents lower than the generally accepted standard 5-ampere rating. Very little published information is available on this subject, other than a description of a few specific installations where such transformers have been applied. The natural question arises as to the advantages and disadvantages resulting from the use of current transformers with secondary ratings below five amperes, and under what circumstances their use should be considered. Because many of the applications of low-current secondaries involved relay protection, the AIEE relay subcommittee appointed a working group in October 1943 to study the problem, and from that study, gives recommended practice for their use.

Applications

The principal application of low-current-secondary current transformers is in those installations involving long runs of secondary leads where the resistance of the leads (utilizing normal size copper conductors) becomes very high, thus imposing on the current transformer excessive lead burden in comparison to the useful burden. A brief summary of the problems to be considered for such installations is covered in this paper.

Another application of current transformers using secondary ratings of other than five amperes, occurs in those installations requiring the paralleling of the secondaries of transformers subject to widely different normal primary load currents. In such cases, the secondary rating is primarily one of convenience and economy. The secondary circuit constants, transformer turn ratios and performance, usually are fixed on a 5-ampere secondary basis. This is dictated by transformers in some of the circuits involved having the standard 5-ampere secondary rating.

Comparison of Solutions

The use of current transformers with secondary ratings below five amperes for the above applications has certain advantages and disadvantages which must be carefully considered in evaluating the gains resulting in the reduction of effective burden of the secondary leads. Any general comparison of these advantages and disadvantages should be made on the common basis of equal volt-ampere energy requirements for the relays, instruments, and meters, irrespective of the secondary rating. Changing the current rating of these devices in no way reduces the energy required for their operation. A reduction in energy is just as desirable on the basis of five amperes as on a lower current rating basis, and minimum operating energy is a controlling factor in the design of this type of equipment.

On the basis of constant volt-ampere energy requirements, a reduction in secondary current rating results in a corresponding increase in secondary voltage rating. The energy consumption in the external devices and the internal losses in the transformer are not materially affected, thus, the only gain is the reduction in energy consumed by the secondary leads between the transformer and external burden.

As an example, if it is assumed that the distance between the current transformer and the instruments or relays is 500 feet, and standard control cable such as one consisting of conductors each having 19 strands of number 22 wire is used, the burden imposed on the transformer by each secondary lead is 11 watts at 5 amperes. Under the same conditions, with a one-ampere secondary, the lead burden would be 1/25 or 0.44 watt per lead at rated current. Thus, in some cases, smaller wire could be used with a resulting saving of copper. Such savings may be limited, however, by the necessity of retaining a larger wire size to obtain mechanical strength. Unless the lead burden is a fair portion of the total burden, this reduction in lead burden materially does not lessen the performance requirements of the current transformer.

In evaluating the benefits gained by the reduction in effective secondary lead burden, consideration must also be given to the effects on the insulation requirements of the secondary circuit, and the availability of standard devices suitable for use on the lower current rating basis.

With low-current secondary currents and the corresponding increase in secondary voltage (assuming equal energy requirements), due consideration must be given to the required increase in secondary voltage. For instance, the present "American Standards for Instrument Transformers" recognize a maximum relaying accuracy classification of 800 volts on the secondary terminals at 100 amperes (20 times rated) secondary current, based on five amperes. On a one-ampere basis, the secondary terminal voltage would be 4,000 volts, and the secondary insulation should be well in excess of this value for safe operation. Furthermore, the present open-circuit voltages on switchboard transformers commonly run from 500 to 5,000 volts crest. The logical basis for consideration of a one-ampere-secondary, therefore, is that the open-circuit voltages will be five times as great, or from 2,500 to 25,000 volts crest. It is apparent that the standard one-minute potential test of 2,500 volts to ground for the secondaries of current transformers should be increased to 12,500 volts for one-ampere secondary ratings. Similarly, relays and instruments used with one-ampere secondary transformers should have the one-minute potential test of 1,500 volts to ground increased to 7,500 volts.

The above requirements for insulation are based on general applications. However, for those applications requiring the use of low-current-secondary current transformers to minimize lead burden, and which will be subjected to considerably less than 20 times normal current, a suitable transformer could be made with an insulation level to meet the actual secondary voltage requirements.

While it is quite true that the secondary voltages existing at normal currents are low, the high voltages occurring on high values of overcurrents and on open circuits sometimes are overlooked. In cases

Paper 46-168, recommended by the AIEE committee on protective devices for presentation at the AIEE summer convention, Detroit, Mich., June 24–28, 1946. Manuscript submitted April 23, 1946; made available for printing May 29, 1946.

This report was prepared by a working group of the relay subcommittee, AIEE committee on protective devices, consisting of S. C. LEYLAND (M '43, *sponsor*), manager, relay section, meter engineering department, Westinghouse Electric Corporation, Newark, N. J.; F. C. POAGE (M '38, *former sponsor*), electrical engineer, engineering department, Ebasco Services, Inc., New York, N. Y.; R. E. NEIDIG (A '38), relay engineer, Metropolitan Edison Company, Reading, Pa.; L. F. KENNEDY (M '39), relay application engineer, General Electric Company, Schenectady, N. Y.; E. C. SCHURCH, (M '35), senior engineer, electrical department, United States Bureau of Reclamation, Denver, Colo.

where only meters or instruments are involved, secondary overvoltage protection may be applied without too much complication. This is particularly true where such protective devices can be permitted to short-circuit the transformer on excessive overvoltage. However, overvoltage protective devices which short-circuit the transformer secondary cannot be used where protective relays are involved, because incorrect relay operation would result. For the foregoing reasons, it is sometimes feasible when considering less than 5-ampere secondary ratings to go to a lower secondary current rating when only meters and instruments are used. When protective relays are used, the problem requires considerable more study.

When considering the use of low secondary current ratings, attention must be given to the use of relays having suitable current ratings. The present complete line of relays (some available with low current taps) was developed to cover the requirements of the field on the basis of the standard 5-ampere secondary transformer ratings. Therefore, their equivalent on a 1-ampere basis does not exist. While a limited number of relays have coils suitable for certain low-current rating applications, to obtain a complete line of such devices with suitably co-ordinated taps and insulation levels would require major development.

In the applications where there is a definite need for a lower secondary current resulting from excessive length of secondary leads, it is desirable to retain standard 5-ampere rating relays and instruments. This may be accomplished by using standard 5-ampere rating main transformers, relays, and instruments with auxiliary current transformers at the main current transformers and the switchboard. It also is possible to use main current transformers with low current secondary rating in conjunction with auxiliary transformers at the switchboard only. It must be remembered, however, that auxiliary current transformers introduce additional burden which tends to offset the gain resulting from reduction in secondary lead burden, and at the same time, lower the accuracy of the over-all transformation because of their own errors. The performance characteristics of the auxiliary current transformers must be as good as those required of the main current transformers, and they should be provided with sufficient insulation to protect the instruments and relays from the higher secondary voltages accompanying the lower currents. Where auxiliary transformers are used, the switchboard circuits should be protected from excessive voltage by the use of suitable short-circuiting devices. Proper consideration must be given to the performance of the auxiliary transformers on a d-c transient having a long time-constant. Auxiliary current transformers fulfilling these requirements increase the cost, require installation space, and reduce the net gain.

Conclusions

In view of the many disadvantages of low current secondaries, compared to the advantage of reduced secondary lead burden or saving in copper, they should not be considered except in special cases. These special cases occur where the secondary lead burden is the major portion of the total burden and definitely causes errors that cannot be tolerated. Then the problem should be studied thoroughly in the light of the foregoing factors. The secondary current rating selected and the secondary circuit arrangements used should be determined as best meets the requirements of the individual application.

The working group feels that the problem of low-current-secondary current transformers is so special that no consideration should be given to standardization at this time.

A Unique Engine-Synchronism Indicator for Aircraft

D. B. PEARSON
ASSOCIATE AIEE

RECENT aircraft design has emphasized multiengine airplanes, especially for commercial transports and military types. Two- and 4-engine planes are commonplace and 6-engine craft are proposed for the near future. Engine synchronism indication, usually between a master engine and each of the others, becomes more important as the number of engines on the airplane increases. It is possible to synchronize two engines by ear, but this method becomes exceedingly difficult for aircraft with more than two engines.

The synchronism indicator, or synchroscope, has been developed to obtain a visual indication of the degree of synchronism that exists between the master and each of the other engines. A discussion of the needs for engine synchronism indication and of the means by which it is obtained, will be presented.

Reasons for Synchroscopes

Perfectly synchronized airplane engines are desirable for several reasons. Better flight efficiency[1] is obtained when the engines are running at the same speed. Planes with constant pitch propellers tend to yaw if the engines are not synchronized exactly. If a condition of near-synchronism exists, such as occurs when synchronizing is attempted with the tachometer indicators alone, a vibration of low frequency is produced. This beat frequency is the arithmetical difference between the high frequency vibrations produced by each engine. Its presence causes high stresses[2] to be set up in the airplane structure which can cause severe damage to the airplane. Fatigue and discomfort for the passengers and crew of the aircraft also are caused by the presence of these vibrations. For example, the Air Forces have found it very desirable to use synchroscopes on transport planes to avoid these harmful vibrations

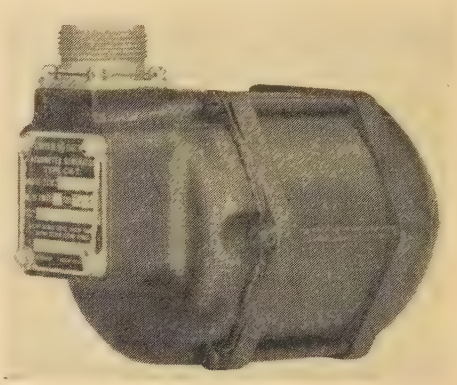

Figure 1. Tachometer generator

Paper 46-148, recommended by the AIEE committee on air transportation for presentation at the AIEE summer convention, Detroit, Mich., June 24–28, 1946. Manuscript submitted April 11, 1946; made available for printing May 15, 1946.

D. B. PEARSON is a development engineer in the aeronautical instrument engineering division, General Electric Company, West Lynn, Mass.

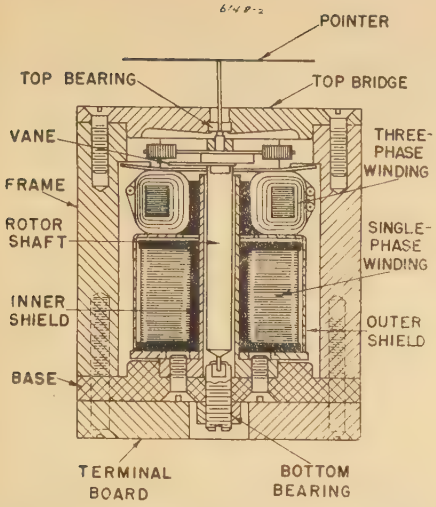

Figure 2. Cross-section view of synchroscope

when carrying sick and wounded personnel.

To promote commercial flying to the greatest degree, passenger comfort is of paramount importance, especially on sleeper-type planes. The synchroscope has been found to be a simple and satisfactory instrument for adjusting engine speeds to obtain efficient flight operation, minimized stresses on the aircraft structure, and to provide a high degree of comfort for the passengers.

Equipment Needed to Indicate Synchronism

No additional source of power or transmitting device is necessary to obtain engine-synchronism indication. Electric tachometer generators[3,4] already installed to operate the tachometer indicators will supply sufficient additional power to operate the synchroscopes. The only additional weight necessary is that of the indicators themselves and the connecting leads.

The most satisfactory tachometer generator has an a-c output with a frequency proportional to engine speed. A typical generator of this kind is illustrated in Figure 1. It is customary to use a reduction gear with a ratio of two to one to drive the generator. Its 4-pole rotor is made of a permanent magnet material such as alnico II. This magnet, as it rotates, induces in the 3-phase winding on the generator stator, a 3-phase a-c voltage having a frequency proportional to the engine speed.

To obtain an indication of the degree of synchronism between two engines, a measurement is made of the frequency difference between the outputs of the generators connected to each engine. To perform this function, the synchroscope uses two stator windings and a rotor. Figure 2 illustrates the mechanical construction of the instrument, while Figure 3 shows the electric circuit. One coil is a 3-phase winding, placed in the form of a toroid on a circular core of high permeability material, such as mu-metal. This winding usually is connected to the generator on the reference, or master engine, which is customarily the one at the extreme left.

Below the 3-phase coil is a single-phase circular stator coil, wound with its axis at

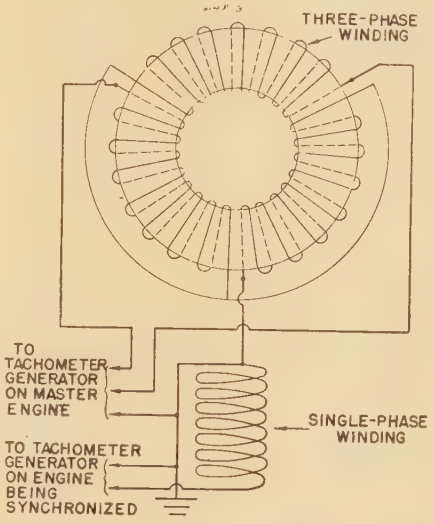

Figure 3. Electric circuit diagram of synchroscope

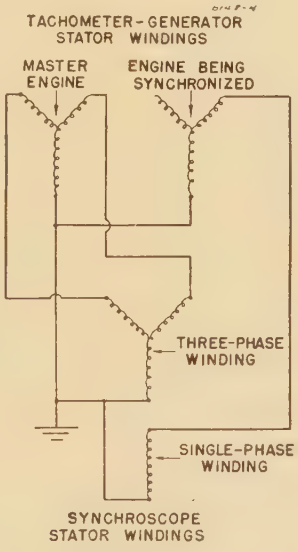

Figure 4. Wiring diagram for synchroscope and tachometer generators

right angles to the plane of the 3-phase winding. This coil is connected to one of the phases of the tachometer generator driven by the engine whose speed is being compared to the master engine.

A rotatable shaft and vane assembly of high permeability material, and supported by suitable bearings, is placed in the instrument so that it can be acted upon by the magnetic fields produced by the two stator windings. A pointer on the shaft gives visual indication of the condition of synchronism that exists between the two engines in question. This construction, embodying two stator coils and a soft-iron rotor, is similar somewhat to that used in switchboard type synchroscopes.[5]

Principle of Operation

When the master engine is running with the synchronism indicator connected as in Figure 4, a rotating magnetic field is produced by the 3-phase winding. This field rotates at the same speed as the engine because the 4-pole tachometer-generator rotor is driven at one-half engine speed. When the engine connected to the single-phase coil is running, there is produced in this winding a magnetic field that alternates at a rate equal to the speed of the connected engine.

As shown in Figure 5, the flux from the single-phase winding crosses the air gap to the shaft and then travels to the vane. After leaving the vane, it passes through the 3-phase core and links with the field from the 3-phase winding. The flux then flows through a washer and a shield of high-permeability material to a second washer at the bottom of the single-phase coil. From the bottom washer the single-phase flux passes to the inner shield, or sleeve, which surrounds the shaft, and then crosses the air gap to the shaft, completing the circuit. All air gaps in this circuit are kept as short as possible to hold the reluctance to a minimum.

When the single-phase winding is energized, its flux, alternating at a frequency proportional to the speed of the engine to

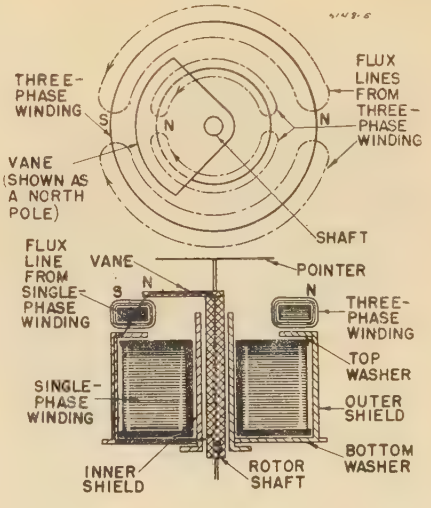

Figure 5. Magnetic circuit diagram of synchroscope

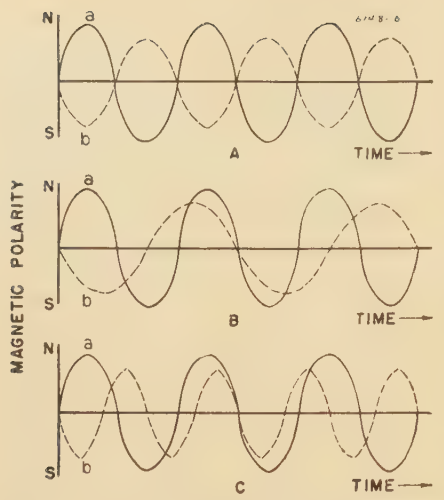

Figure 6. Flux relationships in synchroscope

A—Engines synchronized
B—Second engine running slower than master engine
C—Second engine running faster than master engine
a—Magnetic polarity of a point on the upper surface of the 3-phase winding
b—Magnetic polarity of the rotor vane

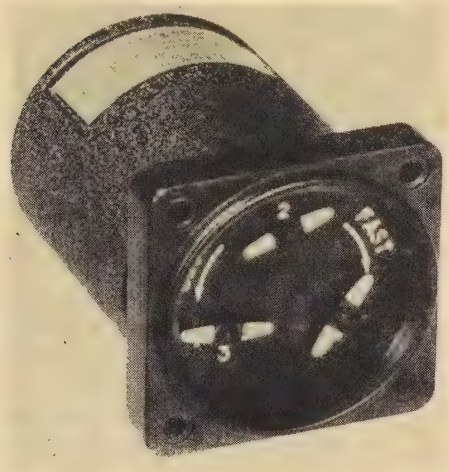

Figure 7. Three synchroscope mechanisms in a 17/8-inch diameter case

Figure 8. Five synchroscope mechanisms in a 23/4-inch diameter case

which it is connected, causes the magnetic polarity of the rotor vane to reverse at the same rate. With the field of the 3-phase winding rotating at a rate proportional to the master engine speed, the rotor assumes a position such that when the vane is a north pole, a south pole from the 3-phase field is at the same point. Figure 6*A* shows the flux relationship in the synchroscope when synchronism exists between the two engines. If the flux in the shaft-and-vane assembly alternates at the same rate as the 3-phase field rotates, the synchroscope rotor will remain stationary, as the fluxes from the two fields produce no rotational forces in the rotor vane. As the vane changes from a north to a south pole, the field from the 3-phase winding rotates 180 degrees from its previous position, so that its south pole is replaced by a north pole.

Figure 6*B* illustrates the flux relationship that exists in the instrument when the engine being synchronized is running slower than the master engine. Under these conditions, the rotating field will have moved more than 180 degrees by the time the vane polarity has changed from maximum north to maximum south. The vane-and-rotor assembly will rotate counterclockwise at a speed sufficiently great to make up the difference in frequency between the two fluxes. This enables the two fields to remain locked together. The torque which causes the rotation is obtained from the forces of attraction and repulsion produced by the two fields acting on the rotor vane.

Figure 6*C* shows the relative position of the two fields that exists in the synchroscope when the second engine is running faster than the master engine. The frequency of the single-phase flux is higher than the frequency of the 3-phase flux, and the rotating field will have moved less than 180 degrees when the vane polarity has changed from maximum north to maximum south. The rotor will turn clockwise at a speed great enough to make up for the difference in frequency between the two fluxes.

For the typical arrangement of 4-pole rotors in generators driven at one-half engine speed, the synchroscope rotor will turn at a speed equal to the difference between the speeds of the two engines. For other arrangements, the synchroscope rotor will turn at a speed proportional to the difference between the speeds of the two engines. The pointer at the end of the rotor shaft, therefore, gives a visual indication of the condition of synchronism that exists between the two engines in question. To synchronize an engine with the master engine, all the pilot need do is to note whether it is running too fast or too slow, as indicated by the direction of rotation of the synchroscope pointer and the markings on the instrument dial, and adjust its speed accordingly until the indicator pointer becomes stationary.

Design Features

Panel space is at a high premium in present day aircraft, and it is very desirable and necessary to reduce the amount of panel space occupied by any instrument. For the synchroscope this has been accomplished by an unusually compact instrument-mechanism design. Figure 7 shows three synchroscope mechanisms in a $1^7/_8$-inch diameter case to provide synchronism indication for 4-engine planes. Figure 8 illustrates five synchroscope mechanisms in a $2^3/_4$-inch diameter case for 6-engine aircraft. If desired, a single mechanism can be used with a selector switch in any multiengine airplane, or it may be incorporated in a dual tachometer indicator.

Figure 9. Disassembled view of synchroscope mechanism showing top of 3-phase winding, top bridge, and rotor assembly

Simplicity of construction and mechanical sturdiness are desirable features for aircraft instruments. These features are illustrated by Figure 9 which shows a disassembled synchroscope mechanism. Placing both windings on the stator, thus eliminating brushes and all other connections to the rotor, permits the synchroscope to be built strongly and yet simply enough to allow easy disassembly. Less than five minutes are required, using only a small screwdriver, to take apart and reassemble the complete mechanism.

Operating Characteristics

Two primary operating characteristics determine how satisfactory a synchroscope is for aircraft applications.[6] First, the rotor should begin to turn when the differential speed between the two engines being synchronized is 150 rpm or more over an engine speed range of 1,400 to 4,500 rpm. It should continue to rotate

until this differential speed has been reduced to zero. Second, when the rotor is turning, it should rotate smoothly, especially when the differential speed is 5 rpm or less.

Smooth operation is dependent on two characteristics of the synchroscope. The natural period of oscillation of the system, made up of the rotor mass and the magnetic coupling between the vane and the rotating 3-phase field, must be above the maximum speed at which the instrument is to operate. The strength of the 3-phase field must be uniform around the periphery of the 3-phase winding. If these conditions do not exist, erratic operation of the rotor assembly will occur. By keeping the moment of inertia of the rotating system as low as possible, and by using a toroidal construction for the 3-phase core and coil assembly as previously described, smooth operation is obtained.

Figure 10 shows typical starting characteristics of a synchroscope built according to the design previously discussed. Small magnetic irregularities in the instrument add to the starting torque in one direction and subtract from it in the opposite direction. For this reason, the starting characteristics vary slightly, depending on the direction in which the rotor is turning.

Figure 10. Starting characteristics of synchroscope at room temperature

A—Rotor turning clockwise
B—Rotor turning counterclockwise
C—Average of *A* and *B*

Figure 11 shows the starting characteristics of the synchroscope at high and low ambient temperature. The torque exerted on the rotor vane is an inverse function of the temperature of the synchroscope windings, as the resistance of the coils is a direct function of their temperature.

To keep the windings at a safe operating temperature, and to prevent fogging of the instrument cover glass, the temperature rise in the instrument must be considered. Table I shows these data obtained on a typical synchroscope sample.

Table I

Time, Hours	Room Temp, C	Max Safe Temp Rise, C	Temperature Rise, C			
			Single Phase Coil	Three Phase Coils		
				AB	BC	AC
0	25		0	0	0	0
1.5	26	40	23	22	25	18

Experience obtained from other instruments indicates that satisfactory service will be obtained at these operating temperatures.

Application Other Than Aircraft

While it has been shown that the synchroscope has a definite aircraft application, its usefulness does not end there. A synchronism indicator such as has been discussed can be used for many other applications where it is necessary to indicate or control the difference in the speeds of two engines.

If 3-phase power is not available, a conventional split-phase[5] design such as is used with some types of single-phase motors can be utilized to operate the synchroscope.

The instrument also can be used as a power-factor or phase-angle indicator when one winding is excited by a voltage in phase with the supply voltage, and the other winding by a voltage in phase with the load current. The position taken by the pointer will be a function of the phase angle between the voltage and current.

Conclusions

Visual synchronism indication has been shown to contribute appreciably to the satisfactory operation of multiengine aircraft. Improved passenger and crew comfort, lessened vibrational stresses in the aircraft itself, and better flight efficiency are among these contributions.

Characteristics of the synchroscope are simplicity of construction, ease of maintenance, small size, and low weight. These features, coupled with the desirable operating characteristics described previously, make the synchroscope a useful addition to the instrument panels of multiengine airplanes.

Figure 11. Starting characteristics of synchroscope at high and low ambient temperatures

A—Synchroscope at −55 degrees centigrade
B—Synchroscope at +25 degrees centigrade
C—Synchroscope at +71 degrees centigrade

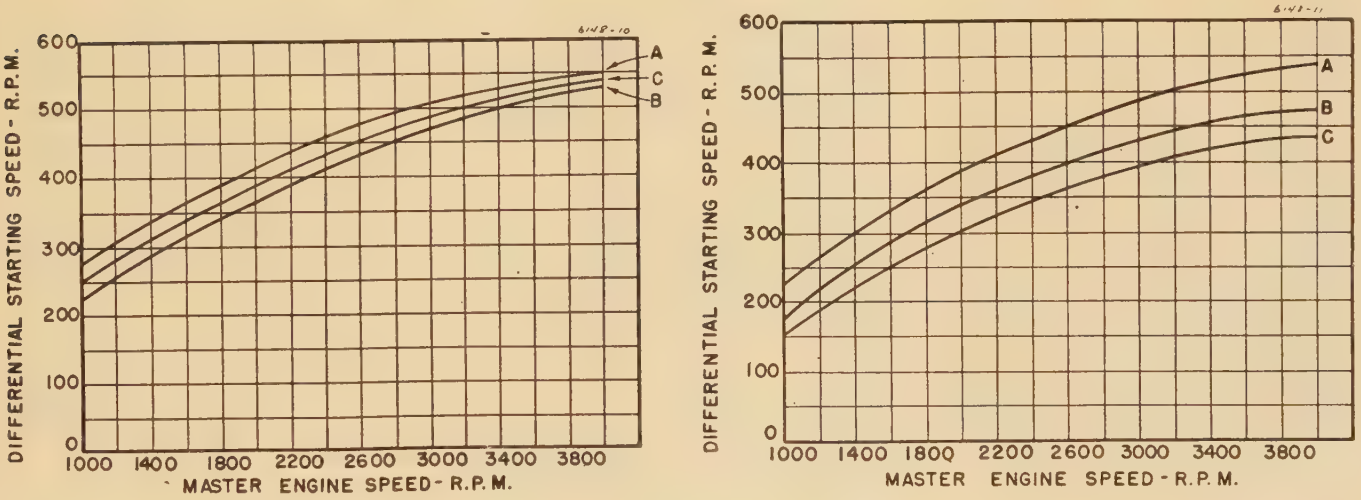

References

1. Flight Instruments (book), **H. W. Hurt, C. A. Wolf.** National Aeronautics Council, Inc., New York, N. Y., pages 20, 22.

2. Aircraft Instruments, Their Theory, Function, and Use (book), **O. E. Patton.** D. Van Nostrand Company, New York, N. Y., page 168.

3. The Magnetic-Drag Tachometer, **R. G. Ballard.** AIEE Transactions, volume 61, 1942. June section, pages 366–8.

4. Recent Advances in Aircraft Tachometer Design, **R. G. Ballard, C. P. Hall.** AIEE Transactions, volume 63, 1944, September section pages 646–8.

5. Design of Long-Scale Indicating Instruments, **A. J. Corson, R. M. Rowell, S. C. Hoare.** AIEE Transactions, volume 61, 1942, June section, pages 318–27.

6. Army Air Forces specification AN-I-20.

Nonlinear Commutating Reactors for Rectifiers

A. SCHMIDT, Jr.
MEMBER AIEE

ONE of the prime objectives in rectifier development during the past 20 years has been the decrease in frequency of arc-back. The factors involved in arc-back have received considerable attention, and it now appears that arc-backs of typical mercury arc rectifiers are caused by the following:

1. Breakdown of the mercury vapor because of inverse voltage.
2. Conditions favorable for cathode spot formation on the anode at the end of the commutation period.

The former cause is not present under normal operating conditions, but may become effective at excessive vapor pressures, as when condensed mercury is permitted to come into contact with a hot anode. The latter cause has been treated in some detail by Kingdon and Lawton.[1]

Phase of Arc-Back

Kingdon has proposed that the cause of arc-back is the charging by positive ions of small insulating particles on the surface of the anode, thereby causing local fields strong enough for runaway field emission. The experiments of Kingdon and Lawton on tubes with 1-centimeter anode-grid spacing indicate that the probability of commutation arc-backs varies with the product of initial inverse voltage and final commutation rate. In a structure with close spacing between the anode and deionizing members, the rate of ion diffusion during commutation is so rapid that the ion density at the end of commutation depends on the rate of change of current at the end of commutation. The number of ions collected by a particle on the anode at the end of commutation determines its resultant potential. This number is proportional to the inverse voltage and the density of ionization.

Hull and Elder have described tests

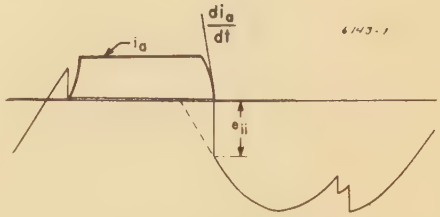

Figure 1. Anode voltage and current in 3-phase rectifier showing elements of rectifier duty

where the factors were controlled so that arc-backs occurred both at commutation and at later times.[2] They concluded that practical rectifiers of correct design will arc-back at the end of commutation rather than some later time, unless conditions are favorable for glow discharge.

There is evidence that the causes of arc-backs in practical rectifiers lead to a distribution of arc-backs throughout the inverse period.[3] A considerable proportion of these occur at the end of commutation. Furthermore, it is common experience that the probability of arc-back at a given load increases with the amount of phase retard and that rectifiers having a rating based on a considerable amount of phase retard can be given a greater rating with no phase retard.

Rectifier Duty

Figure 1 shows the current and voltage in one anode of a 3-phase rectifier and the quantities involved in anode duty. If

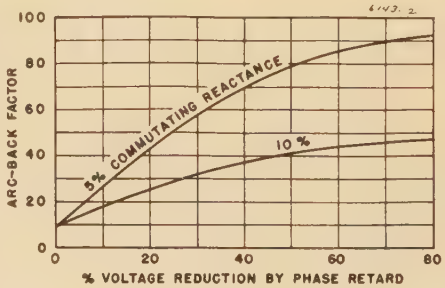

Figure 2. Effect of phase retard and circuit reactance on arc-back factor F_a

$$F_a = e_{ii} \times \frac{di_a}{dt}$$

the effect of residual ionization is denoted by an arc-back factor F_a, then

$$F_a = e_{ii} \times di_a/dt$$
$$= 2\pi f e^2_{ii}/X_c$$

In Kingdon's experiments the frequency of arc-back was approximately proportional to the tenth power of F_a. It will be noted that e_{ii} is an important factor in rectifier duty and that its effect increases rapidly when the rectifier is controlled by phase retard. Figure 2 shows the effect of phase retard on the arc-back factor. Increase of commutating reactance results in a decrease in rectifier duty. This is not a desirable means for reducing duty as increase in reactance results in

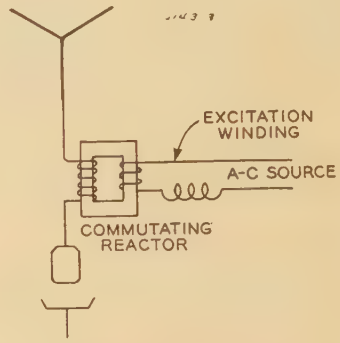

Figure 3. Commutating reactor in anode circuit of rectifier

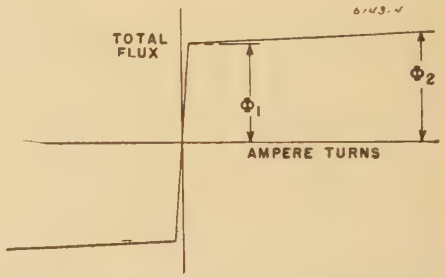

Figure 4. Saturation curve of commutating reactor

increased rectifier regulation and reduced power factor. If the anode current can be "dragged out" or maintained at some low value for a sufficient period just before the end of commutation, a substantial reduction in residual ionization and arc-back probability should result.

Action of Commutating Reactor

A commutating reactor is defined as a reactor used primarily to modify the rate of current transfer between rectifying elements.

A closed core anode reactor having an a-c excitation winding, as shown in Figure

Paper 46-143, recommended by the AIEE committee on electronics for presentation at the AIEE summer convention, Detroit, Mich., June 24–28, 1946. Manuscript submitted April 18, 1946; made available for printing May 14, 1946.

A. SCHMIDT, JR., is in the industrial engineering division, General Electric Company, Schenectady, N. Y.

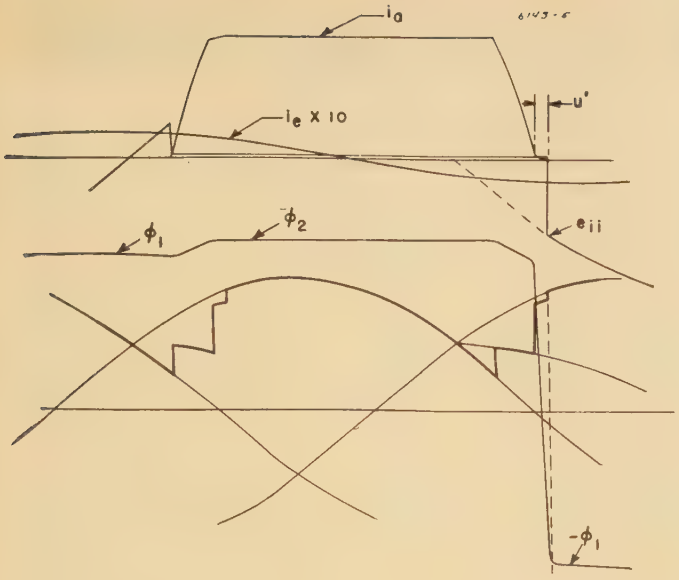

Figure 5. Circuit action of commutating reactor

3, may be used to "drag out" the anode current. Such a reactor preferably would have high permeability below saturation and little flux change beyond saturation, as shown in Figure 4.

Figure 5 shows the circuit action of the reactor. When anode conduction begins, the reactor already is saturated by the excitation winding in the same direction as the anode current, so that the reactor adds relatively little to the commutating reactance. During the anode conducting period, the excitation current i_e reverses.

When commutation to the next anode occurs, it will proceed normally until the anode ampere turns exceed the excitation ampere turns just sufficiently to maintain saturation of the core in the anode current direction. Further decrease in anode current results in desaturation of the reactor. The commutating reactance then will increase, and the anode current will fall slowly at a rate determined by the saturation curve of the reactor and the commutating voltage. This will continue for a time u' until the difference between anode ampere turns and excitation ampere turns is such that the reactor is saturated in the opposite direction, at which time the anode current will fall rapidly the rest of the way to zero.

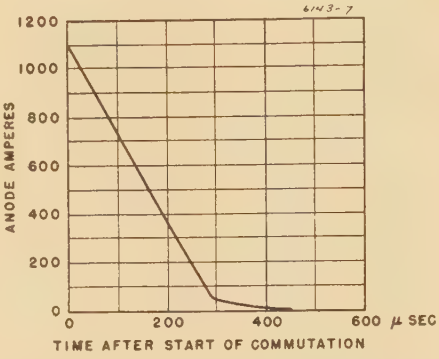

Figure 7. Anode current during commutation with commutating reactor

If the reactor excitation is near the knee of the saturation curve, so that the "drag out" period u' ends at a low value of anode current, then the residual ionization at the end of the conduction period will be reduced. The amount of reduction will depend on the time u'. The value of u' which is needed depends on the arc-back factor and the rate of ion cleanup, which is a function of the geometry of the anode and grid structure of the rectifier.

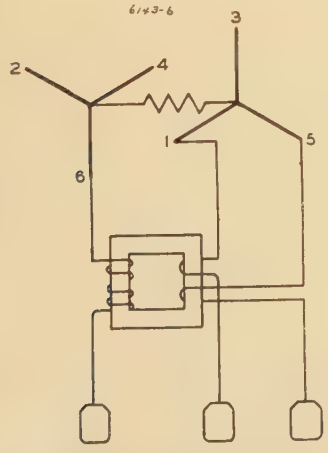

Figure 6. Commutating reactor with excitation by anode currents

Design of Commutating Reactors

The relation $2n\phi_1 \times 10^{-8} = u' \times E_c$ determines the product of anode turns and core section of the reactor. Optimum design requires a minimum ratio of maximum flux to saturating flux in order to reduce the regulation caused by the reactor. The direct voltage loss caused by the reactor is given by

$$E_{xc} = npf(\phi_2 - \phi_1) \times 10^{-8}$$

Since a complete flux reversal occurs in a few electrical degrees, a core design with low eddy loss is needed, otherwise the iron heating will be high and a portion of the drag out period will be consumed in setting up eddy currents in the core structure.

Reactor excitation may be obtained from a separate a-c source, as shown in Figure 3. In this case an impedance is needed in the excitation circuit to limit coupling between the anode circuit and the excitation circuit during the period u', when a high voltage may be induced in the excitation winding. Excitation also may be derived from the currents in other anodes, as shown in Figure 6. If the number of turns in the main winding is so small that this arrangement produces too many excitation ampere turns, suitable current transformers may be used between the anode circuit and the excitation winding.

Operating Results

Figure 7 is typical of the anode current with a commutating reactor in the anode circuit. A record of this current was obtained by placing a small air core reactor in series with the commutating reactor and measuring the amplified voltage across the air core reactor with a cathode ray oscilloscope and camera. A 1,000-cycle sweep was used and was tripped once every 1/60 second so that the record covered 1,000 microseconds. The voltage across the reactor

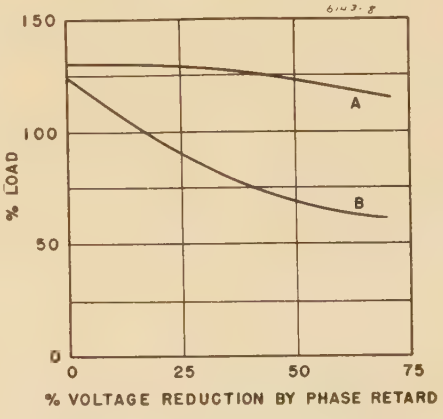

Figure 8. Short time rating of rectifier

A—Commutating reactors
B—No commutating reactors

is proportional to the rate of change of anode current. Since the current at the beginning of commutation was known, the current during commutation could be calculated from the measured rate of change.

Figure 8 indicates the gain resulting from the use of commutating reactors when considerable phase retard is employed. Curve *A* taken with commutating reactors with a drag out time of 350 microseconds at 70 per cent voltage reduction shows that no reduction in rating is needed for phase control. However, a reduction of 40 per cent in rating must be applied in going from 15 to 70 per cent or more voltage reduction without reactors. This is shown in curve *B*. The base load for these curves is the maximum load that can be carried with 15 per cent voltage reduction for a definite time without arc-back.

In this instance it is seen that commutation arc-backs limit the rectifier load both at full and reduced voltages. A minor gain is realized by the use of commutating reactors at full voltage. This becomes a major gain where considerable voltage control is required.

Conclusion

Present day applications of rectifiers call for increasing amounts of voltage control, in many cases to zero voltage. Sustained operation of a rectifier with considerable voltage control usually requires derating of the rectifier. The use of commutating reactors eliminates such derating. They also may prove useful for other cases where high rates of commutation are involved, as at frequencies above 60 cycles.

Appendix. Nomenclature

e_{tt} = initial inverse voltage of anode at end of commutation
di_a/dt = final commutation rate of anode current
u' = drag out time (seconds) of anode current caused by action of commutating reactor
n = turns in anode winding of reactor
ϕ_1 = total flux in reactor at knee of saturation curve
ϕ_2 = total flux in reactor at peak anode current
E_c = average commutating voltage during drag out period
i_e = excitation current in commutating reactor
X_c = commutating reactance per phase
p = number of phases in simple rectifier
f = frequency, cycles per second

Investigation of Porcelain Insulators at High Altitudes

C. V. FIELDS
ASSOCIATE AIEE

C. L. CADWELL
ASSOCIATE AIEE

Synopsis: The use of high voltage apparatus in military aircraft made it necessary to obtain flashover data on capacitor bushings at altitudes up to 50,000 feet. Some of the more pertinent data are presented in this paper which gives a-c and d-c flashover voltages for porcelain bushings having spacings of 5/8 inch to 2 7/8 inches from cap to ring. The tests were made at both normal atmospheric and reduced pressures, but no attempt was made to simulate the frosting conditions as encountered in flying. Correlations are shown between bushing spacings and the effect of pressure change. A single correction curve for pressure changes cannot be used, but a family of curves is required for various spacings of insulators and electrostatic field configuration. This paper shows that the practical use of porcelain insulators is limited to altitudes and voltages well below maximum values proposed for aircraft use. It is recommended that solid insulation be used in such a manner as to obtain the benefit of its puncture strength rather than its flashover at the more extreme conditions of altitude and voltage.

UNTIL RECENTLY the low pressure flashover strength of communication apparatus bushings has received little attention. Previous work, such as that reported by Bellaschi and Evans,[1] covers large gaps and insulators as related to power system operation. More fundamental studies of air strength between various gaps at low air density have been presented by Peek[2] and by Schwaiger and Sorensen.[3]

At the beginning of the war, ignition systems were the chief concern and became rapidly more important with increasing altitudes and severity of operating conditions.[4] This problem was solved by proper use of solid insulating materials.

Concurrently, the tremendous increase in air-borne electric apparatus and the subsequent increase in aircraft distribution voltages brought on many practical problems relative to the operation of all sorts of power apparatus, wiring, and auxiliaries. Several authors[5,6] have measured the permissible breakdown and flashover strength of a variety of gaps and insulators under simulated conditions of aircraft operation. Their work, therefore, was concerned with the adverse affects of dust, icing, temperature extremes, and moisture as well as much greater pressure changes than had previously been studied, and for relatively low voltages only.

Toward the end of the war, certain high voltage air-borne apparatus, particularly radar and communication equipment, began to offer new electrical problems unlike any phase of the previous work. The flashover strength of transformer and capacitor bushings, vacuum tube sockets, and similar apparatus became a major problem. After a cursory investigation, it became apparent that size and weight of insulators required was such that it was impractical to insulate apparatus for voltages over about 5,000 volts at stratosphere aircraft operating conditions, which not only include extreme altitudes, but very rapid changes in temperature and altitude with accompanying moisture condensation.

Pressurization of cabins and apparatus compartments has been accepted as the most satisfactory means of reducing the weight of very high voltage apparatus. There remain, however, many marginal conditions where pressurization may be advantageously or necessarily avoided. Choice of the amount of pressurization

Paper 46-131, recommended by the AIEE committee on air transportation for presentation at the AIEE summer convention, Detroit, Mich., June 24–28, 1946. Manuscript submitted April 19, 1946; made available for printing May 13, 1946.

C. V. Fields, a design engineer in the protective devices engineering department and C. L. Cadwell, a laboratory engineer, are both with Westinghouse Electric Corporation, East Pittsburgh, Pa.

References

1. The Relation of Residual Ionization to Arc-Back in Thyratrons, K. H. Kingdon, E. J. Lawton. *General Electric Review*, volume 42, November 1939, pages 474–8.

2. The Phase of Arc-Back. A. W. Hull, F. R. Elder. *Journal of Applied Physics*, volume 13, March 1942, pages 171–6.

3. Phase Occurrence of Arc-Backs in High-Current Mercury-Arc Rectifiers, W. E. Pakala, W. B. Batten. AIEE Transactions, volume 59, 1940, June section, pages 345–7.

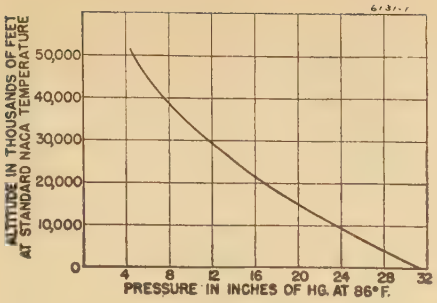

Figure 1. National Advisory Committee for Aeronautics standard altitude corresponding to test chamber pressures at 86 degrees Fahrenheit

or the question of operation in case of pressure failure will depend in part upon apparatus bushing flashover strength. Commercial aircraft will continue to operate at moderate altitudes where pressurization is not warranted. Television and radio equipment will be operated in increasing quantities at moderately high elevations where consideration of the reduction in flashover strength of apparatus bushings caused by reduced pressure will be required.

Previously reported observations of the effects of condensation and frosting on low voltage systems[5] are generally applicable to the high voltage bushings discussed in this paper. That is, unless there is moisture condensation on bushing surfaces, variations in humidity do not affect the breakdown appreciably. Neither is the breakdown affected by frozen moisture. It is to be noted that such factors are of less importance in commercial applications where variations are neither as extreme nor as rapid, and moisture condensation, therefore, less likely to occur. The present work is concerned primarily with the effects of pressure change. All tests were made at room temperature with normal variations in humidity. Omission of a humidity correction seems justified in view of the previous work mentioned.

The National Advisory Committee for Aeronautics standard pressure, temperature, and altitude table generally is accepted for aircraft work. This table gives a standard pressure and a corresponding temperature for each elevation. The curve shown in Figure 1 gives the pressure in inches of mercury (at 86 degrees Fahrenheit) having the same relative air density RAD as the standard altitudes shown as ordinates. Thus the measured pressure of 4.7 inches is seen to correspond to a standard elevation of 50,000 feet, which is in turn equal to 3.4 inches of mercury at the standard temperature of −66 degrees.

This transition from room temperature test conditions to high altitudes is permitted by the principle of similitude,[2] which states in effect that for constant spacing the breakdown voltage will be constant if the ratio of P/T is kept constant, where P and T are the absolute pressure and temperature respectively. Since flashover is substantially proportional[7] to relative air density, the following expression may be used to convert our manometer readings taken at the test temperature of 86 degrees to other temperatures and pressures:

$$RAD = \frac{17.95 \times \text{barometric pressure (inches)}}{460 + \text{temperature (degrees Fahrenheit)}} \quad (1)$$

Test Equipment and Procedure

Most low pressure work previously reported has been conducted with the specimens in a nonmetallic container to reduce field distortion to a minimum. Since it is desirable to test bushings in their normal position mounted on the capacitor, we found it necessary to use a relatively large test chamber. Also, since capacitors usually are surrounded by metal surfaces in practice, it appeared logical to use a metal rather than a glass chamber used by some previous workers testing bushings alone. Capacitor specimens were placed approximately in the center of the tank.

The high voltage lead was brought into the tank through a single hole in the center of the 7/8-inch thick glass cover. The capacitor case was grounded to the tank in bushing-to-ground tests, while the case was insulated and one bushing was grounded for the bushing-to-bushing tests.

The direct voltage was supplied through a 175,000-ohm resistor by a well-filtered rectifier source. A voltmeter was connected directly across the specimen and a dip in the voltmeter reading was taken as the breakdown point. The current was so limited that no apparent damage occurred to the specimen, and a large number of successive readings could be taken without reduction in flashover strength.

The a-c tests were taken on two standard test sets, each with a tertiary voltmeter winding. All points under 50 kv were obtained with a 5-kva 50-kv test set using a hand operated induction regulator. All points above 50-kv were taken with a 50-kva 100-kv test set with a motor driven induction regulator. The wave form conformed to the ASTM Standard D 149.

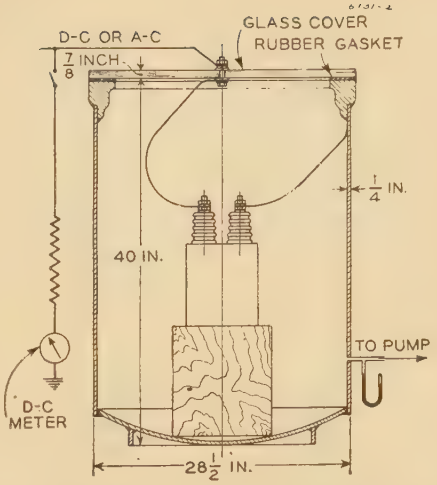

Figure 2. Apparatus for determining capacitor bushing flashover in air at various pressures

Both alternating and direct voltages were raised uniformly at a rate of approximately 10 kv per minute except in the case where the motor driven test set was used, the voltage of which was raised 3 kv per second.

Pressures were measured by a closed tube manometer and a pressure gauge calibrated in inches of mercury absolute. Corresponding altitude values may be obtained by reference to Figure 1 as explained.

Bushing Specimens

These tests were conducted on six typical capacitor bushings shown in Figure 3. All except the gasket sealed bushing *A* were of the "Solder-Seal" metal to porcelain type. They were mounted on conventional capacitor cases with working elements omitted. Leads attached to the top of the bushings were allowed to assume normal positions touching the inside walls of the bushing at random. The leads were clipped off one inch below the bottom of the bushing and were prevented from flashing over inside by filling the capacitor case with Inerteen.*

The bushing size and location and the case dimensions are all commensurate for typical d-c capacitors designed to operate at sea level. Table I gives the major dimensions of the bushings shown in Figure 3 and the covers on which they were mounted.

Summary of Data

The mounting ring on the "Solder-Seal" bushing presents a smooth well-rounded surface, while the cap has rela-

* Chlorinated diphenyl.

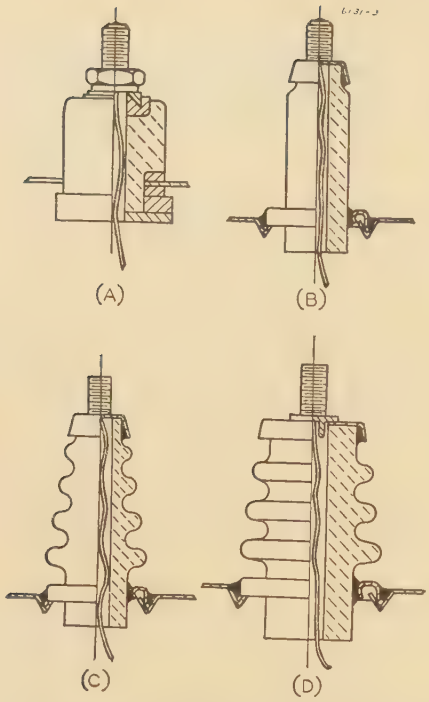

Figure 3. Capacitor bushings tested

Dimensions are shown in Table I

Table I. Major Dimensions of Bushings Shown in Figure 3 and the Covers on Which They Were Mounted

Bushing	Figure	Flashover (Tight-String) Distance in Inches	Diameter (Maximum) in Inches	Striking Distance Between Bushings in Inches	Case Size in Inches: Length	Case Size in Inches: Width	Distance Between Bushing Centers in Inches
A	3A	21/32	3/4	11/16	2 1/2	1 3/16	1 1/4
B	3B	1 3/16	3/4	1 11/32	3 3/4	1 3/4	2
C	3B	1 7/8	15/16	1 1/32	3 3/4	1 3/4	2
D	3C	2 1/16	1 1/2	31/32	4 9/16	3 3/4	2
E	3D	2 3/16	2 3/4	2 9/32	8	4	4 1/2
				4 21/32	13 1/2	4 1/8	6 3/4
F	3D	2 15/16	2 3/4	2 5/32	8	4	4 1/2
				4 17/32	13 1/2	4 1/8	6 3/4

* Bushing *E* is similar to *F* except that the former has only two corrugations.

tively sharp edges but no burrs. Nevertheless, most streamers seem to form on the lower ring, and breakdown voltages seem relatively unaffected by rounding of the edges on the cap. This suggests that the high field intensity at the base of the bushing was a controlling factor in the breakdown mechanism. Most flashovers were observed to occur between the cap and the mounting ring at 1/16 inch or more from the porcelain and rarely seemed to follow the bushing surface.

The bushings tested differ in form as well as height; however, each is of typical configuration for its height. It seemed logical, therefore, to plot curves as a function of height although it is known that the breakdown is partially dependent on diameter and shape. To have all bushings straight sided and of one diameter would make the test academically correct, but of less practical value. Tight-string distance was measured between cap and mounting ring.

No special efforts were made to avoid ordinary variations in the height of liquid or position of the wire inside the bushings, or other normal factors affecting the breakdown voltages. The relatively large spread in flashover, compared to sphere gaps tested in a uniform field, attests to the effect of these variables. Especially at very low pressures, these normal variations in construction may cause unexpectedly large variations in flashover. The data are sufficiently consistent to warrant drawing the curves shown, but seemed to indicate the desirability of testing capacitors or similar apparatus at actual working pressures.

Bushing to case flashover tests were made first on all six bushings with a-c and both polarities of direct voltage. The data in Figure 4 were obtained by evacuating the chamber, then making a series of tests at four or more pressures, each time admitting air to obtain the pressure desired and taking at least five flashover readings after the pressure had become stable at the new value. All points were plotted and smooth curves were drawn through them. Similar smooth curves were drawn for a-c and positive d-c tests on each bushing. However, only the data for the d-c negative flashover tests are shown since they happen to be more conservative at the lower pressures than the values obtained for the d-c positive flashover tests.

Points corresponding to each of the pressures on the curves of Figures 5 and 6 were taken from the smooth curves drawn through the original test points. These latter curves of flashover versus striking distance, therefore, ignore differences between the various bushings, but show clearly how spacing affects flashover at the various pressures. From these curves it is seen to be increasingly difficult to develop high flashover voltage by increasing the bushing size at greatly reduced pressure. The curve for 4.7 inches of mercury clearly illustrates why about 5,000 volts is a logical maximum voltage for any apparatus bushing operated at or near 50,000 feet. An enormous increase in bushing size would be required to double the flashover voltage.

It is noted that the crest a-c values are somewhat lower than either positive or negative d-c breakdown values at

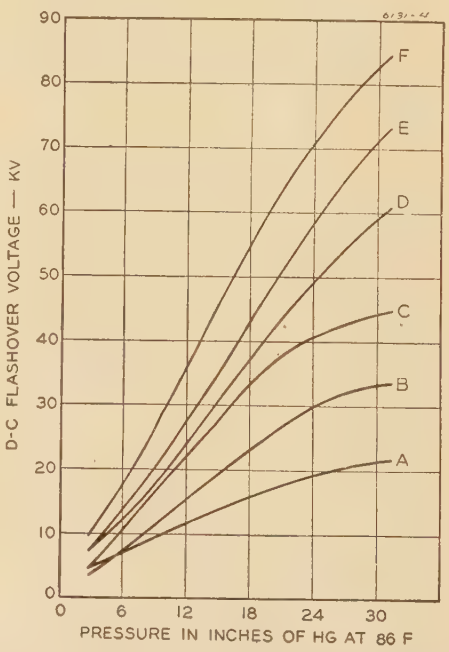

Figure 4. Negative d-c flashover–pressure curves for six bushings tested

Dimensions are shown in Table I

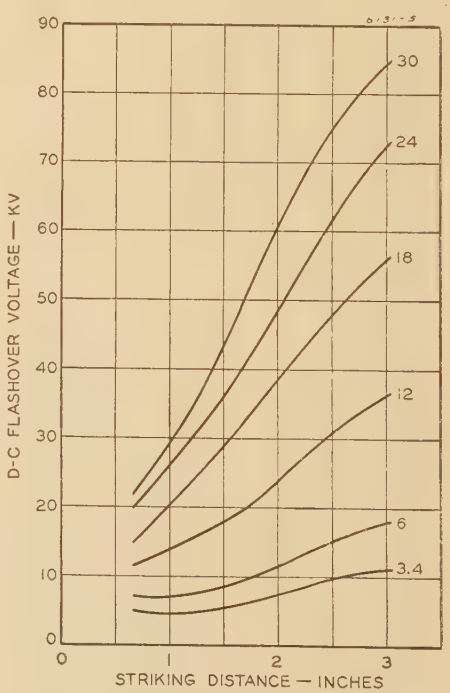

Figure 5. Negative direct voltage required to flash bushings over to case

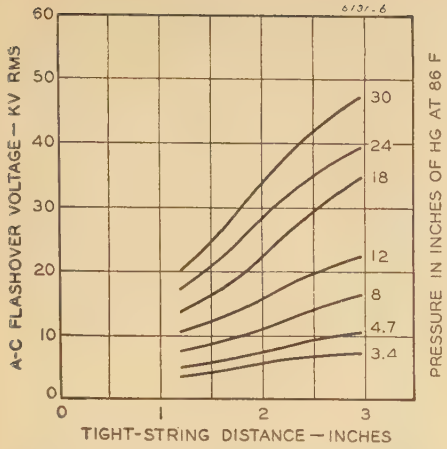

Figure 6. A-c terminal-to-case flashover voltage

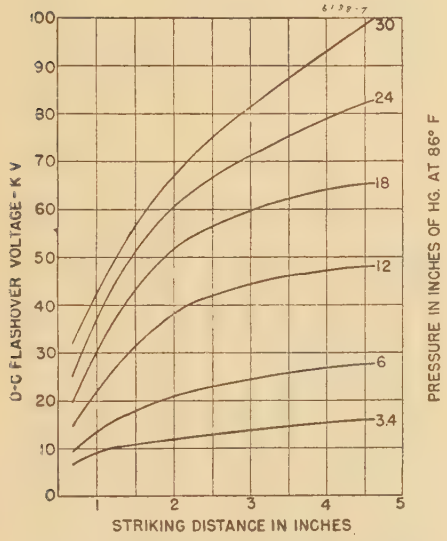

Figure 7. Negative d-c bushing-to-bushing flashover versus spacing

high pressures. This discrepancy is contrary to Berberich's experience in which the peak a-c is higher than d-c values.[5] It is believed that this apparent discrepancy is caused by differences in configuration, both of the field and of the bushings themselves.

A second set of tests was made with the same capacitor bushings mounted as described previously, except that the voltage was applied from bushing to bushing instead of from bushing to case. The flashover values are shown in Figures 7 and 8. Electrostatic fields were assumed to be largely responsible for the considerable rounding of these curves at large spacings.

In order to check the possible relationship between sphere gaps, point gaps, and bushings, the curve in Figure 9 was drawn. From this curve it can be seen that while sphere and point gap flashovers are practically straight lines at sea-level, they flatten out considerably at lower pressures. The bushing to bushing flashover values at 3.4 inches of mercury are intermediate between point and sphere gap values, as might be expected. However, one would not expect the bushing flashover values to fall below those of a point gap. This peculiarity also is believed to be caused by nonuniformity of the field surrounding the capacitor bushings. This explanation is substantiated by a wide variation in flashover voltages of several bushings spaced about the same distance apart, but of different heights.

Ratios of from three to five between sea-level and 45,000-foot altitude flashover voltages found in our work are higher than the 2.7 to 3.7 ratios found by DeLerno[6] in working with smaller gaps.

Table II gives the d-c rated voltage of several capacitors and the flashover voltages taken from the curves for bushings of a size which one would expect to use for high altitude operation. As can be seen, the actual flashover voltages at 45,000 feet are well above the rated values. For comparison, a column is added showing the sea-level test voltage of twice the rated voltage, times 3.7, plus 1,000 volts. It is obvious that the substitution of our maximum ratio of 5 for the 3.7, giving ten times rated voltage plus 1,000 volts, would be nearer the actual sea-level flashover of these particular bushings. However, such a rule would have to be qualified to account for the change in ratio which increases rapidly at large spacings. Furthermore, these sea-level voltages are far higher than could be withstood by the solid insulation used in practice on most apparatus.

Conclusions

1. Our investigations indicate that changes in flashover voltages do not vary in any simple manner with changes in pressure. Ratios of low pressure to high pressure flashover voltages vary considerably with bushing size and configuration, surrounding field, and other factors so that very definite relationships cannot be established.

2. Since the sea-level flashover voltage of most bushings designed for operation at 50,000 feet is far higher than can be withstood by the solid insulation of the apparatus, it appears best to test the completed apparatus in a low pressure chamber to assure proper safety factors at high altitudes. This is particularly true for capacitors because the location of the lead wire and the height of the liquid inside the bushing, and other factors markedly affecting the field change the flashover, especially at very low pressures.

3. The flashover voltage-distance curves for very high altitudes (50,000 feet) are so flat that it is apparent that no reasonable spacing will permit the use of bushings or

Table II. Flashover and Test Voltages for Several High Altitude Capacitor Bushings

Rated Direct Voltage	Bushing Flashover Voltage Distance in Inches	Expected Flashover Voltage at 45,000 Feet*	Actual Flashover Voltage at Sea-Level	Twice Rated Voltage Times 3.7 Plus 1,000 Volts
1,500	13/16	7,000	25,000	12,000
3,000	1 3/16	7,500	33,000	23,200
5,000	1 13/16	10,500	57,500	38,000

* Computed for NACA standard altitude from curves taken at 86 degrees Fahrenheit.

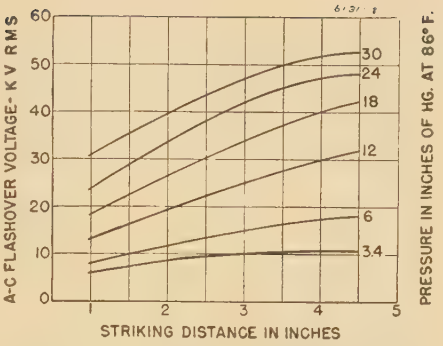

Figure 8. A-c bushing-to-bushing flashover voltage versus spacing

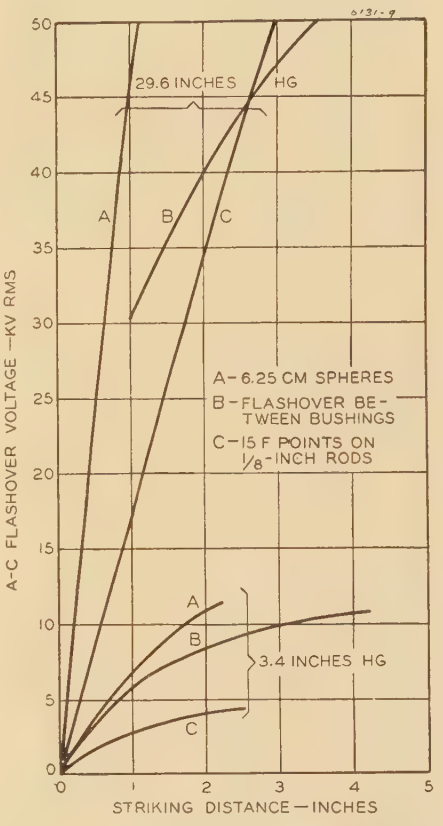

Figure 9. A-c bushing-to-bushing flashover voltages showing relationships to sphere and point gaps with corresponding spacings

Diesel-Electric Synchronous Motor Ship Drives—Propulsion Control Problems

E. FRISCH
NONMEMBER AIEE

Synopsis: Although the many obvious advantages of ship propulsion drives with synchronous motors and generators, and with power supplied by Diesel engines, have been realized for some time, no actual installations were made in this country until a few years ago when a trial installation was completed on a 12,000 horsepower twin-screw vessel. Experience gained from operation of this vessel has established that this type of drive in many respects is superior to other drives, and indications are that it may find extensive use on future vessels. The paper discusses control problems associated with the drive and describes methods of control and types of control equipment which have been found best suited for the drive.

DURING the last 25 years, a rapidly increasing number of naval and merchant vessels has been equipped with electric propulsion equipment, until by now more than 2,000 American vessels are electrically propelled. Primary power for the propulsion motors is supplied by Diesel engines or steam turbines coupled to electric generators. Up to the present time, with very few exceptions, all Diesel engine powered ships have d-c generators and motors, while synchronous generators and motors are used for steam-turbine drives.

The third possibility of using synchronous machines and Diesel engine prime movers for propulsion has been under considerable discussion for years. This type of drive has many obvious merits, but anticipated operating difficulties, especially during maneuvering, delayed actual installations on American vessels for several years. Finally in 1940, with the encouragement of various manufacturing concerns, plans were prepared and an order placed for a trial installation on a twin-screw vessel to demonstrate the practicability of the drive.

The vessel, which was completed in 1942, has two 5,900-horsepower 2,400-volt 3-phase synchronous propulsion motors. Power is supplied by eight 1,600-horsepower Diesel engines direct connected to 1,150-kva generators. The experience gained during sea trials and, through actual operation of the vessel for three years has proved conclusively that this type of drive not only is practical but in many respects is superior to similar drives using d-c equipment. There also is a good possibility that it may offer strong competition to turbine-electric drives for many applications.

Among the advantages of the drive, the following can be mentioned:

1. Synchronous machines weigh less and cost less than d-c machines of the same rating and their efficiency is higher.

2. Synchronous machines are more reliable and easier to maintain than d-c machines.

3. Machines with higher voltage can be used, thereby causing a reduction in cables and bus bars and permitting installation of units with higher ratings than is practical with d-c machines.

4. High speed Diesel engines with greatly increased ratings, now under development, will permit installation of high power Diesel-electric drives on vessels ordinarily powered by steam turbines, thereby dispensing with the bulky and highly vulnerable boiler plants on these vessels. The use of two or more Diesel-electric generating units instead of one larger turbine-electric unit will give additional flexibility and reliability to the propulsion drive.

In view of the above, it is commonly believed that Diesel-electric synchronous motor propulsion drives will be used extensively on future electrically propelled vessels. A brief discussion of problems, type of equipment, and method of control applying to the drives, therefore, should be of interest to a great many people who in some way are connected with the building or operation of ships.

Diesel Engines

Diesel engines for propulsion service, through constant improvements, have attained the high degree of dependability, efficiency, and durability required for this service. The output and speed of the engines have been raised steadily, and engines with a continuous rating of 2,000 horsepower at 800 rpm are now available. Engines of considerably higher rating and speed are under development and should be available in the near future. The engines operate satisfactorily at speeds as low as 30 per cent of rated speed. They develop rated torque down to 50 to 60 per cent speed, but at lower speeds the torque will be reduced gradually to as low as 60 per cent of rated torque at 30 per cent speed.

The engine speed is controlled by governors of the hydraulic type. As a protection against overloading, the governors will automatically limit the amount of fuel which is admitted to the engine per stroke. This amount decreases at low speeds so that the maximum torque, at any speed, will not exceed a safe value for continuous operation. If the torque is exceeded the engines will slow down and unload themselves.

The speed of the engines is adjusted remotely from the propulsion control board. A master speed control transmitter, coupled to the speed lever, serves

---

air insulation appreciably above 5,000 volts. Connectors taking advantage of solid insulation puncture strength, similar to those used in aircraft ignition systems, should be developed if higher voltages are encountered at extreme altitudes.

4. The curves shown represent the conservative averages of a great many tests made under practical conditions, and it is believed that they will serve as a guide in the selection of porcelain bushings falling within the scope of our work.

References

1. Effect of Altitude on Impulse and 60-Cycle Strength of Electrical Apparatus, **P. L. Bellaschi, Paul Evans, Jr.** AIEE Transactions, volume 63, 1944, May section, pages 236–41.

2. Dielectric Phenomena in High Voltage Engineering (book), **F. W. Peck, Jr.** Third Edition, McGraw-Hill Book Company, Inc., New York, N. Y., 1929.

3. Theory of Dielectrics (book), **Schwaiger and Sorensen.** John Wiley and Sons Inc., New York, N. Y., 1932.

4. Simulated-High-Altitude Testing of Aircraft Ignition Cables and Connections, **H. H. Race, A. M. Ross, Jr.** AIEE Transactions, volume 64, 1945, January section, pages 20–6.

5. Effect of Altitude on Electric Breakdown and Flashover of Aircraft Insulation, **L. J. Berberich, G. L. Moses, A. M. Stiles, C. G. Veinott.** AIEE Transactions, volume 63, 1944, pages 345–54.

6. Potential Breakdown of Small Gaps Under Simulated High Altitude Conditions, **M. J. DeLerno.** AIEE Transactions, volume 63, 1944, March section, pages 109–12.

7. Atmospheric Variations and Apparatus Flashover, **P. H. McAuley.** AIEE Transactions, volume 60, 1941, July section, pages 798–803.

Paper **46-149**, recommended by the AIEE committee on marine transportation for presentation at the AIEE summer convention, Detroit, Mich., June 24–28, 1946. Manuscript submitted November 23, 1945; made available for printing May 15, 1946.

E. Frisch is a control engineer with the Westinghouse Electric Corporation, East Pittsburgh, Pa.

to position receivers on the engine governors. Pneumatic or electric positioning devices are available for the speed control. Since the engines must operate in parallel at the same speed, means must be provided to equalize the engine loading. This may be performed automatically or by means of manual vernier speed control transmitters on the control board.

Starting and reversal of the propulsion motor are performed with the engines running at minimum speed. For satisfactory performance the engines must develop the highest possible torque during this period. The torque limitation, imposed on the engines by the governor action, therefore, is removed by energizing of magnetic solenoids provided on the engine governors for this purpose. This will raise the engine torque to a maximum value on the order of 85 per cent of rated torque, which can be delivered for short periods without causing damage.

Motor Starting Torque

During maneuvering periods, when the propulsion motor is being started or reversed, the motor operates as a squirrel cage induction motor with the de-energized field connected in series with a starting resistor. To develop the necessary starting and synchronizing torque, the motor must be provided with heavy damper windings and the associated generators must be overexcited with 200 to 300 per cent normal field current. The motor torque is a combination of two individual components. One component is produced by the current induced in the damper winding while the other component is produced by the current induced in the field coils. The value of the latter component is a function of the value of the starting resistance.

Typical curves, representing the two torque components and the resultant torque as a function of the resistor value, are shown in Figure 1 for 30 per cent generator speed. It will be noted that the peak value of the field torque components *B*1, *B*2, and *B*3 is practically independent of the resistor value but occurs at different motor slips. The starting resistor value should be selected so that a maximum resultant motor torque will be developed at the highest motor slip at which successful synchronizing is possible. The resultant torque curve *C*2 fulfills this requirement. Under certain conditions it may be necessary to bring the motor up to a maximum speed with one resistor value, and then increase the speed further by shorting out part of the resistor before synchronizing is possible. The peak value of the combined torque occurs at 35 to 50 per cent motor slip and should not be less than 50 to 60 per cent of full load torque when all generators are in service and overexcited.

Torque Margin

Torque margin for an electric propulsion drive is defined as the difference between the torque required by the propeller for normal full power running and the torque at which the motor pulls out of step, expressed as a percentage of the propeller torque.

For Diesel-electric drives, a torque margin of 10 to 15 per cent at normal generator and motor excitation is sufficient. This low torque margin is permissible because of the torque limiting feature of modern engine governors. When operating the vessel in rough weather or during periods of acceleration the propeller torque requirement frequently exceeds the pull-out torque.

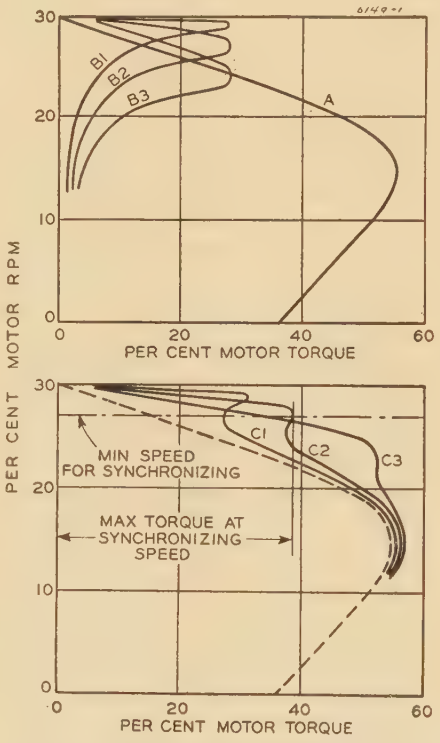

Figure 1. Curves showing the starting torque of a synchronous motor as a function of motor speed for different values of starting resistance

A—Torque developed by damper winding
B—Torque developed by motor field winding
*B*1—Low starting resistance
*B*2—Medium starting resistance
*B*3—High starting resistance
C—Total motor torque
*C*1—Low starting resistance
*C*2—Medium starting resistance
*C*3—High starting resistance

Since the engines cannot develop a torque of this value, however, the result is only a momentary reduction in engine and motor speed and a corresponding reduction in the propeller torque requirement, but the motor will not pull out of step. The transient increase in propeller torque builds up at a relatively slow rate, and the inertia of engines and generators is so low that the engine speed reduces fast enough to prevent the actual occurrence of torques higher than the pull-out value.

This is in contrast to conditions encountered on steam turbine drives. The torque developed by a turbine cannot conveniently be limited by governor action, and may easily exceed rated torque. Furthermore, the turbine inertia is relatively high and its speed cannot be reduced fast enough to prevent occurrence of transient torques, exceeding the pull-out torque, even though the turbine torque was limited. For this reason, the torque margin built into motors and generators for turbine-electric drives must be increased, causing an increase in weight and dimensions, or provisions must be made to increase automatically the pull-out torque whenever required. This is accomplished by a momentary increase in motor and generator excitation.

Dynamic Braking

Typical curves for propeller torque requirements during reversal of a vessel with four propulsion generators are shown in Figure 2. It will be noted that the peak propeller torque, which occurs before the motor stops, actually is higher than the torque required to hold the motor at standstill. This peak torque is of particular interest because it occurs at a point where the available motor torque is low and, in most instances, is not sufficient to overcome the peak torque.

To illustrate this condition, a series of curves representing the available motor torque for two, three, and four generators, operating at 30 per cent speed, have been shown for comparison. Examination of the curves discloses that the propeller cannot be stopped by motor torque alone, even with four generators in service, and that the condition is equally adverse for 2-generator operation, although the propeller torque is reduced, as a result of the lower ship speed in this case.

To stop the propeller preparatory to a reversal, two methods are available:

1. Permit the vessel to slow down without power on the motor until the propeller torque is reduced below the corresponding motor torque at all speed points, and then

apply reverse power. The time required for the slow-down, however, is excessive, especially for large vessels, and this method is not acceptable.

2. Stop the motor by dynamic braking. By this means the motor can be brought to practically standstill and reverse power applied in a few seconds. Since the additional equipment, required for dynamic braking, is relatively inexpensive, this method should be incorporated on all drives of this type as a means for reducing the time required for motor reversal.

Dynamic braking of the motor is produced by connecting a 3-phase resistor to the motor terminals and energizing the motor field with normal field current. The effect of the value of the braking resistance on the braking torque is illustrated in Figure 3, where curves are shown for braking torque as a function of motor speed for three different resistance values. It will be noted that the value of the peak braking torque is practically independent of the resistance value. However, the torque peak occurs at a higher motor speed when the resistance value is increased.

The propeller torque curve for maximum ship speed also is shown to illustrate the relation between this torque and the braking torque. The points of intersection of the curves give the minimum value to which the motor speed will be reduced for different values of braking resistance. The speed decreases with decreasing resistance value. For very low resistance values, however, the braking torque is not sufficient to overcome the propeller torque at higher motor speeds, as illustrated by curve *A*1, and the motor speed will not be reduced below speed *C*. This must be kept in mind when designing the starting resistor, and a check should be made to ascertain that the braking torque is higher than the motor torque at all speeds, as illustrated by curve *A*2.

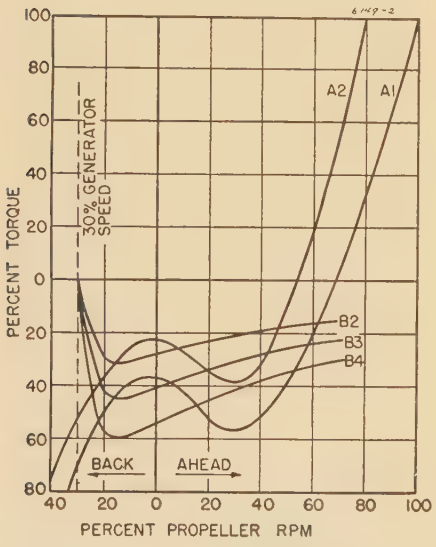

Figure 2. Curves showing motor and propeller torque as a function of motor speed during reversals; vessel moving at full speed ahead

*A*1—Propeller torque, four generators in service
*A*2—Propeller torque, two generators in service
B—Torque developed by propulsion motor
*B*2—Two generators in service
*B*3—Three generators in service
*B*4—Four generators in service

General Control Scheme

A complete propulsion plant consists of two or more Diesel engines directly connected to synchronous generators, a synchronous propulsion motor, an excitation supply, and the propulsion control equipment.

The method of control is very simple and should not vary greatly for different installations. The general description given in this paper gives a fairly complete picture of the type of equipment, control scheme, and operating procedure for most installations. A simplified schematic diagram of a typical control scheme is shown in Figure 4 for a synchronous drive with three generators.

Any combination of the generators can be connected to a common generator bus by means of three high voltage contactor groups. The contactors for generator number one are numbered 1*G*1, 1*G*2, and 1*G*3. The motor can be connected to the same bus by means of reversing contactors *R*1 to *R*4, of which *R*2 and *R*3 close for "ahead" operation and *R*1 and *R*4 close for "astern" or "back" operation. Quick stopping of the motor is made possible by connecting a dynamic braking resistor to the motor terminals by the closing of contactors *R*5 to *R*7.

The excitation for the propulsion machinery is supplied by a motor-generator set with separate exciters for motor and generator excitation. The exciter fields are energized from a constant voltage control bus through a magnetic field contactor *F*, which remains closed for normal operation. The generator and motor exciter fields are energized by the closing of starting switches *S*4 and *S*6. The generator and motor fields are connected to the associated exciter busses by means of field switches as shown. When a field is de-energized, it is connected to a discharge or starting resistor to prevent high inductive voltage peaks.

The cooling of the field coils becomes less effective when the speed of the propulsion motors and generators is reduced. The exciter voltage, therefore, must be decreased for low speed operation, by means of rheostats in the exciter field circuits, to prevent overheating of the coils. The rheostats are coupled to the speed control lever, and so designed that the exciter voltage will be reduced to approximately 75 per cent of normal when the speed lever is moved from the "fast" to the "slow" speed position. The rheostats are shorted by means of starter switches *S*5 and *S*7 during the starting period when maximum excitation is needed to obtain the required starting and synchronizing torques. The generator exciter voltage must be raised to 200 to 300 per cent of normal during this period. A resistor is connected in series with the generator exciter rheostat to reduce the exciter to voltage to normal when switch *S*5 opens in the "run" position.

For the sake of simplicity it is assumed that all contactors and switches, shown in the diagram, are of the cam operated type arranged in groups and controlled manually by means of operating levers in a control stand at the front of the control board. A diagram of the control stand is shown in Figure 5.

Incorrect operation of the starting levers is prevented by means of mechanical interlocking as indicated in the lever diagram. The purpose of the interlocking is as follows:

1. The motor speed lever and the starter lever are interlocked to prevent starting of the motor unless the engine speed is a minimum. It also is necessary to reduce the speed to a minimum before stopping the motor.

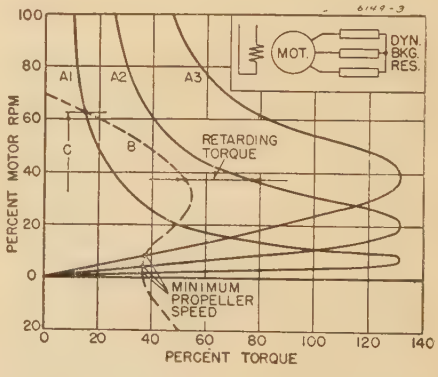

Figure 3. Curves showing dynamic braking torque as a function of motor speed for different values of braking resistance

A—Dynamic braking torque
*A*1—Low dynamic braking resistance
*A*2—Medium dynamic braking resistance
*A*3—High dynamic braking resistance
B—Propeller torque, vessel moving at full speed ahead

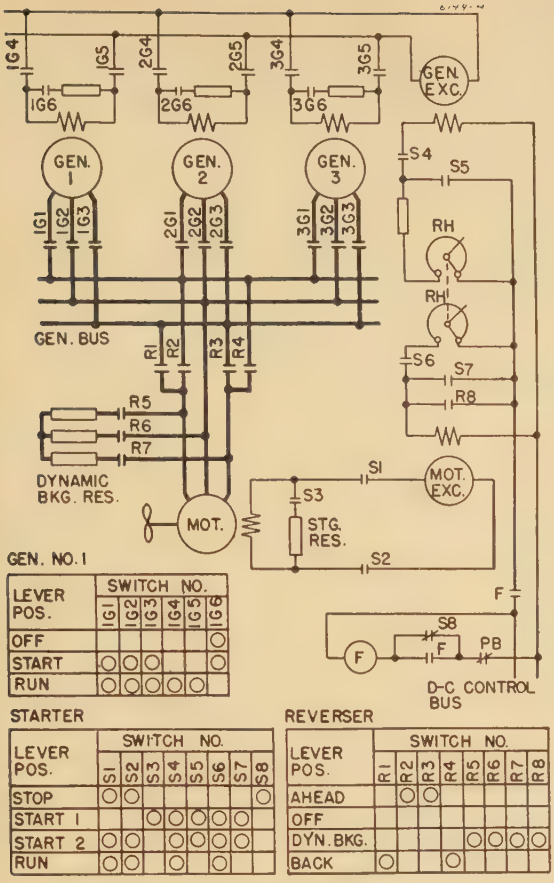

Figure 4. Simplified schematic control diagram for synchronous motor propulsion drive

2. The starter lever and the reverser lever are interlocked to prevent moving the starter lever from the "stop" position, unless the reverser lever is in the "ahead" or the "back" position. Inversely, the reverser lever cannot be moved unless the starter lever is in the "stop" position. Since, in this case, the speed lever must be in the slow speed position, it follows that the reversing contactors cannot be operated unless the generator speed is a minimum and the generator field is de-energized. The operating duty of the contactors, therefore, is considerably lightened.

A speed control transmitter is connected to the speed lever for the purpose of controlling the speed of the engines and, consequently, of the motor over the speed range. Exciter rheostats, required for reduction of generator and motor excitation at reduced speeds, also are coupled to the lever.

Motor Starting

The generators, which will be used for propulsion, are connected to the generator bus by placing the generator levers in the "run" position while the engines are running at idling speed. The generator field switches (1*G*4 and 1*G*5 for generator number one) close and connect the fields to the exciter, which, however, is de-energized since the starter lever is in the "stop" position and switch *S*4 is open. The generators, therefore, will not be synchronized but will run at approximately equal speeds determined by the master speed control transmitter.

As the next step, the reverser lever is moved to the "ahead" position, thereby closing contactors *R*2 and *R*3 and connecting the motor armature to the generator bus. Although motor field switches *S*1 and *S*2 are closed, the motor field remains de-energized since exciter field switches *S*6, *S*7, and *R*8 are open.

Actual starting of the motor takes place when the starting lever is moved to the "start 1" position. Motor field switches *S*1 and *S*2 open and the starting resistor is connected in the field circuit by the closing of switch *S*3. Switch *S*7 closes and applies maximum excitation to the motor exciter in preparation for the motor synchronizing. Simultaneously, the generator fields become overexcited since switches *S*4 and *S*5 close. Although there may be a considerable difference in the speed of the Diesel engines, the synchronizing torque resulting from the overexcitation is sufficient to pull the generators into step and cause synchronization. Following this, the motor starts up as a squirrel-cage induction motor and accelerates gradually to near synchronous speed.

When the motor approaches synchronous speed, the main motor current drops sharply from an almost constant high value during the accelerating period and thereby furnishes an indication that the motor may be synchronized. At this point, the starter lever is moved to the "start 2" position. Switches *S*1 and *S*2 close and connect the motor field to the previously excited motor exciter. Switch *S*3 opens and interrupts the circuit to the starting resistor. As a result the motor becomes energized and begins operating as a synchronous motor. After a few seconds hesitation the starter lever is moved to the "run" position. Switches *S*5 and *S*7 open and reduce motor and generator excitation to normal. The motor speed now may be adjusted to any desired value by means of the speed lever which controls the engine speed control master transmitter.

Discussion of Motor Starting Sequence

The starting sequence, outlined above is unorthodox and probably will be questioned. When first confronted with the problem it would seem more logical first to synchronize and overexcite the generators, connected to the generator bus, and then to start the motor by connecting it to the energized bus. This method is not satisfactory, however, for reasons as outlined as follows.

Before starting the motor, the engines run unloaded at a speed only slightly higher than their minimum stable speed, and the amount of fuel oil, admitted to the engines by the governors, is very low. When connecting the motor to the overexcited generator bus, there will be a se-

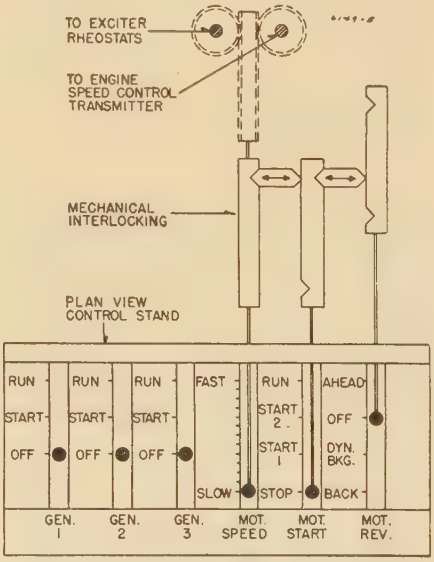

Figure 5. Diagram of lever operating stand with mechanical interlocking

vere and practically instantaneous increase in the generator loading and a corresponding rapid reduction in engine speed. The governors, consequently, will function to increase the amount of fuel oil and the engine torque, but this action is not instantaneous. During the time required to increase the engine torque sufficiently to equal the generator torque, the engine speed frequently will drop below the stable speed and stalling results.

However, when the generators are energized after the motor is connected to the generator bus, the loading increases gradually because of the time constants of exciter and generator fields. The response of the governors is sufficiently fast to follow the load increase, and there is no appreciable reduction in engine speed, and stalling of the engines is prevented.

Motor Reversal

To reverse the propulsion motor when the vessel is making considerable headway, generators and motor first must be de-energized by moving the speed lever to the "slow" position and the starter lever to the "stop" position. The motor now will idle at approximately 70 per cent of normal speed, but is brought quickly to practically standstill by placing the reverser lever in the "dynamic braking" position. Contactors *R5*, *R6*, and *R7* close and connect the braking resistor to the motor terminals. At the same time, switch *R8* closes and applies maximum excitation to the motor field.

As soon as the motor stops, the reverser lever is moved to the "back" position and the starter lever is moved successively to the "start 1," the "start 2," and finally to the run position. The motor starts up in the same sequence as described for normal starting except that the phase rotation is reversed.

Control Problems During Reversal

When making a reversal, the speed of the engines and generators must be reduced to a minimum, since the torque requirement of the motor at synchronizing speed otherwise would become excessive. This presents a serious problem because the engine torque is reduced at low speeds, and also because the engine operates so close to the minimum stable speed that a momentary drop in speed may cause stalling.

To improve conditions, the torque limitation is removed during maneuvering by energizing solenoids on the governors. This will raise the engine torque to 85 per cent or more of normal which can be maintained for short periods. The torque requirement, however, exceeds even the increased engine torque during full power reversals (crash stop) and causes stalling unless special precautions are taken. The condition becomes especially critical where a reversal is attempted with a reduced number of engines. Even normal starting from standstill then may cause stalling.

To obtain a clear picture of the problems involved, curves representing propeller, motor, and engine torques as a function of motor speed are shown in Figure 6. Curve *A1* represents the propeller torque when the vessel is moving ahead at full power speed. *A2* and *A3* are similar curves for reduced ship speeds. Curve *B1* represents the torque developed by the motor at 250 per cent generator excitation and 30 per cent engine speed. *B2* and *B3* are similar curves for reduced generator excitation. The torque required by the engines to produce the corresponding motor torque is represented by curves *C1*, *C2*, and *C3*. It should be noted that the motor torque, as shown, is a function only of the electrical characteristics of motor and generators and has no relation to the propeller torque requirements. The difference between motor and propeller torque is the torque actually available for acceleration. The engine torque is a combination of the motor torque and the considerable electric and mechanical motor and generator losses.

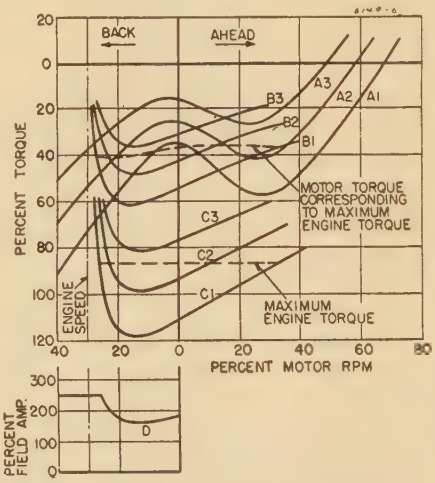

Figure 6. Curves showing propeller, motor, and engine torque as a function of motor speed during reversals

A—Propeller torque
A1—100 per cent ship speed
A2— 85 per cent ship speed
A3— 70 per cent ship speed
B—Propulsion motor torque
B1—250 per cent generator excitation
B2—200 per cent generator excitation
B3—150 per cent generator excitation
C—Engine torques corresponding to above motor torques
D—Generator field current required to maintain maximum engine torque

An examination of the curves discloses that with 250 per cent generator excitation the torque requirement exceeds the maximum available engine torque and the engines will stall. To remedy this condition, the torque requirements must be reduced by reduction of the generator excitation to match the available 85 per cent engine torque. The motor torque available for acceleration of the propeller, of course, is reduced correspondingly, as illustrated.

When reverse power is applied to the motor, after it has been brought to nearly standstill by means of dynamic braking, the reduced torque is sufficient only to raise the reverse motor speed to less than ten per cent where the curve for available motor torque intersects curve *A1*. From this point on, the motor speed increases gradually as the ship speed is reduced, and reaches close to synchronizing speed at 70 per cent ship speed. The generator field current required to maintain 85 per cent engine torque in the accelerating period is represented by curve *D*.

The vessel slows down surprisingly fast as a result of the combined braking effect of hull friction and the reverse propeller thrust, and the time required to accelerate the motor to synchronizing speed is not excessive. The head reach of a vessel with this type of drive compares favorably with the value obtained for similar vessels with d-c drives.

Automatic Torque Control

Satisfactory operation during maneuvering to prevent engine stalling requires automatic control of the generator field current. The current must be maintained at the highest value possible without causing reduction of the engine speed below a permissible minimum value.

A suitable control to meet this requirement is illustrated in the schematic diagram, Figure 7. A small permanent magnet d-c pilot generator *PG* is driven by a 3-phase induction motor, connected to the generator bus through a step-down transformer. The pilot generator voltage is a measure of the main generator frequency and, consequently, of the engine speed. Also coupled to the motor is a regulating exciter *RE* provided with a self-exciting field and a separate control field. A resistor in the self-exciting field circuit is adjusted so that the generator voltage is zero when the control field current is zero, but

will build up to a high value when a very low current is passed through the control field.

The pilot generator is connected in series opposition to a bias voltage across part of a resistor energized from the control bus, and the voltage difference is applied to the control field. The bias voltage is adjusted to equal the pilot generator voltage when the engine speed is 30 per cent of normal. At higher engine speed, the generator voltage exceeds the bias voltage, but current flow through the control field is prevented by a rectifier block. If the engine speed drops as the result of excessive torque requirement, the bias voltage exceeds the generator voltage and a current will flow through the control field in a direction as indicated. The resulting exciter voltage bucks the control bus voltage in the generator exciter field circuit and reduces the field current. This causes a corresponding reduction in main generator excitation and engine torque until stability is regained. The functioning of the torque regulating equipment is illustrated in Figure 7 by a series of curves showing the relative values of the excitation and control voltages as the engine speed decreases.

Torque control is required only until the motor is synchronized, and the regulating equipment is disconnected when the starter lever is moved to the "run" position by the opening of switches $S10$ to $S15$. The de-energized rototrol is bypassed by switch $S9$. The governor solenoids $M1$ and $M2$, which serve to increase the engine torque during the maneuvering period, are de-energized and normal governor function restored by the opening of switch $S11$ when the starter lever is moved to the "run" position.

Paralleling of Generators

When, during normal operation with one or more generators in service, it becomes necessary to increase the power output by connecting an additional generator to the bus, the first step is to start the associated engine and adjust its speed to approximately the same speed as the engines in service by connecting the governor actuator to the master speed control transmitter. The next step is to move the generator lever to the "start" position, thereby connecting the generator armature to the bus, while the de-energized generator field is connected to a field resistor (see Figure 4). The generator as a consequence, will run as a squirrel cage induction motor and will be forced into near synchronism with the other generators. When, as the third step, the generator lever is moved to the "run" position, the generator becomes energized and pulls into step.

To make possible this simple method of synchronizing, the same consideration must be given to the design of damper winding and field resistor for the generators as for the propulsion motor. With correct design, the synchronizing is very positive and it actually is possible, as has been demonstrated, to start an engine from standstill. If the engine starting lever previously has been placed in the "run" position, the engine will start automatically and begin to deliver power simply by advancing the generator lever to the "start" and then to the "run" position.

Operation at Subsynchronous Speeds

The minimum propeller speed possible with synchronous motor operation is limited by the minimum stable engine speed to approximately 30 per cent of normal speed. On a 20-knot vessel, the minimum steady speed will be in excess of six knots. This speed is somewhat high, and it is desirable to operate at lower speed on some classes of vessels.

This is accomplished by operating the motor as a squirrel cage induction motor at subsynchronous speed. The motor speed is controlled by adjustment of the generator excitation below its normal value, while the de-energized motor field is connected to the starting resistor.

Motor torque curves for several values

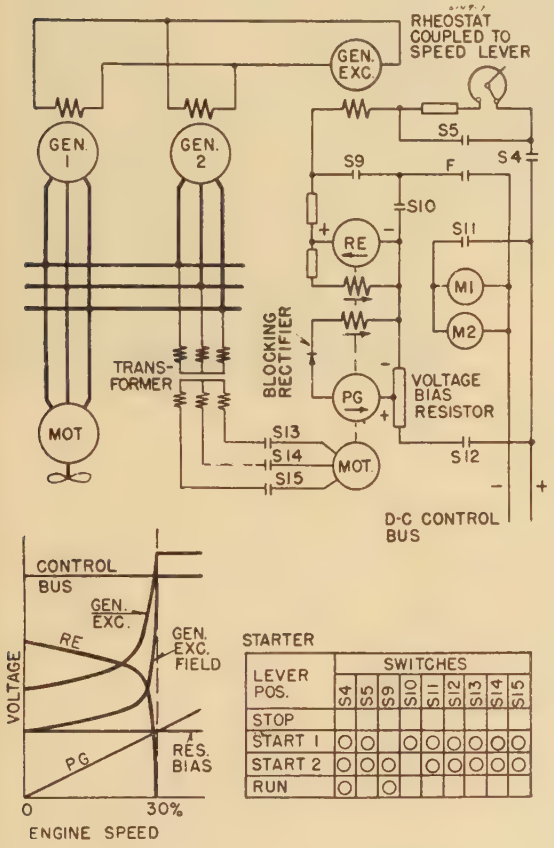

Figure 7. Schematic diagram of automatic engine torque regulation

RE—Regulating exciter
PG—Permanent field pilot generator
M1, *M2*—Engine governor solenoids

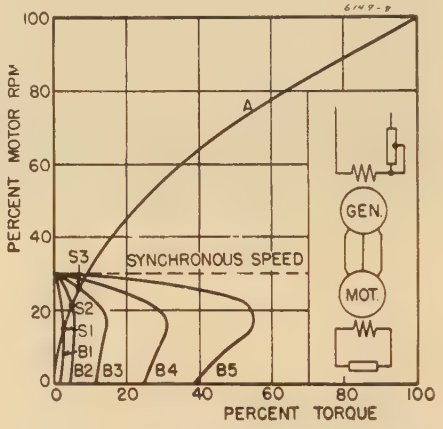

Figure 8. Operation of propulsion motor at subsynchronous speeds

Curves *B1* to *B5* show motor torque as a function of speed for different values of generator excitation. *B1* is for minimum excitation, *B5* is for overexcitation, *A* is propeller torque curve for steady running condition

of generator excitation are shown in Figure 8. The intersections between these curves and the propeller torque curve give the values of the corresponding motor speeds for steady running. To prevent overheating of motor and generators as a result of high magnetizing and damper winding losses, the generator excitation must be reduced considerably below normal value for continuous operation. Operation at speeds between the minimum synchronous speed and 70 per cent of this value, therefore, is not possible. One speed point at approximately 50 per cent of minimum synchronous speed or 15 per cent of maximum motor speed should be sufficient. To permit operation at this speed, the starter lever has an additional position between "stop" and "start 1" positions, in which a field resistor is inserted in the generator exciter field circuit. For satisfactory operation at least 50 per cent of the generators must be in service.

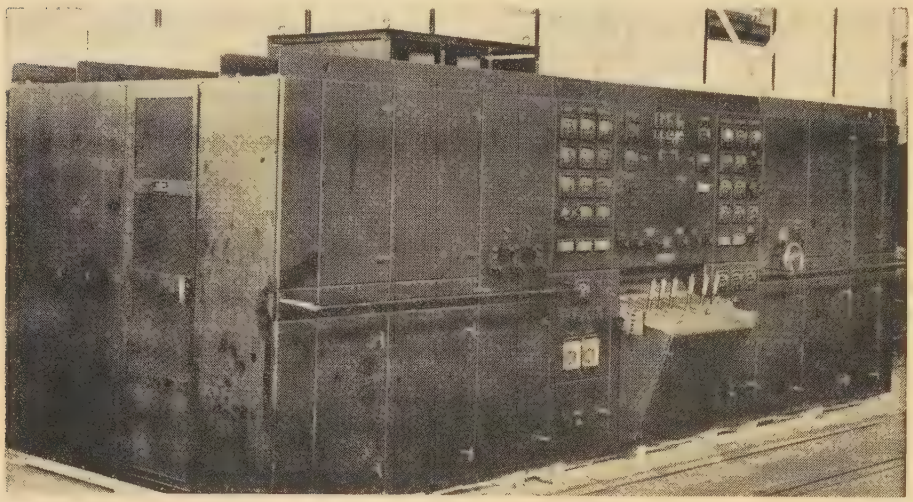

Figure 9. Typical propulsion control board mounted on engine builder's test floor

Protection

The power requirement of a propulsion motor is a function of the propeller speed for any given installation with minor changes caused by the condition of the hull. The motors are designed to supply the necessary torque for the maximum propeller speed and, consequently, cannot be overloaded as long as this speed is not exceeded. The Diesel engines are designed to supply the rated generator output within a narrow margin, thereby precluding overloading of the generators.

Serious overloading of an electric propulsion plant, therefore, is not possible, and, since the equipment is under practically constant supervision when the vessel is under way, normal overload protection is not provided. It is only necessary to protect the main circuits against open circuits and short circuits which occur more frequently than on land installation because of the severe operating conditions.

Phase balance relays in each generator circuit are provided as a protection against this type of fault. The relays trip on a phase unbalance caused by short circuits or open circuits, but are insensitive to the high currents in the circuits during maneuvering. The relay contacts are connected in the coil circuit of a magnetic field contactor and will open and de-energize motor and generators when a fault occurs. The main contactors, therefore, are not required to open short-circuit currents. The contact *PB* of a phase balance relay is shown in diagram, Figure 4. To reset the field contactor after the fault has been cleared, the starter lever must be moved momentarily to the "stop" position when switch *S*8 closes.

Design of Control Boards

The control boards are of the metal enclosed dead front type and should have separate compartments for high and low voltage apparatus if space permits. In accordance with standard marine practice, the main and field contactors are usually of the manually operated type for the sake of reliability. Pneumatically or magnetically operated contactors, however, may be more suitable in many instances, especially on large installations since this permits mounting of switch units in convenient locations remote from the main control station. More positive operation is also possible than with manual switching.

Manual contactors usually are operated by cam shafts, connected mechanically to the operating levers. On installations with pneumatically or magnetically operated contactors, master switches are provided for remote control of the contactors. It may be found desirable to retain the lever operating stand also for this type of control and connect the master switches to the levers. This also simplifies the problem of providing the necessary mechanical interlocking. A control board of this type is shown mounted on the engine builder's test floor in Figure 9.

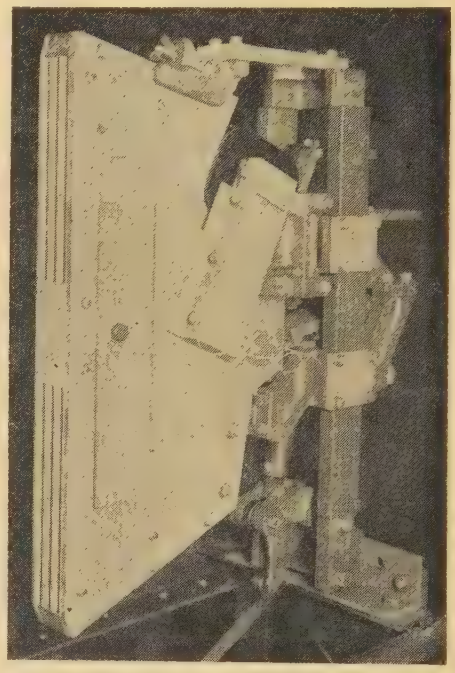

Figure 10. A 2,500-volt 1,500-ampere cam-operated trip-free propulsion contactor

The high voltage main contactors should be of the air break type. They are required to interrupt normal generator and motor currents but not short-circuit currents. When the contactors are of the manual type, it may be necessary to provide trip-free features on the generator contactors to permit remote tripping from the engine gauge boards of associated contactors in case of engine failure. A typical 2,500-volt 1,500-ampere cam-operated trip-free type contactor is shown in Figure 10.

Rectifier Capacity

C. C. HERSKIND
MEMBER AIEE

H. C. STEINER
MEMBER AIEE

THE LOAD CAPACITY of mercury arc rectifiers must be known in order to utilize them to fullest extent and best advantage. Knowledge of the factors affecting rectifier capacity and the relations between them has increased so that it is now possible to specify the rectifier capacity in definite terms.

Mercury arc rectifier tubes (or tanks) are manufactured only in a limited number of types and sizes. A large variety of rectifier units of different ratings and characteristics may be made up from combinations of one or more similar tubes. Information regarding the capacity and characteristics of each tube (or tank) is essential to the design and application of such mercury arc power converters. It is the purpose of this paper to describe the load-time and volt-ampere characteristics of typical mercury arc tubes of the ignitron type and discuss the relations between these characteristics and the factors affecting them. The control and other characteristics of mercury arc tubes will be treated in a companion paper.[1]

The load carrying ability of a mercury pool tube may be limited by arc-back, voltage surges, loss of control, structural failure, or other action. Of these causes, arc-back is generally determining as it imposes a basic limitation on the rectifying action involving fundamental processes in the arc discharge. The limitation in rectifier capacity caused by arc-back is different in nature from the thermal load limitations of most electric machinery in that it usually results in an impairment in reliability, rather than any permanent electrical or structural damage. Furthermore, it is somewhat indefinite because of the random occurrence of arc-back and the complexity and lack of full understanding of the arc processes.

Temperature rise does not provide a measure of the loading on a mercury pool tube or indicate its probable life. However, the operating temperature of the tube does affect its capacity, as it controls the mercury vapor pressure and establishes conditions for the arc discharge. Thermal limitations of essential components, such as seals, studs, grids, also may affect rectifier capacity, although such limitations are usually readily diagnosed and easily surmounted.

As with most electric apparatus, time is an important factor in rectifier capacity, since the short time capabilities are different from those for continuous operation at a steady sustained load. The time required for a mercury pool tube to reach final temperatures is usually short because of the low thermal capacity of its parts. Furthermore, the time required to establish conditions favorable to the occurrence of arc-back involves all the factors affecting the arc action, of which temperature is but one. For these reasons the relation between magnitude and duration of the limiting load of rectifier tubes differs materially from that for other types of conversion equipment.

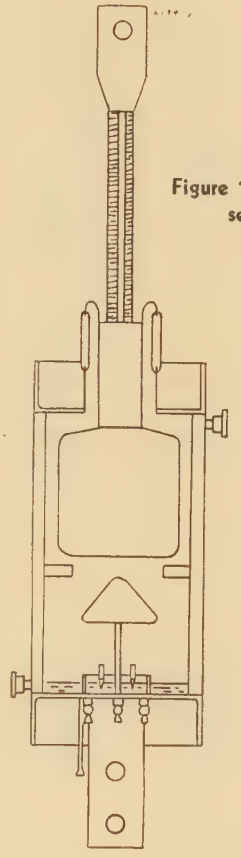

Figure 1. Cross section of sealed ignitron

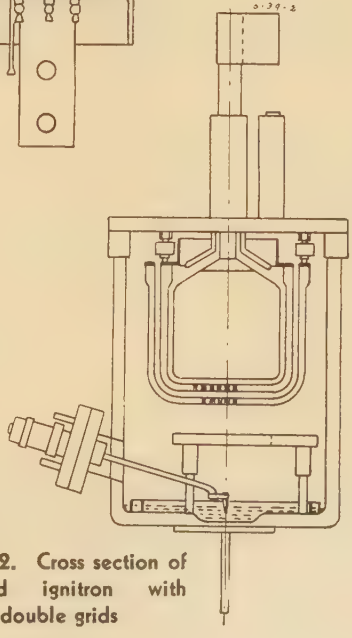

Figure 2. Cross section of pumped ignitron with double grids

Definition of Loading

The loading on a rectifying device may be described in terms of the magnitude and wave form of the current and voltage impressed upon it during a cycle. The loading is the sum of the effects of both separate and concurrent action of current and voltage. Inasmuch as the rectifying device performs only a switching action, the magnitude and wave form of the current and voltage depend almost entirely on the power circuit. The loading imposed upon the rectifying device by the circuit is termed the circuit duty.[2]

The capacity of a rectifying device may be expressed in terms of the circuit duty that it is capable of withstanding without failure. Some of the more important elements of the circuit duty are as follows:

1. Voltage—peak inverse and forward voltage; initial inverse voltage.
2. Current—average, peak, and rms current; final commutation rate.
3. Frequency (of a-c system).
4. Duration of loading.

Circuits differ in the amount of duty they impose upon the rectifying device because of differences in magnitude and form of the current and voltage waves. Also, the various elements of circuit duty have different weightings relative to the over-all loading on the rectifier. Since the effects of the various elements of circuit duty upon rectifier capacity are to a large degree mutually dependent, it is necessary to state the rectifier capacity for several different types of circuit duty in order to fully describe its capabilities.

It is often more convenient to state the rectifier capacity in terms of factors more directly related to the circuit constants and performance characteristics than in the elements of circuit duty. Some of these factors are:

1. Mode of operation (number of rectifier phases).
2. Direct voltage.
3. Direct current.
4. Amount of phase control.
5. Reactance.

Paper 46-139, recommended by the AIEE committee on electronics for presentation at the AIEE summer convention, Detroit, Mich., June 24–28, 1946. Manuscript submitted April 26, 1946; made available for printing May 14, 1946.

C. C. Herskind is with the power rectifier department, and H. C. Steiner is with the electronics department, tube division, both of General Electric Company, Schenectady, N. Y.

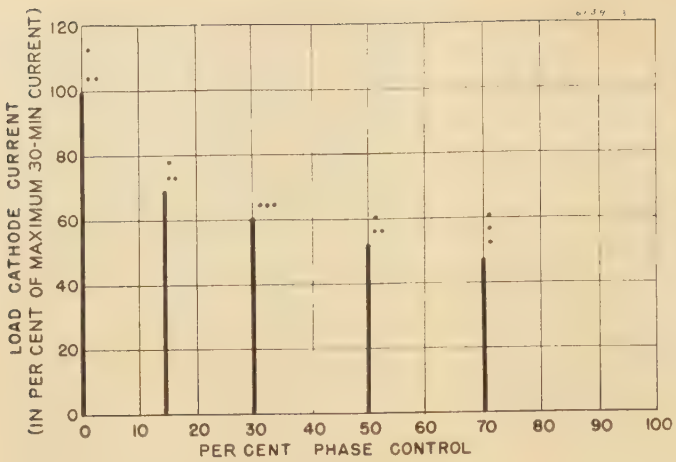

Figure 3. Results of 30-minute load limit tests on six sealed ignitrons

Dots indicate arc-back

A full statement of rectifier capacity also must include the capabilities and limitations under loadings of one cycle duration, that is, the fault current capacity. This capacity is defined as the crest value of current which the rectifying element can carry without incurring voltage surges during the conduction period or arc-back in the succeeding inverse period.

Determination of Capacity

The design of mercury arc rectifiers is based to a large degree on experimental data obtained from tests. As a consequence, each new design requires extensive tests to check its adequacy and determine its capabilities.

Rectifier capacity is determined from load test which consist in operating the rectifier under loads of increasing severity until failure occurs.

Load tests may be made on either a complete unit with a full complement of tubes, or on a section with only enough tubes to obtain the desired circuit action. Accelerated load tests have been termed load limit tests, and the procedure for making them has been described in a previous paper.[3]

Typical load limit test data are presented for the two ignitron tubes shown in Figures 1 and 2. Figure 1 shows a sectional view of a sealed ignitron and Figure 2 illustrates a sectional view of a pumped ignitron with double grids. Load limit data obtained with six sealed tubes connected to a double-Y transformer are shown on Figure 3. Similar data for three pumped ignitrons connected to a single Y are given in Figure 4.

The fault current capacity is determined from short-circuit tests which may be made either on a complete unit or a single tube. The testing procedure consists in increasing the current on successive trials until failure occurs.[3] Typical fault current test results are shown in Figure 5, which gives data for a sealed ignitron.

Characteristic Curves

Rectifier capacity usually is presented in the form of load–time curves, with the load given in amperes and with the other factors determining the load entered as parameters. These curves may be drawn directly from the data obtained on load limit tests, as the usual procedure is to make tests at a given voltage and vary loading by changing the load current.

Load–time curves for the sealed ignitron are shown in Figure 6 and for the pumped ignitron on Figure 7. The load–time curves are plotted most conveniently on a semilogarithmic scale because of the short thermal time constant of the tube and the short duration of the accelerated load limit tests. Values for the 30-minute and 2-hour points on the curves are obtained from the 30-minute load limit tests,* which are made by increasing the load by a fixed increment every half hour. The 30-minute point is then the highest load which was carried successfully without arc-back, and the 2-hour point is taken as the load three increments below. The load–time curves are usually almost straight lines, so values for times longer than two hours may be estimated by extrapolation. Final thermal conditions usually are attained in less than four hours, and experience has shown that the continuous capacity of rectifier tubes does not differ greatly from their 4-hour capabilities. The load capabilities indicated by these curves are limited by arc-back. Where structural features are limiting, different load time relations may be obtained.

A load–time curve may be drawn for each condition of rectifier operation, such as voltage, phase control, reactance, temperature, mode of operation. A complete statement of rectifier capacity therefore requires several families of load–time curves. However, it is frequently desirable to indicate the effect of the other load factors directly. The relationships between some of these factors and rectifier capacity follow.

Voltage

A given mercury pool tube may be operated over a wide voltage range. The load capacity in amperes decreases as the

* Previously designated continuous load limit tests.

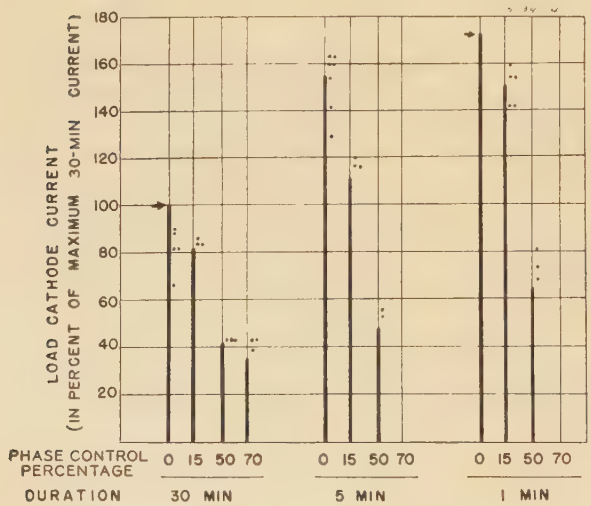

Figure 4. Results of load limit tests on three pumped ignitrons with double grids

Arrows indicate limit of testing facilities
Dots indicate arc-back

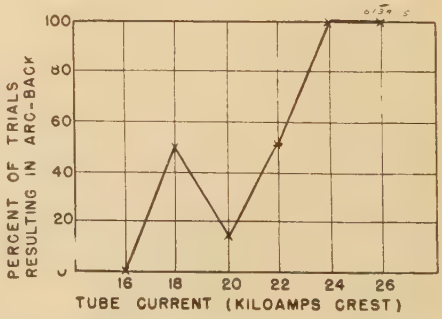

Figure 5. Fault current capacity of sealed ignitron

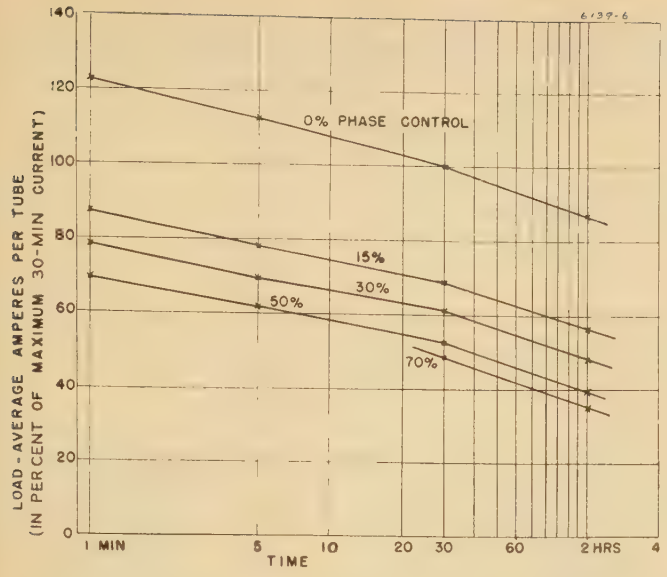

Figure 6. Load–time characteristics of a sealed ignitron

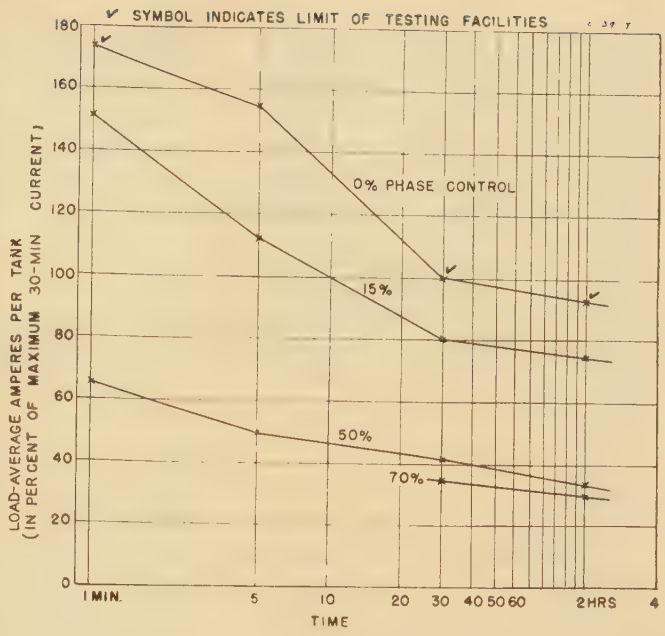

Figure 7. Load–time characteristics of a pumped ignitron with double grids

operating voltage is raised. However, the reduction in current capacity is usually less than the increase in voltage, in that the kilowatt capacity of a rectifier is generally increased as the operating voltage is raised.

These characteristics are shown best by plotting the rectifier capacity as a volt ampere relationship on a logarithmic scale, as in Figure 8. The volt ampere characteristics of both the sealed ignitron and the pumped ignitron are shown. Both have a greater slope than the constant kilowatt curve, indicating an increase in kilowatt capacity as the voltage is raised. Adequate data to establish the volt ampere characteristics as fully as might be desired are not available.

Phase Control

The effect of phase control upon the capacity of certain types of tubes is shown directly by the load limit data in Figures 3 and 4. These curves indicate a reduction in 30-minute current capacity when large amounts of phase control are applied. The percentage phase control is defined as the percentage reduction in output voltage.

Temperature

The rectifier usually is operated at its optimum temperature as determined by load limit tests. The operating temperature or temperature range, therefore, must be included with data on rectifier capacity.

Mode of Operation

The relative effects of the various elements of circuit duty upon rectifier capacity have not been established. Therefore, it is not possible to predict accurately the rectifier capacity for one mode of

Table I. List of Typical Tube Ratings

Tube Type and Description	Class of Service	Rated Output* Kilowatts	Volts	Amperes
Type *A* ignitron	Industrial	150	250	600
		200	600	333
Type *B* ignitron	Industrial	300	250	1,200
		500	600	833
Type *C* ignitron	Industrial	8,100	9,000	900
Type *D* ignitron	Industrial	600	250	2,400
		1,000	600	1,666
Type *E* ignitron	Industrial	1,000	250	4,000
		2,000	600	3,330
Type *F* ignitron	Railway (Classes II and III)	4,000	3,000	1,333
Type *G* ignitron	Industrial	1,500	250	6,000
		3,000	600	5,000

* Rating of six tubes in double-Y circuit.

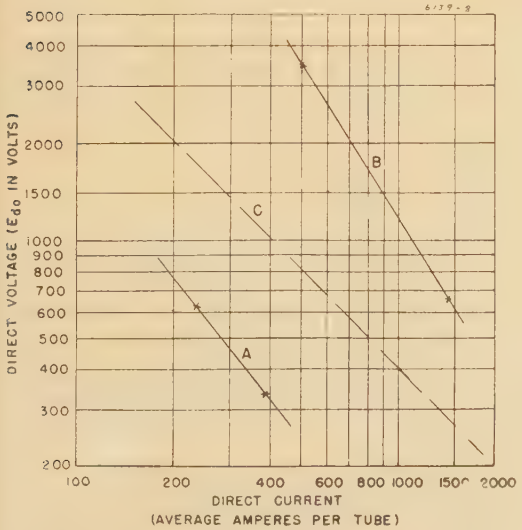

Figure 8. Volt ampere characteristics

A—Sealed ignitron
B—Pumped ignitron with double grids
C—Constant kilowatt

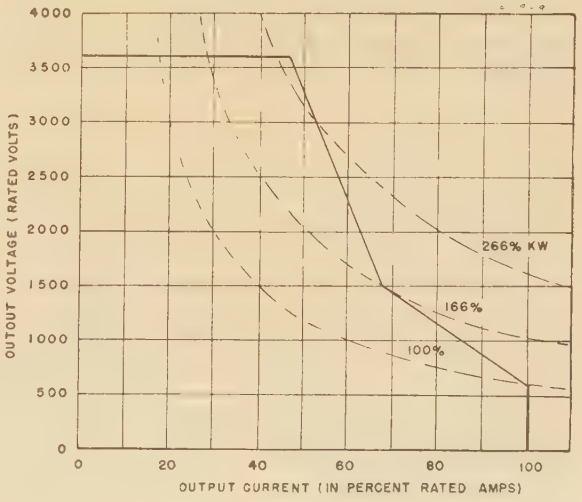

Figure 9. Typical rating curve for pumped ignitron—6-tube unit for railway service, classes II and III

operation from data obtained for another. Most rectifier applications employ circuits having the mode of operation of the double-Y circuit, and tests usually are taken using this circuit.

Research has indicated the importance of the arc phenomena occurring during the initial part of the inverse cycle.[4] The mode of operation, voltage, current, reactance, phase control, and frequency are all factors entering in this action. Our knowledge of this phase of rectifier behavior is not sufficiently complete to permit a complete treatment of these factors at this time.

Application

In the application of data on rectifier capacity as obtained from load limit tests to the design of a rectifier unit a margin must be allowed between the rated or anticipated load and the capacity indicated by tests. This tolerance must be provided to cover the following contingencies:

1. Differences between normal and accelerated loading. It must be recognized that load limit tests are short time or accelerated tests and do not duplicate accurately all the effects of sustained operation in service.

2. Differences in circuit duty. Where load limit tests are made on a set of three tubes, the circuit duty may be less than that incurred on a complete rectifier circuit.

3. Transformer unbalance. Unbalanced transformer reactances may cause unequal tube currents. Transformers usually are designed to permit an unbalance in neutral currents not exceeding five per cent. (The per cent unbalance is defined as the ratio of the difference between actual and rated neutral current to rated neutral current.)

4. Service requirements. The requirements of various applications differ with respect to reliability, depending upon the economic penalties or operational hazards incurred by the occurrence of arc-back.

The amount of the margin will depend upon judgment and experience involving the above factors.

Sizes and Ratings

Table I gives a list of typical tube ratings for some of the ignitron tubes now available.

As the same tube may be used over a wide range of voltages and may be applied to different kinds of service, such a listing does not completely describe its capabilities.

A fuller description of the tube capabilities is provided by rating curves of the type shown in Figure 9.

Mica Capacitors for Carrier Telephone Systems

A. J. CHRISTOPHER
ASSOCIATE AIEE

J. A. KATER
NONMEMBER AIEE

Synopsis: Silvered mica capacitors, because of their inherently high capacitance stability with temperature changes and with age, now are used widely in oscillators, networks, and other frequency determining circuits in the Bell Telephone System. Their use in place of the previous dry stack type, consisting of alternate layers of mica and foil clamped under high pressures, has made possible considerable manufacturing economies in addition to improving the transmission performance of carrier telephone circuits. These economies are the result of their relatively simple unit construction and the ease of adjustment to the very close capacitance tolerance required.

PRESENT DAY carrier telephone systems are placing special demands on capacitors used in frequency determining and frequency sensitive circuits with particular emphasis on initial precision, low a-c losses, and high capacitance stability with temperature and time. In these systems mica capacitors are used in the oscillating circuits and also are used extensively in the electric filters employed to segregate the numerous and closely spaced carrier frequency channels. For these applications the transmission potentials applied to capacitors are quite low and in general do not exceed a few volts. These capacitors, however, must meet very stringent requirements for capacitance tolerance at the time of manufacture, and any subsequent changes in capacitance caused by temperature changes and age must be held to extremely low values to insure high quality transmission for the systems. As a result considerable effort has been expended by the Bell Telephone Laboratories and the Western Electric Company in the development of designs of mica capacitors which would lend themselves to large scale economical production, and at the same time provide high initial precision of capacitance and high capacitance stability over long periods of time under service operating conditions. To meet these exacting demands, mica capacitors having sprayed silver electrodes intimately bonded to the mica laminations were developed and introduced several years ago into the Bell System in quantities to replace the former less stable and more expensive designs.

As a matter of historical interest, silvered mica capacitors were manufactured by the Western Electric Company and used in the Bell System more than 40 years ago as capacitor standards in laboratory measurement work. These silvered mica capacitors were made by the relatively expensive method of chemical deposition of the silver on the mica.

Paper 46-151, recommended by the AIEE committee on communication for presentation at the AIEE summer convention, Detroit, Mich., June 24–28, 1946. Manuscript submitted January 8, 1946; made available for printing May 15, 1946.

A. J. CHRISTOPHER, supervising engineer on capacitor design, and J. A. KATER, capacitor design engineer, are with Bell Telephone Laboratories, Inc., New York, N. Y.

Conclusions

A truly comprehensive statement of tube capabilities directly in terms of the elements of circuit duty is recognized as an ultimate objective. This objective is not fully possible with our present knowledge.

However, a procedure for the description of the load capabilities and limitations of mercury pool tubes has been outlined, and a convenient and useful form for the presentation of such information has been developed. The adoption of a standard form for the specification of tube capacity will help application and operating engineers prepare specifications for tubes which are to be used in rectifier equipment.

References

1. EXCITATION, CONTROL, AND COOLING OF IGNITRON TUBES, C. C. Herskind, E. J. Remscheid. AIEE TRANSACTIONS, volume 65, 1946, October section, pages 632–5.

2. RECTIFIER-CIRCUIT DUTY, C. C. Herskind. AIEE TRANSACTIONS, volume 63, 1944, March section, pages 123–8.

3. THE TESTING OF MERCURY-ARC RECTIFIERS, H. L. Kellogg, C. C. Herskind. AIEE TRANSACTIONS, volume 62, 1943, December section, pages 765–73.

4. THE RELATION OF RESIDUAL IONIZATION TO ARC-BACK IN THYRATRONS, K. H. Kingdon, E. J. Lawton. *General Electric Review*, volume 42, number 11, November 1939.

Physical Construction

Figure 1 illustrates the former type of construction known as the dry stack mica capacitor. In this construction alternate layers of mica and tinned copper foil are held together under high pressure by a clamping arrangement. The unit is maintained in a sealed and nonimpregnated condition by potting in a metal container in a viscous asphaltic compound which does not penetrate the unit appreciably even in its fluid state.

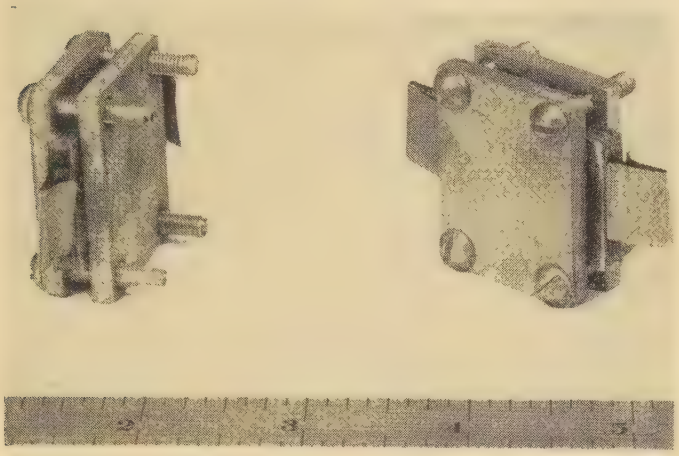

Figure 1. Dry stack mica capacitor units

Two distinct types of silvered mica capacitors were developed for general use in carrier telephone systems. One type known as the potted design was provided for applications where the highest initial precision and highest capacitance stability are required for services involving a limited range in operating temperature usually from about 60 to 100 degrees Fahrenheit. These capacitors are provided in several sizes of extruded nonmagnetic containers and provide for any desired capacitance value up to 0.4 microfarad. The other type is provided with mica filled molded bakelite casings and was developed for applications where small physical size is essential, but where the higher initial precision and higher capacitance stability of the potted types are not required. This type is provided in three physical sizes to cover a capacitance range from a few micromicrofarads up to approximately 20,000 micromicrofarads. A more detailed description of the construction of these two types of capacitors will be given.

Figure 2 shows the area of the mica lamination covered by the silver electrode. This area is coated with a suitable silver solution by spraying after masking the areas required for margins. The laminations then are fired at a high temperature for a short period to form a tight bond between the silver and mica. The laminations then are stacked, as shown in Figure 3, with a continuous strip of lead foil *F* interleaved between silvered surfaces so that one set of silver electrodes is joined electrically together and to the foil. Another strip of foil likewise is connected to the other set of electrodes on the opposite faces of the laminations. The purpose of looping-in the foil instead of using separately laid-in strips of foil is to permit a continuous indication of capacitance during stacking by means of a precise capacitance meter connected to the ends of the foil. Adjustment for capacitance first is made roughly by adding a sufficient number of laminations so that the measured value is somewhat larger than required. Terminals *T* then are crimped tightly over the ends of the foil to the mica stack to complete the unit assembly. The assembled unit of the potted capacitor after drying and coating with a thin layer of mineral wax, then is finally adjusted to close tolerance by removing the silver coating as required from the upper exposed surface shown in Figure 3. This has made possible the provision of capacitors meeting commercial tolerances of ±(0.2%+2 micromicrofarads) after being potted in wax in metallic containers. The molded case capacitor units are treated and adjusted in the same manner except that the wax dipping is omitted and the final adjustment prior to molding is accomplished by removing silver coating from the top lamination in a dry condition. Because of less predictable capacitance shift caused by molding the best commercial tolerance for molded capacitors is ± (0.5 per cent + 1 micromicrofarad). To insure high over-all quality

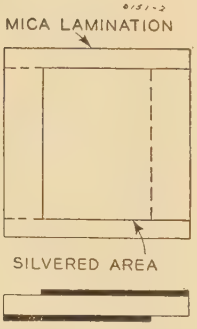

Figure 2. Silvered mica lamination

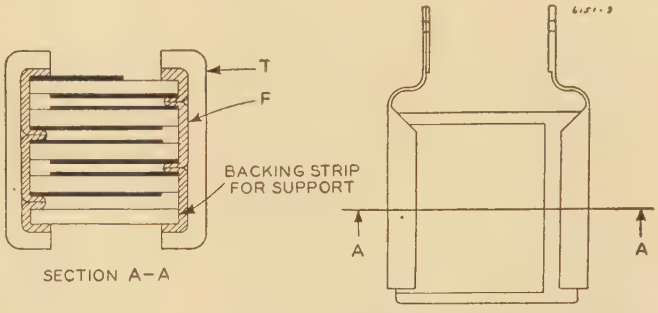

Figure 3. Silvered mica unit construction

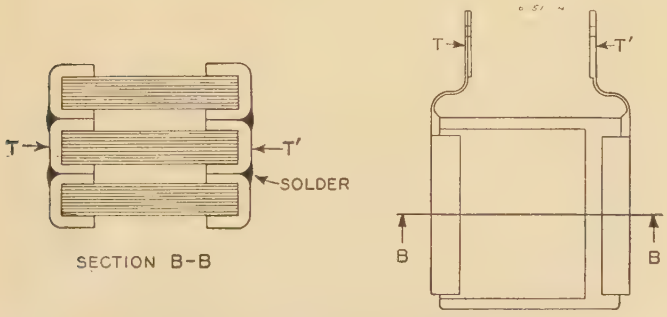

Figure 4. Multiple unit construction

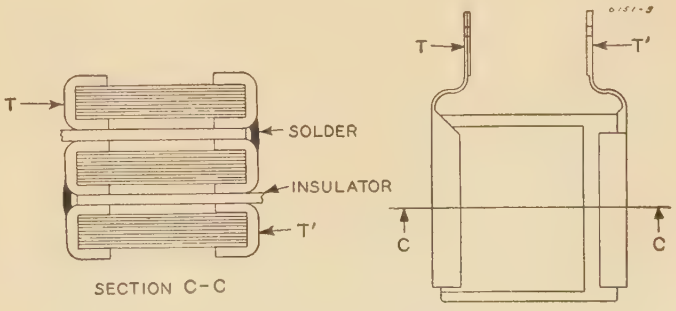

Figure 5. Series unit construction

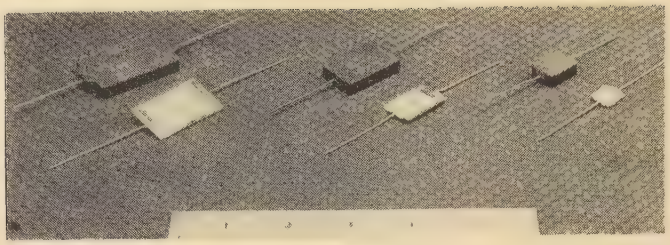

Figure 6. Molded silvered mica capacitors in current production

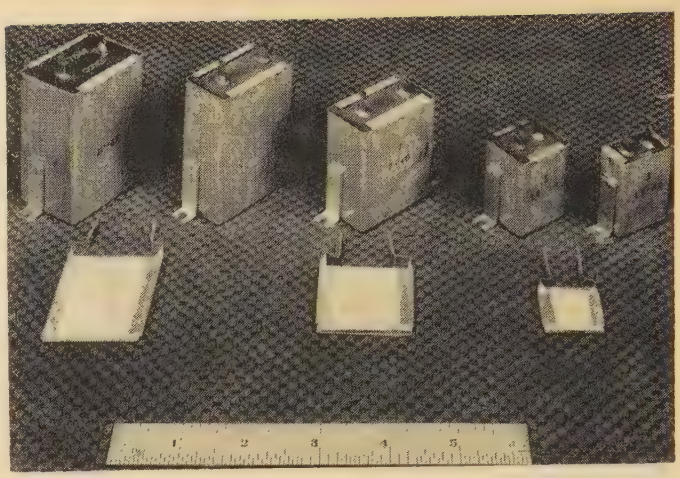

Figure 7 (right). Potted silvered mica capacitors in current production

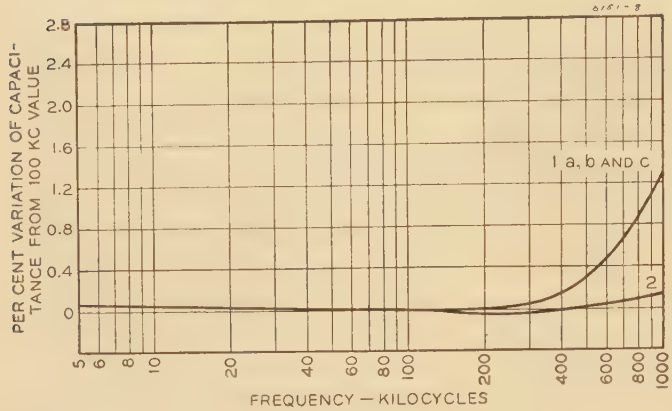

Figure 8. Variation of capacitance with frequency

1*a* = potted silvered mica, 0.01 μf
1*b* = molded silvered mica, 0.01 μf
1*c* = potted dry stack mica, 0.01 μf
2 = same as 1, except 0.001 μf

and performance all assembly operations are carried out in air-conditioned space where the relative humidity is maintained under 40 per cent at 75 degrees Fahrenheit.

Two or more of these unit assemblies are joined together mechanically and electrically to provide for the higher capacitances for the potted designs, as shown by Figure 4. For applications, such as line filters where high surge voltages may be encountered, several sections are connected in series, as shown in Figure 5.

In the case of the molded design, only single units are employed in the assembly because of the high molding pressures. The three sizes are shown in Figure 6. Figure 7 shows the five sizes of the wax potted designs in extruded containers which are provided for use in the Bell System plant.

Electrical and Performance Characteristics

The following discussion will deal with the more important electrical characteristics of dry stack and silvered mica types of capacitors and will cover data obtained on commercially made samples considered to be typical for these two types. Figure 8 shows the variation of capacitance with frequency over a frequency range of 5 to 1,000 kc for potted dry stack, potted silvered mica, and molded silvered mica capacitors of 0.01 and 0.001 microfarad capacitance. The capacitance change shown up to about 200 kc for the larger capacitance value and up to about 400 kc for the smaller value is dependent on the dielectric coefficient of the mica itself. It will be noted that this change is within 0.1 per cent. At higher frequencies the capacitance increases because of the effect of series inductance mainly contributed by the terminals. In the case of capacitors intended for operation at high frequencies, the effect of this inductance must be taken into account and proper allowance made for it where high capacitance precision is required.

Figure 9 shows the change in Q with frequency of 0.026 microfarad dry stack and silvered mica potted capacitors from 1 kc to 100 kc, and Figure 10 shows the change in Q of 0.001 microfarad potted and molded silvered mica capacitors from 5 to 1,000 kc. The average Q of the silvered mica potted design is higher, and the variation of Q with frequency is somewhat less than that of the dry stack design. It is believed that the inherently higher Q of of the silvered mica design results from reduced losses caused by the elimination of asphaltic potting compound and elimination of absorbed hydrocarbon material, as well as small traces of water vapor from the surface of the mica by the very high

Figure 9. Variation of Q with frequency for potted silvered and dry stack mica capacitors

1 = silvered mica, 0.026 μf
2 = dry stack mica, 0.026 μf

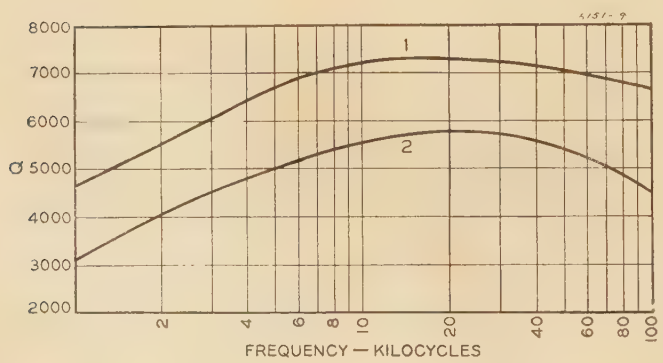

Figure 10. Variation of Q with frequency for potted and molded silvered mica capacitors

1 = potted silvered mica, 0.001 μf
2 = molded silvered mica, 0.001 μf

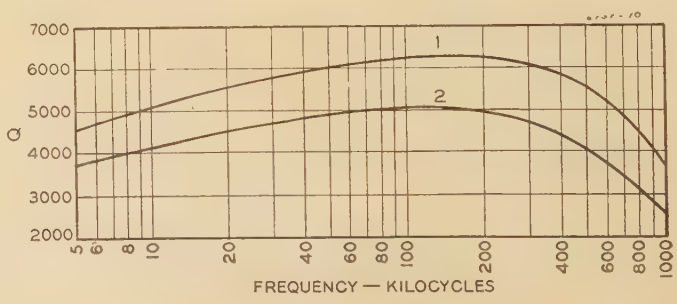

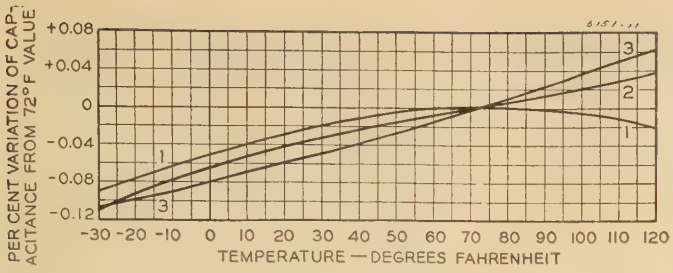

Figure 11. Variation of capacitance with temperature

1 = potted silvered mica, 0.01 μf, 10 kc
2 = molded silvered mica, 0.01 μf, 10 kc
3 = potted dry stack mica, 0.01 μf, 10 kc

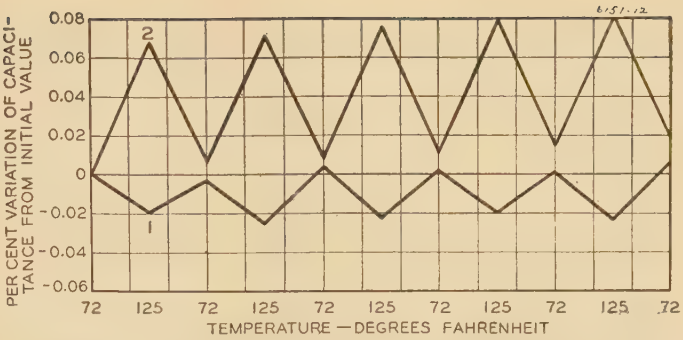

Figure 12. Variation of capacitance with temperature cycling

1 = potted silvered mica 2 = potted dry stack mica

firing temperature. The Q of the potted silvered mica also is higher than that for the molded capacitor of the same capacitance value. The dielectric losses in the phenolic casing and some contamination of the unit from the liberation of vapors during molding probably account for the lower Q of the latter.

Typical changes of capacitance with temperature for the molded and potted types are shown in Figure 11. It illustrates a pronounced difference between the molded and dry stack potted types as compared to the potted silvered mica construction. In the case of the molded and dry stack potted types, the change of capacitance with temperature primarily is caused by changes in the physical dimensions of the unit. These changes are such as to produce a positive temperature coefficient throughout the entire temperature range. In the case of the wax treated and wax potted silvered mica capacitors, the capacitance changes with temperature are caused by changes in the physical dimensions of the unit and also by the effect of the wax, having a high negative temperature coefficient, on the fringing capacitance of the unit. As a result the temperature coefficent is positive up to about 60 degrees and is negative above approximately 80 degrees. Between 60 and 100 degrees, the usual operating temperature range for central office installations, the temperature coefficient is extremely low.

Figure 12 shows the variations in capacitance of a typical potted silvered mica capacitor and also, for comparison, the same characteristic for a typical dry stack potted capacitor with repeated changes in temperature from room temperature to 125 degrees. The drift in capacitance resulting from repeated temperature cycles is caused by such conditions as small permanent displacement of the laminations in the assembly, small changes in the effective separation of the electrodes, and possibly small changes in the effective dielectric constant. Figure 12 illustrates how the drift in capacitance caused by the foregoing conditions, is minimized in the silvered mica capacitors. Data indicate that the potted silvered mica capacitors, also are more uniform from sample to sample in over-all capacitance stability, the extreme variations being one-fourth to one-fifth the magnitude of the variations observed with the dry stack design over the usual central office temperature range. In the case of the molded capacitors, while the average capacitance changes caused by drift as well as temperature coefficient are less than for the dry stack type, their capacitance changes have been found to be approximately double those of the potted silvered mica designs under the same conditons.

Figures 13 and 14 show the third order modulation characteristics for the potted and molded types. This characteristic is a measure of the capacitor's creation of new and unwanted frequencies while transmitting frequencies impressed upon it. In the case of capacitors, the creation of unwanted frequencies is the result of nonlinear effects caused by mechanical vibration and dielectric hysteresis. Un-

Figure 13. Variation of modulation with frequency

1 = potted silvered mica
2 = molded silvered mica
3 = potted dry stack mica

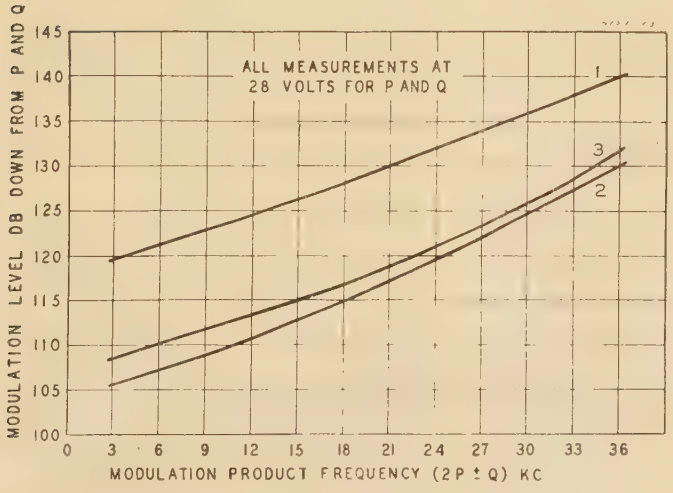

Figure 14. Variation of modulation with applied voltage

1 = potted silvered mica
2 = molded silvered mica
3 = potted dry stack mica

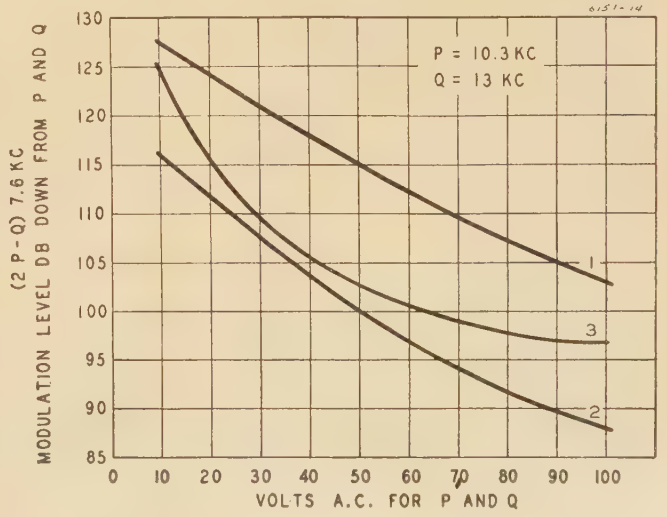

A New Design for the A-C Network Analyzer

J. D. RYDER
ASSOCIATE AIEE

W. B. BOAST
MEMBER AIEE

IN THE PAST FEW YEARS, with the heavy demands made on power systems, an increased interest has developed in network analyzers for public utility use. This has resulted in installation of several new analyzers and design or planning of others. In line with this trend, the Iowa State College has been active in developing and constructing an analyzer for use by utilities of the midwest area. Following general educational policy, the work was undertaken as a research project of the Iowa Engineering Experiment Station to determine the feasibility of applying new equipment and new techniques in improving the design of the a-c network analyzer.

In beginning the work, investigations were made which established a major premise, namely, that higher frequencies than those employed in the past could be used profitably. However, if frequencies are carried higher than previously, conventional instruments become inapplicable, and it is necessary to adopt as a corollary to the major premise, that complete electronic instrumentation will be desirable. As an additional advantage for this system, the instrument burden on the network can be reduced to a desirable minimum, and no longer serves as a major design limit on currents, voltages, and impedances employed.

One reason for raising frequency was a desire to draw on the techniques and apparatus common to electronics and radio, to determine if an amalgamation of the power and radio fields might lead to an improved design. Power levels used in network analyzers are approximately

Paper 46-135, recommended by the AIEE committee on instruments and measurements for presentation at the AIEE summer convention, Detroit, Mich., June 24–28, 1946. Manuscript submitted April 5, 1946; made available for printing May 13, 1946.

J. D. RYDER is an assistant professor, and W. B. BOAST is an associate professor, both of the electrical engineering department, Iowa State College, Ames, Iowa.

less these unwanted frequencies are held to very low energy levels as compared to the energy levels of the desired frequencies, in some cases less than one part in ten billion (100 decibels), crosstalk between carrier channels or noise or both seriously may impair high fidelity transmission of carrier telephone systems. It will be observed that over the frequency and voltage range shown, the silvered mica potted capacitors are approximately 15 decibels better than the molded designs. It is believed that this is because of the damping of mechanical vibration by the wax in the potted designs.

Conclusions

Current practice in the design of carrier telephone and other communication systems is imposing special requirements on capacitors used in frequency sensitive circuits. The exacting requirements of wire communication usually are not encountered to the same extent in other fields of communication engineering. The multiplicity of channels on a single pair of conductors, the large number of elements involved in a long circuit, and the constant use of these channels for years without adjustment or replacement of circuit elements impose very stringent requirements on capacitance tolerance at the time of manufacture, and on permissible change in capacitance subsequent to manufacture, to insure high fidelity transmission of voice and similar signals.

As has been described, two types of silvered mica capacitors were developed to meet these requirements. One type is wax sealed in a seamless metal container and has a practically flat capacitance temperature characteristic over the operating temperature range most commonly encountered, low modulation, and greater uniformity in the commercially manufactured product. The other type is provided in a low loss molded casing and satisfies a demand for small size and low loss capacitors, primarily for application where the higher precision and stability of the silvered mica potted types are not required.

those encountered in electronic equipment. Therefore, much of the standardized high production equipment for electronic service might be incorporated profitably in a network analyzer, instead of using scaled down power machinery and techniques. An example of the advantage of electronic equipment was found in the design of electronic generators for an analyzer. The electronic generator can be built with performance improved over that of the conventional induction motor phase shifter type, and at a much reduced cost.

An important economic factor influencing the decision to operate at a higher than normal frequency was the possibility of lowering cost through use of smaller values of inductance and capacity for given values of reactance. A valuable technical advantage which could be realized at a higher frequency was the elimination of iron cores in the inductive reactors, with consequent improvement in constancy of inductance at all current values and freedom from wave form distortion.

It should be understood that while the network analyzer to be described has proved its ability and the correctness of the fundamental design assumptions, it will continue in an experimental state for a considerable period of time. Built as a small pilot model, to prove the design, and to handle only simple problems, the analyzer may be increased in size by the addition of units in the future. Some modifications based on experience may be necessary, and compromises in equipment choice, forced by wartime conditions, may be eliminated in the larger model.

Fundamental Design Features

In the design of an analyzer in a new frequency range, extrapolated far beyond previous experience, many design decisions had to be made with and without adequate analytical background. Most of the decisions were interdependent and not simply related, but an attempt has been made to give the basis of many of them in the material below.

Choice of Frequency

Since all units are calibrated in terms of resistance, reactance, or susceptance, the actual frequency chosen for operation is independent of the frequency of the system being studied. Previous designs of analyzers have been operated in the 400- to 500-cycle range. In view of certain obvious advantages from the cost standpoint, a higher frequency seemed a desirable choice. These economic advantages

are twofold. Raising the frequency reduces the size of inductors and capacitors required for given reactance values, thus reducing the cost. Also, if the frequency is raised sufficiently, the ratings of many parts become those common to the radio industry, and the high production in this industry further reduces the price. Radio industry components are made in a great variety of sizes and are easily obtainable, which are both desirable advantages. While of somewhat variable quality, it is possible to obtain radio parts which are entirely dependable. This can be accomplished by careful selection of the manufacturer and avoidance of parts obviously built down to a price.

The curve shown in Figure 1 illustrates the variation in price of 100 ohms of capacitive reactance at various frequencies. They are list prices for good quality capacitors, and it is assumed that units of the exact required capacitance could be purchased with no paralleling of small units being necessary. It is probable that inductor costs also would show a considerable drop with frequency, although, as inductors are not common items of commerce, comparable prices cannot be obtained. The curve shown in Figure 1 is not meant to apply to capacitors alone, but is intended to give an indication of the trend in both inductor and capacitor costs with frequency.

Based on this reasoning, a tentative selection of the frequency base for the analyzer was made. This selection was subject, of course, to confirmation or change as other design features were checked. The frequency chosen for the Iowa State College a-c network analyzer was 10,000 cycles per second. This represents a major extrapolation of previous experience. Choice of a frequency substantially below 10,000 cycles per second would have made inclusion of iron cores in the inductors a necessity, and choice of a frequency much higher would have led to difficulties caused by reactance and susceptance of interconnecting leads, as will be discussed. An additional factor in the choice of a frequency of exactly 10,000 cycles per second was the commercial availability of a satisfactory source of low cost.

Frequency Source

As the analyzer was to be operated from a small power system of rather unstable frequency and because a rotary machine of small power rating at 10,000 cycles with sine wave form might be difficult to obtain, all-electronic operation of the analyzer was decided upon. This decision meant the use of a temperature-

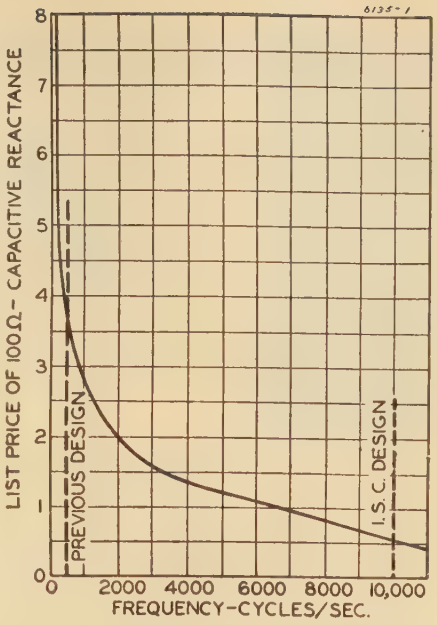

Figure 1. Estimated cost of 100 ohms of capacitive reactance at various frequencies

controlled quartz-crystal standard-frequency oscillator, operating at 100,000 cycles per second as the primary frequency source. By occasional checking against standard frequency signals from radio station WWV of the Bureau of Standards in Washington, this oscillator can be maintained within one cycle at 100,000 cycles, an accuracy in frequency of 0.001 per cent. In actual service, without adjustment, the error has never been found greater than five cycles at 100,000 cycles.

With frequency dividing circuits, the 100,000-cycle signal is subdivided by a factor of ten, yielding a 10,000-cycle output of a few volts, with reasonably good wave form, as the primary frequency source for the analyzer. This voltage then is filtered for wave form improvement and applied to amplifier circuits which are used to develop the power needed in the outputs of the equivalent generating stations of the analyzer.

Choice of *E*, *I*, and *Z* Base Values

With metering limitations somewhat removed in setting base values of voltage, current, and impedance, various other factors to be considered are physical size of units, and electric and magnetic couplings. Also needing consideration are the resistance and reactance drops and susceptance currents in leads connecting the units to busses and transfer jacks.

A low impedance base decreases inductor reactance and reduces the effects of stray shunt capacities. Shunt capacitor ratings are increased, but, in the radio capacitor field, physical sizes are so standardized that an increase in rated capacity over a ten to one range may mean no appreciable change in physical size or cost. Capacitor sizes, and expected effects of shunt lead capacities, indicated that a 100-ohm impedance base would be desirable and it was adopted. To keep electric coupling between circuits within units to a minimum, a voltage of ten volts was selected, resulting in a base current of 0.1 ampere. The power dissipated in the network is so low that small resistors may be used safely without fear of burning out on accidental overloads.

Interconnection of Units

For accurate operation of the analyzer, all leads from units to busses, transfer jacks, and so forth, should introduce negligible resistance, reactance, and susceptance into the circuit. At 10,000 cycles the problem of inductive and capacitive coupling between circuits can be severe unless transposition or shielding is used. Various types and sizes of wire for these lines were investigated with respect to resistance, series reactance, and current taken by the susceptance. Standard tolerances were set up as 0.1 per cent of base values.

Calculations were made on standard types of twisted pair lines used for radio frequency transmission, which indicated that certain types would meet the specifications on resistance and reactance, but might cause larger than desired shunt capacity currents. It was hoped that the twisted pair feature would introduce sufficient transpositions to reduce coupling. A better solution for elimination of inter-circuit coupling was the coaxial cable, and computations indicated that some types would have satisfactorily low circuit values. The complete absence of external field eliminates all circuit coupling, and a $^3/_8$-inch diameter double conductor (Twinax) coaxial cable was adopted for interconnections. The double conductor and shield feature allows input, output, and common ground leads of a line, load, or other unit to be carried in a single cable. The capacity between the two wires then appears shunted across the line or load circuit elements. The error introduced by this capacity across the circuit elements is 0.25 per cent of base value, for the longest lead encountered. The capacity of the two wires to the shield and ground is negligible, causing a current flow of only 0.075 per cent of base current on the longest lead. The resistance of the chosen cable for the longest length is approximately 0.1 per cent of base value.

The reactance of the chosen Twinax line was another limiting factor and for

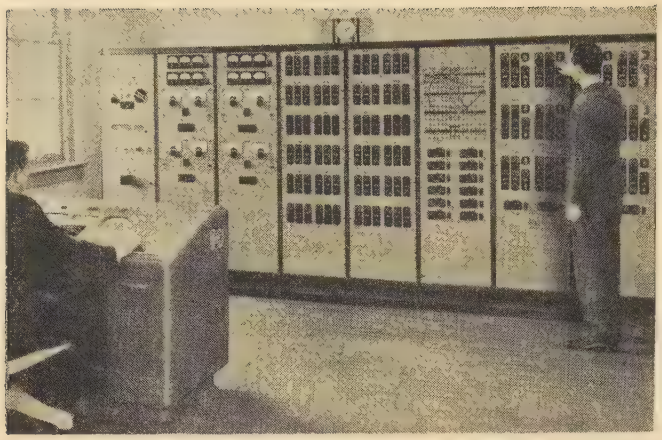

Figure 2. General view of the Iowa State College a-c network analyzer

the longest lead is 0.1 per cent of base value. This fact influenced the choice of 10,000 cycles as base frequency. The magnitude of these limiting factors indicates that a cable design with slightly larger conductors would be desirable. Such a cable was not a commercial product and under wartime conditions it was necessary to design around available equipment.

Inductive Reactances

One of the reasons for the choice of 10,000 cycles as base frequency was the possibility of eliminating all iron in the line and load inductors by the use of air core coils. Use of air core coils removes all anxiety as to wave form distortion by the iron, and constancy of inductance at all current values. Lower losses or higher ratios of reactance to resistance also have been achieved than those mentioned for iron core coils in lower frequency network analyzers.

Air core coil designs have been developed for all sizes of reactors used, which give all inductors phase angles of above 88 degrees, and certain much used load inductor values above 89 degrees. All coils are shielded in mutually perpendicular pairs, and the above phase angle measurements are with shielding in place. The resistance component introduced by any coil of a load unit may be considered as two per cent of the rated reactance, and of any coil of a line unit as four per cent of rated value. Each decade of a reactor group is obtained by series switching of 1-, 2-, 3-, and 4-ohm reactors or multiples of these values.

Accuracy

A definite statement of the accuracy to be expected from such a complex mechanism means very little because of additive and subtractive errors introduced by so many circuit elements in cascade, and to usage of meter readings in various types of calculations. It can be stated that all resistor elements are accurate to better than one per cent of the setting. All inductive reactors have been adjusted to within 0.2 per cent and, because of the air core construction, will maintain that accuracy at all current values. Capacitive susceptors have been assembled to match the 0.2 per cent maximum deviation requirement. The metering system has been calibrated from d-c standards by thermocouple transfer units to one-half per cent or better of full scale values for normal loading conditions.

Use of Standard Radio Equipment

It already has been emphasized that the selections for frequency and impedance bases made possible the use of standard high production radio components and coaxial cable. In addition, the radio and telephone industries have developed a line of standardized instrument racks and panels which have advantages in flexibility and availability. These panels are 19 inches wide with heights in multiples of $1\frac{3}{4}$ inches. The racks are 20 inches wide, six feet high, with mounting holes so arranged that panels can be mounted at any point desired. Such an arrangement will permit easy changes in the future if needed. A view of the complete analyzer is shown in Figure 2.

Control Desk

The main control and metering desk, illustrated in Figure 3, was designed in modern style and finished to harmonize with the panel equipment. Its design permits the operator an easy view of the complete analyzer and houses all instrument amplifiers and certain relays.

The desk combines analyzer controls and master instruments on a sloping panel. The angle of the panel was chosen to be comfortable for the operator in either controlling the analyzer or taking data. On the panel, and accessible to the left hand, are the main 60-cycle power controls, lever keys for connecting the instruments to either input or output circuits of any analyzer unit, a watts-vars switch, and a switch to place the desk instruments in operation.

Also operated by the left hand are the push buttons for preselection of relays by which the desk master instruments may be connected in any circuit. By simply pushing buttons corresponding to the number of the unit to be metered, as on an adding machine, the relay circuits are selected. The capacity of the push button system is 999 circuits which, by reason of the input and output relays on each unit, will permit metering at 1,998 distinct points should that number ever be required. All push buttons are mechanically interlocked to prevent metering two circuits at once. By assigning these controls to the left hand, a pencil held in the right hand for taking data or other work need not be dropped during operation.

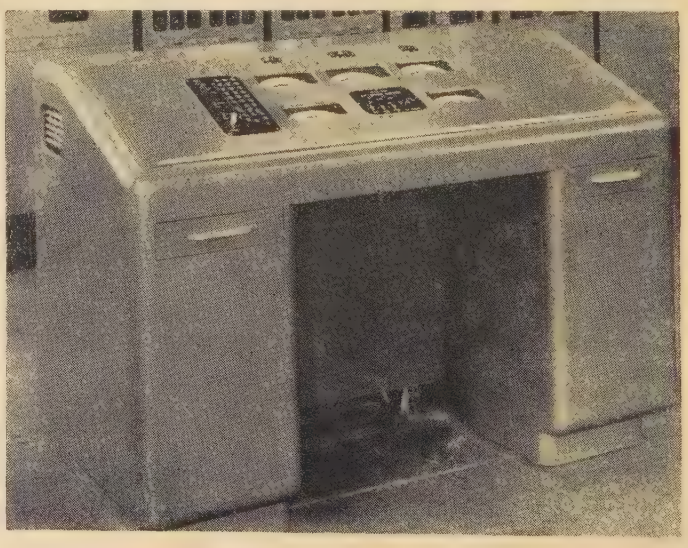

Figure 3. The main metering and control desk

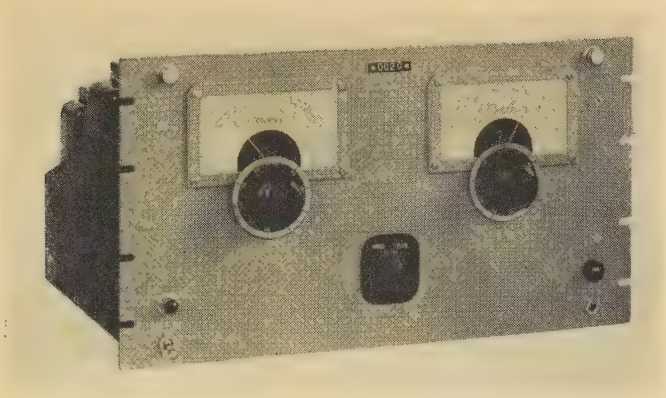

Figure 4. Front panel of a generator unit

The dials are for adjusting voltage and phase angle

The desk instruments are subsurface mounted and internally illuminated with fluorescent lamps, giving a very uniform glareless shadow-free light. The upper and lower rows of instruments are placed at different vertical angles so that an observer of average height will have a line of sight perpendicular to the meter scale for both instrument rows. This materially reduces the fatigue of the operator. Mounted below the instruments are range switches for the ammeter and voltmeter and a reversing switch for the wattmeter. Working in conjunction with the range switches are colored signal lights above the voltmeter, ammeter, and wattmeter, indicating the range multiplier in service at any time.

The instruments used all are operated electronically and comprise a voltmeter, an ammeter, a watt-varmeter, and two phase angle meters. The phase angle meters are at each side in the lower row, the other instruments being placed in the upper row with the wattmeter in the center. Amplifiers for operating these instruments are installed inside the control desk. The voltmeter and ammeter are fairly conventional electronic amplifier types, stabilized by large values of degenerative feedback. The wattmeter is an electrodynamometer type with both current and voltage coils supplied from stabilized amplifiers. A phase shifting circuit converts this to a varmeter. The phase meters are an unconventional feature. One reads angle of the voltage at the metered point and the other reads angle of the current, both with respect to any desired common reference voltage. A switch on the desk allows selection of any generator electromotive force as a reference, or any desired point in the network may be connected as a reference through the transfer jacks. The phase meters employ an electronic circuit[6] which clips and squares the waves before phase comparison, eliminating error caused by amplitude variation.

Insertion of the instruments into the desired circuit is handled by relays, selected by the push buttons. The relays connect the circuits of the desired unit to a Twinax metering bus, which terminates in current shunts and voltage dividers, across which are connected the master instruments of the desk. The shunt introduces a resistance of 0.1 per cent of base value, while the voltage divider inserts a loading of 0.03 per cent on the circuit. The metering bus, connected to all units, inserts some distributed capacity, and the contacts of the switching relays in each unit insert large lumped capacities in the metering system. These all have been compensated for effectively and the resultant error is negligible.

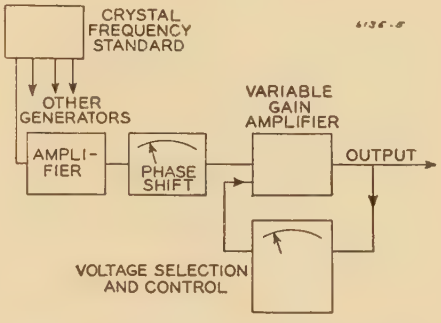

Figure 5. Outline diagram of the generator circuit and operation

Design of Units of the Analyzer

The present Iowa State College a-c network analyzer, although a small pilot model, was designed to handle most advantageously the simpler problems for the utilities of the midwest area. In consultation with these utilities, the following choice of numbers of units of the analyzer was made: 4 generator units, 24 line units, 12 load units, 12 capacitor units, 4 tap changer units, and 4 mutual transformer units. Features of the design of each of these units will be given.

Generator Unit

The standard frequency source has an output of a few volts and negligible power. Each unit simulating a generating station of the analyzer must amplify the voltage to the desired base level or higher and provide sufficient power for input to the loads and lines of a given problem. The generator also must have independent means of adjustment for phase angle and magnitude of voltage output.

The generators for this analyzer consist of vacuum tube amplifiers of power output considerably greater than required for rated base output. A generator is shown in Figure 4. Phase angle control is provided in two 180-degree steps through the left hand dial and the "plus-minus" switch on each generator panel, the control operating in the low level amplifier stages. Voltage selection is possible by the right hand dial on the generator panel. With selection of output voltage, an automatic voltage control circuit is set to adjust the amplifier gain and maintain the desired voltage. A block diagram of a generator is shown in Figure 5.

The performance of the automatic voltage control circuit is shown in Figure 6. The control operates to maintain constant voltage to 250 per cent of base or rated output current into a resistance load. This represents zero internal impedance and zero per cent regulation. Above 250 per cent load current, the generator voltage drops because of an internal impedance of about 4.0 ohms. On either leading or lagging load, the voltage regulation is improved over that for resistive load. Contrasting with the generator performance under control is the performance with no voltage control, as shown by the dashed line in Figure 6.

Connected to each generator is a set of instruments to read generated electromotive force, current, and output power, as shown in Figure 7. The instruments are electronically operated and stabilized by degenerative feedback in order to be entirely independent of changes in tube characteristics and line voltage. All in-

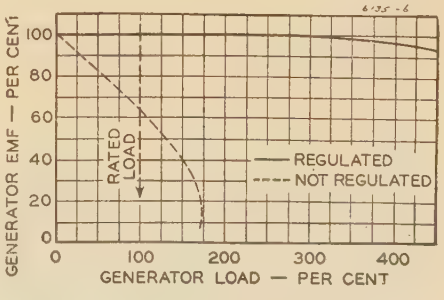

Figure 6. Voltage regulation of the generators for varying output

Figure 7. Individual generator metering panel

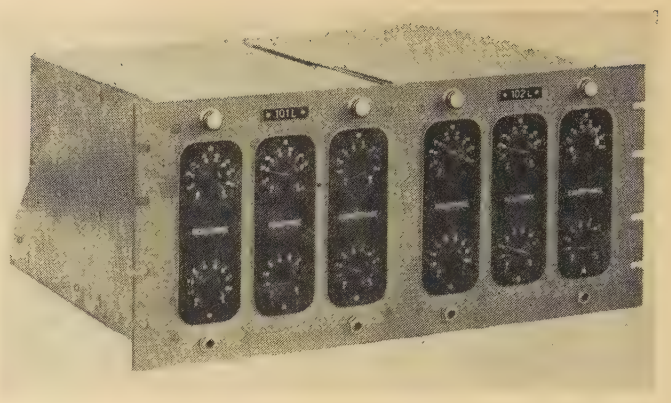

Figure 9 (right). Assembly of a line unit

struments are calibrated in percentage of base values. The wattmeter is arranged with zero center scale so that indications of reverse power flow can be read easily. With the meters permanently connected to each generator output, the loading can be checked continuously, and the effect of adjustments of one generator on the output of other generators in the system can be observed readily.

Mounted below each generator is an inductive reactance panel by which generator reactance up to 99-per-cent base value by 1-per-cent steps may be inserted. Both generator electromotive force and terminal connections are available at the transfer jacks for ready circuit connection.

Line Unit

In reducing an actual system to a model representation on a network analyzer, retention of each line of the system as an entity is highly desirable. In the majority of previous analyzer designs, the series resistance and reactance equivalents have been retained in the analyzer line unit, but shunt susceptance equivalents of all lines emanating from a common bus usually have been added and set up on these analyzers by a single separate capacitive susceptance unit. The direct metering of a line for terminal current conditions, therefore, was impossible. The line unit of the Iowa State College analyzer was designed as an entity containing the shunt capacitive susceptance as well as the series resistance and series inductive reactance. This detail was possible because of the favorable space and cost conditions inherent in the higher frequency design. A schematic wiring diagram of a line unit is shown in Figure 8, and a photograph of a line unit panel is shown in Figure 9.

Either a T- or a π-section design would be electrically satisfactory for the line unit. However, the cost and space requirement of an average capacitive susceptance element is considerably less than that of an average inductive reactance and resistance element, and hence the π-section, requiring one set of reactance and resistance elements and two sets of susceptance elements, was chosen. In each line unit, the two sets of susceptance elements in the π-section are adjusted simultaneously by a 2-gang switch.

The series resistance and reactance are each adjustable from zero to 99 per cent in 1-per-cent steps. The total shunt susceptance is adjustable from zero to 9.9 per cent in one tenth of 1-per-cent steps. Each of these three elements thus was designed in two decades.

Load Unit

The basic elements in the load unit design are resistance and inductive reactance inasmuch as the majority of load conditions in an actual system may be represented by these parameters. In representing load conditions on the analyzer, often the voltage at the load point is an unknown quantity at the time of establishing equivalent resistance and reactance values. If a particular power and power factor are known conditions, an estimate of the voltage usually is made and the corresponding circuit parameters are calculated and set on the analyzer. Measurements then are made of the first approximation of the desired power. If the power is not that desired, a resetting of parameters is necessary. In the Iowa State College analyzer, the resistance and reactance values are viewed electrically through a variable ratio autotransformer, adjustable by 1-per-cent values from 1/1.10 to 1.10. If the first estimate of the resistance and reactance are within approximately plus or minus 20 per cent of the actual values required, the adjustment of the load may be accomplished quite simply by adjusting the turns ratio of the transformer, thus avoiding a recalculation of the individual resistance and reactance parameters. A schematic wiring diagram of a load unit is shown in Figure 10, and photographs of a load unit panel and rear assembly are shown in Figures 11 and 12.

The resistance and reactance elements may be placed either in series or in parallel with one another by the switching plan illustrated in the schematic wiring diagram. This permits more versatility in the application of this unit to a variety of problems.

The resistance and reactance are each adjustable from zero to 9,990 per cent in 10-per-cent steps. Each of these two elements was thus designed in three decades.

The output terminals of the load unit are retained even though for normal load usage this output is closed by a short-circuiting plug. By thus providing the output terminals, the load unit may be used also as a circuit of higher series im-

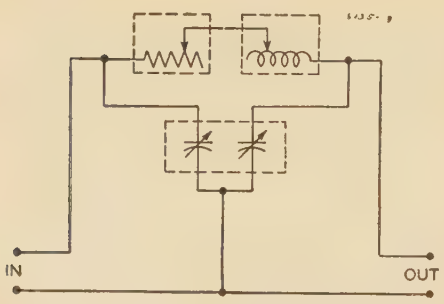

Figure 8. Simplified diagram of the wiring of a line unit

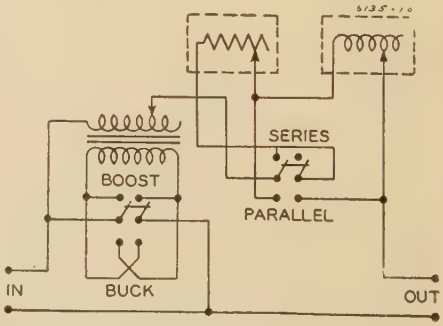

Figure 10. Simplified diagram of the wiring of a load unit

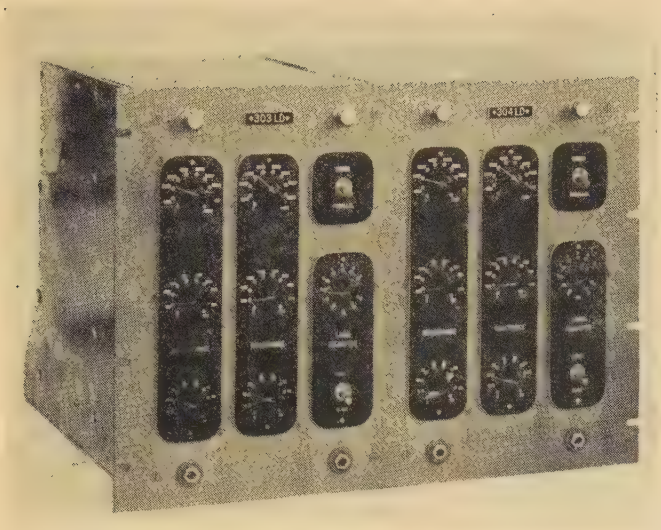

Figure 11 (above). Front panel view of a load unit

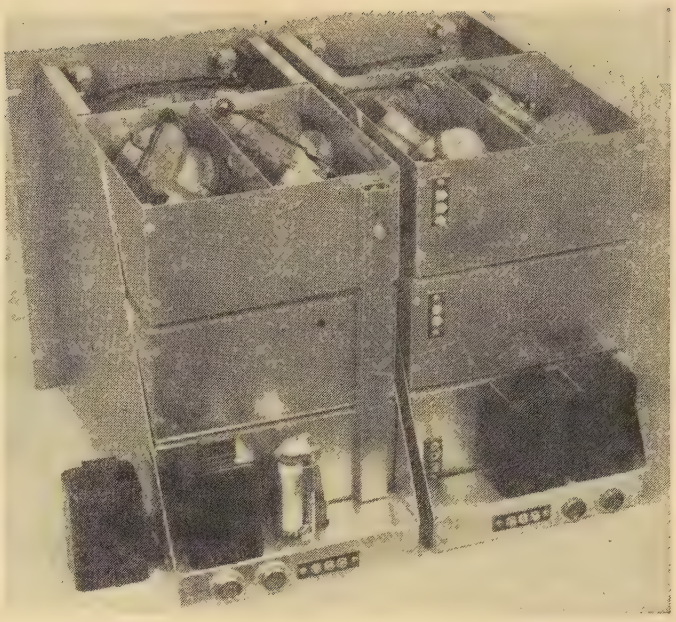

Figure 12 (right). Rear assembly of a load unit

pedance rather than a line unit for those applications where such a circuit may be desirable.

The autotransformer utilizing a high frequency low-loss steel core has an equivalent shunt impedance such that the error introduced by the adjusting transformer when used with the base impedance is approximately 0.6 per cent. The equivalent series impedance of the autotransformer when set at full ten per cent is 0.7 per cent. Each of these errors is comparable to the one-half-per-cent accuracy which was the design goal of this analyzer.

Capacitor Unit

Separate capacitor units are provided on the analyzer for increasing the range of the susceptance built into the line units, adding capacitive loading to the load units, or for representing series or shunt capacitors at any point in a system. A photograph of such a panel is shown in Figure 13.

The capacitive susceptance may be used either as a series or shunt element by a switching plan similar to that used in the load unit. The susceptance is adjustable from zero to 99 per cent in 1-per-cent steps. The element thus is designed in two decades.

Tap Changer Unit

Tap changer units are provided for representing networks which do not possess net unity turns ratios around closed loops. The unit is a variable ratio autotransformer adjustable from 1.000 to 1.295 by 0.005 steps. The transformer has a low-loss steel core and in design is similar to the load adjustor transformer of the load unit. The equivalent shunt impedance is practically identical with that of the other unit. Incorporated also is a reversing switch which changes the turn ratio from a step-up to a step-down basis.

Mutual Transformer Unit

A unity ratio 2-winding transformer with an inductive reactance placed across either side is used for representing mutual coupling between circuits of a power system. The mutual transformer, utilizing a low-loss steel core, introduces losses of approximately 0.4 per cent of base power if used across a 10-ohm reactor at full base current. The equivalent series impedance of the transformer is also 0.4 per cent and introduces negligible error of insertion.

Miscellaneous

The Twinax cable from each unit terminates at the transfer panels in two sets of 2-conductor jacks. One pair of duplicate jacks connect to the common and input conductor of the unit and the other pair to the common and output conductor. By the process of extensions from duplicate pairs, a large bus system may be established.

Associated with the input or output terminals on each unit are separate jacks which permit the interconnection of other units inside the point at which the meters are inserted by the relay system. Thus a single instrumentation of a composite group of units is possible when this is desirable, as for example if capacitive loading were added to a load unit by inserting a capacitor unit inside the metering point of a load unit.

Operating Experience

Although commercial operating experience of the analyzer as a whole is rather limited at the present date, such system problems as have been set up on the analyzer have yielded results which check at nodes and loops quite consistently within the design tolerances previously mentioned.

Several 2- and 3-generator problems which have been calculated have been set up on the analyzer, and measured values on these problems likewise have been within the design tolerances of the units and the instruments.

As elements of the analyzer have been completed over a period of the past 15 months, each has undergone extensive testing in the component form; and, where the experimental measurements did not conform to the design tolerance of one-half-per-cent accuracy, further modi-

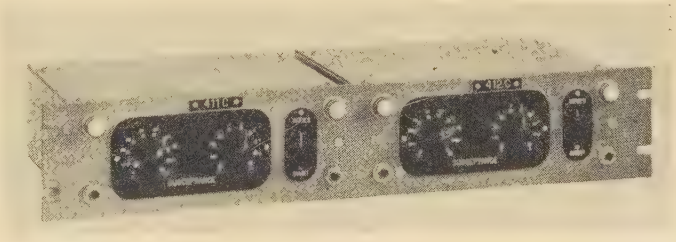

Figure 13. Panel view of a capacitor panel

A 400-Ampere Sealed Ignitron

H. C. STEINER
MEMBER AIEE

H. N. PRICE
NONMEMBER AIEE

Synopsis: As rectifier capacity is increased, it becomes desirable to use larger capacity rectifying elements. The choice of rectifying element size requires careful consideration in order to provide a complete range with a minimum number of units. The sizes of industrial ignitron tubes for welding control and for rectifier service have been chosen on a preferred number scale providing a proportionate increase at each increment. The development of a 400-ampere ignitron for rectifier service was undertaken to provide the next larger size tube in the series. Development work on the 400-ampere ignitron disclosed that design problems become more complex as the physical size of the tube is increased. The ability of a tube to rectify a given current with a minimum number of arc-backs is affected by circuit duty and by control of ionization, particularly at the end of the current commutating period. None of the factors involved have indicated an upper limit in size, but rather a need for a more exact understanding of the phenomena involved.

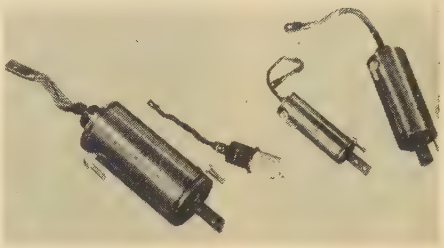

Figure 1. Sealed ignitrons for welder service ranging in capacity from 300 to 2,400 kva at 250 to 600 volts (rms)

THE DEVELOPMENT of the ignitor introduced a new and different concept in the utilization of mercury pool cathodes for mercury arc rectifying devices.[1] The ignitor permitted the starting of a new cathode spot for each conducting period at the precise instant that conduction was desired. With this mechanism it was possible to design mercury pool tubes of the single-anode half-wave type having the control characteristics of the thyratron, the versatility of the half-wave tube in circuit application work, and the very high emission capacity of the mercury pool. This emission capacity seems partly caused by the ability of the cathode spot to divide and subdivide above currents of the order of 15 to 20 amperes until a sufficient number exist to supply the current demand of the circuit in which the rectifying element is connected.

Further recognition of the greater efficiency of the single-anode half-wave design for power conversion work in comparison with the older multianode rectifiers has been made recently in the development of an excitron tube.[2] With this tube, continuous excitation of a cathode spot on the mercury pool is maintained, and control of the starting of the anode current is accomplished electrostatically by means of grids as in the thyratron.

It is the purpose of this paper to review, briefly, the progress that has been made in the development and application of ignitron tubes and to outline some of the design considerations in the development of higher current sealed tubes.

Paper 46-140, recommended by the AIEE committee on electronics for presentation at the AIEE summer convention, Detroit, Mich., June 24–28, 1946. Manuscript submitted April 26, 1946; made available for printing May 14, 1946.

H. C. Steiner and H. N. Price are both with the electronics department, tube division, General Electric Company, Schenectady, N. Y.

Status of Ignitron Tube Development and Application

Pumped Ignitrons

The largest field of application for continuously evacuated ignitron tanks has been in the electrolytic refinement of aluminum and magnesium. Here, large amounts of direct current are required for a single line of reduction cells. Capacities as high as 30,000 kw, 50,000 amperes at 600 volts are needed. Initially, to supply this capacity, individual rectifiers of the order of 3,000 kw were operated in parallel. The rectifying element of each unit consisted of 12 tanks having a continuous average current capacity slightly over 400 amperes per tank. Continued development supplemented by field experience has increased this capacity so that tanks of 1,000 amperes are practicable.

Welding Control Ignitrons

Initial application of permanently evacuated sealed ignitron tubes was made in an entirely new field—that of control and timing for resistance welding.[3]

In resistance welding, two pieces of metal are held together in close contact and a high current passed for a sufficient time to heat the parts to a welding temperature. The parts then are forged together. Control of the time is essential if uniform repetitive welds are to be made. Some progress had been made previously with the use of thyratrons to control the number of cycles in the weld, the current capacity of the thyratron being matched against the welder transformer primary requirements by means of a series transformer. Two ignitron tubes connected in parallel, but with current flow in opposite directions, provide a simple low-inertia switch with sufficient current carrying capacity to conduct the welding transformer primary current directly. In conjunction with thyratrons to initiate conduction, this precise control not only improves the quality of welds in materials

usually fabricated by resistance welding, but also permits materials to be fabricated which heretofore had been considered too difficult to weld. As a result, welding methods have been extended from simple spot welds to line welding (a series of overlapping spots) to sequence control (in which provision is made for preheating, welding, forging, cooling, and annealing periods) and to flash welding. Sealed ignitron tubes developed for this service range in capacity from 300- to 2,400-kva demand for two tubes at supply voltages of 250 to 600 volts (rms). Figure 1 shows the general appearance of the welder ignitrons. All are water-cooled directly except the smallest, in which the heat is transferred to a heavy clamp that in turn may be either air- or water-cooled.

An interesting application of the ignitron contactor principle has been made to provide rapid interruption of the plate power supply in case of arc-over or short circuit in radio transmitters.[4] Ignitron contactors have been placed in each of the three 2,300-volt lines supplying power to the rectifier transformer. Ignition power is supplied through thyratrons. In case of fault, overcurrent operates small high speed d-c relays in the transmitting tube circuits that block the thyratrons, and the ignitron tubes in turn cease conduction. Interruption of fault currents occurs in slightly over one cycle of the 60-cycle supply frequency. Damage to the transmitter equipment from flashover and to the transmitter tubes is negligible.

Rectifier Ignitrons

Rectifier duty is more severe than welder control and it was necessary to modify the design of the sealed tubes somewhat, as discussed later, in order to provide service essentially free from arc-back. Two sizes of tubes were developed which in 300-volt d-c service have continuous average current ratings per tube of 100 and 200 amperes. At 600 volts, the current capacities are 75 and 150 amperes. In addition, overload capacity is required since rectifier equipment for industrial, mine, and railway service has standard 2-hour and 1-minute ratings. These standards vary, depending on the service, from 125 to 150 per cent at the 2-hour point and from 200 to 300 per cent at one minute. To meet these requirements, the continuous or design capacity of the tubes must approach the overload requirements because the mass of the tube electrodes is small, in general, and there is relatively low heat storage capacity.

With these two sizes of tubes, it was possible to provide sealed ignitron rectifier equipment ranging in capacity from 75 to 500 kw at 300 volts, and from 100 to 1,000 kw at 600 volts by proper choice of the circuit and number of tubes.[5] Trial installations were made in the industrial, mining, and electrolytic field, and for building service d-c supply. Sufficient experience had been obtained at the beginning of World War II to provide field tested and proved equipment for the great industrial expansion that took place.

400-Ampere Sealed Ignitron

In the initial development of steel envelope sealed ignitron tubes, there were two predominant considerations—vacuum life and ignitor life. Rectifier duty, in particular, is continuous in nature and it is essential that sealed tubes for this service have a long life to avoid the interruptions of frequent replacements. Experience has demonstrated amply that tubes properly degassed and tightly sealed retain the required vacuum conditions for years. In fact, the action of the arc and the walls of the tube exert a considerable cleanup action which tends to improve the initial vacuum.[6] Under ordinary service conditions, ignitors show very little wear or erosion. Under improper conditions, such as accidental reversal of the ignitor current, the life may be very short—a matter of minutes—since a cathode spot then forms on the ignitor and material is blasted away rapidly. Actual life of some of the tubes in initial installations has exceeded five years with these tubes still in service.

With substantiation through field experience of the basic factors of vacuum and ignitor life and the excellent performance of the higher current rectifiers for aluminum and magnesium reduction, it was felt that development of the next larger size of sealed ignitron tube was desirable and could be undertaken.

Size

It is fully as important to choose a proper series of sizes in electronic tubes as in other electric or mechanical devices. Preferred number scales which provide a proportionate increase in size or capacity at each increment offer a logical means of determining the number of sizes required to serve a given field. Sizes for both the welder and rectifier ignitron tubes were established on this basis. In the case of the rectifier ignitrons, the series 25, 50, 100, 200, 400, 800, 1250, 2500 gives a satisfactory spacing in average current per tube. At the lower end of the scale, 25 amperes and below, thermionic-cathode tubes of the thyratron type are used because of the reduction in required auxiliary equipment. The number of sizes required above the 400-ampere point will depend primarily on application trends. In general, it is preferable to use larger sized tubes rather than increased numbers for increased capacity, provided proper wave shape and induction co-ordination factors are maintained.

Design

Ignitron tubes are basically heat-transfer devices in which maximum temperatures establish the limiting operating conditions as in other forms of electric equipment. The limiting temperatures are not those, in general, at which gradual deterioration or burning takes place, but rather those at which complete failure of the rectifying properties occur. Such failures rarely cause destruction of the rectifying element itself unless the arc-backs are allowed to persist. Normally, restoration of conditions below the limiting ones restores the rectifying action.

The insulating patch theory developed by K. H. Kingdon and E. J. Lawton seems to offer the most reasonable and consistent explanation of the cause of arc-back.[7] Briefly, it is assumed that small microscopic insulating particles exist on the surface of the anode or are carried there by the vapor stream. These patches become charged from the ionization present. If the charge becomes sufficiently great and the distance separating the charge from the anode is sufficiently small, field emission will release enough electrons to establish a glow discharge. The resulting increase in ionization favors the establishment of a cathode spot on the anode, which is followed by arc conduction of current in the reverse direction. The probability of exactly the right conditions occurring depends on the density of ionization in the immediate vicinity of the anode, the rate of ion collection, the frequency of trial, and the size and leakage resistance of the insulating patch. For a given design, the majority of the factors depend on or are related to circuit requirements so that a knowledge of these provides a basis for predicting tube performance.

From the tube design view point, it is difficult to isolate the effects of the factors influencing arc-back since they are interrelated and interdependent. The more important ones are as follows:

1. Vapor pressure.
2. Ionization.
3. Anode current.
4. Anode voltage.
5. Circuit duty.

Vapor Pressure

Energy losses occur in an ignitron tube as a series of pulses. These pulsations are averaged by the mass of the enclosing envelope to an even flow of heat which is removed by the water-cooling. The water temperature therefore determines a base or datum plane above which the instantaneous pressure rises during the conducting cycle. The instantaneous pressures are the result of vaporization of mercury by the action of the cathode spot. Mercury is vaporized at a rate of approximately 7.2×10^{-3} grams per coulomb, and this mercury blast creates pressures during the conducting period far in excess of the pressure determined by the wall temperature. The pressure during conduction is of little importance as regards arc-back, except as its magnitude influences the ability of the condensing walls to reduce the pressure at the end of conduction to a value below the breakdown point. A typical pressure breakdown curve for static conditions in mercury is shown in Figure 2. Since the pressure waves travel with a velocity approximately that of sound, there is a time lag between the current and the corresponding instantaneous pressure at the end of conduction which tends to delay deionization. This lag increases as the size of the tube increases.

In addition to the vaporized mercury, the action of the cathode spot ejects relatively large (visible) mercury droplets which travel at a rate very much slower than the pressure wave. The droplets may be observed in glass tubes by blocking out the glow during conduction with a synchronously rotating slotted disk and by illuminating the vacuum space with the light from a tungsten filament lamp. The initial velocities of individual drops vary widely since droplets are visible at the top of their trajectories over nearly the entire length of the tube. These droplets undoubtedly create high transient pressures when they strike relatively high temperature objects, and because of their random character may account for some of the arc-backs that are found to occur late in the inverse cycle when both the residual ionization and inverse voltage have decreased appreciably from their maximums.

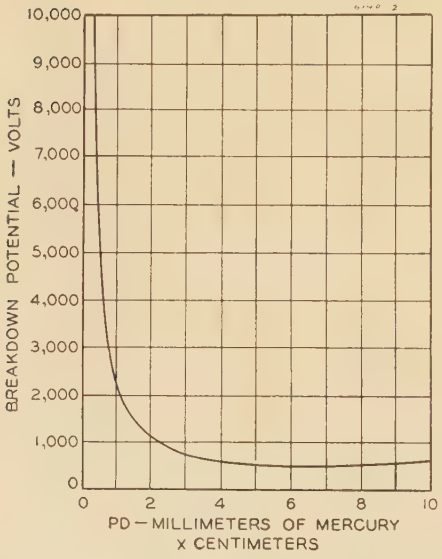

Figure 2. Breakdown voltage between two electrodes in mercury vapor as a function of the product (Paschen's law) of the vapor pressure *P* and the gap length *D*

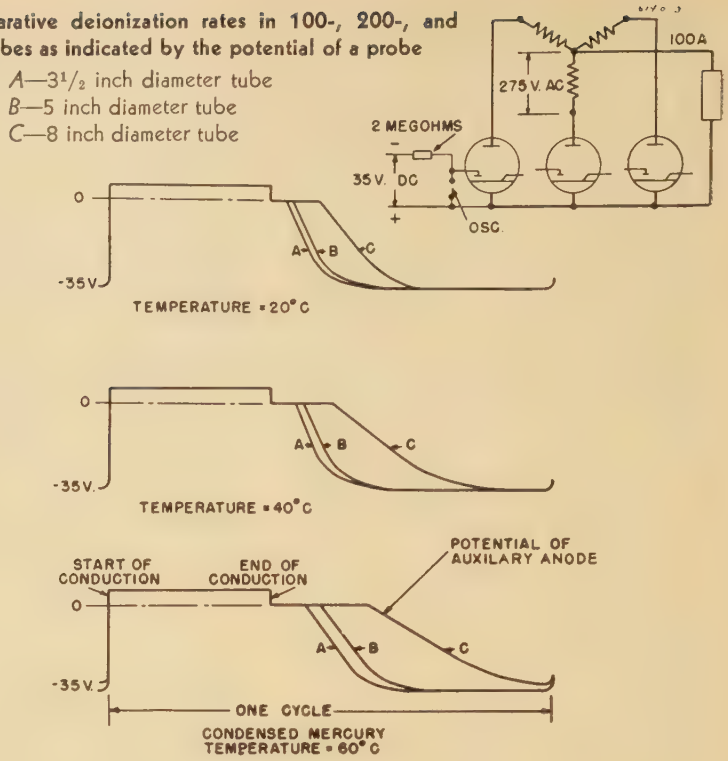

Figure 3. Comparative deionization rates in 100-, 200-, and 400-ampere tubes as indicated by the potential of a probe

Ionization

The problem of ionization becomes increasingly important as the size and capacity of the tube is increased.

Under low pressure conditions, the mean free path of the ions is relatively long, and the arc voltage needed to produce the required ionization is relatively high. Under extremely low pressures, there is a condition in tubes having constricted arc paths where there are insufficient ions to neutralize the space charge and for an instant the tube behaves as though it were a high vacuum tube.[8] The current is reduced abruptly, and this change in conjunction with associated circuit inductance produces high voltage surges. The point at which pressures become low depends largely on the tube design. In tubes of small volume and open construction, the possibility of constriction surges is remote at any temperature above zero degree centigrade (vapor pressure, 0.16 micron) because the action of the cathode spot very rapidly establishes the vapor density required to provide the necessary ions. As the size of the tube increases, and particularly as grids are added to control the ionization, the minimum pressure must be increased. In multiple grid high voltage tubes, minimum pressures of the order of four to eight microns (35–45 degrees centigrade) are required for currents of 4,000 amperes. The minimum pressures usually are determined by the short-circuit current that the tube may be required to conduct, rather than the normal load currents.

At the end of conduction, the intensity of residual ionization becomes extremely important because of its direct relation to arc-back. In tubes of small volume, the deionization rate is rapid and equilibrium between ionization and anode current is reached quickly so that the ion density is relatively low when inverse voltage is applied at the end of commutation, or transfer of current from anode to anode. As the cross section and volume of the tube increase, for higher capacities, the volume of ionized gas increases and the time required for the ions to diffuse to the walls is increased, with the result that the density of ionization at the end of conduction is correspondingly higher. Figure 3 shows the time required for the ionization to decay to a given value for a fixed value of anode current in the 100-, 200-, and 400-ampere sizes of tubes. The curves repre-

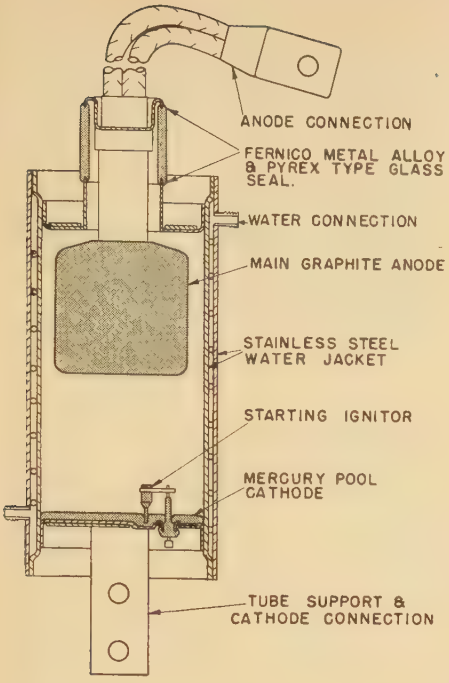

Figure 4. Cross section of a 2,400-kva control ignitron

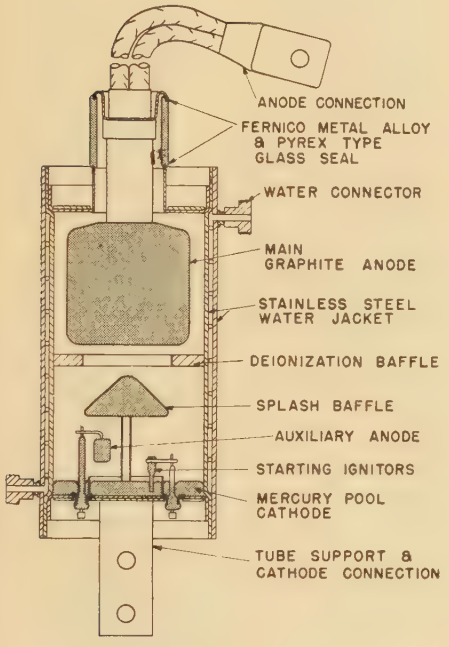

Figure 5. Cross section of a 200-ampere rectifier ignitron

sent the auxiliary anode-to-cathode voltage as seen on a cathode ray oscilloscope, with the auxiliary anode used as a probe and connected to a negative bias to collect positive ions as indicated in the connection diagram insert. The point in the curves at which the auxiliary anode voltage begins to increase negatively indicates the time required for the ionization to decay to a value just at which the probe current can be supplied without an increase in voltage. The effects of increased tube diameter, arc volumes, and particularly increased vapor density are clearly shown.

In the development of the 400-ampere tube, it was expected that the general design of the smaller tubes could be extended to this size. However, operation tests indicated that both the ionization density and time of deionization must be decreased. One of the most effective methods of accomplishing this in the larger tubes is to enclose the anode within a grid. The grid functions primarily as a shield to isolate the anode from the ionization in the arc chamber. The small volume of ionization between the grid and anode insures rapid deionization of this space. Probably of equal importance is the current density level that can be collected on any part of the anode.

Anode Current

The magnitude and wave shape of the anode current influences the magnitude and wave shape of the vapor pressure wave and affects the ionization density. These factors depend, in general, on the mode of operation of the rectifier circuit employed. The delta 6-phase double-Y circuit (proposed AIEE Standards nomenclature) commonly is used and in this circuit there is a ratio of three to one between the peak and average currents. This ratio usually varies from two, three, four, six to one, depending on the type of circuit. At the end of conduction, the current wave shape, and particularly the magnitude of the ionization resulting from the current, depends on both the commutating reactance of the transformer and supply and the voltage that is available to transfer the current from one phase to another.

Anode Voltage

The degree of positive ion bombardment and the thickness of the ion sheathes that form around the anode during the negative part of the cycle are functions of the magnitude of the inverse anode voltage. This voltage therefore influences the factors involved in arc-back directly. The magnitude of the inverse voltage depends on the circuit and is higher for circuits having low ratios of peak-to-average currents and lower for those having high ratios. Two periods in the inverse voltage wave are of particular interest. The initial inverse voltage occurs at the end of commutation at the time the residual ionization is highest. Its magnitude depends on the circuit, the transformer commutating reactance, the current commutated, and the amount of phase control. The maximum inverse voltage depends on the circuit and usually occurs later in the

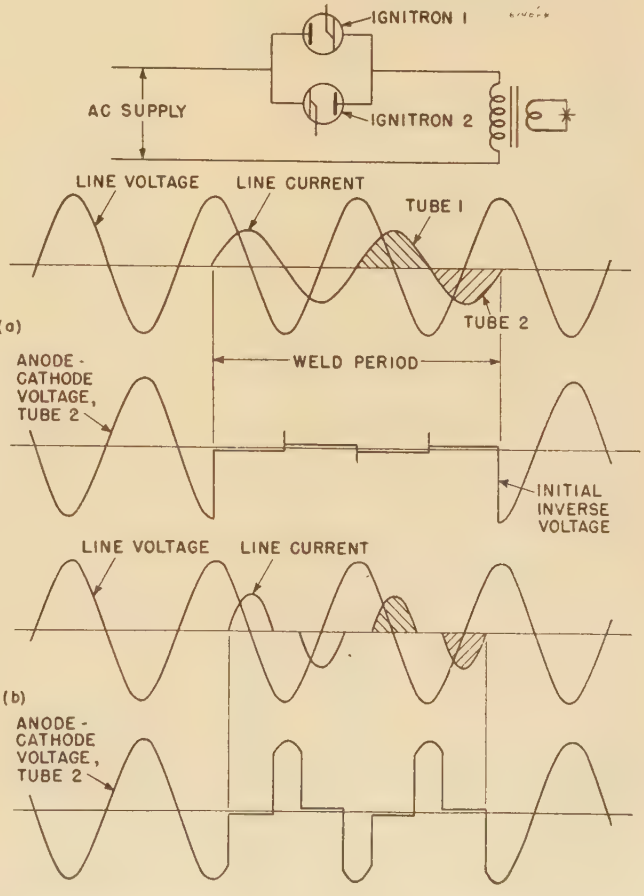

Figure 6. Tube voltage and current wave shapes for welding control operation

(a). No phase retard
(b). Approximately 30 degrees phase retard

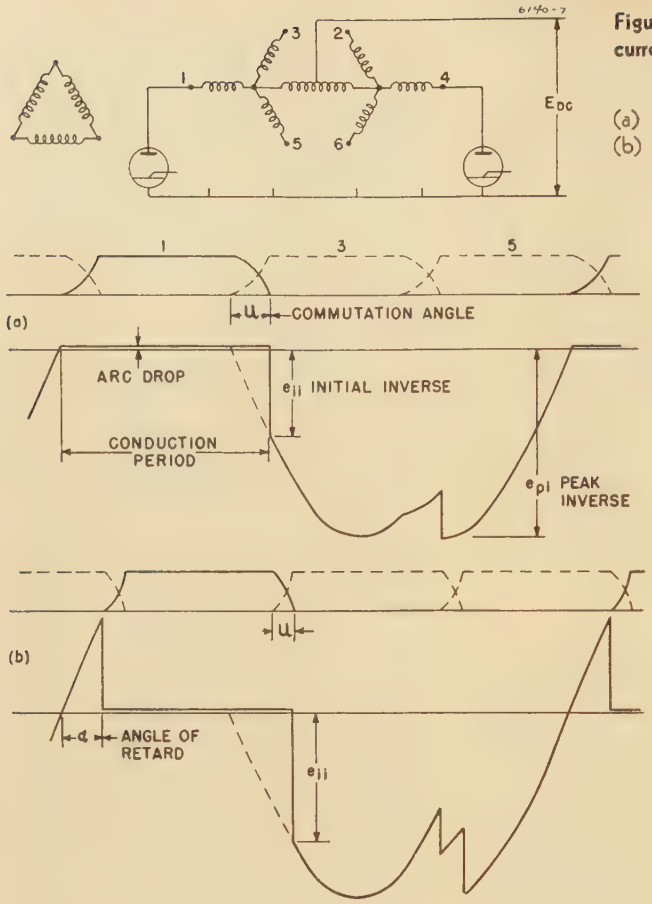

Figure 7. Tube voltage and current wave shapes for rectifier operation

(a) No phase retard
(b) Approximately 30 degrees phase retard

cycle when the residual ionization is reduced. Under large amounts of phase control (70-to 100-per-cent voltage reduction), the initial inverse voltage approaches or equals the maximum in magnitude.

Circuit Duty

The influence of the circuit duty on the tube design is shown in Figures 4 and 5. The figures show, respectively, a sealed ignitron for welder service and one for rectifier service. The two tubes have essentially the same physical dimensions and operate at inverse voltages of about the same magnitude.

In welder service, two tubes are connected back to back to conduct both halves of the a-c wave. The conditions for welder service are shown in Figure 6 for several current cycles in a single spot weld, followed by an off period before the next weld. For the no-phase retard conditions shown in Figure 6a, only the last tube to conduct in the final cycle must withstand an inverse voltage when appreciable ionization is present. Under phase controlled conditions as shown in Figure 6b, the current wave becomes discontinuous so that each tube must withstand commutating conditions in each conducting cycle, and the resulting duty therefore is increased by the increased number of trials. Recognition of this is made in the recommended application practice by reducing the peak current in proportion to the phase control.

In rectifier service, the tubes must withstand successfully commutating conditions in every cycle. Figure 7 shows the tube conditions in a delta 6-phase double-Y rectifier with no-phase retard (a) and phase retard (b). The tube current at commutation is a segment of a short-circuit current wave whose magnitude is limited primarily by the commutating impedance of transformer and by the tube arc-drop. Under phase retard conditions, the voltage that is available to force current transfer from one transformer winding to another is increased, with the result that the transfer time of a current of given magnitude is decreased. The residual ionization at the instant inverse voltage is applied is therefore higher, and this in combination with the higher inverse voltage increases the duty.

In the foregoing discussion of design problems, it should be emphasized that the problem of arc-back has been considered at limiting conditions and that a reasonable reduction in operating conditions below the limit results in performance practically free from arc-back.

Table I. Tube Ratings

	Maximum Anode Current, Amperes	
	300 Volts Direct Current	600 Volts Direct Current
Instantaneous	3,600	2,400
Average		
Continuous	400	300
2-hour	600	450
1-minute	800	600
Surge (0.15 second maximum)	25,000	19,000

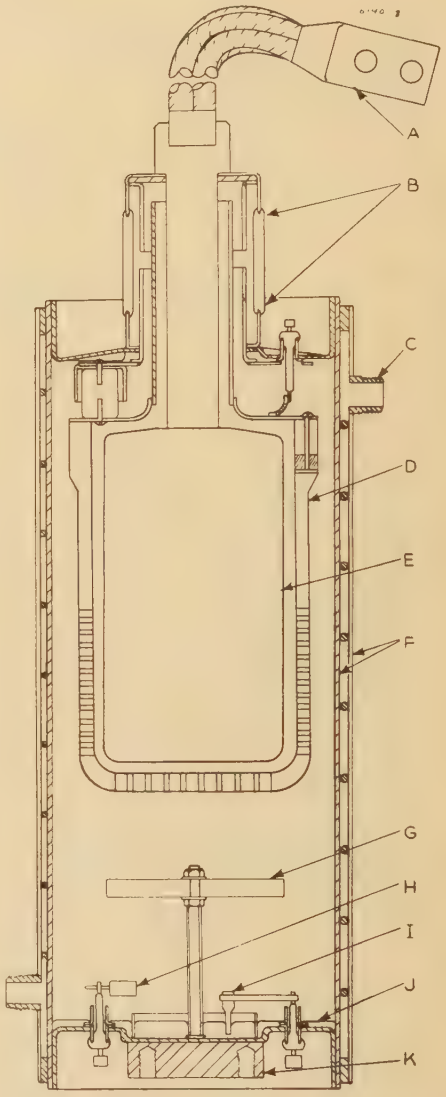

Figure 8. Cross section of the 400-ampere ignitron showing the general design

A—Anode connection
B—Fernico metal alloy and Pyrex type glass seal
C—Water connection
D—Graphite grid
E—Main graphite anode
F—Stainless steel water jacket
G—Splash baffle
H—Auxiliary anode
I—Starting ignitors
J—Mercury pool cathode
K—Tube support and cathode connection

Table II. Combinations of Tubes and Circuits

Kilowatt Output 300 Volts	Kilowatt Output 600 Volts	Number of Tubes	Circuit
400...	750....	6....	Delta 6-phase double-Y
500...	1,000....	6....	Delta 6-phase double-Y
750...	1,500....	12....	Delta, 12-phase quadruple zig-zag Y
1,000...	2,000....	12....	Delta 12-phase quadruple zig-zag Y

Construction

The general design and construction of the 400-ampere tube is shown in Figure 8. The essential materials and general design of the earlier ignitron tubes have been retained. The water-cooling jackets and the inner cylinder forming the vacuum chamber are of stainless steel to minimize corrosion. The anode insulating and supporting bushing is of the fernico-glass sealing combination that has proved very satisfactory, not only from the vacuum tightness standpoint but from the viewpoint of strength and shock resistance as well. Anode and grid are of special graphite. Two ignitors are incorporated again to provide for circuit reversal or other accidents. Only one is required for ignition. An auxiliary anode provides cathode spot stability for anode currents below three to five amperes peak, and permits simplification of the ignition circuit control.

A completed tube is show in Figure 9. The water jacket is approximately nine inches in diameter and 22 inches tall. Over-all height, including the flexible anode lead, is 40 inches, and the tube weight is approximately 95 pounds.

Figure 9. A completed 400-ampere sealed ignitron

In the larger sizes of tubes, the materials used in the construction become an increasing proportion of the tube cost, and, even though warranties protect against loss from early failure, it becomes desirable to provide in the design the possibility of repair. In this tube the header closing welds are of the fusion type rather than resistance seam welds. This permits removal of the headers with relative ease for inspection or repair.

Performance and Rating

Essential ratings of the 400-ampere tube are given in Table I, and Table II shows possible combinations of tubes and circuits to provide industrial rectifiers of standard capacities at the 300- and 600-volt levels.

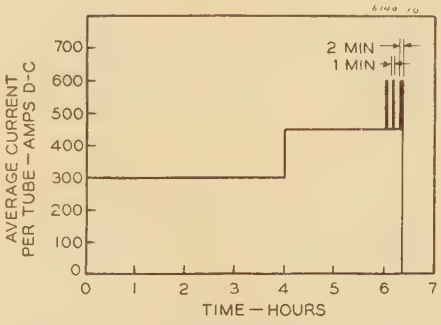

Figure 10. A 600-volt operation test at rated continuous 2-hour and 1-minute load currents for zero phase retard

Rectifier performance tests usually are made on the load increment plan for a chosen water temperature and flow and at the desired operating voltage levels.[9] The commutating impedances are adjusted to give output voltage regulation and short-circuit currents comparable to these expected in actual service. The load usually is absorbed by motor generator sets.

Prior to determining limits, an operation run usually is made to check the performance at rated continuous 2-hour and 1-minute loads. Figure 10 shows the time-current plot of such a run for operation at 600 volts direct current.

Figure 11 shows the general shape of the load limit current curve for the 400-ampere ignitron as the output voltage of the rectifier is reduced progressively to zero by means of phase control. Limits as far as the tubes are concerned are determined by arc-back. Under phase retard conditions, the combined effects of a higher initial inverse voltage and greater ion density produce a higher tube duty, which is reflected by a reduction in load current.

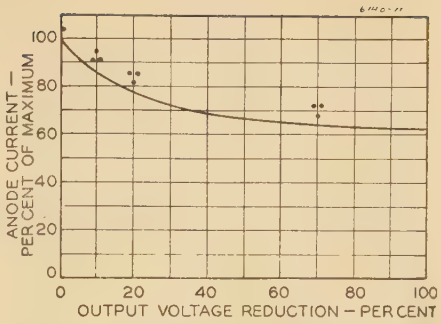

Figure 11. Continuous average anode current, determined by load limit tests, as a function of output voltage reduction by phase control

The dots indicate arc-backs

Conclusion

The development of the 400-ampere sealed ignitron revealed no factors which would tend to limit the size and capacity that could be designed. Undoubtedly, larger tubes would require different treatment and probably different forms. The development did show the very great part played by ionization and the need, in spite of the excellent fundamental work that has been done, for additional work with particular emphasis on the problem of rectification.

References

1. A New Method for Initiating the Cathode of An Arc, **J. Slepian, L. R. Ludwig.** AIEE Transactions, volume 52, 1933, pages 693–8.

2. Development of Excitron-Type Rectifier, **H. Winograd.** AIEE Transactions, volume 63, 1944, pages 969–78.

3. Sealed-Off Ignitrons for Welding Control, **David Packard, J. H. Hutchings.** AIEE Transactions, volume 56, 1937, January section, pages 37–40, 66.

4. Crosley-OWI 200-Kw "Voice of America," **R. J. Rockwell.** *Electronic Industries*, volume 4. 1945, pages 90–172.

5. Sealed-Tube Ignitron Rectifiers, **M. M. Morack, H. C. Steiner.** AIEE Transactions, volume 61, 1942, August section, pages 594–9.

6. The Adsorption of Gases by the Steel Walls of Vacuum Discharge Apparatus and Its Bearing on the Life of Pumpless Mutators, **W. Deck.** *Brown Boveri Review* (Baden, Switzerland), volume 29, number 8, 1942, pages 202–04.

7. The Relation of Residual Ionization to Arc-Back in Thyratrons, **K. H. Kingdon, E. J. Lawton.** *General Electric Review*, volume 42, number 11, 1939, pages 474–8.

8. The Cause of High Voltage Surges in Rectifier Circuits, **Albert W. Hull, Frank R. Elder.** *Journal of Applied Physics*, volume 13. 1942, pages 372–7.

9. The Testing of Mercury-Arc Rectifiers, **H. L. Kellog, C. C. Herskind.** AIEE Transactions, volume 62, 1943, December section, pages 765–73.

The Application of Series Capacitors to Flash Welders

JAMES F. DEFFENBAUGH
ASSOCIATE AIEE

THE APPLICATION of series capacitors to spot, projection, and seam welders no longer presents any difficult problems, and they have been used successfully with these types of welders for several years.

Essentially, enough capacitive reactance is placed in the primary circuit of the welder transformer to neutralize the inductive reactance of the welder. This theoretically produces unity power factor and reduces the kilovolt-ampere demand to the level of the kilowatt demand. Since the voltage across the capacitor units is directly proportional to the current flowing through them, units must be selected with a voltage rating high enough so that this rating is not exceeded unless they are protected by an overvoltage device.

The flash welder, however, presents an entirely different problem since the welding operation is composed of two phases which differ widely in both power factor and kilovolt-ampere demand.

The first phase is termed flashing and occurs when the pieces to be welded are brought in contact and heated to a plastic state by the passage of the current as it flows from one piece to the other. There is some doubt as to whether this current flow is caused by metallic or gaseous conduction. However, we do know that there is not good contact between the two pieces, and we will speak of the condition during current passage as an arc. The flashing kilovolt-ampere demand is less than the final upset phase, the power factor is relatively high, and the wave shape of the current is rather irregular, as shown in Figure 1.

When the plastic temperature has been reached, the upset phase takes place. Here the pieces are forced together quickly and are forged, producing the complete weld. Since the resistance at the weld region is lower at upset than when flashing, the kilovolt-ampere demand is greater, the power factor lower, and because of the absence of arcing, the wave shape of the current is smooth, as illustrated in Figure 2.

An example of this type of machine is the barrel welder. Figure 3 is a simplified drawing of the essential parts. Note that as the cam appearing at the extreme right revolves, the movable platen, in which is clamped one edge of the sheet forming the barrel, moves slowly toward the edge of the sheet which is clamped in the stationary platen. The edges are brought in contact as the cam begins rotating, and, because of the inherent irregularities and minute projections along the edges of the stock, the contact resistance is high and the current flow is restricted to small areas. This produces a flashing action which burns away the multiplicity of projections. It is evident that there are two current paths in parallel: one short path through the weld region and the other, a longer path, through the cylinder. The relatively high resistance offered by these two paths in parallel therefore results in a comparatively low kilovolt-ampere demand and high power factor.

When the upset block on the cam meets the movable platen, the edges of the stock are forced together, the arc extinguished, and, because of the resulting decreased resistance, the current flowing through the weld region increases greatly. The ratio of the resistance to the inductive reactance of the secondary circuit decreases with an accompanying decrease of power factor.

A series of tests were made on a standard 350-kva 440-volt 42-inch barrel welder welding a standard 16-gauge 55-gallon drum to determine the possibility of applying series capacitors to reduce the kilovolt-ampere demand and increase the power factor.

Oscillograms were taken before any power factor correction was attempted and it was found that the demand during flashing was about 350 kva at 92 per cent power factor, and at upset the demand increased to 1,200 kva at a power factor of 48 per cent. The relative magnitudes are shown graphically in Figure 4.

Suppose we add enough capacitance to

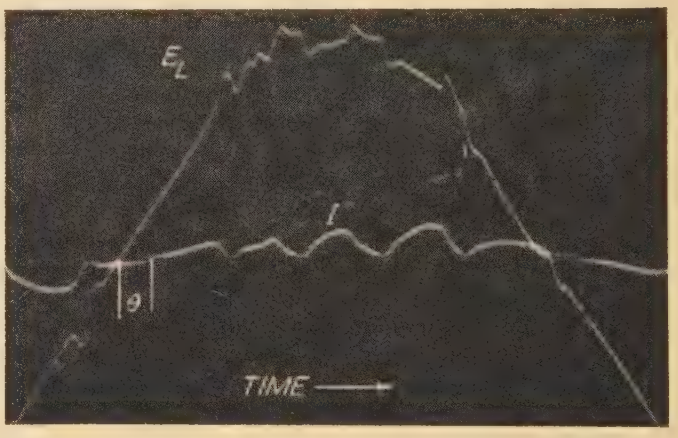

Figure 1. Oscillogram of current and voltage during flashing

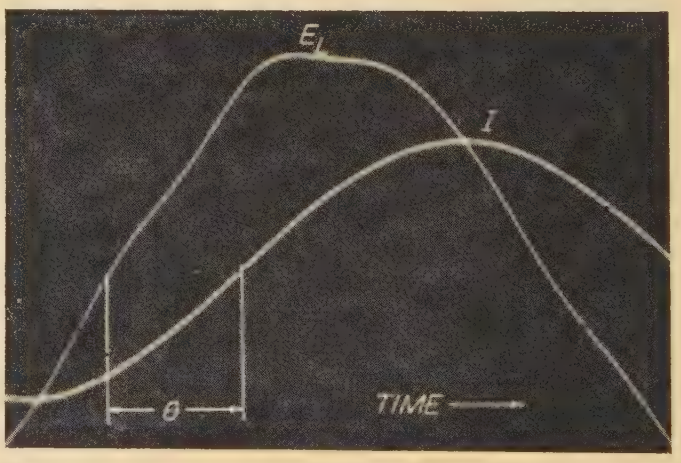

Figure 2. Oscillogram of current and voltage during upset

Paper 46-141, recommended by the AIEE committee on electric welding for presentation at the AIEE summer convention, Detroit, Mich., June 24–28, 1946. Manuscript submitted April 26, 1946; made available for printing May 14, 1946.

JAMES F. DEFFENBAUGH is with The Federal Machine and Welder Company, Warren, Ohio.

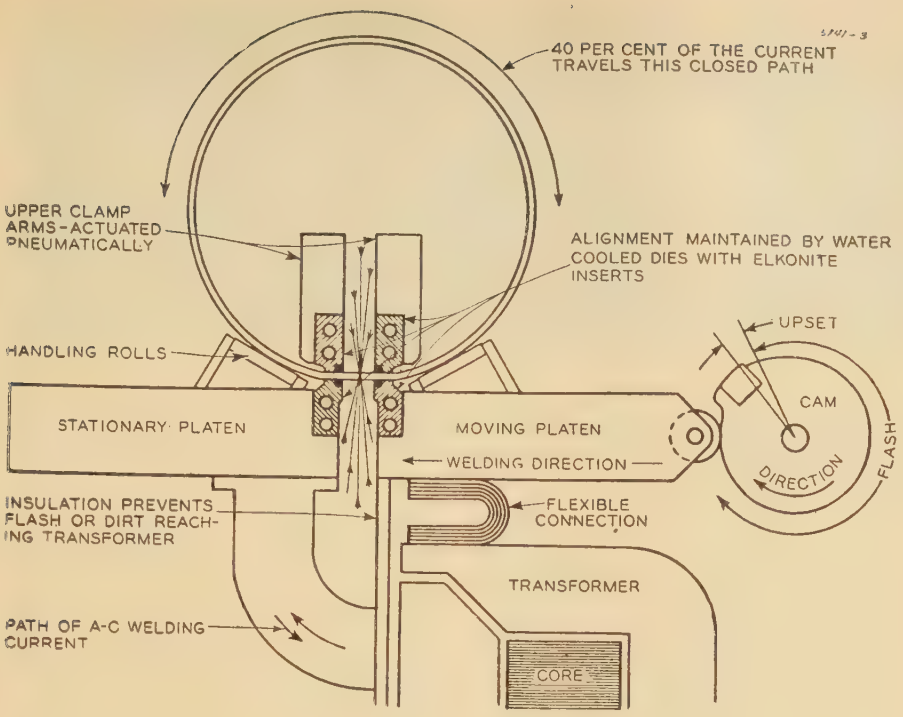

Figure 3. Essential parts of a drum welder

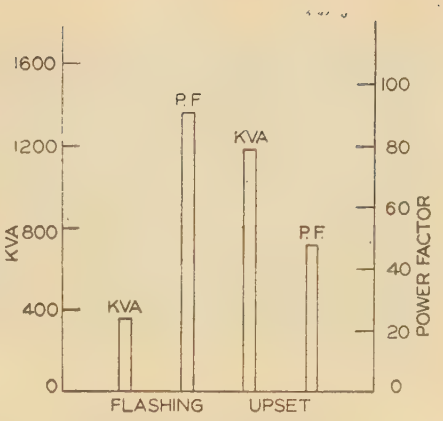

Figure 4. Initial uncorrected values of kilovolt-ampere demands and power factors

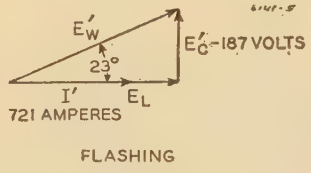

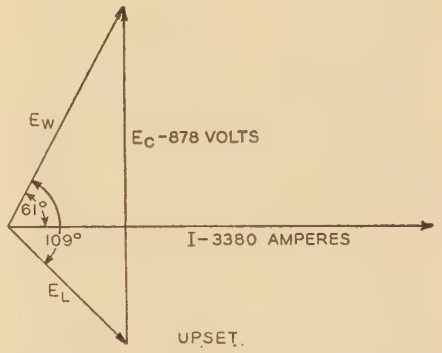

Figure 5. Vector diagrams of currents and voltages existing when the flashing period is corrected to unity power factor

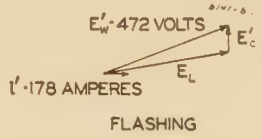

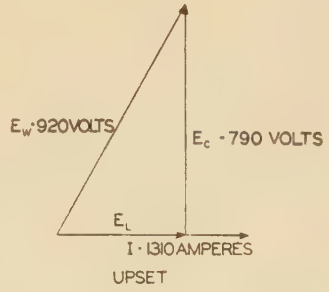

Figure 6. Vector diagrams of currents and voltages existing when the upset period is corrected to unity power factor

the primary circuit of the welder to obtain approximately unity power factor during the flashing period. Proceeding exactly as is done in applying series capacitors to any other type of welder, it is found that 29 230-volt capacitors are required. Figure 5 gives vectorially the voltages existing in the circuit at this time.

During the upset stage of the weld, the current increases, thereby producing a proportional increase in the primary current which now flows through the capacitor bank. This results in a voltage drop across the capacitors which is approximately 150 per cent greater than the maximum permissible voltage of the units. Of course, units with a greatly increased voltage rating could have been chosen initially, but the number required would have been approximately four times that actually selected, so that this is clearly not an economical solution. The demand also has increased to a value approximately 25 per cent greater than it was before the capacitors were applied. The upset portion of Figure 5 gives these values.

Let us now increase the capacitance to that required to correct the upset portion of the weld to unity power factor. We find that it is necessary to use 36 575-volt units. However, the resulting series circuit at upset impresses a voltage of about $2^1/_2$ times the normal supply voltage across the welder transformer, as shown in Figure 6. There are two methods that can be used to maintain the secondary voltage appearing across the platens at the value it was before the capacitors were applied. One method is to increase the welder transformer ratio, and the other is to use a step-down transformer in the supply circuit. In this instance let us choose the first method and increase the transformer ratio.

As shown in the flashing section of Figure 6, we immediately meet complications during the flashing period since the characteristics of the circuit now are such that the voltage impressed on the welder transformer primary is reduced to 60 per cent of that required for proper flashing. This would result in an imperfect weld.

We now are able to conclude that, when there is an appreciable difference between the flashing and upset demands, we will have one of two undesirable conditions present if we apply series capacitors to flash welders, according to conventional theory:

1. Correction of the flashing demand will result in excessive condenser voltage during upset.

2. Correction of the upset demand will result in a welder transformer voltage lower than that required for proper flashing.

Since, in general, it is not economical to use high voltage capacitor units, we will provide a means of increasing the voltage across the welder transformer during the flashing period and use a value of capacitance which will give unity power factor during upset, since

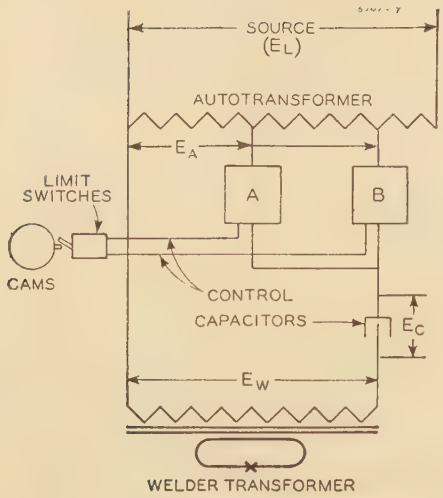

Figure 7. Schematic diagram of circuit used in test

Figure 8. Oscillogram of contactor switching interval

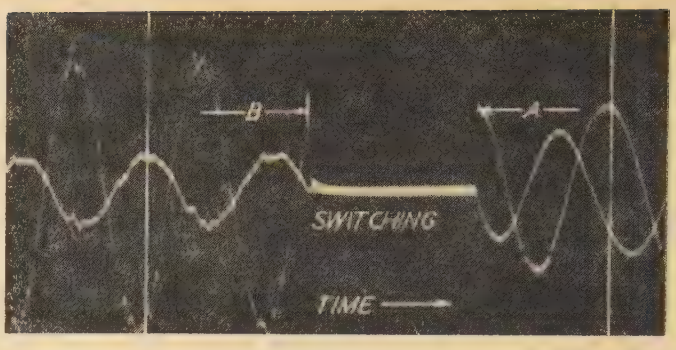

the power factor at flashing is rather high without correction.

In order to accomplish this condition, the circuit shown in Figure 7 was made. A cam has been placed on the shaft which rotates the platen-moving cam, a limit switch which is actuated by this cam has been added, a second tube contactor has been placed in parallel with the original contactor, and an autotransformer has been connected in the supply line. The series capacitors are placed in the circuit between the contactors and the welder transformer primary winding.

The sequence of operation of the circuit is as follows.

When the limit switch is closed, contactor *B* is closed and contactor *A* is left open. The tap on the autotransformer to which contactor *B* is connected is selected so that approximately normal supply voltage is impressed on the welder transformer. This energizes the circuit correctly for the flashing operation. The added cam is adjusted so that contactor *A* is closed and contactor *B* is opened about one cycle before the platen-moving cam starts the upset movement. This adjustment was necessary as there was an interval of one cycle during the switching of contactors in which there was no current flow. However, it is possible to eliminate this period by the use of proper controls. Figure 8 shows this interval. Contactor *A* is connected to a lower voltage tap on the autotransformer and results in normal supply voltage being impressed on the welder transformer during upset.

In order to simplify the calculations, the assumption is made that the source is of infinite capacity. This assumption changes the values slightly from those actually existing during the tests.

The first step is the calculation of the inductive reactance of the welder during upset. This calculation is the value, in ohms, of the capacitive reactance that must be supplied by means of the capacitor units in order to obtain approximately unity power factor at upset. The circuit voltage conditions are as shown by the vector diagram in solid lines in Figure 9. It is evident that the voltage to be supplied by the autotransformer is the welder voltage E_W multiplied by the power factor during upset, plus the tube contactor drop of approximately 15 volts.

The next step is the determination of the circuit constants during flashing. The net reactance is the difference of the capacitive and inductive reactances. This value then is combined vectorially with the flashing resistance to find the resulting impedance. The voltage at the autotransformer then must be equal to this impedance multiplied by the primary flashing current. This current is approximately equal to that occurring during the uncorrected flashing condition. See Appendix II for exact calculation.

The vector diagram composed of broken lines illustrates the voltages existing during flashing. The power factor is slightly lagging because of the fact that the inductive reactance during flashing is greater than during upset. We are not certain as to the exact reason for this change in reactance, but it may be caused by the harmonics present during flashing.

Figures 10 and 11 illustrate oscillograms of the current and voltage as measured at the supply side of the autotransformer after the capacitors had been applied. Note that the power factor during upset is not quite unity and that the power factor during flashing is less than at upset.

Figure 12 shows graphically a comparison between the kilovolt-ampere demand and power factors before and after applying correction in the actual test, the dashed lines giving the corrected values.

It is evident from an examination of Figure 12 that while the low kilovolt-ampere demand and high power factor of the flashing phase has not been altered appreciably, the upset kva demand has been reduced to approximately one-third of its uncorrected value, and the power factor has been increased from 48 to 95 per cent.

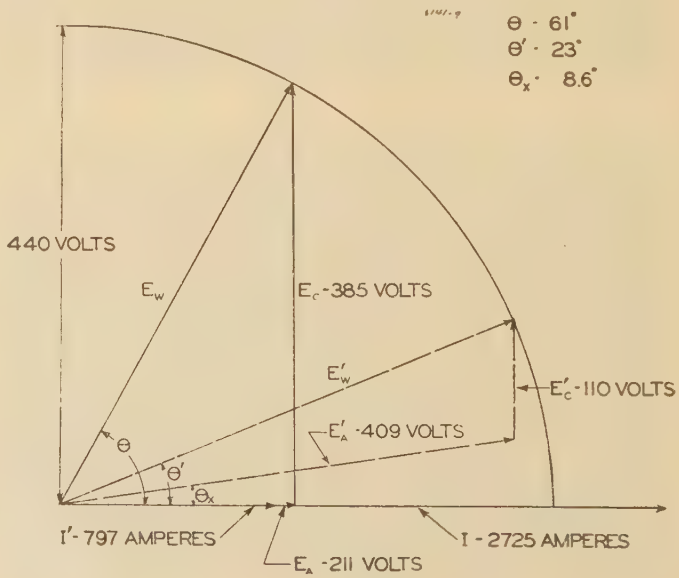

Figure 9. Vector diagram of currents and voltages existing during flashing and upset after capacitors have been applied in final arrangement

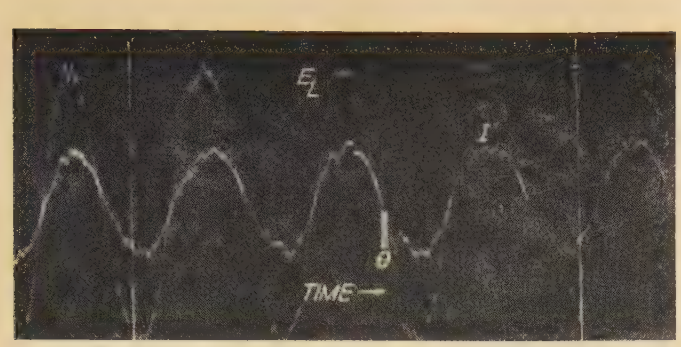

Figure 10. Oscillogram of current and voltage during flashing after addition of capacitors

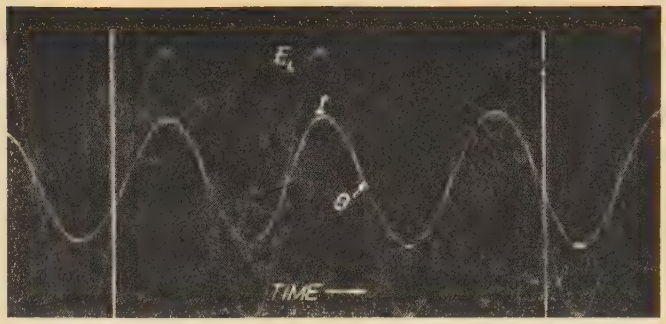

Figure 11. Oscillogram of current and voltage during upset after addition of capacitors

Appendix I. Notation

E_L = supply line voltage
E_A = autotransformer output voltage
E_C = capacitor voltage
I = output current of autotransformer
θ = angular difference between current and voltage in high tension winding of welder transformer

The foregoing refer to upset values. With prime notation they refer to flashing values.

θ_x = phase difference between current and voltage in supply line during flashing after capacitors had been applied

Appendix II. Calculations

Upset period:

$$Z=\frac{E_L^2\times10^{-3}}{\text{kva}}=\frac{440^2\times10^{-3}}{1{,}200}=0.161 \text{ ohm}$$

$$X_L=Z\times \sin 61 \text{ degrees}$$
$$=0.161\times0.875$$
$$=0.141 \text{ ohm}$$

Therefore $X_C=X_L=0.141$ ohm and power factor becomes theoretically unity.

$$E_A=E_L\times \cos 61 \text{ degrees}$$
$$=440\times0.48$$
$$=211 \text{ volts}$$
$$E_C=E_W\times \sin 61 \text{ degrees}$$
$$=440\times0.875$$
$$=385 \text{ volts}$$

$$\text{Corrected kva}=\text{uncorrected kva}\times \cos 61 \text{ degrees}$$
$$=1{,}200\times0.48$$
$$=575 \text{ kva}$$
$$I(\text{corrected})=\frac{\text{kva (corrected)}}{E_A\times10^{-3}}$$
$$=\frac{575}{211\times10^{-3}}$$
$$=2{,}725 \text{ amperes}$$

Flashing conditions:

$$Z'=\frac{E_L^2\times10^{-3}}{\text{kva}}$$
$$=\frac{440^2\times10^{-3}}{350}$$
$$=0.554 \text{ ohm}$$
$$X'_L=Z'\times \sin 23 \text{ degrees}$$
$$=0.554\times0.39$$
$$=0.218 \text{ ohm}$$
$$X_L(\text{net})=X'_L-X_C$$
$$=0.218-0.141$$
$$=0.077 \text{ ohm}$$
$$R'=Z'\times \cos 23 \text{ degrees}$$
$$=0.554\times0.92$$
$$=0.51 \text{ ohm}$$

Thus the power factor with capacitors is

$$\cos^{-1}\tan\frac{X_L(\text{net})}{R'}$$
$$\tan\theta_X=\frac{X_L(\text{net})}{R'}$$
$$=\frac{0.077}{0.51}$$
$$=0.151$$
$$\theta_X=8.6 \text{ degrees}$$
$$\cos\theta_X=0.988$$

Power factor = 98.8 per cent

$$E'_A=\frac{E'_W\times \cos 23 \text{ degrees}}{\cos 8.6 \text{ degrees}}$$
$$=\frac{440\times0.92}{0.988}$$
$$=409 \text{ volts}$$
$$E'_C=E'_W\times \sin 23 \text{ degrees}-E'_A\times \sin 8.6 \text{ degrees}$$
$$=(440\cdot0.39)-(409\cdot0.1495)$$
$$=171-61.2$$
$$=109.8 \text{ volts}$$

$$\text{Kilovolt-amperes (corrected)}=\frac{\text{kva}\times \cos 23 \text{ degrees}}{\cos 8.6 \text{ degrees}}$$
$$=\frac{350\times0.92}{0.988}$$
$$=326 \text{ kva}$$

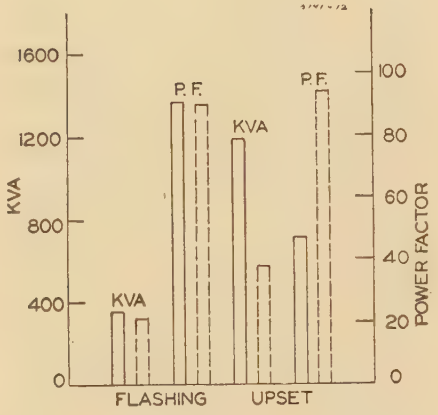

Figure 12. Kilovolt-ampere demands and power factors measured in test after addition of capacitors

Table I. Circuit Constants Before Correction

Circuit Constant	Value
Flashing	
Kva	350
Power factor	92 per cent
θ	23 degrees
E_L	440
Upset	
Kva	1,200
Power factor	48 per cent
θ	61 degrees
Supply voltage	440

$$I \text{ (corrected)}=\frac{\text{kva (corrected)}}{E'_A\times10^{-3}}$$
$$=\frac{326}{409}\times10^{-3}$$
$$=797 \text{ amperes}$$

The actual values of the autotransformer output voltages necessarily will have to be approximately 15 volts greater than the values as calculated to compensate for the voltage drop in the ignitron contactors.

Co-ordination of Insulation and Spacing of Transmission Line Conductors

W. W. LEWIS
FELLOW AIEE

A SURVEY of practice on existing transmission systems shows, for the same operating voltage, wide variations in the insulation used. Also, wide variations occur in the spacing between conductors and from them to grounded members of the supporting structure.

These variations are illustrated in Figure 1, showing practice in the use of pin type insulators;[1] Figure 2, showing practice in the use of suspension insulators;[2,3,4] Figure 3, showing actual spacings between conductors for horizontally arranged lines;[4] and Figure 4, showing actual spacings between conductors for vertically arranged lines.[4,5] These variations possibly reflect to some extent the different degrees of lightning, wind, snow, and sleet encountered in different parts of the country, as well as the difference in experience and conservatism of the designers.

A recent committee report[4] gives data on 35 transmission lines in the 190- to 287.5-kv range. In this report is given a comparison of the impulse flashover of the insulators and the flashover from the conductor to the structure through air, with the conductor swung at 30 degrees from the vertical. In many cases the flashover to the structure through air is considerably less than the flashover of the insulators, indicating a lack of co-ordination in the design.

It is obvious from the preceding discussion that very little guidance can be obtained from existing lines as to the suitable number of insulators and spacings for projected transmission lines of various voltages. The writer, therefore, has undertaken to set up criteria for such insulation and spacings which will offer a guide for those engaged in this work, and which will be consistent for the various voltages.

In order to simplify the problem, the present study will apply mainly to steel tower lines with suspension insulators, although the question of wood pole lines and pin type insulator lines will be touched upon.

Paper 46-175, recommended by the AIEE committee on power transmission and distribution for presentation at the AIEE summer convention, Detroit, Mich., June 24–28, 1946. Manuscript submitted April 11, 1946; made available for printing May 23, 1946.

W. W. Lewis is a transmission engineer with the central station engineering division, General Electric Company, Schenectady, N. Y.

Criteria for Minimum Line Insulation

As a basis for the selection of the minimum line insulation, the following criteria are suggested:

1. The 60-cycle wet flashover must equal or exceed the voltages expected from faults and switching surges. The maximum to be expected from these causes is five to six times normal line-to-neutral voltage. These voltages may be reduced by proper neutral grounding, by the use of breakers with minimum tendency for restriking, and by adequate lightning arrester protection. Under the most advantageous conditions, the upper limit of low frequency voltages may be taken as 3 to 3.5 times normal line-to-neutral voltage, and the 60 cycle wet insulator flashover should equal or exceed this value.

2. The impulse flashover should equal or exceed the standard basic impulse insulation level for the terminal equipment.[6]

In Table I are given the 60-cycle dry and wet and impulse flashover values of standard suspension insulators, ten inches in diameter and spaced $5^3/_4$ inches apart.[7]

In Table II are given 60-cycle and impulse flashover values for standard rod gaps.[7] These values may be used for gaps in air between conductors, between conductors and tower, and so forth.

In Table III, column 2, are given for the standard insulation classes the number of insulator disks spaced $5^3/_4$ inches apart, whose wet 60-cycle flashover will equal or exceed 3.5 times line-to-neutral voltage. This is the smallest number of insulators which will have an impulse flashover equal to or greater than the basic impulse insulation level.

Also given in Table III are the numbers of disks whose wet 60-cycle flashover will equal or exceed 4, 4.5, and 5 times the line-to-neutral voltage. In column 6, for comparison, are given the numbers of disks representing average practice, from Figure 2.

It will be noted that average practice follows column 5 up to and including 115 kv, column 4 for 138 to 230 kv inclusive, and column 3 for 287 and 345 kv. These

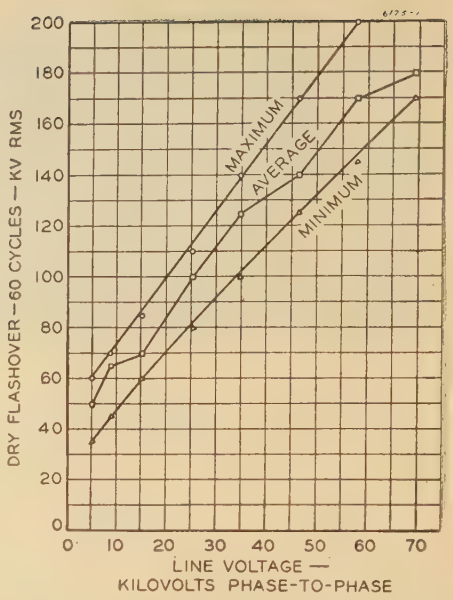

Figure 1. Practice in the use of pin type insulators

average values are from a curve. Actually, the only 287-kv lines in existence have the equivalent of 21 disks spaced $5^3/_4$ inches apart,[4] and so far there are no 345-kv lines. The tendency to use a greater relative insulation at the lower voltages is similar to the tendency to be found in the insulation of apparatus.

Co-ordination of Spacing With Insulation Level

With each level of insulation, there is a proper spacing between conductors and to the steel structure to develop the full strength of the insulator string selected. Let us take the minimum spacing to the steel structure *A* (Figures 5 and 6) as a spacing that will have an impulse flashover ten per cent greater than the impulse flashover of the insulator string.

Spacing *B* (Figures 5 and 6), the horizontal distance from conductor to tower when the conductor is hanging vertically, will be such that when the conductor is swung to 30 degrees from the vertical the impulse flashover from conductor to tower (spacing *A*) will be ten per cent greater than the insulator string flashover. It is assumed that during the summer season, when lightning prevails and there is no ice or snow, 30 degrees is ample to consider for the conductor swing.

Having determined spacing *B* from conductor to tower, spacing *D* between conductors for the horizontal arrangement (Figure 5) becomes two times spacing *B*, plus the width of the tower leg.

For the vertical arrangement (Figure 6), the spacing between horizontal planes through the conductors, spacing *C*, is a

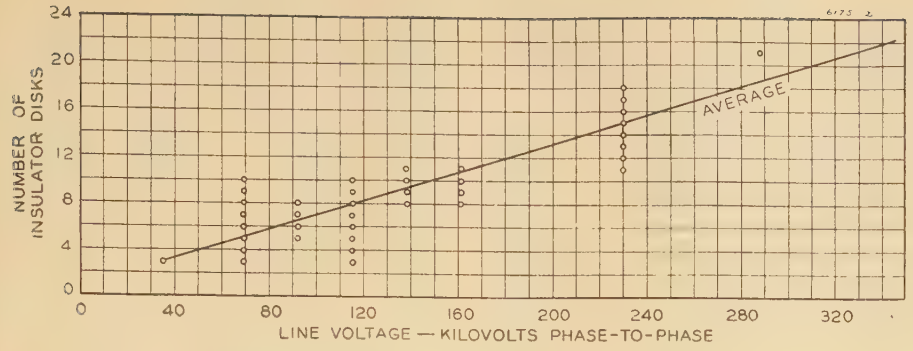

minimum of two times the spacing A, since the insulator string itself has a length approximately equal to spacing A. On the tower illustrated in Figure 6, on account of the slope of the crossarm bracing, the spacing between conductor planes naturally will be somewhat greater than $2A$. In other types of towers without crossarm bracing, this may not be the case, and the minimum spacing $2A$ can be used.

In order that the conductors may be fully shielded from direct strokes, it has been found that the two overhead ground wires are necessary, either for horizontal or vertical arrangement of conductors. If the two ground wires are placed close together, they blanket each other and the full benefit of the two wires is not secured. The effect is much the same as the effect of two rods driven in the ground. If the rods are close together, the combined resistance is only slightly less than that of one rod, but if they are far enough apart, the combined resistance will approach one-half of that of one rod.

In a single circuit line of the usual design, with the conductors horizontally arranged (Figure 5), it works out well mechanically to place the ground wires above the tower legs or above the poles in a wooden H-frame arrangement, that is, on a vertical plane about midway between the two conductors. This has proved in practice to give good protection.

In the double circuit vertical arrangement (Figure 6), the ground wires are well coupled with the top conductors but are more remote from the middle and especially the bottom conductors, so that the coupling factor is rather low. To offset this loss of coupling factor, the ground wires should be spread farther apart. A good position in practice has been found to be about directly above the outermost conductors, which are usually the middle conductors.

The ground wires should be high enough above the conductors to avoid flashover between conductors and ground wires at midspan. However, if the ground wires are too high, the coupling with the conductors will be small and in case the tower voltage is raised above ground by lightning current in the tower, the voltage across the insulator string will be greater than it would have been with the ground wires closer to the conductors.

It has been found by experience that a height of approximately two-thirds the spacing between conductors for the horizontal arrangement and approximately equal to the spacing between conductors for the vertical arrangement is about right to give good coupling to the conductors, and at the same time avoid midspan flashover. Spacing C, Table IV, follows these criteria.

In regions where snow, ice, or sleet are likely to accumulate on the conductors, it happens occasionally on vertical arrangements (Figure 6) that the bottom conductor unloads its snow and ice and swings up level with or above the middle conductor. Also, in case of a coating of ice or sleet and a light wind in the proper direction, sometimes dancing or galloping occurs. In this case, the conductor swings in an oval loop (Lissajous figure). Lightning is not apt to be present under these conditions. Nevertheless, the spacing between conductors when in their closest position should be amply safe, so

Figure 2. Practice in the use of suspension insulators

Table I. Flashover of Suspension Insulators With 10-Inch Diameter and 5 3/4-Inch Spacing

Barometer 30 Inches, Temperature 77 Degrees Fahrenheit, Vapor Pressure 0.6085 Inch

Number of Insulator Units	60 Cycles RMS Dry Kv	60 Cycles RMS Wet Kv*	Impulse Kv
1	80	50	125*–150
2	155	90	250*–255
3	215	130	355
4	270	170	440
5	325	215	525
6	380	255	610
7	435	295	695
8	485	335	780
9	540	375	860
10	590	415	945
11	640	455	1,025
12	690	490	1,105
13	735	525	1,185
14	785	565	1,265
15	830	600	1,345
16	875	630	1,425
17	920	660	1,505
18	965	690	1,585
19	1,010*	720	1,665
20	1,055*	750	1,745
21	1,100	780	1,825
22	1,145	810	1,905
23	1,190	840	1,985
24	1,235	870	2,065
25	1,280	900	2,145
26	1,325	930	2,225
27	1,380	960	2,305
28	1,410	990	2,385
29	1,460	1,020	2,465
30	1,505	1,050	2,550
31	1,550	1,080	2,630
32	1,600	1,110	2,715

From reference 7, except as otherwise noted. Impulse values based on 1.5x40 microseconds positive wave. Values for 21 units and more are extrapolated.

* From Locke Insulator Corporation catalog.

Figure 3. Horizontal arrangement of conductors; actual spacing between conductors and, for comparison, spacing D for average line insulation

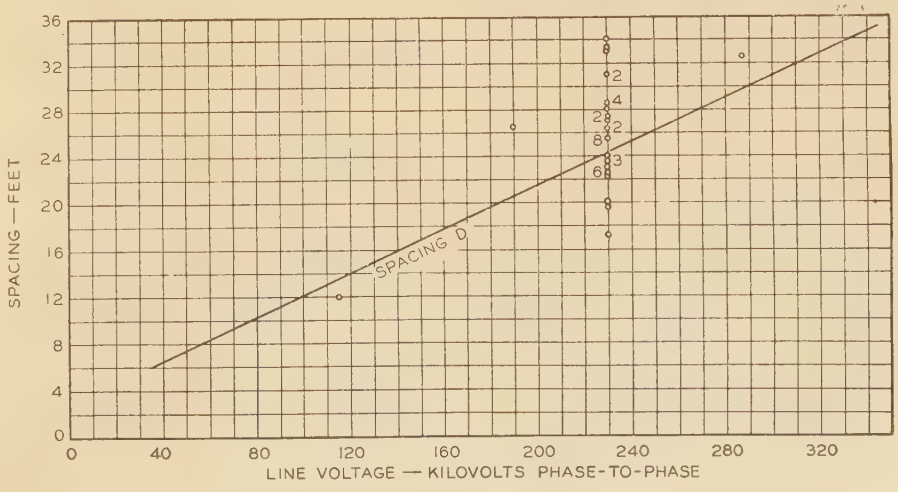

that the dynamic voltage or overvoltages will not flash over. It should be noted in this case that the voltage between conductors is the line-to-line voltage. Spacing E equal to two-thirds A would have a dry 60-cycle flashover approximately 2.5 times the line-to-line voltage, while spacing E equal to A would have a 60-cycle dry flashover approximately 3.5 times the line-to-line voltage. In practice, spacing E may be as small as $0.5A$ for favorable snow and ice regions and up to $1.5A$ for regions where unloading of ice or snow or dancing of conductors may be expected.

Table IV gives the various spacings which co-ordinate with the different numbers of insulator disks, all based on $5^3/_4$-inch spacing between disks. In spacing D the width of the tower leg has been neglected. These values are plotted on Figure 7. If, for example, for a given transmission line seven disks are selected, then the spacings in Table IV corresponding to seven disks will co-ordinate with this number of disks. If for the same line it is desired to use nine disks, then all of the spacings should be increased to those corresponding to nine disks.

On Figure 3 are shown spacings D based on average line insulation from Figure 2, for comparison with the spacings found in practice for horizontal arrangement of conductors. On Figure 4 are shown spacings C based on average line insulation from Figure 2, for comparison with the spacings found in practice for vertical arrangement of conductors.

On lines with pin type insulators, there will be no swing of the conductors at the structure, so that spacing A could be used between conductor and down-lead as far as electric clearances are concerned. However, mechanical considerations may call for larger spacings, and spacing B would be applicable.

Figure 4. Vertical arrangement of conductors; actual spacing between conductors and, for comparison, spacing C based on average line insulation

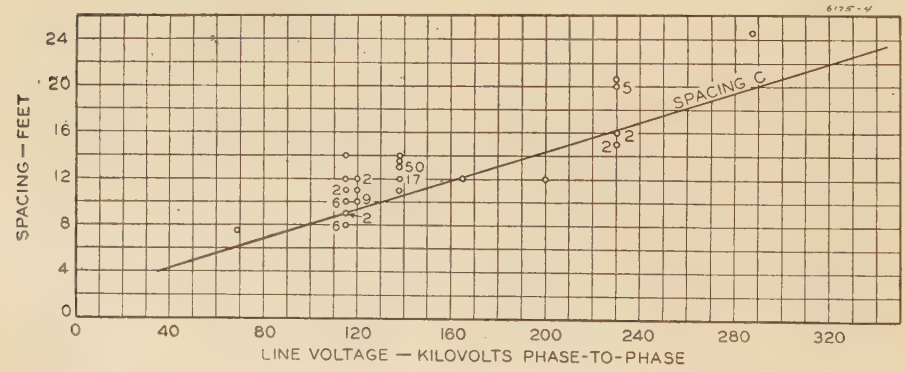

Table II. Flashover of Standard Rod Gaps

Barometer 30 Inches, Temperature 77 Degrees Fahrenheit, Vapor Pressure 0.6085 Inch

Gap Spacing, Inches	60 Cycles RMS Dry Kv	60 Cycles RMS Wet Kv*	Impulse Kv
1	22.5	—	38
2	40	—	60
3	50	—	75
4	58	—	91–95
5	66	—	106–114
6	74	—	128–141
7	—	—	141–155
8	89	—	159–166
9	—	—	175–178
10	105	80	190
15	150	125	275
20	200	170	350
30	295	255	505
40	385	345	650
50	480	430	800
60	575	515	945
70	665	600	1,095
80	755	675	1,240
90	835	755	1,385
100	910*	835	1,530
120	1,055	970	1,820
140	1,200	1,110	2,110
160	1,330	1,230	2,400
180	1,450	1,350	2,690
200	1,560	1,460	2,980

From reference 7, except as otherwise noted. Impulse values based on 1.5x40 microseconds positive wave. Values for spacing above 100 inches are extrapolated.

* From curve of Pittsfield General Engineering Laboratory.

Wood Pole Lines

Wood pole lines with hardware bonded and connected to grounded down-leads would be treated exactly the same as the steel tower lines previously discussed. If the hardware is not bonded, there will be a certain amount of wood insulation in circuit, and the impulse value of this wood when dry may be evaluated at 100 kv per foot, and when wet at 50 kv per foot.[8,9] For conservative design, 50 kv per foot or the equivalent of one-half disk insulator for each foot of wood may be used.

On account of the possibility of wood poles and crossarms splitting from the lightning flashover, it is desirable to have the flashover go from the conductor to the down-lead through air, rather than via the insulator string and crossarm or pole. If the impulse flashover through air is made about the same as the insulator flashover, the added insulation of the wood in series with the insulator will ensure that the flashover will take place through air to the down-lead.

Tower Footing Resistance

The selection of a particular insulation and co-ordinated spacing of conductors does not assure that the line will not flash over because of lightning. Flashover can only be prevented by

1. Shielding the conductors from direct strokes by properly placed overhead ground wires.

2. Low tower footing resistance so that the product of tower current and resistance will not exceed the flashover of the insulation and spacing selected.

Lightning currents to be expected may be determined from reference 10. Experience has shown that flashover usually will not take place if the product of tower current and footing resistance does not exceed the 1.5x40 positive flashover of the insulation or spacing to ground.[11] For example, on a line with seven insulator units having an impulse flashover of 695 kv, and assuming 100,000 amperes tower current, the footing resistance would have to be reduced to about seven ohms in order to prevent flashover. Reference 10 indicates a reduction in footing resistance during surges as compared with the tested resistance. This reduction is greater the larger the lightning current and the larger the normal resistance. The reduction may be considered as a factor of safety when figuring on possible

Figure 5. Single-circuit transmission line with horizontally arranged conductors

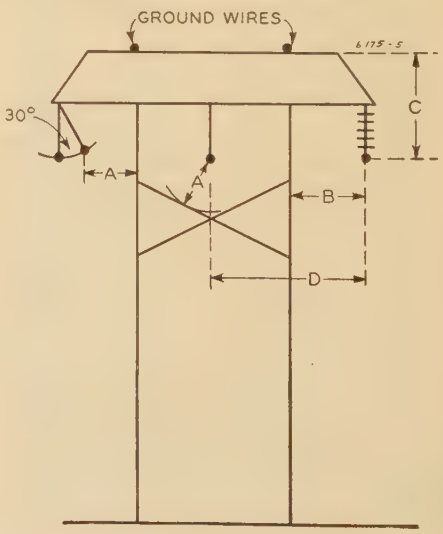

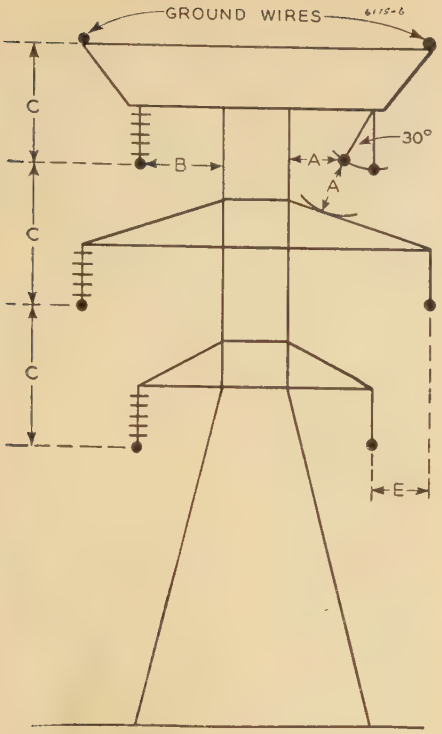

Figure 6. Double-circuit transmission line with vertically arranged conductors

flashover based on the normal resistance. Also, by neglecting the coupling factor an additional factor of safety is secured.

In some locations where the ground resistance is inherently high, it may be necessary to reduce the footing resistance by driven rods or counterpoise wires. Nevertheless, it may not be feasible or economical to obtain footing resistance values low enough. In these cases, it may be desirable to supplement the means already used with ground-fault neutralizers, expulsion protector tubes, or automatic high speed reclosing. These supplementary means have been described amply elsewhere.[12,13,14]

Table III. Minimum Number of Insulator Disks for Transmission Lines Based on 5 3/4-Inch Spacing

(1)	(2)	(3)	(4)	(5)	(6)	(7)
	Number of Disks to Have 60-Cycle Wet Flashover Equal to or Greater Than					
Circuit Voltage Kv	3.5×L-N Voltage	4×L-N Voltage	4.5×L-N Voltage	5×L-N Voltage	Average Practice Number of Disks	Basic Impulse Level Kv
34.5	2	2	2	3	3	200
46	3	3	3	4	4	250
69	4	4	5	5	5	350
92	5	5	6	7	7	450
115	6	7	8	8	8	550
138	7	8	9	10	9	650
161	8	9	11	12	11	750
196	10	11	13	14	13	900
230	12	14	15	18	15	1,050
287	15	18	20	23	19	1,300
345	19	22	25	29	22	1,550

Conclusions

1. The 60-cycle wet flashover of line insulation should equal or exceed the voltages from faults and switching surges, that is, under the most advantageous conditions from 3 to 3.5 times normal line-to-neutral voltage, and under less favorable conditions up to 5 or 6 times normal line-to-neutral voltage. The impulse flashover should equal or exceed the basic impulse insulation level for apparatus.

2. The number of insulators having a wet 60-cycle flashover of 3.5 times line-to-neutral voltage is the minimum number which will meet the basic impulse insulation level.

Figure 7. Relation between number of insulator disks and spacing for transmission lines:

A—Conductor to nearest tower steel
B—Conductor to vertical tower members
C—Between vertical conductors and between conductors and ground wires
D—Between horizontal conductors

3. Spacings between conductors, from conductors to tower, and from conductors to overhead ground wires should co-ordinate with the impulse flashover of the number of insulators chosen.

Spacing *A* from conductor to the nearest tower steel should have an impulse flashover about ten per cent greater than the insulator string flashover. In feet this is roughly equal to $\frac{\text{number of disks}+1}{2}$.

Spacing *B*, the horizontal distance from conductor to tower when the conductor is hanging vertically, equals 1.5*A*.

Spacing *C*, between horizontal planes through conductors in the vertical arrangement, and between the plane of upper conductors and plane of ground wires, equals 2*A*. The same spacing is used between the plane of conductors and plane of ground wires in the horizontal arrangement.

Spacing *D*, between conductors in the horizontal arrangement, is 3*A*.

Spacing *E*, between vertical planes through middle and bottom conductors in vertical arrangement, varies from 0.5 to 1.5*A*, depending on severity of snow and ice, and wind conditions.

4. Immunity from flashover depends not only on the insulation and spacings selected,

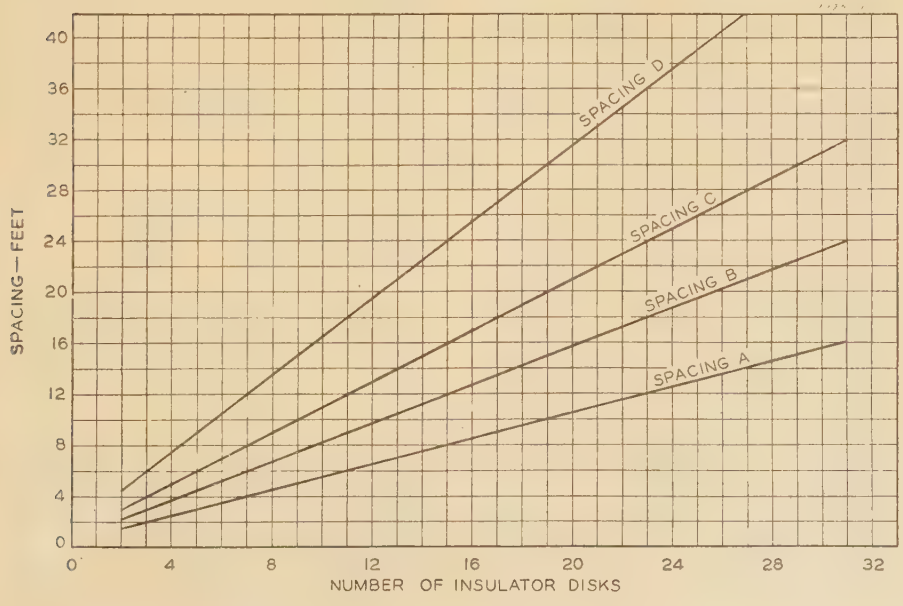

Table IV. Co-ordination of Spacings With Number of Insulator Disks

Number of Insulator Disks*	Spacing A, Feet	Spacing B, Feet	Spacing C, Feet	Spacing D, Feet
3	2	3	4	6
5	3	4.5	6	9
7	4	6	8	12
9	5	7.5	10	15
11	6	9	12	18
13	7	10.5	14	21
15	8	12	16	24
17	9	13.5	18	27
19	10	15	20	30
21	11	16.5	22	33
23	12	18	24	36
25	13	19.5	26	39
27	14	21	28	42
29	15	22.5	30	45
31	16	24	32	48

* Spaced 5 3/4 inches.

Spacings for intermediate numbers of disks may be interpolated.

Refer to Figures 5 and 6 for location of spacings *A*, *B*, *C*, and *D*.

Transmission Rating of Telephone Systems

W. A. CODD
NONMEMBER AIEE

Synopsis: The problem of rating the transmission performance of telephone connections is considered, including a review in considerable detail of a method proposed by J. R. Hughes.[1] With this background, a modification of Hughes' technique is presented with indications of certain attendant advantages.

A TELEPHONE, by definition, is a device for projecting the human voice beyond its normal range. There are other systems, of course, such as broadcasting, public address, paging, and recording-reproducing systems which perform this same general function. Each has its own type of service, the nature of which accounts for the differences in equipment and technique peculiar to each system. The service offered by the telephone system makes it the most complex of all. Each subscriber must have his own telephone set which must have access to all other subscribers individually for 2-way conversation and be able to establish and disengage all possible interconnections. The inherent complexity of establishing the transmission paths may tend to distract attention from the primary function of the system, which is to convey intelligence by means of the spoken word. Since this is the reason for the existence of a telephone system, there should be adequate means of measuring its success in accomplishing this end. This is important both to maintain adequate service and to point the way for progress in the art.

This paper will discuss the methods of rating which have been used from time to time throughout the course of development of telephone systems. Special attention will be given to a technique recently proposed by J. R. Hughes which will be reviewed in considerable detail. With this background, a presentation will be given of a modification of Hughes' technique with certain indicated advantages.

Since this discussion is concerned entirely with the transmission problem, the terms telephone system or connection are to be understood to refer to the equipment which makes up a complete voice transmission path from one subscriber to another.

Basis of Rating Methods

Inasmuch as the fundamental function of the telephone system involves the transmission of voice-produced electric currents over a distance, the first essential for the system is satisfactory transmitting and receiving equipment. With such equipment available it is immediately apparent that the loss in the telephone line (or other connecting medium) is of primary importance since with increased loss the weaker signals, and eventually all signals received, will fall below the audible limit. For that reason, various methods for rating of telephone systems, which have been used throughout the years, use as their unit some measure of the loss in a unit length of line.

Rating Electric Circuit Components

The earliest method used for specifying line losses was to indicate the number of miles of standard cable in the connection. Where lines other than standard (19 gauge) cable were used, the number of miles of standard cable which would give the same reduction of current from input to output at an average frequency of say 800 cycles per second would be the measure of the line loss. When dealing with such lines it was necessary to use some measure of current reduction in the line to determine the length of standard cable which gave equal loss. Accordingly, a further step in development was to state the line losses directly as a function of this current reduction. Thus, the 800-cycle mile was born. It is a unit based on the loss in passing through one mile of standard cable at 800 cycles per second, which is defined mathematically as the natural logarithm of the ratio of the input to output currents in one mile of standard cable (which is 0.109). Thus the formula for determining the number of 800-cycle miles corresponding to any values of input and output current on a properly terminated line is $2.30/0.109 \, [\log_{10} (I \text{ in}/I \text{ out})]$. Other circuit components are then rated in terms of the number of 800-cycle miles corresponding to the current or power reduction resulting from their insertion in the circuit.

Ratings of Transmitters and Receivers

The most difficult problem in telephone transmission rating has been the development of an adequate method for determining and expressing in simple and in-

Paper 46-163, recommended by the AIEE committee on communication for presentation at the AIEE summer convention, Detroit, Mich., June 24-28 1946. Manuscript submitted June 27, 1945; made available for printing May 22, 1946.

W. A. CODD is with the Stromberg-Carlson Company, Rochester, N. Y.

---

but on adequate shielding by overhead ground wires and sufficiently low tower footings resistance. In general, flashover will not be experienced if the footing resistance is less than the 1.5x40 microseconds positive impulse flashover of the insulation, divided by 100,000.

References

1. SELECTION OF PIN-TYPE INSULATORS FOR VARIOUS SERVICE VOLTAGES, **H. A. Frey.** *Distribution*, October 1944, pages 10–11.

2. TRANSMISSION LINE ANALYSIS INDICATES RULING TENDENCIES, **E. B. Kurtz, J. A. Douglas.** *Electrical World*, September 26, 1931, pages 553–5.

3. ENGINEERING DETAILS OF TRANSMISSION LINES IN THE UNITED STATES, *Electrical World*, supplement, September 21, 1929.

4. LIGHTNING PERFORMANCE OF 220-KV TRANSMISSION LINES—II, **AIEE Committee Report.** AIEE TRANSACTIONS, volume 65, 1946, February section, pages 70–6.

5. LIGHTNING PERFORMANCE OF 110- TO 165-KV TRANSMISSION LINES, **AIEE Committee Report.** AIEE TRANSACTIONS, volume 58, 1939, June section, pages 294–304.

6. STANDARD BASIC IMPULSE INSULATION LEVELS, **Joint Committee Report.** ELECTRICAL ENGINEERING, volume 60, March 1941, page 121.

7. FLASHOVER CHARACTERISTICS OF ROD GAPS AND INSULATORS, **AIEE Committee Report.** AIEE TRANSACTIONS, volume 56, 1937, June section, pages 712–14.

8. LIGHTNING STRENGTH OF WOOD IN POWER TRANSMISSION STRUCTURES, **Philip Sporn, J. T. Lusignan, Jr.** AIEE TRANSACTIONS, volume 57, 1938, February section, pages 91–101.

9. WHAT WOOD MAY ADD TO PRIMARY INSULATION FOR WITHSTANDING LIGHTNING, **J. T. Lusignan, Jr., C. J. Miller, Jr.** AIEE TRANSACTIONS, volume 59, 1940, September section, pages 534–40.

10. LIGHTNING INVESTIGATION ON TRANSMISSION LINES—VIII, **W. W. Lewis, C. M. Foust.** AIEE TRANSACTIONS, volume 64, 1945, March section, pages 107–15.

11. LIGHTNING INVESTIGATION ON TRANSMISSION LINES—IV, **W. W. Lewis, C. M. Foust.** AIEE TRANSACTIONS, volume 53, 1934, August section, pages 1180–6.

12. SOME ENGINEERING FEATURES OF PETERSEN COILS AND THEIR APPLICATION, **E. M. Hunter.** AIEE TRANSACTIONS, volume 57, 1938, January section, pages 11–18.

13. PROTECTOR TUBES FOR POWER SYSTEMS, **H. A. Peterson, W. J. Rudge, Jr., A. C. Monteith, L. R. Ludwig.** AIEE TRANSACTIONS, volume 59, 1940, May section, pages 282–8.

14. NINE YEARS EXPERIENCE WITH ULTRAHIGH-SPEED RECLOSING OF HIGH-VOLTAGE TRANSMISSION LINES, **Philip Sporn, C. A. Muller.** AIEE TRANSACTIONS, volume 64, 1945, May section, pages 225–8.

formative terms the performance of transmitters and receivers.

Historically, the earliest attack on the problem is found in the volume or loudness tests. They were based on the fundamental assumption that two over-all connections which would produce equal loudness in the listener's ear were equally satisfactory and, therefore, would be given equal ratings. Observers were asked to judge the relative loudness of two such connections. A series of observations were made with successively different equivalent lengths of a standard trunk in one connection as compared to the other. When settings of trunk were determined which gave equal loudness for the two connections, the difference in equivalent length or attenuation was taken as the difference in rating of the two systems. Thus the performance of over-all connections, including the effects of various subscriber sets, was rated in terms of equivalent trunk losses.

Initially, the standard trunk used for such comparisons was the 19-gauge standard cable (referred to previously) and the ratings were expressed in terms of a number of miles of standard cable. It had the disadvantage of not producing uniform attenuation throughout the frequency range. Consequently, adjustments of the trunk changed not only the level but also the response-frequency characteristic by producing larger changes of attenuation at high frequencies than at low frequencies, thus making equality of loudness difficult to judge. It eventually was decided to replace the standard cable by a 600-ohm distortionless trunk. With the adoption of this trunk, the unit of line loss was replaced by a new unit of approximately the same magnitude, but defined as $10 \log_{10} (P \text{ in}/P \text{ out})$ and called at first the transmission unit (TU) and later the decibel (db).

Quality Differences

In the course of the loudness comparisons which were used in telephone instrument ratings, it often would be apparent to the observers that when the trunk had been adjusted for a loudness match, there was still a difference in the sound of the reproduced voice over the two systems, even when the distortionless trunk was used. Such differences commonly are described as quality differences. It seems evident that when the quality differences are large they so significantly may affect the intelligibility of speech transmitted over the system that volume rating alone becomes inadequate as a performance index.

Judgment Tests

Earliest attempts to take account of quality differences were the judgment tests. In these tests after the systems under comparison had been adjusted for equal volume, various observers were asked to listen to representative sentences transmitted over the system and give their judgment as to which system they preferred. The systems were rated according to the relative number of votes cast for each. A glaring weakness of the method is that the preferences expressed often may be quite unrelated to the actual transmission merits of the system and thus may be definitely misleading.

Articulation Testing

A much more fundamentally sound and informative method of evaluating the effects of quality differences is the articulation test. It has been used since before 1910[2] and its value still is recognized. The test is conducted in the following manner. Each of a number of callers speaks a list of meaningless monosyllables or "logatoms" over each of two systems to be compared. The logatoms preferably are inserted in sentences. A group of observers at the receiving end of the systems record the logatoms as they understand them. The percentage of sounds or logatoms correctly received is called the per cent articulation of the system. Per cent articulation is more significant than volume rating alone in that it does take account of quality differences as well as volume differences. A definite disadvantage, as compared to volume ratings, is that ratings of system components may not be simply combined to determine over-all ratings of connections of varied make-up. It is conceivable, however, that series of articulation tests may be taken on each system in such a manner that their results might finally be expressed in units suitable for this purpose. This will be discussed further in connection with immediate appreciation testing.

Analysis of Quality Differences

The existence of quality differences between systems led to development of other kinds of testing in which the specific objective was to explain the quality differences. Such tests are referred to commonly as objective tests, since they measure the physical characteristics of the system without dependence on the user's judgment or opinion. Their highest development is found in the use of artificial mouth and ear equipment.[3] They are very valuable tests for their intended purpose of analysis of performance. However, they do not afford a straightforward means for the rating of over-all performance in simple terms which are interpreted readily and hence need not receive further consideration here.

The Complete Rating Problem

The preceding discussions have called attention to the fact that one telephone connection may differ from another in the quality of the received speech as well as in volume or loudness. Quality differences may be either in frequency distortion (unsatisfactory balance of response throughout the voice frequency range) or in nonlinear distortion (the introduction by the circuit equipment of additional frequencies not present in the original speech). In addition to these effects, there are differences caused by the fact that the circuit is required to provide 2-way transmission with an invariable circuit, that is, without switching of transmitter and receiver alternately into the circuit for talking and listening, respectively. The result is the condition commonly described as side-tone, that is, a reproduction of a portion of the sound picked up by the transmitter of a given set in the receiver of the same set. During transmitting the presence of this side-tone causes the user to lower his voice, the amount depending on the amount of such side-tone. On receiving, side-tone introduces noise into the listener's receiver picked up from the room in which he is listening, the amount of such noise being dependent on the amount of room noise and the efficiency of the side-tone path.

It is evident that any figure of merit which is intended to serve as a measure of the over-all value of a telephone connection in conveying intelligence in actual service must be obtained in such a way as to include the effects of all of these characteristics of the equipment and their interactions on the users.

The Repetition Rate Test

The repetition rate test[4,5] was conceived and developed in the Bell Telephone System as a practical means of providing such a figure of merit. In this method, the test data are obtained by monitors on actual telephone connections of known make-up who make records of the number of times that the users, in the course of their conversations, give evidence of failure to understand each other. The monitors also observe the elapsed

time for each conversation. The data are summarized to give the number of repetitions required per unit time. This is called the repetition rate for the connection. Such data are statistical in nature and a large number of such observations must be made to give results of acceptable precision. Data are taken on a large number of different connections to cover the range of equipment types to be rated. The repetition rate is taken as the fundamental measure of the degree of success in carrying on conversations. Advantages of the volume rating system are retained by including in these tests measures of the variation of repetition rate with variation of length, or attenuation in decibels, of distortionless trunk included as part of the connection for this group of tests. It is then possible to convert variations of repetition rate caused by changes of any part or component of a telephone connection to equivalent changes in distortionless attenuation expressed in decibels. This gives a rating system in which the performance of any component of a connection may be stated in terms of the number of decibels of effective transmission loss as compared with the corresponding component of a standard reference system.

The basis of these ratings, the repetition rate test, has come to be generally regarded as the ultimate criterion of satisfactoriness of the over-all transmission path of a telephone connection. Disadvantages of this method are that it is essentially a field test, not adaptable to the laboratory, requires a very long time to obtain data, and is not generally practical for operating companies or manufacturers to use because of privacy requirements. The Bell System was able to overcome the latter difficulty by using several hundred stations in the American Telephone and Telegraph Company headquarters building and a like number at the Bell Telephone Laboratories.

The Immediate Appreciation Test

The immediate appreciation test[1] is an attempt to bring the repetition rate test into the laboratory. In other words, it is a proposed means of overcoming the disadvantages of the repetition rate test and still obtaining a rating which will include the effect of all the various system characteristics and the user's reactions to them,

In the application of the method, talking and listening crews speaking over the connection to be rated use lists of 20 sentences, each of about six to ten words, simple and straightforward in type, and extracted from the ordinary news columns

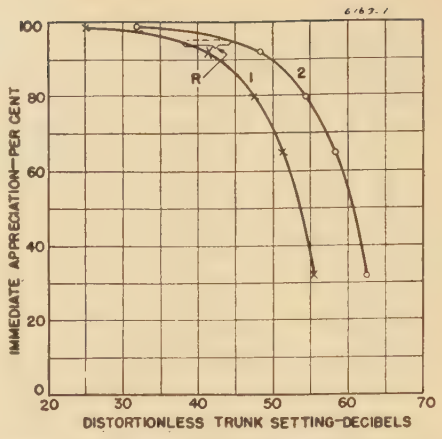

Figure 1. Immediate appreciation test—comparison of transmitting substations

Curve 1—Connection from transmitting substation *A* to receiving substation

Curve 2—Connection from transmitting substation *B* to receiving substation

of a daily newspaper. The listener is simply asked to decide whether or not he *appreciated* the meaning of each sentence *immediately* without any sort of delay or introspection on his part. On this basis he records each sentence as a success or failure. The percentage of successes is the percentage immediate appreciation and is taken as the criterion of performance of the system. It is this particular testing technique which distinguishes the test from other subjective tests. (These are tests which use talking and listening crews.) Other details which will be discussed have to do with means of taking account of the effect of service conditions (that is, speaker's volume level and room noise) and the means of presenting the data and converting it to more useful form.

Assuming the tests are so arranged as to take adequate account of service conditions, it will be seen that the outstanding difference from the repetition rate test is in the fact that the listeners also become observers in the test, so that the test data come directly from them instead of from monitors. The record, however, is based on fundamentally the same reaction, the difference being that the listener, as a result of a failure to appreciate the meaning of what has been transmitted, records this failure instead of requesting a repetition. Advantages are that the tests can be made in the laboratory, the required data can be obtained in a much shorter time since continuity of testing may be obtained, and the sensitivity of the method is higher, thus reducing the amount of required data and testing time. A possible disadvantage is a certain degree of artificiality, a fault of any laboratory test. In this respect, however, the immediate appreciation method has considerable advantage over the articulation test in which meaningless monosyllables constitute the matter transmitted. Here again there is a considerable advantage in time for the appreciation test since consistent results are found to be obtainable with much less matter transmitted. There is also the advantage of practically unlimited source of material in contrast to the limited number of logatoms available, thus reducing practice effects caused by familiarity with the material transmitted. The significant point, however, in the appreciation tests is the fact that the records obtained are intended to indicate specifically and directly the success of the telephone connection in conveying the meaning of connected words (that is, expression of thought) from talker to listener. Aside from these disadvantages of the articulation method, there appears to be no reason why the methods to be presented for rating of systems by application of the immediate appreciation technique might not use equally well the logatom articulation technique.

In the immediate appreciation tests, the direct result of a test run on two systems to be compared will show for the particular test conditions the per cent appreciation for each system. This, in itself, is a valuable indication of the relative performance of two systems. However, in order to enable expression of the results in more useful form, a number of runs are taken on each system, the amount of distortionless trunk in the connection being set at a new value for each run. Resultant data permit the plotting for each system of a curve of per cent appreciation as a function of trunk attenuation. Such curves are shown in Figure 1. Figure 2 shows by block diagram typical circuits which are used in obtaining these data. In Figure 1 the difference R of attenuation in decibels at a given level of per cent appreciation is taken as the difference in effective transmission of the two systems for the given test conditions. Thus, if this per cent appreciation is taken at a value which is agreed upon as representing a satisfactory standard of communication efficiency, it is indicated in the given example that 7.5 decibels more attenuation may be inserted in connection 2 than in connection 1, and still furnish transmission equal to the specified standard. It might be argued that 100-per-cent appreciation should be used. However, for practical reasons, a value somewhat short of this (95 per cent) is used. One reason is that the slope of the curves in this region allows the comparison to be made

more precisely; also, in general, it is not economical to design for perfection.

This method of interpretation of results assumes that it always will be possible to obtain a curve of the type shown in the figure for any system. A little consideration will show that it is a fundamental result of the test method. A difficulty, of course, would be presented by a system of such poor characteristics that 95-per-cent appreciation would be impossible to attain at any attenuation setting. However, there would be no practical interest in trying to rate such a system.

Treatment of Service Conditions

In his article on this method, J. R. Hughes gives extensive discussion of a statistical technique for taking account of the range of service conditions. The statistical method is based on frequencies of occurrence of various values of speaker's volume level and room noise determined from a large number of measurements of these quantities (in the case of room noise at actual subscriber locations). It consists of a procedure for weighting the observed data in accordance with these frequencies of occurrences. In making these tests the talker's volume level has to be treated in such a way that any tendency of the presence of side-tone, which he hears from his own receiver, to influence the loudness of his voice will be permitted to have its normal effect. This means that no artificial control should be exercised, such as the instruction to maintain a constant specified speaking level which is the common procedure in the usual voice-ear volume tests or articulation tests. In lieu of such control, the method of relating the speaking levels of the crew to the range of service distribution is by measurement of their natural speaking level; that is, the level at which they speak most naturally when conversing, without a telephone, in a quiet room.

In obtaining the data for application of this statistical technique, it is necessary to take several families of curves to give the required information on variation of per cent appreciation with service conditions. The several families are taken each for a different fixed value of room noise at the transmitting end of the connection, each curve in a given family being obtained for a different value of room noise at the listening end. Thus each individual curve of each family gives the variation of per cent appreciation with attenuation of distortionless trunk for a different combination of transmitting and receiving end room noises. About four families of four curves each are required. Variations of speaking level are taken as equivalent to variations of distortionless trunk setting.

By application of the statistical technique to these data, a single figure of merit is obtained which indicates how much more attenuation may be inserted in the better of two circuits and still obtain a grade of transmission at least equal to the accepted limiting value (95-per-cent appreciation) on the same percentage of all calls as on the poorer system.

A Modified Technique

In the foregoing discussions of immediate appreciation testing, interpretations of the test data have been made in terms of the excess amount of distortionless attenuation which must be inserted in the better of two systems in order to make the two systems equivalent in their ability to transmit intelligence. In the data discussed in connection with the statistical technique, this equivalence is established on the basis of an equal per cent of calls, enjoying at least 95-per-cent immediate appreciation; and the resultant rating is a composite figure dependent on all combinations (suitably weighted) of room noise levels and speaking levels occurring in service. In contrast to this, in standard Bell System effective ratings, the equivalence of two systems is established on the basis of equal success in conveying intelligence in the presence of a single representative (reference) value of

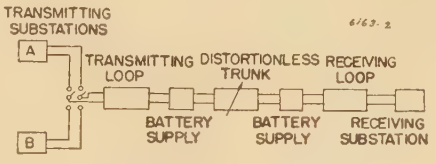

Figure 2. Diagram of connections for a typical immediate appreciation test

room noise existing at each end of the connection in each of the two systems. It seemed desirable in developing a laboratory test for rating telephone systems in this country to express the ratings on this basis.

The adoption of such a basis would result, also, in a very considerable reduction (to about 1/16) in the amount of test data required. This is true since it would mean that the data for determination of the several families of curves discussed in connection with the statistical technique would be reduced to that necessary to give a single curve for each system under test, such as 1 or 2 shown in Figure 1. The full extent of this simplification is not at once evident and may not be permissible always, since the technique employed still must take account of the service range of speaker's volume level, including the effects of side-tone characteristics of the transmitting subsets on this level. Accordingly, these tests must be conducted without instruction to the talkers to maintain any specified speaking level.

In general, it would be necessary to obtain a family of curves of per cent immediate appreciation as a function of distortionless trunk setting for each connection to be rated where the several curves of a family would be taken, each with a different crew having a different natural speaking level. The difference R (Figure 1) between the curves for two systems being compared would be taken for each crew. A weighted average value of R then would be obtained in which the weighting would be in accordance with the frequency of occurrence of the respective values of natural speaking level in service.

The ultimate simplification possible in the use of this method results by applying the fundamental assumption which provides the basis for Hughes' statistical technique. This is derived from his observation that under actual talking conditions amplitude distortion, even in systems using carbon transmitters, is negligible. The corollary to this is that changes in the amount of attenuation in the distortionless trunk may be taken as representing, also, changes of the speaker's volume level. Applying this assumption, for example, to the curves of Figure 1 leads to the following conclusions. Suppose that curves 1 and 2 and the resultant difference R between the two systems have been obtained with a crew having a given natural speaking level. Now suppose that this data were repeated with a crew having, for example, a 10-decibel higher natural speaking level. Application of the foregoing principle leads immediately to the prediction that the new curve 1′ (not shown) for the connection involving transmitting substation A will be obtained from curve 1 by adding ten decibels to the abscissa for each point, that is, the new curve will be displaced horizontally ten decibels to the right from curve 1. The new curve 2′ (not shown) for the connection using transmitting substation B will be obtained in an exactly similar manner from curve 2. Thus the difference R' between curves 1′ and 2′ will be identical to the difference R. Hence the difference R will be independent of the natural speaking level so that

only a single curve of per cent appreciation as a function of distortionless trunk setting need be taken for each connection to be rated.

When the assumption of equivalence of variations of attenuation of distortionless trunk and of speaker's volume level are not substantiated, the method of using several crews having different natural speaking levels should be adopted. This still would require only about one-fourth of the data required by Hughes' complete statistical technique and has the further advantage in this case of taking account of any existing amplitude distortion effects which are neglected by the fundamental assumption of the Hughes' method.

If ratings are desired for other room noise levels, they are obtained by repeating tests of the foregoing type with the room noise adjusted to the required level. As a simplifying approximation, such tests may be taken on a representative system, and the difference between the ratings for average room noise and the required room noise may be applied as a correction to the rating determined on any other system in question at the average (reference) room noise level.

Conclusion

The simpler form of the modified testing technique described has had some application in the rating of transmission performance of subscriber's sets. The limited amount of testing which has been done up to this time indicates this technique to be quite feasible. The immediate appreciation test in this general form, therefore, gives promise of being a very valuable tool in evaluating the overall merit of developments in telephone transmission equipment.

References

1. Comprehensive Assessment of Telephone Communication Efficiency, **J. R. Hughes.** *Journal* of the Institution of Electrical Engineers, Part III—Communication Engineering (London, England,) volume 89, December 1942, pages 195–206.

2. Telephonic Intelligibility, **G. A. Campbell.** *Philosophical Magazine*, volume 19, January 1910 pages 152–9.

3. A Voice and Ear for Telephone Measurements, **A. H. Inglis, C. H. G. Gray, R. T. Jenkins.** *Bell System Technical Journal*, volume 11, April 1932, pages 293–317.

4. Rating the Transmission Performance of Telephone Circuits, **W. H. Martin.** *Bell System Technical Journal*, volume 10, January 1931, pages 116–31.

5. A System of Effective Transmission Data for Rating Telephone Circuits, **F. W. McKown, J. W. Emling.** *Bell System Technical Journal*, volume 12, July 1933, pages 331–46.

Carrier Supervisory Control of Pumping Station Over Power Cable

W. A. DERR
ASSOCIATE AIEE

W. A. KELLER
NONMEMBER AIEE

H. A. W. HEDKE
ASSOCIATE AIEE

THE PROCESSING of starch requires large quantities of water. Thus, when the United States Sugar Corporation recently added the processing of starch to their activities, it was natural to install their new plant, which makes use of sweet potatoes as the raw product, at Clewiston, Fla. Clewiston is located in the Everglades near Lake Okeechobee. Lake Okeechobee is a shallow lake but it covers an area of over 700 square miles, second in area only to Lake Michigan in the United States.

When the new starch plant was planned, it was calculated that the maximum daily demand for water would be 4,000,000 gallons with 3,000,000 of these gallons requiring purification before being used in starch processing. An analysis of the water of Lake Okeechobee indicated that the best source of water for the processing of starch on a purity and temperature basis was four miles from the levee of the lake. These findings resulted in the decision to build a concrete pumping station in Lake Okeechobee, four miles from the levee and a total of seven miles from the water treatment plant where the water is treated before being used in the starch processing.

A view of the pumping station is shown in Figure 1. The inside diameter of the station is 40 feet and the walls are $2^1/_2$ feet thick. The station is slightly over 40 feet from top to bottom with the water level normally being about 15 feet above the lower floor level.

A 24-inch-diameter cast iron pipe carries the water from the pumping station to the water treatment plant. The pipe is buried approximately four feet below the bed of the lake. A 75-horsepower electric motor and a 180-horsepower gasoline engine are used to pump water through the pipe. Electric power is fed to the pumping station from the water treatment plant over a 4,000-volt power cable which is laid in the same trench with the pipe.

The relative inaccessibility of the pumping station led to the decision to provide control of the pumping equipment from the water treatment plant rather than having an operator located in the pumping station.

The remote control of the pumping station could have been accomplished by means of wires in a submarine control cable which would have had to be installed in addition to the power cable, or by means of power-line carrier supervisory control operated over the power cable. Economic considerations led to the application of carrier equipment to the 4,000-volt power cable.

Figure 2 is a single line diagram of the essentials of the power system at the water treatment plant and at the pumping station. The connections of the carrier equipment to the power cable also are indicated.

No carrier line traps were necessary on this installation because the power cable is terminated with the electric motor at the pumping station and with an autotransformer at the water treatment plant.

New Features of Installation

This installation of carrier-operated supervisory control equipment incorporates quite a number of operating and design features not previously employed. Following is a list of these features:

1. Operation of power-line carrier equipment over a submarine cable.
2. The use of standard low voltage capacitors for coupling to the power line instead of standard coupling capacitors, thus making it possible to omit line tuning units.
3. The complete incorporation of power-line carrier equipment including coupling equipment in a metalclad switchgear assembly.
4. Selective telemetering through the

Figure 1. A view of pumping station showing entrance door

Paper 46-174, recommended by the AIEE committee on automatic stations for presentation at the AIEE summer convention, Detroit, Mich., June 24–28, 1946. Manuscript submitted April 19, 1946; made available for printing May 29, 1946.

W. A. DERR is design engineer in the switchboard engineering department of the Westinghouse Electric Corporation, East Pittsburgh, Pa.; W. A. KELLER is meter engineer, Westinghouse Electric Corporation, Atlanta, Ga.; and H. A. W. HEDKE is electrical engineer, United States Sugar Corporation, Clewiston, Fla.

supervisory control equipment over a single-frequency power-line carrier channel without the use of audio tones for modulation of carrier.[1]

5. Establishment of communication circuit over single-frequency power-line carrier channel through supervisory control equipment.

Cable Characteristics

A total of 35,000 feet of 3-conductor power cable is used between the water treatment plant and the pumping station for the transmission of 4,000-volt 3-phase power.

A 22,800-foot length of armored submarine cable is used from the levee on the shore to the pumping station. The armored cable is laid in the same trench with the 24-inch water pipe. The submarine cable has number 4 conductors and is protected with number 8 Birmingham wire gauge galvanized armor. The outside diameter of this cable is approximately 2.06 inches. Figure 3 shows the construction of the armored cable.

A 12,200-foot length of rubber-jacketed cable is used from the levee, where it is spliced to the submarine cable, to the water treatment plant. This cable is laid in trenches across farm land at a depth of approximately four feet. No cover protection is used as this is below cultivating depth.

The characteristic impedance of ordinary high-voltage transmission lines is about 800 ohms for line-to-line channels and about 500 ohms for line-to-ground channels.[2] The characteristic impedance of both the armored and the jacketed cable used on this installation is approximately ten per cent of the usual values for ordinary transmission lines, the line-to-line impedance being approximately 85 ohms and the line-to-ground impedance being approximately 45 ohms.

When the carrier equipment was first placed in operation, the carrier sets were used to obtain a check on the line-to-ground attenuation values for the cable, which had been calculated previously from factory test data.

To obtain data necessary to check the factory test data, the carrier equipment at each location was set on the proper tap of the matching transformer to match the 45 ohms characteristic impedance of the cable. The accuracy of calculated attenuation values is dependent on having the line terminated in its characteristic impedance. The complex nature of the carrier receiver circuit makes it impossible to choose a setting which will provide exactly the right termination for all frequencies. However, because of the relatively high cable losses it was believed that only slight inaccuracies would result from the termination not being exact at all frequencies. The results obtained indicate that the carrier equipment provided satisfactory termination at all frequencies.

The carrier transmitter at the pumping station was adjusted to various frequencies with the high frequency voltage and

Table I. Calculated Decibel Loss for 4,000-Volt Power Cable (22,800 Feet Armored and 12,200 Feet Rubber Jacketed) From Field Data*

Frequency, Kc	Current Input	Voltage Input (E_1)	Voltage Output (E_2)	Impedance, Ohms	Total Decibel Loss	Decibel Loss Per Mile
175	0.515	22.8	0.38	44.3	35.56	5.37
165	0.510	23.2	0.58	45.5	32.04	4.83
150	0.520	23.3	0.79	44.6	29.40	4.43
135	0.520	23.6	1.02	45.4	27.30	4.12
120	0.515	24.5	1.30	47.6	25.50	3.85
105	0.490	23.7	1.95	48.3	21.68	3.28
90	0.510	24.5	2.85	48.0	18.68	2.82
75	0.530	26.4	4.20	49.8	15.96	2.41
60	0.540	26.2	5.50	48.5	13.56	2.05
50	0.535	28.1	7.07	52.5	12.00	1.81
40	0.560	26.2	8.40	46.8	9.88	1.49

* Decibel loss $= 20 \log_{10} \frac{E_1}{E_2}$.

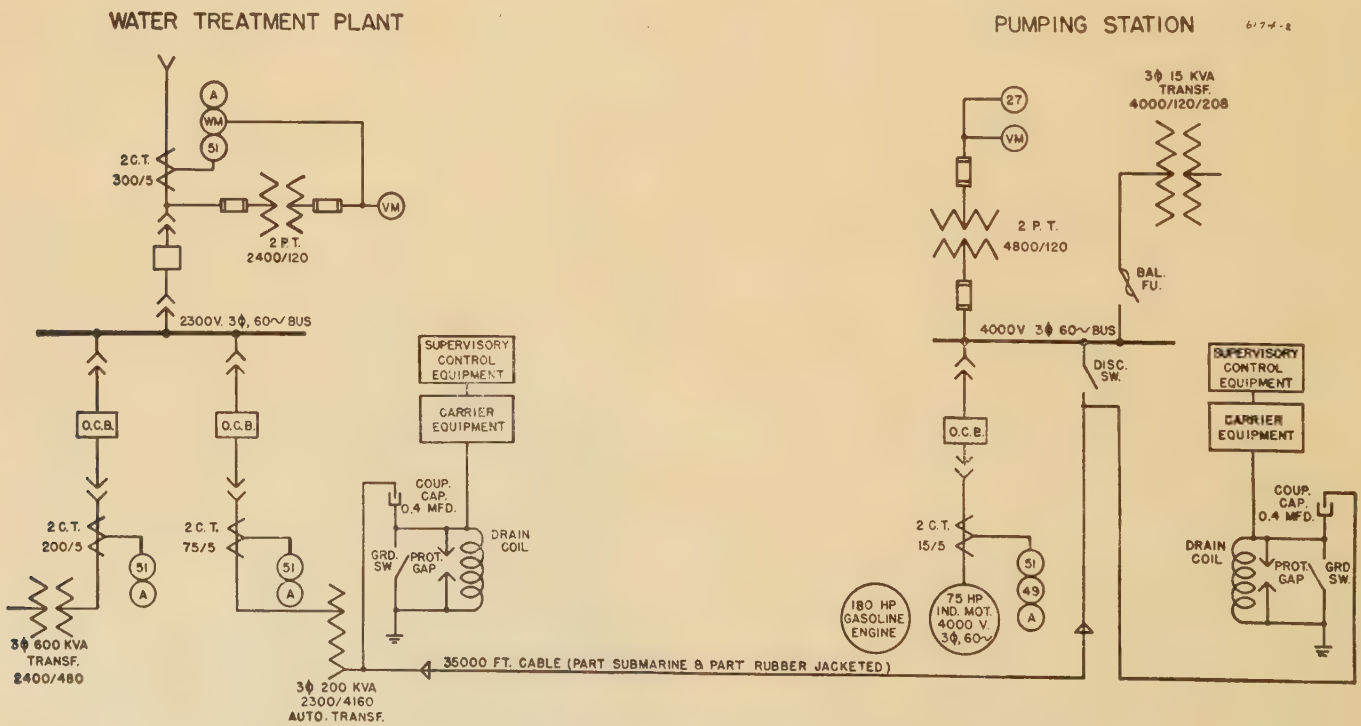

Figure 2. Single line diagram of power system at the water treatment plant and at the pumping station

Figure 3. Cutaway view of armored submarine cable

current values being read for each different frequency. The output voltage also was read at the water treatment plant for each different frequency.

From the test data obtained it was possible to calculate the attenuation values of the cable at the various frequencies. Transmission losses usually are expressed in decibels. The decibel is expressed numerically as follows:[3]

$$db = 10 \log_{10} \frac{P_1}{P_2}$$

where

db = decibel loss (attenuation)
P_1 = power in
P_2 = power out

If the two points at which the voltage is measured have identical impedances, the decibel also can be expressed as follows:[3]

$$db = 20 \log_{10} \frac{E_1}{E_2}$$

where

db = decibel loss (attenuation)
E_1 = voltage input
E_2 = voltage output

Table I shows the readings of current and voltage as well as the calculated values of decibel loss and impedance. The values of impedance which were calculated from the voltage and current input readings indicate that the termination consisting of the carrier receiver at the water treatment plant was not exactly correct for all frequencies since the calculated impedance values should have been the same at all frequencies.

Curve *A* of Figure 4 shows the decibel loss for the entire cable plotted against frequency, the values used being those shown in Table I. The values for the entire cable check well with factory test data obtained prior to installation of the cable. The factory tests indicated somewhat higher losses for the submarine cable alone and somewhat lower values for the jacketed cable alone. Curve *B* of Figure 4 shows the decibel loss per mile of the submarine cable and curve *C* of Figure

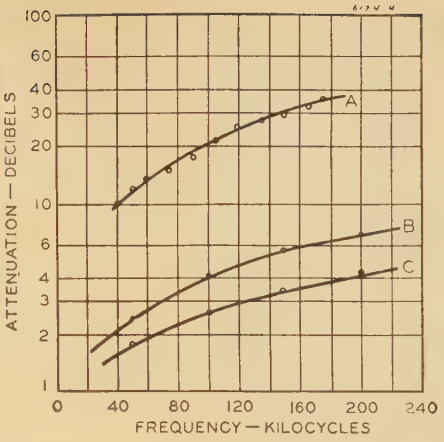

Figure 4. Curves of cable attenuation

A—Total decibel loss for entire cable from field data
B—Decibel loss per mile of submarine cable from factory test data
C—Decibel loss per mile of jacketed cable from factory test data

4 shows the decibel loss per mile of the rubber jacketed cable. Curves *B* and *C* are plotted from factory test data.

Carrier Coupling Equipment

A standard line of coupling capacitors is available for introducing carrier frequencies to power lines.[2] This line of coupling capacitors is available for system voltages from 15 kv to 345 kv. The desirability of keeping these coupling capacitors to a reasonable size resulted in their being designed with low values of capacitance. These low values of capacitance result in a relatively high capacitive reactance for even the carrier frequencies from 45 to 165 kc. Since the carrier sets are designed for matching a line impedance which is essentially resistive, a line tuning unit is used with the standard line of coupling capacitors to cancel the capacitive reactance of the coupling capacitor, thus making it possible to match the carrier sets to a resistive impedance.

The smallest carrier coupling capacitor which could have been used on this installation is for use on 15-kv lines. The size of this unit is such that it could not have been incorporated conveniently in the assembly of metalclad switchgear. Also, a line tuning unit would have been required since the capacitive reactance of this coupling capacitor at a frequency of 50 kc is 320 ohms whereas the characteristic impedance of the cable from line-to-ground is only 45 ohms.

Since the carrier equipment on this installation was to be operated from line-to-ground, it was decided to use a standard 2,300-volt capacitor similar to those used

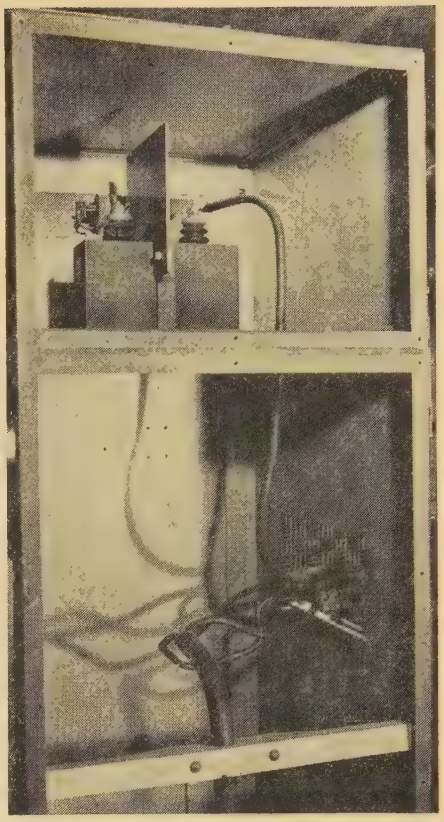

Figure 5. Rear view of metalclad unit with cover removed showing coupling capacitor

for power factor correction to couple the carrier equipment to the power cable. The capacitor chosen has a capacity of 0.4 microfarad. Due to the small size of this capacitor no difficulty was encountered in mounting it in the rear compartment of the metalclad switchgear unit which houses the supervisory control and carrier equipment. Figure 5 shows the capacitor mounted in the metal clad unit at the water treatment plant.

The capacitive reactance of the 0.4-microfarad capacitor which was used is only eight ohms at a frequency of 50 kc. This low value of capacitive reactance made it unnecessary to use a line tuning unit. The use of a 0.4-microfarad capacitor on this low voltage line results in a flow of less than 0.4 ampere of 60-cycle current to ground.

The carrier drain coil, grounding switch, and protective gap as shown in Figure 2, are all mounted on a protective panel mounted on the barrier between the high and low voltage compartments of the metalclad unit. The front of this protective panel can be seen near the top of Figure 6.

Carrier Equipment

The power-line carrier equipment on this installation is of the rack and panel

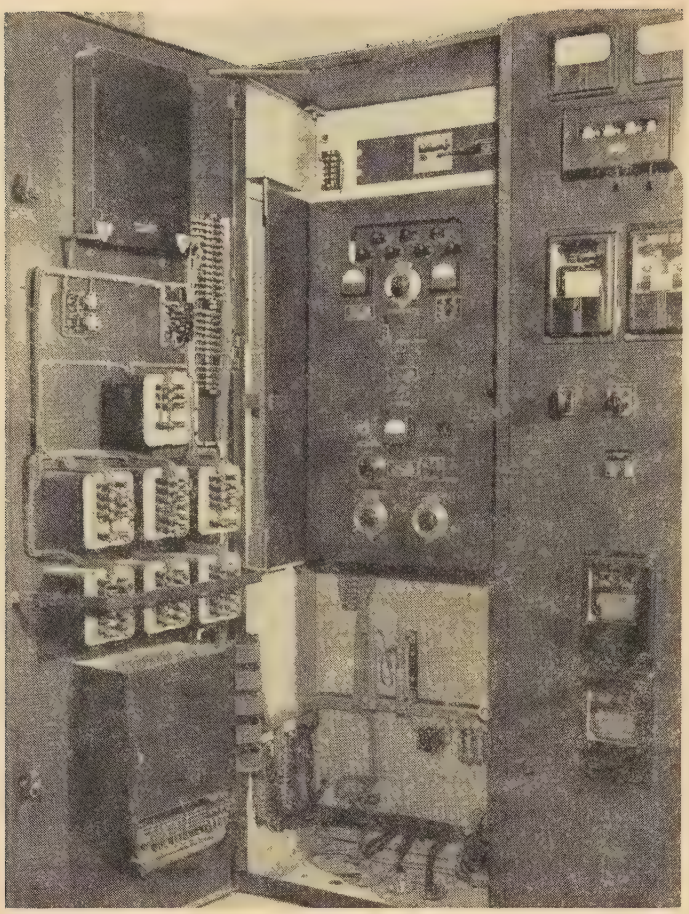

Figure 6. View at pumping station showing front of swinging carrier panel

type.[4] This type of construction makes it possible to build a unit for any carrier application, by making an assembly of the necessary standard panels. In this case a transmitter panel, receiver panel, and modulator panel were required at the pumping station and at the water treatment plant.

The carrier equipment at both locations is mounted on a swinging panel inside of one of the metalclad switchgear units. Figure 6 shows the front of this swinging panel at the pumping station.

The carrier equipment is operated from 125-volt batteries at each location. The carrier transmitters and receivers are adjustable over a frequency range from 45 to 165 kc. The transmitters have a nominal power output of 15 watts and operation is possible with the signal attenuated 30 decibels.

The transmitter panel consists of a Colpitts oscillator (one tube) and of a 6-tube push-pull amplifier. The amplified carrier frequency output is fed into an iron-cored radio frequency transformer whose secondary winding couples the carrier to the line through the coupling capacitor.

The receiver panel consists of a biased detector which is saturated when a satisfactory signal or a stronger than satisfactory signal is received. Thus, the plate current of the receiver is not materially altered for wide variations in received signal strength. The output of the detector supplies rectified current for the supervisory control receiver relay.

The modulator panel includes the matching transformers, resistors, and relays for modulating the transmitter for voice communication, for matching the carrier receiver to the telephone receiver, and for inserting attenuating resistance in the receiver circuit for improved communication.

On this installation both transmitters and both receivers are operated at the same frequency. The equipment is being operated at a frequency of 45 kc, since the attenuation in the cable is considerably less at lower frequencies.

Supervisory Control

The supervisory control equipment on this installation operates by means of coded impulses with each code transmitted being checked by a duplicate code originating at the other station. The impulses are transmitted at the rate of 15 per second and all selection and control impulses are of the same duration.

Carrier impulses are transmitted by the supervisory control equipment by having the supervisory control impulsing contact close the carrier keying circuit. All carrier impulses which are originated at either the pumping station or the water treatment plant result in the carrier receiver relay at both locations being operated since both transmitters and receivers operate on the same frequency. The carrier receiver relay is of the same general type as the rest of the supervisory control relays and is mounted in the supervisory control relay case.

Figure 7 shows the metalclad switchgear unit on which the supervisory control equipment is located at the water treatment plant. This figure shows the individual escutcheons or key and lamp plates for each of the functions performed by the supervisory control equipment as well as the supervisory control relay case and the water flow indicator.

The supervisory control equipment performs the following functions:

1. Start, stop, and supervise electric motor.
2. Start, stop, and supervise gasoline engine.
3. Control and supervise automatic–manual transfer.
4. Supervise electric motor annunciator.

Figure 7. Front view of carrier supervisory control unit at water treatment plant

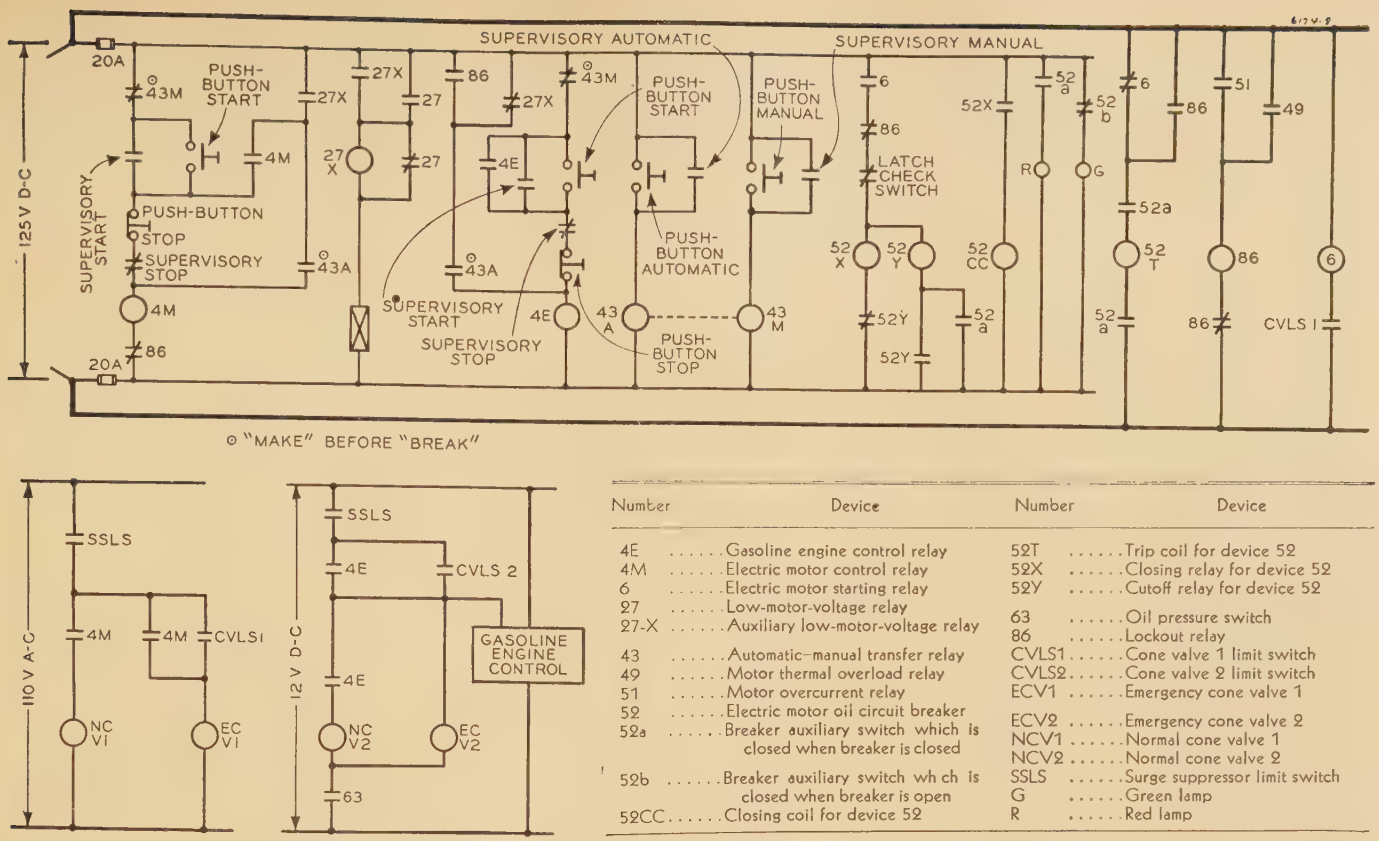

Number	Device	Number	Device
4E	Gasoline engine control relay	52T	Trip coil for device 52
4M	Electric motor control relay	52X	Closing relay for device 52
6	Electric motor starting relay	52Y	Cutoff relay for device 52
27	Low-motor-voltage relay	63	Oil pressure switch
27-X	Auxiliary low-motor-voltage relay	86	Lockout relay
43	Automatic–manual transfer relay	CVLS1	Cone valve 1 limit switch
49	Motor thermal overload relay	CVLS2	Cone valve 2 limit switch
51	Motor overcurrent relay	ECV1	Emergency cone valve 1
52	Electric motor oil circuit breaker	ECV2	Emergency cone valve 2
52a	Breaker auxiliary switch which is closed when breaker is closed	NCV1	Normal cone valve 1
		NCV2	Normal cone valve 2
52b	Breaker auxiliary switch wh ch is closed when breaker is open	SSLS	Surge suppressor limit switch
52CC	Closing coil for device 52	G	Green lamp
		R	Red lamp

Figure 8. Schematic diagram of automatic and manual control of electric motor and gasoline engine

5. Supervise gasoline engine annunciator.
6. Supervise burglar alarm.
7. Selective telemetering of rate of water pumped.
8. Establishment of communication circuits.

Communication

Communication between the water treatment plant and the pumping station is provided over the carrier channel through the supervisory control equipment. Picking up the telephone hand set at either location results in the proper selection codes being transmitted by the supervisory control equipment to ring the telephone bell at the location being called. The telephone bell continues to ring until the call is acknowledged by picking up the telephone hand set at the called location or until the telephone hand set is restored at the calling location. When the telephone hand set is picked up at the called location, the supervisory control equipment automatically locks out and the communication circuits are established. Push-to-talk communication is used since the carrier transmitters and receivers all are adjusted to the same frequency. When communication is established the carrier receivers are operated automatically on the linear portion of the detector tube characteristic curves so that undistorted demodulation can be effected.

The supervisory control equipment remains locked out until the telephone hand sets are restored. When both telephone hand sets are restored, the supervisory control equipment automatically unlocks and is ready immediately for other operations.

Telemetering

A recorder with a 7-day chart is installed in the pumping station to record the rate of water pumped in millions of gallons per day. This recorder operates on impulses received from a telemetering transmitter arranged to measure water flow by a venturi tube connection. The telemetering transmitter which is used to send impulses to the recorder also is connected to the supervisory control equipment so that a selective indication of rate of water pumped can be obtained at the water treatment plant over the supervisory control channel.

The telemetering equipment operates on the duration of impulse principle. Each cycle of the transmitter is divided into an on and an off period. Minimum reading is obtained on the receiver with minimum on period and maximum reading is obtained with maximum on period. The telemetering equipment used on this installation operates on a 5-second cycle. At zero water flow there is an on period of approximately 0.5 second and at a flow of water equal to full scale deflection on the receiver (15,000,000 gallons per day) there is an off period of approximately 0.5 second.

When the telemetering point is selected at the water treatment plant, the telemetering receiver is connected to the carrier receiver at the water treatment plant and the telemetering transmitter is connected to the carrier transmitter at the pumping station. The supervisory control equipment is arranged to be inoperative to the carrier impulses resulting from the operation of the telemetering transmitter, when the telemetering equipment is thus connected to the carrier channel. The indication of the amount of water being pumped may be retained at the water treatment plant as long as desired.

Release of the telemetering indication and restoration of the supervisory control equipment is effected by restoring the pull type selection key just as for the release of other functions. However, in this instance, keying of the carrier transmitter at the water treatment plant for the supervisory control reset impulse is automatically held off until completion of a

telemetering impulse, which may be in progress. The reset impulse is transmitted at the end of the telemetering impulse and operates the supervisory control receiver relay at both the water treatment plant and the pumping station. The duration of the supervisory control reset impulse is approximately one-fifth of a second so that the reset impulse can be completed in the off period of the telemetering transmitter even though the minimum off period of 0.5 second is in effect due to full scale reading being obtained.

The supervisory control receiver relay at the pumping station operates on all telemetering impulses when the telemetering function is selected. Operation of both the telemetering transmitter contact and the supervisory receiver relay does not allow the supervisory control equipment to reset. However, operation of the supervisory control receiver relay with the telemetering transmitter contact open, such as results when the reset impulse is transmitted from the water treatment plant, causes the equipment to reset and restore to normal, releasing the supervisory control equipment for other functions.

Control of Electric Motor and Gasoline Engine at Pumping Station

Figure 8 is a schematic diagram of the automatic and manual control for the 75-horsepower electric motor and the 180-horsepower gasoline engine which are used to pump water from the pumping station to the water treatment plant through the 24-inch pipe.

An automatic–manual transfer scheme which can be operated either from the water treatment plant or the pumping station by means of the supervisory control equipment is employed. A latching type relay 43 is used to effect this transfer. It is to be noted from the schematic diagram that the coils of this relay can be operated either from a push button station located at the pumping station or from supervisory control interposing relays.

When the manual contacts of the transfer relay 43 are closed, the electric motor and the gasoline engine are independently under the control of local push button stations and the supervisory control equipment. Thus, when on manual control, the operator at the water treatment plant can start or stop either the electric motor or the gasoline engine at will. Either unit can be operated to pump water or both units can be operated to pump water at the same time.

Manual Control of Electric Motor

When the electric motor is started on manual control from either the push button station at the pumping station or from the water treatment plant by means of the supervisory control equipment, motor control relay $4M$ is first energized. This relay seals itself in through a make contact of auxiliary voltage relay $27X$. Contacts of motor control relay $4M$ energize the solenoids of the normal and emergency cone values of the pump driven by the electric motor providing there is no surge of water at the time. When the limit switch on the normal cone valve closes, motor start relay 6 is energized. A contact of relay 6 completes the circuit to the motor breaker closing relay $52X$ and relay $52X$ in turn energizes the closing coil of the motor breaker. The motor thus is started and water is pumped.

If the electric motor is stopped by means of the push button at the pumping station, by the supervisory control equipment, or if voltage relay 27 closes its back contact due to loss of voltage or low voltage, motor control relay $4M$ is de-energized. This de-energizes the normal cone valve solenoid of the electric motor pump. When the limit switches on the normal cone valve open, the emergency cone valve solenoid is de-energized and motor start relay 6 is de-energized. A contact of relay 6 energizes the trip coil of the motor breaker, stopping the motor.

Emergency shutdown of the electric motor results if overcurrent relay 51 or thermal overload relay 49 operate. Operation of either of these relays energizes lockout relay 86 which must be manually reset. Relay 86 simultaneously de-energizes motor control relay $4M$ and trips the motor breaker.

Manual Control of Gasoline Engine

When the gasoline engine is started on manual control from either the push button station at the pumping station or from the water treatment plant by means of the supervisory control equipment, engine control relay $4E$ is first energized. This relay then seals itself in. Contacts of engine control relay $4E$ energize the solenoids of the normal and emergency cone valves of the pump driven by the gasoline engine and also complete a circuit to the gasoline engine starting panel, the detailed operation of which is not shown on the schematic diagram. Thus, the cone valves start to open and the gasoline engine starts providing there is no surge on the water line and the oil pressure of the engine is up.

When the gasoline engine is stopped from either the push button station at the pumping station or by the supervisory control equipment, engine control relay $4E$ is de-energized. When relay $4E$ is de-energized it immediately releases the solenoid of the normal cone valve of the pump driven by the gasoline engine.

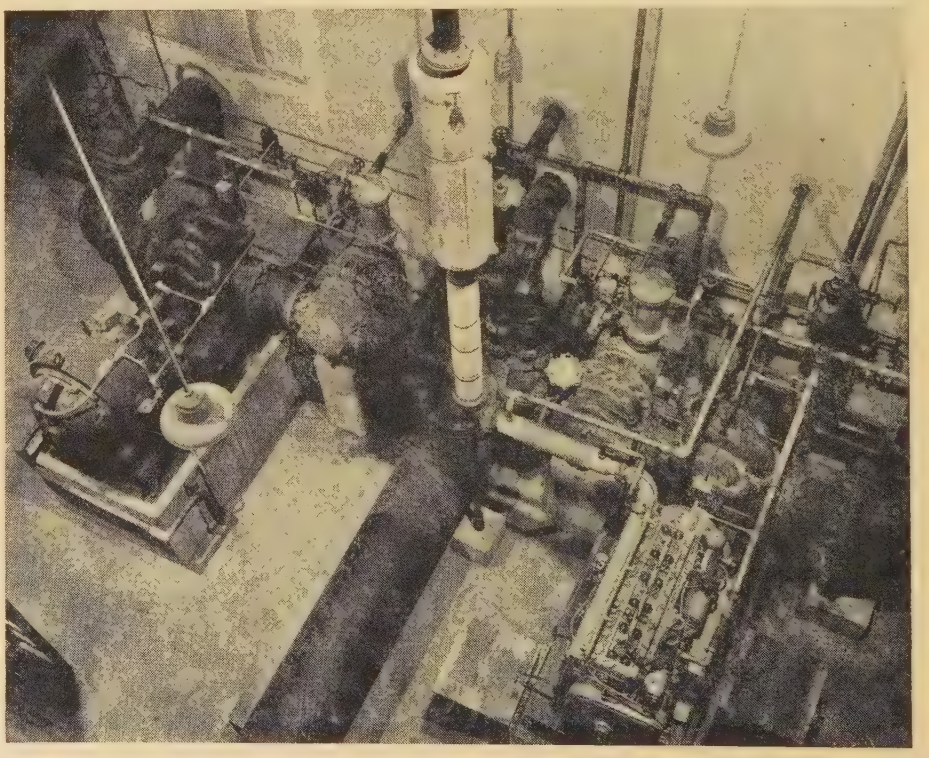

Figure 9. View showing electric motor and gasoline engine in pumping station

When the limit switch on the normal cone valve opens it releases the solenoid of the emergency cone valve and causes the engine control to transfer to the idling cycle.

Automatic Control

With the automatic contacts of the transfer relay closed, the electric motor will be running if there is voltage available and the lockout relay is not operated. When on automatic control the electric motor cannot be stopped from either the push button station or from the water treatment plant by means of the supervisory control equipment. If a transfer from manual control to automatic control is effected from either the pumping station or the water treatment plant the electric motor will start if it was not already running and the gasoline engine will stop if it was running.

If when on automatic control the 4-kv voltage should fail at the pumping station or the lockout relay 86 should operate, the electric motor is stopped and the gasoline engine is started automatically. If the electric motor stops as a result of loss of voltage and voltage again becomes available the gasoline engine automatically stops and the electric motor starts.

When on automatic control, either the electric motor or the gasoline engine will be running if conditions are satisfactory for either to be running, with preference being given to the electric motor. The electric motor and the gasoline engine never will pump water simultaneously when on automatic control.

Conclusions

Power-line carrier equipment has been applied to transmission lines for more than 20 years. The majority of the applications have been for protective relaying and communication with the carrier in most instances being operated over open construction transmission lines rated 33 kv or greater. While there is still much information to be obtained concerning operation of power-line carrier equipment over such lines considerable empirical data have resulted from tests made on some of these applications so that the performance of the carrier equipment usually can be predicted fairly accurately for proposed applications.[2]

Up to the present time there have been very few applications of power-line carrier equipment to low voltage lines. This is especially true in the case of power cable. The possibility of combined functions on carrier channels makes it economically sound to apply carrier equipment to lower voltage lines in many instances, and it is expected that there will be many such applications in the future. The results obtained on the installation described indicate that standard carrier sets which will operate through a 30-decibel loss can be operated over considerable distances of power line cable. There is a need for similar installation data on future applications so that operation over cable can be predicted as accurately as operation over open construction power lines.

This installation of power-line carrier on a low voltage line indicates that there will be many applications of carrier equipment to low voltage lines (either open construction or cable) where it will be desirable to consider coupling means other than the standard line of coupling capacitors from an economic and space standpoint.

Factors Affecting Insulation Resistance of Large D-C Machines

J. S. JOHNSON
MEMBER AIEE

CONRAD WEIL
ASSOCIATE AIEE

INSULATION RESISTANCE of rotating machines was considered by many to be a haphazard collection of unrelated numbers. One reason for this view was that insulation resistance readings rarely were taken under the same conditions. Many of the factors which greatly affect insulation resistance were not known. In the past decade, significant contributions have been made toward a better understanding of the problem.[1-4] The influence of insulation temperature, time of application, and magnitude of test voltage, moisture, and machine size were recognized.

Study of the problem by the AIEE subcommittee on insulation resistance has resulted in the preparation of a proposed "Recommended Practice for Insulation Resistance Testing of A-C Rotating Machines." Its purpose is to summarize existing knowledge, make specific recommendations for test procedures, and give minimum insulation resistance formulas for new machines. Reference to d-c machines was omitted because it was recognized that the problem on these machines in some respects was different, and that further study was necessary. It was hoped, however, that in the near future sufficient progress would be made on the d-c problem to permit extension of the proposed recommended practice to include both classes of machines.

To assist in this problem, insulation resistance data on new d-c machines over 1,000 horsepower have been accumulated by the authors and their associates over a 5-year period. The purpose of the present work has been to determine, from a statistical examination of these data, the relative effect of the principal factors which affect the insulation resistance of d-c machines. In addition to previously recognized factors, such as machine size and insulation temperature, the absolute humidity of the surrounding air has been found to have an important effect on the insulation resistance of commutator type machines. This study has led to the development of an insulation resistance formula for d-c machines which includes all of these factors. It has been recognized

Paper 46-157, recommended by the AIEE committee on electric machinery for presentation at the AIEE summer convention, Detroit, Mich., June 24-28, 1946. Manuscript submitted April 19, 1946; made available for printing May 28, 1946.

J. S. Johnson is an insulation development engineer, a-c engineering department, and Conrad Weil is an insulation engineer, d-c engineering department. Both are in the transportation and generator division of the Westinghouse Electric Corporation, East Pittsburgh, Pa.

The authors gratefully acknowledge the assistance of the following people: A. M. Harrison for engineering guidance; Doctor Casper Goffman for advice and criticism in statistical problems; Henry Glitsch, James Nicalo, and Josephine Garber for assistance in the compilation of the data. All are of the Westinghouse Electric Corporation.

References

1. The Combination of Supervisory Control With Other Functions on Power-Line Carrier Channels, R. C. Cheek, W. A. Derr. AIEE Transactions, volume 64, 1945, May section, pages 241-6.

2. Power-Line Carrier Channels, M. J. Brown. AIEE Transactions, volume 64, 1945, May section, pages 246-50.

3. Reference Data for Radio Engineers (book), Federal Telephone and Radio Corporation, New York, N. Y., 1943.

4. A Versatile Power-Line Carrier System, H. W. Lensner, J. B. Singel. AIEE Transactions, volume 63, 1944, March section, pages 129-32.

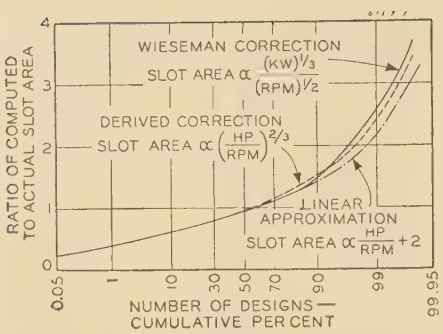

Figure 1. Frequency distribution of the ratio of computed to actual slot area showing correlation of various formulas

Data based on representative designs of 200 d-c machines of 100 horsepower and more

by the authors that for greatest usefulness, such a formula should express the relationship of the various factors in terms of simple arithmetical processes. Accordingly, a linear relationship involving rated horsepower, speed, and the winding insulation dimensions has been developed and compared to the existing formula. The correction factor for the effect of absolute humidity at the time of test, which has been included in the formula, is a new concept.

The factors which affect measured values of machine insulation resistance may be grouped as follows:

1. The nature and condition of the insulation material.
2. The design and construction of the machine.
3. The conditions of test.

Quantitative evaluation of the effect of these influences is difficult because of the complex structure of machine insulation. There is also a lack of basic knowledge of the fundamental processes involved and a lack of control of factors which have an important effect on machine insulation resistance.

Machine Insulation Structure

In general, insulation leakage between machine components may be segregated into two parallel paths, one through the body of the insulation itself, the other over the surface of the insulation. The relative magnitudes of the surface and volume leakage currents depend on the physical proportions of the insulation structure and the extent to which each is affected by existing conditions. It is usually difficult to determine the relative extent that each of these currents contributes to the total insulation leakage. In the case of stator windings of a-c synchronous and induction machines, it is perhaps reasonable to assume that surface leakage currents have a negligible effect on the total leakage current. Experience has shown, however, that at least under normal operating conditions the insulation resistance of d-c machines is determined largely by creepage factors. The same also appears to be true of new d-c machines under certain conditions of atmospheric humidity.

The basic difference between a-c synchronous and induction machines and d-c machines from an insulation standpoint is the existence of relatively large exposed creepage areas which are inherent in the design of d-c machines. This is caused principally by the commutator and to a lesser extent by the brush rigging, series, commutating, and compensating windings. Therefore, it is reasonable to expect that the insulation resistance characteristics of commutator type machines would be different from machines without commutators and that, in general, the commutator type machines would have lower values of insulation resistance.

Scope of Work

The insulation structure of large d-c machines usually consists of armature circuit insulation and shunt field insulation. The insulation resistance of the shunt field winding is usually relatively high. The armature circuit insulation resistance is of principal importance because it is usually lower and more affected by external conditions. The insulation of the armature circuit includes that of the armature winding, brush rigging, series, commutating, and compensating windings. The scope of the present work has been to study and analyze the results of armature circuit insulation resistance measurements of approximately 1,100 d-c machines in the range of 1,000 to 7,000 horsepower. Although insulation resistance data were not available for machines of less than 1,000 horsepower, it was felt by the authors that the dividing line between small and large d-c machines should be 100 horsepower. Therefore, in the development of the size correction which is included in the suggested minimum formula, machines of 100 horsepower and higher were considered.

In this work effort was directed toward estimating from a statistical study of the insulation resistance data known design proportions of the machines and known conditions of test, the probable influence of the principal factors which contribute to the measured value of insulation resistance. A further purpose of this work has been to relate these factors into a simple usable formula for expressing expected insulation resistance of new machines in terms of parameters which are known or easily obtainable. In the development of the ideas advanced in this paper, only general purpose d-c machines of ratings of 100 horsepower or more were considered. The following, therefore, does not necessarily apply to special types of d-c machines such as are used in the traction field.

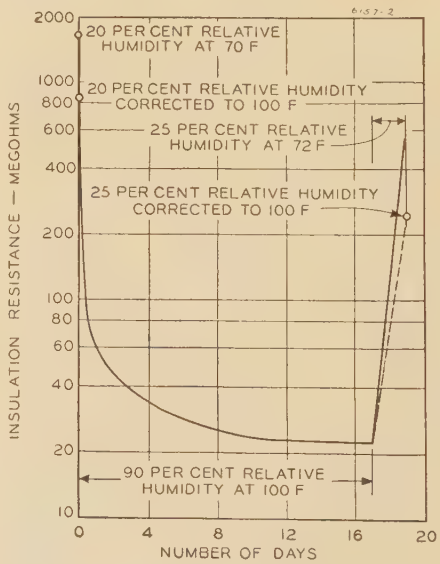

Figure 2. Insulation resistance decrease and recovery of a d-c armature exposed to 90 per cent relative humidity at 100 degrees Fahrenheit

Development of Formula Relating Rated Horsepower and Speed to Machine Size

One of the factors which influences measured values of insulation resistance, which is not related to the nature or condition of the insulation, is the physical size of the machine. A major shortcoming of the present AIEE minimum insulation resistance formula is that it makes no significant allowance for this factor. More rational formulas were proposed in 1934 by Wieseman which take into account effective insulation area and thickness. Although basically sound, these formulas have not enjoyed widespread use, largely because of a general unwillingness to handle formulas involving fractional powers. For greatest usefulness in a practical insulation resistance formula, a relationship among the various factors which involve relatively simple arithmetical processes is desirable. Accordingly, an attempt has been made in this work to develop a linear formula for armature

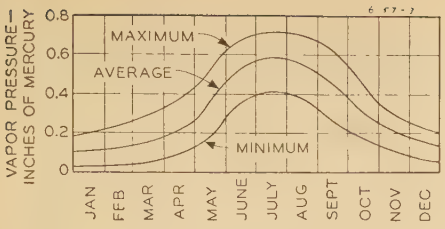

Figure 3. Record of the average and range of the daily vapor pressures for the Pittsburgh area for 1940 to 1946

circuit insulation resistance of d-c machines 100 horsepower and higher which includes the effect of machine size.

Under conditions where surface creepage is negligible, machine insulation resistance would be expected to vary inversely as the ratio of insulation contact area to thickness. Where surface creepage has an appreciable effect, the logic of making a size correction based on contact area, at first glance, would appear questionable. More careful analysis, however, reveals that there is a substantially linear correlation between contact area and effective creepage area. Therefore, even where surface creepage is not negligible, it appears that insulation contact area can be used as a basis for size correction.

The considerations involved and assumptions made in the development of a linear formula, relating machine size to rated voltage, horsepower, and speed are as follows:

1. The total insulation area under consideration includes that of all the windings in the armature circuit. In the development of the formula, only the insulation area in the armature slots is considered. The other areas involved are comparatively small and, in addition, are roughly proportional to the slot contact area.

2. The slot contact area of the armature is equal to the product of the slot perimeter, the number of slots, and the length of the armature iron.

3. Although slot insulation thickness is, in general, a function of voltage, the slot insulation thickness for large d-c machines is substantially constant. Therefore, rated voltage need not be included in the formula.

4. The machine output for a given temperature rise and average conditions of electric and magnetic loading is related to armature size by the following fundamental design relationship:

$$\frac{\text{Horsepower}}{\text{Revolutions per minute}} = K_1 d^2 l$$

where d and l are the armature diameter and length, respectively.

5. The slot depth is approximately constant.

6. An average value is assumed for the slot pitch (center to center distance between slots). Actually, this value may vary by a maximum of plus or minus 30 per cent.

7. An average value is assumed for the ratio of armature length to diameter. This value may vary by as much as plus or minus 80 per cent of the average value. Slot area, however, varies as the cube root of this ratio.

From the foregoing it follows that

$$\text{Slot area} = \frac{K_2 dl}{\text{slot pitch}} = K_3 dl = K_3 a d^2$$

where $a = l/d$.

$$\frac{\text{Horsepower}}{\text{Revolutions per minute}} \propto d^2 l \propto a d^3$$

$$d \propto \left[\frac{\text{horsepower}}{(\text{revolutions per minute})a}\right]^{1/3}$$

where d, l, and slot pitch are in inches, slot area is in square inches.

$$\text{Slot area} = K_4\left[\frac{\text{horsepower}}{(\text{revolutions per minute})}\right]^{2/3} \quad (1)$$

The best linear approximation for equation 1 was determined and is as follows:

$$\text{Slot area} = K_5\left(\frac{\text{horsepower}}{\text{revolutions per minute}} + 2\right) \quad (2)$$

Actually, the values K_4 and K_5 (equations 1 and 2) are not constants because of the assumption of average values for design factors which affect machine size without directly affecting machine output. Average values, however, were obtained by substituting actual slot areas of 200 representative designs into the formula and solving for K_4 and K_5 in equations 1 and 2. The averages thus obtained for K_4 and K_5 were found to be 4,800 and 1,500, respectively.

The validity of the foregoing formula was checked by comparing the ratio of computed to actual slot areas for each formula. The computed ratios for the 200 representative designs were arranged in increasing order and plotted on arithmetic probability paper (see the appendix). Figure 1 shows a comparison of correlation for equations 1 and 2 as well as the Wieseman formula for 200 representative designs of d-c machines in the range of 100 to 7,000 horsepower. For purposes of comparison, a constant for the Wieseman formula was determined in the same manner as K_4 and K_5. It is apparent that the linear formula compares favorably with the other formulas and also has the advantage of simplicity. A size correction based on this linear relationship therefore is included in the minimum insulation resistance formula suggested by the authors.

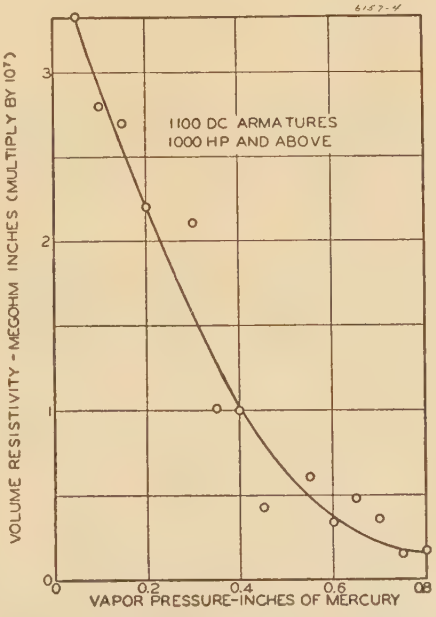

Figure 4. Correlation of median value of volume resistivity with vapor pressure at time of test

Effect of Absolute Humidity

Insulation resistance of all rotating machines is affected by prevailing atmospheric moisture conditions. For this reason, machines built and tested during the winter months, in general, have appreciably higher insulation resistance values than identical machines built and tested during the summer months. This effect is, in general, greater on commutator type machines where large creepage areas from bare copper to ground exist. Study of the data reveals that insulation resistance of the armature circuit of d-c machines is affected by a combination of atmospheric moisture conditions at the time of test, and during the period of manufacture.

The insulation resistance measurements of the armature circuit windings discussed in this work were made shortly after the running test. Since condensation of atmospheric moisture on the insulation surfaces greatly distorts insulation resistance, all tests were made with insulation temperatures five to ten degrees above room conditions. Measurements were made at 500 volts d-c and one minute after voltage application.

The effect of extreme humidity conditions on the insulation resistance of a d-c armature is illustrated in Figure 2. This armature which was initially at equilibrium at 70 degrees Fahrenheit and 20 per cent relative humidity, was exposed to 90 per cent relative humidity at 100

degrees Fahrenheit for 17 days and then returned to the initial ambient conditions. A reduction to 1/13 of the initial resistance after making corrections for temperature was observed at the end of the first day. The temperature correction is based on a ten to one decrease in insulation resistance for a 50-degree-centigrade temperature increase. A further reduction of one half was observed for the succeeding 16 days. Upon returning to room conditions of humidity and temperature, a rapid recovery to approximately one half of the initial insulation resistance value was observed. It, therefore, is apparent that the insulation resistance of a d-c armature is affected greatly by the prevailing atmospheric conditions at the time of test.

To evaluate the effect of atmospheric moisture conditions on insulation resistance, correlations of absolute and relative humidity at time of test with insulation resistivity were attempted. The insulation resistance of the 1,100 machines was corrected for machine size by multiplying the measured values by the ratio of the effective slot area and insulation thickness. The units of insulation resistivity thus obtained were megohm-inches.

Comparison of insulation resistivity with relative humidity at time of test revealed no significant correlation. However, since it was evident from Figure 2 that humidity conditions at time of test should affect the insulation resistance significantly, a correlation between insulation resistivity and absolute humidity was attempted. Absolute humidity differs from relative humidity in that it is a quantitative measure of atmospheric moisture. Relative humidity merely expresses the ratio of actual atmospheric moisture to the maximum or saturation conditions for a given temperature. Since absolute humidity at saturation varies logarithmically with temperature, it is evident that relative humidity by itself is not a measure of atmospheric moisture.

For practical purposes vapor pressure in inches of mercury is a convenient measure of absolute humidity. A record of daily average and range of vapor pressures in the Pittsburgh district for the years 1941 through 1945 is shown in Figure 3.* These observations were made less than five miles from the place of manufacture and were assumed to represent ambient moisture conditions at the plant.

Figure 4 shows the correlation of median insulation resistivity with vapor pressure at the time of test (see the appendix). Based on this correlation, all armature insulation resistivities were corrected to a vapor pressure of 0.1 inch of mercury. Figure 5 shows a comparison of the uncorrected insulation resistance data, the same data corrected for machine size, and the same data again corrected for vapor pressure at the time of test. It is evident from Figure 5 that corrections for machine size and vapor pressure based on the foregoing correlation produce an improvement in the central tendency of the data.

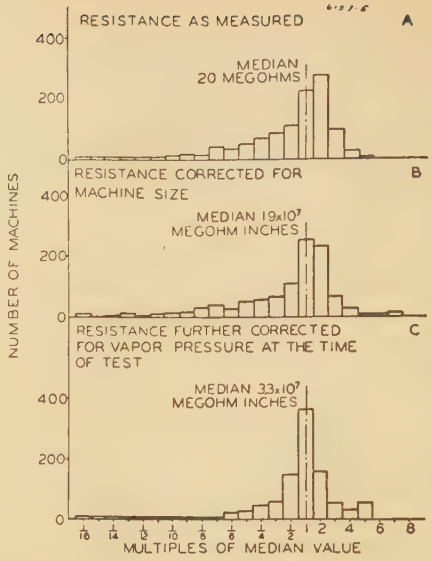

Figure 5. Comparison of insulation resistance frequency distributions before and after corrections—1,100 d-c machines

Although the correlation shown in Figure 4 is based on vapor pressure at time of test, it actually includes the effect of vapor pressure during manufacture. This is true because, in most cases, the average vapor pressure conditions during manufacture and test are substantially the same. For purposes of applying a correction for vapor pressure at the time of test in a minimum insulation resistance formula, it is desirable to separate the effect of vapor pressure during manufacture from that at the time of test.

An examination was made of the insulation resistance of a large number of identical machines which were built at a rate of approximately 50 machines per month over a 15-month period. Table I shows the average insulation resistance of these armatures and the average monthly vapor pressures. If the following assumptions are made, it will be seen from column 3 of Table I that in most cases reasonable approximations for the effect of vapor pressure can be made:

1. Insulation resistance is inversely proportional to vapor pressure at time of test. Figure 2 shows a 13 to 1 initial reduction in insulation resistance for a 13 to 1 increase in vapor pressure.

2. Insulation resistance is inversely proportional to the vapor pressure at time of insulation varnish treatment. In the case of these machines, the time of varnish treatment is assumed to be two months prior to the month of test.

3. The over-all correction for manufacturing and test conditions is the product of the individual corrections for each influence. This assumption was made because it was found from inspection of the data of Table I that a correction of this sort correlated the observed data. Since only the creepage component of insulation resistance is affected by the vapor pressure at the time of test, the foregoing assumption implies that the principal effect of the humidity conditions during manufacture is on the creepage resistance.

Based on the preceding assumptions, a formula for correcting all the observed resistivities to constant vapor pressure conditions of 0.1 inch of mercury is as follows:

$$\text{Corrected resistivity} = \text{uncorrected resistivity} \times \frac{VP_1}{0.1} \times \frac{VP_2}{0.1}$$

where VP_1 and VP_2 are vapor pressures at the time of test and two months prior to the time of test, respectively. Column 3 of Table I indicates that, except for the months of October and November, monthly average resistivities corrected to constant vapor pressure conditions are approximately the same. Corrections, therefore, were made individually to the entire group of machines excluding those tested in October and November. Figure 6 gives a comparison of the frequency distribution of uncorrected and corrected data grouped according to multiples and

Table I. Correlation of Average Resistivity of 700 Identical D-C Armatures by Months, With Average Vapor Pressure at Month of Test and Two Months Prior to Test

Month	Avg Vapor Pressure, In. Hg	Uncorrected Avg Resistivities, Megohm-In. ×10⁷	Avg Resistivities Corrected to 0.1 In. Hg, Megohm-In. ×10⁷
January	0.14	2.9	6.9
February	0.13	2.5	4.8
March	0.15	3.8	8.0
April	0.20	2.7	7.0
May	0.37	1.3	7.2
June	0.57	0.56	6.5
July	0.54	0.58	11.5
August	0.53	0.26	7.8
September	0.36	0.43	8.3
October	0.25	1.7	22.6
November	0.17	2.9	17.7
December	0.12	3.0	9.0
January	0.14	3.5	8.3
February	0.14	3.1	5.2

* Data obtained from original records of the Pittsburgh Weather Bureau.

common fractions of the median value of resistivity. Figure 7 shows a frequency distribution of the corrected data grouped in the usual manner. As shown in Figures 6 and 7, the corrections significantly improve the normality of the observed data. Therefore, the assumptions of the relative effect on insulation resistance of the ambient humidity conditions during manufacture and test appear to be reasonable.

After a machine is in operation, the effect of moisture conditions at the time of varnish treatment would be expected to diminish, and in time the moisture content of the insulation is determined by the prevailing ambient and operating conditions. The real criterion of the moistureproof quality of machine insulation is not necessarily its moisture content, but rather the rate at which moisture is absorbed under given conditions. Under conditions of operation, accumulations of conducting particles on the exposed creepage surface may have a predominating influence on insulation resistance.

Suggested Minimum Formula

The principal requirement for an ideal minimum insulation resistance formula is a simple relationship between the factors which are known to affect the machine insulation resistance. These factors should be in terms of parameters which are known or are easily obtainable at the time of test.

1. *Variation of slot area*, for d-c machines in the range of 100 to 7,000 horsepower, has a maximum range of 100 to 1. A simple relationship between output and speed rating has been developed which makes an average correction with a 27 per cent dispersion. Since slot area varies to a certain extent independently of the output or speed rating, significantly closer correction does not appear possible.

2. *Variation of the exposed creepage surface of the armature* is approximately linearly related to the slot area of the armature so that any corrections made for slot area also will apply to this factor.

3. *Insulation wall thickness*, because of the limited voltage range of d-c machines, may be considered constant.

4. *Insulation temperature* for new d-c machines, where insulation resistance decreases by a factor of approximately ten, increases from 25 to 75 degrees centigrade. There is a relatively small amount of data on temperature-insulation resistance slopes of d-c machines. More data are needed to establish average values and probable dispersions for machines both when new and under operating conditions. In the meanwhile the effect of temperature is minimized best by consistently measuring the insulation resistance at approximately the same temperature. Five to ten degrees above ambient would be a convenient temperature. The possibility of moisture condensation then would be eliminated. If measurements are made at or close to room condition, temperature correction to 25 degrees centigrade, based on an assumed average slope, will introduce relatively small errors.

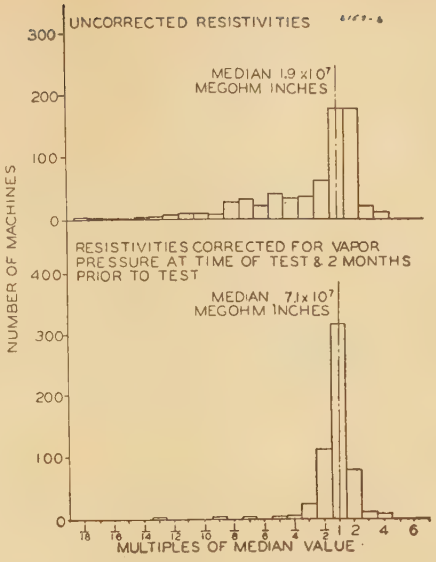

Figure 6. Comparison of insulation resistivity frequency distributions for 700 identical d-c machines before and after corrections for vapor pressure

5. *Absolute humidities immediately preceding the time of test* have been shown to affect the measured insulation resistance by as much as ten to one for variations normally encountered. A simple correction for this factor in terms of ambient temperature and relative humidity at the time of test is possible for this variable.

It might be pointed out here that insulation temperature, as well as absolute humidity, has a d minishing effect on insulation resistance of machines operated in service under conditions where an accumulation of conducting dirt is likely to be deposited on the exposed creepage surfaces.

Assuming that a simple formula which gives the average expected insulation resistance of a d-c armature is possible, the selection of a suitable minimum insulation resistance formula depends upon what this formula thus determined is intended to represent. If the criterion is the value which is safe for application of the proof voltage test, the level of insulation resistivity set by the formula, if moisture is considered to be the contaminating agent, should depend primarily on when the insulation contains a sufficient quantity of moisture to affect adversely the short-time dielectric strength of the insulation. It does not appear possible at the present time to state definitely what this resistivity should be. Exploratory tests for paper-backed sheet-form mica insulation indicate that the short-time breakdown does not begin to be affected significantly until the resistivity is of the order of 1/10,000 or less of the average new machine insulation resistivity. However, while moisture contamination is the principal source of low insulation resistance of new machines, it is not the only possible cause. Values of insulation resistance, which would be considered safe if the assumption could be made that the cause was uniformly distributed moisture, might not be safe if caused by some other factor such as defective or damaged insulation. It should be emphasized that a high value of insulation resistance is no guarantee of adequate dielectric strength for test or operation. Insulation defects are possible which do not affect the insulation resistance. At best, insulation resistance indicates the existence and approximate extent of contaminating influences which affect insulation leakage. It appears that the best procedure possible at the present time in the selection of a minimum formula is to reach some agreement as to

1. What the average resistivity of new machine insulation should be.

2. Some reasonable method by which the minimum insulation resistance shall be calculated from this average value. It should be recognized that the selection of this minimum has no logical basis except that it represents the best estimate possible at the present time.

Table II. Correction Factor for Absolute Humidity at Time of Test in Terms of Ambient Temperature and Relative Humidity

Ambient Temperature, Deg F	Correction Factor*
10	0.18
20	0.30
30	0.48
40	0.70
50	1.00
60	1.47
70	2.15
80	2.95
90	3.90
100	5.50

* f_h = factor × per cent relative humidity.

Based on the foregoing considerations, the following formula is suggested for minimum insulation resistance of new d-c armatures of ratings of 100 horsepower and higher. Essentially, the formula is an expression for the expected average armature circuit insulation resistance of a new machine after correction for machine size, insulation temperature at the time of test, and absolute humidity at the time of test. Since the ground insulation on

d-c machines is essentially the same in both cases, no distinction is made between class *A* and class *B* insulation. Also, for general purpose d-c machines, the voltage range is limited and insulation wall thickness is substantially unaffected by rated voltage. Therefore, the voltage factor has been omitted in the formula.

$$R_i = \frac{4{,}000}{\left(\frac{\text{horsepower}}{\text{revolutions per minute}} + 2\right) f_h}$$

R_i = minimum insulation resistance in megohms at 25 degrees centigrade

f_h = correction factor for absolute humidity at time of test (see Table II)

In addition to this formula, a 2-megohm minimum insulation resistance is suggested for armatures when the calculated value from the formula is below this value. In general, these armatures would be large and important, and there is the ever-present possibility that the low insulation resistance might not be caused by moisture contamination, but might be the result of other localized defects.

Summary and Conclusions

Analysis of insulation resistance data of 1,100 d-c machines in the range of 1,000 to 7,000 horsepower has resulted in the rationalization of the complex factors involved. Consideration and segregation of the principal factors which influence measured values of insulation resistance has enabled a better understanding of the relative effect of each. In addition to previously recognized factors such as material resistivity, insulation temperature, and machine size, the absolute humidity of the surrounding air has been found to affect significantly the insulation resistance of commutator type machines. The total effect of humidity on new machines at the factory has been shown to consist of

1. The effect of prevailing atmospheric humidity during insulation treatment.

2. The effect of atmospheric humidity at the time of test.

Prevailing atmospheric humidity during insulation treatment has only a transitory effect on the machine insulation resistance. Ultimate moisture concentration in machine insulation depends on service conditions. For commutator type machines, absolute humidity at the time of test is a test condition in the same sense as insulation temperature. This effect would be expected to apply also to machines under service conditions, except where accumulation of conducting particles on exposed creepage surfaces has a predominating influence.

The correlation of these various factors has resulted in the development of a simple linear insulation resistance formula which is offered for consideration by the industry.

$$R_i = \frac{4{,}000}{\left(\frac{\text{horsepower}}{\text{revolutions per minute}} + 2\right) f_h}$$

where

R_i = minimum insulation resistance at 25 degrees centigrade for new d-c machines over 100 horsepower

f_h = correction factor for absolute humidity at the time of test

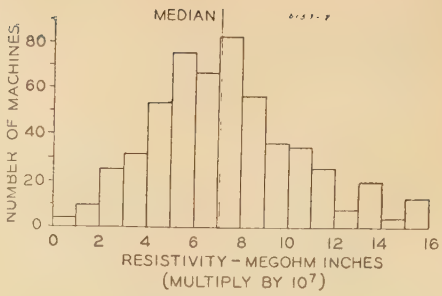

Figure 7. Frequency distribution of volume resistivity of 700 identical machines after correction for vapor pressure at time of test and two months prior to test

Appendix

Correlation of Computed Slot Area by Various Formulas and Actual Slot Area of Representative Designs

In the comparison of the correlation of the several formulas discussed in the text, use was made of graph paper having linear ordinate units and abscissa units arranged in an arithmetical probability scale. The ratio of computed to actual values for each formula was arranged in increasing order and expressed as a cumulative per cent of the total number of designs.

The interpretation of the ratio 1 corresponding to 50 per cent is that one half of the total number of designs have ratios of 1 or less. It is seen, therefore, that for the linear approximation the central 90 per cent of the distribution have ratios between 0.5 to 1.5. The scale of the abscissa is such that normal distributions plot as a straight line. The slope of this line is a measure of the dispersion and a smaller slope indicates smaller dispersion. Per cent dispersion, which for normal distributions is equal to $\frac{\text{standard deviation}}{\text{average}} \times 100$, may be obtained directly from the curve. The standard deviation includes approximately the central two thirds of the area distribution. Therefore, from the curve

$$\text{per cent dispersion} = \frac{(R_{83.7} - R_{50}) \text{ or } (R_{50} - R_{16.3})}{R_{50}} \times 100$$

where $R_{83.7}$, R_{50}, and $R_{16.3}$ are the ratios for the corresponding cumulative percentages in the distribution.

Correlation of Insulation Resistivity and Vapor Pressure at Time of Test

In this correlation the individual values of resistivity were classified according to vapor pressure at the time of test. For each vapor pressure group the median value of insulation resistivity was obtained. The median is defined as the value of the central unit of a distribution. If a distribution contains 101 numbers arranged in order of increasing value, the value of number 51 is the median of the distribution. The median was used as a basis for comparison because it gives less weight to extreme values of a distribution than does the arithmetic average.

Preparation of Table II

Table II lists absolute humidity corrections to be applied in the minimum formula. Absolute humidity is a function of the product of ambient temperature and relative humidity. Since ambient temperature and relative humidities are usually either known or easily determined, the absolute humidity correction is expressed in these parameters.

The table was constructed by considering as unity an average vapor pressure of 0.35 inch of mercury. This corresponds to a temperature and relative humidity of 50 degrees Fahrenheit and 100 per cent. Relative corrections for other temperatures and humidities were obtained from psychometric tables and expressed in terms of the assumed average conditions. In the proposed minimum formula, the average resistivity used is that corresponding to 0.35 inch of mercury.

References

1. Insulation Resistance of Armature Windings, **Robert W. Wieseman.** AIEE Transactions, volume 53, 1934, June section, pages 1010–21.

2. Field Testing of Generator Insulation, **EEI Subject Committee on Generator Insulation and Testing.** AIEE Transactions, volume 60, 1941, December section, pages 1003–11.

3. Insulation Resistance and Dielectric-Absorption Characteristics of Large A-C Stator Windings, **J. S. Askey, J. S. Johnson.** AIEE Transactions, volume 64, 1945, June section, pages 347–51.

4. Use of Dielectric-Absorption Tests in Drying Out Large Generators, **H. C. Marcroft.** AIEE Transactions, volume 64, 1945, February section, pages 56–60.

Properties and Uses of Thermistors—Thermally Sensitive Resistors

J. A. BECKER
FELLOW AIEE

C. B. GREEN
NONMEMBER AIEE

G. L. PEARSON
NONMEMBER AIEE

Synopsis: A new circuit element and control device, the thermistor, or thermally sensitive resistor, is made of solid semiconducting materials whose resistance decreases about four per cent per degree centigrade. The thermistor presents interesting opportunities to the designer and engineer in many fields of technology for accomplishing tasks more simply, economically, and better than with available devices. Part I discusses the conduction mechanism in semiconductors and the criteria for usefulness of circuit elements made from them. The fundamental physical properties of thermistors, their construction, their static and dynamic characteristics, and general principles of operation are treated. Part II of this paper deals with the applications of thermistors. These include: sensitive thermometers and temperature control elements, simple temperature compensators, ultrahigh frequency power meters, automatic gain controls for transmission systems, voltage regulators, speech volume limiters, compressors and expandors, gas pressure gauges and flowmeters, meters for thermal conductivity determination of liquids, and contactless time delay devices. Thermistors with short time constants have been used as sensitive bolometers, and show promise as simple, compact, audiofrequency oscillators, modulators, and amplifiers.

I—Properties of Thermistors

THERMISTORS, or *thermally sensitive resistors*, are devices made of solids whose electrical resistance varies rapidly with temperature. Even though they are only about 15 years old they already have found important and large scale uses in the telephone plant and in military equipments. Some of these uses are as time delay devices, protective devices, voltage regulators, regulators in carrier systems, speech volume limiters, test equipment for ultrahigh frequency power, and detecting elements for very small radiant power. In all these applications thermistors were chosen because they are simple, small, rugged, have a long life, and require little maintenance. Because of these and other desirable properties, thermistors promise to become new circuit elements which will be used extensively in the fields of communications, radio, electrical and thermal instrumentation, research in physics, chemistry and biology, and war technology. Specific types of uses which will be discussed in the second part of this paper include

1. Simple, sensitive, and fast responding thermometers, temperature compensators, and temperature control devices.
2. Special switching devices without moving contacts.
3. Regulators or volume limiters.
4. Pressure gauges, flowmeters, and simple meters for measuring thermal conductivity in liquids and gases.
5. Time delay and surge suppressors.
6. Special oscillators, modulators, and amplifiers for relatively low frequencies.

Before these uses are discussed in detail, it is desirable to present the physical principles which determine the properties of thermistors.

The question naturally arises: Why have devices of this kind come into use only recently? The answer is that thermistors are made of semiconductors and that the resistance of these can vary by factors up to a thousand or a million with surprisingly small amounts of certain impurities, with heat treatment, methods of making contact, and with the treatment during life or use. Consequently the potential application of semiconductors was discouraged by experiences such as the following: two or more units made by what appeared to be the same process would show large variations in their properties. Even the same unit might change its resistance by factors of two to ten by exposure to moderate temperatures or to the passage of current. Before semiconductors could be considered seriously in industrial applications, it was necessary to devote a large amount of research and development effort to a study of the nature of the conductivity in semiconductors, and of the effect of impurities and heat treatment on this conductivity, and to methods of making reliable and permanent contacts to semiconductors. Even though Faraday discovered that the resistance of silver sulphide changed rapidly with temperature, and even though thousands of other semiconductors have been found to have large negative temperature coefficients of resistance, it has taken about a century of effort in physics and chemistry to give the engineering profession this new tool which may have an influence similar to that of the vacuum tube, and may replace vacuum tubes in many instances.

If thermistors are to be generally useful in industry:

1. It should be possible to reproduce units having the same characteristics.
2. It should be possible to maintain constant characteristics during use, the contact should be permanent, and the unit should be chemically inert.
3. The units should be mechanically rugged.
4. The technique should be such that the material can be formed into various shapes and sizes.
5. It should be possible to cover a wide range of resistance, temperature coefficient, and power dissipation.

Thermistors might be made by any method by which a semiconductor could

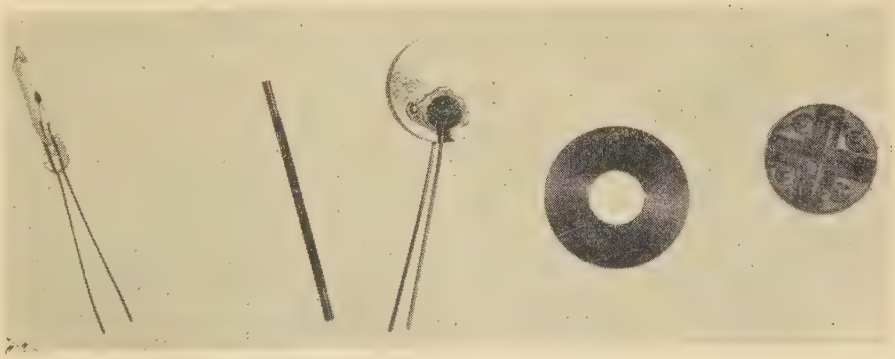

Figure 1. Thermistors made in the form of a bead, rod, disk, washer, and flakes (left to right)

Paper 46-162, recommended by the AIEE committee on communication for presentation at the AIEE summer convention, Detroit, Mich., June 24–28, 1946. Manuscript submitted April 18, 1946; made available for printing May 28, 1946.

J. A. Becker, C. B. Green, and G. L. Pearson are all with the Bell Telephone Laboratories, Inc., Murray Hill, N. J.

The authors acknowledge their indebtedness to J. H. Scaff and H. C. Theuerer for furnishing samples for most of the curves in Figure 4, and to G. K. Teal for the data for the lowest curve in that figure.

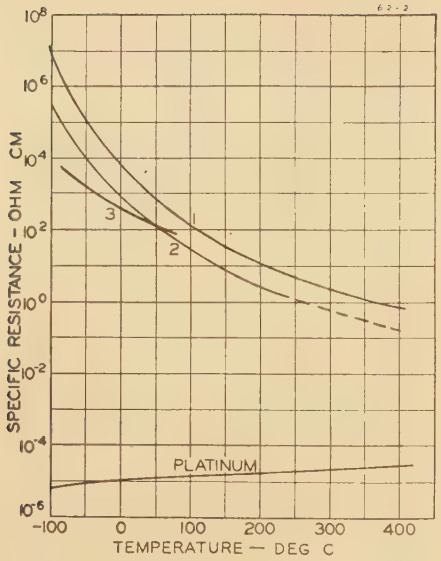

Figure 2. Logarithm of specific resistance versus temperature for three thermistor materials as compared with platinum

be shaped to definite dimensions, and contacts applied. These methods include

1. Melting the semiconductor, cooling, solidifying, cutting to size and shape.

2. Evaporation.

3. Heating compressed powders of semiconductors to a temperature at which they sinter into a strong compact mass, and firing on metal powder contacts.

Although all three processes have been used, the third method has been found to be useful most generally for mass production. This method is similar to that employed in ceramics or in powder metallurgy. At the sintering temperatures, the powders recrystallize and the dimensions shrink by controlled amounts. The powder process makes it possible to mix two or more semiconducting oxides in varying proportions, and obtain a homogeneous and uniform solid. It is thus possible to cover a considerable range of specific resistance and temperature coefficient of resistance with the same system of oxides. By means of the powder process, it is possible to make thermistors of a great variety of shapes and sizes to cover a large range of resistances and power handling capacities.

Figure 1 shows thermistors made in the form of beads, rods, disks, washers, and flakes. Beads are made by stringing two platinum alloy wires parallel to each other with a spacing of five to ten times the wire diameter. A mass of a slurry of mixed oxides is applied to the wires. Surface tension draws this mass into the form of a bead. From 10 to 20 such beads are evenly spaced along the wires. The beads are allowed to dry, and are heated slightly until they have sufficient strength so that the string can be handled. They then are passed through the sintering furnace. The oxides shrink onto the platinum alloy wires and make an intimate and permanent electrical contact. The wires then are cut to separate the individual beads. The diameters of the beads range from 0.015 to 0.15 centimeter with wire diameter ranging from 0.0025 to 0.015 centimeter.

Rod thermistors are made by mixing the oxides with an organic binder and solvent, extruding the mixture through a die, drying, cutting to length, heating to drive out the binder, and sintering at a high temperature. Contacts are applied by coating the ends with silver, gold, or platinum paste such as is used in the ceramic art, and heating or curing the paste at a suitable temperature. The diameter of the rods ordinarily can be varied from 0.080 to 0.64 centimeter. The length can vary from 0.15 to 5 centimeters.

Disks and washers are made in a similar way by pressing the bonded powders in a die. Possible disk diameters are 0.15 to 3 or 5 centimeters, thicknesses from 0.080 to 0.64 centimeter.

Flakes are made by mixing the oxides with a suitable binder and solvent to a creamy consistency, spreading a film on a smooth glass surface, allowing the film to dry, removing the film, cutting it into flakes of the desired size and shape, and firing the flakes at the sintering temperatures on smooth ceramic surfaces. Contacts are applied as described above. Possible dimensions are: thickness, 0.001 to 0.004 centimeter; length, 0.1 to 1.0 centimeter; width, 0.02 to 0.1 centimeter.

In any of these forms, lead wires can be attached to the contacts by soldering or by firing heavy metal pastes. The dimensional limits given above are those which have been found to be readily attainable.

In the design of a thermistor for a specific application, the following characteristics should be considered:

1. Mechanical dimensions including those of the supports.

2. The material from which it is made and its properties. These include the specific resistance and how it varies with temperature, the specific heat, density, and expansion coefficient.

3. The dissipation constant and power sensitivity. The dissipation constant is the watts that are dissipated in the thermistor, divided by its temperature rise in degrees centigrade above its surroundings. The power sensitivity is the watts dissipated to reduce the resistance by one per cent. These constants are determined by the area and nature of the surface, the surrounding medium, and the thermal conductivity of the supports.

4. The heat capacity, which is determined by specific heat, dimensions, and density.

5. The time constant. This determines how rapidly the thermistor will heat or cool. If a thermistor is heated above its surroundings and then allowed to cool, its temperature will decrease rapidly at first, and then more slowly until it finally reaches ambient temperature. The time constant is the time required for the temperature to fall 63 per cent of the way toward ambient temperature. The time constant in seconds is equal to the heat capacity in joules per degree centigrade, divided by the dissipation constant in watts per degree centigrade.

6. The maximum permissible power that can be dissipated consistent with good stability and long life, for continuous operation, and for surges. This can be computed from the dissipation constant and the maximum permissible temperature rise. This and the resistance-temperature relation determine the maximum decrease in resistance.

Properties of Semiconductors

As most thermistors are made of semiconductors, it is important to discuss the properties of the latter. A semiconductor may be defined as a substance whose electrical conductivity at, or near, room temperature is much less than that of typical metals, but much greater than that of typical insulators. While no sharp boundaries exist between these classes of conductors, one might say that semiconductors have specific resistances at room

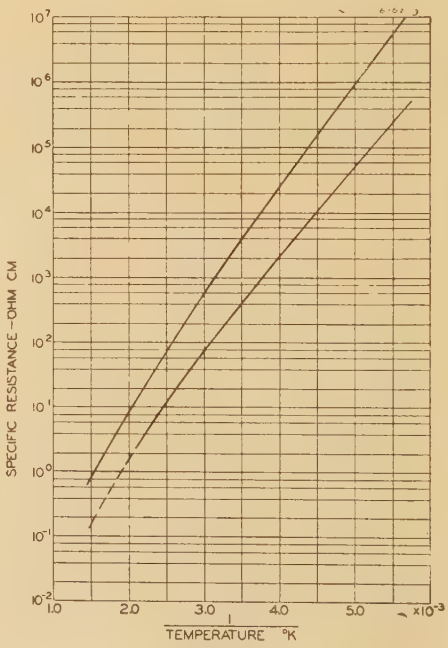

Figure 3. Logarithm of the specific resistance of two thermistor materials as a function of inverse absolute temperature

See equation 1

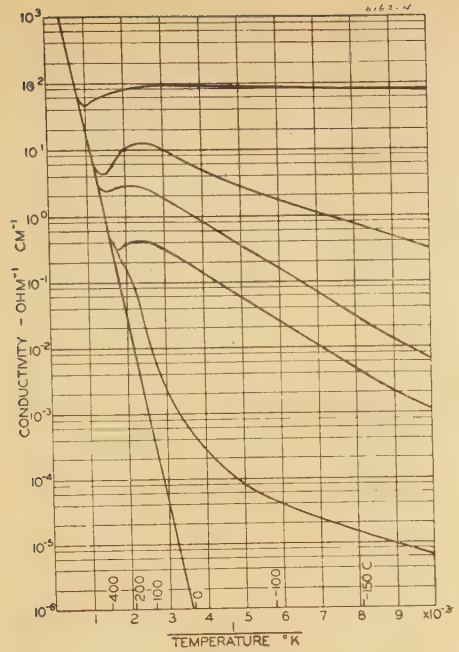

Figure 4. Logarithm of the conductivity of various specimens of silicon as a function of inverse absolute temperature

The conductivity increases with the amount of impurity

temperature from 0.1 to 10^9 ohm-centimeters. Semiconductors usually have high negative temperature coefficients of resistance. As the temperature is increased from 0 degrees centigrade to 300 degrees centigrade, the resistance may decrease by a factor of a thousand. Over this same temperature range the resistance of a typical metal, such as platinum, will increase by a factor of two. Figure 2 shows how the logarithm of the specific resistance, ρ, varies with temperature, T, in degrees centigrade for three typical semiconductors and for platinum. Curves 1 and 2 are for "material 1" and "material 2" which have been used extensively to date. "Material 1" is composed of manganese and nickel oxides. "Material 2" is composed of oxides of manganese, nickel, and cobalt. The dashed part of curve 2 covers a region in which the resistance-temperature relation is not known as accurately as it is at lower temperatures. Curve 3 is an experimental curve for a mixture of iron and zinc oxides in the proportions to form zinc ferrite. From Figure 2 it is obvious that neither the resistance R nor log R varies linearly with T.

Figure 3 shows plots of log ρ versus $1/T$ for "material 1" and "material 2". These do form approximate straight lines. Hence:

$$\rho=\rho_\infty \epsilon^{B/T} \text{ or } \rho=\rho_0\epsilon^{(B/T-B/T_0)} \qquad (1)$$

where T = temperature in degrees Kelvin, $\rho_\infty = \rho$ when $T = \infty$ or $1/T = 0$, $\rho_0 = \rho$ when $T = T_0$, ϵ = Naperian base = 2.718, and B is a constant equal to 2.303 times the slope of the straight lines in Figure 3. The dimensions of B are degrees Kelvin or degrees centigrade. B plays the same role in equation 1 as does the work function in Richardson's equation for thermionic emission. For material 1, B = 3,920 degrees centigrade. This corresponds to an electron energy of 3,920/11,600 or 0.34 volt.

While the curves in Figure 3 are approximately straight, a more careful investigation shows that the slope increases linearly as the temperature increases. From this it follows that a more precise expression for ρ is:

$$\rho=AT^{-c}\epsilon^{D/T}$$

or

$$\log \rho=\log A-c \log T+D/2.303T \qquad (2)$$

The constant c is a small positive or negative number or zero. For "material 1", log A = 5.563, c = 2.73, and D = 3,100. For a particular form of "material 2", log A = 11.514, c = 4.83, and D = 2,064.

If we define temperature coefficient of resistance, α, by the equation

$$\alpha=(1/R)(dR/dT) \qquad (3)$$

it follows from equation 1 that

$$\alpha=-B/T^2 \qquad (4)$$

For "material 1", and T = 300 degrees Kelvin, α = −3,920/90,000 = −0.044. For platinum, α = +0.0037, or roughly ten times smaller than for semiconductors, and of the opposite sign. From equation 2 it follows that

$$\alpha=-(D/T^2)-(c/T) \qquad (5)$$

From equation 3 it follows that

$$\alpha=(1/2.303)\ (d \log R/dT) \qquad (6)$$

For a discussion of the nature of the conductivity in semiconductors, it is simpler and more convenient to consider the conductivity, σ, rather than the resistivity, ρ.

$$\sigma=1/\rho \text{ and } \log \sigma=-\log \rho \qquad (7)$$

The characteristics of semiconductors are brought out more clearly if the conductivity or its logarithm are plotted as a function of $1/T$ over a wide temperature range. Figure 4 is such a plot for a number of silicon samples containing increasing amounts of impurity. At high temperatures, all the samples have nearly the same conductivity. This is called the intrinsic conductivity because it seems to be an intrinsic property of silicon. At low temperatures the conductivity of different samples varies by large factors. In this region silicon is said to be an impurity semiconductor. For extremely pure silicon, only intrinsic conductivity is present and the resistivity obeys equation 1. As the concentration of a particular impurity increases, the conductivity increases, and the impurity conductivity predominates to higher temperatures. Some impurities are much more effective in increasing the conductivity than others. One hundred parts per million of some impurities may increase the conductivity of pure silicon at room temperature by a factor of 10^7. Other impurities may be present in 10,000 parts per million and have a small effect on the conductivity. Two samples may contain the same concentration of an impurity and still differ greatly in their low temperature conductivity. If the impurity is in solid solution, that is, atomically dispersed, the effect is great; if the impurity is segregated in atomically large particles, the effect is small. Since heat treatments affect the dispersion of impurities in solids, the conductivity of semiconductors frequently may be altered radically by heat treatment. Some other semiconductors are not affected greatly by heat treatment.

The impurity need not be a foreign element; in the case of oxides or sulphides, it can be an excess or a deficiency of oxygen or sulphur from the exact

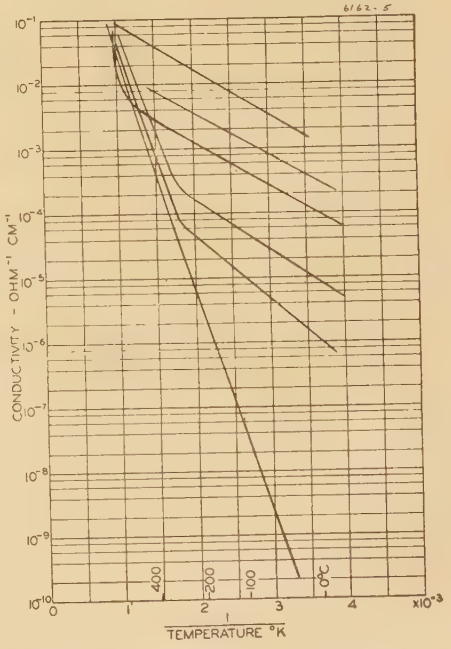

Figure 5. Logarithm of the conductivity of various specimens of cuprous oxide as a function of inverse absolute temperature

The conductivity increases with the amount of excess oxygen above the stoichiometric value in Cu_2O

Data from reference 1

stoichiometric relation. This excess or deficiency can be brought about by heat treatment. Figure 5 shows how the conductivity depends on temperature for a number of samples of cuprous oxide, Cu_2O, heat-treated in such a way as to result in varying amounts of excess oxygen from zero to about one per cent.[1] The greater the amount of excess oxygen, the greater is the conductivity in the low temperature range. At high temperatures, all samples have about the same conductivity.

Semiconductors can be classified on the basis of the carriers of the current into ionic, electronic, and mixed conductors. Chlorides such as NaCl and some sulphides are ionic semiconductors; other sulphides and a few oxides, such as uranium oxide, are mixed semiconductors; electronic semiconductors include most oxides such as Mn_2O_3, Fe_2O_3, NiO, carbides such as silicon carbide, and elements such as boron, silicon, germanium, and tellurium. In ionic and mixed conductors, ions are transported through the solid. This changes the density of carriers in various regions, and thus changes the conductivity. Because this is undesirable, they rarely are used in making thermistors, and hence we will concentrate our interest on electronic semiconductors.

The theoretical and experimental physicists have established that there are two types of electronic semiconductors which can be called *N* and *P* type, depending upon whether the carriers are negative electrons or are equivalent to positive "holes" in the filled energy band. In *N* type, the carriers are deflected by a magnetic field as negatively charged particles would be, and conversely for *P* type. The direction of deflections is ascertained by measurement of the sign of the Hall effect. The direction of the thermoelectric effect also fixes the sign of the carriers. By determining the resistivity, Hall coefficient, and thermoelectric power of a particular specimen at a particular temperature, it is possible to determine the density of carriers, whether they are negative or positive, and their mobility or mean free path. The mobility is the mean drift velocity in a field of one volt per centimeter.

The existence of these classifications is explained by the theoretical physicist[4-2] in terms of the diagrams in Figure 6. In an intrinsic semiconductor, at low temperatures the valence electrons completely fill all the allowable energy states. According to the exclusion principle, only one electron can occupy a particular energy state in any system. In semiconductors and insulators there exists a region of energy values, just above the allowed band, which are not allowed. The height of this unallowed band is expressed in equivalent electron volts, ΔE. Above this unallowed band there exists an allowed band, but at low temperatures there are no electrons in this band. When a field is applied across such a semiconductor, no electron can be accelerated, because if it were accelerated, its energy would be increased to an energy state which is either filled or unallowed. As the temperature is raised, some electrons acquire sufficient energy to be raised across the unallowed band into the upper allowed band. These electrons can be accelerated into a slightly higher energy state by the applied field and thus can carry current. For every electron that is put into an activated state there is left behind a hole in the normally filled band. Other electrons having slightly lower energies can be accelerated into these holes by the applied field. The physicist has shown that these holes act toward the applied field as if they were particles having a charge equal to that of an electron but of opposite sign, and a mass equal to, or somewhat larger than, the electronic mass. In an intrinsic semiconductor, about half the conductivity is due to electrons and half due to holes.

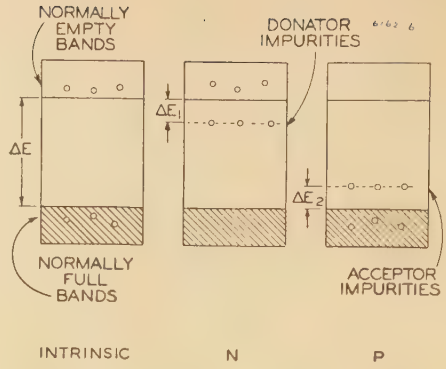

Figure 6. Schematic energy level diagrams illustrating intrinsic, *N*, and *P* types of semiconductors

The quantity ΔE is related to B in equation 1 by

$$2B = (\Delta E)e/k \tag{8}$$

in which B is in degrees centigrade, ΔE is in volts, e is the electronic charge in coulombs, k is Boltzmann's constant in joules per degree centigrade. The value of e/k is 11,600 so that

$$\Delta E = B/5{,}800 \tag{8a}$$

The difference between metals, semiconductors, and insulators results from the value of ΔE. For metals ΔE is zero or very small. For semiconductors ΔE is greater than about 0.1 volt, but less than about 1.5 volts. For insulators ΔE is greater than about 1.5 volts.

Some impurities with positive valencies which may be present in the semiconductor may have energy states such that ΔE_1 volts equivalent energy can raise the valence electron of the impurity atom into the allowed conduction band. See Figure 6. The electron now can take part in conduction; the donator impurity is a positive ion which usually is bound to a particular location and can take no part in the conductivity. These are excess or *N* type conductors. The conductivity depends on the density of donators, ΔE_1, and T.

Similarly, some other impurity with negative valencies may have an energy state ΔE_2 volts above the top of the filled band. At room temperature or higher, an electron in the filled band may be raised in energy and accepted by the impurity, which then becomes a negative ion and usually is immobile. However, the hole which results can take part in the conductivity.

In all cases represented in Figure 6, an electron occupying a higher energy level than a positive ion or a hole, has a certain probability that in any short interval of time it will drop into a lower energy state. However, during this same time interval there will be electrons which will be

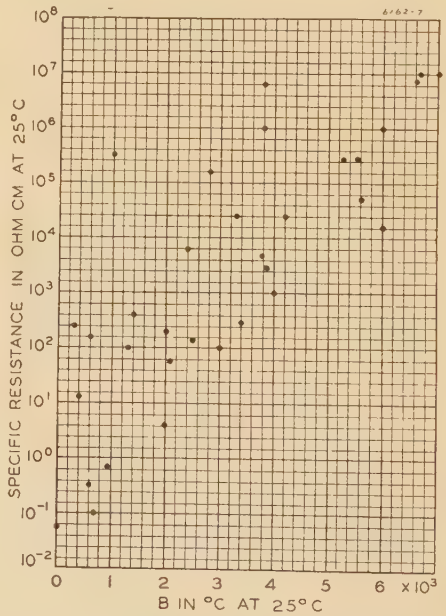

Figure 7. Logarithm of the resistivity of various semiconducting materials as a function of *B* in equation 1

The quantity, *B*, is proportional to the temperature coefficient of resistance as given in equation 4

raised to a higher energy level by thermal agitation. When the number of electrons per second which are being elevated is equal to the number which are descending in energy, equilibrium prevails. The conductivity, σ, is then

$$\sigma = Nev_1 + Pev_2 \qquad (9)$$

where N and P are the concentrations of electrons and holes respectively, e is the charge on the electron, v_1 and v_2 are the mobilities of electrons and holes respectively.

This explains the following experimental facts which otherwise are difficult to interpret:

1. N-type oxides, such as ZnO, when heated in a neutral or slightly reducing atmosphere become good conductors, presumably because they contain excess zinc which can donate electrons. If they then are heated in atmospheres which are increasingly more oxidizing, their conductivity decreases until eventually they are intrinsic semiconductors or insulators.

2. P-type oxides, such as NiO, when heat-treated in strongly oxidizing atmospheres are good conductors. Very likely they contain oxygen in excess of the stoichiometric relation and this oxygen accepts additional electrons. When these are heated in less oxidizing or neutral atmospheres they become poorer conductors, semiconductors, or insulators.

3. When a P-type oxide is sintered with another P-type oxide, the conductivity increases; similarly for two N-type oxides. But when a P type is added to an N type the conductivity decreases.

4. If a metal forms several oxides, the one in which the metal exerts its highest valence is N type, while the one in which it exerts its lowest valence will be P type.[5]

For several reasons it is desirable to survey the whole field of semiconductors for resistivity and temperature coefficient. One way in which this might be done is to draw a line in Figure 3 for each specimen. Before long, such a figure would consist of such a maze of intersecting lines that it would be difficult to single out and follow any one line. The information can be condensed by plotting log ρ_0 versus B in equation 1 for each specimen.[6] The most important characteristics of a specimen thus are represented by a single point and many more specimens can be surveyed in a single diagram. Figure 7 shows such a plot for a large number of semiconductors investigated at these laboratories or reported in the literature. Values for ρ_0 and B are given for T = 25 degrees centigrade. The points form a sort of "milky way." Semiconductors having a high ρ_0 are likely to have a high value of B and vice versa. If a series of semiconductors has points in Figure 7 which fall on a straight line with a slope of

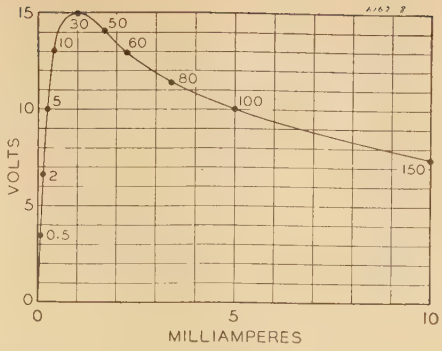

Figure 8. Static voltage–current curve for a typical thermistor

The numbers on the curve are the degrees centigrade rise in temperature above ambient temperature

$1/2.3\ T_0$, they have a common intercept in Figure 3 for $(1/T) = 0$.

Physical Properties of Thermistors

One of the most interesting and useful properties of a thermistor is the way in which the voltage, V, across it changes as the current, I, through it increases. Figure 8 shows this relationship for a 0.061-centimeter diameter bead of "material 1" suspended in air. Each time the current is changed, sufficient time is allowed for the voltage to attain a new steady value. Hence this curve is called the steady state curve. For sufficiently small currents, the power dissipated is too small to appreciably heat the thermistor, and Ohm's law is followed. However, as the current assumes larger values, the power dissipated increases, the temperature rises above ambient temperature, the resistance decreases, and hence the voltage is less than it would have been had the resistance remained constant. At some current, I_m, the voltage attains a maximum or peak value, V_m. Beyond this point, as the current increases the voltage decreases, and the thermistor is said to have a negative resistance whose value is dV/dI. The numbers on the curve give the rise in temperature above ambient temperature in degrees centigrade.

Because currents and voltages for different thermistors cover such a large range of values, it has been found convenient to plot log V versus log I. Figure 9 shows such a plot for the same data as in Figure 8. For various points on the curve, the temperature rise above ambient temperature is given. In a log log plot, a line with a slope of 45 degrees represents a constant resistance, and a line with a slope of -45 degrees represents constant power.

For a particular thermistor, the position of the log V versus log I plot is shifted, as shown in Figure 10, by changing the dissipation constant C. This can be done by changing the air pressure surrounding the bead, changing the medium, or changing the degree of thermal coupling between the thermistor and its surroundings. The value of C for a particular thermistor in given surroundings readily can be determined from the V versus I curve in either Figures 8 or 9. For each point, V/I is the resistance, while V times I is W, the watts dissipated. The resistance data are converted to temperature from R versus T, given by equation 2. A plot is then made of W versus T. For thermistors in which most of the heat is conducted away, W will increase linearly with T, so that C is constant. For thermistors suspended by fine wires in a vacuum, W will increase more rapidly than proportional to T, and C will increase with T. For thermistors of ordinary size and shape, in still air, C/area is equal to from 1 to 40 milliwatts per degree centigrade per square centimeter, depending upon the size and shape factor.

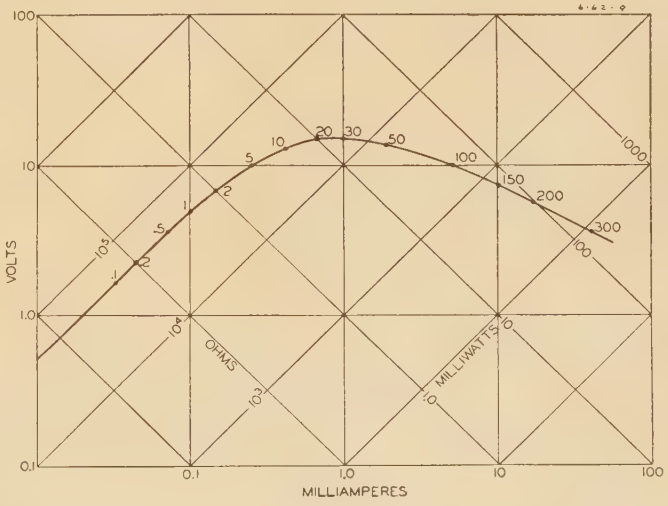

Figure 9. Logarithmic plot of static voltage–current curve for the same data as in Figure 8

The diagonal lines give the values of resistance and power

The user of a thermistor may want to know how many watts can be dissipated before the resistance decreases by one per cent. This may be called the power sensitivity. It is equal to $C/(\alpha \times 100)$ or about one to ten milliwatts per square centimeter in still air. Both C and the power sensitivity increase with air velocity. The dependence of C on gas pressure and velocity is the basis of the use of thermistors as manometers, and as anemometers or flowmeters. Note that in Figure 10 one curve can be superposed on any other by a shift along a constant resistance line.

Figure 11 shows a family of log V versus log I curves for various values of R_o while B, C, and T_o are kept constant. This can be brought about by changing the length, width, and thickness to vary R_o while the surface area is kept constant. If the resistance had been changed by changing the ambient temperature, T_o, the resulting curves would not appear very different from those shown. Note that one curve can be superposed on any other curve by a shift along a constant power line.

Figure 12 shows a family of log V versus log I curves for eight different values of B while C, R_o, and T_o are kept constant. In contrast to the curves in Figures 10 and 11 in which any curve could be obtained from any other curve by a shift along an appropriate axis, the curves in Figure 12 are each distinct. For each curve there exists a limiting ohmic resistance for low currents and another for high currents. For $B = 0$ these two are identical. As B becomes larger, the log of the ratio of the two limiting resistances increases proportionally to B. Note also that for $B > 1{,}200$ degrees Kelvin, the curves have a maximum. For large B values this maximum occurs at low powers and hence at low values of $T - T_o$. This follows as $W = C(T - T_o)$. As B decreases, V_m occurs at increasingly higher powers or temperatures. For $B < 1{,}200$ degrees Kelvin no maximum exists.

The curves in Figures 10 to 12 have been drawn for the ideal case in which the resistance in series with the thermistor is zero, and in which no temperature limitations have been considered. In any actual case there always is some unavoidable small resistance, such as that of the leads, in series with the thermistor, and hence the parts of the curves corresponding to low resistances may not be observable. Also, at high powers the temperature may attain such values that something in the thermistor structure will go to pieces, thus limiting the range of observation. These unobservable ranges have been indicated by dashed lines in Figure 12. The exact location of the dashed portions will of course depend on how a completed thermistor is constructed. In setting these limits we also have considered temperature limitations beyond which aging effects might become too great.

The curves in Figures 9 to 12 have been computed on the basis of the following equations:

$$R = R_o \epsilon^{(B/T)-(B/T_o)} = V/I \tag{10}$$

$$W = C(T - T_o) = VI \tag{11}$$

For these curves the constants R_o, T_o, B, and C are specified. The values of temperature, T_m, power, W_m, resistance, R_m, voltage, V_m, and current, I_m, that prevail at the maximum in the voltage current curve are given by the following equations in which T_m is chosen as the independent parameter. By differentiating equations 10 and 11 with respect to I, putting the derivatives equal to zero, one obtains

$$T_m^2 = B(T_m - T_o) \tag{12}$$

whose solution is

$$T_m = (B/2)(1 \mp \sqrt{1 - 4T_o/B}) \tag{13}$$

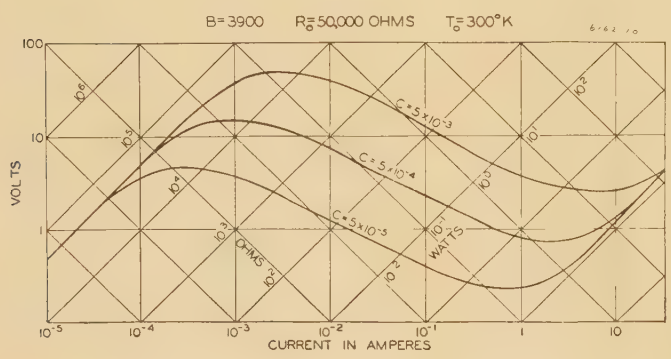

Figure 10 (above). Logarithmic plots of voltage versus current for three values of the dissipation constant C

These curves are calculated for the constants given in the upper part of the figure

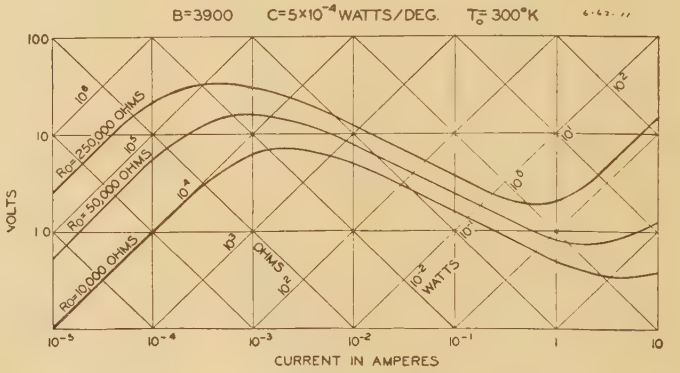

Figure 11 (right, above). Logarithmic plots of voltage versus current for three values of the resistance, R_o, at ambient temperature

These curves are calculated for the constants given in the upper part of the figure

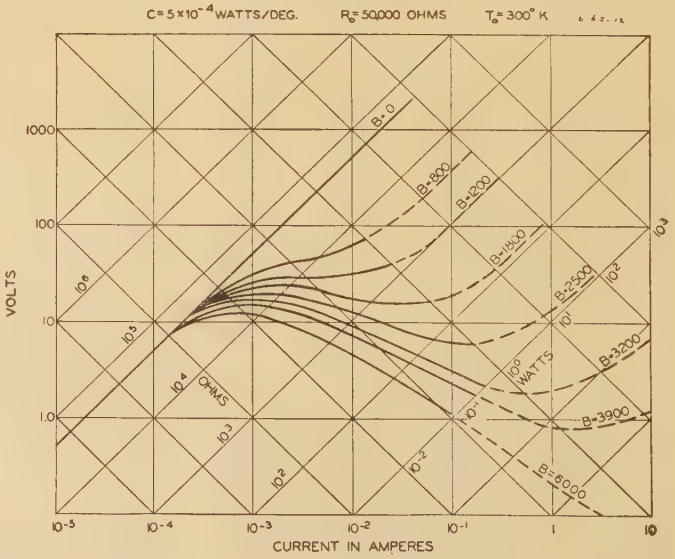

Figure 12 (right). Logarithmic plots of voltage versus current for eight values of B in equation 1

These curves are calculated for the constants given in the upper part of the figure

The minus sign pertains to the maximum in Figures 10 to 12 while the plus sign pertains to the minimum. Note that T_m depends only on B and T_o, and not on R, R_o, or C. From equations 4, 10, and 11 it follows that

$$-\alpha_m(T_m-T_o)=1 \tag{14}$$

$$W_m=C(T_m-T_o) \tag{15}$$

$$R_m=R_o\epsilon^{-T_m/T_0}\doteq R_0\epsilon^{-1}[1-(T_m-T_o)/T_o+(1/2)\{(T_m-T_o/T_o)\}^2-\ldots] \tag{16}$$

$$V_m=[CR_o(T_m-T_o)(\epsilon^{-T_m/T_o})]^{1/2}=\{CR_o(T_m-T_o)\epsilon^{-1}[1-(T_m-T_o)/T_o+(1/2)\{(T_m-T_o)/T_o\}^2-\ldots]\}^{1/2} \tag{17}$$

$$I_m=[(C/R_o)(T_m-T_o)\epsilon^{T_m/T_o}]^{1/2}=\{(C/R_o)(T_m-T_o)\epsilon[1+(T_m-T_o)/T_o+(1/2)\{(T_m-T_o)/T_o\}^2+\ldots]\}^{1/2} \tag{18}$$

Thus far the presentation has been limited to steady state conditions, in which the power supplied to the thermistor is equal to the power dissipated by it, and the temperature remains constant. In many cases, however, it is important to consider transient conditions when the temperature, and any quantities which are functions of temperature, vary with time. A simple case which will illustrate the concepts and constants involved in such problems is as follows: A massive thermistor is heated to about 150 to 200 degrees centigrade by operating it well beyond its peak. At time $t = 0$, the circuit is switched over to a constant current having a value so small that I^2R always is negligibly small. The voltage across the thermistor then is followed as a function of time. From this, the resistance and temperature are computed. Figure 13 shows a plot of log $(T - T_a)$ versus t for a rod thermistor of "material 1", about 1.2 centimeters long, 0.30 centimeter in diameter, and weighing 0.380 gram. In any time interval Δt, there are $C(T - T_a)\Delta t$ joules being dissipated. As a result the temperature will decrease by ΔT given by

$$-H\Delta T=C(T-T_a)\Delta t$$

or

$$(T-T_a)=-(H/C)(\Delta T/\Delta t) \tag{19}$$

where H = heat capacity in joules per degree centigrade. The solution of this equation is

$$(T-T_a)=(T_o-T_a)\epsilon^{-t/\tau} \tag{20}$$

in which $T_o = T$ when $t = 0$, and

$$\tau=H/C \tag{21}$$

where τ is in seconds. It commonly is called the time constant. From equation 20 it follows that a plot of log $(T - T_a)$ versus t should yield a straight line whose slope $= -1/2.303\ \tau$. If H and C vary slightly with temperature, then τ will vary slightly with T and t. The line will not be perfectly straight, but its slope at any t or $(T - T_a)$ will yield the appropriate τ or H/C for that T. As previously described, C can be determined from a plot of watts dissipated versus T. For this thermistor this curve became steeper at the higher temperatures so that C increased for higher temperatures. Table I summarizes the values of C, τ, and H at various T.

When a thermistor is heated by passing current through it, conditions are involved somewhat more since the I^2R power will be a function of time. At any time in the heating cycle, the heat power liberated will be equal to the watts dissipated, or $C(T - T_a)$ plus watts required to raise the temperature, or HdT/dt. The heat power liberated will depend on the circuit conditions. In a circuit like that shown in the upper corner of Figure 14, the current varies with time, as shown by the six curves for six values of the battery voltage E. If a relay in the circuit operates when the current reaches a definite value, a considerable range of time delays can be achieved. This family of curves will be modified by changes in ambient temperature and where rather precise time delays are required, the ambient temperature must be controlled or compensated.

Since thermistors cover a wide range in size, shape, and heat conductivity of surrounding media, large variations in H, C, and τ can be produced. The time constant can be varied from about one millisecond to about ten minutes or a millionfold.

One very important property of a thermistor is its aging characteristic, or how

Table I. Values of C, τ, H as Functions of T for a Thermistor of "Material 1"

Thermistor About 1.2 Centimeters Long, 0.30 Centimeter in Diameter, and Weighing 0.380 Gram. T_a=24 Degrees Centigrade

T, Deg C	C, Watts Per Deg C	τ, Sec	H, Joules Per Deg C	h, Joules Per Gram Per Deg C
44	0.0037	76	0.28	0.75
64	0.0037	74	0.27	0.72
84	0.0038	71	0.27	0.71
104	0.0037	69	0.26	0.68
124	0.0038	68	0.26	0.67
144	0.0038	67	0.26	0.67
164	0.0039	67	0.26	0.69
184	0.0041	66	0.27	0.71
204	0.0042	66	0.28	0.73

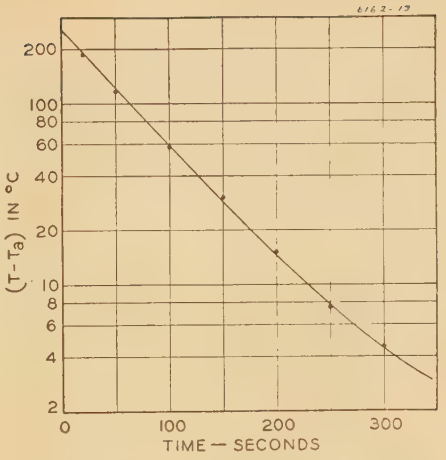

Figure 13. Cooling characteristic of a massive thermistor—logarithm of temperature above ambient versus time

constant the resistance at a given temperature stays with use. To obtain a stable thermistor it is necessary to

1. Select only semiconductors which are pure electronic conductors.
2. Select those which do not change chemically when exposed to the atmosphere at elevated temperatures.
3. Select one which is not sensitive to impurities likely to be encountered in manufacture or in use.
4. Treat it so that the degree of dispersion of the critical impurities is in equilibrium, or else that the approach to equilibrium is very slow at operating temperatures.
5. Make a contact which is intimate, sticks tenaciously, has an expansion coefficient compatible with the semiconductor, and is durable in the atmospheres to which it will be exposed.
6. In some cases, enclose the thermistor in a thin coat of glass or material impervious to gases and liquids, the coat having a suitable expansion coefficient.
7. Preage the unit for several days or weeks at a temperature somewhat higher than that to which it will be subjected.

By taking these precautions, remarkably good stabilities can be obtained.

Figure 15 shows aging data taken on three-quarter inch diameter disks of "material 1" and "material 2" with silver contacts and soldered leads. These disks were measured soon after production, were aged in an oven at 105 degrees centigrade, and were tested periodically at 24 degrees centigrade. The percentage change in resistance over its initial value is plotted versus the logarithm of the time in the aging oven. It is to be noted that most of the aging takes place in the first day or week. If these disks were preaged for a week or a month and the subsequent change in resistance referred to the resistance after

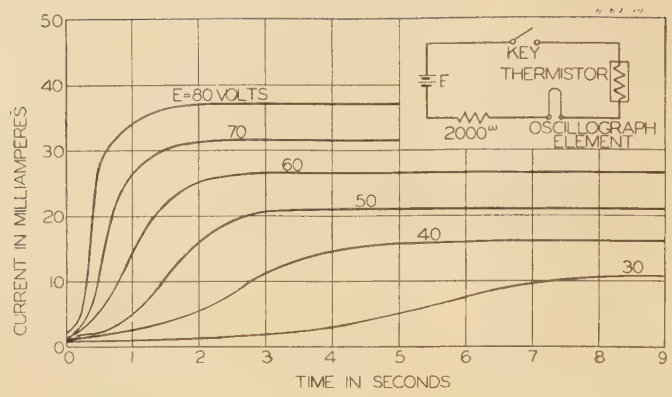

Figure 14. Current versus time curves for six values of the battery voltage in the circuit shown in the insert

preaging, they would age only about 0.2 per cent in one year. In a thermistor thermometer, this change in resistance would correspond to a temperature change of 0.05 degree centigrade. Thermistors mounted in an evacuated tube or coated with a thin layer of glass, age even less than those shown in the figure. For some applications such high stability is not essential, and it is not necessary to give the thermistors special treatment.

Thermistors have been used at higher temperatures with satisfactory aging characteristics. Extruded rods of "material 1" have been tested for stability by treating them for two months at a temperature of 300 degrees centigrade. Typical units aged from 0.5 to 1.5 per cent of their initial resistance. Similar thermistors have been exposed alternately to temperatures of 300 degrees centigrade and −75 degrees centigrade for a total of 700 temperature cycles, each lasting one-half hour. The resistance of typical units changed by less than one per cent.

In some applications of thermistors, very small changes in temperature produce small changes in potential across the thermistor, which are amplified then in high gain amplifiers. If at the same time the resistance is fluctuating randomly by as little as one part in a million, the potential across the thermistor also will fluctuate by a magnitude which will be directly proportional to the current. This fluctuating potential is called noise, and as it depends on the current, it is called current noise. In order to obtain the best signal to noise ratio, it is necessary that the current noise at operating conditions be less than Johnson or thermal noise.[7,8] To make noise-free units it is necessary to pay particular attention to the raw materials, the degree of sintering, the grain size, the method of making contact, and any steps in the process which might result in minute surface cracks or fissures.

All the thermistors discussed thus far either were heated directly by the current passing through them or by changes in ambient temperature. In indirectly heated thermistors, the temperature and resistance of the thermistor are controlled primarily by the power fed into a heater thermally coupled to it. One such form might consist of a 0.038-centimeter diameter bead of "material 2" embedded in a small cylinder of glass about 0.38 centimeter long and 0.076 centimeter in diameter. A small nichrome heater coil having a resistance of 100 ohms is wound on the glass and is fused onto it with more glass. Figure 16 shows a plot of log V versus log I for the bead element at various currents through the heater. In this way the bead resistance can be changed from 3,000 ohms to about 10 ohms. Indirectly heated thermistors ordinarily are used where the controlled circuit must be isolated electrically from the actuating circuit, and where the power from the latter must be fed into a constant resistance heater.

II—Uses of Thermistors

The thermistor, or thermally sensitive resistor, probably has excited more interest as a major electric circuit element than any other except the vacuum tube in the last decade. Its extreme versatility, small size, and ruggedness were responsible for its introduction in great numbers into communications circuits within five years after its first application in this field. The next five year period spanned the war, and saw thermistors widely used in additional important applications. The more important of these uses ranged from time delays and temperature controls to feed-back amplifier automatic gain controls, speech volume limiters, and superhigh frequency power meters. It is surprising that such versatility can result from a temperature-dependent resistance characteristic alone. However, this effect produces a very useful nonlinear volt-ampere relationship. This, together with the ability to produce the sensitive element in a wide variety of shapes and sizes results in applications in diverse fields. The variables of design are many and interrelated, including electrical, thermal, and mechanical dimensions.

The more important uses of thermistors as indication, control, and circuit elements will be discussed, grouping the uses as they fall under the primary characteristics: resistance-temperature, volt-ampere, and current-time or dynamic relations.

Resistance–Temperature Relations

It has been pointed out in part I that the temperature coefficient of electrical resistance of thermistors is negative and several times that of the ordinary metals at room temperature. In thermistor "material 1," which commonly is used, the coefficient at 25 degrees centigrade is −4.4 per cent per degree centigrade, or over ten times that of copper, which is +0.39 per cent per degree centigrade at the same temperature. A circuit element made of this thermistor material has a resistance at zero degrees centigrade which is nine times the resistance of the same element at 50 degrees centigrade. For comparison, the resistance of a copper wire at 50 degrees centigrade is 1.21 times its value at zero degrees centigrade.

The resistance-temperature characteristics of thermistors suggest their use as sensitive thermometers, as temperature

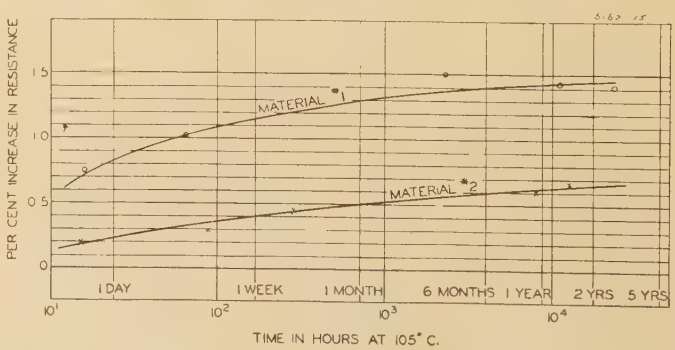

Figure 15. Aging characteristic of thermistors made of materials 1 and 2 aged in an oven at 105 degrees centigrade

Per cent increase in resistance over its initial value versus time on a logarithmic scale

actuated controls, and as compensators for the effects of varying ambient temperature on other elements in electric circuits.

Thermometry

The application of thermistors to temperature measurement follows the usual principles of resistance thermometry. However, the large value of temperature coefficient of thermistors permits a new order of sensitivity to be obtained. This and the small size, simplicity, and ruggedness of thermistors adapt them to a wide variety of temperature measuring applications. When designed for this service, thermistor thermometers have long-time stability which is good for temperatures up to 300 degrees centigrade and excellent for more moderate temperatures. A well-aged thermistor used in precision temperature measurements was found to be within 0.01 degree centigrade of its calibration after two months use at various temperatures up to 100 degrees centigrade. As development proceeds, the stability of thermistor thermometers may be expected to approach that of precision platinum thermometers. Conventional bridge or other resistance measuring circuits commonly are employed with thermistors. As with any resistance thermometer, consideration must be given to keeping the measuring current sufficiently small so that it produces no appreciable heating in order that the thermistor resistance shall be dependent upon the ambient temperature alone.

Since thermistors are readily designed for higher resistance values than metallic resistance thermometers or thermocouples, lead resistances ordinarily are not bothersome. Hence the temperature sensitive element can be located remotely from its associated measuring circuit. This permits great flexibility in application, such, for instance, as wire line transmission of temperature indications to control points.

Table II. Temperature–Resistance Characteristic of a Typical Thermistor Thermometer

Temp, Deg C	Resistance, Ohms	Temp Coefficients B, Deg C	Temp Coefficients α, Per Cent Per Deg C
−25	580,000	3,780	−6.1
0	145,000	3,850	−5.2
25	46,000	3,920	−4.4
50	16,400	3,980	−3.8
75	6,700	4,050	−3.3
100	3,200	4,120	−3.0
150	830	4,260	−2.4
200	305	4,410	−2.0
275	100	4,600	−1.5

Dissipation constant in still air, approximately 4 milliwatts per degree centigrade; thermal time constant in still air, approximately 70 seconds; dimensions of thermistor, diameter approximately 0.11 inch, length approximately 0.54 inch.

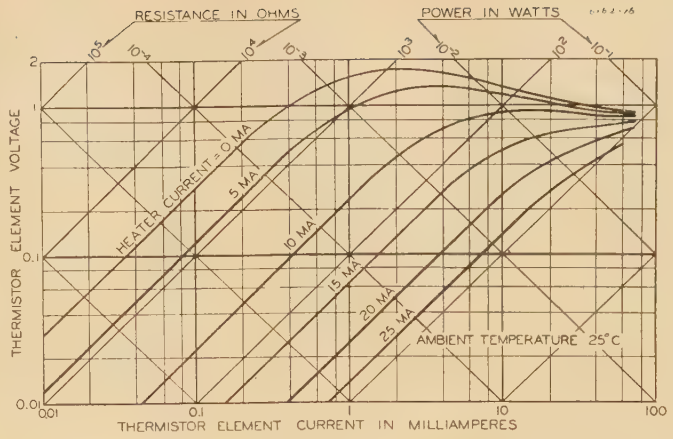

Figure 16. Logarithmic plots of voltage versus current for six values of heater current in an indirectly heated thermistor

Resistance and power scales are given on the diagonal lines

Table II gives the characteristics of a typical thermistor thermometer. The dissipation constant is the ratio of the power input in watts dissipated in the thermistor, to the resultant temperature rise in degrees centigrade. The time constant is the time required for the temperature of the thermistor to change 63 per cent of the difference between its initial value and that of the surroundings. As a sensitive thermometer, this thermistor with a simple Wheatstone bridge and a galvanometer whose sensitivity is 2×10^{-10} amperes per millimeter per meter will indicate readily a temperature change of 0.0005 degree centigrade. For comparison, a precision platinum resistance thermometer and the required special bridge such as the Mueller, will indicate a minimum change of 0.003 degree centigrade with a similar galvanometer.

Several thermistors which have been used for thermometry are shown in Figure 17. Included in the group are types which are suited to such diverse applications as intravenous blood thermometry and supercharger rotor temperature measurement. In Figure 17, *A* is a tiny bead with a response time of less than a second in air. *B* is a probe type unit for use in air streams or liquids. *C* is a meteorological thermometer used in automatic radio transmission of weather data from free balloons. *D* is a rod shaped unit. *E* is a disk or pellet, adapted for use in a metal thermometer bulb. Disks like the one shown have been sweated to metal plates to give a low thermal impedance connection to the object whose temperature is to be determined. *F* is a large disk with an enveloping paint finish for use in humid surroundings. The characteristics of these types are given in Table III.

The temperature of objects which are inaccessible, in motion, or too hot for contact thermometry, can be determined by permitting radiation from the object to be focused on a suitable thermistor by means of an elliptical mirror. Such a thermistor may take the form of a thin flake attached to a solid support. Its advantages compared with the thermopile and resistance bolometer are its more favorable resistance value, its ruggedness, and its high temperature coefficient of resistance. It can be made small to reduce its heat capacity so as to follow rapidly changing temperatures. Flake thermistors have been made with time constants from one millisecond to one second. Since the amount of radiant power falling on the thermistor may be quite small, sensitive meters or vacuum tube amplifiers are required to measure the small changes in the flake resistance. Where rapidly varying temperatures are not involved, thermistors with longer time constants and simpler circuit equipments can be utilized.

Temperature Control

The use of thermistors for temperature control purposes is related closely to their application as temperature measuring devices. In the ideal temperature-sensitive control element, sensitivity to temperature change should be high and the resistance value at the control temperature should be the proper value for the control circuit used. Also, the temperature rise of the control element resulting from circuit heating should be low, and the stability of calibration should be good. The size and shape of the sensitive element are dictated by several factors such as the space available, the required speed of response to temperature changes, and the amount of power which must be dissipated in the element by the control circuit to permit the arrangement to operate relays, motors, or valves.

Because of their high temperature sensitivity, thermistors have shown much

promise as control elements. Their adaptability and their stability at relatively high temperatures led, for instance, to an aircraft engine control system using a rod-shaped thermistor as the control element.[9] The thermistor, mounted in a standard one-quarter inch diameter temperature bulb assembly, operated at approximately 275 degrees centigrade. It was associated with a differential relay and control motor on the aircraft 28-volt d-c system. The power dissipation in the thermistor was two watts. The resistance of a typical thermistor under these high temperature conditions remained within ±1.5 per cent over a period of months. This corresponds to about ± one degree centigrade variation in calibration. Several other related designs were developed using the same control system with other thermistors designed for both higher and lower temperature operation. In the lower temperature applications, typical thermistors maintained their calibrations within a few tenths of a degree centigrade.

In general, gas tube control circuits dissipate less power in the thermistor than relay circuits do. This results in less temperature rise in the thermistor, and leads to a more accurate control. While the average value of this temperature rise can be allowed for in the design, the variations in different installations require individual calibration to correct the errors if they are large. The corrections may be different as a result of variations of the thermal conductivity of the surrounding media from time to time, or from one installation to another. The greater the power dissipated in the thermistor, the greater the absolute error in the control temperature for a given change in thermal conductivity. This follows from the relation

$$\Delta T = W/C \qquad (22)$$

where ΔT is the temperature rise, W is the power dissipated, and C is the dissipation constant which depends on thermal coupling to the surroundings. For the same reason, the temperature indicated by a resistance thermometer immersed in an agitated medium will depend on the rate of flow if the temperature sensitive element is operated several degrees hotter than its surroundings.

The design of a thermistor for a ventilating duct thermostat might proceed as follows as far as temperature rise is concerned:

1. Determine the power dissipation. This depends upon the circuit selected and the required over-all sensitivity.

2. Estimate the permissible temperature rise of the thermistor, set by the expected variation in air speed and the required temperature control accuracy.

3. Solve equation 22 for the dissipation constant and select a thermistor of appropriate design and size for this constant in the nominal air speed. Where more than one style of thermistor is available, the required time constant will determine the choice.

Table III. Thermistor Thermometers

	A	B	C	D	E	F
Nominal resistance, ohms:						
−25 C	—	—	87,500	610,000	—	13,000
0 C	5,000	325,000	37,500	153,000	490	3,200
25 C	2,000	100,000	18,000	48,500	175	950
50 C	900	33,000	9,700	17,300	71	340
75 C	460	13,000	5,500	7,100	32	145
100 C	250	6,000	3,700	3,400	16	70
150 C	95	1,600	—	870	4.5	—
200 C	—	500	—	—	1.6	—
300 C	—	80	—	—	—	—
Temp coefficient α, per cent per deg C at 25 C	−3.4	−4.4	−2.8	−4.4	−3.8	−4.4
Max permissible temp, deg C	150	300	100	150	200	100
Dissipation constant, C, milliwatts per deg C:						
Still air	0.1	1	7	7	—	20
Still water	—	7	—	—	—	—
Thermal time constant, sec:						
Still air	1	30	25	60	—	—
Still water	—	4	—	—	—	—
Shape	Bead	Probe	Rod	Rod	Disk	Disk
Dimensions, inches:						
Diameter or width	0.015	0.1	0.05	0.15	0.2	0.56
Length or thickness (less leads)	0.02	0.6	1.2	0.7	0.1	0.31

Compensators

It is a natural and obvious application of thermistors to use them to compensate for changes in resistance of electrical circuits caused by ambient temperature variations. A simple example is the compensation of a copper wire line, the resistance of which increases approximately 0.4 per cent per degree centigrade. A thermistor having approximately one-tenth the resistance of the copper, with a temperature coefficient of −4 per cent per degree centigrade placed in series with the line and subjected to the same ambient temperature, would serve to compensate it over a narrow temperature range. In practice however, the compensating thermistor is associated with parallel and sometimes series resistance, so that the combination gives a change in resistance closely equal and opposite to that of the circuit to be compensated over a wide range of temperatures. See Figure 18.

A copper winding having a resistance of 1,000 ohms at 25 degrees centigrade can be compensated by means of a thermistor of 566 ohms at 25 degrees centigrade in parallel with an ohmic resistance of 445 ohms as shown in Figure 18. The winding with compensator has a resistance of 1,250 ohms constant to ±1.6 per cent over the temperature range −25 degrees centigrade to +75 degrees centigrade. Over this range the copper alone varies from 807.5 ohms to 1,192.5 ohms, or ±19 per cent. The total resistance of the circuit has been increased only 6.1 per cent at the upper temperature limit by the addition of a compensator. This increase is small because of the high temperature coefficient of the compensating thermistor. The characteristics of such a thermistor are so stable that the resistance would remain constant within less than one per cent for ten years, if maintained at any temperature up to about 100 degrees centigrade. Figure 15 shows aging characteristics for typical thermistors suitable for use in compensators. These curves include the change which occurs during the seasoning period of several days at the factory, so that the aging in use is a fraction of the total shown.

In many circuits which need to function to close tolerances under wide ambient temperature variation, the values of one or more circuit elements may vary undesirably with temperature. Frequently the resultant over-all variation with temperature can be reduced by the insertion of a simple thermistor placed at an appropriate point in the circuit. This is true particularly if the circuit contains vacuum tube amplifiers. In this manner, frequency and gain shifts in communications circuits have been cancelled and temperature errors prevented in the operation of devices such, for instance, as electric meters. The change in inductance of a coil resulting from the variation of magnetic characteristics of the core ma-

terial with temperature has been prevented by partially saturating the coil with direct current, the magnitude of which is directly controlled by the resistance of a thermistor imbedded in the core. In this way the amount of d-c magnetic flux is adjusted by the thermistor so that the inductance of the coil is independent of temperature.

In designing a compensator, care must be taken to ensure exposure of the thermistor to the temperature affecting the element to be compensated. Power dissipation in the thermistor must be considered and either limited to a value which will not produce a significant rise in temperature above ambient temperature, or offset in the design.

Volt-Ampere Characteristics

The nonlinear shape of the static characteristic relating voltage, current, resistance, and power for a typical thermistor was illustrated by Figure 9. The part of the curve to the right of the voltage maximum has a negative slope, applicable in a large number of ways in electric circuits. The particular characteristic shown begins with a resistance of approximately 50,000 ohms at low power. Additional power dissipation raises the temperature of the thermistor element and decreases its resistance. At the voltage maximum, the resistance is reduced to about one-third its cold value, or 17,000 ohms, and the dissipation is 13 milliwatts. The resistance becomes approximately 300 ohms when the dissipation is 100 milliwatts. Such resistance-power characteristics have resulted in the use of thermistors as sensitive power measuring devices, and as automatically variable resistances for such applications as output amplitude controls for oscillators and amplifiers. Their nonlinear characteristics also fit thermistors for use as voltage regulators, volume controls, expandors, contactless switches, and remote control devices. To permit their use in these applications for d-c as well as a-c circuits, nonpolarizing semiconductors alone are employed in thermistors with the exception of two early types.

Power Meter

Thermistors have been used very extensively in the ultra- and superhigh frequency ranges in test sets as power measuring elements. The particular advantages of thermistors for this use are that they can be made small in size, have a small electrical capacity, can be severely overloaded without change in calibration, and easily can be calibrated with d-c or low frequency power. For this application the thermistor is used as a power absorbing terminating resistance in the transmission line, which may be of Lecher, coaxial, or wave-guide form. Methods of mounting have been worked out which reduce the reflection of high frequency energy from the termination to negligible values, and assure accurate measurement of the power over broad bands in the frequency spectrum. Conventionally, the thermistor is operated as one arm of a Wheatstone bridge, and is biased with low frequency or d-c energy to a selected operating resistance value, for instance, 125 or 250 ohms in the absence of the power to be measured. The application of the power to be measured further decreases the thermistor resistance, the bridge becomes unbalanced, and a deflection is obtained on the bridge meter. A full scale power indication of one milliwatt is customary for the test set described, although values from 0.1 milliwatt to 200 milliwatts have been employed using thermistors with different sized beads as shown in Figure 19.

Continuous operation tests of these thermistors indicate very satisfactory stability with an indefinitely long life. A group of eight power meter thermistors, normally operated at 10 milliwatts and having a maximum rating of 20 milliwatts, were operated for over 3,000 hours at a power input of 30 milliwatts. During this time the room temperature resistance remained within 1.5 per cent of its initial value, and the power sensitivity, which is the significant characteristic, changed by less than 0.5 per cent.

When power measuring test sets are intended for use with wide ambient temperature variations, it is necessary to temperature compensate the thermistor. This is accomplished conventionally by the introduction of two other thermistors into the bridge circuit. These units are designed to be insensitive to bridge currents but responsive to ambient temperature. One of the compensators maintains the zero point and the other holds the meter scale calibration independent of the effect of temperature change on the measuring thermistor characteristics.

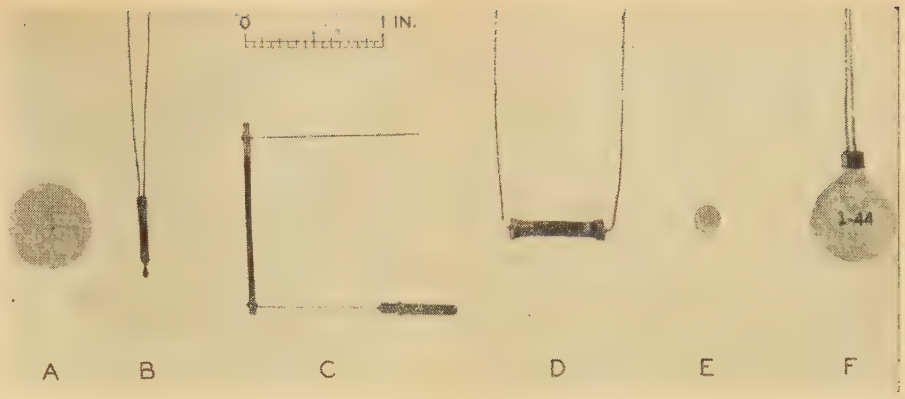

Figure 17. Some forms of thermistors which have been used as resistance thermometers

Automatic Oscillator Amplitude Control

Meacham,[10] and Shepherd and Wise[11] have described the use of thermistors to provide an effective method of amplitude stabilization of both low and high frequency oscillators. These circuits oscillate because of positive feedback around the vacuum tube. The feed-back circuit is a bridge with at least one arm containing a thermistor which is heated by the oscillator output. Through this arrangement, the feedback depends in phase and magnitude upon the output, and there is one value of thermistor resistance which, if attained, would balance the bridge and cause the oscillation amplitude to vanish. Obviously this condition never can be exactly attained, and the operating point is just enough different to keep the bridge slightly unbalanced and produce a predetermined steady value of oscillation output. Such oscillators in which the amplitude is determined by thermistor nonlinearity have manifold advantages over those whose amplitude is limited by vacuum tube nonlinearity. The harmonic content in the output is smaller, and the performance is much less dependent upon the individual vacuum tube and upon variations of the supply voltages. It is necessary that the thermal inertia of the thermistor be sufficient to prevent it from varying in resistance at the oscillation frequency. This is satisfied easily for all frequencies down to a small fraction of a cycle per second. Figure 20 shows a thermistor frequently used for oscillator control, together with its static

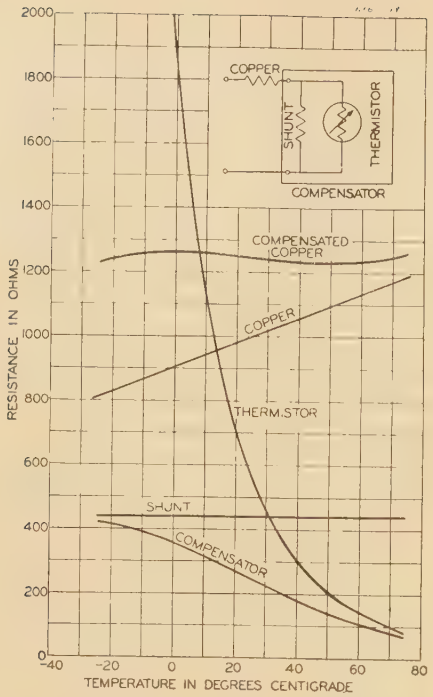

Figure 18. Temperature compensation of a copper conductor by means of a thermistor network

electrical characteristic. This thermistor is satisfactory in oscillators for frequencies above approximately 100 cycles per second. Similar types have been developed with response characteristics suited to lower frequencies, and for other resistance values and powers.

Where the ambient temperature sensitivity of the thermistor is disadvantageous in oscillator controls, the thermistor can be compensated by thermostating it with a heater and compensating thermistor network, as shown in Figure 21.

Amplifier Automatic Gain Control

Since the resistance of a thermistor of suitable design varies markedly with the power dissipated in it or in a closely associated heater, such thermistors have proved to be very valuable as automatic gain controls, especially for use with negative feed-back amplifiers. This arrangement has seen extensive use in wire communication circuits for transmission level regulation, and has been described in some detail elsewhere.[12–14] In one form, a directly heated thermistor is connected into the feed-back circuit of the amplifier in such a way that the amount of feed-back voltage is varied to compensate for any change in the output signal. By this arrangement, the gain of each amplifier in the transmission system is adjusted continually to correct for variations in overall loss due to weather conditions and other factors, so that constant transmission is obtained over the channel at all times. In a carrier system now in extensive use, the system gain is regulated principally in this way. In this system the transmission loss variations due to temperature are not the same in all parts of the pass band. The loss is corrected at certain repeater points along the transmission line by two additional thermistor gain controls: slope, proportional to frequency; and bulge, with a maximum at one frequency. These thermistors are indirectly heated, with their heaters actuated by energy dependent upon the amplitude of the separate pilot carriers, which are introduced at the sending end for the purpose.

In this type of application, the thermistor will react to the ambient temperature to which it is exposed, as well as to the current passing through it. Where this is important, the reaction to ambient temperature can be eliminated by the use of a heater-type thermistor as shown in Figure 21. The heater is connected to an auxiliary circuit containing a temperature compensating thermistor. This circuit is so arranged that the power fed into the heater of the gain control thermistor is just sufficient at any ambient temperature to give a controlled and constant value of temperature in the vicinity of the gain control thermistor element.

Another interesting form of thermistor gain control utilizes a heater-type thermistor, with the heater driven by the output of the amplifier and with the thermistor element in the input circuit, as shown in Figure 22. In this arrangement, the feedback is accomplished by thermal, rather than electrical coupling. A broadband carrier system, now in use, is regulated with this type of thermistor. In this system a pilot frequency is supplied, and current of this frequency, selected by a network in the regulator, actuates the heater of the thermistor to give smooth, continuous gain control.

By utilizing a heater thermistor of different characteristics, the circuit and load of Figure 22 may be given protection against overloads. In this application, the sensitivity and element resistance of the thermistor are chosen so that the thermistor element forms a shunt of high resistance value, so as to have negligible effect on the amplifier for any normal value of output. However, if the output power rises to an abnormal level, the thermistor element becomes heated and reduced in resistance. This shunts the input to the amplifier, and thus limits the output. Choice of a thermistor having a suitable time constant permits the onset of the limiting effect to be delayed

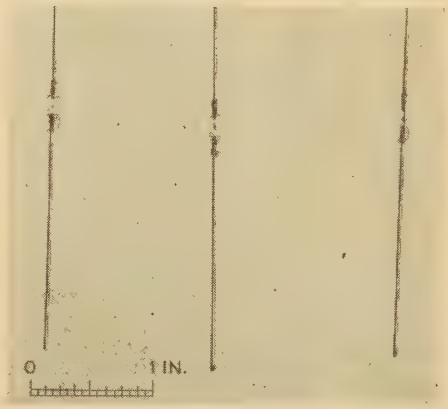

Figure 19. Power measuring thermistors with different sized beads

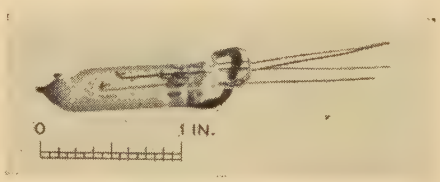

Figure 20A (above). An amplitude control thermistor

The glass bulb is 1.5 inches in length

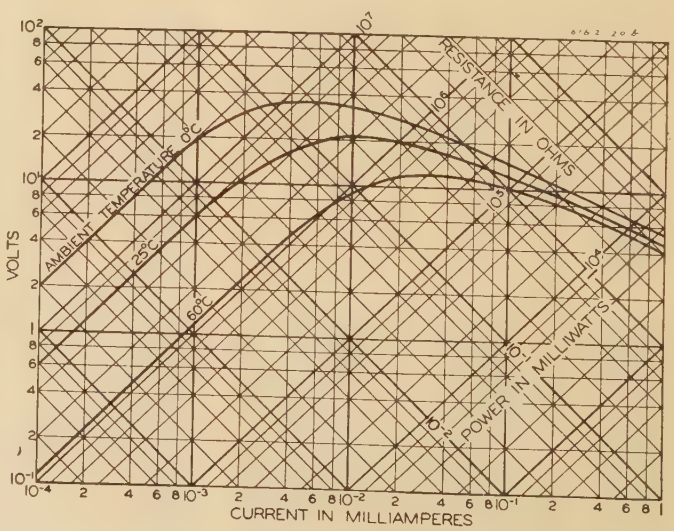

Figure 20B (right). Steady state characteristics of amplitude control thermistor shown in Figure 20A

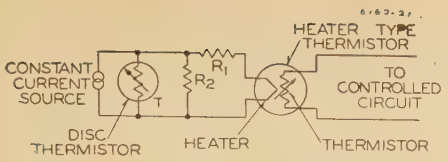

Figure 21. Circuit employing an auxiliary disk thermistor to compensate for effect of varying ambient temperature on a control thermistor

for any period from about a second to a few minutes.

Regulators and Limiters

A group of related applications for thermistors depends on their steady state nonlinear volt-ampere characteristic. These are the voltage regulator, the speech volume limiter, the compressor, and the expandor. The compressor and expandor are devices for altering the range of signal amplitudes. The compressor functions to reduce the range, while the expandor increases it. In Figure 23, curve 1 is a typical thermistor static characteristic having negative slope to the right of the voltage maximum. Curve 2 is the characteristic of an ohmic resistance R having an equal but positive slope. Curve 3 is the characteristic obtained if the thermistor and resistor are placed in series. It has an extensive segment where the voltage is almost independent of the current. This is the condition for a voltage regulator or limiter. If a larger value of resistance is used, as in curve 4, its combination with the thermistor in series results in curve 5, the compressor. In these uses the thermistor regulator is in shunt with the load resistance, so that

$$E = E_o = E_I - IR_S \tag{23}$$

in the circuit diagram of Figure 23. Here E is the voltage across the thermistor and resistor R, E_o is the output voltage, and E_I, I and R_S are respectively, the input voltage, current, and resistance.

If the thermistor and associated resistor are placed in series between the generator and load resistance, an expandor is obtained, and

$$E_o = E_I - E \tag{24}$$

As the resistance R in series with the thermistor is increased, the degree of expansion is decreased, and vice versa.

The treatment thus far in this section assumes that change of operating point occurs slowly enough to follow along the static curves. For a sufficiently rapid change of the operating point, the latter departs from the static curve and tends to progress along an ohmic resistance line intersecting the static curve. For sufficiently rapid fluctuations, control action then may be derived from the resistance changes resulting from the rms power dissipated in the thermistor unit. In speech volume limiters, the thermistor is designed for a speed of response that will produce limiting action for the changes in volume which are syllabic in frequency or slower, and that will not follow the more rapid speech fluctuations with resulting change in wave shape or nonlinear distortion. Speech volume limiters of this type can accommodate large volume changes without producing wave form distortion.[13,15]

Remote Control Switches

The contactless switch and rheostat are natural extensions of the uses just discussed. The thermistor is used as an element in the circuit which is to be controlled, while the thermistor resistance value is, in turn, dependent upon the energy dissipated directly or indirectly in it by the controlling circuit. By taking advantage of the nonlinearity of the static volt-ampere characteristic, it is possible to provide snap and lock-in action in some applications.

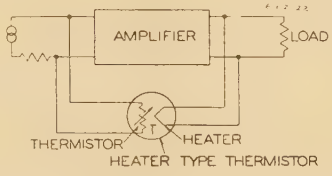

Figure 22. Thermal feed-back circuit for gain control purposes

This arrangement has also been used as a protective circuit for overloads

Manometer

Several interesting and useful applications such as vacuum gauges, gas analyzers, flowmeters, thermal conductivity meters, and liquid level gauges of high sensitivity and low operating temperature are based upon the physical principle that the dissipation constant of the thermistor depends on the thermal conductivity of the medium in which it is immersed. As shown in Figure 10, a change in this constant shifts the position of the static characteristic with respect to the axes. In these applications, the undesired response of the thermistor to the ambient temperature of the medium can, in many cases, be eliminated or reduced by introducing a second thermistor of similar characteristics into the measuring circuit. The compensating thermistor is subjected to the same ambient temperature, but is shielded from the effect being measured, such as gas pressure or flow. The two thermistors can be connected into adjacent arms of a Wheatstone bridge which is balanced when the test effect is zero, and becomes unbalanced when the effective thermal conductivity of the medium is increased. In gas flow measurements, the minimum measurable velocity is limited, as in all hot wire devices, by the convection currents produced by the heated thermistor.

The vacuum gauge or manometer which is typical of these applications will be described somewhat in detail. The sensitive element of the thermistor manometer is a small glass coated bead 0.02 inch in diameter, suspended by two fine wire leads in a tubular bulb for attachment to the chamber whose gas pressure is to be measured. The volt-ampere characteristics of a typical laboratory model manometer are shown in Figure 24 for air at several absolute pressures from 10^{-6} millimeters of mercury to atmospheric pressure. The operating point, in general, is to the right of the peak of these curves. Electrically this element is connected into a unity ratio arm Wheatstone bridge with a similar, but evacuated, thermistor in an adjacent arm as shown in the circuit schematic of Figure

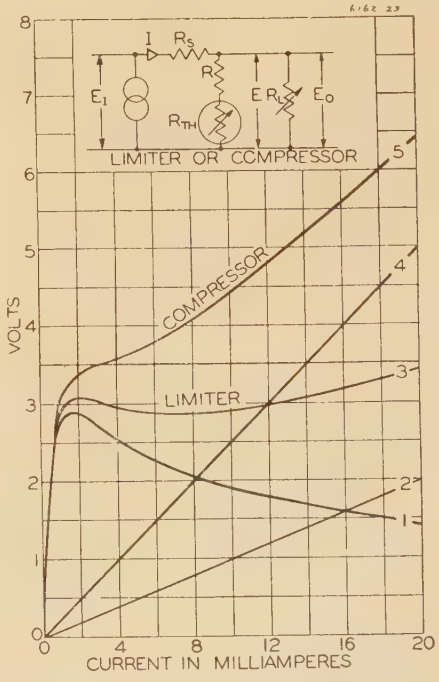

Figure 23. Characteristics of a simple thermistor voltage regulator, limiter, or compressor circuit

25. The air pressure calibration for such a manometer is also shown. The characteristic will be shifted when a gas is used having a thermal conductivity different from that of air. Such a manometer has been found to be best suited for the measurement of pressures from 10^{-5} to 10 millimeters of mercury. The lower pressure limit is set by practical considerations, such as meter sensitivity and the ability to maintain the zero setting for reasonable periods of time in the presence of the variations of supply voltage and ambient temperature. The upper pressure measurement limit is caused by the onset of saturation in the bridge unbalance voltage versus pressure characteristic at high pressures. This is basically because the mean free path of the gas molecules becomes short compared with the distance between the thermistor bead and the inner surface of the manometer bulb, so that the cooling effect becomes nearly independent of the pressure.

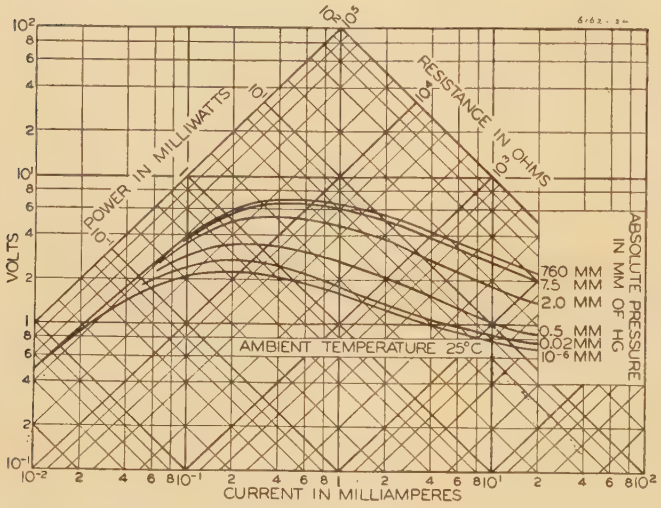

Figure 24 (left). Characteristics of a typical thermistor manometer tube, showing the effect of gas pressure on the volt-ampere and resistance-power relations

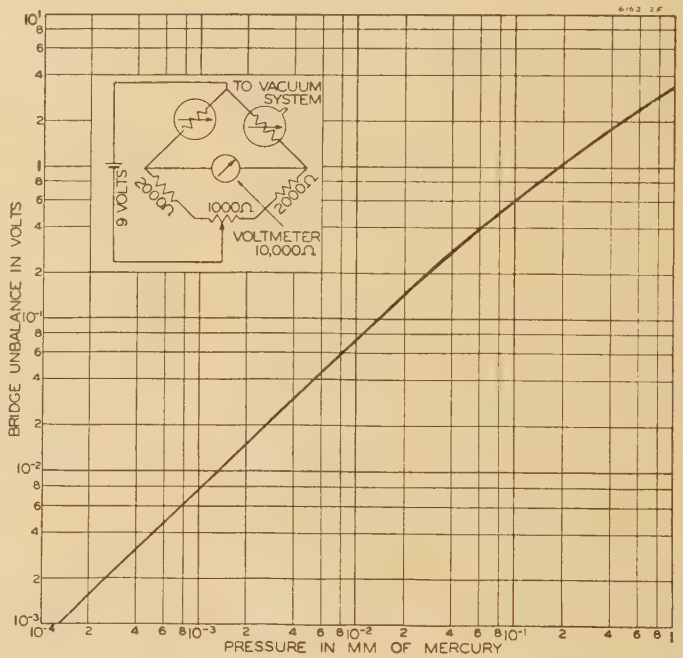

Figure 25 (right). Operating circuit and calibration for a vacuum gauge utilizing the thermistor of Figure 24

The thermistor manometer is specially advantageous for use in gases which may be decomposed thermally. For this type of use, the thermistor element temperature can be limited to a rise of 30 degrees centigrade or less above ambient temperature. For ordinary applications, however, a temperature rise over a range not exceeding 200 degrees centigrade in vacuum, permits measurement over wider ranges of pressure. Special models also have been made for use in corrosive gases. These expose only glass and platinum alloy to the gas under test.

Timing Devices

The numerically greatest application for thermistors in the communication field has been for time delay purposes. The physical basis for this use has been discussed in part I for the case of a directly heated thermistor placed in series with a voltage source and a load, to delay the current rise after circuit closure. This type of operation will be termed the power driven time delay.

By the use of a thermistor suited to the circuit and operating conditions, power driven time delays can be produced from a few milliseconds to the order of a few minutes. Thermistors of this sort have the advantage of small size, light weight, ruggedness, indefinitely long life, and absence of contacts, moving parts, or pneumatic orifices which require maintenance care. Power driven time delay thermistors are best fitted for applications where close limits on the time interval are not required. In some communications uses, it is satisfactory to permit a six to one ratio between maximum and minimum times as a result of the simultaneous variation from nominal values of all the following factors which affect the delay: operating voltage ± five per cent; ambient temperature 20 degrees centigrade to 40 degrees centigrade; operating current of the relay ±25 per cent; relay resistance ± five per cent; and thermistor variations such as occur from unit to unit of the same type.

After a timing operation, a power driven time delay thermistor should be allowed time to cool before a second operation. If this is not done, the second timing interval will be shorter than the first. The cooling period depends on particular circuit conditions and details of thermistor design, but generally is several times the working time delay. In telephone relay circuits requiring a timing operation soon after previous use, the thermistor usually is connected so that it is short circuited by the relay contacts at the close of the working time delay interval. This permits the thermistor to cool during the period when the relay is locked up. If this period is sufficiently long, the thermistor is available for use as soon as the relay drops out. Time delay thermistors have been operated more than half a million times on life test, with no significant change in their timing action

To avoid the limitations of wide timing interval limits and extended cooling periods between operations usually associated with the power driven time delay thermistor, a cooling time delay method of operation has been used. In this arrangement, two relays or the equivalent are employed, and the thermistor is heated to a low resistance value by passing a relatively large current through it for an interval, short compared with the desired time interval. The current then is reduced automatically to a lower value, and the thermistor cools until its resistance increases enough to reduce the current further and trip the working relay.

This part of the operating cycle accounts for the greater part of the desired time interval. With this arrangement, the thermistor is available for reuse immediately after a completed timing interval, or, as a matter of fact, after any part of it. By proper choice of operating currents and circuit values, wide variations of voltage and ambient temperature may occur with relatively little effect upon the time interval. The principal variable left is the cooling time of the thermistor itself. This is fixed in a given thermistor unit, but may vary from unit to unit, depending upon dissipation constant and thermal capacity, as pointed out above.

In addition to their use as definite time delay devices, thermistors have been used in several related applications. Surges can be prevented from operating relays or disturbing sensitive apparatus by introducing a thermistor in series with the circuit component which is to be protected. In case of a surge, the high initial resistance of the thermistor holds the surge current to a low value, provided that the surge does not persist long enough to overcome the thermal inertia of the thermistor. The normal operating voltage, on the other hand, is applied long enough to lower the thermistor resistance to a negligible value, so that a normal operating current will flow after a short interval. In this way, the thermistor enables the circuit to distinguish between an undesired signal of short duration and a desired signal of longer duration, even though the undesired impulse is several times higher in voltage than the signal.

Oscillators, Modulators, and Amplifiers

A group of applications, already explored in the laboratory but not put into engineering use, includes oscillators, modulators, and amplifiers for the low and audio-frequency range. If a thermistor is biased at a point on the negative slope portion of the steady-state volt-ampere characteristic, and if a small alternating voltage is then superposed on the direct voltage, a small alternating current will flow. If the thermistor has a small time constant, τ, and if the applied frequency is low enough, the alternating volt-ampere characteristic will follow the steady-state curve and dV/dI will be negative. As the frequency of the applied alternating voltage is increased, the value of the negative resistance decreases. At some critical frequency, f_c, the resistance is zero and the current is 90 degrees out of phase with the voltage. In the neighborhood of f_c, the thermistor acts like an inductance whose value is of the order of a henry. As the frequency is increased beyond f_c, the resistance is positive, and increases steadily until it approaches the d-c value when the current and voltage are in phase. The critical frequency is approximately given by

$$f_c = {}^1/_{2\tau} \qquad (25)$$

If τ can be made as small as 5×10^{-5} seconds, f_c is equal to 10,000 cycles per second, and the thermistor would have an approximately constant negative resistance up to half this frequency. Point contact thermistors, having such critical frequencies or even higher, have been made in a number of laboratories. However, none of them has been made with sufficient reproducibility and constancy to be useful to the engineer. It has been shown both theoretically and experimentally that any negative resistance device can be used as an oscillator, a modulator, or an amplifier. With further development, it seems probable that thermistors will be used in these fields.

Summary

The general principles of thermistor operation, and examples of specific uses have been given to facilitate a better understanding of thermistors, with the feeling that such an understanding will be the basis for increased use of this new circuit and control element in technology.

References

1. Zur Elektrischen Leitfahigkeit Von Kupferoxydul, **W. P. Juse, B. W. Kurtschatow.** *Physikalische Zeitschrift Der Sowjetunion* (Moscow, U.S.S.R.), volume 2, 1932, pages 453–67.

2. Semi-Conductors and Metals (book), **A. H. Wilson.** The University Press (Cambridge, England), 1939.

3. The Modern Theory of Solids (book), **Frederick Seitz.** McGraw-Hill Book Company, New York, N. Y., 1940.

4. Electronic Processes in Ionic Crystals (book), **N. F. Mott, R. W. Gurney.** The Clarendon Press (Oxford, England), 1940.

5. Die Elektronenleitfahigkeit von Festen Oxyden Verschiedener Valenzstufen, **M. LeBlanc, H. Sachse.** *Physikalische Zeitschrift*, (Leipzig, Germany), volume 32, 1931, pages 887–9.

6. Uber Die Elektrizitatsleitung Anorganischer Stoffe Mit Elektronenleitfahigkeit, **Wilfried Meyer.** *Zeitschrift für Physik* (Berlin, Germany), volume 85, 1933, pages 278–93.

7. Thermal Agitation of Electricity in Conductors, **J. B. Johnson.** *Physical Review*, volume 32, July 1928, pages 97–113.

8. Spontaneous Resistance Fluctuations in Carbon Microphones and Other Granular Resistances, **C. J. Christensen, G. L. Pearson.** *Bell System Technical Journal*, volume 15, April 1936, pages 197–223.

9. Automatic Temperature Control for Aircraft, **R. A. Gund.** AIEE Transactions, volume 64, 1945, October section, pages 730–4.

10. The Bridge Stabilized Oscillator, **L. A. Meacham.** *Proceedings*, Institute of Radio Engineers, volume 26, October 1938, pages 1278–94.

11. Frequency Stabilized Oscillator, **R. L. Shepherd, R. O. Wise.** *Proceedings*, Institute of Radio Engineers, volume 31, June 1943, pages 256–68.

12. A Pilot-Channel Regulator for the K-1 Carrier System, **J. H. Bollman.** *Bell Laboratories Record*, volume 20, June 1942, pages 258–62.

13. Thermistors, **J. E. Tweeddale.** *Western Electric Oscillator*, December 1945, pages 3–5, 34–7.

14. Thermistor Technics, **J. C. Johnson.** *Electronic Industries*, volume 4, August 1945, pages 74–7.

15. Volume Limiter for Leased-Line Service, **J. A. Weller.** *Bell Laboratories Record*, volume 23, March 1945, pages 72–5.

Characteristics of Resistance Welding Transformers

F. E. MURRAY
NONMEMBER AIEE

R. C. JONES
NONMEMBER AIEE

RESISTANCE WELDING as a labor saving production method has made tremendous strides in the past decade. Its widespread recognition during World War II has made it quite evident that this art will be used even more universally in the postwar era.

When one considers that the heart of the resistance welding machine is its transformer, it appears quite logical that an explanation of this type transformer is forthcoming.

It is the purpose of this paper to present the characteristics and functions of the resistance welding transformer in addition to the design problems encountered.

The subject is much too large to enable a detailed discussion and derivation of all the mathematics required to determine the design constants used in this field. Emphasis has been placed on the general problems of design and the effects of deviations from standard practice.

Functions of a Resistance Welding Transformer

The resistance welding transformer, in common with all transformers, is a device for transferring energy by means of electromagnetic induction.

The function of a resistance welding transformer is to furnish relatively large currents at comparably low voltages from the mains of its user's power supply. When delivering load the transformer can be considered, for all practical purposes, as under short-circuit conditions. Its current is limited only by the impedance of the welder plus a small impedance caused by the work.

Standards Governing Resistance Welding Transformers

The Resistance Welder Manufacturers Association has set up standards covering transformers used in resistance welding machines.

The capacity of resistance welding transformers is rated in kilovolt-amperes at 50 per cent duty cycle. The continuous duty rating of such transformers then becomes 0.707 times the name plate rating.

The duty cycle expressed in per cent is considered to be the ratio of weld time in cycles per minute to the total cycles in a minute times 100.

$$\text{Per cent duty cycle on 60 cycles} = \frac{\text{cycles of weld time in a minute}}{3{,}600} \times 100 \quad (1)$$

As the users of resistance welding equipment usually are more concerned with the permissible duty cycle for a given load than they are with the name plate rating, it often is desired to convert as follows:

$$\text{Permissible duty cycle in per cent} = \left(\frac{\text{rated kilovolt-amperes} \times 7.07}{\text{load kilovolt-amperes}}\right)^2 \quad (2)$$

These same standards require that the exciting currents be limited in proportion to the rated current. Transformers rated at less than 100 kva are permitted an exciting current of ten per cent of the rated current, while those rated 100 kva or over are limited to exciting currents of only five per cent of the rated current.

Insulations are required to be able to withstand twice the maximum induced voltage plus 1,000 volts for a period of one minute.

The permitted temperature rise is governed by the type of insulation used. Transformers in which class *B* insulation is used are limited to a temperature rise of 80 degrees centigrade, while those in which class *A* insulation is used are permitted only 60 degrees centigrade rise, as measured by the thermocouple method.

Design Restrictions

The design of resistance welding transformers can be approached only after consideration of several points of limitation.

1. The geometry of the transformer frequently is determined by the available space provided in the welding unit.
2. The limitations as set forth by the RWMA must be met.
3. It is desired to minimize the losses.
4. Economics dictate the manufacture of equipment at a reasonable cost.
5. The number of secondary turns usually is limited to one.

Core Design

The use of high-grade low-watt-loss silicon steel permits the use of higher flux densities for the same hysteresis losses.

Flux densities of from 75,000 to 85,000 lines per square inch (depending on the kilovolt-ampere rating) may be used when it is desired to limit the exciting currents to those values as set forth by the RWMA

From the general formula,

$$E = 4.44NfKBA \times 10^{-8} \quad (3)$$

and assuming a stacking factor of 0.95,

$$B = 395{,}000\frac{E}{NA} \quad (4)$$

when $f = 60$ cycles per second.

$$\frac{\frac{A}{E}}{N} = \frac{395{,}000}{B} \quad (5)$$

This formula gives the area of required core in square inches per volt per turn for a given flux density. Note Figure 1 for flux density versus area.

The core dimensions can be proportioned to suit the available space within certain limitations. A core which takes the form of a square results in a mean turn of minimum length and is the most economical design.

Where space dictates the use of other proportions, the length should not exceed the height by a factor of more than three to one.

Design of the High Voltage Winding

The high voltage winding usually is arranged with eight taps for heat adjustment. Where electronic controls with incorporated heat adjustment facilities are provided, a series-parallel winding without taps is becoming more popular.

The principal advantage of the series-parallel winding is increased duty cycle when less than the maximum load is required. This is true because the copper cross section remains constant as the heat is phased back.

When resistance welding transformers are provided with taps for heat adjustment the copper cross section of the high voltage winding may be reduced as the

Paper 46-156, recommended by the AIEE committee on electric welding for presentation at the AIEE summer convention, Detroit, Mich., June 24–28, 1946. Manuscript submitted April 25, 1946; made available for printing May 28, 1946.

F. E. Murray and R. C. Jones are both design engineers with The Taylor-Winfield Corporation, Warren, Ohio.

square of the open circuit volts across the low voltage winding. In practical design this method of calculating copper densities should be used as a minimum with space dictating how closely it is approached.

Tapering the copper cross section in this manner keeps the permissible duty cycle constant for any tap. Mathematical analysis of this will be shown.

Duty cycle is a function of kilovolt-ampere demand and rating. Then, given a welder of known kilovolt-amperes and duty cycle, it is desired to maintain the duty cycle as the load decreases.

$$\text{Demand kilovolt-amperes} = \frac{E_s I_s}{1000} \quad (6)$$

The low voltage winding current varies directly as its open circuit volts; hence,

$$\frac{E_{s1}}{E_{s2}} = \frac{I_{s1}}{I_{s2}} \quad (7)$$

$$I_{s2} = \frac{I_{s1} E_{s2}}{E_{s1}} \quad (8)$$

$$KVA_1 = \frac{E_{s1} I_{s1}}{1000} \quad (9)$$

$$KVA_2 = \frac{E_{s2} I_{s2}}{1000} \quad (10)$$

Divide one by the other:

$$\frac{KVA_1}{KVA_2} = \frac{E_{s1} I_{s1}}{E_{s2} I_{s2}} \quad (11)$$

Substitute and simplify:

$$\frac{KVA_1}{KVA_2} = \frac{E_{s1} I_{s1} E_{s1}}{E_{s2} I_{s1} E_{s2}} = \frac{E_{s1}^2}{E_{s2}^2} \quad (12)$$

From experience gathered from data on many welding transformers, the following copper densities may be used without exceeding permissible temperature rises for the two types shown:

1. For a pancake type of winding pressed tight against a water-cooled secondary winding insulated from primary winding with mica barriers, a density of 2,500 amperes per square inch may be used at 50 per cent duty cycle rating of transformer.

2. For a layer type of winding, air-cooled and used with a secondary winding not water-cooled, the permissible copper density is 1,500 amperes per square inch. This type of transformer usually has the low voltage winding or secondary made of a laminated copper band built up to the required thickness. The impedance is higher than the pancake type of winding.

Density of Low Voltage or Secondary Winding

The low voltage winding generally is made of cast copper having a minimum of 85 per cent conductivity. Water-cooling pipes are cast into or welded to the outside of the casting. When pipes are cast integral with the secondary, the casting usually is increased in thickness to allow for pipe. When copper tubing is welded to the outside of the secondary section, the thickness can be reduced to the diameter of the tubing. The impedance, therefore, is lowered by using thin sections approximately one-half inch thick and more of them than by the use of a thick section. Under ordinary conditions of cooling water temperature, the density of current in the secondary casting can be 3,200 amperes per square inch at a 50 per cent duty cycle rating.

The secondary winding current will tend to crowd at the corners and the mean turn with respect to current flow will be slightly less than when figured in the conventional manner. The calculated resistance, therefore, will give higher copper loss than actual measurement during impedance test.

Figure 1. Core area versus flux density

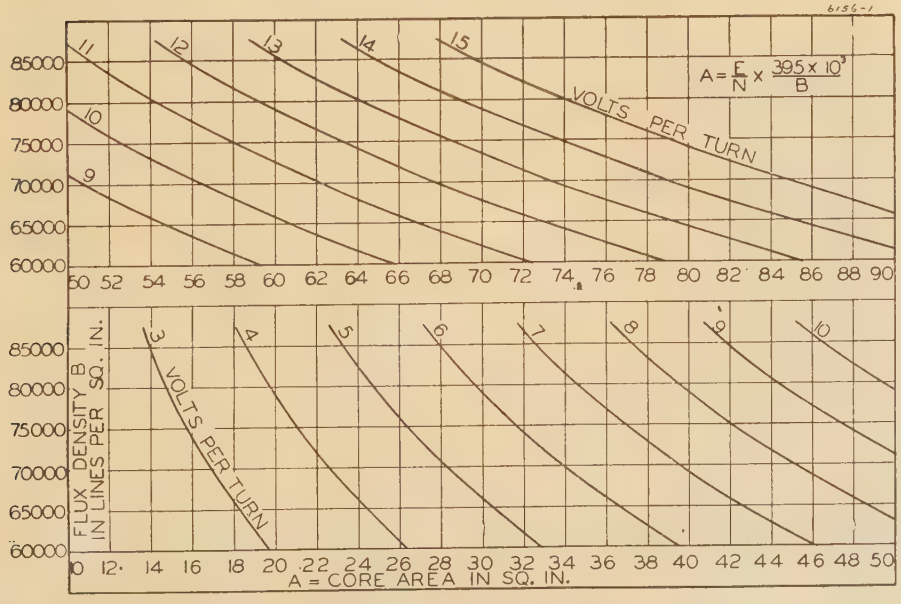

Design of 100-Kva Transformer

This transformer is a 440-volt 60-cycle type with 50 per cent duty cycle. The required open circuit volts (E_s) is 6.67 with 1-turn low voltage winding.

Core Size

B = 77,000 lines per square inch (assumed)

$$A = \frac{E}{N} \times \frac{395{,}000}{B} = \frac{6.67}{1} \times \frac{395{,}000}{77{,}000}$$

$$= 34.2 \text{ square inches} \quad (13)$$

High Voltage or Primary Winding

$$I_p \text{(rated)} = \frac{100{,}000}{440} = 227 \text{ amperes} \quad (14)$$

$$\text{Copper section} = 227 \times \frac{1}{2{,}500}$$

$$= 0.0908 \text{ square inch}$$

$$= 90{,}800 \text{ square mils} \quad (15)$$

$$\text{Number of turns for maximum } E_s = \frac{440}{6.67} = 66 \quad (16)$$

The high voltage winding will be proportioned for a series-parallel arrangement as shown in Figure 11.

The insulation between turns for a class B design can be any one of several materials. In this case the authors would choose 0.020-inch mica.

The width of primary winding copper should be kept as small as practical with one-fourth inch as the minimum. An increase in width will increase the copper loss. A practical width for this design would be 0.625 inch. As the primary winding is split into two sections, the required copper per section is

$$\frac{90{,}800}{2} \text{ square mils} = 45{,}400 \text{ square mils}$$

$$= 0.0454 \text{ square inch} \quad (17)$$

The thickness of the copper per turn is $\frac{0.0454}{0.625} = 0.0728$ inch. Use 0.075 inch $\times$ 0.625 inch for practical reasons.

Therefore, the total height of high voltage winding = $(0.075 + 0.020) \times 33 = 3.13$ inches.

Low Voltage or Secondary Winding

$$I_s \text{ (rated)} = \frac{100{,}000}{6.67} = 15{,}000 \text{ amperes} \quad (18)$$

$$\text{Copper section} = \frac{15{,}000}{3{,}200} = 4.68 \text{ square inches} \quad (19)$$

The secondary winding will be one-half

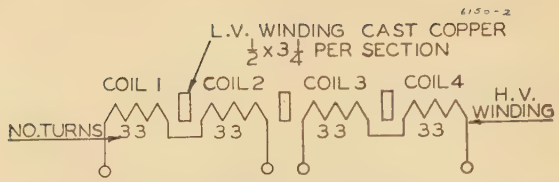

Figure 2. Schematic diagram of transformer winding

0.075×0.625 copper per turn
0.020×0.687 mica between turns

Weight = $[(19^1/_4 \times 10^7/_8) - (7^1/_2 \times 5)] \times 5^7/_8 \times 0.241 =$ 242 pounds

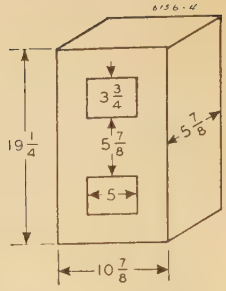

Figure 4. Detail of core

inch wide per section. The area per section = 4.68/3 = 1.56 square inch.

Height of section = 1.56 ÷ 1/2, or 3.12 inches.

Leakage Reactance*

Coil 1 (With Secondary Winding on One Side)[1]

$$L = 3.2 \times T_1^2 \times \frac{MT}{l}\left(S + \frac{d_1+d_2}{3}\right)10^{-8} \quad (20)$$

$$= 3.2 \times (33)^2 \times \frac{37}{3.25}\left(0.125 + \frac{0.625+0.500}{3}\right)10^{-8}$$

$$= 39{,}700 \times 0.500 \times 10^{-8}$$

$$= 19{,}850 \times 10^{-8} \text{ henries}$$

Coil 2 (With Secondary Winding on Each Side)

$$L = 3.2 \times T_1^2 \times \frac{MT}{l}\left(S + \frac{d_1+d_2}{6}\right)10^{-8} \quad (21)$$

$$= 39{,}700 \times 0.3125 \times 10^{-8}$$

$$= 12{,}406 \times 10^{-8} \text{ henries}$$

Total L for coils 1 and 2
$= (19{,}850 + 12{,}406)10^{-8} = 32{,}256 \times 10^{-8}$

Total L for transformer $= \frac{32{,}256 \times 10^{-8}}{2}$

$$= 16{,}128 \times 10^{-4} \text{ henries}$$

$$X_L = 2\pi f L = 377 \times 16{,}128 \times 10^{-8}$$

$$= 0.0608 \text{ ohm} \quad (22)$$

Primary Winding Resistance

Mean turn = 37 inches = l_1
Number of turns per coil = 33 = T_1
Area of copper = $(0.075 \times 0.625)(10)^6 \times 1.27 = 59{,}500$ circular mils

$$R_p = \frac{\rho_1 l_1 T_1}{A \times 12} = \frac{10.37 \times 37 \times 33}{59{,}500 \times 12} = 0.0177 \text{ ohm} \quad (23)$$

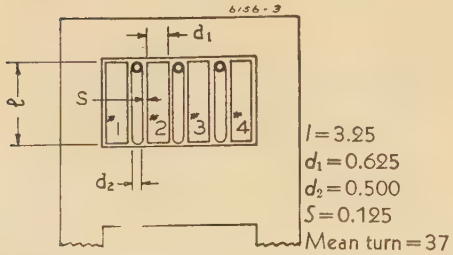

Figure 3. Detail of coil arrangement

Resistance of two coils in series
$= 2 \times 0.0177 = 0.0354$ ohm

Resistance of series-parallel winding
$= \frac{0.0354}{2} = 0.0177$ ohm

$\rho_1 = 10.37$ ohms per circular-mil foot

Secondary Winding Resistance 85 Per Cent Conductivity

Mean turn = 37 inches = l_1
$A = {}^1/_2 \times 3^1/_4 \times 3 = 4.87$ square inches
$= 6{,}190{,}000$ circular mils

$$R_s = \frac{\rho_2 l_1}{A \times 12} = \frac{10.37 \times 37}{0.85 \times 12 \times 6{,}190{,}000}$$

$$= 6.08 \times 10^{-6} \text{ ohms} \quad (24)$$

$\rho_2 = \frac{10.37}{0.85}$ ohms per circular-mil foot

(cast copper)

Equivalent Resistance Referred To Primary Winding

$$R_{eq} = 0.0177 + \left(\frac{66}{1}\right)^2 6.08 \times 10^{-6}$$

$$= 0.0177 + 0.0265 = 0.0442 \text{ ohm}$$

Equivalent a-c resistance (caused by skin effect) = $1^1/_2 \times 0.0442 = 0.0663$ ohm

$$Z_p = \sqrt{R_{eq}^2 + X_L^2} = \sqrt{(0.0663)^2 + (0.0608)^2}$$

$$= 0.09 \text{ ohm} \quad (25)$$

$I_p Z_p$ at rated current of 227A
$= 227 \times 0.09 = 20.43$ volts (26)

Per cent $Z_p = \frac{20.43}{440} \times 100$ per cent
$= 4.64$ per cent (27)

Power factor $= \frac{R_{eq}}{Z_p} = \frac{0.0663}{0.09} = 0.736$ (28)

I^2R loss at rated load $= (227)^2 0.0663$
$= 3{,}420$ watts (29)

Core Loss

Core loss (note Figure 4) at 77,000 lines per square inch equals 0.9 watt per pound from curves furnished by steel manufacturers.

Total core loss $= 242 \times 0.9 = 218$ watts (30)

Total loss $= 3{,}420 + 218 = 3{,}638$ watts (31)

* See Figure 3.

Efficiency at rated load $= \frac{100{,}000}{100{,}000 + 3{,}638}$
$= 0.965$ (32)

Summary

1. Flux densities may be higher than those used in power and distribution transformers.

2. Losses caused by exciting currents have little effect on the over-all efficiency of the welding unit.

3. Losses can be minimized by the use of narrow sections.

4. Variations from optimum conditions can be made without serious effect on over-all efficiency.

5. Pancake type windings are the most efficient for resistance welding transformers.

6. Economics dictate the design of welding transformers having from three to five per cent impedance. The benefits of lower impedance transformers are offset by a greater manufacturing cost.

7. Although no mention has been made of transformers designed for frequencies other than 60 cycles, the same procedure may be followed once the proper flux density is determined.

8. The use of better insulating materials in the future will have a definite effect on present design constants.

Nomenclature

E = volts
N = turns
f = frequency
K = stacking factor
B = flux density in lines per square inch
A = area in square inches
E_s = open circuit volts of low voltage winding
I_s = current in low voltage winding
I_p = current in high voltage winding
L = inductance in henries
T_1 = turns in each high voltage coil
MT = mean turn
l = height of high voltage coil in inches
S = distance between high and low voltage windings
d_1 = width of each high voltage coil in inches
d_2 = width of low voltage coil in inches
X_L = inductive reactance in ohms
ρ_1 = resistivity of copper in ohms per circular mil foot
ρ_2 = resistivity of cast copper in ohms per circular mil foot
R_s = d-c resistance of low voltage winding
R_p = d-c resistance of high voltage winding
R_{eq} = equivalent resistance referred to the primary winding
Z_p = effective impedance referred to the primary winding

Reference

1. Electrical Machine Design (book), Alexander Gray. McGraw-Hill Book Company, New York, N. Y., 1913, page 445.

4,370,000-Kva Short-Circuit Tests on Grand Coulee 230-Kv Bus

W. H. CLAGETT
MEMBER AIEE

W. M. LEEDS
MEMBER AIEE

Synopsis: The unusually large concentration of generating capacity at Coulee Dam makes possible short-circuit power on the 230-kv bus considerably in excess of the rupturing capacity of circuit breakers now available at that voltage. Methods of sectionalizing the bus and segregating the transmission lines to limit the maximum short circuit to less than 3,500,000 kva are described in this paper. A group of fault tests on one of the 230-kv 3-cycle 3,500,000-kva steel tank oil circuit breakers was made with a maximum of six generators connected. Three-phase faults close to the breaker rating and single phase-to-ground short-circuit currents equivalent to 4,370,000-kva 3-phase were cleared with no apparent effort by the breaker. These are believed to be the heaviest short circuits ever interrupted on any power system in the world.

THE GRAND COULEE DAM and power plant is situated on the Columbia River approximately 100 miles west of the city of Spokane, in the heart of the state of Washington. At this point on the river the mean annual runoff is 79,000,000 acre-feet, the mean annual flow is 109,000 second-feet, and the dam provides a mean hydraulic head of 330 feet for operation of the turbines. The power plant is near the center of the vast transmission network of the Northwest Power Pool, which includes 11 major interconnected private and government-owned systems operating in the states of Washington, Oregon, Idaho, Montana, and Utah.

The ultimate power plant installation is to consist of two similar powerhouses, on either side of the river, each housing nine units of 108,000-kw capacity, or a combined total capacity of nearly 2,000,000 kw. The immense size of these waterwheel generators, the largest in service anywhere, is indicated by Figure 1 showing one of the rotors being lowered into place. Associated with the power plant development is an irrigation pumping plant which is situated immediately upstream from the west powerhouse and dam abutment. This pumping development ultimately will consist of 12 65,000-horsepower pumps which will lift the waters of Lake Roosevelt to an irrigation system in the Columbia Basin. Operation of these 12 pumps will be from the first six main unit generators, *L*-1 to *L*-6, through six 5,000-ampere 13.8-kv busses. Because of provisions being made for considerable water storage in the canal system, it will be possible to use these first six generating units for pumping purposes during off-peak load periods, and for commercial load at other times. Figure 2 shows a single-line diagram of the west power plant only, with dotted lines indicating the pump installations.

Such a large concentration of generating capacity introduces unique problems in circuit breaker application and requires special switching arrangements to keep the breaker duty within the rated interrupting capacity. The high speed 3-cycle 230-kv breakers on all outgoing line positions at Coulee Dam have an interrupting rating of 3,500,000 kva, and the 8-cycle generator breakers have an interrupting rating of 2,500,000 kva. The maximum interrupting rating available at the time these breakers were purchased was 2,500,000 kva. The line position breakers subsequently were rebuilt to 3,500,000 kva when interrupters of this increased rating became available.

The power plant installation at the time the fault tests were made in December 1945 consisted of six permanent 108,000-kw units and two smaller 75,000-kw units which had been borrowed temporarily from Shasta Dam, California Central Valley Project, to augment the capacity at Coulee Dam during the war. System calculations of short-circuit currents during a line fault immediately adjacent to the Coulee switchyard indicated that the 3-cycle breaker rating of 3,500,000 kva can be exceeded if more than four units and three lines are connected to the faulted section at any one time. Because of this consideration, it was deemed inadvisable to operate with more than four units on a bus section, and since an adequate synchronizing tie is necessary between the two bus sections for system stability, the interleaved scheme of operation was adopted. Figure 3 shows a simplified diagram of the interleaved line and bus arrangement showing the synchronizing ties provided by parallel line operation to the three load centers: Spokane, Midway, and Columbia. It is not the purpose of this paper to discuss in detail the interleaved scheme and its relation to system stability on the Bonneville Power Administration system, as this was presented previously.[1] However, it should be pointed out that circuit breaker capacity may dictate to a large extent the switching arrangement and method of operation on high capacity systems.

For an example of how limitations in circuit breaker capacity affect switching operations and station capacity, let us suppose that it is desired to overhaul a generator breaker, thus making it necessary to transfer the corresponding unit to

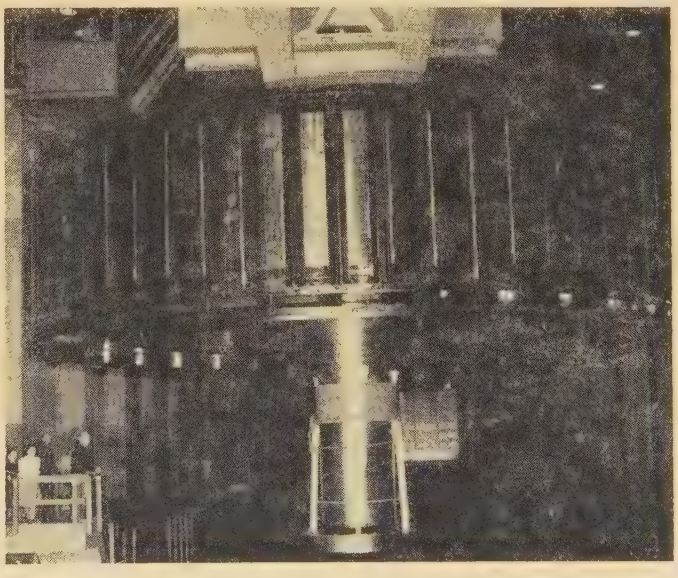

Figure 1. Rotor of 108,000-kva generator being lowered into place at Grand Coulee Dam

Paper 46-177, recommended by the AIEE committee on protective devices for presentation at the AIEE Pacific Coast meeting, Seattle, Wash., August 27–30, 1946. Manuscript submitted June 10, 1946; made available for printing July 8, 1946.

W. H. CLAGETT is assistant chief electrical and mechanical testing and inspection department, United States Bureau of Reclamation, Coulee Dam, Wash. W. M. LEEDS is a development and test section engineer, power circuit breaker engineering department, Westinghouse Electric Corporation, East Pittsburgh, Pa.

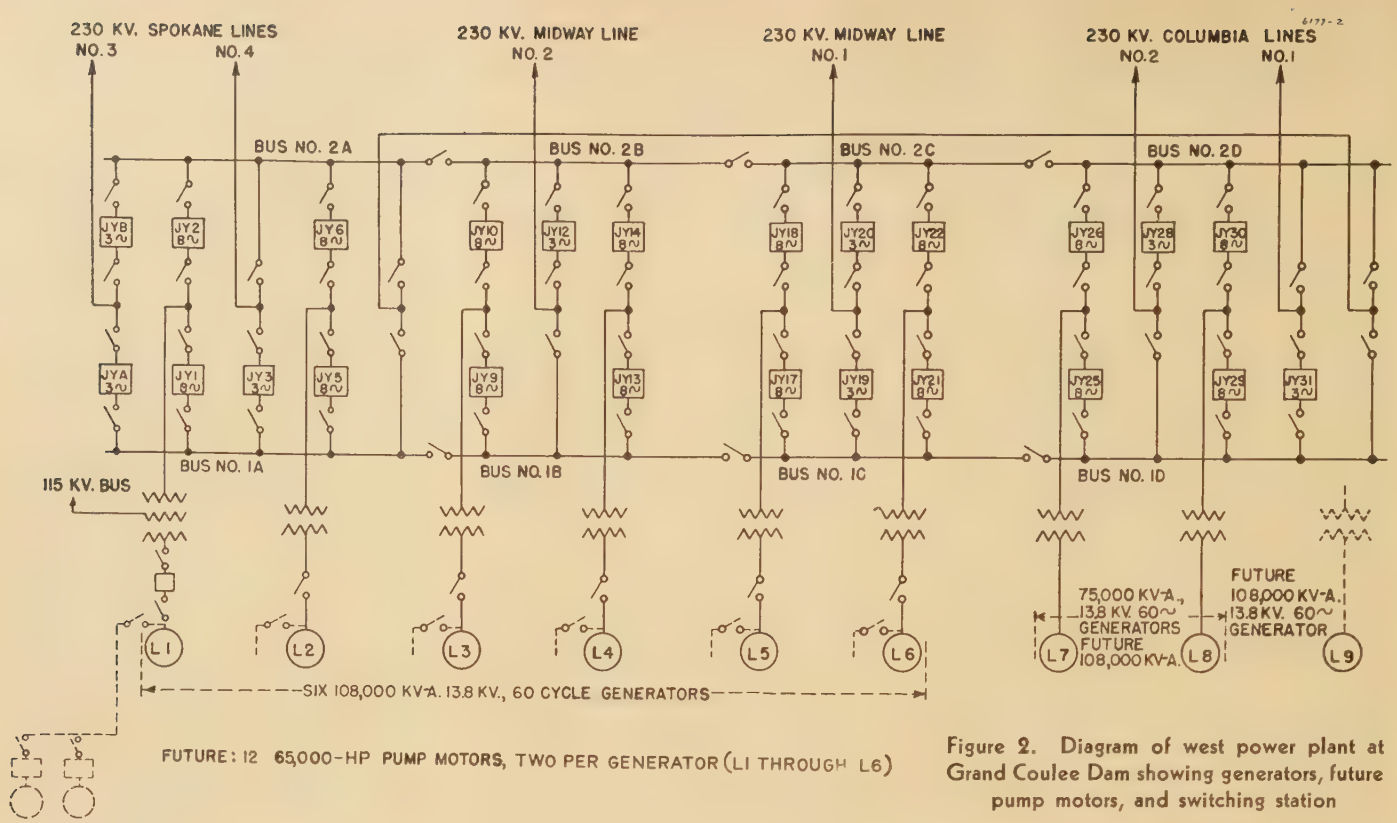

Figure 2. Diagram of west power plant at Grand Coulee Dam showing generators, future pump motors, and switching station

the opposite bus. The first operation would be to unload the unit and open the generator breaker. Before the unit can be placed on the opposite bus, however, a unit on the second bus also must be unloaded and removed from the bus as five units would exceed the interrupting rating of the breakers. This operation requires that 25 per cent of the present plant capacity, or a possible 216,000 kw of capacity must be removed from the system to accomplish the desired switching. Breakers of 5,000,000 kva capacity would make it unnecessary to remove more than one unit at a time.[2]

Fast relaying and circuit interruption during faults play an extremely important role in system stability where there are large concentrations of generating capacity and transmission lines that are heavily loaded. This is accentuated on the system under discussion by the fact that there are lumped loads and lumped generating capacity in the Pacific Northwest, separated by long transmission distances. With over 400,000 kw of generating capacity on one bus at Coulee Dam, a fault on or adjacent to this bus is a major consideration, and will result most surely in a major out-of-step condition on the rest of the system if not cleared promptly. For this reason the fastest circuit breakers available (3-cycle interrupting time) combined with the fastest system of relaying (carrier relaying) is used on the Bonneville System and at Grand Coulee to insure minimum disturbance and maximum stability.

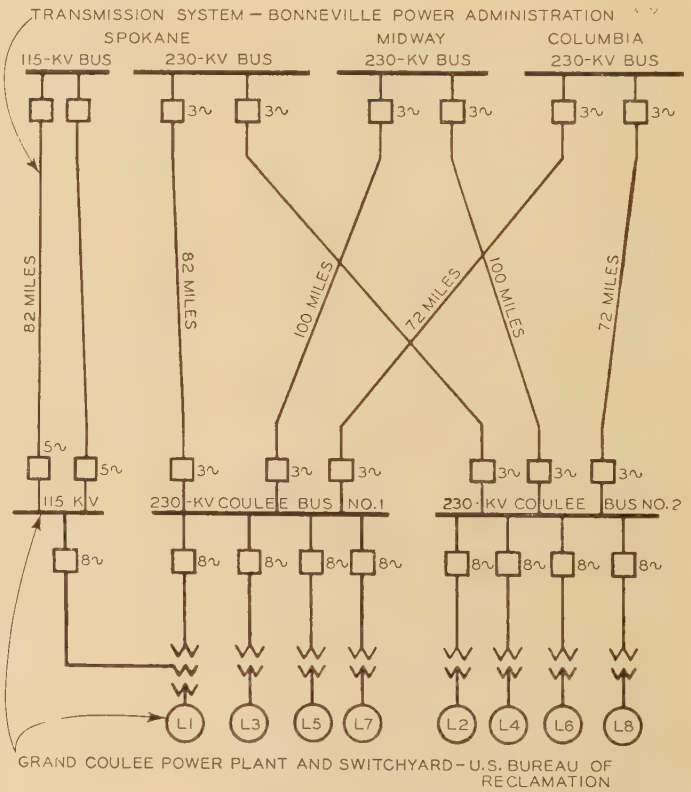

Figure 3. Simplified diagram of interleaved bus arrangement with bus ties through lines to distant stations

The 230-Kv 3-Cycle Oil Circuit Breakers

The principal design features of the 230-kv 3-cycle oil circuit breakers of the type used for the fault tests already have been described.[3] Figure 4 shows a photograph of the test breaker *JYA* which is located at the east end of the 230-kv switchyard and is used for switching one of the lines to Spokane.

The housing on the side of the first tank encloses a compressed air operating

mechanism with tripfree mechanical linkage which is capable of closing the breaker in approximately one-third second using an air pressure of 275 pounds per square inch. The high speed triple latch assembly permits the breaker to part contacts within $1^1/_2$ cycles after energizing the trip coil.

In order to obtain the maximum short-circuit current at the instant of contact parting during this particular series of tests, a special tripping switch was attached to the mechanism frame in such a position that the main lever would close the switch contacts about a cycle before the breaker contacts touched during the closing stroke. This switch can be seen in the close-up view of the mechanism in Figure 5. Thus, when closing against a fault, tripping could be initiated sufficiently in advance of the establishment of the short circuit that the contacts would separate during the first half cycle of fault current.

Each phase of the breaker is built in a steel tank, 108 inches in diameter, with capacitor type bushings having potential taps which were used to obtain an oscillographic record of the transient voltages during the breaker operation. The cross section view of Figure 6 through one of the breaker pole units shows the linkage for operating the main lift rod and crossarm bridging the two interrupting units on the ends of the capacitor bushings.

A sectional view of the multiflow deion grid type of interrupter used in these 3,500,000-kva circuit breakers is shown in Figure 7. The effectiveness of this device is indicated by the fact that only one pressure generating break and one interrupting break per breaker terminal is required for 3-cycle operation at 230 kv. Gas pressure developed in the upper chamber by the short-circuit current sends a flow of oil down two parallel channels and then through pairs of inlets in order to converge on the main arc from opposite directions at four different levels. The flow sweeps axially upward and downward through orifice openings to the vent passages interspersed between the inlets, cooling and deionizing the arc space so that interruption takes place at an early current zero. Arc energy is kept low by avoiding unnecessary lengthening of the arc.

To supplement the self-generated flow during the interruption of line charging current, a spring driven piston is located in the bottom of the contact assembly in such a way as to operate independently of the movement of the lower contact. Oil flow from this piston passes through channels to a single orifice in the top pressure gap and then down the main channels to the interrupting break. During high current interruptions, back pressure holds the piston until after arc extinction. As the pressure falls the piston then completes its stroke, sending a flushing flow of oil through the structure.

A view of two of these multiflow deion grids taken out of the test breaker is illustrated by Figure 8. The shields have been removed to show the contact operating linkage and the vent openings in the side of the grid assembly.

Line Dropping Tests

A series of line dropping tests was made with breaker *JY*-31 opening the charging current of the 183 miles of line from Coulee Dam through Columbia substation to Covington near Seattle. On some of the tests there were single delayed arc reignitions, but the majority of operations were without any restrikes as illustrated by Figure 9, showing complete opening 2.8 cycles after the breaker trip coil was energized.

Of particular interest is the record of voltage E_a directly across the oil circuit breaker terminals. This was measured by means of an amplifier circuit fed from the voltage difference between the potential taps of the two capacitor type bushings on pole *A* of the test breaker. Note that the recovery voltage builds up to double peak value, and then oscillates about an axis displaced by an amount representing the trapped charge on the

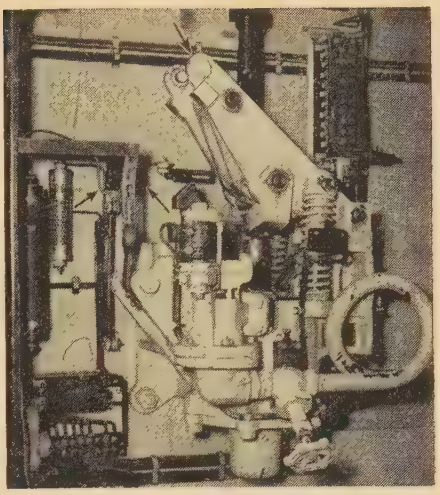

Figure 5. Compressed air operating mechanism for 230-kv test breaker

Arrows point to special pretripping switch

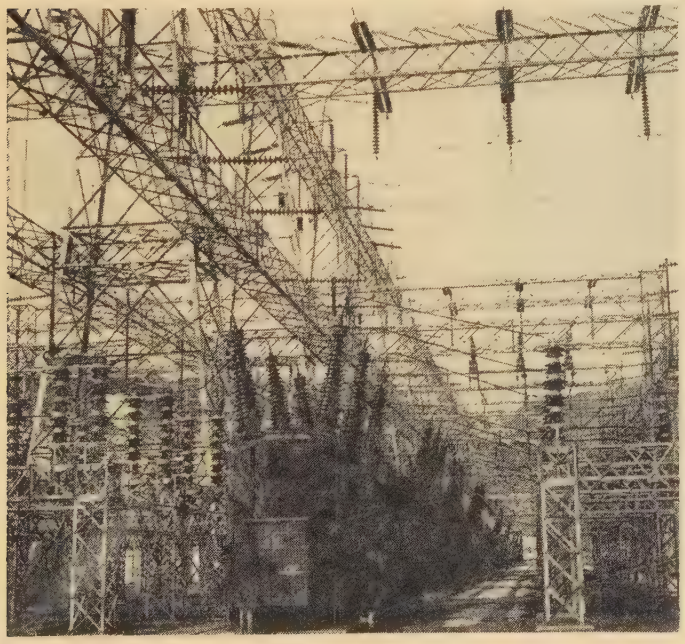

Figure 4 (left). View of Grand Coulee Dam switchyard showing 230-kv oil circuit breakers including test breaker *JYA*

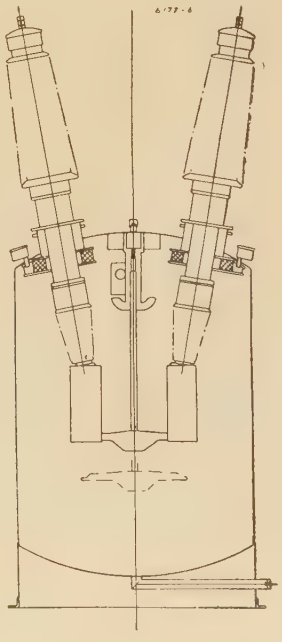

Figure 6 (right). Section through one pole of 230-kv 3-cycle breaker equipped with a pair of interrupting units rated at 3,500,000 kva

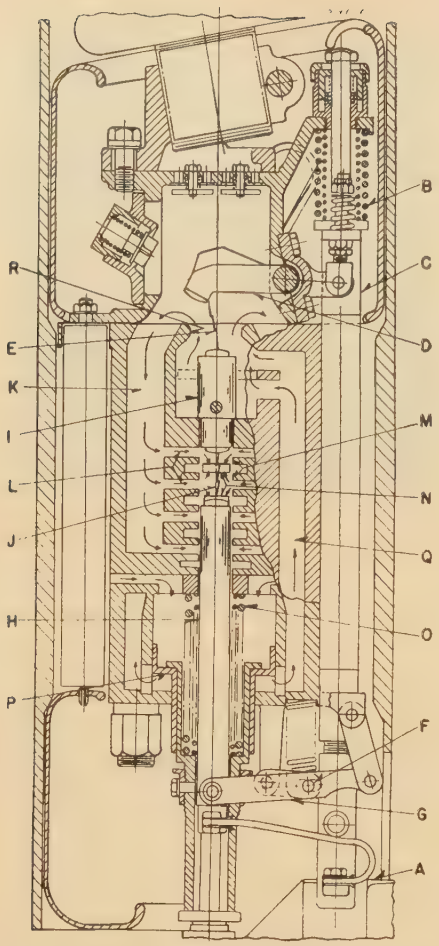

Figure 7. A 230-kv multiflow deion grid interrupting unit showing oil flow path from piston used to interrupt line charging current

Tripping of breaker releases main cross arm *A*, allowing springs *B* to move operating rod *C* down and rotate contact arm *D*, drawing pressure generating arc *E*. Simultaneously, pin *F* swings lever *G* downward, pulling contact *H* away from intermediate contact *I* to draw main arc *J*. Pressure from upper arc *E* drives oil through channels *K* to multiflow inlets *L*, deionizing arc in multiorifice structure *M*, and sending arc products out vents *N*. Springs *O* push piston *P* downward to provide supplementary oil flow for low current arc interruption, flowing oil through channel *Q* to orifice *R* in upper gap and then to main flow channel. Back pressure from high current arcs stops piston until arc is interrupted, when completion of stroke sends flushing oil flow through grid

Table I. Fault Tests—Oil Circuit Breaker *JYA*

December 2, 1945

Generating Units *L*-2, *L*-4, *L*-5, *L*-6, *L*-7, *L*-8*

Duty Cycle	Test Number	Oscillogram Number	Type of Fault	Spokane Number 4 Line	Bus Voltage, Kv	Phase	Instrument Current Transformer	Bushing Current Transformer	Fault Current,‡ RMS Amps	Interrupted Kva on 3-Phase Basis	Interrupting Time, Cycles
CO-15-CO	1	35	3 phase to ground	On	241.5	A	5,000/1		6,908	2,890,000	
						A		300/1	7,000	2,929,000	2.7
						B		300/1	7,425	3,106,000	2.5
						C		300/1	6,240	2,610,000	2.8
	2	36	3 phase to ground	On	241.5	A	5,000/1		5,900	2,470,000	
						A		300/1	6,350	2,658,000	2.4
						B		300/1	5,940	2,485,000	2.7
						C		300/1	6,630	2,770,000	2.6
CO-15-CO	1A	40	Phase A to ground	On	241.5	A	5,000/1		6,360	2,660,000	2.5
	1B	41	Phase A to ground	On	241.5	A	5,000/1		7,840	3,280,000	2.4
CO-15-CO	2A	42	Phase C to ground	Off	241.5	C	5,000/1		10,450	4,370,000	2.7
						C		300/1	†8,866	†3,708,000	
	2B	43	Phase C to ground	Off	241.5	C	5,000/1		10,450	4,370,000	2.7
								300/1	†5,006	†2,094,000	
CO-15-CO	3A	44	Phase B to ground	On	241.5	B	5,000/1		10,015	4,190,000	2.8
								300/1	†7,211	†3,016,000	
	3B	45	Phase B to ground	On	241.5	B	5,000/1		6,535	2,735,000	2.7
								300/1	†6,677	†2,793,000	

* See Figure 10 for bussing arrangement.

† These current values are not reliable because of saturation of the 300/1-ampere bushing current transformers. The 5,000/1-ampere instrument current transformer has a 5,000-ampere primary rating, with a 1-ampere secondary.

‡ These currents are not necessarily the maximum fault currents obtained, but are the currents existing at the instant of mechanical separation of the breaker contacts, upon which the interrupted kva is based.

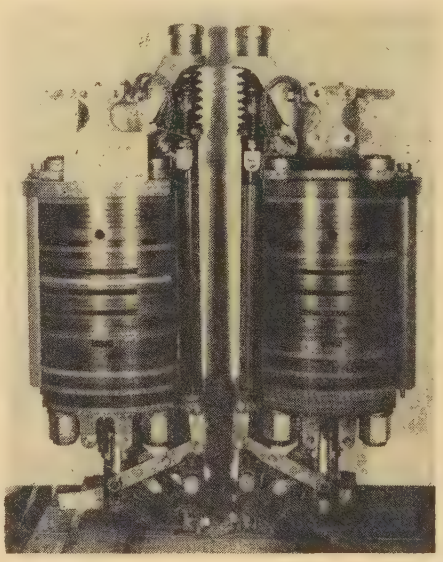

Figure 8. View of pair of 230-kv multiflow deion grid units with shields removed taken after high power fault tests

line which very slowly leaks off. The records of line voltage E_b and E_c, being obtained with conventional potential devices including a step-down transformer, fail to show the sustained charge on the line after being disconnected from the Coulee bus.

Short-Circuit Tests

Single phase tests at 132 kv to ground have been made on a similar breaker in the high power laboratory up to 10,400 amperes, corresponding to a 3-phase fault of 4,300,000 kva. The rate of rise of recovery voltage on this freely oscillating laboratory circuit is approximately 2,500 volts per microsecond, representing a more severe operating condition than is ever likely to be encountered in service.

The 230-kv bus at Coulee Dam, when all transmission lines are disconnected, approximates the laboratory conditions, although it is not likely that maximum generating capacity would be connected to a bus section with only one line carrying load. However, there is more capacitance to ground on the Coulee bus than a laboratory circuit because of the greater number of connected pieces of equipment such as breakers, transformers, bus supports, and coupling capacitors. This is sufficient to reduce the natural frequency of oscillation at the bus, and likewise the voltage recovery rate, to less than 40 per cent of the laboratory circuit.

It should be pointed out that although test breaker *JYA* has been in service for about four years, it was revamped with the present contacts for 3,500,000 kva rupturing capacity about a year and a half before these special tests.

Three-Phase Fault Tests

Following two preliminary tests with one generator and with three generators connected, a standard duty cycle test of two close-open operations separated by a 15-second interval was made under a 3-phase grounded-fault condition with six generators connected. These included four 108,000-kva units and the two 75,000-kva generators as shown in Figure 10. The maximum power interrupted, as indicated by the data of Table I for tests 1 and 2, was 3,100,000 kva, approximately 89 per cent of the breaker rating. The breaker was pretripped as described, permitting the contacts to be separated during the first cycle of short-circuit

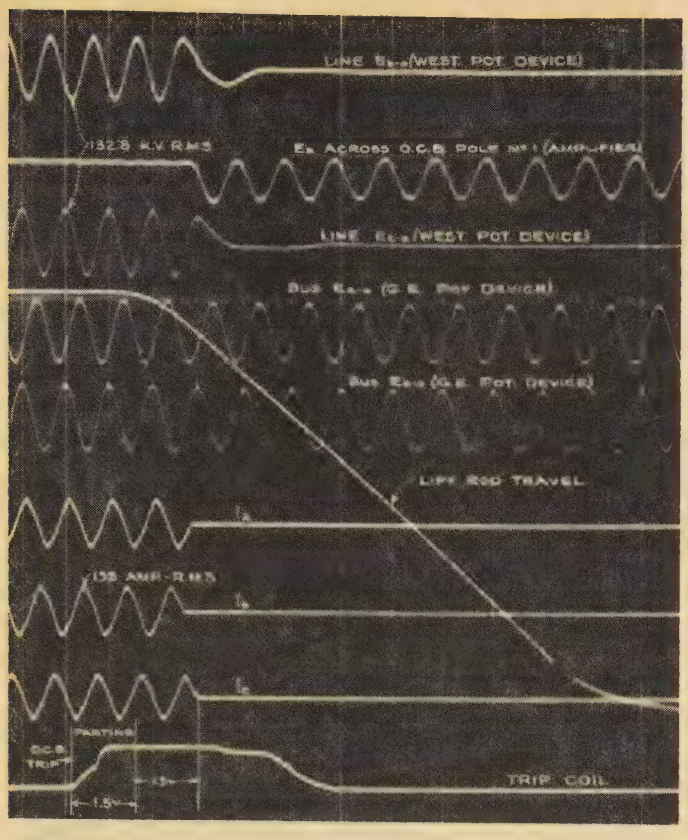

Figure 9. Oscillogram of interruption of charging current to 183 miles of 230-kv line

Record E_a through amplifier shows voltage across pole 1 displaced by charge on line

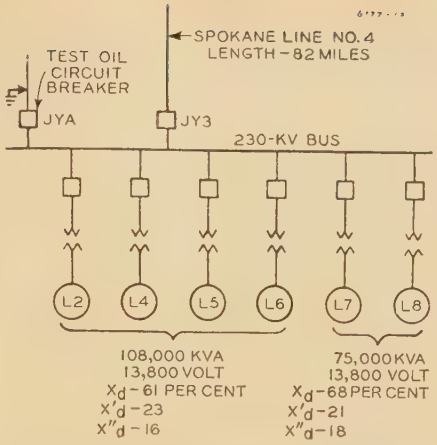

Figure 10. Diagram of connections for short-circuit tests on 230-kv 3-cycle breaker *JYA* using four 108,000-kva generators and two 75,000-kva units in parallel

current (see Figure 11). The performance of the breaker was remarkably quiet, no smoke or jar being evident to the observers.

Before proceeding with the single-phase short circuits at current values up to and above the breaker rating, the oil was removed and an inspection made of the condition of the contacts. So little material was burned away that it was not considered necessary even to smooth up the contact surfaces or make any changes in the contact adjustments. The oil and insulating surfaces were quite clean, so that the breaker was refilled immediately for the remaining tests.

Single-Phase Fault Tests

Each pole of the breaker was given the standard duty-cycle test consisting of two close-open operations separated by a 15-second interval, with a single line-to-ground fault close to the breaker and six generators feeding power to the bus. The pretripping scheme was used again to obtain contact parting as close to the first cycle as possible. Data from the oscillograms of these six interruptions also are given in Table I.

Tests 2*A* and 2*B* form a remarkable pair of almost duplicate interruptions of 10,450 amperes at 241.5 kv bus voltage, corresponding to 4,370,000 kva on a 3-phase basis. The breaker trip coil was energized one cycle before the closing contacts established the fault current which consisted of only three half waves, two large almost completely displaced loops with a small reverse loop between (see Figure 12). The breaker performed quite easily on all of these high power operations, there being very little external evidence of the tremendous short-circuit power cleared by the switch. Since no transmission lines were connected during these two tests, the bus voltage was permitted to oscillate freely, giving a voltage recovery rate estimated from the oscillograms to be close to 1,000 volts per microsecond.

It is interesting to compare the short-circuit current values actually measured with the calculated figures. The maximum asymmetrical 3-phase short-circuit power from four 108,000-kva and two

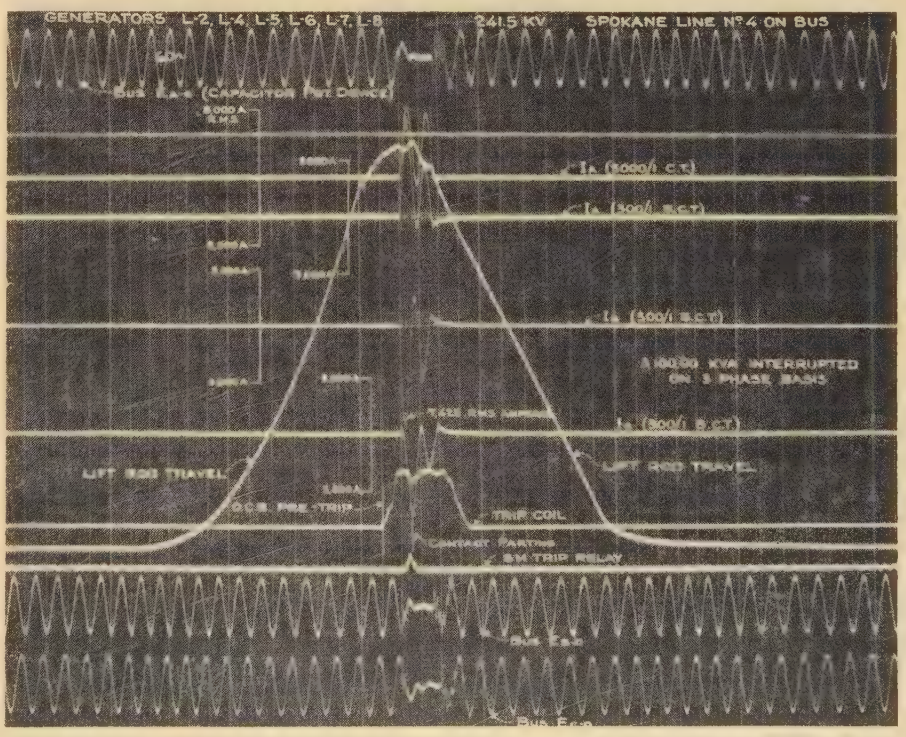

Figure 11. Oscillogram of 3-phase short-circuit test at 241.5 kv interrupting 3,100,000 kva

Breaker pretripped one cycle before fault established by closing contacts

75,000-kva generating units in parallel on the 230-kv bus, with two cycles of decrement, amounts to 2,970,000 kva from Hoard's data.[1] The curve in Figure 13 shows a decrement factor of 1.4 at two cycles, and 1.64 at one half cycle where the breaker contacts actually parted and the current was measured on these tests. Multiplying by the ratio of these two factors raises the short-circuit power to 3,480,000 kva, corresponding to a maximum asymmetrical first-half-cycle current of 8,310 amperes with the power transformers on the 241.5-kv taps used for the tests.

For single-phase faults, with all of the transformer neutrals solidly grounded, the current should be at least 30 per cent higher or 10,800 amperes, which is approximately the maximum current obtained.

On the other four interruptions, the same six generators were connected, but varying degrees of asymmetry in the current wave resulted in short-circuit power between 2,500,000 and 4,000,000 kva on a 3-phase basis. For these tests Spokane number 4 line, 82 miles long, was connected to the high voltage bus, cutting the voltage recovery rate to about a third and damping out overswinging of the initial transient. No consistent effect on the interrupting performance was observed, however, because of this difference in recovery rate, the interrupting times on the six high-power single phase tests being included in the narrow range from 2.4 to 2.8 cycles with an average of 2.65 cycles.

The oil dielectric strength after this heavy duty measured as high as before the tests, and there was only a slight discoloration caused by carbon formation from the arcing. All of the multiflow grid surfaces were quite clean, with no appreciable enlargement of the orifice dimensions as indicated by Figure 14. The silver-tungsten contact tips had lost not more than $1/32$ inch of material over only a part of the surface area, and were still in condition for further service (see Figure 15). The only result of applying these heavy short circuits up to nearly 25 per cent above rating was the cracking off of a small sliver from one of the fiber plate items, and a dislodgement of one intermediate contact sufficient to keep it from falling back into its normal position. With minor design changes to increase the mechanical ruggedness still further there would seem to be no reason why this type of interrupter could not handle satisfactorily short circuits of 5,000,000 kva.

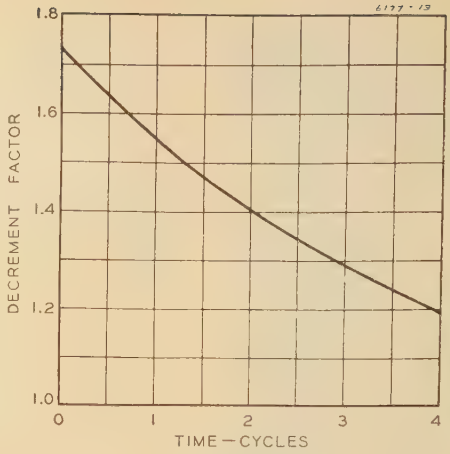

Figure 13. Calculated decrement of maximum asymmetrical fault current for short circuit at Grand Coulee 230-kv bus

Test values checked this curve very closely

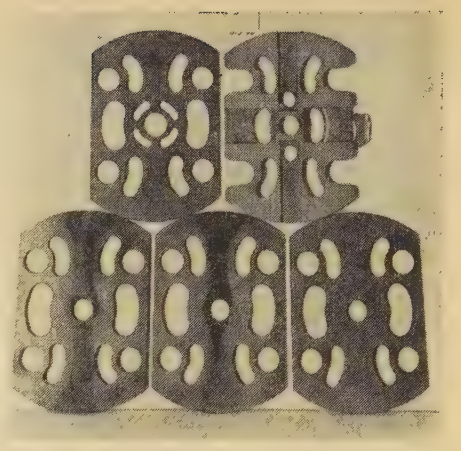

Figure 14. Photograph of fiber grid plates removed from multiflow grid after 4,370,000-kva test showing only slight erosion of orifices

Small chip of fiber was split off upper right plate

Figure 15. Photograph of arcing contacts from pole 2 of 230-kv breaker after 4,370,000-kva test showing only moderate burning of silver-tungsten tips

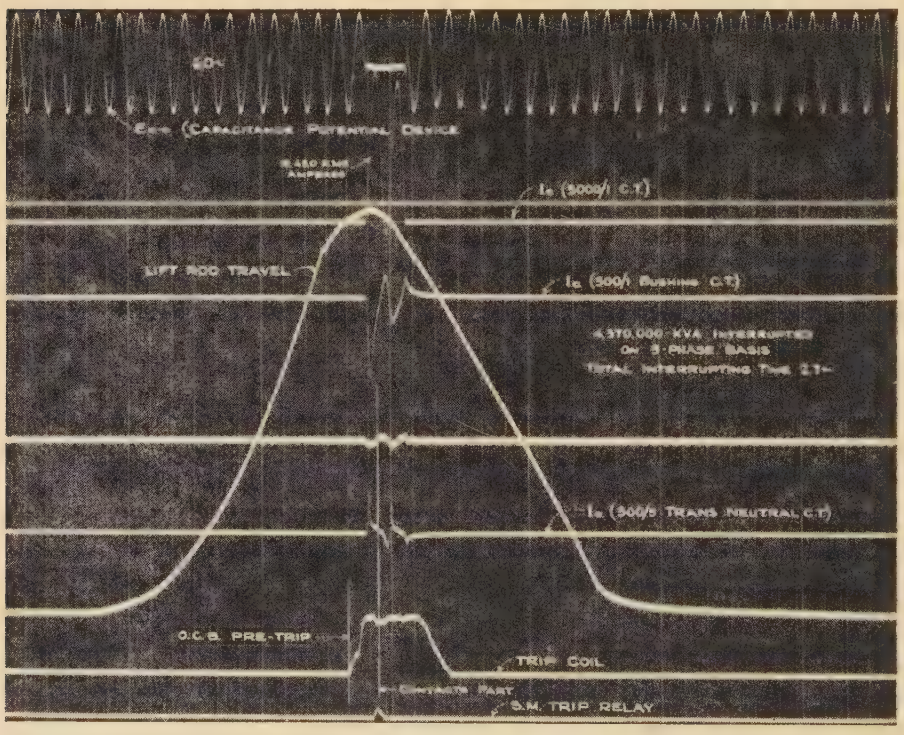

Figure 12. Oscillogram of maximum power single-phase fault interruption, equivalent to 4,370,000 kva at 241.5 kv 3-phase, within 2.7 cycles after energizing breaker trip

No lines connected to bus

Conclusions

These heavy short-circuit tests above 4,000,000 kva on the 230-kv bus at Coulee Dam have served not only as a check on calculations of fault currents, but they also have confirmed high power laboratory test in demonstrating a margin of safety in the rupturing capacity of the 230-kv 3-cycle breakers as rebuilt for a rating of 3,500,000 kva. The relative ease with which the test breaker performed its duty suggests the practica-

Philosophy of Relaying

E. W. KNAPP
MEMBER AIEE

BEN C. HICKS
MEMBER AIEE

PHILOSOPHICALLY the electric power system exists to serve certain human needs and it must serve them better and more economically than they could be served by other methods or it would not be able to continue to exist or to grow. The rendering of service of the required degree of excellence, within economic limitations, is not an inherent attribute of the electric power system but is the result of sustained and carefully co-ordinated effort on the part of all concerned in the rendering of the service, including

1. Precautions taken in the design of equipment to make it trouble free and reliable.

2. Precautions taken in system layout and connections to enable service to be rendered continuously under adverse as well as under favorable conditions.

3. Precautions taken in the operation and maintenance of the system to avoid unnecessary interruptions to service.

When everything economically possible has been done along these lines, however, the system still remains subject to unavoidable defects which result in faults, tending to cause damage to equipment and interruptions to service. Specific measures taken to minimize the detrimental effects of such faults comprise system protection, the fundamental idea of which is to reduce damage to equipment and to improve service to customers. Relay protection cannot prevent faults from occurring on the power system, but it is a means of minimizing the effects of such faults when they do occur. The expenditure which can be justified for protection is a measure of the probable reduction in cost of repairs and of the probable improvement to service which will result from the use of the protection.

Paper 46-172, recommended by the AIEE committee on protective devices for presentation at the AIEE summer convention, Detroit, Mich., June 24–28, 1946. Manuscript submitted January 14, 1946; made available for printing May 23, 1946.

E. W. KNAPP is superintendent, engineering division; BEN C. HICKS is protection engineer, operating department; both of the Shawinigan Water and Power Company, Montreal, Quebec, Canada.

General Principles of Protection

The basic ideas and principles which underlie and determine the policies adhered to in providing protection for the electric power system are relatively few and simple. They may be divided conveniently into two groups.

The immediate object of the electric power system is to make continuously available a supply of energy at approximately constant voltage and frequency. A difficulty encountered in attaining this objective results from the fact that a fault at one point on the system tends not only to destroy or seriously damage the equipment directly affected but also to involve the whole system in serious voltage and frequency disturbances and possibly in widespread interruptions to service; the seriousness of these effects being, in large measure, determined by the length of time that the fault is allowed to remain on the system. This difficulty is met by building the system up of numerous elementary sections joined together at strategic points by suitable automatic circuit-interrupting devices which enable any section to be isolated from the remaining sections without interfering seriously with the essential integrity of the system as a whole. Each of these sections is then provided with appropriate automatic equipment designed to detect faults within the section and to quickly and selectively isolate a defective section from the remainder of the system. In order that no part of the system may remain unprotected the various zones of protection are made to overlap each other at the junction points of the respective sections.

Not only is system protection concerned with the successful isolation of defective sections of the system, it is concerned equally with the determination of fault locations and causes and with the return to service of affected sections in as short a time as possible. For this purpose, therefore, extensive use is made of relay indicators, automatic fault locators, and automatic oscillographs in the analysis of system troubles. Furthermore, experience has shown that the majority of faults on transmission circuits prove to be transient if they are cleared quickly. In such cases automatic reclosing breakers are used as an additional means of improving service.

From the foregoing it may be concluded that, to a very large extent, the protection of a large power system must be a custom built job. The system is analyzed carefully and whenever major modifications or additions take place the necessary fault studies are carried out. As a result of such studies appropriate protective schemes are applied. In general, these schemes are built up in the field, of standardized units of equipment, assembled into the various special combinations necessary to meet the requirements of any situation that may be encountered.

Another fairly obvious conclusion is that, in order to obtain the degree of coordination required for successful functioning, the protection of the whole system must be placed under the control of one centralized authority.

Applications of Principles

When attempting to apply the principles of protection it is necessary to note the physical conditions that can be made use of as the basis of the automatic features of protection. Of primary importance in this respect are the two active quantities of the electric circuit—current and voltage. Intelligently used in appropriate circuits and devices they can be made to represent most of the characteristics that are essential in distinguishing between normal and abnormal conditions on the system. To a more limited extent, various other physical conditions associated with electrical apparatus such as temperature, pressure, gas accumulation, and frequency, may be used also. In ad-

bility of constructing breakers of still higher interrupting rating. The application of such breakers at Coulee Dam would free the system from present operating limitations.

The success of these record breaking tests is the result in no small measure of the excellent co-operation of many members of the engineering and operating personnel of the Bureau of Reclamation, Bonneville Power Administration, and Westinghouse Electric Corporation.

References

1. AN ANALYSIS TO DETERMINE THE OPTIMUM BUSSING ARRANGEMENTS AND TRANSMISSION CAPABILITIES AT GRAND COULEE. **B. V. Hoard, G. W. Bills.** AIEE TRANSACTIONS, volume 63, 1944, pages 1259–64.

2. THE NEXT STEP IN INTERRUPTING CAPACITY—5,000,000 KVA, **A. W. Hill, W. M. Leeds.** AIEE TRANSACTIONS, volume 64, 1945, June section, pages 317–23.

3. HIGH-VOLTAGE OIL CIRCUIT BREAKERS FOR RAPID RECLOSING DUTY, **A. W. Hill, W. M. Leeds.** AIEE TRANSACTIONS, volume 63, 1944, March section, pages 113–18.

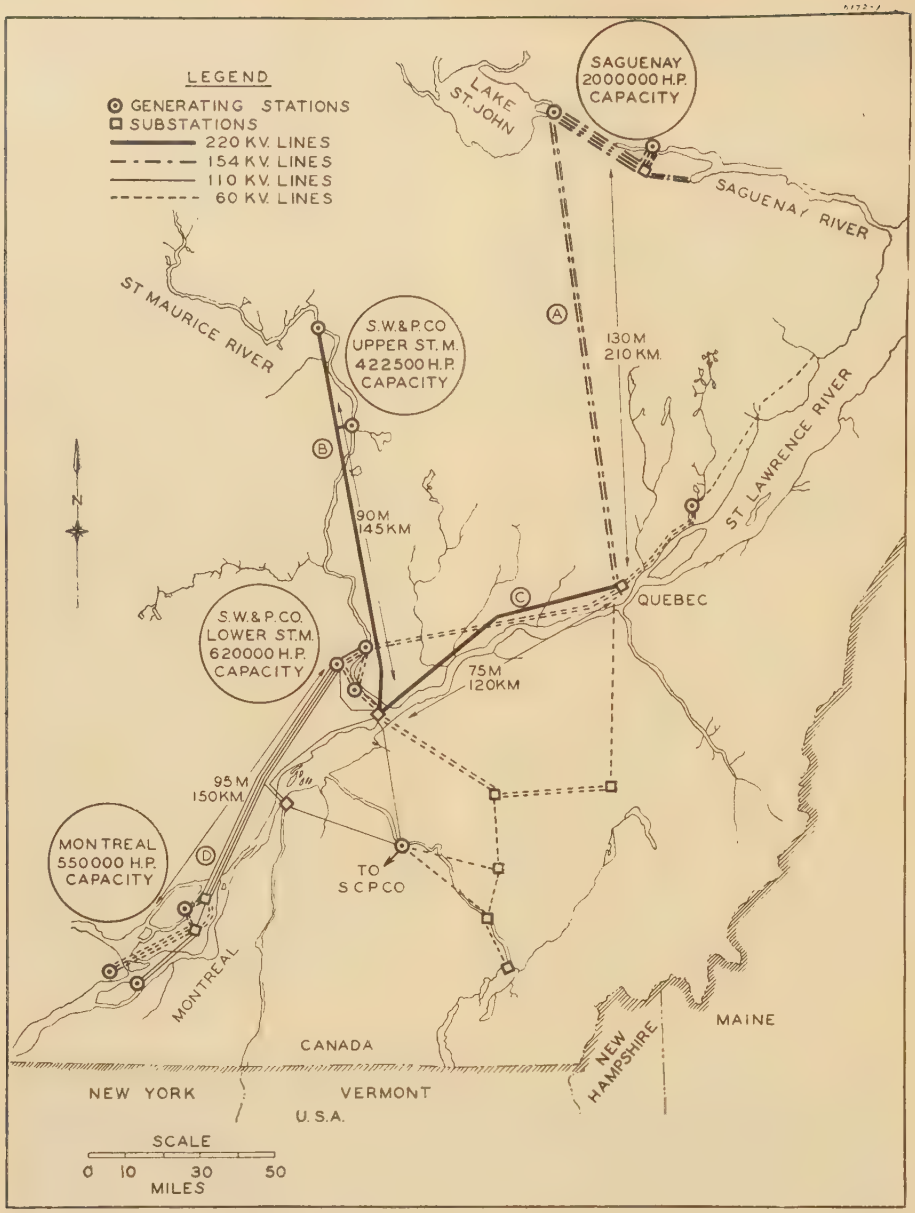

Figure 1. Map showing main transmission lines of interconnected systems, Province of Quebec

dition to these, time is quite generally useful as a co-ordinating factor.

Protection may be considered to be simple or complex depending on whether it makes simultaneous use of one or more of the fundamental quantities available for fault detection. Furthermore, complex protections may possess varying degrees of complexity.

The simplest form of protection is the fuse which utilizes current only and finds extensive applications on a great variety of electric circuits from the lowest voltages up to 138,000 volts. It incorporates in itself both the fault detecting and circuit-interrupting functions. Its great advantages are low cost and simplicity, but its use is limited to circuits carrying a few hundred amperes. An outstanding disadvantage is the more or less prolonged interruption to service required for replacement whenever there is an operation. This may be overcome to some extent by application of the principle of the reclosing fuse. Their somewhat inflexible time–current characteristics may at times be another disadvantage of fuses.

Some of the limitations of fuses may be overcome by utilizing electromagnetic coils energized by the current flowing in the protected circuit. It is then necessary to provide a separate circuit-interrupting device, or circuit breaker, which the coils may actuate. The simplest form of protection associated with a circuit breaker consists of a trip coil on the breaker actuated by the current, or a proportion of the current, which passes through the breaker. Such trip coils may be provided with dash pots to give them an adjustable inverse time–current characteristic. A means is then available for obtaining selective action between circuits on a system so protected. The flexibility of this form of protection may be increased by separating the adjustment and timing features from the trip coil and incorporating them in relays, leaving the trip coil the sole duty of releasing the latch on the circuit breaker.

In these simple forms of current protection there are only two possibilites of obtaining selectivity. One is the possibility that the relative magnitudes of fault currents, at the points between which selectivity is required, will differ by a sufficient amount to inherently provide the required selectivity. The other is the possibility of using time to provide the required selectivity. The former possibility is usually a forlorn hope. The great disadvantage of the latter is the delay involved in clearing faults, which may become several seconds on an extensive system. Another disadvantage is the fact that, in obtaining selectivity by timing, the shortest clearing times are at the ends of branch feeders where fault currents are minimum whereas, from the point of view of limiting damage, the shortest clearing times should be nearest to the power source where fault currents are maximum. Even accepting the kind of selectivity that can be obtained by the use of time and simple current, the method is applicable to radial systems only and not at all to networks.

The field of usefulness of protective features based on current only may be extended very appreciably by associating with it the principle of comparison. This gives rise to such schemes as:

1. Differential current which may be applied to transformers, generators, busses, and short tie lines. Advantages of differential current protections are the fact that the zones protected are clearly and sharply defined providing inherent selectivity; settings may be very sensitive and time instantaneous. Such protections involve problems of current transformer characteristics.

2. Current balance protections such as parallel line and generator split phase. An advantage of the split phase protection is that it can be made very sensitive. Its zone of effectiveness is also clearly defined. Parallel line protections are ineffective for line end faults. On radial lines the zone of ineffectiveness may be a considerable percentage of the line length.

3. Phase sequence networks actuated by current only may be used in conjunction with pilot wires to provide current comparison between the two ends of a transmission line, giving the equivalent of a differential protection.

4. Another method of protecting transmission lines by means of current only is to utilize phase sequence networks in conjunction with carrier current to compare the relative directions of current flow at the two ends of the line.[1]

Also included in the simple protections are

1. Overvoltage, used on generators.
2. Residual voltage, for generator neutrals.
3. Undervoltage.
4. Unbalanced voltage.
5. Gas accumulation, used on transformers.
6. Pressure, used on transformers.
7. Temperature, used on various kinds of equipment.
8. Overfrequency.
9. Underfrequency.

Among the complex protections, impedance is probably the simplest. In principle it uses current and voltage to measure the impedance to a point of fault. When the impedance drops below a critical value operation results. It has the advantage that its distance range, or zone of effectiveness, may be limited at will, within reason. It has the further advantage that it is most sensitive for near-by faults and increasingly insensitive as the end of its zone of effectiveness is approached. Its field of usefulness is in the protection of lines, especially on networks, and for standby or backup protection. It has the disadvantage that its range is altered by power arc voltage and by fault resistance. By associating it with a single time-step effective co-ordination of the protection on a radial system may be obtained without an inordinate increase in time of clearing faults at any point. On network systems it may be associated with directional features of protection to attain an effective co-ordination of the protection of the whole network. In cases where changes of generator capacity connected to the system would affect a simple current protection this limitation is not found with impedance protection.

The disadvantage of having the distance range of an impedance relay affected by fault resistance can be overcome by using a reactance relay. If necessary to attain selectivity a directional impedance or reactance protection may be combined with pilot features by using direct current on metallic conductors or by using carrier on the high voltage line. Under this condition the distance range adjustment need not be critical and simultaneous clearing of both line ends is obtained for all line faults.

On long heavily loaded lines impedance relays may get into trouble by tripping on overload or on power swings. Such a condition may be improved by the use of relays which measure impedance at an angle.

When sections of a large power system tend to pull out of synchronism due to clearing faults, power surges over certain tie lines may cause unnecessary tripping. In such cases when there is the probability that the swings would subside and conditions return to normal, out-of-step blocking may be added to protections that are sensitive to these conditions, to prevent faulty tripping. In cases where it is probable that synchronism cannot be maintained after a swing starts, conditions can sometimes be improved by separating the system at a selected point. For this purpose a system separator can be added to the appropriate protection.

The protective features discussed thus far have been those designed to detect and selectively isolate faults. There remains to be considered, methods of automatically returning circuits to service following the isolation of a fault. In general automatic reclosing is not applicable in the case of equipment failures because defective equipment requires inspection and repair before it can be returned to service. On lines and feeders however the majority of faults are transient and the circuit will remain in service if reclosed immediately. With high speed protection should reclosing take place onto a permanent fault no particular harm would result.

A successful scheme of automatic reclosing can be based on the principle that if a fault is transient the circuit will stay in if it is reclosed immediately after it has cleared. If a fault is permanent the circuit will trip again immediately after it has been reclosed and no further attempts at reclosing should be made. There does not appear to be any practical use in providing more than a single shot recloser. In practice such a recloser is built to lockout should the circuit to which it is applied trip twice within a predetermined time interval, which may be anything from about 2 to 15 or more seconds.

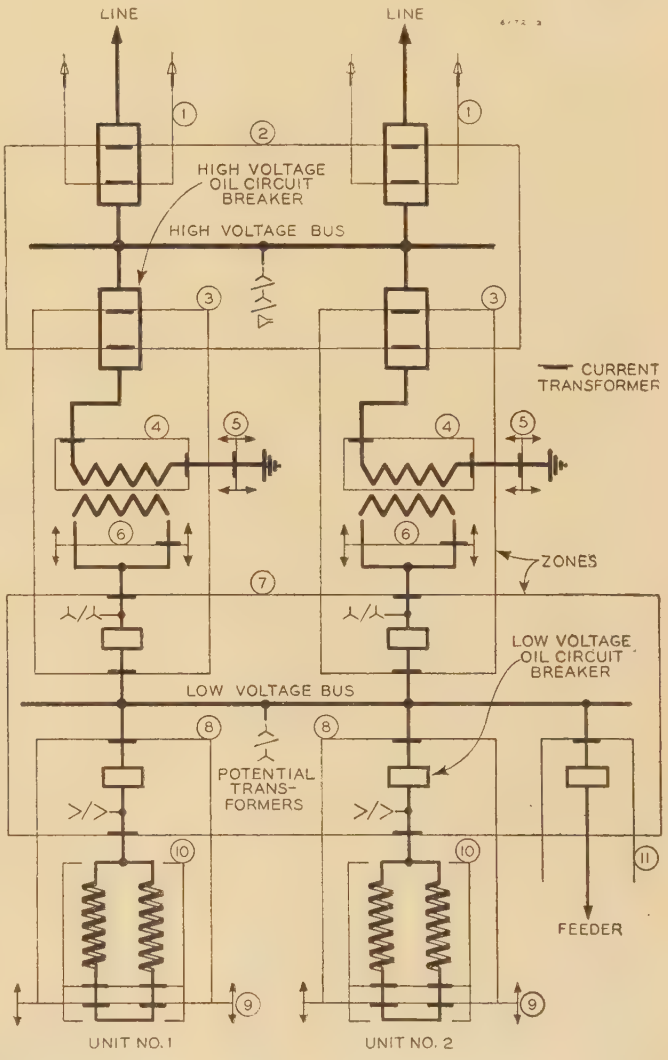

Figure 2. Diagram showing how a power system is covered by overlapping zones of relay protection

Number	Protection
1	Line
2	High voltage bus
3	Transformer differential
4	Transformer high voltage ground differential
5	Transformer high voltage ground stand-by
6	Transformer stand-by
7	Low voltage bus
8	Generator differential
9	Generator stand-by
10	Generator split phase
11	Feeder

Circuit breaker duty ratings have a bearing on automatic reclosing. If circuit breakers have ample capacity the time allowed for resetting the recloser may be short, if not the time must be longer.

Another factor which must be considered in providing automatic reclosing is the condition of synchronism. If a line is a tie between systems it must be decided whether to permit reclosing out-of-phase to take place, depending on the systems to pull into step, or to provide an automatic synchronizer, to operate in conjunction with the automatic recloser.

Practical Aspects of the Art of Protection

Up to this point the problems of protection have been dealt with in broad outlines only. Something now will be said about technical details, remarks along this line being in accord with current practice on the system of the Shawinigan Water and Power Company.

This system is located in the Province of Quebec and serves an area of roughly 30,000 square miles. It comprises a number of hydroelectric generating stations, having a total installed generator capacity of 830,000 kw. There are more than 60 high-voltage lines operating at 44 kv and above, totalling approximately 2,000 miles; in addition to an extensive network of low-voltage distribution lines operating at 33 kv and below which are operated by the distribution department. Much of the power is utilized in heavy industry such as paper mills and mining and electrochemical plants, in addition to that supplied to distribution centers. Interconnections (see Figure 1) are provided with the Saguenay, Hydro-Quebec, and other power companies, comprising a total of approximately 2,500,000 kw of generator capacity for the combined 60-cycle interconnected system.[2]

From the standpoint of protection this extensive system is composed of numerous elements joined together by means of automatic circuit breakers and, to a minor extent, by means of fuses. The various elements of the system are, in the aggregate, provided with a multiplicity of protective schemes which require the use of approximately 10,000 relays of 300 types. As far as possible each element of the system is provided with a protection, the zone of effectiveness of which overlaps the protected zones of adjacent elements. For convenience, relay protection zone diagrams are provided for the various sections of the system. Figure 2 is such a diagram for a small section of the system. This diagram depicts all the main elements of the system, namely, generators, transformers, busses, lines, and feeders; and may be used conveniently as the basis of a discussion of some practical details of protection design.

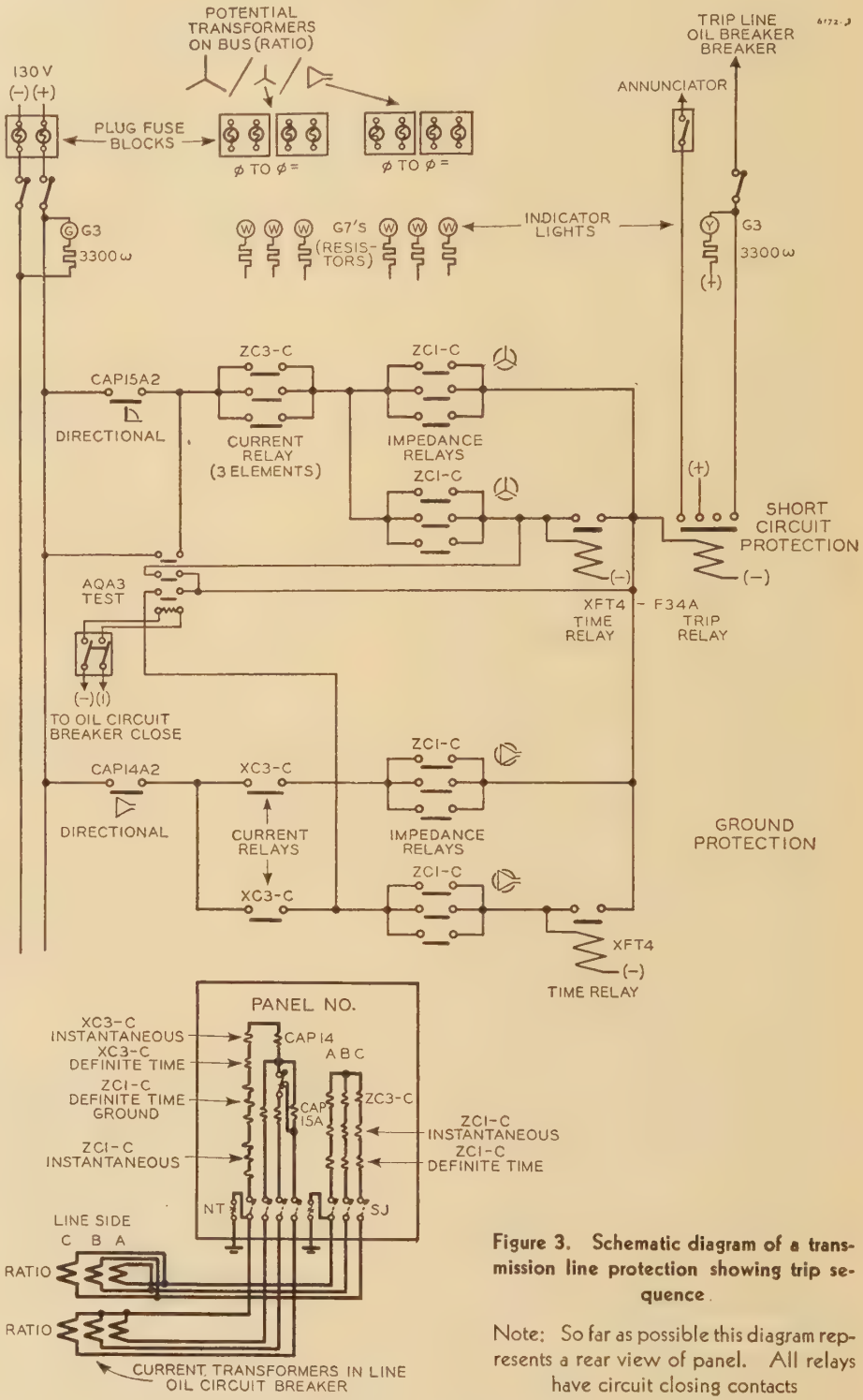

Figure 3. Schematic diagram of a transmission line protection showing trip sequence.

Note: So far as possible this diagram represents a rear view of panel. All relays have circuit closing contacts

The hypothetical section of system shown in Figure 2 is more liberally provided with circuit breakers than is often the case in practice. In some of the older generating stations a main low voltage bus has been provided, but in stations constructed during the past 20 years the tendency is to operate a unit system, each generator and its associated power transformer forming the unit. In some stations transformer banks are not provided with high voltage circuit breakers. High voltage lines, also, sometimes are not provided with high voltage circuit breakers. In all these cases the best expedients available are adopted to make the protection as effective as circum-

stances permit. One of these expedients is the high voltage fuse for transformer protection.

In general high voltage fuses are used on power distribution transformers and on potential transformers. It was formerly the practice to install glass-enclosed lead fuses on small and medium capacity transformers. In case of faults above the rupturing capacity of these fuses, the fault would be transferred to the high voltage line, causing it to open automatically by the action of its protection. Recent practice is to provide fuses of suitable timing characteristics and ample rupturing capacity for the respective location. Both dry and liquid types of fuses are used but preference is now given to the dry types because of their greater convenience and economy in use. Timing characteristics include: high speed fuses for potential transformers and for distribution transformers where selectivity is not required or where selectivity requires fast clearing; medium speed fuses where required for selectivity with other fuses or very fast circuit breakers; and slow acting fuses where selectivity is required with slow operating circuit breakers and relay protection. Fuses should only be used where it is not economically possible to justify the installation of an adequate relay protection.

Where high voltage fuses do not provide an adequate protection and where it is not possible to justify the installation of an automatic circuit breaker automatic grounding switches are used. The operation of the relay protection initiates the closing of the ground switch and this in turn permits the respective main line to be cleared by the action of its protection. Single-pole, 2-pole, and 3-pole switches are in use, either spring operated or motor operated. Experience has indicated that the motor mechanism is more reliable than the spring and that a 2-pole switch is usually adequate.

Protective relays are energized in general by current and potential transformers. Recent practice has been to utilize, as far as possible, bus potential transformers for line relay protection up to and including 110 kv. On systems operating at voltages above 110 kv either capacitor-type potential devices or compensated low voltage potential transformers are used for line relaying. Potential transformers are commonly provided with double secondaries to facilitate obtaining a delta point voltage for ground protection when required. When such a voltage is required and the potential transformers have only one secondary a set of one-to-one ratio auxiliary potential transformers may furnish the required voltage. Occasions also may arise where auxiliary potential transformers furnish a convenient means of correcting phase angle or ratio in the potential supply.

Current transformers quite commonly define the limits of protective zones. This is particularly true in the case of differential protections, but an exception may be noted where a feeder carrying a small load is permitted as a leak in the differential zone. Various justifications may be found for this practice, such as lack of suitable circuit breakers. In the case of directional distance line protections the directional relays permit the current transformers to mark one limit of the zone of effectiveness of the protection, the other limit being determined by the setting applied to the distance relays. On pilot protections current transformers mark both limits of the protected zone.

The most extensively used current transformers are through types installed on the bushings of circuit breakers and transformer banks, or on cables and bus bars when voltages do not exceed 15 kv. Wound primary current transformers are used to some extent on low voltage circuits and on circuit breakers which do not lend themselves to the use of bushing type transformers. Some circuit breaker designs do not permit the use of built-in current transformers and separate oil-filled current transformers are used. In all cases an attempt is made to keep the resistance of the secondary windings of current transformers low, to keep lead burdens low and to use the maximum cross section of iron consistent with space limitations.

In protection design attention is first given to the system diagram, to determine what may be necessary or possible in the way of zones of protection. Then fault studies assist in the co-ordination of the various features of the complete protective scheme. Following this a trip sequence diagram is prepared for each protection, to serve as the basis for the preparation of the main wiring diagrams.

Generators

Generators of 10,000 kva capacity or above usually are provided with several features of protection, including

1. Instantaneous split phase.
2. Instantaneous current differential.
3. Definite time impedance standby.
4. Definite time or inverse time overvoltage.
5. Definite time or instantaneous ground alarm.

The ground alarm is usually provided through the medium of a single potential transformer in the generator neutral or through the installation of a set of star/corner delta potential transformers connected to the generator terminal leads. Thirty per cent of all generators are grounded through a single potential transformer.

In future installations serious consideration will be given to the installation of a small single phase distribution transformer between generator neutral and ground. Differential and split phase protections are set as sensitively as possible to reduce burning of iron laminations and thus avoid restacking. Settings of the order of two per cent of generator rating are attained. By-pass reactors on the relay coils assist in eliminating faulty relay actions due to d-c transients on through faults. Overvoltage protections are set to act instantaneously at about 140 per cent of normal voltage to avoid overstressing insulation following a sudden drop of load. The standby protection acts as a stand-by to the system protection at large and to the generator in case of the differential and split phase features are out of service.

Transformers

Power transformers are usually provided with one or more of the following forms of protection:

1. Inverse-time current differential or 2-step current differential. In some cases impedance relays are used instead of current relays for this feature.
2. Instantaneous residual current ground protection, connected differentially if it appears feasible or advantageous to do so.
3. Gas detector relay to indicate gas accumulation or pressure. In some cases the gas accumulation element is arranged to provide a visual and audible indication only, without actually tripping the respective bank.
4. Impedance stand-by, combined with generator stand-by on the unit system.

Large power transformers are usually provided with some form of differential protection, which either overlaps the generator protection, in the case of a unit system, or the low voltage and high voltage bus protections where busses are used. The aim is to make these protections as sensitive as possible to avoid damage to core iron and to reduce the hazard of oil fires.

In the 2-step form the sensitive feature is set at 30 per cent of bank rating

and 2.5 seconds definite time; the instantaneous feature is set at 225 per cent of bank rating.

Gas detector relays are used more particularly on large 3-phase power transformers and step regulators. Many 3-phase power transformers are equipped for tap changing under load and the gas detector relay provides a measure of protection for this device. Gas detector relays also are used on single phase transformers where they would be more convenient to apply than an adequate excess current or differential protection. Experience with these relays has been reasonably satisfactory and the gas detector element has operated for conditions such as low oil, air in the oil, stoppage of breathers, and overheated connections. Some difficulties have, however, been encountered because of inexperience of operating personnel, oil hammer when attempting to determine the presence of gas, and moisture collecting on the terminal studs of the relay.

Busses

Busses usually are equipped with some form of duplicate differential protection. This usually requires two current transformers per phase, unless a special arrangement is devised.

In some cases a scheme of double differential bus protection has been provided using a single set of current transformers with both impedance and current relays connected so that it requires both features to operate in order to trip the respective bus. Where fault currents exceed the interrupting capacity of low voltage circuit breakers an excess current feature may be added to the respective feeders to insure automatic clearance of the whole bus, rather than rely on the low interrupting capacity of individual circuit breakers. During recent extensions to the power system, it was estimated that fault current in the vicinity of one 110-kv station would exceed the interrupting capacity of existing circuit breakers. There were two 110-kv busses at this station and an arrangement was made to install a high speed circuit breaker between these two busses, equipped with a relay scheme to automatically open the bus tie circuit breaker for nearby faults. It is designed in this manner so that the busses will be separated before a local breaker attempts to clear a nearby fault, thereby reducing the fault current to a value which can be handled by the circuit breaker on the faulted circuit. This feature has operated on several occasions to date with satisfactory results.

Lines

Line protections vary greatly depending among other things on voltage, load, type of system, and type of line. In general the Shawinigan Water and Power Company favors the 2-step impedance and directional scheme for both short circuit and ground protections. The trip sequence diagram of such a protection is shown in Figure 3. This form of protection is particularly applicable to high voltage lines having low ground resistance and operated in either a parallel line or network system.

On lines having high ground resistance, such as wood pole lines, stand-by residual current relays are added to other features. In some cases use has been made of parallel ground relays for wood pole 60-kv lines operating in parallel at both ends. Some difficulty has been experienced in providing a fully satisfactory ground protection for such wood pole lines not equipped with overhead ground wires or other means of reducing ground fault resistance. On short tie lines connected into the main transmission network recent practice has been to provide buried counterpoise wires in order to improve the effectiveness of the impedance ground protections.

All power circuits of 110 kv and above are operated solidly grounded star. All 60-kv circuits are operated "delta isolated neutral" but with small grounding transformers located at strategic points. In some cases transformers of 1,000–3,000 kva capacity used for auxiliary supply are utilized also as grounding transformers. A circuit breaker frequently is installed in the neutral of the grounding transformer and arranged to trip automatically when grounds persist for a definite time of two to three seconds. Most of the high voltage steel-tower lines are provided with either overhead ground wires, buried counterpoise wires, or both. This tends to reduce lightning outages and to keep the ground resistance to a low value, permitting the successful use of impedance ground delays.

The instantaneous step of an impedance protection is ordinarily set to cover 95 per cent to 100 per cent of line length. The second step is set to reach into the next line section with a time delay of 0.5–0.8 second. With high speed circuit breakers and protections it is probable that selectivity can be retained with these time delays reduced to about 0.4 to 0.5 second. On 3-ended lines 3-step impedance protections have been used successfully.

Instantaneous protection over the whole length may be obtained by the use of pilot protection. Three forms are in use

1. A-c 3-wire system using low resistance conductor.
2. D-c 2-wire system using high resistance conductor.
3. Carrier current on the high voltage lines.

Outstanding disadvantages of the a-c pilot wire protection are its high cost limiting its use to very short tie lines and the fact that it does not provide inherently any stand-by or backup protection. The cost of carrier current protection limits its use to high voltage lines and to conditions where adequate protection cannot be obtained otherwise. The d-c pilot protection is used on lines up to 25 miles in length. It usually operates from dry cells of 90–135 volts rating. Conductors vary, depending on local conditions, and include private telephone circuits, leased Bell Telephone circuits, and small-conductor buried cable. All pilot cables are well insulated from ground. The d-c pilot scheme has the advantage that it can be added to a more or less standard line protection and will provide stand-by protection at all times, even when the pilot feature may be out of service.

Automatic Reclosing

There are several automatic reclosing installations in service on transmission systems operating at voltages up to 187 kv. New installations are being completed as rapidly as conveniently possible. Recent practice has been to adopt one immediate automatic reclosure with an automatic reset feature for transient faults and lock-out for permanent faults. Time delay of reclosure is normally kept to a minimum, usually not more than 2.5 seconds. To date, there are no installations of automatic reclosing on lines directly supplying synchronous motor loads. However, installations are now under consideration on a number of 60 kv lines supplying paper mill and mining loads, which include synchronous motor installations. An installation is also being completed on a system consisting of a small generator connected through a tie line to the main system, and on one of the radial lines connected to this there is a synchronous motor. We are looking forward with considerable interest to this development, with a view to extending automatic reclosing to network systems.

Conclusion

It will be realized that the application of protection to the power system does not

Control and Protection of Aircraft D-C Power Systems

B. O. AUSTIN
MEMBER AIEE

D-C POWER SYSTEMS on transport aircraft before World War II were small in capacity as compared to the present requirements. Present wide speed-range generators are 12 to 15 times the ratings used on old DC-3's, and system capacity on new transports may be 30 times greater and capable of sustaining fault currents greater than 5,000 amperes at 30 volts. It is also necessary to consider the increase in the voltage from the smaller system to the larger system. The 12-volt system does not have sufficient potential to maintain an arc or ionize gases so that an arc could be maintained for any length of time, whereas, the 24-volt system does have sufficient potential to maintain an arc or ionize gases. This is a fundamental characteristic of the electric circuit and is quite often forgotten about when voltages greater than the critical arcing values are used. Arcing voltages are in the neighborhood of 18 to 20 volts, depending upon the materials and atmospheric pressures at the electrodes involved. The number of electrically operated devices also has been increased, and many of the electrical requirements which are vital to flight operation are therefore dependent on the continuity of electric power. Study of various means of controlling and protecting electric power systems against failures in the light of these facts has led to some interesting simple developments which are described in this paper.

Paper 46-180, recommended by the AIEE committee on air transportation for presentation at the AIEE Pacific Coast meeting, Seattle, Wash., August 27–30, 1946. Manuscript submitted June 17, 1946; made available for printing July 10, 1946.

B. O. Austin is section engineer in the aviation control division, Westinghouse Electric Corporation, Lima, Ohio.

The author acknowledges the assistance of D. W. Exner, O. C. Walley, C. A. Stump, R. D. Jessee, and R. J. Lusk, all of Westinghouse Electric Corporation, in the development of ideas presented in this paper.

Electric Power and Protective Systems

An aircraft d-c power system like any power system consists of generators, regulators, contactors, protective devices, functional relays, and cable. The simplest system consists of generators, regulators, and reverse current cutouts. This system on multiengine planes using 28 volts definitely has indicated that improvements are desirable from the standpoint of over-all performance, reliability, safety, and full automatic features, both during normal service and under conditions where faults cause serious consequences to the electric power system and perhaps to the airplane itself.

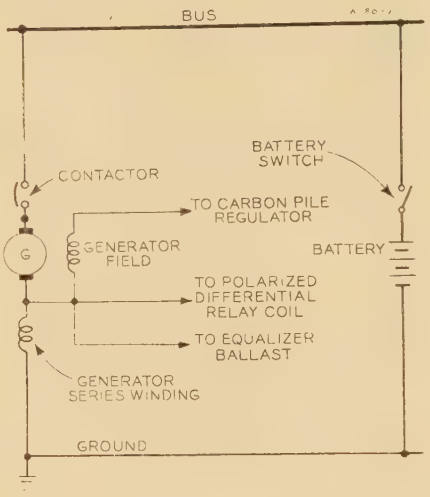

Figure 1. Diagram showing contactor at generator and no fault protection other than reversed currents and polarities

Only two protective features were incorporated in older, low capacity systems. Both were located in the cutout and controlled by the operation of a polarized relay. Polarization of the relay prevented the main contactor from connecting the generator to the bus or battery if its polarity built up incorrectly, and a series coil in the same relay caused the relay to open the main contactor in the event of excessive reverse current, preventing battery discharge.

This system and its two protective features worked reasonably well on low capacity and low voltages. On much higher capacities and higher voltages the results are not as favorable. Generator, contactor and cable faults, and overvoltage resulting from faults have caused complete loss of the electric power supply system, and have damaged batteries and other devices sensitive to power system faults as well as involving fire risks.

Several types of faults are possible and all of them have occurred at one time or another. Power systems having simple protective apparatus against these faults have been developed and are coming into use. In addition to protection against battery drain and reversed generator polarity, protection now can be provided against overvoltage from faults or other causes, grounded generator leads, grounded generators, overheated generators, and low voltage resulting from improper equalizer operation caused by wide generator speed differentials and frozen contactors. Trip-free reset may be provided for fault indications. Although these fault devices may operate infrequently, in case of trouble they are of vital importance.

Details of Protective System

Overvoltage

Overvoltage from one or more generators is caused by excessive current in the shunt field windings for the speed and load conditions under which the generator is operating. In the past, the ratio of generator capacity to the battery capacity was small in comparison to the ratio of the larger generator capacity to the battery

follow rigid rules in all respects. The general aim is to meet the requirements of the particular situations that arise, most effectively. Frequently, perhaps usually, a given end may be attained with equal effectiveness despite considerable variations in the details of accomplishment, so that personal preferences may play some part in the final solution. On the other hand, economic considerations may dictate radically different solutions to apparently similar technical problems at different places. The attempt has been made in this paper to emphasize the rather general aspects of protection; no attempt has been made to analyze technical details exhaustively. It is hoped that we have succeeded in preventing the trees from causing us to lose sight of the forest.

References

1. Phase-Comparison Carrier-Current Relaying, **A. J. McConnell, T. A. Cramer, H. T. Seeley.** AIEE Transactions, volume 64, 1945, December section, pages 825–33.

2. Power System Interconnection in Quebec, **W. R. Way.** AIEE Transactions, volume 61, 1942, pages 841–7.

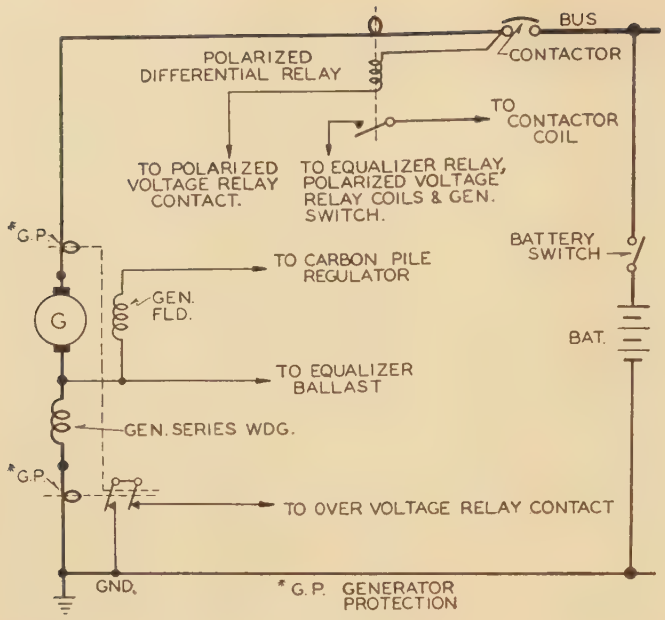

Figure 2. Diagram showing generator and generator lead fault protection

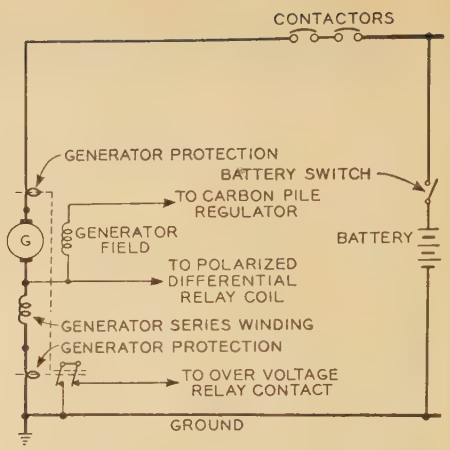

Figure 3. Diagram showing double contactors, generator, and generator lead fault protection

capacity. As a result, the battery of the smaller system could absorb excessive charging current for a much longer time without difficulty and could prevent much increase in voltage. The fault causing the trouble may be sought out and corrected at the next landing. High capacity systems do not have this advantage, and therefore overvoltage protection in larger planes and power systems is certainly desirable and is probably necessary.

Several types of faults are responsible for overvoltage conditions. Wear of carbon pile regulators has been pointed out as an offender. This condition can happen with the older models of this regulator. Design improvements reduced or eliminated this type of fault in modern regulators. However, broken leads, short-circuited terminals, short-circuited leads, or any external fault which will increase the generator field current beyond the control of the regulator will bring about overvoltage.

Relays designed to detect overvoltage operate effectively to remove from the system any generator which is producing overvoltage on the system. Operation of the relay also disconnects the generator field acting through the control devices provided for the purpose. The relay is provided with inverse timing characteristics to prevent transient overvoltage from causing nuisance operation. At 30 to 32 volts its tripping time is one to three seconds, at 60 volts its tripping time is approximately 0.025 of a second. In other words, the higher the overvoltage, the faster the action of the relay. Practically instantaneous operation at extremely high overvoltages is important to avoid damage to electronic equipment such as radio, radar, and similar devices.

After spending considerable time on the investigation of time element relays for overvoltage sensing, a relay with the following description was found which solves the problem in a very reliable manner. It consists of a magnetic piston enclosed within a hermetically sealed nonmagnetic cylinder. The relay coil is wound near the end of the cylinder close to the armature. The piston is hollow, is enclosed at one end, and is normally located toward the end of the cylinder away from the armature. In order for the piston to move, air must flow around the snuggly fitted piston, producing a time lag. When voltage is applied, the piston moves toward the armature, decreasing the air gap. When the piston moves close enough, the armature closes, operating the relay contacts. The higher the applied voltage, the faster the relay operates. A spring returns the piston to its original position when the relay is de-energized.

Multiengine airplanes with one or more generators producing overvoltage will cause the bus voltage to rise, resulting in reverse current to the generators regulated for normal voltage. This condition will cause the main contactors of these generators to trip by the action of the polarized reverse current relay. The voltage of the offending generator will rise still more, resulting in the immediate isolation of the generator from the system. The generators taken off of the bus or battery by the reverse current relay will return to normal operation through the action of the differential relay. Removing the offending generator from the system may clear the fault. The normal operating controls are reset by opening and closing the generator switch. When this is done, the generator will be automatically returned to the system, but if its voltage is still high, the overvoltage relay again

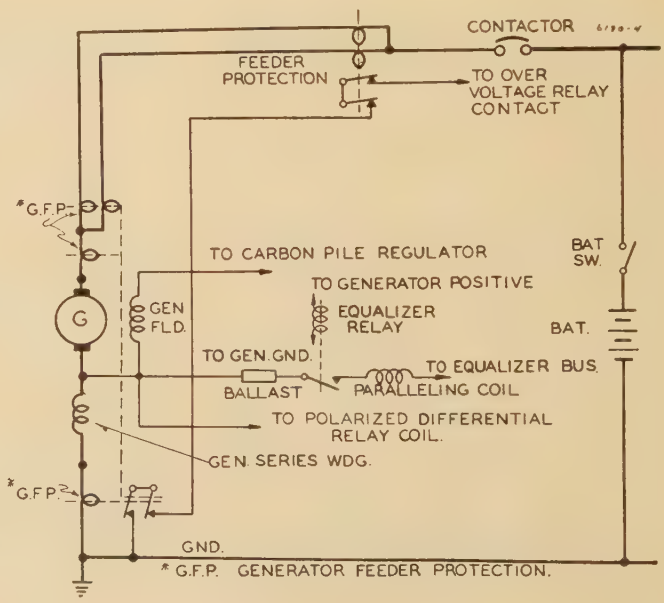

Figure 4. Diagram showing generator, generator lead fault protection plus generator feeder fault protection

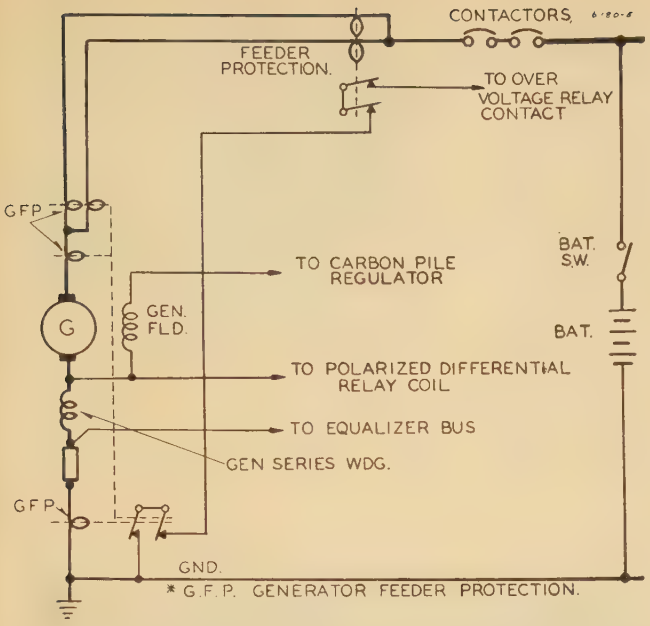

Figure 5. Diagram showing double contactors added to diagram of Figure 4

will remove it from the system. In this case, the flight engineer can decide whether or not he should reset the trip-free control again by opening and closing the generator switch. Two or three trials are considered reasonable.

Generator and Generator Lead Faults

Generator lead faults are infrequent, but probably occur more often than faults within the generator. The generator and generator lead fault protection relay will take care of both types of faults. This relay is usually mounted in the nacelle near the generator. It consists of a single contact operated by two differential series windings on the same magnetic circuit. One of the windings is in series with the positive generator lead, and the second winding is in series with the negative lead. A fault in the generator or at the generator leads unbalances the magnetic circuit of the relay, resulting in the opening of the contacts. This in turn, through the control devices provided for the purpose, isolates the generator and disconnects its field. The trip-free controls may be reset by opening and closing the generator switch. Resetting may be repeated at the judgment of the operator.

Generator Feeder Protection

Faults can occur in cable extending from the generator in the nacelle to the bus in the fuselage. Although such faults are very infrequent in well-installed and maintained generator feeder cables, they are extremely serious when they occur. A two-lead differential method is provided for this protection. Two relays are used, each of the differential-series-coil balanced magnetic circuit type. One is located at the nacelle and the second one is located in the fuselage. Each of the two leads passes through one of the series coils of each relay. A fault of predetermined magnitude in either of the two cables will unbalance the magnetic circuit in one or both of the relays and cause its contacts to open. This will cause the control devices to isolate the fault and, at the same time, will disconnect the field of the generator supplying current to the fault. The trip-free controls can be reset at the option of the operator by opening and closing the generator switch.

Current Balance Versus Reverse Current Circuit Breaker

Some degree of generator feeder protection may be obtained by using a reverse current circuit breaker adjacent to the main contactor. When a major generator feeder fault occurs while the main contactor is closed, the circuit breaker will trip on a very heavy reverse current entering the feeder from the bus or the battery. This trip setting is normally about 50 per cent greater than the rating of the generator with a time delay, and instantaneous at currents 100 per cent above the trip setting. The high minimum trip current and the time delay feature are necessary to prevent false tripping during momentary reverse current conditions imposed by system voltage errors or by generator re-

Figure 6. Schematic diagram showing the complete control and protection of a single aircraft d-c generator

BR	Ballast resistor
BS	Battery switch
C	Contactor
CP	Carbon pile regulator
DR	Damping resistor
EDR	Equalizer disconnecting relay
FP	Feeder protection
FR	Fixed resistor
G	Generator
GF	Generator field
GFP	Generator feeder protection
GFR	Generator field relay
GS	Generator switch
GSW	Generator series winding
OTI	Overtemperature indicator
OVR	Overvoltage relay
PC	Paralleling coil
PDR	Polarized differential relay
PVR	Polarized voltage relay
RC	Regulator coil
TI	Trip indicator
VJ	Voltmeter jack
VR	Variable resistor

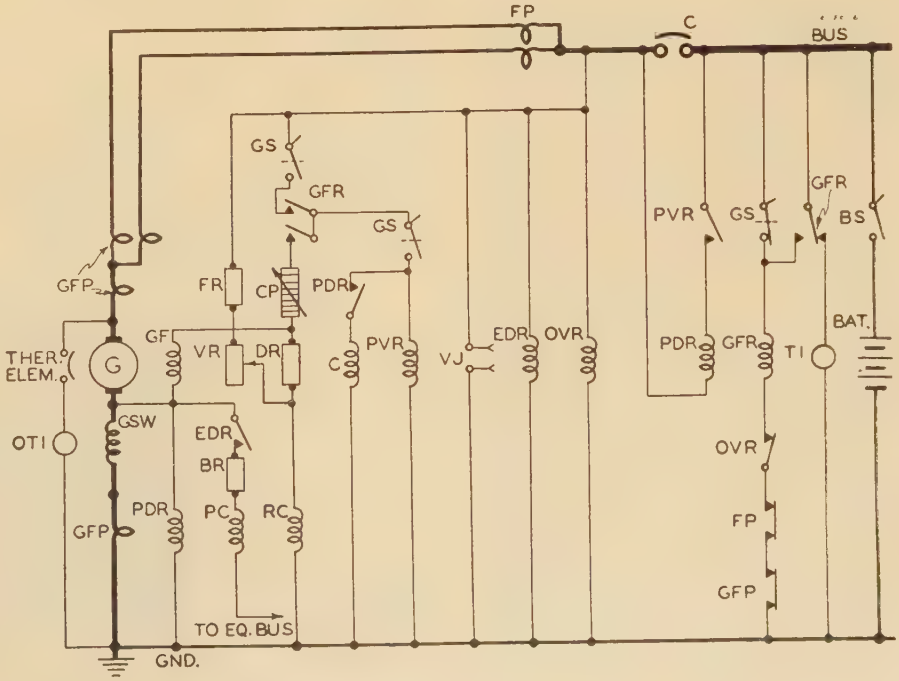

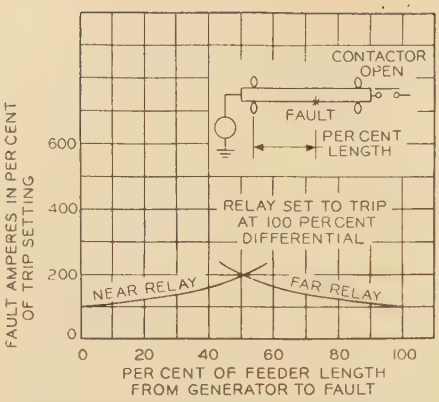

Figure 7. Curves showing fault amperes in per cent of trip setting of the protective relays for a typical generator feeder

weight than current balance and double contactors having remote reset control.

Double Break in Generator Bus Feeder

A single main contactor for connecting the generator to the bus or battery has been used extensively. There are important reasons for using two identical contactors in series with their operating coils in parallel. Because of slight manufacturing differences in magnetic circuits, springs, and mechanical parts they never may open and close at the same instant. One of them normally will operate, leaving the other as a backup unit.

The backup contactor will be available for instantaneous operation if the other unit fails to open. Frozen contacts may not cause trouble during flight, but after landing and shutdown of engines the pilot may fail to open the battery switch. In such a case the frozen single contactor will cause complete discharge of the battery. This might not damage the generator; however, if an airport power supply is plugged in, the generator is certain to burn out.

Contactors having new features which reduce the chances of freezing are in use. They have high pressure at the contacts, inertia backup during closing, and a very low voltage drop-out. With such contactors, danger of freezing of contacts is slight and, for all practical purposes, the use of double contactors will eliminate these risks to the electric power system.

Ballast Equalizer Connections

A system with two or more generators requires provisions for satisfactory parallel operation. The only methods now in use consists of coil windings in each regulator, operated from the drop across an external resistor in series with the generator or indirectly from a series winding inside the generator. The series resistor usually provides one-half of a volt drop at full load current and has been used extensively for military aircraft. Paralleling has been moderately satisfactory. However, paralleling for commercial transports should be good enough to prevent the overloading of one or more generators in flight or ground operations. Stand-by loads for 2-engine airplanes require reasonably accurate paralleling because this operating condition is likely to heat the generators more than any other phase of operation as a result of limited generator cooling air. Four-engine airplanes require paralleling to be reasonably accurate for all operating conditions because three generators must run at full output

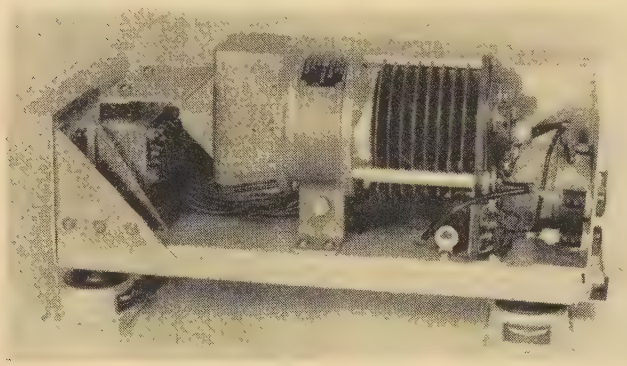

Figure 8. Control panel including regulator plugged into shock mount

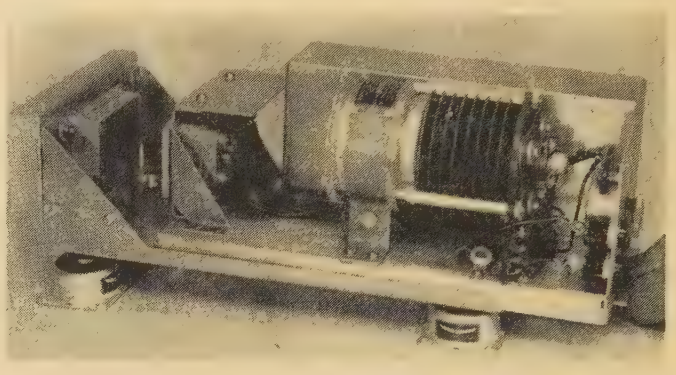

Figure 9. Control panel shown in Figure 8 being removed as a single unit from the shock mount

Note separation of plug and receptacle

covery characteristics following an external load circuit fault. As a consequence, it is quite possible to have a generator feeder fault of a magnitude that will open the contactor by reverse current action before the circuit breaker can trip. If this occurs, the generator field will not be opened and the generator will continue to feed the fault. A similar condition will exist if a fault occurs while the contactor is open, or if the generator builds up on a faulted generator feeder.

The well-known current balance feeder protection is not subject to these errors. Because it is not responsive to normal load current, reverse current, or external fault conditions, it can be set to trip on faults considerably lower in magnitude than the current setting limitation of the reverse current circuit breaker. Most important, current balance protection operates without dependence on reverse current relay sequence, timing devices, or main contactor status. If the contactor is already open, the protective relay proceeds to open the generator field, and thus prevents feeding the fault. Manual reverse current circuit breakers are slightly less in

Figure 10. Control panel shock mount showing clamp and receptacle

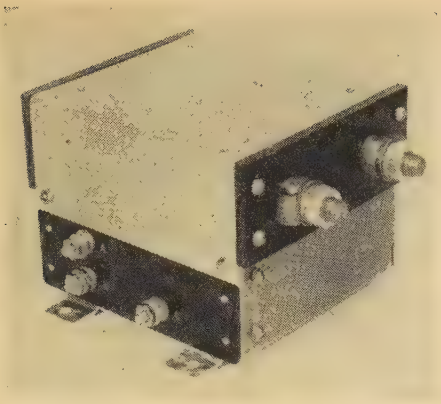

Figure 11. Nacelle type contactor and ground protection relay box

in case of the failure of any one generator.

Commercial transports are subject to delayed ground operations at many airports. The equal loading of each generator under these conditions is important. Increased equalizer voltage increases the sensitivity of the regulator to unbalanced current conditions and provides much better parallel operation. Full voltage is being taken from across the series winding of the generator and is approximately $1^1/_2$ volts.

Increased equalizer voltage also results in a lower system voltage when the speed of one or more generators is lowered to the idling value. This is an unfavorable condition, and it is corrected to some extent by a nonlinear ballast in the equalizer circuit, which limits the equalizer current under wide generator speed differences.

An equalizer disconnecting relay is also provided which opens the equalizer connection between regulators when fault protective devices operate or when the generator switch is opened. This then permits all other generators to operate at normal voltage when any one or more generators are cut out as a result of faults or shutdown. The relay is a simple voltage operated 2-position type.

Generator Thermal Indication

Overheating of the generators may be caused by overloading or insufficient ventilation at normal loads. Insufficient ventilation usually occurs under stand-by conditions. Analysis has shown that the only satisfactory device for indicating overheating of the generators is a thermal indicator sensitive to temperature and independent of current or load. The generator is not disconnected from the system when overheating is indicated, as modern insulation permits the generator to operate until the nonessential loads can be removed and the cause investigated at the next landing.

Stabilized Voltage Regulators

This type of regulator consists of a stack of carbon and graphite disks contained in a heat-radiating cylinder and a solenoid, or regulating coil, matched over a wide range to a spring which is arranged to apply varying pressure on the carbon pile in accordance with the voltage in the generator circuit. The carbon pile is connected in series with the generator field circuit so that the resistance variation through the carbon pile causes variations in the generator field current, thus obtaining constant generator voltage regardless of connected load or speed. The stability of the regulator is achieved by a damper mechanism employing both air and spring damping. Tests have demonstrated stable operation throughout the life of the regulator.

Control Apparatus Assembly And Locations

For elementary systems used on military aircraft and some commercial transports, the regulator is usually mounted in the fuselage, and the differential relay and ground resistor mounted in the engine nacelle. This is a reasonably satisfactory arrangement for this type of apparatus.

Systems provided with protective devices as described in this paper are designed with considerable flexibility as to the assembly of each unit and the mounting locations. Regulators and relays are preferably assembled on a plug-in base similar to the plug arrangements used with radio panels and racks. With this arrangement the major control units can be replaced in a few seconds. The assembly of the fault protection relays and the contactors are generally in single units and are located to the best advantage in the particular airplane being constructed.

Conclusions

Many of the simple principles used in the aircraft d-c power and protective systems are those used extensively in land power systems where continuity of service is of first degree importance.

Cable, generator, overvoltage, frozen contactor, and generator overheating faults are isolated or indicated during all operating conditions. Otherwise the system functions normally and fully automatically to connect and disconnect the generators from the battery bus as required. Satisfactory operation under conditions of humidity, sand, dust, vibration, altitude, explosive gas fumes, and acceleration normal to aircraft has been achieved by designing with these extreme conditions in mind.

Means for quick removal and replacement of the complete control panel by using standard radio plugs and receptacles provides the ultimate ease in maintenance and involves no compromises with performance. Contactors for any given power system are designed and applied so that they will interrupt successfully without undue stress any top current value that can be obtained on the system at the point where the contactor is located.

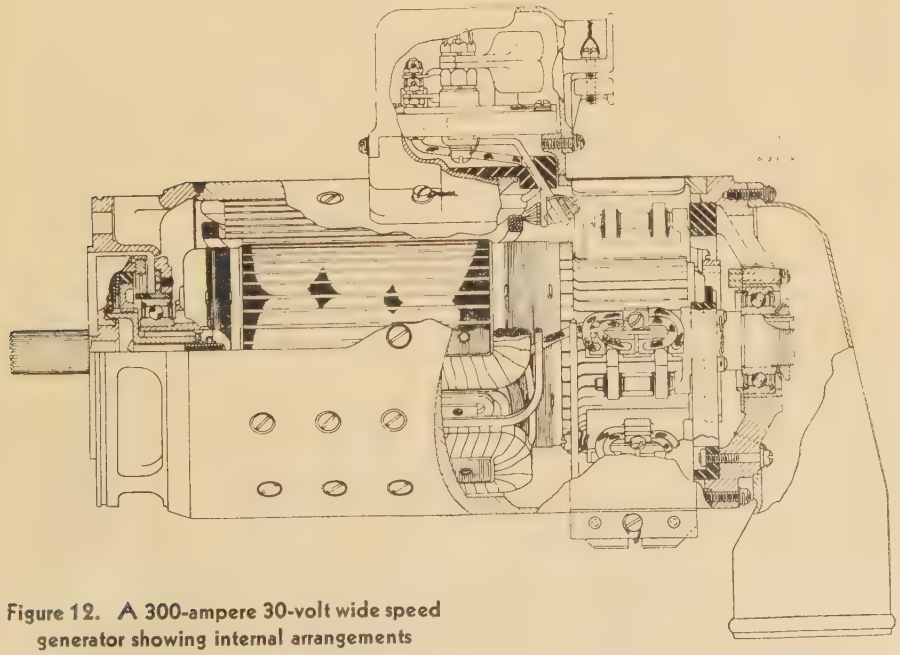

Figure 12. A 300-ampere 30-volt wide speed generator showing internal arrangements

Reference

1. An Aircraft Differential-Voltage Cutout O. C. Walley. AIEE Transactions, volume 63 1944, September section, pages 632-4.

Protection of Powerhouse Auxiliaries

AN AIEE COMMITTEE REPORT

THE AIEE relay subcommittee has reviewed the protection of generating stationauxiliary power motors and supply systems. The study was made to obtain information on auxiliary power systems now in use and the protective methods being applied, and to make recommendations on preferred practices.

In order to obtain basic information, a questionnaire was sent to approximately 30 engineers interested in this subject. These questionnaires covered data on the supply systems used, various forms of protection applied, and a summary of the experience obtained with these systems. Answers to the questionnaire were received from various representative companies covering both steam and hydro stations and a wide range in station sizes. The answers submitted represented the modern practice of each company. This subject also was discussed in a conference session held during the 1946 winter convention.

Summary of Information Received

Following is a brief summary of the information received on the various points covered by the questionnaire.

Supply Systems Used

In most cases, transformers are being used for auxiliary power supply. Values of 2,300 and 440 are the principal voltages used, with motors higher than approximately 100 horsepower being supplied by the higher voltage system. In most cases the systems operate ungrounded, although some companies prefer to operate grounded, either solidly or through impedance.

Paper 46-169, recommended by the AIEE committee on protective devices for presentation at the AIEE summer convention, Detroit, Mich., June 24–28, 1946. Manuscript submitted April 19, 1946; made available for printing May 29, 1946.

This report was prepared by a working group on powerhouse auxiliaries of the relay subcommittee, AIEE committee on protective devices, consisting of E. L. Michelson (M '44, sponsor), senior engineer, Commonwealth Edison Company, Chicago, Ill.; A. H. Burkhalter (M '41), electrical engineer, design and construction department, Ebasco Services, Inc., New York, N. Y.; R. E. Cordray (M '43), in charge of relay engineering, General Electric Company, Philadelphia, Pa.; E. H. Klemmer (A '42), switchgear engineer, Westinghouse Electric Corporation, East Pittsburgh, Pa.; W. E. Marter (A '40), assistant relay protection engineer, Duquesne Light Company, Pittsburgh, Pa.; C. L. Smith (A '28), relay engineer, electric distribution department, Rochester Gas and Electric Corporation, Rochester, N. Y.

The protection of the auxiliary power transformers includes, in most cases, differential relays with time delay overcurrent protection for backup purposes. In many installations there are two sources of primary supply with an automatic throwover arrangement, initiated by undervoltage relays, which connects the reserve supply if the primary source is lost.

On busses supplied by auxiliary generators, the problem of bus protection is complicated by the decrement in fault current supplied by the generator. The decrement causes a rapid reduction of fault current to a point approaching normal load current, so that it is difficult to obtain bus protection with time delay overcurrent relays. In such cases differential or fault bus relays provide the most desirable method for bus protection.

Motor Protection

In the majority of cases, the 2,300-volt motors are protected by long-time-delay overload relays set at 125 to 150 per cent of full load current and instantaneous overcurrent relays on the cable leads which are set above the starting inrush current. The smaller motors are in general protected by thermal tripping elements for overload, and an instantaneous trip device for short circuits.

There is some variation in the treatment of essential and nonessential motors. In most cases, the essential and nonessential motors are protected by similar relays. However, in a few cases the circuit breakers feeding essential motors are not tripped by the time delay overload relays. These relays give an alarm only in the event of an overload condition.

Essential motors are defined as those motors whose failure results in the shutdown of generating capacity. Examples of this class of motors include the circulating pump, boiler feed pump, and induced and forced draft fans.

Other Forms of Protection

In most cases where the systems are operated ungrounded, ground detectors are available for detecting grounds.

In powdered fuel plants, it is necessary to interlock the sequence of starting and stopping certain motors. For example, the induced draft fan is started first, and is followed in sequence by the forced draft fan, the exhauster, the pulverizer, and the feeder. If any piece of equipment in this series is stopped, provision is made to stop automatically all of the motors ahead of it.

Experience and General Conclusions

The answers received indicated that as a whole the protective schemes now in use are satisfactory. The only indication of unsatisfactory performance has been with the thermal relays used on the smaller motors. Various types of troubles have been reported, such as lack of thermal capacity to withstand fault currents, and lack of sensitivity. One company uses oversize thermal elements to avoid difficulties which have been experienced with the sizes recommended by manufacturers.

In general, the importance of auxiliary power in generating stations is so fundamental that simple and rugged relaying schemes are to be desired. In almost every case the auxiliary power supply is the last element of the system which should be shut down, and therefore the relaying systems used should be as free from trouble as possible.

Recommended Preferred Practices

Supply Systems

For ungrounded systems or grounded systems where the ground fault current is limited to a few amperes, ground detector relays should be used.

For systems grounded solidly or through low impedance, residual current relays should be used on individual circuits.

Transformers supplying essential auxiliary power busses should be protected with differential relays, and time delay overcurrent relays should be used for backup protection.

Bus protection should be provided by overcurrent, differential, or fault bus relays. Overcurrent relays on auxiliary generators should not be relied upon for bus protection.

Motor Protection

The 2,300-volt motors should use long-time-delay phase overcurrent relays for overload and internal motor faults set at approximately 150 per cent of rated current. They also should be equipped with instantaneous overcurrent relays for short-circuit protection set above maximum inrush current.

On essential motors the time-delay overload relays may be used for alarm purposes only, and the instantaneous relays used to trip. In this case, the time-delay relays can be set more sensitively than 150 per cent of rated current.

Low voltage motors (208, 440, 550 volts) should use thermal device for overload protection, and an instantaneous trip device for short-circuit protection.

The thermal device may be built into the contactor supplying the individual motor, and one circuit breaker may provide short-circuit protection for a group of motors.

On essential motors the thermal element may be used for alarm purposes only.

Answers to Questionnaires

Following in a summarized form are the individual answers received.

Company Number 1

Supply System Used. This company uses transformers for supplying power to 2,300- and 440-volt busses. The transformers are operated ungrounded.

The transformers are protected by overall differential relays with time delay overcurrent protection on the low voltage output and time delay phase and instantaneous ground protection on the primary.

Motor Protection. Motors of 75 horsepower and higher use 2,300 volts. These motors have long-time-delay induction overload relays set at about 150 per cent of full load. Instantaneous relays also are used and are set to exceed slightly the maximum starting inrush current.

The 440-volt motors all are protected by circuit breakers with thermal tripping elements.

Other Forms of Protection. Static type ground detectors or lamps are used to detect grounded circuits, which are located by opening the circuits in turn.

Most essential auxiliaries are equipped with dual drive.

Both 2,300- and 440-volt busses are arranged for automatic throwover to adjacent sections in case of loss of potential, although the throwover will not function in case of a fault on the bus. Throwover is initiated when the voltage drops to about 65 per cent.

Experience. As a whole the protection has been satisfactory.

General Conclusions. It is felt that the ideal type of auxiliary power motor protection would consist of an instantaneous relay sensitive to all motor faults but insensitive to overloads, plus an overload relay with good correlation between its operating characteristic and motor temperatures.

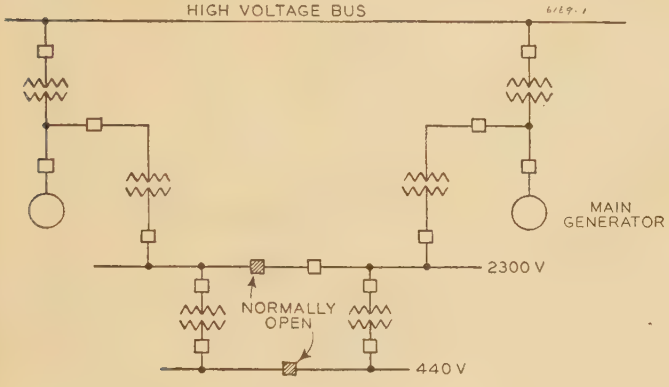

Figure 1. The supply system used by company number 2

Differential and overcurrent protection on auxiliary transformer. Differential closes bus tie when transformer breaker trips

Company Number 2

Supply System Used. The supply system used is illustrated in Figure 1.

Motor Protection. Motors 75 to 100 horsepower are supplied at 2,300 volts. On 2,300-volt essential motors, the protection consists of instantaneous overcurrent plunger relays for short-circuit protection. Thermal relays give visual indication only. On nonessential motors, the protection consists of 40-second overcurrent induction relays with instantaneous attachments.

On 440-volt essential motors, the protection consists of small instantaneous air circuit breakers. Thermal elements of motor contactors only light lamps. The nonessential 440-volt motors have the same protection except that the thermal elements trip the motors.

Other Forms of Protection. Ground detector relays are used on the 2,300-volt system and lamps on the 440-volt system.

An interlocking system between motors is used on the boiler auxiliaries to protect the boiler against motor failures.

Experience. The reliability of modern motors justifies a minimum of protection and maximum freedom from undesired tripping.

Relays for 2,300-volt breakers are satisfactory, but contactor elements, small air circuit breakers, and so forth, for 440-volt service are not sufficiently reliable.

Many applications require "latched-in" contactors to prevent disconnection on voltage surges.

Company Number 3

Supply System Used. The supply system used is illustrated in Figure 2.

Motor Protection. Motors up to 125 horsepower are connected to the 440-volt bus.

All 2,300-volt motors are protected by differential relays using instantaneous overcurrent relays set for approximately 50 per cent of full load current.

On the 440-volt system, feeders from the main bus are used to supply subbusses throughout the plant. These feeders use circuit breakers with a series trip set for 200 to 400 per cent of the rating of the breaker. These breakers protect against faults on the subbusses and heavy faults on the feeders to the 440-volt motors. Each motor is protected individually by a contactor with a thermal relay set for 30 seconds at 150 per cent load.

Other Forms of Protection. Lamps are used for ground detecting system. Grounds are removed by disconnecting portions of the system until the ground is located. The location of grounds is delayed until it is convenient to take equipment out of service.

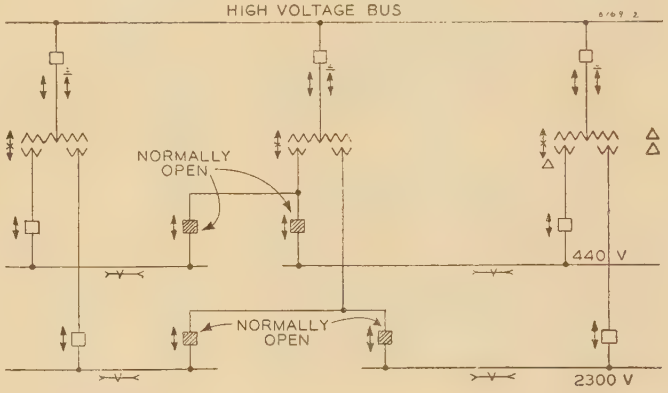

Figure 2. The supply system used by company number 3

Undervoltage relays throwover to reserve transformer

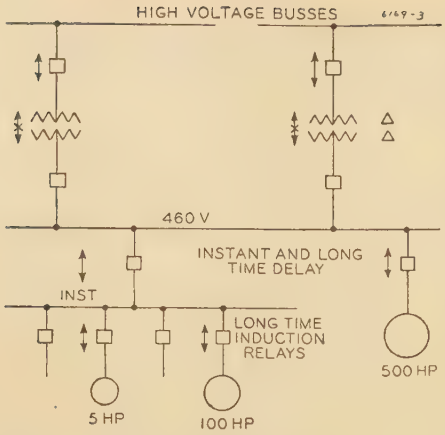

Figure 3. The supply system used by company number 5

Experience. High speed clearing of faults has resulted in very satisfactory operating conditions and has proved advantageous in limiting the extent of damage caused by motor faults.

Lack of thermal overcurrent protection on 2,300-volt motors has resulted in some difficulty with detecting cases of overload on mill motors.

Operation of thermal elements on 440-volt motors has been satisfactory.

General Conclusions. While differential protection on 2,300-volt motors has proved to be advantageous, it is questionable whether their use is economically justifiable. Future installations will use overcurrent relays.

Company Number 4

Supply System Used. The supply to auxiliary power is from transformers 13.8/2.3 kv, delta-Y connected. The 2.3-kv neutral is grounded solidly. Smaller motors are supplied from a 575-volt system, which in some cases is grounded and in other cases ungrounded. The transformers are protected by differential and induction type overcurrent relays.

Motor Protection. Motors up to 100 horsepower are supplied from the 575-volt system.

Motors are protected by a 40-second induction-type relay with instantaneous attachment. The time delay element is set at approximately half way between the ordinates of the motor full load temperature curve and the curve representing motor thermal limitations. The instantaneous trip is set just over "locked rotor" current. In some instances, thermal relays are used which are set in the same manner as for the induction relays.

No distinction is made between methods employed for protection of essential and nonessential motors except that the instantaneous auxiliary overcurrent relays set at approximately 115 per cent of the rated current are applied to pulverizer motors. These relays stop the coal feeder motors upon overload of the pulverizer until the pulverizer motor current drops back to normal.

Other Forms of Protection. Very elaborate interlock systems are used between induced and forced draft fans, pulverizers, boiler feed water pumps, and so forth.

Ground lamps are used for ground protection. No grounds have developed to date.

Experience. Performances of protective and control schemes have been excellent. All thermal relays of a certain make have had to be dismantled and reassembled in our laboratory before being placed in service because of poor factory workmanship.

Speeds of clearing faults have been very satisfactory; all cable and motor fault currents have been of a magnitude high enough to operate the 1-cycle relays. Iron and winding damage has been negligible.

General Conclusions. The simplicity of the 40-second induction overcurrent relays with instantaneous current trip features makes this scheme a slight favorite over the thermal combination for 2.3-kv motors. The manufacturer's standard protection on 575-volt cubicle switchgear has been found satisfactory.

Company Number 5

Supply System Used. The supply system used is illustrated in Figure 3.

Motor Protection. All motors are supplied at 460 volts (5 to 500 horsepower).

The 40-second induction overcurrent relays are used on almost all auxiliary motors. Current settings are from 125 to 150 per cent of motor rating. Time settings are generally about one second minimum time.

Instantaneous trips are used on all group breakers to clear any short circuit of sufficient magnitude to affect the operation of other motors.

Other Forms of Protection. Mill motors and exhauster fans are interlocked. Coal conveyer systems are all interlocked.

A set of ground indicating lamps with series resistors is installed on each auxiliary bus. Ground is established, for test, by a push button. This is a routine test performed by the operator on each shift. A ground is a rare occurrence on these 440-volt busses, but as soon as one does occur it is usually possible to cut in duplicate equipment and clear the trouble.

Experience. Our experience with thermal relays has not been satisfactory. The testing and maintenance cost has been extremely high. We have found that the long time induction overcurrent relay, though slightly more expensive initially, is far more reliable, maintains its calibration, and is easy to test. Quite a few of these motors are equipped with thermoguard protection. We have not used these devices for tripping, but have considered the possibility of doing so.

General Conclusions. Differential protection is not justified on 440-volt auxiliary motors because winding failures are rare.

Instantaneous tripping should be provided for every group or feeder circuit breaker which is connected to the main auxiliary bus.

Company Number 6

Supply System Used. The supply system used is illustrated in Figure 4.

A 440-volt system is used which is fed from either of the 2,300-volt busses.

Motor Protection. On motors fed from the 2,300-volt service, long time overcurrent relays with instantaneous elements are used. Long time overcurrent relays having a time delay up to 40 seconds are used and can be set for 110 to 125 per cent of full load current and with sufficient time delay to ride over the starting inrush. The instantaneous elements are set above starting inrush and furnish protection for faults on motor leads and circuit.

The main 440-volt motors are equipped with individual circuit breakers with thermomagnetic overload protection. This

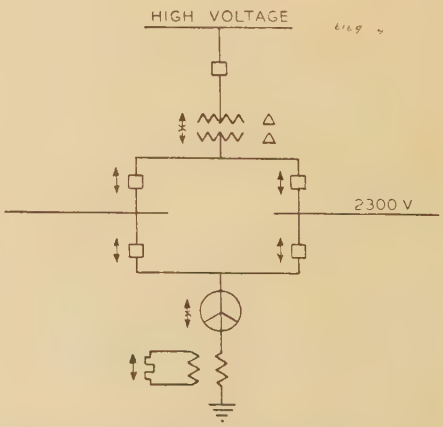

Figure 4. The supply system used by company number 6

provides both overload and short-circuit protection for these motors. Time delay undervoltage type *CV* relays are used on the 2,300-volt motors.

Other Forms of Protection. Automatic transfer of busses from the transformer to the generator source is provided to transfer load in case of voltage failure. The transfer scheme is interlocked to prevent paralleling of busses or to transfer after an overload relay operation.

The 440-volt busses have automatic transfer between transformers connected to the two 2,300-volt bus sections and have interlocks similar to the 2,300-volt busses.

Experience. The protective schemes used have given very satisfactory service and no load curtailment or shut down has occurred because of station service failures. The equipment described is new and few failures have occurred.

Table I

Motor Voltage	Max Hp	Min Hp	Protected by
2,300	1,000	300	Individual circuit breakers
550	250	50	Individual circuit breakers
550	50	1/2	Magnetic contactors

General Conclusions. The long time overcurrent relays with instantaneous attachments seem to offer satisfactory protection for the 2,300-volt motors since they can be set low enough to prevent roasting of insulation on overload, and the instantaneous elements provide quick clearing for severe faults.

Company Number 7

Supply System Used. The auxiliary power is supplied by transformers at 2,300 and 550 volts. The supply busses are operated ungrounded.

Protection consists of differential relays on the transformer banks and time delay induction overcurrent relays on all supply transformer circuit breakers.

Motor Protection. Motors are supplied as indicated in Table I.

Motors controlled by individual circuit breakers have

1. Instantaneous overcurrent relays set slightly above motor starting current.

(*a*). On 2,300-volt motors these are plunger type relays actuated from current transformers.

(*b*). On 550-volt motors these are built into breaker housing.

2. Time delay overcurrent relays set to pick up at 125 per cent of motor rated current and with sufficient time delay so as not to trip during motor starting.

(*a*). On 2,300-volt motors these are induction type operated from current transformers.

(*b*). On 550-volt motors these are thermal devices built into the breaker.

3. Thermal devices built into the motor structure which open a contact when the motor temperature exceeds a safe value and sound an alarm.

Motors controlled by magnetic contactors have

1. Air circuit breaker for instantaneous short-circuit protection.

2. Thermal overload built into the magnetic contactor.

All motors controlled by circuit breakers are treated as the foregoing.

1. Essential motors controlled by magnetic switches have thermal overload two sizes above that recommended for the size of motor involved.

2. Nonessential motors controlled by magnetic switches have thermal overload one size above that recommended for the size of motor involved.

Other Forms of Protection. An alarm is provided on each ungrounded bus to inform operator when a ground occurs. It consists of double-Y potential transformers with the neutral grounded on the high voltage side and overvoltage plunger type instantaneous relays connected from phase-to-neutral of the secondary winding. When a ground occurs the two relays on the ungrounded phases pick up and sound an alarm.

Experience. Fortunately the occurrences of short circuits on the auxiliary power system have been few and far between. In cases where short circuits have occurred, the instantaneous overcurrent relays in general have operated to clear the circuit with very little resulting damage to the equipment. Also, for *overload* conditions few cases have been experienced, for in general the size of motors chosen have had ample capacity to take care of the maximum mechanical load demanded. In the few cases where overload conditions occurred, the time delay induction overcurrent relays have done a good job without serious damage to the motors. In case of the thermal devices the experience has not been quite as good but not serious enough to change the scheme of protection.

General Conclusions. The use of ungrounded auxiliary power system employing a ground fault detecting system and eliminating the ground immediately after it occurs reduces to a minimum the number of short circuits that occur on the system. Further, the use of instantaneous overcurrent relays do a very satisfactory job when such short circuits do occur. In the use of instantaneous overcurrent relays, care should be taken that they are set at their minimum pickup value (that is just a little above the starting current) and not the general value sometimes recommended of ten times the circuit breaker rating. Also, the employment of induction overcurrent relays set at 125 per cent of motor rated current appears to be more reliable than other forms of overload protection.

Company Number 8

Supply System Used. The supply system used is illustrated in Figure 5.

Motor Protection. The 2,300-volt system supplies motors from 175 to 600 horsepower, the 440-volt system 1/2 to 200 horsepower.

Motor protection consists of the following:

1. On all 2.3-kv equipment—one overcurrent long-time relay with instantaneous attachments and two instantaneous overcurrent relays, two current transformers with an overcurrent relay connected in the residual circuit of the two current transformers.

2. On all 440-volt equipment—air circuit breakers (deion) with time delay and instantaneous relays.

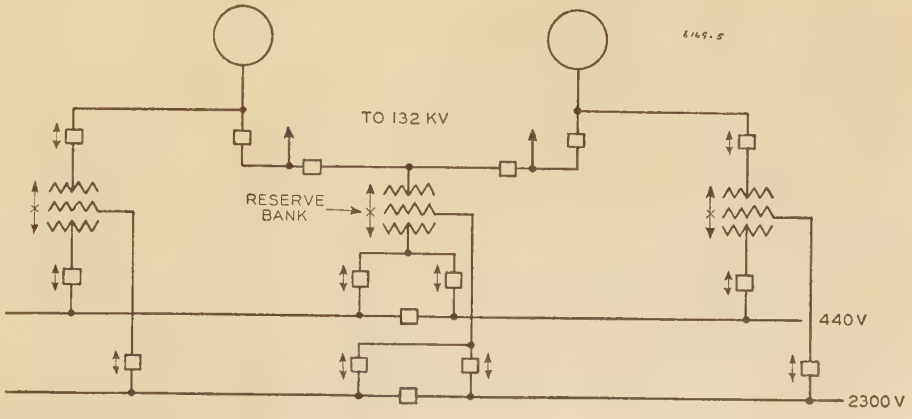

Figure 5. The supply system used by company number 8

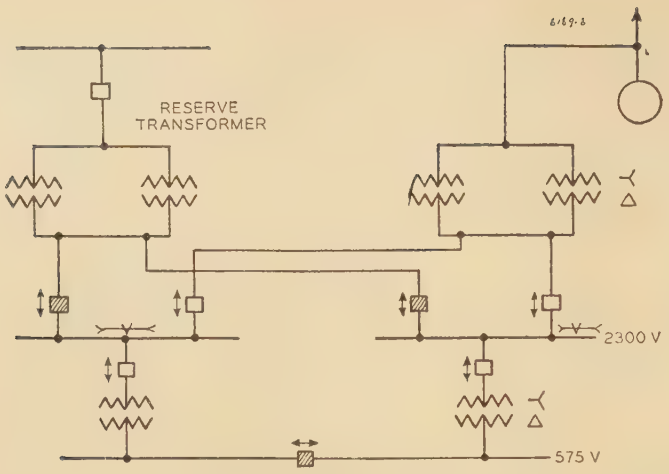

Figure 6. The supply system used by company number 9

Undervoltage relays throwover to reserve transformers

3. Undervoltage type *CV* relays on 440-volt bus trips pulverizer mills.

4. Most 440-volt motors have individual air circuit breakers with thermal trips.

No preference is given between essential and nonessential circuits on relaying procedure.

Automatic throwover of both 2.3-kv and 440-volt busses is provided.

Other Forms of Protection. Interlocks are used on pulverizers and coal scales, also on forced draft and induced draft fans.

Ground detectors are located on both 2.3-kv and 440-volt busses.

Experience. Present relays are very satisfactory. However, those originally installed (two overcurrent standard relays with instantaneous attachments) could not be set to co-ordinate properly with motor starting. Faults have been cleared very quickly and no extensive damage has resulted to motors or cables.

General Conclusions. The afore-mentioned scheme (one overcurrent and two instantaneous overcurrent relays) seems to us to be a very workable and efficient scheme.

Company Number 9

Supply System Used. The supply system used is illustrated in Figure 6.

Motor Protection. The 2,300-volt system supplies motors over 100 horsepower. All 2,300-volt motors have instantaneous overcurrent relays for short-circuit protection. The essential motors have a long-time-delay relay for overload protection which gives an alarm only. On nonessential motors the long-time-delay overload relay trips the motor. On the 575-volt motors, there is an instantaneous trip for short-circuit protection and a thermal trip for overload.

The instantaneous relays are set approximately ten per cent above maximum motor inrush current, that is, ten per cent above asymmetrical peak value occurring in the first half cycle.

Other Forms of Protection. Boiler fan motors and mill motors are interlocked for sequence starting and stopping.

Ground relays on 2,300-volt and 575-volt busses operate an annunciator. Grounds are removed by disconnecting one motor feeder at a time until the ground is located.

Experience. Provision has been made to trip almost all of the motors immediately in case of a short circuit in the feeder or the motor. In faults of this nature the amount of damage is limited by the quick tripping. In a recent case of motor failure it was possible to remove the faulted coils from the circuit by using jumpers and keep the motor in service.

Some difficulty is experienced in co-ordinating the instantaneous direct acting trips of the 575-volt circuit breakers. Where these breakers are cascaded a short circuit usually trips all of them in the cascade with loss of unfaulted motors or feeders. Dashpot devices have not proved satisfactory for this purpose. A simple device, such as an adjustable escapement, on the instantaneous trips for a few cycles timing would be of material benefit in solving the problem.

General Conclusions. In general, the protective scheme adapted is considered reasonably economical and simple and has performed satisfactorily with the exception of the cascading referred to in the foregoing paragraph.

Company Number 10 (Hydroeletric)

Supply System Used. The supply system used is illustrated in Figure 7.

Motor Protection. All motors are supplied at 550 volts. The motors are supplied through individual "Non-fuz" breakers. Between each of the breakers and the individual motors, there are magnetic switch starters with a suitable thermal relay for overload protection.

Other Forms of Protection. The station service is not grounded and there is no means of detecting and removing grounds.

Experience. No difficulty has been experienced with any part of the station service.

Company Number 11 (Hydroeletric)

Supply System Used. All auxiliary power motors are supplied at 550 volts. The supply is from transformers that are fed from house generators. These transformers are protected by overcurrent relays. The auxiliary power supply system is grounded solidly.

Motor Protection. All auxiliary motor circuits are protected by overcurrent inverse time relays, plus overcurrent instantaneous elements at a higher setting.

Other Forms of Protection. No other forms of protection are used.

Experience. Experience in operating for 13 years with this protection system has not shown any defects in the method. However, no essential auxiliary motors or circuits have developed a fault thus far. The crane motor-generator set and two sump pumps are the only equipment to develop any trouble, and the trouble was not extensive. A coil or two short-circuited

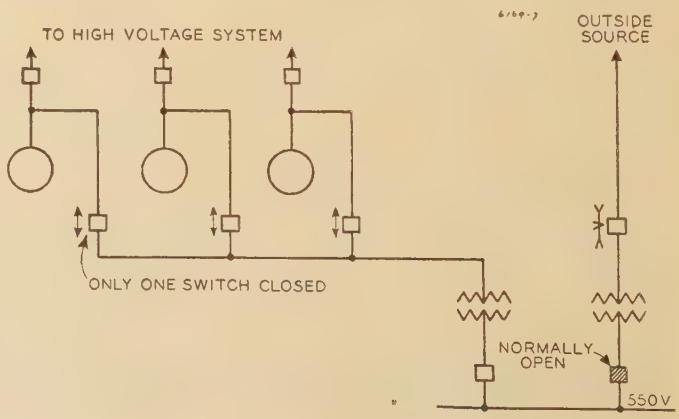

Figure 7. The supply system used by company number 10

Six Years' Experience With Factory-Built Unit-Type Substations

E. F. MILLER
MEMBER AIEE

R. B. MILLER
ASSOCIATE AIEE

THE Iowa-Illinois Gas and Electric Company installed its first unit-type substations late in 1939. At the present time, there are installed in the various operating districts of the company nine unit-type substations. We are outlining the reasons for the choice of this type of substation and the distribution system into which the substations are being fitted. This paper will cover our operating experience with six of this type of substation located in the quad-city area of Davenport, Iowa; Rock Island, Moline, and East Moline, Ill. The reasons given for the selection of this type of substation, the design of the distribution system served by the substation, and operating experience so far encountered are typical also of the other districts in which the additional three substations are located.

The quad-city area comprising the cities outlined above occupies two states, Iowa and Illinois. The division between states and cities is made by the Mississippi River. Davenport, Iowa, and its suburban towns, occupying the north bank of the Mississippi River and located in the State of Iowa, comprise a total population of approximately 90,000. The cities of Rock Island, Moline, and East Moline, Ill., with their attendant suburbs located on the south bank of the Mississippi River, comprise a total population of approximately 114,000.

Because of the advantages offered by the Mississippi River, the bulk of industry is concentrated along the river banks. The cities of course started their growth on the banks of the river and have expanded outward. Greatest load concentrations are along both banks of the river with the residential load being located in an approximate semicircular area around the outside of the industrial area. Original substations are located close to the river in the heavy industrial and commercial areas.

Polyphase alternating current was introduced into the quad-city area in 1888, six years after the first electric service was installed. This early a-c system was 2-phase, and, as a result, all growth on the quad-city system for many years was 2-phase. This 2-phase service was utilized in two ways.

1. The 2-phase 4,800-volt primary circuits were used to supply industrial customers.
2. The 2-phase 2,400-volt circuits were used to supply lighting customers.

The 2,400-volt system was utilized throughout much of the residential area as single phase primaries. The distribution system remained single phase 2,400-volt and 2-phase 4,800-volt until late in 1939. In the meantime, a backbone transmission and subtransmission system of 69-kv and 13.8-kv 3-phase circuits was built which served the complete quad-city area.

The later load growth has tended to be away from the river to keep pace with the expanding residential areas and some smaller outlying industrial areas. Because of growth of the communities, the load center of residential load kept shifting out away from the river and the original manually attended substation locations. This change in load center was followed by lengthening of the distribution lines until the long lines introduced poor regulation despite the use of induction feeder voltage regulators. Interruptions of service on these long feeders involved a large number of customers. As the areas grew, a number of small outlying commercial areas developed in which only single phase service was available. This offered many disadvantages to the merchants located in these areas as much of the equipment which they purchased normally came equipped with 3-phase motors.

The requests for polyphase service were each of relatively small electrical demand and scattered over fairly large areas. As a result, it was uneconomical to construct long polyphase feeders from the existing substation locations to serve the widely diversified loads of small magnitudes. The many requests for polyphase service received from the outlying areas required that consideration be given to the establishment of polyphase primaries in these localities. The location of the existing substations and number of circuits already leaving those stations made it difficult to get out additional circuits without going considerable distances underground, thereby raising the cost of each of the outgoing circuits which would be required.

Paper 46-176, recommended by the AIEE committee on power transmission and distribution for presentation at the AIEE summer convention, Detroit, Mich., June 24–28, 1946. Manuscript submitted April 26, 1946; made available for printing May 20, 1946.

E. F. Miller and R. B. Miller are both engineers with Iowa-Illinois Gas and Electric Company, Rock Island, Ill.

in the sump pumps which caused tripping by the overload protection during running, and clearing took place quickly enough to prevent any spreading of the fault. The crane motor-generator set became defective because of broken coil leads caused by insufficient bracing to withstand line start operation. The overload relays occasionally would trip out during the starting period for some time before the condition developed in enough bars to prevent satisfactory operation. No burning or spreading of the damage resulted, and it was difficult to locate the flaws which had occurred in the winding.

It should be remembered that in line start operation of motors the overload relay moves toward closing its contacts every time the motor is started, and the timing preferably is adjusted originally by trial to be just great enough so that tripping is not completed. The timing thus determined experimentally, while the desired pickup value for the relay is not changed, then is applied to all other similar circuits.

The frequent movement of the moving element of the relay, during each starting period, is felt to be an advantage in preventing any tendency to stickiness and insuring that the relays remain in operating condition. After the original calibration and conditioning following installation, recalibration checks are required infrequently since operating conditions can be proved roughly by simply observing the amount of contact travel during the starting up of equipment. Actually, subsequent checks have never shown an appreciable divergence from the original values.

General Conclusions. The conclusions reached are not new and only agree with the general idea of providing instantaneous tripping devices to operate on fault currents plus low-pickup-value inverse-time relays for satisfactory clearing of prolonged overloads or low current internal winding faults.

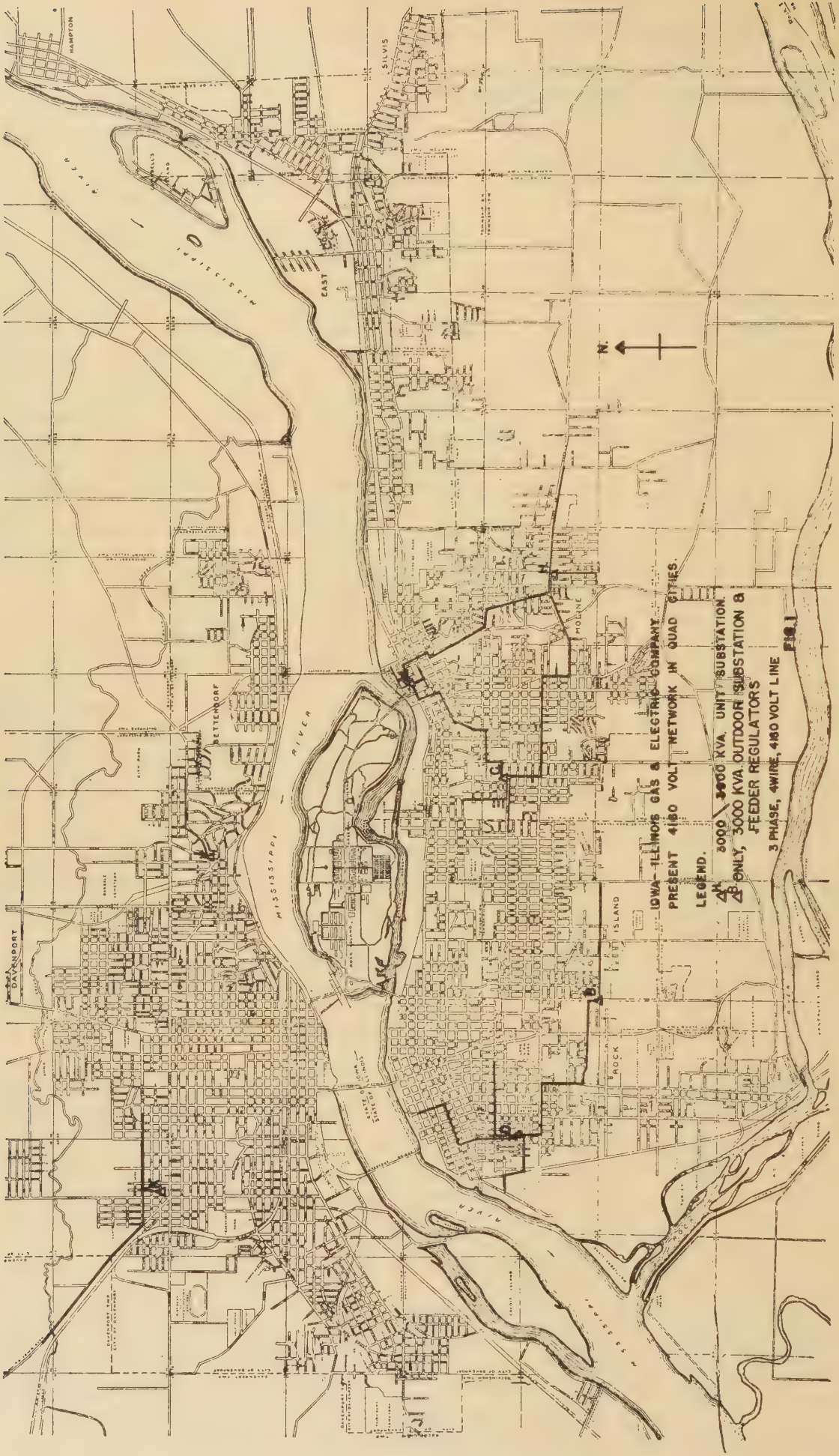

Figure 1. Present 4,160-volt 3-phase 4-wire network in quad cities

Δ^H—3,000/3,900-kva unit substation
Δ^B—only 3,000-kva outdoor substation and feeder regulators

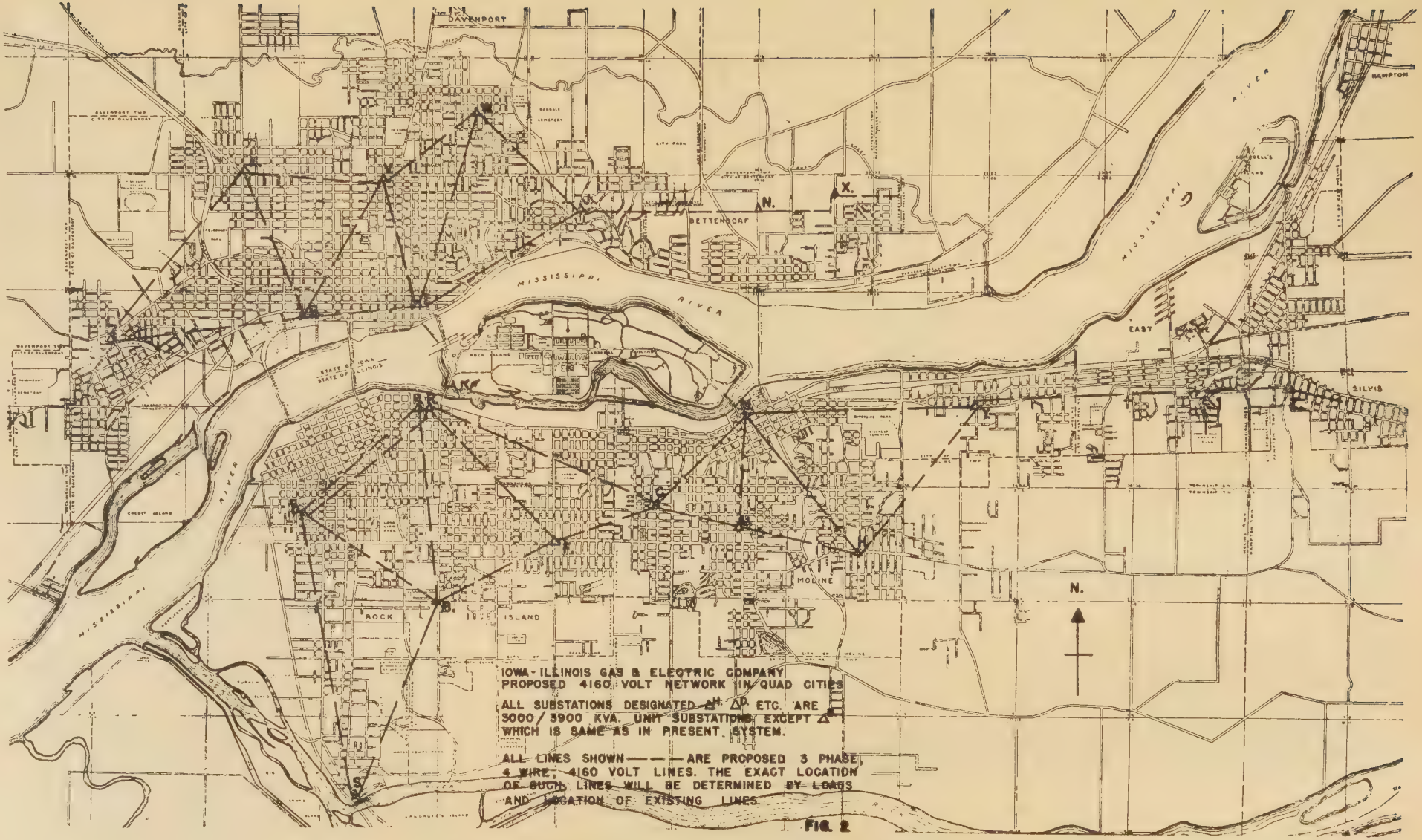

Figure 2. Proposed 4,160-volt 3-phase 4-wire network in quad cities

All substations designated Δ^H, Δ^D, and so forth, are 3,000/3,900-kva unit substations, except Δ^B which is the same as in the present system

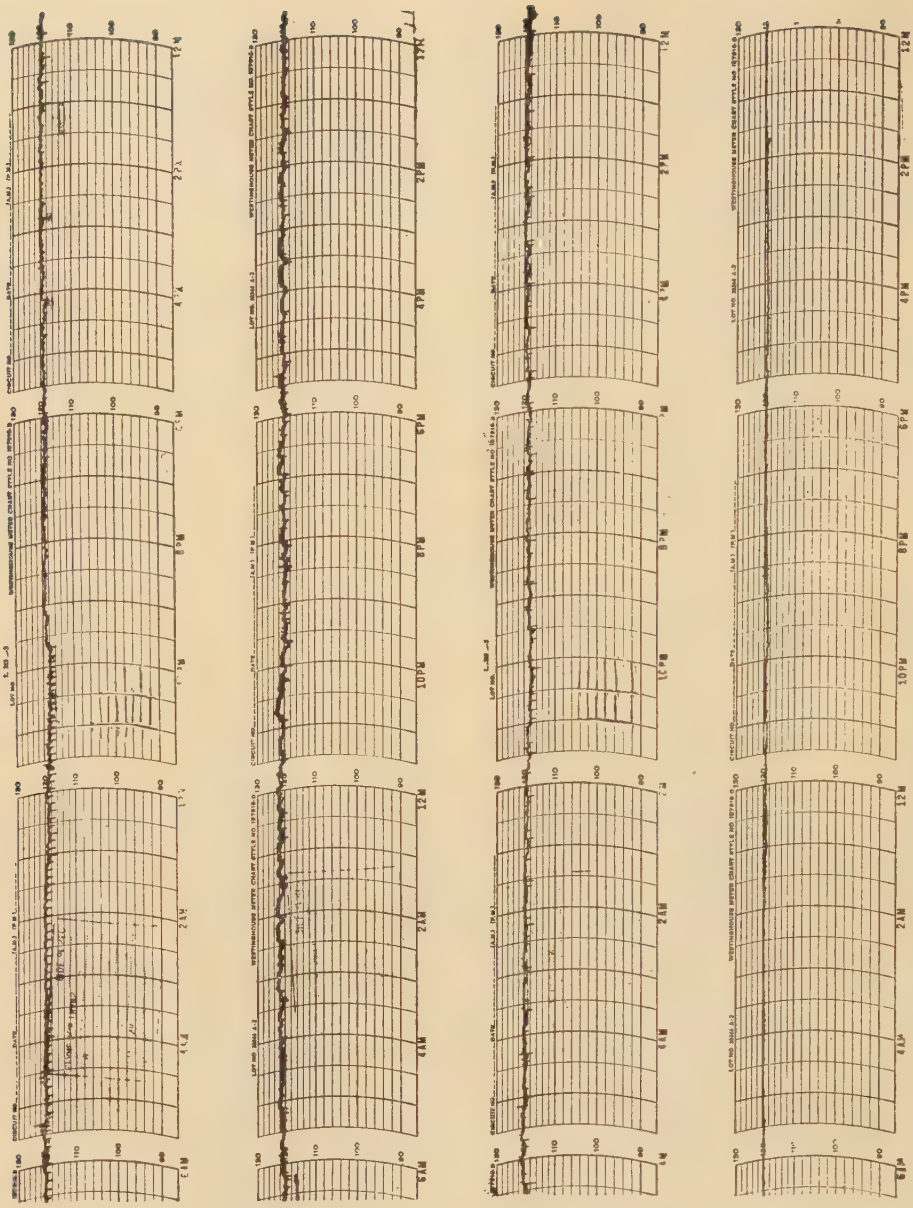

Figure 3. Typical voltage charts taken from secondary circuit approximately three spans from transformer

Transformers are located approximately one mile from the unit substation at center of 4-kv tie

Increased loads on existing substations required that additional larger capacity supply lines be constructed to those substations. The increased line capacity supplied through the larger number of step-down transformers raised the short-circuit duty on all existing station equipment. As a result much of the present station equipment became inadequate in interrupting capacity and thermal capacity. In addition, the fact that much of the existing station equipment was 2-phase also made it obsolete.

In 1939 it was decided to modernize the distribution system. After careful study of various types of distribution systems, it was decided that 4-kv primary networks would be instituted independently for the communities on each side of the Mississippi River. Because of the width of the river, it was deemed not advisable to join the 4-kv networks on opposite sides of the river. Involved in the study of the type of distribution system to be constructed was the matter of the type of substation to be utilized with the distribution system. After considerable study it was decided to use factory-built unit-type outdoor substations, these substations to be supplied from the 13-kv system and to be 3-phase 4-kv on the output side.

The majority of these substations will serve the residential areas, outlying commercial and small industrial areas. In general, no industrial customers will be served whose original demand exceeds 300 kva. In the areas where 13-kv circuits are available as well as 4-kv circuits, industrial customers having demands in excess of 100 kva will be supplied from the 13-kv system.

The type of substation decided on has the following description: 3,000/3,900 kva, equipped with transformer secondary breaker, four 3-phase 4-kv feeder compartments, and necessary auxiliary compartments for metering equipment, operating transformers, and other essential equipment. The individual feeders are equipped with overcurrent relays having instantaneous attachments. Three shot reclosers are used on each feeder, automatic reclosing being set for 15, 30, and 45 seconds with lockout on the fourth outage. All substations are equipped with air circuit breakers, the original two substations being equipped with stationary breakers and group operated disconnecting switches. The four later substations are equipped with drawout circuit breakers. The transformer secondary breaker, in addition to being equipped with overcurrent relaying for bus fault protection and transformer failure protection, is also equipped with network and phasing relays which will connect the 4-kv bus to the transformer and to the 13-kv circuit any time voltage of proper magnitude and proper phase quality is applied to the 13-kv circuit. Individual breakers are rated as 600 amperes, 7.5 kv with an interrupting rating of 150,000 kva.

Originally, two substations were purchased in 1939, one of which had a cable entrance on the 13-kv side, the other having an overhead entrance through cover bushings with lightning arresters mounted directly ont he transformer cover. Experience with bushing flashover on this substation within the first month after it was placed in service caused a decision to be reached that all future substations would have 13-kv cable entrance. No switching equipment is provided on the 13-kv side except a pole-top switch on one of the last poles before the 13-kv circuit goes underground.

The accompanying diagram, Figure 1, shows substation locations and indicates the portions of the primary network which so far have been tied together. The unit substations are supplied either by a radial 13-kv feeder from one of the attended substations or generating stations, or from a tap onto an existing 13-kv tie line. The 13-kv tie lines make up a part of the network of that voltage embracing the generating stations and all attended substations of the quad-city area. Only one unit substation is connected onto either a tie line or a radial feeder. The secondary side of

each substation is tied into the 4-kv primary network. Each substation has at least two of its feeders, and ultimately will have all of its feeders, tied into other substations in the network. Radial load in the area through which each 4-kv tie line passes is balanced on the three phases of the tie line. This includes both the residential as well as the small commercial and small industrial load which already have been mentioned.

Actual construction of the primary network was delayed by the war. In addition to the substations now in service, one other substation has been on order since May 1945, and we contemplate the installation of six additional unit-type substations in the next 5-year period. The accompanying diagram, Figure 2, shows the ultimate network as planned with the future substations shown dotted. Substations are located in the small commercial areas adjoining residential districts. Where possible under zoning ordinances, substations will be located in the residential area. All 4-kv feeders are taken out underground, the actual underground distance being determined by the varying conditions at each substation site. The 4-kv tie circuits between unit substations are constructed as follows: outgoing riser cables with a 300,000-circular-mil single conductor and either paper-insulated lead-covered, or rubber-insulated with a Neoprene jacket. Where paper-insulated lead-covered cables are used and the neutral conductor is pulled in the same duct with the phase conductors, insulated wire is used. Generally, this has been a copper conductor of 4/0 size with a single layer of paper insulation and a lead sheath, although we have used some rubber-insulated braid-covered wire when wartime restrictions prohibited the use of lead on conductors insulated for less than 2,500 volts. The overhead conductors consist of three 4/0 phase conductors and a 1/0 neutral. The neutral wire is marked by means of white porcelain insulators and the phase conductors are always placed in sequence with the neutral as a marker. Construction, in general, is made to conform with the surrounding neighborhood. In some cases underground feeders have been run as far as two city blocks before rising to meet the overhead system.

Spacing of unit-type substations is determined by load in areas to be served, length of tie lines to other unit substations, planned future additions to the network, and by regulation based on the fact that bus regulation is used. Because the bus is regulated instead of the individual feeders, we have determined that no ties between stations will be over $2\frac{1}{2}$ miles long. In general, substations are spaced from 2 to $2\frac{1}{4}$ miles apart, and voltage regulation has been very satisfactory as shown by the accompanying charts, Figure 3.

Maintenance on the substations has been very slight. A regular weekly visit is made to each substation at which time all equipment is inspected, dust and dirt are removed by means of an electric vacuum cleaner and blower combination, records are made of kilowatt-hours and demand, and readings of the various operation counters are noted. A weekly inspection report is made out on each substation covering the various data taken, and space is provided for notes covering unusual maintenance, record of relay operations as indicated by targets and other matters of interest. A single spare circuit breaker is on hand which can be used to replace any of the existing breakers which require maintenance. For the circuits which are supplied from both ends, such as ties between substations, it is a simple matter to change circuit breakers without having interruption of service. For circuits which are strictly radial feeders, a time is chosen to interrupt service while the breaker is being changed which will cause the least inconvenience to the customer involved. In the six years of operation with these substations, only two minor cases of repairs in circuit breakers have been necessary.

We believe that the primary network

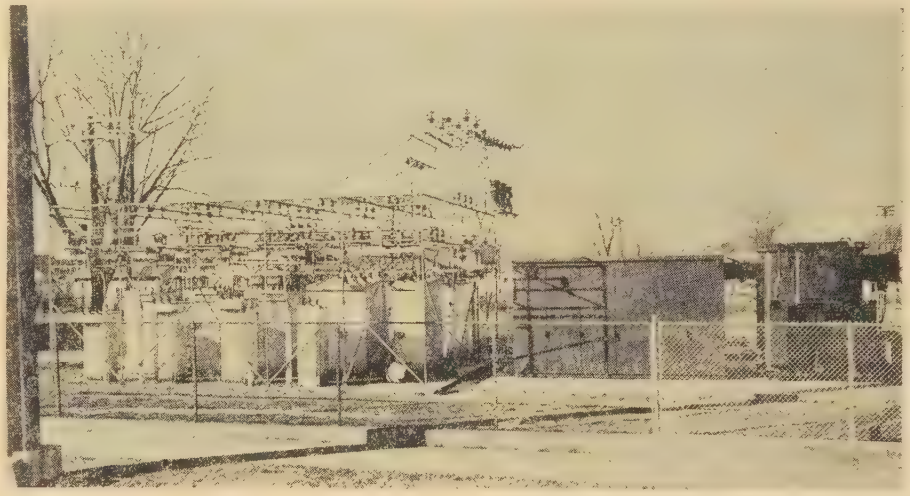

Figure 4. A 3,000/3,900-kva unit substation located in the same lot with a 1,500-kva substation of the open conventional design

The 1,500-kva open type substation was later removed and the material used at other locations

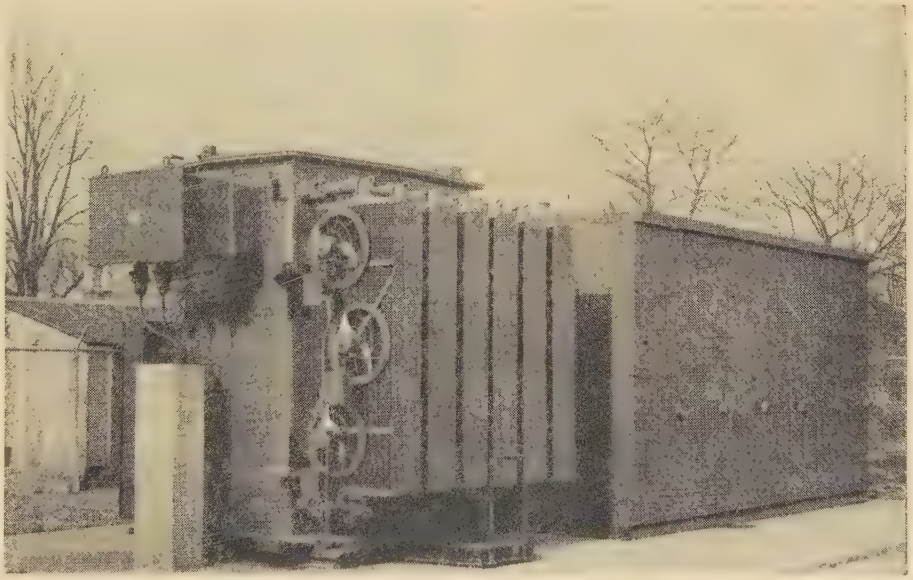

Figure 5. Close-up view of one of the standard 3,000/3,900-kva unit substations

and the use of unit substations have a number of advantages over the radial type of system. The location of the substation close to the load center keeps losses to a low value and provides for better regulation. The bulk of the energy is supplied at the subtransmission voltage which insures better system regulation and a more economical source of energy. The 3-phase low voltage lines provide better regulation with lower losses. The use of 3-phase tie circuits makes it easy to supply polyphase service to small commercial areas and outlying industrial locations. Spare transformer capacity is not required as in the conventional radial system. Voltage charts taken on the substation busses and on the customers' premises indicate that for the most part a smaller variation in voltage is maintained than where induction voltage regulators are used on radial-type feeder circuits. This of course accounts for better operation of appliances, particularly fluorescent lighting units, greater customer satisfaction, and increased revenue. Continuity of service through the use of primary network is excellent. The absence of induction feeder voltage regulators lowers maintenance costs as well as first costs, and operating and maintenance costs have been much lower than they are for the identical radial system.

We have found that a standard design of unit substation can be utilized to work out in the quad-city area as well as in the smaller outlying districts which incorporate a 3,000/3,900-kva transformer with one transformer secondary breaker and four feeder breakers. This size of transformer was chosen on the basis of cost per kilovolt-ampere and load density which we encounter in the area served, coupled with a reasonable distance between substations. Air blast equipment is supplied on the transformers when they are purchased and they provide an economical reserve capacity which is required occasionally in the event of other substations in the network being out of service at times of peak load.

In addition to the relays and other control equipment already mentioned as being standard with the substation used, we use a recording wattmeter, a recording varmeter, three recording ammeters, and a recording voltmeter of the strip chart variety to give us a continuous record of those quantities. These instruments are all connected into the leads of the transformer secondary so that the quantities measured pertain to the substation as a whole. A voltmeter switch is used to get a record of individual phase to ground voltages. A 1-week record per phase to ground quantity is normally obtained. No indicating or recording instruments are provided on the individual feeders. Test blocks are provided, however, on the control panel for each feeder to permit easy installation of portable recording instruments where checks need to be made for magnitude and division of load on each circuit.

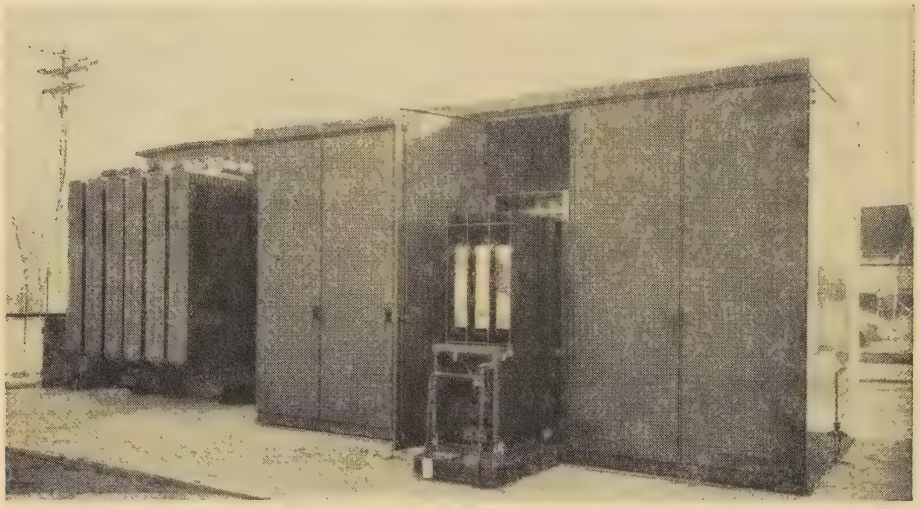

Figure 6. View of substation with air circuit breaker in drawn out position

Figure 7. View of one of the units set in edge of residential area, showing landscaping used

Provisions for future expansion are excellent. It is possible to add additional unit substations at any time at the points of maximum load growth and it is also possible to move a substation in its entirety if load shifts dictate, thereby salvaging the bulk of the investment in a substation installation. System planning through the use of a-c network calculators has permitted the selection of the most economical size of unit-type substation, the most economical number of circuits, proper loading of the various substations, proper control of regulation for the complete distribution system through the use of bus regulated substations, and adequate provision for future growth.

Frequent use is made of the a-c network calculator to keep ahead of network growth, to anticipate the requirements for additional substations, and to check the operation of the existing network. In this way we are able to check substation locations with respect to load growth and to anticipate well in advance the locations where future substations must be installed, and to plan network changes and additions to meet system requirements in the best way.

Systems Development of Military Communications

THOMAS R. PUTNAM
MEMBER AIEE

Synopsis: It is the purpose of this paper to set forth the broad phases of the problems involved in establishing a telephone and telegraph landline system in a military theater of operations, the manner in which these problems were met, and the results obtained in the North African Theater of Operations. The aspects reviewed are those involving the unification of the theater-wide wire facilities into a single system including maximum integration of civil plant and military installations, with centralized supervisory control of the available resources.

IN the North African Theater of Operations the landline communications system handled thousands of telephone calls and thousands of telegraph messages daily, over many hundreds of miles of telephone and telegraph channels involving distances, in some cases, greater than the distance between New York and Chicago. To provide an adequate system of communications for the Armed Forces in the field requires the fullest exploitation of the available communications resources, both personnel and equipment, if satisfactory service is to be furnished with maximum economy in the employment of these resources. The system communications problem involves a landline network and radio and submarine cable circuits operated as links in the landline network, both telephone and telegraph. To accomplish the mission of providing these communications, it is essential that an appreciation of the system philosophy be acquired by all concerned with the planning, engineering, installation, and operation of these facilities.

It might be worth while to consider for the moment the basic nature of the communication service required by the Armed Forces in areas in which extensive land and land-based air operations are carried out. In smaller units, perhaps up to and including division level in the ground forces, the primary purpose of communications is for fire control. That is to say, communications are required between commands posts, forward observers, observation posts, gun and infantry positions, and armored elements, to bring fire power to bear on the enemy when and where needed. Communications for this purpose have been largely on a point to point basis, especially in fast moving situations. However, as a given situation tends to become stabilized, a larger share of the traffic over the circuits is for administrative and supply service purposes, the number of users increases, the number of points required to be reached by telephone or telegraph increases, and switching facilities and system operation become a necessity.

Above division or perhaps corps level, the physical plant required begins to take on the appearance of a system network rather than a series of point to point routes. Many main routes are required, oftentimes passing through the areas of control of several commanders. For example, the requirements of the air forces for long haul circuits for intercept, tactical, and strategic air operations are governed by the deployment of the air forces. The location of the air installations depends not only upon the current tactical situation, but broad geographical and other considerations as well. Other governing factors in the location of main routes in the rear areas are the locations of ports of supply and other large administrative and supply centers. For these reasons the communications required to serve these areas must be considered as a system with many of the same problems we find in commercial operations.

In this connection, it seems desirable to look into the experience of commercial communications organizations and certain inherent features of their operations. The commercial operation of a landline communication service and its associated radio and submarine cable links has been described as a natural monopoly for the reason that the greater the number of facilities integrated into a single system, the greater is the value of the service to the users. It is on this basis that the need for a strong centralized control of the over-all operation is primarily recognized. This same necessity and reason exists in the development of a system of military communications. In addition, only by means of an integrated communication organization can the required flexibility in allocation of resources be attained to provide facilities when and where needed.

A major difference between the opera-

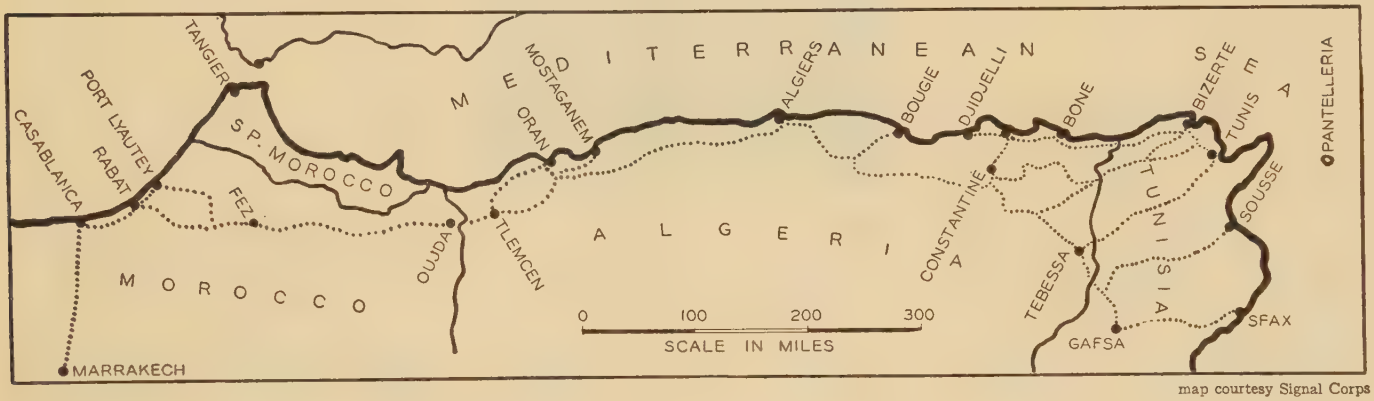

map courtesy Signal Corps

Figure 1. Map showing main landline routes in French North Africa

Approximate route distances, miles:	
Algiers–Oran	340
Algiers–Casablanca	890
Algiers–Constantine	320
Algiers–Bizerte	580
Casablanca–Marrakech	150
Casablanca–Bizerte	1,470

Paper 46-161, recommended by the AIEE committee on communication for presentation at the AIEE summer convention, Detroit, Mich., June 24–28, 1946. Manuscript submitted April 22, 1946; made available for printing May 27, 1946.

THOMAS R. PUTNAM is with the New York Telephone Company, New York, N. Y.

tion of a military communication system in the field and commercial operations, however, is the method by which the requirements are limited with respect to the available supply of facilities. In general, the normal peacetime demands on a commercial service are kept in reasonable balance with the available supply of facilities by virtue of the cost of the service to the users, which in turn is related to the investment. This means of regulating the needs of military users, however, is not applicable in areas of military operations, which is another reason for centralizing appropriate technical control of communications at the highest level of military authority in the area served by the system.

Another major difference between military and commercial systems is the fact that the development of a commercial system is usually characterized by an orderly change of requirements, with time factors permitting the installation of an economical, well-designed plant. However, the pressure of limited time in the development of a military network in a theater of operations seldom permits the thorough co-ordination of all concerned to the extent desired.

System Philosophy

The need for centralized control of communications facilities becomes apparent when we realize how closely the activities of a communications installation at one location must be co-ordinated with those of the installations at other locations. Satisfactory electrical communication has been established between two points only when a conversation can be held between the two, or a message can be transmitted from one point to the other with such quality and dispatch as will satisfy the user. Delays due to unwarranted interruptions or lack of co-operation between those responsible for operations at various points in the system are evidence of unsatisfactory service.

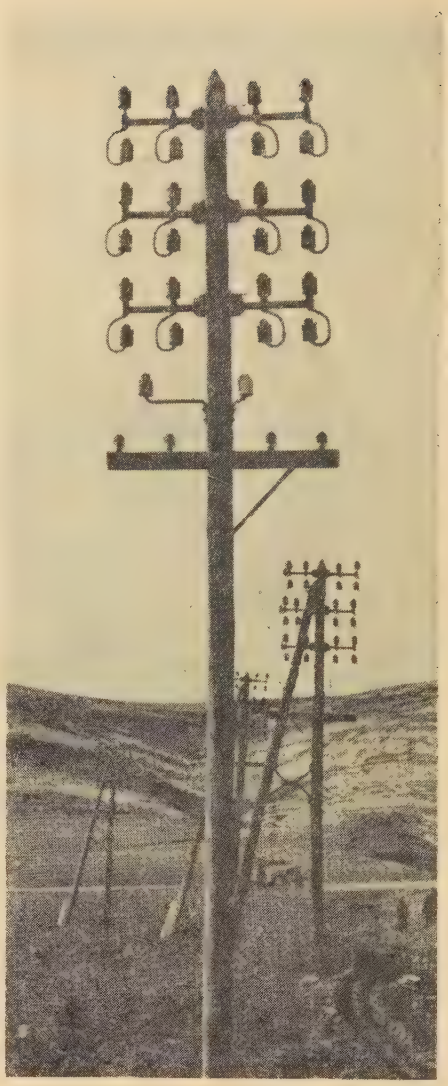

Signal Corps photo

Figure 2. Four-pin crossarm constructed by the Signal Corps on French civil open wire lead during combat in Tunisia

It is not sufficient that all individuals and organizations place and splice field wire or lead-covered cable; construct and maintain pole lines; place open wire; install and line up carrier terminal and repeater equipment; install, maintain, and operate telephone and telegraph switchboards and radio installations in accordance with the same manuals of instructions. These activities must be carried out by organizations and personnel in several commands at the same time. The only way this possibly can be done without delay and confusion is by adopting basic principles of military signal communication organization which will permit the designation of a single agency in advance to be responsible for laying down the ground rules under which this work is to be accomplished. Furthermore, these ground rules must be binding on all commands whose communications are an integral part of the system as a whole.

It may be accepted as axiomatic that rarely will sufficient resources be available in a theater of war to satisfy the communications requests of all users. It therefore becomes incumbent upon those responsible for providing this service to exercise the utmost in judgment and skill to bring about maximum economy in the employment of these resources. In view of the technical aspects involved in the interconnection and interoperation of the various equipment located hundreds of miles apart in many cases, it is easy to see why the centralized control of technical administration by an experienced and highly specialized staff assumes an important role in systems development.

To consider that it is only necessary to provide communications within the chain of command, that is, from superior to subordinate commanders, is to fail to appre-

Signal Corps photo

Figure 3. Signal Corps personnel operating a French civil switchboard with French interpreters at Oran

Signal Corps photo

Figure 4. Signal Corps personnel operating Creed teleprinters (British) at Allied Force Headquarters in Algiers

ciate the realities of modern operations. Were this the case, the provision of communications would be relatively simple. The problem is to provide a single network for use of all commanders and staffs of all elements of the armed forces occupying a given area, and it is under these conditions that complexity is added to the system. A further complication is added and in no small degree, in the provision of communications for joint operations involving the land, sea, and air forces of not only our own, but allied nations as well, utilizing the native resources of each, including civil systems.

In those overseas theaters in which organizational difficulties were encountered in systems development of communications during World War II, these difficulties stemmed from a basic deficiency in signal communications doctrine as promulgated by the War Department. Briefly stated, this doctrine sets forth the principle that every commander controls the system of communication required for his command. This principle of control by the several subordinate commanders must not be confused with the concept that the technical control of the single system of physical plant must be exercised by the common superior of these commanders. These two concepts of control are complementary and not inconsistent. For this reason they must be treated coequally in any pronouncement of signal communication doctrine for the Armed Forces.

Experience in the North African Theater of Operations—May to November 1943

Following the surrender of the Axis land forces in Tunisia in May 1943, the landline communication system of the Allies extended from Marrakech and Casablanca to Tunis and Bizerte in French North Africa, covering a maximum distance of about 1,600 miles. Communications operations expanded considerably following the cessation of ground combat operations for the mounting and support of two major amphibious operations, Sicily in July, and Italy (Salerno) in September 1943. To give some idea of the magnitude of the facilities required, following is a tabulation of the long haul channel mileages operated during the fall of 1943:

	Channel Miles	
1943	Telephone	Telegraph
September	26,500	29,300
November	38,300	34,400

The outside plant making up this network consisted of existing French civil (Services des Postes des Telegraphes et des Telephones) open wire leads and buried cable, American 10-pin and 8-pin open wire leads, American spiral four cable, and buried cable placed by both the American and British forces. Many of the French civil open wire leads in Tunisia had to be rehabilitated following combat operations in that area.

The equipment used to derive the long haul channels included French civil systems and varieties of American and British equipment available at the time. The French installations consisted chiefly of 1- and 3-channel telephone carrier systems operated over the open wire leads between Rabat and Oran. American telephone carrier equipment consisted of types *H* and *C* Western Electric systems, providing one and three carrier frequency channels, respectively; and Signal Corps type CF-1 which provides one voice frequency telephone channel and three carrier frequency telephone channels. British equipment consisted of the so-called "one plus one" (one voice frequency telephone channel plus one carrier-frequency telephone channel) and "one plus four" (one voice frequency telephone channel plus four carrier frequency telephone channels) tactical systems, and British SOS and SOT (three carrier frequency telephone channels) commercial systems.

Both American and British voice frequency telegraph systems were employed for long haul telegraph (teletypewriter and teleprinter) use. American types consisted of type 40-C-1 Western Electric (12 channels) equipment and the Signal Corps CF-2 (4 channels) tactical system. British voice frequency telegraph systems used, were the "speech plus simplex," "speech plus duplex," and "6 channel duplex" tactical systems. The "speech plus duplex" (S plus Dx) and "speech plus simplex" (S plus Sx) systems are designed to derive carrier telegraph from a portion of the frequency band used by a telephone channel while retaining the use of the channel for speech transmission. In the S plus Dx system the band from about 1,500 to 2,000 cycles is eliminated from the speech transmission circuit and used for telegraph purposes. The carrier midband frequencies employed are 1,680 cycles for one direction of transmission and 1,860 cycles for the other direction. Carrier is transmitted for marking and interrupted for spacing. The S plus Sx system provides service in both directions on a circuit but in only one direction at a time (American half

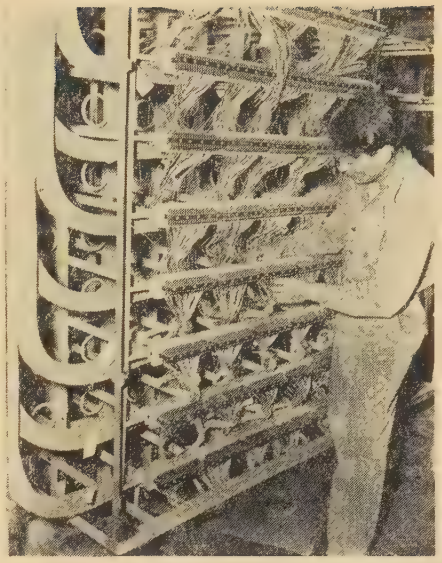

Signal Corps photo

Figure 6. Main distributing frame of the Freedom Exchange installed by the Signal Corps at Algiers

Signal Corps photo

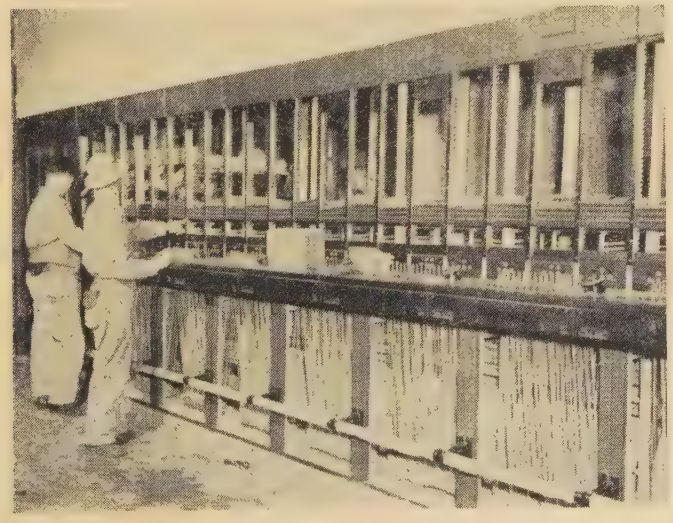

Figure 5. Switchboard installers of the Signal Corps at work on an 8-position Western Electric 11 type switchboard at Algiers

Duplex). A choice of carrier frequencies is available in this latter system depending on which of the three types of the equipment is used. Numbers 1 and 2 are arranged to use frequencies of 300, 900 or 2,300 cycles per second. The number 3 equipment uses frequencies of 300, 1,740, or 2,300 cycles per second.

Multichannel very high frequency radio equipment as developed and later used in other overseas military areas as links in landline systems was not available in the North African Theater; and a discussion of the point to point radio operations is outside the scope of this paper. In the fall of 1943 a limited amount of broadcasting was done over transmitters in the vicinity of Tunis from studios in Algiers, using landline program supply channels. Although these channels were not high quality, they did serve the purpose. Musical programs of the Special Services and foreign language news were broadcast for short periods at night. Also, on several occasions news broadcasts picked up at points in Tunisia were carried over landlines to Algiers where they were transmitted by radio to this country for broadcast.

The Mediterranean area has a rather well-developed civil network of submarine cables which proved to be extremely useful to the Allied Forces. A considerable volume of intratheater telegraph traffic was carried over these circuits particularly after the islands in the Mediterranean between French North Africa and Italy were occupied. In respect to security considerations, submarine cable circuits are unique in that they are acceptable for transmission of military telegraph traffic in clear text, including messages classified as secret, providing the water areas through which the cables pass are in complete control of friendly forces. In view of the shortage of automatic cryptographic equipment, the advantage of this was that arrangements could be made if the condition just mentioned were fulfilled, for the clearing of large volumes of telegraph traffic without the time-consuming burdens of manual cryptography.

To develop a theater-wide system of communications involving complex operating features as just described, it soon was found that staff responsibility without technical administrative authority over the operating personnel of the various subordinate commands was entirely unsatisfactory. The solution to this problem in French North Africa was to activate liaison offices called long lines district offices, in Oran, Algiers, Constantine, and Bizerte to be under the direct control of the wire division of the signal section, Allied Force Headquarters. This action was taken in September 1943. Signal Corps officers and enlisted men were assigned to these offices who were entirely familiar with the "big picture" of the system and who were technically competent to analyze maintenance and operations results.

Figure 7. Signal Corps personnel operating an 8-position Stromberg-Carlson 18 type switchboard at Constantine

Signal Corps photo

Telephone Operations

In September 1943 it was found necessary to restrict the number of telephones having access to the long distance service. Long distance calls were permitted from about 50 per cent of all the telephones connected to military switchboards. The effect of this policy was an immediate improvement in the service, and by October between 85 and 90 per cent of all long distance calls which were placed were completed on the first attempt on a non-hang-up basis.

The principal headquarters telephone switchboards completed an average of approximately 69,000 calls per day in the month of November 1943. Conservatively estimating the number of calls handled in addition on smaller switchboards for which records were not available, the total number of telephone connections was probably in excess of 150,000 per day.

Table I

Location and Switchboard Designation	November 1943 Type of Board*	Number of Positions	Number of Calls Per Day
Algiers			
Algiers long distance	WE 11	6	5,570
Freedom (local)	WE 11	10	20,457
Bizerte			
Bizerte (combination local and long distance)	TC-1	5	5,557
Eagle (local Eastern Base Section)	TC-1	3	5,003
Casablanca			
Beacon (combination Atlantic Base Section)	WE 550	3	6,589
Constantine			
Constantine (combination)	SC 18	8	5,829
Oran			
Merit long distance	TC-1	6	3,675
Merit local (Mediterranean Base Section)	WE 11	8	16,086
		Total	68,766

* WE—Western Electric; TC-1—Signal Corps nomenclature; SC—Stromberg-Carlson.

Table II. Landline Telegraph (Teletype) Traffic Data* for Certain of the Major Signal Centers in French North Africa—June and November 1943

Month	Allied Force Headquarters	Atlantic Base Section	Mediterranean Base Section	Eastern Base Section
June	95,638	27,379	42 938	18,650
November	114,057	9,886	52,187	27,926

* Daily average—incoming and outgoing words (excluding press).

The record of calls passed on the principal boards as recorded from actual peg counts is shown in Table I.

Telegraph Operations

The first voice frequency telegraph system in French North Africa using American equipment was installed in March 1943. Signal Corps CF-2 four channel equipment was installed in Algiers and Oran and operated over a French civil underground cable circuit. Prior to that time all voice frequency telegraph channels were provided by means of British equipment of the type mentioned earlier. Also, in the same month of March, sufficient teletype switchboards (Signal Corps BD-100) had become available to establish a common user telegraph printer network. Switchboards of this network were installed at Oran (Mediterranean base section), Algiers (Allied Force Headquarters, Air Force, port, and other service organizations), and at Constantine (Eastern Base Section); and at later dates the system was extended to include Casablanca, Tunis, and Bizerte.

The telegraph traffic load of several of the larger headquarters in French North Africa for June and November 1943 is shown in Table II.

Technical Administration

The development of a network of communications into an efficient system requires a scheme of technical administration which will enable each member of the communication team to know not only what his own duties and responsibilities are to carry out a given function, but also what other members of the team at distant points should be doing. For routine matters this is best accomplished through the medium of a set of uniform practices or instructions issued under a competent order to all concerned. A few of the activities which must be covered in this way are service order and trouble reporting routines, and long distance circuit order and facility record practices. These instructions must take into account all the conditions affecting the operation of the communication system, such as the communication procedures of all the military and civil agencies and commands involved in the operation, and the numerous types of equipment and organizations available to the military forces and civil communication administration. Instructions of this kind are applicable only to the communication system of a particular area of operations, and for this reason they must be prepared in the field by the agency responsible for the operation of the system. In the North African Theater of Operations these instructions were issued as "Operating and Maintenance Instructions," by the wire division of the signal section, Allied Force Headquarters.

By the fall of 1943, plant operations showed considerable improvement over earlier results. Contributing largely to this improvement were the extensive inside and outside plant preventive maintenance programs which were put into effect during the summer, the introduction of universal patching facilities, and the substantial on-the-job training acquired by the maintenance personnel. In addition, of major importance was the improved operation of the plant on a system basis following the activation of the afore-mentioned long lines district offices. For example, during the two months immediately following the establishment of these offices, telephone carrier troubles of one hour or more duration decreased 40 per cent, and similar telegraph carrier troubles decreased 50 per cent during the same period. These improvements in carrier maintenance operations provide strong evidence as to the soundness of the system doctrine applied to military communications operation. The over-all experience in the operation of the landline system in French North Africa leads inevitably to the conclusion that a single chain of command must exist from the very top down through all signal communication organizations involved in providing a communications system for military operations in a theater of war.

Frequency Compensated A-C Ammeters and Voltmeters

J. M. WHITTENTON
MEMBER AIEE

C. A WILKINSON
NONMEMBER AIEE

Synopsis: The increased use of a-c instruments over a frequency range of 25 to 3,000 cycles for aircraft and industrial applications has imposed new requirements on instrument design. It is recognized that the standard type of a-c ammeters and voltmeters normally calibrated for use at a given frequency are subject to errors in indication when used at other frequencies. This paper describes the manner in which one line of a-c ammeters and voltmeters can be compensated to have minimum errors resulting from changes in frequency over a range of 25 to 3,000 cycles. Errors found in the uncompensated and compensated types of instruments with changes in frequency are shown, and a practical means of determining the amount of compensation and its application to ammeters and voltmeters is presented.

FOR many years the conventional types of a-c ammeters and voltmeters have been designed for operation over a small range of power frequencies from 25 to 125 cycles per second and have been used primarily on 25-, 50-, and 60-cycle circuits. In recent years, however, the operating frequency range has been extended[1] and instruments have been designed with improved magnetic materials to operate accurately over a range of 15 to 12,000 cycles. Some of the more common frequencies encountered in the extended range have been 180 cycles for portable machine tools and high speed motors, 400 and 800 cycles for aircraft, 960 to 3,000 cycles for electric furnace applications, and from 8,000 to 12,000 cycles for industrial heat treatment use.

The more general method of instrument adjustment has been to calibrate at 60 cycles for use at 25 to 125 cycles and at the specified operating frequency for higher ranges. This procedure in the past has proved satisfactory and, generally speaking, variations up to 20 per cent of the calibrated frequencies have not produced objectionable errors. A rapidly increasing demand, however, has developed recently for instruments to be used over much wider frequency ranges. For example, in aircraft there have been applications for instruments for use on not only 400 but 800, 1,200, 1,600, and 2,100 cycles. The problem of equipping these airplanes and maintaining replacement supplies would be simplified greatly if an instrument calibrated at one frequency

Paper 46-155, recommended by the AIEE committee on instruments and measurements for presentation at the AIEE summer convention, Detroit, Mich., June 24–28, 1946. Manuscript submitted February 21, 1946; made available for printing May 24, 1946.

J. M. WHITTENTON is assistant design engineer and C. A. WILKINSON is an engineer in the electrical instrument engineering division of General Electric Company, West Lynn, Mass.

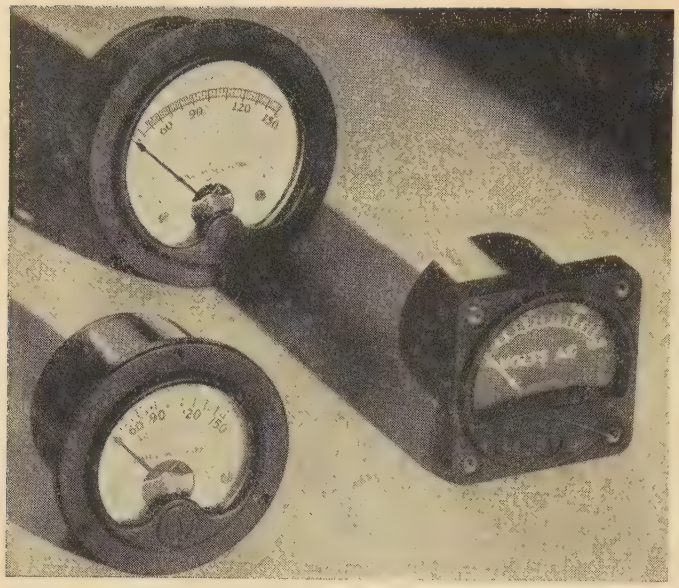

Figure 1 (left). Representative panel type a-c instruments for industrial and aircraft applications

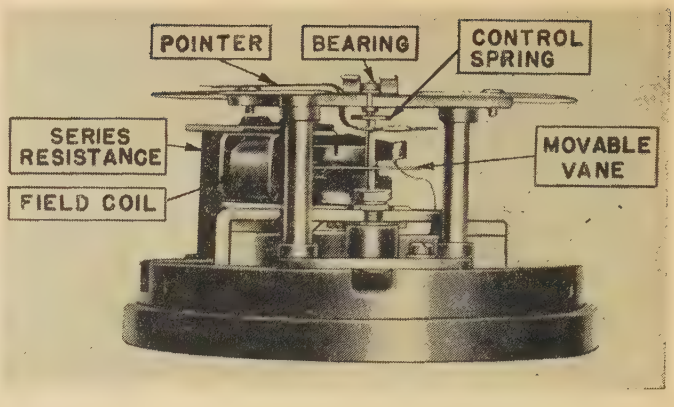

Figure 2 (above). Instrument assembly showing mechanism and internal construction

also would perform accurately over the complete range. Similarly, in many modern industrial and electronic applications the operating frequency may vary over ranges much in excess of 20 per cent of the calibrating frequency. These conditions have created a need for instruments which are compensated over a wide frequency range. A method of compensation and the results obtained are described in this paper.

Errors in Uncompensated Voltmeters and Ammeters

The moving iron instrument of the attraction type used for many a-c ammeters and voltmeters is shown in Figure 1 in typical sizes. Briefly, the mechanism of this instrument consists of a vane of high permeability material moving within a fixed coil and mounted on a nonmagnetic shaft which carries the indicating pointer and is supported in suitable bearings. When current flows in the fixed coil, a magnetic field is set up which tends to pull the magnetic vane into the coil. The rate with which the vane is pulled into the coil is controlled by a flux distributor, and the movement is opposed by the torque of a control spring attached to the shaft. The internal construction of this type of instrument is shown in Figure 2.

This mechanism is used in ammeters by allowing the current to be measured to flow through a field coil. For voltage measurements, the mechanism is connected across the line and in series with a fixed resistance, to permit a current proportional to voltage to flow through the field coil. The electrical circuit of a standard uncompensated voltmeter is shown in Figure 3.

The voltmeter is subject to frequency errors which are caused by changes in the inductive reactance of the field coil and of the series resistor, and in the effective a-c resistance of the coil. The impedance of this typical design at 60 and at 3,000 cycles is shown vectorially in the two diagrams in Figure 4. While the change in inductive reactance is directly proportional to the change in frequency, the relation of the change in effective resistance with frequency is more complex. It has been shown previously[2] that the eddy current losses in magnetic circuits vary as a nonlinear function of the frequency, and have the same effect as a resistance which shunts the field coil and decreases the current through it. The combined effect of these two factors is to increase the circuit impedance and decrease the indication for a given voltage as the frequency increases.

An example of errors in an uncompensated voltmeter of this type is shown by the calibration check of a typical 150-volt voltmeter in Table I. The instrument was calibrated at 60 cycles and checked over a frequency range of 60 to 3,000 cycles. The differences in readings at 60 cycles and other designated frequencies are expressed in per cent of full scale voltage. This rating of voltmeter has a series resistance of 14,000 ohms which limits the current through the field coil to 10 milliamperes.

The frequency error in ammeters of the moving iron type is caused only by the change in eddy current losses and is not affected by inductive reactance changes which merely cause a change in the voltage drop across the coil, but not in the current through it. As a result, the overall error is considerably less than that found in voltmeters. For example, the error of a 5-ampere ammeter, similar in general design to the 150-volt voltmeter described and adjusted on 60 cycles, does not exceed minus 3 per cent at full scale indication on 3,000 cycles.

Method of Frequency Compensation for Voltmeters

A study of frequency errors shown in Table I, indicates that voltmeters should be compensated for frequency changes when calibrated at one frequency and used over a wide range of different frequencies. The ideal, from the users standpoint, would provide compensation to hold the magnitude of the total effective impedance constant even though the values of the resistive and reactive components change as the frequency varies. A study of prior methods[3,4] has shown that compensation can be obtained by shunting all of the series resistance with a capacitor of required value if the resistance of the series resistor is relatively large as compared with that of the field coil.

This method is very undesirable for use in quantity production, as the value of capacitance must be held within much closer limits than the standard plus or minus 20 per cent tolerance in the micro-

Table I. Uncompensated Instrument Errors Over Frequency Range

Expressed in Per Cent of Full Scale Value

Standard Voltage	Cycles				
	60	400	1,200	2,000	3,000
60	0	−0.8	−2.3	− 4.9	− 8.9
90	0	−1.1	−3.6	− 7.6	−11.2
120	0	−1.1	−4.7	− 9.3	−14.8
150	0	−1.5	−5.1	−12.0	−22.0

farad values of capacitors which are available in quantity, and in the dimensions required. Furthermore, such capacitors will be subject to peak voltages which are more than can safely be impressed on them. For example, a capacitor which shunts 14,000 ohms of a 15,000-ohm instrument circuit would be subjected to a peak voltage of 198 volts at full scale indication, and to even much higher values for intermittent overloads to which instruments may be subjected.

These difficulties, however, can be overcome largely by shunting only a portion of the series resistor and varying the resistance value of this portion to match the actual capacitance of a given capacitor. Since the value of this resistance is determined during the test procedure, and the resistor spool then is wound to the required resistance, it is not necessary to maintain a large inventory of these resistor spools, and commercial tolerance capacitors can be used without difficulty in quantity production. In addition, the voltages likely to occur across them are reduced to safe values.

With this method, the amount of compensation and, therefore, the magnitude of the remaining error in a given voltmeter, depends upon the per cent of the series resistor which is shunted and the value of capacitance used. The effect of different per cents of series resistor shunted, and the magnitude of errors over a 60- to 2,500-cycle frequency range, is indicated in Figure 5. As shown, shunting 58 per cent of the resistor with a 0.004-microfarad capacitor reduces the errors to a maximum of 1/4 per cent over the frequency range. If, however, this compensation is used on 3,000 cycles, a 1 per cent error will occur. On the other hand, errors over the range extended to 3,000 cycles can be made negligible by shunting 75 per cent of the resistor with 0.003 microfarad.

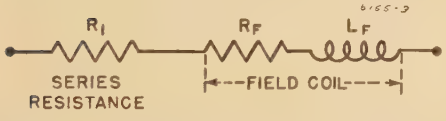

Figure 3. Schematic diagram for uncompensated moving iron type voltmeter

R_F—Field coil resistance
L_F—Field coil inductance
R_1—Series resistance

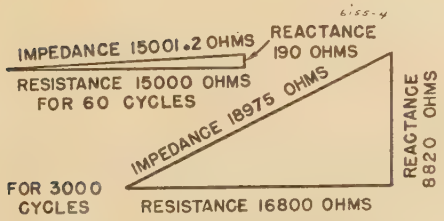

Figure 4. Vector diagrams showing how internal impedance varies with frequency

Application of Method to Actual Voltmeters

It is important to note that the preceding values are for an individual voltmeter and will differ slightly with each instrument as a result of the tolerances which must be allowed in the components. The different values of series resistance which were shunted by a fixed value of capacitance in order to fully compensate a group of six instruments are shown in Table II.

Table II. Variations in Resistance Shunted by Fixed Capacitance

Capacitor Rating, μf	Resistance Shunted, Ohms	Resistance Unshunted, Ohms	Per Cent Shunted
0.003	10,300	3,700	73.6
0.003	10,385	3,615	74.1
0.003	10,390	3,610	74.1
0.003	10,520	3,480	75.3
0.003	10,715	3,285	76.6
0.003	10,880	3,120	77.7

This method of shunting a portion of the series resistance approaches closely the ideal compensation by maintaining nearly constant the magnitude of the total effective impedance over wide frequency ranges. This is shown in Table III for which the equivalent resistance R_e and the equivalent reactance X_e have been computed from measured values for each component by using the following equations:

$$R_E = R_F + R_1 + \frac{R_2}{R_2^2\omega^2C^2+1} \text{ ohms}$$

$$X_E = j\omega\left(L_F - \frac{R_2^2C}{R_2^2\omega^2C^2+1}\right) \text{ ohms}$$

where R_F, L_F, R_1, R_2, and C refer to the components shown in Figure 6. The vector relationship of these values at 3,000 cycles is shown in Figure 7.

The data in Table III were taken for the full scale point only, and other points on the scale will vary slightly as a result of changes in the demagnetizing effects in the magnetic circuit resulting from the movement of the vane in and out of the field coil. The magnitude of such changes is shown in Table IV and is considered satisfactory for the applications previously mentioned. It is significant to note that the scale distribution changes with frequency and that such changes are more pronounced at the higher frequencies.

The application of this method of frequency compensation to large quantity production of voltmeters is entirely practical. The voltmeter first is adjusted at 60 cycles with the fixed coil in series with the resistance required for full scale. The frequency then is changed to 3,000 cycles, which increases the instrument impedance and decreases the pointer indication. A commercially available capacitor of approximately the right value then is connected across a sufficient amount of series resistance to bring the pointer again to the full scale point. This adjusting technique can be adapted easily to simplified test procedure by using standard resistors of different values which can be quickly connected to the instrument circuit by a selector switch.

Compensation of Lower Range Voltmeters

The discussion thus far has been restricted to voltmeters rated 0–150 volts. Lower range voltmeters can be compensated in the same manner if certain new problems are solved. In order to assure adequate factors of merit and temperature compensation, it is necessary to maintain a given number of ampere-turns for the field coil, and a definite ratio of the resistance of the copper in the

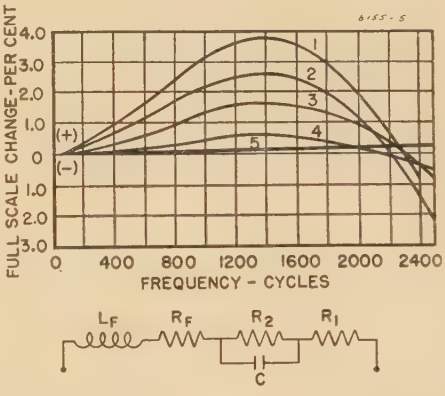

Figure 5. Degree of compensation for different percentages of series resistor shunted by specified value of capacitance

Decade Box For Resistors R_2 and R_1

Curve	Ohms R_F	Ohms R_2	Ohms R_1	μf C
1	1,000	3,645	10,650	0.025
2	1,000	3,300	10,700	0.025
3	1,000	4,200	9,800	0.015
4	1,000	5,750	8,250	0.008
5	1,000	8,100	5,900	0.004

field coil to that of the series resistor which is wound with negligible temperature coefficient material. These and other factors result in the series resistance decreasing more rapidly than the field coil impedance, as the full scale voltage rating is reduced. As a result, voltmeters in ranges below 75 volts do not have sufficient series resistance to be shunted for correct frequency compensation. It is necessary, therefore, either to make some sacrifice in performance or to design special high frequency instruments for such ratings to obtain effective compensation.

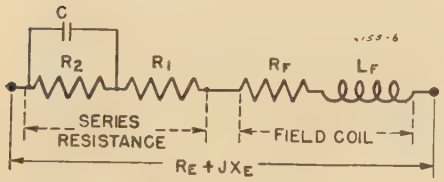

Figure 6. Schematic diagram for compensated moving iron type voltmeter

R_F—Field coil resistance
L_F—Field coil inductance
R_1—Unshunted series resistance
R_2—Shunted series resistance
C—Capacitor

Compensated Ammeters

It has been pointed out previously that the frequency errors in the ammeters are relatively small as compared with those found in voltmeters and principally are a result of eddy current losses. These losses can be reduced to a minimum by the use of high resistivity material such as phosphor-bronze for the field coil form and high permeability material such as permalloy, mumetal, and nicaloi in proper combination in the magnetic circuit. As a result, errors in ammeters are reduced to negligible values over the frequency range of 60 to 3,000 cycles.

Table III. Variation of Total Effective Impedance With Frequency

Frequency, Cycles Per Sec	R_E, Ohms	X_E, Ohms	Z_E, Ohms	Per Cent Variation of Z_E From Value at 60 Cycles*
60	15,030	70	15,030	0
400	15,090	493	15,090	+0.40
1,200	15,030	1,280	15,080	+0.33
2,000	14,820	2,130	14,970	−0.40
3,000	14,300	4,290	14,960	−0.50

* With the sign reversed these values are equal to the per cent error at full scale caused by frequency variation.

Table IV. Typical Scale Errors Over Frequency Range in Per Cent of Full Scale

Standard Voltage	Cycles 60	400	1,200	2,000	3,000
150	0	0	0	0	0
120	0	+0.1	+0.2	+0.6	+1.4
90	0	−0.3	−0.8	−0.1	+1.1
60	0	+0.4	−1.1	−1.1	−0.7

Conclusions

A practical technique of frequency compensation has been developed which can be applied easily to standard a-c instruments. The compensation has been accomplished first, by the use of improved magnetic materials in the ammeter and voltmeter, and secondly, by the addition of a commercially standard capacitor to the voltmeter.

By the application of these simple improvements in existing designs it is possible to use instruments normally adjusted for accuracy to within plus or minus two per cent of full scale value for one frequency, over a wide range of 25 to 3,000 cycles without incurring additional errors in excess of two per cent.

It is hoped that this work will encourage the use of frequency compensated a-c instruments to replace those now calibrated for a standardized frequency of either 60, 400, or 800 cycles as well as those calibrated for other specific frequencies. This will insure more accurate measurement of current and voltage over a wide range of frequencies.

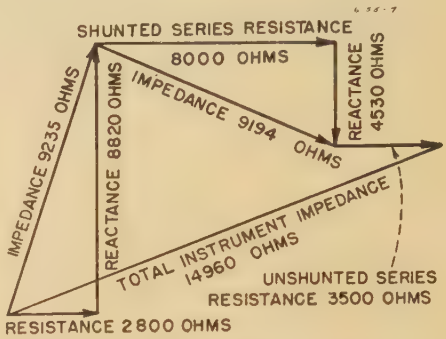

Figure 7. Vector diagram showing total instrument effective impedance at 3,000 cycles

References

1. Performance of Conventional Indicating Instruments on Frequencies up to 3,000 Cycles, S. C. Richardson. *General Electric Review*, volume 46, October 1943.

2. Alternating Current Circuits (book), R. M. Kerchner, G. F. Corcoran. John Wiley and Sons, Inc., New York, N. Y., 1938.

3. Electrical Measuring Instruments, volume 1, C. V. Drysdale, A. C. Jolly. D. Van Nostrand Company, New York, N. Y., 1924.

4. Electrical Measurements and Measuring Instruments (book), E. W. Golding. Sir Isaac Pitman and Sons, Ltd., London, England, 1942.

Sensitive Ground Relay Protection for Complex Distribution Circuits

LLOYD F. HUNT
FELLOW AIEE

Synopsis: Protection engineers always have desired to obtain a system of ground fault protection that will discriminate and actually trip out only the ground faulted circuit of a complex distribution network. This has been a difficult chore because the magnitude of the ground current often varies so greatly as to be out of the range of the normal protective relay settings. A system is proposed here that not only has proper discrimination, but also operates on very low amounts of ground current with the maximum ground current held to such a low value that practically no harm or damage is done by the ground fault. This development was encouraged by the necessity of joint use of poles by lines of communication circuits and distribution circuits. This method comprises the installation of a small bank of grounding transformers at each of the stations where the lines originate or terminate. With these small ground banks the maximum ground fault current is very small. Adequate relays and systems are used to isolate only the faulted sections of line. The installation of one 11-kv and one 16.5-kv loop will be described. These two systems have had several years of successful operation.

Conclusions

THIS type of sensitive ground relay protection will discriminate on ground currents in the order of one per cent of the current transformer ratings, that is, with a 200–5 current transformer on the circuit, a fault of two amperes ground current will cause proper tripping.

The maximum ground current can be arranged to be from 40 to 60 amperes. This low current can do little harm as compared to the damage caused by a current of several thousand amperes that may occur in the solid grounded neutral systems. It has been found by years of operating experience that the damage done on ground faults with this type of protection is negligible.

Tests have been made with tree grounds and it has been shown that conductor contacts on green trees do not pass sufficient current to trip the lines out from this cause. Years of operating experience have confirmed this fact.

The operation of this relay scheme can be made very fast, thus eliminating ground faults rapidly. Since the control of the ground relays can be used to control the phase relays, phase-to-phase short circuits also can be cleared rapidly.

Introduction

Continuity of service to the customers of electric power utilities always has been one of the main problems of the protection engineer. Complex and interconnected high voltage circuits have been common for a long time. The protection of these circuits has been satisfactory and is improving continually. The lower voltage circuits have the same advantage of giving better continued service when interconnected. This has been done for some time but there has been no reliable way of isolating ground-faulted feeders correctly when the range of ground current has been so great. Therefore development of such a system was begun. Various standard types of relays were applied to many systems and no reliable discrimination could be obtained.

Then two further requirements became apparent:

1. If successful operation is to be obtained in joint pole use, the distribution line upon contacting the telephone circuit should be isolated rapidly and with as small amount of current as necessary to properly clear the distribution circuit. It is important to both the telephone utility and the power utility to make these fault damages a minimum as they both serve the same customers and continuity of both services is important.

2. The damage to property and the hazard caused by fallen live wires makes it necessary to isolate and de-energize them as rapidly as possible and with as small amount of ground current as necessary.

It can be seen that the same relay system can accomplish each type of ground fault isolation. During many years, ground tests were conducted with many types of relay systems and many improved ones were developed, but most of them were not adequate to service a complex distribution system. The system described here was finally suggested and tried. Although rather complicated for distribution circuits, it has proved successful with years of experience. Several improvements have been made to facilitate operation. The system herein described is now in service on some of the

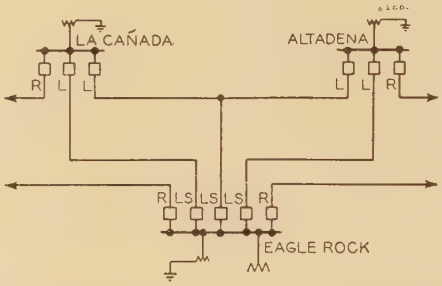

Figure 1. Eagle Rock substation 16-kv loop system

Figure 2 (below). Katella and Fairview substations 11-kv loop system

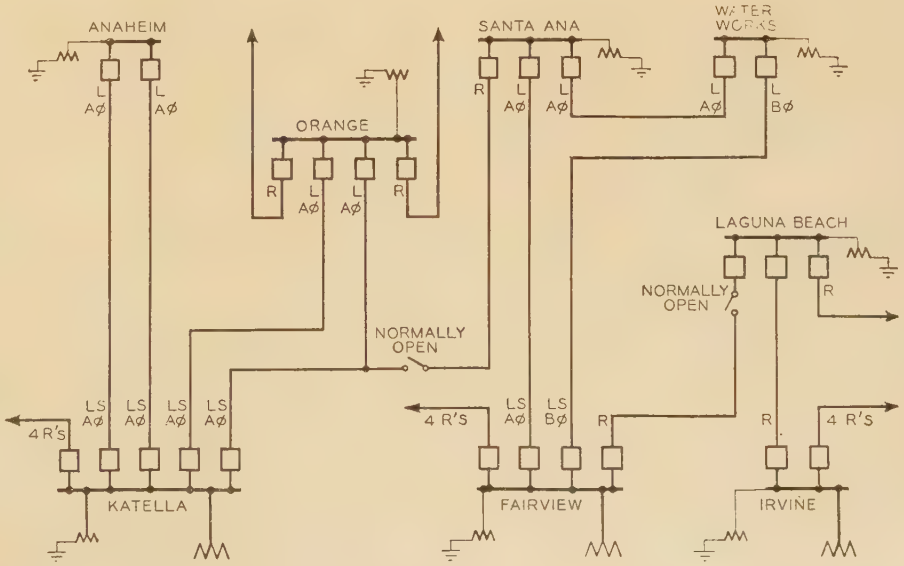

Paper 46-200, recommended by the AIEE committee on protective devices for presentation at the AIEE Pacific Coast meeting, Seattle, Wash., August 27–30, 1946. Manuscript submitted June 14, 1946; made available for printing July 24, 1946.

LLOYD F. HUNT is chief electrical engineer, Southern California Edison Company Ltd., Los Angeles, Calif.

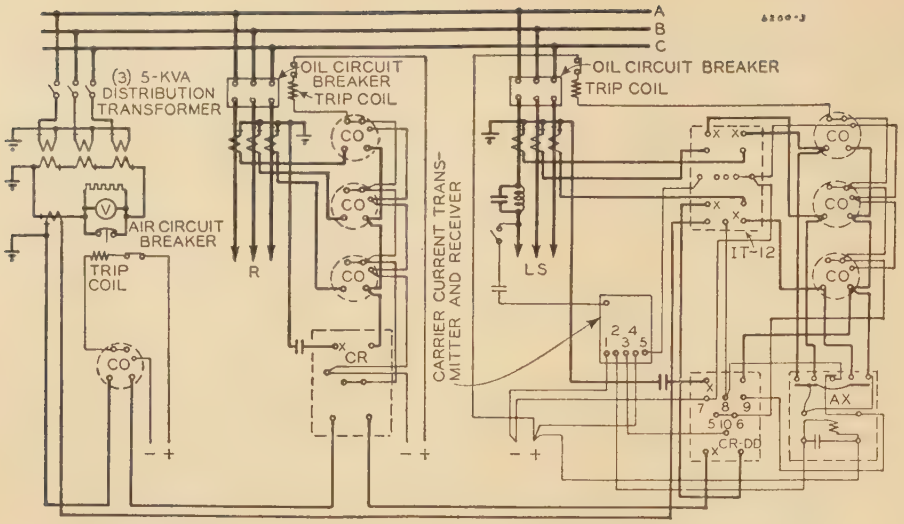

Figure 3. Source station relay system

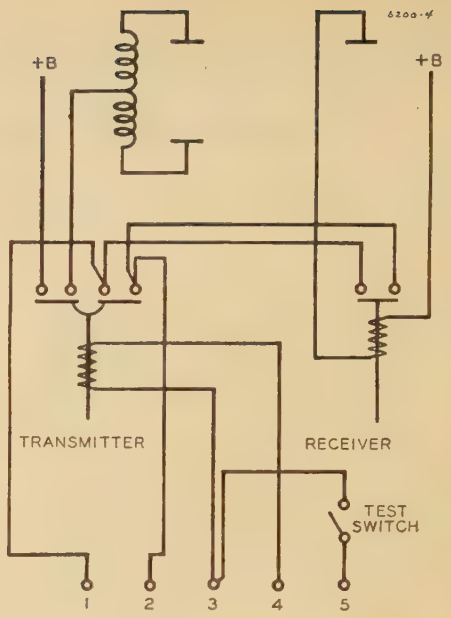

Figure 4. Carrier set relay system

distribution circuits of the Southern California Edison Company Ltd.

Complex Distribution Systems

The sensitive relay systems were applied to one 16-kv network as shown in Figure 1 and a more complicated 11-kv network as shown in Figure 2.

At each station a small grounding bank of three 5-kva distribution transformers is installed.

It can be seen that a separate type of protection is required for:

1. Radial feeders, designated by *R*.
2. Loop feeders at the source station, designated by *LS*.
3. Loop feeders at the receiving stations, designated by *L*.

Relay Systems

The diagram in Figure 3 shows the relay protection, type *R* and *LS* required for source stations such as Eagle Rock substation shown in Figure 1, and Katella and Fairview substations shown in Figure 2. This diagram shows only one radial feeder and one loop feeder. Additional feeders are exact duplicates of one of these types. Figure 4 is a schematic wiring diagram of the relays used in conjunction with the transmitting and receiving sets. Figure 5 is an internal diagram of the special fault detecting relay *IT-12*. The radial feeder relay system is the same as that described in a previous paper.

It can be seen (Figure 3) that the grounding bank consists of three 5-kva distribution transformers. The primary windings of these transformers used in Figure 1 are 16.5 kv, the secondary windings, 115 volts; and the ones used in Figure 2 are 12 kv to 120 volts.

The grounding bank secondary delta is closed by an air circuit breaker which is controlled by an over-current relay. In the event the relay protection takes longer than a predetermined time to clear a ground fault, the over-current relay will operate, thus opening this delta circuit breaker. When the circuit breaker is open a voltmeter across the delta indicates percentage ground faults. Only at the source station is there a resistor of such conductivity as to prevent resonance, thus preventing high voltages when the system becomes ungrounded.

Because the grounding banks at the various stations are small, their impedance is high in relation to the line impedance. Therefore a ground fault at any location will cause all grounding banks to produce almost the same amount of ground current. The maximum ground current depends upon the number of ground banks used in a given system when a solid ground fault occurs. The magnitude of ground fault current then will range from a minimum to this maximum, inversely as the resistance in the ground fault.

Since the line impedance is so low, the problem of discriminating by time is impossible. It therefore is necessary to use a blocking method to prevent improper ground relay action. In the two locations shown in Figures 1 and 2, carrier current sets[2] are used to send the necessary lockout signals. Pilot wires could be used for the signal channel but at the above locations the carrier sets proved more economical.

The directional ground relay type *CR-DD* is made as shown by the internal connection diagram, Figure 6. This relay is similar to a directional-controlled single-phase power directional relay except that the directional contacts have duodirectional function. When contact 8 closes to contact 10, it activates a transmitting relay sending a signal to the remote end of that circuit to lock out the tripping relays, thus preventing them from operating. When contact 8 is closed in the opposite direction, the relay is in tripping condition.

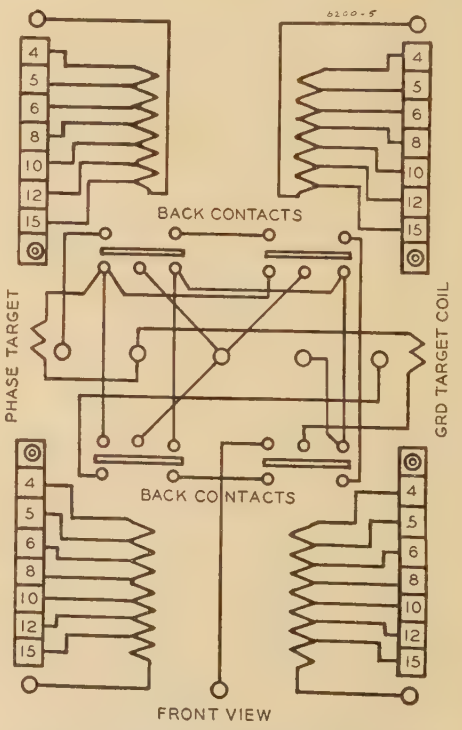

Figure 5. Internal connections of special fault detecting relay type *IT-12*

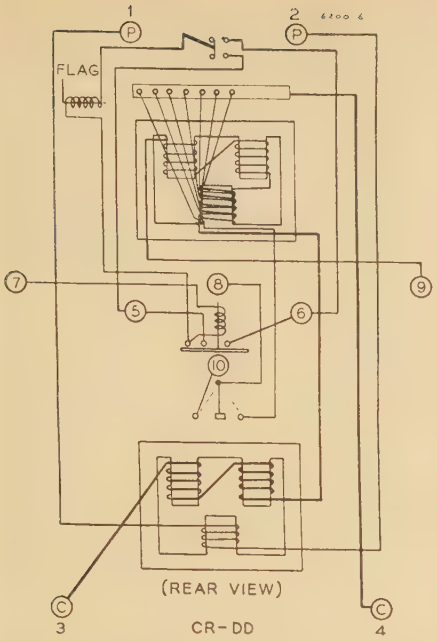

Figure 6. Internal wiring diagram of special ground relay type *CR-DD*

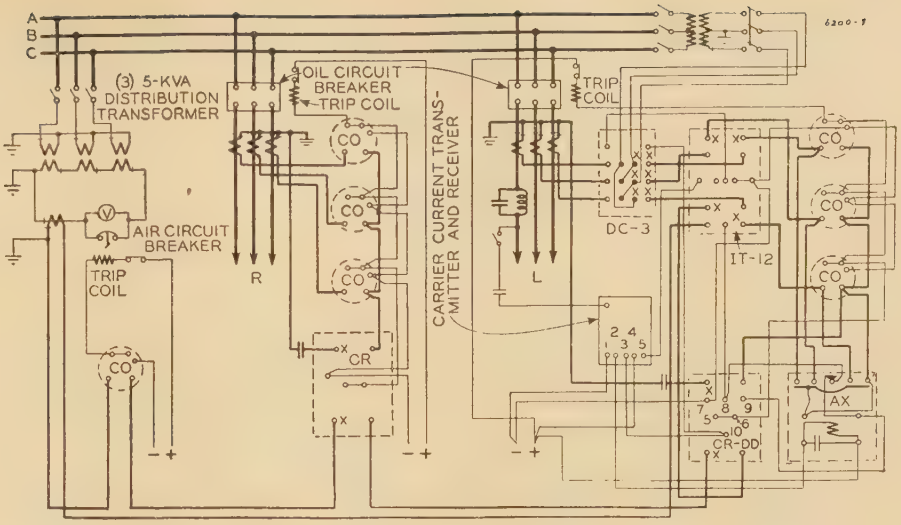

Figure 7. Receiving station relay system

Figure 7 is a diagram of the relay setup at receiving stations consisting of one radial feeder and one loop feeder. This setup is different in that there is no limiting resistor in the secondary delta circuit and a phase directional relay has been added for phase protection. The reason no phase directional relay is necessary at the source station is apparent in that any phase-to-phase short-circuit current is away from the station and not toward the station. The over-all operation of the system is simple and makes use of the fact that if fault current flows through a feeder toward a station bus, that feeder is unfaulted and should not relay. Therefore in Figures 1 and 2, ground current faults can flow toward any station in the loop feeders while phase-to-phase current can flow in the feeders only toward receiving stations. For example, should a ground fault occur on the radial feeder out of Katella, a source station, ground current will flow toward Katella on the two feeders from Orange and the two feeders from Anaheim. If a phase-to-phase occurred on this radial feeder, no short-circuit current would flow on these four feeders. If a ground fault occurred on a radial feeder out of Orange substation, ground current would flow in the two Orange circuits in the opposite direction from the foregoing case, while the current in the two Anaheim lines still would flow toward Katella. However, if a phase-to-phase fault occurred on this feeder, short-circuit current would flow toward Orange on its two circuits and none on the Anaheim lines.

This relay system will cause a directional relay to close contacts when fault current is flowing toward a station bus. If the fault is phase-to-phase it will cause the polyphase directional relay *DC-3* to close contacts, and if the fault is phase-to-ground it will cause the ground directional relay *CR-DD* to close contacts. If the fault current is of sufficient magnitude it will cause the fault detector relays *IT-12* to operate its contacts. The contacts of each of these two sets of relays are in series and energize the transmitting relay which causes the carrier set to transmit, sending a signal to the remote end of the distribution circuit to prevent the relays at that end from tripping. This is accomplished by having the receiver relay energize the lockout relay *AX*. The lockout relay short-circuits the operating coils of the over-current phase tripping relays and opens the directional control of the ground tripping relay, thus preventing the operation of the tripping relays. This is done also at the transmitting end by energizing the lockout relay directly from the transmitting relay *TR*. Figure 6 is an across-the-line diagram to show schematically the connections of these various relays.

Because the receiving substations are all unattended, it became necessary to devise a method of routine testing of the entire carrier relay circuits. The receiver relays are set to operate at two milliamperes current and the second receiver relay has a setting of five milliamperes. This second relay is used normally as a signal relay so that when reception is below five milliamperes, it will not function. Therefore, the scheme of testing must have the operator at the source substation transmit on one of the loop circuits. This will cause the signal receiver relay at the remote or receiving substation to operate, which in turn causes the transmitter of the other circuit at the receiving substation to transmit to the signal receiving relay at the source substation energizing a pilot light. This gives a positive check on carrier operation in that direction. By energizing the other transmitter at the source substation, a positive check is made for carrier transmission in the opposite direction. In Figure 1, if the transmitter is energized on the Altadena line at Eagle Rock, the receiver relays of the other two circuits should indicate proper transmis-

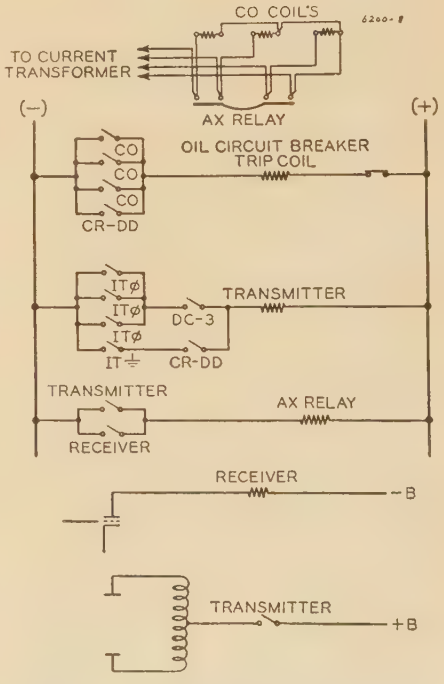

Figure 8. Across-line diagram of relay system

Application Ratings of Indoor Power Circuit Breakers

O. B. VIKOREN
MEMBER AIEE

Synopsis: Increased cost involved in serving electric power to customers, and the aim to lower rates, have accelerated the need for most efficient utilization of existing generating and distribution equipment. The paper describes a method for loading power circuit breakers on a temperature basis for the purpose of taking advantage of their inherent current carrying ability. Several years of practical application of the basic theory has proved entirely satisfactory on various types of electric equipment and has, in many cases, established considerable savings on new investments. While these savings apply to a lesser degree to circuit breakers than to other major power equipment, their application in accordance with temperature, rather than name plate rating, has put the use of new and existing facilities on an equally sound engineering basis.

AS A RESULT of the increasing need for better utilization of high-voltage line capacities, the question arose some years ago as to what maximum safe overloads could be carried on existing line equipment during emergency conditions. It is the practice to consider the firm capacity of a load distribution center as the summation of the capacities (ratings) of all associated supply lines except one, assuming for discussion purposes that the characteristics of all lines under consideration are the same, so far as current carrying ability is concerned. Heretofore, the individual lines had been loaded to less than 100 per cent of their published ratings under normal operating conditions, and slightly overloaded only during emergency. This is not to imply that rational overloading of equipment had never been practiced before; in fact, certain transformers had been operated on a temperature basis for a number of years. However, the temperature limits used were, as a rule, those which were set up for the entire industry by the AIEE, or in a few isolated cases, determined by tests on the system. Certain power circuit breakers also had been included in these tests, but a practice of overloading equipment in general, on a true temperature basis, had not been firmly established. In the proposed setup, the optimum conditions would be to operate each line normally at 100 per cent of its true rating and apply correspondingly heavier overload during emergencies, even if a small percentage of the equipment life had to be sacrificed at each occurrence. The emergencies were estimated to last for relatively short periods of time in the majority of cases, that is, a relatively heavy overload might be expected for the first two hours, but after that time some relief would be provided by load transfer, and after four hours the load per line would, as a rule, be expected to be reduced to the normal capacity of the line.

Before such a setup could be adopted, however, various pieces of equipment, comprising a line from the source to the receiving end had to be investigated; thus also, power circuit breakers. In the early attempts to load equipment on a true temperature basis, very little information could be obtained from current literature on the effect of overload on circuit breakers, and the manufacturers were cautious in their statements regarding overload capacity because they were becoming aware of the fact that, among older types of circuit breakers, only those with practically new contacts would stay within the temperatures permitted by the AIEE Standards under full load conditions. The manufacturers were fearful that overload of 2- and 4-hour durations might tend to weaken the contact structure and, in the case of most types of oil circuit

Table I

Circuit-Breaker Name Plate Ratings	Per Cent Service Factor	
	Copper Contacts	Silver Contacts
2.4-kv and 4-kv service		
600–1,200 amperes	75	100
2,000 amperes and above	65	90
All types of metalclad switchgear		100
13-kv service		
600–1,200 amperes	80	100
2,000 amperes and above	75	90
All types of metalclad switchgear		100

1. When circuit breakers, except for metalclad units, are installed in open air, these service factors are to be multiplied by a compartment factor of 1.1, and when installed in tight compartments with no ventilation, the service factors are to be multiplied by 0.9.

2. A service factor of 100 per cent is to be used for metalclad switchgear as long as conventional installations are adhered to, or in cases where a single metal-enclosed unit is installed in an existing concrete cell with restricted air flow on three sides. Where metal-enclosed units are installed, either as a single unit or in the conventional way, but where in both cases the head room is seriously restricted, an arbitrarily chosen service factor of 95 per cent should be used. The fact that the units have tightly fitting doors should be disregarded because, where in the manufacturer's judgment extra ventilation is required, they are designed with louvers, or openings are provided in places where they are most effective. In other words, the compartment factor is one.

3. The maximum temperature of copper directly connected to circuit-breaker terminals is to be limited to 70 degrees centigrade under normal conditions, and 90 degrees centigrade under emergency conditions lasting two days or less, except for metalclad switchgear where the limits should be 85 degrees centigrade under normal conditions and 105 degrees centigrade under similar emergency conditions.

4. The maximum temperature of copper directly connected to circuit-breaker terminals is to be limited to 80 degrees centigrade under emergency conditions lasting for more than two days, except for metalclad switchgear where the limit should be 95 degrees centigrade.

Paper 46-134, recommended by the AIEE committee on protective devices for presentation at the AIEE summer convention, Detroit, Mich., June 24–28, 1946. Manuscript submitted April 4, 1946; made available for printing May 13, 1946.

O. B. VIKOREN is an engineer in the electrical engineering division, Philadelphia Electric Company, Philadelphia, Pa.

sion. This is true of the other two transmitters at Eagle Rock substation.

Operating Experience

The systems in Figures 1 and 2 have been in operation for six years, and very few difficulties have been uncovered. In one heavy severe rain and wind storm there were over 200 operations, none of which were unnecessary. These 200 operations consisted of many ground faults and phase-to-phase faults.

There has been trouble with the *CR-DD* relays in that they have operated with current in only one circuit. This should not occur and sometimes it is very difficult to adjust these relays to prevent such operation. The wave trap capacitors absorb moisture causing difficulty with the carrier operation. This seems to be the greatest cause of trouble in all carrier relay systems of the Edison Company.

With these years of operating experience it can be said that this scheme is a practical solution to the ground fault problem. A less complicated system may be developed in the future.

References

1. SENSITIVE GROUND PROTECTION FOR RADIAL DISTRIBUTION FEEDERS, **Lloyd F. Hunt, J. H. Vivian.** AIEE TRANSACTIONS, volume 59, 1940, February section, pages 84–7.

2. NEW PILOT PROTECTION GIVES RELIABILITY, **Lloyd F. Hunt.** *Electrical World*, volume 106, September 26, 1936.

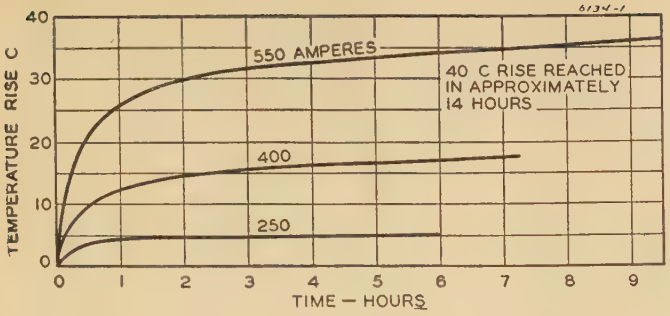

Figure 1. Temperature rise versus time curves for 500-ampere power circuit breaker

Main contacts in air

breakers, heat the oil to such an extent that the circuit breakers might catch fire if called upon to interrupt short-circuit current while in the overheated condition.

The only way really to determine what circuit breakers could do under overload conditions would be to make tests on typical units of various makes in the compartments in which they were operating.

Test, Evaluation, and Application

In view of the efforts made to provide for good housekeeping and proper maintenance of equipment, it was quite a surprise when tests revealed that the temperature rises on some of the circuit breakers substantially exceeded 30 degrees centigrade at full load (name plate rating) when tested in the "as found" condition. Some circuit breakers would not carry full load even when the main contacts were replaced with completely new assemblies obtained from stock. The loads at which the tested circuit breakers had 30 degrees centigrade temperature rise ranged from 45 per cent to 80 per cent of name plate rating in the "as found" conditions, and from 70 per cent to 100 per cent when reconditioned, depending on the type.

From the tests it could be stated quite conclusively that no oil circuit breaker with copper to copper contacts was able to carry current equal to its name plate rating without exceeding the standard 30 degrees centigrade temperature rise, except when in as good as new condition, and operating in open air or in a well ventilated compartment. Copper contacts, in particular, deteriorate after initial installation or subsequent overhauling, because of cumulative oxidization and the resulting increased temperatures.

It logically may be asked why this condition had not been discovered before tests were made. The answer is that circuit breaker ratings often exceeded cable ratings when single cable per line was used, that in the previous operating setup circuit breakers were called upon to carry full load only under rare emergency conditions, and under normal conditions the load currents were low enough so as not to make contact maintenance particularly excessive and thus did not arouse the suspicion of those in charge.

This is substantiated by the tests, and Figure 1 shows a typical example of the temperature rise of the main current-carrying contacts versus time, for three different load currents on a 15-kv 500-ampere oil circuit breaker of a type on which the main contacts are in air.

Deterioration of contacts due to cumulative oxidization, accidental burning during fault current interruption, gradual annealing and reduced contact pressure are all factors which tend to increase the temperature rise of a circuit breaker. The factor contributing the most, however, is probably oxidization. This means that in order to maintain rated temperature rise, the true rating of a circuit breaker ought to be decreased as a function of time after each reconditioning, but, since this is impractical, the ratings have been set up on an approximate basis, to secure rated temperature rise on the circuit breakers at the elapse of about one-half of the time between maintenance periods. This rating is referred to as the nominal rating.

Obviously, tests could not be conducted on all the various types of circuit breakers which are in service on the system, and they were therefore confined to eight units of the types most commonly used.

The method adopted for determining nominal ratings of circuit breakers, to be applied over a normal period between maintenance overhaulings, employs an assigned service factor and compartment factor dependent upon the circuit-breaker type, type of contact structure, and type of installation. The product of these factors and the name plate rating, will give a true rating for continuous load at which the circuit breaker is expected to have 30 degrees centigrade contact temperature rise above ambient temperature outside the breaker compartment, on the time basis explained above.

The list of service factors had to be chosen with considerable conservatism, particularly for metalclad switchgear, because operating experience with that type of equipment was considerably less at that time than it is today. In view of the fact that silver surfaced contacts are used in metalclad switchgear, and silver does not develop current-resisting oxides to the same degree as copper, experience has taught that there is less reason for conservatism with this equipment than with other types of switching equipment. The service factors now in use, excepting those of especially weak circuit breakers, are as listed below. These factors apply to circuit breakers in ventilated compartments, and are subject to modifications as stated in the notes supplementary to the list. Some of the factors recently have been increased slightly, and may be modified further if future experience so permits.

The purpose of the tests conducted on the eight circuit breakers mentioned was not only to determine the temperature versus time curves for these particular units, but also to give sufficient basic information so that the equations for such curves could be derived, and thereby a method established, by means of which the temperature rise for any combination of load and time could be calculated. The reader may sense that the entire analysis of this problem is rather involved. The practical application has been greatly simplified, however, by developing diagrams similar to Figure 2 for typical load cycles and for various types of circuit breakers.

Example: Normal* and typical emergency ratings are to be assigned to a 500-ampere 15-kv circuit breaker of the type used in the test, assuming that the ambient temperature is 40 degrees centigrade, the service

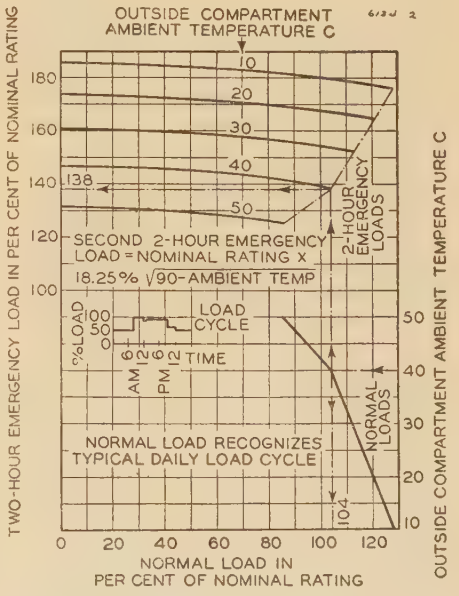

Figure 2. Permissible normal and emergency loads in per cent of nominal rating on indoor oil-poor and oilless power circuit breakers

Main contacts in air

Table II

Time, Hrs	Tested Temp Rise at 550 Amp	Calculated Temp Rise at 400 Amp	Tested Temp Rise at 400 Amp
0.5	21.2	11.25	9.5
2	29.8	15.8	14.5
5	33.5	17.7	16.7
7.5	35.0	18.5	17.5

factor is 0.8, and the compartment factor is 0.9; in other words, a circuit breaker with copper to copper contacts, mounted in a tight compartment and having a nominal rating of

500 amperes $\times 0.8 \times 0.9 = 360$ amperes

Following the guide on Figure 2 the results are

Normal rating $= 360 \times 1.04 = 375$ amperes
Two hour emergency rating $=$
$360 \times 1.38 = 496$ amperes

Second 2 hour emergency rating is calculated from the formula

$360 \times 0.1825\sqrt{90-40} = 466$ amperes

The basic theory on operation of electric equipment on a temperature basis as used in the Philadelphia Electric Company was developed by members[1-3] of this company's engineering department. The general equation has the form

$$\theta = A(1-\epsilon^{-at}) + B(1-\epsilon^{-bt}) \quad (1)$$

where θ is the temperature rise, and A, B, a, and b are the equivalent of the factors which appear in the first two terms of an infinite series expressing the reaction of a thermal circuit to applied energy. These two first terms give a close approximation of the total series. Referring to the temperature rise curve in the 550-ampere test shown in Figure 1, and taking the slope of the curve at the times $t_2 = 3$, $t_3 = 6$, and $t_4 = 12$ hours, values designated $X_2 = 1.317$, $X_3 = 0.688$, and $X_4 = 0.425$ were obtained, which in turn give values for the parameters $A = 28$, $B = 12$, $a = 2.65$, and $b = 0.14$. Inserting these values in equation 1 gives the following numerical expression for the temperature rise versus time for this particular test:

$$\theta = 28(1-\epsilon^{-2.65t}) + 12(1-\epsilon^{-0.14t}) \quad (2)$$

It may be noted from the curve that the final temperature rise in this test went to 40 degrees centigrade, and the preceding equation also satisfies this condition for high values of t. However, as it is desirable to limit the rise to AIEE standard value of 30 degrees centigrade, the equation for that condition becomes

$$\theta = 21(1-\epsilon^{-2.65t}) + 9(1-\epsilon^{-0.14t}) \quad (3)$$

retaining the general shape of the curve while shifting its location. This step is justified by the tests because the temperature rise varies practically as the square of the current over the major portion of the curves, as will be seen from Table II and by referring to the temperature rises in the 400-ampere and 440-ampere tests. Following the same reasoning, the current which will cause a 30 degree centigrade temperature rise is therefore

$$I = 550\sqrt{\frac{30}{40}} = 475 \text{ amperes}$$

In the majority of cases when dealing with overload, the question is not so much one of finding out what temperature rise a circuit breaker will have when starting "cold," as it is to determine what total temperature it will reach at a given ambient temperature after having carried a certain amount of load prior to the application of overload. After all, it is the total temperature which sets the limit at which a circuit breaker can operate safely, and once this limit has been chosen, the corresponding current can be calculated.

If

X_t represents total contact temperature in degrees centigrade as a function of time, that is, temperature rise plus ambient temperature,

A represents ambient temperature in degrees centigrade,

t represents time in hours,

θ_{1_0} and θ_{2_0} represent the initial temperature rise in degrees centigrade of the component parts of total temperature rise before application of a load whose ratio to nominal rating is R,

θ_{1_f} and θ_{2_f} represent the final temperature rises in degrees centigrade of the component parts of total temperature rise at sustained load whose ratio to nominal rating is R,

then the equation for the total temperature can be written:

$$X_t = A + \theta_{2_0} + \theta_{1_0} + (\theta_{2_f} - \theta_{2_0})(1-\epsilon^{-2.65t}) + (\theta_{1_f} - \theta_{1_0})(1-\epsilon^{-0.14t}) \quad (4)$$

where

$$\theta_{2_f} = 21R^2 \quad (5)$$

$$\theta_{1_f} = 9R^2 \quad (6)$$

and

$$R = \frac{\text{sustained load}}{\text{name plate current rating} \times \text{per cent service factor} \times \text{per cent compartment factor}} \quad (7)$$

It may be noted that equation 4 becomes identical with equation 3 if the temperature rise is limited to 30 degrees centigrade, the initial temperature of the circuit breaker is the same as the ambient temperature, that is, $\theta_{1_0} = 0$, $\theta_{2_0} = 0$, and $R = 475/475 = 1$.

Since the tests, of which the results are show in Figure 1, were conducted on a circuit breaker whose main contacts are surrounded by air, equations 4 through 7 are believed to be accurate enough for practical application on any type of power circuit breaker whose main contact structure is in air.

To clarify the application of equation 4, let it be assumed that the 500-ampere test circuit breaker had carried 400 amperes continuously at 40 degrees centigrade ambient temperature, that the product of the service factor and compartment factor is 80 per cent, and that it is desired to find the total temperature which the circuit breaker will reach when carrying 200 amperes additional load for two hours. Graphically, the problem is shown in Figure 3 and the numerical solution is found as follows.

Because of the fact that the circuit breaker has been carrying 400 amperes continuously, prior to the application of the 600-ampere load, and its temperature, thereby, has reached a steady state, it is immaterial what the initial temperature rises were when the 400-ampere load was first applied. Equation 4 can therefore be written as follows for the steady state condition.

$$X_t = 40 + 0 + 0 + (\theta_{2_f} - 0)(1-0) + (\theta_{1_f} - 0)(1-0)$$

and inserting the values for θ_{2_f}, θ_{1_f} and R

$$X_t = 40 + 21\left(\frac{400}{500\times 0.8}\right)^2 + 9\left(\frac{400}{500\times 0.8}\right)^2$$
$$= 40 + 21 + 9 = 70 \text{ degrees centigrade}$$

These values, 21 and 9, become the initial temperature rises of the component parts so far as the following two hours are

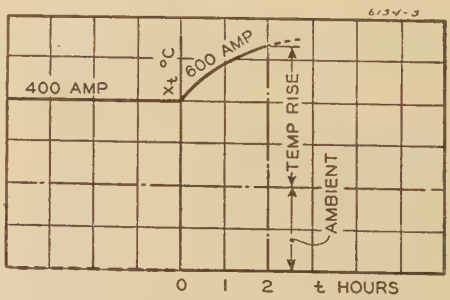

Figure 3. Total temperature of circuit breaker with 200-ampere load superimposed for two hours on 400-ampere normal load

* The normal rating is equivalent to the load which a circuit breaker can carry day in and day out without exceeding a total temperature of 70 degrees centigrade at 40 degrees centigrade ambient temperature, 60 degrees centigrade at 20 degrees centigrade ambient temperature, and 55 degrees centigrade at 10 degrees centigrade ambient temperature, recognizing the typical daily load cycle. Emergency loads equivalent to emergency ratings may be carried immediately following normal load.

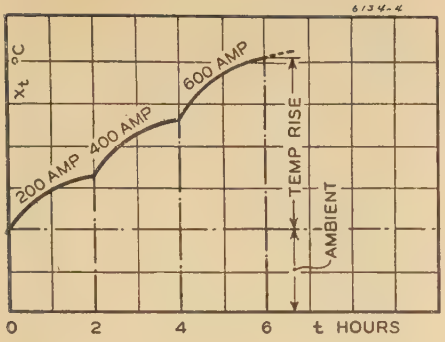

Figure 4. Total temperature of formerly idle circuit breaker after successive application of 200-ampere, 400-ampere, and 600-ampere load for two hours each

concerned, during which time the load is 600 amp. Therefore, equation 4 for that condition can be written:

$$X_t = 40+21+9+\left\{21\left(\frac{600}{500\times0.8}\right)^2-21\right\}\times(1-\epsilon^{-5.3})+\left\{9\left(\frac{600}{500\times0.8}\right)^2-9\right\}\times(1-\epsilon^{-0.28})=98.9 \text{ degrees centigrade}$$

If, however, the conditions had been as shown on Figure 4, that is, the circuit breaker had been idle and had assumed the same temperature as the surrounding air before loads of 200 amperes, 400 amperes, and 600 amperes were applied at two hour intervals, the solution would be as follows:

First two hours

$$X_t = 40+21\left(\frac{200}{500\times0.8}\right)^2(1-\epsilon^{-5.3})+9\left(\frac{200}{500\times0.8}\right)^2(1-\epsilon^{-0.28})=40+5.2+0.5$$

Second two hours

$$X_t = 40+5.2+0.5+\left\{21\left(\frac{400}{500\times0.8}\right)^2-5.2\right\}\times(1-\epsilon^{-5.3})+\left\{9\left(\frac{400}{500\times0.8}\right)^2-0.5\right\}\times(1-\epsilon^{-0.28})=40+21+2.1$$

Third two hours

$$X_t = 40+21+2.1+\left\{21\left(\frac{600}{500\times0.8}\right)^2-21\right\}\times(1-\epsilon^{-5.3})+\left\{9\left(\frac{600}{500\times0.8}\right)^2-2.1\right\}\times(1-\epsilon^{-0.28})=93.7 \text{ degrees centigrade}$$

It will be noted that by using equations 4 to 7, inclusive, and a step by step method of calculation, temperatures or ratings of oilless and oil-poor circuit breakers can be calculated for any type of load cycle, provided that in the first case, the load currents are known, and in the second case, the temperature limits are chosen.

For oil circuit breakers with all of the contact structure under oil, the same reasoning as above can be applied to the test results obtained on these types, and the total temperature of the contacts can be expressed by the equation

$$X_t = A+\theta_1+\theta_{2_0}+(\theta_{2_f}-\theta_{2_0})(1-\epsilon^{-t/3}) \quad (8)$$

where

$$\theta_1 = 4.5R^2 \text{ for } t = \text{two hours or more} \quad (9)$$

$$\theta_1 = 7.5R^2 \text{ for } t = \text{less than two hours} \quad (10)$$

$$\theta_{2_f} = 25.5R^2 \quad (11)$$

and

X_t represents total contact temperature in degrees centigrade as a function of time, that is, temperature rise plus ambient temperature

A represents ambient temperature in degrees centigrade

t represents time in hours

θ_1 represents contact temperature rise above oil temperature in degrees centigrade

θ_{2_f} represents final oil temperature rise in degrees centigrade under load whose ratio to nominal rating is R

θ_{2_0} represents initial oil temperature rise in degrees centigrade before application of load whose ratio to nominal rating is R

While some of the temperature limits now in use when rating circuit breakers have been stated in connection with the service and compartment factors, the selection of these and others needs to be justified.

The various tests were conducted on circuit breakers mounted in compartments which were either tightly closed with doors or partially ventilated, and the ambient temperature on which the temperature rises are based, was taken outside the compartment to make the basis consistent. For circuit breakers in tight compartments with no ventilation, it was found that the ambient temperature inside the compartment and thus the circuit breaker total temperature was approximately five degrees centigrade higher than for the same circuit breaker with the same load in a compartment with some ventilation. Based on this observation, the rating for circuit breakers in tight compartments should be approximately 0.9 times the rating of circuit breakers in ventilated compartments. Further, since the ambient temperature inside the compartment was approximately five degrees centigrade higher than outside the compartment, a circuit breaker installed on a structure without compartmentation, with little or no restrictions to the air flow, could carry approximately 1.1 times the load of the same circuit breaker when installed inside a ventilated compartment.

Table III. Average Ambient Temperature

Calculated (Deg C)	Use (Deg C)
17.5–22.5	20
22.5–27.5	25
27.5–32.5	30
32.5–37.5	35
37.5–42.5	40

Ambient Temperatures

Before any rating based on temperature can be assigned to a circuit breaker, it is necessary to arrive at an average ambient temperature at its location. In attended places, this is done by taking daily thermometer readings in the room every four hours during two seasons of the year, one season termed summer lasting from April through October and containing 214 days, the other termed winter lasting from November through March and containing 151 days. The daily maximum readings on the same thermometer are added over each of the two seasons and divided by 214 and 151 days respectively, thus arriving at a daily average ambient temperature for the summer, and likewise for the winter. If several thermometers are located in the same room the highest value calculated on the above basis is considered the average ambient temperature for that room. However, in any event, for the purpose of simplifying rating calculations, the average is rounded off as shown in Table III.

Continuous and Normal Load Conditions

Both terms cover day in and day out operation, except that the latter recognizes the typical daily load cycle for the individual problem.

The temperature rise of a circuit breaker is, as shown in Table II, nearly proportional to its I^2R loss. However, oxidization produces a steadily increasing contact resistance, particularly on copper to copper surfaces, and thus an increasing loss and temperature rise. If the total temperature is held constant and the time involved is not too long, this temperature will produce the same rate of oxidization, whether it is a result of high ambient temperature and low temperature rise, or vice versa. To clarify, compare the values in Table IV where it is assumed that under condition A, two identical circuit breakers are operating at different loads, at different ambient temperatures, but at the same total temperature when initially put in service. For a while the contacts are going to oxidize at the same rate, and let it be assumed that

after some time the contact resistance has increased 20 per cent. While initially there was no difference in total temperature, this no longer is true as the resistance increases with time, even though the ambient temperatures and the loads are held constant. This is shown under condition *B*.

Under conditon *B* it will be noted that circuit breaker 1 is four degrees centigrade hotter than circuit breaker 2. It will get progressively hotter, in fact, the heating is actually somewhat worse than indicated in the tabulation because the two circuit breakers will oxidize at different rates as soon as the smallest difference in total temperature appears.

From this analysis the conclusion can be drawn that, for circuit breakers operating on a continuous or normal basis, the allowable total temperature limits should be lowered with decreasing ambient temperature, although not necessarily in direct ratio. Stated in another way, the permissible temperature rise should be restricted with decreasing ambient temperatures. This restriction has been chosen as one-half of the amount between the actual ambient temperature and 40 degrees centigrade, as long as the ambient temperature is below the latter value. At 40 degrees centigrade ambient temperature and above, the total temperature has been limited to 70 degrees centigrade because, so far, no higher value appears justified under normal load conditions. It will be noted under condition *C* in Table IV that, in order not to exceed the permissible total temperature limits of circuit breaker 1 while operating continuously at loads exceeding its nominal rating, several remedies can be employed. These will be considered in the same order as tabulated under condition *C*.

Remedy 1. Reduce the load current. This may or may not be possible and would mean revenue loss unless it could be picked up on other less loaded circuits.

Remedy 2. Reduce contact resistance below original value. This means either to rebuild the circuit breaker for the next higher current rating, which generally is feasible only on circuit breakers rated below 1,200 amperes, or to replace the circuit breaker with one of higher rating. (It has been assumed that the new contact structure would have 20 per cent less resistance than the original in order to fit into this picture.)

Remedy 3. Reduce the ambient temperature by means of ventilation. As a result of ventilation, the compartment factor will change, which in turn will increase the nominal rating, and thus reduce the percentage overload (shown in parentheses, Table IV) for the same actual current. Thus, in this example, the contacts could, at least on a theoretical basis, be permitted to deteriorate until their resistance reached 150 per cent of the original before permissible temperature limits would be exceeded. Since the needs for overhauling, under the assumed conditions, would seem to be only a matter of time, the contacts might just as well be reconditioned and at the same time silver surfaced, which would permit carrying the same ampere load without resorting to drastic reduction of ambient temperature. (Remedy 4 refers to this alternate condition. Economy, of course, will dictate which of the two steps should be taken, because ventilation may in some cases be required for other equipment in the same room.)

Remedy 4. Recondition contacts. As already indicated in the preceding paragraph, reconditioning of contacts combined with silver surfacing proves as effective as, and is often much simpler than, any of the other remedies discussed, because it does not necessarily involve extra capital expenditure or loss of revenue. Since the silver surfacing will change the service factor, which in turn will increase the nominal rating, the percentage overload actually will be less for the same ampere load. (Figure in parentheses refers to this.) The same reasoning can be applied to circuit breaker 2 for silver surfaced contacts.

Silver surfaced contacts have much less cumulative oxidization than copper contacts because silver oxide is a relatively good conductor, while copper oxide is a relatively poor one. For this reason the service factors, determined on the basis of the tests, are higher for silver than for copper contacts. While all but the earliest tests actually were conducted on reconditioned circuit breakers, as good as new copper contact assemblies were used, and during the relatively short durations of the tests, these assemblies had practically the same contact resistance as silver surfaced contacts, although with time, they would deteriorate much more rapidly.

Short Time Emergency Conditions, Maximum Duration Two Days

As a result of the fact that contact oxidization under short time emergency overloads will be considerably less than that during long time overloads, 90 degrees centigrade total temperature limit at any ambient temperature has been chosen for emergency conditions lasting two days or less. This is on the safe side so far as effect of oxidization is concerned, but has been so chosen in order not to anneal the contacts, particularly where these are of laminated brush types. According to the circuit breaker manufacturers, the annealing of spring contacts is quite rapid at higher than 90 degrees centigrade, and oil will begin to smoke at about 100 degrees centigrade. Therefore, in order not to impair the interrupting ability of power circuit breakers while in over-heated condition, the 90 degree centigrade total temperature limit seems to be wisely chosen. This excludes metalclad switchgear. If oilless circuit breakers are used, 105 degrees centigrade is believed to be permissible. If oil circuit breakers are used in metalclad gears, special consideration will be given to the problem.

Since the 90 degree centigrade limit applies to emergencies of two days or less, the question may be raised as to what load a circuit breaker can carry for two days if the 90 degree centigrade limit is reached, for example, within the first two hours. Referring to equations 4 and 8, these take the form $X_t = 30R^2 + A$ under this condition. Solving for R, realizing that X_t already has reached 90 degrees centigrade and may continue at this value up to two days, the answer is

$$\text{Nominal rating} \times \sqrt{\frac{1}{30}(90 - A)}$$

Long Time Emergency Conditions

Under long time emergency operation lasting more than two days, the total

Table IV

Condition	Circuit Breaker	Per Cent Resistance of Contacts	Continuous Load in Per Cent of Nominal Rating	Ambient Temp, C	Temp Rise, C	Total Temp, C	Remarks
A	1	100*	129	20	50	70	Exceeds permissible temp rise
	2	100*	100	40	30	70	Permissible total max temp
B	1	120†	129	20	60	80	Exceeds permissible total max temp
	2	120†	100	40	36	76	Exceeds permissible total max temp
C	1	120†	115	20	40	60	Limited by permissible total max temp
	1	80	129	20	40	60	Limited by permissible total max temp
	1	150†	129 (115)	0	50	50	Limited by permissible total max temp
	1	100‡	129 (115)	20	40	60	Limited by permissible total max temp
	2	100‡	100 (90)	40	30	70	Limited by permissible total max temp

* New or reconditioned copper contacts. † Oxidized copper contacts. ‡ Silver surfaced copper contacts.

temperature limit for power circuit breakers has been chosen at 80 degrees centigrade in order to avoid excessive contact oxidization. Similarly, metalclad switchgear with oilless circuit breakers is limited to 95 degrees centigrade. In metalclad gears, the contacts always are silver surfaced, and springs which furnish contact pressure are not depended on so far as current carrying ability is concerned. Again oil circuit breakers in metalclad gears are given special consideration.

Temperature Limits of External Connections

The total temperature limits for external copper directly connected to power circuit breakers have been so chosen that heat will not be carried into the circuit-breaker contacts. When apparent deviations occur at low ambient temperatures, they are not believed to be serious, as the circuit-breaker terminal structure has been found to act as a choke. The values are stated in Table I.

In the preceding discussion, except where applied to metalclad switchgear, the conventional 30 degrees centigrade rise over 40 degrees centigrade ambient temperature has been assumed in referring to circuit-breaker name plate ratings. Since the name plate ratings for metalclad switchgear are based on 45 degrees centigrade rise over 40 degrees centigrade ambient temperature, the temperature limits chosen under overload conditions for this type of equipment have been raised by 15 degrees centigrade, as compared with the limits applying to other types of switching equipment. Except for this difference, the same formulas and procedure are used on all types of indoor power circuit breakers.

Conclusion

The preceding discussion is believed to be comprehensive enough to enable those who have not yet tackled the problem of loading circuit breakers on a temperature basis to do so without difficulty. The basic problem is the same for all users, and while some of the details may vary, these details should be relatively easy to collect once the requirements are known.

In case of new circuit breakers, the calculated normal and emergency ratings may exceed name plate values by moderate amounts depending on the physical arrangement and the ambient temperature. On older types of circuit breakers, however, the name plate values will seldom be exceeded unless the units are equipped with silver surfaced contacts and ambient temperature, as well as the physical arrangements, are favorable.

The specific method described has been used on circuit breakers for several years on the Philadelphia Electric Company system and has given results which are believed to be entirely safe. The same general method also has been applied to other types of major power equipment and has resulted in considerable savings on capital investments. These savings have contributed to the maintenance of low rates in spite of the steadily rising costs involved in serving electric power to customers.

References

1. Notes on Emergency Ratings, A. H. Kidder. Appendix A. AIEE Transactions, 1939, November section, pages 599–610. (The practical application of this theory was carried out by R. J. Woodrow.)

2. Designs of Current Carrying Contacts in Modern Switchgear, R. Paxton, H. E. Strang. *General Electric Review*, volume 36, December 1933, page 524.

3. Hydro Maintenance, C. P. Rhine. *Electrical West*, volume 83, October 1939, page 43.

Power System Development for Service to Hanford Plutonium Plant

B. V. HOARD
MEMBER AIEE

J. R. CURTIN
ASSOCIATE AIEE

EARLY IN 1943 a number of engineers in the Bonneville Power Administration were informed of a new "mystery load" which was to be added to the BPA system. Later this load became known as the Hanford Engineer Works of the Manhattan District. We, of course, were warned that the new load was one of the war's top secrets. The product to be made, about which no one seemed to know anything, the location of the plant and its general arrangement, the amount of power to be taken by the plant, the location of the transmission lines which were to supply it, and the additional important fact that the power to be supplied had to have the utmost reliability were subjects which were not to be discussed unless absolutely necessary. It is our feeling that all these secrets were well-kept. For while BPA engineers had the responsibility of arranging their system to provide reliable service to this new load, there were times when we despaired of ever obtaining sufficient general technical information regarding the apparatus to be used by the Hanford Engineer Works to make possible the best co-ordinated system design.

At the time this new load first was considered on the BPA system slightly more than one year of war had passed. Materials and labor were critical, and the system had started serving many large war loads, including the reduction of aluminum and power for shipyards. Commitments also had been made to supply power to other large war factories, the plants for which were still under construction. A number of calculating board studies had been made previously of the transmission system including these future loads, and it was realized that the transmission system, heavily loaded as it would be, could not supply the type of reliable service which would be required by the new "mystery load." Accordingly, it was decided to determine by a series of a-c calculating board studies what system additions and changes would be necessary in order to obtain a reliable source of supply to the Hanford Engineer Works' load. These studies were started and included load-flow diagrams, transient stability studies, and relay studies, so that all possible contingencies could be taken care of.

Paper 46-178, recommended by the AIEE committees on power generation and power transmission and distribution for presentation at the AIEE Pacific Coast meeting, Seattle, Wash., August 27–30, 1946. Manuscript submitted June 12, 1946; made available for printing July 9, 1946.

B. V. Hoard is chief of the a-c calculating board studies group, system engineering staff, and J. R. Curtin is an engineer on the system engineering staff, both of Bonneville Power Administration, Portland, Oreg.

Location of the Hanford Engineer Works' Load on the BPA System

Geographically, the BPA's transmission system serves three major load areas —the Puget Sound, Portland, and Spokane areas. Figure 1 indicates the geographic location of 230-kv and 115-kv transmission lines, major substations, and generating stations as of June 1946.

The system peak load during the war was 1,427,000 kw. But in February 1943, when the Hanford Engineer Works first

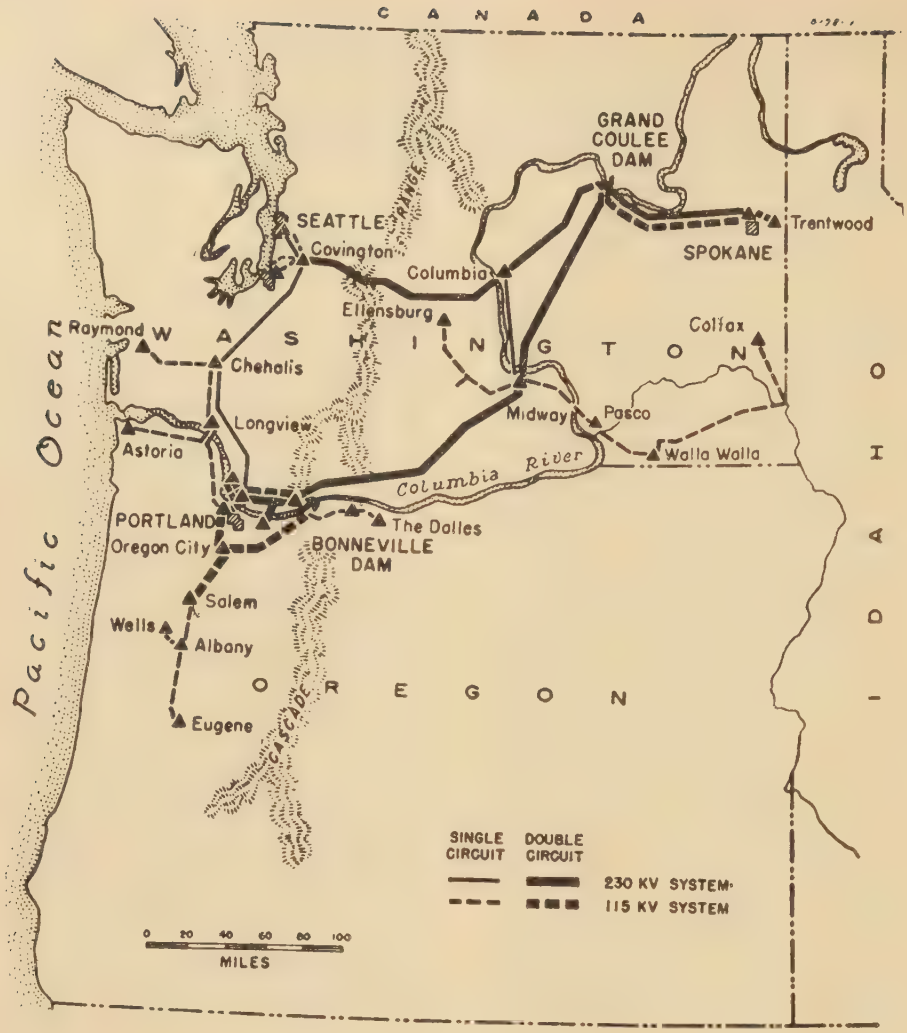

Figure 1. Bonneville Power Administration 230-kv and 115-kv transmission grid

was being considered as an additional load, the BPA system had not grown to its present size. A simplified schematic diagram of the BPA 230-kv transmission system as of February 1943 is indicated in Figure 2. This diagram shows a 230-kv loop with two large generating stations, Grand Coulee and Bonneville, and two large load centers, the Portland area and the Puget Sound area, connected to the loop. At this time there were three 108,000-kva generators installed at Grand Coulee and four 60,000-kva generators installed on the 230-kv system at Bonneville. But before the Hanford Engineer Works' load would be able to start operation, there would be eight Grand Coulee generators operating with two new 230-kv lines to Spokane and a large load at Spokane connected to the system.

The Grand Coulee generating station is constructed and operated by the United States Bureau of Reclamation; the Bonneville Power Plant is constructed and operated by the United States Army Engineers; and power from these two stations is transmitted to load centers over the transmission system of BPA. Two parallel 230-kv transmission lines connect the two generating stations through an intermediate switching station at Midway which is 100 miles from Grand Coulee and 134 miles from Bonneville. The Hanford Engineer Works' load was to be supplied from Midway, as this station had a source of supply either from Grand Coulee through two 230-kv lines or from Bonneville through two 230-kv lines.

The Problem

At that time the process to be used at the Hanford Engineer Works never had been tried fully so that knowledge of how it would work was very limited. In view of this lack of information and present-day knowledge of the destructiveness of atomic bombs, it is not surprising that extreme precautions were taken to maintain a source of supply of power to the load. We now know this power drove large pumps to supply cooling water to the uranium piles, and now can understand that the loss of power for even a short time might have brought about serious operational difficulties. Accordingly, it was decided, in addition to other less stringent reliability requirements, that the BPA system should be arranged to maintain power supply to Midway substation even for the remote probability of simultaneous or near simultaneous faults on both Coulee–Midway lines.

However, the following limitations were found with the 230-kv system as shown in Figure 2:

1. When all new loads and generation had been added to the system, loads in the Puget Sound and Portland areas would be very large in comparison with the transmission capacity, so that any double-line-to-ground fault on the Coulee–Covington line or on a Coulee–Midway line would result in the system being unstable. It would break apart, and in so doing would cause low voltage at Midway which was considered dangerous to the Hanford Engineer Works' process.

2. Power normally flows from Grand Coulee to Bonneville and the Portland area. After the system breakup occurred, with Grand Coulee separated from Midway, there was not sufficient generation at Bonneville to supply both the Portland area and the Midway loads so that the frequency and voltage at Midway would drop rapidly. Such drop in frequency also was considered dangerous to the Hanford Engineer Works' process. Similar difficulties would be encountered in case of a simultaneous fault on both Coulee–Midway lines.

3. At the beginning of the war, Grand Coulee had only one generator installed. Before August 1944 when the Hanford Engineer Works' load was to be energized, there would be eight generators installed with a maximum overload capacity of approximately 930,000 kw, and if all 230-kv lines and eight generators were to be connected to the same bus the short-circuit duty on 230-kv circuit breakers would approach 5,000,000 kva. Existing circuit breakers had an interrupting rating of 2.5 million kva while the largest available breaker, which was developed after the war started, had only a 3.5-million kva interrupting rating. Accordingly, the Grand Coulee bus had to be split up, and it was decided after considerable study that more reliable service could be supplied to the Hanford Engineer Works if one Coulee–Midway line was to be connected to each of the two new busses at Grand Coulee. This design of the Grand Coulee bus, which utilizes an interleaved arrangement of the transmission lines on two busses, has been covered in a previous paper.[1]

4. It already has been indicated how the system load, generation, and transmission lines had grown since the start of the war. Orders for high-speed carrier-current relaying had been placed for each end of all major 230-kv lines, but because of higher priorities of Army and Navy equipments, not one of some 22 sets ordered had been delivered. Without high speed clearance of faults at both ends of a faulted 230-kv line as provided by these relays, the system could

not be made stable without a greater number of reinforcements being required than otherwise would be the case. All such reinforcements, of course, had to be justified to the War Production Board because of shortages of critical material and labor.

Solution of the Problem

Extensive and intensive studies were conducted to determine the minimum system additions needed to obtain reliable service. Over 150 transient stability studies were made using several bussing arrangements at Grand Coulee and assuming faults at various locations on the system. The transmission system as shown in Figure 3, which finally was selected as satisfying the Hanford Engineer Works' load requirements for reliability as well as having sufficient capacity to supply other system loads, consists of the 230-kv loop with generation supplied at two points, while major loads are supplied from the loop at five other points. System characteristics were determined during transient stability swings following the clearance of a faulted line to be certain that relays would operate correctly when called upon to do so during these transient swings as well as during the faults. In this respect the war had forced transmission line loadings that were very high, and it was found that standard carrier type relays on some lines had to be modified before they would be completely satisfactory.

Because of the transmission loop arrangement, it was found that out-of-step blocking was undesirable, for instability might be initiated between any two major substations depending on the fault location, the initial system load division, or generation division, as well as circuit breaker and relay operating time. If such out-of-step operation did occur as a result of any cause, it was necessary to make certain that the system breakup would not produce low frequency or excessively low voltage at Midway except that low voltage would occur unavoidably for the few cycles (five to ten) between the time when a fault first occurred near the Midway bus and when it was cleared.

System Changes Needed

As a result of the foregoing and other studies, the following system changes and additions were made from February 1943 (Figure 2) to August 1945 (Figure 3). Important steps also are listed which are not shown easily on Figure 3.

1. Change in bussing arrangement at Grand Coulee.[1]

2. Addition of Coulee–Covington line number 2.

3. Arrangement for bus tie and bus sectionalizing breakers at Midway. Power to Hanford Engineer Works fed from both ends of the bus to prevent outage in case of a bus fault at the Midway substation.

4. Installation of carrier relays on all 230-kv transmission lines. Priority assistance to obtain delivery was needed most as most of the sets previously had been ordered.

5. Installation of a transfer tripping scheme at Coulee, Midway, and North Bonneville to provide an alternate source of supply from Bonneville generating station without drop in frequency or low voltage in the event of a double line outage of the two Coulee–Midway lines. (Until installation of Columbia–Midway 230-kv line.)

6. Installation of Columbia switching station (in Coulee–Covington lines) and Columbia–Midway 230-kv line.

7. Special relay studies.

(*a*). Resulting in modification of carrier relays.

Figure 2. Schematic 1-line diagram of BPA 230-kv system in February 1943

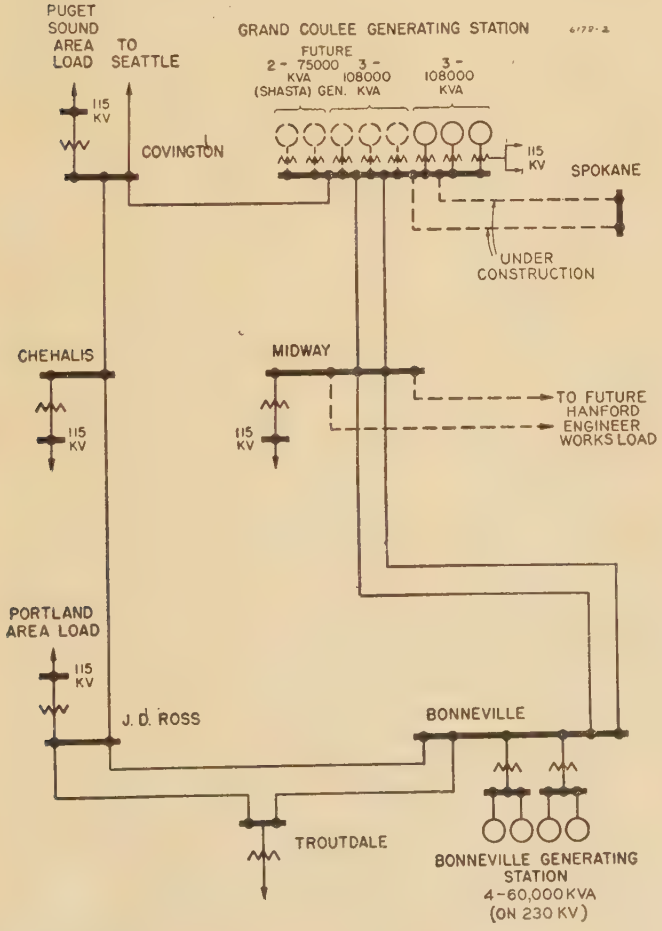

Figure 3. Schematic 1-line diagram of BPA 230-kv system in August 1944, approximate time when Hanford Engineer Works started operations

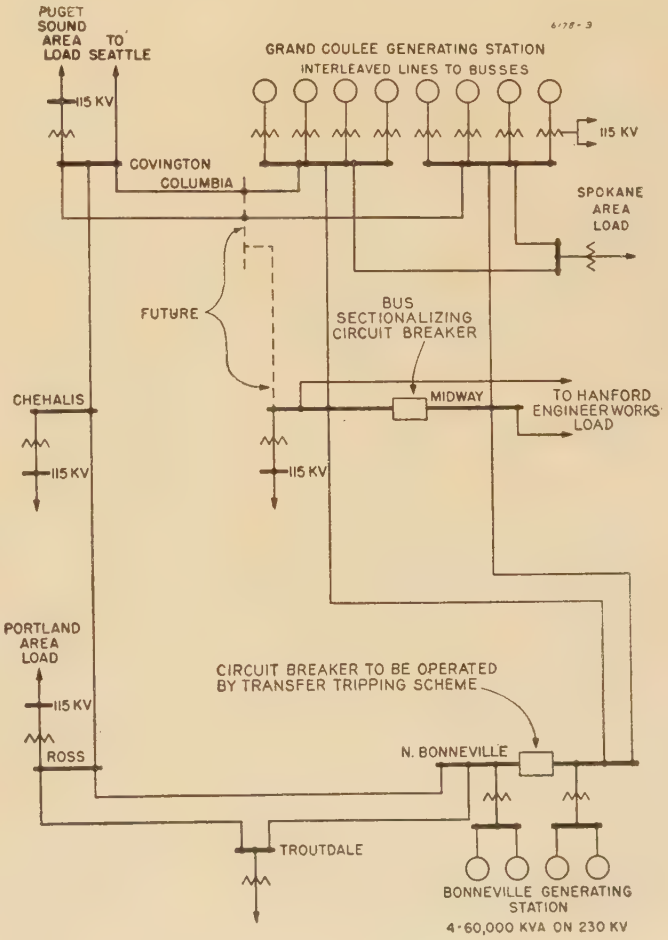

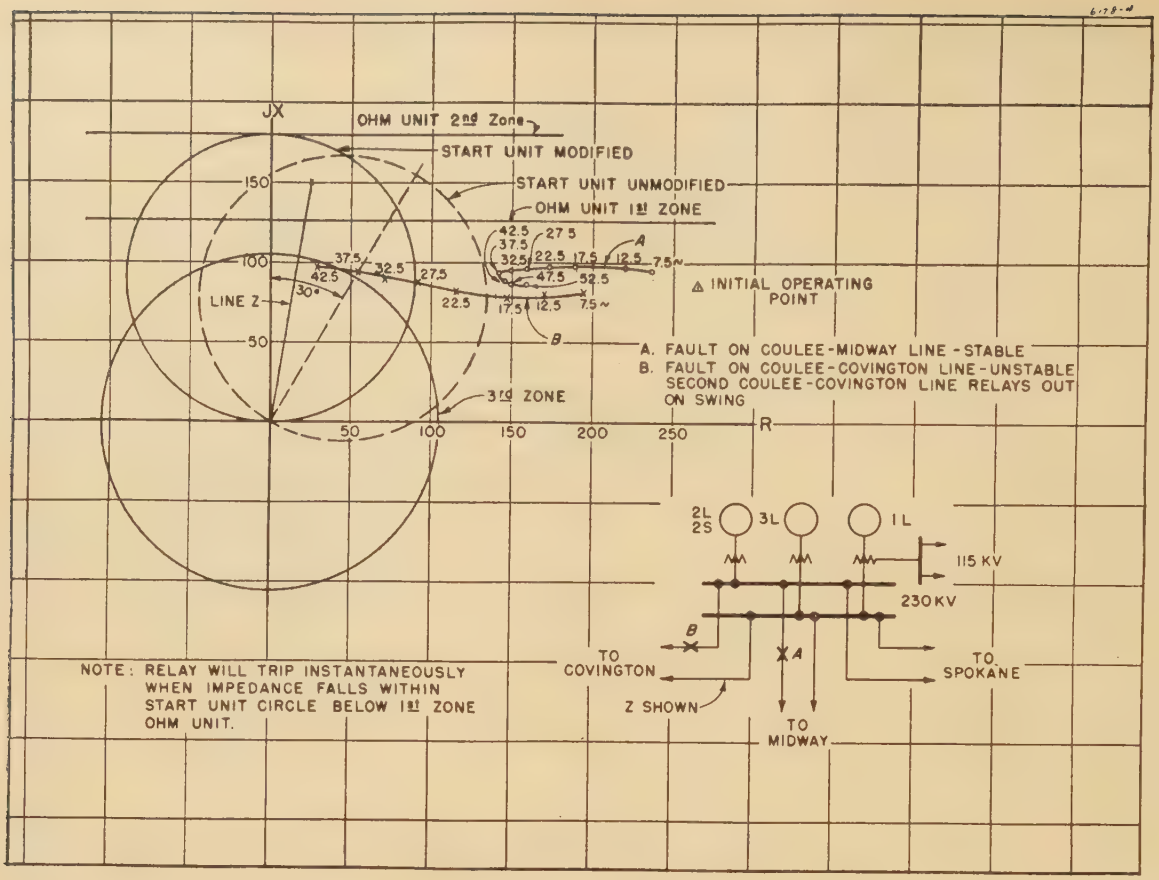

Figure 4. Impedances seen by Coulee end *GCX* and *HDX* relays in Coulee – Covington line during stability swings

(*b*). Resulting in nonstandard relay settings.

(*c*). Special backup arrangements on relays.

8. System tests.

This list is rather imposing. Items 1, 2, and 4, and the Columbia switching station previously had been planned, but even though the load had grown enormously, lack of materials had stopped all construction and expansion except that so absolutely necessary that the War Production Board would grant priorities for the additions. A few of the foregoing additions and changes are of sufficient interest to be discussed more in detail.

Coulee–Covington Line

Repeated efforts had been made to obtain a second Coulee–Covington line long before anything was known about the Hanford Engineer Works' load; however, it had not been approved by the War Production Board because of scarcity of materials. When it became known that the Hanford Engineer Works' load would be connected, approval was expedited. However, before this line could be built and before the Hanford load was connected to the system, extremely heavy loads were carried on the first Coulee–Covington line. A peak value of 240,000-kw input at Grand Coulee was obtained. A board study previously had determined the static-stability limit of this line when connected to the system at Covington with two 108,000-kw generators connected at Grand Coulee at approximately 265,000-kw input. Hence the foregoing loading corresponded to 90 per cent of the static limit. For literally days at a time the line was loaded to 230,000-kw input (210,000-kw output at Covington). Over this period several faults occurred on the 115-kv system in the vicinity of Covington but several miles out from the bus. Nevertheless, the line was operating so near to the stability limit that the two generators connected to the line at Grand Coulee lost synchronism with the system for these faults, even though the fault normally would be considered remote from the generators. The circuit breaker at Grand Coulee would open for these conditions while the circuit breaker at Covington would remain closed. Further investigation showed that the relay characteristic needed to be modified at Grand Coulee to prevent tripping up to the maximum transient swing for which this portion of the system still would remain stable.

System Stability

With the Hanford load scheduled to be added to the Bonneville system, the procurement of carrier equipment, as well as all other materials and equipment needed to safeguard that load, became greatly facilitated. The original carrier relaying equipment consisted of standard distance relays (*HZ* and *GCX*), high speed carrier ground relays, and auxiliary carrier relays and equipment. These were to be arranged in well-known directional comparison schemes for high speed tripping of line faults by either first zone or carrier relays, and backup by other zones and by independent slower directional ground relaying. Ground-current balance relays also were provided on parallel line sections. As mentioned previously, it was decided not to use relays which would block tripping on out-of-step conditions, but to do everything possible to avoid transient instability, and in those cases where instability was inevitable to permit the system to split where it would. Accordingly, transient stability studies were made of the system as shown in Figure 3, with the object in mind of determining the limit to which the system could swing and still remain stable, and the critical load and fault conditions which would produce such swings. During these studies the loci of apparent impedances seen by line relays were plotted on R-X diagrams and compared with the relay impedance characteristics.

It was learned that the 230-kv loop with generation at some points and loads

at other points would produce complicated loci of apparent impedances seen by line relays during these transient swings. An example of this is shown in Figure 4, on which is drawn the characteristics of a modified start unit and the unmodified start unit (shown dotted), for the *GCX* and *HDX* relays located at Grand Coulee in a Covington line. The loci of impedances, as seen by the relay during two transient swings, are drawn on this figure. Curve *A* corresponds to a fault on a Coulee–Midway line which after clearing was found to be stable, but the locus very closely approaches the unmodified circle before it turns away. The reversal of direction of this characteristic indicates that transient stability could be maintained by the system provided the relay does not trip. If the impedance had moved within the start unit circle, undesirable instantaneous tripping would be indicated. Curve *B* corresponds to a fault on one Coulee–Covington line, which after clearing was found to produce instability. It will be observed that the relays in the remaining Coulee–Covington line will trip this circuit when the apparent impedance has progressed until it is within the start unit circle. Numbers on each curve represent cycles elapsed after the fault first occurred; the first point was at 7.5 cycles because of calculating board technique. In all these studies, the fault was assumed cleared at both ends in five cycles through use of carrier relaying and 3-cycle breakers. As a result of these studies, the start unit was changed to the foregoing modified 90-degree characteristic instead of the standard 60-degree characteristic as shown dotted, since the 90-degree angle conforms more closely to the average impedance angle of BPA 230-kv lines ($81^1/_2$ degrees) than the 60-degree angle.

Another example of the transient impedance characteristics of the system, in this case compared with the *HZ* impedance relays at the Midway end of a Coulee–Midway line is shown in Figure 5. Curve *A* represents the impedance seen by the relay for a fault on the other Coulee–Midway line and is stable since the curve reverses direction. The curve actually progresses into third zone tripping (modified to be nondirectional) except that there is a time delay of 45 cycles before actual tripping can occur, and the system has moved out of danger before the necessary time can elapse. The directional element eliminates the possibility of the second zone tripping during this period.

Curve *B* shows corresponding values for a fault on a Coulee–Covington line which was unstable. It would appear that this relay also would trip; however, analysis of other relays on the system shows that the system breaks up between Coulee and Covington and between Midway and North Bonneville. Hence Hanford is left with power supply from Grand Coulee.

In Figure 5 it may be observed that the average reach of the second and third zones is rather short, being approximately 120 per cent of the line section. These were reduced in order to avoid tripping on transient swings from which the system can recover. These swings are shown in the figures as impedance loci which reverse direction, and it was to avoid having these swings get within the tripping areas for any appreciable time that the second and third zone areas were reduced.

In order to permit the reduced settings mentioned and at the same time obtain as much reach as possible for third zone backup time delay relays, these relays were made nondirectional. By this means the third zones of all breakers on a bus provide backup for any particular breaker, rather than depending upon remote breakers. They are better able to perform this function with the necessary reduced settings because they are one line section closer to the fault, and backup tripping tends to be localized to the affected bus section.

Special Backup Relaying

A time delay backup arrangement has been added in major stations which has definite advantages in meeting the re-

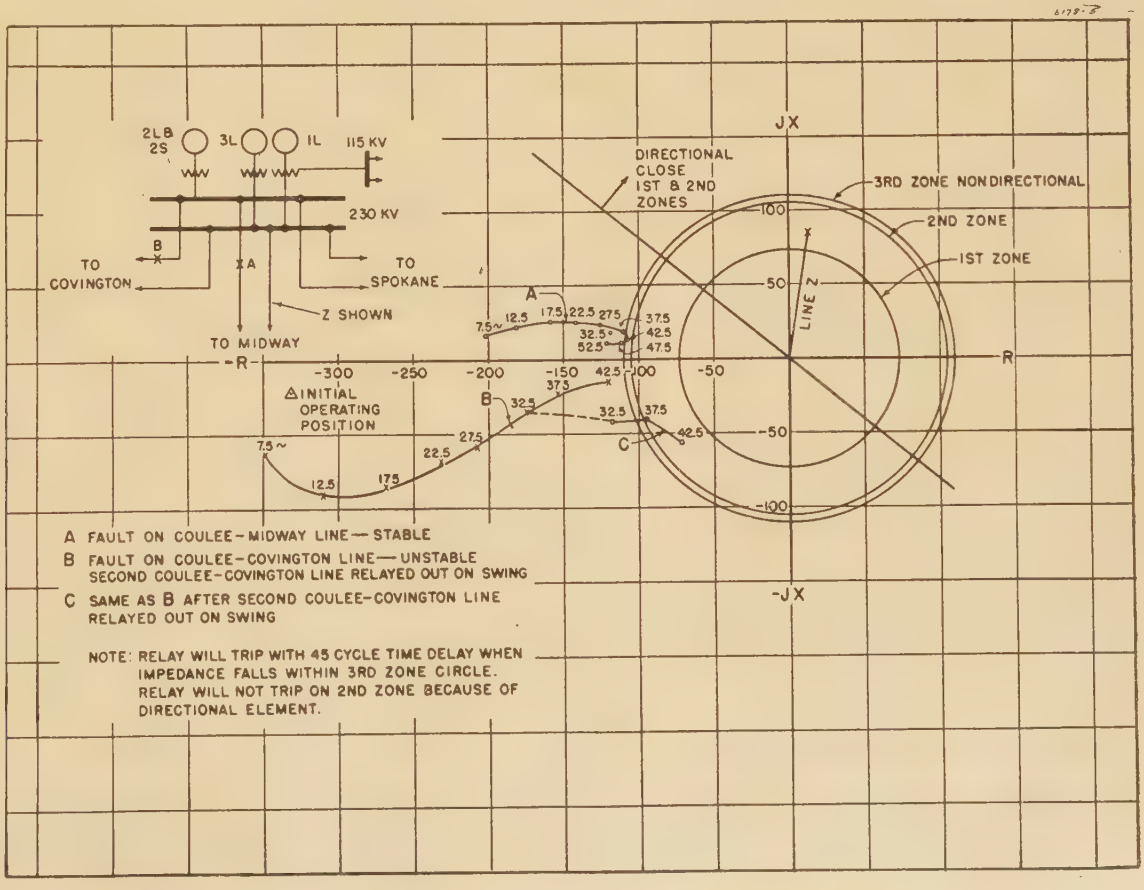

Figure 5. Impedances seen by Midway end *HZ* relay in Coulee–Midway line during stability swings

quirements of the system. This scheme, in the event that a breaker fails to open, operates the bus differential auxiliary relay associated with that breaker in 6 to 12 cycles after the breaker trip coil has been energized. (These are 3-cycle breakers.) This scheme tends to isolate trouble before second zone operations occur in other substations and is consistent with the attempt to localize backup tripping to the affected station as much as possible. Another important aspect of this backup feature, in cases where several sources can feed into a faulted line, is that it does provide backup where the normal type of overlapping directional impedance relays with time delay would fail to do so. The fact that the currents in the unfaulted lines are small percentages of the total fault current, because of multiple feeds, makes the impedance apparent to relays in the unfaulted lines often much larger than the settings of their backup zones. Since the normal backup scheme is not suited to the conditions, it was decided to use the special scheme described, the operation of which is initiated directly by the failure of the breaker to trip in the faulted line.

In order to provide more reliable service to the Hanford Engineer Works, at Midway substation only, the second zone distance trip circuits are connected to auxiliary relays arranged to trip any selected group of breakers. Since any second zone operation at Midway probably would be accompanied by system instability, this arrangement was made so that the system could be split to provide service to Midway from at least one line.

The third zone trip circuits of the Coulee and Bonneville lines at Midway are wired to trip one of the two bus differential auxiliary relays. The selection of the particular bus differential auxiliary to be tripped is made by directional relays on the bus sectionalizing breaker. Since both Midway–Bonneville lines are tripped by either bus differential auxiliary relay, this final backup arrangement of the Coulee lines. Similar backup for the Hanford lines is provided by instantaneous overcurrent relays which are operated by the sum of the two Hanford line currents. These relays cut out the third zone trip circuits but produce tripping through the directional relays and a timer, which is set for a longer time than the third zone delay of relays on the Hanford circuits.

Miscellaneous Relay Arrangements

A 1-cycle time delay has been added to all ground carrier trip circuits to decrease the possibility of false tripping because of gap flashover in carrier sets or sequential pole operation of oil circuit breakers.

Overcurrent fault detectors have been added in the first zone and carrier trip circuits of all the relays on the Hanford loop and many on the Bonneville system to prevent tripping caused by loss of potential.

Transfer Tripping Scheme

Certain network analyzer stability studies showed that the loss of both Coulee–Midway lines, before the installation of the Columbia–Midway line, during a critically heavy load period might result in system instability, that is, Coulee would run ahead of Bonneville and separate from the Portland area. As a result of this, Bonneville would be loaded heavily by the Portland area with resultant low voltage and frequency at Midway. To safeguard against this contingency, a bus sectionalizing breaker has been installed at North Bonneville (Figure 3) and a transfer tripping scheme arranged which can be used to isolate two Bonneville generators on the lines to Midway whenever both Coulee–Midway lines are opened.

This scheme is designed to operate as follows. If either line breaker is opened at Coulee, one of two audio tones is transmitted over the line carrier relaying channel to Midway. At Midway, tone relay contacts and pallet contacts on the Coulee breakers are arranged so that whenever both Coulee lines are opened at either end an auxiliary relay will initiate the transmission of two additional tones, both over the two carrier relaying channels to Bonneville. At Bonneville the audio components are filtered and brought to their respective tone relays. These relays have their contacts in series, and are also in series with a power directional relay, which is closed for power flow toward Midway, and with a 6-cycle time delay relay. This arrangement was made to prevent any possible misoperation of the transfer trip relays because of arcing on disconnects, which can cause the tone relays to operate.

To date, system loads have not approached the critical condition for which this scheme might have been necessary, and it actually is not in service.

Conclusions

Since the inception of the Hanford Engineer Works' load on the BPA system, no change on the 230-kv system or addition of any importance was contemplated without a consideration of its effect and the requirements of that load. The result has been the development of the afore-mentioned transmission and relaying system which was designed to supply continuous service to the Hanford Engineer Works, if necessary at the sacrifice of other loads on the system.

The extreme contingencies resulting from line faults, bus faults, or circuit breaker failure for which the system was designed have not occurred. The worst of this type which has occurred was a simultaneous outage caused by lightning of both Midway–Grand Coulee lines. This occurred twice in May 1946. However, the system was loaded lightly at the time, so that these faults, although severe, were not equal to the worst condition for which the system was designed. The Hanford operators noticed the voltage dip at the time, but they continued to operate normally, apparently without ill effects. The transfer tripping scheme was not in service because of a previous determination that it would be unnecessary under present system conditions, that is, with the Columbia–Midway line in service.

A more severe condition, not a result of a line fault, occurred in March 1946, when the excitation was lost accidently on five Grand Coulee generators, all that were operating at that time, and they pulled out of step from the rest of the system. The result was a drop in frequency to 94 per cent and in voltage to 72 per cent of the normal. Design information on the pumps and motors at Hanford indicates that even at this lowered voltage and frequency, sufficient power could have been supplied to keep the pumps operating. However, during this disturbance the pumping load was taken over automatically by a standby source of power within the Hanford area, thereby avoiding this critical test of apparatus.

Numerous other line outages, caused by a variety of line faults, have occurred without incident at Hanford other than momentary voltage fluctuations.

It is difficult to evaluate a transmission and relaying scheme when the goal is absolute continuity of service. Practical design considerations have been based on assumptions of very severe conditions, many of infrequent occurrence, through which service would have to be maintained, but there are always a number of imaginable disasters which unavoidably would result in loss of service. Generally speaking, it is believed that this scheme, as incorporated into the system, has met and probably will continue to meet the requirements of this load.

Reference

1. An Analysis to Determine the Optimum Bussing Arrangements and Transmission Capabilities at Grand Coulee, B. V. Hoard, G. W. Bills. AIEE Transactions, volume 63, 1944, pages 1259–64.

An Electronic Frequency Meter and Speed Regulator

ELLIS LEVIN
ASSOCIATE AIEE

AN electronic frequency meter and speed regulator has been developed to measure and hold the speed of a small steam turbine within plus or minus one-half of one per cent of any speed between 10,000 and 100,000 rpm.

This equipment fills a need for precise measuring and speed control apparatus required in the development and testing of very high speed machinery. In addition, the new circuits are of such basic nature that they readily can serve other applications for which no suitable commercial equipment is available. The frequency meter in its present form can be used as a general purpose laboratory instrument for the precise measurement of frequency or the accurate indication of small deviations from a given frequency. It gives an indication which is stable to about one or two rpm under normal line voltage variations, and its accuracy can be made to approach one-tenth of one per cent.

For use on machinery operating at speeds up to 100,000 rpm, the measuring instrument must not unbalance (and in some cases must not load) the moving part; therefore a photoelectric speed pickup is employed which requires no mechanical connection to the turbine shaft. The speed pickup, which can be placed several inches away from the turbine, merely "looks at" alternate black and polished areas on the surface of the turbine shaft and produces an electric signal whose frequency is some known multiple of the rotational frequency of the shaft.

Then in place of counting the revolutions per minute of the shaft we have the problem of measuring the frequency of an electric signal. The frequency meter used for this purpose must meet the following requirements:

1. Accurate within plus or minus one-half of one per cent or better.
2. Continuously adjustable over a frequency range of at least ten to one.
3. Capable of operating from an input signal having a very distorted wave form such as would be provided by a photoelectric or magnetic pickup.
4. Capable of providing an error signal proportional to deviation from any desired frequency to operate a servomechanism for regulating the turbine speed.

None of the commercial frequency meters are able to meet all of these requirements. A new frequency measuring circuit therefore has been devised which is essentially an electronic frequency meter of the recurrent capacitor discharge type but modified to operate as a "null-balance" circuit instead of a direct-reading device. By this simple modification the accuracy is increased from plus or minus two per cent to the order of one-tenth of one per cent and means are provided for obtaining a d-c or an a-c error voltage proportional to variation of shaft speed from the desired value. This voltage is used for indicating speed variations and for automatic speed regulation. It also operates a protective relay which will stop the machine in the event of an excessive speed deviation.

General Description

The desired speed is set up on a 3-dial decade speed selector having increments of 10,000, 1,000, and 100 rpm. The difference between selected speed and measured speed is called speed error. Its magnitude and algebraic sign are indicated on a large speed error meter, which has two ranges: plus or minus 250 rpm and plus or minus 1,000 rpm. A small speed meter, 0 to 100,000 rpm, is provided to show the approximate speed at which the turbine is running.

An electropneumatic servomechanism actuated by a speed error signal operates a steam control valve to regulate the steam pressure at the input to the turbine and hold the turbine speed at the desired value. The servomechanism is provided with a proportional air pressure "follow-up" and a manual reset control called the air pressure control dial. The steam control valve also is provided with proportional pressure follow-up so that the valve reproduces output pressure rather than valve position. In addition, the speed error signal contains a certain amount of error "anticipation" to minimize the response time of the system. By holding down a "bat handle" on the control panel the operator at any time can disconnect the speed error signal and assume manual control of the turbine speed, which he regulates by means of the air pressure control dial.

A block diagram of the complete speed control system is shown in Figure 1. The general scheme of operation is as follows: The turbine operator sets the speed selector dial to the number of revolutions per minute at which he desires the turbine to run. By means of the air pressure control dial he manually brings the turbine up to speed while watching the approximate turbine speed indicated by the speed meter. When the turbine speed comes within 4,000 or 1,000 rpm (operator's choice) of the desired preset value, the system switches into automatic control and the air pressure control dial becomes a fine speed adjustment. The operator trims the air pressure to make the speed error meter stabilize at zero. The frequency meter and servomechanism then hold the speed within plus or minus one-half of one per cent of the desired value. When a major load change is made, the operator retrims the air pressure control dial to return the speed error to zero, and the system regulates about the new control

Paper 46-188, recommended by the AIEE committees on air transportation and instruments and measurements for presentation at the AIEE Pacific Coast meeting, Seattle, Wash., August 27–30, 1946. Manuscript submitted July 1, 1946; made available for printing July 18, 1946.

ELLIS LEVIN is an engineer with the physical research unit, engineering department, Boeing Aircraft Company, Seattle, Wash.

The author wishes to acknowledge the contributions of Doctor C. K. Stedman, for his suggestion of the frequency measuring circuit; G. H. Stoner, for joint design of the complete frequency meter and regulator; and other persons who assisted in the work.

point. To measure a given speed at which the turbine is running, the operator adjusts the speed selector until the speed error meter read zero, and then reads the setting of the speed selector dial.

If for any reason the actual turbine speed goes either above or below the selected speed by more than 1,000 or 4,000 rpm (operator's choice), automatic protection circuits will shut off the steam supply and stop the turbine. In addition, the turbine automatically will be shut down by failure of any of the electric circuits. The speed error meter and automatic protection circuits function regardless of whether the system is in automatic or manual control.

The operator's control panel is shown in Figure 2. At the top is the frequency meter chassis with the speed selector in the center. On the left is the speed meter and an indicator light which shows when sufficient speed signal is present. On the right is the speed error meter, its range switch, and a light which indicates when the speed error is less than 1,000 or 4,000 rpm. Below the frequency meter is a panel containing steam and air pressure gauges. The next lower chassis contains the servo and automatic protection circuits, with the "bat handle" in the center and the air pressure control dial on the right. At the very bottom is the power supply chassis, with switch, fuses, and a monitor voltmeter.

At the present time, the turbine is being driven by high pressure air instead of steam, involving no changes, however, in the speed control equipment.

The Basic Frequency Measuring Circuit

The basic null-balance frequency measuring circuit is shown in Figure 3. It consists of a pair of push-pull connected triode switching tubes (V_1 and V_2) capacitor coupled to a diode bridge rectifier. The negative end of the bridge output resister R_B is grounded to the negative end of the common triode cathode resistor R_K and the negative side of battery B_1.

A square wave voltage, derived by the use of suitable shaping or trigger circuits from the signal whose frequency is to be measured is applied to the input terminals A and B in such a way that during one half-cycle the potential of terminal B is sufficiently negative to drive tube V_1 to cutoff. During the period of cutoff no voltage drop caused by tube current occurs in the resistor R_{L1}, and the capacitor C_1 will become charged to approximately the potential of battery B_1. The charging path is from ground, through battery B_1, resistor R_{L1}, capacitor C_1, diode tube V_4, rectifier output resistor R_B, and back to ground.

During the next half-cycle the signal applied to terminal B is within the operating range of tube V_1, and terminal A is sufficiently negative to drive tube V_2 to cutoff, so that tube V_1 will conduct and allow the potential of its anode to drop by an amount IR_{L1}, where I is the steady state plate current of the tube. The potential across the capacitor C_1 will drop by the same amount IR_{L1}, the discharge path being to ground through tube V_1 and resistor R_K in parallel with resistor R_{L1} and thence back to the capacitor C_1 through battery B_2 and diode V_5.

Since the electronic circuits are symmetrical, a similar charging and discharging of capacitor C_2 produces identical current pulses at alternate half-cycle intervals of the driving signal voltage, with the result that the charging current for the capacitors C_1 and C_2 flows through the resistor R_B in the manner illustrated in Figure 3a, and the discharging current of the capacitors C_1 and C_2 flowing through the resistor R_K takes the form shown in Figure 3b. The resistor R_B, therefore, carries only the transient charging current of capacitors C_1 and C_2, while the resistor R_K carries the steady current of the tubes V_1 and V_2 in addition to part of the transient discharge current of the capacitors C_1 and C_2.

In order to utilize this circuit as a frequency meter, it is only necessary to adjust discharge resistor R_K so that the average voltage developed across this resistor equals the average voltage across the rectifier output resistor R_B. When this has been done the voltmeter V will indicate zero.

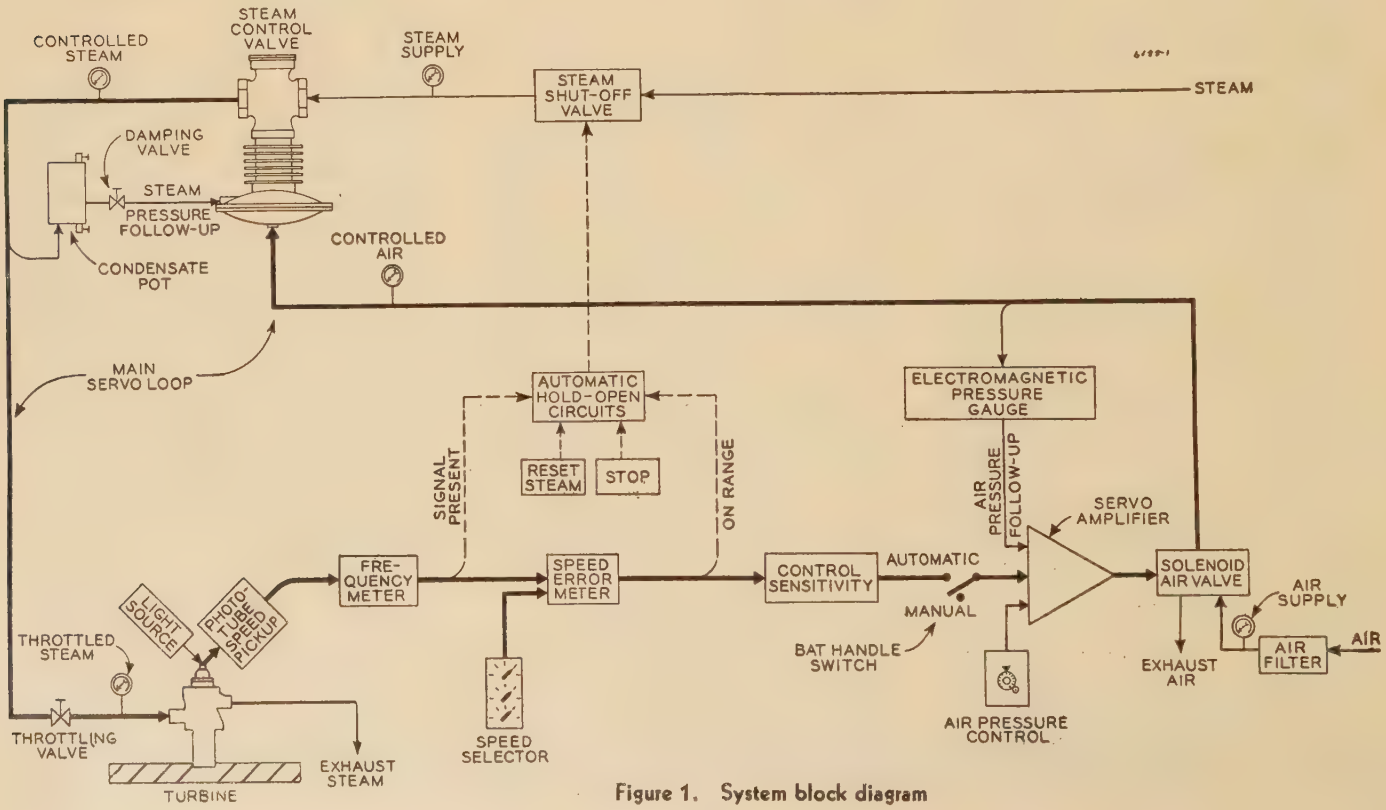

Figure 1. System block diagram

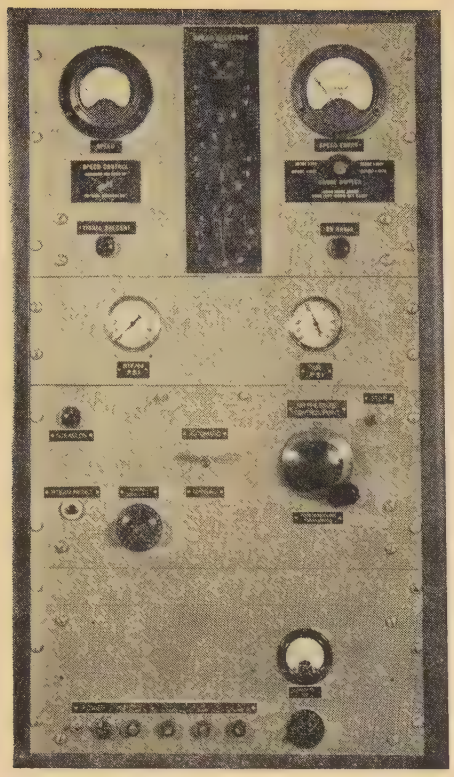

Figure 2. The control cabinet

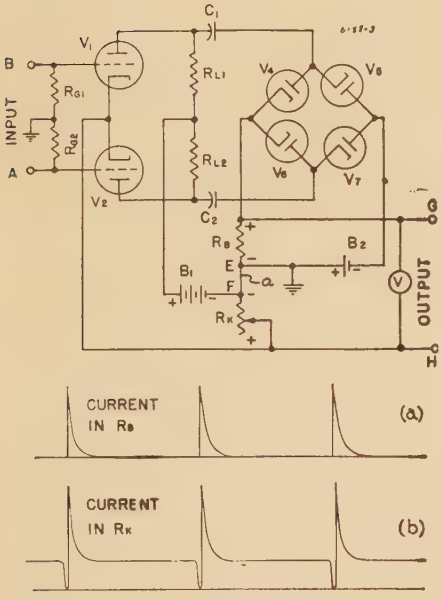

Figure 3. The basic null-balance frequency measuring circuit

If the frequency of the driving voltage applied to terminals A and B is raised, the heights and durations of the peaks in Figures 3a and 3b will not change, but will move closer together. The average current through resistor R_B is thus proportional to the frequency. However, the average current in resistor R_K is practically independent of frequency because the area of the discharge current peaks is only a fraction of the total area under the curve shown in Figure 3b. Consequently, the value of the resistor R_K required to balance the voltmeter V to zero will be very nearly proportional to the frequency of the signal applied to the input terminals A and B.

The equation of balance now will be derived. Since the circuit is symmetrical, either of the identical wire-wound resistors R_{L1} or R_{L2} can be represented by the single symbol R, and either of the high-stability mica capacitors C_1 and C_2 can be represented by the symbol C. R_p indicates the anode resistance, I the steady state anode current of either of the tubes V_1 and V_2, f the frequency of the signal voltage applied to the terminals A and B, R_B the value of the rectifier output resistor, and R_K the value of the discharge resistor required to balance the voltmeter V to zero. Each time a capacitor C is charged its voltage rises by an amount IR, and its charge rises by an amount CIR. The number of such charging pulses passing through R_B per second is $2f$. Thus the average voltage across R_B is

$$2fCIRR_B \tag{1}$$

Similarly, it can be shown that the average voltage across R_K is

$$R_KI+\left[\left(\frac{IR_KR^2}{R+R_p+R_K}\right)C\times 2f\right] \tag{2}$$

If R_K is adjusted until the voltmeter V reads zero, then these two average voltages are equal, and

$$2fCIRR_B=R_KI+\left[\left(\frac{IR_KR^2}{R+R_p+R_K}\right)C\times 2f\right] \tag{3}$$

Solving for f,

$$f=\frac{R_K}{2RC\left[R_B-\dfrac{RR_K}{R+R_p+R_K}\right]} \tag{4}$$

Since the expression $RR_K/(R+R_p+R_K)$ in the denominator varies with R_K from zero to a very small percentage of the resistance of R_B, the calibration curve of f as a function of R_K is very nearly a straight line, or

$$f\propto\frac{R_K}{2RCR_B} \tag{5}$$

If the circuit is to be used as a frequency meter, it is only necessary to vary the discharge resistor R_K until the voltmeter V reads zero, and then compute the input signal frequency by means of equation 4 or 5, or obtain the frequency value directly from the calibration curve previously prepared by comparison with a frequency standard.

Such a circuit can be used as a speed regulator control if discharge resistor R_K is adjusted so that the voltmeter V reads zero when a pickup device on the shaft rotating at the desired speed is supplying substantially square wave voltage impulses via a suitable trigger circuit to the signal input terminals A and B. Variations in speed of the shaft then will produce a pulsating d-c error voltage at the output terminals G and H which can be smoothed by a suitable electric filter and impressed upon a servo amplifier for speed control purposes.

Equation 5 shows that the only components which materially affect the calibration are the capacitor C and the resistors R_K, R_B, and R (R_{L1} and R_{L2} in Figure 3). If these components are stable and have low temperature-coefficients, the performance of the circuit as a frequency meter or as a speed regulator will be accurate and stable. The stability of the circuit also is increased by the fact that the voltages across resistors R_B and R_K are both proportional to the steady state anode current I so that variations caused by tube characteristics and battery voltages cancel out. The battery B_2 reduces to a low value the current which initial velocities of electrons in the diodes would cause to flow through the diodes and R_B. Changes in the contact potentials of the tubes resulting from changes

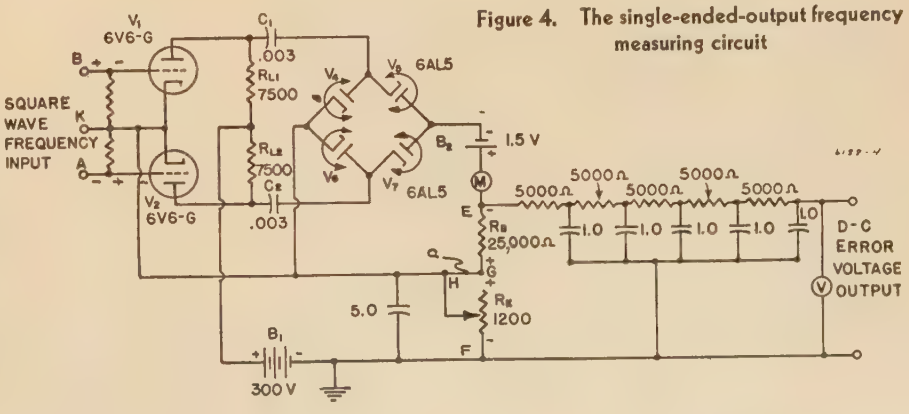

Figure 4. The single-ended-output frequency measuring circuit

in heater voltage are small compared with the charging potential of the battery B_1. Equation 4 shows that moderate variations in the anode resistance R_p of the tubes V_1 and V_2 have only a minor effect on the frequency calibration.

The Single-Ended Frequency Measuring Circuit

The circuit shown in Figure 3 and discussed thus far utilizes a double-ended input signal balanced to ground and produces an error voltage such that neither output terminal is grounded. A single-ended input can be utilized, if desired, by eliminating half of the symmetrical capacitor charging and discharging circuit, namely, V_2, R_{L2}, C_2, V_6, V_7, and R_{G2}. The output circuit can be modified to produce an error voltage with one output terminal grounded, by interchanging the wire a (Figure 3) with the voltmeter V, so that terminals G and H are joined together when the voltmeter is connected between terminals E and F.

The turbine speed control system described in this paper employs the frequency measuring circuit arranged for a double-ended input and grounded output, as shown in Figure 4. In this modified circuit the voltmeter V is connected between terminals E and F, and the terminals G and H are connected together. This joins the two measuring resistors R_B and R_K at their positive voltage ends rather than at their negative ends (as was done in Figure 3). In the circuit of Figure 4 at the bridge output, resistor R_B will conduct capacitor discharging current instead of charging current, but the circuit performance will be substantially the same as in the basic circuit which is shown in Figure 3.

Also in Figure 4, a milliammeter M has been inserted to measure the current in R_B. As this current will be proportional to the input frequency but subject to errors caused by variations in line voltage and tube characteristics, the meter M is used only for an approximate indication of the input frequency or speed. But the value of R_K required to balance the voltmeter V to zero at a given input frequency will be independent of variations in line voltage and tube characteristics to an accuracy approaching one-tenth of one per cent. The setting of R_K which gives zero output error voltage is used as a precise measure of the input frequency. The capacitor connected across the cathode resistor R_K, and the five RC sections connected to output terminals E and F serve to filter the pulsating output voltage into a steady d-c error signal.

Figure 5. Block diagram of the complete frequency meter

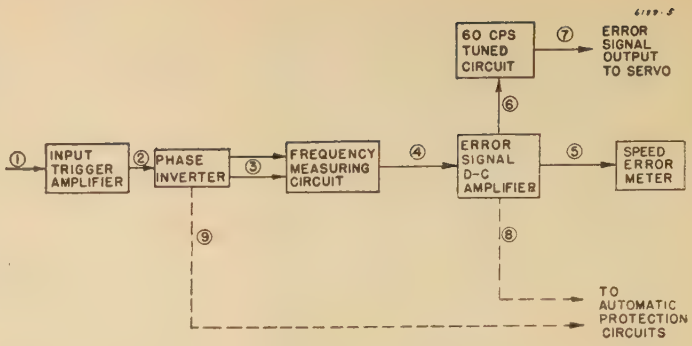

Figure 6 (below). The error signal d-c amplifier circuit

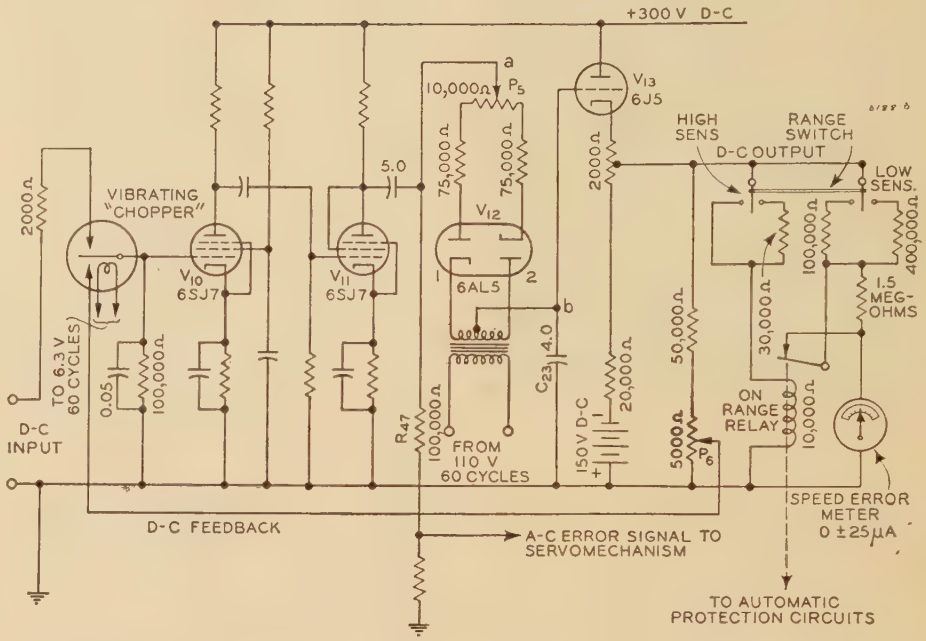

The Complete Frequency Meter

A block diagram of the complete frequency meter is shown in Figure 5. An input trigger amplifier converts the low level input frequency signal (this can be of sine, square, or distorted wave form) into high level single-ended square wave which is applied to a phase inverter. Output from the phase inverter is double-ended square wave which drives the two switching tubes in the frequency measuring circuit.

Full scale d-c error signal from the frequency measuring circuit is about 25 volts for 100,000-rpm speed error or 0.25 millivolts per revolution per minute deviation from the selected speed. In order to achieve a measuring and control accuracy of plus or minus one-half of one per cent if any speed between 10,000 and 100,000 rpm the circuit should be sufficiently sensitive to indicate changes of at least 0.1 to 0.05 per cent. For 0.1 per cent speed deviation the d-c output error voltage is 2.5 millivolts at 10,000 rpm and

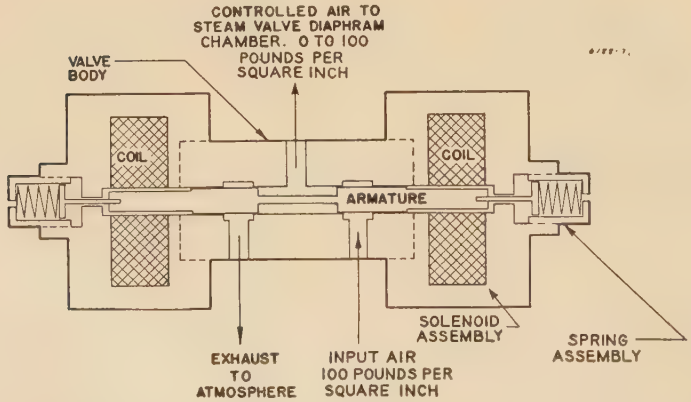

Figure 7. Schematic diagram of the solenoid air valve

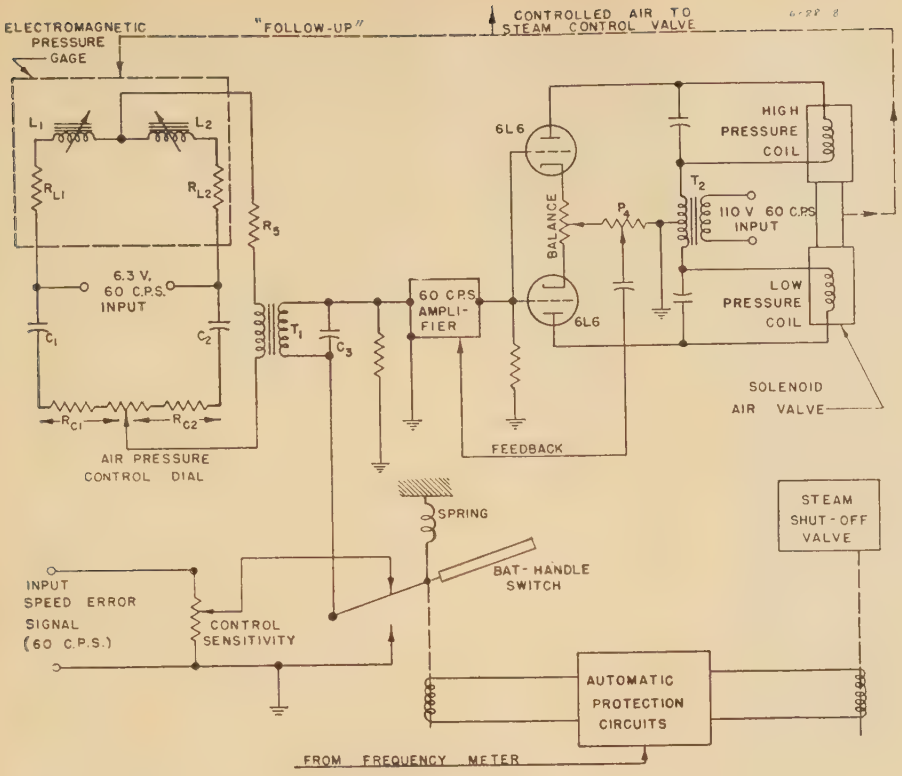

Figure 8. The servo circuit

25 millivolts at 100,000 rpm, which is not sufficient signal to operate a high resistance d-c voltmeter directly. Therefore the output voltmeter V shown in Figures 3 and 4 should be a vacuum tube voltmeter, which generally employs an amplifier to drive a panel type d-c microammeter or milliammeter.

The Error Signal D-C Amplifier

Because of the instabilities associated with conventional direct-coupled amplifiers a special stabilized, sensitive, discriminating d-c amplifier was devised for use in this frequency meter. This amplifier utilizes the established technique of "chopping" the d-c signal into square wave alternating current and passing it through a more easily stabilized a-c amplifier; but in addition it employs a familiar phase-discriminating rectifier to change the alternating current back to high level direct current, and incorporates d-c negative feedback to produce a high degree of over-all stability.

The circuit of the error signal d-c amplifier is shown in Figure 6.

The input d-c "chopper" is effectively a single-pole double-throw mechanical switch which opens and closes continuously at the rate of 60 cycles per second. It consists of a vibrating reed contactor driven between two stationary contacts by means of a 6.3-volt 60-cycle-per-second exciter coil. As the reed oscillates between the two fixed contacts it assumes the potential of the upper contact for approximately one-half of the 1/60-second cycle and the potential of the lower contact during the other half of the cycle. Therefore, when a direct voltage is applied between the two fixed contacts it will be converted to a 60-cycle-per-second square wave voltage across the vibrator output impedance connected between the reed and the lower fixed contact. The output alternating voltage will be in phase with the 110-volt 60-cycle-per-second line when the applied direct voltage is of a given polarity (say positive) and 180 degrees out of phase with the line when the input direct current is of the opposite polarity (negative).

Consider for the present that the lower fixed contact is grounded. Then the amplitude of the 60-cycle-per-second square wave from the vibrator will be approximately equal to the d-c error voltage and proportional to speed error. The phase will reverse when the speed error goes through zero. Connected across the 100,000-ohm vibrator output resistor is a 0.05-microfarad capacitor which serves to by-pass the high frequency transient peaks which occur during the "make" and "break" switching intervals.

The low level a-c error voltage is amplified in the conventional 6SJ7 stages V_{10} and V_{11}, and then impressed upon the phase-discriminating half-wave rectifier V_{12}, which operates as follows: Via the injection transformer T_1, the 110 volt a-c line voltage switches the two diodes of V_{12} on and off at the rate of 60 cycles per second and in synchronism with the 60-cycle-per-second vibrating reed in the d-c "chopper" at the input to the error signal amplifier.

The 60-cycle-per-second speed error voltage applied between point a and ground cannot reach point b when the diodes are cutoff; but during the half-cycle of line voltage that the diodes conduct there is a path of finite resistance from a to b allowing pulsating direct cur-

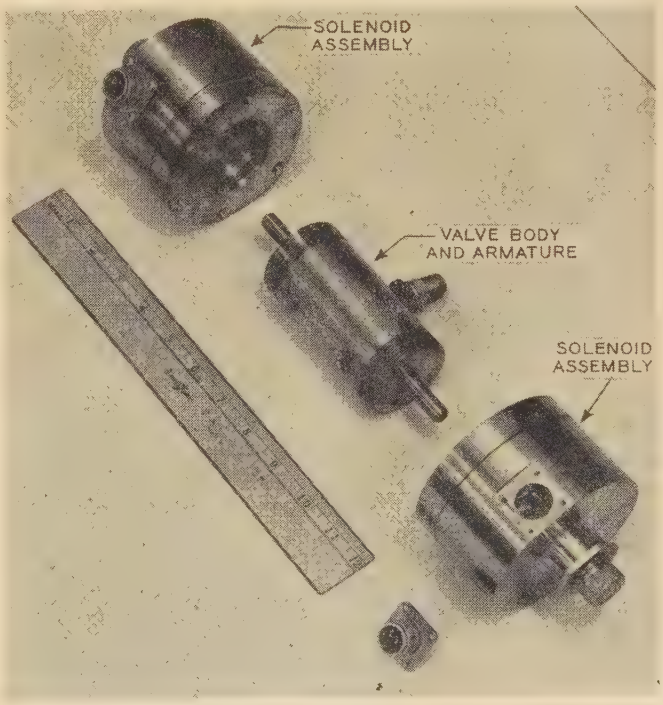

Figure 9. The solenoid air valve partly disassembled

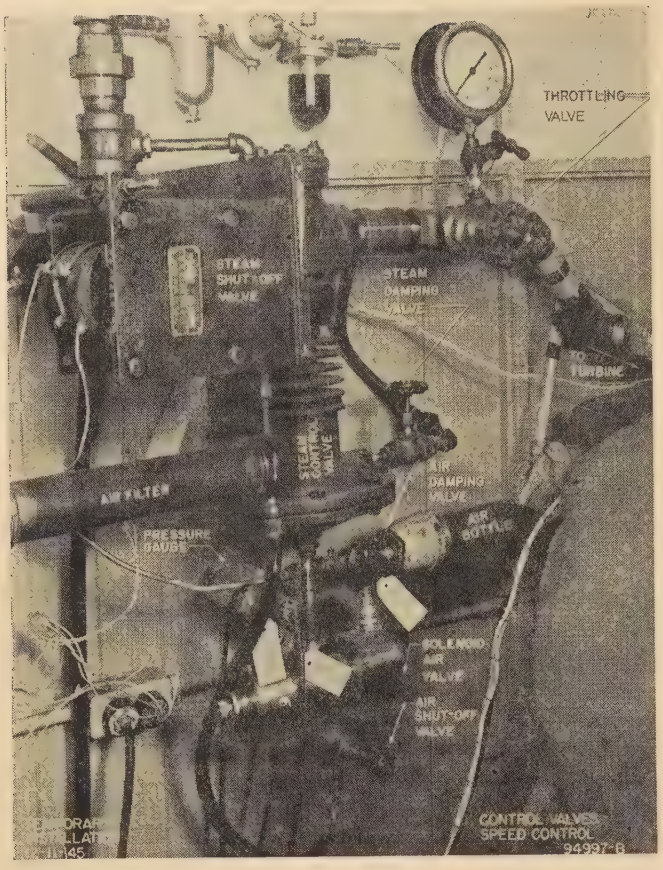

Figure 10. Temporary control valve installation with turbine operated by high pressure air instead of steam

rent to be fed to capacitor C_{23} through two parallel paths, each consisting of one-half of P_5, one $75K$ resistor, one diode, and one-half of the secondary winding of T_1. (The diodes are balanced so that the switching voltage from T_1 causes no potential difference between points a and b.) Because it comes from the d-c chopper, the a-c signal applied to point a is either in phase or 180 degrees out of phase with the 110-volt 60-cycle-per-second line. If a becomes positive when the diode plate 2 becomes positive the pulsating direct current will flow from a to b and through C_{23} to ground, producing across C_{23} an output voltage such that point b is positive with respect to ground. Similarly if point a is driven negative when diode plate 2 is negative, then the pulsating direct current will flow from ground through C_{23} and from b to a, producing across C_{23} an output voltage such that point b is negative with respect to ground. Capacitor C_{23} smooths the pulsating direct current to give a steady output voltage of the same polarity but greater magnitude than the d-c speed error signal applied to the d-c chopper at the input to the amplifier. The output high level d-c error voltage is impressed upon the cathode follower V_{13} which drives the zero-centered speed error meter to the right or left of zero to indicate positive or negative speed deviations.

By means of a voltage divider connected across the cathode follower output terminals, a portion of the d-c output voltage is fed back to the lower fixed contact of the input "chopper." The circuit is phased, by means of T_1, so that the potential at h is of the same polarity as the input potential at the upper fixed contact

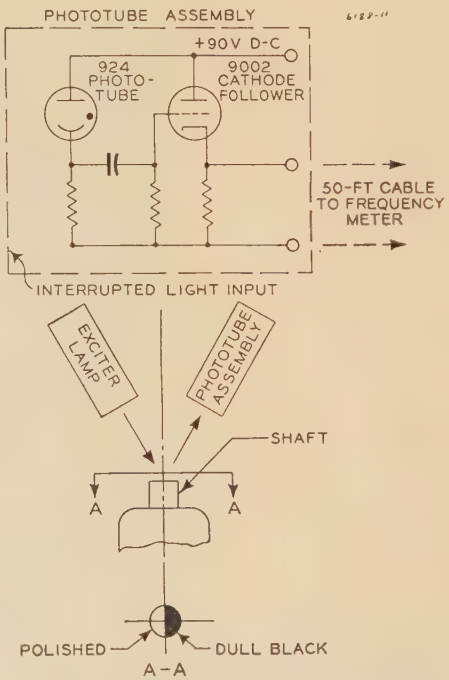

Figure 11. The speed pickup arrangement

of the vibrator. Therefore, as the vibrating reed assumes during one half-cycle of 60-cycle-per-second line voltage the input potential of the upper fixed contact and during the other half-cycle the feedback potential of the lower fixed contact, the magnitude of the alternating voltage output from the vibrator is reduced by the d-c feed-back voltage. This reduces the over-all gain of the error signal amplifier but serves to stabilize the amplifier output against changes in supply voltages and tube characteristics. The amount of feedback, and consequently the gain of the amplifier, is adjusted by means of P_6.

Also connected across the d-c output is the on-range relay which actuates the automatic protection circuits when the speed error exceeds 1,000 or 4,000 rpm, depending upon the setting of the range switch. When energized it also inserts a 1.5-megohm protective resistor in series with the speed error meter.

The Input Trigger Amplifier

There are various shaping amplifiers which can be used to operate the frequency measuring circuit. The one selected for this frequency meter is a new reliable "go–no go" circuit. That is, when the input speed signal amplitude exceeds a critical minimum voltage of about 0.15 volt (at any frequency from zero to at least 5 kc), the amplifier will trigger and provide high level square wave output of constant amplitude and one-half the input frequency. If the input signal amplitude falls below the critical value, the circuit will give no output at all. This feature is utilized by the automatic protection circuits to stop the turbine and summon the operator in the event of erratic or insufficient input signal from the photoelectric speed pickup.

The circuit diagram is shown in Figure 13. The input tube V_0 is an amplifier to feed the required 10,000-ohm input to the first trigger tube V_1. With the plate, cathode, and grid resistance values as shown, V_1 can be set up to have two stable operating points. The bias and feed-back resistors are adjusted until the tube is operating in one equilibrium condition and almost at the point where it will change to the second equilibrium condition. Then a small input signal will trigger the tube from one operating condition to the other. Output can be taken between ground and either the plate or the number 2 grid.

Although the tube will be triggered by either a rising or decreasing wave front as soon as the amplitude crosses a given

critical value, better square wave results when the triggering impulse is a sharp pulse, in which case a small capacitor connected between the plate and the number 1 grid adds to the reliability of operation.

The output from the number 2 grid of V_1 has squared sides but not a perfectly flat top and bottom. This signal is differentiated in the output *R-C* branch (25 micromicrofarads, 10,000 ohms) to obtain sharp pulses for tripping a second trigger tube V_3.

The differentiated output appears at the number 1 grid of V_2 as a series of alternate positive and negative pulses. But the time interval between a given positive pulse and the adjacent negative pulse might be different in length from the interval between the negative pulse and the following positive pulse if the speed input signal has unequal positive and negative half cycles such as might be provided by a photoelectric speed pickup. Therefore the blanking amplifier V_2 removes alternate pulses (by successive positive and negative blanking), producing at its second cathode a new series of equidistant pulses that are positive only. These are differentiated in the output *R-C* branch (10 micromicrofarads, 500,000 ohms) to obtain very sharp double-ended pulses which are used to fire the second trigger tube V_3. A given pulse triggers the tube in one direction and the following pulse trips it in the opposite direction. The resultant output from V_3 is a good square wave voltage having equal positive and negative half cycles. Its frequency is exactly half that of the input speed signal. This single ended square wave is fed to a 6N7-G phase inverter which produces double-ended square wave to drive the two switching tubes V_1 and V_2 in the frequency measuring circuit.

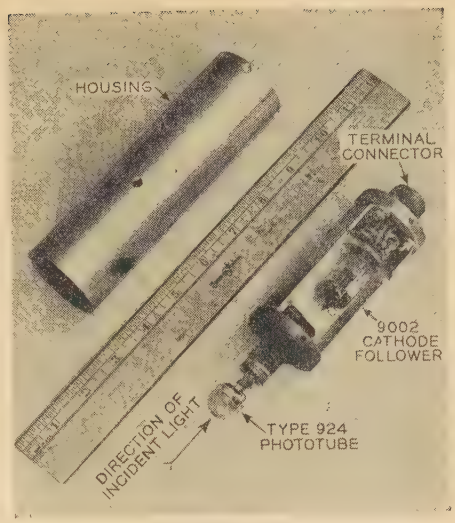

Figure 12. The phototube assembly

The Servomechanism

As shown in Figure 1, the diaphragm-actuated steam control valve is operated by an electropneumatic servomechanism, which receives 60-cycle-per-second speed error signal from the frequency meter unit. To supply regulated air to the steam control valve, at 0 to 100 pounds per square inch, the servomechanism utilizes a solenoid air valve shown schematically in Figure 7.

The air valve contains a balanced armature that slides in a cylinder which is provided with an annular metering port on each end and a central "controlled pressure" outlet connected to the diaphragm chamber of the steam control valve. At each end of the cylinder housing, a solenoid and adjustable spring assembly is provided to position the armature within the cylinder. When the armature is moved to the right far enough to open the inlet port, high pressure air will flow around the undercut middle section of the armature and through the center outlet to the diaphragm of the steam control valve. The pressure built up in the diaphragm chamber will depend upon how much and how long the inlet port is open. When the armature is returned to the neutral position so that both ports are closed, the output pressure will remain at the built-up value until the armature is moved to the left to open the exhaust port or until the air leaks out around the armature bearing surfaces. Thus by proper positioning of the armature, the output pressure can be set to any value between 0 and 100 pounds per square inch.

Each of the solenoid coils is connected as the plate load of a 6L6 power output tube in a phase-discriminating servo amplifier shown in Figure 8. The two 6L6 plate circuits are energized, 180 degrees out of phase, by the 60-cycle-per-second line via the high voltage transformer T_2 whose secondary is grounded at its center-tap. At zero a-c input to the 6L6 grids, the tubes are balanced to supply equal plate currents to the two solenoid coils. A 60-cycle-per-second error signal applied to the grids such that it is in phase with the plate voltage of the upper tube will be out of phase with the plate voltage of the lower tube; therefore the plate current of the upper tube will increase and that of the lower tube will decrease. This will result in a differential magnetic pull on the valve armature, which will move the armature toward the inlet port to increase the output air pressure. Similarly, if the phase of the input error signal is reversed, the lower tube will conduct more plate current than the upper one, moving the armature toward the exhaust port to decrease the output air pressure.

The current in each solenoid is half-wave rectified 60-cycle-per-second, partly smoothed by means of a 0.5-microfarad shunt capacitor. The remaining a-c component of coil current is utilized to buzz the armature at 60 cycles per second and minimize static friction in the valve bearings. A portion of the second-harmonic cathode voltage is fed back to the input voltage amplifier to provide added stability and an over-all gain control.

The 60-cycle-per-second sine-wave input to the servo amplifier consists of speed error signal (coming in through a "control sensitivity" attenuator and the bat handle switch) in series with air pressure follow-up signal (from the pressure gauge bridge circuit via transformer T_1). The electromagnetic pressure gauge consists of two

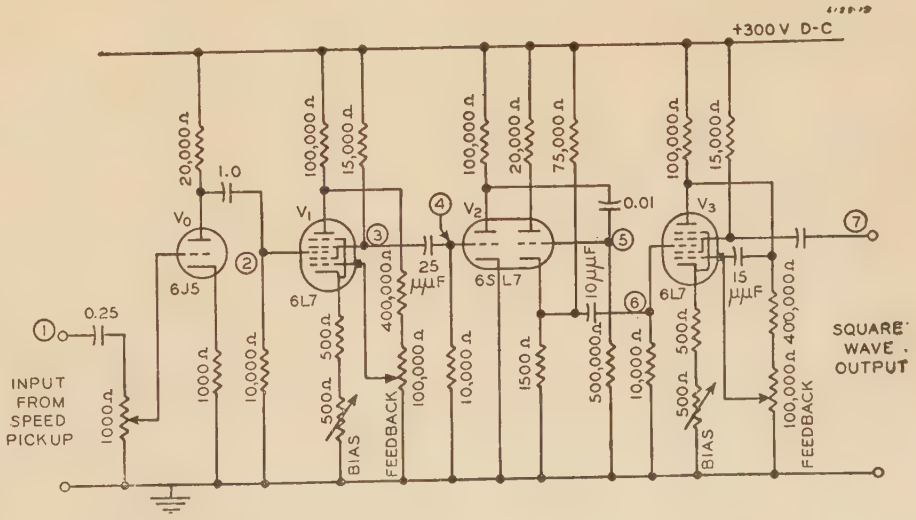

Figure 13 The input trigger amplifier

Electrical Anti-icing of Aircraft Windshields

J. D. McCRUMM
ASSOCIATE AIEE

PREVENTION of ice formation on the aircraft windshield presents difficult problems. In addition to optical quality, the thermal and structural characteristics of suitable transparent materials, such as glass and certain plastics, must be given careful consideration. Further, an important design criterion for an aircraft windshield is its ability to withstand impact loads such as those which result when a large bird strikes the windshield. Contemporary windshield design practice usually calls for a laminated structure, commonly consisting of a layer of polyvinyl butyral, encased between two plates of tempered glass. The impact resistance of such a construction has been shown to be dependent upon the vinyl temperature, the optimum temperature being of the order of 110 degrees Fahrenheit. Direct correlation thus exists between impact resistance and anti-icing ability in windshield design. The regulations of the Civil Aeronautics Board specify that the windshield and supporting structure of a transport airplane shall be designed to resist the impact of a 4-pound bird when the airplane is flying at sea level cruising speed.[1] It is apparent, therefore, that it may be necessary to supply heat to a laminated windshield continuously, regardless of the prevalence of icing conditions, and further that the amount of heat must be controlled within the limits specified by impact resistance as well as deicing.

Five schemes or combinations thereof have been advanced for the prevention of ice formation on the windshield:

1. Fluid and wiper.
2. Hot air.
3. Resistance wires embedded in the windshield.
4. Radiant heat (infrared).
5. A transparent electrically-conductive coating.

It is the purpose of this paper to examine the basic considerations for the design of a windshield anti-icing system, and to discuss in some detail the pertinent characteristics peculiar to each scheme. The design will be considered primarily as a windshield ice-prevention problem, with impact resistance as the major secondary consideration.

Paper 46-190, recommended by the AIEE committee on air transportation for presentation at the AIEE Pacific Coast meeting, Seattle, Wash., August 27–30, 1946. Manuscript submitted June 24, 1946; made available for printing July 18, 1946.

J. D. McCRUMM, formerly an electrical engineer at the Douglas Aircraft Company, Santa Monica, California, is an associate professor of electrical engineering at Swarthmore College, Swarthmore, Pa.

The author wishes to acknowledge the assistance of the air conditioning group and research laboratories of the Douglas Aircraft Company in the described investigation and the co-operation of the Pittsburgh Plate Glass Company in supplying design data. Appreciation is expressed for permission to reproduce from reference 2 the data shown in Figure 1.

Heat Requirements

Thermal energy is removed in several ways from a heated windshield which is being flown in an icing environment. Assuming flight through a dense formation of super-cooled water droplets, effective anti-icing will be achieved by maintaining the outer surface of the windshield at a temperature above freezing, say 35 degrees Fahrenheit. The heat absorbed from the surface can be grouped into four basic categories:

1. The loss by forced convection and radiation.
2. The heat of liquid required to raise the temperature of the water droplets striking the surface.
3. The loss by evaporation of that portion of water required to maintain 100 per cent vapor saturation in the surface boundary layer.
4. The edge losses by conduction to the structure.

A fifth category, kinetic heating,* should be considered, representing a gain of heat.

The relative importance of kinetic heating is dependent upon the amount of free water in the cloud. For a low water density and small droplets, the droplets may be evaporated entirely before they strike the windshield surface. For a higher water concentration, water will strike the surface and at once be vaporized so that the surface remains dry; in this case, the kinetic heat equals or exceeds the heat losses. Insufficient kinetic heating is characterized by a sharp reduction in the temperature of the surface (with a consequent icing over) unless auxiliary heat is supplied. Complete wetting of the surface will be brought about by a relatively high concentration of water, and all five factors plus auxiliary heat achieve importance in an anti-icing heat balance analysis.

The relative magnitude of the thermal losses for a given airplane and windshield are dependent upon the outside air temperature, water droplet size, amount of water per unit volume, altitude, and aircraft velocity. Two other determining factors, the surface boundary layer velocity distribution and amount of water catch, are influenced by those structural conditions which determine the aerodynamic flow characteristics over the windshield. Briefly consider each previously mentioned heat loss.

Loss by forced convection in wet air is greater than in dry air because of the higher specific heat of wet air; the radiation loss is relatively small. The heat of liquid required to raise the water temperature is dependent upon the amount of water catch on the windshield and the temperature differential through which it is raised. The loss by heat of evaporation

* In wet air Prandtl's number approaches unity, and kinetic heating becomes proportional to the airplane velocity squared.

similar coils whose inductances are varied equal amounts but in opposite directions by changes in servo output air pressure. These coils are connected along with the air pressure control dial into a 60-cycle-per-second bridge circuit. By means of the air pressure control dial, the bridge can be balanced to zero at any given operating air pressure. Then any change in pressure will produce a bridge unbalance and a proportional output error voltage, which will energize the servo amplifier to return the air pressure to its original value and rebalance the bridge. If, however, the air pressure control dial is displaced, the servo will stabilize the output pressure at the new value required to rebalance the bridge at the new setting of the control dial.

By means of the resistor R_5 and capacitor C_3 the follow-up voltage at the secondary of T_1 is phased exactly with the speed error signal from frequency meter.

When the bat handle is held down, the speed error signal is disconnected and the servo responds only to the bridge circuit, so that the air pressure control dial can be used for manual speed control.

requires more detailed explanation. As the temperature of the air in the boundary layer over the windshield increases, because of the acquisition of auxiliary heat, it possesses a greater ability to absorb water. If the air at the initial temperature is considered 100 per cent saturated, a lower degree of saturation will exist at the higher temperature. Because of the resulting differential vapor pressure conditions, liquid will be evaporated from the water droplets and the wet windshield surface, and a considerable amount of thermal energy will be extracted in the process. Loss by conduction at the frame is a function of the frame configuration and thermal contact at the glass edge.

The temperature specifications for maximum impact strength have been mentioned. Figure 1, taken from reference 2, indicates a maximum strength when the vinyl plastic is maintained at 110 degrees Fahrenheit, but little deviation from the maximum strength results over a temperature range of from 100 to 120 degrees Fahrenheit. When the vinyl is at a temperature corresponding to that of cabin air, say 70 degrees Fahrenheit, the impact strength based on penetration velocity is reduced by about 45 per cent. This is a serious diminution. The data of Figure 1 refer to a specific windshield and frame design. Other similar designs will have different absolute maximum impact resistance, but the maximum will occur at about the same vinyl temperature.

It is evident that if impact resistance be considered a design criterion of an anti-icing windshield, the thermal requirements will be influenced accordingly. This is particularly true when the time schedule of operation is considered, since adequate impact resistance may require application of heat continuously while the airplane is in flight; anti-icing may be required only at infrequent intervals. The relative heat demand is modified by variations in glass and vinyl thickness, method of heat application, and plane at which heat is developed initially, as well as differences in the flight atmosphere.

Design Considerations

Definite factors influence the adoption and design of a windshield anti-icing scheme:

1. Anti-icing ability.

2. Impact resistance. Proper structural design is involved, possibly supplemented by heat.

3. Weight.

4. Optical properties. Freedom from annoying reflections, adequate light transmission, freedom from optical distortion, and so forth, are necessary.

5. Ease of control. The arrangement must lend itself to a reasonably simple and reliable control system with rapid response characteristics.

6. Transient thermal properties. The system should be able to commence effective anti-icing quickly from an initially unenergized state.

7. Structural factors. Depending upon the source of heat, the structure must be adapted to the primary needs of the system. A simple structural and interior layout is desirable.

8. Fundamental means for ice prevention. Other than fluid deicing, four thermal systems are available. Selection of a system must include consideration of the influence of the deicing system on the functional behavior of other components of the airplane.

9. Reliability and safety.

10. Aerodynamic considerations. The velocity distribution over the windshield surface and the amount of water catch will be determined by the air flow characteristics over the nose and upper front fuselage. Thermal requirements are affected directly.

11. Pilot comfort. A high temperature at the inner windshield surface will result in excessive radiant heat on the pilot. Discharging large amounts of warm air in the cockpit enclosure from a hot air system is likewise undesirable.

12. Maintenance and ease of servicing.

13. Fabrication of windshield. A means of ice removal requiring a panel difficult to manufacture and correspondingly costly is to be avoided. Replacement as well as initial cost would be high.

14. Defogging and defrosting. Collection of fog or frost on the interior windshield surface also must be avoided, the simplest means being to maintain the inner surface above the dew point temperature for the given cockpit air humidity, density, and temperature.

Miscellaneous factors arise from other sources. For example, one air line is considering the addition of a thermal deicing system on a modified Douglas C-54 airplane. Since the line figures a revenue loss of over 1,000 dollars for each day the airplane is out of service, a system which can be installed quickly is highly desirable, even though a weight penalty of several pounds is exacted.

A discussion of the possible methods of supplying heat to the windshield will assist in forming a decision as to the most desirable scheme for a given airplane.

Nonelectrical Methods

Two nonelectrical deicing systems are in common use and will be discussed briefly for comparison with electrical methods. The earliest and most widely used method consists of a mechanical wiper which also distributes an alcohol fluid freezing point depressant over the wiping surface. There are definite limits to the deicing ability, and of course no protection at all is afforded after the supply of fluid is exhausted. The system is, however, simple and reasonably light in weight, and may be applied readily to most structural configurations without modification. Curved

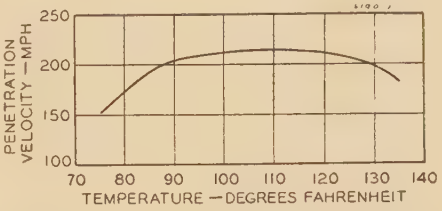

Figure 1. Variation of bird penetration velocity with temperature of a laminated glass and vinyl plastic windshield

windshields present an obvious problem. Other advantages and disadvantages are evident and will not be enumerated.

Hot air anti-icing has received much attention since 1940.[3] The most commonly used arrangement consists of two panes with an air gap of from 0.1 to 0.2 inch. The heated air is introduced at one edge, passes between the two panels, and is discharged directly into the cockpit, over other windows for defogging, or elsewhere. The inner panel is usually of impact resistant construction and the outer designed for maximum heat transfer consistent with adequate strength. One heated air scheme introduces the air to the windshield on the outside surface in the form of an artificial boundary layer.

The hot air system is reasonably light in weight, although the weight of a second panel is appreciable. Optically, the double windshield is poorer than a single pane arrangement because of the multiplicity of light images, both transmitted and reflected, occasioned by the two additional prime surfaces. A distinct disadvantage is the high temperature and mass of air flow required to provide the necessary thermal energy for combatting a severe icing atmosphere. This may overheat any vinyl plastic present, causing permanent small bubbles to form, and also appreciably reduce the impact strength of a laminated panel. Further, the resulting hot inner surface radiates excessive heat to the pilot's face. The glass may crack because of the high thermal gradients. However, the system has been adopted for numerous military and commercial aircraft, largely because of the relative ease in obtaining heated air, either from waste exhaust heat or primary

combustion heaters, compared with the difficulty of procuring sufficient electric power and specially designed windshields.

Embedded Wires

Perhaps the most obvious electrical method of developing heat at the windshield surface is by means of embedded resistance wires. This idea is not new. Rodert describes experiments in which a series of wires were mounted in a space between two glass panels with the intervening region filled with liquid ethylene glycol.[4] The method proved unsatisfactory because of the difficulty in sealing the configuration against leaks of glycol liquid. A windshield of laminar construction with a layer of vinyl plastic sandwiched between two panes of tempered glass conceivably could have wires embedded in either the glass or the vinyl. Because of fabrication difficulties, however, it is impracticable to embed the wires in the glass. One air frame manufacturer has intensively pursued an investigation of panels having the fine wires situated at the interface of the glass and plastic.

The wires must be of a material which can be drawn to a diameter of about one mil or less and still possess adequate tensile strength. The resistance must be correlated with the required deicing power per square foot, wire spacing, and operating voltage. The wire surface should be dull to avoid reflections. Several materials are suitable, such as copper, platinum, copper encased in platinum for strength, beryllium-copper, or nickel. During manufacture the wires are bonded to the vinyl while under tension. Wire buckling and kinking thus is prevented both during panel fabrication and while being heated electrically. The ends are soldered to a bus, usually running horizontally at the top and bottom of the windshield with the wires contained vertically. Visual distraction is less with this arrangement than with the wires mounted horizontally.

A typical design will be described. Beryllium-copper wire one mil in diameter is embedded at or very near the interface between the outer pane and the vinyl. The thicknesses of glass and plastic depend upon the impact strength desired, except that a sufficiently thick front glass pane is required to permit a uniform temperature distribution over the outer face. Three-quarter tempered glass panels 3/16 inch thick, with 1/8 inch to 1/4 inch vinyl are typical dimensions for a windshield 15 inches by 30 inches over-all. Assuming an anti-icing heat demand of 1,740 Btu per hour per square foot with a five-per-cent loss into the pilot enclosure, 535 watts per square foot must be developed by the heated wires. Mounting the wires vertically, and allowing a one-half-inch-wide horizontal bus at top and bottom, the wires will be 14 inches long. One mil beryllium-copper has a resistance of about 60 ohms per foot, and at 27 volts each wire will dissipate 10.4 watts. Thus 60 wires will be necessary per foot of panel, or a wire spacing of 0.2 inch.

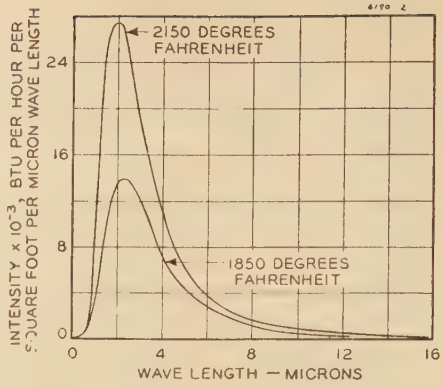

Figure 2. Dependence of radiation intensity upon wave length for a black body

A German windshield, reported by a technical observer of the "Combined Intelligence Objectives Subcommittee" under the British and United States Armies, is described as having 0.015 millimeter (0.6 mil) of copper wire embedded in a plastic middle layer, with a very narrow spacing of the order of 0.05 inch.

The deicing ability of an embedded wire panel should be good, but will be limited by the temperature developed in the vinyl. Exceeding the temperature for maximum impact strength is one consideration; another is a 200-degree-Fahrenheit limit imposed by the tendency of the plasticizer to vaporize above this temperature, forming permanent small bubbles. Values much higher than the critical limit for bubble formation must be developed at the wire surfaces to produce a lower required average vinyl temperature.

The important factors favoring hot wire windshields are the light weight associated with operation on 28 volts, their reliability, and the efficient manner in which the developed heat energy is dissipated.

The disadvantages of the scheme are fundamental and serious. Optically, there are two deterrents. First is the necessity for looking through the closely spaced fine wires with the concomitant eye fatigue. Viewed from a distance of two feet, with eyes focused on objects beyond the windshield, the visual distraction is slight but not insignificant. Second, and of greater importance, is the optical distortion caused by the local heating of the vinyl sheath about each wire. The resulting localized variation of the index of refraction will distort severely objects viewed through the panel. The extent of distortion is proportional to the temperature gradient, and provision of sufficient heat for anti-icing under moderate to extreme conditions may render the windshield optically useless. This condition is tempered by virtue of an outside visibility of zero during icing conditions anyway, but the significant time required for the distortion to fade away after the panel is de-energized may be serious. The distortion produced by the heat necessary in clear air for interior defogging and for impact strength further establishes the seriousness of the situation.

The necessary construction renders the windshield difficult and expensive to manufacture, and the deicing ability is limited by local overheating of the vinyl. If the necessity for supplying heat in clear air conditions (for impact strength and defogging) or the inadvisability of so doing (because of distortion) are disregarded, a complication is introduced by the thermal lag of the system. The time which elapses between the application of power and the inception of ice removal could be serious in an emergency.

Infrared Radiation

Radiant thermal energy directed on a solid body will be absorbed to a varying degree. Most solids are sensibly opaque to infrared radiation, but because of the characteristic similarity between energy in the visible spectrum and in the near infrared spectrum, visually transparent substances such as windshield constituents will pass a certain portion of the energy entering the surface. Because of surface reflection, only a part of the radiation impinging on the surface will enter any material.

The amount of energy reflected or absorbed by a receiver is a function of the wave length of the radiations emitted by the source.[5] The visible spectrum is included within the range of from 0.35 to 0.8 micron. The infrared spectrum is divided arbitrarily into the near infrared spectrum ranging from 0.8 micron to around 25 microns, and the far infrared spectrum ranging above 25 microns. In general, thermal radiation at all wave lengths is emitted by hot solid bodies, the total emission depending upon the temperature, the material, and the condition of the surface. Typical radiation

patterns for a body at two temperatures is shown in Figure 2. A small fraction of the total energy is in the visible range but the greatest portion is in the near infrared spectrum. At higher temperatures the peak of the curve is shifted to a lower wave length, the position of the maximum being inversely proportional to the absolute temperature.

The dependence upon wave length of the total energy absorbed by an optically transparent receiver is indicated in Figure 3. Ordinary glass and vinyl plastic readily pass the visible frequencies. The very near infrared spectrum is largely passed by the glass, but strongly absorbed by the vinyl. Thermal radiation at frequencies above 2.8 microns is absorbed by both materials. Special glasses are available which are opaque to visible radiation, but which transmit most of the infrared rays from one to four microns. Conversely, others transmit most of the visible rays, but strongly absorb all wave lengths above 0.8 micron.

An anti-icing scheme using infrared rays is apparent. A grid consisting of electrically heated wires or a series of specially constructed radiant heat lamps are practical as a source. A polished metal reflector will assist in concentrating or distributing the energy on the windshield. An infrared filter may be incorporated, depending upon the amount of visible light developed (a direct function of source temperature) and the necessity for eliminating it. Directing the radiation on the windshield will cause it to rise in temperature, and if sufficient energy is supplied, effective ice prevention may be accomplished.

Most of the heat is developed within the windshield because of the relatively strong absorptive characteristic of the vinyl. The proportional amount for a specific case may be determined from Figure 3. The heat then is transmitted by conduction to the outside. The amount of energy passing on through the assembly may be reduced by using a heat absorbing glass as the outer pane, thus collecting more heat energy in this plane. However, radiation energy passing completely through the windshield will be absorbed by ice or water which may have collected on the surface. Laboratory tests show that a layer of ice so irradiated tends to "mush-up" and melt throughout the layer, a phenomenon readily explained by the penetrating power of the radiation.

A similar layer melted only by heat conducted through the glass displays a tendency to melt away at the glass surface, leaving an ice bridge over the windshield but separated from it by a small air or water filled space.

Suitably locating the source of the infrared rays is one of the major problems presented by this system. Pilot vision must not be impaired, but a reasonably uniform distribution of heat must be secured. These conditions are difficult to meet except for highly sloping windshields, since the incident radiation should strike the windshield at as near 90 degrees as possible. Any solution for windshield configurations similar to the DC-3 or DC-6 is apt to be awkward, and require considerable skill in overcoming the inherent spatial problem. The ratio of source space required to power emanated is of the order of one to two cubic inches per watt. The applicability of radiant heating thus is seen to be greatly dependent upon the structural configuration of the cockpit.

One answer to the space question is to locate the source outside of the airplane. Some form of retractable mounting for hermetically sealed source could be employed in conjunction with a filter to eliminate the visible light. The slope of the windshield may make it desirable to mount the source above the windshield rather than on the nose. This or other factors combined with the high space-to-power ratio again emphasize the fundamental awkwardness of the scheme based on infrared radiation.

Advantages of a radiant heating scheme are light weight and ability to operate on 28 volts. A special windshield design is unnecessary, and the appropriate plastic temperature for satisfactory impact strength may be maintained, although this temperature will not be synonymous with the all anti-icing heat requirements. Indeed, because of the absorbtive capacity of the vinyl in the near infrared spectrum and its low thermal conductivity, an inside source may overheat seriously the inner plane of plastic in an attempt to transmit sufficient heat to the outer glass.

Major disadvantages are the cumbrous installation demands, the difficulty of obtaining even heat distribution over the windshield, and the fire hazard inherent in operating the source at a suitably high temperature. The over-all energy efficiency is poor because of heat losses at the source by convection and conduction plus the loss in a filter should one be necessary. There are also practical limits to the amount of heat energy that can be developed by the source, and to the amount the windshield can absorb without undue temperature gradients within the glass and vinyl sections. The former condition is more of a limitation than the latter, and is related to the space and safety requirements and thermal efficiency. Either factor may make it impossible for the infrared radiation system to provide sufficient protection against the expected icing environment.

Transparent Electric Conductor

A transparent electrically conductive coating on glass, a coating of unique properties, recently has been developed and introduced by a major glass manufacturer.* The importance and application of such a coating for windshield deicing is at once obvious. A coating of this general description is not new; a film of high electrical resistance has been used in the past on glass surfaces for the prevention of electric charge collection, or electrostatic shielding. The new coating, however, exhibits the very important advantages of relatively low resistance and indestructibility. Instead of resistivities of the order of megohms, the new so-called *NESA* coating, can be produced with a resistivity as low as 100 to 120 ohms per square, this being the resistance measured between opposite sides of a square sheet of any linear dimension. Some idea of the thinness of the *NESA* coating is gained by considering that a film of copper having a resistivity of 100 ohms per square would be only seven billionths of an inch thick (assuming that the dimensional resistance properties are maintained for very thin sections, which may not be the case). This is about 0.03 of one per cent of the wave length of light.

The exact nature of the *NESA* film is not known to the author, but its physical properties and limitations can be described. The basic material is applied to a glass surface and processed at relatively high temperatures. It cannot be applied to such materials as Plexiglas (because of the high processing temperature, and possibly other factors). The film has excellent abrasive resistance properties, being of the nature of the glass itself. The coated glass may be partially tempered, but a high temper presents some difficulties. A laminated panel can be made with the coating next to the vinyl plastic if so desired. A *NESA* coating within a laminated panel will introduce a loss in light transmission of around four per cent largely by reflection loss caused by the difference in the index of refraction of the glass or vinyl and the *NESA*. A coating on the outer glass surface will double this loss and occasion more objectionable reflections. The index of refraction of the

* The Pittsburgh Plate Glass Company.

NESA is approximately two. When viewed by transmitted light, the panel imparts no noticeable reflections or color. By reflected light, the reflections from the *NESA* surface are sharp and possess a greenish or reddish caste. The coating appears mottled under close inspection and formed of small splotches reflecting red and green.

Electrical connection is established by means of a narrow opaque bus applied as a coating to the surface of the *NESA* film and usually running lengthwise along opposite edges of a panel. A copper strip may be soldered to the bus and brought out to serve as a terminal connection point.

The uniformity of the *NESA* coating on an aircraft windshield is important, since a nonuniform film will produce localized hot and cold spots. Several large laminated panels, with the coating either on the outer glass surface or next to the vinyl, have been laboratory tested for thermal variance. The results show a maximum deviation from the average of about plus or minus three degrees Fahrenheit for spot checks at points two inches apart over the entire windshield surface. These data were obtained with the horizontally mounted panel in still air with a steady state average surface temperature of approximately 100 degrees Fahrenheit.

A windshield has been designed for a pressurized Douglas airplane which is expected to provide freedom from icing under the most severe anticipated conditions at any operating speed or altitude of the plane. Further, impact resistance of significant excess over the minimum requirement may be incorporated at all times. The panel is approximately 13 inches wide, 28 inches long at the top and 31 inches long at the bottom. A maximum power of 3,100 Btu per hour per square foot is to be dissipated by the *NESA* film which has a resistivity of 120 ohms per square. The heat requirement was computed by methods previously described as that required to anti-ice for the severest expected atmospheric conditions at minus ten degrees Fahrenheit, sea level, and 270 miles per hour, and assuming that the outer surface of the windshield is maintained at 35 degrees Fahrenheit. The average vinyl temperature will be controlled at 110 degrees plus or minus ten degrees Fahrenheit for greatest impact strength, and will not exceed 125 degrees Fahrenheit under this maximum power demand condition.

First considerations in the design were the location of the *NESA* layer, and the glass and vinyl thicknesses. For the most

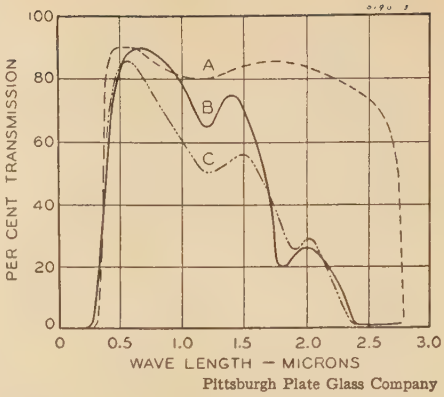

Figure 3. Transmission characteristics as a function of wave length

A—Polished plate glass, 6.17 millimeters
B—Vinyl plastic, 3.1 millimeters
C—Laminated panel, 0.120-inch vinyl plastic encased between two $^{7}/_{64}$-inch glass panes

rapid response and most effective deicing, the coating should be put on the windshield outer surface. This, however, introduced the problem of protecting the bus from abrasion, a safety hazard because of the exposed coating, and necessitated other means, such as another interior coating, for maintaining a warm vinyl and for defogging. The best compromise was a *NESA* coating on the inner surface of the outer pane. The power of 3,100 Btu per hour per square foot will be conducted through the outer pane at a negative temperature gradient of 465 degrees per inch, neglecting edge conditions. A glass panel 3/16 inch thick will transmit this thermal energy at a temperature difference of 87 degrees Fahrenheit, thus requiring 122 degrees Fahrenheit at the vinyl-glass interface, a figure which is approximately the upper limit for maximum impact strength. A thinner front pane would be satisfactory thermally and more desirable from the standpoint of rapid transient response, but strength and glass temper considerations lead to the selection of the greater thickness. The same thickness was adopted for the inner pane, and 1/8 to 3/16 inch adopted for the vinyl. The temperature difference across the vinyl under operating conditions will be only a few degrees.

The described windshield incorporates a 5/16-inch bus running horizontally at the top and bottom edges behind the mounting frame. The heated area is 2.65 square feet requiring 2.4 kw at 3,100 Btu per hour per square foot. This amount of power will be developed by 350 volts for a coating resistivity of 120 ohms per square.

Control may be effected by maintaining a vinyl temperature appropriate for high impact resistance. At 110 degrees Fahrenheit nearly all icing environment can be countered; for the most severe conditions the control setting can be increased to 120 or 125 degrees Fahrenheit. Only a minor sacrifice in impact strength will be introduced by maintaining the temperature in the upper range, and full anti-icing ability will be provided at all times. Or, if sufficient strength is developed at a lower temperature, say 70 degrees Fahrenheit, control could be maintained at this point with a corresponding improvement in pilot comfort in a warm cockpit. Several schemes for control have been advanced which will not be enumerated here. The design will depend largely upon the following three factors:

1. The source of electric power and type of generating equipment.
2. The type of temperature sensing element incorporated with the windshield.
3. The transient thermal response of the windshield and associated components.

At the maximum flying speed in cold clear air, sufficient power must be supplied to the windshield to maintain the optimum vinyl temperature. The previously quoted figure of 3,100 Btu per hour per square foot will suffice to maintain a vinyl temperature of 120 degrees Fahrenheit for an outside air temperature of minus 70 degrees Fahrenheit at 270 miles per hour.

Provision for stand-by in case of control or generating equipment failure may be obtained by using two control units and two alternators or inverters. Alternating current is the most logical type of power because of the high voltage requirement and absence of disturbing unidirectional fields. One generator may be of a capacity that is sufficient to do the whole job, with a second machine for stand-by; or two generators of half capacity may be used with a switching arrangement to allow application of power to the pilot's windshield system only, should his generator or control fail. Thus at least half of the pilot's enclosure could be kept ice-free in an emergency, and for light icing conditions the one generator could deice the entire windshield system.

The transparent electrically conducting coating of low resistance appears to be an ideal solution to the windshield icing and impact proofing problem. The maximum amount of heat required for the worst conditions may be supplied easily and used efficiently. The system lends itself readily to control both from anti-icing and impact resistance considerations. A *NESA* coated windshield possesses satisfactory optical characteristics at all times. It is relatively simple to manufacture, not subject to failure in operation, and alleged

Moisture Equilibrium Between Gas Space and Fibrous Materials in Enclosed Electric Equipment

JOHN D. PIPER
NONMEMBER AIEE

THE USE of an inert gas in enclosed electric equipment has increased considerably in recent years. In transformers an inert gas is used in the space provided above the transformer fluid to allow for its volumetric expansion with temperature rise. There the function of the gas is to provide an inert medium by which the pressure at the surface of the transformer fluid is kept slightly above atmospheric. Thus the fluid is not exposed to the moisture and oxygen of the air, as it is with the so-called "open-breather" or "oil-conservator" types unless the latter communicate with the outside atmosphere through chemical agents. In gas pressure cables, however, the inert gas is used at pressures up to approximately 15 atmospheres in order that the cables may operate successfully at electric stresses that are higher than otherwise would be possible.[1–3]

The purpose of this paper is to call attention to a phenomenon that occurs in enclosed electric equipment in which both an inert gas and fibrous material are present. The systems involved tend to establish an equilibrium between the moisture content of the fibrous materials and that in the gas space. Consideration, therefore, should be given to the moisture content of the fibrous materials present as well as that of the gas itself. A quantitative method is suggested for predetermining the equilibrium condition for both unimpregnated and impregnated fibers. It is believed that use of the method may assist in the solution of manufacturing and operating problems.

Paper 46-160, recommended by the AIEE committee on power transmission and distribution for presentation at the AIEE summer convention, Detroit, Mich., June 24–28, 1946. Manuscript submitted March 29, 1946; made available for printing May 28, 1946.

JOHN D. PIPER is in the research department of The Detroit Edison Company, Detroit, Mich.

Field Experience and Data

The increasing of the moisture content of dry nitrogen by the transfer of moisture from fibrous materials has been observed in The Detroit Edison Company in transformers and in the 120,000-volt gas-pressure cable.[1–3] This increasing of the moisture content of the gas can be of practical significance only if the dew point of the gas is reached at local cool spots over considerable periods of time, thus causing progressive transfer of moisture from the warmer fibrous materials, and if the resulting condensate drops upon a vulnerable part of the equipment. Any condensation that takes place as a result of an over-all cooling of the equipment or of a cool spot of short duration is of no significance because the water content of the gas is relatively low.

During severely cold weather, it is probable that some condensation occurs in all of the transformers that have been investigated. Moreover, it is probable that, in certain transformers, condensation occurs during the cool part of the day nearly every day of the year. Apparently the condensate usually drops in locations where it does no harm. Condensate has been found, however, on the terminal board inside transformers. Whether or not service failures actually have been caused by condensate on vulnerable parts is unknown, but there seems little question that such condensation constitutes a potential source of trouble.

In the case of the 120,000-volt gas-pressure cable, in which the paper-insulated unsheathed cables rest on the bottom of a steel containing-pipe, nearly all locations are vulnerable to attack by liquid water should condensation occur at local cool spots. Such cool spots might occur at a terminal, a length that crosses

---

to be free from deterioration caused by aging, sunlight, overheating, and abrasion. During operation the inner surface of the windshield is not excessively hot, which improves pilot comfort by minimizing the radiant heat. The installation should prove reliable and safe. Structurally, a clean design should result, the only complication being the means for attaching the power wires and control elements.

There are disadvantages to the scheme, however. Most important is the weight, which may be high because of the necessity for using high voltage alternating current delivered by inverters or engine driven alternators. The control system adds significant weight, although a unit to effect the same order of regulation in other ice prevention schemes would be of comparable weight. Inability to operate the *NESA* film directly from the ship's 28-volt power supply and provide the necessary power is a disadvantage. The requisite high voltage introduces a safety hazard, although placing the *NESA* coating next to the vinyl will tend to mitigate the danger. Windows or shields made of plastics such as Plexiglas cannot be deiced or defogged by this method since the *NESA* coating cannot be applied to their surface, at least not by present techniques.

Conclusions

1. Aside from anti-icing, an additional prime reason for heating aircraft windshields is evident. For a given weight and construction, vastly improved impact resistance can be obtained by using a laminated panel with the vinyl plastic maintained at about 110 degrees Fahrenheit.

2. The method of heating a windshield will depend greatly upon the structural configuration of the cockpit and of the windshield system. Availability of heated air and (or) electric power are equally important factors.

3. Use of the transparent electrically conductive coating on glass is the most desirable electrical method for providing heat at the windshield. Indeed, unless operating experience proves otherwise, this method appears to be suited ideally for the purpose of windshield anti-icing. For most airplanes, it ultimately should supplant other presently known systems.

References

1. AIRPLANE AIRWORTHINESS, TRANSPORT CATEGORIES. Manual 04, Civil Aeronautics Board, Washington, D. C. Section 04.38013.

2. IMPACT RESISTANT WINDSHIELD CONSTRUCTION, George L. Pigman. *Aeronautical Engineering Review*, volume 4, January 1945, pages 9–25.

3. AN AIRCRAFT DOUBLE WINDSHIELD—ITS DEVELOPMENT AND USE, R. L. McBrien. *Journal*, Society of Automotive Engineers, volume 51, October 1943, pages 350–5.

4. AN INVESTIGATION OF THE PREVENTION OF ICE ON THE AIRPLANE WINDSHIELD, L. A. Rodert. National Advisory Committee for Aeronautics, *Technical Notes*, number 754, March 1940.

5. INDUSTRIAL HEAT TRANSFER (book), A. Schack, H. Goldschmidt, E. P. Partridge. John Wiley and Sons, New York, N. Y., 1933, pages 173–207.

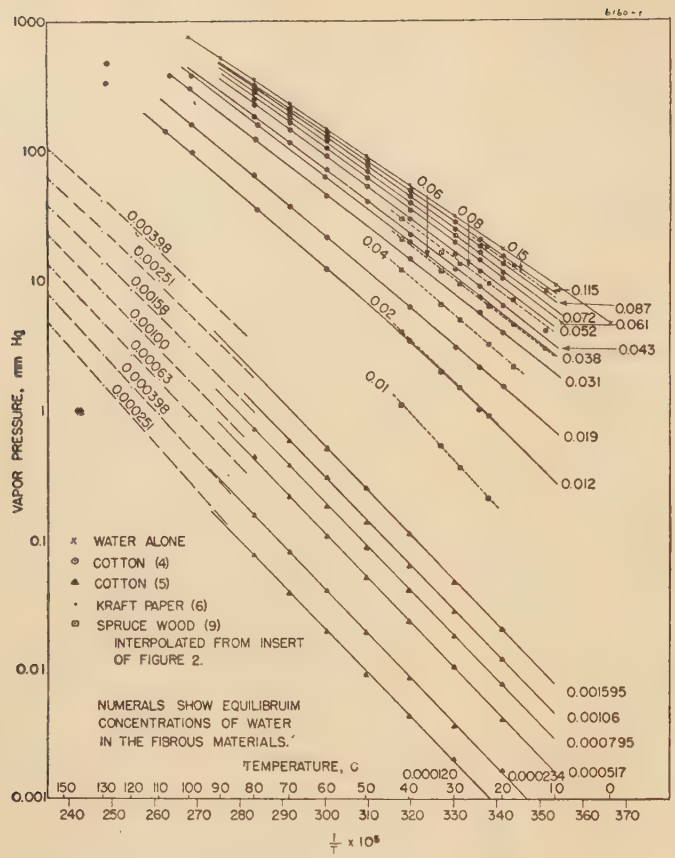

Figure 1. Vapor pressure of water alone and in fibrous materials; data from literature

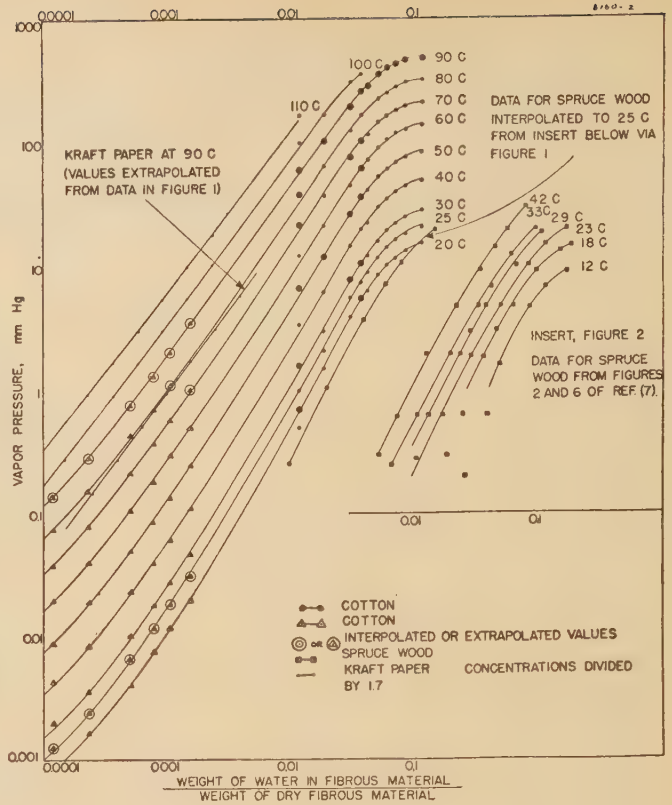

Figure 2. Equilibrium between water concentrations in fibrous materials and vapor pressure at selected temperatures

a canal, or a location in proximity to a water main. For this reason when it was found during the progress of the installation that the moisture content of the dry nitrogen gas, which was introduced immediately after the cable-pulling operation, was beginning to increase, steps were taken co-operatively by the manufacturer and user to determine the cause and corrective measures necessary. These efforts were completely successful as demonstrated both by the data herein contained and by the performance of this circuit since it was energized in December 1941. The data concerning this cable are presented in this paper only because they indicate that a predictable equilibrium exists between the moisture content of the fibrous material, even when impregnated, and that of the gas space.

As has been described elsewhere[1,2] the 120,000-volt gas-pressure cable is of preimpregnated-tape construction; that is, the cable was taped in an air-conditioned room with tapes that previously had been impregnated and from which the excess impregnant had been removed. Over the taped insulation two layers of metallized-paper shielding tapes were applied and over these a thin bronze tape intercalated with an impregnated muslin tape. This was followed by two layers of paraffin-impregnated canvas* to provide mechanical protection during installation. After a spiraled skid wire was wrapped over the canvas and the assembly coated with petrolatum for lubricant during installation, the cable was enclosed in a temporary lead sheath that was stripped within a few feet of the entrance tube to the pipe line as the cable was being installed.

When the dry nitrogen, which was introduced into the steel pipe line with the cable and held at slightly over atmospheric pressure by temporary plugs, began to show the presence of moisture, the source of the moisture was sought. The pipe was known to be dry. No water was found in the petrolatum grease but from 2.4 to 5.0 per cent of water** was found in the impregnated muslin and canvas tapes,* based upon the weight of dry fabric. The average for 14 samples was 3.3 per cent. Two steps were taken to minimize the moisture content of the muslin and canvas tapes.

1. The manufacturer modified his process in such a manner that the moisture content of the muslin and canvas tapes on further shipments of cable was reduced to an average of 1.67 per cent as judged by tests on six samples in which the content varied from 1.0 to 2.0 per cent.

2. Evacuation of the completed line, which is a normal procedure in the installation of this type of cable, was extended for eight days while the cable was heated by conductor heating to give a tape temperature of between 40 and 42 degrees centigrade.[3] The water removed was collected in a carbon-dioxide-alcohol trap and measured. From the average water concentrations and the weight of water removed, the average moisture content of the protective tapes as the line was placed in operation was calculated to be 1.73 per cent. Presumably, most of the water that was removed came from the wetter tapes.

In order to determine whether these efforts to prevent the possibility of condensation were successful, periodic determinations were made of the moisture concentrations† or the dew points of the gas space and of the temperature at various points along the line. During the first year of operation the dew points rose until late summer when at the more moist locations, which contained cable not given the special factory treatment, they were above the winter operating

* This type of construction no longer is used by the manufacturer and hence it does not follow that dew point problems are inherent in other gas-pressure-cable installations.

** As determined by Dean-Stark apparatus and boiling toluene.[4]

† Originally the moisture concentrations were determined gravimetrically at atmospheric pressure and the results calculated to line pressure. Later dew points were determined at line pressure using a dew-point apparatus.

temperature of the pipe line. In winter, however, the dew points fell to values safely below the winter operating temperature.

Inasmuch as the rise and fall, with temperature change, of the vapor pressures that corresponded to the several dew points or moisture concentrations followed the vapor pressure rule for liquids, within experimental error, it became evident that an equilibrium existed between the moisture content of the gas space and that of the tapes. This behavior, coupled with the change in dew points of transformers with temperature change, led to a search of the literature to determine whether quantitative data existed concerning this equilibrium for the fibrous materials generally used in the electrical industry. Literature on the subject revealed that although there are many articles describing the water concentrations of various fibrous materials under various relative humidities, only a few show the effect of temperature change. Fortunately two such sets of data were available for cotton and one each for kraft paper and spruce wood. From these data an equilibrium chart has been prepared that is useful for predicting and interpreting the behavior of the moisture within electric equipment containing fibrous materials and a gas space.

Preparation of the Equilibrium Chart

Figure 1 shows the data as obtained from the literature. In this figure the vapor pressures, on a logarithmic scale, are plotted against the reciprocals of the absolute temperatures on a linear scale. The top curve is for water alone. The long solid curves below the top curve represent the data of Urquhart and Williams[5] for cotton containing over one per cent of water. The data for each concentration are represented as a continuous curve instead of as the two intersecting straight lines used by the original authors. As thus represented, the curves for the higher concentrations are nearly parallel to, and have nearly the same curvature as, the curve for water. With diminishing concentration of water, the curves become more divergent and their slopes approach that of the curve for ice. This curve for ice is not shown in Figure 1. The solid curves at the lower right hand corner of the figure represent the data of Neale and Stringfellow[6] for cotton of low moisture content. These curves are straight, parallel lines having the slopes of the vapor pressure curve for ice. The curves that appear to extend as broken lines from the curves representing Neale and Stringfellow's data represent the data of Houtz and McLean[7] for kraft paper of low moisture content at elevated temperatures. The data for the samples having the higher moisture concentrations are best represented by curved lines whereas the data for the samples of lower concentrations fall along straight lines as shown. The latter are not parallel with each other. For the data of Urquhart and Williams, the slopes of the curves become steeper as the moisture concentrations of the samples represented diminish. The fourth set of data is that of Pidgeon and Maass[8] for spruce wood. These data appear in the same region as those of Urquhart and Williams. Because the temperature range for the investigation on spruce wood was narrow, it is not clear whether the data are best represented by straight or curved lines. The slopes of the lines are approximately the same, however, as those of the adjacent curves for cotton.

In using the four sets of data to prepare a general equilibrium chart, no effort was made to distinguish between absorption and desorption data. The difference, where shown by the original authors, is small as compared with the effect of temperature change, which is the primary concern of this paper, and probably is also small as compared with the effect of the previous history of the samples.[9]

The data for the equilibrium chart for cotton were obtained essentially by interpolation, for selected temperatures, of the vapor pressures that correspond to chosen concentrations of moisture. The principal object of the interpolation, of course, was to bridge the gap between the data of Urquhart and Williams and those of Neale and Stringfellow in the concentration range between 0.0016 and 0.012 gram of water per gram of dry cotton. Interpolation was carried out by means of Figure 2, where the vapor pressures and concentrations of water in cotton are both plotted on logarithmic scales for selected temperatures to give the long S-shaped curves that represent both the data of Urquhart and Williams and those of Neale and Stringfellow. In order to obtain the 90-degrees-centigrade curve of Figure 2, the data of Neale and Stringfellow were extrapolated from 80 to 90 degrees centigrade by extending the straight lines as shown in Figure 1.

Because only one set of data was available for kraft paper‡ and that at high temperatures only, interpolation similar to that described for cotton could not be carried out. Instead, the curves in Figure 1 for the data of Houtz and McLean were extrapolated downward from 100 to 90 degrees centigrade, and the resulting values of vapor pressure were plotted against their respective concentrations in Figure 2. The straight line that resulted when the extrapolated values for kraft paper at 90 degrees centigrade were plotted on the double-log scale of Figure 2 lies slightly below the curve for cotton at 80 degrees centigrade as shown. Next, it was reasoned that inasmuch as kraft paper often is made from spruce pulp, possibly the equilibrium in kraft paper and spruce pulp might be related. For this reason the data of Pidgeon and Maass,[8] shown in the insert of Figure 2, were in-

Figure 3. Comparison between the concentration of water in cotton and that in kraft paper or spruce wood required to give the same vapor pressure at the same temperature

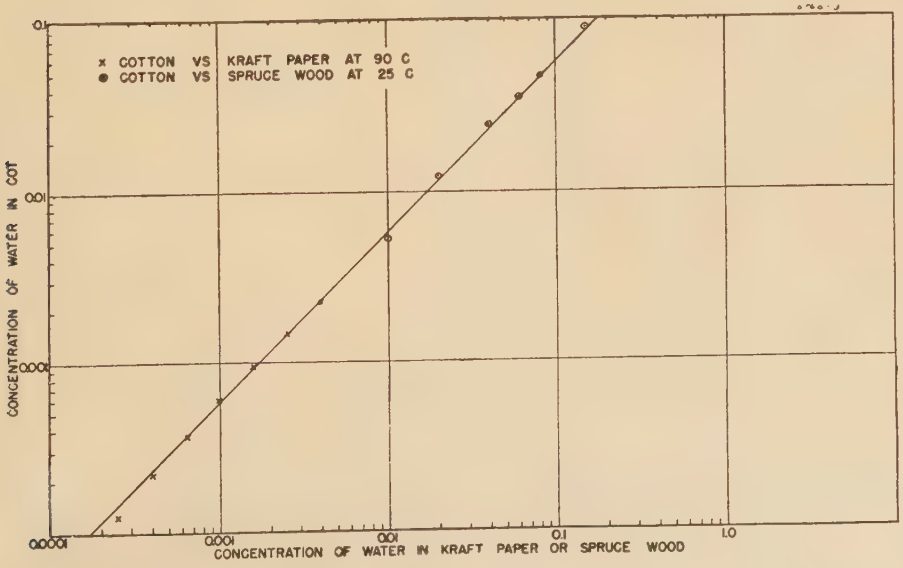

‡ Vincent and Simons[10] evidently investigated the field over a wide range of temperatures and moisture concentrations but unfortunately did not include in their publication data suitable for preparing an equilibrium chart.

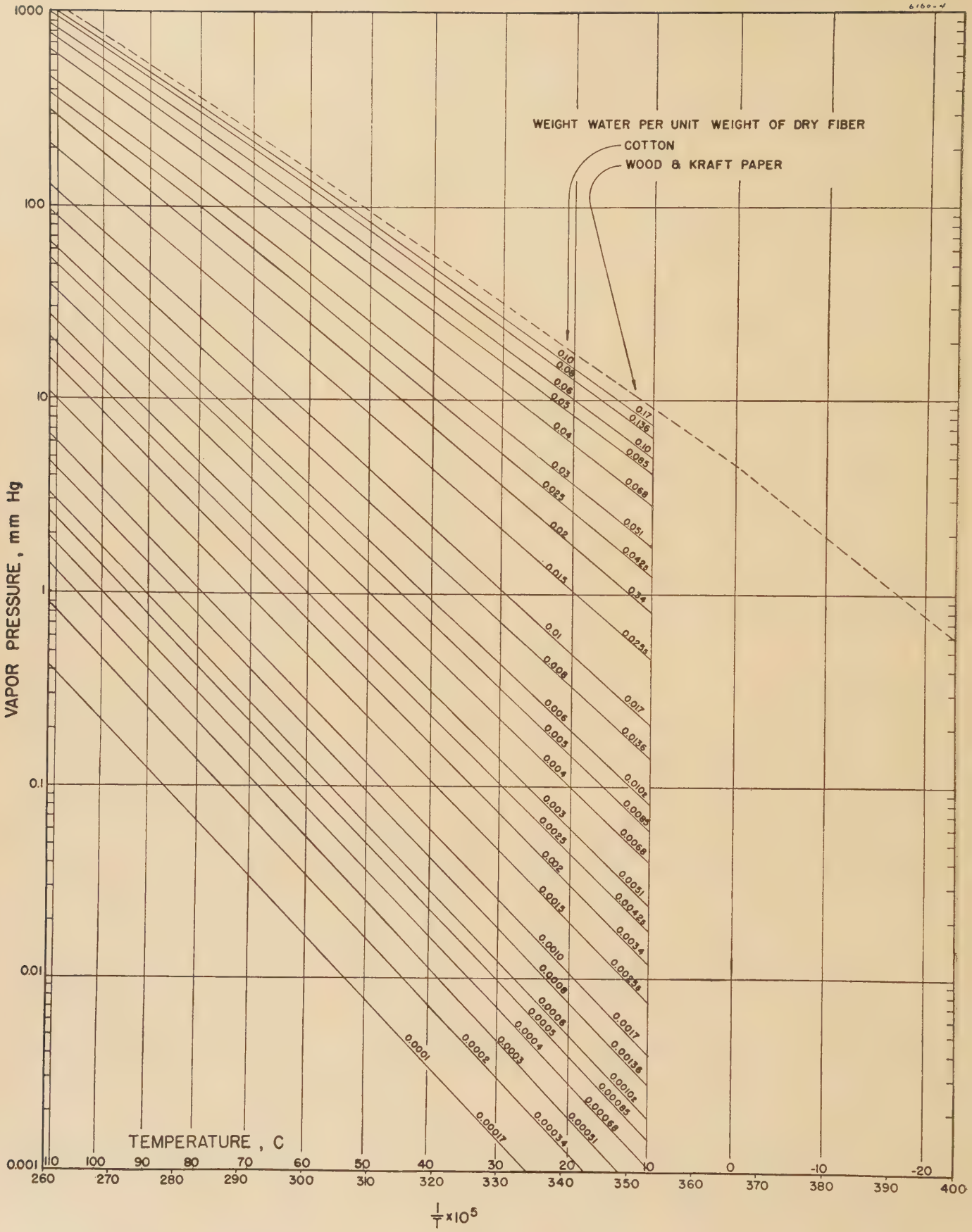

Figure 4. Equilibrium chart showing the relationship between the water concentration in fibrous materials and the vapor pressure of water in space at temperatures between 10 and 110 degrees centigrade

terpolated by the use of Figure 1 to 25 degrees centigrade. Finally, the concentrations of water in cotton required to give the same vapor pressure at 90 degrees centigrade as are given by selected concentrations of water in kraft paper and those concentrations required to give the same vapor pressure at 25 degrees centigrade as are given by selected concentrations of water in spruce wood were plotted on a double-log scale as shown in Figure 3. The straight line through these points indicates that the relationship between the water concentrations that are required to produce the same vapor pressures in cotton and in either kraft paper or spruce wood is simply the ratio 1 to 1.7.

By dividing the concentrations of water in kraft paper, as given in Houtz and McLean's data, by 1.7, an estimate was made of the vapor pressures that would result from low concentrations of water in cotton at 100 and 110 degrees centigrade. These data were combined with the experimental data of Urquhart and Williams in that temperature range to produce the top two curves of Figure 2.

The equilibrium chart was prepared by plotting the vapor pressures for cotton, as given from the curves of Figure 2 for selected concentrations, on a logarithmic scale against the reciprocals of the absolute temperatures, similarly to Figure 1. This chart is shown in Figure 4. All of the curves are extrapolated from 20 to 10 degrees centigrade. Those for concentrations above 0.03 gram of water per gram of dry cotton also are extrapolated for temperatures above 80 degrees centigrade. For this extrapolation, the gentle curvature of the vapor pressure curve for water, shown as the broken line constituting the top curve, was followed.

The equilibrium concentrations of water in cotton that were selected for the preparation of the equilibrium chart are shown by the numerals of each curve in the left-hand column. The numerals in the right-hand column represent the equilibrium concentrations of water in kraft paper or spruce wood, as obtained by multiplying the respective values for cotton by 1.7.

Effect of an Impregnant

Although the practical value of an equilibrium relationship, such as that described in this paper, has been recognized previously for unimpregnated fibrous materials,[10] there seems to be no record of its application to impregnated fibers. Indeed, to many who have tried to dry impregnated fibers that have absorbed moisture, it might appear that impregnated fibers behave entirely differently from unimpregnated ones. The data for the paraffin-impregnated cotton protective tapes of the 120,000-volt cable previously described provide a comparison between the behavior of commercially made American impregnated-cotton tapes and that of the two sets of laboratory-prepared unimpregnated-cotton fibers made in England.

The comparison between the impregnated and the unimpregnated cotton samples is given in Figure 5. The solid lines in this figure, and the numerals arranged in a column upon them, are reproduced for cotton from Figure 4. The crosses represent the average conditions at three locations at which the higher moisture concentrations were found in the gas space as the average temperature of the pipe line rose and fell with seasonal and load change. The low-temperature point was determined while the line was not in operation. The circles represent the average conditions at two locations at which the lower moisture concentrations were found. It is evident that, regardless of whether the fibers are impregnated or not, the change of the vapor pressure of water in the gas space is essentially the same function of temperature change. It is also evident that although equilibrium had not been reached when some of the data on the cable line were obtained, especially those taken in September 1942, the moisture concentrations in the cotton, as indicated by the chart for different dates and temperatures, are nearly the same. Even including the September 1942 data, the indicated concentrations ranged only between 2.2 and 2.6 per cent for the tapes in the more moist regions and between 1.2 and 1.5 per cent for those in the drier locations. Data taken during the initial operation of the cable in the winter of 1942, however, fall far below the equilibrium values shown.

It does not necessarily follow, that because the vapor pressure changes in the same manner with the temperature change regardless of whether the cotton is impregnated or unimpregnated, that the equilibrium concentration of water in the cotton is the same in impregnated cotton as in unimpregnated. Naturally it was impractical to obtain samples of the tapes in the completed 120,000-volt cable line after the evacuation treatment in order to determine whether the impregnant alters the equilibrium. Nevertheless, a means for obtaining a qualitative answer exists. As previously stated, the average concentration of water in the impregnated cotton tapes of the completed line, as calculated from the analytical results and from the quantity of water removed, was 1.73 per cent. The points indicated by dots in Figure 5 show the concentrations of water in cotton at each of the 30 joints at which the samples were taken. These were determined with the equilibrium chart from the average temperature of the line and the vapor pressures that correspond to the dew points that were determined in September 1944. The values, which because they were determined by the chart are for unimpregnated cotton, ranged between 0.9 and 2.65 per cent and averaged 1.68 per cent. The agreement between 1.73 and 1.68 per cent is much closer than the analytical methods warrant. The agreement indicates that it is safe to use the equilibrium chart for impregnated cotton at least in the solution of practical problems in which an error of perhaps plus or minus two in the second significant figure can be tolerated.

No data are available to show whether impregnation with insulating oil changes the equilibrium temperature for kraft paper. The data for the paraffin-impregnated cotton support the belief that although the impregnant greatly slows down the diffusion process by which equilibrium is attained, the equilibrium concentration of water in a fibrous material is not affected greatly by an organic impregnant. It seems probable that the equilibrium conditions shown for unimpregnated kraft paper in Figure 4 will apply approximately for oil-impregnated kraft paper as well.

Use of the Equilibrium Chart

The following examples are intended to illustrate a few of the uses that may be made of the equilibrium chart in the electrical industry. The first three of these examples concern cable of the type discussed.

Example 1

Did the precautionary treatments of protective tapes (previously described) effect any substantial reduction in the dew point of the gas?

This question is answered by the information in Figure 6, which also shows the method of using the equilibrium chart. As previously stated, before the drying treatments the maximum moisture concentration was 5.0 per cent, and the average 3.3 per cent. After the factory treatment on the part of the cables and evacuation of the entire line, the maximum concentration as determined from the dew points was 2.65 per cent and the average concentration from both the dew point measurements and the calculated residual water concentration was

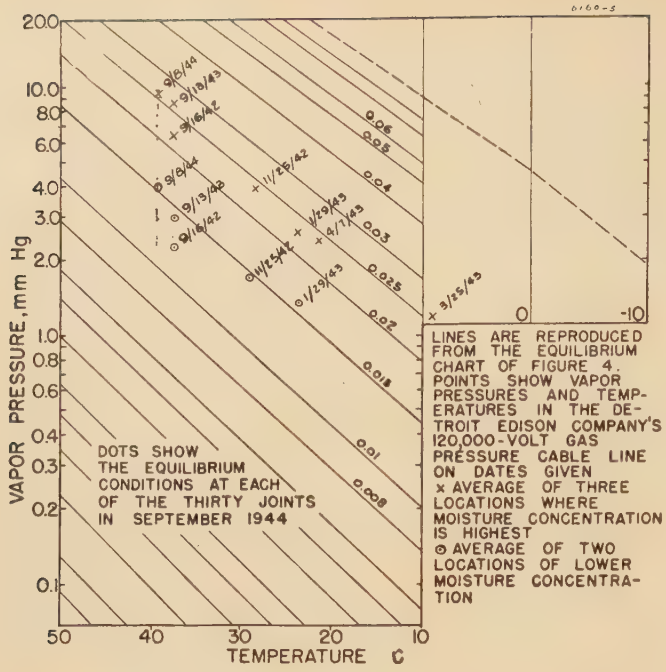

Figure 5. Similarity in equilibrium behavior between impregnated and unimpregnated cotton

1.7 per cent. The dew point of the gas space corresponding to a point that represents a given moisture concentration and selected temperature of the fibrous material is obtained by drawing a horizontal line from that point to the curve for water as shown by the arrows in Figure 6, and obtaining the dew point temperature as given by the point of intersection. Thus the chart shows that the dew point in the vicinity of tapes having the maximum moisture content of 5.0 per cent would be 26 degrees centigrade when the summer temperature of the cable line averages 38 degrees centigrade, and nine degrees centigrade when the winter temperature of the line averages 20 degrees centigrade. Thus it is shown that the drying treatments reduced both the maximum and the average dew points by approximately 15 degrees centigrade over the entire operating temperature range of the line, as shown.

EXAMPLE 2

What concentration of water would a cotton protective tape acquire if the cable on which the tape is wrapped stands, until equilibrium takes place, in a room air conditioned to a relative humidity of 20 per cent at 30 degrees centigrade, and the cable thereafter is sheathed?

A 20-per-cent relative humidity at 30 degrees centigrade is equivalent to a moisture content of 6.0 grams per cubic meter which corresponds to a vapor pressure of 5.7* millimeters of mercury. A point representing 5.7 millimeters and 30 degrees centigrade on the chart indicates a moisture content of 2.6 per cent based upon the weight of dry unimpregnated cotton.

* Because the concentration of water in grams per cubic meter and the vapor pressure are nearly the same numerically up to 50 degrees centigrade, only a small error is introduced by multiplying the vapor pressure shown on the chart by the relative humidities to obtain the equilibrium vapor pressures. In this case, instead of 5.7 millimeters, a value of 20 per cent of 32 or 6.4 millimeters would be obtained.

EXAMPLE 3

What concentration of water would preimpregnated kraft paper tapes acquire if they were exposed in the air-conditioned room described in example 2 long enough for equilibrium to be reached?

The point representing 507 millimeters of mercury and 30 degrees centigrade on the chart indicates a moisture concentration of 4.4 per cent in kraft paper.

The foregoing example does not imply that the moisture content of a preimpregnated paper insulation is high just because the equilibrium moisture content is high for the humidities that feasibly may be maintained in the taping room. Under conditions of normal operation the time of exposure is too short to allow significant absorption. For example, the average moisture content of the insulation of the cable previously mentioned was not 4.4 per cent but only 0.055 per cent, which is essentially the same as that for other well-made cables impregnated in a conventional manner. An equilibrium value that low would require, according to the chart, the relative humidity at 30 degrees centigrade to be of the order of 0.017 per cent. Obviously, the low rate of moisture absorption is of much more importance to the manufacturer of this type of cable than is the equilibrium concentration.

The two examples that follow illustrate the use of the equilibrium chart for problems involving condensation in transformers. For given equilibrium moisture content in the fibrous material, most of which is of wood origin, the probability of condensation is greater than for gas-pressure cable. The reason is that the top of the transformer casing may be only a few degrees above outdoor temperature while the fibrous material is at the oil temperature, which may reach a daily maximum of 50 to 60 degrees centigrade. The equilibrium for transformers is more complicated than for the paraffin-impregnated tapes because the amount of water in the large mass of oil is not negligible as compared with that in the much smaller mass of fibrous materials. It is probable that a definite relationship also can be established for the equilibrium between the moisture content of oil and that of the gas space. Until such information is available, however, it is not possible to estimate the water content of the oil from dew point data. In the following the oil is considered only as a barrier that markedly reduces the rate at which equilibrium becomes established between the moisture contents of the gas and fiber.

EXAMPLE 4

The gas in a new transformer had a dew point of ten degrees centigrade when operating at an oil temperature of 50 degrees centigrade while the outdoor temperature was well above the dew point of the gas. What was the probable moisture content of the kraft paper insulation within it?

A dew point of ten degrees centigrade corresponds to a vapor pressure of 9.2 millimeters of mercury, which at 50 degrees centigrade is shown by the chart to be in equilibrium with a moisture content of approximately 2.7 per cent in the insulation.

EXAMPLE 5

The gas in a reconverted oil-conservator type of transformer had a dew point of 20 degrees centigrade when operating at an oil temperature of 42 degrees centigrade while the outdoor temperature was well above the dew point of the gas. How much water would have to be removed from the fibrous insulation of the transformer in order for the gas to have a dew point of minus ten degrees centigrade while the oil temperature was 50 degrees centigrade?

A dew point of 20 degrees centigrade, or a vapor pressure of 17.5 millimeters of mercury, indicates an equilibrium moisture concentration of 5.4 per cent at 42 degrees centigrade, according to the chart. A dew point of minus ten degrees centigrade or 1.95 millimeters of mercury indicates a concentration of 1.05 at 50 degrees centigrade. Thus it would be necessary to reduce the water content by approximately 4.35 per cent based upon the weight of the paper fibers. For a transformer containing 3,000 pounds of such insulation, it therefore

would be necessary to remove approximately 130 pounds or 15.6 gallons of water which does not include the amount that would have to be removed from the oil to reach the same equilibrium conditions.

Vapor Barriers

Consideration of the information given by the equilibrium chart leads to the conclusion that, if no vapor barrier existed between the cotton and the kraft paper tapes of the cable previously mentioned, equilibrium ultimately should become established between the moisture content of the cotton and kraft tapes with resultant reduction in the dew point of the gas space. The two kinds of tapes are present in the fiber-weight ratios of 22 to 485. Considering the region in which the final concentration of moisture in the cotton tapes was highest (2.65 per cent), if equilibrium were established with the kraft types, which had an average concentration of 0.055 per cent, the final moisture concentration of the cotton tapes would be 0.1 per cent and of the kraft tapes 0.17 per cent. The equilibrium vapor pressure at a temperature of 38 degrees centigrade then would be, according to the chart, approximately 0.05 millimeter of mercury, and the corresponding dew point approximately minus 45 degrees centigrade. Although establishment of the equilibrium between the moisture contents of the cotton and kraft tapes would be expected to be slow, there was no evidence that any exchange had taken place in over $2^1/_2$ years of operation. This is remarkable when it is realized that the conditions are the same as though the cable had been exposed continuously for over two years to a relative humidity of approximately 30 per cent. Furthermore, exposure for several months of unsheathed samples of the cable to Detroit's humid summer atmosphere out of direct contact with rain resulted in no apparent increase in moisture content of the kraft insulation. Of three samples of cable so exposed before the line was completed, the moisture concentrations were 0.01, 0.01, and 0.05 per cent, respectively, all of which values happened to be less than the average for unexposed samples. The author's interpretation of the reason the insulation does not become moist is that the metallized-paper shielding tapes bar the diffusion of water vapor into the insulation. This fact is believed to be of further practical significance, for no longer can it be said that plastic cable sheaths cannot be used for oil-impregnated cables on the basis that all such sheaths, although they provide a barrier for liquid water, are too permeable to water vapor. It seems entirely possible that if an elastomer can be developed to have suitable life in contact with oil on one side and ground water and air on the other, it should be a suitable sheathing for cables provided the outside of the insulation of each conductor is shielded by metallized paper or thin metal tapes. The latter without some sort of sheath are not adequate because they will not keep out liquid water nor provide mechanical protection. Use of a corrosion and abrasion-resistant elastic material that can be applied competitively with lead seems worthy of investigation, particularly for solid type cables. The elaborate "sandwich" scheme of Rihl and Heering[11] to use a plastic sheath seems unnecessary.

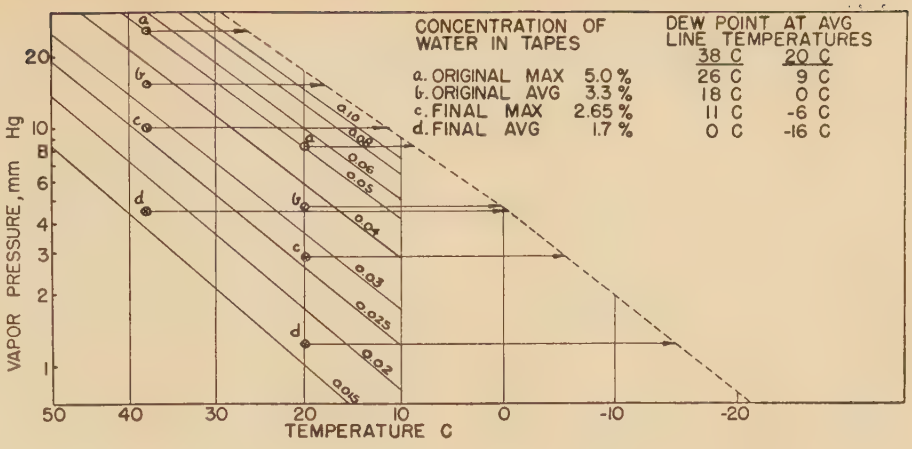

Figure 6. Use of the equilibrium chart in estimating the reduction in dew point that was effected by reducing the water concentration in impregnated cotton tapes

Conclusions

An equilibrium chart has been prepared from data from the literature to relate the equilibrium concentration of water in cotton or kraft paper with the vapor pressure of water, over a temperature range of 10 to 110 degrees centigrade. The concentrations of moisture covered by the chart range from 0.01 to 10 per cent for cotton and 1.7 times those values for kraft paper.

Although the equilibrium chart was prepared from data for unimpregnated fibers, data taken on The Detroit Edison Company's 120,000-volt gas-pressure cable line show that the chart is also valid for impregnated materials, at least for cotton impregnated with paraffin.

Examples are given of the use of the chart in predicting the equilibrium moisture content that fibrous materials will acquire when exposed to atmospheres of various relative humidities and temperatures, in predicting the dew points of the gas in enclosed electric apparatus, and in employing dew point measurements as a nondestructive analytical tool for determining the moisture content of fibrous materials in electric equipment.

Metallized-paper electrical shielding tapes placed over fibrous materials are shown to be remarkably effective in preventing diffusion of water into these materials. The significance of this phenomenon in connection with the use of an elastomer as a sheathing material, particularly for solid-type cables, is pointed out.

References

1. 120-Kv High-Pressure Gas-Filled Cable, **I. T. Faucett, L. I. Komives, H. W. Collins, R. W. Atkinson.** AIEE Transactions, volume 61, 1942, pages 658–65.

2. Detroit Pioneers With 120-Kv Pipe-Type Gas-Filled Cable—I, **G. B. McCabe, F. M. Hull.** *Electrical World*, volume 117, 1942, page 2214.

3. Detroit Pioneers With 120-Kv Pipe-Type Gas-Filled Cable—II, **G. B. McCabe, F. M. Hull.** *Electrical World*, volume 118, 1942, page 278.

4. Scott's Standard Methods of Chemical Analysis, **N. H. Furman, editor.** Fifth edition, volume 2, D. Van Nostrand Company, Inc., New York, N. Y., 1939, page 1342.

5. The Moisture Relations of Cotton, the Effect of Temperature on the Absorption of Water by Soda-Boiled Cotton, **A. R. Urquhart, A. M. Williams.** *Journal*, Textile Institute (Manchester, England), volume 15, 1924, page T559.

6. The Primary Sorption of Water by Cotton, **S. M. Neale, W. A. Stringfellow.** *Transactions*, Faraday Society (London, England), volume 37 1941, page 525.

7. Adsorption of Water by Papers at Elevated Temperatures, **C. C. Houtz, D. A. McLean.** *Journal of Physical Chemistry*, Baltimore, Md., volume 43, 1939, pages 309–21.

8. The Adsorption of Water by Wood, **L. M. Pidgeon, O. Maass.** *Journal*, American Chemical Society, Washington, D. C., volume 52, 1930, page 1053.

9. Heat of Adsorption of Water by Papers, **C. C. Houtz, D. A. McLean.** *Journal of Physical Chemistry*, Baltimore, Md., volume 45, 1941, pages 111–27.

10. A Sensitive Method for the Determination of Moisture, Applied to Electrical Insulating Materials, **R. S. Vincent, A. Simons.** *Proceedings*, Physical Society (London, England), volume 52, 1940, pages 489–500.

11. Cable Sheath, **W. Rihl, H. Heering.** *Elektrotechnische Zeitschrift* (Berlin, Germany), volume 62, 1941, page 1917.

A Multichannel Microwave Radio Relay System

H. S. BLACK
FELLOW AIEE

J. W. BEYER
MEMBER AIEE

T. J. GRIESER
NONMEMBER AIEE

F. A. POLKINGHORN
MEMBER AIEE

Synopsis: An 8-channel microwave relay system is described. Known to the Army and Navy as *AN/TRC*-6, the system uses radio frequencies approaching 5,000 megacycles. At these frequencies, there is a complete absence of static and most man-made interference. The waves are concentrated into a sharp beam and do not travel along the earth much beyond seeing distances. Other systems using the same frequencies can be operated in the near vicinity. The transmitter power is only one four-millionth as great as would be required with nondirectional antennas. The distance between sets is limited but by using intermediate repeaters communications are extended readily to longer distances. Short pulses of microwave power carry the intelligence of the eight messages utilizing *pulse position modulation* to modulate the pulses and *time division* to multiplex the channels. The eight message circuits which each *AN/TRC*-6 system provides are high-grade telephone circuits and can be used for signaling, dialing, facsimile, picture transmission, or multichannel voice frequency telegraph. Two-way voice transmission over radio links totaling 1,600 miles, and one-way over 3,200 miles have been accomplished successfully in demonstrations.

THE *AN/TRC*-6 is a combined transmitter and receiver designed specifically for radio relay purposes and includes multiplex facilities for providing eight two-way high-grade message circuits between points separated by an unobstructed optical path. Acknowledgment is made of the impetus and assistance given in this development by those concerned in a somewhat similar British development (British Wireless Set Numbet 10) conducted by the Ministry of Supply on behalf of the British Army.

In military use, one *AN/TRC*-6 set usually is transported by truck, and can be set up and placed in operation on a favorable site in a few hours. Figure 1 depicts an arrangement used by the Army in tactical movements, with the operational units housed in a truck. All of the microwave equipment is atop the 50-foot tower. Simultaneous two-way communication is obtained by the use of different radio frequencies for the two directions of transmission. Using separate antenna systems, the microwave transmitter and receiver-converter are mounted directly behind their respective 5-foot parabolic reflectors.

A sharply focused and highly directive microwave beam whose frequency is nearly 5,000 megacycles is used to carry the intelligence of the eight messages. This extremely high frequency affords communication channels free from static and most man-made interference. By the use of beamed radiation and reception, the transmitter power is only one four-millionth as great as would be required with nondirective antennas. Sharply beamed transmission combined with the absence of external noise means a small amount of transmitter power is adequate for communication over optical paths of considerable length. A peak power of a few watts serves for jumps as great as 100 miles. This power is obtained from a small tube no larger than an ordinary radio receiving tube, operating as a reflex velocity modulated oscillator ("reflex klystron").

Because of the sharp beam, because of the type of modulation used, and because transmission must be over an unobstructed optical path other sets using the same frequency can be operated in the near vicinity.

The sets were designed to be used in pairs to form a radio repeater, and it is practical to operate a considerable number of radio links in tandem. Because of the line-of-sight over which the system operates, the distance between sets is limited by the curvature of the earth, but by using intermediate sets as repeaters, communications are extended readily to hundreds and even thousands of miles.

When the set is used for military purposes, essential units are supplied in duplicate, as indicated by Figure 2 which is a close-up of the operational units. The portable test oscilloscope is for conveni-

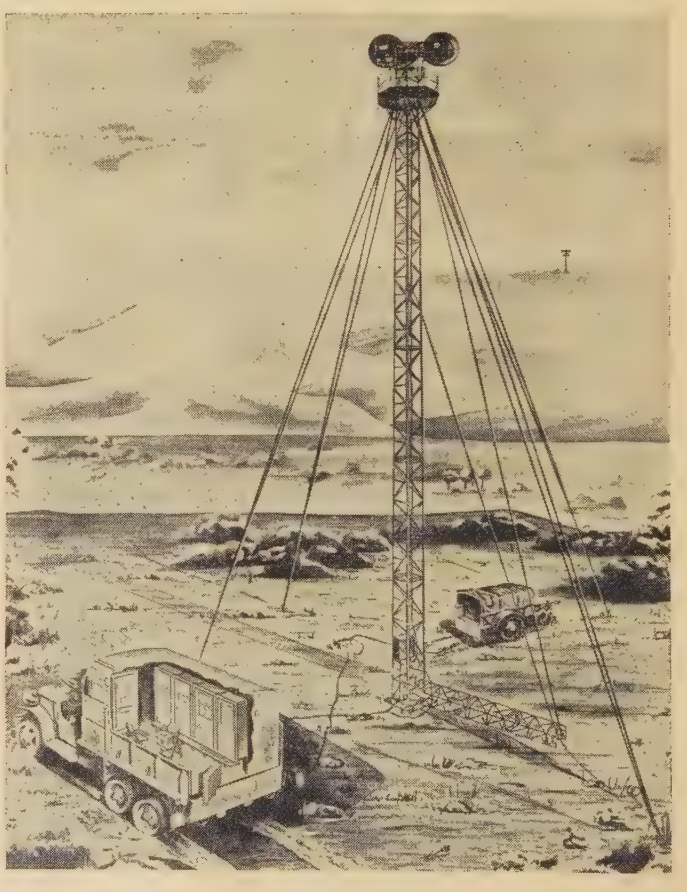

Figure 1. *AN/TRC*-6 with operational units in a truck

Paper 46-205, recommended by the AIEE committee on communication for presentation at the AIEE Great Lakes District meeting, Indianapolis, Ind., October 9–11, 1946. Manuscript submitted August 26, 1946; made available for printing September 17, 1946.

H. S. BLACK is high frequency transmission engineer, transmission development department, J. W. BEYER, T. J. GRIESER, and F. A. POLKINGHORN, are members of the technical staff, Bell Telephone Laboratories, Inc., New York, N. Y.

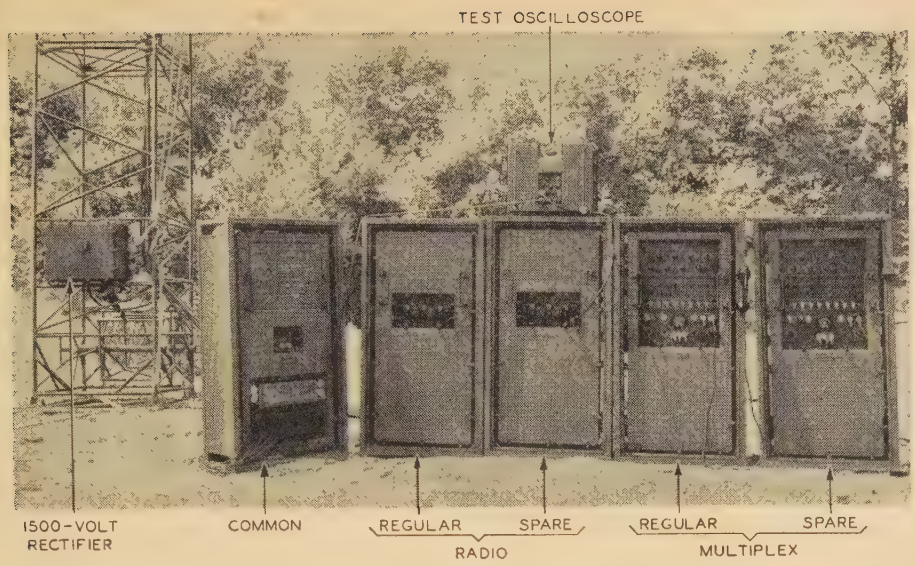

Figure 2. *AN/TRC*-6 set up as a field terminal

ence in monitoring. A high voltage rectifier for the transmitter is located at the bottom of the tower.

An optional and improved arrangement representing a recent development and known as *AN/TRC*-6 (*XC*-4) is now available. This improved equipment features one antenna instead of two, a lighter weight tower presenting a less conspicuous target, and the location of the microwave transmitter and receiver-converter on the ground instead of atop the tower. The radio transmitter and receiver-converter connect through wave guide filters to a single antenna system also located on the ground. The parabolic ground reflector (Figure 3) is beamed on a wire mesh 48-degree plane reflector atop the lightweight 50-foot mast. The extra loss introduced by the single antenna system is about three decibels.

Unlike conventional communication equipment which transmits a continuously modulated wave, *AN/TRC*-6 makes use of pulse modulation. In such a system, the transmitter is caused to emit short pulses of microwave power. These microwave pulses are substantially constant in amplitude and frequency. Eight 1-microsecond pulses (Figure 4), one for each channel, are transmitted in sequence and are preceded by a 4-microsecond synchronizing pulse called a marker. This sequence of marker plus eight channel pulses repeats itself 8,000 times a second and is called a frame.

The intelligence of each channel is conveyed by varying the exact position in time of the channel pulses. The phrase pulse position modulation has been applied to this method. The eight channels share the operating time of the transmitter, each using the radio path in turn. Such a sharing process utilizes a multiplexing principle that for many years has been known as time division. Pulse modulation, therefore, not only provides for position modulating the pulses but also permits multiplexing the channels by time division. No detectable distortion of the recreated message in the final receiver need be inherent in this method of transmission, nor is the scheme limited to eight channels. Systems using these same principles could be designed readily for many more channels.

In carrying out the pulse modulation method, the voice wave of each incoming message is sampled 8,000 times a second. Each sampling subsequently results in a pulse of microwave power leaving the transmitting antenna. With no voice input, the pulse associated with a particular channel recurs 8,000 times a second or every 125 microseconds. When the channel is busy, the pulse occurs earlier or later, depending on whether the voice wave is positive or negative. The exact displacement of a pulse from its unmodulated position is linearly proportional to the magnitude of the voice wave at the time of sampling.

The modulation of channel 2 in this manner is illustrated in Figure 5 for the case of a particular sinusoidal input of 1,000 cycles. When the input signal is zero, namely, at points *A*, *E*, and *I* in the figure, the channel pulse will occur at the middle of the position allocated to the channel. Successive diagrams depict the change in the relative position in time of the channel-2 pulses from frame to frame for nine successive frames.

The eight voice circuits connect to the common unit (Figure 6) and go to the transmitting portion of the multiplex which generates marker and channel pulses. These pulses are cabled to the transmitter and are used to turn the transmitter (transmitter-oscillator) on or off for intervals of time corresponding to the length of each pulse. Thus, d-c or video pulses from the transmitting multiplex are translated into pulses of microwave power. These microwave pulses are conducted to the focal point of the transmitting paraboloid where they radiate to illuminate the reflector, the pattern of the reflected radiation being sharply beamed.

Attenuated microwave pulses from the distant transmitter are picked up by the receiving parabolic reflector (Figure 6) and go to the receiver (receiver-converter). The converter changes the microwave pulses to *IF* (intermediate frequency) pulses centered about 58.5 megacycles. After amplification, the *IF* pulses go to the remainder of the radio receiver located on the ground.

Here the *IF* pulses are amplified further, detected; and the resulting video pulses fed to an amplifier. The receiver has automatic tuning so that it is at all

Figure 3. *AN/TRC*-6 featuring two-way transmission with a single antenna

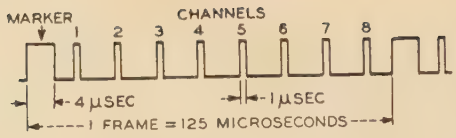

Figure 4. Pulse array at output of transmitting multiplex or input to receiving multiplex

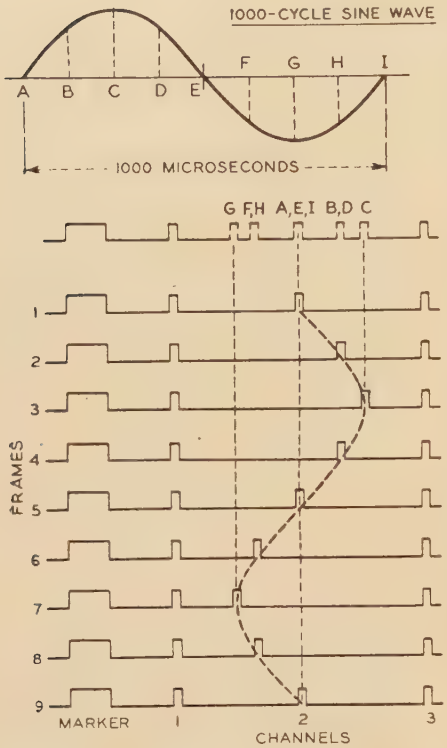

Figure 5. Modulation of channel-2 pulses

times correctly tuned to the distant transmitter. The receiver also has automatic volume control so that the output pulses are substantially constant despite fading.

The receiver has a special feature termed a slicer or double clipper whose function is to carve out a narrow slice (about 5 per cent) from each received pulse. The slicer (Figure 7) substantially frees the pulses of noise.

The output of the slicer goes to the receiving multiplex. Here the marker pulse is identified because of its greater length and causes the receiving multiplex to operate "start–stop."

The sequence of events triggered off by recognition of the marker opens, successively, electronic "gates" to each of the eight channels in turn. After a particular channel gate is opened, the next pulse passes through and is caused to trigger another circuit which starts a direct current flowing. This flow of direct current continues until stopped by the closing of the gate. The starting and stopping of a direct current in this manner generates a length modulated pulse

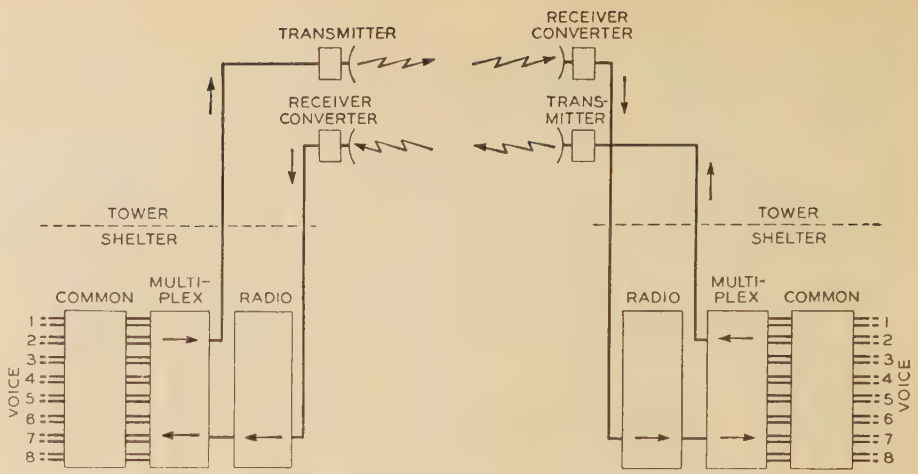

Figure 6. Block diagram of single link system

whose trailing edge is fixed but whose leading edge depends upon the exact timing of the received channel pulse. This represents the conversion of pulse position modulation to pulse length modulation. The voice signal is derived by passing the length modulated pulses through a low-pass filter.

Specific Embodiment

Method of Operation of the Multiplex

Figure 8 is a block diagram of the transmitting section of the multiplex. An 8,000-cycle oscillator fixes the frame frequency and produces a rectangular wave for starting the marker pulse generator and eight pulse position modulators.

The marker pulses are generated by differentiating the oscillator output and applying the resulting pulses to a tube so operated as to be insensitive to positive pulses. Each negative pulse produces an output pulse which, when limited or clipped, results in a nearly rectangular 4-microsecond pulse at the start of each frame.

Except for channel 1, which will be described separately, short positive pulses are required for starting the pulse position modulators. For channels 7 and 8 it is possible to derive these directly from the oscillator by a differentiating circuit. Exciter circuits, similar in design to the marker generator, start channels 2 to 6. Use of separate exciters for odd and even numbered channels reduces interchannel crossstalk.

Except for channel 1, each position modulator is a multivibrator. This multivibrator is a 2-stage resistance-capacitance coupled amplifier with its output fed back to the input. The circuit is so operated that the first stage normally is cut off and the second conducts. Application of a positive trigger pulse to the grid of the first stage causes it to conduct and cut off the second stage. After an interval of time, depending mainly upon the time constant of the *R-C* circuit which connects the two stages, the multivibrator relaxes, that is, returns to its original condition with the first stage cut off and the second conducting. Each trigger pulse results in an output pulse, the duration of which is determined primarily by the time constant. The time constants are adjusted so that each multivibrator relaxes at the time assigned to that particular unmodulated channel pulse.

Although the time of relaxation of the multivibrator is controlled primarily by its time constant, this time also can be altered by superposing a varying voltage on the grid of the second stage. This grid is the point at which voice frequency voltage is applied from the voice amplifier of that particular channel. Consequently, the trailing edges of the pulses developed by the multivibrator are position modulated by the voice input. A 1-microsecond pulse, produced in a generator common to four channels,

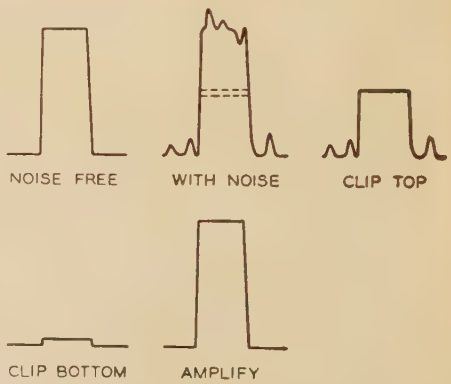

Figure 7. Reduction of noise by slicer or double clipper

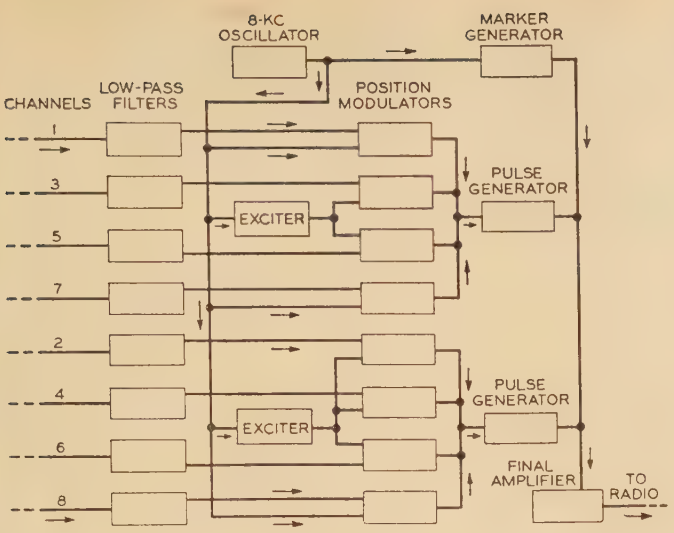

Figure 8. Block diagram of transmitting multiplex

is derived from this trailing edge. The two groups of channel pulses and the marker are combined and go to the radio transmitter.

Because little time exists between the marker and the first channel pulse, channel 1 differs from the other channels in that it does not require a multivibrator to delay the channel pulses. For this channel, therefore, a simpler circuit is possible. This circuit produces a length modulated pulse by clipping a saw-tooth shaped pulse at a voltage determined by the voice sample. The desired channel-1 pulses are derived from the leading edges of these length modulated pulses.

In the receiving section of the multiplex (Figure 9), video pulses from the radio are amplified and the circuit branches into two paths, one of which serves to select the marker pulse. The marker selector is so arranged that its output voltage is proportional to the duration of an input pulse. Marker pulses produce voltage peaks about four times those resulting from channel pulses. The marker amplifier is negatively biased so that the channel pulses do not cause plate current to flow. Therefore only the marker is passed. A new pulse derived from the trailing edge of the selected marker is fed to a multivibrator (called square wave generator) which thus is synchronized accurately with the marker. This symmetrical square wave is used either directly or through intervening sweep generators to operate the gate generating circuits.

To separate the channels, properly timed gate pulses are used. Each gate is a rectangular pulse 13 microseconds long. The gates must be delayed by varying amounts from the edges of the square wave. This is accomplished by generating sweep or saw-tooth voltages and starting the gate pulses at the time the respective sweep voltages cross a reference voltage. The circuit constants for the various channels are different so as to vary the rate of rise of the sweep voltage and thereby locate each gate at its assigned time.

It was noted previously that the received video pulses branch into two paths, one of which selects the marker. The second path includes a 2-stage amplifier which produces new pulses derived from the trailing edges of the received pulses.

These new pulses are fed to the input of the eight channel converters. To each converter is fed also the output of the appropriate gate generator. The gate pulse voltage plus its corresponding channel pulse voltage is appreciably greater than the voltage of the other channel pulses. For example, gate 1 voltage plus channel 1 voltage is greater than channel pulses 2 to 8. Channel 1 is separated from the other channels and this position modulated pulse is converted to a length modulated pulse by a multivibrator so operated that it can be triggered by the combined gate and channel pulse voltages but not by either alone. This circuit not only separates the channels but also converts pulse position modulation to pulse length modulation. When the channel pulse is superposed on the gate pulse, sufficient voltage is obtained to start the multivibrator so that the first stage conducts and remains conducting for the remainder of the gate pulse interval. At the end of the gate pulse, the first stage in the multivibrator circuit is cut off, thereby returning the multivibrator to its original condition. Because the multivibrator is started at a variable time dependent upon the position of the channel pulse and is cut off at a fixed time established by the end of the gate pulse, the output pulses vary in length in accordance with the instantaneous position of the input pulses. By passing these length modulated pulses through a low-pass filter, the audio signal is obtained and all modulation products above the highest audio frequency are eliminated.

Special Radio Features

While two radio frequencies suffice for operation over a single link, a choice of four frequencies is available as a further means of reducing interference between systems or between sets of the same system when repeaters are operated in tandem. Although designed to operate on fixed frequencies, the equipment is capable of being adjusted continuously to operate at any frequency between the extremes. Both transmitter and receiver-converter use small oscillator tubes of the reflex velocity-modulated type

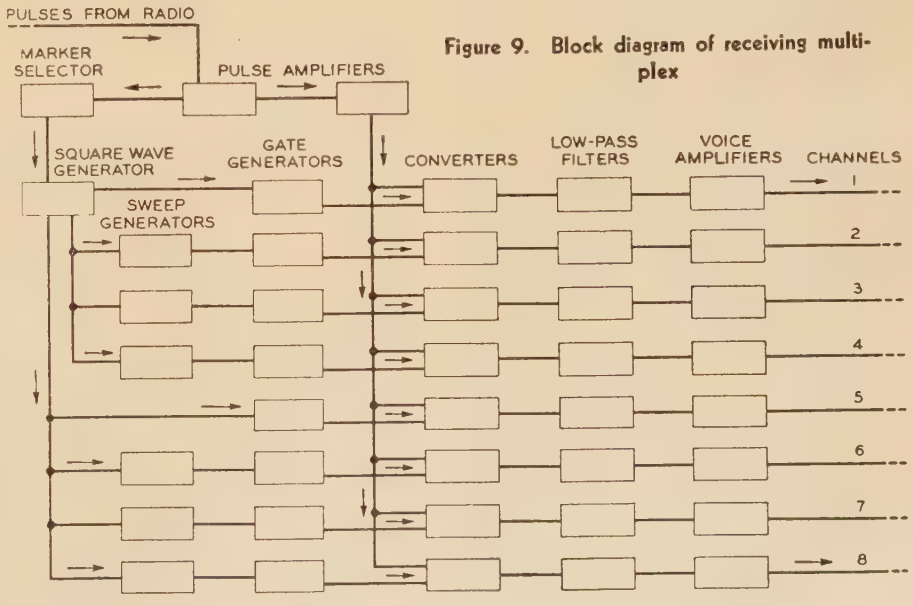

Figure 9. Block diagram of receiving multiplex

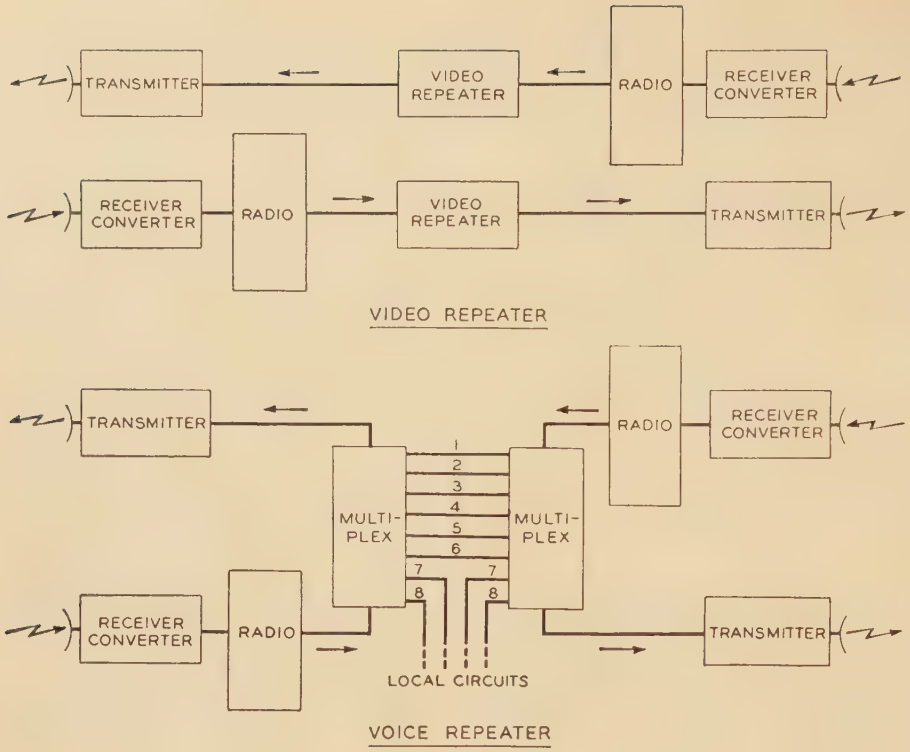

Figure 10. Alternative repeater arrangements

having a flexible cavity which is mechanically varied to get the approximate frequency. The exact frequency is obtained by varying the repeller potential.

Each antenna has a gain of approximately 33 decibels over a simple half-wave antenna. The polarization is normally horizontal but vertical polarization can be used if desired.

A feature of a pulse modulated oscillator is that because power is not generated continuously, the heating of the tube is less than for a continuous wave system and advantage may be taken of this by increasing the applied voltages so as to get increased power during the pulsing intervals.

The radio transmitter is a simple self-excited oscillator which oscillates or not depending on whether a pulse is present. This oscillator is pulsed by a modulator tube whose plate connects to the cathode of the oscillator. The repeller electrode is pulsed simultaneously with a fixed fraction of the voltage applied to the cathode in order to reduce frequency modulation to a minimum. A peak pulse power of 2 to 10 watts is obtained depending upon the type of tube and frequency.

Radio frequency power from the oscillator passes through a short coaxial lead which radiates into a wave guide through an impedance matching arrangement. The wave guide is tuned with a plunger at one end and delivers power to the antenna at the other end. A coupling arrangement is provided on the latest model to permit in-service measurement of microwave power without affecting the power delivered to the antenna. Microwave power is measured with a portable direct-reading power meter.

In the latest model of the receiver-converter, the beating oscillator is fed to a wave guide through an attenuator and coupling arrangement which permits amplitude adjustments or frequency measurements without regard to the impedance presented to the beating oscillator by the antenna.

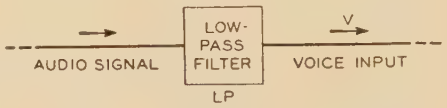

Figure 11

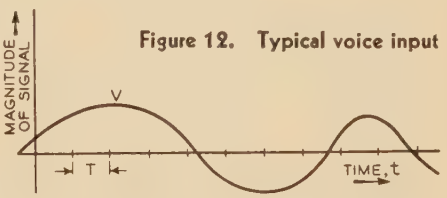

Figure 12. Typical voice input

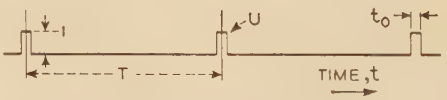

Figure 13. Unit sampling function, *U*

$$U = k + 2k \sum_{m=1}^{\infty} A_m \cos mCt$$

$$f_c = \frac{C}{2\pi} \qquad \frac{1}{f_c} = T$$

$$k = \frac{t_0}{T} \qquad A_m = \frac{\sin mk\pi}{mk\pi}$$

Video Repeater

The two radio sets forming a repeater can be joined either at voice or video frequencies (Figure 10). Joining at voice frequencies is a convenient arrangement if message circuits are dropped or added.

When sets are joined at video frequencies, there is a saving in equipment because the multiplex boxes are not required. Instead, a video repeater is used. Located in the common box, this repeater provides order wire facilities for monitoring and modulating channel 1 so that a relay attendant will be able to signal and talk to any other station along the route. In addition, the received pulses are lengthened to compensate for their having been shortened, chiefly by the preceding transmitter.

Special Equipment Features

The mechanical and equipment features of *AN/TRC-6* were governed largely by Signal Corps specifications. Important objectives such as ruggedness, portability, maintenance, storm-proofing, ease of setup, weight, and dependability were given proper balance to obtain a set suitable for military use.

The 50-foot sectionalized welded aluminum tubing tower consists of six 8-foot sections from two to three feet square with provision for omitting sections to obtain lesser heights. The four intermediate sections are tapered and may be telescoped together for shipping. The top section rests in the base section together with the hoisting boom during shipment.

With the tower properly guyed, the movement of the antenna beam pattern is restricted to a fraction of a degree even in a 60-mile wind. The sets have oper-

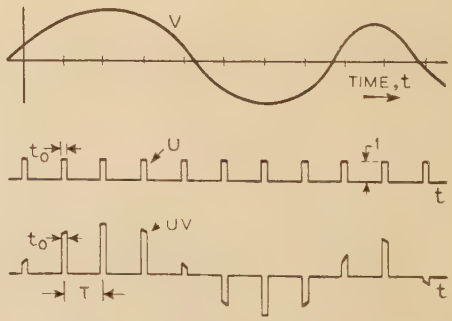

Figure 14. Diagram of *V* and *U*

UV is the result of sampling *V*

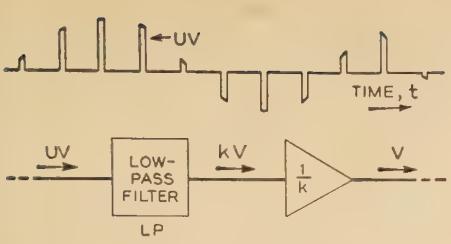

Figure 15. Passing *UV* through a low-pass filter and amplifier to obtain *V*

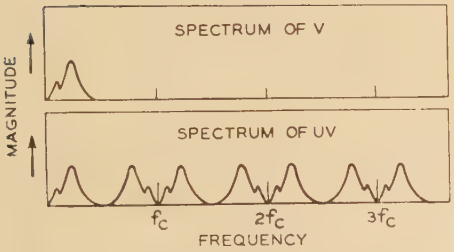

Figure 16. Spectrum analysis of *V* and *UV*

ated successfully through two hurricanes. The electrical and mechanical performance have proved satisfactory in actual field usage even when the antennas, top beam section, platform, tower, and guys were coated with more than three-quarters of an inch of ice.

Pulse Modulation Principles

The discussion to follow is a treatment of pulse modulation including the sampling principle and time division. To enumerate important features:

1. It is the sampling principle which specifies the least number of points required to reproduce a changing voice wave.

2. It is the job of the modulated pulses to carry this information to the distant receiver.

3. Pulse position modulation, like frequency modulation, reduces noise at the expense of band width.

4. A method of scaling is described whereby time division is regarded as a scale model of a single channel system.

In carrying out the pulse modulation method, the voice signal usually is passed first through a low-pass filter (Figure 11) to cut out all frequencies above an upper limit which is less than one-half the sampling frequency, f_c. After filtering, the signal is designated V and termed voice input.

V (Figure 12) is the instantaneous value of a short portion of a voice signal which might have passed the low-pass filter of Figure 11. The sampling principle teaches that if V is sampled instantaneously at regular intervals T, where T is less than a half period of the highest frequency in V, then the samples contain all of the information of the original signal. The magnitude of a sample is the information a modulated pulse is required to carry to the distant receiver.

The unit sampling wave (Figure 13) is designated U and will be used presently to sample the voice. Mathematically U is regarded as equal to a d-c term plus harmonics of the sampling frequency, f_c. The interval between pulses is designated T and equals $1/f_c$. The ratio of pulse length to the interval between pulses is designated k.

The voice input and unit sampling wave are repeated at the top of Figure 14. Because U is either one or zero, the product UV is an analytical process for sampling the voice. The result is a series of positive and negative pulses. When U is one, the product is equal to the voice input and at all other times zero.

Because UV is similar in appearance to amplitude modulated pulses (Figure 15), it is not surprising to find that an attenuated replica of V is obtained simply by passing UV through a low-pass filter. In the process of sampling and filtering, V is reduced by a factor k. Amplifying by a factor $1/k$ restores V to its original value.

To bring out more concretely that passing UV through a low-pass filter produces the original signal, Figure 16 presents a spectrum analysis of V and also UV. The upper diagram is the spectrum of V. After sampling V becomes UV. The spectrum of UV is the spectrum of V, small but exact, together with upper and lower sidebands about harmonics of f_c.

Remembering UV is the result of sampling, we can draw a conclusion; if, in a communication system, the resultant sampling UV is transmitted to the distant receiver either by direct transmission or by conversion to pulse position modulation, the voice signal can be derived simply by passing through a low-pass filter followed by an appropriate amplifier.

The simple physical concepts of pulse position modulation (Figure 17) will be reviewed by considering an idealized 1-channel system. With no voice input, pulses of fixed amplitude and length recur at regular intervals T. When the channel is busy, each pulse is displaced from its unmodulated position and occurs earlier or later depending on whether the voice signal is positive or negative. The exact displacement is linearly proportional to the instantaneous value of the voice wave at the time of sampling. With full input, the maximum excursion, neglecting the length of the pulse, is plus or minus $T/2$ or $\pm 1/2\, f_c$.

Figure 7 illustrates the reduction of noise by the slicer or double clipper. A practically noise-free pulse is delivered by the transmitting multiplex. A long radio path attenuates the pulse and noise is introduced by the receiver, producing a typical pulse with noise as indicated. The double clipper works in two steps. First, the top of the wave is shaved off reducing noise superimposed on the pulse. Second, the bottom of the wave is chopped off leaving a nearly noise free but attenuated pulse. This is amplified

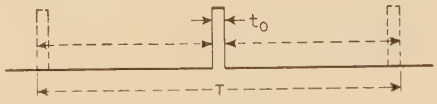

Figure 17. Single-channel pulse-position-modulation system

$$\pm\frac{T}{2}=\pm\frac{1}{2f_c}$$

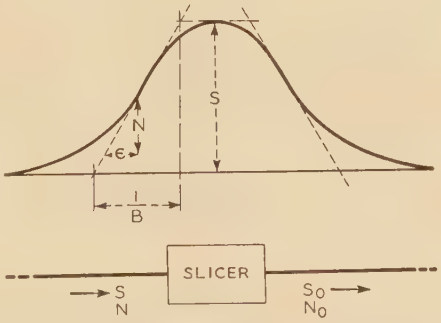

Figure 18. Equation for signal-to-noise improvement resulting from slicer

$$\frac{S}{N}=\frac{1}{B\epsilon} \qquad \frac{1}{\epsilon}=\frac{SB}{N}$$

$$\frac{S_0}{N_0}=\frac{1}{2\sqrt{2}\epsilon f_c} \qquad \frac{S_0}{N_0}=\frac{S}{N}\times\frac{B}{2\sqrt{2}f_c}$$

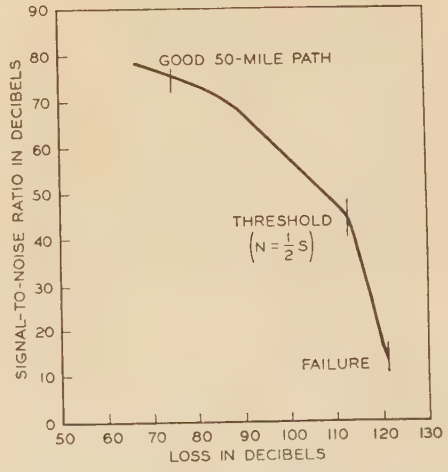

Figure 19. Decibel signal-to-noise ratio versus path loss

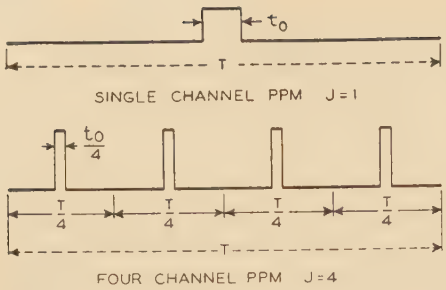

Figure 20. Formation of J channels by time division

and delivered to the receiving multiplex. It should be noted that whereas the effects of noise on amplitude can be practically eliminated by the slicer, nevertheless, the effects of noise on the exact timing of the pulse remain. However, the magnitude of this error in timing can be reduced by increasing the band width.

Because the exact time of occurrence of these nearly noise-free pulses is changed by the presence of noise at the input to the slicer, this effect, namely, the variation in exact time of occurrence of the pulses, will register as additional noise in the final receiver. This additional noise is evaluated by an approximate formula (Figure 18) for the signal-to-noise improvement due to the slicer (see Appendix). $B/2\sqrt{2f_e}$ is the improvement where B is the IF band.* This is the improvement for a single channel system whose maximum excursion approaches plus or minus $T/2$.

Because of the slicer, noise affecting the remainder of the system is restricted substantially to that which occurs during the time that the pulse amplitude is within the range of the slicer, provided the peak amplitude of the noise is less than one-half the peak amplitude of the signal. As the noise exceeds this limiting value or threshold, the ability of the receiver to distinguish between noise pulses and signal pulses begins to deteriorate (Figure 19). For values of peak noise below the threshold, the improvement in signal-to-noise ratio resulting from the slicer is constant.

A feature of pulse position modulation is that for fixed average power out of the transmitter, the peak power can be increased as the pulse length is reduced. Thus, if the band width is increased K-fold, it is assumed the pulse length is divided by K and that the pulse power is increased K-fold. Assuming the noise has characteristics similar to resistance noise, the signal-to-noise ratio at the input to the slicer and, therefore, the threshold, are independent of band width. Because of the K-fold wider band, the maximum rate of rise and fall of the pulse will be increased K-fold, and consequently the signal-to-noise ratio at the output of the slicer further is increased K-fold which corresponds to a further improvement in decibels of $20 \log_{10} K$. This is in contrast to a conventional frequency modulation system where, over a path of specified attentuation, the threshold represents a limitation on the signal-to-noise ratio obtainable with a given amount of carrier power.

Passing to the theoretical concept of time division, a time division multiplex can be treated by first considering an idealized 1-channel system. Assuming one channel and maximum excursion of the pulse, the band width will depend upon the signal-to-noise improvement sought. For double sideband transmission, the IF band will be twice the video. The band width of the transmitter should equal that of the receiver. The pulse should be as short as the band width of the system will tolerate.

To provide J channels by time division (Figure 20), all significant band widths are increased J-fold; the length of each pulse is divided by J; the peak power of each pulse is multiplied by J; J pulses appear in each frame; the average power of the transmitter is increased J-fold; and the modulation or maximum excursion of each pulse is divided by J. Forming a scale model in this fashion, the J-channel system will have the same threshold and same signal-to-noise ratio as the idealized 1-channel system.

Transmission Performance

Microwave propagation at frequencies of 4,000 to 5,000 megacycles is subject to fading, and observed diurnal and seasonal effects are evidence of a close connection between microwave propagation and local meteorological conditions.

Figure 21. Typical transmission–frequency characteristic

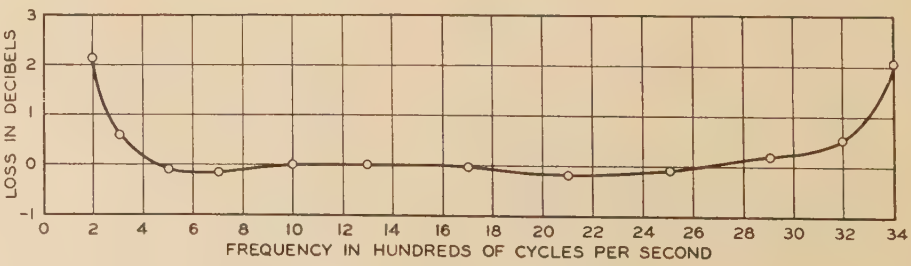

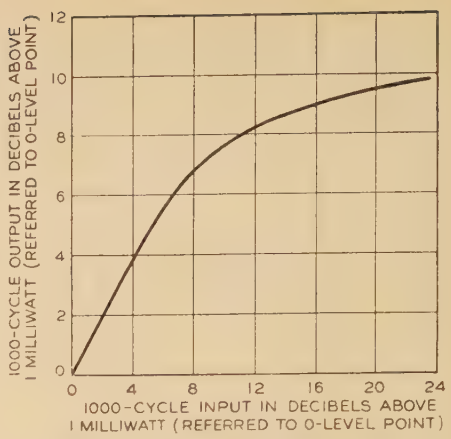

Figure 22. Typical load performance

However, the presence of rain or snow in the transmission path has given no evidence of causing serious increases in attenuation. Although the radio propagation may vary by very substantial amounts, the transmission stability of the message circuits is extremely good.

The eight message circuits which each *AN/TRC*-6 system provides are high quality telephone circuits and meet commercial standards for long distance telephone transmission. The individual message circuits may be terminated 2-wire or 4-wire and may be used to transmit signaling, dialing, facsimile, pictures, or multichannel voice frequency telegraph. In the latter instance, a single message circuit will handle as many as 18 separate teletypewriter facilities.

As indicated by Figure 21, the transmission–frequency characteristic of each of the eight channels varies less than one decibel from 300 to 3,300 cycles, and, as shown by Figure 22, each channel is capable of handling inputs up to about plus eight decibels above a milliwatt at the zero level point (2-wire input) without appreciable overloading. The load capacity of the receiving multiplex is sufficient so that when terminated 4-wire, the circuit can be adjusted to nine decibels gain. Receiving potentiometers provide a continuous adjustment of channel gain over a 15-decibel range.

Inspection of Figure 23 shows that the circuit noise observed on a single link is dependent upon the attenuation in the

* An evaluation of the signal-to-noise ratio that is similar in principle is included in an article entitled "Pulse Time Modulation" by E. M. Deloraine and E. Labin in Electrical Communication, volume 22, 1944, number 2, pages 91–8.

path. For a many link system, this noise increases with the number of repeaters. However, the individual message circuits are particularly quiet. For example, over a good 50-mile path, the noise in the absence of fading is approximately six decibels above reference noise when measured at a receiving level nine decibels below zero level. In terms of rms signal-to-noise ratio, assuming the signal is plus eight decibels above a milliwatt at zero level, this corresponds to a signal-to-noise ratio of 75 decibels. Further inspection of Figure 23 will show that on a 50-mile path, a margin against failure of approximately 48 decibels has been built into the set, and fades approaching this magnitude can be encountered before the system fails.

The intervals of time that are significant in determining the exact position in time of a channel pulse are small. For example, in Figure 23, if the relative random jitter in the trailing edge of the channel pulses had been as great as one thousandth of a microsecond, the noise meter readings for sufficiently low values of path attenuation would have been slightly more than 3 decibels higher than the experimental values observed.

Two-way voice transmission over radio links totalling 1,600 miles and one-way

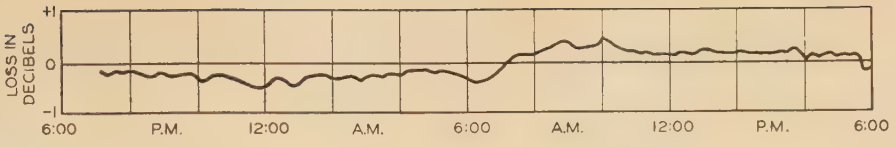

Figure 24. Transmission stability of 3,200-mile circuit

over 3,200 miles have been accomplished successfully in demonstrations. To do this, ten radio sets were set up to form five two-way 8-channel systems each operating simultaneously over the same 40-mile air path. The five links were connected in tandem to form a two-way 8-channel system 200 miles long with four intermediate repeaters. By connecting all channels in tandem a two-way 1,600-mile circuit was obtained. Finally, by connecting both directions together, excellent 1-way transmission was obtained over an air path 3,200 miles long. To illustrate the over-all stability of the 3,200-mile circuit, Figure 24 is a typical 24-hour recording of the received level of a 1,000-cycle test tone and it can be seen that the maximum variation is less than plus or minus 0.5 decibel.

Figure 23. Message circuit noise for a single link versus path loss

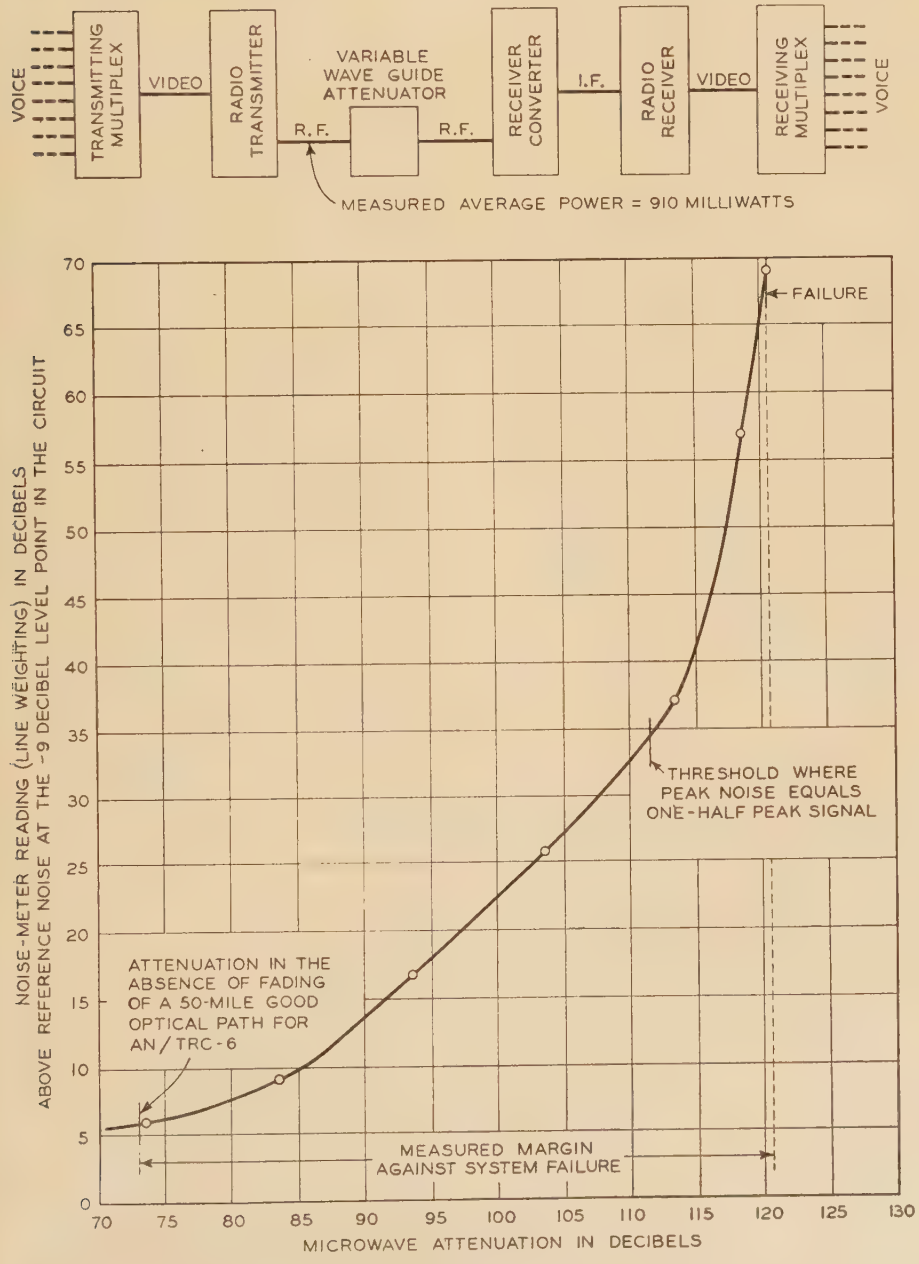

Conclusion

Although this equipment was designed for military use, its basic principles and design features can be used to provide telephone and other communications to the public. Sharply beamed radiation and reception, pulse modulation and time division multiplex are all factors which tend to make such systems attractive and their economic field in competition with other alternatives needs to be determined.

Appendix

Noise will modify the times at which the incoming pulses reach the slicing or triggering level. Figure 18 shows how a small noise voltage N, superimposed on a video pulse of amplitude S, changes the triggering time by an amount ϵ. From the geometry of the figure, $S/N=1/B\epsilon$. After passing the IF amplifier of band width B and second detector, the approximate slope of the leading edge of the pulse at the slicing level is SB and the corresponding "time of rise" is $1/B$. When the output of the slicer is passed to the receiving multiplex, the error in timing ϵ will cause a noise voltage N_0 in the output of the receiving multiplex.

Assuming a 1-channel system (Figure 17) and supposing that the maximum excursion of a pulse can assume its limiting value of plus or minus $1/2f_c$, plus or minus $1/2f_c$

An Improved Azimuth Indicating System for Aircraft

E. E. LYNCH
MEMBER AIEE

R. A. PFUNTNER
NONMEMBER AIEE

Synopsis: Because of the violent maneuvering possibilities in modern aircraft, the usefulness of azimuth indicators in avigation depends on circumstances not existing in marine navigational applications. New problems in direction indicating instruments therefore have been introduced, such as the perplexing problem of obtaining indication after loops or rolls. Azimuth indicating systems now used in aircraft have not given a completely satisfactory solution to such problems.

This paper summarizes the progress from the direct reading compasses to monitored gyroscopes and concentrates on the unique problems in aircraft where space limitations, reliability, and operation at all altitudes are important. It indicates how azimuth indicators and auto pilot controls close to the ideal are obtainable by the use of special features including a novel "nontumbling" mechanism and an electromagnetic type of gimbal adjusting device.

DURING the past few years more emphasis has been placed on the development of a directional indicating and control system which will meet the new rigid requirements for avigation as well as the older well-established needs of navigation which are still used in guiding aircraft. The first systems for use in aircraft followed the natural development trend towards improvement of navigational compasses. However, the rotational and translational accelerations which are experienced in modern aircraft bring forth new and, until recently, unsolved problems in azimuth indication. A major and perplexing problem is that of obtaining indications during steep banks, rolls, and loops. It is the purpose of this paper to point out the principal features needed in an azimuth system for use in modern aircraft and to indicate how some of the major problems can be solved. It will be shown how a modern measurement system has been designed which closely approaches the ideal.

Paper 46-192, recommended by the AIEE committees on air transportation and instruments and measurements for presentation at the AIEE Pacific Coast meeting, Seattle, Wash., August 27–30, 1946. Manuscript submitted November 23, 1945; made available for printing July 18, 1946.

E. E. LYNCH and R. A. PFUNTNER are both with the General Electric Company, Lynn, Mass.

Existing Systems

Before stating the ideal characteristics, it is desirable to review briefly some of the systems utilized for indicating and controlling aircraft directions. The direct reading compass is simple, rugged, light in weight, and small in size. Under favorable conditions it is reliable and accurate. Because its indications often fluctuate rapidly and are influenced by proximity to magnetic fields or magnetic materials, its use is often limited to emergencies. It also displays the northerly turning errors which are well known to pilots and others familiar with compasses.[1] The remote indicating compass helps to solve the difficulty resulting from magnetic fields and materials by locating the direction sensitive element in a position where such influences are minimized. However, it does not solve the problems of northerly turning errors or pointer oscillation.

In certain cases the stabilization of the magnetic compass has been found desirable[2] in order to eliminate the effect of the vertical component of the earth's field which is responsible for the northerly turning errors. This is done in the gyrostabilized compass by mounting the direction sensitive element on a vertical axis gyroscope. The element thus is maintained in a level position during maneuvers and while flying in rough air. However, because the vertical gyroscope is kept vertical by gravity control, it will have some errors during maneuvers of long duration since centrifugal forces influence the apparent direction of the gravitational force. It also has the disadvantage of heavy weight and large size in the forms that are generally available. Although in this general design the compass transmitter including the gyroscope can be located remotely to minimize magnetic effects, its location must be selected carefully to provide sufficient space and to be sure that vibration will not damage the gyroscope bearings. Modern high speed airplanes allow only a few inches of height in the wing tips where it is often desirable to locate the transmitter.

Another class of azimuth indicator is the directional gyroscope which in its electric form[3] has been used mainly as an indicating and control instrument in a relief type of autopilot.[4] This device gives an indication that is well-stabilized but is subject to gradual drifting or wandering and must be reset frequently to the magnetic compass heading. A part of the drift may be the result of gimbal bearing friction, unbalance, or mechanical imperfections, but a more fundamental cause is the rotation of the earth which produces an apparent drift depending on the geographical location and heading of the directional gyroscope. Resetting is inconvenient and may result in an error if the compass happens to be under the influence of temporary accelerations when the heading is transferred from the compass to the gyroscope.

To avoid these difficulties the directional gyroscope can be reset automatically and continuously to agree with the compass.[5] Such an arrangement utilizes a remote compass transmitter and thus minimizes magnetic difficulties. Because it utilizes a directional gyroscope, its indication is stable. However, there still remains an unsolved problem in conventional directional gyroscopes, whether compass controlled or not. This is the

---

represents the peak modulation (displacement in time) of a pulse from its unmodulated position. The corresponding rms displacement when the pulses are modulated fully by a single frequency test tone approaches $1/2\sqrt{2}f_c$. If S_0 denotes the corresponding rms signal voltage in the output of the multiplex, $S_0=K/2\sqrt{2}f_c$ where K is a constant factor of proportionality.

In Figure 18, N can be regarded as the voltage of an instantaneous noise sample taken at the time of triggering and ϵ as the corresponding error in timing caused by the noise sample. N can vary from sample to sample. The approximate rms value of ϵ can be taken as the rms value of N divided by SB. In this case N_0 will denote the rms noise voltage in the output of the multiplex. If the noise voltage at the input to the slicer has the characteristics of resistance noise, its rms value will equal the rms value of the instantaneous noise samples N.

Since

$$S_0=K/2\sqrt{2}f_c$$

and

$$N_0=KN/SB$$

then

$$\frac{S_0}{N_0}=\frac{S}{N}\times\frac{B}{2\sqrt{2}f_c}$$

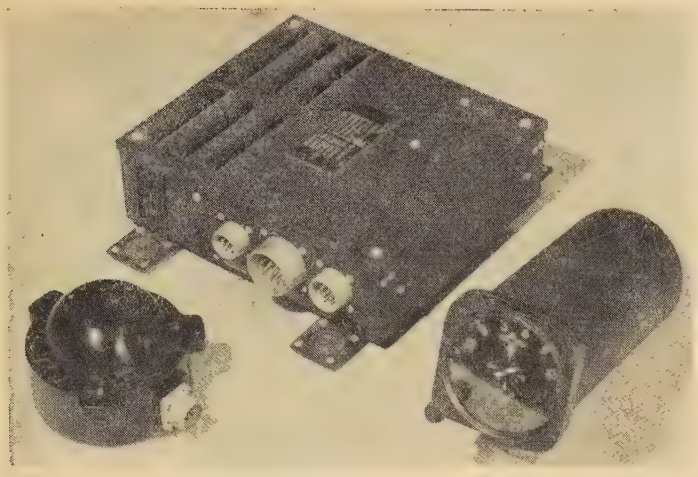

Figure 1. Components of azimuth indicating system

elimination of the error in indication or complete loss of indication caused by the upsetting of the gyroscope motor because of insufficient freedom of movement within its gimbal mounting. With modern aircraft violent maneuvers are possible and loops or rolls must be expected with military planes. These maneuvers will cause normal directional gyroscopes to upset.

Ideal Characteristics of a Modern Azimuth Indicating System for Aircraft

From the foregoing discussion of the limiting features in existing arrangements, it can be seen that an ideal azimuth indicator or control system for use on modern aircraft must meet certain requirements to avoid the difficulties described. Without attempting to cover all the requisites,[6] one may state that such a measurement system should be light and small, and should occupy minimum panel space. Such a system should have provision for minimizing the effects of magnetic fields or magnetic materials, and its accuracy should meet the requirements of the application. It should produce an indication which is stable. Its reading should not be excessively disturbed by normal or even violent maneuvers. It also should have some provision for minimizing turning and acceleration errors. For many applications it should have provision for transmitting the indication to a number of remote stations and it also should provide the necessary signals for azimuth stabilization or azimuth autopilot control. An additional feature considered of much importance is an emergency compass, so that if the gyroscope fails there will still remain a readable indication which is independent of local magnetic effects. A further very important feature is the characteristic of "safe failure" if anything should go wrong with the system.

Figure 2. Schematic diagram of azimuth indicating and control system

B—Selsyn detector
D—Torque motor
F—Auto pilot "pick-off"
H—Subtransmitter
J—Winding
K—Alnico bar magnet
L—Magnetic vane mounted on shaft
M—Vanes
N—115-volt 400-cycle source
O—Switch
P—Copper cylinder
Q—4-pole disk magnet
R—Motor shaft
S—Main gimbal

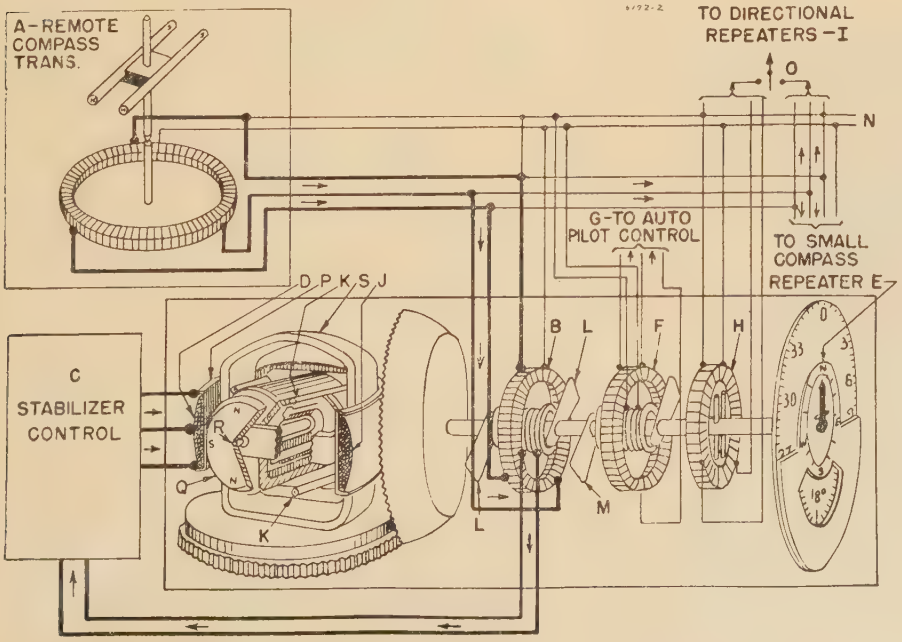

Important Features for an Ideal System

Three important features which help to meet these requirements are compass control, automatic gimbal adjustment, and nontumbling action. The first tends to hold the gyroscopic indication in agreement with the average compass position regardless of any natural tendency to drift. The second continuously tends to adjust the gimbals to a position at right angles to each other so that they will not drift into line and cause an upsetting condition. The third feature makes it possible to operate satisfactorily even during violent maneuvers by eliminating the undesirable tumbling action which occurs in normal limited angle directional gyroscopes.

General Description of an Improved System

The following will show how an azimuth control system, which very closely approaches the requirements of the ideal, has been obtained by the controlling or monitoring of a small nontumbling directional gyroscope by means of a remote magnetic compass. The basic devices required are shown in Figure 1 and will be discussed in detail under "Operating Principles."

In order to overcome the tendency of the gyroscope to drift in azimuth, a magnetic compass transmitter of the remote indicating type corrects the heading of the gyroscope continuously, but at a very slow rate. By this means both the natural tendency of the gyroscope to wander and the large oscillations of the compass are reduced to negligible values.

A second harmonic signal from the remote compass transmitter *A*, as shown in Figure 2, is applied to a Selsyn detector *B* located on the azimuth axis of the gyroscope. Any angular difference between the compass and gyroscope is translated

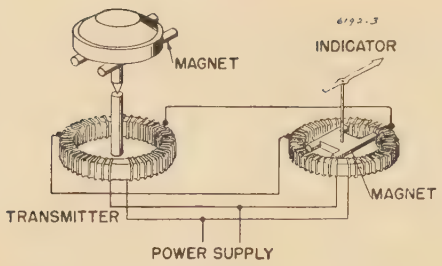

Figure 3. Basic diagram of Selsyn repeater circuits

into a voltage which is amplified in a stabilizing control box *C* and used to correct the gyroscope heading. The control is accomplished in a torque motor *D* attached to the gyroscope.

The headings of the compass transmitter and the gyroscope instrument at any instant may be compared by means of a small compass repeater *E* located in the face of the directional gyroscope. This repeater, which is connected directly to the remote compass transmitter, provides both a check on the correct functioning of the system and a very important stand-by instrument in case of a failure of the gyroscope or automatic control.

An inductive type polyphase electromagnetic "pick-off" *F* generates alternating voltages *G* capable of azimuth control of an automatic pilot or other equipment.

Because many airplanes require several simultaneous indications of direction in various parts of the airplane, a subtransmitter *H*, as shown in Figure 2, which is similar in principle to the remote indicating compass transmitter, also is provided. This is capable of operating a number of light compass repeaters *I* located as desired about the aircraft. Normally these repeaters duplicate the signal of the directional gyroscope and therefore are not subject to the usual compass errors or oscillations. Should the gyroscope fail, however, they may be connected directly to the compass transmitter by switch *O* shown in Figure 2. With this connection they provide a conventional remote compass system.

Operating Principles

A system such as the one described has many features which are responsible for its satisfactory operation. Included in a list of such features are

1. The Selsyn detector to determine the difference between compass and gyroscopic indications.
2. The stabilizer control unit that detects which direction the torque motor should run and controls that motor.
3. The torque motor for correcting the gyroscopic reading.
4. The gyroscope motor.
5. The repeater circuits which make possible the transmission of the stabilized gyroscopic indication to a large number of directional repeaters.

The operating principle of units furnishing these features will be outlined before discussing the details of the very important automatic gimbal adjustment and nontumbling action features.

Remote Compass System

The compass transmitter and repeater usually are connected in a circuit similar to that shown in Figure 3. Double frequency voltages are generated in the transmitter windings by the interaction of the d-c flux from the north-seeking compass magnets and the a-c flux from the power source in a saturatable core material. The generation of double frequency voltages by this saturating means and their use in repeater instruments already has been described adequately.[7]

The distribution of the voltages about the core is determined by the angular position of the transmitter magnets relative to the core and coils, and since the magnets are free to align themselves with the earth's magnetic field, double frequency voltages are obtained whose relative magnitudes are a function of magnetic heading of the aircraft. The usual practice is to impress these voltages upon an indicator whose magnetic construction is similar to that of the transmitter. In the indicator the interaction of the a-c flux from the power source and the double frequency flux from the compass transmitter generate a d-c field across the diameter of the indicator core. Since the angular position of this d-c field is a function of the transmitter heading, it is used to hold the indicator magnet to which the indicating pointer is attached in agreement with the transmitter heading.

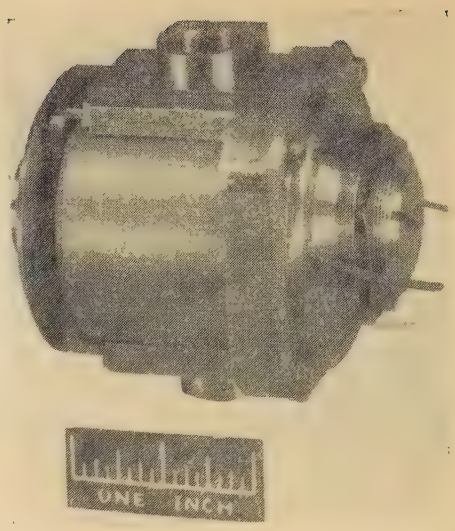

Figure 5. Gyroscope motor for compass controlled directional gyroscope

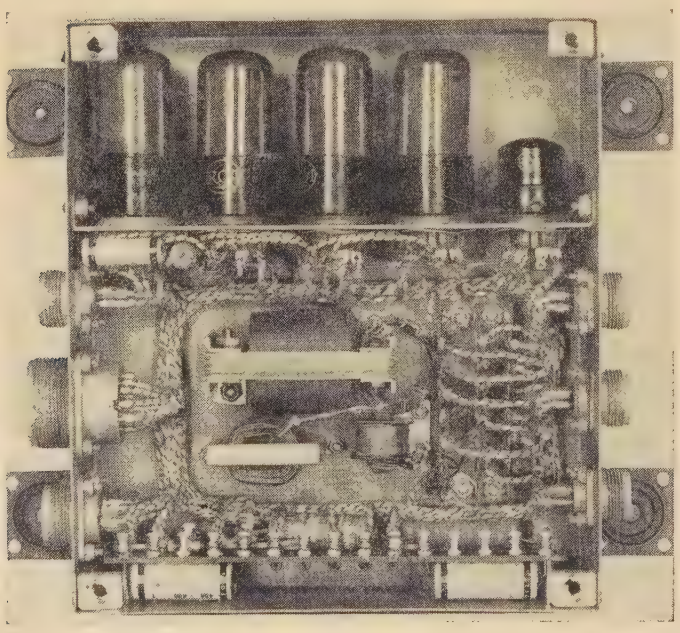

Figure 4. View of stabilizer control with cover removed

Selsyn Detector

In the control of the directional gyroscope the compass transmitter is connected to the Selsyn detector. In the detector the polyphase coils and core differ from those of the conventional compass indicator or repeater by the fact that saturation of the core does not occur. Thus a double frequency flux with a direction depending on the voltage pattern of the transmitter is obtained instead

of a d-c field. Two magnetic vanes mounted on a shaft, as shown by L in Figure 2, can pick up this flux and guide it through a detector coil to detect the angular position of this double frequency flux. If the vanes are exactly in line with the a-c field, a maximum voltage will be induced in the coil, but if the vanes are turned 90 degrees from this position, zero voltage will be induced. By mounting the vanes on the gyroscope azimuth shaft the zero voltage position is used to detect when the gyroscope azimuth axis is in agreement with the compass heading. Any voltage present in the detector coil indicates an error in the gyroscope heading, the direction of which is determined by the polarity (in phase or 180 degrees out of phase from a reference voltage) of the alternating voltage.

Stabilizer Control Unit

The detector output is impressed upon an electronic control unit which amplifies and rectifies the signal to give a d-c output for operation of the torque motor to bring the gyroscope to the correct heading. A photograph of the stabilizer control unit with the cover removed is shown in Figure 4. The signal first is amplified in a conventional 2-stage amplifier circuit. It then is rectified. During rectification it is combined with a properly phased master voltage to obtain a direct current which reverses if the polarity of the input reverses. This direct current in turn is amplified and used to control the torque motor.

Torque Motor

The torque motor D, Figure 2, is operated by direct current from the stabilizer control unit circulating between the center tap and either end of a winding J. The current in the coil produces a magnetic field inside it parallel to the gyroscope main gimbal axis and in a direction determined by the direction of the correction required. Four alnico bar magnets K are placed on the sides of the motor frame with their axes parallel to the motor shaft. The magnetic field from the coil reacts with these magnets to produce a torque in such a direction that precession will take place about the azimuth axis. Precession will continue until the compass and gyroscopic indications are in agreement.

Gyroscope Motor

The gyroscope motor shown in Figure 5 is a 3-phase 2-pole hysteresis-type motor which operates synchronously at 24,000 rpm and is capable of furnishing a powerful starting torque. Adequate moment of momentum is provided by means of an external rotor shell of a tungsten alloy, and this together with the high rotating speed gives the necessary stabilizing torque. Special bearings designed to withstand high vibration accelerations give these motors improved characteristics.

Repeater Systems

In order to utilize the stabilized directional gyroscope for other purposes than as an individual indicator, additional repeater systems are employed. One of these is the subtransmitter H shown in Figure 2. In principle this transmitter is equivalent to that of the remote compass except that the transmitter magnet is attached to the gyroscope azimuth axis. By means of a circuit similar to that shown in Figure 3, the heavily damped gyroscope subtransmitter signal may be used to actuate a number of standard remote directional repeaters located conveniently about the aircraft.

A second system is the autopilot azimuth control which is initiated by a signal from a polyphase "pick-off" mounted around the gyroscope azimuth shaft as shown at F of Figure 2. The construction of this "pick-off" is similar to that of the Selsyn detector, but its operation is somewhat different. The power supply frequency is supplied to the single center coil and the vanes M distribute the flux to the outer polyphase coils in accordance with the angular heading of the gyroscope. Voltages produced in the polyphase coil are therefore a function of the gyroscope heading. These voltages may be used for accurately controlling and stabilizing various directional devices.

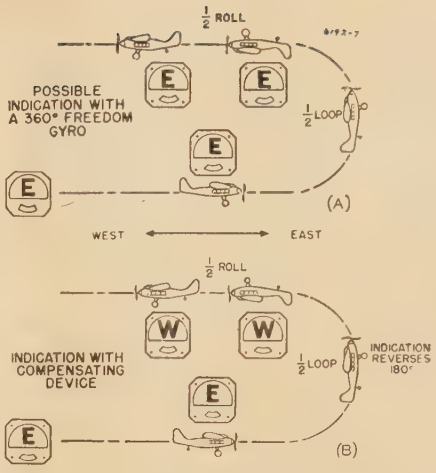

Figure 7. Indication during an Immelman turn

A. Without a compensating device
B. With a compensating device

Automatic Gimbal Adjustment

A very important feature is used in this compass-controlled gyroscope system. An automatic method of keeping the gimbals at right angles to each other prevents the horizontal gimbal from precessing into line with the main gimbal. Such a lineup of the gimbals causes the gyroscope to upset. Figure 2 shows the construction schematically. A copper cylinder P is attached to the instrument frame in such a manner that it surrounds the gyroscope motor and its axis coincides with the main gimbal axis. In the actual design illustrated, this cylinder also serves as the mechanical support for the torque motor coil. A 4-pole disk magnet Q is attached to the end of the motor shaft R and turns with the motor rotor at 24,000 rpm. Eddy currents are induced in the copper ring by the spinning magnet and produce an electromagnetic drag acting on the motor rotor.

As it revolves the upper part of the magnet moves in one direction with respect to the cylinder, and the lower part

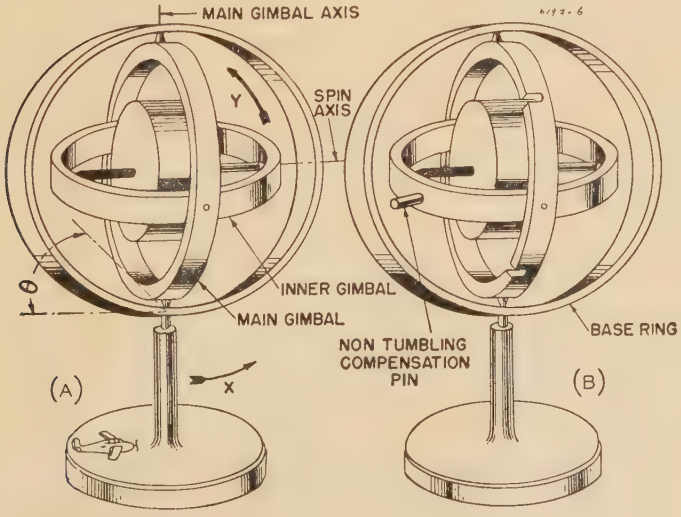

Figure 6. Typical toy gyroscope

A. Standard type
B. Special type equipped with non-tumbling compensation

moves in the other direction. The torques caused by the upper and lower parts of the magnet are, therefore, symmetrical when the spin axis is level, and no resultant drag exists about the vertical axis. When the motor axis becomes tilted with respect to the plane of the copper cylinder, the forces become unbalanced because one-half of the magnet disk is closer to the cylinder than the other. This force unbalance results in a torque about the vertical axis of the gyroscope which causes precession about the horizontal axis and prevents gyroscopic upset by keeping the spin axis at right angles to the main gimbal S.

Nontumbling Gimbal Reversal Feature

It previously has been pointed out that the system should indicate correctly after all the maneuvers that an aircraft may be expected to perform. The maneuvers include loops and rolls which cause conventional directional gyroscopes to upset because the angular movement of the spin axis in the main gimbal is limited. Universal freedom mounting can be designed to reduce the hazard of upset. A toy gyroscope such as shown in Figure 6A illustrates the general construction. Problems arise, however, which make it impractical or, at least, undesirable.

One major problem is illustrated by the fact that with 360 degrees freedom it is possible to go through certain maneuvers such as an Immelman turn where, after coming out of the maneuver, the instrument will read incorrectly by 180 degrees as shown in Figure 7A. This is further complicated by the fact that when going through a similar maneuver at a slightly different heading, this reversal will not be present.

In order to clarify this principle, consider Figure 6 which illustrates schematically a directional gyroscope. There are two conditions limiting the directional gyroscope's proper use.

1. The spin axis is fixed in direction.

2. The base is fastened to the aircraft and is upright in normal flight.

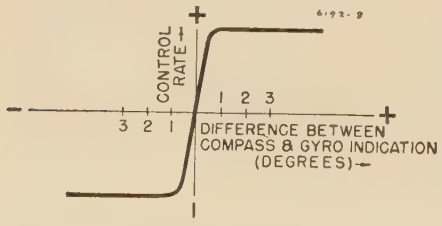

Figure 8. Typical control rate for gyroscope azimuth precession

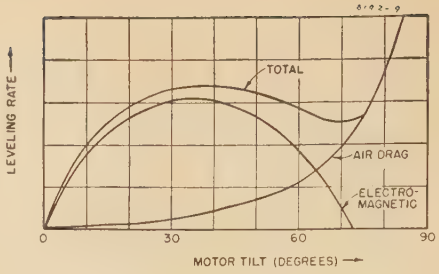

Figure 9. Typical control rate for leveling gyroscope gimbal

The angle θ, Figure 6A, between the plane of the base ring and the plane of the main gimbal is a measure of the gyroscopic indication. It is evident that with only these two limitations, the angle θ can have two values differing by 180 degrees for a particular heading of the gyroscope base ring, since besides the position illustrated, we can turn the spin axis as shown by arrow Y, continuing it through the main gimbal, and then we can bring the black end of the spin axis back to the left hand side by rotating it about the main gimbal axis. Thus for the same heading of the aircraft, we have two azimuth readings differing by 180 degrees.

The fact that both of the foregoing readings can exist is verified during an Immelman turn, which is illustrated by the following experiments. If the aircraft is considered heading in the direction shown on the gyroscope base in Figure 6A, and if the base is rotated as shown by the arrow X (keeping the spin axis in the plane of the base ring) until the base is upside down, the angle θ will not change. If the base then is returned to normal by rotating about the spin axis, θ still will be unchanged.

If the experiment is repeated in a similar manner, but if the spin axis intentionally is kept slightly off the plane of the base ring, then a phenomenon occurs which at first thought may seem strange. The main gimbal rotates 180 degrees on its own axis as the base turns upside down. This phenomenon is caused by the gyroscope's tendency to keep its spin axis pointed in one direction. When the gyroscope is mounted in gimbals with axes at right angles to each other, the main gimbal must turn in the manner described in order to allow the spin axis to hold its direction. This action is referred to as gimbal error action in less violent maneuvers.

The problem is to eliminate the possibility of having two different indications for the condition where the aircraft is upright and headed in one particular direction. A stop to prevent the spin axis passing through the main gimbal prevents the possibility of two such indications, and the arrangement is schematically shown in Figure 6B. During a loop, when the pin hits the gimbal, it is engaged only momentarily since gyroscopic action turns the main gimbal to free the pin, and therefore no undesirable tumbling action takes place.

The stop is placed so that the inner gimbal cannot quite line up with the main gimbal, and two additional desirable results are attained.

1. Since the inner gimbal will not rotate 360 degrees, spirals can be used to lead current into the motor rather than slip rings. This eliminates undesirable friction.

2. Since the axis of the inner and main gimbal never can line up exactly, the maximum undesirable effects of "gimbal lock" are eliminated. "Gimbal lock" is the condition where the spin axis lines up with the main gimbal axis, and in this position friction of the motor bearings will tend to turn the main gimbal and thus start the directional gyroscope indicator dial spinning.

Operating Characteristics

There are certain operating characteristics of especial interest in the compass-controlled directional gyroscope. Some of these may be called design characteristics since they are easily adjustable in design. These would include the precession rate of the gyroscope azimuth correction, and the leveling rate of the gyroscope gimbal automatic adjustment.

Precession Rate

The advantage of a high rate for correcting the gyroscope indication lies in the faster return of the gyroscope when large errors occur, and also in a reduction in errors caused by the drift of the gyroscope that is being compensated for, as shown in the appendix. However, because the compass may have large errors during turns, a high rate might cause greater gyroscopic errors than a low rate. Figure 8 illustrates a typical control rate curve where the amplifier is designed to change from zero to the maximum current very quickly, and thus give a high correction rate for small angles of deviation. It has an approximately constant rate for all larger angles of deviation in order to reduce turn errors.

Leveling Rate

Another characteristic is the leveling rate of the automatic gimbal adjustment. With the construction shown in Figure 2, characteristics similar to those illustrated by Figure 9 are obtained where the maximum value may be varied by the strength

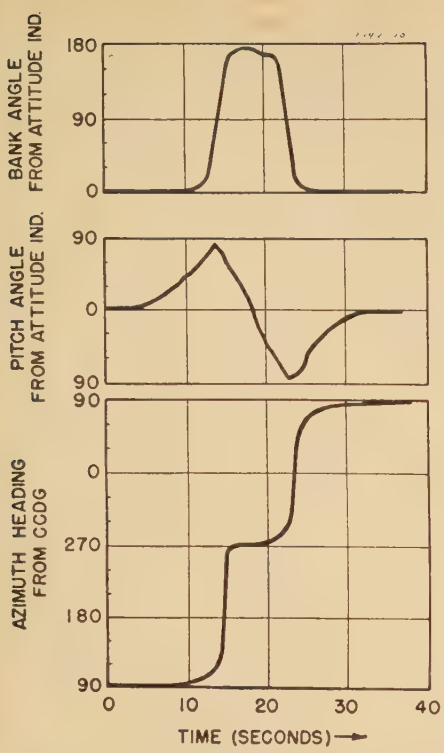

Figure 10. Data typical of actual results during a complete loop

of the alnico bar magnet. Since the dip of the motor normally is not transmitted to the dial, the shape of this curve is not particularly critical. Ordinarily there is nothing to upset the motor to a position outside the range of the copper ring, but if considered necessary, air drag on the motor rotor may be used as a leveling means for the high angles.

Flight Data During Violent Maneuvers

Very important operating characteristics are shown by actual flight data. Figure 10 shows the data taken during a loop starting on a 90-degree heading in a typical flight test.

Conclusions

This system will give satisfactory overall operation covering a wide range of voltage, frequency, temperature, and attitude conditions. For optimum performance, however, the frequency should be kept within ten per cent of its rated value, and volts per cycle within a similar range.

As fast as instrumentation and control of aircraft in azimuth have posed new problems to solve, new techniques have been developed to meet the requirements. Magnetic compasses, stabilized compasses, and compass-controlled gyroscopes have all been steps in the evolution of direction indication but have failed in the past to be adequate for the violent maneuvers which modern fast airplanes can perform. It has been shown, however, that one form of compass-controlled directional gyroscope when supplied with the new "nontumbling feature" can provide satisfactory operation for these applications. Not only can this be accomplished, but the weight and size are such that the gyroscope indicator can be mounted in a standard $3^1/_8$-inch-diameter AN-size instrument panel cutout, a feature which is extremely desirable.

Appendix. The Servomechanism System of an Improved Azimuth Indicator

With reference to Figure 2, the primary detector of the directional measuring system is a permanent magnet which seeks a north-south direction in the remote compass transmitter A. A voltage pattern is produced which is transmitted to the compass repeater E and, if desired, can be transmitted to the directional repeaters I. The main function of the voltage pattern, however, is to act as the "desired behavior" of a regulatory loop or closed casual servo system. A paper on this subject, entitled "Unified Symbolism for Regulatory Control" by G. A. Philbrick, was presented at the December 1945 meeting of the American Society of Mechanical Engineers. Figure 11 shows a graphical or symbolic diagram of the servo system.

This voltage pattern produces an a-c flux in the Selsyn detector B that has a direction determined by the pattern. Using the symbolism of Brown and Hall[8] this direction can be represented functionally by $\Theta_i(t)$. The gyroscope itself positions pickup vanes in the Selsyn detector, the direction of which can be represented functionally by $\Theta_o(t)$. The difference between the compass reading (corresponding to the flux direction) and the gyroscopic reading (corresponding to the vane direction) then is represented by $\Theta_i(t) - \Theta_o(t)$ and this corresponds to the error signal voltage $\xi(t)$ induced in the pickup coil.

This error signal voltage $\xi(t)$ isthe input to a stabilizer control C, the outputs of which are direct currents. These currents flow through the coils of a torque motor D to produce a torque which can be represented functionally by $T_c(t)$. If the combined operator is $C_c(p)$, then the torque $T_c(t)$ is the result of $C_c(p)$ operating on the input $\xi(t)$. This output torque $T_c(t)$ combines with disturbance torques $T_o(t)$ such as those causing drifts to cause precession of the gyroscope in a direction to reduce the error signal. This precession operator $H_o(p)$ operating on the torques determines the position of the pickup vanes.

$$H_o(p)[T_c(t)+T_o(t)]=\Theta_o(t)$$

Figure 11 easily can be recognized as a standard simple servomechanism. The operator $C_c(p)$ can be considered a constant K for small values of $\xi(t)$ because in this region the stabilizer is a proportional amplifier, and the torque from the precession coils is essentially proportional to the current. However, for large values of $\xi(t)$, the amplifier saturates, and $C_c(p)$ has the necessary value to keep $T_c(t)$ or $C_c(p)\xi(t)$ essentially constant. The differential operator $H_o(p)$ is essentially an integral operator $1/p$ since the speed of gyroscope precession, or $(d\Theta_o)/dt$, is proportional to the torque $T_c(t) + T_o(t)$.

From this discussion it is apparent that the standard simple servomechanism equations which are covered fully in another paper[8] can be used to predict errors and stability of such systems.

The three basic equations can be written as follows, omitting (t) where convenient:

$$\left.\begin{aligned}&\xi(t)=\Theta_i(t)-\Theta_o(t)\\ &\text{or}\\ &\xi=\Theta_i-\Theta_o\end{aligned}\right\} \quad (1)$$

$$\left.\begin{aligned}&T_c(t)=C_c(p)\xi(t)\\ &\text{or}\\ &T_c=K\xi\end{aligned}\right\} \quad (2)$$

$$\left.\begin{aligned}&\Theta_o(t)=H_o(p)[T_c(t)+T_o(t)]\\ &\text{or}\\ &\Theta_o=1/p[T_c+T_o]\end{aligned}\right\} \quad (3)$$

Subtracting Θ_i from each side of equation 3 and substituting equation 2 in equation 3,

$$\Theta_i-\Theta_o=\Theta_i-1/p[K\xi+T_o]$$

which from equation 1 gives

$$\xi=\Theta_i-1/p\ K\xi-1/p\ T_o$$

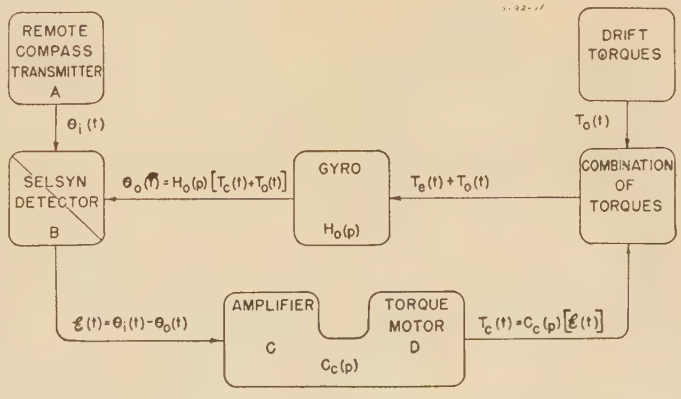

Figure 11. Graphical and symbolic diagram of compass controlled directional gyroscopic servo mechanism

or

$$\left.\begin{aligned}\xi &= \frac{\Theta_i - 1/p\ T_o}{1+1/p\ K} \\ &= \left[\frac{p\Theta_i - T_o}{p+K}\right]\end{aligned}\right\} \quad (4)$$

The use of this den ator as an over-all system operator h en recognized in servomechanism design for years.

Thus $(p+K)^{-1}$ summarizes the system behavior over the range that K is a constant. Since $(p+K)^{-1}$ is the Laplacian transform for ϵ^{-Kt} its characteristic is an overdamped system without oscillation and with a time constant determined by K. From equations 1, 2, and 3

$$\Theta_o(t) = \frac{C_c(p)H_o(p)\Theta_i(t) + H_o(p)T_o(t)}{1+C_c(p)H_c(p)}$$

or

$$\Theta_o = \frac{K\Theta_i + T_o}{p+K}$$

or

$$\frac{d\Theta_o}{dt} = K(\Theta_i - \Theta_o) + T_o$$

For "steady" conditions

$$\frac{d\Theta_o}{dt} = 0$$

and

$$\Theta_i - \Theta_o = \xi = -T_o/K \quad (5)$$

Equation 5 leads to the conclusion that the basic error of the system can be kept small by increasing the gain represented by K and by reducing the undesired torque T_o. Equation 4 which indicates a nonoscillating system with a time constant determined by K also indicates that K may be large without producing undesirable characteristics.

If K is to be large over the range that it is a constant, and if the precession rate is to be limited beyond this range in order to reduce errors that result from the gyroscope following the compass during the period that turn errors are present in the compass, a characteristic curve as shown in Figure 8 results.

With this characteristic, errors caused by normal undesirable torques are negligible and normal turn errors are small. If existing turn errors are objectionable, the compass control can be disconnected during turns.

References

1. Northerly Turning Error of the Magnetic Compass for Aircraft, C. S. Draper, W. H. Cook, W. McKay. *Journal of the Aeronautical Sciences*, July 1938.

2. Electrically Operated Gyroscopic Instruments, H. Konet. AIEE Transactions, volume 63, 1944, October section, pages 735–8.

3. Electrically Driven Gyroscopes for Aircraft, H. M. Witherow, Albert Hansen, Jr. AIEE Transactions, volume 63, 1944, April section, pages 204–8.

4. Electrical Control in Automatic Pilots, C. M. Young, E. E. Lynch, E. R. Boynton. AIEE Transactions, volume 63, 1944, December section, pages 939–43.

5. The Gyrosyn Compass, O. E. Esval. AIEE Transactions, volume 63, 1944, November section, pages 857–60.

6. Automatic Pilot—Past, Present and Future, Robert L. Johnson. *Aeronautical Engineering Review*, September 1946.

7. Magnesyn Remote Indication, Robert S. Childs. AIEE Transactions, volume 63, 1944, September section, pages 679–82.

8. Dynamic Behavior and Design of Servomechanisms, G. S. Brown, A. C. Hall. *Transactions*, American Society of Mechanical Engineers, volume 68, July 1946, pages 503–24.

Some Aspects of Polyphase Motor Design—The Design and Properties of the Magnetic Circuit

T. C. LLOYD
MEMBER AIEE

HOWARD B. STONE
ASSOCIATE AIEE

N a preceding paper,[1] an attempt was made to present a design point of view, indicating that the criterion for a design method is its direct ability to provide the construction data whereby desired machine specifications are met. The idea was illustrated by a procedure for polyphase motor design, stripped of refinements, and employing a magnetic circuit of fixed contour. Such a condition arises through the use of standard laminations in which designs are made. The questions naturally arise as to how these laminations are proportioned and what affect the proportions have on performance. It is with such matters that the present paper is concerned, directed chiefly at motors with semiclosed slots of 50 horsepower or less.

An investigation of the various proportions and dimensions which can be used in the magnetic circuit of an electric motor leads to some interesting relationships. Unfortunately, these readily can become of academic rather than practical interest unless several underlying facts of industrial and commercial importance are kept in mind.

Faced with the requirements of designing a suitable stator and rotor lamination for one definite horsepower and speed rating for a polyphase induction motor, it can be imagined readily that the relation of slot area to tooth area, and rotor diameter to stator diameter (and several other proportions) could be set up in useful ratios so as to obtain minimum copper, or minimum material cost, maximum efficiency, or any one of several other desideratum. This is a process of designing a lamination for a particular rating. In contrast to this is the process of designing a lamination for a given frame. The distinction is important enough to bear further explanation.

It has been pointed out that while a motor manufacturer sells horsepower, in reality he sets up to build frames. In some instances, a special frame or a special design may be made for one application, bearing one rating only, and planned for very large production. In such a case, the design of a "best" lamination for the case at hand may be justified.

Table I

Horsepower	RPM	Horsepower	RPM
General purpose, open type, 60 cycles			
10	3,600	1½	600
7½	1,800	1	514
5	1,200	¾	514
3	900	¾	450
2	720		
Totally enclosed			
3	1,800	2	900
General purpose, open type, 25 cycles			
5	1,500	2	500
3	750	1½	500

In the majority of cases, a lamination is to be provided for a given frame and made as widely useful as possible for all ratings which expect to be sold in that frame size. Suppose, for instance, NEMA* frame 284 is considered. Standardized ratings in Table I indicate the horsepower and speeds which all are expected from this

Paper 46-166, recommended by the AIEE committee on electric machinery for presentation at the AIEE summer convention, Detroit, Mich., June 24–28, 1946. Manuscript submitted April 15, 1946; made available for printing May 28, 1946.

T. C. Lloyd and Howard B. Stone are both engineers with Robbins and Myers, Inc., Springfield, Ohio.

* National Electrical Manufacturers Association.

"container" of more or less fixed dimensions.

From a commercial point of view, all ratings shown should be obtained from exactly the same lamination, stacked to the same axial length. Such a practice would mean that any order for such ratings could be filled from a stock of built-up unwound bodies and fields, modifying only the stator windings and the end ring sections of the squirrel cage. This ideal state cannot be realized but it can be approximated, and the attempt has a great effect upon lamination design and the functions of the designer.

Considering the foregoing facts, an attempt to design a "best" lamination can be of interest only in the exceptional case. If the lamination is to be widely useful, the proportions determined as best for one rating readily may prove undesirable for another. The result is a series of compromises, based on the minimum number of laminations for any given frame, which will yield all of the standardized (and some special) ratings as required, without serious interference with the accepted standards of performance.

Dealing with lamination contours for such purposes, it is reasonable to take a pragmatic viewpoint. Accordingly, we will investigate first the proportions of a series of laminations which, through refinements of practice, have been known to yield useful results.

Method of Fixing Stator Proportions

A total of 108 stator and rotor laminations were used to determine lamination proportions. These varied in rotor diameter from 3 to 15 inches. Their proportions had been determined initially by investigations or as manifestations of the individual tastes of a number of designers over a period of years. As a first step in determining proportions, a series of points were plotted using diameter to the bottom of the stator slots versus rotor diameter. With surprisingly little variation these points fell on a straight line which can be expressed by the equation (see Figure 1)

$$D_1 = 1.175D + 0.647 \tag{1}$$

To determine the outside diameter of the stator, relative flux densities of teeth and stator yoke will be used. Maximum tooth densities and average yoke densities will be determined.

Maximum stator tooth density is

$$B_{max} = \frac{1.57 \times \text{poles} \times \text{flux per pole}}{\text{number of slots} \times t_w \times L} \tag{2}$$

The tooth width (t_w) is assumed to be the narrow straight portion shown in Figure 1.

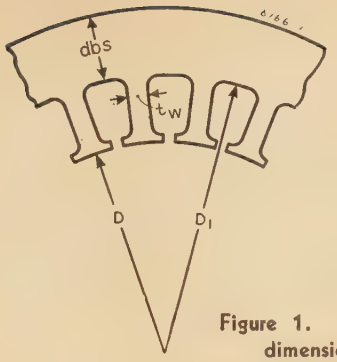

Figure 1. Stator dimensions

Average density in the yoke is

$$B_{ave} = \frac{0.5 \times \text{flux per pole}}{\text{radial yoke length} \times L} \tag{3}$$

The radial yoke length or depth below slot will be abbreviated *dbs*.

As a working basis, it will be assumed that a reasonable magnetic circuit results from proportions giving a maximum stator tooth density of 120 per cent of the average yoke density. This ratio can vary somewhat with few bad effects. It is obvious that if tooth densities were kept constant on say both 4- and 8-pole designs, the yoke densities would reduce to half in the latter case. As will be shown in dealing with compromise laminations, over-all densities may well be adjusted. The effect of other ratios is investigated briefly in the appendix. From the 120-per-cent ratio,

$$\frac{1.57\phi P}{S_1 t_w L} = 1.20\frac{0.5\phi}{L(dbs)} \tag{4}$$

Solving for depth below slot,

$$dbs = 0.382\frac{S_1 t_w}{P} \tag{5}$$

Twice the depth below slot, plus D_1 represents the outside diameter of the stator laminations. It would be convenient to obtain this in terms of rotor diameter, and to do so the following method was employed.

The portion of the stator lamination lying just within the circle swept out by D_1 obviously fulfills the double purpose of supplying both the magnetic and the electric circuits. The division of this ring between slots and teeth affects the performance and results in an iron or a copper design. The effect is illustrated briefly in the appendix, but at this point it is sufficient to point out that a motor requiring low current densities (as a totally enclosed design with a cooling problem) might require a greater portion of this area for copper. Conversely, a design requiring high maximum torque, and intended for intermittent service, can be shown to require an increased tooth width. Our interest, however, is to determine a working value which is useful for general purpose designs, and hence the average for a group of existing laminations were investigated. When ($S_1 \times t_w$) versus rotor diameters were plotted for the 108 laminations, the results spread over a band which gave a clearly defined straight line. The equation is

$$S_1 t_w = 1.35D \tag{6}$$

Substituting in equation 5,

$$dbs = 0.515\frac{D}{P} \tag{7}$$

Then

$$OD = 1.175D + 1.03\frac{D}{P} + 0.647 \tag{8}$$

Solving for D,

$$D = \frac{OD - 0.647}{1.175 + \frac{1.03}{P}} \tag{9}$$

This equation, along with equation 1, is plotted in Figure 2 against rotor diameter. Based entirely upon average relationships observed from a number of laminations used in practice, and a few fundamentals, it fixes the main proportions of a stator lamination. Its validity as a working method will be checked later.

Compromise Dimensions

To illustrate the use of these curves or formulas, assume that laminations were to be provided for a frame which could accommodate a lamination diameter of ten inches. By these rules, Table II can be made.

Table II indicates that for each number of poles a different lamination would be necessary, and hence this practice represents the very requirement which is least desirable commercially. The point is, however, that by an examination of the dimensions, progressing in a logical manner, an intelligent compromise of dimensions can be made. Any such compromise

Table II

Poles	D, In.	D_1, In.	dbs, In.
2	5.53	7.14	1.42
4	6.53	8.32	0.84
6	6.94	8.80	0.595
8	7.16	9.06	0.46
10	7.32	9.25	0.377
12	7.42	9.36	0.317
14	7.49	9.45	0.276
16	7.55	9.52	0.242
18	7.59	9.56	0.217
20	7.62	9.60	0.196

involves a grouping of numbers of poles, and a consideration of mechanical strength of the yoke, in cases of many poles.

A 2-pole lamination usually represents an isolated design, not used for any other speed. This distinction is obvious, as the flux density in the yoke is only half of that obtained for a 4-pole machine, if the two designs are attempted in the same lamination. This change is always proportionately less as the poles increase in number. Table II illustrates this point.

No absolute rules can be laid down as to the grouping to be followed, partially because the relative production in various lines represents an individual problem. Thus compromise dimensions might be set up between the 4- and 6-pole designs, planning all production of a greater number of poles in one lamination. However, it might prove feasible to plan 4-, 6-, and 8-pole production in a compromise lamination, using a different design from 10-pole up. If 36 stator slots are used, fractional slot winding obviously would be required on the 8-pole designs. Grouping the 8-pole requirements with the lamination designed for the greatest number of poles, and using 72 slots, results in comparatively few fractional slot windings from 8 to 20 poles. Three-phase cases are emphasized here.

Granted that the grouping is an individual problem, it is of interest to observe the general effects on performance which would result in using a lamination designed by these rules for 4-pole use, when applied to 6-pole motors and vice-versa. Such results are tabulated in the appendix and are contrasted with other designs made in compromise laminations.

Stator Tooth Shape

Shape of the tooth tip and contour of the slot bottom are necessary for the completion of the stator lamination design. Relative values of d' and e' are important to the performance (see Figure 3). Too small a value of e' may make insertion of the windings difficult or impossible; too large a value increases the tooth flux fringing, the effective gap length, and the surface losses. An increased value of d' shows up chiefly in the increased slot leakage reactance.

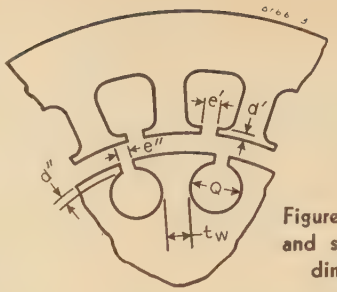

Figure 3. Rotor and stator tooth dimensions

A suggested working basis is to calculate

$$e' = 0.0143D + 0.0643 \quad (10)$$

In designs with an unusually great number of slots for comparatively small diameters, the value of e' given by this formula may prove quite large. Any modification should be made towards reducing this value.

The depth d' should be chosen so that

$$d'/e' = 0.3 \text{ (approximately)} \quad (11)$$

The bottom of the slot can be made semicircular, tangent to the circle swept out by D_1; or it can be made flat, with rounded corners. No recommendations can be made on this choice, aside from the comment that a die maker usually prefers the former practice.

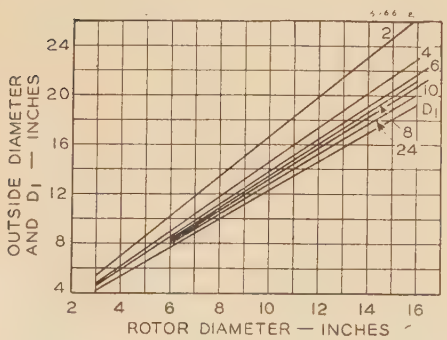

Figure 2. Values of outside diameter and D_1

The former varies with the number of poles when plotted as a function of rotor diameter

Area of Stator Slots

The toroid between D and D_1 represents an area from which total tooth area can be subtracted to give gross slot area. Such a calculation gives the following expression for gross area of all slots:

$$\text{Area (sq in)} = 0.18D^2 + 0.758D + 0.33 \quad (12)$$

Note that this is independent of the number of slots. Actually, because of rounding off corners, the net useful area per slot for laminations designed by these rules is approximately

$$\frac{0.9 \text{ gross area}}{S_1} = \text{actual slot area} \quad (13)$$

Gross area is plotted in Figure 4.

Rotor Lamination Design

Items to be considered in the design of squirrel cage rotor laminations are the number and size of slots, and the dimensions of the slot openings. Common practice makes use of the following two forms of construction:

1. The round slot used with copper bars.
2. The deeper slot used with die cast cages.

The general problem will be considered in more detail for the first case.

It already has been pointed out that the stator slot opening can be obtained through the empirical relationship of equation 10. A useful value for the rotor opening is 70 per cent of e' or

$$e'' = 0.01D + 0.045 \quad (14)$$

Modification usually should occur on the low, rather than the high side.

The slot constant K_s'' expresses the effective linkages per ampere per inch of length for a given slot shape. As a working basis, it will be assumed that this should always be 1.3. Now, since

$$K_s'' = 0.623 + d''/e'' \text{ (for round bars)} \quad (15)$$

it follows that

$$d''/e'' = \frac{d''}{0.01D + 0.045} \text{ or } 0.677$$

Hence

$$d'' = 0.00677D + 0.0304 \quad (16)$$

Both d'' and e'' are now fixed by these equations

The diameter of the slot remains to be determined. A working basis for deciding on slot diameter, and hence tooth width, involves a consideration of flux densities in the teeth. For field laminations the tooth width was fixed thus:

$$t_w = \frac{1.35D}{S_1}$$

In the same manner, if equal flux densities in the stator and rotor teeth are desired,

$$t_w'' = \frac{1.35D}{S_2} \quad (17)$$

where S_2 = the number of rotor teeth or slots.

When round slots are used, the assumption that t_w'' indicates the tooth width at the narrow neck usually permits higher densities in the rotor than in the stator (see Figure 3). A figure of 118 per cent is useful and hence

$$t_w'' = \frac{1.35D}{1.18S_2} \quad (18)$$

For cast rotors in which the tooth is commonly longer, equal flux densities in stator and rotor teeth are more desirable.

The magnetizing ampere turns required for rotor teeth otherwise may become excessive.

While the foregoing relationship enables the designer to determine the tooth width, a more direct calculation for fixing the diameter of the slot (and hence the bars) is very useful. This problem will be instigated further.

Our first concern is with an expression for the slot or bar circle diameter. A distinction must be made concerning diameter D as to whether it is used as the true rotor diameter or the stator bore. If considered as the stator bore, the air gaps immediately enter the calculations. While practices as to suitable gap lengths vary considerably, a reasonable basis is

$$\Delta = 0.0016 \times D + 0.0072 + 0.001L \qquad (19)$$

If modified, this usually would be increased for higher speed motors.

This gives the radial length of air gap in inches, as a function of both diameter and stack length. For our purposes it will be sufficiently accurate to assume a gap resulting from an average stack of three inches, leaving gap length as a function of diameter only.

To determine the slot diameter, we can make use of the following relationship:

$$\text{Diameter across slot centers} = D - 2\Delta - 2d'' - Q \qquad (20)$$

where Q = diameter of slot in inches. (This equation is in error to the extent that d'' is not measured on the diameter D, but is offset by the amount of one-half e''.)

Expanding equation 20, by equations 19 and 16 we obtain

$$\text{Diameter across slot centers} = 0.9833D - 0.0752 - Q$$

From which it follows that the diameter of the slot is

$$\frac{1.95D - 0.236}{S_2 + \pi} = Q \qquad (21)$$

It is of interest to note how the total area of the rotor slots varies as a function of their number. These areas are shown in Figure 5.

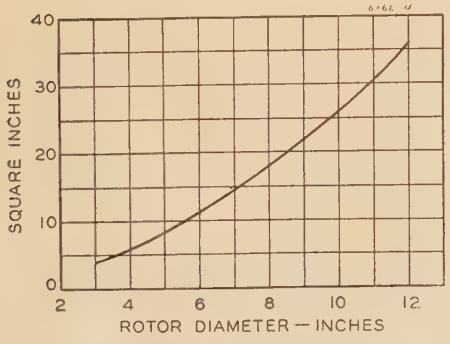

Figure 4. Total area of all stator slots as a function of rotor diameter

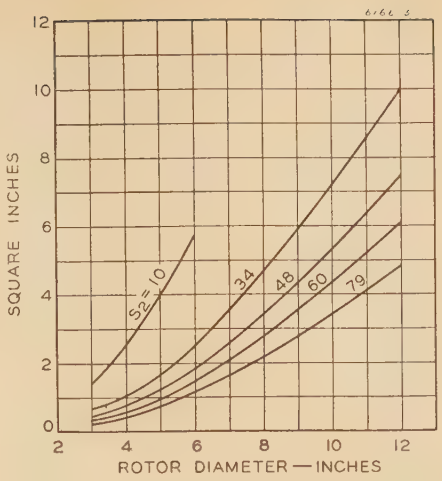

Figure 5. Total area of all rotor slots for various numbers of slots

Recapitulation

The foregoing rules are all that are required to determine the dimensions for stator and rotor laminations, once the outside diameter and the number of poles are known. Yet, it must be kept in mind that perhaps the greatest use of such formulas occurs through the design of general purpose or average laminations which are intended for use for a variety of designs, involving various numbers of poles. The assumption is that if one wishes to design a lamination for 4-, 6-, and 8-pole use the procedure would involve the preliminary design for 4- and 8-pole, and thus make an intelligent compromise between the known limits.

No data on recommended numbers of slots are given here as that involves other factors not relevant to this paper.

Lamination Capacity

It cannot be emphasized too strongly that once a set of laminations has been proportioned the maximum torques available from all motors built with these laminations have been fixed. Aside from the slight variation possible by a change in pitch, or the working of the magnetic circuit at various densities, a given stack of laminations results in a fixed value of maximum torque.

These facts give rise to the interesting possibilities of determining the inherent maximum torque of a given lamination when designed by the method evolved here and when designed according to any or no method.

It is possible to set up expressions for all motor constants in terms of the dimensions resulting from the rules given here. Then, by selecting a flux density for the teeth, the maximum torque for an entire line of laminations can be determined. Such calculations, while not shown here, can be used as the basis for empirical equations for maximum torque as functions of stack length and rotor diameter. By such a method, 4-pole 60-cycle designs of full pitch windings, and with a maximum stator tooth density of 96,000 lines per square inch, display maximum torques of

$$T_m = KL^{1.4}D^{1.87} \qquad (22)$$

where stator and rotor slots are, respectively, 24 and 34, K equals 0.21; 36 and 48, K equals 0.31; and 48 and 60, K equals 0.40.

Similarly, for 2-pole motors designed in these laminations according to the foregoing standards,

$$T_m = KL^{1.59}D^{1.63} \qquad (23)$$

where stator and rotor slots are, respectively, 10 and 12, K equals 0.10; 24 and 34, K equals 0.34.

These constants will vary as the square of the ratios of the densities, for any other values chosen.

It is of interest to compare the result of these empirical expressions with the actual design carried through in some detail in Appendix I. A maximum torque of 52.9 pound-feet was obtained therein. By equation 22

$$T_m = 0.31 \times 3^{1.4} \times 6.875^{1.87} = 53.5 \text{ pound-feet}$$

Maximum Torque of Any Lamination

Calculation of the maximum torque of any polyphase induction motor involves the determination of the stator winding resistance, the leakage reactance, and the leakage factor. Basically, these all are calculated from certain physical dimensions of a lamination stack and the windings which can be provided in the laminations.

Such expanded expressions obviously can be substituted in the maximum torque equation to obtain an equation in terms of dimensions. As this substitution is straightforward, it requires no derivation here. The final equation is

$$T_m = 0.029\left(\frac{1 - P^2K_a}{K_d}\right)\frac{B_k^2L^2}{K_aP} \times \frac{1}{\frac{K_g}{f}\left(\frac{K_h}{P} + L + K_c\right) + K_aL + \frac{K_m}{P^2}} \qquad (24)$$

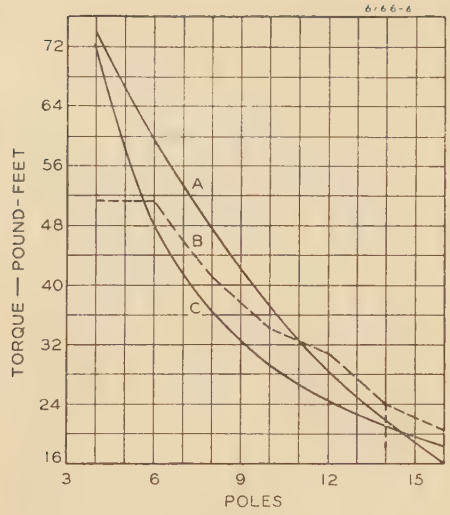

Figure 6

A—Inherent maximum torque of a lamination with constant flux density in the teeth

B—Maximum torque of standardized NEMA ratings (225 per cent ratio)

C—Inherent volt-amperes of a lamination with constant current densities. Scale not shown, as only the relative slopes and positions of the curves are significant

where

$$K_a = 3.60(0.625p + 0.375)\left(\frac{K_s'}{S_1} + \frac{K_s''}{S_2}\right) + \frac{7.5DK_z}{S_1S_2\Delta}(0.8p + 0.2)$$

$$K_z = \left(\frac{t' + t''}{\lambda' + \lambda''} - 0.5\right)^2$$

$$K_c = 0.2D$$

$$K_d = 0.845\frac{DK_w^2}{\Delta K_1}$$

$$K_1 = \frac{\lambda' \times \lambda''}{t' \times t''}$$

$$K_e = \frac{328}{(K_w t_w S_1)^2}$$

$$K_g = \frac{0.153 \times 10^8}{AkS_1}$$

$K_h = 4.4p(D + \text{stator tooth length})$

$K_m = 1.57D(1.25p - 0.25)$

and

P = number of poles

p = pitch as a decimal fraction

B_k = maximum flux density in the stator tooth in kilolines per square inch

f = frequency in cycles per second

$K_s' + K_s''$ = primary and secondary slot constants, respectively

$S_1 + S_2$ = number of primary and secondary slots, respectively

Δ = the radial air gap length in inches

$t' + t''$ = the effective tooth face in inches for primary and secondary, respectively. These are wider than the actual circumferential tooth widths by the effect of fringing

$\lambda' + \lambda''$ = the tooth pitches of primary and secondary, respectively

K_1 = the air gap constant. Greater than unity to allow for fringing effect

t_w' = the effective stator tooth width in inches

A = slot area in circular mils

k = the space factor for the slot (0.25 to 0.30)

Fortunately, these constants are properties of a given lamination and need not be recalculated for various designs. Specifically, they are unaffected by changes in stack length, frequency, flux density, or voltage. If the change in winding factor with the number of poles is neglected in making rough calculations for estimates, the constants are unaffected. To be more exact, K_a, K_d, K_e, K_h, and K_m must be adjusted for each change in pitch and winding factor.

A detailed example of this calculation is given in Appendix IV. However, its significance can be shown by assuming that one were interested in investigating design possibilities of everything from 4- to 16-pole motors in exactly the same lamination and stack. The inherent maximum torque of the lamination used in the appendix is shown plotted in Figure 6. The relation of such torques to the torque ratings required of the motors built in a corresponding NEMA frame also are indicated by these curves. Minimum ratios of maximum torque to full load torque are fixed at 200 per cent by NEMA, but the plotted values are at 225 per cent.

Volt-Ampere Rating of a Lamination

The volt-ampere capacity of a lamination is a fixed quantity only if allowable flux and current densities are chosen. The relationship can be derived as follows:

$$\text{Circular mils per conductor} = \frac{AkS_1}{nC} \quad (25)$$

For a given maximum flux density in the teeth of B_k kilolines,

$$C = \frac{1}{L}\left(\frac{EP \times 70.9 \times 10^3}{B_k f S_1 t_w K_w}\right) \quad (26)$$

All terms have been defined previously.

If the allowable current density in circular mils per ampere is D_c, it follows that

$$\text{Volt-amperes (all phases)} = \frac{AkS_1^2 LB_k t_w f K_w}{D_c P \times 70.9 \times 10^3} \quad (27)$$

The foregoing formula holds for any lamination, but if the given rules are followed, the following simplifications result for laminations designed accordingly. Since

$$t_w = \frac{1.35D}{S_1}$$

$$\text{Volt-amperes} = DL\frac{AkS_1B_k f K_w}{D_c P} \times 1.9 \times 10^{-5} \quad (28)$$

Assuming an average space factor for the slot of 0.28, useful slot area can be expressed by the approximate relationship

$$AkS_1 = 0.28 \times 0.9 \times D^{1.41} \times 1{,}273{,}000$$

Then

$$\text{Volt-amperes} = D^{2.41}L\frac{B_k}{D_c}\text{rpm} \times K_w \times 0.051 \quad (29)$$

Comparing this equation with the empirical expression for maximum torque, it becomes clear that as the diameter of the rotor (or correspondingly, the outside diameter of the laminations) increases,

Table III. Four-Pole Design

Lamination Outside Diameter 10.5 Inches, Slots 36/48, Stack 3 Inches
Full Load Torque: 7 1/2-Horsepower 4-Pole Motor, 22.9 Pound-Feet

	1	2	3
Nominal rotor, D	6.875 in.	7.75 in.	6.5 in.
Depth below slot, dbs	0.885 in.	0.84 in.	1.0 in.
Tool width, t_w	0.257 in.	0.30 in.	0.225 in.
Slot constant, K_s'	1.295 in.	0.857 in.	1.3 in.
Slot area (sq in.)	0.355 in.	0.184 in.	0.400 in.
Wire weight (lbs)	15.6	8.1	17.6
Stator tooth density	96,000	96,000	96,000
Stator yoke density	80,000	98,000	62,000
Stator winding resistance	0.452 in.	0.64 in.	0.525 in.
Rotor slot constant, K_s''	1.3	1.3	1.3
Maximum torque	52.9	57.0	42.6
No-load values			
Amperes	6.3	8.0	5.04
Copper loss	53.6	123.0	40.0
Iron loss	150.8	178.0	128.7

Notes: Column 1—"Average" method.
Column 2—Large D, t_w.
Column 3—Small D, t_w.

the volt-ampere capacity of the laminations increases more rapidly than the maximum torque. The inverse of this has been noted by any designer of small polyphase motor parts, which are generally capable of yielding comparatively high maximum torque values. Attempting to give such parts their corresponding horsepower ratings can be done only at a sacrifice of circular mils per ampere.

The motors used in Appendix IV are calculated for inherent volt-ampere capacity and plotted in Figure 6. An allowance of 425 circular mils per ampere was used for the stator winding.

Appendix I

To illustrate the application of the formulas for the average lamination, assume that a lamination is to be designed for an outside diameter of 10.5 inches. As a working basis, the maximum stator tooth density of 120 per cent of average yoke density will be used.

From equation 7

$D = 6.875$ inches (4 poles)

Selecting 36 stator slots, we obtain the tooth width from equation 5:

$t_w' = 0.257$ inch
$dbs = 0.885$ inch

From equation 10, we obtain the slot opening:

$e' = 0.162$ inch

For $d/e = 0.3$,

$e = 0.049$ inch

"Rounding off" the corners of the slots yields a slot area of 0.355 square inch. This completes the stator lamination design, determined not as a fair lamination for say both 4- and 6-pole designs, but based on 4-pole calculations only.

For the rotor, using 48 slots and a gap of 0.025 inch (which is subtracted from the nominal diameter), the diameter of the rotor slot is 0.255 inch.

For semiopen slots, e'' equals seven-tenths of e', or 0.11 inch; and d'', when the rotor is ground, will be such that the slot constant is 1.3. The tooth width at the narrow portion is now 0.164 inch.

These laminations will be used for a design of a $7\frac{1}{2}$-horsepower motor, using the principles derived in the first paper on this subject.[1] Selecting a maximum to full load torque ratio of 225 per cent, and a suitable stator tooth density as 96,000 lines per square inch, the required stacking will be 3.0 inches.

For a full pitch winding, the complete performance is given in Table III, column 1.

The solution of the foregoing problem represents purely a routine task, of little significance beyond the indication that the lamination design method results in reasonable values. It leaves unanswered the following questions:

1. What would happen had a larger or a smaller rotor diameter been chosen?

2. What would be the effect of upsetting the ratio set up between tooth and slot areas in the stator?

To investigate, assume that a rotor diameter of 7.75 inches were chosen, along with a tooth width of 0.30 inch. The flux densities in stator core and teeth are now practically equal and are kept at 96,000 lines per square inch, as before. The lamination design, in general, is what would follow if 1.2 were changed to 1.0 in equation 4. The completed performance is tabulated in column 2 of Table III and bears out the conclusion that such a procedure results in a "flux motor" with high maximum torque, but overworked copper. Such a lamination design may represent a cooling problem, but might be useful for intermittent duty service with high torque demand.

In the other direction, suppose a lamination had been designed for a rotor diameter of 6.5 inches with a tooth width of 0.225 inch. The attempt to limit the flux density in the stator teeth to 96,000 lines now results in a weak motor, with maximum torque below the 200 per cent ratio if a $7\frac{1}{2}$ horsepower rating is expected. The increased slot area naturally results in less copper loss. Performance items are shown in column 3 of Table III.

Appendix II

Examples given previously were based on the use of a lamination intended primarily for 4-pole operation. Using the same principles, but designing the lamination for 6-pole operation only, results in a rotor diameter of 7.315 inches with a tooth width of 0.274 inch. The resulting performance items are shown in Table IV, column 1. The 6-pole rating in this same stack represents a 5-horsepower motor. It will be noted that this motor is somewhat weaker in torque ratios than the one designed in Appendix I. A slight increase in densities brings about an equivalent value of maximum torque, with performance as shown in column 3.

While the data are not shown, a modification of this "average" lamination to yield equal densities in stator yoke and teeth, or to increase the tooth densities beyond the 120 per cent ratio setup, results in exactly the same trends already indicated in Appendix I.

In attempting to judge the validity of these lamination designs, one of the most effective means is to determine the effect of not following the rules. Thus, while average laminations have been designed for 4- and 6-pole use, it would be of interest to show how satisfactory a 6-pole design could be made in the lamination intended for 4-pole service.

The lamination of Table III, column 1 yields a 6-pole design as shown in Table IV, column 2. A flux density of 96,000 lines in the stator teeth again was chosen as a basis for calculation. As compared to the "average" lamination for 6-pole use, a sharp reduction in maximum torque results, along with an increase in copper loss.

This comparison bears out the fact that as an increased number of poles is used with a given lamination, the available torque always is reduced so long as tooth densities are maintained constant. This effect is exaggerated here, because the laminations had been deliberately designed for 4- or 6-pole duty respectively. In practice, the contrast would not have been so marked if the lamination dimensions had been compromised between 4- and 6-pole requirements, or if constant tooth densities were not maintained. Since an increase in the number of poles always results in reduced stator yoke densities (on a given lamination), an increase in tooth density then is not unreasonable. This may result in no great increase in core loss nor magnetizing current, and this practice does reduce the slope of the maximum torque versus number of poles curve for a given lamination.

Appendix III

It has been indicated in Appendix I that a 4-pole lamination for the outside diameter required should have a rotor diameter of 6.875 inches, and that the resulting performance was reasonable. Similarly in

Table IV. Six-Pole Design

Laminations Outside Diameter 10.5 Inches, Slots 36/48, Stack 3 Inches
Full Load Torque: 5-Horsepower 6-Pole Motor, 22.9 Pound-Feet

	1	2	3
Nominal rotor, D	7.315 in.	6.875 in.	7.315 in.
Depth below slot, dbs	0.628 in.	0.885 in.	0.628 in.
Tooth width, t_w	0.274 in.	0.257 in.	0.274 in.
Slot constant, K_s'	1.28	1.295	1.28
Slot area (sq in.)	0.386	0.355	0.386
Wire weight (lbs)	14.3	12.6	14.3
Stator tooth density	96,000	96,000	98,000
Stator yoke density	80,000	53,300	81,700
Stator winding resistance	0.659	0.814	0.630
Rotor slot constant	1.3	1.3	1.3
Maximum torque	50.2	42.9	52.6
No load values:			
Amperes	6.42	5.83	6.68
Copper loss	72.0	85.2	84.0
Iron loss	130.0	111.8	134.0

Column 1—"Average" method for 6-pole lamination.
Column 2—"Average" 4-pole lamination with 6-pole design.
Column 3—6-pole lamination with redesign of windings for higher value of maximum torque.

Table V. Four- and 6-Pole Designs

Laminations Outside Diameter 10.5 Inches, Slots 36/48, Stack 3 Inches

	4-Pole		6-Pole	
	1	2	3	4
Full load torque	22.9 lb-ft	—	22.9 lb-ft	
Inside stator bore	7.00 in.	—	7.00 in.	
Depth below slot, *dbs*	0.826 in.	—	0.826 in.	
Tooth width	0.265 in.	—	0.265 in.	
Slot constant, K_s'	1.31	—	1.31	
Slot area	0.34	—	0.34	
Wire weight (lbs)	15.1	15.1	12.2	12.2
Stator tooth density	96,000	97,500	96,000	104,000
Stator yoke density	88,000	89,500	59,000	64,000
Stator winding resistance	0.374	0.385	0.708	0.602
Rotor slot constant, K_s''	1.3	1.3	1.3	1.3
Maximum torque	51.2	53.0	43.8	51.0
No load values:				
Amperes	6.6	6.8	6.1	7.3
Copper loss	51.0	55.0	83.0	101.0
Iron loss	155.0	161.0	116.0	129.0

Appendix II, a 6-pole lamination has been shown with a nominal diameter of 7.315 inches. Performance was acceptable, but when the 4-pole lamination was used on a 6-pole design, results were less satisfactory.

To illustrate that these rules are of aid in achieving a compromise design, let us assume that one lamination were to be used for both, and that its dimensions are selected as being between the two extremes.

Between nominal diameters of 6.875 and 7.315 inches, we will select 7 inches for the stator bore.

Between stator tooth widths of 0.257 and 0.274 inch, select 0.265 inch which follows from equation 6.

By equation 1, $D_1 = 8.847$ inches and $dbs = 0.826$ inch.

The 4- and 6-pole designs made in this compromise lamination are tabulated in Table V. The significance of the statement that compromise laminations require adjustments in flux densities is apparent at once in examining columns 1 and 3 of this table. While the 4-pole motor suffers slightly in maximum torque, the 6-pole design is below the 200 per cent minimum, if the 96,000 density is used. Columns 2 and 4 show the results of adjusting the designs for the values of maximum torque obtained previously. The resulting performances do not compare too unfavorably with those obtained from the laminations made for individual designs.

Appendix IV

To illustrate the application of the inherent maximum torque of a lamination, we will consider a sample lamination designed without reference to the rules shown here, and displaying the following properties:

Outside diameter = 11.75 inches
Inside diameter = 7.50 inches
Slots = 48
Useful slot area = 123,000 cubic centimeters
Slot constant = 1.94
Tooth width = 0.23 inch
Tooth length = 1.125 inches
Rotor outside diameter = 7.445 inches
Air gap = 0.0275 inch
Slots = 60
Slot constant = 1.3
Gap constant = 1.27
B_k (assumed) = 85
Stack length, $L = 3.00$ inches

Assume that this set of laminations was used for designs from 4 to 16 poles inclusive, using a fractional slot winding in the necessary cases. The initial calculations will be made with a pitch of 0.75 and a winding factor of 0.88 used as constant throughout.

Then

$K_a = 0.271$
$K_c = 1.50$
$K_g = 2.60$
$K_m = 8.10$
$K_d = 141.0$
$K_e = 3.45$
$K_h = 28.5$

By equation 24,

T_m (4-pole design) = 73.8 pound-feet

Other values are plotted in Figure 6.

It is obvious that with the increase in the number of poles, the winding factor cannot remain constant, and the appropriate terms must be changed. The nature of the error resulting can be illustrated by comparing the results on the 16-pole design in which the winding factor is assumed first to be 0.88 and finally to be unity. In the latter case,

$K_a = 0.3198$
$K_c = 1.50$ (unchanged)
$K_d = 180.0$
$K_e = 2.72$
$K_g = 2.60$ (unchanged)
$K_h = 38.0$
$K_m = 11.8$

T_m (16 poles) = 18.2 pound-feet versus 16 by uncorrected winding factor

The use of the same lamination for all of these poles hardly would be practicable because of the fractional slot windings which might result, and the poor slot combinations and unfavorable harmonic conditions on some designs. The curve of inherent maximum torque is chiefly useful to observe the trend. It must be kept in mind, also, that all designs were made for the same tooth density, and that with an increase in numbers of poles the yoke densities decrease. As previously mentioned it is sometimes practicable, and reasonable, to increase the densities slightly with pole increase. This would result in raising the lower portion of the curve.

As this set of laminations was intended for frame 284 it is of interest to compare the maximum torque expected of standardized ratings (4 to 16 poles) in this NEMA frame, with that inherent with this lamination. While standardization requires a maximum torque of only 200 per cent of full load torque, this curve is plotted with a reserve, using 225 per cent ratio. These are the points connected by dotted lines in Figure 6. Between this reserve, and the flattening effect of the inherent torque curve brought about by flux density adjustment with pole change, inherent maximum torques can be kept safely above the values expected of the standardized ratings. Similar investigations on other diameters of laminations indicates the theoretical soundness of the ratings called for in standardized frames. However, the inherent torque reserve of some horsepower ratings over others is very marked in a few cases.

Reference

1. Some Aspects of Electric-Motor Design—Polyphase-Induction-Motor Design to Meet Fixed Specifications, T. C. Lloyd AIEE Transactions, volume 63, 1944, January section, pages 14–20.

Effects of Thermal Characteristics of Aircraft Generators on Load Analysis

STANLEY ROGERS
ASSOCIATE AIEE

Synopsis: The elaborate electric systems in modern long-range aircraft have made accuracy of load analysis more important than ever before. A more precise evaluation of the adequacy of proposed generating equipment can be made by averaging expected loads over several different periods which are chosen on the basis of the generators' thermal characteristics. These averages are compared graphically with curves which show the maximum overloads generators can tolerate without damage.

AS AIRCRAFT have increased in size and complexity, so have their electric systems. The problem of establishing a precise relationship between system size and the anticipated electric loads has become more and more important.

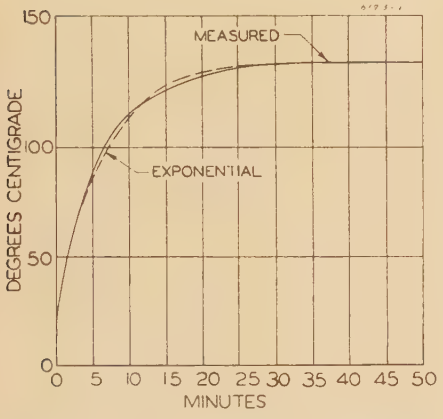

Figure 1. Simple exponential curve (broken line) compared with measured generator-winding heating curve (solid line)

Inadequate capacity may result in failure of the electric system with the consequent possible loss of the airplane, its crew, and its passengers. Too large a capacity, however, decreases pay load. Not only is extra fuel required to haul the useless weight, but additional fuel is needed to transport the fuel consumed in hauling this dead weight.

For airplanes with small electric systems, it may be sufficient to add up the power requirements of the various units of electric equipment and choose a generator which is estimated to be adequate. For somewhat larger systems, average power over various periods of time has been used as the basis for selecting generators. Later it was recognized by the more progressive manufacturers of large aircraft that peak loads and short time average loads are also important.

The most recent contributions to the making of an adequate load analysis include the following:

1. Loads should be averaged over not one or two, but several periods of time or "load intervals."
2. These periods of time depend on the overload thermal characteristics of the generator.
3. There is a maximum period of time over which loads may be averaged reasonably. The length of this maximum period depends on the generator.
4. A direct comparison between the maximum anticipated demand for electric power and the capacity of the generating system to meet that demand is essential to an adequate load analysis.

It is the purpose of this paper to explain why these propositions are true and to show how they are applied practically in determining the adequacy of an aircraft electric power system. The first step will be a consideration of the manner in which generator temperatures vary.

Temperature and Overloads

A typical aircraft generator is heated principally by the flow of electric current through its windings and is cooled by a blast of air under low pressure. The transfer of heat from the windings to the air follows the laws of thermodynamics, that is, the rise and fall of temperature occur exponentially. In most practical cases, the exact exponential function is complicated, but a simple function may be used as a first approximation. In Figure 1 a measured generator-winding heating curve (solid line) is compared with such a simple exponential curve (broken line). The close similarity between the two curves is apparent. In the analysis which follows it is assumed that the simple function is sufficiently accurate for practical purposes.

Experience has shown that a generator can stand a heavy overload for a short time without raising the temperature above a safe value. The less severe an overload is, the longer it can be tolerated without unwarranted damage. The length of time various overloads can be tolerated under a given set of operating conditions can be plotted. Figure 2 shows a typical curve. The curve is called a "permissible overload curve." The magnitude of overload (in terms of rated continuous-duty load) is plotted against the time for which the overload can be sustained without damage to the generator.

The permissible overload curve should be based on tests conducted by the manufacturer and should represent the guaranteed performance of the generator when

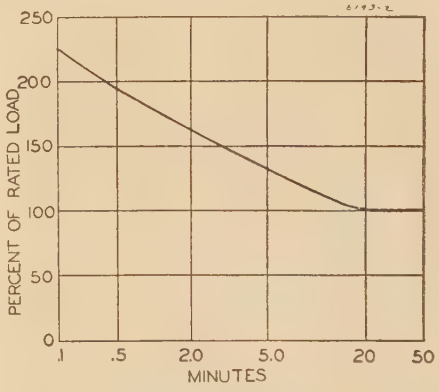

Figure 2. Typical permissible overload curve

subjected to overload. The curve rests on a specified set of conditions (generator speed, air pressure, air temperature, humidity, and so forth) and on assumed loading prior to the application of the overload. A family of such curves, representing performance under different conditions, would be even better. A conservative assumption is that thermal equilibrium under full-rated continuous-duty load has been attained before the overload is applied. Different conditions could be assumed, and curves based on them may be determined by test.

Unfortunately, manufacturers generally do not supply permissible overload curves of the type here suggested. It therefore has been necessary to develop a method for estimating them as accu-

Paper 46-193, recommended by the AIEE committee on air transportation for presentation at the AIEE Pacific Coast meeting, Seattle, Wash., August 27–30, 1946. Manuscript submitted June 24, 1946; made available for printing July 18, 1946.

STANLEY ROGERS is a research engineer and head of the analytical section of the radio and electrical laboratories, Consolidated Vultee Aircraft Corporation, San Diego, Calif.

The approach utilized in the mathematical derivations in the appendix was suggested by Doctor George L. Shue, and the form and organization of the mathematical treatment is largely the work of B. D. Abramis, both of Consolidated Vultee Aircraft Corporation, San Diego, Calif.

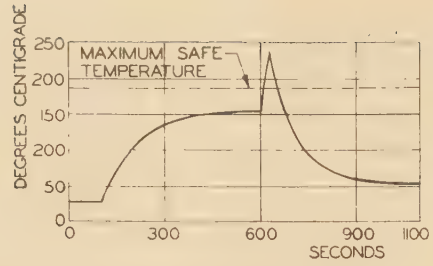

A. Armature temperature curve

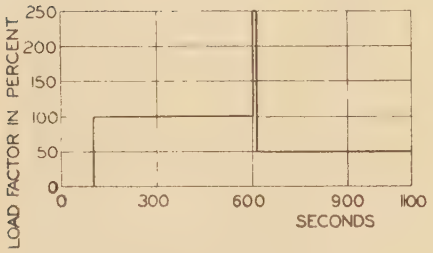

B. Corresponding load profile

Figure 3

The overload lasts five seconds. Load factor is the ratio of actual load to rated continuous-duty load

rately as possible. How this was done is set forth in detail in the appendix. Attention now is directed to the first of the four propositions which have been stated.

Why Loads Should Be Averaged Over Several Load Intervals

A number of load intervals are generally essential to a satisfactory analysis of loads on the generating system of a large airplane because averages taken over periods which differ substantially from the length of a damaging overload may give no indication of danger. This will be shown by means of two examples.

Figure 3A illustrates the variation of armature temperature with load. A cool generator is heated under rated load (as shown in Figure 3B) to full normal operating temperature. Thereupon a heavy overload is applied for five seconds, after which the load is reduced to one-half of full rated value. The attending rise and fall of temperature are shown in Figure 3A. It will be seen that during the overload the temperature quickly passes the maximum safe value and that about 25 seconds elapse before it decreases to a safe value. It will be noted that the graphs employ load factor as a parameter. It is the ratio of armature overload current (or power) to rated continuous-duty current (or power).

In Figure 4 the average load over intervals of 5, 15, 60, 180, and 600 seconds is plotted, the average always being taken so as to have the greatest possible value. The permissible overload curve is plotted to the same scale on this graph. The only average which exceeds the permissible overload curve is that for the 5-second interval. All the other averages lie on or below the curve and so do not indicate damage to the generator.

In Figures 5A, 5B, and 6, another case is illustrated in which a moderate overload is applied for 60 seconds. The armature reaches higher temperatures than in the first case and remains above the maximum safe value for more than a minute. This load is averaged over the same intervals of time as were used previously, and the averages again are compared with the permissible overload curve. Note that all the averages, except that for 60 seconds, lie below the permissible overload curve and give no warning of danger.

While the two cases chosen for purposes of illustration are not likely to be encountered in practice, experience has shown that when five well-chosen load intervals are used, excessive overloads may appear in only one or two of them, while the averages for the other load intervals appear to be safe.

From the foregoing considerations, it is evident that one or two periods of integration, regardless of their lengths, easily may fail to reveal the presence of damaging overloads. To discover with certainty every excessive overload, it would be necessary to use as many load intervals as there are different lengths of intermittent loads on the generating system; this would involve an impractical amount of work. Experience indicates that if the worst possible distribution of the intermittent loads is assumed, the use of four or five load intervals is usually adequate.

Load Intervals Chosen on the Basis of Permissible Overload Curve

If, several periods of integration must be used in order to make a load analysis which will reveal a dangerous overload, regardless of its duration, how long should each of the periods be? This question can be answered best by an example.

Figure 7 illustrates an overload characteristic curve for a large (40-kva) aircraft generator. Five periods over which loads may be averaged are indicated. These were chosen by the following criteria:

1. The shortest load interval should be somewhat longer than the shortest intermittent load worth considering and is usually of the order of five seconds. (Manufacturers sometimes supply overload ratings for such short times. It would be very helpful if a 5-second rating were furnished for all aircraft generators.)

2. The longest load interval should be equal to the shortest time for which the continuous-duty load ratings apply. Occasionally a manufacturer will supply this information. If he is unable to do so, the time may be estimated as being equal to three or four times the period of one cooling time constant.*

3. One of the intermediate load intervals should approximate the manufacturer's specified overload rating time (usually between one and five minutes).

4. The remaining intermediate load intervals should be so chosen as to make the differences between permissible overloads for successive intervals roughly equal.

5. The interval lengths chosen according to the foregoing rules should be modified enough to make the calculations easy.

It will be noted that the intervals indicated in Figure 7 are simply related to each other and that the overloads which correspond to them approximate an arithmetic progression as shown in Table I.

For one type of 6-kw aircraft generator, load intervals of 0.1, 0.5, 2.0, and 10 minutes are satisfactory. It is obvious that these load intervals would be unsatisfactory for use in analyzing loads on a 40-kva generator because of the marked difference in their thermal characteristics.

It follows, then, that before an adequate load analysis can be begun, the type of generator to be used first must be selected. Its thermal characteristics then are determined, and the load intervals are chosen. Loads may be averaged over each of these intervals, and the averages compared with the permissible overload (as indicated by the overload curve for the particular generator chosen). If the generators are not selected before the load intervals are chosen, a sufficient

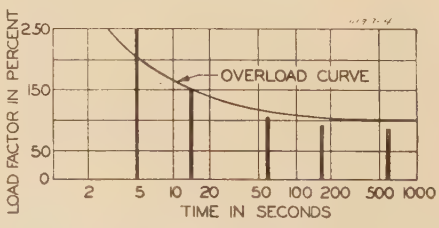

Figure 4. Values of load of Figure 3B averaged over periods of 5, 15, 60, 180, and 600 seconds

*This time constant may be determined experimentally as follows: The generator is heated under standard conditions until it reaches thermal equilibrium under full rated continuous-duty load. With the machine rotating and the standard conditions maintained, the load is removed, and armature temperature is plotted against time as the machine cools. The cooling time constant is approximately the time required for the armature temperature to drop through the first 63.2 per cent of the difference between cooling air temperature and the armature's full load operating temperature.

number of different intervals must be analyzed to insure adequate coverage of the overload characteristics of all types of generators which might be used.

Maximum Time of Averaging Loads

Periods of one or two hours have been used in taking averages of loads on small generators. Some aircraft electrical engineers have been inclined to base all load intervals on the probable duration of each flight condition or aircraft operating condition (such as take-off, climb, cruise, land, and taxi) without regard to the thermal characteristics of the generators.

The duration of take-off, for example, is short and, for the analysis of loads during take-off, does justify limiting the longest load interval to a relatively short time. But it does not follow therefore

Table I. Load Intervals and Corresponding Loads for 40-Kva Aircraft Generator

Load Interval Length, Min	Permissible Percentage of Full-Rated Continuous-Duty Load	Difference in Percentages
0.1	222	
0.5	190	32
3	158	32
15	125	33
60	100	25

that, because an airplane may cruise for hours, the longest load interval for use in analyzing cruising loads should be one or more hours. On the contrary, the maximum length of a useful load interval is dependent, as will be shown, on the thermal characteristics of the generating equipment.

As the generator's heat is transferred to the cooling air, its temperature drops unless new heat is added to offset the losses to the air. The transfer to the air of the heat present in the generator at any particular moment takes place exponentially. The amount of heat available for transfer is limited by the temperature difference between the generator and the air. In the simplest case, 63.2 per cent of this heat will be transferred to the air after one time constant, 86.5 per cent after two time constants, 95.0 per cent after three time constants, and 98.2 per cent after four time constants.** Thus the cooling of the generator causes it to "forget" how hot it was at an earlier time.

Whenever the load on the generator changes, the temperature rises or falls exponentially. If the new load is maintained for three or four times constants, generator temperature will reach a value substantially independent of its previous magnitude.

The fact that the generator "forgets" how hot or cold it was is illustrated in Figure 8, in which four different load and temperature conditions are graphed. In each case the abnormal load ends at the point marked zero time constants. The restoration of normal operating temperatures proceeds exponentially. After three time constants the four curves are very close together, and after five time constants they merge. These curves show that

1. Temperature at any particular time is not affected materially by the temperature at any time more than three or four time constants earlier.

2. The temperature at a particular instant depends on those loads and only those loads which occurred during the immediately preceding three or four time constants.

3. Averaging loads over a period greater than three or four time constants may result in hiding a damaging overload by averaging it with an underload so far removed in time that it could have no effect on temperatures reached during the overload.

Choice of RMS or Average Values of Loads

A comparatively recent development in electric load analysis is the proposed use of rms values of load in place of average values. This proposal is based on excellent theoretical foundations. Since the load on aircraft generators is variable, its mean heating value is proportional to the average of the current squared. The suuare root of this value is a truer index of generator heating than is the average current. It has been found, however, that there is no significant difference between rms and average values in most practical cases. Since the rms values are much harder to calculate than average values, they rarely are justified in practice.

Direct Comparison of Anticipated Loads and System Capacity

The permissibe overload curve indicates the magnitude of overload which, under specified conditions, may be applied for a given time without damaging the generator. A direct comparison of the

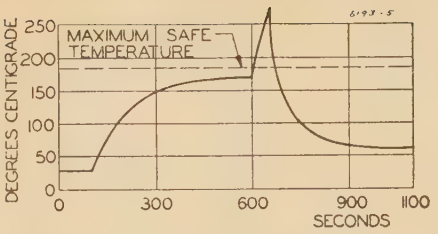

A. Armature temperature curve

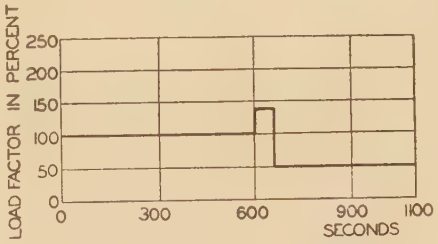

B. Corresponding load profile

Figure 5

Overload lasts 60 seconds

curve with the greatest anticipated average (or rms) loads for each load interval is obtained by plotting the calculated averages to scale on the graph of the permissible overload curve.

Such a graphical comparison is illustrated in Figure 9. The average loads appear as vertical bars. The height of each bar is proportional to the average value of the load it represents. The location of the bar on the time axis of the graph indicates the length of the period over which the average was taken. One graph is made for each flight condition (take-off, cruise, and so forth) that is analyzed.

A glance at the graph indicates whether there are any dangerous overloads, and, if there are none, what margin of safety the chosen generator provides. By examining a set of graphs for the most important flight conditions, those conditions which merit special study may be chosen. These graphs convey a great deal of information in simple easily-understood form.

Load Analysis Procedure

After the type of generator to be used has been selected tentatively, a curve representing its thermal characteristics on overload is obtained or calculated. Such a curve is shown in Figure 9. This curve is based on the assumption that the generator is heated fully under full load before the overload is applied. The curve shows the time for which any given steady overload then may be applied without causing excessive damage to the insula-

**In the expression $(1-e^{-t/B})$, where t represents time, B is the time constant. This expression states the portion of the transferrable heat which has been conveyed to the air in time t.

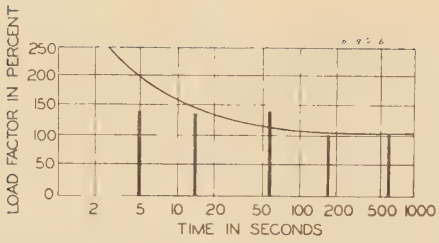

Figure 6. Values of load of Figure 5B averaged over periods of 5, 15, 60, 180, and 600 seconds

tion. The foregoing assumption is conservative since the chances are that, before and after an overload, the load on the generator is less than full rated capacity.

From the permissible overload curve four or five periods of integration or load intervals are chosen. These vary from a few seconds to 15 minutes or longer. They are selected in order to cover the range of permissible overloads in fairly even steps such as 100, 75, 50, and 25 per cent overload and no overload (full rated continuous-duty load). For convenience the lengths of the load intervals are made simple multiples or factors of each other.

The flight conditions or airplane operating conditions which are to be analyzed then are chosen. The most important ones are those in which the most severe electrical loads occur. These generally include take-off, cruise maximum, heavy combat, land, and ground operation.

Loads are tabulated and averaged for each flight condition and each load interval. The averages are plotted to scale as vertical bars on graphs of the overload characteristic of the generator. The resulting load analysis graph is illustrated in Figure 9. This graph not only summarizes the most important data, which conventionally are presented in tabular form on the load analysis chart, but also shows the relationship between calculated loads and available generator capacity.

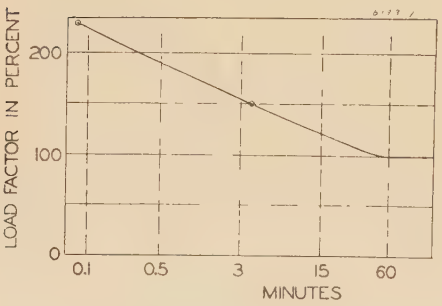

Figure 7. Permissible overload curve for 40-kva aircraft generator (calculated by method described in the appendix)

Five load intervals suitable for analyzing loads on this generator are indicated

While the propositions and method explained were applied to the analysis of loads on aircraft generators, the same principles may be used in analyzing many other types of electrical loads.

Appendix. Estimating the Permissible Overload Curve

Because manufacturers at present generally do not supply curves showing the time for which various overloads may be applied safely to the generator under specified conditions, a mathematical analysis of the thermal behavior of overloaded aircraft generators was undertaken.

The following simplifying assumptions have been made:

1. Heating and cooling occur as simple functions.
2. The armature heats and cools uniformly, and temperature gradients usually may be disregarded.
3. The highest temperatures occur in the armature winding.

An exact evaluation of the effect of field heating on armature temperature and of radiation and metallic conduction losses is not attempted.

The analysis made in this paper is necessarily approximate. The goal toward which it is directed is the expression of the time for which a given overload may be tolerated in terms of the load factor L (the ratio of actual load to rated continuous load) and a set of constants which can be evaluated. The analysis is divided into five operations.

1. Solution of the differential equation for rate of temperature change.
2. Expression of the temperature T in terms of the load factor L and time t.
3. Obtaining the expression for the permissible duration of a given overload.
4. Evaluating the ratio of the effective thermal capacity C to the coefficient of cooling K and incorporating the result into the final equation for permissible overload duration.
5. Drawing the permissible overload curve.

All temperatures are expressed in degrees absolute. The symbols and units used in the course of the analysis are explained as they occur.

Analysis of the thermal behavior of the armature winding is approached best by considering the rate of change of temperature. The truth of the following statement is evident:

$$\text{Rate of change of temperature} = \frac{\text{rate of heating} - \text{rate of cooling}}{\text{effective thermal capacity}}$$

Stated in mathematical terms, this becomes

$$\frac{dT}{dt} = \frac{HT - K(T - T_a)}{C} \qquad (1)$$

where

T = Kelvin temperature of the armature winding
t = time in seconds
H = rate of heating per degree absolute and equals I^2R'/T' watts per degree Kelvin
I = armature current in amperes
R' = armature resistance in ohms at reference temperature T'
K = coefficient of cooling (watts per degree Kelvin)
T_a = Kelvin temperature of the cooling air
C = effective thermal capacity (joules per degree Kelvin)

This equation is based on the following reasoning:

1. For permissible generator temperatures the resistance R of copper varies roughly as its absolute temperature, $R = R'(T/T')$. Hence the rate of liberation of heat is proportional not only to the current squared, but also to the absolute temperature of the copper, $I^2R = (I^2R'/T')T$. The rate of heating is, therefore, HT.
2. The rate of cooling follows Newton's law of cooling and is proportional to the difference in temperature between the winding and the cooling air. It is represented by the expression $K(T - T_a)$ in which K is the factor of proportionality. This factor is presumed to be constant for a given installation under a given set of cooling conditions and is independent of H.
3. The rate of change of temperature varies inversely as the effective thermal capacity C.

Inasmuch as it is difficult to evaluate the constant K in practical cases, a solution in terms of temperature and load is desirable. The analysis will proceed as follows:

1. The differential equation 1 is solved (equations 2 and 3).
2. In the following steps (through equation 11), the ratio H/K is expressed in terms of the load and known temperature constants.
3. After expressing the temperature equation in a simplified parametric form (equation 13), the equation is solved for time t' (equation 14). The new equation contains a factor C/K which remains to be evaluated. This is accomplished by substituting two known boundary conditions in the overload time expression and solving the resultant equations simultaneously.

Operation I—Solution of the Differential Equation

$$\frac{dT}{HT - KT + KT_a} = \frac{dt}{C} \qquad (2)$$

The solution of this equation is

$$T = \left(T_o + \frac{KT_a}{H - K}\right)\epsilon^{(H-K)t/C} - \frac{KT_a}{H - K} \qquad (3)$$

where T_o is the initial temperature.

Note, that when $H = K$, equation 2 becomes

$$\frac{dT}{KT_a} = \frac{dt}{C} \qquad (2a)$$

the solution of which is

$$t = \frac{C}{K} \times \frac{T - T_o}{T_a} \qquad (3a)$$

Operation II—Expression of T in Terms of L and t

In the following steps equations 3 is expressed in terms of the ratio H/K. This ratio then is stated in terms of the load factor L and of S, a function of known temperature constants. The variable H thus is eliminated.

Letting $P = H/K$, equation 3 becomes

$$T = \left(T_o + \frac{T_a}{P - 1}\right)\epsilon^{K(P-1)t/C} - \frac{T_a}{P - 1} \qquad (4)$$

When P is less than unity, that is, when H is less than K, the exponential term vanishes as t approaches infinity. This is clearly the case when the generator is carrying its full rated load. Letting the subscript n denote value at full rated continuous-duty load, the final steady state temperature is T_n

where

$$T_n = T_a/(1-S) \tag{5}$$

and

$$S = P_n = H_n/K = (T_n - T_a)/T_n \tag{6}$$

For overload conditions it may be assumed that H, the power consumed per degree absolute in heating the armature winding, is proportional to the square of the armature current. Letting L equal the ratio of load current to rated continuous-duty load current,

$$H = QL^2 \tag{7}$$

where Q is the factor of proportionality.

At full rated load, L equals 1, and H has its "normal" value of H_n. Therefore

$$Q = H_n \tag{8}$$

and

$$H = H_n L^2 \tag{9}$$

Substituting equation 6 in equation 9 and dividing each side by K,

$$H/K = H_n L^2/K = SL^2 = P \tag{10}$$

Substituting equation 10 in equation 4,

$$T = \left(T_0 + \frac{T_a}{SL^2-1}\right)\epsilon^{(K/C)(SL^2-1)t} - \frac{T_a}{SL^2-1} \tag{11}$$

Let T_s be the asymptote of this equation. Its value is that of the constant term of equation 11.

$$T_s = \frac{T_a}{1-SL^2} \tag{12}$$

Using the parameter T_s, equation 11 becomes

$$T = T_s - (T_s - T_0)\epsilon^{-(K/C)(T_a/T_s)t} \tag{13}$$

Note, that for the special case in which $H = K$,

$$T = T_0 + T_a(K/C)t \tag{13a}$$

Operation III—Solution for the Permissible Duration of an Overload

Solving equation 13 for time t when T equals T_p, the peak permissible winding temperature, and T_0 equals T_n, the normal full rated continuous load (assuming that the generator is fully heated under rated continuous load before the overload is applied),

$$t' = \frac{C/K}{T_a/T_s} \ln \frac{T_s - T_n}{T_s - T_p} \tag{14}$$

For the case in which $H = K$,

$$t' = (C/K)(T_p - T_n)/T_a \tag{14a}$$

where t' is the permissible overload duration, that is, the time the given overload will require to raise armature temperature from its normal value T_n to the peak permissible value T_p, and T_s is the variable (see equation 12).

When t' is plotted against the load factor L, it is seen that the curve is asymptotic to the line

$$L = \sqrt{(T_n/T_p)(T_p - T_a)/(T_n - T_a)}$$

Therefore equation 14 is useful only for load factors greater than this value. In practice typical usable values of L usually range from 1.5 to 2.5.

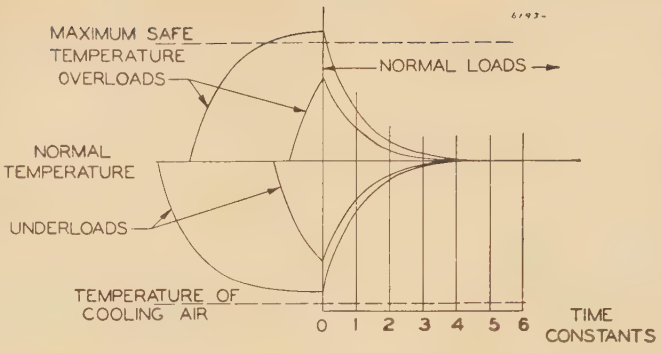

Figure 8. Temperature versus time curves showing that, regardless of deviations caused by underloads and overloads, temperatures return to normal a few time constants after normal load is restored (at time equals zero time constants)

Operation IV—Evaluation of C/K and Statement of Final Solution

Attention now is directed to the quantity C/K. In the foregoing equations the thermal capacity C was assumed to be a constant. Actually, the effective thermal capacity is a function of both t and L. Taking into account the variation of C with time would have resulted in a more complicated differential equation and solution. Because of the uncertainty as to the nature of that variation, equations including this variation (some of which were set up and solved) were found to be of little value. However, treating C as a function of the load factor L only, does not affect the preceding analysis. The results obtained on this basis are in better agreement with experimental evidence than is an oversimplified solution in which the thermal capacity C is regarded as a constant.

The maximum value of C cannot exceed the thermal capacity of the material heated by the generator. There also must be a minimum value of C which holds only for a very brief period immediately following the application of a large overload. In so short a period there is no time for heat to be transferred from the copper of the armature winding to surrounding material. Because of variations in the resistance of different parts of the armature winding (a result of temperature differences for example) the effective minimum value of C may be far below the thermal capacity of the entire armature winding. The rate of heating at the hot spots is accelerated by the local increase in resistance caused by the increase in temperature.

Several assumptions as to the nature of the variation of C/K (K being a constant) were tried. The resultant permissible overload curves were plotted for a 40-kva aircraft generator for which two overload ratings were specified, one for five seconds and the other for five minutes. The following assumptions were evaluated from an examination of the curves:

1. C/K = constant.
2. $C/K = ML$.
3. $C/K = M/L + N$.
4. $C/K = M/(L + NL^2)$.
5. $\log C/K = N(M - L)$.

M and N represent constants, and L is the load factor. Only the last of these assumptions was found to be workable. Each of the other four either produced negative values of C/K for some range of values of L or failed to permit the permissible overload curve to pass through both specified rating points.

Letting t_q and t_r denote the durations of the two specified overloads and letting L_q and L_r respectively represent their load factors, by simultaneous equations we find

$$M = \frac{aL_r - bL_q}{a-b} \tag{15}$$

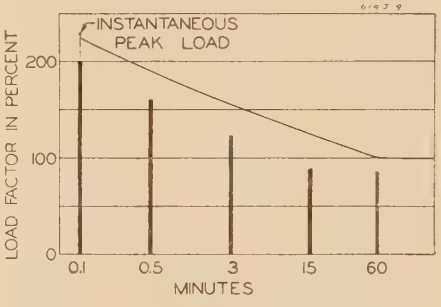

Figure 9. Typical load analysis graph

Bars represent average (or rms) values of load taken over periods of 0.1, 0.5, 3.0, 15, and 60 minutes

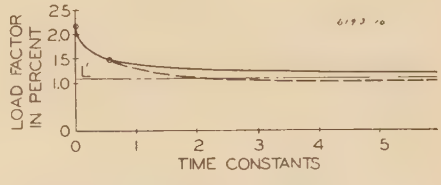

Figure 10. Illustration showing manner in which estimated (broken line) curve is joined to the calculated (solid line) permissible overload curve

The curve which is used consists of the estimated curve plus that portion of the calculated curve which lies to the left of the junction of the two curves

$$N = \frac{a-b}{L_r - L_q} \tag{16}$$

where

$a = \log (t_q / U_q)$
$b = \log (t_r / U_r)$

When $L = L_q$

$$U_q = \frac{T_s}{T_a} \ln \frac{T_s - T_n}{T_s - T_p} \tag{17}$$

When $L = L_r$

$$U_r = \frac{T_s}{T_a} \ln \frac{T_s - T_n}{T_s - T_p} \tag{18}$$

To evaluate equations 17 and 18, refer to equations 12 and 6.

Operation V—Drawing the Permissible Overload Curve

The permissible overload curve is calculated on the basis of known values for the following quantities:

T_a = absolute temperature of cooling air
T_n = normal hot spot insulation temperature (absolute) for rated continuous duty load
T_p = maximum permissible insulation temperature (absolute)
t_q = time for which an overload of load factor L_q can be applied to the generator and bring the hot spot insulation temperature exactly to T_p*
t_r = time for which an overload of load factor L_r can be applied to the generator and bring the hot spot insulation temperature exactly to T_p*

Figure 10 shows a calculated overload curve (solid line) and the two known overload rating points used in its determination. This curve is asymptotic to the line L-equals-L'. This is the magnitude of load which will just raise the temperature to T_p after an infinitely long time. Equation 14 indicates that this load can be carried indefinitely, but the generator manufacturer's rating for continuous duty is represented by the line L equals 100 per cent. For reasons already discussed, after three to four time constants have elapsed, the manufacturer's rating applies (refer to Figure 8). Hence the estimated curve (broken line) is added. It joins the calculated line below the lower of the two known overload rating points-and in the vicinity of three to four thermal time constants merges with the L-equals-100-per-cent line. It is recommended that the overload curve be plotted on semi-log paper and that the estimated curve be drawn in with a French curve.

Because of the composite nature of the permissible overload time curve, an inflection point may occur in the vicinity of the joint between the estimated and calculated sections. This point is especially likely to happen when the curve is plotted on semi-log paper

*In practice it may be assumed that t_q and t_r are the rated times for which overloads L_q and L_r may be applied.

Field Tests on Power-Line Carrier-Current Equipment

R. H. MILLER
ASSOCIATE AIEE

E. S. PRUD'HOMME
ASSOCIATE AIEE

Synopsis: This paper briefly describes a series of field tests made on the power line carrier current telephone system of the Pacific Gas and Electric Company, covering both amplitude and frequency modulated equipment. A discussion of various tests and test results is given, with a comparison of performance of the amplitude and frequency modulated equipment.

THE Pacific Gas and Electric Company has used carrier current telephone equipment on its high voltage transmission network for 23 years. Severe noise problems exist on some parts of the 230-kv transmission system because the lines have high corona losses. Early attempts to provide satisfactory carrier current communication over these lines were unsuccessful and led to the development of single-side-band power-line carrier-telephone equipment, some of which has been in service since 1927 and has been described previously.[1]

Major additions of hydroelectric generation and transmission facilities were made in 1944 requiring a considerable extension to the carrier current communication system. As some of the channels of the new carrier telephone system were to operate over the high corona lines, the noise problem required careful consideration. The use of frequency modulated carrier equipment[2] was proposed as a solution to the noise problem and an installation of this type equipment was made over a part of the system.[3] The complete carrier current telephone additions made in connection with the power system expansion in cluded four 2-frequency-duplex amplitude-modulated channels and one 2-frequency-duplex frequency-modulated channel on the Pacific Gas and Electric Company system. In addition, another 2-frequency-duplex amplitude-modulated channel was installed by the United States Bureau of Reclamation between Shasta Dam power house and the Pacific Gas and Electric Company Shasta substation. The carrier current telephone channels on the 230-kv system, with connecting channels, are shown in Figure 1.

The power system expansion was made to meet wartime requirements, and it was impossible to make complete tests of the carrier current equipment in the field at the time of installation because of the shortage of personnel, test equipment, and time. After the installation was completed, it was thought that maximum performance was not being realized from the system. Listening checks resulted in differences of opinion on the performance of various parts of the system. An extensive investigation of the characteristics of the system was undertaken to obtain quantitative data of the performance, and to make any adjustments found necessary to provide improvements.

Description of Tests

Data were taken to determine

1. The carrier frequency response of the equipment.
2. The audio frequency response.
3. The effects of transmitter output power level on the received signal and signal-to-noise ratio.
4. A comparison of frequency and amplitude modulation signal-to-noise ratios.
5. The effects of percentage modulation on signal-to-noise ratio.
6. Audio frequency attenuation of wire line and cable extensions used with the carrier current equipment.

The carrier frequency response gives an indication of the correctness of the tuning of the transmitter output stages, the line tuning units, and the receiving equipment. Carrier frequency response data were obtained by reading the transmitter output voltage, the coupling capacitor current, carrier output current (measured at the transmitter), received voltage, and receiver limiter current as the transmitter oscillator frequency was varied. From

Paper 46-199, recommended by the AIEE committee on power system applications of carrier current for presentation at the AIEE Pacific Coast meeting, Seattle, Wash., August 27–30, 1946. Manuscript submitted July 1, 1946; made available for printing July 19, 1946.

R. H. Miller, an assistant engineer with the Pacific Gas and Electric Company, San Francisco, Calif. is now on a temporary assignment with the United States Navy.; E. S. Prud'homme is an electronics engineer with the General Electric Company, San Francisco, Calif.

The authors wish to acknowledge assistance in the tests given by R. W. Beckwith of the General Electric Company, Syracuse, N. Y., and L. L. Creighton and A. K. Worthington of the Pacific Gas and Electric Company, San Francisco, Cal.

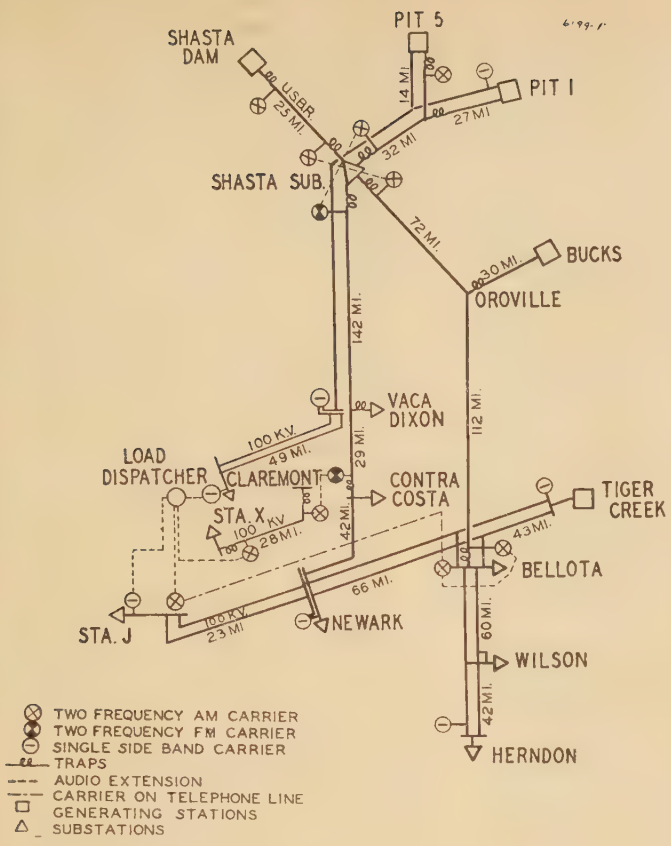

Figure 1 (left). Carrier current telephone channels on the Pacific Gas and Electric Company 230-kv transmission system

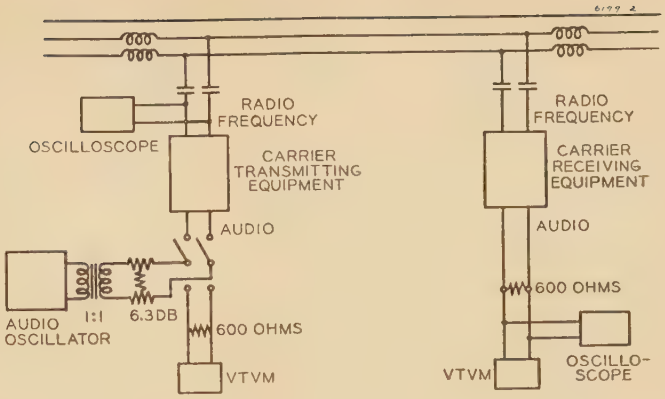

Figure 2 (above). Circuit used to obtain audio frequency response characteristics

these data it was possible to plot and observe the frequency response of each part of the equipment through which the carrier frequency signal passed.

Audio frequency response was obtained by supplying constant level audio frequency tones to the transmitter modulator and measuring the receiver output voltage. These tests were carried out after the correct carrier frequency adjustments had been established. The circuit used for the audio frequency response measurements is shown in Figure 2. These measurements were made on each channel of the system and over several channels in cascade. The input level of the audio tones was set to provide a high percentage modulation, approximately 75 per cent for normal voice, as determined by observation with an oscilloscope of the carrier frequency output. With this setting the modulation limiter would prevent overmodulation on peaks. Both the carrier frequency and audio outputs were observed with an oscilloscope to determine whether or not distortion was present.

Noise measurements were made on all channels and the signal-to-noise ratios were determined. Noise and signal measurements were made with a vacuum-tube voltmeter, and noise measurements are unweighted. Weighted noise measurements were taken on some channels, but an insufficent number are available for comparison and will not be presented.

Received signal and signal-to-noise ratios were observed as the transmitter power output was varied.

Frequency and amplitude modulation signal-to-noise ratios were compared on the same power transmission line section in order to obtain actual field data on the effectiveness of frequency modulation as a means of overcoming noise in carrier current telephone systems.

Audio frequency attenuation of the audio frequency extensions on the carrier system were obtained. As the extensions were of considerable length, their characteristics were considered to be a factor in over-all performance.

Results

It was found that considerable improvement was possible in some parts of the system, and data and curves showing the characteristics of some of the channels, both before and after readjustments, will be presented.

Carrier Frequency Response

Figure 3 shows the carrier frequency response of the frequency modulation channel with its original adjustment. These curves show a considerable dissymmetry about the 75-kc operating frequency, which was apparent as distortion in the receiver output. Careful retuning of the line tuning equipment resulted in doubling the transmission line current, a considerable increase in received voltage, and symmetrical variations about the operating frequency as indicated by the curves of Figure 4.

Audio Frequency Response

Considerable audio frequency response data were obtained. The manufacturer had guaranteed that the audio characteristics of the individual channels would be within plus or minus five decibels between 300 and 3,000 cycles. It was possible to come well within these limits on each channel. Audio characteristics of the 75-kc frequency modulation channel operating between Shasta and Contra Costa substations are shown in Figure 5. The audio response curve for the 85-kc amplitude modulation channel between Shasta substation and Pit 5 power house is illustrated in Figure 6. This curve is typical of the response of the amplitude modulation equipment.

One of the amplitude modulation re-

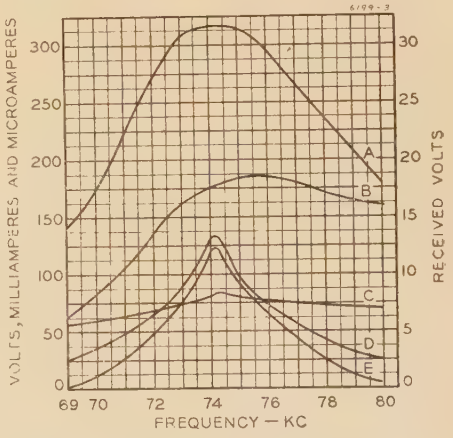

Figure 3. Carrier frequency response of 75-kc frequency modulation channel with improper line tuning

A—Output current at transmitter (milliamperes)
B—Transmitter output voltage
C—Coupling capacitor current (milliamperes)
D—Received voltage
E—Receiver limiter current (microamperes)

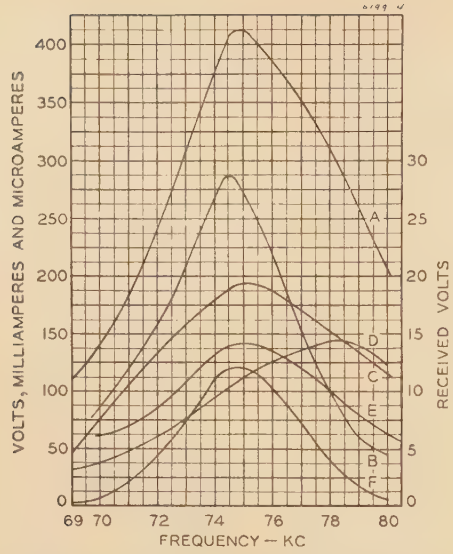

Figure 4. Carrier frequency response of 75-kc frequency modulation channel with correct line tuning

A—Output current at transmitter (milliamperes)
B—Received voltage (high *Q*)
C—Coupling capacitor current (milliamperes)
D—Transmitter output voltage
E—Received voltage (low *Q*)
F—Receiver limiter (high *Q*) current (microamperes)

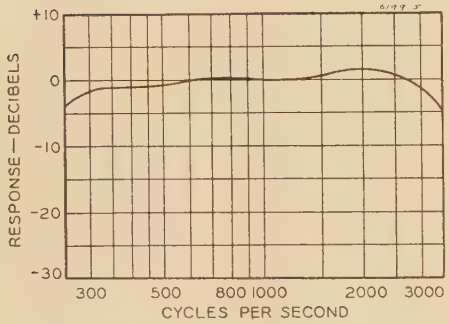

Figure 5. Audio frequency response of 75-kc frequency modulation channel

ceivers had been aligned for maximum detector current at the carrier frequency, and the effect on the audio characteristic is shown in curve *A* of Figure 7. When the intermediate frequency amplifiers were realigned for the correct band pass, the audio characteristic was improved considerably as indicated by curve *B* of Figure 7. At carrier frequencies the required band pass is a relatively greater percentage of the carrier frequency than in ordinary space radio applications. As in any highly selective receiver employing band pass circuits, tuning adjustments must be made carefully.

A limiting factor in audio frequency response, in this case of 2-frequency-duplex carrier system with interphase coupling using only 0.001-microfarad coupling capacitors, was found to be the resonance characteristics of the line tuning equipment. It was possible to improve the audio frequency response at the expense of received signal volts by reduction of the *Q* of the receiver line tuning equipment. Broadening of the audio frequency response resulted in some loss in signal-to-noise ratio. The effect on carrier frequency response is shown in the "low *Q* received volts" curve of Figure 4. An indication of the effect on the audio characteristics by broadening the band pass of the line tuning equipment is shown in Figure 8. Curve *A* shows the audio characteristics with high *Q* line tuning elements on the receiver input. Curve *B* shows the increased response to high frequencies with broadened receiver line tuning.

Over-all audio characteristics of three channels in cascade are shown in Figure 9. This system includes one frequency modulation and two amplitude modulation channels between station *X*, Oakland, and Pit 5 power house. The over-all response nearly meets the plus or minus 5-decibel limits set for one channel.

Power Output

The effects of the variation of transmitter output on the received signal and signal-to-noise ratio for the 75-kc frequency modulation channel are given in Table I. Received volts in Table I are signal plus noise. These results indicate the effectiveness of the frequency modulation receiver in maintaining the signal-to-noise ratio with large variations in the transmitter output and the received signal. It was possible to maintain communication over a 175-mile 230-kv line when using only the exciter unit of the frequency modulation transmitter with a power output of two watts.

Frequency and Amplitude Modulation Signal-to-Noise Comparison

A comparison of frequency and amplitude modulation signal-to-noise ratios is given in Table II. From these data it is apparent that the frequency modulation equipment is capable of maintaining a

Table I

Transmitter Output, Volts	Receiver Input, Volts	Signal-to-Noise Ratio, Decibels
50	3.6	29.5
25	2.2	27.8
10.8	1.6	24.5
4.8	1.5	24.5

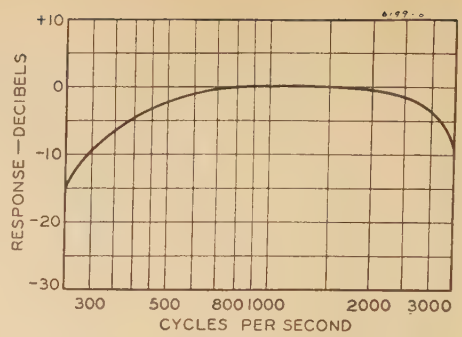

Figure 6. Audio frequency response of 85-kc amplitude modulation channel

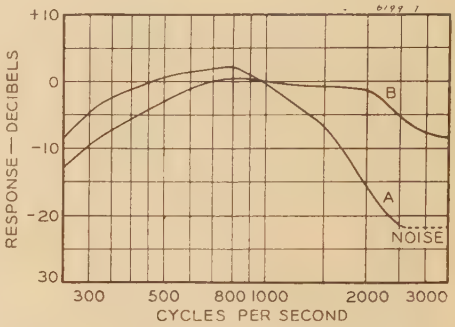

Figure 7. Audio frequency response of 140-kc amplitude modulation channel

Curve *A*—Receiver aligned for maximum detector current at carrier frequency
Curve *B*—Receiver aligned for correct band-pass

high signal-to-noise ratio even as the carrier signal approaches the noise level, and consequently communication can be maintained under conditions when a conventional amplitude modulation system would be inoperative.

Effects of Modulation Level on Signal-to-Noise Ratio

On the frequency modulation channels with a deviation ratio of less than one-to-one, the signal-to-noise ratio was reduced considerably. Checks were made with deviation ratios of approximately one-third to one, and one-to-one, with the result that the signal-to-noise ratio was increased from 22 decibels with the lower to 34.5 decibels with the higher level of modulation. With a small deviation ratio, the phase modulation resulting from noise becomes appreciable relative to the desired frequency modulation and the noise output is proportionally higher. With the modulation correctly adjusted for normal voice input, overswing on peaks is limited by means of the modulation limiter which tends to maintain the deviation ratio near the correct value. A discussion of deviation ratios, band-width requirements, and noise considerations is given in reference 2. One of

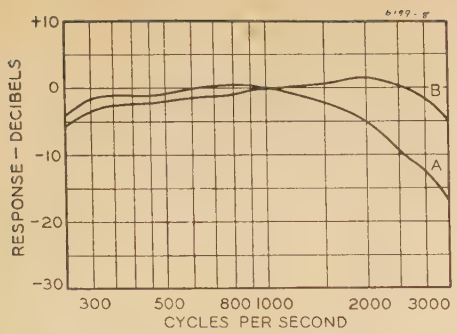

Figure 8. Audio frequency response curves showing the effect of the band pass of line tuning equipment

Curve *A*—High *Q* line tuning equipment
Curve *B*—Low *Q* line tuning equipment

Table II

Transmitter Output, Watts	Frequency Modulation Signal-to-Noise, Decibels	Amplitude Modulation Signal-to-Noise, Decibels	Frequency Modulation Over Amplitude Modulation Decibels
10	36.2	22.5	13.7
5	36	22.5	13.5
1	32.4	22.4	10.0
0.2	24.8	17.5	7.3

the early difficulties in the field adjustment of the frequency modulated carrier equipment was lack of a simple field check of deviation. With amplitude modulation equipment it is possible to observe the modulation envelope with an oscilloscope to check percentage modulation and the presence of distortion. A similar procedure for the frequency modulation equipment was suggested by R. W. Beckwith. With the carrier output connected to an oscilloscope with internal synchronization, a change of frequency will cause the pattern to move horizontally on the screen. By calibrating the horizontal movement versus frequency swing, a simple but sufficiently accurate method of measuring deviation is obtained, and the performance of the frequency modulation transmitter can be observed conveniently.

Audio Characteristics of Wire and Cable Extensions

The carrier terminals are located at high voltage substations at a considerable distance from the dispatcher and general offices of the company. The carrier telephone system was installed primarily to provide communication for the dispatchers to the generating plants, but also is used by others in carrying on business incidental to the operation of the power system. It was recognized that an investigation of the carrier system should include the characteristics of the extensions because they are a part of the complete communication system. The extensions to the dispatcher's office includes both open wire line and cable. Audio frequency characteristics of one of these extensions are shown in curve *A* of Figure 10. The extension from the dispatcher's office to the general offices is by submarine cable across the San Francisco Bay. The audio frequency characteristics of this cable are shown in curve B of Figure 10. There is in this cable a rapid cutoff of the frequencies above 2,500 cycles. The measured attenuations at 1,000 cycles were approximately two decibels for curve *A* and nine decibels for curve *B*, but the curves have been plotted through zero at 1,000 cycles for a better comparison of their shapes.

Listening tests also were made to compare various types of telephone instruments, and although no quantitative data were obtained, it was apparent that there was a large difference in the performance of different instruments, and that improvements could be made in some cases by providing modern high quality telephone instruments for use with the carrier equipment.

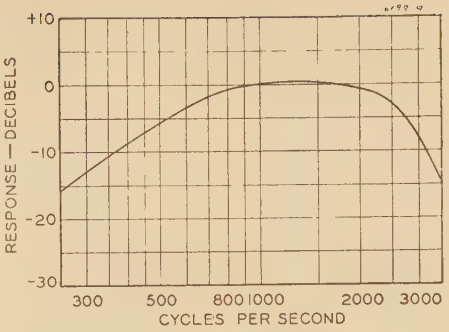

Figure 9. Over-all audio response of three carrier current channels in cascade

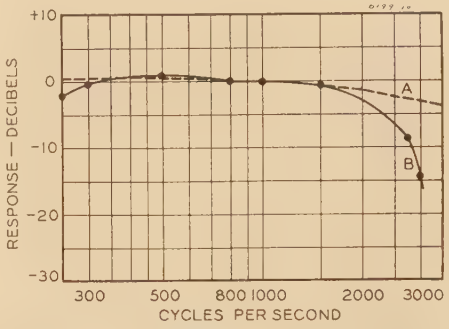

Figure 10. Characteristics of audio frequency extensions to carrier current channels

Conclusions

Tests such as those described in this paper provide information to evaluate properly the performance of the various parts of a carrier telephone system, and to make adjustments for optimum performance. Specifically it can be concluded that

1. Care in the adjustment of carrier current communication equipment will provide the maximum in performance, and adjustments cannot be made correctly without the use of proper instruments and a logical procedure.

2. Good audio frequency response is possible by correct adjustment of the equipment, and is particularly important where several sets are to be cascaded by means of audio coupling. Audio frequency response may be limited by characteristics of the line tuning equipment. In practice, a compromise between audio frequency response and signal-to-noise ratio must be accepted.

3. Frequency modulation equipment is capable of maintaining a high signal-to-noise ratio with large variations of carrier signal.

4. The frequency modulation system provides a definite advantage over amplitude modulation equipment insofar as signal-to-noise ratio is concerned, which permits successful carrier current operation on lines with noise levels so high as to preclude the use of conventional amplitude modulated equipment.

5. In frequency modulation, as in any carrier system, it is important to maintain a high level of modulation in order to realize the maximum signal-to-noise ratio.

6. Audio extensions from the carrier terminal equipment enter into the over-all consideration of the system, and can be limiting factors in the performance of a system.

Data such as those collected in the tests described are also invaluable in maintenance work on the system. The actual performance of the equipment can be compared with the test results from time to time, and any marked deviations can serve as guides in finding and correcting troubles.

References

1. Problems in Power-Line Carrier Telephony, **W. V. Wolfe, J. D. Sarros.** AIEE Transactions, volume 48, 1929, pages 107–13.

2. Frequency Modulation for Power-Line Carrier Current, **E. W. Kenefake.** AIEE Transactions, volume 62, 1943, October section, pages 616–20.

3. Pacific Gas and Electric Company Pioneers in FM Power Line Carrier Current. *Electrical West*, volume 93, August 1944, pages 54–6.

Teaching Electricity and Magnetism

V. P. HESSLER
FELLOW AIEE

Synopsis: A discussion of a method for presenting the fundamental relations of the science of electricity and magnetism is presented including a brief description of the various absolute unit systems. Most of the fundamental relations of electricity and magnetism are presented in general form. The relations are called general in the sense that they are complete and correct for use with any consistent unrationalized unit system. The relations are presented in a logical and rigorous sequence, that is, the basis of each relation is found in the preceding relations.

THE fundamental relations of electricity and magnetism form the basis of analysis for all analytical problems of electrical circuits and equipment. The primary objective of the formal training in engineering is to develop skill in engineering analysis. Thus it is very important that the electrical engineer have excellent training in his major basis for analysis, electricity and magnetism. Skill in engineering analysis demands an understanding of the field of application and limitations of basic relations which can be gained only through a well-organized study of the science involved.

The purpose of this paper is to present the author's approach to such study and training in electricity and magnetism. The organization presented has evolved through many revisions while presenting the material to sophomore electrical engineering students. It was developed on the basis of maintaining sequential rigor at the sophomore level of comprehension. Electrostatic field theory is developed toward the end of the organization instead of at the beginning because the average student has little background in this field and can gain essential background through the study of circuits and magnetic fields. For example, in accordance with the above principles potential difference is defined as work per unit charge instead of the line integral of field intensity.

Experimental, Defined, and Derived Relations, and Generalizations

The classification of the relations or formulas of electricity and magnetism into experimental, defined, or derived relations and generalizations was suggested to the writer by Professor Edward Bennett and forms an essential part of the organization of the text of which Professor Bennett is the coauthor.[1]

To comprehend fully the significance and limitations of each of the relations, formulas, and rules which make up the body of a science it is necessary to understand clearly the basis upon which each was obtained. All of the relations of electricity and magnetism can be classified under one or another of the four headings. The headings are so descriptive as to hardly need further exposition.

Experimental relations are those which are determined directly by experiment, such as Coulomb's law of force between charges and Ampere's law of force between parallel wires. Relations which are termed experimental were usually so determined historically but this does not imply that all relations which were originally determined experimentally should be so termed. For example, Joule's law concerning power dissipation in a resistor is considered derived in this presentation. It is also important to understand the actual experimental background for experimental relations because they must not be extrapolated too far beyond the experimental evidence on which they are based. Students of electronics are well aware of the limitations of $F = ma$ in cathode ray tube theory. For a presentation of original experimental procedures see Magie[2], and for a discussion of the limitations of experimental relations see Bridgman.[3]

Defined relations include all those which define units, conventions, and physical quantities. It is especially important to understand which quantities or relations are defined because a defined quantity must not be given properties beyond those involved in the definition. Failure to understand that the magnetic field is a defined quantity often leads to fruitless discussions concerning the mechanism of induced voltage. Also it is important that a given quantity be defined in one way only lest inconsistencies appear in succeeding analysis.

Derived relations are determined analytically usually through the combining of experimental and defined relations. Again familiarity with their source is important because all derived relations are circumscribed by the limitations of the experimental and defined relations upon which they are based.

Generalizations or postulates are relations which are assumed to be universally true because no exception to them has ever been observed. The law of conservation of energy is an example. Here again the engineer must understand that the law of conservation of energy based on the Macro measurements of engineering cannot be extrapolated into the realm of atomic physics.

Absolute Measure

A clear understanding of the origin and structure of unit systems is essential in engineering analysis. All electrical unit systems are based on absolute measure, that is, measurement based on the fundamental units of length, mass, time, and a fourth arbitrarily assigned quantity called the permeability of free space. Gauss laid the foundation for absolute measure in the 1830's by measuring the earth's magnetic field in terms of the moment of inertia and period of oscillation of one magnetized needle and of the deflection of a second magnetized needle in the vicinity of the first.[2] The pole strengths of both magnets cancel out of the equations thus giving the strength of the earth's field in terms of length, mass, time, and the permeability of free space tacitly assumed as unity in Gauss' experiments. Thus it was possible to duplicate magnetic measurements without a standard magnetic needle. All electrical units are based on similar measurements. The actual experimental work is very complicated involving difficult adjustments and corrections, but the basic academic definitions of the processes are quite simple as will be shown later.

The CGS Electromagnetic System

The cgs electromagnetic system is based on the centimeter, gram, second, and the permeability of free space taken as unity. It is the standard unit system in the field of physics and is the basis of the practical system of electrical units.

The International or Practical System

The early telegraph engineers did not find the cgs electromagnetic units a con-

Paper 46-187, recommended by the AIEE committee on education for presentation at the AIEE Pacific Coast meeting, Seattle, Wash., August 27–30, 1946. Manuscript submitted September 23, 1944; made available for printing July 16, 1946.

V. P. Hessler is chairman of the electrical engineering department, University of Kansas Lawrence, Kan.

venient size so they developed the practical system whose units differed from the cgs electromagnetic units by various multiples of ten. However, the practical system embraced only circuit phenomena and was not extended to cover mechanics, or magnetic or electrostatic field theory. This was perhaps the greatest source of misunderstanding and confusion in the study of electricity and magnetism since any analysis involving mechanical force or electric or magnetic fields and electric circuits involved borrowing units from other unit systems and resulted in innumerable multiplying factors. Also, no relation could be considered complete without a statement of the particular assortment of units for which it was designed. Giorgi provided the solution in 1903 by the invention of the mks unit system. The system was adopted as the international standard in 1935.

The MKS System

Giorgi's invention of the mks system consisted of extending the practical system into a complete absolute system embracing all of mechanics and electric and magnetic field theory and at the same time retaining all of the circuit units of the practical system. This was done by choosing units of length and mass of such size as to make the unit of mechanical work equal to the unit of work in the practical system (the joule) and by assigning a numerical value to the permeability of free space ($\mu_v = 10^{-7}$) which would result in a unit of current equivalent to the ampere. These ideas will be expanded in the process of setting up the fundamental relations.

General Electrodynamic Equations

The foregoing discussion indicates the possibility of writing a complete set of fundamental relations in electricity and magnetism with no need for supplementary statements concerning the appropriate units. Units of the mks system are inserted on the right of a relation and the answer is known to be in units of the same system. It may not be quite as evident, however, that these same expressions serve equally well in any other consistent unit system. That is, the identical relations apply equally well in the mks, cgs electromagnetic, and cgs electrostatic systems.

With this approach, beginning students show equal facility in solving problems in any of the three unit systems mentioned. Often one or the other of the cgs systems will handle a given problem with greater convenience than the mks system. Experience has demonstrated that students can use three or more systems interchangeably without confusion. However, it is imperative that only one system be used in a given problem or relation.

The Fundamental Electrical Quantities

Electric Charge

The development of the fundamental relations presented herein is based on the concept of the electron as a charged particle, that is, charge is considered real and field is considered a condition which is produced in the vicinity of charge. The reverse of this may be a more exact picture of nature but the charged particle concept seems to lend itself more readily to the development of the science of electricity and magnetism.

Forces on Electric Charge

The science of electricity and magnetism deals with forces between electric charges at rest and in motion. We know from experiment that electric charges exert forces upon each other because of their positions, their velocities, and their accelerations.[4] The first effect is the basis of electrostatics, the second of generated voltages and magnetic forces, and the third of induced or transformer voltages and radio transmission.

Electric Fields

Even though it is possible in many cases to calculate the forces of electric charge in terms of "action at a distance," that is in terms of the force of one charge upon another, it is almost always simpler and more effective to assume that one charge or group of charges produces a field which in turn exerts a force on other charges in the vicinity. Forces between electric charges resulting from their relative positions are calculated in terms of electrostatic fields, and forces between charges in motion are calculated in terms of magnetic fields. The transmission of radio signals is usually calculated in terms of the electromagnetic field, but the calculations also can be made in terms of "vector potentials" which make no use of the magnetic field concept. The defining relations for the various field quantities are presented in the following section.

The Fundamental Electrodynamic Relations and Quantities

The fundamental electrodynamic relations and quantities are herein developed in a rigorous sequence. The source of each relation whether experimental, defined, derived, or generalization is so indicated. Space limitations prevent giving more than an outline of each derivation, or of stating the complete significance of all terms of all of the relations. The prime purpose in presenting the sequence of quantities and relations is to illustrate the logical manner in which the relations of electricity and magnetism may be developed. The reader should refer to standard text books in the field for details of specific relations. Units given are of the mks unrationalized system.

Basic Mechanics

1. l—length, meters (defined)
2. m—mass, kilograms (defined)
3. t—time, seconds (defined)
4. v—velocity, meters per second (defined)
5. a—acceleration, meters per second per second (defined)
6. Newton's law of force

$F = ma$ (experimental)

7. F—force, newtons (defined)

A newton is that force which will give a mass of one kilogram an acceleration of one meter per second per second.

8. W—work, joules (newton-meter) (defined)

$W = Fl$

9. P—power, watts, (joules per second) (defined)

$P = W/t$

Electric Circuit Quantities

10. Ampere's law of force between parallel wires (experimental)

$$F = \frac{K\mu_r I_1 I_2 l}{d}$$

where μ_r is the relative permeability of the medium between the wires, I_1 and I_2 are the currents in the two wires, l is the length of the wires, d the distance between centers, and K is a constant which determines the unit system. To establish an unrationalized system

$K = 2\mu_v$

where μ_v is called the absolute permeability of free space. It is really a number which determines the size of the electrical units.

11. μ_v—absolute permeability of free space, (defined, fundamental mks unit)

$\mu_v = 10^{-7}$

12. $\mu_r\mu_v$—absolute permeability of a medium (defined)

13. I—electric current, ampere (defined)

Unit current is defined in terms of Am-

pere's law of force between parallel wires

$$F=\frac{2\mu_r\mu_0 I_1 I_2 l}{d}$$

The ampere is that current which will produce 2×10^{-7} newtons of force per meter of length between two parallel wires spaced one meter apart in air.

14. Q—electric charge (defined)

When two bodies attract each other with a force other than that of gravitation or repel each other with no material connection, they are said to be charged electrically.

15. Relation between electric current and charge (experimental)

$$Q=It$$

Rowland showed in 1876 that electric current was time rate of redistribution of charge.

16. Q—charge, coulomb (defined)

One coulomb of charge passes a given point in a circuit each second when the current is one ampere.

17. Potential difference (defined)

Potential difference is the action which tends to set up a current in an electric circuit. The unit is defined in terms of work per unit charge.

18. E, V—potential difference, volts (defined)

A potential difference of one volt is said to exist between the points a and b if one joule of energy is required to carry one coulomb of charge from a to b. The point b is at a higher potential than a if positive work is done on a positive charge.

$$V_{ba}=\frac{W}{Q}$$
$$=-\int_a^b \frac{F}{Q}\cos(F, dl)dl$$

where V_{ba} is the potential of the point b with respect to the point a, F is the electric force on the test charge, and (F, dl) is the angle between the direction of the electric force and dl.

19. Resistance (defined)

Resistance is that property of a circuit which opposes current flow.

20. Ohms Law (experimental)

$$I=E/R$$

21. R—resistance, ohms (defined)

A circuit is said to have a resistance of one ohm if a potential difference of one volt sets up a current of one ampere in it.

22. Resistance of a conductor (experimental)

$$R=\frac{\rho l}{A}$$

where ρ is the resistivity of the conductor material, l is the length of the conductor, and A its cross-sectional area.

23. G—conductance, mhos (defined)

Conductance is defined as the reciprocal of resistance.

24. Power in an electric circuit (derived)

$$P=VI$$

This relation is derived from the definition of potential difference, and of current considered as time rate of redistribution of charge.

25. Power in electric circuits (derived)

$$P=I^2R$$
$$=V^2/R$$

Derived from (24) and Ohm's law.

26. Energy in electric circuits (derived)

$$W=VIt$$
$$=I^2Rt$$
$$=V^2t/R$$

27. Law of conservation of charge (generalization)

28. Law of conservation of energy (generalization)

29. Kirchhoff's laws (derived)

$$\Sigma E's=0$$
$$\Sigma I's=0$$

These relations are derived on the basis of conservation of energy and conservation of charge.

30. Resistances in series (derived)

$$R_t=R_1+R_2+\ldots+R_n$$

31. Resistances in parallel (derived)

$$R_t=\frac{1}{\frac{1}{R_1}+\frac{1}{R_2}+\ldots+\frac{1}{R_n}}$$

Magnetism

Considering Ampere's law (13) let us assume that the current I_1 produces a stress in space which exerts a force on the current I_2. This assumption is the basis of the concept of magnetism. Let us say that the stress sets up a quantity called flux Φ (magnetism) usually represented by lines, and that the number of lines per unit area is flux density B.

32. Flux density (defined)

$$F=BlI\sin(B, l)$$

Flux density, a vector quantity, is defined by this relation where (B, l) is the angle between the direction of the flux lines and the direction of the wire.

33. B—flux density, webers per square meter (defined)

The flux density of a field is said to be one weber per square meter if a wire carrying a current of one ampere and perpendicular to the field experiences a force of one newton per meter of length.

34. Φ—flux, webers (defined)

$$\Phi=BA$$

or

$$\Phi\int B\cos(B, n)dA$$

The total flux passing through a plane area is equal to the product of flux density B and the area A if the flux density is uniform and perpendicular to the area. In case of nonuniform fields the summation must be determined by integration. In the integral, (B, n) is the angle between the direction of flux density and the direction of the normal to the differential area dA.

35. Flux density about a long straight wire (derived)

$$B=\frac{2\mu_r\mu_0 I}{x}$$

where x is the distance in meters from the center of the wire.

36. Field intensity (defined)

$$B=\mu_r\mu_0 H$$

Field intensity, a vector quantity, is defined by this relation. It is the agency which produces flux density; that is, the flux density at any point in a field is proportional to and directed along the field intensity vector.

37. H—field intensity, pragilberts per meter (defined)

A field intensity of one pragilbert per meter sets up a flux density of 10^{-7} webers per square meter in free space.

38. Field intensity about a long straight wire (derived)

$$H=\frac{2I}{x}$$

39. Magnetomotive force (defined)

$$M=\int H\cos(H, dl)dl$$

Magnetomotive force is defined as the line integral of field intensity. It is the total magnetic action along a given path. (H, dl) is the angle between the direction of H and the differential length of path dl.

40. M—magnetomotive force, pragilberts (defined)

A magnetomotive force of one pragilbert will set up a field intensity of one pragilbert per meter in a path one meter long.

41. Magnetomotive force about a long

straight wire (derived)

$$M=\int_0^{2\pi d}\frac{2I}{x}\cos(H, dl)dl$$
$$=4\pi I$$

It can be shown that the result is independent of the path of integration.

42. Magnetomotive force of a coil (derived)

$$M=4\pi NI$$

N is the number of turns in the coil which is carrying the current I.

43. Field intensity resulting from a current element (generalization)

$$dH=\frac{I\sin(r, dl)dl}{x^2}$$

where dH is the field intensity set up at a distance x from a differential length of conductor dl which is carrying a current I.

This relation must be considered true because no contradictory evidence has been discovered.

44. Field intensity about a wire of finite length (derived)

$$H=\frac{I}{r}(\sin\alpha_1+\sin\alpha_2)$$

Set up (43) for particular case and integrate. x is the perpendicular distance from the point at which H is evaluated to the axis of the wire. α_1 and α_2 are the angles between the perpendicular and the two ends of the wire.

45. Field intensity on the axis of a concentrated circular coil

$$H=\frac{2\pi r^2NI}{(r^2+x^2)^{3/2}}$$

where r is the radius of the coil and x is the distance from the plane of the coil.

Note. (44) and (45) become expressions for flux density by multiplying by $\mu_r\mu_v$.

46. Total flux produced in a toroid of cross-sectional area A and mean length l (derived)

$$\Phi=\frac{4\pi NI\mu_r\mu_vA}{l}\text{ (approximately)}$$

Ratio of length to area must be large.

47. Reluctance (defined)

The reluctance of a magnetic path is defined as the ratio of the magnetomotive force across a path to the flux set up in the path.

48. $\mathcal{R}$—reluctance, pragilberts per weber (defined)

Definition follows from name of unit.

49. Reluctance of a path (derived)

$$\mathcal{R}=\frac{l}{\mu_r\mu_vA}$$

Generated and Induced Voltages

50. Electromagnetic induction (experimental)

Faraday discovered that a voltage is generated whenever a conductor is moved across a magnetic field or whenever there is a change in the number of flux lines linking a coil. The first is a case of forces between moving charges and the second of forces between accelerated charges.

51. Voltage generated by a moving conductor (derived)

$$V=Blv\sin(B, v)$$

The derivation is made in terms of an elementary generator and the law of conservation of energy. Wire is considered moving perpendicular to its axis v is the velocity of the conductor and (B,v) is the angle between the direction of the flux and the velocity.

52. Flux linkages, weber-turn (defined)

$$\lambda=N\Phi$$

53. Voltage generated by changing flux linkages (experimental)

$$e=N\frac{d\Phi}{dt}$$

Note. The lower case letter e is used in this and subsequent relations to indicate instantaneous values. Instantaneous current is indicated in a corresponding manner.

54. Inductance (defined)

Inductance is that property of a circuit which tends to prevent a change in current.

55. L—inductance, henries (defined)

$$L=e/(di/dt)$$

A circuit is said to have an inductance of one henry if current changing at the rate of one ampere per second induces an emf of one volt.

56. Inductance in terms of flux linkages per ampere (derived)

$$L=N(d\Phi/di)$$

57. Inductance in terms of circuit dimensions (derived)

$$L=\frac{4\pi\mu_r\mu_vN^2A}{l}\text{ (approximately)}$$

Derived from (56) and (46).

58. Inductance of two long straight wires.

Distance d between centers, wire radius r, and length of circuit l (derived)

$$L=l\left(4\mu_v\log_e\frac{d}{r}+\mu_r\mu_v\right)$$

59. L_m—mutual inductance (defined)

$$L_m=e_1/(di_2/dt)$$

60. k—coefficient of coupling of two coils (defined)

$$k=k_1k_2$$

where $k_1=\Phi_{12}/\Phi_1$ and $k_2=\Phi_{21}/\Phi_2$. Φ_{12} is the part of flux Φ_1 which also links coil 2 and Φ_{21} is the part of flux Φ_2 which also links coil 1.

61. Mutual inductance in terms of self inductance (derived)

$$L_m=k\sqrt{L_1L_2}$$

62. Energy stored in inductive circuits (derived)

$$W=\frac{LI^2}{2}$$
$$=\frac{N\Phi I}{2}$$

63. Energy stored per unit volume in magnetic fields (derived)

$$\frac{W}{v}=\frac{\mu_r\mu_vH^2}{8\pi}$$
$$=\frac{BH}{8\pi}$$
$$=\frac{B^2}{8\pi\mu_r\mu_v}$$

where v is the volume in cubic meters.

64. Pull of an electromagnet (derived)

$$F=\frac{B^2A}{8\pi\mu_v}$$

Electrostatics

The following relations are concerned with forces experienced by electric charges resulting from their relative positions.

65. Coulomb's law of force between charges (experimental)

$$F=\frac{Q_1Q_2}{\epsilon_r\epsilon_vx^2}$$

where ϵ_r is the relative permittivity of the medium between the charges, also known as the dielectric constant. ϵ_v is the absolute permittivity of free space or more exactly a number the magnitude of which is determined by the unit system. (In an

Table I

Unit System	Permeability of Free Space	Permittivity of Free Space
Mks unrationalized...	10^{-7}	$..1.113\times10^{-10}$
Cgs electromagnetic...	1	$..1.113\times10^{-21}$
Cgs electrostatic.....	1.113×10^{-21}..	1
Mks subrationalized..	$4\pi10^{-7}$	$..8.854\times10^{-12}$

electrostatic system it is chosen arbitrarily and determines the size of the electrical units.)

66. ϵ_v—permittivity of free space (experimentally determined constant)

$\epsilon_v = 1.113 \times 10^{-10}$

The value may be determined by placing a known charge Q_1 at a given distance from another known charge Q_2 and measuring the force.

67. $\mathcal{E}$—Field intensity (electrostatic) (defined)

$$\mathcal{E} = \frac{F}{Q}$$

Similar to the case of parallel wires, let us assume that one charge produces a condition in space which exerts a force on the other charge. The condition is called field intensity and is defined by the foregoing relation.

68. $\mathcal{E}$—field intensity, newtons per coulomb (defined)

Unit field intensity exerts a force of one newton per coulomb on a point charge.

69. Field intensity in terms of space rate of change of potential, volts per meter (derived)

$$\mathcal{E} \cos(\mathcal{E}, dl) = \frac{-dE}{dl}$$

This relation is derived from the defining relations of field intensity and potential difference.

70. Field intensity about a point charge (derived)

$$\mathcal{E} = \frac{Q}{\epsilon_r \epsilon_v x^2}$$

71. D—electrostatic displacement density or flux density, pracoulombs per square meter (defined)

$D = \epsilon_r \epsilon_v \mathcal{E}$

Displacement density is set up by field intensity and is defined by the foregoing relation.

72. ψ—electrostatic displacement or flux, pracoulombs (defined)

$\psi = DA$

or

$\psi = \int D \cos(D, n) dA$

Table II

Quantity	Replace	By
Permeability	μ_v	$\mu_{rv}/4\pi$
Permittivity	ϵ_v	$4\pi\epsilon_{rv}$
Magnetomotive force	M	$4\pi M_r$
Field intensity	H	$4\pi H_r$
Displacement density	D	$4\pi D_r$
Displacement	ψ	$4\pi\psi_r$
Reluctance	R	$4\pi R_r$

where n is the direction of the normal to the surface. Also see 34.

73. Displacement from a point charge (derived)

$\psi = 4\pi Q$

74. Displacement from any charge (derived)

$\psi = 4\pi Q$

from Gauss' theorem.

75. Capacitor (defined)

If a potential difference is applied to two conductors separated by an insulator, charge is observed to flow from one plate to the other. This arrangement is called a capacitor.

76. C—capacitance, farads (defined)

$C = Q/V$

A capacitor is said to have a capacitance of one farad if one coulomb is transferred from one plate to the other by a potential difference of one volt.

77. Capacitance of a parallel plate capacitor (derived)

$$C = \frac{\epsilon_r \epsilon_v A}{4\pi x}$$

78. Capacitance of a concentric cylinder capacitor (derived)

$C = \epsilon_r \epsilon_v l / 2 \log_e (r_2/r_1)$

where l is the length of the cylinder, r_2 the radius of the outer cylinder, and r_1 the radius of the inner cylinder.

79. Energy stored in a capacitor (derived)

$W = {}^1/_2 CV^2$

80. Energy stored per unit volume in an electric field (derived)

$$\frac{W}{v} = \frac{\epsilon_r \epsilon_v \mathcal{E}^2}{8\pi} = \frac{D^2}{8\pi \epsilon_r \epsilon_v} = \frac{\mathcal{E} D}{8\pi}$$

81. Force between parallel plates (derived)

$$F = \frac{2\pi\sigma^2 A}{\epsilon_r \epsilon_v}$$

σ = charge density.

82. Capacitor current (derived)

$i = c(de/dt)$

83. Capacitor voltage (derived)

$$e = \frac{1}{C} \int i \, dt$$

Values of Permeability and Permittivity

Table I gives the values of absolute permeability and absolute permittivity in the four common unit systems. In the cgs electrostatic system the permittivity is assigned the value unity by definition and the value for permeability is experimentally determined. The other three, being electromagnetic systems, have the values of permeability assigned arbitrarily and the permittivity values are experimentally determined.

Examples

The application of various unit systems to the fundamental relations may be illustrated by a few simple examples.

Example 1. Calculate the force per meter of length between two long straight wires spaced 10 centimeters apart and carrying 500 amperes.

Mks (unrationalized)

$$F = \frac{2\mu_r \mu_v I_1 I_2}{r} = \frac{2 \times 1 \times 10^{-7} \times 500 \times 500 \times 1}{0.1}$$

$= 0.5$ newton

Cgs electromagnetic

$$F = \frac{2 \times 1 \times 1 \times 50 \times 50 \times 100}{10}$$

$= 50{,}000$ dynes

Cgs electrostatic

$$F = \frac{2 \times 1 \times 1.113 \times 10^{-21} \times 500 \times 3 \times 10^9 \times 500 \times 3 \times 10^9}{10}$$

$= 50{,}000$ dynes

The solutions check since one newton equals 10^5 dynes. The expression does not apply to the rationalized system.

Example 2. Calculate the flux density at 10 centimeters from a long straight wire carrying 50 amperes.

Mks unrationalized

$$F = \frac{2\mu_r \mu_v I}{r} = \frac{2 \times 1 \times 10^{-7} \times 50}{0.1}$$

$= 1 \times 10^{-4}$ weber per square meter

Cgs electromagnetic

$$F = \frac{2 \times 1 \times 1 \times 5}{10}$$

$= 1$ gauss

$= 1$ maxwell per square centimeter

The calculation can be made similarly for the electrostatic system but there is no

accepted name for magnetic flux density in the electrostatic system. The results check again since gausses $\times 10^{-4}$ equals webers per square meter.

Example 3. Calculate the capacitance of a parallel plate capacitor consisting of two plates 50 centimeters square and separated by one centimeter. Neglect fringing.

Mks unrationalized

$$C=\frac{\epsilon_r\epsilon_0 A}{4\pi d}$$

$$=\frac{1\times 1.113\times 10^{-10}\times 0.25}{4\pi\times 0.01}$$

$$=2.22\times 10^{-10} \text{ farads}$$

Cgs electrostatic

$$C=\frac{1\times 1\times 50^2}{4\pi\times 1}$$

$$=198.8 \text{ stat-farads}$$

Cgs electromagnetic

$$C=\frac{1\times 1.113\times 10^{-21}\times 50^2}{4\pi\times 1}$$

$$=2.22\times 10^{-19} \text{ abfarads}$$

See Hudson[5] for a complete list of conversion factors.

Fundamental Rationalized Relations

The fundamental relations can be changed to the rationalized form by making the substitutions indicated in Table II wherever any of the quantities listed appeared in the relations.

The question of the choice between the rationalized and unrationalized systems is not the subject of this paper.

Unit Magnetic Pole

The unit magnetic pole has not been used in connection with the organization because the approach to magnetism through forces on current carrying conductors seems more satisfactory to the writer. Too often the student is introduced to electrical and magnetic quantities through the concept of impossible experiments with unit poles. However, it is granted that the concept may be useful in certain field analyses and there is no objection to defining a unit pole for this purpose just as we have defined magnetic fields for the purpose of simplifying the calculation of forces between electric charges in motion.

Summary

Most of the fundamental relations in electricity and magnetism are presented in general form. The relations are called general in the sense that they are complete and correct for use with any consistent unrationalized unit system. The basis of each relation is clearly indicated and the relations appear in a logical sequence of development. That is, the basis of each succeeding relation is found in the preceeding relations. Such an organization presents the beginning student with the means of acquiring a fundamental understanding of the science of electricity and magnetism, and also forms his basic training in engineering analysis.

150,000 Horsepower Applied to Aeronautical Research

JAMES A. WHITE
ASSOCIATE AIEE

BEHIND THE SCENES of the rapid development of aeronautics in this country during recent years are the aeronautical research laboratories. In addition to their part in the development of aeronautics, these laboratories are of interest because of the variety of electric devices they employ and the surprising magnitude of their electric power loads. One of the largest aeronautical laboratories in terms of electric power is the Ames Aeronautical Laboratory of the National Advisory Committee for Aeronautics, located at Moffett Field, Cal. This laboratory, on which construction was started in 1939, has developed rapidly to the point where it is now the largest single connected load on the Pacific Gas and Electric Company's system. With completion of wind tunnels now under construction this laboratory will have over 150,000 connected horsepower.

The Ames Aeronautical Laboratory is one of three laboratories of the National Advisory Committee for Aeronautics (NACA) the other two laboratories being at Langley Field, Va., and Cleveland, Ohio. The National Advisory Committee for Aeronautics consists of 15 members appointed by the President and serving without pay. This committee serves in an advisory capacity and is charged with the responsibility of studying the fundamental problems of flight with a view to their practical solution. A large supporting staff of full-time employees under the director of aeronautical research operates the facilities just mentioned, and carries out all types of appropriate basic studies of interest to not only the military services and the industry but also to the air lines and private flyers. The Ames laboratory includes several of this country's most up-to-date and highest powered wind tunnels, as well as a highly developed flight research department.

Paper 46-197, recommended by the AIEE committees on air transportation and electric machinery for presentation at the AIEE Pacific Coast meeting, Seattle, Wash., August 27–30, 1946. Manuscript submitted June 25, 1946; made available for printing July 24, 1946.

JAMES A. WHITE is chief of the service division, National Advisory Committee for Aeronautics, Moffett Field, Calif.

The author acknowledges the assistance of the General Electric Company, the Westinghouse Electric Corporation, and the Allis-Chalmers Manufacturing Company by supplying the detail design of the various drive systems and for their ingenuity and co-operativeness in recommending suitable types of equipment to meet the requirements of the Ames Aeronautical Laboratory.

Wind Tunnels

The largest users of power at the Ames laboratory are the wind tunnel fan drives. From the standpoint of control requirements and novel applications of electric machines they are also among the most interesting. A wind tunnel is simply a device for circulating air past an airplane or model of an airplane to simulate the conditions which occur in flight. A schematic sketch of a typical wind tunnel is shown in Figure 1. The propeller, or fan, circulates air around the continuous closed air passage in the direction shown. The air speed is increased to a maximum at the test section, where the model is

References

1. INTRODUCTORY ELECTRODYNAMICS FOR ENGINEERS (book), E. Bennett, H. M. Crothers. McGraw-Hill Book Company, Inc., New York, N. Y., 1926.

2. SOURCE BOOK IN PHYSICS (book), W. F. Magie. McGraw-Hill Book Company, Inc., New York, N. Y., 1935.

3. THE LOGIC OF MODERN PHYSICS (book), P. W. Bridgman. The Macmillan Company, New York, N. Y., 1927.

4. THE FUNDAMENTALS OF ELECTROMAGNETISM (book), E. G. Cullwick. The Macmillan Company, New York, N. Y., 1939.

5. THE ENGINEERS MANUAL (book), R. G. Hudson. John Wiley and Sons, Inc., New York, N. Y., 1939.

mounted, by the nozzle-like shape of the air passage at the approach to the test section. Beyond the test section the passage gradually is expanded again to reduce the air velocity and minimize friction losses.

The airplane or model undergoing tests is supported on a balance system so that the forces of the wind on the model may be measured to determine its lift, drag (resistance to forward motion), pitching moments, and so forth. In addition to the over-all forces on the model, forces on individual components may be measured by suitable techniques such as pressure-distribution measurements or by special measuring devices built into the model. The wind tunnel provides a simple device in which controlled test conditions are readily obtainable, and the effects of changes to the model may be studied quickly, accurately, and without the hazards of experimental flight testing. Figure 2 shows a powered model mounted in the 7-by-10-foot wind tunnel.

The power required to operate a wind tunnel ranges from a few horsepower up to many thousands of horsepower, depending upon the size and the air speed produced. The ideal wind tunnel would test full size airplanes at maximum flying speeds. However, such a wind tunnel would require over 400,000 horsepower; consequently, all wind tunnels to date have represented compromises, either as to size or maximum air speed, or both. In the early days of aeronautics much valuable information was obtained from small low speed wind tunnels of a few horsepower. As progress in aeronautics has demanded more and more attention to details the scale-effect errors of such small low speed tunnels no longer can be tolerated. Moreover, as the speed of flight approaches or exceeds the speed of sound (approximately 765 miles per hour at sea level) important phenomena caused by compressibility of the air occur which cannot be simulated in a wind tunnel except by operation at the same high speeds. Thus one finds at the Ames laboratory, for example, the following wind tunnels:

1. The 40-by-80-foot full scale wind tunnel with a test section 80 feet wide by 40 feet high capable of testing actual full size airplanes up to about 70-foot wing span at air speeds up to 250 miles per hour.

2. The 16-foot high speed wind tunnel (16-foot-diameter test section) which tests relatively large models up to about 90 per cent of the speed of sound.

3. The 1-by-3-foot supersonic wind tunnel which tests small models at speeds equivalent to 1,600 miles per hour at sea level.

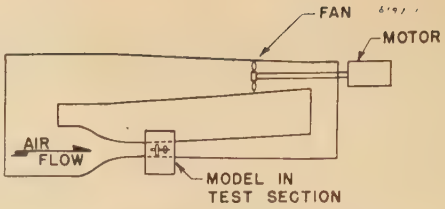

Figure 1. Schematic sketch of the essential features of a wind tunnel

These tunnels require, respectively, 36,000, 27,000, and 10,000 horsepower. Four other wind tunnels of various particular characteristics make a total connected wind-tunnel-fan horsepower of 87,950. An additional 50,000-horsepower supersonic wind tunnel now under construction, plus the miscellaneous laboratory equipment, will bring the total connected horsepower of the Ames laboratory to well over 150,000 horsepower. Figure 3 shows the 27,000-horsepower 16-foot high-speed wind tunnel.

The requirements for the drive system for a wind tunnel are quite exacting in that they usually require adjustable speed over a very wide range and steady speed at any given speed setting, while at the same time often requiring tremendous motor sizes. Operation is intermittent and the equipment must withstand frequent starting, stopping, and speed changing. In large sizes, power factor of the drive system may be important, and starting surges or surges during speed changing may be a critical factor for large wind tunnels.

Of the various types of adjustable speed drives available, the d-c adjustable voltage system (in which the propeller is driven by a d-c motor supplied by a separate generator, and the speed control is obtained by varying the voltage of the generator) has been almost ideal for these applications because of its simplicity of control, wide speed range without discontinuities, and adaptability to automatic control. This system has been used for most small and medium sized wind tunnels. Various other types of systems have been used for larger tunnels, either in an attempt to decrease the cost over that of the d-c adjustable-voltage system or to avoid problems which arise in applying the d-c system in very large sizes. In recent years what is sometimes called the modified Kraemer system has been used very successfully on several large wind tunnel drives, including the Ames 36,000- and 27,000-horsepower tunnels. In this system the main propeller motor is a wound-rotor induction motor, and speed control is obtained by impressing a voltage of controllable frequency on the rotor of the induction motor.

Modified Kraemer Adjustable Speed Drive

To understand the operation of the modified Kraemer system, it might be well to consider first the action of the wound-rotor induction motor with conventional speed control by means of secondary resistance. The voltages and power in the rotor circuit are indicated in Figure 4a. For ease in understanding, the rotor circuit is shown in Figure 4 as though single phase, and, in determining components of power, internal losses are neglected. As the resistance connected across the rotor is increased, the rotor must slip a greater amount in respect to the rotating stator flux in order to generate sufficient voltage in the rotor circuit. This circulates sufficient current in the rotor to develop the necessary torque, resulting in a decrease in speed. By varying the rotor resistance a range of speeds may be obtained. The current and voltage in the rotor circuit will be alternating at a frequency corresponding to the slip between the rotor and the stator flux. As far as the rotor circuit is concerned, the motor acts like a generator and, neglecting motor internal losses, induction motor theory shows that

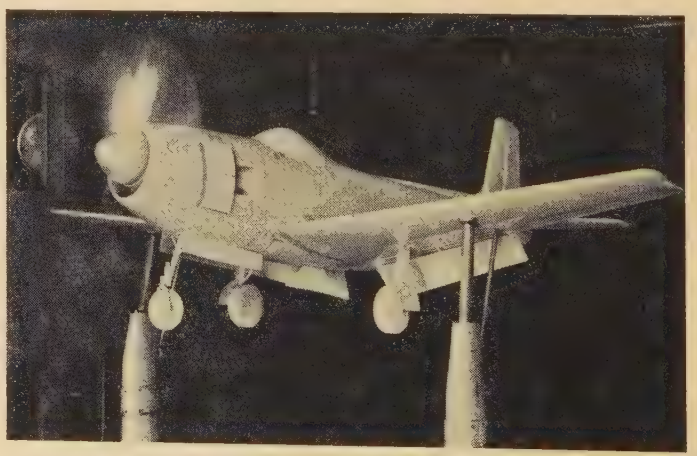

Figure 2. A powered model mounted in the 7-by-10-foot wind tunnel at the NACA Ames Aeronautical Laboratory, Moffett Field, Calif.

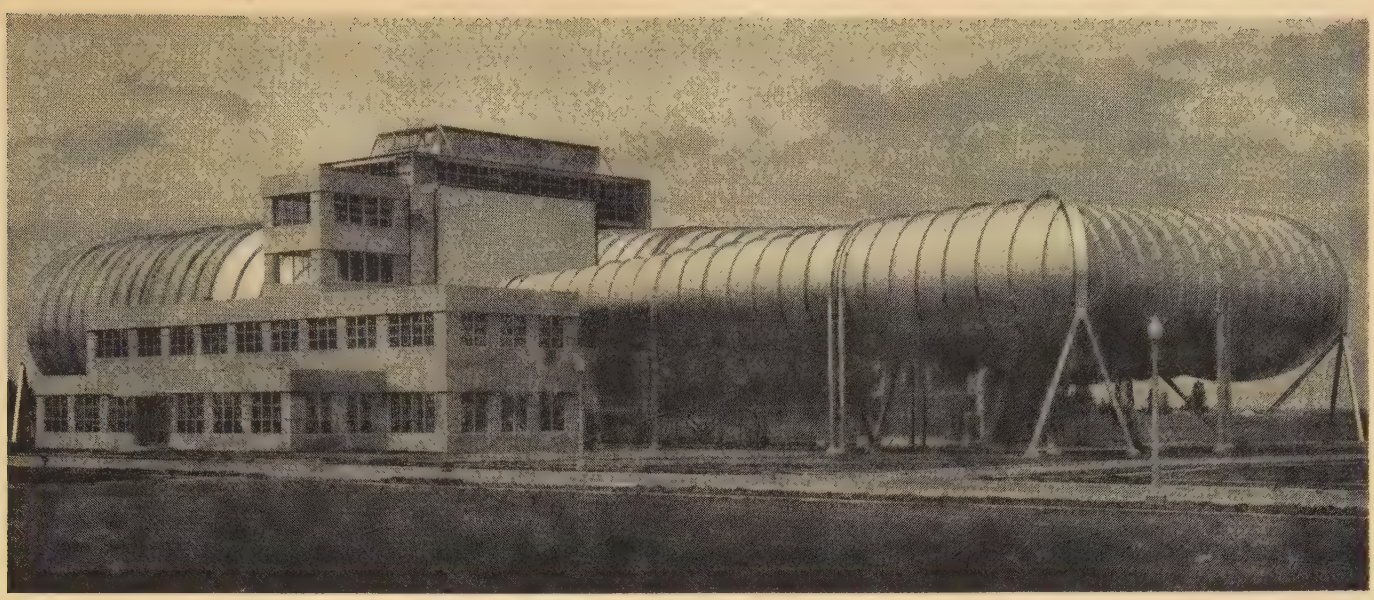

Figure 3. The 27,000-horsepower 16-foot high speed wind tunnel at the NACA Ames Aeronautical Laboratory

an amount of power is dissipated in the resistor equal to Ps, where P is the power input to the motor and s is the slip in fraction of synchronous speed. Thus power is wasted, resulting in a low efficiency which cannot exceed $(P - Ps)/P = 1 - s$ = speed in fraction of synchronous speed.

If it were possible to generate a voltage whose frequency would at all times be equal to the slip frequency of the motor and in the proper phase relationship, it would be possible to substitute this generated voltage in place of the voltage drop across the resistor. An alternator may be considered as a source for such a voltage. At first glance it would seem impracticable, in replacing the resistance by an alternator, to keep the generated frequency the same as the rotor frequency so that the generated voltage at all times would be exactly opposite in phase to the voltage induced in the rotor circuit. However, upon studying the arrangement further, it will be found that any tendency for the alternator voltage to change in frequency or phase in respect to the rotor voltage will result in a circulating current which will produce a synchronizing torque tending to prevent the two from getting out of phase. This action is very similar to that which occurs in the case of a synchronous motor which, within the limits of its pull-out torque, always will remain with its internal generated voltage in phase opposition to the line voltage. If the frequency of the alternator is decreased by decreasing the alternator speed, the synchronizing current induced between the alternator and the induction motor rotor will increase the motor torque causing the rotor to speed up, thus decreasing the slip frequency and permitting the two to remain in step. Conversely, if the alternator frequency is increased, the resulting circulating current will cause the induction motor to decrease in speed so that the increased slip frequency still matches the alternator frequency. Thus, the speed of the induction motor may be controlled over the operating range by varying the speed of the alternator connected to the rotor. Similarly, as the main motor is loaded and tends to slow down, the corresponding phase shift between the rotor voltage and the alternator voltage causes a circulating current to flow which produces the necessary torque to support the load. The same circulating current flowing through the alternator tends to speed up the alternator, causing it to act as a motor. The flow of power is shown in Figure 4b.

The speed of the alternator can be adjusted most readily by driving it by a d-c motor supplied from a d-c generator with adjustable voltage speed control. The complete system is outlined in Figure 5 for the case of a single fan motor.

The alternator must be of sufficient size to handle the full load rotor current of the induction motor, and must be able to produce, at the primary frequency, a voltage equal to the rotor voltage of the induction motor at standstill; although, with a fan load, the conditions of maximum current and maximum voltage never occur simultaneously. The power which must be handled by the motor-generator sets under any particular condition of load and speed must be equal to the power in the induction motor rotor circuit which otherwise would have been dissipated in a secondary resistance. This power, as previously stated, is equal to Ps, or, in terms of the motor output, the rotor power is $P_o[s/(1-s)]$, where P_o is the power output. For a fan load varying as the cube of the speed, such as is encountered in the usual wind tunnel drive, the rotor power reaches a maximum value at two-thirds synchronous speed equal to approximately one-seventh of the motor horsepower rating. Thus, it may be seen that most of the auxiliary machines are much smaller in size than would be the motor-generator set for a straight d-c adjustable-voltage system.

This modified Kraemer system is considerably more complicated in the number of machines involved and the complexity of the control than a straight d-c adjustable-voltage system. In fact, it involves, in addition to the wound-rotor motor, a complete adjustable-voltage system for secondary frequency control. The advantage of the modified Kraemer system on extra large drives lies in the reduced size of the d-c machines, and the fact that the equipment may be started with less disturbance to the power system than in the case of starting the adjustable-voltage d-c system. This system has essentially all the desirable control characteristics of the d-c adjustable-voltage system, including ready control of power factor and good efficiency.

In the usual starting sequence the constant speed motor–generator set is first started. This set is quite small compared with the rating of the main motor and offers no difficulties from the standpoint of starting surge. The variable speed set then is brought up to speed with the alternator excited until the alternator frequency is 60 cycles. Since

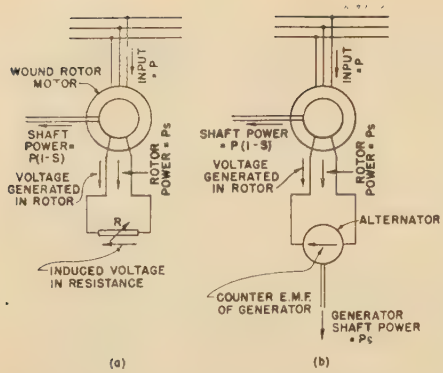

Figure 4. Voltage and power relations in the circuit of a wound-rotor induction motor

(a.) With resistance in secondary circuit
(b.) With counter electromotive force of an alternator in secondary circuit

the alternator is connected to the main motor rotor at all times, a voltage appears on the primary of the motor. By adjusting the alternator speed the motor stator voltage may be synchronized with the line voltage and the motor primary breaker closed with no attendant power disturbance. The motor then may be caused to rotate at any desired speed by reducing the speed of the alternator. With this system a 27,000-horsepower motor can be brought onto the line with no more disturbance than that incurred in starting a 5,000-horsepower synchronous motor.

While exciting the main motor from the secondary side prior to synchronizing, the d-c machine of the constant speed set is generating, driving the variable speed set. After synchronizing, when the alternator frequency is reduced and the main motor starts rotating and picking up load, the flow of power is reversed. Thus the various machines operate sometimes as generators and at other times as motors, and the terms generator or motor are meaningless.

Figure 5 shows a single fan motor. The modified Kraemer system functions equally well if the load is divided among two or more motors with their rotors connected to a single alternator. In fact the 36,000-horsepower wind tunnel, because of its tremendous size, actually uses six 6,000-horsepower motors and fans arranged aerodynamically in parallel in a double row of three above three (Figure 6). The motors are mounted in the air stream, housed in the faired enclosures immediately in front of the propellers. Since all motors are connected to a common frequency on the stator side and to another common frequency on the rotor side, they operate in exact synchronism with each other. In the 16-foot wind tunnel the 27,000 horsepower is divided between two 13,500-horsepower motors driving separate counterrotating fans in tandem (Figure 7). The two motors are mounted back to back in the steel enclosing drum between the two fans.

A doubly fed induction motor is similar to a synchronous motor in that it has a revolving stator field and a separately excited rotor field, the two fields being locked into step by the synchronizing torque. As a synchronous motor tends to oscillate, or hunt, so also does the doubly fed induction motor. A damper winding cannot be used on the induction motor, as on the synchronous motor, because the magnetic flux normally rotates in respect to the rotor at slip frequency and would generate a high voltage in the damper winding even though there were no hunting. Thus the hunting problem demands careful attention on the part of the designer. Where there is a single motor, damping can be incorporated in a damper winding in the variable-frequency alternator. However, if two or more induction motors are connected in parallel to a single alternator, it is possible for the motors to oscillate in respect to each other without affecting the alternator, thus obtaining no help from the damper winding. In the 16-foot wind tunnel with its two motors, the manufacturer avoided independent oscillations between the motors by connecting the variable frequency alternator in series in the rotor circuit between the two motors so that circulating current between the two motors also must pass through the alternator. In the 40-by-80-foot wind tunnel with its six motors there was no alternative to the parallel connection, and hunting was prevented only by careful attention to damping factors in the design.

Figure 8 shows the control motor–generator sets at the 16-foot wind tunnel.

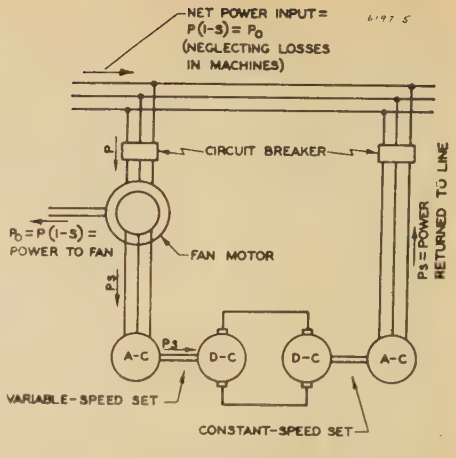

Figure 5. Connection diagram for a complete modified Kraemer system

Two d-c machines are seen on each set because it was impracticable to handle the full power in a single d-c machine. Figure 9 shows a view of the associated switchgear. Modern metal clad switchgear is used throughout, using oil circuit breakers of 500,000 kva interrupting capacity. Controls are semiautomatic so that the wind tunnel operator can devote his full attention to the test under progress. Only such simple controls as a "start-stop" switch and a speed control switch are required to give the operator complete control of the massive wind tunnel drive equipment. When starting a run the operator simply turns the start-stop switch to "start." Without further attention on his part the equipment automatically goes through the sequence of starting the various auxiliary machines and motor–generator sets and automatically synchronizing them with the line. When the main motors are on the line a red light is illuminated on the control panel signalling to the operator that the equipment is on the line ready for him to adjust the speed as needed. The complete start consumes approximately four minutes.

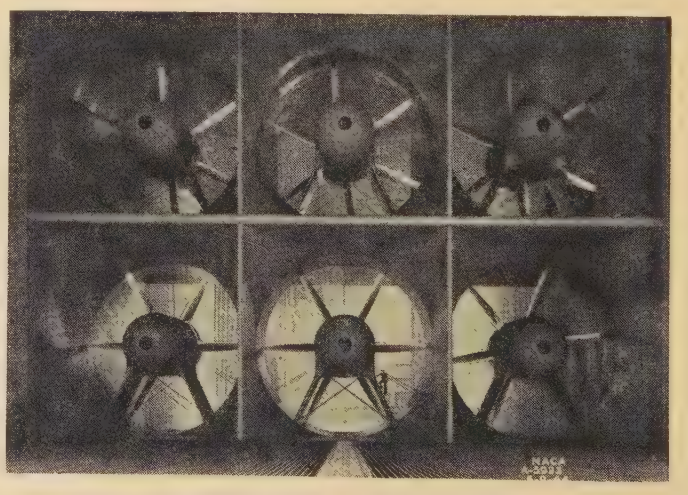

Figure 6. View looking upstream at fans of the NACA 40-by-80-foot wind tunnel—six fans, each driven by a direct - connected 6,000 - horsepower motor

Combination Slip-Regulator and D-C Drive

The 12-foot pressure wind tunnel, with 10,250 fan horsepower, uses to advantage a combination of d-c adjustable-voltage control and wound-rotor induction motor with secondary resistance control. The fan drive unit consists of a 1,250-horsepower d-c motor and a 9,000-horsepower wound-rotor induction motor in tandem. A motor–generator set supplies adjustable voltage direct current for the d-c motor, while a liquid rheostat provides an adjustable resistance for the induction motor rotor circuit. Since the fan load of a wind tunnel varies approximately as the cube of the speed, a tunnel requiring 10,250 horsepower at full speed would require only 1,280 horsepower at one-half speed. Thus the 1,250-horsepower d-c motor provides ample power up to almost half speed. Above half speed the induction motor is energized and its secondary resistance adjusted so that it carries the excess load. At full speed both motors are carrying full load. Sensitive automatic speed regulation is maintained at all speeds through the d-c motor to prevent fluctuations in speed.

Supersonic Tunnel Drives

The wind tunnels discussed thus far all operate at test air speeds below the speed of sound. Wind tunnels designed for operation at test section air speeds in excess of the speed of sound, that is, supersonic wind tunnels, exhibit some quite different characteristics.

1. In the supersonic tunnel the volume of air handled is relatively small and pressure differences relatively high; consequently, the "fan" of a supersonic tunnel has less of the characteristics of an ordinary fan or airplane propeller and is more like a turbine or air compressor. In fact, the 1-by-3-foot supersonic wind tunnel uses commercial centrifugal type air compressors to move the air.

2. At supersonic speeds, an attempt to increase the air speed by speeding up the blower results primarily in an increase in air density at the test section rather than an increase in air speed. Hence air speed control in this class of wind tunnel must be obtained by changing the nozzle contours and the cross sectional area of the test section, and a constant speed motor may be used to drive the blower.

The 10,000 horsepower 1-by-3-foot supersonic wind tunnel utilizes four 2,500-horsepower synchronous motors driving individual compressors. The 50,000-horsepower supersonic wind tunnel now under construction will utilize two 25,000-horsepower wound-rotor induction motors driving an axial-flow compressor. However, wound-rotor motors were selected instead of synchronous motors, not for speed control, but rather from considerations of starting of large machines with high WR^2 load.

Variable Frequency Systems

In conjunction with the wind tunnels another major application of electric power is in the operation of model propellers on models undergoing tests. The rapid increase in the engine power in airplanes in recent years has made the effects of the propeller slipstream and propeller thrust so important an item in the characteristics and control of the airplane that it is no longer possible to obtain sufficiently useful test information on the model without duplicating the action of the propellers. In a full-scale wind tunnel it is usually convenient to use the actual service engine and propeller when testing airplanes. In models, however, it is necessary to provide some other source of propeller power. When a small-scale model is scaled down from the actual airplane, it generally is found that the space available for a motor to provide the motive power for the propeller on the model is much too small for any standard motor. Also, the rotational speed required for the propeller is very high. In scaling down the propeller operation from a full-scale airplane to a small model, it is necessary that the tip speed of the propeller on the model be the same as the tip speed on the full-scale propeller. This necessitates that the propeller speed be increased in proportion to the decrease in its diameter. Thus, if a full-scale propeller operates at 1,500 rpm, the propeller on a 1/10-scale model would have to turn at 15,000 rpm.

To meet these difficult conditions, the most practical solution has been the use of 3-phase squirrel cage induction motors, since this type of motor is simplest in construction and smallest in size for its

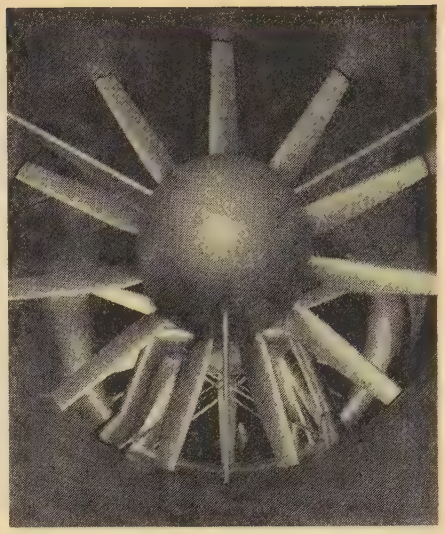

Figure 7. View looking upstream at fans of NACA 16-foot high speed wind tunnel at the Ames Aeronautical Laboratory—two fans, each direct connected to a 13,500-horsepower motor

horsepower rating. Even then, in order to get the power within the available space, all possible means must be taken to keep size at a minimum. Consequently, the motors are water cooled and are operated at temperatures which would not be tolerated in ordinary motors, but which give a reasonable length of life for such test purposes. A few small motors have even used carbon dioxide from high pressure cylinders as a refrigerant for cooling. As examples of what can be obtained in motors of this type, motors rated 22 horsepower at 12,000 rpm and measuring only $4^1/_2$ inches in diameter by 12 inches long and motors rated 100 horsepower at 10,000 rpm measuring 8 inches in diameter by $16^1/_8$ inches in length are typical of water cooled models. A motor 2 inches in diameter by $7^5/_8$ inches long is available rated 4 horsepower at 18,000 rpm with combined water and carbon dioxide cooling. Figure

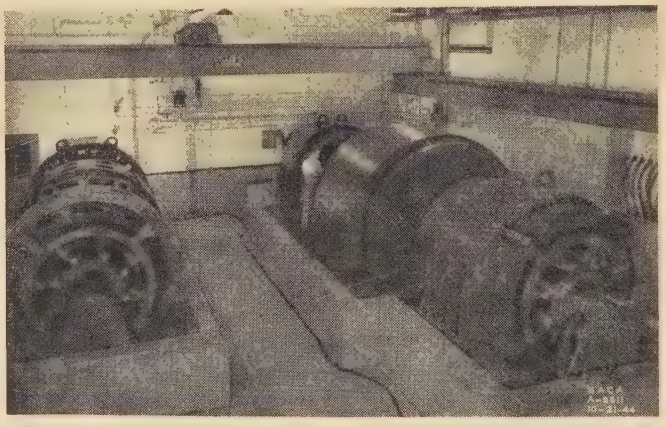

Figure 8. Control motor – generator sets for NACA 16-foot wind tunnel drive system at the Ames Aeronautical Laboratory

Figure 9. Switchgear for control of the NACA 16-foot wind-tunnel drive at the Ames Aeronautical Laboratory

10 shows the 4-horsepower and 100-horsepower motors with a conventional 1-horsepower general purpose motor for comparison. These motors for models usually are designed to carry their rated load for approximately 20 minutes, which allows sufficient time for the average test. They have been built in ratings from 2 horsepower at 18,000 rpm to 1,000 horsepower at 2,400 rpm. The aeronautical laboratories continually are attempting to produce smaller and more powerful motors.

On these high-power high-speed motors, bearings are a major problem. Thus far, antifriction bearings have been used exclusively. A major addition to bearing troubles arises from the dissipation of the heat from the rotor of the motor. The stator is readily water-cooled, but there is no way of applying water to the rotor. Consequently, any heat generated in the rotor tends to travel along the shaft and heat the bearings. The point has not been reached where the bearings can be depended upon completely. However, it has been found necessary to provide the bearings with considerable internal looseness of the balls in the races in order to allow the inner race to expand without causing the bearing to become tight.

In nearly all tests using model propellers, it is essential to be able to vary the propeller speed over a wide range. Since the motors are of the squirrel cage induction type, the only means available for varying their speed is to change the frequency of the power supply from which they are operated. Thus, a variable frequency power supply is a necessary accessory for power-on tests. These variable frequency power supplies consist of either an alternator or a frequency changer driven at any speed over a wide speed range by a d-c motor supplied from a separate d-c generator with adjustable voltage control. In order to obtain the necessary high speeds with squirrel cage induction motors, it is necessary to operate them on high frequencies. Thus approximately 300 cycles per second are required for 18,000 rpm. There are seven separate variable frequency systems at the Ames laboratory of ratings from 100 kw at 400 cycles to 1,800 kw at 150 cycles. The motors usually are operated at a constant ratio of voltage to frequency because this results in a constant magnetic flux in the motor and gives approximately a constant value of current for a given torque throughout the speed range. However, different values of volts per cycle are required for different motors.

The distribution of the output of each variable frequency set to several points of utilization offers interesting problems. The ordinary a-c power distribution system is a simple parallel system—the voltage and frequency are constant, the circuit is energized at all times, and motors and equipment necessarily are provided with any features required for starting on a full voltage system. Any number of loads can be manipulated independently without appreciably affecting each other. On variable frequency systems, however, only a single load can be served at a given time from one variable frequency set since each load requires individual control of voltage and frequency. Controls must be provided at each point of utilization for varying the voltage and frequency, and interlocking must be provided to insure that only one station has control at any one time, all other loads being disconnected. Variable frequency motors normally are started on reduced frequency and voltage without auxiliary starting equipment. This necessitates interlocking equipment to prevent application of the power unless the voltage and frequency are at low values. These requirements result in rather involved systems when one variable frequency set must serve several different load stations, or when provisions are required for paralleling sets for added capacity. Distribution problems are complicated further by high voltage drop in cables because of high reactance at the high frequencies involved.

The same line of high speed motors and variable frequency supply systems is used to drive blowers, instead of propellers, to simulate the jet from a jet engine. The testing of jet propulsion combinations has introduced a new need for extremely high speed motors in high horsepower ratings.

Power Supply and Distribution System

Electric power is delivered to the laboratory at 110,000 volts from the Pacific Gas and Electric Company's large sub-

Figure 10. Two typical motors for powered aircraft models shown in comparison with a conventional general purpose motor

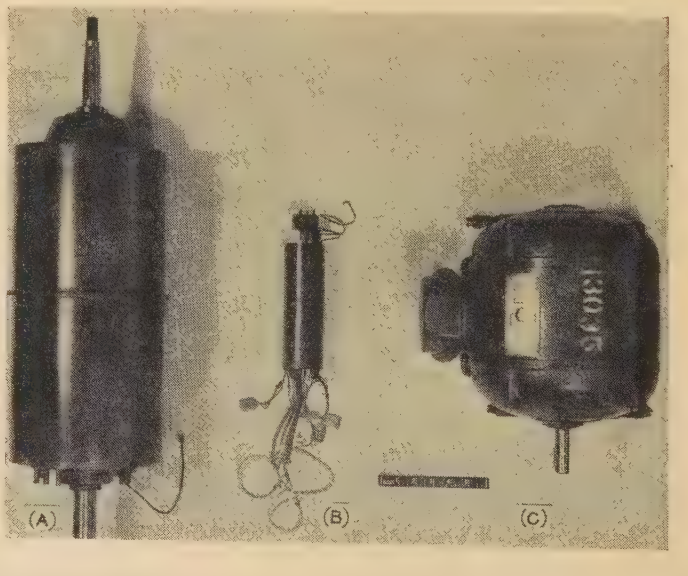

A. A 100-horsepower 10,000-rpm water cooled motor

B. A 4 - horsepower 18,000-rpm water- and carbon-dioxide - cooled motor

C. A 1 - horsepower 1,725-rpm conventional general purpose motor (shown for comparison)

Fault-Current Measuring Device

MARTIN J. LANTZ
ASSOCIATE AIEE

IN electric power system operation numerous problems are encountered in analyzing the results of short circuits and in the physical location of the trouble. Some devices now available for analyzing short circuits in a-c circuits are the oscillograph, the annunciator ammeter, and a magnetic link device requiring rectifiers. The oscillograph is the most accurate device but is expensive. The annunciator ammeter provides a limited amount of data; however, it offers a high electric burden to the circuit and does not have closely graduated steps of reading.

When a short circuit occurs on a power system, the current normally increases immediately in the faulted area. The device that records the phenomena must be very rapid and positive in action. It must not interfere with the electrical characteristics of protective apparatus in the same circuit, and it must be prepared to operate automatically, recording values that may be interpreted later. To be extensively applied, the device must be inexpensive, reasonably accurate, and reliable.

The fault-current measuring device described in this paper meets these requirements.

Paper 46-179, recommended by the AIEE committees on instruments and measurements and protective devices for presentation at the AIEE Pacific Coast meeting, Seattle, Wash., August 27–30, 1946. Manuscript submitted March 26, 1946; made available for printing July 9, 1946.

MARTIN J. LANTZ is in the system engineering section of the Bonneville Power Administration, Portland, Oreg.

Description of Device

The fault-current measuring device for use in a power circuit consists of one or more coils of insulated copper wire with magnetic links snugly fitted within them, and a standard high-speed voltage relay with low resistance and normally closed contacts shunting the coils (Figures 1–3). The use of a surge-crest ammeter and a demagnetizing coil is required to read the magnetization of the links and to demagnetize them after energization. The surge-crest ammeter is a special device used principally in lightning investigation for measuring the degree of magnetization of magnetic links. The magnetic link consists of three or four small magnetic laminations enclosed in a small tube. The device may be built with one or more coils to cover the desired current range. It is designed to operate in the secondary circuit of current transformers and is placed in series with the regular current-operated system protective relays or in the metering circuits. The burden of the device is low.

The high-speed by-pass relay is used with the device to minimize the effect of the initial d-c offset that may occur when the magnitude of an inductive alternating current is suddenly increased. In the field test application the by-pass relay was energized from the same direct voltage circuit that energized the tripping circuit of the oil circuit breaker. The by-pass relay which operates as a result of action by the system protective relays then opens its normally closed contacts across the coils one cycle or more prior to the zero point of the interrupted wave, allowing the current to be measured to flow through the coils and magnetize the links. The magnetic links are in the electric circuit when used with the by-pass relay only after the relay is energized and the by-pass contacts are open. Figure 4 is a typical schematic installation of the device. After operation of the device a target shows, the coils are again by-passed, and the by-pass relay locks out to prevent a second operation. A second device may be placed in service automatically if desired.

One device designed and tested covers a current range of approximately 4 to 60 amperes rms alternating current and consists of a 12- and a 56-turn coil in series. Assuming a 600/5 ratio current transformer, a primary current range of approximately 500 to 7,200 amperes is covered.

Theory

The magnetic link is placed in the coil and is magnetized by an alternating current flowing through the coil. This alternately magnetizes the link in one direction and then the other, the magnetism following the link's hysteresis loop. Each half cycle of symmetrical current demagnetizes the magnetism resulting from the previous half cycle and remagnetizes the link in the opposite direction. The electrical principle of the device is based upon the hysteresis loop of the small magnetic link and the interruption of the current at the zero point

station at Newark, Cal. A 50,000-kva and a 5,000-kva transformer bank reduce the voltage to 6,600 volts for distribution to the various loads which all are located relatively close to the substation. For the 50,000-horsepower supersonic tunnel under construction, an additional 62,500-kva transformer bank is being installed.

Owing to the large concentration of power, careful consideration has been required to keep the short-circuit capacity on the 6,600-volt feeders under 500,000 kva. To exceed the 500,000-kva limit would increase the cost of motor-control switchgear greatly as well as increase the probable extent of the damage in case of a fault. To keep within the 500,000-kva limit it was found necessary to avoid interconnecting the 6,600-volt busses of the proposed 62,500-kva bank and the existing 50,000-kva bank and install a small amount of reactance in the feeders to the 50,000-horsepower supersonic tunnel. The machines of the large wind tunnel drive systems make appreciable contributions to the short-circuit capacities on the 6,600-volt busses.

Power is distrubuted at 6,600 volts to the various buildings for small power and lighting. Y-connected 120/208-volt systems, on which 120-volt single phase loads may be distributed on all three phases, are used to advantage in the buildings, where the loads are a combination of lights and 3-phase motors. In a new hangar and shop building of much larger size than previous buildings, a 440-volt system was installed for building distribution and for motor loads with 440- to 120/208-volt dry-type transformers at load centers for lighting and convenience outlets.

Wind tunnels always operate intermittently, and much of the time at less than maximum rated power. Consequently, by staggering operation of several wind tunnels, it is possible to operate under a maximum kilowatt demand limit much less than the total kilowatt rating of the apparatus. In order to make most efficient use of power within the established maximum demand limit without unnecessarily delaying any wind tunnel, a totalizing and telemetering system is being installed which will indicate at all times at each wind tunnel control desk and at a central dispatcher's office the total kilowatt demand for the entire laboratory.

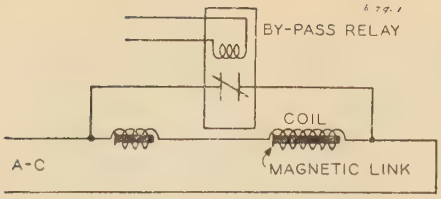

Figure 1. Schematic diagram of basic device for fault-current measurement

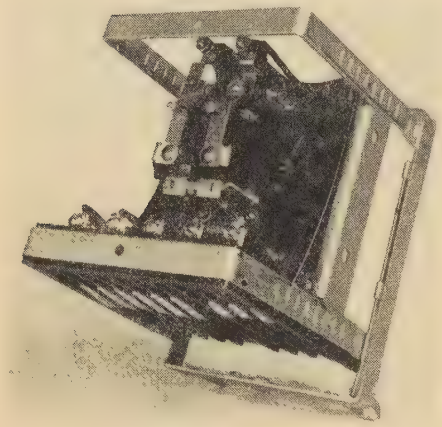

Figure 2. Rear view of preliminary sample of fault device showing relays

Device is mounted in cradle of standard single element protective relay

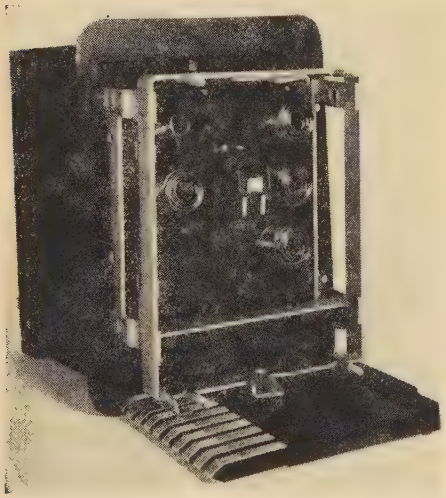

Figure 3. Front view of preliminary sample of fault device showing coils and links

(Figure 5). The residual magnetism retained by the magnetic link is proportional to the peak or crest magnitude of the last half cycle of the current, providing the last two half cycles are approximately equal in magnitude. This magnetism is then measured with a surge-crest ammeter. A calibration curve is obtained by plotting surge-crest ammeter readings against alternating current values. This provides a direct means for determining the last half cycle of alternating current through the coil by interrupting the current at zero and reading the degree of link magnetization by the surge-crest ammeter.

If the current is asymmetrical containing a d-c component, the magnetism of the link is affected and records a value which will not compare with a calculated or measured symmetrical value. The initial surge of direct current may place an amount of magnetism in the link that cannot be wiped out before the circuit is interrupted by the successive half cycles of opposite direction. The by-pass relay effectively eliminates the d-c component from the link as long as it is by-passed and then applies a reduced d-c component to the link, resulting in a more accurate determination of the magnitude of the last half cycle. By placing in series with the coils a 0.2- to 0.3-ohm resistance, the current is diverted to the by-pass relay contacts. This is a precaution against contact resistance and adds only a small burden to the circuit during the time the by-pass contacts are open. The illustrated replica of a test oscillogram demonstrates the action of this by-pass relay (Figure 6).

Use and Advantages

The basic device, which is considered to be the coil and link, will record automatically the magnitude of the last half cycle of an alternating current wave preceding its interruption at current zero by an oil circuit breaker. To obtain data of practical value on power systems with high-speed oil circuit breakers which may not allow time before opening for the d-c component effect to neutralize itself in the link, the by-pass relay is a necessary adjunct to the device. The data obtained by the device will aid greatly in determining the actual current values from short circuits on power systems.

Table I. Summary of Laboratory Tests on Fault-Current Measuring Device

Number of Turns in Coil	Number of Readings	Max Deviation, Per Cent	Average Deviation, Per Cent	Current Range, Amperes
45	6	−10.7	+2.1, −6.3	5.3–17
20	4	+ 8.7	+4.5, −4.2	9.4–38
12	12	+ 9.8	+3.3, −4.8	15.6–61
10	7	−10.6	+5.3, −7.8	18.8–77
5	6	+10.5	+8.7, −5.3	38.5–84

The following is a list of some of the advantages over devices which accomplish similar purposes, such as the automatic oscillograph and the annunciator ammeter:

1. Simplicity. There are no moving parts in the recording portion of the device, therefore no mechanical failures resulting from restrained movement can occur. The by-pass relay is considered as auxiliary to the basic device.

2. Instantaneous operation. There is no mechanical inertia in the recording portion of the device. It requires no mechanical action and is ready at all times for instant record.

3. Durable record. It is desirable to read the device soon after its operation but the reading may be deferred a number of hours.

4. It records a value proportional to the magnitude of alternating current without resorting to initial rectification.

5. Used in conjunction with a by-pass relay to record the last half cycle of a transient asymmetrical wave, the effect of the possible high initial d-c offset resulting from short circuits is materially reduced.

6. The device has a low electric burden and does not jeopardize the operation of protective devices.

7. The device may be automatically locked out of the circuit after operating.

8. The readings obtainable from the device are a continuous graduation of values obtained from a calibration curve allowing more accurate analysis to be made than is possible from a step-reading device such as the annunciator ammeter.

9. The device is inexpensive, making it

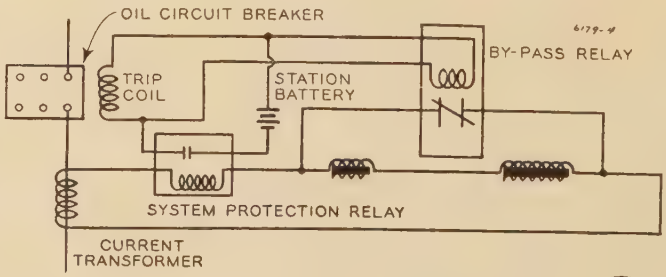

Figure 4. Schematic diagram of typical installation of fault-current device

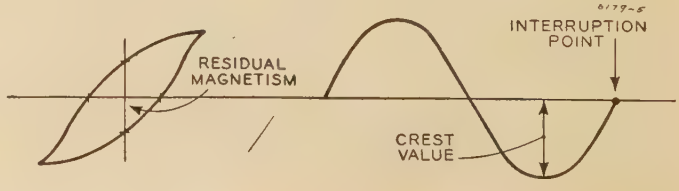

Figure 5. Hysteresis loop and sine wave

possible to distribute them extensively about the system to obtain operational records. As a fault-locating device and indicator of the type of fault, it can be applied to many lines where a more expensive device is not feasible.

Results of Tests

A series of tests using the magnetic link was made by the Bonneville Power Administration's electrical laboratory. These constituted both laboratory and field tests.

Laboratory Tests

The laboratory tests provided a-c and d-c magnetic link calibrations for various turn coils and tests to determine the effectiveness of the by-pass relay on asymmetrical waves. Data were secured for 5-, 10-, 12-, 20-, and 45-turn coils.

Figure 7. Fault device laboratory test on 5-, 10-, and 20-turn coils

⊙—A-c calibration
△—Link reading short-circuited by relay
⊡—Link reading not short-circuited by relay

Curve	Link	Turns of Coil	Max Deviation, Per Cent	Avg Deviation, Per Cent	Current Range, Amp
A	8	20	8.7	4.5, −4.2	9.4 to 38.5
B	6	10	10.6	5.3, −7.8	18.8 to 77
C	4	5	10.5	8.7, −5.3	38.5 to 84.8

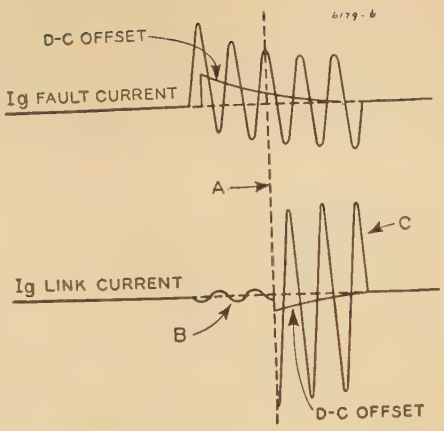

Figure 6. Replica of oscillogram showing results of use of by-pass relay across coil during system test

A—Current through coil when by-pass relay contacts are opened
B—Current through coil when by-pass relay contacts are closed
C—Last one-half cycle current measured by link

The a-c calibration data were obtained by adjusting the current with a variable resistive load. The energized circuit was closed through a circuit breaker into a resistance load, the circuit breaker opening at the zero point of current. Oscillographic records were obtained for all tests so that the results could be correlated. The a-c calibration points are indicated in Figure 5 by the circles. Peak amperes divided by the square root of two are plotted against surge-crest ammeter readings.

To determine the effect of the by-pass relay on offset currents, the resistance load was replaced with an inductive load. The current was passed through two coils in series, one of which was by-passed for a few cycles. The points in the squares, Figure 7, indicate the link readings containing the effect of d-c offset. The points in the triangles indicate the link readings in the by-passed coil. Shunting most of the d-c offset current around the link causes the link reading to move closer to the calibration curve.

Similar data are shown in Figure 8 for the 12- and 45-turn coils. Since the surge-crest ammeter readings are more accurate above 18 and below 70, these values were used as the limits of reliability.

Figure 8. Fault device laboratory test on 12- and 45-turn coils

⊙—D-c calibration
△—Link reading short-circuited by relay
⊡—Link reading not short-circuited by relay

Curve	Link	Turns of Coil	Max Deviation, Per Cent	Avg Deviation, Per Cent	Current Range, Amp
A	8	45	10	2.1, −6.3	5.3 to 17.2
B	6	12	9.8	3.3, −4.8	5.6 to 61.1

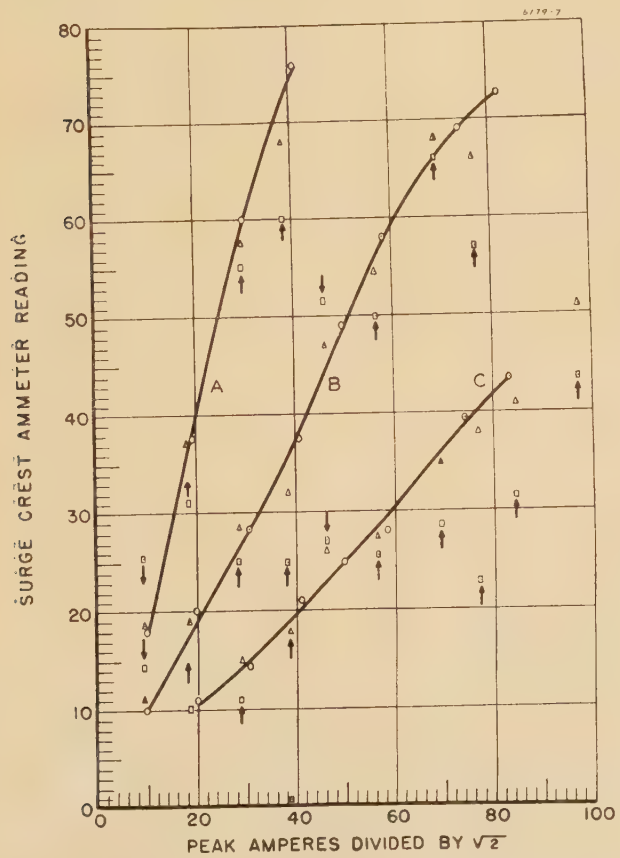

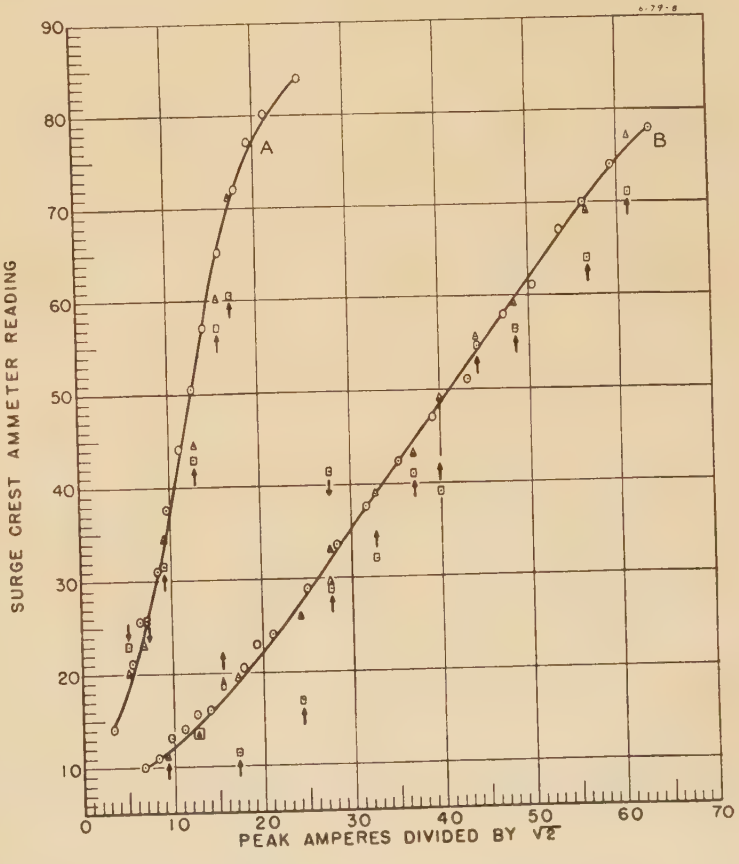

The relationship between actual oscillographic measured current values and current values measured by means of the magnetic link are expressed in Table I as percentages of the link reading.

Theoretically the magnetic link should be magnetized in proportion to the peak value of current for a sinusoidal wave. Tests show the magnetic link d-c calibration curve to lie slightly higher than the corresponding a-c calibration curve which is to be expected after the first half cycle of magnetization.

All tests conducted should give link readings corresponding to the a-c calibration curve. However, the tests conducted in the laboratory corresponded more closely to the d-c calibration curves. This was probably the result of a higher percentage of harmonics introduced by the highly reactive test load used.

Tests in the field corresponded more closely to the a-c calibration curve as expected. The a-c calibration curve was used as the basis for determining the field test currents.

Field Tests

A series of staged system fault tests was made in May 1945, including single-phase-to-ground, two-phase-to-ground, and phase-to-phase faults. A fault-current measuring device with a by-pass relay was installed during the tests. The data resulting from these tests are shown in Figure 9. The test data were plotted on the a-c calibration curve for the 12-turn coil. All data were compared with oscillographic records taken during the test.

Figure 9. Fault device field test on 12-turn coil

⊙—A-c calibration data
⊡—Link reading without by-pass
△—Link reading with by-pass relay

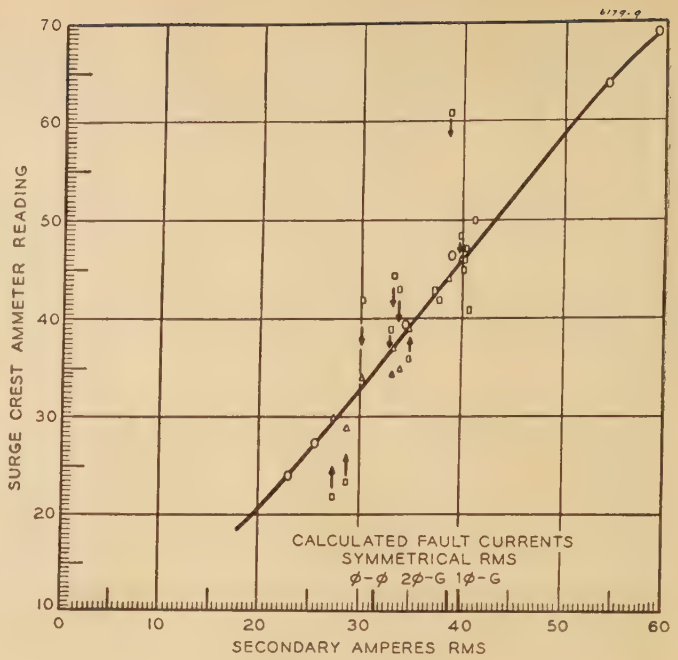

The oscillograms of the tests show a higher degree of d-c offset present than normally would be expected for system faults. Several tests resulted in a rather large amount of d-c offset still present at the time of interruption.

A second field test was conducted in January 1946, during which thirteen single-phase-to-ground faults were made on the system. The results of this test are summarized in Table II. A maximum deviation from the oscillographic record was 12.1 per cent with an average deviation of minus 3.9 per cent and plus 4.8 per cent. One failure was recorded. A possible explanation for this failure was that a d-c transient caused by the collapsing flux of a saturated current transformer demagnetized the link causing it to read low. A d-c transient of opposite direction to the last half cycle shows on the oscillogram after current interruption.

Table II. January 20, 1946, Midway Substation Single-Line-to-Ground Short-Circuit Tests

Results Obtained Using Fault-Current Measuring Device With By-Passed 12- and 45-Turn Coils

Test Number	Amperes Rms Last Half Cycle: Magnetic Link	Magnetic Oscillograph	Per Cent† Deviation
1	4,960	5,250	−5.9
2	4,770	4,770	0
2R	4,860	4,680	+3.7
*3	3,700	5,840	
4R	5,380	5,220	+3.0
5	1,295	1,290	+0.3
6	1,295	1,305	−0.8
7	2,305	2,030	+11.8
7R	2,400	2,170	+9.5
8	1,655	1,660	−0.3
8R	1,655	1,660	−0.3
9	1,645	1,845	−12.1
10	1,260	1,190	+5.6
		Average	−3.9, +4.8

* Failure to record correct value. Possible explanation in the text under field tests.

† $\frac{I_{oscillograph} - I_{link}}{I_{link}}$.

Conclusions

The magnetic link fault-current measuring device shows excellent correlation between its readings and corresponding values from oscillograms for both laboratory and field tests. The accuracy displayed on all the tests indicates a maximum deviation from the oscillographic record of approximately plus or minus 12 per cent and an average deviation of approximately plus or minus 5 per cent for the accepted design.

The tests conducted utilized a magnetic link and a surge-crest ammeter which were designed for a different purpose. Possibly a redesigned magnetic link and magnetism detecting device could be developed that would improve the operation of this device for the application to a-c measurements.

Magnetic Link Data. Midway Test May 20, 1945

Type of Fault	Number of Readings	Max Deviation,* Per Cent	Avg Deviation,* Per Cent
1ϕ-G	5	−10.5	2.7, −3.7
2ϕ-G	5	− 2.3	0.9, −1.5
ϕ-ϕ	6	6.6	3.3, −4.2

* Compare to asymmetrical rms current values.

The device may be used extensively on a system because of its simplicity and low cost.

Since it is a current-operated device, it may be used on lines or feeders of any voltage using the proper current transformers.

There are several advantages of the device, one being improvement over the accuracy of the annunciator ammeter for use as a fault locator using the current-ratio method. It may be used as a check on relay target operation when additional coils are used in the separate phases to determine the type of fault and phases involved. It is believed the device has very good capabilities for use on power systems for the determination of the magnitude of fault currents. It provides a method for determining the interruptoin current of an oil circuit breaker during a fault. The latter may be of value in scheduling maintenance for oil circuit breakers. The device measures the magnitude of the last half cycle of current being interrupted. The difference between the magnitude of the last half cycle cur-

Frequency Performance of Thyratrons

HUBERT H. WITTENBERG
ASSOCIATE AIEE

Synopsis: The frequency performance of small thyratrons is investigated by supplying anode voltage from a variable frequency electronic generator of 1,400 watts output capacity. At high audio frequencies there is a departure from the 60-cycle-per-second performance; the grid control characteristic resolves itself into two characteristics—a starting characteristic and an extinguishing characteristic. The starting characteristic is shown to be a function of grid–anode capacitance and grid resistance. The extinguishing characteristic is determined by deionization effects and so is a function of frequency, grid resistance, anode current, tube geometry, and gas pressure.

THERE are many applications for thyratrons at frequencies above the power frequency of 60 cycles per second. Inverters, servo controls, relaxation oscillators, radar modulators, and grid-controlled rectifiers for airborne equipment are examples of such applications. The frequency range is from a few hundred to 50,000 cycles per second. Although the circuits used in these applications are well understood, the exact nature of ionization and deionization effects on thyratron performance generally has not been known. This paper reports an investigation of such effects as affected by anode-supply frequency. A sinusoidal wave shape was used for the various tests because it frequently is used in actual circuits and because it is easy to generate. Wave shape affects thyratron performance, but performance with other wave shapes can be extrapolated from the results obtained with sine waves.

Paper 46-203, recommended by the AIEE committee on electronics for presentation at the AIEE Great Lakes District meeting, Indianapolis, Ind., October 9–11, 1946. Manuscript submitted May 13, 1946; made available for printing August 29, 1946.

HUBERT H. WITTENBERG is an engineer with RCA Victor Division, Radio Corporation of America, Lancaster, Pa.

In the tests the sinusoidal voltage is applied to the anode circuit of the tube under test; hence the voltage source must have considerable power capability. A high-power electronic audio-frequency generator capable of supplying 1,400 watts of power at 115 volts in the frequency range of 300 to 3,500 cycles per second was used in this investigation.[1] By means of an external signal generator, the equipment also could be used as a power amplifier to produce reduced power at frequencies up to 20,000 cycles per second. The output voltage of the generator is maintained at a preset level independent of load by means of a regulating circuit having a time constant of about one second.

Figure 1 shows a block diagram of the test setup. T is a stepup transformer to supply the anode voltage for the tube under test. R_L is a load resistor to limit the average anode current $\bar{I}_b$. Filament power for the tube under test comes from the 60-cycle power line. Peak anode voltage is measured with a diode type peak voltmeter. Wave forms of both current and voltage are monitored on a cathode-ray oscilloscope. Grid voltage is supplied by a 90-volt battery.

One type of thyratron, 3D22, was selected to be run through all the tests in which conditions would be subject to control by the user. The type 3D22 is a xenon-filled shield-grid thyratron rated for a peak forward voltage of 650 volts, a peak inverse voltage of 1,300 volts, and an average current of 0.75 ampere. Its control ratio is 150.

However, other tube types were put through some of the tests. The results reveal the effects of tube geometry and gas pressure, which are subject to control by the user, and thus aid the user in selecting the proper tube type for a given application.

An additional test shows the effect of change in gas pressure, a characteristic which is subject to control by the user only in the case of mercury thyratrons.

Thyratron Control Phenomena

Transition to On-Off Control

At a low frequency (60 cycles per second), the average current through a thyratron can be controlled by the grid and can be calculated from the following equation,[2] which neglects tube drop:

$$\bar{I}_b = \frac{\hat{E}_{bb}}{2\pi R_L}(1+\cos\theta)$$

$\hat{E}_{bb}$ = peak anode supply voltage (sinusoidal)
R_L = load resistance
θ = phase angle at which conduction begins

When the grid voltage is zero in a negative grid thyratron, θ is zero, conduction starts at the beginning of the anode voltage cycle, and maximum average current flows. With increasing negative grid voltage, θ approaches 90 degrees and the current is reduced to one-half the maximum average value. With only direct voltage on the grid, 0 to 90 degrees is the maximum range of variability since making the grid still more negative cuts off the current completely.

When the anode supply frequency is increased sufficiently, this mechanism breaks down. The grid no longer is able to vary the anode current; it becomes simply an on-off control, the current being established only by the external anode circuit. Figure 2 shows this transition in the case of the type 3D22 thyratron. The explanation of this form of operation is that ions remaining from the previous conduction cycle interfere with the grid control. At low frequency the interference is small and the extinction current is

Figure 1. Test setup for audio frequency testing of thyratrons

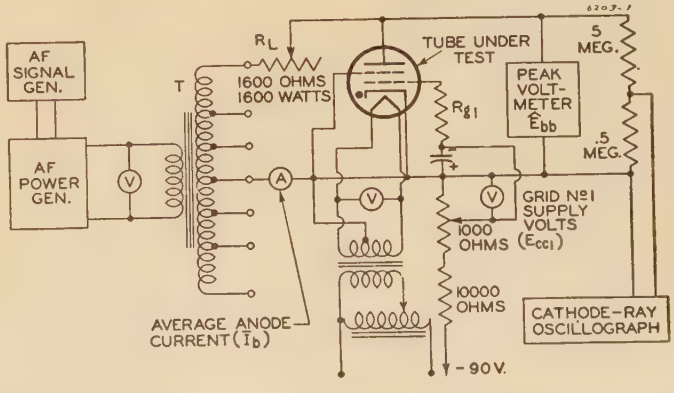

$\bar{I}$ = average current
$\hat{E}$ = peak voltage
Rating of transformer T:
Primary = 115 volts
Secondaries = 3,500/1,750 volts, 2,000/1,000 volts, and 1,000/500 volts
Volt-amperes = 2,120/2,750
Frequency = 0.3 to 3.5 kc

rent and the current at the time the contacts part, which is defined as the interrupted current, is usually negligible. This may not be true in the case of very fast circuit breakers opening before the d-c component has decayed to a non-critical point, for restrikes, nor for low-voltage circuit breakers where the arc voltage is sufficient to choke down the last half cycle of current. The instances in which the device will be subjected to these conditions probably will be infrequent.

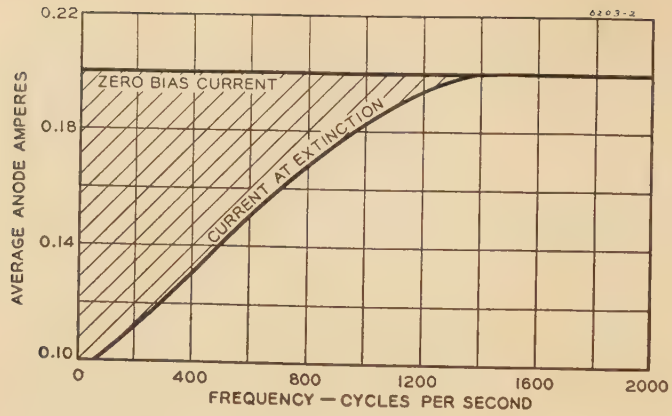

Figure 2. Extinguishing current versus frequency for type 3D22 thyratron

R_{g1} = 0.1 megohm
E_{cc2} = 0
R_{g2} = 0
E_{bb} = 650 volts

therefore nearly half the maximum current. As the frequency is increased, this interference increases, the extinction current increases until it reaches the maximum average value, and we have solely on-off control.

However, if one desires to obtain a variable anode current at frequencies beyond 1,500 cycles per second for the type 3D22 thyratron one can use the d-c bias-phase-control method.[3] In this case the grid voltage consists of a combination of direct voltage plus a 90 degrees lagging alternating voltage. This method is successful in controlling the average anode current at higher anode supply frequencies whereas the direct voltage method alone would fail. The explanation is that the alternating grid voltage sweeps out ions while swinging negative. Figure 3 gives the conditions under which this control may be applied to the type 3D22 thyratron at a frequency of 2,000 cycles per second where d-c grid voltage alone would not permit variable control.

Two Control Characteristics—Starting, Extinguishing

It became apparent as these tests progressed that there is not one but two control characteristics. One characteristic describes the relation between anode voltage and grid voltage on starting.

Table I. Capacitance Measurements of the Type 3D22 Thyratron

Tube Component	Capacitance, $\mu\mu$f
Socket	0.229
Grid–anode (inside envelope)	0.094
Effective base pin (tube in socket)	0.126
Total	0.449

This is the initial conduction of current and is not to be confused with the every cycle starting which accompanies an a-c anode supply. The other describes this relation for extinction or cutoff of the discharge. By cutoff is meant failure to reignite on successive cycles. Figure 4 shows how the extinguishing characteristic has shifted considerably in the negative direction at 2,500 cycles per second. This shift is caused by a lack of complete deionization. At a low frequency (60 cycles per second) the extinguishing characteristic is coincident with the starting characteristic.

To the author's knowledge the first investigator to indicate that there are two control characteristics was W. G. Shepherd of the Bell Laboratories. In 1943 Shepherd published a paper describing work on deionization effects in thyratrons.[4] He differentiated between a static and dynamic characteristic. The work was done with alternating voltage on the grid, and the dynamic characteristic was in terms of peak a-c grid swing necessary for stable operation.

However, it is believed that the concept of extinction control characteristic as herein presented is closer to the accepted definition of control characteristic.[5]

The Extinguishing Control Characteristic

As would be expected the extinguishing characteristic is a function of frequency. Figure 5 shows how this characteristic shifts with frequency for the type 3D22 thyratron. At 3,500 cycles per second the grid cutoff voltage is nearly ten times the 60-cycle value. The shift is increasing at a rate faster than proportional to frequency. Nevertheless, the grid is still potent as a control electrode, and in none of these tests did the grid lose control completely. If the grid voltage is made sufficiently negative it will sweep out the ions at a rate such that it can prevent reignition on the next positive cycle. The limit is reached, however, when the sum of the negative grid voltage plus the peak anode voltage exceeds the cold breakdown value between grid and anode; in other words Paschen's law is operating.

The Starting Control Characteristic

The starting control characteristic for the type 3D22 thyratron was found to be constant for frequencies from 60 to 3,500 cycles per second. However, this condition is a special case; usually the starting control characteristic is a function of fre-

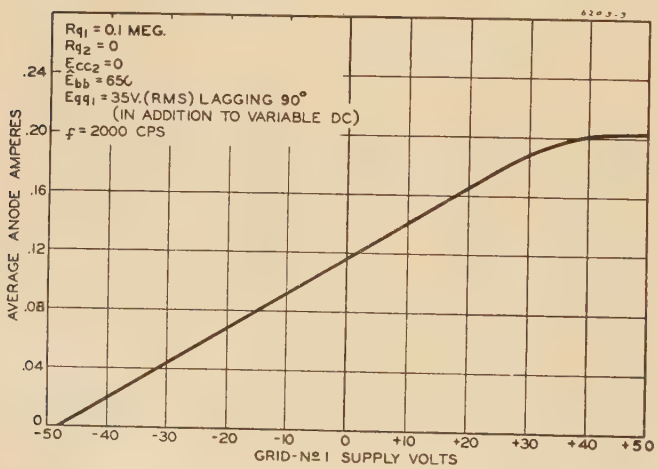

Figure 3. Thyratron control of type 3D22 combined direct voltage and 90-degree lagging alternating voltage

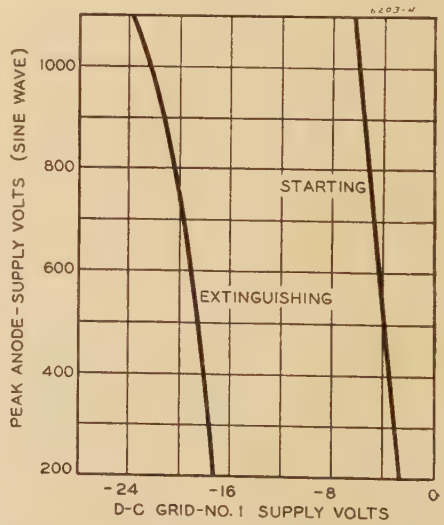

Figure 4. Control characteristics of type 3D22 thyratron starting and extinguishing

R_{g1} = 0.1 megohm R_{g2} = 0
I_b = 0.2 ampere at E_{cc1} = 0 E_{cc_2} = 0
Frequency = 2,500 cycles per second

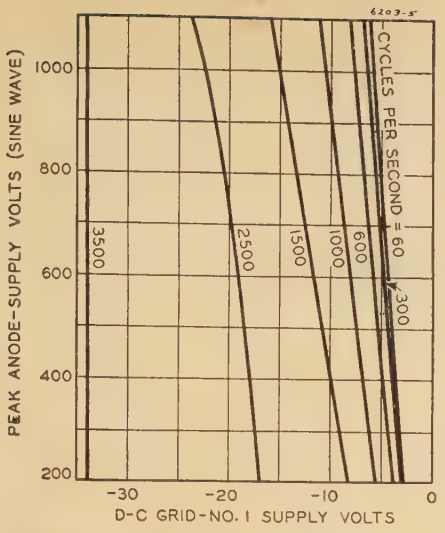

Figure 5. Typical extinguishing control characteristic of type 3D22 thyratron

R_{g1}=0.1 megohm R_{g2}=0
$\bar{I}_b$=0.2 ampere at E_{cc1}=0 E_{cc2}=0

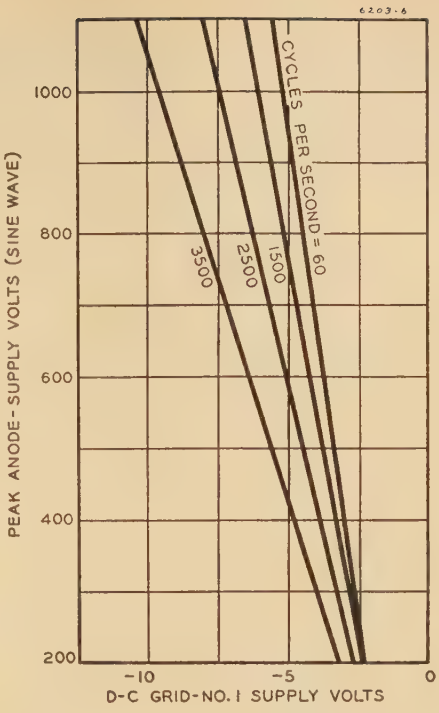

Figure 6. Typical starting control characteristic of type 2050 thyratron

R_{g1}=0.1 megohm R_{g2}=0 E_{cc2}=0

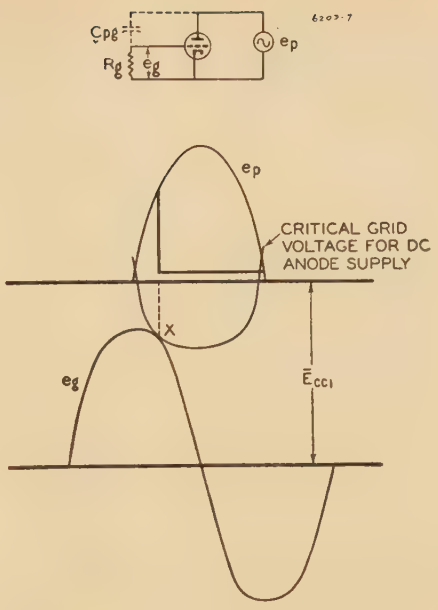

Figure 7. Anode–grid coupling in thyratron

quency. In order to illustrate the general case consider the type 2050 thyratron. The type 2050 is a xenon-filled shield-grid thyratron similar to the type 3D22 but smaller in size. The ratings are a peak forward voltage of 650 volts, a peak inverse voltage of 1,300 volts, and an average current of 0.1 ampere. Its control ratio is 250. Figure 6 gives the starting control characteristic as a function of frequency for this type. One may observe that, like the extinguishing characteristic, the shift is toward the negative grid voltage but that the shift is not as great. This shift is not caused by ionization but by coupling to the grid through the anode–grid capacitance shown in Figure 7.

The anode–grid capacitance C_{pg} is small and therefore its reactance is large in comparison with the grid resistance. Hence the induced grid voltage is nearly 90 degrees ahead of the anode voltage. This induced voltage becomes tangent to the critical grid voltage at point x. As the frequency of the anode supply is increased the induced voltage increases, and thus conduction begins at a more negative d-c grid voltage.

Control Versus Grid Resistance

The tests presented thus far all were made at one value of grid resistance, namely 0.1 megohm. Figure 8 shows the effect of varying this grid resistance at a fixed frequency of 1,000 cycles per second. Both the starting and extinguishing grid voltages become more negative as the grid resistance is increased.

It is now clear why no shift in starting characteristic was observed in the case of the type 3D22 thyratron. The grid resistance chosen (0.1 megohm) was not sufficiently large.

The explanation of the starting shift has been given. To check the data in Figure 8, capacitance measurements were made on the type 3D22 thyratron and its socket with the results as given in Table I. It is interesting to note that only one-fourth of the capacitance is contributed by the tube electrodes. Tube capacitance as published by tube manufacturers includes neither the interbasepin capacitance nor the socket capacitance.

The capacitive reactance of 0.449 micromicrofared at 1,000 cycles per second is 354 megohms. The peak induced grid voltage for the conditions of Figure 8 at five-megohm grid resistance is 9.18 volts The induced grid voltage does not cut the critical grid voltage at the peak of the induced voltage, but it is close to this value. Reading the data from the curve of Figure 8, we find that the shift in control grid bias from 60 to 1,000 cycles per second is from minus 4.5 to minus 16.5 or 12 volts. The remainder of the shift is caused by direct current resulting from leakage or grid emission.

The shift in extinguishing characteristic increases with grid resistance because of the effects just described plus deionization effects. Increasing the grid resistance decreases the effectiveness of the grid as a deionizing agent. The grid is able to sweep out fewer ions between conduction periods

Control Versus Anode Current

It is a common conception that the control characteristic is independent of current. At high audio frequencies this is not true. The cutoff bias is a linear function of the average anode current as Figure 9 shows.

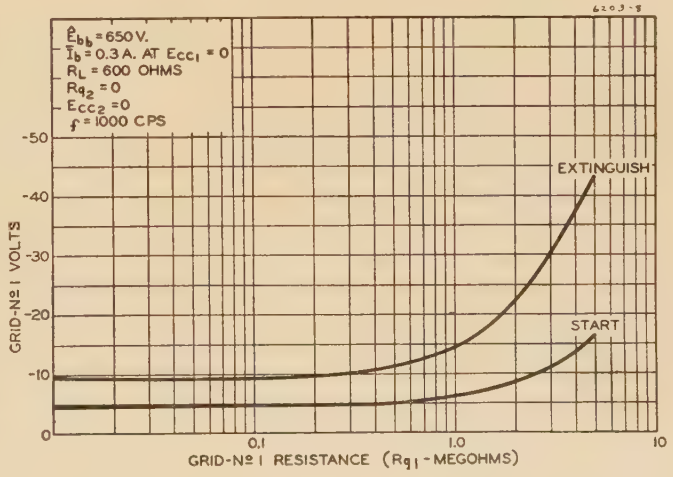

Figure 8. Critical grid bias versus grid resistance of type 3D22 thyratron

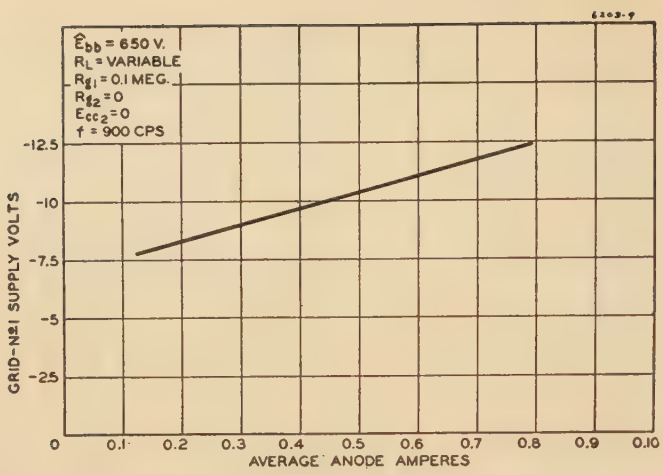

Figure 9. Extinguishing grid voltage versus average anode current for type 3D22 thyratron

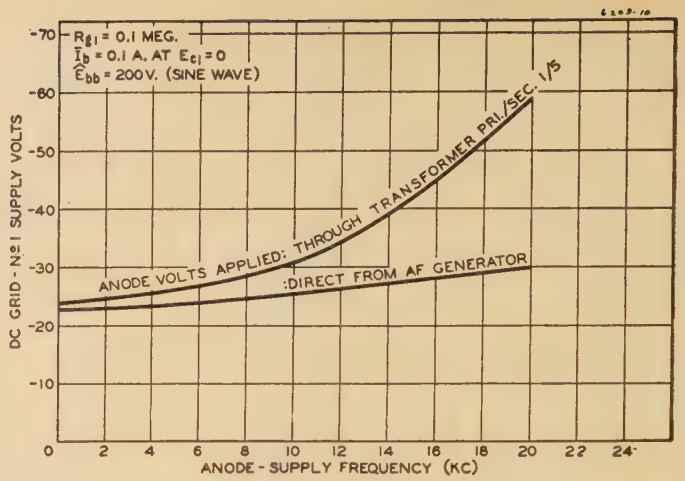

Figure 10. Effect of inductance in anode supply on extinction for type 884 thyratron

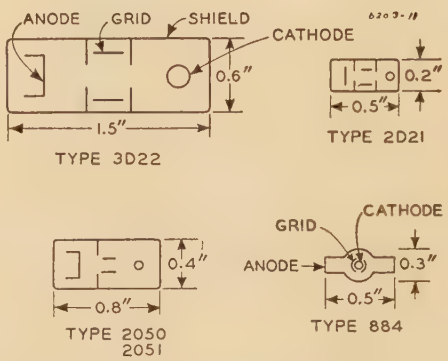

Figure 11. Thyratron constructions

Such a linear relationship would be expected if the following train of events are considered. The number of positive ions in the discharge is proportional to the current that has passed. Between conduction cycles the quantity of ions decays exponentially at a fixed rate, so that at a fixed time after current ceases in the external circuit the number of ions is proportional to the current that flowed. The negative grid, being the most effective deionization agent, sweeps the ions out at a rate approximately proportional to the negative applied voltage. At the beginning of the next cycle, if the grid has reduced the ions below a critical number, the anode rising in voltage will not be able to initiate a discharge.

Because of these relationships the anode current must be specified when the control characteristic at high frequency is given.

Effect of Inductance

When there is inductance in the load, the current persists after the anode voltage has dropped to zero. The solution[8] for a pure inductive load is

$$i_b = \frac{\hat{E}}{\omega L}(\cos\theta - \cos\omega t)$$

The generator produces a sinusoidal voltage of angular frequency ω and peak value $\hat{E}$. θ is the angle of firing as set up by E_{cc}, the d-c grid supply.

This persistence of current beyond 180 degrees results in a larger number of ions in the tube at the beginning of the next conduction cycle and hence requires a larger negative grid bias to sweep these ions out and to allow the grid to regain control. The effect may be seen in Figure 10 where a more negative curve was obtained when a transformer was inserted between the audio generator and the tube under test.

In taking these data the transformer ratio, resistive load, and voltage were selected to minimize the effect of transformer inductance.

Comparative Data on Different Thyratrons

Types 2051, 2D21, and 884 also were tested in this investigation in addition to types 3D22 and 2050. Ratings of these types appear in Table II. Figure 11 illustrates the construction of each one of these types. The cross sections are shown accurately to scale; the dimensions given are inside values. Note the similarity among the three types 3D22, 2050, and 2D21. Each of these types is a xenon-filled shield-grid thyratron. Types 2051 and 884 are argon-filled.

Starting Control Characteristic

In Figure 12 the starting control characteristics are compared for the four high-control-types. Types 2050 and 2051 have a high anode–grid capacitance and therefore exhibit a large shift. The 2D21 thyratron has the smallest grid–anode capacitance and hence the smallest shift. The frequency has to be increased to 15,000 cycles per second before a shift is observed in the 2D21.

Figure 14 gives the starting characteristic for type 884. This thyratron has a large grid–anode capacitance but its control ratio is so low that the shift is not excessive even at high audio frequencies.

Extinguishing Characteristic

The extinguishing control characteristic for the type 3D22 thyratron is shown in Figure 5. In Figure 13 the extinguishing characteristics are compared for the four high-control-ratio types. The shift in control is roughly proportional to the cross-sectional area of the type. Table III gives another indication that the phenomena are effects of deionization.

Although the type 2051 thyratron is a

Table II. Comparative Ratings of Thyratron Tubes

Type	Peak Forward Voltage, Volts	Peak Inverse Voltage, Volts	Average Current, Amperes	Anode–Grid Capacitance (Including Socket), $\mu\mu f$	Control Ratio
3D22	650	1,300	0.75	0.45	150
2050	650	1,300	0.100	0.60	250
2051	350	700	0.075	0.60	250
2D21	650	1,300	0.100	0.25	250
884	350	350	0.075	6.4	10

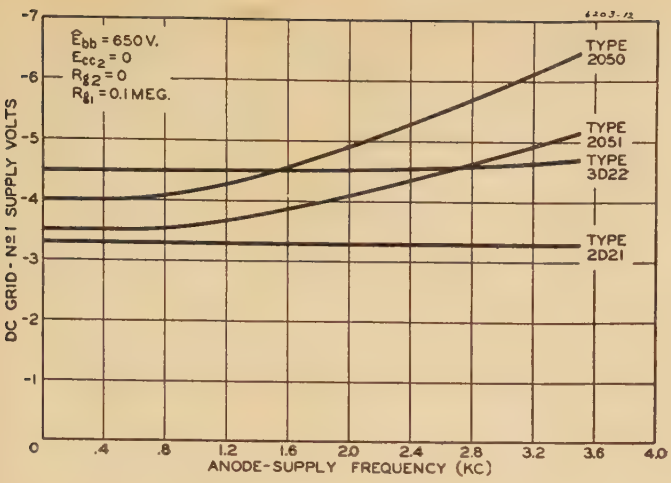

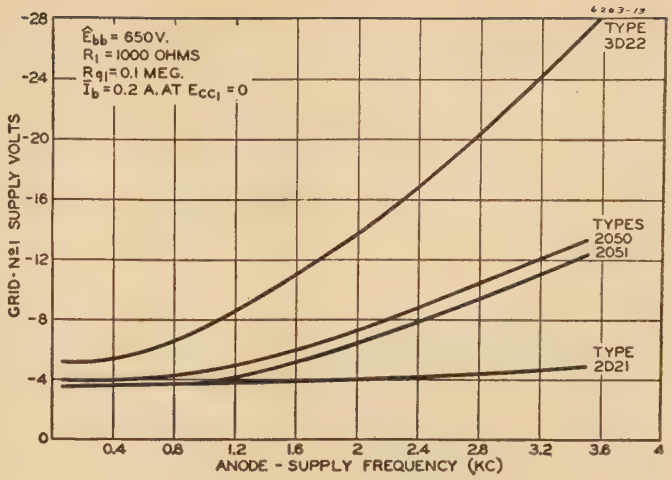

Figure 12. Comparison of starting grid voltages for types 2D21, 3D22, 2050, and 2051 thyratrons

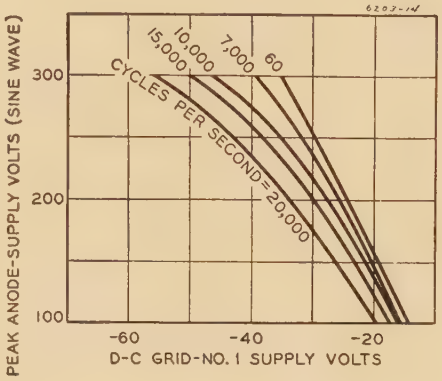

Figure 14. Starting and extinguishing characteristic of type 884 thyratron

R_{g1} = 0.1 megohm $\bar{I}_b$ = 0.1 ampere at E_{cc1} = 0

renewal type, not to be specified for new equipment, it was tested because it was expected that the use of the lighter gas argon in place of xenon would lower its deionization time. However, the gas pressure is nearly three times greater in the latter tube and therefore counteracts the difference between gases.

Referring to Figure 14 for the type 884, it may be seen that the starting and extinguishing characteristics are identical. One must conclude that the effect of deionization on the control characteristic is negligible even up to 20,000 cycles per second. The whole shift is caused by grid-anode coupling; consequently, the type 884 is the most desirable tube for high frequency work.

Effect of Pressure

Starting Control Characteristics

A number of type 2050 tubes were made with pressures ranging from 25 to 250 microns of xenon. The starting characteristics of these tubes were measured, but there is no definite shift with pressure. Had the pressure range been extended down to about five microns a shift probably would have been observed since this is the pressure range in which mercury thyratrons exhibit a large shift in control characteristic.[6] The explanation for this shift in starting control characteristic of a thyratron with pressure will be considered in order to distinguish it from the other shift phenomena observed in this paper. It is the same as the explanation for Paschen's breakdown curve of a gas diode. As the pressure is increased each electron makes more collisions and produces more ions in crossing the tube. Thus the critical anode current for the formation of a discharge with the given anode voltage is reached at a lower initial electron current or at a greater negative grid voltage.

Extinguishing Control Characteristic

It is known that deionization time is a function of pressure[7] so that, if the shift in extinguishing control characteristic is a deionization effect, the shift should be a function of pressure. The results of the test for extinguishing characteristic are elegant as Figure 15 will attest. The curves fall in order toward the negative grid voltage as pressure is increased.

Conclusions

The following conclusions can be drawn about the performance of thyratrons at high audio frequencies:

1. The grid loses control over the average anode current but is still potent enough to shut off the discharge.

2. There are two control characteristics instead of one—a starting characteristic and an extinguishing characteristic.

3. The starting characteristic shifts negatively with increasing frequency as a result of coupling through grid–anode capacitance.

4. The extinguishing characteristic shifts negatively with increasing frequency because of coupling through grid–anode capacitance as well as because of deionization effects.

5. The extinguishing characteristic shifts negatively with increasing grid resistance.

6. The extinguishing characteristic shifts negatively with increasing anode current.

7. A comparison of tubes of similar construction indicates that the shift of extinguishing characteristic with frequency is roughly proportional to the cross-sectional areas of the tube cage.

8. The starting characteristic may shift

Figure 13. Comparison of extinguishing grid voltages for types 2D21, 3D22, 2050, and 2051 thyratrons

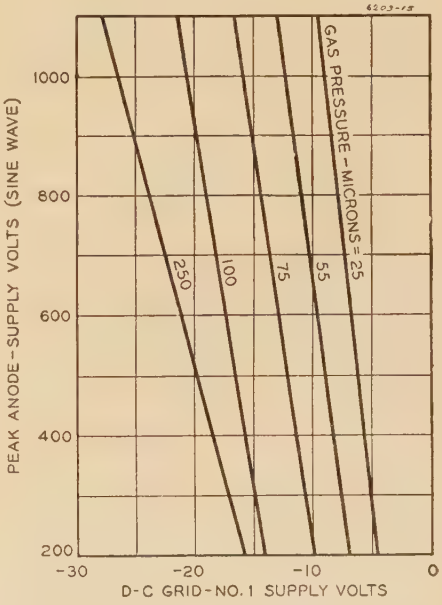

Figure 15. Extinguishing characteristic versus pressure for type 2050 thyratron

R_{g1} = 0.1 megohm R_{g2} = 0
$\bar{I}_b$ = 0.200 ampere at E_{cc1} = 0 E_{cc2} = 0
Frequency = 3,500 cycles per second

Low Reactance Flexible Cable for Induction Heating

MYRON ZUCKER
MEMBER AIEE

THERE has been a demand for a flexible cable to carry single phase current for induction heating at frequencies up to 10 kc. Tests on an interleaved type of cable, used widely in portable spot welding, indicate its usefulness in carrying thousands of amperes at potentials under 1,000 volts at the higher frequencies.

The flexibility of the cable has been sought for two purposes in induction heating:

1. For convenience of installation in the generator-transformer-coil circuit and for occasional shifting of the machinery.

2. For ability to carry currents (generally at low voltages) to coils that may be frequently or even continuously in motion.

In some cases, maneuverability is so important that it is advisable to use water cooled conductors in order to minimize cable size. Especially in such cases, it is logical to consider an adaptation of an interleaved type cable now widely used to carry heavy currents to portable spot welders. The basic problems of low reactance, high flexibility, and water tightness have been solved in this cable. The principal new requirement for induction heating is higher electric insulation. This has been attained for several hundred volts, and the cable is being used with and without water cooling.

The purpose of this paper is not to describe the cable (which has been covered elsewhere from the welding viewpoint[1,2]), but to estimate and give test values for some physical and electrical characteristics pertaining to its use at higher frequencies. The material offered here is not exhaustive, but introduces the characteristics of this type of cable which appears to have advantages in economy, low reactance and resistance, and flexibility compared with coaxial cable. Interleaved cable should not be used where its external field would be troublesome, unless it is shielded. Coaxial cable, described in many articles where studies of coaxial cables were made for other purposes,[3,4,5] may be preferable in such cases.

This presentation is limited to interleaved type cable. Physical dimensions are covered. They affect flexibility (cables of larger diameter being stiffer) and must be known for calculation of inductive reactance. The latter is covered in some detail since it is the major element of impedance of the cable at the frequencies involved. Some data are given on resistance, capacitance, and leakage losses. Cable ratings are not considered here since further information is needed on increased resistance losses at high frequencies in order to extend welding application data.[2] Also, more data are required on heating time constants at low water rates to evaluate heating and cooling of the cable under intermittent operations.[6]

Paper 46-153, recommended by the AIEE joint sub committee on induction and dielectric heating for presentation at the AIEE summer convention, Detroit, Mich., June 24–28, 1946. Manuscript submitted April 29, 1946; made available for printing May 16, 1946.

MYRON ZUCKER is a vice-president of Mackworth G. Reese, Inc., Detroit, Mich.

Description of Cable

The essence of this cable design is that each conductor is broken up into a number of "ropes" (see Figure 1) placed around a central nonconducting core in a manner similar to the outer groups of the ordinary concentric-lay stranded electric cable. Ropes of alternate polarity lie next to each other except for a thickness of insulation between them. Since water cooling is desired each conductor is bare, and the insulation takes the form of a tube of irregular cross section that is formed in place inside half of the conductors and outside of the other half. The whole mass is held in a

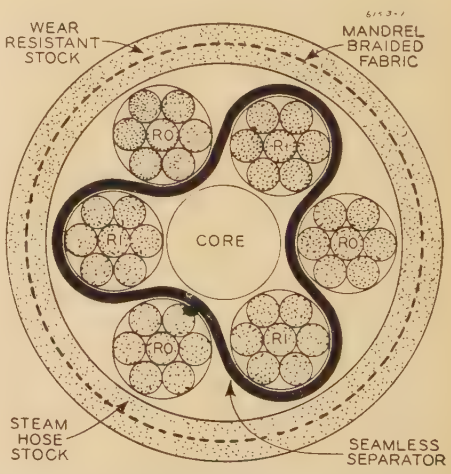

Figure 1. Cross section of interleaved cable for six ropes, three per electric side

negatively with increasing gas pressure because of increased ionization efficiency.

9. The extinguishing characteristic will shift negatively with increasing gas pressure because of increased ionization efficiency as well as for reasons of longer deionization time.

Appendix. Nomenclature

$\bar{I}$ = average current
$\hat{E}$ = peak voltage
E_{cc1} = d-c supply voltage for number 1 grid
E_{cc2} = d-c supply voltage for number 2 grid
R_{g1} = resistance in series with number 1 grid
R_{g2} = resistance in series with number 2 grid
E_{c1} = voltage at number 1 grid
E_{c2} = voltage at number 2 grid
E_{gg1} = a-c (rms) supply voltage for number 1 grid
$\hat{E}_{bb}$ = peak supply voltage for anode
$\bar{I}_b$ = average anode current
f = frequency of anode supply

Note: All voltages are referred to cathode.

Table III. Extinguishing Control Characteristics of Thyratron Tubes

Type	Cross Section, Square Inches	Shift in D-C Supply Voltage for No. 1 Grid E_{cc1}, Volts
3D22	0.818	22
2050	0.284	9
2D21	0.118	2

60–3,500 cycles per second; $\hat{E}_{bb}$ = 600 volts.

References

1. A Variable Frequency Electronic Generator, **D. A. Griffin.** *Electronics*, New York, N. Y., September 1943, page 130.

2. Theory and Applications of Electron Tubes (book), **H. J. Reich.** McGraw-Hill Book Company, New York, N. Y., 1939, page 444.

3. Electronics (book), **J. Millman, S. Seeley.** McGraw-Hill Book Company, New York, N. Y., 1941, page 434.

4. Deionization Considerations in a Harmonic Generator Employing a Gas Tube Switch, **W. G. Shepherd.** *Proceedings*, Institute of Radio Engineers, New York, N. Y., volume 31, February 1943, pages 66–74.

5. Standards on Electronics, Institute of Radio Engineers Standard 2E3. 1938.

6. Applied Electronics (book), **Massachusetts Institute of Technology Staff.** John Wiley and Sons, Inc., New York, N. Y., 1943, page 236.

7. Hot Cathode Thyratrons, **A. W. Hull.** *General Electric Review*, New York, N. Y., volume 32, April 1929, pages 221–2.

8. Gaseous Conductors (book), **J. D. Cobine.** McGraw-Hill Book Company, New York, N. Y., 1941, page 482.

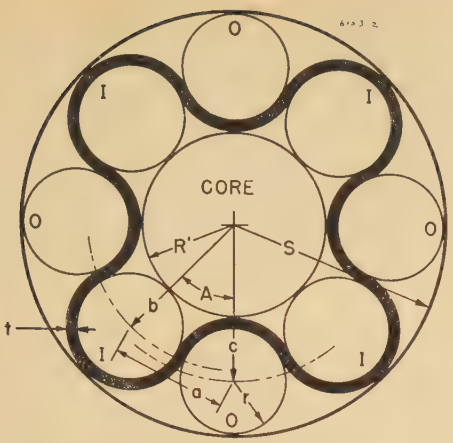

Figure 2. Symbols for analysis of cable section

regular pattern by means of an outer covering.

Some of the computations that follow are based on this arrangement. Then simpler formulas are derived from an approximate pattern in which all the conductors are on the circumference of one circle with radial insulating partitions. It is evident that the more ropes that are provided, the lower will be the reactance and the skin effect, which becomes important at higher frequencies. More ropes entail a larger core.

The core is a nonconductor which has been adopted for mechanical reasons even though the use of copper in the core would result in a smaller over-all cable diameter. The question is how great a price in terms of bulk must be paid for the lower impedance obtained by subdividing the copper.

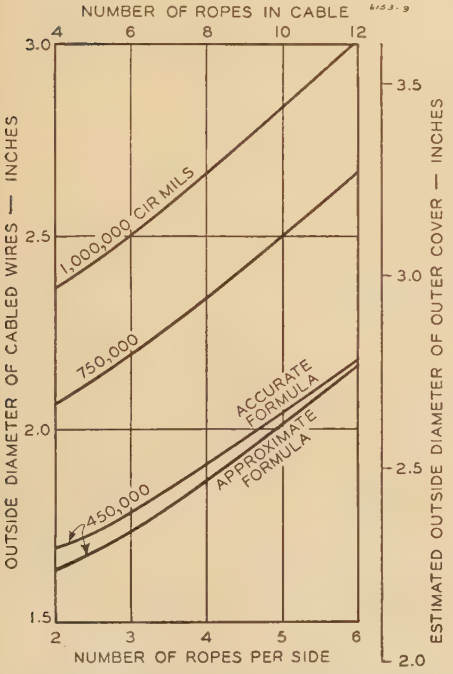

Figure 3. Calculated dimensions versus number of ropes in three sizes of interleaved cable

Cable Dimensions

The size of the cable is important not only because it determines flexibility, but also because the electrical characteristics depend on the size and the distance between conductors.

The geometry is somewhat complicated by the fact that the conductors are on the circumferences of two circles. The ropes *O* outside the insulating separator are on one circle; the ropes *I* that are inside are on another circle (see Figure 2).

Let

r = radius of each conducting rope

R' = radius of insulating core

t = thickness of insulating separator

Then let

a = straight line distance between centers of adjacent ropes $= 2r+t$

b = radius of circle upon which *I* ropes center $= R'+r$

c = radius of circle upon which *O* ropes center $= R'+r+t$

To solve the triangle abc, let

$$S=\frac{a+b+c}{2}$$

Then

$$S=\frac{2r+t+R'+r+R'+r+t}{2}=R'+2r+t$$

which, by coincidence, equals the radius of a circle around the cable.

If n equals the total number of ropes, then the angle between the centers of adjacent ropes is $A=360°/n$.

Since

$$\sin\frac{A}{2}=\sqrt{\frac{(S-b)(S-c)}{bc}}$$

we obtain, by substituting for A, S, b, and c from the foregoing expressions,

$$\sin^2\frac{A}{2}=(\sin^2)\frac{180°}{n}=(S-b)(S-c)/bc$$
$$=\frac{(r+t)r}{(R'+r+t)(R'+r)}$$

This may be solved for the diameter of the core:

$$2R'=-(2r+t)\pm\sqrt{(2r+t)^2-4r(r+t)\left(1-\frac{1}{\sin^2\frac{180°}{n}}\right)} \quad (1)$$

Then the diameter D of the composite, which is also the inside diameter of the outer covering (neglecting clearances required for assembly), may be expressed as follows in terms of r, t, and n:

$$D=2S=2R'+4r+2t$$
$$=2r+t+\sqrt{(2r+t)^2-4r(r+t)\left(1-\frac{1}{\sin^2\frac{180°}{n}}\right)} \quad (2)$$

The values of D for several sizes of cable (with 4 to 12 ropes) are shown in Figure 3.

A simpler approach is to assume that the centers of the ropes are on the circumference of one circle of radius R. The circumference of this circle is

$$2\pi R=n(2r+t)$$

whence

$$R=n\frac{(2r+t)}{2\pi}* \quad (3)$$

The outer diameter of the array is taken as the diameter of this circle plus the diameter of a rope and one thickness of the separator. Thus

$$D=2R+2r+t$$
$$=n\frac{(2r+t)}{\pi}+2r+t \quad (4)$$

The closeness of this approximation when insulation thickness is small compared with the size of conductors is shown in Figure 3. These curves are based on theoretical values of r. In actual cases sizes may vary considerably because of different stranding and cabling practices. The curves are within reason, however, and illustrate the effect of varying the amount and subdivision of copper area in this design.

Electrical Characteristics

Inductive Reactance

The induced voltage in each rope is the line-to-neutral reactive drop. Using the method of counting flux linkages up to some distance u outside of the cable, the voltage induced in rope 1 per centimeter length is found to be

$$E_{L-N}=\omega i 10^{-8}\times$$
$$\left[\frac{1}{20}+0.2\ln\left(\frac{u}{r}\cdot\frac{u}{a_3}\cdot\frac{u}{a_5}\cdots\frac{a_2}{u}\cdot\frac{a_4}{u}\cdot\frac{a_6}{u}\cdots\right)\right]$$

where a_n is the distance between the center of rope 1 and the center of the nth rope and i is the current per rope.

* More accurately,

$$R=\sqrt[n-1]{\frac{a}{n}}=\sqrt[n-1]{\frac{2r+t}{n}}$$

Through the following eight simple transformations, we obtain the value of X_{LL}:

1. Change to common units of volts per foot (2.54×12 multiplier).
2. Line-to-line voltage $E_{LL}=2E_{LN}$.
3. Total current $I=ni/2$.
4. Use $\omega=2\pi f$.
5. Cancel the common u in the parentheses.
6. Convert from natural to common logarithms.
7. Coalesce 0.05 with the logarithmic term by use of conductor geometric mean radius $GMR=r/0.78$.
8. Transform to reactance: $X_{LL}=E_{LL}/I$.

Through these steps we obtain

$$X_{LL}=\frac{7.68f\times10^{-6}}{n}\times 0.46\log\frac{a_2a_4\ldots a_n}{0.78ra_3a_5\ldots a_{n-1}} \quad (5)$$

This cumbersome form was found (as shown in the appendix) to reduce to

$$X_{LL}=\frac{3.53f\times10^{-6}}{n}\times\log\frac{4R}{0.78nr}\text{ ohms per 1,000 feet} \quad (6)$$

This may be stated in terms of basic dimensions by substituting the value of R from equation 3. Then

$$X_{LL}=\frac{3.53f\cdot10^{-6}}{n}\log\frac{2(2r+t)}{0.78r} \quad (7)$$

or, since

$$r=\sqrt{\frac{2CM/n}{2{,}000}} \quad (8)$$

$$X_{LL}=\frac{3.53f\times10^{-6}}{n}\log 5.1\left(1+\frac{1{,}000t}{\sqrt{2CM/n}}\right)$$

ohms line-to-line per 1,000 feet (9)

where

f = frequency in cycles per second

t = thickness of insulation between ropes

n = the total number of ropes in the cable

CM = circular mils of conductor in each electric side of the cable; that is, half the total copper in the cable

Equation 9 shows that the reactance is nearly inversely proportional to the number of ropes per conductor, and only slightly dependent upon conductor dimensions.

This relationship is illustrated in Figure 4 at 10 kc for one thickness of separator, a range of common cable sizes, and two to six ropes per side.

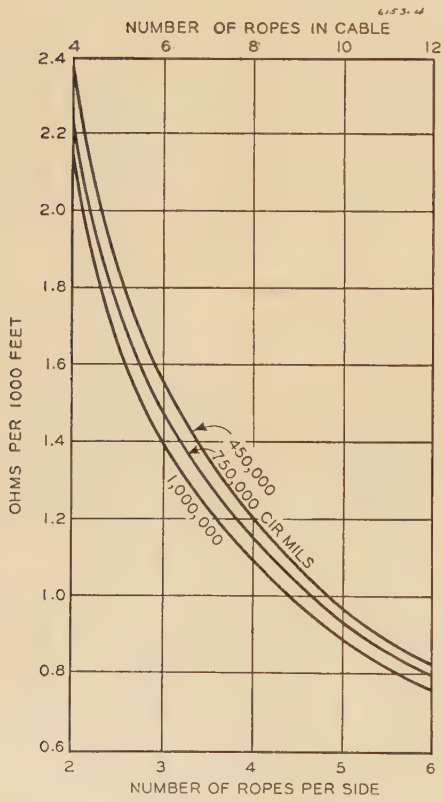

Figure 4. Inductive reactance at 10 kc versus number of ropes in three sizes of interleaved cable

Resistance

No calculations have been made on skin effect or proximity effect of the array of conductors under discussion here. It is evident that the breaking up of the conductor and the interaction between ropes will produce a better distribution of current than in ordinary conductors, and so decrease the resistance.

Tests have been made on 6-rope cables at high power levels with direct current and at 60, 890, and 9,600 cycles. The latter were rather crude and are included only because they furnish an "order of magnitude" value. More accurate tests are planned at various frequencies and with different cable sizes and numbers of ropes.

From available tests, the approximate ratio of a-c resistance to d-c values are shown in Figure 5.

Capacitance

The capacitance between the two electric sides of the cable depends upon whether it is dry or filled with water. An estimate is made most easily under the latter conditions, since the high dielectric constant of the water permits the first approximate assumption that the voltage stress is distributed uniformly across the rubber separator whose perimeter is p. This is the equivalent of a plate capacitor of width p and of length equal to the length of the cable.

Since the perimeter of the separator is equal to that of insulators completely encircling half the ropes, $p = 2\pi nr/2 = \pi nr$, the capacitance, therefore, is

$$C=0.224kp/t=0.224k\pi nr/t \text{ micromicrofarads per inch length} \quad (10)$$

where

t = thickness of the separator

k = specific inductive capacitance of the separator

Taking $k = 5$ for a rubber insulator, using a 1/16-inch thickness, changing to one foot of cable length, and substituting the value of r from equation 8, we get

$$C=0.34\sqrt{n}\sqrt{2CM} \text{ micromicrofarads per foot of cable length}$$

Considering this as a lumped capacitance,

$$X_c=\frac{1}{2\pi fc}=\frac{1}{2\pi f\times0.34\sqrt{n}\sqrt{2CM}}=\frac{0.47\times10^6}{f\sqrt{n}\sqrt{2CM}}\text{ megohm-feet of cable} \quad (11)$$

Figure 6 gives reactances calculated from this formula.

An idea of charging current is obtained by taking 500 volts across a 10-foot length of 6-rope 450,000-circular-mil cable at 10 kc:

$$I_c=\frac{500\times10}{20{,}000}=0.25\text{ ampere}$$

Although much greater than the charging current for ordinary cables, this is still negligible. Tests indicate that this current value is reduced by about ten in the dry cable.

Leakage Losses

There are two causes of loss:

1. Current through the water when the cable is water cooled.
2. Dielectric losses in the rubber insulation.

In the standard cable, the current has a direct path through the water in the "caps" of the two terminals. The d-c resistance of these paths in parallel is about 6,000 ohms in good city water. This resistance can be increased by special construction if required. In dry cable the leakage resistance of a 6-foot long assembly is about 300,000 ohms.

The dielectric losses of insulation depend, of course, upon the material used. Neglecting losses in the water, a reasonably high value for present inferior insula-

tion, is ten per cent of the charging current which has been derived previously:

$$\text{Dielectric loss} = \frac{0.10E^2}{X_c} \qquad (12)$$

For example, in the typical case of a 10-foot 6-rope 450,000-circular-mil cable, the dielectric loss at 500 volts, 10 kc will be

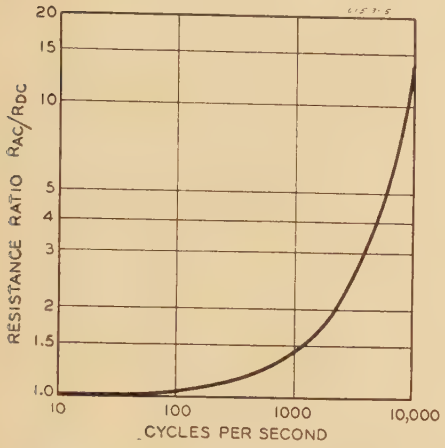

Figure 5. Approximate resistance ratio versus frequency for 6-rope interleaved cable

about $0.10 \times 500 \times 500/20{,}000 = 12$ watts.

These losses are small enough so they can be neglected in most cases.

Conclusion

The electrical impedances of water cooled interleaved cables in the range of frequencies up to 10 kc are approximately

$$Z_{series} = \text{resistance ratio} \times \frac{23L}{CM} + j\frac{3.53f \times 10^{-9} L}{n} \times \log 5.1\left(1 + \frac{1{,}000t}{\sqrt{2CM/n}}\right) \text{ohms} \qquad (13)$$

$$Z_{shunt} = 6{,}000 - j\frac{0.47 \times 10^{12}}{fL\sqrt{n}\sqrt{2CM}} \text{ ohms} \qquad (14)$$

where

L = cable length in feet
CM = circular mils of conductor in each electrical side of cable
f = frequency in cycles per second
n = total number of ropes in the cable
t = thickness of separator in inches

As an example, when operating a 10-foot length of 6-rope 450,000-circular-mil cable at 10 kc,

$Z_{series} = 0.0064 + j0.0155$,
$Z_{shunt} = 6{,}000 - j2{,}000$

If carrying 2,000 amperes at 500 volts, voltage drop $= 12.8 + j\,31 = 33.6/\underline{168°}$, and leakage current $= 0.1 + j\,0.2$

In this frequency range, leakage is unimportant, and estimates may be made on the basis of equation 13. This is borne out by installations at 900 cycles and at 10,000 cycles where production economy demanded a flexible conductor.

Any modification from the commercial 6-rope cables, that are considered for the purpose of decreasing the voltage drop, must be viewed in the light of decreased flexibility because of larger diameter, and increased cost as a result of more difficult and nonstandard manufacture.

Appendix

Another method of deriving equation 6 is through geometric means, that is,

$$L_t = 2\,ln\,\frac{G_{to}}{G_{ti}} \qquad (15)$$

where

L_t = inductance associated with the inner ropes
G_{to} = geometric mean distance between all the inner ropes and all the outer ones
G_{ti} = geometric mean distance of the inner ropes with respect to themselves

To state the G's in terms of cable dimensions the simplest approach, suggested by H. B. Dwight, is to apply Guye's theorem which states that for m points or circles spaced equally around a circular line of radius R, the geometric mean distance of one from the others is

$$g = Rm^{\frac{1}{m-1}} \qquad (16)$$

(In this development, g is used for the distance from one rope to others, G denoting the distance between a group of conductors and others.)

First consider the inner ropes, letting m equal the number of inner ropes. Then the geometric mean distance from one inner rope to the other inner ropes is

$$g_{to} = Rm^{\frac{1}{m-1}} \qquad (17)$$

To find the geometric mean distance of the complete array with respect to itself, we also refer to the well-known relation that for a circle

$$g_{ts} = re^{-1/4} = 0.78r = r' \qquad (18)$$

Then the geometric mean distance of the inner set of ropes is obtained from

$$G_{ti}{}^m = g_{ts}g_{ti}{}^{m-1} \qquad (19)$$

$$= r'\left(Rm^{\frac{1}{m-1}}\right)^{m-1}$$

$$= mr'R^{m-1} \qquad (20)$$

Having found the "self" geometric mean distance G_{ti}, we proceed to the "mutual" geometric mean distance G_{to} between inner and outer wires. This is done indirectly (since Guye's theorem gives a direct solution for arrays of equidistant points like . . *iii.* or . . *ioio* . ., but not for . . *ooioo* . . .) by finding $g_{t(t+o)}$, the geometric mean distance from i to all other ropes, and then combining that with g_{ti} to obtain G_{to} from equation 22.

That is, using equation 16 with $2m$ = total number of ropes,

$$g_{t(t+o)} = R(2m)^{\frac{1}{2m-1}} \qquad (21)$$

Now because of the symmetry of the array, $g_{t(t+o)}$ also could be obtained by the process

$$g_{t(t+o)} = \sqrt[2m-1]{g_{ti}{}^{m-1}G_{to}{}^m} \qquad (22)$$

which gives

$$G_{to}{}^m = g_{t(t+o)}{}^{2m-1}/g_{ti}{}^{m-1} \qquad (23)$$

where G_{to} is the geometric mean distance of all the inner ropes with respect to all the outer ones. Substituting equations 17 and 21 in equation 23,

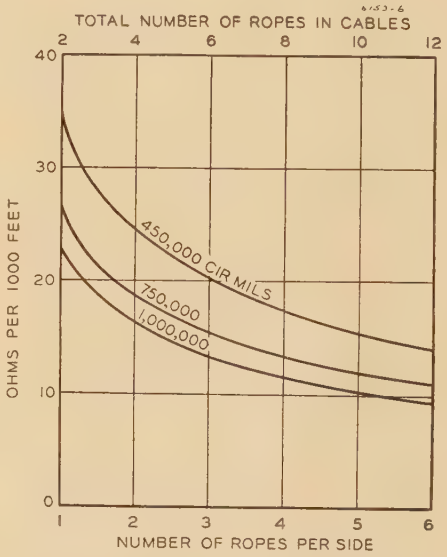

Figure 6. Calculated capacitive reactance at 10 kc versus number of ropes in three sizes of interleaved cable

$$G_{to}{}^m = R(2m)^{\frac{1}{2m-1}}/Rm^{\frac{1}{m-1}} = 2mR^{2m-1}/mR^{m-1} = 2R^m \qquad (24)$$

Combining equations 24 and 20,

$$\left(\frac{G_{to}}{G_{ti}}\right)^m = \frac{2R^m}{mr'R^{m-1}} = \frac{2R}{mr'} \qquad (25)$$

$$m \cdot ln\frac{G_{to}}{G_{ti}} = ln\frac{2R}{mr'} \qquad (26)$$

Since $m = n/2$,

$$ln\frac{G_{to}}{G_{ti}} = \frac{2}{n}ln\frac{4R}{mr'} = \frac{2}{n}ln\frac{4R}{0.78mr} \qquad (27)$$

Influence of Magnetic Materials on the Welding Characteristics of Resistance Welding Machines

J. J. RILEY
NONMEMBER AIEE

C. E. SMITH
MEMBER AIEE

MOST MEN associated with resistance welding machines are conscious of the fact that the introduction of magnetic material into the throat of such equipment causes a reduction of the welding current. The degree of reduction and simple mathematical tools for estimating it are contained in this paper.

Steel sheets and products fabricated from them constitute the majority of welding applications. It was of interest to determine the effect on the welding current by changing

1. The thickness of the sheets.
2. The length inserted into the welder throat.
3. The position in the welder throat.
4. The width of the sheets.
5. The actual current used for welding.

All of these factors could react to reduce the welding current, some more severely than the others.

The change in welding current was evaluated by measuring the reactive and resistive voltage components caused by the steel sheets in the welder throat. These voltage components in combination with the short-circuit impedance constants of the welding machine provide the necessary information.

Consequently, with a knowledge of these impedance constants and the nomogram indicating the effect of steel, it is a brief routine operation to calculate the change in welding current caused by the insertion of magnetic material into the secondary welder loop.

The apparent loss of current arises from the more intense magnetic field or increase in flux linkages and from the core loss resulting as heat generated in the steel sheets, a natural consequence of being subjected to an alternating magnetic field. Some effort was directed toward determining the magnitude and distribution of these flux linkages so that a better basic understanding of the influence of magnetic materials could be realized.

The magnitude of the magnetic field produced in the welder throat will depend primarily on the welding current. It is realized that a wide range of welding current can be used to make spot welds in mild or low carbon steel. The desirable maximum and minimum points of this range, together with other associated welding variables, are given in Table I. Figure 1 summarizes the welding variables for seam welding of low carbon steel. Figure 2 lists the welding variables for spot welding of austenitic stainless steels.[1] The data shown in both Figures 1 and 2 are the tentative recommended practices of the American Welding Society.

These combinations of welding variables produce satisfactory spot welds and seam welds, and justify their use for further work of the influence of magnetic materials.

Paper 46-137, recommended by the AIEE committee on electric welding for presentation at the AIEE summer convention, Detroit, Mich., June 24–28, 1946. Manuscript submitted March 11, 1946; made available for printing May 14, 1946.

J. J. RILEY and C. E. SMITH, a chief electrical engineer, are both of the Taylor-Winfield Corporation, Warren, Ohio.

Apparatus

The welding was performed on a Resistance-Welder-Manufacturers-Association size-2 press welder manufactured by the Taylor-Winfield Corporation and capable of being used as a spot and projection welder. A cross sectional view along the length of the welder throat is shown in Figure 3. Area and position of the current carrying members vary at different lengths in the welder throat.

Procedure

It was desirable to make the necessary electrical measurements while making actual welds with the steel sheets inserted in the welder throat. However, the slight distortion of the current wave form caused by the volume of steel added to the circuit and the attempt to accurately read the small changes in power factor from a watt-galvanometer oscillographic trace made it imperative to separate the resistance caused by making a weld from the resistive component caused by the presence of steel sheets. It was evident that the welding resistance R_w was much larger than the resistive component R_{rs}, especially in thin sheets.

Measurement of Welding Resistance R_w

The welding resistance R_w is the resistance from electrode to electrode across

Using equation 26 in equation 15, we find that

$$L_i = \frac{4}{n} ln \frac{4R}{0.78nr} \text{ abhenries per centimeter} \quad (28)$$

Appropriate changes to practical units and conversion to reactance produce equation 6.

References

1. Low-Reactance Cables for Portable Resistance Welders, **Myron Zucker.** *Welding Journal*, volume 23, October 1944, page 911.

2. War-Proved Advances in Low-Reactance Cables, **Myron Zucker.** *Welding Journal*, volume 24, November 1945, page 1022.

3. High-Frequency Coaxial-Line Calculations, **H. H. Race, C. V. Larrick.** AIEE Transactions, volume 61, 1942, July section, pages 526–30.

4. Transmission Characteristics of the Coaxial Structure, **J. F. Wentz.** *Bell Laboratories Record*, volume 16, February 1938, page 196.

5. Electrical Engineers Handbook (book), **Harold Pender.** Third edition, John Wiley and Sons, Inc., New York, N. Y., 1936, section 14, page 46, part 2.

6. Rating of Electric Equipment Under Intermittent Load, **Myron Zucker.** AIEE Transactions, volume 63, 1944, November section, pages 778–83. Discussion, pages 1382–4.

7. Electric Power Transmission and Distribution (book), **Woodruff.** Second edition, John Wiley and Sons, Inc., New York, N. Y., 1938.

8. **C. E. Guye.** *Comptes Rendus des Séances*, Académie des Sciences (Paris, France), volume 118, 1894, page 1329.

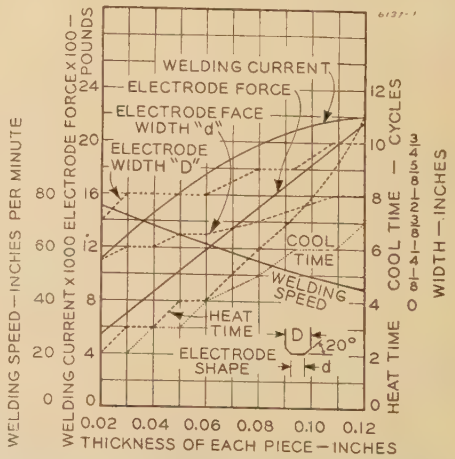

Figure 1. Low carbon steel seam welding data

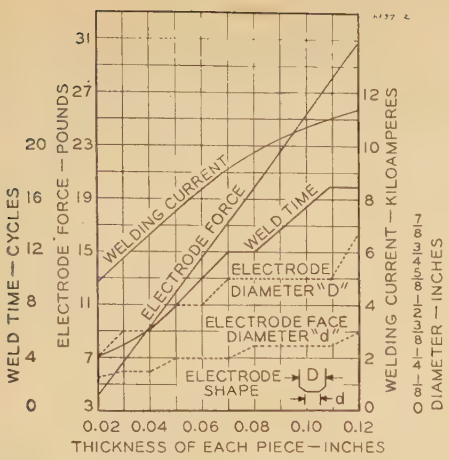

Figure 2. Austenitic stainless steel spot welding data

the work pieces when welding small coupons. It is the resistance added to the electrical circuit by welding operation itself and is independent of steel that extends into the welder secondary loop. R_w differs from the resistance R used in making the weld by that energy or heat that is dissipated into the work pieces and at the electrode faces.

Expressed mathematically

$$\text{Energy for welding} = I^2Rt + \text{losses} = I^2R_wt$$

where

I = welding current
t = time of current flow
R = resistance used for welding
R_w = effective resistance present to the flow of welding current caused by welding

The value of R_w is the important quantity in welder operational characteristics, and it is fortunate that it can be measured easily while R is impossible to determine accurately.

The resistance R_w was measured when making a weld in small coupons by taking the voltage drop across the two electrodes at two points as close to the weld as possible and dividing this voltage by the secondary current. When welding stainless steel, the drop from the top of one sheet to the bottom of the other one (sheet to sheet resistance, V_2) also was measured. A schematic diagram of the setup is shown in Figure 4. The inductive pickup was minimized by carefully twisting the voltage leads together and holding them perpendicular to the electrodes.

Simultaneous oscillographic records were taken of the voltage drops, primary current, and watts. The primary current was converted into the secondary or welding current by multiplying by the turns ratio of the welding transformer. The magnetizing current was neglected being less than two per cent in the most exaggerated case.

The variations of R_w with time during spot welding for several thicknesses of low carbon steel with different combinations of welding variables is shown in Figures 5 and 6. A less comprehensive picture of the variation of R_w with time for austenitic stainless steel is shown in Figure 7. A similar set of data for seam welding low carbon steel is presented in Figure 8. By selecting average values of R_w for spot welding low carbon steel and stainless steel under the conditions specified by Table I and Figure 2, the variation of R_w with sheet thickness results as shown in Figure 9.

The mild steel used in this investigation was covered with a slight film of oil to prevent rusting, being previously hot rolled and pickled. Before welding the steel was wiped with a clean rag to remove any dirt that accumulated during storage. The surface was still perceptibly oily after wiping. This type of surface condition, most often used in production applications, increases R_w beyond that expected from degreased sheets.

Measurement of Resistive Voltage Component, V_{rs} and Reactive Voltage Component, V_{xs} Caused by the Insertion of Magnetic Material or Steel into the Welder Throat

These voltage increments were measured without involving the welding resistance R_w. A hole two inches in diameter with its center two inches from the front edge and midway across the width was drilled in two equal thicknesses of steel sheet (Figure 10). The sheets were insulated from each other by a sheet of

Figure 3. Side view of welder throat construction showing copper and copper-alloy current conducting members

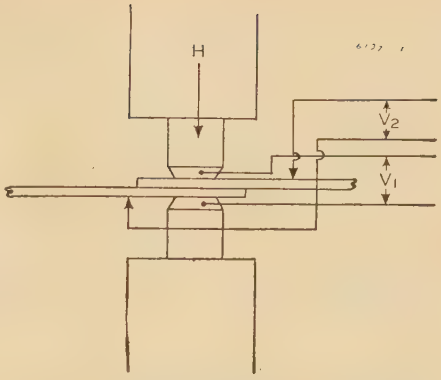

Figure 4. Electrode setup for measurement of welding resistance and sheet-to-sheet resistance

$$\text{Welding resistance } R_w = \frac{V_1}{I}$$

$$\text{Sheet resistance } R_{ss} = \frac{V_2}{I}$$

paper, inserted in the welder throat midway between the welder horns, and locked in position with wooden blocks in order to counteract the magnetic force when the welder current was applied. A water-cooled copper tube was inserted through the hole in the sheets and connected to the welder horns. With the steel in place, the current necessary to make a weld and form an equivalent magnetic field was passed through the secondary circuit of the welder. A magnetic contactor, manually controlled, allowed interruption of the current whenever desired. The frequency of the applied voltage was 60 cycles per second.

Electrical values were measured using instruments equipped with pointer stops and capable of reading the rms values of distorted wave forms. Readings were taken of primary voltage, primary current, primary power, welder transformer turns ratio, and depth of steel in welder throat.

The steel sheets were prepared initially to extend the maximum depth into the welder throat. After each set of measurements six inches would be sheared off the

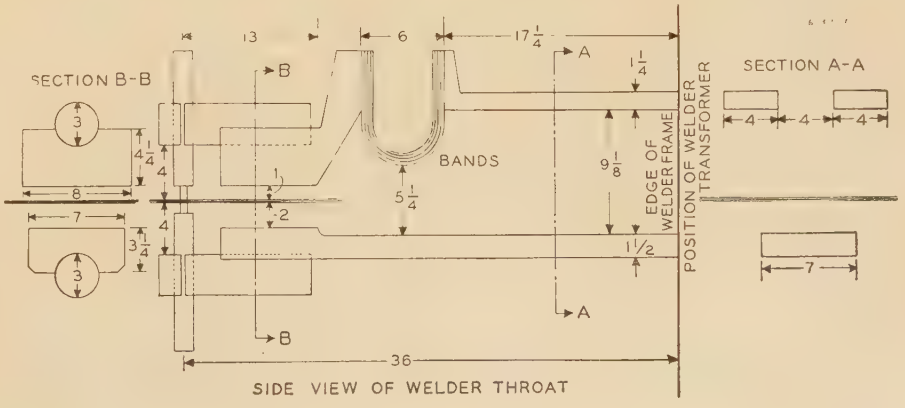

Table I. Low Carbon Steel Spot Welding Data

Data Common to All Classes of Spot Welds						Welding Variables for Best Quality Class-A Weld					Welding Variables for Better Quality Class-B Weld					Welding Variables for Good Quality Class-C Weld				
Thickness of Thinner Outside Piece		Electrode Diam and Shape (See Figure 1)		Min Weld Spacing, Center Line to Center Line, In.	Min Contacting Overlap (Note 8), In.	Weld Time Single Impulse, Cycles	Min Weld Strength and Electrode Force		Approx. Current, Amps	Approx. Diam of Fused Zone, In.	Weld Time, (Note 8), Cycles	Min Weld Strength and Electrode Force		Approx. Current, Amps	Approx. Diam of Fused Zone, In.	Weld Time (Note 7), Cycles	Min Weld Strength and Electrode Force		Approx. Current, Amps	Approx. Diam of Fused Zone, In.
T, In.	United States Standard Gauge	Max ρ, In.	Min D, In.				Force, Lbs	Load, Lbs				Force, Lbs	Load, Lbs				Force, Lbs	Load, Lbs		
0.010	32	1/8	3/8	1/4	3/8	4	200	200	4,000	0.13	5	130	170	3,700	0.12	15	65	130	3,000	0.11
0.021	25	3/16	3/8	3/8	7/16	6	300	450	6,100	0.17	10	200	390	5,100	0.16	22	100	320	3,800	0.14
0.031	22	3/16	3/8	1/2	7/16	8	400	840	8,000	0.21	15	275	770	6,300	0.20	29	135	680	4,700	0.18
0.043	19	1/4	1/2	3/4	1/2	10	500	1,300	9,500	0.23	21	360	1,160	7,500	0.22	38	180	1,050	5,600	0.21
0.049	18	1/4	1/2	7/8	9/16	12	650	1,550	10,300	0.25	24	410	1,420	8,000	0.23	42	205	1,320	6,100	0.22
0.061	16	1/4	1/2	1 1/16	5/8	14	800	2,050	11,600	0.27	29	500	1,900	9,000	0.26	48	250	1,770	6,800	0.25
0.077	14	5/16	5/8	1 3/8	11/16	21	1,100	2,800	13,300	0.31	36	650	2,620	10,400	0.30	58	325	2,420	7,900	0.28
0.092	13	5/16	5/8	1 5/8	3/4	25	1,300	3,550	14,700	0.34	44	790	3,450	11,400	0.33	66	390	3,160	8,800	0.31
0.107	12	3/8	5/8	1 13/16	1 3/16	29	1,600	4,600	16,100	0.37	50	960	4,350	12,200	0.36	72	480	4,050	9,500	0.35
0.123	11	3/8	5/8	2	7/8	30	1,800	6,000	17,500	0.40	60	1,140	5,550	12,900	0.39	78	570	5,200	10,000	0.37

Notes:

1. Type of steel SAE 1010.
2. Material free from grease, scale, and dirt.
3. Welding conditions determined by thickness of thinnest outside piece T.
4. Data for total thickness of pileup not exceeding $4T$.
5. Minimum spacing is that spacing for two pieces for which no special precautions are necessary to compensate for shunting of adjacent welds. For 3 pieces increase spacing 30 per cent.
6. Electrode material, class 2, minimum conductivity, 75 per cent copper; minimum hardness, 75 per cent rockwell B.
7. Weld times from 1 to 30 cycles consisted of a single impulse, from 32 to 60 cycles consisted of two equal impulses, and from 63 to 90 cycles consisted of three equal impulses.
8.

previous length until five inches extended into the welder throat.

The short-circuit constants or welder electrical constants without any steel in the welder throat but with the proper horn spacing were checked after each set of measurements. The resulting values of impedance, reactance, and resistance referred to the secondary side are designated as Z_o, X_o, and R_o, respectively.

The values of the voltage components caused by the addition of steel in the welder throat were determined in the conventional manner (Appendix I). The voltages V_{rs} and V_{xs} are the resistive and reactive components referred to secondary circuit.

These components are plotted for several thicknesses of sheet and different horn spacings in Figure 11. The components were the same for 8- and 16-inch horn spacing within the accuracy of measurement. The effect of sheet width on the voltage components is shown in Figure 12. The change of resistive and reactive voltage components with welding current for one gauge of sheet is illustrated in Figure 13.

In order to establish the extent to which cold-working the austenitic stainless steel made it magnetic because of the formation of small areas of the metallurgical constituent ferrite, two sheets of the largest thickness available were checked at various dimensions in the welder throat. Values of V_{rs} and V_{xs} are shown in Figure 14.

Measurement of Flux Patterns

While the absolute values of resistive and reactive voltage components caused by steel in the welder throat are the working tools in electrical characteristics calculations, a study of the changes in flux and flux pattern in the welder throat circuit is most beneficial to understanding the phenomenon and applying an engineering analysis to the problem.

The flux was measured by evaluating it from the voltage induced in a search coil. The method used for calculating flux from the induced voltage is described in Appendix III. In all tests two equal thicknesses of steel sheet 12 inches long were placed in the welder throat so that the front edge was two inches from the edge of the shorting bar, and the width was distributed equally on each side of the horn center line. The influence of the width of the sheet on the variation of maximum flux density along width of the sheet is shown in Figure 15.

As saturation of the low carbon steel sheets would occur at flux densities of approximately 125,000 lines per square inch, it is obvious that the normal welding current saturated the sheets at the center, or midway between the current carrying conductors. In order to determine how much the welding current could be decreased before the steel directly between the conductors would not saturate, two of the thickest sheets used in past work were subjected to different currents and the maximum flux density measured

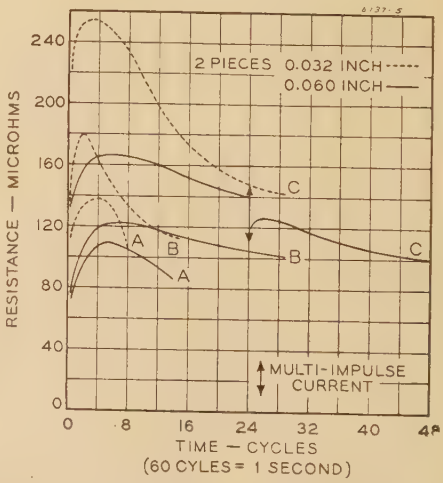

Figure 5. Variation of welding resistance with time in spot welding low carbon steel sheet

A, B, and C refer to classes of welds

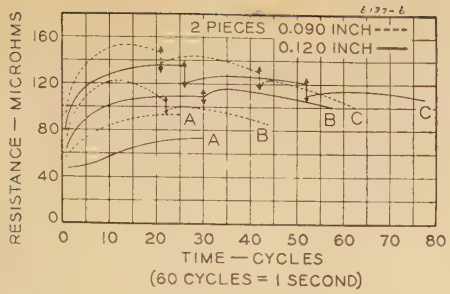

Figure 6. Variation of welding resistance with time in spot welding low carbon steel sheet

A, B, and *C* refer to classes of welds

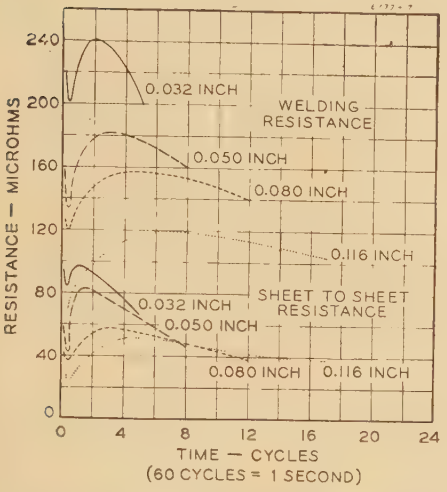

Figure 7. Variation of welding resistance and sheet-to-sheet resistance with time in spot welding austenitic stainless steel sheet of half-hard temper

(Figure 16). The thickest sheets were selected for this test as the ratio of welding current to sheet thickness decreases with increasing sheet thickness. Saturation still exists at the lowest value of current selected

Results

Welding Resistance R_w

The welding resistance R_w consists of two main components

1. The resistance from electrode to sheet.
2. The resistance from sheet to sheet.

The first component consists primarily of contact resistances. The second component consists of a contact resistance between the sheets and the resistance of the sheets themselves. From the test results on spot welding stainless steel in which these components were measured individually, it is notable that the resistance from sheet to sheet is approximately only 40 per cent of the total. It is expected that a similar relationship also would prevail for mild steel. Some past investigations[2–4] have indicated this approximate relationship. It is evident that the contact resistance between electrode and work piece is an appreciable part of the welding resistance and causes considerable heat generation at the electrode faces. Such being the case, it is very essential to cool the electrodes adequately in spot welding to prevent excessive deformation and to have the data apply.

While it is instructive to determine the components of the welding resistance R_w individually, the basic effect on the electric circuit is summarized in the value of R_w. From past experience it would be anticipated that R_w would be a function of the current density at the electrode face and the force density or pressure at the electrode face. As the variation of R_w with time could not be related satisfactorily to these two factors, average values of R_w were selected from Figures 5 and 6. Using these values and the associated data contained in Table IV, the following empirical relationship was determined for spot welding low carbon steel:

$$R_w = 333\,\frac{(D^{15}+1.7)}{P+2}$$

where

R_w = welding resistance in microhms
D = current density in (amperes per square inch) $\times 10^{-5}$
P = pressure in (pounds per square inch) $\times 10^{-3}$

The agreement between the calculated and measured values of R_w also is shown in Table IV. The equation gives passable results and point out that the heat generated in welding increases more rapidly than the square of the current, and reduction in electrode force causes appreciable increase in welding resistance.

In the empirical equation for R_w, the resistivity of the steel is not shown explicitly. However, it is erroneous to assume that the resistivity has no effect on welding resistance. In spot welding stainless steel, the values of R_w are considerably larger than those for mild steel of like gauges. The difference in resistivity,

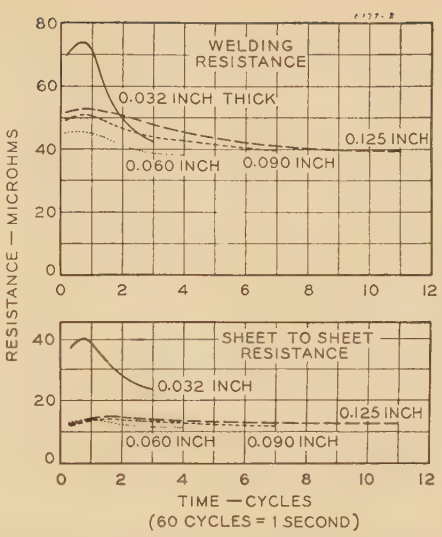

Figure 8. Variation of welding resistance with time in seam-welding low-carbon steel sheet

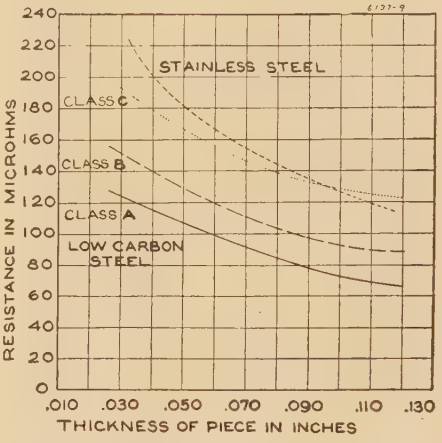

Figure 9. Variation of average welding resistance with thickness of sheet in spot welding

12.3 and 73 microhms per centimeter cube, and surface condition between commercial hot rolled pickled and oiled mild steel and bright finished stainless steel, account for the marked differences in welding resistance between these materials.

The values of welding resistance in seam welding should depend on the same factors as in spot welding but the different nature of the electrode contact area while welding and the shunting effect of

Table II. Materials Used in Welding Investigation

Type of Steel	Approximate Chemical Composition							Ultimate Tensile Strength, Lbs Per Sq In.
	C	Si	Mn	Cr	Ni	P	S	
Commercial-quality cold-rolled steel sheet	0.08	0.34	0.35			0.01	0.01	45,000
Austenitic stainless steel, half-hard temper	0.10	0.50	1.1	17.3	7.3	0.015	0.006	160,000

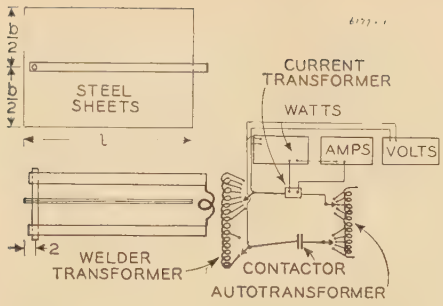

Figure 10. Circuit for measuring impedance of steel work pieces inserted in welder throat

the previous welds in a pressure tight seam cause deviations from the values of R_w measured in spot welding. It was rather surprising to discover that both the welding resistance R_w and the sheet to sheet resistance R_{ss} were almost equal in the range of thicknesses from 0.060 to 0.120 inch.

The emphasis on the determination of welding resistance was justified entirely as the resistive voltage component caused by it is of much greater magnitude than the resistive voltage component V_{rs} caused by the eddy current loss in the steel sheets inserted into the welder throat. If this factor were assumed carelessly, the final application of the data of V_{rs} would have given avoidable erroneous results. The values of R_w are so high in some cases that many resistance welders in operation today probably are functioning at higher power factors than normally assumed.

The Reactive Voltage Component V_{xs} and the Resistive Voltage Component V_{rs} Caused by the Presence of Steel in the Welder Throat

Engineers making electric circuit calculations are familiar with the procedure of considering a resistance welder secondary loop in terms of reactive and resistive impedance constants. These are combined with impedance values evaluating the welding effect and the totals placed as the loaded secondary circuit of the welder transformer. This procedure

Table III. Impedance of Welding Machine and Welding Transformer at a Frequency of 60 Cycles Per Second

Horn Spacing, Inches	Throat Depth, Inches	Impedance Z_o, Microhms	Reactance X_o, Microhms	Resistance R_o, Microhms
8	36	273	268	54
11	36	344	340	56

Note: There is no measurable change in impedance constants at secondary currents of 10,000 and 20,000 amperes.

and much factual data on welder secondary circuits are contained in an article by J. H. Cooper.[5] This practice must be altered when evaluating the presence of steel in the welder throat as ohmic values of reactance and resistance. These impedances change with the welding current. The effect of steel in the throat is to produce reactive and resistive voltage components opposing the applied secondary voltage of the transformer. These voltage components are almost independent of current over the normal welding range (Figure 14). Thus

$$V_{xs} = IX_s = C_1 \qquad V_{rs} = IR_s = C_2$$

Consequently, if ohmic values of reactance and resistance are desired to express the presence of steel in the welder throat, the values must be selected in combination with the welding current to give the correct voltage drop.

Saturation of the steel sheets by the welding current is the prime reason why V_{xs} and V_{rs} remain almost independent of current. An elementary study of the flux changes in the steel sheets is instructive in pointing out the limitations of the data.

The magnetic field in air betwen two parallel conductors is shown in Figure 17. This field will be distorted when steel sheets are added, but the flux still will concentrate at the section of steel directly between the conductors. It must be realized that the effect of the steel sheets in distorting the air flux field as well as the effect of causing more flux linkages have been combined to evaluate V_{xs} and V_{rs}. In other words, the values of welder shortcircuit impedance constants X_o and R_o have been assumed constant in spite of the air field distortion and the higher harmonics in the welding current caused by the presence of steel sheets in the welder throat. This assumption is valid providing V_{xs} and V_{rs} do not become too large a part of the applied secondary voltage as will be the case in most welder secondary circuit construction.

The steel sheets are saturated by the magnetizing force caused by the welding current. The relationship of welding current, flux, induced voltage, and the flux-current curve for a specific thickness and length of steel are shown diagrammatically in Figure 18. As the welding current increases, the flux hardly increases as the intrinsic flux density B_i ($B - \mu_o H = B_i$) has reached its limiting value.* The area of the induced voltage curve is a measure of the maximum flux, and as the maximum flux under saturated conditions will be almost constant the average value of induced voltage will be almost

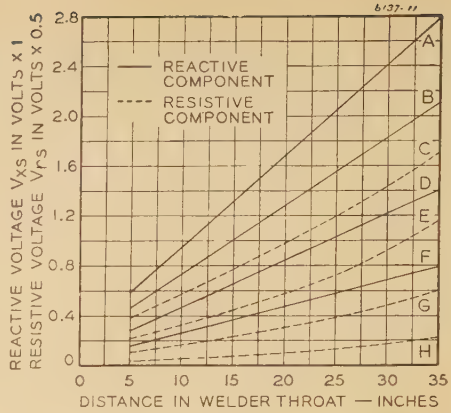

Figure 11. Variation of reactive and resistive voltage components caused by the presence of steel in the welder throat with distance in throat

A and *C*. Two pieces 0.119 inch thick, 18,000 amperes

B and *E*. Two pieces 0.090 inch thick, 15,000 amperes

D and *G*. Two pieces 0.060 inch thick, 12,000 amperes

F and *H*. Two pieces 0.032 inch thick, 8,300 amperes

Duplicate results for 8-and 16-inch horn spacings

most constant. The effect of change of welding current should be to change the wave form of flux and the wave form of the induced voltage. In circuit calculations it is the effective value and not the average value of induced voltage that must be investigated. The measurements indicated that both the effective and average values of induced voltage stayed almost constant, in spite of change of welding current. In order to have this condition prevail with such wave forms of induced voltage as recorded, it is necessary to have the flux current relationship change with different magnetizing forces.

The value of V_{xs} is proportional to the increase in length of steel in the welder throat. Under saturated conditions the maximum flux density is constant, and the increase in induced voltage is the result of the increase in flux caused by the increase in cross-sectional area provided by the additional length for a specific thickness.

Horn spacing or the distance between the throat bars does not influence V_{xs} appreciably. The steel sheets become saturated at any specific position in almost the same length of time from the zero point of the current wave. There is no

* The intrinsic flux density B_i is a measure of that part of the flux density attributable to the ferromagnetic characteristic of the material. When the material becomes saturated, it can make no further contribution to the flux density. As the magnetizing force H is increased beyond the value which saturates the material, the slope of the B–H curve becomes μ_o, the permeability of free space, and B_i becomes constant.

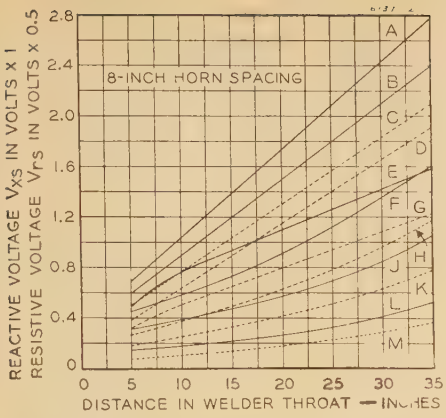

Figure 12. Variation of reactive and resistive voltage components with distance in throat and width of sheet

A, *B*, and *E*. Reactive voltages for two pieces 0.118 inch thick and widths of 36, 18, and 9 inches, respectively

F, *J*, and *L*. Resistive voltages under the above conditions

C, *D*, and *G*. Reactive voltages for two pieces 0.090 inch thick and widths of 36, 18, and 9 inches, respectively

H, *K*, and *M*. Resistive voltages under the same conditions

need to have the sheets equally spaced between welder horns to have the data apply.

It might be anticipated that V_{xs} would be independent of the width of the steel sheet if the steel were saturated at the section under the center line of the welder horns and thus limited the flux. By considering the air flux pattern, it is clear that narrow sheets will coerce less flux lines to enter the sheet than wide ones. As the current and magnetizing force change with time in the normal periodic manner, the flux will follow a similar pattern. As the saturation density is reached the preference for flux to pass into the sheet is eliminated. However, with narrow sheets it takes a longer period of time of a half-cycle of current flow to reach the saturation density. The resulting induced voltage is smaller as the rate of change of flux with time is smaller. It would be anticipated that after a certain width of sheet is reached, greater widths would cause negligible increase. This factor is associated with the distance between throat conductors or horn spacing and shape of conductors. The correction factors in Figure 20 are based on 8-inch horn spacing.

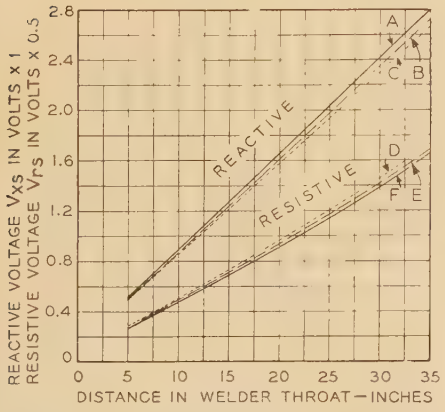

Figure 13. Variation of reactive and resistive voltage components with distance in throat and welding current. Two pieces of low carbon steel 0.118 inch thick and 36 inches wide

A and *F*. 19,000 amperes
B and E. 15,000 amperes
C and *D*. 10,000 amperes

Austenitic stainless steel is considered nonmagnetic, but cold working the steel causes the formation of small areas of iron or ferrite. These areas of ferrite would certainly reach saturation under the magnetizing force caused by the welding current. However, for the half-hard condition, the resulting values of V_{xs} and V_{rs} are small. The full-hard condition would have raised V_{xs} and V_{rs}. A word of caution is advisable in considering the magnetic effect in stainless steel. Those which are austenitic can be considered nonmagnetic for all practical purposes. However, those which are ferritic will be magnetic and should be considered having effects similar to mild steel.

The resistive voltage component multiplied by the secondary current represents the real power or core loss in the steel sheets. The great thickness of the sheet implies that the principle loss will be in the form of eddy currents. In the measurements, one steel sheet was insulated from the other, which means that the eddy currents would reach their maximum value near the outer surfaces of the sheets. If the sheets were in such intimate contact that the contact resistance between them could be considered zero, the resistive voltage component would increase theoretically to four times its former value. In most welding conditions the first case is more likely to exist than the second one, although some discretion should be used in applying the data.

The resistive voltage component caused by the presence of steel in the welder throat is normally a small part of the total resistive component composed also of the welder component $I_t R_o$ and the component finished by the welding resistance $I_t R_w$.

Application of the Data

After making an analysis of the data and the limitations imposed upon them,

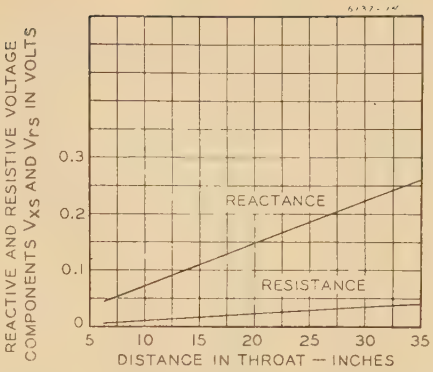

Figure 14. Variation of reactive and resistive voltage components with distance in throat for two pieces of austenitic stainless steel 0.109 inch thick, 24 inches wide and half-hard temper

it was desirable to compile these data into usable form. The values of V_{xs} and V_{rs} in Figure 11 were examined. By drawing straight lines for the V_{rs} variation with length, the empirical formulas and the resulting nomogram shown in Figure 20 were derived. The value of V_{rs} does not include the effect of welding resistance. The correction for width was obtained from Figure 12. The correction for difference in welding current from the base current was obtained from Figure 13.

The nomogram can be used for either spot welding or seam welding. For this reason, the effect of welding resistance is not included. The value of resistive voltage caused by the welding resistance can be selected from Figure 19. It is advisable to compare the desired welding technique with the technique outlined in Table I and Figures 1 and 2 so that a satisfactory choice of welding resistance voltage can be made.

Two examples of application of the data are shown in Appendix II.

Conclusions

1. The steel plates inserted in a welder throat will be saturated by the magnetic field produced by the welding current under normal conditions of operation.

2. The effect of the presence of steel plates (magnetic material) in the welder throat is measured best by expressing it as a reactive and a resistive voltage component. These voltage components are almost independent of welding current over the normal spot welding range.

3. The normal procedure of expressing the electric circuit of a welder in terms of resistance and reactance should be altered when the effect of steel plates is included. The circuit should be expressed in terms of reactive and resistive voltage drops, only some of which will be proportional to the current.

4. The effect of welding resistance and its

Table IV. Comparison of Calculated and Measured Values of Welding Resistance and Factors Affecting Welding Resistance

Thickness of Each Piece, Inches	Welding Current, Amperes	Electrode Force, Pounds	Force Density, Pounds Per Square Inch	Current Density, Kiloamperes Per Square Inch	Welding Resistance R_w, Microhms	
					Measured	Calculated
0.032	8,000	425	15,400	291	125	128
0.032	6,400	280	10,300	233	150	146
0.032	4,730	135	4,900	172	190	189
0.060	11,500	800	16,300	234	102	97
0.060	9,000	490	10,000	183	115	116
0.060	6,850	245	5,000	139	140	158
0.090	14,300	1,250	16,300	187	78	78
0.090	11,400	770	10,000	149	102	98
0.090	8,520	380	5,000	112	132	137
0.120	17,120	1,800	16,300	155	69	66
0.120	12,800	1,110	10,000	116	90	82
0.120	10,000	550	5,000	91	126	122

resulting voltage component is normally larger than the resistive voltage component caused by the presence of steel sheets for gauges less than 0.125 inch. As the thickness increases the effect of welding resistance voltage drop decreases and the resistive effect of the sheets becomes the predominating factor.

5. The effect of magnetic material in the welder throat is a function of the thickness and width of the sheets and of the secondary circuit constants of the welder. Resistance welders with large horn spacing are less influenced than welders with small horn spacing for the same throat depth. In other words, the larger the secondary voltage to supply a necessary welding current, the less the influence of the constant bucking voltage caused by the steel sheets.

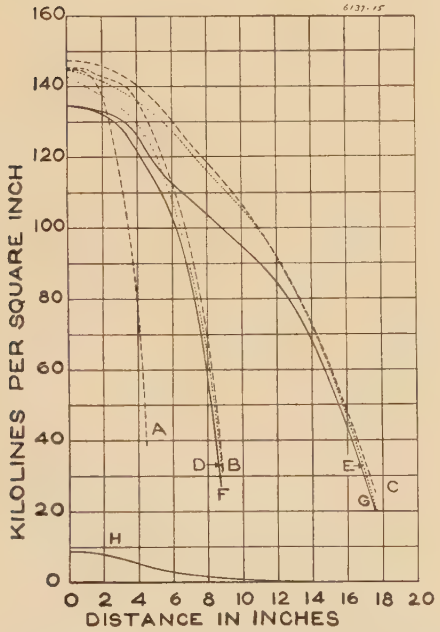

Figure 15. Variation of maximum flux density with distance from center line of electrodes at right angles to the welder throat

A, B, and *C.* Sheets 0.120 inch thick and 9, 18, and 36 inches wide, respectively, at 18,000 amperes

D and *E.* Sheets 0.090 inch thick and 18 and 36 inches wide, respectively, at 15,000 amperes

F and *G.* Sheets 0.032 inch thick and 18 and 36 inches wide, respectively, at 8,300 amperes

H. For magnetic field in air at 17,500 amperes

Appendix I. Determination of V_{rs} and V_{xs} from Instrument Readings

V_p = primary voltage, volts
I_p = primary current, amperes
W_p = primary power, watts
l = depth of steel in throat, inches
a = transformer turns ratio
V_t = secondary voltage, volts
I_t = secondary current, amperes
W_t = secondary power, watts
Z_p = impedance referred to primary winding, ohms
R_p = effective resistance referred to primary winding, ohms
X_p = reactance referred to primary winding, ohms
R_t = impedance referred to secondary winding, ohms
R_t = effective resistance referred to secondary winding, ohms
X_t = reactance referred to secondary winding, ohms
Z_s = impedance (for a specific current) of steel sheets referred to secondary winding, ohms
X_s = reactance (for a specific current) of steel sheets referred to secondary winding, ohms
R_s = resistance (for a specific current) of steel sheets referred to secondary winding, ohms
V_{rs} = resistive voltage component caused by steel sheets, volts
V_{xs} = reactive voltage component caused by steel sheets, volts
Z_o = impedance of welder secondary circuit under short-circuit conditions, ohms
X_o = reactance of welder secondary circuit under short-circuit conditions, ohms
R_o = resistance of welder secondary circuit under short-circuit conditions, ohms

$$Z_p = V_p/I_p = a^2(Z_o + Z_s) \quad (1)$$
$$Z_s = (Z_p/a^2) - Z_o \quad (2)$$

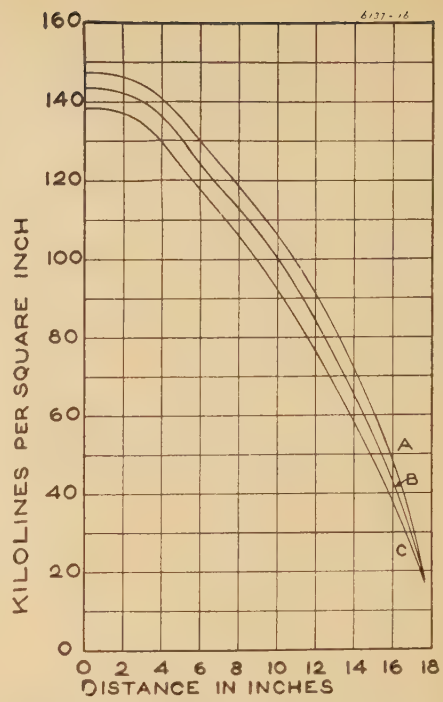

Figure 16. Variation of maximum flux density with distance from center line of electrodes at right angles to the welder throat and with welding current for two pieces 0.120 inch thick, 36 inches wide

A. 18,500 secondary amperes
B. 14,400 secondary amperes
C. 10,000 secondary amperes

$$R_p = W_p/I_p^2 = a^2(R_o + R_s) \quad (3)$$
$$R_s = (R_p/a^2) - R_o \quad (4)$$
$$X_p = \sqrt{Z_p^2 - R_p^2} = a^2(X_o + X_s) \quad (5)$$
$$X_s = X_p/a^2 - X_o \quad (6)$$
$$I_t = I_p(a) \quad (7)$$
$$V_{rs} = I_t R_s \quad (8)$$
$$X_{xs} = I_t X_s \quad (9)$$

The foregoing equations are used for the calculations of two sheets 0.118 inch thick, 18 inches wide, and inserted 35 inches in the welder throat.

$a = 52$
$X_o = 268 \times 10^{-6}$ ohm

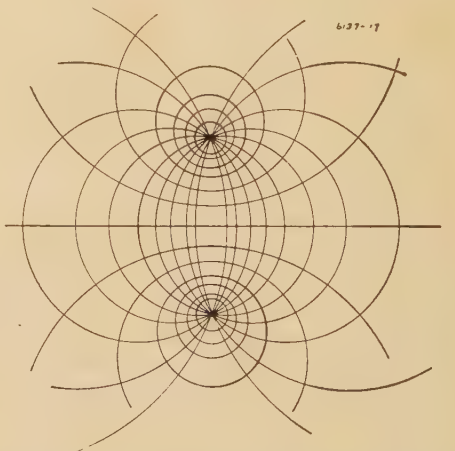

Figure 17. Graphical flow map of magnetic field in air between two parallel conductors

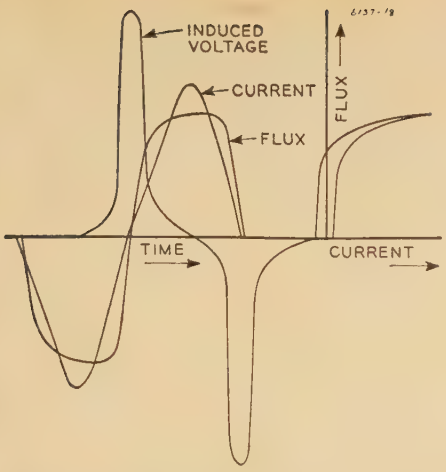

Figure 18. Schematic diagram of induced voltage, welding current, and flux in a saturated steel sheet

$R_o = 54 \times 10^{-6}$ ohm
$Z_o = 273 \times 10^{-6}$ ohm
$Z_p = 375/349$
$= 1.075$ ohms
$Z_s = 1.075/(52)^2 - 273 \times 10^{-6}$
$= 128 \times 10^{-6}$ ohm
$R_p = 26{,}700/(349)^2$
$= 0.219$ ohm
$R_s = 0.219/(52)^2 - 54 \times 10^{-6}$
$= 27 \times 10^{-6}$ ohm
$X_p = \sqrt{(1.075)^2 - (0.219)^2}$
$= 1.05$ ohms
$X_s = 1.05/(52)^2 - 268 \times 10^{-6}$
$= 121 \times 10^{-6}$ ohm
$I_t = 349(52)$
$= 18{,}100$ amperes
$V_{rs} = 18{,}100(27 \times 10^{-6})$
$= 0.488$ volt
$V_{xs} = 18{,}100(121 \times 10^{-6})$
$= 2.19$ volts

Appendix II. Applying Data to Specific Problems

Problem 1

Find the increase in secondary voltage necessary to maintain 18,000 amperes welding current in spot welding two sheets 0.120 inch thick and 36 inches wide when one inch and then 36 inches is inserted in the welder throat. Welder short-circuit constants are

$Z_o = 273 \times 10^{-6}$ ohm
$X_o = 268 \times 10^{-6}$ ohm
$R_o = 54 \times 10^{-6}$ ohm

From Figure 20

$I_t R_w = 1.26$ volts

From Figure 21

$V_{rs} = 0.86$ volt
Welder resistance drop $= I_t R_o$
$= (18{,}000)(54 \times 10^{-6})$
$= 0.97$ volt

Total resistive voltage drop $= V_r$
$= 3.09$ volts
Welder reactance drop $= I_t X_o$
$= (18{,}000)(268 \times 10^{-6})$
$= 4.82$ volts

From Figure 21

$V_{xs} = 2.87$ volts

Total reactive voltage drop $V_x = 7.69$ volts
Adding vectorially, $V_r + V_x = V_t$

$V_t = \sqrt{V_r^2 + V_x^2}$
$= 8.3$ volts at 36 inches
Voltage at start (one inch in throat) in which V_{rs} and V_{xs} are not effective
$= 5.32$ volts
Increase in voltage $= 8.3 - 5.3$
$= 3.0$ volts

Problem 2

The question is the same as in problem 1 except that the sheets are 18 inches wide, welding current is 10,000 amperes. The sheets are welded in the same welder. From Figure 20

$I_t R_w = 1.23$ volts

From Figure 21

$V_{rs} = 0.86$ volt

From this same chart this value must be corrected to

$K_1 \cdot V_{rs} = 0.65\ (0.86)$
$= 0.559$

because the sheet is only 18 inches wide. This value should be corrected further for change in base current, $K_3 = 1.05$.

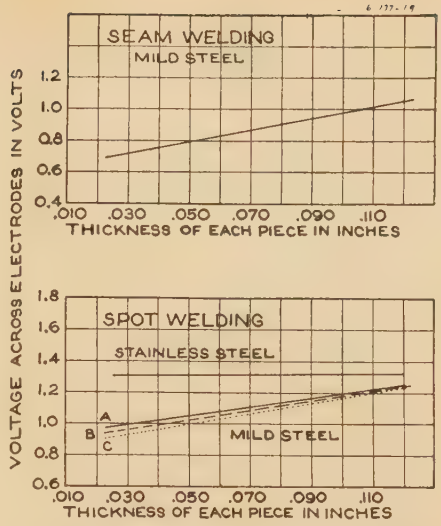

Figure 19. Resistive voltage drop across the electrodes caused by the welding resistance when welding small coupons

$K_1 \cdot K_3 \cdot V_{rs} = (0.65)(1.05)(0.86)$
$= 0.587$ volt
Welder resistance drop $= I_t R_o$
$= 10{,}000(54 \times 10^{-6})$
$= 0.54$ volt
Total resistive voltage drop $= V_r$
$= 2.36$ volts

Figure 20. Reactive and resistive voltage components caused by two thicknesses of low carbon steel 36 inches wide in welder throat

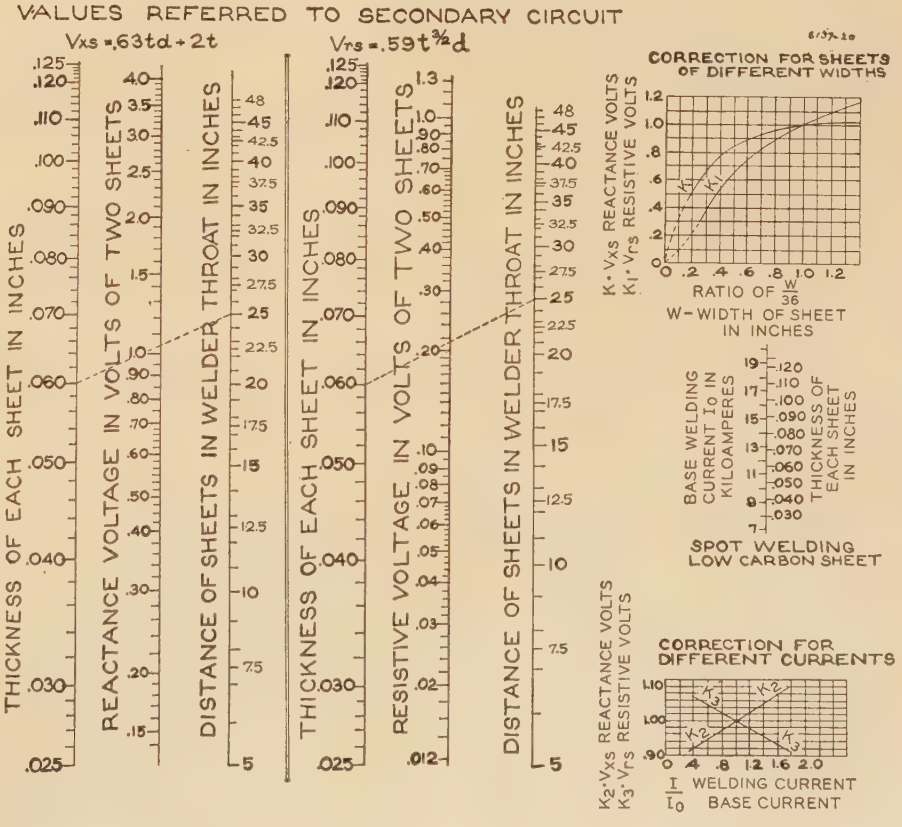

Welder reactance drop $= I_t X_o$
$= 10{,}000\ (268 \times 10^{-6})$
$= 2.68$ volts

From Figure 21

$K \cdot K_2 \cdot V_{xs} = 0.84(0.94)(2.87)$
$= 2.27$ volts

Total reactive voltage drop $= 4.95$ volts

$V_t = 5.48$ volts at 36 inches

Voltage at start (1 inch in throat) in which V_{rs} and V_{xs} are not effective $= 3.21$ volts

Increase in voltage $= 5.48 - 3.21$
$= 2.27$ volts

Appendix III. Determination of Flux and Flux Density From the Induced Electromotive Force or Voltage Wave

Basically

$$e = -N \frac{d\phi}{dt}\ 10^{-8}$$

$$d\phi = \frac{-1}{N}\, e \cdot dt\, \frac{1}{10^{-8}}$$

$$\phi = \frac{-10^8}{N} \cdot \int_{t_1}^{t_2} e \cdot dt$$

where

N = number of turns on search coil
e = instantaneous voltage, volts
$\frac{d\phi}{dt}$ = rate of change of flux with time
ϕ = flux, maxwells or lines
t = time, seconds

The integral $\int_{t_1}^{t_2} e.dt$ represents the average voltage over the time interval considered. When the maximum value of flux is desired, as it was in this work, it is necessary to measure the area under the voltage wave e for one-half cycle by means of a planimeter,

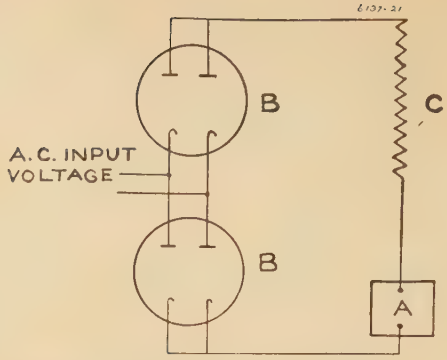

Figure 21. Rectifier unit for converting a-c input voltage to average direct voltage

A. D-c millivoltmeter, 1,000 millivolts, full scale, 5,000 ohms resistance
B. 6H6 tube
C. 100,000-ohm resistor

divide it by two, and substitute in the expression

ϕ_M(flux in lines or maxwells) =

$$\frac{\text{area of one-half of voltage wave in square inches}}{\text{number of turns on search coil}} \cdot \left(\frac{\text{volts}}{\text{inch}}\right)^* \cdot \left(\frac{\text{seconds}}{\text{inch}}\right)^* \cdot 10^8$$

The maximum flux density B_m is found by dividing the flux by the area of steel that the coil encloses. This assumes that the flux is confined entirely to the steel or that the magnetic field in air is small compared to the magnetic field in the steel sheets.

$$B_m = \frac{\phi_m}{A}$$

where

A = area in square inches
B_m = maximum flux density in lines per square inch

* These are calibrations measured from the oscillogram of the voltage wave.

A direct reading meter can be made to evaluate $\int_{t_1}^{t_2} e.dt$ or the average voltage. It was possible to measure this integral for determination of ϕ_m by using a bridge-type full-wave rectifier (Figure 22) and suitable d-c meter. The rectified direct voltage is approximately 1/20 of the alternating voltage input. A search coil of ten turns of number 22 wire was used with the instrument setup.

$$\phi_m = \frac{E_{avg}}{240N} \times 10^8$$

where

$\frac{1}{240}$ = one-fourth of a cycle of a 60-cycle system
E_{avg} = average volts

References

1. Proposed Recommended Practices for Resistance Welding. *Welding Journal*, New York, N. Y., volume 23, August 1944.

2. Data on the Spot Welding of Low Carbon Steel, **W. F. Hess, R. L. Ringer.** *Welding Journal*, New York, N. Y., volume 18, April 1939.

3. Spot Welding of Automobile Grade Mild Steel, **W. F. Hess, R. A. Wyant.** *Welding Journal*, New York, N. Y., volume 18, October 1939.

4. Spot Welding of Low Carbon and Stainless Steel, **W. F. Hess, R. L. Wyant.** *Welding Journal*, New York, N. Y., volume 18, October 1939.

5. The Electrical Characteristics of Resistance Welders, **J. H. Cooper.** *Welding Journal*, New York, N. Y., volume 21, February 1942.

6. Surface Polish and Contact Resistances, **W. B. Kouwenhoven, J. Tampico.** *Welding Journal*, New York, N. Y., volume 20, October 1941.

7. Magnetic Circuits and Transformers (book), **Electrical Engineering Staff of Massachusetts Institute of Technology.** John Wiley and Sons, Inc., New York, N. Y., 1944, pages 18–25.

8. Empirical Equations and Nomography (book), **Dale S. Davis.** McGraw-Hill Book Company, Inc., New York, N. Y., 1943, pages 70–91, 104–110.

Radio Telemetering for Testing Aircraft in Flight

CARL L. FREDERICK
MEMBER AIEE

Synopsis: A brief résumé is given of the factors which necessitated the development of thoroughly practicable and reliable telemetering equipment for dynamic testing of high-speed aircraft in flight. An outline of a radio telemetering system is presented which was developed under contract and accepted as suitable for structural flight testing by the United States Navy Bureau of Aeronautics in April 1945. Emphasis is placed upon the electric system and circuits which are of most interest to Institute members. These include the stabilized amplitude modulated subcarrier oscillators, the master amplifier, the air-borne regulated power supply, the frequency modulated transmitter, the automatic frequency controlled frequency modulated receiver, the heterodyne analyzer, and the mobile receiving station.

AN accurate knowledge of the amplitude, frequency, and relative phases of dynamic strains, pressures, and accelerations to be experienced by aircraft in flight is of vital importance in its design. In the past, much of this information could be calculated or determined by wind tunnel tests on small models. To meet the recent demands for speeds near the velocity of sound, or greater, it has become increasingly difficult, if not impossible, to extrapolate wind tunnel data. Means for telemetering this information from experimental aircraft and recording the data on the ground then became a necessity. With the advent of wind tunnels capable of testing powered models having spans up to 12 feet under conditions of pressure up to four atmospheres, and air velocities up to the speed of sound,[1] aerodynamic knowledge as to the effects of compressibility will be expanded greatly. However, the demand for even higher speeds makes the most modern wind tunnels incapable of furnishing all the required aerodynamic knowledge. A continued need for telemetering is therefore indicated, not only because it is the only practicable method of testing full scale remotely controlled aircraft designed to operate at nearsonic or supersonic speeds, but experience has indicated considerable savings in cost and manpower over other methods of testing larger and slower airplanes.

As often happens when research projects are undertaken to meet an urgent demand for one use, many other applications present themselves. Since the telemetering equipment has been completed, requests have come to use it in modified form for testing extremely high-speed compact flying bodies, for medical research to learn the effects on the human body when separated from high-speed aircraft flying at high altitudes, for testing and monitoring wind tunnels, and for observing and recording at the same time many items of information at remote points in large industrial plants or railroad yards.

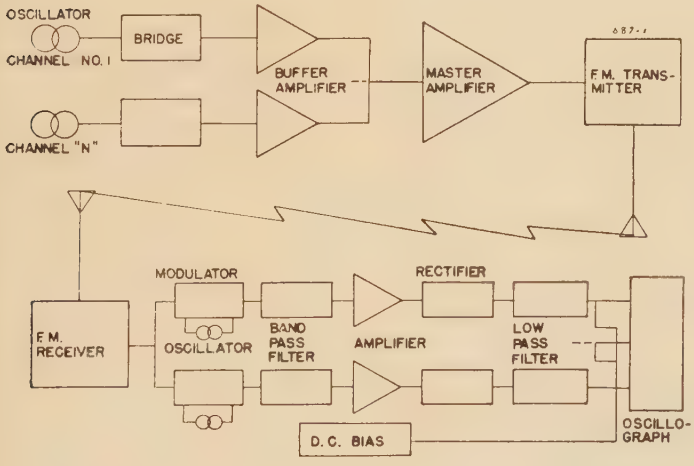

Figure 1. Block diagram of radio telemetering

As indicated, any number of channels (*N*) up to 14 may be included and simultaneously operated in the radio telemetering system

In planning the radio telemetering system herein described, established carrier telephone art was employed freely. As early as March 1916, R. A. Heising, of the Western Electric Company, filed an application for a patent on plural channel signaling. Numerous improvements have been made during succeeding years, and many of these are incorporated in the telemetering system designed by the Cornell Aeronautical Laboratory. The main point to be emphasized here is that this basic system was considered to be the most promising for development from the standpoint of proved reliability and simplicity, and the most likely to yield a practicable aircraft telemetering instrument with the minimum expenditure of time and manpower.

General Scheme of the Radio Telemetering System

This system may be described as an amplitude modulated subcarrier and frequency modulated radio carrier system as shown in Figure 1. The 14 subcarrier oscillators supply alternating current of frequencies from about 10 to 50 kilocycles to Wheatstone bridges incorporating strain-sensitive wires. These may be of the bonded-type or the unbonded-type gages with strain-sensitive wires incorporated in the instruments to measure pressures, accelerations, or forces. The variation in the resistance of the strain-sensitive wires changes the amplitude of the subcarrier oscillator. These changes from subcarrier channels are then amplified, collected, further amplified by the master amplifier, and then sent to the radio transmitter. The radio transmitter changes the amplitude modulated signals to a frequency modulated signal, the modulation of which is transmitted and detected by the radio receiver. Heterodyne analyzers are provided in a mobile receiving station to separate the individual signals and direct them to the

Paper 46-87, originally presented at the AIEE North Eastern District meeting, Buffalo, N. Y., April 24–26, 1946; recommended for publication by the AIEE committees on air transportation, communication, and instruments and measurements. Manuscript submitted March 6, 1946; made available for printing March 21, 1946.

CARL L. FREDERICK is vice-president of Fredric Flader, Inc., Air and Power Research Engineers, North Tonawanda, N. Y. He was formerly chief, physics department, Cornell Aeronautical Laboratory, Cornell Research Foundation, Inc., Buffalo, N. Y.

Contributions made by various members of the physics department of the Cornell Aeronautical Laboratory to the design of the components herein described are gratefully acknowledged. The author is particularly indebted to Karl D. Swartzel and Edward R. Dye, assistant department heads, for their supervision of the project and to C. F. Curtis, consulting engineer, Hazeltine Electronics Corporation, for his work on the automatic frequency control circuits of the frequency modulated receiver.

appropriate galvanometer in the recording oscillograph where 14 lines are drawn on sensitive paper ten inches wide.

Stabilized Oscillators, Bridge Circuits, and Buffer Amplifiers

The schematic diagram of the stabilized oscillators and bridge circuit is shown in Figure 2. As indicated previously, it is necessary that any required flight information be first converted to some form of electric change prior to its transmission to the ground receiving station. This conversion is effected by oscillator bridge units used in conjunction with either a bonded strain gauge attached to the structural member or an unbonded strain-sensitive element incorporated into the indicating mechanism of a flight instrument. The oscillator generates a signal whose amplitude, when introduced into a resistance bridge circuit containing the strain-testing element, is modulated by an amount proportional to the strain involved, that is, to actual flight data. The oscillator and bridge units are essentially the nerve centers of the entire radio telemetering system. Each consists of three separate components built into a single small aluminum chassis. These components are

1. An oscillator circuit, providing the subcarrier signal.
2. Two arms and necessary balance control of a resistance bridge circuit.
3. A buffer amplifier.

The most critical of the three components is the oscillator circuit itself. The nature of its use is such that it must maintain nearly constant amplitude and frequency for all operating conditions of voltage and temperature. Since the strain-gauge circuits will transmit information directly proportional to amplitude, the output voltage level of each oscillator must be held to close limits of stability, consistent with the accuracy of the data to be telemetered. In our case, a regulation of about one per cent was attained. This stability is achieved by a circuit in which the amplitude is controlled by a thermal element used as one arm of the oscillator feedback bridge. Thus, when an increase in output drives the bridge harder, unbalance is reduced tending to hold the oscillator output voltage constant. The over-all stability of the oscillator is accomplished through

1. The action of the hot filament balance lamps.
2. The control of ambient temperature within the definite limits of from 80 to 120 degrees Fahrenheit.

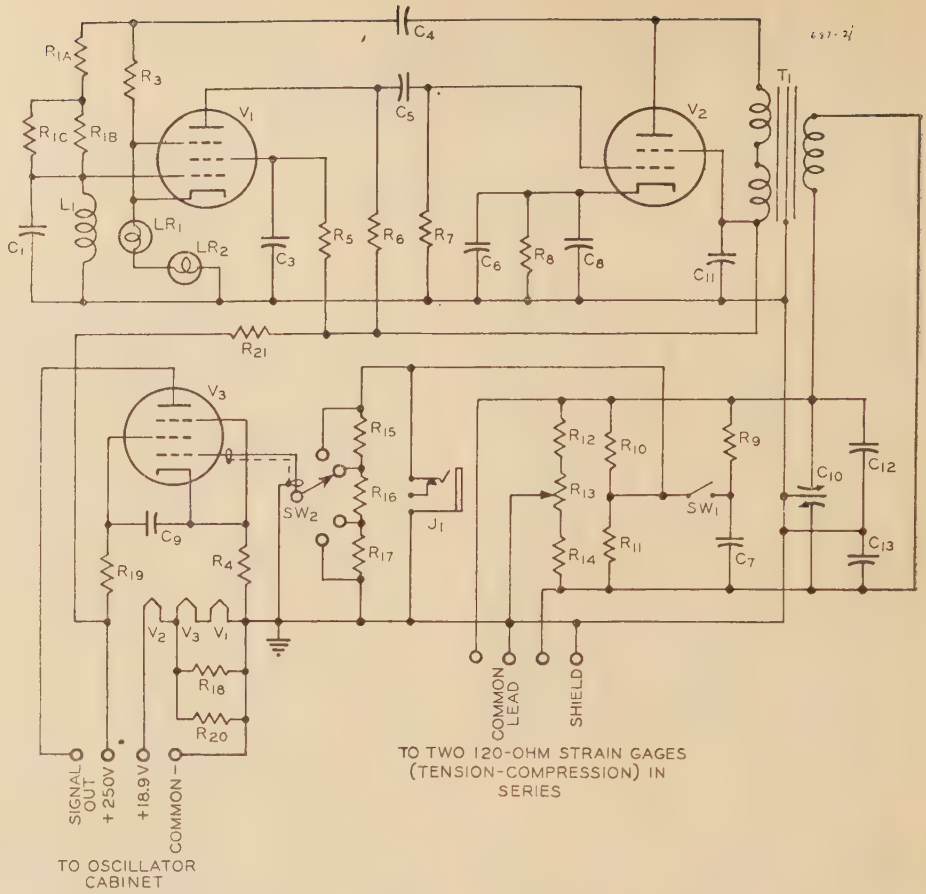

Figure 2. Schematic wiring diagram of oscillator and bridge balance unit

Components Common to All Channels

Symbol	Description	Symbol	Description	Symbol	Description
R_{1C}	20,000 ohms, 1 w	R_{15}	1,250 ohms, 0.1%	C_9	0.05 μf, 400 v
R_4	1,250 ohms, 10%	R_{16}	750 ohms, 0.1%	C_{10}	140 μμf
R_5	1 megohm, 10%	R_{17}	500 ohms, 0.1%	C_{11}	0.25 μf, 400 v
R_6	0.1 megohm, 10%	R_{18}	100 ohms, 10%	V_1	6SJ7
R_7	0.5 megohm, 10%	R_{19}	1 megohm, 10%	V_2	6V6
R_8	750 ohms, 10%	R_{20}	500 ohms, 10%	V_3	6SJ7
R_9	48,000 ohms, 0.1%	R_{21}	250 ohms, 10%	LR_1	6 w, 115 v
R_{10}	120 ohms, 0.1%	C_3	0.25 μf, 400 v	LR_2	6 w, 115 v
R_{11}	120 ohms, 0.1%	C_4	0.1 μf, 400 v	SW_1	Single pole, single throw
R_{12}	2,000 ohms, 1%	C_5	0.05 μf, 400 v	SW_2	Single pole, 4-position
R_{13}	10,000 ohms potentiometer	C_6	0.5 μf, 400 v	J_1	Jack-Mallory A2A
R_{14}	2,000 ohms, 1%	C_8	0.001 μf, 600 v	T_1	Altec-Lansing TM205

Components Varying With Channels

Channel Number	Frequency Cycles Per Second	L_1 Megohms	R_{1A} Ohms	R_{1B} Ohms	R_3 Ohms	C_1 (Approximate) μμf	C_7 μμf	C_{12} μμf	C_{13} μμf
1	10,833	40	22,000	10,000	1,870	5,600	50	—	100
2	13,333	20	17,300	10,000	1,850	7,100	20	—	50
3	15,833	20	26,800	15,000	1,920	5,000	10	—	100
4	18,333	10	17,500	10,000	2,000	7,500	5	—	50
5	20,833	10	21,000	12,000	1,740	5,800	20	250	—
6	23,333	10	50,000	30,000	2,500	4,700	25	—	100
7	25,833	5	15,000	10,000	2,220	7,600	25	—	50
8	28,333	5	26,100	15,000	2,500	6,300	15	50	—
9	30,833	5	30,000	15,000	2,500	5,400	20	—	100
10	33,333	3	15,000	8,500	1,820	7,500	15	500	100
11	35,833	3	25,000	12,500	2,500	6,600	15	—	—
12	38,333	3	18,000	10,000	1,770	5,700	15	—	100
13	40,833	3	21,000	12,000	1,670	5,100	10	250	—
14	43,333	2	10,000	7,500	1,670	6,600	15	—	100

3. By the adjustment of the effective temperature coefficient of the resistor designated R_1.
4. By moderately close control of the plate and heater voltages.

The balance lamps adequately suppress the amplitude changes associated with supply voltage variations up to plus or minus ten per cent. Regulation of the 22-volt supply is adequate to control plate and heater supply within this range. The balance lamps, however, are not

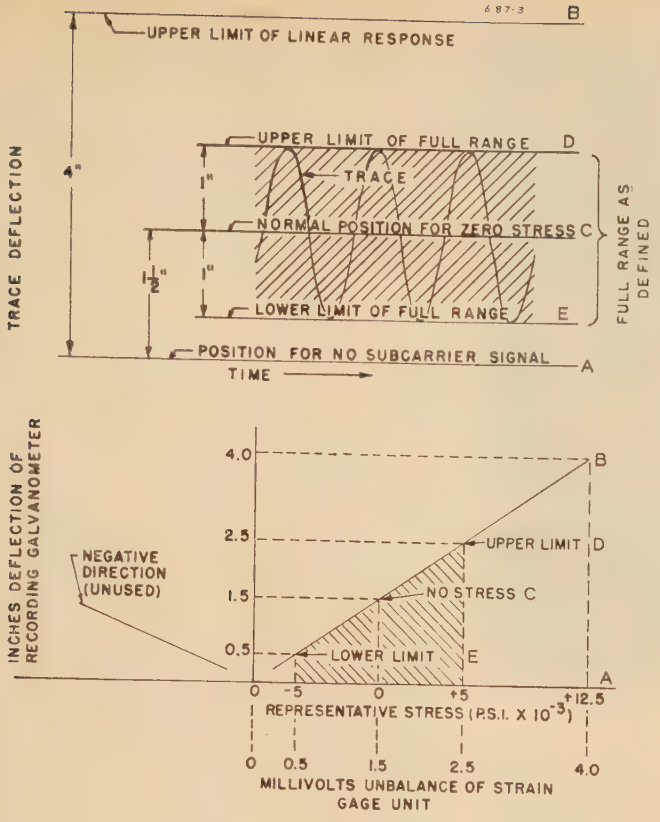

Figure 3 (left). Diagrams of signal ranges and the response of a recording galvanometer element to these changes

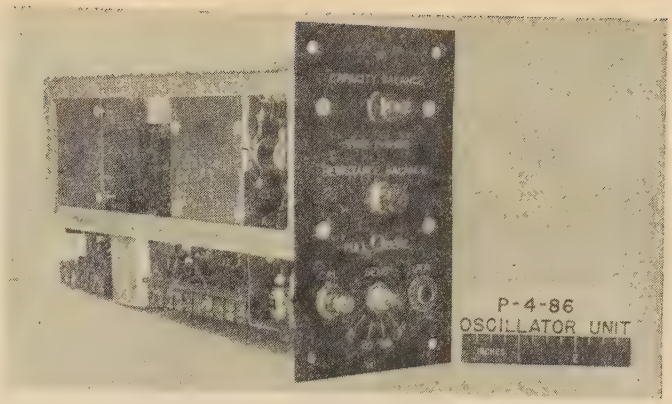

Figure 4 (above). Oscillator unit

capable of stabilizing the changes in the tuned circuit resistance associated with the alteration in Q value of the coil L_1 caused by temperature changes. To overcome this difficulty, the 14 oscillator and bridge units are housed in a single cabinet whose temperature is held within the temperature limits mentioned. To prevent this last increment of amplitude change, a temperature compensating resistor consisting of a series-parallel combination of a highly negative coefficient resistor and two positive coefficient resistors are chosen so as to give an overall temperature coefficient which will supply the required compensation. The compensating network is mounted within the shield of the coil L_1 so that its effect will change at the same time rate as the Q of the coil. In theory it is possible to adjust for zero amplitude change for various temperatures. Control is not quite that accurate in practice; it has been possible to adjust and hold to less than two per cent change for a 40-degree Fahrenheit temperature rise permitted within the cabinet.

Because of the high Q of the tuned circuit, the frequency is relatively independent of plate and heater voltages. Through a plate voltage range of 250 plus or minus ten volts or for a change in heater voltage of ten per cent, the frequency change is less than two cycles per second. Frequency change with temperature is less than two cycles from 80 degrees to 120 degrees Fahrenheit because of the existing favorable temperature balance between the duo-lateral coils L_1 and the silver mica capacitors C_1.

Two arms of the strain-gauge resistance bridge are built into each circuit. The other two arms completing the bridge are formed by the strain-sensitive elements attached to the airplane. The necessary balance controls for both amplitude and phase adjustments must be included as part of the bridge unit. In this design it is imperative that drift of the bridge balance be prevented, since the indicated strain is proportional to the change in the bridge balance. The transformer T_1, connecting the oscillator to the strain-gauge circuit, has a balanced secondary to facilitate securing strain-gauge bridge balance and to reduce noise pickup. Two strain gauges attached to the structure under test are connected to the unit, one for receiving strain and the other as a temperature balancing element. The resistors R_{10} and R_{11} are fixed resistors built into the amplifier and oscillator assembly as discussed later. A potentiometer, R_{13}, is incorporated for balancing the resistive components to the bridge. R_{12} and R_{14} limit the total range of adjustment available on R_{13}. The capacitor C_{10} is for adjusting the reactive component of the bridge balance. As has been explained before, the carrier signal does not show readily the sense of the measured stress. For this reason the bridge is operated off-balance by an amount depending on the anticipated strain. At the receiving point, the nature of the response to the signal from a bridge adjusted in this manner is illustrated in Figure 3. The signal ranges are shown in the upper diagram with conservatively defined full range values and maximum linear response range. The lower diagram shows the response of a recording galvanometer element to the above signal

Figure 5. Telemetering cabinet, 14-channel
The rule is 18 inches long

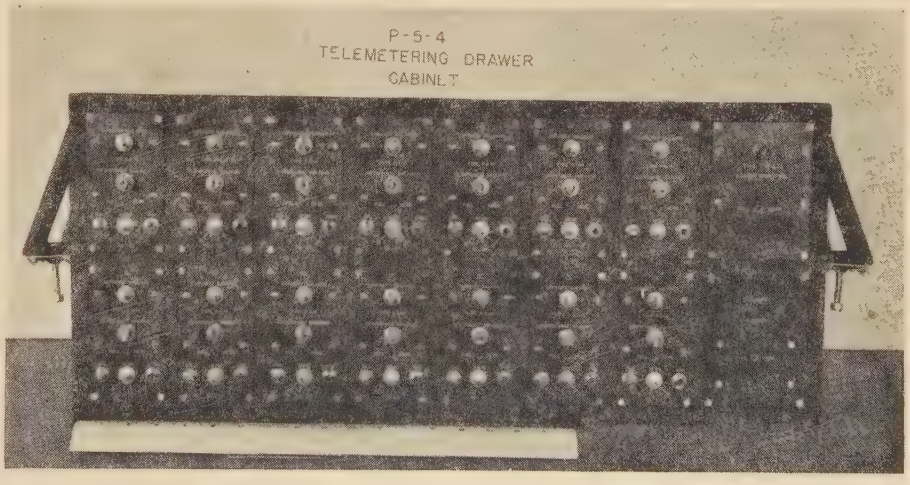

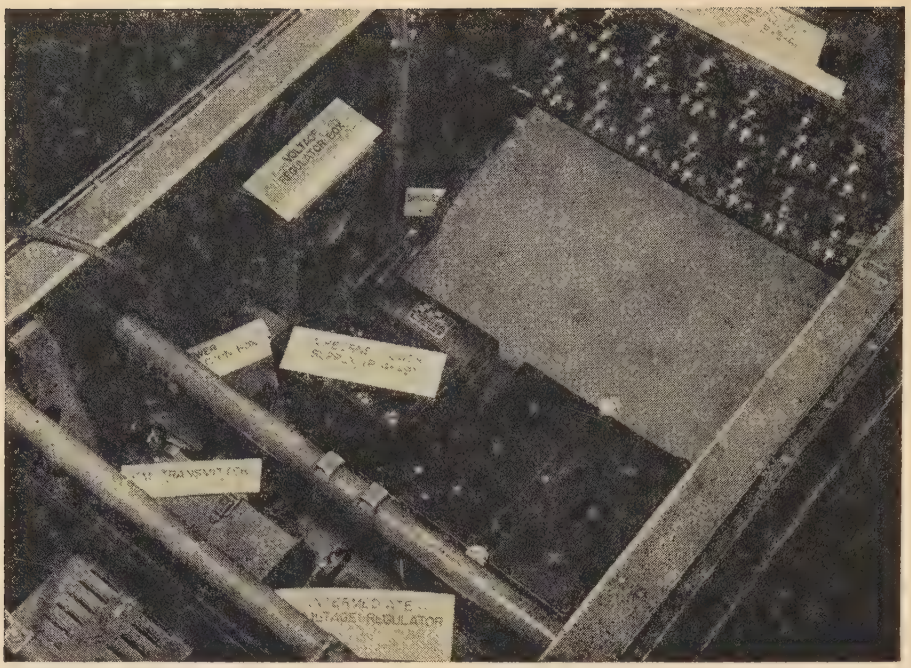

Figure 6. Equipment installation in SB2A-4 airplane

ranges as received from a strain gauge connected to transmit stress information.

The principal considerations controlling the buffer amplifier design were that it must not cause cross modulation between various signals, and its gain must be held constant within extremely narrow limits. The buffer amplifier also serves the purpose of preventing undesirable coupling between the several strain-gauge circuits. Negative feedback reduces harmonic distortion and stabilizes the gain. The harmonic distortion of the circuit shown is less than 0.2 per cent with a 10-millivolt signal on the grid. The normal signal level is only 1.5 millivolts. During performance tests of this circuit, the gain varied two per cent as the plate voltage was changed from 200 to 300 volts and varied one per cent as the heater voltage varied from 5.5 to 7.0 volts. The 14 buffer amplifiers have a common plate feed resistor so that their signals are all added together in the common output circuit.

In selecting the oscillator frequencies, it was found in preliminary tests that distortion was relatively large in the frequency region below ten kilocycles. Therefore the subcarrier oscillator frequencies were all set above ten kilocycles, as shown in the table in Figure 2. The frequency of 10,833 cycles per second was chosen as a starting point so that an inharmonic relationship would exist between subcarriers, but noise caused by other modulation products may be just as serious as that caused by harmonics of subcarrier frequencies. It is almost impossible to allocate 14 frequencies so that all the modulation products will be outside of the transmission bands. However, it was found that the set of frequencies chosen reduced the amount of noise on the recording oscillograph to a satisfactory minimum. A spacing of 2.5 kilocycles between subcarriers was chosen because of the characteristics of the crystal filter units used in the heterodyne analyzer receiving circuits in the mobile receiving station. The mid-frequency of the crystal filter band pass units is located at 92 kilocycles, and a frequency 2.5 kilocycles from the center of any pass band lies at or near the region of maximum attenuation. A discrimination of more than 50 decibels between subcarriers of adjacent channels is maintained.

The bridge elements, the oscillator components, and the buffer amplifier for each assigned subcarrier frequency channel were designed to mount together as a unit in the form of a drawer, as illustrated in Figure 4. These drawers are designed to be inserted into a cellular cabinet, as shown in Figure 5. After removal of four screws in the front panel, each drawer can be withdrawn without unsoldering any leads, since connections are established through separate connecting plugs at the back of the drawer

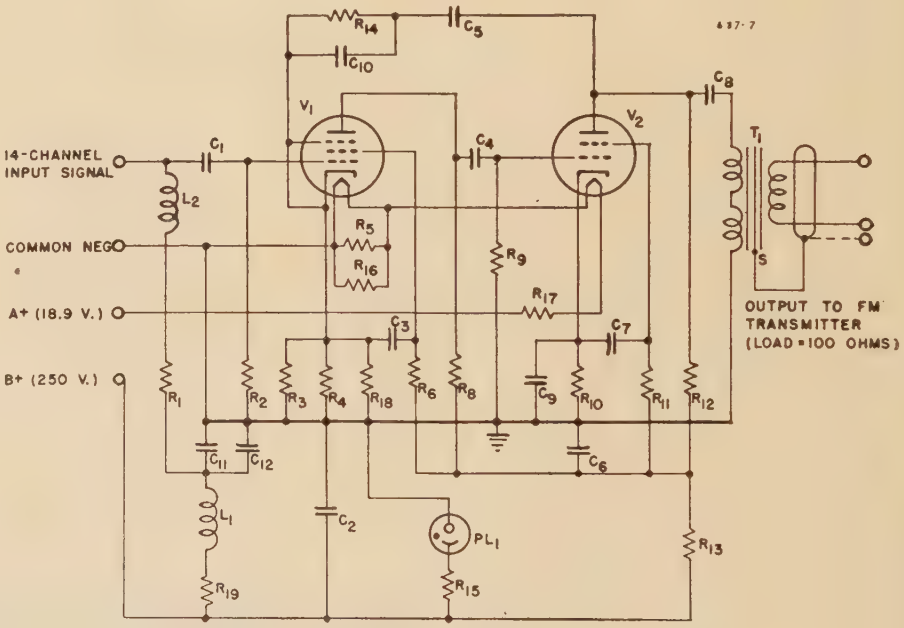

Figure 7. Schematic wiring diagram of master amplifier

Components Common to All Channels

Component Description	Component Description	Component Description
V_1—6SJ7	R_{11}—0.15 megohm, IRC BT-1	C_5—0.01 μf
V_2—6V6, GTIG	R_{12}—0.015 megohm, IRC BT-1	C_6—0.5 μf
P_1—AN 3102-14S-2P (reworked)	R_{13}—2,250 ohms, IRC BW-1	C_7—0.1 μf
S_1—AN3102-14S-75	R_{14}—0.075 megohm, IRC WW-4	C_8—0.01 μf
R_1—0.01 megohm, IRC* ABA	R_{15}—0.5 megohm, IRC BT-1	C_9—0.1 μf
R_2—0.5 megohm, IRC BT-1	R_{16}—250 ohms, IRC BW-1	C_{10}—5 μf
R_3—2,250 ohms, IRC BW-1	R_{17}—15 ohms, IRC ABA	C_{11}—0.5 μf
R_4—2,250 ohms, IRC BW-1	R_{18}—0.01 megohm, IRC ERIE	C_{12}—0.5 μf
R_5—50 ohms, IRC ABA	R_{19}—0.001 megohm IRC BW-1	L_1—40 mh, Delta R.**
R_6—0.5 megohm, IRC BT-1	C_1—0.01 μf	L_2—30 mh, Delta R.
R_8—0.05 megohm, IRC BT-1	C_2—0.5 μf	PL_1—1/25-w neon lamp
R_9—0.5 megohm, IRC BT-1	C_3—0.25 μf	T_1—Altec*** TM205
R_{10}—200 ohms, IRC BW-1	C_4—0.0001 μf	

*International Resistance Company. ** Delta Radio Corporation. *** Altec Lansing Corporation.

Each drawer weighs 2.75 pounds. The cabinet with drawers mounted, including the master amplifier and the temperature controlling unit, weighs 60 pounds and occupies 2.25 cubic feet. The cabinet, together with its associated voltage regulator, power supply, and frequency modulated transmitter, is shown in Figure 6 installed in the rear observer's cockpit of the SB2A-4 airplane.

Master Amplifier

The function of the master amplifier, shown schematically in Figure 7, is to receive and superpose the comparatively weak signals from the 14 buffer amplifiers, described previously, and to raise the composite signal level to an optimum value for input to the frequency modulated transmitter. The 2-stage resistance-capacitance coupled amplifier with a large negative feedback provides 17 ±0.5 decibel of gain with less than 0.25 per cent total distortion over the frequency range from 10 to 50 kilocycles.

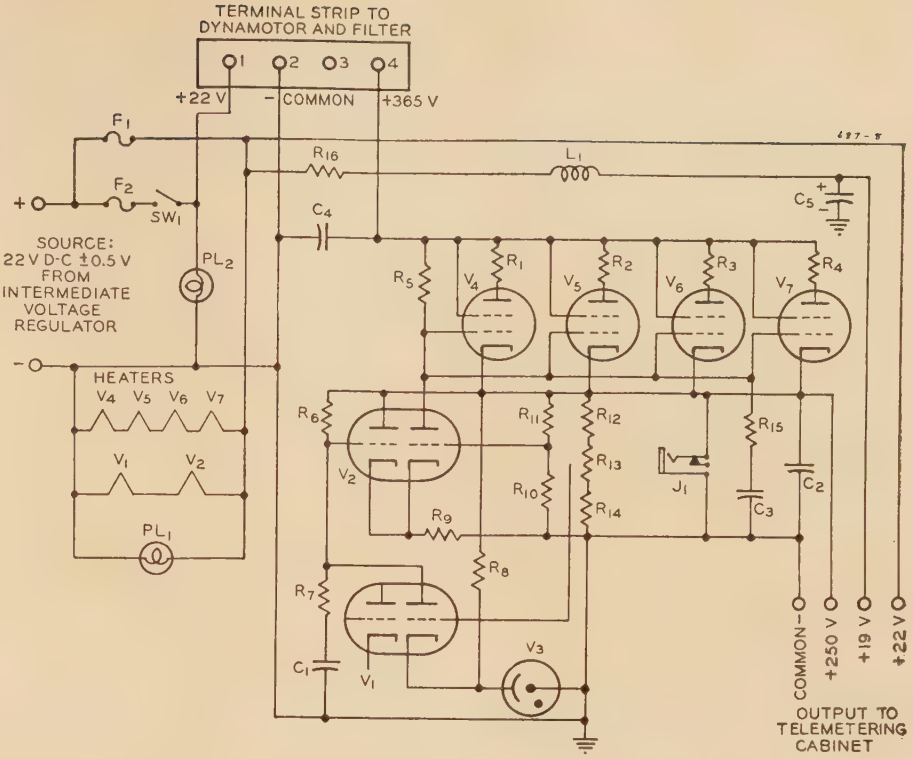

Air-Borne Regulated Power Supply

The accuracy and stability of the air-borne radio telemetering equipment depend upon a high degree of stability of the plate supply. It was therefore necessary to develop an extremely well-regulated 250-volt source to supply the vacuum tubes in the oscillator cabinet. As is well known, the voltage supply by an airplane under test may vary from 20 to 30 volts depending upon the maneuver. An intermediate-voltage regulator was designed using a series of extremely fast-acting relays to supply a primary power source of 22 plus or minus 0.5 volt direct current for the air-borne regulated power supply. Space will permit only a brief description of the air-borne regulated power supply, shown schematically in Figure 8, and its regulation characteristics in Figure 9. The circuit is a direct-coupled amplifier having a gain of 55 decibels and a negative feedback of 44 decibels. The input to the amplifier is derived by balancing a portion of the output voltage against a

Figure 8. Schematic wiring diagram of air-borne power supply

Components Common to All Channels

Component Description	Component Description
R_1, R_2, R_3, R_4—100 ohms	(0.01 and 0.003 in parallel)
R_5—0.3 megohm	C_2, C_4—2.00 μf, 600 v
R_6—1.5 megohms	C_3—0.00075 μf
R_7—5,000 ohms	C_5—25 μf, 50 v
R_8—10,000 ohms	V_1, V_2—12SL7GT
R_9, R_{10}—0.1 megohm	V_3—VR-75
R_{11}—0.15 megohm	V_4, V_5, V_6, V_7—6Y6G
R_{12}—0.25 megohm	PL_1, PL_2—28-v pilot lamps
R_{13}—0.05 megohm	SW_1—Single pole, single throw, 30 amps, 28 v
R_{14}—0.1 megohm	J_1—Standard phone jack
R_{15}—25,000 ohms	F_1—20 amps, Littelfuse 4AG
R—Ten 5-ohm, 10-w resistors parallel	F_2—40 amps, Littelfuse 4AG
C_1—0.013 μf	L_1—100 mh

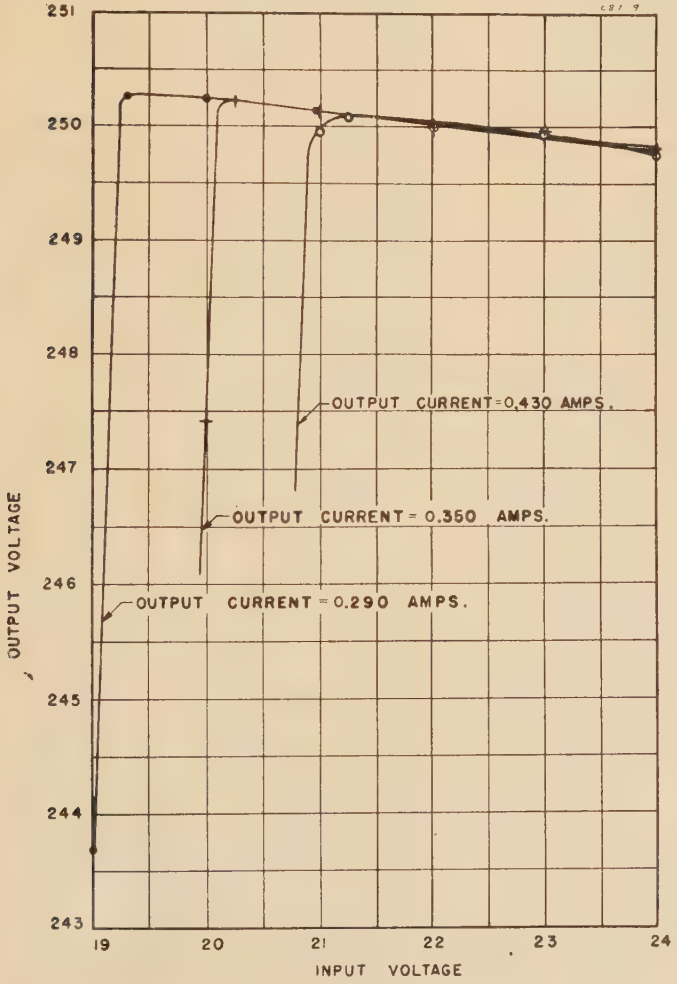

Figure 9. Regulation characteristics of air-borne power supply

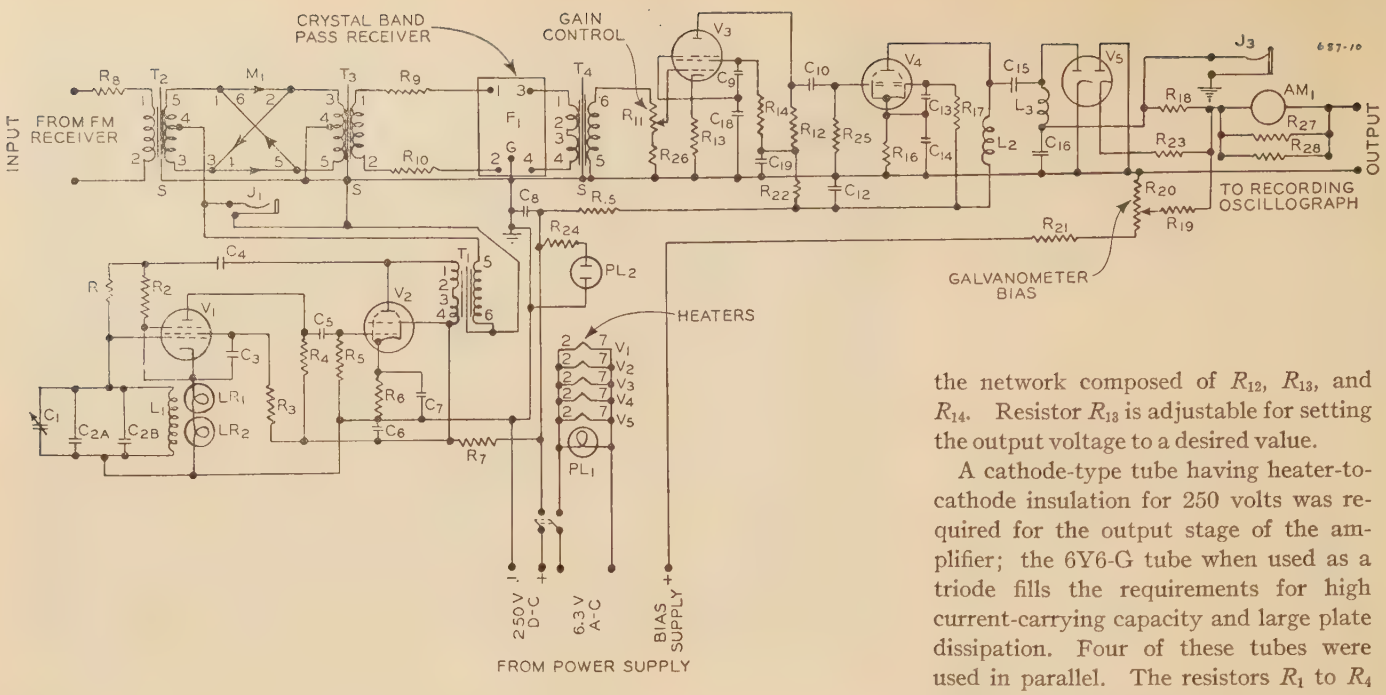

Figure 10. Schematic wiring diagram of heterodyne analyzer

Components Common to All Channels

Component Description	Component Description	Component Description
R_1*—IRC BT-1	R_{23}—1,000 ohms, IRC BT-1	C_{12}—0.1 μf, 400 v, paper
R_2—2,500 ohms, IRC BW-1	R_{24}—0.5 megohm, IRC BT-1	C_{13}—0.05 μf, 400 v, paper
R_3—0.5 megohm, IRC BT-1	R_{25}—0.5 megohm, IRC BT-1	C_{14}—0.05 μf, 400 v, paper
R_4—0.025 megohm, IRC BT-1	R_{26}*—IRC BT-1	C_{15}—0.05 μf, 400 v, paper
R_5—0.5 megohm, IRC BT-1	R_{27}—50 ohms, IRC BW-1	C_{16}—0.05 μf, 400 v, paper
R_6—750 ohms, IRC BW-1	R_{28}—150 ohms, IRC BW-1	C_{18}—0.05 μf, 400 v, paper
R_7—1,000 ohms, IRC BW-2	T_1—Specifications, Altec TM206	C_{19}—0.1 μf, 400 v, paper
R_8—600 ohms, IRC WW-3	T_2—WE 146F	L_1—0.5 megohm, Delta R.
R_9*—150 ohms, IRC WW-3	T_3—WE 146F	L_2—20 megohm, Delta R.
R_{10}*—150 ohms, IRC WW-3	T_4—WE 151B	L_3—40 megohm, Delta R.
R_{11}—0.03-megohm potentiometer, wire wound	PL_1—6.3-v 0.15-amp pilot lamp	LR_1—6 w, 120 v, Mazda lamp S-6
R_{12}—0.2 megohm, IRC BW-1	PL_2—1/25-w neon lamp	LR_2—6 w, 120 v, Mazda lamp S-6
R_{13}—1,000 ohms, IRC WW-4	C_1†—Variable, Budd	V_1—6SJ7
R_{14}—1 megohm, IRC BT-1	C_2A—Silver mica	V_2—6V6
R_{15}—1,000 ohms, IRC BW-2	C_2B‡—Silver mica	V_3—6SJ7
R_{16}—500 ohms, IRC WW-4	C_3—0.05 μf, 400 v, paper	V_4—6V6
R_{17}—0.02 megohm, IRC BT-1	C_4—0.01 μf, 300 v, mica	V_5—6H6
R_{18}—1,000 ohms, IRC WW-4	C_5—0.05 μf, 400 v, paper	AM_1—Milliammeter, Simpson 127
R_{19}—1,000 ohms, IRC WW-4	C_6—0.1 μf, 400 v, paper	M_1—Varistor, WE D97 428
R_{20}—2,000-ohm potentiometer, wire wound	C_7—25 μf, 50 v, electrolytic	F_1—Filter, WE D168 159
R_{21}—0.02 megohm, IRC WW	C_8—0.1 μf, 400 v, paper	J_1—Jack, Mallory A2A
R_{22}—0.01 megohm, IRC BT-1	C_9—0.05 μf, 400 v, paper	J_2—Jack, Mallory A2A
	C_{10}—0.0005 μf, mica	SW_1—Toggle switch, double-pole single-throw

* Adjust according to test specifications. † See the following table. ‡ As determined by text.

Channel Number	Frequency, Cycles Per Second	C_1 Max, μμf	C_2 (Approximate), Total, μμf	R_1 (Approximate)	C_2A, μμf
1	102,833	100	4,800	25,000	4,000
2	105,333	100	4,500	26,400	4,000
3	107,833	100	4,300	27,500	3,500
4	110,333	100	4,200	28,800	3,500
5	112,833	100	4,000	29,800	3,500
6	115,333	100	3,900	30,700	3,500
7	117,833	100	3,700	32,000	3,000
8	120,333	50	3,500	33,000	3,000
9	122,833	50	3,400	34,400	3,000
10	125,333	50	3,300	35,400	3,000
11	127,833	50	3,100	36,400	2,500
12	130,333	50	2,900	37,900	2,500
13	132,833	50	2,800	39,000	2,500
14	135,333	50	2,700	40,300	2,000

constant d-c potential of 75 volts determined by the gas-filled tube V_3. The first stage of amplification makes use of one triode section of V_1 and has a gain of 30 decibels. The second stage uses both sections of V_2 to obtain a gain of 30 decibels with no phase reversal. The output of the amplifier is a cathode follower stage using vacuum tubes V_4 to V_7 inclusive in parallel. The output stage has a loss of approximately six decibels. Negative feedback is obtained through the network composed of R_{12}, R_{13}, and R_{14}. Resistor R_{13} is adjustable for setting the output voltage to a desired value.

A cathode-type tube having heater-to-cathode insulation for 250 volts was required for the output stage of the amplifier; the 6Y6-G tube when used as a triode fills the requirements for high current-carrying capacity and large plate dissipation. Four of these tubes were used in parallel. The resistors R_1 to R_4 inclusive, in series with the plate leads, suppress any high frequency parasitic oscillations.

Power for the vacuum tube heater circuits in the oscillator cabinet (seven amperes direct current at 19 volts) is obtained from the 22-volt input through a series dropping resistor R_{16}. The coil L_1 and capacitor C_5 reduce the dynamotor interference in the heater supply.

Frequency Modulated Transmitter

The transmitter was especially designed to transmit signal frequencies in the range of from 10,000 to 50,000 cycles and to reduce cross modulation products to a value low enough to produce clean traces on the recording oscillograph. It was purchased from the F. M. Link Corporation, New York, and modified by the Cornell Aeronautical Laboratory in minor respects for the particularly severe stability requirements imposed on electronic equipment used in aircraft testing. The modifications consisted mainly in strengthening the frame and component supports to reduce the relative movement of the parts under the high acceleration forces and the replacement of a few elements with others designed for stability under the extreme temperature ranges encountered. In the course of development, adequate tests were performed to establish the optimum level of the composite subcarrier signal. This input level must be approximately 0.35 volt in order to assure a minimum background from modulation products during the transmission of flight data.

The transmitter is used with a crystal operating on 71.5 megacycles. Its more

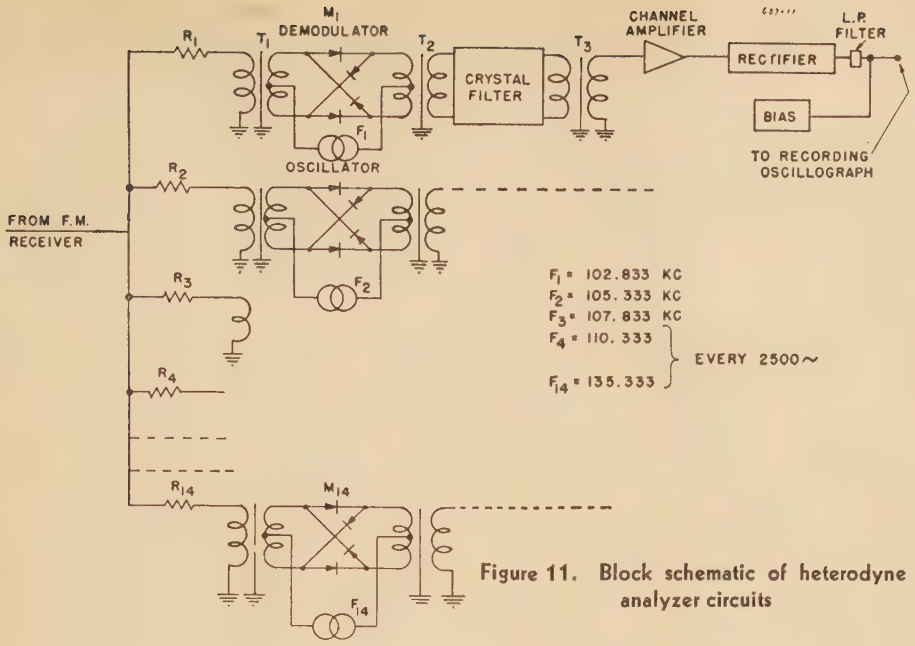

Figure 11. Block schematic of heterodyne analyzer circuits

important characteristics are as follows:

Power output	50 watts
Frequency range	65 to 72 megacycles
Frequency deviation	±150 kilocycles
Audio response	±1 decibel 1,000–50,000 cycles per second (overall; transmitter-receiver)
Modulation stability	Within one per cent for primary source variation between 21.5–22.5 volts
Mounting	Shock mounted on base
Size	16½ by 8¼ by 7⅞ inches
Power required	7.5 amperes at 28 volts direct current
Output impedance	50–100 ohms into concentric line

The transmitter is self-contained with its dynamotor power supply. Both filament and dynamotor currents are obtained through the remote control box which is equipped with separate switches and pilot lights for each. A metering jack on the front panel permits measuring the audio input level. A meter and selector switch also are provided on the front panel to permit measuring grid currents in all necessary stages when making adjustments.

Automatic Frequency Controlled Frequency Modulated Receiver

The frequency modulated receiver used was purchased from the F. M. Link Corporation, New York, N. Y., and modified for automatic frequency control. The automatic frequency control feature is not required for many applications where precise crystal control may be obtained in the transmitter. However, the requirements on the frequency stability of the transmitter may be greatly reduced if automatic frequency control is used in the receiver. (In fact, crystal control of the transmitter is not feasible in many applications of telemetering for compact flying bodies.) The output circuit has been modified to furnish a suitable subcarrier signal level to the heterodyne analyzer circuits.

The receiver may be adjusted manually over the approximate range of 66 to 74 megacycles and automatically over the range of plus or minus 0.5 megacycle from the manual setting. It has been designed especially to receive signal frequencies in the range of 10,000 to 50,000 cycles with sufficient fidelity of reproduction, holding cross modulation products to a value low enough to permit the recording of clean traces on the recording oscillograph paper.

The more important characteristics of the modified receiver are

Frequency range	65 to 72 megacycles
Type of signal	Frequency modulated ±150 kilocycles maximum deviation
Audio response	±1 decibel, 10,000–50,000 cycles per second (overall; transmitter-receiver)
Output stability	Within one per cent for primary source variation between 24–28 volts
Power required	3 amperes at 28 volts direct current
Output impedance	100 ohms
Output power	1/2 watt maximum

Heterodyne Analyzer

The composite signal which appears at the output of the frequency modulated radio receiver is analyzed, or separated into its 14 separate components, by means of a heterodyne analyzer system of 14 similar units, one for each subcarrier channel. The principal parts of each unit shown in Figure 10 are

1. A copper-oxide ring modulator.
2. A vacuum tube oscillator to provide the best frequency for the subcarrier.
3. A crystal filter for selecting the modulated signal on that subcarrier frequency.
4. An amplifier and detector combination for each channel, the output of which is applied to its assigned recording-oscillograph galvanometer.

An adjustable amount of regulated direct current is added to the signal as galvanometer bias to compensate for that portion of the detected current which represents the signal level of the subcarrier in the absence of strain on the gage at the transmitter. A milliammeter in series with the output gives visual indication of the signal level.

The block schematic shown in Figure 11 will serve to present the general plan of the analyzer. The 14 modulated subcarriers appear on the primary winding of the transformers, T_1. It was considered advisable to use identical crystal filters for each channel because procurement was simplified and also because changes in subcarrier frequencies were facilitated when desirable. Frequencies for the 14 local oscillators then were chosen to permit the desired side band to pass through the filters as shown. For example, the local oscillator frequency of F_1 is chosen of the value 102.833 kilocycles to apply to demodulator M_1. The subcarrier T_1 of frequency 10.833 kilocycles then combines with F_1 to produce a difference frequency of 92.000 kilocycles which passes through the crystal filter. It will be noticed that the attenuation characteristic shown in the insert of

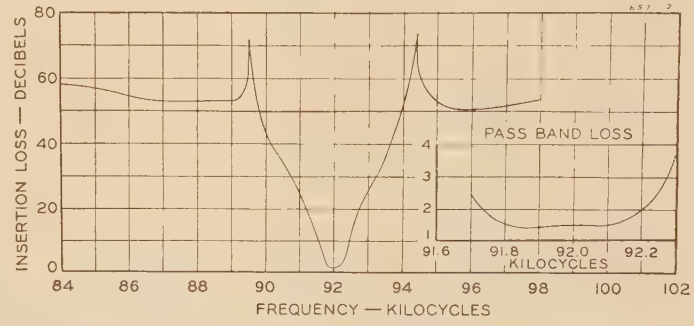

Figure 12. Crystal filter characteristic

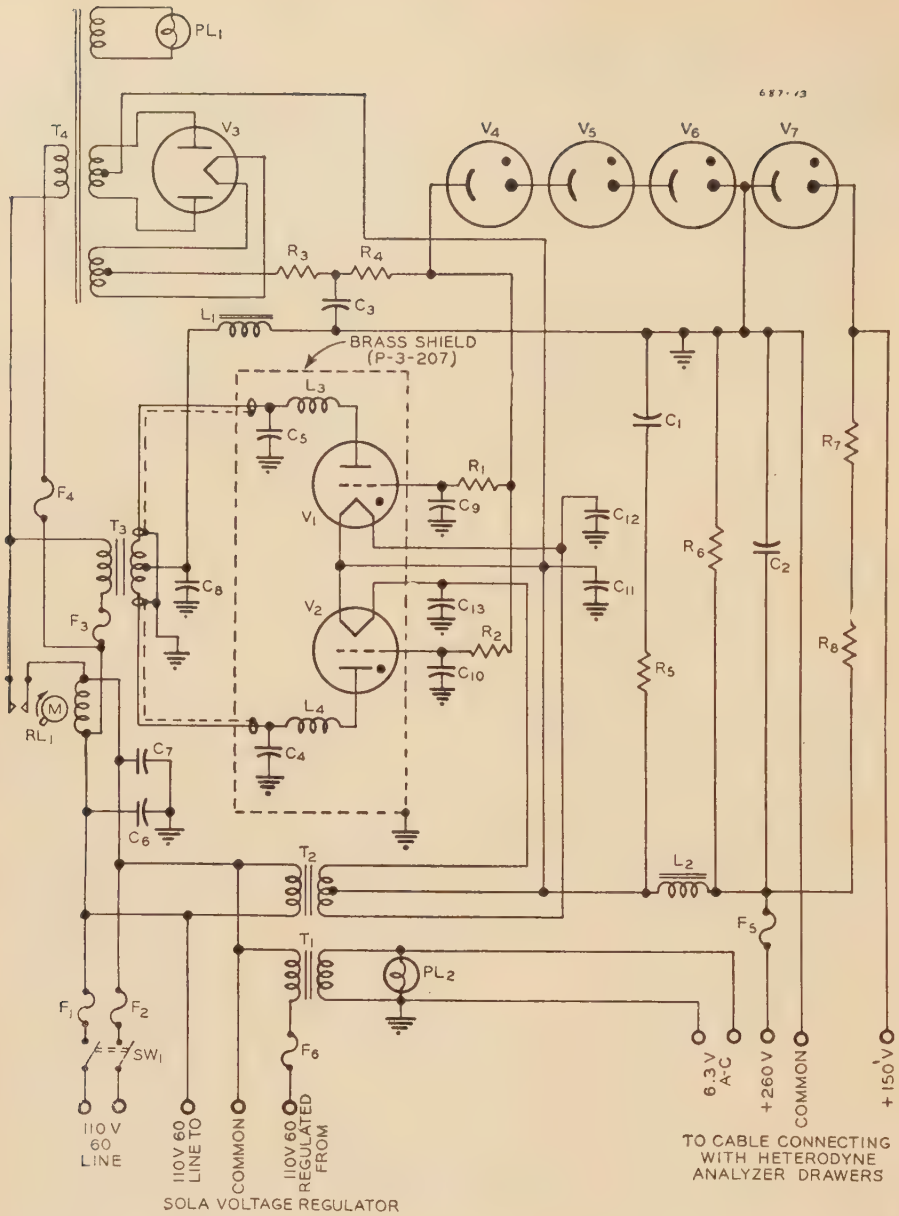

Figure 13. Schematic wiring diagram and components of power supply for heterodyne analyzer

Component Description	Component Description
R_1—0.05 megohm, 1 w	T_1—Filament transformer, Jeffries 1,290
R_2—0.05 megohm, 1 w	T_2—Filament transformer, Thordarson T-19F-84
R_3—0.01 megohm, 10 w	T_3—Power transformer, Jeffries 1,288
R_4—0.01 megohm, 2 w	T_4—Bias supply transformer, Stancor P6,010
R_5—10 ohms, 10 w	V_1—393 A
R_6—0.02megohm, 25 w	V_2—393 A
R_7—750 ohms, 25 w	V_3—5W4GT-G
R_8—50 ohms, 10 w	V_4—VR90
C_1—400 μf, 450 v	V_5—VR90
C_2—400 μf, 450 v	V_6—VR105
C_3—40 μf, 450 v	V_7—VR150
C_4—0.01 μf, 2,000 v	PL_1—6.3 v, 0.15 amp
C_5—0.01 μf, 2,000 v	PL_2—6.3 v, 0.15 amp
C_6—0.1 μf, 600 v	RL—Time delay relay, Hayden
C_7—0.1 μf, 600 v	SW—Double-pole single-throw switch
C_8—0.005 μf,1,200 v	F—15 amp, 4AG
C_9—0.02 μf, 1,200 v	F_2—15 amp, 4 AG
C_{10}—0.02 μf, 1,200 v	F_3—5 amp, 4 AG
C_{11}—0.01 μf, 1,200 v	F_4—1 amp, 4AG
C_{12}—0.005 μf, 1,200 v	F_5—2 amp, 4 AG
C_{13}—0.005 μf, 1,200 v	F_6—5 amp, 4AG
L_1—4h choke	
L_2—4h choke	
L_3—Radio frequency choke, 1 amp (P-1-055)	
L_4—Radio frequency choke, 1 amp (P-1-505)	

Adjust time delay of RL_1 to 50 seconds ±10 seconds. Connect capacitors C_9, C_{10}, C_{11}, C_{12}, and C_{13} as close as possible to sockets of V_1 and V_2.

Figure 12 has a pass band flat to within plus or minus 0.1 decibel over a frequency range of at least 200 cycles per second. The operator of the receiving station readily can adjust the oscillators to attain uniform attenuation and phase transmission of all frequencies represented in the modulation of the air-borne subcarrier oscillators produced by the instruments from which data are desired.

Each modulator unit, shown in Figures 10 and 11, consists of four copper-oxide rectifier elements arranged in a lattice structure. The input signal is applied through a transformer from the 1-ohm impedance in the output of the frequency modulated receiver. It is therefore attenuated sufficiently in passing through the input resistor R_8 of 600 ohms and the primary impedance of the transformer T_2, which is also 600 ohms, to prevent appreciable crosstalk from the modulator in a specified channel to the other analyzers which are connected in parallel. Since the input of each signal channel to the modulators is about 50 millivolts rms, the composite signal amplitude of the 14 channels is about 700 millivolts, which is about ten decibels below the 1-volt output of the oscillators. Increase in the signal level may result in overmodulation and increase the noise level of the oscillator output. The temperature characteristics of the copper-oxide rectifiers in the modulators are such that temperature regulation beyond that provided for the comfort of the operators of the mobile receiving station is not required.

Since the voltage level of the crystal filter output is low, 2-stage resistance-coupled amplifiers are employed in each channel as shown. There is sufficient variation in the performance of commercial 6SJ7 tubes to cause considerable difference in the crystal filter response curve for different volume control settings in the first amplifier grid circuit. By selecting for use only tubes with closely similar characteristies, this difficulty has been minimized.

To obtain the envelope containing the signal from the 92 kilocycles amplitude

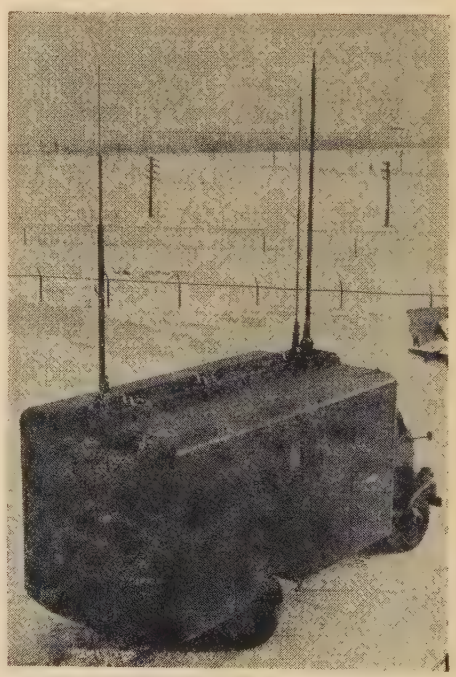

Figure 14. Exterior view of mobile receiving station for radio and television telemetering

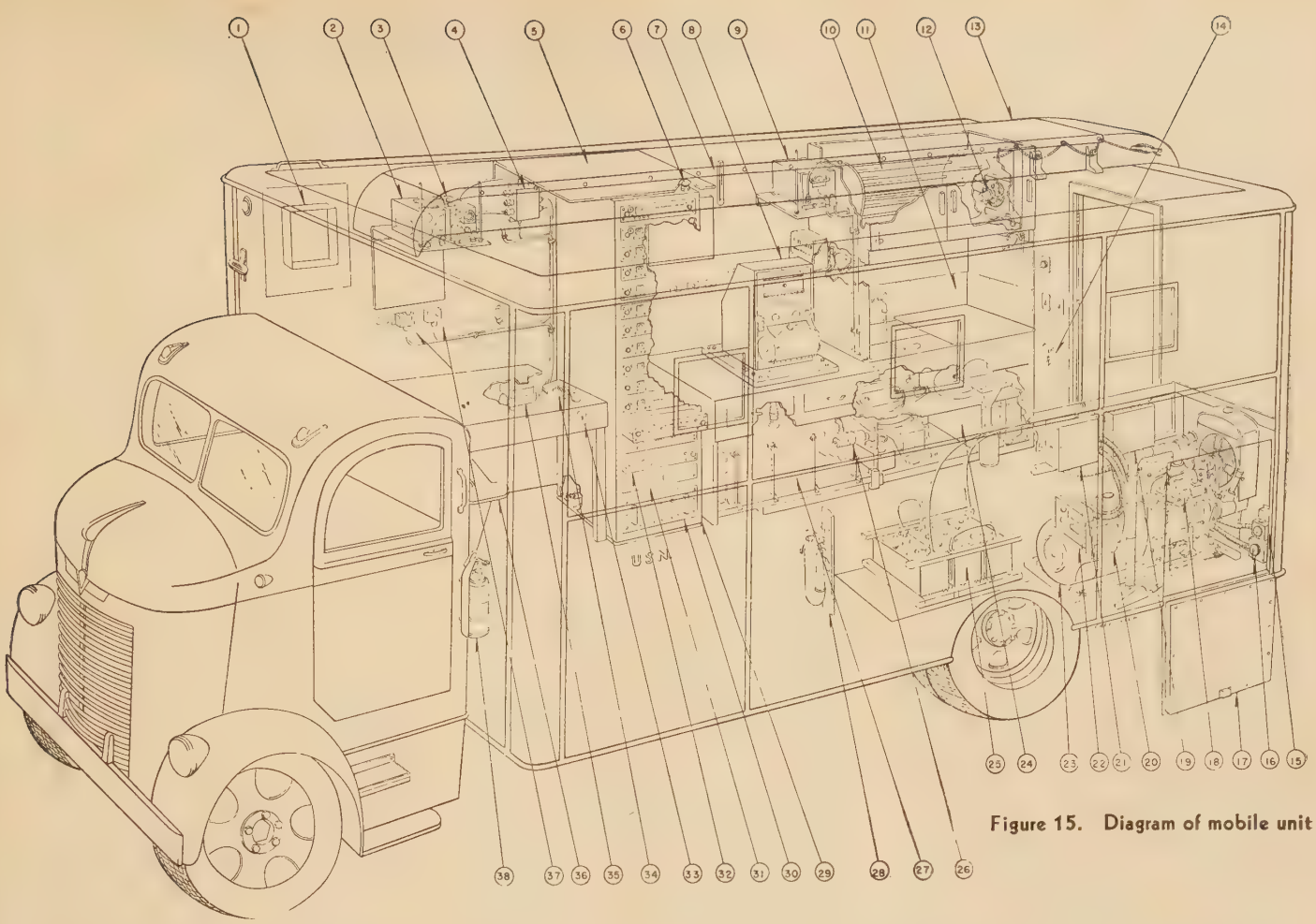

Figure 15. Diagram of mobile unit

modulated wave received from the amplifier, a 6H6 diode detector is used in a bridge-type half-wave detector circuit balanced to reduce the effect of variations in filament voltage. The carrier frequencies present in the rectifier output are suppressed by a low-pass filter system with an adequate attenuation above 300 cycles per second. Filters have been designed to reduce the frequency response of the telemetering system to any desired value. For example, in studying certain types of low frequency flutter, higher frequencies sometimes referred to as "aerodynamic hash" may be eliminated from the record, thus facilitating the analysis of the particular quantity under study.

Figure 16. Interior of mobile unit

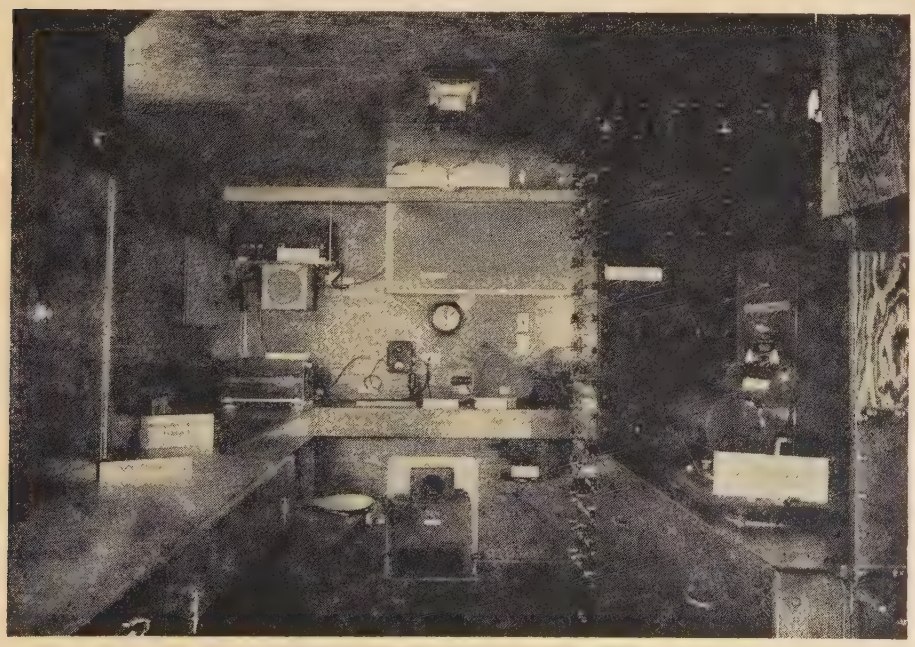

As mentioned previously, an a-c bias is applied in the subcarrier oscillator and bridge unit for the purpose of identifying the direction or sense of change in strain-gauge circuits connected with the airborne radio transmitter. Zero strain is represented by a signal of half strength, plus strain by more than half, and minus strain by less than half. To remove the effect of this bias at the receiving station, a d-c bias obtained from the heterodyne analyzer power supply is applied to the galvanometers which record the signals received from the rectifiers. Since the 150 volts direct current from the power supply is constant within ±0.2 per cent, the galvanometers can be adjusted accurately and permanently for zero on the scale. The bias current is attenuated so that a current of zero to five milliamperes is available to balance the detected zero level signal. Galvanometer sensitivity is such that a 1-inch deflection results from about 67 per cent modulation.

Heterodyne Analyzer Power Supply

Accuracy and dependability of operation of the heterodyne analyzer unit re-

quire a high degree of stability in the potential sources supplying the electronic circuits. The heterodyne analyzer supply shown in Figure 13 was developed and constructed to energize the plate and heater circuits of the vacuum tubes in the analyzers and to provide a source of direct current to bias the galvanometers in the recording oscillograph. The combined heater load of the vacuum tubes is 27 amperes alternating current at 6.3 volts. The plate circuits require 1.0 ampere direct current at 250 volts, constant to within ±1 per cent, while for galvanometer bias a current of 0.1 ampere at 150 volts direct current, constant to ±0.2 per cent, is needed. The available input potential to the power supply is 115 ±5 volts alternating current at 60 ±5 cycles per second, derived from the generator in the mobile receiving station.

The regulator circuit uses two type-393A thyratrons, V_1 and V_2, as full-wave grid-controlled rectifiers. These tubes were selected because of their large current rating, their dependable operation at all anticipated temperatures, and their positive starting characteristics at temperatures below freezing.

By operating the rectifier grids at a fixed potential, the output voltage is maintained constant within narrow limits regardless of variations in input potential or load current. The fixed grid potential is obtained from three voltage-regulator tubes connected in series, V_4, V_5, and V_6. An auxiliary power supply composed of T_4, V_3, R_3, and C_3 provides sufficient potential to ionize the VR tubes and maintain fairly constant current through them.

A filter is used to smooth the ripple content in the rectifier output. It is important to note that the first filter choke, L_1, is in the negative lead, thus reducing the ripple in the voltage appearing between the rectifier cathodes and the point which fixes their grid potential.

Mobile Receiving Station

The mobile receiving station, shown in Figures 14, 15, and 16, was designed for efficient and reliable use in the field. Large savings in cost of flight testing can be effected if time can be saved during field tests because a large crew is generally involved, and flying time is very costly. Provisions were made for a specially designed 5-kilowatt engine-driven generator to furnish both alternating and direct current, heating and cooling units to keep the interior within a temperature range of plus or minus ten degrees Fahrenheit, complete facilities for developing oscillograph paper and 16-millimeter film, and means for erecting the antennas from within the body. Storage space for all instruments, spares, and tools for making minor repairs also were included. In addition to the radio telemetery equipment described in the paper, a television telemetering system also was developed to transmit 54 slowly varying items of data (400 cycles per minute). A synchronizing system was developed so that the data recorded from both systems could be correlated for a given instant of time.

Many special instruments were developed in connection with the telemetering project.

Reference

1. New Features of Latest Wind Tunnels, *Aero Digest*, July 1, 1945, pages 59–64.

Negative Resistance Effects in Saturable Reactor Circuits

J. M. MANLEY
NONMEMBER AIEE

E. PETERSON
MEMBER AIEE

Synopsis: Sustained oscillations exhibiting many of the properties of free oscillations are found in saturable reactor circuits under appropriate conditions. The frequencies of such oscillations are classified in relation to that of the driving source as

1. Incommensurable.
2. Subharmonic, and multiples thereof.
3. Harmonic.

General properties of the oscillations classified are elucidated by reference to an analysis of R. V. L. Hartley's, dating back to 1917. In part I a comparatively simple form of analysis is used to demonstrate the development of negative resistance by what is essentially a modulation process. Applications are then made to the three classes of oscillations listed. Some of the simplifying assumptions of part I are removed in part II to approximate practical conditions more closely for the evaluation of a specific product, the third subharmonic. Quantities evaluated over wide ranges of the variables involved include the impedance of the nonlinear coil to the subharmonic, the subharmonic amplitude, its stability, and the conditions required for starting and maintaining the oscillation. Experimental data are found in general agreement with the results of computation.

Part I

THE GENERATION of subharmonics in saturable reactors has had just one commercial application[1] so far as the authors know—the production of 20-cycle telephone ringing current from 60-cycle power. Interest in the phenomenon is far more widespread than the comparatively small field of application would suggest however, as subharmonics may be encountered whenever an attempt is made to tune circuits which include saturable reactors.[2] In fact, subharmonics represent but one of the several classes of sustained oscillations exhibiting similar performance features which may be generated in such circumstances. These classes are arranged according to the ratio of the oscillation frequency to the frequency of the driving a-c source as

1. Incommensurable.
2. Subharmonic, and multiples thereof.
3. Harmonic, both even and odd.

Their performance features differ sharply from those of the more familiar coexistent forced oscillations which include the fundamental and its odd harmonics, assuming the driving source sinusoidal and the nonlinear core unpolarized. To list some of these differences, the oscillations classified can be generated only where the impressed electromotive force falls within a definite range of amplitudes and where the load impedance, too, is located within a restricted region. While the amplitude of any of these oscillations varies continuously with impressed electromotive force or load impedance over a certain range, it falls suddenly and irreversibly to zero when the range is exceeded. Thus the voltage of the generated oscillation goes to zero when the load circuit is opened.

These oscillations have characteristics similar to those of free oscillations in vacuum tube circuits, for example, and

Paper 46-120, recommended by the AIEE committee on basic sciences for presentation at the AIEE summer convention, Detroit, Mich., June 24–28, 1946. Manuscript submitted January 16, 1946; made available for printing May 8, 1946.

J. M. Manley and E. Peterson are with the Bell Telephone Laboratories, Inc., Murray Hill, N. J.

The authors are indebted to a number of their associates in these laboratories, and especially to S. O. Rice and Doctor L. A. MacColl for constructive criticisms and suggestions.

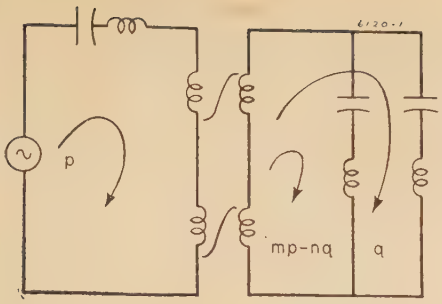

Figure 1. Circuit used by Heegner for developing self-oscillations

The two nonlinear coils are oppositely poled. Resonances are provided at the supply frequency $p/2\pi$, and at the two oscillation frequencies $(mp-nq)/2\pi$ and $q/2\pi$

have been referred to in the literature as free[3] and as self-excited[4] or self oscillations. In any one of the three classes, however, the frequency is related to that of the driving source, a property commonly thought of as an attribute of forced oscillations. Since the oscillations classified therefore have aspects associated with both free and forced oscillations, it might be preferable to designate them by a term indicative of that fact, such as free-forced, combined, composite, or quasi-free. Conforming to previous usage we shall refer to them as free, keeping the reservation just noted in mind.

To provide a physical picture of the way in which free oscillations can be generated in saturable reactor circuits, as well as to exhibit the relationship between the three classes of free oscillations, we shall use the results of a circuit analysis worked out by R. V. L. Hartley[5] in 1917. For this purpose we consider a circuit consisting of a nonlinear coil in series with an external impedance which is assigned suitable values at significant frequencies. The input is supplied by two a-c generators which, for convenient reference, are designated carrier and signal, the term signal being used arbitrarily for the lower of the two input frequencies. With the two input currents flowing through the coil, a whole series of modulation product voltages is generated. The external impedance then is assumed to permit just two of the generated components to flow, the impedance being taken as infinite for the other products.

Solution of the circuit equations permits us to study the effective impedance of the nonlinear coil to the signal. It is found that the flow of certain products introduces a positive resistance, but the flow of certain other products introduces a negative resistance into the signal path. These introduced resistances arise through the intermodulation of the several current components flowing through the coil. The appearance of a negative resistance opens possibilities for the existence of free oscillations. For if the negative resistance can be made large enough to annul the positive circuit resistance at any frequency, and if the circuit reactance can be tuned out at that frequency, the necessary requirements for oscillation are fulfilled.

Because it is fundamental to the operation of magnetic self-oscillating circuits, a brief derivation of the negative resistance (Hartley) effect will be outlined in its simplest form. The results will be compared with corresponding modulation effects in nonlinear resistance circuits. Applications then follow to explain how the three groups of free oscillations can be made to arise. Following this general discussion in part I, the production of a typical subharmonic will be treated quantitatively in part II.

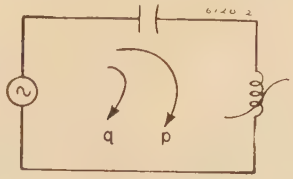

Figure 2. Circuit used by Fallou for frequency reduction

A single resonance is provided for the self-oscillation

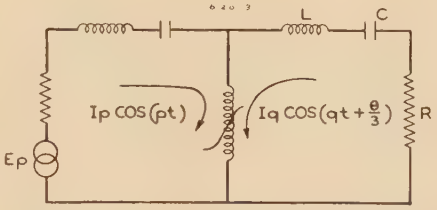

Figure 3. Circuit used for subharmonic analysis with resonances provided at input and subharmonic frequencies

All other current components suppressed

The Hartley Effect

Perhaps the simplest equation we can use to exhibit the relation between flux density and magnetizing force in the saturable reactor is

$$B = a'_1 H + a'_3 H^3 \qquad (1)$$

This relation exhibits saturation when the nonlinear term is negative, and when the maximum excursion of the magnetizing force is limited to regions in which the slope of equation 1 is positive. With the magnetizing current and magnetizing force linearly related, the voltage developed across the coil may be written

$$v = KB = Ki(a_1 + a_3 i^2) \qquad (2)$$

The coil is connected in series with a linear impedance and with two independent sine wave generators, their frequencies being $p/2\pi$ and $q/2\pi$, the carrier and signal, respectively. Because of the nonlinearity exhibited by equation 2, new frequencies are generated—in general there are many such components. The frequency of any component may be expressed as $(mp \pm nq)/2\pi$, m and n being integers. Its order is the sum of absolute values of the frequency coefficients $m + n$. This sum will be restricted to odd integers since equation 1 is an odd function and the core is unpolarized. For present purposes there are two nonlinear components in which we are interested primarily. These are the two third-order* side frequencies $(p \pm 2q)/2\pi$. To reduce the work to its essentials, we assume networks connected in circuit which permit the flow of just the four components—two impressed by external sources and two gen-

* Two other third-order side frequencies ($m=2$ $n=1$) are included in the products which meet a high circuit impedance and are therefore assumed to produce negligibly small current flow.

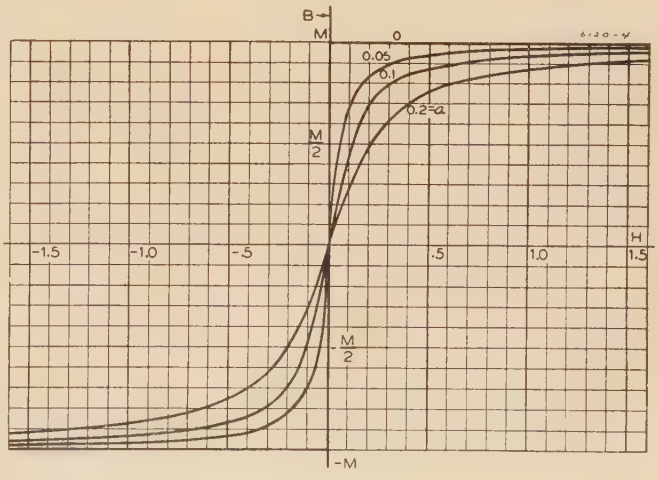

Figure 4. Plot of the equation $B=(2M/\pi)\tan^{-1}(H/a)$ with a as parameter

This parameter is equal to the magnetizing force at which the flux density reaches half its saturation value M

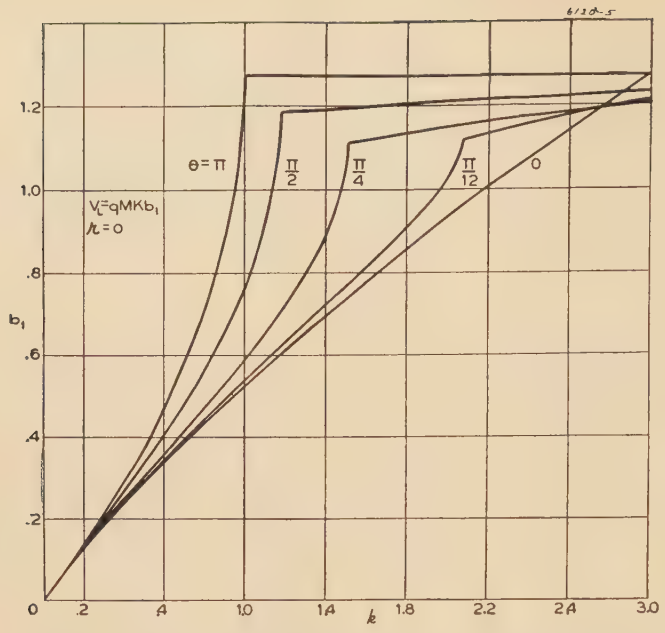

Figure 5. Here a two-component wave of magnetizing force. $H=P\cos 3qt+Q\cos(qt+\theta/3)$ is assumed to act on the magnetic characteristic ($a=0$) illustrated in Figure 4

The inductive coil voltage component of frequency $q/2\pi$ is plotted as a function of $k=Q/P$ for several values of θ; $b_1(\theta)=b_1(-\theta)$

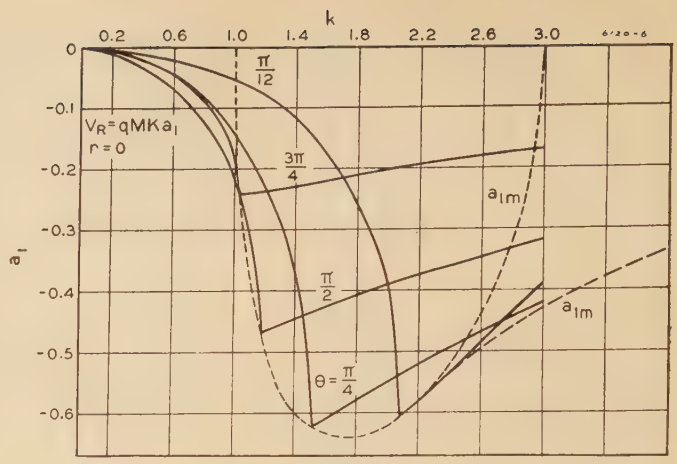

Figure 6. The resistive coil voltage component of frequency $q/2\pi$ shown here was obtained for the conditions specified in Figure 5

$a_1(\theta)=-a_1(-\theta)$, $a_1=0$ for $\theta=0,\pi$

erated by nonlinearity. Accordingly

$$i=I_p\cos pt+I_q\cos qt+I_+\cos[(p+2q)t+\theta_+]+I_-\cos[(p-2q)t+\theta_-] \quad (3)$$

Here the phase angles $\theta_\pm$ permit necessary phase displacements with respect to the input waves.

The circuit equation may be expressed as

$$\Sigma e_\gamma=\Sigma_\gamma Z_\gamma' i+v \quad (4)$$

where the subscript γ is used to indicate values effective to a particular component p, q, or $p\pm 2q$ in the present case. Σe_γ refers to the externally impressed electromotive forces, v refers as before to the voltage components across the nonlinear coil given by equation 2, and $Z_\gamma' i$ refers to the potential drops across the linear impedance.

Putting equation 3 in equations 2 and 4, we arrive at an equation for each of the four current components. Taking the carrier substantially greater in amplitude than the other components, only simple linear operations are encountered from this point on, so that the results may be expressed concisely in the notation of complex algebra. Thus for the two side-frequencies, equation 4 becomes

$$\left.\begin{aligned} 0&=Z_+I_+\epsilon^{j(\theta_++\varphi_+)}+j(p+2q)\kappa I_pI_q^2\\ 0&=Z_-I_-\epsilon^{j(\theta_-+\varphi_-)}+j(p-2q)\kappa I_pI_q^2\end{aligned}\right\} \quad (5)$$

Here φ_γ represents the phase angle of Z_γ the total circuit impedance to the component indicated by the subscript, and κ includes the nonlinear coefficient and other coil constants. If again to simplify matters we assume the side frequency impedances to be purely resistive—reactances tuned out—then the φ's are zero, and the side frequency amplitudes and phase angles are

$$\left.\begin{aligned} \theta_+&=\theta_-=-\pi/2\\ I_+&=(p+2q)\frac{\kappa I_pI_q^2}{R_+}\\ I_-&=(p-2q)\frac{\kappa I_pI_q^2}{R_-}\end{aligned}\right\} \quad (6)$$

These relations permit evaluation of the impedance reaction into the fundamental or input paths. For the lower of the two impressed frequencies, after substituting equation 6 in equations 3 and 4, and again assuming reactances tuned out,

$$E_q=R_qI_q+q4\kappa I_pI_q(I_+-I_-) \quad (7)$$

Similarly for the higher input frequency,

$$E_p=R_pI_p+p\kappa I_q^2(I_+-I_-) \quad (8)$$

From equation 7 it is apparent that in the signal path the upper side-frequency introduces a positive resistance, whereas the lower side-frequency introduces a negative resistance. In the carrier path as given by equation 8, each side-frequency introduces a positive resistance.†

Extensions of the Analysis

The same general result holds for other products. For example, the other third order side frequencies $2p+q$ and $2p-q$ produce positive and negative resistance effects in much the same way as the components $p+2q$ and $p-2q$, respectively. Since the same type of result is found with side frequencies of any order,* the statement following equation 8 can be generalized as follows:

The flow of a lower side-frequency of any order introduces negative resistance into the signal path and positive resistance into the carrier path; the flow of upper side-frequency of any order introduces positive resistance into both paths.

Inasmuch as the term negative resistance is used to describe a source of energy, another way to express this result is to say that the flow of lower side-frequency in a magnetic modulator circuit causes energy to be abstracted from the carrier and delivered to the signal; flow of upper side-frequency abstracts energy from both inputs. Taking into account the transfer of energy from one path to another, it is a straightforward matter to show that energy is conserved.

For subsequent use we can generalize the quantitative results of equations 6 and 7 to fit any order of modulation. Confining attention to the lower side-frequency throughout, equation 6 shows the amplitude of the third order product $(p-2q)$ to be proportional to $I_pI_q^2$. The product of order $m+n$

$$s=mp-nq$$

has an amplitude I_- proportional to $I_p^mI_q^n$, the conclusion following directly from a power series expansion. Equation 7 includes a q voltage component produced by the modulation of the third order product $(p-2q)$ with the two fundamentals to form the product

$$|(p-2q)-p+q|=q$$

This is again a third order process, in-

† Analogous effects appear in variable capacitor circuits.[6,7]

* Hartley's original analysis dealt with second order side-frequencies, the nonlinear core being polarized.

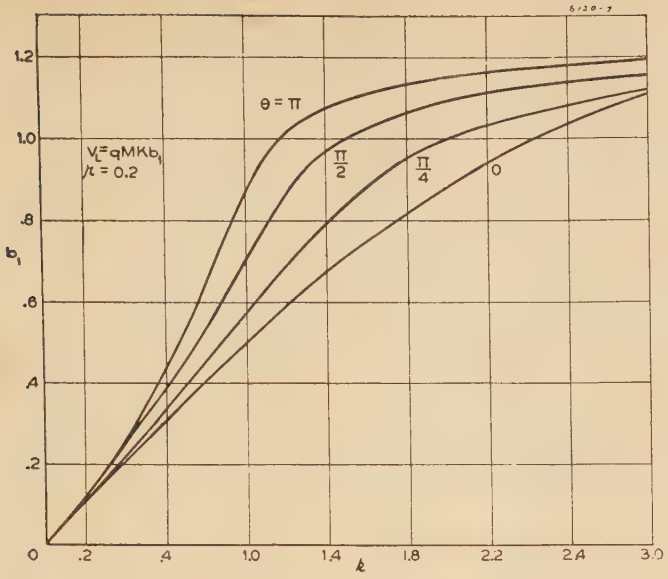

Figure 7. The inductive coil voltage component of frequency $q/2\pi$ corresponds to the condition of Figure 5 except that here $r = a/P = 0.2$, $b_1(\theta) = b_1(-\theta)$

volving three components this time, the amplitude of the reaction term being proportional to $(I_p I_q^2)(I_p)(I_q)$. In general, to get the required q reaction from a modulation involving s, we have to subtract $s-q$, or

$$|(mp-nq)-mp+(n-1)q|=q$$

The amplitude of this product, following the rule previously set forth, is proportional to

$$(I_-)(I_p)^m(I_q)^{n-1}$$

The order of this process is given by the sum of the exponents, $1, m, n-1$, or $m+n$.

Comparison of Nonlinear Reactive and Resistive Circuits

It is interesting to compare these results with analogous ones found in nonlinear resistance circuits such as diode and copper oxide modulators. Carrying out the work in much the same way as for the nonlinear inductance, it is found,[8,9] that both side-frequencies introduce negative resistance terms into the signal path. Sustained free oscillations never are observed in these circuits, nor are they observed in any circuit in which the slope of the current–voltage characteristic of the nonlinear resistance is always positive. Evidently this differs from the findings of the nonlinear reactance case, and the reason can be stated simply. In the nonlinear reactance case, the negative resistance is produced by a reactance variation; positive resistance components resulting from losses are incidental and comparatively small so that the total circuit resistance can be made negative. Further, the average reactance can be tuned out. In the other case of a resistance variation, the introduced negative resistance is always less than the positive resistance component in any passive element.[8,9] Thus the resistance of the nonlinear element itself is always positive, that of the external circuit adds to it, and the total circuit resistance remains positive.

Free Oscillations

Having established the factors controlling the generation of negative resistance, the next step is to consider applications to some of the consequent oscillation phenomena. First it will be desirable to prevent the flow of the upper side-frequency in order to have as large a negative resistance as possible. Thus we now are considering the current to have just three sinusoidal components in response to the carrier and signal sources. If the external resistance to the side-frequency is now reduced from a large value, the total signal circuit resistance approaches zero.

When this point is reached at a particular value of signal amplitude, the external signal source can be removed[10] and the three components will continue to flow if the circuit reactance is tuned out. Thus, two frequencies are being generated, incommensurable in general with that of the carrier source, the oscillations being of class 1. If, however, the tuning is set so as to make q and p commensurable, the oscillations are of class 2 or of class 3. An interesting point to be noted here is that even harmonics and subharmonics are generated by a purely odd order process,[11] no external polarization being used. Another point is that we may regard the q component as the lower side-frequency in the modulation of p and s, and, similarly, s may be regarded as a lower side-frequency in the modulation of p and q; hence negative resistances are developed in both q and s paths. It should be remarked that no precise adjustment of the reactances is necessary as the circuit is self-adjusting to a certain extent, with the coil impedance depending upon current amplitudes and phases.

It is possible to have negative resistance and oscillation in a circuit in which only two components flow. The process is the same as that outlined previously when we consider that here the signal and side-frequency components have merged to produce an oscillation of class 2 or class 3. Explicitly

$$mp-nq=\pm q$$

or

$$q=mp/(n\pm 1) \qquad (9)$$

Whether free oscillations in any case start from rest or from a finite threshold amplitude can be determined by inspecting the negative resistance term for the q component. This term from the foregoing discussion involves the signal amplitude in the form I_q^{n-1}. Evidently there is just one positive integral value of n (unity) which makes this term independent of I_q and which in turn permits oscillations to start from zero amplitude. Otherwise, with the negative resistance depending upon some positive power of the amplitude, a threshold always will exist below

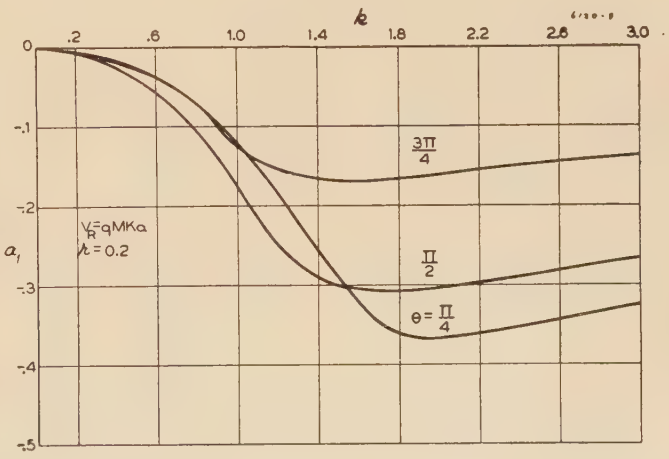

Figure 8. The resistive coil voltage component of frequency $q/2\pi$ plotted here is a companion piece to the inductive component of Figure 7

$a_1(-\theta) = -a_1(\theta)$,
$a_1 = 0$ for $\theta = 0, \pi$

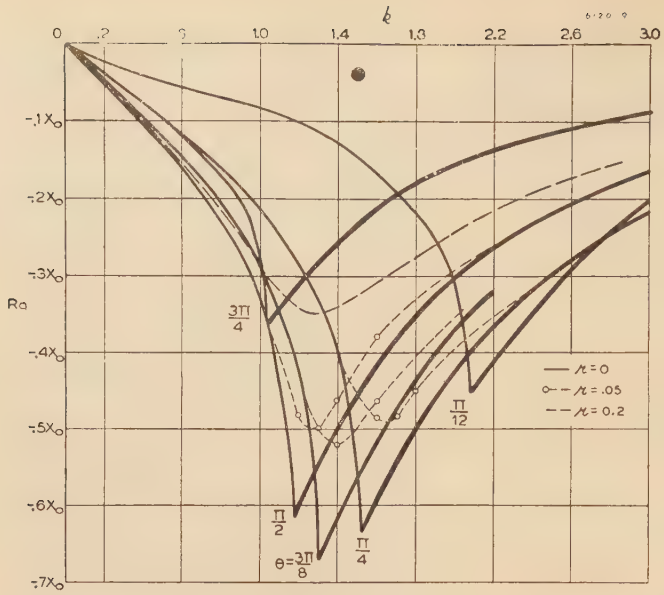

Figure 9. For comparative purposes the resistance of a nonlinear coil at the frequency $q/2\pi$ has been computed for three values of $r=a/P$

The quantity X_0, in terms of which the resistance is expressed, is the coil reactance to the q component when Q is small
$Rq=X_0\lambda a_1/k=0$ for $\theta=0, \pi$

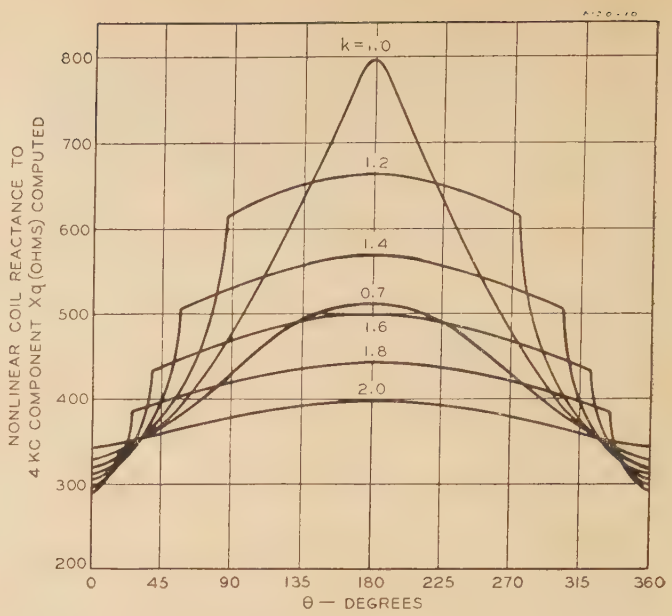

Figure 10. Computed coil reactance to the lower of two impressed frequencies of ratio 1/3, plotted in terms of the phase angle between the two components

The parameter is the ratio of the two component amplitudes. The magnetic characteristic for a zero is used here, and the family of curves shown corresponds to the amplitude specified for the higher frequency component
$H=P\cos pt+Q\cos(qt+\theta/3)$
$p/2\pi=12$ kc, $q/2\pi=4$ kc
$P=0.96$ oersted

which the total circuit resistance is positive so that free oscillations cannot be sustained. Applying this conclusion to the case of merged components, we have from equation 9 that $q=mp/2$. As $m+n$ is odd and n is unity, m must be an even number. Thus only class 3 oscillations are self-starting where only a single free oscillation flows. But where two individual free oscillations flow, only those oscillations of classes 1 and 2 are self-starting which have the angular velocities $mp-q$ and q.

A vacuum tube circuit yielding results corresponding to equation 9 is the regenerative (resistance) modulator.[12] In that circuit the gain around the feed-back loop must equal unity, and the phase shift around the loop must be zero for steady-state oscillation to exist. Further, a product of modulating the feed-back current with the input must coincide in frequency with that of the feed-back current. Here the input frequency corresponds to the carrier and the feedback to the signal. With a passive resistance modulator, an amplifier must be included in the feed-back loop to make the equivalent negative resistance big enough.

Applications to Circuits

Specific circuit arrangements used to develop free oscillations can be interpreted in the light of the preceding analysis.

A saturable reactor circuit used by Heegner[4,13] is shown in Figure 1. There two distinct nonlinear coils are provided, but the two may be combined in a single somewhat more complex magnetic structure. The use of two nonlinear coils in a balanced circuit permits an easy separation of components. In this arrangement the primary circuit may be tuned to the input frequency. If one of the secondary meshes is tuned to q, the other is tuned to $mp-nq$. With the cores unpolarized, $m+n$ is restricted to odd integers. The balanced coil connection requires m to be even, and so n must be odd. Since, generally speaking, p and q are incommensurable, the oscillations are of class 1.

Another circuit used by Heegner for developing harmonics utilizes just one secondary circuit instead of the two foregoing. This corresponds to merged oscillations in which equation 9 holds. Restricting n to unity yields oscillations of class 3. Allowing n to take higher odd integral values yields, in addition, oscillations of class 2.

The simple circuit used by Fallou[3,14] for frequency reduction is shown in Figure 2. Here again we have a case of merged oscillations and the same relation exists in equation 9 as in Heegner's circuit, except that no limitation is imposed upon m or n individually. As a consequence, a lower order of modulation is required of Fallou's circuit for odd subharmonics. As used by Fallou, oscillations of class 2 are involved but those of class 3 can be made to appear as well.

Wave Forms and Wave Components

Our discussion up to this point and indeed throughout the paper, is based upon the resolution of waves into their Fourier components. This approach is particularly useful where only a few components have to be considered. A different approach, valuable in tracing the minutiae of the starting process, for example, or in dealing with large numbers of components, considers wave forms[16] rather than their components.* In this procedure general principles such as those previously discussed are not discernible, and the analysis is limited to computation of specific numerical cases. The computations are necessarily lengthy as in each case a large number of cycles must be covered to indicate whether or not the oscillation reaches a steady state. When the numbers initially selected result in an oscillation close to the boundary between stable and unstable states, and especially when errors of computations are cumulative, the work is practically interminable. The use of mechanical aids is particularly valuable here. It may be remarked that the great bulk of the literature dealing with wave forms in circuits of the type under discussion is devoted to experimental studes.[2,15]

* Investigation of this method was carried out by L. W. Hussey and S. O. Rice of these laboratories in 1935.

Part II

The analysis of part I has been designed to present the most important effects in comparatively simple form. Conclusions drawn from this simplified analysis cannot be applied quantitatively to practical cases. Two outstanding reasons are that the B–H relation in ferromagnetic materials is not accurately represented by the simple cubic, and that, in general, the significant generated currents are not small compared to those impressed.

Accordingly, we proceed to set up a situation more closely approximating practical conditions which can be analyzed quantitatively.† To facilitate analysis the circuit of Figure 3 is adopted which requires consideration of just two current components, one impressed and the other generated. The generated component, typical of class 2, is a subharmonic one-third the impressed frequency. After the circuit equations are set up in general form, a specific form is introduced for the B–H relation. The complexity of the resulting equations makes analytical solution impossible except for limiting cases, and most of the evaluation is graphical. The conclusions are subjected to test in several directions. First the impedance of the nonlinear coil with the two harmonically related frequencies impressed is derived and compared with the results of bridge measurements. Next the self oscillation amplitudes are computed for a variety of circuit conditions and input amplitudes, and compared with measured values. Finally the stability of the oscillations and the conditions required to start them are similarly checked.

Equations for Two-Frequency Magnetization

In this section relations generally valid for two-frequency magnetization are set up under the restrictions previously noted to provide the basis for an analysis of the third subharmonic case. Expressions for the impedance of the nonlinear coil are formulated in terms of Fourier coefficients for the flux density, followed by circuit equations for the oscillation in terms of the same coefficients. The circuit equations permit the oscillation amplitude and phase to vary with time so that stability and starting conditions may be studied.

The magnetizing force acting on the nonlinear core is accordingly

$$H=P\cos pt+Q\cos(qt+\varphi)$$
$$=P\cos\beta\omega t+Q\cos\left(\alpha\omega t+\frac{\alpha\theta}{\beta}\right) \qquad (10)$$

where α and β are integers and $\alpha/\beta=q/p$ represents the frequency ratio expressed in its lowest terms.

The flux density now can be expressed as a Fourier series having $\omega/2\pi$ for fundamental frequency. Factoring out the saturation value M of the flux density,

$$B(H)=M\sum_{n=1}^{\infty}[a_n\sin n(\omega t+\theta/\beta)+ b_n\cos n(\omega t+\theta/\beta)] \qquad (11)$$

The voltage across the coil has a component of frequency $q/2\pi$ equal to

$$v_q=K\left[\frac{dB(H)}{dt}\right]_q$$
$$=qMK\times\left[a_\alpha\cos\left(qt+\frac{\alpha\theta}{\beta}\right)-b_\alpha\sin\left(qt+\frac{\alpha\theta}{\beta}\right)\right]$$

and the corresponding q component of current is

$$i_q=(Q/\Upsilon)\cos\left(qt+\frac{\alpha\theta}{\beta}\right)$$

where $\alpha\omega=q$, $K=NA\ 10^{-8}$, $\Upsilon=0.4\ N/d$,

† Preliminary work along these lines was done by S. O. Rice in 1934.

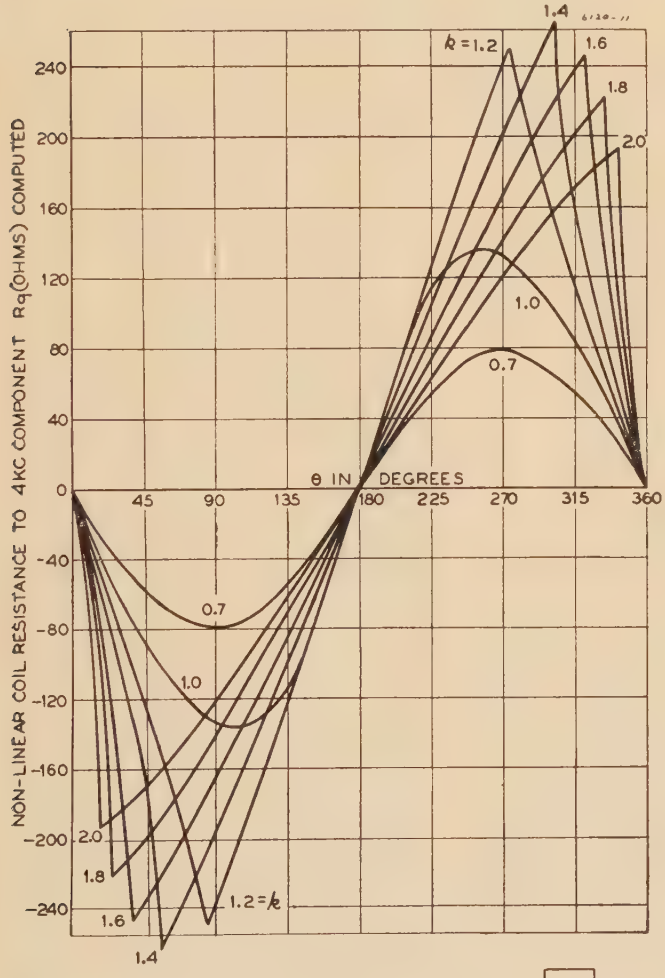

Figure 11. Computed coil resistance to the lower of two input frequencies of ratio 1/3, plotted in terms of the phase angle between the two components

This is a companion piece to Figure 10
$P=0.96$ oersted

Figure 12 (below). Bridge setup for measuring the impedance components of a nonlinear coil to the lower of two impressed frequencies of ratio 1/3

A phase shifter serves to vary the phase angle between the two input currents

Auxiliary tuned circuits are used to reduce all other current components to a value at least 20 db down on the input currents. Preliminary balance is obtained with switch S closed

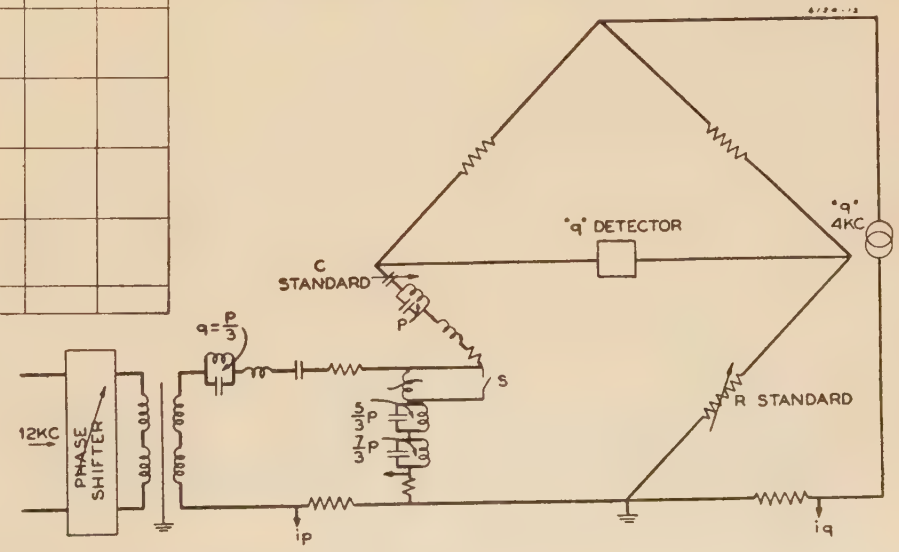

and N is the number of conductor turns around the toroidal core of diameter d. From these the impedance of the coil to the q component is defined

$$Z(H) \equiv \frac{v_q}{i_q}$$
$$= qMK\Upsilon\left[\frac{a\alpha}{Q} + j\frac{b\alpha}{Q}\right]$$
$$= R_q + jX_q \qquad (12)$$

Defining $Q/P \equiv k$, we have

$$R_q = \frac{X_0 \lambda a_\alpha}{k} \qquad (13)$$

$$X_q = \frac{X_0 \lambda b_\alpha}{k}$$

where

$$X_0 = qL_{q0}$$
$$= \operatorname{Lim}_{Q \to 0} (X_q)$$
$$= \frac{qMK\Upsilon}{\lambda P} \qquad (14)$$

and λ is specified later in terms of a specific B–H relation. Thus the impedance components of the saturable coil are expressed in terms of L_{q0}, its inductance to a small signal amplitude in the presence of a comparatively large carrier.

Now consider the oscillation q to exist when just one external generator of frequency $p/2\pi$ is connected. Referring to Figure 3, the differential equation for the right-hand mesh, to which the free oscillation is confined, is

$$RS + L\frac{dS}{dt} + \frac{1}{C}\int S\,dt + \Upsilon K \frac{d}{dt}\Big[B(H)\Big]_s = 0 \qquad (15)$$

where S is the magnetizing force of the oscillation. Three questions are to be considered:

1. What are the circumstances for which the steady oscillation

$$S = Q\cos\left(qt + \frac{\alpha\theta}{\beta}\right) \qquad (16)$$

is a solution?
2. Is the solution stable?
3. What conditions must be satisfied to start the oscillation?

We can get at the stability of a solution by finding whether small changes in its amplitude and phase will build up or die away in the course of time after the cause of the changes has been removed. For the question of starting, it is an initial rather than a normal steady-state value which provides the starting point. Hence for these investigations, Q and θ must be considered as functions of time. It will be assumed that the amplitude and phase vary slowly compared with cos qt. Thus $\frac{dQ}{dt}/pQ$ and $\frac{d\theta}{dt}/q$ are small so that higher order derivatives and products of derivatives can be neglected. It may be seen later that this assumption is consistent with the results. Equations 16, 11, and 14 are inserted into equation 15 and the term $\int (S/C)\,dt$ is changed into an expression involving derivatives through two successive integrations by parts. Then equating coefficients of sine and cosine terms separately to zero, we obtain the two differential equations

$$Rk + \lambda X_0 a_\alpha + \alpha\frac{\lambda X_0 a_\alpha}{\beta q}\frac{d\theta}{dt} + \frac{X_1}{q}\frac{dk}{dt} + \frac{\lambda X_0}{q}\left(\frac{\partial b_\alpha}{\partial k}\frac{dk}{dt} + \frac{\partial b_\alpha}{\partial \theta}\frac{d\theta}{dt}\right) = 0 \qquad (17)$$

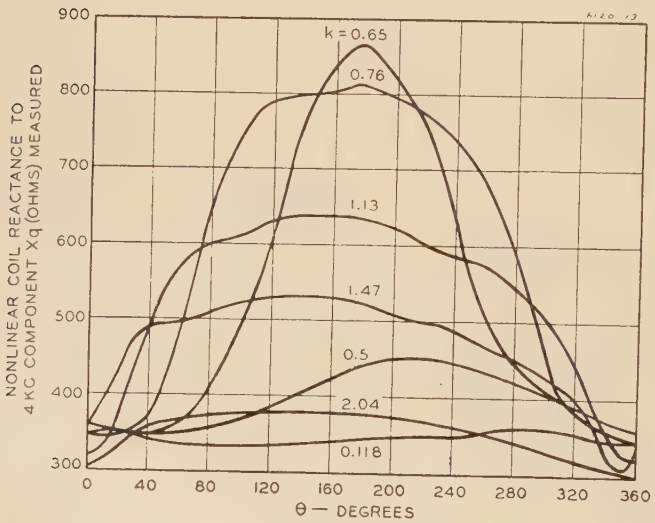

Figure 13. Measured coil reactance at 4 kc with 12 kc superposed, as function of the phase angle between the two components

Amplitude ratio of the two components is the parameter
$P = 0.96$ oersted
$H = P\cos pt + Q\cos(qt + \theta/3)$

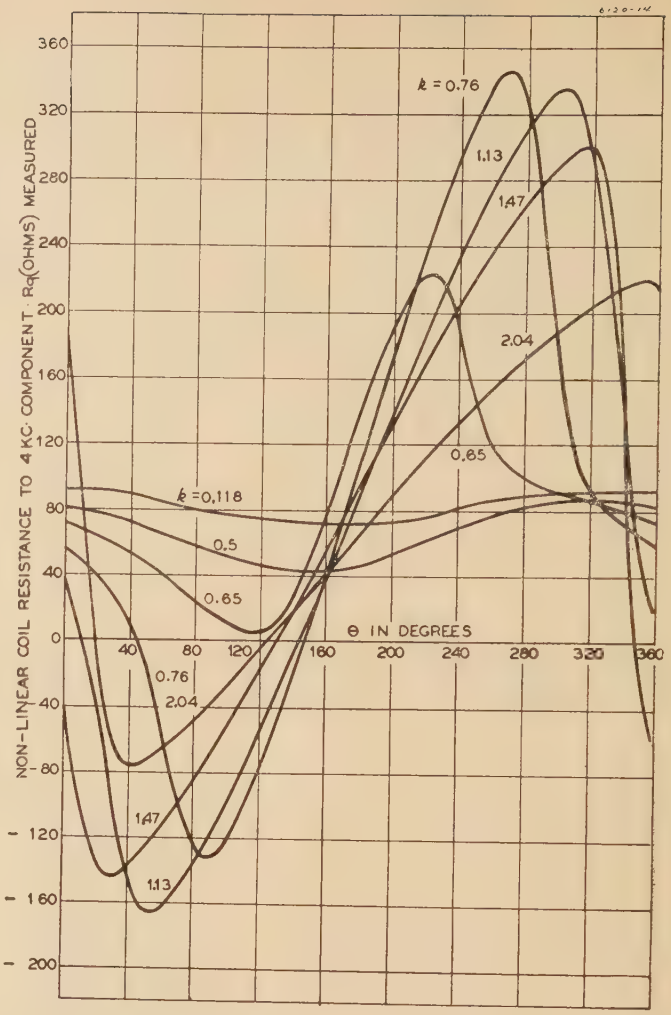

Figure 14. Measured coil resistance at 4 kc with 12 kc superposed, as function of the phase angle between the two components

Amplitude ratio of the two components is the parameter. This is a companion piece to Figure 13
$P = 0.96$ oersted

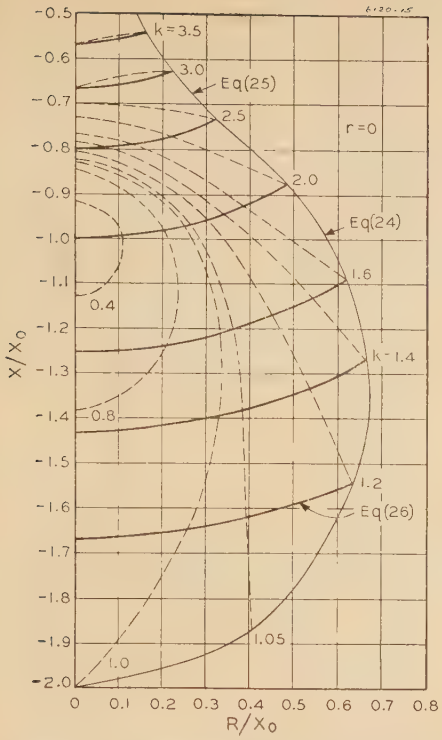

Figure 15. Computed map of external impedance region within which the one-third subharmonic can be generated

For any particular ratio of subharmonic to input amplitude indicated by the parametric numbers, two solutions are found represented by the two branches which join at the boundary. The branch heavily lined represents stable states, the dashed branch represents unstable ones; $r=0$

$$Xk+\lambda X_0 b_\alpha+\alpha\frac{\lambda X_0 b_\alpha}{\beta q}\frac{d\theta}{dt}+\frac{\alpha k}{\beta q}X_1\frac{d\theta}{dt}-\frac{\lambda X_0}{q}\left(\frac{\partial a_\alpha}{\partial k}\frac{dk}{dt}+\frac{\partial a_\alpha}{\partial\theta}\frac{d\theta}{dt}\right)=0$$

Here R and $X=qL-1/qC$ represent the resistance and reactance of the external circuit and $X_1=qL+1/qC$. Equations 17 are simultaneous first order differential equations in Q and θ because higher order derivatives and products of derivatives are negligibly small under the conditions mentioned before. Although we are not able to solve these nonlinear equations completely we can extract from them enough information for our needs.

Steady-state solutions are those for which amplitude and phase remain invariable with time so that dk/dt and $d\theta/dt$ are zero in equation 17. They are to be considered in the next section before taking up stability and starting considerations which require the full equations.

Fourier Coefficients for the Third Subharmonic

We now proceed to calculate the Fourier coefficients b_α and a_α required in the foregoing equation from a particular form of B–H characteristic. The impedance of the saturating coil and the conditions for oscillation then may be determined. As our attention is to be centered upon the third subharmonic representative of class 2 oscillations, we have $\alpha=1$ and $\beta=3$ in equations 10 to 17.

A satisfactory approximation to the form of the B–H relation on each branch of a symmetrical hysteresis loop is given by

$$B(H)=\frac{2M}{\pi}\tan^{-1}\frac{H}{a} \qquad (18)$$

M being the saturation value of flux density and a a scale factor for the magnetizing force.* This relation is shown in Figure 4 with a as parameter. It may be noted that in the limit for a zero, the assumed B–H relation approximates an ideal limiter. An approximation sufficiently close for our purposes is to use the same single-valued B–H characteristic for both branches of the hysteresis loop, provided that a supplementary resistance is included in the oscillation circuit to account for hysteresis and eddy losses. This resistance will be treated conveniently as part of the external circuit.

The coefficients a_1 and b_1 of the Fourier series for $B(H)$ are expressed by the usual definite integrals.** When $k\ll 1$, analytical expressions can be derived for the coefficients. These are

$$b_1=\frac{2}{\pi}\frac{k}{\sqrt{1+r^2}}\left[1-\frac{k\cos\theta}{4(1+r^2)}+\cdots\right]$$
$$a_1=\frac{2}{\pi}\frac{k}{\sqrt{1+r^2}}\left[-\frac{k\sin\theta}{4(1+r^2)}+\cdots\right] \qquad (19)$$

where $r=a/P$, and $k\ll 1$. When k is not restricted, the values of b_1 and a_1 for the one-third subharmonic are obtained directly from the definite integrals by computing and plotting values of the integrand as a function of qt for several values of k and θ, and then planimetering the resulting curves. When a or r is zero, the arc tangent characteristic takes the form of a step function changing between $-M$ and $+M$ at zero magnetizing force. In this case the integrals for a_1 and b_1 are computed easily after the values of qt are found for which the magnetizing wave H in equation 10 becomes zero.†

Values of a_1 and b_1 computed in this way are shown in Figures 5, 6, 7, and 8 for two values of r, namely zero and two-tenths, respectively. For accuracy we need to consider an extended range of values of r as the input amplitude P changes. This would involve much labor. The experimental work to be described later centers about a value of r in the neighborhood of 0.05. Examination of significant quantities in this region indicates their rate of variation with r to be fairly small however. This permits us to base our work for the most part on the limiting case of r zero, although on occasion effects introduced by other values of r will be brought in. Further evidence on the consequence of varying r is given in Figure 9, which shows how the derived values R_q/X_0 of equation 13 vary as a function of k, with r and θ as parameters. Three values of r are included: 0, 0.05, and 0.2.

In carrying through the work for $r=0$ as outlined in the appendix, it was found possible to obtain equations for a_1 and b_1 at the salient points of the curves shown in Figures 5 and 6

$$\left.\begin{aligned} a_{1m}&=-\frac{1}{\pi k}[(9-k^2)(k^2-1)]^{1/2}\\ b_{1m}&=\frac{1}{\pi k}(k^2+3)\end{aligned}\right\}\quad k<3 \qquad (20)$$

A plot of a_{1m} is shown dotted in Figure 6. This is the locus of maximum values of a_1 valid for k less than $\sqrt{5}$. For larger values of k, maximum values of a_1 are represented by the dashed line of the figure for which

$$a_{1M}=-4/\pi k$$
$$b_{1M}=\frac{4\sqrt{(k^2-1)}}{\pi k} \qquad (21)$$

Equations 20 and 21 will be found useful in establishing the boundary between stable and unstable states.

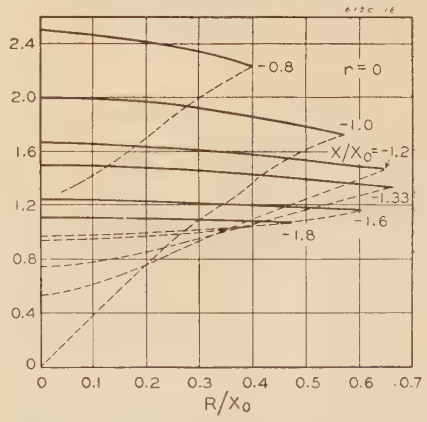

Figure 16. Sections of the map in Figure 15 taken normal to the X-axis

The ratio of subharmonic to input current amplitudes is plotted as a function of the external resistance, with external reactance as parameter

Heavy lines represent stable states, dashed lines represent unstable ones

* Incidentally, a is a function of frequency when eddy currents are appreciable.

** See Appendix I, equation 31.

† Appendix I.

Coil Impedance to the Oscillation

In this section the values of b_1 and a_1 just found are used to evaluate the resistance and reactance of the coil effective at the signal frequency. The results will be compared with corresponding measured values to provide an estimate of the validity of the approximations used up to this point.

The small signal values of b_1 given by equation 19 may be used to evaluate λ in equation 14

$$\lambda=\frac{\pi}{2}\sqrt{1+r^2} \tag{22}$$

This is nearly independent of the fundamental input P so long as $P^2 \gg a^2$. Thus the effective inductance to a small signal, by equation 14,* is inversely proportional to the carrier amplitude

$$L_{q0}=\frac{2\Upsilon KM}{P\pi\sqrt{1+r^2}}$$

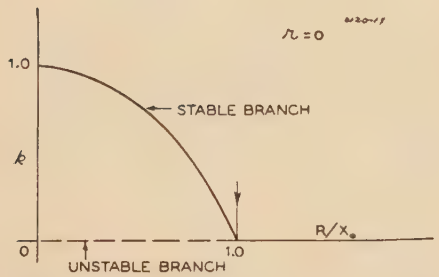

Figure 17. Amplitude curve for a typical class 3 product showing unstable branch lying along the X-axis so that at any external resistance less than the critical, the oscillation can start from rest and grow until it reaches the stable branch

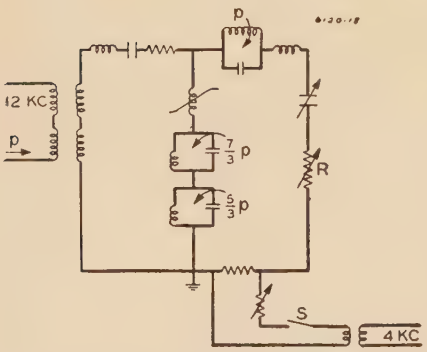

Figure 18. Experimental setup for subharmonic production with resonances provided in input and subharmonic paths

Trap circuits are included to keep the input frequency out of the subharmonic path as well as to suppress unwanted components
S is a starting switch

From the curves of Figures 5 and 6 we may compute the resistance and reactance components given by equation 13. These are plotted in Figures 10 and 11 in terms of the phase angle θ between the two components.

It appears that the effective resistance is negative when the phase angle lies in the first and second quadrants. Inspection of the curves, as well as of the limiting analytic forms, shows that R_q is zero for any order of subharmonic when the oscillation amplitude vanishes, and this is the case for merged oscillations of class 1 or class 2.

Comparison of Calculated and Measured Coil Impedances

Bridge measurements of the impedance components (R_q, X_q) of a saturable coil** were made for comparison with the values calculated previously. Two magnetizing components were supplied by two external generators which were derived from a single source so that the input frequencies of 4 kc and 12 kc were accurately in the 1 to 3 ratio. The 12-kc source, corresponding to the $3q$ component, was introduced through separating tuned circuits into that arm of the bridge which included the saturable coil. The 4-kc source, corresponding to the q component for which the bridge was to be balanced, was introduced at the normal bridge input. Other current components through the coil were reduced to low values by action of the tuned circuits shown in Figure 12. The amplitudes of the two components were individually adjustable, and the phase angle between them was set at will by means of a variable phase shifter. The results are shown in Figures 13 and 14 where R_q and X_q are plotted against θ for various values of k. Comparing them with the computed values of Figures 10 and 11 for r zero shows general agreement in form. The residual resistance resulting from hysteresis, eddy, and copper losses, which may be called R_{q0}, is discernible in the experimental curve for k small as something in the neighborhood of 80 ohms. Supplementary calculation of the coil loss resulting from hysteresis using the arc tangent form for the B–H relation and a suitable value for the carrier amplitude yields the value 60 ohms.

Thus measurements show that under certain conditions the saturating coil develops a negative resistance, which is a function of the two magnetizing current amplitudes and of the phase angle between them. This result and in fact the general course of variation of the coil impedance can be approximated roughly by the methods of calculation previously outlined.

Steady-State Oscillation Amplitudes

With the general agreement between calculated and measured impedances evidenced, we proceed to the determination of the steady-state oscillation amplitude.

As shown previously the steady-state conditions for the present case are solutions† of equation 17, in which $\alpha=1$, $\beta=3$, and both dQ/dt and $d\theta/dt$ are zero

$$\left.\begin{aligned} Rk+X_0\lambda a_1=0 \\ Xk+X_0\lambda b_1=0 \end{aligned}\right\} \tag{23}$$

In these equations R is the external resistance and X is the external reactance of the oscillation circuit as indicated in Figure 3. It may be noticed that these equations have the same form as those of any oscillating circuit in which each impedance component to the free oscillation must be zero. We want to solve these equations simultaneously for the oscillation amplitude Q in terms of R and X. This may be done graphically by plotting against each other the values of R/X_0 and X/X_0 satisfying the equations for a particular value of Q or k. When this is done in a number of cases, there results the family of curves shown in Figure 15. For $k<\sqrt{5}$ solutions are found in a region bounded by the circle

$$(R/X_0)^2+(X/X_0+4/3)^2=(2/3)^2 \tag{24}$$

while for $k>\sqrt{5}$ the boundary is given by

$$\left(\frac{R}{X_0}-1\right)^2+\left(\frac{X}{X_0}\right)^2=1 \tag{25}$$

Equation 24 is obtained by putting equation 20 into equation 23; and equation 25 similarly by inserting equation 21 in equation 23. From equation 24 the largest value of external resistance R at which oscillations can be sustained is

$$R_m=\frac{2}{3}X_0$$

---

* Another relation valid for k small connects L_{q0} with L_{p0}, the inductance of the coil to the p component

$$\frac{L_{p0}}{L_{q0}}=2\left[1+r^2-r\sqrt{1+r^2}\right]$$

As r approaches zero, the ratio approaches two. Note that the inductance ratio is independent of the frequency ratio q/p. A similar relation exists between the corresponding resistance components of a resistance limiter.

** Coil Data:
Core material molybdenum permalloy
Core weight = 1 gram
Tape thickness = 0.6 mil
Core inside diameter = 1.43 centimeters
Core outside diameter = 1.63 centimeters
Cross-sectional core area = 2.4 square millimeters
Number of turns = 200

† One solution of equation 17 is $Q=0$.

which requires $X=-(4/3)X_0$. Under these conditions $k=1.34$.

It may be remarked that as r increases, the region in which the subharmonic is sustained shrinks. For $r=0.2$, R_m/X_0 is half that for $r=$ zero, and for $r=0.05$, R_m/X_0 is eight-tenths that for $r=$ zero. The region also shrinks as the subharmonic order increases. Thus for the fifth subharmonic and $r=$ zero, R_m is about $^2/_5 X_0'$, X_0' being the initial coil reactance at the oscillation frequency $(1/5)(p/2\pi)$. This amounts to

$$\frac{2}{5}\times\left(\frac{3}{5}X_0\right)$$

Substituting into equation 23 the values of a_1 and b_1 given in Appendix I, equation 34, the heavily lined branches of Figure 15 are represented by the family of circles

$$(R/X_0)^2+(X/X_0)^2=4/k^2 \qquad (26)$$

Inspection of Figure 15 shows that there are two possible values of k for each pair of values of R and X. The situation may be clarified by taking sections through the family of curves, and plotting k against R/X_0 with X/X_0 constant. The double-valued character of the solution is shown clearly in Figure 16. It will be shown later that points on the upper branch (solid line) represent stable solutions, while those on the lower branch (dashed line) are unstable. In using these curves, the coil loss resistance R_{q0} is to be treated as part of the external resistance R. After further inspection of the family of curves of Figure 15 and the method of sectioning, it appears that the stable solutions of Figure 16 are represented by the circles of equation 26.

The average value of oscillation power delivered to the circuit resistance is

$$W_q=\frac{I_q^2R}{2}$$

$$=I_p^2X_0^2\frac{2R}{R^2+X^2}$$

which includes the power lost in the residual resistance R_{q0}. Of course only those values of R/X_0 and X/X_0 lying within the boundary circles of equations 24 and 25 permit oscillations to exist so that the power equation is valid only within the bounded region. For any given value of reactance X, the maximum power is obtained for that value of resistance which is at the boundary of the stable region. From equation 24 the maximum of these limiting powers occurs for $X/X_0=-0.8$ at the value

$$W_{qm}=I_p^2X_0$$

In the case of even harmonics ($\beta=1$) a wholly similar procedure yields the k versus R curve of Figure 17 (solid line). There it is found that if the circuit resistance is less than the critical value

$$R_m=X_0e^{-\frac{2r}{\alpha}}$$

even harmonics can be developed. It is interesting to note that the following relations are roughly valid: for harmonic oscillations, $k<1$, and for subharmonic oscillations, $k>1$.

Comparison of Calculated and Measured Oscillation Amplitudes

Oscillation amplitudes observed in the circuit of Figure 18 were compared with the calculations detailed in the preceding section. The nonlinear coil used for the impedance measurements was used here. Auxiliary tuned circuits were included in circuit so that unwanted current components were at least 20 decibels below the input current. Figure 19 shows typical calculated and measured curves for a constant value of fundamental input current and it is seen that the two are comparable. While these results apply to the one-third harmonic, they are typical of class 2 oscillations in a circuit like that of Figure 18. This is borne out by experimental determinations on higher order subharmonics and their multiples, such as the products one-fifth, one-seventh, and four-fifths the fundamental frequency.

Stability and Starting

To investigate the stability of the preceding steady-state solutions, a procedure ordinarily used in dynamics[17] will be followed. The variables k and θ are given values slightly different from the steady-state solutions and differential equations in these small variations are derived. These differential equations then are studied to find out whether in the course of time the variations die away or build up. If they die away so that k and θ return to the steady-state values under investigation, this steady state is said to be stable; if not, it is unstable. In this way the desired answers are obtained without solving equation 17 explicitly.

Accordingly, k and θ are displaced from their steady-state values k_s and θ_s by Δk and $\Delta\theta$ respectively so that

$$k=k_s+\Delta k$$
$$\theta=\theta_s+\Delta\theta \qquad (27)$$

k_s and θ being obtained from equation 23, that is

$$Rk_s+\lambda X_0a_{1s}=0$$
$$Xk_s+\lambda X_0b_{1s}=0 \qquad (23)$$

In the neighborhood of the steady state values, b_1 and a_1 may be expressed as

$$b_1=b_{1s}+\frac{\partial b_1}{\partial k}\Delta k+\frac{\partial b_1}{\partial\theta}\Delta\theta$$

$$a_1=a_{1s}+\frac{\partial a_1}{\partial k}\Delta k+\frac{\partial a_1}{\partial\theta}\Delta\theta \qquad (28)$$

Putting equations 23, 27, and 28 into equation 17 with $\alpha=1$, $\beta=3$ and neglecting quantities involving higher powers of the variations than the first, two simultaneous differential equations in Δk and

Figure 19. Comparison of measured and computed subharmonic amplitudes as function of external circuit resistance; external circuit reactance as parameter

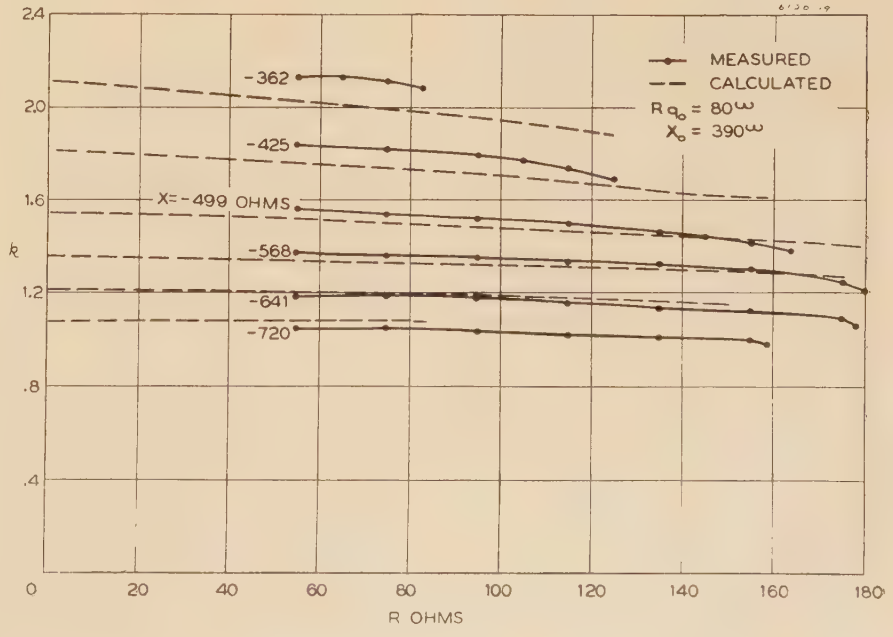

$\Delta\theta$ are obtained.* These equations are linear with constant coefficients with solutions of the form

$$\Delta k = Ae^{ut}$$
$$\Delta\theta = Be^{ut} \qquad (29)$$

Upon inserting these assumed solutions in the differential equations, we get two algebraic equations in A and B, the coefficients of which are functions of u. In order to obtain solutions other than $A=B=0$, it is necessary that the determinant of the coefficients vanish. Setting this determinant equal to zero yields a quadratic equation in u**

$$g_2u^2+g_1u+g_0=0 \qquad (30)$$

the solution of which determines u in equation 29. The quantities A and B depend on the initial value of the perturbation, but since their specific values are not needed they will be considered no further.

The character of the roots u of equation 30 determines the stability or lack of it in the steady state. If both roots are negative or have negative real parts, then by equation 29 the variations die away and the steady state is stable. If either of the roots is positive or has a positive real part, then the variations will build up and the steady state is unstable. To investigate the stability of any steady-state solution we must first obtain the corresponding characteristic equation 30 and then determine the nature of its roots.

Consider first the steady-state solutions which are represented by the upper branches (solid lines) of the curves in Figure 16. A study† of quadratic equation 30 shows that for all these solutions, the three coefficients g_2, g_1, and g_0 are positive if $X_1/X_0>0.1$; thus both roots u are negative and this group of steady-state solutions is stable. For the lower branches (dashed lines) of Figure 16, it is found that g_2 is positive and g_0 is negative; hence at least one root is positive no matter what the sign of g_1, and these solutions are unstable.

If the oscillation amplitude Q is initially zero we have $k_s=0$, which is one of the steady-state solutions of equation 23. After the conditions accompanying this solution are applied to the differential equations in Δk and $\Delta\theta$,† a first degree equation in u is obtained with the result that u is negative. Hence a zero initial amplitude of oscillation is stable, and the oscillation is not self-starting. In fact the oscillation will decrease to zero if k is initially less than the value on the lower branch, and will increase if k is initially greater than this value. In both cases there is a positive u, but the variations are opposite in sign. Another way of expressing these facts is to say that the oscillating circuit has a negative resistance for amplitudes between the stable and unstable values, and a positive resistance outside this range; the oscillation builds up when the over-all resistance is negative. A study of this resistance when R/X_0 is increased beyond the limiting value (0.65 for $X/X_0=-1.2$), shows that it is positive for all values of k, and so an oscillation will die away no matter what the initial amplitude may be. These considerations account for the necessity of providing starting means in this circuit. The same requirement has been established experimentally by Fallou[14] for his single-mesh circuit.

The limitation $X_1/X_0>0.1$ mentioned previously is not restrictive as in any practical case it is necessary for X_1/X_0 to be substantially greater than unity in order that the oscillation may be sinusoidal as assumed in equation 10. From the definitions of X_1 and X, we have

$$X_1/X_0=2qL/X_0-X/X_0$$

so that X_1 increases with the series inductance L. In the experimental work $qL=2X_0$ approximately, hence $X_1/X_0=3$ nearly. When X_1/X_0 is of this magnitude, the roots u of equation 24 are roughly proportional to X_0/X_1. In particular, if $X_1/X_0>3$, then $u<0.1\,q$ and thus $\frac{1}{qk}\frac{dk}{dt}$ and $\frac{1}{q}\frac{d\theta}{dt}$ are small. Therefore the assumption made before in deriving equations 17 is justified.

We conclude that when the tuning inductance L is large enough as specified previously, the upper branches of the solutions shown in Figure 16 are stable solutions and the lower branches are unstable. To have the oscillation start, it must be given an initial amplitude at least as large as the value of the corresponding unstable branch. If R is increased beyond the point where the two branches meet, the oscillation dies away.

This point was checked by measuring the minimum input amplitude necessary to start the oscillation. The measurement is difficult to make accurately, but the results indicate a starting curve of the same form as that depicted by the dashed lines of Figure 16, although somewhat lower in amplitude than the calculated lower branches.

Table I

	$0\le\theta\le\pi$	
	$k<k_0$	$k>k_0$
$\partial b_1/\partial k$	+	+
$\partial a_1/\partial k$	−	+

For the even harmonic case, a typical k versus R curve is found to look like the one shown in Figure 17. So long as the circuit resistance is less than the critical value, any small disturbance will build up to the upper (stable) branch as the R axis ($k=0$) corresponds to the lower unstable branch. Hence the oscillation is self-starting, as found experimentally.

It may be concluded, therefore, that the general picture of oscillating amplitudes, stabilities, and starting conditions is reproducible by the methods of calculation employed.

It should be emphasized that our discussion has been confined to the particular case in which just one generated current component is permitted to flow. When additional products flow, complications appear because some introduce positive, and others negative resistance effects which may cause the circuit performance to change radically. For example, if with the one-third subharmonic flowing a low impedance path is provided for its fifth harmonic, the oscillations are made self-starting.[18]

Appendix I

The coefficients a_1, b_1 of the Fourier series for $B(H)$ in equation 11 are expressed by the usual integrals after inserting equation 10 in equation 18, that is,

$$b_1=\frac{2}{\pi^2}\times\int_0^{2\pi}\tan^{-1}\left[\frac{\cos 3qt+k\cos(qt+\theta/3)}{r}\right]\times\cos(qt+\theta/3)\,dqt$$

$$a_1=\frac{2}{\pi^2}\times\int_0^{2\pi}\tan^{-1}\left[\frac{\cos 3qt+k\cos(qt+\theta/3)}{r}\right]\times\sin(qt+\theta/3)\,dqt \qquad (31)$$

where $r=a/P$. By simple transformations it may be shown that

$$b_1(-\theta)=b_1(\theta)$$
$$a_1(-\theta)=-a_1(\theta)$$

Alternatively we could compute and sum all the modulation products of frequency $q/2\pi$. This is equivalent to expanding equations 31 in Fourier series in θ. The direct method is the more desirable because

* See Appendix II, equations 35.

** See Appendix II, equation 36.

† See Appendix II.

‡ For convenience in computation, the phase angle θ was transferred to the $3qt$ term here.

it gives a complete result, whereas the second usually requires the summation of a large number of terms for a comparable result. When $k \ll 1$ in equation 31, the analytical expressions in equation 19 can be derived for the coefficients by expanding the arc tangent function of the integrand in a power series in $k \cos(qt+\theta/3)$.

In computing a_1 and b_1 by the direct method when $r=0$, we have instead of equation 31‡

$$b_1 = \frac{2}{\pi}\int_0^{\pi} \pm \cos y \, dy$$
$$a_1 = \frac{2}{\pi}\int_0^{\pi} \pm \sin y \, dy \qquad (32)$$

The positive sign is used when H in equation 10 is positive and the negative sign when H is negative. In general, there are three values of qt between 0 and π at which $H=0$, designated as y_1, y_2, and y_3. For $k<k_0$, k_0 being a function of θ, the positive sign is used from 0 to y_1 and from y_2 to y_3, and the negative sign from y_1 to y_2 and from y_3 to π. Carrying through the indicated operations, we get

$$b_1 = (4/\pi)(\sin y_3 + \sin y_1 - \sin y_2)$$
$$a_1 = (-4/\pi)(\cos y_3 + \cos y_1 - \cos y_2) \qquad (33)$$

As k approaches k_0, y_3 and y_2 approach each other until at $k=k_0$, $y_3=y_2$ and a_1 and b_1 are at the salient points as shown on the curves. For $k>k_0$ there is only one value y_1 at which H is zero. In this case as at $k=k_0$,

$$b_1 = (4/\pi)(\sin y_1)$$
$$a_1 = (-4/\pi)(\cos y_1) \qquad (34)$$

To facilitate calculation, y_1, y_2, and y_3 were computed and curves were plotted as functions of k and θ.

At the point where $y_3=y_2$ and the salient points of a_1 and b_1 appear, we have $dk/dy=0$ and $dH/dy=0$. Expressing this with the aid of equation 10 and solving simultaneously with $H=0$ enables us to get analytical expressions for $\sin y_1$ and $\cos y_1$ at these points and hence the expressions in equation 20 for a_1 and b_1.

For values of $k>\sqrt{5}$, these salient points are not the maximum values for a_1. The maximum values, a_{1M} in equation 21, were found by setting $da_1/\partial\theta=0$.

Appendix II

The two differential equations in Δk and $\Delta\theta$ mentioned just preceding equation 29 are

$$\left(R+\lambda X_0\frac{\partial a_1}{\partial k}\right)\Delta k+\left(\frac{X_1}{q}+\frac{\lambda X_0}{q}\frac{\partial b_1}{\partial k}\right)\frac{d}{dt}(\Delta k)+\lambda X_0\frac{\partial a_1}{\partial\theta}\Delta\theta+\left(\frac{\lambda X_0}{q}\frac{\partial b_1}{\partial\theta}-\frac{1}{3}\frac{k_s R}{q}\right)\times\frac{d}{dt}(\Delta\theta)=0 \qquad (35)$$

$$\left(X+\lambda X_0\frac{\partial b_1}{\partial k}\right)\Delta k-\frac{\lambda X_0}{q}\frac{\partial a_1}{\partial k}\frac{d}{dt}(\Delta k)+\lambda X_0\frac{\partial b_1}{\partial\theta}\Delta\theta+\left[\frac{k_s}{3_q}(X_1-X)-\frac{\lambda X_0}{q}\frac{\partial a_1}{\partial\theta}\right]\frac{d}{dt}(\Delta\theta)=0$$

Explicitly equation 30 is

$$\frac{u^2}{q^2}\left[\frac{k_s}{3}\left(\frac{X_1}{X_0}-\frac{X}{X_0}\right)\left(\frac{X_1}{X_0}+\frac{\lambda\partial b_1}{\partial k}\right)-\frac{\lambda X_1}{X_0}\frac{\partial a_1}{\partial\theta}-\frac{\lambda k_s}{3}\frac{R}{X_0}\frac{\partial a_1}{\partial k}+\lambda^2\left(\frac{\partial b_1}{\partial\theta}\frac{\partial a_1}{\partial k}-\frac{\partial b_1}{\partial k}\frac{\partial a_1}{\partial\theta}\right)\right]+\frac{u}{q}\left[\frac{k_s}{3}\frac{R}{X_0}\frac{X_1}{X_0}+\lambda\left(\frac{X_1}{X_0}-\frac{X}{X_0}\right)\times\left(\frac{\partial b_1}{\partial\theta}+\frac{k_s}{3}\frac{\partial a_1}{\partial k}\right)+\frac{\lambda R}{X_0}\left(\frac{k_s}{3}\frac{\partial b_1}{\partial k}-\frac{\partial a_1}{\partial\theta}\right)\right]+\left[\frac{\lambda R}{X_0}\frac{\partial b_1}{\partial\theta}-\frac{\lambda X}{X_0}\frac{\partial a_1}{\partial\theta}+\lambda^2\left(\frac{\partial b_1}{\partial\theta}\frac{\partial a_1}{\partial k}-\frac{\partial b_1}{\partial k}\frac{\partial a_1}{\partial\theta}\right)\right]=0 \qquad (36)$$

As shown here, stability considerations require determination of the signs of g_2, g_1, and g_0, which are the coefficients in equation 36. A brief outline of this determination and some of the intermediate results are given here.

The partial derivatives of a_1 and b_1 were found graphically except in the region near $k=k_0$ where they are large for $k<k_0$. Supplementary expressions for a_1 and b_1 in the neighborhood of $k=k_0$ were worked out and derivatives computed. The Jacobian

$$\frac{\partial b_1}{\partial\theta}\frac{\partial a_1}{\partial k}-\frac{\partial b_1}{\partial k}\frac{\partial a_1}{\partial\theta}$$

which appears in both g_0 and g_2, is zero for $k>k_0$ as may be verified by means of equation 34; for other values of k, it is small and negative. The term X/X_0 is always negative because b_1 is positive and the two are connected as shown in equation 23.

The signs of the partial derivatives are given in Tables I, II, and III.

In Table II θ_0 is the value of θ corresponding to the salient point for a given value of k, and θ_1 is that value for which $\partial a_1/\partial\theta=\partial b_1/\partial\theta=0$.

Applying all the information just mentioned to equation 36, it is found that when $X_1/X_0>0.1$, g_2, g_1, and g_0 have signs as shown in Table III.

Thus the dividing point between stable and unstable solutions occurs at the point where $\partial a_1/\partial\theta$ changes sign. As seen from the table of derivative signs, this point occurs at the salient point (k_0, θ_0) when $k<\sqrt{5}$ and at $\theta_1[\cos\theta_1=(3-4/k^2)/k]$ when $k>\sqrt{5}$. A distinction is made between the two regions because $\partial a_1/\partial\theta$ changes sign discontinuously at the salient points. Referring to the curves k versus R/X_0, X/X_0 constant, shown in Figure 16, θ increases as k increases and R/X_0 increases as a_1 increases. Hence the upper branches of these steady-state curves are stable and the lower branches are unstable.

Table II

	$k<\sqrt{5}$		$k>\sqrt{5}$		
	$\theta<\theta_0$	$\theta>\theta_0$	$\theta<\theta_0$	$\theta_0<\theta<\theta_1$	$\theta>\theta_1$
$\partial b_1/\partial\theta$	+	+	+	−	+
$\partial a_1/\partial\theta$	−	+	−	−	+

Table III

	$\partial a_1/\partial\theta>0$	$\partial a_1/\partial\theta<0$
g_2	+	+
g_1	+	
g_0	+	−

For the steady state $k_s=0$, we have from equation 19

$$\partial a_1/\partial\theta=\partial a_1/\partial k=\partial b_1/\partial\theta=0$$
$$\partial b_1/\partial k=2\pi$$

Putting these in the differential equations for Δk and $\Delta\theta$, we find

$$u=\frac{-R_q}{X_1+X_0}<0$$

so that the zero amplitude solution is stable.

References

1. Approved Maintenance Practices, Part XXXV, **Seitz.** *Telephony*, December 1944, page 19. See also "Sub-Cycle," the New Ringer for Exchanges, **Seitz.** *Telephony*, July 1936, page 30.

2. An Experimental Investigation of Subharmonic Currents, **John D. McCrumm.** AIEE Transactions, volume 60, 1941, pages 533–40.

3. Sur un démultiplicateur de fréquence statique, **Fallou.** *Revue Generale de l' Electricité* (Paris, France), volume 19, 1926, page 987.

4. Über Selbsterregungserscheinungen bei Systemen mit gestörter Superposition, **Heegner.** *Zeitschrift für Physik* (Berlin, Germany), volume 29, 1924, page 91.

5. Atomic Physics and Circuit Theory, **Peterson.** *Bell Laboratories Record*, volume 7, 1929, page 231.

6. Oscillations in Systems with Non-Linear Reactance, **Hartlay.** *Bell System Technical Journal*, volume 15, 1936, page 424.

7. Oscillations in an Electromechanical System, **Hussey, Wrathall.** *Bell System Technical Journal*, volume 15, 1936, page 441.

8. Impedance of a Nonlinear Circuit Element, **Eugene Peterson.** AIEE Transactions, volume 46, 1927, pages 528–34; Figure 8.

9. Equivalent Modulator Circuits, **Peterson, Hussey.** *Bell System Technical Journal*, volume 18, 1939, page 32.

10. Quelques nouvelles expériences de demultiplication de fréquence dans un circuit oscillant dont la bobine est a noyau de fer, **Rouelle.** *Revue Generale de l' Electricité* (Paris, France), volume 40, December 1936, page 811.

11. Zur Geschicte der Erzeugung gerader und gebrochener Relativfrequenzen mit Eisendrosseln ohne Vormagnetisierung, **Kasarnowski.** *Zeitschrift für Physik* (Berlin, Germany), volume 30, 1924, page 225.

12. Fractional-Frequency Generators Utilizing Regenerative Modulation, **Miller.** *Proceedings*, Institute of Radio Engineers, volume 27, 1929, page 446.

13. United States patent 1,656,195. **Heegner,** January 17, 1928.

14. United States patent 1,633,481. **Fallou,** June 21, 1927.

15. Sustained Subharmonic Response in Non-Linear Series Circuits, **Spitzer.** *Journal of Applied Physics*, volume 16, 1945, page 105.

16. Subharmonic Circuits Containing Iron-Cored Inductors—II, **Irven Travis.** AIEE Transactions, volume 58, 1939, pages 735–42.

17. Advanced Rigid Dynamics (book), **Routh.** Part II, chapter 6.

18. United States patent 2,272,246. **Manley,** February 10, 1942.

Rotating Electric Machine Time Constants at Low Speeds

C. CONCORDIA
MEMBER AIEE

THE use of the concept of time constants in the analysis of a-c rotating electric machine transients is well known.[1] It is also well known that the short-circuit time constants of machines running at normal speed are not at all like those of the same machines at rest. The purposes of this paper are to show the continuous nature of the variation of the machine characteristics in the range of speed from zero to rated speed, and to determine the limits of applicability of the full-speed and standstill values and the behavior at low speed.

Rated-Speed Characteristics

In the analysis of transient currents and voltages in induction motors and synchronous motors and generators operating at rated speed, a procedure is more or less well established.[1] In the case of induction motors,* there is a d-c time constant for the decay of the d-c component of current given by the ratio of the transient (short-circuit or standstill) reactance to the stator resistance; there is also an a-c time constant, for the decay of the a-c component of current, given by the ratio of the transient reactance to the rotor resistance. In the case of synchronous machines, there are similarly a d-c (or armature) time constant and two a-c (a subtransient and a transient or field short-circuit) time constants. The two a-c or rotor time constants used most frequently are the direct-axis quantities, the quadrature-axis rotor time constant being considered to have only a secondary effect on short-circuit conditions. The d-c time constant is given by the ratio of the negative-sequence reactance (or the average of the direct- and quadrature-axis subtransient reactances) to the armature resistance; the direct-axis subtransient time constant

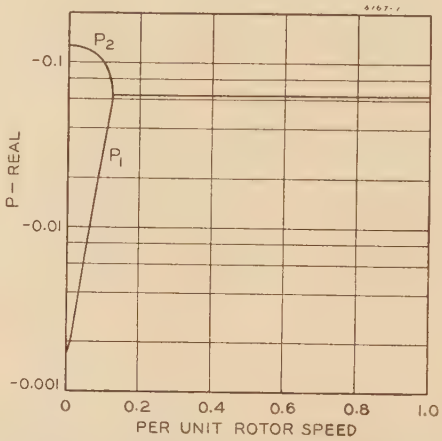

Figure 1. Induction motor—decrement factors as functions of rotor speed

(Real parts of roots of equation 4)

$x_1 = x_2 = 0.08$
$x_m = 3.00$
$r_1 = r_2 = 0.01$

is given by the ratio of the short-circuit reactance viewed from the direct-axis amortisseur to the (direct-axis) amortisseur resistance; the field short-circuit time constant is given similarly by the ratio of the short-circuit reactance viewed from the field (and neglecting the amortisseur) to the field resistance. One notes in all of these definitions the rather remarkable simplifying feature that each time constant depends on only one resistance; there is apparently no interaction between stator and rotor resistances. The reason for this lies in the relative motion of the rotor and stator. All of these time constants are fundamentally d-c time constants for the circuit in question, and a d-c or slowly decaying current in any winding corresponds to an alternating (or speed frequency) current in a winding which is rotating with respect to the first. The resistance in the winding containing the alternating current is usually negligible compared to the reactance at the frequency in question. The apparent separation of the field and direct-axis amortisseur resistances is qualitatively quite different and arises only because of the usually very large difference in magnitude between these two resistances; it is not a generality and would not be true for an unusually high field resistance or an unusually low amortisseur resistance.

Standstill Characteristics

When the machine is at rest the situation is entirely different and the rated-speed time constants have no meaning. In the case of an induction motor the d-c time constant, like that of a transformer, ordinarily is considered to be given by the ratio of the short-circuit reactance to the sum of the stator and rotor resistances, and thus may be less than half of the full-

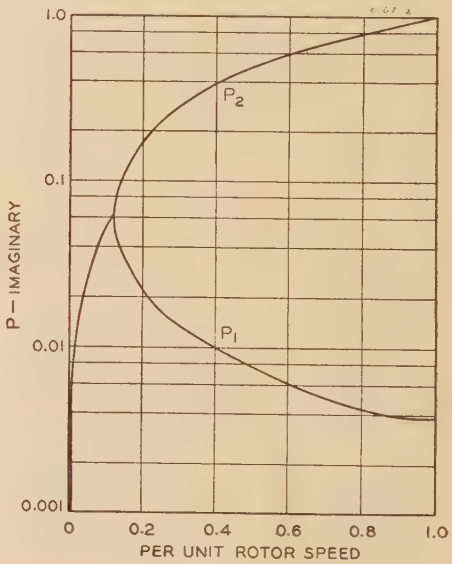

Figure 2. Induction motor—natural frequencies as functions of rotor speed

(Imaginary parts of roots of equation 4)

$x_1 = x_2 = 0.08$
$x_m = 3.00$
$r_1 = r_2 = 0.01$

speed value. Actually there are two d-c time constants, one defined in the preceding sentence, or more nearly by the ratio of the sum of the stator and rotor leakage reactances to the sum of the stator and rotor resistances, the other given approximately by the ratio of the sum of the mutual (magnetizing) reactance plus the paralleled stator and rotor leakage reactances to the paralleled stator and rotor resistances. The first time constant is the only one apparent in an oscillogram of the starting current. The second time constant

Paper 46-167, recommended by the AIEE committee on electric machinery for presentation at the AIEE summer convention, Detroit, Mich., June 24–28, 1946. Manuscript submitted April 29, 1946; made available for printing May 29, 1946.

C. CONCORDIA is with the central station engineering department, General Electric Company, Schenectady, N. Y.

* It tacitly is assumed here and in the discussion of synchronous machines that stator currents rather than rotor currents are being computed, and that the machine is either connected to an infinite system or has all three phases short-circuited. Further, we are dealing entirely with calculated values, and the time constants discussed are defined in terms of the calculation required to obtain them. A practical definition must, of course, admit of determination by a not too complicated measurement, and may be incompatible except as an approximation with the abstractions dealt with here. This question is discussed in reference 2.

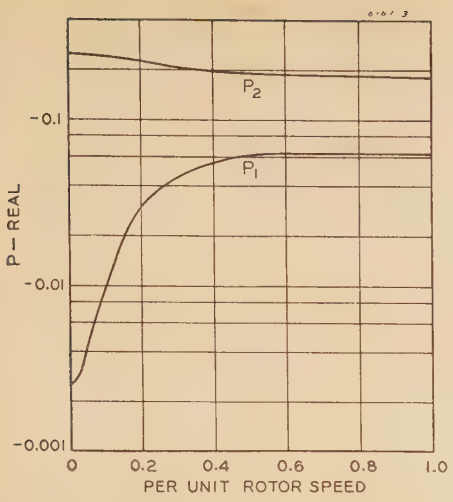

Figure 3. Induction motor—decrement factors as functions of rotor speed

(Real parts of roots of equation 4)

$x_1 = x_2 = 0.08$
$x_m = 3.00$
$r_1 = 0.01$
$r_2 = 0.03$

applies to only a very small component of stator or rotor current, which is however a magnetizing current and corresponds to a rather large flux and torque.[4]

For a synchronous machine, similar but more complex conditions apply. Even the most elementary considerations for a machine with no amortisseur will show that there are two armature (stator) d-c time constants, one for each rotor axis. In the direct axis the time constant is given by the ratio of the transient reactance (or more nearly the sum of the armature and field leakage reactances) to the sum of the armature and field resistances; in the quadrature axis it is given by the ratio of the quadrature-axis reactance to the armature resistance. These values may differ by a factor of two or more to one. There is also, as in case of the induction motor, a direct-axis flux time constant given by the ratio of the sum of the mutual reactance plus the paralleled armature and field leakage reactances to the paralleled field and armature resistances.

Low-Speed Characteristics

The procedures at full speed and at rest are relatively clear and straightforward. However, because the conclusions differ so markedly the question naturally arises as to what happens at very low speeds, and where the transition between the two forms takes place, if there is any such definite speed. In order to show the continuity of the characteristics as functions of speed and to determine the lowest speed at which the full-speed concepts may be used, this paper presents in Figures 1–12 the results of calculations of the various short-circuit time constants at all speeds from zero to full speed for several more or less typical machines.

The figures show decrement factors (reciprocals of the time constants) and natural frequencies calculated from the complete system equations. Figures 1 and 2 are for an induction motor with equal stator and rotor resistances. Figures 3 and 4 are for the same motor except that the rotor resistance is now three times as great as before. These figures show that strictly speaking there is really no such thing as a d-c time constant when the machine is running. The component that may appear in an oscillogram as a decaying direct current has actually a period at full speed ($\omega = 1.0$) of about 250 normal cycles for the case of Figure 2 (a rotor resistance of 0.01), and 100 cycles for the case of Figure 4 (a rotor resistance of 0.03). Similarly, the normal frequency transient component has really only a nearly normal frequency, being necessarily of such a frequency that the sum of the frequencies of the two components equals rotor speed. The real oscillatory nature of the d-c component becomes more pronounced at low rotor speeds, the case of equal stator and rotor resistances (Figure 2) being especially remarkable in that the frequencies of both transient components become exactly equal to one-half rotor speed below a speed of about 12 per cent. The value 12 per cent is seen to be a critical speed below which the frequencies are equal and above which the decrements are equal (Figure 1). Moreover, the

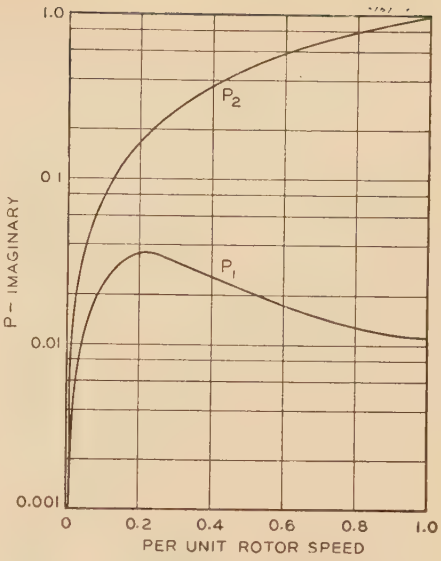

Figure 4. Induction motor—natural frequencies as functions of rotor speed

(Imaginary parts of roots of equation 4)

$x_1 = x_2 = 0.08$
$x_m = 3.00$
$r_1 = 0.01$
$r_2 = 0.03$

decrements in this case are given exactly by the ratio of the transient reactance to the stator (or rotor) resistance, although ordinarily this formula must be regarded as only approximate.

The full-speed time constants are given approximately by the relations

$$\text{Stator time constant} = \frac{x_1 + \dfrac{x_2 x_m}{x_2 + x_m}}{r_1} = \frac{x'}{r_1} \qquad (1)$$

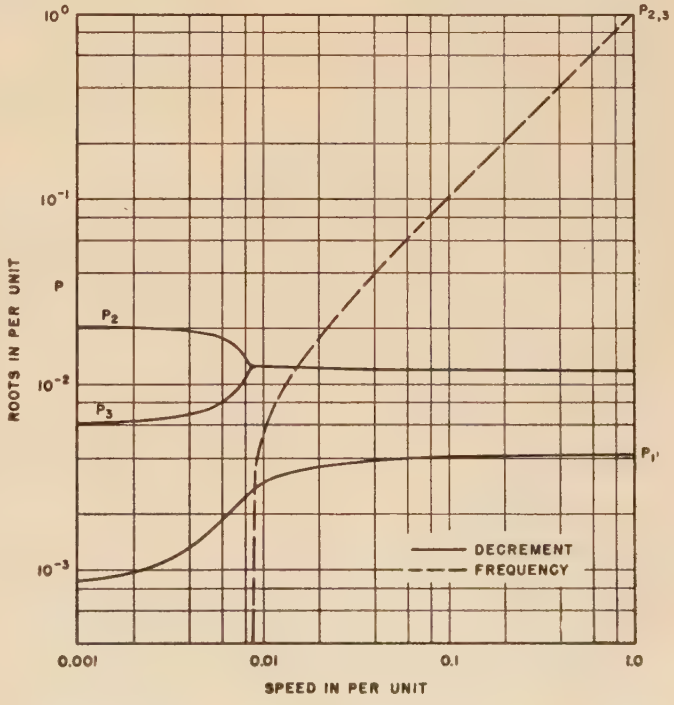

Figure 5. Synchronous machine—decrement factors and natural frequences

(Roots of the characteristic equation 9)

No amortisseur
$x_q = 0.8$
$x_d = 1.2$
$x_d' = 0.2909$
$T_o = 1{,}000$
r_a 0.005

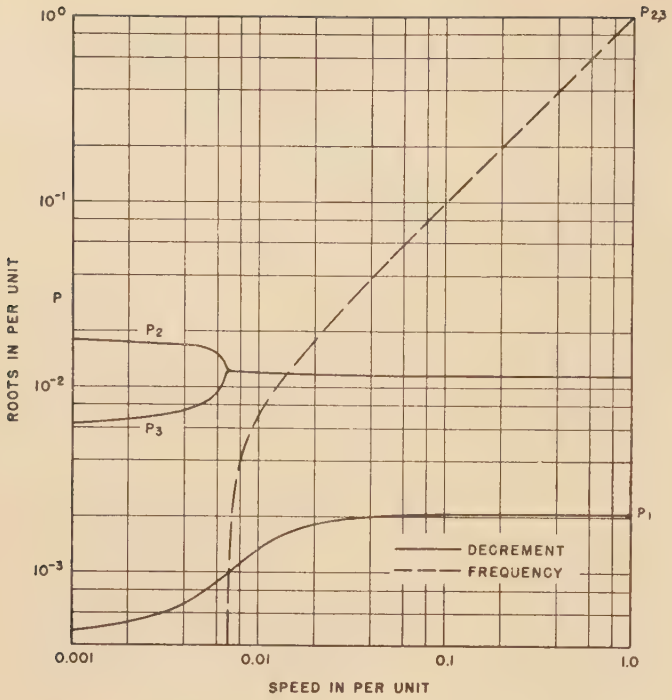

Figure 6. Synchronous machine—decrement factors and natural frequencies

(Roots of the characteristic equation 9)

No amortisseur

$x_q = 0.8$
$x_d = 1.2$
$x_d' = 0.2909$
$T_o = 1{,}000$
$r_a = 0.005$

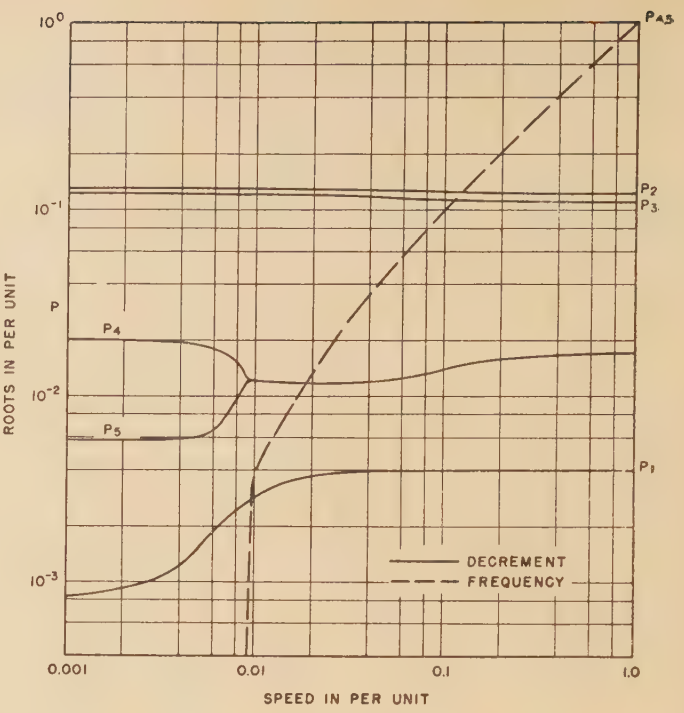

Figure 7. Synchronous machine—decrement factors and natural frequencies

(Roots of the characteristic equation 9)

With amortisseur

$x_l = 0.2$
$x_{aq} = 0.6$
$x_{ad} = 1.0$
$x_{kq} = 0.2$
$x_{kd} = 0.1$
$x_f = 0.1$
$r_a = 0.005$
$r_{kq} = 0.04$
$r_{kd} = 0.02$
$r_f = 0.0011$

$$\text{Rotor time constant} = \frac{x_2 + \dfrac{x_1 x_m}{x_1 + x_m}}{r_2} \qquad (2)$$

where

x_1 = stator leakage reactance
x_2 = rotor leakage reactance
x_m = mutual magnetizing reactance
r_1 = stator resistance
r_2 = rotor resistance
x' = transient or short-circuit reactance

The machine equations from which the roots plotted in Figures 1–4 were obtained are, in the notation of reference 3,

$$(L_1 p + r_1)\boldsymbol{I} + Mp\boldsymbol{i} = \boldsymbol{E}$$
$$M(p - j\omega)\boldsymbol{I} + [L_2(p - j\omega) + r_2]\boldsymbol{i} = \boldsymbol{e} \qquad (3)$$

where

L_1 = stator self inductance = $x_1 + x_m$
L_2 = rotor self inductance = $x_2 + x_m$
M = mutual inductance between stator and rotor = x_m
ω = rotor speed
$\boldsymbol{I} = I_\alpha + jI_\beta$ = stator current
$\boldsymbol{i} = i_\alpha + ji_\beta$ = rotor current
$\boldsymbol{E} = E_\alpha + jE_\beta$ = stator voltage
$\boldsymbol{e} = e_\alpha + je_\beta$ = rotor voltage
$p = d/dt$ (t = time)

All quantities are in per unit on a common base.

The characteristic equation of the coefficients of these performance equations is

$$(L_1 p + r_1)(L_2 p + r_2) - M^2 p^2 - j\omega L_2(L_1 p + r_1) + j\omega M^2 p = 0 \qquad (4)$$

Conclusions for Induction Motors

The results shown here indicate that the full-speed decrements are more or less effective from full speed down to rather low speeds (about 10 to 40 per cent). In the low-speed range the more nearly correct values given here must be used for accurate work. The oscillatory character of the nominally d-c component is not perceptible at rated speed because of the relatively very rapid decay.

Synchronous Machines at Low Speed

Figures 5–8 show the results of calculations for four different synchronous machines, considered either as short-circuited or as connected to an infinite bus. The machines differ by having two values of field open-circuit time constant, T_0 = 1,000 per unit (Figures 5 and 7) and T_o = 2,000 (Figures 6 and 8) and by being considered with (Figures 7 and 8) and without (Figures 5 and 6) and amortisseur. These figures show that for the synchro-

Table I

Short-Circuit Time Constant	Assumption r_a	r_f	r_{kd}	r_{kq}
Field	0*	r_f	∞	r_{kq}
Direct-axis amortisseur	0*	0	r_{kd}	r_{kq}
Quadrature-axis amortisseur	0*	r_f	r_{kd}	r_{kq}
Armature	r_a	0	0	0

* In these cases, instead of assuming $r_a = 0$ it is possible to assume $\omega = \infty$.

Table II. Short-Circuit Time Constants

Machine		Figure 5	Figure 6	Figure 7	Figure 8
Field	Exact	242	485	248	490
	Approximate	242	485	242	485
Direct amortisseur	Exact			7.94	8.0
	Approximate			8.125	8.125
Quadrature amortisseur	Exact			8.75	8.75
	Approximate			8.75	8.75
Armature	Exact	85.3	85.4	58.2	58.4
	Approximate	85.3	85.3	58.0	58.0

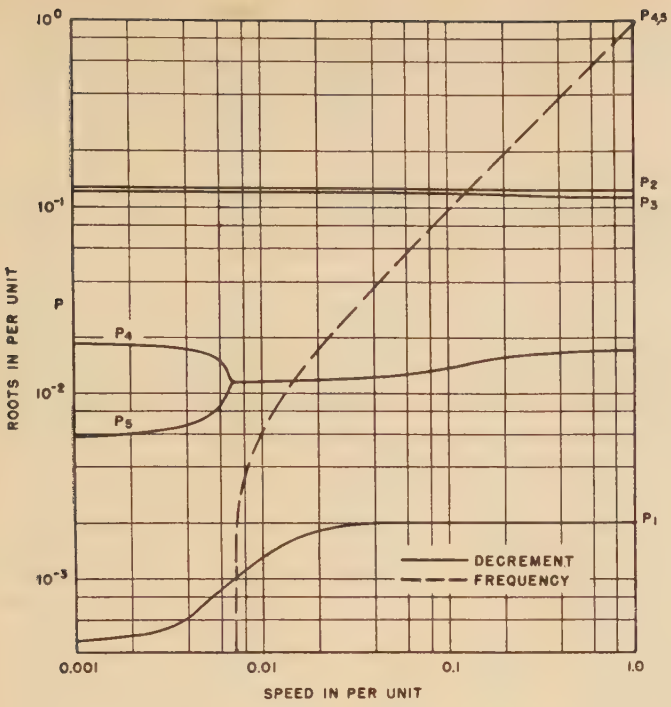

Figure 8. Synchronous machine—decrement factors and natural frequencies

(Roots of the characteristic equation 9)

With amortisseur

$x_l = 0.2$
$x_{aq} = 0.6$
$x_{ad} = 1.0$
$x_{kq} = 0.2$
$x_{kd} = 0.1$
$x_f = 0.1$
$r_a = 0.005$
$r_{kq} = 0.04$
$r_{kd} = 0.02$
$r_f = 0.00055$

$$\text{Field time constant} = \frac{1}{r_f}\left[x_f + \frac{x_l x_{ad}}{x_d}\right] \quad (5)$$

$$\text{Direct-axis amortisseur time constant} = \frac{1}{r_{kd}}\left\{x_{kd} + \left[\frac{1}{x_f} + \frac{1}{x_{ad}} + \frac{1}{x_l}\right]^{-1}\right\} \quad (6)$$

$$\text{Quadrature-axis amortisseur time constant} = \frac{1}{r_{kq}}\left[x_{kq} + \frac{x_l x_{aq}}{x_q}\right] \quad (7)$$

$$\text{Armature time constant} = \frac{2}{r_a}\left[\frac{x_d'' x_q''}{x_d'' + x_q''}\right] \quad (8)$$

where

x_l = armature leakage reactance
x_f = field leakage reactance
r_f = field resistance
r_{kd} = direct-axis amortisseur resistance
r_{kq} = quadrature-axis amortisseur resistance
x_{kd} = direct-axis amortisseur leakage reactance
x_{kq} = quadrature-axis amortisseur leakage reactance
r_a = armature resistance
x_{ad} = direct-axis mutual reactance (assumed to be the same for armature, field, and amortisseur)*
$x_d = x_{ad} + x_l$
x_{aq} = quadrature-axis mutual reactance between armature and amortisseur
$x_q = x_{aq} + x_l$

nous machines considered, the decrement factors, and thus the time constants, have nearly their full-speed values down to a very low speed (from about one to five per cent). Below about one per cent speed all of the roots become real. It should be noted that, because the machine equations are set up in terms of axes fixed in the rotor, the armature d-c decrements (P_2 and P_3 in Figures 5 and 6, P_4 and P_5 in Figures 7 and 8) are the real parts of the complex roots, and correspond to the speed-frequency oscillations of direct- and quadrature-axis currents.

It is interesting to compare the values of short-circuit time constant found at full speed from the rigorous solution of the characteristic equation with the values found from the usual approximate formulas, which may be written as

* This may be accomplished by choice of rotor current bases as in definition 4 of reference 5.

Figure 9. Synchronous machine—decrement factors and natural frequencies

(Roots of the characteristic equation 9)

With amortisseur

$x_l = 1.2$
$x_{aq} = 0.6$
$x_{ad} = 1.0$
$x_{kq} = 0.2$
$x_{kd} = 0.1$
$x_f = 0.1$
$r_a = 0.005$
$r_{kq} = 0.04$
$r_{kd} = 0.02$
$r_f = 0.0011$

Figure 10. Synchronous machine—decrement factors and natural frequencies

(Roots of the characteristic equation 9)

With amortisseur

$x_l = 1.2$
$x_{aq} = 0.6$
$x_{ad} = 1.0$
$x_{kq} = 0.2$
$x_{kd} = 0.1$
$x_f = 0.1$
$r_a = 0.005$
$r_{kq} = 0.04$
$r_{kd} = 0.02$
$r_f = 0.00055$

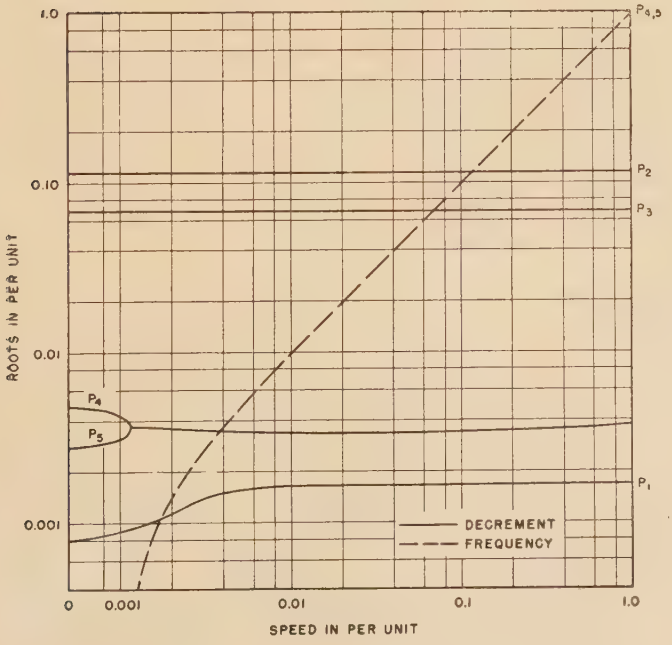

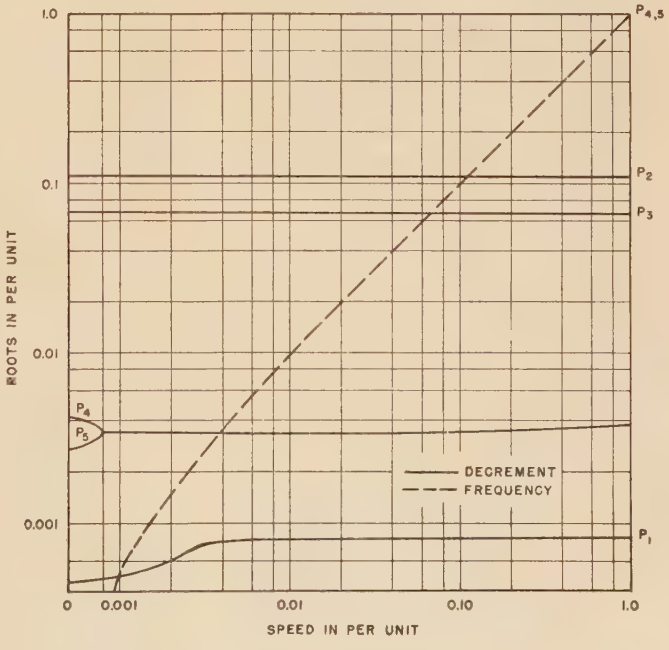

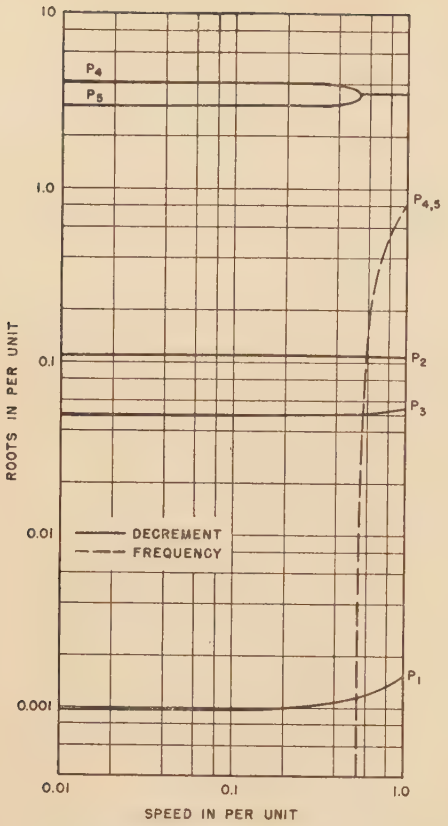

Figure 11. Synchronous machine—decrement factors and natural frequencies

(Roots of the characteristic equation 9)

With amortisseur

$x_l = 0.2$	$x_f = 0.1$
$x_{aq} = 0.6$	$r_a = 1.005$
$x_{ad} = 1.0$	$r_{kq} = 0.04$
$x_{kq} = 0.2$	$r_{kd} = 0.02$
$x_{kd} = 0.1$	$r_f = 0.0011$

All quantities are in per unit on a common base.

These approximate formulas are obtained by making assumptions as indicated in Table I.

Table II gives the comparison of the exact and approximate short-circuit time constants at full speed, and shows that there is very little difference between them.

The exact decrements are found from the roots of the equation

$$[r_a + px_d(p)][r_a + px_q(p)] + \omega^2 x_d(p) x_q(p) = 0 \tag{9}$$

where, for the machine with no amortisseur,

$$x_d(p) = \frac{x'_d T_o p + x_d}{T_o p + 1} \tag{10}$$

$$x_q(p) = x_q \tag{11}$$

and for the machine with an amortisseur,

$$x_d(p) = x_l + \left[\frac{1}{x_{ad}} + \frac{1}{x_f + \frac{r_f}{p}} + \frac{1}{x_{kd} + \frac{r_{kd}}{p}} \right]^{-1} \tag{12}$$

$$x_q(p) = x_l + \left[\frac{1}{x_{aq}} + \frac{1}{x_{kq} + \frac{r_{kq}}{p}} \right]^{-1} \tag{13}$$

Values of the various reactances and resistances are given on the figures.

Conclusions for Short-Circuited Synchronous Machines

The full-speed short-circuit time constants of synchronous machines are valid down to speeds of only a few per cent. At very low speeds the armature time constant separates into two different quantities applying separately to the direct and quadrature-axis and depending also on the rotor resistances.

Effect of Load or Tie Line

The results discussed previously apply to a synchronous machine connected to an infinite bus or short-circuited. In this section there are given the results of calculations with external armature inductance and resistance. The inductance may represent an extreme case of a reactive tie line and the resistance may represent a load.

Figures 9–12 show the results obtained. Only the machine with an amortisseur was considered. Figures 9 and 10, for an external reactance of unity, show that for this case the full-speed values are valid down to even smaller speeds with external reactance. Figures 11 and 12, for an external resistance of unity, show that for this case the full-speed values are only approximated at any speed. The field decrement P_1 changes rapidly, and the armature decrement is valid only above about 55 per cent speed.

The formulas of equations 5–8 may be used to compare the exact full-speed time constants with the conventional approximate values for the case of an external reactance (Figures 9 and 10), but for an external resistance (Figures 11 and 12) it is necessary to use the formulas

$$T_{d3}' = T_{do}' \left(\frac{x_d' x_q + r_a^2}{x_d x_q + r_a^2} \right) \tag{14}$$

$$T_{d3}'' = T_{do}'' \left(\frac{x_d'' x_q + r_a^2}{x_d' x_q + r_a^2} \right) \tag{15}$$

$$T_{q3}'' = T_{qo}'' \left(\frac{x_q'' x'_d + r_a^2}{x_q x_d' + r_a^2} \right) \tag{16}$$

The first formula for the short-circuit field time constant T_{d3}' in terms of the field open-circuit time constant T_{do}', is well known, the second and third, for the direct T_{d3}'' and quadrature T''_{q3} axis subtransient time constants in terms

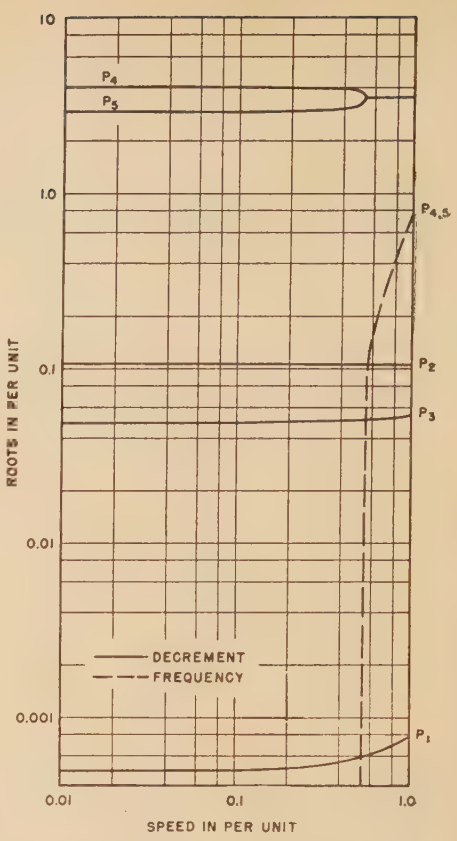

Figure 12. Synchronous machine—decrement factors and natural frequencies

(Roots of the characteristic equation 9)

With amortisseur

$x_l = 0.2$	$x_f = 0.1$
$x_{aq} = 0.6$	$r_a = 1.005$
$x_{ad} = 1.0$	$r_{kq} = 0.04$
$x_{kq} = 0.2$	$r_{kd} = 0.02$
$x_{kd} = 0.1$	$r_f = 0.00055$

of the corresponding open-circuit values T_{qo}'' and T_{do}'' are written simply by analogy to the first. All the exact values are found to check the approximate values within a few per cent at full speed.

For example, by the approximate formulas, with $r_a = 1.005$, $x_d' = 0.2909$, $x_d'' = 0.2476$ and $x_q'' = 0.35$,

$$T_{d3}'' = 9.28 = \frac{1}{0.1078}$$

$$T_{q3}'' = 17.9 = \frac{1}{0.0559}$$

$$T_{d3}' = 631 \text{ or } 1262$$

$$= \frac{1}{0.001585} \text{ or } \frac{1}{0.000792}$$

All of these are in good agreement with Figures 11 and 12.

For the case of Figures 9 and 10, we similarly find

$$T_{d3}' = 587 \text{ or } 1174$$

$$= \frac{1}{0.00170} \text{ or } \frac{1}{0.00085}$$

Design of Induction Heating Coils for Cylindrical Magnetic Loads

J. T. VAUGHAN
ASSOCIATE AIEE

J. W. WILLIAMSON
ASSOCIATE AIEE

Synopsis: Equations are presented whereby the authors' previous paper[1] is extended to the design of coils for heating magnetic loads, where the load remains in a fixed position relative to the coil during the heat. In heating magnetic materials, there is considerable variation in impedance of the coil circuit as the load temperature changes. The present paper first develops certain general principles by which a variable impedance circuit may be designed to absorb a predetermined maximum power, on the basis of constants determining the maximum and minimum impedance. Methods then are given by which these constants may be calculated for carbon steel loads of types SAE 1015 to SAE 1045, or their equivalent. In practice, these methods apply to most through heating and some surface heating applications. The accuracy of calculations is substantiated experimentally.

WITH the advent of considerable application of magnetic induction in heating steel for forging, it becomes more essential that the designer is able to precalculate the power, kilovolt-amperes, and efficiency variations during the heat in order to determine the required coil turns, capacitor values, and heating rates. It is the purpose of the present paper to outline methods by which these variations may be calculated and coil turns and capacitor values determined.

Numerous attempts have been made to adapt the theory of the induction heating of nonmagnetic loads to magnetic loads by assuming a constant permeability. However, unless some means is given of determining the value of permeability to use, the results are ambiguous. Baker[2] has shown that a value

$$\mu = 1.8 B_M / H_M$$

where B_M is the maximum flux density (taken in Baker's paper as 18,000 lines per square centimeter) and H_M is the peak magnetic intensity at the outside of the load may be used to calculate the power input to thin moving steel strip. Kinn[3] proposes an almost identical formula for permeability for use with loads of various shapes. His value for B_M, however, is 16,000 lines per square centimeter. Kinn's paper is confined mainly to practical applications and, therefore, does not give theoretical derivation or experimental confirmation of the formulas supplied.

The conventional induction heating circuit used with rotating generators is shown in Figure 1. The purpose of the capacitor is to adjust the power factor at the generator terminals. In heating operations where the load remains in fixed position during the heat, the capacitor usually is adjusted to give a power factor at generator terminals in the range of unity to 0.9 leading while the load is in the magnetic state. As the load temperature rises above the Curie or critical point, there is an increase in current and lagging kilovolt-amperes to the induction heating coil.

If the generator voltage output is held constant by means of a regulator, usually the power output will decrease, but the increase in lagging kilovolt-amperes to the induction heating coil may cause an increase in generator output current to a value above its rating. In this case it is necessary to add capacitance in order to keep the generator output current within its rating. In typical applications the power output after the load temperature passes critical may decrease to as low as 30 per cent of the peak output occurring during the heat.

If there is no voltage regulator on the generator, as the load temperature rises above the critical point the resulting lagging power factor load on the generator causes a decrease in the generator output voltage. In this case it is desirable to add capacitance to keep the generator output voltage up to a value near its rating.

Usually, the number of coil turns is so selected that with rated generator terminal voltage the maximum power absorption during the heat is equal to the generator output rating. However, in cases where the power at the end of the heat is considerably less than the peak during the heat for a given coil voltage, fewer coil turns may be used, resulting in a maximum power absorption equal to generator output rating with a voltage less than the generator rating. In this case the generator output voltage is reduced by operating with a lagging power factor while the load is below the critical point. Then the generator output voltage is increased by addition of capacitance after passing the critical point. By this means it is sometimes possible to realize a higher average power during the heat and hence reduce heating time compared to that which would be obtained with a coil designed to absorb a maximum power output equal to generator rating at rated voltage.

Changes as Load Heats

In the definitions which follow, A, B, C, D, E, F, and G are defined implicitly to save space. For example, $R_P = N^2 A$ is equivalent to $A = R_P/N^2$.

N = number of turns
$R_P = N^2A$ = resistance of inductor coil itself (ohms)
$R_S = N^2B$ = resistance of load as reflected in inductor coil (ohms)
$R = N^2(A+B) = N^2F$ = resistance of inductor coil with load (ohms)
$X_P = N^2C$ = reactance caused by flux between inside and outside radius of inductor coil (ohms)
$X_S = N^2D$ = reactance caused by flux within the load as reflected in inductor coil (ohms)
$X_o = N^2E$ = reactance caused by flux in air gap between coil and load (ohms)
$X = N^2(C+D+E) = N^2G$ = reactance of inductor coil with load (ohms)
E_L = voltage across inductor coil terminals AA (volts)
I_L = current through inductor coil (amperes)
P_L = power input to inductor coil and load (watts)
P_S = power dissipated in load (watts)

These may be compared to P_1 of Figures 9 and 10.

References

1. THREE-PHASE SHORT-CIRCUIT SYNCHRONOUS MACHINES—V, **R. E. Doherty, C. A. Nickle.** AIEE TRANSACTIONS, volume 49, 1930, pages 700–14.

2. INHERENT ERRORS IN THE DETERMINATION OF SYNCHRONOUS-MACHINE REACTANCES BY TEST, **C. Concordia, F. J. Maginniss.** AIEE TRANSACTIONS, volume 64, 1945, June section, pages 288–94.

3. AN ANALYSIS OF THE INDUCTION MACHINE **H. C. Stanley.** AIEE TRANSACTIONS, volume 57, 1938, pages 751–5

4. Discussion by C. Concordia of TRANSIENT PERFORMANCE OF INDUCTION MOTORS. AIEE TRANSACTIONS, **F. J. Maginniss, N. R. Schultz,** volume 63 1944, pages 1457–8.

5. PER-UNIT IMPEDANCES OF SYNCHRONOUS MACHINES—II, **A. W. Rankin.** AIEE TRANSACTIONS, volume 64, 1945, December section, pages 839–41.

Paper 46-124, recommended by the AIEE subcommittee on induction and dielectric heating for presentation at the AIEE summer convention, Detroit, Mich., June 24–28, 1946. Manuscript submitted April 15, 1946; made available for printing May 9, 1946.

J. T. VAUGHAN is a research and development manager and J. W. WILLIAMSON is a research engineer, both of the Tocco division of The Ohio Crankshaft Company, Cleveland, Ohio.

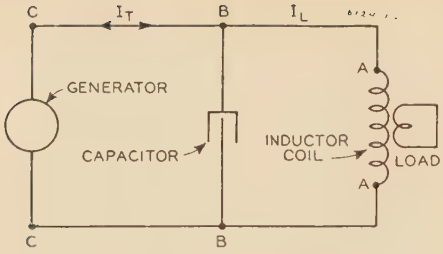

Figure 1. Conventional induction heating circuit using motor generator set

The required number of turns for any given total power to the coil and for any given terminal voltage may be calculated by means of equation 2.

In analyzing the changes which occur in a variable impedance circuit, it is convenient to represent the variation of reactance with resistance by a plot in rectangular co-ordinates. Referring to Figure 2, the total resistance R and reactance X of an induction heating coil with its load at room temperature are represented by the co-ordinates of point P_1. Since R_p, X_p, and X_o are nearly constant, the principal changes which occur in R and X as the load heats are caused by variations in the load resistance and reactance, R_S and X_S. When the power first is applied, R_S and X_S increase because of the increasing resistivity of the load with rising temperature. The load impedance, therefore, follows a locus such as $\overline{P_1P_2}$.

After a portion of the load reaches the critical temperature, R and X drop off rapidly. Let P_3 represent the impedance calculated by taking the entire load to be above the critical temperature and nonmagnetic with resistivity corresponding to final conditions. The assumption will be made that after the point of maximum impedance is reached R and X follow the straight line locus P_2P_3. This assumption has been checked experimentally and found to be reasonably accurate.

Suppose E_L, the inductor coil terminal voltage, is held constant as the load heats. The locus of inductor coil current I_L corresponding to impedance locus P_2P_3 is the circular arc I_2I_3.[4] The center of the circle OI_2I_3 lies on the line OQ, which makes the same angle α with the vertical as P_2P_3 makes with the horizontal. The power factor angle θ is equal to the angle OP makes with E_L. With conditions as shown in Figure 2, maximum power to the coil occurs at the point of maximum impedance, represented by P_2, since the component of inductor current that is in phase with E_L is greatest at this point.

The current locus of Figure 2 would result from a relatively large air gap reactance X_o. Under this condition the current through the inductor coil does not change greatly during the heating operation. However, if the air gap reactance is small, the magnitude of this current may change sufficiently so that maximum power to the coil occurs when the impedance is less than the maximum value. With the impedance locus shown in Figure 3, maximum power occurs when I_L is represented by OI_4, where Q is the center of the current locus and QI_4 is parallel to E_L. By plane geometry $\theta_4 = \angle QI_4O$, and $90°+\alpha = \angle QI_4O + \angle QOI_4 = 2\angle QI_4O$. Therefore,

$$\theta_4 = 45° + \alpha/2 \tag{1}$$

The angle which OP_4 makes with E_L may be determined, therefore, by plotting P_2P_3 and measuring the angle α which this line makes with E_L. The intersection P_4 of OP_4 with P_2P_3 gives the values of R and X for maximum power to the coil. If θ_4 as defined by equation 1 is less than θ_2 or greater than θ_3, the intersection of OP_4 with P_2P_3 extended does not represent an impedance which actually occurs during the heating operation. If θ_4, or $45° + \alpha/2$, is less than θ_2, as in Figure 2, maximum power corresponds to maximum impedance. If θ_4 should be greater than θ_3, maximum power would occur at the end of the heating operation where the impedance is minimum.

Since F and G are proportional to the total resistance and reactance of the coil ($R = N^2F$ and $X = N^2G$), P_2P_3 in Figures 2 and 3 represents not only the locus of X versus R but, to a different scale, the locus of F versus G. The values of F and G used to determine the number of turns usually are based on conditions for maximum power to the coil. For $\theta_2 > 45° + \alpha/2$ (Figure 2), maximum power to the load corresponds to maximum impedance, or the values of F and G plotted at P_2. For $\theta_2 < 45° + \alpha/2$ (Figure 3), maximum power to the load occurs when F and G are determined by the co-ordinates of P_4.

Circuit Equations and Their Limitations

For any given total power P_L to the coil and coil terminal voltage E_L, the required number of turns is

$$N = E_L\sqrt{\frac{F}{P_L(F^2+G^2)}} \tag{2}$$

By definition,

$$F = A + B \tag{3}$$

$$G = C + D + E \tag{4}$$

Formulas are given in the authors' previous paper[1] for the calculation of A, C, and E, and for the calculation of the load resistance and reactance coefficients B and D at the end of the heating operation, if the load is in the nonmagnetic state. The same limitations as given previously apply in the use of these formulas. These equations for resistance and reactance coefficients for nonmagnetic loads may be applied with reasonable accuracy to SAE 1010 to 1045 steel above 1,600 degrees Fahrenheit. For convenience, curves of resistivity versus temperature for SAE 1010 and SAE 1045 steels are given in Figure 4.

For the load in the magnetic state and at the temperature for maximum impedance, B and D may be calculated by

$$B = \left(\frac{3.14a_oK_1^2}{L}\right)\sqrt{f}K_7\times10^{-8} \tag{5}$$

$$D = 0.65B \tag{6}$$

K_7 is plotted against $P_S/(3.14\,a_oL)\sqrt{f}$, the watts per square inch of cylindrical surface of load within coil divided by the square root of frequency, in Figure 5. The ranges of extrapolation are indicated by dotted lines. For convenience the function

$$K_8 = \sqrt{f}\,K_7 \tag{7}$$

is given as a function of $P_S/3.14\,a_oL$ for f = 10,000, 3,000, and 1,000 cycles per second in Figure 6. To determine B and D, it is first necessary to find P_S. The portion of the total coil power input absorbed by the load is $B/F = B/(A + B)$. Therefore, the power to the load is

$$P_S = \left(\frac{B}{A+B}\right)P_L \tag{8}$$

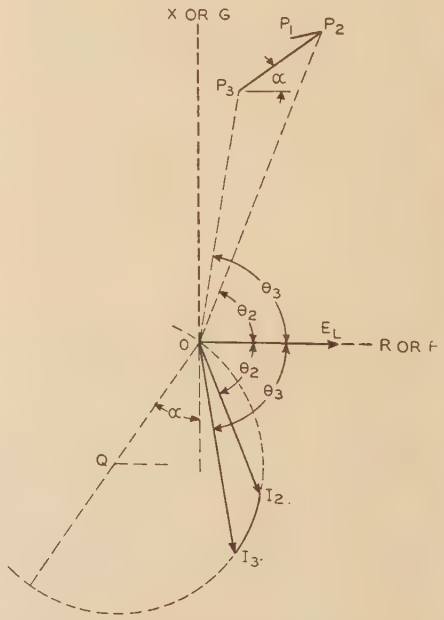

Figure 2. Impedance and current changes as load heats

B and F cannot be determined until P_s is known. However, the ratio B/F usually lies within the range 0.80 to 0.95. P_s, therefore, may be calculated first from equation 8 on the basis of any reasonable value of this ratio. An approximate value for $\sqrt{f}\,K_7$ or K_6 then can be obtained, which may be substituted into equation 5 to obtain a first approximation for B. Actually, a three per cent error in estimating P_s results in only a one per cent error in B, so that this first approximation is often sufficiently accurate for practical purposes. However, if greater accuracy is desired, the first approximation for B

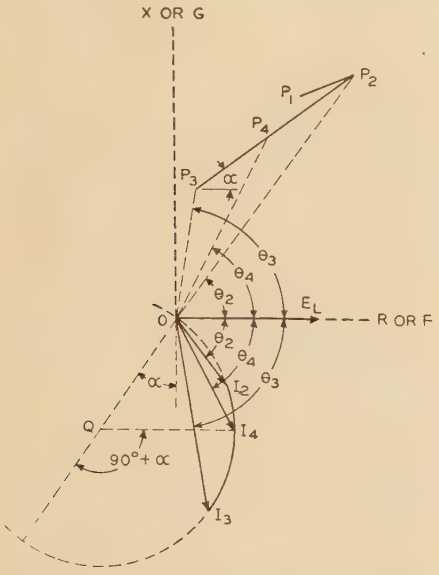

Figure 3. Impedance and current changes as load heats

may be used to obtain a more accurate value of $B/(A + B)$ and the foregoing process repeated.

LIMITATIONS

1. Taking the resistivity of the load as 40×10^{-6} ohm-inch at the temperature for maximum impedance, the maximum depth which magnetic flux and current penetrate into the load, or the depth of zone in which energy is induced (from equation 34) is

$$\delta_M = \frac{0.064}{K_6} \text{ (inches)} \qquad (9)$$

If the load is hollow, its wall thickness should be at least as great as δ_M for the given equations to apply.

2. For an accuracy of plus or minus ten per cent, the ratio a_o/δ_M should be at least 8.0.

3. The correction for coil shortness should depend on the ratio of inside diameter of the induction heating coil to its length, the ratio of the outside diameter of the load to the inside diameter of the coil, and probably the ratio

$$\sqrt{R_s^2+X_s^2}/X_o = \sqrt{B^2+D^2}/E$$

of impedance associated with flux in the load to impedance associated with flux in the air gap. If this ratio is of the order of magnitude of 1.0 or greater, the flux through the load is appreciable in relation to the flux in the air gap, and the total flux is therefore considerably greater than the flux through the air gap alone. Consequently, a larger number of ampere turns is required to overcome the flux reluctance drop in the portion of the magnetic circuit external to the coil, or for any given number of ampere turns the magnetic intensity inside the coil is less than would result with a nonmagnetic load of the same dimensions. However, in the majority of applications in which a steel load is heated with a multiturn coil the effect of coil shortness is so small that it is believed that the equations given may be used with reasonable accuracy. The constant K_1, by which the actual ampere turns per inch must be multiplied to obtain the ampere turns per inch which would produce the same average power density if the coil were infinitely long, is derived (for nonmagnetic loads) in the authors' previous paper.[1]

Derivation of Expressions for B and D

The equations for B and D given in the foregoing text are based on experimental data and relations derived and checked experimentally under "More Exact Derivations," by means of which these data may be extended to other frequencies. The "Approximate Theory" is included to provide an understanding of certain physical principles in the induction heating of magnetic materials and to establish limitations for small diameters and wall thicknesses. The assumption made in the latter section does not limit the generality of the remainder of this paper.

Let

Subscript o refer to outside of load
Subscript M denote maximum values
δ = distance from outside of load (centimeters)
a_o = outside diameter of load (centimeters)
r = distance from axis of load (centimeters)
i = instantaneous current density in load (abamperes per square centimeter)
I_{ins} = instantaneous current in coil (abamperes)
I = rms current in coil (abamperes)
ϕ = instantaneous magnetic flux within radius r (maxwells)
e = instantaneous voltage per turn to bring about time rate-of-change of flux within load $= d\phi_o/dt$ (abvolts)
β = magnetic flux density (maxwells per square centimeter)
H = magnetic intensity
ρ = resistivity (abohms per centimeter)
t = time (seconds)

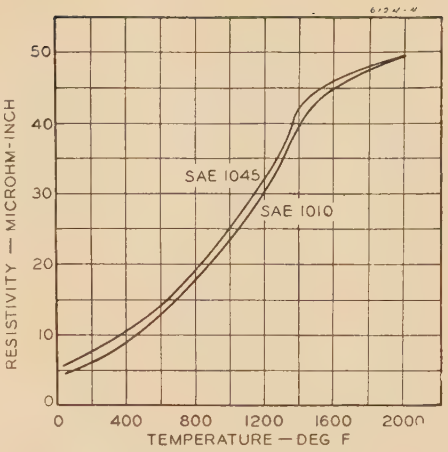

Figure 4. Resistivity versus temperature for SAE 1010 and SAE 1045 steel

f = frequency (cycles per second)
$\omega = 2\pi f$
L = length of coil (centimeters)
N = number of turns

The total flux within a circle of radius r is, by definition,

$$\phi = 2\pi \int_o^r r\beta dr \qquad (10)$$

By Ohm's law, with positive directions as indicated in Figure 7,

$$2\pi r\rho i = \frac{\partial \phi}{\partial t} \qquad (11)$$

Providing, as will be assumed, that the radius of the load is sufficiently great so that r is nearly equal to the outside radius over the region in which β and i are appreciable, equation 10 may be written

$$\phi = \pi a_o \int_o^r \beta dr = \pi a_o \int_\delta^{a_o/2} \beta d\delta \qquad (12)$$

where $\delta = a_o/2 - r$ is the distance from the outside of the load. Equation 11 may be written

$$\rho \pi a_o i = \partial\phi/\partial t \qquad (13)$$

Consider only coils and loads of large length to diameter ratios. Then, as in the induction heating of nonmagnetic materials, the magnetic intensity is equal

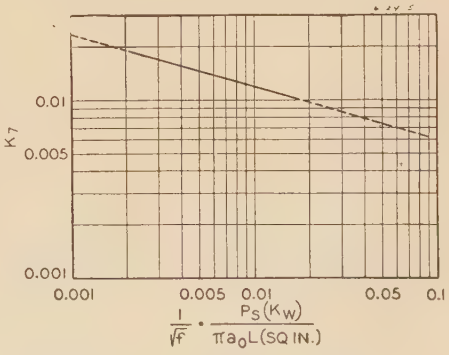

Figure 5. Load resistance coefficient K_7

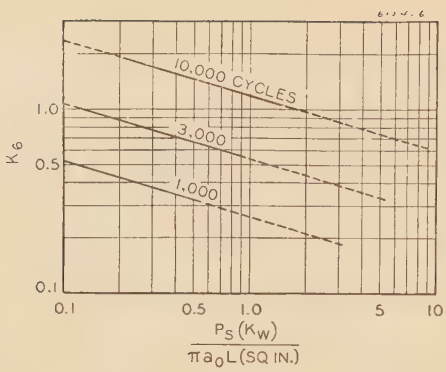

Figure 6. Load resistance coefficient K_δ

to 4π times the total current per unit axial length outside the given radius. The current per unit axial length in the coil is $(N/L)\,I_{ins}$. Therefore,

$$H=4\pi\left[\frac{N}{L}I_{ins}-\int_0^{\delta} i\,d\delta\right] \tag{14}$$

The minus sign before the integral results from the choice of positive direction for i (Figure 7). Differentiating equation 13 with respect to δ and substituting equation 12 for ϕ,

$$\frac{\partial i}{\partial \delta}=-\frac{1}{\rho}\cdot\frac{\partial \beta}{\partial t} \tag{15}$$

Approximate Theory

Most induction heating applications require inductor coil current densities such as to produce high saturations near the outside of the load. Therefore, in the present section assume the $\beta-H$ curve shown in Figure 8, in which $\beta=\pm\beta_M$ or zero. Positive directions are indicated in Figure 7. Take the instant $t=0$ when the current in the inductor coil is zero after having been negative. Assume that at this instant the flux density β is negative (or to the left) between $\delta=0$ and $\delta=\delta_M$, where δ_M is the maximum depth of penetration to be determined later. The flux through the load at $t=0$ is

$$\phi_o|_{t=0}=-\pi a_o \delta_M \beta_M \tag{16}$$

The portion of the voltage per turn utilized in bringing about a time rate-of-change of flux within the load is

$$e=\frac{d\phi_o}{dt} \tag{17}$$

Since ϕ_o is negatively maximum at $t=0$, e is zero at $t=0$, but positive after this instant. Therefore, assuming this voltage varies sinusoidally with time, which is the case at least if the voltage applied to the coil is sinusoidal and the air gap between the coil and load is sufficiently small,

$$e=e_M \sin \omega t \tag{18}$$

Equation 15 shows that at any instant the current density in the load varies with δ only where the flux density β is changing with time. By assumption, β can have only three values: β_M, $-\beta_M$, and zero. At any given time, i can change only where β is going from one to another of these values.

The magnetic intensity at the outside of the load is

$$H_o=4\pi(N/L)I_{ins} \tag{19}$$

Consequently, at the instant $t=0$ at which the current in the coil becomes positive, the direction of magnetization at the outside of the load also becomes positive. Denote the depth of positive magnetization by δ_+. The total flux within the load is

$$\phi_o=\pi a_o[\delta_+\beta_M+(\delta_M-\delta_+)(-\beta_M)]=\pi a_o\beta_M(2\delta_+-\delta_M) \tag{20}$$

Integrating equation 17 and substituting equation 18 for e,

$$\phi_o=\int_o^t e\,dt+\text{constant}=-(e_M/\omega)\cos\omega t+\text{constant} \tag{21}$$

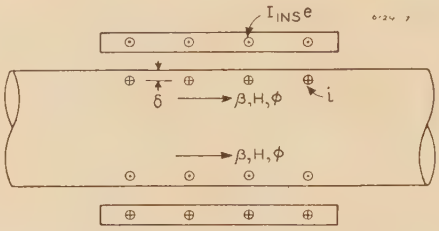

Figure 7. Current and flux directions—positive

Combining equations 20 and 21, and noting that $\delta_+=0$ at $t=0$,

$$\delta_+=(e_M/2\pi a_o\beta_M\omega)(1-\cos\omega t) \tag{22}$$

δ_+ is plotted against time in Figure 9.

The time rate-of-change of flux $\partial\phi/\partial t$ is independent of position for $\delta<\delta_+$, and zero for $\delta>\delta_+$. Therefore, from equation 13,

$$\left.\begin{aligned} i&=\frac{1}{\rho\pi a_o}\cdot\frac{d\phi_o}{dt} \quad \text{for } \delta<\delta_+\\ &=0 \qquad\qquad\quad \text{for } \delta>\delta_+\end{aligned}\right\} \tag{23}$$

The total current per unit length in the load is

$$\int_o^{a_o/2} i\,d\delta=i\delta_+ \tag{24}$$

β is zero for $\delta>\delta_M$ by assumption. Therefore, H is also zero. Substituting $\delta=a_o/2$ into equation 14, therefore, gives

$$I_{ins}=(L/N)i\delta_+ \tag{25}$$

Substituting equations 23 and 21 for i and equation 22 for δ_+

$$I_{ins}=\frac{L}{N}\cdot\frac{e_M^2}{2\pi^2\rho a_o^2\beta_M\omega}\sin\omega t(1-\cos\omega t) \tag{26}$$

$e=0$ at $\omega t=\pi$. Therefore, from equations 17 and 13, $d\phi/dt=0$ and the current density i is zero; i was also zero at $t=0$. The conditions at $\omega t=\pi$, therefore, are identical (except for directions) with the conditions assumed at $t=0$. During the remaining half cycle a wave of negative magnetization enters the load. The phenomena of the first half cycle are repeated with changes in polarity, as shown in Figure 9. The maximum depth of penetration of electrical energy is obtained by substituting $\omega t=\pi$ into equation 22.

$$\delta_M=e_M/\pi a_o\beta_M\omega \tag{27}$$

Equation 26 applies only to the intervals during which e is positive. From equations 18 and 26, the instantaneous input per turn to the load during the first half cycle is

$$eI_{ins}=\frac{L}{N}\cdot\frac{e_M^3}{2\pi^2\rho a_o^2\beta_M\omega}\sin^2\omega t(1-\cos\omega t) \tag{28}$$

The average power per turn to the load obtained from equation 28 is

$$w=\frac{L}{N}\cdot\frac{e_M^3}{4\pi^2\rho a_o^2\beta_M\omega} \tag{29}$$

From equation 26 the rms coil current during the first half cycle, which is equal to the rms coil current, is found to be

$$I=\sqrt{\frac{5}{8}}\cdot\frac{L}{N}\cdot\frac{e_M^2}{2\pi^2\rho a_o^2\beta_M\omega} \tag{30}$$

Comparing equations 29, 18, and 30, the ratio of abwatts to abvolt-amperes or watts to volt-amperes is

$$\frac{w}{0.707e_MI}=\sqrt{0.8}=0.895 \tag{31}$$

Solving equation 30 for e_M and substituting into equation 29, the power to the load per turn is

$$w=3.16a_o\sqrt{\rho\beta_M\omega}\cdot\sqrt{\frac{N}{L}}\cdot I^{1.5} \tag{32}$$

or the total power to the load is

$$Nw=7.92a_o\sqrt{\frac{\rho\beta_M f}{L}}\cdot(NI)^{1.5} \tag{33}$$

Table I

	Kilowatts Per Square Inch to Load	Ratio (Watts Divided By Volt-Amperes) to Load
Calculated	0.244	0.895
Measured	0.239	0.802

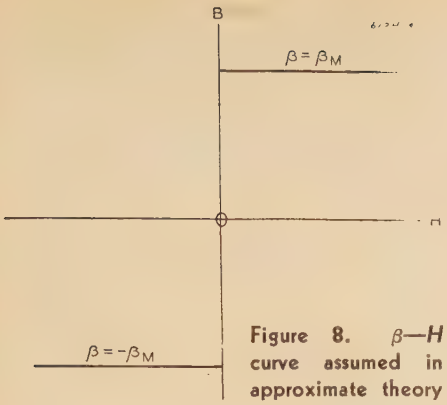

Figure 8. β—H curve assumed in approximate theory

Making use of equations 27, 30, 33, 5, and 7 and converting all quantities to the ohm-inch system, it can be shown that

$$\delta_M = 1.595 \times 10^3 \frac{\rho}{K_6} \tag{34}$$

For a given density of power to the load, the maximum depth of penetration should be nearly independent of the air gap. Therefore, the expression used for K_6 in deriving equation 34 was obtained by putting $K_1 = 1$ in equation 5.

Table I gives a comparison of experimental results with theoretical calculations, the latter based on the approximate theory. An SAE 1015 steel load was heated to 210 degrees Fahrenheit by means of a closely fitting coil. The frequency was 10,000 cycles per second. The measured coil current was such as to produce 486 ampere turns (rms) per inch axial length of coil. In the theoretical calculation, the resistivity of SAE 1015 steel at 210 degrees Fahrenheit and the flux density β_M were taken respectively as 6.75×10^{-6} ohm-inches and 18,500 lines per square centimeter.

The following conclusions may be drawn from the analysis so far presented:

1. The total depth of penetration of electrical energy in the magnetic state is usually small. Table II gives values of δ_M corresponding to two kilowatts per square inch to the load and the temperature for maximum impedance with constant current; ρ is taken as 40×10^{-6} ohm-inch, and K_6 in equation 34 is obtained from Figure 6.

2. The power density is approximately proportional to the 1.5 power of current. This relation was observed by Rosenberg.[5,6,7] As noted by Baker,[2] however, Rosenberg's explanation is not very satisfactory.

3. It frequently has been assumed that the resistance and reactance of an induction heating coil with a magnetic load could be calculated by assuming "some" constant value of permeability. This is not strictly true, since any constant value of permeability would result in a ratio of watts to volt-amperes to the load of 0.707 at sufficiently high frequencies.

4. With power densities as used in induction heating practice and with δ_M small compared to the load diameter, the load power caused by hysteresis is usually negligible. For instance, considering a 1-inch diameter load of SAE 1020 steel with a power density of 500 watts per square inch of load surface at 10,000 cycles, the power caused by hysteresis would be less than 22 watts per square inch of load surface, or four per cent of the total power. This is based on an assumed maximum flux density of 100,000 lines per square inch and a hysteresis energy of 0.05 joule per cubic inch per cycle,[10] which is from data with the steel at room temperature. Further data indicate a decrease in hysteresis loss as temperature is increased, the hysteresis loss approaching zero as the critical temperature is approached.[9]

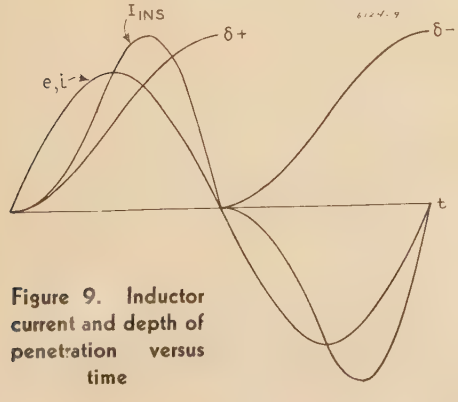

Figure 9. Inductor current and depth of penetration versus time

More Exact Derivations

The saturation flux densities of carbon steels usually treated by induction heating are known at present only at room temperature. In order to design coils for heating above the critical point, however, the values of the load resistance and reactance coefficients B and D must be determined at the temperature of maximum impedance, about 1,200 degrees Fahrenheit. The present section provides a means of accomplishing this, and at the same time affords a more accurate theory which avoids the assumption that $\beta = \pm$ constant. Use is made of experimental information which is readily obtainable.

Again consider loads of sufficient radius so that the distance from the axis may be taken as the outside radius $a_0/2$ at all points for which the magnetic intensity H, the flux density β, and the current density i are appreciable. Neglect hysteresis. Then for any given value of H there exists one and only one value of β or, mathematically,

$$\beta = \phi_{(H)} \tag{35}$$

Differentiating equation 14 twice with respect to δ and substituting into equation 15,

$$\frac{\partial^2 H}{\partial \delta^2} = \frac{4\pi}{\rho} \cdot \frac{\partial \beta}{\partial t} \tag{36}$$

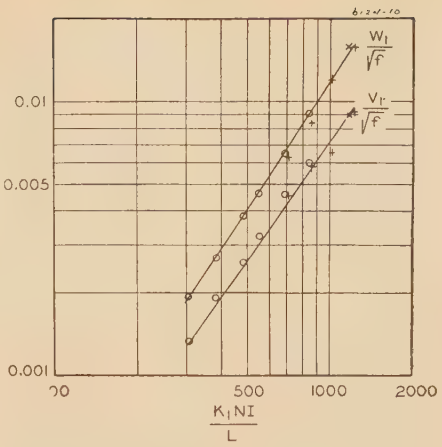

Figure 10. Plot of experimental data

⊙—Coil 1, 10,000 cycles
+—Coil 2, 10,000 cycles
×—Coil 3, 3,000 cycles

Making use of equation 35,

$$\frac{\partial^2 H}{\partial \delta^2} = \frac{4\pi}{\rho} \mu'_{(H)} \frac{\partial H}{\partial t} \tag{37}$$

where $\mu'_{(H)}$ is the differential permeability defined by

$$\mu' = \frac{dB}{dH} \tag{38}$$

Since for any given distance δ from the outside of the load and time, there exists one and only one value of H:

$$H = \psi_{(\delta,\ t)} \tag{39}$$

As $\psi_{(\delta,\ t)}$ is a solution of equation 37, it can be shown that $H' = \psi_{(k\delta,\ k^2 t)}$ is also a solution. At the outside of the load $\psi_{(\delta,\ t)} = \psi_{(o,\ t)}$ and $\psi_{(k\delta,\ k^2 t)} = \psi_{(o,\ k^2 t)}$. Suppose for a given peak magnetic intensity H_{OM} at the outside of the load and a given frequency f_1, H is represented by $\psi_{(\delta,\ t)}$. Then for the same magnetic intensity H_{oM} at the outside of the load and a frequency $k^2 f_1$, the magnetic intensity is represented by $\psi_{(k\delta,\ k^2 t)}$.

With a frequency f_1,

$$\beta = \phi_{(H)} = \phi_{(\psi(\delta,\ t))} = \Omega_{(\delta,\ t)} \tag{40}$$

With the same peak magnetic intensity at the outside of the load and a frequency $k^2 f_1$,

$$\beta = \phi_{(H')} = \phi_{(\psi(k\delta,\ k^2 t)} = \Omega_{(k\delta, k^2 t)} \tag{41}$$

Since the flux density is assumed negli-

Table II

Frequency in Cycles Per Second	Depth of Penetration in Inches
10,000	0.066
3,000	0.145

gible except for very small values of δ, the upper limit in equation 12 may be taken as infinity. Therefore,

$$\phi_o = \pi\pi a_o \int_o^\infty \beta d\delta \tag{42}$$

Substituting equations 40 and 41 into equation 42, with a frequency f_1,

$$\phi_o = \pi a_o \int_o^\infty \Omega_{(\delta,\ t)} d\delta \tag{43}$$

or, with a frequency $k^2 f_1$,

$$\phi'_o = \pi a_o \int_o^\infty \Omega_{(k\delta,\ k^2 t')} d\delta$$
$$= \pi a_o / k \int_o^\infty \Omega_{(\delta,\ k^2 t')} d\delta \tag{44}$$

At corresponding times, $k^2 t'$ in equation 44 is equal to t in equation 43. Therefore, the total flux in the load is proportional to $1/k$ or $1/\sqrt{f}$. The load impedance is proportional to the product of the magnitude of this flux multiplied by frequency, or

$$(1/\sqrt{f})f = \sqrt{f}$$

Let

w_1 = kilowatts per square inch to the load
v_1 = reactive kilovolt-amperes per square inch to the load
$K_1 NI/L$ = effective ampere turns per inch (rms)

Then from the foregoing reasoning, w_1 and v_1 may be written in the form

$$w_1 = \sqrt{f}\, F_1(K_1 NI/L) \tag{45}$$

$$v_1 = \sqrt{f}\, F_2(K_1 NI/L) \tag{46}$$

where the functions F_1 and F_2 are independent of frequency. To determine these functions for SAE 1015 steel at the load temperature for maximum impedance and to show experimentally that $w_1/\sqrt{f}$ and $v_1/\sqrt{f}$ are independent of frequency for any given $K_1 NI/L$, data were taken at 10,000, 9,600, and 3,000 cycles per second. The results are shown in Figure 10. The variations in $w_1/\sqrt{f}$ and $v_1/\sqrt{f}$ between 9,600 and 10,000 cycles per second were negligible for a given $K_1 NI/L$. Dimensions of coils and loads are given in Tables III and IV. In each reading the current through the induction heating coil was held constant by varying the voltage. This current was measured through a current transformer by a dynamometer type ammeter. Readings were taken at the instant of maximum coil terminal voltage. The power to the coil also was found to be maximum at this instant. To measure this power as accurately as possible, the capacitor at BB (Figure 1) was adjusted for approximately unity power factor at the generator terminals CC for the instant readings were taken. The generator output was measured by a wattmeter connected at CC.

The power to the load was obtained by subtracting the calculated coil copper loss.[1] After making a slight correction for conductor wall thinness at 3,000 cycles per second (no correction was required at 10,000 cycles per second), the maximum ratio of calculated coil I^2R loss to generator output was 0.04. Capacitor and bus losses between the wattmeter and coil terminals were negligible. The voltage at the terminals of the induction heating coil was measured by a voltmeter connected at AA. It was assumed that the reactive volt-amperes to the coil could be determined from the watts and volt-amperes by the usual method. Experience indicates that, after making allowance for the reactance of the bus, the reactive volt-amperes so calculated agree closely with the volt-amperes of capacitance required to balance to unity power factor at the generator terminals, even though the wave form of the current through the inductor coil is not truly sinusoidal. The reactances associated with the time rate-of-change of flux in the coil copper and air gap are, respectively, N^2C and N^2E. The reactive volt-amperes to the load were obtained by subtracting $I^2N^2(C+E)$ from the reactive volt-amperes to the coil. The watts per square inch and vars per square inch to the load then were found by dividing the power and reactive volt-amperes by the load surface within the coil $\pi a_o L$.

With a frequency of 9,600 cycles only, the foregoing experiments were repeated with SAE 1020 and SAE 1045 loads. No significant differences could be detected from the results with SAE 1015 steel. At 1200 degrees Fahrenheit, the difference in resistivities between SAE 1015 and SAE 1045 steels is about three per cent. According to equation 33, if the magnetic properties of the two steels were identical, the load resistances should differ by about two per cent. This variation would be negligible in most induction heating calculations.

By definition,

$$B = R_s/N^2 = I^2 R_s/(NI)^2 \tag{47}$$

Table III. Description of Induction Heating Coils

	Coil 1	Coil 2
Total turns, N	35	19
Inside diameter, inches	3.29	3.20
Length over turns, L, inches	14.62	7.05
Conductor:		
Dimension parallel to axis of coil, inches	0.375	0.297
Dimension perpendicular to axis of coil, inches	0.25	0.25
Wall thickness, inches	0.045	0.048
Resistivity, microhm inches	0.73	0.73

Table IV. Description of Loads

	Load 1	Load 2	Load 3
Outside diameter, inches	2.51	2.50	2.50
Type steel, SAE number	1015	1020	1045

But I^2R_s is the power to the load in watts. Since w_1 is expressed in kilowatts per square inch, $I^2R_s = \pi a_o L w_1 \times 10^3$. Therefore,

$$B = \frac{\pi a_o L w_1 \times 10^3}{(NI)^2}$$
$$= \frac{\pi a_o k_1^2}{L} \sqrt{f}\, K_7 \times 10^{-3} \tag{48}$$

where

$$K_7 = \frac{w_1 \times 10^6/\sqrt{f}}{(K_1 NI/L)^2} \tag{49}$$

From equation 45 $w_1/\sqrt{f}$ is a function of $K_1(NI/L)$, or $K_1 NI/L$ is a function of $w_1/\sqrt{f}$. Therefore, K_7 is also a function of $w_1/\sqrt{f}$. Similarly, it may be shown that

$$D = \frac{\pi a_o K_1^2}{L} \sqrt{f}\, K_8 \times 10^{-3}$$

where

$$K_8 = \frac{v_1 \times 10^6/\sqrt{f}}{(K_1 NI/L)^2}$$

is a function of $K_1 NI/L$ or $w_1/\sqrt{f}$. However, Figure 10 indicates that within the range of $K_1 NI/L$ covered by experiments, the ratio of reactive volt-amperes to watts is nearly constant and equal to 0.65. Therefore, it is sufficiently accurate at the load temperature for maximum impedance to determine D from B by means of equation 6.

References

1. Design of Induction-Heating Coils for Cylindrical Nonmagnetic Loads, **J. T. Vaughan, J. W. Williamson.** AIEE Transactions, volume 64, 1945, August section, pages 587–92.

2. Induction Heating of Moving Magnetic Strip, **R. M. Baker.** AIEE Transactions, volume 64, 1945, April section, pages 184–9.

3. Vacuum-Tube Radio-Frequency Generator —Characteristics and Application to Induction-Heating Problems, **T. P. Kinn.** AIEE Transactions, 1944, volume 63, pages 1290–1303.

4. Elementary Electric Circuit Theory (book), **Richard H. Frazier.** McGraw-Hill Book Company, Inc., New York, N. Y. 1945, pages 246–9.

5. Wirbelstrome in Massivem Eisen, **E. Rosenberg.** *Elektrotechnische Zeitschrift* (Berlin, Germany), May 31, 1923, pages 513–18.

6. Eddy Currents in Iron Masses, **E. Rosenberg.** *The Electrician* (London, England), August 24, 1923, pages 188–91.

7. Properties and Testing of Magnetic Materials (book), **Thomas Spooner.** McGraw-Hill Book Company, Inc., New York, N. Y., 1927, pages 98–103.

8. Reference 7, pages 138–9.

9. Reference 7, pages 174–6.

10. Electro-Magnetic Devices (book), **H. C. Roters.** John Wiley & Sons, Inc., New York, N. Y., 1941, page 57.

Formulas for Calculating the Inductance of Channels Located Back to Back

WILLIAM G. SCHWANTZ
ASSOCIATE AIEE

THOMAS JAMES HIGGINS
ASSOCIATE AIEE

IN 1937 Arnold[1] published an analytic procedure enabling the designer of a single-phase 2-conductor bus to determine combinations of conductor spacing and cross section that render proximity and skin effects (a-c resistance, eddy-current losses, and current density distortion) a minimum. For explicit details the reader is referred to Arnold's paper. For our purpose it suffices to remark:

1. In general the designer is afforded an unlimited number of combinations of conductor spacing and cross section.

2. As the theoretical cross sections are infinitely thin, it is necessary, in practice, to use finitely thick structural shapes whose mean perimeters approximate the theoretical shapes.

3. As the ratio of conductor spacing to perimeter of theoretical cross section increases, the approximately equivalent structural shape associated with a particular spacing shifts from rectangular strap to channel to circular or square tubular conductor.

4. Although the infinitely thin theoretical cross sections produce zero proximity and skin effects, such is not true of the finitely thick conductors actually used: for though the proximity effect is effectively yet zero, unavoidably there is introduced minimum skin effect.

5. The skin effect losses, and hence the a-c resistance, can be calculated from a given simple formula.

6. The accuracy of this formula and the correctness of the general theory are verified by experimental data set forth in Arnold's paper.

Despite, however, the availability and the obvious usefulness of this general theory, it would seem that no considerable use, if any, has yet been made of it. In some part, no doubt, this neglect is due to lack of knowledge of it: Arnold's paper was published in the *Journal* of the Institution of Electrical Engineers, a British periodical which in this country enjoys but little circulation outside of engineering libraries or the technical departments of a few of the larger public libraries. In other part, however, this neglect doubtlessly can be attributed to the fact that, largely, a-c industrial-bus design is polyphase and has as its desideratum the achievement of minimum inductance and hence minimum reactance voltage drop. Designs achieving this end involve closely spaced conductors and thus greater than minimum eddy-current losses, whereas practical designs achieving minimum eddy-current losses involve fairly widely spaced conductors and thus increased reactance voltage drop.

When, however, single-phase busses are to be designed and minimum reactance is not so much the desideratum as is minimum eddy-current loss (for example, very heavy current busses where eddy-current loss is the predominant factor in design), Arnold's theory affords preferred designs. In consequence, it is of interest to the designer of such busses that there be available to him formulas enabling calculation of the electrical and mechanical performance of designs stemming from Arnold's theory. This, as already mentioned, yields conductor cross sections to be approximated by standard structural shapes: rectangular strap, channel, and circular or square tubular conductors.

Now formulas for calculating the a-c resistance, a-c inductance, mutual electromagnetic forces on short circuit, and other conductor parameters essential to knowledge of the electrical and mechanical (short-circuit) performance of the bus are available for rectangular strap and for circular and square tubular conductors.[2] As regards (uniformly thick) channel conductors located back to back, Arnold[1] has advanced a formula for calculating the a-c resistance and Higgins[3,4] has advanced formulas for calculating the mutual electromagnetic forces exerted between the conductors on short circuit. But explicit formulas for the inductance as a function of the geometrical parameters specifying conductor spacing and cross section have not been published hitherto. Yet, inasmuch as among the various combinations of conductor spacing and cross section afforded by Arnold's theory, that combination which affords the best all-around design is usually one comprised of moderately spaced channels located back to back, it is most desirable to have formulas for the inductance.

Such formulas are derived in this paper, it being assumed that the conductors are nonmagnetic, are of such length that end effects are negligible, are right-cornered, are uniformly thick, and carry currents uniformly distributed over their cross sections.

Of these five conditions, the first and second commonly are satisfied in practice. Right-corneredness, however, though essential to tractable analysis, is not always true in practice: channels built up of strap conductors are usually right-angled, whereas channels drawn, rolled, or otherwise formed in one piece usually have rounded edges. However, error introduced by neglecting the rounded edges is usually quite small; moreover, where necessary the increase in inductance can be approximated by use of semi-empirical formulas derived by Dwight and Wang.[5] Uniform thickness, on the other hand, is true both of channels built up of strap conductor and (except for possible slight variation in the immediate vicinity of a rounded edge) of most commercial channels. Finally, in designs based on Arnold's theory, proximity effect is practically obviated and skin effect minimized; though this minimum skin effect tends to produce an inductance slightly less than the d-c value, the actual change is practically negligible (see, for example, the discussion following reference 5 or the experimental results published in reference 6); whence the assumption of uniform current distribution is consistent with fact, introduces negligible error, and enables solution of an otherwise intractable problem.

If these five postulates are granted, derivation of the desired formulas, though lengthy, is not particularly difficult. The conductor cross sections can be considered, in various fashions, as combinations of parallel-sided rectangular areas. By virtue of the fundamental theorem of geometric mean distance theory, the inductance can be expressed in terms of the geometric mean distances between these rectangular areas. These geometric mean distances can be calculated from known formulas[7,8] as shown under "Some General Relationships." Accordingly, determination of the inductance as a function of the parameters

Paper 46-119, recommended by the AIEE committee on basic sciences for presentation at the AIEE summer convention, Detroit, Mich., June 24–28, 1946. Manuscript submitted January 9, 1946; made available for printing May 8, 1946.

WILLIAM G. SCHWANTZ is an engineer, line design division, Commonwealth Edison Company, Chicago, Ill., and a graduate student, department of electrical engineering, Illinois Institute of Technology, Chicago. THOMAS JAMES HIGGINS is an associate professor of electrical engineering, Illinois Institute of Technology, Chicago.

defining the (spacing and cross sections of the conductors of the) bus reduces, in essence, to specific formulation of these geometric mean distances and substitution of them in the general equation for the inductance (see "Derivation of the General Formula"). To check the correctness of the resulting formula, we note that the channels can be (1) so proportioned or (2) so located relative to each other that the bus reduces to one comprised of rectangular strap conductors. Corroboratively, the known formula[9,10] for the inductance of this latter bus is yielded by the general formula for channels back to back ("Corroboration of Equation 10").

This general formula contains some 75 terms. A much simpler formula, similarly derived—but on the assumption that the conductors can be considered as comprised of line segments (Figure 5)—facilitates computation preliminary to final choice of cross section. To check the correctness of this formula, we note that if the flanges are taken to be of zero width, the bus reduces to one comprised of infinitely thin strap conductors. Corroboratively, the known formula[9,10] for the inductance of this bus is yielded by the general formula for line segment channels back to back "(Approximations to the General Formula").

The desired formulas having been obtained and checked, their use is illustrated by the numerical solution of a typical problem in bus design ("Some Illustrative Examples"). Additionally, this illustrative example reveals certain precautions that must be observed in the use of the approximate formulas based on line segment channels ("Remarks on the Approximate Formula").

Some General Relationships

From well-known theory we have that the inductance of a bus comprised of two long parallel cylindrical nonmagnetic conductors, each of uniform but otherwise arbitrary cross section, is

$$L = 2 \log \frac{D_{ab}^2}{D_{aa} D_{bb}} \qquad (1)$$

wherein D_{aa} and D_{bb} are the self geometric mean distances of the conductor cross sections and D_{ab} is the geometric mean distance between the cross sections.

If each of the two conductors is comprised of several component conductors connected in parallel, m comprising that with cross section S_a and n that with cross section S_b, equation 1 can be written[8]

$$L = -\left(\frac{2}{I^2}\right) \sum_{i=1}^{m+n} \sum_{j=1}^{m+n} w_i w_j S_i S_j \log D_{ij} \qquad (2)$$

wherein I is the conductor current; w_i the current density in the ith component of cross sectional area S_i, taken positive for current flow in one direction and negative for current flow in the opposite direction; and $D_{ij} \equiv D_{ji}$ is the geometric mean distance between areas S_i and S_j.

If $S_i = RS$ and $S_j = R'S'$ are two arbitrarily located parallel-sided rectangular areas (Figure 1), the geometric mean distance between them is given by

$$S_i S_j \log D_{ij} = -\left(\frac{25}{12}\right) S_i S_j - \left(\frac{1}{24}\right) \sum_{p=1}^{4} \sum_{q=1}^{4} (-1)^{p+q} K(A_p, B_q) \qquad (3)$$

wherein

$$K(A_p, B_q) = (A_p^4 - 6A_p^2 B_q^2 + B_q^4) \times \log (A_p^2 + B_q^2)^{1/2} - 4A_p B_q^3 \times \tan^{-1} \frac{A_p}{B_q} - 4A_p^3 B_q \tan^{-1} \frac{B_q}{A_p} \qquad (4)$$

and

$$A_1 = |D+R+R'|; \quad A_2 = |D+R|; \quad A_3 = |D|; \quad A_4 = |D+R'| \qquad (5)$$

$$B_1 = |P+S+S'|; \quad B_2 = |P+S|; \quad B_3 = |P|; \quad B_4 = |P+S'| \qquad (6)$$

Derivation of the General Formula

Consider a bus comprised of two identical channels back to back (Figure 2). Each of the channels can be taken as comprised of two component conductors: one of full rectangular cross section wherein current exists in the same direction as in the channel; the other of smaller rectangular cross section having current in opposite direction. Hence $m = n = 2$, and from equation 2,

$$L = -\left(\frac{2}{I^2}\right) \sum_{i=1}^{4} \sum_{j=1}^{4} w_i w_j S_i S_j \log D_{ij} \qquad (7)$$

By definition of geometric mean distance, $D_{ij} \equiv D_{ji}$. By virtue of the geometric symmetries in Figure 2,

$$D_{11} = D_{44}; \quad D_{22} = D_{33}; \quad D_{12} = D_{34}; \quad D_{13} = D_{24}$$

Further,

$$S_1 = S_4; \quad S_2 = S_3; \quad w_1 = -w_2 = w_3 = -w_4 = I/(S_1 - S_2)$$

In consequence of these relationships, we have from equation 7

$$L = -\left(\frac{4}{A^2}\right) [S_1^2 (\log D_{11} - \log D_{14}) + S_2^2 (\log D_{22} - \log D_{23}) - 2S_1 S_2 (\log D_{12} - \log D_{13})] \qquad (8)$$

wherein

$$A = (S_1 - S_2) = [rs - (r-t)(s-2t)] \qquad (9)$$

Corroboratively, if $S_2 = S_3 = 0$, we have rectangular strap conductors of cross section $S_1 = S_4$ and equation 8 reduces to the known formula,

$$L = 4 \log \frac{D_{14}}{D_{11}}$$

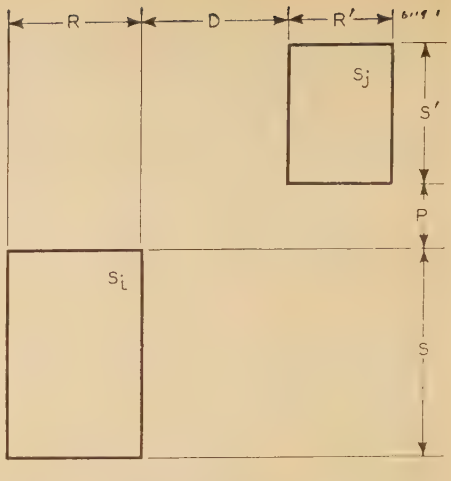

Figure 1. Relative location of two parallel-sided rectangles

Determining the six geometric mean distances in the right-hand member of equation 8 by use of equations 3–6—the explicit expressions are to be found in Appendix I—substituting appropriately in equation 8, and rearranging terms, we have

$$L = -\left(\frac{1}{6}\right) [rs - (r-t)(s-2t)]^2 \{ 4r^4 \log r + 4s^4 \log s - 12t^4 \log t - 2d^4 \log d + 4(r-t)^4 \log (r-t) - 4(s-t)^4 \times \log (s-t) + 4(s-2t)^4 \log (s-2t) + 4(d+r)^4 \log (d+r) - 4(d+2r)^4 \times \log (d+2r) - 2(d+2t)^4 \log (d+2t) + 4(d+r+t)^4 \log (d+r+t) - 2(r^4 - 6r^2 s^2 + s^4) \log (r^2+s^2) - 2(r^4 - 6r^2 t^2 + t^4) \log (r^2+t^2) - 2[(r-t)^4 - 6(r-t)^2 t^2 + t^4] \log [(r-t)^2 + t^2] - 2[(s-t)^4 - 6(s-t)^2 t^2 + t^4] \log [(s-t)^2 + t^2] + (d^4 - 6d^2 s^2 + s^4) \log (d^2+s^2) + 2[(d+t)^4 - 6(d+t)^2 t^2 + t^4] \log [(d+t)^2 + t^2] + 2[r^4 - 6r^2 (s-t)^2 + (s-t)^4] \times \log [r^2 + (s-t)^2] + 2[(r-t)^4 - 6(r-t)^2 (s-t)^2 + (s-t)^4] \times \log [(r-t)^2 + (s-t)^2] - 2[(r-t)^4 - 6(r-t)^2 (s-2t)^2 + (s-2t)^4] \times \log [(r-t)^2 + (s-2t)^2] - 2[(d+r)^4 - 6(d+r)^2 s^2 + s^4] \log [(d+r)^2 + s^2] + [(d+2r)^4 - 6(d+2r)^2 s^2 + s^4] \times \log [(d+2r)^2 + s^2] - 2[(d+r)^4 - 6(d+r)^2 t^2 + t^4] \log [(d+r)^2 + t^2] + 2[(d+2r)^4 - 6(d+2r)^2 t^2 + t^4] \times \log [(d+2r)^2 + t^2] - 2[(d+r+t)^4 - 6(d+r+t)^2 t^2 + t^4] \times \log [(d+r+t)^2 + t^2] + 2[(d+r)^4 - 6(d+r)^2 (s-t)^2 + (s-t)^4] \times \log [(d+r)^2 + (s-t)^2] - 2[(d+2r)^4 - 6(d+2r)^2 (s-t)^2 + (s-t)^4] \times \log [(d+2r)^2 + (s-t)^2] - 2[(d+t)^4 - 6(d+t)^2 (s-t)^2 + (s-t)^4] \times \log [(d+t)^2 + (s-t)^2] + [(d+2r)^4 - 6(d+2r)^2 (s-2t)^2 + (s-2t)^4] \times \log [(d+2r)^2 + (s-2t)^2] + [(d+2t)^4 -$$

$6(d+2t)^2(s-2t)^2+(s-2t)^4]\times$
$\log\ [(d+2t)^2+(s-2t)^2]+2[(d+r+t)^4-6(d+r+t)^2(s-t)^2+(s-t)^4]\times$
$\log\ [(d+r+t)^2+(s-t)^2]-2[(d+r+t)^4-6(d+r+t)^2(s-2t)^2+(s-2t)^4]\times$
$\log\ [(d+r+t)^2+(s-2t)^2]+16rs^3\times$
$\tan^{-1} r/s+16r^3s\ \tan^{-1} s/r+16rt^3\times$
$\tan^{-1} r/t+16r^3t\ \tan^{-1} t/r+$
$16(r-t)t^3\ \tan^{-1}(r-t)/t+16(r-t)^3t\times$
$\tan^{-1} t/(r-t)+16(s-t)t^3\times$
$\tan^{-1}\ (s-t)/t+16(s-t)^3t\times$
$\tan^{-1} t/(s-t)-8ds^3\ \tan^{-1} d/s-$
$8d^3s\ \tan^{-1} s/d-16(d+t)t^3\times$
$\tan^{-1}\ (d+t)/t-16(d+t)^3t\times$
$\tan^{-1} t/(d+t)-16r(s-t)^3\ \tan^{-1} r\div$
$(s-t)-16r^3(s-t)\ \tan^{-1}\ (s-t)/r-$
$16(r-t)(s-t)^3\ \tan^{-1}\ (r-t)/(s-t)-$
$16(r-t)^3(s-t)\ \tan^{-1}\ (s-t)/(r-t)+$
$16(r-t)(s-2t)^3\ \tan^{-1}\ (r-t)\div$
$(s-2t)+16(r-t)^3(s-2t)\times$
$\tan^{-1}\ (s-2t)/r(-t)+16(d+r)s^3\times$
$\tan^{-1}\ \ (d+r)/s+16(d+r)^3s\times$
$\tan^{-1} s/(d+r)-8(d+2r)s^3\times$
$\tan^{-1}\ (d+2r)/s-8(d+2r)^3s\times$
$\tan^{-1} s/(d+2r)+16(d+r)t^3\times$
$\tan^{-1}\ (d+r)/t+16(d+r)^3t\times$
$\tan^{-1} t/(d+r)-16(d+2r)t^3\times$
$\tan^{-1}\ (d+2r)/t-16(d+2r)^3t\times$
$\tan^{-1}\ \ t/(d+2r)+16(d+r+t)t^3\times$
$\tan^{-1}\ (d+r+t)/t+16(d+r+t)^3t\times$
$\tan^{-1}\ t/(d+r+t)-16(d+r)(s-t)^3\times$
$\tan^{-1}\ \ (d+r)/(s-t)-16(d+r)^3\times$
$(s-t)\ \tan^{-1}\ (s-t)/(d+r)+16(d+2r)(s-t)^3\ \tan^{-1}\ (d+2r)/(s-t)+$
$16(d+2r)^3(s-t)\ \tan^{-1}\ (s-t)\div$
$(d+2r)-8(d+2r)(s-2t)^3\times$
$\tan^{-1}(d+2r)/(s-2t)-8(d+2r)^3\times$
$(s-2t)\ \tan^{-1}\ (s-2t)/(d+2r)+$
$16(d+t)(s-t)^3\ \tan^{-1}\ (d+t)/(s-t)+$
$16(d+t)^3(s-t)\ \tan^{-1}\ (s-t)/(d+t)-$
$8(d+2t)(s-2t)^3\ \tan^{-1}\ (d+2t)\div$
$(s-2t)-8(d+2t)^3(s-2t)\times$
$\tan^{-1}\ (s-2t)/(d+2t)-16(d+r+t)\times$
$(s-t)^3\ \tan^{-1}\ (d+r+t)/(s-t)-$
$16(d+r+t)^3(s-t)\ \tan^{-1}\ (s-t)\div$
$(d+r+t)+16(d+r+t)(s-2t)^3\times$
$\tan^{-1}\ (d+r+t)/(s-2t)+$
$16(d+r+t)^3(s-2t)\ \tan^{-1}\ (s-2t)\div$
$(d+r+t)-8t^4(\pi+\log 2)\}$ (10)

Corroboration of Equation 10

In other fashion each of the channels can be considered as comprised of three component conductors, each of rectangular cross section, and all having current in the same direction (Figure 3). Thus $m=n=3$.

By virtue of the geometric symmetries in Figure 3,

$$D_{11}=D_{33}=D_{44}=D_{66};\ D_{22}=D_{55};\ D_{12}=D_{23}=D_{45}=D_{56};\ D_{13}=D_{46};\ D_{16}=D_{34};\ D_{15}=D_{35}=D_{24}=D_{26};\ D_{14}=D_{36}$$

Further,

$$S_1=S_3=S_4=S_6;\ S_2=S_5;$$

$$w_1=w_2=w_3=-w_4=-w_5=-w_6=\frac{I}{A}$$

Figure 2. Cross section of channel bus comprised of four superimposed strap conductors

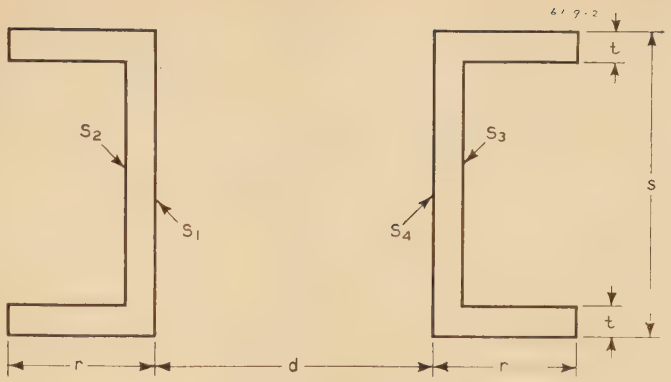

In consequence of these relationships, we have from equation 2

$$L=\left(-\frac{4}{A^2}\right)[2S_1^2\ (\log D_{11}+\log D_{13}-\log D_{14}-\log\ D_{16})+S_2^2\ (\log\ D_{22}-\log\ D_{25})+4S_1S_2\ (\log D_{12}-\log\ D_{15})] \quad (11)$$

Corroboratively, if $S_1=S_3=S_4=S_6=0$ we have rectangular strap conductors of cross section $S_2=S_5$ and equation 11 reduces to the known formula,

$$L=4\ \log\ \frac{D_{25}}{D_{22}}$$

Determining the eight geometric mean distances in the right-hand member of equation 11 by use of equations 3–6—the explicit expressions are to be found in Appendix II—substituting appropriately in equation 11, and rearranging terms we obtain, as is to be expected, equation 10.

Although this verification most certainly ensures that the algebra involved in the derivation of the geometric mean distances given in Appendixes I and II and in the subsequent substitution of these expressions in equations 8 and 11 has been carried through correctly, certain additional checks are made easily.

1. If $r=0$, we have a bus comprised of strap conductors of width t and height s, spaced distance d between adjacent faces. Corroboratively, we obtain from equation 10 the known formula[9,10] for this case.

2. If $d=-r$, the conductor cross sections are located as in Figure 4; over the superimposed areas the current density is uniform and opposite; whence effectively we have the cross section of a bus comprised of strap conductors (cross-hatched) of width t and height $s-2t$, spaced distance $r-2t$ between adjacent faces. Corroboratively, we obtain from equation 10 the known formula[9,10] for this case.

Approximations to the General Formula

The general formula for the inductance comprises 75 terms: of these, 32 are logarithmic, 42 arctangentic, and 1 algebraic. This is a formidable number. But the work incidental to computation of the inductance of a specified bus can be carried through without difficulty provided in calculating one employs proper technique (judicious use of the trigonometric identity, $\tan^{-1} X+\tan^{-1} X^{-1}=\pi/2$; factoring, in so far as is possible, logarithmic arguments into prime numbers; and so forth) and suitable tools (an electric calculating machine; the 15-place Works Projects Administration tables[11] of natural logarithms and arc tangents having 0.0001 and 0.001 increment arguments). Admittedly, the task of computation is lengthy. In a sense, however, this is no drawback if, the final dimensions of the bus having been decided on, it is imperative to determine (as accurately as possible) the inductance for some specified purpose: say, to enable computation of the bus impedance for use in calculating voltage regulation or fault conditions. But in calculations leading to the choice of final bus dimensions, it is obviously desirable to have formulas that will enable rapid determination of the approximate inductances of the several designs under consideration.

A possible means of deriving such formulas is suggested by an earlier investigation of the inductances of busses comprised of hollow rectangular conductors.[12] It was found that for conductor thicknesses used in practice the inductance calculated from the formula taking conductor thickness into account and the inductance calculated from much simpler formulas derived by Dwight and Wang[5] on the basis that the conductor is infinitely thin—that is, that the cross section is comprised of line segments—differed only slightly. Although for reasons discussed in "Remarks on the Approximate Formula" such excellent agreement does not attend a similar treatment of channel conductors, it does afford formulas sufficiently satisfactory for preliminary calculations.

Consider, then, each conductor as com-

prised of three line segments (Figure 5). Thus, $m=n=3$. From the geometric symmetries of Figure 5,

$$D_{11}=D_{33}=D_{44}=D_{66};\ D_{12}=D_{23}=D_{45}=D_{56};\ D_{13}=D_{46};\ D_{14}=D_{36};\ D_{16}=D_{34};\ D_{22}=D_{55}$$

Further,

$$S_1=S_3=S_4=S_6;\ S_2=S_5;\ w_1=w_2=w_3=-w_4=-w_5=-w_6=\frac{I}{(2S_1+S_2)}$$

In virtue of these relationships, we have from equation 2

$$L=\left(\frac{-4}{B^2}\right)[2S_1^2\ (\log D_{11}+\log D_{13}-\log D_{14}-\log D_{16})+S_2^2\ (\log D_{22}-\log D_{25})+4S_1S_2\ (\log D_{12}-\log D_{24})] \quad (12)$$

wherein

$$B=(2S_1+S_2)=2x+y \quad (13)$$

Corroboratively, if $S_1=S_3=S_4=S_6=0$, we have infinitely thin strap conductors of linear cross section $S_2=S_5$, and equation 12 reduces to the known formula,

$$L=4\ \log\frac{D_{25}}{D_{22}}$$

Determining the eight geometric mean distances in the right-hand member of equation 12—the explicit expressions are to be found in Appendix III—and substituting appropriately in equation 12 yield

$$L=[2/(2x+y)^2]\{-4x^2\log x-6y^2\log y+4d^2\log d-4(d+x)^2\log(d+x)+2(x^2+2xy-y^2)\log(x^2+y^2)+2(d+2x)^2\log(d+2x)-4dy\log(d^2+y^2)-2[(d+x)^2-2(d+x)y-y^2]\times\log[(d+x)^2+y^2]+[(d+2x)^2-y^2]\times\log[(d+2x)^2+y^2]+4[x^2-2xy-y^2]\times\tan^{-1}x/y+4(d^2-y^2)\tan^{-1}d/y-4[(d+x)^2+2(d+x)y-y^2]\times\tan^{-1}(d+x)/y+4(d+2x)y\times\tan^{-1}(d+2x)/y+2\pi d(2x+y)\} \quad (14)$$

If $x=0$, we have a bus comprised of infinitely thin strap conductors of height y, spaced distance d. Corroboratively, we obtain from equation 14 the known formula[9,10] for this case. Again, if $d=-x$, the cross sections fall on one another; the superimposed flanges have equal and opposite currents densities; whence effectively we have a bus comprised of infinitely thin strap conductors of height y, spaced distance x. Corroboratively, we obtain from equation 14 the known formula[9,10] for this case.

The advantages of equation 14 over equation 10 in regard to computation are considerable. Whereas the general formula comprises 72 terms, this approximate formula comprises only 14: 9 logarithmic, 4 arctangentic, and 1 algebraic. Again, the coefficients and arguments of these terms are simpler than those of the corresponding terms of equation 10. In consequence, a calculation with this formula, if effected with the tools of computation mentioned above, requires but a short time. Unfortunately, for reasons discussed in "Remarks on the Approximate Formula," this approximate formula is, as mentioned above, not as accurate as that of the corresponding formula for hollow rectangular conductors.

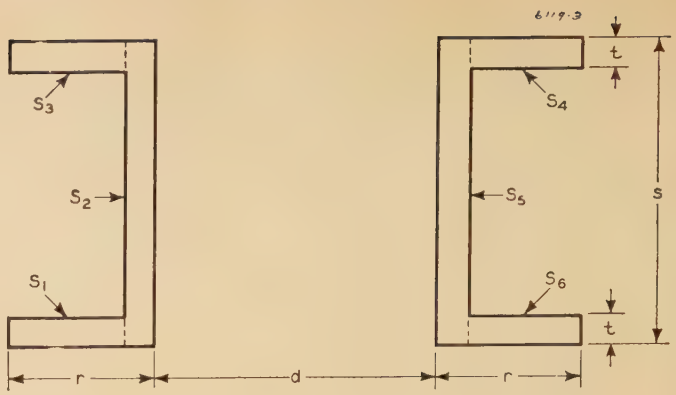

Figure 3. Cross section of channel bus comprised of six strap conductors

By means of the trigonometric identity, $\tan^{-1}X+\tan^{-1}X^{-1}=\pi/2$, the right-hand members of equations 10 and 14 can be expressed in various equivalent forms. However, in that the best use of this identity hinges on the numerical values associated with a given bus design—to avoid tedious interpolation with finite differences or computation with infinite series, this identity should be employed so that the maximum number of arctangent arguments are tabulated in the Works Projects Administration tables—there is little point in writing out any of the multitude of alternative forms.

Inasmuch as the right-hand members of equations 10 and 14 are dimensionless, we note that in substituting in these equations, r, s, t, x, y, and d can be measured in any like unit of length. But otherwise the units of all quantities mentioned to this point are in the absolute system: bus dimensions in centimeters; current I in abamperes; inductance L in abhenries per centimeter of bus length. Multiplying abhenries per centimeter by 3.048×10^{-5} yields millihenries per foot; multiplying by 11.48×10^{-6} yields 60-cycle reactance in ohms per foot.

Some Illustrative Examples

To illustrate use of the general formula and to gain knowledge of the accuracy to be expected of values calculated with the approximate formula, we consider the following problems:

EXAMPLE 1

To calculate the inductance of a bus comprised of (approximately) standard aluminum channels: web, $s=12$ inches; flange width, $r=3$ inches; thickness, $t=0.4$ inch; spaced back to back, $d=6$ inches (Figure 3):

Substituting these values in equation 10, collecting and rearranging numerical terms, obtaining values of the logarithmic and arctangentic terms from the Works Projects Administration tables, and effecting all calculations with an electric calculating machine, we obtain

$$L=2.58567_2 \text{ abhenries per centimeter of bus length} \quad (15)$$

Obviously, as by virtue of the assumptions underlying derivation of the general formula, it is unlikely that L represents the inductance of the hypothetical bus to more than plus or minus several in the second or third decimal place, the last several digits have no physical significance. They are given merely to emphasize that in so far as the numerical computation is concerned, the value of L is correct to this number of places. For all logarithmic and arctangentic terms were taken to nine decimal places; values stemming from consequent arithmetic manipulations were held to six places of decimals. In that the value given in the equation above stems from a final algebraic addition of some two score terms, the largest of which approximates 227,000 and the smallest 0.3, it is essential that some such degree of preciseness be held. In that the resulting value of L is significant to only two or three decimal places, it is not unlikely that study of the number of decimal places to be held in the various stages of computation would reveal that a smaller number than actually used would yet be satisfactory. Inasmuch, however, as 15-place tables were employed and the calculation was per-

formed on a 10-digit electric calculating machine, the added labor is negligible and there is no uncertainty as to the effect of cumulative errors on the accuracy of first few digits of L.

EXAMPLE 2

To calculate the inductance of a bus comprised of channels having "external" dimensions and spacing as in example 1 ($s=12$ inches, $r=3$ inches, $d=6$ inches) but with thickness, $t=0.1$ inch.

Substituting appropriately in equation 10 and effecting computation as previously, we have

$L=2.53_8$ abhenries per centimeter of bus length (16)

Thus, as the thickness is decreased from 0.4 inch to 0.1 inch, the "external" dimensions and spacing of the channels being held constant, the inductance decreases slightly. Accordingly, it is tempting to conjecture that further reduction in thickness from 0.1 inch to indefinitely thin (line-segment) conductors will result in a correspondingly slight decrease in the inductance. That decrease in the thickness of the channels to line-segment

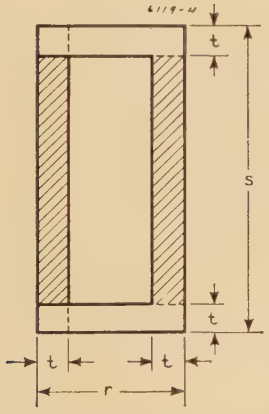

Figure 4. Cross section of rectangular strap bus comprised of two superimposed channels

channels does not result in a corresponding decrease in inductance is evidenced by the following example.

EXAMPLE 3

To calculate the inductance of a bus comprised of line-segment channels having "external" dimensions and spacing as in examples 1 and 2 ($y=12$ inches, $x=3$ inches, $d=6$ inches):

Substituting appropriately in equation 14 and effecting computation as before yield

$L_e=3.51_7$ abhenries per centimer of bus length (17)

Figure 5. Cross section of bus comprised of six infinitely-thin strap conductors

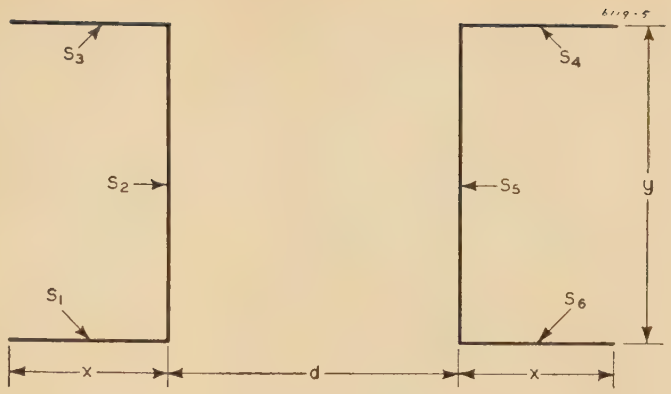

This value is considerably larger than that of equation 16.

Remarks on the Approximate Formula

Noting that the inductance of the line-segment bus is considerably larger than that of the original bus of example 1 gives rise to a question regarding the best use of the approximate formula to calculate the inductance of busses of finite thickness such as actually occur in practice. Thus, the "external" dimensions and spacing of the bus of example 1 are used in example 3. But if the "mean" or the "internal" dimensions and spacing were to be used, would not the resulting values of inductance be closer to those of example 1? To settle this point we calculate the inductances indicated.

EXAMPLE 4

To calculate the inductance of line-segment busses having (1) the "mean" and (2) the "internal" dimensions and spacing of example 1:

1. $x=2.8$ inches; $y=11.6$ inches; $d=6.4$ inches
2. $x=2.6$ inches; $y=11.2$ inches; $d=6.8$ inches

Substituting appropriately in equation 14 and effecting computation as before yield

$L=3.97_7$ abhenries per centimeter of bus length (18)

$L_i^m=4.38_7$ abhenries per centimeter of bus length (19)

We find, therefore, that the best approximation to the inductance of the bus of example 1 stems from use of the "external" dimensions and spacing.

From analysis of these four examples we conclude:

1. If the inductance of a bus is to be approximated by use of equation 14, the best result will stem from use of the "external" dimensions and spacing as in example 3.
2. Comparatively large changes in the thickness of the channels apparently result in slight changes in the inductance.
3. Though the approximate value will be somewhat larger than the actual inductance, it is yet of use in actual design.

For example, in the course of determining the best dimensions of a bus it is often necessary to determine whether or not the inductance of a number of proposed designs exceeds a certain allowed maximum—say that which specifies the maximum allowable voltage drop for a given load current. If of one or more of these designs it is found that the inductance calculated from the approximate equation is less than the allowed maximum, the exact value is even more so: whence the lengthy exact computation need not be undertaken.

Again, in much design work only an approximate knowledge of the inductance is needed; whence a value 20 or 30 per cent larger than the actual value is yet sufficiently accurate.

Appendix I

The geometric mean distances indicated in equation 8 follow from equation 3 by substitution therein of the following values of the parameters A_p, B_p, these being obtained by inspection of Figure 2.

$S_1^2 \log D_{11}$: $A_1=A_3=r$, $A_2=A_4=0$; $B_1=B_3=s$, $B_2=B_4=0$

$S_1^2 \log D_{14}$: $A_1=d+2r$, $A_2=A_4=d+r$, $A_3=d$; $B_1=B_3=s$, $B_2=B_4=0$

$S_2^2 \log D_{22}$: $A_1=A_3=r-t$, $A_2=A_4=0$; $B_1=B_3=s-2t$, $B_2=B_4=0$

$S_2^2 \log D_{23}$: $A_1=d+2r$, $A_2=A_4=d+r+t$, $A_3=d+2t$; $B_1=B_3=s-2t$, $B_2=B_4=0$

$S_1S_2 \log D_{12}$: $A_1=r-t$, $A_2=t$, $A_3=r$, $A_4=0$; $B_1=B_3=s-t$, $B_2=B_4=t$

$S_1S_2 \log D_{13}$: $A_1=d+2r$, $A_2=d+r$, $A_3=d+t$, $A_4=d+r+t$; $B_1=B_3=s-t$, $B_2=B_4=t$

Substituting these parameters in equation 3 yields:

$$S_1^2 \log D_{11} = -(25/12)S_1^2+(1/24)[4r^4\times \log r+4s^4 \log s-2(r^4-6r^2s^2+s^4)\times \log (r^2+s^2)+16rs^3 \tan^{-1} r/s+ 16r^3s \tan^{-1} s/r]$$

$$S_1^2 \log D_{14} = -(25/12)S_1^2+(1/24)\times \{2d^4 \log d-4(d+r)^4\times \log (d+r)+2(d+2r)^4\times \log (d+2r)-(d^4-6d^2s^2+s^4)\times \log (d^2+s^2)+2[(d+r)^4-6(d+r)^2s^2+ s^4] \log [(d+r)^2+s^2]-[(d+2r)^4- 6(d+2r)^2s^2+s^4] \log [(d+2r)^2+s^2]+ 8ds^3 \tan^{-1} d/s+8d^3s \tan^{-1} s/d- 16(d+r)s^3 \tan^{-1} (d+r)/s-16(d+ r)^3s \tan^{-1} s/(d+r)+8(d+2r)s^3\times \tan^{-1} (d+2r)/s+8(d+2r)^3s\times \tan^{-1} s/(d+2r)\}$$

$$S_2^2 \log D_{22} = -(25/12)S_2^2+(1/24)\{4(r-t)^4\times \log (r-t)+4(s-2t)^4 \log (s-2t)- 2[(r-t)^4-6(r-t)^2(s-2t)^2+ (s-2t^4] \log [(r-t)^2+(s-2t)^2]+ 16(r-t)(s-2t)^3\tan^{-1}(r-t)/(s-2t)+ 16(r-t)^3(s-2t)\times \tan^{-1} (s-2t)/(r-t)\}$$

$$S_2^2 \log D_{25} = -(25/12)S_2^2+(1/24)\{2(d+ 2r)^4 \log (d+2r)+2(d+2t)^4 \log (d+ 2t)-4(d+r+t)^4 \log (d+r+t)- [(d+2r)^4-6(d+2r)^2(s-2t)^2+ (s-t)^4] \log [(d+2r)^2+(s-2t)^2]- [(d+2t)^4-6(d+2t)^2(s-2t)^2+(s- 2t)^4] \log [(d+2t)^2+(s-2t)^2]+ 2[(d+r+t)^4-6(d+r+t)^2(s-2t)^2+ (s-2t)^4] \log [(d+r+t)^2+(s-2t)^2]+ 8(d+2r)(s-2t)^3\times \tan^{-1} (d+2r)\div (s-2t)+8(d+2r)^3(s-2t) \tan^{-1} (s- 2t)/(d+2r)+8(d+2t)(s-2t)^3\times \tan^{-1} (d+2t)/(s-2t)+8(d+2t)^3\times (s-2t)\times \tan^{-1} (s-2t)/(d+2t)- 16(d+r+t)(s-2t)^3\tan^{-1}(d+r+t)\div (s-2t)-16(d+r+t)^3(s-2t)\times \tan^{-1} (s-2t)/(d+r+t)\}$$

$$S_1S_2 \log D_{12} = -(25/12)S_1S_2+(1/24)\times \{4t^4(\pi+ \log 2)+6t^4 \log t+2(s-t)^4\times \log (s-t)+(r^4-6r^2t^2+t^4)\times \log (r^2+t^2)-[r^4-6r^2(s-t)^2+ (s-t)^4] \log [r^2+(s-t)^2]+ [(r-t)^4-6(r-t)^2t^2+t^4]\times \log [(r-t)^2+t^2]+[(s-t)^4- 6(s-t)^2t^2+t^4] \log [(s-t)^2+t^2]- [(r-t)^4-6(r-t)^2(s-t)^2+(s-t)^4]\times \log [(r-t)^2+(s-t)^2]-8rt^3\times \tan^{-1} r/t-8r^3t \tan^{-1} t/r-8(r-t)t^3\times \tan^{-1} (r-t)/t-8(r-t)^3t \tan^{-1} t\div (r-t)-8(s-t)^3t \tan^{-1} t/(s-t)- 8(s-t)t^3 \tan^{-1} (s-t)/t+8r(s-t)^3\times \tan^{-1} r/(s-t)+8r^3(s-t) \tan^{-1} (s- t)/r+8(r-t)(s-t)^3 \tan^{-1} (r-t)\div (s-t)+8(r-t)^3(s-t) \tan^{-1} (s-t)\div (r-t)\}$$

$$S_1S_2 \log D_{13} = -(25/12)S_1S_2+(1/24)\times \{[(d+t)^4-6(d+t)^2t^2+t^4] \log [(d+ t)^2+t^2]-[(d+r)^4-6(d+r)^2t^2+t^4]\times \log [(d+r)^2+t^2]+[(d+2r)^4-6(d+ 2r)^2t^2+t^4] \log [(d+2r)^2+t^2]- [(d+r+t)^4-6(d+r+t)^2t^2+t^4]\times \log [(d+r+t)^2+t^2]-[(d+t)^4- 6(d+t)^2(s-t)^2+(s-t)^4] \log [(d+t)^2+ (s-t)^2]+[(d+r)^4-6(d+r)^2\times (s-t)^2+(s-t)^4] \log [(d+r)^2+ (s-t)^2]-[(d+2r)^4-6(d+2r)\times (s-t)^2+(s-t)^4] \log [(d+2r)^2+ (s-t)^2]+[(d+r+t)^4-6(d+r+t)^2\times (s-t)^2+(s-t)^4] \log [(d+r+t)^2+ (s-t)^2]-8(d+t)t^3 \tan^{-1} (d+t)/t- 8(d+t)^3t \tan^{-1} t/(d+t)+8(d+r)t^3\times \tan^{-1}(d+r)/t+8(d+r)^3t \tan^{-1} t\div (d+r)-8(d+2r)t^3 \tan^{-1} (d+2r)/t- 8(d+2r)^3t \tan^{-1} t/(d+2r)+ 8(d+r+t)t^3 \tan^{-1} (d+r+t)/t+ 8(d+r+t)^3t \tan^{-1} t/(d+r+t)+ 8(d+t)(s-t)^3 \tan^{-1} (d+t)/(s-t)+ 8(d+t)^3(s-t) \tan^{-1} (s-t)/(d+t)- 8(d+r)(s-t)^3 \tan^{-1} (d+r)/(s-t)- 8(d+r)^3(s-t) \tan^{-1} (s-t)/(d+r)+ 8(d+2r)(s-t)^3\tan^{-1}(d+2r)/(s-t)+ 8(d+2r)^3(s-t)\tan^{-1}(s-t)/(d+2r)- 8(d+r+t)(s-t)^3 \tan^{-1} (d+r+t)\div (s-t)-8(d+r+t)^3(s-t)\times \tan^{-1} (s-t)/(d+r+t)\}$$

Appendix II

The geometric mean distances indicated in equation 11 follow from equation 3 by substitution therein of the following values of the parameters A_p, B_q, these being obtained by inspection of Figure 3.

$S_1^2 \log D_{11}$: $A_1=A_3=r-t$, $A_2=A_4=0$; $B_1=B_3=t$, $B_2=B_4=0$

$S_1^2 \log D_{13}$: $A_1=A_3=r-t$, $A_2=A_4=0$; $B_1=s$, $B_2=B_4=s-t$, $B_3=s-2t$

$S_1^2 \log D_{14}$: $A_1=d+2r$, $A_2=A_4=d+r+t$, $A_3=d+2t$; $B_1=s$, $B_2=B_4=s-t$, $B_3=s-2t$

$S_1^2 \log D_{16}$: $A_1=d+2r$, $A_2=A_4=d+r+t$, $A_3=d+2t$; $B_1=B_3=t$, $B_2=B_4=0$

$S_2^2 \log D_{22}$: $A_1=A_3=t$, $A_2=A_4=0$; $B_1=B_3=s$, $B_2=B_4=0$

$S_2^2 \log D_{25}$: $A_1=d+2t$, $A_2=A_4=d+t$, $A_3=d$; $B_1=B_3=s$, $B_2=B_4=0$

$S_1S_2 \log D_{12}$: $A_1=r$, $A_2=t$, $A_3=0$, $A_4=r-t$; $B_1=s$, $B_2=s-t$, $B_3=t$, $B_4=0$

$S_1S_2 \log D_{15}$: $A_1=d+r+t$, $A_2=d+r$, $A_3=d+t$, $A_4=d+2t$; $B_1=s$, $B_2=s-t$, $B_3=t$, $B_4=0$

Substituting these parameters in equation 3 yields

$$S_1^2 \log D_{11} = -(25/12)S_1^2+(1/24)\{4t^4\times \log t+4(r-t)^4 \log (r-t)-2[(r-t)^4- 6(r-t)^2t^2+t^4] \log [(r-t)^2+t^2]+ 16(r-t)t^3 \tan^{-1} (r-t)/t+16(r- t)^3t^3 \tan^{-1} t/(r-t)\}$$

$$S_1^2 \log D_{13} = -(25/12)S_1^2+(1/24)\{2s^4\times \log s-4(s-t)^4 \log (s-t)+2(s-2t)^4\times \log (s-2t)-[(r-t)^4-6(r-t)^2x^2+ s^4] \log [(r-t)^2+s^2]+2[(r-t)^4- 6(r-t)^2(s-t)^2+(s-t)^4] \log [(r-t)^2+ (s-t)^2]-[(r-t)^4-6(r-t)^2(s-2t)^2+ (s-2t)^4] \log [(r-t)^2+(s-2t)^2]+ 8(r-t)s^3 \tan^{-1} (r-t)/s+8(r-t)^3s\times \tan^{-1} s/(r-t)-16(r-t)(s-t)^3\times \tan^{-1} (r-t)/(s-t)-16(r-t)^3\times (s-t) \tan^{-1} (s-t)/(r-t)+ 8(r-t)(s-2t)^3 \tan^{-1} (r-t)/(s-2t)+ 8(r-t)^3(s-2t) \tan^{-1} (s-2t)/(r-t)\}$$

$$S_1^2 \log D_{14} = -(25/12)S_1^2-(1/24)\{[(d+ 2r)^4-6(d+2r)^2s^2+s^4] \log [(d+2r)^2+ s^2]^{1/2}-[(d+2r)^4-6(d+2r)^2(s-t)^2+ (s-t)^4] \log [(d+2r)^2+(s-t)^2]+ [(d+2r)^4-6(d+2r)^2(s-2t)^2+ (s-2t)^4] \log [(d+2r)^2+(s-2t)^2]^{1/2}+ [(d+2t)^4-6(d+2t)^2s^2+s^4]\times \log [(d+2t)^2+s^2]^{1/2}-[(d+2t)^4- 6(d+2t)^2(s-t)^2+(s-t)^4]\times \log [(d+2t)^2+(s-t)^2]+[(d+2t)^4- 6(d+2t)^2(s-2t)^2+(s-2t)^4]\times \log [(d+2t)^2+(s-2t)^2]-[(d+t)^4- 6(d+t)^2(s-t)^2+(s-t)^4]\times \log [(d+t)^2+(s-t)^2]+[(d+t)^4- 6(d+t)^2(s-2t)^2+(s-2t)^4]\times \log [(d+t)^2+(s-2t)^2]-[(d+r+t)^4- 6(d+r+t)^2(s-t)^2+(s-t)^4]\times \log [(d+r+t)^2+(s-t)^2]+[(d+r+ t)^4-6(d+r+t)^2(s-2t)^2+(s-2t)^4]\times \log [(d+r+t)^2+(s-2t)^2]-4(d+ 2r)s^3 \tan^{-1} (d+2r)/s-4(d+2r)^3s\times \tan^{-1} s/(d+2r)+8(d+2r)(s-t)^3\times \tan^{-1} (d+2r)/(s-t)+8(d+2r)^3\times (s-t) \tan^{-1} (s-t)/(d+2r)-4(d+ 2r)(s-2t)^3 \tan^{-1} (d+2r)/(s-2t)- 4(d+2r)^3(s-2t) \tan^{-1} (s-2t)/(d+ 2r)-4(d+2t)s^3 \tan^{-1} (d+2t)/s- 4(d+2t)^3s \tan^{-1} s/(d+2t)+ 8(d+2t)(s-t)^3 \tan^{-1} (d+2t)/(s-t)+ 8(d+2t)^3(s-t) \tan^{-1} (s-t)/(d+2t)- 4(d+2t)(s-2t)^3 \tan^{-1} (d+2t)\div (s-2t)-4(d+2t)^3(s-2t)\times \tan^{-1} (s-2t)/(d+2t)+ 8(d+r+t)s^3 \tan^{-1} (d+r+t)/s+ 8(d+r+t)^3s \tan^{-1} s/(d+r+t)- 16(d+r+t)(s-t)^3 \tan^{-1} (d+r+t)\div (s-t)-16(d+r+t)^3(s-t)\times \tan^{-1} (s-t)/(d+r+t)+8(d+r+t)^3\times (s-2t)^3 \tan^{-1} (s-2t)/(d+r+t)+ 8(d+r+t)^3(s-2t) \tan^{-1} (s-2t)\div (d+r+t)\}$$

$$S_1^2 \log D_{16} = -(25/12)S_1^2+(1/24)\times \{2(d+2r)^4 \log (d+2r)+2(d+2t)^4\times \log (d+2t)-4(d+r+t)^4\times \log (d+r+t)-[(d+2r)^4- 6(d+2r)^2t^2+t^4] \log [(d+2r)^2+t^2]- [(d+2t)^4-6(d+2t)^2t^2+t^4]\times \log [(d+2r)^2+t^2]+2[(d+r+t)^4- 6(d+r+t)^2t^2+t^4\times \log [(d+r+t)^2+t^2]+8(d+2r)t^3\times \tan^{-1} (d+2r)/t+8(d+2r)^3t\times \tan^{-1} t/(d+2r)+8(d+2t)t^3\times \tan^{-1} (d+2t)/t+8(d+2t)^3t\times \tan^{-1} t/(d+2t)-16(d+r+t)t^3\times \tan^{-1} (d+r+t)/t-16(d+r+t)^3t\times \tan^{-1} t/(d+r+t)\}$$

$$S_2^2 \log D_{22} = -(25/12)S_2^2+(1/24)\{4s^4\times \log s+4t^4 \log t-2(s^4-6s^2t^2+t^4)\times \log (s^2+t^2)+16st^3 \tan^{-1} s/t+ 16ts^3 \tan^{-1} t/s\}$$

$$S_2^2 \log D_{25} = -(25/12)S_2^2+(1/24)\{2d^4\times \log d-4(d+t)^4 \log (d+t)+2(d+ 2t)^4 \log (d+2t)-(d^4-d^2s^2+s^4)\times \log (d^2+s^2)+2[(d+t)^4-6(d+t)^2s^2+ s^4] \log [(d+t)^2+s^2]-[(d+2t)^4- 6(d+2t)^2s^2+s^2] \log [(d+2t)^2+s^2]+ 8ds^3 \tan^{-1} d/s+8d^3s \tan^{-1} s/d- 16(d+t)s^3 \tan^{-1} (d+t)/s-16(d+ t)^3s \tan^{-1} s/(d+t)+8(d+2t)s^3\times \tan^{-1} (d+2t)/s+8(d+2t)^3s\times \tan^{-1} s/(d+2t)\}$$

$$S_1S_2 \log D_{12} = -(25/12)S_1S_2+(1/24)\times \{2t^4(\pi+ \log 2)+r^4 \log r-s^4 \log s+ 2t^4 \log t-(r-t)^4 \log (r-t)+(s-t)^4\times \log (s-t)-(r^4-6r^2s^2+s^4)\times \log (r^2+s^2)^{1/2}-(r^4-6r^2t^2+t^4)\times \log (r^2+t^2)^{1/2}+(s^4-6s^2t^2+t^4)\times \log (s^2+t^2)^{1/2}+ [(r-t)^4-6(r-t)^2s^2+s^4]\times \log [(r-t)^2+s^2]^{1/2}+ [(r-t)^4-6(r-t)^2t^2+t^4]\times \log [(r-t)^2+t^2]^{1/2}-[(s-t)^4-$$

$$6(s-t)^2t^2+t^4]\log[(s-t)^2+t^2]^{1/2}+$$
$$[r^4-6r^2(s-t)^2+(s-t)^4]\times$$
$$\log[r^2+(s-t)^2]^{1/2}-[(r-t)^4-$$
$$6(r-t)^2(s-t)^2+(s-t)^4]\times$$
$$\log[(r-t)^2+(s-t)^2]^{1/2}+$$
$$4rs^3\tan^{-1}r/s+4r^3s\tan^{-1}s/r+$$
$$4rt^3\tan^{-1}r/t+4r^3t\tan^{-1}t/r-$$
$$4st^3\tan^{-1}s/t-4s^3t\tan^{-1}t/s-$$
$$4(r-t)s^3\tan^{-1}(r-t)/s-4(r-t)^3s\times$$
$$\tan^{-1}s/(r-t)-4(r-t)t^3\times$$
$$\tan^{-1}(r-t)/t-4(r-t)^3t\times$$
$$\tan^{-1}t/(r-t)+4(s-t)t^3\times$$
$$\tan^{-1}(s-t)/t+4(s-t)^3t\times$$
$$\tan^{-1}t/(s-t)-4r(s-t)^3\times$$
$$\tan^{-1}r/(s-t)-4r^3(s-t)\times$$
$$\tan^{-1}(s-t)/r+4(r-t)(s-t)^3\times$$
$$\tan^{-1}(r-t)/(s-t)+4(r-t)^3\times$$
$$(s-t)\tan^{-1}(s-t)/(r-t)\}$$

$$S_1S_2\log D_{15}=-(25/12)S_1S_2-(1/24)\times$$
$$\{(d+r)^4\log(d+r)-(d+t)^4\times$$
$$\log(d+t)+(d+2t)^4\log(d+2t)-$$
$$(d+t+r)^4\log(d+t+r)-$$
$$[(d+r)^4-6(d+r)^2s^2+s^4]\times$$
$$\log[(d+r)^2+s^2]^{1/2}-[(d+r)^4-$$
$$6(d+r)^2t^2+t^4]\log[(d+r)^2+t^2]^{1/2}+$$
$$[(d+t)^4-6(d+t)^2t^2+t^4]\times$$
$$\log[(d+t)^2+t^2]^{1/2}-[(d+2t)^4-$$
$$6(d+2t)^2t^2+t^4]\log[(d+2t)^2+t^2]^{1/2}+$$
$$[(d+t)^4-6(d+t)^2s^2+s^4]\times$$
$$\log[(d+t)^2+s^2]^{1/2}-[(d+2t)^4-$$
$$6(d+2t)^2s^2+s^4]\log[(d+2t)^2+s^2]^{1/2}+$$
$$[(d+r)^4-6(d+r)^2(s-t)^2+(s-t)^4]\times$$
$$\log[(d+r)^2+(s-t)^2]^{1/2}-[(d+t)^4-$$
$$6(d+t)^2(s-t)^2+(s-t)^4]\times$$
$$\log[(d+t)^2+(s-t)^2]^{1/2}+[(d+2t)^4-$$
$$6(d+2t)^2(s-t)^2+(s-t)^4]\times$$
$$\log[(d+2t)^2+(s-t)^2]^{1/2}+$$
$$[(d+r+t)^4-6(d+r+t)^2t^2+t^4]\times$$
$$\log[(d+r+t)^2+t^2]^{1/2}+[(d+r+t)^4-$$
$$6(d+r+t)^2s^2+s^4]\log[(d+r+t)^2+$$
$$s^2]^{1/2}-[(d+r+t)^4-6(d+r+t)^2$$
$$(s-t)^2+(s-t)^4]\times\log[(d+$$
$$r+t)^2+(s-t)^2]^{1/2}+4(d+r)s^3$$
$$\tan^{-1}(d+r)/s+4(d+r)^3s\times$$
$$\tan^{-1}s/(d+r)+4(d+r)t^3\times$$
$$\tan^{-1}(d+r)/t+4(d+r)^3t\times$$
$$\tan^{-1}t/(d+r)-4(d+t)t^3\times$$
$$\tan^{-1}(d+t)/t-4(d+t)^3t\times$$
$$\tan^{-1}t/(d+t)+4(d+2t)t^3\times$$
$$\tan^{-1}(d+2t)/t+4(d+2t)^3t\times$$
$$\tan^{-1}t/(d+2t)-4(d+t)s^3\times$$
$$\tan^{-1}(d+t)/s-4(d+t)^3s\times$$
$$\tan^{-1}s/(d+t)+4(d+2t)s^3\times$$
$$\tan^{-1}(d+2t)/s-4(d+r)(s-t)^3\times$$
$$\tan^{-1}(d+r)/(s-t)-4(d+r)^3\times$$
$$(s-t)\tan^{-1}(s-t)/(d+r)+4(d+t)\times$$
$$(s-t)^3\tan^{-1}(d+t)/(s-t)+$$
$$4(d+t)^3(s-t)\tan^{-1}(s-t)\div$$
$$(d+t)+4(d+2t)^3s\tan^{-1}s/(d+2t)-$$
$$4(d+2t)(s-t)^3\tan^{-1}(d+2t)\div$$
$$(s-t)-4(d+2t)^3(s-t)\times$$
$$\tan^{-1}(s-t)/(d+2t)-4(d+r+t)t^3\times$$
$$\tan^{-1}(d+r+t)/t-4(d+r+t)^3t\times$$
$$\tan^{-1}t/(d+r+t)-4(d+r+t)s^3\times$$
$$\tan^{-1}(d+r+t)/s-4(d+r+t)^3s\times$$
$$\tan^{-1}s/(d+r+t)+4(d+r+t)\times$$
$$(s-t)^3\tan^{-1}(d+r+t)/(s-t)+$$
$$4(d+r+t)^3(s-t)\tan^{-1}(s-t)\div$$
$$(d+r+t)\}$$

Appendix III

The geometric mean distances indicated in equation 12 are given by equations 11 and 13 of reference 7. Appropriate substitution therein yields

$$S_1^2\log D_{11}=x^2(\log x-3/2)$$

$$S_1^2\log D_{13}=(x^2-y^2)\log(x^2+y^2)^{1/2}+y^2\times$$
$$\log y+2xy\tan^{-1}x/y-3x^2/2$$

$$S_1^2\log D_{14}=1/2[(d+2x)^2-y^2]\log[(d+2x)^2+$$
$$y^2]^{1/2}-[(d+x)^2-y^2]\log[(d+x)^2+$$
$$y^2]^{1/2}+[(d^2-y^2)/2]\log(d^2+y^2)^{1/2}+$$
$$(d+2x)y\tan^{-1}(d+2x)/y-$$
$$2(d+x)y\tan^{-1}(d+x)/y+dy\times$$
$$\tan^{-1}d/y-3x^2/2.$$

$$S_1^2\log D_{16}=1/2\{(d+2x)^2\log(d+2x)-$$
$$2(d+x)^2\log(d+x)+d^2\log d-3x^2\}$$

$$S_2^2\log D_{22}=y^2(\log y-3/2)$$

$$S_2^2\log D_{25}=(y^2-d^2)\log(d^2+y^2)^{1/2}+d^2\times$$
$$\log d+2dy\tan^{-1}y/d-3y^2/2$$

$$S_1S_2\log D_{12}=1/2\{xy\log(x^2+y^2)+x^2\times$$
$$\tan^{-1}y/x+y^2\tan^{-1}x/y-3xy\}$$

$$S_1S_2\log D_{24}=1/2\{(d+x)y\log[(d+x)^2+$$
$$y^2]-dy\log(d^2+y^2)+(d+x)^2\times$$
$$\tan^{-1}y/(d+x)+y^2\tan^{-1}(d+x)/y-$$
$$d^2\tan^{-1}y/d-y^2\tan^{-1}d/y-3xy\}$$

References

1. The Transmission of Alternating-Current Power With Small Eddy-Current Losses, **A. H. M. Arnold.** *Journal*, Institution of Electrical Engineers (London, England), volume 80, 1937, pages 395-400.

2. The Design of Busbar Industrial Distribution Systems: an Epitomization of Available Data, **T. J. Higgins.** AIEE Transactions, volume 64, 1945, pages 385–400; discussion, pages 486–8.

3. Formulas for Calculating Short-Circuit Forces Between Conductors of Structural Shape, **T. J. Higgins.** AIEE Transactions, volume 62, 1943, October section, pages 659–63.

4. Formulas for Calculating Short-Circuit Forces Between Channels Located Back to Back, **T. J. Higgins.** AIEE Transactions, volume 63, 1944, October section, pages 710–12.

5. Reactance of Square Tubular Bus Bars, **H. B. Dwight, T. K. Wang.** AIEE Transactions, volume 57, 1938, pages 762–5; discussion, pages 765–6.

6. The Inductance of Linear Conductors of Rectangular Section, **A. H. M. Arnold.** *Journal*, Institution of Electrical Engineers (London, England), volume 70, 1931–1932, pages 579–86.

7. Formulas for the Geometric Mean Distances of Rectangular Areas and of Line Segments, **T. J. Higgins.** *Journal of Applied Physics*, volume 14, 1943, pages 188–95.

8. Formulas for the Calculation of the Inductance of Linear Conductors of Structural Shape, **T. J. Higgins.** AIEE Transactions, volume 62, 1943, pages 53–8.

9. Reactance of Strap Conductors, **H. B. Dwight.** *Electric Review*, volume 70, 1917, pages 1087–8.

10. Reactance Values for Rectangular Conductors, **H. B. Dwight.** *Electric Journal*, volume 16, 1919, pages 255–6.

11. Tables of Natural Logarithms; Tables of Arctangents (book), Works Projects Administration. Columbia University Press, New York, N. Y.

12. Formulas for the Inductance of Rectangular Tubular Conductors, **T. J. Higgins.** AIEE Transactions, volume 60, 1941, December section, pages 1046–50.

Improvements in Performance of Hydroelectric Generating Units on the 2,000,000-Horsepower Saguenay System

F. L. LAWTON
MEMBER AIEE

THE large number of similar high-capacity hydroelectric generating units in the power plants of the Saguenay system have afforded an unusual opportunity to effect improvements in efficiency, reliability, and output of such units. Well organized operating records, thorough engineering studies and experimentation, and farsighted management all have contributed to this result.

Following a brief review of the major features of the Saguenay system, criteria affecting rate of wastage of water-wheel-runner metal by pitting, and costs of repairs are discussed. The advantages of operating water wheels at best gate, and means of accomplishing this by gate position indicators, are noted. Increases in water-wheel efficiency and capacity effected through model and prototype tests are set forth. Methods employed to ensure maximum energy generation from available storage water are described. The effect of dirt on generator stator-winding temperature rise is investigated. Improved generator performance arising from better application of stator-winding insulation, superior stranding, transposition of stator coils, use of high-silicon stator iron, and better ventilating systems, is discussed at some length.

The Saguenay System

The Saguenay system, a 60-cycle system based on the Isle Maligne and Shipshaw hydroelectric developments, has been built to a capacity of 2,000,000 horsepower during the last quarter century. The Isle Maligne plant, when placed in service, was possibly the largest water-power development completed in one step. Isle Maligne has an installed capacity of 540,000 horsepower, and Shipshaw 1 (Chute-a-Caron), 300,000 horsepower. Shipshaw 2 plant has a capacity of 1,200,000 horsepower.

The Saguenay system is located in the valley of the Saguenay River and the broad basin of Lake St. John lies at its head. The watershed tributary to the Saguenay (Figure 1) is about 30,000 square miles in extent, and is richly endowed with water-power resources. Useful storage in Lake St. John and two other storage reservoirs, one completely artificial, now totals 400 billion cubic feet.

Early power developments in the area were located on the smaller and more easily harnessed tributaries of Lake St. John and the Saguenay River, rather than on the Saguenay itself. These plants were built principally to supply mills of the pulp and paper industry. There were 13 scattered plants with a total capacity of some 67,000 horsepower by 1925 when Isle Maligne was placed in service. It contains 12 45,000-horsepower units.

The transmission network of the Saguenay system came into being as the aluminum, pulp, and paper industries were attracted to the area by the presence of cheap power and raw materials, with the construction of the Isle Maligne development. It was expanded with the addition of Shipshaw 1 in 1931 and brought to its present stage, as shown by Figure 2, with the completion of Shipshaw 2 in 1943.

Although the complete Shipshaw power development had been planned when the river closure and spillways associated with Shipshaw 1 station were started, the depression of the '30s precluded construction, so it was not until the ever increasing need of aluminum for military aircraft had exhausted all quickly available power resources in Canada and the United States that actual construction of Shipshaw 2 was put in hand. The first unit was placed in service November 23, 1942, just 18 months and 8 days after the start of construction. Additional units were put into operation at a steady rate until December 24, 1943, when the twelfth and last unit went into service. Shipshaw 2 is one of the greatest single hydroelectric powerhouse in the world, capable of generating 1,200,000 horsepower at maximum capacity.

The addition of Shipshaw 2 to the Saguenay system necessitated careful planning to limit fault currents to values interruptible by available circuit breakers having a capacity of 2,500,000 kva at seven to eight cycles interrupting time. A high degree of reliability was required on account of the large d-c aluminum reduction load of 890,000 kw, and the necessity of maintaining synchronism with other power systems hundreds of miles away for power exchange for seasonal and daily load-factor equalization. A flexible system was also an imperative requirement to facilitate obtaining optimum efficiency in conversion of storage water during the winter period of low river flow.

A ring bus at generator voltage at Isle Maligne and a unit system at each Shipshaw plant, whereby one generator feeds a 154-kv transmission circuit with step-up and step-down transformers, directly supplying a block of the aluminum plant load substantially equal to its capacity, and with the surplus or deficiency handled over the 154-kv busses, provides reliability and flexibility. It also permits economy in usage of storage water. Fault currents are limited by splitting the 154-kv system into three subsystems which which can be paralleled through three 90,000-kva transformer banks onto a 13.2-kv bus at Arvida substation, or through three 56,250-kva transformer banks onto a 13.2-kv bus at Shipshaw 1.

Saguenay System Loads

Loads on the Saguenay system are almost entirely industrial, concentrated in large blocks, with very high daily load factors. Yearly system load factor was 74.7 per cent in 1939 and 78.8 per cent in 1945.

The aluminum industry's load in the Saguenay area reached 890,000 kw during the war, of which about 745,000 kw was converted to direct current by mercury-type rectifiers, most ignitrons, and an additional 88,000 kw was converted by synchronous converters. Local paper mills required 100,000 kw. At times, 285,000 kw have been delivered to and 204,000 kw received from a double-circuit line connecting the Saguenay system with the Shawinigan Water and Power Company's system in the St. Maurice Valley, 200 miles away.

During periods of high and normal flow in the Saguenay, and when aluminum production is below normal, secondary power is available for the generation of steam. Electric steam generators on the system

Paper 46-144, recommended by the AIEE committee on power generation for presentation at the AIEE summer convention, Detroit, Mich., June 24–28, 1946. Manuscript submitted April 1, 1946; made available for printing May 15, 1946.

F. L. LAWTON is with the Aluminum Company of Canada, Ltd., Montreal, Quebec, Canada.

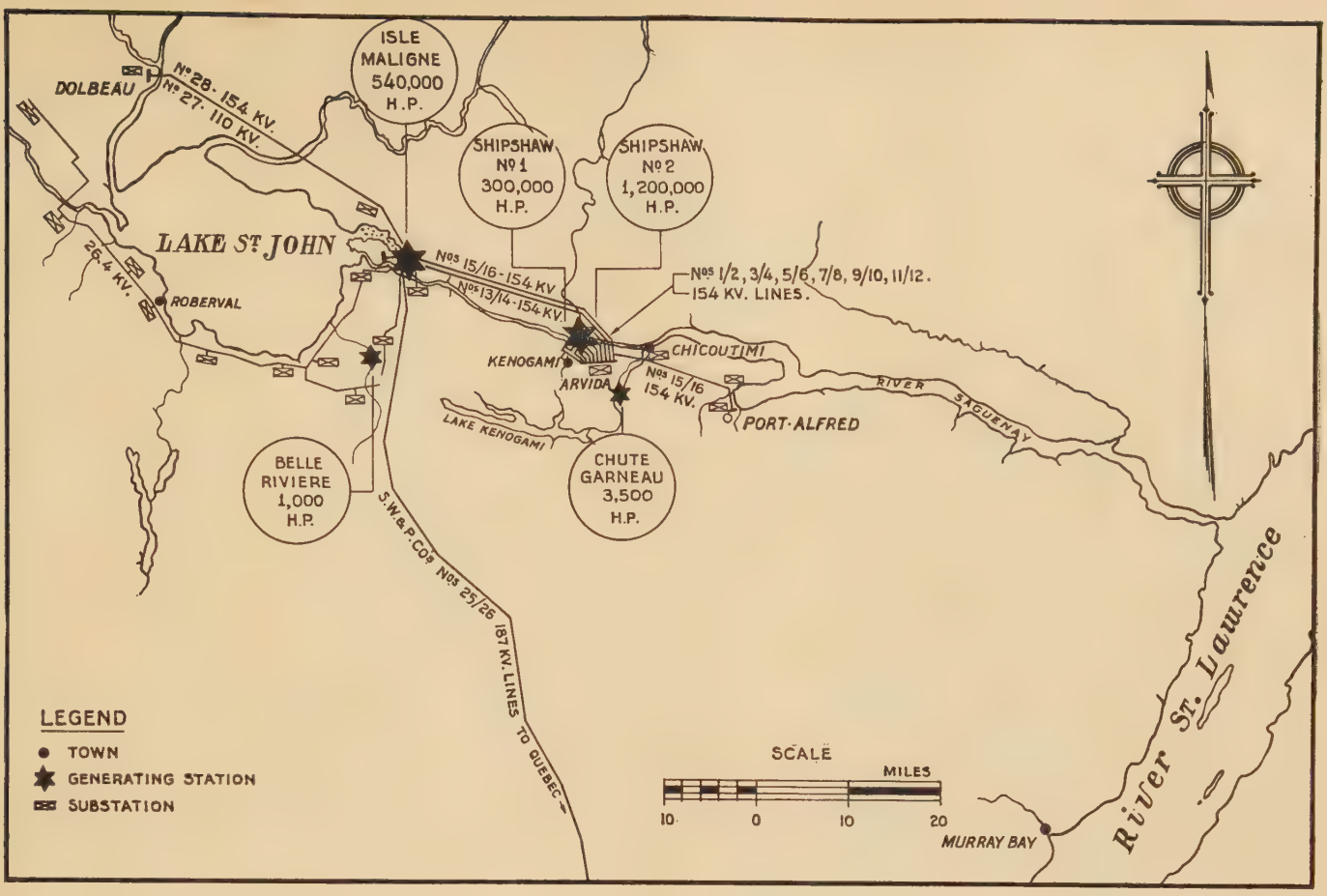

Figure 1. Map showing Saguenay system

have a total capacity of 360,000 kw. Primary power and occasionally a considerable amount of surplus power, for water storage purposes and for steam generation, is applied to the Shawinigan system.

Isle Maligne Generating Station

Isle Maligne generating station,[1] the first hydroelectric development on the Saguenay River, is located about nine miles below the outlet of Lake St. John. Owned and operated by Saguenay Power Company, Ltd., it contains 12 vertical Francis water wheels, each rated 45,000 horsepower, 112.5 rpm, 110 feet head, with direct-connected 35,000-kva 13.2-kv generators. A typical cross section of the plant is shown by Figure 3.

The generators are ventilated by an open system, cool air being taken from over the tailrace, through the wheel pits and generators to the generator room, whence it is discharged to atmosphere through the generator room windows and roof ventilators. During cold weather, part may be recirculated back through the generators by way of generator floor openings in order to maintain temperatures in the plant at comfortable levels.

Water-Wheel-Runner Pitting and Repairs

The water-wheel runners, measured at the middle of the guide case, have a diameter of 128 inches. A homologous runner, with 30.2 inch diameter, gave 93.3 per cent efficiency on a Holyoke test. The specific speed is 67, which the specific-speed experience curve indicates is in excess of the limiting value for freedom from pitting. Operating experience has confirmed this, considerable pitting having occurred.

The original runners were cast iron. Fatigue stresses in the vanes, where they join the crown plate, were increased by the removal of metal near the junction of the vanes and shroud ring through pitting. The net result was the gradual development of cracks in the vanes near the crown plate, starting from the discharge edges of the vanes and working outward. These cracks have been repaired by electric welding and mechanical clamps. All but one of the original 12 cast-iron runners are still in service. However, four cast-steel runners have been purchased. Three runners are always in the repair bay, which allows time for unhurried maintenance. Thirty-six hours' time is ample for exchanging runners.

Careful operating and inspection records were kept from the inception of operation. These included

1. Runner number.
2. Water-wheel number in which installed.
3. Date of inspection.
4. Number of hours in operation since last inspection.
5. Average operating load since last inspection.
6. Average operating gate opening since last inspection.
7. Average operating gross head since last inspection.
8. Average operating static draft head since last inspection.
9. Average effective draft head since last inspection.
10. Hours in operation with gate openings equal to or in excess of seven-tenths.
11. Hours in operation with load equal to or in excess of 30,000 kw.
12. Cracks.
13. Extent of pitting, plotted on standard forms for each vane, with contours showing area and depth, see Figure 4.
14. Cost of repairs.

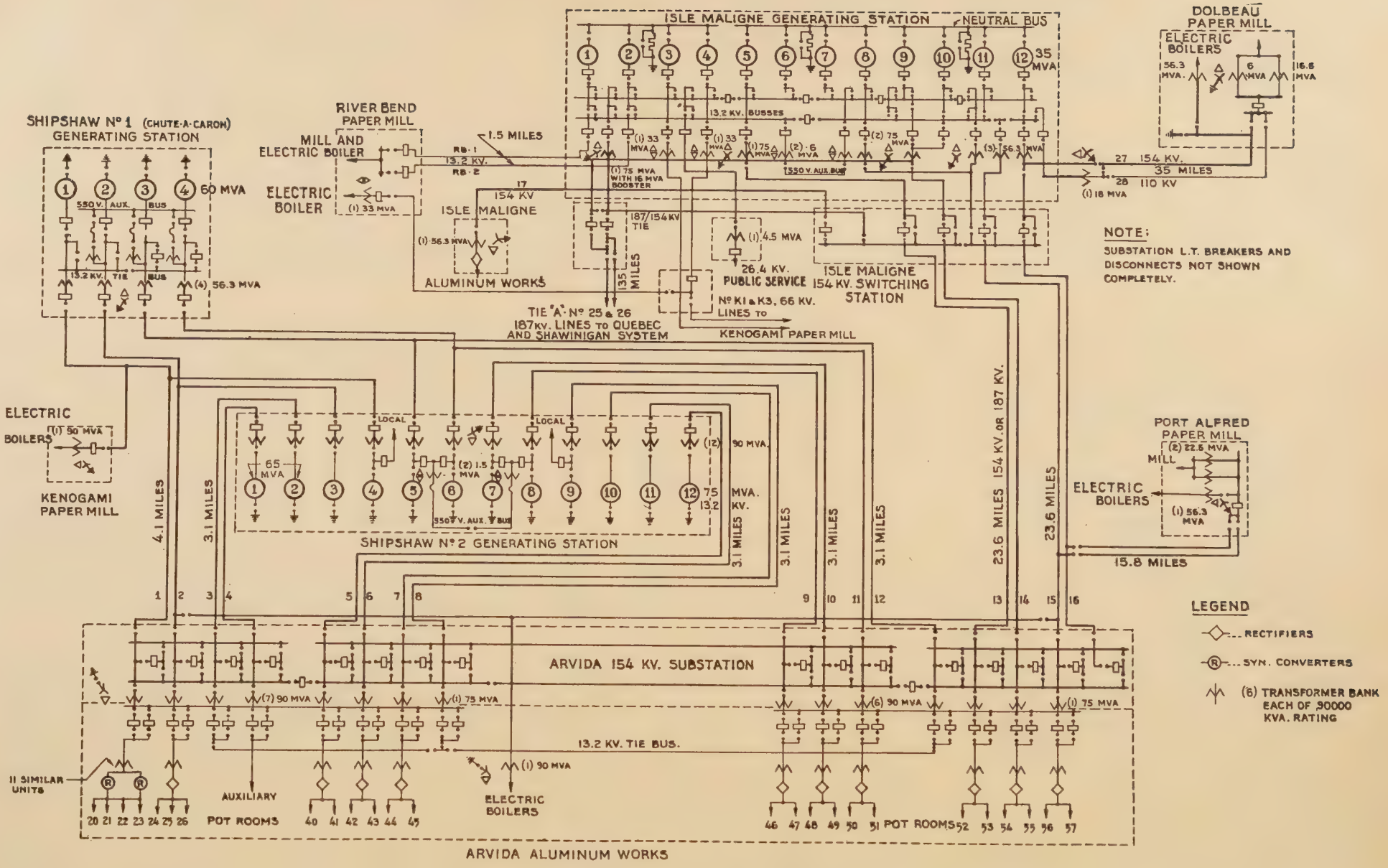

Figure 2. Saguenay system diagram

Substation low-voltage breakers and disconnecting switches not shown completely

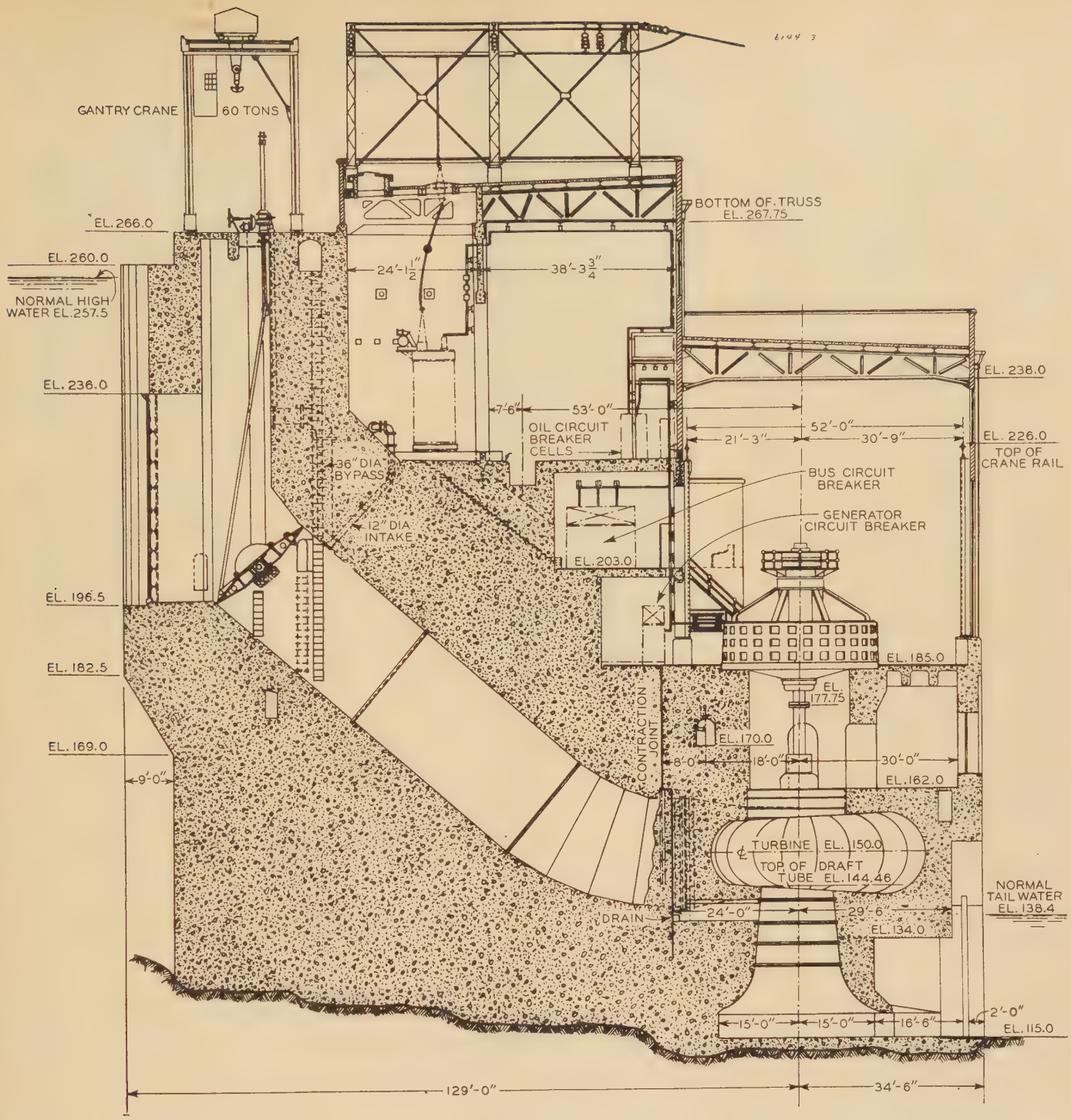

Figure 3. Typical cross section through Isle Maligne power plant

15. Cost of welding cracks and pitted areas.
16. Electrodes used for item 15, in pounds.
17. Cost of special work.
18. Electrodes used for item 17, in pounds.
19. Runner outage for repairs, in hours.
20. Labor on repairs for item 14, in man-hours.
21. Cost per pound of electrodes used for repairing pitting and cracks.

The records show the wastage of metal due to pitting is closely proportional to hours of operation under either of two criteria during periods between repairs. These are:

1. Hours of operation at gate openings over seven-tenths.
2. Hours of operation over 30,000-kw load.

There is a definite variation between runners but for a given runner the foregoing is true.

Figure 5, derived from 4.5 years operation of a cast-steel runner, otherwise identical with the original cast-iron runners, illustrates the variation in wastage of metal due to pitting with gate opening. The wastage rapidly increases above seven-tenths gate. It may be noted seven-tenths gate is approximately best gate, at which maximum efficiency is obtained.

Salient data from the Isle Maligne experience on wastage of metal in water-wheel-runner vanes resulting from pitting, are embodied in Table I. During the period 1925 to 1938, inclusive, the group of cast-iron runners lost metal some 5.5

times as rapidly as the cast-steel group on a weight basis, or about six times as fast on a volume basis. There was a greater range of wastage in the cast-steel group than for the cast-iron group, but this was a result of the excellent performance of a cast-steel runner designed for minimum pitting. Average cost of welding repairs was $2.30 per pound of electrode used for the repairs to the cast-iron runners, 18 per cent more than for the cast-steel runners. During the period 1939–1944, inclusive, when the average static draft head was 3.4 feet lower than during 1925–1938, inclusive, the same group of cast-iron runners lost weight three times as rapidly as the cast-steel runners, but only 36 per cent as quickly as previously, whereas the cast-steel runners lost weight at 67 per cent of the previous value during a given period. It is noteworthy that the spread between maximum and minimum pitting increases sharply with the lower static draft head.

Also, pitting practically ceased on the cast-steel runner designed for minimum pitting. It is interesting to observe the decrease of over 30 per cent in welding repair costs associated with the less extensive pitting of the 1939–1944 period.

Table I. Water-Wheel Pitting Experience Data at Isle Maligne

Type of Runner	Period (Inclusive)	Wastage of Metal, Lb Per Year* Max	Min	Avg	Cost of Repairs Per Lb of Electrode Used
Cast iron	1925–1938	744	144	411	$2.30
Cast steel	1925–1938	177	17	75	$1.95
Cast iron	1939–1944	509	61	149	$1.59
Cast steel	1939–1944	97	1.5	50	$1.33

* 8,760 hours of operation at gate openings over seven-tenths.

Water-Wheel Gate-Opening Position Indicators

During the late fall and winter months, the generating stations of the Saguenay system operate on water released from storage. During extremely dry years, which occur about once in seven years, storage water may be required during about nine months. Efficient usage of available water is particularly important during such storage drawdown periods. This necessitates operating hydroelectric units at their optimum efficiency, ordinarily termed best gate.

As previously noted, pitting damage on the Isle Maligne runners increases rapidly with time, during which the units are operated at gate openings in excess of the best gate. Consequently, normal operating procedure provides for operating the units at the gate openings corresponding to best gate for each unit.

To facilitate this, a water-wheel gate-opening position indicator was devised. This consists of a Selsyn transmitter mechanically actuated by a rack on the water-wheel servomotor crosshead. A movement of the crosshead imparts a motion of rotation to the transmitter directly proportional to the guide-vane opening. This rotation of the transmitter causes unequal voltages to be set up in the circuit linking the transmitter and receiver, so that the receiver rotor moves to a position matching the transmitter rotor, indicating on the scale the exact gate opening with a maximum error of plus or minus one per cent. The receiving indicator for each unit is mounted in the control room in full view of the operators. The point of best gate for each unit is marked on the dial of the indicator for that unit and any deviation may be detected instantly.

A Gibson efficiency test on one unit and careful index tests on the other units provided the necessary information from which curves similar to Figure 6 could be worked out for each unit. These, used in conjunction with the gate-opening position indicators, afford an effective means of securing maximum energy from storage water and minimizing pitting damage because actual generation per shift can be compared with anticipated generation as derived from head and unit gate-opening records. These daily records are worked out by the shift operators and instill a spirit of competition, thus securing best results.

Effect of Dirt on Generator Temperature Rise

Hydroelectric generators with open ventilating systems, even though operating in a clean atmosphere, pick up an

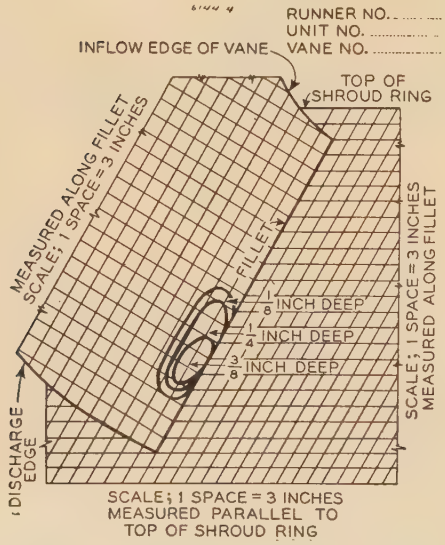

Figure 4. Water-wheel-runner pitting inspection form

Typical pitting for cast-iron runner shown by contours

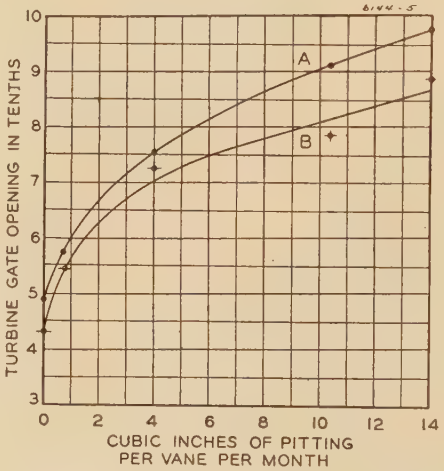

Figure 5. Effect of gate opening on wastage of water-wheel-runner metal caused by pitting

A—Average gate opening during operating time with Sunday and holiday light load periods deducted

B—Average gate opening during total operating time

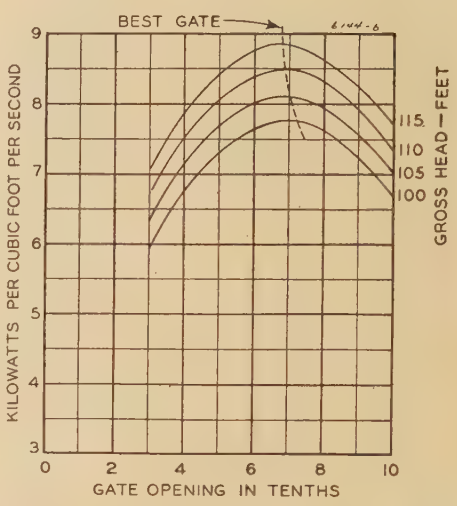

Figure 6. Relationship between kilowatts per cubic foot per second water usage and water-wheel gate opening for various heads

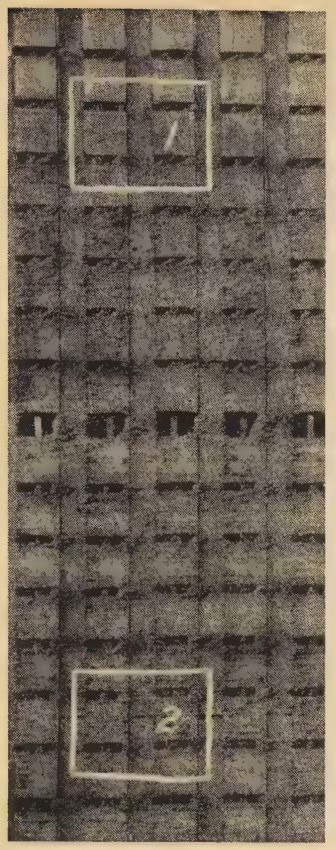

Figure 7 (left). Dirt deposits at locations 1 and 2 on the stator of a 30,000-kva water-wheel generator operated for 5.67 years between thorough cleanings

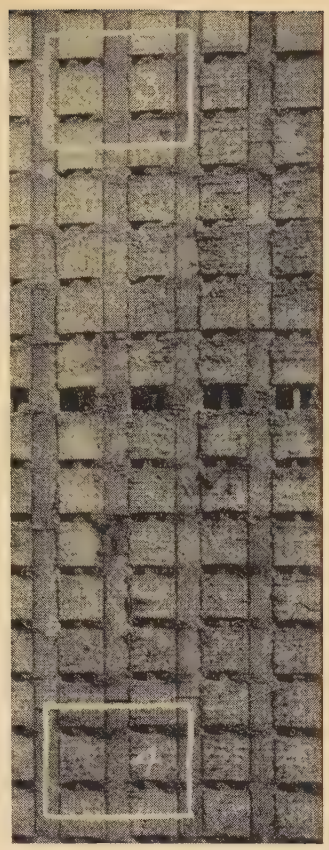

Figure 8 (right). Dirt deposits at locations 3 and 4 on the stator of the same 30,000-kva water-wheel generator as shown in Figure 7

amazing amount of dirt which is deposited in the ventilating ducts and to a lesser extent on exposed portions of the windings. Combined with a slight amount of oil vapor which escapes from the guide bearings even with the most perfect seals, these deposits have sufficient coherence to adhere tightly and cannot be removed satisfactorily or completely with compressed air. These deposits interfere with the transfer of heat and reduce the amount of ventilating air. Cleaning practices vary but the most satisfactory appears to be about as follows.

When windings are dry and dusty, they can be blown out with dry compressed air and wiped down. The dirt in the ventilating ducts can be loosened up with rectangular-shaped pieces of fiber or suitable brushes and blown out. For moderately dirty windings with some oil, the coils can be wiped off with cloths dampened with varsol and dried by natural air currents. When windings are excessively dirty, with oil, they can be sprayed and flushed down with varsol, after which they can be blown out and wiped down. In such cases, the winding should be placed on dry out until the insulation resistance to ground returns to normal, as indicated by ohmmeter readings.

At Isle Maligne, it was found that the most satisfactory cleaning could be done when a unit was taken down for an exchange of runners. In one instance, a unit was operated 5.67 years between thorough cleanings of the stator ventilating ducts and winding. During this period, dirt deposits in the stator ducts built up as illustrated by Figure 7 and Figure 8.

In order to ascertain the effect of such deposits on the volume of cooling air passing through the ventilating ducts, a cylinder 36 inches long was fitted carefully over a typical area on the air gap side of the stator. At the end remote from the stator, dry compressed air under close control was admitted in a direction at right angles to the longitudinal axis of the cylinder, from an air receiver. Pressures were measured in a plane $2^5/_8$ inches away from the air gap face of the stator iron by a suitable probe and draft gauge. On the opposite side of the stator iron, and covering the same relative area, the air passing through the ducts was measured by a 4-inch diameter vane anemometer fitted in a $9^1/_2$-inch long cylinder. Suitable shoes and gaskets on the cylinders precluded any loss of air.

Tests at the four locations, indicated in Figures 7 and 8, gave closely similar results. Figure 9 is a plot of the variation in volume of air passing through the ducts in one square foot of stator surface, with respect to static pressure on the air gap face. The effect of the dirt deposits is readily apparent.

Careful anemometric tests, before and after thoroughly cleaning the generator, showed a reduction of 22.5 per cent in the total volume of cooling air passing through the generator, as a result of the 5.67 years' accumulation of dirt deposits.

The effect of these dirt deposits on the stator winding and iron temperatures is plotted in Figure 10, from which it will be noted the capacity of the generator was reduced by

1. 3,450 kva, or 11.5 per cent of the original 30,000 kva rating, for the same maximum winding temperature rise.
2. 5,800 kva or 19.3 per cent for the same average winding temperature rise.

Extensive studies on all elements of the generator ventilating circuit were made for the Isle Maligne units as a result of which worthwhile improvements were effected in the rotor baffling, as well as externally. This latter consisted of doubling the entry areas for the cooling air taken from over the tailrace by enlarging the turbine floor windows.

Generator Insulation

The original Isle Maligne generator windings are illustrated by the typical section in Figure 11. Winding failures began to occur after about five years

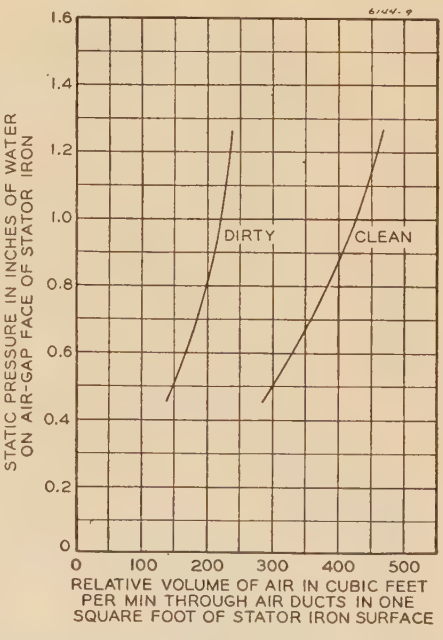

Figure 9. Variation in relative volumes of cooling air passing through stator ventilating ducts with static pressure on air gap face

Measured at locations 1, 2, 3, and 4 of Figures 7 and 8

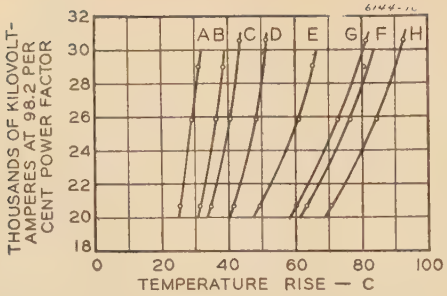

Figure 10. Effect of 5.67 years' accumulation of dirt deposits on stator iron and winding temperature rises of 30,000-kva generator

A—Average stator iron after cleaning
B—Maximum stator iron after cleaning
C—Average stator iron before cleaning
D—Maximum stator iron before cleaning
E—Average stator coil after cleaning
F—Maximum stator coil after cleaning
G—Average stator coil before cleaning
H—Maximum stator coil before cleaning

service and with increasing frequency. Cause of failures was found as follows:

1. Cotton and paper tape used to bind together the five turns which comprised a coil, before the application of the class B insulating jacket shrank and became brittle as a result of

2. High temperature accelerated by corona on the coils near the machine terminals where the voltage to ground was in excess of 7,000 rms volts.

3. Vibration, always potentially present, began to take place in the space provided by the shrinkage and the displacement of the embrittled insulation.

4. Eventually the mica strip between two turns was worn through or a strand worked around the edge of the strip, causing a short circuit of a turn, which heated the copper to the melting point. The insulating jacket next failed as a result of the heat and pressure of the molten copper.

An improved design of coil was worked out which almost eliminated the cellulose tape binding beneath the insulating jacket. It also contained 15 per cent more copper than the original coil with the same over-all thickness of insulation. This was accomplished by the use of less cellulosic carrier for the mica and a denser application, eliminating voids. Superior transposition of the winding was effected by the use of new series connectors. The new coil design, shown in Figure 11, also gave corona protection in the form of an Aquadag-treated asbestos outer wrapper. This design of stator winding was installed in all units and has given every indication of superior life.

Table II. Water-Wheel Performance at Shipshaw 2 Generating Station

Item	Unit 8, With Original Design of Runner	Unit 10, With Runner Cut Back on Inlet Edges	Unit 9, With Runner Cut Back on Inlet and Discharge Edges
Output at best gate, horsepower	82,000	88,000	86,000
Output at full gate, horsepower	96,700	101,360	105,160
Efficiency at best gate, per cent	93.3	94.4	94.5
Efficiency at full gate, per cent	84.7	85.3	86.4
Water usage at best gate, cubic feet per second	3,727	3,953	3,859
Water usage at full gate, cubic feet per second	4,844	5,039	5,164

Figure 11. Typical section through slot portions of original and new Isle Maligne generator stator windings

The whole coil is impregnated with asphalt compound (crude oil specially processed, practically a synthetic asphalt)

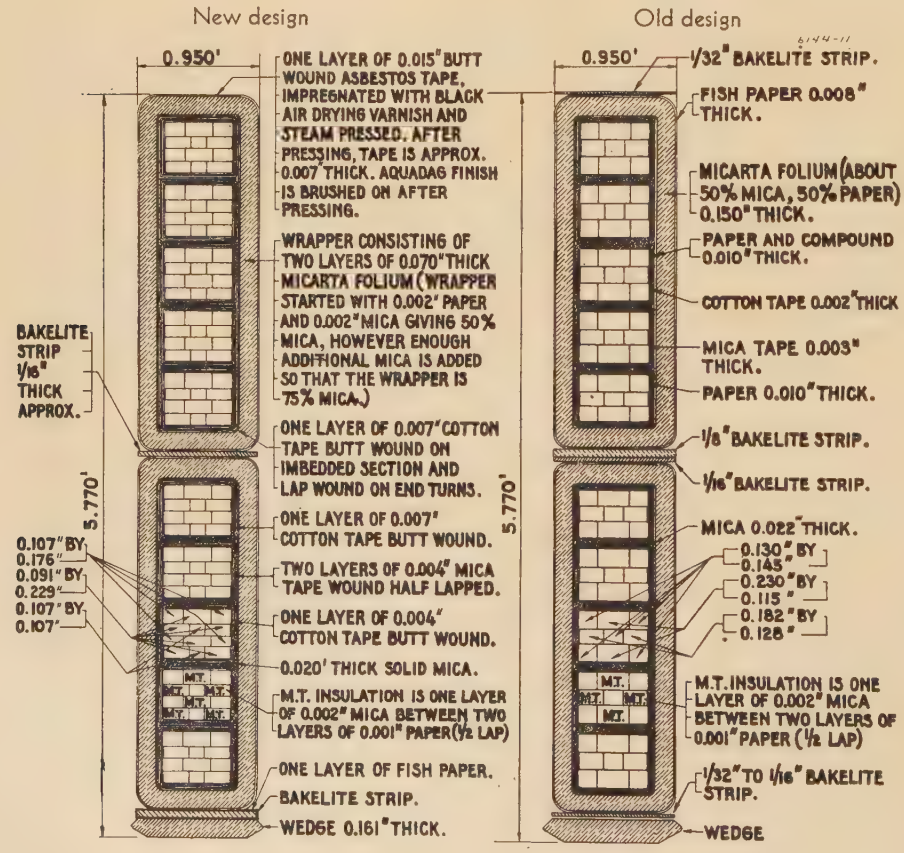

Isle Maligne Generator Losses

Together with an efficiency test by the Gibson method on the last water wheel installed, efficiency tests were made on

1. A generator with the original stator iron (2.2 silicon) and the original stator winding.

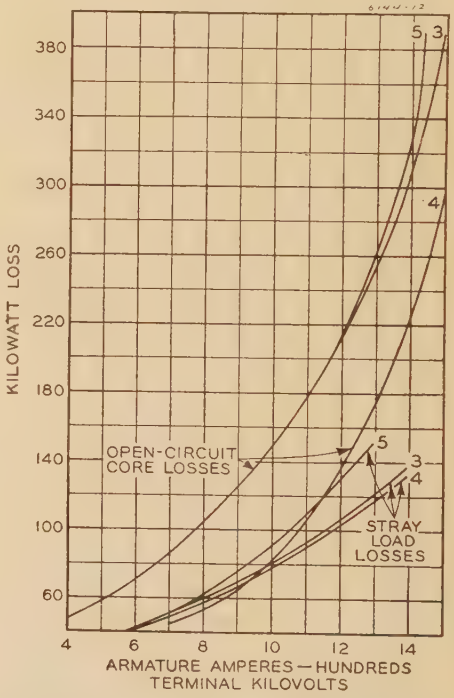

Figure 12. Improvement in core and stray-load losses of Isle Maligne generators resulting from use of higher silicon iron and new design of stator windings

Generator 3—Original iron and new stator winding
Generator 4—New iron and stator winding
Generator 5—Original iron and stator winding

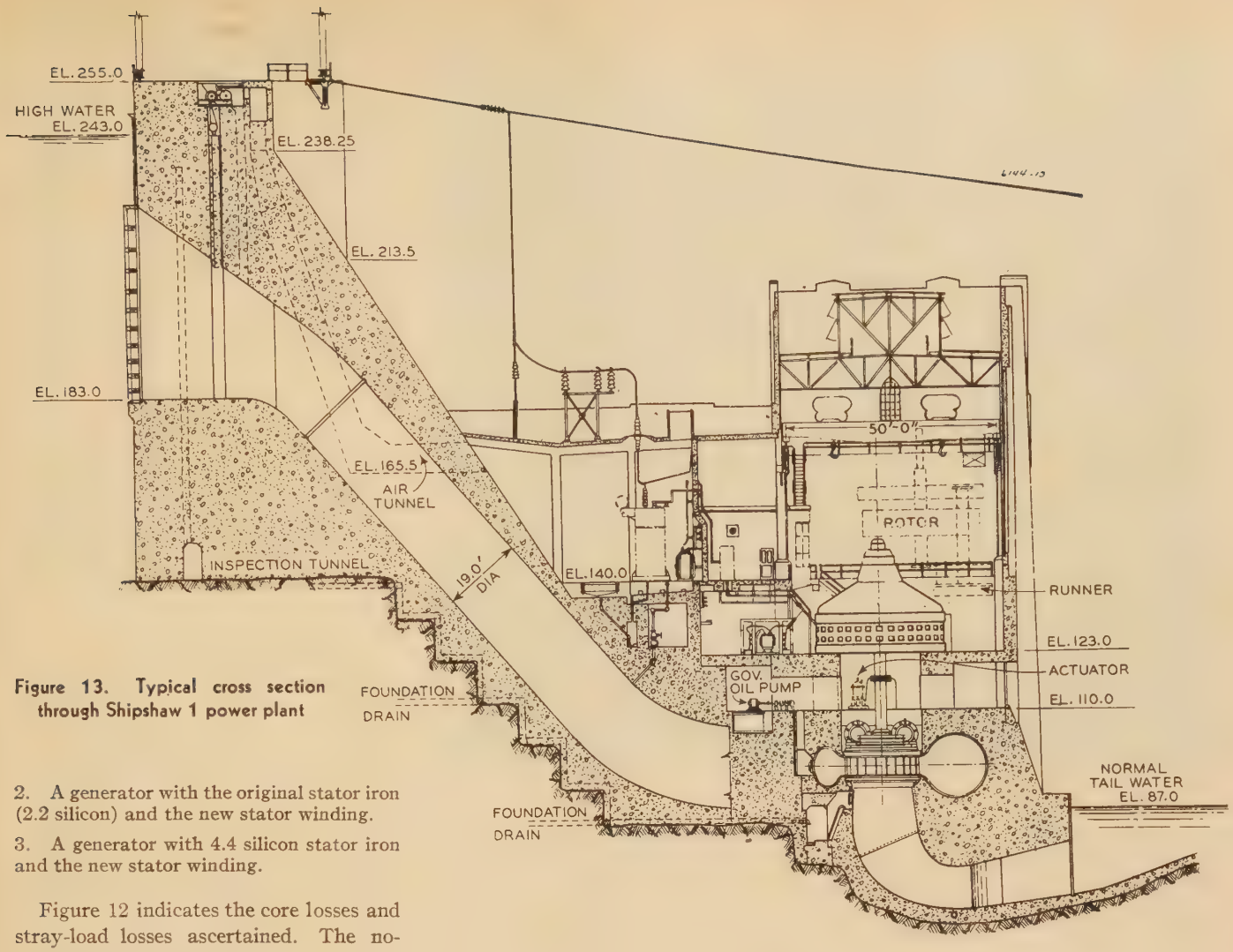

Figure 13. Typical cross section through Shipshaw 1 power plant

2. A generator with the original stator iron (2.2 silicon) and the new stator winding.

3. A generator with 4.4 silicon stator iron and the new stator winding.

Figure 12 indicates the core losses and stray-load losses ascertained. The notable improvement in core loss due to the use of the 4.4 silicon iron and in stray-load loss as a result of the new design of stator winding is significant of the improvements which frequently can be obtained with existing units by taking advantage of new materials, manufacturing technique, and design. The new windings and improved ventilation at Isle Maligne increased the output of each of the generators by 5,000 kva for the same temperature rise.

Shipshaw 1 Generating Station

Shipshaw 1 generating station, frequently called Chute-a-Caron, is located on the Saguenay River 20 miles below Isle Maligne. The first stage of the complete Shipshaw power development, owned by the Aluminum Company of Canada, Ltd., it contains four vertical Francis water-wheel units developing about 75,000 horsepower each, under 155 feet head, with 60,000-kva 13.2-kv 120-rpm generators. These generators have an open ventilating system, with cooling air being taken in from above the tailrace, as indicated by Figure 13, and have been rewound with improved coils similar to the new windings used at Isle Maligne.

Prior to the completion of the Shipshaw development by the construction of Shipshaw 2, the discharge from Isle Maligne plant was about 50 per cent in excess of the requirements at Shipshaw 1. Although the specific speed of 56 for the water wheels at the original rating of 65,000 horsepower was in excess of the value indicated by the experience curve for pitting, no pitting of any importance was encountered in operation. Also, it was known from test that the generators and transformers could carry safely at least 15 per cent overload.

Consequently, model tests were carried out to develop a runner capable of developing maximum output rather than maximum efficiency. These tests disclosed that a runner identical with the original design but with the diameter at the center line of the guide case reduced from 155 inches to 144.7 inches, could develop safely an additional 10,000 horsepower. New runners of the improved design were installed in all units, between November 1940 and October 1941, and operated with little pitting and efficiencies at wide gate openings better than the original runners.

Shipshaw 2 Generating Station

The Shipshaw 2 generating station, taking water from the same forebay as Shipshaw 1, is located about 1.5 miles down the Saguenay River from Shipshaw 1, as shown by the aerial view of Figure 14. Six 30-foot diameter shafts and tunnels each supply two single-runner, vertical, Francis-type water wheels originally specified to have 85,000 horsepower capacity at or near best gate, operating at 128.6 rpm. Eight units of one make are rated at 100,000 horsepower each and four of another make are rated at 85,000 horsepower each. Each turbine is directly connected to a three-phase generator having a specified capacity of 75,000 kva at 80-per cent power factor, 60-degree-centigrade maximum temperature rise, except two, which had been temporarily installed in an extension to Shipshaw 1 station, re-

Figure 14. Aerial view of Shipshaw power development, showing Shipshaw 2 plant in foreground and Shipshaw 1 plant (Chute-a-Caron) in left background

tained their 65,000 kva rating when relocated. Figure 15, a typical cross section through the headblock, water passages, and powerhouse, illustrates the general arrangement of the plant.

The scroll cases of the Shipshaw 2 water wheels,[2] including the connections to the cast-steel flanges of the speed rings, were welded completely. Complete application of welding to the scroll cases, with an inlet diameter of 16 feet and a maximum outside diameter of 49 feet 8 inches, resulted in greatly expediting field construction and very smooth casing outlines. All welding was done under extensometer and test-bar control. The former provided control of locked up stresses and eliminated the necessity of stress-relieving by controlled peening. The latter was taken care of by impact testing of sections cut daily from the actual welds of every operator.

Table III. Weights of Component Parts of 75,000-Kva Generators at Shipsaw 2

	Generator A, Lb	Generator B, Lb
Exciter armature	12,800	11,500
Exciter stator	19,900	15,000
Air casing, louvres	35,000	35,000
Upper guide bearing and bracket	96,450	105,000
Lower guide bearing and bracket	18,600	35,000
Shaft, 35 in. diameter	76,000	63,000
Rotor, spider	121,850	60,000
Rotor, poles and coils	200,500	173,000
Rotor, copper	96,700	53,000
Rotor, net	766,300	623,000
Stator copper	33,500	39,000
Stator laminations	144,000	125,000

The general requirement was 30 foot-pounds (Charpy). The smooth casing lines with flush joints undoubtedly contributed substantially to the high efficiencies secured on field test, as noted later.

Shipshaw 2 Water-Wheel Performance

Field tests on the first unit particularly were gratifying, there being so little vibration, resonance, and other indications of overstressing, that the manufacturer of eight of the water wheels offered to increase the maximum capacity of the water wheels still under manufacture by opening up the runners. It was estimated that the full-gate capacity could be increased about 5,000 horsepower by cutting back the inlet edges of the runner vanes and a further 3,000 horsepower by cutting back on the discharge edges. It also was anticipated this in-

Figure 15. Typical cross section through Shipshaw 2 power plant

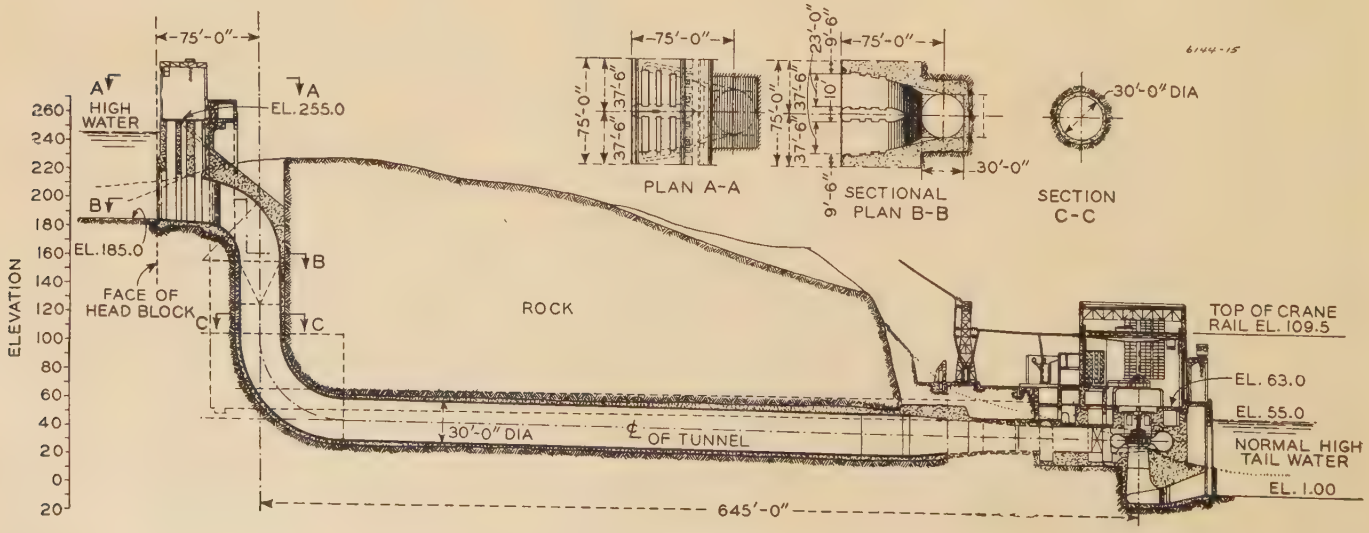

crease in full-gate capacity would not be detrimental to the best-gate efficiency. No definite assurance could be given as to the effect on pitting, vibration, and resonance, but since the demand for more power was paramount, the runner of one unit was cut back on the inlet edges and that for a second unit was cut back on the inlet and discharge edges. After these were installed, efficiency tests using the Gibson method were made, with the results shown in Table II, from which it will be noted the expected increase in capacity was obtained. Following that, eight runners were trimmed on the inlet and discharge edges of the buckets. To date, after two years service, pitting has been very mild and efficiencies excellent.

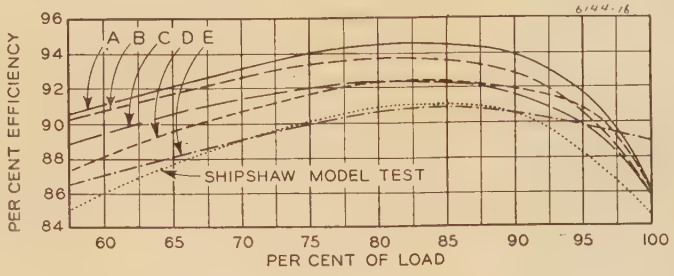

Figure 16. Comparative efficiencies of Shipshaw 2 and other outstanding water wheels in North America

Curve	Unit	Hp Rating	Ft. Head	Specific Speed, Rpm
A	Shipshaw unit 9	105,200	208	52
B	Niagara unit 21	88,000	213.5	39
C	Grand Coulee unit L7	115,500	330	33
D	Osage unit 3	37,000	90	78
E	Boulder unit 5	125,000	520	21

The relative efficiency of the Shipshaw and other outstanding water wheels in North America, all determined by the Gibson method, is illustrated by Figure 16. Note the striking correspondence between the actual field performance at Shipshaw and the model tests on a 14-inch 100-horsepower runner under a head of about 100 feet.

Generator Ventilation

In order to maintain the extremely close schedule under which Shipshaw 2 was built, it was necessary to utilize the manufacturing facilities of the only two Canadian manufacturers capable of building the generators. The order was divided equally, on the understanding all differences in electrical design and characteristics would be ironed out satisfactorily and that all units would be identical in outline and exterior dimensions.

A closed ventilating system was decided on, partly because of experience with the open ventilating systems at Isle Maligne and Shipshaw 1, and partly because the low temperature of the cooling medium, water from the forebay, would permit maximum utilization of the generator capacity at all seasons of the year. Moreover, the use of the closed ventilating system eliminated the necessity for otherwise lengthening the turbine shafts about 8 feet and providing an additional reinforced concrete floor over the space occupied by the main units to furnish necessary duct capacity. Actually, the whole structural layout was simplified and the cost decreased appreciably. Moreover, the lower, controllable ambient temperature permitted an actual increase of about 100,000 kva capacity for the station for the guaranteed temperature rise of 60 degrees centigrade.

The air housings for the generators[3] are arranged so that two doors at each corner can be opened, closing off the adjacent coolers and deflecting the hot air to the generator room for heating in cold weather. In the United States, it is usual practice to seal off the generator, but at Shipshaw this is accomplished by doors in the entrances to the wheel pits. The air from the generator rotor and stator is circulated through the water-cooled heat exchangers, whence it is discharged to the water-wheel pit and through the rotor to the stator.

The advantage of this method is the ease of access to the lower end turns of the stator winding, or the rotor guide bearing, without having to remove the sealing pans normally fixed to the generator lower bracket. In the case of the generators built by manufacturer *B*, the lower end turns are readily accessible in event of fire, without having to remove the baffles. Under actual conditions, the units built by manufacturer *A* take 135,000 cubic feet of cooling air per minute, whereas the others take 200,000 cubic feet per minute. These units have excess thermal capacity, and in all probability about 150,000 cubic feet of air per minute would have met requirements.

The rotating parts of the generator and turbine are carried on a single thrust bearing with one turbine and two generator guide bearings. Two types of thrust bearings are used, Kingsbury bearings and spring-thrust bearings. All thrust bearings, except one, are tin-base babbitt. On one thrust bearing, owing

Figure 17. Stator of 75,000-kva generator built by manufacturer *B* for Shipshaw 2

Note the curved ribs or spacer plates

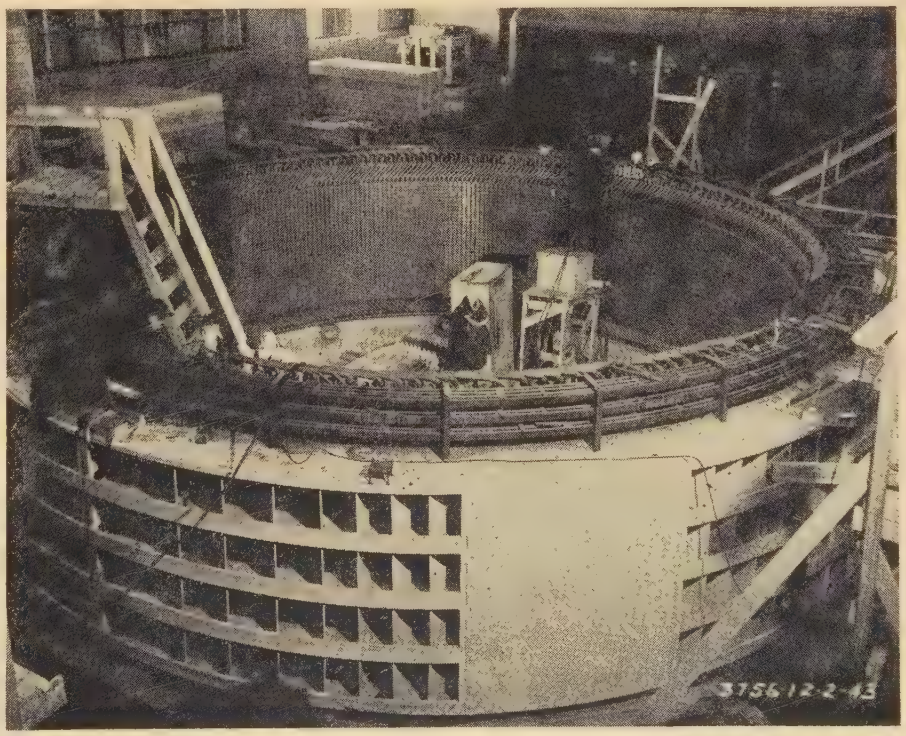

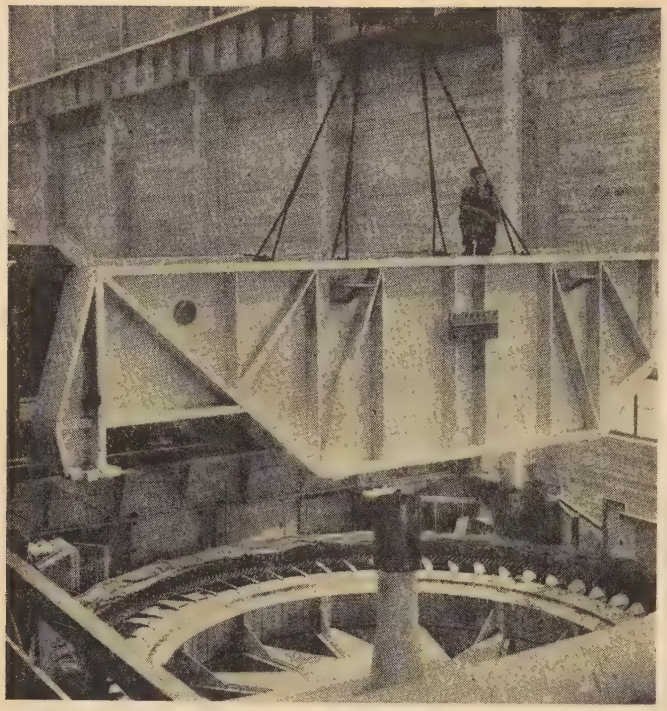

Figure 18. View of rotor and stator of 75,000-kva generator built by manufacturer *B*

The air coolers can be seen at the corners of the housing

to the difficulty in obtaining tin, it was decided to try an arsenical lead babbitt which so far has proved satisfactory.

Manufacturer *A* used the conventional generator design with spider-type upper bracket and semidepressed oil pot around which the air casing was built and the coolers installed. The rotor is of standard design with cast-spider and conventional baffles. Manufacturer *B* employed a stator design which resulted in an open machine providing free circulation of air, and by shaping the spacer plates tended to control the direction of air flow towards the coolers. Note Figure 17. He used a depressed bridge-type girder upper-bracket arrangement with fully depressed thrust-bearing oil pot. A totally fabricated rotor was used, with the sections built up by welding steel plate. By means of specially designed slot wedges in the stator and special fan blades on the rotor, air flow through the stator is controlled without the use of baffles, leaving a very open machine on which the end turns, both upper and lower, are readily accessible. See Figure 18. This illustration shows the coolers at the corners of the housing.

The two different designs resulted in considerable difference in weight of materials, as shown in Table III. Table IV illustrates the comparative performance of the two types of generators.

In the generators built by manufacturer *B*, the greater part of the cooling air is supplied to the stator ducts through ducts in the rim of the rotor feeding the interpolar spaces, and then directly into the stator ducts, instead of the conventional manner wherein fans on the ends of the rotor blow air into the spaces between the poles. Thus the air entering the stator ducts is at the same temperature throughout the core, resulting in maximum and average temperatures closely alike. Scoop-type fans at the ends of the rotor ventilate the end turns and prevent recirculation of air. Actually, about 50 per cent more air than required to limit its temperature rise to the 18-degree-centigrade value desired, was circulated through the machine. This obviously resulted in a greater windage loss than otherwise would have been the case.

After a year of service, during the completion of construction of the plant, about 6.5 cubic feet of dirt were deposited on the inside of the rotor rim, but the stator ducts and duct entrances remained clean.

The *B* machines are designed for a different method of replacement of a few stator coils than the conventional method of dismantling the unit and removing the rotor.

The field coils and poles are arranged so they can be disconnected readily at the top. The pole keys are pulled out by the crane, and the rotor poles lifted out by the same means. The stator coil, or coils, are then removed by heating the adjacent group of coils electrically to soften the insulation, removing the slot wedges, and pulling the group out into the gap left by the withdrawn poles, and then lifting out the damaged coil or coils. New coils are installed by reversing this process. The working time required to make the replacement of a coil which failed was approximately 56 hours.

Table IV. Comparison of Shipshaw 2 *A* and *B* Generators Operating Under Full Load at Unity Power Factor

	Generator A	Generator B
Kilovolt-amperes or kilowatts	75,000	75,000
Stator current, amperes	3,280	3,280
Field current, amperes	740	855
Stator I^2R, kilowatts	244	199
Field I^2R, kilowatts	110	125
Open-circuit core loss, kilowatts	290	465
Short-circuit core loss, kilowatts	190	220
Windage and friction, kilowatts	325	555
Total losses, kilowatts	1,159	1,564
Output, kilowatts	75,000	75,000
Input, kilowatts	76,159	76,564
Efficiency, per cent	98.48	97.98

References

1. Hydroelectric Development of the Saguenay River, **W. S. Lee.** AIEE Transactions, volume 44, 1925, pages 722–36.

2. The Design of the Shipshaw Power Development, **H. G. Acres.** *The Engineering Journal* (Montreal, Canada), volume 27, 1944, pages 221–33; discussion, pages 449–58.

3. Electrical Equipment at Shipshaw, **R. A. H. Hayes.** *The Engineering Journal* (Montreal, Canada), volume 27, 1944, pages 250–60.

The Electrical Performance of Ceramic Dielectrics at Elevated Temperatures

H. A. FREY
MEMBER AIEE

J. M. JESATKO
ASSOCIATE AIEE

Synopsis: Some recent developments have emphasized the need for information concerning the temperature at which dielectrics can be operated without electrical breakdown. This paper deals primarily with porcelain, but some data are included on the performance of steatite, glass, and zircon compositions. Data are presented on the variation in resistivity of the materials with varying temperature and also with varying voltage gradient. From the temperature–resistivity curves a method is developed for approximating the combination of temperature and voltage gradient which will result in electrical failure. Supporting data in the form of breakdown tests, made at various temperatures, are included. These tests include practical insulator forms as well as prepared test specimens.

IT IS WELL KNOWN that the electrical resistance of most of the commonly used insulating materials diminishes with increasing temperature. The actual performance of ceramic insulating materials at temperatures above the normal atmospheric level, and the factors affecting the ultimate breakdown at these temperatures, have not been the subject of much investigation. Recent requirements for insulators to operate at high temperatures and high voltages have indicated the need for such information.

There have been several insulator failures in precipitator applications which are directly attributable to the combination of high voltage and high temperature operation. Perhaps even more important is the development of certain new industrial processes which require that insulators be used at high temperatures. This investigation was undertaken for the purpose of obtaining fundamental design information on the high temperature electrical performance of ceramic materials and to develop suitable special materials for such applications.

Apparatus and Method

It was necessary to provide a suitable test chamber in which the specimens could be mounted and held at any desired temperature while voltage was applied. Accordingly, a thermally insulated box or furnace was built. The electrical heating elements in the back of the box were separated from the test chamber by a 1-inch thick thermally insulating partition in order to prevent direct heating of the specimens by radiant heat. The heated air was circulated by means of a fan through ports at each end of the test chamber. The fan also served to maintain air turbulence in the test chamber and thus prevent stratification. Temperature measurements were made by commercial gas thermometer, and automatic controls were provided for holding any desired temperature between minus 100 and plus 1,000 degrees Fahrenheit. With this arrangement temperatures could be held within five degrees Fahrenheit of the desired level. Provision also was made for removing the heating elements from the back of the box and substituting racks of dry ice in order to obtain low temperatures.

Most of the tests were made with direct voltage in order to eliminate the difficulty of separating conduction currents from charging currents. The voltage source was a full-wave high-voltage kenetron rectifier with suitable capacitors for the elimination of the 60-cycle pulse.

The direct voltages were measured by means of a suitable known resistance connected in series with a microammeter.

Most of the test specimens were prepared in the form of plates of various thicknesses. Some specimens were made from standard suspension insulator shells using the head section, ground down to the desired thickness, as the test area.

Electrodes of circular shapes were applied to the opposite sides of each test specimen. Guard rings also were provided to eliminate the effect of surface leakage and corona and to preserve a more nearly uniform field through the test zone. The electrodes and guard rings were of silver ceramicly bonded to the surface of the dielectric to avoid entrapped air between the dielectric and its electrode.

Resistance measurements were made by connecting one electrode to the voltage source and grounding the opposite electrode through a microammeter or milliammeter of proper scale range for the current involved. Suitable selector switches were provided for switching quickly from one instrument to another. The guard ring connections were shunted around the ammeters to ground. Resistance was determined from the ratio of voltage to current.

Before each measurement was made, the specimen was allowed to stand in the test chamber at zero voltage and constant temperature for a sufficient length of time to be sure that it was heated uniformly throughout its volume.

Materials

The greater part of this investigation is concerned with porcelain, although some data have been obtained on two kinds of glass, a steatite composition and a zircon composition.

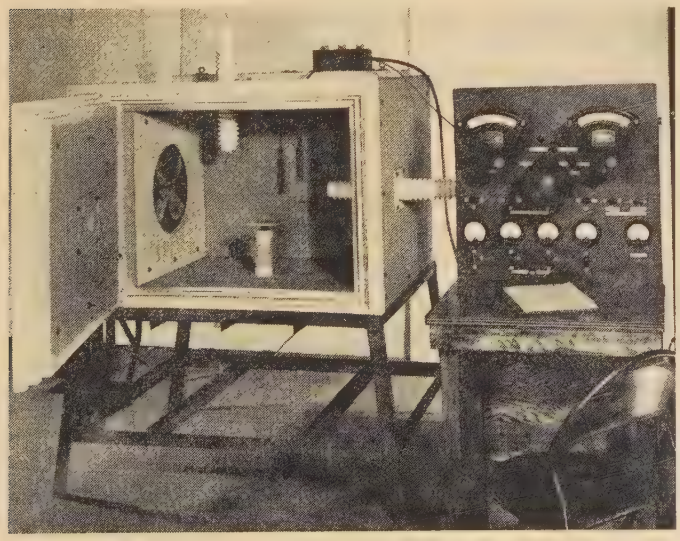

Figure 1. Test chamber and operating panel with specimen mounted in position

Paper 46-117, recommended by the AIEE committee on power transmission and distribution for presentation at the AIEE summer convention, Detroit, Mich., June 24–28, 1946. Manuscript submitted March 5, 1946; made available for printing May 8, 1946.

H. A. FREY and J. M. JESATKO are both with the Locke Insulator Corporation, Baltimore, Md.

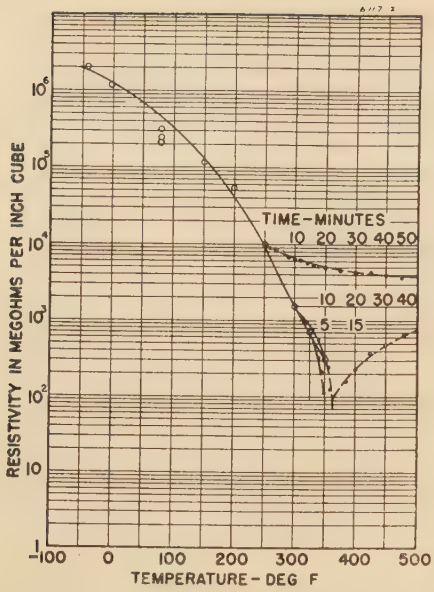

Figure 2. Temperature versus resistivity, wet process electrical porcelain

Voltage gradient 40 volts per mil direct current, thickness 0.8 inch, electrode area 30 square inches

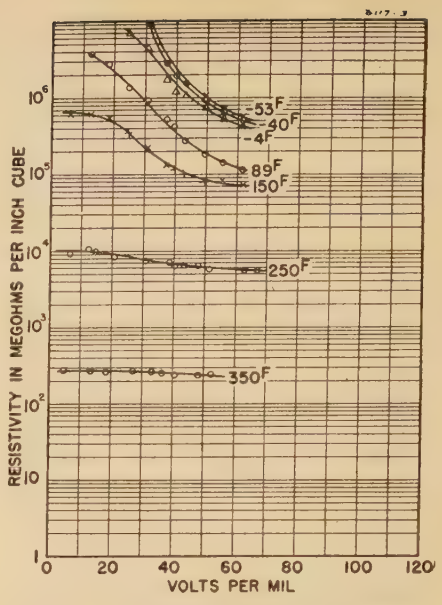

Figure 3. Voltage gradient versus resistivity, wet process electrical porcelain

Thickness 0.8 inch, electrode area 30 square inches

These are all generic names, and there is considerable latitude in composition and in physical structure within each category.

The porcelain specimens involved all were made of wet process feldspathic porcelain of the type commonly known as electrical porcelain. Samples of such porcelain as made by three different manufacturers were used.

The steatite specimens were a magnesia-alumina-silicate composition maturing at a firing temperature of about 2,250 degrees Fahrenheit. The zircon specimens were composed basically of zirconia silicate with a calcium-zirconium-silicate flux compounded to mature at 2,250 degrees Fahrenheit. This composition was developed particularly for high temperature applications.

Two types of glass specimens were included: a borosilicate glass of the type used in the manufacture of high voltage insulators, and a lead glass also sometimes used in certain classes of insulators.

Discussion of Data—Porcelain

Many measurements were made on a variety of specimens of varying shapes and thicknesses, at temperatures ranging from minus 70 to plus 900 degrees Fahrenheit and at voltage gradients up to 700 volts per mil. A gratifying degree of consistency in results was obtained. Typical data illustrating the results obtained are presented herein. As an example, the curve shown in Figure 2 is typical of the measurement made to determine the variation of resistivity with temperature and to determine the temperature at which final breakdown would occur. In plotting the curve, the measured total resistances have been reduced to resistivity in megohms per inch cube. It should be noted that as the temperature was increased the resistivity steadily declined but remained stable (within the limits of measurement) at each point up to 250 degrees Fahrenheit. At 250 degrees Fahrenheit, on this particular specimen, it was found that with constant voltage the resistivity declined slowly with time, finally becoming stable at a lower level after about 45 minutes. This change in resistivity with time is indicated in Figure 2 by superimposing a time axis on the curve. The variation in resistivity with time, for a constant ambient temperature corresponding to that at zero time, is indicated by a broken line. This decline in resistance with time undoubtedly is caused by the internal heating of the specimen above the surrounding air because of the I^2R loss. It represents an average internal temperature rise of about 20 to 25 degrees Fahrenheit.

When the test chamber temperature was raised to 300 degrees Fahrenheit and held constant, the resistivity, with constant applied voltage, diminished with increasing rapidity until after 12 minutes the specimen no longer would support voltage and, for all practical purposes, had failed electrically. At this point voltage was removed, but the test chamber still was held at a constant temperature of 300 degrees Fahrenheit. At intervals of five minutes the same voltage was reapplied momentarily, and readings quickly were taken. It should be noted that as the specimen cooled internally the resistivity recovered along a typical cooling curve.

The test chamber temperature then was raised to 325 degrees Fahrenheit and the same voltage reapplied. The resistivity again declined still more rapidly with time, and within five minutes reached the point where voltage could not be supported. Voltage then was removed, and the piece again was allowed to recover. The test chamber temperature was raised to 350 degrees Fahrenheit and a momentary reading taken as indicated on the curve. The test chamber was allowed to cool back to room temperature, and the resistivity again was measured checking the value determined at the start of the test.

On this particular specimen, voltage was removed in each case as soon as a runaway condition was observed as indicated by current increasing more and more rapidly. On some other specimens, voltage was not removed promptly, and power was delivered to the piece for several seconds after the runaway phenomenon was observed. In such cases the dielectric was cracked or a fused path developed through it resulting in a permanent failure.

The curve shown in Figure 2 illustrates the variation of resistivity with temperature for one particular porcelain specimen at a constant voltage gradient. At any temperature level, the resistivity may vary also with changing voltage gradient. This effect was studied on a number of porcelain specimens, and Figure 3 shows a typical plot of the data obtained on one particular specimen—the same specimen appearing in Figure 2. It should be noted that at the lower temperatures resistivity diminishes rather rapidly with increasing voltage gradient, but at temperatures above 250 degrees Fahrenheit the resistivity becomes nearly independent of voltage gradient.

The results of all measurements made on porcelain to determine the variation of resistivity with temperature were plotted on one composite curve (Figure 4). At the higher temperature it was necessary to make all tests at relatively low voltage gradients in order to obtain stable measurements. Thus at 900 degrees Fahrenheit the measurements were made on a specimen approximately 0.8 inch thick with voltage applied from a 45-volt battery equivalent to about 0.05 volt per mil. At these higher temperatures the resistivity changes but little with chang-

ing voltage gradient so this limitation does not impair the usefulness of the information contained in Figure 4.

An examination of Figure 4 shows that data conform with reasonable accuracy to a single curve for all temperatures above about 250 or 300 degrees Fahrenheit. At lower temperatures the composite data spread widely as indicated by the envelope shown. This spread of the data at the lower temperatures is caused primarily by two factors:

1. The influence of voltage gradient on resistivity at lower temperature.
2. The influence of specimen thickness.

The influence of voltage gradient already has been illustrated. In testing specimens of different thicknesses, it was observed that at low temperatures the apparent resistivity was lower for thick specimens than for thin ones. The influence of thickness on resistivity diminished with increasing temperature so that for temperatures above about 250 or 300 degrees Fahrenheit the apparent resistivity was relatively independent of thickness. The apparent effect of thickness on resistivity is believed to be caused by the variation of the true voltage gradient from the average voltage gradient. As the specimen thickness is increased it becomes more and more difficult to maintain a truly uniform voltage gradient through it.

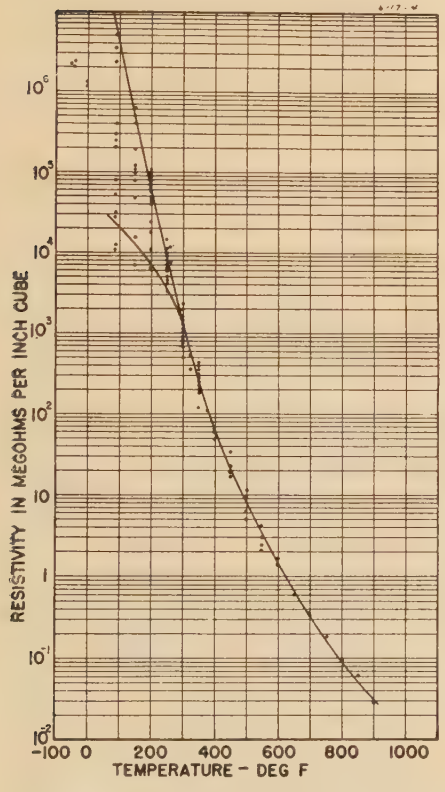

Figure 4. Composite curve, temperature versus resistivity of wet process electrical porcelain

It has been pointed out that porcelain made by three different manufacturers was used in the investigation. No significant difference was found among the three porcelains. Figure 5 shows a typical comparison of dimensionally identical pieces as made by two manufacturers. These two pieces were tested simultaneously. The change in resistivity with time (because of internal heating and cooling) is shown on the curve in the same manner as in Figure 2. At 300 degrees Fahrenheit, voltage was applied for ten minutes at which time the resistivity had become stable. Voltage then was removed and the specimen allowed to cool back to the test chamber temperature. Voltage then was reapplied, and a duplicate heating curve was obtained. At 325 degrees both specimens drifted toward breakdown. Specimen *B* actually refused to support voltage, but specimen *A* was well on the way to the same condition and doubtless would have failed in another minute or two had the test been continued. It should be noted that at 325 degrees both of the resistivity drift curves pass through a definite flex point where the shape of the drift curve changes from concave upward to concave downward. After the breakdown at 325 degrees, the pieces were allowed to cool, and the test chamber temperature was raised to 350 degrees. At this level both specimens drifted rapidly to breakdown in about three minutes.

Effect of Glaze

All data which have been discussed up to this point have been obtained on unglazed specimens. In order to determine the effect of glaze on the high temperature performance of porcelain, two cylinders were prepared $1^1/_8$ inches in diameter and $2^1/_4$ inches long. One of these cylinders was glazed with a standard glaze of the type normally applied to high voltage insulators. The other cylinder was left unglazed. Silver electrodes were applied and ceramicly bonded to each end of each cylinder. The silver coatings were carried over the ends and extended down the side walls on each end for a distance of $^5/_{16}$ inch. This was done in order to place the highest voltage gradient along the outer glazed surface. Figure 6 shows the results of a simultaneous test made on these two pieces. The resistance of the two was practically the same throughout the test, and both pieces drifted to failure at 410 degrees Fahrenheit. Note that this curve is plotted with total resistance and not resistivity as ordinates.

Some Practical Insulators

In addition to prepared test specimens, a number of tests have been made on practical insulators of various types and forms. Figure 7 shows the results of two such tests made on a standard 23-kv heavy duty 2-shell outdoor switch insulator. The insulator was tested with its regular metallic parts cemented in place in the usual manner. A direct correct voltage of 14 kv was applied between cap and pin; this voltage is numerically the same as the rms normal service voltage to ground. Note that in Figure 7 the total resistance to ground is plotted as a function of temperature. In this insulator the conduction path from top to bottom metallic elements passes through three layers of portland cement and two layers of porcelain. It should be noted that the initial measurement made at 80 degrees Fahrenheit is considerably below the curve as drawn and also is lower than the second point at 150 degrees. This peculiar performance is believed to be caused by the variation in resistance of the cement. Portland cement is quite hygroscopic and when slightly moist is a fairly low resistance conductor. As the water is driven off, however, its resistance increases so that at elevated temperatures it adds in some measure to the total resistance of the insulator. The high temperature end of the curve is 2-pronged, representing the results from two separate tests. Note that drift curves became measurable on one curve at 350 degrees and on the other

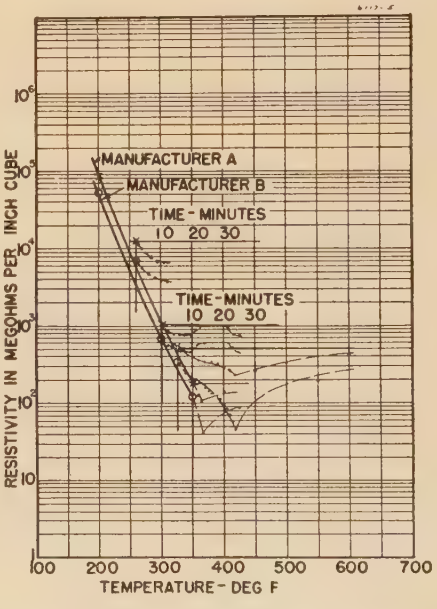

Figure 5. Temperature versus resistivity, comparison of two manufacturers of wet process electrical porcelain

Voltage gradient 20 volts per mil, specimen thickness 0.55 inch

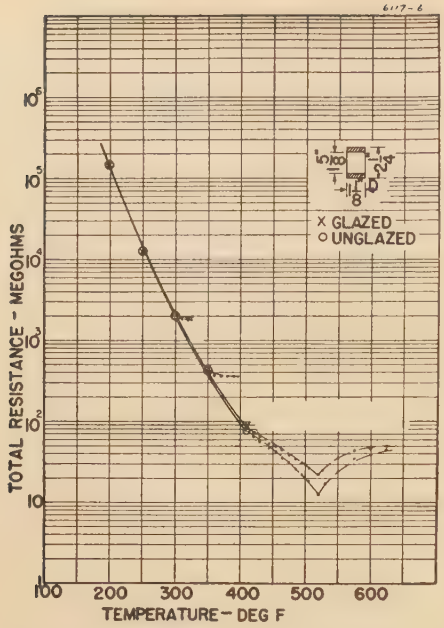

Figure 6. Temperature versus resistance, comparison of glazed and unglazed wet process electrical porcelain

Total voltage applied 5,000 volts direct current

at 400 degrees, reaching stability in each case after about 40 minutes. At 450 degrees the insulators drifted to failure in 20 and 30 minutes, respectively.

A similar insulator was subjected to test at 14 kv rms 60 cycles. This test was made by raising the temperature in 50-degree steps and holding the voltage and temperature constant for one hour at each step. Because of the difficulties of separating conduction from charging currents, no resistance measurements were made. The unit failed after 54 minutes at 400 degrees Fahrenheit. A number of other a-c tests have been made on other porcelain samples, the results of which will be discussed later.

Discussion of Data—Glass

In Figure 8 are plotted the measurements of the resistivity of borosilicate glass as a function of temperature. This particular glass specimen was the glass element only of a suspension insulator. Silver electrodes with guard ring were applied to the head area. At 85 volts per mil and 350 degrees Fahrenheit, the specimen drifted to breakdown in about three minutes. At the instant of failure the specimen was shattered by the forces of differential expansion.

In Figure 9 the variation of resistivity of the same specimen is shown as a function of voltage gradient.

Similarly, Figures 10 and 11 show the performance of a specimen made of a lead glass. This specimen drifted toward failure at 40 volts per mil and 600 degrees Fahrenheit after about three minutes, but upon cooling recovered and was not permanently injured. At 650 degrees and 20 volts per mil, the same specimen showed a definite downward drift in resistivity because of internal heating but stabilized after about ten minutes. At 650 degrees and 30 volts per mil, the piece drifted to failure in about eight minutes. In this case power was not removed quickly enough, and a permanent failure occurred taking the form of a fused path through the glass.

Discussion of Data—Steatite

The results of tests on two steatite specimens are shown in Figure 12. Note that for two voltage gradients, 20 and 40 volts per mil, the curves virtually coincide. Both specimens initially drifted toward failure after 15 and 17 minutes, respectively, at 700 degrees Fahrenheit and 40 volts per mil. The pieces were cooled back to test chamber temperature and recovered. At 750 degrees, both specimens failed at 20 volts per mil after nine and ten minutes, respectively.

There are not sufficient data to plot the variation in resistivity of this steatite composition as a function of voltage for various temperature levels. In Figure 13 such data are plotted for one temperature, only.

Discussion of Data—Zircon

Several zircon compositions were investigated, and it was found that the high temperature electrical characteristics of the several compositions varied radically. The particular zircon composition included in this paper is the one having the best characteristics of the group tried. Figure 14 gives the variation in resistance as a function of temperature with a voltage gradient of 40 volts per mil. Figure 15 shows the variation in resistance as a function of voltage gradient for various temperture.

There are two characteristics of this material which are worthy of particular note.

1. It is observed that in certain ranges increasing voltage gradient results in slight increases in the measured resistance. Such a condition was not observed on any of the other materials, nor even on the other zircon specimens having slightly different composition.

2. It was observed that, at any fixed temperature above about 400 degrees Fahrenheit when a constant voltage was applied, an initial current was measured which diminished with time, finally stabilizing at a value lower than the initial. In other words the measured resistance increased with time. This is exactly opposite to the performance of the other materials. At the lower temperatures, around 500 degrees, this upward drift of resistance reached stability in about one minute with a rise in resistance of about three to four per cent. At higher temperatures, about 800 degrees, the upward drift of resistance reached stability in several minutes with rise in resistance of about 30 per cent. At 800 degrees and at higher voltage gradients, 60 volts per mil, stability was reached only after 20 minutes with a rise of more than 100 per cent of the initial value.

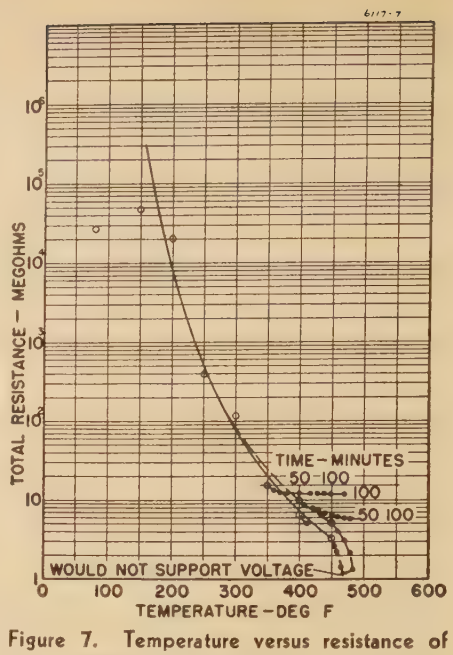

Figure 7. Temperature versus resistance of 23-kv NEMA standard outdoor switch and bus insulator

Total voltage applied 14 kv direct current

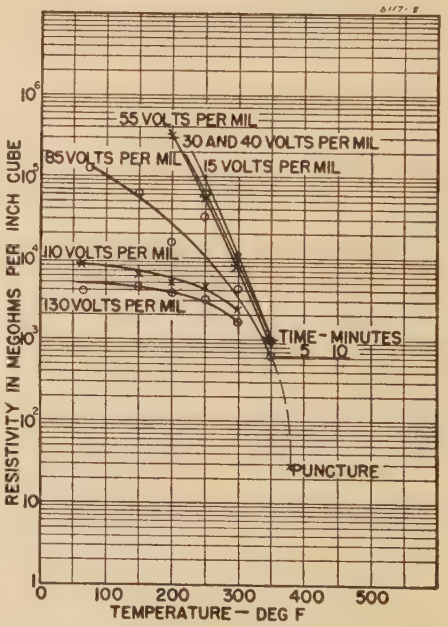

Figure 8. Temperature versus resistivity, borosilicate glass

Thickness 0.36 inch

This characteristic continued up to 900 degrees, the upper limit of the test, and no breakdowns were obtained.

These two unusual characteristics of this material are believed to be caused by dielectric polarization. The curves shown in Figures 14 and 15 are plotted to show the resistance at each level for the polarized or stable condition.

Theoretical Considerations

From an engineering standpoint, it is most important that one be able to determine the temperature and voltage at which a particular insulator may be operated safely without failure. To accomplish this with some reasonable knowledge of the margin of safety, the end point conditions should be predictable. Therefore, some theoretical discussion of the mechanism of breakdown is in order.

From the data it seems reasonably conclusive that, at least at elevated temperatures (250 degrees Fahrenheit and above), breakdown is a thermal phenomenon. When voltage is applied to a dielectric, a leakage or conduction current flows through the material and the I^2R loss results in internal heating above the ambient temperature. This increase in internal temperature results in a reduction of resistivity with consequent increase in internal heating, if a constant applied voltage is maintained. As the internal temperature rises above the ambient, heat is dissipated from the stressed volume. In most practical applications thermal conduction is the principal means of heat dissipation from the stressed volume. The power dissipated as heat from any point in the stressed volume is therefore a function of the internal temperature rise. If the power dissipated as heat increases more rapidly as the temperature rises than does the power input, the time rate of temperature rise will diminish and a condition of stability will be obtained. If the reverse condition occurs, the temperature will rise with increasing rapidity until the dielectric fuses or is is cracked by differential expansion stresses.

Consider the elemental cube (Figure 16) in the dielectric body. Let the volume of this cube be ΔV and the edge dimensions be ΔX, ΔY, and ΔZ. Let the direction of voltage gradient be parallel to the Y axis through the elemental cube. If the voltage gradient through the cube in volts per inch is E and if the resulting current density is I amperes per square inch, then P_{T1}, the total power input to the cube, is

$$P_{T1}=(E\Delta Y)(I\Delta X\Delta Z)=EI\Delta V$$

If the resistivity of the material is r ohms per inch cube,

$$P_{T1}=\frac{E^2}{r}\Delta V$$

The power input per unit volume is

$$P_1=\frac{P_{T1}}{\Delta V}=\frac{E^2}{r} \qquad (1)$$

If the total power output from the cube in the form of heat is P_{T2}, then

$$P_{T2}=\int_s K\nabla T\cdot \boldsymbol{n}d\sigma$$

where

T = the temperature rise of the cube above the ambient temperature
∇T = the temperature gradient outward from the cube
$d\sigma$ = any element of surface of the cube
$\boldsymbol{n}$ = a unit vector normal to that element of surface
K = the thermal conductivity of the material

The power output per unit volume is

$$P_2=\frac{P_{T2}}{\Delta V}$$

$$=\frac{K}{\Delta V}\int_s \nabla T\cdot \boldsymbol{n}d\sigma$$

Taking the limit as ΔV approaches zero

$$P_2=K\nabla^2 T \qquad (2)$$

The term $K\nabla^2 T$ cannot be evaluated exactly from theoretical considerations alone. However, this term merely represents the power output in the form of heat from a small element in the stressed volume. In any practical insulator, as soon as a voltage is applied some element within the stressed volume begins to heat slightly faster than its immediate surroundings. This may be because the element is at the center of the volume where heat loss is the slowest, because of variations in voltage gradient, or because of variations in the homogeneity of the material. As soon as the element in question begins to rise in temperature above that of the surrounding stressed volume, its resistivity diminishes and consequently its rate of heating is increased further. A "hot spot", therefore, is established quickly, and it is this hot spot which is of

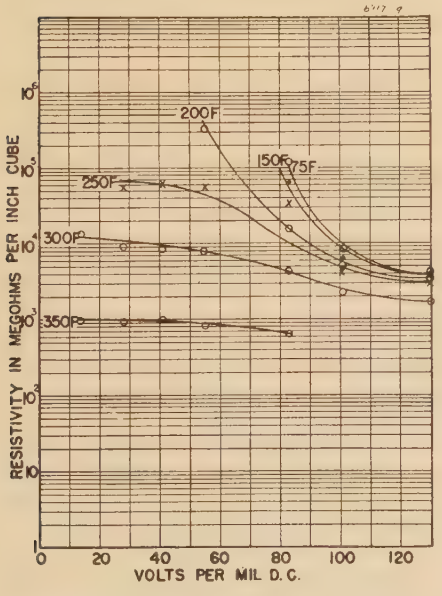

Figure 9. Voltage gradient versus resistivity, borosilicate glass

Thickness 0.36 inch

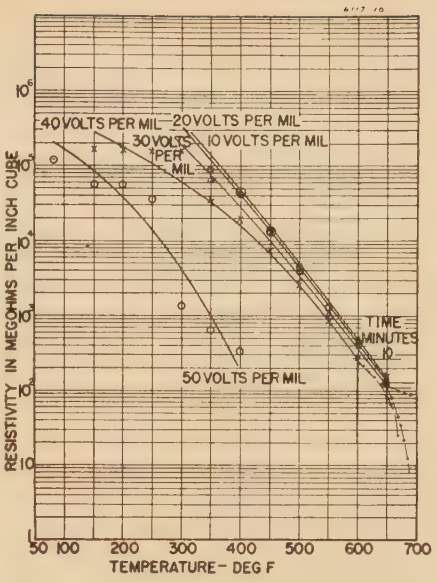

Figure 10. Temperature versus resistivity, lead glass specimen

Thickness 0.50 inch

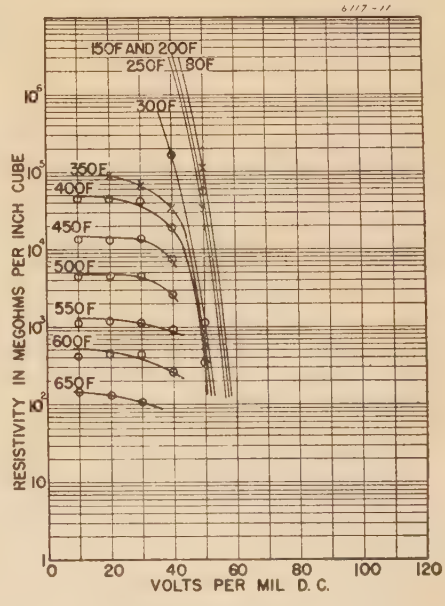

Figure 11. Voltage gradient versus resistivity, lead glass

Specimen thickness 0.50 inch

primary concern. Equation 2 may be applied to represent the heat loss from the critical element and by making certain reasonable assumptions may be reduced to a more useful form. Since the surface area of any practical insulator is relatively large and since the thermal conductivity of the material under consideration is relatively small, it may be assumed that the rate of heat loss from the critical volume is directly proportional to the temperature rise above the ambient. For these assumptions equation 2 may be written

$$P_2 = K\alpha T \tag{3}$$

where

T = the temperature rise of the element
α = the factor of proportionality

At any point of stability P_2 must equal P_1.

When voltage is first applied, $T=0$, and consequently $P_2=0$. As T increases, P_1 and P_2 both increase. If, with increasing temperature T, P_1 continuously increases faster than P_2, stability can never be reached, and the temperature will continue to rise until failure occurs. Conversely, if P_2 continuously increases faster than P_1, a condition of equilibrium will ultimately be reached where $P_2=P_1$.

The rate of increase of P_1 with respect to temperature T is

$$\frac{\partial P_1}{\partial T} = -\frac{E^2}{r^2}\frac{\partial r}{\partial T}$$

Since, for the materials under consideration, $\partial r/\partial T$ is negative, this shows a positive value for the product $-\frac{E^2}{r^2}\frac{\partial r}{\partial T}$.

The rate of increase of P_2 with respect to temperature is

$$\frac{\partial P_2}{\partial T} = K\frac{\partial(\nabla^2 T)}{\partial T} \backsimeq K\alpha \tag{4}$$

The conditions leading to ultimate breakdown are illustrated in Figure 17. The power input when voltage first is applied at ambient temperature T_0 is represented by P_1. As the internal temperature rises, the power input increases as shown. The power output is initially zero but increases as internal temperature rises. If the P_2 curve intersects the P_1 curve, stability is reached. If the P_2 curve fails to intersect the P_1 curve, runaway and breakdown ultimately occur.

If the power input (P_1) curve is concave upwards, the critical point will be reached when the starting temperature T_0 is such as to make the P_2 curve reach the P_1 curve at a point of tangency. This occurs at some critical temperature T_c and with power input P_1'', as illustrated in Figure 17.

At this point

$$\frac{\partial P_1}{\partial T} = \frac{\partial P_2}{\partial T}$$

or

$$-\frac{E^2}{r^2}\frac{\partial r}{\partial T} = K\alpha \tag{5}$$

The initial ambient temperature T necessary ultimately to reach the critical condition is lower than T_c by an amount equal to P_1'' divided by $K\alpha$.

If the power input curve P_1 is concave downward, the P_2 curve always will intersect it at some point and with some theoretical finite temperature rise above the ambient. Whether or not failure occurs then depends upon whether the temperature at this point of intersection is within the range which the dielectric can stand without fusing, cracking, or charring. It is perfectly possible that the power input curve may be in some zones concave upward and in other zones concave downward with a flex point as illustrated by the broken line in Figure 17.

Equation 5, therefore, may be applied only when the second derivative of power input with respect to temperature is positive at the critical point.

$$\frac{\partial^2 P_1}{\partial T^2} = -\frac{E^2}{r^2}\frac{\partial^2 r}{\partial T^2} + \frac{2E^2}{r^3}\left(\frac{\partial r}{\partial T}\right)^2$$

This term is always positive when $\frac{\partial^2 r}{\partial T^2}$ is negative. If $\frac{\partial^2 r}{\partial T^2}$ is positive, the term is positive only when

$$\frac{E^2}{r^2}\frac{\partial^2 r}{\partial T^2} < \frac{2E^2}{r^3}\left(\frac{\partial r}{\partial T}\right)^2$$

$$\frac{\partial^2 r}{\partial T^2} < \frac{2}{r}\left(\frac{\partial r}{\partial T}\right)^2 \tag{6}$$

The values of r and of the first and second partial derivatives can be determined physically from the temperature–resistivity curve of any material. For porcelain, the steatite composition, and the two glasses equation 6 is satisfied within the range investigated. For zircon the second derivative of r with respect to T is negative up to about 350 degrees Fahrenheit. Above 350 degrees equation 6 is satisfied up to about 700 degrees. Above 700 degrees, the power input curve is concave downward, and stability always can be reached theoretically at some temperature rise. In this respect above 700 degrees zircon will behave more like a very high resistance conductor than an insulator.

Hence equation 5 can be applied to porcelain, the two glasses, and the steatite composition within the range for which data exist. It also can be applied to the zircon up to 700 degrees Fahrenheit. The values of thermal conductivity K for these materials are given approximately in Table I.

For most of these materials, the thermal conductivity increases somewhat with increasing temperature. By neglecting

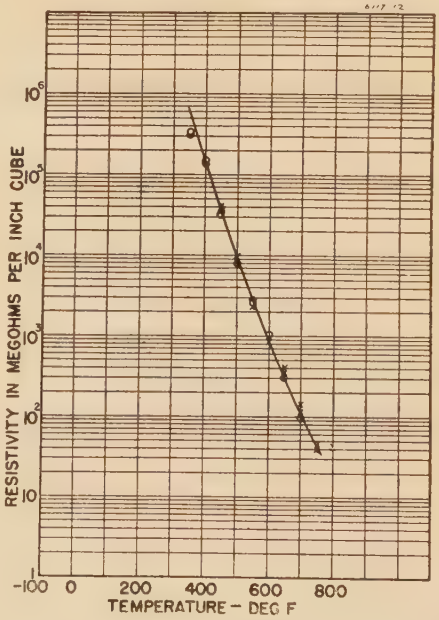

Figure 12. Temperature versus resistivity, wet process steatite

Voltage gradient 20 and 40 volts per mil, specimen thickness 0.188 inch and 0.203 inch

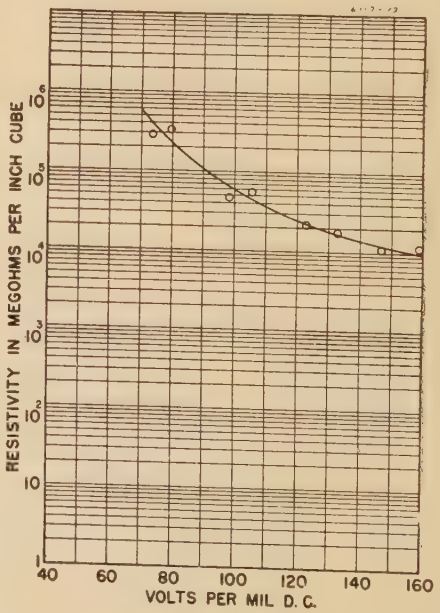

Figure 13 (right). Voltage gradient versus resistivity, wet process steatite

Temperature 84 degrees Fahrenheit, specimen thickness 0.188 inch and 0.203 inch

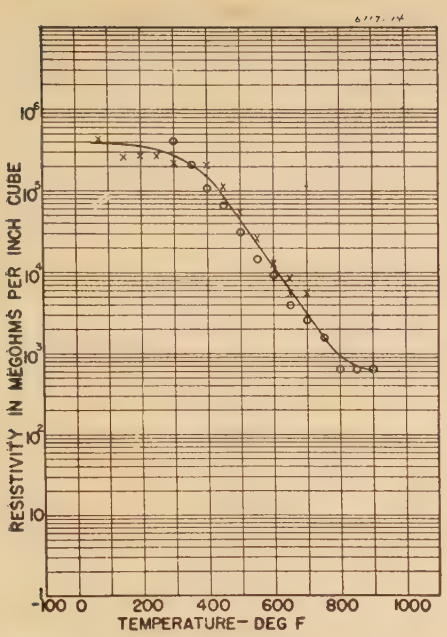

Figure 14. Temperature versus resistivity, zircon

40 volts per mil, 2-square-inch electrode 0.489 inch thick and 1-square-inch electrode 0.196 inch thick

this change using the values given in Table I throughout, conservative results will be obtained.

In order to evaluate equation 5 numerically, the value of the factor α must be determined. The points of ultimate failure with direct voltage for all porcelain test specimens are listed in Table II. The theoretical values for $-\frac{E^2}{r^2}\frac{\partial r}{\partial T}$ are shown for each case. It again should be noted that the data in Table II were obtained by applying constant voltage and raising the ambient temperature in steps. In many cases failure probably would have occurred at some lower temperature if smaller steps had been used. For this reason those tests have been discounted on which failure occurred in less than three minutes. For the remaining tests, the average value of the term $-\frac{E^2}{r^2}\frac{\partial r}{\partial T}$ is 0.067 with a range from 0.0189 to 0.124. The last column in Table II shows a word symbol indicating whether or not the drift curve to failure passed through a flex point. Those tests marked "flex" showed a definite flex point in the drift curve. For those points marked "no", the drift curve continued with increasing acceleration to failure with no flex point. For cases where no flex point occurred in the drift curve, the starting temperature must have been at some point above T_c. For those tests where a flex point appeared, the starting temperature must have been between T_0 and T_c. The values of $-\frac{E^2}{r^2}\frac{\partial r}{\partial T}$ for those tests which passed through a flex point range from 0.0189 to 0.0925, with an average value of 0.0398. For those tests which did not show a flex point on the drift curve, the value of $-\frac{E^2}{r^2}\frac{\partial r}{\partial T}$ ranged from a high of 0.124 to a low of 0.023, with an average of 0.0725. By inspection it appears that the value of the function $-\frac{E^2}{r^2}\frac{\partial r}{\partial T}$ should be about 0.06 at the flex point. If 0.06 is taken as the approximate numerical value of the function at the flex point, then this may be substituted in equation 5, and the factor α may be evaluated as approximately three for porcelain. This evaluation is not very precise, but it should be noted that an error of even three to one in the value of α produces an error of only about 50 degrees Fahrenheit in the theoretical end point temperature.

For porcelain the resistivity varies but little with voltage gradient for temperature above 250 degrees Fahrenheit. A reasonably accurate general solution, therefore, can be obtained for temperatures above 250 degrees. For temperatures below 250 degrees, some confusion exists probably because of the variation of resistivity with voltage gradient, and sufficient data are not available for an accurate analysis. As a matter of interest, equation 5 has been evaluated for porcelain below 250 degrees using the two extremes of the resistivity curve shown in Figure 4.

Table I. Thermal Conductivity

Material	Watts Per Sq In. Per In. Per Deg F
Porcelain	0.0203
Steatite	0.0285
Borosilicate glass	0.0182
Lead glass	0.0182
Zircon	0.031

This yields the theoretical internal temperature T_c at which runaway actually starts for any particular voltage gradient. In Figure 18 the values of T_c have been plotted against voltage gradient. The starting ambient temperature T_0, from which the critical internal temperature T_c ultimately may be reached, also has been plotted in Figure 18 taking

$$T_c - T_0 = \frac{\text{watts per cubic inch input at } T_c}{K\alpha}$$

Any point to the left of the T_0 curve should be safe for continuous operation. Points to the right of the T_0 curve should result in failure if given sufficient time.

In Table III the actual breakdown points for several practical insulators are shown. These values also have been plotted on Figure 18.

For the materials other than porcelain, there are not sufficient data to make a determination of α by the method used

Table II. Breakdown Points of Porcelain Test Specimens, Direct Voltage

Electrode Area, Sq In.	Specimen Thickness, In.	Volts Per Mil D-C	Temperature at Beginning of Failure, Deg F	Resistivity at Beginning of Failure, Megohms Per In. Cube	Time Required for Failure, Min	$\frac{E^2}{r^2}\frac{\partial r}{\partial T}$ Watts Per Cu In. Per Deg F	Characteristic of Drift Curve
1	0.131	382	95	Approximately 200,000	5	0.021	No
1	0.122	410	150	Approximately 50,000	7	0.094	No
1	0.075	440	200	Approximately 58,000	Less than 0.02	0.087	No
1	0.275	136	250	5,000	28.5	0.0925	Flex
1	0.258	194	250	Approximately 3,000	2.5	0.287	No
1	0.605	40	300	495	15	0.077	No
1	0.609	40	300	870	15	0.0442	No
30	0.81	39.5	300	1,630	12	0.023	No
1	0.172	87	300	2,150	7.5	0.084	No
1	0.172	87	300	2,150	7.5+	0.084	No
1	0.797	40	300	892	16	0.043	Flex
2	0.535	20.6	325	516	19	0.0189	Flex
2	0.528	20.6	325	348	19	0.0282	Flex
0.785	0.97	30.8	350	193	3+	0.108	No
0.785	0.98	30.8	350	183	3+	0.114	No
1	0.791	20.2	350	405	44	0.0222	Flex
0.44	0.282	35.5	350	285	4	0.0975	No
0.44	0.282	35.5	350	285	4+	0.0975	No
1	0.172	43.5	350	335	6	0.124	No
1	0.172	43.5	350	335	6+	0.124	No
1	0.81	9.87	400	60	62	0.034	Flex
0.785	0.97	10.25	400	66	15.5	0.0336	No
0.785	0.98	10.25	400	57	15.5	0.0387	No
0.785	0.975	20.4	400	47	2.5	0.186	No
0.785	0.980	20.4	400	47	2.5+	0.186	No

Table III. Breakdown Points of Practical Porcelain Insulator Shapes, Alternating and Continuous Voltage

	Continuous Voltage					Alternating Voltage
	Cylindrical Smooth Walled Standoff Insulator	Cylindrical Corrugated Standoff Insulator	Standard 23-Kv Heavy Duty Outdoor Switch and Bus Insulator	Tube $2^3/_4$ by $1^3/_4$ by 20 In. Long, Smooth Walled	3-Unit $5^3/_4$ by 10 In. Suspension Insulator	Standard 23-Kv Heavy Duty Outdoor Switch and Bus Insulator
Total porcelain thickness, in.	1.62	5.12	1.25	20	2.06	1.25
Total voltage applied, volts	15,000	40,000	14,000	46,000	46,000	14,000 rms
Average volts per mil	9.25	7.8	11.2	2.3	22.3	11.2 rms
Temperature at beginning of failure, deg F	410	400	405	550	350	400
Total resistance at beginning of failure, megohms	79	82	3.26–5.2	24.8	82.2	Approximately 2.7
Approximate average resistivity at beginning of failure, megohms per in. cube	48.7	50.4	81–128	4.36	461	Approximately 66
Time required for failure, min	21	45	17–35	49	112	54
$\frac{E^2}{r^2}\frac{\partial r}{\partial T}$ watts per cu in. per deg F	0.036	0.025	0.0254–0.0162	0.0205	0.0237	0.032
Characteristics of drift curve	Flex	Flex	No	Flex	Flex	—

for porcelain. It is difficult to see why the value of α should differ materially from that for porcelain. If we assume that α is the same for the steatite, glass, and zircon compositions as for porcelain, then theoretical breakdown curves can be plotted for these materials. Such curves for the four other materials are plotted in Figure 18 within the range of the existing data. For borosilicate glass no data area vailable above 350 degrees Fahrenheit, and for temperatures below 250 degrees the resistivity varies greatly with voltage as indicated in Figures 8 and 9. The curve for borosilicate glass, therefore, can be generalized from this data over only a short range. In Figure 18 the borosilicate glass curve is shown in broken lines so that it may be distinguished from the porcelain curve.

Examination of Figures 10 and 11 will show that the lead glass curve can be generalized from existing data only within the temperature range from 350 to 650 degrees Fahrenheit and for voltage below 40 volts per mil.

No data are available on the steatite composition to show the variation of resistivity with voltage at the higher temperatures. There is every indication, however, that, like porcelain, the resistivity of steatite becomes essentially independent of voltage at temperatures above 250 degrees Fahrenheit. The plot for steatite in Figure 18 is based on this assumption.

For the zircon composition, it appears that above about 140 volts per mil resistivity will vary considerably with voltage. Also, above 700 degrees stability, theoretically, always can be reached. The generalized zircon plot is therefore quite short but does indicate adequately the relative position of this material. Above 700 degrees there is some question as to whether at any particular voltage gradient the material will stabilize before the internal temperature rise becomes excessive. The experimental evidence indicates that for d-c gradients up to 40 volts per mil the zircon composition can be operated successfully at 900 degrees and possibly higher.

As a practical check on these theoretical predictions, Tables II, III, IV, and V give the actual measured breakdown points for a number of specimens. The individual points from these tables have been plotted on the curves in Figure 18 for direct comparison. As would be expected, all actual breakdown points fall to the right of the theoretical curve.

Some actual breakdown points for porcelain are included for temperatures below 250 degrees Fahrenheit. It has been pointed out that at these lower temperatures the generalized curves are of doubtful value. It is interesting to note, however, that the actual low temperature breakdown points are at least of the proper order relative to the theoretical curves. Some breakdown points obtained with alternating voltages also are included in Tables III and IV, and are plotted on the curve in Figure 18. In each case these have been listed and plotted in rms rather than crest volts, since the heating effect is a function of the former. These seem to fit the curves equally as well as do the d-c points, but the amount of a-c data available are relatively small. No actual resistance measurements were made with alternating current and the resistivities listed in Table IV are taken from Figure 4.

Despite the fact that the temperature–resistivity curves were obtained from test specimens with relatively uniform voltage gradients, the theoretical break-

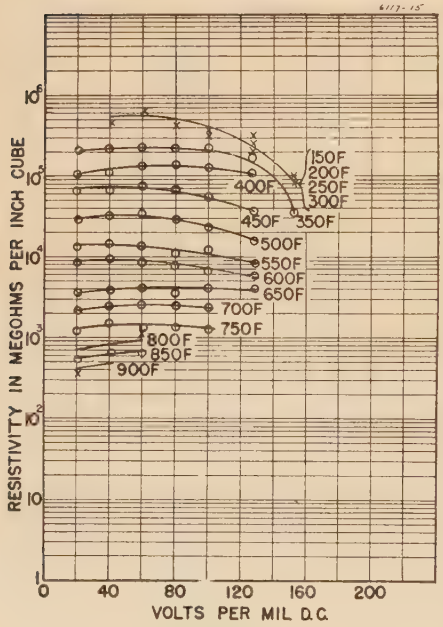

Figure 15. Voltage gradient versus resistivity, zircon

1-square-inch electrode, specimen thickness 0.196 inch

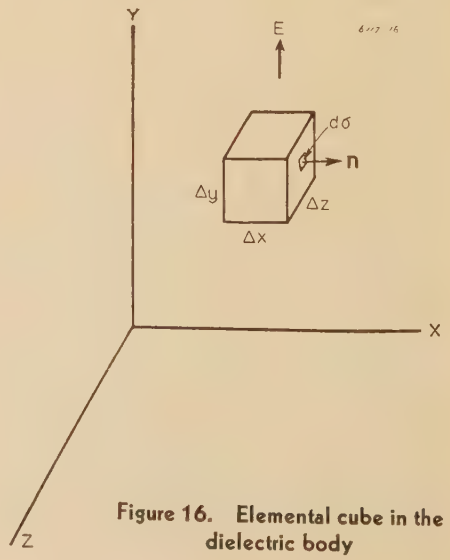

Figure 16. Elemental cube in the dielectric body

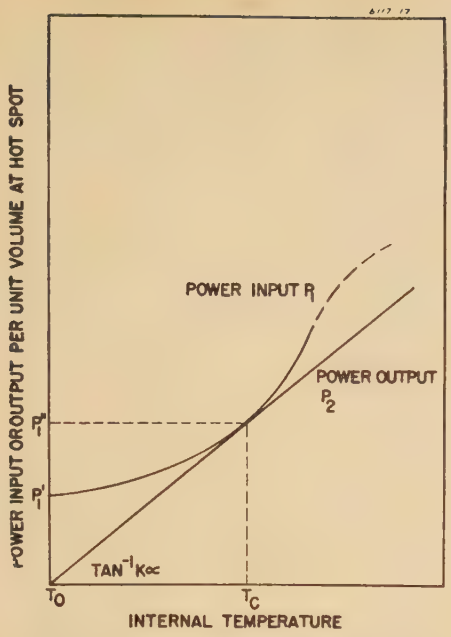

Figure 17. Power imput and power output conditions leading to ultimate breakdown

down curve for porcelain applies with reasonable accuracy to practical insulator shapes at the higher temperatures. This is shown by the actual breakdown tests on practical insulators as listed in Table III.

It seems probable that at temperatures above 250 degrees the reduction in resistivity of the porcelain results in more nearly uniform voltage gradients in the practical insulators.

No actual breakdowns were obtained on the zircon composition even though temperatures were carried up to 900 degrees at 40 volts per mil direct current. The tendency of the zircon to increase in resistivity with time at constant ambient temperature and voltage is believed to be caused by dielectric polarization. At any constant temperature and voltage, the more mobile negative ions (or possibly electrons) drift away from the negative electrode, leaving a super abundance of the less mobile positive ions in this area. This results in an apparent increase in the resistivity of the material. When such polarization occurs to a marked degree, it would be expected that the breakdown temperature with alternating current would be lower than with direct current.

Conclusions

The electrical resistivity of all of the ceramic insulating materials tested diminishes not only with increasing temperature but also, at the lower temperatures, with increasing voltage gradient. The rate of change of resistivity with voltage appears to diminish with increasing temperature so that for porcelain above 250 degrees the resistivity is nearly independent of voltage.

From the shape and level of the temperature resistivity curves, it is possible to predict the temperature at which an insulator will fail under any particular voltage gradient. While these predictions are based primarily on high temperature measurements, it appears as though the thermal effect may be a major factor in

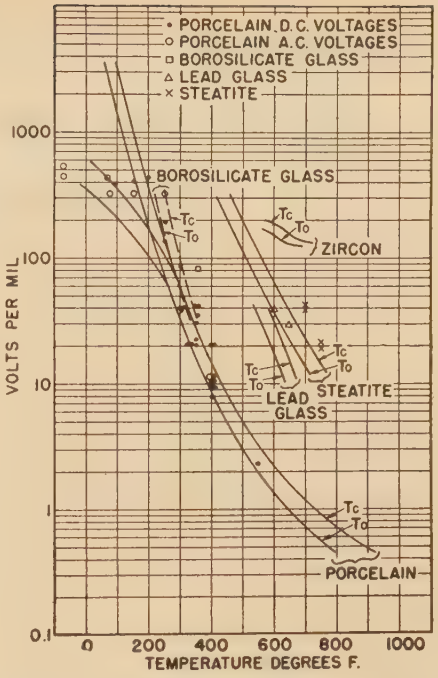

Figure 18. Temperature versus voltage gradient for breakdown

insulator breakdowns even at low temperatures. The existing data do not permit definite determination at low temperature, however.

The breakdown curves shown in Figure 18 are believed to be applicable for 60-cycle alternating as well as direct voltage for all of the materials except zircon. For zircon the a-c breakdown temperatures may be somewhat lower.

There is also some question as to whether these curves are applicable to high frequency alternating voltages. At high frequencies other forms of dielectric loss may become of important magnitude, so that failure may occur at lower temperature levels. This has not been investigated.

There seems to be no appreciable difference in the high temperature electrical performance of wet process electrical porcelain as made by several well-known United States manufacturers.

The presence of glaze on porcelain does not seem to affect the high temperature performance.

The high temperature performance of glasses, steatite, and zircons may be expected to vary widely with different compositions. The one zircon composition which thus far appears to be best can be operated at 900 degrees Fahrenheit at 40 volts per mil direct current without failure.

Table IV. Breakdown Points of Porcelain Test Specimens With Alternating Voltage

Electrode Area, Sq In.	Specimen Thickness, In.	RMS Volts Per Mil	Temperature at Beginning of Failure, Deg F	Calculated Resistivity at Beginning of Failure, Megohms Per In. Cube	Time Required for Failure, Min	$\frac{E^2}{r^2}\frac{\partial r}{\partial T}$, Watts Per Cu In. Per Deg F
1	0.113	531	−70	600,000	0.25	0.0118
1	0.125	448	−70	1,200,000	5.5	0.0042
1	0.137	438	71	50,000	1.5	0.077
1	0.150	347	77	100,000	18	0.024
1	0.121	346	150	80,000	2.25	0.030
1	0.117	342	250	5,000	0.116	0.469

Table V. Breakdown Points of Glass and Steatite Test Specimens

Material	Electrode Area, Sq In.	Specimen Thickness, In.	Volts Per Mil D-C	Temperature at Beginning of Failure, Deg F	Resistivity at Beginning of Failure, Megohms Per In. Cube	Time Required for Failure, Min	$\frac{E^2}{r^2}\frac{\partial r}{\partial T}$, Watts Per Cu In. Per Deg F	Characteristic of Drift Curve
Borosilicate glass	0.6	0.36	83.3	350	625	3	0.6	No
Lead glass	0.442	0.50	40	600	272	14	0.109	No
Lead glass	0.442	0.50	30	650	110	7.25	0.22	No
Steatite	0.785	0.188	21.3	750	43.9	13	0.188	Flex
Steatite	0.785	0.203	19.7	750	42.5	13	0.166	Flex
Steatite	0.785	0.188	42.5	700	104.5	1.5	0.285	No
Steatite	0.785	0.203	39.4	700	101.3	3	0.252	No

References

1. Insulation Failure—A Pyroelectric Effect, J. L. R. Hayden, C. P. Steinmetz. *Electrical World*, volume 80, 1922, page 865.

Tennessee Valley Authority Hydroelectric Stations—Electrical and Mechanical Design

R. A. HOPKINS
FELLOW AIEE

H. J. PETERSEN
NONMEMBER AIEE

Synopsis: Design policies have been developed and established during the building and operating of 14 major hydroelectric generating stations since 1934. Turbines, governors, generators, transformers, switchgear, and other major equipment have been selected generally in accordance with normal manufacturers' designs except in specific cases where operating experience has indicated a definite need for improvement. Many of the improvements subsequently have become standardized by the manufacturers. Switching, bussing, control, relaying, wiring, piping, auxiliary equipment, and other station features have been developed by the Tennessee Valley Authority, using manufacturers' standard components as far as possible. The bases for selection of equipment and for development of station designs undoubtedly are applicable to other hydroelectric projects.

A REPORT was made in December 1941[1] on the electrical design of the Tennessee Valley Authority's new hydroelectric generating stations after six of the new stations were in operation. Today with 14 new stations operating, this supplemental report brings the record up to date, adds the mechanical design features, and outlines the fundamental electrical and mechanical design practices which have controlled the new generating station designs.

The Tennessee River system drains an area of 40,910 square miles, lying in the states of Tennessee, Virginia, North Carolina, Georgia, Alabama, Mississippi, and Kentucky. From the highest headwater in the mountains of North Carolina to the lowest tailwater in the western corner of Kentucky there is a total fall of 3,188 feet in 714 river miles. Mean annual rainfall on the watershed averages 52 inches and run-off averages 44 per cent. The unregulated stream flow at Kentucky Dam, the dam nearest the mouth of the Tennessee River, ranged from a minimum of 4,500 cubic feet per second to a probable flood of 960,000 cubic feet per second.

The Tennessee Valley Authority now owns and operates 26 hydroelectric plants with 89 units aggregating 1,777,580 kw, and 12 fuel plants with 37 units aggregating 430,400 kw. By agreement with the Aluminum Company of America, the authority dispatches the water and the power at eight Alcoa dams with a total installed capacity of 311,120 kw of hydroelectric power, and by agreement with Memphis Power and Light Company, it leases 20,000 kw of steam power, thus bringing the total installed capacity now controlled by the Authority to 2,539,100 kw of which 82.3 per cent is hydroelectric.

The principal transmission lines, between generating stations and large load centers (Figure 1), consist of about 2,000 circuit miles of 154-kv lines and 1,000 circuit miles of 110-kv lines. Although the generation and the load are scattered fairly well over the entire area, the hydroelectric generation in the eastern portion of the system is mostly of a storage nature, while that in the central and western portion is generally run-of-river. This condition causes a considerable transmission of energy eastward during the storage season and westward during release and requires rather heavy east-west lines. These heavy lines, together with several interconnections with adjacent power systems, result in unusually economical generation and distribution of energy, not only within the Authority's system but also in the adjoining systems. Many of the turbines are either set above tailwater or are provided with compressed air facilities to depress tailwater so they can be motored as synchronous condensers when not needed for energy or when reservoirs are being filled. This provides potential sources of synchronous capacity widely scattered over the entire system. When a unit is motored, the controls are set to pick up load immediately upon sudden demand.

Load has grown steadily along with the development of generating facilities and much of the time has grown faster than generation could be provided. During the fiscal year ended June 30, 1945, the Authority-controlled plants generated 11,935,000,000 net kilowatt-hours of energy, of which 85.4 per cent was from the hydroelectric station. The maximum hourly demand was 1,933,000 kilowatts.

Generating Stations

The 14 new hydroelectric stations and the six new units at existing Wilson Dam are listed with their principal characteristics in Table I. With their variations in flow, head, storage, ratings, topography, and transmission connections these developments represent three general types of development and several plant arrangements.

Enclosed conventional generator rooms with indoor cranes (Figures 2 and 3) are provided at eight of the 15 plants At Wheeler, where the tailwater is especially low, the generators are outdoors in weatherproof housings, and an outdoor gantry crane serves the main units after removing the housings and serves the erection bays through removable hatch covers. At the remaining six plants an open-deck design (Figure 4) is used with an outdoor gantry crane serving the generating units and erection bays through removable hatch covers.[2]

Transformers are located alongside the

2. HIGH-VOLTAGE INSULATION, **J. L. R. Hayden, Charles P. Steinmetz.** AIEE TRANSACTIONS, volume 42, 1923, pages 1029–41.

3. A THEORY OF IMPERFECT SOLID DIELECTRICS, **Michel G. Malti.** AIEE TRANSACTIONS, volume 46, 1927, pages 616–32.

4. THE ELECTRICAL RESISTIVITY OF INSULATING MATERIALS, **Harvey L. Curtis.** AIEE TRANSACTIONS, volume 46, 1927, pages 1039–47.

5. ELECTRIC STRENGTH OF SOLID AND LIQUID DIELECTRICS **W. A. DelMar, W. F. Davidson, R. H. Marvin.** AIEE TRANSACTIONS, volume 46, 1927, pages 1049–61.

6. THE THEORY OF THERMAL BREAKDOWN OF SOLID DIELECTRICS, **P. H. Moon.** AIEE TRANSACTIONS, volume 50, 1931, pages 1008–21.

7. LOW LOSS CERAMICS, **R. Russell, Jr., F. J. Berberich.** *Electronics*, May 1944.

8. BREAKDOWN OF GLASS WITH ALTERNATING POTENTIALS, **N. D. Kenney, A. M. Luery, J. D. Moriaty.** AIEE TRANSACTIONS, volume 51, 1932, pages 404–8.

9. PREDETERMINATION OF THE A-C CHARACTERISTICS OF DIELECTRICS, **J. B. Whitehead, Alfredo Banos, Jr.** AIEE TRANSACTIONS, volume 51, 1932, pages 392–402.

Paper **46-108**, recommended by the AIEE committee on power generation for presentation at the AIEE summer convention, Detroit, Mich., June 24–28, 1946. Manuscript submitted March 29, 1946; made available for printing May 1, 1946.

R. A. HOPKINS and H. J. PETERSEN are head electrical engineer and head mechanical engineer, respectively, technical staff, design department, Tennessee Valley Authority, Knoxville, Tenn.

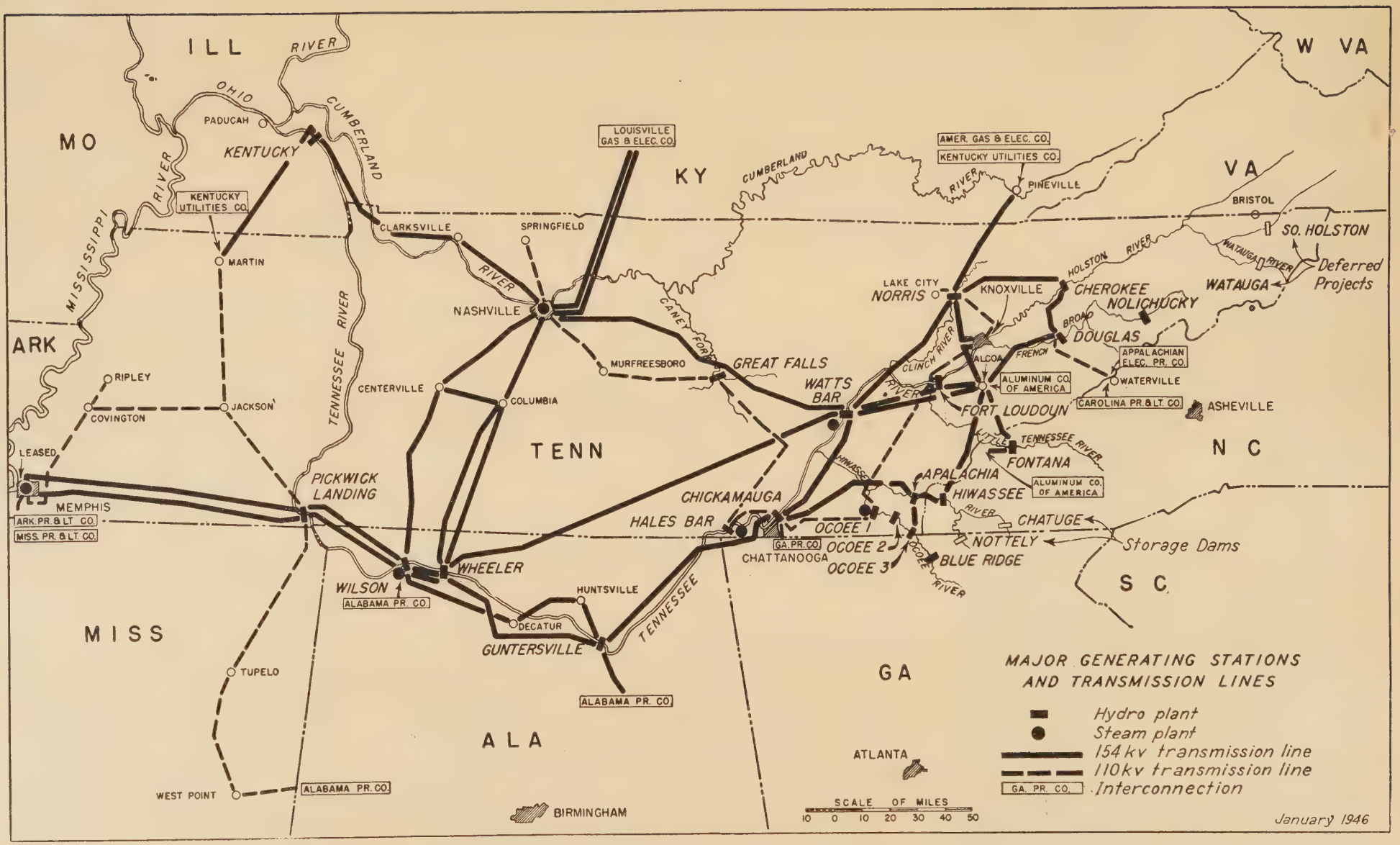

Figure 1. Transmission map, January 1946

generator room at three plants and adjacent to the switching structures at 12 plants. The control room is preferably located between the powerhouse equipment and the switchyard equipment to minimize the lengths of control circuits and to reduce the radius of operation. At 11 of the plants the control room is located in the end or corner of the powerhouse nearest the switchyard. At Apalachia the control room is located alongside the generator room and the governor cabinets are located within the control room, thereby reducing manpower requirements.

At Watts Bar an unusual topography presented a steep rocky bluff at the shore end of the powerhouse (Figure 5). The transformers, the switchyard, and a separate control house are all located 126 feet above the generator floor. The control house is connected to the powerhouse by means of a vertical shaft with elevators and a horizontal corridor at the powerhouse level. This switchyard and control room handle also the output of the 240,000-kw Watts Bar Steam Plant located 3,500 feet downstream.

The 30,000-kva single-unit Ocoee 3 Hydroelectric Plant with remote supervisory control by cable[3] was added to the system in 1943. Operation has proved entirely satisfactory, and three other generating units of similar size for other plants on the system are now under design also for supervisory control. Two will be controlled by cable and one by carrier.

The Authority has made every effort to specify for all of its generating and auxiliary equipment, characteristics and construction which are fairly well standardized by all the manufacturers so as not to demand special features. This policy which was established early in the program demonstrated its value very forcibly during the war when at one time as many as 20 major hydroelectric units were in manufacture and erection, and practically all the standard practices previously developed were successfully maintained.

Turbines

Kaplan-type movable-blade propeller turbines are used in the main-river plants except at Wheeler, where the small variations in headwater and tailwater elevations made a fixed-blade propeller turbine more desirable, and at Wilson where the relatively higher head dictated Francis turbines. Francis turbines are used at all the tributary storage plants and at the tunnel and surge-tank plants because of their high heads.

Specific speed, peripheral coefficient, and critical sigma for cavitation are factors in determining the sizes, speeds, and settings of all turbines.[4] In some plants which operate over extreme ranges of head, a specific speed was selected which would be mechanically safe for the runner when operating at the highest head. Turbines are usually rated at full gate, normal head.

In the main-river plants where propeller-type turbines are used, it was necessary in order to prevent excessive cavitation to set the runners below normal tailwater, thus obtaining a negative static draft head. Draft tube water-depressing systems are installed on certain units to lower the tailwater below the runner to reduce the power losses when these units are operated as synchronous condensers.

Runners are cast steel. The high first cost of cast-steel runners over cast-iron runners is more than offset by their greater resistance to cracking or disintegrating after years of operation under fluctuating loads. Cast steel has the further advantage that cavitation can be retarded and can be repaired with comparative ease by welding, while welding on cast-iron runners is a very expensive and unsatisfactory operation. To retard cavitation, areas on runners which experience has proved to be subject to excessive cavitation are prewelded at the factory with a one-eighth-inch layer of stainless steel.

Guide vanes are steel castings. In the high-head plants during off-peak hours and during storage periods, it is desirable to operate one or more units as synchronous condensers. During this operation, with the guide vanes closed and full headwater in the scroll case, the leakage past the tops and bottoms of the guide vanes has been found to cause some erosion similar to a scouring action. To minimize this erosion in the later plants, strips of stainless steel were welded to the guide vanes at this point.

Scroll cases at the main-river plants are concrete. In the high-head tributary and surge-tank plants the higher pressures dictated the use of steel scroll cases. Throat rings are rolled steel, as this material has proved more resistant to pitting than cast steel.

Water-lubricated main bearings are used in the low-head main-river plants which have relatively high tailwater conditions. Both lignum vitae and rubber wearing surfaces were used in some of the earlier plants, but Insurock has been used in the majority. The shafts are fitted with stainless steel sleeves where they pass through these bearings. The high-head units have smaller wheels operating at higher speeds, and their main bearings are oil-lubricated, babbitt-lined, and bear directly on the polished steel of the shafts.

Shafts are open-hearth, carbon or alloy

Table I. Generating Station Statistics

Station	Average Flow, CFS	Useful Storage, Acre-Ft	Rated Head, Ft	Number of Units at Present	Number of Units Ultimately	Turbine Rating, Hp	Type	Speed, Rpm	Generator Rating, Kw	Number of Generators Per Transformer Bank	Transmission Voltages, Kv	Powerhouse Type	Switchyard Type
Main-River Developments													
Chickamauga	38,410	329,400	36	3	4	36,000	Kaplan	75.0	27,000	1	154, 110, 44	Enclosed	Low
Fort Loudoun	14,300	109,300	65	2	4	44,000	Kaplan	105.8	32,000	2	154, 110	Open-deck	Low
Guntersville	41,400	162,900	36	3	4	34,000	Kaplan	69.2	24,300	1	154, 110, 44	Enclosed	Low
Kentucky	63,620	4,010,800	48	4	5	44,000	Kaplan	78.3	32,000	1, 2	154, 66	Open-deck	Low
Pickwick	55,000	418,400	43	4	6	48,000	Kaplan	81.8	36,000	1	154, 110	Enclosed	High
Watts Bar	26,400	337,600	52	5	5	42,000	Kaplan	94.7	30,000	1	154	Open-deck	Low
Wheeler	50,000	348,900	48	4	8	45,000	Fixed	85.7	32,400	2	154	Outdoor	High
Wilson*	52,000	52,500	92	6	10	35,000	Francis	100.0	25,200	2	154, 110	Enclosed	High
Tributary Storage Developments													
Cherokee	4,650	1,473,100	100	2	4	41,500	Francis	94.7	30,000	2	154, 66	Open-deck	Low
Douglas	6,700	1,419,700	100	2	4	41,500	Francis	94.7	30,000	2	154, 110	Open-deck	Low
Fontana	3,970	1,154,300	330	2	3	91,500	Francis	150.0	67,500	1	154	Enclosed	Low
Hiwassee	2,150	364,700	190	1	2	80,000	Francis	120.0	57,600	1	154, 44	Open-deck	Low
Norris	4,600	2,281,000	165	2	2	66,000	Francis	112.5	50,400	1	154, 110	Enclosed	High
Tunnel and Surge-Tank Developments													
Apalachia	2,240	37,500	360	2	2	53,000	Francis	225.0	37,500	1	154	Enclosed	High
Ocoee 3	1,270	9,400	280	1	1	33,500	Francis	200.0	27,000	1	154, 66	Enclosed	High

* New units in existing plant.

steel forgings, heat-treated, and machine-finished. They have renewable sleeves where they pass through the water-lubricated guide bearings and the stuffing boxes in the head covers. They are all hollow-bored to allow for internal inspection. The upper ends of the shafts for Kaplan wheels are belled out to receive the blade-tilting servomotors.

Governors

The governing system for each turbine is of the hydraulic relay valve actuator type, with motor-driven governor head, auxiliary control mechanism, restoring mechanism, oil-pressure system, pipe, and, in the case of the Kaplan units, the control valve for runner blade adjustment. The governing mechanism and pumping units are mounted in a cabinet (Figure 6), the lower part of which forms the oil sump and the front face of which is the turbine instrument and control board. Governors for either one or two units are mounted in one single or one double cabinet as the powerhouse arrangement dictates.

The governors are designed for a normal maximum operating oil pressure of 300 pounds per square inch. Each governor is provided with a separate vertical cylindrical oil storage tank, with sufficient compressed air space above the oil to operate the turbine wicket gates through one complete cycle. Oil-pressure systems are interconnected, and sufficient spare pumps are provided to permit operation of all governors in the plant during outage of one of the pumping units.

Gate operating time, as controlled by the governor, is adjusted from a minimum of six seconds to a maximum of ten seconds at the various plants. Speed-level controls are provided to control the speed of the turbine from 85 per cent of rated speed at no load and zero speed droop to 105 per cent of rated speed at full load and maximum speed droop. Speed droop adjustment is from zero to six per cent.

Generators

Generator characteristics and construction were developed at the beginning of the program in consultation with the engineers of the manufacturers on the basis of meeting system requirements and at the same time keeping within the manufacturers' normal designs and practices as far as possible. A few compromises were necessary on both sides, and over the years a few improvements have been developed mutually. Principal features which are practically uniform for nearly all the 44 generators installed to date are:

1. Power factor, 0.9.
2. Short circuit ratio, 1.1.
3. Condenser capacity, 55 per cent.
4. Line-charging capacity, 80 per cent.
5. Noncontinuous damper windings giving reactance ratio, 1.35.
6. Flywheel effect based on 30 per cent speed rise with full-load rejection and gate closure in five seconds resulting in 120 to 180 per cent of normal flywheel effect.
7. Excitation voltage, 250.
8. Ceiling, 325.
9. Response ratio, 1.
10. Direct-connected main and pilot exciters partially telescoped.
11. Thrust bearing below the rotor and usually one guide bearing also below the rotor.
12. Shaft flanged at top to rest on thrust bearing and to support the rotor.

An important shop test required by the authority consists of assembling the generator and turbine shafts and their bearing surfaces and checking the complete assembly in a lathe. It is specified that the running surface of the thrust bearing runner shall be perpendicular to the axis of the generator and turbine guide bearing journals within a tolerance of 0.0005 inch at every point. After erection in the powerhouse, each generating unit is given a mechanical rotation check to ensure that the thrust bearing surface is perpendicular to the axis of the generator and turbine guide bearings within the tolerance allowed in the shop test and that the shaft is plumb to within a tolerance of 0.001 inch in about five feet.

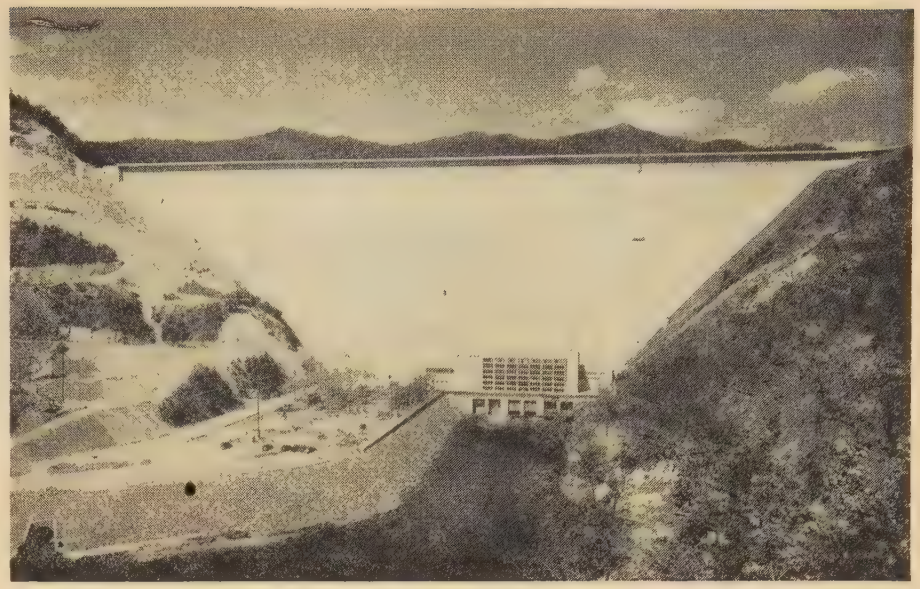

Figure 2. Fontana Dam
Enclosed generator room

Carbon - dioxide fire - extinguishing equipment for the enclosed generators has been improved through the years. Spare cylinders originally were kept on hand to renew an exhausted bank. These cylinders now are racked and piped to form a reserve bank always ready for instant use. A systematic test procedure has been developed wherein a few cylinders are released and the carbon-dioxide concentration is measured over a period of 30 minutes with the generator running. This provides a basis of judging the airtightness of the generator housing and for adjusting the time intervals at which the delayed discharges should be released. The tests also have demonstrated that with a reasonably tight housing fewer cylinders are required in both the initial and the delayed banks than were considered necessary on the earlier units before these tests were developed.

Transformers

Fundamental features originally selected have been carried through to date with minor improvements in keeping with the advances in manufacturing practice.

Three-winding transformers with load-ratio control from the switchboard (Figure 7) have been installed at Ocoee 3 and Kentucky in addition to those previously reported. It has become general practice to provide spare transformers

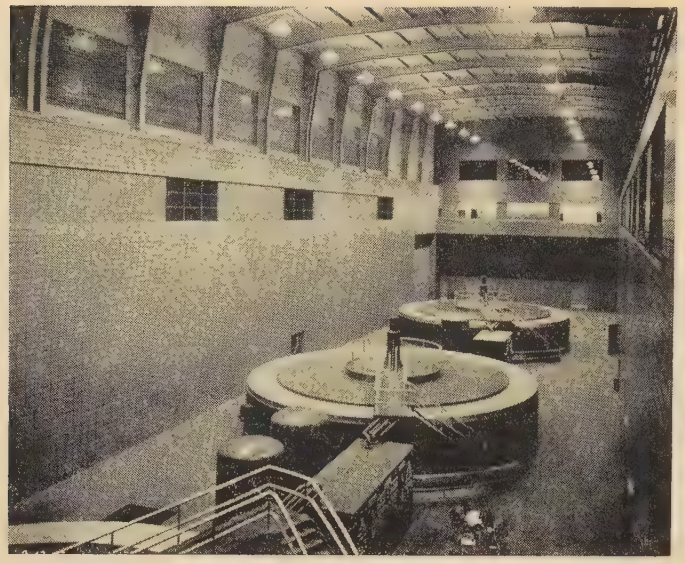

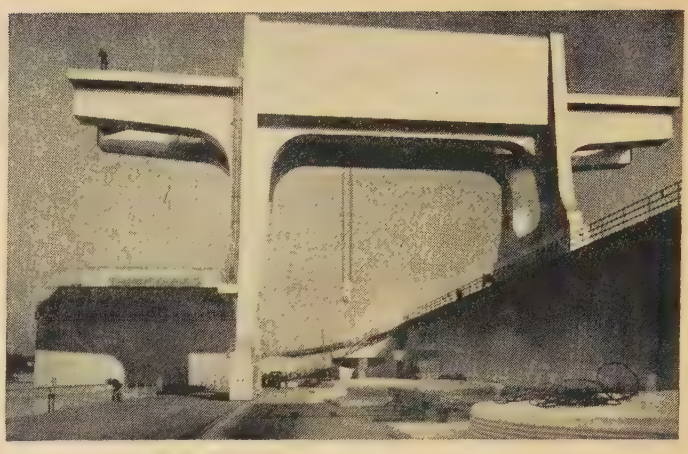

Figure 4 (above). Kentucky Dam
Open-deck station with double-trolley gantry crane

Figure 3 (left). Chickamauga enclosed generator room

only for important ties and system interconnections where outage would cause loss of load, but not for generation stepup.

Fire protection for transformers has not been installed except at Wheeler, Pickwick, and Wilson, where the transformers are located adjacent to the powerhouse structures. These three systems employ fixed fog nozzles arranged to envelop the transformers. Flow of water is initiated manually by remote control or automatically by thermostats and differential relay operation depending on local conditions.

Main Electrical Connections

Operation to date has indicated the general adequacy of the bussing and switching scheme established at the beginning of the power program. While no fundamental changes have been necessary, a number of minor improvements have become possible as the power system has grown.

At Watts Bar the connection of the four new 60,000-kw steam turbine generators to the hydro bus increased the generation in the Watts Bar area to the point where it no longer was felt necessary to provide separate 154-kv switching for each of the five 30,000-kw generators. Furthermore, space was required in the 154-kv yard for more 154-kv lines than originally had been anticipated. Consequently hydroelectric units 1 and 2, which were already installed, with their individual 3-phase transformers, were paralleled solidly on the high-voltage side and switched as a 60,000-kw unit to the 154-kv bus. Units 4 and 5, installed later, similarly were connected and switched. This provides six 60,000-kw and one 30,000-kw generator circuits on the 154-kv bus with six existing lines and space for two future lines. Synchronizing breakers were installed between hydroelectric generators 1, 2, 4, and 5 and their transformers. The retaining of the individual 3-phase transformers provides flexibility and uniformity, while the group switching to the 154-kv bus conserves breakers and switchyard space.

At Guntersville, where an additional line was needed urgently during war-time restrictions, generators 1 and 2 with their 3-phase transformers, which were already in operation, also were paralleled on the high-voltage side and switched as a 48,600-kw unit to the 154-kv bus. Synchronizing breakers were added between the generators and their transformers. While this conservation of steel structures, high-voltage breakers, and equipment was particularly desirable during the war, the power system had grown to the point where the common switching of the two generating units could be justified as a permanent arrangement.

In a few cases it has been found that system operation does not require as many 154-kv bus-sectionalizing disconnects as originally planned, and fewer disconnects have been provided, particularly in the transfer busses.

The ring-bus arrangement has been used successfully in the initial 154-kv installations at several plants, including Kentucky, Fort Loudoun, Fontana, Douglas, and Cherokee. As pointed out in the previous report, the standard switchyard design provides for a ring-bus arrangement for three or four circuits, and the construction is such that the ring bus is converted readily to a main-and-transfer-bus arrangement when more circuits are added. This conversion has been made in a number of cases.

At Fontana a departure was necessary from the established policy of avoiding local distribution at generator voltage. Since there were no nearby power lines of a voltage lower than 154 kv, and since there was a demand of some 3,000 kw in village load, it was considered expedient to avoid excessive stepdown transformation by taking the village service from the 13.8-kv delta busses of the two stepup transformer banks of generators 1 and 2. A 13.8–12.5-kv transformer bank and a step-type regulator in the village feeder, together with station-type arresters, guard the generator circuits against voltage surges from lightning.

Generator-Voltage Switchgear and Connections

Air blast circuit breakers have been given consideration during recent years, but up to the present time conventional oil circuit breakers have been used exclusively. The conventional top-connected breakers are well adapted structurally to the Authority's standard switchgear designs, and because of the small number of indoor breakers required, never more than two per generator, the oil fire hazard is not considered serious.

Cables from generators to switching cubicles for many of the later installations have been insulated with varnished-cambric tape instead of corona-resisting rubber compound. They are shielded with copper tape. The ducts generally are drained and ventilated and in this case the cables are provided with an outer cover of tape and braid. In any case where moisture may be expected, the cables are covered with Neoprene jackets. Creepage terminals are formed in much the same way as with rubber insulation except that particular attention is given to the excluding of all moisture

by finishing the exposed insulation with several coats of Glyptol varnish and by filling the end of the stranded conductor with solder. The cables are designed for operation at a conductor temperature not exceeding 78 degrees centigrade.

Cables from switching cubicles to transformers are in most cases paper-insulated and lead-covered, as previously reported, but two exceptions will be noted. At Watts Bar Dam, where a 126-foot difference in elevation exists between the two ends of the circuits, varnished-cambric insulation with nonmigrating compound is used instead of oil-impregnated paper insulation. At Wilson Dam and at Kentucky Dam, where distances up to 1,475 feet were required and where the circuits were carried through areas where conventional duct lines would have congested available space, Oilostatic cable circuits were installed. The Oilostatic circuit, which consists of paper-insulated cables with the three phases installed in a steel pipe filled with oil, used about 75 per cent of the copper and 50 per cent of the space which would have been required for conventional duct lines.

Bare structural shapes have been used to advantage in three recent installations where rather heavy circuits were required between the switching cubicles and the transformers. At Apalachia, one $2^1/_2$-inch iron-pipe-size copper tube per phase was used for the 1,927-ampere circuits outdoors. At Fort Loudoun, two $2^1/_2$- by-$2^1/_2$- by-3/16-inch copper angles per phase forming a square with vertical ventilation were used for the 3,420-ampere circuits on the ceilings of concrete tunnels with Transite barriers and bottom covers and with forced ventilation at full load. At Fontana two $3^1/_2$- by-$3^1/_2$- by-1/4-inch copper angles per phase forming a square with vertical ventilation were used for the 3,610-ampere circuits on the side walls of concrete tunnels with Transite barriers and front covers and with natural ventilation. These three installations represent copper economies of 1,220, 1,950, and 1,100 amperes per square inch, respectively.

Transmission-Voltage Switchgear and Connections

Oil circuit breaker ratings on the 154-kv system have been improved at many of the older stations from 2,500,000 kva, 8-cycle opening, 35-cycle reclosing, to 3,500,000 kva, 5-cycle opening, 20-cycle reclosing, with pneumatic operators; and recently all new breakers have been purchased with the higher ratings. Likewise, the few 1,500,000-kva breakers originally installed at certain earlier stations have been improved to 2,500,000 kva.

Air blast breakers have been given considerable study, but during war restrictions it was necessary to use the conventional oil breakers, and so far they have been able to meet all essential requirements.

Automatic reclosing at 20 cycles without synchronism check now is being used on some of the 154-kv tie lines.

Currents in excess of 600 amperes have developed on certain 154-kv heavy tie lines and busses, requiring the continued use of 1,200-ampere breakers, the reinforcing of certain disconnecting switches, and the changing of some of the steel pipe conductors to copper tubing.

Lightning Protection

The arresters located at the terminals of the stepup transformers now are rated 145 kv for the 154-kv system, 121 kv for the 110-kv system, and 73 kv for the 66-kv system. At Apalachia, the 154-kv switchyard where the lines terminate is approximately 1,000 circuit feet from the arresters at the transformers, and consequently station-type arresters are provided also in the switchyard. These arresters are rated 169 kv, which is considered adequate for the protection of the switchgear.

Relaying

Generator protection against faults to ground, particularly near the neutral ends of the stator windings, has been improved in some of the later stations by use of a low-energy short-time overcurrent relay connected as a differential ground relay to compare the residual current in the generator main leads with the current in the generator neutral lead. This relay is now used in place of the ground backup relay with low-current long-time setting previously used.

Most of the 154-kv lines now are provided with distance phase relays and directional overcurrent relays controlled by carrier pilot relays. The directional overcurrent ground backup relays also are used as originally. The recent type GCY and HZM relays are being used on the longer lines.

Annunciation

The operation recorder previously mentioned now has become standard equipment at all new generating stations. It records on a strip chart the important manual and switching operations and all abnormal conditions usually annunciated. One or two recorders, depending on the station requirements, are located on the operator's desk alongside the telephone turret (Figure 8). With the recorder equipment, it is no longer necessary to provide the large array of annunciator windows along the top of the instrument board as installed at a few of the earlier plants. The particular annunciations which require immediate attention of the switchboard operator are arranged in small windows on the recorder housing on the operator's desk, and those requiring immediate attention of the turbine opera-

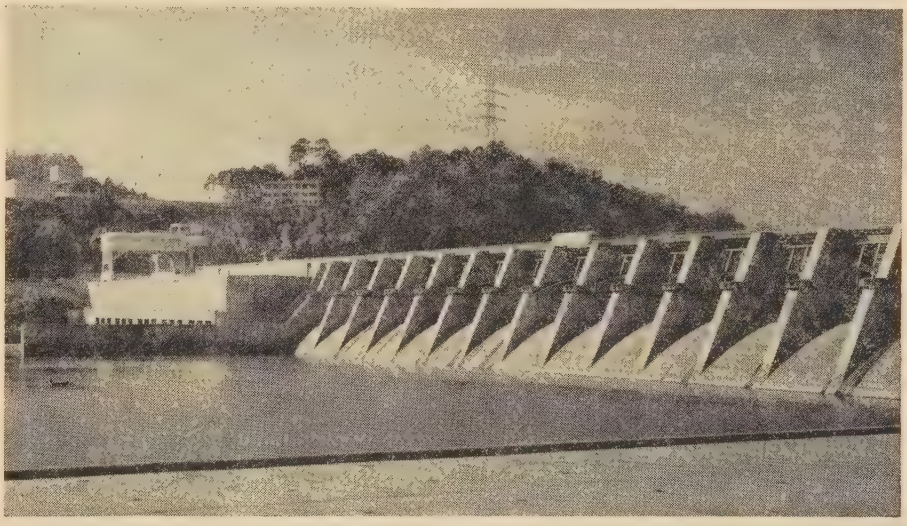

Figure 5. Watts Bar project

Two elevations

tor are arranged in windows on the governor actuator panels.

Communication

Power line carrier telephone channels now provide direct communication between all generating stations and the dispatcher's office. Most of the stations are also connected to the dispatcher's office by telephone lines which are owned or leased by the authority. These telephone lines carry both voice and carrier channels.

Telemetering by power line carrier recently has been installed for transmitting the load on each tie connection with other utilities from the point of interconnection to the dispatcher's office in Chattanooga. Here the loads are recorded, totalized, and retransmitted to the dispatcher of one of the neighboring utilities or are used to control automatically the impulses of a master system load controller. These impulses are broadcast over the entire Tennessee Valley Authority system by a frequency-shift type carrier equipment and can be received at all of the larger hydroelectric stations for regulating the governors of local generators in response to load changes on a distant tie-line interconnection. The total generation at the major stations also is transmitted to the dispatcher's office by means of the carrier telemetering channels. Equipment is being installed at the two largest generating stations, Wilson and Watts Bar, to enable these two stations to carry a definite proportion of the regulating load when operating in parallel under the control of the master controller. These stations then will share the load in the same manner as the generators within a station share the load when operating under proportionate load control.

Carrier-current equipment now is being located generally in the air-conditioned telephone rooms, although earlier carrier relay sets were located in the switchyard. The inspection and servicing of this type of equipment are facilitated greatly by having the equipment indoors.

Switchboards and Controls

Within the control room the general arrangement of boards, panels, and equipment, as previously described, has become standardized with few exceptions. At Apalachia, a 2-unit particularly compact station, and at Ocoee 3, a 1-unit unattended station, the controls and instruments are mounted on a common vertical board, and a bench is not required.

Switchboards in the more recent stations (Figure 9) instead of being black are finished in generally light colors blending with the finish of the control room, while all equipment has contrasting standard black finish. This combination presents a very pleasing appearance and improves vision. Draw-out type relays with built-in test facilities are becoming standard.

Wiring of the switchboards constantly is becoming simpler and more accessible. In most of the later stations, except the largest ones, terminal blocks have been mounted very successfully on wing panels extending back from main panel intersections, and the control cables are carried through rectangular steel ducts to asbestos trays in the room below. This eliminates the 3-story arrangement, with terminal cabinets on the intermediate floor, which is used at the larger plants. At the plants where the terminal blocks and other devices are located in cabinets on the floor below the switchboard, the wiring was made continuous from the terminals on the switchboard equipment to the terminal blocks and was therefore installed by the Authority. With the terminal blocks on the wing panels, the wiring can be installed either at the factory or in the field. In cases where time has been available to get all wiring requirements into the hands of the manufacturer in time for him to do the wiring, it has been done in the factory; but in many cases of extreme urgency, time has been gained by having the boards shipped unwired and installing the wiring in the field. Control cables recently have been insulated with oil-base compound containing Buna S and have been jacketed with Neoprene.

Automatic oscillographs have proved very useful in analyzing line faults, and in stations having a large number of lines, two 6-element oscillographs have been installed.

Station Auxiliaries

Indoor overhead cranes of capacities up to 300 tons are provided in all stations having conventional enclosed generator rooms for erection, dismantling, and maintenance of the generating units. They also are used for handling transformers in those stations where the transformers can be rolled into the generator room for untanking. Most of these cranes have two trolleys, each with a main hoist and an auxiliary hoist. A lifting beam on the two main hooks is used to handle the heavier loads. Bridge drive is by two motors mounted near the center of the bridge and connected through individual cross-craneway shafts to at least 50 per cent of the wheels on each rail. One drive is provided with a hydraulic-operated service brake and the other with a time-delay thrustor-released spring brake. Trolley drive is by one motor mounted on the trolley connected to one wheel at each side of the trolley and provided with a solenoid-operated

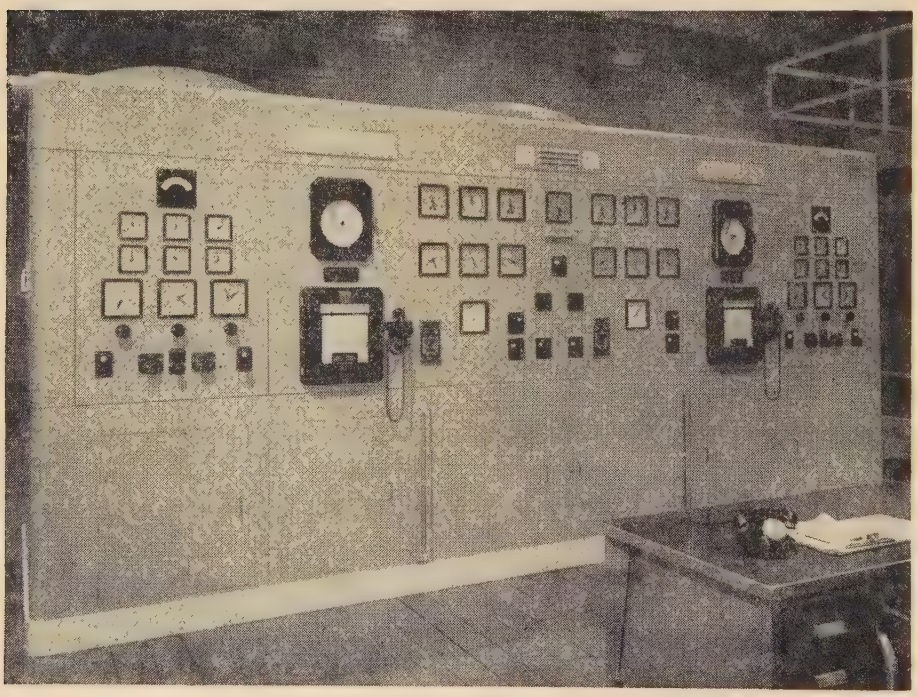

Figure 6. Double governor cabinet at Watts Bar

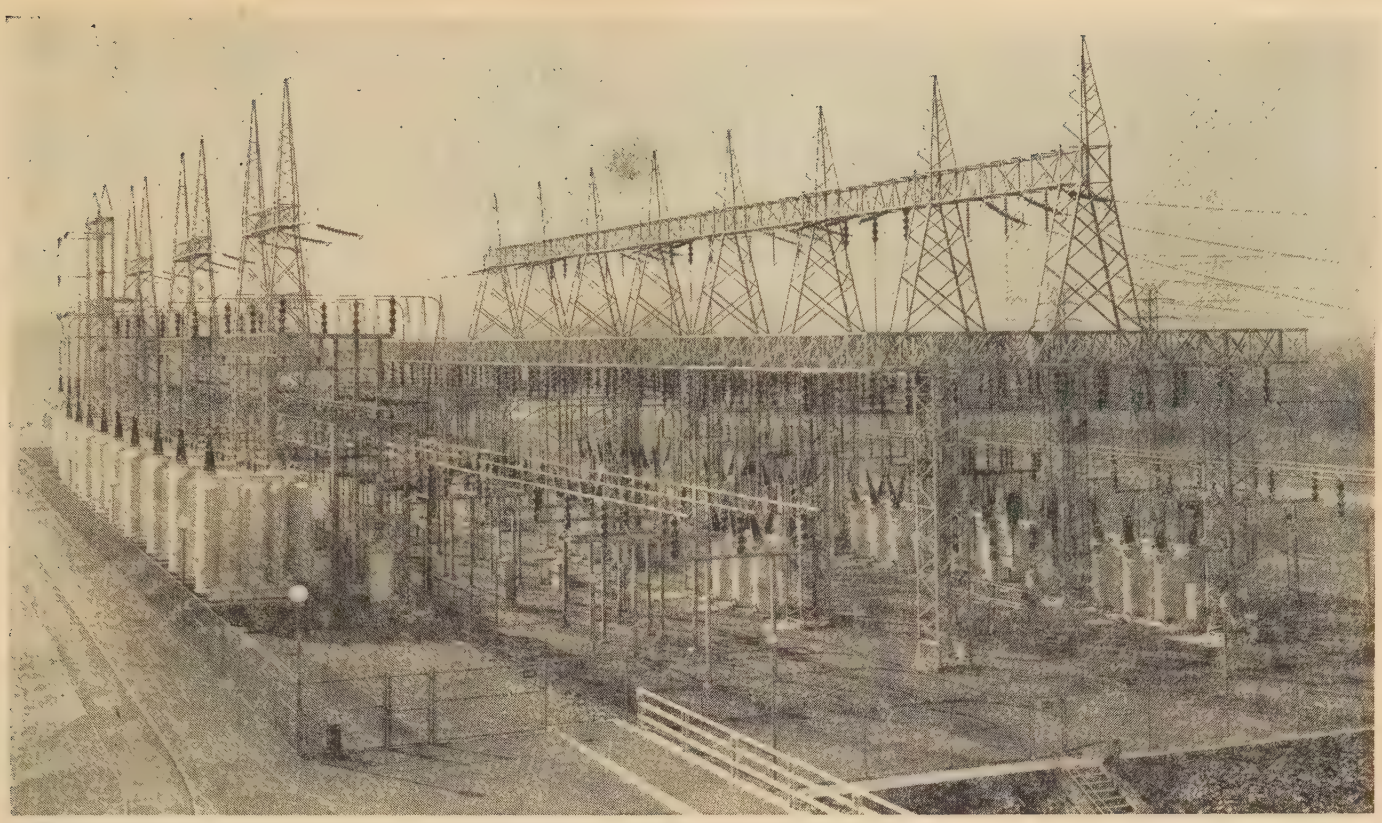

Figure 7. Three-winding transformers and low-type switchyard at Chickamauga

brake. The main and auxiliary hoists have individual motors which are identical and interchangeable and are provided with thrustor-released spring brakes. All motors are 440-volt 3-phase ball or roller bearing crane type. All are wound-rotor type except the trolley drive motors which are squirrel-cage type. Controls of bridge travel, trolley travel, and hoisting are arranged for independent control of these three motions and to permit only one motion at a time. Acceleration is by adjustable definite-time automatic control. The control provides for movements from rest of less than 1/16 inch for the main and auxiliary hoists and less than 1/4 inch for the bridge and trolley travels. The controls are of magnetic type with master switches in the operator's cab. Power supply for the crane is at 440 volts, 3-phase, by steel or copper angles in the runway and sliding shoes on the crane. Power and control connections to the trolleys are by steel angle conductors on the bridge girders and sliding shoes on the trolleys.

Light overhead single-beam cranes, of capacities up to five tons, operated from the floor by cord switches are provided in several of the erection bays and machine shops.

Unloading cranes and derricks are provided at a number of the plants for receiving materials coming in by river.

Outdoor double-trolley gantry cranes (Figure 4) of capacities up to 275 tons are provided over the generator rooms and erection bays at Wheeler and at all stations of the open-deck design for erection, dismantling, and maintenance of the generating units. These cranes also are used for handling transformers in those stations where the transformers can be rolled under the gantry crane and lowered into the erection bay for untanking. These gantries are in most cases provided with overhanging bridges or with boom hoists to permit handling of tail gates. Each of the two trolleys has a main hoist and an auxiliary hoist. Gantry drive is by means of four motors, one at each corner of the gantry and operated through a common control. Trolley drive is by one motor mounted on each trolley and connected to one wheel on each side of the trolley. Each of the four hoists has an individual motor, all four motors being identical. The motors, brakes, and controls are essentially the same as for the indoor overhead cranes. Power supply for the gantry is by flexible cable and motor-driven cable reel from polarized receptacles installed along the runway except at Kentucky, where collector angles are used. Power and control connections to the trolley are by steel angle conductors on the gantry and sliding shoes on the trolleys. All machinery is protected from the weather by a steel housing, and particular attention was given to the streamlining of the crane structures and the housings, since the large gantry is one of the prominent features at each site.

Outdoor single-trolley gantry cranes of capacities up to 100 tons are provided at most of the stations for handling spillway gates, intake gates, stop logs, emergency bulkheads, trash gates, and trashracks. An important design practice at most of the stations is to build the deck at the same elevation across the spillway and intake sections so that the cranes can operate over both these sections. The trolley has a short travel over the two slots of a gate. It is provided with a hoist and with latching attachments for handling the gates. Drive motors, brakes, and controls are essentially the same as for the double-trolley gantry, and the machinery is covered. Power supply to the gantry is normally by means of conductors under deck and collector shoes on the crane. In emergency, power is supplied by flexible cable and motor-driven reel from polarized receptacles installed along the runway. Power and control connections to the trolley are by flexible cable looped between a terminal box on the gantry and one on the trolley.

Spillway gates[5] at Watts Bar, Fort Loudoun, Cherokee, and Douglas are of

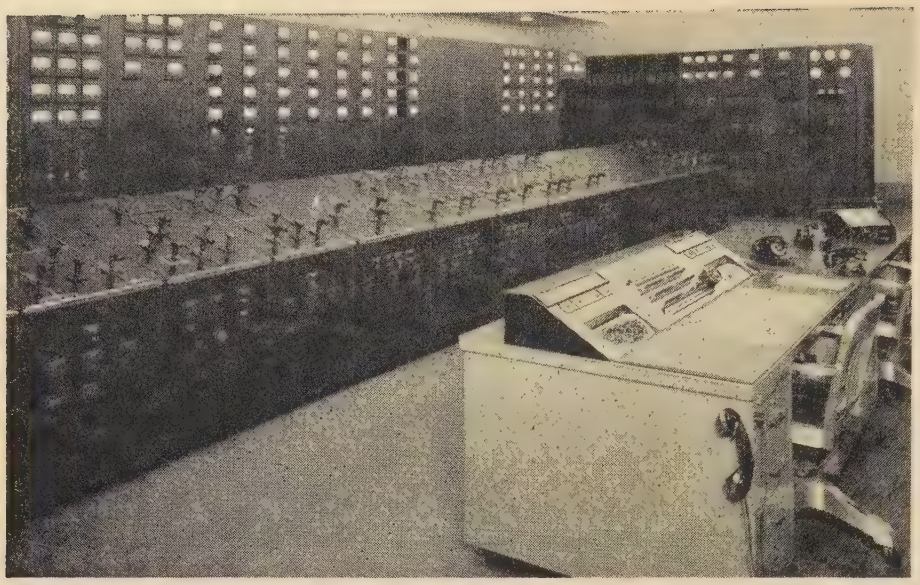

Figure 8. Control desk with operation recorders and telephone turret at Chickamauga

Figure 9 (right). Control room with asymmetrical indirect lighting and colored switchboards at Fort Loudoun

the radial type and are raised and lowered by means of two traveling hoists (Figure 5) running on rails on the deck for the full length of the spillway. Each hoist consists essentially of two chain drums driven by a single motor, the whole mounted on a 4-wheeled carriage. The hoist motor is squirrel-cage type, and the control makes use of regeneration while lowering. A separate squirrel-cage motor is provided for driving the carriage. The equipment is enclosed in a streamlined housing. Power supply is by flexible cable and motor-driven reel from polarized receptacles installed along the runway. At Apalachia Dam, where radial spillway gates also were used, individual fixed hoists were installed in order to provide remote control at a later date.

Intake gates at high-head plants are of the roller type and are operated by fixed hoists located in chambers near the tops of the dams. They are controlled by local push buttons, and emergency close buttons are provided at the governor control boards.

Compressed air[6] at 100 pounds per square inch is provided in all stations for tools, generator brakes, various pneumatic controls in the ventilating system, and turbine grease lubrication. The usual practice is to install one stationary 105 - cubic - foot - per - minute compressor and one portable 100-cubic-foot-per-minute compressor in each plant. Several plants are provided with additional air compressor capacity to depress the tailwater below the turbine runners while motoring the units and in one plant to prevent the formation of ice on the spillway gates. Black steel uninsulated pipe with welded or screwed fittings is used for all air lines.

One kind of lubricating oil is used both for the governor pressure system and for bearing lubrication. It has a viscosity of 300 Saybolt-second units at 100 degrees Fahrenheit. The oil is purified by a 350-gallon-per-hour centrifuge provided in each plant. Two tanks are provided, one for clean oil and one for dirty oil. When space permits, these tanks are located in the powerhouse adjacent to the oil-purification room. Where no such space is available, the tanks are buried in the fill outside the powerhouse wall. One clean-oil pump and one dirty-oil pump are furnished to handle the oil between the purifier, the tanks, and the generating units. The pumps are standard positive-displacement type with built-in relief valves, and each is rated 30 gallons per minute when pumping oil at a temperature of 50 degrees Fahrenheit. Black steel uninsulated pipe with welded joints is used for the oil lines.

One kind of insulating oil is used for transformers and circuit breakers, but oil once used in a breaker is never used in a transformer. The insulating oil is purified and handled (Figure 10) by a separate system in each plant similar to the lubricating-oil system. The purifier is a 900-gallon-per-hour combination centrifuge and filter press with electric heater, and the pumps are 100 gallons per minute each. The supply and return lines are not connected permanently to the transformers and breakers, but a valve is located in each line near the equipment, and flexible hose is used when filling, draining, or circulating.

Runner hub oil is required for lubricating the runner blade operating mechanisms in the Kaplan turbines. This oil has a viscosity of approximately 1,700 Saybolt-second units at 100 degrees Fahrenheit. Each hub contains about 1,500 gallons of oil. Whenever the runner is dismantled for inspection or repair, it is necessary to remove this oil, and it is salvaged for reuse.

Portable pumping facilities and tanks are provided to handle and transport this oil, but no purification equipment is installed.

Raw water is used in coolers for the main generators, the air compressors, and the air-conditioning equipment. In some plants it is used for fire protection, lubricating the turbine guide bearings, and as makeup for the treated-water

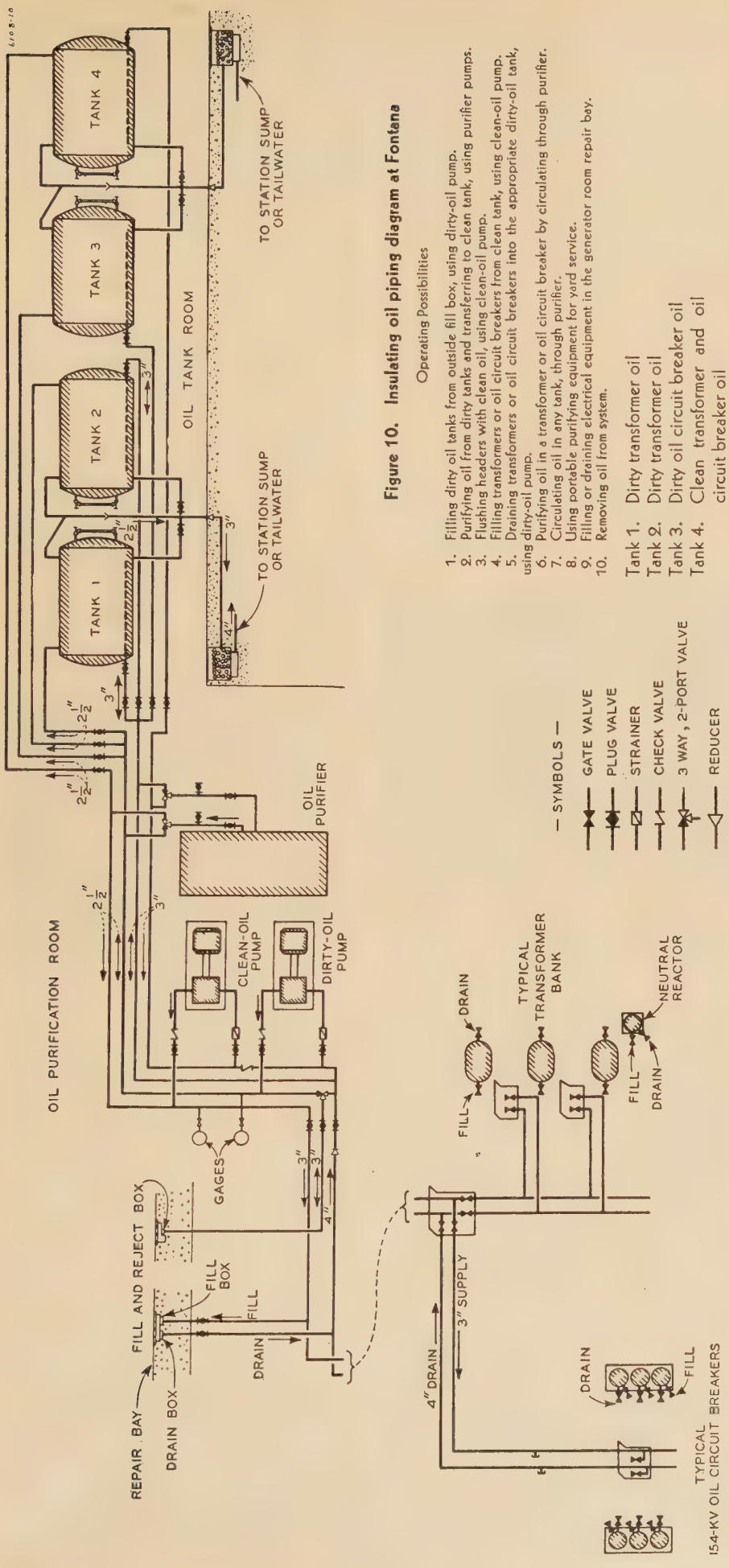

Figure 10. Insulating oil piping diagram at Fontana

Operating Possibilities

1. Filling dirty oil tanks from outside fill box, using dirty-oil pump.
2. Purifying oil from dirty tanks and transferring to clean tank, using purifier pumps.
3. Flushing headers with clean oil, using clean-oil pump.
4. Filling transformers or oil circuit breakers from clean tank, using clean-oil pump.
5. Draining transformers or oil circuit breakers into the appropriate dirty-oil tank, using dirty-oil pump.
6. Purifying oil in a transformer or oil circuit breaker by circulating through purifier.
7. Circulating oil in any tank, through purifier.
8. Using portable purifying equipment for yard service.
9. Filling or draining electrical equipment in the generator room repair bay.
10. Removing oil from system.

Tank 1. Dirty transformer oil
Tank 2. Dirty transformer oil
Tank 3. Dirty oil circuit breaker oil
Tank 4. Clean transformer and oil circuit breaker oil

system. In the low-head plants, water is taken from the scroll case in each unit and pumped through a multiple basket strainer, having 3/16-inch openings, to a header leading to the station system. The pumps are horizontally split double-suction single-stage volute-type centrifugal units. Specifications require enclosed bronze impellers with wearing rings, bronze shaft sleeves through the stuffing box, water seal piping, and deep stuffing boxes. Experience has proved that this type of pump will give years of service with little maintenance except occasional repacking and lubrication of the bearings. For the high-head plants, a separate intake from each unit penstock is connected to a central manifold from which the individual systems are supplied through pressure-reducing valves as required. An air cushion chamber is installed on the manifold to absorb any water hammer caused by the operation of the system.

Treated water is used in the various hydroelectric plants for all sanitary services and in some plants for fire protection. Wherever possible, treated water is obtained from a nearby community, even at the expense of laying a mile or two of pipe line. Where this is not possible, filter plants are installed. At projects requiring considerable water to supply an operators' village as well as the hydroelectric station, a conventional-type rapid sand gravity filter plant with mixing chamber, coagulation basin, dry chemical feeders, and chlorinators is usually provided. At projects where the demand is light, pressure-filter plants are installed. System pressure often is obtained by use of elevated storage tanks which usually are left standing from the construction activities at the project.

The station sumps in most plants are unwatered by two 300-gallon-per-minute float-controlled deep-well-type vertical-shaft turbine pumps operating in echelon. This type of pump keeps the motor above the wet conditions of an open sump and prevents possibility of flooding out caused by high tailwater conditions. Very little sand or abrasive matter is present in the water, so enclosed or semi-enclosed impellers are specified. The pumps are bronze-mounted and are oil-lubricated automatically by a solenoid valve energized with the motor circuit. In plants where sufficient head is available from the reservoir, water jet eductors are usually installed in lieu of pumps. Since the pressure water for operation of eductors comes from the unit penstocks and since it is possible for the penstocks to be empty, drainage

eductors are usually supplemented by one motor-driven sump pump.

Each draft tube is connected to the station sump with a large size line containing a sectionalizing valve. Most plants have two deep-well-type vertical unwatering pumps which range in capacity from 2,500 to 5,000 gallons per minute according to the volume of the draft tube. They are operated manually and can augment the station sump pumps in an emergency. In high-head plants, water jet eductors are usually provided for unwatering.

Fire protection uses raw water at all plants where the minimum lake level provides sufficient pressure. A pressure of 40 pounds per square inch at the hose nozzle has been adopted as the minimum for this service, but a pressure of 60 to 70 pounds per square inch is preferred and is used when obtainable. In plants where the minimum pressure is not obtainable from the lake, fire protection is obtained from the treated-water system or by means of a hydropneumatic system employing a raw-water booster pump. Valves and hydrants with hose racks are provided at strategic points in the powerhouse and in the switchyard. Fog-type hose nozzles which produce a highly atomized spray are provided for use around electrical hazards.

Portable carbon-dioxide extinguishers of 4 to 15 pounds are provided in the powerhouse, and wheeled truck extinguishers of 200-pound capacity are provided in the switchyards. Fixed automatic carbon dioxide systems, with banks of cylinders similar to those provided for the generators, are installed for the protection of oil-treating rooms, oil-storage rooms, and the gas-engine generator rooms.

Heating to 72 degrees Fahrenheit is provided only for those areas where attendance is required. Other spaces are heated only as required for relief of dampness and excessive chill. All heating is by electric resistance heaters except for the air-conditioned areas. Heaters in general are thermostat-controlled fan-type 440-volt 3-phase units with auxiliary on-off-auto-manual switches. The ventilation is provided in several areas of each plant according to the need for human comfort, dissipation of heat from equipment, dissipation of solar radiation, and relief of dampness.

Air conditioning is provided in certain spaces of each powerhouse for the protection of delicate electrical equipment and for human comfort. The general areas served by air conditioning include the control room and its related spaces, the office area, the public areas including the lobby and entrance vestibules, the telephone room, the laboratory, the assembly room, and the first-aid station. Electric blast heaters are used for heating, and their operation is thermostatically regulated. Humidification is provided by discharge of live steam generated by an electric immersion heater in an open pan in the plenum of each system. Cooling is by finned surface coolers using chilled water in the coils. In the high-head plants where reservoir water is available at 55 degrees Fahrenheit or less, it is used. In other plants, water is chilled by mechanical refrigeration.

A permanent machine shop is provided at each plant, usually located just off the erection area on the generator floor. The size of the machine shop and the amount of equipment are chosen in accordance with the proximity of outside repair service. Even in the isolated plants which have maximum complement of machine tools, it is not intended that they shall be able to make all major repairs. A central repair shop capable of handling a great variety of work, including large water-wheel repairs and transformer rewinding, is maintained at Wilson Dam.

Elevators are provided at most of the plants where considerable differences exist in elevation between operating areas. In several projects separate elevators are provided for employees and for the public. Elevators are traction type usually with d-c drive and motor-generator supply. Automatic control and self-leveling features are provided.

Motors driving station auxiliaries are general-purpose National Electrical Manufacturers Association standard, with class A insulation. Motors driving constant-speed equipment, such as pumps, compressors, and ventilating fans, are squirrel-cage induction type with normal torque and starting current; those for variable speed and torque, such as cranes and hoists, are wound-rotor slip-ring type. A few auxiliaries, such as emergency turbine guide bearing lubricating oil pumps and important valves, are provided with 250-volt d-c motors operated from the station-control battery. Motors in locations where windings might become damaged by water or oil are provided with moistureproof insulation and splashproof or dripproof frames. In very damp locations it has been found necessary to apply strip-type heaters or to circulate a small amount of current through the motor coils when idle.

Controls are centralized on auxiliary power switchboards for groups of related equipment. Each motor circuit contains a manually operated disconnecting switch, a set of fuses as protection against short circuit, and a magnetic contactor for full-voltage starting and thermal overload protection. Push-button stations for manual control generally are located at or near the motors. Motors under automatic control also have push-button stations which provide manual control for inspection.

Auxiliary Power Supply

The sources, switching, and distribution of power for station auxiliaries have been standardized as previously described and illustrated.

Wiring, principally on account of loss of rubber during the war, has undergone an evolution. As an outcome, the auxiliary power wiring in most of the recent plants has been insulated with oil-base compound containing Buna S and has been jacketed with Neoprene.

Lighting and Heating

The normal lighting and heating sources and distribution, as previously described, have become standard. Unique illumination carefully co-ordinated with the architecture has been provided to assist operation to the utmost and to enhance the general appearance. Appearance has always been considered important, since these are publicly owned plants and are inspected critically by the public. During 1941, the last year before war restrictions, the number of visitors varied from 26,000 to 1,300,000 at individual plants and totaled 2,700,000 at ten of the new plants.

The emergency lighting system has undergone some revision, partially due to the war. As previously discussed, the emergency lighting load was carried normally by the motor-generator sets which charge the control battery, and it was supported by the battery in case of loss of a-c input to the motor-generators. This eliminated all throw-over switches but required that the lamps must have a voltage rating as high as possible, since the battery floats normally at about 258 volts and many of the emergency lamps burn continuously. With 260-volt lamps the lamp life was acceptable, but when the 250-volt lamps became the highest rating available, they required such frequent replacement that it was necessary to install automatic throw-over switches. The emergency lamps now operate normally at 230 volts alternating current and only rarely at 258 volts direct current.

Electronic Control of Frequency Converter Sets for Testing Aircraft Models

G. W. HEUMANN
MEMBER AIEE

W. F. STRONG
ASSOCIATE AIEE

THE TESTING of airplane scale models in wind tunnels has brought about a demand for variable frequency a-c power for controlling the speed of power model motors used to drive the propellers of the plane models. To obtain aerodynamic data on the plane model which are equivalent to the expected performance of the actual plane, it is necessary to drive the model propellers at speeds greatly in excess of propeller speeds of the actual plane. During tests in the wind tunnel, it must be possible to control propeller speed and to measure accurately the speed as well as power input into the propeller.

Squirrel cage induction motors, capable of speeds up to 80,000 rpm at 1,330 cycles, have been developed. To start and control the speed of such motors, it is necessary to have available a power supply system the frequency of which can be varied and regulated. To permit model motors of various sizes and manufactures to be used, the a-c output voltage of the system must be adjustable. When using a motor over a wide frequency range, the ratio of voltage to frequency (volts per cycle) must be held constant to obtain constant air gap flux. Thus it is necessary that the volts per cycle of the power supply system be regulated.

The frequency and voltage supply system must be fast in response, unvarying in frequency and voltage at the test point, and flexible for maximum variety of tests to be made. Such a system frees the operator to concentrate on the various other quantities to be held constant during the course of the test, such as air velocity, air temperature, and many others.

The aircraft designer is interested in speed and torque input into the propeller. Torque may be measured directly on the model, or it may be deduced from the electric input data by calibrating the model motors. A set of calibration curves for each motor is then taken on a dynamometer or torque stand, correlating input watts from the variable frequency system and output torque at various speeds.

Use of variable frequency a-c power systems is not restricted to plane model testing. Research work on propellers, either inside or outside of a wind tunnel, superchargers, gas turbines are but a few examples of applications which require high speed motors with a wide range of speed control.

Figure 1. View of United Aircraft wind tunnel in East Hartford, Conn., at which power model testing equipment is installed

Scope

It is the object of this paper to describe a frequency converter installation at the United Aircraft Corporation wind tunnel laboratory operated by the Research Department at East Hartford, Conn. Variable frequency power is utilized for model testing in the wind tunnel, for propeller testing inside and outside the tunnel, and for testing work in the thermodynamics laboratory. Electronic regulators are used for the following control purposes:

1. To adjust and regulate frequency.
2. To adjust and regulate volts per cycle.
3. To maintain parallel operation of two converter sets.
4. To maintain current limit during acceleration and deceleration.
5. To limit alternating voltage available at high volts per cycle settings.

Power Conversion Equipment

Figure 3 is a 1-line diagram of the power circuits of the system. Variable frequency power is supplied to the utilization network by two frequency converter sets *A* and *B*, each consisting of:

One 300-kw 24-pole 1,700-rpm wound rotor converter, 440-volt 3-phase 60-cycle primary, 720-volt 3-phase 400-cycle secondary.

One 400-horsepower, 1,700-rpm 250-volt d-c adjustable speed shunt wound motor.

References

1. TENNESSEE VALLEY AUTHORITY HYDROELECTRIC STATIONS—ELECTRICAL DESIGN, **R. A. Hopkins,** AIEE TRANSACTIONS, volume 60, 1941, pages 1281–93.

2. DESIGN OF HYDROELECTRIC STATIONS, **G. P. Palo, C. R. Marks III.** *Proceedings,* American Society of Civil Engineers, volume 71, October 1945, pages 1209–23.

3. SUPERVISORY CONTROL OF 30,000-KVA HYDROELECTRIC PLANT, **C. W. Bohner, A. P. Maness.** AIEE TRANSACTIONS, volume 65, 1946, June section, pages 337–42.

4. HYDRAULIC TURBINE PRACTICE OF THE TVA, **H. J. Petersen, J. F. Roberts.** *Mechanical Engineering,* April 1943, page 237.

5. SPILLWAY GATES AND EQUIPMENT ON TVA PROJECTS, **Kenneth C. Roberts.** *Civil Engineering,* volume 16, January 1946, pages 13–16.

6. THE DESIGN OF MECHANICAL AUXILIARIES FOR TVA HYDROELECTRIC PLANTS, **H. J. Petersen.** *Transactions,* American Society of Mechanical Engineers, volume 68, October 1946, pages 663–73.

Paper 46-129, recommended by the AIEE committees on air transportation and industrial control devices for presentation at the AIEE summer convention, Detroit, Mich., June 24–28, 1946. Manuscript submitted April 9, 1946; made available for printing May 13, 1946.

G. W. HEUMANN is with the control engineering division and W. F. STRONG is with the industrial engineering division, both of General Electric Company, Schenectady, N. Y.

The authors wish to acknowledge that the system of providing variable frequency by means of induction frequency converter sets with electronic field control was first proposed by C. C. Clymer, industrial engineering division, General Electric Company.

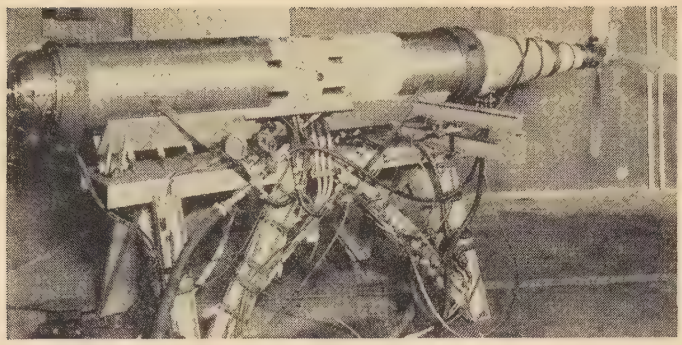

Figure 2. Two 375-horsepower dual rotation model motors mounted on torque stand in calibration room

Two sets are used so that two independent tests can be run when the combined output of the system is not required.

Output frequency of the converters is varied between 65 and 400 cycles by varying the speed of the d-c driving motors between 25 and 1,700 rpm. Variable voltage control of motor speed is employed. Operation at standstill, or 60-cycle output, is prevented by the control in order to avoid burning of the slip rings. The rotor of each converter contains the primary windings, and the stator the secondary windings. The stator windings have two circuits per phase, the total volts per cycle range is 0.5 to 4. With parallel connection of the circuits of each phase, a range of 0.5 to 2 volts per cycle is obtained; with series connection, the range is one to four volts per cycle. The range selection is made by manual knife switches, to suit the rating of model motors under test.

To supply power to and control the converter sets, a 6-unit constant speed motor generator set is used, consisting of:

One 800-horsepower 1,200-rpm 2,300-volt 3-phase 60-cycle synchronous driving motor.

Two 250-kw 250-volt shunt-wound d-c generators to supply variable armature voltage to the d-c motors of sets *A* and *B*.

Two 156-kva 440-volt 3-phase 60-cycle alternators to supply excitation to the frequency converters.

One 20-kw 125/125 volt compound wound d-c exciter to supply a constant voltage control bus.

Synchronous motor and d-c motor fields are energized from the constant voltage d-c exciter bus. The field excitation of the d-c generators is supplied by thyratron rectifiers from the 60-cycle power system. The field strength, which determines the speed and output frequency of the converters, is controlled by electronic regulators. Similarly, the field excitation of the alternators is obtained from thyratron rectifiers with electronic regulators, providing control of the volts per cycle of the converter output. Included in Figure 3 is a block diagram of the principal electronic field control circuits.

Power Distribution System

Output power from the frequency converters is fed through a distribution system to various points of utilization. From each converter power flows through a line switch and a transfer switch to either the wind tunnel or the thermodynamics laboratory. In the wind tunnel laboratory, each converter bus (*A* and *B*) is split into three channels. Thus six channels are available in the tunnel for testing a model having six propellers. One channel off each bus can be connected to the calibration room, and another pair of channels can be routed to a small pilot tunnel for preliminary test work. Knife switches are used to select the channels.

For tests requiring the combined output of both converter sets, the two converter busses can be paralleled through a paralleling contactor. During parallel operation, voltage and frequency of the system is determined by the control of set *A* which acts as the master. Set *B* then automatically matches set *A* and acts as the follower.

Overcurrent Protection

As the impedance of the converters and the distribution system is comparatively high, the short-circuit capacity of the system is low, and contactors are adequate for interrupting short-circuit current. The short-circuit current flowing in the secondary winding of either frequency converter reflects itself in the primary winding in inverse ratio of coil turns. Instantaneous overload relays, connected in the primary side of the converters, trip out line contactors 1*MA* and 1*MB*. This removes excitation from the converters and reduces their secondary voltage to zero.

Excess power output in the secondary circuit of either converter results in a high current in the loop circuit of the corresponding d-c machines. Therefore, instantaneous overload relays in the loop circuits trip d-c line contactors 2*MA* and 2*MB*.

Protection against sustained overloads is obtained by thermal relays with resistance type heaters in each of the six channels. Each relay is connected in the secondary side of a current transformer. Since the heaters carry only a small amount of current, they are wound of fine wire. The effect of frequency within the system working range on the relay tripping current is negligible. These relays protect the system, and, by proper selection of heater sizes, also protect the model motors.

Metering

In order to obtain an accurate record of the power input into the model motors, precision wattmeters are provided which permit measuring power with an accuracy of repetition of 0.10 per cent. Because of the wide range in current and voltage measured, the wide range in frequency, and the high accuracy required, multitap current and potential transformers are used.

As it is not necessary to meter all channels simultaneously, a separate metering channel may be connected to each bus in series with any one of the three channels. For instance, if contactor 1*A* is closed, channel 1 is connected directly to bus *A*. If contactors 1*B* and 1*C* are closed and contactor 1*A* is open, channel 1 is connected through the metering channel. Control is so interlocked that only one channel can be connected to either metering channel at one time.

In addition to the precision wattmeters, switchboard type voltmeters and ammeters are connected to the instrument transformers. At the beginning of a test, the precision instruments are disconnected, and the operator selects the instrument transformer ratio so that the pilot instruments are within proper reading range. Pilot wattmeters, connected to each metering channel through their own sets of instrument transformers, give the tester a direct indication of power.

Precision tachometers, actuated by tachometer generators built into the model motors, are used to read model motor speed during a test. As these instruments are apart from the power system, their details will not be discussed in this paper.[1] Frequency of the system is indicated by switchboard type d-c voltmeters, calibrated in cycles and connected to tachometer generators which are coupled to the converter sets.

Volts per cycle is measured by a volts per cycle meter which can be connected to either converter. This instrument is an ammeter which measures the current flowing through an inductance, the impedance of which is proportional to frequency. Switchboard type ammeters indicate the load on either converter.

Electronic Control

Of first importance in the testing of a model motor is the frequency and voltage applied to the motor. These quantities are adjusted and held constant during a given test by comparing each quantity to a reference voltage and maintaining the difference between the quantity and its reference as small as possible. For example, in the case of frequency control, a d-c tachometer generator directly connected to the converter produces a direct voltage which is a function of frequency. This voltage is matched against a reference voltage in the electronic circuit to hold frequency constant as long as the reference voltage is unchanged.

Each d-c generator field and each alternator field is excited by a pair of thyratron tubes in a biphase half-wave circuit in which the thyratron firing angle is controlled by resistance variable inductance bridge circuits. The inductance of the bridge is in the form of a saturable reactor whose d-c winding is supplied from a regulated d-c source and controlled by a high vacuum tube. This is shown in Figures 4, 5, 6, 7, and 8, which are simplified diagrams of the various control circuits. Each of the quantities to be adjusted or held constant is controlled by a closed loop regulating system.

Figure 3. One-line diagram of power model supply system

Frequency Control Circuit

In Figure 4a the essential elements of the frequency regulators are shown. The tachometer generator produces a direct voltage of 50 volts per 1,000 rpm of the converter. The tachometer generator

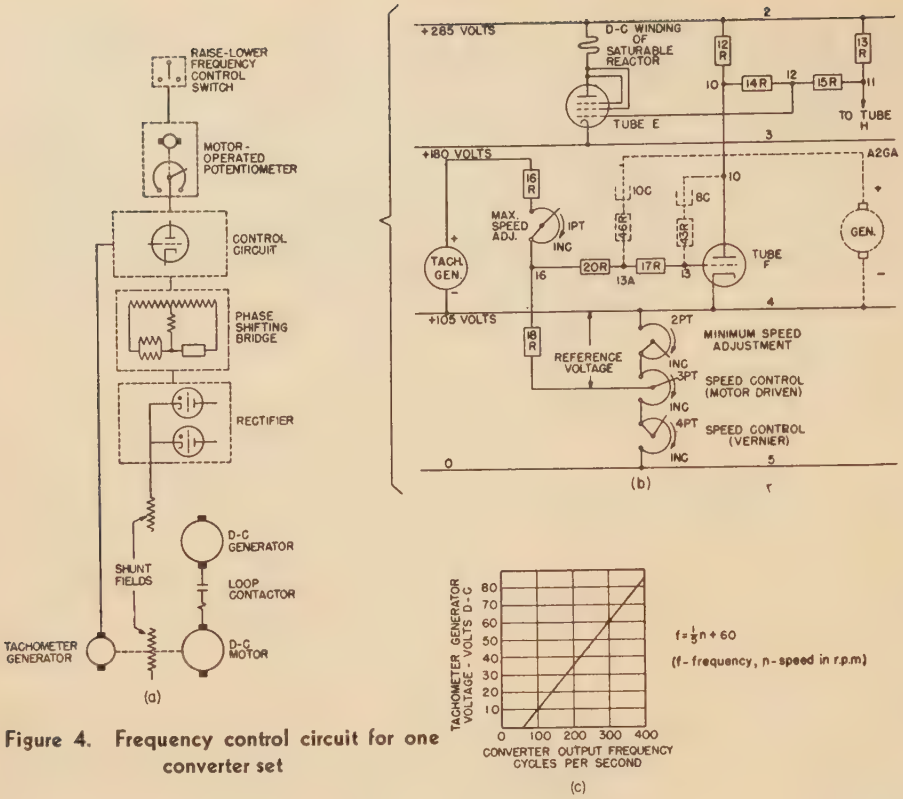

Figure 4. Frequency control circuit for one converter set

voltage, therefore, is a function of frequency. The 24-pole converter produces a frequency

$$f = 60 + 24n/120 \qquad (1)$$
$$= 60 + n/5$$

where n is the speed of the converter in revolutions per minute. Since the tachometer generator voltage follows the formula

$$V_T = (50/1{,}000)n \qquad (2)$$
$$= n/20$$

where V_T is the tachometer generator voltage, then

$$V_T = 5(f - 60)/20 \qquad (3)$$
$$= f/4 - 15$$

This is shown graphically in Figure 4c. By comparing V_T with an adjustable reference voltage, the value of which is set by the position of the motor operated potentiometer, a signal is obtained which governs the amount of generator field excitation. This controls the motor speed which in turn determines frequency.

Figure 4b is described best by following the circuit as it would operate under typical conditions. Assume that the converter is running at 100 cycles and it is desired to increase frequency to 150 cycles. The operator throws the frequency control switch to the raise position which starts the motor operated potentiometer turning in such a direction as to increase the reference voltage. This action causes the potential of point 16, and consequently point 13 to become more negative with respect to the cathode of tube F, which decreases the plate current of this tube. Neglecting for the moment the resistor capacitor circuits in phantom and assuming the potential of point 11 to be held constant at approximately 40 volts positive with respect to bus 4, decreasing the plate current of tube F raises the potential of point 10, and likewise the potential of point 12 with respect to bus 3 and cathode of tube E. As the plate current of tube E increases, the reactor becomes more saturated and the thyratron firing angle is advanced. As the generator field excitation is thus increased, the converter set accelerates to a new speed. This speed is determined by the amount the tachometer generator voltage must increase to offset the increase in reference voltage. When the tachometer generator voltage has increased to its new value, points 16, 13A, and 13 will have returned to within a fraction of a volt of their original values. Likewise, the tube currents and the potentials of points 10 and 12 will be very near their original values. These differences are those required to hold the frequency at the value of 150 cycles. The phantom lines represent feedback circuits

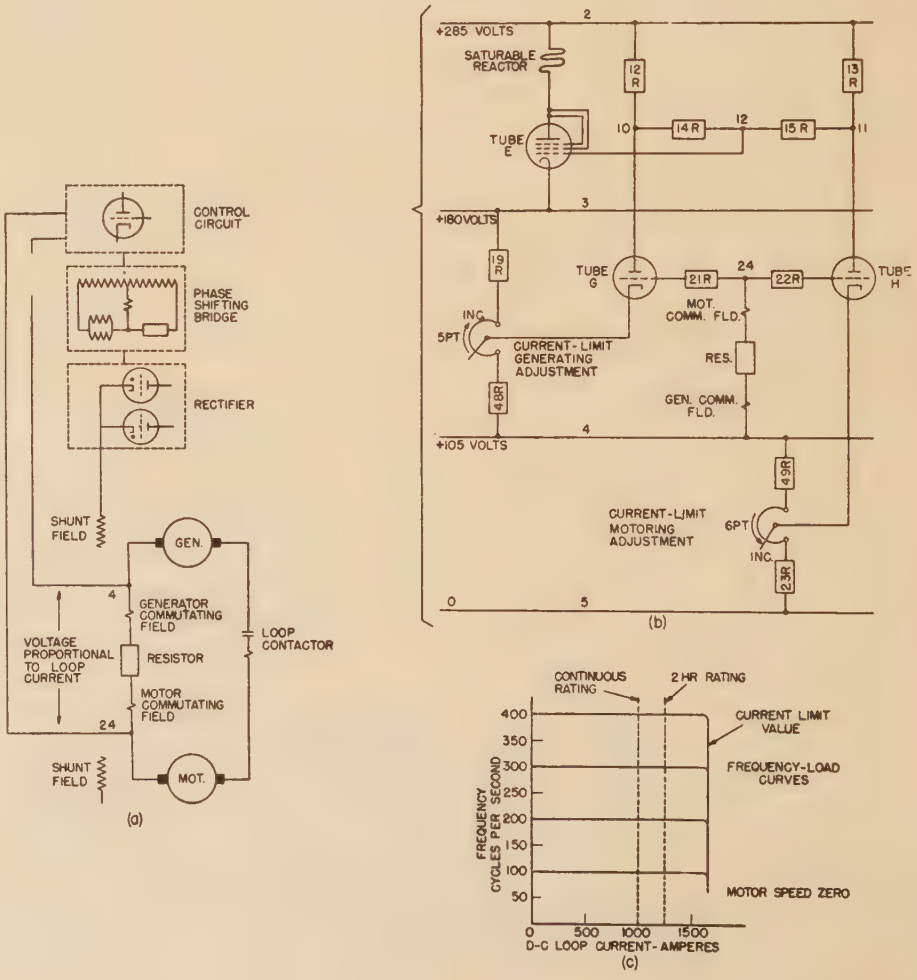

Figure 5 (below). Current limit control circuit for one converter set

which assure stable operation at all times and maximum speed of response with minimum overshoot under transient changes of load or frequency.

Current Limit Control Circuit

In any system consisting of a d-c motor energized from a d-c generator very high current may flow in the loop circuit between the generator and motor armatures. Although instantaneous overcurrent protection is provided to shut down the motor in the event of high overcurrents it is sometimes desirable to prevent the existence of currents above a chosen value. Figure 5a presents the method of regulating current at the current limit value. An IR drop proportional to loop current is compared with two adjustable reference voltages in the control circuit. When power flow is from generator to motor, point 24 is positive with respect to point 4, and tube G (Figure 5b) becomes the amplifier for the current signal. When point 24 rises in potential, as the loop current increases, to a point approximately one volt negative with respect to the cathode of tube G, whose potential is determined by the current limit adjustment $5PT$, the plate current of tube G increases, and the potential of point 10 decreases. Since the potential of point 11 is fixed by the tube H which is turned full on except at current limit motoring, the decrease in potential of point 10, and consequently of point 12 with respect to bus 3, will decrease the plate current of tube E thus reducing the generator field excitation as described under the foregoing heading. If the generating current limit action is brought about by rapid motor acceleration, the effect of reducing the generator field by the current limit control circuit is to retard the rate of acceleration of the motor.

If the motor is running at a given speed and the frequency reference voltage is suddenly reduced, the generator field voltage will be decreased, and the motor acting as a generator will supply power to the generator acting as a motor. Under this condition the potential of point 24 becomes negative with respect to point 4, and the current limit motoring control circuit begins to function. As point 24 becomes negative with respect to the cathode of tube H, the plate current of tube H will decrease, and points 11 and 12 will rise in potential. This action increases the plate current of tube E, which increases the generator field excitation to a value sufficient to hold the loop current at the preset current limit value.

Volts Per Cycle Control Circuit

The volts per cycle ratio is controlled by comparing the converter output voltage to the tachometer generator voltage which is a function of frequency. In this case the tachometer generator voltage is the reference determined by the frequency control setting. Figure 6a shows a 1-line diagram of this circuit, and Figure 6b the control circuit. Since the frequency is proportional to the tachometer generator voltage, plus a constant, some means must be provided to add a constant direct voltage to the tachometer generator voltage. By connecting the grid of tube M to a point sufficiently negative with respect to bus 4, the cathode of tube M will be negative in the control range. This has the desired effect of adding a constant voltage to the tachometer generator circuit. The constancy of volts per cycle over the complete frequency range is determined by the setting of the bias adjustment. The range adjustment provides a means of varying simultaneously the maximum and minimum volts per cycle ratios obtainable.

Tube N in Figure 6b limits the maximum voltage available from the converter regardless of frequency. As the converter voltage increases, the cathode of tube N becomes less positive with respect to the

Figure 6. Volts per cycle and voltage limit control circuit for one converter set

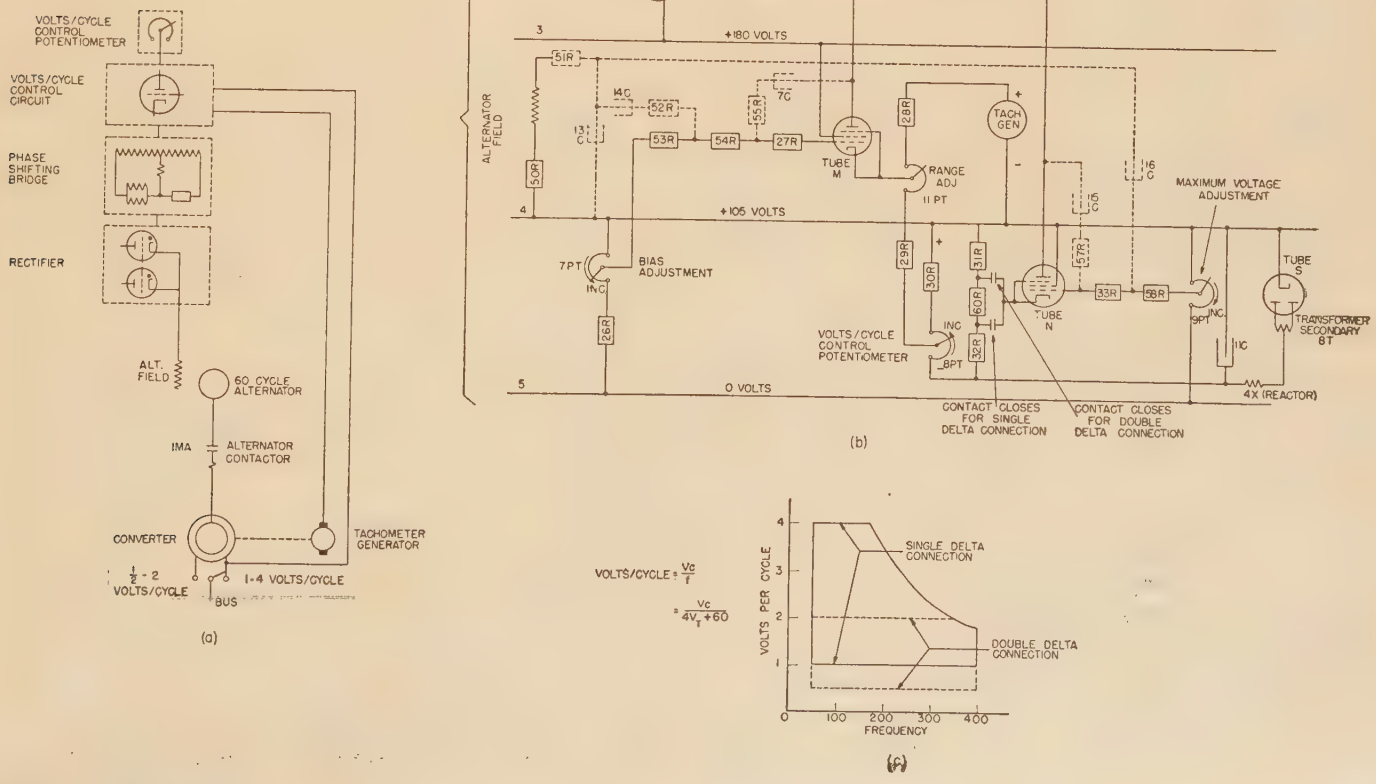

grid, until the tube begins to pass current which restrains the alternator field, thus limiting the converter voltage to a predetermined value.

Figure 6c presents the range of volts per cycle obtainable at each frequency. The curved portion indicates the maximum volts per cycle obtainable at the higher frequencies because of limitations imposed by the maximum converter voltage rating of 720 volts. For the single delta connection, maximum volts per cycle is 4.0 up to 180 cycles and $720/f$ above 180 cycles. For the double delta connection, maximum volts per cycle is 2.0 up to 360 cycles and $720/f$ above 360 cycles.

Parallel Operation

Figure 7 shows the method of comparing IR drops in the d-c generator motor loop circuits to balance the currents in these circuits during parallel operation of the converters. The d-c IR drop is a true measure of converter load, since at a given frequency the division of power between the d-c motor and the alternator, neglecting losses, is fixed in accordance with the formulas:

$$\frac{\text{D-c motor power}}{\text{Converter power}} = \frac{fc - fa}{fc}$$

$$\frac{\text{Alternator power}}{\text{Converter power}} = \frac{fa}{fc}$$

where

fa = frequency of alternator, which is 60 cycles

fc = frequency of converter, which may be 65 to 400 cycles

For example, when the converter is running at 150 cycles and supplying 75 kw to a load, the alternator load is

$$\frac{60}{150} \times 75 = 30 \text{ kw}$$

and the d-c motor load is

$$\frac{150 - 60}{150} \times 75 = 45 \text{ kw}$$

Thus, since the ratio of d-c motor load to total converter load is fixed, by the converter frequency, the d-c loop current, which is a function of d-c motor load, is a measure of total converter load. When the two converters are running in parallel, the load on converter B is made equal to the load on converter A by making the d-c loop current of set B equal to the d-c loop current of set A.

Figure 7b indicates an adjustment included to balance the two loop currents. This adjustment also provides a means of introducing a small direct voltage to compensate for the grid to cathode voltage of tube F in the control range.

Power Factor Balance—Parallel Operation

When the two converters are running in parallel, the d-c current balance circuit insures the equal division of actual load between the two sets. In addition, for highest efficiency, equalization of heating and maximum pull out torque, some means must be provided to balance the power factor of the two converters. There are several methods of accomplishing power factor balance. Possible methods are as follows:

1. Balance total load current of one converter against the other.
2. Balance reactive component of load current of one converter against the other.
3. Balance total current of one alternator against the other.
4. Balance the reactive component of load current of one alternator against the other.
5. Balance the d-c field current of one alternator against the other.

During parallel operation with equalized power and power factor, all of the foregoing currents will be balanced, however, the last mentioned proved to be most satisfactory from the standpoint of stability and circuit simplicity. This is shown in Figure 8.

Figure 8b gives the method of measuring field current by using the voltage drop across a resistor in series with the alternator field. The strength of alternator A field is determined by the volts per cycle setting, and the control circuit of set B acts to amplify the difference between the two alternator field currents and to control alternator B field in such a direction as to reduce the difference to zero. Potentiometer $12PT$ provides the grid bias voltage for tube M and a means for adjusting the field current of alternator B

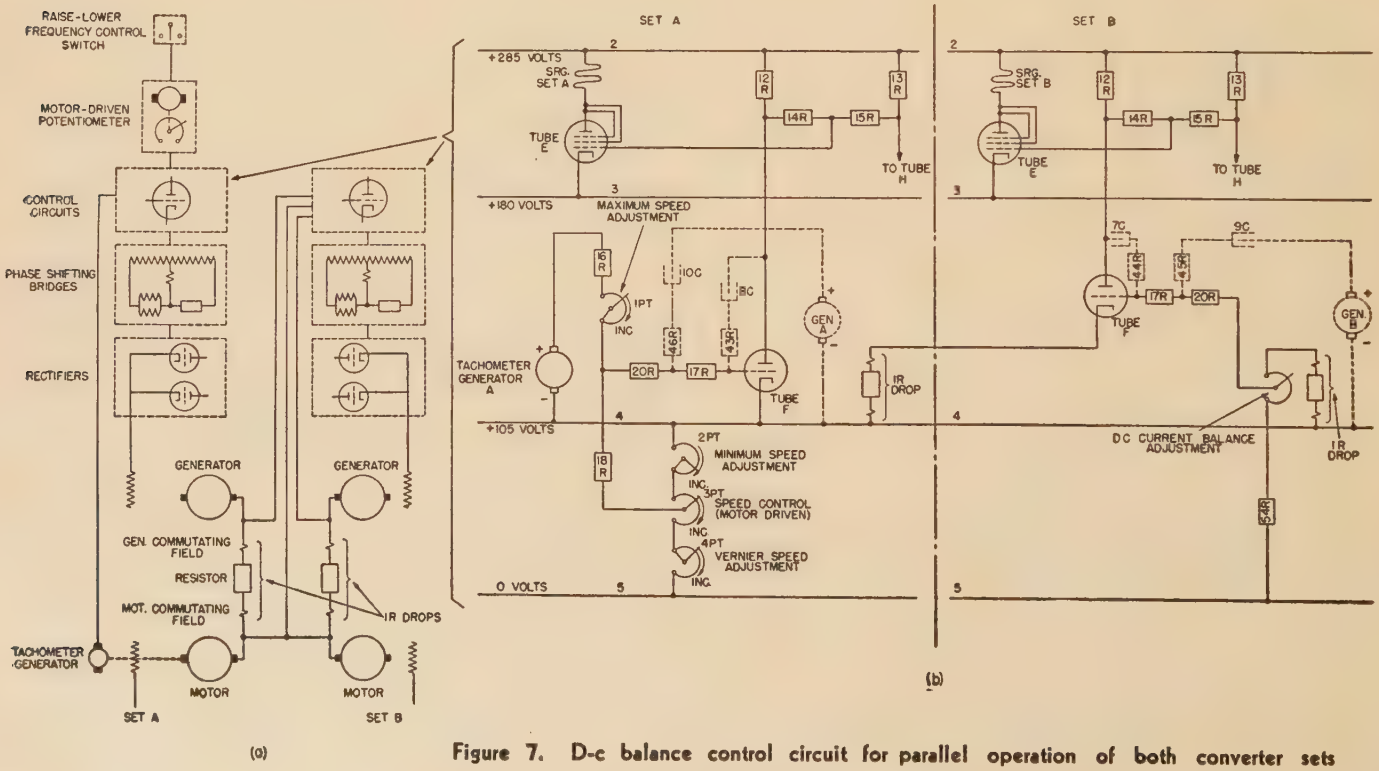

Figure 7. D-c balance control circuit for parallel operation of both converter sets

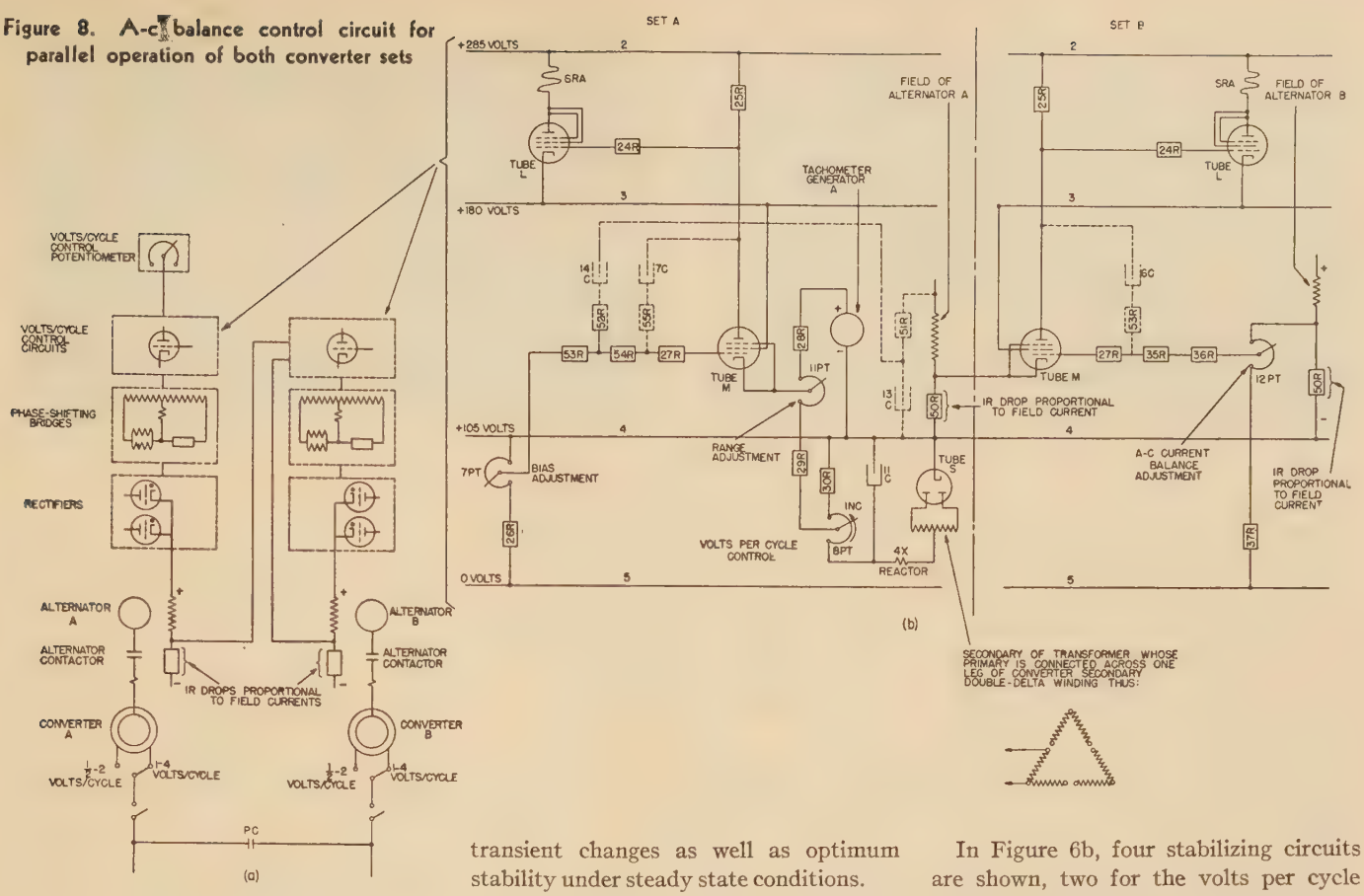

Figure 8. A-c balance control circuit for parallel operation of both converter sets

with respect to the field current of alternator *A*.

Stabilizing Circuits

The complete system uses six regulators to control the d-c generator and alternator fields. These are the following:

1. Frequency regulator (tachometer generator signal compared to an adjustable reference voltage).

2. Current limit regulator (a voltage proportional to d-c loop circuit current compared to an adjustable reference voltage).

3. Volts per cycle regulator (a direct voltage proportional to converter voltage compared to tachometer generator voltage).

4. Maximum converter voltage (a direct voltage proportional to converter voltage compared to an adjustable reference voltage).

5. D-c balance-parallel operation (d-c loop circuit current of set *B* compared to d-c loop circuit current of set *A*).

6. A-c balance-parallel operation (field current of alternator *B* compared to field current of alternator *A*).

As in many regulators, these circuits tend to have a regular hunting frequency under normal running conditions. Thus it is necessary to introduce stabilizing circuits to eliminate oscillations under steady state operating conditions. These circuits are chosen to give fast response to transient changes as well as optimum stability under steady state conditions.

The dotted portion of Figure 4b represents the stabilizing elements for the frequency control circuit. A capacitor and resistor connected from plate to grid of tube *F* feeds a signal back to the grid of the tube, which is leading in phase angle with respect to any steady oscillating voltage from plate to cathode of the tube. Such a circuit reduces the gain of the amplifier with respect to the a-c hunting component of grid voltage without sacrificing d-c or steady state sensitivity. The circuit also has the characteristic of attenuating any high frequency ripple voltage on tube *F* grid caused by tachometer generator ripple or stray voltages induced in the leads. In general, the practical effect of the plate to grid stabilizing circuit is to slow down the transient response of the system. To offset this, a resistor capacitor feedback from the positive d-c generator lead to the tube *F* grid is used. Once a suitable combination of resistance and capacitance for plate feedback is found by trial, a generator voltage feedback circuit can be found which will eliminate steady state oscillations and provide the transient response desired.

The current limit circuit is sufficiently stable without the use of stabilizing circuits. The current limit amplifier has a much lower gain than the amplifier of other circuits, which accounts for the inherent stability of this circuit.

In Figure 6b, four stabilizing circuits are shown, two for the volts per cycle regulator and two for the maximum converter voltage regulator. In each case the plate-to-grid circuit is combined with the alternator field voltage feedback circuit to produce maximum speed of response and stability. In this case, since the alternator field is energized from a controlled thyratron rectifier, a resistor capacitor filter is used to produce a smooth d-c voltage for use as a feedback signal.

It is to be noted that the stabilizing circuits have little or no effect on the accuracy of the system. Under normal running conditions, the various voltages in the vacuum tube circuits are d-c voltages; hence the stabilizing capacitors charge up to the voltage impressed on them and remain at that charge until the voltage changes. Thus the gain of each circuit and the established adjustments are unaffected by the stabilizing circuits.

Control Panels and Console

Contactors, relays, electronic regulators, knife switches, and transformers, required to control the power system, are mounted on two enclosed dead front switchboards located in the machinery room with the converter sets (see Figure 9). Switchboard *A* contains the starter for the synchronous motor and all other controls for the constant speed and the converter sets, including the electronic regulators (see Figure 10). Switchboard

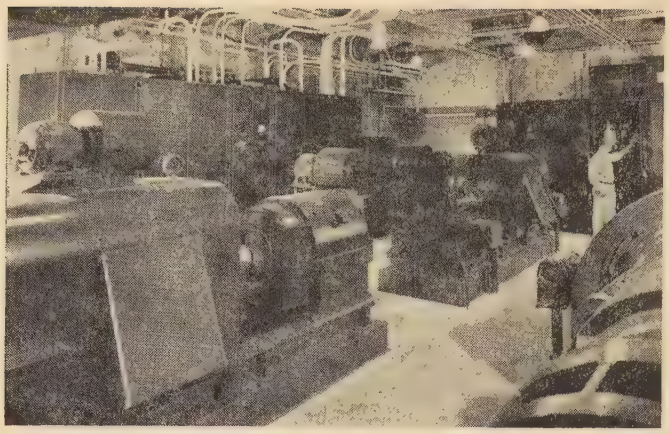

B controls the output circuits from the converters and includes all devices used in conjunction with the utilization and metering channels.

Pilot control switches, indicating lights, and instruments, which the operators require to control the system, are arranged on the console which is located in the control room above the machinery room, level with the wind tunnel test chamber (see Figure 11). The console is of semicircular design with an elongated center section. The right half controls the wind tunnel itself, and the left half controls the power model testing equipment (see Figure 12).

The console is so arranged that the operator in charge of power model testing can read all instruments and operate all control switches from one position. Instruments are mounted on a raised inclined section. Control switches and indicating lights are mounted on the horizontal section, which also provides writing space for keeping test records. The back is sufficiently low so that the operator can observe the wind tunnel test chamber through a window.

Figure 9 (left). General view of motor generator set room with switchboard *A* in background and switchboard *B* on left side

Figure 11 (right). Control room with operators seated at console, tunnel test chamber visible through window in background

Operation

Before a power model test is started, the operator closes the knife switches to the channels to which power model motors are connected; he closes the converter range switches in the position for proper volts per cycle. Then he starts the constant speed motor generator set from the machinery room. When the "ready" light on the console glows, indicating that the thyratron tube filaments are at operating temperature, full voltage is applied to the d-c motor fields, the alternator and d-c generator field circuits to the electronic regulators are closed. The operator then takes over from the console and goes through the following steps:

1. With the motor operated speed rheostat in the position for minimum converter speed, and the volts per cycle rheostat in the minimum voltage position, the operator closes the bus energizing switches, thereby closing the a-c line contactors and the d-c

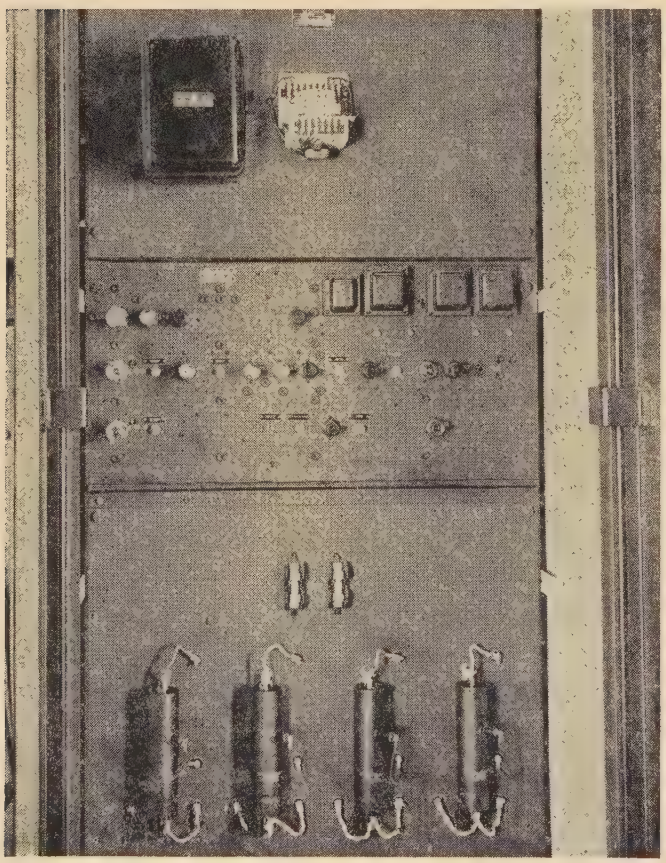

Figure 10 (left). Section of switchboard *A* containing electronic control equipment

Figure 12 (below). Left section of control console containing instruments and control switches for power model testing equipment

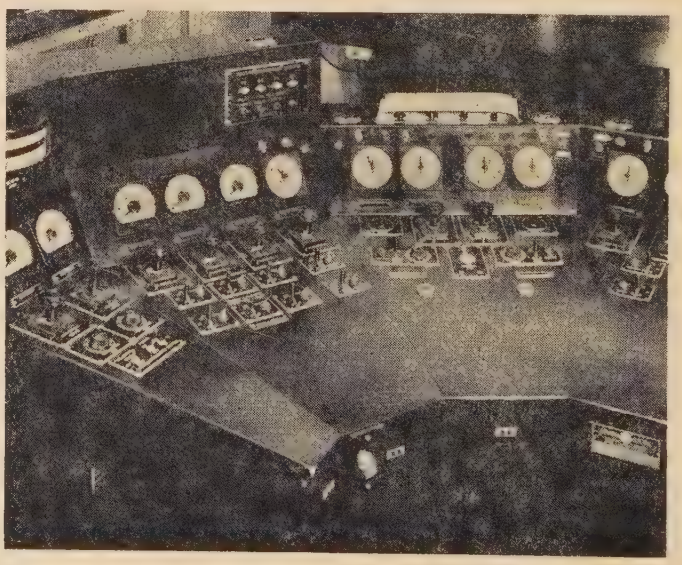

loop circuit contactors, and thus starting the converter sets. The converter sets turn at minimum speed.

2. Volts per cycle is adjusted by turning the rheostat up, until volts per cycle corresponds to the rating of the model under test.

3. When model motors are tested from standstill, the operator now closes control switches, which in turn control contactors (1*A* to 6*A*) connecting the selected channels to their bus. When model motors are tested in the tunnel and their propellers are windmilling, the operator first raises the frequency to a value corresponding to the windmilling speed, so that power is applied to the motors at a low slip.

4. Model motor speed then is adjusted to the desired value by adjusting the system frequency. A control switch permits raising and lowering the motor operated rheostat, and a manually operated rheostat serves as a vernier adjustment.

5. In order to meter any channel, the operator closes the metering switch of that channel. This causes the *B* and *C* contactors of that channel to close and the *A* contactor to open. Next, the operator turns the transformer ratio selector switches until the pilot voltmeter and ammeter are reading up scale. Closing a test switch connects the precision wattmeter in the metering circuit.

6. Any or all channels are de-energized by tripping out the busses, since the channel contactors cannot interrupt power. If an individual channel is to be dropped during a test, a push button may be pressed which reduces volts per cycle to zero. The channel contactor then can be tripped, and, when the push button is released, voltage returns to the previously set value.

When the two converter sets are to be operated in parallel, the paralleling contactor is closed from the console with the converter sets at standstill. The secondaries of the converter sets are connected in parallel. When starting the converter sets, the operator momentarily raises volts per cycle, and the two converter sets lock in step. Frequency and volts per cycle controls for set *A* control both sets during parallel operation.

Conclusions

The control system described in this paper realizes the following operating advantages:

1. Accurate control of system frequency permits accurate adjustment of model motor speed.

2. Accurate volts per cycle control over the frequency range prevents damage to model motors on account of voltage drift during a test.

3. Current limit and maximum voltage controls prevent damage to the rotating machines.

4. Splitting the system into two sections provides flexibility, as either two tests with half system power or one test with full system power may be scheduled. Also two independently adjustable power supplies are available for studies on counter rotating propellers.

5. During parallel operation, the electronic control balances the two converters with respect to load and power factor, thereby freeing the operator from continually readjusting the two converter sets by hand.

6. Providing several channels on one power bus and one metering channel per bus permits precision metering of several model motors with the investment of only one set of precision metering equipment.

Reference

1. Precision Speed Measurements for Wind Tunnels, **R. K. Fairley, H. L. Clark.** *Transactions*, American Society of Mechanical Engineers, volume 68, October 1946, pages 719-22.

Modern Excitation Systems for Large Synchronous Machines

J. B. McCLURE
ASSOCIATE AIEE

S. I. WHITTLESEY
ASSOCIATE AIEE

M. E. HARTMAN
NONMEMBER AIEE

AN EXCITATION SYSTEM consists essentially of an exciter and means for its regulation. Originally, manual control of voltage was used widely. With the development of power systems using modern apparatus, automatic control, in general, has come to play an important part in the progress of the electric power industry. Therefore, it is in keeping with this progress that voltage regulators have been used increasingly and have become an important factor in making possible further economies and improvements in system reliability. The increased use and acceptance of voltage regulators has been a great stimulus to the advancement of the art with the result that with the past few years several new types have been developed, placed in regular service, and are performing successfully.

The need for automatic regulation of voltage for water wheel generators and synchronous condensers has long been recognized. One of the important factors which has directed attention recently to the problems of automatic regulation of excitation has been the desirability of obtaining increased capacity in large 3,600-rpm turbine generator sets. The physical size of the generating element for a given capacity is determined largely by its short-circuit ratio. Reduction in short-circuit ratio makes more desirable the use of automatic regulation, and at the same time increases the importance of the excitation system reliability. With this a desire also has come to provide sources of excitation other than the direct-driven exciter for the higher speed units.

This paper reviews the principles and characteristics of existing widely used excitation systems and discusses some of the more recently developed excitation systems. These systems and the solutions of the general excitation problem discussed in this paper are identified primarily with the company with which the authors are associated. Any terms used are based on either American Standards Association definitions or on generally accepted industry terminology.

Types of Excitation Systems

The present day practice in excitation systems is to use the unit system which consists of an individual exciter and regulator for each a-c machine. In this general type of system, the voltage of each a-c machine is automatically and independently controlled by its own regulator, and the division of reactive current among machines is automatically controlled by alternating current compensation of the individual regulators. There is no problem of load division among exciters, as each exciter is operated and controlled independently. Each of the excitation

Paper 46-152, recommended by the AIEE committee on power generation for presentation at the AIEE summer convention, Detroit, Mich., June 24–28, 1946. Manuscript submitted April 29, 1946; made available for printing May 23, 1946.

J. B. McClure and S. I. Whittlesey are with the central station engineering division, and M. E. Hartman is with the control engineering division, all of General Electric Company, Schenectady, N. Y.

The authors wish to acknowledge the contributions of L. W. Thompson and F. E. Crever and their associates of the General Electric Company in the development of the improved types of voltage regulators discussed in this paper. The authors also wish to acknowledge the helpful suggestions and constructive criticisms of S. V. Travis and S. B. Crary of the same company.

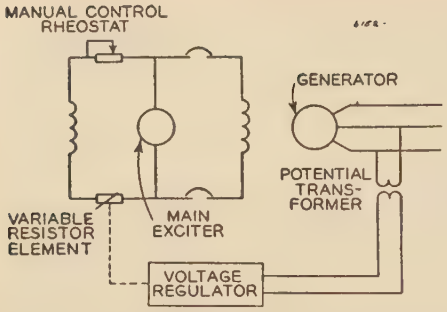

Figure 1. Elementary diagram of an excitation system consisting of a main exciter and a direct-acting rheostatic-type voltage regulator

systems discussed is designed to operate as a unit system.

Self-Excited Main Exciter and Direct-Acting Rheostatic-Type Regulator

One of the simplest types of excitation systems consists of a self-excited main exciter and a direct-acting rheostatic-type regulator.[2] The essential elements of such a system are shown schematically in Figure 1. The exciter is a shunt wound d-c machine and supplies excitation to the field of the main synchronous machine through a field breaker. In normal operation the voltage regulator detects changes in the controlled a-c voltage and mechanically changes the resistance in the exciter field circuits to produce the required exciter voltage. This regulator can be taken out of service and the exciter placed on manual control of voltage by using the rheostat provided for this purpose.

Main and Pilot Exciters and Indirect-Acting Rheostatic-Type Voltage Regulator

An excitation system which has been used with the larger machines for the past few years consists of a main and pilot exciter and an indirect-acting rheostatic-type regulator. The essential elements of such a system are shown schematically in Figure 2. The main exciter is a separately excited d-c machine and supplies excitation to the field of the main synchronous machine through a field breaker. The pilot exciter is a compound-wound self-excited d-c machine designed to hold essentially constant voltage. The field of the main exciter is energized by the pilot exciter through a motor-operated Wheatstone-bridge rheostat. In normal operation the voltage regulator detects changes in the controlled a-c voltage and adjusts the position of the rheostat to vary the output voltage of the main exciter. This regulator can be taken out of service and the rheostat placed under manual control.

Main Exciter and Static Voltage Regulator With Rotating Amplifier

One of the more recently developed excitation systems consists of either a separately- or a stabilized self-excited main exciter and a static voltage regulator with a rotating amplifier. The essential elements of this system, when using a self-excited main exciter, are shown schematically in Figure 3. The main exciter is a self-excited d-c machine and supplies excitation to the field of the main synchronous machine through a field breaker. In normal operation the voltage regulator detects changes in the controlled a-c voltage and adjusts the output of the rotating amplifier to either decrease or increase the exciter field voltage, which in turn controls the output voltage of the main exciter. The static voltage sensitive element can be of either the impedance or the electronic type. The rotating amplifier can be taken out of service and the exciter placed on manual control by using the rheostat provided for this purpose.

This system was developed after several installations of electronic regulators and electronic exciters on hydrogen-cooled synchronous condensers indicated that the cost of the electronic equipment would be considerably more than that of a standard excitation system with rotating exciter. Studies indicated that the performance of the electronic system could be duplicated by the static regulator and rotating exciter, which has a cost comparable to the standard excitation system. Experience over a period of five years has amply confirmed the expected performance.

Electronic Exciter and Electronic Voltage Regulator

Another type of excitation system consists of an electronic exciter and an electronic voltage regulator. The essential elements of such a system are shown schematically in Figure 4. The electronic exciter is a power tube rectifier, complete with its required control equipment and supply transformer, and supplies excitation to the field of the main synchronous machine through anode breakers which act as a field breaker. In normal operation, the voltage regulator detects changes in the controlled alternating voltage and adjusts the firing time of the tubes to give the required exciter output voltage. Provision also is made for operating the electronic exciter on hand control.

Exciters

The exciter for any large synchronous machine must meet certain minimum performance requirements. These requirements have not been formulated specifically on an industry wide basis, but practice and experience have demonstrated

Figure 2 (below left). Elementary diagram of an excitation system consisting of a main and pilot exciter and an indirect-acting rheostatic-type voltage regulator

Figure 3 (below right). Elementary diagram of an excitation system consisting of a main exciter and a static voltage regulator with a rotating amplifier

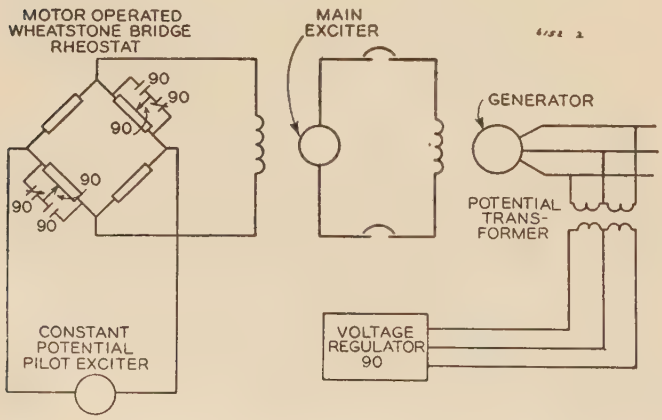

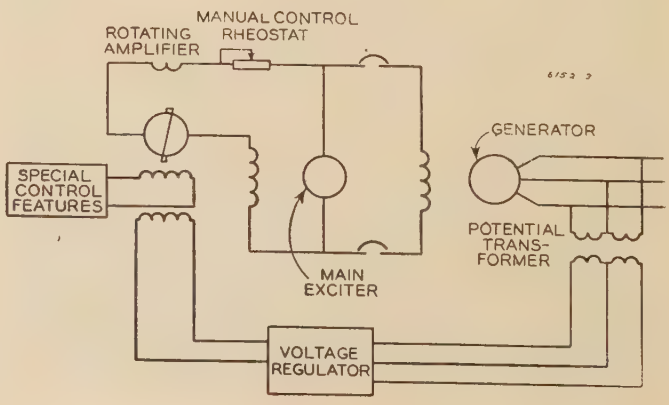

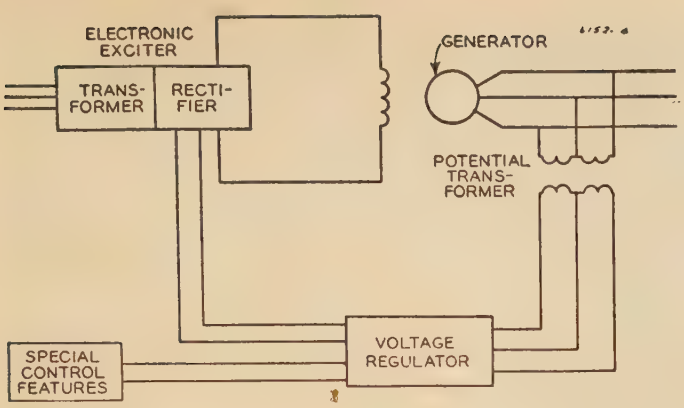

Figure 4. Elementary diagram of an excitation system consisting of an electronic exciter and an electronic voltage regulator

what they should be. As applied, present day exciters have conservative current and voltage ratings and a reasonable ceiling voltage. The over-all excitation system is designed to have a moderately quick response. The foregoing requirements have been arrived at largely through experience with shaft-driven exciters, and, in cases where other than shaft-driven exciters are used, the excitation system should be designed to give the same actual performance under certain assumed adverse system operating conditions.

Shaft-Driven Exciters

Shaft-driven exciters have been generally used for many years with turbine generators, water wheel generators, synchronous condensers, and frequency changers. The outstanding advantage of a shaft-driven exciter is its ability to ride through severe system disturbances while continuing to maintain the excitation. The main disadvantage of a shaft-driven exciter is that maintenance must be done either by shutting down the main machine or by incurring the hazard of maintenance while the machine is operating.

Hydrogen-Cooled Exciters

In the past motor-driven exciters were generally accepted for use with hydrogen-cooled synchronous condensers and frequency changers. This practice allowed the main machines to be built with a simple hydrogen-tight shell with no running-shaft hydrogen seals.

During the last five years, successful experience has been obtained with direct-connected main exciters on hydrogen-cooled synchronous condensers operating up to speeds of 900 rpm. In each of these installations, the exciter operates in a hydrogen-filled compartment which is a part of the main shell. When the machine is at rest, the exciter compartment can be isolated from the main shell and opened for inspection and maintenance. The use of a direct-connected pilot exciter in these applications would have required major structural changes and a longer shaft extension, which would have materially increased the cost.

Special Motor-Driven Exciters

The increased use of high-speed turbine generators of larger capacity has accentuated some of the problems of the shaft-driven exciter. These problems have been largely met by both improvements in design of high-speed exciters and also by the use of geared exciters for the larger sizes. However, with the trend during the past few years toward still larger capacity high-speed turbine generators, there has been an increasing inclination to provide excitation from sources other than shaft-driven exciters. A special motor-driven exciter has been developed primarily for use with large high-speed turbine generators, and also may find more general application for other types of synchronous machines. There are some obvious advantages for such a motor-driven exciter set.

1. The foundation of the main turbine generator set is simplified.
2. A low speed commutator is obtained without the use of gears.
3. Maintenance can be readily accomplished without shutting down the main unit when a spare exciter is provided.

Such a motor-driven exciter can obtain its power from the station auxiliary bus and be considered as one of the essential station auxiliaries. When the station auxiliary power is provided by either shaft generators for separate house generators, the exciter set does not need to be particularly special in design. However, most steam electric stations obtain auxiliary power either from the main generator terminals or from the main station bus, and the auxiliary power system is subjected to reduction in voltage for all main system disturbances. It is essential, therefore, to design the motor-driven exciter set to carry on through such system disturbances. It has been shown[5] that it is possible to design a motor-driven exciter set which gives the same main generator and system performance as is obtainable with a direct-connected exciter for sustained system voltage as low as 70 per cent of normal and severe faults of 12 to 15 cycles duration.

The essential features of such a motor-driven exciter set are as follows:

1. The inertia of the set is increased by using a flywheel located between the motor and generator. An inertia constant of five based on the exciter nameplate kw rating is conservative.
2. The induction motor should have a high maximum torque to enable it to carry the output of the exciter at ceiling voltage. This will be accomplished by using a motor with a maximum torque approximately equal to five.
3. The exciter should have a normal ceiling sufficient to realize a ceiling of not less than 120 per cent when the driving motor is operating, with approximately 70 per cent voltage applied to its terminals.

Exciter Stability

The ability of the exciter to maintain its voltage without appreciable drift with time has been actively discussed[14] as a requirement for the manual control of rotating self-excited exciters. When automatic voltage regulators are in use, such a requirement is not particularly pertinent. Even when under manual control, such a requirement is not necessary for short periods of operation such as transfer from one source to another. It may be important, however, when the a-c generator is left unsupervised under manual

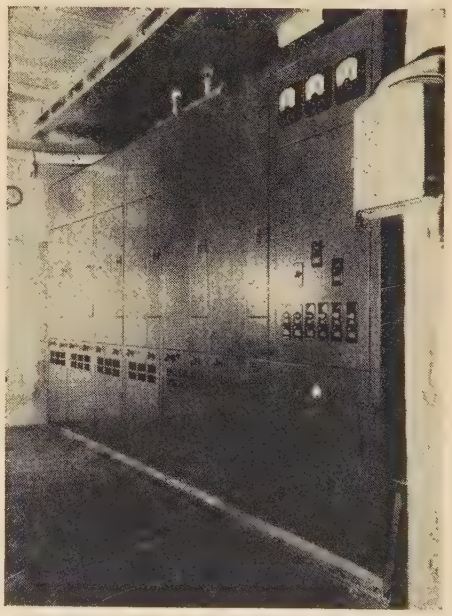

Figure 5. Electronic exciter for a synchronous condenser

control of its excitation for prolonged periods, particularly at light loads.

Electronic Exciters

The electronic exciter offers another solution for the elimination of the direct-connected exciters. Electronic exciters offer similar advantages to those already outlined for motor-driven exciters.

Electronic exciters have been supplied for differing applications. Three large synchronous condensers using electronic exciters and supplied by one manufacturer have been in operation each for 11, 9, and 7 years, respectively. One of these electronic exciters is shown in Figure 5. Functionally, these electronic exciters with their electronic regulators have given an outstanding performance. They are equipped with water-cooled ignitron power tubes having ample capacity and arranged for changing tubes while the set is in operation. Although initially the tube life did not measure up to expectations, progress in the art has resulted in reasonable tube life. Based on present experience, such an electronic exciter obtaining power through a suitable transformer from the auxiliary source in the station will have a considerably higher initial cost and higher maintenance than either the shaft- or motor-driven exciters.

Some users have insisted that the supply for an electronic excitation source should be a shaft-driven a-c generator on the main set. This brings back most of the structural disadvantages of a direct-driven excitation source and makes such a solution even more expensive.

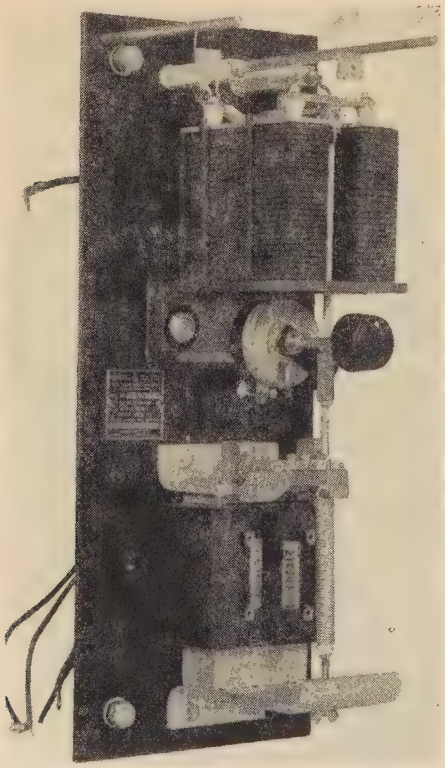

Figure 6. Direct-acting rheostatic-type voltage regulator

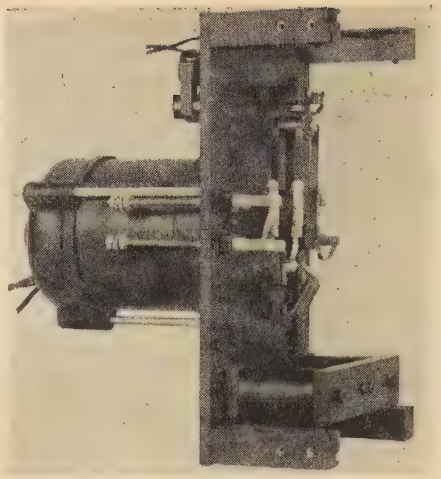

Figure 7. Indirect-acting rheostatic-type voltage regulator

When the power for an electronic exciter is obtained from the main alternator terminals or the system, it is important to design the transformer supplying the electronic exciter with a turn ratio such that high ceiling voltages are available. This is necessary for two reasons.

1. To realize at least 120 per cent ceiling with 70 per cent alternating voltage available.
2. To realize a reasonable response during a system disturbance.

The experience with electronic exciters on synchronous condensers has demonstrated that they can be applied successfully with other types of synchronous machines.

Voltage Regulators

In recent years, the use of voltage regulators has increased considerably. The main function of these regulators is to respond to any changes in the controlled voltage and to instigate the necessary changes in the excitation system to restore the controlled voltage to its original value. The required performance of the voltage regulator can be stated quite simply in terms of its band of voltage regulation which, broadly speaking, includes dead band, inherent regulation, accuracy, and stability. The various types of regulators which have been developed employ different basic principles, as will be described.

Direct-Acting Regulators

One of the simplest voltage regulators is the direct-acting rheostatic type,[2] as shown in Figure 6. In this regulator the voltage sensitive element is an electromagnet, the armature of which is balanced against a spring. The resistance element which is in the exciter field circuit is connected directly to the armature and is a part of the regulator assembly. When there is a change in the controlled voltage, the armature will change position and adjust the resistance element in such a way as to restore the controlled voltage. This type of regulator is compact and simple to install, operate, and maintain. At present, it is not designed to handle high exciter field currents and, therefore, its use is limited to small and medium size machines. This regulator is of the continuously-acting type and has a narrow band of voltage regulation.

Indirect-Acting Regulators

The indirect-acting rheostatic-type voltage regulator is well suited for use in excitation systems having both a pilot and a main exciter and is shown in Figure 7. The voltage sensitive element of this regulator may be a polyphase torque motor, the torque of which is proportional to the approximate average 3-phase voltage. The torque of the motor is balanced against the pull of a spring so that for each value of voltage there is a definite position of the motor rotor to which is attached a contact assembly. The contact assembly has two sets of contacts, the first set operates intermittently for small changes in voltage to control the pilot motor of the motor-operated Wheatstone-bridge rheostat (Figure 8), which in turn adjusts the resistance of the rheostat. Both sets of contacts operate for large changes in voltage, the second set controlling the temporary switching of all the regulating resistance in the rheostat, while the first set of contacts controls the final position of the rheostat. Thus, for large changes in voltage, there is an extremely rapid change in the excitation field resistance which increases the response of the entire excitation system.

This type of regulator is rugged and reliable. When used with the Wheatstone-bridge-type rheostat, rapid response is obtained, and practically no limit need be placed on the field currents it will successfully control. For some applications where severe fluctuating loads are encountered, the dead-band principle in conjunction with the intermittent control feature, is not the ideal type of regulator.

Impedance Regulator

The impedance regulator is one of the more recent developments in the voltage regulator field and is shown in Figure 9. It is a static-type regulator and is nor-

mally used with a rotating amplifier. The function of the rotating amplifier is to respond to changes in the controlled voltage as detected by the regulator and modify the voltage in the field circuit of the main exciter in such a manner as to restore the controlled voltage.

The impedance voltage regulator consists essentially of a linear and nonlinear impedance. The 3-phase voltage to be controlled is passed through a positive-sequence network and the resulting single-phase voltage, which is the approximate average of the 3-phase voltage, is impressed on both the linear and nonlinear impedances. The linear impedance supplies rectified current to the control field of the rotating amplifier in such a direction as to raise the output voltage. The nonlinear circuit also supplies rectified current to the control field of the rotating amplifier, but in such a direction as to lower the output voltage. The volt-ampere characteristics of the two impedances are such that they intersect at some value of control voltage at which point there is no net current in the control field of the rotating amplifier. For a change in the controlled voltage, there will be a net current in the control field which is in the direction to restore the controlled voltage to its previous value.

The impedance voltage regulator is simple in operation, has no moving parts, and no inherent dead band, and is of the continuously acting type. Special control features can be added readily to this type of regulator by the use of additional control fields in the rotating amplifier. The use of this type of regulator results in fast smooth response of the excitation system with a narrow band of voltage regulation.

Electronic Regulator

Another static type of voltage regulator is the electronic regulator which is shown in Figure 10. It can be used either with a rotating amplifier in an excitation system with rotating exciters or directly with an electronic exciter to control the grids of the firing tubes, which in turn control the firing point of the main power tubes.

The electronic regulator consists essentially of a constant voltage glow tube and the necessary rectifier and control tubes. The 3-phase voltage is rectified and compared with the voltage across the glow tube. Any difference in these voltages is amplified and produces a change in the grid of the tubes supplying power to the control fields of the rotating amplifier. The tubes used are radio type, and, to give reliable operation, two tubes in parallel are used so that tubes can be checked or changed without shutting down the regulator.

The electronic regulator has the same features as the impedance regulator. In this type of regulator, special control features can be added directly to the regulator. Its use also will result in fast smooth response[1] of the excitation system with a narrow band of voltage regulation.

The outstanding performance of several installations with electronic exciters and electronic regulators, in maintaining smooth voltage control at locations where severe fluctuating loads exist, was caused primarily by the characteristics of the regulator and not by the electronic exciter. It is well recognized that a voltage regulator of the continuously acting type andwithout dead band gives the ideal type of control. These regulating characteristics are now available for using with rotating exciters.[1]

General

Rheostats

Pilot exciter field rheostats are usually of the manually-operated dial type. They are used initially to obtain the proper pilot exciter voltage and once that is done need not be changed.

Main exciter field rheostats should be chosen to suit the application. In general, they will be motor-operated so that they may be controlled from a central location. When the main exciter is operated self-excited with a voltage regulator, the rheostat will be used for short intervals only while maintenance work is being done. In this case, a relatively simple and inexpensive dial type rheostat may be used.

When the main exciter is excited separately and the motor-operated Wheatstone-bridge-type rheostat is used in conjunction with a rheostatic-type voltage regulator, such a rheostat is of the face-plate type as shown in Figure 8. This rheostat is simple and rugged and able to successfully withstand the frequent operations required by the regulator.

Several years ago, it was considered general practice to use main generator field rheostats. There were two reasons for requiring these rheostats.

1. More than one synchronous machine often was excited from a common d-c source and the rheostat equalized any difference in the excitation requirements.

2. The excitation systems were not designed for operation at the low voltages required for line charging and for synchronous generators with low short-circuit ratios.

In modern practice, the unit system of excitation is used almost universally and the entire excitation system is capable of operating down to low voltages. Thus the need for main generator field rheostats has practically disappeared.

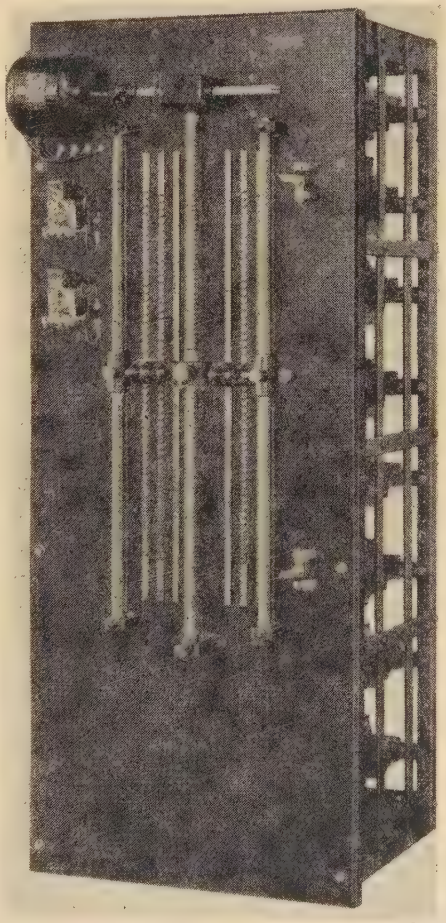

Figure 8. Motor-operated Wheatstone-bridge rheostat

Dynamic Stability

The possibility of operating above the ordinary steady state stability limits by using a special excitation system has been recognized for some time, although it has not been ordinarily necessary to require operation in this region. This requirement together with equipment which is capable of so operating may be desirable during emergency conditions in order to allow for safe operation with smaller stability margins and, therefore, with higher transmission system loadings. An interesting application of this principle has been made to electric ship propulsion.[12]

Reference 12 shows, in general, the factors which need to be taken into account in order to provide for stable operation. A desirable characteristic is small voltage dead band with small excitation system time lags.

Lower Excitation Limit

If the unit is under automatic control of voltage, it may be desirable to use a fixed

or variable lower limit. A variable limit for generators preferably should be made a function of prime mover torque, which can be obtained conveniently from the position of the mechanism which controls prime mover input. Such a variable limit allows for a greater range of regulator operation than if a fixed lower limit is used and insures against the possibility of reducing the excitation below the point where instability may result.

The critical value of excitation, below which instability may result, does not depend greatly upon the external system. It is, therefore, possible by means of a variable lower limit to insure an adequate amount of excitation for a wide range of system conditions. This lower limit is insurance against an error in setting the voltage adjusting rheostat or other errors which incorrectly may reduce the excitation.

Salient-pole synchronous condensers may be provided with a fixed lower limit of negative polarity and possibly biased by terminal voltage in order to take advantage of the saliency torque, and thereby increase the lagging capacity.[13] Frequency changer sets, however, may require an adjustable lower limit which can be adjusted as determined by operating conditions.

A fixed lower limit of generator excitation is often used. With the use of a low short-circuit ratio generator, this lower limit necessarily must be set at a value higher than that required for synchronizing. Therefore, during synchronizing the limit must be removed or synchronizing obtained under manual control of the excitation.

Upper Excitation Limit

An upper excitation limit has been used for some applications based on limiting either the excitation voltage, alternator field current, or armature current. A common method in supervised stations is to ring an alarm when either the excitation voltage or current exceeds a given amount for a predetermined time. Also, for synchronous condenser installations, a limit on the excitation has been based on the average field temperatures (from resistance measurement) exceeding that obtained from rated or normal field excitation. It should be noted here that such a limit should not be based on allowable temperature for insulation used, but rather should be based on the total temperature obtained with nominal or rated excitation and the existing ambient. Although many variations of the use of an upper limit are possible, it probably is necessary only to sound an alarm in supervised stations when the excitation exceeds for a given time delay a limiting amount. In unsupervised stations it may be desirable to limit the excitation to the rated value and allow for a corresponding drop in voltage at the regulated bus. This need be the only requirement necessary for 0.8- to 0.9-power-factor generators since their rated field excitation will be normally sufficient to carry the maximum kw output of the prime mover.

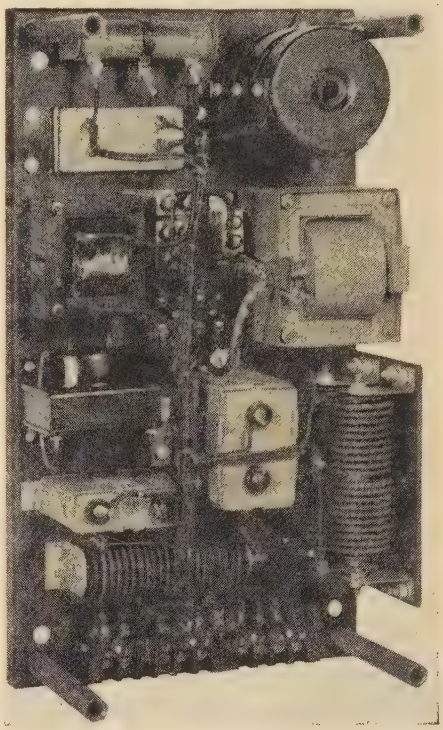

Figure 9. Impedance-type voltage regulator

Application Guides

The following discussion summarizes what may be considered modern practices for successful excitation systems of the larger synchronous machines. In present day practice, rotating exciters are almost exclusively used, and therefore, the preferred field of application of electronic exciters will be left until such time as they can be justified on an economical basis and until they are more generally accepted. The unit system of excitation, that is an independent exciter and regulator for each synchronous machine, is assumed throughout.

Turbine Generators

For several years it has been considered standard practice to control and supply the excitation of the larger turbine generators with a main exciter, pilot exciter, Wheatstone-bridge rheostat, and indirect-acting-type voltage regulator. This system has proven to be a reliable one, but experience has indicated that there are some fundamental disadvantages. The inherent dead band requires greater droop to obtain accurate division of reactive current between machines, which in turn required more frequent adjustment of voltage levels to maintain voltage at some desired location on the system. Special control features cannot be added readily to this type of regulator.

One other solution for the small and medium sized generators has been to apply the direct-acting-type regulators. In this way the pilot-exciter and Wheatstone-bridge-type rheostat are eliminated. The continuous-type regulator gives good division of reactive current and smooth response. The regulator has the disadvantage that at present it cannot handle high exciter field currents, and, therefore, its use is limited to generators not in excess of 25,000 kva. It is also difficult to add special control features to this type of regulator.

Experience indicates that a universally applicable regulating system for the larger turbine generators is a static-type regulator with a rotating amplifier. Smooth fast response is obtained; the continuous-type regulator with no dead band gives accurate division of reactive current, and low energy control circuits make it possible to add automatic limits. In addition, this type of regulator is readily applied to existing main exciters and in this way any excitation system can be modernized conveniently.

For those who still prefer shaft-driven exciters for their high speed units, present day conservative practice would suggest gear-driven exciters for the larger units and direct-driven for the smaller units up to 25,000 kva. However, with the improvements in system relaying and auxiliary power system arrangements, the possible simplifications, flexibility, and performance resulting from the use of a special motor-driven exciter make its use particularly attractive for large turbine generators. It is expected that the acceptance of motor-driven exciters in these applications will increase rapidly.

Water Wheel Generators

It is almost universal practice on all of the larger water wheel generators to control and supply their excitation with a main exciter, pilot exciter, Wheatstone-bridge rheostat, and indirect-acting-type voltage regulator. Hydro stations usually feed radially into a system so that any disadvantage of the inherent dead band

in the regulator is not very important. The high speed feature of the bridge rheostat makes it ideal for controlling voltage during loss of load, and the ability to operate at very low excitations makes it ideal for line charging requirements.

Because of the additional advantages of the static-type regulators and a rotating amplifier, it can be expected that this type of regulating system eventually

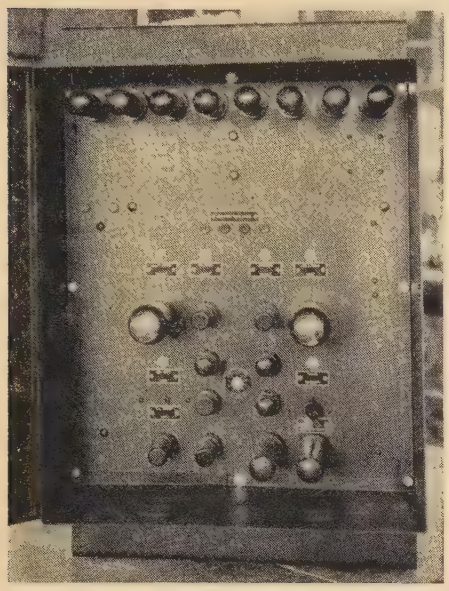

Figure 10. Electronic-type voltage regulator

will be applied to water wheel generators.

Direct-connected exciters are used almost universally in hydro installations, and maintenance has not proved excessive in these slow speed exciters.

Synchronous Condensers

Several years of experience with static-type regulators and rotating amplifiers on synchronous condensers, indicates that this is practically the ideal regulating system for such applications. The continuous-acting-type regulator with no dead band makes it particularly suited to the type of voltage control expected of synchronous condensers.

During this same time, direct-connected hydrogen-cooled exciters have been operating successfully with several synchronous condensers. As a result of this experience, all moderate and low speed synchronous condensers, both air-cooled and hydrogen-cooled, may now be equipped with direct-connected exciters.

Frequency Changers

The requirements of an excitation system for a frequency changer set will vary between that of a synchronous condenser and water wheel generator, depending upon the location of the set on the system. Most of the existing frequency changers are equipped with main and pilot exciter Wheatstone-bridge rheostats and indirect-acting voltage regulators. This type of excitation system has given successful performance. Where system conditions require close control of voltage, a static-type regulator and rotating amplifier can be used to advantage.

As a result of the successful experience with hydrogen-cooled exciters on synchronous condensers, all frequency changers, both air-cooled and hydrogen-cooled, now may be equipped with direct-connected exciters.

Conclusions

1. The general use of automatically controlled excitation systems makes it possible to operate existing equipment at higher loadings and to design more economical system extensions.

2. Improved division of reactive currents and improved system performance are made possible by applying voltage regulators, which have a narrow band of voltage regulation now available in modern regulators of the continuously acting type.

3. The advantages of providing limits with voltage regulators are recognized, and these limits may be readily applied when static-type voltage regulators are used.

4. Excitation systems which do not include pilot exciters may be readily modernized by applying a rotating amplifier and a static-type voltage regulator.

5. Special motor-driven exciters may be successfully used in place of large high speed shaft-driven exciters.

6. Shaft-driven hydrogen-cooled main exciters have been successfully used for moderate speed synchronous machines.

7. Co-ordinated excitation systems are now available for all types of application requirements.

References

1. The Development of Modern Excitation Systems for Synchronous Condensers and Generators, **F. M. Porter, J. H. Kinghorn.** AIEE Transactions, volume 65, 1946, pages 1020–7.

2. The Direct-Acting Generator Voltage Regulator, **W. K. Boice, S. B. Crary, Gabriel Kron, L. W. Thompson.** AIEE Transactions, volume 59, 1940, March section, pages 149–57.

3. Regulation of A-C Generators With Suddenly Applied Loads, **E. L. Harder, R. C. Cheek.** AIEE Transactions, volume 63, 1944, June section, pages 310–18.

4. Voltage Variation of Suddenly Loaded Generators, **H. C. Anderson, Jr.** *General Electric Review*, August 1945, pages 25–33.

5. Motor-Driven Exciters for Turbine Alternators, **R. B. Bodine, S. B. Crary, A. W. Rankin.** AIEE Transactions, volume 65, 1946, May section, pages 290–7.

6. Discussion by **J. F. Miller** of Motor-Driven Exciters for Turbine Alternators. AIEE Transactions, volume 65, 1946, page 516.

7. Progress in Power Apparatus Development, **A. C. Monteith.** *Edison Electric Institute Bulletin*, June 1945, pages 169–72.

8. Power Systems for Auxiliary Drives in Steam-Electric Stations, **J. B. McClure, S. I. Whittlesey.** AIEE Transactions, volume 64, 1945, December section, pages 844–51.

9. Electric Drives for Steam-Electric Generating-Station Auxiliaries, **W. R. Brownlee, S. A. Elzi.** AIEE Transactions, volume 64, 1945, November section, pages 741–5.

10. Stability Characteristics of Turbine Generators, **C. Concordia, S. B. Crary, J. M. Lyons.** AIEE Transactions, volume 57, 1938, pages 732–41.

11. Preferred Standards for Large 3600 RPM, Three-Phase, 60 Cycle Condensing Steam Turbine-Generators. AIEE Standards 601 and 602, May 1945.

12. Steady-State Stability of Synchronous Machines as Affected by Voltage-Regulator Characteristics, **C. Concordia.** AIEE Transactions, volume 63, 1944, May section, pages 215–20.

13. Power System Stability (book), **S. B. Crary.** John Wiley and Sons, Inc., New York, N. Y. Volume I, section 103.

14. Exciter Instability, **R. E. Doherty.** AIEE Transactions, volume 41, 1922, pages 767–80.

High Vacuum Leak Testing With the Mass Spectrometer

W. G. WORCESTER
ASSOCIATE AIEE

E. G. DOUGHTY
NONMEMBER AIEE

THE DETECTION of small leaks in large all-metal vacuum systems has long been a troublesome manufacturing problem for which there was no satisfactory solution. All of the generally used techniques of leak detection are cumbersome or have serious limitations such as lack of sensitivity, lack of selectivity, poor response, dependence upon vacuum conditions, uncertainty of interpretation of response, or usefulness being restricted to certain materials. Experience with many methods of leak detection on all sizes of apparatus has shown that an ideal leak detector must have the following characteristics:

(*a*). *High sensitivity.* The instrument must be able to detect small leaks.

(*b*). *Accuracy.* To facilitate repairs to the system the leak must be accurately located.

(*c*). *Response.* The instrument must respond quickly when a leak is located and must "clean up" quickly when the leak has been passed. Too much lag interferes with the accurate location of leaks.

(*d*). *Selectivity.* The leak detector must be capable of locating large or small leaks in the presence of many other leaks.

(*e*). *Certainty of response.* The instrument must always respond to a leak and must not be subject to spurious effects or false signals.

(*f*). *Versatility.* The method should be applicable to large or small systems constructed of metal, glass, or other materials. Usefulness of the method should not depend too much upon vacuum conditions, since it is usually not convenient to obtain a high vacuum in the test sample.

(*g*). *Simplicity.* Operation of the leak detector must be sufficiently simple that it can be performed by unskilled personnel.

(*h*). *Portability.* Since many vacuum systems are permanent installations, the leak detector must be portable.

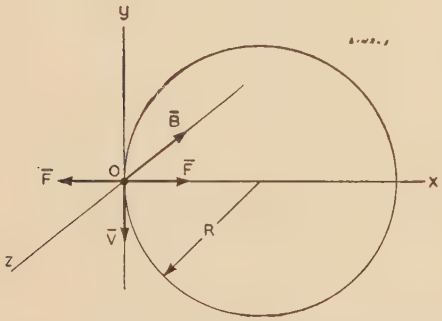

Figure 1. Forces acting on a charged particle in a magnetic field

It is the object of this paper to describe a special mass spectrometer, designed for use as a leak detector, which fulfills these requirements to a higher degree than any previously known form of leak detector.

This leak detector design is based on the mass spectrometer experience of Doctor A. O. C. Nier of the University of Minnesota,[1] who also shared in a major way in the problems of design and manufacture of the leak detector.

The Mass Spectrometer

The mass spectrometer is a device which utilizes electric and magnetic fields to sort out ionized gas molecules according to their molecular weights (or to be exact, according to mass-to-charge ratio, or *specific mass*). The instrument is therefore capable of measuring the partial pressure of each gas in a mixture of gases in a vacuum system. The device is thus inherently selective, which immediately suggests its use as a detector of some gas which can be used as a tracer in a mixture of gases. In the present application, the tracer gas would be allowed to flow through a leak, and its presence in the vacuum system would be detected by the mass spectrometer, irrespective of the presence of other gases. It remains to determine whether the other requirements of an "ideal leak detector" can be met.

Paper 46-142, recommended by the AIEE committee on instruments and measurements for presentation at the AIEE summer convention, Detroit, Mich., June 24–28, 1946. Manuscript submitted April 12, 1946; made available for printing May 14, 1946.

W. G. WORCESTER and E. G. DOUGHTY are in the general engineering and consulting laboratory of the General Electric Company, Schenectady, N. Y.

The authors wish to extend credit to Professor A. O. C. Nier, of the University of Minnesota, whose many contributions to the field of mass spectrometry have been of outstanding importance. They also wish to acknowledge the contributions of Doctor R. B. Jacobs in the application of the mass spectrometer to the problems of leak detection. The mass spectrometer type leak detector and methods of application of the instrument were developed by Professor Nier and Doctor Jacobs who also co-operated with the General Electric Company in solving the problems of design and manufacture of the commercial model.

Theory

In order to understand the principle of operation of the mass spectrometer, let us consider the forces acting on a charged particle moving at right angles to a magnetic field as shown in Figure 1. In vector notation, the electromagnetic force acting on the particle will be

$$\boldsymbol{F}=q\boldsymbol{v}\times\boldsymbol{B} \tag{1}$$

where $\boldsymbol{F}$, $\boldsymbol{v}$, and $\boldsymbol{B}$ are vectors representing force, velocity, and magnetic induction respectively, and q is the charge on the particle.

Since the force is always perpendicular to the velocity, there will be no linear acceleration; but there will be constant angular acceleration, so that the path of the particle will describe a circle in the x-y plane with the center at (R, 0, 0) as shown, where R is the radius of curvature.

From elementary mechanics, a particle of mass m moving with a velocity v along a curved path of radius R will experience a centrifugal force

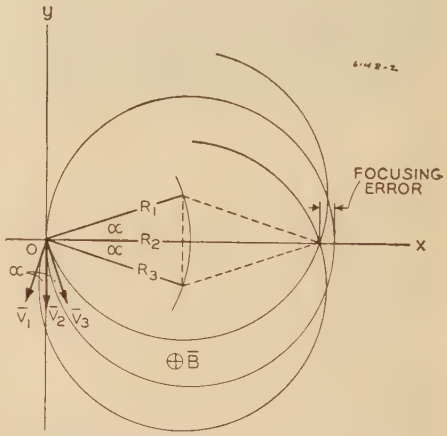

Figure 2. Focusing property of magnetic field

$$F'=\frac{mv^2}{R} \tag{2}$$

Since F and F' are equal in magnitude but opposite in direction, we can write

$$qvB=\frac{mv^2}{R}$$

or

$$qB=\frac{mv}{R} \tag{3}$$

Let us assume that the charged particle acquired its velocity by falling through an electrostatic potential V, in

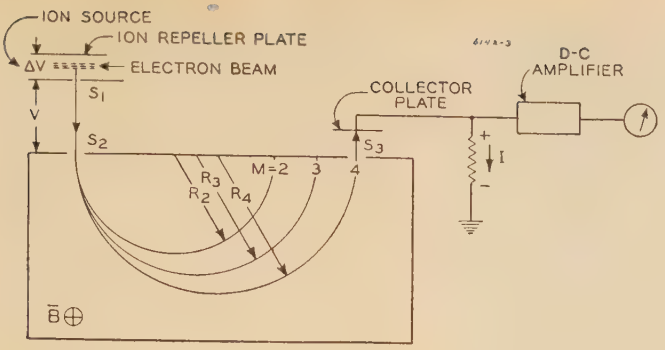

Figure 3 (above left). Mass spectrometer

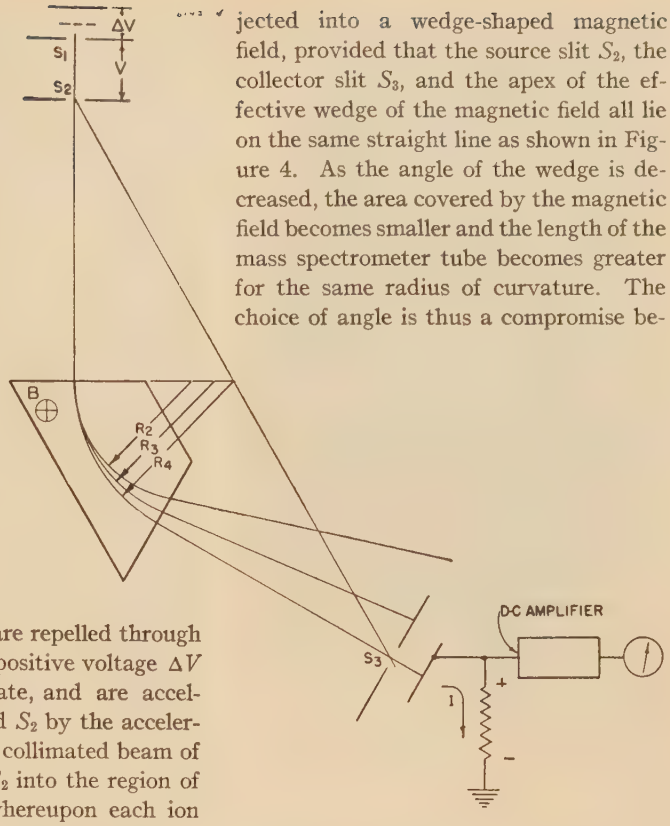

Figure 4 (right). Sixty degree mass spectrometer

which case the potential energy would be

$$PE = qV \tag{4}$$

which must be the same as the kinetic energy after acceleration

$$KE = \frac{mv^2}{2} \tag{5}$$

Setting equation 4 equal to equation 5 and solving for v, we get

$$v = (2qV/m)^{1/2} \tag{6}$$

Substituting this value for v in equation 3, and solving for the mass-to-charge ratio, we obtain

$$m/q = B^2R^2/2V \tag{7}$$

From this we can see that charged particles having different mass-to-charge ratios will follow paths of different radius, and that the radius for any particular particle can be controlled by choosing the proper values of magnetic field and accelerating voltage.

Let us now consider the effect of the magnetic field on charged particles whose velocities at the origin differ in direction by the small angle α, but which are identical in all other respects. A simple geometrical construction as shown in Figure 2 demonstrates that there will be a point, lying on the x axis, at which the three paths are closest together, or at which the originally divergent paths are refocused. The "focusing error" is seen to be

$$\text{Focusing error} = 2R(1 - \cos \alpha) \tag{8}$$

where

$$R = R_1 = R_2 = R_3$$

Obviously the focusing error can be made as small as desired by making the angle α small.

The mass spectrometer utilizes the principles that we have discussed in a manner illustrated diagrammatically in Figure 3. Gas molecules are introduced at low pressure to the ion source, where part of the gas is ionized by bombardment with electrons which have been accelerated through a potential of the order of 150 volts. The ions are repelled through the slit S_1 by a small positive voltage ΔV on the ion repeller plate, and are accelerated between S_1 and S_2 by the accelerating potential V. A collimated beam of ions passes through S_2 into the region of the magnetic field, whereupon each ion will follow a circular path according to equation 7. By proper adjustment of the magnetic field and the accelerating voltage, ions of any specific mass

$$M = m/q = B^2R^2/2V \tag{9}$$

can be made to pass through a third slit S_3 and will discharge on the collector plate, causing a positive current to flow through the high resistance to ground. The voltage drop across the resistor is amplified and measured.

If it is assumed that the electric and magnetic fields are adjusted to bring ions of specific mass $M = 4$ into focus on the collector plate, ions of specific mass 3 and 2 will follow paths of smaller radius as shown in Figure 3.

In an actual mass spectrometer, since the slits must have a finite width, the beam of ions entering the magnetic field will have a width determined by S_1, and divergence depending upon the geometry of the ion source and slit system. Therefore the collector slit S_3 must be made somewhat wider than the source slit in order to collect all ions of any specific mass. In addition, it is impossible to accelerate all ions through exactly the same electric potential, and the collector slit width must be increased somewhat to collect ions of slightly differing energies.

Up to this point we have discussed only a mass spectrometer in which the path of the ion is bent through a total angle of 180 degrees. It can be shown that the same principles apply when the ions are projected into a wedge-shaped magnetic field, provided that the source slit S_2, the collector slit S_3, and the apex of the effective wedge of the magnetic field all lie on the same straight line as shown in Figure 4. As the angle of the wedge is decreased, the area covered by the magnetic field becomes smaller and the length of the mass spectrometer tube becomes greater for the same radius of curvature. The choice of angle is thus a compromise between minimum tube size and minimum magnet size, and an arbitrary value convenient for manufacturing is generally used. The angle of deflection for the leak detector described in this paper is 60 degrees.

Definitions and Units

For the purpose of discussing the theory of the mass spectrometer, we have dealt somewhat loosely with such units as mass and charge. In order to facilitate discussion of the special instrument which will hereafter be referred to as the leak detector, it will be useful to redefine the units as follows:

q is always a small integral multiple of the charge of the electron. For the remainder of this paper we will assume that q is one electronic charge

m is the mass of the ion in atomic weight units

$M = m/q$ = specific mass in atomic weight units per electronic charge

B is the magnetic field strength in gauss

V is the accelerating voltage in volts

R is the radius of curvature in centimeters

We now can rewrite equation 7 in terms of these practical units, putting in the constant of proportionality

$$M = 4.8 \times 10^{-5} B^2R^2/V \tag{10}$$

The Leak Detector

The leak detector is a small portable mass spectrometer of all-metal construc-

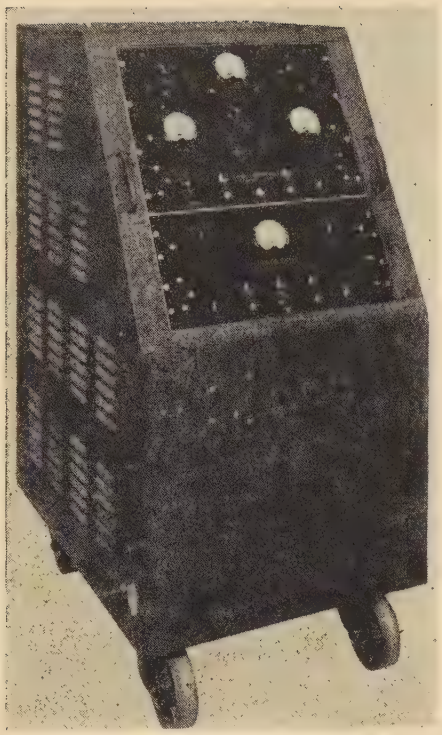

Figure 5. Mass spectrometer leak detector

tion designed to detect minute quantities of helium. The instrument continuously draws a sample of gas from the system being leak tested and indicates the partial pressure of helium in the sample. As portions of the test system are exposed to a helium jet, any helium entering the system through a leak causes an increase in the output current of the amplifier, thus indicating the presence of the leak. To insure that it will find very small leaks, the instrument has been designed for the highest sensitivity compatible with ruggedness and simplicity. An over-all view of the leak detector is shown in Figure 5.

The value of the method in actual use will depend upon the ability of the mass spectrometer to detect minute quantities of the tracer gas in a mixture of air and other gases and to detect small changes in the amount of tracer gas.

As an illustration, suppose that we have a vessel with a large number n leaks of equal size. We wish to locate each leak accurately by the use of our leak detector. If we completely cover one leak with the probe gas and leave the remainder exposed to air, the ratio of the flow of probe gas into the vessel to the flow of air is $1/(n-1)$ (assuming equal rates of flow for the different gases). In order to detect the leak, we must admit a detectable quantity of helium to the leak detector, and at the same time we must be able to admit $(n-1)$ times as much air without causing damage to the instrument.

Since the minimum detectable ion current is fixed by the state of the art of d-c amplifier design, it is desirable to obtain as many ions per second as possible at the collector plate. In the ion source the sample pressure and the electron emission from the filament will be as high as is commensurate with reasonable filament life. The slits S_1 and S_2 will be made as wide as possible, resulting in a relatively large angle of divergence of the ion beam and consequently a large focusing error. By referring to Figures 2 and 3 it can be seen that a limitation on slit width and beam divergence is imposed by the relative values of specific masses that are collected and those that are excluded. Examination of equation 10 shows that the separation in space of neighboring masses is greater for low values of specific mass than for high values. For example, the separation between masses 3 and 4 would be

$$\Delta R = R_4(1-3/4)^{1/2} = 0.134R_4 \qquad (11)$$

whereas the separation between masses 39 and 40 would be only

$$\Delta R = R_{40}(1-39/40)^{1/2} = 0.013R_{40} \qquad (12)$$

It is obvious that a mass spectrometer with a small radius of curvature and the widest possible slits is most adaptable to use with low specific masses, and that such an instrument would not be expected to separate neighboring high masses.

The foregoing considerations suggest the choice of helium as the most suitable gas for use as a "probe" or "tracer" gas. Since helium is inert and is rare in the atmosphere, being present to the extent of about one part in 200,000 parts of air at sea level, we would not expect to find an appreciable background signal because of residual helium present in the mass spectrometer tube or leakage of air through any other leaks that may be present. It is also significant that there are not likely to be other gases present which could give an apparent, or spurious, helium signal due to the loss of two or more electrons in the ionization process. For example, the probability of triple charging of carbon-12, or quadruple charging of oxygen-16 in detectable quantities is very small. It is hardly necessary to point out that helium is a gas at all temperatures and pressures to be considered and therefore will not plug leaks or contaminate the system. Neither will it react with any other materials which may be present. The requirements of versatility and certainty of response are seen to be fulfilled by the use of helium as the probe gas. The further requirements of simplicity and portability also are brought closer to realization.

Component Parts of the Leak Detector

In addition to the basic element of the leak detector, the mass spectrometer tube, a number of auxiliary components

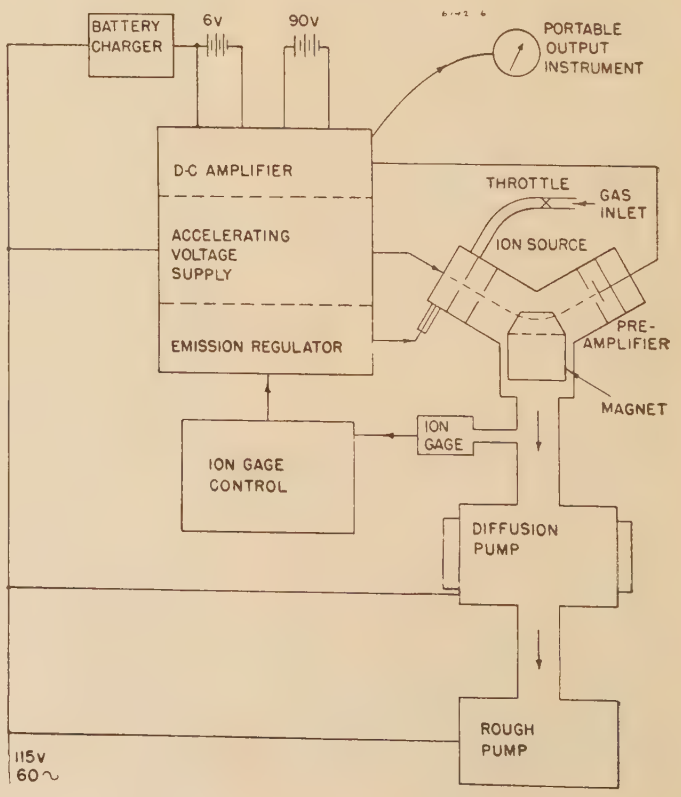

Figure 6. Leak detector block diagram

are required for control purposes. These are shown diagrammatically in the block diagram of Figure 6 and can also be seen in the back view of the instrument shown in Figure 7. The chief parts are as follows:

1. Mass spectrometer tube.
2. Emission regulator.
3. Accelerating voltage supply.
4. D-c amplifier.
5. Ion gauge.
6. Diffusion pump.
7. Rough pump.
8. Throttle valve.

The gas sample from the system under test is introduced to the spectrometer tube through a throttle valve in order that the pressure in the spectrometer tube can be regulated to a suitable value. Some of the gas molecules in the ion source are ionized by bombardment with an electron beam, which is held constant by an electronic emission regulator circuit. The ions are accelerated through a series of plates by an adjustable voltage obtained from the accelerating voltage supply, and are deflected by the field of a permanent magnet with trapezoidal pole pieces which is mounted inside the mass spectrometer tube. The ions which pass through the collector slit are discharged on the collector plate, and the ion current is amplified and measured by the d-c amplifier.

Output current of the amplifier can be read either on a panel instrument or on a portable instrument which is readily placed in view of the operator. While it would be possible to use a well regulated power pack to operate the amplifier, batteries are used for plate and filament voltages in this equipment.

The pressure in the spectrometer tube is measured by a standard ionization gauge with an a-c operated control panel. A protective feature is incorporated in the ion gauge control to automatically turn off the ion gauge and spectrometer tube filaments if the pressure accidentally is allowed to rise above a safe operating limit.

The oil diffusion pump and cold trap, backed by a mechanical rough vacuum pump, will reduce the spectrometer tube pressure to a safe operating value within about an hour after the pumps are started.

The Mass Spectrometer Tube. Figure 8 is a diagram showing the essential parts of the mass spectrometer tube. The permanent magnet produces a field of about 900 gausses, and the tube is designed for a 5-centimeter radius of curvature. Inserting these values in equation 10 we find that helium, of specific mass 4 will be focused on the collector slit with an accelerating voltage of 243 volts. It is also interesting to note that for a constant radius, which is fixed by the slit system, and a constant magnetic field, the product of specific mass and accelerating voltage is a constant, in this case 4×243 or 972, so that equation 10 reduces to $M = K/V$.

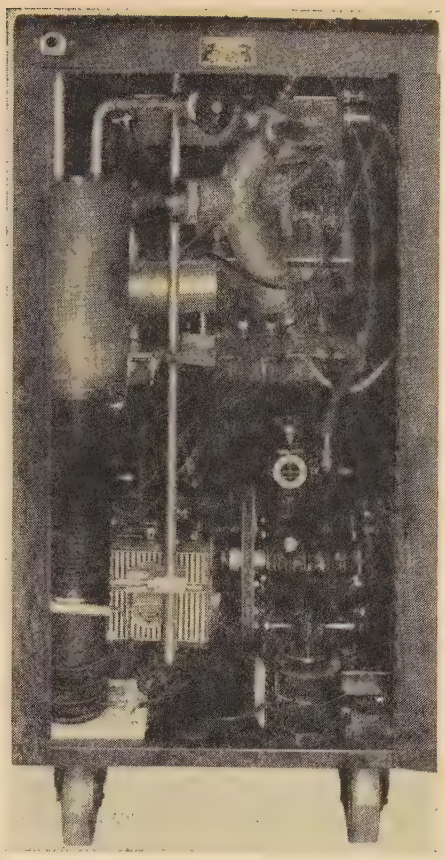

Figure 7. Rear view of leak detector showing arrangement of parts

This fact simplifies the problem of identifying other ions that may be collected at different values of accelerating voltage.

The ion source is somewhat more complicated than is indicated in Figures 2 and 4 due to the addition of an ion lens, consisting of two focusing half-plates which can be separately adjusted to the proper potentials to concentrate the ion beam at slit S_2 and to center the beam on the slit. Referring to the ion lens diagram, Figure 9, if the potential gradient E_b is greater than E_a the ion lens will be converging with a focal length equal approximately to $2V/(E_b - E_a)$, and can be treated in much the same manner as a thin optical lens of the same focal length.[2] Use of such an ion lens increases the intensity of the ion beam, and therefore increases the sensitivity of the leak detector.

The ion source is separated from the remainder of the spectrometer tube by a baffle located at the second source slit. The purpose of the baffle is to introduce additional pumping resistance so that the source pressure will be higher than the tube pressure, and more ions will be formed. The net result is greater sensitivity. This will become apparent if we consider the pressure limitations in the tube.

Any mass spectrometer must be operated under high vacuum conditions for two reasons. First, the average ion must not suffer a collision with gas molecules or other ions while travelling from the ion source to the ion collector, that is, the mean free path must be greater than the length of the mass spectrometer tube. Otherwise the beam will be scattered,

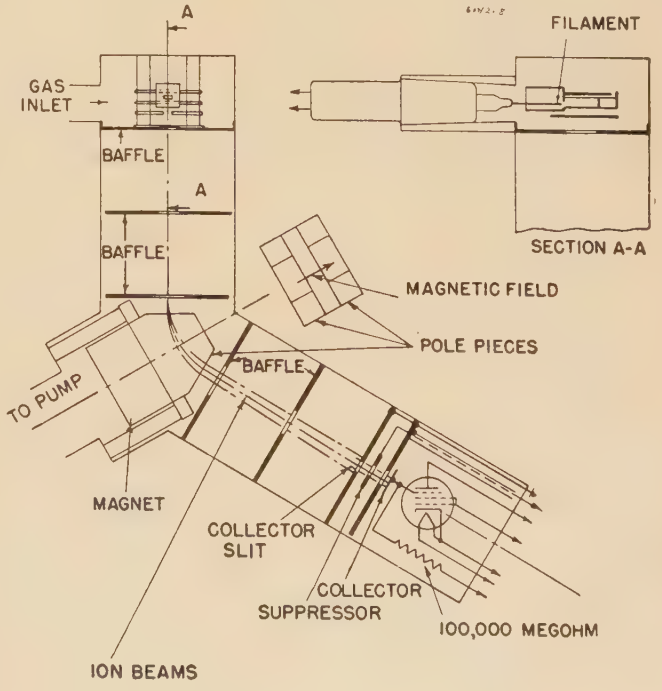

Figure 8. Mass spectrometer tube diagram

with resulting lack of sensitivity, and under certain circumstances a background ion current can appear at the collector. The second reason for the high vacuum is that a tungsten filament is used as a source of electrons, and the life of the filament would be very short at pressures above about 10^{-3} millimeter mercury (1 micron).

Experimental results show that satisfactory filament life under normal operating conditions can be obtained if the source pressure is limited to about 3×10^{-4} millimeter with a filament emission current of five milliamperes. At this pressure, however, the mean free path for air molecules would be less than the length of the path through the spectrometer tube. This condition is obviously unsatisfactory, since more than half of the ions would suffer a collision before reaching the collector. Tests on an actual tube have shown that it is necessary for the mean free path to be more than ten times the length of the spectrometer tube for satisfactory operation, and even in this case an appreciable portion of the ions will suffer collisions.

Use of the baffle allows us to maintain maximum source pressure for highest possible sensitivity and still have a low enough pressure in the major portion of the spectrometer tube to prevent scattering of the ion beam by collisions with air molecules.

The ion collector arrangement indicated in Figures 3 and 4 consists of a slit and a collector plate. Again the actual arrangement used is somewhat more complicated, as shown in the tube diagram Figure 8. A suppressor plate is introduced between the slit and the collector, and a shield is provided to guard the collector from fluctuations in suppressor plate potential. With no voltage on the suppressor plate the actual arrangement is equivalent to that indicated in Figure 4. If we were to operate the instrument under these conditions with a small amount of helium mixed with air at the maximum allowable tube pressure, we would obtain a spectrum in the region of helium as shown by the upper curve of Figure 10. The sloping background curve is due to ions which have been slowed down or deflected by collisions during the transit from the ion source, and which therefore happen to pass through the collector slit. All such ions will have less than normal energy, since each collision results in loss of energy for the high-speed particle. We can erect a potential barrier through which these scattered ions cannot pass by applying a positive potential, essentially equal to the accelerating voltage, on the suppressor plate. We then obtain a spectrum similar to the lower curve of Figure 10, in which it is apparent that the presence of the same amount of helium is much more easily discerned than in the upper curve.

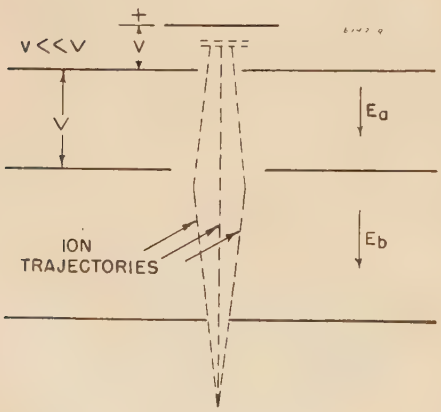

Figure 9. Ion lens

A typical spectrum in the neighborhood of the helium peak for a mixture of 1 part helium in 50,000 parts air is shown in Figure 11.

Production of Ions. Ions are formed in the ionization chamber by bombarding gas atoms or molecules with electrons which have been accelerated through a potential of about 145 volts. The electrons are emitted from an incandescent tungsten filament located behind a slit in the ionization chamber. Since the emission current varies rapidly with changes in voltage, changes in heat conductivity of the surrounding gas, changes in the surface conditions of the filament due to the presence of different gases, and other similar causes it is desirable to hold the emission constant with some kind of an automatic regulator.

The scheme used in the leak detector for emission regulation is shown schematically in Figure 12. A transformer having a high amount of voltage regulation, due to an adjustable resistor in series with the primary winding, is used to supply two secondary loads; the spectrometer tube filament, which operates at a few volts and a few amperes, and a variable load due to the triodes T_3 and T_4 operating at a few hundred volts and a few hundredths of an ampere. The filament is operated emission limited. Due to the high regulation of the transformer, an increase in either of the secondary loads will cause the voltages of all three windings to decrease; thus the voltage on the filament winding may be held at any desired value by controlling the load on the high-voltage secondary winding. This is done automatically as follows:

Let us assume that the filament emission current increases above its normal value. The voltage at the grid of the amplifier tube T_1 will increase due to the increased drop across the emission control resistor; but the cathode voltage of T_1 is held at a constant value by the voltage regulator tube T_2. Therefore T_1 conducts more current, reducing the potential at its plate and lowering the cathode potential of loading tubes T_3 and T_4 with respect to their fixed grid potential. The loading tubes are therefore more conducting and constitute an increased load on the transformer, so that the voltages of all three windings will drop. Since the filament is operating emission-limited and is very sensitive to voltage changes, the emission current will be reduced to a value only very slightly higher than the normal value. In other words, the emission current is regulated at a value determined by the *IR* drop across the emission control resistor. By changing this resistor, any desired value of emission current can be selected. The circuit is adjusted to the regulating range by means of the adjustable series resistor in the transformer primary. A regulator of this type will hold the emission current constant within less than one-half of one per cent.

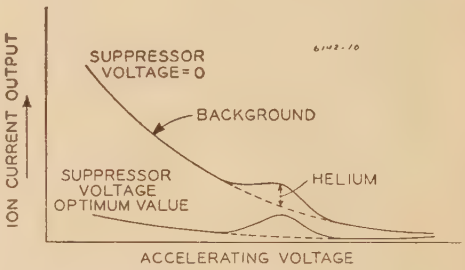

Figure 10. Background characteristics in the region of the helium peak

All voltages shown in Figure 12 are relative values referred to the slit 1 plate, which may be at any value from 0 to 370 volts above ground potential.

The supply voltages for the emission regulator are actually tapped from the ion accelerating voltage supply.

Accelerating Voltage Supply. The ion accelerating and focusing potentials are obtained from a conventional full-wave rectifier with voltage regulator tubes for d-c output voltage regulation and a simple voltage divider circuit shown schematically in Figure 13. The accelerating voltage (between slit 1 and ground) is adjusted with potentiometer R_1, which actually consists of a coarse and a fine adjustment. This adjustment is used to bring helium ions through the collector slit.

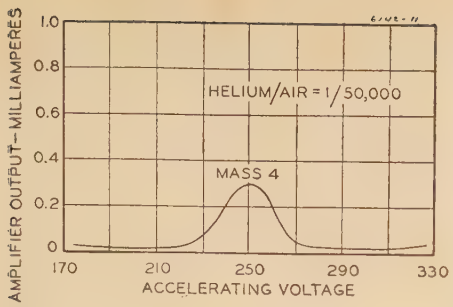

Figure 11. Typical helium spectrum from leak detector

Ion Current Measurement. Attainment of maximum over-all sensitivity implies the use of the most sensitive available method of ion current detection; but the detector must also meet the important requirements of ruggedness, simplicity of operation, and portability. A d-c amplifier with 100-per-cent feedback meets these requirements satisfactorily, although it is somewhat less sensitive than certain other methods, such as an electrometer tube and sensitive galvanometer. The amplifier, when used with an input impedance of 10^{11} ohms and an output instrument rated 30 millivolts full scale, is capable of measuring ion currents of the order of 10^{-14} ampere.

The amplifier consists of an acorn tube connected as a space-charge tetrode followed by two stages of voltage gain and a cathode follower output tube. The output appears on an ordinary panel-type milliammeter rated one milliampere full scale, and having a resistance of 30 ohms. The amplifier circuit is shown schematically in Figure 14A. Such an amplifier possesses the valuable characteristic that the output voltage is equal to the input voltage, but reversed in sign. This can be shown to be the case by consideration of Figure 14B. We will define input voltage as the voltage drop across the input resistor R_i due to the flow of ion current I, where the input resistance is very high (of the order of 100,000 megohms) and the ion current is very small (less than one micromicroampere), so that so far as the ion current is concerned the negative side of the input resistor is grounded through the low impedance millivoltmeter circuit. The output voltage is defined as the voltage from B to ground, which is equal to the voltage at C minus the output battery voltage E_B. The output voltage can be balanced to zero when there is no ion current flowing by adjusting the plate potentiometer in the first stage of the amplifier until the voltage at C is equal to the battery voltage.

An ion current I flowing through the input resistor will produce an input voltage V_i, and point A will go positive by an amount ΔV which for the moment we will assume to be any value not greater than V_i. By reference to Figure 14A we can see that since the last stage is a cathode follower, the amplifier will behave as if it had an odd number of stages, and there will be a phase reversal. Therefore the voltage at C will decrease by an amount $\mu\Delta V$, where μ is the over-all voltage gain of the amplifier, provided by the second and third stages. The voltage at C changes from the initial value E_B to a new value $(E_B-\mu\Delta V)$, and the voltage at B, which is controlled by the stiff output circuit, changes from zero to a new value

$$V_0=-\mu\Delta V \tag{13}$$

Applying Kirchhoff's law to the circuit from ground to B to A and back to ground, we obtain

$$-\mu\Delta V+IR_i-\Delta V=0$$

or

$$IR_i=(1+\mu)\Delta V \tag{14}$$

If the gain μ is much greater than unity this becomes

$$IR_i=\mu\Delta V \tag{15}$$

But IR_i is defined as the input voltage, and $\mu\Delta V$ is the negative output voltage. Therefore we write

$$V_0=-V_i \tag{16}$$

It is apparent that ΔV is very small in comparison with the input voltage, which means that point A will always remain at essentially ground potential, so that the apparent input resistance of the amplifier taken from A to ground will be less than the actual resistance by the factor $1/\mu$. The time constant of the input circuit is reduced accordingly by the same factor, which is an important feature in improving the over-all response of the leak detector. It is also evident that the output voltage cannot exceed the battery voltage E_B, since the voltage at C cannot have a negative value. The output instrument therefore is protected against excessively large input signals.

The first stage of the amplifier is mounted inside the mass spectrometer tube as shown in Figure 8 in order to keep the high resistance and the grid connections dry to minimize leakage currents, to keep the leads as short as possible from collector plate to the grid of the first tube, and to provide electrostatic shielding for the input stage. The remainder of the amplifier is mounted in the top part of the leak detector control panel, as indicated in Figure 6.

Ionization Gauge Tube and Control. The pressure in the high vacuum system is measured with a standard ionization gauge (Distillation Products type VG1-A) and an electronic control circuit. The gauge tube consists of a hairpin filament surrounded by a grid which is wound in a double helix with wide turn spacing, and a plate or collector consisting of a platinized layer on the pyrex glass envelope of the tube. Both ends of the grid are brought out, so that the grid can be outgassed by passing current through it.

Electrons emitted by the incandescent filament are accelerated through the grid, which operates at positive potential with respect to the filament. Since the collector is at a negative potential with respect to the filament, the electrons will return to the grid and be collected. Some of the electrons will collide with gas molecules, causing ionization in the space between the grid and the collector. The ions are drawn to the collector and discharged. With constant emission current and constant grid potential, the ion current is a linear function of pressure for any gas, although the calibration will vary somewhat for different gases.

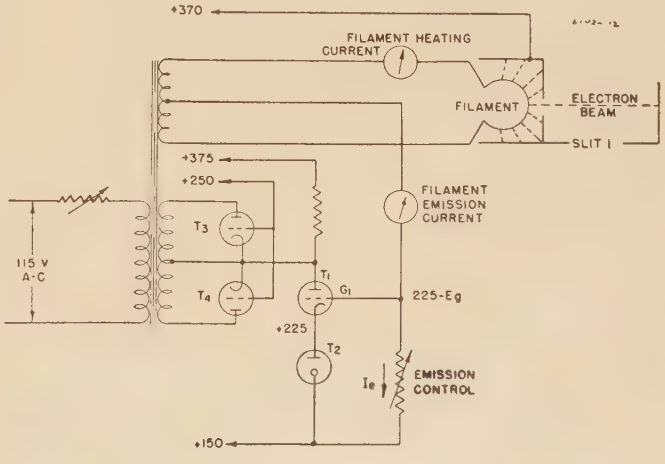

Figure 12. Emission regulator

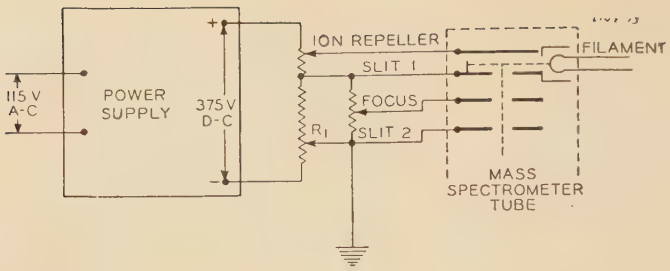

Figure 13. Accelerating voltage supply

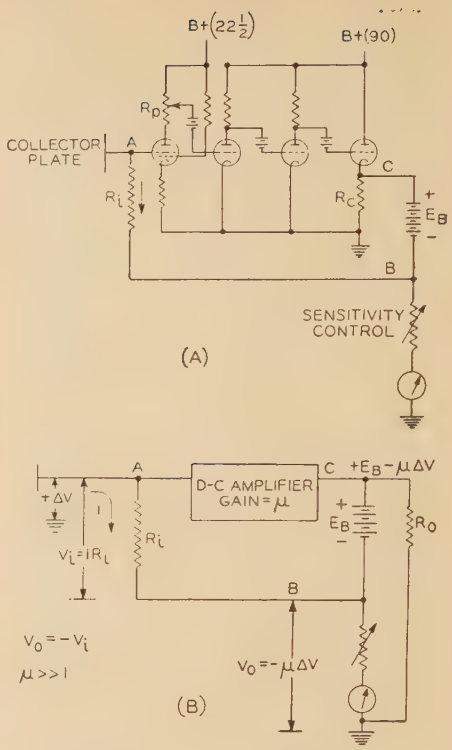

Figure 14. D-c amplifier

The ion gauge control is an a-c operated unit which performs four functions:

1. Voltage supply for ionization gauge tube.
2. Emission regulation and emission current measurement.
3. Ion current measurement.
4. Vacuum relay to operate if the pressure in system exceeds a predetermined value.

The direct voltage supply is a conventional full-wave rectifier, with an output of several milliamperes at 400 volts.

The emission regulator circuit is essentially the same as shown in Figure 12.

The ion current is measured with a simple vacuum tube microammeter circuit shown in Figure 15. A full-scale deflection on the highest sensitivity corresponds to one-half-microampere input.

The vacuum relay circuit is also shown schematically in Figure 14. The relay is used to turn off the ion gauge and spectrometer tube filaments in the event that the pressure accidentally rises above a safe operating point. Since samples are continually connected to and removed from the leak detector in normal operation, it is inevitable that the wrong valve will eventually be left open. This relay has saved many filaments.

Pumping System. The vacuum in the leak detector is maintained by an oil diffusion pump with a cylindrical dry ice trap. The speed of this combination is about 30 liters per second. The diffusion pump requires about 3 cubic centimeters per second of tap water for cooling. By means of a thermal switch the diffusion pump heater is shut off if the flow of cooling water is not sufficient. Normal heater operation requires about 350 watts from a 110-volt power line. The fore vacuum is obtained with a small mechanical vacuum pump.

Characteristics of the Leak Detector

The leak detector is characterized by compactness and ruggedness, simplicity of operation, high sensitivity, and adaptability. It possesses the unique feature of selectivity, that is, it can detect a small leak in the presence of a large leak, or it can detect a leak in the presence of thousands of other leaks of the same size. It is therefore a very useful method for testing very large vacuum systems which may have a multitude of leaks.

The sensitivity of the leak detector is such that it will detect the helium in normal air (1 part helium in 200,000 parts air). Under these conditions the partial pressure of helium in the leak detector is only 5×10^{-11} millimeter Hg measured at the ion gauge tube. The quantity of helium flowing through the spectrometer tube is about 1.5×10^{-9} liter-millimeter per second, which is roughly equivalent to a flow of 1 cubic centimeter in 16 years at standard temperature and pressure.

Since the response of the leak detector depends only upon the presence of helium in sufficient quantities, and not upon the purging of the system by the probe gas, the response of the instrument when used on small systems is almost instantaneous for practical purposes. The signal will disappear as fast as the helium is pumped from the system, which is usually a matter of a few seconds but depends upon the size and pumping characteristics of the sample system. Test methods will be discussed in the following section on applications.

Applications of the Mass Spectrometer Leak Detector

The full degree of flexibility of the mass spectrometer as a leak detector cannot be visualized without consideration of its applications. Its advantages are more apparent when compared with the limited applications of the other commonly used methods of leak testing. To aid in this comparison, a brief discussion of some of these methods and their limitations is presented.

Other Methods of Leak Testing. A rather crude method of leak testing which is often used is that of building up the internal pressure of the test system and searching for escaping gas. The escaping gas is usually detected by immersing the test system in water and observing the bubbles as the gas escapes. This observation is sometimes made more sensitive by adding chemicals to the water to reduce the surface tension.

If certain gases are used to pressurize the system, the escaping gases may be observed by noting a change in color of a gas flame used as a probe. This method is restricted to large leaks in systems which can withstand internal pressures of several atmospheres.

Several methods of leak testing are in use which depend upon the detection of gases leaking into an evacuated system. The means of detecting these leaks are as varied as the properties of gases themselves. Mention need be made of only the few which have been found most useful.

One method of detecting such leaks makes use of the color of the glow discharge of different gases. If the system under evacuation has an air leak, a glow discharge induced by a high-frequency high-voltage supply will have the characteristic pink color which indicates the presence of nitrogen in the system. The leak may be found by observing the change in color of the discharge as the leak is covered by a gas or liquid which has a glow of different color. Examples are the grayish glow of oxygen and the blue glow of ether. This method is applicable primarily to glass systems in which the glow discharge can be easily initiated and observed. It is limited to pressures that will maintain a glow discharge, and therefore cannot be applied to leaks large enough to give pressures greater than a few millimeters of mercury or to leaks in a system where the pressure is lower than a few microns. If multiple

leaks exist the discharge is masked by air leakage and the sensitivity is decreased. Due to its low sensitivity, the glow discharge method cannot be applied to the location of small leaks. However, indications that small leaks exist may be obtained by the following procedure. The system is evacuated to a good vacuum, in which the glow discharge cannot be initiated, and then sealed off. If a later check shows a pink discharge, an air leak is assumed to exist. This may be used to indicate very small leaks, but often requires storage of the evacuated system for several weeks. Also, observed results sometimes are difficult to interpret.

A leak in a system under evacuation sometimes may be located by covering the leak with water or other liquid having a vapor pressure of less than one atmosphere and observing the pressure drop in the system. This method is limited by the accuracy with which a small pressure change can be detected and does not apply at all to small leaks. Indicated results are often doubtful or misleading.

If the system being evacuated has a pressure greater than 0.1 micron, the heat conductivity of the gas is sufficient to produce a detectable cooling of a heated filament. Since the heat conductivities of hydrogen and helium are about six times that of air, large leaks may be found by observing the change in resistance of a heated filament when one of these gases is used for probing. In addition to being limited to large leaks and certain pressure conditions, this method requires differentiating between heat conductivity changes due to the probing gas and heat conductivity changes due to changes in pressure.

The temperature-limited emission from a tungsten filament depends upon the condition of the surface of the tungsten. In a good vacuum, a small increase in the concentration of oxygen will produce an observable decrease in this emission. Therefore, leaks may be found by observing the decrease in emission from a constant temperature filament while using oxygen as a probing gas.[3] Under favorable conditions this method of leak testing is very sensitive. For this reason it has found wide application to laboratory vacuum systems. Its disadvantages are that an extremely good vacuum is required, the filament must be initially clean, and the quantity of oxygen and water vapor evolved from the walls of the vacuum system must be very small. Although this method of leak testing has high sensitivity, it is not as sensitive as the mass spectrometer method.

Another method often used is that of making repeated checks on the rate of pressure rise in a sealed-off system after successively painting small areas with compounds which will plug the leaks. This method is time consuming and the results are not conclusive.

Mass Spectrometer Leak Detector. The characteristics of the mass spectrometer as a leak detector already have been discussed. The absence of the limitations of the other methods make it applicable to many new fields of leak testing. In fields where other methods have been used, it provides an easier, faster, and more reliable means of leak testing.

Leak Test Vacuum Systems. The use of the mass spectrometer leak detector requires a vacuum manifold and an auxiliary pumping system. The design of the vacuum manifold and pumping system is determined by the leak test requirements. Some of the factors which influence the design are

1. Size and shape of test objects.
2. Number of objects to be tested.
3. Expected evolution of gas from the test objects.
4. Sensitivity required.
5. Time allotted to leak testing.

Several general types which meet the majority of applications will be discussed.

Figure 16 is a block diagram showing the simplest form of leak test manifold. In using a manifold of this type, the procedure is to first evacuate the test objects by opening the exhaust valve and the isolating valves. In well-designed manifolds of moderate size, this rough evacuation takes less than 30 seconds. The throttle valve is then opened as far as possible without exceeding the permissible pressure in the spectrometer tube, and the system is ready for leak testing. Since the response to a leak is proportional to the rate at which helium passes through the spectrometer tube, the greatest sensitivity is obtained by opening the throttle valve and closing the exhaust valve to maintain the maximum permissible pressure in the spectrometer tube. The ultimate sensitivity is obtained when the throttle valve is wide open and the exhaust valve is closed entirely. All of the gas from the test manifold and test objects then passes through the spectrometer tube.

The two obstacles to obtaining this ultimate sensitivity are large leaks and the evolution of gas from the walls of the test objects and test manifold. In the first case, the ultimate sensitivity is not required and the leaky test objects can be located and removed from the system by closing their isolating valves. In the second case, a liquid air or dry ice trap in the line between the test manifold and the spectrometer tube will collect the condensable gases, but not helium, and thus allow a larger portion of the helium to be passed through the spectrometer tube. The amount of gas evolved is reduced by using a smaller test manifold. With a small manifold the ultimate sensitivity can be obtained without the cold trap mentioned above. This type of manifold is thus seen to be particularly applicable to high sensitivity requirements on vacuum systems where the amount of evolved gas is not great.

In applications where the maximum sensitivity is not required, but the time allotted to leak testing is short, a larger manifold having a more elaborate pumping system is better adapted. A system to meet these requirements is shown in Figure 17. This system is really two manifolds served by a single set of pumps and a single leak detector. The method of operation is quite similar to that of the simple manifold. Assume that initially

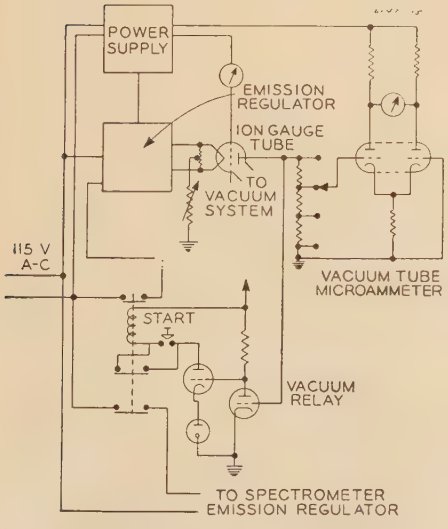

Figure 15. Ion gauge control

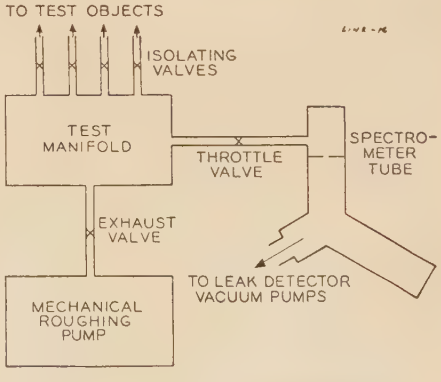

Figure 16. Simple leak test manifold

both roughing valves, both exhaust valves and the throttle valve are closed. Test objects are placed on manifold number 1 and evacuated to a rough vacuum by opening the isolating valves and the number 1 roughing valve. When the pressure in the manifold is reduced to a few microns, roughing valve number 1 is closed and exhaust valve number 1 is opened. The throttle valve then is adjusted to give the maximum allowable pressure in the spectrometer tube and manifold number 1 is ready for leak testing. While leak testing continues on manifold number 1, test objects are placed on manifold number 2 and evacuated to a rough vacuum by opening the isolating valves and the number 2 roughing valve. Thus the rate of leak testing can be more than double that obtained with only one of the manifolds.

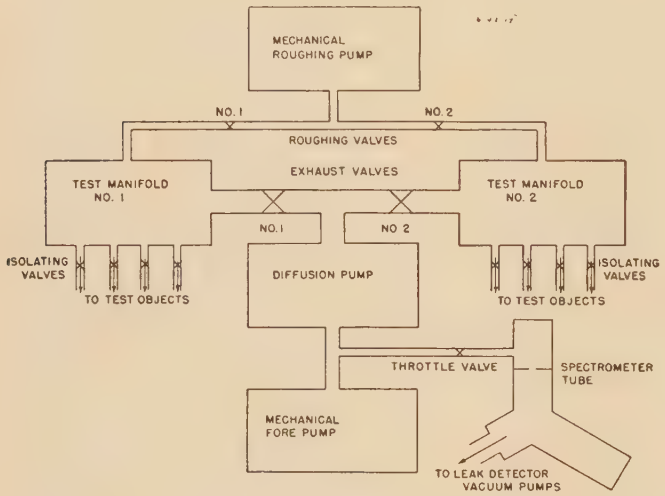

Figure 17. Dual leak test manifold for high speed testing

On systems of the type just described, the manifolds usually are made large so that a large number of test objects can be accommodated. With these larger manifolds it is advantageous to use a diffusion pump to increase the speed of response to a leak. If the leak detector is connected between the manifold and the diffusion pump, the pressure in the manifold may be low enough to prevent passing the maximum allowable amount of gas through the leak detector. Therefore the leak detector usually is connected between the diffusion pump and the fore pump, where the pressure is higher and the gas composition is very little different from that in the manifold. The pumps should be chosen so that it will not be necessary to adjust the fore pump valve to obtain the maximum allowable flow of gas through the leak detector. A liquid air or dry ice trap in the line connecting the leak detector to the manifold system will collect the condensable gases. Since helium will not be condensed, the gases passing into the leak detector will contain a greater proportion of helium and the system will have greater sensitivity.

The vacuum system for the leak testing of large tanks, climatized chambers, and so forth, does not differ greatly from those shown in Figures 16 and 17 if the manifolds are replaced by the tank to be tested. The time of response to a leak increases with increase in volume and decreases with increase in speed of the pumping system. For this reason, it is desirable to use high speed vacuum pumps when testing large systems. In designing the pumping system for these applications, proper consideration should be given to the number of objects to be tested.

A method of leak testing which is well adapted to certain production line manufacture, requires the evacuation of the test objects to a rough vacuum and sealing them off. The evacuated test objects are passed into a chamber containing a high concentration of helium and left there for a specified time. They then are removed and each one checked on the leak detector to determine if helium has leaked into its vacuum. The sensitivity of this method increases with the length of time the test objects are left in the helium chamber. After leaky test objects have been found by this method, the leaks can be located accurately by probing with a helium jet. This method may be extended to locating test objects with very minute leaks, if they are left in the helium chamber for a long time. However, the point of leakage cannot be located by probing if the leakage rate is less than 2×10^{-9} cubic centimeter of air per second (measured at 0 degrees centigrade and 760 millimeters pressure).

Other methods of using the leak detector for leak testing have been tried and still others are possible, but their applications seem too limited to merit description at present.

Analogy of Vacuum Systems to Electric Network. In the design of vacuum manifolds for leak testing, two considerations are predominant. The response to a leak should be fast and the percentage of helium from the leak passing through the leak detector should be high. These two considerations are not always independent and a compromise based on the particular application must be made. In the analysis of the vacuum system and its effect upon leak testing, it is often advantageous to think of the vacuum system in terms of its electric network analogue. A list of corresponding terms is given.

Electrical Entity	Vacuum Equivalent
Voltage, V (volts)	Pressure, P (microns)
Quantity of electricity, Q (coulombs)	Quantity of gas, PV (micron-liters)
Current, $I = dQ/dt$ (amperes)	Rate of gas flow, $Q = d(PV)/dt^2$ (micron-liters per second)
Conductance, G (mhos)	Conductance, F, S (liters per second)
Capacitance, C (farads)	Volume, V (liters)
Inductance, L (henrys)	Inertia of gas (negligible in vacuum)

In using this analogy there are several things which should be noted. First, the symbols generally used may occur in both systems of units, but do not necessarily represent corresponding entities. Second, in vacuum terminology, speed and conductance are not separate entities and are often used interchangeably. However, speed generally is used to denote the conductance of a pump or the net conductance of a pump and connected system. For example, a pump of speed S, connected through a pipe of conductance F, has a resultant speed of S_R given by

$$\frac{1}{S_R}=\frac{1}{S}+\frac{1}{F}$$

Third, the vacuum conductances cannot be considered as being independent of pressure except at very low pressures. They are different for different gases and except at very low pressures depend upon the mixture of gases in the system. They also vary with temperature. Methods of calculating the conductances of pipes, orifices, and other components of the vacuum system are given in a number of books treating the subject of vacuum and the kinetic theory of gases.[4,5] The speed-pressure characteristics of pumps can be obtained from the pump manufacturers.

In calculating the speed of response of a leak test manifold, the pressure and

temperature may be considered as constant during the leak testing. The conductances may be calculated for the pressure and temperature considered and treated as constants. Since the leak detector signal is proportional to the partial pressure of helium in the manifold, the rate at which the helium pressure builds up and decays may be taken as the speed of response of the manifold. Consider the simple system shown in Figure 18A, consisting of a pump of speed S liters per second connected to a volume of V liters in which the pressure P microns, remains uniform. Assume that this system has a constant leak of Q micron liters per second. The electrical analogue is shown in Figure 18B. It is a capacitor of C farads with a discharge resistor of R ohms and a constant charging current of I amperes. Applying the charging current when the voltage is zero, the voltage build-up is given by

$$V = IR\left(1 - \epsilon^{-\frac{1}{RC}t}\right)$$

When the charging current is removed from the fully charged capacitor the voltage decay is given by

$$V = IR\epsilon^{-\frac{1}{RC}t}$$

In the vacuum system the application of the helium jet to the leak and its removal give the corresponding equations

$$P_{He} = \frac{Q_{He}}{S}\left(1 - \epsilon^{-\frac{S}{V}t}\right)$$

and

$$P_{He} = \frac{Q_{He}}{S}\,\epsilon^{-\frac{S}{V}t}$$

where P_{He} and Q_{He} refer, respectively, to the partial pressure and rate of leakage of helium. When considering long pipes in vacuum systems, the pressure is not uniform throughout the length of the pipe. The electrical analogue is a d-c transmission line with distributed resistance and capacitance.

Fields of Leak Detector Application

It is impossible at this time to compile a comprehensive list of the different fields in which the leak detector will be applicable. However, a list of those fields in which its application has been studied will serve to show the scope.

Vacuum valves	Vacuum tubes
Vacuum bellows	Power rectifiers
Vacuum seals	Hermetically sealed instruments
Vacuum chambers of all sizes	Vacuum pumps
Pressure containers	Laboratory vacuum systems
Refrigerators	Cyclotrons
Pressure gauges	High voltage accelerating tubes
Pressure instruments	
Vacuum instruments	
Vacuum welds	

The leak detector may be used to reject defective parts or it may be used to accurately locate leaks so that parts may be repaired. It finds additional application as an aid in selecting production methods and in locating faulty processes. These applications are well illustrated by an actual example.

In the manufacture of a large power tube, rejections due to leaks were excessive. Investigation by older methods of leak testing were slow and results were inconclusive. The application of the leak detector provided a fast and reliable method of investigation. Practically all of the leaks were found to occur in one of the small subassembly parts. Pre-leak testing of this subassembly was initiated

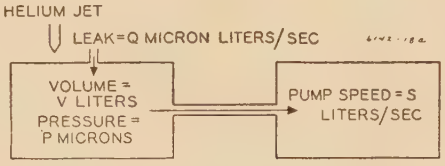

Figure 18A. Simple vacuum system

and rejections were made on the relatively inexpensive subassembly instead of on the completed tube. Accurate locating of leaks in the subassembly led to improved methods in its manufacture so that very few rejections occurred. The over-all result was increased production, lower manufacturing cost, and improved quality of the product.

Special Leak Testing Considerations

On large manifold systems where rapid testing of a large number of objects is required, it has been found that testing time can be reduced by the use of a testing hood to surround the entire test object with an atmosphere of helium. This eliminates probing time and gives a response proportional to the total leakage if several leaks exist. The possibility of missing leaks by careless probing is also removed. After locating leaky test objects the hood may be removed and the leaks located accurately by probing with a small jet of helium. A valuable adjunct to the testing hood is a thermal conductivity gauge calibrated to read directly the concentration of helium in the hood.

For most probe testing, probes made from 4-inch metal capillary tube of 5- to 20-mil diameter with one pound pressure of helium have been satisfactory. However, when testing in confined spaces where the helium cannot readily diffuse away, the helium concentration may become sufficient to give a reading when the probe is some distance away from the leak. In this case a special probe may be made which will withdraw the excess of helium. Spurious signals may sometimes be caused by air currents carrying helium from the probe to a large leak some distance away. These are recognized easily by their erratic nature and may be

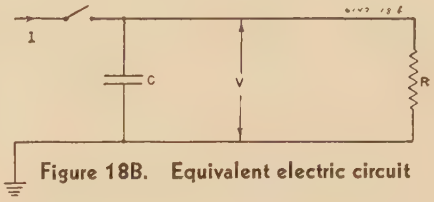

Figure 18B. Equivalent electric circuit

eliminated by locating the leak causing the trouble and isolating it from the system.

Very small leaks are sometimes temporarily plugged by dust particles or water vapor and may escape detection at the time of leak testing. Heating seems to be the most effective way of reopening these leaks.

Results obtained by the leak detector are repetitive and the leak detector can be used to measure rate of leakage by comparison with a calibrated leak. Also, the sensitivity of a particular leak test system may be obtained by observing the magnitude of the signal from a calibrated leak attached to the system.

Other applications of leak detectors are indicated in which helium may be used as a tracer gas. These would include investigation of flow in ventilating systems, velocity and distribution of flow in piping systems, turbulence, and other similar problems.

References

1. A Mass Spectrometer for Routine Isotope Abundance Measurement, **A. O. C. Nier.** *Review of Scientific Instruments*, volume 11, page 212.

2. Principles of Electricity and Magnetism (book), **G. P. Harnwell.** McGraw-Hill Book Company, New York, N. Y., 1938.

3. An A-C Operated Leak Detector and Ionization Gauge, **R. B. Nelson.** *Review of Scientific Instruments*, 1945, volume 16, page 55.

4. High Vacuum, **S. Dushman.** *General Electric Review*, 1922.

5. High Vacua (book), **G. W. C. Kaye.** Longmans Green and Co., New York, N. Y., 1927.

Current and Torque of D-C Machines on Short Circuit

T. M. LINVILLE
MEMBER AIEE

Synopsis: This paper presents formulas, in terms of easily evaluated coefficients, for the armature current, field current, and torque of d-c machines on short circuit. The method of the paper makes it unnecessary to calculate the mutual inductance between the armature and field windings. Heretofore, this mutual inductance (between the two windings which normally are in quadrature with each other) has made it exceedingly difficult to calculate current and torque on short circuit. Under short-circuit conditions, the armature and field windings are not, in effect, in quadrature with one another and are mutually inductive partly because of saturation of the flux path at one side of the poles and partly because of commutation phenomena. These circumstances create difficulties uniquely overcome in the paper. A basic feature of the paper is the expression for the relation between flux, armature amperes, and field amperes. Calculations cannot be made without establishing this relationship (plotted for a specific case in Figure 9) and a simple expression for it has not been presented before to the author's knowledge. Another important feature, also believed to be new, is the development of an expression for the resistance to current flow created by the reactance voltage of the alternating current in the armature winding. A third feature is a formula for estimating the time constant of the armature circuit using an average coefficient of inductance. The results are applied to several machines and the calculated performance compared with test data. In most cases, particularly with large machines having bar windings, approximate calculations can be made without need of manufacturer's data.

PROTECTION must be provided for d-c machines and d-c distribution circuits against the large currents which flow on short circuit. Otherwise, machines, switchgear, instruments, and bus structures will be damaged by overheating, flashing, and burning. When machines are connected in parallel to a common bus, as in the case of continuous rolling mills or shipboard distribution circuits, the electromagnetic forces between current-carrying parts of the equipment may be astonishingly large. Also, it has happened that the sudden high torque of the machines has twisted shaft keys breaking coupling hubs. In applying circuit breakers, it has been necessary to calculate the current and voltage at the time of interruption for various types of breakers of different operating speeds. It has been equally important to build all machines strongly enough to withstand mechanical stresses and, therefore, to calculate maximum torque and forces on the windings and their supports at maximum current. These calculations have been uncertain and stresses assumed beyond those which actually exist, in spite of the fact that size, weight, and cost are sometimes determining factors in the selection of machinery and its successful application.

It is helpful to recognize that at the moment when the current reaches its maximum the internal voltage of the average d-c machine is a high fraction of the voltage before short circuit. As there is no large immediate collapse of internal flux and voltage, the maximum current is determined chiefly by the resistance of the windings and by the a-c reactance voltage in the armature winding which causes an equivalent large d-c brush contact voltage. It is the purpose of this paper to emphasize and establish these phenomena, and to develop formulas for calculating the current and torque.

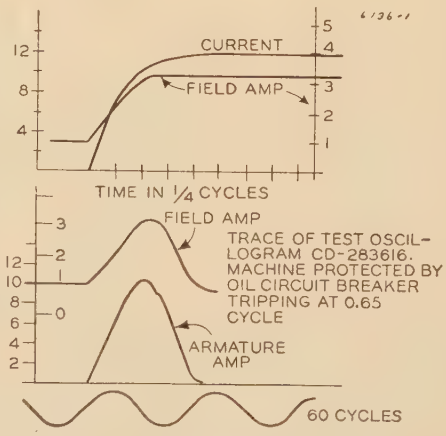

Figure 1. Currents on short circuit of d-c generator

Type *MCF*, 8 poles, 1,500 kw, 514 rpm, 1,500 volts

$$i_a = 3.3 + 9.2\epsilon^{-1.5t} - 12.5\epsilon^{-206t}$$
$$i_f = 1 + (3.3 - 0.7)(\epsilon^{-1.5t} - \epsilon^{-206t})$$
$$\rho = 0.17,\ n_f = 0.15,\ R = 0.040,$$
$$K_1 = 6.4,\ K_2 = 0.2,\ \phi_o = 1$$
Armature axis shift = $1\frac{1}{4}b$

The calculation of peak current is given particular attention because the sustained current is not reached until induced current in the exciting winding has died out. Exciting windings of d-c machines are notoriously slow, and the induced field current takes more time to disappear than is needed for operating even slow acting breakers. Moreover, large machines will flash over if the current is not interrupted quickly, and damage will be done to circuits, apparatus, and instruments. Therefore, circuit breakers are used nearly always in the armature circuit, capable of opening peak short-circuit current. Consequently, the sustained current is not often of practical importance. However, for completeness, calculation of the sustained current is included in the paper.

The results of the paper and general experience show that the maximum current on "dead" short circuit is 7 to 15 times rated current and maximum torque 5 to 12 times normal torque. In general, the higher values are encountered with 600- to 1,500-volt machines, and the lower values with 125- and 250-volt machines. Slow speed machines generally give lower values than high speed machines. Machines with pole face windings have higher values than those without. Also, values are higher if the shape of the armature is a cylinder of short length rather than long.

That the current is not much higher is surprising in view of the high internal electromotive force immediately after short circuit and the low normal resistance of the windings. Ordinarily, rated voltage divided by the normal resistance gives 25 to 50 times rated current. This indicates the importance of the reactance voltage produced by the alternating current in the armature winding, in limiting the current, a major feature treated in the paper.

Evidence that the electromotive force does not collapse immediately is obtained from observations of the behavior of the field current on many short-circuit tests. Many of these have been made over the years in connection with tests of circuit breakers using d-c machines for power. Usually the field current rises to not more

Paper 46-136, recommended by the AIEE committee on electric machinery for presentation at the AIEE summer convention, Detroit, Mich., June 24–28, 1946. Manuscript submitted April 25, 1946; made available for printing May 14, 1946.

T. M. LINVILLE is with the motor and engineering division, apparatus department, General Electric Company, Schenectady, N. Y.

Appreciation is expressed to Robert W. Wieseman for providing Figures 12, 13, and 14. Grateful acknowledgment is made to S. B. Crary and P. L. Alger, for reviewing the paper and giving helpful suggestions, and to B. H. Caldwell, for making helpful comments and assisting in securing test oscillograms.

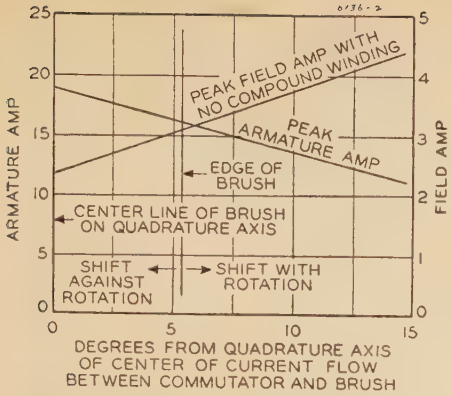

Figure 2. Effect of brush arcing (shifting axis of armature magnetomotive force) on armature and field currents

Type *MCF*, 8 poles, 1,500 kw, 514 rpm, 1,500 volts

than three times its value before short circuit. Also, it is well known that except for small or special machines the leakage flux linkages of the exciting winding, producing no electromotive force in the armature, are a small part (15 per cent or less) of those producing electromotive force. Therefore, to illustrate the evidence with numbers, the total linkages before short circuit may be taken as 115 per cent. Then, assuming the field current rises to three times the initial value after short circuit, the leakage flux interlinkages increase correspondingly to 45 per cent, and the flux which produces electromotive force, according to the constant flux linkage theorem, is 115 per cent minus 45 per cent, or 70 per cent. Thus the electromotive force after short circuit is 70 per cent of the initial electromotive force, until the unsupported field current decays. This decay occurs after the maximum current has been reached. In fact, the field and line currents rise to a maximum at the same instant.

This may make it appear to the practical minded person that all one needs to do to calculate the maximum current is to take 70 per cent of the rated voltage and divide by the resistance of the windings. For a rough approximation, the calculation is as simple as this provided one allows for the a-c reactance voltage in the armature. Then the maximum torque may be estimated in per cent of rated torque simply by taking the maximum current in per cent of rated current and taking 70 per cent of it.

G. E. Frost recently presented a paper[1] in which it was shown that the armature and excitation circuits are coupled together magnetically with a coefficient of mutual inductance M. In normal operation the armature magnetomotive force and flux are in the cross or quadrature (interpole) axis with respect to the excitation (field) magnetomotive force and flux in the direct or field pole axis. Therefore, the armature and excitation circuits ordinarily are not coupled if there is no compound winding. M becomes a real quantity only when the armature magnetomotive force becomes large with overload current, causing saturation of the armature teeth at one side of the main pole with an appreciable shift in the effective position of the main pole axis of the machine. Furthermore, when the commutating poles become saturated and their flux is no longer sufficient to hold the current collection from the commutator central under the brushes, the axis of armature magnetomotive force shifts to reduce its angle with the effective main pole axis still more. The factors which Frost used account for these phenomena, but it is difficult to evaluate them numerically by calculation or to measure them by test. The present paper builds on this essential basic theory. In doing so, machines with and without pole face windings are kept in mind, making the method applicable to all types. Pole face windings hold the armature and field circuits in a more nearly true quadrature relationship, making it difficult to account for test results by the theory of mutual coupling between these circuits. The viewpoint from machines with pole face windings leads directly to recognition of the major factors which determine the maximum (peak) current.

Assumptions

1. There are no shunts across pole face or commutating pole windings.

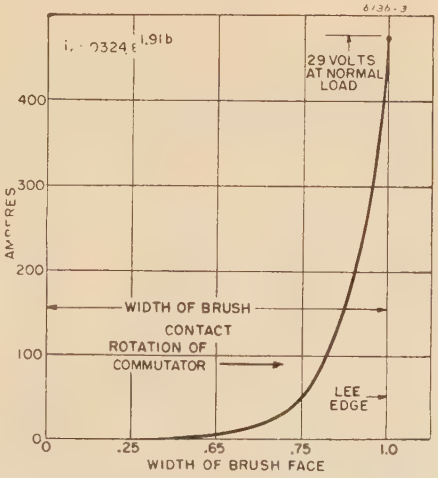

Figure 3. Distribution of current in brush face of d-c generator

Type *MCF*, 8 poles, 1,500 kw, 514 rpm, 1,500 volts

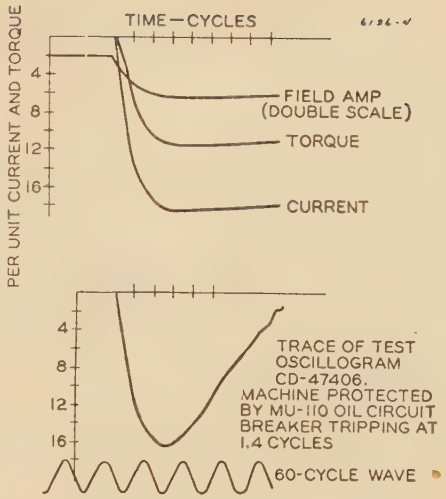

Figure 4. Currents and torque on short circuit of d-c generator

Type *MCF*, 6 poles, 750 kw, 600 rpm, 1,500 volts

$\rho = 0.215$, $n_f = 0.15$, $R = 0.033$
$K_1 = 6.5$, $K_2 = 0.24$, $\phi_o = 1$
$i_a = 8.2 + 11.4\epsilon^{-1.5t} - 19.6\epsilon^{-143t}$
$i_f = 1 + 2.3(\epsilon^{-1.5t} - \epsilon^{-143t})$
$T = 0.033 i_a^2$

2. Saturation other than in armature teeth and pole face teeth is neglected.

3. Leakage flux interlinkages of the field winding are proportional to field amperes.

4. Center of current flowing between brushes and commutator is at lee edge of the brushes. However, provision is made for modification of this assumption in exceptional cases.

5. Speed of the machine is maintained.

Per-Unit Quantities

Per-unit quantities, used throughout the paper, have the following base or unit values:

V = unit voltage = rated voltage
I_{a1} = unit armature amperes = maximum continuous rated amperes
I_{f1} = unit field amperes = field amperes for rated voltage at rated base speed, no load
M_{f1} = unit magnetomotive force ampere turns = field magnetomotive force at unit field amperes
ϕ_1 = unit flux = field flux corresponding to unit field amperes (excluding field leakage flux)

Formulas for Current and Torque

Complete formulas for armature current, field current, and torque, each as a function of time, are derived in Appendix I. The method used consists of the following steps:

1. Develop the general equation for the relation between exciting flux, armature amperes, and field amperes (equation 23).

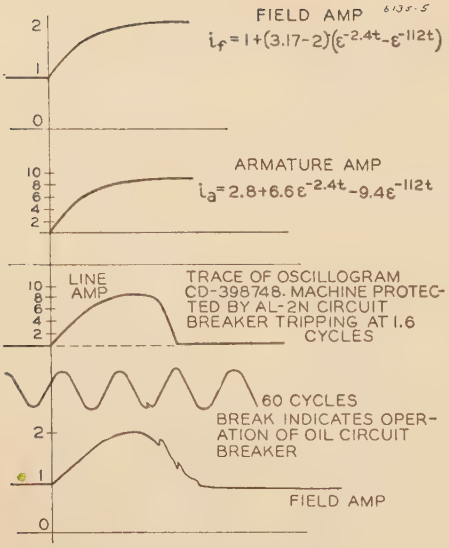

Figure 5. Currents on short circuit of d-c generator

Type *MPC*, 6 poles, 300 kw, 1,200 rpm, 120/240 volts

$\rho = 0.186$, $R = 0.070$, $n_f = 0.107$

$K_1 = 2.06$, $K_2 = 0.214$, $\phi_o = 1$

Line and circuit breaker inductance = 0.26 per unit

2. Equate the field linkages immediately after short circuit (at the instant of peak current) to those immediately before short circuit in accordance with the constant linkage theorem (equation 27).

3. Write the equation summing the voltages in the armature circuit (equation 28).

4. Solve the equations simultaneously for the currents.

5. Combine the currents with their respective decrement factors governing their rise and decay. These decrement factors are the reciprocals of the time constants for the armature and field circuits derived in Appendix II.

The results follow.

For armature current:

$$i_a = I_a - I_a'\epsilon^{-\sigma_a t} + (I_a' - I_a)\epsilon^{-\sigma_f t} \quad (1)$$

For field current:

$$i_f = I_f - (I_f - I_f')(\epsilon^{-\sigma_f t} - \epsilon^{-\sigma_a t}) \quad (2)$$

For torque:

$$T = \frac{Rn_1}{n} i_a^2 \quad (3)$$

where

$$I_a' = -\frac{C_1}{2} + \sqrt{\frac{C_1^2 + 4C_2}{4}} \quad (4)$$

$$I_f' = \frac{(1+n_f)\phi_o - I_a' R}{n_f} \quad (5)$$

$$I_a = -\frac{C_3}{2} + \sqrt{\frac{C_3^2 + 4C_4}{4}} \quad (6)$$

$$C_1 = \frac{K_1 RB + 2K_1 n_f bP - BK_2(1+n_f)\phi_o}{Rn_f B + K_2 RB + 2K_2 n_f bP} \quad (7)$$

$$C_2 = \frac{BK_1(1+n_f)\phi_o}{Rn_f B + K_2 RB + 2K_2 n_f bP} \quad (8)$$

$$C_3 = \frac{2K_1 bP - BK_2}{RB + 2K_2 bP} \quad (9)$$

$$C_4 = \frac{K_1 B}{RB + 2K_2 bP} \quad (10)$$

$$K_1 = \frac{\phi_i p_a p_p}{p_b(p_a M_{a1} + p_p M_{b1})} \quad (11)$$

(When there is no pole face winding, $p_b = p_a$ and $M_{b1} = 0$)

$$K_2 = \rho K_t = \frac{gK_\lambda C_s C_d}{0.85(g + d_s)} K_t \quad (12)$$

$$R = r_w + r_b = r_w + \frac{E_R b + V_c}{V} \quad (13)$$

When E_R is not known, it may be estimated at rated load (expressed in kilowatts) and rated speed by

$$E_R = \frac{C_r \times \text{kilowatts}}{d_a} \quad (14)$$

Definitions of symbols are given in Appendix VI. All of the foregoing quantities are per unit. The decrement factors σ_a and σ_f are the reciprocals of the time constants T_a and T_f, respectively, where

$$T_a = \frac{19.1 C_x}{(r_w + r_b)(n_1 \times P)} \text{ seconds} \quad (15)$$

$$T_f = \frac{N\phi_1 K_i P(1+n_f)10^{-8}}{V_f} \text{ seconds} \quad (16)$$

$(r_w + r_b)$, ϕ_1, and V_f are in ohms, maxwells, and volts, respectively. With heavy armature current, the normal time constants are reduced because of additional saturation. For this condition the "saturated" time constants are

$$T_{as} = T_a \frac{\rho + n_f}{1 + n_f} \quad (17)$$

$$T_{fs} = T_f \frac{\rho + n_f}{1 + n_f} \quad (18)$$

When short circuit occurs at full voltage only the "saturated" time constants T_{as} and T_{fs} are considered effective. When short circuit occurs at less voltage, the rise of current is governed by the normal time constants at first and later by the "saturated" time constants. In such cases the current-time curves are plotted for both sets of time constants. Then a judicious transition is drawn in from one to the other. For general calculations, only the "saturated" constants should be used.

Comparison of Calculated and Test Results

Calculated results are presented for comparison with test oscillograms for three machines on which short-circuit tests have been made. In making the tests, the machines are protected with circuit breakers interrupting the current almost as quickly as the peak is reached.

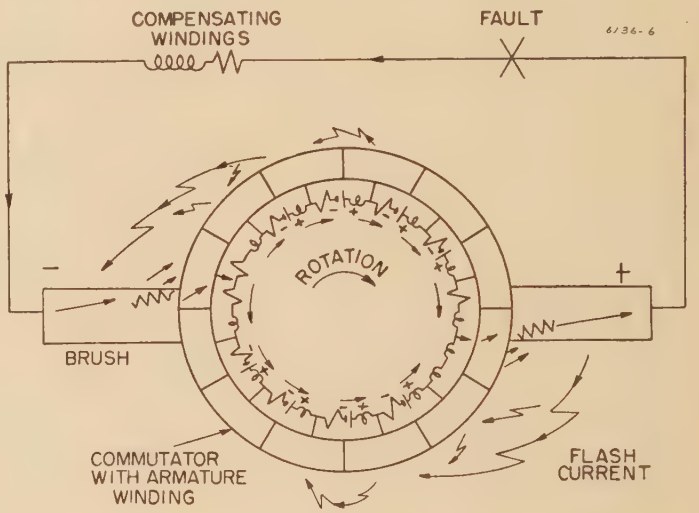

Figure 6. Current between commutator and brush—diagram showing that flash current flows opposite in direction to brush current

In Figure 1 comparison is made between calculated and test results for a 1,500-kw 1,500 volt railway generator. Both the field and armature currents are shown. The calculations are made considering arcing at the brush edges such that the equivalent brush position is $1\frac{1}{4}$ brush widths from the quadrature axis. The machine is equipped with flash barriers whose location determines this allowance. Figure 2 is plotted to show the effect of shifting the armature magnetomotive force, and shows that if arcing is neglected the short-circuit peak current is 36 per cent higher, and the field current 26 per cent lower. It is obvious from Figure 3 that severe arcing will occur. There is little commutating pole flux at

the moment of peak current. Therefore, the current in the brush face shifts drastically to the lee edge and causes the brush contact voltage to reach roughly 29 volts to accomplish commutation at rated load. Under heavy overload current, there is more than sufficient voltage for severe arcing.

In spite of these circumstances, the calculations are made for other machines taking the brushes to be centered on the quadrature axis with the center of current at the lee brush edge. This is the general condition similar to the distribution shown by Figure 3. Practical calculations can be made on this basis with good results, as Figures 4 and 5 show. Machines, in general, do not have the high voltage and high armature reactance peculiar to the machines of Figure 1.

Figure 4 is for another railway generator, 750-kw 1,500-volt, having brushes 26 per cent narrower than for the machine of Figure 1 and about 51 per cent less armature reactance voltage at rated load (without commutating pole flux). The calculated results show no large error in this case. The test oscillogram shows about 16 times normal current which is high for d-c machines in general and is caused chiefly by the 150-per-cent 2-hour load rating and 300-per-cent temporary load rating, for which the machine is designed. Hence unit current for the machine is an underrating relative to machines in general.

Both of these machines have pole face windings unlike the machine of Figure 5, which has interpole windings only. The latter machine is rated 300 kw, 250 volts, and shows slightly less than nine times rated current for the maximum. The machine has a series winding of one turn per pole which is taken into account in the calculation of field current. On this test the circuit breaker and cables have inductance of 0.26 per unit and resistance of 0.009 per unit (measured). These factors are included in the calculations.

In the calculations for Figures 1 and 4, the per-unit inductance of the machines is taken as 0.15 and for Figure 5 as 0.60 (see Table I). Winding resistances are measured values corrected to 75 degrees centigrade. Comparison of calculations and tests show good agreement of time constants.

These results, and calculations for other large motors and generators, show maximum currents from approximately 7 to 11 times rated current for machines with interpole windings only, and up to 14 for normally rated machines with both interpole and pole face windings. Such currents are most unlikely to occur in service, as faults without arcing or of zero resistance are rare. Maximum machine torque, in general, is less than 12 times rated torque (shown calculated and plotted for example in Figure 4). This is not difficult to take care of with safe margins in constructing machines. The weakest part is usually the coupling hub and key.

Discussion of Results

Fault Resistance

The formulas do not include fault resistance as such. When this exists it is included with the winding resistance of the machine. The effect of fault inductance can be allowed for fully by including it in the circuit inductance. Arcing faults are evaluated by allowing an average arc impedance or by calculating the results for "dead" short circuit and judiciously tempering the results.

Self-Excitation and Compound Excitation

Self-excited machines on "dead" short circuit have negligible sustained field current and the same formulas applying, except that I_a and I_f, the sustained currents, are zero.

Compound wound machines give the same peak current, exciting flux, and torque as the basic separately excited machines. However, the peak field current is increased by an increment equal in per-unit terms to the ampere turns of the compounding winding per pole, divided by unit field ampere turns. The sustained field current is the same as in the separate or self-excited cases, respectively, but the sustained flux and armature current are different. Although the method can be extended to include these conditions, special formulas are not presented. Peak values are most important and are given by formulas 1, 2, and 3 for all types of machines except series wound. Occasionally, the method will need to be extended for compound wound machines when knowledge of sustained torques is necessary to study stresses in shafting, assuming that the field circuit instead of the armature circuit is interrupted and that overload relays are slow in acting or time must be allowed for dissipation of field energy to prevent excessive voltage. In any case, the reliability of the steady state results is affected by flashing between commutator segments creating multiple short-circuit current paths. In this connection some observations about flashing are important.

Flashing

A distinction is made between flashing current and arcing current. Flashing current is current flowing to or from the brush on the lee side having opposite direction of flow with respect to the arcing current flowing between brush and commutator on the same side. This is illustrated by Figure 6, making it clear that arcing at the lee brush edges cannot be carried around by the commutator to cause flashing current and actually is extinguished by reversal of the bar-to-bar voltage as the bars move away from the brushes. However, ionization of the air allows the armature electromotive force to strike new arcs across the commutator micas resulting in flashing current. Even with "dead" short circuit, there is substantial voltage around the commutator surface sufficient to cause flashing. Between brush arms this voltage is equal to the voltage across the commutating pole and pole-face windings

Table I. Tests and Calculations to Determine C_x for Large Machines

Poles	Kw	Rpm	Volts	Test*	Calculated	Equation 1†	C_x
6	75	257	250	—	0.0062	0.0062	0.6
6	100	225	250	—	0.0042	0.0053	0.6
6	125	225	250	—	0.0043	0.0043	0.6
8	150	200	250	—	0.0020	0.0030	0.6
8	200	200	250	—	0.0023	0.0022	0.6
8	250	200	250	—	0.0018	0.0018	0.6
8	250	185	250	—	0.0017	0.0019	0.6
8	300	200	250	—	0.0016	0.0015	0.6
8	500	300	250	—	0.0008	0.00060	0.6
10	300	150	250	—	0.0016	0.0016	0.6
10	500	150	250	—	0.0011	0.00096	0.6
10	470	150	250	0.000958	—	0.00102	0.6
6	500	400	600	0.000700	—	0.00086	0.15‡
8	1,250	750	600	0.000132	—	0.00014	0.15‡
8	750	600	250	0.00020	0.00020	0.00020	0.6

* Test data are the a-c impedance at 25 cycles (checked at 60 cycles) measured between line terminals with the resistance of brush and brush contact short-circuited by copper jumpers and normal direct current in the shunt field winding.

† Equation 1: $L = \frac{E}{I} \frac{19.1 C_x}{(\text{rpm}) P}$

‡ Machines have pole face windings.

plus the brush contact voltage. The latter voltage includes voltage equivalent to the a-c reactance voltage in the armature. The sum of these voltages is a substantial part of the voltage existing before short circuit.

These observations make evident the value of flash barriers[2] which sweep the ionized gas off the commutator and interfere with the flash path. They indicate that appreciable time is required to ionize the air and distribute it sufficiently to start flashing. Speaking of time in terms of 60 cycles per second, the current may rise to its peak in less than one cycle (see Figures 1, 4, 5). However, one-half cycle at machine frequency is taken for rotation of the armature through one pole pitch to carry ionized gases to the next brush arm. Most large d-c machines have frequencies less than 60 cycles so that breakers starting to interrupt current in one-half cycle (based on 60 cycles) should and actually do prevent flashover. Such breakers together with flash barriers give machines maximum protection.

Brush Arcing

Apart from flashing, arcing at the lee brush edges continues as the commutator bars leave the brush until current reversal in the respective coils is completed. The bar-to-bar voltage supports this arcing until polarity reverses some distance from the brush. This results in a shift of the armature magnetomotive force producing a component in the direct axis, increasing the field current, and shifting more field flux to the leakage paths reducing the armature electromotive force. If the amount of shift can be estimated, the effect may be included fully as provided for in Appendix I. However, in practice it is recommended that calculations be made assuming that the center of current flow between brushes and commutator is effectively at the lee edge of the brushes, knowing that arcing will reduce the current as, for example, in Figure 2. In general, the calculations will be pessimistic but not far wrong, as is shown by comparison of results with tests. Figure 3 illustrates the concentration of current at the lee edge of the brushes when there is negligible commutating pole flux. In Appendix IV it is shown that the effective brush contact resistance is the same with or without arcing so long as the bar-to-bar voltage, if appreciable, is considered consumed in the arcs. On this basis, brush arcing does not affect the circuit resistance materially, having its chief effect as a result of armature magnetomotive force shifted into the direct axis. As a basis for judgment in particular cases, it is helpful to understand the voltage required to support arcing.[3]

Transient and Steady State Resistances

The formulas may be expressed in a form similar to the well-known formulas for synchronous machines[4,5] by letting $I_a' = 1/r_d'$ and $I_a = 1/r_d$, where r_d' and r_d are, respectively, transient and steady state effective resistances for short circuit with unit voltage on the machine. These resistances may be compared with the reactances x_d' and x_d, respectively, of synchronous machines; r_d' and r_d are affected by saturation and commutation and are variables. Unlike x_d', r_d' is not a definite coefficient widely useful in problems of transient voltage stability of generators or transient speed stability of motors. Generally, in d-c machines the armature magnetomotive force is held in quadrature with respect to the field magnetomotive force, and the armature and field windings are independent. Hence only winding resistance and self-inductance are effective in transient problems other than short-circuit performance. Of course, mutual inductance between series and shunt field windings always must be accounted for.

Appendix I. Derivation of Current and Torque Formulas

Consider for the moment a machine operating at normal voltage without load to be suddenly short-circuited, with no external resistance, and with constant speed maintained. The armature current rises very rapidly, but the rise of flux in the commutating poles is relatively slow because of the solid magnet frame. This flux rises fast in the skin of the frame, but, as saturation forces it to penetrate deeper into the solid steel, its rise is slowed. Accordingly, when maximum armature current is reached, the machine commutates substantially without benefit of commutating pole flux. Therefore, there is negligible compensation for the a-c reactance voltage in the armature winding, and an equivalent d-c voltage drop shows up at the brush contacts. This voltage is more than directly proportional to ordinary reactance voltage, as in a machine without commutating pole flux the current collection is crowded to one side of the brush faces with an effective reduction in width of brush face. The consequent change in wave shape of the current reversal in the armature conductors increases the reactance voltage. The equivalent direct voltage is determined and added to the RI drop of the windings and this sum equated to the electromotive force of the armature, giving an equation for the sum of the voltages in the armature circuit.

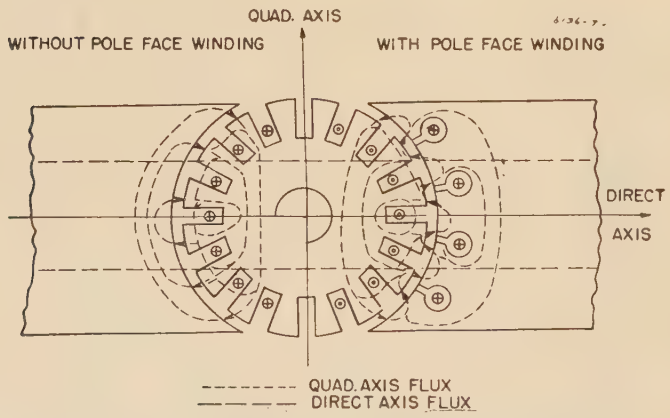

Figure 7 (above). Definition of axes and flux paths in machines with and without pole face windings

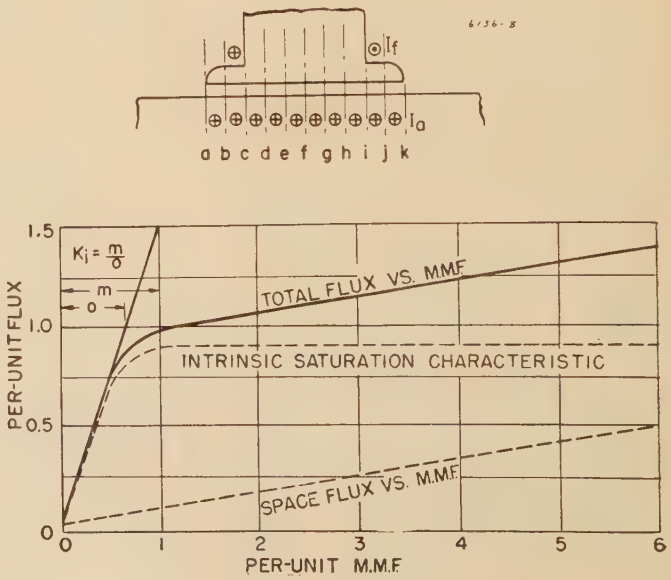

Figure 8 (right). Calculation of net direct axis flux resulting from combined direct and quadrature axes magnetomotive forces

See Table II for calculated data

Table II. Calculated Data for Figure 8

		Net Mmf Acting on Section											Flux of Each Section										
I_a	I_f	a	b	c	d	e	f	g	h	i	j	k	a	b	c	d	e	f	g	h	i	j	k	ϕ_d
0	1.	1	1	1	.1	.1	.1	1	1.	1	1	1	.1	.1	.1	.1	.1	.1	1	1	1	1	.1	
2.5	1.	3.5	3.0	2.5	2.0	1.5	1.0	0.5	0.	−0.5	−1.0	−1.5	1.21	1.17	1.12	1.08	1.04	1.0	0.75	0	−0.75	−1.0	−1.04	0.461
5.0	1.	6	5	4	.3	.2	.1	0	−1.	−2	−3	−4	1.42	1.33	1.25	1.17	1.08	1.0	0	−1.0	−1.08	−1.17	−1.25	0.25
7.5	1.	8.5	7.0	5.5	4.0	2.5	1.0	−0.5	−2.0	−3.5	−5.0	−6.5	1.63	1.50	1.38	1.25	1.12	1.0	−0.75	−1.08	−1.21	−1.33	−1.49	0.186
10	1.11	9	7	.5	.3	.1	−1	−3.	−5	−7	−9		1.83	1.67	1.5	1.33	1.17	1.0	−1.0	−1.17	−1.33	−1.5	−1.67	0.168
15	1.16	13	10	.7	.4	.1	−2	−5.	−8	−11	−14		2.25	2.0	1.75	1.5	1.25	1.0	−1.08	−1.33	−1.58	−1.83	−2.08	0.168

Although the build-up of the commutating pole flux is delayed, this is not so for the slot, end, and gap fluxes set up by the armature current in the laminated armature core and main pole shoes. These fluxes and what happens to the exciting flux are illustrated by reference to Figures 7 and 8. Figure 7 defines the direct and quadrature axes and shows the paths of flux under consideration. Figure 8 shows the pole of a machine without pole face windings and for simplicity with a uniform air gap. For illustration, the ampere turns of rated armature reaction at each pole tip are taken equal to the field ampere turns for the gap and teeth at normal voltage with no load. Then the magnetomotive force of armature reaction is divided into ten steps under the pole (not necessarily slots). At five times normal load amperes ($I_a=5.0$), the magnetomotive force per step is equal to the no-load normal-voltage gap and teeth ampere turns. Using per-unit terminology, this is unit magnetomotive force numerically equal to one. For any direct axis magnetomotive force applied to the gap and teeth, exciting flux (direct axis flux) and cross flux (quadrature axis flux) can be determined if the saturation curve for each section of the air gap is drawn as in Figure 8. Very large magnetomotive forces have to be handled, and this is done by fixing the slope of the upper part of the curve equal to that of an air gap whose length is equal to the normal air gap plus the depth of tooth. The basis for this is the well-established fact that above the density of "intrinsic" saturation limit (about 125,000 lines per square inch), the teeth act as though they were nonmagnetic to further increase in flux. In Table II calculated results for the direct axis flux (net exciting flux) are tabulated for direct axis magnetomotive force of 1, 2, 3, and 4 per unit and cross axis magnetomotive force of 0, 2.5, 5, 7.5, 10, and 15. These results are plotted in Figure 9 showing the relation between exciting flux field current and armature current.

To express the relationships by mathematical formula, the flux is divided into components. One of these is the flux existing in the gap and tooth space, taking the teeth to be nonmagnetic. This is the "space" component or "space" flux. The other component is the flux carried by the teeth at the intrinsic saturation limit. This is the "iron" component or "iron" flux. In calculating this with tapering teeth, the average width of the teeth is used. It is only necessary to calculate the flux for a single tooth and divide by the slot pitch to determine the "iron" flux per inch of pole arc. From the geometry of Figure 10, the following results are apparent:

$$\text{Quadrature axis (cross) iron flux} = \frac{b}{p_a}\phi_i = \frac{c}{p_a}\phi_i \quad (19)$$

where

ϕ_i/p_a = iron flux per inch of pole arc (= iron flux per tooth divided by slot pitch)

$$\text{Direct axis (exciting) iron flux} = \frac{a\phi_i}{p_a} = \frac{M_f' p_p}{M_a' p_a}\phi_i \quad (20)$$

where

p_a = pole arc (inches)
p_p = pole pitch (inches)
M_f' = peak transient field magnetomotive force
M_a' = simultaneous peak transient armature magnetomotive force

It is important to observe from Figure 10 that the portion of the arc (dimension a) which carries the net direct axis flux is acted on by magnetomotive force greater than that required for the intrinsic saturation limit. Sections of the pole arc b and c, where the iron may not be at this density, contribute only to the cross flux.*

The total direct axis (exciting) flux is determined by adding the space flux to the iron flux.

$$\text{Space flux} = M_f' \rho \frac{\phi_1 K_i}{M_{f1}} \quad (21)$$

where

ϕ_1 = flux producing armature electromotive force equal to rated voltage at base speed, no load
M_{f1} = field ampere turns for rated voltage, no load
K_i = ratio gap and tooth ampere turns to gap ampere turns at flux ϕ_1
ρ = ratio of permeance of air gap with nonmagnetic teeth to that of the normal air gap

With pole face windings, the quadrature axis flux in the gap and teeth is as shown in Figure 7. The combined magnetomotive force of the armature and pole face windings is distributed across the pole arc as shown in Figure 11A. Its distribution across the arc between pole face bars is shown in Figure 11B where the magnetomotive force is that acting between the two windings from top of pole face copper to top of armature copper, rather than from bottom of pole face slot to bottom of armature slot as in Figure 11A.

The method used for determining the direct axis flux and the corresponding electromotive force under the influence of the strong quadrature flux is the same as for machines without pole face windings, except that the pitch between pole face slots is substituted for the pole arc and the magnetomotive force of the pole face winding is added to the armature magnetomotive force over the pole face slot pitch. Distortion of the flux distribution corresponding to the magnetomotive force distribution of Figure 11B exists at the top of the teeth because of criss-cross flux in the air gap and tooth-tip leakage flux. There is very little distortion at the bottom of the slots if the pole face magnetomotive force is well distributed and equal to the armature magnetomotive force. Magnetomotive force distributed as in Figure 11A is likely to be insufficient to saturate the teeth full depth, and in some cases the magnetomotive force acting on the tooth tops as in Figure 11B may be below that required to reach the intrinsic saturation limit of the iron over some part of dimension a. However, even in these special cases, negligible error in the results is caused by calculating the "iron" flux at the intrinsic saturation limit in the mean section of the armature teeth and dividing it into quadrature and direct axis components by the magnetomotive force ratio shown in Figure 11B. Then the direct axis iron flux is

$$\phi_{id} = \frac{a\phi_i}{p_b} = \frac{M_f' p_a \phi_i}{p_b\left(\frac{p_a M_a'}{p_p} + M_b'\right)} \quad (22)$$

This method takes care of machines with incomplete compensation and with varying number of pole face slots. If the pole face winding is removed, p_b becomes p_a and the formula reduces to equation 20.

The formula for space flux is the same as equation 21. Because the pole face slot tips saturate, ρ is the ratio of permeance of normal air gap to that with nonmagnetic

* It will be noted from Figure 10 that the average magnetomotive force acting on section a is $p_a M_a'/p_p$. When the flux caused by this magnetomotive force is derived for this section alone, the answer is identical with equation 20 plus equation 21. However, the factor ρ is derived to include with the "space" flux the fringing flux outside the pole arc. In this way, the fringing flux is not neglected.

armature teeth plus nonmagnetic pole face tooth tips.

From equations 21 and 22, the total exciting flux at the instant of maximum current is

$$\phi_d' = \frac{M_f' p_a \phi_i}{p_b\left(\frac{p_a M_a'}{p_p} + M_b'\right)} + M_f' \rho \frac{\phi_i K_i}{M_{f1}} \qquad (23)$$

This has the unknowns ϕ_d', M_f', M_a', and M_b'. There are also the following equations holding simultaneously:

$$M_f' = \frac{M_{f1}}{I_{f1}} I_f' \text{ per unit} \qquad (24)$$

where

I_f' = maximum field amperes
M_{f1} = base field magnetomotive force
I_{f1} = corresponding base field amperes

Similarly,

$$M_a' = \frac{M_{a1}}{I_{a1}} I_a' \text{ per unit} \qquad (25)$$

$$M_b' = \frac{M_{b1}}{I_{a1}} I_a' \text{ per unit} \qquad (26)$$

where

M_a' = maximum armature magnetomotive force
M_{a1} = armature magnetomotive force at rated amperes
I_{a1} = rated armature current
M_b' = maximum pole face winding magnetomotive force
M_{b1} = pole face winding magnetomotive force at rated armature current
I_a' = maximum armature current

Also, since the field linkages immediately after short circuit at the instant of peak current will be equal to those immediately before short circuit in accordance with the constant linkage theorem,

$$\phi_d' + n_f \frac{\phi_1}{I_{f1}} I_f' = \phi_o(1+n_f) \qquad (27)$$

where ϕ_o is the initial field flux producing armature electromotive force. Since both sides of the equation are multiplied by the same number of turns to obtain linkages, this multiplier is omitted and the flux equation written directly. The term n_f is the fraction of ϕ_o which when multiplied by the same number of turns represents the remainder of the total field linkages, being that part which is caused by leakage flux not creating armature electromotive force.

The final necessary simultaneous equation is

$$I_a' = \frac{(\text{emf})'}{r_w + r_b} = \frac{1}{r_w + r_b} \phi_d' \frac{V}{n_1 \phi_1} \frac{60}{2\pi} \frac{d\theta}{dt} \qquad (28)$$

where

r_w = resistance of windings (plus fault if necessary)
r_b = resistance of brush contact (equivalent to a-c reactance voltage of armature winding)
V = armature electromotive force (= rated voltage)
n_1 = rpm (= rated base speed)
ϕ_1 = flux producing unit electromotive force at unit speed
θ = angular displacement in radians
t = time in seconds

The paper is limited to the case of constant speed on the assumption that the drop in speed at the instant of peak current is negligible in all cases. For the sustained conditions, the results are limited to cases where the speed is maintained by the driving machine or reverse power flow to the driven machine.

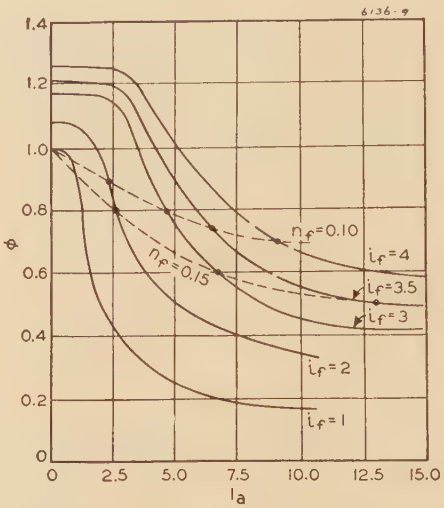

Figure 9. Relation between flux, armature current, and field current for machine represented by Figure 8

Circles and dashed lines connecting them are from equation 27

The equations give the following solutions:

$$I_a' = \frac{K_2\phi_o(1+n_f) - RK_1}{2R(K_2+n_f)} + \sqrt{\frac{K_1(1+n_f)\phi_o}{R(K_2+n_f)} + \left(\frac{RK_1 - K_2\phi_o(1+n_f)}{2R(K_2+n_f)}\right)^2} \qquad (29)$$

$$I_f' = \frac{\phi_o(1+n_f)I_a'}{K_1 + (K_2+n_f)I_a'} \qquad (30)$$

$$T' = \phi_d' I_a' = (K_1 + K_2 I_a')I_f' \qquad (31)$$

$$P' = (I_a')^2 R \qquad (32)$$

where, in terms of per-unit quantities,

$$K_1 = \frac{\phi_i p_a p_p}{p_b(p_a M_{a1} + p_p M_{b1})} \qquad (33)$$

$$K_2 = \rho K_i \qquad (34)$$

$$R = r_w + r_b \qquad (35)$$

The steady state results are obtained by solving the equations, excluding equation 27, which does not hold for steady state conditions. I_f, the sustained field current, is substituted for I_f'. For separately excited machines, I_f is the same as the initial field current I_{f0}. For self-excited machines on "dead" short circuit, $I_f = 0$. The solution for the steady state gives

$$I_a = \frac{K_2 I_f}{2R} + \sqrt{\frac{K_1}{R} I_f + \left(\frac{K_2 I_f}{2R}\right)^2} \qquad (36)$$

$$T = (K_1 + K_2 I_a) I_f \qquad (37)$$

The effect of shift of the axis in armature magnetomotive force mentioned under "Brush Arcing" can be included by replacing M_f' in equation 23 with M_d', where

$$M_d' = \frac{M_{f1}}{I_{f1}} I_f' - \frac{2bP}{B} \frac{M_{a1}}{I_{a1}} I_a' \qquad (38)$$

and using this equation in place of equation 24

b = brush width in number of segment pitches
P = the number of poles
B = total number of commutator segments

This gives the formulas presented in "Formulas for Current and Torque." Any shift from the quadrature axis measured in equivalent number of commutator segments can be accounted for by replacing b by twice the number of segments of shift.

To develop complete current-time formulas, time constants for the armature and field circuits are developed in Appendix II. The reciprocals of these time constants give the corresponding decrement factors. Then, if

σ_a = decrement for armature circuit
σ_f = decrement for field circuit
I_a' = peak armature current
I_a = sustained armature current

The armature current has the following components:

Rise:

$$I_a'(1 - \epsilon^{-\sigma a t})$$

Decay:

$$-(I_a' - I_a)(1 - \epsilon^{-\sigma_f t})$$

The time constants are so dissimilar that the components may be put together directly with negligible error. Therefore,

$$I_a = I_a - I_a'\epsilon^{-\sigma a t} + (I_a' - I_a)\epsilon^{-\sigma_f t} \qquad (39)$$

Similarly,

$$i_f = I_f - (I_f - I_f')(\epsilon^{-\sigma_f t} - \epsilon^{-\sigma a t}) \qquad (40)$$

Appendix II. Time Constants

The field time constant is

$$T_f = \frac{L_f}{R_f} = \frac{N\phi_1 K_i P(1+n_f)10^{-8}}{V_f} \text{ seconds} \qquad (41)$$

where N is the number of turns per coil, and V_f is the field voltage including rheostat. ϕ_1 is in maxwells.

The armature time constant is

$$T_a = \frac{L_a}{r_w + r_b}$$

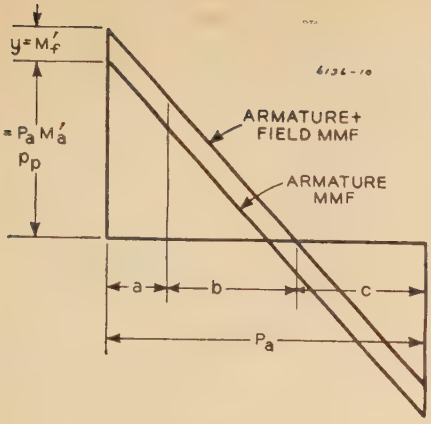

Figure 10. Distribution along air gap showing net exciting magnetomotive force over section a

$$c:(x-y)=(a+b):(x+y)$$
$$b=c;\ P_a=a+b+c$$
$$\text{Therefore, } \frac{a}{P_a}=\frac{y}{x}=\frac{M_f'P_p}{M_a'P_a}$$

L_a = armature circuit inductance $=\dfrac{k_1T^2p_q}{a^2P}$, neglecting slot and end leakage (42)

where

T = total number of armature turns
p_q = total gap permeance for armature magnetomotive force
a = number of circuits in armature winding
P = number of poles

Also,

$$\frac{E}{I}=\frac{k_2T\,(\text{rpm})\,p_d\,(\text{field mmf})\,P}{aI} \tag{43}$$

where

E = rated volts
I = rated amperes
p_d = excitation permeance
rpm = rated base speed

Let field magnetomotive force be proportional to armature reaction:

$$\text{Field magnetomotive force}=\frac{k_3TI}{aP} \tag{44}$$

and let p_d be proportional to p_q. Then, substituting equation 44 in equation 43 and substituting the result in equation 42,

$$L_a=\frac{E}{I}\,\frac{C_x}{P(\text{rpm})} \tag{45}$$

This indicates that under the assumptions L_a is equal to unit resistance divided by machine frequency and multiplied by a coefficient C_x. The value for C_x, representative of some d-c machines, has been determined from test data and calculations shown in Table I. Using this quantity it is possible to estimate the inductance and, therefore, to specify the approximate time constant. When resistance is expressed in per unit,

$$T_a=\frac{19.1C_x}{(r_w+r_b)(\text{rpm})P}\ \text{seconds} \tag{46}$$

Saturated Time Constants

The rise of current is governed at first by the normal armature time constant, but finally any change in flux linkages of either the armature or field circuits for a given change in their respective currents is substantially in proportion to the space permeance illustrated in Figure 8. Calculations similar to those of Figure 8 demonstrate this. Therefore, the saturated time constants are

$$T_{as}=\frac{\rho+n_f}{1+n_f} \tag{47}$$

and

$$T_{fs}=\frac{\rho+n_f}{1+n_f} \tag{48}$$

Equation 47 is an approximation for the armature winding taking the portion of the flux linkages not affected by saturation to be the same percentage of total linkages as is the case for the field winding.

Appendix III. Permeance Ratio ρ

The normal air gap permeance is (omitting numerical coefficients)

$$P_n=\frac{A}{gK_\lambda C_sC_d} \tag{49}$$

where

A = area of gap = pole arc × pole length
g = average length of air gap
K_λ = ratio flux under pole arc to total gap flux, Figure 12 (fringing factor for boundaries of pole face)
C_s = slot fringing factor, Figure 14
C_d = duct fringing factor, Figure 13

The space permeance with nonmagnetic teeth is

$$p_n'=\frac{A}{(g+d_s)K_\lambda'} \tag{50}$$

where

d_s = depth of slot
K_λ' = 0.85 (very nearly constant for very large gaps)

Therefore,

$$\rho=\frac{p_n'}{p_n}\,\frac{gK_\lambda C_sC_d}{0.85(g+d_s)} \tag{51}$$

In cases with pole face windings, add to d_s the depth from pole face to top of copper in pole face slots.

Appendix IV. A-C Reactance Voltage of Armature and Equivalent Brush Contact Resistance r_b

Assuming that the machine operates momentarily without commutating pole flux because of the extremely rapid rise of armature current, all of the reactance voltage appears as an equivalent brush contact voltage. However, the normal reactance voltage is increased by crowding the current to the edge of the brush, in turn increasing the rate of current reversal in the coil and the reactance voltage. Under these circumstances the equivalent brush drop voltage is arrived at in the following way.

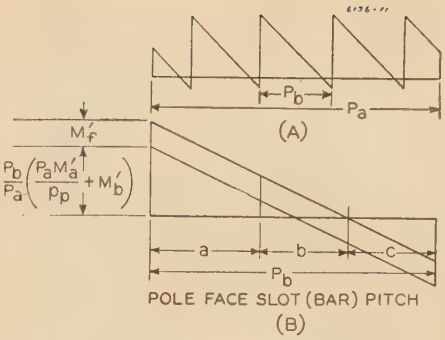

Figure 11. Difference in combined magnetomotive force distribution acting at top and bottom of slots in machines with pole face windings

A—Acting across space from bottom of pole face slot to bottom of armature slots ($=M_f'+M_a'-M_b'$)
B—Acting across space from top of pole face copper to top of armature copper

If a reactor of negligible resistance is suddenly connected in parallel with a resistor which is part of a circuit containing a driving voltage and a steady circulating current, the current will shift from the resistance path to the inductive path. While this shift is happening, the energy lost in the resistor is equal to the change in energy stored in the reactor. The resistor is analogous to the net brush contact resistance and the reactor to the armature coil. The energy change in a coil can be calculated and, since the number of coils rotating past the brush per second is known, the equivalent watts at the brush contact can be determined. It will be assumed that the *average* reactance voltage per coil E_R is known or is measured as in Appendix V. Then the inductance per coil is

$$L_c=\frac{E_Rb}{I_bf_s}\times10^8 \tag{52}$$

where

I_b = amperes per brush arm
f_s = segments per second (= number of segments times revolutions per second)
b = brush overlap (= width brush face in number of segment pitches)

The energy change per coil is

$$\Delta\epsilon=\tfrac{1}{2}L_cI_b^2=\frac{E_RbI_b}{2f_s} \tag{53}$$

The equivalent watts are

$$f_s\Delta\epsilon=\frac{E_RbI_b}{2} \tag{54}$$

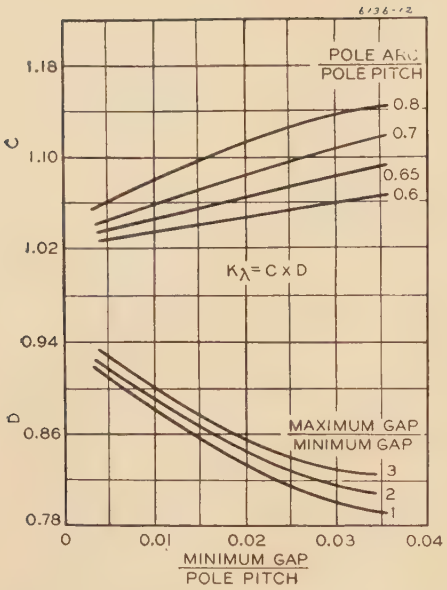

Figure 12. Fringing factor for boundaries of pole face K_λ

and the equivalent brush contact resistance for plus and minus brushes is

$$r_b = \frac{E_R b}{I_b} \tag{55}$$

This is the minimum brush resistance, assuming all the brush contact voltage counteracts reactance voltage with constant contact resistance. If L_c is nearly constant, this is also the minimum contact resistance for either arcing contact or for brush contact resistance varying with current. But in all cases, all the voltage produced is needed to counteract reactance voltage. The true voltage is more than this minimum because it is known that arc voltage consists of a "constant" base voltage plus a variable voltage depending on arc length and current.[3] The "constant" base voltage is surplus and cannot counteract reactance voltage as only the voltage difference between segments can do this. Moreover, the author has found the resistance of carbon brush contacts at high density to be nearly equivalent to a base voltage plus a constant times the brush current. Undoubtedly, there is some surplus voltage in the brush contact with or without arcing, and, therefore, the contact loss of brushes under rated conditions assuming perfect commutation is added to allow for it approximately. The final result for r_b on a per-unit basis is

$$r_b = \frac{E_R b + V_c}{V} \tag{56}$$

where

V_c = approximate contact drop of the plus and minus brushes at rated load current density

V = rated voltage

Equation 56 is approximately true whether or not arcing is involved in commutation, so long as the effective self-inductance of the armature coils is not affected. A correction factor sometimes needed for equation 56 and an expression for the distribution of current in the brush face are derived by solving the basic equation of a coil undergoing commutation. This equation says that the reactance voltage is equal to the difference in brush contact voltage between the brush and the two segments to which the coil is connected or, from Figure 15,

$$L\frac{d}{dt}i_c = \frac{(Rt_b)}{(t_s)}t_s\frac{d}{dt}i_s \tag{57}$$

$$i_s = t_s\frac{d}{dt}i_c \tag{58}$$

from which

$$\frac{d}{dt}i_s - \frac{L}{Rt_b t_s}i_s = 0 \tag{59}$$

where

$RI_b = V_c$ = normal brush contact voltage

$\frac{Rt_b}{t_s}$ = brush contact resistance/segment

$L = E_R t_b / I_b$

The solution to equation 59 is

$$i_s = A\epsilon^{pt}$$

where

$$p = L/Rt_b t_s$$
$$= E_R/RI_b t_s$$
$$= \frac{E_R f_s}{V_c}$$

and A is found from

$$\text{Average } i_s = \frac{1}{t_b}\int_o^{t_b} i_s dt$$
$$= \frac{A}{t_b}\frac{(\epsilon^{pt_b}-1)}{p}$$
$$= \frac{I_b t_s}{t_b}$$

from which

$$i_s = \frac{E_R\epsilon^{pt}}{R(\epsilon^{pt_b}-1)} \tag{60}$$

This equation is plotted for a 1,500-kw 1,500-volt generator in Figure 3.

The watts loss in the brush contact is

$$\frac{1}{t_s}\int_o^{t_b} i_s^2\frac{(Rt_b)}{(t_s)}dt = \frac{t_b E_R I_b}{2t_s}\times\frac{(\epsilon^{2pt_b}-1)}{(\epsilon^{pt_b}-1)^2}$$
$$= I_b^2 R_b \tag{61}$$

where

R_b = effective brush contact resistance

The total brush contact resistance is in per-unit

$$r_b = 2R_b I_b/V$$
$$= \frac{E_R b}{V}\left(\frac{\epsilon^{2x}-1}{\epsilon^{2x}-2\epsilon^x+1}\right) \tag{62}$$

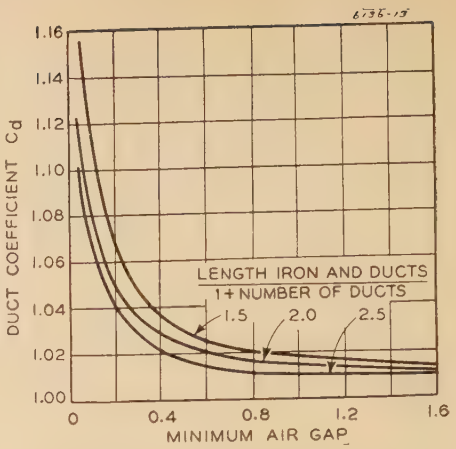

Figure 13. Duct fringing factor C_d

where

$$x = \frac{E_R b}{V_c}$$

If x is small in some cases so that the bracketed factor is appreciably greater than one, the first term of equation 56 should be increased accordingly.

Appendix V. Constants From Test Measurements

In many cases the results may be used without reference to manufacturer's data.

ϕ_i may be taken as equal to 1.0 in large machines because the tooth density at normal voltage will approach 125,000 lines per square inch. For small machines ϕ_i may be as much as 1.25. An error does not affect the results seriously for peak armature current and torque as, in any case, the exciting flux is stoutly maintained unless the field leakage flux is unusually large ($n_f > 0.15$).

The term ρ may be determined by measuring the air gap and the depth of slot with gauge and rule. Then by using equation 51, taking $K_\lambda = 0.93$, $C_s = 1.1$, and $C_d = 1.04$, the value of ρ may be computed. These are representative values for large machines.

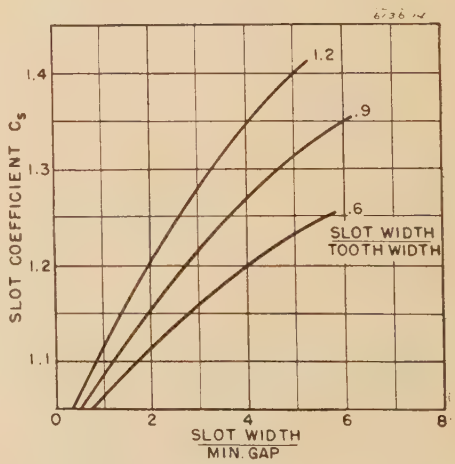

Figure 14. Slot fringing factor C_s

Average or representative values for K_1 and K_t for large machines with pole face windings are 4.0 and 1.3, respectively. Without pole face windings, K_1 averages about 1.0 with no change in K_t. The field leakage coefficient n_f may be taken as 0.12 (an average figure).

All these factors chiefly influence the induced field current required to maintain the field flux linkages, and when n_f is small they have relatively little influence on the peak armature electromotive force, current, and also torque. If n_f were zero, they would have no influence at all.

The remaining factor of major importance is the resistance r_b dependent on E_R. This can be determined from equation 13 and the relation

$$E_R = 6.38 \times AT \times 1/g \times l \times S \times 10^{-8} \qquad (63)$$

where

AT = net difference in the ampere turns at rated load of the armature and compensating windings determined by counting their respective turns from inspection
g = measured length of the commutating pole air gap and nonmagnetic shims
l = measured length of the armature core in inches
S = revolutions per second times the measured periphery of the armature in inches

Another method for estimating E_R is from the relation

$$E_R = \frac{C_r \text{ times } K_w}{d_a} \qquad (64)$$

where

C_r = reactance voltage coefficient averaging about 0.12 for large machines
K_w = rated kilowatts
d_a = armature diameter in inches

If a fluxmeter or ballistic galvanometer is available it may be connected to an exploring coil around the tip of the commutating pole to measure the flux, which when multiplied by f_s/b and by 10^{-8} will give E_R (roughly) for a half coil turn. Similarly, an exploring coil around the base of the main pole and another around the pole face can be used to measure n_f approximately.

Appendix VI. Nomenclature

AT = net difference between armature ampere turns and ampere turns of commutating pole plus pole face windings at maximum rated continuous current
b = width of brush contact face in commutator segments
B = total number of commutator segments
C_d = flux fringing coefficient for armature ducts (Figure 13)
C_r = reactance voltage coefficient (=0.12 for large machines)
C_s = flux fringing coefficient for armature slots (Figure 14)
C_x = average per-unit inductance of d-c machines (see Table I)
d_a = armature diameter in inches
d_s = depth of armature slot in inches
E_R = rated load average reactance voltage at speed for which short circuit is calculated
f_s = commutator segments per second passing brush arm
g = main pole average air gap in inches
I_a = steady state short-circuit armature amperes
I_{a1} = maximum rated continuous armature amperes
I_a' = maximum or peak transient short-circuit armature amperes
I_b = rated amperes per brush arm
I_{f1} = field amperes for rated voltage at base speed, no load
I_f' = maximum or peak transient field amperes on short circuit
K_1 = "iron" flux constant, equation 11
K_2 = "space" flux constant, equation 12
K_t = air gap plus tooth ampere turns divided by air gap ampere turns at rated voltage, base rated speed, no load
K_λ = pole arc air gap flux divided by total gap flux (Figure 12)
l = length of iron core portion of armature including ducts in inches
M_{a1} = total armature ampere turns per pole at maximum rated continuous current (equals current times total turns divided by circuits, divided by poles)
M_a' = peak transient armature ampere turns per pole on short circuit
M_{b1} = pole face winding ampere turns per pole at rated current
M_b' = maximum transient ampere turns of pole face winding per pole on short circuit
M_{f1} = field ampere turns at rated voltage, rated base speed, no load
M_f' = maximum transient field ampere-turns on short circuit
n = speed for which short circuit is calculated
n_1 = rated base speed in revolutions per minute
n_f = field leakage flux linkages divided by field linkages from flux generating armature electromotive force
N = number of field winding turns per pole
p_a = pole arc in inches
p_b = pole face slot pitch (average) in inches
p_p = pole pitch in inches
P = number of poles
r_b = equivalent resistance of brush contacts
r_w = resistance of machine windings
$R = r_w + r_b$ = total effective resistance of circuit
S = revolutions per second times armature circumference in inches
t = time in seconds
T = torque as function of time
T' = maximum transient torque on short circuit
T_a = time constant of armature circuit in seconds
T_{as} = saturated time constant of armature circuit
T_f = time constant of field circuit
T_{fs} = saturated time constant of field circuit
V = rated voltage
V_c = normal load brush and brush contact voltage drop
V_f = field voltage including rheostat
θ = angular displacement in radians
ρ = ratio permeances: air gap plus nonmagnetic teeth to normal air gap
σ_a = armature decrement factor (reciprocal of T_a or T_{as})
σ_f = field decrement factor (reciprocal of T_f or T_{fs})
ϕ_0 = flux before short-circuit generating armature electromotive force
ϕ_1 = flux per pole generating rated voltage at rated base speed
ϕ_d' = flux generating electromotive force immediately after short circuit

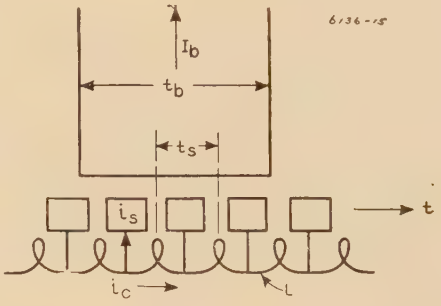

Figure 15. Circuit diagram for equation governing current reversal in armature coils and flow of current between segments and brush

ϕ_t = "iron" flux (=pole arc times mean section of tooth times 125,000 lines per square inch divided by slot pitch)

References

1. Short Circuit Characteristics of D-C Generators, G. E. Frost. AIEE Transactions, volume 65, 1946, June section, pages 394–402.

2. Protection From Flashing for Direct-Current Apparatus, J. J. Linebaugh, J. L. Burnham. AIEE Transactions, volume 37, 1918, pages 341–52.

3. Einfuhrung in die Physik der Gasentladunger (book), R. Seeliger. J. A. Barth (Leipsig, Germany) 1927, page 286 (second edition, 1934, page 375).

4. Synchronous Machines—IV, R. E. Doherty, C. A. Nickle. AIEE Transactions, volume 47, 1928, pages 457–87.

5. Three-Phase Short Circuit Synchronous Machines—V, R. E. Doherty, C. A. Nickle. AIEE Transactions, volume 49, 1930, pages 700–13.

6. Graphical Determination of Magnetic Fields, R. W. Wieseman. AIEE Transactions, volume 46, 1927, pages 141–8.

Temperature Limits for Short-Time Overloads for Oil-Insulated Neutral Grounding Reactors and Transformers—II

V. M. MONTSINGER
FELLOW AIEE

J. E. CLEM
FELLOW AIEE

Synopsis: In part I, published in 1938,[1] the principal question considered was the effect of ventilating coils on temperature limits for ground faults greater than one minute, for which it was assumed that 160 degrees centigrade based on all heat stored in copper was the correct limit.

Since 1938 considerable new data have been obtained. This paper presents the new data and shows that:

1. For heating periods of one minute or less, practically all aging of insulation occurs during the cooling period. It is shown that temperature limits can be based on the rate of cooling rather than on the heating period.

2. In the heating-up period of one minute or less, 25 to 45 per cent of the loss is dissipated from the copper to the insulation and oil. Formulas are developed for calculating the temperatures during the heating and cooling periods.

3. Temperature limits above 160 degrees centigrade for one minute are permissible for both nonventilated and ventilated coils, being approximately 200 degrees centigrade for windings which cool sufficiently rapidly.

THE earlier paper[1] gave data on the heating of coil stacks with and without ducts, and served as the basis of selecting 160 degrees centigrade as a suitable limiting temperature for short-time rating of grounding devices using class A insulation. The standard for neutral grounding devices, AIEE Standard 32, is undergoing revision, and this paper is being presented to give data to serve as the basis of selecting suitable temperature limits.

The heating time intervals generally accepted for neutral grounding devices are ten seconds and one minute. For such short heating periods, the cooling time is more effective on the aging of the insulation than the heating time. Accordingly, the temperature limit for a 10-second coil can be only a few degrees higher than the limit for a 1-minute coil.

Previous calculations of the short-time heating of neutral grounding devices have been made on the basis of all heat stored in the copper. This practice results in calculated rises appreciably higher than actual, and, in reality, furnishes no experience at all in reference to the suitability of 160 degrees centigrade as a temperature limit.

In the transformer standard American Standards Association C-57, the temperature limit is 250 degrees centigrade with the calculations based on all the heat being stored in the copper, the same as for neutral grounding devices, and with full sustained voltage applied to the transformer. Again this gives no clue as to what temperature might be considered safe for neutral grounding devices because it is definitely known that the 250 degrees centigrade limit never is reached, nor even approached very closely.

Accordingly, the question of the selection of suitable limits for neutral grounding devices must be approached directly on its own merits. Several papers on aging have been published, and it is more or less generally agreed that the rate of aging doubles for a definite temperature increment. In a recent paper by F. M. Clark,[2] he shows that the increment of temperature for which doubling occurs is relatively small at 95 degrees centigrade and is practically 8 degrees centigrade for temperatures upward from approximately 115 degrees centigrade. This confirms the value originally reported by V. M. Montsinger.[3] Some authors have given values up to 10 degrees centigrade. However, the value of 8 degrees centigrade as the increment generally is accepted for transformer insulation.

In Clark's paper there are data indicating that 16 doubles in aging effect occur over the temperature range from 100 to 200 degrees centigrade, and it seems reasonable to use this rate of aging

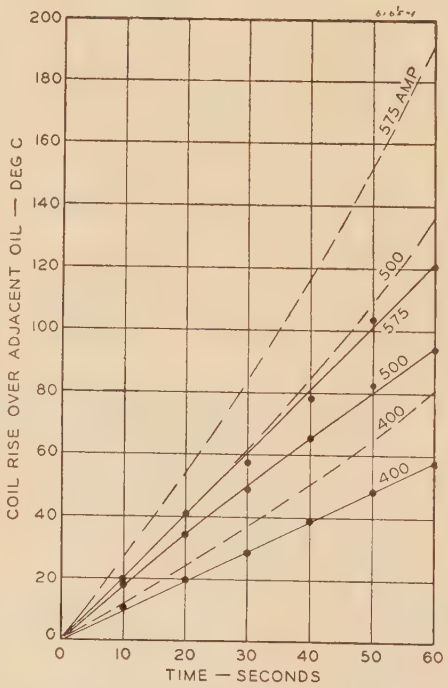

Figure 1. Curves of tested and calculated temperature rises during 60-second duration in 24-degree-centigrade oil

--------- Calculated, all heat stored in copper only
——— Line through test points
Size of conductor, 0.435 by 0.095 inch

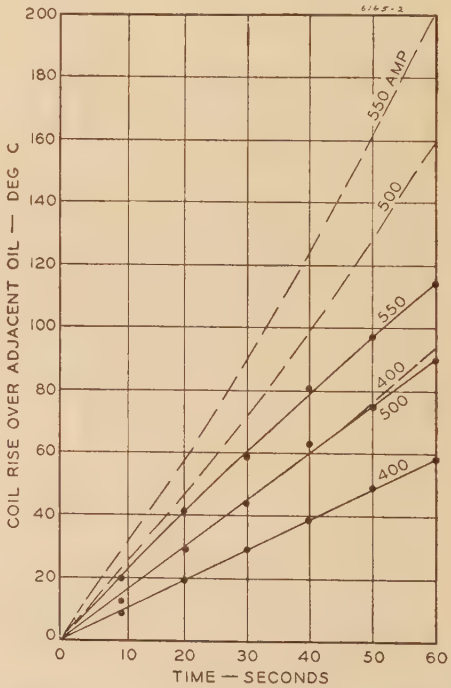

Figure 2. Curves of tested and calculated temperature rises during 60-second duration in 71-degree-centigrade oil

--------- Calculated, all heat stored in copper only
——— Line through test points
Size of conductor, 0.435 by 0.095 inch

Paper 46-165, recommended by the AIEE committee on electric machinery for presentation at the AIEE summer convention, Detroit, Mich., June 24–28, 1946. Manuscript submitted April 26, 1946; made available for printing June 4, 1946.

V. M. MONTSINGER is a research engineer in the power transformer engineering department, General Electric Company, Pittsfield, Mass.; J. E. CLEM is in the central station engineering division, General Electric Company, Schenectady, N. Y.

The authors wish to acknowledge the assistance given by Miss J. Shipton in the calculation of data and to C. J. Lamberton for conducting the tests.

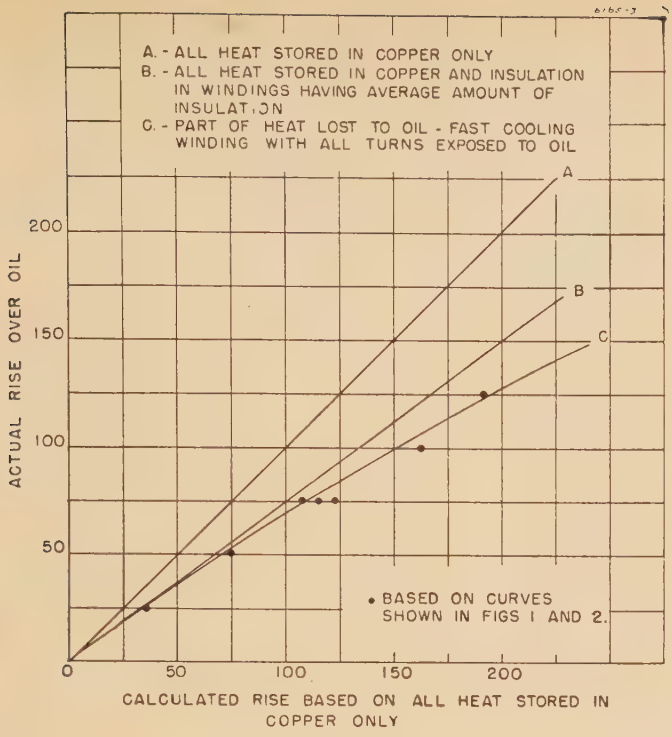

Figure 3. Curves of calculated temperature rise and hot-spot temperature rise under 1-minute fault condition

increase in estimating suitable temperature limits for neutral grounding devices. It should be borne in mind, however, that aging tests are tests of a mechanical nature in that loss of mechanical strength is measured. Such tests give no clue as to the actual length of life to be expected in transformers or similar devices. The aging tests, however, do furnish a means of making comparisons so that we can say that greater or less life can be expected at lower or higher temperatures. Further, the deviations in the results of life tests are quite large so that we must talk of relative aging in rather broad terms. The translation of the results of aging data into life estimates must be made cautiously and with common sense and judgment.

Quite obviously, the selection of the temperature limit will depend upon the answer to the question, "How much aging can be allowed for each operation?" This could be answered if we knew how many faults would occur per year. However, lacking that knowledge, it is necessary to make the best estimate possible on the basis of the data we have. After considerable investigation it appears that the temperature limit should be selected on the basis that the relative aging of a neutral grounding device during one year be the same as that of a power or distribution transformer during the same period, operating at rated load in the reference ambient temperature, and also that ten events (faults at full rated current) occur per year.

Since most of the aging occurs during the cooling of the coil, it appears quite obvious that the higher the rate of cooling, the higher can be the temperature limit. The cooling time varies directly as the thermal capacity associated with one pound of copper, varies inversely in an exponential manner as the watts per pound required to produce a given ultimate temperature rise, and is a direct function of the heating characteristics of the winding, that is, the temperature rise for one watt per sound. Obviously a multitude of limits might be established depending upon the correlation of these factors, but this does not seem desirable.

Designation of Windings Used in Neutral Grounding Devices

Since as much as 45 per cent of the heat escapes to the insulation and oil during a 1-minute fault in windings having cooling ducts between all coils, it is desirable to have some easy means of distinguishing between these windings and windings with no cooling ducts from which no heat escapes to the oil.

For purposes of identification in this paper the usual well-ventilated coils will be designated as "fast cooling windings" and the "no duct" or poorly-ventilated coils will be designated as "slow cooling windings," without consideration of grammatical correctness.

Heating Period Under Fault Condition

Fast Cooling Windings

In the past it has been assumed that for a short-time fault condition all heat is stored in the copper, that is, the thermal capacity of the conductor insulation was neglected. However, recent tests have shown that for windings having each conductor exposed on both edges to the oil, between 25 and 45 per cent of the copper loss is dissipated at the end of 60 seconds.

The tests referred to previously were made on horizontal disk coils having 0.435-by-0.095-inch conductors with a two-sides thickness of turn insulation of 0.019 inch. The radial build of the coils was 2.625 inches. The hot-spot temperature was measured by a thermocouple embedded under a spacer and between turns of the next to top coil. All temperature rises were based over the adjacent oil, 1.5 inches away from the coil containing the thermocouple.

The temperatures were read on an automatically balanced indicating type of potentiometer. The lag in temperature was quite small because the temperature started falling within one to two seconds after the current was removed. The direction of the current was reversed in alternate coils to reduce stray loss to a minimum. The measured loss was practically the same as the I^2R.

Figures 1 and 2 show curves of meas-

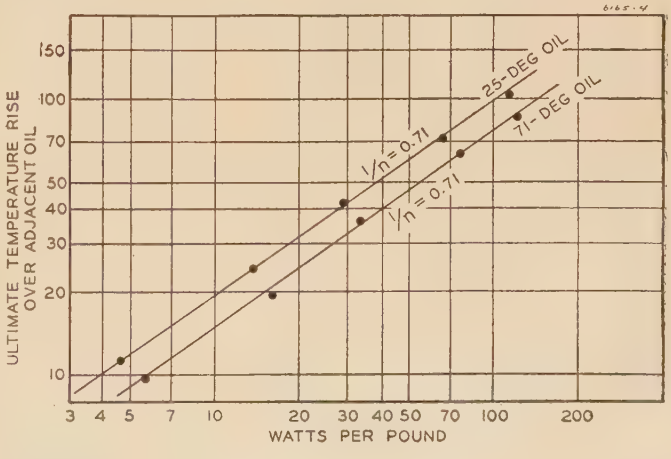

Figure 4. Ultimate hot-spot temperature rise versus watts per pound of disk coils

Disk coils have 0.435-by-0.095-inch conductors, 2.625 inches radial build, 3/8-inch oil ducts between coils, and are immersed in 25- and 71-degree-centigrade oil

Table I. Tested Rises in Per Cent of the Calculated Rises

Approximate Oil Temp, Deg C	Amp	Temp Rise at End of 60 Sec Over Adjacent Oil, Deg C		Tested Rise in Per Cent of Calculated Rise
		Calculated*	Tested	
25	400	80	57	71
25	500	135	94	70
25	575	191	120	63
71	400	93	58	62.5
71	500	150	90	56.0
71	550	201	114	57.0

*On basis all heat stored in copper.

ured temperature rises, holding three different values of amperes for 60 seconds on coils immersed in approximately 24- and 71-degree-centigrade number 10-*C* oil. The dashed lines show the temperature rises that would have been attained if all the heat had been stored in the copper. The formula for calculating these rises is shown in Appendix I.

These tests show that the temperature rise of fast cooling coils under a 1-minute fault can be assumed to be approximately 65 per cent of the rise based on all heat stored in copper only. For the higher oil temperatures, the value is less than 65 per cent. Fifty-five to 65 per cent would be more nearly correct, so 65 per cent is conservative.

Figure 3 shows the relationship between calculated and actual rises in windings ranging from fast cooling to the slowest cooling.

Slow Cooling Windings

Under slow cooling windings may come

1. Windings having no oil ducts between individual coils.
2. Windings or coils heavily taped.
3. Windings having several layers between oil ducts.

For windings coming within the above classifications, it can be assumed that the temperature rise within a period of 60 seconds is close to that resulting from all heat stored in the copper and adjoining insulation.

Where the adjoining insulation is all on the conductors, the rate of heat storage in copper and its insulation can be calculated close enough for practical purposes by assuming that the thermal capacity of the insulation is "by volume" one-half that of the copper.[4] That is, the temperature rise calculated on the basis of all heat stored in the copper should be multiplied by the factor

$$\left(\frac{2a}{A+a}\right)$$

where

A = cross-sectional area of copper plus insulation
a = cross-sectional area of copper

Cooling Period Following a Fault

Because most of the aging of the insulation even in fast cooling windings occurs during the cooling period following a 1-minute fault as shown later, it is important to be able to calculate the cooling of various kinds of coils.

To calculate the cooling of a winding that has not reached ultimate conditions requires that the initial temperature rise (at start of the cooling period) be translated into terms of watts per pound to cause an ultimate rise equal to the initial rise. Unless the internal coil gradients are materially different, cooling down from a given maximum temperature rise occurs in the same manner, regardless of whether the rise is obtained under transient or ultimate conditions.

Ultimate Temperature Rise Tests

Since the oil in neutral grounding reactors is at room temperature at the start of a fault, and the oil in grounding transformers on account of continuous core loss is (by assumption in the Standards) at 75 degrees centigrade at the start of a fault, ultimate heat runs were made in different oil temperatures to determine the effect of the viscosity of the oil on the temperature rises.

The results of the tests are given in Figure 4. The test values can be expressed by the formula

$$\Theta = k W_c^{\frac{1}{n}} \mu^{0.25} \qquad (1)$$

where

Θ = temperature rise, degrees centigrade
k = constant
W_c = watts per pound of copper at ultimate temperature
μ = viscosity of the average temperature of the oil film expressed in centipoises
n = empirical exponent of temperature rise Θ versus W_c

Figure 4 shows the relationship between ultimate tested temperature rise and watts per pound of copper. For these curves, when viscosity is not factored $1/n$ = approximately 0.70. When viscosity is factored, $1/n = 0.75$ in the formula. Similar tests were made on other sizes of conductors and conductor insulation of two-sides thickness up to and including 0.073 inch. The tests made on one size of conductor and insulation are given in Table II. These values are plotted in Figure 4.

Table II. Summary of Tests Made on Coils for Ultimate Temperature Rises in Different Oil Temperature

(0.435-by-0.095-inch) P .012 C .007 Insulation

Amp	Watts Per Pound, W_c	Hot-Spot Temp, Deg C	Adjacent Oil, Deg C	Hot-Spot Temp Rise Over Oil, Deg C Test
25-deg-C oil				
60	4.88	36.9	24.9	12.0
100	14.2	50.3	24.9	25.4
140	29.6	67.6	25.0	42.2
202	68.0	98.5	25.7	72.8
250	113.8	129.4	27.3	102.1
70.5-deg-C oil				
60	5.66	80.0	70.5	9.5
100	16.3	90.8	70.8	19.5
140	33.6	106.3	70.5	35.7
207	79.8	137.5	70.2	67.1
250	122.4	156.7	71.2	85.5

Cooling After Fault Condition

Where temperature rise varies directly with the loss, the cooling can be calculated by the formula

$$\Theta = \Theta_i \epsilon^{-t/B} \qquad (2)$$

where

Θ = temperature rise at any time t
Θ_i = initial temperature rise over oil
t = time of cooling in minutes
B = time constant, for time in minutes

$$B = \frac{\Theta_i C}{W_0}$$

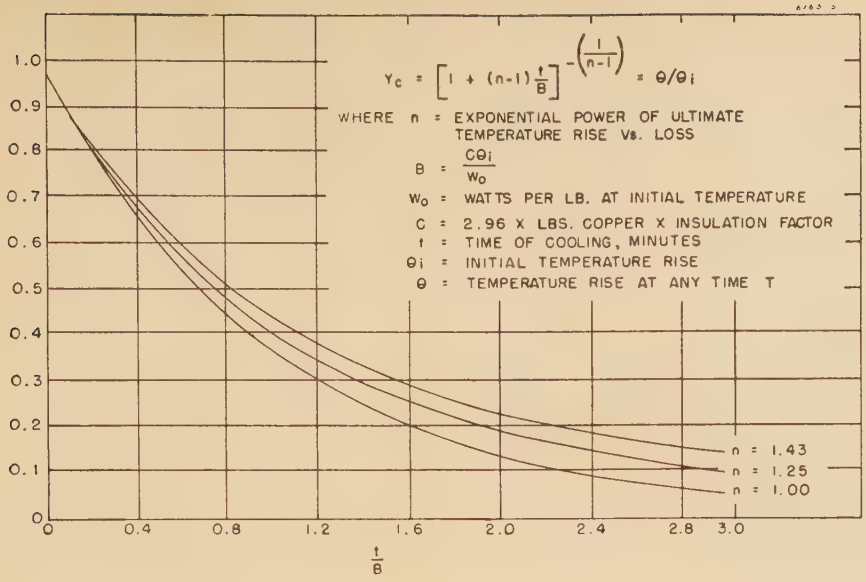

Figure 5. Cooling curves for windings in which loss = $k\Theta^n$, where n varies from 1 to 1.43

C = thermal capacity of one pound in watt-minutes of copper plus adjacent insulations

W_0 = watts per pound of copper required to produce an ultimate rise equal to Θ_i

However, when temperature rise varies with loss raised to a power in the order of 0.8 or less, equation 2 does not apply, and an equation of the following form applies:

$$Y_C^* = \left[1 + (n-1)\frac{t}{B}\right]^{\frac{-1}{n-1}} \qquad (3)$$

where

$Y_C = \Theta/\Theta_i$

n = exponent of ultimate temperature rise Θ versus loss

$$B = \frac{C\Theta_i}{W_0}$$

Figure 5 gives a plot of Y_C versus t/B when $n = 1.43$, that is, 1/0.7, 1.25, and 1.0.

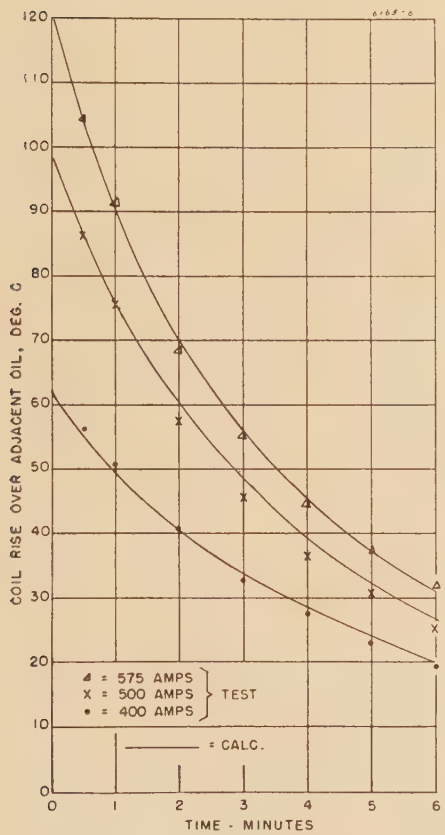

Figure 6. Curves of tested and calculated cooling after 1-minute heating tests

Tests made in 24-degree-centigrade oil
Size of conductor, 0.435 by 0.095 inch
Solid line calculated by equation 3

Example of Calculated Cooling

Assume a temperature rise of 67 degrees centigrade in 71-degree-centigrade oil. At the end of an overload where 67 degrees centigrade is the initial rise for the cooling cycle, the copper loss by Figure 4 is 80 watts per pound.

The value of C (thermal capacity of copper and insulation) for (0.435 inch by 0.095 inch) conductors with 0.019-inch two-sides thickness of turn insulation, is by previous statement

$$C = 2.96\left(\frac{0.0518+0.0408}{2\times 0.0408}\right) = 3.36$$

Other tests not reported in this paper show that the spacers add approximately 10 per cent to the thermal capacity. That is,

$$C = 3.36\times 1.1 = 3.7$$

*See Appendix II for derivation.

Therefore

$$\frac{1}{B} = \frac{80}{3.7\times 67} = 0.322$$

A comparison between the tested and calculated values (by equation 3) is shown in Table III.

Table III

t	$\frac{t}{B}$	Y_C	Temp Rise, Deg C $Y_C\Theta_i$ Calculated	Test
0	0	1.0	67.0	67.0
½	0.161	0.86	57.5	57.0
1	0.322	0.735	49.2	49.0
2	0.644	0.565	38.0	38.5
3	0.966	0.445	30.0	30.8
4	1.288	0.353	23.6	25.4

Figures 6 and 7 give the tested and calculated cooling curves for six different tests made in 25- and 71-degree-centigrade oil.

Cooling of Windings Having Few or No Cooling Ducts

Tests made on a typical poorly ventilated coil stack consisting of a number of coils of 3.625 inches radial build, assembled without cooling ducts and having several thermocouples embedded between the coils, gave maximum ultimate internal temperature rises as shown in Table IV. The wire size was 0.400 by 0.040 inch with 0.021-inch two-sides thickness of turn insulation.

Then

$$O = 2.96\left(\frac{A+a}{2a}\right)$$

$$= 2.96\left(\frac{0.0416}{0.032}\right)$$

$$= 3.85$$

and

$$\frac{1}{B} = \frac{9.8}{3.85\times 115}$$

$$= 0.0222$$

The value of 0.0222 for $1/B$ should be about the minimum that would occur in poorly ventilated coils.

The hot-spot temperature rise over oil versus watts per pound shown in Table IV is given in Figure 8. The rises for 30-degree-centigrade oil were corrected by varying the tested rises as the one-fourth power of the viscosity of the average oil film. The slope of the corrected curve is the same ($1/n = 0.7$) as that for ventilated coils, which is reasonable since a large part of the hottest-spot

Table IV

Amp Per Square Inch	Watts* Per Pound of Copper	Oil Temp, Deg C	Outside Surface Rise Over Oil, Deg C	Hottest Spot or Maximum Internal Temp Rise Over: Outside Surface Temp, Deg C	Hottest Spot or Maximum Internal Temp Rise Over: Oil Temp, Deg C
1,000	2.55	22.3	28	22	50
1,740	9.80	39.5	50.5	65	115.5

*At point of maximum temperature.

temperature rise over oil is in the oil film on the outside surface of the coils.

Maximum Temperature Limits for 1-Minute Faults as Governed by Aging of Insulation

Two cases have been worked out—one that cools rapidly, and one that cools slowly—with temperatures to produce the same aging of insulation in 30-degree-centigrade oil. These cases are given in Figure 9. The formula for calculating the aging by the 8-degree-centigrade rule is,

$$\text{Aging} = t\left[\frac{\epsilon^{0.0865T_2} - \epsilon^{0.0865T_1}}{0.0865(T_2 - T_1)}\right] \qquad (4)$$

where

t = time in minutes

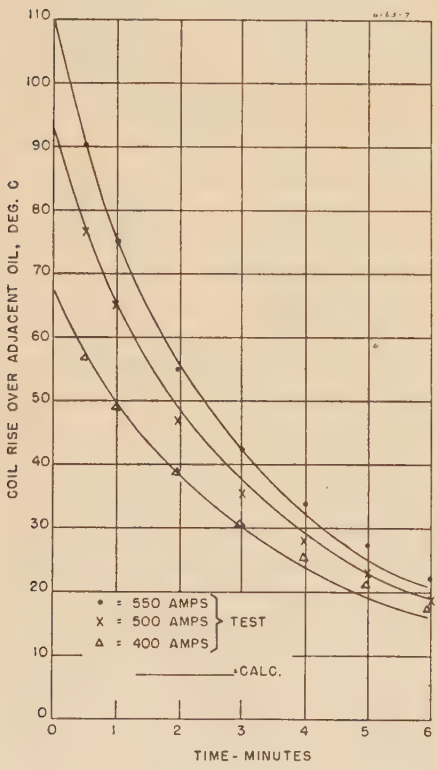

Figure 7. Curves of tested and calculated cooling after 1-minute heating tests

Tests made in 71-degree-centigrade oil
Size of conductor 0.435 by 0.095 inch
Solid line calculated by equation 3

T_2 = maximum temperature
T_1 = minimum at some value below which the aging is negligible (as for example, 100 degrees centigrade in these conditions)

The calculation of the aging for the areas represented by cooling curves A and B are as follows:

Curve A (fast cooling)

$$\text{Aging} = 2.4\left[\frac{\epsilon^{0.0865\times 202} - \epsilon^{0.0865\times 100}}{0.0865(202-100)}\right]$$
$$= 10.2\times 10^6$$

Curve B (slow cooling)

$$\text{Aging} = 27\left[\frac{\epsilon^{0.0865\times 170} - \epsilon^{0.0865\times 100}}{0.0865(170-100)}\right]$$
$$= 10.7\times 10^6$$

The quantity 10.7×10^6 is approximately 1/250 of that resulting for the time (0.0085 weeks or 86 minutes) to reduce the insulation when aged at 200 degrees centigrade to 50 per cent of initial strength as shown in Figure 4 of Clark's paper.[2] That is,

$$\text{Aging} = \frac{86\epsilon^{0.0865\times 200}}{250}$$
$$= 10.9\times 10^6$$

In other words, by Clark's data, 250 applications (10 per year for 25 years) would reduce the tensile strength to approximately half its initial value.

Curves A and B in Figure 9 shows

1. Three-quarters of the aging of the fast cooling windings occurs during the cooling period, while practically 100 per cent of the aging of the slow cooling windings occurs during the cooling period.

2. A difference of approximately 30 degrees centigrade temperature limit should be allowed between a fast cooling and the slowest cooling windings.

3. The temperature limit should be approximately the same for heating periods or faults of one minute or less duration.

Aging Curves and Temperature Limits

Figures 10A, B, C, and D show four aging curves, two for an ambient temperature of 30 degrees centigrade and two for an ambient temperature of 75 degrees centigrade, two for 0.019-inch insulation and two for 0.073-inch insulation. These curves show the relative aging on a per unit basis for one event, for varying temperatures, and both for a 10-second and a 1-minute heating time. On a basis of ten events per year, the relative aging per event would be 0.1 and the corresponding temperature limits are as follows:

Insulation	Temp Limit, Deg C: For 30-Deg-C Oil Temp	Temp Limit, Deg C: For 75-Deg-C Oil Temp
0.019	205	201
0.073	196.5	192.5

The coil having 0.019 insulation may be looked upon as a representative of a fast cooling winding so that actual temperature rises of 175 and 125 degrees centigrade may be permitted for 30 and 75 degrees centigrade ambient temperatures respectively.

However, the temperature rise for the 0.073 insulation coils does not represent adequately the performance of a slow cooling coil. In Figure 11 are shown the cooling curves of these four cases with the temperature limit for a relative aging of 0.1 marked by a dot. It is quite evident that the coils both are cooling rapidly.

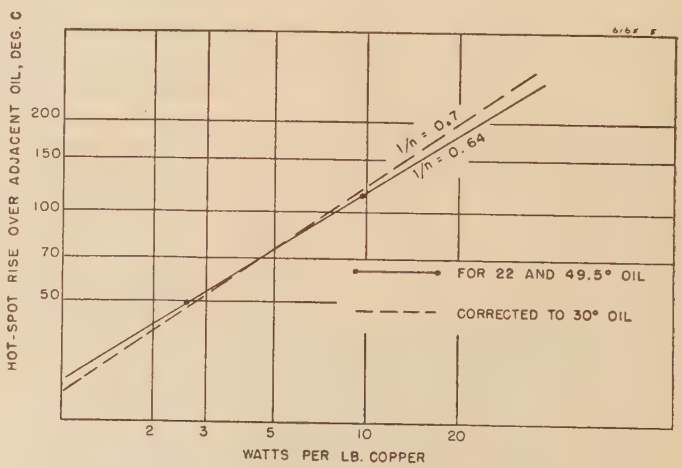

Figure 8. Ultimate temperature rise of disk coil stack having no oil ducts—slow cooling winding

Conductor size, 0.400 by 0.040 inch, 0.021-inch insulation
Radial build of coils 3.625 inches
Hottest-spot temperature determined by thermocouples between coils

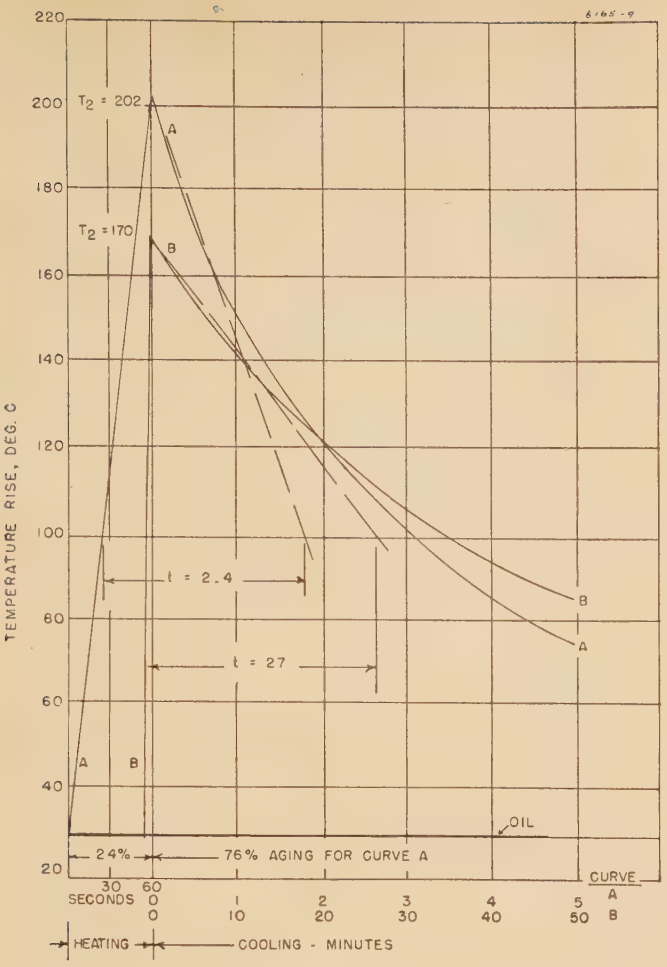

Figure 9. One-minute heating and cooling of windings to produce same amount of aging of insulation

Aging by equation 1
A—Fast cooling winding, 10.2 × 10^6 units
B—Slow cooling winding, 10.7 × 10^6 units
Note:
Heating assumed a straight line
Cooling calculated by equation 3
Initial loss taken from Figure 4 for *A*, and from Figure 8 for *B*

It has been proposed in the current revision of AIEE Standard 32 that coils without ducts be restricted to a rise 25 degrees centigrade less than that obtained for coils with ducts (well-ventilated), or as they may be termed, fast cooling coils. However, this decrement should be taken below the value for the 0.073-inch insulated coils, and the temperature rises then would be 140 and 90 degrees centigrade for ambient temperatures of 30 and 75 degrees centigrade respectively. These permissible temperature rises give ultimate temperatures of 170 and 165 degrees centigrade, slightly higher than those formerly allowed in AIEE Standard 32 when no distinction was made in reference to the rate of cooling.

Basis for Setting Temperature Limits Under Fault Conditions

Temperature limits for windings having any rate of cooling can be based on the initial rate of cooling as determined by the thermal capacity of the windings and the relationship of loss and ultimate rise as shown in the following discussion.

Since practically all the aging occurs during the cooling part of the cycle, it is logical to associate the temperature limit requirements with the rate of cooling. A reasonable criterion for the rate of cooling to determine the suitability of the windings for the temperatures proposed in AIEE Standard 32 is that the time to cool a specified initial part of the cooling range be no greater than a specified amount when calculated by a standardized method.

According to curves *A* and *B*, Figure 9, the time to cool the first ten per cent of the cooling range can be estimated close enough for practical purposes by the following formula:

$$t = k\left(\frac{\Theta_i C}{W}\right) \qquad (5)$$

where

t = time in minutes
k = 0.11 (representing ten per cent cooling + one per cent factor)
Θ_i = initial temperature rise over oil
C = thermal capacity of copper + insulation
W = watts per pound of copper dissipated at a temperature of Θ_i

For example, for curve *A*, Figure 9

where

Θ_i = 172 degrees centigrade (202 − 30)
C = 3.7
W = 225 (Figure 4)

$$t = 0.11\left(\frac{172 \times 3.7}{225}\right)$$

= 0.31 minute, or 18.6 seconds as compared with 18 seconds, curve *A*, to cool 17.2 degrees centigrade

For curve *B*

where

Θ_i = 140 (170 − 30)
W = 12 (Figure 8)
C = 3.85

$$t = 0.11\left(\frac{140 \times 3.85}{12}\right)$$

= 4.95 minutes as compared with 4.8 minutes, curve *B*, to cool 14 degrees centigrade

Appendix I. Short-Time Heating Calculations

For a constant current, and when all heat is stored in copper or in copper plus associated insulations, the increase in temperature of copper can be calculated by the following formulas:

Based on Watts Per Pound of Copper

The time t required to produce any temperature rise may be calculated by the following expression:

$$t = \left[\frac{C}{W_0(1-E_0)a_0}\right] \times \frac{1}{2}\log_e\left[(1+a_1\Theta)^2(1-E_0)+E_0\right] \qquad (6)$$

in which

t = time to heat up to a temperature rise of Θ degrees centigrade from a starting temperature of Θ_0
C = thermal capacity of one pound of copper and associated insulations (if C is in watt-seconds t is in seconds, if C is in watt-minutes t is in minutes)
W_0 = total loss in watts per pound at the starting temperature
E_0 = eddy current loss at starting temperature per unit in reference to W_0
a_0 = temperature coefficient of copper at starting temperature
Θ = temperature rise, degrees centigrade

$$\frac{1}{a_0} = 234.5 + \Theta_0$$

$$1 + a_0\Theta = \frac{234.5 + \Theta + \Theta_0}{234.5 + \Theta_0}$$

Θ_0 = starting temperature

The calculations will be simplified and on the conservative side if the measured loss is used for W_0 and the eddy current loss neglected. The expression then becomes

$$t = (234.5 \times \Theta_0)\frac{C}{W_0} m \log\left(\frac{234.5 + \Theta_0 + \Theta}{234.5 + \Theta_0}\right) \qquad (7)$$

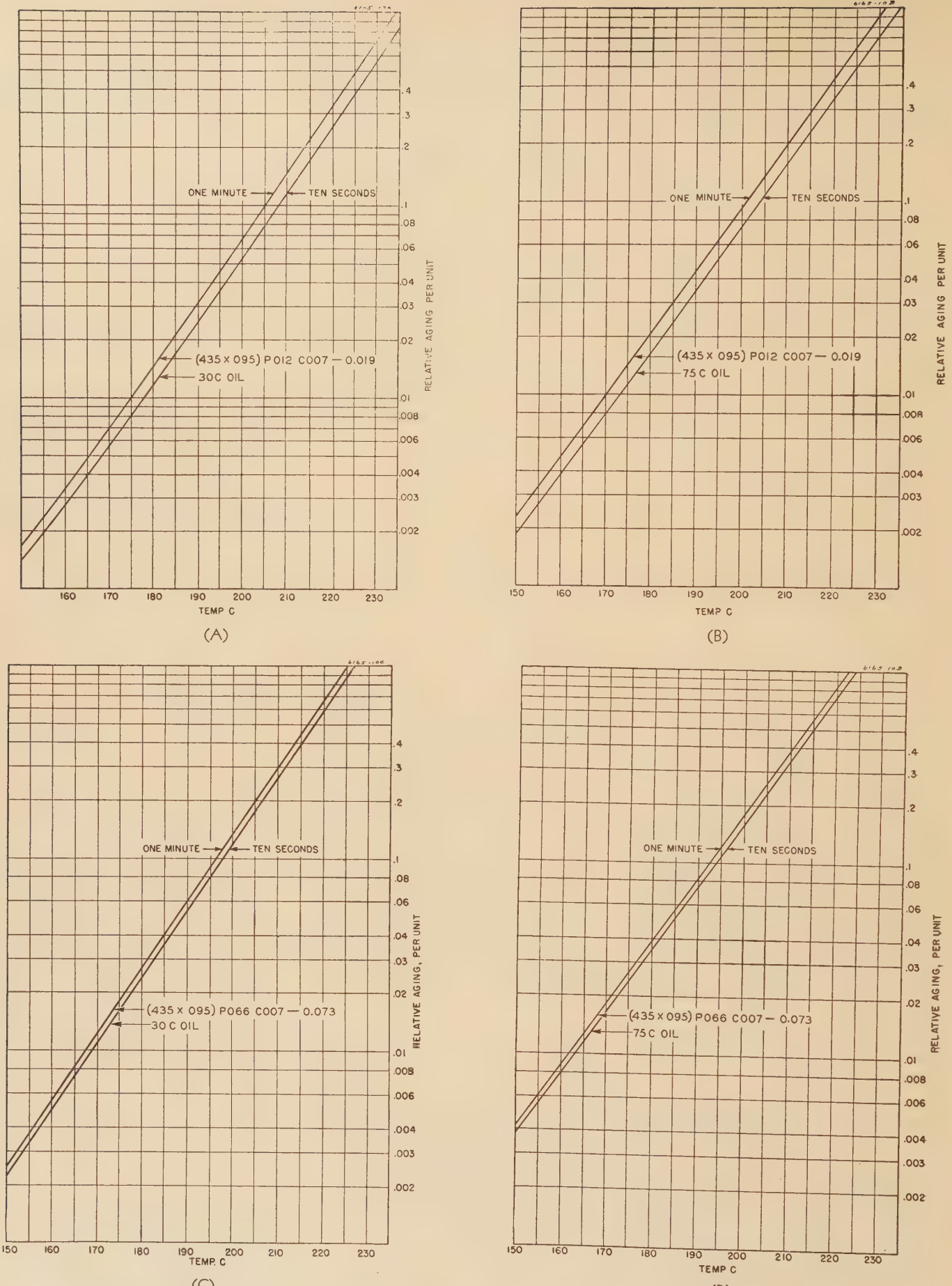

Figure 10. Relative aging curves for two thicknesses of conductor insulation at 30- and 75-degree centigrade oil

Relative aging—one unit = one year at 95 degrees centigrade

or

$$\Theta=(234.5+\Theta_0)\left[\log^{-1}\left(\frac{tW_0}{mC(234.5+\Theta_0)}\right)-1\right] \quad (8)$$

in which

t = time in minutes
C = thermal capacity of copper and associated insulation in watt-minutes per pound of copper
W_0 = watts per pound of copper at starting temperature Θ_0, total based on loss measurement

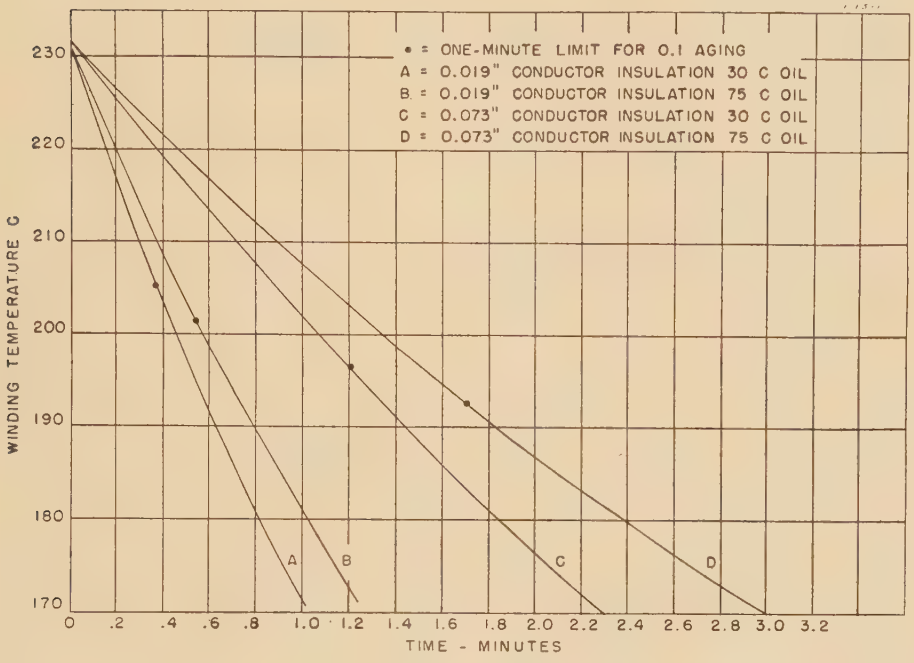

Figure 11. Cooling curves for coils shown in Figure 10

Θ_0 = starting temperature
Θ = temperature rise at end of time interval t
log = common logarithm
m = conversion factor from common to natural logarithms = 2.3026

Based on Amperes Per Square Inch

When the eddy loss is negligible and the current density is known, the temperature rise can be calculated by

$$\Theta=\log_{10}{}^{-1}\left[2.00D^2t10^{-11}+\log_{10}(\Theta_0+234.5)\right]-(234.5+\Theta_0) \quad (9)$$

where

Θ = temperature rise over the starting temperature, Θ_0
D = current density in amperes per square inch
t = time in seconds
Θ_0 = initial temperature, degrees centigrade

When the adjacent insulation absorbs some heat

$$\Theta_c=R_c\Theta$$

where

Θ_c = temperature rise with insulation factored
R_c = ratio of thermal capacity of copper to that of copper plus adjacent insulation when conductor insulation only is factored

$$R_c=\frac{2a}{A+a}$$

where

A = cross section of insulated conductor
a = cross section of bare conductor

Appendix II. Cooling Calculations

Following is the derivation of formulas for calculating the cooling of a winding where the ultimate rise is not directly proportional to the loss:

C = heat storage capacity of winding, watt-minutes per pound per degree centigrade
K = heat transfer coefficient, winding to oil, watts per pound (per degree centigrade)$^{n'}$
Θ = temperature rise of winding, degrees centigrade
Θ_i = initial temperature rise of winding at start of cooling period
t = time after start of cooling, minutes
n = exponent of ultimate temperature rise Θ versus loss
$K\Theta^n$ = heat loss, winding to oil, watts per pound

Differential equation:

$$K\Theta^n dt=-Cd\Theta$$

$$\frac{d\Theta}{\Theta^n}=-\frac{K}{C}dt \quad (10)$$

Solution:

$$\frac{\Theta^{1-n}}{(1-n)}=\frac{\Theta_i{}^{1-n}}{(1-n)}-\frac{K}{C}t$$

$$\left(\frac{\Theta}{\Theta_i}\right)=\left[1+\frac{(n-1)K\Theta_i{}^n}{C\Theta_i}t\right]^{\frac{-1}{1-n}} \quad (11)$$

If W_0 = watts per pound to maintain steady-state temperature rise Θ_0, then

$$W_0=K\Theta_i{}^n$$

and equation 11 becomes

$$\Theta=\Theta_i\left[1+(n-1)\frac{t}{B}\right]^{\frac{-1}{n-1}} \quad (12)$$

where

$$B=\frac{\Theta_i C}{W_0}$$

References

1. Temperature Limits for Short-Time Overloads for Oil-Insulated Neutral Grounding Reactors and Transformers, **V. M. Montsinger.** AIEE Transactions, volume 57, 1938, January section, pages 39-44.

2. Factors Affecting the Mechanical Deterioration of Cellulose Insulation, **F. M. Clark.** AIEE Transactions, volume 61, 1942, pages 742–9.

3. Loading Transformers by Temperature, **V. M. Montsinger.** AIEE Transactions, volume 49, 1930, pages 776–90.

4. Cooling of Oil-Immersed Transformer Windings After Shutdown, **V. M. Montsinger.** AIEE Transactions, volume 36, 1917, pages 711–30.

Long-Distance Power Transmission as Influenced by Excitation Systems

C. CONCORDIA
MEMBER AIEE

S. B. CRARY
FELLOW AIEE

F. J. MAGINNISS
ASSOCIATE AIEE

THE renewed attention now being given to transmission of power from hydroelectric sites located at moderate and long distances from their load areas requires a re-evaluation of some of the factors affecting power system stability. This paper shows that the electrical loadings of long distance transmission systems may be increased a significant amount by the use of automatically controlled excitation and proper co-ordination of the apparatus characteristics.

About 20 years ago, particularly during the years 1924, 1925, and 1926, many papers and discussions were presented before the AIEE dealing with the problems of long distance transmission. During this period most of the important factors which influenced the problem, particularly stability, were discussed and methods of analysis described. Much attention[1-7] was given to the use of intermediate synchronous condensers provided with quick acting voltage regulators of the vibrating type.

Since this earlier period, several developments have taken place which make it desirable to reconsider the use of automatically controlled field excitation as a means for increasing the stability power limits of transmission systems. Most important of these has been the development of the continuously acting static type of voltage regulator.[8] During the last war, such voltage regulating means were applied successfully to an important type of naval vessel using electric propulsion.[9] Prior and subsequent to this application, analyses[10] and tests were made which bore out the practicability of using lower short-circuit ratio synchronous machines for this type of drive than would be possible without a specially designed excitation system. Following this experience, tests were made on hydroelectric generators indicating that the static type of continuously acting voltage regulator with a properly co-ordinated excitation system can increase substantially the power limits. This progress, combined with methods of analysis now available, lends encouragement to realizing higher power loadings on long distance a-c transmission systems, and can be expected to bring to fulfillment the predictions of the earlier investigators. Furthermore, it is now possible to determine the power limits of a system as influenced by automatic control devices more readily and accurately by making use of available a-c network and differential analyzers.[11, 12]

This paper presents an analysis of two types of systems. The first is a system which transmits power a moderate distance of 200 miles over two parallel lines with one intermediate switching station. This analysis shows the relative benefits to be realized from quick fault clearing and excitation response. This study was made using a differential analyzer[13] for determining the characteristics of the system with various excitation system parameters. The second system analyzed transmits power over a single-circuit 600-mile transmission line with intermediate synchronous condensers using controlled field excitation, and compares these results with those obtainable without such compensation. This latter part of the study was made with the aid of an a-c network analyzer[14] and is an extension of previous work presented in reference 15. The effect of intermediate synchronous condenser capacity, its location along the line, reactance, and excitation system characteristics are studied. It is shown that with low-transient-reactance synchronous condensers with properly controlled field excitation, an entirely practical method of increasing the power limit becomes available which requires consideration along with other methods of increasing the stability limits. This method of compensation by intermediate synchronous condensers becomes practical because of the ability now to design reliable voltage regulating means which will, in effect for stability purposes, closely approach holding the field flux linkages constant and under some circumstances the terminal or regulated voltage point.

Summary and Discussion of Results

The two systems selected for study are typical of two types of long distance transmission. The first, consisting of a 200-mile double circuit line with an intermediate switching station, is representative of a system designed for reliable power delivery from a hydroelectric site to a load area. The second, consisting of a 600-mile single circuit line, may be taken as representative of long distance transmission when full advantage is taken of the reserve generating capacity of the load area to minimize the cost of such transmission. Such a system may be given careful consideration because of the greatly improved reliability of high voltage transmission lines and the general necessity for reserve generating capacity in the load area.

Although space limitations do not allow a full detailed presentation of the results of these studies, a few selected cases will be used for illustration.

200-Mile Double-Circuit Line

Four typical differential analyzer runs will be described to illustrate the performance of the system of Figure 1 following a 3-phase fault near the generator

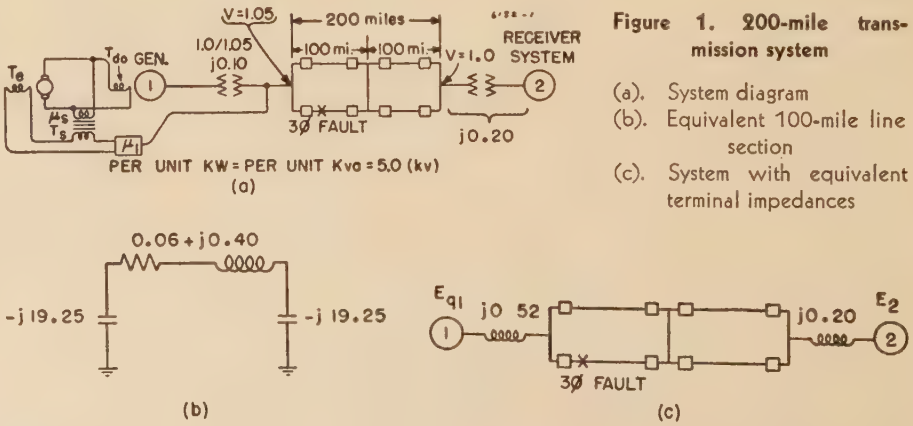

Figure 1. 200-mile transmission system

(a). System diagram
(b). Equivalent 100-mile line section
(c). System with equivalent terminal impedances

Paper 46-182, recommended by the AIEE committees on power generation and power transmission and distribution for presentation at the AIEE Pacific Coast meeting, Seattle, Wash. August 27–30, 1946. Manuscript submitted June 21, 1946; made available for printing July 11, 1946.

C. Concordia, S. B. Crary, and F. J. Maginniss are with the central station engineering divisions, General Electric Company, Schenectady, N. Y.

The authors wish to acknowledge the assistance given them by Miss Phyllis Fox, Mrs. Doris Stupp, Mrs. Shirley Sutphen, and members of the a-c network analyzer and differential analyzer staffs.

high-voltage bus. See discussion under "Analysis" for a description of method and system quantities. The system per unit kilowatt and kilovolt-ampere base is 5.0 × (kv)² which for a 230-kv system corresponds to 264,500 kw and kva, and for 360 kv corresponds to 650,000 kw and kva.

For each differential analyzer run the following plots were made:

1. Relative electrical angular displacement between the generator and receiving end system versus relative angular velocity, that is, δ_{12} versus $\frac{d\delta_{12}}{dt}$.

2. Relative electrical angular displacement between the generator and receiving end system versus time, that is, δ_{12} versus t.

3. Generator electrical angular displacement versus time, that is, δ_1 versus t.

4. Generator field flux linkages versus time, that is, e_{q1}' versus t.

5. Generator field current versus time, that is, e_{f1} versus t.

Figures 5 to 8 inclusive show the differential analyzer plots for the four runs summarized in Table I.

Figure 5 as indicated by Table I is for the case of the generating station initially carrying unit power with no regulator and having a total fault clearing time of 0.07 second. Figure 5A shows the oscillation between the per unit relative angular velocity and the relative angular displacement. As shown, the system is initially stable and has a damped oscillation which is decaying to about 90 degrees. From this plot stability may or may not be maintained, depending upon whether or not the field flux linkages will be reduced further. Figures 5B and 5C show the oscillation of δ_{12} versus time and δ_1 versus time. As shown by Figure 5B, the relative angular displacement indicates a damped oscillation, but the average value gradually is increasing. Figure 5C indicates the decrease in speed which results from the increased losses in the transmission line and which has not been compensated for by governor action, as change in prime mover torque was neglected during this initial period of the disturbance. Figure 5D shows the decay in field flux linkages. Initially, the decay is relatively rapid because of the fault. Following the clearing of the fault, the linkages continue to decrease and, as indicated, still are decaying gradually at the end of 5.5 seconds. This continual decay of flux linkages indicates that stability will be ultimately lost although it was maintained during the first three swings. Figure 5E shows the oscillation in generator field current. Initially there is a rise in the d-c component of field current induced by the short circuit (the a-c components were neglected), and then an oscillation following the clearing of the fault resulting from the rotor oscillation. As shown, the average field current is above the initial value indicating that there is a component of induced current resulting from the gradual increase in relative angular displacement of the rotor. All of these results confirm the indication that stability cannot be maintained even for this loading if no regulator is used. Other runs show that with a regulator, even if the excitation response is very low, stability can be maintained for such a case as Figure 5.

Table I. Summary of Differential Analyzer Runs Used for Illustration

Figure	Run Numbers	P_t	T_e, Sec	t_s, Sec	Remarks
5	48, 76	1.00	∞	0.07	No regulator
6	83	1.05	∞	0	No regulator
7	51, 57	1.10	0.73	0.03	Regulator and stabilizer
8	51, 58	1.10	0.73	0.04	Regulator and stabilizer

Figure 6 is similar to Figure 5 in that no regulator is used. The loading has been increased to 1.05 per unit. The fault clearing time is zero corresponding to "no fault" or merely opening a generator-end transmission-line section. As indicated by Figure 6A, although stability is maintained during the first three swings of the oscillation, it is subsequently lost because the angular displacement after the third swing increases indefinitely. The curves of Figure 6 can be compared with those of Figure 5 to show the effect of a slightly higher initial loading with a reduced switching time. As shown by Figure 6D the field flux linkages show a definite trend downward. Figure 6E shows the induced field current resulting from the oscillation and the displacement of the average current from the initial value resulting from the gradual increase in average relative angular displacement.

It is evident from a comparison of Figures 5 and 6 that the conditions of Figure 5 are less unstable but may be considered to be very near the critical load when no regulator is used. Both of these cases, as is shown by other runs, are stable even with a relatively slow excitation system response.

Figure 7 is for the case of higher loading ($P = 1.1$) than for the cases of Figures 5 and 6. For $P = 1.1$, a regulator using an excitation system stabilizer is used and the excitation system time constant is of moderate value ($T_e = 0.73$ second). This corresponds to a per unit excitation system response of approximately 1.0. During the first swing and subsequently stability is maintained, the oscillation being damped out toward a final steady-state value. This is borne out by the other curves of Figure 7, with the field flux link-

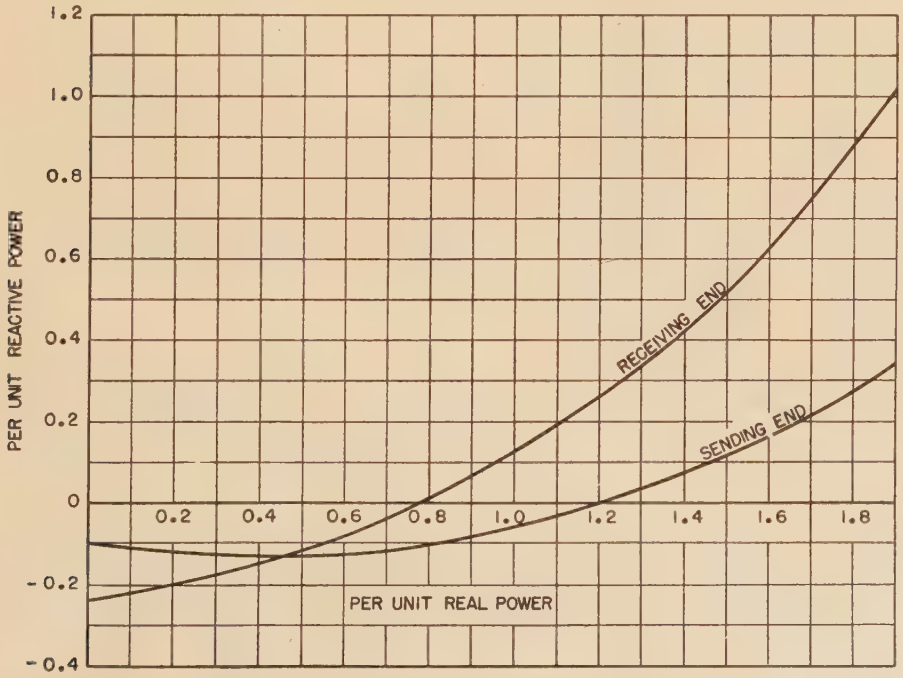

Figure 2. Transmission line real power and reactive power circle diagram for all line sections of both lines in operation

System of Figure 1

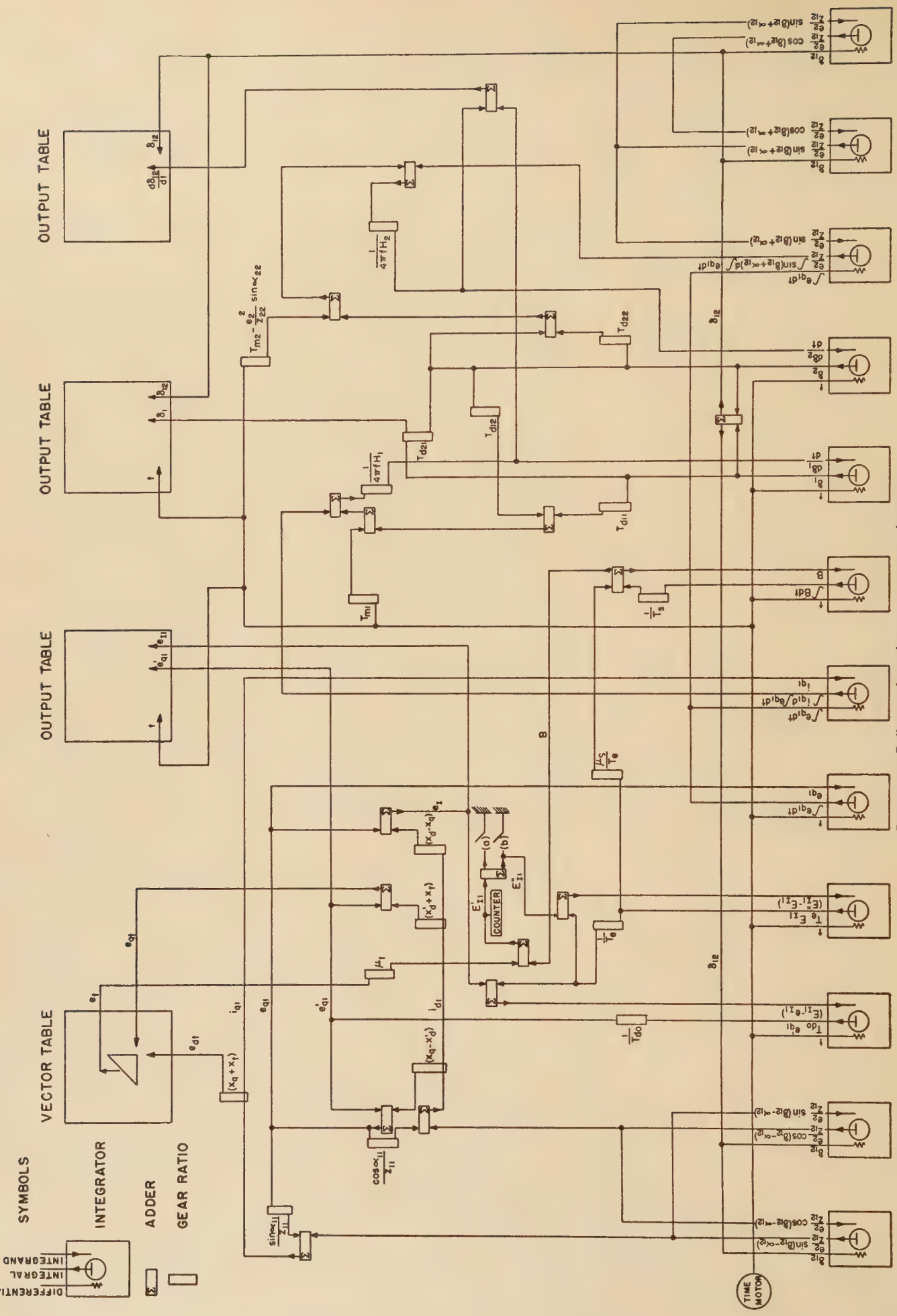

Figure 3. Differential analyzer connection diagram

ages and field current settling out to new sustained values.

Figure 8 is for a case similar to Figure 7 except that the switching time has been increased from 0.03 to 0.04 second. Stability is lost on the first swing although the field flux linkages actually are increased following the fault period resulting from the response of the excitation system.

From the results of many runs similar to these Figure 9 was obtained which shows the change in transient power limit with fault clearing time and with excitation system response. It is interesting to note that for a practical switching time for the assumed system, that is, $t_s \approx 0.08$ second or 4.8 cycles, the excitation system response does not influence appreciably the maximum power that can be carried. However, with more rapid fault clearing times, the effect of the excitation system response is more pronounced. These results may be interpreted for less severe faults by assuming the 3-phase fault to be of shorter duration than the actual switching time. That is, for a line-to-ground fault actually switched in 4.8 cycles, it would be expected that the resulting performance would be essentially not much different from that obtained with zero switching time, as the severity of a line-to-ground fault is relatively small. Also, for faults located at a distance from the high-voltage bus, the fault severity would be decreased correspondingly. The results can be interpreted therefore to indicate that greater benefits can be expected by the more rapid response excitation systems for faults of reduced severity than for very severe faults.

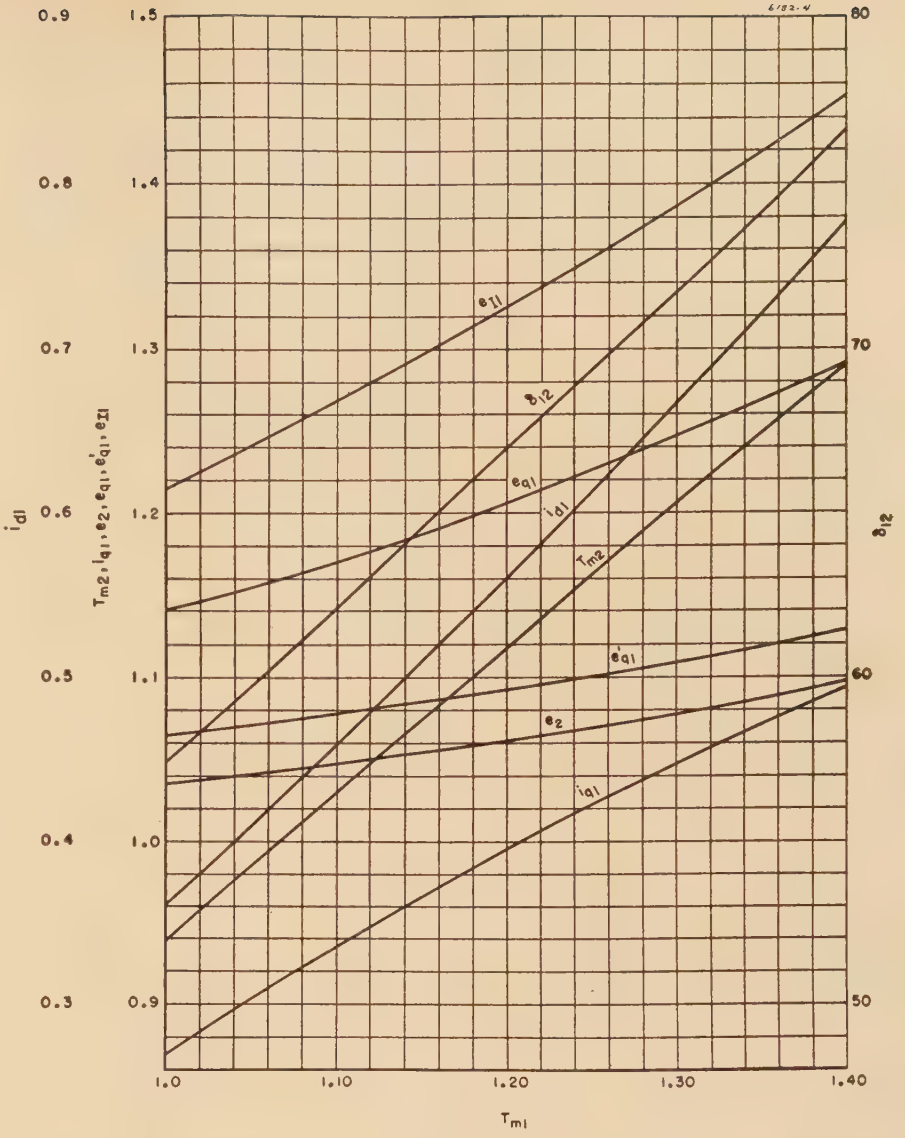

Figure 4. Initial quantities before fault

600-Mile Single Circuit Transmission

The most significant results of the study made of the effect on steady-state stability of synchronous capacity along a single circuit 600-mile transmission system are shown on Figures 15 and 16. The constants and methods used are described in more detail under Analysis and by information in the figure titles.

Figure 15 shows that for relatively low line loadings the synchronous capacity is more effective in increasing the stability limit if it is concentrated at the sending and receiving ends of the line. On the other hand, if relatively higher loadings are to be used, the same synchronous capacity is more effective if it is distributed between the sending and receiving end and the intermediate stations. Although Figure 15 illustrates the relative advantages of distributing capacity along the line to attain high transmission system loadings, it is only of theoretical interest because it is difficult to realize such an equal distribution in practice.

Figure 16, however, is of practical interest because it shows the relative advantage of distributing intermediate synchronous condenser capacity along the line for given generator and receiving system reactances. Figure 16 indicates that it is possible to transmit without intermediate condensers and typical terminal system reactances, a receiver power approaching as a limit 1.9 $(kv)^2$ or for a 230-kv line, $1.9 \times 230^2 = 100{,}000$ kw. If three intermediate synchronous condensers having a reactance including their high voltage transformer of 25 per cent on their rating with a total rating of $2.5 \times 230^2 = 132{,}000$ kva are placed along a line, their total per unit admittance is 4.0 and the steady-state power limit is increased to $2.85 \times 230^2 = 151{,}000$ kw. Such a loading is quite reasonable for a 230-kv line. If the line is operated at 360 kv, the corresponding power limit would be 369,000 kw with an intermediate synchronous capacity of 324,000 kva. Such an amount of intermediate synchronous capacity is entirely reasonable and practical.

The practicability of this method depends upon obtaining a low effective reactance as a result of being able to use a voltage regulator which in effect will hold the voltage behind transient reactance of specially designed low transient reactance synchronous condensers. If, however, it were not possible to build such low transient reactance synchronous condensers, or if it were not possible to depend on the voltage regulator characteristics, the required synchronous condenser capacity would be increased three to four times, making such a method uneconomical in comparison with other methods of line compensation.

If the total admittance of the intermediate condenser stations is increased to

12.0 per unit, then according to Figure 16 for a 360-kv line, a total synchronous capacity of about 1,000,000 kva with 25 per cent reactance would be required to increase the power limit of the 360-kv line to 475,000 kw. Table II shows the relative synchronous condenser capacity required for both a 360- and 230-kv 600-mile line for different loadings if it is assumed that special synchronous condensers may be used having a total effective reactance of 25 per cent to the high-voltage bus including the high-voltage transformer; whereas a conventional synchronous condenser would have a reactance of about 100 per cent to the high-voltage bus, or four times that of the special condenser. The synchronous capacity need not be added until the system loadings have been increased, and can be located at points which ultimately may be used as interconnection points to load areas. Because the required synchronous condenser capacity is large with respect to the reactive kilovolt-amperes required for the transmission lines, the intermediate synchronous condenser capacity also may be used for power factor correction of the tapped loads. The building of low transient reactance synchronous condensers with special excitation systems now appears entirely practical and makes it necessary to consider such a method in the design of any new long distance transmission system. However, if it were not possible to attain the special features, the required synchronous condenser capacity would become extremely large, making this method uneconomical compared with other methods.

A 600-mile line has an appreciable line charging capacity, approximately 166,000 kva for a 230-kv line and 405,000 kva for a 360-kv line. The intermediate synchronous condenser capacity also may provide the required underexcited capacity during periods of light load and thereby maintain normal voltage levels along the line.

It also is evident from Figure 16 that it may not be desirable economically to locate the synchronous condensers along the line in any more than two or three locations because of the diminishing gain realized by increasing the number of intermediate stations. Because of the relatively large required capacity, however, it becomes economically possible to locate the synchronous condensers at more than one location. A margin in the steady-state stability under automatic control may be taken so as to allow for failure of any one condenser or its excitation system and also to allow the system to ride through transient faults in the terminal systems. The required margin will depend on the requirements of the particu-

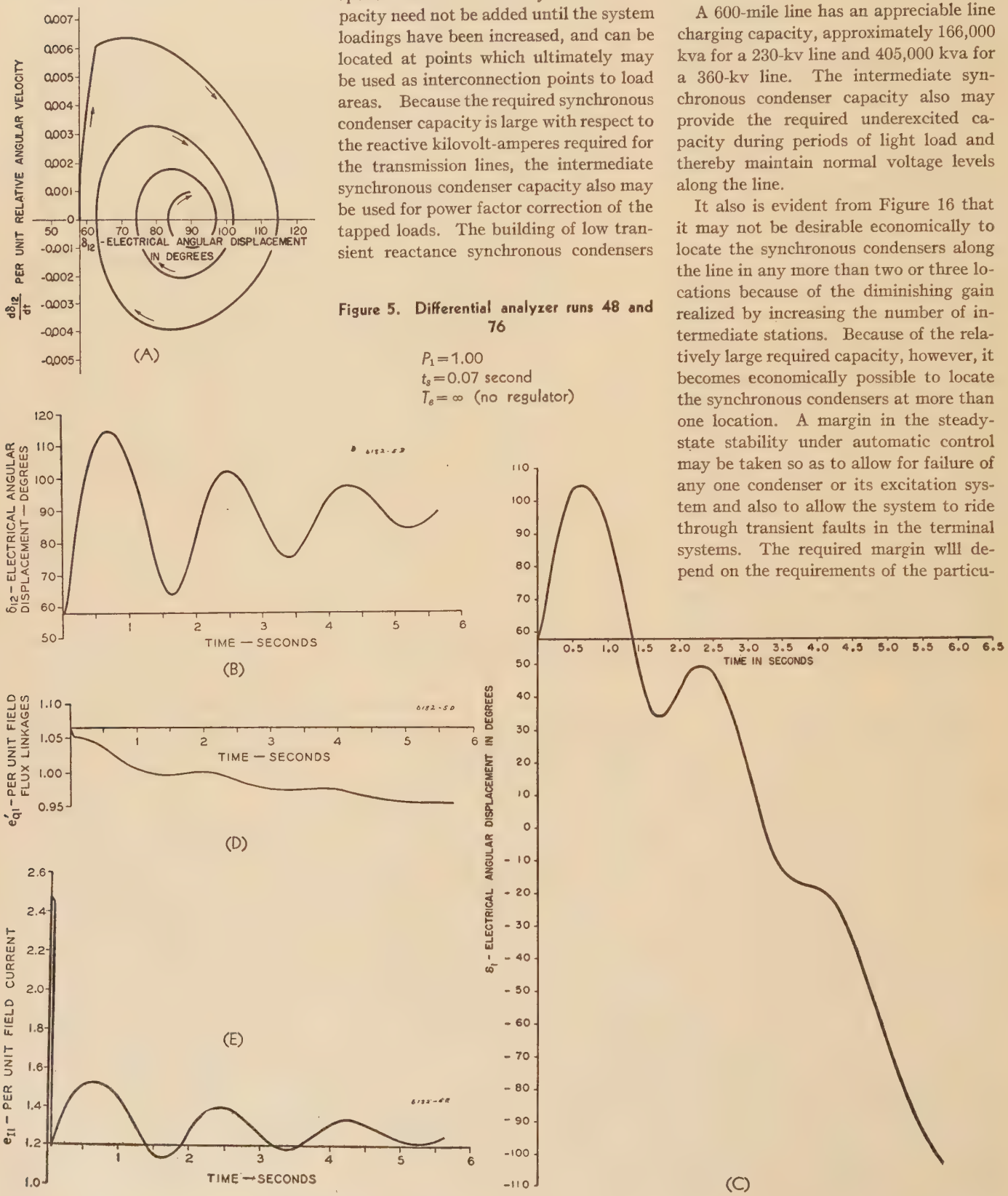

Figure 5. Differential analyzer runs 48 and 76

$P_1 = 1.00$
$t_s = 0.07$ second
$T_e = \infty$ (no regulator)

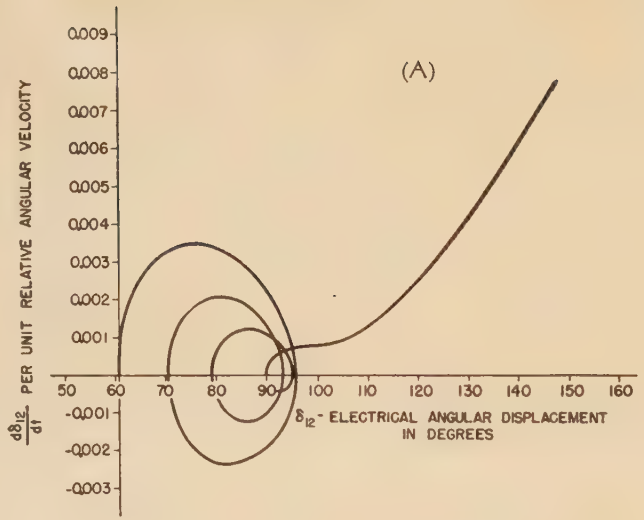

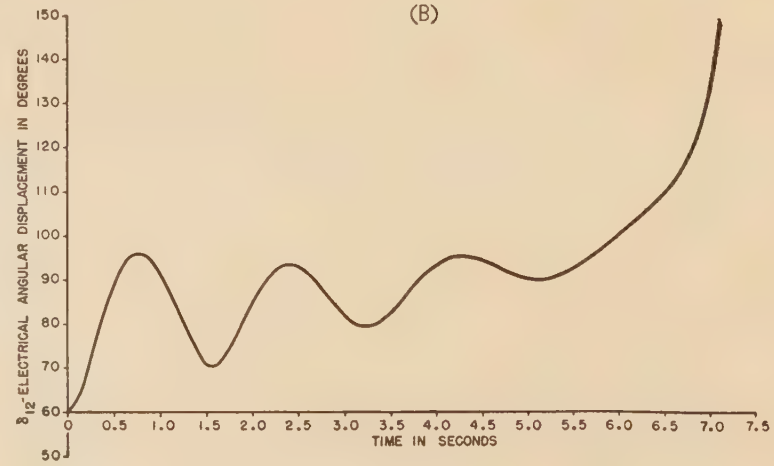

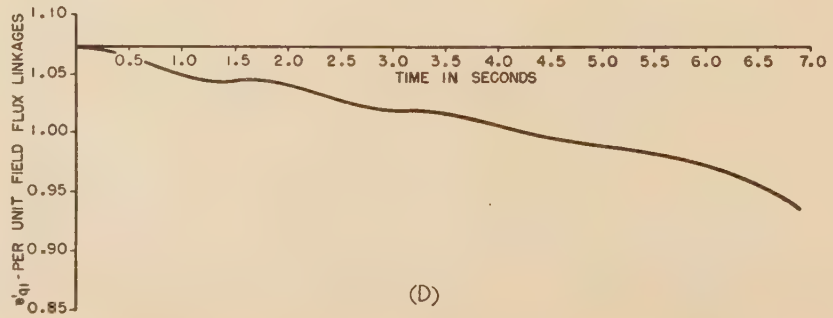

Figure 6. Differential analyzer run 83

$P_1 = 1.05$
$t_s = 0$ second
$T_e = \infty$ (no regulator)

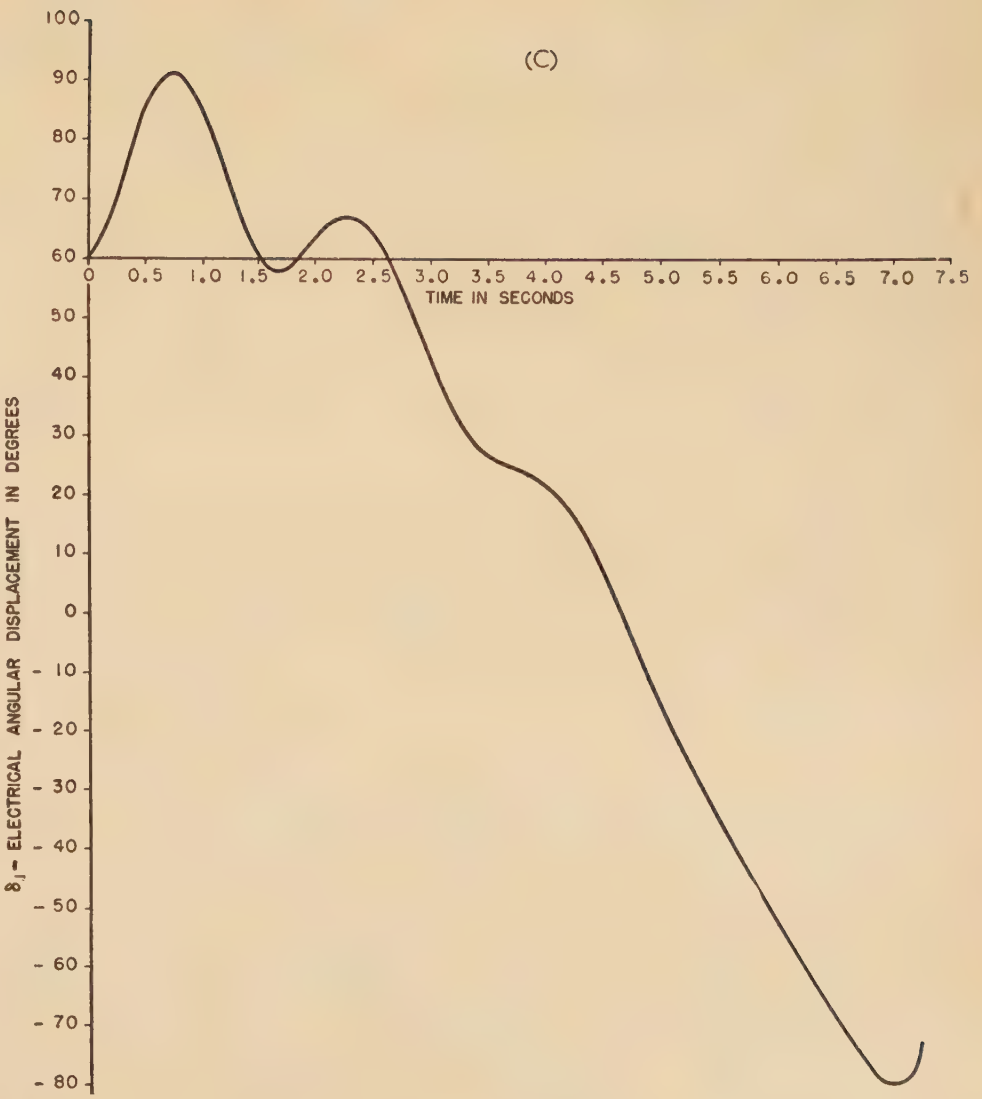

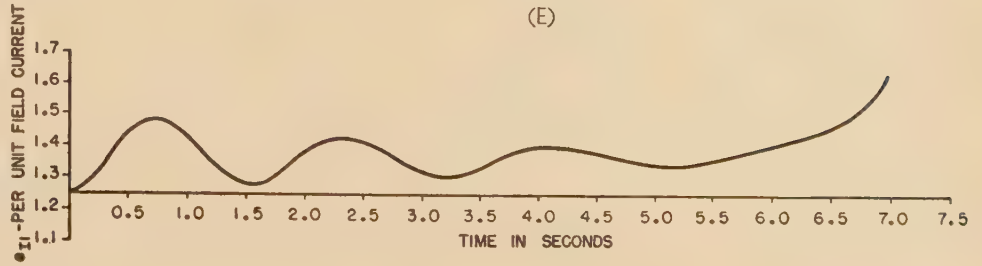

lar case under consideration and can be determined by analysis.

Conclusions

The following conclusions have been drawn from these studies:

1. For severe faults on a line section cleared as quickly as five to six cycles, little additional benefit or increase in power limit can be realized by the use of a quick response excitation system for a typical system using parallel transmission lines.

2. For less severe faults or faults of shorter duration some benefit can be realized by using high rates of excitation response. The power limit can be increased as much as 5 to 10 per cent by increasing the response from 0.5 to 2.0 per unit.

3. For a system of the type studied with parallel lines and a fault on one of the line sections, the transient resulting from switching out of a line section places a more severe limitation on the reliable or sustained power delivery than the final steady-state stability limitation corresponding to the condition of one line section out.

4. With a properly stabilized excitation system, stability will be maintained, in general, on subsequent swings if it is maintained on the first swing.

5. For a 600-mile single circuit line, special intermediate low transient reactance synchronous condensers with properly coordinated regulators and excitation systems can be used to provide a practical method for increasing the stability limits.

6. For a given synchronous condenser capacity, greater benefit is obtained if the condensers are distributed along the line. However, the improvement diminishes with increased number so that for a 600-mile line, the optimum economic number probably will be two or three.

7. A more nearly equal distribution of synchronous capacity along and at the terminals of a long distance transmission system allows for higher loadings than if this same synchronous capacity were not distributed so equally.

Analysis

The analysis given in this paper is devoted to two types of typical systems.

The first system consists of a hydroelectric station and two transmission lines with one intermediate switching station delivering power 200 miles to a load area. Consideration is given to the relative effect of fault clearing time, excitation system response, and other more detailed excitation system characteristics on both the steady-state and transient stability power limits.

The second system to be analyzed consists of a hydroelectric station delivering

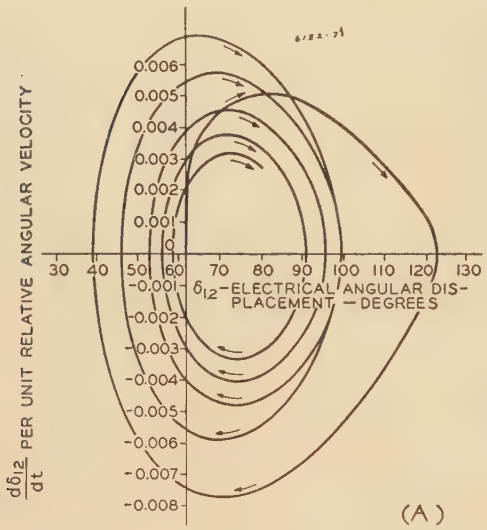

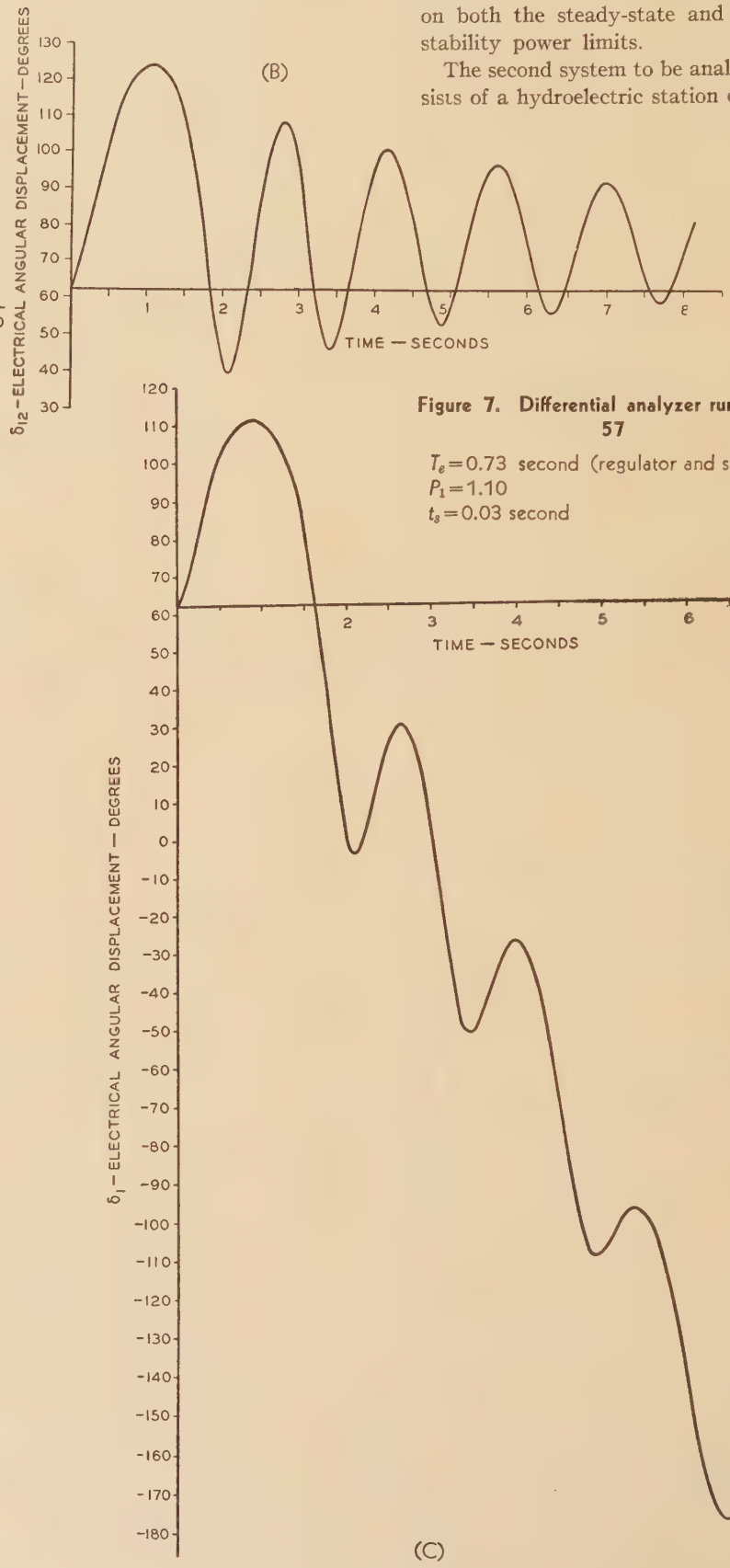

Figure 7. Differential analyzer runs 51 and 57

T_e = 0.73 second (regulator and stabilizer)
P_1 = 1.10
t_s = 0.03 second

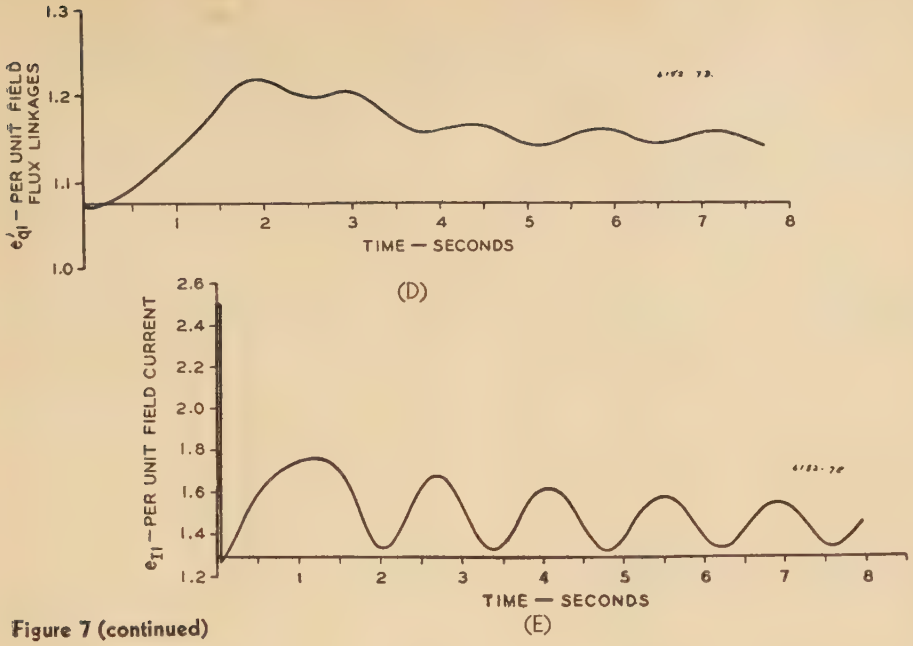

Figure 7 (continued)

power over a single 600-mile transmission line to a load area. Consideration is given to the effect of intermediate synchronous condenser stations and their location along the line on the steady-state stability limits.

Although the analysis presented in this paper is limited to these two types of systems, the results will help indicate the factors which are worthy of careful consideration in order to obtain the maximum transmission or system loading with a given amount of equipment. An economic study is not attempted because the economics depend on many local and special factors which are not always generally known. Also, the economic factors change with time and progress in the art.

200-Mile Double Circuit Transmission

The system analyzed is shown in Figure 1, consisting of a hydroelectric station delivering power to a receiver system over two 200-mile lines with one intermediate switching station. The hydroelectric station is represented by a salient pole generator with step-up transformer and an excitation system. Generator saliency is included but generator saturation is neglected. The excitation system is represented by an exciter with a given ceiling excitation voltage and lower limit of negative excitation and an exciter field time constant T_e which is varied in the study. The regulating system is represented by a regulator amplification factor of μ. This amplification factor is the ratio of the increase in per unit exciter voltage to the per unit decrease in voltage applied to the voltage sensitive element of the regulator to produce this increase in exciter voltage. For example, if 0.01 per unit change in voltage applied to the voltage-sensitive element produces a 0.10 per unit change in the exciter voltage, $\mu = 10.0$. An excitation system stabilizer is represented by an amplification of μ_s and a time constant of T_s.

The transmission line constants are typical for a 60-cycle high-voltage overhead line. The receiver system is represented by a reactance of 20 per cent and is assumed to be unregulated during the disturbance studied. The type of disturbance used as a basis for testing the system for stability is a 3-phase fault of varying duration near the generator high-voltage bus.

The assumption is made that the power angle equations may be used for determining the electric torque, which neglects the subtransient effects and the effect of the small changes from synchronous speed during the disturbance. Damping torques are introduced as independent terms and in this way the effect of change in speed on both the electrical and mechanical torque is included.

The method of analysis is outlined briefly by the following steps. A study of the data and equations will provide an understanding of the basis for the analysis.

1. System diagram, Figure 1.
2. System data, Appendix II.
3. Transmission line circle diagram (both lines, all sections in), Figure 2.
4. Characteristic system impedances, Appendix III.
5. System equations, Appendix IV.
6. Differential analyzer equations, Appendix V.
7. Different analyzer diagram, Figure 3.
8. Plot of initial conditions, Figure 4.
9. Typical differential analyzer output curves, Figures 5, 6, 7, and 8.
10. Graphical summary of results, Figure 9.

The system of Figure 1 was analyzed also for the steady-state power limit with one of the sending end transmission line sections opened, corresponding to the condition after the fault was removed. The same system equations (Appendix IV) were used to obtain relations for the condition of small variations. The system then was tested for stability by Routh's criterion and the stable and unstable regions determined for various conditions. Typical results obtained are shown by Figure 10, which shows the stable and unstable regions of generator power as a function of the regulator amplification factor μ. The system parameters for this case were the same as indicated previously except as noted in the caption of Figure 10.

600-Mile Single Circuit Transmission

Analyses of steady-state stability similar to those presented in reference 10 and in Figures 10 and 11 indicate that it is possible to operate at appreciably higher power loadings under steady-state conditions with excitation systems designed to raise the steady-state stability limits. These results indicate, in general, two limits or levels, one which readily can be realized corresponding to holding the voltage back of transient reactance, and one which is more difficult to realize corresponding to holding the regulated

Table II. Steady-State Stability Limits

600-Mile 60-Cycle Single Circuit System

230 Kilovolts			360 Kilovolts		
Power Received, Kw	Synchronous Condenser Kva		Power Received, Kw	Synchronous Condenser Kva	
	Special	Conventional		Special	Conventional
101,000	0	0	247,000	0	0
156,000	132,000	528,000	383,000	324,000	1,296,000
195,000	264,000	1,056,000	475,000	648,000	2,592,000

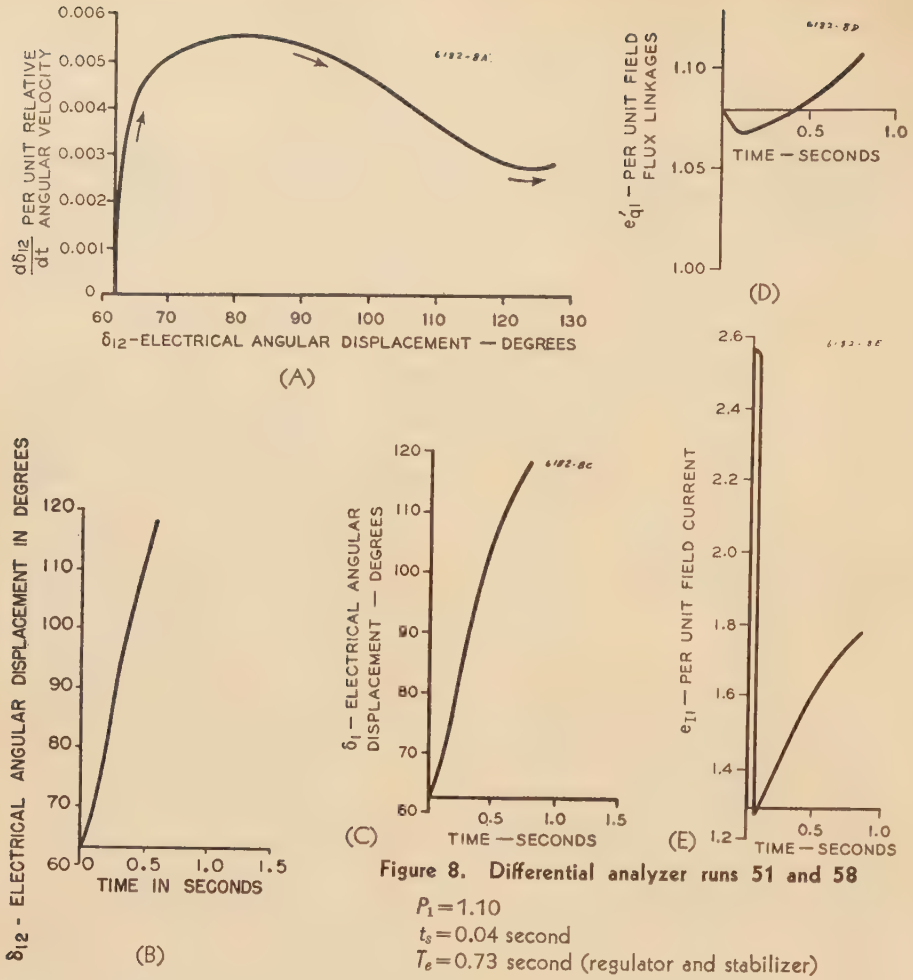

Figure 8. Differential analyzer runs 51 and 58

$P_1 = 1.10$
$t_s = 0.04$ second
$T_e = 0.73$ second (regulator and stabilizer)

function of the intermediate station and terminal systems' equivalent or effective reactances. The effect or increase in power limit caused by decreasing this effective reactance then can be studied to determine the possible gain in stability resulting from the regulating systems as well as the effect of locating the synchronous condensers along the line.

Results of a study of a 600-mile line with one and two intermediate synchronous condenser stations are given in reference 15. These results were extended by studying for the same line constants the case of three intermediate stations located along the line. The system was set up on an a-c network analyzer and the steady-state stability limit determined by the methods of reference 16 or criterion *C* of reference 17.

The titles of the figures give a summary of the system characteristics studied. Figure 12 gives the power angle characteristic, where δ_{12} is the angular displacement between the sending and receiving terminals of the line. The required reactive power for the intermediate synchronous condensers and the line terminals is shown also. The vertical lines indicate the steady-state stability limit for the indicated values of station reactances when $X_G = X_M = X_{c1} = X_{c2} = X_{c3}$. This shows the change in power limit and reactive

voltage constant. The results shown by Figure 11 obtained for the analysis in Appendix I indicate that an intermediate condenser station may be used to raise the limit of the transmission system to a level corresponding to holding approximately the intermediate synchronous condenser's voltage back of transient reactance or with high amplification factors approximately the regulated voltage point in the system. This suggests the desirability of studying the power limits of a long line with intermediate synchronous condensers as a

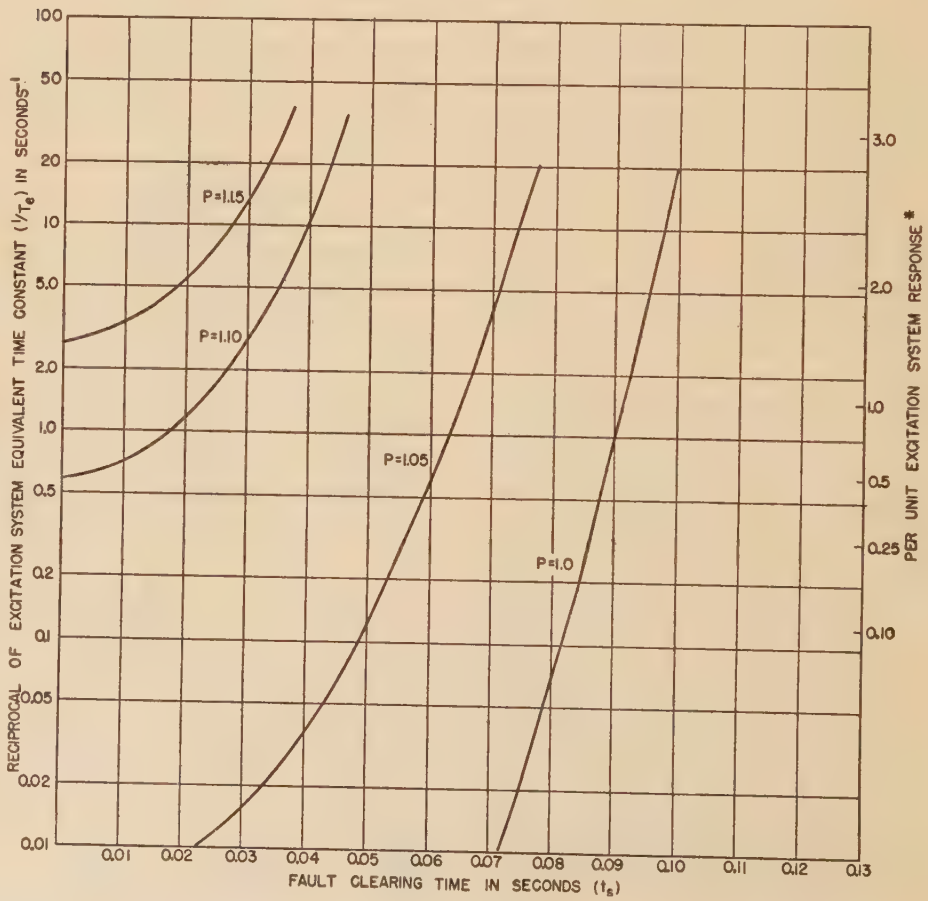

Figure 9. Summary of portion of differential analyzer results showing relation between transient power limit P_1, fault clearing time t_s, and excitation system response for 200-mile transmission system for Figure 1

These results are based on drawing curve of critical switching time for constant initial power between stable and unstable differential analyzer run points

Per unit excitation system response as plotted on right hand scale is the average rate of increase of exciter voltage during the first half second following a sudden drop in a-c regulated voltage expressed as a ratio of exciter volt-seconds and initial exciter voltage. For this scale, initial exciter voltage was taken corresponding to an initial load of $P_1 = 1.0$ and $e_{f1} = 1.217$. For an initial load of $P_1 = 1.15$ rather than 1.0 the per unit excitation response decreases only slightly, for example, from a response of 1.0 to 0.91 per unit for $1/T_e = 1.5$

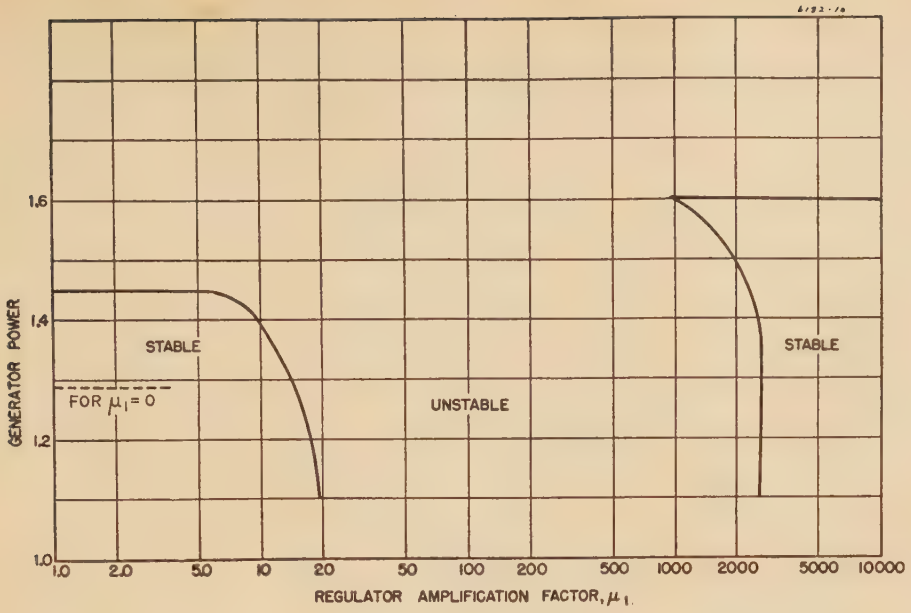

power requirement with changes in station effective reactance.

Figure 13 is similar to Figure 12 except that the sending and receiving system reactances are kept constant and the abscissa is the total angular displacement δ_{GM}. The vertical lines indicate the power limit and reactance power requirements with change in the intermediate station terminal reactance. Figure 14 is a summary of the results obtained from reference 15 and Figure 13. Figure 14 shows the change in power limit with change in intermediate synchronous condenser reactance. Figure 15 is a summary of the results obtained from reference 15 and Figure 12 with total station admittance as abscissa. This abscissa indicates the total synchronous machine capacity required if it were distributed equally between the terminal and the intermediate stations. This indicates that for higher loadings the synchronous capacity is more effective in raising the stability limit if it is distributed more equally along the line. However, for lower loadings it is more effective if it is concentrated at the ends. Figure 16 is a summary of results from Figure 14. This figure indicates that for given sending and receiving end reactances, the power limit is increased with increase in the number of intermediate condenser stations along the line for the same total synchronous condenser capacities.

Figure 10. Steady-state power limits of system of Figure 1 with one generator line section out corresponding to system condition following clearing of fault, showing effect of generator voltage regulator amplification factor

System data same as shown in Appendix II with following exceptions:

$T_{d11} = T_{d12} = T_{d21} = T_{d22} = 3.0$
$T_s = 200$ radians or 0.53 second
μ_1 = variable

Figure 11. Steady-state power limits of 3-machine stability system of Figure 17

Data as given in Appendix I

A—T_{d1} 0, $T_{d2} = 3.0$
B—$T_{d1} = 3$, $T_{d2} = 0$
C—$T_{d1} = 3$, $T_{d2} = 3.0$
D—$T_{d1} = 0$, $T_{d2} = 0$

D has only one stable region above $P = 0.6$

Nomenclature

The nomenclature used here follows that which has been established generally by previous usage. All machine and system quantities are in per unit of the designated bases unless otherwise specified.

e = voltage
e_{dt} = direct-axis component of regulated voltage
e_I = quadrature-axis voltage proportional to field current
e_q' = quadrature-axis voltage proportional to field flux linkages
e_{q1} = quadrature-axis voltage of generator back of $x_{q1}i_1$
e_{qt} = quadrature-axis component of regulated voltage
e_t = regulated voltage
E_I = quadrature-axis voltage corresponding to field voltage
f = frequency in cycles per second
H = inertia constant in kilowatt-seconds per kilovolt-ampere
i = armature current
i_d = direct-axis component of armature current
i_q = quadrature-axis component of armature current
$p = d/dt$ = differential operator
t = time in electrical radians or seconds
T = torque
T_d = damping torque
T_{do} = generator open-circuit time constant in radians or seconds
T_e = electric torque
T_m = mechanical torque
T_s = synchronizing torque or excitation system stabilizer time constant
x_d = direct-axis synchronous reactance
x_d' = direct-axis transient reactance
x_q = quadrature-axis synchronous reactance
x_t = transformer reactance
Z_{nm} = transfer impedance
Z_{nn} = driving point impedance
$\alpha = \pi/2 - \theta$
δ = electrical angular displacement in radians or degrees
θ = impedance angle
μ = regulator amplification factor
μ_s = excitation system stabilizer amplification factor

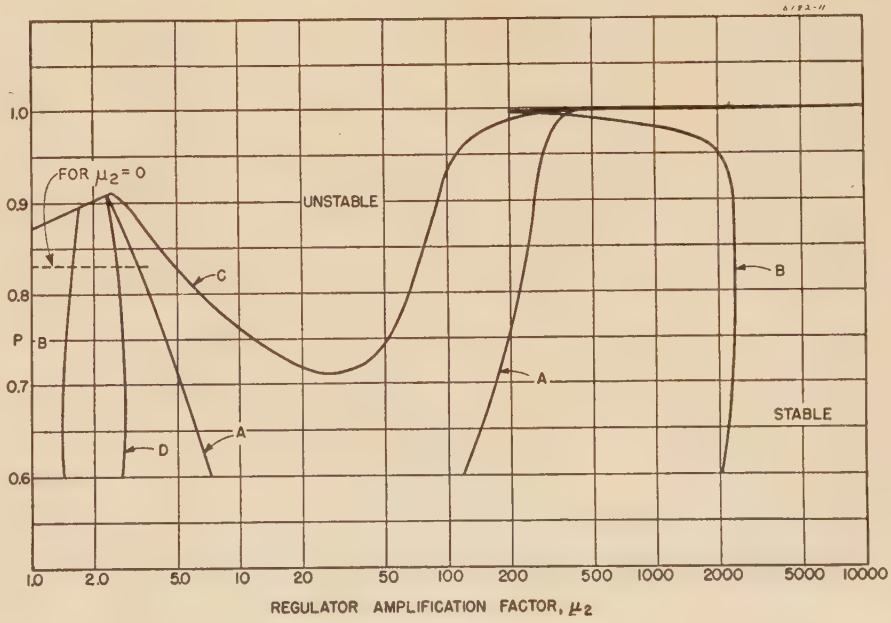

General Subscripts

d = direct-axis
q = quadrature-axis
t = regulated voltage point
1 = generator or sending end system
2 = intermediate synchronous condenser or receiving end system
0 = initial value

Appendix I. Intermediate Synchronous Condenser With Automatic Voltage Regulator

The following analysis is made to determine the effect of a voltage-regulated intermediate synchronous condenser on the steady-state stability limits of a simple type of system. Previous analyses have indicated the gains to be realized for the simple 2-machine case, whereas this analysis is for a 3-machine case.

The system to be analyzed is shown in Figure 17, only machine 2 is assumed to have transient saliency ($x_d'/x_q \neq 1.0$) and only machine 2 has controlled excitation.

The equations for the system, in accordance with the usual assumptions that the electric torque is expressible by the steady-state equation for power flow, are as follows:

$$M_1\frac{d^2\delta_1}{dt^2}+T_{d1}\frac{d\delta_1}{dt}=T_{m1}-T_{e1} \quad (1)$$

$$M_2\frac{d^2\delta_2}{dt^2}+T_{d2}\frac{d\delta_2}{dt}=T_{m2}-T_{e2} \quad (2)$$

where

$M=4\pi fH$

t = time in electrical radians at normal frequency, and

$$T_{e1}=\frac{e_1e_{q2}}{x_{12}}+\frac{e_1e_3}{x_{13}}\sin\delta_{13} \quad (3)$$

$$T_{e2}=\frac{e_{q2}e_1}{x_{12}}\sin\delta_{21}+\frac{e_{q2}e_3}{x_{23}}\sin\delta_{23} \quad (4)$$

$$pe_{q2}'=\frac{1}{T_{do2}}(E_{I2}-e_{I2}) \quad (5)$$

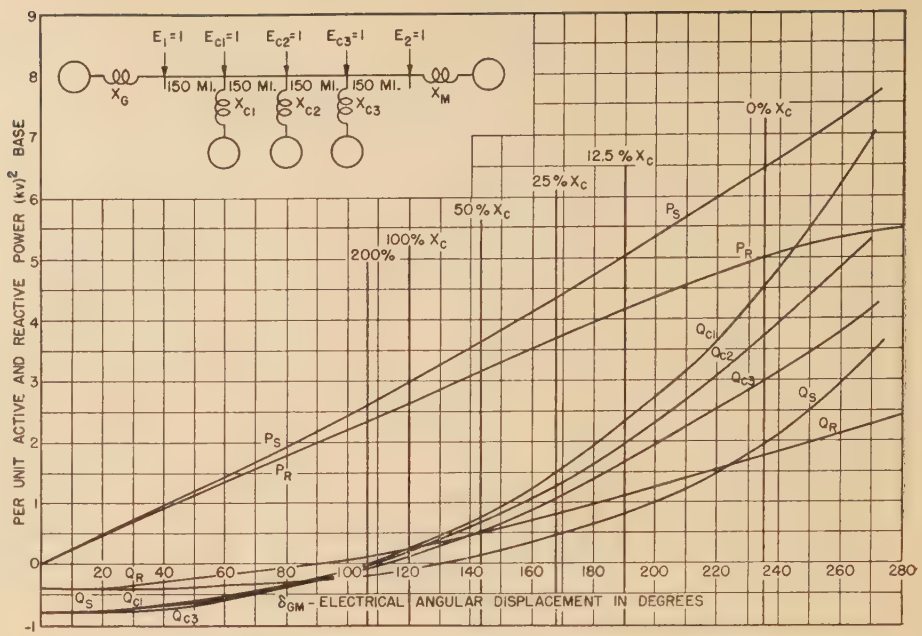

Figure 13. Characteristics of 600-mile 60-cycle transmission line with synchronous terminal equipment and three intermediate synchronous condensers

Per unit kva = per unit kw = $(kv)^2$, $x=0.8$ ohm per mile, $r=0.08$ ohm per mile, $b=5.2\times10^{-6}$ mho per mile, $X_G=0.40$ per unit based on 2.5 $(kv)^2$ (0.16 per unit based on $(kv)^2$). $X_M=0.25$ per unit based on 2.5 $(kv)^2$ (0.10 per unit based on $(kv)^2$) $X_{c1}=X_{c2}=X_{c3}$ and $E_1=E_2=E_{c1}=E_{c2}=E_{c3}=1.0$. Vertical lines give steady-state stability limits with intermediate station reactances based on kva = 2.5 $(kv)^2$

Figure 12. Characteristics of 600-mile conventional 60-cycle transmission line with synchronous terminal equipment and three intermediate synchronous condenser stations

Per unit kva = per unit kw = $(kv)^2$, $x=0.8$ ohm per mile, $r=0.08$ ohm per mile, $b=5.2\times10^{-6}$ mho per mile. Vertical lines give steady-state stability limits with equal terminal and intermediate station reactance as indicated based on $(kv)^2$

$$X_G=X_M=X_{c1}=X_{c2}=X_{c3}$$
$$E_1=E_2=E_{c1}=E_{c2}=E_{c3}=1.0$$

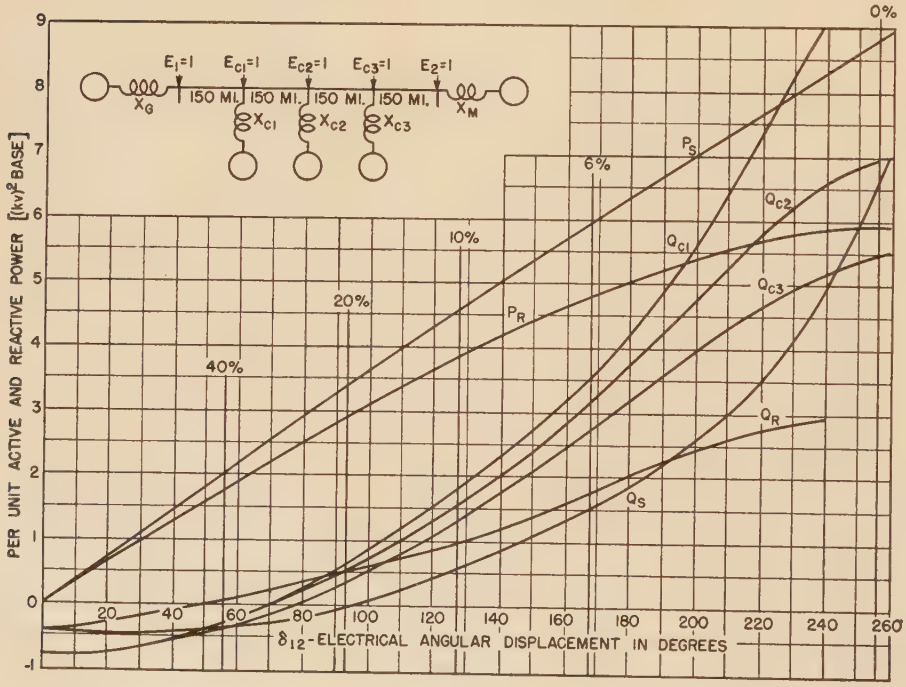

$$e_{q2}'=e_{q2}-i_{d2}(x_{q2}-x_{d2}') \quad (6)$$

$$e_{I2}=e_{q2}+i_{d2}(x_{d2}-x_{q2}) \quad (7)$$

$$E_{I2}-E_{I20}=-\mu_2(e_t-e_{t0}) \quad (8)$$

$$e_{dt2}=-i_{q2}x_{q2} \quad (9)$$

$$e_{qt2}=e_{q2}-i_{d2}x_{q2} \quad (10)$$

$$i_{d2}=\frac{e_{q2}}{x_{22}}-\frac{e_1}{x_{12}}\cos\delta_{21}-\frac{e_3}{x_{23}}\cos\delta_{23} \quad (11)$$

$$i_{q2}=\frac{e_{q2}}{x_{12}}\sin\delta_{21}+\frac{e_3}{x_{23}}\sin\delta_{23} \quad (12)$$

Equations 1 to 12 were solved for the condition of small oscillations and the resulting characteristic denominator tested for stability by Routh's criterion.

Figure 11 is representative of the results obtained for the system of Figure 17 and the following initial conditions.

Constants

$e_1=1.0$
$e_3=1.0$
$x_{12}=3.0$
$x_{23}=3.0$
$x_{13}=3.0$
$x_{22}=1.5$
$M_1=4{,}000$

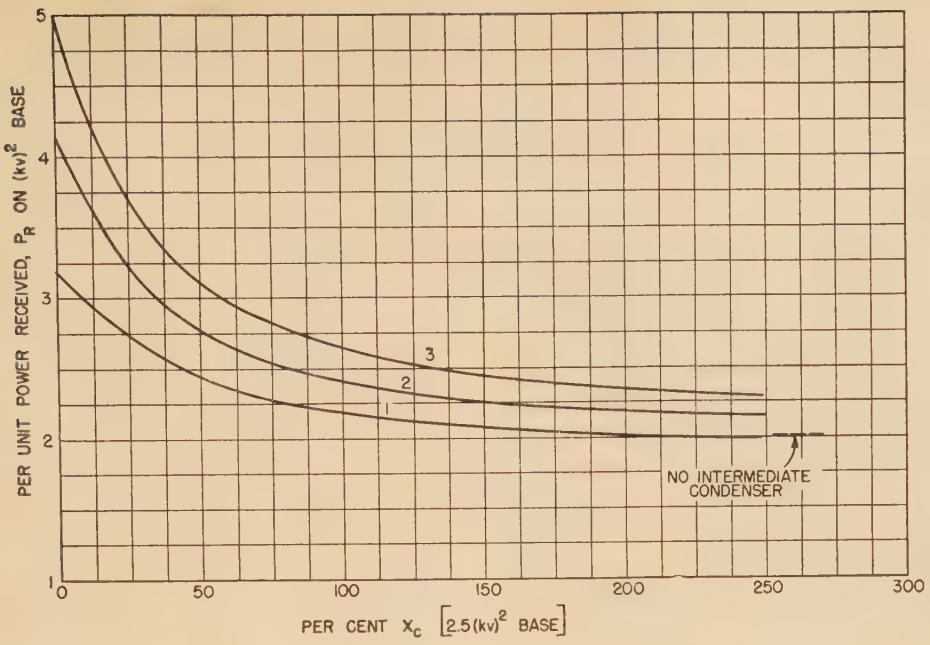

Figure 14. Receiving end power at steady-state limit for 600-mile 60-cycle conventional line with one, two, and three intermediate synchronous condenser stations equally spaced along the line as affected by intermediate station reactances

$X_G = 40$ per cent [2.5 (kv)^2 base]
$X_M = 25$ per cent [2.5 (kv)^2 base]
$x = 0.8$ ohm per mile
$r = 0.08$ ohm per mile
$b = 5.2 \times 10^{-6}$ mho per mile
1—One intermediate condenser station
Line in two 300-mile sections
$E_1 = E_2 = E_{c1} = 1.0$
2—Two intermediate condenser stations
Line in three 200-mile sections
$E_1 = E_2 = E_{c1} = E_{c2} = 1.0$
$X_{c1} = X_{c2}$
3—Three intermediate condenser stations
Line in four 150-mile sections
$E_1 = E_2 = E_{c1} = E_{c2} = E_{c3} = 1.0$
$X_{c1} = X_{c2} = X_{c3}$

$M_2 = 1{,}500$
$x_{q2} = 1.0$
$x_d'_2 = 0.30$
$T_{do2} = 2{,}000$
$e_{t2} = 1.0$
$e_{qt2} = 1.0$
$e_{dt2} = 0$
$T_{d1} = T_{d2} = 0$ (curve D, Figure 11)
$T_{d1} = 3.0$, $T_{d2} = 0$ (curve B, Figure 11)
$T_{d1} = 3.0$, $T_{d2} = 3.0$ (curve C, Figure 11)
$T_{d1} = 0$, $T_{d2} = 3.0$ (curve A, Figure 11)
$\sin \delta_{12} = \sin \delta_{23} = P$
$\cos \delta_{12} = \cos \delta_{23} = \sqrt{1-P^2}$
$\cos \delta_{13} = 1 - 2P^2$
$e_2 = 1 + 2\left(1 - \sqrt{1-P^2}\right)$

Appendix II. System Data

Generator Data

Rated power factor = 0.95
Kilowatt rating = $5.0 \times (kv)^2$
Kilovolt-ampere rating = $5.27 \times (kv)^2$
$x_d = 0.60$, $x_q = 0.40$, $x_d' = 0.20$ } on $5.27 \times (kv)^2$ or generator kilovolt-ampere base
$x_d = 0.63$, $x_q = 0.42$, $x_d' = 0.21$ } on high voltage and system base of $5.0 \times (kv)^2$ ($x_{gen} \times 0.95 \times \frac{}{1.05^2}$)
$T_{do} = 1{,}885$ radians or 5.0 seconds
$H = 5.0$ kilowatt-seconds per kilovolt-ampere

Line Data

$x = 0.8$ ohm per mile
$r = 0.12$ ohm per mile
$y = 5.2$ micromhos per mile

System Data (On System Base)

$H_2 = 50.0$ kilowatt-seconds per kva
$T_{d11} = 4.0$, $T_{d12} = 3.0$, $T_{d21} = 3.0$, $T_{d22} = 18.0$ } damping torque coefficients

Excitation System Data (Per Unit on System Voltage Base)

Ceiling excitation voltage, $E_{I(max)}'' = 2.25$
Minimum excitation voltage limit, $E_{I(min)}'' = -0.304$

Figure 15. Receiving end power at steady-state limit for 600-mile 60-cycle conventional line with one, two, and three intermediate synchronous condenser stations, equally spaced along the line as affected by total synchronous capacity of terminal and intermediate stations expressed as the summation of the station equivalent per unit admittances on 2.5 (kv)^2 base

$x = 0.8$ ohm per mile
$r = 0.08$ ohm per mile
$b = 5.2 \times 10^{-6}$ mho per mile
$X_G = X_M = X_C$
1—One intermediate synchronous condenser station
Line in two 300-mile sections
$E_1 = E_2 = E_{c1} = 1.0$
$X_c = X_{c1}$
2—Two intermediate synchronous condenser stations
Line in three 200-mile sections
$E_1 = E_2 = E_{c1} = E_{c2} = 1.0$
$X_c = X_{c1} = X_{c2}$
3—Three intermediate synchronous condenser stations
Line in four 150-mile sections
$E_1 = E_2 = E_{c1} = E_{c2} = E_{c3} = 1.0$
$X_c = X_{c1} = X_{c2} = X_{c3}$

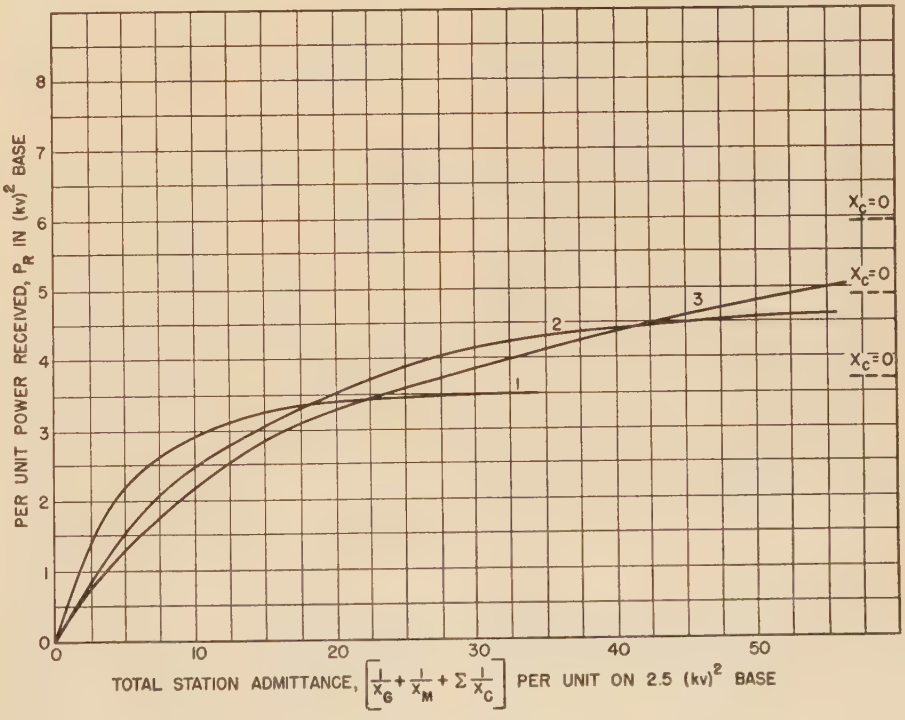

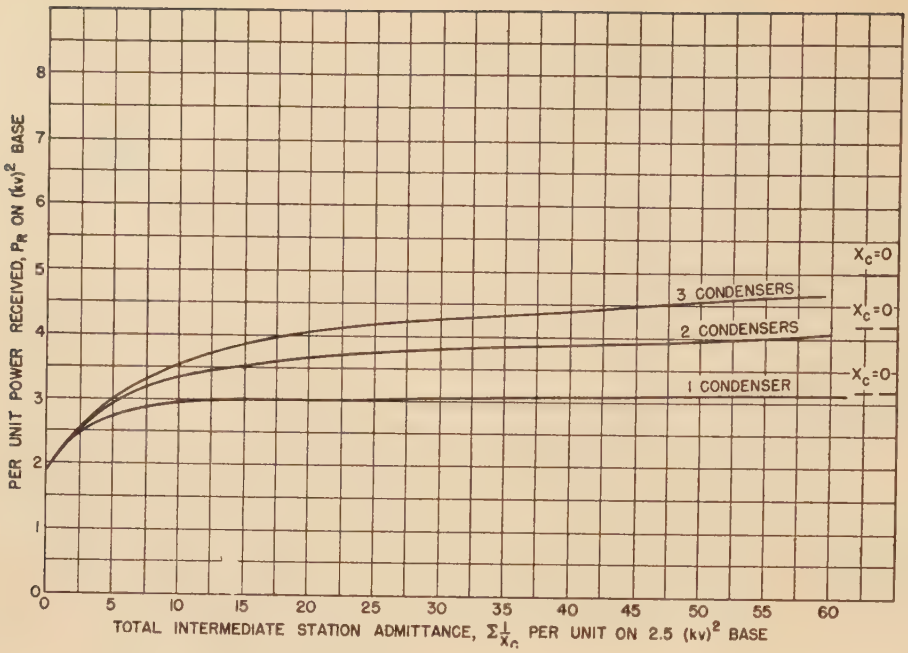

Figure 16. Receiving end power at steady-state limit for 600-mile 60-cycle conventional line with one, two, and three intermediate synchronous condenser stations, equally spaced along the line, as affected by total intermediate station capacity expressed as the summation of the intermediate station equivalent per unit admittance on 2.5 (kv²) base

$x=0.8$ ohm per mile
$r=0.08$ ohm per mile
$b=5.2\times10^{-6}$ mho per mile
$X_G=40$ per cent [2.5 (kv²) base]
$X_M=25$ per cent [2.5 (kv²) base]
1—One intermediate condenser station
Line in two 300-mile sections
$E_1=E_2=E_{c1}=1.0$, $X_c=X_{c1}$
2—Two intermediate condenser stations
Line in three 200-mile sections
$E_1=E_2=E_{c1}=E_{c2}=1.0$, $X_c=X_{c1}=X_{c2}$
3—Three intermediate condenser stations
Line in four 150-mile sections
$E_1=E_2=E_{c1}=E_{c2}=E_{c3}=1.0$, $X_c=X_{c1}=X_{c2}=X_{c3}$

Regulator excitation system amplification factor, $\mu_1=20.0$
Stabilizer amplification factor, $\mu_s=4.0$
Stabilizer time constant,
$T_s=176$ radians or 0.466 second

Appendix III. Characteristic System Impedances

Kva base $=5.0\times(\text{kv})^2$
Fault on (3-phase near sending end high-voltage bus)

$Z_{11}=0.015+j0.52=0.52\ /88.3°$

$Z_{22}=0.632\ /84.29°$

A resistance of 0.015 was assumed for the sending-end terminal impedance during the fault on period to approximate the 3-phase short-circuit loss.

Faulted Line Section Cleared

$Z_{11}=1.39\ /85.0°$ $\alpha_{11}=4.2°$

$Z_{22}=1.69\ /85.0°$ $\alpha_{22}=5.0°$

$Z_{12}=1.22\ /86.4°$ $\alpha_{12}=3.6°$

Appendix IV. System Equations

$$4\pi f H_1\frac{d^2\delta_1}{dt^2}=T_{m1}-T_{e1} \tag{13}$$

$$4\pi f H_2\frac{d^2\delta_2}{dt^2}=T_{m2}-T_{e2} \tag{14}$$

$$T_{e1}=T_{d11}\frac{d\delta_1}{dt}-T_{d12}\frac{d\delta_2}{dt}+T_{s1} \tag{15}$$

$$T_{e2}=-T_{d21}\frac{d\delta_1}{dt}+T_{d22}\frac{d\delta_2}{dt}+T_{s2} \tag{16}$$

$$i_{d1}=\frac{e_{q1}}{Z_{11}}\cos\alpha_{11}-\frac{e_2}{Z_{12}}\cos(\delta_{12}-\alpha_{12}) \tag{17}$$

$$i_{q1}=\frac{e_{q1}}{Z_{11}}\sin\alpha_{11}+\frac{e_2}{Z_{12}}\sin(\delta_{12}-\alpha_{12}) \tag{18}$$

$$T_{s1}=i_{q1}e_{q1} \tag{19}$$

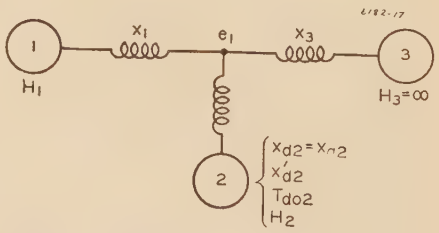

Figure 17. Three-machine system analyzed in Appendix I

Machine 1—Generator
Machine 2—Intermediate synchronous condenser
Machine 3—Infinite inertia receiver system

$$T_{s2}=\frac{e^2_2}{Z_{22}}\sin\alpha_{22}-\frac{e_2e_{q1}}{Z_{12}}\sin(\delta_{12}+\alpha_{12}) \tag{20}$$

$$e_{dt}=-i_{q1}(x_q+x_t) \tag{21}$$

$$e_{qt}=e_{q1}'-i_{d1}(x_d'+x_t) \tag{22}$$

$$e_t=\sqrt{e_{dt}^2+e_{qt}^2} \tag{23}$$

$$\frac{de_{q1}'}{dt}=\frac{1}{T_{do}}(E_{I1}-e_{I1}) \tag{24}$$

$$e_{q1}'=e_{q1}-i_{d1}(x_q-x_d') \tag{25}$$

$$e_{I1}=e_{q1}+i_{d1}(x_d-x_q) \tag{26}$$

$$E_{I1}''=f(E_{I1}') \tag{27}$$

$$=E_{I1}'-E_{I10}'$$
$$=-\mu_1(e_t-e_{to})-B \tag{28}$$

$$B=\frac{\mu_sT_sp}{T_sp+1}E_{I1}$$

$$\frac{dE_{I1}}{dt}=\frac{1}{T_e}(E_{I1}''-E_{I1}) \tag{29}$$

Appendix V. Differential Analyzer Equations (Derived From Appendix IV)

$$\frac{d\delta_1}{dt}=\frac{1}{4\pi fH_1}\{T_{m1}t-T_{d11}\delta_1+T_{d12}\delta_2-\int i_{q1}d\int e_{q1}dt\} \tag{30}$$

$$\frac{d\delta_2}{dt}=\frac{1}{4\pi fH_2}\left\{\left(T_{M2}-\frac{e_2^2}{Z_{22}}\sin\alpha_{22}\right)t+T_{d21}\delta_1-T_{d22}\delta_2+\frac{e_2}{Z_{12}}\int\sin(\delta_{12}+\alpha_{12})d\int e_{q1}dt\right\} \tag{31}$$

$$i_{q1}=\frac{e_{q1}}{Z_{11}}\sin\alpha_{11}+\frac{e_2}{Z_{12}}\sin(\delta_{12}-\alpha_{12}) \tag{32}$$

$$e_{q1}=e_{q1}'+(x_q-x_d')i_{d1} \tag{33}$$

$$e_{q1}'=\frac{1}{T_{do}}\int(E_{I1}-e_{I1})dt \tag{34}$$

$$e_{I1}=e_{q1}+(x_d-x_q)i_{d1} \tag{35}$$

$$i_{d1}=\frac{e_{q1}}{Z_{11}}\cos\alpha_{11}-\frac{e_2}{Z_{12}}\cos(\delta_{12}-\alpha_{12}) \tag{36}$$

$$E_{I1}'-E_{I10}'=-\mu_1(e_t-e_{to})-B$$

$$B=\mu_sE_{I10}-\frac{1}{T_s}\int B\,dt \tag{37}$$

$$E_{I1}''=f(E_{I1}') \tag{38}$$

$$E_{I1}=\frac{1}{T_e}\int(E_{I1}''-E_{I1})dt \tag{39}$$

$$e_t=\sqrt{e_{dt}^2+e_{qt}^2} \tag{40}$$

$$e_{dt}=-(x_q+x_t)i_{q1} \tag{41}$$

$$e_{qt}=e_{q1}'-(x_d'+x_t)i_{d1} \tag{42}$$

References

1. Voltage Regulation and Insulation for Large Power, Long Distance Transmission Systems, F. G. Baum. AIEE Transactions, volume 40, 1921, pages 1017–77.

2. The Limitations Output of a Power System Involving Long Transmission Lines, E. B. Shand.

Functional Analysis of Measurements

I. F. KINNARD
FELLOW AIEE

HISTORY tells us that measurement has been one of the principal foundations upon which the material progress of mankind has been based. It is only by carefully comparing or measuring the unknown in terms of some known quantity or unit that real knowledge is advanced. As our modern way of living increases in complexity and as our knowledge of science and technology expands, measurements and measuring equipment have progressively increased in diversity and in complication. Better measurements have vitally aided our progress in understanding physical laws, in designing and operating new and improved machines, and in automatic control of processes and operations. In all fields of applied arts and sciences, our rich store of knowledge is largely the result of our ability to measure.

Measurements were once simple and relatively few. With the development of practical applications of all branches of science, however, the number of quantities requiring accurate measurement has increased greatly and is now almost without limit. Measurements on a large scale have graduated from the laboratories to our workshops, factories, and even our homes. They have become in one way or another a real and necessary part of our daily lives. Much measuring apparatus has become exceedingly complex. This is caused by a number of factors, including the necessity of performing new measurements inherently more difficult and the need of greater accuracy and sensitivity.

Electrical means for assisting in the measurement of a large number of physical quantities are now quite generally utilized. Their use provides a number of outstanding advantages, such as ready availability of measurement energy and superior flexibility. Moreover, electricity readily lends itself to remote operation of indicators, recorders, or controllers. This trend has further complicated measuring equipment, however, by adding many complex measurement systems and devices that have been designed for a great variety of purposes.

The method of analysis and classification described in this paper concerns itself largely with the measurement of electrical or other physical quantities by methods employing electrical means, but the principles involved are not limited to electrically operated equipment. It was developed after several years of study in order to provide a clear presentation of the various functional parts of any measurement system or device, and to make available a common language of measurement terms and nomenclature for the group of measurement engineers with which the author is associated. Other benefits have accrued from the study which will be outlined later. It is hoped that the material herein presented will be of assistance to all designers and users who are interested in this very important and rapidly expanding field.

General Functional Classification

All measurement systems, simple or complex, can be considered as being composed of not more than three principal functional parts or groupings, namely, a primary detector, one or more intermediate means, and an end device. This conception is illustrated by the diagram shown in Figure 1. The sequence of the measurement is from left to right and all functional steps in the over-all operation logically fall into one of these groups. In many types of measurements, no intermediate means is necessary in order to accomplish the desired result. Very frequently, however, all three general functional classifications are required to analyze a complete system or measurement operation.

End Device and Primary Detector

A particular quantity is measured to obtain either an indication of its present value, a record showing time of occurrence, or to initiate a control operation. For practical purposes, therefore, a mechanism or assembly that embodies one or all of these functions is called the end device. This represents the result of the measurement and is of primary interest to the user of the equipment. Everything else involved is for the purpose of suitably actuating the end device in proper relation to the quantity being measured.

For classifying purposes, definite and recognized names can be applied to the various types of indicating and recording end devices, and these are well understood. Some further explanation, however, should be made in regard to the control initiator. In those cases where a measurement is made in whole or in part for the purpose of controlling the measured quantity or variable, there is some definite point in the measurement sequence where the control operation can be said to be initiated. This may be in the form of suitable make-and-break contacts, or it

AIEE Transactions, volume 43, 1924, pages 59–70.

3. Fundamental Considerations of Power Limits of Transmission Systems, **R. E. Doherty, H. H. Dewey.** AIEE Transactions, volume 44, 1925, pages 972–84.

4. Studies of Transmission Stability, **R. D. Evans, C. F. Wagner.** AIEE Transactions, volume 45, 1926, pages 51–80.

5. An Investigation of Transmission-System Power Limits, **C. A. Nickle, F. L. Lawton.** AIEE Transactions, volume 45, 1926, pages 1–21.

6. Automatic Voltage Regulators, **C. A. Nickle, R. M. Carothers.** AIEE Transactions, volume 47, 1928, pages 957–69.

7. Static Stability Limits and the Intermediate Condenser Station, **C. F. Wagner, R. D. Evans.** AIEE Transactions, volume 47, 1928, pages 94–121.

8. Modern Excitation Systems for Large Synchronous Machines, **J. B. McClure, S. I. Whittlesey, M. E. Hartman.** AIEE Transactions, volume 65, 1946, pages 939–45.

9. Excitation Systems on Turbine-Electric Drive Ships, **F. V. Smith.** *Marine Engineering and Shipping Review*, New York, N. Y., volume 49, December 1944, pages 179–83.

10. Steady State Stability of Synchronous Machines as Affected by Voltage Regulator Characteristics, **C. Concordia.** AIEE Transactions, volume 63, 1944, May section, pages 215–20.

11. Analyzers, **H. A. Peterson, C. Concordia.** *General Electric Review*, New York, N. Y., volume 48, September 1945, pages 29–37.

12. Differential Analyzer Applications, **F. J. Maginniss.** *General Electric Review*, New York, N. Y., volume 48, May 1945, pages 54–9.

13. A New Differential Analyzer, **H. P. Kuehni, H. A. Peterson.** AIEE Transactions, volume 63, 1944, May section, pages 221–7.

14. A New A-C Network Analyzer, **H. P. Kuehni, R. G. Lorraine.** AIEE Transactions, volume 57, 1938, February section, pages 67–73.

15. Stability Limitations of Long-Distance A-C Power-Transmission Systems, **Edith Clarke, S. B. Crary.** AIEE Transactions, volume 60, 1941, pages 1051–9.

16. Power Limits of Synchronous Machines, **Edith Clarke, R. G. Lorraine.** AIEE Transactions, volume 53 ,1934, pages 1802–09.

17. Power System Stability (book), **S. B. Crary.** John Wiley and Sons, Inc., New York, N. Y., 1945.

Paper **46-133**, recommended by the AIEE committee on instruments and measurements for presentation at the AIEE summer convention, Detroit, Mich., June 24–28, 1946. Manuscript submitted April 23, 1946; made available for printing May 13, 1946.

I. F. Kinnard is works engineer at General Electric Company, West Lynn, Mass.

The material in this paper represents part of a study directed by the author and undertaken largely for administrative purposes. Various members of his staff have assisted in this project, but special acknowledgment is given H. C. Dickinson for his keen interest and valuable assistance.

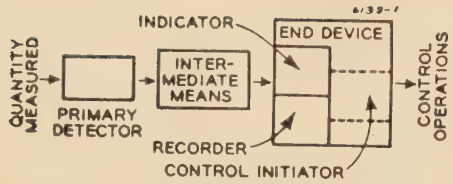

Figure 1. Schematic diagram of general functional classification

may consist of pickup coils and other types of basic elements. The control initiator usually is included in the end device, but it may be associated with the primary detector or intermediate means.

The first operation in the measurement sequence is of particular interest. The basic element or elements here involved must respond quantitatively to the measured quantity or variable in such a manner that the operational result can be used to actuate the end device directly or indirectly. This element or group of elements has been termed the primary detector associated with the measurement apparatus under consideration. It should be emphasized that this conception of a primary detector is purely functional and that some specific basic elements may or may not be primary detectors, depending upon where they are used in the measurement sequence.

As previously indicated, a primary detector and end device may constitute the entire measurement. This is particularly true of the simpler measurement systems. In Table I a number of measurement devices and systems are listed that can be classified suitably in these two functions. In some cases the primary detector may be a self-contained device functioning independently of the actual end device, as illustrated by the first three items in Table I. However, it may constitute an important functioning part of the end device itself, as in the last four devices listed in Table I.

Intermediate and Auxiliary Means

In many instances the output or operational result of a primary detector is not suitable to operate the necessary end device either because of its nature or because of its remote location. It, therefore, becomes necessary to convert this output or operational result into some different quantity, to supply measurement energy, or to modify or amplify it in such a manner that it becomes suitable to accomplish the purpose in hand. All such intermediate operations are classified as intermediate means. They are provided for, where necessary, by a proper selection of specific functional basic elements. The location and physical housing of the intermediate means are determined by convenience. It may be included with the primary detector or the end device, or it may consist of separate devices interconnected mechanically or electrically. The thoughtful designer will use a minimum of such transformations or additional operations, since, in general, some measurement precision may be lost in the process. Certainly there is added complexity and cost. Much greater flexibility and sensitivity often can be realized by their use, however,

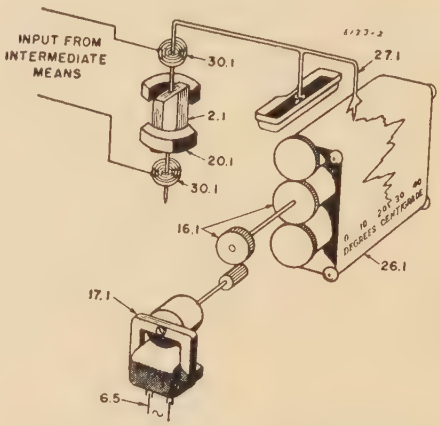

Figure 2. Specific functional classification, D'Arsonval recorder

Basic elements:

2.1—Moving coil
6.5—A-c standardized frequency source
16.1—Gearing
17.1—Timing motor
20.1—Stationary field magnet
26.1—Chart for marking
27.1—Curve-drawing means
30.1—Restoring-torque springs

and in many cases the nature of the measurement is such that one or more intermediate means are necessary for its accomplishment. In Table II a number of measurements systems are listed that require intermediate means.

Occasionally it may be necessary to change the magnitude of the measured quantity so that its level is better suited to the primary detector. Equipment used for this purpose includes instrument transformers, preamplifiers, and shunts, and is classified in a subordinate grouping as auxiliary means. It is located in front of the primary detector and may be either a separate unit or built in as part of a measurement device. Typical examples are the current and potential transformers used in connection with watthour meters, and also the built-in type of transformers used for conventional thermal watt demand meters.

The auxiliary means constitutes important and necessary equipment for some measurements, but its function is to prepare suitably for the proper operation of the primary detector. It actually does not perform the initial step or quantitative response in the measurement sequence, since it merely changes the level of the measured quantity.

Comments on General Functional Analysis

As has been stated, all measuring devices or systems can be classified in accordance with the 3-part functional analysis that has been explained. This has been done for hundreds of different types of measurements and the results tabulated. In general, a rather limited number of functional types of indicating and recording end devices is used. There is a larger list of primary detectors that are available and, undoubtedly, more will be invented. A complete tabulation of the measuring systems that have been analyzed is not included in this paper, but Tables I and II show a few typical cases and will serve to illustrate the manner in which this method can be applied.

The type of analysis shown in Tables I and II provides a means for considering any line or field of measurement apparatus in an orderly manner. Lists of primary detectors, intermediate means, and end devices can be prepared and should be very useful to designers and users of this class of equipment. Such a classification reduces to a relatively few fundamental types what otherwise might appear to be

Table I. General Functional Classification of Simple Measurement Devices and Systems

Measurement Device or System	Quantity Measured	Primary Detector	End Device
Temperature meter (thermocouple type)	Temperature	Thermocouple	D'Arsonval indicator
Light meter	Illumination	Light cell	D'Arsonval indicator
Aircraft synchroscope	Aircraft-engine synchronism	A-c generator	Rotating field and vane indicator
Directional gyroscope	Direction	Horizontal axis gyro	Directional gyro indicator
Interval timer	Time	Timing motor	Time switch
D-c ammeter	Direct current	D'Arsonval mechanism	D'Arsonval indicator
A-c wattmeter	A-c power	Electrodynamic mechanism	Electrodynamic indicator

, an almost endless variety of measurement apparatus.

Specific Functional Classification

The term basic element has been used in the text as indicating that measurement devices are composed of certain units which perform specific and definite functions in the measurement sequence. It is quite evident that the classification into general functions does not supply sufficient information to obtain a clear and precise understanding as to the real nature of the various devices under consideration. By further analyzing these devices, therefore, and identifying each specific functional operation in the measurement chain, some very interesting results are obtained. For example, a typical D'Arsonval recorder may be broken down into components or units which perform necessary and distinct steps in the sequence of the measurement operation, as shown in the schematic diagram, Figure 2. There are actually eight functional units as listed that are essential to complete the over-all operation of recording the value of the quantity measured on the chart. For the purposes of exact nomenclature, the units that perform such specific and distinct functions are termed basic elements, and represent the smallest steps in the measurement sequence that it is convenient to consider. These basic elements in a sense may be termed the "building blocks of measurement."

It is now possible to analyze each device or assembly in any measuring apparatus or system and break it down into the basic elements of which it is composed. This has been done for all of the measuring equipment that has been considered from the standpoint of the general functional analysis previously described, and the basic elements identified were listed and classified. In Table III all basic elements thus far considered are grouped into 34 general types, and these expanded into 92 specific types. A decimal index system is used for convenience of reference and for adding new elements as may be required. In preparing diagrams and tabulations, the number of the specific type is always shown, since this definitely identifies the function involved.

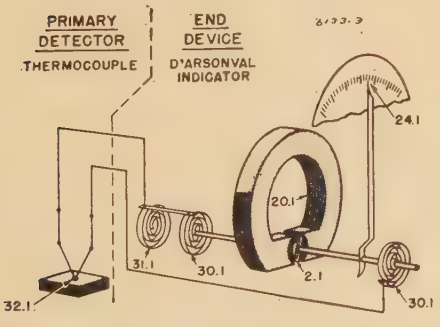

Figure 3. Temperature meter, thermocouple type

Basic elements:

2.1—Moving coil
20.1—Stationary field magnet
24.1—Moving pointer, fixed scale
30.1—Restoring-torque springs
31.1—Bimetallic actuator
32.1—Contact thermocouple

Table II. General Functional Classification of Systems Requiring Intermediate Means

Measurement Systems	Quantity Measured	Primary Detector	Intermediate Means	End Device
Temperature meter (resistance type)	Temperature	Resistance temperature detector	Resistance bridge	Moving-magnet ratio indicator
Photoelectric temperature recorder	Temperature	Thermocouple	Galvanometer, optical transmission, electronic amplifier	D'Arsonval recorder
Remote indicating compass	Direction	Compass mechanism	Induced second harmonic transmission	Induced second harmonic indicator
Liquid-level gauge (capacitance type)	Liquid quantity	Capacitor	Electronic oscillator	Moving-magnet ratio indicator
Watt-demand recording system	A-c power demand	Watthour-meter mechanism	Electric-impulse transmission	Demand recorder

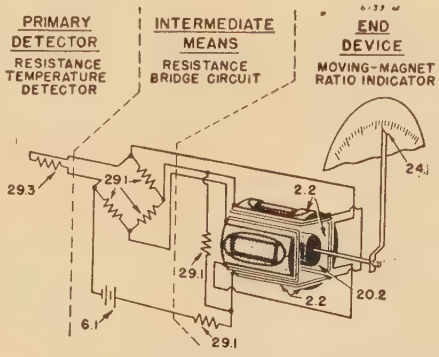

Figure 4. Temperature meter, resistance type

Basic elements:

2.2—Fixed coils
6.1—D-c source
20.2—Moving-field magnet
24.1—Moving-pointer, fixed scale
29.1—Fixed resistors
29.3—Temperature sensitive resistor

While only 92 specific types are needed to analyze the measuring equipment thus far considered, it is realized that this list cannot be considered as complete. Additions will have to be made as new types are encountered in existing apparatus, and also as new inventions are made. The number added, however, probably will be small, since experience has shown that nearly all new measuring systems analyzed fit into the pattern of classification that has been established.

It is quite feasible to subdivide further these specific types of basic elements into major and minor variations for purposes of classifying actual physical constructions that are used. The decimal system lends itself to this extension very nicely, and, by this means, types of construction, material used, and actual size and shape may be identified with particular decimal numbers. This actually has been done for some of the basic elements listed and is being extended, since it provides an excellent system for purposes of systematic filing and indexing of data.

Complete Analysis and Classification

It is now possible to show on one schematic diagram a complete measurement system utilizing the methods of analysis that have been described. This provides a standard method of presentation and also a basis for naming, listing, and statistically analyzing all the functional parts of which measurement apparatus is composed, namely, basic elements, primary detectors, intermediate means, and end devices. The secondary classification of auxiliary means can be noted and listed also, as required. In making such an analysis, care should be taken to follow the exact meaning of these terms as closely as possible. Definitions of these and other measurement terms frequently used have been carefully worked out and are given in the following section.

Some of the measurement systems or devices that have been previously mentioned now will be shown in diagrammatic form by combining the general and specific functional classification. Each significant step in the measurement sequence is clearly indicated by identifying the basic elements involved and marking them in accordance with the decimal numbers shown in Table III. The order of the tabulation, in general, corresponds to the flow of measurement energy from the first operation to the end result.

The measurement systems or devices

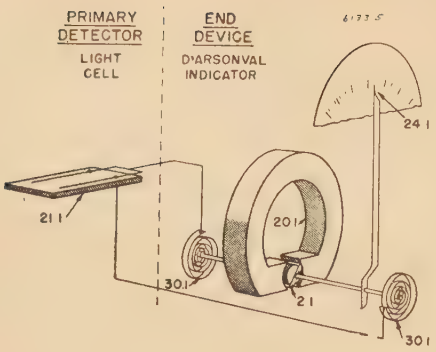

Figure 5. Lightmeter

Basic elements:

2.1—Moving coil
20.1—Stationary field magnet
21.1—Photovoltaic cell
24.1—Moving-pointer fixed scale
30.1—Restoring-torque spring

selected for illustrating the complete functional analysis method are shown in Figures 3 through 10, and their principles of operation should be self-explanatory if the foregoing material has been carefully considered.

The complete analysis and classification data can be tabulated in compact form for purposes of reference and statistical study. This has been done for a large part of the equipment involved in the electrical measurement field, including apparatus for measuring both electrical and nonelectrical quantities. It is not feasible to show the complete results of this study in this paper, but a skeleton table has been prepared, Table IV. This table shows a number of typical measurements and illustrates how such a tabulation can be built up. A column could be added showing control initiator, if desired, and this is done in considering measurements closely connected with control apparatus. In Table IV the general functional groupings are listed by recognized names associated with their respective functions, and the basic elements of which they are composed are shown by the numbers in parentheses, which refer to the listing of specific types in Table III.

A tabulation such as shown in Table IV can be made quite complete for the measurement of electrical quantities which are relatively few in number, but when extended into the field of measurement of nonelectrical quantities by electrical means, the list is very much larger and is constantly increasing. This clearly shows the growing application of electrical methods to the measurement of physical quantities other than electricity.

Separate lists have been made of basic elements, primary detectors, intermediate means, and end devices. Such data are of considerable importance statistically and as a means of ready reference, as will be explained later.

One mental picture given by a tabulation such as shown in Table IV is the very real significance of the term "building blocks of measurement" as applied to basic elements. It is easy to see at a glance those devices that are complicated and have many steps in the measurement sequence, as compared to those that are simple and have few steps. The point also is brought out that the same basic elements are used in various com-

Table III. List of Basic Elements

General Group	Specific Type
1—Capacitor	1.1—Fixed capacitor
	1.2—Varying dielectric capacitor
	1.3—Variable capacitor
2—Coil, air core	2.1—Moving coil
	2.2—Fixed coil
3—Coil, ferromagnetic core (See also inductor-15)	3.1—Electromagnet
	3.2—Electromagnet stator
	3.3—Electromagnet rotor
4—Contacts	4.1—Make-and-break contacts
	4.2—Commutator
5—Eddy-current disk sector or member	5.1—Braking disk
	5.2—Drag disk
6—Electric source	6.1—D-c source (nonstandardized)
	6.2—D-c standardized-voltage source
	6.3—A-c source (nonstandardized)
	6.4—A-c standardized-voltage source
	6.5—A-c standardized-frequency source
7—Electrodes	7.1—Nonmetallic electrodes
	7.2—Metallic electrodes
	7.3—Thermoelectric electrodes
8—Electronic tube (See also photosensitive cells-21 and rectifier-28)	8.1—Grid-controlled electronic tube
	8.2—Gaseous discharge tube
	8.3—Cathode-ray tube
9—Ferromagnetic moving member	9.1—Ferromagnetic vane
	9.2—Ferromagnetic plunger or lever
10—Float	10.1—Liquid-level float
11—Fluid-quantity converter	11.1—Eccentric-piston pump
12—Fluid velocity converter	12.1—Orifice
	12.2—Pitot tube
13—Frequency standard (See also Piezoelectric crystal-23)	13.1—Tuning fork
	13.2—Resonant circuit
14—Gyroscope	14.1—Electrically driven gyro rotor
15—Inductor or reactor	15.1—Fixed inductor
	15.2—Variable inductor
	15.3—Mutual inductor
	15.4—Saturating reactor
16—Mechanical linkage	16.1—Gearing
	16.2—Lever
	16.3—Clutch
	16.4—Cam
	16.5—Crank
	16.6—Pawl and ratchet
17—Motor	17.1—Timing motor
	17.2—Servo motor
18—Optical component	18.1—Lense
	18.2—Mirror
	18.3—Filter
19—Pendulum	19.1—Free pendulum
20—Permanent magnet	20.1—Stationary field magnet
	20.2—Moving field magnet
	20.3—Braking, drag or damping magnet
	20.4—Motion transmitting magnet
	20.5—Holding, lifting, or pulling magnet
21—Photo-sensitive cells	21.1—Photovoltaic cell
	21.2—Photoconductive cell
	21.3—Photoemissive cell
22—Photo-radiation source	22.1—Electric lamp
23—Piezoelectric crystal	23.1—Frequency-standard crystal
	23.2—Pressure-conversion crystal
24—Pointer and scale	24.1—Moving-pointer, fixed-scale
	24.2—Fixed-pointer, moving-scale
	24.3—Light-beam, fixed-scale
25—Pressure converter	25.1—Expanding vessel
	25.2—Liquid column
	25.3—Microphone diaphragm
26—Record charts	26.1—Chart for marking or printing
	26.2—Photo-sensitized chart
27—Record-making means	27.1—Curve-drawing means
	27.2—Printing means
	27.3—Light-beam means
28—Rectifier	28.1—Blocking-layer rectifier
	28.2—Electronic rectifier tube
29—Resistor	29.1—Fixed resistor
	29.2—Variable resistor
	29.3—Temperature-sensitive resistor
	29.4—Moisture-sensitive resistor
	29.5—Strain-sensitive resistor
	29.6—Vibration-sensitive resistor
30—Spring	30.1—Restoring torque spring
	30.2—Positioning spring
	30.3—Stress strain member
31—Temperature converter (See also resistor-29 and thermocouple-32)	31.1—Bimetallic actuator
	31.2—Vapor tension bulb
32—Thermocouple	32.1—Contact thermocouple
	32.2—Radiation thermocouple
33—Transformer	33.1—Instrument transformer
	33.2—Coupling transformer
	33.3—Saturating core transformer
	33.4—Biased transformer
	33.5—Power-supply transformer
34—Weight	34.1—Solid weight

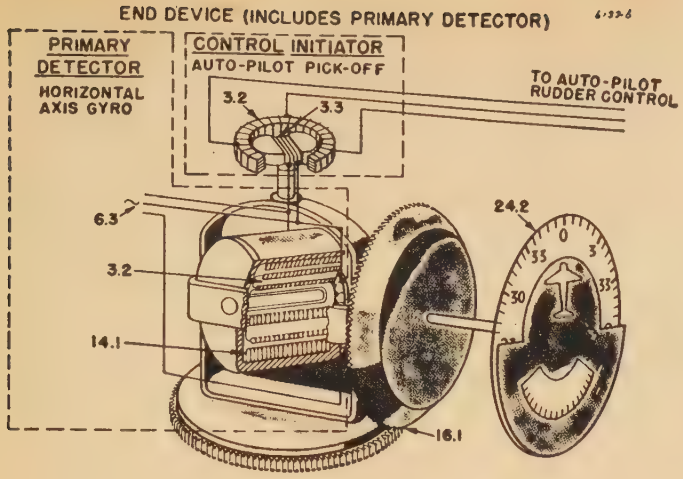

Figure 6. Directional gyroscope

Basic elements:

3.2—Electromagnet stator
3.3—Electromagnet rotor
6.3—A-c source
14.1—Electrically driven gyro rotor
16.1—Gearing
24.2—Fixed-pointer, moving scale

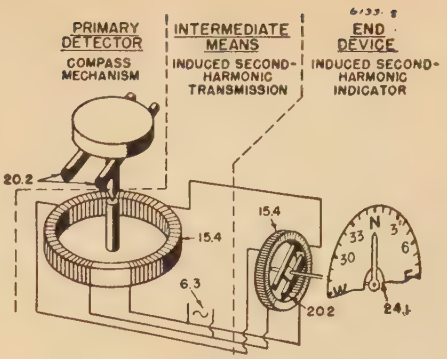

Figure 8. Remote indicating compass

Basic elements:

6.3—A-c source
15.4—Saturating reactor
20.2—Moving field magnet
24.1—Moving-pointer, fixed scale

binations to accomplish widely different results.

Definitions of Measurement Terms

It will be helpful at this point to give specific definitions for the various terms that are used to describe the proposed method of analysis. These definitions are carefully worded and are intended to facilitate the actual analysis and classification of measurement devices or systems. Some of these terms are new ones designating somewhat new conceptions, and others are terms that are in general use but to which it is necessary to ascribe more specific meanings.

New terms, which have been selected specifically for the functional analysis and classification of measurements, are as follows:

A primary detector is the first basic element or group of elements that responds quantitatively to the quantity measured and performs the initial measurement operation. A primary detector performs the initial conversion or control of measurement energy and does not include transformers, amplifiers, shunts, resistors, and so forth, when these are used as auxiliary means.

An end device is the assembly of basic elements that responds quantitatively to the quantity measured and performs the final measurement operation. An end device performs the final conversion of measurement energy to an indication, record, or the initiation of control.*

The intermediate means includes all basic elements that are used to perform necessary and distinct operations in the measurement sequence between the primary detector and the end device. The intermediate means, where necessary, adapts the operational results of the primary detector to the input requirements of the end device.

A measurement component is a general term applied to parts or subassemblies that are used primarily for the construction of measurement apparatus. It is used to denote those parts made or selected specifically for measurement purposes and does not include standard screws, nuts, insulated wire, or other standard materials.

A basic element is a measurement component or group of components that performs one necessary and distinct function in a sequence of measurement operations. Basic elements are single purpose units and provide the smallest steps into which the measurement sequence can be classified conveniently.

An auxiliary means is a basic element or group of elements which changes the magnitude but not the nature of the quantity being measured to make it more suitable for the primary detector. In a sequence of measurement operations, it usually is placed ahead of the primary detector.

Control initiation is the function introduced into a measurement sequence for the purpose of regulating any subsequent control operations in relation to the quantity measured. The basic element or group of elements comprising the control initiator usually is included in the end device but may be associated with the primary detector or the intermediate means.

Existing terms, which are specifically defined for use in the functional analysis and classification of measurements, are as follows:

A measurement device is an assembly of on

* It should be noted that end devices, as defined under new terms, are frequently, but not always, complete measurement devices in themselves, since they often are built in with all, or part, of the intermediate means or primary detectors to form separate self-contained units.

Figure 7. Photoelectric temperature recorder

Basic elements:

1.1—Fixed capacitors
2.1—Moving coil
6.3—A-c source
6.5—A-c standardized-frequency source
8.1—Grid-controlled electronic tubes
16.1—Gearing
17.1—Timing motor
18.1—Lenses
18.2—Mirrors
20.1—Stationary field magnet
21.3—Photoemissive cells
22.1—Electric lamp
26.1—Chart for marking
27.1—Curve-drawing means
28.2—Electronic rectifier tube
29.1—Fixed resistors
30.1—Restoring torque spring
32.1—Contact thermocouple
33.5—Power supply transformer

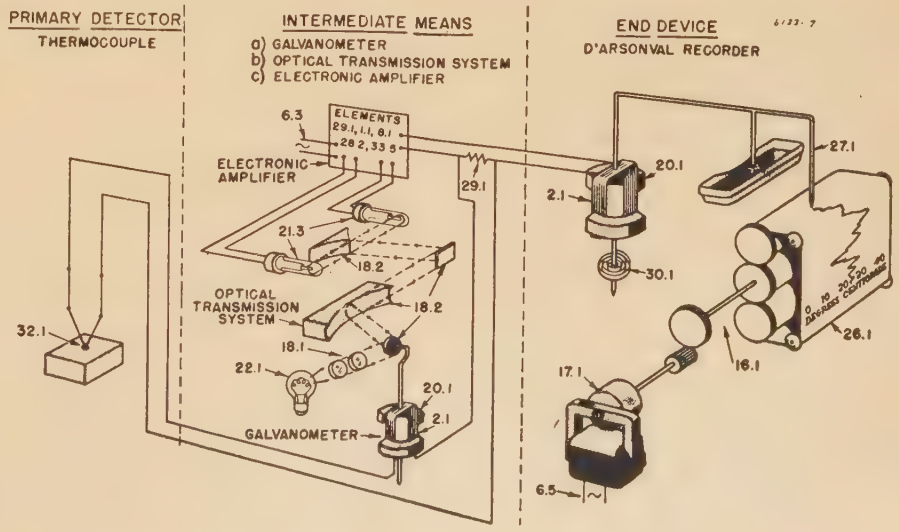

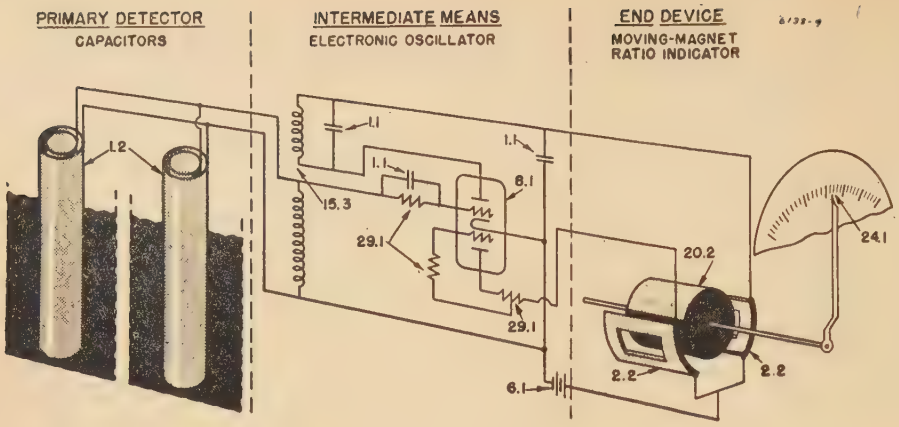

Figure 9. Liquid-level gauge, capacitance type

Basic elements:

1.1—Fixed capacitors
1.2—Varying dielectric capacitor
2.2—Fixed coils
6.1—D-c source
8.1—Grid-controlled electronic tube
15.3—Mutual inductor
20.2—Moving field magnet
24.1—Moving-pointer, fixed scale
29.1—Fixed resistors

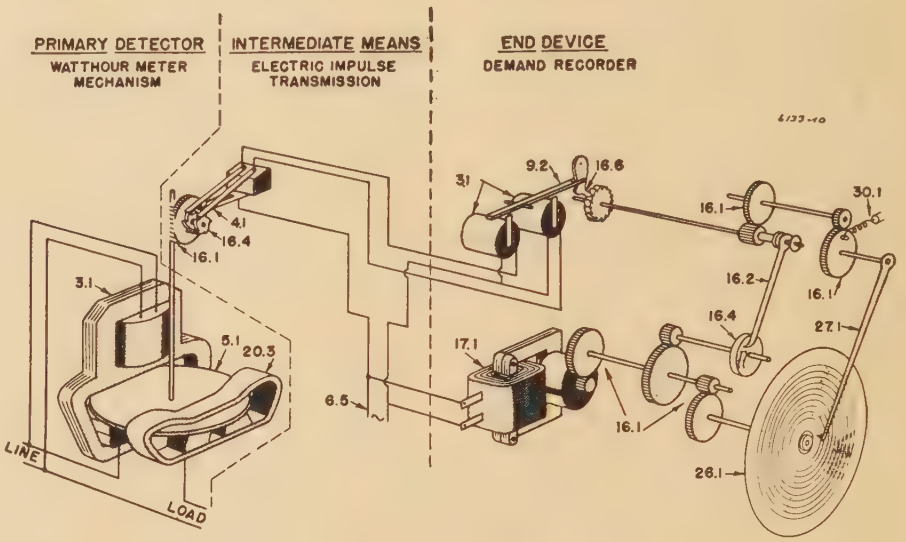

Figure 10 (right). Watt-demand recording system

Basic elements:

3.1—Electromagnet
4.1—Make-and-break contacts
5.1—Eddy current disk
6.5—A-c standardized-frequency source
9.2—Ferromagnetic lever
16.1—Gearing
16.2—Lever
16.4—Cams
16.6—Pawl and ratchet
17.1—Timing motor
20.3—Braking magnet
26.1—Chart for marking
27.1—Curve-drawing means
30.1—Restoring torque spring

or more basic elements with other components and necessary parts to form a separate self-contained unit for performing one or more measurement operations. It includes the protecting, supporting, and connecting as well as the functioning parts, which are all necessary to fulfill the application requirements of the device.

A measurement system consists of one or more measurement devices and any necessary auxiliary or intermediate means interconnected to perform a complete measurement from the first operation to the end result. A measurement system can be divided into general functional groupings, each of which consists of one or more specific functional steps or basic elements.

Measurement energy is the energy required to operate a measurement device or system. Measurement energy can be obtained either from the quantity being measured, from an external source, or from both.

Measurement equipment is a general term applied to any assemblage of measurement components, devices, apparatus, or systems.

A measurement mechanism is an assembly of basic elements and immediate supporting parts for performing a mechanical operation in the sequence of measurement. For example, it may be a group of components required to effect the proper motion of an indicating or recording means and does not include such parts as bases, covers, scales, and accessories. It also may be applied to a specific group of elements by substituting a suitable qualifying term, such as time switch mechanism or chart drive mechanism.

Related Terminology and Literature

Wherever practical, the foregoing terms and definitions, as well as the names of the devices and elements used in the tables and illustrations, have been kept in agreement with the established terminology of measurement.[1] Modifications and adaptations, however, have been necessary in developing the method of functional analysis. For example, the new term primary detector may at first seem an unwarranted departure from primary element, which is the name that has been used for some time in connection with industrial process instrumentation for the initial functional unit in a measurement sequence.[2,3] This change was made, however, because in the method of analysis described the primary detector may consist of more than one basic element, and because the term basic element is used to cover functional units anywhere in the measurement sequence and is not limited to the initial operation. Primary detector, therefore, is used to avoid confusion and to be more consistent with the names of the other two general functional groupings, the intermediate means and the end device.

Functional analyses of measurement and automatic control systems have appeared previously in technical literature.[3,4,5] While these analyses emphasize the value of considering measurements from the functional point of view, they have been limited, in general, to only a part of the whole measurement field and have been made to facilitate detailed discussions of the particular part involved. The functional analysis method presented herein is intended to be universally applicable to every device and system in the measurement field.

Uses of Method and Conclusions

The method of analysis and classification of measurements that has been described was developed to provide an orderly approach to the problem of understanding and properly classifying the fundamentals of modern measurement systems. The many ramifications and the apparent complexity of this type of equipment make it imperative that terms be standardized more specifically

than at present, and a co-ordinated nomenclature, therefore, is suggested.

The principal beneficial results obtained from this study may be summarized as follows.

Clearer Understanding

It seems obvious that a useful medium is made available to depict or illustrate individual measurement systems or devices, showing in a systematic manner and in the proper sequence just how they function. As a corollary, a specific use of words and phrases connected with measurement leads to verbal or written technical treatment that can be understood easily and commonly. It is hoped that this may have some helpful influence on future standardization activities.

By identifying common functional elements or assemblies of elements, a convenient method is provided for exploring and evaluating the whole measurement field and determining fundamental relationships in equipment having widely different applications. It is also of value in studying various designs of measurement apparatus intended for the same purpose and determining fundamental differences and similarities. This all can be accomplished by carefully listing the basic elements, primary detectors, intermediate means, end devices, auxiliary means, or control initiators of which the apparatus under consideration is composed.

Co-ordination and Standardization

As a result of a clearer understanding of the exact nature and purpose of the various functional parts of a measurement system or device, engineers can co-ordinate more effectively the design of specific basic elements, parts, or mechanisms. Co-ordination here is used in the sense of insuring that specific parts having a particular function be used as widely as possible in different apparatus wherever that function is required. Wasteful duplication thus is prevented by minimizing minor variations in parts or mechanisms intended to perform the same or very similar operations.

The interrelation of basic elements, primary detectors, and other functional parts of a system has been emphasized in connection with Table IV. This also is indicated clearly by the fact that only 92 basic elements (Table III) are required to build up many hundreds of greatly diversified systems and devices. Of course

Table IV. Partial Listing of Functional Analysis and Classification of Measurements

Quantity Measured	Primary Detector		Intermediate Means		End Device	
	Name	Basic Elements	Name	Basic Elements	Name	Basic Elements
Group I—Electrical quantities						
D-c amps and volts	D'Arsonval mechanism	(2.1)(20.1)	None	—	D'Arsonval indicator	(2.1)(20.1)(30.1)(24.1)
	D'Arsonval mechanism	(2.1)(20.1)	None	—	D'Arsonval recorder	(2.1)(20.1)(30.1)(17.1)(6.5)(16.1)(26.1)(27.1)
A-c amps and volts	Moving iron mechanism	(3.1)(9.1)	None	—	Moving iron indicator	(3.1)(9.1)(30.1)(24.1)
	Thermocouple converter	(29.3)(32.1)	None	—	D'Arsonval indicator	(2.1)(20.1)(30.1)(24.1)
	Electronic rectifier	(29.1)(1.1)(8.1)(28.2)(33.5)(6.3)	None	—	D'Arsonval indicator	(2.1)(20.1)(30.1)(24.1)
A-c power	Electrodynamic mechanism	(2.1)(2.2)	None	—	Electrodynamic indicator	(2.1)(2.2)(30.1)(24.1)
A-c energy	Watthour meter mechanism	(3.1)(5.1)(20.3)	None	—	Watthour meter	(3.1)(5.1)(20.3)(16.1)(24.1)
A-c power demand	Watthour meter mechanism	(3.1)(5.1)(20.3)	Elec impulse transmission	(16.1)(16.4)(4.1)(6.5)	Demand recorder	(3.1)(9.2)(16.6)(16.1)(17.1)(16.2)(16.4)(30.1)(27.1)(26.1)
	Bimetallic actuator	(33.1)(31.1)	None	—	Thermal demand indicator	(33.1)(31.1)(16.1)(24.1)
Totalized a-c power demand	Watthour meter mechanism	(3.1)(5.1)(20.3)	Elec impulse transmission	(16.1)(16.4)(4.1)(6.5)	Demand recorder	(3.1)(9.2)(16.6)(16.1)(17.1)(16.7)(16.4)(30.1)(27.1)(26.1)
			Totalizing relay	(3.1)(9.2)(16.6)(16.1)(16.4)(4.1)(6.5)		
Group II—Nonelectrical quantities						
Speed	A-c generator	(20.2)(3.2)	Synchronous motor	(3.2)(20.2)	Magnetic drag disk indicator	(20.3)(5.2)(30.1)(24.1)
	A-c generator	(9.1)(20.1)(3.2)	Frequency sensitive rectifying network	(33.3)(28.1)(29.1)	D'Arsonval indicator	(2.1)(20.1)(30.1)(24.1)
Aircraft-engine synchronism	A-c generator	(20.2)(3.2)	None	—	Rotating field and vane indicator	(3.2)(9.1)(24.1)
Temperature	Resistance temperature detector	(29.3)	Resistance bridge	(29.1)(6.1)	Moving mag ratio indicator	(29.1)(2.2)(20.2)(24.1)
	Thermocouple	(32.1)	None	—	D'Arsonval indicator	(2.1)(20.1)(31.1)(30.1)(24.1)
	Thermocouple	(32.1)	Galvanometer	(2.1)(20.1)	D'Arsonval recorder	(2.1)(20.1)(30.1)(17.1)(6.5)(16.1)(26.1)(27.1)
			Optical transmission	(22.1)(18.1)(18.2)(21.3)		
			Electronic ampl.	(29.1)(1.1)(8.1)(28.2)(33.5)(6.3)		
Pressure	Bellows mechanism	(25.1)	Induced 2nd harmonic transmission	(20.2)(15.4)(6.3)	2nd harmonic ratio indicator	(15.4)(20.2)(20.1)(24.1)
Flow	Pump mechanism	(11.1)(20.4)	Selsyn transmission	(4.2)(6.1)(29.1)(3.2)(20.2)	Magnetic drag disk indicator	(20.3)(5.2)(30.1)(24.1)(16.1)(24.2)
Liquid level	Float mechanism	(10.1)(16.1)(20.4)	D-c Selsyn transmission	(29.2)(6.1)	D-c Selsyn indicator	(3.2)(20.2)(24.1)
	Capacitor	(1.2)	Elec oscillator	(15.3)(1.1)(29.1)(8.1)(6.1)	Moving mag ratio indicator	(2.2)(20.2)(24.1)
Direction	Horizontal axis gyro	(14.1)(3.2)(6.3)	None	—	Directional gyro indicator	(14.1)(3.2)(6.3)(16.1)(24.2)
	Compass mechanism	(20.2)	Induced 2nd harmonic transmission	(15.4)(6.3)	2nd harmonic indicator	(15.4)(20.2)(24.1)
Time	Timing motor	(17.1)(6.5)	None	—	Time switch	(16.1)(24.2)(16.4)(16.2)(30.2)(4.1)
Light	Light cell	(21.1)	None	—	D'Arsonval indicator	(2.1)(20.1)(30.1)(24.1)

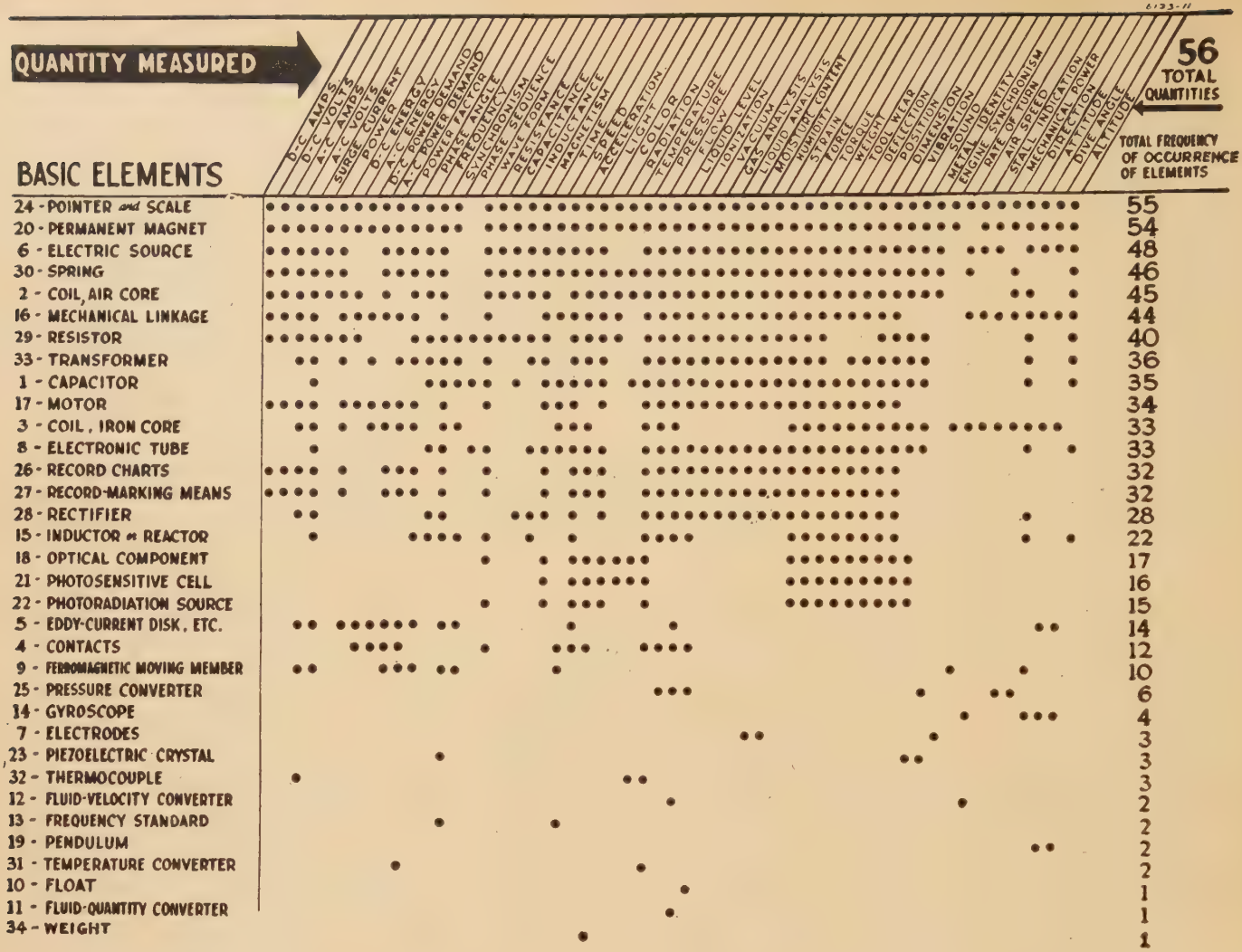

Figure 11. Frequency of occurrence of basic elements

many varieties of these have been developed for specific purposes, probably many more than are economically sound. It would seem that engineers are concerned mostly with designing some modifications of existing basic elements and regrouping them in order to accomplish a desired result. It rarely happens that a really new one is added.

In order to get a rough idea of the extent to which each basic element that has been identified actually is used for various types of measurements, the tabulation shown in Figure 11 has been prepared. Apparatus suitable for measuring 56 of the more important electrical and non-electrical quantities was analyzed and the necessary basic elements listed. In Figure 11, basic elements involved are shown in the order of their frequency of occurrence. This arrangement is useful in emphasizing those elements that probably require most attention for co-ordination purposes. It is not claimed, however, that this tabulation is complete, nor entirely accurate. It is a generalization and presents a point of view that may be useful.

All progress that can be made in co-ordinating and standardizing functional parts of devices and systems will be, of course, a powerful influence in arriving at better standardization of measuring equipment as a whole.

Research and Development

Well-arranged lists of basic elements and the general functional parts of all known measurement apparatus or equipment are very helpful to research and development engineers. They indicate clearly what is available and where new development or inventions are required. Furthermore, the general viewpoint and over-all understanding that can be gained from an analysis such as outlined enables an engineer to focus his attention directly on a desired specific objective and to see it in proper relation to the general problem in hand and the entire measurement field.

Application and Service

In the selection of measurement equipment for a specific purpose, the functional analysis method can be quite helpful in several ways. In the first place, the simplified functional diagrams should aid in understanding and choosing the proper instrumentation and in maintaining it in service. Evaluations and comparisons made possible by the system described aid materially in answering such questions as the following. How direct is the measurement? Is there undue complexity, especially in intermediate means? Are the basic elements inherently simple and reliable? Is the design well co-ordinated? What auxiliary means, or power supply, is necessary? Correct answers to these and other pertinent questions can be expedited if the application engineer is familiar with the idea of functional analysis and uses it carefully as an aid to his investigations.

Data and Statistics

Considerable use already has been made of the systematic classifications and tabulations of measurement functional parts for purposes of filing and cross-indexing.

Simplicity in Protective Relaying

LLOYD F. HUNT
FELLOW AIEE

SIMPLICITY is of paramount importance when designing and laying out protective relay circuits. These circuits are called upon to operate so infrequently that they should be more reliable than the apparatus or lines they protect. Certain limiting conditions and requirements requested by circuit designers generally cause false tripping and make the circuits less reliable. A simple protective system with all the extra devices left out operates so satisfactorily that the reasons for its good operation are often forgotten. The simple rules concerning protective systems in use on the Southern California Edison System that have made it possible to attain such a high standard service to its customers are reviewed in this paper.

A short study of fault conditions reveals that by far the majority of failures are faults to ground. On very high voltage transmission lines on steel towers ground faults approximate 98 per cent of all faults. On lower voltage transmission lines and higher voltage distribution lines on wood poles, ground faults drop to about 90 per cent. For rotating machines and transformers ground faults reach 98 per cent. Therefore the task for protection engineers is to design protection to isolate ground faults first. If a perfect system of only ground fault protection were used, the service record of relay performances would be an excellent one. It is therefore important that the added protection necessary for faults other than those to ground should be simple.

Conclusions

This paper presents the principles that have guided the application of protective systems over a period of the last 20 years. It is evident from the above-average record of operation that they have paid in equipment saved, and outages and false tripping prevented.

Because all these principles have been based on simplicity and reliability, the results of continued service have justified their practices.

Though many relay applications have been pioneered on the Edison system, the trend has been to apply protection primarily for the majority of faults. Elimination of complicated schemes for protection against less important faults has resulted in a system that has been designed and maintained easily. The record of approximately 99 per cent perfect relay operations over a long period of time indicates the justification of these principles of simplicity and reliability.

Paper 46-173, recommended by the AIEE committee on protective devices for presentation at the AIEE summer convention, Detroit, Mich., June 24–28, 1946. Manuscript submitted April 15, 1946; made available for printing May 24, 1946.

L. F. HUNT is with Southern California Edison Company, Ltd., Los Angeles, Calif.

Introduction

The Southern California Edison Company, Ltd. has primarily a transmission type system. It is expanding continuously to meet the needs of a very rapidly growing community serving 17,500 square miles in southern California. Its present transmission system is shown in Figure 1. From this diagram it can be seen that the backbone of the system is the 220-kv line starting at Big Creek and Boulder power plants, running through or to the major stations and ending at Long Beach number 3 steam plant.

The load is supplied through the 66-kv subtransmission system. The 66-kv system is divided into many sections. At each major substation where 220 kv is stepped down to 66 kv, the 66-kv system is a unit by itself, not normally paralleled with any other 66-kv group. Even at some of these major substations the 66-kv busses are split to form two of these groups. For example, the 66-kv system at Eagle Rock can be paralleled or it can be separated, each part being supplied from one transformer bank. It is not clearly shown in Figure 1 where the separation of the 66-kv lines are made between 66-kv systems. This is variable according to load conditions. For example, the 66-kv system of Eagle Rock

---

Data on primary detectors and end devices, for example, can be indexed in accordance with the quantities to which they respond, as well as by their names on the charts. Intermediate and auxiliary means can be indexed relative to the function they perform and also the specific names assigned to them. Basic elements are specifically and conveniently listed on the chart and each one can be subdivided into detailed variations as far as desired. All technical information available can be so indexed that it is readily identified with the pertinent basic element. These examples will serve to point out the usefulness of this method in organizing and indexing technical information.

General

The benefits realized by the functional analysis and classification of measurement systems and devices that has been described will depend a great deal upon how much it is really studied, understood, and applied in a given organization or industry. In this paper it has been possible to present only a small part of the work that has been done on the subject. It is also likely that the point will be raised that nothing really new or radical has been presented. In one sense this is true. What has been attempted, however, is to collect, analyze, systematize, and organize information, methods and nomenclature that have been used in the art, but used in an unsatisfactory and indefinite manner. In doing this it was found necessary to coin some new words and phrases and to give these, as well as those commonly used, specific meanings and definitions. It is felt, too, that a complete analysis consistently and systematically carried out from the functional viewpoint is new. Actually, it has already proved very useful in a practical manner. Although little thought has been given to the matter, it is also probable that the methods described in this paper can be extended advantageously to apparatus and equipment quite outside of the measurement field.

References

1. AMERICAN STANDARD DEFINITIONS OF ELECTRICAL TERMS, ASA-C42-1941. American Standards Association, 1942.

2. FUNDAMENTALS OF INSTRUMENTATION (book), **M. L. Behar.** Instruments Publishing Company, New York, N. Y., 1932.

3. PROCESS CONTROL TERMS, *Mechanical Engineering*, volume 66, March 1944, pages 205–06.

4. GENERAL PRINCIPLES OF INSTRUMENT ANALYSIS, **C. S. Draper, G. V. Schliestett.** *Instruments*, volume 12, number 5, May 1939.

5. ELECTRIC MEASURING INSTRUMENTS, **D. M. Nielsen.** *Electrical Engineering*, volume 65, February 1946, pages 66–74.

and Laguna Bell normally do not operate in parallel.

Figure 1 shows 1,506 circuit miles of 220-kv lines and 2,130 circuit miles of 66-kv lines supplied by 872,200 kw of hydroelectric generating capacity and 436,250 kw of steam and other generating capacity. The total frequency-changer capacity for 50 to 60 cycles and vice versa is 185,000 kw. Synchronous condenser capacity is 573,000 kva. The maximum peak load to date is 1,025,200 kw. The daily load factor during last year reached as high as 87 per cent, and the yearly load factor was over 70 per cent.

Protection Features

It is the duty of large electric systems to supply continuous service to their customers. If a perfect system could be built economically, no relaying systems would be required. This being impossible, it is important that the protection group study the problem from several viewpoints; first, of preventing faults on the system; second, of studying behavior of faults with emphasis placed on troubles that affect the system as a whole; third of directing design of protective systems by which the type and location of faults can be determined and possibly be remedied without de-energizing circuits in which the dropping of load or generation is involved; and fourth, of relaying the smallest portion of the system in order to isolate the fault.

The protection group in the Edison organization has a great deal of influence on system planning, station layout, and design. It has pointed out factors in design which were potential weaknesses and which consequently were avoided. In the layout of stations it is possible to make slight modifications to limit the amount of equipment tripped out in the case of a fault, also to arrange oil circuit breakers to give flexible operation and over-all protection. Recording devices such as automatic oscillographs, Hall recorders and disturbance recorders have been installed at strategic locations.[1] The records of these devices are used for studying methods of better protection. The recorders also are used in the determination of the location of faults. This has aided materially the field forces in checking the condition and damage of the transmission lines.

Protection of Transmission System

Because the prime purpose of protection is to maintain service to customers and to do as little relaying as possible to accomplish this without leaving the facilities in a hazardous condition, it behooves the protection men to use systems of simple circuits.

In the initial application of relays to the Edison system, many individual design engineers took it upon themselves to make up circuits for installations upon which they were working. It was soon found that every job had its distinctive style of connections without any co-ordination of relays. The protection group no longer could be satisfied with studying the behavior of relays but had the duty of dictating types and styles to fit in the system as a whole.

In the original circuit designs the relays operated annunciators, bells, and flags without much regard to tripping circuit breakers. This soon led to a simple standard rule that has continued through the years. That is, the trip circuits of relays are to be the simplest for direct tripping and that only the necessary knife switches be included to facilitate relay testing. Because switches can open from causes other than by means of the trip coil, it was decided, and still is an Edison standard, to have an auxiliary switch on circuit breakers to operate the alarm circuits. Earthquakes and passing trains have caused circuit breakers to trip without signals to the operator under normal setup; however, with the momentary closing of an auxiliary switch upon the opening of the circuit breaker, an alarm is set off. All tripping circuits should be locked in until the auxiliary switch on the circuit breaker has released the trip-coil current. In many locations, as shown on Figure 1, it is necessary to trip two circuit breakers. This is done with double-trip relays. Figure 2 shows schematically the standard tripping and alarm circuits. When more than two circuit breakers are tripped, as in the case of differential protection, an auxiliary relay is used with a sealing-in circuit as shown in Figure 3. This type has a separate reset circuit which is common for tripping all auxiliary relays in the station, thus requiring the operator to use only one reset button for his entire station. A special alarm is used on each auxiliary relay, and thus the operator knows he must reset it before any switching is done. This seems apparent, but the less operators have to remember about such things during system disturbances, the better is the operating record. Many years ago, a hand-reset tripping-relay caused a very long system outage. The operator had no signal to inform him that this relay had not been reset and in the excitement of the trouble he forgot to reset the relay. When the circuit breaker was closed it tripped out immediately, and it was assumed the line (the only 220-kv line left) had a permanent fault. Since this disastrous outage occurred the rule is that all tripping circuits are to be released automatically as in Figure 2, or released manually with an alarm on the relay as in Figure 3.

The relay system on the 220-kv lines is differential from one end to the other, without adjacent section backup, and without overload protection. The word

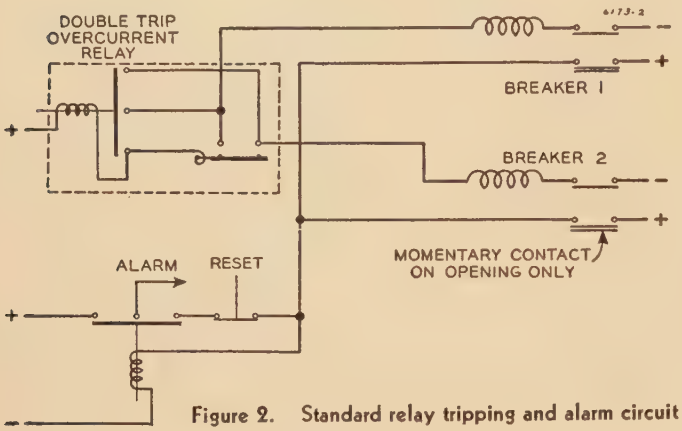

Figure 2. Standard relay tripping and alarm circuit

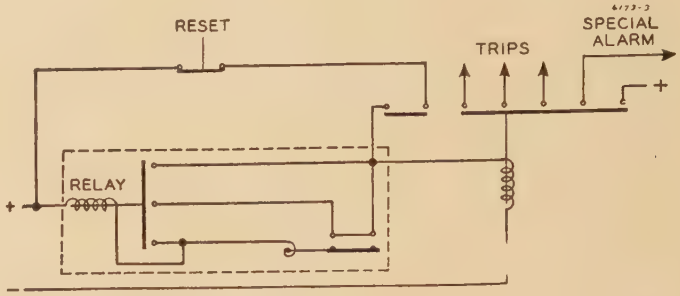

Figure 3. Standard auxiliary relay tripping circuit

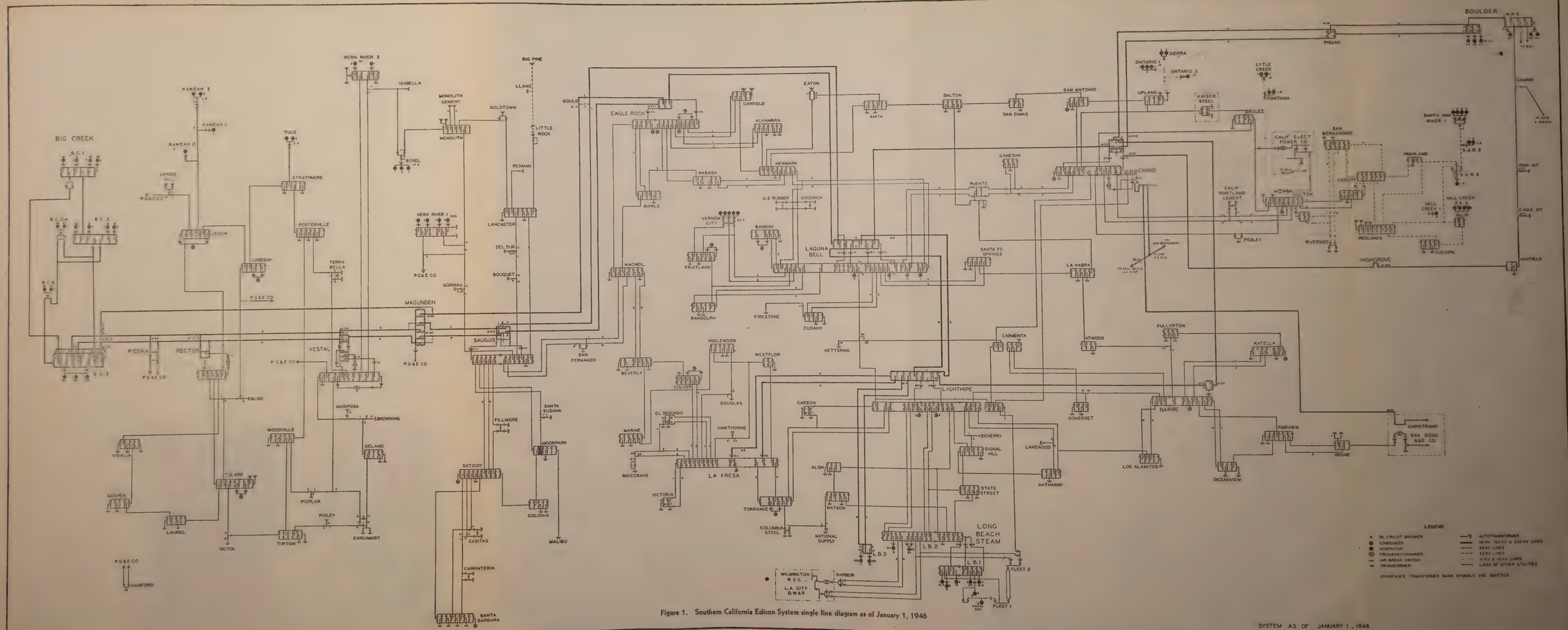

Figure 1. Southern California Edison System single line diagram as of January 1, 1946

differential is used in the broad sense rather than literally. All of the relays are not connected differentially, but are arranged so as not to trip when faults occur in adjacent sections. The primary protection for all 220-kv line sections, is of instantaneous overcurrent type. All 220-kv terminals are equipped with three phase, and one ground element relay as shown by Figure 4. The ground elements are set to operate on slightly above maximum through ground current. In these cases the ground elements will trip on sequence when the fault is close to one end, and simultaneously when the fault is in the center section. The phase elements are set to operate on just above out-of-step currents. On long sections this setting covers about 40 per cent of the distance from the station. In the shorter sections when all lines are in service these settings generally cover 100 per cent of the line in sequential tripping. To secure tripping for the remaining portion of the lines, or when some lines are out of service, a carrier system of relaying is used when necessary. Otherwise, on long lines where blocking is not essential, the relay scheme of carrier is used without the carrier blocking

The Edison system's first 220-kv carrier-current relay system was started in 1926. This system was very complicated and the record of its operation was unsatisfactory. There were more false tripouts than correct tripouts. In fact, more cases of internal faults were cleared on this line section by the alternate group of relays because it was necessary to have the carrier relay group out for repairs.

The next line section that was equipped with this type of carrier system had a 100 per cent performance record on both internal and external faults, but the record of the very complicated system changed to about 50 per cent operation because of many unnecessary tripouts. This complication, excessive maintenance, time out of service, and replacement costs, required an investigation of a simple and more reliable system. The system which was developed[2] utilizes a lockout carrier or pilot wire and is very simple, because the short circuits on the 220-kv system were mostly ground faults, a few phase-to-phase or phase-to-phase-to-ground, it was believed that simplicity justified leaving out the instantaneous 3-phase fault protection. The phase protection consists of a balanced-current relay for tripping, that is, A phase is balanced against B phase, B phase against C phase, and C phase against A phase. If an unbalance of ten per cent occurs at short-circuit values of current, the relay will trip. It can be seen readily that no complication is needed for guarding against tripping on out-of-step conditions.

For parallel lines, only balanced-current ground relays are used. With high-speed circuit breakers, high-speed balance relays are used and slower relays still are used with slower circuit breakers. This protection has discriminated successfully on all short circuits. With many staged short-circuit tests at Laguna Bell and Saugus substations[3] tied into the system, the whole 220-kv relay setup had an excellent test and no false tripping occurred.

The most difficult work connected with any carrier system is the maintenance of the radio sets. It became necessary to devise a transmitting and receiving set with a minimum of parts, especially capacitors and radio-frequency choke coils. The result was a set employing push-pull oscillator and push-pull power-amplifier stages, using a total of four tubes plus rectifier tubes. These sets proved economical in first cost and operated with reliability.

The terminal protection on the 220-kv system consists of an instantaneous overcurrent relay, carrier, and an auxiliary group consisting of instantaneous overcurrent and time-delay relays. Because there are no normal backup relays, it is being tested and adjusted. This is necessary because distances between installations are great, and it is desirable when highly trained test engineers are making routine tests that the relays be available for inspection.

The switching from one group of relays to another is required for all terminals when the lines cannot be taken out of service for tests. As mentioned before, in major stations on which the relays trip two breakers, push buttons are supplied so that while testing one switch at a time it may be tripped from the relays being tested.

The 66-kv system is protected by the use of inverse time setting of overload and directional relays. However, at the major supply stations such as Eagle Rock, Laguna Bell, and Lighthipe the 66-kv lines also are equipped with the same 4-element instantaneous-overcurrent relays shown in Figure 4. In these installations they are set for approximately 90 per cent of the line length. With this setting these relays have operated in many cases on the whole line after the switch had opened at the remote end.

Even the simple overcurrent directional relay has three features that make it difficult to apply.

1. It was discovered that much false tripping occurred by changing direction of flow after one end of the faulted line relayed. Study of the problem revealed that it was necessary to govern the overload element by only allowing it to close contact when the direction was correct. In those early days the Edison system built a few sets of directional-controlled relays, which were placed in service at a location where considerable

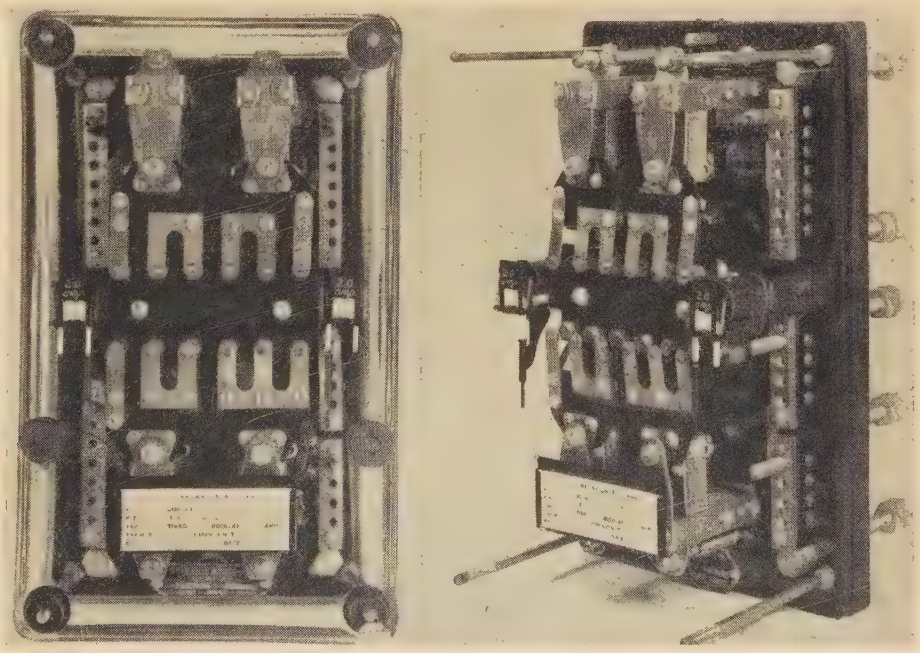

Figure 4. Four-element instantaneous overcurrent relay

difficulty with false tripping had occurred. The results were gratifying. However, it took personal contact with the factory to prove that it could be done and was necessary. It is self sufficient to say that all inverse-directional overcurrent relays are now directionally controlled.

2. The application of single-phase directional overcurrent relays must be watched. If the currents in the unfaulted phases of a ground fault reach values above minimum trip setting of the relays, one of the unfaulted-phase relays on unfaulted lines will be in the direction of trip and will cause unnecessary tripouts.

3. In all directional schemes operated by potential it is possible to have a short circuit that will reduce the voltage to a value so low that the relays will not function. Rigid inspection is required to keep relays in condition to operate at very low voltages. In fact, a very thorough study was made several years ago about changing the 66-kv type of protection. This study revealed that if the directional elements of the relays were modernized according to our requirements, we would have as good an operating system with the existing circuit breakers as possible. As a result the directional elements were modernized with about $35,000 worth of parts. The results have proved the study was right because it is now very seldom that a short circuit occurs which reduces the voltage sufficiently to cause false tripping.

At present a program of rebuilding all 220-kv circuit breakers so that they will range from three to five cycles in opening time is under way. This will require slight changes in our relay system. The time-delay balanced-current relays will be replaced with high-speed balanced-current relays, and in some places the carrier will be speeded up slightly by using higher speed directional-relays. Another program of speeding up all 66-kv switches is being started and when that is done, changes in relays will be made to keep up with the progress.

Relays and relay systems using an electric circuit for preventing tripping has been avoided. The simple rule used is that a relay must act to complete a circuit to cause tripping, and it must be activated by a definite minimum fault current. The simple tripping circuit of Figure 2 holds true in our carrier schemes. It is very easy to have something happen to a holding circuit thus allowing the tripping of unnecessary switches. This perhaps is the main reason for not using distance relays. In several places where these were used in interconnections with other systems, outages occured more from false tripping than by actual faults. Much has been said about tripping currents of less than full-load value. In many 66-kv faults when the current was reduced by the opening of the first switch, the arc went out before the second end of the line could relay. Recently one 66-kv line grounded several times without maintaining an arc long enough to trip any of the circuit breakers.

Two instantaneous 3-phase short circuits have occurred on the 220-kv system, both caused by an operator closing a 3-phase gang-operated grounding switch on a hot line. The first occurred before the addition of instantaneous overcurrent relays and automatic separation. This caused a severe hydroelectric system outage and a much longer steam system outage. The other was tripped out by instantaneous relays at the end closest to the station. Because it happened on a

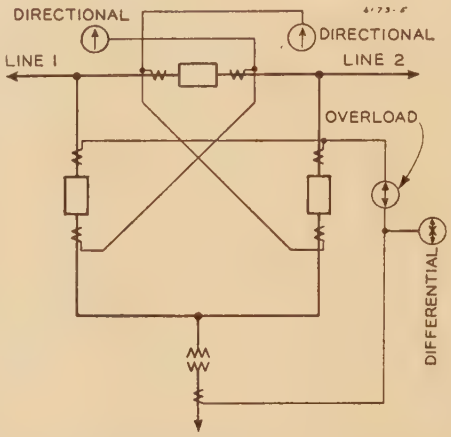

Figure 5. Station layout for one transformer bank and two lines

long section of line, the other end did not relay, therefore the automatic separation of the system allowed the steam to carry its load without interruption. The operator cleared the line with an apparent heavy load on it and the hydroelectric system suffered only a slight interruption. This clearly illustrates the advantages of these two devices. It might be interesting to analyze the action of the normal carrier systems that rely upon voltage directional relays for tripping under these same conditions. In these cases with the voltage ratio of 2,000 to 1, not even a trace of voltage would appear across the voltage coils of the relays. This means there is no tripping with the normal setting. If the relays were biased to operate under these conditions, then all the lines would relay, as in the previously mentioned cases, and the entire hydroelectric load would be dropped. Because these two cases are the only instantaneous 3-phase short circuits on record to date, it is apparent that not much risk is being taken in an over-all operation. Another fact that sometimes is overlooked, is that when some flashovers do go 3-phase it is possible that the arc will go out of its own accord on the first or second slip cycle because of reduction of voltage.

The separation system[4] used operates on three slip cycles, and is adjustable for two to five slip cycles. Prearranged tripping setups are made so that Big Creek hydroelectric plant has its load, Boulder hydroelectric plant has its load, and Long Beach steam plant has its load to carry when they are separated. Many tripping operations have taken place without interruption of load and with all points resynchronized in two minutes.

Protection for Equipment

Synchronous machines generally are equipped with only the normal induction percentage differential relays for generator use. Even though generators have split windings no additional relays are used. All synchronous machines operate with neutrals ungrounded. A potential transformer connected from neutral to ground is used to initiate an alarm when faults occur.[5] In all major generating plants the unit system of generator and transformer installation is used. In some locations two generators are used with one bank of transformers. This is also true with synchronous condensers. No distribution circuits are taken directly from generator leads. The exception has occured at small unimportant generating stations. The alarm is sounded when a ground of ten per cent or more has occurred. A ground detector then is used by the operator to determine the magnitude of the ground fault. There has been much comment about using only a potential transformer for this purpose, but experience[6] has shown that it is more than justified. To date the results of operation with ungrounded neutrals have been most gratifying, and this practice has resulted in operation that has allowed use of a lower amount of spinning reserve because the chances of losing a machine have been reduced to a minimum.

J. E. Allen and S. K. Waldorf of Baltimore are to be complimented on their very valuable contribution to this subject by their work.[7] The Edison system has had all forms of ground failures since the use of ungrounded neutrals and concurs in their findings. At the present time nothing is available to alter the operating setup.

The advantages of this method of operation can be explained best by two actual cases. One midafternoon, ground alarms occurred indicating trouble on a 60,000-kva steam unit. Because the unit was required through the evening peak, it was left in service. During this

time visual inspection was made of as much of the installation as possible. It was discovered that a bus support-insulator had failed. All the necessary equipment for repair was gathered and as soon as the machine could be released the repair was made in short order. If this machine had been operated with solidly grounded neutral, a heavy fault would have occurred doing much damage and the machine would have been tripped off immediately. It would have been difficult to pick up its load immediately from other sources and, of course, the unit would not have been available for that evening's peak.

In the other case, an 80 per cent ground occurred on a 45,000 kw hydroelectric generator. It was taken off the line as soon as it could be spared. Upon test, one phase was found to be solidly grounded. This 80 per cent-indicated ground showed the fault to be about 80 per cent from the neutral to the terminal. Upon removing the faulted coil a burned spot the size of a silver dollar between coils was discovered. The lower coil showed some damage too, but had not failed yet. The coils were replaced. If this machine had had a solidly grounded neutral it would have been damaged seriously. Also the instantaneous dropping of that amount of generating capacity would have caused system trouble. Many other gratifying cases could be listed.

As a result of this satisfactory record of operation a study has been started regarding new installations without direct generator protection and with only the over-all transformer and generator differential protection. By doing this, all current transformers are eliminated from generator leads, all being connected on the neutral end of the generator. The question is, do the current transformers present more of a hazard on the leads than the value gained by using the more sensitive generator protection?

Transformers are protected by induction percentage-differential relays with good results. It is pleasing to note that the manufacturers are doing something about the weakest point in transformers. Most faults on recent transformers have occurred in high-voltage bushings. Bushings have been redesigned completely for transformers for 69 kv use and above.

Protection of Distribution

The normal inverse-time-delay relays, both plain overload and directional overload, are used for phase tripping. The most difficult faults to isolate are ground faults. There is and perhaps always will be a discussion on merits of ungrounded and grounded systems. The Edison system has many of both kind. Those operating very satisfactorily ungrounded use a ground detector[8] for giving an alarm and a grounded feeder-selector[9] for indication of a faulted feeder. This method certainly gives the maximum service to customers with equal facilities, because a fault can be run down without de-energizing the line.

The grounded-neutral system has its disadvantages in that the fault-to-ground resistance[4] varies so greatly that it is impossible to have a relay sensitive enough for all conditions. This fact led to the development of sensitive ground relaying.[10] This scheme permits tripping on one per cent of current transformer rating; that is, with 100 to 5 wound current transformers, the line can be tripped with one ampere primary ground current. The maximum ground current is limited to approximately ten times minimum trip current. The two requirements for this sensitive ground protection are for when the lines run in hazardous territory and for when higher voltage circuits are used jointly with communication circuits. In the latter case tests have been made showing that upon contact, lines will trip out without even blowing subscribers' fuses. Where power and telephone utilities are serving the same customers, much is gained in taking advantage of the economy of joint use of pole lines. Hundreds of circuits are equipped with sensitive ground relaying and the almost perfect results have justified the small extra cost of installation.

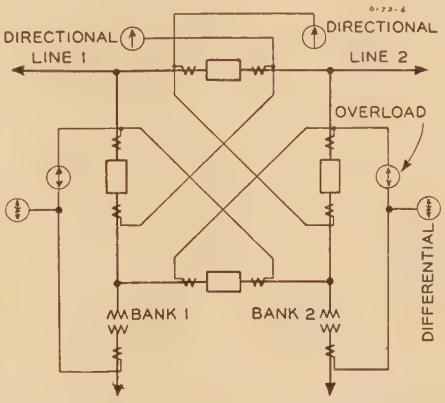

Figure 6. Station layout for two transformer banks and two lines

Station Layouts

As previously stated, the protection group has had considerable influence on station designs and layouts. Figure 5 shows the switch arrangement for a station with two lines and one transformer bank, and Figure 6 shows the switch arrangement for a station with two lines and two transformer banks. It can be seen readily that from a protection standpoint with overlapping current transformers all electrical parts are protected without the addition of bus differential protection, thus simplifying the over-all protection problem.

If five circuits are required and two are alike, such as shown for Eagle Rock substation in Figure 1 where three lines and two transformer banks are used, the six-switch setup is used. Here the bus is included in the transformer differential. For Boulder, two lines and three transformer banks are shown, and the bus is included in the line protection. With use of suspension busses a very economical installation is possible. The suspension bus requires a minimum of insulator strings, thus cutting failure hazards to a minimum.

In many station layouts long current transformer leads have been necessary. The burden of these leads has been excessive. To prevent such losses in the leads one-ampere secondary transformers are used.[11] There is a 25 to 1 gain using the same leads. The smallest size conductors from a mechanical standpoint are used which permits a considerable saving in copper and yet there is very little lead burden.

Relay Testing

All types of facilities have been tried for the testing of relays. As early as 1925 a plug-in relay was developed and studies were made to determine its value. The relay was all right, but the problems encountered in its application were more than could justify its complication. The most satisfactory method and the one that is standard in all installations in Edison stations is very reliable. On all important lines which are required to be kept in service while the relays are being tested two sets of relays with a roto-switch for switching from one group to another are installed. Where lines can be de-energized one set of relays is used with a roto-switch for testing. No lines are left in service without protection. In many installations, the second group of relays is identical to the first group; in other installations, the second group has somewhat fewer but adequate protective features. For machine differential protection the relays are inspected and adjusted during overhaul periods, but in some cases it has been justifiable to put in an alternate set of relays for machines which operate for long periods.

Electromechanical Transient Performance of Induction Motors

C. N. WEYGANDT
ASSOCIATE AIEE

S. CHARP
ASSOCIATE AIEE

Synopsis: This paper is the result of a differential analyzer study of the starting characteristics of 2-phase induction motors. The prototype of the motors investigated is the small 2-phase machine commonly used in closed cycle control systems. The performance equations of the induction motor are solved, and summary curves based upon the conclusions reached are presented in a form useful to motor designers. No published data of this type have come to the attention of the authors. It is hoped that the results herein reported can be utilized in the design of better motors for servo applications.

EARLY in the course of development of a new closed cycle control system for a-c motors, it became apparent to the authors that there was not sufficient information available about the transient performance of induction motors. High speed performance of a servomechanical system requires that the drive motor come up to required speed in as short a time as possible. At the same time other desirable features of motor design should not be subordinated.

The performance of an induction motor can be represented adequately by the set of equations derived by H. C. Stanley.[1] Since the publication of his results, relatively little work has been done on the evaluation and solution of his equations. This failure has been mainly because of the mathematical complexity which is involved in the solution of a set of simultaneous nonlinear differential equations subject to arbitary boundary conditions.

It is the purpose of this paper to present some solutions of the Stanley equations for the case of suddenly applied voltages. Previous investigators solved these equations for the case of a motor with infinite inertia,[2] a somewhat unphysical case; or they were concerned primarily with the effects of mechanical transients;[3] or they used constants typical of large motors.[4]

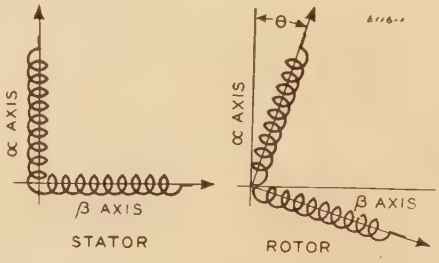

Figure 1. Stator and rotor coils showing instantaneous angular position

The motors studied have their prototype in the small 2-phase squirrel cage induction motor used in low power servomechanisms, in particular, approximately the 4-watt size. In the analysis this theoretical motor is started from rest by applying voltage to the two phases, the rotor being accelerated to synchronous speed in the case where there is no external or friction load or to some steady state speed in the case of an external or friction load.

The differential analyzer plotted the rotor speed, stator and rotor currents, and the applied voltage as functions of time. Machine parameters were varied and the results studied to determine design parameters for a motor which could start and stop in an extremely short time interval. This characteristic is necessary for successful application to a closed cycle control system.

Experimental verification for one of the motors investigated has been obtained to a degree which makes valid the broad conclusions drawn from the remainder of the work.

Assumptions

In accordance with the limitations of the performance equations for the induction motor, the following simplifying assumptions were made in this analysis:

1. Both rotor and stator have symmetrical windings.
2. The coefficient of mutual inductance is

Paper 46-116, recommended by the AIEE committee on electric machinery for presentation at the AIEE summer convention, Detroit, Mich., June 24–28, 1946. Manuscript submitted April 9, 1946; made available for printing May 8, 1946.

C. N. WEYGANDT and S. CHARP are chief project engineer and project engineer, respectively, at the Moore School of Electrical Engineering, University of Pennsylvania, Philadelphia, Pa.

The authors wish to acknowledge the assistance of the differential analyzer laboratory of the Moore School and of Chuan Chu, who assisted with the experimental work. This paper is part of the results obtained in work under contract between the Bureau of Ordnance, Navy Department, and the University of Pennsylvania.

All relays are given careful inspection by test engineers. The 220-kv line protection is given a routine check twice a year and others are inspected for periods varying from one complete secondary and tripping test a year to one every other year.

The two group relay setups have proved valuable many times when system operating conditions changed. At such times one group of relays was set for one condition of operation while the other was set for another.

All important switches are given a trip test by the operators each month according to a prearranged schedule. With all this precaution and continual checkup the comparatively simple relaying system of the Edison Company has performed most satisfactorily.

References

1. SOME PRACTICAL MEASURING DEVICES, **Lloyd F. Hunt.** AIEE TRANSACTIONS, volume 59, 1940, pages 765–8.

2. NEW PILOT PROTECTION GIVES RELIABILITY, **Lloyd F. Hunt.** *Electrical World*, New York, N. Y., volume 106, September 26, 1936.

3. DETHERMALIZING ARC QUENCHERS, **Lloyd F. Hunt, Fred H. Cole.** AIEE TRANSACTIONS, volume 62, 1943, November section, pages 720–4.

4. SOME RECENT RELAY DEVELOPMENTS, **Lloyd F. Hunt, A. A. Kroneberg.** ELECTRICAL ENGINEERING, volume 53, April 1934, pages 530–5.

5. MINIMIZING FAULT DAMAGE WITHIN GENERATOR, **Lloyd F. Hunt.** *Electrical World*, New York, N. Y., volume 94, December 29, 1929.

6. OPERATING GENERATORS AND SYNCHRONOUS CONDENSERS WITH UNGROUNDED NEUTRALS, **J. H. Vivian.** *Electric Light and Power*, Chicago, Ill., September 1943.

7. ARCING GROUND TESTS ON A NORMALLY UNGROUNDED 13-KV 3-PHASE BUS, **J. E. Allen, S. K. Waldorf.** AIEE TRANSACTIONS, volume 65, 1946, May section, pages 298–306.

8. GROUND DETECTORS WARN OF DANGEROUS CONDITIONS, **Lloyd F. Hunt.** *Journal of Electricity*, volume 56, April 1 and 15, 1926.

9. SIMPLE SELECTIVE INDICATION FOR GROUNDED FEEDERS, **Lloyd F. Hunt.** *Journal of Electricity*, volume 57, December 1, 1929.

10. SENSITIVE GROUND PROTECTION FOR RADIAL DISTRIBUTION FEEDERS, **Lloyd F. Hunt, J. H. Vivian.** AIEE TRANSACTIONS, volume 59, 1940, February section, pages 84–7.

11. ONE AMPERE CURRENT TRANSFORMER PROPOSED, **Lloyd F. Hunt, J. H. Vivian.** *Electrical World*, New York, N. Y., volume 121, June 24, 1944.

a cosinusoidal function of the electrical angle between the rotor and stator axes.

3. The rotor is smooth, and the self-inductances of all windings are independent of rotor position.

4. The effects of saturation, hysteresis, and eddy currents in the iron circuits are neglected.

5. The machine impedances are independent of rotor speed.

6. The motor is connected to an infinite bus through zero impedance.

7. All electrical switching is accomplished in zero time.

8. The stator and rotor neutrals are ungrounded.

Conclusions

1. The performance of an induction motor may be specified completely by five parameters.

τ_s = the stator time constant
τ_r = the rotor time constant
τ_m = the mechanical time constant
k = the coefficient of coupling
T_L = the load torque

2. The mechanical time constant, τ_m, should be small for rapid acceleration of the rotor. Methods for making τ_m small are discussed in a subsequent paragraph.

3. The stator and rotor time constants have optimum values for the rise time to be a minimum. The ratio of the optimum time constants is approximately unity.

4. The rise time is independent of shaft loads which are proportional to the velocity.

5. A small air gap reduces the rise time, but a point of diminishing returns can be reached between further decreases in air gap and decreases in rise time.

6. Starting an induction motor by applying voltage to one phase when the other phase has been previously energized yields the same rise time as if both phases were energized at the same time, within the range of parameters investigated.

Units Used in Analysis

In the analysis of problems involving many parameters it is usually convenient to rewrite the equations in terms of dimensionless variables. This is done commonly in electric machinery analysis, and the equations so derived are said to be in a per unit system. Common kilovolt-ampere and time bases are chosen in the usual per unit system, and voltage bases are chosen for each part of the system. In this paper it was more convenient to choose as a common voltage base the voltage actually applied to the machine and separate impedance bases for the rotor and stator. Base time was chosen as the time in seconds for the revolving field to move 2π electrical radians as in the usual per unit system. Per unit values as used in this paper mean the actual values divided by the appropriate base values. Thus, per unit current means the ratio of the actual current in amperes to the current that would be obtained if the voltage actually applied to the machine were applied to an impedance equal to the base value of impedance. Therefore, base values are not necessarily coincident with name plate ratings of the machine.

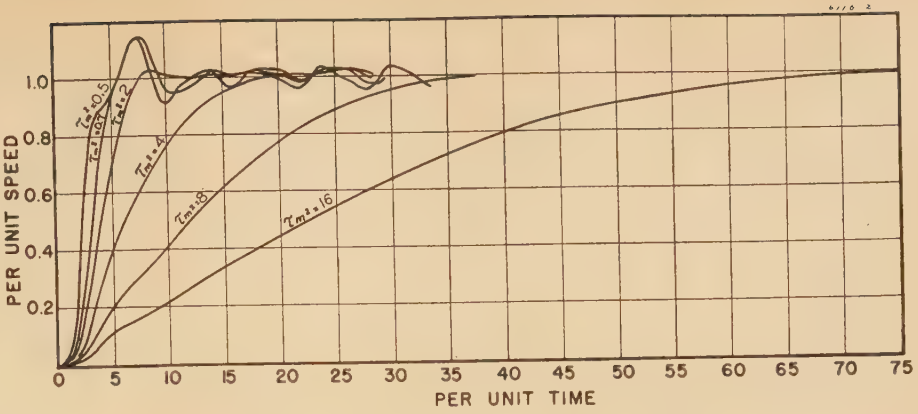

Figure 2. Effect of varying τ_m

$\tau_s = 4$ $\quad k = 0.75$
$\tau_r = 2$ $\quad T_L = 0$

Results From the Differential Analyzer

The differential analyzer plotted directly the stator current, the α and β components of rotor currents, and the rotor speed as functions of time. Hereafter, the α and β components of rotor current will be called simply rotor currents. Typical curves are shown in Figures 2 through 8.

Effect of Mechanical Time Constant

Figure 2 indicates clearly that when the mechanical time constant τ_m is decreased, there is a corresponding decrease in the rise time. For purpose of definition, rise time is taken to mean the time required to reach 85 per cent of full steady state speed. In the case of no load, this corresponds to a slip of 15 per cent. There does not seem to be any uniformity on definition of rise time for motors. In fact, there is not much agreement among workers in closely allied fields, the general opinion being to define rise time to best suit a particular problem. The square of the mechanical time constant for the 2-phase machine is defined as

$$\tau_m^2 = \frac{\omega^4 JL}{2q^2E^2k^2}$$

It is seen to be a function of six different quantities. Of these, only five can be varied at will without changing the other significant machine constants. In particular, the curves shown can represent linear changes in the rotor inertia or the stator inductance; or the curves can show changes inversely proportional to the square of the product of applied voltage, number of pairs of poles, and coefficient of coupling. The curves are sufficiently general to admit interpretation in either direction.

It can be seen from these curves that an induction motor at normal voltage does not rise to speed in a smooth fashion. This can be explained by the fact that during the starting period there exists a damped oscillation in the electric torque.

Effect of Rotor and Stator Time Constants

The magnitude and duration of the induced voltage and current in the rotor circuit would be obviously a function of the rotor parameters. In the case of a squirrel cage rotor it is virtually impossible to measure inductance and resistance. However, it is possible by a series of physical measurements (Appendix III) to compute a number which can represent the ratio of the rotor inductance to the rotor resistance. The product of this ratio and the angular frequency is termed the rotor time constant and is given by the relationship $\tau_r = \omega l/r$.

Figure 3 illustrates the effect of changes in this time constant, keeping other machine parameters fixed. It is seen that there is an optimum value for the rotor time constant in so far as rapid rise time is concerned. The rather large oscillations in speed, not at fundamental frequency, are oscillations at the natural period of the system, determined by the inertia and the electric torque acting as a spring.

This figure also shows the variations of the rotor and stator currents as functions

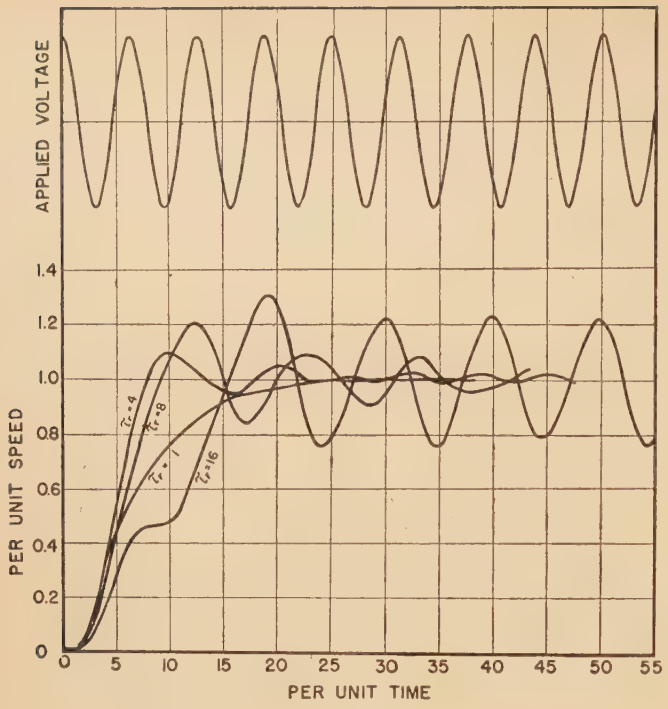

(a)

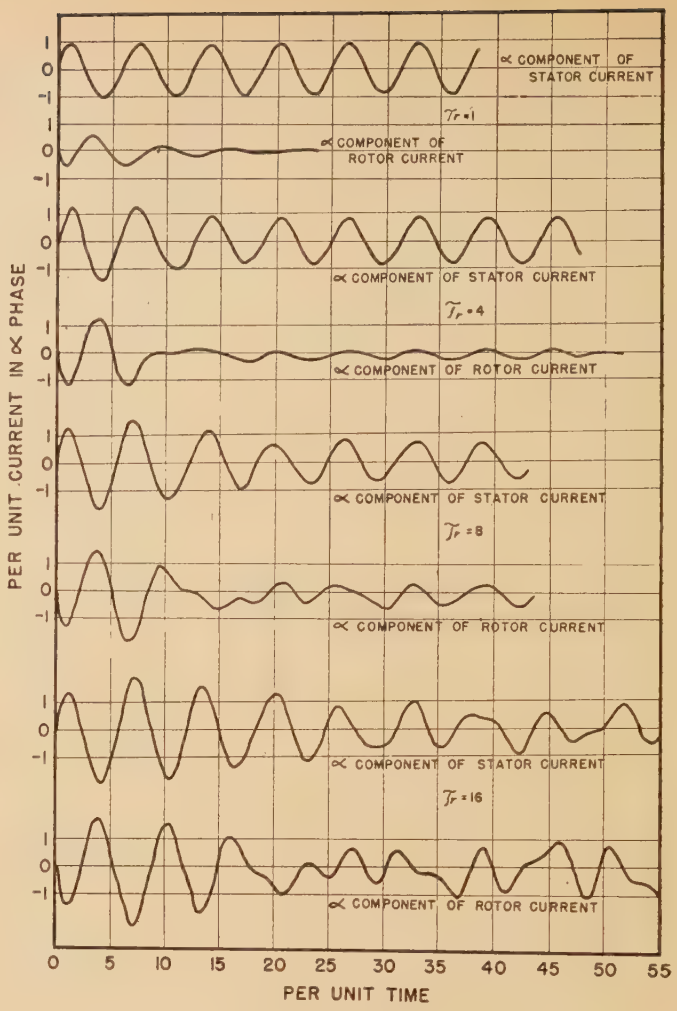

(b)

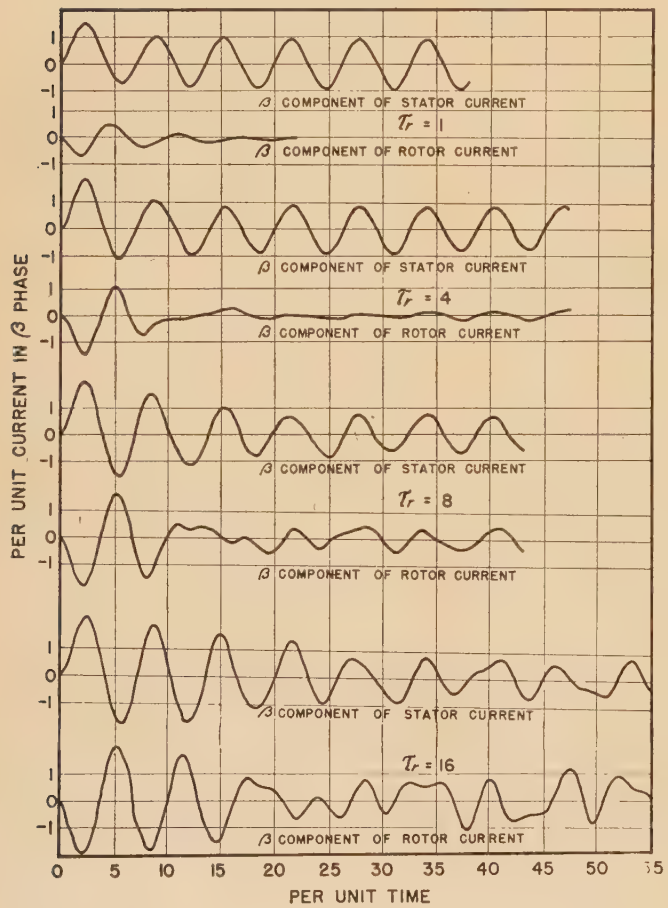

(c)

Figure 3. Effect of varying τ_r

τ_m^2=2.5 k=0.75
τ_s=4.0 T_L=0

(a). Per unit speed and applied voltage versus per unit time
(b). Per unit current in α phase versus per unit time
(c). Per unit current in β phase versus per unit time

of time. It is seen that when the rotor currents have decreased to a small value, the rotor has gone up to synchronous speed. The current surges in the rotor rarely last for more than one cycle. Therefore, little attention need be given to its peak heat dissipating properties.

The stator inductance and resistance combine in an analogous manner to form the stator time constant $\tau_s=\omega L/R$. Figure 4 shows the motor speed as a function of time. It can be observed that there is an optimum value of τ_s for this machine, other constants being equal.

Effect of Friction Load

In the majority of applications of servo motors used in low power controls, there is little or no load on the motor. The curves previously discussed were all for the case of no load. In certain other applications, however, a damping load proportional to velocity is of importance. The effect of a load on the performance of an actual motor is illustrated by the speed response curves shown in Figure 5. The time to reach steady speed is almost independent of the load. Of course, the final speed is dependent upon load. It is interesting to see from this curve that for most loads encountered in servo work, even up to a friction torque coefficient equal to the base torque of the machine, there is no appreciable change in the speed–time curve. It is only for the much higher values of load that there is a decided drop in speed.

Effects of Switching

A servomechanism must have rapid response in accordance with variations in

input signal. Consequently, a servo motor must be able not only to rise to a steady state speed rapidly, but also to reverse in a short time. An investigation was made of the reversing or switching of a motor, with possible application to plugging a motor to zero speed. Typical results are shown by the solid lines in Figure 6, where the variable parameter is τ_m. The parameters used in this set of curves are those of an actual motor. It is seen that the lower the value of τ_m, the shorter can be the reversing time. Here again is observed the decided oscillation in the motor speed after the reversal. In this study, reversal of the motor was accomplished by shifting instantaneously the phase angle of the voltage applied to one phase of the motor by 180°. The effect of this switching on the currents can be observed clearly.

The β phase was switched in this investigation. It is seen that the rotor and stator currents reverse in phase and go through a transient period, in which the magnitude of the transient current may be several times the normal steady state value. During this transient period, the α phase currents likewise change, due to induced effects, but here there is a change of magnitude only, accompanied by a time lag due to the electrical constants of the machine. The initially large rotor currents result in a large value of electric torque in a reverse direction; hence, the motor speed starts to drop almost instantaneously. The acceleration during this period never can be infinite because of circuit time lags, but it can be extremely large. For example, the average acceleration of the steepest speed curve shown in Figure 6 is approximately 1. This means that the motor comes to rest from full speed in one direction in an interval of time of 1 unit, which for a 60-cycle voltage is 1/377 second or 2.65 milliseconds. In terms of cycles, this is 0.159 cycle or about 1/6 cycle. Response of this order of magnitude is desirable for a rapid servomechanism.

Sequential Energizing of Phases

Most applications of servomechanisms which use a 2-phase induction motor for the output are operated with one phase permanently connected to a source, the second phase responding to a signal. Figure 7 proves that better over-all operation of the motor may be achieved by connecting both phases simultaneously. In Figure 7, the initial conditions were as follows:

1. Both phases were connected at the same time, and the motor accelerated up to synchronous speed.
2. With the motor at rest, the α phase was energized, and the β phase was short-circuited. This latter condition was continued for three cycles of the applied voltage. Then full voltage was applied to the β phase. The speed response of the motor as a result of sequential application of voltage, was exactly the same as if both voltages were applied at the same time.

As a result, it would seem desirable not to operate a motor with one phase always energized, if for no other reason than to keep the motor from heating when not in useful operation.

In order not to confine this study to a small motor, a set of curves is shown in Figure 8 representative of a much larger machine. For the constants chosen, it is seen that the motor accelerates unevenly, and when the average steady state is reached an oscillation in speed at approximately fundamental frequency occurs. Presumably, had the solution been carried further, these oscillations would have died out. The rotor and stator currents are particularly interesting for this set of parameters. The transients are prolonged and of higher value than in the motors previously considered. A decided d-c component in the rotor and stator circuits is seen to be present.

Analysis of Differential Analyzer Results

The general results of this study may be summarized in a set of curves showing the over-all effects of varying the time constants and physical dimensions of the induction motor. Typical summary sheets are shown in Figures 9 through 14.

The time for the experimental motor to accelerate from rest to 85 per cent of its steady state speed and the time for the current to decay to steady state value are plotted in Figure 9 as functions of the square of the mechanical time constant τ_m. After steady state was reached, for each of the values of τ_m the voltage applied to one phase was reversed, resulting in a reversal of the rotor rotation. This reversal introduced a transient current. The time curves for the speed to change to 85 per cent speed in the reverse direction are shown as a dotted line in Figure 9. The broken lines are drawn to represent a motor having a slightly different value of τ_s and τ_r.

The effect of a low value for the mechanical time constant can be obtained by increasing the applied voltage above normal. But in a machine this variation is limited by insulation difficulties and by a saturation, an effect wholly neglected in the present study.

The coefficient of coupling k cannot be changed to any great extent, even by machine design, but the number of pairs of poles q can be changed. Since this factor does not appear in any other machine parameter, it is reasonable to say that increasing the number of pairs of poles to a limit bounded by the physical size of the machine is to be preferred to increasing the voltage.

Of course, when the number of poles is increased, the synchronous speed is decreased and the torque increased in direct proportion. Servo motors usually drive a load through a step-down gear ratio, so that the output speed can be kept the same by reducing this ratio. This results in more efficient over-all operation. When the number of poles is increased, the rotor inertia probably must be increased also. If the ratio of the new moment of inertia to the original moment of inertia is less than the square of the increase in the number of pairs of poles, τ_m will be reduced.

The theoretical results obtained on the

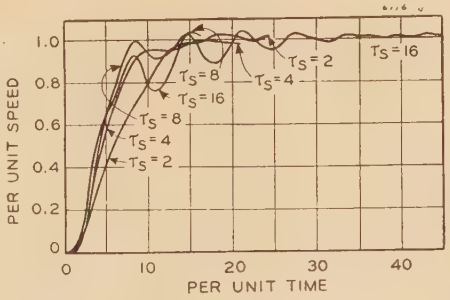

Figure 4 (above). Effect of varying τ_s

$\tau_m^2=2.5$ $k=0.75$
$\tau_r=2.0$ $T_L=0$

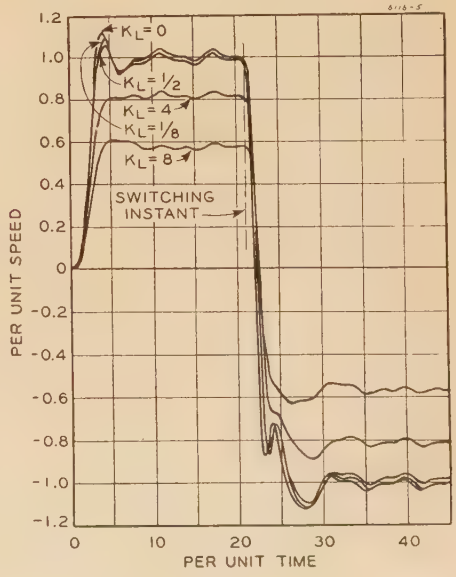

Figure 5 (right). Effect of varying K_L

$\tau_s=2.35$ $\tau_m^2=0.356$
$\tau_r=3.50$ $k=0.815$

Figure 6a. Comparison of theoretical and experimental curves for various τ_m's

$\tau_s = 2.35$ $\quad k = 0.815$
$\tau_r = 3.50$ $\quad T_L = 0$

Per unit speed and applied voltage versus per unit time. The dotted curves were determined experimentally

differential analyzer were verified experimentally in the case of variations in applied voltage or τ_m. The parameters of an actual motor were used on the differential analyzer, the results of which are shown in Figure 6. For an experimental check, this motor was shaft coupled to an a-c rate generator with one phase of the generator excited with 1,000 cycles. The voltage induced in the second phase was proportional to the speed of rotation of the motor rotor. The generator output was fed to a cathode ray oscilloscope, and a photographic record was made of this voltage as the motor accelerated from standstill. Measurements were made for applied voltages of one, two, and four times normal. The envelopes of the resulting curves are plotted on Figure 6 as a dashed line. It is seen that at voltages above normal there is better agreement between the theoretical and experimental result. For all voltages, the time to rise to full speed is approximately the same for the theoretical and experimental tests, agreement being within 30 per cent at full speed.

Some differences exist between the motor theoretically studied and that used in the experimental setup. The added inertia due to the rate generator rotor increases the effective inertia of the motor by 13.3 per cent. The effect of this increased parameter increases the square of the mechanical time constant by a like amount. As seen from the summary curve *d* of Figure 9, this increased inertia has the effect of increasing the rise time by a like amount.

Measurements on the experimental motor indicated that the time constants of the stator and the rotor changed with variations in applied voltage. These changes were not recognized in the analytical study, since the effects of saturation were neglected. It should be observed, however, that Figure 6, which compares the speed-time curves of the analyzer and actual systems, shows better agreement at the higher voltages, at which points it would be expected that saturation of the motor would enter the problem. As with the analyzer solution, the variation of rise time with mechanical time constant is linear in the case of the experimental motor. This is shown in Figure 9.

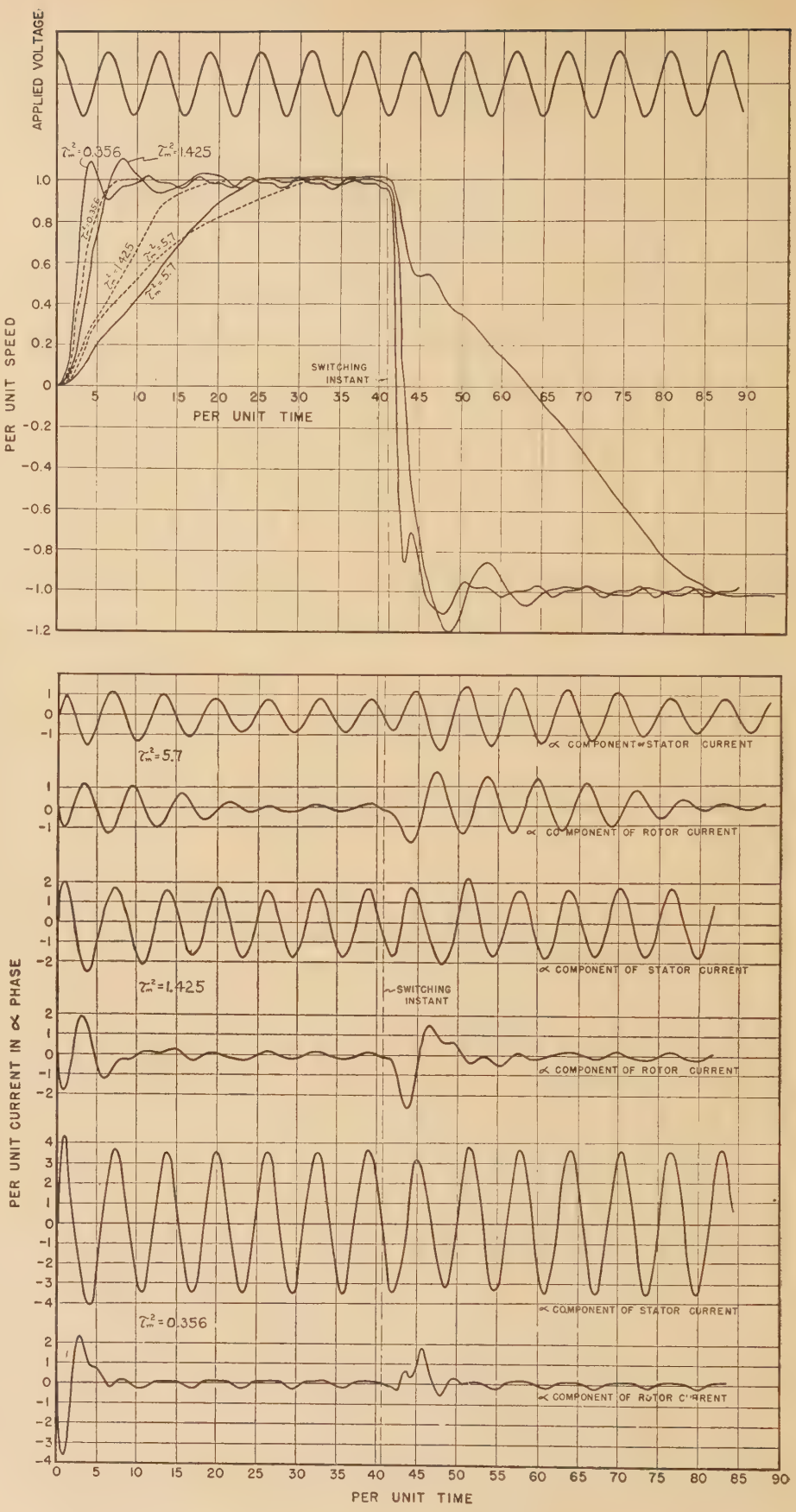

At first thought, it would be desirable that the rotor time constant be made as small as possible. The argument for this small value is that the rotor currents would die out rapidly, and, therefore,

Figure 6b. Comparison of theoretical and experimental curves for various τ_m's

$\tau_s = 2.35$ $\quad k = 0.815$
$\tau_r = 3.50$ $\quad T_L = 0$

Per unit current in α phase versus per unit time

the motor at no load would reach synchronous speed in a short time. Inspection of the summary curve in Figure 10 shows that this is not the case. For a fixed set of machine parameters, other than the rotor time constant, it is seen that there is an optimum value to the rotor time constant, which will result in a minimum rise time. This value is not defined well. For the machine parameters whose curve is shown, the range of time constants would be from two to six. From other observed data, a general rule would be that $\tau_r < \tau_s < 3\tau_r$ for short rise times. The rotor time constant, $\tau_r = \omega l/r$, is rather difficult to ascertain theoretically in the design of a rotor, because in the case of a squirrel cage machine the effective values of the self-inductance and rotor resistance are functions of the applied voltage. Of course, a wound rotor can be designed to fit any desired design parameters. The low values of τ_r desired can be interpreted either as due to a low value of self-inductance or to a large value of rotor resistance.

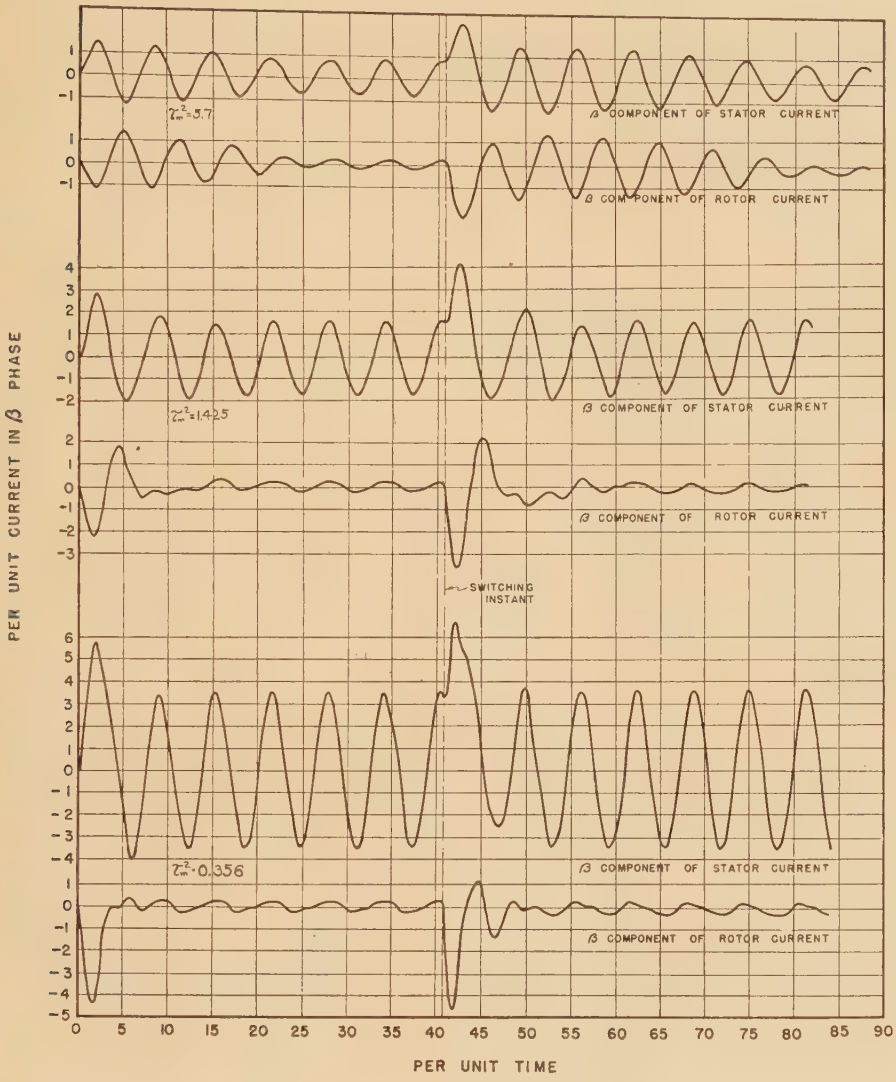

Figure 6c. Comparison of theoretical and experimental curves for various τ_m's

$\tau_s = 2.35$ $\quad k = 0.815$
$\tau_r = 3.50$ $\quad T_L = 0$

Per unit current in β phase versus per unit time

The effect of low rotor time constant is reflected back to the stator, as can be seen in the curve showing the time for the current to reach its steady state value. The low value of τ_r or the high value of rotor resistance is transferred to the stator, which then has an increased effective resistance or a decreased time constant. This in turn tends to shorten the period of the transient stator current.

The rise time of the induction motor is a function of the stator time constant in much the same way as it is a function of the rotor time constant; namely, in the presence of an optimum value of stator time constant there is a minimum rise time. For the curve shown in Figure 11, $\tau_s \backsimeq 3\tau_r$. This is in the range of τ_s, as indicated from the τ_r variation curve. Although the rise time increases with further decrease in stator time constant, the actual time for the stator current to reach its steady state value decreases with a decrease in stator time constant. This is understandable, because a low value of τ_s may be interpreted as an increased stator resistance, and hence a shorter transient period.

Figure 12 shows some rather surprising results. This summary curve shows over-all results for changes in friction load torque coefficient. The product of friction load torque coefficient K_L and speed is the total damping torque. It is seen that the motor reaches 85 per cent of its final speed in a time independent of the load torque. Furthermore, the time for the current to decay to a steady state value is also independent of load conditions. The final speed obtained by the motor for each load is shown. It is seen that even for a load torque coefficient eight times base value the final speed is as high as 55 per cent of synchronous speed.

It is apparent that changing the air gap will alter the magnetic structure in such a way as to reflect this change upon the parameters of the stator and the rotor. Although the inductance coefficients are related to the coefficient of coupling by the relationship $k = M/\sqrt{Ll}$, it is not sufficient to change only k in considering changes in air gap. That this is so may be seen from the following rather approximate analysis.

The magnetic circuit for both the stator and the rotor may be thought of as being composed of two flux paths, one through the iron structure itself, mutual to the stator and the rotor, designated by a permeance P_m, and the other a flux leakage path, different for the stator and the rotor, designated by permeances P_{ls} and P_{lr} for the stator and rotor, respectively. On the further assumption that the inductance coefficients are proportional to the square of a factor N, the number of turns, there can be written

$$L = N_s^2(P_m + P_{ls}) \tag{1}$$

$$l = N_r^2(P_m + P_{lr}) \tag{2}$$

$$M = N_s N_r P_m \tag{3}$$

The coefficient of coupling then becomes

$$k = \frac{M}{\sqrt{Ll}} = \frac{P_m}{\sqrt{(P_m + P_{ls})(P_m + P_{lr})}} \tag{4}$$

If $P_{ls} = P_{lr} = P_l$, a not too approximate

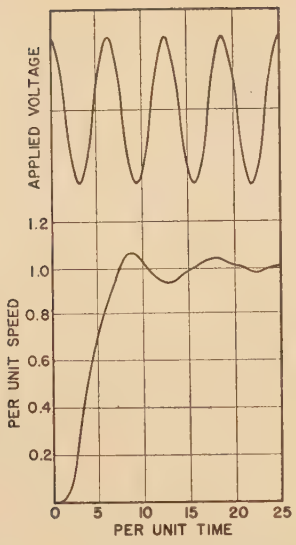

Figure 7a. Per unit speed and applied voltage versus per unit time

$\tau_s = 7.00$ $\quad k = 0.857$
$\tau_r = 3.50$ $\quad T_L = 0$
$\tau_m^2 = 3.85$

assumption, the coupling becomes

$$k = \frac{P_m}{P_m + P_l} = \left(1 + \frac{P_l}{P_m}\right)^{-1} \tag{5}$$

$$k \approx 1 - \frac{P_l}{P_m} + \left(\frac{P_l}{P_m}\right)^2 \cdots\cdots \tag{6}$$

This term is seen to be dependent upon the ratio of the permeance to leakage flux to the permeance to mutual flux. For most cases it is sufficient to consider only the first two terms. The self-inductance of the stator and rotor now can be written

$$L = N_s^2 \frac{P_m}{k} \tag{7}$$

$$l = N_r^2 \frac{P_m}{k} \tag{8}$$

The mutual permeance, being dependent upon the magnetic path through the rotor and the stator, must include the effect of the air gap. The mutual permeance can then be written as

$$P_m = \frac{1}{\frac{1}{P_i} + \frac{1}{P_{\text{gap}}}} = \frac{P_i P_{\text{gap}}}{P_i + P_{\text{gap}}} \tag{9}$$

and, because the permeance is proportional to the factor μ/l, where μ is the permeability and l is the effective length of the magnetic path, it is seen that to a first approximation, $P_i >> P_{\text{gap}}$, and

$$P_m = P_{\text{gap}} \alpha \frac{l}{l_{\text{gap}}} \tag{10}$$

Therefore, from equations 7 and 8, we have

$$N_s^2 = kLl_{\text{gap}} \tag{11}$$

$$N_r^2 = kll_{\text{gap}} \tag{12}$$

These relationships were used to vary theoretically the parameters of the prototype motor under investigation. A summary curve of the effect of changing the air gap spacing is shown in Figure 13.

As would be anticipated, decreasing the air gap decreases the rise time. Cutting the air gap in half decreases the rise time by 21 per cent. Since the air gap in the prototype motor as presently manufactured is greater than required from physical considerations, it would seem desirable to revise the design of such motors to decrease the air gap and so decrease the rise time. There is, however, a point of diminishing returns. If the air gap were made infinitely small, even zero, there would be a finite rise time, for zero gap would, on our assumptions, result in the coefficient of coupling approaching unity and in a complete revision of the performance equations. The greatest effect would seem to be the finite inertia of the rotor, which, in itself, would not allow a rise to full speed in zero time. The stator currents, it is seen, do not die out rapidly when the air gap is decreased. In fact, the tendency is to increase the length of the transient current with a decrease in the air gap.

The prototype machine was investigated for changes in applied frequency. The applied frequency enters into the definition of the machine constants τ_r and τ_s, varying linearly with frequency, and τ_m, varying as the square of the frequency. For the constants chosen, the minimum rise time occurred at a frequency of 60 cycles, with an almost linear increase in rise time with increase in frequency.

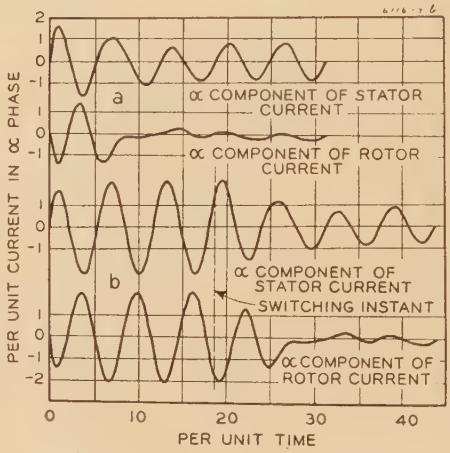

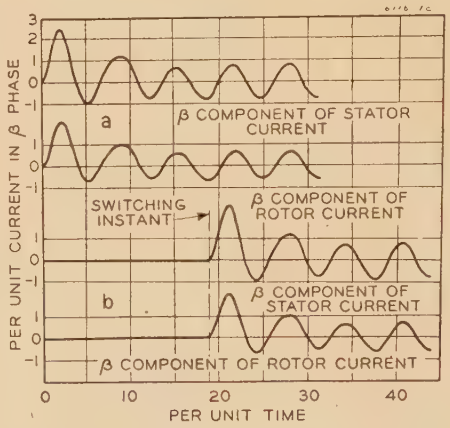

Figures 7b and 7c. Per unit current versus per unit time, showing effect of energizing one or both phases

(b). In α phase
(c). In β phase

Curve *a* is for the case when both phases were energized at the same time

For curve *b*, the α phase was energized for three cycles of the applied voltage with the β phase short circuited. Then the β phase was energized

$\tau_s = 7.00$ $\quad k = 0.857$
$\tau_r = 3.50$ $\quad T_L = 0$
$\tau_m^2 = 3.85$

Appendix I. Nomenclature of Terms Used in the Analysis

E = voltage applied to the motor, volts
L = stator phase inductance, henrys
l = rotor phase inductance, henrys
M = mutual inductance between rotor and stator, henrys
R = stator phase resistance, ohms
r = rotor phase resistance, ohms
p = number of phases
q = number of pairs of poles
ω = angular frequency of applied voltage, radians per second
J = rotor moment of inertia, watt seconds cubed
t' = actual time, seconds
θ_m = rotor position with respect to the stator, mechanical degrees
θ = rotor position with respect to the stator, electrical degrees
T_L' = actual total load torque, watt seconds
I_α', I_β' = actual stator currents in positive α and β axes, respectively, amperes
i_α', i_β' = actual rotor currents in positive α and β axes, respectively, amperes
I_α', I_β = per unit stator current in positive α and β axes, respectively
i_α', i_β = per unit rotor current in positive α and β axes, respectively
T_L = per unit load torque
K_L = load torque coefficient; $T_L = K_L \frac{d\theta}{dt}$

$\tau_s = \frac{\omega L}{R}$ = stator time constant

$\tau_r = \frac{\omega l}{r}$ = rotor time constant

$\tau_m = \omega \left(\frac{J}{qT_n}\right)^{1/2}$ = mechanical time constant

$T_n = \frac{pqE^2k^2}{\omega^2 L}$ = base torque, watt seconds

$I_n = \frac{E}{\omega L}$ = base stator current, amperes

$i_n = \frac{EM}{\omega L l}$ = base rotor current, amperes

$t = \omega t'$ = base time

Appendix II. Derivation of Equations Solved on the Differential Analyzer

The Stanley equations for the operation of a 2-phase induction motor can be written as follows:

$$RI_\alpha' + L\frac{dI_\alpha'}{dt'} + M\frac{di_\alpha'}{dt'} = E\cos\omega t' \tag{13}$$

$$RI_\beta' + L\frac{dI_\beta'}{dt'} + M\frac{di_\beta'}{dt'} = E\sin\omega t' \tag{14}$$

$$M\frac{dI_\alpha'}{dt'} + ri_\alpha' + l\frac{di'_\alpha}{dt'} + (MI_\beta' + li_\beta')\frac{d\theta}{dt'} = 0 \tag{15}$$

$$M\frac{dI_\beta'}{dt'} + ri_\beta' + l\frac{di_\beta'}{dt'} - (MI_\alpha' + li\alpha')\frac{d\theta}{dt'} = 0 \tag{16}$$

$$J\frac{d^2\theta_m}{dt'^2} = \frac{qp}{2}M(I_\beta' i_\alpha' - I\alpha' i_\beta') - T_L' \tag{17}$$

Define now a base stator current, $I_n = E/\omega L$, and a base rotor current, $i_n = EM/\omega Ll$. Then, dividing equations 13 and 14 by these base values, there results

$$\frac{R}{\omega L}I_\alpha + \frac{dI_\alpha}{dt} + \frac{M^2}{Ll}\frac{di_\alpha}{dt} = \cos t \tag{18}$$

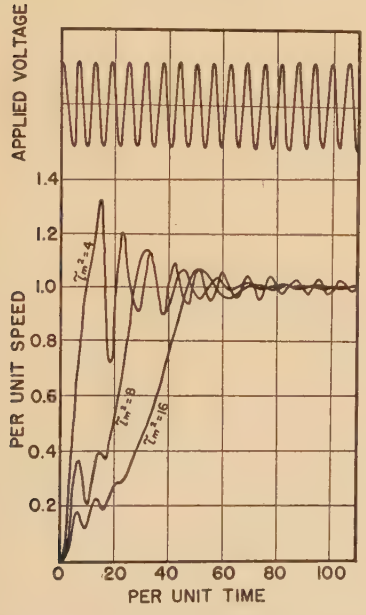

Figure 8a. Per unit speed and applied voltage versus per unit time

$\tau_s = 32$ $\quad k = 0.815$
$\tau_r = 16$ $\quad T_L = 0$

Figure 8b(below). Per unit current in α phase versus per unit time

$\tau_s = 32$ $\quad k = 0.815$
$\tau_r = 16$ $\quad T_L = 0$

Figure 8c (right). Per unit current in β phase versus per unit time

$\tau_s = 32$ $\quad k = 0.815$
$\tau_r = 16$ $\quad T_L = 0$

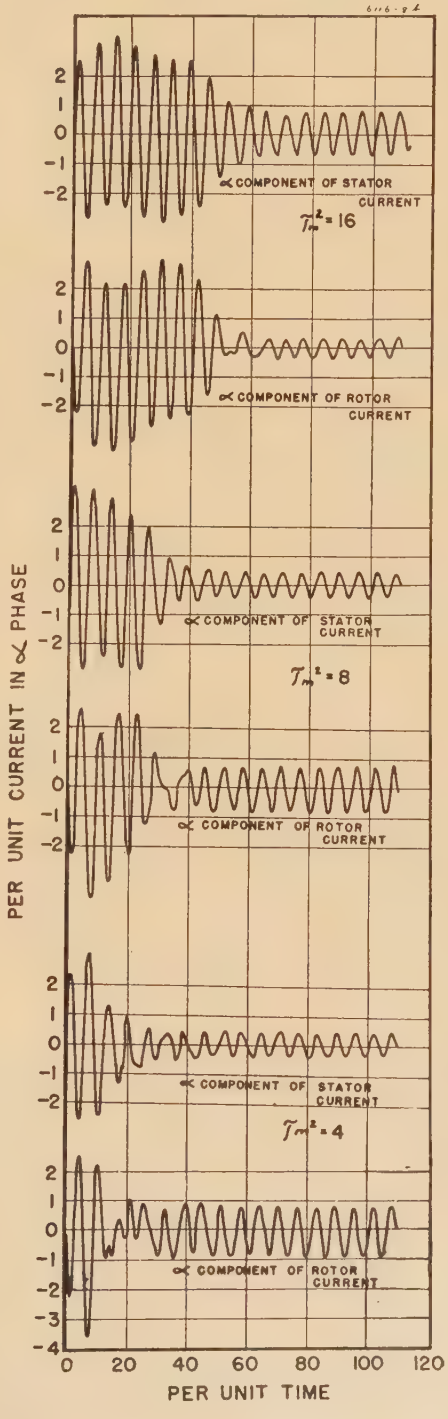

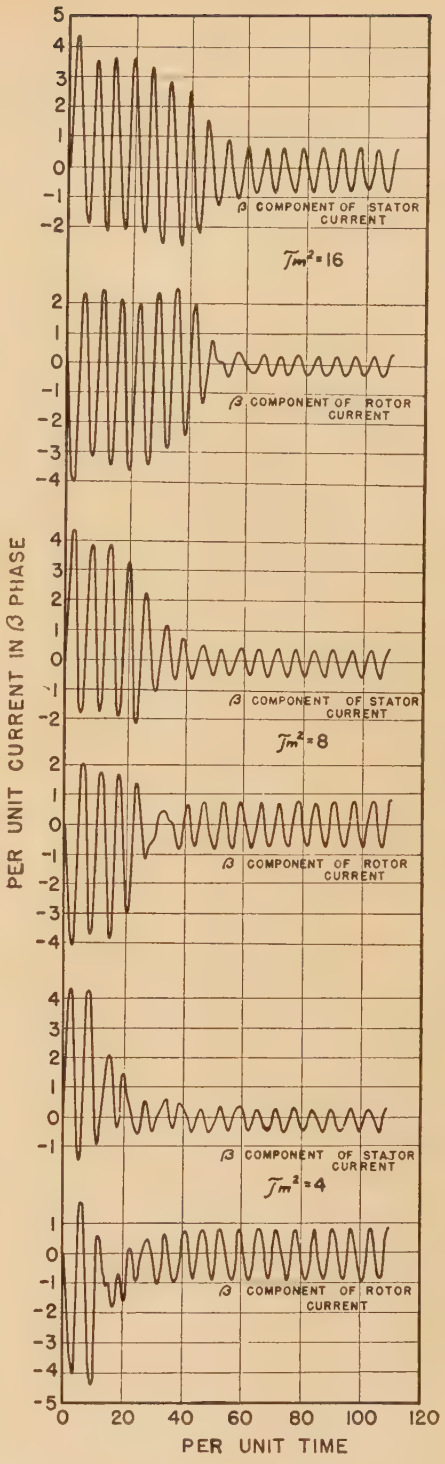

$$\frac{R}{\omega L}I_\beta + \frac{dI_\beta}{dt} + \frac{M^2}{Ll}\frac{di_\beta}{dt} = \sin t \tag{19}$$

In a similar manner equations 15 and 16 transform to

$$\frac{dI_\alpha}{dt} + \frac{r}{\omega l}i_\alpha + \frac{di_\alpha}{dt} + (I_\beta + i_\beta)\frac{d\theta}{dt} = 0 \tag{20}$$

$$\frac{dI_\beta}{dt} + \frac{r}{\omega l}i_\beta + \frac{di_\beta}{dt} - (I_\alpha + i_\alpha)\frac{d\theta}{dt} = 0 \tag{21}$$

The developed electric torque and the load torque are balanced by the product of the moment of inertia of the rotor and its

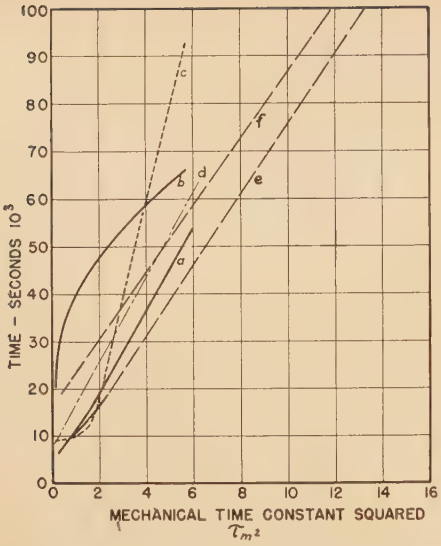

Figure 9. Rise time and decay time versus mechanical time constant squared

(a)—Rise time from 0 to 85 per cent full speed
(b)—Time for current transient to disappear
(c)—Rise time from 100 per cent to −85 per cent full speed
(d)—Rise time from 0 to 85 per cent full speed (experimental)

$\tau_s = 2.35$ $\quad k = 0.815$
$\tau_r = 3.50$, $\quad \omega = 377$ $\quad T_L = 0$

(e)—Rise time from 0 to 85 per cent full speed
(f)—Time for current transient to disappear

$\tau_s = 4$ $\quad k = 0.75$
$\tau_r = 2$ $\quad \omega = 377$ $\quad T_L = 0$

acceleration. Hence, for the whole machine (p phases),

$$\frac{J}{q}\frac{d^2\theta}{dt'^2} = \frac{pq}{2}M(I_\beta' i_\alpha' - I_\alpha' i_\beta') - T_L' \tag{22}$$

$$\frac{\omega^2 Jl}{pq^2\left(\frac{ME}{\omega L}\right)^2}\frac{d^2\theta}{dt^2} = {}^1/_2(I_\beta i_\alpha - I_\alpha i_\beta) - \frac{T_L' l}{pq\left(\frac{ME}{\omega L}\right)^2} \tag{23}$$

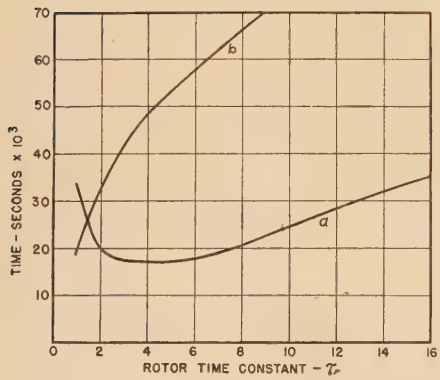

Figure 10. Rise time and decay time versus rotor time constant

(a)—Rise time from 0 to 85 per cent full speed
(b)—Time for current transient to disappear

$\tau_m^2 = 2.5$ $\quad k = 0.75$
$\tau_s = 4.0$ $\quad T_L = 0$
$\omega = 377$

$$\frac{\omega^2 J}{qT_n}\frac{d^2\theta}{dt^2} = {}^1/_2(I_\beta i_\alpha - I_\alpha i_\beta) - T_L \tag{24}$$

Equations 18 through 21 and equation 24 describe the performance of the induction motor on a per unit base, in accordance with our definitions of base values. If these equations are rewritten in terms of the time constants defined in Appendix I, we have

$$\frac{I_\alpha}{\tau_s} + \frac{dI_\alpha}{dt} + k^2\frac{di_\alpha}{dt} = \cos t \tag{25}$$

$$\frac{I_\beta}{\tau_s} + \frac{dI_\beta}{dt} + k^2\frac{di_\beta}{dt} = \sin t \tag{26}$$

$$\frac{dI_\alpha}{dt} + \frac{i_\alpha}{\tau_r} + \frac{di_\alpha}{dt} + (I_\beta + i_\beta)\frac{d\theta}{dt} = 0 \tag{27}$$

$$\frac{dI_\beta}{dt} + \frac{i_\beta}{\tau_r} + \frac{di_\beta}{dt} - (I_\alpha + i_\alpha)\frac{d\theta}{dt} = 0 \tag{28}$$

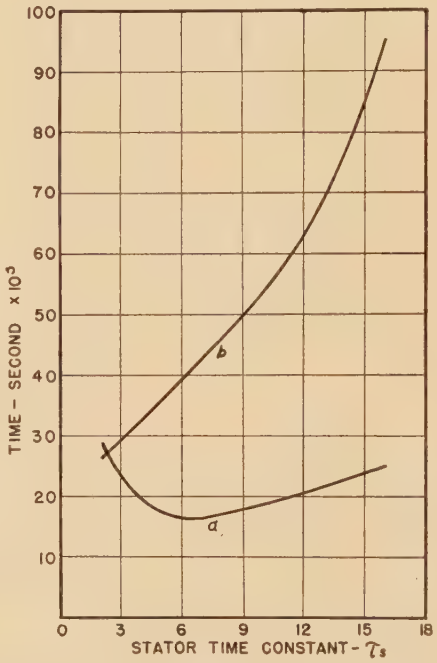

Figure 11. Rise time and decay time versus stator time constant

(a)—Rise time from 0 to 85 per cent full speed
(b)—Time for current transient to disappear

$\tau_m^2 = 2.5$ $\quad k = 0.75$
$\tau_r = 2.0$ $\quad T_L = 0$
$\omega = 377$

$$2\tau_m^2\frac{d^2\theta}{dt^2} = (I_\beta i_\alpha - I_\alpha i_\beta) - 2T_L \tag{29}$$

It is now convenient to define the currents x_α and x_β

$$x_\alpha = I_\alpha + i_\alpha \tag{30}$$

$$x_\beta = I_\beta + i_\beta \tag{31}$$

Equations 25 through 29 now may be written

$$\frac{I_\alpha}{\tau_s} + \frac{dx_\alpha}{dt} + (k^2 - 1)\frac{di_\alpha}{dt} = \cos t \tag{32}$$

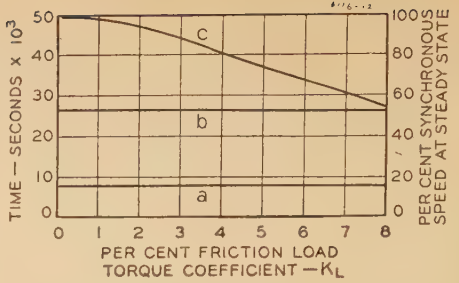

Figure 12. Rise time and decay time versus friction load torque coefficient

(a)—Rise time from 0 to 85 per cent full speed
(b)—Time for current transient to disappear
(c)—Per cent synchronous speed at steady state

$\tau_m^2 = 0.356$ $\quad k = 0.815$
$\tau_s = 2.35$ $\quad \omega = 377$
$\tau_r = 3.50$

$$\frac{I_\beta}{\tau_s} + \frac{dx_\beta}{dt} + (k^2 - 1)\frac{di_\beta}{dt} = \sin t \tag{33}$$

$$\frac{i_\alpha}{\tau_r} + \frac{dx_\alpha}{dt} + x_\beta\frac{d\theta}{dt} = 0 \tag{34}$$

$$\frac{i_\beta}{\tau_r} + \frac{dx_\beta}{dt} - x_\alpha\frac{d\theta}{dt} = 0 \tag{35}$$

$$2\tau_m^2\frac{d^2\theta}{dt^2} = (I_\beta i_\alpha - I_\alpha i_\beta) - 2T_L \tag{36}$$

Upon integrating once with respect to time, we have

$$\frac{1}{\tau_s}\int I_\alpha dt + x_\alpha + (k^2 - 1)i_\alpha = \sin t \tag{37}$$

$$\frac{1}{\tau_s}\int I_\beta dt + x_\beta + (k^2 - 1)i_\beta = -\cos t \tag{38}$$

$$\frac{1}{\tau_r}\int i_\alpha dt + x_\alpha + \int x_\beta d\theta = 0 \tag{39}$$

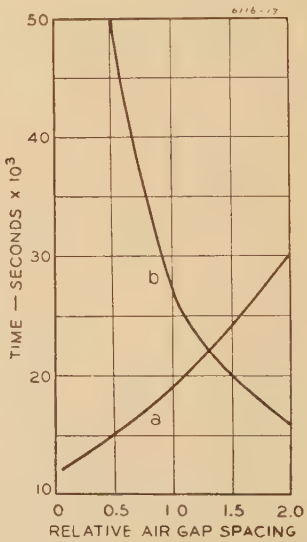

Figure 13. Rise time and decay time versus relative air gap spacing

(a)—Rise time from 0 to 85 per cent full speed
(b)—Time for current transient to disappear

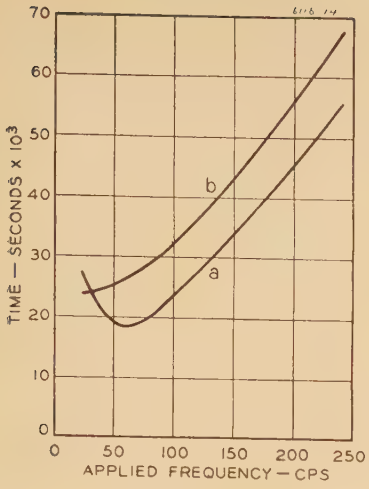

Figure 14. Rise time and decay time versus applied frequency

(a)—Rise time from 0 to 85 per cent full speed
(b)—Time for current transient to disappear

$$\frac{1}{\tau_r}\int i_\beta dt + x_\beta - \int x_\alpha d\theta = 0 \tag{40}$$

$$2\tau_m{}^2\frac{d\theta}{dt} = \int I_\beta i_\alpha dt - \int I_\alpha i_\beta dt - 2\int T_L dt \tag{41}$$

$$\theta = \int \frac{d\theta}{dt}\,dt \tag{42}$$

Equations 37 through 42 were solved on the differential analyzer, subject to various boundary conditions and various sets of parameters as discussed in the body of the paper.

Appendix III. Experimental Determination of Machine Constants

The range of parameters to be investigated was determined by making the standard blocked rotor and free rotor tests, under the assumptions that the motors had no hysteresis or iron circuit losses.

The equivalent circuits for these tests are shown in Figures 15a and b. From the first of these figures, for the blocked rotor case, the equivalent input impedance is given by

$$Z_{in} = \left(R + \frac{\omega^2 M^2 r}{r^2+\omega^2 l^2}\right) + j\left(\omega L - \frac{\omega^3 M^2 l}{r^2+\omega^2 l^2}\right) \tag{43}$$

If measurements of the current I_B, voltage E_B, and power P_B are now made, there result

$$\frac{P_B}{I_B{}^2} = R + \frac{\omega^2 M^2 r}{r^2+\omega^2 l^2} \tag{44}$$

$$\sqrt{\left(\frac{E_B}{I_B}\right)^2 - \left(\frac{P_B}{I_B{}^2}\right)^2} = \omega L - \frac{\omega^3 M^2 l}{r^2+\omega^2 l^2} \tag{45}$$

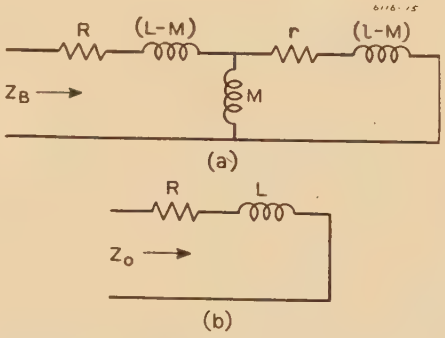

Figure 15. Equivalent circuits for one phase of an induction motor

(a)—Rotor blocked
(b)—Rotor free

For the free rotor case shown in Figure 15b, similar measurements are made, with like quantities designated by the subscript o. There result

$$\frac{P_o}{I_o{}^2} = R \tag{46}$$

$$\sqrt{\left(\frac{E_o}{I_o}\right)^2 - \left(\frac{P_o}{I_o{}^2}\right)^2} = \omega L \tag{47}$$

Combining the results of the blocked rotor and the free rotor tests, we have the ratio $\tau_r = \omega l/r$, the rotor time constant. The coefficient of coupling can be determined from these same measurements as follows:

$$A = \frac{\omega^3 M^2 l}{L(r^2+\omega^2 l^2)} = \frac{M^2}{Ll}\left(\frac{\omega\tau_r{}^2}{1+\tau_r{}^2}\right) \tag{48}$$

Since the quantity A can be computed from the test measurements, we have immediately that the coefficient of coupling is given by the square root of the term

$$k^2 = \frac{M^2}{Ll} = A\left(\frac{1+\tau_r{}^2}{\omega\tau_r{}^2}\right) \tag{49}$$

References

1. An Analysis of the Induction Motor, **H. C. Stanley.** AIEE Transactions, volume 57, 1938, pages 751–5.

2. Transient Torques in Squirrel-Cage Induction Motors With Special Reference to Plugging, **E. S. Gilfillan, E. Kaplan.** AIEE Transactions, volume 60, 1941, pages 1200–09.

3. Transient Starting Torques in Induction Motors, **A. M. Wahl, L. A. Kilgore.** AIEE Transactions, volume 59, 1940, November section, pages 603–07.

4. Transient Performance of Induction Motors, **F. J. Maginniss, N. R. Schultz.** AIEE Transactions, volume 63, 1944, September section, pages 641–6.

Oscillations of a High-Voltage Secondary Winding

A. BOYAJIAN
FELLOW AIEE

THE PHYSICAL THEORY of the characteristic oscillations of a high-voltage winding as a primary, that is, when the voltage disturbances are impressed directly across its terminals, is now well known.[1] However its behavior as a secondary with respect to the disturbances is not as well known. Although papers[2–4] have been published on this latter subject, this paper presents a physical theory believed to be novel and helpful.

The theory is of interest not merely as basic knowledge of transformer transients, but also as having applications to design. For instance, contrary to what generally is assumed, it is found that depending on its constants, the same oscillatory winding may develop higher transient voltages as a secondary than as a primary winding. This has a bearing on the design of both windings and ratio adjusters, the latter for the reason that taps from the various parts of the winding are brought together into a small space.

While the main feature of the present theory is the physical picture which it yields, it is not merely qualitative, but is fully quantitative and is formulated in terms of constants with which designers are familiar and which may be calculated or tested by methods well known to them.

General Nature of Theory

As a primary the characteristic modes of oscillation of a winding with the neutral end grounded are half waves (and their multiples). As a secondary they are neither half waves nor quarter waves but intermediate fractions of a wave. They might be described as chopped half waves—chopped at the isolated end of the winding. That is, the half wave is longer than the winding, and its extension beyond the winding is chopped off. In general, the higher the harmonic the greater percentage of the wave is chopped so that the oscillation approximates the quarter-wave mode. The lower the harmonic, the smaller is the fraction of the wave which is chopped, and thus the fundamental wave may be nearer to a half-wave length than to a quarter-wave length.

The leakage reactance of the transformer causes these modes of oscillation, a fact that cannot be ignored. If an ideal transformer were assumed with no reactance, magnetizing current, and so forth, no difference would be found between the oscillations of a winding as primary and those as secondary.

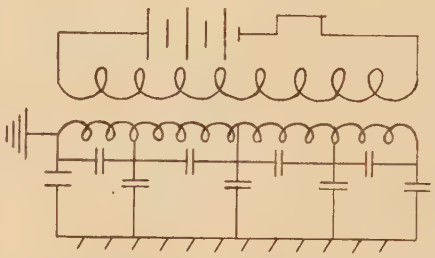

Figure 1. Essential elements of a transformer of the type here considered; considerable distributed capacitance in the secondary winding, negligible capacitance in the primary winding. Primary suddenly closed through a battery circuit

In the case of an oscillation that is intermediate between a quarter wave and a half wave, the maximum voltage to ground is in the interior, not at the terminal, of the winding. If the ratio of the maximum internal voltage (to ground) to the terminal voltage (to ground) be represented by μ_n for the nth harmonic and if the actual angular length of that oscillatory wave of the harmonic on the winding be represented by θ_n, then

$$\mu_n = 1/\sin\theta_n$$

This might be called the amplification factor of the harmonic voltage.

The angular length θ_n of the harmonic wave on the winding is found to be a certain function of the ratio of the nth-harmonic oscillatory leakage inductance L_n of the winding to the normal leakage inductance L_o of the winding, therefore if L_n/L_o equals 50, 20, 10, 5, 2, and 1, then μ_n equals respectively, 19, 6.6, 3.3, 2.2, 1.1, and 1. The conclusion follows that in order to keep μ_n low, the ratio L_n/L_o must be kept low.

The magnitudes of the various harmonic voltages for a rectangular wave are determined as follows:

1. Determine the angular length θ_n of each harmonic. This is a characteristic mode of the winding.

2. Determine the turn-ratio voltage distribution of the secondary winding, which will be a straight line stretching from zero at the grounded end to the maximum turn-ratio voltage at the other end of the winding. This sloping line is the normal (magnetic) initial voltage of the secondary winding. Because the presence of capacitance along the winding makes the actual initial voltage along the winding zero, the various harmonics at each point must initially add up (algebraically) to a value equal and opposite to the normal voltage at that point.

3. Choose as many points along the winding as the number of the harmonics desired to write enough simultaneous equations to determine the unknown magnitudes of the desired harmonics.

An example is shown in Figure 19.

The Circuit

Figure 1 illustrates the actual circuit. Its features are

1. One end of the high-voltage winding is grounded, the other isolated.

2. The high-voltage winding is associated with a network of coil-to-coil and coil-to-ground capacitances.

3. The voltage rating of the low-voltage winding is assumed so low that its associated capacitive kilovolt-amperes, varying as the square of the voltage, is negligible compared

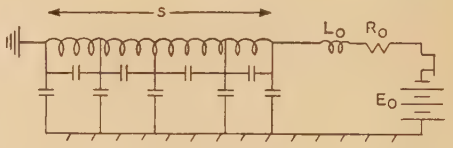

Figure 2. Tentative equivalent circuit of the transformer and of an analogous transmission line

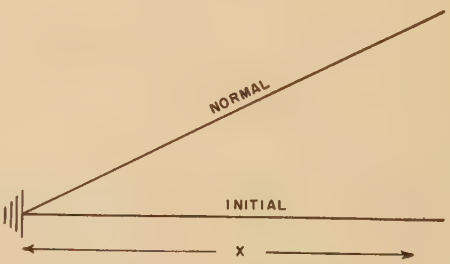

Figure 3. Initial and final distributions of rectangular voltage wave

Paper 46-164, recommended by the AIEE committee on electric machinery for presentation at the AIEE summer convention, Detroit, Mich., June 24–28, 1946. Manuscript submitted April 18, 1946; made available for printing May 27, 1946.

A. BOYAJIAN is with the power transformer engineering division, General Electric Company, Pittsfield, Mass.

with that of the high-voltage winding. Hence no low-voltage capacitance network is shown.

4. The magnetizing current, whether primary or secondary, is ignored.

5. The resistances and leakage reactances are to be given quantitative consideration.

6. Excitation consists of a long-tail rectangular wave, like voltage from a battery, impressed across the low-voltage terminals.

7. The battery impedance is negligible.

Method of Analysis

The 2-winding system described can be replaced tentatively by an equivalent single-circuit network as shown in Figure 2. L_o is the leakage inductance between the two windings and R_o their effective resistance expressed in terms of the high-voltage circuit. Similarly, E_o is the battery voltage stepped up by the turn ratio. Although Figure 2 is not an exact equivalent of the transformer for these phenomena, it is very helpful in suggesting a simpler analogous problem in transmission lines to develop certain physical conceptions. After these conceptions have been developed the transformer equations will be based rigorously on Figure 1.

The problem is to formulate the transient phenomena of the high-voltage circuit following the closing of the battery switch, Figures 1 and 2.

Considering Figure 2, when the switch is closed the capacitance network evidently will behave as a short circuit momentarily and the entire voltage then will be consumed by the leakage inductance L_o so that the actual initial voltage distribution along the entire high-voltage winding will be zero, Figure 3. The normal voltage distribution, in the absence of the capacitance network, would have been along some slanting line like that shown in the same figure and will be the same for the secondary as for the primary winding, corrected for turn ratio. The normal voltage distribution of a winding frequently is spoken of also as the final distribution, and in the present case this may appear to be ultimately zero along

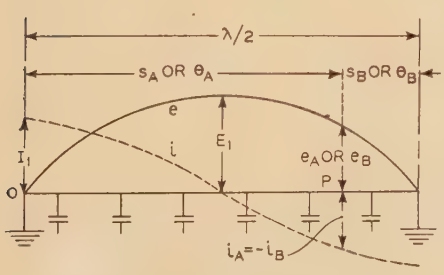

Figure 4. Standing wave in a transmission line which is grounded at both ends, as viewed from a point *P* on the line

all of the secondary winding. But as the transient is the result of the simultaneous magnetic and capacitive action and not the result of a prophetic vision of this winding into the distant future, a final voltage distribution can be a factor in calculation only in so far as it represents a component that was present at the beginning to co-operate with the other factors to control every detail of the transient phenomena. When so considered the desired reference axis for the oscillation will be recognized as the inductive-voltage distribution. The inductive voltage in the secondary winding does diminish with time but very slowly and for the present purpose may be considered as constant. This may be verified as follows.

The average value of a harmonic wave is 90 per cent of its rms value. Therefore if starting with zero flux in the core a battery voltage equal to the rated rms

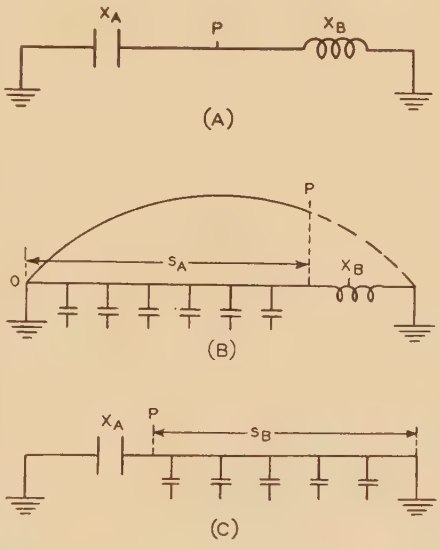

Figures 5A, B, C. Three equivalent oscillatory networks of Figure 4 as viewed from the point *P* on the line

voltage is impressed across a 60-cycle transformer winding, it will be transformed magnetically to a secondary winding for at least a quarter of a cycle (4,000 microseconds) without drawing a magnetizing current sufficient to cause a noticeable voltage regulation through resistance drop. If a rectangular impulse voltage 20 times as large as the rated rms voltage of the winding is impressed under the same conditions, the inductive voltage transformation from the primary to the secondary winding will be as good as before for 200 microseconds. That is, it will be time enough for the maxima of the natural oscillations of many transformer windings to be exhibited fully.

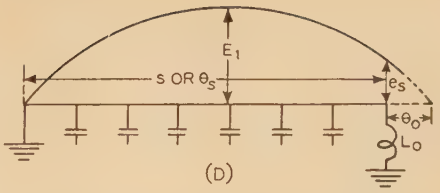

Figure 5D. Fundamental oscillatory wave length on a transmission line solidly grounded at one end and grounded through an inductance at the other end

The transition phenomena from initial to normal voltage distribution is then the crux of the problem. These will consist of a complex set of oscillations, but the question is what kind. So far as mathematics is concerned, the difference between the initial and the final curves of Figure 3 can be resolved into a set of harmonics in an infinite number of different ways, but only one of those sets would be acceptable, namely, that set of which each component constitutes a stable single-frequency mode of oscillation of the system. The modes of oscillation of the high-voltage as a primary winding as developed in reference 1 cannot be applied here unmodified for reasons as follows.

The fundamental mode of oscillation of the secondary as a secondary winding cannot be a half wave because

1. One end of the winding is open, Figure 1.

2. Such an oscillation in the secondary winding would not produce a voltage across the primary terminals and therefore it could not be produced in its turn by a voltage across the primary terminals. Also, the secondary oscillation cannot be a quarter wave because if the leakage reactance between the primary and secondary windings is zero or negligible, the oscillation would become short-circuited. If the leakage reactance is not negligible the oscillation will be short-circuited through that reactance and proportionately modified.

The first task evidently is to determine the normal modes of oscillation of the system in the presence of a leakage reactance L_o. In order to keep physics and mathematics together, and build the mathematics on the physics as far as possible, some pertinent basic physical conceptions first will be developed by considering the simpler problem of the analogous phenomena of a transmission line. These conceptions then will be developed further to adapt them to the transformer phenomena.

Analogous Problem in Transmission Lines

The system represented by Figure 2 is grounded at both ends and its oscillatory

characteristics therefore must be related to those of a line grounded at both ends. We therefore start with the consideration of the line shown in Figure 4. It does not contain an L_o but that will be introduced after some conceptions are developed based on this simpler circuit.

Let the line of Figure 4 be assumed to oscillate at its fundamental mode—a half-cycle wave in space, not in time. The voltages to ground are zero at both ends, maximum in the middle. The conductor current is zero in the middle, maximum at the two ends, positive at one end and negative at the other. It should be borne in mind that we are dealing with a standing wave, not a traveling wave, which is alternating in time but stationary on the wire.

Let us make some observations and deductions at an intermediate point P on this line.

Looking from P into section A towards O, we find at P a voltage e_A and a current i_A.

$$e_A = E_1 \sin [2\pi(s_A/\lambda)] \cos [2\pi(c/\lambda)t] \quad (1a)$$
$$= E_1 \sin \theta_A \cos \omega t \quad (1b)$$
$$i_A = -(E_1/X_1) \cos [2\pi(s_A/\lambda)] \times \sin [2\pi(c/\lambda)t] \quad (2a)$$
$$= -(E_1/X_1) \cos \theta_A \sin \omega t \quad (2b)$$

where

E_1 = the maximum of the voltage wave
s_A = the length of section A in linear measure
θ_A = the length of section A in angular measure
λ = the wave length in linear measure
c = the velocity of wave propagation along the line in the same linear measure (per second) as used in measuring λ
X_1 = the surge impedance of the line

For ease of reference

$$\theta_A = 2\pi s_A/\lambda$$
$$\omega = 2\pi c/\lambda$$

The negative sign in equations 2a and 2b follows from the consideration that at a short distance from ground, θ_A small, the current must appear as lagging behind the voltage.

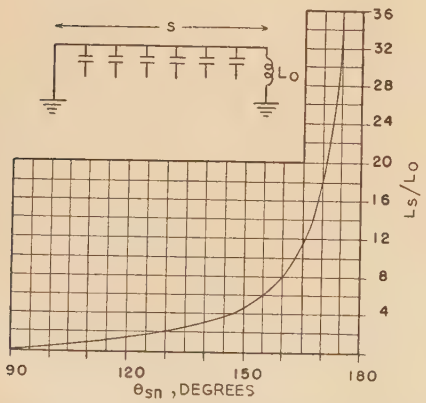

Figure 6A. Angular wave length of the fundamental oscillation of the line of Figure 5D

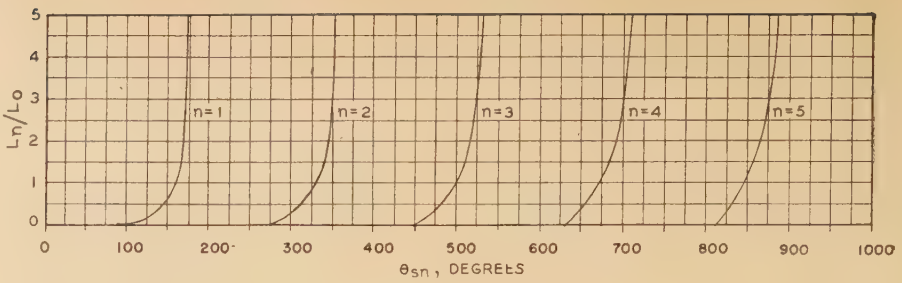

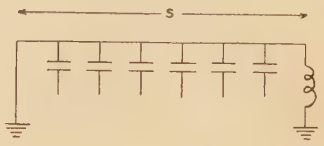

Figure 6B. Angular wave length of the various harmonic oscillations of the line of Figure 5D

Looking from P into section B toward the other end of the line, the same voltage will be found as before but an opposite current. It is opposite because the current is flowing from section A into section B or vice versa. Accordingly

$$e_B = E_1 \sin [2\pi(s_B/\lambda)] \cos [2\pi(c/\lambda)t] \quad (3a)$$
$$= E_1 \sin \theta_B \cos \omega t \quad (3b)$$
$$= E_1 \sin \theta_A \cos \omega t \quad (3c)$$
$$i_B = -(E_1/X_1) \cos [2\pi(s_B/\lambda)] \sin [2\pi(c/\lambda)t] \quad (4a)$$
$$= -(E_1/X_1) \cos \theta_B \sin \omega t \quad (4b)$$
$$= (E_1/X_1) \cos \theta_A \sin \omega t \quad (4c)$$

From the fact that θ_A and θ_B are supplementary angles it follows that equation 3c is equal to equation 3b, and equation 4c is the opposite of equation 4b. The sines of supplementary angles are alike, the cosines opposite.

Based on these current and voltage observations, we are justified in deducing that no matter what the actual structure of the two sections A and B of the circuit may be, viewed from the chosen point P, they offer the effective impedances X_A and X_B defined by

$$X_A = \frac{E_1 \sin \theta_A}{I_1 \cos \theta_A} \quad (5a)$$
$$= X_1 \tan \theta_A \quad (5b)$$
$$= -X_1 \tan \theta_B \quad (5c)$$

$$X_B = \frac{E_1 \sin \theta_B}{I_1 \cos \theta_B} \quad (6a)$$
$$= X_1 \tan \theta_B \quad (6b)$$
$$= -X_1 \tan \theta_A \quad (6c)$$

X_1, equal to E_1/I_1, will be recognized as the surge impedance of the line to the fundamental wave of the line. Although the surge impedance of a transmission line is the same to all waves, for the sake of generality (to be utilized later in transformer windings) the subscript will be retained.

The signs of these equations are so chosen that positive X means a lagging reactance, negative leading.

If θ_A is more than 90 degrees as shown in Figure 4, X_A, the reactance of section A effective at the point P, will be negative, that is, equivalent to a capacitive reactance. θ_B will be less than 90 degrees and therefore X_B will be positive, equivalent to an inductive reactance.

Thus considered from the standpoint of our chosen point of observation P, the oscillating system can be represented by any one of three equivalent networks.

1. Figure 5A consisting of a massed capacitive reactance X_A and a massed inductive reactance X_B.

2. Figure 5B consisting of a distributed line of length s_A at the left terminating through a massed inductive reactance X_B at the right.

3. Figure 5C consisting of a massed capacitive reactance X_A at the left and a line of length s_B on the right.

Conversely, if we have an actual circuit as illustrated in Figures 5A, B, or C, it can be represented by a transmission line of length $\lambda/2$, Figure 4, with no massed reactance anywhere.

Fundamental Mode of Oscillation of a Line Terminating in a Massed Inductance

Several important general conclusions and novel concepts follow from the foregoing text.

(*a*). The fundamental mode of oscillation of a line of linear length s, Figure 5D, terminating through a massed inductance L_o and grounded at both ends is not a half wave but a fractional or stub-ended wave of angular value θ_s given by

$$1/\tan \theta_s = -X_1/\omega L_o \quad (7a)^*$$
$$\theta_s/\tan \theta_s = -L_1/L_o \quad (7b)^*$$

L_1/L_o is the ratio of the distributed

*Note that X_1, is the surge impedance of the line, not its inductive reactance. Therefore X_1, is not equal to ωL_1 but to $\omega L_1/\theta_s$, as defined by equation 7e.

inductance L_1 of the line to the massed inductance L_o at the end. The values of θ_s corresponding to given values of L_1/L_o can be obtained from Figure 6A.

Equations 7a and 7b are derived from equation 6c by substituting into the latter the following relationships.

$$X_B=\omega L_o;\ \omega=2\pi c/\lambda;\ \lambda=2\pi s/\theta_s$$

Therefore

$$\omega=c\theta_s/s$$

Let L and C be the line constants per unit length, so that L_1 equals sL. Then

$$c=1/\sqrt{LC}$$

Therefore

$$C=1/Lc^2 \qquad (7c)$$

$$X_1=\sqrt{L/C}=Lc \qquad (7d)$$

Hence

$$X_1/\omega=Lc/(c\theta_s/s)=L_1/\theta_s \qquad (7e)$$

Substituting equation 7e into equation 6c and remembering that X_B is also equal to ωL_o, we obtain

$$\theta_s/\tan\theta_s=-L_1/L_o \qquad (7b)$$

Just as θ_s is the portion of the wave (in angular measure) subtended by the line, $\theta_o(\theta_o=\pi-\theta_s)$ is the portion of the wave subtended by the massed inductance L_o. Substitution of $\theta_s=\pi-\theta_o$ into equation 7b yields

$$(\pi-\theta_o)/\tan\theta_o=+L_1/L_o \qquad (8)$$

With increasing values of L_1/L_o, θ_o becomes smaller approximating the value

$$\theta_o\approx\frac{1}{L_1/L_o} \qquad (8a)$$

As equations 7b and 8 are solved for θ_s and θ_o conveniently with the help of the curves of Figure 6A, equation 8a need not be resorted to except for a rough estimate.

It can be seen from either the equations or the curves that no matter how large L_o may be, its angle θ_o will be less than 90 degrees and θ_s between 90 and 180 degrees.

As a matter of theoretical interest, if the line terminates through a massed capacitance instead of inductance, these relations between the two θ's will be interchanged. θ_s will be between 0 and 90 degrees, θ_o between 90 and 180 degrees.

(*b*). A line of length s terminating through a massed inductance and grounded at both ends oscillates as if it were part of a line of a greater length s' supporting a full half wave.

$$s'=s(\pi/\theta_s) \qquad (9a)$$
$$\lambda=2s'$$

(*c*). The frequency of oscillation of such a standing wave is given by

$$\omega=2\pi c/\lambda=c\theta_s/s \qquad (10)$$

This means that series massed inductance lowers the frequency of oscillation of a line in the ratio of π to θ_s.

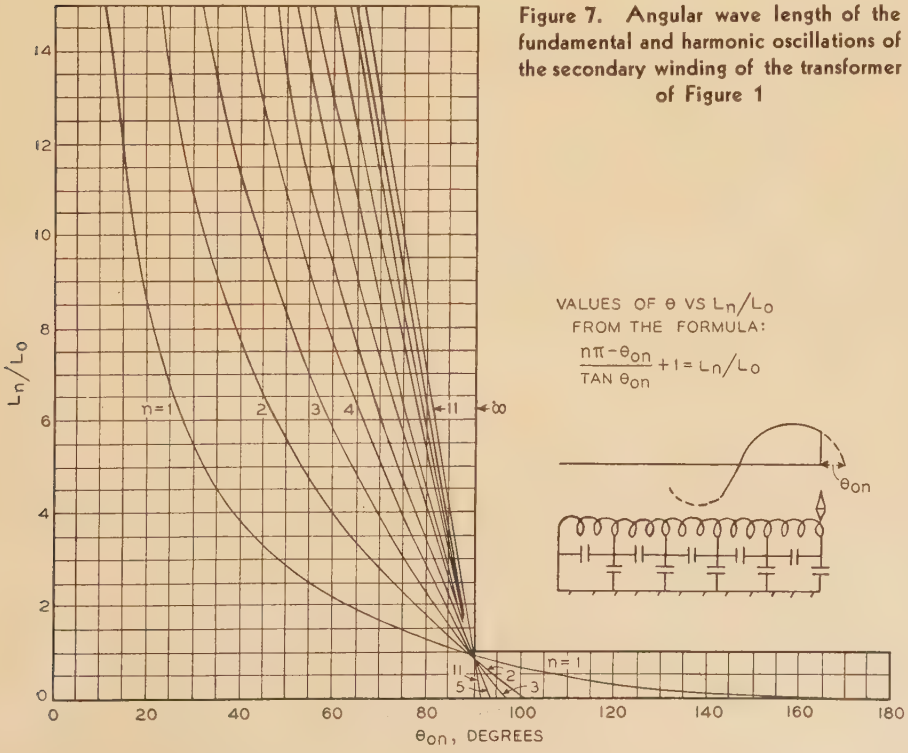

Figure 7. Angular wave length of the fundamental and harmonic oscillations of the secondary winding of the transformer of Figure 1

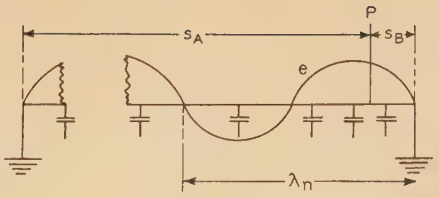

Figure 8. Harmonic wave on a transmission line grounded at both ends

(*d*). If the circuit conditions are such as to fix the line terminal voltage e_s Figure 5D and to compel E_1 to adjust itself to it, then there will be a voltage amplification along the line in the ratio of E_1 to e_s given by the equation

$$\mu_1=E_1/e_s=1/\sin\theta_s=1/\sin\theta_o \qquad (11)$$

Since in equation 8 the larger the ratio L_1/L_o the smaller is θ_o and for small values of θ, $\sin\theta=\theta=\tan\theta$, the substitution of this into equations 8 and 11 yields the approximation

$$\mu_1\approx L_1/(L_o\pi) \qquad (11a)$$

That is, the higher values of harmonic amplification are of the order of one-third of L_1/L_o.

Higher Harmonic Modes

In Figure 8 the transmission line of Figure 4 is shown as oscillating under a standing wave of the nth space-harmonic of wave length λ_n. Observations made as before will lend to the same general equations as before for current and voltage and therefore for X_A, X_B, θ_s (equation 7b), θ_o (equation 8), and μ (equation 11) by substituting the appropriate value of λ for the desired harmonic and by multiplying π by n in equation 8.

Of major interest are θ_o and μ for the line of Figure 5D for the nth harmonic.

Equation 7b for θ_s does not seem to have provision for different harmonics although it does inasmuch as it has an infinite number of solutions, one for each harmonic. Figure 6A shows only a fragment of the complete plot—just enough to cover the fundamental mode. Figure 6B shows a more extended one with the curves of θ_s up to the fifth harmonic; and Figure 7 is in terms of θ_o up to the eleventh harmonic. Thus it is seen that equation 7b (or equation 8 modified) defines all of the infinite number of different possible normal modes of oscillation of a line terminating through a massed inductance and grounded at both ends.

General Formulas

We now put the more important formulas in a form applicable to all harmonics of the transmission line, including the

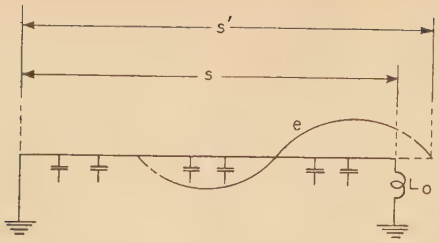

Figure 9 (above). Harmonic wave on a transmission line solidly grounded at one end and grounded through an inductance at the other end

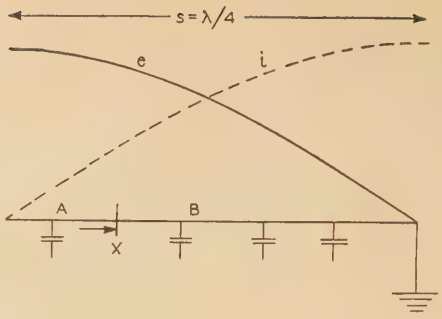

Figure 10 (top right). Fundamental wave on a line open at one end, grounded at the other end

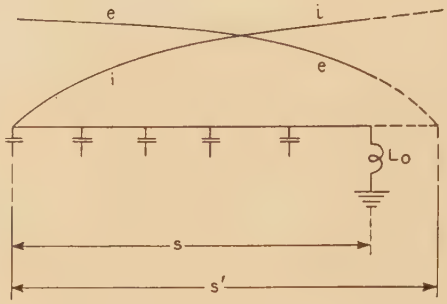

Figure 11 (bottom right). Fundamental wave on the line open at one end, grounded through an inductance at the other end

fundamental (half wave) for which $n=1$.

$$\theta_{sn}/\tan\theta_{sn} = -L_n/L_o \tag{12}$$

and

$$\theta_{on} = n\pi - \theta_{sn} \tag{13}$$

θ_{sn} can be obtained more conveniently from Figure 6B, or

$$\frac{n\pi-\theta_{on}}{\tan\theta_{on}} = +L_n/L_o \tag{14}$$

and

$$\theta_{sn} = n\pi - \theta_{on} \tag{15}$$

Also

$$\mu_n = 1/\sin\theta_{sn} = 1/\sin\theta_{on} \tag{16}$$

$$\omega_n = c\theta_{sn}/s = \theta_{sn}/(s\sqrt{LC}) = c(n\pi-\theta_{on})/s \tag{17}$$

$$s'_n = s(n\pi/\theta_{sn}) \tag{18}$$

$$\lambda_n = 2s'_n/n = 2\pi s/\theta_{sn}$$

The fact that the equations for θ_{on} and θ_{sn} are transcendental forbids any expectation that s'_n, that is, the equivalent length of the system will be the same for all harmonics.

Open Line

The stable modes of oscillation of an open line like those shown in Figures 10 and 11 are analogous to those of the isolated high-voltage winding and are analyzed in Appendix II. Equations 20–27 also will be found there.

Other Combinations

A line may have stable modes of oscillation with massed reactances introduced at intermediate points as in Figures 14 and 15. These are discussed in Appendix III.

Applications to the Transformer

Constraints of the Transformer

It will be shown now how a fractional standing wave, like that of Figure 5D for instance, is also the normal mode of oscillation of the secondary winding of a transformer satisfying its current and voltage constraints.

Current Constraints of the Secondary. The voltage wave of Figure 5D is reproduced in Figure 16 as e_x. The current wave appropriate to Figure 5D is shown in Figure 16 as i'_x with the value i'_s at the stub end. This current wave does not satisfy the terminal conditions of the winding of Figure 16 because it is entirely open at the end in question and cannot have any current at that point. The winding current therefore must be an offset wave like i_x, zero at s. This is equivalent to the addition of a uniformly distributed current $-i'_s$. Then the current i_x along the winding will consist of two components.

$$i_x = i'_x + i''_x \tag{29a}$$

$$= I_{max}\{\cos[(x/s)\theta_s] - \cos\theta_s\} \tag{29b}$$

Because all of the current in the high-voltage winding must flow into its capacitance network as a distributed load, the question arises how this new i_x in the conductor is to be fitted to the current and voltage of the capacitance network.

The distribution of i_x in the winding represents no different current distribution in the capacitance network than the distribution of i'_x in the winding. The former means that the current of the right-hand portion of the capacitance network, instead of flowing through the winding toward the right (toward the open end) to return, flows toward the left (the closed end) to return to the ground.

The component i'_x produces the voltage e_x while i''_x contributes to the leakage reactance voltage across the primary or low voltage.

Primary (Low-Voltage) Current. A complete half wave of current in the high-voltage winding, like that shown in Figure 4, would call for no current i_p in the low-voltage primary winding, but one similar to either the unsymmetrical i'_x (with unequal half cycles) or the offset i_x would do so, by the general formula,

$$i_p = -(1/s)\int_o^s i_x dx \tag{30a}$$

As all turns are in series in the primary winding and there are no shunt paths, this current i_p will flow in all of its turns uniformly, not as a function of x.

Substituting equation 29b into equation 30a and integrating,

$$i_p = -I_{max}\left[\frac{\sin\theta_s}{\theta_s} - \cos\theta_s\right] \tag{30b}$$

and

$$i_p/i_s = -i_p/I_{max}\cos\theta_s = -\left(\frac{\tan\theta_s}{\theta_s} - 1\right) \tag{31}$$

As the low-voltage terminals are connected to a zero-impedance source, the total oscillatory voltage at its terminals must be zero. This consists of two components: e_s and $i_p\omega L_o$ where L_o is the leakage inductance. Hence

$$e_s + i_p\omega L_o = 0 \tag{32a}$$

or

$$e_s = -i_p\omega L_o \tag{32b}$$

We see that the same applications can be made here as in the case of the transmission line except for the numerical value of the current causing a drop through L_o. In the transmission line the current was $I_{max}\cos\theta_s$ and in this case it is given by equation 30b. How this affects θ_o and θ_s will be determined.

Equations for θ_o and θ_s. Developing equation 32b by substituting into it the value of i_p from equation 30b,

$$e_s = E_1\sin\theta_s = (E_1/X_1)\left[\frac{\sin\theta_s}{\theta_s} - \cos\theta_s\right]\omega L_o \tag{33a}$$

or dividing through by $E\sin\theta_s$

$$1 = (1/X_1)[1/\theta_s - \cot\theta_s]\omega L_o \tag{33b}$$

$$X_1/\omega L_o = (1/\theta_s) - (1/\tan\theta_s) \quad (33c)$$

Equation 7e stated

$$X_1/\omega = L_1/\theta_s$$

which when substituted into equation 33c and interpreted for the nth harmonic yields

$$(\theta_{sn}/\tan\theta_{sn}) - 1 = -L_n/L_o \quad (34)$$

and

$$\frac{n\pi - \theta_{on}}{\tan\theta_{on}} + 1 = (L_n/L_o) \quad (34a)$$

Given L_n/L_o, θ_{on} can be obtained conveniently from Figure 7.

L_n is involved also in the formula for the frequency of the oscillation of the harmonic and will be formulated under that topic. Meanwhile for the purposes of equations 34 and 34a, the following thought may be found helpful.

In these equations the ratio, not the absolute values, of L_n and L_o is needed. Therefore factors like $(4\pi/10)$ that enter into all inductance formulas can be cancelled out from both numerator and denominator leaving finally

$$L_n/L_o = 1.25\frac{A_n}{A_o}\times\frac{h_o}{h_n}$$

where

A = the effective cross section of the leakage path
h = the effective length of the leakage path
1.25 = a factor derived in the following text

The impedance condition to which A_n and h_n apply are illustrated in Figure 21 for the first three harmonics with current-flow diagrams familiar in transformer design practice.

Comments on Figure 7. Figure 7 shows that, with varying values of L_n/L_o, θ_{on} varies over a wide range for the fundamental, and narrower ranges with the increasing order of the harmonics. As L_n/L_o itself gets smaller with the increasing order of the harmonics for a given winding, it follows that the reduction in range is even more pronounced than it appears at first sight. For instance, to a rough approximation (Appendix V) L_n may be assumed to vary inversely as the square of the order of the harmonic, and on that basis the exhibit in Table I for two values of L_1/L_o may be enlightening.

It is seen that the oscillation approaches the quarter-wave type for all harmonics above the fundamental in case 2 and above the second in case 1. It can be less than $\pi/2$.

Aside from the visual picture this gives of the character of the various harmonics, it also affords an opportunity for simplification of the harmonic analysis of complex waves by approximation.

General Equations of the High-Voltage (Secondary) Winding

Based on the foregoing analyses the equation of the voltage to ground along the secondary winding, at a distance x from neutral, with a rectangular voltage impressed across the primary, and with allowance also for damping, will be of the form

$$e_x = E_o(x/s) + \sum_1^n E_n\epsilon^{-k_n t}\sin[(x/s)\theta_{sn}]\times\cos\omega_n t \quad (35)$$

This involves the unknowns E_n, k_n, θ_{sn}, and ω_n. Of these θ_{sn} already has been defined and is obtainable from Figure 7 in terms of θ_{on}. As k_n, the damping exponent, is influenced strongly by stray inductive and dielectric losses difficult to formulate, it is better to estimate it from experience. That leaves two unknowns to formulate—E_n and ω_n.

Amplitude of Harmonics, E_n

Given the initial actual and the normal voltage distributions Fig. 3, how are the amplitudes of the fundamental and the higher harmonics to be determined?

The well-known Fourier analysis does not apply here because, if the integration is done for the actual winding length s, the waves are incomplete. If the integration is done for s', that is, the equivalent length, then s' is not the same for each harmonic.

Still, the harmonics can be obtained by one of several different methods.

Method 1. Calculate θ_{Lo} (or θ_s) for as many harmonics as desired and plot the waves, each with 100-per-cent maximum amplitude, together with the final voltage distribution curve. If this is done on co-ordinate paper, then at any point along the winding it is seen at a glance that a certain percentage of the fundamental harmonic plus certain other percentages of the various harmonics at the first instant must be equal and opposite to the local value of the final voltage distribution. Therefore with the help of the plot equations may be written for as many points of the winding as the number of the simultaneous equations needed, that is, the number of the harmonics.

Table I

Harmonic	Case 1: $L_1/L_o = 9$ L_n/L_o	Case 1: θ_{on}, Degrees	Case 2: $L_1/L_o = 5$ L_n/L_o	Case 2: θ_{on}, Degrees
Fundamental	9	20	5	32
Second	2.25	76	1.25	88
Third	1.0	90	0.55	94
Fourth	0.56	95	0.31	93
Fifth	0.36	93	0.25	92
Infinite	0.00	90	0.00	90

Method 2. A set of simultaneous equations can be written without the initial plot of method 1 as follows.

Let it be assumed that only three harmonics are required. At $x = s$, the transient component of $e_x = -E_o$. Hence

$$E_1\sin\theta_{o1} + E_2\sin\theta_{o2} + E_3\sin\theta_{o3} = -E_o \quad (39)$$

In all cases at $x = s'_2/2$ the second harmonic is zero, and the transient component of voltage is $-(s'_2/2s)E_o$. Hence

$$E_1\sin[(s'_2/2s)\theta_{s1}] + E_3\sin[(s'_2/2s)\theta_{s3}] = -(s'_2/2s)E_o \quad (40)$$

Finally, at $x = s'_3/3$, the third harmonic is zero, and the transient component of

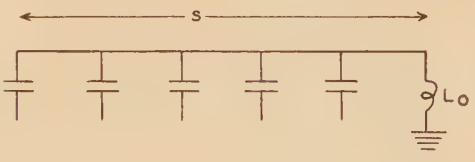

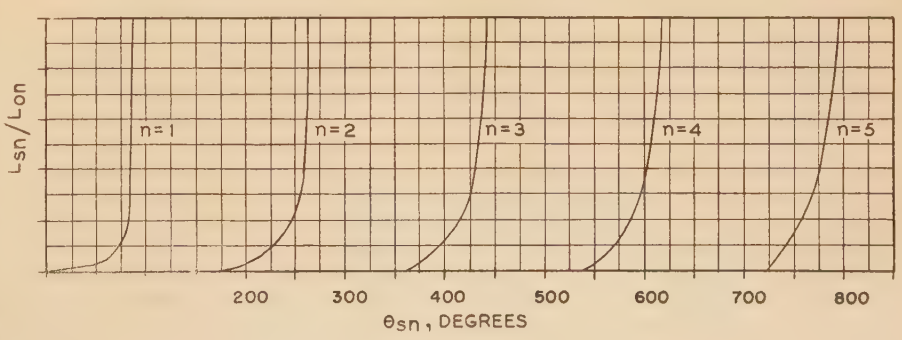

Figure 12. Angular wave length of the various harmonic oscillations of the line open at one end and grounded through an inductance at the other end

the voltage is $-(s'_3/3s)E_o$. Hence

$$E_1 \sin [(s'_3/3s)\theta_{s1}]+E_2 \sin [(s'_3/3s)\theta_{s2}] = -(s'_3/3s)E_o \quad (41)$$

Thus we have three equations to determine the three unknowns E_1, E_2, and E_3.

When few harmonics are considered, for example three, both methods are approximate and the answers depend on the choice of points used for setting up the equations.

Example — Calculation of Harmonics. For simplicity only three harmonics will be considered.

Let

$L_1/L_o=5$
$L_2/L_o=2.8$
$L_3/L_o=1$

Then

$\theta_{o1}=30°$
$\theta_{o2}=70°$
$\theta_{o3}=90°$
$\theta_{s1}=150°$
$\theta_{s2}=290°$
$\theta_{s3}=450°$
$\sin \theta_{s1}=0.5$
$\sin \theta_{s2}=-0.94$
$\sin \theta_{s3}=1$

The plotting of the harmonics by method 1 is facilitated by laying out the scale of angles for each harmonic as shown in Figure 19A. The bottom scale is for the fundamental harmonic, the middle scale for the second harmonic, and the top scale for the third harmonic. The waves with 100 per cent amplitude are not reproduced there in order to avoid confusion with the actual curves of the harmonics.

At the open end

$$E_1 \sin 150° \text{ (or } 30°)+E_2 \sin 290° \text{ (or } 70°)+E_3 \sin 450° \text{ (or } 90°) = -100 \text{ per cent}$$

That is,

$$0.50E_1+0.94E_2+E_3=-100 \text{ per cent} \quad (39a)$$

At 60, the fundamental degrees, the third harmonic is zero. Hence

$$0.86E_1-0.9E_2=-40 \text{ per cent} \quad (39b)$$

Finally, at 90, the fundamental degrees,

$$-E_1+0.1E_2+E_3=-60 \text{ per cent} \quad (39c)$$

Solving these three equations simultaneously,

$$E_1=-85 \text{ per cent}; \quad E_2=38 \text{ per cent}; \quad E_3=-22 \text{ per cent} \quad (40)$$

These waves are plotted in Figure 19A.

As a check the initial actual voltage distribution which these three harmonics represent is shown in Figure 19B which is seen to be a crude sort of a zero line because only three harmonics are utilized.

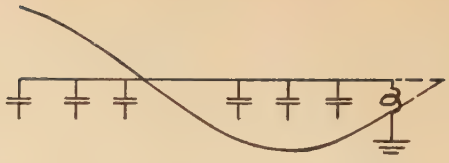

Figure 13. Higher harmonic wave on the line open at one end, grounded through an inductance at the other end

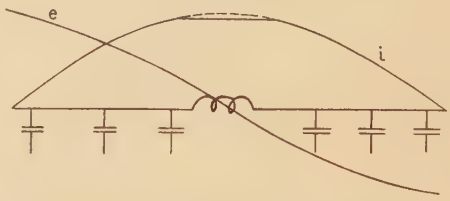

Figure 14. Oscillation of a line having a massed series inductance in the middle

Example—Voltage Distribution a Half Cycle Later. To determine the resultant voltage distribution a half cycle (of the fundamental) later, let it be assumed first that $\omega_2=3\omega_1$, that the third harmonic is almost damped out, and the fundamental and second harmonic are substantially undamped. The result is shown in curve *A* of Figure 19C. The maximum voltage to ground is 188 per cent of the impressed (turn-ratio) voltage. The maximum gradient is near the middle and is about 3.2 times that corresponding to uniform distribution.

As an alternative and more realistic assumption, let it be assumed that the third harmonic will be damped out 100 per cent, the second harmonic 75 per cent, and the fundamental 30 per cent. The resulting distribution is shown by curve *B*, Figure 19C. The maximum voltage is now 142 per cent instead of 188 per cent; and the maximum gradient is 2.2 instead of 3.2 times that corresponding to uniform distribution of the turn-ratio impulse voltage.

The amplitudes and wave shapes of these subsequent voltages vary widely with varying assumptions of relative frequencies and damping. The foregoing example is intended to be nothing more than illustrative.

Frequency of Oscillation, Inductance, and Surge Impedance

Frequency of Oscillation and Inductance. In a standing wave of unit amplitude, Figure 20, with C_s and C_g representing constants per unit length,

$$e_g = \sin [(2\pi/\lambda)x] \quad (41a)$$
$$e_s = (2\pi/\lambda) \cos [(2\pi/\lambda)x] \quad (41b)$$
$$i_g = \omega C_g e_g = \omega C_g \sin [(2\pi/\lambda)x] \quad (42)$$
$$i_s = \omega C_s e_s = \omega C_s (2\pi/\lambda) \cos [(2\pi/\lambda)x] \quad (43)$$

$$i_L = i_s + \int_x^{\lambda/4} i_g dx \quad (44a)$$
$$= \omega(C_s 2\pi/\lambda + C_g \lambda/2\pi) \cos [(2\pi/\lambda)x] \quad (44b)$$

It may be recognized in equation 44b that $C_s(2\pi/\lambda)$ represents the series capacitance per radian and may be symbolized by $-C'_s$. Similarly, $C_g(\lambda/2\pi)$ is ground capacitance per radian and may be symbolized by C'_g. Equation 44b then may be written as

$$i_L=\omega(C'_s+C'_g) \cos [(2\pi/\lambda)x] \quad (44c)$$

It may be interesting to observe that when the series and ground capacitances are entered per radian they enter additively to each other with equal weight, as equivalent to each other, or interchangeable, so to say. We therefore might represent $C'_s+C'_g$ by the single symbol C' as the total effective capacitance per radian.

The physical meaning of this is that a C_s distribution of one microfarad per radian constitutes identically the same burden on the winding as a C_g distribution of one microfarad per radian.

Now we must determine what value of ω (if any) will enable the i_L of equation 44c to produce the e_s of equation 41b through whatever inductive effect the winding may offer to it.

Let

N = the number of turns per unit length
h = the effective length of the harmonic-flux path

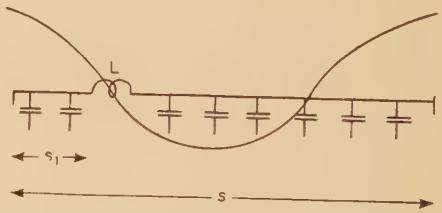

Figure 15. Oscillation of a line having a massed series inductance at a voltage node other than midpoint

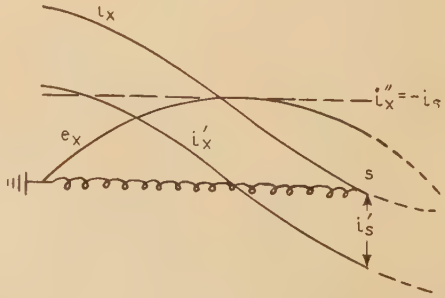

Figure 16. Components of current wave to satisfy the primary and secondary terminal conditions of Figure 1

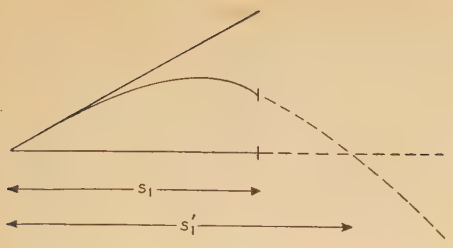

Figure 17. Actual fractional wave and corresponding complete half wave

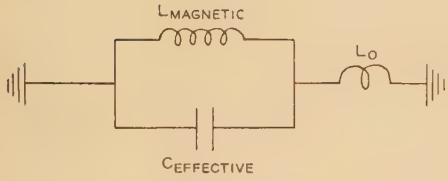

Figure 18. Equivalent inductance and capacitance network of shielded transformer

p = the mean perimeter of the winding

Then

$$B=(4\pi/10)(N/h)\int_o^x i_L dx \tag{45}$$

$$d\phi=1.26(Np/h)\int_o^x i_L dx \tag{46}$$

$$\frac{de_s}{dx}=1.26\times10^{-8}(N^2p/h)\omega\int_o^x i_L dx \tag{47}$$

$$e_s=1.26\times10^{-8}(N^2p/h)\omega\int_x^{\lambda/4}\int_o^x i_L dx^2 \tag{48a}$$

Substituting the value of i_L from equation 44c,

$$e_s=1.26\times10^{-8}(N^2p/h)\omega^2(C'_s+C'_g)\times\int_x^{\lambda/4}\int_o^x \cos[(2\pi/\lambda)x]dx^2 \tag{48b}$$

$$=1.26\times10^{-8}(N^2p/h)(\lambda/2\pi)^2\omega^2(C'_s+C'_g)\cos[(2\pi/\lambda)x] \tag{48c}$$

If e_s is multiplied by $\lambda/2\pi$, it becomes volts per radian. Doing this to both members of equation 48c,

$$(\lambda/2\pi)e_s=1.26\times10^{-8}(N^2p/h)\times(\lambda/2\pi)^3\omega^2(C'_s+C'_g)\cos[(2\pi/\lambda)x] \tag{49a}$$

$$=\omega L'\omega(C'_s+C'_g)\cos[(2\pi/\lambda)x] \tag{49b}$$

$$=\omega L' i_L \tag{49c}$$

in which

$$L'=1.26\times10^{-8}(N^2p/h)(\lambda/2\pi)^3 \tag{49d}$$

From equation 49c it is clear that L' is the effective inductance of the winding per radian under a sinusoidal current wave.

To solve for ω we equate the e_s in equation 41b to the e_s in equation 49b. Cancelling similar factors from both sides leaves

$$1=\omega^2L'(C'_s+C'_g) \tag{50}$$

Hence

$$\omega=\frac{1}{\sqrt{L'(C'_s+C'_g)}} \tag{51a}$$

$$=\frac{1}{\sqrt{L'C'}} \tag{51b}$$

where in per-radian quantities

$$C'=C'_s+C'_g \tag{51c}$$

Because the values of both L' and C' vary with the harmonic, it is better to write the constant with the subscript n to make this thought more explicit so that equation 51b would be written as

$$\omega_n=\frac{1}{\sqrt{L'_nC'_n}} \tag{51d}$$

Because L'_n is the inductance per radian and L_n in previous equations was the total inductance of the winding, it follows that

$$L_n=\theta_{sn}L'_n \tag{51e}$$

where θ_{sn} is in radians.

It may be recognized that equations 51b and 51d also are applicable to transmission lines. By expressing the constants of the system per radian, we have secured a generality of formula applicable to any harmonic whether on a transmission line or on a transformer winding. This also is true of surge impedance.

Inasmuch as it is not practical to secure a sinusoidal distribution of current for the experimental determination of the inductance at low frequencies, it may be well to determine the relationship of L' to the nearest quantity that can be determined by test and with the conception of which we may be familiar.

The nearest familiar inductance concept to L' is the leakage inductance L'' corresponding to an ampere-turn distribution that has the same wave length but is triangular instead of sinusoidal, with equal current in each turn. A half group with triangular magnetomotive-force distribution corresponds to (though does not equal) the sinusoidal half wave. We assume that the current is one ampere in each turn in the triangular magnetomotive-force case and one ampere maximum in the sinusoidal case.

The leakage inductance L″ of such a half group of length $\lambda/2$ with triangular ampere-turn distribution is

$$L''=1.26\times10^{-8}(N^2p/h)\lambda^3/96 \tag{52}$$

L'' can be either calculated or measured. Calculation may sometimes involve the uncertainty of the effective value of h and direct measurement then is desirable.

As the half group corresponds to π ra-

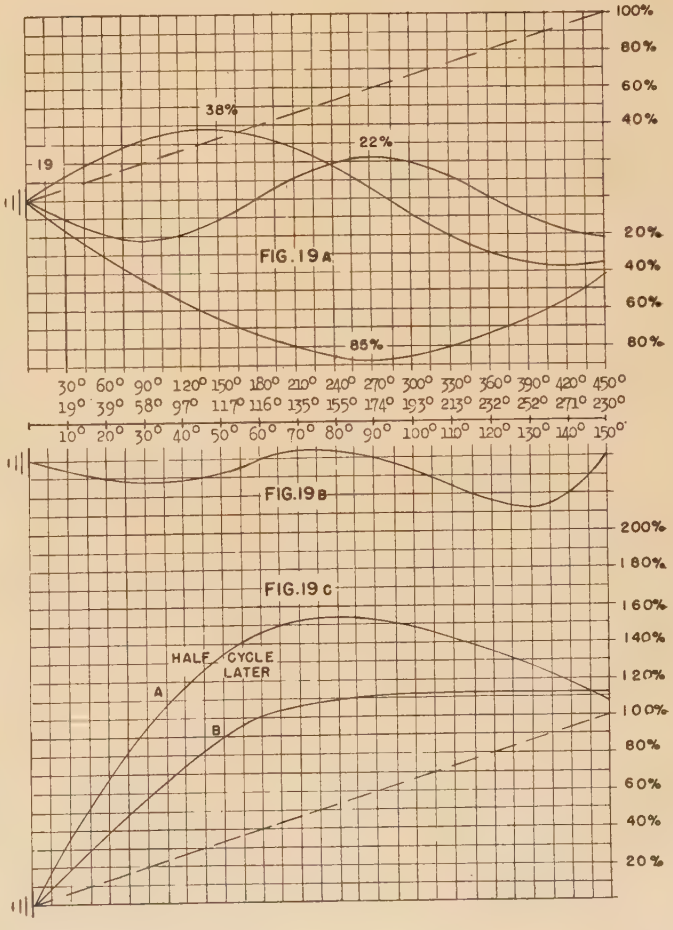

Figure 19

A. Angular wave length of three harmonics of a transformer

B. The 3-harmonic initial resultant voltage distribution

C. Voltage distribution a half cycle after start

dians, the equivalent value of the inductance per radian will be the L'' of equation 52 divided by π.

$$L''_{\text{per radian}} = L''/\pi \quad (53a)$$
$$= 1.26\times10^{-8}(N^2p/h)\lambda^3/96\pi \quad (53b)$$

Comparing equations 53 and 50, it may be seen that

$$L' = (12/\pi^2)L''_{\text{per radian}} = 1.2515L''_{\text{per radian}} \quad (54)$$

This is an interesting result. The effective inductance per radian for a sinusoidal distribution of magnetomotive force is $12/\pi^2$ or 1.2515 times that for a triangular distribution of magnetomotive force.

Based on equations 51e and 54, L_n for the whole winding is given by

$$L_n = 1.25L''_{\text{per radian}} \times \theta_{sn} \quad (55a)$$
$$= 1.25L''\theta_{sn}/\pi \quad (55b)$$

When θ_{sn} is almost a whole multiple of π, there are n half groups and

$$L_n = 1.25nL'' \quad (55c)$$

When making measurement it is desirable to do so for complete waves and then interpolate for fractional waves.

Measuring the Inductance. Three inductances have been discussed.

1. L'_n, the harmonic inductance per radian.

2. L_n, the harmonic inductance of the whole winding.

3. L'', the inductance of a half-group for uniform current.

It also has been pointed out that the harmonic inductance is 1.25 times the uniform-current inductance. It follows therefore that $L_n/1.25$ can be measured directly in accordance with the illustrative impedance diagrams of Figure 21 for the fundamental, the second, and the third harmonics. Then

$$L'_n = L_n/\theta_{sn} \quad (55d)$$

where θ_{sn} is in radians.

Surge Impedance. The surge impedance Z_n of an oscillatory system for the nth harmonic is the ratio of the voltage maximum to the current maximum for that harmonic. Therefore, from equations 41a and 44c,

$$Z_{n\ \text{surge}} = \frac{e_{g\ \max}}{i_{L\ \max}} = \frac{1}{\omega_n(C'_s+C'_g)_n} = \frac{1}{\omega_n C'_n} \quad (56a)$$

Substituting the value of ω_n from equation 51d into equation 56a,

$$Z_{n\ \text{surge}} = \sqrt{\frac{L'_n}{C'_n}} \quad (56b)$$

which also applies for transmission lines and for all harmonics. This generality also is secured by expressing the constants per radian. In the transmission line the values of L' and C' vary similarly with wave length and therefore their ratio, the surge impedance, is constant for all harmonics. In the transformer winding the values of L' and C' vary as different functions of the wave length and accordingly the surge impedance varies with the harmonic. It is the more creditable for equation 56b therefore that it fits both cases.

Oscillations of a Shielded Secondary

Because a shielded secondary maintains the same voltage distribution along its capacitance network as along its inductive circuit, there is no tendency for cross currents to flow from one to the other at their intermediate cross connections. These intermediate cross connections therefore may be opened (on paper) leaving only the end connections intact without modifying the phenomena. With the intermediate cross connections open, the capacitance network becomes equivalent to a single massed capacitance C_{eff} and the system equivalent to that shown in Figure 18. If the magnetizing current is assumed zero and the magnetizing inductance infinite, then we have a simple circuit consisting of C_{eff} in series with the leakage inductance of the transformer having only one possible mode of oscillation

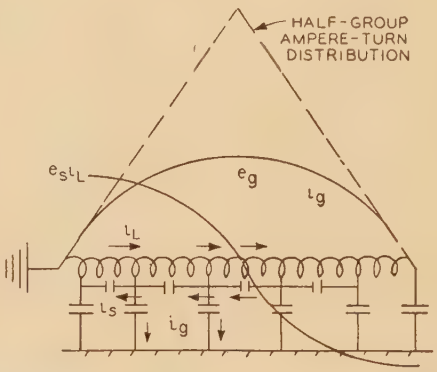

Figure 20. Ampere turn distributions—sinusoidal and triangular

$$\omega = 1/\sqrt{L_o C_{eff}} \quad (57)$$

The effective capacitance will be somewhat larger than $\sqrt{C_g C_s}$ of the unshielded transformer because of the capacitance introduced by the shielding.

As the inductance in the formula for ω is the normal leakage inductance and the capacitance is of the same order as (though greater than) that of the unshielded transformer, the frequency of oscillation of the shielded transformer may be higher than that of the fundamental of the unshielded design.

Under a rectangular impulse and with no damping, this system will oscillate between zero voltage and double the impulse voltage, both to ground and across the coils, maintaining uniform distribution all the time.

While damping data have to be obtained experimentally, 50 per cent damping per cycle (or even per half cycle) may be expected. Hence, as a rough estimate, increases in gradients and major insulation stresses may be of the order of 50 per cent.

Inasmuch as all internal stresses of a shielded design are proportional to its terminal voltage, whenever it is assured that the terminal voltages will be held down to a safe value, no greater concern need be felt for the simple shielded winding when acting as the secondary than when acting as the primary winding.

Appendix I. Velocity of Propagation in Transformer Windings

The concept of velocity of propagation is ill-fitting to the concept of a standing wave—bad enough in the case of a transmission line, worse in that of the transformer windings. Therefore any symbol that may be taken for velocity of propagation will be interpreted in terms of standing waves.

In some of the early equations of a transmission line, a velocity of propagation c was utilized because originally (in classical analyses) the standing wave is derived as the resultant of two waves traveling in opposite directions. But after the concept of a standing wave has been established, c may as well be given a new interpretation better fitting the standing wave concept. As c appears in our formulas for ω, and $\omega = 2\pi f = 2\pi c/\lambda$, it follows that $c = f\lambda$; and for $f = 1$, $c = \lambda$. That is, c is the wave length of a standing wave oscillating at one cycle per second.

If the frequency of oscillation has constant proportionality to the reciprocal of the wave length, as in a transmission line, the foregoing formula gives the same value of c reckoned from any harmonic $c = f_n\lambda_n$. Since the ratio of f to $1/\lambda$ is not constant for all wave lengths in the case of windings, c will have a different value c_n as reckoned from different harmonics, $c_n = f_n\lambda_n$.

The meaning of c_n in windings then is that wave length which a standing wave would have to have in order to oscillate at one cycle per second if the winding had linear characteristics proportional to those of the nth harmonic. Thus the 1-cycle-per-second wave length is different as reckoned from different harmonics.

Appendix II. Transmission Line Completely Open at One End

This is a further discussion of "Open Line" of the text. The circuit is illustrated in Figure 10 and is analogous to the isolated high-voltage winding.

Fundamental Mode of Oscillation

The standing wave of the longest possible wave length on such a line is a quarter of a wave length ($\lambda=4s$), and the voltage and current equations referred to the open end as origin are

$$\left.\begin{aligned} e_x &= E_1 \cos [2\pi(x/\lambda)] \cos [2\pi(c/\lambda)t] \\ &= E_1 \cos \theta_x \cos \omega_1 t \end{aligned}\right\} \quad (20)$$

$$\left.\begin{aligned} i_x &= -(E_1/X_1) \sin [2\pi(x/\lambda)] \\ &\qquad \sin [2\pi(c/\lambda)t] \\ &= -(E_1/X_1) \sin \theta_x \sin \omega_1 t \end{aligned}\right\} \quad (21)$$

The algebraic sign is so assumed as to make the current lead the voltage.

At any point x along the line, the effective reactances of the two sections of the line will be

$$X_A = e_x/i_x = -X_1 \cot \theta_x \quad (22)$$

It follows that

$$\omega = c\theta_s/s \quad (25c)$$

which is the same as equation 10.

The substitution of equation 25c into equation 24b yields

$$X_1 s/cL = \theta_s/\cot \theta_s = \theta_s \tan \theta_s = L_s/L_o \quad (26)$$

This equation is solved conveniently with the help of Figure 12.

From equation 20 we obtain for μ

$$\left.\begin{aligned} \mu_1 &= E_1/e_s \\ &= 1/\cos \theta_s \\ &= 1/\sin \theta_o \end{aligned}\right\} \quad (27a)$$

and from equation 25b

$$s' = s(\pi/2)/\theta_s \quad (27c)$$

It may be observed that Figure 10 also may be considered as one-half of Figure 4, because the line of the latter could be cut in two without altering the oscillation of the system in any way. The foregoing equations differ from those of the closed line only because the origin of co-ordinates now corresponds to the middle of the line of Figure 4. The equations of the open and closed lines could be correlated along this idea, but no space will be devoted to it here.

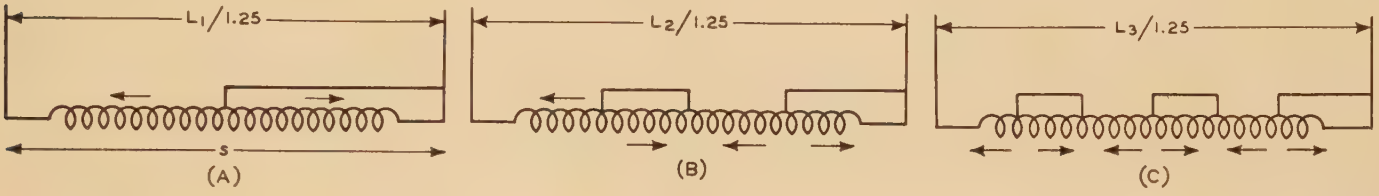

Figure 21. Connection to measure the inductance offered to various modes

A. The fundamental oscillation
B. The second harmonic oscillation
C. The third harmonic oscillation

$$X_B = -X_A = X_1 \cot \theta_x \quad (23a)$$

$$= -X_1 \tan \left(\frac{\pi}{2} + \theta_x\right) \quad (23b)$$

As $\theta_x < 90$ degrees and all trigonometric functions are positive in the first quadrant, X_A will be negative or capacitive and X_B positive or inductive.

A massed inductance connected to the open end (but without closing the circuit to ground) can have no current and no voltage drop and therefore no effect whatever on the oscillation of the line. However, if inserted at the grounded end, Figure 11, it becomes equivalent to an extension of the line from s, the actual length, to s', an equivalent length, derived as follows.

If the terminating reactance is capacitive, the circuit cannot oscillate to a quarter wave length of any modified dimensions because two capacitive reactances cannot oscillate—cannot resonate—with each other. Oscillation can take place, however, under a harmonic wave for which the line subtends an angle between 90 and 180 degrees and becomes positive or lagging.

From equations 23a

$$X_L = X_1 \cot \theta_s \quad (24a)$$

$$\omega L = X_1 \cot \theta_s \quad (24b)$$

But

$$\omega = 2\pi c/\lambda \quad (25a)$$

and

$$\lambda = 4s' = 4s(\pi/2)/\theta_s \quad (25b)$$

Higher Harmonic Modes of the Open Line

Equations 20 and 21 apply to harmonic voltages and currents by substituting the appropriate value of λ. Therefore equations 24a and 26 which are derived from them also apply to the higher harmonics, Figure 13, and can be calculated with the help of the curves of Figure 12. When θ_s is determined for any harmonic, μ_n for it follows from equation 27b.

Appendix III. Other Combinations of Transmission Line and Massed Inductance

Although not all combinations of lines with massed inductances are capable of supporting standing waves, there is an enormous number that can. A few comments here on the general principles of these may be interesting and helpful.

1. For a stable standing-wave oscillation, the massed inductance must be adjacent to a voltage node (zero). Conversely, only those oscillations are possible as standing waves which bring the massed inductance to a voltage node.

2. As the current at both ends of a massed inductance has to be the same, such an inductance can be inserted into an interior nodal point only when the current and voltage of the inductance can be fitted to both sides of the circuit. For instance, a line open at both ends, Figure 14, with a massed inductance in the middle can oscillate in the manner shown. Figure 15 illustrates a possible case in which the massed inductance is located at approximately a quarter of the line and the oscillation is a full wave.

3. Figure 15 might be analyzed as a repetitive extension of Figure 11. In Figure 15, if s_1 is the short section of the line, s the total, and s_L the equivalent additional length of line introduced by L_o, then for a stable standing-wave oscillation like that shown, s_1 will not be $s/4$ but

$$s_1 + (s_L/2) = (s+s_L)/4$$

Appendix IV. Effect of Massed Capacitance at Transformer Terminals

If one high voltage terminal is grounded, as assumed in the foregoing text, and the other not entirely isolated but connected to an idle network of appreciable capacitance, not large enough to be considered a short circuit to the transient phenomena, the situation is as if the winding is grounded through a capacitive reactance, and the foregoing equations are modified as follows.

Now i_x will not be zero at $x=s$ but some value i_s determined by

$$\left.\begin{aligned} i_s &= -e_s/X_c \\ &= -E_1 (\sin \theta_s)/X_c \\ &= -I_{\max} (\sin \theta_s)(X_1/X_c) \end{aligned}\right\} \quad (42)$$

Equations 29a and 29b now become

$$i_x = i'_x + i''_x + i_s \quad (43a)$$

$$= I_{\max} \{\cos [(x/s)\theta_s] - \cos \theta_s - (\sin \theta_s)(X_1/X_c)\} \quad (43b)$$

Then

$$i_p = -(1/s)\int_o^s i_x dx \quad (44a)$$

$$= -I_{\max}\left[\frac{\sin \theta_s}{\theta_s} - \cos \theta_s - (\sin \theta_s)(X_1/X_c)\right] \quad (44b)$$

Equation 33a now becomes

$$E_1 \sin \theta_s = (E_1/X_1)\left[\frac{\sin \theta_s}{\theta_s} - \cos \theta - (\sin \theta_s)(X_1/X_c)\right]\omega L_o \quad (45a)$$

$$1 = (1/X_1)[1/\theta_s - \cot \theta_s - X_1/X_c]\omega L_o \quad (45b)$$

The Development of Modern Excitation Systems for Synchronous Condensers and Generators

F. M. PORTER
MEMBER AIEE

J. H. KINGHORN
MEMBER AIEE

DURING the past 15 years and particularly in the past ten years, there have been many major developments in excitation systems for synchronous condensers and generators. These changes and improvements were stimulated in 1928 by the introduction of the hydrogen-cooled synchronous condenser which necessitated a reconsideration of the excitation arrangement and brought about a change from a direct-connected exciter to separate excitation. This, together with the desire to obtain maximum speed of response and to eliminate maintenance caused by moving parts associated with rotating exciters and with mechanical regulators, led to the trial of electronic applications on the systems of the American Gas and Electric Company A development program along these lines was carried on over a period of approximately 15 years and included specifically 15 exciter applications on large generators and condensers. About six years ago a review of the performance and operating experience on the machines involved in this plan resulted in the design and trial of a system using a direct-connected exciter with amplidyne control for excitation of a large synchronous condenser. Following this, four similar installations were provided. Thus there has been obtained a wide variety of experience with excitation systems and associated equipment. It is the purpose of this paper to recount these developments, describe typical installations, and discuss the operating results obtained with them.

Paper 46-154, recommended by the AIEE committee on power generation for presentation at the AIEE summer convention, Detroit, Mich., June 24–28, 1946. Manuscript submitted April 18, 1946; made available for printing May 16, 1946.

F. M. PORTER is electrical equipment engineer and J. H. KINGHORN is protection engineer in the American Gas and Electric Service Corporation, New York, N. Y.

The authors wish to acknowledge the fine spirit of co-operation and great amount of work carried out by the engineering staffs of both the General Electric Company and Westinghouse Electric Corporation, who between them designed and constructed all of the equipment discussed in this paper. The authors also express their indebtedness to the organizations of the Appalachian Electric Power Company, Indiana and Michigan Electric Company, Kentucky and West Virginia Power Company, Inc., Ohio Power Company, and the Scranton Electric Company, upon whose systems these machines were installed. Had it not been for the patient co-operation of all concerned in solving miscellaneous problems incident to the initial trials and later operation of the various excitation systems described in this paper, the development program covering this equipment could not have been brought to its unusually successful conclusion.

History of Development and Description of Installations

Introduction of Hydrogen-Cooled Condensers

Until 1928 the conventional type of excitation system used with synchronous condensers consisted of a direct-connected or motor-driven exciter with mechanical regulator. Although satisfactory performance was, and still is, being obtained from rotating exciters, periodic shutdowns of the equipment were necessary for maintenance purposes. Also, the wear on the moving parts of the mechanical type voltage regulators necessitated frequent adjustments and replacements. In addition the quality of the performance of the regulating system was limited by the characteristics of the regulator and by the time lag of the exciter. At this time the first large hydrogen-cooled synchronous condenser, a 20,000-kva unit, was placed in service at the Turner station of the Appalachian Electric Power Company. The complication involved in attempting to build a gas tight machine with a direct-connected exciter discouraged the use of such an arrangement, and therefore a motor-driven exciter with a vibrating type regulator was provided.

In 1930 and 1931, four additional hydrogen-cooled synchronous condensers ranging in size from 15,000 to 30,000 kva were installed. This was discussed in a previous paper.[1] The excitation system for each of these machines likewise consisted of a motor generator set with mechanical type regulator.

Electronic Pilot Exciters

The possibility of taking advantage of high speed response characteristics of a tube type regulator had been studied for some years. To obtain experience with such an arrangement, an electronic pilot exciter and regulator, the first installations of this kind, were placed in service in 1930 with a 15,000-kva outdoor air-cooled synchronous condenser at the Howard station of the Ohio Power Company. The field of the motor-driven exciter of this unit is excited by means of a thyratron rectifier arrangement as described about ten years ago.[2] Pertinent data covering this machine and exciter are included in Table I, which lists all of the machines and excitation systems involved in this development program carried out on the systems of the American Gas and Electric Company.

Satisfactory performance obtained from this initial installation resulted in providing two similar thyratron pilot exciters and regulators for the direct-connected exciters of two large turbogenerators at the Glen Lyn station of the Appalachian Electric Power Company. These equip-

$$L_{s1}/L_0 = 1 - \theta_s/\tan\theta_s - \theta_s^2 C/Cs \qquad (45c)$$

in which

C = the line capacitance connected to the transformer

C_s = the effective winding capacitance (analogous to L_s) for the harmonic under consideration

These two constants L_s and C_s are related to each other by the X_1 and the ω of the winding for the harmonic

$$X_n = \sqrt{L_{sn}/C_{sn}};\ \omega_n = \theta_{sn}/\sqrt{L_{sn} \times C_{sn}} \qquad (46)$$

If X_n, ω_n, and θ_{sn} are obtained by test, L_{sn} and C_{sn} can be calculated.

References

1. ABNORMAL VOLTAGES WITHIN TRANSFORMERS, L. F. Blume, A. Boyajian. AIEE TRANSACTIONS, volume 38, 1919, pages 577–614.

2. EFFECT OF TRANSIENT VOLTAGES ON POWER TRANSFORMER DESIGN—IV, K. K. Palueff, J. H. Hagenguth. AIEE TRANSACTIONS, volume 51, 1932, pages 601–15.

3. LIGHTNING SURGES TRANSFERRED FROM ONE CIRCUIT TO ANOTHER THROUGH TRANSFORMERS, P. L. Bellaschi. AIEE TRANSACTIONS, volume 62, 1943, December section, pages 731–8.

4. TRANSIENT OSCILLATIONS OF MUTUALLY COUPLED WINDINGS, L. V. Bewley. AIEE TRANSACTIONS, volume 51, 1932, pages 299–308.

ments were placed in service in April 1931 and were installed primarily to prevent the occurrence of out-of-step conditions following severe faults. This is accomplished by employing a regulating system which maintains a steady bus voltage by controlling it continuously. This arrangement is provided with a grid-controlled 3-phase thyratron rectifier in place of a separate pilot exciter. The thyratron grids are energized by a 60-cycle voltage which lags the anode voltage by 90 degrees, and on this voltage is superimposed the variable direct voltage output of an electronic regulator.

Figure 1 shows the electronic regulator panel at Glen Lyn and Figure 2 is a schematic diagram of the circuit employed which is typical for both exciters as well as for the one at Howard. The diagram does not include filter circuits which are not essential to an understanding of the principles involved. The regulator employs a Wheatstone bridge having two legs of thyrite and two of standard resistors. The 3-phase voltage to be regulated is rectified and impressed on two terminals of this bridge. Because of the characteristics of thyrite, small changes in this impressed voltage produce relatively large changes in the voltage across the other two bridge terminals. This latter voltage is applied to the grid of a pliotron, producing an amplified voltage across a resistor in the pliotron plate circuit. This amplified voltage is used as the variable d-c grid control voltage for the thyratron rectifier. The thyratron tube heaters are supplied from the same potential transformers which supply the regulator. A means is provided for transferring the main exciter from electronic pilot excitation to self-excitation when necessary to change tubes or to work on the regulator pilot exciter system.

Electronic Main Exciters

The desire to obtain the maximum benefit from an electronic system following the satisfactory performance of the tube type pilot exciters previously mentioned resulted in the installation in August 1933 of the first all tube regulator and thyratron excitation system at Scranton, Pa. This equipment was placed in service with a 15,000-kva hydrogen-cooled synchronous condenser and has been described elsewhere.[3] In the original installation the six power tubes were air-cooled thyratrons, but they were replaced several years later with water-cooled ignitrons.

A similar combined electronic exciter and regulator of improved type were installed at Fostoria, Ohio, on a 36,000-kva synchronous condenser in 1936.[1] The outstanding feature of this machine was its design for operation at a gas pressure of 15 pounds per square inch, utilizing for the first time the advantage of more efficient cooling, obtainable by operating at higher gas pressure.

Satisfactory performance of the electronic exciter at Fostoria as well as the one at Scranton led to the installation of a third exciter for a similar 36,000-kva synchronous condenser at the Torrey Station of The Ohio Power Company. This equipment was provided in 1939 for maintaining the voltage of a 22-kv bus which serves a highly fluctuating load consisting primarily of large electric furnaces. Figure 3 shows a front view of the Torrey electronic excitation equipment which is mounted on the three left panels of the switchboard. The tube compartments were designed as an integral part of this switchboard, two tubes being mounted behind each panel. Access for changing tubes is from the rear and the anode circuit breaker must be tripped before the compartment door can be opened. Furthermore, the main field circuit which is normally ungrounded must be tested for grounds, and if it is found clear the cathode bus must then be

Table I. Typical Synchronous Condensers and Generators Associated With Development of Excitation Systems

Listing as of February 1, 1946

			Synchronous Machine				Main Exciter			
								Rating		
Location	Operating Company	Starting Date	Type	Kilovolt-Amperes	Revolutions Per Minute	Cooling Medium	Type	Kilowatts	Volts	Field Supply or Control
Howard, Ohio	The Ohio Power Company	March 1930	Condenser	15,000	900	Air	Motor driven	80	250	Electronic pilot exciter
Glen Lyn, Va.	Appalachian Electric Power Company	*April 1931	Turbogenerator	25,000	1,800	Air	Direct connected	100	250	Electronic pilot exciter
Glen Lyn, Va.	Appalachian Electric Power Company	*April 1931	Turbogenerator	31,250	1,800	Air	Direct connected	150	250	Electronic pilot exciter
Scranton, Pa.	The Scranton Electric Company	August 1933	Condenser	15,000	900	Hydrogen	Electronic	78	150	
Fostoria, Ohio	The Ohio Power Company	November 1936	Condenser	36,000	1,200	Hydrogen	Electronic	175	200	
Fostoria, Ohio	The Ohio Power Company	*February 1938	Condenser	5,000	600	Air	Direct connected	54	125	Electronic pilot exciter
Torrey, Ohio	The Ohio Power Company	July 1939	Condenser	36,000	1,200	Hydrogen	Electronic	175	200	
Claytor, Va.	Appalachian Electric Power Company	October 1939	Hydrogenerator	20,833	138.5	Air	Direct connected	150	250	Electronic pilot exciter
Claytor, Va.	Appalachian Electric Power Company	October 1939	Hydrogenerator	20,833	138.5	Air	Direct connected	150	250	Self-excited amplidyne control
New Carlisle, Ind.	Indiana and Michigan Electric Company	March 1940	Condenser	30,000	3,600	Hydrogen	Electronic	125	250	
Muncie, Ind.	Indiana and Michigan Electric Company	May 1941	Condenser	18,750	900	Hydrogen	Direct connected	120	250	Self-excited amplidyne control
Danville, Va.	Appalachian Electric Power Company	August 1942	Condenser	18,750	900	Hydrogen	Direct connected	120	250	Self-excited amplidyne control
Lima, Ohio	The Ohio Power Company	October 1943	Condenser	18,750	900	Hydrogen	Direct connected	120	250	Self-excited amplidyne control
Beaver Creek, Ky.	Kentucky and West Virginia Power Company, Inc.	January 1945	Condenser	18,750	900	Hydrogen	Direct connected	120	250	Self-excited amplidyne control
Anderson, Ind.	Indiana and Michigan Electric Company	January 1946	Condenser	18,750	900	Hydrogen	Direct connected	120	250	Self-excited amplidyne control

* Electronic pilot exciters placed in service on this date on machines installed previously.

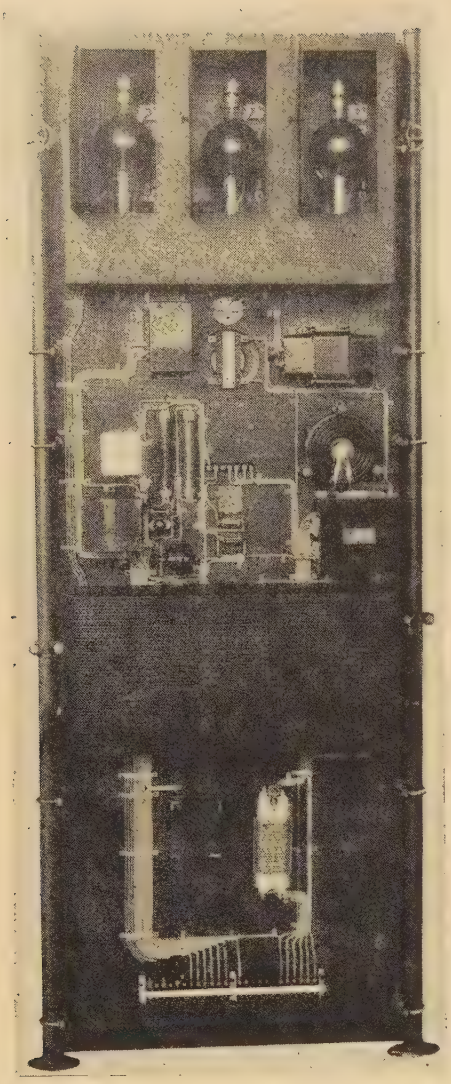

Figure 1. Back view of electronic pilot exciter and regulator

Glen Lyn 31,250-kva generator of the Appalachian Electric Power Company

grounded before the door can be opened. With these precautions tubes may be changed without shutting down the machine. A means is provided for cutting out the electronic regulator and leaving the exciter itself on manual control.

Figure 4 is a schematic diagram showing the circuit employed for this unit. As in the case of the pilot exciters, all filter circuits not essential to an understanding of the fundamentals of the control are omitted. The rectifier is 6-phase and the point at which the igniters fire is controlled by six thyratrons, the grids of which are energized from a grid transformer which supplies a voltage lagging the anode voltage by 120 degrees. On this voltage is superimposed a variable d-c output voltage from the electronic regulator in a manner similar to that employed for the electronic pilot exciters. Each power tube has an individual anode circuit breaker provided with reverse current protection.

The regulator employs a glow tube which provides a constant voltage against which variations in regulated voltage are compared. The 3-phase voltage to be regulated is rectified and impressed on the glow tube through a resistor. The voltage across the glow tube provides a constant potential for the cathode of a pliotron tube whose control grid voltage is obtained from a potentiometer connected across the rectified regulated voltage. Small changes in regulated voltage therefore produce changes in control grid voltage, which are amplified by the pliotron, producing large changes in the voltage across a resistor in its plate circuit. As in the case of the bridge-type regulator, this amplified voltage is applied to the thyratron firing tube grids to control their output and the output of the ignitron rectifier. Although omitted from the diagram for simplicity, all tubes in the regulator are provided in duplicate and connected in parallel so as to provide protection against tube failures.

A fourth installation of an electronic main exciter and electronic voltage regulator was completed in 1940 on a 30,000-kva synchronous condenser at New Carlisle, Ind. As reported elsewhere,[1] this condenser was designed to take maximum advantage of the low density of hydrogen gas by using for the first time a speed of 3,600 rpm. This rating of the machine is based on operation at a gas pressure of 15 pounds per square inch. Figure 5 shows a front view of the exciter installation. The three panels at the left of the switchboard are used for the control of the condenser and its switching. As in the case of Torrey, the power tubes may be changed without shutting down the machine. The regulator which supplies variable d-c bias for the thyratron tube control works on a somewhat different principle from that of Torrey. The control grid voltage for the pliotron tube is made up of two components. The first is a rectified voltage which varies directly with the regulated voltage and which therefore acts similarly to the Torrey arrangement. The second is a voltage drop across a hot cathode tube which varies with the filament voltage. The filament voltage of this tube is obtained from the regulated voltage. A change in regulated voltage therefore produces an instantaneous change in the pliotron control grid voltage, followed by a somewhat slower further change as the tube filament temperature changes. This arrangement is designed to keep hunting at a minimum

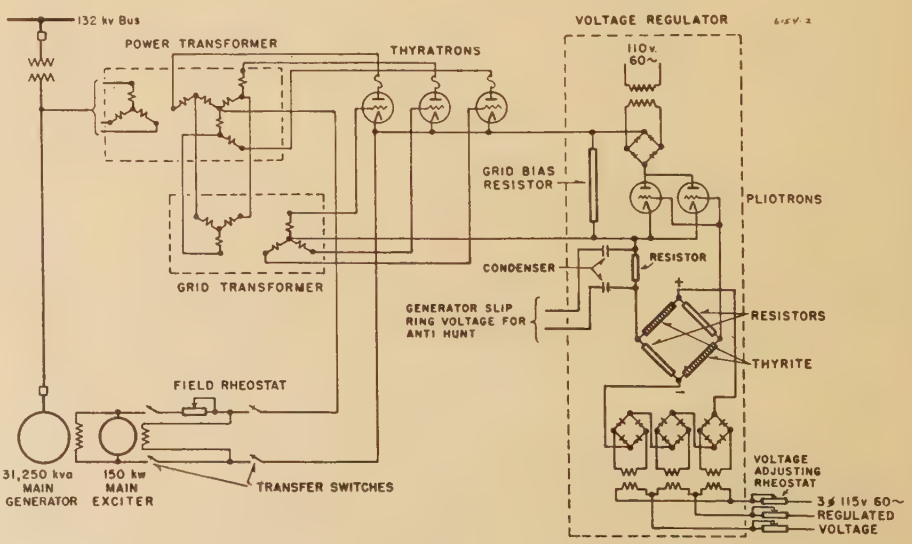

Figure 2. Schematic diagram of electronic pilot exciter and regulator

Glen Lyn 31,250-kva generator

Miscellaneous Direct-Connected Exciter Systems

In October 1939, four 20,833-kva hydrogenerators were placed in service at the Claytor station of the Appalachian Electric Power Company. All of these machines were provided with direct-connected exciters, but in order to obtain comparative experience on various types of pilot exciters and regulators, two of the machines were supplied with direct-connected pilot exciters and rheostatic type voltage regulators, and one was equipped with an electronic pilot exciter similar to those previously installed at Glen Lyn and Howard and with a regulator similar to that at Torrey. An amplidyne excitation system with a static type voltage regulator was provided for controlling excitation of the fourth machine. This was the first time that an amplidyne excitation system had been provided for a syn-

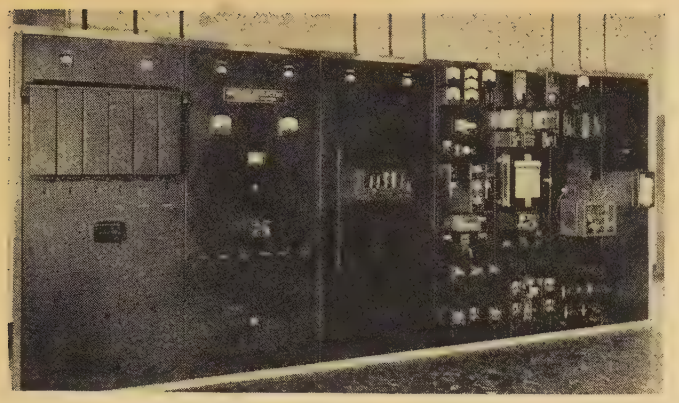

Figure 3. Front view of electronic main exciter and regulator

Torrey 36,000-kva synchronous condenser of The Ohio Power Company

chronous generator. An explanation of this type of arrangement is included later.

During the period from 1930 to 1940, other waterwheel generators and turbo-alternators were installed which were provided with the customary arrangement of direct-connected or gear-driven exciter and pilot exciter. Also air-cooled synchronous condensers in capacities up to 7,500-kva were placed in service at various locations and these were provided with direct-connected exciters and improved types of mechanically operated voltage regulators. During this time there was considerable development on regulator applications for the purpose of obtaining greater reliability and better performance.

Review of Development Up to 1940

In 1940 the performance record of, and operating experience obtained with, all of the synchronous condensers and generators and their excitation and regulation systems previously described were reviewed in order to determine whether definite conclusions could be reached as to an ideal arrangement. The excellent performance anticipated from the electronic exciter facilities was demonstrated without question. However, the initial cost of such equipment in addition to the heavy expense of making tube replacements offered objections to continuing this arrangement. The superior performance and reliability of the electronic regulator definitely had been proved. Difficulties resulting from operating synchronous condensers at speeds of 1,200 and 3,600 rpm indicated the desirability of returning to the previously conventional speed of 900 rpm. The use of hydrogen at gas pressures up to 15 pounds per square inch was established definitely as being a highly satisfactory and desirable practice, and therefore consideration was given to the design of a machine suitable for still higher gas pressure operation. Also, the possibility of providing a direct-connected exciter for a hydrogen-cooled unit had been given considerable study by the manufacturers, and there was reason to believe that a satisfactory design could be made. The superiority of a direct-connected arrangement, as far as electrical performance is concerned, could be obtained in this way. Furthermore, such a design would offer the many advantages of hydrogen atmosphere operation for the exciter as well as for the condenser. The amplidyne excitation arrangement at Claytor was providing excellent performance and therefore was given due consideration in the final decision for obtaining the most suitable excitation arrangement for a synchronous condenser.

Direct-Connected Exciters With Amplidyne Control

As a result of this careful survey of the whole problem, an entirely new type synchronous condenser running at 900 rpm was designed by one of the manufacturers and placed in service in 1941 at the Muncie station of the Indiana and Michigan Electric Company. This is a hydrogen-cooled machine and its rating at one-half pound-per-square-inch hydrogen pressure is 18,750 kva. It was designed for operation at gas pressures up to 25 pounds per square inch and a maximum capability of approximately 25,000 kva is obtained on this basis. This capability is realized partly because of the advantages of operating at the increased hydrogen pressure and partly because of the margins which exist in the machine at the one-half pound rating. The outstanding development in connection with this unit is that for the first time a direct-connected exciter is provided in a hydrogen ventilated machine. The normal air-cooled rating of this exciter is approximately 100 kw but by utilizing the efficient cooling effect of hydrogen at a gas pressure of 25 pounds per square inch, the capacity is increased to approximately 150 kw. The amplidyne regulation system was provided for controlling the excitation to the condenser field and an electronic regulator was installed for controlling the amplidyne generator. Thus an ideal arrangement for an excitation system for a synchronous condenser is obtained when consideration is given to the various factors involved such as greatest reliability, best performance, highest economy, and least maintenance. Along with this improvement there evolved a superior design for the condenser itself.

A schematic diagram showing the electrical connections for this installation is shown in Figure 6. Excitation is controlled by the amplidyne generator which is connected as a source of voltage in series with the field of the main exciter, and which is provided with two control fields. Its buck field is supplied with constant excitation by a small rectifier while its boost field is supplied by the same rectifier through a pliotron tube, the grid of which is controlled by the output of an

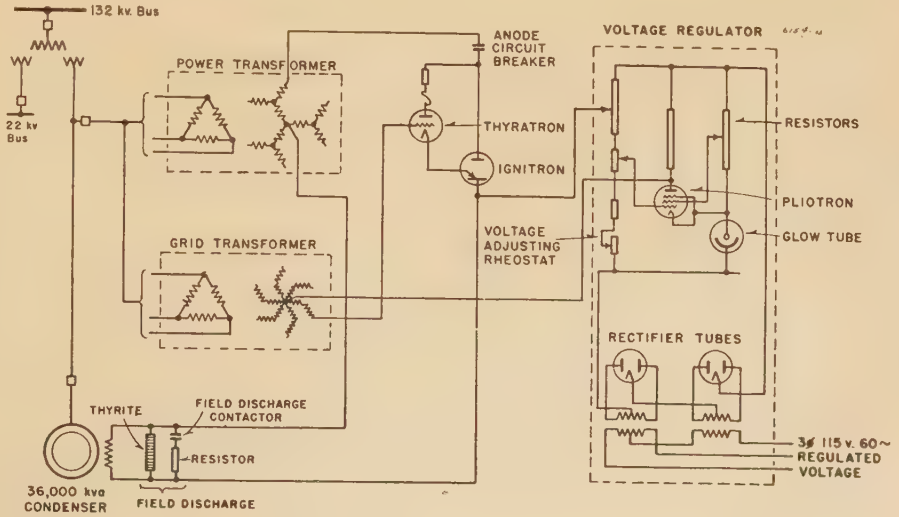

Figure 4. Schematic diagram of electronic main exciter and regulator

Torrey 36,000-kva synchronous condenser

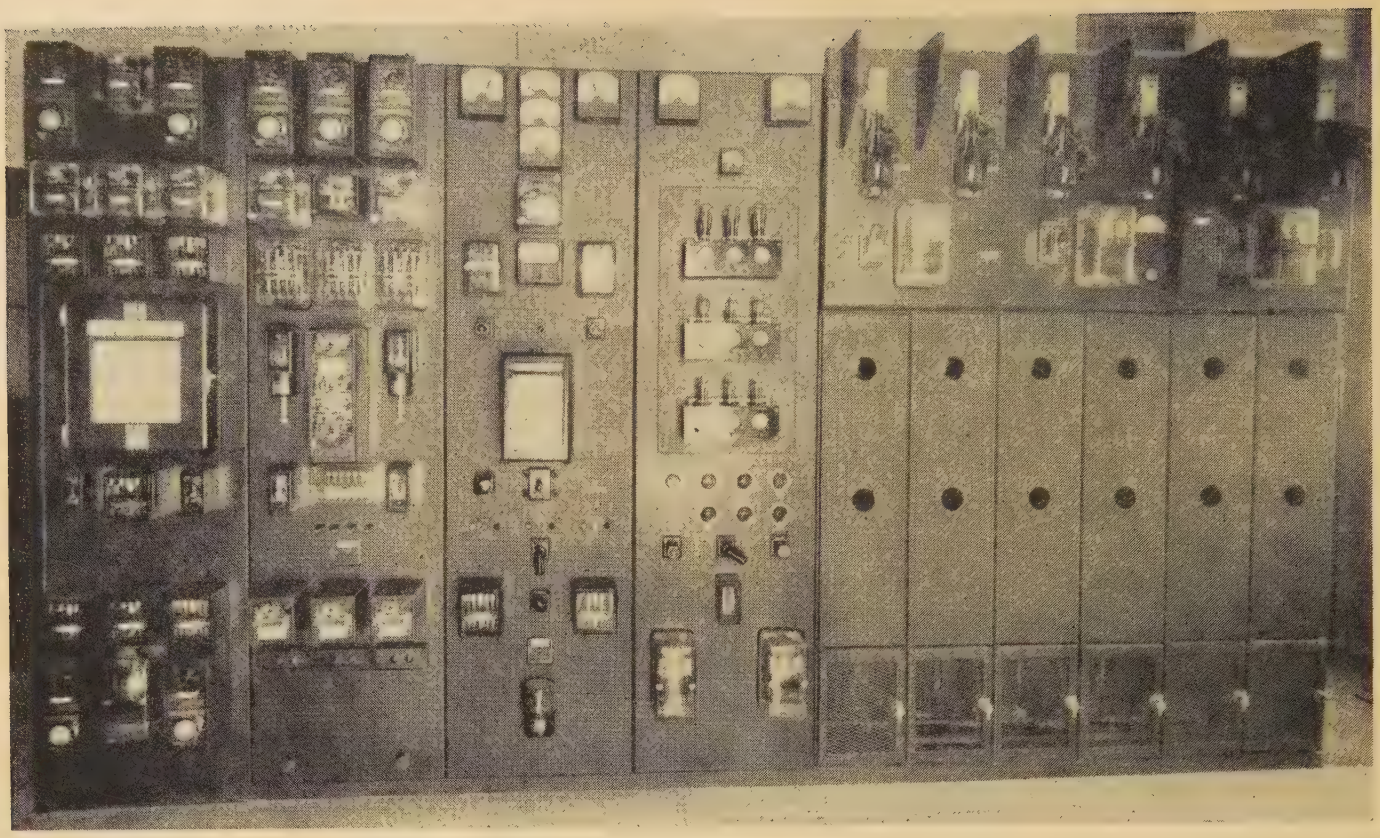

Figure 5. Front view of electronic main exciter and regulator

New Carlisle 30,000-kva synchronous condenser of The Indiana and Michigan Electric Company

electronic voltage standard type regulator similar to that shown in Figure 3 for Torrey. Thus the amplidyne serves as the final step of amplification of the variations in regulated voltage and provides the necessary power to change the field current of the main exciter quickly. The amplidyne driving motor power source is taken from the station auxiliary power supply. It may be noted from Figure 6 that a fixed resistance is connected in series with the amplidyne. This resistance limits the voltage which the main exciter will attain as a self-excited exciter to a value only slightly in excess of normal voltage, and therefore makes accidental loss of amplidyne motor driving power not immediately serious.

As a result of the fact that initial tests and operation over a short period of time indicated that this new combination of hydrogen-cooled synchronous condenser, direct-connected exciter, and amplidyne excitation system was superior to any of the previous arrangements, there resulted the installation of a similar machine at Danville, Va., in 1942. This was followed by three more condensers with excitation systems of the same kind, which were placed in operation at Lima, Ohio; Beaver Creek, Ky.; and Anderson, Ind.; during the past four years.

It is interesting to note that following the satisfactory performance of the amplidyne excitation arrangement on one hydrogenerator and five condensers over the past six years, the same system is being utilized for a 32,500-kva turbogenerator which will go into service this year at Atlantic City, N. J. A similar arrangement is being provided for another 32,500-kva turbogenerator now being built for installation at Scranton, Pa.

Operating Experience and Performance Data

Electronic Pilot Exciters

An idea of the performance characteristics of the electronic pilot exciters is given in Table II. With normal voltage supply to the thyratron power transformer the exciter is capable of applying to the main exciter field a voltage of about 170 per cent of the main exciter rated voltage. A 3-phase short circuit on a line a short distance away from the high voltage bus produces the lowest thyratron power transformer voltage during which the generator or condenser excitation must be maintained. Under this condition the transformer voltage is 14 per cent at Claytor and 35 per cent at Glen Lyn, giving a voltage applied to the main exciter field of 25 per cent at Claytor and 60 per cent at Glen Lyn. This is equivalent to about full load excitation in the case of Claytor. There have been no cases of loss of synchronism resulting from excitation failure at either plant.

It must be borne in mind that 3-phase faults are comparatively rare and, in addition, that such a fault on any line at either station will be cleared in a maximum of nine cycles. Furthermore, at Claytor it is possible to operate two machines simultaneously connected to the low voltage side of the transformer bank and this is a normal operating condition whenever the stream flow permits. In this case the maximum pilot exciter output voltage would be about 50 per cent of the main exciter voltage rating. Likewise at Howard where the maximum instantaneous pilot exciter output voltage for a 3-phase high voltage fault is 30 per cent of the main exciter rating, there has been no indication of loss of synchronism. In this case where the machine is a synchronous condenser, momentary loss of synchronism might go undetected because there is no out-of-step relay for protection.

Table II shows the types of thyratron tubes employed and the life obtained from them. At Howard it can be noted that two types of tubes have been used. The original tubes were chosen conservatively to have about five times as much current carrying capacity as was required.

Table II. Application Data and Performance Record of Electronic Pilot Exciters

Listing as of January 1, 1946

Location	Per Unit Reactance: Generator or Condenser X''_d	Main Transformer X	Pilot Exciter Max Output Volts	Thyratron Tubes: Type	Rated Plate Amp	Total Tube Failures	Average Operating Hours Per Tube Failed	Total Operating Days of Pilot Exciter
Howard (original)	0.226	0.048	425	FG-29	12.5	13	9,998	1,745
Howard (modernized)	0.226	0.048	425	FG-95	2.5	19	13,632	3,650
Glen Lyn units 2 and 4 (original)	0.16	0.086	425	FG-29	12.5	18	23,016	7,625
Glen Lyn units 2 and 4 (modernized)	0.16	0.086	425	FG-172	6.4	5	12,613	
Fostoria	0.20	0.029	160	FG-172	6.4	9	10,033	2,942
Claytor	0.271	0.044	440	FG-172	6.4	24	3,376	1,208
Average							11,735	
Total						88		17,170

The tubes now used have a current rating about equal to the exciter field requirements. In spite of this difference the original tubes did not give as good service as the new ones. However, these original tubes were subjected to more severe service because of the type of control circuit used which caused unbalanced tube currents with relatively small changes in grid characteristics. A similar change in tubes but not in control was made at Glen Lyn, and in this case the performance of the original tubes appears to be almost twice as good as that of the new ones. However, this change has been made quite recently, and it will be noted that only five of the new tubes have failed so far.

At both Glen Lyn and Howard the tube life record for the original installation includes the operating hours of the tubes which were in service but had not failed when the exciter was modernized. The tubes now in service at Glen Lyn have an average operating record of over 17,000 hours, and it therefore appears that the average operating hours of the tubes which fail will increase considerably as time goes on. The record for the thyratrons of the Claytor exciter is not as satisfactory as that for the other machines. The exciter field ampere requirements are well within the tube ratings and so far no explanation has been found for this relatively shorter life.

Aside from expense for replacement of thyratron tubes, the maintenance cost of these exciters has been negligible. Because tubes may be installed without shutting down the machine, tube replacement does not represent an operating hardship. From the data in Table II it will be noted that the average operating time per tube for all installations has been 11,735 hours. There have been about 2.2 tubes required per exciter for each year of actual operation and it is expected that further operation will reduce this figure. Total combined operating time for all electronic pilot exciters as of January 1, 1946 was 17,170 days or approximately 47 years.

Electronic Main Exciters

The performance characteristics of electronic main exciters are given in Table III. With normal voltage supply to the excitation power transformer the exciter has a ceiling voltage of 275 per cent of maximum continuous slip-ring voltage rating in the case of Torrey, Fostoria, and New Carlisle; and of 244 per cent in the case of Scranton. When a 3-phase short circuit occurs on the high voltage bus, the output voltage varies from 127 per cent of slip-ring voltage in the case of New Carlisle to 41 per cent in the case of Scranton. As in the case of the electronic pilot exciters, there has been no indication of loss of synchronism on any of the machines equipped with this type of exciter. Figure 7 shows regulated voltage of the 22-kv bus and condenser loading for a portion of a typical day's operation at Torrey. The 36,000-kva condenser is connected through a 3-winding 48,000-kva transformer bank to the 132- and 22-kv station busses as shown in Figure 4. The condenser load may be seen to vary between 40,000 kilovar out and 11,000 kilovar in, the latter being the zero field current load, with variations in regulated voltage of less than one per cent. These charts are typical of those obtained from the other machines. The Torrey unit was chosen for illustration because it is subjected to frequent large changes of load caused by the fluctuating nature of the arc furnace load served from the 22-kv bus.

Table III shows the types of thyratron and ignitron tubes employed and the tube

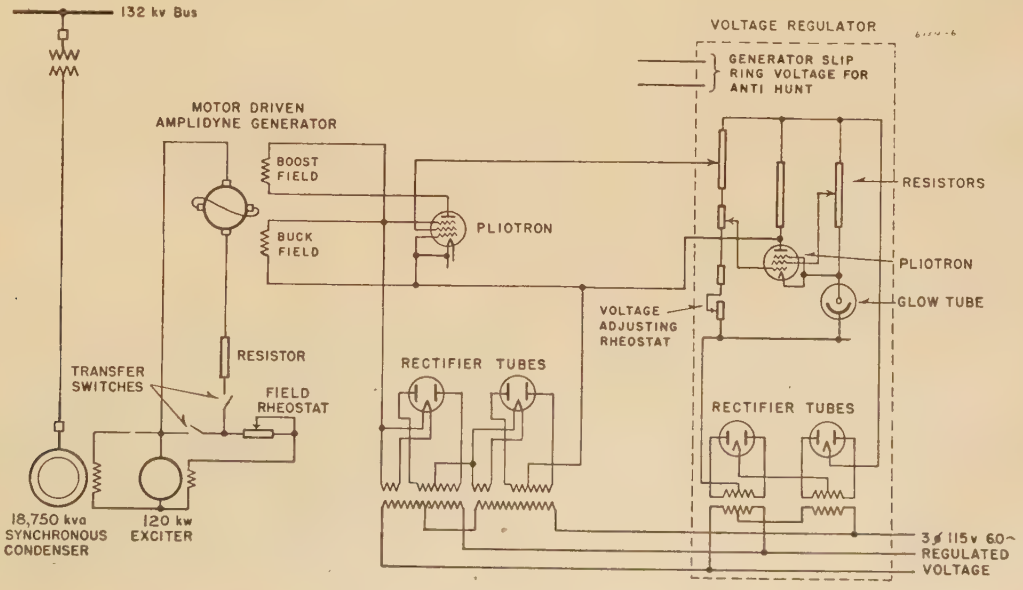

Figure 6. Schematic diagram of direct connected exciter with amplidyne control

Muncie 18,750-kva synchronous condenser of The Indiana and Michigan Electric Company

Table III. Application Data and Performance Record of Electronic Main Exciters

Listing as of January 1, 1946

Location	Per Unit Reactance		Condenser		Thyratron Firing Tubes				Power Tubes					
	Condenser X'_d	Main Transformer X	Exciter Max Output Volts	Max Continuous Slip-Ring Volts	Max Continuous Field Amps	Type	Rated Plate Amp	Tubes Failed	Avg Operating Hrs Per Tube Failed	Type	Rated Plate Amp	Tubes Failed	*Avg Operating Hrs Per Tube Failed	Avg Operating Hrs of Tubes in Service	Total Operating Days of Exciter
Scranton (original)	0.25	0.05	280	115	475	FG-95	2.5			FG-53	100	10	22,029	}	3,494
Scranton (modernized)	0.25	0.05	280	115	475	FG-172	6.4	16	8,651	FG-259	100	8	18,045	17,683	3,021
Fostoria	0.32	0.076	435	160	740	FG-172	6.4	23	13,277	FG-238	150	16	12,940	19,651	2,310
Torrey	0.32	0.088	435	160	740	FG-172	6.4	14	17,678	FG-238	150	8	25,736	15,563	1,917
New Carlisle	0.109	0.093	580	217	500	KU-676	6.4	20	9,314	WL-653	150	3	5,900	36,389	10,742 (Total)
								73 (Total)	12,021 (Avg)			45 (Total)	16,340 (Avg)		

* Failures during first year of exciter operation are omitted.

life obtained from them. In the case of the power tubes, failures during the first year of operation have been omitted because in each case this proved to be a trial period during which various modifications were made to improve performance. In the case of the firing thyratrons, the entire life of the exciter is included because the initial trial period made little difference in the averages. In order to indicate the trend of averages with further operation, the average operating hours of the power tubes now in service have been included. These figures indicate that much longer tube life is to be expected both at Fostoria and New Carlisle where the tube designs have been improved and the tube failure hours have been influenced by the record of those of earlier design as well as by a few defective tubes which failed with comparatively short service records. The record for the original installation at Scranton includes the tubes which were in service but had not failed when the exciter was modernized.

As in the case with the pilot exciters, the maintenance cost of these exciters has been negligible with the exception of the expense for tube replacements. From the data in Table III it will be noted that the average operating hours per power tube is 16,340 and per firing tube is 12,021. Since six tubes of each type are employed per exciter there have been 3 power tubes and 4.4 firing tubes required for each year of actual operation, and it appears that further operation should produce a substantial improvement in the record for the power tubes. The total combined operating time for the four electronic main exciters as of January 1, 1946 was 10,742 days or approximately 29 years.

Amplidyne Excitation Systems

The amplidyne excitation system performance has been similar to that obtained from the electronic pilot and main exciters. From the standpoint of power system operation, no essential difference has been observed on the condenser installations between the performance of excitation systems with ultrahigh speed response and those having more conventional speeds. For small changes in regulated voltage the speed of response of the amplidyne system is comparable to that of the electronic pilot exciter. This is true because the controlling factor in both cases is the amount of antihunt which must be introduced to produce stable operation. The ceiling voltage of the amplidyne generator is not affected by large dips in system voltage because its driving motor is designed with considerably more power than normally required and, in addition, its inertia contributes to the total energy required for quick changes in excitation. Figure 8 is an oscillogram of a special test made at Muncie in June 1941, and shows the rate of response of the amplidyne generator to a sudden change of $2^1/_2$ per cent in regulated voltage starting with a slip-ring voltage of 45. The measured maximum rate of response of slip-ring voltage as obtained

Figure 7. Typical charts of regulated voltage and condenser load

Torrey 36,000-kva synchronous condenser of The Ohio Power Company

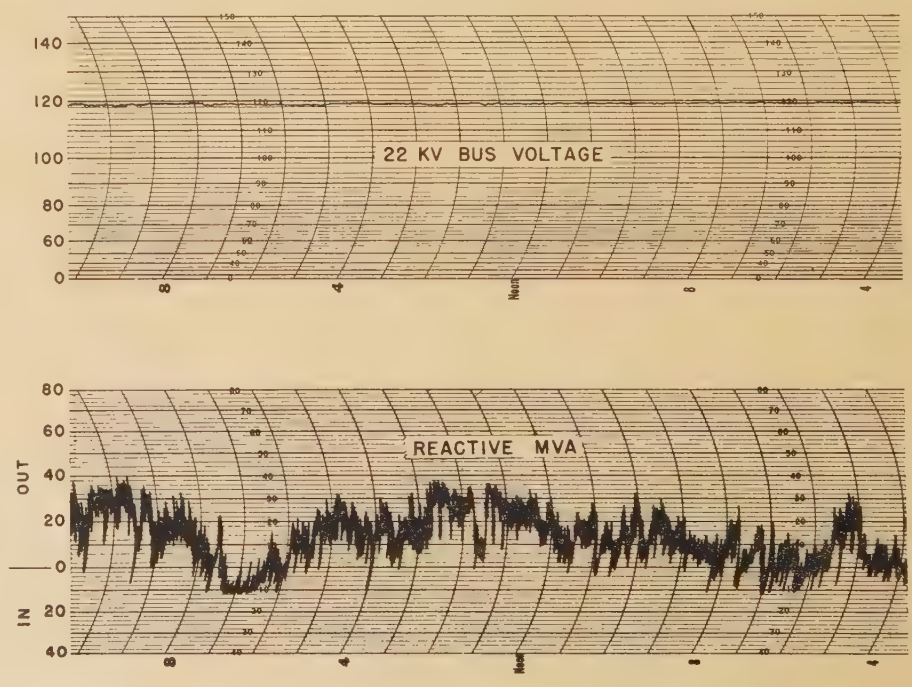

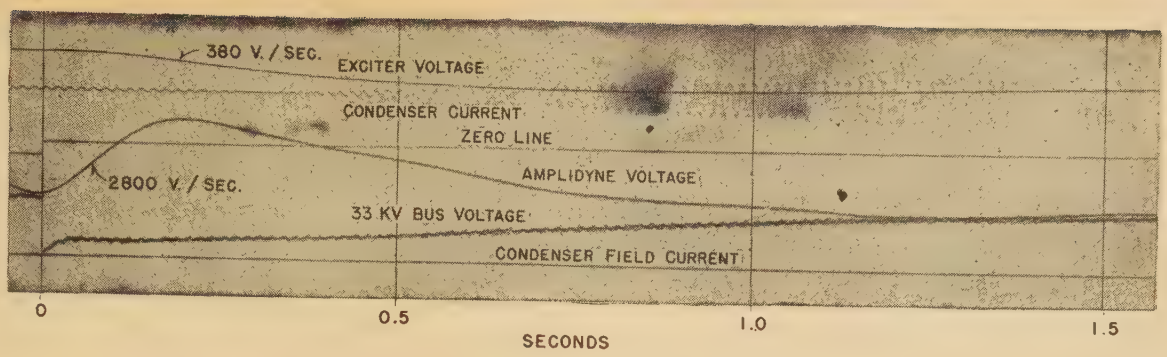

Figure 8. Oscillogram showing response of amplidyne control system

Muncie 18,750-kva synchronous condenser of The Indiana and Michigan Electric Company

from this oscillogram is 380 volts per second. The maximum rate of response of the amplidyne generator voltage was 2,800 volts per second.

Because the amplidyne generator can produce either a buck or a boost voltage, it is suited ideally to produce a reversed slip-ring voltage by which additional lagging capacity can be obtained from the condenser. This feature is made use of in all cases and gives an increase in capacity of about 18 per cent above that obtained with zero slip-ring voltage, without approaching the point at which the condenser would slip a pole. This feature cannot be obtained with an electronic exciter and can be obtained with an electronic pilot exciter only by the addition of a differential field and some source of excitation for it.

Maintenance of an amplidyne excitation system is essentially the same as for other arrangements using rotating exciters. The amplidyne generator driven by an ordinary induction motor requires very little attention. The direct-connected exciter operating in hydrogen has given very satisfactory results. The absence of external dirt and oxygen in the cooling gas for the exciter compartment has simplified the maintenance problem. Periodic cleaning and inspection of the exciter compartments is made three times a year, with the total annual outage for this reason amounting to approximately one day. As of January 1, 1946, these five machines have operated for a combined total time of 3,994 days or approximately 11 years.

Electronic Regulators

The performance of both types of electronic regulators described has been excellent. Both are capable of holding regulated voltage within about three-quarters of one per cent while varying the condenser loading from maximum kilovars in to rated kilovars out. The bridge type is somewhat more sensitive to large changes in ambient temperature, but as all are installed in heated control rooms, this is of little practical importance. The tubes used in these regulators have given long life and their replacement cost is low. As stated, charts of regulated voltage and condenser loading are similar for all the excitation systems described, and this is the case because all are controlled by sensitive electronic regulators which have no dead band and respond to the slightest change in regulated voltage. Aside from tube changes, only a few minor replacements of parts have been required. In two cases copper oxide rectifiers have been replaced and in one case a voltage adjusting rheostat of the conventional slide wire type was changed.

The electronic regulator lends itself readily to the addition of special features when desired. Some of those which have been employed are as follows:

1. A definite slip-ring voltage set automatically for transferring the condenser from starting to running.
2. A definite maximum slip-ring voltage set automatically when the condenser approaches a dangerous temperature.
3. Adjustable amounts of droop obtained in regulated voltage.
4. Adjustable maximum reverse slip-ring voltage used in the case of amplidynes.

Its accuracy and the fact that it has no dead band make the electronic regulator readily adaptable to parallel operation in that compensator or droop settings can be made with minimum attention to errors in the regulator itself.

However, the primary purpose of a voltage regulator when used with a synchronous condenser or generator is to control voltage, and the more sensitive and accurate the regulator is the more nearly this aim can be realized. From a maintenance viewpoint an ideal regulator would have no moving parts and require no periodic adjustments or renewal of parts. Although the electronic regulator does require periodic replacement of tubes its absence of moving parts brings maintenance attention to a much lower level than is the case with any of the various types of mechanical regulators. The total combined operating time as of January 1, 1946 for the 14 electronic regulators installed on the exciters previously discussed amounts to approximately 87 years.

Conclusions

Operating experience with 5 electronic pilot exciters, 4 electronic main exciters, 14 electronic regulators, and 6 amplidyne excitation systems on 15 large synchronous generator and condenser applications, dating as far back as 1930, permits the drawing of rather definite conclusions.

1. More than 47 machine years of operation of electronic pilot exciters have demonstrated the reliability and satisfactory performance of this type of excitation when used with either generators or condensers on a large power system.
2. Operating experience with four electronic main exciters over a combined period of approximately 29 years has demonstrated the excellent performance and reliability of this excitation arrangement.
3. Initial cost of electronic exciter equipment and the heavy expense of making tube replacements offer objections to use of this otherwise most desirable equipment. It is hoped that further developments in the design of more satisfactory tubes for this purpose will occur which will reduce original and maintenance costs thus making the electronic system more attractive.
4. Approximately 11 machine years of satisfactory operation of five hydrogen-cooled direct-connected exciters indicates that the many benefits and fine results now being obtained by the operation of numerous generators and condensers in a hydrogen atmosphere can be duplicated in the case of exciters. The feasibility of gas pressure operation up to 25 pounds per square inch has been demonstrated. This results in increased capacity for both the exciter and the synchronous condenser to which it is connected.
5. More than 87 machine years of operation of electronic regulators applied on 14 large rotating machines have proved the reliability and the desirable characteristics of this method of control.
6. The performance of the amplidyne control system with direct-connected exciters has been essentially equal to that obtained

Performance Criteria for Current-Limiting Power Fuses—I*

C. L. SCHUCK
ASSOCIATE AIEE

POWER fuses are used at many locations on transmission and industrial power systems to insure the prompt interruption of serious short-circuit currents. An engineer making such an application primarily desires assurance that the fuses will be capable of safely interrupting all magnitudes of short-circuit current up to the maximum the system can produce.

This available short-circuit interrupting capacity may be expressed either in terms of 3-phase symmetrical kilovolt-amperes, or as maximum rms current. In computing the latter, the initial symmetrical alternating component of current is multiplied by the factor 1.6 to provide for the maximum practicable d-c component which may be involved in the short circuit.

Either or both of these ways of expressing the interrupting requirements may be compared with manufacturers' interrupting ratings for power fuses. The maximum current method of rating has been in use longer, but in recent years increasing use has been made of the 3-phase kilovolt-ampere rating, to facilitate direct comparison with the ratings given circuit breakers. In making reference to such ratings, the user is relying on the manufacturer to have made adequate and sufficiently severe tests on the fuse units to insure that they will interrupt safely fault current such as may occur within their interrupting ratings.

The proving of the interrupting ratings of power fuses usually is done in a short-circuit testing laboratory, where all factors affecting the test severity can be controlled and measured. Figure 1 shows power fuses arranged for test in the short-circuit cell of a high power testing laboratory. If practicable, tests on an actual power system are valuable to demonstrate the ability of the fuses to interrupt fault current at the location where their use is proposed. Such tests are likely to be less severe than those made in a short-circuit testing laboratory because of the presence of line resistance, and because the operating voltage usually will be less than the voltage rating of the fuse unit for the same voltage class. At the laboratory, it is also possible to vary all factors contributing to test severity, and to measure their separate effects on fuse performance. One important device available at the testing laboratory is the synchronous closing switch, with which it is possible to explore the regions of fault starting angle which analysis indicates might be severe. Such facilities permit the rapid accumulation of useful data, which could be obtained only with considerably greater difficulty by making tests at random closing angles, as would be necessary on a power system where synchronous closing means are not available. With laboratory facilities, the fuse designer can carry interruption tests to the point of destruction of his developmental fuse samples to disclose critical design factors. It is necessary to have such data to design power fuses having a factor of safety above the required interrupting ability.

Modern power fuses are of two principal types; those that permit approximately the full available short-circuit current to flow during the first half cycle, and those which have a substantial current-limiting effect.

The latter is the more recently developed type[2] and is a more efficient interrupter because the considerably smaller energy dissipated within the fuse unit can be absorbed there without external disturbance. In fuses which do not have this current limiting effect, the arc energy released in the fuse is usually so high that it must be expelled to the outer atmosphere or into a chamber where the ionized gases can be condensed. As might be expected, the interrupting ability of fuses of the expulsion type is limited as compared to the interrupting ability of fuses of the current-limiting type. Figure 2 shows oscillograms taken during interruptions by both these types. Symbols have been added to the oscillograms appearing in this portion of the paper to assist in their interpretation. These symbols are defined in Appendix I, and are defined and used similarly in the analytical study presented in part II of this paper.[1]

Of the two types, the current-limiting fuse lends itself better to the study of severity. This results primarily from the prompt action in interrupting the available current, and from the fact that an oscillogram taken during the test will show very definitely whether the current was interrupted easily or with difficulty.

Increasing severity can be detected both by oscillographic records and by the visible evidence of distress shown by the fuse test sample. Figure 3 shows four test samples of current-limiting power fuse units after tests at the same voltage, but with progressively increasing available short-circuit current. In these, the excess filler has been removed, showing the "fulgurites" or fused tubes of granular quartz where the elements were before they were melted. These formations seemingly have become heavier as severity increased, and in the case of sample 4,

Paper 46-170, recommended by the AIEE committee on protective devices for presentation at the AIEE summer convention, Detroit, Mich., June 24–28, 1946. Manuscript submitted April 26, 1946; made available for printing May 24, 1946.

C. L. SCHUCK is designer, high voltage fuses, device and relay division, General Electric Company, Philadelphia, Pa.

*Part II of this paper[1] was prepared by E. W. Boehne.

from the electronic main or electronic pilot applications.

7. The evolution of an ideal combination consisting of a standard speed synchronous condenser with direct-connected exciter operating in a hydrogen atmosphere at 25 pounds gas pressure and with amplidyne control and electronic regulator, illustrates the interdependence of a machine and its associated equipment and shows what can be accomplished by a co-ordinated development program over a period of years.

References

1. APPLICATION OF AND OPERATING EXPERIENCE WITH HYDROGEN-COOLED SYNCHRONOUS CONDENSERS AND ALTERNATORS, **Philip Sporn, F. M. Porter.** AIEE TRANSACTIONS, volume 59, 1940, pages 890–907.

2. THYRATRON VOLTAGE REGULATORS, **Philip Sporn, G. G. Langdon.** *Electrical World*, New York, N. Y., volume 105, 1935, pages 1182–4.

3. THYRATRON-EXCITED CONDENSER, **Philip Sporn, G. G. Langdon.** *Electrical World*, New York, N. Y., volume 105, 1935, pages 1582–4.

4. DYNAMOELECTRIC AMPLIFIER FOR POWER CONTROL, **E. F. W. Alexanderson, M. A. Edwards K. K. Bowman.** AIEE TRANSACTIONS, volume 59, 1940, pages 937–8.

5. THE DESIGN CHARACTERISTICS OF AMPLIDYNE GENERATORS, **Alec Fisher.** AIEE TRANSACTIONS, volume 59, 1940, pages 939–44.

6. INDUSTRIAL APPLICATIONS OF AMPLIDYNE GENERATORS, **D. R. Shoults, M. A. Edwards, F. E. Crever.** AIEE TRANSACTIONS, volume 59, 1940, pages 944–9.

7. MODERN EXCITATION SYSTEMS FOR LARGE SYNCHRONOUS MACHINES, **J. B. McClure, S. I. Whittlesey, M. E. Hartman.** AIEE TRANSACTIONS, volume 65, 1946, pages 939–45.

enough damage was done to the interior of the sample by the arcing to cause the tube to break. Differences in test severity such as those between samples 1, 2, and 3 cannot be judged accurately from the remains of test samples, but oscillograms of the tests give dependable comparisons. For this reason, oscillograms of power fuse tests are included in part I of this paper to illustrate differences in severity resulting from changes in the variable circuit factors.

The severity of an interruption test on a power fuse depends on the following factors or variables of the test circuit:

1. Generated voltage.
2. Available current.
3. Fault starting angle.
4. Voltage angle at melting.
5. Frequency.
6. Power factor.
7. Number of phases.

It is the purpose of this portion of the paper (part I), to appraise the separate effect on severity of each of these variables, with the object of arriving at recommendations for the testing of power fuses.

Generated Voltage

The circuit voltage at which interruption tests are made directly affects test severity, other factors remaining constant, as will be noted from the oscillograms shown in Figure 4. These record three tests on the same developmental design of test sample with progressive increases in circuit voltage. At 110 per cent of rated voltage (Figure 4A), the fuse had no difficulty in developing enough arc voltage drop to more than exceed the generated voltage and bring the current down to zero within one-quarter of a cycle. The arc current, i, was substantially constant during the first portion of the arcing period and then was forced down to zero without apparent difficulty. At 115 per cent voltage (Figure 4B) the fuse apparently had greater difficulty in interrupting the circuit because the arc current reached a higher value than the melting current, and lasted somewhat longer than at 110 per cent voltage. In both these tests the fuse interrupted with no external disturbance.

At 120 per cent voltage (Figure 4C) the arc voltage drop developed by the fuse was insufficient to exceed this higher test circuit voltage, and after an initial dip the arc current i was permitted to rise to substantially the available short-circuit values. The resulting high release of energy within the fuse test sample caused the tube to break, arc current of short-circuit magnitude persisted, and the circuit had to be opened by the backup circuit breaker. In these tests, different degrees of severity were imposed upon a fuse unit of given design capable of developing only a given arc voltage drop. In part II of this paper,[1] the arc current is determined analytically, assuming certain ratios of fuse arc voltage to the circuit voltage, the results showing the same trend as the empirical results of Figure 4. These observations emphasize the importance of making interruption tests of power fuses at the rated voltage of the fuse units in accordance with established standards.

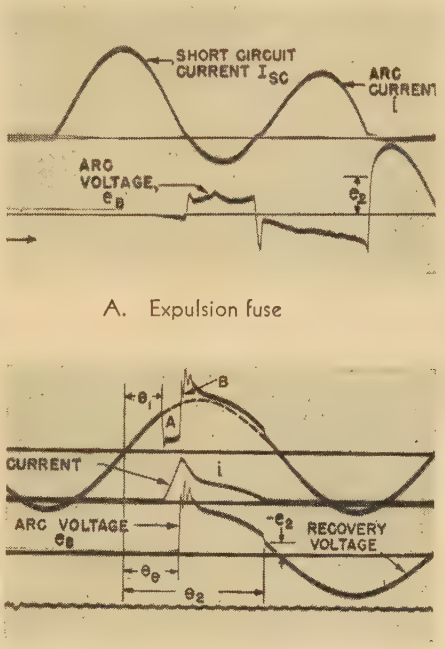

Figure 2. Typical oscillograms of short-circuit interruptions by the two principal types of power fuses

Available Current

Short-Circuit Current

As a result of the fact that the heat capacity of the current responsive element of a power fuse is relatively small, melting by a high short-circuit current can take place early in the first half cycle. The

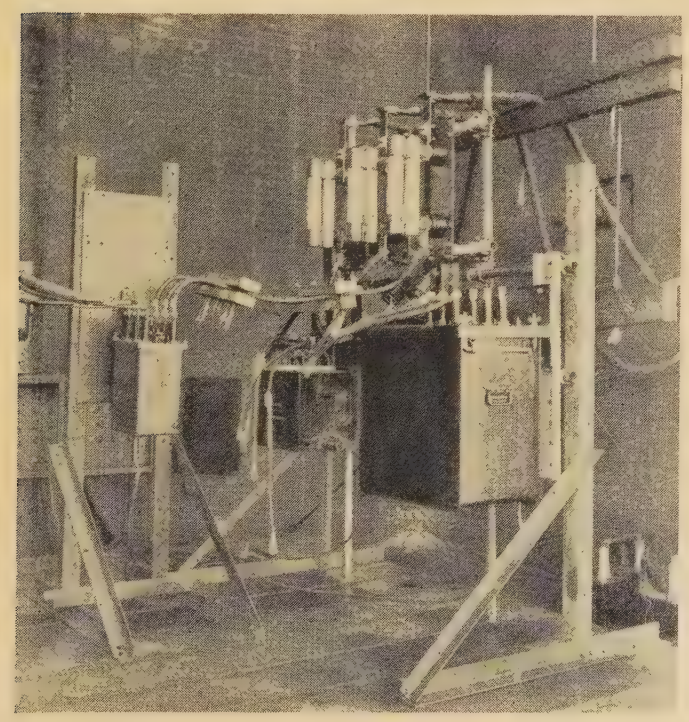

Figure 1 (left). Power fuses connected in circuit at short-circuit testing laboratory

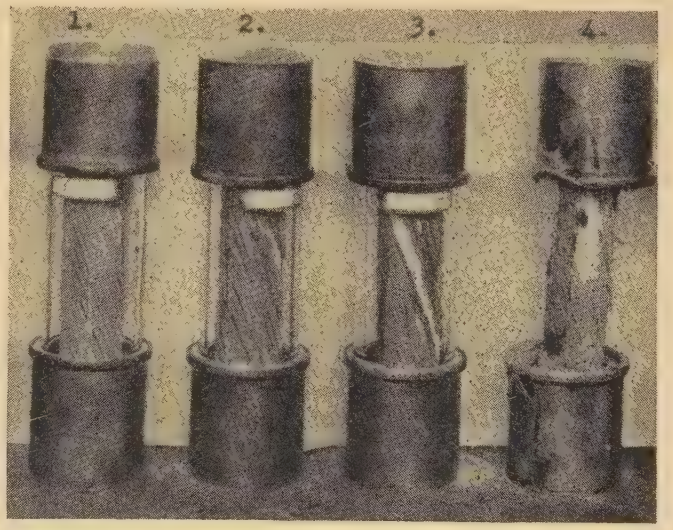

Figure 3 (above). Current-limiting power fuse units after interruption tests of progressively greater severity

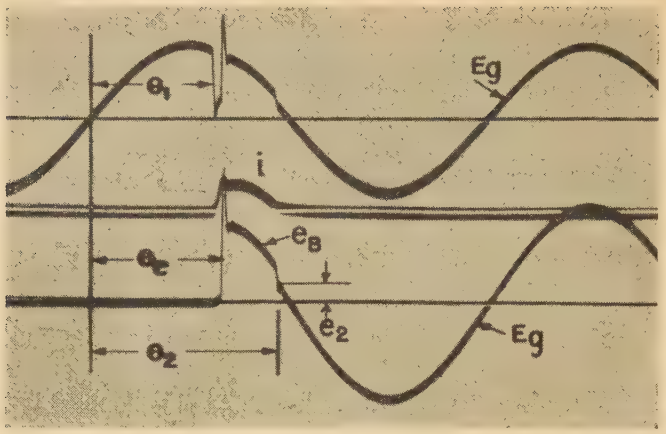

(A)

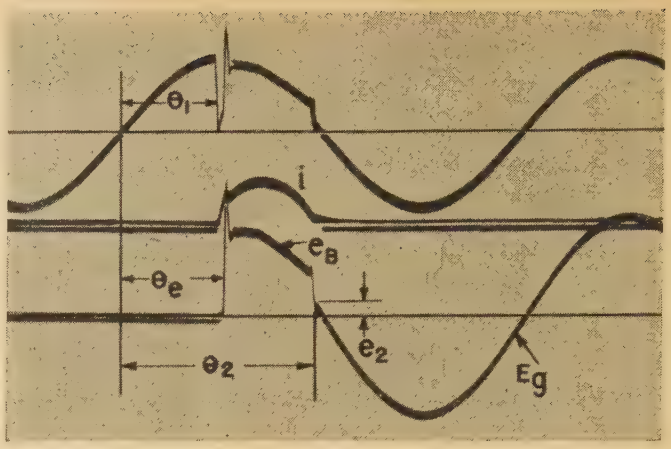

(B)

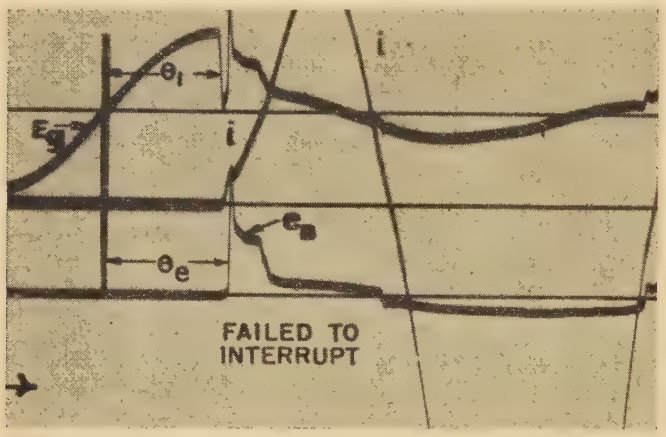

(C)

Figure 4. Illustrating progressive increase in test severity resulting from increasing test voltage

Developmental test samples

A. 110 per cent of rated voltage
B. 115 per cent of rated voltage
C. 120 per cent of rated voltage

melting time and the instantaneous value of current when melting takes place can be calculated with a high degree of accuracy.[1] The factors affecting the melting point are

1. The material and cross section of the current responsive element.
2. The frequency.
3. The available short-circuit current.
4. The degree of asymmetry of the available current.

The magnitude of an available symmetrical short-circuit current implies a certain initial rate of rise of current. The initial slope of the current-time curve is zero when considering a fully displaced asymmetrical current. For a symmetrical current, the peak current admitted by a fuse unit of low ampere rating varies directly as the cube root of the available short-circuit current, and for asymmetrical current, directly as the fifth root. For larger ampere ratings, a more involved calculation is necessary to obtain exact values of peak current. This results from the fact that the sine wave veers away from a linear rise, the departure making significant differences for greater melting angles than 30 degrees. A detailed treatment of this subject is contained in part II of this paper.[1]

The peak current at melting is one of the most important factors contributing to test severity. In view of this alone, it would be expected that higher available short-circuit current leads to greater severity in interruption. Existing standards[13] state that tests to establish time–current characteristics should be made at room temperature with no initial load current. Similarly, interruption tests should be made with no preloading, which would cause a reduction in the peak current at melting and in the melting time. However other factors contribute to the severity, notably, the magnitude of the circuit voltage during the early arcing period. It is during this time that a current-limiting power fuse either succeeds or fails to develop sufficient arc resistance, hence arc voltage drop, to exceed the generated voltage and cause the current to be brought back to zero. The arc voltage must exceed generated voltage during this critical interval in order to effect a reduction of arc current and subsequently create the current zero necessary for interruption. It is possible for arc voltage to be less than generated voltage for short intervals during the arcing period and still obtain interruption. The arc current increases during such an interval, as in the borderline interruption of Figure 4B. Test records of this type are invaluable to the fuse designer, as they indicate the threshold of safe operation and the direction in which design features must be changed to provide the desired factors of safety.

The energy released in the fuse during the arcing period is another important severity factor and may be computed by integrating the product of arc voltage and arc current over the arcing period. Arc energy is not necessarily a maximum at the maximum available short-circuit current, and for this reason it is recommended that interruption tests be made not only at the current representing the interrupting rating of the fuse unit, but at several intermediate values to cover any variations in the energy released in the fuse unit itself. A full discussion of the effect of circuit variables upon the energy absorbed by the fuse is included in part II of this paper.[1]

Low Current Operation

The ability to interrupt low available currents barely capable of causing fuse operation, is expected of power fuses manufactured to meet existing standards.[13] Depending on its heat capacity, a fuse may require between a few minutes and an hour to reach its final temperature and have its element melted.

Existing National Electrical Manufacturers Association Standards, call for the assignment of ampere ratings on the basis shown in Table I.

A sufficient number of interruption tests should be made in the range of such low available currents to prove the ability of the fuse unit to interrupt under these conditions. The most likely causes for prolonged overload currents of such magnitudes are internal transformer faults, usually in the insulation between turns of the primary winding, leading to a progressive drop in primary impedance. It is estimated that the power factor of such

Table I

Ampere Ratings	Per Cent of Rated Current	Melting Time, Minutes
Up to and including 100 *E* amperes*	200–240	5
125 *E* amperes* and above	220–264	10

*Current ratings include the letter *E* to denote conformance with the standards.

faults will be at least 20 per cent; hence it is recommended that the test circuit have a power factor of 20 per cent maximum.

Fault Starting Angle

The angle of the generated voltage, at the instant of inception of the short circuit, has an important influence on severity. Until melting occurs, the only effect of this fault starting angle is to produce displacement of the available current. If a highly inductive circuit is closed at an instant when voltage is zero, the displacement will be the maximum, and the available current will be fully asymmetrical (Figure 5). With the fault starting at 90 degrees (peak voltage), symmetrical available current will result. For intermediate starting angles, the displacement will be partial, and a "major loop" of available current will be obtained. A starting angle greater than 90 degrees (or after peak voltage) will result in a "minor loop" of current which affects the fuse as a symmetrical current of smaller magnitude and higher frequency.

In Figure 5 the degrees of asymmetry are compared for different fault starting angles. The available short-circuit current is 20,000 symmetrical rms amperes, and peak currents obtained are indicated for typical current limiting fuses of various ampere ratings.

For a fuse of low ampere rating, maximum peak current is obtained on a symmetrical short circuit since its initial rate of rise is greater than could be obtained with any asymmetry. Although the symmetrical current has the greatest initial rate of rise, the melting angle of fuses of large ampere ratings can be so great that the departure from a linear rise becomes significant, this effect taking place over the same range of voltage angles at which the asymmetrical current is approaching its maximum slope. Thus, if the ampere rating of the fuse is large enough, the peak current obtainable on an asymmetrical current can be even greater than that obtained on a symmetrical current. In the case of the 200-ampere fuse unit (Figure 5) melted on a circuit capable of producing 20,000 symmetrical rms amperes, slightly higher peak currents can be obtained when the current is asymmetrical than when it is symmetrical. It is also interesting to note that in the range between, in which major loops of short-circuit currents are obtained, the currents can be slightly higher than either of these values because the effective slope is higher during the melting interval.

Melting Angle

It is to be expected, and it has been borne out by tests, that maximum severity occurs in fuse units of low ampere rating if melting takes place at, or slightly before, peak voltage. For such a fuse, this is also the closing angle producing maximum peak currents. This would call for closing the circuit at approximately 80 degrees for such ratings. The higher ampere ratings require a considerable number of degrees to melt. An example of this is the case of the 200-ampere fuse in Figure 5 which requires approximately 76 degrees to melt on the 20,000-ampere asymmetrical short circuit. It has been found empirically and it is shown analytically in part II of this paper,[1] that maximum severity is obtained if the circuit is closed at such a voltage angle as to cause melting to take place in the region between 70 and 80 degrees. This results in high effective generated voltage during the critical early arcing period.

In Figure 6 oscillograms are shown of three tests on the same circuit, on three developmental fuse samples of high current rating, the circuit being closed at different angles after voltage zero. The test of Figure 6A was evidently the most difficult, as the short-circuit current was not interrupted, and the fuse sample broke apart as a result of the high release of energy inside the fuse tube. In this test, the circuit was closed at 11 degrees and melting took place at 68 degrees. At this time, circuit voltage was approximately 90 per cent of maximum and still increasing. The subsequent attempt on the part of the fuse to produce arc voltage equal to effectively maximum circuit voltage was unsuccessful. In Figure 6B the circuit was closed at 90 degrees of voltage producing a symmetrical current, but melting did not occur until 138 degrees, when voltage was already down to 67 per cent of maximum voltage. In Figure 6C the oscillogram shows a relatively easy interruption resulting from closing the circuit after voltage maximum, resulting in a minor loop of current, with melting occurring in the following half cycle. Although circuit voltage was near maximum when melting did take place, the melting current was somewhat less in this test and alleviated the severity. None of the possible fault starting angles after 90 degrees have been found to cause as much test severity as those before 90 degrees.

Circuit Frequency

The frequency of the test circuit determines the time interval between voltage zeros and therefore has an important bearing on test severity. This leads to the recommendation that interruption tests be made at rated frequency. In the time between melting and the subsequent voltage zero, a current limiting power fuse must develop enough arc voltage drop to force the current down to zero before excessive energy is released within the fuse tube.

On a circuit of lower frequency, the longer time between voltage zeros brings with it an increase in test severity, other factors being equal. This is reflected in

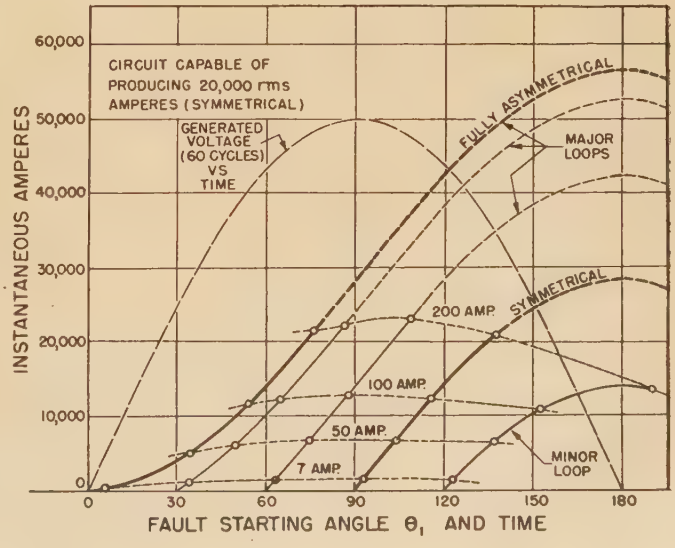

Figure 5. Effect of fault starting angle on displacement of available current

Melting peak current of typical current limiting power fuses of 7-, 50-, 100-, and 200-ampere ratings

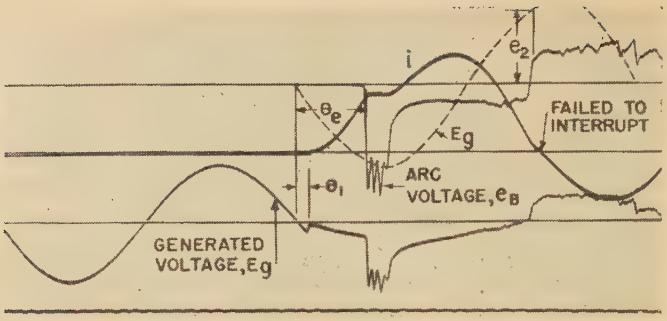

(A)

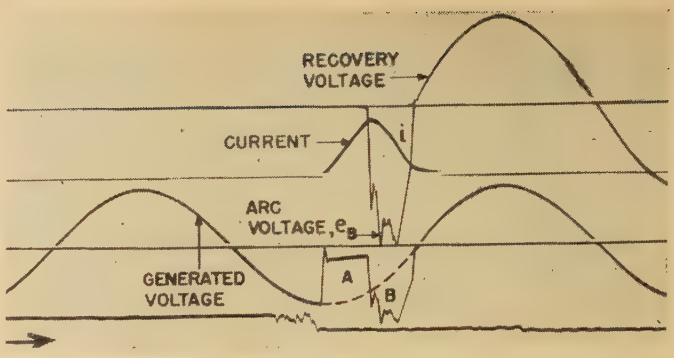

(B)

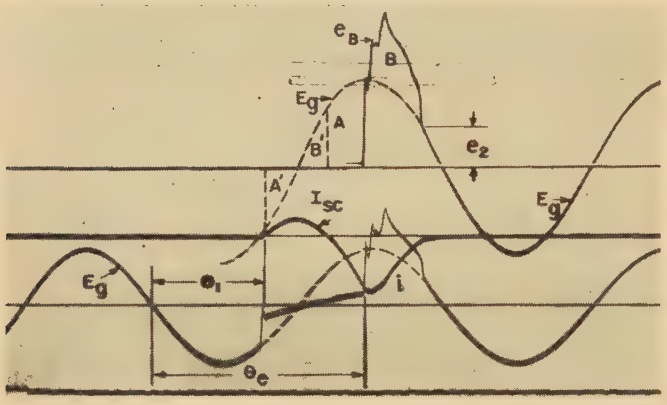

(C)

Figure 6. Influence on test severity of voltage angle at melting of a current limiting power fuse

Developmental test samples

A. Melting at 68°
B. Melting at 138°
C. Melting at 260°

lower interrupting ratings at 25 cycles than at 60 cycles for many present-day high current rated fuses. Figure 7 shows oscillograms of tests made at 25 and 60 cycles at the same circuit voltage, on the same design of a high current rated fuse test sample. In all other respects except frequency, the 60-cycle test would be regarded as more severe because the available and melting currents were higher, and because melting occurred nearer maximum voltage. However, the lower frequency test was clearly more severe, as evidenced by the higher arc current (Figure 7A) following melting and the longer arc duration.

A d-c circuit is the extreme case of low frequency. Here the fuse must force a current zero without any help from voltage zeros. A full treatment of the relative severity of a-c and d-c test circuits is beyond the scope of the present paper, but a few observations may be made.

For a fuse of low ampere rating, the a-c test probably will be more severe because the peak of generated voltage bears a $\sqrt{2}$ ratio to the same nominal value of d-c voltage. In the d-c case, the same nominal current may be available as in the a-c circuit, but the time constant of the d-c circuit may cause a faster or a slower rise of current than in the a-c case. Thus for d-c circuits some description of the circuit time constant, such as the initial rate of rise of current, must be specified. For a fuse of high current rating, indications are that the d-c test might be more severe on account of the absence of voltage zeros.

Power Factor

To some extent the power factor of the test circuit will have an effect on severity. At a low power factor with a symmetrical short-circuit current, a fuse of low ampere rating which melts quickly will have nearly a 90-degree wait until the next voltage zero. At higher power factors, with the current and voltage more nearly in phase, the delay of the subsequent voltage zero is even longer, up to the maximum of 180 degrees. For a fuse of high current rating, severe test conditions apparently will result if the power factor is such that voltage is in the critical 70- to 80-degree region at melting. Tests have been made at high power factors by inserting resistance in an otherwise highly inductive circuit. The results of such tests indicate that the interrupting duty is not as severe as that of low power factor tests made at full short-circuit current.

If very low available currents are to be interrupted, the power factor has a greater importance, as mentioned previously under "Low Current Operation."

Number of Phases

It generally is agreed that a single-phase test made with full line-to-line voltage across a single fuse sample is more severe than a 3-phase test, made more or less simultaneously on three fuse samples. Since a power fuse is essentially a single-phase interrupter, it is logical to compare the severity experienced by a fuse unit interrupting in any phase of a 3-phase system with the severity if tested on a single-phase circuit. Examination of the possible faults on a 3-phase system yields few possible cases as severe as a single-phase test at full line-to-line voltage, because the recovery voltage across any one fuse is usually less than this value. Also, the operation of at least two fuses of the three in rapid succession greatly decreases the possibility of obtaining conditions of maximum severity on either fuse. In Figure 8A oscillograms are shown of a 3-phase interruption of a triple line-to-ground fault (generator windings connected in delta with no ground connections) by current-limiting power fuses, and Figure 8B is the record of a single developmental sample fuse of the same design tested line-to-line on the same circuit. The single-phase test was more severe, because it resulted in failure, and because the records of current in each phase show (Figure 8A) definite current-limiting action. In the 3-phase test there were no signs of high arc current, a characteristic of difficulty in interrupting. Although the short circuit was closed with a 3-phase circuit breaker, not all the poles closed exactly at the same time. Even with simultaneous closure of the three lines at the fault, unbalanced currents generally would result because of phase differences in the generated voltages. In the 3-phase test of Figure 8, the fuse in phase one operated first and opened phase one before the fuse in phase two melted, and at approximately the same time as the fuse in phase three melted. This left the fuses in phases two and three effectively in series, and they then assisted each other in clearing the circuit, the burden being apparently more on the fuse in phase three, as may be noted from the small rise in arc current after melting, and the corresponding dips in arc voltage in phase three. Phase two apparently cleared easily as may be noted

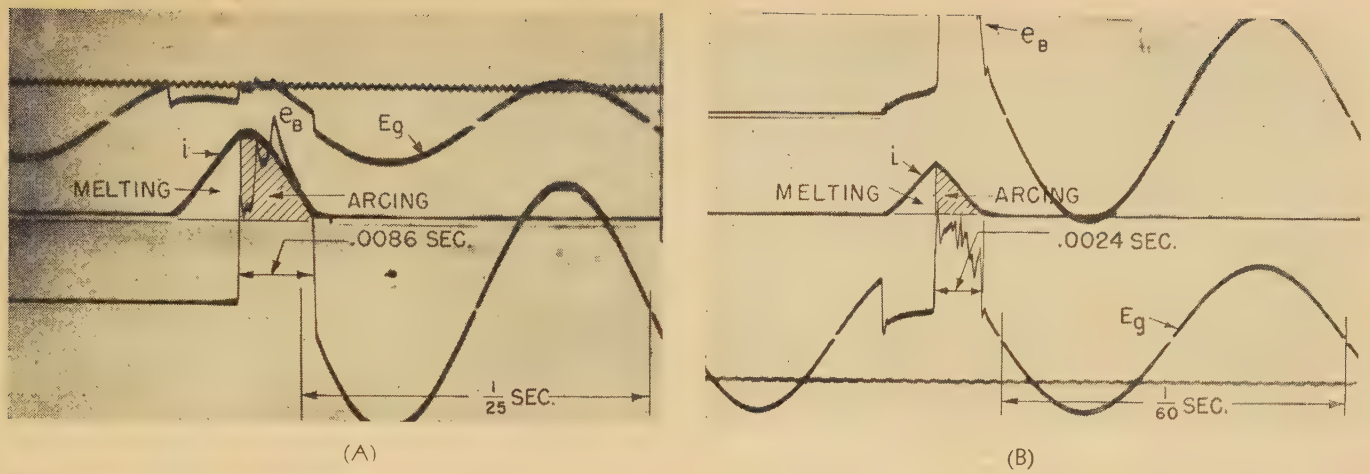

Figure 7. Effect of circuit frequency on test severity

	A	B
Circuit frequency	25 cycles	60 cycle
Test voltage (rms)	2,500 volts	2,500 volts
Available current (rms)	20,000 amp	25,000 amp
Current at melting	18,000 amp	28,000 amp
Angle of inception	62°	50°
Angle at melting	136°	108°
Arcing time	0.0086 sec	0.0024 sec

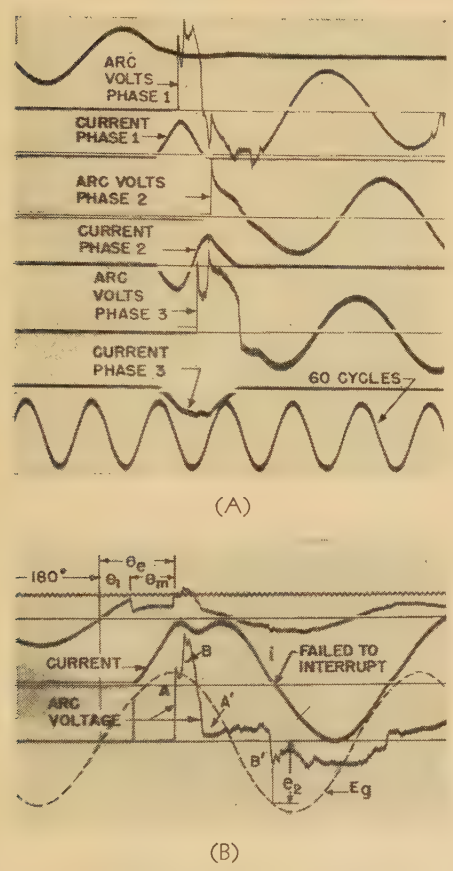

Figure 8. Single-phase and 3-phase interruption tests on the same current-limiting power fuse design showing the greater severity of the single-phase test

	A 3-Phase	B Single-Phase
Frequency, cycles	25	25
Test voltage (rms), volts	2,500	2,500
Available current (rms) including displacement, amperes	Phase 1—39,000 Phase 2—30,000 Phase 3—25,000	28,000
Peak amperes at melting (instantaneous)	Phase 1—21,000 Phase 2—12,200 Phase 3—13,400	19,800
Series reactance, ohms	Phase 1, 2, 3; 0.04	0.04
Performance	Fuses in all three phases interrupted without disturbance	Fuse failed to interrupt the circuit

from the concave shape of the arc current and the resultant arc volts which remained well above generated voltage from melting onward. This mutual assistance by the phases is characteristic of 3-phase tests, and in many similar tests has resulted in the ability to interrupt a greater nominal kilovolt-amperes than the 3-phase kilovolt-amperes computed from single-phase interrupting ability.

The symmetrical rms short-circuit current obtainable by making single-phase tests phase-to-phase on a 3-phase generator is only 86 per cent of the line current obtainable in a 3-phase short circuit. It is recommended that the 3-phase kilovolt-ampere interrupting ability be computed from the measured current interrupted by a single fuse tested line-to-line. It is believed that this basis of rating will cover all short-circuit conditions (whether faults are single line to ground or phase-to-phase) and justify the use of the maximum rms ampere rating, including cases where single-phase applications are proposed, and the single-phase interrupting requirements are known.

Specific Applications

In some cases, a given rating of power fuse is designed for a specific application rather than being made available for general use. Typical cases are

1. Fuses for high voltage motor controls. For such cases, not only the interrupting capacity of the fuse unit itself must be determined, but tests must be made with the contactor and current transformer in the circuit to check the ability of these devices to windstand the let-through current of the fuse, both from a thermal and magnetic standpoint. The phrase let-through current implies not only the peak current permitted by the current limiting action of the fuse, but also the magnitude and duration of arc current until interruption is completed.

2. Fuses for use with banks of capacitors. For these, safe limits of application must be determined, within which the fuse let-through current will not cause the case of a faulted capacitor unit to be ruptured, endangering apparatus and personnel, and possibly allowing the fault to become external and spread to the other phases.

Conclusions

In establishing the interrupting ability of current-limiting power fuses, it is recommended that tests be made as follows:

1. In a short-circuit testing laboratory where circuit variables can be controlled and measured. Tests on systems may give additional data, providing adequate control and measuring means are used.

2. Single-phase.

3. At the fuse unit rated voltage in accordance with established standards.

4. With the starting angle of the short-circuit current at zero of voltage to justify the maximum rms ampere interrupting rating (asymmetrical—including d-c component) to be assigned.

5. With the starting angle of the short-circuit current near 90 degrees after voltage zero (preferably earlier) in the case of fuse units of low ampere ratings, and at such a current as to cause melting of the fusible element between 70 degrees and 80 degrees on the voltage wave, for fuses of high ampere ratings.

6. At several other values of short-circuit current less than the interrupting rating, the angle of inception being in each case such as to cause melting somewhat before maximum voltage. Three-phase kilovolt-ampere interrupting ability, when assigned, to be calculated from the symmetrical a-c component of short-circuit current I, successfully interrupted single-phase as in pre-

ceding 4 and 5, that is, kilovolt-amperes = $\sqrt{3} \times$ kilovolts $\times I$.

7. At rated frequency.

8. On a circuit of low power factor, for short-circuit tests.

9. At low available currents in the region of those specified by existing standards[13] for the assignment of ampere ratings, and on a circuit the power factor of which is 20 per cent maximum.

10. In conjunction with other devices with which their application is intended.

Appendix I. Definitions of Symbols Shown on Oscillograms

E_g = generated voltage
e_B = arc voltage of fuse
I = available symmetrical rms short-circuit current
I_{sc} = short-circuit current
i = actual circuit current
θ_1 = fault starting angle
θ_e = arc voltage angle
$\theta_m = \theta_e - \theta_1$ = melting time of fuse in degrees
θ_2 = angle when arc current becomes zero (interruption)
e_2 = instantaneous generated voltage at θ_2
A, B, A', B' = volt–time areas

References

1. Performance Criteria for Current-Limiting Power Fuses—II, **E. W. Boehne,** AIEE Transactions, volume 65, 1946, pages 1034 44.

2. The Current-Limiting Power Fuse, **D. C. Prince, E. A. Williams, Jr.** AIEE Transactions, volume 58, 1939, January section, pages 11–18.

3. A New Current-Limiting Fuse, **H. L. Rawlins, A. P. Strom, H. W. Graybill.** AIEE Transactions, volume 60, 1941, February section, pages 77–80.

4. Control of the Switching Surge Voltages Produced by the Current-Limiting Power Fuse, **E. A. Williams, Jr., C. L. Schuck.** AIEE Transactions, volume 60, 1941, May section, pages 214–17.

5. The Quenching of Arcs in the Granular Fillers of High Voltage Fuses, **H. Lapple.** *Elektrotechnische Zeitschrift* (Berlin, Germany), April 8, 1937, pages 369–72, and April 22, 1937, pages 426–8.

6. The Arc Produced Upon the Melting of Fusible Elements in Sand, **Helmut Kroemer.** *Archiv Fur Elektrotechnik* (Berlin, Germany), volume 36, number 8, August 1942, article 1055, pages 455–70.

7. High Rupturing Capacity Cartridge Fuse, With Special Reference to Short-Circuit Performance, **J. W. Gibson.** *Journal*, Institution of Electrical Engineers (London, England), volume 88, part II, February 1941, pages 2–40.

8. High Voltage Fuses, **K. A. Lohausen.** *Allgemeine Electricitats Gesellshaft Mitteilungen* (Berlin, Germany), March 1935, pages 71–3.

9. Criteria of Severity in the Short-Circuit Testing of Fuses, **A. W. Metcalf.** *Beama Journal* (London, England), August 1938, pages 38–43.

10. A New Three-Element Current-Limiting Power Fuse, **H. L. Rawlins, H. H. Fahnoe.** AIEE Transactions, volume 63, 1944, April section, pages 156–9.

11. A Current-Limiting Fuse for Aircraft Applications, **A. H. Powell.** AIEE Transactions, volume 64, 1945, July section, pages 541–4.

12. Excess Current Protection, by H.R.C. (High Rupturing Capacity) Fuses on Medium Voltage Circuits, **R. T. Lythall.** *Journal* Institution of Electrical Engineers (London, England), part II, October 1945, pages 419–29.

13. Distributation Fuse Cutout and Power Fuse Standards. NEMA Publication 44-93, National Electrical Manufacturers Association, New York, N. Y., September 1944.

14. AIEE Standard 25 for Fuses Above 600 Volts, March 1945.

15. The Geometry of Arc Interruption, **E. W. Boehne.** AIEE Transactions, volume 60, 1941, pages 524–32.

16. The Geometry of Arc Interruption—II Current Zero Phenomena, **E. W. Boehne** AIEE Transactions, volume 63, 1944, pages 375–87. Discussion, pages 447–50.

17. Anode-Circuit-Breaker Design and Performance Criteria, **E. W. Boehne, W. A. Atwood.** AIEE Transactions, volume 64, 1945, June section, pages 337–45.

18. Coupe-circuit à grand pouvoir de coupure, **J. Grillet.** *Revue Générale de L'Eléctricité* (Paris, France), volume XLIII, number 20 May 14, 1938, pages 623–37.

19. High Power Fusible Cutout, **L. C. Grant.** *Journal*, Institution of Electrical Engineers (London, England), September 1926, pages 920–59.

Performance Criteria for Current-Limiting Power Fuses—II*

E. W. BOEHNE
FELLOW AIEE

THIS PAPER is part of an analytical study conducted for the purpose of establishing a sound fundamental interpretation of observed performance characteristics of high interrupting-capacity power fuses of the current-limiting type. Some of the more important conclusions, which have been verified by a study of test performance, are presented and discussed in the foregoing part of this paper by C. L. Schuck. In another sense this paper is an application of the analytical methods developed in the two papers on "Geometry of Arc Interruption."[15,16] This application to fuse performance is particularly fitting since the interval from the inception of a short circuit until the arc voltage of the fuse is introduced, may be predetermined quite accurately from the melting characteristics of the fuse. Conductor heating and energy equations are presented for the first time which include all the essential variables to predetermine the arc energy to be developed by the interrupter for various magnitudes of arc voltage, degrees of circuit asymmetry, and melting times of the fuse.

Although the analytical methods used in this paper are applied to the analysis of current-limiting power fuse performance, they are by no means restricted to this application. When applied to a circuit breaker, for example, the so-called melting time of the fuse (Θ_m) becomes the contact parting time of the circuit breaker. Indeed, many high speed interrupters[17] whose contact parting times may be predetermined accurately are subject, in some degree, to the analysis and conclusions here presented. One such application of this treatment to power circuit breakers for rectifier service has been presented previously[17] before the AIEE.

In particular, this paper approaches the problem of fuse performance on an analytical basis, to establish certain fundamental trends which result as one or more of the circuit variables is altered. The work is carried out on a quantitative basis in such a way as to enable the equations and curves to be applied to any single-phase circuit regardless of the frequency, voltage, or current magnitudes. No attempt is made to enter into a discussion of the physics of the arc within the interrupter or to explain the methods used to develop the arc voltage characteristics essential to good current-limiting fuse performance. The study is of particular value to the testing and application of the interrupter as well as rendering considerable data of use to the fuse designer. Regions of maximum circuit severity may be predicted and test programs arranged to explore these regions. It is particularly fortunate that the straight forward application of the fundamental concepts of linear circuit theory may be applied to solve what otherwise appears as a nonlinear circuit problem. In several places this analytical study sheds new light on the performance characteristics of current-limiting power fuses and clears up what otherwise might ap-

Paper 46-171, recommended by the AIEE committee on protective devices for presentation at the AIEE summer convention, Detroit, Mich., June 24–28, 1946. Manuscript submitted April 26, 1946; made available for printing May 24, 1946.

E. W. Boehne is research engineer, engineering general division, General Electric Company, Philadelphia, Pa.

The author wishes to acknowledge the contributions of D. C. Robertson, H. R. Castenschoild, and M. J. Jang for their computation of much of the data presented in this paper.

*Part I of this paper was prepared by C. L. Schuck.

pear to be inconsistencies in the laboratory and field performance of this interrupter.

Assumptions and Nomenclature

Any quantitative analytical treatment which is devoid of empirical data reincorporated into the analysis is restricted by certain assumptions which usually are made to facilitate the treatment. In spite of these assumptions, however, it is the duty of the analyst to render a solution which indicates the salient trends to be found in the device under study, although it is recognized that no one single performance ever will be duplicated exactly in the analytical study. In the study under consideration, it will be shown, for example, that the ratio of the magnitude of the arc voltage developed by the interrupter to the generated voltage is a controlling factor in its performance. For this reason the study includes a solution for numerous assumed ratios of arc voltage to generated voltage and such results are plotted with this ratio as the variable.

Because the study at hand is concerned with fuses applied for the interruption of short-circuit currents, the assumption of a zero power factor circuit is made for the great majority of the data developed. It is to be made clear, however, that the analytical method employed is not limited to the zero power factor circuit. Moreover, it is not to be implied that zero power factor always presents the most severe condition in all cases.

Field, laboratory, and analytical studies all confirm that the fuse experiences its most difficult tasks when clearing single-phase short circuits. For this reason (as discussed more fully in the foregoing part I of this paper by C. L. Schuck), the analytical treatment presented here is concerned entirely with single-phase interruptions.

In order that the relations developed might be applied to circuits of any voltage, any current, and any frequency, a per unit system of nomenclature was selected which expresses the arc energy as a coefficient k which must be multiplied by the circuit MVA (based upon a symmetrical current) to obtain the true arc energy in watt hours. Similarly, the time scales are expressed in degrees in order that the results might be applied to circuits of any frequency. The reference point for measuring the major angles, namely, Θ_1, Θ_e and Θ_2, as listed following, is the zero of the generated voltage. This has many advantages in the mathematical treatment. The salient nomenclatures

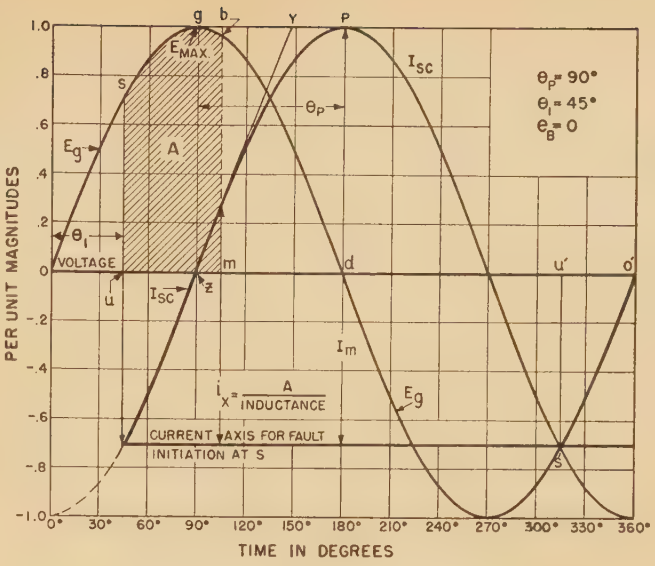

Figure 1. Relationship between volt-time areas and short-circuit current in a single-phase zero-power-factor a-c circuit

The short-circuit current i_x is equal at all times to the volt-time area under the generated voltage. Note that the current axis depends upon the angle Θ_1

as used in the paper are

Θ_p = power factor angle
90 degrees = all inductive, no resistance
Θ_1 = fault starting angle (measured from voltage zero)
90 degrees = symmetrical fault current when $\Theta_p = 90$ degrees
0 degrees = fully displaced current
Θ_e = arc voltage angle (measured from voltage zero)
$\Theta_m = (\Theta_e - \Theta_1)$ = melting time of fuse
Θ_2 = angle when final current zero occurs (measured from voltage zero)
$\Theta_B = (\Theta_2 - \Theta_e)$ = arcing time
$\Theta_f = (\Theta_2 - \Theta_1)$ = fault duration
E_g = generated voltage (single-phase, rms)
E_m = crest of generated voltage
e_B = arc voltage of interrupter in per unit of E_m
e_2 = instantaneous generated voltage at interruption in per unit of E_m
I = available symmetrical, rms, short-circuit current (no arc voltage)
I_{sc} = short-circuit current available (includes d-c component)
I_m = peak value of available current
i_B = current that would flow if e_B acted alone in the circuit
i = actual current in the circuit = $I_{sc} - i_B$
i_m = peak value of actual current
Q = the integral of arc current over the arcing time
L = inductance of the circuit in henries
$MVA = E_g \times I \times 10^{-6}$ = available, symmetrical, zero-power-factor, megavolt-amperes
k = arc energy coefficient, watt-hours per megavolt amperes (60-cycle circuit)
k_L = maximum inductive energy in circuit in watt-hours per megavolt-amperes
W = arc wattage in watt-hours = $k \times$ megavolt amperes (60-cycle circuit)
$\omega = 2\pi f$
f = circuit frequency
$\Sigma i^2 t$ = summation $i^2 t$ of a fuse. This is obtained from the basic fuse design data and concerns the material and cross section of the fusible element. See equation 7

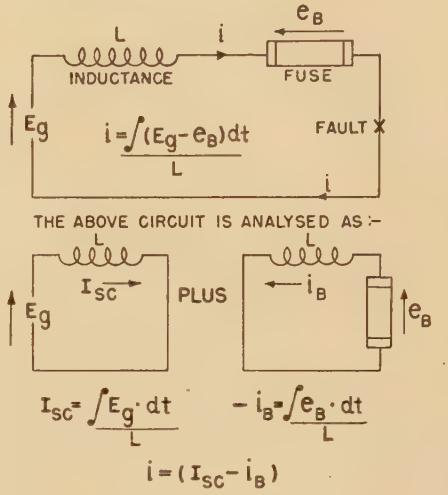

Figure 2. Fundamental circuits used in the analytical determinations in this paper

Here the principle of superposition is used to show the concept of a backward moving or cancellation current produced by the fuse voltage

$H = \frac{\Sigma i^2 t \times \omega}{I^2}$ = heating function (equation 5)

x_L = inductive ohms of circuit
$= \omega L = E_g / I$

A, A', B, B', C = voltage-time areas

Analytical Approach

The student of short-circuit protection will achieve a clear insight into the behavior of interrupting devices by applying a few fundamental laws of circuit theory. The simplest of these concerns the voltage-current relationship in a purely inductive circuit. The majority of a-c short circuits is limited primarily by the inductive reactance of the circuit. Short-circuit current calculations on transmission systems usually neglect circuit re-

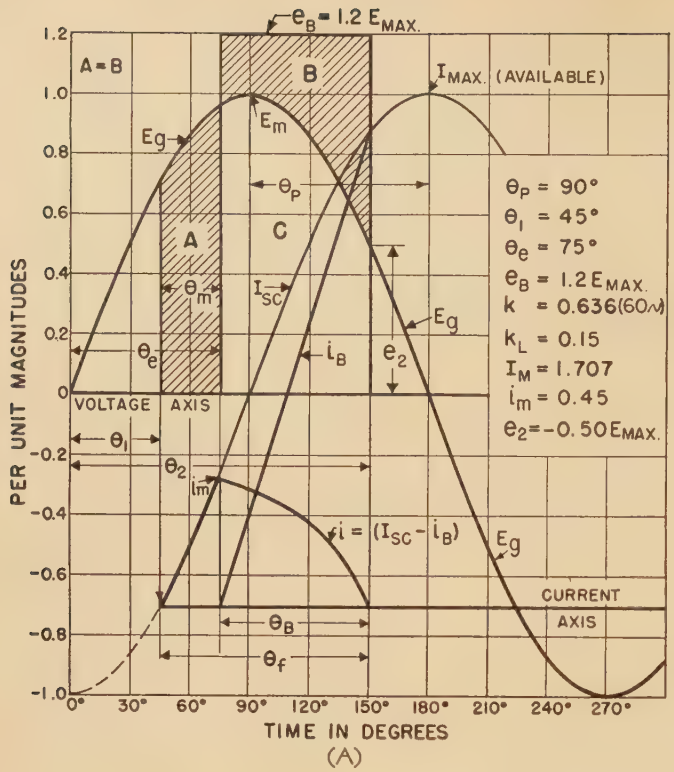

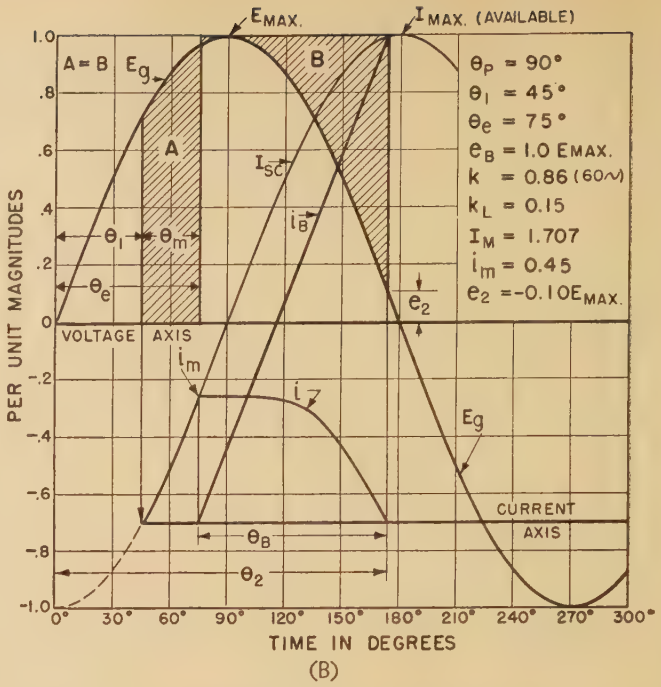

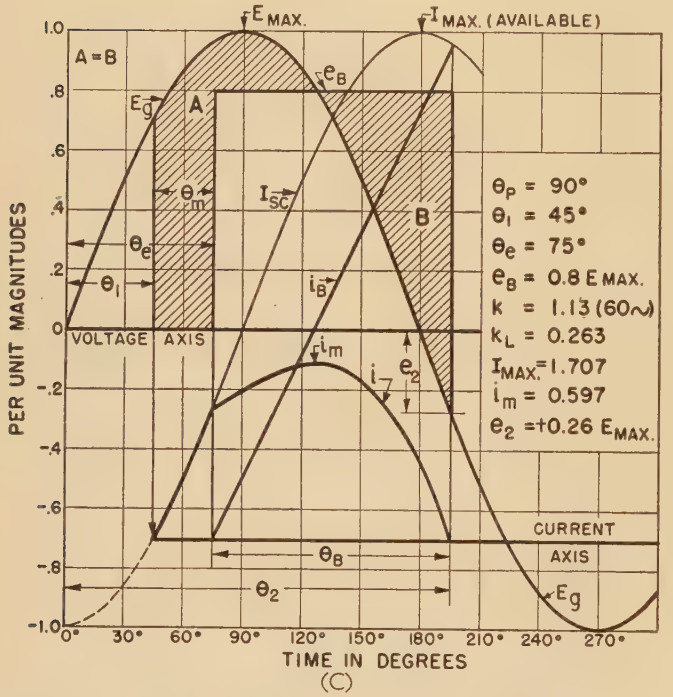

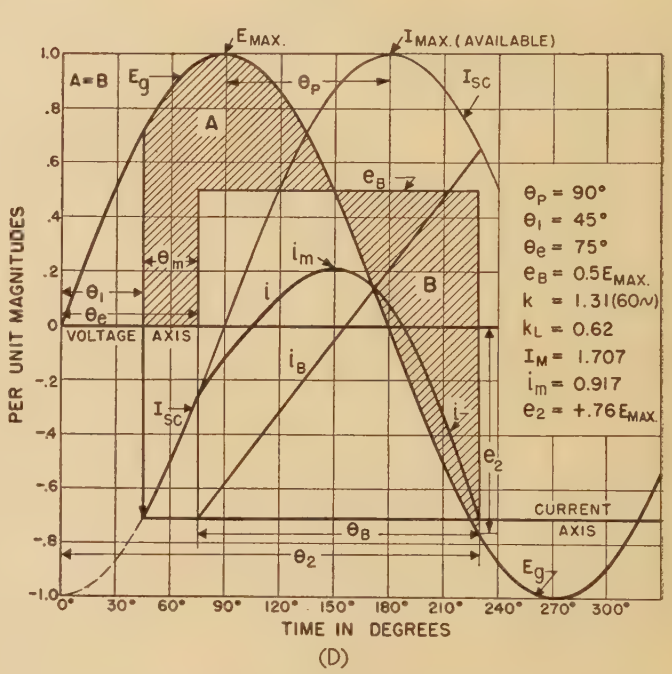

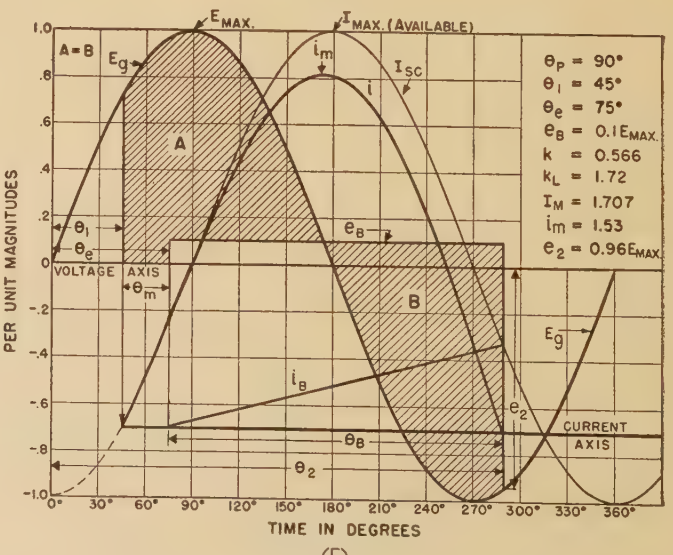

Figure 3. Graphical interpretation of the circuit of Figure 2 when the arc voltage e_B of the fuse is considered as a rectangular or flat top voltage drop introduced 75 degrees following a voltage zero and 30 degrees following the inception of the short-circuit current

The cancellation current produced by the fuse is the linearly rising current i_B. The effect of various ratios of arc voltage to generated voltage peaks is shown in the various parts of the figure. Particular attention should be paid to the relative arc energy k as the arc voltage is modulated

A. Arc voltage of $1.2E_m$
B. Arc voltage of $1.0E_m$
C. Arc voltage of $0.8E_m$
D. Arc voltage of $0.5E_m$
E. Arc voltage of $0.1E_m$

sistance and can do so with a high degree of accuracy. Although the most pessimistic conditions cannot be predicted always on the basis of the purely reactive circuit (zero power factor), nevertheless a working understanding of the purely inductive circuit forms the foundation of this phase of the protection engineers' art. Just as the current in a noninductive circuit is given by E/R so the current in the purely inductive circuit may be expressed as the voltage-time area divided by the circuit inductance. The fundamental equation of current in the purely inductive circuit hence becomes

$$i = \frac{\int e \times dt}{L} \qquad (1)$$

This is just another way of expressing the well-known voltage drop in an inductance, namely,

$$e = L\frac{di}{dt}$$

This volt–time area concept is only applicable to the purely inductive circuit and is the foundation of a simple geometry which requires that from current zero to current zero the net area under the circuit voltages is zero. Figure 1 shows this law applied to the generation of the reactive short circuit in a purely inductive circuit, giving a pictorial understanding of the cause of the asymmetrical short circuit. The voltage E_g in Figure 1 is the fixed sinusoidal a-c generated voltage with its fixed axis. The current I_{sc} is the short-circuit current, the current axis being determined by the instant of short-circuit initiation. For example, if the fault starts at s, on the generated voltage, a vertical from the voltage to the current determines the current axis for that condition. The magnitude of the current at any instant is then proportional to the volt–time area from fault inception up to that instant. The current i_x, for example, is equal to the volt–time area A = s-b-m-u-s divided by the circuit inductance as defined in equation 2. It follows that in this case, peak current I_m will occur at a voltage zero, its magnitude being dependent upon the volt–time area s-d-u. Hence current zero will occur when an equal area under the negative voltage has been covered, that is, when area $s'du'$ = s-d-u. The magnitude of the minor loop of current which follows will be proportional to the area $s'o'u'$. Inspection will reveal now that a fault starting at voltage peak will produce a symmetrical fault current (constant inductance) having a peak value d-P. Similarly a fault starting at a voltage zero will produce a fully displaced short-circuit current having a peak twice this magnitude. These area concepts therefore produce results which agree with other approaches to the same problem and will be extended now in simple graphical form to cover the performance of fuses.

When more than one voltage acts within a circuit, the current resulting from each source can be determined independently and the resulting currents added to determine the net current. A study of Figure 2 reveals this principle applied to the problem at hand. This superposition of currents is well known and often applied to the solution of circuits in cases when the multiple source of voltages are all generated electromotive forces and batteries. The broadening of the superposition principle to consider voltage drops acting in the circuit just as if they were generated electromotive forces generally is not used and its power is not appreciated fully. This extension of the fundamental superposition principle, as an analytical tool, finds its greatest usefulness in the analysis of many circuits containing devices whose voltage drops are nonlinear, such as tubes, circuit interrupters, arc furnaces and welders. This is particularly true when the performance of these devices depends upon their voltage drops and this characteristic, in turn, can be controlled by the designer. Such is the case with most circuit interrupters and in particular with power fuses of the current-limiting type.

The voltage drop characteristics of a power fuse determine the energy liberated in the fuse, the recovery voltage which appears following interruption, its current-limiting ability and, in general, controls the performance of the fuse. These facts may be demonstrated most easily by considering the voltage across the fuse to take a rectangular shape following the melting of the current-responsive element in a zero power factor circuit. The current i_B (Figure 2) produced by a rectangular or d-c voltage, e_B, in a purely inductive circuit is, as outlined before, proportional to the area under the voltage. This current, i_B, is hence a linearly rising current, at a rate e_B/L, and given in this case by the equation

$$-i_B = \frac{\int e_B dt}{L} = \frac{e_B \times t}{L}$$

The scale of this current, for graphical analysis, is obtained most readily from Figure 1 by observing that, for a symmetrical fault originating at crest voltage, E_m = zg, a linearly rising current zy would have resulted in one radian (57.3 degrees) had the crest voltage E_m been maintained over the interval. When the fuse voltage, e_B, is rectangular, it produces a current which rises at a rate e_B/E_m times the slope of zy on Figure 1. It follows

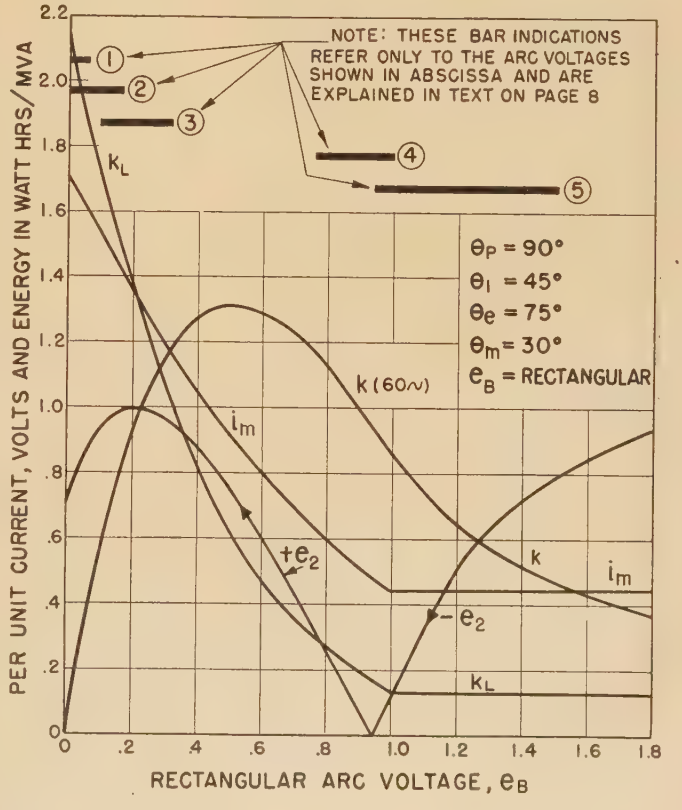

Figure 4. Master plot of the essential data from Figure 3 as a function of the magnitude of the ratio of arc voltage to generated voltage crest

Note that peak arc energy occurs for an arc voltage whose magnitude is about 0.5 of the crest of the generated voltage. The horizontal bar lines at the top of the figure pertain only to the nominal relative arc voltage range of the following interrupters:

1. Air blast breaker
2. Oil circuit breakers
3. Expulsion fuses
4. Magne - blast breakers
5. Current - limiting power fuses

that the current i_B, so developed as a result of the fuse voltage e_B, is a current which flows in opposition to the short-circuit current I_{sc} (see Figure 2) and is plotted in all figures in a positive sense to visualize better its algebraic addition to I_{sc}. A typical example of such an analysis is shown in Figure 3A which will be described in detail as a demonstration of the method used to determine all the analytical data developed in this paper. Here a fault is assumed to originate in a zero power factor circuit (Θ_p = 90 degrees) at an interval of Θ_1 = 45 degrees following the voltage zero. This would have produced a short-circuit current, I_{sc} rising to 1.707 times the normal symmetrical current crest. At an interval of 30 degrees following current initiation, the current-responsive element in the fuse melts (Θ_m = 30 degrees) and gives rise to an assumed rectangular arc voltage e_B of 1.2 times the generated voltage peak. This arc voltage accordingly would produce the linearly rising cancellation current i_B which rises at a slope of 1.2 times the slope of the short-circuit current at maximum voltage (1.2 *zy* on Figure 1). When this current i_B becomes equal to the short-circuit current I_{sc}, that is where the two currents intersect on the diagrams in this paper, current zero occurs. The fuse current i, following the melting of the current-responsive element, is therefore the difference between the two currents I_{sc} and i_B. This resulting current is shown plotted on the current axis. As current zero is reached, and if interruption occurs, the voltage which appears across the fuse is naturally the generated voltage. Hence at interruption the arc voltage e_B drops to the generated voltages E_g at this point as revealed on all the figures and oscillograms in part I of the paper. It might be advisable, to point out here that high frequency recovery voltage oscillations at interruption, such as accompany the operation of oil and air blast breakers, are not associated with current-limiting fuse operation. This is borne out further by the fact that current-limiting fuse performance is essentially independent of the amount of capacitance to ground associated with the circuit in which the fuse operates. Hence the recovery voltage across the fuses, discussed here, is the generated voltage. The fuse, however, does recognize the initial magnitude of the generated voltage e_2 at interruption, particularly if the generated voltage is rising following interruption. This fact becomes an important element in determining the severity of the operation and will be discussed more in detail later. In Figure 3A the initial recovery voltage e_2 is $-0.50E_m$, the minus sign indicating that the current zero leads the voltage zero or that the generated voltage is falling. This represents a favorable operation.

Area Criterion

Since current is proportional to the volt–time area covered in the purely inductive circuit, it follows that equal volt–time areas must have been covered by both the generated voltage E_g and the arc voltage e_B at the instant the two currents become equal. The volt–time area $A+C$ must be equal, therefore, to the volt–time area $C+B$ in Figure 3A, and accordingly $A=B$. This fact finds mathematical expression in the equations found in Figure 2. From these facts emerge some of the more obvious general conclusions as can be deduced by the reader by an inspection of Figure 3A, namely,

1. The arc voltage of the fuse must exceed the generated voltage and remain above the generated voltage for a time sufficiently long to create a volt–time area B equal to the volt–time area A developed during the melting time of the fuse.

2. Fuses of low current rating and thus having small melting times (θ_m) will produce a small volt–time area A and accordingly make it easier to create the neutralizing area B resulting from fusion.

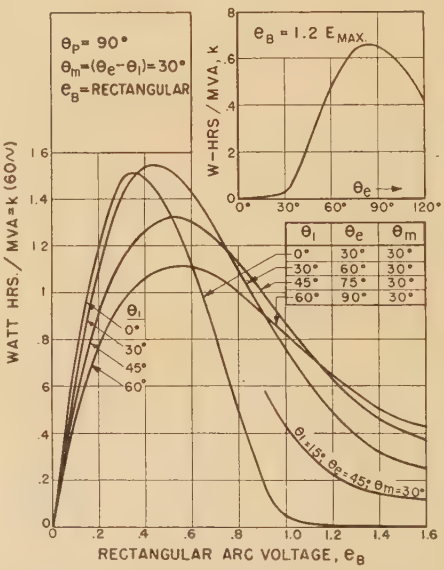

Figure 5. Relative arc energies for various fault initiating angles Θ_1 plotted with respect to the magnitude of a rectangular arc voltage ratio e_B

The curve for Θ_1=45 degrees is replotted from Figure 4. In the upper right-hand corner is shown the relation between arc energy and the arc voltage angle Θ_e for a melting angle of 30 degrees. Note that peak energy occurs when fusion takes place just before the peak of generated voltage

3. Because the arc voltage is controlled by the fuse design, it follows that fuses applied in circuits having higher than the rated voltage of the fuse will make it difficult to create the area B and in any event the current zero will be delayed.

These facts will be made clearer and some of the less obvious facts will emerge with the modulation of some of the variables associated with fuse performance.

Arc Energy

The energy released by a current-limiting fuse preferably is absorbed within the fuse without any display of expelled gases or mechanical breakage. This is one of the reasons why the energy released is important to the fuse designer. Of more importance, however, is the influence of the energy released upon the interrupting ability of the fuse. Arc voltages of sufficient magnitude are maintained by cooling the arc path at a rate faster than the energy generation. Experience shows that the more energy released per conductor, the lower the arc voltage becomes; and, as will be shown, the lower the arc voltage, the more energy is released. The fuse designer, therefore, must proportion the materials so as not to produce too high a voltage surge at fusion, yet produce as nearly as possible the optimum arc voltage characteristic for over-all fuse performance. This is done by the proper choice of multiple conductors, their materials, diameter, length, and arrangement, as well as the material and grain size of the fuse filler.

Returning now to Figure 3A, the arc wattage is the product of arc voltage e_B and the arc current i. Because the arc voltage is constant in this case, the wattage is proportional to the arc current i and hence is not replotted. The arc energy is proportional to the watt–time area, that is, the area under the wattage curve. For those cases where the arc voltage is constant during the arcing period, the arc energy liberated by the interrupter in a 60-cycle zero power factor circuit, is given by

$k=\left[1.4736\times e_B\times\int_{\Theta_e}^{\Theta_2} i\,dt\right]$ watt-hours per megavolt-ampere per half cycle of arc. (see equation 13)

This integral of arc current and time is termed Q and is shown in Appendix I to be the following function of the angles of the circuit

$$Q=\int_{\Theta_e}^{\Theta_2} i\,dt$$

$$=\tfrac{1}{2}\Theta_B(\cos\Theta_1+\cos\Theta_2)-(\sin\Theta_2-\sin\Theta_e) \quad (2)$$

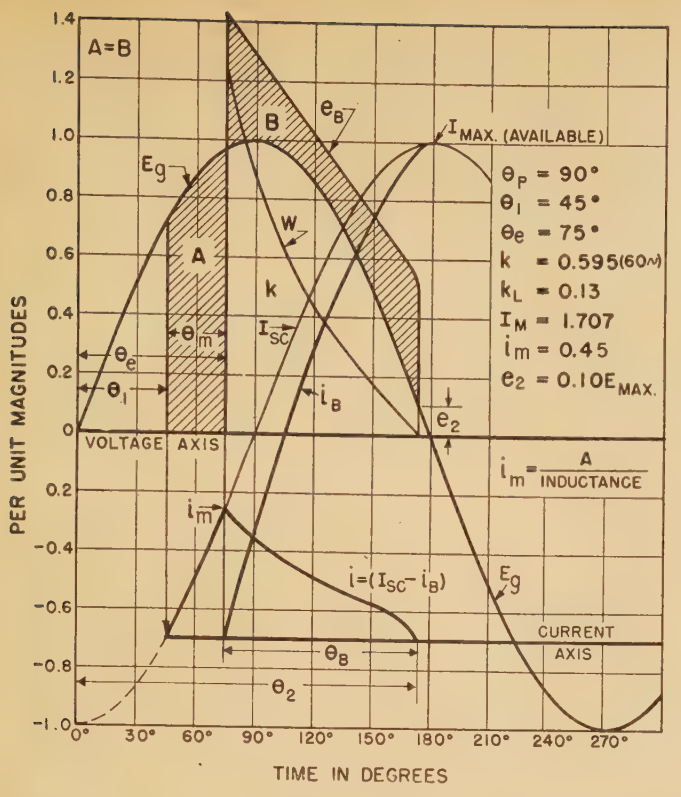

Figure 6. Although the arc voltage e_B differs from a rectangular shape, the area criterion ($A=B$) must hold from current zero to current zero in a zero-power-factor circuit

Here the interrupting current zero was chosen to take place at the same time as found in Figure 3B. Note that the arc energy above is less than in Figure 3B, all other factors being identical save the arc voltage wave shape. Figure 7 shows what happens, however, when such a characteristic is used in a 25-cycle circuit. See Figure 6C in part I for oscillogram showing these characteristics

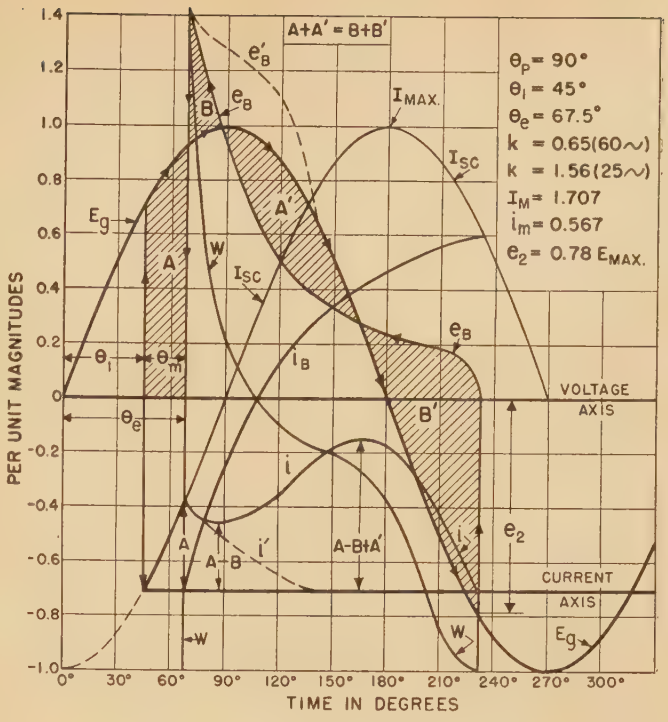

Figure 7. When the fuse characteristic of Figure 6 functions in a 25-cycle circuit, the melting angle is only 22.5 degrees

The drooping arc voltage wave shape however causes the arc voltage to dip below the generated voltage as indicated by the area A'. During the interval A', therefore, the arc current must rise and only come to zero as the area B' is created such that $A+A'=B+B'$. Note that the arc energy k and the initial recovery voltage e_2 both represent more severe conditions than the corresponding 60-cycle values on Figure 6. See Figure 8B in part I for oscillogram showing these characteristics on a 25-cycle circuit

A more general expression of arc energy which applies for any frequency is given in Appendix I, equation 12, and repeated here

$$\text{arc energy} = 555\frac{e_B Q}{\omega} \text{ watt-hours per mega-volt-ampere} \quad (12)$$

The conditions for which these arc energy equations are valid are indicated clearly in Appendix I.

The use of these equations requires the determination of the angle θ_2, or the terminating angle of the current. An inspection of Figure 3 will show that this angle is related to the arc voltage e_B by the following relationship

$$e_B = \left(\frac{\cos\theta_1 - \cos\theta_2}{\theta_B}\right) \quad (3)$$

Because $\theta_B = (\theta_2 - \theta_e)$ it follows that no exact solution for θ_2 is possible because of the transcendental nature of the equation. Graphical methods, as disclosed in Figure 3, will give a very close approximation to θ_2. A more exact determination can be achieved quickly with one or two insertions in the preceding equation. Mass calculations assuming θ_2 as the variable and later cross plotting for e_B are quite useful. The preceding arc energy relations are plotted in Figure 9 as a function of the melting time of the fuse for a particular arc voltage e_B of $1.2E_m$ in a 60-cycle circuit. The actual energy W developed by the fuse is accordingly

$$W = k \times MVA \text{ watt-hours}$$

The arc energy represented by Figure 3A is 0.636 watt-hour per megavolt-ampere. Hence a fuse operating on the pattern of Figure 3A in a 60-cycle circuit interrupting 36,000 amperes at 2,800 volts would develop 64 watt-hours. The peak energy stored in the circuit inductance during this operation is $1/2Li_m^2$ and is termed the maximum inductive energy k_L. This is given on Figure 3A as 0.15 watt-hour per megavolt-ampere. Hence the energy developed within the fuse exceeded the stored energy by 425 per cent.

The preceding energy values come into proper perspective with a few limiting values indicated. Consider a single-phase zero power factor circuit, representing a definite short-circuit megavolt-ampere, and allow a linear resistance of ohmic value equal to the inductive ohms to be added in series with the inductance. Such a resistor will develop 1.16 watt-hours per megavolt-ampere per half cycle of current (60 cycles). This is the maximum energy which can be liberated per half cycle in the conventional linear R–L circuit on a steady-state basis in a 60-cycle circuit. The maximum inductive energy for this case is 0.3684 watt-hour per megavolt-ampere. Note that $1.16/0.3684 = \pi = 3.1416$. The maximum possible energy which can be liberated on a transient basis approaches the limiting value of 2.9473 watt-hours per megavolt-ampere per half cycle (exact value $= 1000/108\pi$). This is the maximum stored energy in the circuit inductance in a zero power circuit under full asymmetrical conditions. This is exactly eight times the maximum inductive energy in the conventional R–L circuit proportioned for maximum resistance wattages, that is, $2.9473 = 8 \times 0.3684$.

The arc energy liberated by the fuse is one of the primary ingredients contribu-

ting to the severity of its performance. The magnitude of the actual energy liberated is dependent upon the megavolt-amperes being interrupted. In general, the energy liberated increases as the megavolt-amperes increase; however, very important cases will be shown in which the energy actually decreases as the megavolt-amperes are increased.

Circuit Variables

Among the factors which influence the energy as well as the initial recovery voltage e_2 (the two primary ingredients of performance severity) may be listed the following:

1. Magnitude of the ratio of arc voltage to the circuit voltage, e_B/E_m.
2. Shape of the arc voltage.
3. Melting time of the fuse Θ_m.
4. The MVA available at the time of the short circuit.
5. Frequency of the circuit.
6. Power factor of the circuit.
7. Single-phase or 3-phase performance.
8. The displacement angle of the short circuit (Θ_1).

Only the first two of these factors are under the control of the fuse designer, and to some extent he is able to control the melting time Θ_m for any specific current rating. The last of these factors, however, is a purely random phenomenon. It behooves the fuse designer to have a thorough understanding of the influence of all eight of these factors, as well as their interrelation, in order to satisfactorily test fuses in the laboratory to meet all the requirements which may be encountered in their field application.

It is, of course, beyond the scope of this paper to present all the combinations and permutations in which these eight factors might occur to produce the most severe operating condition. Furthermore, no attempt will be made to wed the two most important elements of severity, arc energy k and recovery voltage e_2, into one severity factor inasmuch as these elements of severity seldom bear the same relative relationship for all fuses. Instead, it seems more practical at this time to show how both of these quantities vary by changing only one of the eight variables at a time. Some of the more exact quantitative values, as determined analytically, will be sacrificed in the interest of simplicity by an analytical treatment which approximates the actual fuse characteristics yet maintaining the same relative magnitudes and trends. A sufficient number of oscillograms of fuse performance are presented in part I of this paper to confirm the validity of the trends established by analytical means.

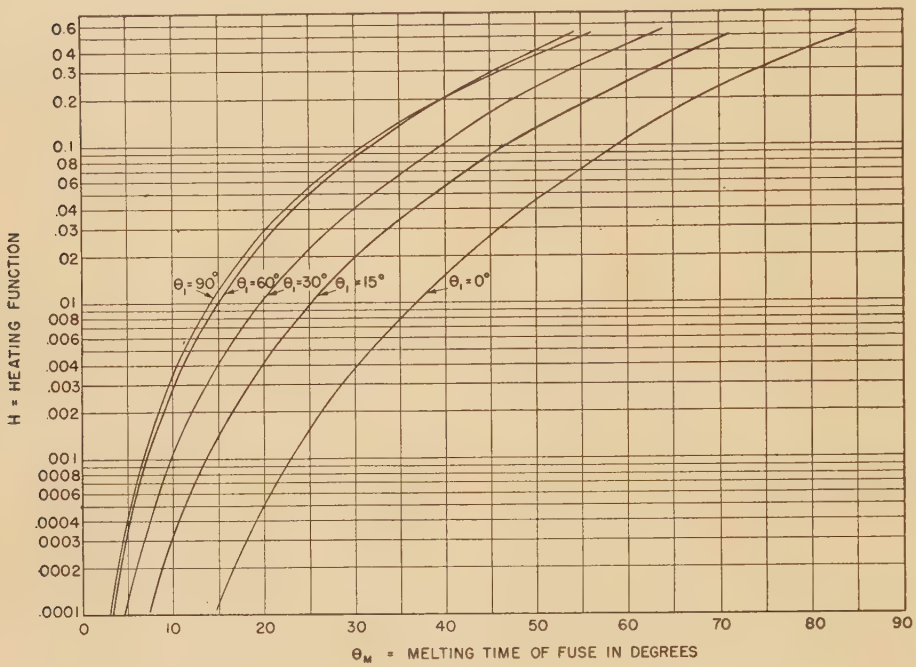

Figure 8. Basic heating function characteristics H for short time currents for various angles of asymmetry in a zero-power-factor circuit

These curves enable the melting angle Θ_m to be determined when the H value is computed from equation 7 in the text. The curves in the figure are a plot of equation 5

Effect of Arc Voltage—Generated Voltage Ratio

The single-phase performance of an interrupting device as effected by a variation in the magnitude of the applied voltage or in the magnitude of an assumed rectangular arc voltage e_B is presented in the five parts of Figure 3. Here rectangular arc voltages whose magnitudes represent 1.2, 1.0, 0.80, 0.50, and 0.10 times the crest of the generated voltage are presented. A discussion of Figure 3A already has been presented to enable a full understanding of the method used to determine the quantities presented on these diagrams. For the diagrams of Figure 3, the following factors are held constant at the values indicated:

1. Power factor of circuit assumed zero (Θ_p = 90 degrees).
2. Displacement angle of the short circuit (Θ_1) of 45 degrees which gives rise to an available per unit current peak I_m of 1.707.
3. Melting time of fuse (Θ_m) equal to 30 degrees thus causing fusion to take place at 75 degrees = $\Theta_e = (\Theta_1 + \Theta_m)$.
4. Shape of arc voltage assumed rectangular.

On each diagram is given the arc energy coefficient k in watt-hours per megavolt-ampere as would be developed in a 60-cycle circuit. The quantity k_L represents the maximum stored energy in the circuit inductance. The magnitudes of peak current i_m as experienced by the interrupter during the interrupting process as well as the instantaneous recovery voltage e_2 at time of current zero are tabulated also.

The essential data from Figure 3 are plotted in Figure 4 as a function of the magnitude of the rectangular arc voltage. This shows that the full current-limiting effect of the fuse under these conditions is not realized unless the arc voltage exceeds the crest of the generated voltage. The initial recovery voltage e_2, an essential ingredient in determining the relative severity of the performance, is shown in such a way as to indicate not only the magnitude, but the direction of the generated voltage following interruption.

Although the data presented in Figure 4 represent the relative performance under the conditions as specified, it is representative enough to serve as a means of indicating roughly where the different types of circuit interrupters function with respect to the magnitude of their arc voltages. This is considered timely here in order that the reader may see in what position of the over-all interrupting spectrum a fuse of the current-limiting type lies, and at the same time to point out that the analytical methods presented are applicable to any type of circuit interrupter. The bar indications at the top of Figure 4 thus show approximately the

Table I

I 1,000	H	Θ_m	k	MVA	W
3	2.78	103.3	2.36	7.5	17.7
4	1.57	86.2	2.18	10.0	21.8
5	1.00	75.7	1.93	12.5	24.1
10	0.2507	50.5	1.22	25.0	30.5
15	0.1114	40.3	0.84	37.5	31.5
17.5	0.082	37.3	0.73	43.75	31.92
20	0.0627	33.9	0.63	50.0	31.5
25	0.0401	29.8	0.44	62.5	27.5
30	0.0278	26.6	0.347	75.0	26.0
40	0.0157	22.4	0.205	100.0	20.5
50	0.0100	19.6	0.132	125.0	16.5
60	0.00697	17.6	0.093	150.0	14.0
80	0.00392	14.8	0.053	200.0	10.6
100	0.002507	13.0	0.036	250.0	9.0

relative arc voltages associated with the following types of circuit interrupters.

1. Air blast circuit breakers.
2. Oil circuit breakers.
3. Expulsion type fuses.
4. Magnetic type air circuit breakers.
5. Current-limiting fuses.

The curves of Figure 4, when considered in this light, hence represent only relative values and describe the arcing period only. In a circuit breaker, Θ_m represents the contact parting time as measured from the previous current zero.

Because arc voltage is expressed, in this paper, in per unit of generated voltage crest, it follows that the diagrams of Figures 3 and 4 also represent the change that takes place as the generated voltage is increased, which in turn is equivalent to decreasing the arc voltage for a given fuse. Such use of these diagrams demonstrates the flexibility of the use of the per unit system adopted. It also follows that if both k and the circuit megavolt-amperes are increased as the generated voltage is increased, then the actual arc energy ($k \times$megavolt-amperes) will increase faster than the increase in k alone.

Effect of Displacement Angle, Θ_1

The arc energy coefficient curve k on Figure 4 is replotted in Figure 5 together with similar curves representing three other displacement angles, keeping the melting angle fixed at 30 degrees. These curves describe, better than words, the relative arc energies as the displacement angle is varied. For the low arc voltage interrupters, the relative arc energies are progressively lower as the fault starting angle is increased. For high arc voltages (above 1.2) the liberated energy is reversed from that of the low arc voltage devices. In the upper right-hand corner of Figure 5 are shown the relative arc energies plotted with respect to Θ_e or $(\Theta_1+\Theta_m)$ for a specific arc voltage of 1.2. This shows that the peak energy released occurs when the current-responsive element melts just prior to the peak of the generated voltage. This fact has been determined empirically by other investigators,[7] but is subject to qualifications which will develop under other headings.

In the testing of fuses, therefore, the choice of a displacement angle which permits the current-responsive element to melt prior to the generated voltage crest will be, in general, one of the regions of severity which should be explored to demonstrate satisfactorily the adequacy of the fuse to meet its rating.

Arc Voltage Wave Shape

Seldom does the arc voltage of a fuse follow the pattern of a rectangular wave shape, although this simple assumption serves adequately to determine analytically the relative trends in fuse severity. The arc voltage e_B, shown in Figure 6 is more representative of one type of arc voltage found in the current-limiting fuses. Because the power factor still is assumed to be zero ($\Theta_p=90$ degrees), it follows that the areas A and B still must be equal from current zero to current zero. The cancellation current i_B resulting from the arc voltage is no longer a straight line, but is dependent upon the volt–time area under the arc voltage. The quantities in the diagram of Figure 6 were so chosen as to place the current interruption Θ_2 at the same point as occurred in Figure 3B for the rectangular arc voltage whose magnitude was $1.0E_m$. Hence the initial recovery voltage in both Figures 6 and 3B is $-0.10E_m$. The energy liberated by the fuse in the case of Figure 6, however, is only 70 per cent of that for the case shown in Figure 3B. This apparently makes the drooping arc voltage of Figure 6 a more desirable characteristic. This is true of the two cases shown. However, conclusions on this point should be reserved until the effect of circuit frequency has been covered in the next paragraph.

Circuit Frequency Versus Arc Voltage Wave Shape

When the fuse which has the arc voltage characteristic shown in Figure 6 is applied to a zero power factor 25-cycle circuit (Figure 7) and a fault is initiated at $\Theta_1=45$ degrees as in Figure 6, the current-responsive element will melt in 22.5 degrees instead of the 30 degrees as in the 60-cycle circuit. This is to be expected and is shown thus in Figure 7 to give a

Table II

I	H	Θ_m	k	MVA	W
500	0.437	59.5	1.49	1.25	1.86
800	0.1713	45.0	1.03	2.00	2.06
1,000	0.1092	40.2	0.84	2.50	2.10
1,100	0.0906	38.3	0.77	2.75	2.11
1,200	0.0760	36.4	0.70	3.00	2.10
1,400	0.0560	33.2	0.58	3.50	2.03
1,700	0.0379	29.1	0.433	4.25	1.84
2,000	0.0274	26.3	0.335	5.00	1.68
2,500	0.0176	23.1	0.227	6.25	1.42
3,000	0.0122	20.7	0.158	7.50	1.19
4,000	0.00684	17.5	0.091	10.00	0.91
5,000	0.00438	15.3	0.059	12.50	0.738

fair comparison between the two frequencies under the conditions assumed. The arc voltage of Figure 6, however, when applied to the 25-cycle scale of Figure 7, drops so rapidly that the area B is not large enough to neutralize the area A, and accordingly the arc current i stops its descent and again starts to rise and continues to do so as long as the arc voltage e_B is below the generated voltage. Peak arc current then occurs when the area A' is more than B and takes place as the arc voltage again crosses the generated voltage. The magnitude of the peak arc current is then equal to volt–time areas $A+A'-B$ divided by the circuit inductance. (Inductance is unity in the per unit system.) Current zero eventually occurs when the area B' has been supplied such that $A+A'=B+B'$. The energy developed by this performance in a 25-cycle circuit is $k=1.56$ watt-hours per megavolt-ampere or 2.62 times the energy represented in Figure 6 for the same arc voltage acting in a 60-cycle system of the same *megavolt-ampere*. The severity of the performance shown in Figure 7, however, is further complicated by the high positive value of the initial recovery voltage e_2 of $+0.78\ E_{max}$. Such a combination of high energy and high recovery voltage would make interruption difficult. A study of Figures 6A and 8B of part I of this paper[1] will confirm the validity of the analysis shown in Figure 7 of this paper.

Had the arc voltage of Figure 3B been applied to the 25-cycle conditions of Figure 7, the arc energy coefficient k still would have been in the neighborhood of 1.5, but the initial recovery voltage e_2 would have been leading at about $-0.25\ E_m$. One of the factors favoring the 25-cycle system which tends to compensate for the apparently high arc energy is the fact that the recovery voltage rises much slower and the peak is reached much later. This advantage can be enjoyed, however, only when interruption occurs in the neighborhood of voltage zero. This analysis explains in part why heavy cur-

Table III

Starting angles, Θ_1..	0°	..30°	..60°	.. 90°
Arc voltage angle Θ_e for max energy, as shown in Figure 10.....	67.5°	..68.0°	..78.5°	..112.5°

rent fuses usually are derated when applied to 25-cycle circuits.

Determination of Melting Time

The performance of all high-speed interrupting devices are affected by the magnitude of the circuit current at the time the arc voltage is introduced into the circuit. This is particularly true of those interrupters which must permit only one pulse of arc current before interruption. In a circuit breaker, this interval is determined by the contact parting time and this time can be predetermined accurately only in very high-speed devices.

In a fuse, however, this interval is determined by the fusion time of the fusible element and accordingly may be predetermined quite accurately for large currents from the design data of the fuse. When the currents are large and the fusion times are less than one cycle, it can be shown that the total i^2t absorbed by the fuse is the true criterion of its fusion characteristics regardless of the manner in which this i^2t is introduced into the circuit. This fact is predicated upon the assumption that in this short interval, no heat is dissipated from the fusible element. It follows, therefore, that the melting time of the fuse may be predetermined if the i^2t of the short-circuit current is available for all conditions which may be experienced. This has been determined in Appendix II in such a way as to be applicable for all currents and all frequencies. Here it is shown that

$$\sum i^2t = \frac{H \times I^2}{\omega} \qquad (4)$$

where

Σi^2t is known from the fuse data (equation 7)

I = the available symmetrical value of the zero power factor short-circuit current being considered

$\omega = 2\pi f$

f = circuit frequency

H = a dimensionless trigonometric heating function whose general equation for the single phase zero power factor circuit is expressed as

$$H = 2\Theta_m + \Theta_m \cos 2\Theta_1 + {}^1/_2 \sin 2\Theta_e + {}^3/_2 \sin 2\Theta_1 - 4 \cos \Theta_1 \sin \Theta_e \qquad (5)$$

This heating function is extremely useful and is plotted for various fault starting angles Θ_1 using as the abscissa the melting time Θ_m of the fuse. The melting angle of any fuse can be determined therefore, by first determining H from

$$H = \frac{\Sigma i^2t \times \omega}{I^2} \qquad (6)$$

and in turn referring to the H function curves to determine the melting angle Θ_m which in turn may be converted to time if desired.

For a multiconductor fuse, the value of Σi^2t is given by

$$\sum i^2t = F_m \times d^4 \times n^2 \qquad (7)$$

where

n = number of conductors in multiple

d = their diameter in mils

F_m = a constant depending upon the metal of the fuse conductor

Effect of Melting Time of the Fuse

From the heating function characteristics H shown in Figure 8, it is observed that as H is decreased by raising the short-circuit current I, the melting time Θ_m decreases. It is observed also from Figure 9 that as the melting time Θ_m is decreased, the magnitude of arc energy function k is decreased; although the megavolt-amperes (by which k is multiplied to produce the actual arc energy) increases proportional to the current. Because the melting time decreases as the current is raised, the question naturally arises concerning the relationship between the actual liberated energy W and the symmetrical fault current, as the latter is increased without limit for a particular fuse design. This problem is approached in the following text for a fuse which has an Σi^2t of 66,500.

By selecting a single-phase generated voltage of 2,500 volts and assuming a per unit rectangular arc voltage of 1.2 or 4,250 volts and further selecting the closing angle Θ_1 of the zero power short circuit at 30 degrees for each current applied, these curves are entered to obtain the solution which is tabulated in Table I for a 60-cycle circuit.

From Table I it becomes apparent that for the assumed condition of a flat top or rectangular arc voltage of 1.2 times the crest of the generated voltage together with a closing angle of 30 degrees in a 60-cycle zero power factor circuit, the maximum energy absorbed by the fuse (under these conditions) will occur in the neighborhood of 17,500 amperes. The energy developed under these conditions will be 31.92 watt-hours. As the fault current is increased above 17,500 amperes, the developed energy decreases until at 100,000 amperes only 9.0 watt-hours of energy is available, the arc voltage, of course, being assumed constant at 1.2 times the crest of the generated voltage as the current is increased.

This problem is presented again in Table II for a smaller fuse having an Σi^2t of 290 and for the same assumed conditions as for the preceding case.

The two arc wattage characteristics W tabulate in Tables I and II are plotted in the master curve of Figure 10 as the $\Theta_1 =$ 30-degree curve together with the corresponding current–energy variations for fault starting angles of $\Theta_1 = 0$ degrees, $\Theta_1 = 60$ degrees, and $\Theta_1 = 90$ degrees. The curves of Figure 10 apply for any fuse operating in a zero power factor circuit at any frequency, but assumes a rectangular arc voltage of 1.2 times the crest of the generated voltage. The fact that one such master energy curve exists for all fuses for all frequencies for a specific arc voltage ratio e_B, is a natural consequence of the choice of parameters which made possible this interesting observation.

Figure 10 teaches that for an assumed arc voltage of 1.2 times the crest of the generated voltage, maximum energy conditions occur for a fault starting angle of $\Theta_1 = 0$ degrees. Similar master characteristics for other arc voltage-generator voltage ratios e_B, shown in the discussion of this paper, reveal that the fully displaced fault does not always give rise to the maximum possible energy. For example, when the ratio e_B is 1.0 instead of 1.2, maximum energy conditions are indicated for a fault starting angle of about 50 degrees and the energy levels are approximately 50 per cent higher than for the e_B ratio of 1.2.

As the rectangular arc voltage e_B drops below 1.0 to, say, 0.95 or 0.90 E_m and below, the arc energy characteristic as a function of megavolt-amperes no longer decreases for high available fault currents, but rises with the megavolt-amperes. The tendency for the arc voltage of the fuse to decrease with increasing circuit current hence may bring about a rising arc energy characteristic at very high currents, and thus establish a ceiling on the interrupting capacity of the fuse. The critical angle of such a characteristic occurs for a Θ_1 between 50 and 70 degrees. A slow rise of the arc voltage of the fuse will contribute materially to this phenomenon, particularly for fuses of the low continuous ampere capacity. These conclusions may be confirmed easily by the use of the equations or graphical methods presented in this paper.

Of considerable interest is the fact that,

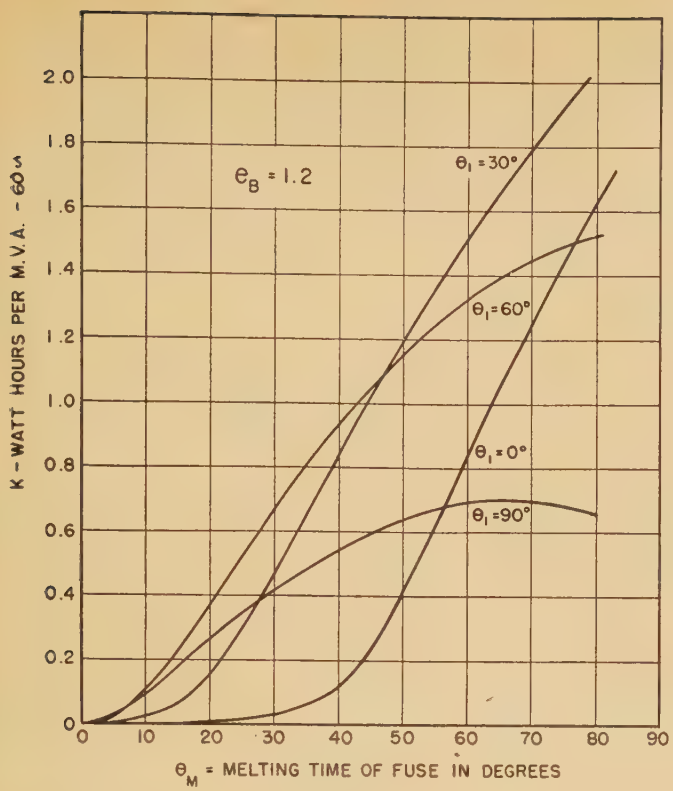

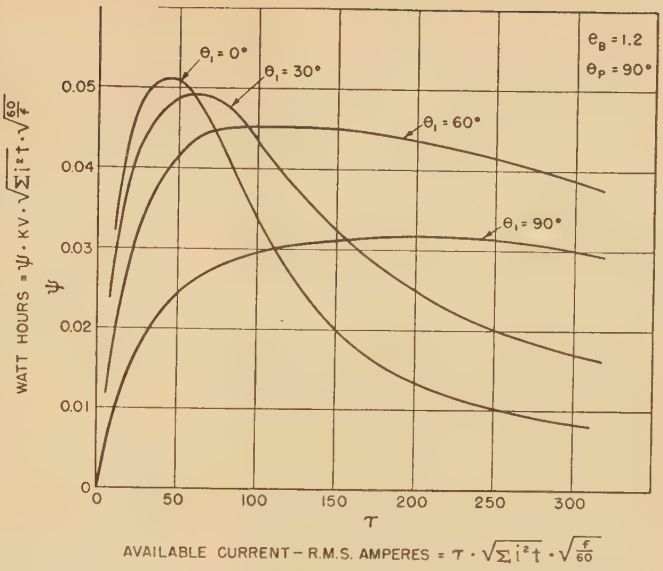

Figure 10 (above). Master energy characteristics for fuses, as a function of single-phase symmetrical zero-power-factor short-circuit currents

These relations are valid only for rectangular arc voltages (or their equivalent) with a nominal magnitude of 1.2 times the crest of the generated voltage. They may be used for any frequency or applied voltage under these conditions. See equation 13

Figure 9 (left). Typical arc energy curves for a 60-cycle zero-power-factor system computed for a rectangular arc voltage which is 1.2 times the crest of the generated voltage

as shown in Figure 10, maximum available energy does not occur necessarily at maximum available rms current. The peak energies of Figure 10 occur when the arc voltage angles are as shown in Table III for $e_B = 1.2$ and $\Theta_p = 90$ degrees.

This confirms the empirical observation made in part I of this paper and reference 7 that one region of maximum severity occurs when melting of the fusible element occurs between 70 degrees and 80 degrees of the voltage wave, that is, just prior to the voltage peak (see Figure 5). This feature is discussed more fully in part I of this paper.

It also is revealed in Figure 10 that the relative energies to be absorbed by fuses of various sizes increase as the square root of the $\Sigma i^2 t$ and directly with the voltage of the application, provided that the arc voltage ratio e_B is maintained constant.

Effect of Circuit Frequency

Figure 10 also teaches that the maximum energy conditions for various circuit frequencies vary as the square root of the ratio of the frequencies. For example, in a 25-cycle circuit, the increase energy available to be absorbed by the fuse, under the conditions of maximum severity, would be $\sqrt{60/25}$ or 1.55 times that for a 60-cycle circuit. It is imperative that the assumption under which this is true be kept firmly in mind; namely, that in both cases, a rectangular arc voltage of the same relative magnitude is maintained throughout the arcing time of the fuse.

In practice, the possible energy ratios for the two frequencies exceeds 1.55 because of the phenomena discussed in connection with Figure 7.

Circuit Power Factor

It is beyond the scope of this paper to include equations and curves which expand this treatment to circuits of various power factors. Such an extension has been indicated clearly,[15,17] and although slightly more complicated, should result in curves similar to those presented in this paper. A few comments regarding the broad conclusions drawn from calculations made for circuits of various power factors are:

1. In general, if the short-circuit calculations are made neglecting all resistance, regardless of its presence, and circuit interrupters are applied which are capable of interrupting the zero power factor megavolt-ampere so determined, the arc energy released, in general, will be less than the values indicated in this paper. On this basis the applications will be on the conservative side.

2. If the short-circuit determinations are made by test, the actual power factors also should be available and the above zero power factor megavolt-ampere readily determined.

3. If the applications of interrupters are made up to their full rated megavolt-amperes, using currents determined from test or calculation which include sufficient resistance to produce currents which lag the voltage by 60 to 75 degrees, then the arc energy released by high speed interrupters, especially of the current-limiting type, will be increased above those indicated by the curves and equations in this paper.

(a). Devices which operate on the right hand side of the master energy characteristics of Figure 5, that is, high arc voltage devices of a high speed nature, will be more likely to experience an increase in circuit severity under these conditions.

(b). High speed devices which operate on the left-hand side of the master energy characteristics of Figure 5, that is, low arc voltage devices, will experience a small increase in developed energy over the zero power factor circuit (constant megavolt-amperes). Such interrupters, however, usually are sensitive to the recovery voltage transient and must consider this voltage in their severity problem. For this reason such interrupters are likely to experience an over-all reduced severity resulting from the damping of the recovery voltage transient offered by the presence of the circuit resistance.[16] This feature will be modulated to a considerable extent depending upon the natural frequencies of the recovery voltage oscillation associated with the circuit.[16] The performance of expulsion fuses is likely to fall into this classification.

Discussion

It has been possible in the preceding treatment to discuss the effect of only one circuit variable at a time. It will become clear to the reader that when, for example,

the arc voltage is changed from $1.2E_g$ to $1.0E_g$, the arc energies for all cases will rise as indicated by comparing Figures 3A and 3B. Moreover, the relative currents at which maximum energy is developed may be expected to shift. It follows that the fuse designer and in particular the fuse tester should have a working knowledge of what regions in this multidimensional space he may expect to test the fuse to determine its ability to handle the most severe field condition which may be imposed upon his interrupter. It also will become apparent to the ultimate fuse user that the controlled conditions of the high power testing laboratory where the current, frequency, power factor, and closing angle all can be predetermined for the test, is the most reliable means of proving the adequacy of power fuses to meet all field conditions.

It should be re-emphasized here that the curves and relationships shown are predicated upon assumed magnitudes of arc voltage of a fuse and do not represent a tabulation or plot of any particular fuse data. In fact, no fuse to our knowledge will produce exactly a rectangular arc voltage. For these reasons, the results obtained on this analytical basis can be used only as a guide to the trends which more or less do take place as described in part I of this paper. Experience shows that as the current at melting increases, the magnitude of the arc voltage tends to decrease. Hence we have what is akin to a volt–ampere characteristic for a particular fuse. With such a characteristic established, the true severity ratios for a particular fuse might be determined more accurately by the application of the curves presented in this paper.

The reader is directed particularly to part I of this paper where oscillograms will be found which demonstrate the principles presented in this paper. The nomenclature on the oscillograms is identical to that used in both papers. The volt–time area relationships are indicated clearly.

An analytical approach to the problem of current-limiting fuse performance has been presented which suggests a method of attack which holds much promise of extension to conditions not presented in this paper. The method has a firm foundation on fundamental principles of circuit theory. Only a little region of a multidimensional circuit problem has been covered in this paper, but sufficient to indicate the essential trends in a quantitative manner for a particular interrupter. The use of superposition principles affords the opportunity of a clear geometrical visualization of the relative importance of each of the circuit variables as exhibited in Figures 3, 6, and 7. Although applied specifically to the current-limiting fuse, the methods employed are applicable to other interrupters and for a wide range of circuit conditions. This is revealed by the fact that the general arc energy equations here presented for the zero power factor circuit are applicable to any interrupter whose arc voltage characteristic can be approximated by a rectangular arc voltage.

Appendix I. Derivation of the Arc Energy Function k, for Rectangular Arc Voltages, Acting in a Zero Power Factor Circuit and Delivering Asymmetrical Short-Circuit Currents

Arc energy is fundamentally the product of the arc current i and the arc voltage e_B, integrated over the arcing time from Θ_e to Θ_2 (see Figure 3). Because the arc voltage is to be held constant, it follows that

$$\text{arc energy} = e_B \int_{\Theta_e}^{\Theta_2} i \, d\Theta \tag{8}$$

This integral will be observed to represent the area between I_{sc} and i_B between Θ_e and Θ_2 in all cases, as shown in Figure 3. Inspection will reveal this area to be represented by

$$\int_{\Theta_e}^{\Theta_2} (\cos\Theta_1 - \cos\Theta) d\Theta - {}^1/_2\Theta_B(\cos\Theta_1 - \cos\Theta_2) \tag{9}$$

The solution becomes

$$\int_{\Theta_e}^{\Theta_2} i \, d\Theta = [{}^1/_2\Theta_B(\cos\Theta_1 + \cos\Theta_2) - (\sin\Theta_2 - \sin\Theta_e)] \tag{10}$$

To obtain the true magnitudes of current the foregoing instantaneous per unit value must be multiplied by $\sqrt{2}I$. Similarly the per unit arc voltage e_B must be multiplied by $\sqrt{2}E_g$ to give the actual arc voltage. Moreover, because $\Theta = \omega t$, it is necessary to divide the preceding integral by ω to convert the area to ampere-seconds. Making these additions and at the same time allowing the foregoing bracketed term to be represented by the symbol Q, there results

$$\text{arc energy} = \frac{2 \times E_g \times I \times e_B \times Q}{\omega} \text{ watt-seconds} \tag{11}$$

Converting to watt-hours per megavolt-ampere, this becomes

$$\text{arc energy} = 555 \frac{e_B \times Q}{\omega} \text{ watt-hours per megavolt-ampere} \tag{12}$$

For the 60-cycle circuit, where $\omega = 377$, this energy equation becomes

$$k = 1.4736 e_B \times Q \text{ watt-hours per megavolt-ampere (60 cycles)} \tag{13}$$

where

$$Q = [{}^1/_2\Theta_B(\cos\Theta_1 + \cos\Theta_2) - (\sin\Theta_2 - \sin\Theta_e)]$$

These relations are valid for any single-phase interrupter acting in a zero power factor circuit whose arc drop may be approximated by a rectangular characteristic. The value of k is the energy per MVA produced by one pulse of current in a 60-cycle current. If arcing persists for more than one-half cycle, the energy in subsequent half cycles may be determined in a similar manner (Figure 10, reference 15).

Appendix II. Derivation of the Heating Function H for Zero-Power-Factor Asymmetrical Short-Circuit Currents

For short time heating of electric conductors, during which time it can be assumed that no heat is lost to the medium surrounding the conductor, the quantity $\Sigma i^2 t$ is the true measure of the heating (including melting and vaporization) of the conductor. This is particularly valid for fuses when interrupting short-circuit currents in a fraction of a cycle. It is the purpose of this section to derive the expression for the total $\Sigma i^2 t$ of the general asymmetrical zero power factor current. Referring to Figure 1, it can be noted that the general zero-power-factor short-circuit current may be expressed

$$I_{sc} = \sqrt{2}I(\cos\Theta_1 - \cos\Theta) \tag{14}$$

It follows that the total or summation Σ of $i^2 t$ over the melting interval may be obtained from the integration of $i^2\Theta$ between the limits Θ_1 and Θ_e; namely

$$\sum i^2\Theta = 2I^2 \int_{\Theta_1}^{\Theta_e} (\cos\Theta_1 - \cos\Theta)^2 \, d\Theta \tag{15}$$

The solution of this equation is

$$\sum i^2\Theta = I^2\{2\Theta_m + \Theta_m \cos 2\Theta_1 + {}^1/_2 \sin 2\Theta_e + 1{}^1/_2 \sin 2\Theta_1 - 4\cos\Theta_1 \times \sin\Theta_e\} \tag{16}$$

where

$$\Theta_m = (\Theta_e - \Theta_1)$$

Allowing the bracketed trigonometric function of equation 16 to receive the symbol H, there results

$$\sum i^2\Theta = I^2 H \tag{17}$$

But $\Theta = \omega t$ (radian measure), hence

$$\sum i^2 t = \frac{I^2 H}{\omega} \tag{18}$$

and

$$H = \frac{\Sigma i^2 t \times \omega}{I^2} \tag{19}$$

H is termed the zero power factor heating function and is computed from equation 16 and plotted in Figure 8 as a function of the melting angle of the fuse in degrees for various fault starting angles, Θ_1. Because the $\Sigma i^2 t$ is available from the fuse design (see equation 7), and the circuit frequency and symmetrical short-circuit current are known, it follows that the melting angle of any fuse can be determined from Figure 8 or its extension by the use of equations 16 and 22. The presence of ω (which is $2\pi f$) in these rela-

The Use of Business Machines in Determining the Distribution of Load and Reactive Components in Power Line Networks

PHILIP D. JENNINGS
NONMEMBER AIEE

GEORGE E. QUINAN
FELLOW AIEE

THE ANALYZER BOARDS available at various points in the United States have afforded welcome relief from the tedious calculations which are ordinarily necessary in determining the distribution of load and reactive component in electric power networks. Since, however, they frequently are located inconveniently, power engineers still have to use longhand methods on their current problems and often have to content themselves with approximate methods, yielding less information than they would like to have. Help in the solution of these problems that arise between visits to the analyzer board can be had by making use of accounting machines of the IBM* type, which usually are available to members of the light and power industry. These machines greatly expedite the calculations while retaining full accuracy of the classical method.

AIEE defines network[1] as follows:

"An electric network is a system of interconnected admittances.

The point at which three or more admittances meet is called a junction point of the network. An admittance connecting any two junction points is called an arm or branch of the network. A mesh within a network is a closed path through three or more junction points."

For the purpose of this paper we will use the expression mesh in the sense of the foregoing definition but with the limitation that a mesh will be in its simplest form, that is, containing no smaller meshes.

The determination of the distribution of load and reactive component in the branches of a network can be accomplished by the solution of a group of simultaneous complex linear equations, with one equation for each mesh of the network; but the large amount of labor involved ordinarily makes this procedure impracticable for networks involving more than three or, at the most, four meshes. Simultaneous equations are solved most easily by the method of determinants. IBM machines are used in the solution of the determinants since they are designed specially to automatically carry through schematic sequences of operations involving multiplication, addition, and subtraction.

For reasons of simplification, a typical 2-mesh network, requiring a determinant of the second order, is shown in Figure 1. Power is fed into the network by two generating stations, 1 and 2, and power is taken out from the network at points *a*, *b*, and *c*. It is assumed that generating station 2 is operating at a fixed load and substantially fixed excitation. Generating station 1 is doing the load regulating.

The vector load currents $\boldsymbol{I}_a$, $\boldsymbol{I}_b$, and $\boldsymbol{I}_c$ and generator current $\boldsymbol{I}_d$ are known with respect to a common reference axis, which in this case is assumed to be the potential $\boldsymbol{E}_0$ (which also is known) at generating station 1. The given vector impedances of each of the branches of the network are represented by the $\boldsymbol{Z}$ values shown in the diagram.

The key to the problem is to determine the two unknown branch currents $\boldsymbol{I}_1$ and $\boldsymbol{I}_2$ in branches *o–f* and *f–d*, respectively, from which the complete solution readily follows. It will be observed from the equations of the currents of the other five branches that they are all functions of known currents and one or both of the two unknown currents $\boldsymbol{I}_1$ and $\boldsymbol{I}_2$.

Referring to Figure 1, the usual solution of a typical 2-mesh network is carried through by means of a second order determinant, as shown in equations 1 to 13. The end product of this procedure is represented by equations 11, 12, and 13, which involve the real and imaginary *M* and *N* quantities used directly in the solution of the values $\boldsymbol{I}_1$ and $\boldsymbol{I}_2$. The right hand members of equations 8, 9, and 10 are developed by the determinant routine, and it is with these that the machines deal.

For example, equation 8 consists of eight terms of two factors each, four of these are real and four of them are imaginary terms. The machines obtain the products of the factors in each term and the final algebraic summation of the terms, keeping the real terms and the imaginary terms separate.

In the case of a 3-mesh network, in which three simultaneous equations are required, each determinant has 48 terms of three factors each. In general the order of the determinant will be the same as the number of meshes in the network

tions permits their use for any frequency. The determination of Θ_m is necessary to determine the arc energy of the interrupter from Figure 9 and derived in Appendix I.

Equation 19 is the foundation of the abscissa of Figure 10 in the observation that

$$I = \sqrt{\Sigma i^2 t}\sqrt{\omega} \times \frac{1}{\sqrt{H}} \qquad (20)$$

$$I = \sqrt{\Sigma i^2 t}\sqrt{\frac{f}{60}} \times \sqrt{\frac{377}{H}} \qquad (21)$$

where in Figure 10,

$$\tau = \sqrt{\frac{377}{H}}$$

Approximation Formula

When the melting angles are very small (up to 0.1 radian) the bracketed portion of equation 16 reduces to the approximate formula

$$H \leqq \{ {}^{2}/_{3} \sin^2 \Theta_1 \times \Theta_m{}^3 + {}^{1}/_{4} \sin 2\Theta_1 \times \Theta_m{}^4 + {}^{1}/_{10} \cos^2 \Theta_1 \times \Theta_m{}^5 \} \qquad (22)$$

For the symmetrical case, when $\Theta_1 = \pi/2$, this reduces to

$$H \leqq {}^{2}/_{3} \Theta_m{}^3 \qquad (23)$$

For the asymmetrical case, when $\Theta_1 = 0$, the heating function becomes

$$H \leqq {}^{1}/_{10} \Theta_m{}^5 \qquad (24)$$

These relations are quite useful when the currents are high enough to cause melting in a few degrees.

References

(See page 1034.)

Paper 46-195, recommended by the AIEE committee on basic sciences for presentation at the AIEE Pacific Coast meeting, Seattle, Wash., August 27–30, 1946. Manuscript submitted June 26, 1946; made available for printing July 24, 1946.

PHILIP D. JENNINGS, associate engineer, and GEORGE E. QUINAN, chief consulting engineer, are both of the Puget Sound Power and Light Company, Seattle, Wash.

* International Business Machines.

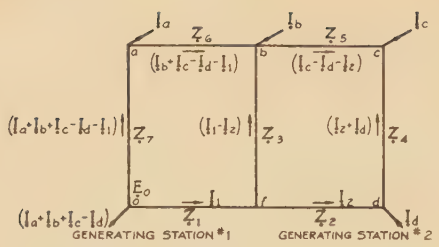

Figure 1. Typical 2-mesh network

and any complex determinant of the nth order will have $(2^n\ n!)$ terms of n factors each.

Experience shows that the solution of a 4-mesh network by the usual method takes from three to ten days, depending on whether or not any errors are made in the 7,680 calculations and 9,600 determinations of signs. The machines will do the same work in four to six hours, requiring only the attention of the regular machine operator. The only errors that can arise in the machine method will be caused by supplying incorrect coefficient data to the master cards (subsequently described). This can be avoided by being careful that the coefficients are correct. This part of the work is not difficult or lengthy, but requires careful checking. If no preliminary work has been done, it will take approximately one day to supply the coefficients for a 4-mesh network. This part of the calculation is the same for the usual method and the machine method.

The process of solving complex determinants by means of the machines is essentially as follows: The accounting machine people punch a so-called formula deck for solving a particular order of determinant. Each factor will be represented by a card in this deck for each term in which the factor appears. For example, in a determinant of order 2 there are eight factors, each of which appears in two terms, making 16 cards in all. A determinant of the fourth order has 32 factors, each of which appears in 48 terms, requiring 1,536 cards; and a determinant of the fifth order has 50 factors, each appearing in 384 terms, requiring 19,200 cards. In addition there will be almost as many blank cards as formula cards. These are punched automatically in the calculating process, one for each term of the determinants. The cost of the cards is nominal. An examination of equation 8 will show substantially what is accomplished by the formula deck. Each card of the deck is punched with certain coded signal numbers that indicate to the various machines the process to be followed. In equation 8 the formula cards will start the sequence of operations required by the determinant, as $a_1 \times a_4$, $b_1 \times b_4$, $a_2 \times a_3$, and so forth, and will signal the sorting machine in its turn to sort the real values separately from the j values. In this way the tabulating machine can make the proper additions and subtractions of terms to give the M and N values of equations 11, 12, and 13.

The formula deck is, in reality, a signal deck capable of producing a definite sequence of multiplications and additions and is not concerned with numerical values. It will solve any determinant of the order for which it was designed, provided the numerical values are assigned. These values for any particular problem are assigned to the formula deck by the use of so-called master cards, on which have been punched the numerical values of the real and j coefficients of the fundamental equations 3 and 4. A determinant of the fourth order requires 32 of these cards, and a determinant of the fifth order requires 50 cards. The master cards are arranged in the formula deck in a definite order, and all the cards then are run through a machine which punches on the cards of the formula deck the numerical values carried by the master cards. Duplicates of the original formula deck are produced automatically by machine, and these duplicates are used in the solution of particular problems, the original deck being used over and over in this way.

The duplicate formula deck, with numerical values assigned, then is run through the various machines for sorting, multiplication of factors, summation of terms, and so forth. Our information indicates that the machines will handle determinants up to the fifth order at least, and their use therefore makes practicable the solution of many network problems which otherwise would have to wait until they could be set up on an analyzer board.

The detailed procedures involved in hand punching, machine punching, and running the cards have not been discussed since all of these are matters of routine with machine operators. The purpose of this paper merely is to call attention to the adaptability of the machines for the solution of complex determinants using a method developed for the Puget Sound Power and Light Company by the Seattle office of IBM Company.

Appendix

Given

$\boldsymbol{I}_a$, $\boldsymbol{I}_b$, and $\boldsymbol{I}_c$ = vector load currents
$\boldsymbol{I}_d$ = vector generator currents
$\boldsymbol{E}_0$ = vector generator potential
$\boldsymbol{Z}_1$, $\boldsymbol{Z}_2$, and so forth = vector impedance operators

$$\boldsymbol{I}_0 = \boldsymbol{I}_a + \boldsymbol{I}_b + \boldsymbol{I}_c - \boldsymbol{I}_d$$

The problem is to find the vector line currents $\boldsymbol{I}_1$ and $\boldsymbol{I}_2$.

From Kirchhoff's laws

$$\boldsymbol{I}_1\boldsymbol{Z}_1 + (\boldsymbol{I}_1 - \boldsymbol{I}_2)\boldsymbol{Z}_3 = (\boldsymbol{I}_a + \boldsymbol{I}_b + \boldsymbol{I}_c - \boldsymbol{I}_d - \boldsymbol{I}_1)\boldsymbol{Z}_7 + (\boldsymbol{I}_b + \boldsymbol{I}_c - \boldsymbol{I}_d - \boldsymbol{I}_1)\boldsymbol{Z}_6 \quad (1)$$

$$(\boldsymbol{I}_1 - \boldsymbol{I}_2)\boldsymbol{Z}_3 + (\boldsymbol{I}_c - \boldsymbol{I}_d - \boldsymbol{I}_2)\boldsymbol{Z}_5 = \boldsymbol{I}_2\boldsymbol{Z}_2 + (\boldsymbol{I}_2 + \boldsymbol{I}_d)\boldsymbol{Z}_4 \quad (2)$$

Collecting coefficients of $\boldsymbol{I}_1$ and $\boldsymbol{I}_2$ in equations 1 and 2 we have

$$\boldsymbol{I}_1(a_1 + jb_1) + \boldsymbol{I}_2(a_2 + jb_2) = c_1 + jd_1 \quad (3)$$

$$\boldsymbol{I}_1(a_3 + jb_3) + \boldsymbol{I}_2(a_4 + jb_4) = c_2 + jd_2 \quad (4)$$

where

$$a_1 + jb_1 = \boldsymbol{A}_1 = \boldsymbol{Z}_1 + \boldsymbol{Z}_3 + \boldsymbol{Z}_6 + \boldsymbol{Z}_7$$
$$a_2 + jb_2 = \boldsymbol{B}_1 = -\boldsymbol{Z}_3$$
$$c_1 + jd_1 = \boldsymbol{Q}_1 = \boldsymbol{I}_a\boldsymbol{Z}_7 + (\boldsymbol{I}_b + \boldsymbol{I}_c - \boldsymbol{I}_d)(\boldsymbol{Z}_6 + \boldsymbol{Z}_7)$$
$$a_3 + jb_3 = \boldsymbol{A}_2 = \boldsymbol{Z}_3$$
$$a_4 + jb_4 = \boldsymbol{B}_2 = -\boldsymbol{Z}_2 - \boldsymbol{Z}_3 - \boldsymbol{Z}_4 - \boldsymbol{Z}_5$$
$$c_2 + jd_2 = \boldsymbol{Q}_2 = \boldsymbol{I}_d(\boldsymbol{Z}_4 + \boldsymbol{Z}_5) - \boldsymbol{I}_c\boldsymbol{Z}_5$$

Putting the equivalent coefficients of $\boldsymbol{I}_1$ and $\boldsymbol{I}_2$ from equations 3 and 4 into determinant form,

$$\boldsymbol{S}_0 = \begin{vmatrix} \boldsymbol{A}_1 & \boldsymbol{B}_1 \\ \boldsymbol{A}_2 & \boldsymbol{B}_2 \end{vmatrix} = \boldsymbol{A}_1\boldsymbol{B}_2 - \boldsymbol{A}_2\boldsymbol{B}_1 \quad (5)$$

$$\boldsymbol{S}_1 = \begin{vmatrix} \boldsymbol{Q}_1 & \boldsymbol{B}_1 \\ \boldsymbol{Q}_2 & \boldsymbol{B}_2 \end{vmatrix} = \boldsymbol{Q}_1\boldsymbol{B}_2 - \boldsymbol{Q}_2\boldsymbol{B}_1 \quad (6)$$

$$\boldsymbol{S}_2 = \begin{vmatrix} \boldsymbol{A}_1 & \boldsymbol{Q}_1 \\ \boldsymbol{A}_2 & \boldsymbol{Q}_2 \end{vmatrix} = \boldsymbol{Q}_2\boldsymbol{A}_1 - \boldsymbol{Q}_1\boldsymbol{A}_2 \quad (7)$$

$$\boldsymbol{I}_1 = \boldsymbol{S}_1/\boldsymbol{S}_0$$
$$\boldsymbol{I}_2 = \boldsymbol{S}_2/\boldsymbol{S}_0$$

Then equations 5, 6, and 7 could be written, respectively, as follows:

$$\boldsymbol{S}_0 = (a_1 + jb_1)(a_4 + jb_4) - (a_3 + jb_3)(a_2 + jb_2) = (a_1a_4 - b_1b_4 - a_2a_3 + b_2b_3) + j(a_1b_4 + a_4b_1 - a_3b_2 - a_2b_3) \quad (8)$$

$$\boldsymbol{S}_1 = (c_1 + jd_1)(a_4 + jb_4) - (c_2 + jd_2)(a_2 + jb_2) = (a_4c_1 - b_4d_1 - a_2c_2 + b_2d_2) + j(a_4d_1 + b_4c_1 - b_2c_2 - a_2d_2) \quad (9)$$

$$\boldsymbol{S}_2 = (c_2 + jd_2)(a_1 + jb_1) - (c_1 + jd_1)(a_3 + jb_3) = (a_1c_2 - b_1d_2 - a_3c_1 + b_3d_1) + j(a_1d_2 + b_1c_2 - b_3c_1 - a_3d_1) \quad (10)$$

From equations 8, 9, and 10 let

$$a_1a_4 - b_1b_4 - a_2a_3 + b_2b_3 = M_0$$
$$a_1b_4 + a_4b_1 - a_3b_2 - a_2b_3 = N_0$$
$$a_4c_1 - b_4d_1 - a_2c_2 + b_2d_2 = M_1$$
$$a_4d_1 + b_4c_1 - b_2c_2 - a_2d_2 = N_1$$
$$a_1c_2 - b_1d_2 - a_3c_1 + b_3d_1 = M_2$$
$$a_1d_2 + b_1c_2 - b_3c_1 - a_3d_1 = N_2$$

$$\boldsymbol{S}_0 = M_0 + jN_0 \quad (11)$$

$$\boldsymbol{S}_1 = M_1 + jN_1 \quad (12)$$

$$\boldsymbol{S}_2 = M_2 + jN_2 \quad (13)$$

Reference

1. Definitions of Electrical Terms. American Standard C42, 1941. Section 05.45.089.

Dielectric Strength of Station and Line Insulation to Switching Surges

P. L. BELLASCHI
FELLOW AIEE

L. B. RADEMACHER
ASSOCIATE AIEE

THE STRIDES achieved since the early thirties in the field of system-insulation rationalization are well known in recent technical literature[1–7] and need not be reviewed here. However, a point to emphasize is that further progress in this industry-wide problem can be attained only through continued research and studies directed particularly to the remaining major questions. In this manner it will be possible to pursue in future developments the principles of system-insulation rationalization to their fullest economic possibilities.

A survey of these future developments would indicate the need for a greater knowledge of the conditions resulting from system transients and, correspondingly, more comprehensive data on the performance of insulation to these conditions. Much has been published on system overvoltages, and there have been some contributions[8–11] relating to the strength of insulation to switching surges and other transients, but the fact remains that more comprehensive data are required in view of the future developments. It is the purpose of this paper to fill in the existing gap by presenting recently established data on the strength of station and line insulation to switching surges, and also to discuss and analyze the new findings with previously determined data in relation to the over-all problem.

Importance of Switching-Surge Data

It would be well to review briefly the significance of system overvoltages in relation to the insulation requirements. This may be done considering several representative cases in which switching surges appear to assume particular importance. Insulation may be proportioned on circuits not exposed to lightning with reference to the system overvoltages entirely, of course, in addition to the normal operating voltages. The data presented here therefore should be helpful in applications of this character.

For systems exposed to lightning, it is a fact that the insulation is applied primarily from a lightning or impulse viewpoint and, in so doing, the requirements arising from system overvoltages as well as other requirements usually are fulfilled, or more than fulfilled, simultaneously. Almost invariably this is the case for systems of modern design which operate with the neutral solidly grounded. However, this approach cannot be accepted

Figure 1. General view of and circuit arrangement for switching-surge tests on medium voltage apparatus

C_s—Surge-voltage generator, 0.083 microfarad
C_l—Load capacitance, 0.042 microfarad
R—Load resistance, 384,000 ohms
L—Series inductance, 1.06 henries
G—25-centimeter sphere gap
B—Apparatus tested
CD—Capacity divider
CRO—Cathode-ray oscillograph

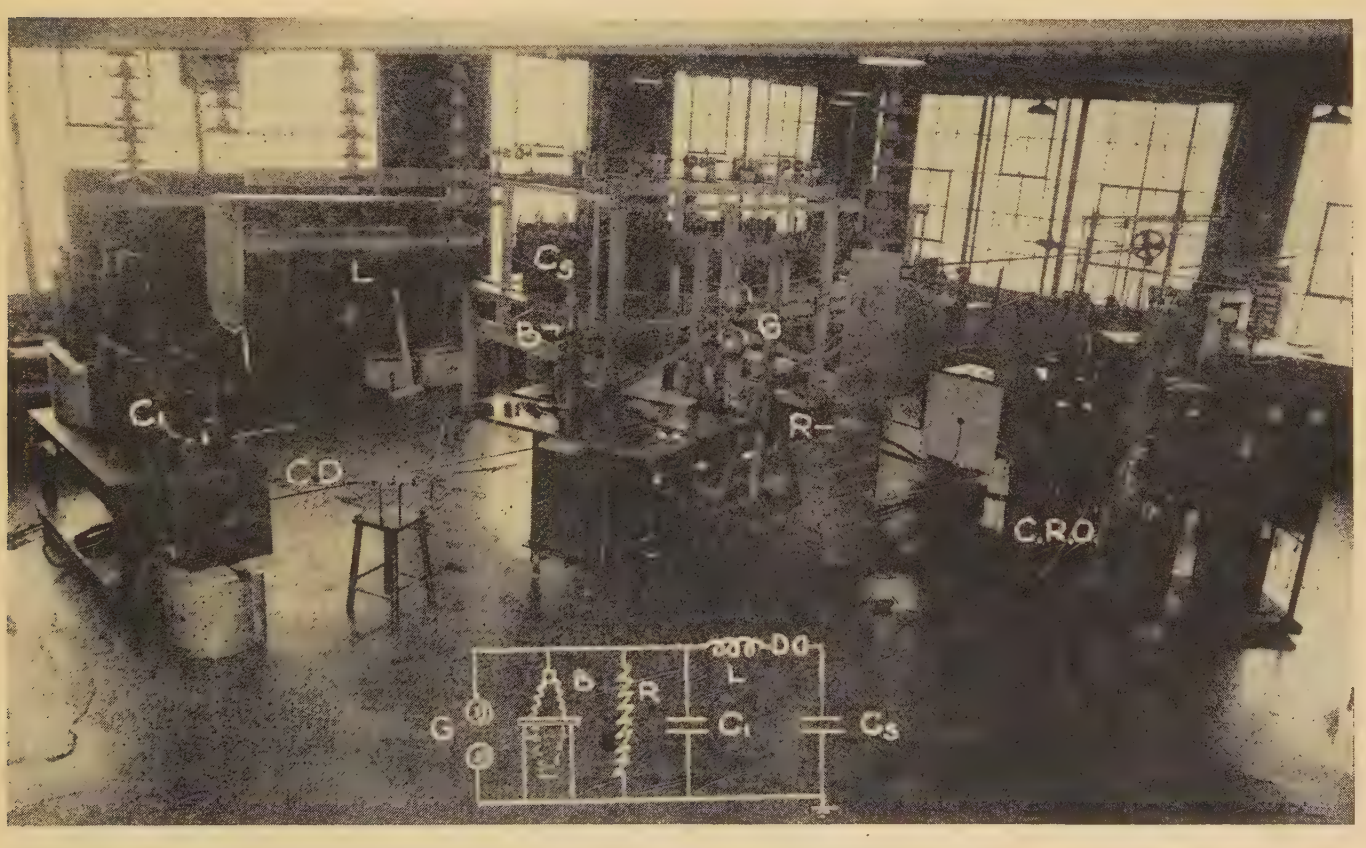

Paper 46-189, recommended by the AIEE committee on electric machinery for presentation at the AIEE Pacific Coast meeting, Seattle, Wash., August 27–30, 1946. Manuscript submitted June 7, 1946; made available for printing July 18, 1946.

P. L. BELLASCHI, a development engineer, and L. B. RADEMACHER, an electrical engineer, are both of the Westinghouse Electric Corporation, Sharon, Pa.

The authors wish to acknowledge the assistance rendered by Paul Evans, Jr., and R. E. Armington.

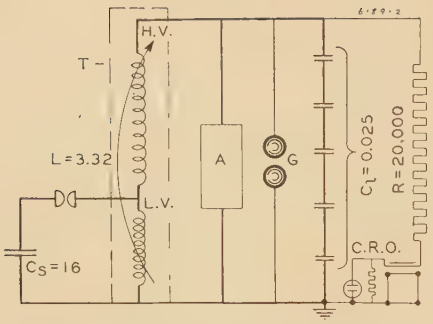

Figure 2. Circuit for switching-surge tests on high voltage power apparatus; *R* in ohms, *C* in microfarads, *L* in henries

C_s—Surge-current generator
C_l—Load capacitance
G—200-centimeter sphere gap
A—Apparatus tested
R—Resistance divider
T—2,500-kva power transformer
HV—230/$\sqrt{3}$-kv winding (230-kv insulation class)
LV—13.8-kv winding (15-kv insulation class)
L—Effective 60-cycle inductance referred to high voltage side

axiomatically in all cases even for grounded-neutral systems. For instance, on grounded-neutral systems where reduced rated arresters are applicable, power transformers in the next lower insulation class have been applied in increasing number because of the economic advantage. In the event future developments indicate possibilities of greater reduction in the insulation than now is considered good practice, then system overvoltages correspondingly will require greater attention.

Surge overvoltages inherently are higher on systems which operate with the neutral isolated and may attain five to six times the line-to-neutral crest voltage, whereas on a solidly grounded neutral the surge overvoltages seldom will exceed it $3^1/_2$ times. It is apparent that on systems which operate with the neutral isolated correspondingly more attention must be given to the insulation from a surge-overvoltage standpoint.

The foregoing considerations assume even greater importance when attention is turned to systems for operation at extra high voltages, for instance 400 kv, as have been proposed. In view of the excellent service record of present 230- and 287-kv transmission systems,[12,13] it would appear that from a consideration of lightning alone the impulse-insulation levels of these systems should be satisfactory at 345 or 400 kv. In other words, the insulation requirements from a switching-surge viewpoint will require attention at the extra high voltages. At these voltages economic advantages most certainly will dictate a grounded neutral system.

In short, there is a distinct need for fundamental data relating to the switching-surge strength of station and line insulation to supplement the present impulse data which in general may be considered reasonably complete.

Characteristics of Switching Surges

The tests of this investigation were conducted with surges of the duration and wave form given in Figures 4 and 5. The periods of these surges are in excess of 1,000 and 3,000 microseconds, respectively. Even on extensive systems, switching overvoltages seldom reach durations greater than a few thousand microseconds. Fundamentally, a longer period would mean that the system would be operating close to 60-cycle resonance, a condition rarely, if ever, attained in service. A survey of the recent contributions on system transients[14–21] indicates that periods within the range of 20 to 2,000 microsecond microseconds comprehend practically all conditions of service.* The surges selected for this investigation are adequately long and therefore, from a dielectric standpoint, correspond in effect to switching surges in the field. Furthermore, the test voltages applied to the equipment extended up to 900 kv crest. An overvoltage of this amplitude corresponds to nearly five times line-to-neutral crest voltage on a 230-kv system and to $3^1/_3$ times on 345 kv. In this respect, too, the wide scope of this investigation is apparent.

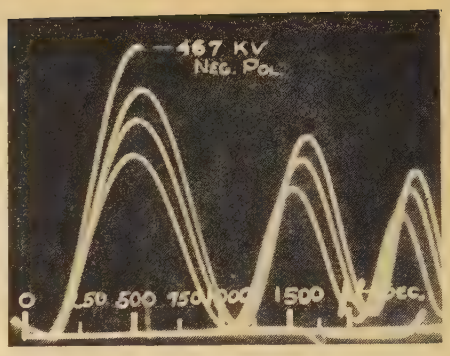

Figure 4. Typical oscillograms of switching surges applied to 46-kv bushing

Apparatus Tested

The apparatus tested in this investigation are listed in Table I; some are shown in Figures 1 and 3. The list comprehends some of the more typical electric apparatus encountered in stations and on lines. For instance, switching-surge tests were conducted on outdoor apparatus bushings in the 46-, 115-, 161-, and 230-kv insulation classes. Representative of porcelain equipment are the 6-unit suspension insulator string and the 3-unit apparatus-insulator assembly. Inasmuch as air gaps are common to practically all outdoor

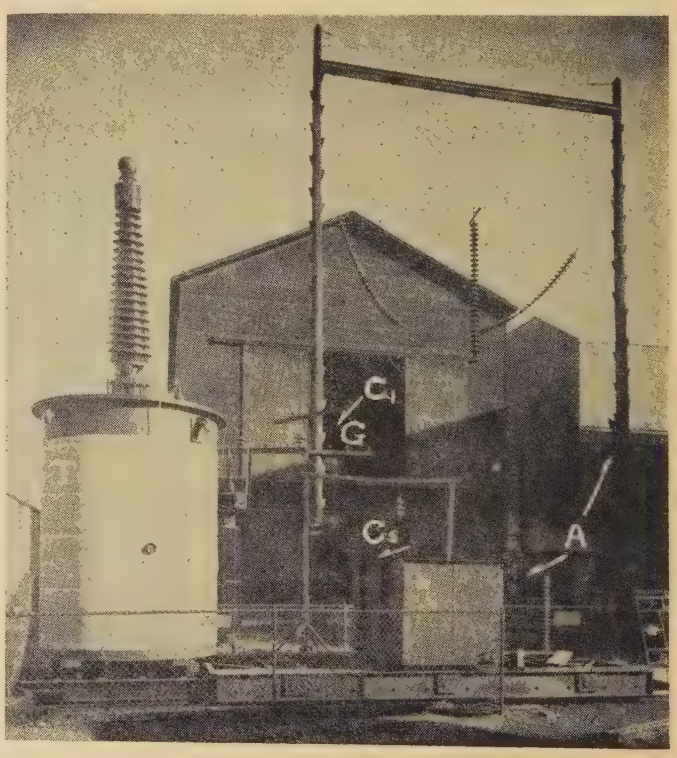

Figure 3. Partial view of switching-surge setup for testing high voltage power apparatus (refer to Figure 2 for circuit)

* Figure 1 of reference 21 is an example of a switching surge recorded on a power system. Other typical examples are found in various technical papers (for example, AIEE and International Conference on Large Electric High-Voltage Systems) relating to faults and circuit-interruption investigations on power systems.

apparatus, standard rod gaps at 10-, 20-, and 40-inch spacings were tested. In the same manner, completely assembled power transformers in the 138- and 230-kv insulation class were the object of extensive switching surges in the course of this investigation and in its forerunner.[8] In view of the importance of oil as a criterion of the internal strength of station apparatus, tests on oil for representative electrode arrangement and spacings are reported here. Some of the tests were made on the apparatus dry (bushings, insulators, and so forth), others under artificial rain (wet test), and still others under condition of heavy dew. For comparison purposes impulse tests were made simultaneously on some of the equipment, and were omitted on others for which standard data are available. In short, it was the intent that the investigation be conducive to practical results and, to this end, apparatus as used in service was tested in nearly all instances.

Test Methods

All switching surges in this investigation were produced by the two methods shown diagrammatically in Figures 1 and 2. The method of Figure 1 closely follows the previous investigation.[8] It consists of a generator C_s which discharges into a load capacitance C_l through an inductance L. The duration and wave form of the surge across the apparatus tested is fixed by the constants of the circuit, and the magnitude is controlled by the charging voltage applied to the generator. Typical oscillograms of the surges developed by this method are given in Figure 4. The maximum voltage available for test was 500 kv. Furthermore, other limitations restricted this test method to the small equipment not exceeding the 69-kv class.

Most of the tests of this investigation were conducted according to the method of Figure 2. In this method, a capacitor bank of 16 microfarads is charged to the desired voltage, and then discharged into the low voltage winding of a power transformer. The high voltage winding connects from the high voltage terminal (230-kv insulation class) to a load capacitance C_l and to a resistance divider R. Thus, through autotransformer action, switching surges of much higher amplitude than had been attained heretofore in the laboratory could be generated. The circuit constants were proportioned to produce surges of desired wave form and duration. Typical oscillograms of tests are shown in Figure 5.

Figure 3 gives a view of the testing equipment that was used. The capacitor banks C_s and C_l normally a part respectively of a high current and a high voltage impulse generator are located in the laboratory. The 230-kv power transformer T is of standard design, except that provision is not made for radiators which for the purpose of this paper are not necessary. With radiators and cooling devices the transformer would have a load capacity substantially above its present nominal rating of 2,500 kva. Therefore, electrically, the circuit elements in these tests compare favorably with major component parts encountered on large power systems. For instance, at the full charge of 100 kv the capacitance C_s has stored energy corresponding to a 30,000-kilovar capacitor

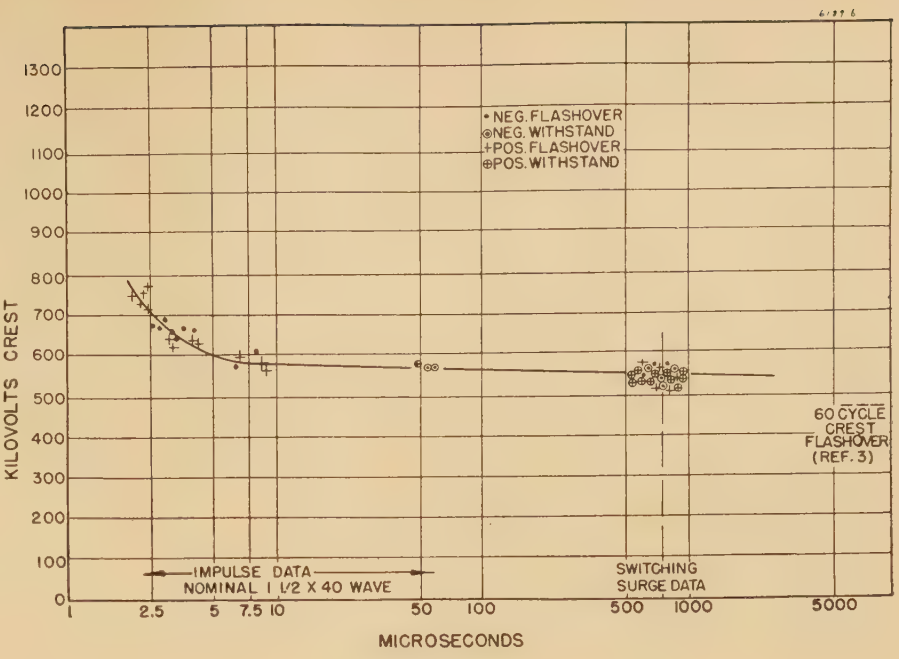

Figure 6. Switching-surge and impulse characteristics of 6-unit suspension insulator string

Relative air density = 1.00
Absolute humidity (grains per cubic foot):
Switching data, 5.1 to 8.5
Impulse data, 3.4 to 6.2

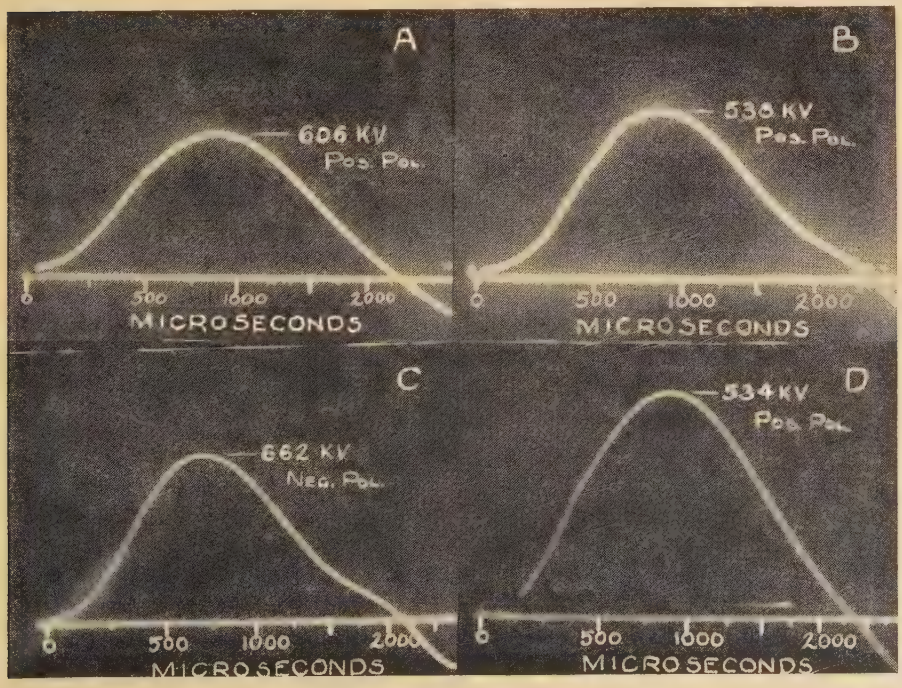

Figure 5. Oscillograms of switching surges

Surge applied to

A. 3-inch oil gap
B. 6-unit suspension insulator string
C. 115-kv bushing
D. 3-unit apparatus insulator assembly

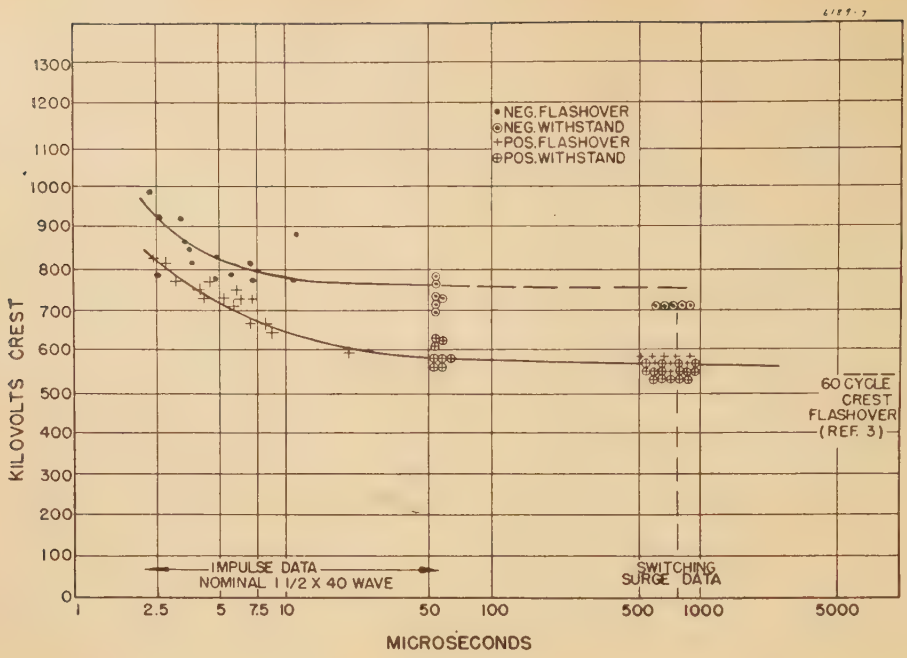

Figure 7. Switching-surge and impulse characteristics of 3-unit apparatus insulator assembly

Relative air density = 1.00
Absolute humidity (grains per cubic foot):
Switching data, 6.8
Impulse data, 7.1

bank on a 60-cycle system. The significance of these tests is borne out even more emphatically by the fact that the switching surges produced are comparable in magnitude and duration to the values recorded on power systems.

In the arrangement of Figure 2, the magnitude of the voltage developed at the apparatus tested A is controlled by the charging voltage applied to the capacitor bank C_s. The procedure in testing was as follows. At the start, the surge voltage would be well under the withstand value of the apparatus and then gradually would be raised, usually by 5-per-cent steps, either to the full withstand value or to critical flashover. All testing on large and small apparatus alike, both dry and wet, was outdoors in the yard adjacent to the laboratory (Figure 3). All measurement equipment is located in the laboratory. Measurements of the wave form and magnitude of the surge were effected by the recognized standard method which consists of the cathode-ray oscillograph in combination with a wire-wound resistance divider shown schematically in Figure 2. Some check tests were made between the resistance divider and a capacitance divider; these showed very close agreement in wave form between the two methods. To expedite the testing, frequently the voltage amplitude alone would be measured with a standard 200-centimeter sphere gap, using standard calibration data.[22] However, in the course of the investigation some check tests of the 200-centimeter sphere gap were made with the resistance-divider cathode-ray oscillograph method. The two methods of voltage measurement in most cases agreed within three or four per cent.

Test Data

Table I summarizes the switching-surge tests conducted in this investigation. Figures 6, 7, 8, and 9 present positive and negative switching-surge data respectively for a 6-unit suspension-insulator string, a 3-unit apparatus-insulator assembly, a standard 115-kv bushing, and and for a 1-inch oil spacing between a ball and plate. During the investigation, impulse tests were made on the apparatus using an identical setup; these results are presented in the curves for comparison purposes. In each case, the combined data serve to link the impulse and switching characteristics into a single volt–time curve.

In like manner, Tables II and III present data for 46-, 115-, 161-, and 230-kv bushings. Switching-surge data on standard rod gaps for 10-, 20-, and 40-inch spacings are reported in Table IV. No impulse tests were made on the rod gaps because data are generally available; the impulse data in the tabulation are standard reference values. The effect of dew formation and rain on switching-surge flashover of apparatus, such as in bushings and insulators, is apparent from the data in Tables II and V. Other tests of this character both on switching surge and impulse were conducted; these results are not readily conducive to tabulation and will be discussed in the following section. It will be noted that the data in these tables and figures are corrected to

Table I. Switching-Surge Tests Conducted on Station and Line Insulation

Insulation Tested	Type	Test Method	Typical Oscillograms	Polarity of Surges and Test Conditions: Positive	Polarity of Surges and Test Conditions: Negative	References and Comments
Bushing, 46-kv						
Without gap	Station	Figure 1	Figure 4	Dry and dew	Dry and dew	Tables II and III
With 15-inch gap	Station	Figure 1	Figure 4	Dry	Dry	Tables II and III
Bushing, 115-kv, without gap	Station	Figure 2	Figure 5	Wet and dry	Wet and dry	Tables III and V; Figure 8
Bushing, 161-kv, without gap	Station	Figure 2	Figure 5	Dry	Dry	Table III
Bushing, 230-kv, with 48 1/4-in. gap	Station	Figure 2	Figure 5	Dry	Dry	Table III
Suspension insulator, 6-unit string (10-in. diam × 5 3/4 in. spacing)	Station and line	Figure 2	Figure 5	Wet and dry	Dry	Figure 6 and Table V
Apparatus insulator, 3-unit assembly (17-in. diam × 14 1/2 in. spacing)	Station and line	Figure 2	Figure 5	Wet and dry	Dry	Figure 7 and Table V
Standard rod gap (air), 10-, 20-, and 40-in.	General	Figure 2	Figure 5	Dry	Dry	Table IV
Oil gap, 1 to 8 in. (6-in. diam bushing ball to tank)	General	Figure 2	Figure 5			Figure 9
Power transformer						
138-kv insulation class	Station	Reference 7	Reference 7			Subjected to more than 500 surges up to 530 kv
230-kv insulation class	Station	Figure 2	Figure 5			Subjected to more than 800 surges up to 900 kv

Table II. Critical Flashover of 46-Kv Bushing to Impulse and Switching Surges

Test Condition of Bushing	Impulse, Kv* (1½x40 Wave)		Switching Surge, Kv* (Figure 4)	
	Positive	Negative	Positive	Negative
Bushing with 15-in. gap	260	350	240	330
Bushing without gap	285	380	290	380
Bushing without gap, dew on porcelain**			290	360

* Relative air density = 1.00 (corrected). Humidity range = 5.3 to 7.1 grains per cubic foot.

** Air terminal of bushing chilled with dry ice, resulting in heavy frost with subsequent dew formation on porcelain.

unity air density, but no attempt has been made to correct for the standard humidity reference since correction factors are still uncertain. The humidity range during the test is indicated in each test.

In addition, switching-surge tests were made in this investigation on the 230-kv 2,500-kva transformer and on a 138-kv 1,000-kva transformer as reported in the previous investigation.[8] The extent of these tests is apparent from the last column in Table I. Likewise, impulse tests up to the respective levels were made on the transformers.

Discussion of Results

With the one exception in Table II, the test data in Tables II, III, and IV and in Figures 6, 7, and 8 correspond to apparatus that is dry and in a reasonably clean condition. Compared to the full-wave impulse strength, the data invariably show little or no reduction in insulation strength to switching surges. For instance, the difference is only five per cent for either the suspension-insulator string, or the apparatus-insulator assembly, and practically none for the 46- and 115-kv bushings. Although impulse tests were not conducted on the 161- and 230-kv bushing or on the rod gaps, a comparison can be made with reference to the available impulse data on this equipment. In this case, too, little or no difference is found between the switching-surge and impulse values.

The data for the dry tests indicate good consistency throughout. As expected, the data in Figures 6 and 7 show a perceptible polarity effect for the apparatus-insulator assembly and practically none for the suspension insulator string. The small polarity effect in the 115-kv bushing data (Figure 8) apparently indicates a similar electrode arrangement at line terminal and ground for the setup. Because of the pronounced dissymmetry which exists for the 46-kv bushing between line terminal and the large ground plate (see Figure 1), the polarity effect becomes particularly marked. From the foregoing, it can be stated that the positive switching-surge strength comprises the data of greater interest since in general the strength of the insulation is lowest for this polarity.

The 60-cycle dry flashover values in Figures 6, 7, and 8 are from design tests on identical equipment or from well-recognized reference data. They are presented here for comparison with the impulse and switching-surge data.

Wet test data on switching-surges for the 115-kv bushing, the apparatus-insulator assembly, and the suspension-insulator string are reported in Table V. In these tests, the rate of water precipitation was close to the standard reference value of 0.20-inch per minute, except for the suspension-insulator string which was 0.26-inch per minute. Compared to the dry flashover, the switching-surge wet flashover values for the precipitation indicated are 20, 8, and 15 per cent lower for the bushing, apparatus-insulator assembly, and suspension-insulator string, respectively. It might be noted that the resistivity of the water in these tests was less than one-half the standard. In these rain tests, it was observed further that the strength of the insulation would recover to the dry test value immediately upon removal of the water spray, even though the porcelain and other component parts still would be dripping wet. For instance, the positive critical flashover of the bushing rose from 450 to 590 kv the instant the water was shut off. Similarly, the insulator string increased in flashover from 460 to 530 kv. An attempt was made to establish test data for precipitations under 0.20-inch per minute, but because of a breeze blowing and lack of time the tests were not disposed entirely and therefore the results can be considered useful only as a guide. They do indicate, however, that for the more usual precipitation encountered, for example 0.10 inch per minute, the switching-surge strength of outdoor apparatus is unlikely to be affected by the rain more than five to ten per cent.

The findings noted on the dripping wet insulators and bushings just reported, correlate quite well with the results of tests conducted on the 46-kv bushing to determine the effect of heavy dew forma-

Table III. Critical Flashover of Power Apparatus Bushings to Switching Surges

Rating, Kv	Gap, In.	Switching Surge, Kv* Positive	Switching Surge, Kv* Negative
46	None	290	380
46	15	240	330
115	None	590	610
161	None	750	
230	48¼	760	**

* Relative air density = 1.00 (corrected). Humidity range = 5.3 to 7.6 grains per cubic foot.

** Maximum voltage applied to 230-kv bushing was 900 kv (negative), the limit of the switching-surge generator.

Figure 8. Switching-surge and impulse characteristics of standard 115-kv bushing

Relative air density = 1.00
Absolute humidity (grains per cubic foot):
Switching data, 5.3 to 5.5
Impulse data, 6.5 to 7.2

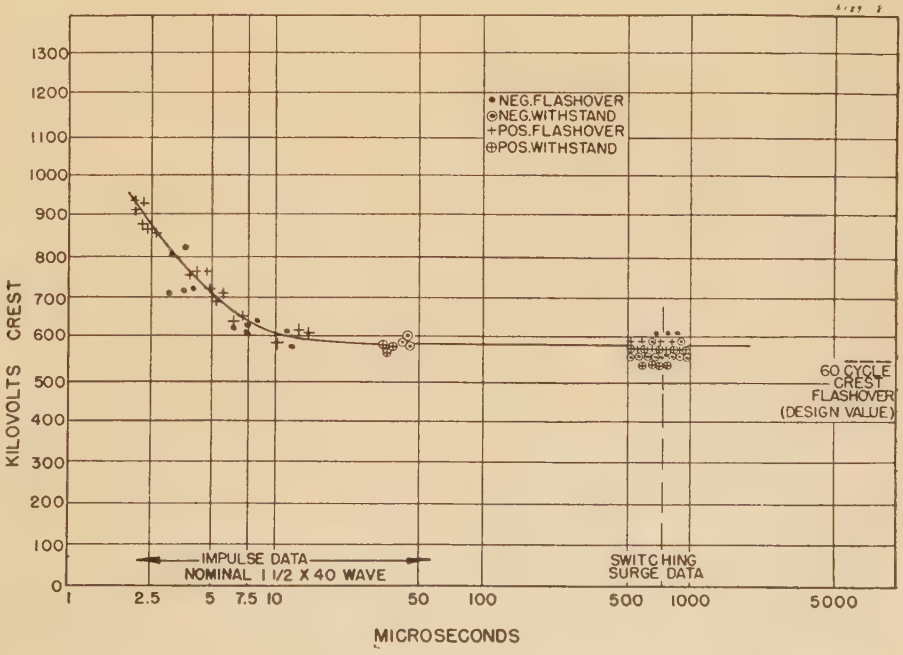

Table IV. Comparative Critical Flashover of Standard Rod Gaps to Impulse and Switching Surges*

Gap Spacing, In.	Impulse, Kv ($1^1/_2$x40 μ sec Wave)		Switching Surge, Kv (Figure 5)	
	Positive	Negative	Positive	Negative
10	190	225	175	225
20	350		330	
40	645		655	

* Switching-surge data are from this investigation. Relative air density = 1.00 (corrected). Humidity range = 5.1 to 6.9 grains per cubic foot. Impulse values taken from American Standard C68.1.

tion, reported in Table II. The tests show that the switching-surge strength is practically unaffected by dew as compared to the strength when the bushing is dry. However, it should be noted carefully that insulation which operates in a heavily polluted atmosphere, or near the sea, or that which is subjected to heavy fogs following a long dry dusty season may be affected adversely. The effect of surface contamination on the flashover of insulation will be discussed in the next section.

For comparison purposes, wet impulse-test data also were secured on the 115-kv bushing, the apparatus-insulator assembly, and on the suspension-insulator string. Again, the bushing tests presented similar difficulties as mentioned previously because of a breeze affecting the direction of spray. Therefore, only the data on the remaining equipment are presented here. At an average water precipitation of 0.17 inch per minute, the critical full-wave positive flashover of the apparatus-insulator assembly and the suspension-insulator string is, respectively, 530 and 480 kv, compared to 590 and 570 kv in the dry state, a reduction of 10 and 15 per cent. It appears then that the reduction suffered by outdoor insulation when subjected to rain is no greater for switching surges than for impulses.

For comparison purposes typical data on the volt–time characteristics of pressboard and oil, taken from the previous investigation,[8] are reproduced in Figure 10. From these data it was concluded that the strength of pressboard and oil essentially is the same for switching surges as for impulse voltages at full wave. The test data on oil in this investigation, reported in Figure 9, fully support in a practical sense this conclusion though, to be exact, the strength for switching surges is about five per cent lower. It is well to note that the present tests correspond to a condition of more uniform stress at the electrodes (ball-to-plate) compared to the preceding tests (disk-to-plate), and in addition the tests are carried to higher voltages. The present tests therefore give support and general acceptance to the foregoing conclusion.

Though tests on oil and solid insulation provide a criterion with which to evaluate the internal strength of oil-immersed apparatus, actual tests on the complete apparatus when possible are even more conclusive in this respect. The switching-surge tests summarized at the bottom of Table I therefore have particular significance. The tests on the 138-kv power transformer were reported in the previous investigation. All told, this transformer received over 500 switching surges, some approaching the flashover of the bushing (530 kv). This transformer also had received successfully on various occasions, American Standards Association impulse tests corresponding to its insulation class as well as front-of-wave tests. In this investigation, the 230-kv power transformer being a part of the test circuit (Figure 2) received repeated switching surges which, according to the record, exceeded 800 applications. The bulk of these surges were between 500 to 750 kv, a small number from 750 to 850 kv, and a few approached 900 kv, the limit of the switching-surge generator. Previous to and during this investigation, this transformer also received successfully American Standards Association impulse tests at full 230-kv level as well as front-of-wave tests up to 1,400 kv. Since 1939 this transformer has been part of the high voltage laboratory equipment and had been used extensively in the course of prior impulse and 60-cycle investigation as well as for the purpose of excitation in commercial impulse tests.

Table V. Wet Critical Flashover of Bushing and Station Insulators to Switching Surges*

Apparatus	Switching Surge, Kv Positive	Switching Surge, Kv Negative	Rate of Water Precipitation, In. Per Min
Bushing, 115-kv	450	495	0.23
	450		0.18, 0.18, 0.20
Apparatus insulator, 3-unit	525		0.22, 0.20, 0.18
Suspension insulator, 6-unit	460		0.25, 0.27, 0.28

* In these tests, relative air density = 1.00 (corrected) and water resistivity = 2,400 ohms per cubic inch. For corresponding dry critical flashover, refer to Figures 6, 7, and 8.

Strength of Insulation to Switching Surges

This and the previous investigation show that the switching-surge strength of insulation does not differ appreciably from the impulse strength. For example, in the directly comparative data for bushings and other high voltage insulation in air (Figures 6, 7, and 8), the switching-surge strength, in no instance, is less than 95 per cent of the impulse. Likewise, the internal strength of oil-immersed apparatus is nearly as high on switching surge as on impulse tests. In this connection, it is well to point out that stresses in the winding proper are likely to be distributed much more uniformly for switching surges. The foregoing conclusions are based on switching surges of long duration as in Figures 4 and 5. Furthermore, they apply for conditions referred to in standards as "usual." The switching-surge strength of equipment, otherwise conforming to usual conditions, is not affected by rain or dew to a greater degree than the impulse. This investigation thus establishes that the strength of station and line apparatus to switching surges in

Table VI. Comparative Data on Critical Flashover of Insulators (For Source of Data See Reference 10)

Apparatus Tested			Critical Flashover on Positive Polarity in Per Cent of Dry Flashover of 1x50 μsec Wave		
Description	50-Cycle Flashover, Kv RMS	Condition*	1x50 μsec	1x1,000 μsec	One-Half Cycle Wave of 5,500 μ Sec Duration Above One-Half Amplitude
Bushing	102	Dry	100	97	97
		Dew	98	90	80
		Rain	80	79	76
Insulator assembly, 2-unit pillar type (11-in. diam)	224	Dry	100	96	96
		Dew	92	86	84
		Rain	99	89	76
Suspension insulator string, 4-unit (10-in. diam)	227	Dry	100	99	97
		Dew	93	93	82
		Rain	85	76	72

* Insulators clean. Water precipitation (rain) = 0.12 inch per minute. Water resistivity (rain and dew) = 4,000 ohms per cubic inch. Dew applied with vaporizer.

most cases is as high as 90 to 95 per cent of the impulse strength.

Important studies on the flashover voltage of insulators in air in the range intermediate between impulse and operating frequency have been reported by W. Wanger and his associates.[10,11] The insulators tested differ from similar equipment of United States design, and the wave form of the voltages in the two investigations also differ. Consequently, it is not possible to compare the results of

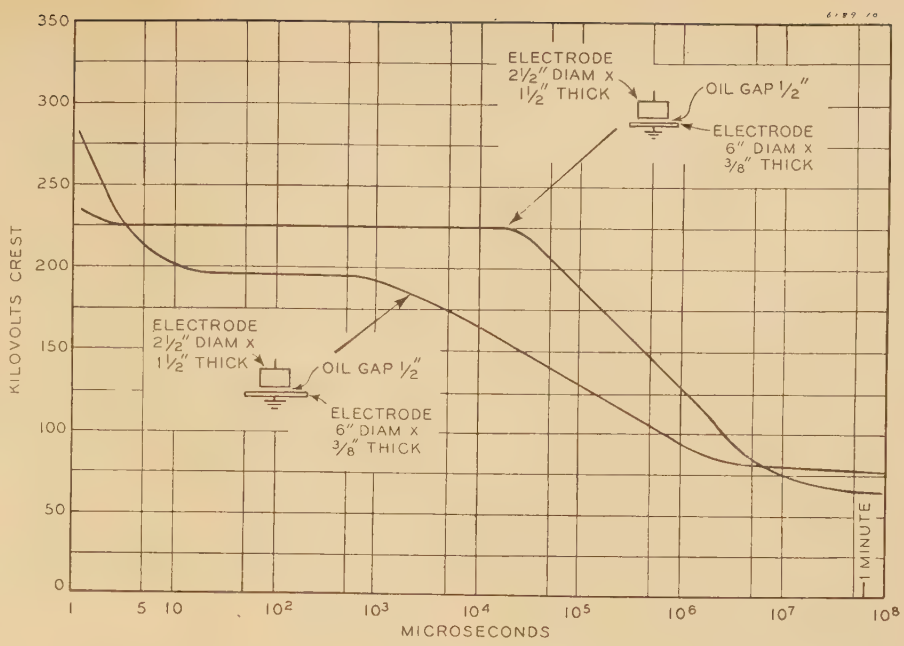

Figure 10 (right). Volt–time breakdown curves for transformer oil and oil-impregnated pressboard in oil (reference 7)

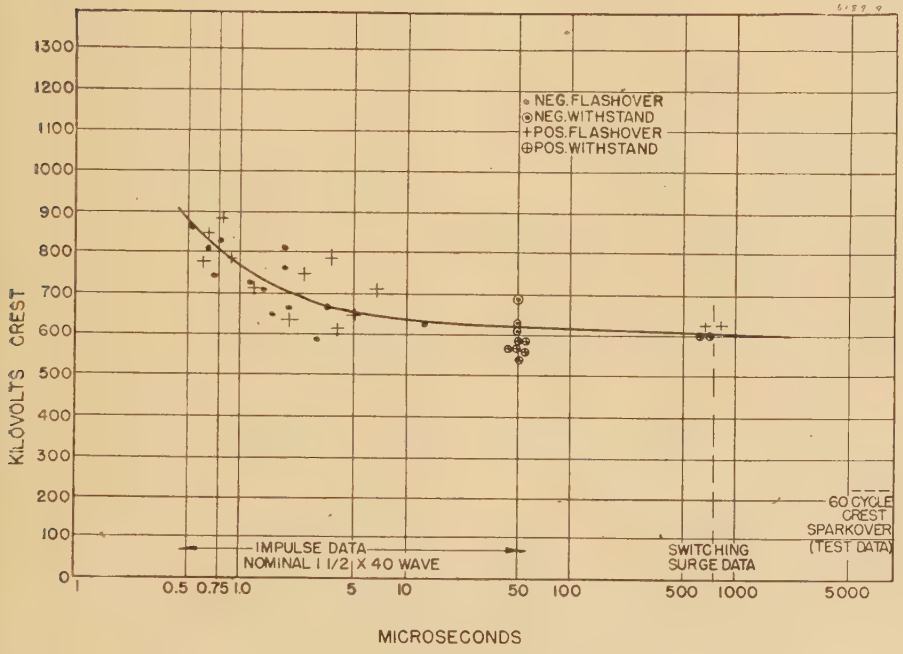

Figure 9 (below). Switching-surge and impulse characteristics of 1-inch oil gap from 6-inch-diameter bushing ball of 161-kv bushing to tank wall

the foregoing contributions directly with the data in this paper. However, the data in Table VI are of interest as they provide a general comparison regarding the effect of wave form, rain, and dew on insulator flashover. The tabulation is in reasonably good agreement with the relationship established in this investigation. The research by Wanger also contributes useful data on the effect of various voltages on insulator flashover resulting from heavy contamination of the surface with soot coating, salt, and cement dust in combination with rain and dew. Under these unusual conditions, it is well-known from operating experience that the strength of insulators is reduced materially. According to his tests, in general, a pronounced reduction begins to take place for voltages of duration beyond approximately 1,000 microseconds. When unusual conditions as these prevail, the practice is to clean the insulators at frequent intervals or, in case such measures are not feasible, to provide insulation specifically to meet these conditions.

As the duration of the voltage applied is extended into the range from one-tenth to one second, the characteristics of the insulation approach more and more the low frequency test values. For overvoltages of such long duration (as might develop on systems with the neutral isolated, on hydro systems, from accidental contacts between high and low voltage lines, and so forth), the performance of insulation should be assessed more with reference to the low frequency test data as well as the rating of the apparatus for continuous voltage operation.

Conclusions

1. The switching-surge strength of station and line insulation, in most cases, is 90 to 95 per cent of the corresponding impulse value.

2. For insulation in air and conforming to usual conditions, the switching-surge strength is not affected by rain or dew to a greater degree than impulse.

3. Additional studies on the effect of unusual conditions upon the strength of insulation in air appear desirable, particularly at short and medium 60-cycle durations and for sustained operation.

4. The fundamental data presented here should be conducive to a more effective utilization of insulation.

References

1. Basic Impulse Insulation Levels, **Philip Sporn, C. A. Powel.** AIEE Transactions, volume 59, 1940, October section, pages 596–8.

2. Rationalization of Transmission-System Insulation Strength—III, **Philip Sporn, I. W. Gross.** AIEE Transactions, volume 59, 1940, October section, pages 591–5.

3. Coordination and Protection of Station Insulation Against Lightning, **P. L. Bellaschi.** International Conference on Large Electric High-Voltage Systems (CIGRE), Paris, France, 1939, report 317.

4. Progress in Power-Transformer Insulation and Protection, **P. L. Bellaschi.** International Conference on Large Electric High-Voltage Systems (CIGRE), Paris, France, 1946.

5. The Co-ordination of Electrical Equipment With Basic Insulation Levels, **J. H. Foote, J. R. North.** AIEE Transactions, volume 59, 1940, October section, pages 585–9.

6. Application of Spill Gaps and Selection of Insulation Levels, **H. L. Melvin, R. E. Pierce.** AIEE Transactions, volume 56, 1937, June section, pages 689–94.

7. Insulation Coordination, **A. C. Monteith.**

Comparisons of Railway Motive Power for Operations in the Pacific Northwest

T. M. C. MARTIN
ASSOCIATE AIEE

RECIPROCATING steam, Diesel-electric, and electric locomotives compete today for the main-line freight and passenger assignments of Pacific Northwest railways. It is doubtful if the present struggle for dominance among the three will be influenced greatly by other types of locomotives. Reciprocating steam locomotives have occupied a position of leadership here as elsewhere in the United States since the coming of the railroad, but it is apparent that their days of unchallenged leadership are over. On the basis of physical ability to perform present and prospective tasks as well as on the basis of operating economy, steam locomotives face strong competition from Diesel-electric and electric motive power.

There have been other times when competition for steam locomotives appeared about to materialize, but each time something intervened to remove the immediate threat to their leadership. Between 30 and 40 years ago it was predicted freely that electrification was coming into recognition. Several things happened. World War I was fought and labor and materials that might have been invested in a great network of electrified railroads was used for other things. The natural advocates of electrification failed to agree among themselves on the question of what kind of a system of electrification should be encouraged. Fundamental objectives were lost sight of in the more heated than enlightened debates over the merits of alternating versus direct current. Enough uncertainty was cultivated in the minds of already steam-minded railroad officials to cause indefinite postponement of most electrification plans.

Paper 46-186, recommended by the AIEE committee on land transportation for presentation at the AIEE Pacific Coast meeting, Seattle, Wash., August 27–30, 1946. Manuscript submitted June 21, 1946; made available for printing July 15, 1946.

T. M. C. Martin is an electrical engineer with the Bonneville Power Administration, Portland, Oreg.

Diesel-Electric Progress

It is only a little more than ten years ago that Diesel-electric passenger locomotives first appeared in main-line service. They came with the early streamliners and to many casual travelers the words streamliner and Diesel are synonymous. It is likewise only about five years ago that the first of the so-called 5,400-horsepower 4-cab Diesel-electric main-line freight locomotives was delivered. Diesel-electric switching locomotives were in use quite a few years before either of the main-line classes, but the history of all three can be studied fairly well by going no further back than 1929. Table I is a summary of locomotive orders during the past 17 years.

Prior to the depression very few Diesel locomotives were ordered; the steam locomotive has as yet no important competition. By 1937 the Diesel was approaching equality with steam in the competition for new orders, and commencing in 1938 it assumed a leadership which has not been relinquished. Figure 1 illustrates graphically the struggle between the two from 1929 to 1946. Although the Diesel remained a poor competitor until 1940, it took but two years for it to overhaul and then exceed the cumulative lead of the steam locomotive established over the preceding decade. This is quite an

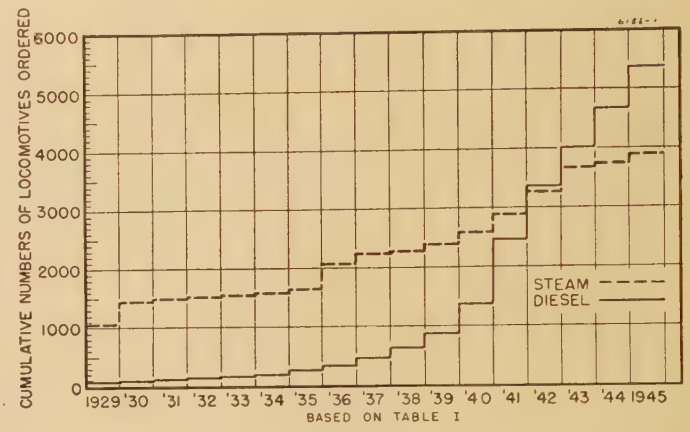

Figure 1. Cumulative trend of orders for new steam and Diesel locomotives from 1929 to 1945 inclusive

H. R. Vaughan. *Electrical Transmission and Distribution Reference Book*, Westinghouse Electric Corporation, chapter 14.

8. Dielectric Strength of Transformer Insulation, P. L. Bellaschi, W. L. Teague. AIEE Transactions, volume 56, 1937, January section, pages 164–71.

9. Breakdown Curve for Solid Insulation, V. M. Montsinger. AIEE Transactions, volume 54, 1935, December section, pages 1300–01.

10. The Flashover Voltage of Dirty and Wet Insulators When Subjected to Impulses of Varying Duration, W. Wanger. International Conference on Large Electric High-Voltage Systems (CIGRE), Paris, France, 1939, report 209.

11. Flashover Voltage of Insulators and Spark Gaps in the Intermediate Range Between Impulse-Voltage Testing and Voltage Testing at Operating Frequency, W. Wanger, W. Huber. *Brown Boveri Review* (Baden, Switzerland), volume 27, December 1940.

12. An Eight-Year Investigation of Lightning Currents and Preventive Lightning Protection on a Transmission System, E. Hansson, S. K. Waldorf. AIEE Transactions, volume 63, 1944, May section, pages 251–8.

13. Symposium on Operation of the Boulder Dam Transmission Line—Insulation and Lightning Protection, Bradley Cozzens. AIEE Transactions, volume 58, 1939, April section, pages 140–6.

14. Transient Recovery-Voltage Characteristics of Electric-Power Systems, H. P. St. Clair, J. A. Adams. AIEE Transactions, volume 61, 1942, September section, pages 666–9.

15. Transient Recovery Voltages and Circuit-Breaker Performance, R. C. Van Sickle. AIEE Transactions, volume 61, 1942, November section, pages 804–13.

16. Power-System Transients Caused by Switching and Faults, R. D. Evans, A. C. Monteith, R. L. Witzke. AIEE Transactions, volume 58, 1939, August section, pages 386–94.

17. Power-System Voltage-Recovery Characteristics, Harold A. Peterson. AIEE Transactions, volume 58, 1939, August section, pages 405–11.

18. Survey of High-Capacity Testing Stations for Alternating-Current Tests on Circuit Breakers, E. Juillard. International Conference on Large Electric High-Voltage Systems (CIGRE), Paris, France, 1939, report 136.

19. Surges on Chicago 12-Kv System, F. O. Wollaston, H. J. Plumley. AIEE Transactions, volume 60, 1941, June section, pages 260–5.

20. Traveling Waves Initiated by Switching, L. V. Bewley. AIEE Transactions, volume 58, 1939, January section, pages 18–26.

21. Discussion by T. J. Carpenter of Traveling Waves Initiated by Switching, AIEE Transactions, volume 58, 1939, January section, page 26.

22. Standard for Measurement of Test Voltage in Dielectric Tests. American Standard C68.1, March 1943.

accomplishment when it is remembered that during the greater part of these 17 years the available Diesel units were confined to switching and high-speed passenger types. Not until 1942 were road service freight units generally available. The fact is that main-line types are still relative newcomers to motive-power rosters, and the major statistical gains have been achieved by switching units. It is clear that the reciprocating steam engine has yielded to the Diesel in the field of switching service. For several years the orders for steam locomotives have included few or none of the switching type, whereas Diesel orders have run strongly to switching units. In 1945, for example, of the 148 steam locomotives ordered only 3 or about 2.0 per cent were switchers, while 478 or about 68.0 per cent of the 702 Diesels ordered were switching units.

Technical and economic factors that have enabled Diesel switching units to cause obsolescence among parallel steam types are operative in the field of main-line motive power and therefore warrant brief recital.

1. Diesel-electric units are able to motorize all their weight and hence produce relatively much greater tractive effort or hauling ability than otherwise comparable steam units.

2. With no fires to clean, ashes to dump, boilers to wash, and with less lost time for assorted other reasons, Diesels have demonstrated a higher degree of availability and reliability.

3. Diesel-electric switching units have demonstrated that they can replace steam switchers and almost invariably do a better job cheaper.

Savings are realized chiefly in the items of fuel and running repairs. It has been established that Diesel units can cut repair costs in half and reduce fuel expense by two-thirds when they replace steam. Recent studies reported by the Committee on Railway Location and Operation of the American Railway Engineering Association under the chairmanship of L. K. Sillcox[1] suggest that savings of from one to two dollars per yard-locomotive-hour are common where Diesels replace steam locomotives. Since in yard service less total investment frequently is required for a pool of Diesel switching locomotives it can be seen that there are many situations where continued steam operations are plainly uneconomic.

Table I. Locomotives Ordered for Domestic Use, 1929–1945[7]

Year	Steam	Diesel	Electric	Total
1929	1,055	80	95	1,230
1930	382	18	21	421
1931	62	21	91	174
1932	5	7		12
1933	17	25		42
1934	72	37	76	185
1935	30	60	7	97
1936	435	77	24	536
1937	173	145	36	354
1938	36	160	29	225
1939	119	249	32	400
1940	207	492	13	712
1941	302	1,104	38	1,444
1942	363	894	12	1,269
1943	413	635		1,048
1944	74	680	3	757
1945	148	702	6	859

Note: United States Government purchases excluded for years 1942–1944.

Table II. Principal Weights, Dimensions, and Proportions of the Steam Locomotive Used for Comparative Purposes

Class of Locomotive—4-6-6-4 Single Expansion, Articulated

Weights in working order, pounds:	
On drivers	404,000
On front truck	101,000
On trailing truck	122,000
Total engine	627,000
Tender fully loaded	437,000
Engine and tender fully loaded	1,064,000
Weights of supplies carried, pounds:	
25,000 gallons water	208,000
28 tons coal	56,000
Lengths:	
Driving wheel base	12 feet 2 inches
Total engine wheel base	60 feet 4.5 inches
Engine and tender wheel base	106 feet 8 inches
Engine and tender, coupler to coupler	119 feet
Driving wheel diameter, inches	69
Boiler and firebox details:	
Steam pressure, pounds per square inch	280
Length of combustion chamber, inches	106
Length over tube sheets, inches	240
Grate area, square feet	132.2
Direct heating surface, firebox and combustion chamber, square feet	500
Circulators (5-security), square feet	81
Total direct, square feet	581
Indirect (tubes and flues), square feet	4,214
Superheater (Elesco type E), square feet	2,162
Total evaporative and superheater, square feet	6,957
Cylinders:	
Number	4
Diameter, inches	21
Stroke, inches	32
Rated tractive force of engine at 24.1 per cent adhesion, pounds	97,350
Ratios, per cent:	
Weight on drivers to engine weight	64.4
Weight on drivers to total weight (engine and tender fully loaded)	38.0

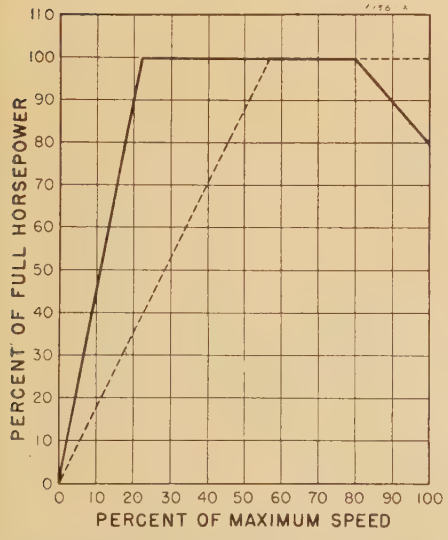

Figure 2. Percentage of full horsepower available at various percentages of maximum speeds in motor-generator and a-c series motor type locomotives

——— Motor-generator locomotives
- - - - - A-c series motor locomotives

Electrification Affected by Trend Toward Diesel

Paradoxically the trend toward Diesel-electric switching units has advanced the cause of main-line electrification. Prior to the advent of the Diesels, it was necessary to erect a great deal of trolley before a railroad could achieve full benefits from electrification. Unless electric locomotives could operate over a relatively large mileage of industrial and classification yard trackage some other kind of motive power was necessary. The capital cost of providing relatively little-used trolley facilities was excessive, and yet if both steam and electric motive power were to be required at many intermediate and all principal terminals many of the important arguments for main-line electrification were weakened. If main-line movements only were to be handled electrically, leaving yard movements to be made with steam, the opportunities for smoke abatement would be reduced seriously. Since steam and electric locomotives differ markedly in certain types of repair and service facilities many of the best opportunities for savings in operating expenses would be lost.

Development of Diesel-electric switching power has improved the basis for main-line electrification. It no longer is considered proper, much less necessary, to erect trolley over any track not clearly essential to the operation of main-line trains. Operations over other trackage are within the recognized sphere of the Diesel switching unit. A Diesel-electric locomotive is related more closely to an electric locomotive than either of them is

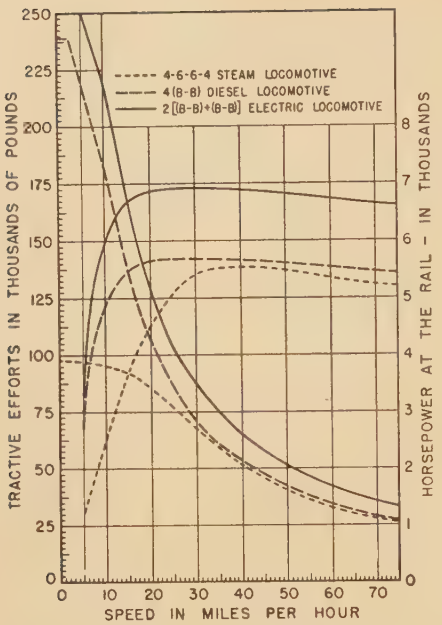

Figure 3. Tractive effort and horsepower at the rail versus speed; steam, Diesel, and electric locomotives chosen for comparison

to a steam locomotive, and joint use of many kinds of facilities and maintenance staffs is entirely practicable. A railroad company contemplating main-line electrification with a corollary use of Diesel power for yard service now can look forward to complete elimination of facilities such as coal and ash handling equipment, water service treating plants, tanks, penstocks, boiler washing facilities, turntables, and much heavy shop equipment largely useful in repairing steam locomotives. Modern Diesel and electric locomotives can utilize similar electrical maintenance facilities. Maintenance of Diesel prime movers will require specialized equipment, but the over-all shop layout is simplified and cleaned up when steam units are withdrawn. A combination of electrification and dieselization offers the next best thing to complete electrification in the reduction of smoke and fumes.

Fundamental Differences in Motive Power

Comparisons of motive power are not easy to make and will not prove satisfying or acceptable to everyone. Physical comparisons are complicated and produce differences of opinion which are not lessened when the subject is extended to include economic phases of motive power utilization.

A steam locomotive and a Diesel locomotive can be compared without too much trouble. The electric locomotive causes most of the difficulties when comparisons are attempted. This is because both steam and Diesel locomotives are so-called independent units, requiring only coal or oil to burn and track to run on to ready them for service. The electric locomotive is a dependent unit and in addition to track requires suitable central station, transmission, and trolley facilities to generate and bring electric energy to its pantographs. Except for the location of the primary source of energy, modern Diesel road locomotives and modern electric locomotives are quite similar. Both of them are in reality electric locomotives. In fact, motor-generator type electric locomotives closely resemble late model Diesel-electric road units in many important respects. One leading manufacturer is using the same type of d-c traction motors on both locomotives. The d-c generators of the two locomotives also are not too different. The chief difference in the machines lies in the means of driving these generators. Generators on Diesel locomotives are connected directly to the Diesel engines, whereas on motor-generator locomotives they are connected directly to synchronous motors which receive their energy from a relatively high voltage a-c trolley.

Basic Factors Governing Comparisons

Railroads in the Pacific Northwest are comparatively long thin lines of relatively low traffic density. A large part of all mileage is single-tracked, heavy grades are commonplace, and there is a substantial amount of horizontal curvature. In all of this region there is very little of what rightfully could be called high speed track. High speed track here is track that will permit 75.0 miles per hour with safety and comfort, and there are not too many opportunities for sustained running at that speed. Another characteristic of importance is the fact that the roads in this region are predominately used as freight carriers. This is a further reason why extremely high speeds are neither necessary nor desirable, and it is a circumstance that suggests the wisdom of choosing a kind of motive power that will deliver high tractive efforts at reasonable speeds rather than offer large horsepower outputs at speeds which are seldom attainable under actual operating conditions.

Table III. Principal Weights, Dimensions and Proportions of Diesel-Electric Locomotive Used for Comparative Purposes

Class of Locomotive—4 (*B-B*)

Weights in working order, pounds:*	
On drivers	954,000
Total locomotive fully loaded	954,000
Supplies carried and weights, pounds:	
4,800 gallons Diesel oil	36,000
3,200 gallons water	26,700
580 gallons lubricating oil	4,000
76 cubic feet sand	7,600
Lengths, feet:	
Driving wheel base	9.0
Total coupler to coupler	193.0
Diameter driving wheels, inches	40
Engine: four 16-cylinder V-type 2-cycle, rated 1,500 horsepower each	
Generator: four nominal 600-volt direct current, single bearing direct-connected to engine crankshaft	
Traction motors: 16 d-c roller bearing truck-mounted	
Gear ratio	3.53/1.00
Rated tractive force of locomotive at 25 per cent adhesion, pounds	238,500
Minimum speed (at continuous output), miles per hour	17.0
Maximum speed, miles per hour	75.0
Ratio of weight on drivers to total locomotive weight, per cent	100.0

* Electric brakes and train heating equipment included.

It is necessary to limit the scope of the comparisons to be made, and it is believed that this can be accomplished best by considering but a single locomotive from each of the classes. This imposes a considerable burden upon anyone who chooses the particular locomotives to represent each of the classes. It is obvious that the one who picks the locomotives and selects the bases of comparison can in some measure determine the outcome. Unfortunately subjective influences cannot be cancelled out entirely, and the only practical course is to strive for as much objectivity as possible.

There are a few general principles that guided the choice of locomotives for this particular comparison.

1. The units selected should be up to date—typical of the latest and best practice of the builder's art in each case.

2. The locomotives chosen should be capable of interchangeable passenger or freight service. This factor is of controlling importance in the selection of the steam locomotive only, since either the Diesel or the electric easily can meet this requirement.

3. The size of the respective units should be reasonably comparable. Both the Diesel and the electric types can be controlled in multiple units, and hence it would be possible to group so many cabs under the control of one crew that comparisons with a single steam locomotive would be quite unfair.

Motive Power Terminology

Tractive effort and horsepower at the rail are the fundamental characteristics that determine almost everything else. Tractive effort is merely the force produced by the torque of the locomotive driving wheels. It is exerted tangentially

to the driving wheels and is limited by the torque and by the adhesion factor existing between wheel and rail.

In general

$$\text{Power} = \frac{\text{force} \times \text{distance}}{\text{time}}$$

or

$$\text{Power} = \text{force} \times \text{velocity}$$

If tractive effort is substituted for force and everything is expressed in proper units an expression defining rail horsepower can be obtained.

Let

V = speed in miles per hour
RHP = rail horsepower
TE = tractive effort in pounds

Then

$$RHP = TE \times V \times \frac{5{,}280}{33{,}000 \times 60}$$

$$RHP = TE \times \frac{V}{375} \quad (1)$$

$$TE = \frac{375}{V} \times RHP \quad (2)$$

On western mountain grades it is customary to consider only the continuous rail horsepower of locomotives having electric traction motors. The Association of American Railroads in their 1930 recommendations regarding traction motor ratings specified that the 1-hour output be determined with the motors starting "cold" (the ambient temperature). The temperature rises permitted vary with the class of insulation but are only 15 degrees centigrade higher for the 1-hour than for the continuous ratings. It is clear therefore that the hour ratings might be useful in flat country but in a mountainous region traction motors are worked at or near their continuous rating most of the time leaving little likelihood of using short-time ratings except at the start of engine runs. Even downgrade operation affords no relief since regenerative braking produces temperature rises of the same order of magnitude as does motoring. Steam locomotives present no problem of traction motor limitations, and hence for any given speed whatever rail horsepower is available will be continuously available.

Other terms used rather freely are defined in the following paragraphs.

Drawbar Pull

Drawbar pull is the force (either push or pull) which is exerted at the drawbar or coupler of the locomotive. It is produced by the movement of the locomotive and is equal to the tractive effort diminished by the tractive resistance of the locomotive considered as a car. Being dependent upon tractive effort it is limited also by the adhesion factor. Thus, for example, when for any reason a locomotive's drivers slip, its drawbar pull instantly and drastically is reduced. The only function of a locomotive is to create drawbar pull which can be applied to a train of cars and cause them to be accelerated into motion.

Adhesive Weight

That part of the total weight of a locomotive which is carried on the drivers is described as adhesive. In the case of a steam locomotive it is always less than the total weight of the locomotive. In electric and Diesel locomotives, it may or may not be equal to the total weight depending upon whether or not there are unpowered axles.

Adhesion Factor

The adhesion factor is the ratio between the adhesive weight of a locomotive and the maximum tractive effort that can be exerted without slipping the drivers. This ratio is dependent for the most part upon the coefficient of friction between wheel and rail which is in turn largely dependent upon the condition of the rail. It usually is stated in reverse order or as the maximum percentage of the weight on drivers that can be utilized as tractive effort under varying rail conditions. This ratio varies with speed, is a maximum at starting, and drops rapidly to a value which is maintained fairly well throughout the practical speed range of a locomotive. Generally accepted values at starting are as follows:[2]

1. Clean dry well-sanded rail and rolled steel wheels—30 per cent.
2. The same conditions and cast-iron wheels—25 per cent.
3. Clean dry rail with either kind of wheels—20 per cent.
4. Wet greasy rail—15 per cent.

Running adhesions are considerably less. Most authorities agree that 16 or 18 per cent is all that ought to be assumed in rating locomotives. Higher running adhesions are possible under ideal rail conditions and liberal sanding but should not be relied upon.

Table IV. Principal Weights, Dimensions, and Proportions of Straight Electric Motor-Generator Type Locomotive Used for Comparative Purposes

Class of Locomotive—2 [(B-B)+(B-B)]

Weights in working order, pounds:*	
On drivers	1,034,000
Total locomotive fully loaded	1,034,000
Supplies carried and weights, pounds:	
2,400 gallons water	20,000
1,000 gallons fuel oil	7,000
Lengths, feet:	
Driving wheel base	8.5
Coupler to coupler	148.0
Motor-generator sets, number	2
Traction motors, number	16
Gear ratio	3.75/1.00
Rated tractive forces of locomotive at 25 per cent adhesion, pounds	258,500
Minimum speed (at continuous output), miles per hour	17.0
Maximum speed, miles per hour	75.0
Diameter of driving wheels, inches	42
Ratio of weight on drivers to total locomotive weight, per cent	100.0

* Train heating equipment included.

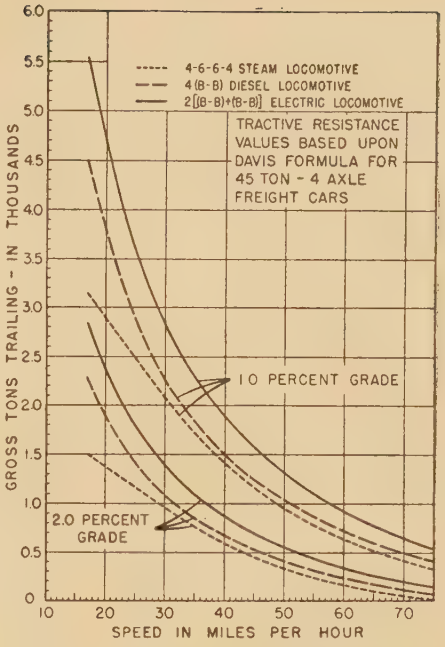

Figure 4. Gross tons trailing versus speed for 1.0- and 2.0-per-cent grades, steam, Diesel, and electric locomotives chosen for comparison

Tractive Resistance

Tractive resistance is the sum total of the forces which oppose motion in both the train and locomotive. It is made up of several different components which are caused respectively by

1(a). Journal resistance.
1(b). Flange resistance.
1(c). Air resistance.
2. Grade resistance.
3. Curve resistance.
4. Acceleration.

The first three are usually grouped and called net resistance on straight level track at uniform speed in still air. The latter has been measured empirically by many investigators and curves based upon the work of one of the most widely ac-

cepted authorities have been used in these comparisons.[3]

Grade Resistance

Grade resistance is the component of force required to lift a train up a rising gradient. Where the gradient is expressed in terms of percentage rise (or feet per hundred) and train weights are expressed in tons, grade resistance is equal to 20 pounds per ton per one per cent of grade. Obviously grade resistance may be either additive or subtractive depending upon whether movement is against or with the grade.

Table V. Maximum Loadings and Speeds With Steam, Diesel, and Electric Motive Power

	Steam	Diesel	Electric
Maximum gross tons trailing at 17.0 miles per hour*			
Level track	5,625**	5,625**	5,625**
1.0 per cent	3,140	4,510	5,550
1.5 per cent	2,090	3,080	3,810
2.0 per cent	1,500	2,280	2,850
Maximum speeds of freight trains, miles per hour*			
1,500 gross tons trailing*			
Level track	75.0	75.0	75.0
1.0 per cent grade	38.5	40.5	46.5
1.5 per cent grade	27.0	30.0	35.5
2.0 per cent grade	17.0	23.5	28.0
2,280 gross tons trailing*			
Level track	65.0	68.0	75.0
1.0 per cent grade	27.5	30.0	35.0
1.5 per cent grade	‡	21.5	26.0
2.0 per cent grade	‡	17.0	20.5
2,850 gross tons trailing*			
Level track	60.0	62.0	68.0
1.0 per cent grade	21.0	25.0	30.0
1.5 per cent grade	‡	18.0	21.5
2.0 per cent grade	‡	‡	17.0
Maximum speeds of passenger trains, miles per hour*			
1,200 gross tons trailing†			
Level track	75.0	75.0	75.0
1.0 per cent grade	44.0	46.0	53.0
1.5 per cent grade	33.0	35.0	41.0
2.0 per cent grade	24.0	28.0	33.0

* Resistance for 45-ton 4-axle freight cars. Speed is the minimum permissible for continuous operation at maximum rail horsepower output.

** Limited by train length to 125 45-ton cars.

† This train could be composed of 16 75-ton standard weight cars, 20 60-ton lightweight cars, or various combinations. The speeds shown for passenger trains are somewhat conservative since freight train car resistance was used in their calculation.

‡ Overloaded.

Curve Resistance

Where the gradient is constant there is an increase in resistance going around a curve which is roughly proportional to the degrees of curvature. Curve resistance also has been the subject of many empirical investigations. Western roads generally employ a figure of about 0.7 pound per ton per degree of curvature.

Compensated Grade

If mountain railroads were to have uniform gradients, operation over them would be very difficult since the element of curve resistance would introduce a persistent variable into the equation of total tractive resistance. Western railroads have found it better to plan their vertical and horizontal alignments so that, over a given section, the summation of the components of grade and curve resistance will be constant. Practically this is done by fixing a uniform average gradient of say 2.2 per cent for a section of track and then reducing this grade around all curves by an amount which for most trains nearly will balance the extra resistance imposed by the curve. If curve resistance is taken at 0.7 pound per ton per degree, since grade resistance per ton per cent is equal to 20 pounds, the equivalent grade reduction on a 6.0-degree curve would be $\frac{0.7\times6.0}{20}=0.21$.

The greatest advantage of employing compensated gradients is in safer, steadier operation, but it offers a further advantage to railroad students. They can forget all about curve resistance in their calculations—it has been "compensated," and the net resistance caused by both grade and curve is as though it were all concentrated in the grade. One further thing needs to be noted regarding compensated grades and that is their directional limitations. The grade can be compensated in one direction only. It is the practice to compensate the grade for upgrade movement. It necessarily follows that on down-grade movements there will be some slowing effect on curves because curve resistance is now subtractive from the component caused by grade.

Resistance to Acceleration

The resistances previously mentioned apply to movement without acceleration. A force is required to accelerate a mass and the amount of acceleration produced will be roughly proportional to the magnitude of the force and inversely proportional to the mass, $F=ma$.

In railroading the forces resisting acceleration are not computed easily. It is usually the practice to add all other resistances together and subtract their sum from the total tractive effort available at any given speed (it is different for each speed), and the remainder is the force available for acceleration. Thus by an integration process the time–distance relationships involved in acceleration are calculable.

Table VI. Evaluation of Physical Characteristics and Hauling Abilities of Steam, Diesel, and Electric Motive Power Units Selected for Comparison

	Steam	Diesel	Electric
1. Total weight of locomotive fully loaded, tons*	532	477	517
2. Total length of locomotive and tender, feet*	119	193	148
3. Rail horsepower continuously available at 17.0 miles per hour**	4,098	5,582	6,800
4. Pounds per horsepower [(line 1×2,000)/(line 3)]	260	171	152
Index, electric = 100	171	112	100
5. Feet per 1,000 horsepower [(line 2×1,000)/(line 3)]	29.0	34.6	21.8
Index, electric = 100	133	159	100
6. Maximum gross tons trailing on 1.0 per cent grade†	3,140	4,510	5,550
7. Maximum gross tons trailing on 2.0 per cent grade†	1,500	2,280	2,850
8. Hauling efficiency on 1.0 per cent grade, gross tons trailed per ton of locomotive (line 6/line 1); index, steam = 100	5.9 100	9.45 160	10.74 182
9. Hauling efficiency on 2.0 per cent grade, gross tons trailed per ton of locomotive (line 7/line 1)	2.82	4.78	5.51
Index, steam = 100	100	170	195

* From Tables II, III, and IV.
** From Figure 3.
† From Figure 4 and Table V.

Minimum and Maximum Speeds—Gearing

Electric-traction-motor locomotives require two speed limitations in connection with their ratings—a maximum and a minimum. The upper limit is absolute and is fixed by the banding of traction motor armatures. The lower limit is not absolute but depends upon the load being drawn. The series motors commonly used for traction purposes have the characteristic of increasing torque as speed drops. But as speed drops, armature current and consequently temperature rises. When series motors are turning out their continuous horsepower rating there is a certain minimum speed that must not be violated. When speed falls to the critical value and excessive amperage beings to flow, the unit is overloaded and there is no alternative but to unload

the motors by reducing the trailing tonnage. Obviously, a railroad ordinarily does not dispatch trains on an experimental basis figuring that when they have stalled because of overloading they will set out excess tonnage and continue their runs. Each class of locomotive is rated; that is, it is assigned a maximum number of trailing tons that it will be permitted to depart with from a given terminal.

Locomotive Ratings

The rated tonnage of a locomotive is the maximum trailing load it can handle over its district. It is not based upon ideal conditions of weather, rail, or fuel, but upon average everyday experience with some allowance perhaps for even worse circumstances. Locomotive ratings are not equal over all districts of a railroad, but vary with what is known as the ruling grade of the particular district. The ruling grade is the maximum grade against which movement must be made save in rather exceptional cases where maximum grades are of such short duration and so located that momentum may be relied upon to assist trains over them. In this case the ruling grade will be the next heaviest grade. On all parts of a district having less than the ruling gradient a locomotive will be able to do either or some of both of two things.

1. Pull faster the same number of trailing tons it is rated for on the ruling grade.
2. Pull an increased number of tons at the same speed as on the ruling grade.

A railroad generally likes to load a train with respect to available motive power so that a reasonable mileage may be run without changing the loading. In general then the tendency will be to use the remaining power potential of a locomotive operating on less than the ruling grade in the production of more speed rather than in trying to add trailing tons. It is also clear that for this reason the determination of how much territory to include in a given locomotive district is very important. If a district is so chosen that the ruling grade, though heavy, is of short duration, and the remainder of the profile

Table VIII. Fuel and Energy Requirements and Equivalents

	Freight	Passenger	Total
Steam operations			
Pounds of coal per train	109,440	78,900	
Number of trains per day	11.4	6.0	17.4
Pounds of coal per day	1,247,616	473,400	1,721,016
Pounds of coal per year	455,379,840	172,791,000	628,170,840
Tons of coal per year	227,690	86,395	314,085
Diesel operations			
Gallons Diesel oil per train	2,476.8	1,542.0	
Number of trains per day	7.5	6.0	13.5
Gallons of Diesel oil per day	18,576.0	9,252.0	27,828.0
Gallons of Diesel oil per year	6,780,240	3,376,980	10,157,220
Electric operations*			
Purchased kilowatt hours per train	51,970	20,720	
Number of trains per day	6.0	6.0	12.0
Purchased kilowatt hours per day	311,820	124,320	436,140
Purchased kilowatt hours per year	113,814,300	45,376,800	159,191,100
Fuel and energy equivalents			
Pounds of coal per kilowatt hour	4.00	3.81	3.95
Pounds of coal per gallon of Diesel oil	67.16	51.17	61.84
Kilowatt hours per gallon of Diesel oil	16.79	13.44	15.67

* All electric energy is measured at the low side of the 3-phase 60-cycle transformers supplying the frequency changer stations.

Table VII. Time Table Comparing Maximum Performances of Steam, Diesel, and Electric Locomotives With Tonnage Freight Trains and First-Class Passenger Trains Over a Hypothetical 400-Mile District of Mountain Railroad*

				Freight Trains						First Class Passenger Trains					
				Steam Locomotives 1,500 Gross Tons Trailing		Diesel Locomotives 2,280 Gross Tons Trailing		Electric Locomotives 2,850 Gross Tons Trailing		Steam Locomotives 1,200 Gross Tons Trailing		Diesel Locomotives 1,200 Gross Tons Trailing		Electric Locomotives 1,200 Gross Tons Trailing	
Mile-post	Station	Average Compensated Grade	Mileage Interval	Time, Hours and Minutes	Average Speed, Mph	Time, Hours and Minutes	Average Speed, Mph	Time, Hours and Minutes	Average Speed, Mph	Time, Hours and Minutes	Average Speed, Mph	Time, Hours and Minutes	Average Speed, Mph	Time, Hours and Minutes	Average Speed, Mph
0.0	Eastwood			0:00		0:00		0:00		0:00		0:00		0:00	
		0.0	140.0		75.0		68.0		68.0		75.0		75.0		75.0
140.0	Garnet			1:54		2:06		2:06		1:54		1:54		1:54	
		+1.0	30.0		38.5		30.0		30.0		44.0		46.0		53.0
170.0	Kenton			2:42		3:06		3:06		3:36		2:36		2:30	
		+1.5	21.5		27.0		21.5		21.5		33.0		33.0		41.0
191.5	Mercer			3:30		4:06		4:06		3:18		3:12		3:00	
		+2.0	8.5		17.0		17.0		17.0		24.0		28.0		33.0
200.0	Summit			4:00		4:36		4:36		3:36		3:30		3:18	
		−2.0	8.5		21.2		21.2		21.2		28.0		28.0		28.0
208.5	Trail			4:24		5:00		5:00		3:54		3:48		3:36	
		−1.5	21.5		30.7		30.7		30.7		36.0		36.0		36.0
230.0	Unity			5:06		5:42		5:42		4:30		4:24		4:12	
		−1.0	30.0		43.0		43.0		43.0		50.0		50.0		50.0
260.0	Vernon			5:48		5:24		6:24		5:06		5:00		4:48	
		0.0	140.0		75.0		68.0		68.0		75.0		75.0		75.0
400.0	Watertown			7:42		8:30		8:30		7:00		6:54		6:42	
Average speed over district					51.9		47.1		47.1		57.1		58.0		59.7
*KGTML***					812.8		1,102.8		1,346.8		692.8		670.8		686.8
Fuel and energy requirements															
Coal, pounds					109,440						78,900				
Diesel oil, gallons							2,476.8						1,542.0		
Kilowatt hours									51,970						20,720
Fuel and energy ratios															
Coal per *KGTML*, pounds					135						114				
Diesel oil per *KGTML* gallons							2.25						2.30		
Kilowatt hours per *KGTML*									38.6						30.2

* Westbound movements only are shown, but since the profile is symmetrical, the eastbound movements are identical.

** *KGTML* = thousands of gross ton miles including locomotives.

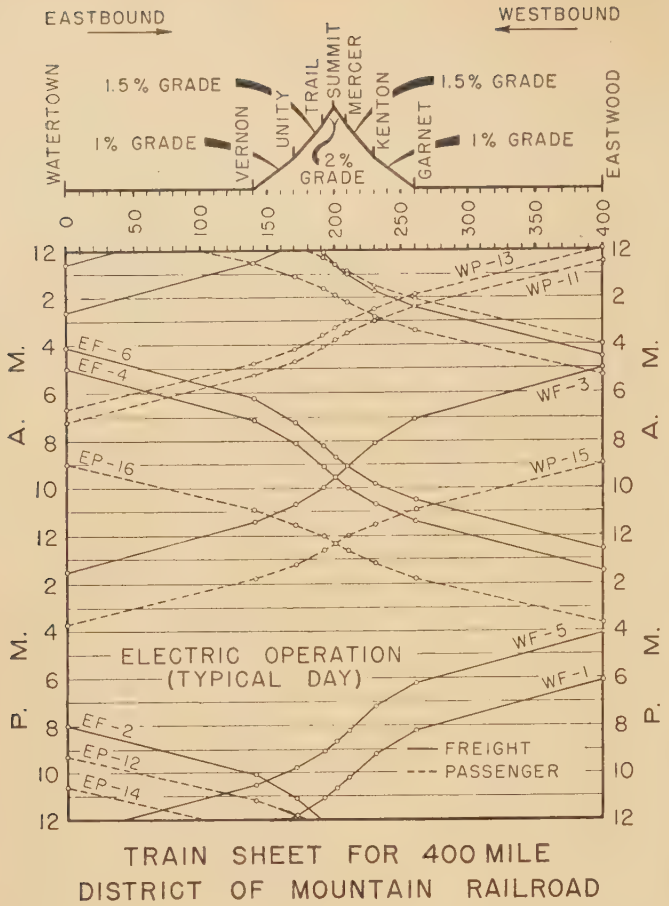

Figure 5 (above). Train sheet for hypothetical 400-mile district of mountain railroad

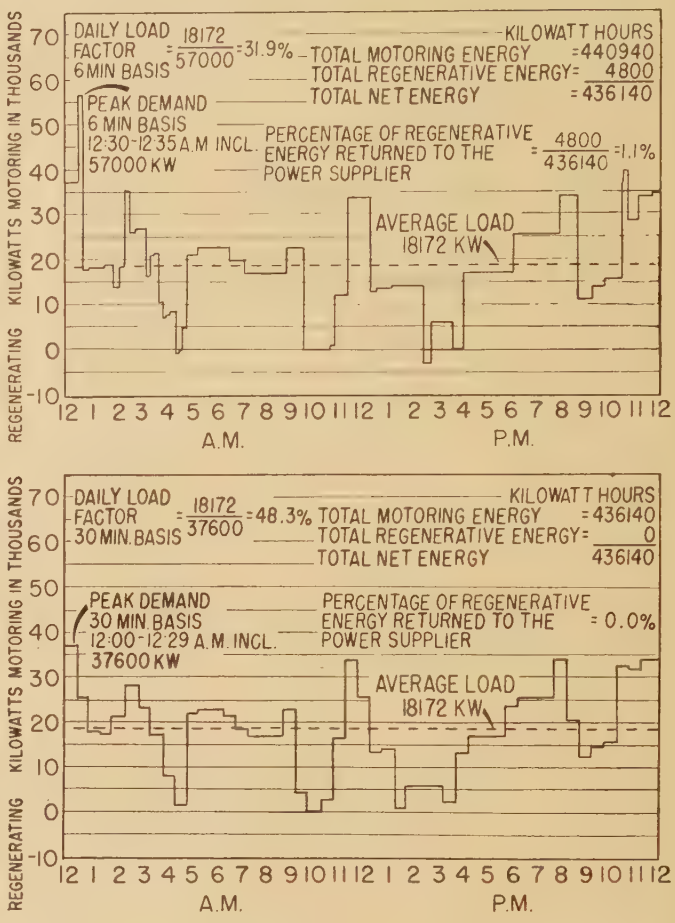

Figure 6 (below). Substation load charts for typical maximum day of electrified operation shown in Figure 5

is relatively easy as to gradient but is not high speed track, then the efficiency of motive power utilization will be reduced considerably. The trailing tons will be less than could be handled over most of the district aside from the small section embracing the ruling grade and the speed will not be increased sufficiently to use up the power potential of the locomotive. The working load factor of the locomotive will be low suggesting inefficient utilization.

Helper District

It is this general situation which gives rise to what are known as "helper" districts. The theory is to load a locomotive for some gradient less than the ruling grade, thus permitting it to take an increased number of trailing tons. When the ruling grade section is reached a "helper" locomotive is added which is capable of supplying sufficient additional drawbarpull to negotiate the hill. A helper district is nothing more than an expedient to avoid the necessity of breaking trains into smaller units for negotiation of short sections of profile. It is usually cheaper to run one train than two since although an additional engine crew may be required there is no, or at least a very minor, increase in train crew and other operating costs. Notwithstanding these favorable aspects, helper districts are nuisances and are resorted to only where they cannot be avoided.

Motive Power Chosen for Comparison

Characteristic curves and basic performance data used in these comparisons were assembled from a number of sources and are believed to be factual and fair. For obvious reasons exact identification of the locomotives used has been withheld.

Steam Locomotive

Table II is a brief description of the steam locomotive selected for this comparison. Known in motive power circles by its wheel arrangement as a 4-6-6-4 it is of the single expansion articulated type. It is a 4-cylinder engine, in reality two separate engines served by one boiler and under the control of one engine crew. It bears the closest resemblance to multiple unit control available where electric motors are not used for traction purposes. With a driving wheel diameter of 69 inches a reasonable compromise is had between the objectives of high tractive effort demanded in freight service and high maximum speeds requisite to passenger operations. The top speed of the engine should be about 75.0 miles per hour and it appears to be about as satisfactory a universal passenger-freight type as is available for use in this part of the country.

Diesel Locomotive

There are at least four manufacturers building so-called 6,000-horsepower Diesel-electric locomotives at the present time. The one chosen here is of the 4-cab type with each cab having a B-B wheel arrangement. Table III lists the principal facts regarding its weight, size, and so forth. The gearing was selected with the purpose of limiting its top speed to approximately match the top speed of the steam locomotive chosen or 75.0 miles per hour. This fixes the minimum speed under continuous output conditions at about 17.0 miles per hour. It should be

noted that if the steam locomotive chosen actually will not run this fast, the use of the 3.53 to 1.00 gearing chosen will penalize the Diesel slightly. For example, if the top speed could be taken as 70.0 miles per hour a ratio of about 3.81/1.00 could be used which would permit the minimum speed under continuous output to be dropped back to 15.5 miles per hour. This might not seem important, but it actually would afford about a 10-per cent increase in the continuous tractive effort of the Diesel and an equal augmentation of its hauling ability. The assumption therefore is that all of these locomotives will be able to attain top speeds of 75.0 miles per hour. Oil fired steam generators have been included for passenger train heating purposes.

Table IX. Motive Power Availability and Utilization

	Steam Operation			Diesel Operation			Electric Operation		
	Freight	Passenger	Total	Freight	Passenger	Total	Freight	Passenger	Total
1. Road time required by one train, hours	7.7	7.0		8.5	6.9		8.5	6.7	
2. Number of trains per day	11.4	6.0	17.4	7.5	6.0	13.5	6.0	6.0	12.0
3. Total road hours per day	87.78	42.00	129.78	63.75	41.40	105.15	51.00	40.20	91.20
4. Total road hours per year	32,040	15,330	47,370	23,269	15,111	38,380	18,615	14,673	33,288
5. Assumed utilization of availability, per cent*			50			50			50
6. Total hours locomotives should be available for assignment			94,740			76,760			66,576
7. Number of locomotives			15			11			9
8. Total potential locomotive hours per year			131,400			96,360			78,840
9. Derived availability factor, per cent (line 6/line 8)			72.1			79.7			84.4

* This factor permits calculation on a uniform basis for all three classes of motive power, of the difference between actual time spent in trains on the road, and the total time the pool of locomotives is available for work assignments. It accounts for all differential time except that required for running and classified repairs.

Electric Locomotive

A somewhat more detailed explanation of the choice made in the case of the electric locomotive seems appropriate. It is obvious that the selection of the electric locomotive also implies selection of the type of system to be employed. What kind of electricity will be placed on the catenary for the pantographs to pick up? It also should be obvious that it is entirely beyond the scope of the present paper to delve into the ramifications of a choice of system. The purpose here was to compare some electric locomotive with the best available steam and Diesel motive power under parallel operating conditions. Naturally, it was desired to select an electric locomotive equal to the competition. It would be pointless to pick one either physically or economically deficient.

Regarding the choice of system, the primary criterion was the ability to deliver at least 15,000 kw to a point on the trolley system. If enough substations could be built there would be no particular bar to delivering such an amount of power, but, as even the casual observer knows, railway power supply facilities cost a great deal and there are few opportunities to be lavish with substations if over-all economics mean anything. Under the circumstances the use of a low voltage trolley system appears to be impractical. To keep power supply facilities, including both the elements which normally are railroad-owned and those normally owned by the power supplier, at a minimum it seems essential to keep the trolley potential up to at least 12 kv. From the immediate practical standpoint this definitely suggests the necessity of choosing a 12-kv 25-cycle trolley system.

The choice of a frequency of 25 cycles requires explanation. There are many reasons why the frequency should be lower than 60 cycles, but few if any of them can be cited to justify the choice of 25 cycles. The Swiss and Germans appear to have made a wiser choice with their $16^2/_3$-cycle equipment. American practice probably would be better had a simple 3/1 or 4/1 ratio to the basic 60 cycles been established a long time ago. There are now too many precedents and too much installed equipment to be upset to suggest 15 or 20 cycles, and even a switch to 24 cycles, which would permit substantial improvements in frequency changers, appears difficult. Be this as it may, the necessity of lowering frequency from 60 cycles is virtually unchallenged. It is necessary because of at least two things.

1. The excessive reactance of 60 cycles.
2. The single phase unbalance that would be sustained by a power supplier attempting to feed 60 cycles to a railroad for direct application to the trolley. Changing frequency permits the assembly of what otherwise would be single-phase low-power-factor loads into a 3-phase unity-power-factor load.

With the choice of the trolley system fixed at 12 kv, 25 cycles, it is necessary to choose between two types of motive power.

1. Locomotives using single phase a-c motors of the series commutator type for traction.
2. Locomotives using d-c series motors for traction with d-c generators directly connected to synchronous motors supplied from the a-c trolley.

Fortunately the choice between these two is comparatively easy in this part of the country. The a-c traction motor locomotive has certain characteristics that make it a relatively inferior performer in a region where heavy gradients prevail and where freight forms a large part of total traffic. In such circum-

Table X. Summaries of Train Crew and Locomotive Maintenance Expenses

	Steam	Diesel	Electric
Traffic statistics			
Number of freight trains per day	11.4	7.5	6.0
Freight train miles per day	45,600	30,000	24,000
Freight train miles per year	1,664,000	1,095,000	876,000
Number of passenger trains per day	6.0	6.0	6.0
Passenger train miles per day	24,000	24,000	24,000
Passenger train miles per year	876,000	876,000	876,000
Total locomotive miles per year (Line 3 plus line 6)	2,540,400	1,971,000	1,752,000
Train crew costs per year*			
Freight train miles at $.80 per mile	$1,313,200	$ 876,000	$ 700,800
Passenger train miles at $.33 per mile	$ 289,080	$ 289,080	$ 289,080
Total train crew costs	$1,620,280	$1,165,080	$ 989,880
Locomotive maintenance costs per year**			
Steam locomotive repairs at $.55 per locomotive mile	$1,397,220		
Diesel locomotive repairs at $.55 per locomotive mile		$1,084,050	
Electric locomotive repairs at $.32 per locomotive mile			$ 560,640

* Assumed on basis of comparable wage rates prevailing in the Pacific Northwest. Freight crews consist of engineman, fireman, conductor, and three brakemen. Passenger crews consist of engineman, fireman, conductor, and two brakemen.

** Locomotive maintenance costs assumed on the basis of the best available experience that is believed credible.

stances the prime requirement of motive power is the ability to provide high tractive effort at relatively low speeds. This in turn means that the horsepower characteristic of a locomotive must be such that full horsepower is available in the speed range where it can be used effectively. Figure 2, which follows recent analyses of F. E. Wynne of the Westinghouse Electric Corporation, illustrates the nature of the horsepower characteristics of the motor-generator and a-c commutator type locomotives.[4]

It should be noted that full horsepower is available in the case of the motor-generator locomotive in the range from 22 to 80 per cent of full speed, whereas in the case of the a-c commutator locomotive the full horsepower range extends from 56 to 100 per cent of full speed. At 22 per cent of full speed the a-c commutator machine achieves only about 40 per cent of its full horsepower. Since the tractive effort of a locomotive at a particular speed varies directly with its rail horsepower, it is evident that at 22 per cent of full speed a motor-generator locomotive would have 2.5 times the tractive effort of an a-c commutator locomotive of equal nominal horsepower. Such a deficiency in tractive effort means a corresponding decrease in the number of trailing tons which the locomotive could be loaded with for operation over the ruling grade. So long as the major premise of the desirability of the relatively low speed operation of freight trains in a region such as the Pacific Northwest is granted, it is hard to see that any choice other than the motor-generator locomotive is warranted. There are compelling reasons for the supplier of power to prefer the motor-generator locomotive, but it is believed unnecessary to labor this point when there appears to be no logical reason for a railroad to have a contrary preference.

Table IV includes the principal dimensions of the motor-generator type electric locomotive selected. The important points to be noted are

1. The complete motorization of all weight.
2. The gearing of 3.75/1.00 which on 42-inch wheels gives about the same maximum and continuous speeds as the Diesel, that is, 75.0 and 17.0 miles per hour respectively.
3. The provision of oil fired train heating equipment.

Table XI. Assumed Capital Cost of Facilities Affected by Type of Motive Power

400-Route-Mile District of Mountain Railroad

Affected Items	Steam	Diesel	Electric
Electrification fixed properties			
480 track miles of trolley and single phase transmission construction			$ 5,760,000
Frequency changer apparatus and trackside substations			3,650,000
Communications and signal changes and other contingencies			590,000
Total fixed properties (electrification)			$10,000,000
Motive power			
15 (4-6-6-4) steam locomotives at $250,000 each	$ 3,750,000		
11 Diesels at $600,000 (61,400 continuous rail horsepower at $107.49 per horsepower)		$6,600,000	
9 motor-generator electric locomotives at $525,000 each (61,200 continuous rail horsepower at $77.21 per horsepower)			4,725,000
Total affected capital costs	$3,750,000	$6,600,000	$14,725,000
Incremental investment over that required for steam operation		$2,850,000	$10,975,000

Table XII. Assumed Annual Operating Expenses of Facilities Affected by Type of Motive Power

400-Mile District of Mountain Railroad—Case 1

Affected Accounts	Steam	Diesel	Electric
Operating expenses			
Maintenance of way and structures, electrification fixed properties			$125,000
Maintenance of equipment, locomotive repairs*	$1,397,220	$1,084,050	560,640
Transportation rail lines, train crew expenses*	1,620,280	1,165,080	989,880
Fixed charges			
Depreciation			
Electrification fixed properties, 33⅓-year life—3.0 per cent			300,000
Steam locomotive, 25-year life—4.0 per cent	150,000		
Diesel locomotive, 16⅔-year life—6.0 per cent		396,000	
Electric locomotive, 20-year life—5.0 per cent			236,250
Interest, total affected investment—5.0 per cent	187,500	330,000	736,250
Total affected expenses except for fuel and energy	$3,355,000	$2,975,130	$2,948,020
Fuel and energy expenses**			
314,085 tons of coal at $2.00 per ton	628,170		
10,157,220 gallons of Diesel oil at 6.0 cents per gallon plus 20.0 per cent for engine lubricating oil		731,320	
159,191,100 kilowatt-hours at 4.0 mills per kilowatt hour			636,764
Total affected expenses	$3,983,170	$3,706,450	$3,584,784
Annual savings over steam operation		$ 276,720	$ 398,386

* From Table X.

** Quantities from Table VIII.

Horsepower and Tractive Effort Comparisons

Figure 3 is the starting point for analyses. Included are characteristic rail horsepower and tractive effort curves. Attention is called to the point at which substantially full horsepower becomes available in the different locomotives. It will be noted that in the case of both the Diesel and the electric locomotives this occurs at about 17 miles per hour but is not reached until 30 miles per hour in the case of the steam. At first this may not seem a serious defect in the makeup of the steam locomotive, but it probably will become gradually apparent that it is organic. Even if there were some assured means of shifting the characteristic so that full horsepower were to be available earlier, it probably would be found that the adhesion would not be sufficient to permit full utilization of the additional tractive effort. As it is the steam locomotive chosen for comparison is credited with about 90,000 pounds tractive effort at 17.0 miles per hour. Since the weight on drivers is but 404,000 pounds this would be equivalent to a working adhesion of 22.2 per cent, and it scarcely can be presumed that anything more would be possible even with clean dry rail and liberal sanding.

Hauling Efficiency of Locomotives

Probably the most important single criterion for judging these locomotives is their ratings in terms of the trailing loads each of them could handle on various ruling grades. These ratings have to be based upon assumed average conditions of tractive resistance, and accordingly the Davis formula for 45-ton 4-axle freight cars has been used. Drawbar pulls for

various grades were computed and loading curves prepared. Space permits the inclusion in Figure 4 of curves for the 1.0- and 2.0-per-cent grades only. The curves show gross tons trailing versus speed where the trailing load is composed of 45-ton 4-axle freight cars, but can be taken as applicable to other trailing loads averaging similar tractive resistance. Table V contains a summary of freight and passenger loadings and speeds for different grades. Table VI contains a summary of the more important data that facilitate appraisal of the physical performance of these locomotives. With a weight efficiency of 260 pounds per continuous rail horsepower at 17.0 miles per hour the steam locomotive is 71 per cent heavier than the electric locomotive which weighs but 152 pounds per continuous rail horsepower. In the length efficiency comparisons the Diesel locomotive shows to less advantage requiring 59 per cent more length of cab per 1,000 continuous rail horsepower.

It is the hauling efficiency comparisons that are the epitome of most of the observations that can be made of the physical abilities of these locomotives. It should give pause for thought that on a 2.0-per-cent grade the steam locomotive will haul only 2.82 tons for each one ton of its own weight. It is seen that the Diesel locomotive will handle 4.78 tons and the electric 5.51 tons per each ton of their respective weights. In addition to the inefficiency included in this comparison, steam locomotives spend sizeable portions of their useful lives engaged in the nonrevenue task of hauling their own fuel back and forth to various fueling stations. If this were measured easily it would impair still further the hauling comparisons with electric motive power which requires no allowance for such nonrevenue trailing loads.

Economic Generalizations Hazardous

As stated earlier economic comparisons are difficult. Extreme variations in the physical conditions encountered make generalizations risky. Each railroad presents a somewhat different situation and often different divisions of the same railroad pose completely different operating problems. Actual case studies of the economics of motive power utilization require time and money and must be applied to specific sections of railroad. In view of space requirements, it is obviously impossible to analyze adequately economic factors surrounding the use of the locomotives described in the previous sections. It seems worthwhile to present some comparison however inadequate and hypothetical it may be in order to indicate the nature and general magnitude of the factors that affect the economics of motive power utilization at the present time and to suggest how changes in these factors could affect future comparisons.

Table XIII. Effect of Changes in Price of Fuel and Energy Upon Annual Expenses Shown in Table XII

	Steam	Diesel	Electric
Total affected expenses except for fuel and energy	$3,355,000	$2,975,130	$2,948,020
Case 2			
314,085 tons of coal at $2.00 per ton	628,170		
10,157,220 gallons of Diesel oil at 7.0 cents per gallon, plus 20.0 per cent for engine lubricating oil		853,206	
159,191,100 kilowatt hours at 4.0 mills per kilowatt hour			636,764
Total affected expenses	$3,983,170	$3,828,336	$3,584,784
Annual savings over steam operation	$	$ 154,834	$ 398,386
Case 3			
314,085 tons of coal at $2.00 per ton	628,170		
10,157,220 gallons of Diesel oil at 7.42 cents per gallon, plus 20.0 per cent for engine lubricating oil		904,399	
159,191,100 kilowatt hours at 4.0 mills per kilowatt hour			636,764
Total affected expenses	$3,983,170	$3,879,529	$3,584,784
Annual savings over steam operation	$	$ 103,641	$ 398,386
Case 4			
314,085 tons coal at $2.50 per ton	785,162		
10,157,220 gallons of Diesel oil at 9.00 cents per gallon, plus 20.0 per cent for engine lubricating oil		1,096,980	
159,191,100 kilowatt hours at 4.0 mills per kilowatt hour			636,764
Total affected expenses	$4,140,162	$4,072,110	$3, 584,784
Annual savings over steam operation	$	$ 68,052	$ 555,378

Hypothetical Operating Section

The method employed here had to be hypothetical and greatly oversimplified. A theoretical 400-mile operating district of a mountain railroad was devised. To save time a greatly simplified and symmetrical profile was assumed with all gradients combined into four classes—0.0, 1.0, 1.5, and 2.0 per cent. Contrary to actuality, grades were assumed to be compensated equally in both directions. A sketch of the profile appears in Figure 5.

A uniform daily traffic was assumed as follows:

1. Freight, 8,550 gross tons trailing in each direction.

2. Passenger, 3,600 gross tons trailing in each direction.

This traffic was assumed to be handled at maximum performance by each kind of locomotive. No allowances were made for acceleration time, station stops, meets with other trains, in short no delays of any kind; just maximum performance from terminal to terminal was assumed. Also no helper service was assumed. Each locomotive takes its rated tonnage (fixed by the 2.0-per-cent grade) and uses up any excess horsepower available on the lesser grades in additional speed.

Table VII is a time table illustrating maximum performance of freight and passenger trains. A rather curious fact revealed here is that the tractive effort characteristics of the steam locomotive are such that when it is loaded to its maximum rated tonnage for the 2.0-per-cent or ruling grade it can run faster with that load on any lesser grade than the Diesel or electric locomotives can run with their rated tonnages. Care must be exercised in interpreting this fact. It does not mean that the steam engine can run faster with the same trailing load. This is revealed clearly in the average speeds attained by the passenger trains. It does mean that the steam locomotive in freight service can trail 1,500 gross tons over these 400 miles at an average speed of 51.9 miles per hour, whereas the Diesel and electric locomotives are able to handle their rated tonnages at but 47.1 miles per hour. The trailing loads handled by the Diesel and electric locomotives, however, are 2,280 and 2,850 tons respectively. Tables VIII, IX, and X are included to summarize essential data necessary in the calculation of operating expenses.

The principal comment that is required here relates to the rather remarkable savings in maintenance that are evident in the case of the electric locomotive. It seems to be true that on an equated rail horsepower–mileage basis, an electric locomotive of the type selected here can be maintained for from 40 to 50 per cent of the corresponding cost of a Diesel of the type selected. This can be explained quite well on the basis of the work necessary. The electrical and running gear

maintenance of the two will be nearly identical. Maintenance of the Diesel engine accounts for the chief difference. It can be seen that the difference in crew costs is purely a function of the relative hauling ability of the three types. Use of electric locomotives reduces the number of train miles that have to be run to a minimum that is nearly half that required by steam locomotives, and only about 80 per cent of that necessary for Diesel locomotives.

Capital and Operating Costs Compared

Table XI shows the assumed capital cost of those facilities which are affected

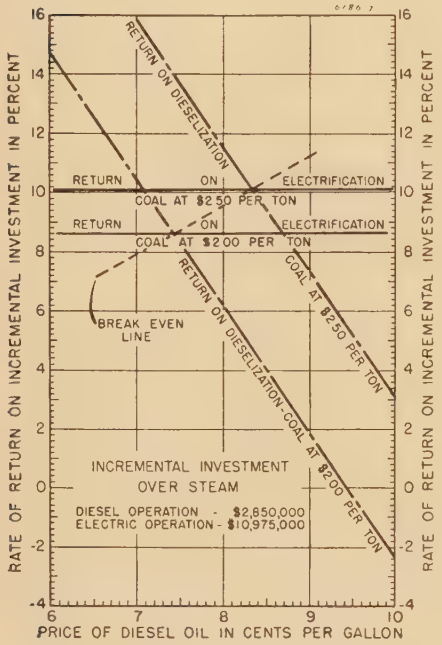

Figure 7. Effect of changes in the price of Diesel oil and coal upon the rate of return from incremental investments made for dieselization and electrification

by the type of motive power. Obviously these are not the entire capital costs of building such a section of railroad, but only the costs of the items which would vary with the different types of motive power. Considerable simplification will be noted in these assumed data. Investments other than for motive power have been eliminated from the steam and Diesel figures. Fixed properties therefore appear only in the case of the electric. This is not actually true, but it is an assumption that works no particular hardship on the steam and Diesel locomotives. The prices that have been assumed like all prices in troubled times are subject to uncertainties, but the comparison between types of locomotives is believed to be realistic and fair.

The affected operating expenses as of the present time are presented in Table XII. Here, as in the case of the capital costs, there is room for differences of opinion. The objective has been to use the best data and experience available that seemed to be free from bias. Table XII reveals that on the basis of present prices annual savings of $276,720 are possible where Diesels are substituted for steam locomotives at an incremental cost of $2,850,000 and annual savings of $398,396 are possible by electrification at an incremental cost of $10,975,000. With the 5.0-per-cent interest previously charged this is equivalent to returns of 14.7 and 8.6 per cent respectively on the incremental investments made for dieselization and electrification respectively. If this were all that could be said for the two alternatives it would appear that a case had been made for dieselization, for on this basis about a 6.0-per-cent greater return could be earned on money spent for modernization.

Effect of Diesel Oil Price Changes

That this would be a dangerous conclusion to reach hurriedly is evident upon examination of Table XIII where an attempt has been made to show how the annual savings of the different plans of operation are affected by changes in the price of Diesel oil and coal. For example, note that in case 3 where the price of Diesel oil has been assumed at 7.42 cents per gallon, an increase of not quite 25 per cent, the annual savings on Diesel operation are reduced to $103,641. This reduces the return on the incremental investment in dieselization to 8.6 per cent, exactly equal to that obtainable from electrification. Whether it should be assumed that Diesel oil will increase in price without assuming a corresponding increase in the price of coal can be debated. There are nearly as many opinions available on the future price of both commodities as there are authorities to be quoted. There does seem to be some evidence to suggest that the long term price trends of the two are different. The supply of coal though limited is fairly well known, while the supply of oil is both limited and unknown. It can be argued that both commodities are likely to increase in price with respect to their present bases but that the factor of increasing demand is more likely to produce a disproportionate increase in the case of Diesel oil. Demands for Diesel oil and all other petroleum products are increasing by leaps and bounds while the bituminous coal industry is organizing to combat what they view as the possibility of gradually decreasing demands.

Electrification Offers Hedge Against Inflation

Figure 7 has been prepared to indicate the effect of price changes in both Diesel oil and coal upon the relative economy of dieselization and electrification. It is believed that a substantial case for electrification can be inferred from the relationships shown. The reasoning probably would be as follows:

1. The present attractiveness of Diesel-electric locomotives as replacements for steam locomotives has both a physical and an economic foundation.

2. Physically, the electric locomotive has no equal—there is nothing the Diesel locomotive can do to outclass the steam locomotive that the electric unit cannot improve upon.

3. Measured economically, dieselization has considerable present margin over steam.

4. Measured economically, electrification also offers a margin over steam although the returns on incremental investments are not so large as offered by the Diesel on the basis of present prices.

5. The crux of the contest between dieselization and electrification lies in the question of which of the two is more likely to maintain or increase its present margin over steam, and this depends almost entirely upon the future price of respective energy sources.

6. The price of electric energy over the next decade or two may not decrease markedly, but it is hardly likely to rise. This largely is based on the fact that the supply can and very probably will keep pace with the demand.

7. There is no corresponding assurance of the maintenance of present prices for Diesel oil, and most authorities apparently anticipate gradual increases.

8. If the price of coal does not increase beyond present levels (in the view of many a strictly possible result of decreasing demand), an increase in the price of Diesel oil of 25 per cent approximately would equalize the return from investments in electrification and dieselization.

9. Should coal rise about 25 per cent in price a rise of 40 per cent in Diesel oil prices again would equalize dieselization and electrification.

10. In view of the foregoing, electrification appears to offer railroad mangements the most likely hedge against inflation of operating costs. By electrifying main lines and dieselizing yard operations, it appears feasible for them to achieve some assurance of reasonable costs during the next 20 years.

References

1. Locomotive Economics, **L. K. Sillcox.** *Railway Mechanical Engineer*, New York, N. Y., volume 120, May 1946, pages 249–53.

Specific Engineering Problems in Rural Electrification and Electroagriculture

M. M. SAMUELS
FELLOW AIEE

A DISTINCTION is made between "rural electrification" and "electroagriculture," the former being the art and the business of bringing electric service to the rural area and to the individual consumer in that area, the latter being the art and the business of using electric power for farming.

In both of these fields there are specific problems for the electrical engineer, some old, some new, some partly solved, others as yet unsolved, and still others which have not been definitely stated yet.

There are collateral problems between the two fields. One of the problems is the case of industrial loads supplied from rural lines. Offhand it would seem that a sharp line of demarcation between industrial load on the farm and that in urban areas would be important only for the purpose of statistics and economics but not for engineering purposes. However, occasionally specific engineering problems arise in connection with industrial loads on the farm. Even though very few such specific problems have been crystallized as yet, indications are that many new ones will arise as the farm load grows. Therefore a few specific items will be referred to.

While specific solved or partly solved problems in both fields will be presented, the main purpose is to point to problems yet to be solved, to others yet to be stated, and to stimulate and challenge the electrical engineer, particularly the young electrical engineer, to tackle them.

The sum and substance of all engineering problems in both fields can be stated thus: continuity of service on the farm is more important than in the city. This applies both to the continuity of the power supply and the continuity of operation of the individual piece of equipment. An outage of a few hours in the city may be a mere inconvenience. One can go to the movies, eat in a restaurant, or relax in the dark. But when a farmer uses electric milking, electric water pumping, or electric cooling or freezing equipment and the power is off for a few hours, he may experience a serious financial loss. This continuity of service however, must be rendered at a low cost. Furthermore, when a computation in large power systems is completed and the problem is known, the necessary diversity of circuit breakers, relays, regulators, and other devices generally can be selected from a catalog to solve the problem, or new relays can be designed. But in the case of the rural primary circuits, there is no such diversity; there is only the fuse, the circuit breaker with a series coil, and possibly a thermal tripping device. Thus the engineering problem of the rural circuit is in some respects more difficult to solve than that of the 460,000-volt line.

Shall a power system study the load requirements and provide a supply system to satisfy these loads, or shall it promote loads which will help build up the system? The answer is that it should do both and should not waste time discussing the question of whether the chicken or the egg was first. For practical purposes the load conditions will be discussed here first, followed by a discussion of power supply problems. What kind of specific loads are there on the farm? A list of possible uses of electrical service on the farm, prepared by J. P. Schaenzer, is presented in the appendix. It is no doubt incomplete, but it is sufficient to indicate the great diversity.

It is evident that we are dealing here with a new industry, the electroagriculture industry. A new industry calls for new engineering treatment. Only a few years ago few items of electric equipment for specific use on the farm were manufactured for the market by quantity production methods. American manufacturers thought that there was no market for such items. Competent hard-working men in agricultural colleges developed some fine designs, but there were no manufacturers willing to produce them. The best they could do was to send farmers the designs and specifications for homemade equipment. How many farmers can read blue prints, particularly when the drawings are not prepared by experienced draftsmen? How many farmers have the time for it? It became evident that if the American farm was to be electrified, it would have to be done by American manufacturers. But there was such a great diversity of ideas among agricultural experts and agricultural colleges that manufacturers hesitated to invest in tooling up for quantity production of any one design. It may be recorded that the American manufacturing industry finally did create this new industry during the war years, the most difficult imaginable time for such a creation. How did it come about? A few cases will serve best as a general demonstration.

A few years ago, few manufacturers were on the market with combination quick-freeze and zero-storage units suitable for the farm and at a price which the farmer could afford to pay. A brief survey was made among farmers. Based on this survey, a functional specification was prepared and distributed among manufacturers. Recently, several hundred manufacturers announced such models.

Manufacturers found it difficult to embark upon quantity production of pig brooders because practically every state agricultural college had a different design. An investigation was made among agricultural colleges and full co-operation was furnished by many professors. A careful study of all the diversity of designs resulted in one basic design for a pig brooder which met practically all the requirements. A report was prepared and made available to manufacturers. As a result, several manufacturers now advertise models at low prices, because they are manufactured by quantity production methods.

During the war the electric welder became a very important tool on the farm for the repair of damaged equipment because the farmer was unable to get

2. THE STEAM LOCOMOTIVE (book), **Ralph P. Johnson.** Simmons-Boardman Publishing Corporation, New York, N. Y., 1942.

3 THE TRACTIVE RESISTANCE OF ELECTRIC LOCOMOTIVES AND CARS, **W. J. Davis, Jr.** *General Electric Review*, New York, N. Y., volume 29, October 1926, pages 685–707.

4. COMPARABLE LOCOMOTIVE RATINGS, **F. E. Wynne.** *Railway Age*, New York, N. Y., volume 120, February 9, 1946, pages 316–18.

5. LOCOMOTIVES OF TOMORROW, **Charles Kerr, Jr.** *Railway Mechanical Engineer*, New York, N. Y., volume 120, May 1946, pages 239–44 and 256.

6. LOCOMOTIVES, PRESENT AND FUTURE, **Charles A. Scarlott.** *Westinghouse Engineer*, East Pittsburgh, Pa., volume 6, May 1946, pages 78–83.

7. **Arthur J. McGinnis,** *Railway Age*, New York, N. Y., volume 120, January 5, 1946, page 88.

Paper 46-184, recommended by the AIEE committee on domestic and commercial applications for presentation at the AIEE Pacific Coast meeting, Seattle, Wash., August 27–30, 1946. Manuscript submitted May 31, 1946; made available for printing July 15, 1946.

M. M. SAMUELS is chief, technical standards division, Rural Electrification Administration, Washington, D. C.

either new equipment or repair parts. No data were available to advise the manufacturers of the type of welders which could be supplied properly from rural power lines. In many instances the welder loads caused distribution transformers to burn out, disturbances of voltages, and similar nuisances. An investigation was made on which was based a specification prepared in co-operation with manufacturers and this specification eventually was accepted by the National Electrical Manufacturers' Association (publication 45-105, September 1945). Now the manufacturer can proceed with quantity production and the farmer can get a welder which will not disturb the power system.

A survey was made among colleges in search of new developments which might be ready for manufacturers to develop for quantity production. The report was distributed among manufacturers and several items now are being studied by them. Here one of the difficulties encountered is the policy of some schools not to permit members of the faculty to secure patents on inventions. It is done with the best intention. They feel that a devleopment made in a public institution should be available to everyone. However, this very policy prevents many a good idea from being put to general use. No invention is ever ready for the market. Expensive development usually is called for. A manufacturer cannot be expected to spend great sums on such development unless he has some exclusive patent protection. This applies also to a so-called public patent on which everyone could secure a free license. Some institutions, such as Purdue University, have a very sound policy in this respect. Other schools should give this problem the consideration which it deserves.

Numerous items are now in the development stage but the new electroagricultural industry already has arrived and is here to stay. It offers a challenge and an opportunity to the electrical engineer.

In an industry such as this, which is still partly in *statu nascendi*, it would be premature and inadvisable to establish rigid standards which might interfere with the creative imagination of the engineer and inventor or with creative competition which is needed for progress. However, some basic standards for performance as well as size and quality of material are needed to make it possible for the buyer to judge quality. Commercial test procedures also are needed for determining the service the buyer may expect an item to render. It is suggested that a special AIEE committee be set up for this purpose. Co-operation with committees of other bodies should not be too difficult. But most of the pending problems seem to be of an electrical engineering nature.

Attention may be called to a few specific items for which there is immediate need. Two hundred years ago sanitation was not as important as it is today, as is evidenced from the requirements of a French boarding school, then patronized by the French nobility. In its catalog to parents of prospective female pupils it includes the following revealing information:

> Pupils are entitled to have one set of underclothing, one pair of stockings and two handkerchiefs per month. Towels: Pupils, one every week; nuns, one every two weeks. Foot baths: Pupils, one a month; nuns, only by special authorization of the superior. Complete baths: Three a year (May, June and July). Pupils unable to take their baths on the appointed day must wait until the following month.

Today, no one will dispute that sanitation is one of the most important requirements of human beings if they are to live on a level higher than that of pigs.

The most important need is perhaps for a small electrically driven water pump, simple and low priced, to make it possible to introduce a minimum amount of sanitation even in the poor farm shack.

A small milk pasteurizer for the farmer who has only a few cows is needed badly. The present difficulty is that in most places a curve-drawing thermometer is required which costs more than the whole pasteurizer would. The problem is either to develop a cheap temperature recorder or an electronic pasteurizer which does not require temperature recording and on which it would be possible to secure approval upon presentation of competent test reports.

No adequate data are available as yet which could be used as a basis for a functional specification for a competent electric egg cooler. Research now is being carried on, and it is hoped that it soon will be possible to furnish manufacturers the necessary fundamental information for the design and quantity production of such a cooler.

The problem of control of off-peak water heating on the farm has not been solved yet. For various reasons, clock control has not become popular. What is needed is a device which will disconnect the water heater upon the expiration of a definite time after the total load on the service transformer has reached a prescribed limit, and to reconnect the water heater as soon as other loads have been reduced. This would permit control regardless of the time of day or night. The principal difficulty in solving this problem is the fact that the device would have to be both simple and inexpensive to be suited for farm use. It is hoped that the development work now carried on by some manufacturers will result soon in a competent device.

Off-peak house heating has been tried, but in some cases it turned out to be peak-load. This definitely calls for further study. In many parts of the country the heat pump eventually may become the best method of heating and cooling farm houses and other farm buildings.

Another item for which there is a definite demand is a competent, automatic, electric high-pressure cooker.

Fire hazard on the farm is far more serious than in the city. Many farmers would like to eliminate overhead secondary distribution lines between buildings, because of the hazards of lightning, icicles, trees falling on the conductors, and roosting chickens or other birds. For single-phase circuits it is conceded generally that an underground cable made up of one insulated conductor and one parallel bare conductor would offer the best lightning protection. Manufacturers are now busy at work on the development of an economical conductor of this nature, and it is hoped they soon will be able to place one on the market which will meet the approval of the authorities. This cable should be ratproof and gopherproof. It also should be frostproof, to make it unnecessary to dig below frost line.

Perhaps the field of freezing and cooling offers greater opportunities than other items for invention, improvement, and development. It is important to repeat that while centuries have been devoted to the engineering of controlling temperatures upwards, the engineering of controlling temperatures downwards is of comparatively recent origin.

According to the United States Department of Agriculture Circular 423, January 1937, an estimated total of 60,000,000 rats on the farm cost the American farmer about $65,000,000 a year. It is indeed surprising that with this enormous amount of money involved, to say nothing of the danger to human health, American engineers have not tackled the problem yet. At least two types of electric rat catchers are known to exist and are reported to have given satisfactory results. American manufacturers should concentrate on the study of this problem and attempt to develop electric rat catchers which could be manufactured by quantity production methods

and made available to the electrified farm at reasonable prices.

The study of the possibility of a small storage-battery-driven tractor has been delayed by the fact that some new lightweight batteries developed during the war are still military secrets. As soon as such batteries are available, the study should be continued. The convenience of electrical control certainly promises considerable advantages. Storage-battery charging would be excellent night load.

The application of high frequency to various purposes on the farm has not been studied sufficiently yet; neither has that of ordinary light or infrared and ultraviolet radiations.

At present, freezing, cooling, heating, lighting, water pumping, and similar electrical applications on the farm are mere adaptations of developments made for city use. Engineers should begin to place themselves in a state of mind of never having seen any of these applications, crystallize the specific problem of farm use, and then proceed to develop equipment for the specific purpose. Good results would be inevitable. Numerous specific problems no doubt soon will be crystallized in relation to the electric motor and the motor control equipment on the farm. The problem of power factor control, limitation of starting current and similar specific problems are now ready for investigation in a similar manner as the welding problem was investigated. One item, the need for which has been known for some time, is a simple and inexpensive means for stopping a motor automatically when the load is finished, as for instance for feed grinding and sawing wood, where time clocks are not suitable. One or more such devices are already on the market. But more designs for quantity production are needed.

Electroagriculture offers a challenge and an opportunity to the electrical engineer. A great deal has been done by basic research, and many results of this research are available for the engineer to pick up for industrializing. It is surprising to find how little engineering has been applied to the problem of food production, food distribution, and food preservation. This art is only in the process of becoming engineering. On the whole our food production still depends on the climate and the weather as it did many centuries ago. Freezing and air transportation are in the process of bringing about drastic changes. As freezing and high-speed air transportation become economical, it no longer will be necessary to raise everything everywhere. Fresh fruits and vegetables may be raised only in places where they can be raised with the least effort and delivered fresh to large consumption centers in a matter of hours. It is the job of the engineer to make this economical. But this is not enough. It is the ultimate job of the engineer eventually to make food independent of climate and independent of weather. It is not expected that such a revolution will be brought about in a day or a year, and it would be premature to suggest at this time how this will be brought about. But when hundreds or thousands of engineers begin to think about it seriously and continue thinking about it for 25, 50, or even 100 years, they eventually will solve the problem as they have solved many more difficult problems in the past. But the time is definitely at hand to begin engineering thinking.

It is evident that the farm load and demand diversity are, and will continue to be, of such uncertain nature as to make circuit computation difficult. But this is the time to start the study of the characteristics of this diversity and to continue it. The present cost of the numerous demand meters which would be required makes such a study practically impossible. It is necessary to resort to statistical interpretation, and very little has been done even by statisticizing. The great accuracy of the present meters, which were developed for different purposes would not be required. If a simple, cheap, recording ammeter were to be brought out, there would be a quantity market for it.

All of these features and many others must be given consideration in the planning of rural electrification (supplying power for rural areas). A layman, or even the average engineer, when observing a typical rural circuit from the window of a railroad train, will be surprised to hear that the simple little pole with a pair of small insulators, carrying a pair of conductors and occasionally a small transformer with its accessories, offers any engineering problem at all. It is therefore of some importance to show that there are engineering problems, that many of these problems have not been solved yet, and that others have not been stated. The crystallization of these problems and their solution are essential if the farmer is to have eventually the degree of continuity of service which the character of the load calls for or will call for in the future when more items of electric equipment for farming are made available. In fact, the speed with which many new uses of electric service will be introduced on the farm will depend to a great extent on the speed with which many engineering problems will be stated and solved.

Most of the primary circuits in rural areas are single-phase multigrounded 60-cycle 7,200-volts phase-to-ground. There is a main conductor and a neutral conductor. The primary and secondary windings of each distribution transformer are grounded together to the neutral, and a ground wire generally is carried down the pole to a ground rod at each distribution transformer. Grounds also are installed frequently on intermediate poles. The secondary windings are carried to the house or other building, and there usually is located another ground connection. Thus, a multiplicity of parallel grounds exist along the line, primary and secondary. Anyone who ever tries to trace the various paths that the current could take loses himself in what appears to be a hopeless maze. This is one of the most complex circuits in electrical engineering. The question as to why this specific circuit was selected instead of a delta circuit would be beside the point at this time, because there are already hundreds of thousands of miles of such circuits and the time has definitely arrived to establish a mathematical foundation for them. After consulting many outstanding authorities, to the best of the author's present knowledge, the general differential equation for the multigrounded single-phase circuit has not been set up yet. After it eventually is set up, it no doubt will be of a series character with numerous variables, and very likely it will not be possible to integrate it generally. It very likely will become necessary to assume some variables as constants for different purposes and establish a different integration for each purpose. The mathematical study is now under way, and the indications are that the basic differential equation soon will be available. Until it is available, problems of short circuit, voltage regulation, hazards brought about by voltage gradients on the surface of the soil, and similar problems cannot be solved to the full satisfaction of electrical engineering.

What goes on in the soil in the proximity of such a circuit? Very few test data or analytical data are available. The answer will not be at hand until many more tests are made and interpreted in the light of the basic formula yet to be set up. It is known that the circuit in the ground does not flow in the direction of the line from ground rod to ground rod. Tests show that the voltage distribution in the soil is nearly uniform in each direction from each ground rod. It

is evident that soil capacitance will have to be given consideration in addition to soil resistance. Observations made so far indicate that the voltage gradient on the surface of the soil can be modified considerably with multiple grounds of various designs. But the available data are inadequate as a foundation for definite designs in definite cases. It is evident that a great amount of testing superimposed on mathematical analysis will be required before a definite engineering foundation is available for the solution of many related problems.

This naturally leads to the question of the ground return line, a single-phase circuit made up of one wire, the earth forming the return. On one hand there are statements about great hazards, and on the other hand the question is raised why such circuits are not used more extensively. Circuits of this nature have been used in various places, and to the best of the author's present knowledge have not resulted in accidents.

Two types of hazards are mentioned. The first is the possibility of a break in the conductor which runs down the pole to the ground. In this case there would be practically full voltage across the break even though two or more such ground conductors generally are carried down the pole. The protective covering of the conductors would have to be broken to result in this hazard. The second is the possibility of dangerous voltages on the surface of the soil. It is evident from the foregoing remarks that no definite statements of a quantitative nature can be made at this time which would serve as a guide for those who are considering the use of such circuits. Neither is there sufficient evidence to prove or disprove that there are real hazards, what their degrees are, and how to overcome them. Those who use such circuits have to exercise caution after a thorough familiarity with soil conditions and load conditions in each case. The National Electric Safety Code states in relation to such circuits:

> In urban districts supply circuits shall not be designed to use the ground normally as the sole conductor for any part of the circuit. It is recommended that such use be avoided in rural districts.

It is to be noted that in urban areas it "shall not be used" but in rural areas it is "not recommended." However, a responsibility is involved in recommending it because in case of a jury trial for criminal negligence relating to an accident, the recommendation of the National Electric Safety Code no doubt would carry considerable weight.

Analytically the ground return circuit is a special case of the general multigrounded circuit. Once the formula for the general circuit is available, the ground return circuit can be developed by making the neutral impedance equal infinity.

It is evident from this discussion that the least that can be done is to provide the best possible grounds everywhere and to inspect and test the grounds periodically, first to make sure that they are intact, and second to accumulate as much data as possible on the electrical characteristics of the specific soil. However, our present methods of testing grounds are cumbersome, and the testing equipment is too expensive. Here too the great accuracy for which the various instruments were designed is not required. With lower accuracy it should be possible to develop simple low-cost instruments for quantity production, so that each farmer who has a worth-while electrical installation could himself periodically test not only all his electric circuit grounds, but also all his lightning rod grounds. Simpler methods of attaching the testing instruments to the circuits also are required. There will be very little testing if the present procedure is to be continued, which makes it necessary in each case to dig up the soil at each ground rod, disconnect the ground lead from the rod, connect the instruments to the rod, disconnect it after the test, reconnect the ground lead to the rod, and then refill the soil. What specific engineering problems are implied in the little distribution transformer used on rural circuits? Surprising as it may seem, there are numerous complex problems. It has not been possible yet and will not be possible until the previously referred to recording ammeters are available in quantity to determine the best range of sizes of distribution transformers. The sizes now used are those originally determined for urban purposes. The weight is important because of the handling difficulties in farm areas. Numerous accessories have been added to the little transformer, such as lightning arresters, gaps, and cutouts, which make it resemble a Christmas tree. A great deal of competent design study still is called for before a reasonably satisfactory arrangement will be had.

A number of small transformers in a rural area with unsatisfactory $I \cdot T$ products may result in inductive interference, which may call for considerable expenditures in testing to determine the location of the cause of the interference and to design remedial measures altogether out of proportion to the cost of the transformers. It is essential that manufacturers are made to realize that it is more important for a rural transformer to have a satisfactory $I \cdot T$ product than it is for an urban transformer. This also applies as well to small generators in isolated areas. The cost of the remedy is less than the cost of the investigation. It is gratifying to report that most manufacturers appreciate this problem and are doing their best to reduce harmonic troubles.

One of the most important features is the need for low core losses. An urban transformer may have a diversity of loads with a reasonably good over-all load factor. A rural transformer generally has only one consumer. The copper loss load factor may be as low as 15 or 20 percent, whereas the core loss load factor is always 100 percent. There are cases where the billed kilowatt-hours are less than the core loss kilowatt-hours which are not billed. The Kelvin law, in any one of its forms, could be set up to determine the economy of the ratio of core losses to copper losses. But the problem can be stated simply without any formula. There are three criteria.

1. The lower the fixed charges, the more investment is justified on the saving of core losses and replacing them by a corresponding amount of copper losses.
2. The higher the cost of energy is on the primary winding side, the more can be invested on the reduction of core losses.
3. The lower the load factor is on the individual transformers, the more can be invested on the reduction of core losses.

It is realized that the reduction of core losses is not a simple problem for the transformer designer if the over-all efficiency is not to be reduced, if the resulting exciting current is not to bring about troublesome harmonics, and if the voltage regulation is not to be made worse. Nevertheless, manufacturers advise that there is hope for a considerable reduction in core losses in the near future. To indicate the great strides already made in improving rural transformer design, it is only necessary to report what one large manufacturer accomplished in a short time. The weight of the $1^1/_2$-kva transformer was reduced from 275 pounds in 1936 to 200 pounds in 1937, 145 pounds in 1943, and 120 pounds in 1945. Its core losses were reduced from 24 watts to 22 watts. The core losses of the 3-kva transformer were reduced during that same time from 36 watts to 30 watts and those of the 5-kva unit from 51 watts to 48 watts. This is progress indeed. But

it is not enough. Considering the fact that the cost of core losses on rural distribution transformers amounts to several million dollars per annum, further reductions definitely are called for. It is reasonable to assume that they will be forthcoming.

It was mentioned before that the absence of a diversity of relays and electrically operated circuit breakers makes circuit control in rural areas difficult. In addition, the small circuit breaker available for sectionalizing primary rural circuits has to be automatic reclosing. And yet, the performance of this little circuit breaker is nothing short of being miraculous. S. R. Faris, manager of Illinois Rural Electric Company, Winchester, Ill., reports:

During the heavy rains and floods of the spring of 1944 a landslide occurred on a bluff parallel to our line at a point about three miles west of the oil circuit breaker. Small trees of from three to six inches in diameter were carried into our line and the oil circuit breaker went to work. The landslide occurred about eight o'clock one morning and our members reported that our lights had been coming and going from that time until four the next afternoon when we finally discovered the condition.

We discovered the condition during a patrol of the line along the river. The land on which the line was built was almost all about eight feet under water. During this patrol the linemen stopped at the oil circuit breaker installation and could hear it operating once or twice every five to ten minutes. No reports of trouble had been received by our members on this line.

Upon arriving at the location of the landslide, our patrolmen found that the neutral wire was broken and that quite a few of the smaller trees had been burned off and cleared the phase wire. One tree, approximately four inches in diameter, had also been burned off and cleared, and another tree about six inches in diameter was up against the phase wire and it was about half burned in two. The power was still on, however, and it was necessary to kill the line before making repairs.

Upon reading the counter on the circuit breaker, we determined that it had operated approximately 93 times during this fault. After repairs were made and the trouble cleared up, the writer visited several members receiving service from the section of line controlled by this circuit breaker and questioned them as to why they hadn't reported the condition. The answers were all the same—they didn't think they should report an outage as long as the power kept coming and going and they felt sure it would clear up soon.

This is quite an accomplishment for a little circuit breaker.

The same system which installed 60 circuit breakers in 1942 reports:

Average number of operations per year per circuit breaker 12.12 with an average of 0.25 lockouts per month. The total operating expense saved by each circuit breaker per year is estimated as over $26.00. This is based on straight time pay, even though actually about 50 per cent of the outages had to be taken care of by overtime at time and a half. The cost of fuse replacements is offset by the cost of maintaining the circuit breaker.

However, even this investment is too high for minor primary tap lines. Two manufacturers therefore now are bringing out still smaller circuit breakers at considerably lower cost because this small circuit breaker requires practically no rupturing capacity. One manufacturer, for instance, furnishes the following description:

The sectionalizer is designed so that its contacts do not open during the time that a short circuit exists on the system. The actual clearing of line faults and interrupting of short-circuit current is performed by a backup recloser. The sectionalizer operates to disconnect the branch line only after one, two, or three operations of the backup recloser have failed to clear the line fault.

When a permanent line fault occurs beyond a sectionalizer which is backed up by a recloser, the short-circuit current flowing through the sectionalizer will prepare it for an opening operation. The short-circuit current which also flows through the recloser will cause it to operate in an attempt to clear the fault. During the time which the recloser is open, the sectionalizer moves forward one position toward the opening of the contacts. The second operation of the recloser again prepares the sectionalizer for an opening operation and during the time that the recloser is open the sectionalizer again moves forward another position toward opening. After the third operation of the recloser, the contacts of the sectionalizer are opened during the time that the recloser is open. In this way the faulted branch line is disconnected and when the recloser energizes the system after the third operation, the fault has been removed, allowing service to be continued to the balance of the system.

If the line fault is of a temporary nature, it will be cleared by the first or second operation of the recloser, and service to the entire system will be restored. Following this, the recloser and the sectionalizer will reset themselves automatically for another complete cycle of operations.

The sectionalizer may be adjusted to open on a permanent line fault after one, two, or three operations of the backup recloser. Inasmuch as the sectionalizer opens its contacts only during the no voltage period while the backup recloser is open, the sectionalizer is not required to interrupt short-circuit current. Consequently, there is no appreciable wear of the sectionalizer contacts or contamination of the insulating oil.

Even for the primary and secondary sides of the little distribution transformer manufacturers have been at work developing automatic devices to replace fuses. The type of transformer with internal primary fuse and internal secondary circuit breaker has become very popular. One manufacturer recently placed on the market a "fuseless cutout." This device is said to produce a dead short circuit to ground on the primary side when a heavy overload occurs on the secondary side or within the transformer, resulting perhaps in a heavy arc on the primary side. The main reclosing circuit breaker then trips. As soon as this happens the arc is extinguished. When the main reclosing circuit breaker recloses, the arc is out; the individual faulty transformer is disconnected; the reclosing circuit breaker remains closed; and the whole system, except for one consumer, again has service.

One reason against the latter two types is that every time there is a fault on the tap line or on the individual transformer, the main sectionalizing circuit breaker will open for a short period and many farmers will have to reset their clocks. But a farmer would much rather have to reset a clock than be without service for a considerable period.

Anyone who is familiar with the history of switchgear knows that no item of electrical equipment has been undergoing such a continuous process of change and improvement as has the circuit breaker. No circuit breaker design ever is finished. The need for major and minor improvements continually is revealed by continuous co-operation of manufacturer and operating man. No one therefore needs to be unduly disturbed if operating experience calls and will continue to call for improvements in the design of the rural sectionalizing circuit breaker which already meets unprecedented demands. It is certain that as the need for improvement is revealed, manufacturers will introduce them.

When the load on a line has been disconnected for any appreciable length of time and the line is re-energized, a large current, several times the normal value, flows. This current decreases with time but does not return to the normal value for an appreciable period sometimes running into minutes. This re-energizing phenomenon has been termed inrush current and is caused by the current inrush into resistance type loads, and more particularly by the starting requirements of direct connected motors.

The early types of reclosers used on rural circuits had a very short opening time delay. Consequently, in many cases when the recloser was closed back in on the load for re-energization purposes, the inrush current retripped the recloser.

In many cases the recloser had to be by-passed temporarily in order to pick up the load.

Some later designs have greater opening time delay, overcoming pickup difficulty to some extent. However, the exact shape or characteristic of the inrush current as it varies with time is not yet sufficiently known. Moreover, the rapid increase in the use of motors on the farm promises to make the problem much more serious.

Tests now are being carried on to determine the shape of the inrush current time curve and to predict the ultimate shape with the load growth. Preliminary tests on one section of rural line indicate an inrush current of less than 200 per cent of the normal peak after an outage of a few seconds. After an outage of one hour the inrush current was 400 per cent of the normal peak. But in all cases the inrush currents decayed to roughly one-third of their initial values in the first two seconds. It is hoped that results of further tests will be available soon.

Small rural generating plants run fewer machines at light load than at full load. The full load current at peak, therefore, may be more than the fault current during off-peak hours. The power factor of the load current is not vastly different from that of the fault current. Inexpensive devices are needed that will distinguish between load and fault currents, and which could be applied to pole-mounted reclosers.

In some cases of transformer failures the line sectionalizing devices may operate to lock out the lines before the transformer fuses blow. The transformer then may be very difficult to find. There seems to be a vast difference in characteristics of internal fuses furnished by different manufacturers. There is a need for standardization of internal fuses and development of recloser and fuse characteristics to co-ordinate more properly.

Voltage regulation problems on rural circuits are not vastly different from those on any circuit. They are only more aggravating, first because the rural circuits extend comparatively great distances from the source, and second because line investment must be kept to a minimum.

Original estimates of load on rural systems were difficult because very little experience was available as to rural power consumption. Later experience on rural systems has shown that the original estimates were too low, and a great deal of engineering is called for on many systems to bring the voltage regulation within acceptable limits. Now that the farmer is learning how to use electric power for production, experience shows that load estimates need to be revised sharply upward.

As already mentioned, the solution of the problem of voltage regulation is first of all waiting for the setting up of the basic circuit formula. Inexpensive low-capacity regulators with small steps are needed for regulating long branch lines. The rapid changes in load characteristics which may be expected in the near future would seem to make it imperative for manufacturers to explore the possibility of inexpensive secondary regulators. Perhaps some device eventually will be incorporated in the distribution transformer.

The rapid growth of motor power on rural systems indicates an eventual need for low cost capacitor installations to switch on and off automatically with load. Series capacitors no doubt would solve many a problem, but a competent system of protection for such capacitors still remains to be developed.

The problem of fault locating is as old as the electric circuit itself. Aggravating as a long delay in locating a fault may be in urban areas, it is even more aggravating in rural areas. And again the problem is aggravated by the imperative demand to do the job at low cost.

Rural distribution systems extend into remote areas which are frequently inadequately served with telephone facilities or have no telephone service at all. Outages in such areas may be prolonged because of lack of communication with the power maintenance office. There are cases on record in which the maintenance office was notified of outages by postal card and letter. Needless to say, such loads as milking machines, coolers, chick brooders, and water pumps make prolonged outages intolerable.

A carrier current outage recorder was manufactured experimentally and was undergoing field tests at the outbreak of the war. Further work on this equipment was suspended for the duration of the war. It consisted of a small low-cost carrier current transmitter located at each important sectionalizing point and an associated receiver located at the maintenance office. When an outage occurred a coded impulse from the appropriate transmitter was sent to the receiver, which activated a punch type paper strip recorder and time stamp. Thus, the location and time of the outage were recorded immediately. Provisions were made for another operation of the recorder when service was restored so that a complete record of the outage could be maintained.

After the end of the war the study was resumed. Several schemes which offer the possibility of being simpler and more reliable than the original one are being considered now. One of these schemes may make use of the radar pulse technique for detecting circuit irregularities and discontinuities. Another scheme may make use of the change in circuit impedance when an outage occurs.

It appears today that some competent means for reporting and recording outages automatically will be solved in the not too distant future.

Mention already has been made of the fact that the main problem of inductive co-ordination in rural areas is the cost of investigation. With the great amount of research and development over many years and the unusually high degree of co-operation by power system engineers and communications engineers, there is as yet no cut and dried method either for locating the source of trouble or for designing the remedy. Each case is still practically an individual research job, and each remedy still has to be practically a tailor-made job. Special equipment is required for testing, and it takes a good engineer a considerable time as an assistant on actual cases before he can take charge of investigating a case on his own and designing the remedy. This applies equally to telephone interference, telegraph interference, and railway signal interference. A complete visualization of the simultaneous functioning of an interconnected power system is called for, superimposed on a visualization of the functioning of the communications system, in addition to a familiarity with the functioning of each part of each system. The ability for such a visualization cannot be acquired in a day. It is utterly impossible and no doubt will continue to be impossible to do such a job from a text book, even if a good text book were available, which is not yet the case. Neither could the best special college course prepare an engineer to be able to assume the responsibility without first having served as an assistant on several actual cases.

With the exception of radio, full co-operation prevails between the engineers of power systems and those of communication systems, so that neither side is called upon to carry alone the burden of the investigation and the design and installation of the remedy. Power systems and communication systems both find it advisable to have specially trained engineers available. These engineers on both sides generally communicate with each other and tackle the job jointly. It is suggested respectfully that every young

electrical engineer who makes power his career make every effort to find an opportunity to participate in at least two or three inductive co-ordination investigations from the first report of the trouble, through the tests, the preparation of the report, and the installation and testing out of the remedy. It will help him acquire a visualization of the functioning of a power system. Not only do the engineers on both sides co-operate after a case of interference actually is reported, they also consult with each other when a power system or a communication system is being designed and thus prevent in advance as much as possible the appearance of interference. Research laboratories and manufacturers of power and communication equipment likewise render their services and co-operation.

In the field of radio such co-operation has not yet been established, and this applies not only to rural systems but to all power systems. When a case of radio interference is reported, the whole burden of locating the source of trouble and designing and installing the remedy has to be carried by the power system. It is hoped that it will be possible soon to establish between the engineers of power systems and those engaged in broadcasting, radio research, and radio manufacturing the same degree of co-operation that now prevails in other fields of communication.

There is now a great need for a simple, practical, and inexpensive radio interference locating instrument, specifically for rural areas. It is hoped that radio research institutions soon will bring out not just one such instrument, but a diversity of instruments. Here, as in most fields, competition will result in progress. There is definitely a quantity market for such an instrument.

In addition to the previously referred to possible use of carrier for the automatic recording of outages, carrier recently has been tried out on some rural power systems for communication purposes for power system maintenance. Here too the difference between carrier on high voltage lines and carrier on rural lines is principally one of permissible cost. The developments have not gone far enough for a competent analysis on the AIEE platform.

This applies also to 2-way radio as an auxiliary to maintain the rural power system. Some interesting and promising developments are taking place now, but they do not yet lend themselves to a competent AIEE presentation. Possibly, leased radio channels furnished by telephone systems will be the best answer, just as leased telephone wires were found by many power systems to offer advantages over private telephone circuits on the transmission towers or on separate poles.

All of this relates only to communication problems for the power system itself and not to the problem of communication for the farmer. Particularly in the case of carrier there has been some confusion of the two, and it is important to establish the distinction. Recently an unprecedented demand for telephone service developed among farmers throughout the country. This probably was brought about partly by the enormous increase in the use of mechanical and electric equipment on the farm. The challenge was taken up and is being attacked rigorously from three angles.

1. There is a great activity in the extension of direct wire communication to farms.

2. Intensive studies are being made and experiments carried on in the joint wire use of power poles for telephone and telephone poles for power.

3. Intensive experiments are being carried on in the joint use of carrier telephone on power lines to render telephone service to farmers who have electric power service.

The latter two developments are not yet ready for a competent AIEE presentation. It is sufficient to mention that numerous intricate engineering problems, some apparently picayune but actually very difficult and annoying, are involved in joint wire use and joint carrier use. In connection with carrier it is important to mention that there is a great difference between the incidental use of a carrier phone by a lineman to talk to his headquarters and the continuous use of telephone service by a domestic or commercial telephone subscriber. Several years of research at great cost have been devoted to the latter problem, both in the laboratory and in the field, before the first experimental instruments were installed in farm homes. Here again, the cost is of extreme importance. One of the bottlenecks of cost was the coupling capacitor. For a long time the cost appeared to be prohibitive, until a progressive American manufacturer developed a capacitor for a 7,200-volt line, with a dry impulse flashover of about 200 kv and at a cost of around $10. It is reasonable to say that without this development carrier telephones in quantity would not be an immediate prospect for the American farmer. They are definitely so now.

This is about all which is considered practical to present within the scope of a single paper. But it is hoped that it will serve the purpose of bringing about a realization in the electrical engineering profession that the humble rural circuit offers important engineering problems worthy of the serious consideration of the electrical engineer. It is hoped that it will result in a much broader realization of the utter necessity of co-operation between system design engineers, operating engineers, manufacturing engineers, and research engineers.

Appendix. Applications of Electricity for the Farm

Farm Home

Air conditioner
Air sterilizer
Alarm
  Burglar
  Fire
Amplifier
Aquarium heater
Attic fan
Bell
Bell ringing transformer
Biscuit baker
Blanket
Bottle
  Sterilizer
  Warmer
Bread mixer
Broiler
Bun warmer
Can opener
Casserole
Cauterizer
Chafing dish
Chimes
Cigar lighter
Clippers
Clock
  Household
  Time
Coal stoker
Coffee
  Maker
  Mill
Communication system
Corn popper
Cream whipper
Croup kettle
Curling iron
Dehydrator
Dishwasher
Door opener
Double boiler
Doughnut kettle
Dumb-waiter
Egg
  Beater
  Cooker
  Poacher
Evaporative cooler
Fan
Floor
  Polisher
  Sander
  Waxer
Flour and cereal mill
Flour sifter
Fly trap
Food
  Chopper
  Mixer
  Warmer
Freezer
  Cabinet
  Walk-in
Fruit and vegetable juicer
Fruit corer and peeler
Frying pan
Furnace fan
  Circulating
  Forced draft
Games
Garbage disposer
Grill
Hair drier
Hand drier
Heating pad
Hedge clipper
Hot plate
Humidifier
Ice cream freezer
Ice maker
Insect
  Trap
  Eradicator
Iron
Ironer
Laundry drier
Lawn
  Edger
  Mower
Lights
  Building
  Decorative
  Photoflood
  Yard
Massager
Meat
  Cooker
  Grinder
Milk shaker
Motion picture projector
Necktie presser
Oil furnace
Organ
Oven
Oven (infrared)
Paint sprayer
Pants presser
Percolator
Phonograph
Photoenlarger
Player piano
Pottery kiln

Pump jack
Radiation
  Infrared
  Ultraviolet
Radio
Range
Razor
Refrigerator
  Household
  Walk-in
Roaster
Room heater
Sausage
  Grinder
  Stuffer
Scissors
Screen
Sewing machine
Shoe polisher
Siren
Slicer—food
Space heater
Steam iron
Steam radiator
Straw flower drier
Sump pump
Teakettle
Televisor
Toaster
Tooth brush
Toys
Vacuum cleaner
Vaporizer
Ventilator
Vibrator
Waffle iron
Washing machine
Water
  Chlorinator
  Cooler
  Heater
  Pail
  Softener
Water system
  Deep well
  Jet
  Shallow well
Wiener roaster
Woodburner—decorative

Farm Equipment

Crop Processing

Baler
Blower
  Grain
  Roughage
Bulb cooker
Caster bean huller
Clover huller
Cider mill
Conveyer
Corn
  Cracker
  Sheller
Dehydrator
  Fruit
  Vegetable
Drier
  Grain
  Hay
  Hop
  Nut
  Seed
Elevator
  Grain
  Roughage
Ensilage cutter
Fanning mill
Feed
  Carrier
  Chopper
  Cooker
  Grinder
  Mixer
Filbert huller
Flour and cereal mill
Freight elevator
Fruit
  Apple butter maker
  Cleaner
  Grader
  Washer
  Waxer
Grain sprouter
Green feed chopper
Hay
  Chopper
  Crusher
  Hoist
Husker—shredder
Irradiator—seed
Metal removing magnet
Molasses heater
Oat huller
Pea and bean huller
Pea viner
Peach defuzzer
Potato
  Grader
  Seed cutter (Idaho)
  Washer
Root
  Chopper
  Shredder
Seed
  Cleaner
  Duster
  Germinator
  Grader
  Scarifier
Storage
  Fruit
  Vegetable
Straw chopper
Sugar cane press
Sweet potato
  Curer
  Shredder
Thresher
Tobacco curer
Vegetable
  Grader
  Tier
  Washer
Walnut separator

Dairy

Agitator
  Cheese vat
  Milk can
  Milk cooler
  Pasteurizer
Air conditioner
Alarm
Barn cleaner
Boiler
Bottle washer
Bottling machine
Brine pump
Bull exerciser
Butter worker
Calf weaner
Cheese maker
Churn
Clippers
Cream
  Ripener
  Separator
Fan
Feed
  Carrier
  Grinder
  Mixer
Fence
Fly
  Screen
  Trap
Groomer
Heating cable—water pipe
Homogenizer
Ice cream
  Freezer
  Stirrer
Insect sprayer
Irradiator
Lights
  Building
Liquid manure pump
Litter carrier
Manure
  Carrier
  Drier
  Pump
Milk
  Pump
  Tester
Milk cooler
  Dry
  Immersion
  Surface
Milking machine
Ox-grub remover
Pasteurizer
Prod
Radiation
  Infrared
Radio
Silage unloader
Space heater
Steam accumulator
Sterile lamp
Stock tank heater
Utensil sterilizer
Ventilator
Water heater
Water pail

Farm Shop

Air compressor
Alarm
  Burglar
  Fire
Battery charger
Buffing wheel
Concrete
  Mixer
  Vibrator
Drill
  Portable
  Press
Emery wheel
Forge blower
Glue pot
Grinder
  Implement
  Tool
Grindstone
Hoist
Lathe
  Metal
  Wood
Lights—building
Paint
  Brush cleaner
  Drier
  Mixer
  Sprayer
Planer
Portable motor
Pump
  Gas
  Grease
Sander
Saw
  Band
  Buck
  Circular
  Cross-cut
  Hack
  Jig
Shaper
Soldering
  Iron
  Pot
Space heater
Vulcanizer
Welder
Wood
  Saw
  Splitter

Field Operations

Cultivator
Irrigation
Manure pump
Stump
  Burner
  Puller
Tractor
Truck

Horticulture

Bleacher—vegetable
Bulb
  Drier
  Grader
Cider mill
Cultivator
Elevator
  Box or crate
  Fruit
  Vegetable
Fans—orchard
Fruit
  Drier
  Grader
  Storage
  Washer
Greenhouse
  Fan
  Heater
  Ventilator
Hotbed heater
  Cable
  Lamp
Humidifier
Insect
  Sprayer
  Trap
Irrigation pump
Lights
  Building
  Greenhouse
  Plants
Pollinator
Seed germinator
Soil
  Shredder
  Sifter
  Sterilizer
Soil heating cable
  Greenhouse
  Hotbeds
Soilless culture
  Pump
  Solution heater
Stationary spray plant
Sweet potato curer
Vegetable
  Drier
  Grader
  Storage
  Tier
  Washer
Viner—pea
Water heater

Insect

Comb wire imbedder
Fly
  Screen
  Trap
Hive heater
Honey extractor
Insect sprayer
Insect trap
  Field
  Fish feeding
  Home
  Orchard

Livestock

Animal prod
Branding iron
Brooder
  Lamb
  Pig
Bull exerciser
Clipper
Feed
  Cooker
  Grinder
  Mixer
Groomer
Hog caller
Lamb docker
Lights
  Building
Litter carrier
Manure
  Carrier
  Drier
Meat processing
  Brine pump
  Fat cooker
  Fat cutter
  Freezer
  Grinder
  Hoist
  Refrigerator
  Saw
  Sterile lamp
Ox-grub remover
Radiation
  Infrared
Sheep shears
Stock tank heater

Miscellaneous

Fish barrier
Limestone pulverizer
Well drill
Worm getter

Poultry

Alarm
  Burglar
  Fire
  Temperature
  Voltage
Bone grinder
Brooder
  Battery
  Hover
  Room
Caponizer
Cleaner
  Dropping board
  Incubator
  Poultry house
Debeaker
Egg
  Candler
  Cleaner
  Cooler
  Grader
  Washer and dryer
Electrocutioner
Foot piercer
Grain sprouter
Grinder
  Bone
  Shell
Hatcher
Heating cable—water pipes
House heater
Incubator
Lights
  Building
  Poultry
Manure shredder—grinder
Mash warmer
Picker
Radio
Scalder
Singeing device
Time clock
Ultraviolet

Self-Excited Electromagnetic Drive for a Resonant Fatigue Machine

ABNER R. WILLSON
MEMBER AIEE

Synopsis: This paper describes the development of low frequency and self-synchronous electric drive equipment for fatigue life testing machines. These test machines simulate the vibrating loads that result from reciprocating engines, variable air loads, and so forth. The self-synchronous feature is important because the inherent high mechanical Q of the system amplifies some 10 to 50 watts of drive power into 2,000 to 5,000 pounds of vibrating load at frequencies from 7 to 40 cycles per second. Mechanically driven types lack sufficient speed stability to maintain resonance, and this results in poor control of the specimen test load. The power requirements for large loads at high speeds are excessive. An experimental 5,000-pound machine with self-excited electromagnetic drive is described. This electric drive is low in both original and maintenance costs. The specimen load is controlled as simply as the volume on a radio receiver. A 100,000-pound machine is nearing completion and is discussed briefly.

DURING the past few years the testing of alloy metals and structures under vibrating loads has assumed an ever increasing importance, especially in the manufacture of structures subject to the vibration of high power reciprocating engines, variable air loads, and imperfectly balanced rotating machinery. Fatigue testing has been practiced by most structural test laboratories to some extent for many years. The common practice has been to apply the vibrating loads by rotating eccentric weights or mechanically driven vibrating cantilever beams. These mechanical systems have inherent limitations which prevent accurate control of the applied force and vibrating frequency. Maintenance costs have been high, and interruptions because of mechanical failures have been too frequent.

The several types of electric drive systems which have been used, all have had characteristics that were not adequate for the type of fatigue testing described in the foregoing paragraph.

1. One type required an alternator with a complex type of frequency control.[1]

2. Another required that the test specimen be a bar of limited dimensions.[2]

3. A third was a separate drive solenoid motor which was connected mechanically to the specimen and excited by a separate oscillator and amplifier. The load limit was considerably below the requirements.[3]

4. A self-resonant type was adapted to the vibration testing of large beams suspended so as to vibrate at their natural frequencies.[4]

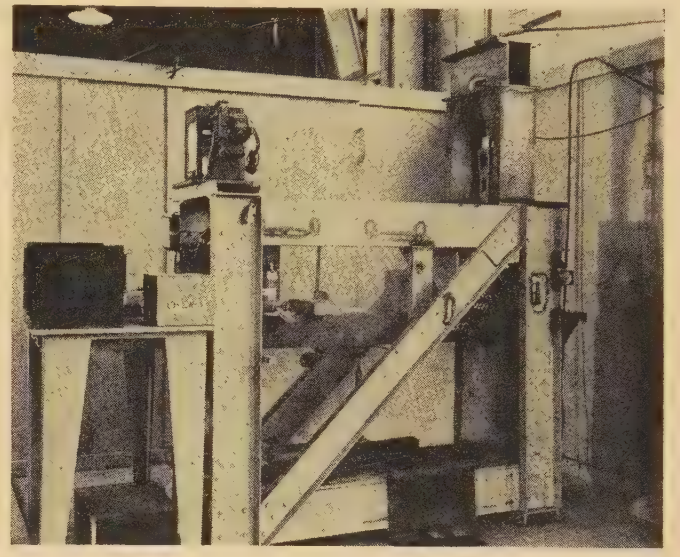

Figure 1. A 5,000-pound fatigue machine, amplifiers, recording meter, actuator solenoid assembly, vibrating beam, and test specimens

In order to design equipment which would meet the requirements of the proposed test program an experimental model was developed which provided a maximum peak-to-peak vibrating load change of 5,000 pounds. The preload may be adjusted to 7,500 pounds which results in a maximum specimen load of 10,000 pounds (refer to Figure 1). A second fatigue machine has been designed and constructed for 100,000-pound maxi-

Ventilator
Water warmer
Waxer
Wax remelter

Referen

1. ERDSTROEME (book), **F. Ollendorff.** Julius Springer, Berlin, Germany, 1928.

2. ERDUNG, NULLUNG, UND SCHUTZSCHALTUNG (book), **Oscar Loebel.** Julius Springer, Berlin, Germany, 1933.

3. GROUNDING PRINCIPLES AND PRACTICE, I—FUNDAMENTAL CONSIDERATIONS ON GROUND CURRENTS, **Reinhold Rüdenberg.** *Electrical Engineering*, volume 64, January 1945, pages 1–13.

4. GROUNDING PRINCIPLES AND PRACTICE, II—ESTABLISHING GROUNDS, **Claude Jensen.** *Electrical Engineering*, volume 64, February 1945, pages 68–74.

5. GROUNDING PRINCIPLES AND PRACTICE, IV—SYSTEM GROUNDING, **W. R. Bullard.** *Electrical Engineering*, volume 64, April 1945, pages 145–51.

6. INDUCTIVE CO-ORDINATION OF REA LINES AND BELL SYSTEM LINES, **Lee M. Moore, H. R. Huntley.** *Electrical World*, October 13, 1945.

7. INDUCTIVE CO-ORDINATION OF REA DISTRIBUTION SYSTEMS AND TELEPHONE SYSTEMS, **W. T. Smith, K. J. Plucknett, T. A. Taylor.** AIEE TRANSACTIONS, volume 60, 1941, pages 586–95.

8. CARRIER INDICATOR REPORTS RURAL OUTAGES, **D. E. Basler, J. F. Atkinson.** *Electrical World*, February 22, 1941.

9. NEW IDEAS IN RURAL ELECTRIFICATION ENGINEERING, **M. M. Samuels.** *Agricultural Engineering*, March 1941.

10. NEW ENGINEERING AND A NEW INDUSTRY, **M. M. Samuels.** *Electrical Engineering*, volume 61, October 1942, pages 517–20.

11. EXPERIENCE WITH OIL CIRCUIT RECLOSERS ON REA SYSTEMS, **Lee M. Moore, B. O. Watkins.** AIEE TRANSACTIONS, volume 62, 1943, August section, pages 531–5.

12. USES AND SOURCES OF ELECTRIC POWER, **M. M. Samuels.** *The Annals of the Academy of the Political and Social Science*, November 1945.

13. ELECTRO-AGRICULTURAL EQUIPMENT FOR WAR AND PEACE, **J. P. Schaenzer.** *Agricultural Engineering*, November 1943.

14. ESSENTIALS OF A FARM TYPE FROZEN FOOD CABINET, **E. C. Meyer.** *Agricultural Engineering*, March 1943.

15. ENGINEERING FARM REFRIGERATION, **J. P. Schaenzer.** *Agricultural Engineering*, August 1945.

Paper **46-194**, recommended by the AIEE committee on industrial power applications for presentation at the AIEE Pacific Coast meeting, Seattle, Wash., August 27–30, 1946. Manuscript submitted June 25, 1946; made available for printing July 19, 1946.

ABNER R. WILLSON is an electrical test engineer, structural test department, Boeing Aircraft Company, Seattle, Wash.

The author expresses appreciation to H. L. Adams, chief of the Boeing structural test unit for valuable assistance in the design of the mechanical portions of the electric system, and to Ray C. Fisher and Robert M. Wisner of the physical research unit for assistance in the design of portions of the electric system.

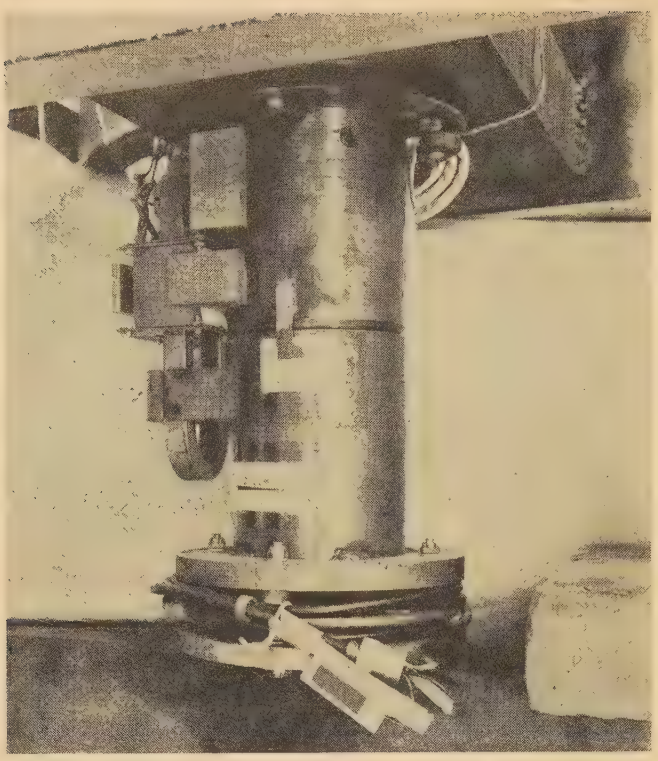

Figure 2. Electromagnetic actuator and pickup, strain gauges and shielded cable, and wedge for indicating vibration amplitude

mum loads. The electric drive is nearing completion (June 1946) but performance data are not yet available. These machines may be adjusted so that the specimen may be vibrated in tension alone, in compression alone, or in a combination of tension and compression.

The Mechanical Problem

The problem was to design and construct a relatively low cost fatigue machine of the resonant type which would provide large vibrating loads and require a minimum of operating supervision and maintenance expense. The resonant type was chosen because of the inherent large amplification of the synchronous drive force into the specimen load.

Rotating beam and other small standard machines were not acceptable because of the limitations in size and shape of test specimens. These machines were designed primarily for test coupons of small dimensions to determine the fatigue life of test specimens of various materials. The requirements for the equipment were not to establish the fatigue lives of present materials but rather to determine the comparative fatigue lives of proposed or actual existing airplane construction members. Typical test problems include the comparative performance of various types of rivets and bolts alone and rivet and bolt patterns on assembled structural sections. Comparative fatigue data also are required for various types of welds and new materials.

The vibrating load demands were to be from a few hundred to 5,000 pounds. These loads would be the peak-to-peak loads as shown in Figure 11. That is, the specimen would be preloaded statically in excess of half the total vibrating load, and the resulting maximum and minimum specimen loads then would be the preload plus or minus one-half of the peak-to-peak vibrating load change. For the example shown in Figure 11 the preload was 2,350 pounds, and the vibrating load change was 3,766 pounds. The maximum specimen load was 4,233 pounds, and the minimum was 467 pounds.

The 5,000-Pound Machine

The development model of the Boeing fatigue machine is illustrated in Figure 1. The vibrating beam is a pair of 6-inch commercial steel channels supported at the right end by flexure pivots. The beam is vibrated by the actuator solenoid assembly shown at the left end of the beam in Figure 1 and also in Figure 2. This actuator is in two sections. The top half is bolted to the framework, and the lower part is fastened to the vibrating beam with four one-quarter-inch aluminum-alloy bolts on which are mounted strain gauges.[5] Copper tubing electrostatically shields and mechanically protects the gauges and their leads. The shielded cable shown coiled around the lower shell connects the gauges to a

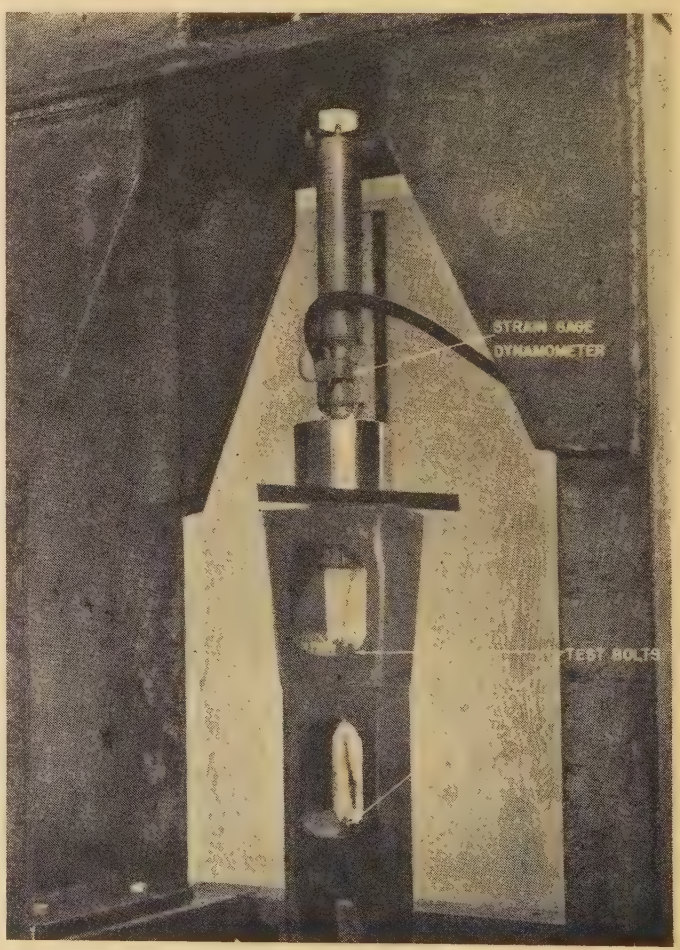

Figure 3. Test bolts and strain gauge dynamometer

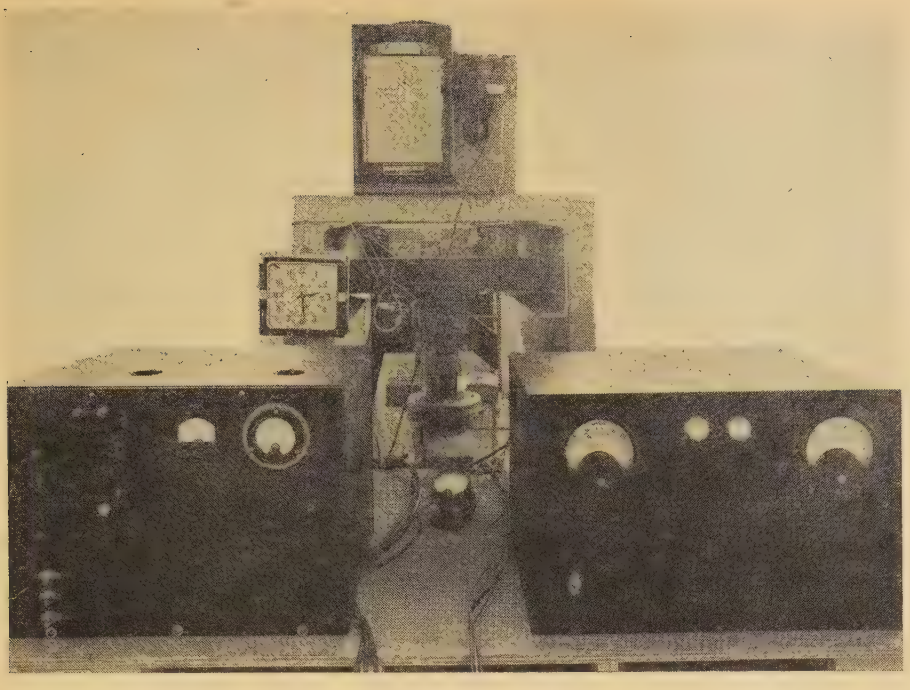

Figure 4. Amplifiers for 5,000-pound fatigue machine

The recording amplitude meter shows the preliminary adjustment of preload and adjustment of impedance matching transformers. The machine was operating with a specimen load of about 3,000 pounds

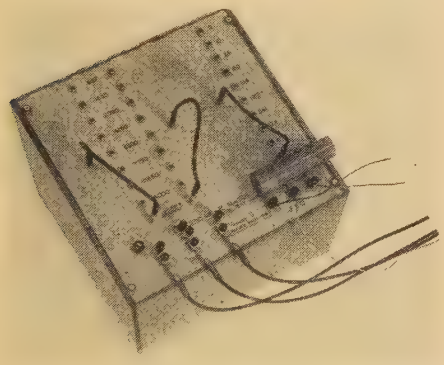

Figure 5. Impedance matching transformer for 5,000-pound fatigue machine

vacuum tube voltmeter and recording oscillograph to indicate and record the driving force.

The test specimen is attached between the fixed support shown at the upper right in Figure 1 and a point on the vibrating beam near the flexure joint to give a 9.5-to-1 mechanical advantage. The test specimens illustrated in Figures 1 and 3 are 5/16-inch special alloy steel bolts. The bolt heads and nuts are shown at the bottom and top of the O jigs. Strain gauges are mounted on the top adjustment bar. These gauges are for measuring the loads in the specimen, both static and dynamic. These specimens were preloaded with the flat spring and turnbuckle shown in the lower part of Figure 1. The preload is measured statically by the strain gauge output into a d-c bridge-type instrument which is calibrated directly in pounds per square inch. This instrument with its white dial is shown at the lower center in Figure 12. The recording strip chart meter shown at the top of Figure 4 indicates the amplitude of beam vibration and is therefore an indication of the load in the specimen. The broken curve on the strip chart shows the preliminary calibration of the meter and adjustments of the amplifier output and impedance matching for the bolt test. The exciting voltage is generated by the pickup (Figure 2), amplified by the equipment shown in Figure 4, and fed through the impedance matching transformer (Figure 5) into the actuating solenoid (Figure 2). Each of these electric components is to be described.

The Electric Circuit

The electric circuit may be considered as that of an oscillator with the output sufficiently amplified to drive the vibrating beam (refer to Figures 2, 4, and 6). The exciting voltage is generated by a permanent magnet attached to the vibrating beam and vibrating into fixed coils (Figure 2). The pickup voltage is usually in the order of three to six volts. It is fed to the input circuit of the amplifiers (Figure 4). The amplifier output is impedance matched to the actuator winding by a special transformer designed for the 7- to 40-cycle-per-second frequencies (Figure 5). The polarizing coils are energized by the rectified power supply for the 6L6 amplifier. A filter separates the polarizing current from the plate voltage supply to the amplifier tubes.

The recording meter, Figure 4, indicates the amplitude of the vibration of the beam. It is a 0–1.4-volt 1,400-ohm d-c voltmeter. It is connected to the output of the pickup coil through a series calibrating resistor and a small dry rectifier. The meter reading follows the amplitude of the beam vibration with sufficient range and accuracy for any one test frequency and load condition. The strip chart gives a continuous record of specimen load and operating time. The vibrating specimen loads first are measured with strain gauges and an oscillograph. The recording meter then is calibrated for that test condition. The record on the strip chart meter shows a gradual decrease slightly before the specimen fails.

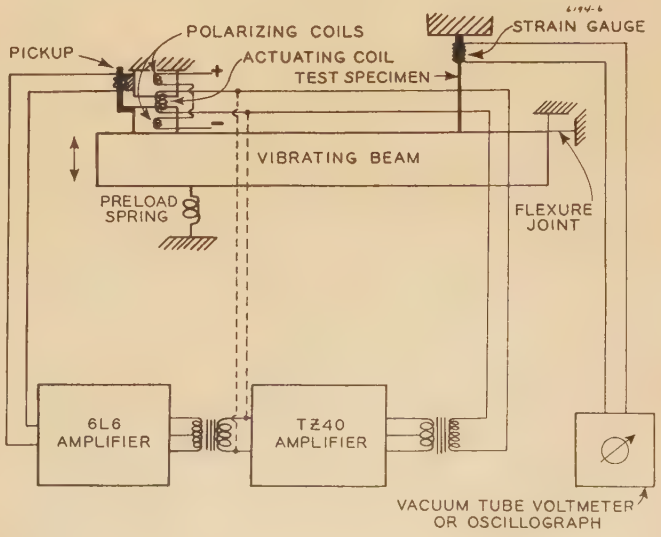

Figure 6. Electric circuit of the 5,000-pound fatigue machine

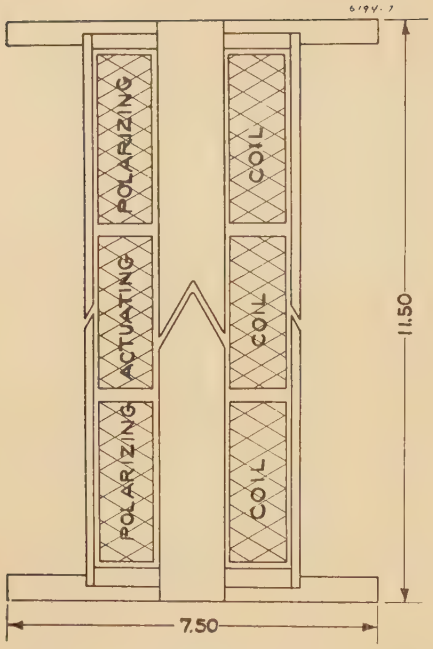

Figure 7. Cross section of the actuator solenoid assembly

After the failure of the specimen the beam falls on a limit switch which opens all electric circuits including the electric drive on the strip chart.

The Actuator System

A cross section of the actuator system is shown in Figure 7. A polarizing magnetic field is induced by the top and bottom coils. They are wound with number-30 enameled magnet wire and usually are worked at about 2,500 ampere turns. The central coil corresponding to the voice coil in a loud speaker, supplies the actuating force. This coil, the load for the output of the amplifier, usually is worked at an alternating current density of 150 to 350 milliamperes and at frequencies between 12 and 30 cycles per second. The impedance characteristics of the actuator coil will be discussed.

Motional Impedance of the Actuator Solenoid

Measurements were made of the vibrating and blocked impedance components of the actuating coil with the normal 50-milliampere polarizing current in the field coils. The exciting alternating voltage was from an audio oscillator. The test set up was as shown in Figure 8, and the vector relationships of the quantities measured were as shown in Figure 9.

The voltages across *BD* and *ED* were measured at the resonant vibrating frequency of the mechanical system (19.6 cycles per second) and also at other frequencies from 18 to 50 cycles per second. The impedance components were calculated and plotted as shown on the curves in Figure 10. From these data the motional impedance[6] and the drive efficiency of the actuator coil were determined.

The impedance values for the 19.6-cycle-per-second natural mechanical resonant frequency are listed in Table I.

Motional impedance = 365 ohms

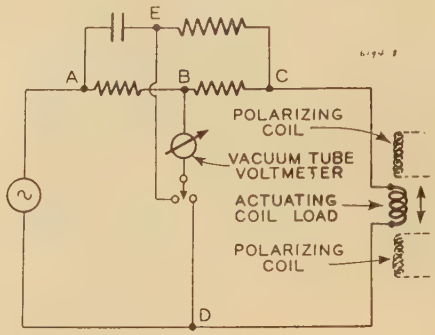

Figure 8. Setup for measuring motional impedance

For vector relations refer to Figure 9

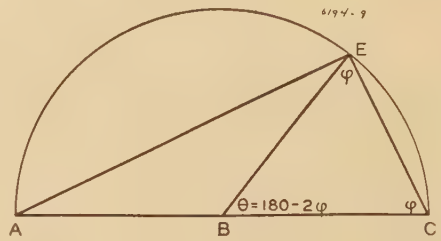

Figure 9. Vector relations of the voltages in Figure 8

The motional impedance is the difference between the 666-ohm resistive component of the vibrating impedance and the 301-ohm resistive component of the blocked impedance.

Efficiency $(666 - 301)/(666) = 55$ per cent

This efficiency may be defined as the ratio of output power to input power when the load resistances for these quantities are considered as

$$\frac{\text{Vibrating resistive component} - \text{blocked resistive component}}{\text{vibrating resistive component}} = 55 \text{ per cent}$$

The sharp resonance curves show the importance of operating the electric drive at the mechanical resonant frequency. The power into the actuator coil is obviously a maximum when the motional resistive component is a maximum.

Amplifier

The amplifier is in two sections. The first has a 6J5 tube input, and a push-pull 6L6 output with transformer coupling between the 6J5 plate and the 6L6 grids. When the specimen loads are less than 2,000 pounds the output of the 6L6 plates is fed through a special impedance matching transformer directly to the actuator coil. For greater loads the 6L6 output drives the second amplifier section which has push-pull TZ40 tubes. The output is coupled to the actuator through a second special impedance matching transformer (Figure 5). The output of the 6L6 amplifier directly into the load at 12 to 30 cycles per second is 15 to 30

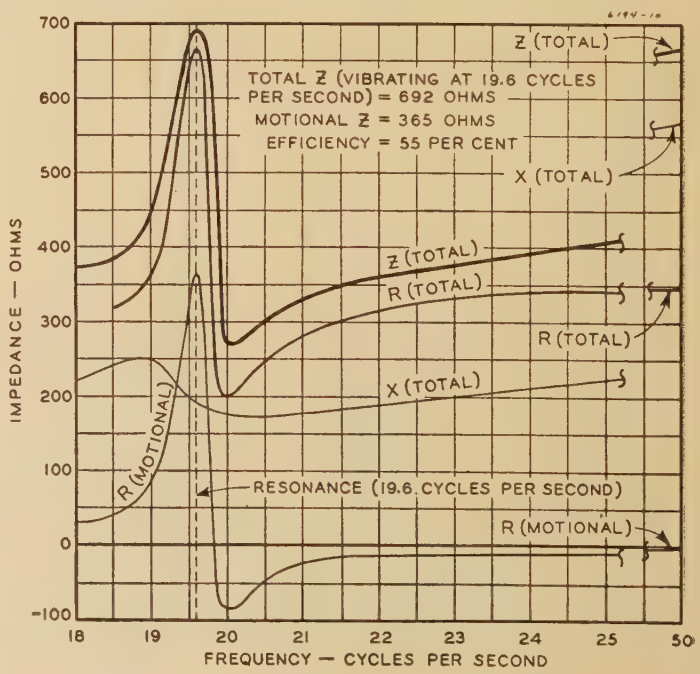

Figure 10. Variation of impedance components with frequency

Because the driving power is a function of the resistive component it is evident that a small departure from resonance means a large loss in power

watts. For greater specimen loads the TZ40 amplifier delivers 30 to 90 watts at the same frequencies. In this case the 6L6 amplifier supplies only the three to six watts required to drive the TZ40 grids.

Low Frequency Transformers

When one considers the comparative sizes of conventional power transformers of equal kilovolt-ampere and voltage ratings to operate on 400-, 60-, and 25-cycle circuits it will be evident that the 7- to 40-cycle power requirements of the vibrating machine demand transformers with much copper and iron in order to face both the tube output and the actuator input circuits with sufficient inductance to transfer the low frequency energy with reasonable transformer losses and proper impedance matching.

The impedance matching transformer illustrated in Figure 5 is used to match the TZ40 push-pull plates to the actuator coil. For vibrating the specimens shown in Figure 3 the plate-to-coil impedance ratio was 59 to 1. The frequency for this test was 12.5 cycles per second.

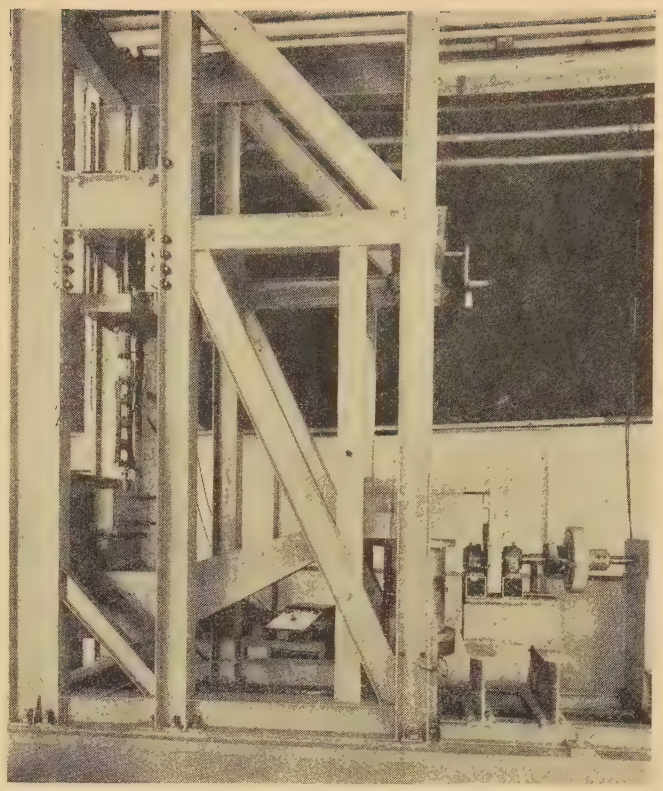

Figure 12. A 100,000-pound fatigue machine

The vibrating beam weighs 1,100 pounds and the actuator coil assembly weighs 440 pounds; five-eighths-inch heat treated bolt specimens are being fatigue tested

Performance

A typical test setup is shown in the illustrations. The test specimens were 5/16-inch special alloy bolts. The initial preload and vibrating load in the specimen was measured by the output of the specimen strain gauges. The force produced by the actuator solenoid was measured by a second set of strain gauges. The oscillograph curves reproduced in Figure 11 show the static preload and the magnitude and phase relation of the force supplied by the electric drive system and the resulting vibrating load change in the test bolts. The over-all Q of the system was 100. This 100-to-1 ratio of the 3,766-pound load in the specimen bolts to the 27.7-pound driving force results from the 9.5-to-1 mechanical advantage of the application points of the driving force and specimen load and the amplification which results from operating the beam system at its natural resonant frequency.

Table I. Impedance of the Actuator Solenoid

Component	Impedance, Ohms
Total vibrating, 15.7° phase angle	692
Resistive	666
Reactive	184
Total blocked, 34.5° phase angle	365
Resistive	301
Reactive	206

The lead weight shown clamped to the beam in Figure 1 lowered the natural frequency of the beam system as it was moved away from the pivot point. Lowering the frequency increased the specimen load but decreased the transformer efficiency. The optimum frequency for this test condition was 12.5 cycles per second.

Measurements were made of the various voltages and currents while operating with a 3,000-pound load change in the specimens. These rms voltages and currents are listed in Table II. When operating with a 4,000-pound load in the specimens the actuator alternating current was 250 milliamperes.

The 100,000-Pound Vibrating Machine

A vibrating machine was designed for a maximum specimen load of 100,000 pounds. This is 50,000 pounds vibrating load change and 50,000 pounds preload. The mechanical portion has been completed and temporarily is being driven for light specimen loads by a mechanical eccentric until completion of the electric drive (Figure 12). Three five-eighths-inch bolts were being tested in the O jigs at the left. Directly above the specimens is shown a copper cylinder which electrostatically shields and also mechanically protects the strain gauges which measure specimen loads. The static prestress is measured on the d-c

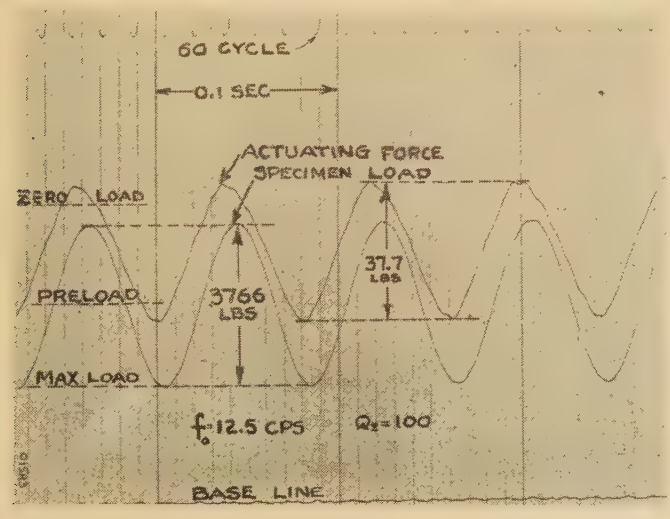

Figure 11. Oscillograph record of the actuating force and resulting load in the specimen

A Q of 100 was obtained for this test at 12.5 cycles per second

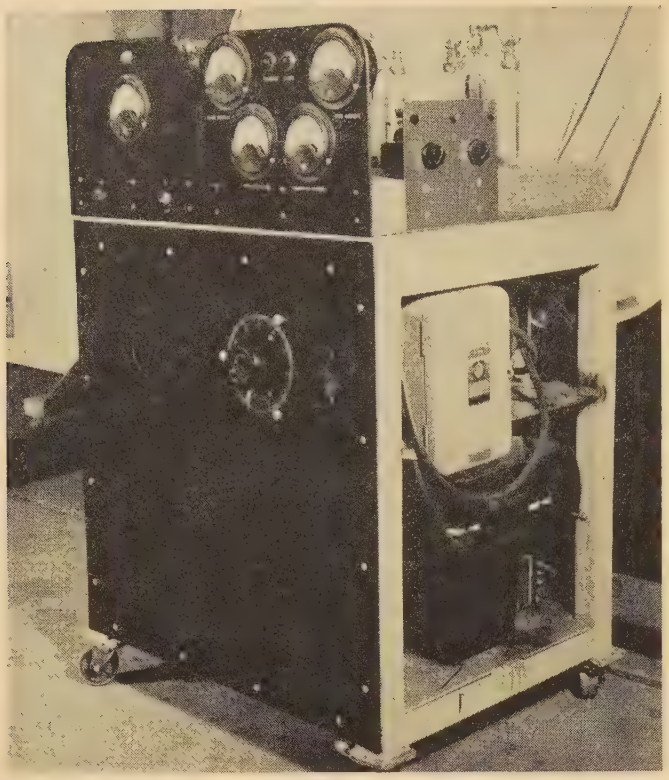

Figure 13. Amplifiers for 100,000-pound fatigue machine

Table II. Voltages and Currents at 3,000-Pound Load Change

	Rating
Pickup voltage	5
Coupling transformer primary voltage	150
Coupling transformer secondary voltage	78
Output transformer primary voltage	530
Output transformer secondary (load) voltage	84
Load current (ma)	130
Polarizing current (ma)	40

bridge shown at the central rear. Dynamic loads are measured with a vacuum tube voltmeter and oscillograph as in the measurements for the 5,000-pound machine. The lower specimen mounting is fastened near the pivot point of the 1,100-pound offset beam. The 12-inch cylindrical sections which house the polarizing and actuator coils are shown at the right end of the beam. The top section vibrates with the beam, and the lower section is fastened to the framework. A large helical preload spring is mounted directly above the actuator assembly and is adjusted by the hand crank shown at the upper right. The preload also may be adjusted by the specimen adjusting bolts shown at the upper left.

The actuator assembly consists of the 12-inch steel shells, the enclosed polarizing coils at the top and bottom, and the actuating coil at the center. The weight of the copper wire is 170 pounds, and the steel shell and core assembly weighs 270 pounds. The polarizing coils will be operated at 2,000 to 5,000 ampere turns, and for maximum load conditions the actuator is expected to require about 400 watts. A permanent magnet and a solenoid attached respectively to the stationary and moving shell sections will furnish the synchronous exciting voltage to the amplifier input. The driver amplifier is a 6L6 type similar to the one described for the 5,000-pound machine. The power amplifier stage contains push-pull RK63 power tubes rated at 200 watts plate dissipation. Special low frequency transformers couple the two amplifiers and match the output of the power stage to the actuator solenoid. Preliminary tests have indicated that the operating frequencies will be from 7 to 40 cycles per second.

References

1. Testing Material in the Resonance Range, **R. K. Bernhard.** *Proceedings*, American Society for Testing Materials, volume 41, 1941, pages 747-57.

2. Reflex Fatigue Machine. Baldwin Southwark Company, Philadelphia, Pa., Bulletin 145, 1944.

3. Electronic Vibration Exciting Equipment. Rollen Company, Pasadena, Calif., Bulletin 35, 1945.

4. Acceleration of Fatigue Tests, **R. A. Hudson, J. E. Chick.** *Aero Digest*, September 1937.

5. SR-4 Strain Gage. Baldwin Southwark Company, Philadelphia, Pa., Bulletins 164 and 171.

6. Dynamical Analogues (book), **H. F. Olson.** D. Van Nostrand Co., Inc., New York, N. Y., 1943, chapter VIII.

Application of Compandors to Telephone Circuits

C. W. CARTER, Jr.
MEMBER AIEE

A. C. DICKIESON
MEMBER AIEE

D. MITCHELL
NONMEMBER AIEE

Synopsis: Prior to the war a compandor was developed for general use on telephone circuits of the Bell System. This equipment provides power range compression at the transmitting end and power range expansion at the receiving end of a telephone channel. The resulting crosstalk and noise reductions of about 25 decibels are large enough to make useful circuits out of channels which otherwise would be unworkable. This paper considers engineering problems in the application of compandors and describes the circuit principles involved in the equipment.

GOOD transmission characteristics of a communication channel are primarily the result of care exercised in the original design and construction of the communication system of which the channel is a part, whether it be cable, open wire, radio, or mixtures of these. In the designs allowance is made for growth, so that future added channels will meet noise and crosstalk limits themselves and at the same time not react on the earlier installations. There are economic limits to such anticipatory design, however, and sometimes demands for additional channels arise more rapidly than was expected. It then may prove either physically difficult or expensive to provide the relief needed. For example, the obvious measure of adding a 12-channel carrier system to another pair of wires of an open-wire line might require elaborate reassignment of all the pairs in the lead, retransposition, and retensioning to avoid undue crosstalk from system to system.

The compandor to the present time has found its main field of use in meeting such situations. The principles involved are sufficiently general, however, to suggest that circuit designers will find it advantageous to consider the application of compandors, in some form, in the over-all planning of new systems. It then becomes a question of economics as to whether this, or other methods, or both should be employed to meet noise and crosstalk limits.

The compandor described is a voice-frequency device, applied channel by channel where needed, which enables noise and crosstalk reductions up to about 25 decibels to be obtained. Its first application to wire lines in the Bell System was made early in 1941 on the Charlotte–Miami and Charlotte–West Palm Beach routes. It proved of value during the war in permitting rapid additions to cope with some of the demands stimulated by military installations. Circuits which otherwise would have been unworkable were brought to satisfactory standards. The number of compandors in use at the present time is over a hundred, on the routes mentioned and in other locations, and substantial additions are to be made during the current year.

A compandor was applied to the long-wave New York–London radio circuit some years ago.[1,2] At that time vacuum tube circuits were utilized for compression and expansion, but the general theory stated then still is applicable to the present compandors, in which there are vario-lossers formed of copper-oxide varistors. An experimental model using varistors was installed in 1938 on the Boston–Provincetown circuit, which is partly wire and partly radio; this is still in operation. Other applications of compandors outside the Bell System have been made by the British Post Office.[3]

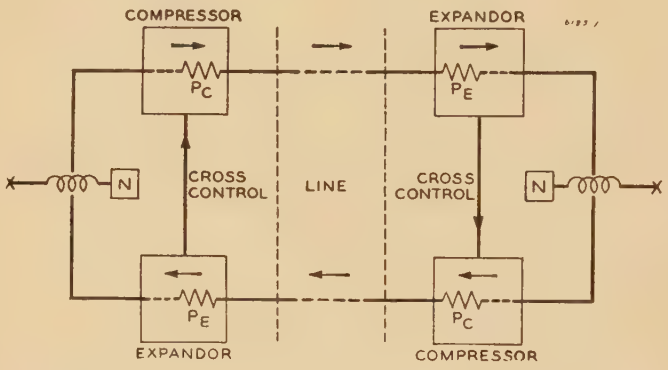

Figure 1. Compandors applied to 4-wire telephone circuit

Functional Description

Circuit Application

A compandor consists of two units, a compressor and an expandor, from which it obtains its name. Each is a piece of equipment of about one-half cubic foot in volume. The units are one-way devices operated at voice frequencies so that they are installed, as Figure 1 indicates, on the 4-wire side of the circuit. The 4-wire circuit is converted to 2-wire by the standard hybrid coil and balancing network arrangements indicated. The compressor is installed at the transmitting end of a one-way channel and the expandor at the receiving end.

The line between the two terminals may be voice frequency or carrier and it may include a radio link. The channels may be equipped with compandors in each direction of transmission, or only in one direction, as required. The functions of the attenuating pads P_C and P_E and of the cross controls shown in Figure 1 will be discussed later.

Compression and Expansion

The compressor and the expandor complement each other; what one does the other reverses. If the compressor inserts amplification in the channel the expandor inserts an equal attenuation. The noise reduction afforded by these complementary units comes about because the compandor allows a basic principle to be pushed further than is possible otherwise. This is the old proposition that if the transmitting level of a circuit is increased, a loss can be inserted at the receiving end without changing the net loss, but reducing noise coming into the line between terminals by the amount of the inserted loss. Usually transmitting levels cannot be increased without overloading the line amplifiers by the stronger signals. The compandor avoids this difficulty by giving no gain, or even a loss to the strongest signals, and by giving the maximum gain to the weakest signals, which although so amplified are well below the overload point.

Paper 46-183, recommended by the AIEE committee on communication for presentation at the AIEE Pacific Coast meeting, Seattle, Wash., August 27–30, 1946. Manuscript submitted April 18, 1946; made available for printing July 12, 1946.

C. W. Carter, Jr., A. C. Dickieson, and D. Mitchell are members of the technical staff of Bell Telephone Laboratories, Inc., New York, N. Y

The variable gains and losses in the compressor and expandor are controlled automatically by the syllabic envelope of the signal itself, which ordinarily is speech. There are rapid variations in speech power and these produce an incessant variation in the gains and losses of the two units. It is simpler to consider the action of the compandor in terms of steady-state testing power.

Figure 2 shows input-output characteristics of the compressor and expandor, measured separately. The input power was applied in each case at the toll switchboard or other zero-level points ahead of the device. The output power was measured at a zero-level point beyond the device. (Zero-level points in a toll circuit are those points at which the net loss as measured from the toll switchboard is zero; these points are designated before insertion of the compandor.)

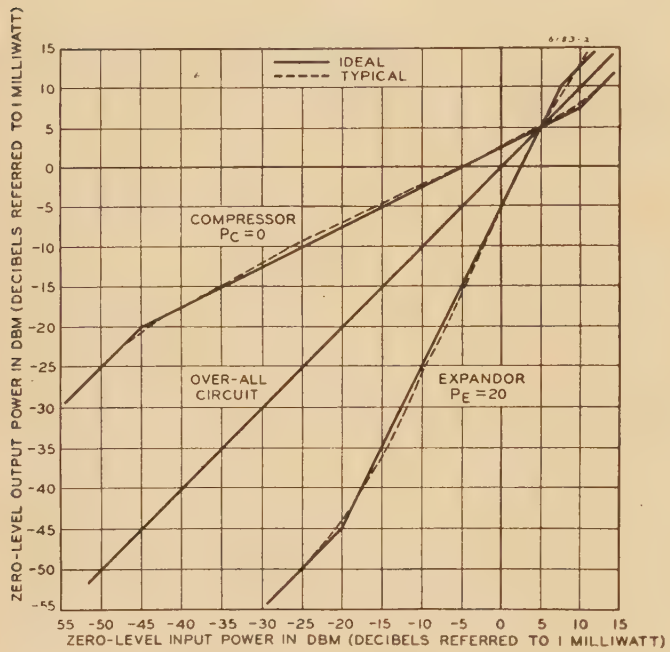

Figure 2. Input–output characteristics of compressor and expandor

The 45-degree slopes at the extremes of the curves mean that the devices are ordinary amplifiers at those values. The companding action takes place in the range between called the companding range. In this range the slope of the compressor curve is one-half. A range of input power of 55 decibels (minus 45 to plus 10 "dbm" is converted by the compressor to an output range of 27.5 decibels. (This electric power is expressed in decibels referred to the commonly used base of one milliwatt. In the Bell System this unit generally is abbreviated "dbm" and for the sake of convenience the abbreviation will be used throughout this paper.) The slope of the expandor curve is two, and it converts an input range of 27.5 decibels to an output range of 55 decibels.

Power Levels

In the usual communication circuit two input powers, differing by 30 decibels, for example, will remain 30 decibels apart from one end of the circuit to the other. This condition is changed when a compandor is inserted, as is shown in Figure 3. This indicates graphically how a range of input power is reduced by the compressor for transmission and then restored by the expandor.

In Figure 3 the power levels and level changes in a compandored circuit are shown at three points.

1. A zero-level input point.
2. A zero-level output point.
3. A point between the compressor and expandor which would be a zero-level point if the devices were not there.

One input power only (for this compandor it is plus five "dbm") goes through the system unchanged. The top of the companding range, plus ten "dbm" is attenuated by 2.5 decibels in the compressor and thus is transmitted over the line at a level lower than normal. Input powers between plus five and minus 45 "dbm" are amplified by amounts equal to half the separation in decibels between the input power and plus five "dbm." Zero-"dbm" testing power, for example, is amplified by 2.5 decibels and a power of minus 30 "dbm" by 17.5 decibels. Powers that were 30 decibels apart at the input thus are transmitted 15 decibels apart. Powers at the bottom of the compounding range, minus 45 "dbm," and below are amplified 25 decibels. The whole companding range, 55 decibels, thus is transmitted as a range of 27.5 decibels. At the receiving end the expandor restores the original separation between the powers.

Since the maximum gain of the compressor is 25 decibels, the maximum loss of the expandor is also 25 decibels, and this is the maximum possible noise reduction. Ordinarily the crosstalk reduction is slightly less than this figure, but under some circumstances to be discussed later it may be considerably more. More noise reduction could have been obtained if the value of power which receives neither gain nor loss had been put at the top of the companding range, for then the maximum loss would have been 27.5 decibels, one-half the whole range. This was found to be undesirable for it increased the frequency of occurrence of high speech peaks on the line, thus reducing the overload margin.

Noise and Crosstalk Reduction

When a compandor is installed on a circuit to reduce noise, crosstalk, or both, adjustments can be made to suit various circumstances by selecting the values of the attenuation pads P_C and P_E indicated in Figure 1. In the compandor described in this paper, the sum of these losses ($P_C + P_E$) must be kept at 20 decibels to maintain the complementary relation between compressor and expandor. Thus there is only one independent adjustment to be made.

Formulas describing the relations between steady-state input and output powers are helpful in understanding the basis for selecting the values of P_C and P_E. Referring to Figure 2, the slope for the straight line representing the compressor characteristic is one-half, and the output power for an input of 0 "dbm" is 2.5 "dbm." The pad P_C of the compressor will reduce further the output power. Thus, in "dbm," the output power C_{OUT} is related to the input power C_{IN} as follows:

$$C_{OUT} = \frac{1}{2} C_{IN} + 2.5 - P_C \qquad (1)$$

The slope for the expandor is two, and the output power for an input of zero "dbm" is minus five "dbm" when the pad P_E is 20 decibels. If the value of P_E is decreased from 20, the output will be increased by twice the change in P_E, since P_E is in the input side. Thus the output power E_{OUT} is related to the input power E_{IN}.

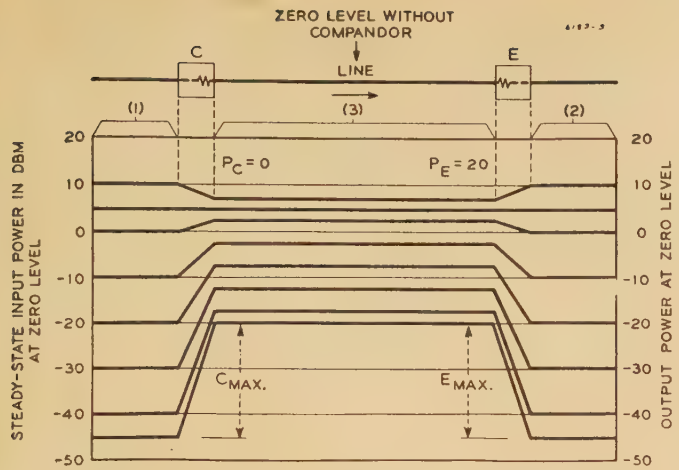

Figure 3. Power levels in telephone circuit with compandor

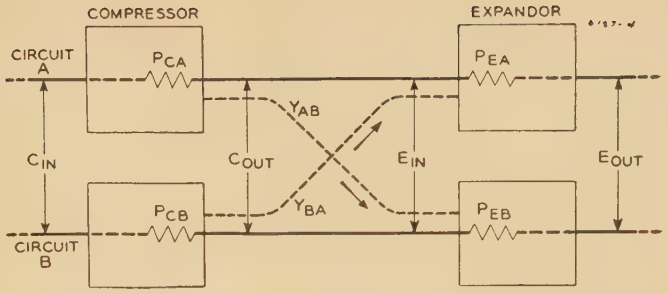

Figure 4. Losses in crosstalk paths between telephone circuits with compandors

$$E_{OUT} = 2E_{IN} - 5 + 2(20 - P_E) \quad (2)$$

As stated in the foregoing text, to preserve complementary action,

$$P_C + P_E = 20 \quad (3)$$

Thus, choosing P_C for the independent adjustment, the expression for E_{OUT} becomes

$$E_{OUT} = 2E_{IN} - 5 + 2P_C \quad (4)$$

If E_{IN} is made equal to C_{OUT}, by substitution from equation 1 it will be found that $E_{OUT} = C_{IN}$; the over-all net loss is unaffected.

The maximum gain inserted by the compressor occurs when $C_{IN} = -45$ "dbm." At this value $C_{OUT} = -20 - P_C$, and the gain $C_{OUT} - C_{IN}$ at this value is $(25 - P_C)$ decibels. This maximum gain is matched by the complementary loss in the expandor, so that the maximum loss in the expandor, designated E_{MAX}, is

$$E_{MAX} = 25 - P_C \quad (5)$$

Noise Reduction

If noise is induced in the line between its terminals, the maximum loss is desired at the receiving terminal. To obtain this, the compressor pad P_C is made zero, and the expandor pad P_E is made 20 decibels. The power levels then correspond to Figure 3. In general, the noise advantage is E_{MAX}; thus, if for any reason P_C is not zero, the noise advantage becomes $(25 - P_C)$ instead of 25 decibels.

There is an upper limit to the amount of noise with which the expandor can deal. If the noise is high enough it will operate the expandor controls and the loss inserted will be less than 25 decibels. The upper limit is quite high, however. As Figure 2 shows, any noise corresponding to a power of minus 20 "dbm" or less will not operate the expandor controls and therefore will be attenuated by the full loss. A single frequency noise of minus 20 "dbm" would read plus 70 decibels on a Western Electric type 2 noise measuring set,[4] unweighted. The corresponding figure for noise spread over the frequency band, such as static, is about 55 to 60 decibels above reference noise, with message weighting. Noise of this value also is reduced by the expandor to 30 to 35 decibels at the zero level, or 20 to 25 decibels at a minus 10-decibel level, which is within satisfactory limits.

Crosstalk Reduction

The crosstalk problem usually differs from the noise problem in that whole groups of channels need to be considered in relation to each other. These may be, for example, all of the channels of the same frequency allocation and direction of transmission in several carrier systems in the same cable. Nothing is gained in this case by raising all of the transmitting levels and inserting compensating losses at the receiving end, since the couplings between channels are not changed.

The crosstalk advantage provided by the compandor is a result of its selectivity with respect to amplitude. The range of talking volumes applied to a telephone circuit is about 40 decibels; of these, it is the louder ones which constitute the sources of crosstalk. The compressor can be arranged to discriminate against these by lowering the level for high talking volumes while raising the level for low talking volumes. The compressor therefore can be used to control crosstalk into other channels. A further crosstalk reduction is provided by the expandor on the receiving end of the disturbed circuit. This can be used to control crosstalk from other channels. Ordinarily it is desirable to gain the maximum advantage at the expandor end, since this also provides the maximum noise reduction. In special cases it may be more useful to work the compandor in such a way as to gain a large advantage at the compressor end. For example, the total advantage may be divided between two circuits. The choice of values for the compressor and expandor pads P_C and P_E depends on such considerations.

Table I

No. of Channels Being Equipped	Value of P_C For Which $CXA = 0$
1	5
5	4
40	2
All	0

Compressor Crosstalk Advantage

The compressor crosstalk advantage CXA for test tone is the reduction in the power transmitted to the line caused by the compressor, or

$$CXA \text{ (for test tone)} = C_{IN} - C_{OUT} = \frac{1}{2}C_{IN} - 2.5 + P_C \quad (6)$$

For input powers less than plus five "dbm" this is negative, that is, a disadvantage unless P_C is made greater than zero.

In speech the power varies widely during the time one talker is speaking, and the averages for different talkers cover a wide range of volumes. Also there are often several possible disturbing sources. For these reasons the compressor crosstalk advantage for speech requires a statistical evaluation. This has been done, with the results listed in Table I.

The number of channels being equipped signifies the quantity which have such frequency allocations as to be potential crosstalk disturbers, and in which compandors are being installed.

Designating the figures in the right hand column as P'_C, the crosstalk advantage formulation for speech then becomes

$$CXA \text{ (for speech)} = P_C - P'_C \quad (7)$$

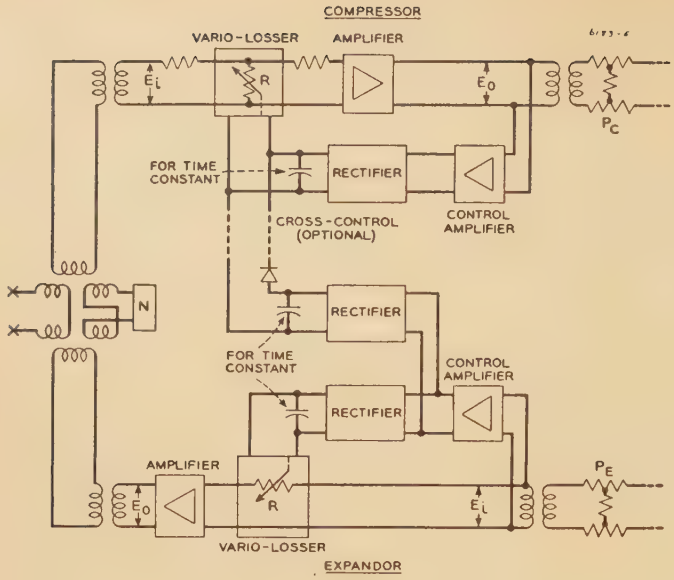

Figure 5. Schematic diagram of compandor at one end of a 4-wire telephone circuit

In ordinary practice, P_C is made equal to P'_C so that CXA is zero, that is, the circuits with compandors are no more disturbing to other circuits than previously. In special cases, it may be desirable to reduce the disturbing effect to other circuits and this is done by making P_C greater than P'_C.

Expandor Crosstalk Advantage

Since crosstalk of manageable proportions is too weak to operate the expandor controls, the expandor crosstalk advantage is the maximum loss in the expandor E_{MAX}, or

$$EXA = 25 - P_C \tag{8}$$

The formula shows that it is desirable to make P_C as small as possible. As previously indicated, however, this is limited by the disturbing effect of the circuit to which the compandor is applied.

Total Crosstalk Advantage

Total crosstalk advantage from one circuit to another is the sum of the compressor crosstalk advantage CXA of the disturbing circuit and the expandor crosstalk advantage EXA of the disturbed circuit. In the usual cases with P_C made equal to P'_C, the value of CXA is zero, so that the total crosstalk advantage from circuits either with or without compandors to a circuit with a compandor is EXA, or $25 - P'_C$ or from 20 to 23 decibels.

In special cases where specific couplings are known the crosstalk advantages may be distributed in other ways. For example, assume a situation as in Figure 4 where there are only two circuits. The values of P_C can be chosen so as to equalize the crosstalk loss in the two directions, even though the couplings are not equal. Assume that

$$Y_{BA} = Y_{AB} + D \tag{9}$$

where the Y's indicate the attenuations through the crosstalk paths from B to A and A to B, and D is the difference between them. In the A–B direction the total advantage is

$$CXA_A + EXA_B \tag{10}$$

and in the B–A direction the subscripts are interchanged. It is desired to have

$$CXA_A + EXA_B = CXA_B + EXA_A + D \tag{11}$$

so that a greater advantage in the A–B direction will compensate for the fact that there is less attenuation to crosstalk in that direction. Using equations 7 and 8, with added subscripts to denote terminals.

$$P_{CA} - P'_C + 25 - P_{CB} = P_{CB} - P'_C + 25 - P_{CA} + D \tag{12}$$

Therefore

$$P_{CA} - P_{CB} = \frac{D}{2} \tag{13}$$

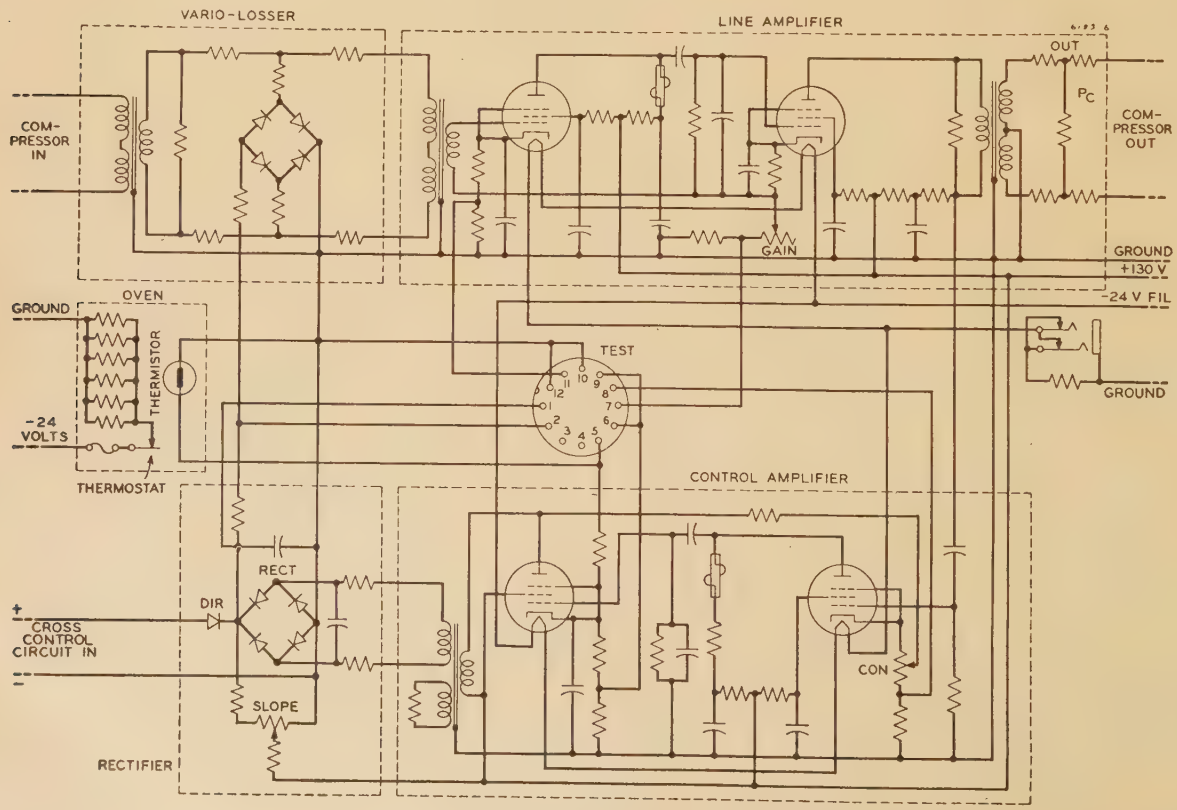

Figure 6. Schematic diagram of compressor, Western Electric type 1A

Assume, for example, that $D = 20$ decibels. Since there are only two circuits and both are equipped, $P'_C = 0$, so that P_{CB} can be made zero. Then, by equation 13, P_{CA} should be ten decibels. The corresponding values of P_{EB} and P_{EA} are 20 and 10 decibels, respectively. The total advantage in the A–B direction is $10 + 25 = 35$ decibels, while that in the B–A direction is $0+15=15$ decibels. The same formula (13) also can be derived from equations 6 and 8 for test tone. It is of some interest that in a situation of this kind the total advantage in one direction can exceed E_{MAX}, since the advantage is the sum of the value of CXA on one circuit and EXA on the other.

Transmission Considerations

Net Loss Variations

Net loss variations in a communications channel are deviations from the nominal or assigned value of over-all net loss. These may occur from a variety of causes, but on wire lines primarily from fluctuations of weather. A positive variation, which increases the net loss, is undesirable because the loudness of the speech heard by the subscribers is reduced. Negative variations, though improving the loudness of the speech, also may be undesirable if too great. Speech reflected from the far end of a circuit then may be audible as an annoying echo. If the negative variation is extreme the circuit finally may become unstable and sing.

The compandor accentuates the problem of net loss variations. Equation 4 shows, for powers within the companding range, that if the input power to the expandor is changed by a line loss variation, the change in output power is twice as great. For this reason, compandors are applied to most advantage on circuits which have good regulation of net loss.

Effect of Cross Control on Echo and Singing

When both sides of a 4-wire circuit are equipped with compandors the effect of the increased net loss variations on the round trip path can be avoided by means of cross controls from the expandor to the compressor at each terminal. These are indicated in Figure 1. By means of the cross control, when the expandor is inserting gain in its own path it simultaneously inserts an equal loss in the compressor at the same terminal. This is a unilateral action, since a directional element prevents the control current of the compressor from reaching the expandor. Bilateral controls also have been tested, but were found to be unnecessary. However, in most applications to modern well-regulated carrier circuits the unilateral control is not needed either, so that its use is made optional.

When cross controls are used in a 4-wire circuit equipped with compandors in both directions, the echo conditions are better in some circumstances than on the same circuit without compandors. This advantage is most pronounced when the compandors are at the terminals and the circuit is not switched to other circuits to distant cities at either end. The echo then returns so quickly that it passes through the compressor while the cross control from the expandor at the same terminal is inserting a loss in it, and the net loss to the echo in the return path thereby is increased as compared with a return path not having a compandor. If there is a long connecting circuit the echo may return after such an interval that the cross control has ceased its action, so that this echo improvement no longer is obtained.

With respect to singing, the cross control tends to cancel the effect of the increased net-loss variations introduced by the expandor, since a compensating loss or gain is inserted in the return path.

Quality Considerations

The Compandor, a Dynamic Device

For simplicity, the preceding sections have described the properties of the compandor in terms of steady-state testing power. Its primary purpose, however, is to transmit speech, which is a constantly varying quantity. The wide fluctuations of power during speech cause continual variation of loss in both compressor and expandor. In these circumstances it was not easily predictable that speech powers could be compressed, transmitted over a telephone line of limited frequency range,

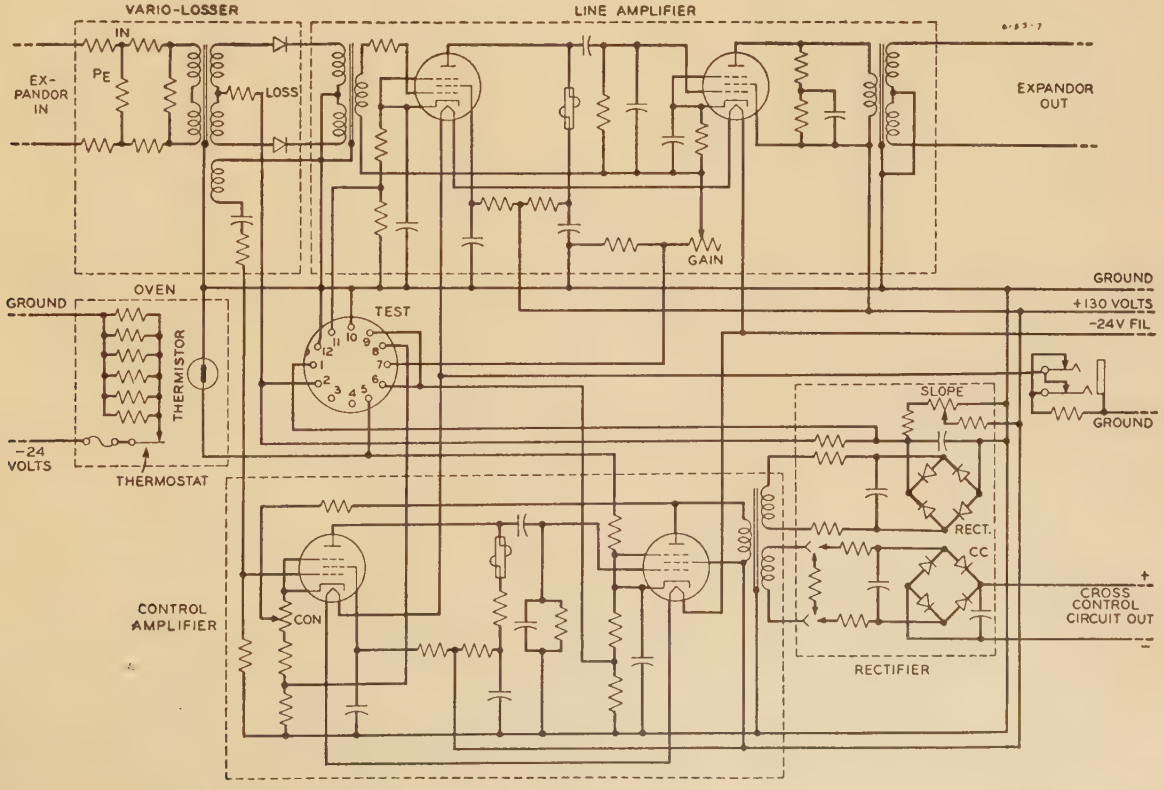

Figure 7. Schematic diagram of expandor, Western Electric type 1A

and then themselves guide the expandor in such a way as to reproduce the original dynamic pattern sufficiently well to be acceptable to the ear.

The quality characteristics depend on close matching of the characteristics of the vario-lossers at the two terminals, and on the selection of the proper attack and recovery times in the control circuits. Attack time is the interval required, after the sudden application of a steady testing signal, for the gain of the compressor or of the expandor to reach substantially its final value. Recovery time is the analogous interval after the interruption of a steady testing signal. If the attack and recovery action is too abrupt, modulation products may be created which may be heard as distortion and noise. If the attack time is too slow there may be mutilation of the initial part of a syllable. If the recovery time is too slow the loss of the expandor is not inserted fully between syllables. Talking and listening tests established that attack times on the order of ten milliseconds and recovery times on the order of 50 milliseconds gave satisfactory quality on good toll circuits.

Noise Advantage in the Absence of Speech—Aural Tests

When speech is not being transmitted, the expected improvement, as discussed in preceding sections, is equal to the loss inserted by the expandor. Measurements of this improvement have been made with a noise measuring set and also by ear balance comparisons for noises both below and above the threshold of expandor operation. In the ear balance tests, each of a group of observers listened alternately with the expandor in and out of the circuit, adjusting the noise in the latter condition until he judged the two noises to sound equally loud. The results are shown in Table II.

The noises were inserted between compressor and expandor and measured at zero-level points. It is of interest that the ear balance measurements check the meter measurements quite closely and that the full improvement is obtained up to values of noise measuring nearly 60 decibels.

Noise Advantage in the Presence of Speech—Aural Tests

When speech is being transmitted along with the noise the explanation of the noise improvement is not so simple, and the figures are somewhat different. This is because of the fact that during speech the vario-losser of the expandor is being varied by the speech. Consider first the case of a noise measuring less than 60 decibels above reference noise at a zero-level point. Between syllables the expandor attenuates this 25 decibels. During a syllable the speech operates the expandor, removing loss, perhaps to the extent of 25 decibels. Thus the attenuation given the noise during speech varies according to the strength of the syllables. If the recovery times of the control circuits are not chosen carefully the variation of the background noise may be quite audible; from its nature this effect has been named "hush-hush." The recovery times chosen disguise the hush-hush on a message circuit from all but the most critical listener.

Table II. Noise Improvement—Compandor In Versus Out

Magnitude of Noise, Db			Noise Improvement, Db	
	With Compandor			
Without Compandor	Noise Measuring Set	Ear	Noise Measuring Set	Ear Balance
49	24	25		
58	33	32	25	26
68	47	48	21	20
77	65	66	12	11

Table III. Noise Improvement in the Presence of Speech

Talking Volume at Zero Level, vu	Ear Balance Tests		
	Zero Level Noise, Db		Noise Improvement, Db
	Without Compandor	With Compandor	
No speech	58	32	26
−10	58	34	24
+ 8	58	37	21

Although with these adjustments the speech syllables mask the noise variations it is a fact that the noise actually is present in greater or less amounts and presumably is interfering with the syllables. That being so it is reasonable to ask whether the noise improvement is the same when speech is present as when it is absent. This is a matter for listening tests, which indicate that when speech is present the appraisal of noise improvement indeed is affected, but to a small extent. This is shown in Table III.

As a matter of orientation minus ten vu represents about the average volume which reaches the toll switchboard for transmission, while plus eight vu is attained by only one in about 10,000 talkers. It is apparent that over the practical range of talking volumes nearly the full improvement is maintained, even though the noise may rise many decibels during the transmission of a syllable. Suppression of the noise during intervals between syllables seems to be of controlling importance, which probably is related to the relief of the ear from fatigue. That the improvement is no mere illusion of judgment has been shown by articulation tests. It also has been demonstrated in a striking way by an experimental arrangement such that the noise without the compandor not only interfered with but completely obliterated the speech, whereas with the compandor the speech was intelligible.

Circuit Description

Compressor and Expandor

The functional elements of a compandor are shown in Figure 5 as they are arranged at one terminal of a 4-wire circuit. The other end of the circuit is equipped similarly.

The talking path through the compressor consists of a vario-losser followed by an amplifier. The control path works from the output of this amplifier back to the vario-losser. In the control path there is an amplifier followed by a rectifier, the current from which controls the loss of the vario-losser.

Let E_i be the input voltage, and E_o be the output voltage of the compressor. Since the vario-losser consists of a variable resistance R bridged across a circuit of considerably higher resistance, the voltage across R is proportional to the value of R and to the input voltage. Thus $E_o = K_1 R E_i$. The relationship desired for a 2/1 compressor is $E_o = K E_i^{1/2}$. This relationship will be met if R is inversely proportional to E_o. If the variable element is a copper oxide varistor, this relationship is approximated. The current-voltage characteristic of copper oxide varistors can be approximated over a considerable range by the expression $I = a\epsilon^{bE}$, where I and E are current and voltage, a and b are constants.

$$\frac{1}{R} = \frac{dI}{dE} = ba\epsilon^{bE}$$

whence

$$R = 1/bI$$

If the control system is linear, so that $I = K_2 E_o$, then, as desired.

$$R = 1/K_3 E_o$$

In the expandor the talking path also contains a vario-losser followed by an amplifier, but in this case the control amplifier-rectifier is connected ahead of the vario-losser. The latter is a variable

resistance R in series with a circuit of considerably lower resistance. Thus the current through the circuit is determined mainly by R. The voltage across the low output impedance is proportional to this current so that $E_o = E_i/K_1R$. As before, the rectifier is linear, and the varistor is copper oxide, so that $R = K_2/E_i$, whence $E_o = KE_1^2$, as desired for a 2/1 expandor.

The cross control consists of another rectifier connected to the expandor control amplifier, with the d-c output connected through a one-way element to the vario-losser of the compressor. Thus at the same time that the expandor loss is being reduced by input, an approximately equal loss is being added to the compressor. The one-way device at the output of the cross control, a copper oxide varistor, makes the action unilateral.

Matching Characteristics

The compressor and the expandor should be exactly complementary, so that the over-all circuit will have a constant loss at all amplitudes. It was a design objective to keep deviations from this relation to less than one decibel for all causes, including manufacturing tolerances, aging, temperature, and power supply variations, with the added condition that any compressor must work with any expandor.

The variations contributed by amplifiers are made negligible by designing both line and control amplifiers with about 35 decibels of negative feedback, which reduces any individual variation by a factor of 50 or more.

As ordinarily used, copper oxide varistors are subject to relatively large variations because of manufacturing tolerances, aging, and temperature changes. As used here, the copper oxide disks are superaged in the factory. It is estimated that this produces an aging effect equivalent to about 75 years of ordinary service, and that further changes will be of the order of three per cent in resistance over a 20-year period. After this process, the disks are selected by individual tests, high and low resistance disks being combined so that the four arms of the vario-lossers are balanced.

To minimize variations caused by ambient temperature changes, the varistors are mounted in a small oven, the temperature of which is controlled by a thermostat to an accuracy of about plus or minus three degrees Fahrenheit.

Because of the design precautions taken, the control rectifiers are closely alike; however, their input-output characteristic is not strictly linear. For this reason, the rectifiers are adjusted to work over the same portion of the curve by adjusting their output currents to be equal at a normal testing tone input of zero "dbm" at a zero-level point in the circuit. It is found by experience that varistors differ most in resistance at low control currents. For this reason, an additional adjustment is made by means of a potentiometer at a circuit input corresponding to the bottom of the companding range. This adds a small direct current derived from the 130-volt plate battery to the current produced by the control rectifier, thus making the input-output curve cross the ideal again at this input.

Performance

Figure 2, which shows the input-output characteristics of idealized compressors and expandors, contains dashed lines which show typical measured characteristics for comparison. These are matched to a degree such that the over-all circuit loss measured at different input amplitudes will not vary more than plus or minus one decibel, and in the usual case will be in the range plus or minus 0.25 decibel. These figures include all variations except the effect of loss variations in the circuit between compressor and expandor.

Frequency characteristic distortion, modulation products, and noise from apparatus sources all have been reduced to the point of contributing only a negligible amount on a high-grade 200–3,500-cycle message channel.

Detailed Description

Figures 6 and 7 show the circuits of the compressor and expandor in some detail. The line and control amplifiers each comprise two stages, impedance coupled, with about 35 decibels of negative feedback for gain stabilization. Screwdriver controlled potentiometers in the feed-back path are used for fine adjustment of gain. Heater-type pentode tubes are used throughout.

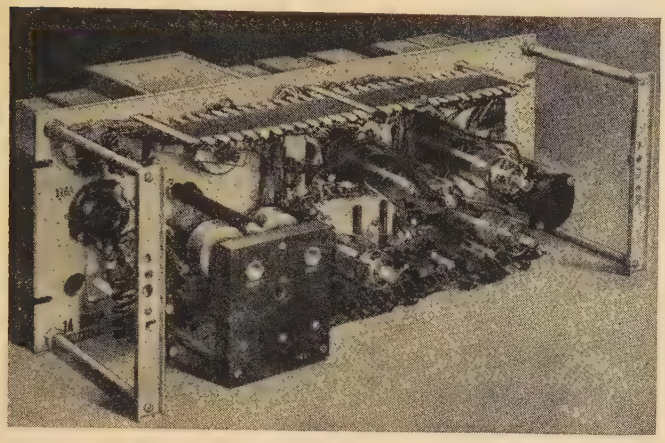

Figure 8. Front view of compressor (cover removed), Western Electric type 1A

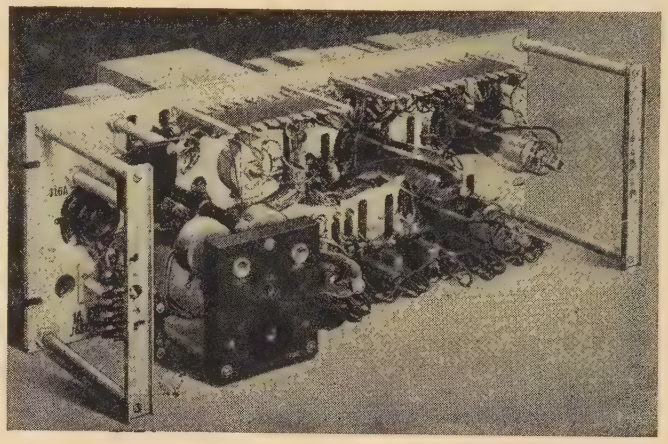

Figure 9. Front view of expandor (cove removed), Western Electric type 1A

The temperature inside the oven may be measured by means of a thermistor disk about the size of a dime, which is inside the potting can holding one of the vario-lossers. This thermistor is a portion of a Wheatstone-bridge circuit, the other arms being made up of resistances in a vacuum-tube cathode circuit. The condition of balance of the bridge, which is an indication of the oven temperature, may be determined by the same testing equipment[5] used to maintain other circuits in the telephone office. The currents flowing in the various cathode circuits and in the control rectifier output are measured also with this same test set by connection to the receptacle "test" on the panel.

In case of a thermostat failure causing permanent closure, damage to the

An Oscillograph for Recording Transient Recovery Voltages

W. G. HOOVER
ASSOCIATE AIEE

THE importance of the effects of the magnitude and rate of rise of the transient recovery voltage upon the difficulty of arc interruption in circuit breakers has been recognized for a number of years. It is known that differences in the interrupting performance of circuit breakers may be obtained at different locations in power systems, even though the power-frequency voltages and short-circuit currents involved may be similar.[1] In general, the greater the rate at which the transient recovery voltage builds up and the greater the final value that it attains across the arc space as the arc extinction process occurs, the more difficult it is for the circuit breaker to clear the circuit. There is not, however, any simple quantitative relationship between these transient values and the arcing time of a circuit breaker or its interrupting capacity limit. Individual short-circuit interruptions with a given circuit breaker and circuit conditions may show considerable variations in arcing time. For such and other reasons the added complication of transient recovery-voltage rate and magnitude limits has not been added to circuit breaker interrupting capacity ratings or specifications.[2]

Interrupting capacity ratings applied by manufacturers to circuit breakers generally are intended to be sufficiently conservative to hold under the most severe recovery conditions likely to be encountered in practice. In the larger ratings, test verification of this assumption may be difficult or impossible to obtain. In certain applications full rating short circuits result in low recovery-voltage rates. Such a condition well might be considered in specifying interrupting capacity requirements, especially where the choice otherwise lies between adjacent standard ratings.

Although the transient recovery characteristics of circuits in which circuit breakers are connected may be calculated,[3,4] the numerical results desired may be obtained in many cases only after the expenditure of considerable effort and the making of a number of simplifying assumptions. Indirect tests at low voltages may be made to deter-

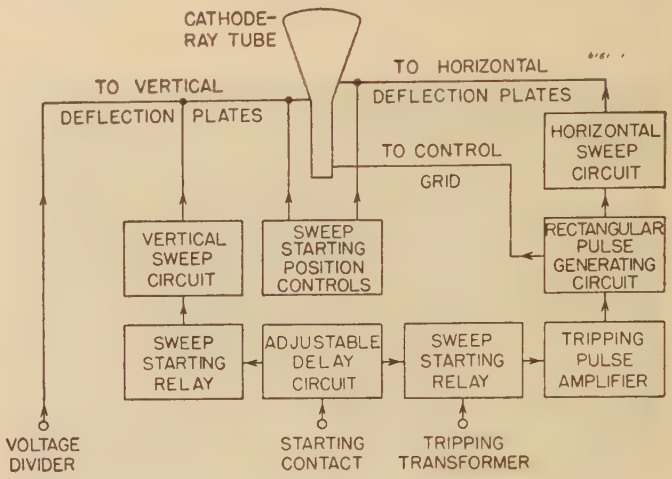

Figure 1. Block diagram of main circuits in oscillograph

Paper 46-181, recommended by the AIEE committees on instruments and measurements and protective devices for presentation at the AIEE Pacific Coast meeting, Seattle, Wash., August 27–30, 1946. Manuscript submitted June 17, 1946; made available for printing July 10, 1946.

W. G. HOOVER is associate professor of electrical engineering, Stanford University, San Francisco, Calif.

The author acknowledges the assistance of the Pacific Electric Manufacturing Corporation in making possible the construction of this oscillograph and carrying out tests to check its performance.

---

varistors is prevented by a temperature operated fuse which opens the heater circuit when the oven temperature becomes greater than 140 degrees Fahrenheit.

The pads "out" (Figure 6) and "in" (Figure 7) are the adjustment pads P_C and P_E previously discussed. They are arranged to plug into tube sockets, and may be selected in 0.25-decibel steps from 0 to 20 decibels. The losses of the two pads in one direction of transmission always must sum up to 20 decibels to maintain complementary action in this compandor.

Physical Description

The compressor and the expandor, which are shown in Figures 8 and 9, are 7-by-19-inch panels designed to mount on relay racks. Stud-mounted components are on the rear while wiring and vacuum tubes are on the front of the panels. Front covers have cutouts for access to testing jacks and controls. Each panel weighs approximately 25 pounds. Shop-wired bays normally include 12 units, which may be compressors, expandors or a combination of both. Patching and monitoring jacks, a 4-wire monitoring and talking panel, and miscellaneous trunks as required also are provided in the bay.

The power supplies required are 130 volts for plates, 24 volts for filaments, and 24 volts for the ovens. A power panel is also available so that the filament circuit and oven heaters may be operated from an a-c source, if desired. It is a $10^1/_2$-inch panel with sufficient capacity to supply 12 units. The total power required is about 40 watts for each unit.

References

1. THE "COMPANDOR"—AN AID AGAINST RADIO STATIC, **R. C. Mathes, S. B. Wright.** AIEE TRANSACTIONS, volume 53, 1934, June section, pages 860–6.

2. THE VOICE-OPERATED COMPANDOR, **N. C. Norman.** *Bell Laboratories Record*, New York, N. Y., volume 13, December 1934, pages 98–103.

3. THE REDUCTION OF CROSSTALK ON TRUNK CIRCUITS, BY THE USE OF THE VOLUME RANGE COMPRESSOR AND EXPANDOR, **J. Lawton.** *Post Office Electrical Engineers Journal* (London, England), volume 32, April 1939, pages 32–8.

4. A NEW NOISE METER, **J. M. Barstow.** *Bell Laboratories Record*, New York, N. Y., volume 15, April 1937, pages 252–6.

5. A CARRIER TELEPHONE SYSTEM FOR TOLL CABLES, **C. W. Green, E. I. Green.** AIEE TRANSACTIONS, volume 57, 1938, May section, pages 227–36.

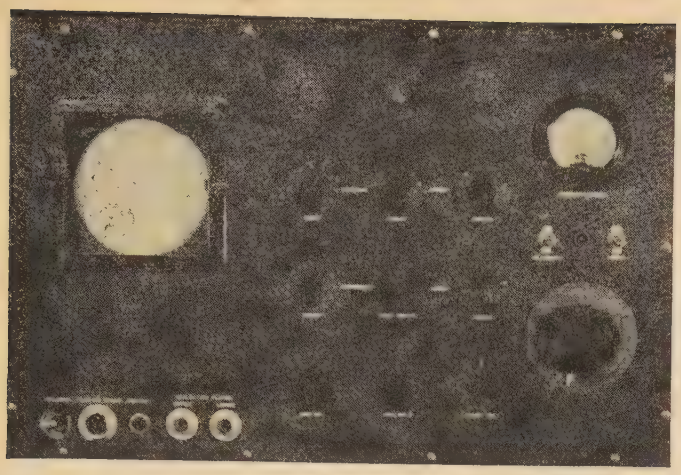

Figure 2 (left). Front panel of oscillograph

Figure 3 (below). Oscillograph with camera and tripping transformer

mine transient performance of circuits viewed from the circuit breaker location.[5,6] Such tests require that the circuits involved be de-energized during the test. They do not indicate any modifications of the recovery-voltage transient resulting from circuit breaker arc voltage or residual arc conductivity after the main current zero. Where interruption tests are made, either in the field or in the high-power test laboratory, there is considerable interest and satisfaction in directly measuring these voltages. Such measurements lie within the field of application of the moderate or high-speed recording cathode ray oscillograph.

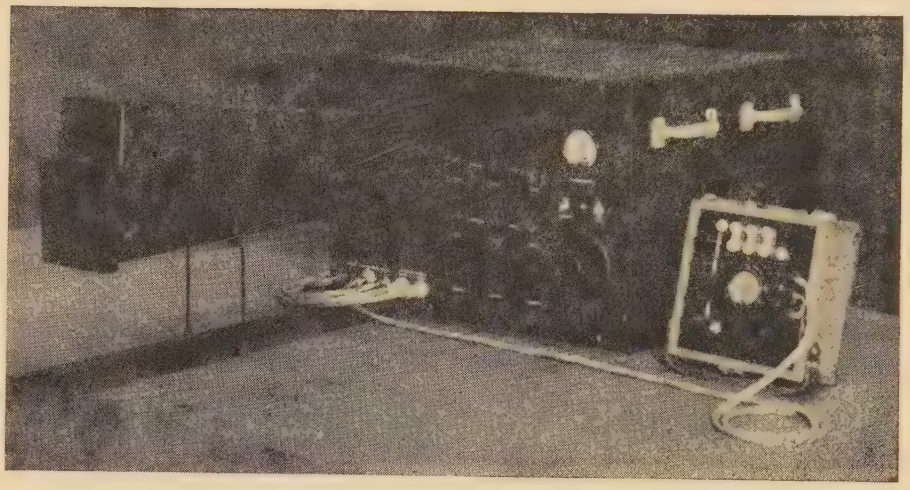

Methods of Measurement

A requirement peculiar to these recovery-voltage measurements involves the ability to record transient voltage variations occurring in a few microseconds, and maintaining this high recording speed sensitivity over a time interval of several cycles of power frequency. Two basically different methods have been employed for timing the record on the photographic film and obtaining a sufficiently expanded time scale.

One method utilizes a moving film oscillograph.[7,8] The film is attached to a drum which is rotated at speeds up to several thousand revolutions per minute. The cathode ray beam is deflected by the variations of voltage across the circuit breaker along an axis at right angles to that of the film travel. The beam is energized for a period of time sufficient to include the interruption process. During this exposure time the film may complete a number of revolutions with the result that a similar number of overlapping traces appears on the record. The separate traces are usually distinguishable, and since the total length of trace on the film is several feet, low and moderate transient recovery-voltage frequencies and rates of rise can be resolved satisfactorily. With this method the complete history of the arc voltage in the circuit breaker from the beginning of the arc to its final extinction is available on the oscillogram. For most purposes, however, the important parts of the record are only those regions in the immediate vicinity of the current zeros, wherein the transient recovery voltages appear. The moving-film oscillograph is electrically relatively simple, and timing the period of recording is easily accomplished. There are, nevertheless, a number of disadvantages. The maximum speed at which the film may be driven is limited by mechanical considerations to a value in the order of 0.005 centimeter per microsecond. This is not sufficient for easy or accurate resolution of the higher frequency components that may exist under some test conditions. For example, one cycle of a 100,000-cycle wave would appear 0.5 millimeter long at this speed. The high-speed revolving drum with its necessary accurate balancing, film supporting means, and motor drive involve mechanical complications not present in oscillographs using a stationary film.

In the other method of recording transient recovery voltages the cathode-ray beam is deflected in a direction perpendicular to that caused by the voltage being measured to give the time axis.[1,9] The oscillogram is produced on stationary film. The total deflection distance in the time axis direction is limited to a few inches in this case. Without difficulty the speed of deflection may be made much greater than obtainable with mechanically driven film. A relatively intensive examination of a small fraction of the total interruption process is thus possible. The main difficulty encountered is that of timing the start of this high speed short duration time sweep to occur at the proper instant to include the transient recovery voltage at the end of the last half cycle of arcing. Probably the most satisfactory solution so far employed for this problem involves the use of a saturating-core current transformer to produce a voltage peak in the secondary winding at approximately current zero in the primary. In another case,[10] the beam is swept back and forth by a sine-wave power-frequency deflection voltage of much greater peak value than necessary to move the beam across the fluorescent screen width. The timing is arranged so that the arc extinction period occurs during the time the beam is on the screen. A number of sweeps appear on the same part of the record, and the right and left-hand travel is somewhat difficult to follow.

Description of Oscillograph

The oscillograph described in this paper utilizes a high-voltage sealed-off cathode-ray tube of the same kind as used for impulse testing.[11] The record is produced on a stationary film. The

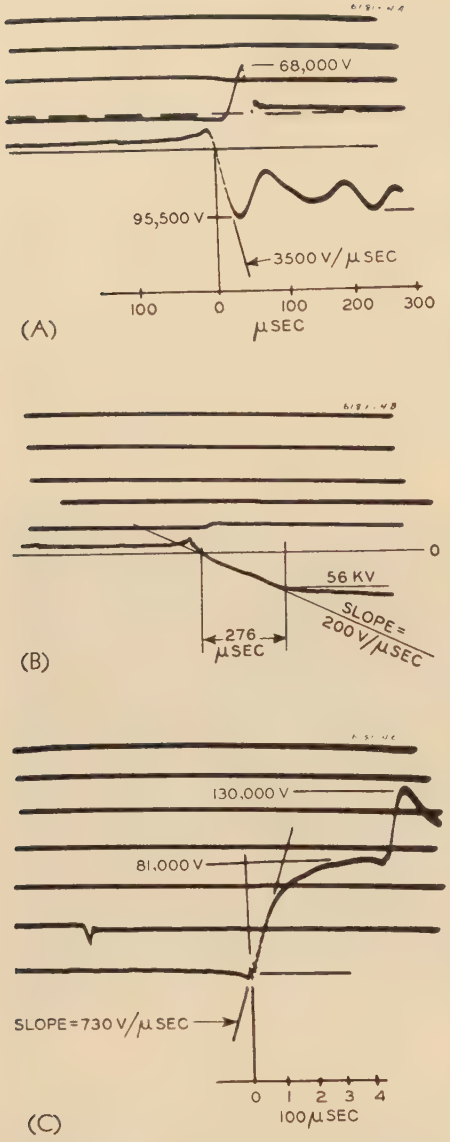

Figure 4. Recovery voltage oscillograms taken on 110-kv line-to-ground short-circuit tests at Newark substation of Pacific Gas and Electric Company

A. Test at 8,290 amperes. The 60-cycle crest recovery volts = 88,000
B. Test at 14,400 amperes
C. Test at 5,200 amperes

necessary high time-sweep speed is obtained by moving the beam horizontally across the screen in a short period of time in the region of current zero. This sweep is repeated once each half cycle from a time definitely before the arcing contacts of the circuit breaker separate until the final arc interruption. The successive horizontal sweeps are separated by superimposing them on a relatively slow uniform downward sweep or drift of several cycles duration. The time interval between the horizontal sweeps, when the screen is dark, is nearly a half cycle. The complete record thus appears as a series of spaced horizontal lines with vertical deviations produced by the voltage across the circuit breaker. The last and lowest line contains the recovery-voltage transient at the final current zero.

This method of operation permits use of a high intensity beam with about the same time integral of beam power to the fluorescent screen per horizontal sweep as when the tube is used in oscillographs for impulse testing. This is possible because the actual fraction of the time the beam is energized is very small and because in the successive sweeps the beam does not retrace the same screen area. Because the film is stationary the usual medium-persistence screen may be used. The advantages of a simple fixed camera are apparent. The camera used in this case allows simultaneous visual observation and photographic recording of the traces on the screen. This opportunity of visual observation has been found very useful in giving immediate information about the duration of arcing, the polarity at interruption, the shape of the recovery voltage transient and the effect of the residual arc conductivity in modifying it.

Although the circuits contained in this instrument are more complex than necessary with the moving-film type of oscillograph, most of the extra equipment is made up of easily available radio receiving tubes and parts. The oscillograph and auxiliary equipment are sufficiently compact and portable to be transported easily to test locations in a passenger automobile.

A block diagram of the main component circuits is shown in Figure 1. The cathode-ray tube used is an RCA-912. This tube may be operated with a total beam accelerating voltage of 15,000 volts. It was decided in this case to use a maximum value of 10,000 volts since the recording speeds necessary are considerably below the tube limit. The lower voltage power supply is lighter in weight and more compact.

The sequence of operation may be summarized as follows:

1. Initiation of the vertical and horizontal sweep actions depends upon the closing of an external starting contact a short time (a few cycles) before the circuit breaker arcing contacts separate. This contact should remain closed during a portion of the opening stroke of the circuit breaker sufficient to include the interruption process.

2. Actual initiation of the afore-mentioned sweeps follows the closing of two small fast-acting relays within the oscillograph. To aid in timing the starting of the two sweeps, an adjustable delay circuit is interposed between these relays and the external starting contact. The vertical sweep starts immediately upon the closing of its starting relay. On closing the horizontal sweep-starting relay simply completes the circuit from the externally mounted tripping transformer to the horizontal sweep voltage generating circuit. This tripping transformer produces a sharp peak of voltage once each half cycle of the test current at a few degrees (adjustable) before current zero. The successive horizontal sweeps are initiated by these voltage pulses and are thus properly timed to include the current zero region.

3. The control grid of the cathode ray tube is normally maintained at a bias voltage sufficiently negative to prevent the formation of an electron beam. For the short duration of the individual horizontal sweep, however, the beam is released by the application of a rectangular positive voltage pulse from the horizontal sweep circuit.

4. The recovery voltage appearing across the test circuit breaker is reduced to a lower and accurately proportional value by means of a capacitance-type voltage divider. This voltage is fed through a shielded transmission line from the circuit breaker location to the oscillograph deflection plates.

Figures 2 and 3 show the oscillograph, tripping transformer, and camera. Controls brought out to the front panel of the instrument are for adjusting the starting position of the beam at the beginning of the sweeps, the speeds of both the vertical and horizontal sweeps, the sweep-starting time delay, the cathode-ray tube beam focus and intensity, and the total beam accelerating voltage. This last quantity is indicated by a meter on the panel. A push button for producing a test sweep also is provided. Input terminals shown at the lower left of the panel are for the 115-volt 60-cycle power source, the secondary of the tripping

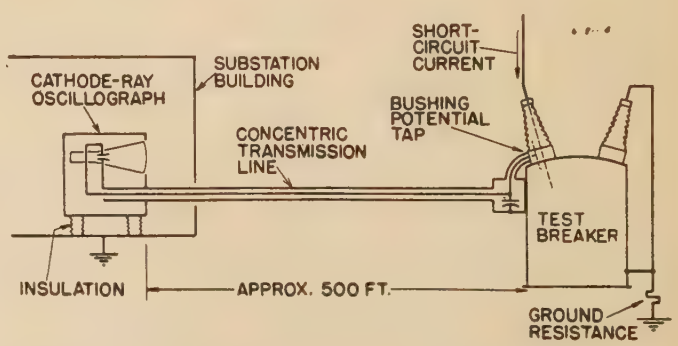

Figure 5. Connection of cathode-ray oscillograph to test circuit breaker for Newark tests

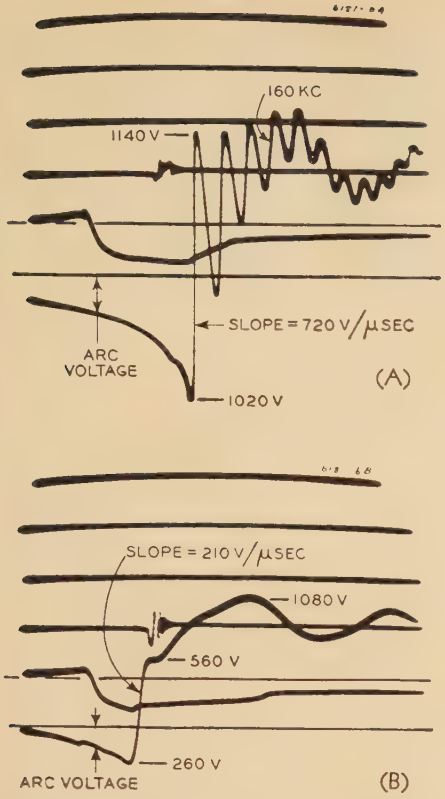

Figure 6. Recovery voltage oscillograms taken on short-circuit tests with laboratory generator at Stanford University

A. Recovery showing high-frequency oscillation

B. Recovery showing damping due to arc-space conductivity

transformer, a connection for the external sweep-starting contact, and one concentric cable terminal for each vertical deflection plate.

Test Results

This oscillograph has been used on interruption tests on power systems and as a key instrument in laboratory studies of arc-extinction phenomena.

Figure 4 shows oscillograms taken during short-circuit tests made at the Newark substation of the Pacific Gas and Electric Company, July 8 and 15, 1945. The single-pole test circuit breaker was connected from a section of the 110-kv bus to ground. Figure 4A is the oscillogram obtained for a current of 8,290 amperes rms, corresponding to an equivalent 3-phase interruption of 1,600,000 kva. The current in this case was limited principally by reactance of transformers within the substation grounds. The rate of rise of recovery voltage obtained was high. It is interesting to note the restriking voltage built up across the arc space on the previous half cycle. In another test, Figure 4B, the interrupted current was 14,400 amperes and the equivalent 3-phase interruption was 2,720,000 kva. In this test the current was limited mainly by the impedance of several long transmission lines feeding into the substation. The voltage at the receiving end of these lines was pulled down to a low value during the flow of current. A relatively low recovery rate was obtained, as a result of the time required for restoration of normal voltage on these lines after the current ceased to flow. Figure 4C was obtained for a test on a smaller circuit breaker. The test current was limited to 5,200 amperes with reactance at the substation. In order to reduce the severity of the recovery-voltage conditions, an open-ended 110-kv transmission line was connected in parallel with the circuit breaker. The length of this line was about 40 miles. The oscillogram shows the returning wave front reflected from the open end of the line.

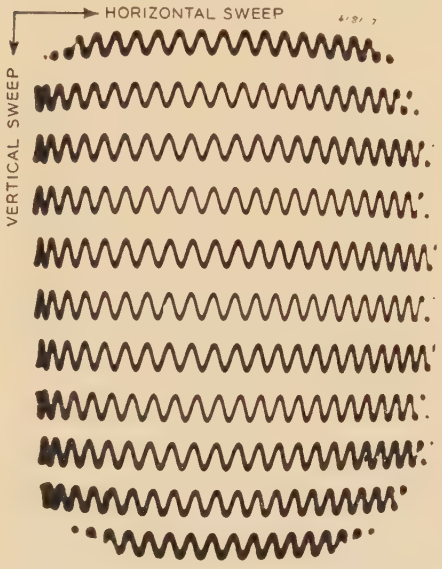

Figure 7. Test sweep with same oscillograph adjustments as for Figure 6

200-kc timing wave

Figure 5 shows the connections between the test circuit breaker and the cathode-ray oscillograph used in the foregoing tests. Since the short circuits were line to ground there was possibility of a considerable difference of potential between the ground connection at the location of the circuit breaker and grounds at other parts of the substation. For reasons of safety and convenience all measurement and control equipment was centered in the substation building about 500 feet from the test circuit breaker. A connection to the capacitance tap in the line-side bushing of the circuit breaker was brought through a concentric transmission line to one of the vertical deflection plates of the cathode-ray oscillograph. The outer conductor of this line was connected solidly to the circuit breaker tank. The oscillograph housing and the other vertical deflection plate were connected to the other end of the outer conductor. A capacitive division of the voltage across the circuit breaker was obtained according to the ratio of the capacitance between the bushing tap and the bushing center conductor to the capacitance of the transmission line center conductor, the bushing tap, the deflection plate circuit, and an auxiliary shunting capacitor to ground. The cathode-ray oscillograph was mounted on insulating supports and the 115-volt 60-cycle power required for its operation supplied through a low capacitance insulating transformer. In this way the potential of the oscillograph housing was allowed to follow freely that of the circuit breaker ground and only the difference of voltage across the circuit breaker caused deflection of the beam. Actually, the voltage appearing between the oscillograph housing and the ground connection near by was only about 200 volts during the test current flow of 14,000 amperes.

Two oscillograms taken in laboratory

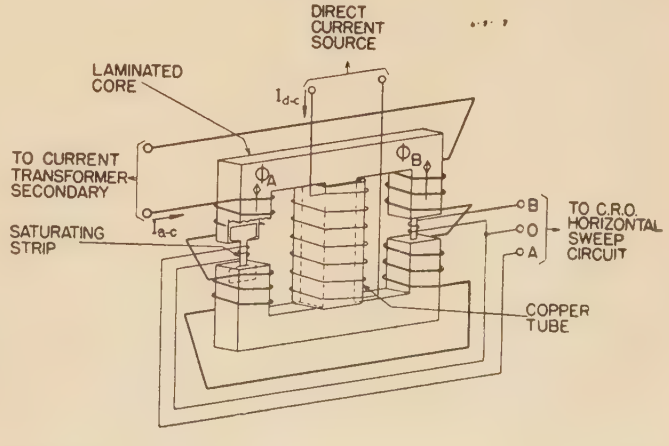

Figure 8. Diagram of core and windings of tripping transformer

short-circuit tests of a small circuit breaker are shown in Figure 6. The circuit voltage was 1,300 volts and the interrupted current 600 amperes. The oscillogram in Figure 6A shows a large high-frequency oscillation with relatively low damping. Figure 6B was obtained for another test interruption several minutes later under identical circuit conditions. In this case the effect of the arc conductivity during the extinction period is indicated by the complete damping of the high-frequency oscillation and the reduced rate of rise of the recovery-voltage transient. Simultaneous records of the current in the arc space during this critical period of time show for the first test practically no current flow after the normal zero, but a considerable amount, in the order of two amperes, for a short time in the second test. Results of these current measurement tests will be reported at a later date.

The oscillograms of Figure 6 were taken with a fast horizontal sweep. They represent periods of approximately 2 degrees of the 60-cycle power-frequency wave. Figure 7 shows a 200-kc timing wave test with the same oscillograph adjustments as used for Figure 6. The horizontal sweeps were tripped by passing a steady 60-cycle current through the primary of the tripping transformer.

Circuit Details

Tripping Transformer

The principle of operation of the saturating-core peaking or horizontal-sweep tripping transformer is illustrated by Figures 8 and 9. The primary winding consists of four coils, two on each outside leg of the core. Each coil has 22 turns of number 14 wire. The coils may be connected in series, series-parallel, or parallel. The operating range is approximately 3 to 30 amperes per coil. The impedance of the primary winding with the series connection is about 0.5 ohm. The secondary windings each have 250 turns of number 38 wire. They are wound on single strips of 0.007 inch thick silicon steel, 0.05 inch wide by 0.25 inch long. Ends of the saturating sections flare out to 0.5 inch width for good magnetic contact with the main core. The center leg of the core has a d-c bias winding of 1,200 turns of number 26 wire. The current in this winding may be adjusted up to a maximum value of 100 milliamperes by means of a potentiometer and indicating meter on the panel of the transformer housing. The copper sleeve around the center core leg is to reduce the effect of any unbalance of the a-c magnetomotive force upon the d-c winding circuit.

Figure 9 shows wave forms, somewhat idealized, applying to the tripping transformer. The result desired is to produce sharp pulses of voltage at a controllable small angle before the current zeros in the primary winding. The net fluxes Φ_A and Φ_B in the outside core legs may be considered as the sums of component fluxes resulting from the a-c primary and d-c bias magnetomotive forces. The magnetic strips through the secondary windings are saturated except during short periods in the vicinities of the next flux reversals. The corresponding induced voltage peaks have a maximum value in the order of two volts and a width of about two degrees at half amplitude. Only the negative pulses are used; the input to the oscillograph

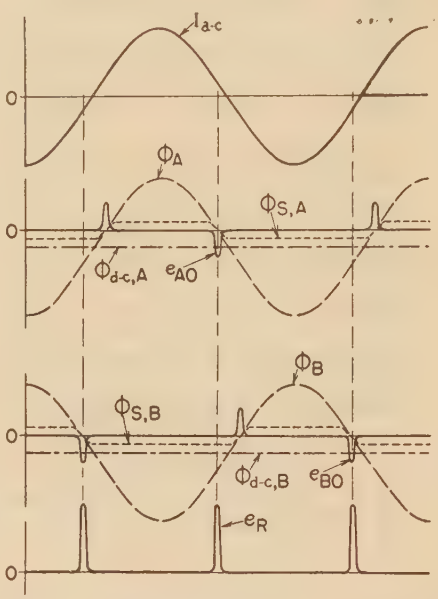

Figure 9. Idealized wave forms in tripping transformer

Φ_A, Φ_B, net fluxes in outside core legs
$\Phi_{d\text{-}c,\,A}$ $\Phi_{d\text{-}c,\,B}$, d-c components of flux in outside core legs
$\Phi_{S,\,A}$, $\Phi_{S,\,B}$ fluxes in saturating strips
e_{AO}, e_{BO}, induced voltages in secondary windings

contains a stage of voltage amplification and rectification, with a result indicated by the peaked voltages e_R in Figures 9 and 10. An increase in the d-c bias current causes the peaks e_R to lead the alternating current zeros by a larger angle and causes the recovery-voltage transient to appear farther to the right on the horizontal sweep.

The above construction of the tripping transformer is used not only to provide horizontal sweep timing control, but to insure satisfactory timing with a considerable (as much as 10 per cent at maximum primary current) d-c component in the main short-circuit current wave at the time of interruption. If the d-c component at the time of clearing may be appreciable, a high-accuracy current transformer must be used to supply both components of current to the tripping transformer primary.

Horizontal Sweep

Figure 10 shows some idealized wave forms applying to different stages of the horizontal sweep circuit. The amplified and rectified voltage peaks e_R are used to trip a pulse-sharpening stage employing a type 884 gas thyratron. The sharp negative peaks A then trigger a "flip-flop" or "one-shot" rectangular pulse generating circuit.[12] This circuit consists of two tubes with the plate of each coupled to the grid of the other. The tube into which the triggering pulse is fed normally carries considerable plate current at a low plate voltage. The other tube is biased beyond cutoff. Upon triggering, the plate voltage of the first tube rises quickly to full plate supply value and remains there for a period of time during which the second tube carries current. The duration of this high plate voltage ends abruptly when the circuit restores itself to the original condition. The length of the practically rectangular pulse of plate voltage B on the first tube is mainly a function of the time constants of the grid-plate coupling circuits.

The control grid of the cathode-ray tube normally has a sufficiently negative voltage with respect to the cathode to prevent the formation of an electron beam. It is coupled through a capacitor to the rectangular pulse generating circuit, so that the grid potential rises in the positive direction with the rectangular pulse. The amplitude of this change of grid voltage D, about 150 volts, allows the production of a strong beam current C. The actual beam intensity is adjusted by controlling the original negative bias on the control grid.

The rectangular pulse of voltage B also is applied to a resistance and capacitance in series. The resistance is high enough so that the capacitance is charged to but a small fraction of the amplitude of the rectangular pulse at the end of the pulse. The rate of change of the voltage E across the capacitance is very nearly constant under these conditions. The voltage E is supplied to a push-pull voltage amplifier, the output of which is

connected to the horizontal deflection plates of the cathode-ray tube to produce a nearly linear horizontal time-sweep. Any one of four different sweep speeds may be selected by means of a multicontact switch operated from the front panel. The times available for a complete horizontal sweep are approximately 20, 10, 5, and 2 degrees on a 60-cycle basis.

Vertical Sweep

Two 0.05 microfarad capacitances, one charged to +1,250 volts and the other to −1,250 volts with respect to ground, are discharged in series through a type 6AC7 pentode upon the closing of the sweep-starting relay. The constant-current characteristic of the pentode produces a nearly uniform rate of change of voltage across these capacitances. This voltage is supplied to the vertical deflection plates through 2-megohm resistances in each lead. Voltages to be measured are fed to the vertical deflection plates through 0.015 microfarad capacitances. The rate of change of vertical sweep voltage is low enough to change the charge on the 0.015 microfarad capacitances without much voltage drop in the 2-megohm resistances. Though the continuous voltage rating of the 6AC7 pentode is exceeded greatly in this circuit, the duration of application is so short that no trouble has been experienced over more than a year of frequent use. Different vertical-sweep speeds are obtained by varying the cathode bias resistance for the 6AC7 pentode.

Other Circuits

Four rectified d-c power supplies are built into this oscillograph. Accelerating and focusing voltages for the cathode-ray tube are obtained from a voltage-doubling circuit using type 2X2 rectifier tubes. Voltage for the vertical sweep circuit and for the last amplifier stage of the horizontal sweep circuit is obtained from a 2,500-volt supply with midpoint grounded. Two conventional 300-volt rectifier and filter combinations are used, one for the amplifier circuits, and the other for the sweep-starting relay circuit. These relays are operated by current flow in the plate circuit of a type 884 thyratron. The tripping grid voltage for this thyratron is developed across a capacitance which is charged through an adjustable resistance in series with the external sweep-starting contact. Steps of this charging resistance controlled from the front panel may be set to cause delays of 0 to 6 cycles in 1-cycle intervals.

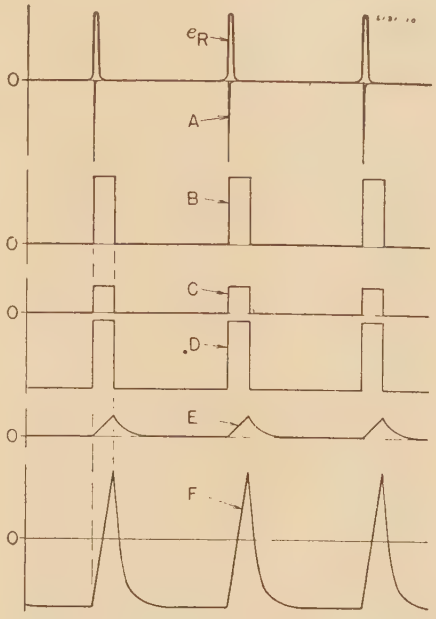

Figure 10. Idealized wave forms in horizontal sweep circuit

References

1. Circuit Breaker Recovery Voltages, **R. H. Park, W. F. Skeats.** AIEE Transactions, volume 50, 1931, pages 204–38.

2. Power-Circuit-Breaker Ratings, **R. C. Van Sickle.** AIEE Transactions, volume 60, 1941, September section, pages 882–4.

3. Determination of Circuit Recovery Rates, **E. W. Boehne.** AIEE Transactions, volume 54, 1935, May section, pages 530–9.

4. Transient Recovery-Voltage Characteristics of Electric-Power Systems, **H. P. St. Clair, J. A. Adams.** AIEE Transactions, volume 61, 1942, September section, pages 666–8.

5. Recurrent-Surge Oscillographs and Their Application to Short-Time Transient Phenomena, **K. J. R. Wilkinson.** *Journal*, Institution of Electrical Engineers (London, England), volume 83, 1938, pages 663–72.

6. The Recovery-Voltage Analyzer for Determination of Circuit Recovery Characteristics, **G. W. Dunlap.** AIEE Transactions, volume 60, 1941, November section, pages 958–62.

7. Arc Extinction Phenomena in High Voltage Circuit Breakers, **R. C. Van Sickle, W. E. Berkey.** AIEE Transactions, volume 52, 1933, pages 850–7.

8. Breaker Performance Studied by Cathode Ray Oscillograms, **R. C. Van Sickle.** AIEE Transactions, volume 54, 1935, February section, pages 178–84.

9. Oil Circuit Breaker and Voltage Recovery Tests, **E. J. Poitras, H. P. Kuehni, W. F. Skeats.** AIEE Transactions, volume 54, 1935, February section, pages 170–8.

10. Dielectric Recovery by an A-C Arc in an Air Blast, **T. E. Browne, Jr.** AIEE Transactions, volume 65, March section, pages 169–76.

11. A New High-Speed Cathode-Ray Oscillograph, **H. P. Kuehni, Simon Ramo.** AIEE Transactions, volume 56, 1937, June section, pages 721–8.

12. Multivibrator Circuits, **M. V. Kiebert, A. F. Inglis.** *IRE Proceedings*, volume 33, 1945, pages 534–9.

Asynchronous and Single-Phase Operation of Synchronous Machines

A. W. RANKIN
MEMBER AIEE

ASYNCHRONOUS operation of synchronous machines has been the subject of numerous articles in the technical literature, for example, the articles of Fechheimer,[1] Hay and Mowdawalla,[2] Putman,[3] Park,[4] Linville,[5] Lauder[6]. The fact that articles on this subject continue to be of primary interest to design and operating engineers is attributable to the importance of satisfactory operation at asynchronous speeds. It is only through a precise knowledge of the conditions present in asynchronous operation that machines can be designed for and operated through these asynchronous periods satisfactorily. As examples of the extreme conditions which can arise during asynchronous operation, it should be noted that stalling a synchronous machine with the field voltage applied can result in pulsating torques greater than those obtained by inadvertent synchronizing 180° out of phase;[6] or that the currents in the damper bars on the trailing half of a pole can be considerably greater than the currents in the corresponding bars on the leading half of the pole, and the resulting unequal heating will influence the design of the damper winding to a considerable degree. Because of the importance of these and similar phenomena, the problem of asynchronous operation must be studied continuously until a complete, easily visualized, and easily applied solution is obtained.

The analysis of asynchronous operation, however, is quite involved, and the number of pertinent variables is so large that heretofore the physical aspect of the problem has tended to become submerged completely in the mathematical manipulations involved. The first of the major steps by which the design engineer was extricated from this maze of mathematical transformations was due to Park, whose generalized 2-reaction theory was applicable directly to asynchronous phenomena. A further step was the application of the equivalent-circuit concept by Linville. The next major step was the application by Lauder of the tensor symbolism of Kron[7] by which the multiple mathematical equations could be handled by groups rather than individually.

Important as these latter steps were, however, the calculations were still too time-consuming and labyrinthine to permit their application to routine design problems. The most promising solution to these difficulties appears to be the generalized equivalent circuits of Kron.[7,8,9] With these circuits the problem is reduced to the determination of currents and voltages in relatively simple networks. This not only eliminates the distracting mathematical transformations heretofore employed but also presents an easily visualized method in which the physical characteristics retain their importance and are not submerged in the mathematics.

It is accordingly the purpose of this article to present an analysis of the asynchronous and single-phase operation of a synchronous machine based on the generalized equivalent circuits of Kron. The fundamental equations of Park will be used as the starting point, but the succeeding mathematical operations will be guided by the aforementioned tensor publications of Kron. The asynchronous torque and current relations will be presented in terms of the currents and voltages of simple equivalent circuits, and, in addition, a numerical comparison will be given of the asynchronous and single-phase operating characteristics of synchronous machines with complete and incomplete end rings on the damper windings. This comparison has direct value in design engineering not only as a study of the various torques, but also as a picture of the distribution of the damper-bar currents in the leading and trailing pole halves.

The methods here presented are intended for use with the a-c network analyzer,[10] and all the torque and current expressions are given directly in terms of current and voltage readings obtained from the network analyzer.

This paper is divided into the following four main parts:

A. Derivation of the equivalent circuits for constant-speed asynchronous operation.

B. Numerical example of the application of the equivalent circuits of *A*.

C. Derivation of the equivalent circuits for constant-speed single-phase operation.

D. Numerical example of the application of the equivalent circuits of *C*.

This article is based upon three recent papers by the author,[11–13] which were published to provide a sound basis for the present study. It will be assumed that the reader is familiar with their contents.

The equivalent circuits for asynchronous operation are based on the circuits of reference 8, while the equivalent circuit for single-phase operation is based

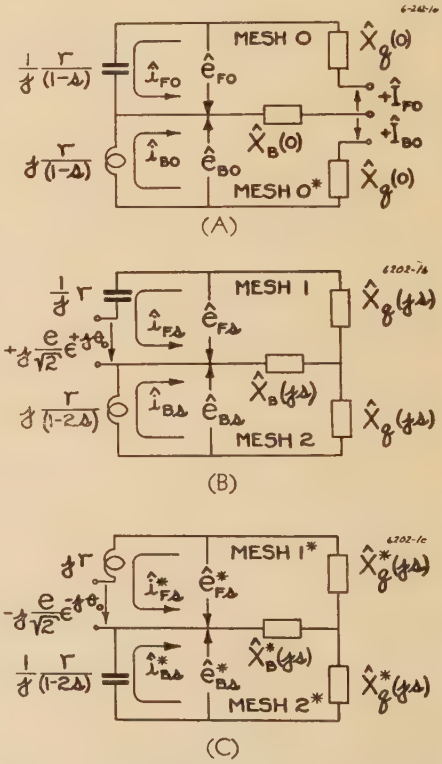

Figure 1. Equivalent circuits for constant-speed asynchronous operation

A. Rotor excitation only
B. Stator excitation only
C. Stator excitation only

Paper 46-202, recommended by the AIEE committee on electric machinery for presentation at the AIEE Great Lakes District meeting, Indianapolis, Ind., October 9–11, 1946. Manuscript submitted May 31, 1946; made available for printing September 9, 1946.

A. W. RANKIN is with the turbine-generator engineering division of General Electric Company, Schenectady, N. Y.

The author acknowledges the co-operation and contributions of his associates in the General Electric Company in the study presented in this paper, S. B. Crary for his suggestions and constructive criticisms, C. E. Kilbourne for his stimulating interest and for placing at the author's disposal several unpublished studies of asynchronous operation by the members of his division, and C. Concordia for his contributions to the single-phase study. Particular appreciation and thanks are extended to Gabriel Kron whose published and unpublished papers on tensor analysis and equivalent circuits guided the mathematical analysis presented here.

on the circuits of the primitive machine presented in reference 9.

Results

Figure 1 gives the equivalent circuits (spin circuits) from which the asynchronous operating characteristics of a synchronous machine may be determined by meter readings of the currents, voltages, and powers. The formulas by which the machine characteristics are expressed in terms of the spin-circuit quantities are given in part *A*.

A comparison of the calculated operating characteristics of synchronous machines with complete and incomplete end rings is given by Figures 2A–15. These figures are discussed in part *B*. From these curves it is evident that by means of the spin circuits, a solution to the problem of asynchronous operation at constant speed has been obtained which, for ease of application, elimination of mathematical transformations, and completeness of treatment, surpasses the solutions previously published for this problem. The numerical example itself possesses immediate practical value. The curves showing current distribution in the damper windings present a picture of the unequal heating which the damper winding must be designed to handle satisfactorily, while the torque curves illustrate the dangerous torque pulsations which exist not only at stalling speeds but throughout the entire speed spectrum.

Figure 17 gives the equivalent circuit from which the single-phase operating characteristics of a synchronous machine may be determined by meter measurements of the various currents, voltages, and powers. The type of single-phase loading is shown in Figure 16. The formulas which express the machine operating characteristics in terms of the spin-circuit quantities are given in part *C*. Note that this spin circuit permits the direct determination of the harmonic currents and torques to any harmonic order.

A numerical example of the calculated single-phase operating characteristics of the synchronous machines described in part *B* is given by part *D*. It is shown there that even in single-phase operation, a considerable difference exists in the loading of the leading and trailing damper bars. In the case of the machine with incomplete end rings on a pure resistance load, the 240-cycle currents and torques are of the order of ten per cent of the corresponding 120-cycle quantities.

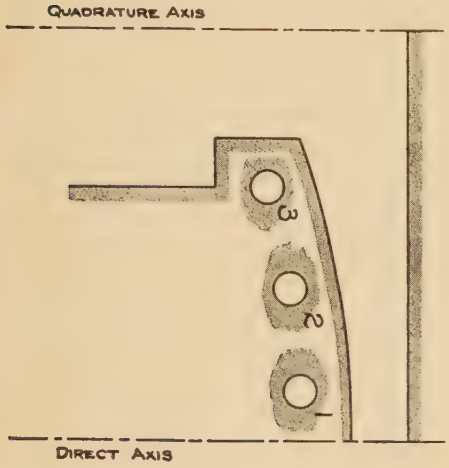

Figure 2A. Numbering of damper bars

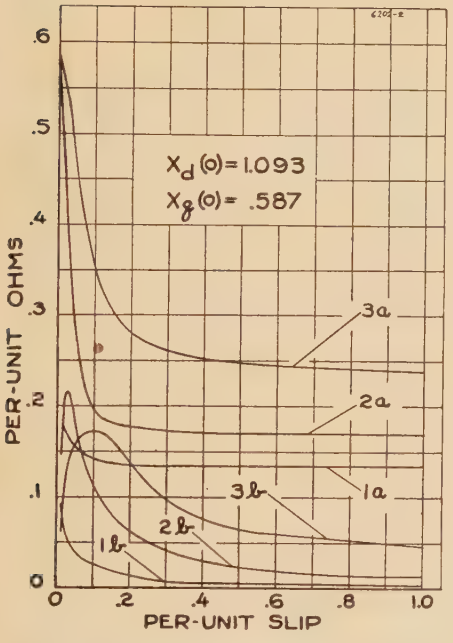

Figure 2B. Impedance functions $\hat{x}_d(js)$ and $\hat{x}_q(js)$ for the synchronous machines used in the numerical examples

$\hat{x}(js) = x - jR$ with x and R given by these curves
a—real component (x)
b—imaginary component (R)
1—direct-axis quantities; complete and incomplete end rings
2—quadrature-axis quantities; complete end rings
3—quadrature-axis quantities; incomplete end rings
As an example, $\hat{x}_q(js)$ for the machine with complete end rings at 0.5 slip is $0.170 - j0.024$

Unit Currents

All currents in the following study are expressed in per unit. Such dimensions are adequate in studying machine operation, but for design and manufacture the actual ampere values must be known. That the stator currents are in per unit of the rated stator current is obvious, but

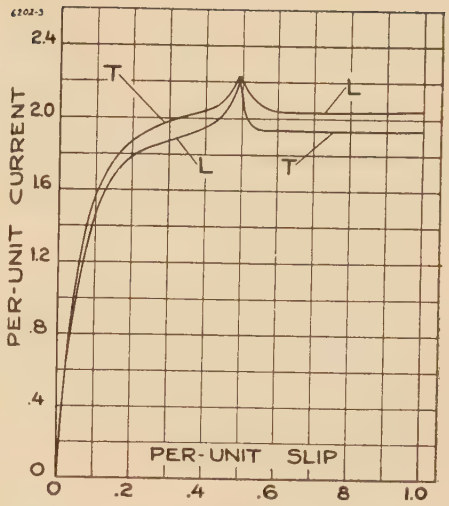

Figure 3. Current in damper bar 1 of machine with complete end rings

T—Trailing
L—Leading

the unit values of the rotor-circuit currents are not at all obvious. In references 11 and 12, the author points out that unit rotor-circuit currents are entirely arbitrary, but that after they are selected the per-unit rotor-circuit impedances must be calculated accordingly. In this article, the x_{ad} bases of reference 12 are used.

Unit field current is that current which at synchronous speed will induce in each stator phase a voltage $x_{ad} i_{ao}$. This current is expressed in amperes by equation 35*a* in terms of i_{ao} and the machine design constants. Unit current for the additional rotor circuits, both direct and quadrature axes, is that current which when flowing in a damper-bar circuit of 100 per cent pitch will induce in each stator phase, at synchronous speed, a voltage $x_{ad} i_{ao}$. This current is expressed in amperes by equation 35*b* in terms of i_{ao} and the machine design constants.

$$\frac{I_{fdo}}{(3/2)\, i_{ao}} = \frac{4}{\pi} \frac{A_{d1}}{F_{d1}} \frac{N}{K_p K_d P_1} \frac{1}{N_{fd}} \text{ (peak)} \quad \textbf{(35a)}$$

$$\frac{I_{xdo}}{(3/2)\, i_{ao}} = \frac{4}{\pi} \frac{A_{d1}}{D_{d1x}} \frac{N}{K_p K_d P_1} \frac{1}{N_{xd}} \text{ (peak)} \quad \textbf{(35b)}$$

All impedances are calculated with the base-current ratios, equations 35*a* and 35*b*. Formulas for the impedances, using these base-current ratios, were derived in reference 13.

The various current expressions are in per unit instantaneous rather than effective values, but these instantaneous values are in per unit of the unit currents,[11] equations 35*a* and 35*b*. Hence, when it is desired to determine the effective value of a slip-frequency current, it must

be taken in per unit of the effective values of the base currents equations 35*a* and 35*b*.

A. Derivation of the Equivalent Circuits for Constant-Speed Asynchronous Operation

Equivalent Circuit for Stator Excitation Only

The fundamental relations between the axis quantities are given by equations 8, 9, and 10 of reference 4. Assuming a constant rotor speed of v per unit and a balanced 3-phase system, these equations reduce to the following:

$$e_d = p\psi_d - ri_d - v\psi_q \quad (1a)$$

$$e_q = p\psi_q - ri_q + v\psi_d \quad (1b)$$

Let the following complex spin quantities be defined.

$$\hat{\psi}_F = \frac{\psi_d + j\psi_q}{\sqrt{2}} \quad (2a)$$

$$\hat{\psi}_B = \frac{\psi_d - j\psi_q}{\sqrt{2}} \quad (2b)$$

Let the spin quantities $\hat{e}_F$ and $\hat{e}_B$, $\hat{\imath}_F$ and $\hat{\imath}_B$, be defined analogously in terms of their corresponding axis quantities. Since the axis quantities are real, it is evident that the spin quantities are conjugate complex quantities.

Since all the rotor-circuit voltages are assumed zero, the axis linkages are given by the following operational functions of the axis currents. The first of these relations, equation 3*a*, was given by equation 8*a* of reference 13, and the second is obtained in an analogous manner.

$$\psi_d = -x_d(p)i_d \quad (3a)$$

$$\psi_q = -x_q(p)i_q \quad (3b)$$

The spin linkages are obtained in terms of the spin currents by substituting equations 3*a* and 3*b* into equations 2*a* and 2*b*. Equations 4*a*, 4*b*, 5*a*, and 5*b* thereby are obtained.

$$\hat{\psi}_F = -x_F(p)\hat{\imath}_F - x_B(p)\hat{\imath}_B \quad (4a)$$

$$\hat{\psi}_B = -x_B(p)\hat{\imath}_F - x_F(p)\hat{\imath}_B \quad (4b)$$

$$x_F(p) = \frac{x_d(p) + x_q(p)}{2} \quad (5a)$$

$$x_B(p) = \frac{x_d(p) - x_q(p)}{2} \quad (5b)$$

Substituting the spin equations of the type given by equations 2*a* and 2*b* back into the axis equations 1*a* and 1*b* will give the fundamental spin relation of equations 6*a* and 6*b*.

$$\hat{e}_F = (p + jv)\hat{\psi}_F - r\hat{\imath}_F \quad (6a)$$

$$\hat{e}_B = (p - jv)\hat{\psi}_B - r\hat{\imath}_B \quad (6b)$$

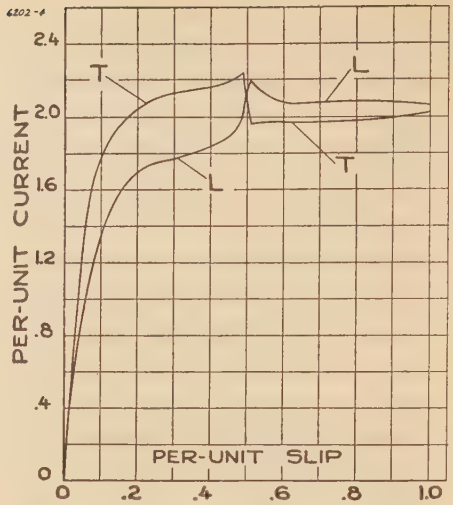

Figure 4. Current in damper bar 2 of machine with complete end rings

T—Trailing
L—Leading

Substituting equations 4*a* and 4*b* into equations 6*a* and 6*b* gives the operational equations 7*a* and 7*b*.

$$-\hat{e}_F = (p + jv)[x_F(p)\hat{\imath}_F + x_B(p)\hat{\imath}_B] + r\hat{\imath}_F \quad (7a)$$

$$-\hat{e}_B = (p - jv)[x_B(p)\hat{\imath}_F + x_F(p)\hat{\imath}_B] + r\hat{\imath}_B \quad (7b)$$

Assuming that balanced 3-phase voltages are applied with the machine running at a constant slip, the phase voltages are as given by equations 8*a*–8*c*; the angular position is as given by equation 9; and the axis voltages are as given by equations 10*a* and 10*b*. These latter voltages are obtained by means of equation 6 of reference 4.

$$e_a = e\cos t \quad (8a)$$

$$e_b = e\cos(t - 120) \quad (8b)$$

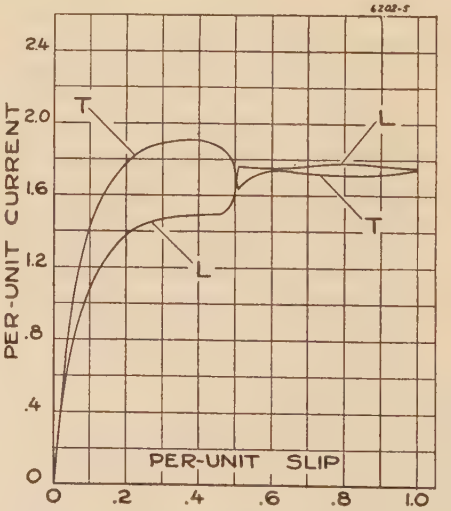

Figure 5. Current in damper bar 3 of machine with complete end rings

T—Trailing
L—Leading

$$e_c = e\cos(t + 120) \quad (8c)$$

$$\theta = (1 - s)t - \theta_0 \quad (9)$$

$$e_d = e\cos(st + \theta_0) \quad (10a)$$

$$e_q = e\sin(st + \theta_0) \quad (10b)$$

Substituting equations 10*a* and 10*b* into the voltage equations analogous to equations 2*a* and 2*b* gives the spin voltages equations 11*a* and 11*b*.

$$\hat{e}_F = 0.707e\epsilon^{+j(st+\theta_0)} \quad (11a)$$

$$\hat{e}_B = 0.707e\epsilon^{-j(st+\theta_0)} \quad (11b)$$

With the spin voltages given by equations 11*a* and 11*b*, it is evident from equations 7*a* and 7*b* that the steady-state values of the spin currents can contain only exponentials of the type given by equations 11*a* and 11*b*. Because it is also evident from the current equations analogous to equations 2*a* and 2*b* that the spin currents are conjugate quantities, it is permissible to assume solutions for the spin currents as given by equations 12*a* and 12*b*. The subscript s is used here to identify these spin currents as belonging to the solution for constant-speed asynchronous (slip) operation.

$$\hat{\imath}_F = \hat{\imath}_{Fs}\epsilon^{+jst} + \hat{\imath}_{Bs}{}^*\epsilon^{-jst} \quad (12a)$$

$$\hat{\imath}_B = \hat{\imath}_{Bs}\epsilon^{+jst} + \hat{\imath}_{Fs}{}^*\epsilon^{-jst} \quad (12b)$$

Substituting equations 12*a* and 12*b* and equations 11*a* and 11*b* into equations 7*a* and 7*b*, grouping the terms containing like exponentials, and equating these groups to zero will result in equations 13*a* and 13*b* and equations 14*a* and 14*b*.

$$+0.707je\epsilon^{+j\theta_0} = \left[\hat{x}_F(js) + \frac{r}{j}\right]\hat{\imath}_{Fs} + \hat{x}_B(js)\hat{\imath}_{Bs} \quad (13a)$$

$$0 = \hat{x}_B(js)\hat{\imath}_{Fs} + \left[\hat{x}_F(js) - \frac{r}{j(1-2s)}\right]\hat{\imath}_{Bs} \quad (13b)$$

$$-0.707je\epsilon^{-j\theta_0} = \left[\hat{x}_F{}^*(js) - \frac{r}{j}\right]\hat{\imath}_{Fs}{}^* + \hat{x}_B{}^*(js)\hat{\imath}_{Bs}{}^* \quad (14a)$$

$$0 = \hat{x}_B{}^*(js)\hat{\imath}_{Fs}{}^* + \left[\hat{x}_F{}^*(js) + \frac{r}{j(1-2s)}\right]\hat{\imath}_{Bs}{}^* \quad (14b)$$

Equations 13*a* and 13*b* can be solved electrically by means of the a-c network of Figure 1B; equations 14*a* and 14*b* can be solved similarly by the a-c network of Figure 1C. It is evident that the circuit of Figure 1C is the conjugate of the circuit of Figure 1B, and that the currents and voltages of the former are the conjugates of the corresponding quantities in the latter. For this reason the circuit of Figure 1C at present may seem superfluous. Actually, however, both these

circuits are needed simultaneously for the determination of the torques as will be shown in a following section.

Equivalent Circuit for Rotor Excitation Only

The equivalent circuit from which the steady-state currents and voltages due to rotor excitation alone may be obtained is derived as follows. Let the subscript O be used to designate all quantities due to the rotor excitation.

If the machine is connected to a balanced unexcited system, the line currents will be balanced, but their frequency will correspond to the machine speed. Assuming operation at speed v, the phase currents are as given by equations 15a–15c; the angular position is as given by equation 16; and the axis currents are as given by equations 17a and 17b. These latter currents were obtained by means of equations 3 and 3a of reference 4.

$$i_a = i_O \cos vt \tag{15a}$$

$$i_b = i_O \cos (vt-120) \tag{15b}$$

$$i_c = i_O \cos (vt+120) \tag{15c}$$

$$\theta = vt - \theta_0 \tag{16}$$

$$i_{dO} = i_O \cos \theta_0 \tag{17a}$$

$$i_{qO} = i_O \sin \theta_0 \tag{17b}$$

Assuming that the d-c rotor excitations in the direct- and quadrature-axis field circuits are I_{fdO} and I_{fqO}, respectively, the stator axis linkages are given by equations 18a and 18b. These expressions are taken directly from equation 16a of reference 11. It is evident that no currents are flowing in any of the additional rotor circuits because the machine now is assumed to be connected to a balanced unexcited system.

$$\psi_{dO} = x_{afd} I_{fdO} - x_d i_{dO} \tag{18a}$$

$$\psi_{qO} = x_{afq} I_{fqO} - x_q i_{qO} \tag{18b}$$

Substituting spin relations of the form of equations 2a and 2b into equations 18a and 18b gives the spin linkage equations 19a and 19b with the spin rotor excitations and spin reactances defined by equations 20a and 20b and equations 21a and 21b, respectively.

$$\hat{\psi}_{FO} = \hat{I}_{FO} - \hat{x}_F(0)\hat{i}_{FO} - \hat{x}_B(0)\hat{i}_{BO} \tag{19a}$$

$$\hat{\psi}_{BO} = \hat{I}_{BO} - \hat{x}_B(0)\hat{i}_{FO} - \hat{x}_F(0)\hat{i}_{BO} \tag{19b}$$

$$\hat{I}_{FO} = 0.707(x_{afd} I_{fdO} + j x_{afq} I_{fqO}) \tag{20a}$$

$$\hat{I}_{BO} = 0.707(x_{afd} I_{fdO} - j x_{afq} I_{fqO}) \tag{20b}$$

Substituting equations 19a and 19b back into the fundamental spin relations, equations 6a and 6b, gives equations 22a and 22b.

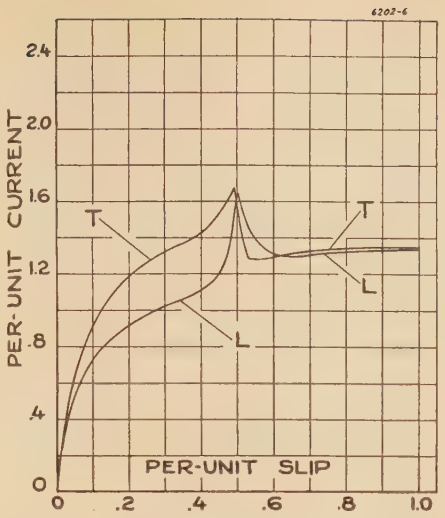

Figure 6. Current in damper bar 1 of machine with incomplete end rings

T—Trailing
L—Leading

$$\hat{x}_F(0) = \frac{x_d(0)+x_q(0)}{2} = \frac{x_d+x_q}{2} \tag{21a}$$

$$\hat{x}_B(0) = \frac{x_d(0)-x_q(0)}{2} = \frac{x_d-x_q}{2} \tag{21b}$$

$$\frac{\hat{e}_{FO}}{jv} = \hat{I}_{FO} - \left[\hat{x}_F(0) + \frac{r}{jv}\right]\hat{i}_{FO} - \hat{x}_B(0)\hat{i}_{BO} \tag{22a}$$

$$\frac{-\hat{e}_{BO}}{jv} = \hat{I}_{BO} - \hat{x}_B(0)\hat{i}_{FO} - \left[\hat{x}_F(0) - \frac{r}{jv}\right]\hat{i}_{BO} \tag{22b}$$

If the machine is connected to a balanced unexcited infinite system, the voltages $\hat{e}_{FO}$ and $\hat{e}_{BO}$ are zero, and the reactance expressions include only the machine reactances. If the system is of finite magnitude, the voltages $\hat{e}_{FO}$ and $\hat{e}_{BO}$ still are to be considered zero, but the system reactance then must be added to the machine reactances. In either case equations 22a and 22b will reduce to equations 23a and 23b.

$$\hat{I}_{FO} = \left[\hat{x}_F(0) + \frac{r}{jv}\right]\hat{i}_{FO} + \hat{x}_B(0)\hat{i}_{BO} \tag{23a}$$

$$\hat{I}_{BO} = \hat{x}_B(0)\hat{i}_{FO} + \left[\hat{x}_F(0) - \frac{r}{jv}\right]\hat{i}_{BO} \tag{23b}$$

It is evident that equations 23a and 23b can be solved electrically by the a-c network of Figure 1A.

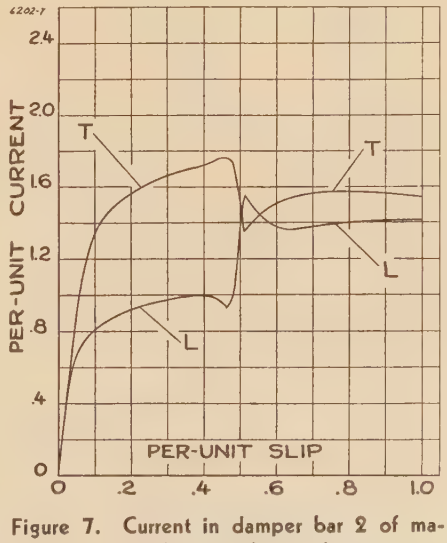

Figure 7. Current in damper bar 2 of machine with incomplete end rings

T—Trailing
L—Leading

Determination of Rotor and Stator Currents

The rotor and stator currents during constant-speed asynchronous operation at slip s are obtained from the spin circuits of Figures 1A, 1B, and 1C as follows.

From expressions analogous to equations 2a and 2b, the spin currents are obtained in terms of the axis currents by means of equations 24a and 24b.

$$\sqrt{2} i_d = \hat{i}_F + \hat{i}_B \tag{24a}$$

$$j\sqrt{2} i_q = \hat{i}_F - \hat{i}_B \tag{24b}$$

Substituting equations 12a and 12b into equations 24a and 24b and adding the currents due to rotor excitation gives i_d and i_q in terms of the spin-circuit currents as in equations 25a and 25b.

$$i_{ds} = \frac{\hat{i}_{Fs}+\hat{i}_{Bs}}{\sqrt{2}}\epsilon^{+jst} + \frac{\hat{i}_{Fs}^*+\hat{i}_{Bs}^*}{\sqrt{2}}\epsilon^{-jst} + \frac{\hat{i}_{FO}+\hat{i}_{BO}}{\sqrt{2}} \tag{25a}$$

$$i_{qs} = \frac{\hat{i}_{Fs}-\hat{i}_{Bs}}{j\sqrt{2}}\epsilon^{+jst} - \frac{\hat{i}_{Fs}^*-\hat{i}_{Bs}^*}{j\sqrt{2}}\epsilon^{-jst} + \frac{\hat{i}_{FO}-\hat{i}_{BO}}{j\sqrt{2}} \tag{25b}$$

The damper-winding currents in the direct and quadrature axes are obtained by means of the above equations and the current moduli $\hat{U}_{nds}$ and $\hat{U}_{nqs}$. These current moduli were introduced in equations 9a–9c of reference 13. $\hat{U}_{nds}$ is defined as the a-c current (in complex notation) in the nth bar of the direct-axis circuit (Figure 1, reference 13) at slip s when the terminal current i_{ds} of the direct-axis circuit (Figure 1, reference 13) is $1.00\ \underline{/0}$. $\hat{U}_{nqs}$ is defined analogously for the quadrature-axis circuit. The currents in the nth bar of the direct- and quadrature-axis circuits are then as given by equations 26a–26d. The subzero currents of equations 25a and 25b obviously cause no currents to flow in the damper windings because the frequency of these currents corresponds to the rotor speed.

$$\hat{U}_{nds}=\hat{I}_{nds} \quad \text{for } \hat{i}_{ds}=1.00\underline{/0} \tag{26a}$$

$$\hat{U}_{nqs}=\hat{I}_{nqs} \quad \text{for } \hat{i}_{qs}=1.00\underline{/0} \tag{26b}$$

$$I_{nds}=\frac{\hat{i}_{Fs}+\hat{i}_{Bs}}{\sqrt{2}}\hat{U}_{nds}\epsilon^{+jst}+\frac{\hat{i}_{Fs}^{*}+\hat{i}_{Bs}^{*}}{\sqrt{2}}\hat{U}_{nds}^{*}\epsilon^{-jst} \tag{26c}$$

$$I_{nqs}=\frac{\hat{i}_{Fs}-\hat{i}_{Bs}}{j\sqrt{2}}\hat{U}_{nqs}\epsilon^{+jst}-\frac{\hat{i}_{Fs}^{*}-\hat{i}_{Bs}^{*}}{j\sqrt{2}}\hat{U}_{nqs}^{*}\epsilon^{-jst} \tag{26d}$$

I_{nds} and I_{nqs} may be expressed more concisely as in equations 27*a* and 27*b*.

$$I_{nds}=\sqrt{2}\Re[(\hat{i}_{Fs}+\hat{i}_{Bs})\hat{U}_{nds}\epsilon^{+jst}] \tag{27a}$$

$$\sqrt{2}\Im[(\hat{i}_{Fs}-\hat{i}_{Bs})\hat{U}_{nqs}\epsilon^{+jst}] \tag{27b}$$

Equations 27*a* and 27*b* give the axis bar currents as real functions of time, and complex quantities are not present.

The preceding expressions have given the axis currents. The true currents in the physical bars are given by the following expressions which are taken from equations 9*d* and 9*e* of reference 13.

Bars on trailing pole halves

$$I_{ns}=+I_{nds}+I_{nqs} \tag{28a}$$

Bars on leading pole halves

$$I_{ns}=-I_{nds}+I_{nqs} \tag{28b}$$

Due consideration must be given to the bar numbering system described in reference 13 by which the direct-axis bars are numbered from the direct axis and the quadrature axis bars are numbered from the quadrature axis.

It is evident from equations 28*a* and 28*b* that, in general, there is unequal loading of the bars in the trailing and leading pole halves. The degree of this inequality depends upon the pole saliency and lack of symmetry between the direct and quadrature axes. Equal loading of the trailing and leading pole halves exists only when I_{nds} and I_{nqs} are in time quadrature. A quantitative illustration of this unequal loading is given in the following part *B*.

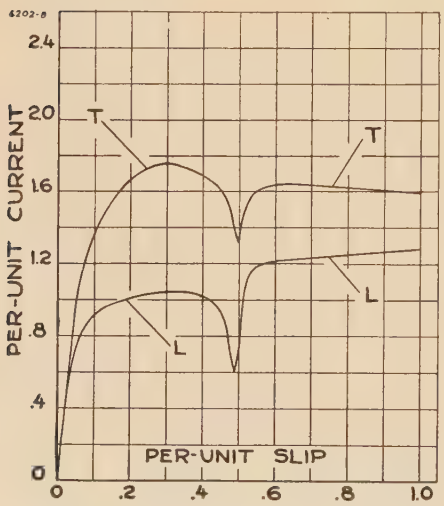

Figure 8. Current in damper bar 3 of machine with incomplete end rings

T—Trailing
L—Leading

The currents I_{fds} and I_{fqs} may be obtained from expressions analogous to equations 27*a* and 27*b*. The concept of a quadrature axis field winding is somewhat academic but, as discussed in reference 13, its introduction simplifies considerably the analysis of the quadrature axis. If such a winding were present, however, it would not be a part of the direct-axis field winding, and expressions such as equations 28*a* and 28*b* could not be written for the field circuit. The alternating currents in the direct and quadrature axis field-winding circuits are given by equations 27*a* and 27*b* directly. The rotor excitation currents I_{fdo} and I_{fqo} must be added to these, of course, to obtain the total current.

The stator line currents are obtained, as follows, directly from the spin currents of Figures 1A and 1B. At a constant slip *s*, the line current i_a in the *a*-phase is expressed in terms of the axis currents as in equations 29*a* and 29*b*. (See equation 14, reference 4.)

$$i_a=i_{ds}\cos\theta-i_{qs}\sin\theta \tag{29a}$$

$$i_a=i_{ds}\cos[(1-s)t-\theta_0]-i_{qs}\sin[(1-s)t-\theta_0] \tag{29b}$$

Substituting equations 25*a* and 25*b* into equations 29*a* and 29*b* and noting that $\hat{i}_{FO}=\hat{i}_{BO}^{*}$ simplifies the latter into equation 30*a*.

$$i_a=\sqrt{2}\Re[\hat{i}_{Fs}\epsilon^{+(jt-\theta_0)}+\hat{i}_{FO}\epsilon^{+j[(1-s)t-\theta_0]}+\hat{i}_{Bs}\epsilon^{-j[(1-2s)t-\theta_0]}] \tag{30a}$$

It is immediately evident that three frequencies exist in the line current, namely, system frequency, system frequency times $(1-s)$, and system frequency times $(1-2s)$. The magnitudes of the currents of these three frequencies are given explicitly by equation 30*a*. If zero time is selected so as to make $\theta_0=0$, then equation 30*a* reduces to equation 30*b*.

$$i_a=\sqrt{2}\ \Re[\hat{i}_{Fs}\epsilon^{+jt}+\hat{i}_{FO}\epsilon^{+j(1-s)t}+\hat{i}_{Bs}\epsilon^{-j(1-2s)t}] \tag{30b}$$

Determination of Torques

The rotor torques during constant-speed asynchronous operation at slip *s* are obtained from the spin circuits of Figure 1 as follows.

In terms of the axis quantities, the rotor torque is given by equation 31*a*. (See equation 19, reference 4.)

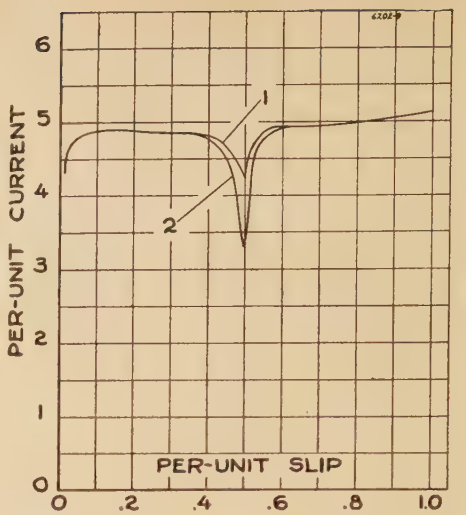

Figure 9. Slip-frequency current in direct-axis field winding

1—Complete end rings
2—Incomplete end rings
The exciting current I_{fdo} must be added to these curves to obtain the total current

$$T=i_q\psi_d-i_d\psi_q \tag{31a}$$

Substituting the spin quantities defined by equations 2*a* and 2*b* and analogous expressions into equation 31*a* will give the general torque equation in terms of spin quantities.

$$T=j[\hat{i}_B\hat{\psi}_F-\hat{i}_F\hat{\psi}_B] \tag{31b}$$

The currents and linkages used in equation 31*b* must include the effects of both rotor and stator excitation. The linkages due to the stator excitation are given by equations 4*a* and 4*b*; the currents due to the stator excitation are given by equations 12*a* and 12*b*; the linkages due to the rotor excitation are given by equations 19*a* and 19*b*; and the currents due to the rotor excitation are simply $\hat{i}_{FO}$ and $\hat{i}_{BO}$. Substituting these equations into equation 31*b* will give the torque expressions of equations 32*a*–32*g*, 33*a*–33*f*, and 34*a*–34*d*. Note that the torques now are known directly in terms of the currents and voltages of the spin circuits of Figures 1A, 1B, and 1C.

Zero-Frequency Torque T_{0s}

$$-T_{0s}=(V_{00}-V_{0^*0^*})+(V_{11}-V_{22})-(V_{1^*1^*}-V_{2^*2^*}) \tag{32a}$$

$$(\hat{e}_{FO})^{*}\hat{i}_{FO}=0+jV_{00} \tag{32b}$$

$$(\hat{e}_{BO})^{*}\hat{i}_{BO}=0+jV_{0^*0^*} \tag{32c}$$

$$(\hat{e}_{Fs})^{*}\hat{i}_{Fs}=W_{11}+jV_{11} \tag{32d}$$

$$(\hat{e}_{Fs}^{*})^{*}\hat{i}_{Fs}^{*}=W_{1^*1^*}+jV_{1^*1^*} \tag{32e}$$

$$(\hat{e}_{Bs})^{*}\hat{i}_{Bs}=W_{22}+jV_{22} \tag{32f}$$

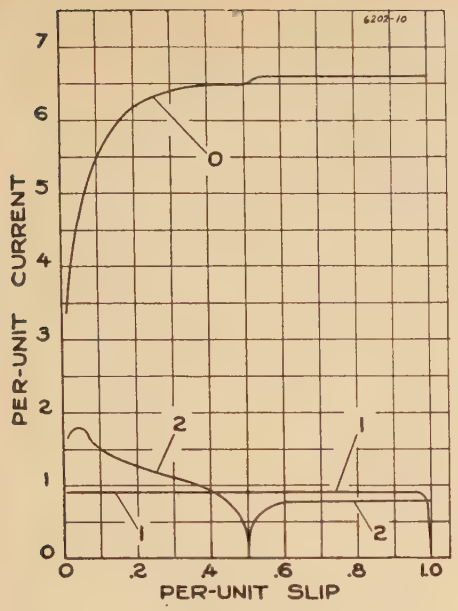

Figure 10. Stator current in machine with complete end rings

0—Current of system frequency
1—Current of system frequency times $(1-s)$
2—Current of system frequency times $(1-2s)$

$$(\hat{e}_{Bs}{}^{*})^{*}\hat{i}_{Bs}{}^{*}=W_{2*2*}+jV_{2*2*} \tag{32g}$$

Slip-Frequency Torque T_{1s}

$$T_{1s}=2\sqrt{(W_{01}-W_{0*2}+W_{20*}-W_{10})^{2}+(V_{01}-V_{0*2}-V_{20*}+V_{10})^{2}} \tag{33a}$$

$$-T_{1s}=2(W_{01}-W_{0*2}+W_{20*}-W_{10})\times\sin st+2(V_{01}-V_{0*2}-V_{20*}+V_{10})\times\cos st \tag{33b}$$

$$(\hat{e}_{FO})^{*}\hat{i}_{Fs}=W_{01}+jV_{01} \tag{33c}$$

$$(\hat{e}_{BO})^{*}\hat{i}_{Bs}=W_{0*2}+jV_{0*2} \tag{33d}$$

$$(\hat{e}_{Fs})^{*}\hat{i}_{FO}=W_{10}+jV_{10} \tag{33e}$$

$$(\hat{e}_{Bs})^{*}\hat{i}_{BO}=W_{20*}+jV_{20*} \tag{33f}$$

Double-Slip-Frequency Torque T_{2s}

$$T_{2s}=2\sqrt{(W_{12*}-W_{21*})^{2}+(V_{12*}-V_{21*})^{2}} \tag{34a}$$

$$T_{2s}=2(W_{12*}-W_{21*})\times\sin 2st-2(V_{12*}-V_{21*})\cos 2st \tag{34b}$$

$$(\hat{e}_{Fs})^{*}\hat{i}_{Bs}{}^{*}=W_{12*}+jV_{12*} \tag{34c}$$

$$(\hat{e}_{Bs})^{*}\hat{i}_{Fs}{}^{*}=W_{21*}+jV_{21*} \tag{34d}$$

The method of writing the products of complex numbers as used above is necessary in order to clarify the $W+jV$ readings taken on the network analyzer. If the analyzer flow conventions are such that positive flow of reactive power is opposite to the positive flow of real power, then the analyzer is wired internally so that the product $e^{*}i$ is obtained by plugging the voltage e (not its conjugate) to the voltage terminals and the current i to the current terminals. In order to maintain the forementioned flow convention, the $W+jV$ meter will reverse the angle of the voltage automatically and will give $e^{*}i$. Hence, on the voltages in the foregoing expressions, the (*) outside the parentheses refers to the conjugation automatically performed by the meter. The potential terminals of the meter are to be plugged to the voltage inside the parentheses.

The forementioned currents and voltages are indicated on the spin circuits of Figures 1A, 1B, and 1C. The determination of the various torques during constant-speed-asynchronous operation has been reduced to the measurement of the real and reactive power in these spin circuits.

B. Numerical Example of the Application of the Equivalent Circuits of Part A

As a numerical example illustrating the application of the equivalent circuits developed in part *A*, part *B* will present the calculated operating characteristics of the synchronous machines described in the following paragraph when operating asynchronously on an infinite system.

SYNCHRONOUS MACHINE

937.5 kva, 750 kw
779 volts line-line
695 amperes line current
6-pole, 1,200-rpm
3-phase, 60-cycle
six damper bars per pole

$e_{ao}=636$ volts per phase, peak
$i_{ao}=983$ amperes line, peak
$x_{ao}=0.647$ ohm

$r=0.008$
$x_d=1.093$
$x_q=0.587$

The impedance functions $\hat{x}_d(js)$ and $\hat{x}_q(js)$, as defined by equation 8*b* of reference 13 and Figure 1 of the same reference, are shown in Figure 2B as functions of the per-unit slip. Two end-ring conditions are shown by these curves. Curves 1 and 2 show $\hat{x}_d(js)$ and $\hat{x}_q(js)$, respectively, for the case of complete end rings, and curves 1 and 3 show the same functions for the case of incomplete end rings. Since it is physically impossible to open the end rings between poles completely, the incomplete end ring condition was simulated by making the impedances X_{e11q} and R_{e11q} of the incomplete ring ten times the corresponding values for the complete ring. It should be noted that $\hat{x}_d(js)$ and $\hat{x}_q(js)$ for unit slip are in satisfactory agreement with normal subtransient reactance values.

The impedance operators $\hat{x}_d(js)$ and $\hat{x}_q(js)$ as given in Figure 2B were obtained by a-c network analyzer measurements of the equivalent circuits shown in Figure 1 of reference 13. The impedances used in these circuits were calculated by the per-unit impedance formulas of the same reference. These per-unit formulas, in turn, are based upon the x_{ad} base-current ratio recommended in reference 12 as a preferred standard, and evaluated in equations 1*c* and 1*d* of the same reference. These base-current ratios are as follows.

$$\frac{I_{fdo}}{(3/2)i_{ao}}=\frac{4}{\pi}\frac{A_{d1}}{F_{d1}}\frac{N}{K_pK_dP_1}\frac{1}{N_{fd}} \tag{35a}$$

$$\frac{I_{xdo}}{(3/2)i_{ao}}=\frac{4}{\pi}\frac{A_{d1}}{D_{d1x}}\frac{N}{K_pK_dP_1}\frac{1}{N_{xd}} \tag{35b}$$

Substituting the required design constants in the foregoing formulas gives the following for the unit currents in the field and damper windings:

$$I_{fdo}=24.70 \text{ amperes} \tag{35c}$$

$$I_{xdo}=5{,}300 \text{ amperes} \tag{35d}$$

As discussed in reference 13, I_{xdo} is the base current for the damper-winding circuits in both the direct and quadrature axes. By this means, the per-unit values of I_d and I_q may be added directly.

The operating characteristics of the two synchronous machines defined by the foregoing constants and the impedance operators of Figure 2 are given by Figures 3–15 inclusive. These characteristics describe asynchronous operation at a constant slip, with the direct-axis field winding carrying unit excitation, with no quadrature axis field winding, and with

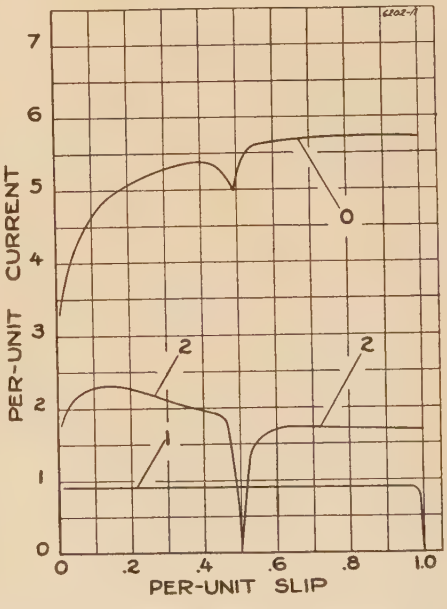

Figure 11. Stator current in machine with incomplete end rings

0—Current of system frequency
1—Current of system frequency times $(1-s)$
2—Current of system frequency times $(1-2s)$

the machines connected to an infinite system of unit voltage and synchronous frequency.

Figures 3, 4, and 5 show the magnitudes of the slip-frequency currents in damper bars 1, 2, and 3, respectively, for the machine with complete end rings; the curves marked T and L refer to the trailing and leading bars, respectively. The numbering system which defines the physical location of the damper bars in the pole is given on Figure 2A. It should be noted from Figures 3, 4, and 5 that above half speed, the trailing bar is loaded more heavily while below half speed the leading bar carries a heavier load. The inequality is greater above half speed, however, and the trailing bar in general must carry a much heavier load than the leading bar.

Figures 6, 7, and 8 show corresponding curves for the machine with incomplete end rings. In this case, the trailing bar carries a heavier load than the leading bar almost continuously, this inequality being especially marked for bar 2 and bar 3. The unequal heating which is concomitant with this unequal current distribution influences the design of the damper winding to an appreciable degree.

Figure 9 shows the slip-frequency current in the direct-axis field windings for both complete and incomplete end rings. Except at the half-speed point, there is little difference between the two cases.

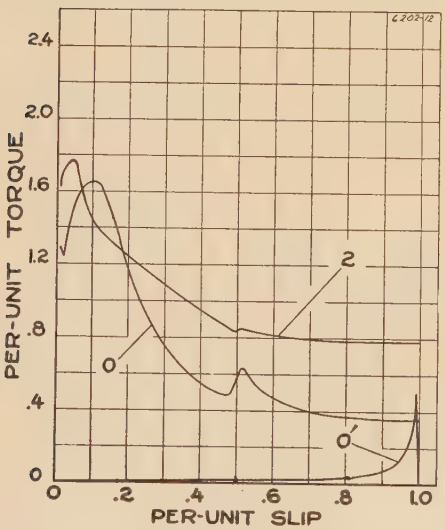

Figure 12. Torques of machine with complete end rings

0—Unidirectional torque with stator excitation only
0—Unidirectional torque with rotor excitation only
2—Double-slip-frequency torque with stator excitation only
The unidirectional torques 0 and 0′ are opposite in sign

It should be remembered that to obtain the total current in the field winding, the rotor-excitation current $I_{fdo}=1.0$ must be added to the curves of Figure 9.

Figures 10 and 11 show the stator-current curves for complete and incomplete end rings, respectively. The system-frequency current for the case of incomplete end rings is less than the same current for the case of complete end rings almost in the ratio of the average of the $x_d(j\omega)$ and $x_q(j\omega)$ impedances, as expected. The currents labeled 2, which are of system frequency times $(1-2s)$, are larger for the case of incomplete end rings due to the greater inequality between the d and q axes. The currents labeled 1, which are of system frequency times $(1-s)$, are exactly the same for the two cases because these currents are caused by the rotor excitation only.

The torque characteristics are given by Figures 12–15, inclusive. Figure 12 shows the torques of the machine with complete end rings with stator and rotor excitation applied separately, but not concurrently. The curve marked 0 gives the unidirectional torque caused by stator excitation alone, and the curve marked 0′ gives the unidirectional torque due to rotor excitation alone. These two torques are naturally opposite in sign. The small dip in the 0 curve around half speed indicates little tendency to lock at this speed. The curve marked 2 gives the double-slip-frequency torque due to stator excitation alone. Note that this torque exceeds the maximum of the unidirectional torque.

Figure 13 corresponds to Figure 12 but is for the case of incomplete end rings. Note that the unidirectional torque 0 due to stator excitation alone is less than that of Figure 12 and has an extreme dip at half speed. The double-slip-frequency torque 2 is very large, indicating extreme torque pulsations. The unidirectional torque 0′ due to rotor excitation alone is identical with the corresponding curve of Figure 12.

Figure 14 shows the effect of applying rotor and stator excitation concurrently for the machine with complete end rings. The unidirectional torque 0 is similar to that of Figure 12 but becomes negative at very low speeds. The double-slip-frequency torque 2 is identical with that of Figure 12. The slip-frequency torque 1, however, has increased considerably, because the flux caused by rotor excitation has reacted with the currents resulting from stator excitation. At standstill this slip-frequency torque reaches a value of 5.8 per unit. The danger in inadvertently stalling a synchronous machine while rotor excitation is maintained is shown vividly by this figure.

Figure 15 corresponds to Figure 14 but is for the case of incomplete end rings. The pronounced dip in the unidirectional torque curve at half speed is still present, and in addition, this torque becomes negative at very low speeds. The double-slip-frequency torque 2 is identical with that of Figure 13. The slip-frequency torque 1 has increased considerably but not as much as for the case of complete end rings, because the currents due to stator excitation are less for the case of incomplete end rings. Nevertheless, at stalling a slip-frequency torque of 4.70 per unit is obtained.

C. Derivation of the Equivalent Circuit for Constant-Speed Single-Phase Operation

Derivation of Equivalent Circuit

The equivalent circuit from which the machine characteristics during constant-speed single-phase operation can be obtained will be derived in this section. The single-phase operation studied in this section is of the type shown in Figure 16. A load is connected across two of the machine terminals, but the machine is not connected to any system. The single-phase load is simulated by putting an impedance Z in each line and then tying two phases together with the third open. The

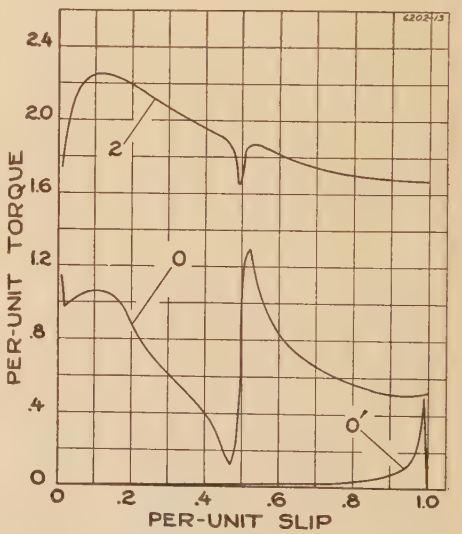

Figure 13. Torques of machine with incomplete end rings

0—Unidirectional torque with stator excitation only
0′—Unidirectional torque with rotor excitation only
2—Double-slip-frequency torque with stator excitation only
The unidirectional torques 0 and 0′ are opposite in sign

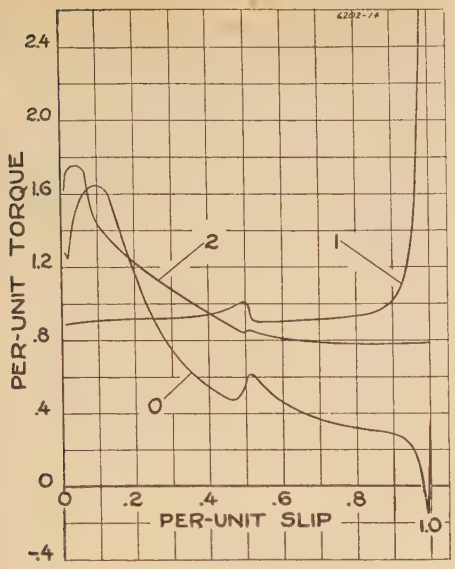

Figure 14. Torques of machine with complete end rings with stator and rotor excitations of 1.0 each applied concurrently

0—Unidirectional torque
1—Slip-frequency torque
2—Double-slip-frequency torque
The slip-frequency torque reaches a maximum of 5.80 at 1.00 slip

load impedance Z is lumped with the machine impedance, and the machine terminal voltage discussed below is the voltage external to the load impedance. Such single-phase operation is defined by equations 36*a*–36*d*.

$$i_a = 0 \tag{36a}$$

$$i_b = -i_c = i \tag{36b}$$

$$e_a = e_a \tag{36c}$$

$$e_b = e_c = e \tag{36d}$$

The axis linkages are given by equations 37*a* and 37*b*. Note that these linkages differ from those of equations 18*a* and 18*b* because the constant rotor excitation in this case can produce currents of frequencies different from that corresponding to the machine speed.

$$\psi_d = x_{afd} I_{fdo} - x_d(p) i_d \tag{37a}$$

$$\psi_q = x_{afq} I_{fqo} - x_q(p) i_q \tag{37b}$$

The spin linkages, as obtained from equations 2*a* and 2*b* and analogous equations, are given by equations 38*a* and 38*b*.

$$\hat{\psi}_F = \hat{I}_{FO} - x_F(p)\hat{\imath}_F - x_B(p)\hat{\imath}_B \tag{38a}$$

$$\hat{\psi}_B = \hat{I}_{BO} - x_B(p)\hat{\imath}_F - x_F(p)\hat{\imath}_B \tag{38b}$$

Substituting equations 38*a* and 38*b* into the general voltage equations in the spin system, equations 6*a* and 6*b*, gives equations 39*a* and 39*b*.

$$\hat{e}_F = (p+jv)[\hat{I}_{FO} - x_F(p)\hat{\imath}_F - x_B(p)\hat{\imath}_B] - r\hat{\imath}_F \tag{39a}$$

$$\hat{e}_B = (p-jv)[\hat{I}_{BO} - x_B(p)\hat{\imath}_F - x_F(p)\hat{\imath}_B] - r\hat{\imath}_B \tag{39b}$$

The spin currents may be expressed as follows.[14]

$$\hat{\imath}_F = \frac{\sqrt{2}}{3}[i_a\epsilon^{-j\theta a} + i_b\epsilon^{-j\theta b} + i_c\epsilon^{-j\theta c}] \tag{40a}$$

$$\hat{\imath}_B = \frac{\sqrt{2}}{3}[i_a\epsilon^{+j\theta a} + i_b\epsilon^{+j\theta b} + i_c\epsilon^{+j\theta c}] \tag{40b}$$

Analogous equations for the spin voltages can be written.

Assuming operation at a constant rotor speed of v per unit, equations 40*a* and 40*b* can be reduced to equations 41*a* and 41*b*.

$$\hat{\imath}_F = \frac{\sqrt{2}}{3}\epsilon^{-jvt}(i_a + i_b\epsilon^{+j120^\circ} + i_c\epsilon^{-j120^\circ}) \tag{41a}$$

$$\hat{\imath}_B = \frac{\sqrt{2}}{3}\epsilon^{+jvt}(i_a + i_b\epsilon^{-j120^\circ} + i_c\epsilon^{+j120^\circ}) \tag{41b}$$

Introducing the single-phase definitions of equations 36*a*–36*d* will reduce equations 41*a* and 41*b* and the analogous voltage equations to equations 42*a*–42*d*.

$$\hat{\imath}_F = +ji\sqrt{2/3}\epsilon^{-jvt} \tag{42a}$$

$$\hat{\imath}_B = -ji\sqrt{2/3}\epsilon^{+jvt} \tag{42b}$$

$$\hat{\imath}_B = -\hat{\imath}_F\epsilon^{+j2vt} \tag{42c}$$

$$\hat{e}_B = +\hat{e}_F\epsilon^{+j2vt} \tag{42d}$$

Substituting equations 42*a* and 42*b* into equations 39*a* and 39*b* and equating the two equations by means of equations 42*c* and 42*d* will give the single-phase spin equation 43.

$$\begin{aligned}\epsilon^{+jvt}(p+jv)x_F(p)i\epsilon^{-jvt} - \epsilon^{+jvt}(p+jv)x_B(p)\times\\ i\epsilon^{+jvt} - \epsilon^{-jvt}(p-jv)x_B(p)i\epsilon^{-jvt} +\\ \epsilon^{-jvt}(p-jv)x_F(p)i\epsilon^{+jvt} + 2ri =\\ \sqrt{3/2}v[\hat{I}_{FO}\epsilon^{+jvt} + \hat{I}_{BO}\epsilon^{-jvt}]\end{aligned} \tag{43}$$

To obtain a solution of equation 43, assume that i can be expressed as in equation 44.

$$\begin{aligned}i = A_1\cos vt + A_3\cos 3vt + \ldots +\\ A_m\cos mvt + \ldots + A_1'\sin vt +\\ A_3'\sin 3vt + \ldots + A_m'\sin mvt + \ldots\end{aligned} \tag{44}$$

The assumed current i can be expressed in complex form as in equation 45*a*, with the complex coefficients defined as in equations 45*b* and 45*c* in terms of the real coefficients of equation 44.

$$\begin{aligned}i = \hat{\imath}_1\epsilon^{+jvt} + \hat{\imath}_3\epsilon^{+j3vt} + \ldots + \hat{\imath}_m\epsilon^{+jmvt} + \ldots +\\ \hat{\imath}_1{}^*\epsilon^{-jvt} + \hat{\imath}_3{}^*\epsilon^{-j3vt} + \ldots + \hat{\imath}_m{}^*\epsilon^{-jmvt}\\ + \ldots\end{aligned} \tag{45a}$$

$$\hat{\imath}_m = \frac{A_m - jA_m'}{2} \tag{45b}$$

$$\hat{\imath}_m{}^* = \frac{A_m + jA_m'}{2} \tag{45c}$$

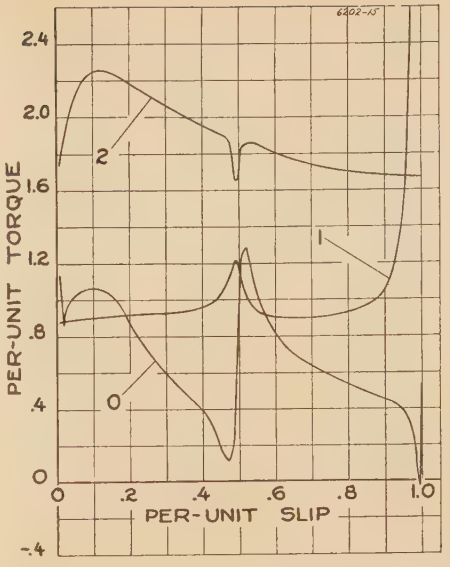

Figure 15. Torques of machine with incomplete end rings with stator and rotor excitations of 1.0 each applied concurrently

0—Unidirectional torque
1—Slip-frequency torque
2—Double-slip-frequency torque
The slip-frequency torque reaches a maximum of 4.70 at 1.00 slip

Consider the general term given by equation 46. Note that for negative values of m, the conjugate coefficient $i_m{}^*$ is to be used instead of i_m.

$$i = \hat{\imath}_m\epsilon^{+jmvt} \tag{46}$$

Substitute equation 46 into the single-phase spin equation 43, group together the terms containing like exponentials, and equate these groups to zero. An infinite number of equations, corresponding to the infinite number of values of m thereby will be obtained. The equations for $m=+1$ and $m=-1$ are given by equations 47*a* and 47*b*, while the general equation for all other values of m is given by equation 47*c*.

Let $m=+1$

$$\begin{aligned}\left[\hat{x}_F(0) + \hat{x}_F(j2v) + \frac{2r}{jv}\right]\hat{\imath}_1 - \hat{x}_B(0)\hat{\imath}_1{}^* -\\ \hat{x}_B(j2v)\hat{\imath}_3 = \frac{1}{j}\sqrt{\frac{3}{2}}\hat{I}_{FO}\end{aligned} \tag{47a}$$

Let $m=-1$

$$\begin{aligned}\left[\hat{x}_F(0) + \hat{x}_F{}^*(j2v) - \frac{2r}{jv}\right]\hat{\imath}_1{}^* - \hat{x}_B(0)\hat{\imath}_1 -\\ \hat{x}_B{}^*(j2v)\hat{\imath}_3{}^* = j\sqrt{\frac{3}{2}}\hat{I}_{BO}\end{aligned} \tag{47b}$$

Let $m = m$ (positive or negative)

$$\begin{aligned}\left\{\hat{x}_F[j(m-1)v] + \hat{x}_F[j(m+1)v] + \frac{2r}{jmv}\right\}\hat{\imath}_m -\\ \hat{x}_B[j(m-1)v]\hat{\imath}_{m-2} - \hat{x}_B[j(m+1)v]\times\\ \hat{\imath}_{m+2} = 0\end{aligned} \tag{47c}$$

When the value of m in equation 47c is such as to make the subscript negative, the conjugate current and conjugate impedance are to be used. Comparing equations 47a through 47c with the single-phase spin circuit of Figure 17, it is immediately evident that the latter is an electrical means of solving these equations. The efficacy of the equivalent-circuit solution is evident in this example, as this equivalent circuit provides a direct means of determining the harmonic currents to any desired order. The efficacy of the equivalent-circuit method of solution is still more evident in the following section on the rotor torques during single-phase operation.

Determination of Rotor and Stator Currents

Assume that the following currents and their conjugates have been obtained from the single-phasing circuit of Figure 17.

$$\hat{\imath}_1 = i_1/\underline{\delta_1} \tag{48a}$$

$$\hat{\imath}_3 = i_3/\underline{\delta_3} \tag{48b}$$

$$\hat{\imath}_m = i_m/\underline{\delta_m} \tag{48c}$$

Substituting equations 48a–48c into equation 45a will give the stator current as in equations 49a and 49b.

$$i = 2\mathcal{R}[\hat{\imath}_1\epsilon^{+jvt} + \hat{\imath}_3\epsilon^{+j3vt} + \ldots + \hat{\imath}_m\epsilon^{+jmvt} + \ldots] \tag{49a}$$

$$i = 2i_1\cos(vt+\delta_1) + 2i_3\cos(3vt+\delta_3) + \ldots \tag{49b}$$

The axis currents in the damper bars are obtained by means of i_d, i_q, $\hat{U}_{ndm}$, and $\hat{U}_{nqmm}$ as follows. Substituting equations 48a–48c, 42a and 42b back into the current equations analogous to equations 2a and 2b will give the axis currents equations 50a and 50b.

$$i_d = \frac{1}{j\sqrt{3}}[-\hat{\imath}_1 + (\hat{\imath}_1 - \hat{\imath}_3)\epsilon^{+j2vt} + (\hat{\imath}_3 - \hat{\imath}_5)\epsilon^{+j4vt} + \ldots + \hat{\imath}_1^* - (\hat{\imath}_1^* - \hat{\imath}_3^*)\epsilon^{-j2vt} - (\hat{\imath}_3^* - \hat{\imath}_5^*)\epsilon^{-j4vt} - \ldots] \tag{50a}$$

$$i_q = \frac{1}{\sqrt{3}}[+\hat{\imath}_1 + (\hat{\imath}_1 + \hat{\imath}_3)\epsilon^{+j2vt} + (\hat{\imath}_3 + \hat{\imath}_5)\epsilon^{+j4vt} + \ldots + \hat{\imath}_1^* + (\hat{\imath}_1^* + \hat{\imath}_3^*)\epsilon^{-j2vt} + (\hat{\imath}_3^* + \hat{\imath}_5^*)\epsilon^{-j4vt} + \ldots] \tag{50b}$$

Introducing the current moduli $\hat{U}_{ndm}$ and $\hat{U}_{nqm}$ permits the axis currents in the damper bars to be written as in equations 51a and 51b.

$$I_{nd} = \frac{2}{\sqrt{3}}\mathcal{I}[(\hat{\imath}_1 - \hat{\imath}_3)\hat{U}_{nd2}\epsilon^{+j2vt} + (\hat{\imath}_3 - \hat{\imath}_5)\hat{U}_{nd4}\epsilon^{+j4vt} + (\hat{\imath}_5 - \hat{\imath}_7)\hat{U}_{nd6}\epsilon^{+j6vt} + \ldots] \tag{51a}$$

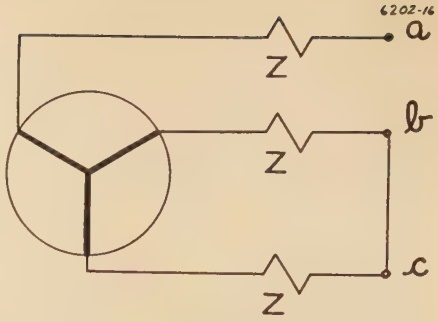

Figure 16. Single-phase loading

Z—System impedance

$$I_{nq} = \frac{2}{\sqrt{3}}\mathcal{R}[(\hat{\imath}_1 + \hat{\imath}_3)\hat{U}_{nq2}\epsilon^{+j2vt} + (\hat{\imath}_3 + \hat{\imath}_5)\hat{U}_{nq4}\epsilon^{+j4vt} + (\hat{\imath}_5 + \hat{\imath}_7)\hat{U}_{nq6}\epsilon^{+j6vt} + \ldots] \tag{51b}$$

The physical currents in the various damper bars are obtained from the axis currents equations 51a and 51b by means of equations 28a and 28b. The subscript s, denoting slip operation, may be dropped from these equations when using equations 51a and 51b.

Determination of Torques

The rotor torques during constant-speed single-phase operation can be obtained from the spin circuit of Figure 17.

Substituting the spin linkages of equations 38a and 38b into the general spin torque expression, equation 31b, will give the single-phase torque expression, equation 52.

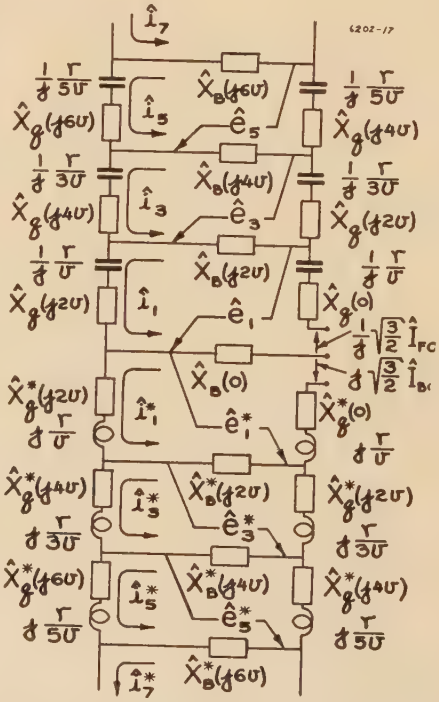

Figure 17. Equivalent circuit for constant-speed single-phase operation of the type defined by Figure 16

$$T = j\hat{\imath}_B[\hat{I}_{FO} - x_F(p)\hat{\imath}_F - x_B(p)\hat{\imath}_B] - j\hat{\imath}_F[\hat{I}_{BO} - x_B(p)\hat{\imath}_F - x_F(p)\hat{\imath}_B] \tag{52}$$

Substituting equations 42a and 42b into equation 52 will give the torque in terms of the current i. Substituting equation 45a will give then the torque in terms of the current harmonics. This torque is composed of a unidirectional component plus an infinite series of harmonic components. These torques are given by the following expression.

Unidirectional Torque T_0; Frequency = 0

$$T_0 = -{}^1/_3[V_{11} + V_{33} + V_{55} + V_{77} + \ldots - V_{1*1*} - V_{3*3*} - V_{5*5*} - V_{7*7*} - \ldots] \tag{53a}$$

$(\hat{e}_1)^*\hat{\imath}_1 = W_{11} + jV_{11}$
$(\hat{e}_3)^*\hat{\imath}_3 = W_{33} + jV_{33}$
$(\hat{e}_5)^*\hat{\imath}_5 = W_{55} + jV_{55}$
$(\hat{e}_7)^*\hat{\imath}_7 = W_{77} + jV_{77}$
$(\hat{e}_1^*)^*\hat{\imath}_1^* = W_{1*1*} + jV_{1*1*}$
$(\hat{e}_3^*)^*\hat{\imath}_3^* = W_{3*3*} + jV_{3*3*}$
$(\hat{e}_5^*)^*\hat{\imath}_5^* = W_{5*5*} + jV_{5*5*}$
$(\hat{e}_7^*)^*\hat{\imath}_7^* = W_{7*7*} + jV_{7*7*}$

Second-Harmonic Torque T_2; Frequency = 2vt

$$T_2 = {}^8/_3\sqrt{[W_{13} + W_{35} + \ldots - W_{1*_3} - W_{3*1*}\ldots]^2 + [V_{13} + V_{35} + \ldots - V_{1*1} - V_{3*1*} - \ldots]^2} \tag{54a}$$

$(\hat{e}_1)^*\hat{\imath}_3 = W_{13} + jV_{13}$
$(\hat{e}_3)^*\hat{\imath}_5 = W_{35} + jV_{35}$
$(\hat{e}_5)^*\hat{\imath}_7 = W_{57} + jV_{57}$
$(\hat{e}_7)^*\hat{\imath}_9 = W_{79} + jV_{77}$
$(\hat{e}_1^*)^*\hat{\imath}_1 = W_{1*_1} + jV_{1*_1}$
$(\hat{e}_3^*)^*\hat{\imath}_1^* = W_{3*1*} + jV_{3*1*}$
$(\hat{e}_5^*)^*\hat{\imath}_3^* = W_{5*3*} + jV_{5*3*}$
$(\hat{e}_7^*)^*\hat{\imath}_5^* = W_{7*5*} + jV_{7*5*}$

$$T_2 = -{}^8/_3[(W_{13} + W_{35} + \ldots - W_{1*_1} - W_{3*1*} - \ldots)\sin 2vt + (V_{13} + V_{35} + \ldots - V_{1*1} - V_{3*1*} - \ldots)\cos 2vt]$$

Fourth-Harmonic Torque T_4; Frequency 4vt

$$T_4 = {}^8/_3\sqrt{[W_{15} + W_{37} + \ldots - W_{1*_3} - W_{3*1} - \ldots]^2 + [V_{15} + V_{37} + \ldots - V_{1*_3} - V_{3*_1} - \ldots]^2} \tag{55a}$$

$(\hat{e}_1)^*\hat{\imath}_5 = W_{15} + jV_{15}$
$(\hat{e}_3)^*\hat{\imath}_7 = W_{37} + jV_{37}$
$(\hat{e}_5)^*\hat{\imath}_9 = W_{59} + jV_{59}$
$(\hat{e}_1^*)^*\hat{\imath}_3 = W_{1*_3} + jV_{1*_3}$
$(\hat{e}_3^*)^*\hat{\imath}_1 = W_{3*_1} + jV_{3*_1}$
$(\hat{e}_5^*)^*\hat{\imath}_1^* = W_{5*1*} + jV_{5*1*}$

$$T_4 = -{}^8/_3[(W_{15} + W_{37} + \ldots - W_{1*_3} - W_{3*_1} - \ldots)\sin 4vt + (V_{15} + V_{37} + \ldots - V_{1*_3} - V_{3*_1} - \ldots)\cos 4vt]$$

The foremention currents and voltages are indicated on the spin circuit of Figure 17, and the determination of the torques during constant-speed single-phase operation is reduced to the direct

measurement of real and reactive power in this network. The torques of higher harmonic order can be obtained from the preceding equations by analogy.

The discussion given after equations 34*c* and 34*d* concerning the method of writing the products of complex numbers also applies to the above expressions.

D. Numerical Example of the Application of the Equivalent Circuit of Part C

As a numerical example of the application of the equivalent circuit of part *C*, the synchronous machines described in part *B* were subjected to various single-phase loads, of the type defined by Figure 16, while running at synchronous speed. The torques and rotor and stator currents so obtained are given below. In each case, the field current was adjusted to give unit fundamental stator current through the single-phase loads. The single-phase loads were of unit magnitude (per phase) of either pure reactance or pure resistance.

COMPLETE END RINGS, PURE REACTANCE LOAD

Rotor d-c excitation $I_{fdO} = 1.85$
Stator line current i = 1.00 (60 cycles)
Rotor-circuit currents
bar 1, trailing = 0.196 (120 cycles)
leading = 0.182 (120 cycles)
bar 2, trailing = 0.194 (120 cycles)
leading = 0.174 (120 cycles)
bar 3, trailing = 0.190 (120 cycles)
leading = 0.114 (120 cycles)
field winding = 0.407 (120 cycles)
Second-harmonic torque = 0.758 (120 cycles)

COMPLETE END RINGS, PURE RESISTANCE LOAD

Rotor d-c excitation $I_{fdO} = 1.31$
Stator line current i = 1.00 (60 cycles)
Rotor-circuit currents
bar 1, trailing = 0.207 (120 cycles)
leading = 0.194 (120 cycles)
bar 2, trailing = 0.195 (120 cycles)
leading = 0.173 (120 cycles)
bar 3, trailing = 0.157 (120 cycles)
leading = 0.143 (120 cycles)
field winding = 0.413 (120 cycles)
Undirectional torque = 0.678 (0 cycles)
Second-harmonic torque = 0.670 (120 cycles)

INCOMPLETE END RINGS, PURE REACTANCE LOAD

Rotor d-c excitation $I_{fdO} = 1.87$
Stator line current i = 1.00 (60 cycles)
Rotor-circuit excitations
bar 1, trailing = 0.184 (120 cycles)
leading = 0.169 (120 cycles)
bar 2, trailing = 0.168 (120 cycles)
leading = 0.158 (120 cycles)
bar 3, trailing = 0.118 (120 cycles)
leading = 0.118 (120 cycles)
field winding = 0.411 (120 cycles)
Second-harmonic torque = 0.812 (120 cycles)

INCOMPLETE END RINGS, PURE RESISTANCE LOAD

Rotor d-c excitation $I_{fdO} = 1.34$
Stator line current = 1.00 (60 cycles)
0.063 (180 cycles)
Rotor-circuit currents
bar 1, trailing = 0.180 (120 cycles)
= 0.019 (240 cycles)
leading = 0.160 (120 cycles)
= 0.006 (240 cycles)
bar 2, trailing = 0.175 (120 cycles)
= 0.011 (240 cycles)
leading = 0.142 (120 cycles)
= 0.010 (240 cycles)
bar 3, trailing = 0.125 (120 cycles)
= 0.007 (240 cycles)
leading = 0.119 (120 cycles)
= 0.008 (240 cycles)
field winding = 0.425 (120 cycles)
= 0.024 (240 cycles)
Unidirectional torque = 0.700 (0 cycles)
Second-harmonic torque = 0.690 (120 cycles)
Fourth-harmonic torque = 0.071 (240 cycles)

All harmonics of orders higher than those given are negligible, and their magnitudes are less than five per cent of the values given. In the first and third cases the unidirectional torques are zero because the loads are purely reactive.

Nomenclature

All quantities are in per unit unless in boldface type, in which case they are in the ampere-inch-second system (amperes, volts, and inches). Quantities such as N, P_1, and so forth for which it obviously is unnecessary to distinguish the ampere-inch-second values by a special script, are in standard type only.

All vector quantities are indicated by a circumflex (^) over the symbol. All conjugate quantities are indicated by an asterisk (*). The d-c rotor-excitation currents and in parts *A* and *B* the stator current due to the d-c rotor-excitation currents are indicated by the subscript *O*. The subscript s indicates constant-speed asynchronous operation at slip s, and the subscript m (which takes the values 1, 2, 3. . .) identifies the harmonic quantities obtained during constant-speed single-phase operation. The subscript 0 identifies the unit values of the various currents and voltages.

The d and q functions, by which the various quantities are resolved into components in line with the direct and quadrature axes, are termed the axis quantities.

The axis quantities are grouped into vector quantities which in this paper are identified by the subscript F and B.

The F and B quantities are equivalent to vectors rotating at slip speed, and for this reason these quantities are termed the "spin" quantities.

A double subscript rotation is used for the $W+jV$ measurements. The first subscript locates the mesh in which the voltage is to be measured, and the second subscript locates the mesh in which the current is to be measured.

A_1, A_3, A_5 = current harmonics obtained during single-phase operation (see equation 44)
A_{d1} is defined in references 12 and 13
D_{d1x} is defined in references 12 and 13
e = phase voltage
e_a, e_b, e_c = phase voltages
e_d, e_q = axis voltages of reference 4
$\hat{e}_F$, $\hat{e}_B$ = spin voltages defined by equations analogous to equations 2*a* and 2*b*
e_{ao} = peak value of rated stator phase voltage
F_{d1} = defined in references 12 and 13
i = line current
i_a, i_b, i_c = phase currents
i_d, i_q = axis currents of reference 4
$\hat{i}_F$, $\hat{i}_B$ = spin currents defined by equations analogous to equations 2*a* and 2*b*
$\hat{i}_1$, $\hat{i}_3$, $\hat{i}_5$ = current harmonics obtained during single-phase operation (see equation 45*a* and Figure 17)
i_{ao} = peak value of rated line current in amperes
I_{fd}, I_{fq} = direct- and quadrature-axis field-winding currents
I_n = current in nth damper bar
I_{nd}, I_{nq} = axis currents in nth damper bar
$\hat{I}_F$, $\hat{I}_B$ = spin currents defined in equations 20*a* and 20*b*
$\mathbf{I}_{fdO}$ = unit current in amperes for field-winding circuit
$\mathbf{I}_{xdO}$ = unit current in amperes for damper bars
$\mathcal{I}$ = imaginary part of . . .; $\mathcal{I}(a+jb) = b$
$j = \sqrt{-1}$
K_p, K_d = pitch and distribution factors (greater than 1.0)
m = order of harmonic during single-phase operation
N = stator series turns per phase
N_{fd}, N_{xd} = turns per pole of field winding and xth additional circuit, respectively, ($N_{xd} = 1.0$ for damper-winding circuits)
p = differential operator $\frac{d}{dt}$
P_1 = number of poles
r = stator resistance per phase
$\mathcal{R}$ = real part of . . .; $\mathcal{R}(a+jb) = a$
s = slip
t = time in radians per second
T = torque
T_{0s}, T_{1s}, T_{2s} = torques obtained during asynchronous operation; unidirectional, slip frequency, and double slip frequency, respectively
T_0, T_2, T_4 = harmonic torques obtained during single-phase operation; unidirectional, second harmonic, and fourth harmonic, respectively

Characteristics of a 400-Mile 230-Kv Series-Capacitor-Compensated Transmission System

B. V. HOARD
MEMBER AIEE

SERIES capacitors have been recognized for some time as a means of increasing the amount of power transmitted over a long transmission line and as a means of increasing the distance that alternating-current power can be transmitted economically.[1] The basic concept of neutralizing any portion of the series inductive reactance of a long transmission system by means of series capacitors is theoretically sound. The practical application of series capacitors for such service introduces several new and interesting problems of system design and operation, which while capable of solution will require the attention of engineers of both the equipment manufacturers and the operating companies. It is the objective of this paper to outline system characteristics encountered when series-capacitor compensation is used, with a view toward solving the problems arising therefrom. No attempt will be made to reexamine the relative cost of transmission with and without series compensation. In fact, the cost of the compensated system will be influenced to a certain degree by the methods used to solve the problems arising through use of series compensation.

A brief discussion of some of the major factors that must be considered in the application of series capacitors on any system will present the problems involved and suggest methods of solution. Series capacitors are connected into a transmission line in series with the line reactance in order to neutralize or compensate a portion or possibly all of the line reactance. With greater capacitive reactance, it is theoretically possible, but for several reasons not practical to compensate also a part of the reactance of the terminal equipment at each end of the line. It would be desirable from an operation and protective-relaying standpoint to insert the capacitors uniformly along the line in a large number of small units; however, it is not practical from an economic standpoint to do so because of high overvoltages on the capacitors during system faults and because of the higher cost of a large number of small capacitor stations.

From the standpoint of electrical performance, assuming capacitors are distributed uniformly along the line and are in operation at all times, a 400-mile line with 50 per cent compensation would become the equivalent of a 200-mile line but would have a higher resistance and more line-charging current than the standard conductor used in the line. The electrical performance of such a 200-mile line could be represented exactly by an equivalent hollow-core conductor of rather large diameter and small cross section which would give both the higher resistance and larger charging current.

System Characteristics During Faults

A simple example consisting of a 400-mile line in which the line reactance is assumed to be 100 per cent compensated, but with no compensation of reactance of terminal equipment, will illustrate some of the compensated system characteristics

Paper 46-196, recommended by the AIEE committee on power transmission and distribution for presentation at the AIEE Pacific Coast meeting, August 27–30, 1946. Manuscript submitted July 8, 1946; made available for printing July 19, 1946.

B. V. HOARD is chief of the a-c calculating board studies group, Bonneville Power Administration, U.S. Department of the Interior, Portland, Oreg.

The author wishes to acknowledge the assistance given by Lewis Weiner and other associates in obtaining and preparing data for this paper from a series of a-c network analyzer studies, and to E. C. Starr for suggestions on the arrangement of the paper.

$\hat{U}_{nd}$, $\hat{U}_{nq}$ = current moduli defined in equations 26*a* and 26*b* and in reference 13

v = speed ($v = 1 - s$)

V = reactive-power component of $W + jV$

W = real-power component of $W + jV$

x as a subscript denotes the 100-per-cent-pitch damper-winding circuit; defined in reference 13

x_{afd}, x_{afq} = mutual reactances between stator and field windings in direct and quadrature axes; evaluated in reference 13

x_d, x_q = synchronous reactances; evaluated in reference 13

$x_d(p)$, $x_q(p)$ = operational impedances in the axis system; evaluated in reference 13

$x_F(p)$, $x_B(p)$ = operational impedances in the spin system; defined in equations 5*a* and 5*b*

x_{ao} = base stator impedance in ohms

$$x_{ao} = \frac{e_{ao}}{i_{ao}}$$

Z = system impedance defined by Figure 16

δ_1, δ_2, δ_3 = phase angles of the harmonic currents obtained during single-phase operation; see equations 48*a*–48*c* and Figure 17

θ = space angle between stator and rotor axes; defined in reference 4

ψ_d, ψ_q = axis linkages defined in reference 4

$\hat{\psi}_F$, $\hat{\psi}_B$ = spin linkages defined by equations 2*a* and 2*b*

References

1. SELF-STARTING SYNCHRONOUS MOTORS, C. J. Fechheimer. AIEE TRANSACTIONS, volume 31, 1912, pages 529–85.

2. STARTING CONDITIONS OF SYNCHRONOUS MACHINES, A. Hay, F. N. Mowdawalla. AIEE TRANSACTIONS, volume 38, 1919, pages 1713–55.

3. STARTING PERFORMANCE OF SYNCHRONOUS MOTORS, H. V. Putman. AIEE TRANSACTIONS, volume 46, 1927, pages 39–57.

4. TWO-REACTION THEORY OF SYNCHRONOUS MACHINES, R. H. Park. AIEE TRANSACTIONS, volume 48, 1929, pages 716–27.

5. STARTING PERFORMANCE OF SALIENT-POLE SYNCHRONOUS MOTORS, T. M. Linville. AIEE TRANSACTIONS, volume 49, 1930, pages 531–45.

6. SALIENT POLE MOTORS OUT OF SYNCHRONISM, A. H. Lauder. AIEE TRANSACTIONS, volume 55, 1936, June section, pages 636–49.

7. THE APPLICATION OF TENSORS TO THE ANALYSIS OF ROTATING ELECTRICAL MACHINERY, Gabriel Kron. *General Electric Review*, Schenectady, N. Y., volume 38, 1935, pages 181–91, and volume 39, 1936, pages 108–16.

8. EQUIVALENT CIRCUIT OF THE SALIENT-POLE SYNCHRONOUS MACHINE, Gabriel Kron. *General Electric Review*, Schenectady, N. Y., volume 44, 1941, pages 679–83.

9. EQUIVALENT CIRCUITS OF THE PRIMITIVE MACHINE WITH ASYMMETRICAL STATOR AND ROTOR, Gabriel Kron. AIEE TRANSACTONS, volume 66, 1947.

10. A NEW A-C NETWORK ANALYZER, H. P. Kuehni, R. G. Lorraine. AIEE TRANSACTIONS, volume 57, 1938, February section, pages 67–73.

11. PER-UNIT IMPEDANCES OF SYNCHRONOUS MACHINES, A. W. Rankin. AIEE TRANSACTIONS, volume 64, 1945, August section, pages 569–73.

12. PER-UNIT IMPEDANCES OF SYNCHRONOUS MACHINES—II, A. W. Rankin. AIEE TRANSACTIONS, volume 64, 1945, December section, pages 839–41.

13. THE DIRECT- AND QUADRATURE-AXIS EQUIVALENT CIRCUITS OF THE SYNCHRONOUS MACHINE, . W. Rankin. AIEE TRANSACTIONS, volume 64, 1945, December section, pages 861–8.

14. RELATIONS AMONG TRANSFORMATIONS USED IN ELECTRICAL ENGINEERING PROBLEMS, C. Concordia. *General Electric Review*, Schenectady, N. Y., volume 41, 1938, pages 323–5.

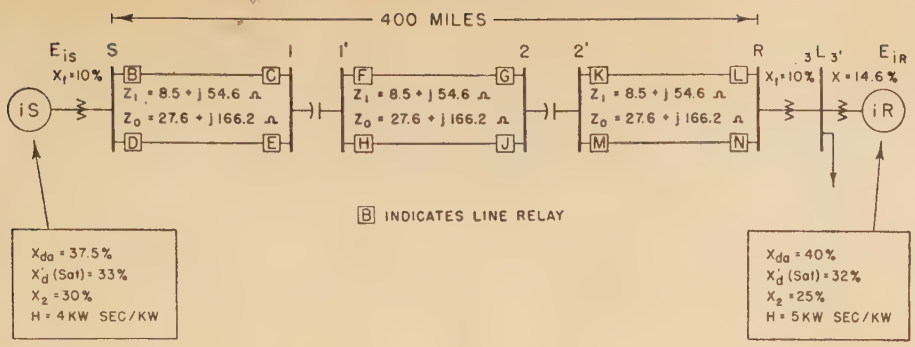

Figure 1. Characteristics of a 400-mile 230-kv compensated transmission system

General conditions

1. Line characteristics
   230 kv, double circuit, 400 miles with 795,000-circular-mil aluminum-cable-steel-reinforced at 27 feet flat spacing and two intermediate sectionalizing stations
2. Terminal equipment rating
   Transformer *R* capacity = kva delivered
   Generator and transformer *S* capacity = rating transformer *R* plus line losses
   Receiver end transformer and generator capacity = 2 times rating transformer *R* (impedances on same base as transformer *R* are $^1/_2$ of those specified)
   Load = approximately 3 times rating transformer *R* at unity power factor
3. Series capacitors
   X_c of compensating capacitors was changed for the various studies but is expressed as a percentage compensation of the total line reactance between buses *S* and *R*, normally with all line sections in service or during emergencies when a faulted line section is out of service
4. Equipment reactances
   X_{da} = adjusted synchronous reactance. Sending end generator is assumed to be hydro-electric. Receiving end generator is assumed to consist of system containing hydro-electric and turbo generation. Reactance of receiver end system (X = 14.6 per cent) assumed to include both transformer and distribution system

Equipment Rating

Case No.	Generator and Transformer *S*	Transformer *R*	Receiver End Generator and Transformer
1–8*	375,000 kva	320,000 kva	640,000 kva
9†	185,000 kva	185,000 kva	370,000 kva

* Ratings based on conductor thermal limit (900 amperes) with one line section out of service.
† Ratings based on static stability limit with 15 per cent margin, with one line section out of service.

during faults. Such a compensated line would have a net line impedance consisting of resistance only, so that any fault current would be limited almost entirely by the impedance of the terminal equipment. Therefore, approximately the same magnitude of fault current would be supplied from the sending-end generators whether a fault was at the generating station high-tension bus or at the receiver bus 400 miles away. In practice full 100-per-cent line compensation probably would not be used; however, this simple example illustrates the fact that fault current tends to be limited more by impedance of terminal equipment rather than by line impedance as the per cent compensation is increased. Hence, if a 100-per-cent-compensated line is connected to a high capacity system having low terminal impedance which could supply a fault current ten times the maximum full load current of the compensated line, then all series capacitors in the line would be subjected to ten times normal voltage for a fault occurring near the receiver bus. Even if the above line is connected to generators and step-up transformers having a total of 40 per cent reactance, the fault current flowing through the capacitors when 100-per-cent compensation is used would result in 2.5 times normal full load capacitor voltage and 6.25 times normal capacitor kilovolt-amperes. In many cases such an increase in momentary kilovolt-ampere capacity and the resultant cost of capacitors cannot be economically justified, so that the capacitors will be installed in two or three large units with protective equipment which short-circuits them as soon as the excessive overvoltage occurs during the fault.

When the capacitors are concentrated in a few large units, they will be placed at intermediate stations in the line as indicated in Figure 1 which shows three line sections but only two capacitor stations. When the per-cent compensation is sufficiently high, the capacitive reactance located in a station becomes greater than the inductive reactance of a line section, because there is always one less capacitor station than the number of line sections. Then, for a fault just beyond a capacitor station a net capacitive reactance is obtained between the fault point and the high-voltage bus of the generating station which causes partial neutralization of the reactance of terminal equipment. This produces a larger fault current for a fault located beyond the capacitor station than for a fault located at the generating station high-voltage bus. For the system shown in Figure 1 a line compensation greater than two-thirds of the line reactance will result in partial neutralization of terminal reactance when the fault is located as described previously. For a 75 per cent compensation of the line and the fault located at point 2′, practically all of the sending-end transformer reactance is neutralized by the net capacitive reactance obtained out to the fault point. Similar conclusions are obtained for the components of fault current supplied from the receiver end of the line when the fault occurs on the sending-end side of a capacitor.

Capacitors have quite definite maximum voltage ratings, the magnitude depending on the period during which the capacitor is subjected to overvoltages. Table I specifies four emergency ratings in terms of the allowable voltage, the time interval of application, and the corresponding kilovolt-amperes obtained in the capacitor.

With the two conflicting requirements of a maximum allowable voltage across the capacitor and voltages above normal during system faults, it is desirable for purposes of comparison in this study to assume the capacitor equipment constructed in one of two ways which will be designated hereafter as design *A* or *B*.

A. Construct the capacitor to withstand the maximum momentary voltage to which the capacitors will be subjected during faults. Capacitor cost will increase almost directly with the kilovolt-amperes or as the square of the maximum voltage so that for many cases this design cannot be justified from

Table I. Emergency Ratings of Capacitors

110 per cent of normal voltage continuously, 121 per cent of normal kilovolt-amperes
135 per cent of normal voltage up to 30 minutes 182 per cent of normal kilovolt-amperes
150 per cent of normal voltage up to 5 minutes, 225 per cent of normal kilovolt-amperes
*200 per cent of normal voltage up to $^1/_2$ cycle, 400 per cent of normal kilovolt-amperes

* Protected by spark gap set at twice normal voltage.

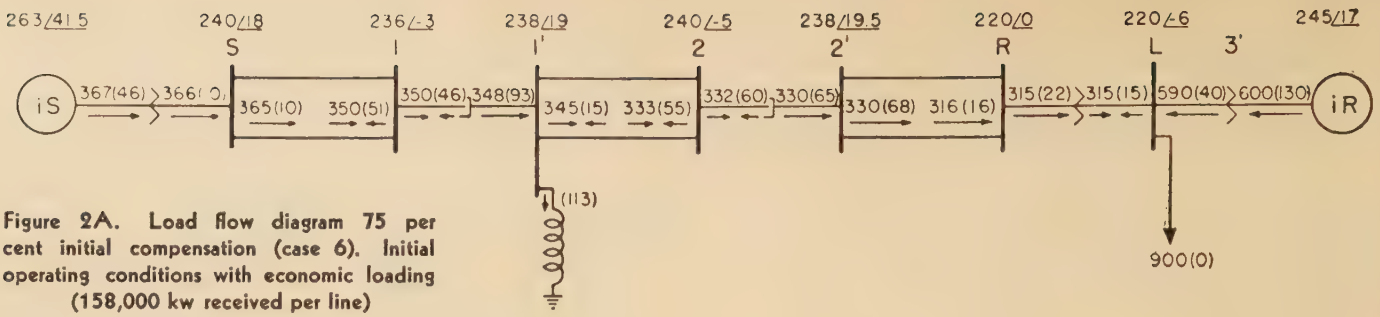

Figure 2A. Load flow diagram 75 per cent initial compensation (case 6). Initial operating conditions with economic loading (158,000 kw received per line)

Power and reactive flow is indicated thus—
kw/1,000 (kilovars/1,000)
Arrows in same direction indicate lagging power factor

an economic standpoint. In general, this design should be investigated when the reactance of terminal equipment at each end of the line is relatively high, and when the per-cent compensation is relatively low. When this design is investigated, consideration should be given to the short-time overvoltage ratings of series capacitors. For example, if manufacturers will allow a maximum capacitor voltage of approximately twice rated value during the short period of the fault, a system having a maximum fault current through the capacitors of 2.2 to 2.4 times maximum load current may use this design economically in comparison with the design in which the capacitors are short-circuited during the fault.

B. Provide protective equipment such as a spark gap or short-circuiting breaker to short-circuit the capacitors during a fault, and a contactor or circuit breaker to clear the spark gap as soon as the fault is removed so that the capacitive reactance will be reinserted rapidly in the line. This design would be used when the terminal impedance is low and the per-cent compensation is high. The short-circuiting of the capacitors during the fault plus the effects of the short but important time interval needed to reinsert the capacitors into the line after the fault is cleared make it necessary, in obtaining a given power limit, to use a higher percentage compensation but in general not as high a kilovolt-ampere rating as for design *A* for the same degree of initial line loading.

If design *A* is used, it may be possible and is desirable to have several small capacitor stations in the line. If design *B* is used, the cost of protective equipment dictates the need for a few capacitor stations of relatively large capacity.

Transient Stability Considerations

It can be shown that the most economical loading of a 60-cycle 230-kv 200-mile uncompensated line is approximately 175,000 kw delivered. Similarly, the most economical loading of a 230-kv 400-mile line may be of the order of 165,000 kw delivered. If transient stability is considered, it is possible by proper design to approach the above economical loading on lines of 200-mile length without series compensation, but it is not possible to obtain both stability and the most economical loading on 400-mile lines without using relatively large series compensation. In fact, without compensation on the 400-mile lines, other system design being equal, the transient stability limit may be of the order of 75,000 kw per circuit for a system similar to that shown in Figure 1, except uncompensated. Compensation of lines longer than 400 miles also will show large relative increases in power transmitted without loss of stability.

The determination of the allowable loading of lines and the transient stability limit becomes a major design and operat-

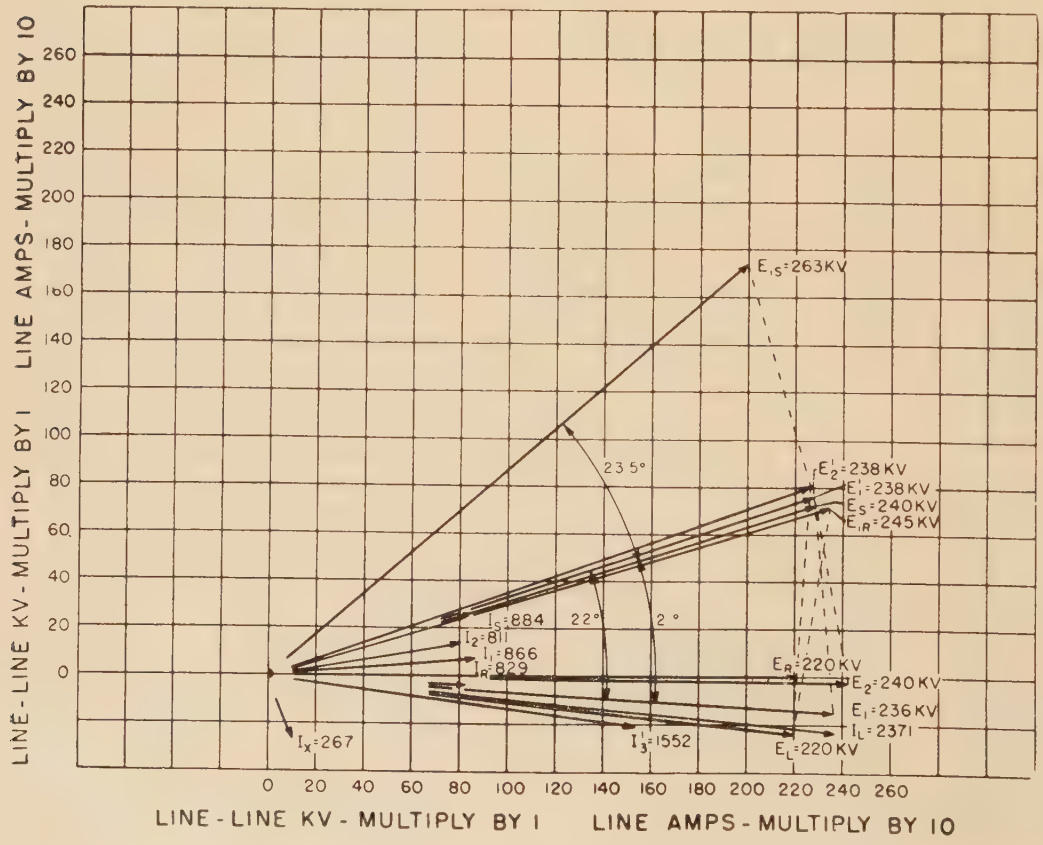

Figure 2B. Vector diagram, 75 per cent initial compensation (case 6). Initial operating conditions with economic loading (158,000 kw received per line)

Equipment rating

Generator *S*—375,000 kva
Transformer *R*—320,000 kva
System *R*—640,000 kva

ing problem for all long lines supplying firm power whether they are compensated or uncompensated. But by increasing the compensation used, the stability-limit loading can be increased and will approach the most economical loading of the line.

Determining transient stability introduces a number of other important factors such as type of system, how connected, type of assumed fault and where located, time of clearing of fault, and percentage of transmission capacity removed when the faulted line section is cleared. Series compensation using design *B* also involves short-circuiting of capacitors during the fault and then reinserting them. If the capacitors are not reinserted at the instant the fault is cleared, a reduction in the stability limit occurs. Assume for example a line with 50-per-cent compensation after the faulty line section has been removed; then for the length of the period of delay in reinserting the capacitors the transmission line reactance is doubled, and this becomes a major factor in maintaining stability. Likewise, less synchronizing power can be transmitted during the period of the fault if the capacitors are out of the circuit than if they remain in the circuit. It is obvious that the period of time the capacitors are short-circuited must be cut to the minimum. The time required to clear the fault, that is, whether sequential tripping must be used or whether it can be assumed that simultaneous tripping can be obtained through a reliable over-all carrier relaying design, is similarly an important factor in determining the stability. To summarize, for design *B* for any specified initial load on the transmission system, there are three important factors which will make it necessary to increase the compensation required to maintain stability, first, removal of the capacitors during the fault; second, increase in fault clearing time; and third, increase in the time required to reinsert the capacitors after the fault is cleared. For design *A* only the second factor applies.

System Analyzed

In order to obtain more specific data on system characteristics resulting when series compensation is used, the system shown in Figure 1 was studied extensively on an a-c calculating board. It will be observed that this system consists of a 2-circuit 230-kv 400-mile line using 795,000-circular-mil aluminum-cable-steel-reinforced conductors with sectionalizing stations at two intermediate points 1–1′ and 2–2′ and with series capacitors placed at these points. It was decided to load the line initially to approximately 900 amperes at the sending end, corresponding to the thermal limit of one line section if the other parallel section were not in service. This assumption also resulted in a delivered power of approximately 160,000 kw per line, which is considered fairly close to the most economical

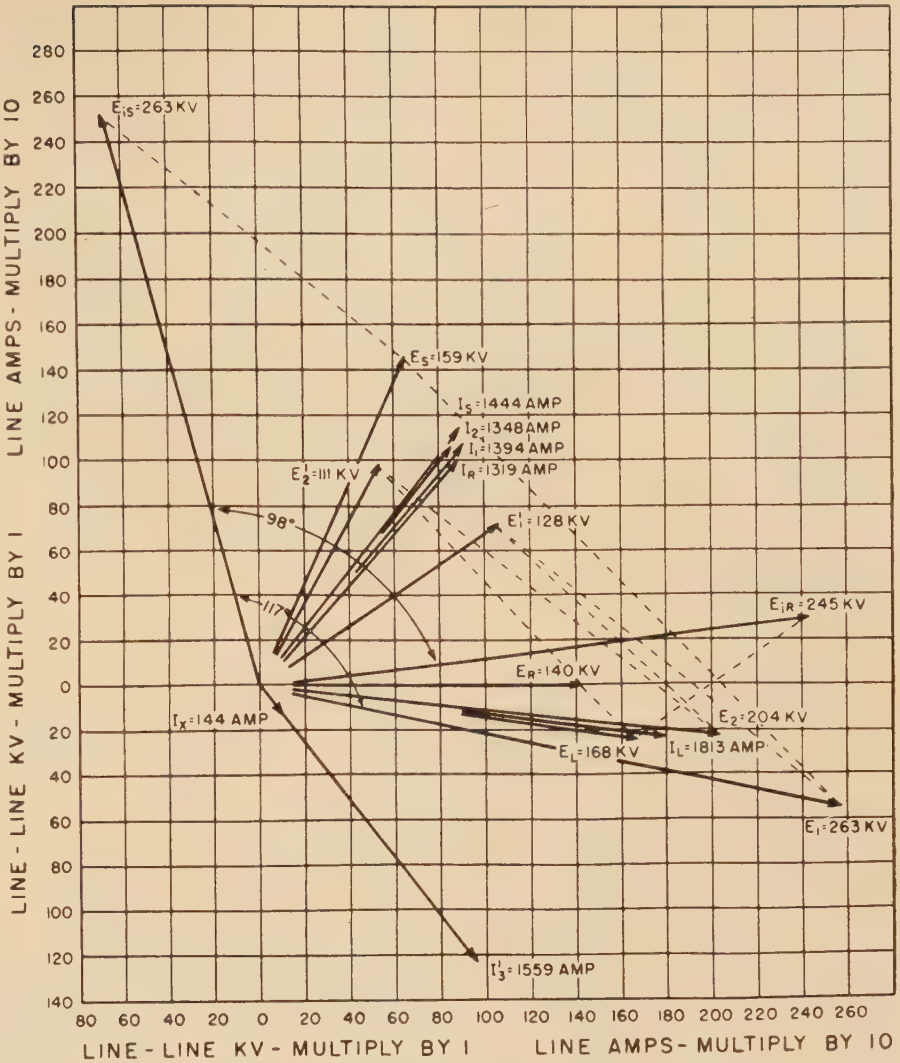

Figure 3. Vector diagram at angle of maximum transient swing (case 6). 75 per cent initial and final compensation

Conditions

1. Initial loading as per Figure 2A
2. 2-phase ground fault on one line near point 1. Near end breaker open at 3.5 cycles. Fault cleared at 7 cycles
3. Capacitors short-circuited during fault periods and reinserted at 10.5 cycles

Angular Difference, Degrees		Ratio $I/I_{initial}$		System Z** Each Line—Ohms		Per Unit Current Through Capacitor	
$E_{iR}-i_S$	98	S	3.26*	S	110/13.5		
E_{R-S}	66	1	3.22*	1	−188/−62		
E_{iS-L}	−113	1′	1.78	1′	178/−21		
E_{iR-L}	−15	2	1.66	2	−302/−58	1	1.55†*
E_{S-1}	−78	2′	1.66	2′	165/10	2	1.50†
E_S-I_S	−13.5	R	1.59	R	212/−49		
E_1-I_1	62	L	0.77				
$E_1'-I_1'$	21	3′	1.00				
E_2-I_2	58						
$E_2'-I_2$	−10						
E_R-I_R	49						

* Line current carried by single line with faulted section removed.
** Negative Z indicates I in nontripping direction.
Negative θ indicates capacitive reactance.
† Based on 900-ampere rating.

line loading. As indicated in Figure 1, the delivered kilovolt-amperes plus line losses determined the capacity of the sending-end equipment. The receiver-end system, to the right of the load bus L, was assumed to have a capacity twice that of R and the resultant load L (unity power factor) to be three times the power delivered by the compensated lines. Various reactances and inertia constants are also specified in Figure 1. Load-flow diagrams were obtained with 240-kv sending-end voltage (bus S) and 220-kv load bus voltage (bus L).

Most of the transient stability studies

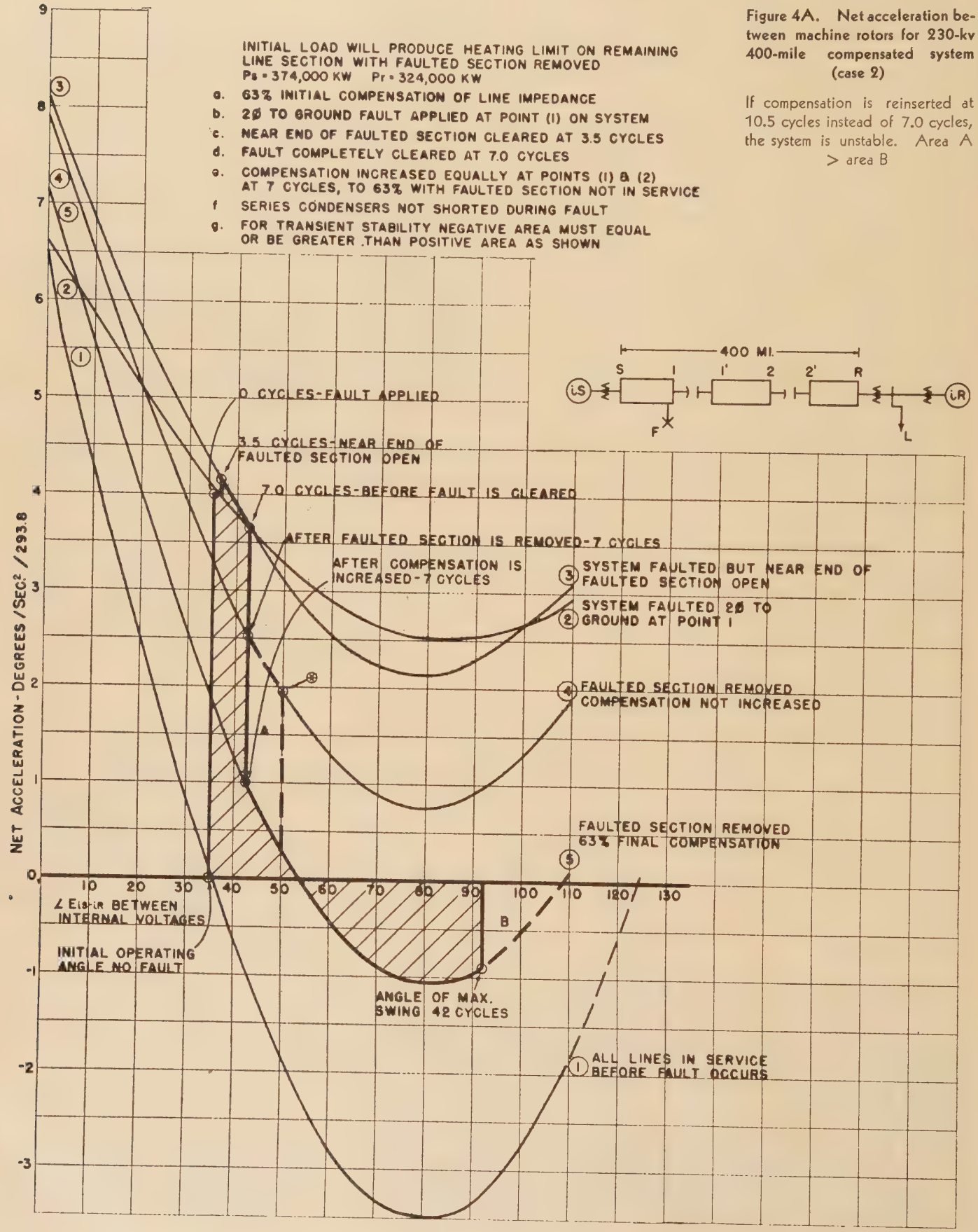

Figure 4A. Net acceleration between machine rotors for 230-kv 400-mile compensated system (case 2)

If compensation is reinserted at 10.5 cycles instead of 7.0 cycles, the system is unstable. Area A > area B

assumed a double-line-to-ground fault applied on one line near point 1, Figure 1. Checks were made which showed that the transient shock was more severe for a fault on the sending-end line section as compared to other sections and was slightly more severe for a fault at the sending-end bus than at the point 1 bus. However, because a considerable amount of data had been obtained previously for faults at point 1, it was decided to continue the study with the fault location at this point.

Relaying Characteristics

Both the time required to clear the fault and that required to reinsert the capacitors are of major importance in maintaining stability. These periods are tied up intimately with the protective relaying of the lines and the control of the series capacitors. Of the standard relay schemes available, studies indicate that a high-speed current-balance scheme would provide proper protection for the lines. Other standard relay schemes show limitations which will require major modifications to the schemes before they can be used. In view of the many new factors to be considered, it is planned to make laboratory tests in the future to confirm these results.

It will be shown from examples studied here that relay requirements which must be met, namely, to trip the faulted line section and to block tripping on the unfaulted line sections are such that the standard methods of impedance relaying cannot be used. The following reasons are given:

(*a*). When the compensation is high so that the compensating reactance "reaches" part way into the transformer and generator reactance, faults located beyond the capacitor stations produce greater fault currents, and lower impedances may be seen by impedance relays than when the fault is located near the generator bus.

(*b*). Before the gaps have flashed over, some relays may be called upon to operate on the basis of a small resistance and large capacity reactance. After the gaps have flashed, they must operate on the basis of a small resistance and a large inductive reactance. This produces a shift in phase angle between voltage and current approaching 160 to 170 degrees before and after gap flashover. This system characteristic is critical for a relay scheme using conventional directional relays or their equivalent since it allows only a 10- to 20-degree band between tripping and blocking. Other shifts in phase of voltage and current between a 3-phase fault and unbalanced faults may eliminate completely the simple directional relay since it may not indicate the true direction of the fault when series capacitors are both short-circuited and not short-circuited.

For these reasons if impedance relays or these relays with carrier current are to be used, it will be assumed that the first zone impedance relay will have to be eliminated, and modifications of existing directional relays will be necessary. With these modifications, perhaps existing carrier relays can be depended upon to obtain fast and reliable tripping; or perhaps a high-speed back-up scheme should be included also. Assuming carrier, it is estimated that omission of the first zone impedance element may add from 0.5 to 1.0 cycle to the clearing time of the circuit breaker nearest the fault because of the longer operating time required by the carrier relays. Such an increase in relay time would be disadvantageous. It might be overcome by substituting high-speed current-balance relays for the discarded first zone impedance relay. The current-balance relays would provide high-speed sequential tripping and would back up the carrier relaying and vice-versa. Or after possible improvements in the relatively new phase-comparison carrier relaying scheme have been made, this scheme might prove satisfactory. For the present, the phase-comparison scheme is relatively slow and cannot be applied where the minimum 3-phase fault currents are only slightly greater than maximum load current, and therefore this scheme is not considered applicable.

With the foregoing considerations in mind, it was decided that a reasonably safe assumption of clearing time for use in the stability studies would be 3.5 cycles for the relay and circuit breaker nearest the fault and 7.0 cycles for the equipment at the far end. Such sequential tripping was used in the study, although with carrier relays, simultaneous tripping of both ends might result in clearing in about 4.5 cycles, which would produce slightly less shock to the system than the sequential tripping assumed.

No accurate data were available for time required to reinsert the capacitors in the circuit after clearance of a fault. Therefore, two values for reinsertion were assumed, either 7.0 or 10.5 cycles after the occurrence of the fault, and the amount of compensation required to obtain transient stability for each assumed time was determined. Thus a comparison is obtained showing the increase in compensation required for the same power transmitted when the reinsertion is delayed from 7.0 to 10.5 cycles.

Results and Discussion

Table II lists some of the results of a number of the studies made. For the first six cases listed, a constant percentage of compensation was used both before and after the faulted line section is removed, which assumes more compensation added

Table II. Summary of Stability Studies

Case Number		1	2	3	4	5	6	7	8	9
1. Constant per cent compensation. See item 5. (Before and after fault)	Initial per cent	60	63	63	65	66	75			
	Final per cent	60	63	63	65	66	75			
2. Constant ohmic value of compensation. (Before and after fault. No additional compensation added on removal of fault)	Initial per cent							100	100	0
	Final per cent							75	75	0
3. Compensation removed during fault		No	No	Yes	No	Yes	Yes	Yes	Yes	
4. Compensation reinserted after start of fault (cycles)				7.0	7.0	10.5	7.0		10.5	
5. Additional compensation added after start of fault (cycles). (Equally at both capacitor stations)		7.0	7.0	7.0	10.5	7.0	10.5			
6. Initial loading at receiver end (kw/1,000)		311	324	324	325	314	315	324	324	150
7. Initial operating angle between E_{is} and E_{ir} (degrees)		32.5	34	34	34.5	29	24.5	12.5	12.5	28.5
8. Maximum angle of swing (degrees)		102	91	Unstable	Unstable	91	98	102	Unstable	91.5
9. Shunt reactor (kilovars/1,000)*						109	113	114	114	

* Installed at point 1′ (see Figure 1) to reduce maximum voltage at point 1 and to neutralize a portion of line charging current and decrease current flowing in section *S*-1 below thermal limit.

Fault type, location, and clearing time: Two phase to ground at point 1 (see Figure 1). Near end cleared in 3.5 cycles, far end in 7.0 cycles.

Table III. Net Acceleration Ratios Obtained. Fault at Point 1

Case No.	Initial Per Cent Compensation	Generator Rating, Kva/1,000 S	Generator Rating, Kva/1,000 R	Initial Power Output, Kw/1,000 S	Initial Power Output, Kw/1,000 R	*Accelerating Power, Kw/1,000 S	*Accelerating Power, Kw/1,000 R	*Acceleration, Degrees per Second² S	*Acceleration, Degrees per Second² R	*Acceleration, Degrees per Second² Net	*Acceleration Ratio Case 9 = 1.00
1†	60	375	640	359	634	229	172	1,645	581	1,064	0.97
2†	63	375	640	376	624	241	172	1,735	581	1,154	1.05
3	63	375	640	375	618	241	−28	2,020	−95	2,115	1.93
4†	65	375	640	375	618	240	166	1,730	561	1,169	1.07
5	66	375	640	373	604	273	−32	1,965	−108	2,073	1.89
6	75	375	640	367	600	274	−24	1,970	−81	2,051	1.85
7 and 8	100	375	640	377	590	302	−20	2,175	−68	2,243	2.05
9	0	185	370	164	390	113	95	1,650	554	1,096	1.00
10‡	0	185	370	164	390	152	147	2,215	858	1,357	1.24‡

* At instant fault is applied.

† Capacitors not short-circuited during fault; for other cases, capacitors short-circuited during fault.

‡ 3-phase fault applied; for all other cases 2-phase-to-ground fault applied.

after the faulted line section is cleared. This assumption was made to determine if there were any appreciable increase in power limit if a portion of the compensation is added after the fault is removed. Such addition of compensation at all capacitor stations after the fault is cleared may introduce another problem because of the distance between stations. A transfer tripping scheme using additional carrier channels probably would be needed to obtain the high speed of operation that would be necessary.

In some of the cases listed the compensation is removed completely during the fault; in others it is left in the circuit. In cases 7 and 8 a constant ohmic value of compensation is used before and after the faulted section is cleared. With constant ohmic value, the per cent compensation is decreased when the faulted line section is removed from service. For comparison purposes, case 9 shows results for the system of Figure 1 but without any compensation, so that the power delivered has to be reduced materially (to approximately one-half) to maintain stability as compared to the compensated systems. Proportionately reduced size of terminal equipment corresponding to the reduced power transmitted is used in case 9. Table II also lists the power delivered for each case and the initial operating angle before the fault is applied. In some cases a shunt reactor is included at point 1′ in Figure 1, which was placed there to keep the line voltage at point 1 from being excessive and to reduce the line-charging current flowing through the sending-end section, thereby increasing the delivered power without exceeding the thermal current-carrying capacity of the conductor when one line section is out of service. Incidentally, the reactor also increases the stability of the system.

A comparison of cases 1 and 5 of Table II indicates that approximately 10-per-cent increase in capacitor impedance, voltage, and kilovolt-ampere capacity is needed, or an increase of 6 per cent of line compensation is needed when the capacitors are removed from service during the fault period of 7.0 cycles. A comparison of cases 5 and 6 shows that the extra 3.5 cycles of delay in getting the capacitors back into service after the fault is cleared require another 13.5-per-cent increase in capacitor kilovolt-amperes or 9-per-cent increase in line compensation. Both of these effects require from 20- to 25-per-cent increase in capacitor kilovolt-amperes, or about 15-per-cent increase in line compensation over that needed if the capacitors were not taken out of the circuit for the 10.5 cycles.

For 325,000 kw delivered and on the basis of constant capacitor ohms (case 7), 75-per-cent final line compensation or 100-per-cent initial compensation (when only two capacitor stations are employed) is required when the capacitors are removed from service during the fault and are reinserted at the time the fault is cleared. It will be observed that the initial operating angle between the internal voltages of sending and receiver machines decreases with increasing compensation. Such a decrease in initial operating angle apparently does not change materially the amount of power which can be transmitted with stability, provided the final percentage compensation is identical for two otherwise similar cases. Hence, there is no real advantage from a stability standpoint of introducing the complication of switching in a portion of the compensation at each capacitor station after the fault is removed.

Figure 2A is a load-flow diagram of the conditions of initial loading for the system of Figure 1 using 75-per-cent initial compensation (case 6). The figure is included to show the various bus voltages and reactive power flow through the various lines and capacitor stations. Figure 2B is a vector diagram of the system under these loading conditions. It is of special interest to observe the relative phase angles obtained in machines, lines, and series capacitors. Figure 3 is a vector diagram of the system after the faulted line section between points S and 1 has been removed, the capacitors reinserted, and the system has swung to the maximum phase angle. Note the large phase angle, 117 degrees, between E_{ts} and point 1, and the corresponding low values for E_s, 66 per cent of normal, and for E_2', 47 per cent of normal. The current through the remaining line section has increased from its initial value of 450 amperes to 1,444 amperes or 3.26 times the initial value. It is also of interest to observe that the voltage across the capacitors at station 1 is 155 per cent of rated value.

It is desirable to compare the relative net accelerations between machine rotors at the instant the fault occurs for the various cases studied. Table III lists the net accelerations assuming double-line-to-ground faults for compensated lines with and without compensation removed. For further comparison, acceleration for completely uncompensated lines (case 9) and for a 3-phase fault on uncompensated lines (case 10) is included. Using the net acceleration for the uncompensated line and a double-line-to-ground fault (case 9) as a standard of comparison, it will be observed that for cases 1, 2, and 4 in which the compensation is not removed, the acceleration ratio varies from 0.97 to 1.07. In other words, the shock to the system is almost directly comparable with case 9. However, when the compensation is short-circuited during the fault, the acceleration ratio varies from 1.85 to 2.05, or the shock to the system is approximately double that for an uncompensated line as for a system in which the capacitors are left in during the fault. For the uncompensated system and a 3-phase fault (case 10) the shock to the system is only 24 per cent greater than the double-line-to-ground fault in case 9. These relative accelerations are an indication why additional compensation is needed in order to maintain stability in cases where the compensation is removed during the fault.

As further comparison, sets of net acceleration-angle curves are shown in Figures 4A and 4B. Figure 4A shows acceleration-angle areas for case 2 in which the compensation was not removed during the fault. With respect to these curves, it can be shown that the positive

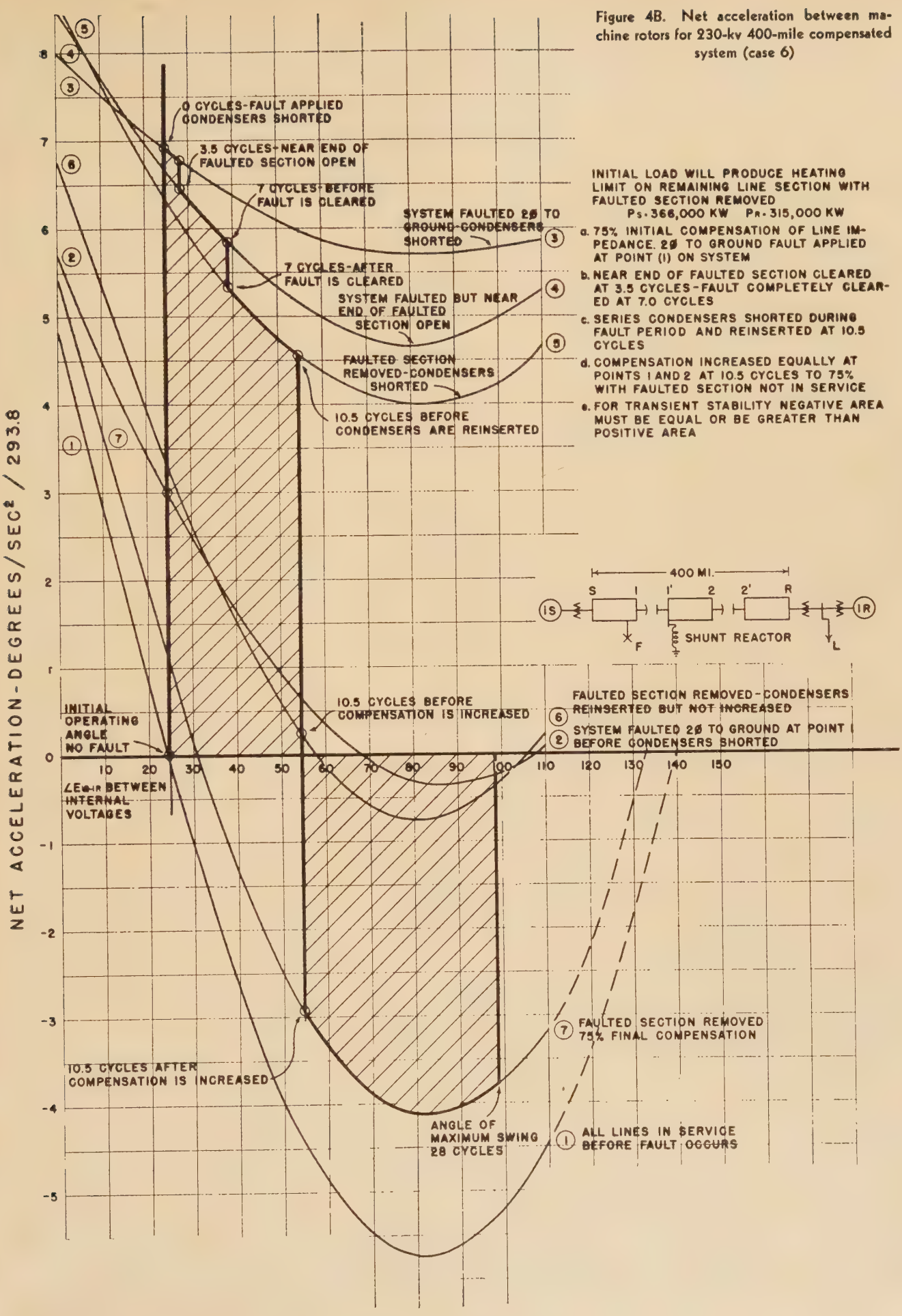

Figure 4B. Net acceleration between machine rotors for 230-kv 400-mile compensated system (case 6)

Table IV. Fault Current Analysis and Control of Capacitors by Overcurrent Elements. Assumptions: Two Times Normal Current Causes Gaps to Flashover

Drop to Below Normal Current Initiates Reinsertion of Capacitors

3-Phase Fault At	Special Conditions: Capacitors In	Capacitors Out	Near End Open	Fault Cleared	Supplied From	Component of Load Current: Measured at	Units of Load Current*: 63 Per Cent Compensation Case No. 2†	75 Per Cent Compensation Case No. 6	100 Per Cent Compensation Case No. 7 and 8
S	x	or x			S	S	2.26 (a)	2.45 (a)	
	x	or x	x		S	S	0.61 (a)	0.56 (a)	
	x	or x		x	S	S	0.76 (a)	0.45 (a)	
	x				R	1 and 2	1.20	1.38 (b)	
		x			R	1 and 2		0.63 (g)	
	x		x		R	1 and 2	0.91		
		x	x		R	1 and 2		0.48 (g)	
	x			x	R	1 and 2	0.72		
		x		x	R	1 and 2		0.47 (g)	
1	x	or x			S	S	1.24 (a)	1.34 (a)	1.26 (a)
	x	or x	x		S	S	1.01 (a)	0.99 (a)	0.87 (a)
	x	or x		x	S	S	0.76 (a)	0.54 (a)	0.37 (a)
	x				R	1 and 2	2.05 (d)	3.14 (c)	3.99 (c)
		x			R	1 and 2		0.90 (f)	0.85 (f)
	x		x		R	1 and 2	0.66		
		x	x		R	1 and 2		0.37	0.30
	x			x	R	1 and 2	0.73		
		x		x	R	1 and 2		0.56	0.47
1′	x				S	1	1.97	2.37 (c)	
		x			S	1		1.38	
	x		x		S	1	0.64		
		x	x		S	1		0.60 (f)	
	x			x	S	1	0.72		
		x		x	S	1		0.53	
	x				R	2	1.24	1.32 (b)	
		x			R	2		0.87 (g)	
	x		x		R	2	0.99		
		x	x		R	2		0.63 (g)	
	x			x	R	2	0.71		
		x		x	R	2		0.43 (g)	
2	x				S	1	1.22	1.46 (b)	
		x			S	1		1.01 (g)	
	x		x		S	1	1.02		
		x	x		S	1		0.82 (g)	
	x			x	S	1	0.72		
		x		x	S	1		0.53 (g)	
	x				R	2	2.40 (d)	2.77 (c)	
		x			R	2		1.33	
	x		x		R	2	0.62		
		x	x		R	2		0.39 (f)	
	x			x	R	2	0.71		
		x		x	R	2		0.43	
2′	x				S	1 and 2	1.80	2.37 (c)	
		x			S	1 and 2		1.01	
	x		x		S	1 and 2	0.63		
		x	x		S	1 and 2		0.50 (f)	
	x			x	S	1 and 2	0.71		
		x		x	S	1 and 2		0.50	
	x	or x			R	R	1.30 (e)	1.28 (e)	
	x	or x	x		R	R	0.97 (e)	0.79 (e)	
	x	or x		x	R	R	0.74 (e)	0.45 (e)	

(a)—No current from S through capacitors.
(b)—Gap at this capacitor station will not flash over.
(c)—Gap at this capacitor station will flash over.
(d)—Capacitors required capable of withstanding more than twice normal voltage.
(e)—No current from R through capacitors.
(f)—Reinsertion of capacitors will start and may be reinserted too soon.
(g)—For comparison only since gap at this capacitor station will not flash over.

* Load expressed in per unit of full load (900 amperes).

† For case 2 it was assumed that capacitors would be designed to withstand excessive voltages during faults and would not be removed from service.

shaded area is proportional to the excess of kinetic energy stored in the sending-end machine rotors compared to the receiving machine rotors. The negative shaded area represents the absorbing of this excess kinetic energy. The system is stable provided the negative area is greater than the positive area. A comparison of positive area produced during the swing from 0 to 7 cycles (case 2) to that produced during the swing from 0 to 10.5 cycles (case 4) indicates why the system is unstable if additional compensation is inserted at 10.5 cycles instead of at 7.0 cycles.

Figure 4B shows acceleration curves for case 6 in which the compensation is removed during the fault. A much larger positive area is produced by removal of the compensation. It must be offset through increase in compensation over those cases in which capacitors were not removed during the fault so as to increase the negative area available. These curves also show the need for removing the fault as rapidly as possible and the need for reinserting the capacitors as rapidly as possible after clearance of the fault.

Table IV lists ratios of currents through capacitors and spark gaps in terms of rated current of the capacitors (900 amperes) during 3-phase faults at various points. This table was compiled to find out if a suggestion to control operation of the capacitors and gap breakers by overcurrent relays were feasible. The table lists 3-phase faults at S, 1, 1′, 2, and 2′ (points shown on Figure 1). For most of the conditions studied, data are tabulated assuming capacitors are first in the system; second, short-circuited; third, the breaker nearest the fault is cleared; and finally, the fault is completely cleared. Values are given for 63-, 75-, and 100-per-cent initial compensation. Based on spark-gap flashover at twice normal capacitor voltage, it will be observed that for conditions marked with note *b* the gaps at the capacitor station will not flash over. For other conditions marked with note *c* the gap will flash over at or above twice normal capacitor voltage. Conditions marked with note *f* may result in faulty operation because capacitors may be reinserted before the fault is completely cleared and the protective gaps will flash over again. Then for the period of time required for the gap circuit breaker to go through a complete opening and closing cycle, the capacitors cannot be reinserted. Therefore, it is important to prevent either premature capacitor reinsertion or to have a protective scheme for the capacitors which is capable of the reinserting them several times with practically no time delay between the reinserting cycles. It will be observed from the data in Table IV that there are conditions in which only a small difference in current must cause the overcurrent relay to pick up or drop out. A relay is needed which will operate rapidly under these small differences in current.

Quantities available for relaying the system are tabulated in Table V for 75-per-cent initial compensation and 3-phase faults located at points specified. Relay locations are shown on the sketch in the table. Voltage, current, and impedance, as seen by the relay, are tabulated. One relaying problem which may result in faulty operation of directional relays at points K and M occurs for a fault near point 1. Both relay elements should

Figure 5. Starting transient in an *L-R-C* series circuit

$$i = \frac{E_m}{Z}\sin(\omega t + \lambda - \theta) + I_1 \epsilon^{-\alpha t}\sin(\beta t - \sigma)$$

$$\text{or } i = \frac{E_m}{Z}\sin(\omega t + \lambda - \theta) + \frac{E_d}{\beta L}\epsilon^{-\alpha t}\sin\beta t - \frac{E_m}{Z}\sin(\lambda-\theta)\epsilon^{-\alpha t}\cos\beta t$$

$$\text{Where } E_d = E_m \sin\lambda - \frac{Q_0}{C} - \frac{E_m \omega L}{Z}\cos(\lambda-\theta) - \frac{E_m R}{2Z}\sin(\lambda-\theta)$$

$Q_0 = 0$ charge on condenser at $t = 0$

$\omega = 377$ radians per seconds (60 cycles)

$\alpha = \frac{R}{2L}$ λ = angle of E at $t = 0$

$\beta = \sqrt{\frac{1}{LC} - \frac{R^2}{4L^2}}$ θ = impedance angle

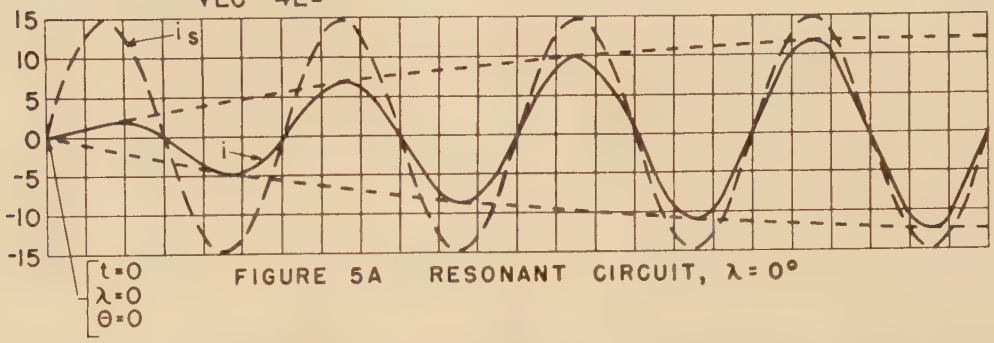

FIGURE 5A RESONANT CIRCUIT, $\lambda = 0°$

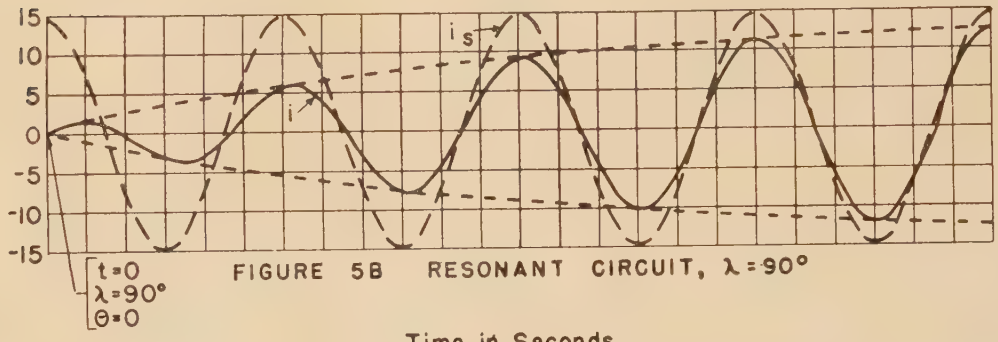

FIGURE 5B RESONANT CIRCUIT, $\lambda = 90°$

i_s = Steady State Current
i = Total Instantaneous Current
Amperes/1000

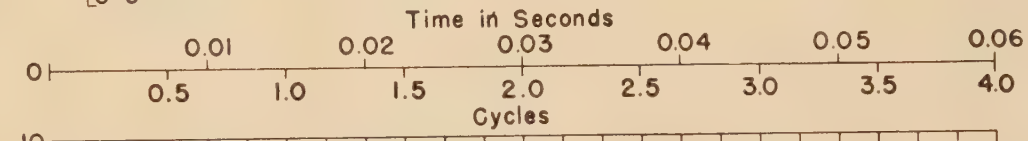

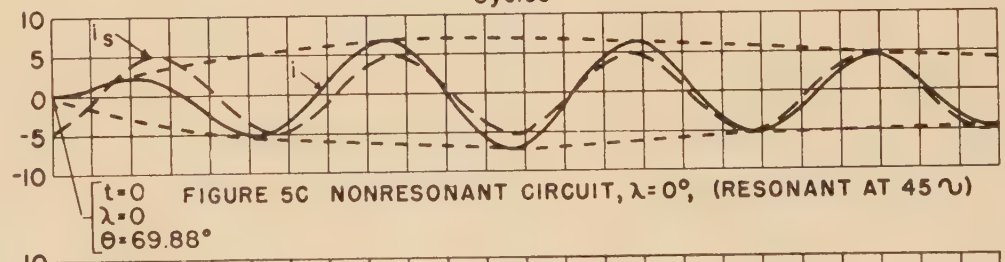

FIGURE 5C NONRESONANT CIRCUIT, $\lambda = 0°$, (RESONANT AT 45 ∿)

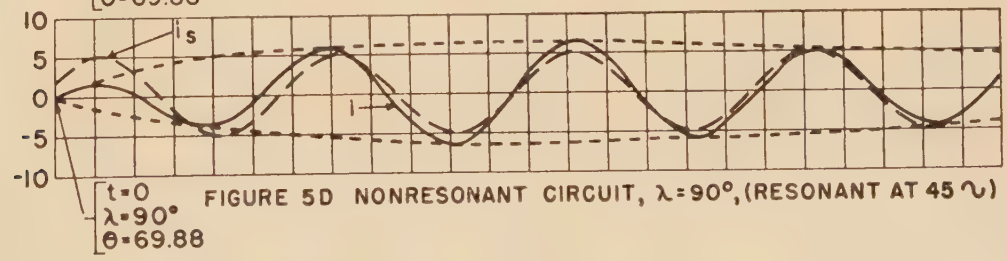

FIGURE 5D NONRESONANT CIRCUIT, $\lambda = 90°$, (RESONANT AT 45 ∿)

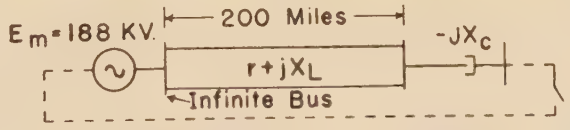

Fig. No.	r	jX_L*	$-jX_C$*	% Neutralized
5a & 5b	12.9 Ω	82 Ω	82 Ω	100%
5c & 5d	12.9 Ω	82 Ω	46.5 Ω	57%

* At 60 CYCLES

Table V. 75-Per-Cent-Initial-Compensation Economic Loading (Case 6). System Impedance as Seen by Line Relays Under Fault Conditions

Current at Each Point Taken as Reference Vector

3-Phase Fault At	Special Conditions: Capacitors In	Special Conditions: Capacitors Out	Special Conditions: Near End Open	Special Conditions: Fault Cleared	Relay B** I*	Relay B** E‡	Relay B** Z†	Relay C** I*	Relay C** E‡	Relay C** Z†	Relay D*** I*	Relay D*** E‡	Relay D*** Z†	Relay E*** I*	Relay E*** E‡	Relay E*** Z†	Relays F and H I*	Relays F and H E‡	Relays F and H Z†	Relays K and M I*	Relays K and M E‡	Relays K and M Z†
Initial loading, amperes, kv, ohms					442	240/0	.542/0	−433	236/−8.5	−544/−8.5	442	240/0	.542/0	−433	236/−8.5	−544/−8.5	416	240/−4.5	579/−4.5	406	240/9.5	592/9.5
(a)S	x				6.24	0	0	1.44	0.53	202/80	−1.41	0	0	1.44	0.53	202/80	−1.49	0.08	−29/−13	−1.48	0.15	−60/−17.5
		x			5.46	0	0	0.66	0.25	203/81	−0.65	0	0	0.66	0.25	203/81	−0.77	0.24	−183/81.5	−0.69	0.49	−416/81
		x	x		0			1.53	0.54	193/83	1.14	0.88	.420/55	−1.17	0.54	−253/34	0.63	0.53	488/−50.5	0.53	0.68	748/−55
		x		x	0			0			0.91	1.02	.607/18	−0.99	0.91	−502/12	0.52	0.89	996/−20	0.48	0.92	1,133/−7
(b)1	x				1.37	0.50	.197/81	7.89	0	0	1.37	0.50	.197/81	−1.40	0	0	−2.99	1.22	−234/−87	−3.24	1.32	−240/−81.5
		x			1.37	0.50	.199/81.5	3.00	0	0	1.37	0.50	.199/81.5	−1.40	0	0	−0.98	0	0	−0.96	0.33	−203/81.5
		x	x		1.96	0.69	.192/82.5	0			0.74	0.69	.504/5	−0.76	0.73	−523/−17.5	0.50	0.72	821/−44	0.40	0.80	1,195/−36
		x		x	0			0			0.91	1.02	.607/18	−0.99	0.91	−502/12	0.52	0.89	996/−20	0.48	0.92	1,133/−7

3-Phase Fault At	Special Conditions: Capacitors In	Special Conditions: Capacitors Out	Special Conditions: Near End Open	Special Conditions: Fault Cleared	Relay F** I*	Relay F** E‡	Relay F** Z†	Relay G** I*	Relay G** E‡	Relay G** Z†	Relay H*** I*	Relay H*** E‡	Relay H*** Z†	Relay J*** I*	Relay J*** E‡	Relay J*** Z†	Relays C and E I*	Relays C and E E‡	Relays C and E Z†	Relays K and M I*	Relays K and M E‡	Relays K and M Z†
Initial loading, amperes, kv, ohms					416	240/−4.5	579/−4.5	−406	241/−10.5	−594/−10.5	416	240/−4.5	579/−4.5	−406	241/−10.5	−594/−10.5	−433	236/−8.5	−544/−8.5	406	240/9.5	592/9.5
(c)1′	x				6.25	0	0	1.47	0.51	205/82	−1.43	0	0	1.47	0.51	205/82	−2.46	0.96	−212/−88	−1.47	0.07	−29/−16
		x			3.71	0	0	0.96	0.32	200/82.5	−0.94	0	0	0.96	0.32	200/82.5	−1.44	0	0	−0.96	0.32	−200/82.5
		x	x		0			1.74	0.56	193/82.5	0.93	0.77	.476/38	−0.95	0.56	−352/15	−0.62	0.78	−682/56	0.70	0.57	477/−59
		x		x	0			0			0.95	0.93	.563/1	−0.96	0.91	−563/−7	−0.55	0.94	−936/32	0.48	0.91	1,130/−7
(d)2	x				1.43	0.50	.202/81	7.50	0	0	1.43	0.50	.202/81	−1.46	0	0	−1.52	0.11	−38/−50	−3.07	1.09	−210/90
		x			0.99	0.34	.200/81.5	3.73	0	0	0.99	0.34	.200/81.5	−1.01	0	0	−1.05	0.35	−180/82	−1.48	0	0
		x	x		1.70	0.57	.193/84	0			0.85	0.57	.385/−23	−0.87	0.74	−504/−47	−0.85	0.58	−370/53	0.43	0.74	1,011/−47
		x		x	0			0			0.95	0.92	.561/0	−0.96	0.91	−565/−7	−0.55	0.94	−932/31	0.48	0.92	1,134/−7

3-Phase Fault At	Special Conditions: Capacitors In	Special Conditions: Capacitors Out	Special Conditions: Near End Open	Special Conditions: Fault Cleared	Relay K** I*	Relay K** E‡	Relay K** Z†	Relay L** I*	Relay L** E‡	Relay L** Z†	Relay M*** I*	Relay M*** E‡	Relay M*** Z†	Relay N*** I*	Relay N*** E‡	Relay N*** Z†	Relays C and E I*	Relays C and E E‡	Relays C and E Z†	Relays G and J I*	Relays G and J E‡	Relays G and J Z†
Initial loading, amperes, kv, ohms					406	240/9.5	.592/9.5	−414	221/3	−535/3	406	240/9.5	.592/9.5	−414	221/3	−535/3	−433	236/−8.5	−544/−8.5	−406	241/10.5	594/−10.5
(b)2′	x				6.07	0	0	1.39	0.53	204/81	−1.42	0	0	1.39	0.53	204/81	−2.46	1.00	−222/−83.5	−2.54	0.91	−213/−89.5
		x			3.28	0	0	1.39	0.52	202/82	−1.42	0	0	1.39	0.52	202/82	−1.05	0.35	−180/81.5	−1.05	0	0
		x	x		0			2.01	0.73	193/81.5	0.94	0.83	.526/27.5	−0.92	0.73	−423/6	−0.51	0.92	−969/42	−0.47	0.83	−1,052/27.5
		x		x	0			0			0.98	0.95	.575/9	−0.98	0.96	−525/2.5	−0.52	0.99	−1,035/27	−0.49	0.95	−1,151/9
(a)R	x				1.53	0.52	.199/81.5	7.67	0	0	1.53	0.52	.199/81.5	−1.50	0	0	−1.53	0.17	−60/−33	−1.53	0.07	−29/−22.5
		x			0.82	0.28	.199/81	7.15	0	0	0.82	0.28	.199/81	−0.80	0	0	−0.84	0.54	−352/82.5	−0.82	0.27	−199/81
		x	x		1.67	0.55	.193/82	0			0.90	0.55	.358/−35.5	−0.88	0.84	−507/−58	−0.70	0.71	−551/55	−0.66	0.54	−488/40
		x		x	0			0			0.98	0.95	.574/10	−0.98	0.96	−524/2	−0.52	0.99	−1,035/27	−0.49	0.95	−1,150/10

* Negative denotes current in nontripping direction. Per unit of initial loading current.

† Negative Z denotes current in nontripping direction. Negative θ denotes capacitive impedance.

‡ Per unit of initial operating voltage.

* Relays on faulted line.

*** Relays on line paralleling faulted line.

(*a*)—Neither gap will flash over.

(*b*)—Both gaps will flash over.

(*c*)—Gap at capacitor station 1 will flash over. Gap at capacitor station 2 will not flash over.

(*d*)—Gap at capacitor station 1 will not flash over. Gap at capacitor station 2 will flash over.

Note: Table gives conditions existing on the system assuming both capacitor gaps flash over before the first circuit breaker opens. Actually such will not always be the case. See footnotes (*a*)–(*d*).

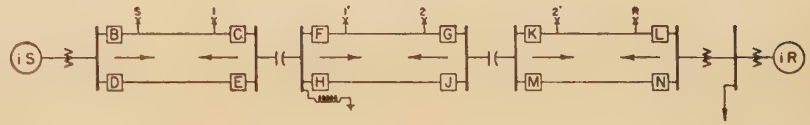

block tripping for this fault. Before the gaps flash over, relays K and M see a high capacity reactance with voltage lagging the current by over 80 degrees in the blocking direction. After the gaps flash, the voltage leads the current by over 80 degrees (in blocking direction). However, these relays should trip for a fault near the receiver bus in which case the voltage is leading the current by over 80 degrees (tripping direction). Hence, this relay should have a torque–phase angle characteristic which will cause it to trip for the voltage leading the current by 80 degrees, but it must block for the voltage leading the current by 100 degrees. It is believed that existing standard directional elements will need to be improved to obtain both high-speed and positive contact closing when operating so near the zero torque characteristic curve. Similar requirements must be met by relays F and H for a fault near point 1. Additional studies will be needed to determine the effects of unbalanced faults on this phase shift. Also the effects of unbalanced impedances in case individual spark gaps are used for each phase of the compensating capacitor must be studied.

The effects of transients in the series L-R-C circuit are of importance. When such a circuit is energized, the instantaneous current i which is produced includes two components, a damped a-c transient which oscillates at the natural or resonant frequency of the circuit, and the steady-state a-c wave which is forced to oscillate at the 60-cycle supply frequency. The summation of these two components produces the instantaneous current i. Figures 5A and 5B show starting current and steady-state current projected backward to zero time for resonance at 60 cycles and for λ, the phase angle at which the voltage first is applied, equal to 0 and 90 degrees, respectively. Figures 5C and 5D show similar currents when the natural frequency of the circuit is 45 cycles. Assuming no system load initially, the system shown in Figure 1 when using 75-per-cent line compensation and assuming a fault occurring at point 1′ would produce starting transient currents similar to those shown in Figures 5C and 5D.

The transient and steady-state components of current are in opposing phase at the beginning; hence, there is a relatively slow build up of the instantaneous current to the final steady-state value. Another way of stating this phenomena is that it takes time to store energy in the dielectric and magnetic fields through the resistance of the circuit; hence, the current is larger the second half cycle than it is the first half cycle. The time constant of this build up is from 2.5 to 3.5 cycles, which is of course appreciable in terms of gap flashover time and of operating time of high-speed relays. A factor which may be important from a directional relaying standpoint (Figures 5C and 5D), is the shift in phase angle during the first two cycles of the total current wave i as compared to the steady-state wave. These factors must be investigated further with respect to their effects on relays.

Operating Requirements of Equipment

With respect to the operating requirements and design of control equipment for capacitors, it is believed that highest speed of operation cannot be obtained by use of three pieces of conventional equipment, namely, relays, a circuit breaker or contactor, and a spark gap. Instead, the functions of this equipment should be combined in fewer pieces of apparatus.

From a system performance standpoint the ideal arrangement might have somewhat similar characteristics to those of a rotary spark gap or lightning arrester which would flash over when the voltage became greater than twice normal, continue to flash over during each half cycle of the fault, and seal off during the next half cycle after the voltage across the capacitor had dropped to a predetermined amount, perhaps normal value or 150 per cent of normal value. Such a device might tend to reinsert the capacitor during each half cycle of the fault but would fail to do so because of the high voltage obtained. However, it would fulfill the important operating condition that the capacitor would be reinserted immediately following clearance of the fault. Investigation of oscillations in the system which might be produced by such a device should be made with a view toward damping them out, or otherwise minimizing any system or apparatus troubles which such oscillations might produce.

Protection of the line sections can be obtained by a high-speed current-balance scheme which will provide sequential tripping of a faulted line section when parallel lines are involved. However, there are good reasons for trying to modify the existing standard-carrier relaying scheme or to improve the characteristics of the phase-comparison carrier scheme so that one or the other can be used with series compensation. With respect to developing a directional relay characteristic to be used with the standard carrier scheme, it may be possible to combine the capacitor voltage with the regular line voltage and current to obtain proper phase-angle characteristics. This seems to be promising since it is the capacitor voltage which causes the trouble in the first place.

Conclusions

The results of this study indicate

(a). That compensation is very effective in increasing the allowable line loading.

(b). Building the capacitors to withstand the high voltages during short circuits in most cases cannot be justified. However, for system arrangements having relatively high terminal impedance at both ends and a relatively low percentage of line compensation (produces a relatively low ratio of maximum fault current to maximum load current), design A which does not remove the capacitors from service during a fault may have distinct advantages over design B and, therefore, although a more expensive installation, may be economically feasible where firm power is a consideration.

(c). If capacitors are removed during the fault period of seven cycles, approximately ten per cent increase in capacitor kilovolt-amperes or six per cent increase in line compensation is required for the particular system studied to obtain the same line loading with stability, as compared to system quantities in which the compensation is not removed.

(d). If capacitors are removed during the fault period of 7.0 cycles plus an additional delay of 3.5 cycles for reinserting them after the fault is cleared, approximately 25-per-cent increase in capacitor kilovolt-amperes or 15-per-cent increase in line compensation is required for the same line loading on the particular system studied, as compared with the compensation required if the capacitors are not removed.

(e). Due to high machine accelerating powers produced during the fault, especially if the capacitors are removed, fast clearing of the fault when compensation is used is considerably more important than in conventional systems. Fast reinsertion of capacitors after the fault is cleared is extremely important. To obtain increased speed in clearing the fault and reinserting the capacitors in the system, increased costs of relays and circuit breakers may be justified. Similarly, higher inertias of machines are desirable and may be economically justified.

(f). Assuming that modification of the existing standard relay schemes is not practical, a highspeed current-balance relay scheme appears to fulfill the line protection requirements more completely than any other existing scheme. The relatively new phase-comparison schemes are slow and not completely applicable on systems where fault currents may be lower than maximum load current.

(g). Considerable further study, design, and test of special apparatus seem to be in order to obtain equipment characteristics which will meet best the new problems encountered when series compensation is used.

References

1. Series Capacitors for Transmission Cir-

CUITS, **E. C. Starr, R. D. Evans.** AIEE TRANSACTIONS, volume 61, 1942, pages 963–73.

2. STEADY-STATE AND TRANSIENT-STABILITY ANALYSIS OF SERIES CAPACITORS IN LONG TRANSMISSION LINES, **J. W. Butler, J. E. Paul,** and **T. W. Schroeder.** AIEE TRANSACTIONS, volume 62, February section, pages 58–65.

3. POWER SYSTEM STABILITY, volume 1, STEADY-STATE STABILITY, **S. B. Crary.** John Wiley and Sons, Inc., New York, N. Y., 1945.

4. FIRST REPORT OF POWER-SYSTEM STABILITY, **An AIEE Committee Report.** AIEE TRANSACTIONS, volume 56, 1937, February section, pages 261–82.

5. EFFECT OF ARMATURE RESISTANCE UPON HUNTING OF SYNCHRONOUS MACHINES, **C. F. Wagner.** AIEE TRANSACTIONS, volume 49, 1930, pages 1011–24.

6. ANALYSIS OF SERIES CAPACITOR APPLICATION PROBLEMS, **J. W. Butler, C. Concordia.** AIEE TRANSACTIONS, volume 56, 1937, August section, pages 975–88.

7. THE SERIES-CAPACITOR INSTALLATION AT BALLSTON, NEW YORK. **E. K. Shelton.** *General Electric Review*, Schenectady, N. Y., August 1928, pages 432–4.

8. THE EFFECT OF SERIES CAPACITORS UPON STEADY-STATE STABILITY OF POWER SYSTEMS, **E. J. Allen, J. L. Cantwell.** *General Electric Review*, Schenectady, N. Y., May 1930, pages 279–82.

9. STABILITY LIMITATIONS OF LONG-DISTANCE A-C POWER TRANSMISSION SYSTEMS, **Edith Clarke, S. B. Crary.** AIEE TRANSACTIONS, volume 60, 1941, pages 1051–9.

Maintenance of Rectifiers on Electrochemical Installations

Discussion of paper 46-96 by J. E. Housley and G. N. Hughes, presented at the AIEE Southern District meeting, Asheville, N. C., May 14–16, 1946, and published in AIEE TRANSACTIONS, 1946, July section, pages 436–41.

H. G. Harvey and **T. J. Woth** (Westinghouse Electric Company, Atlanta, Ga.): Industry often does not have the opportunity to benefit from such a wealth of experience that has been obtained during the past few years at the Aluminum Company of America plant and as described by J. E. Housley and G. N. Hughes. The experience gained by the operation of such a large number of units varying in type, construction, and circuit design, most certainly should serve as a valuable guide in future installations.

The designer, to a large extent, depends upon operating problems to guide him in his development and research activities. If we can look forward to receiving such a valuable operating report periodically, and I believe we can, we should feel confident that the rapid progress that has been made during the past years in electronic conversion equipment will continue.

During the war, the installation of rectifiers other than electrochemical declined somewhat. However present indications are that rapid expansion will be made in the use of these devices, especially to supply, street railway, trolley buses, and mining loads. Although the load factor involved in these applications probably will average as low as 25 per cent as compared to more than 90 per cent for the electrochemical applications, the majority of these units will be of single-anode, multiple-tank continuously-pumped type. Operating experience with a limited number of ignitron rectifiers installed before the war, operating under the rapidly varying railway load conditions, indicates that highly successful operations can be expected.

Recent experimental work in connection with artificial arc-backs has cast some new light on the arc-back problem and should be helpful in still further reducing this trouble in the future.

The main cause of arc-backs, as described by the authors, is assumed to be the formation of a cathode spot on the anode. However, experimental work during the development of the ignitron principle indicated that if the source of ionized vapor could be eliminated entirely during the negative half cycle, it should reduce the number of arc-backs greatly. This was accomplished by the use of the ignitor circuit which made it possible to eliminate entirely the separate d-c-excited keep-alive anodes. The absence of ionized vapor in the ignitron unit, except during the conduction period, undoubtedly accounts for the much lower arc-back rate for this type of unit.

All standard rectifiers are designed so that a voltage reduction of approximately 15 per cent can be obtained by delayed firing.

There are however a number of disadvantages which, as the authors have pointed out, make it desirable to operate normally with zero firing delay or as near to this point as possible. In addition to the increased tendency to backfire, and lower power factor, it should be pointed out that the magnitude of harmonic currents increases rapidly with the number of degrees of firing delay. Although this item may be of minor importance in the large multiphase installations, it is generally an important consideration in the smaller individual applications. In most of these cases, the high-voltage transformer taps can be arranged so that normal operation with zero firing delay will be satisfactory and the voltage control feature used only in emergencies or for the degassing operation.

The many helpful suggestions made by the authors in regard to special pressure tests for finding gas leaks, caution that should be used in making repairs, and critical performance during the degassing operation should be extremely helpful to the operators who now are planning initial installations of rectifier equipment.

Inductive Co-ordination Aspects of Rectifier Installations

Discussion of paper 46-105, an AIEE committee report, presented at the AIEE summer convention, Detroit, Mich., June 24–28, 1946, and published in AIEE TRANSACTIONS, 1946, July section, pages 417–36.

R. D. Evans (Westinghouse Electric Corporation, East Pittsburgh, Pa.): The contents of this paper should prove to be of great usefulness to the industry. In the preparation of this report special efforts have been made to provide a discussion of a method which could be used generally by application engineers of industrial organizations and power companies as well as by engineers of the electrical manufacturing and telephone companies. It is believed that this report is sufficiently self-contained and explicit to permit its use by a much wider group of engineers than was possible by previous technical reports on this subject.

The body of the report is basically simple in character, and this fact should not be disregarded by the presence of the appendixes which contain supplementary material of considerable interest and usefulness in special cases.

The report contains the term "commutating reactance," and the proposed standard for pool cathode mercury-arc power converters (AIEE Standard 6, June 1946) includes a definition of commutating reactance. A discussion of the meaning and significance of commutating reactance may be of interest.

For many years specialists in the application of rectifiers have used the term commutating reactance in all theoretical methods for estimating the performance of rectifier circuits from the standpoint of regulation and harmonics. Nevertheless, rectifier transformer nameplates in the past have not included commutating reactance, but instead have given another reactance which frequently has been referred to as nameplate reactance. The use of these two reactances of a rectifier transformer has been a source of confusion and to a considerable extent has limited the application of analytical methods for estimating harmonics in the circuits of rectifiers. This particular difficulty would be avoided in the future by the methods presented in this paper and in the treatment included in the proposed rectifier standards.

Nameplate reactance of a rectifier transformer may be obtained by applying polyphase voltage to the primary of a rectifier transformer with all secondary terminals short-circuited. Commutating reactance of a rectifier transformer is half of the reactance in the circuit involving the anodes between which commutation takes place. Commutating reactance may be measured by applying single phase voltage to the rectifier transformer terminals between which commutation takes place with the a-c line terminals of the rectifier transformer short-circuited. The two reactances may be converted from primary to secondary voltage bases, or vice versa, by using the well-known conversion methods. It is important, however, to recognize that these two reactances for a particular rectifier transformer will have, in general, different numerical values. These differences arise from the circumstances which cause the mutual effects of the windings to be different for the two circuit conditions. Thus the difference between nameplate reactance and commutating reactance depends in part upon the circuit connections and in part upon winding construction which affects the mutual inductance between the windings. Because of these circumstances it is not feasible to provide a simple equation relating the numerical values of these reactances. In the future the commutating reactance will be given on the nameplates of rectifier transformers. For existing transformers this information can be obtained by tests in the field or may be supplied by the manufacturer of the transformer who usually makes such a test in the factory or can estimate the reactance from design proportions. Nameplate reactance is of use principally in connection with the calculation of maximum short-circuit current in the rectifier transformer.

Protection of Powerhouse Auxiliaries

Discussion and closure of paper 46-169, an AIEE committee report, presented at the AIEE summer convention, Detroit, Mich., June 24–28, 1946, and published in AIEE TRANSACTIONS, 1946, November section, pages 746–51.

W. R. Brownlee (The Commonwealth and Southern Corporation, Jackson, Mich.): While this report is based on a relatively small number of replies, it is believed that a representative cross section of experience has been secured. On many aspects of the problem a majority concurrence is indicated, but there are a number of cases of sharp divergence in practice. It is felt that this also holds true when a large number of cases are considered. For example, most users omit undervoltage protection, although some have retained it. Many con-

nect motor thermal overload elements to operate an alarm for essential motors, but several connect the thermal devices to trip the motors. A large proportion of users rely on transformers for station service supply, but a few utilize shaft generators or even house turbines.

In order to provide the reliability which it generally is agreed is so necessary in station auxiliary performance, it is believed that close attention is required to these points

1. Eliminate all (or almost all) undervoltage protection even of the time delay type on all essential motors.

2. Connect thermal relay elements to provide alarm or indication for essential motor circuits, using elements with generous settings to trip nonessential motors only.

3. Provide station auxiliary sources from transformers, preferably connected at generator voltage, with proper co-ordination of control and protection.

Several factors have contributed to the trend toward these principles in the treatment of station auxiliaries. Undervoltage protection was at one time required because of the use of compensator starting or slip-ring induction motors. With modern designs all essential motors may be of the squirrel-cage line-starting type so that undervoltage protection is not required for this purpose. The desirability of safety interlocking was responsible for the use of undervoltage protection in the past, but recent plants make use of safety devices responding to the driven quantity, such as differential air pressure relays in the exhauster pipes, and time lagged pressure relays in the induced draft fan systems. Similarly the present day practices in central stations differ from the typical industrial plant in that special attention is given to the co-ordination of motors with the drive characteristics, maintenance is performed on a program basis, and close surveillance by station operators eliminates many causes of motor overloading.

With a co-ordinated system of station auxiliaries as outlined in a foregoing paragraph, a highly reliable and efficient system may be provided. Tests on such a co-ordinated scheme have been described[1] showing that the system is immune to external short circuits since a total interruption of auxiliary power for as much as five seconds does not interfere with boiler and turbine performance. Test also have shown that in severe emergencies voltage may drop as low as 60 per cent of normal for a sustained interval without loss of flame or reduction in capacity. With such a system of electrical auxiliaries, the margin for emergencies in boiler and turbine operations is inherently greater than can be provided in the interconnected transmission system to withstand extreme voltage reductions, so that the over-all system emergency capability need not be limited because of station auxiliaries.

REFERENCE

1. ELECTRIC DRIVES FOR STEAM-ELECTRIC GENERATING-STATION AUXILIARIES. **Wm. R. Brownlee, J. A. Elzi.** AIEE TRANSACTIONS, volume 64, 1945, November section, pages 741–5.

E. L. Michelson (sponsor, relay subcommittee, AIEE committee on protective devices): W. R. Brownlee's discussion emphasizes the desirability of simple and reliable relaying methods for powerhouse auxiliaries. It is necessary for the auxiliary power system to be more reliable than any other component of the power system, because of the greater hazard which accompanies the loss of auxiliary power in the generating station.

The recent trend toward the use of motor driven exciters further increases the need of reliable system of auxiliary power. Since the loss of supply to the exciter set for even a brief interval may result in the loss of excitation to the main generating unit, continuity of service to the exciter set is even more important than the supply to other auxiliary services.

Brownlee mentions that the use of undervoltage relays largely has been eliminated for the protection of auxiliary power motors. It should be noted that these relays are being used in many installations for the purpose of restoring service to an auxiliary power bus which has lost its normal source of supply.

Mica Capacitors for Carrier Telephone Systems

Discussion of paper 46-151 by A. J. Christopher and J. A. Kater, presented at the AIEE summer convention, Detroit, Mich., June 24–28, 1946, and published in AIEE TRANSACTIONS, 1946, October section, pages 670–4.

N. N. Babcock (Western Electric Company Kearny, N. J.): As mentioned in the paper by Christopher and Kater silvered mica capacitors have been made for many years, but only in the past decade with the development of new materials and methods have they proved desirable from either a design or a manufacturing standpoint. The first metalized mica capacitors were made basically by one of three processes.

1. Chemically depositing silver or other metal.
2. Cathode sputtering.
3. Evaporation of metals in a vacuum.

In general, such capacitors, in addition to being quite expensive to manufacture, tended to be unstable with variable voltage and temperature[1] and to possess undesirable frequency characteristics caused chiefly by the thinness and discontinuity of the coatings serving as the electrodes.

The application of metallic coatings, especially those of gold and silver, to ceramics by the method of firing on a glasslike matrix containing the finely divided metal or its salts is an ancient art. Leyden jars have been made in this manner for a long time. The extension of the method to mica capacitors seemed obvious, but the china decorators' pastes fired at temperatures too high to be tolerated either electrically or mechanically by the mica. Anticipating that many advantages might be gained, the Western Electric Company initiated a development about ten years ago which, in co-operation with commercial manufacturers of ceramic decorators' pastes, resulted in improved silver pastes firing at lower temperatures and possessing the desirable characteristics of good adherence to mica, ease of application, and controllable thickness of coating which now form the basis of the silvered mica capacitor industry.

The silver solutions now used by the Western Electric Company have been developed particularly for spray application. The silver is in finely divided metallic form with carefully controlled amounts of low melting point glass of special composition and an extender suspended in a suitable vehicle. Firing of the silver coating after spraying on the mica plates is accomplished in a well-ventilated electrically heated conveyor furnace. The electrical properties of the silvered mica plates or laminations have been found to be affected noticeably if the composition of the silver formulation is not controlled closely.

The assembly of the units, whether intended for use in the potted types or the molded phenolic encased capacitors, is essentially the same. In the case of the molded types the relatively small effect of pressure on the silvered mica unit allows a reliable prediction to be made of the capacitance rise that will take place during the molding operation. Consequently in commercial production capacitance tolerances of plus or minus the quantity (0.5 per cent plus one micromicrofarad), without resorting to selection methods, regularly are obtained. Three sizes of the molded type capacitor with wire leads are manufactured. The capacitance range covered by this group is two micromicrofarads to 0.02 microfarad. For the potted types, in which the silvered mica unit is placed in an extruded aluminum can filled with wax, there are three basic sizes of mica laminations used. From these basic unit sizes five different sizes of finished capacitors may be built up. The cans themselves may carry mounting lugs or not, depending upon the end application of the capacitor.

The testing equipment used in the manufacture and final inspection of these capacitors necessarily is designed and calibrated to a high order of accuracy. The capacitance and conductance of every capacitor is checked carefully in final inspection on precision bridges. The dielectric strength and insulation resistance requirements are checked on 100 per cent of the product. Temperature coefficient of capacity, drift, and quality of seal against the effects of humid atmospheres are checked on a sampling inspection basis.

It has been found advantageous at the Western Electric Company to carry out all assembly operations on silvered mica capacitors and the final testing as well, in an atmosphere of not over 45 per cent relative humidity and at a temperature held close to 75 degrees Fahrenheit. The adverse effects of adsorbed moisture on the mica laminations making up a capacitor are recognized widely. Air conditioning tends to minimize difficulties of that nature and at the same time assures maximum stability and reduced maintenance for the precision testing equipment. These factors together with the over-all improvement in the amount of production and quality level of the product more than justify the cost of air conditioning.

Among the advantages resulting from the adoption of the silvered mica construction from the manufacturing viewpoint perhaps the most important was the marked reduction in the number of operations and the time required to effect final capacitance ad-

justment. This is accomplished readily on silvered mica by scraping off a portion of the electrode area while the unit is connected to a capacitance bridge. Adjusting to close tolerances in the case of clamped mica-foil types was an exceedingly tedious job requiring considerable skill. Another advantage of silvered mica is the fact that stacking to the desired capacity value may be carried out with considerable precision and with no necessity for close thickness limits on the mica. Manufacturing yields were greatly improved, the cost was reduced, and difficulties caused by aging out of limits almost were eliminated by the adoption of silvered mica.

In an article by Doctor A. T. Chapman the manufacture of these capacitors is discussed in more detail.[2]

References

1. Mica Condensers as Standards of Capacity, **Harvey L. Curtis.** United States Bureau of Standards, Washington 25, D. C., reprint 137, April 22, 1910.

2. Manufacture of Silvered Mica Capacitors, **A. T. Chapman.** *Electronics*, McGraw-Hill Publishing Company, New York, N. Y., November 1945.

Electronic Register Control for Multicolor Printing

Discussion and author's closure of paper 46-132 by W. D. Cockrell, presented at the AIEE summer convention, Detroit, Mich., June 24–28, 1946, and published in AIEE TRANSACTIONS, 1946, August–September section, pages 617–22.

S. L. Burgwin (Westinghouse Electric Corporation, East Pittsburgh, Pa.): I wish to compliment W. D. Cockrell upon the clarity and organization of his paper. I found it unusually easy to read and his method of illustrating the operation of the electronics circuits is very easy to follow.

Early in this paper Cockrell states that the register must be within three thousandths of an inch to be acceptable. We, at Westinghouse, in developing apparatus for similar application in conjunction with the Cline Electric Company have adopted the same value as an objective, although it is my personal opinion that the average reader will not be disturbed unduly until the mis-register exceeds ten thousandths of an inch. I would like to ask Cockrell how he obtained this particular value.

In our early development at Westinghouse we likewise found vibration of the scanning head to be a serious problem and we likewise were forced to shock-mount our amplifier. It is amazing how nearly similar our early designs were to that shown in this paper. However, such shock-mounting resulting in a slight uncertainty or variability of position of our scanner which made it difficult to reduce vibration to a satisfactorily low level and still realize the goal of three thousandths of an inch register. Consequently, we found it advisable in a later design to develop other methods of solving the vibration problem. Perhaps Cockrell has been more fortunate than we have been in this respect.

In our early development we ran into considerable difficulty in maintaining the steep wave front of the voltage pulses generated by the change of light on the phototube, resulting from interelectrode capacity of the first amplifier tube. This resulted in a decreased amplification and a greater sensitivity of register to line voltage changes. Although our circuit differed considerably from that described in this paper, the circuit shown may be subject to the same difficulties.

In Figures 8 and 9 of the paper, voltages produced by web and cylinder scanners are assumed to change instantaneously. Cockrell no doubt has made this assumption to simplify his explanation. I would like to point out that in a more rigorous analysis the actual rates of change would have to be taken into account as they depend upon the width of the slits in front of the phototubes, which are not negligible, and to some extent upon interelectrode capacity of the amplifier tubes, which also may not be negligible. While Cockrell has not stated the widths of these slits I assume that they are in the order of half the width of the register mark. If so, the pulses from the web scanner will be more nearly triangular than square and the error indication would be more nearly proportional to the square of the error than the first power. On this basis the regulator cannot be classified strictly as a proportional regulator but lies between the proportional and dead zone types.

Only a statistical study of the register of a large number of specimens can prove whether the objective of three thousandths of an inch has been attained, and even the results of such a study might not be conclusive as there is always some change in dimensions of the paper from one printing cylinder to another. Whether or not this objective of three thousandths of an inch register has been attained, observation of the operation of the register control described by Cockrell leaves little room for doubt that it is a considerable improvement over manual control.

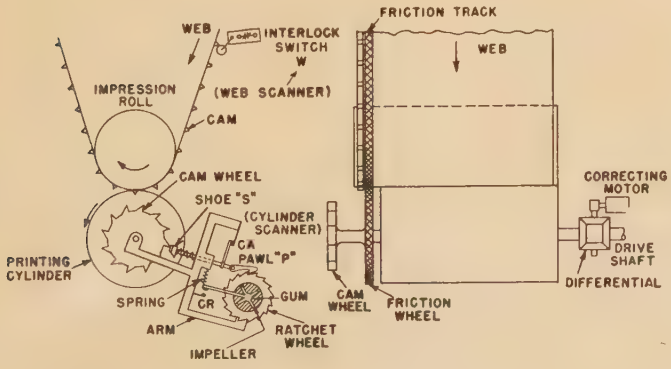

Figure 1. The impression and printing cylinders with imaginary electromechanical equipment for automatic color register

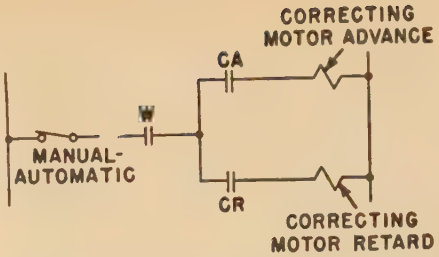

Figure 2. The wiring circuit of the contacts shown in Figure 1

CA. Cylinder advance contact
CR. Cylinder retard contact
W. Web interlock switch

K. P. Grenfell (General Electric Company, Schenectady, N. Y.): It might be of some assistance in understanding the action of the photoelectric color register control, described in Cockrell's paper, to visualize an electromechanical analogy. The problem is to provide a means of keeping the web in a definite longitudinal relationship to the printing cylinder so that the cylinder will superpose its impression exactly over that printed on the web at the previous cylinder.

Suppose it were possible to attach a friction track on the web, as shown in Figure 1 of this discussion, and to have this mesh with a friction wheel on the cylinder shaft. Once the proper relationship were established, register would tend to be locked in, as the web would be geared to the printing cylinder.

In order to get this gearing into phase, and to keep it there whenever it tried to slip, devices would be needed to detect out-of-register conditions. Imagine a series of teeth or cams attached at regular intervals to the edge of the web. These correspond to the web register marks. An interlock switch or web scanner marked *W* has its contacts closed for a brief interval each time a cam passes under its roller.

Picture again a wheel or scanner disk solidly connected to the printing cylinder, with equally spaced cams on its periphery. The number of cams on the wheel equals the number of cams on the web passing per revolution of the printing cylinder. The passage of a cam under shoe *S* momentarily closes contact *CA*, and advances pawl *P* on its ratchet wheel. The ratchet wheel carries a container of gum. When the trailing edge of shoe *S* slips sharply off the trailing edge of the cam, contact *CA* opens, pawl *P* turns the ratchet wheel, and the gum closes contact *CR* by means of an imbedded impeller. Contact *CR* is drawn open again by a spring after a time interval approximately equal to the closed time of contact *CA*. The *CA* contact, pawl, ratchet wheel, and *CR* contact are mounted on an arm which is adjustable about the cylinder axis. The *CA* contact and its operating mechanism correspond to the cylinder scanner phototube and optical system. The ratchet wheel and *CR* contact create the live zone for retarding correction—a function actually performed in the mixing panel.

The three contacts are wired up as shown in Figure 2 of this discussion. The coil causing the correcting motor to advance the

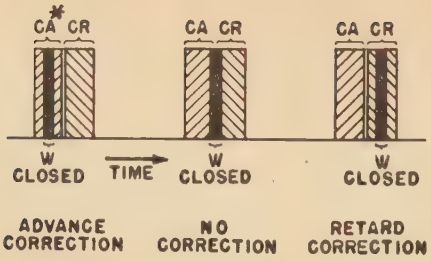

Figure 3. The zones of correction

*Contacts closed

printing cylinder with respect to the web is energized when both W and CA contacts are closed. The coil for retarding operates when both W and CR are closed. Under a condition of correct register at the printing cylinder, the arm should be so positioned that shoe S drops over the trailing edge of the cam at an instant exactly half way through the closed interval of contact W. Reference to Cockrell's paper will show that in the electronic equipment the *trailing edge* of the cylinder disk slits is the indicating point. Under this condition the correcting motor will receive first an impulse to advance, followed immediately by an impulse of equal duration to retard. The net correction will be zero.

Suppose the gearing slips for some reason, and the printing cylinder drops back slightly with respect to the web. Contact W now will be closed predominantly during the time that CA is closed, and the correcting motor will advance the cylinder till register is restored. Similar reasoning applies to retard corrections. Figure 3 of this discussion illustrates this action. As Cockrell explains, a single correcting pulse lasts only a matter of microseconds. The electronic equipment therefore must integrate these to obtain a signal long enough to operate the correcting motor.

Starting a new run on the press can be visualized easily with this mechanical analogy. With the automatic equipment disconnected by a switch in series with interlock W, the operator brings the various colors into register by manual control of the correcting motor. Inspection of the product is his guide. He then moves the arm until shoe S slips over the trailing edge of the cam at the same instant that the arm of interlock switch W reaches its maximum deflection. Register operation then is switched over to automatic.

W. D. Cockrell: In reply to S. L. Burgwin's question about the 0.003 inch register tolerance which I mentioned, I can say only that it was a compromise, arrived at after discussion of the various types of reproductions to be registered. If the cut consists of fine lines such as the reproduction of an etching or engraving, a difference of even 0.001 inch is noticeable. However, for other reproductions, such as that of a water color having broad areas which blend, 0.010 inch register will be permissible. However, for the usual Kodachrome reproduction, 0.003 inch to 0.005 inch register will do a satisfactory job. The equipment described should hold better than 0.003 inch under constant speed conditions with uniform paper and humidity, but it is believed that the guarantee of 0.005 inch will cover most conditions of constant speed operation encountered in the average color printing plant.

The high sensitivity demanded requires that we shock-mount our electronic equipment. This is shown in Figure 7 in the paper. However, in order to obtain the greatest accuracy of register, the optical system is mounted as rigidly as possible, since it is the position of the optical system (which ends with a slit through which the light is transmitted to the phototube) that determines the accuracy.

Obtaining the proper shape of electric wave front requires careful circuit design and co-ordination with the optical system. However, present day television practice requires the passage of much shorter signals and a much wider range of frequencies. Hence, the circuit requirements, while difficult, are not at all impossible. The projected width of slit is less than one-fourth that of the register mark so that the rounding of the signal resulting from the optical system is not too great a handicap and a reasonably square wave-form results. The control is of the proportional type with a dead zone determined by the low torque required to break the correcting motor starting friction.

K. P. Grenfell's mechanical analogy of the timing and synchronizing principles is quite interesting, and is a reasonably accurate picture of the action taking place. Since most press operators have mechanical rather than electrical training, analogies of this type should be very useful in presenting to them the theory of operation of the register control.

Electrical Accuracy of Selsyn Generator-Control Transformer System

Discussion of paper 46-113 by Harold Chestnut, presented at the AIEE summer convention, Detroit, Mich., June 24–28, 1946, and published in AIEE TRANSACTIONS, 1946, August–September section, pages 570–6.

C. Concordia (General Electric Company, Schenectady, N. Y.): A paper such as this is valuable first in showing

1. The deviations of the actual component of a control system, the Selsyn, from the ideal proportionality assumed in so many studies.

2. The smallness of these deviations.

It is difficult to obtain in small machines the good wave form ordinarily obtained in large machines by proper winding distribution and pole shaping, and it may not be worth while in view of the deviation magnitudes shown.

Another point that should be mentioned is that it is not possible to make deviations of any magnitude completely negligible simply by gearing the Selsyn system in order to make it run at a sufficiently high speed, since a reasonable accuracy of the gears has to be considered, and there is some optimum division of effort between work devoted to improving Selsyn accuracy and that devoted to improving gear accuracy.

A New Approach to Probability Problems in Electrical Engineering

Discussion and author's closure of paper 46-128 by H. A. Adler and K. W. Miller, presented at the AIEE summer convention, Detroit, Mich., June 24–28, 1946, and published in AIEE TRANSACTIONS, 1946, October section, pages 630–2.

Philip Doane (Consolidated Edison Company of New York, Inc., New York, N.Y.): If we assume infinitely small time intervals so that no two events occur within the same time interval, then origination of a period with r events existing can occur only by an increase or decrease of one event from a state with $(r-1)$ or $(r+1)$ events existing. The numer of periods with r or more events then will be equal to the number with r events existing which originate as increases from the status with $(r-1)$ events existing. For $r>0$ this will be, provided the average length and the frequency of the successive occurrences of any one event are the same for all events,

$$N_r=\frac{n!}{(r-1)!(n-r)!}t^{r-1}(T-t)^{n-r}/T^n=\frac{r}{pT}P_r$$

The average length as a fraction of the total time T of periods with r or more events existing is then

$$t_R/T=(P_n+P_{n-1}+\ldots+P_{r+1}+P_r)p/rP_r$$

It should be noted that, as in all of the equations of the paper, the ending of a period with r events existing followed in the next time interval by the beginning of another period with r events existing is considered a division between two different periods.

Equation 12 apparently requires qualification as neglecting those cases in which successive originations of an event occur in time intervals immediately following the end of prior occurrences thereby occupying time intervals otherwise designated as intervals originating periods with the next lower number of events existing. In most practical cases the error would be negligible.

H. A. Adler: In view of several questions and special requests, the following additional background information seems desirable for clarification of the formulas presented in the paper. As an example, if there is a certain probability that four out of n events occur simultaneously, then it is obvious that, in general, it will be much less probable that all four events start and end simultaneously. For events which can change position in time continuously or in small steps, most overlaps will be only partial ones. All degrees of overlaps from small ones to complete ones are possible, and each has its own probability. From all possible overlaps and their probable frequencies the average overlap or average duration of simultaneous occurrences can be calculated.

This average overlap may be of practical importance in engineering problems as can

Table I. Summary of Enumerations for $n = 3$, $t = 4$, $T = 10$

Length of Occurrence in Units	No Occurrence		Single Occurrence		Double Occurrence		Triple Occurrence	
	Number of Times	Total Duration	Number of Times	Total Duration	Number of Times	Total Duration	Number of Times	Total Duration
1	300	300	780	780	660	660	180	180
2	240	480	600	1200	480	960	120	240
3	180	540	420	1260	300	900	60	180
4	120	480	270	1080	90	360	10	40
5	60	300						
6	10	60						
Total	910	2160	2070	4320	1530	2880	370	640

be seen from the following two examples. If a certain probability of simultaneous outages of say four machines on a system were determined, it would make a considerable difference for reserve planning purposes whether the average duration of such an outage were expected to be a matter of a few hours or a few days. Similarly a simultaneous operation of a number of welders on a circuit would have obviously little effect upon voltage flicker if the average overlap were only a small portion of a cycle. Of course for cases where events can change position only in steps equal to their duration, or, in other words, if only complete or no overlaps are possible, then the binomial law gives the complete answer. For these special cases the equations presented in the paper reduce to the binomial formulas. The binomial law is, therefore, a special case of the new equations.

The formulas have been derived empirically by enumeration of a variety of cases. Following is an example to illustrate the method. Consider the case of three events each lasting four consecutive units of time and occurring recurrently once in ten units of time. It is apparent that these three events can take 10^3 or 1,000 different positions in the period of ten units if the events can change position in steps of unit length. Figure 1 shows an analysis of the first 20 of the possible 1,000 positions. On the left side the positions of the three events are shown graphically. The next column shows graphically the consequent amplitude and duration of occurrences. In these graphical illustrations it should be understood that the period T is a recurring measure of time such as hours or years and not a confined length. An event occurring near the end of T then merely would extend into the next period T or it could be considered reappearing at the start of the same period T as it has been done, to save space, in Figure 1. The right side columns of Figure 1 enumerate the duration and amplitude of the occurrences.

The results of the complete analysis of this case are summarized in Table I. It should be noted that the numerals in the last line under the headings "Total Duration" are identical with the numerical value of the numerator of equation 2 for $n = 3$, $t = 4$, $T = 10$, and $r = 0, 1, 2, 3$ while the numerals in the last line in the columns "Number of Occurrences" are identical with the value of the denominator of equation 2 for these cases. Equation 2 has been derived by a systematic analysis of a variety of enumerations such as the one discussed. Analogous methods were used for the duration of the other unit step formulas. The analyses included a number of extreme borderline cases where the formulas might have been expected to break down. However, the formulas were found to be consistent with the enumerations of even such cases.

With regard to Doane's comments, the method of statistical equilibrium suggested by him leads to an equation which is identical with equation 5, although this equation has been derived by a different method. He is correct in stating that the ending of a period of r events followed by a period of r events of which at least one is new is considered a division between different periods, see, for example, positions 15, 16, and 18 of Figure 1.

As stated in the paper with regard to equation 12, individual length and order of occurrences of repeated events have no effect on the results. Therefore successive occurrences following immediately the end of a prior occurrence should not influence the accuracy of the results.

Figure 1. The first 20 out of 1,000 positions for $n = 3$, $t = 4$, $T = 10$

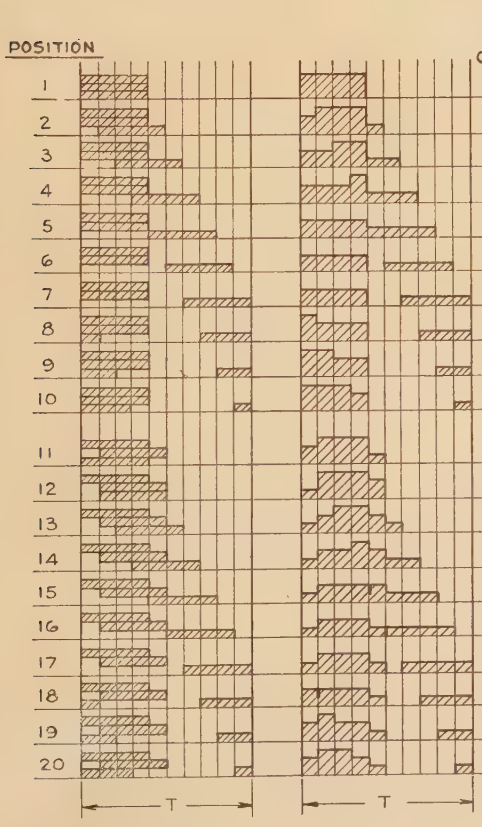

POSITION	LENGTH IN UNITS: NO OCCURRENCE	SINGLE OCCURRENCE	DOUBLE OCCURRENCE	TRIPLE OCCURRENCE
1	6	0	0	4
2	5	1	1	3
3	4	2	2	2
4	3	3	3	1
5	2	4	4	0
6	1+1	4	4	0
7	2	4	4	0
8	3	3	3	1
9	4	2	2	2
10	5	1	1	3
11	5	1	1	3
12	5	1	1	3
13	4	1+1	1+1	2
14	3	2+1	2+1	1
15	2	3+1	3+1	0
16	1	1+1+4	3	0
17	1	1+1+4	3	0
18	2	1+3	3+1	0
19	3	2+1	2+1	1
20	4	1+1	1+1	2

4,370,000-Kva Short-Circuit Tests on Grand Coulee 230-Kv Bus

Discussion and authors' closure of paper 46-177 by W. H. Clagett and W. M. Leeds, presented at the AIEE Pacific Coast meeting, Seattle, Wash., August 27–30, 1946, and published in AIEE TRANSACTIONS, 1946, November section, pages 729–34.

T. M. Blakeslee (Water and Power Department, City of Los Angeles, Los Angeles, Calif.): The scheme used to obtain maximum short-circuit current by arranging the test breaker contacts to part within the first half cycle of fault current is a clever method of squeezing out maximum kilovolt-ampere capacity from the available test setup. It is understood that this idea has been used for many years in the Westinghouse high-current laboratory. Nevertheless, if the scheme were known more generally, it would promote a more extensive use of power systems for circuit-breaker testing.

Operating engineers have been somewhat adverse to the use of the power system as a laboratory for short-circuit tests. This aversion is probably justified, because it arises from the idea that there are enough voltage dips in the normal course of events without worrying about deliberately imposed short circuits.

With this anticipated-tripping scheme, breaker tests will produce voltage dips of such short duration that they will not be noticed by the customer. Experience with the 287-kv Boulder circuits, which clear faults within three to four cycles, indicates that these short-duration faults are not

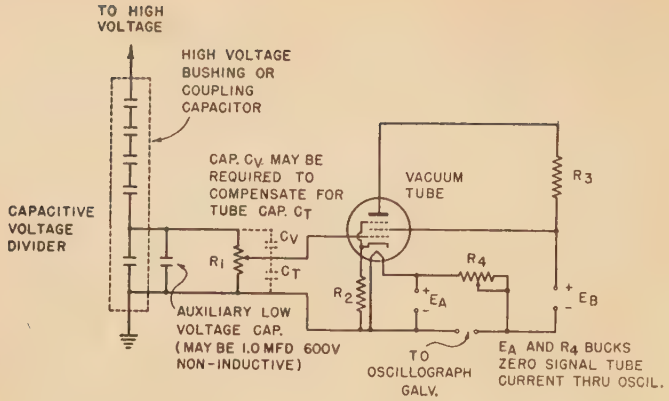

Figure 1. Bonneville Power Administration oscillograph amplifier basic circuit

noticed. Now, the test engineer using this scheme of Clagett and Leeds can guarantee to the operating force that the deliberately imposed short circuit for circuit-breaker testing will not disturb the customers. This guarantee must be predicated, of course, on the assumption that the breaker test will be successful. The industry should benefit from any scheme that will promote greater use of power systems as laboratories for circuit-breaker testing.

Figure 9 of the paper shows the interruption of 138-ampere charging current at 230-kv. This oscillogram shows the charging current passing continuously through two current zeros following contact parting before interruption takes place at third current zero. Normally breakers interrupt capacitive currents at the first current zero following contact parting, but all breakers, of course, do not maintain this current cut-off without subsequently restriking This interruption at the first current zero is attributable to the fact that no voltage exists across the breaker contacts at this time as a result of the ability of the capacitor (line or cable) to remain charged at system crest voltage. This interruption at first current zero, even though it may be only momentary, has occurred always in the department's experience with high-voltage charging-current interruption. What is the explanation for the performance exhibited by Figure 9?

Harold L. Levinton (Bonneville Power Administration, Portland, Oreg.): In describing tests of the interruption of short-circuit currents having a magnitude above the present highest rating of 230-kv oil circuit breakers, the authors cover a subject which will be of greater concern as operating companies continue to grow. I concur with the authors regarding the general practicability of constructing 230-kv oil circuit breakers rated above 3,500,000 kva. Also, I believe that in developing breakers suitable for higher ratings, interrupter and operating mechanism improvements will result in even better and more reliable breakers. Operating companies are to be commended for the encouragement they provide designers and manufacturers in co-operative testing which has resulted in more reliableand often in faster breakers than the latest present-day relay systems which often require a longer period to operate than the breakers which they control.

There are two points of general interest which I wish to discuss.

1. The definition of "interrupting time" provided in present standards is not sufficiently complete to cover some types of breakers now manufactured. For example, the 1945 American Standard *C*37.4, paragraph 4-5.7.4 on "interrupting time" states

A. "The interrupting time of a circuit breaker is the interval existing between the energizing of the trip coil at rated voltage and the interruption of the circuit." A further explanatory note contains the following:

B. "This (interrupting time) is the summation of the opening time and the arcing time."

The "opening time" is defined by the American Standards Association as the interval between the energization of the trip coil and the parting of the arcing contacts, and the "arcing time" as the interval between the parting of the arcing contacts and the extinction of the arc.

The two quotations given above are contradictory where resistors are introduced into the current-carrying circuit during the interruption, in that the extinction of the arc between the arcing contacts (see quote *B*) does not result in interruption of the circuit (see quote *A*); the circuit is not interrupted until the resistor current is broken. My question then is, "Is the interrupting time of a breaker the interval between the energizing of the trip coil and the interruption of the arc in the arcing contacts, or does it extend to the complete interruption of the circuit including any period of resistor current?"

2. From observation of many tests on the Bonneville Power Administration system, I believe that the question of the interruption of line-charging or capacitive current by circuit breakers is about as important as the interruption of high values of fault current because of the possible damage to the breaker (which has been observed more than once) and to connected system equipment, damage that can occur as a result of voltage stresses which can be present as a result of restriking during the interruption of line-charging current. In my opinion, any high-voltage breaker test should include a large number of tests covering the interruption of line-charging current for both short and long lines in order to establish definitely the performance of the test breaker in this important service. Furthermore, I believe that the standards should contain data regarding this important service and that breaker-rating classifications should contain definite minimum requirements with regard to line-charging current interruption.

For use in oil circuit breaker tests and in other tests where appropriate, the Bonneville Power Administration developed a small, inexpensive electronic amplifier device which in connection with the capacitor voltage divider tap of bushings can give an accurate replica of the high voltage on the bushing over a range of frequencies from direct current to 100 kc or more. As normally used, without frequency-correcting capacitors the amplifier is linear from direct currents to well beyond the 10,000-cycle range of high-frequency electromagnetic oscillographs. One of these amplifiers was used in the subject tests to give an oscillographic record of the voltage across the breaker contacts during the interruption of line-charging current. Other uses have included oscillographic recording of the trapped voltage on a transmission line during line-charging current interruption, accurate representation of line and bus voltages during fault conditions, and transient voltages present in static capacitor installations. The device which is made of inexpensive radio components is a simple direct-coupled amplifier. Its basic circuit is shown in Figure 1 of this discussion. Tests have shown it to be considerably superior to capacitor potential devices and to have applications where potential transformers are not suitable. Its cost is less than that of a capacitor potential device. When appropriately used with a suitable electromagnetic oscillograph, it is believed to give results which from a practical standpoint, except for impulse testing, approach those of cathode ray equipment for power system testing.

Philip Sporn and **H. P. St. Clair** (American Gas and Electric Service Corporation, New York, N. Y.): The authors of this paper and the organizations they represent are to be commended for carrying out a courageous job of circuit-breaker testing and thereby making a definite contribution to the circuit-breaker art. The interruption of 10,500 amperes at 230 kv, representing a new high in kilovolt-amperes, seems to offer no difficulty with a modern highly efficient interrupting device. Since substantially higher currents, over 14,000 amperes, have been cleared successfully at 138 kv, and since modern high-voltage interrupters are acknowledged to be essentially current-interrupting devices, there does not appear to be any reason why ratings even higher than 5,000,000 kva at 230 kv cannot be realized. It will be recalled that the need for developing 5,000,000 kva 3-cycle breakers was suggested in a paper,[1] as well as in the closing discussion pertaining to this paper, presented before the Institute on January 1945. In subsequent papers Leeds also indicated his confidence in the feasibility of developing breakers not only for 5,000,000 kva but for possibly as high as $7\frac{1}{2}$-million kva as well.

The situation at Grand Coulee, which necessitated extensive bus sectionalizing to limit the concentration of short-circuit capacity on any one bus section as dictated by limitations of circuit-breaker interrupting capacity, is one that we may be facing increasingly in the future with the inevitable growth of power systems. We agree fully with the authors of this paper that important advantages in operating flexibility will be obtained by having available circuit breakers of sufficient interrupting capacity to avoid the necessity of using more or less complicated bus-sectionalizing schemes. As we have pointed out in other discussions, already we have had occasion to feel the lack of operating flexibility in the sectionalizing scheme we were forced to employ at our Philo plant in order to keep interrupting duties within the maximum of 2,500,000 kva, which at that time was the largest capacity available at 138 kv. We should like to emphasize again that in order to meet future requirements it is none too soon to consider the development of 5,000,000-kva breakers at this lower voltage.

In carrying out these tests at Grand Coulee, the authors have made an interesting deviation from the procedure we have followed in making full-scale circuit-breaker tests in the field. The individual testing of each pole of the breaker by line-to-

ground tests undoubtedly insures a greater likelihood within a given number of shots of giving each pole a test somewhere near maximum severity. At the same time, this method may have the advantage that the shock or disturbance from a system standpoint is somewhat less than that involved in 3-phase tests. On the other hand, we have felt that the carrying out of a larger number of full 3-phase tests, with the likelihood that in one or more of these tests each of the three poles would be stressed close to maximum severity, would provide the best over-all series of tests for the breaker. If the total number of tests is to be limited, as appears to have been the case at Grand Coulee, the method adopted of testing each pole individually may be the best procedure.

We have observed also that the tests were confined to the standard duty cycle with a 15-second interval between shots. Without attempting in any way to depreciate the value of these tests it appears to us, in the light of the increasing use and importance of ultra high-speed reclosing, that an even greater contribution to the circuit-breaker art would have been made had it been possible to arrange for rapid reclosing tests at these high short-circuit values. Beginning with the first major field test which we carried out in 1925, we invariably have included at least a series of shots as closely spaced as our control arrangements would permit. While true ultra high-speed intervals were achieved only in later tests, these intervals were always much smaller than 15 seconds. It is our hope, therefore, that if another series of tests of this nature is carried out, it will include either a number of shots typical of the full ultra high-speed reclosing duty cycle or at least a series of tests at much closer intervals than 15 seconds.

REFERENCE

1. FIELD TESTS AND PERFORMANCE OF HEAVY-DUTY HIGH-SPEED 138-KV CIRCUIT BREAKERS—OIL AND AIR-BLAST, Philip Sporn, Harry P. St. Clair. AIEE TRANSACTIONS, volume 64, 1945, pages 401–10.

W. H. Clagett and **W. M. Leeds:** Blakeslee refers to Figure 9 of the paper showing the interruption of line-charging current and asks for an explanation of the absence of any attempt to interrupt at the first current zero after contact parting. This is accounted for by the purposely delayed pumping action of the oil flow piston in the interrupter, which begins to function only after the contacts have separated approximately one inch. Because only two interrupting units are used per pole, the voltage gradients across the contact gaps are correspondingly higher than for multi-break designs, so that even a small voltage is sufficient for arc reignition before the oil flow is started. Another factor involved is the small high frequency transient appearing across the breaker contacts at current zero attributable to the shift in bus potential by the amount of the voltage rise through the series inductive reactance of the generators and transformers. In the case in question, this rise measures about 10 per cent of the generated voltage, and, assuming 100 per cent overswing in a 1,000-cycle frequency oscillation, a build-up of 40 kv crest in 500 microseconds would be possible. This could cause an arc reignition within an interval too small to observe on the magnetic oscillogram.

Levinton asks whether the definition of "interrupting time" of a circuit breaker should include specifically the time to interrupt the current through special resistors inserted momentarily in the circuit by the sequence of contact opening. Where the residual resistor current is comparable in magnitude to load or line-charging currents, it would seem logical to include the disconnection of the resistors in the interrupting time. In any case, we agree that it is a matter which should receive attention by the Standards committee for clarification.

As Levinton suggests, it is very desirable to include in any program of field testing of high-voltage circuit breakers a considerable number of line-dropping tests, interrupting the charging current to both short and long lines. The Bureau of Reclamation is well aware of the importance of such testing and has made many series of line-dropping tests on the breakers in the Coulee Dam switchyard. In the absence of a cathode ray oscillograph, the accurate measurement of line and bus transient voltages has been greatly facilitated by the use of the amplifier developed by the Bonneville Power Administration and described in Levinton's discussion.

Sporn and St. Clair seem to favor 3-phase testing over separate tests on individual poles as providing the best over-all check on breaker performance. Where the maximum fault power desired is obtainable as a 3-phase short circuit, this is certainly the case. However, it should be pointed out that the principal reason for including single phase tests at Grand Coulee, in addition to full power 3-phase tests, was the 30 per cent increase in current obtainable on single line-to-ground short circuits as compared with 3-phase faults.

The recommendation that high-speed reclosing duty cycles be included in future high-power field tests of this nature is in line with the trend in high-voltage system operation. While the operating mechanisms on the line breakers in the Coulee Dam switchyard are not designed for high speed reclosing, consideration has been given to revamping them for such duty. In view of current discussions concerning the appropriateness of present de-rating factors for circuit breakers operating on high-speed reclosing duty cycles, the inclusion of such tests wherever possible in field testing programs should be of real value to both operating engineers and circuit breaker designers.

Simplicity in Protective Relaying

Discussion and author's closure of paper 46-173 by Lloyd F. Hunt, presented at the AIEE summer convention, Detroit, Mich., June 24–28, 1946, and published in AIEE TRANSACTIONS, 1946, pages 995–1000.

E. E. George (Ebasco Services Incorporated, New York, N. Y.): This most interesting and valuable paper by L. F. Hunt should be required reading for all relay engineers and all planning engineers.

Without derating the qualifications of Hunt or his associates, it may be suggested that a large part of their success in protection is due as much to their influence on system planning as to the simplicity of their relay schemes.

With due modesty, the discusser may recall his often repeated statement that it is easy to design power systems that cannot be relayed by experts.

Heretofore, relay engineers generally have had too little interest and influence in planning bus layouts and allocating circuit breakers. Hunt's statement that relay engineers should prevent as well as minimize system faults is unanswerable. And what method of prevention is more effective than proper planning of bus and switching facilities? Complicated, expensive, and unreliable relaying is unavoidable if the system plan includes such things as

1. Three-terminal lines.
2. Bus tie or transfer circuit breakers.
3. Transfer or by-pass disconnecting switches.
4. Insufficient line circuit breakers.
5. Slow-operating circuit breakers.

Experience on other transmission systems confirms Hunt's comments on the advantages of

1. Sensitive ground protection.
2. Reduction of backup protection.

Figure 1 of the paper shows several interesting features.

1. The use of ring busses on the newer stations (see also Figures 5 and 6).

2. The use of loop transmission with line circuit breakers at junctions.

3. The use of circuit breakers on lines rather than on equipment.

The suggested use of over-all generator and transformer protection may be questioned by some engineers if it leads to the omission of the generator circuit breaker. The time constant of large generators is sufficient to do considerable damage in case of transformer trouble.

The suggested bell alarm scheme is better than the use of a series bell relay, but not as good as a combination of both—particularly in older stations, where trip coils, batteries, and circuit-breaker mechanisms are none too reliable.

Without forgetting that some of the newer and more complicated relays are essential for certain popular layouts on many systems, it would appear that the Southern California Edison Company is planned and relayed by engineers who know system maintenance and system operation.

W. R. Brownlee (The Commonwealth and Southern Corporation, Jackson, Mich.): The author has presented an interesting review of the relaying systems which have been developed for application to the conditions encountered by his company. It is agreed generally that simplicity in itself is highly desirable, but the so-called simpler devices are capable of performing only relatively simple functions under ideal conditions. For example, the author has avoided the use of distance relays, the inference being that there are no intermediate steps between a plain overcurrent relay and carrier current relay protection. It seems that much better over-all simplicity could be secured by using distance relays, which may be more complicated in theory but not in

actual operation, rather than to face the necessity of having station operators transfer the protection of transmission lines from one set of relays to another (as described by the author) whenever system generating conditions change.

Reference is made to sensitive ground protection of distribution circuits. While adequate methods for sensitive protection of 3-wire systems, or 4-wire systems with the neutral grounded at one point only, have been available for many years, the sensitive protection of the almost universal 4-wire multigrounded distribution system is still a most difficult problem, and it is believed that the author's scheme does not apply to these more common systems.

Reference is made to a distribution protection sensitivity of 1-ampere primary with a statement that one of the requirements for this type of protection is for the condition where higher voltage distribution circuits are used jointly with communication circuits. Such an inference is most unfortunate because representatives of the power industry and the telephone industry have agreed that positive protection which will operate on a current of 50 amperes or less at a time of not longer than five seconds is entirely adequate for the higher voltage joint use installations.

A performance record of 99 per cent is mentioned. Is this based on the principles outlined in the report "Uniform Records of Electrical Operation of Power System?"[1] This method of judging performance considers the over-all system and not just the relay. For example, if a relay of the overcurrent type operated precisely on its characteristic to trip a circuit breaker unnecessarily merely because the generating conditions in effect were not those considered when setting the relay, this report would consider the operation incorrect on a system basis.

One of the objections cited by the author to distance relays, or even directional relays, is the uncertain performance of older types of directional elements at low voltage. As early as 1930, directional distance relays were available which would operate positively with all three conductors of a high voltage line tangled together within the first span from the station. The case of a 3-pole gang-operated grounding switch causing practically zero voltage at a station readily has been taken care of elsewhere by providing an auxiliary switch on such a line grounding device to trip the associated circuit breaker without the necessity of any relay action.

Naturally, different fundamental conditions may result in differences in relaying methods. For example, the isokeraunic level of the Southern California Edison system is indicated as between 5 and 10, whereas corresponding values for the midwestern area are from 35 to 55. This and other factors may account for the following items in which our practice differs from the author's:

1. Phase faults must have positive protection.

2. The economical operation of plants, especially where steam power is a heavy proportion of the total, requires that relaying systems be able to meet constantly changing conditions.

3. A radial or simple loop system is relatively easy to relay but may be very costly in the major equipment required to serve a given load.

4. Many applications are found where distance relays are the proper solution, these usually being of the restricted circle variety.

5. The large increase in cost to provide carrier current relaying usually is not justifiable merely to provide simultaneous clearing of both ends of lines which are too long for pilot wire protection, but are justifiable to insure maximum load carrying and swing current ability.

6. Stability studies including a-c calculating board readings of relaying quantities are highly desirable to insure that the relaying system does not become the limiting factor in transmission system emergency capability.

Finally, it is believed that the pendulum has swung somewhat away from having all system planning depend quite so heavily on relaying principles. Many years ago system planning in general paid little attention to relaying or even to emergency operating methods, and experience demonstrated that these must be planned together. Based on progress in the relaying art at that time, rather severe limitations sometimes were imposed on system planning by relaying considerations, and this resulted in uneconomical major expenditures in certain cases. With improvements in relays and methods, and with reasonable co-ordination in planning, it is possible to plan economical power systems in which the relay system will not cause any substantial limitation in emergency system capability.

REFERENCE

1. UNIFORM RECORDS OF ELECTRICAL OPERATION OF POWER SYSTEMS, National Electric Light Association publication 289-52.

Ben C. Hicks (Shawinigan Water and Power Company, Montreal, Quebec, Canada): Agreement no doubt will be quite general regarding the importance, within reason, of simplicity in protective relaying, but a question arises as to what constitutes simplicity and how it best may be attained. In striving for simplicity, sight should not be lost of the fact that the fundamental aim is to secure the most effective over-all protection possible within economic limits. It is doubtful if this end can be achieved by selecting and codifying a few principles of protection, enforcing adherence to these principles alone and disregarding all others. On the contrary, it is probable that the many and often complex problems of system protection can be solved most successfully if approached with an open and untrammelled mind, aware of all the ramifications of the problems that may arise and equally aware of and free to use any of the multitudinous resources that may be available to aid in their solution.

L. F. Hunt's outline of practice on the Southern California Edison Company system presents both similarities and contrasts to practice on the system of the Shawinigan Water and Power Company. Among the similarities may be noted:

1. It is considered to be of vital importance that the control of all system protection be centralized under one authority.

2. It is considered to be impracticable to protect the system completely against all conceivable hazards, and hazards that are likely to have only a minor effect on the security of the system at large often are accepted.

3. Considerable attention is given to the attainment of uniformity in the design and handling of details of protection. An effort also is made however to prevent any attempt at the achievement of uniformity from interfering with effectiveness.

The contrasts are more numerous and include among others, the following:

1. Engineers of the Shawinigan Water and Power Company do not consider it essential that all trip circuits should be locked in.

2. The use of hand reset trip relays is avoided entirely.

3. Little or no justification is found for providing an alarm, actuated by an auxiliary switch, to indicate the opening of circuit breakers.

4. An effort is made to avoid the use of a multiplicity of alarms, which would tend to be confusing to the operators. As far as possible, a common alarm bell is used, often supplemented by some form of annunciator scheme.

5. Considerable importance is attached to the provision of backup protection.

6. Distance relays are used extensively for line and stand-by protections. Current relays alone are not considered adequate for the protection of any important transmission line, except in the case of a few short tie lines which are provided with pilot wires and a differential current protection.

7. Either or both differential and split phase protections are used on synchronous machines.

8. An effort is made to approach simultaneous tripping of both line ends, and tripping in sequence is avoided whenever possible.

Hunt states that approximately 99 percent perfect relay operation has been obtained over a long period of time. This is a most enviable record. It would be interesting to know the basis of reckoning used in arriving at this figure.

L. F. Hunt: It is gratifying to have such liberal discussion on this paper. E. E. George has read between the lines and understands the intent of this paper and fully appreciates the difficult problems involved.

There is not nearly the discrepancies between the relay protection systems of the Southern California Edison Company and others as brought out by W. R. Brownlee and Ben C. Hicks. If all the references were read a similarity would be appreciated more. As brought out in the paper, the prime purpose of protective relays is to trip circuit breakers to isolate faults. The alarm circuits are not as important. It is agreed that multiplicity of bell alarms is not good; it has been standard setup for 20 years on the Edison system to use only one audible alarm with annunciators for individual indication. The use of hand reset relays individually is not tolerated. As brought out in the paper, only one reset is used for all differential tripping relays in one station. This form is more reliable than the the complication of automatically resetting these relays.

Carrier relaying started on the Edison system in 1926, which is about six to eight years before other applications were used. During this time a carrier system which is very simple was developed by the engineers of the Edison Company. Brownlee is quite correct, relative to the choice of relay systems having no immediate step between plain or balanced current protection and carrier current relay protection. The carrier current relay system developed by the Edison Company has practically the same cost as the so-called distance relay system. The cost of the coupling capacitor can be charged justly to line potential and synchronizing. Therefore it is agreed with Brownlee that carrier current protection is better than the distance relays systems.

The percentage indicated is a very simple result of arithmetic. If all faults are cleared perfectly without any extra switches trip-

ping, the result would be 100 per cent. The longest time at this value was eight consecutive months of operation. However, if 100 faults occur and on one fault the isolation was correct, but an extra switch opened even though no extra load was dropped, the record would be 99 per cent correct. In other words the percentage equals the number of correct fault isolations divided by the number of faults.

As Brownlee states the case, "but the so-called simpler devices are capable of performing only relatively simple functions under ideal conditions," may be true, but with no major system outage in ten years and a record of 99 per cent correct isolation by simple relays seems answer enough.

Transmission Rating of Telephone Systems

Discussion and author's closure of paper 46-163 by W. A. Codd, presented at the AIEE summer convention, Detroit, Mich., June 24–28, 1946, and published in AIEE TRANSACTIONS, 1946, October section, pages 694–8.

Arthur Bessey Smith (Automatic Electric Laboratories, Inc., Chicago, Ill.): In general there are two plans for testing the transmission of a telephone system.

1. Compare an unknown with something similar which is for the time regarded as the standard, at least for the purpose of measurement. The unknown may be judged to be better or worse than the standard of reference.

2. Test the performance of an unknown system without comparing it to anything else and rate it by an independent number or per cent.

The first voice and ear tests followed the first method. The repetition rate, immediate appreciation, and syllabic tests follow the second method as well as some of the machine tests.

In common with others we formerly used only voice and ear tests both for research and development and for factory inspection. But even in those days, mere loudness was never satisfactory to me. For that reason I worked out, adopted, and applied for many years the use of three carefully selected words: three, six, and eight. They were selected because they contain a large number of frequencies which are essential to clear articulation and understanding. These three words are of about equal loudness, a factor of great importance to the listener. They were pronounced carefully and with the same loudness, first on circuit *A* then on circuit *B*. The listener was asked to listen with this aspect in mind: "If I had to receive an important message and get it correctly at once, which circuit would I prefer?" He was directed not to choose the circuit which was the more pleasing to him. The choice of which circuit delivered the message more certainly was made entirely on a utilitarian basis.

Moreover, the voice of the speaker in the tests had to be of the ordinary volume which would be used by the public as far as we at that time could determine it.

For a long time this method gave excellent results, which agreed well with the performance of systems in public use.

Though it was a comparison method, it is evident that it duplicated some of the features of the immediate appreciation test described by Hughes (reference 1 of the paper).

For the many who cannot afford the very expensive and time-consuming repetition-rate method, the immediate appreciation method deserves careful study.

W. A. Codd: Doctor Smith has pointed out that the articulation, repetition rate, and immediate appreciation tests give figures of merit which express performance in absolute terms as a rate or percentage for a given set of conditions and therefore is not inherently dependent upon comparison to a standard or reference system. This has some value in that it gives an indication of the degree of approach to perfection in terms of the criterion adopted. It should be noted, however, that in the application of the results of the repetition rate tests and also of the immediate appreciation technique, as proposed in the present paper, a comparison method is used. This is evident from the fact that interpretations of the test data to obtain effective ratings are made in terms of the decibels attenuation of distortionless trunk, which when added to or taken from a given system will make its performance in terms of the given criterion equal to that of a reference system. The significant difference between these tests and the older comparison type tests, such as the voice-ear volume tests, is in the test criterion adopted, namely, some measure of intelligibility instead of volume or loudness.

Dangerous Electric Currents

Discussion and author's closure of paper 46-112 by Charles F. Dalziel, presented at the AIEE summer convention, Detroit, Mich., June 24–28, 1946, and published in AIEE TRANSACTIONS, 1946, August–September section, pages 579–85.

J. J. Smith (General Electric Company, Schenectady, N. Y.): We are indebted to Professor Dalziel for his contribution in this paper to further knowledge of what constitutes dangerous electric currents. A better picture of this question is being obtained gradually from such studies. Some points still are missing in the spectrum of the effects of the electric currents. As I see it, there are several thresholds in which we are interested.

The first is the threshold of feeling. This is of interest because it is essential that the person using an electric appliance must not get the sensation of a shock. Experimental work has shown that if the current is limited to 0.3 milliampere the danger of such a sensation of shock is small. This limiting value of 0.3 milliampere has been adopted by a joint committee of Edison Electrical Institute, National Electrical Manufacturers Association, and Radio Manufacturers Association and is covered in NEMA publication 105.

The next threshold is the "let-go" threshold. This is of interest because below this level the person experiencing the shock is able to let go freely, although he may experience a very distinct sensation of shock. Thus, if the current did not exceed this value, a person might feel more free in handling it, than is the case in which there is a possibility of higher currents. This threshold has been given by Professor Dalziel as approximately nine milliamperes in men and seven milliamperes in women.

The next threshold in which we are interested is not quite so clear. This is a result of the lack of good data in the region between 10 milliamperes and 100 milliamperes. In his tests, Professor Dalziel subjected some subjects to shocks up to 25 milliamperes with no ill effects when they were released from the current, which was on only a short time. I have heard of cases where people were subjected to 50 milliamperes with no lasting effects. It would be desirable to have definite data to show whether shock in any part of the region between 10 milliamperes and 100 milliamperes is liable to cause cessation of breathing so that artificial respiration must be applied. Some of those with whom I have discussed this question were of the opinion that such currents applied momentarily could stop respiration, others felt it could not. Whether this does or does not occur in this region is of importance in connection with men who normally work on electric circuits under suitable precautions but because of the nature of their work, they are liable to come in contact with these circuits once in a while. They normally would have another man working with them who can remove the power quickly should they be unable to let go.

The next threshold is that of ventricular fibrillation which has been estimated by Ferris and Williams at about 100 milliamperes. In the present paper Professor Dalziel extends our knowledge of this to include the effect of the duration of the shock. I understand that ventricular fibrillation does not occur often when the current through the body is greater than about one ampere but would like Professor Dalziel's comment on this point.

The next threshold is that for which fibrillation does not occur but where the current is large enough to render the victim unconscious, so that artificial respiration must be applied. I wonder if Professor Dalziel has any figures he could suggest on this subject.

The next is the threshold for burning. It would seem desirable to have an estimate of the amount of current which when passed through the body for even a short time might be expected to cause burns.

Because the use of 60 cycles is so common, it would be well to have all these thresholds first established for this frequency. At a later date similar thresholds might be given for direct current and various other frequencies.

With the development of radar during the war, it would be desirable to have similar thresholds in connection with such pulsed currents.

L. P. Ferris (New York, N. Y.): Professor Dalziel's paper is based practically wholly on the data presented in the 1936 paper by Williams, King, Spence, and myself (reference 4 of the paper). No new experimental data are presented on this subject, Professor Dalziel confining himself to a reanalysis of our data and the presentation of the results in the form of mathematical equations. No single

conclusion of the 1936 basic paper is invalidated or altered by Professor Dalziel's reanalysis. Despite this gratifying fact, I must take exception to some applications of Professor Dalziel's methods to our data. It undoubtedly would be convenient if the results could be expressed in simple mathematical form. Professor Dalziel has done this, but I question his justification, particularly when applying it to the data on effect of shock duration on threshold current, Figure 14 of the 1936 paper. The authors of the earlier paper were hopeful of discovering some simple correlation between minimum fibriliating current and shock duration. We could not, however, draw a straight line on log-log paper which we thought would correctly represent the experimental data presented by our Figure 14. However, Professor Dalziel seems to have done this in his Figure 6. He throws out in his analysis the experimental data which we designated as mode *A*. I cannot take much exception to this because inspection of our Figure 14 shows that we gave but little weight to the mode *A* data in drawing our curve. Professor Dalziel also chooses to omit certain other experimental points, namely our 0.47-second shock tests on sheep. Whether or not this is justified, we should have further experimental evidence before the effect of duration is represented as a simple exponential function.

It should be remembered that in changing the duration of shock from several seconds to a fraction of a second, entirely different conditions are encountered. The several-second shocks blanket one or more complete heart cycles, whereas shocks of a small fraction of a second duration are only effective in causing fibrillation when they occur during the partial refractory phase of the heart cycle, which is about 20 per cent of the whole. In passing from one of these conditions to the other, it should not be surprising if the curve of fibrillating current versus shock duration changes slope.

It is to be hoped that Professor Dalziel and other investigators may be able to carry further the experimental investigation of electric shock. Further data on the effect of wave form and frequency of shock current, as well as shock duration, would be desirable. Also desirable would be a study of resuscitation in cases of known ventricular fibrillation with and without electric counter-shocks. Progress with measuring instruments and in the electronic art in the last ten years should make it possible to control and measure shocks with greater precision than was possible before 1936.

Charles F. Dalziel: J. J. Smith's definitions and discussion of the significance of the various current thresholds are exceedingly valuable. His discussions are stimulating because the answers to many of his questions are unknown. With the exception of one paper (reference 4 of this paper) very little data are available for currents in excess of about 25 milliamperes.

In 1936 letters were sent to several neon sign manufacturers in the attempt to determine the hazard from 30-milliampere high reactance 5- to 15-kv sign transformers. No fatal accidents were reported. L. T. Jones, a manufacturer, reported as follows:

> From personal experience in the industry I believe it is safe to assume that in each plant, each day, some one or more persons receives a shock from a 30-milliampere transformer. Insofar as I have been able to determine, not one person has been injured . . and I have been able to find no record of a fatality.

In preparation of this closure I communicated with major sign manufacturers and others in the San Francisco area who are cognizant of accidents in this field. Although accidents involving burns were mentioned, no one could recall a single fatality on 30-milliampere equipment.

Observations during the let-go experiments indicated that currents in excess of about 20 milliamperes from hand to hand were very painful and the accompanying muscular contractions made breathing difficult if not impossible during the shock; however respiration resumed automatically upon interruption of the current.

Determination of the threshold currents required to produce respiratory inhibition or unconsciousness would be a difficult but valuable undertaking. The threshold current producing burns is probably very low, as feeble sparks, if continued for more than a few moments, cause burns. Dr. W. B. Buchanan, Hydroelectric Power Commission of Ontario, reports that under suitable conditions 0.35 milliampere will cause some carbonization of wooden insulator pins, but with 0.7 milliampere the action was much more definite. Reference 4 and Figure 16 of the paper and the accompanying discussion is offered in reply to the question regarding the decrease in likelihood of inducing ventricular fibrillation at currents considerably in excess of the threshold.

Perhaps the best reply to L. P. Ferris is to state that in the beginning of many engineering analyses approximations often are tolerated pending completion of conclusive research. Certainly conclusions based on limited data are open to question, and especially where human life may be at stake. Future investigations may indicate that fibrillating currents cannot be expressed accurately by simple mathematical relations or as straight lines. In the meantime, a tentative answer may be better than no answer, especially if it is based on a conservative analysis of all available experimental data. Attention was called to the uncertainties of the analysis in the paper, and I should like to repeat that application to man is entirely conjectural. However, only one out of the 99 experimental points in Figure 6 of this paper falls below the one-half per cent line for the 57.4-kilogram sheep. With this single exception the proposed fibrillating current thresholds, as indicated by the one-half per cent lines of Figures 5 and 6 of the paper, include a reasonable factor of safety. It would be a simple matter to draw other lines having a greater factor of safety, if other investigators thought this advisable.

The same data were used in the preparation of Figure 14 by Ferris, King, Spence, and Williams, as in Figure 6 by the author. The dissimilarity of the figures is because of the method of plotting the data, and although log-log scales were used in both, the presentations are sufficiently different to preclude direct comparison. In Figure 14 the minimum current causing fibrillation was plotted versus the ratio of the duration of the shock to the length of the heart beat. Throughout my paper I took the fibrillating current equal to 1/2 (minimum current causing fibrillation plus the maximum current not causing fibrillation). In Figure 6 fibrillating currents were plotted versus shock duration in seconds. Hence the differences in appearance of the two figures and resulting curves do not represent as wide a divergence of opinion as might be concluded from casual inspection.

Although the original data designated as mode *A* and the 0.47-second shock tests on sheep were not used in either the statistical analysis or in determining the deviation curve of Figure 3, for the reasons discussed in the paper, these data were included in Figure 6. Without exception all the data furnished the author by L. P. Ferris and associates were included in Figures 5 and 6. All data were considered when deciding just where to draw the best line to represent the general trend of the responses.

It might be well to mention that the purpose of evaluating fibrillating current thresholds is to establish (if even only approximate) the most dangerous current threshold to permit a more accurate analysis of accidents, and to add to the general fund of knowledge on electric shock. Considering the various factors and their uncertainties, the author still believes that the proposed analysis may be used without excessive error to estimate the probable fibrillating hazards for large groups. The analysis should not be used to calculate an individual's chance of survival or to excuse a careless workman. Because of the limited information on fibrillating currents, and the lack of any data on the currents causing respiratory inhibition and unconsciousness, no human should be exposed purposely to electric currents approaching fibrillating thresholds.

The author appreciates the many suggestions and comments given this research, and would welcome receipt of factual information regarding serious accidents. This invitation is made with the hope that eventually sufficient quantitative data may be assembled to permit arriving at more accurate answers to some of these questions.

Carrier Supervisory Control of Pumping Station Over Power Cable

Discussion and author's closure of paper 46-174 by W. A. Derr, W. A. Keller, and H. A. Hedke, presented at the AIEE summer convention, Detroit, Mich., June 24–28, 1946, and published in AIEE TRANSACTIONS, 1946, November section, pages 699–705.

Abe Tilles (Pacific Gas and Electric Company, San Francisco, Cal.): The establishment of a satisfactory carrier channel over power cable, as here reported, is a development of great interest. It arouses further concern because some earlier attempts in this direction gave very unfortunate results.

In making use of a line-to-ground channel the path provided by the power conductor is excellent. The return path, except where there is an uninterrupted lead sheath, is quite a different matter. For a conductor not enclosed in steel pipe or fer-

rous armor, general ground paths are likely to be available. This is particularly true for underwater cable.

For cable without continuous lead sheath and enclosed in ferrous armour or pipe, the return path is comprised of several parallel paths none of which are favorable. These include

1. The high reactance paths outside of the iron.
2. A thin path on the inner surface of the iron.
3. A thin path spiraling around the cable along any shielding tapes.
4. A path lengthwise down the cable along shielding tapes which overlap or spiral in contrary directions and contact in a basket weave effect.

If a path of type 4 of relatively low impedance is presented, the 60-cycle losses may be increased to an undesirable degree.

In view of the pioneer nature of this installation it would be very useful if the authors, or the cable suppliers, in discussion could add to this paper by giving in detail the physical characteristics of the cable. What kind and thickness of lead sheath, shielding tape, and so forth, are each of the two pieces? What are the test or calculated data showing where the return current of the carrier channel goes? How were the losses calculated in design?

W. A. Derr: The construction of the two sections of cables used on this installation is as follows:

1. *Armored submarine cable* (22,800 feet in length), three conductor, American wire gauge 4, 19 strands of 0.0469-inch copper, $^{12}/_{64}$ inch Buna *S* insulation. Each conductor taped with a rubber-filled cloth cable tape, conductors cabled with jute fillers, double wrap of cable tape, layer of saturated jute. Birmingham wire gauge 8 galvanized-steel wire armor

2. *Jacketed cable* (12,200 feet in length), three conductor, American wire gauge 4, 19 strands of 0.0469-inch copper, $^{12}/_{64}$ inch wall of Buna *S* insulation. Each conductor taped with cable tape, cabled with jute fillers, layer of cable tape, $^{8}/_{64}$-inch rubber sheath over-all.

The construction of both cables was determined mainly for 60-cycle power operation. Prior to manufacture of the cable, the phase-to-phase attenuation at carrier frequencies was calculated from the following formula:

$$\text{Decibel loss per loop mile} \approx 4.34 \sqrt{C} \times \sqrt{\frac{R^2}{L}\left(1+\frac{\overline{PF}^2}{2}\right)+\omega^2 L \overline{PF}^2+2\omega R\overline{PF}}$$

where

C = mutual capacity in farads per mile
R = resistance in ohms per loop mile
L = inductance in henries per loop mile
PF = power factor
$\omega = 2\pi$ times frequency in cycles

Table I. Cable Constants Used in Calculating Cable Losses

	60 Kc	100 Kc	150 Kc
Resistance (ohms/loop mile)	11.6	15.7	17.9
Inductance (henries/loop mile)	0.00123	0.00123	0.00123
Mutual capacity (μf/mile)	0.148	0.148	0.148
Power factor	0.010	0.010	0.010

Note: Method and values for calculated losses were obtained from the Okonite Company, Passaic, N. J.

In any calculation of attenuation the main difficulty is in establishing proper constants. Table I gives the choice of cable constants used in calculating cable losses for both of these cable sections.

The calculated losses were low enough to assume that satisfactory carrier operation could be effected from phase to ground despite additional loss in the ground return circuit. No attempt was made in calculations or tests to determine the actual path of the carrier currents in the ground circuit.

Our experience with cables has indicated that discontinuities in metallic sheaths result in very high attenuation as mentioned by Tilles. However, where there is a continuous sheath, whether lead or iron, the attenuation is not excessive.

It is expected that the carrier ground current in the submarine cable portion of this installation flows along the sheath with relatively small loss. The carrier ground current in the jacketed cable portion of this installation probably flows some distance from the cable, the actual path being determined by the reactance and resistance involved. The loss on this installation in the ground return circuit for the jacketed cable is not excessive since the over-all attenuation is not exceptionally high.

Fault Location and Relay Performance Analysis by Automatic Oscillographs

Discussion and author's closure of paper 46-109 by H. P. Dupuis and W. E. Jacobs, presented at the AIEE summer convention, Detroit, Mich., June 24–28, 1946, and published in AIEE TRANSACTIONS, 1946, July section, pages 442–6.

G. D. Floyd (Hydro-Electric Power Commission of Ontario, Toronto, Canada): Automatic oscillographs have been used on the 230-kv network of the Hydro-Electric Power Commission of Ontario for about 15 years to provide a record of system performance including relay behavior and to locate faults. At the present time there are four such oscillographs installed at three of the six terminal stations of the network. Four additional oscillographs are on order. The average length of the trunk lines forming this network is about 200 miles.

Our experience has been much the same as that of the authors in that we found when preparing sets of fault current–distance curves from network analyzer data that mutual induction between circuits had a marked effect on the current distribution. One of our difficulties always has been to provide for the wide difference in current to be measured on a faulty circuit from the near, and far ends, and on parallel and sound circuits. The ratios may be in the order of 40 to 1. Consequently, the deflections obtained for the smaller of the two currents may be very small with a relatively large error in their measurement. It is this source of error, which is inherent, that may limit the application of the method of ratios, suggested by the authors, in our case. This method is sound where it can be applied and overcomes the error caused by fault and tower footing resistance. We agree that this source of error is usually present. Our method of decreasing this error has been to use residual currents on tie lines other than the circuit involved in the fault and to record total transformer bank ground current at two of the stations where oscillographs are located. The indicated locations of fault from all these readings are averaged. The number of faults located during the three years that this method of fault location has been given a serious trial is much better than expected considering the possible sources of error.

The usual rapid clearance of faults on this 230-kv network gives only one or two cycles of record before the first circuit breaker clears. The rapid clearance permits us to use the initial values of current, obtained from the analyzer, without modification. Figure 8 of the paper shows that currents were read after 19 cycles of fault, at which time some decrement in current would be expected. A further advantage in the use of the ratio of currents is indicated, although not claimed by the authors, in that the error introduced in the direct measurement by decrement is eliminated. Our experience has been that a great deal of valuable data may be obtained by use of these instruments at the cost, however, of considerable effort in their application and maintenance.

W. E. Jacobs: The operating department is interested in oscillographs mainly from the operating standpoint. That is, they are interested so far as the information obtained will make it easier in locating faults and analyzing system disturbances. The confidence which the operating men have in the oscillograph reports has been growing steadily with the improvements in the methods of interpreting the oscillograms.

It is the practice of the Consumers Power Company to make an inspection of a line as soon as practicable after a fault. This inspection usually will be made before the oscillograms can be developed and analyzed. If no evidence of the fault is located on this inspection, then another inspection of a short section is made after the location is calculated from the oscillogram. This second inspection covers a section two to three miles each side of the calculated location and is made very carefully, using a high power glass and at times climbing towers. Usually this inspection is made on a bright day. In case of a single line-to-ground fault, the field man can be told the position of the faulted conductor. The primary purpose of this second inspection is to find hidden damage and to determine whether there is some condition that can be corrected to prevent a recurrence of the fault.

We have found it very convenient when specifying the fault locations to use tower numbers as well as the miles from the terminals and have made-up charts showing tower numbers by miles. When the damage is found, the report lists the tower number which gives an accurate check on the calculated location. Since many tower lines run diagonally across country, this designation of fault location by miles alone may be subject to considerable error.

The servicing and calibrating of the oscillograph is handled by relay maintenance men. However, certain other men are instructed in taking the film out of the oscillograph and placing it in special mailing containers. These men are members of the plant organization where the instrument is located and are readily available to send the film for developing immediately after a storm. These men remove and mail the film after each storm or disturbance or when specially requested to do so by the dispatcher. Occasionally one storm will operate the oscillograph more than once. Each instrument is equipped with a station identification letter and a clock stamp which are both very necessary for identifying films after they are developed. A log of the oscillograph operation is kept for each instrument and supplements the time stamp. A signal bell is connected to sound when the oscillograph operates.

The films are developed at our laboratory at Jackson, but since one of the instruments is nearly 150 miles from Jackson it may require two or three days before films are received and developed. Consideration has been given to having the films developed locally and telephoning the measured value to the dispatcher to speed up the fault analysis. However, the number of permanent faults has been low and in most cases of permanent fault other lines are available to maintain service. Therefore the need for this method has not been great. We would welcome discussion on how other companies arrange this service and also on the methods used to develop the films. Our present method of developing the films, especially the longer rolls, is not entirely satisfactory from the standpoint of the time required.

As evidence of the speed of clearing faults, exactly 50 per cent of the 256 faults analyzed in the past five years caused so little damage that they could not be located by the initial field inspection. Part of those faults which are not located on the initial inspection are located at the end of the lightning season when a pole-top inspection is made. In the past two years a factor equal to kiloamperes squared times cycles has been calculated for each fault. We have termed this "damage factor". No definite conclusions have been drawn, but a broad general statement can be made that if the damage factor is below 50 there probably will be no visible damage, and if it is above 200 the damage probably will be found. Further experience may show that these limits can be closer. This is a burning factor and at the present time we have no data to correlate it with insulator breakage.

Of the 256 faults 96 per cent involved ground current. Only four per cent of the faults were phase to phase. Lightning caused 80 per cent of the faults; outside interference such as birds and machinery, caused nine per cent; and wind accounted for 7.4 per cent. Approximately four tripouts were caused by lightning per 100 miles of line per year for this 5-year period, and approximately five tripouts resulted from all causes.

In the operating department we feel that the greatest value of the oscillograph other than its value in locating faults is the information that is obtained when a fault is not cleared properly. In most cases these data definitely point to the cause of incorrect operation or failure to operate so that immediate steps can be taken to prevent their recurrence.

High Voltage D-C Testing of Rubber-Insulated Wire

Discussion of paper 46-121 by W. N. Eddy and W. D. Fenn, presented at the AIEE summer convention, Detroit, Mich., June 24–28, 1946, and published in AIEE TRANSACTIONS, 1946, August–September section, pages 576–8.

C. T. Hatcher (Consolidated Edison Company of New York, Inc., New York, N. Y.): The authors have presented data on d-c testing of rubber-insulated cables at the factory in order to eliminate inherent defects in the insulation. This method appears to be a step in the right direction as any test method which does not affect the insulating qualities of the rubber insulation, but still acts as a means for eliminating defects, is quite desirable.

C. E. Betzer (Commonwealth Edison Company, Chicago, Ill.): This paper gives some valuable information on the suitability and effects of voltage tests for factory process and acceptance testing. It indicates that such tests might leave undetected some serious imperfections in the insulation. Since the operating stresses for rubber-insulated cable are very low and breakdowns in service are caused mainly by oxidation (either by natural aging or by corona) and not by electrical puncture (except by lightning), these serious imperfections have not attracted attention in service. However, as the ability to withstand oxidation is improved, there should be an increasing necessity to eliminate these inperfections and then to reduce insulation thicknesses.

The Insulated Power Cable Engineers Association specifications for ozone-resistant type of insulation require an a-c acceptance test for cable rated at five kv and higher of about 90 volts per mil, or a d-c test of about 270 volts per mil after 24 hours immersion in water. The authors show that insulation with a fine needle puncture might withstand this test and with a U-knife cut easily could pass the test if squeezed in the manner common on a reel containing several turns of wire. Furthermore, it is shown that insulation with air pockets leaving only ten per cent of sound rubber withstood tests at 340 volts per mil direct current after 12 days of immersion, which indicates that it would have had a very large margin over the required test after one day of immersion. In another case insulation with an iron chip through two-thirds of the thickness withstood three tests at 570 volts per mil direct current during 12 days immersion.

Defects in rubber insulation almost never are found after the wire is shipped from the factory. The operating stresses are less than five volts per mil for low voltage wire or cable, 12 to 15 volts per mil for 5-kv cable operated at four kv, 22 to 25 volts per mil for 15-kv cable operated at 12 kv. Failures caused by electrical puncture by operating voltage (other than oxidation) almost never occur. When they do occur the cause seldom is found. Carbonized paths cannot be seen in the black insulation, and the insulation cannot be opened to view in the same manner as paper or varnished cambric insulation.

This paper suggests that some upward revisions of the acceptance test voltages for rubber insulation would be helpful.

The Electrical Performance of Ceramic Dielectrics at Elevated Temperatures

Discussion and authors' closure of paper 46-117 by H. A. Frey and J. M. Jesatko, presented at the AIEE summer convention, Detroit, Mich., June 24–28, 1946, and published in AIEE TRANSACTIONS, 1946, pages 911–20.

C. M. Sherer and **D. I. Smith** (Pennsylvania Water and Power Company, Holtwood, Pa.): One of the practical accomplishments of this investigation was to provide a satisfactory solution to a problem of porcelain failures where porcelain was used as an insulator across high voltage in the hot stack gases of electrostatic precipitators.

Drive shafts made of glazed porcelain were used between the electrode rapping device and driving motor in the Cottrell precipitators installed at the Holtwood steam plant. The shafts were 54 inches long, and had a 5-inch outside diameter with a $1\frac{1}{2}$-inch hole through the center. Operating voltage across the shafts was nominally 70,000 volts direct current, and operating temperature was of the order of 500 degrees Fahrenheit. Average life of the shafts was $2\frac{1}{2}$ to three months, and when failure occurred it was usually in the form of a clean shear break or in the nature of shattering. The breakages at first were thought to be caused by mechanical stresses, and it was hoped to reduce them by shortening the shafts. Whether or not a shorter shaft would be dielectrically satisfactory with respect to flashover was to be determined by wiring strips of sheet

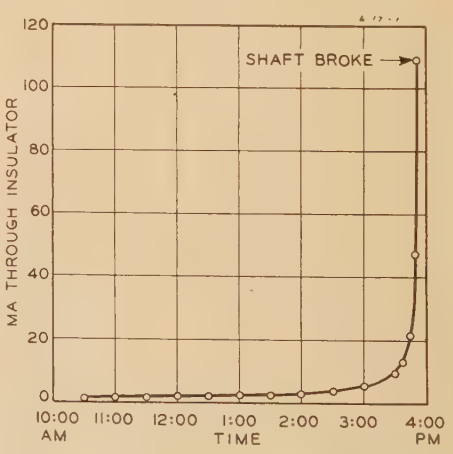

Figure 1. Dielectric failure of porcelain shaft in Holtwood precipitator 3

Boiler started at 3:17 a.m., April 23, 1945

metal to the sides in such a manner that half the length of the shaft would be short-circuited. Two shafts so treated and placed in service were found broken three days later, the exact time of failure not being determined. A third one is known to have failed sometime during the first day, and still another seven hours after being placed in service. Fusible temperature pellets which had been placed on two of these shafts showed that the porcelain under the metal strips had been at a temperature of between 500 and 550 degrees Fahrenheit, which was the same as the ambient gas temperature. The bare portion of the shafts, however, had reached a temperature of between 650 and 700 degrees Fahrenheit, thus indicating a dielectric failure because of runaway as found by Frey and Jesatko in their experiments. This half in each instance shattered into many small fragments in contrast with the shielded half which remained intact.

It now appeared that the failures were produced electrically rather than mechanically, and the cause was assumed to be a thermal runaway effect initiated by conduction current through the porcelain at the elevated operating temperature. As proof of this an idle shaft with half its length similarly short-circuited was placed in the hot gases without mechanical load and the normal operating potential of 70,000 volts applied across it. A recording milliammeter was connected in series with the shaft on the ground side to obtain a graphic record of the conduction current. The bare half of the shaft shattered 12½ hours after the boiler was fired. The curve in Figure 1 shows the progressive increase in conduction current for the last 5½ hours preceding the failure of the shaft. During this interval of time current increased from 1.33 to 109 milliamperes, or 8,000 per cent, with most of the increase occurring in the final minutes before failure. The runaway effect thus is shown clearly.

An experimental shaft made of zircon then was installed in regular service in place of a porcelain shaft. It was somewhat different in design from the porcelain shafts, being 4⅝ inches square with a 3½-inch hole through it. When it was installed, half of its length was shorted out in order to duplicate the conditions under which the porcelain was tested. Under the same operating conditions as the porcelain, this shaft lasted 28 days or 672 hours as compared with ten hours for porcelain (average of two for which the time of failure is definitely known). On the strength of this, all the porcelain shafts were replaced with shafts of zircon. Three of these now have been in service for periods of 7½, 13, and 14 months, and to the present time there have been no failures.

Our operating experience therefore supports the findings of Frey and Jesatko. Zircon has shown its superiority over porcelain under the temperatures and potentials encountered in the Holtwood precipitators. The authors are to be commended for having established the characteristics of ceramic dielectrics so that their performance can now be predicted at elevated temperatures and operating voltages.

Julius J. Torok (Corning Glass Works, Corning, N. Y.): This is a very welcome paper as there is very little information available on the electrical performance of various ceramic bodies at elevated temperatures. The authors are to be complimented on their analysis of their test results.

Table I

Temperature, Deg F	Resistivity, Megohms
400	5.1×10^{7}
600	2.0×10^{5}
800	4.1×10^{3}

Their data on glass checks roughly those obtained at the Corning Glass Works laboratories. The deviations are probably caused by the lower voltage gradients used in the Corning tests. Tests at Corning have been made on all glasses used by the electrical industries for such applications as radio tubes and lamps. Since in many of these applications the glasses are subject to high temperature uses, it was necessary to make such tests as well as develop new glasses which would give satisfactory results under a wide range of requirements.

One of the borosilicate glasses which has good electrical characteristics at elevated temperatures has resistivity characteristics as given in Table I.

It can be seen that the resistances of this glass is much higher than that of the general purpose borosilicate glass tested by the authors.

An analysis of the data presented by Frey and Jesatko on glass indicates that the borosilicate glass which shattered at the instant of failure was a tempered piece of glass. Highly tempered glass will shatter if a deep penetration into the volume of the glass occurs. If the authors still have some of the pieces of that glass it would be desirable if they would send them to Corning for stress analysis.

Paul M. Ross (The Ohio Brass Company, Barberton, Ohio): The authors have performed a meritorious job in contributing basic data on the temperature–resistance performance of porcelain. Figure 3 presents the voltage gradient versus resistivity characteristics of wet process electrical porcelain. In the normal operating temperature region for porcelain insulators, 150 degrees Fahrenheit and lower, the resistivity of the porcelain varies markedly with change in voltage gradient. Will the authors explain this characteristic?

Several of the specimens were carried to electrical failure at elevated temperatures.

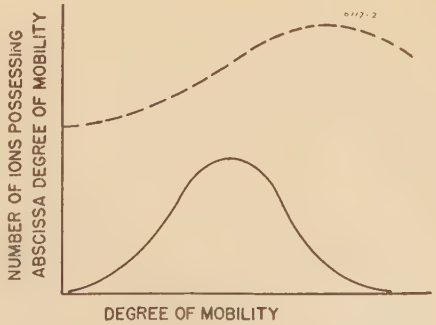

Figure 2. Distribution of ion mobility at normal and elevated temperatures

Was the type of failure obtained similar to that found on service insulator failures which involved attachment parts and external surface leakage conditions in addition to internal porcelain conduction?

While a discussion of the oil puncture test, as described in American Standard C29.1-1944, paragraph 4.7, is not contained as a part of this paper, do the authors find any evidence from their temperature versus voltage tests that explains puncture locations outside of the enclosed head section of suspension insulators as obtained on the oil puncture test? Do the authors' tests indicate that such puncture locations may be indicative of the electrical quality of the porcelain?

H. A. Frey and **J. M. Jesatko:** The authors wish to thank the discussers for their interest and for the pertinent facts brought out in their discussions.

C. M. Sherer has shown the practical application of these data to the solution of a baffling problem involving the failure of precipitator shafts operating at high temperature and high voltage. The curve of leakage current versus time presented by Sherer shows very clearly the characteristic of a long time runaway. The point of upward break in this curve corresponds to the point at which some element in the dielectric has exceeded the critical temperature T_c. The physical breakage resulted from the forces of differential expansion.

Paul M. Ross has asked several pertinent questions. The first of these requests an explanation of the variation of resistivity with voltage gradient. Any such explanation must be hypothetical. We know that the situation exists but at present we only can theorize as to its fundamental cause. As Doctor Torok has pointed out in his discussion, the conductivity of these dielectrics is believed to be caused by an ion drift. Let us suppose that there are in the dielectric body ions of varying degrees of mobility. If the relative mobility of the ions is distributed at random it would be expected that the distribution would follow a normal distribution curve as shown in Figure 2. Ions possessing a high degree of mobility would be influenced by very small voltage gradients while those having lower degrees of mobility would require higher voltage gradient.

Also as the temperature is raised the mobility of all ions is increased and some of those which are fixed relatively firmly at low temperature succeed in breaking loose from these bonds resulting in a shift in the distribution curve as indicated by the broken line in Figure 2. If these suppositions are made it will be seen that a resistivity voltage gradient curve will be obtained for any temperature having the typical form illustrated in Figure 3 of the paper.

Ross also asks whether the failures obtained at high temperature resemble those found on service insulator failures. Some of the tests described in the paper were made on actual service insulators of the type to which Ross refers. The failures on such insulators were exactly like low temperature punctures in such insulators. The point of failure was marked by a fused path in the dielectric sometimes accompanied by radial cracks. The location of the punctures in these cases were always inside the metal

enclosed head. On some long insulators, such as typical standoff insulators used in radio applications, the failure more nearly resembled a mechanical break and is caused by differential expansion. These failures were much like those described by Sherer.

The authors are inclined to believe that the punctures in oil outside of the enclosed head to which Ross refers are caused by either dielectric defects or localized stresses set up by the presence of the oil.

Parallel Circuits in Servomechanisms

Discussion and author's closure of paper 46-107 by H. Tyler Marcy, presented at the AIEE summer convention, Detroit, Mich., June 24–28, 1946, and published in AIEE TRANSACTIONS, 1946, August–September section, pages 521–9.

D. G. Soergel (nonmember; Washington University, St. Louis, Mo.): This paper is a very complete study of the solution of servo design problems through the use of inverse transfer functions. In particular, Marcy has been very general in his approach and has assumed a general feedback transfer function $K_f G_f(j\omega)$ which is characteristic of many industrial applications, for example, automatic temperature control where the characteristic periods of the controlled element and the measuring feed-back element are often of different values. The analysis is complete in that the author has derived and plotted inverse system functions to indicate static stability and has also shown how a knowledge of the quantities α, ζ, and μ_n is necessary to estimate the system transient responses. The results are plotted in nondimensional form, making them applicable to any problem.

I believe that nondimensionalized system transfer charts plotted for basic lead controllers, integral controllers, combined integral and lead controllers and tachometer derivative stabilized controllers with $\beta = -1$ would be of much help in assisting designers in the design of controllers for a variety of servomechanism applications. Marcy's paper has illustrated the approach to use to develop such charts and opens the way to a systematized procedure to follow for rapid controller design. Problems involving different feed-back transfer functions would become a special design problem, but experience in application may show in the future which types (such as the process illustrative example of Marcy's) would merit and would lend themselves to chart design.

All in all, Marcy's paper is a definite contribution to the engineering phase of servo design, and a utilization of his approach to the problem should result in data which will fit very well into high production design methods. The analysis used is of course characterized by a great deal of mathematics, and it should not be required that production engineers spend time developing the basic equations used. Rather, they are more concerned with the results to be expected of a particular system and whether or not the results are compatible with the particular application they have in mind. This information should be available in chart form.

It is agreed generally that since all physical systems are nonlinear systems, the design criterion arrived at through a mathematical analysis based on linear parameters is at the best a close approximation. The important thing, however, is a knowledge of the system trends caused by a change in one of the system parameters. This information is generally available either in the mathematical expressions describing the system or may be obtained from the nondimensionalized charts applicable to the particular system.

H. Tyler Marcy: I should like to thank D. G. Soergel for his interesting discussion of this paper. It is particularly interesting that he believes that the charts can be of engineering use in the design of industrial controllers. The availability of such charts certainly would be more convincing than a recommendation of the normally optimum relationships of circuit time constants. The charts tell at a glance how critical the controller adjustments are.

A word of caution is advisable, however, in recommending the use of charts. Only when the number of variable parameters represented is small can the relationship between them be presented adequately on a single sheet of paper. Thus, control processes that respond to sudden changes of the controller in an oscillatory manner are difficult to treat in a concise way because they can be described only by a statement of sensitivity, undamped natural frequency (or resonant frequency, if easier), and ratio of actual to critical damping (or degree of resonance, if easier). For this type of process a simple proportional controller, aided perhaps by tachometric feedback or lead networks, may not represent the usual complexity of the controller. However, the problem already has become difficult to treat with the aid of charts.

Determination of Cable Temperatures by Means of Reduced-Scale Models

Discussion and authors' closure of paper 46-103 by Andrew Gemant and Joseph Sticher, presented at the AIEE summer convention, Detroit, Mich., June 24–28, 1946, and published in AIEE TRANSACTIONS, 1946, July section pages 475–82.

R. W. Atkinson (General Cable Corporation, Bayonne, N. J.): The reduced-scale-model testing for determining temperature by Gemant and Sticher is another of the clever methods for the cable industry that has come from the laboratories of the Detroit Edison Company. There is little doubt that, like the earlier contributions, this one will be the source of valuable information to the industry. The reduced time constant accompanying the reduced dimensions is one of the very important advantages that might have been overlooked in a casual consideration.

I have been glad to learn that we may expect to have further data from the setup at Detroit. My further remarks will relate to suggestions toward such future work.

The important data that can be learned from a system such as these authors have developed are not concerned with what happens in the cable itself or in the immediate vicinity but rather with what happens in the surroundings—the duct structure or the earth around a buried cable. The performance of the cable and its immediate surroundings, specifically its performance within the duct, readily can be superposed on the data showing rise of duct structure. I have been urging this since 1913 and thus may be prejudiced somewhat, but the plan is so logical that it has come to be generally followed.

To study the rise of the underground structure as contrasted with that of the cable above its immediate surroundings it is necessary to provide test conditions where a larger part of the total rise is that of the structure. In general, this means making tests where many loaded cables, instead of only one, are placed in a duct bank. It is pertinent also that it is usually only in duct banks where several cables are installed that significant current limitations are imposed by the heating of underground cable. Where a cable is not heated by adjacent cables, the underground portion will operate, during most of the year, at a much lower temperature than the end portions.

It also will be very desirable when making these determinations on the model setup to arrange a comparison with a heavily loaded bank of commercial cables. While the theoretical basis for correlation of the model tests with commercial sized installations seems sound and it is perhaps adequate, the authors themselves have recognized the desirability of having an experimental verification of this correlation. The experimental comparison shown in the paper does not give a basis for indicating that a good correlation will exist between model tests and the performance of a loaded commercial duct bank.

It has been of interest to note that the indicated rise of sheath temperature over adjacent duct wall is considerably lower than I have indicated or than generally has been accepted. This is in large part because most of the tests reported cover ducts purposely made wet, but data are shown that suggest that the accepted constants should be subject to review even for dry ducts. However, it will be well for the authors to consider the desirability of giving greater attention to making tests in which there is no free water in the ducts. It can be argued that many ducts or that most ducts are wet. However, in most cities I believe that the serious problems of current limitation occur in ducts that are fairly dry, or in others when they are dry though they often may be wet.

I have gone into detail in these suggestions because I believe the proposed method is suitable for a practical solution of a wide variety of problems relating to the current rating of cables. In a way it may be considered as a mathematical instrument or an integrator set up for solving our special cable thermal problems. It serves this purpose, however, which is not accomplished by the purely mathematical calculators. It does, by its physical setup, what is required

of a mathematical physicist in setting up the mathematical equations to be solved by the mechanical calculating machines.

Herman Halperin (Commonwealth Edison Company, Chicago, Ill.): Anyone who has to do frequent work on current rating of cables and is faced with the uncertainties of some thermal constants will welcome such research as covered in the paper by Gemant and Sticher.

As pointed out by the authors, reduction in the dimensions of model installations is permissible accurately only where conduction alone is involved, while for thermal circuits including convection and radiation the conditions are more complicated. For example, the International Power Cable Engineers Association standard on current ratings provides that the thermal surface resistivity of lead sheath shall be expressed as follows:

"A straight line from 650 at cable diameter equal to zero inch to 1,200 at cable diameter equal to 1.75 inches. For diameters larger than 1.75 inches, a flat value of 1,200 degrees centigrade per watt per square centimeter is used."

It is apparent, therefore, that a reduction in size of a model would give erroneous results. Similar limitations apply to cables in pipes or three cables in a tube, and other problems of this nature for which information is important.

The size of the cable is also important in electrical problems where proximity and skin effects are a factor, for example, for three cables installed in an iron pipe.

The authors have recognized that corrections need to be made in adapting results of tests with models to field conditions, and I am mentioning these points just as a matter of emphasis.

With regard to the use of a box 15 feet long, five feet wide, and four feet high, filled with soil, we wonder whether such a model actually represents the current flow under field conditions. Especially during the summer months, the level of the ground water may be an important factor affecting heat dissipation.

It would be of interest if test results with these models could be compared with the usual formulas used in the industry so that, if necessary, corrections could be made in the constants used in this formula.

For a given conduit cross section and occupancy by cables, it has been found in many field surveys that the heating constants will vary considerably. This variation is a function of the type of soil, the percentage of moisture in it and other things. In Chicago we have found that the variation might be three to one or even more, excluding conduits that are submerged. It therefore has seemed necessary to make field surveys of conduit temperatures, particularly during the summer months, in order to avoid using excessively high heating constants of the conduits in determining load ratings.

C. T. Hatcher (Consolidated Edison Company of New York, Inc., New York, N. Y.): The determination of cable temperatures in duct banks is a problem which all operating engineers have to determine. System investments are affected materially by proper determination of cable temperatures because it is quite important not to install more copper than is required and, conversely, it is important that sufficient copper is used in order that the life of cables is not shortened. Any method which will help in determining proper temperatures is quite desirable.

The authors have outlined a very interesting development and it provides a relatively quick and inexpensive method of obtaining almost exact thermal limits for particular cables in specified buried duct structures under various load cycles. The data may be used for transient as well as steady state determinations. The method does not appear to be flexible enough to permit its use economically for determining loading limits on wide varieties of duct configurations such as are met in station cable designs.

The proposed method apparently can be used for determining short time ratings of important feeder installations where the limiting structure can be determined by observation. It would be quite desirable to be able to extend this method to the determination of cable ratings in complicated station duct structures where little data are now available. The authors have presented considerable data but the form in which it has been assembled requires considerable study to obtain logical conclusions.

L. F. Roehmann (Anaconda Wire and Cable Company, Hastings-on-Hudson, N. Y.): The aim of the authors' method of reduced-scale-model tests is to determine, versus time, the temperature of cables installed in a duct bank under transient or steady state conditions. According to the authors, a reduction of the linear cross-sectional dimensions by a factor α (α smaller than unity) and a reduction of the load currents by the same factor α produces a time contraction by α^2 but leaves the temperatures unchanged. These relations are valid if the thermal parameters of the model are the same as for the full-size installation. They disregard convection and radiation in the duct bank, and magnetic and dielectric losses in the cables.

There are cases in which magnetic and, particularly, dielectric losses may not be disregarded without introducing serious errors. This limitation might be avoided by loading the model cables so that their loss in watts per foot is equal to the loss of the real cables.

Regarding the amount of experimental equipment involved there seems to be little saving as compared with tests on life-size cables installed in a life-size duct bank. Both cases require sources of adjustable current (as many sources as there are cables), thermocouples, recorders, and so forth. A laboratory duct bank has to be cast in a laboratory soil box and laboratory-size cables linearly reduced to about one-fifth natural size have to be manufactured specially.

It would seem to us that either full-scale installations should be tested or, if models are required because of space and time limitations the scale reduction should be greater than one-fifth. If there is a real interest in sheath temperature–time curves, in addition to conductor temperature–time curves, the duct bank should be set up with the cables in natural size thereby avoiding the errors inheren tin a model reduction. However, it may be sufficient to obtain at somewhat reduced accuracy conductor temperature–time curves for transient and steady-state conditions. In that case a model of much smaller dimensions will be adequate. The cables can be represented by heater wires, and the loads can be controlled with small laboratory-size equipment, for example, variable-primary transformers.

R. J. Wiseman (The Okonite Company, Passaic, N. J.): I have had the good fortune to be acquainted with this research since its beginning, discussing the theoretical aspects and later analyzing its test results. I think Gemant and Sticher have introduced a method for studying the heat characteristics of cable systems, both buried and in ducts, which can go a long way to help us solve many of the problems which have confronted us for years.

Discussing first the buried cable case, we have the well-known Kennelly log 4 L/D formula for the steady state case. Some of us think that perhaps a cylindrical log formula will apply equally as well. Also the formula for the transient temperature of a cable before arriving at a steady state as given in the authors' paper is complicated and not easily understood except by mathematical experts. One cannot visualize easily that which is taking place. The authors have shown that a buried cable will follow the exponential integral formula. A few years ago I was interested particularly in the transient temperatures of a buried cable system such as the Bennett oilostatic system. I approached the problem from a cylindrical field viewpoint and had tests conducted by Doctor Paschkis of Columbia University on his thermal bridge. I was able to set up empirical formulas based on the cylindrical log formula which reproduced the actual curves. Later I took the exponential integral formula and also reproduced the curves obtained by Doctor Paschkis. Now I feel that I safely can use either method for determining transient temperatures of a buried cable, but my empirical method is easier to calculate and also gives a better picture of that which takes place. I am hoping, as soon as I have time, to prepare a paper on our investigation.

As the authors point out, it is impossible to express by means of a formula the case for cables installed in ducts. However, the error from the assumption that a cable model will give the desired information empirically is not great as shown by the results if one is willing to accept a difference of three to four degrees centigrade between actual field results and laboratory tests. This error is partially caused by some errors in assumption, for example, the radiation from the surface of a cable and a cable model are not exactly comparable because the emissivity of the surface is a function of the diameter.

The study of the influence of blowing air through a duct or allowing water to flow through is very helpful in proving their desirability where conditions sometimes warrant heavily overloading cables, or where hot spots develop and a quick method must be found to prevent excessive cable temperatures.

The authors are interested primarily in what cables will do under overload condi-

tions, that is, how long a cable will operate at a given load before reaching a limiting temperature or what load is permissible for various times before reaching a limiting temperature. I believe the authors have given us a means in a laboratory for checking the duct heating constants which now are used. At the present time we use values which are not related to the kind of soil or its moisture content; yet for a direct buried cable we want to take into consideration all the variables. This is logical for buried cable systems; why isn't it equally logical for duct systems? By setting up model duct systems with varying numbers of ductways we can make load-temperature tests and then estimate the heating constants. By varying the kind of soil and moisture content we can determine the influence of both.

I wish to congratulate the authors on their unique method for determining the transient temperature of cables without resorting to complicated calculations and a means for investigation of other temperature problems pertaining to power cable systems.

Andrew Gemant and **Joseph Sticher:** We appreciate Atkinson's constructive comments. At present, additional tests on our model setup are under way that meet some of the requirements which he stresses in his comments. In particular, various tests are being carried out on a heavily loaded duct bank which contains eight 3-conductor cables. Part of these tests also involve comparison of model and field data, insofar as these latter are available. Other tests are carried out with one of the ducts dry and the other ducts wet in order to reveal loading limitations in dry ducts as compared with wet ones.

Halperin correctly points out that certain factors, such as skin effect and radiation, require the use of correction factors when determining field temperatures from model data. We recently developed the correction term to be used in reference to radiation, and this term is being used, for instance, in our present tests involving dry ducts. We further believe that our test box is sufficiently large to represent field conditions, since the temperatures in the field are not affected beyond a 12-foot distance from the cable (2.5 feet in the model). However, a larger box could be used easily, if wanted, and water simulating ground water conditions also could be introduced in the model. Halperin's suggestion concerning the use of the model for a redetermination of present-day duct constants will be commented upon in our answer to Doctor Wiseman.

Hatcher emphasizes that our method is not flexible enough to take care of complicated station duct structures. If he has in mind open troughs in which the majority of the heat is lost through radiation, then his statement is correct. For all cases in which radiation inside a duct does not carry more than, say, 40 per cent of the total heat, the model in combination with a correction term can be used.

Roehmann finds only little saving in a model equipment as compared with a field test. It is difficult to agree with this opinion, considering the amount of information now being assembled from model tests which needed about two weeks to carry out, tests which would require a whole year's work in the field. Roehmann further states that conductor temperature data could be obtained from a model much smaller than ours, utilizing heating wires for cables. This statement probably is based on a misunderstanding since theory clearly shows that conductor temperatures can be obtained only if the cable itself is reproduced accurately on a scale reduction basis.

Doctor Wiseman in his comments mentions an investigation of his own which is concerned with establishing an empirical formula for evaluating transient temperatures. We are looking forward to the opportunity of discussing Doctor Wiseman's method more in detail, when his paper will be published. He also emphasizes the possibility of using the model method for checking existing duct heating constants, a suggestion made also by Halperin. We welcome this suggestion as the model method is certainly well-suited for such type of work. We think that it would need careful planning and also a general agreement among various interested companies as to the advisability of such research before steps to carry it out are undertaken.

Dynamic Braking Control of D-C Series Motors—Calculation of Stability Limit

Discussion and authors' closure of paper 46-130 by G. W. Heumann and W. P. Smith, presented at the AIEE summer convention, Detroit, Mich., June 24–28, 1946, and published in AIEE TRANSACTIONS, 1946, July section, pages 454–7.

J. D. Leitch (Electric Controller and Manufacturing Company, Cleveland, Ohio): The authors are to be complimented on a very fine paper containing data of great importance to the designer of d-c crane hoist control. They have chosen to express their results in the per unit system which makes their curves useful over a wide range of motor frame sizes. By an interesting choice of units they have been able to express the torque per ampere of armature current, and the counter electromotive force per rpm for various values of field current in a single motor saturation curve. This should reduce greatly the time required in calculating the speed–torque characteristics of any hoist circuit using a d-c series motor.

The authors point out that they have chosen the one-half hour rating of the motors in defining their base units. This is in accordance with the practice on general purpose cranes and it is important that the motor rating be defined carefully in determining the stability limits of a hoist controller when lowering a heavy overhauling load. In the case of more severely worked cranes, such as bucket cranes, it is customary to choose the motor sizes on the basis of their one-hour ratings while on standby cranes, such as are used in a power station, the one-quarter-hour ratings sometimes are employed. Obviously, in designing controllers for those cranes on which the motors have been chosen on the basis of the one-quarter-hour ratings, greater care must be exercised in assuring that the stability limits are not exceeded.

Using the published characteristic curves for a wide range in sizes of mill type motors we have endeavored to plot the K_s and K_t curves on a per unit basis and found considerable variation between motors of different frame sizes. Though there appeared to be a definite trend as we considered motors of larger sizes, this trend was contradicted in a number of cases. We acknowledge however that we were compelled to perform a certain amount of extrapolation of the characteristic curves and that the accuracy of the method could at best be approximate only. In the light of the authors' work with a wide range in motor sizes and with actual test data at their disposal, would they care to give us some information regarding the variation in the K curves (Figures 2 and 4 of the paper) for the range of motors investigated?

The authors show very clearly the importance of a series resistor R_s (Figure 7) as a means of increasing the stability limit. Would they care to discuss the value, if any, from a stability point of view, to retaining a small amount of resistance in the armature circuit?

G. W. Heumann and **W. P. Smith:** D-c series motors as used on cranes are generally mill or crane type motors for which manufacturers' handbooks publish the ratings not only on a one-half-hour basis, but also on a one-hour and one-quarter-hour basis. It should be noted that although different time ratings may be assigned to a motor, its speed–torque curves and stability limit in terms of rpm and pound-feet are not altered thereby. A given set of motor test

Table I

For Curve Shown in Figure 2 of the Paper

Per Unit Field Amperes	Maximum K / Minimum K
0.30	1.24
0.50	1.11
0.80	1.03
1.00	1.00
1.20	1.03

Table II

For Curves Shown in Figure 4 of the Paper

Per Unit Armature Amp	Max K/Min K: 1.00 PU Field Amp	0.5 PU Field Amp	0.3 PU Field Amp
Generating			
2.0	1.2	1.35	1.93
1.5	1.19	1.17	1.38
1.0	1.15	1.26	1.25
0.5	1.11	1.25	1.30
0.0	1.07	1.20	1.29
Motoring			
0.5	1.04	1.10	1.20
1.0	1.00	1.08	1.30
1.5	1.03	1.20	1.60
2.0	1.07	1.28	1.64

data which are carried out far enough to permit calculation of the limit of stability may be expressed in per unit to any base. The per unit values of either test data or subsequently calculated data may be changed to any other base by the relation:

$$PU_2 = PU_1 \times \frac{B_1}{B_2}$$

where

PU_2 = per unit value of given quantity on base quantity, B_2

PU_1 = per unit value of given quantity on base quantity, B_1

It was hoped, when work was first started on this paper, that it would be possible to arrive at average per unit curves which would be sufficiently accurate to apply to a large range of motor sizes. It was found, however, that the curves of individual motors are so different as to preclude this possibility. It also was found that, while there were some definite trends as larger motor sizes were considered, the curves, especially the K curves of the type shown in Figure 4, were of many different shapes. The resulting variations in K value were often so large as to be totally misleading. To illustrate the magnitude of these variations the data shown in Table I and Table II of this closure are presented.

As might be expected, variations are greater for weak field strengths than for heavy field strengths. The general trend with motor size of saturation curves, such as Figure 2, is for larger motors to have lower than average K at field strengths less than 1.0 PU, and higher than average K at field strengths above 1.0 PU. Smaller motors exhibit the opposite tendency Exceptions, however, are notable and frequent. No definite trend with motor size is noted with curves of the type shown in Figure 4.

Resistance in series with the armature only has no effect on the steady-state stability limit. According to equation 11 of the paper, torque is solely a function of armature current. Resistance in series with the armature determines the electromotive force according to equations 12 and 13, and consequently the speed according to equation 10. Therefore, if a circuit were used similar to Figure 6, except with resistance in series with the armature, the maximum torque would not change, but it would occur at a higher speed.

Adding resistance in series with the armature increases the slope of the speed–torque curve so that, with a given no-load speed and a given stability limit, a higher full-load speed is obtained. When switching from the last point to preceding points during deceleration, the presence of resistance in series with the armature has a beneficial effect in that transient current peaks are reduced; therefore it can be said that armature resistance increases the transient stability of the motor during deceleration.

Another advantage is gained by the use of resistance in series with the armature when two motors are connected to a large hoist, forming a duplex drive. Armature resistance will cause the two motors to share their load more evenly than without armature resistance. On a duplex drive the combined stability limit is given by the motor carrying the higher load, and for this reason it may be stated that resistance in series with the armature has the tendency of increasing the stability limit of a duplex controller.

Circuit Cushioning of Gas-Filled Grid-Controlled Rectifiers

Discussion of paper 46-146 by D. V. Edwards and E. K. Smith, presented at the AIEE summer convention, Detroit, Mich., June 24–28, 1946, and published in AIEE TRANSACTIONS, 1946, October section, pages 640–3.

Roman Pogorzelski (Power Equipment Company, Detroit, Mich.): An experience with one of our rectifiers in the field demonstrates very significantly the effectiveness of circuit cushioning as presented in this paper.

The rectifier under discussion uses xenon-gas-filled grid-controlled tubes operated much of the time at approximately 30 per cent of their rating and approaching the initial inverse voltage conditions given in test 6 of Table II of the paper. Without a cushion circuit the tube life did not exceed 500 hours in any case. After the cushion circuit, suggested by D. V. Edwards, was added, the rectifier has operated well over 11,000 hours to the present date with no tube failures. The cushion circuit consisted of an 0.6-microfarad capacitor in series with a 300-ohm resistor across each tube.

With regard to measurements to determine the values of constants in the cushion circuit, it was found expedient to use a method that permits the calculation of these values. Outlined briefly, the method is as follows. The maximum current commutation rate is calculated from the maximum commutating voltage obtainable in the plate transformer and the leakage inductance as measured by a short-circuit test. The value of A_{10} is then computed, and the maximum safe rate of rise of initial inverse voltage is determined for the given tube type. The values of resistance and capacitance are derived from consideration of the transient response of the series R, L, C circuit formed by the cushion circuit and leakage inductance to the suddenly applied electromotive force at the end of the commutation.

J. W. Picking (Reliance Electric and Engineering Company, Cleveland, Ohio): We have designed our standard electronic variable voltage d-c motor drive controller to incorporate-xenon-filled grid-controlled rectifiers as manufactured by the authors' company.

Our original life tests and actual sample installations indicated we could expect an average normal life in excess of 5,000 hours on 6.4-ampere *C6J* grid-controlled rectifiers. These tests were based on single-phase full-wave rectifiers supplying power to a d-c motor armature. In all cases the load was such as not to require continuous current conduction throughout the normal operating range.

One of the sample installations was used to drive the work spindle of a precision universal grinder. After operating for several months it was noticed that chatter marks were set up on the ground surface especially on large diameter work. The cause of these marks was traced to angular vibration set up in the driving motor by the discontinuous pulses of rectified current.

To eliminate this trouble sufficient inductance was added in the form of a reactor in series with the motor armature so that current in the circuit was continuous for all values of load and speed. Within one month, approximately 450 hours of operation, both tubes had failed. Tube tests indicated high arc drop. Results were similar on a second and third set of replacement tubes.

D. V. Edwards was contacted and cushioning as covered in this paper was suggested. This was tried and this original set of tubes still are operating, having passed the 8,000-hour point recently.

On the basis of this and similar results on other installations it has become the standard practice of our company to apply cushioning circuits to all grid-controlled rectifiers, either gas- or mercury-filled where continuous conduction is expected at any point in the operating range.

This practice has caused us to redesign all of our anode transformers, adjusting the leakage reactance. Because the amount of cushioning required is a function of transformer leakage reactance we have found that a satisfactory compromise between voltage regulation and required cushioning can be obtained so that the maximum cushioning per tube will be less than 1.0 microfarad in series with less than 150 ohms for all sizes of rectifiers up to 25 amperes at 230-volts output.

Considerable difficulty was experienced in obtaining oscillographic readings for determining the current ten microseconds before cessation of current and the rate of rise of initial inverse voltage. Using a pulse driven sweep oscilloscope of the Dumont 248 type has reduced the taking of these readings to a matter of minutes and is recommended to those interested in studying these circuits in detail. As a warning, distributed capacity of the leads and instrument must be neutralized carefully as the wave fronts are very steep.

D. V. Edwards and E. K. Smith are to be complimented on developing a practical solution to a very difficult problem.

The Frequency Response of Automatic Control Systems

Discussion and author's closure of paper 46-114 by Herbert Harris, Jr., presented at the AIEE summer convention, Detroit, Mich., June 24–28, 1946, and published in AIEE TRANSACTIONS, 1946, August–September section, pages 539–46.

D. G. Soergel (nonmember; Washington University, St. Louis, Mo.): Harris has presented a very clear description of a servomechanism analysis technique which very easily can be applied to engineering practice.

It would be an agreeable situation if all

information needed to evaluate transient responses could be obtained from steady state frequency response data. Harris' statement that the resonant frequency persisting after a transient condition could be determined from a transfer loci plot and that an increase of frequency response would result in a more rapidly damped system seems very reasonable. However, specific information necessary for the synthesis of a controller such as the system attenuation constant α, the actual time necessary to reach a steady state condition, and the magnitude of initial overshoot would require a transient analysis of the system. Unfortunately, as was stated in the paper, the analytical determination of transient data often involves more work than is practical. The usual procedure then is to design the system from a stability approach and make laboratory corrections for faulty transient operation. If laboratory setups are physically impossible, the only recourse is a mathematical analysis.

A design criterion of 1.5 for the value of M is a good choice and can be determined most easily from a comparison of constant M and inverse loop transfer plots. Harris discussed and illustrated inverse loop transfer functions to some extent but his paper largely was concerned with the determina- and calculation of direct loop transfer functions and the determination of system responses from them. We believe that advantages realized from the use of inverse functions justify their use over direct functions for the reasons given by the author and also for the simple fact that concentric M circles and straight-line constant phase angles are plotted more easily.

A standard procedure to follow is to derive the inverse system transfer function and then separate the constant gain factor from the frequency variant portion. The product then is plotted and the approach of the locus to the M equals 1.5 constant M circle is noticed. If the locus is not tangent, the gain factor may be increased accordingly until tangency is reached, and the intersection of the system locus and constant M circles and constant phase angle lines will determine the system characteristics.

The treatment of inherent controller delays and compensating or antihunt networks is also of interest since it indicates to the designer an approximate order of antihunt values, and also the correct direction for a contemplated circuit change.

In conclusion, the paper does not present anything noticeably different in the treatment of servo design and seems to treat the most convenient approach to the problem, inverse system functions, merely as another way to solve the problem. Actually inverse functions should rate first attention. The paper, is written however, in clear engineering language and discusses quite ably the physical significance of the mathematics needed to calculate loop transfer functions. This is a very welcome bridge in the gap between the high mathematics needed to solve servo problems and the actual values and parameters used to approach physically the ideal expressed by mathematical quantities.

Herbert Harris, Jr.: Soergel points out the difficulties involved in trying to correlate the frequency response parameters such as resonant peak amplitude and frequency with transient response parameters such as attenuation constant and response time. This is a recognized difficulty but it loses much of its importance as the servomechanism designer becomes experienced in comparing the two solutions. With this experience, it is just as easy to think in terms of the frequency response as it is in terms of the transient response. The saving in calculation time is certainly worth considerable effort in achieving a new point of view.

It is true, with some exceptions, that the inverse transfer functions are easier to use than the direct transfer functions presented in the paper. Historically, however, they came into general use several years after my original presentation of this method in a National Defense Research Council report dated December 1941, and consequently there exists much experimental and design data in the form of direct transfer functions. H. T. Marcy has described the use of inverse transfer functions in more detail.[1]

REFERENCE

1. PARALLEL CIRCUITS IN SERVOMECHANISMS, H. Tyler Marcy. AIEE TRANSACTIONS, volume 65, 1946, August–September section, pages 521–9.

The Influence of the Concentration and Mobility of Ions on Dielectric Loss of Insulating Oils

Discussion of paper 46-110 by Bun Po Kang presented at the AIEE summer convention, Detroit, Mich., June 24–28, 1946, and published in AIEE TRANSACTIONS, 1946, July section, pages 403–07.

Andrew Gemant (The Detroit Edison Company, Detroit, Mich.): Bun Po Kang is to be commended for having obtained a reasonable amount of information on the ionic conductivity of oils, notwithstanding the fact that he had only a 60-cycle power factor bridge and a viscometer at his disposal. His unit of poise-watts which is used as a measure of the ion content of an oil clearly indicates the inherent limitation of power factor measurements. By this means one obtains only the product of ion content times mobility, and a separation of the two in order to obtain absolute values for both is not possible without additional information. This is the reason why the discusser has been for the past few years engaged in a research of introducing electrochemical electromotive-force measurements into the study of insulating oils. It is to be hoped that by this means, just as in aqueous solutions, more complete information on the concentration and mobility of ions may be obtained.

Attention also should be called to the fact that the phenomenon discussed in connection with Figure 6 has been familiar to those who have investigated mixtures of insulating liquids (see Association of Edison Illuminating Companies minutes for 1934, pages 475–8).

Dimensionless Analysis of Servomechanisms by Electrical Analogy

Discussion and author's closure of paper 46-150 by S. W. Herwald and G. D. McCann, presented at the AIEE summer convention, Detroit, Mich., June 24–28, 1946, and published in AIEE TRANSACTIONS, 1946, October section, pages 636–9.

W. M. Pickslay (Allis-Chalmers Manufacturing Company, Milwaukee, Wis.): This paper presents an interesting new tool for the analysis of regulating or closed cycle systems. Most of the work in this new type of analysis has occurred with angular position servomechanisms of comparatively small powers. This is natural because the development of the analysis coincided with the war demand for such particular servomechanisms.

Previous papers of the AIEE including one by men from the same manufacturer have shown that the performance of larger generators subjected to sudden load changes is substantially independent of the voltage regulator. The main factors affecting regulation are the design characteristics of the generator and up to a certain speed, the exciter speed of response. This being the case, I would like to ask if the use of this new tool has resulted in any significant improvement of performance of voltage regulating systems through alteration of the regulator or servomechanism parts or circuits.

G. D. McCann: W. M. Pickslay's question can be answered best by stating that a very comprehensive study of voltage regulating systems has been made recently with the transients analyzer. These data are being presented in a future paper.

Tennessee Valley Authority Hydroelectric Stations—Electrical and Mechanical Design

Discussion and author's closure of paper 46-108 by R. A. Hopkins and H. J. Petersen, presented at the AIEE summer convention, Detroit, Mich., June 24–28, 1946, and published in AIEE TRANSACTIONS, 1946, pages 920–31.

S. H. Mortensen (Allis-Chalmers Manufacturing Company, Milwaukee, Wis.): A brief discussion of the design of the Chickamauga generators shown in Figure 3 of Hopkins' and Petersen's paper may be of interest to AIEE membership. The generators shown in cross section in Figure 1 of this discussion are duplicates rated 30,000 kva, 90 per cent power factor, three phase, 60 cycles, 13,800 volts, 75 rpm, class B insulated and guaranteed to carry rated load with temperature rise not exceeding 60 degrees centigrade over 40 degrees centigrade air.

Their design is of the overhung or umbrella type with the thrust and single guide bearings supported on a bracket below the generator rotor. This construction, suitable for large diameter slow speed machines with narrow cores, facilitates inspections and repairs as it permits generator rotor removal without disturbing shaft and bearing alignment, as well as dismantling of the bearing housing shafts and bearings in one piece without changing the unit alignment. It also reduces generator head room requirements to a minimum. With the thrust and guide bearings both mounted in a single water cooled oil bath, no provisions for oil circulation are required. The flat adjustable 8-segment Kingsbury thrust bearing 93 inches in diameter supports the combined weight of the unit's rotating parts as well as its hydraulic thrust, which combined amounts to 2,050,000 pounds. The 85-inch diameter by 14-inch long single guide bearing is made in sections free to pivot and bearing upon a smooth finished surface of the thrust block. The lower portion of the bearing is submerged in the oil bath, and the rotation of the shaft establishes an oil flow through longitudinally spiraled bearing oil grooves adequate for bearing lubrication. The construction of the oil container in conjunction with that of the sectionalized cooling coils and guide and thrust bearings permits removal of the latter through normally covered openings in the container sides.

For shipping reasons the rotors were built with fabricated arms bolted to a shaft-mounted hub. Flanges on the arms support the punched floating type rotor rim that carries the field poles and coils.

The dovetailed field poles have copper damper bars silver-soldered into the pole end plates. The latter are fitted tightly into the spider rim and the two combined completes the winding circuit.

A break rim with replaceable segments is supported on the spider arms.

For shipping reasons the generator stator was made in four sections which were stacked at the factory and wound at the destination. Shims provided between yoke joints provide means for adjustment of core pressure at splits.

The generator ventilating system is of the enclosed circulating type and designed for CO_2 fire protection. Two rotor mounted fans circulate 75,000 cubic feet of ventilating air per minute over the coil and core surfaces through the yoke and eight fin-type water-cooled heat exchangers which absorb the heat losses. From the coolers the air is discharged into an air housing which surrounds the stator and from there it returns to the rotor fans. The air housing which also encloses generator leads and piping allows space for inspections. Access is gained by means of a number of doors sufficiently tight to hold CO_2 when admitted to the ventilating system for fire protection.

The direct driven 300-kw main and 28-kw pilot exciters mounted on a separate bridge are ventilated independently of the main generator by means of separate fans as shown in Figure 1 of this discussion.

A few dimensions and weights of the Chickamauga generators may be of interest. The stator bore is 380 inches; the outside diameter of the air housing is 557 inches; the net stator weight is 194,000 pounds; the net rotor weight with alternator shaft is 579,500 pounds; the air housing weighs 82,000 pounds. These weights combined with those of bearings, brackets, exciters and sole plates bring the total machine weight up to 1,200,000 pounds. The rotor $WR^2 = 75{,}000{,}000$ pound-feet-squared, and it is designed for a runaway speed of 207 rpm.

The characteristics of the Chickamauga generators and exciters which were built some years ago conform to the recent Tennessee Valley Authority specifications given in Hopkins' and Petersen's paper except for the construction of the thrust block, which is a separate casting, and the mounting of the rotor on the generator shaft. The difference between this design and that corresponding to the recent Tennessee Valley Authority specifications becomes apparent by comparing Figures 1 and 2 of this dis-

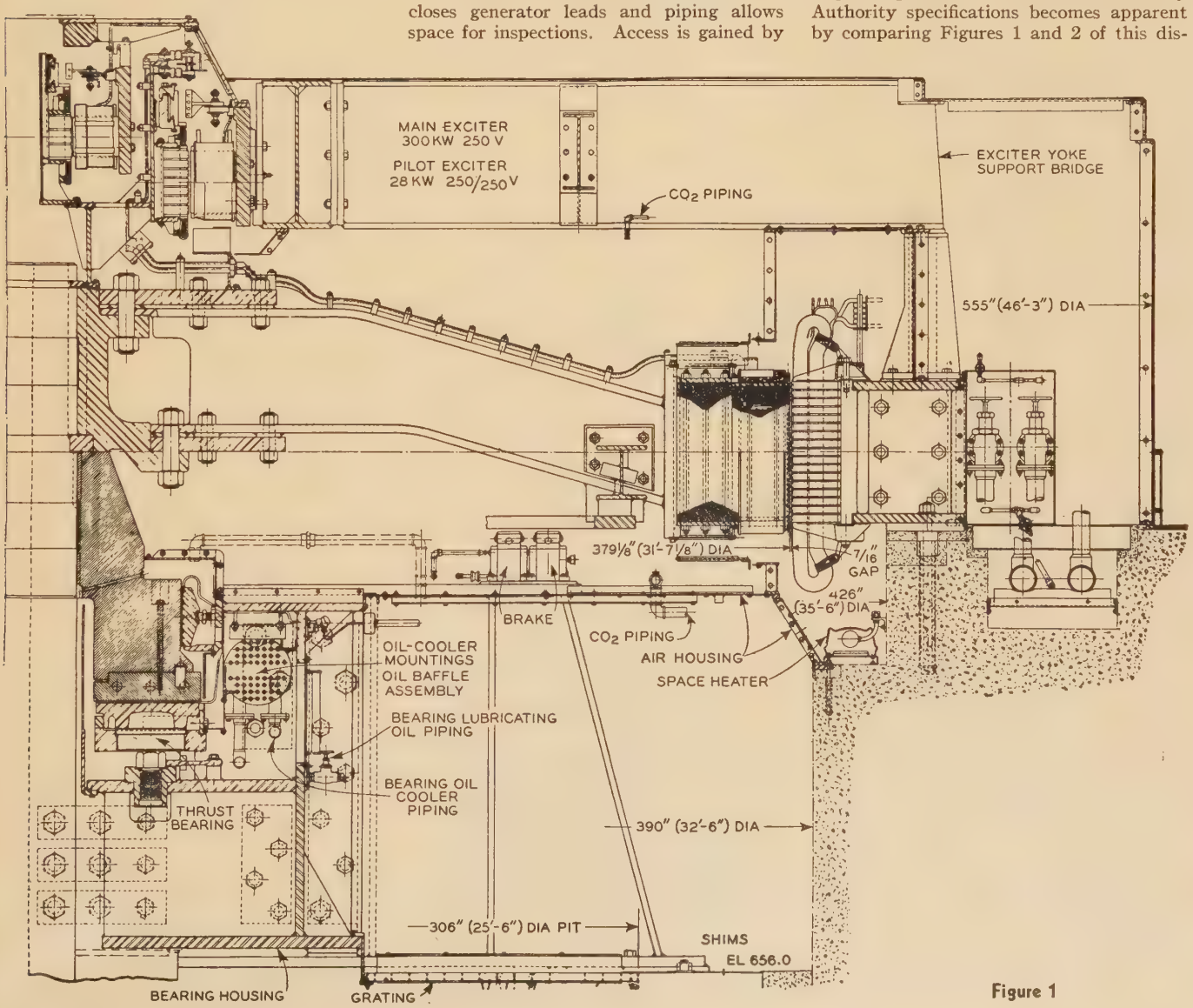

Figure 1

cussion. The latter is a cross section of the 35,500-kva 90-per-cent-power-factor 3-phase 60-cycle 105.8-rpm 13,800-volt umbrella-type generators built by Allis-Chalmers Company for Tennessee Valley Authority's Fort Loudon Station. The Fort Loudon design follows that of the Chickamauga generators except for the thrust block being integral with the rotor shaft and the generator rotor being mounted on and keyed to the top surface of the thrust block. This construction reduces the generator shaft length and simplifies rotor erection and dismantling.

On the other hand the large diameter shaft flanges may introduce difficulties in obtaining acceptable shaft forgings.

In conclusion I want to compliment the authors on their very able paper.

S. B. Griscom (Westinghouse Electric Corporation, East Pittsburgh, Pa.): This paper and its predecessor of the same subject[1] are of great value to the industry. In designing a power station, many decisions must be made between alternate plans which individually will satisfy the basic requirements, yet which differ in intangible respects such as reliability and flexibility. In such instances, the engineers' old stand-by—the economic comparison—is unavailing, and the answer must be obtained by judgment based on experience.

The authors have studied over a period of years many individual problems, resolved them to their fundamentals, and formulated standard practices applying specifically to the Tennessee Valley Authority conditions, but of general value on similar projects. The compilation of these practices will be of great assistance to design engineers for a long while to come by affording comparison of conclusions. Particularly noteworthy is the general use of normal manufacturers standards.

The omission of spare transformers for generating stations and operating more than one generator per high voltage circuit breaker are of particular interest. This reflects two important changes from past practice. First, that transformer and circuit breaker reliability have been improved greatly, and secondly, that systems (including interconnections) have become so large that if a unit is dropped occasionally as a result of apparatus failure, it will not affect service. The unit system as applied to generators is quite a departure from the double-bus double-circuit-breaker generator and high voltage busses with spare transformers which were in vogue some time ago.

The use of automatic reclosing on some of the 154-kv lines is of interest. I would like to know if this has made it possible to defer construction of new 154-kv circuits, or whether its principal use has been to improve reliability of the high voltage network.

The adoption of an isolating 13.8/12.5-kv transformer bank for supply of 3,000 kw of village load is an unusual application, wherein the maximum possible protection is offered to the 67,500-kva generators. While increasing the cost somewhat, this procedure no doubt will turn out to have been a good investment during the life of the station.

REFERENCE

1. TENNESSEE VALLEY AUTHORITY HYDROELECTRIC STATIONS—ELECTRICAL DESIGN, **Raymond A. Hopkins.** AIEE TRANSACTIONS, volume 60, 1941, pages 1281–93.

Figure 2

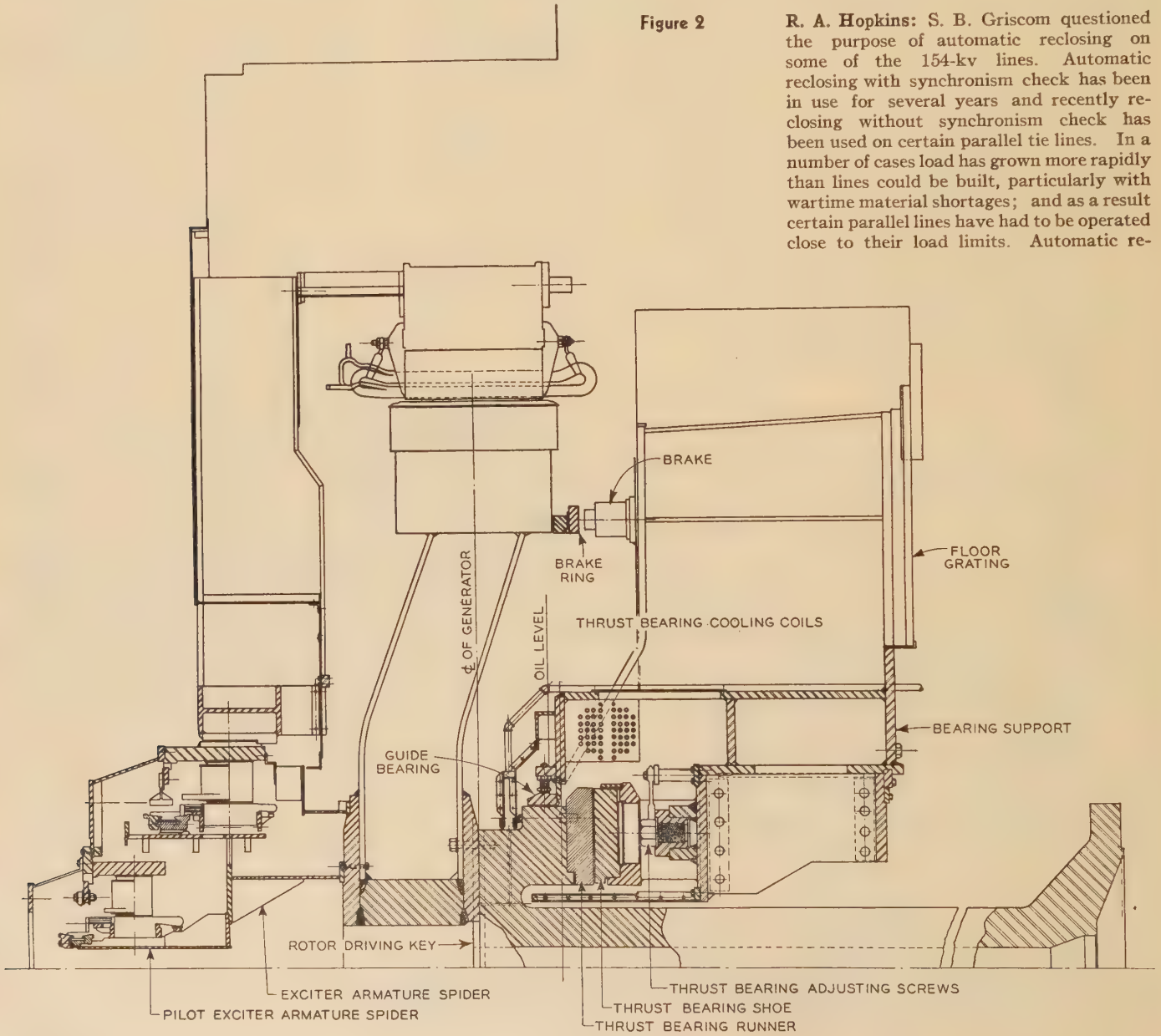

R. A. Hopkins: S. B. Griscom questioned the purpose of automatic reclosing on some of the 154-kv lines. Automatic reclosing with synchronism check has been in use for several years and recently reclosing without synchronism check has been used on certain parallel tie lines. In a number of cases load has grown more rapidly than lines could be built, particularly with wartime material shortages; and as a result certain parallel lines have had to be operated close to their load limits. Automatic re-

closing under these conditions often results in immediately re-establishing parallel operation after a trip-out of one of the lines.

Philosophy of Relaying

Discussion and authors' closure of paper 46-172 by E. W. Knapp and Ben C. Hicks, presented at the AIEE summer convention, Detroit, Mich., June 24–28, 1946, and published in AIEE TRANSACTIONS, 1946, November section, pages 735–40.

Eric T. B. Gross (Illinois Institute of Technology, Chicago, Ill.): I think that all relay engineers should read this paper very carefully and give its contents plenty of thought. The authors have presented the real basis of simplicity in modern relaying, and their conclusions are not restricted in their general application.

It is noticeable that ground fault protection of generators through high impedance grounding and residual voltage relays is recommended, and that the practical experiences have been very satisfactory. There is much reason to give this kind, or some other sort of high resistance grounding, preference in comparison with low reactance grounding of generators. If we would ask ourselves more often, "Why do we ground the neutral of systems and which of the possible answers is to be given preference in each particular case?" many a mistake could be avoided.

It is very interesting indeed, that gas detector relays (indicating the accumulation of gas resulting from incipient faults, and tripping resulting from pressure when more severe internal faults occur) have been used and found very satisfactory. The application of this kind of transformer protection has been wide and successful abroad, but the number of installations in the United States seems to be limited. It should be helpful if the authors would comment more in detail on their experiences with this type of protection, and would include the means which eliminated some of the earlier difficulties mentioned in the paper. It would be of interest to know how many such gas detector relays are in the use in the system of the Shawinigan Water and Power Company, and if other utilities and companies in Canada also use this kind of transformer protection.

E. W. Knapp and Ben C. Hicks: In reply to Eric T. B. Gross, the Shawinigan Water and Power Company has in use 40 gas detector relays on transformers and regulators aggregating 600,000-kva capacity, and we understand that other large utilities in Canada use these relays, some more and some less extensively. The chief difficulties that we have encountered in the use of these reays are the following:

1. When an accumulation of gas is released, oil hammer will occasionally cause the pressure element to operate. It has, therefore, been made a rule to block the pressure element whenever releasing gas from the gas accumulation element.

2. Two instances of ruptured diaphragms have been encountered, one in service and one after a shop test. This suggests the advisability of inspecting the diaphragm whenever there is reason to suspect that the relay may have been subjected to excessive pressure.

3. In a few instances, grounds or short circuits have occurred on the relay terminals as a result of moisture accumulating in the terminal chamber. On existing relays this hazard has been overcome by providing a small drain hole in the bottom of the chamber. On new relays the drain hole is provided by the manufacturer and, in addition, the design of the terminal chamber has been improved.

4. Newly filtered oil in a transformer will release trapped air for a period of a few weeks. During this period the relay is used for alarm purposes only.

Our operating experience with gas detector relays extends over the past nine years. Actual operations of the relays during this period have been relatively few. Internal faults on two transformers and one regulator have been detected correctly. In addition to these, a number of miscellaneous conditions, such as low oil, freezing of breathers, and defects in the cooling system have been indicated. There has been no instance of a failure to detect a fault.

Regarding the question of protection in general, our attention has been drawn to the fact that the paper contains no reference to single-phase-switching or Petersen coils. We have had no operating experience with either, but both, when properly applied, undoubtedly have a definite field of usefulness, in clearing ground faults resulting from flashovers on transmission lines without loss of load or loss of synchronism. For this purpose the former is used in conjunction with instantaneous automatic reclosing.

Short-Time Current Ratings for Aircraft Wire and Cable

Discussion and authors' closure of paper 46-145 by B. W. Jones and J. A. Scott, presented at the AIEE summer convention, Detroit, Mich., June 24–28, 1946, and published in AIEE TRANSACTIONS, 1946, October section, pages 644–8.

R. H. Kaufmann (General Electric Company, Schenectady, N. Y.): The results of investigations presented in this paper fill a long felt want in aircraft application technique. The entire practical application significance has been condensed into one simple graph which defines the permissible current-time boundary for the normally encountered variety of conductor sizes over the entire range of current and time. Appropriate test procedures also have been outlined by which other investigators may extend the scope of knowledge. The authors are to be credited with a valuable contribution to the aircraft electrical art.

The results of this work clearly emphasize the need of automatic fault protectors in aircraft electric circuits and make evident the hazards of non-trip-free circuit breakers and manual over-ride features. It can be noted that the flow of a 3,000-ampere fault current will elevate in 0.2 second the temperature of a number 8 copper conductor to the maximum safe value. If current flow be continued for another 0.2 second, violent evolution of smoke will occur, and in less than one second total elapsed time, the conductor will be elevated to the ignition temperature of volatile materials in its insulation. The extremely short time which is available in which corrective action is to taken is entirely beyond the ability of a human being to respond.

A vivid demonstration of the evolution of large quantities of smoke from aircraft cable was performed inadvertently during laboratory tests in which a length of number 4 cable was used to simulate a resistance fault. After several successive intervals of approximately 5,000-ampere fault current flow, each of about one-half second duration, there suddenly occurred a tremendous evolution of smoke throughout the entire length of the conductor which filled the laboratory room and caused several other laboratory attendants promptly to vacate the premises. Once this effect is witnessed, there no longer will be any doubt that such an occurrence positively must be prohibited on aircraft electrical systems in flight.

L. G. Levoy (General Electric Company, Schenectady, N. Y.): This paper should prove to be of substantial value and interest to designers of aircraft electrical systems, and fills a long felt need in the industry. The authors are to be congratulated on providing useful basic data, and pointing the way for obtaining a more rational basis for short-time current ratings of wires than heretofore has been available.

On some aircraft installations, after periods of use, it was observed that the conductor insulation on certain wires appeared to have slipped back, exposing the bare conductor for one-half inch or more near the end, and it seemed unlikely that the insulation was cut back that far at the time of installation. This phenomena may be a result of the longitudinal thermal expansion and contraction of the conductor, and the lack of bond between the conductor and insulation. I would be interested in knowing whether or not the authors observed this effect, and under what conditions it can be expected to appear.

In the zone labeled "smoke starts," the lower boundary apparently represents the lower limit at which smoke was observed on any sample, and the upper boundary of this zone represents the upper limit above which all sample conductors smoked. Is this difference a result of the different types of insulation tested, or of the difficulty of detecting accurately the beginning of visible smoke?

B. W. Jones and J. A. Scott: L. G. Levoy mentions the apparent shrinkage of the wire insulation, which takes place most noticeably with heavy current surges and consequent rapid conductor heating. The wire expands rapidly as its temperature rises, it separates from and protrudes out of the insulation which responds more slowly. On subsequent cooling the wire shrinks but carries the insulation back with it, with a net result that looks like slippage.

The width of the "smoke starts" zone is a result of the difficulty of detecting accurately the time at which smoke first starts, or more accurately expressed, reaches a noticeable rate of evolution, for the rate at which smoke is given off changes rapidly with the temperature once it starts.

F-3 Lead Alloy—An Improved Cable Sheathing

Discussion and authors' closure of paper 46-115 by L. F. Hickernell and C. J. Snyder, presented at the AIEE summer convention, Detroit, Mich., June 24–28, 1946, and published in AIEE TRANSACTIONS, 1946, August–September section, pages 563–9.

Herman Halperin (Commonwealth Edison Company, Chicago, Ill.): For the past 16 years, I actively have been looking for and assisting in the development of a lead alloy for improved cable sheathing. The development of the F-3 lead alloy is, I believe, the first lead alloy that has substantially better quality in all properties than ordinary commercial leads, without having any particular disadvantages. The authors and their associates deserve great praise for the development.

Considerable work on field conditions has been done in Chicago during the past 20 years to avoid premature sheath cracking in manholes incidental to bending caused by variations in daily loading. This work included

1. Enlarging manholes to provide more room for cable movement.
2. Improving the cable training.
3. Modifying the cable fireproofing in the manholes.

The troubles caused by sheath cracks were reduced, but are still a major item. As brought out in an earlier paper,[1] the life of the sheath to cracking in the manhole is in many cases substantially less than the life of the insulation.

Our interest in the development of a new alloy has been accentuated in recent years mainly because we expect to continue the trend of increasing the loading of cables in order to obtain the maximum feasible usage of investment. Recently, the prices of cable have increased roughly one-third. The costs of conduits and manholes have increased even much more in the past seven years. Altogether, such sharp increases in costs emphasize the necessity for carrying heavy loads in underground cable systems, especially since there seems to be no particular tendency to allow electricity rates to increase.

The bending amplitude of the sheaths in the manholes is increased with increased loading. Furthermore, the ability of the sheaths to withstand a given amount of bending is decreased by the higher temperatures at which the sheaths will operate.

We changed a few years ago from belted type cable to shielded type 3-conductor cable for 12-kv service. Then we found that the life of the sheath of shielded cable before cracking in dummy manhole tests was roughly 40 per cent less than for the sheath of the belted type cable. Therefore, we were going forward as far as the insulation is concerned and backwards as far as the sheath was concerned.

We have investigated several types of alloys on an experimental basis, and we are continuing these co-operative investigations with the manufacturers. Two of the alloys that seemed attractive initially subsequently were found to be unsuitable. These two materials age hardened and then had no advantage, and perhaps some disadvantages as far as resistance to manhole fatigue was concerned.

Over the past four years, we have made extensive studies on the F-3 alloy sheath in Chicago and at the University of Illinois. According to our tests, this alloy does not harden with age, and its ductility is retained with age even better than that of chemical lead. Also, the F-3 alloy seems to be suitable for use at considerably higher hoop stresses than ordinary leads in use.

A comparison of the life to fracture of the F-3 alloy to that of ordinary lead in the dummy manhole is shown in Figure 1 for a variety of conditions. All of the tests represented were made on 500,000-circular-mil 3-conductor 12-kv cable of several types having practically the same diameters. In some cases the samples are from the same factory, so that they differed only in type of sheath or binder.

These data indicate that with equal conditions of temperature and movement, F-3 sheaths can withstand about three times the number of bending cycles that copper bearing lead sheaths can withstand. The graph also shows how sharply the life of sheaths decreases when the sheath temperature is increased from room temperature to merely 43 degrees centigrade (110 degrees Fahrenheit). That temperature represents a high average temperature for sheaths in manholes during maximum day-in-and-day-out loading and is the temperature we selected about 12 years ago for some of the research at the University of Illinois.

For some cables an increase of 200 per cent or more in sheath life, as indicated for the F-3 sheath, is quite desirable. For example, the 200-per-cent improvement is essential for some uses of 3-conductor shielded type cable with metallic binder. Based on these laboratory data and related field experience, for equivalent life to sheath fracture for cables having over-all diameters greater than about 1.75 inches, it is estimated that the new alloy will permit an increase of about 25 per cent in daily loading. Some other factors, such as the deterioration of the insulation or system conditions, might reduce the extent to which this advantage can be applied.

These bend tests were made at a rate of about one cycle per minute, whereas the bending in service is at about one cycle per day. In the research on cable sheathing at the University of Illinois, some information is being obtained on the effect of the speed on the life to fracture, for strip specimens are held horizontally at points eight inches apart while the middle is moved up and down. The average number of cycles to fracture with 10-minute cycles for lead was 51 per cent less than the number of cycles with 1-minute cycles, while the decrease was only 37 per cent for the F-3 alloy. Tests with longer cycles are in progress, but results are not available now. If this trend persists to 24-hour cycles in service, then the superiority of F-3 alloy over lead in this respect is even greater than that indicated by the graph.

Incidentally, our co-operation with the Anaconda Wire and Cable Company in testing and otherwise investigating the F-3 alloy started six years ago. We did not place any commercial order for cable with the F-3 alloy until November 1944. These time periods are mentioned to indicate that the investigations of the suitability of a new lead alloy take years.

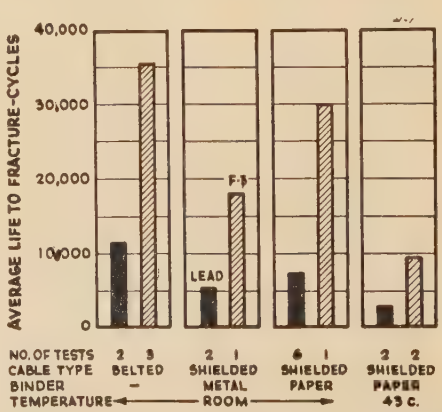

Figure 1. Life of sheath in dummy manhole—0.5-inch movement

Reference

1. Load Ratings of Cable, Herman Halperin. AIEE Transactions, volume 58, 1939, October section, pages 535–52.

C. T. Hatcher (Consolidated Edison Company of New York, Inc., New York, N. Y.): The authors have presented data on a subject which is of extreme importance to the industry at the present time. A lead sheath is being offered which apparently answers many of the disturbing problems which we are encountering today. If field experience confirms the laboratory test data, then a great contribution has been made.

The authors list oil filled cable operating at 10 to 15 pounds pressure as one of the places where this type of lead could be used advantageously. A more specific requirement for the use of this lead in oil filled cable systems is where the pressures may be in excess of 15 pounds, and therefore double sheath cable is required. Elimination of double sheath cable is one of the things which we always attempt to do in the initial design of an oil filled system. I have attempted to obtain this end during the past number of years, and if the new lead will answer this problem a considerable contribution has been made.

A lead sheath which will give longer life under loading conditions causing expansion and contraction of cables is needed. We have had several experiences in recent years where the cable sheath has been broken on gas and oil filled cables because of cable movement in manholes where proper racking conditions could not be obtained, and if a sheath is available that will help this situation it certainly will be helpful.

Abe Tilles (Pacific Gas and Electric Company, San Francisco, Calif.): As the authors state, improvement in dielectric of cables has made the lead sheath more and more of a limiting factor in the life of the cable. Accordingly, the very fine qualities reported in the paper for the lead alloy described are of great interest to all users of lead covered cable.

It would be of interest to know how much of such sheathing has been placed in com-

mercial use and which operating companies have made major installations. It also would be of interest to know if this sheathing has been, or is being, applied to higher voltage, for example, 120-kv cable.

T. H. Haines (Boston Edison Company, Boston, Mass.): During the past few months, the Boston Edison Company has been testing F-3 lead sheath at its own laboratory. Three 10-foot samples of 3-conductor 350,000-circular-mil cable having 260 mils of paper insulation and 125 mils of F-3 lead were bent to a radius of 42 inches. One end was fixed and the other was moved back and forth by a motor driven arm which made ten 2-inch strokes per minute. An air valve and pressure relay were attached to each test specimen. During the test the cable sample operated with an internal air pressure of five pounds per square inch. When the sheath cracked, the relay operated, stopping the test. The number of cycles of bending was read on a counter.

For comparison, three samples of cable sheathed with commercial or copper bearing lead were tested in the same way. These were chosen to have as nearly as possible the same weight, outside diameter, and lead thickness as the Anaconda Wire and Cable Company sample. One was a piece of 3-conductor number-4/0 15-kv split sector cable and the other two were cut from a length of 3-conductor 350,000-circular-mil 28-kv type-H cable. The number of cycles required for failure with the F-3 samples were 20,260; 25,695; and 19,484. The number of cycles required for failure with the control samples were 9,931; 6,061; and 8,307.

In each case it was noted that the F-3 lead cracked between the bulges developed by the test, while the other sheaths cracked on the bulged surface.

Another type of test was tried which consisted of placing strips of sheath between strips of brass and clamping the assembly jaws six inches apart. The centers of the strips were vibrated with a 7/32-inch stroke at a frequency of 240 cycles per minute. We have not had this device in use long enough to have established a standard reproducible test, but in the few runs which were made the strips of F-3 lead remained intact longer than the other samples.

Howard S. Phelps (Philadelphia Electric Company, Philadelphia, Pa.): Physical tests have been made on limited samples of F-3 lead alloy cable sheathing and sheathing pipe by the Philadelphia Electric Company.

Internal Pressure Hydraulic Bursting Tests

Time-to-Burst. Hydraulic bursting tests at constant internal pressure[1] at 110 degrees Fahrenheit on sample of F-3 lead alloy sheathing pipe indicate this alloy has characteristics quite different from those of lead sheathing alloys heretofore tested. The time-to-burst versus initial stress data substantially corroborate the F-3 curve of Figure 5 of the authors' paper for stresses of 2,400 and 1,600 pounds per square inch. Present indications are that the time-to-burst for a specimen of approximately two inches internal diameter and 9/64-inch nominal thickness may be of the order of 40 years at 100 pounds per square inch internal pressure (720 pounds per square inch initial stress). This contrasts with a number of other alloys tested, none of which appears to be very much longer lived than commercially pure lead at stresses of the order of 300 to 400 pounds per square inch.

Type of Failure. It has been found characteristic of lead sheathing having appreciable percentages of alloying elements (that is, more than one-tenth per cent), that the bursts occur in the welds. The F-3 sheathing pipe appears to be no exception. The failures of the specimens tested at 2,400 and 1,600 pounds per square inch initial stress occurred in die welds.

Total Stretch. The total stretch of F-3 sheathing at failure, as indicated by the authors in Figure 9, increases with decreasing stress, but appears to be of the order of 15 per cent increase in diameter. In the Philadelphia Electric Company tests, the total stretch for the specimen stressed at 2,400 pounds per square inch was 2.8 per cent, and 4.0 per cent for the specimen stressed at 1,600 pounds per square inch. This corroborates the tendency toward increasing total stretch at failure with decreasing stress, indicated by the authors. However, in the Philadelphia Electric Company tests the total stretch was considerably less than for copper lead or chemical lead for the same stresses, indicating the F-3 sheathing is less ductile at high stresses.

In 66-kv single conductor solid type cables, the pressures developed by thermal expansion can become very great. Although A.S.T.M. grade leads (not alloyed) are quite ductile at high stresses, a considerable proportion of failures of such cables are attributed to sheath bursts by internal pressure, despite the relief afforded by stretching of the sheath. It would appear that for this type cable, the reduced ductility of F-3 lead alloy at the higher stresses may result in more internal pressure failures.

Bending Resistance

Philadelphia Electric Company has made limited dummy manhole bending tests[2] on cables sheathed with F-3 lead alloy. The results indicate that the life of cable sheathed with this alloy is of the order of three times that for the same type of cable sheathed with the types of lead generally used commercially.

Hardness

Hardness tests of F-3 alloy lead indicate it to be intermediate in hardness between Asarco (0.26 per cent tin, 0.03 per cent magnesium, 0.025 per cent calcium, and 0.02 per cent bismuth) and the leads in general commercial use.

References

1. Internal Hydraulic Bursting Tests of Lead Cable Sheathing, **H. S. Phelps, A. M. Gates, F. Kahn.** *Proceedings*, American Society for Testing Materials, volume 40, 1940, page 885.

2. Cyclic Movement of Cable—Its Causes and Effects on Cable Sheath Life, **Clement S. Schifreen.** AIEE Transactions, volume 63, 1944, pages 1121–30.

G. B. McCabe (Detroit Edison Company, Detroit, Mich.): The new F-3 alloy of the Anaconda Wire and Cable Company appears to have many desirable properties that appeal to utility operators of cables, who are always glad to welcome and adopt any proved new development that insures longer and more troublefree life for cable. If actual field experience under a variety of operating conditions supports the test results and the many claims made for the new alloy, there undoubtedly will be a demand by the operators for the more universal use of it as sheathing of cables to be installed on their systems.

The primary purpose of my discussion is to correct an erroneous conclusion which the authors drew from reference 9 of their paper.

In using this reference, the authors stated that calcium alloys (0.025 to 0.031 per cent) are difficult to extrude (very drossy) and undergo slow and serious age hardening, which has caused troubles to develop in a few years of service due to brittleness and early cracking in the manholes.

The authors have used the term calcium alloy, whereas a distinction should be made between straight calcium lead cable sheathing and other alloys of lead containing calcium. I wish to make it clear that we have had no adverse experience with straight calcium lead sheathing in five years of service.

The article referred to dealt principally with trouble experienced with a quinary alloy composed of magnesium, tin, bismuth, calcium, and lead, which was designated as alloy B. Cable sheathed with this alloy, which originally was installed in 1940, developed innumerable cracks through the sheath upon being reinstalled. A large circumferential crack also was discovered in the expansion loop of an aerial line of cable sheathed with this alloy. A similar crack was uncovered in a slight offset two feet from a joint in a heavily loaded underground cable.

Laboratory examinations of sections of the sheath indicated that the failure of the sheath was caused by age hardening, with resultant loss in ductility as manifested by a marked intercrystalline brittleness and decrease in bending strength.

Also in 1940 there was installed a considerable quantity of cable sheathed with calcium lead containing a nominal content of 0.027 per cent of calcium.

This cable, which was of the 350,000-circular-mil shielded 3-conductor 24-kv type, was installed in various parts of the system in order to obtain operating experience under a variety of conditions, such as on aerial construction, on the feed from a large base-load generator to a switching station, and in cable transmission lines subjected to heavy load cycles.

During the service of more than five years for this cable, there has been no sign of distress in the sheathing at any point. Samples taken from a length, on which three installations were simulated, revealed no evidence of even surface checking of the sheath.

Figure 2 of this discussion indicates the influence of calcium content on tensile strength. It also shows the relatively short time necessary for calcium alloys to approach their ultimate tensile strength. The calcium lead (0.025 per cent) starts out with a tensile strength of about 3,000 pounds per square inch (curve 2) and attains values in excess of 3,600 pounds per square inch within 20 days (curve 3). Alloy B, however, required about one year's aging before it approached its ultimate value (curve 1). The

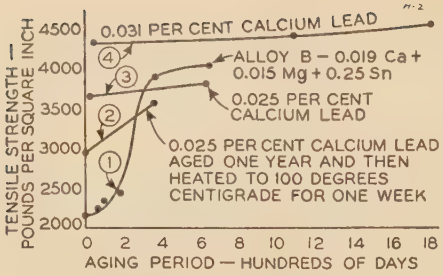

Figure 2. Increase in tensile strength of alloy sheath after aging

Samples represented by curves 3 and 4 were 21 and 48 days old before the first test was made

data for the calcium lead, which incidentally were received largely from the Anaconda Wire and Cable Company laboratory, do not agree with the curve on Figure 1 of the present paper, which shows that it takes almost two years instead of a few weeks for 0.025-per-cent calcium lead to attain a tensile strength of 3,600 pounds per square inch.

Figure 3 of this discussion shows the uniformity of bending strength with time for calcium lead, compared to the large decrease for alloy B in less than one year.

In those tests reported in the paper by Hickernell and Snyder, in which data were obtained on calcium lead composed of 0.025 per cent calcium, there appeared to be but little difference between it and the F-3 alloy, particularly as shown in Figures 2, 4, and 12.

Metallurgical consideration indicates that the calcium content could be reduced to 0.020 per cent and thus improve the important property of ductility without significant reduction in tensile strength, and resistance to creep, fatigue, and abrasion. A 0.020-per-cent calcium lead probably would have a tensile strength of about 3,200 to 3,300 pounds per square inch, approximately that of the new F-3 alloy.

While I am in no position to question the statements of the authors with reference to extrusion difficulties encountered with calcium alloys, their data fail to support the implication that poor service is an inherent quality of calcium lead cable sheath.

Data on copper bearing lead reveals tensile strength of about 1,950 pounds per square inch. It would appear that F-3 alloy, which has a tensile strength of 3,250 pounds per square inch according to Figure 1 of the paper, would be at least 65 per cent stronger than copper bearing lead instead of "not much stronger" as stated in the paper. Also, the Brinell hardness number of F-3 alloy is almost double that of copper lead.

On the occasion of previous developments by a cable manufacturer, such as compact stranding, carbon dioxide cleansing of impregnating tanks, supercalendered paper insulation, shielded construction, gas filled cable, and the like, agreements have been effected between the various manufacturers concerned for the incorporation of such new developments in cables produced by them. What is the probability of the new F-3 alloy becoming available soon to the other cable manufacturers so that the users may benefit from the claimed and proved advantages of such an improved sheathing on their future cable purchases?

How will the cost of cable sheathed with F-3 alloy compare with those sheathed with copper-bearing lead and the alloys of tin or antimony?

REFERENCE

1. AGE HARDENING PROVES FATAL TO LEAD-ALLOY CABLE SHEATH, G. B. McCabe. *Electrical World*, October 13, 1945.

C. R. Bond and **F. W. Nimmer** (Ohio Edison Company, Akron, Ohio): Hickernell and Snyder are to be complimented on the excellence of their paper. There appears to be a substantial contribution to the reliability of electric power cables by the development of a new lead alloy to be used in cable sheathing. They have tried to take into consideration all of the essential requirements for lead sheath demanded by the cable users at this time. It also is interesting to note that a good deal of time seems to have been devoted to the accompanying research problems in order that essential properties might be given adequate consideration, prior to the presentation of a definite recommendation of superiority of any given type of cable sheathing. Not only has the technical research work been done, but actual commercial installations have been made which have been in service for a period of several years in particularly critical locations, in order to determine the variations between laboratory test and practical commercial installations.

In the interest of completeness, we suggest that two additional items be considered; namely, any new alloys used for lead sheathing should not affect the insulating properties of the various insulating materials to be employed, and, also, such lead sheathing should have good thermal conductivity. Up to the present time, we have not been concerned particularly about these features, but as new alloy sheathings are developed, we must be certain that deterioration of the cable will not result from a lack of recognition of these features.

If this new F-3 lead alloy fulfills the requirements as well as we hope that it will, Hickernell and Snyder will have made a very substantial contribution to the cable art.

Earle E. Schumacher (Bell Telephone Laboratories, Murray Hill, N. J.): I have read with interest the paper by Hickernell and Snyder and consider the work which they have done a valuable contribution to the cable sheath art. My major comment concerns the authors' statements regarding lead alloys containing 0.025 to 0.031 per cent calcium. The embrittlement behavior cited in their reference 9 actually concerns a complex lead calcium alloy containing magnesium rather than the binary lead calcium alloy. It is well-known that magnesium is likely to induce brittleness in lead. The paper by G. B. McCabe emphasizes that the binary lead calcium alloy is not subject to this embrittlement and states that ". . . a reel of lead calcium alloy sheathed cable, that had been installed and operated for $2\frac{1}{4}$ years and later removed from the duct, was subjected to re-reeling twice at the cable plant. No evidence whatsoever of even surface checking of the sheath was found."

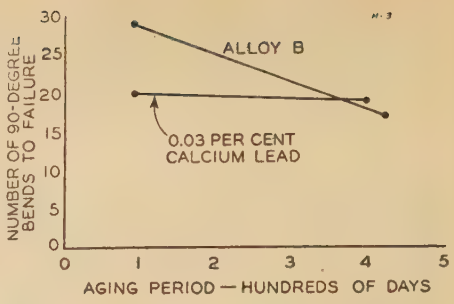

Figure 3. Decrease in bend strength of alloy sheath after aging

These sheaths were extruded in the latter part of April 1940, but were not tested until nearly three months later

This confirms Bell system experience with lead alloys containing 0.025 to 0.031 per cent calcium. Hundreds of miles of telephone cable sheathed with this alloy have shown no evidence of failure because of embrittlement.

With regard to the authors' statement about dross in lead calcium sheath, microscopic examination of a great number of samples of the binary alloy have shown this type of sheath to be as free from dross as other types of lead alloy sheath extruded on intermittent presses.

My other comments deal with the interpretation of creep and fatigue data in general. Creep tests at the Bell Telephone Laboratories carried out over a period of eight years have shown that data taken at stresses of 400 or 500 pounds per square inch are not necessarily a reliable indication of the behavior of the same alloys stressed at 100 or 150 pounds per square inch. The slope of the stress-rupture curve often changes at the low stresses, and this may change the relative rating of the alloys.

With respect to fatigue data on lead cable sheath alloys, we have found as a result of extensive studies that frequently the relative merit of different materials is dependent upon the speed of testing. Since the major deflections of sheath in service are in most instances of the order of one or two cycles per day, there is a substantial reason for testing at speeds much lower than 700 cycles per minute. Accordingly, most of our tests now are made at a speed of 15 cycles of reversed deflections per hour. Also, since the forces which produce cyclic sheath deformations in service are so great that sheaths regardless of their properties tend to be deflected similar amounts, there is considerable merit in making fatigue comparisons on a deflection cycle basis rather than on a stress cycle basis.

G. B. Shanklin (General Electric Company, Schenectady, N. Y.): F-3 alloy is undoubtedly a step forward in the art of cable sheath construction. It is one of a group of arsenical alloys, all of which have similar characteristics. There are a number of relatively hard high strength lead alloys available for cable sheathing. Most of these are age hardening but some are age softening (self-annealing). The arsenical alloys belong in the latter class, and this explains their higher bending fatigue life, which is their outstanding characteristic.

Any type of hard high-strength lead-sheath alloy requires exceptionally close metallurgical and foundry practice control to assure that neither age hardening nor age softening will become objectionable or dangerous after a long period of service. In underground power cable work, the two most important characteristics that need control throughout the life of the cable are bending fatigue and long-time creep strength. These two characteristics oppose each other, however. High bending fatigue resistance requires an age softening alloy, while high creep strength resistance requires an age hardening alloy. The obvious goal is to obtain an alloy that neither age softens nor age hardens but retains complete stability of characteristics throughout its life. Everyone who has had experience with the high strength alloys knows how difficult it is going to be to reach this goal. With this in mind, it might be well to review briefly the major sheath requirements for the different types of high voltage cable used in this country.

For solid type cable, especially up to 18-kv rating, resistance against sheath fatigue caused by cable movement is an outstanding requirement with high creep strength a lesser requirement. Practically all sheath fatigue troubles have occurred in this type and voltage range of cable and are primarily caused by high operating temperature range and small manholes with inadequate bends and offsets. As the voltage rating of solid type cable increases, bending fatigue becomes of lesser importance and creep strength of greater importance, because of the fact that the operating temperature range decreases, and more liberal bends and offsets in the manholes generally are used. Also, oil filled joints and reservoirs increase the importance of high creep strength.

During the past 19 years, something like 4,000,000 feet of standard low pressure oil filled cable have been installed in this country. As far as sheath failures caused by cable movement are concerned, the record is remarkable, in fact practically perfect. Most of this cable has copper bearing single sheath, and this service record plainly indicates that there is still plenty of latitude for load and cable movement increase before there will be any serious problem of bending fatigue. The reason for this is that the manholes always have been large to accommodate the accessories, and the bending radius and offsets always have been quite liberal. This experience shows that there is no real need of a high bending life alloy as far as oil filled cable is concerned. There is some need, however, for a high creep strength alloy sheath for oil filled cable, particularly on steep grades where hydrostatic head pressure builds up. The economic over-all saving that this would represent, however, is much less than most engineers realize. For average profiles usually encountered, it would mean a few less stop joint manholes. This in turn would in average cases mean only a few per cent saving in over-all cost. In return it would mean a definite commitment to high hoop stress operation of the sheath. Hickernell and Snyder are not exactly correct when they say that copper bearing sheath is limited to a hoop stress of 125 pounds per square inch. This limit actually applies to two-per-cent tin alloy sheath at full operating temperature. Long experience has shown that copper bearing sheath can be worked safely to a hoop stress of 150 pounds per square inch without noticeable creep in service. To show any appreciable economic gain, an alloy sheath would have to be used which would allow a hoop stress of at least 300 pounds per square inch, and resistance to creep under this stress must be retained throughout the life of the cable. In the case of age softening alloys such as F-3, we would have to be absolutely sure that these limits could be met. There would be little doubt about it with age hardening alloys such as Asarco, but it is yet to be proved with age softening alloys, where the relative decrease in creep strength with increase in time and temperature is more marked.

With low pressure gas filled cable, there has been a limited amount of trouble with sheath fatigue caused by cable movement, but this has been only at 15 kv and for the reasons already outlined for similar trouble with solid type cable. This type of cable is used under much the same conditions as solid type, and there is no question but that high bending fatigue life is desirable at the lower voltage ratings. High creep strength is even more important, however, since the present low pressure gas filled cable with copper bearing sheath is limited to a working gas pressure in the order of 15 pounds per square inch. If this could be doubled, it would allow a reduction in insulation thickness and actually become a medium pressure system. It would, however, mean that a hoop stress in the order of 300 pounds per square inch would have to be accepted. There is an open question whether an age softening alloy could withstand this working stress indefinitely at full allowable operating temperature and with the cable movement that will be superimposed. So far, we have used only the double reinforced type of sheath for medium pressure systems. We have hesitated to offer Asarco sheath unconditionally for this purpose, not because there was any doubt about its permanently high creep strength, but because of its tendency to age harden. For the present at least, we would hesitate to offer an age softening alloy for reverse reasons, and feel that a good deal more must be learned about the stability of long-time creep strength before such extreme limits of hoop stress are adopted on a wide scale. Until these points are cleared, the logical field of use for F-3 alloy is in taking advantage of its bending fatigue resistance as required by solid type cable.

A systematic research program is being carried out by our laboratories, and presumably by others. Based on results to date, we feel that it is only a question of time before improved lead sheath alloys having high creep strength stability become available.

R. J. Wiseman (The Okonite Company, Passaic, N. J.): Hickernell and Snyder have presented a most interesting paper on a lead alloy which they have developed to meet the problems which confront us today in the operation of impregnated paper cables. They list the factors which determine if a lead is good or bad. All of us for several years have been studying lead alloys as we have come to recognize that to meet the demands of the electrical industry for a long life lead sheath, it is necessary to turn to alloys. Some have been promising in the beginning, but because of age hardening have failed to prove in. Others are good in some physical respects, yet fail in other respects, so we have been hesitant to try them out on a large scale. It appears that the authors have a very promising alloy and even though their tests give every indication of successfully meeting the all-around physical properties of good sheathing, we all know that field experience will be the final criterion after a large production of pipe with the variability of foundry practice present.

There is one interesting fact to me which my company, in its study of this subject, found to be significant. You will note that the authors do not use a large amount of an alloying metal, but small amounts of several metals. We found this to be favorable in our studies. We have studied the same metals as the authors report and also others, but in all cases small amounts were used. In some cases there seems to be a limit to the amount which is helpful, beyond this the alloyed lead loses its promising properties. There are some metals, even in small amounts, which are undesirable. As many of us have been working on this problem for years, we can expect a disclosure, from time to time, of other alloys of lead also approaching the ideal sheath to meet the increasing demands of the utilities for higher operating temperatures without sheath failures, which is the major cause of cable failures today.

L. F. Hickernell and C. J. Snyder: In general, the experimental data presented by the discussers corroborate data in the paper. In evaluating the several properties and in the possible applications of the new alloy, some differences in opinion exist. This is to be expected with any new material and serves to indicate the value of free and open discussions on engineering matters as afforded by the forums of professional societies.

Specifically, in reply to the discussers, we offer the following:

(*Halperin*) We greatly appreciate the encouragement of Halperin in this development and are indebted to him and his engineering associates, the Commonwealth Edison Company, Utilities Research Commission, and University of Illinois for their painstaking research program and evaluation of this new alloy. We hope at some future time he will present more of these interesting and valuable data.

Although not strictly on the subject of the paper, we cannot refrain from pointing out in his figure the increase in life on bending obtained on shielded cable by replacing the metal binder with a paper binder. This superior mechanical performance is obtained without any sacrifice in electrical characteristics by constructing the binder of carbon black tapes which have transverse (radial in the cable) as well as longitudinal conductance and hence form a short effective conducting path from the individual shielded conductors to the sheath.

(*Haines*) On the basis of average values, we note that the life of F-3 alloy was approximately three times that of the copper lead sheath, thus verifying results obtained by others. This confirmation is of special

interest because the bending of the cable samples was conducted on a different type of test equipment.

(*Hatcher*) As pointed out in the paper, the higher working stress of F-3 alloy will permit the use of single instead of double sheath in certain installations. We hope that a trial installation can be made to study its operating performance in this service.

(*Tilles*) Up to August 1, 1946, about 140,000 feet of cable (or 600,000 pounds of alloy) are on order or have been shipped to Commonwealth Edison Company, Kansas City Power and Light Company, Duquesne Light Company, Consolidated Gas Electric Light and Power Company of Baltimore, Pittsburgh Plate Glass Company, Detroit Edison Company, and Arkansas Power and Light Company. The highest voltage cable rating to date is 45 kv.

(*Phelps*) With reference to bursting strength, we have experienced no failures in over four years of F-3 alloy at stresses 1,000 pounds per square inch or lower in samples on test. Other alloys tested are not appreciably better than copper lead at low stresses (see Figure 5). We are glad to note confirmation of this desirable performance.

In our experience, bursts occur at the thinnest portion of the specimen, which is quite likely to be in the region of the top or bottom weld. This is a limitation of present extrusion equipment rather than an inherent property of any material. Despite this, reference to Figure 5 indicates that at 1,600 pounds per square inch time-to-burst of F-3 alloy is approximately 500 times that of copper lead.

In discussing inherent properties of these materials, it is important to note that most alloys are characterized by a difference in the grain structure at the weld areas compared to the remaining structure, which is the cause of their relatively low bursting strength. However, F-3 alloy has uniform grain structure throughout (see Figure 4 of this discussion). Accordingly, F-3 alloy inherently has the same unit strength in the weld areas as elsewhere in the structure.

As shown in Figure 9, F-3 alloy is less ductile than copper lead at the same stresses. However, in the case of 66-kv solid type cable, operated with oil reservoirs, we do not see quite how the use of a material with greatly superior bursting strength would lead to more internal pressure failures.

(*McCabe*) In view of his favorable operating experience with 0.025 per cent calcium lead alloy, it would appear that our reference 9 is in error. However, it is well-recognized that calcium lead does age harden as indicated by McCabe's curve 2, Figure 2 of his discussion. This age hardening ultimately lowers the bursting strength and bending resistance.

Curve 3 (obtained from our laboratory in 1941) in McCabe's Figure 2 was based on data from cable sheath. Our Figure 1 is based on tubes. The mechanical working in tightly applying the sheath onto the cable core rapidly ages an age sensitive material. Consequently, the initial tensile values on a sheath are approximately the same as those on a tube after a considerable period of aging.

Referring to McCabe's Figure 3 of his discussion, the principal purpose of the IPCEA* bending machine is to check quality at the factory by disclosing poor welds, lamination, and so forth. We believe it is not sufficiently sensitive to differentiate aging characteristics between materials.

As stated, 0.025 per cent calcium lead is about the same as F-3 alloy in our Figure 2 (creep resistance), Figure 4 (creep rate), and Figure 12 (vibration fatigue). However, after aging calcium lead lacks bending resistance and bursting strength (Figure 5) of importance in power cable service.

The licensing of other manufacturers to use this patented cable sheathing material is a matter of negotiation between commercial departments.

Based on present market conditions, it is expected that F-3 alloy will cost no more, and perhaps somewhat less than two per cent tin or three-fourths-per-cent antimony alloy. Obviously, the exact differential between any of these alloys is dependent upon the metal market at the time of quotation.

(*Bond and Nimmer*) With reference to thermal conductivity, we have made no determinations, but we would not expect it to differ appreciably from other lead sheathing material. In current-carrying-capacity calculations, thermal resistance of the lead sheath is assumed to be negligible. Thermal emissivity depends primarily upon the condition and color of the sheath surface and has been standardized as one value for all sheathing materials.

Regarding the effect on the insulation, we find that the chemical composition of the sheath material makes little difference in the formation of lead soaps. Of course, in our type CB cable design, any formation of copper or lead soaps is neutralized completely by the adsorption properties of carbon black.

(*Schumacher*) Our statement regarding the effects of age hardening of calcium lead alloy was based primarily upon the results of dummy manhole tests and some operating experience in power cable service. Apparently, our reference 9 to the McCabe paper was unfortunate. We never have questioned the adequacy of 0.025 per cent binary calcium alloy for telephone service. As a matter of fact, until the development of our new alloy, we recognized this calcium alloy as the equal or superior to the customary alloys used for power cable service.

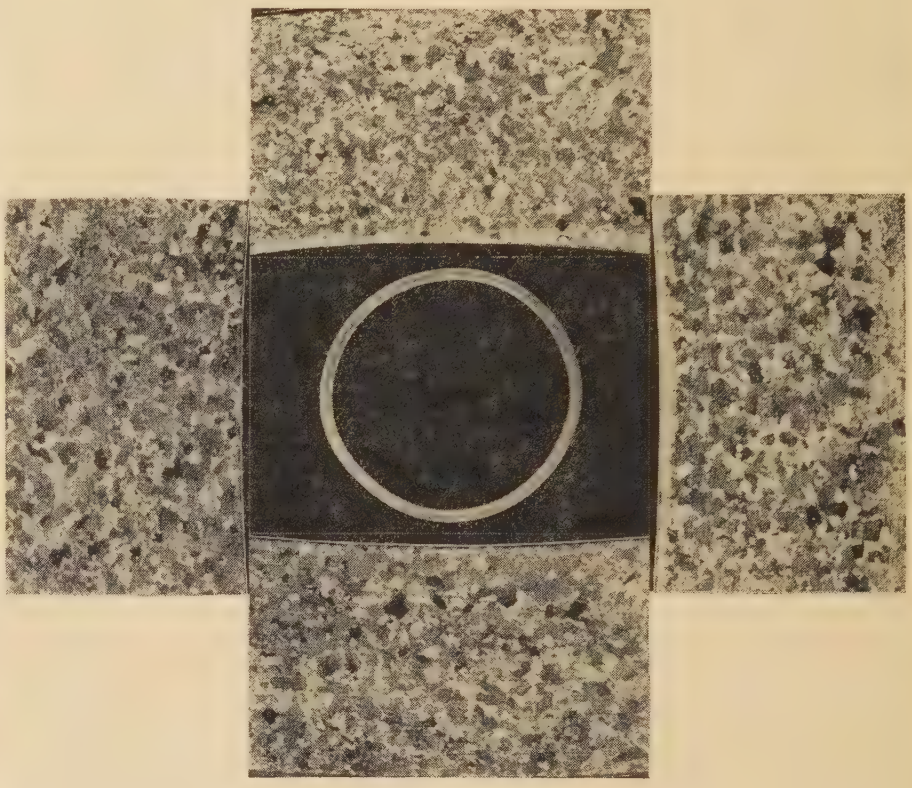

Figure 4. Structure of F-3 alloy

Upper and lower microphotographs show weld areas

Two side microphotographs show nonweld areas

When melted, calcium alloy forms surface dross much more readily than other alloys because of oxidation of the calcium. This is undesirable from an extrusion standpoint because

1. The dross, if not thoroughly removed, may be extruded inadvertently in the finished sheath.
2. The calcium content must be replenished frequently.

Consequently, additional process and metallurgical control is required. This can be accomplished, as demonstrated by Western Electric Company and our plants, but at increased cost. F-3 alloy does not dross readily, in fact it forms less dross than copper lead, and its chemical composition remains stable when melted.

In our paper we have designated high frequency test results as vibration fatigue and low frequency as bending resistance. We agree that the latter is the more important for power cable in ducts. In his discussion of

* Insulated Power Cable Engineers Association.

our paper, Halperin has reported his results on 1-minute (60 per hour) and 10-minute (6 per hour) cycles in addition to his dummy manhole tests at 70-second (51.4 per hour) cycles.

(*Shanklin*) In assuming that F-3 alloy is age softening because it contains arsenic, Shanklin apparently has overlooked the fact that it also contains tin and bismuth. In over four years of testing, we have found no age softening except for a very slight amount in the first few months (see Figure 1). F-3 alloy is stable in properties, purposely so designed, and, in our opinion, meets the goal of "an alloy that neither age softens nor age hardens but retains complete stability of characteristics throughout its life".

We do not agree that "high bending fatigue resistance requires an age softening alloy, while high creep strength resistance requires an age hardening alloy". Calcium alloy has comparatively good bending resistance and antimony alloy has poor creep resistance, yet both are age hardening materials.

Practically all power cables undergo daily load cycles and hence are subjected to bending. A sheath which has higher bending resistance should improve cable life (or conversely, permit higher loading for the same life) whether solid, oil filled, or gas filled type. Whether or not the additional cost of such an alloy sheath is justified economically depends upon the individual installation and operating duty.

With respect to oil filled cable, may we suggest that present specification operating temperatures have been selected with the limitations of previously available sheath materials in mind which has contributed to the good operating record of present installations.

Experimental data indicate that copper lead sheath can not be operated safely at 150 pounds per square inch at *maximum permissible temperatures* for normal and emergency service. This is recognized in the AEIC† specifications which limit the stress to 125 pounds per square inch for standard sheath thicknesses. For cases where the stress exceeds 125 pounds per square inch, the thickness of sheath and composition of lead should be as agreed mutually between purchaser and manufacturer.

We have reason to believe that very few oil filled cables in this country actually are operating at 150 pounds per square inch; also, that most of them are operating at moderate temperatures. In several installations, when loaded to permissible temperature limits, sheath cracks have developed.

At the present time, we have suggested 200 pounds per square inch as a conservatively safe working stress for F-3 alloy. We anticipate that operating experience will indicate that this value can be increased.

Granted that this stress would not permit a reduction in insulation thickness of low pressure gas filled cable, we believe the use of F-3 alloy sheath would improve its performance by reducing the sheath troubles which have been experienced in the field with this type of cable.

(*Wiseman*) We are pleased to have the chairman emphasize the importance of small amounts of alloying elements on the properties of sheathing materials and to point out that an alloy is required to improve cable performance.

† Association of Edison Illuminating Companies.

Fundamental Properties of the Vacuum Switch

Discussion of paper 46-126 by R. Koller presented at the AIEE summer convention, Detroit, Mich., June 24–28, 1946, and published in AIEE TRANSACTIONS, 1946, August–September section, pages 597–604.

Jerome J. Taylor (The Detroit Edison Company, Detroit, Mich.): Perhaps everyone has speculated to himself about vacuum breakers, and there has been much experimental work on them. Comparatively little has been published. The author develops the problem in an incisive manner, and derives definite results on many interesting points. The paper itself lacks a few statements as to conditions under which the tests were performed. Curves show current points up to 100 amperes, but oscillograms are all in the 10- to 25-ampere range, and corresponding values of test circuit voltage and inductance are not presented. From a design standpoint, factors that cause failure of a switch to interrupt, and sequence of events when it does not, are of first importance. These are not discussed with the same attention as are the successful operations.

The small contact separation required in vacuum breakers raises the question whether for a-c service they could not be timed to open at current zero and be separated fast enough to prevent subsequent breakdown of the gap. There then would be realized the dream of opening high-power circuits without release of explosive energies within the breaker. If internal breakdown strength of a high vacuum switch is assumed to be of the order of 10^6 volts per centimeter separation of the contacts (limited by cold-cathode emission), an opening speed of 10^2 centimeters per second results in a nominal recovery-voltage strength of 10^2 volts per microsecond. This is not necessarily the limit in contact speeds and begins to compare favorably with many actual circuit characteristics.

T. E. Browne, Jr. (Westinghouse Research Laboratories, East Pittsburgh, Pa.): Doctor Koller has presented some experimental results obtained with a vacuum switch in a relatively low power d-c circuit. While these are of considerable scientific interest and are of value for the design of low power switches such as vacuum relay contacts, a word of caution seems to be needed against trying to extrapolate these results to the design of a high power vacuum circuit breaker. First, as is well-known, the problems involved in interrupting large alternating currents are such that studies of the interruption of small direct currents are applicable to them in only an indirect way. In stating that the literature contains no explanation for the lack of success of vacuum switches in power circuits, Doctor Koller apparently has overlooked such an explanation given by Dr. Slepian in a paper originally presented at the International Electrical Electrical Congress in Paris in 1932.[1] In this paper the action of the vacuum switch in interrupting alternating currents is analyzed briefly but completely. The principal difficulty is shown to be the finite thermal lag of the vapor emission from the electrodes, particularly but not exclusively the cathode.[2] In spite of the high rate of dispersion (not true diffusion) of vapor in an evacuated vessel, this "after-boiling" results in a considerable vapor density between the switch contacts at and just after a current zero. Under favorable conditions the restored voltage causes breakdown in this vapor only to a glow which loses its conductivity with the subsequent disappearance of the vapor blast. The weakness of the switch is, however, that such a glow shows a tendency, increasing with vapor density, current, and voltage,[3] to change over suddenly to an arc. Under such conditions the probability of this glow-arc transition (similar to the arc-back of a mercury arc rectifier) is high, and the switch is not a reliable interrupter.

Doctor Koller, however, in studying d-c interruption has focused his attention on the opposite phenomenon, the transition of an arc to a glow. His oscillograms, like those of some other investigators,[4] show many rapidly repeated transitions back and forth between arc and glow with the arc-to-glow transition finally "winning out", so to speak, when his interruptions were successful. This arc-to-glow transition tendency, or arc instability, is actually a source of trouble in an a-c breaker since, if it occurs too long before a normal current zero (at too large a current) in an inductive circuit, it can produce troublesome and possibly dangerous high voltage surges of very steep wave front. In the commonly-used low-current vacuum contacts, capacitor shunts often are required to absorb these surges.

Even if the delayed vapor blast could be controlled or eliminated entirely, the application of the vacuum switch to high voltage circuits still would face the difficulty of the apparently inherent lack of reliability of an evacuated space as an insulator which gives rise to random arc-back even in high vacuum thermionic rectifier tubes operated at high voltage. It appears that the glow-arc transition retains, at high voltage gradients, a finite probability of occurrence even at vacuum pressures where glows are invisible and so ordinarily are not imagined.

I should like to ask Doctor Koller for a fuller explanation of his suggestion of the use of multiple contacts for interruption of higher currents and voltages with vacuum switches. It seems very doubtful to me that contacts can be operated in parallel to increase the current interrupting limit, since, even with perfect contact synchronization, separate arcs ordinarily cannot exist in parallel with each other. A series arrangement of contacts undoubtedly would improve the voltage interrupting ability provided the voltage be distributed evenly among the breaks. Furthermore, experiments with the effect of series operation on the arc-back probability of mercury vapor rectifiers[5] indicate that the reliability of a series connection of breaks might be very much greater than that of a single break at the same per-break voltage. This follows from the observed random nature of the glow-arc transition.[3]

References

1. The Electric Arc in Circuit Interrupters, J. Slepian. *Journal*, Franklin Institute, Lancaster, Pa., volume 214, 1932, page 430. Section VIII.

2. High Velocity Streams in the Vacuum Arc,

E. C. Easton, F. B. Lucas, F. Creedy. AIEE TRANSACTIONS, volume 53, 1934, November section, pages 1454–60.

3. BACKFIRES IN MERCURY ARC RECTIFIERS, J. Slepian, L. R. Ludwig. AIEE TRANSACTIONS, volume 51, 1932, pages 92–104.

4. ÜBER RASCHE VORGÄNGE IM QUECKSILBERVACUUMBOGEN, O. Engelbrecht. *Archiv fuer Elektrotechnik*, Berlin, Germany, volume 36, 1942, page 515.

5. ARC-BACKS IN IGNITRONS IN SERIES, J. Slepian, W. E. Pakala. AIEE TRANSACTIONS, volume 60, 1941, June section, pages 292–4.

O. K. Marti (Allis-Chalmers Manufacturing Company, Milwaukee, Wis.): In spite of the fact that during the last few years many different kinds of vacuum switches have been put on the market, the literature still does not give any theoretical explanations of the various phenomena which occur during the interruption of an arc in vacuum. I am sure, therefore, that many investigators in this field will appreciate the splendid and thorough work done by Doctor Koller and that they also will feel indebted to Professor L. B. Loeb of the University of California who fostered this research. I had the good fortune during my stay in California to be able to follow some of this work from time to time and also to see the switch in operation under different conditions.

When studying the present circuit breaker art, especially the means employed for arc interruptions, one is impressed very much by the ingenious methods and contraptions which are being used to increase the rate recovery of the dielectric strength of the medium in the arc path. This is chiefly caused by the fact that it is very difficult to fill the space between the parting contacts with the dielectric medium, be it oil or air, in a very efficient way, and this is especially difficult if the opening speed of the contacts is very high as is the case in all modern breakers. The only other way to accomplish this same thing was by pushing the arc out of the space traveled by the contact. It easily can be seen that in connection with the vacuum breaker this difficulty does not exist because the dielectric medium used for interrupting the arc is present, nothing has to be forced or injected between the contacts, nor are any means necessary to force the arc to travel. In addition it has to be realized that vacuum has a dielectric strength far greater than any other interrupting medium in use.

I am in full agreement with the author that since in connection with the development of sealed tube rectifiers the art of removing gases from tube walls and internal parts has been perfected, it should be much easier to develop a high capacity vacuum switch consisting of a glass or steel container with bushings or inlets as used with sealed tube rectifiers.

Some of the most important results obtained during these investigations are

1. Very good interruptions still could be relied upon at a vacuum of 10^{-4} millimeter of mercury, which is quite significant considering the fact that at a vacuum of 10^{-7} millimeter of mercury there are still about 10^{9} gas molecules per cubic centimeter present. From experience with rectifiers, especially sealed tube rectifiers, such vacuums can be obtained easily in glass or steel vessels if properly evacuated and heat treated.

2. The pumping action and getter action of this type of switch was such that the vacuum did not seem to decrease after hundreds of operations if the contacts and shields were designed properly in spite of the fact that some of the material is removed from the contact during each operation. Some of these favorable results have been obtained probably also because that part of the gases released from the anode and cathode spots have been absorbed by them after each single arcing episode.

3. The arrangement and shape of the anode and cathode contributes a great deal to the performance during an interruption.

4. The amount of material which is being removed from the cathode depends, as could be expected, on the type of contact material but is extremely small if the vacuum is maintained below 10^{-4} millimeter of mercury. It also should be noticed that the cathode and not the anode loses material.

However, it seems to me that the author made the most valuable contribution to the understanding of arc interruptions by his analysis of the mechanism of the arc on the basis of much data collected by means of special cathode-ray oscillograph and high speed camera setups which required very painstaking work. An excellent understanding of the arcing episodes can be obtained from a study of Figure 7. Following his theoretical outlines it easily can be imagined that the operation would differ materially from that of a high vacuum tube as there is no longer a clear path for the electrons, especially at the time of contact separation, because of many the emitted electrons will collide with gas molecules, a condition which will improve naturally after each successive episode.

At the end of the paper the author gives some of the essential design features which could be tested by future investigators. It would seem that a breaker built on his present layout could handle only currents up to 200 amperes per single contact. However, it has to be realized that these interrupting tests were made with direct current and it therefore can be assumed that a proper arrangement of the opening mechanism may permit the interruption of much higher current values in case of alternating current.

It is hoped that this investigation, which was carried out with somewhat limited facilities, will stimulate some further work along this line and I am sure further investigators will be glad to have, as a basis, Doctor Koller's results and the scheme for opening the contacts as well as the splendid optical method for measuring the speed of separation of the electrodes.

Co-ordination of Insulation and Spacing of Transmission Line Conductors

Discussion and author's closure of paper 46-175 by W. W. Lewis, presented at the AIEE summer convention, Detroit, Mich., June 24–28, 1946, and published in AIEE TRANSACTIONS, 1946, October section, pages 690–4.

L. M. Robertson (Public Service Company of Colorado, Denver, Colo.): The electrical industry owes an expression of gratitude to Doctor Lewis for obtaining the data and presenting this paper. It will be a very valuable guide for transmission line designers and for a review of practice by operators who may wish to improve the operation of transmission lines.

There are a few factors which might be mentioned in connection with this subject in addition to those in the paper.

The experience of the Public Service Company of Colorado has indicated that contamination of insulators is a factor which must be considered in determining the size of pin type units or the number of disks in a string. Altitude also should be considered since an increase of altitude requires an increase of insulation on lines and stations.

It also has been determined that the use of wood in crossarms and crossarm braces may be of considerable value in line insulation and operation. This applies to lightning difficulties as well as those caused by birds. A 44-kv double-circuit line with pin type insulators on steel arms on steel poles and with overhead ground wire had a poor operating record. When the steel arms were replaced with wood arms and braces the troubles were eliminated.

A spacing between conductors and between conductors and ground wires may not be satisfactory in some cases where the terrain is hilly or mountainous and the winds blowing in such a direction and nature as to produce severe upcast of the conductors. Contact between ground wire and conductors has been obtained on a line of horizontal configuration where the phase spacing is 18 feet and the ground wire six feet above the plane of the conductors.

In general we have found that the data presented conform closely to that which has proved to be satisfactory in most cases in this territory.

M. S. Oldacre (Commonwealth Edison Company, Chicago, Ill.): The paper gives an excellent summary of transmission line practice and co-ordination of insulation that will serve as a useful starting point in transmission line design. It should be realized that the recommendations are based on the average of many averages. The actual design should be engineered completely with due consideration to the various limiting elements of line construction. This will allow for clearance as it is required and will give the most efficient use of material with the best operating results.

A comparison of recommendations in the paper with the dimensions of two existing lines may be helpful in considering how satisfactory the recommendations may be. The 230-kv line was built in 1940 and has had a very low outage rate because of lightning or dancing conductors. The other line, which was built in about 1928, has had a consideralby higher outage rate, and wherever possible alterations have been made to obtain better performance. The data are shown in Table I of this discussion.

The effect of ice or snow on the conductors is mentioned too briefly, and the effect during foggy weather of dirt accumulation on the insulators should be considered.

There seems to be a very large amount of literature on the subject of ice and snow on conductors and the frequently resulting dancing of conductors, but a critical study of it will produce no definite answer that will serve as a design basis.

If adequate allowance is not made for dancing conductors, there may be a loss of the lines at the time they are needed most

or else some expensive mitigative measure may be required. Such a measure might be increased current loading of part of the lines while parallel lines are taken out of service, or might be the short-circuiting of a line and supplying it directly from the bus or from a separate transformer or generator depending on the line characteristics. Either one of these methods is an expensive one both from an investment and operating point of view.

The amount of clearance to allow for dancing conductors cannot be determined adequately from present data. The amplitude of the conductor movement may be nearly twice the sag of the conductor, if there is only one loop of dancing per span, but may have a maximum amplitude about equal to the sag if there are two loops. If there are more than two loops per span the amplitude will be reduced. The dancing conductor with one loop per span sometimes is designated as vibrating at its fundamental frequency and other times at the first harmonic. Therefore it is more definite as a practical matter to speak of the number of loops of vibration per span.

The conductors frequently dance in an elliptical orbit, but there are reports of conductors dancing vertically up and down. Thus the amplitude and direction of the dancing are important elements to consider in selecting conductor clearance.

It would be advantageous if anyone having helpful data on dancing conductors would make the information generally available by publication or correspondence between interested operating engineers.

Possibly further investigation would develop mitigative measures or devices that could be applied to the conductors to reduce dancing to an amount that will not cause serious trouble. No specific methods are offered but only the speculation that something might be developed.

The dirt and fog question is well worth more consideration than it has received. This trouble usually is concentrated in rather small areas and additional construction costs in such cases may be justified.

On some particular lines, the combination of dirt and fog is more of a menace than lightning. That is, there have been more outages caused by dirt and fog than by lightning.

It seems a hopeless and useless task to try to prevent all flashovers resulting from dirt and fog, but some remedies are available that have been satisfactory.

1. Cleaning the insulators by hand, either on the line or after replacement.

2. Washing the insulators with a high pressure water stream while the line is alive.

3. Providing additional insulation that may be sufficient to eliminate all dirt and fog flashovers or else eliminate them if the insulators are washed once a season just before the usual foggy weather.

There are good indications that the last method can be accomplished successfully with special insulators having increased creepage distance, particularly in surface that remains relatively dry. An alternate method is an increased number of insulator disks where suspension insulators are used. This may be relatively expensive if clearance to towers is maintained.

All of the foregoing text can be summarized by saying

1. The possibility of dancing conductors must be considered and allowed for where necessary.

2. The effect of dirt and fog must be considered and provided for.

3. Additional observation and investigation by those having trouble because of dancing conductors, dirt, and fog would be very valuable to the industry as a whole to obtain a better design basis for future lines or for possible alterations to existing lines.

Abe Tilles (Pacific Gas and Electric Company, San Francisco, Calif.): In applying the basic considerations of insulation co-ordination to the detailed selection and design of an insulator string and supporting structure a great variety of considerations need careful attention. When one tentatively has selected a design and wishes by way of check to make a general comparison to other lines, he is likely to find, as documented by the author, that a great variety of usages are in existence and that a limited comparison is confusing and may be very misleading. Accordingly, the comprehensive assemblage of data here presented and simplified is very welcome and useful as a general comparison and guide, as well as being very helpful as a rapid first cut in design in many instances.

Those who have labored in detail with the considerations involved will appreciate how skillfully and compactly the author has assembled and simplified, in gross outline, the various factors involved in the problem.

In a recent design of a major 230-kv line, because of the existing dust and weather conditions together with quite low footing resistance, wet flashover at 60 cycles was controlling at critical wind conditions. A somewhat different proportion of spacings than that listed by the author was selected accordingly. The loan by the author of a preliminary copy of his paper was of interest as a general check and was appreciated greatly.

H. A. Frey (Locke Insulator Corporation, Baltimore, Md.): Doctor Lewis has presented a very interesting and practical rationalization of transmission line insulation. It should be noted that his insulation levels are established principally by the balance between the voltage expected from switching surges and the wet flashover values of the insulators. The user thus is left free to select a particular insulation level corresponding to the magnitude of switching surges which may be probable on the system in question. In so doing it must be borne in mind that the rated wet flashover values of insulators result from an arbitrary yard stick. They are not necessarily the lowest voltages at which the insulators will flashover. The rated wet flashover voltage is merely the average value at which flashover will occur when tested in accordance with the standards of the AIEE.[1] In service under varying condition of precipitation and with the insulator surface fouled with dirt to varying degrees, it is quite possible that lower wet flashover voltages may be obtained. Under some conditions it therefore may be desirable to use more conservative insulation levels.

REFERENCE

1. INSULATOR TESTS. American Standard C29.1. 1944.

W. W. Lewis: One purpose of the paper is to give a means for quickly estimating the minimum insulation that should be used on a transmission line. In practice this insulation may be increased somewhat to allow for local conditions such as excessive lightning, high footing resistance, dirt and fog. Finally when the number of disks is selected, all spacings to grounded members of the tower between conductors and to overhead ground wires should be co-ordinated in order to prevent a weak spot for flashover and prevent waste of insulation or spacing. The paper gives a method of readily selecting the co-ordinated spacings.

Table I. Comparison of Recommended Practice and Actual Line Dimensions

	138-Kv Line		230-Kv Line	
	Recommendations in Paper	Data From Actual-Line	Recommendations in Paper	Data From Actual Line
Minimum number of insulator disks	7		12	
Maximum number of insulator disks	10		18	
Number of disks for average practice	9	12 (5-inch spacing)	15	18
60-cycle wet flashover, kilovolts	375	450	600	690
Impulse flashover, kilovolts	860	1,000	1,345	1,585
Clearances, feet				
Figure 5A			9.5	9.5 min.
Figure 5B			14.25	15.0
Figure 5C			19.0	28.8 to 37.5(d)
Figure 5D			28.5	33.3
Distance between ground wires, feet			28.5	46.3
Clearances, feet				
Figure 6A	5.0	6.75	9.5	10.4
Figure 6B	7.5	9.25 min.	14.25	15.+
Figure 6C (conductor to conductor)	10.0	15.0	19.0	20.5 to 26.0†
Figure 6C (ground wire to top conductor)	10.0	12.0	19.0	23.0 to 39.0‡
Figure 6E	2.5 to 7.5	5.0* / 4.5** / 8.0†	4.75 to 14.25	4.0
Location of ground wires	Over outer conductor		Over outer conductor	Over outer conductor

* Top conductor inset from center conductor.

** Bottom conductor inset from center conductor.

† Ground wire inset from center conductor.

‡ Dimension *C* is larger for the longer spans.

In selecting the insulation, switching surges and wet flashover have been given the main consideration. However, as brought out by all of the discussers, the effect of dirt, dust and other contamination during foggy or wet conditions may lower the flashover of the insulators considerably and require more conservative insulation levels, special insulators with large creepage distances, or a program of periodic washing.

M. S. Oldacre stresses the phenomenon of dancing conductors and mentions the large amount of literature on the subject which does not produce a definite answer that will serve as a design basis. This phenomenon seems to be localized in a belt adjacent to the Great Lakes. The experience of companies operating in this region is teaching the designers how to lay out their lines to cope with this trouble. Companies in a somewhat wider and longer belt experience trouble caused by the accumulation of snow, ice, or sleet on conductors, not usually accompanied by dancing. They also have learned by experience how to overcome this trouble and to continue in operation. As Oldacre states, an actual design should be engineered with due consideration to all of the local limiting features.

The author wishes to thank each one who so kindly has offered a discussion of the paper.

Current and Torque of D-C Machines on Short Circuit

Discussion and author's closure of paper 46-136 by T. M. Linville, presented at the AIEE summer convention, Detroit, Mich., June 24–28, 1946, and published in AIEE TRANSACTIONS, 1946, pages 956–65.

B. Litman (Westinghouse Electric Corporation, East Pittsburgh, Pa.): T. M. Linville's paper does much to systematize the calculation of short-circuit currents in d-c machines and introduces the previously neglected factor of the a-c reactance voltage which opposes current flow. Apparently this factor has been overlooked in the past because on high voltage machines it exerts only a minor influence on the magnitude of the short-circuit current. In order to check the actual magnitude of this voltage, short-circuit oscillograms have been taken on a comparatively low voltage generator which had probe coils wound about the main pole tips to determine the actual loss in flux. The values obtained, which are listed in the following text, indicate fairly good agreement if a correction is made for saturation of the teeth in the commutating zone.

In equation 27 of Appendix I application is made of the theorem of constant flux linkages, and the field leakage coefficient n_f is introduced. It appears that this should be the over-all effective leakage coefficient introduced by G. E. Frost[1] in order to include the effect of armature leakage flux which reduces the air gap flux and yet does not link the main field winding.

We wish to introduce a somewhat different explanation for the equivalent contact drop caused by a-c reactance voltage. The differential equation for a coil undergoing commutation (equation 59 of Appendix IV) is solved to give

$$i_s = A\epsilon^{pt}$$

and the constant A is calculated by assuming that the total current adds up to the line current per arm. This tacitly assumes that the brush contact drop is large enough to accomplish this successful commutation, and that if the reactance voltage were twice as large, the contact resistance drop somehow would be twice as large so that commutation still would be successful. Actually, very little current will be collected through the brush and most of the current will appear in an arc at the trailing edge.

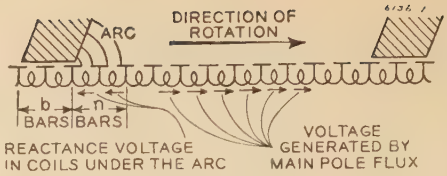

Figure 1

Figure 1 of this discussion shows such an arc at the trailing edge extending effectively over n bars. The current in these coils thus is changing from peak value in one direction to peak value in the other direction over a span of n bars, whereas if normal commutation existed this change could take place under the brush in a span of b bars. These coils therefore have an average reactance voltage of $E_R \times b/n$ per coil, and as the figure indicates there are n of these coils in series with their voltages opposing the generated voltage. Therefore the generated voltage should be reduced by a total amount $E_R \times b$ and the equivalent brush contact resistance is $E_R b/I$ ohms which is the same answer as given in equation 55, Appendix IV of Linville's paper.

The calculation of an equivalent resistance from the value of E_R at rated load assumes that this reactance voltage changes linearly with load current. Actually the slot leakage fluxes which give rise to the major portion of this reactance voltage will saturate the teeth before short-circuit current is reached. On the machine tested, this saturation is reached at less than half the peak short-circuit current so that the equivalent brush contact resistance is only a little more than half the value which otherwise would be expected. The values obtained on test are

Machine rating = 1,500 kw, 250 volts, 5,000 amperes, 514 rpm

Flux before short circuit = 1.0 = 250 volts

Flux loss during short circuit = 0.511 = 128 volts

Net flux after short circuit = 0.489 = 122 volts

Calculated equivalent brush contact drop caused by a-c reactance voltage (neglecting saturation) at 10.2 times rated current, which is the actual short-circuit current obtained = 103 volts

In obtaining the latter value, the magnitude of E_R was obtained from equation 63 of Appendix V.

Since this voltage is almost as large as the net generated voltage after short circuit, it is evident that a correction for saturation is necessary. In making this correction we have assumed that the teeth are equivalent to air paths for flux densities above the saturation value of the iron. The value then obtained for this voltage drop is 54 volts.

Net voltage available = 122 − 54 = 68 volts

Armature circuit resistance = 0.00113 ohms

Peak short-circuit current = 68/0.00113 = 60,000 amperes

The actual value of current obtained was 61,000 amperes.

Reference

1. The Short-Circuit Characteristics of D-C Generators, G. E. Frost. AIEE Transactions, volume 65, 1946, June section, pages 394–402.

T. M. Linville: B. Litman's comments are interesting and very much appreciated. He disagrees with the paper in saying that the a-c reactance voltage exerts only a minor influence on the magnitude of the short-circuit current in high voltage machines. The analysis made in the paper and the author's tests make it evident that the a-c reactance voltage actually is a major factor opposing the current flow and generally the largest factor in all machines, including high voltage ones.

This is made apparent by recognizing that with linear commutation at ten times normal current the reactance voltage would be ten times as much as at rated current. Then consider that at the instant of this peak current the commutating pole flux has not had time to rise and the nonlinear commutation shown in Figure 3 exists. Then one has to think of reactance voltage in terms of 50 times normal. As a matter of fact the multiplying factor on account of nonlinear commutation is equal to the brush overlap in segments according to equation 55 which Litman substantiates. Generally the brush overlap on high voltage machines is large so that the effect of a-c reactance voltage opposing the current flow on these machines is large.

Litman suggests that the effective over-all leakage coefficient given in Frost's paper should be used in Equation 27 in order to include the effect of armature leakage flux on the air gap flux. The method of the paper in effect develops Frost's theory to a point where calculations from machine dimensions can be made. This is done by determining separately the air gap flux (or pole to armature flux) and the flux across the space from pole to pole. The former is a function of armature current and field current and is determined by equation 23. To derive this equation the field magnetomotive force and armature magnetomotive force are combined and multiplied by the magnetic permeance. In effect this product is integrated around the air gap taking into account the varying values of magnetomotive force and permeance. This then determines the net air gap flux. The pole-to-pole flux is determined by the second term of equation 27 considering it proportional to the field current.

Litman is believed to be saying that all of the net air gap flux between pole and armature, equation 23, does not link the field winding as assumed in equation 27.

This is the same as saying that all of the flux going directly from pole to pole does not link the field winding.

For these statements to be true there would have to exist in the pole iron a molecular magnetomotive force which acts with the same polarity as the field magnetomotive force and becomes effective as the iron of the pole shoe saturates. This is improbable because the over-all change in the magnetic permeance of the pole shoe caused by saturation acts to oppose the field magnetomotive force always. Furthermore, if equation 27 does not truly represent the field linkages because some part of the air gap flux ϕ_d goes directly from pole to pole without linking the field, then that portion of the pole-to-pole flux which does link the field must be greater than what is accounted for in equation 27. Such an error in the method would make the transient field current calculated by the paper smaller than actual. Therefore the justification of the paper lies not only in its logic but also in comparison of the calculated field current with test results. Figures 1, 4, and 5 show a good check substantiating the method of the paper.

It is considered that there is no appreciable change in flux in the commutating pole circuit, affecting the armature electromotive force, in the time interval between the instant of short circuit and the moment of peak current.

It seems axiomatic that the brush contact drop, or arc drop, from brush arm to commutator always at least must equal the reactance voltage caused by current reversal in the armature coils when the flux of the commutating pole is negligibly small. Otherwise current reversal would not occur. This equivalent brush contact drop, or arc drop, is calculated in the paper and when divided by the peak short-circuit current is equal to the equivalent resistance r_b. Litman is to be thanked for demonstrating that the expression for r_b, equation 55, is independent of the number n of bars over which the arc between brushes and commutator extends. The paper states this fact without demonstrating it.

Litman's figures for the machine he tested cause him to conclude that the value of r_b should be corrected for saturation of the armature teeth. Otherwise the set of figures given are not consistent. The author does not believe that this is true. The armature teeth underneath a commutating pole at the instant of peak short-circuit current carry substantially only the flux crossing the armature slots caused by magnetomotive force in the slots. It is the reversal of this flux which causes the reactance voltage E_R, which determines r_b. In some machines saturation is present in the teeth at the beginning and end of this reversal period but in between the reactance voltage reaches the full unsaturated value. In general this saturation has small influence and no correction should be made. The results of the paper substantiate this conclusion.

It seems that the value for r_b obtained by Litman using the method of the paper is more nearly the correct value. The incompatibility in his set of figures evidently is caused by the value used for the flux loss during short circuit which is the measured loss during short circuit but not at the immediate instant of peak armature current. The paper is believed to be correct in assuming that the maximum current is reached so quickly that there is negligible loss in the flux linkages of the field circuit in this time interval, that is, the theorem of constant flux linkages can be applied. If so, the immediate loss of flux cannot be 0.511 because to hold constant flux linkages in the field this loss of air gap flux must be balanced by at least an equal gain of pole-to-pole flux. As the pole-to-pole flux of the machine with normal excitation should not be more than about ten per cent of normal exciting flux and the permeance of the pole-to-pole path is fairly constant until after peak armature current is reached, it is apparent that the field current must rise to more than six times normal to hold constant linkages. So great a rise in field current never has been observed to the author's knowledge. However, sometime after maximum current when the induced field current has diminished, the loss of air gap flux and field flux linkages will be as great as 0.511. It should be re-emphasized that r_b is derived to represent the effective brush arm to commutator resistance at the instant of maximum short-circuit current (maximum current is the important calculation to be made), and thereafter it will be too large a quantity. The following set of figures are possibly correct for Litman's machine at the moment of peak current:

Exciting flux before short circuit = 1.0 = 250 volts

Exciting flux loss at moment of maximum short-circuit current = 0.312 = 78 volts

Net flux at moment of maximum current = 0.688 = 175 volts

Calculated brush arm to commutator drop = 103 volts

Net voltage available = 172 − 103 = 69 volts

Armature circuit resistance = 0.00113 ohm

$$\text{Peak short-circuit current} = \frac{69}{0.00113} = 61{,}000 \text{ amperes}$$

Field leakage flux linkages = 0.1 times normal exciting flux linkages

Initial field linkages = 1.1

Leakage linkages at maximum current = 1.1 − 0.688 = 0.422 ampere

Maximum transient field current = 0.422/0.1 = 4.22 amperes

Four times normal field current is much more consistent with tests made by or reported to the author.

Semiconducting Shielding for A-C Power Cable

Discussion and author's closure of paper 46-118 by Edwin J. Merrell, presented at the AIEE summer convention, Detroit, Mich., June 24–28, 1946, and published in AIEE TRANSACTIONS, 1946, August–September section, pages 605–09.

R. W. Atkinson (General Cable Corporation, Bayonne, N. J.): The data given by Edwin J. Merrell should be very convenient for use in determining conditions resulting when there is a considerable voltage drop along the length of a semiconducting shield. I am inclined to feel, however, that the approach generally should be along another direction, namely that the total voltage drop should never be permitted to be more than a relatively small fraction (say ten per cent) of the full voltage of the cable. When this is the case no significant error is introduced by calculating the current in the shield as though it were metallic. In this simple calculation any slight error is on the safe side and is insignificant in any event in terms of the engineering data.

There seems no real reason to use a shielding tape and then let it only partly perform its function by permitting a voltage to ground that is a large fraction of what would exist without the shield. Moreover, there seems no excuse for permitting a loss in the region of the grounding contacts sufficient to produce even a slightly significant effect on the temperature rise and available carrying capacity. These points are emphasized when it is remembered, as the author points out, that the loss and the voltage drop are proportional to the square of the spacing of the ground points and thus that these are under rather simple control. This view seems not to be in conflict with that of the author except for emphasis.

E. W. Greenfield (Anaconda Wire and Cable Company, Hastings-on-Hudson, N. Y.): It is gratifying to see this paper finally published. More than five years have passed since the author first indicated his work on semiconducting jackets at the National Research Council meeting in Williamsburg, Va.

Independently, the writer had come to the conclusion that voltage gradients along a semiconductive jacket could be interpreted best on the basis of distributive infinitesimal parameters. In our work on nonmetallic conductive jackets, we have used transmission-line differential equations which are similar in most respects to those shown by the author. However, we do not form an artificial term of RL^2 as parameter but instead we use the conventional terms for the cable, namely propagation constant and characteristic impedance.

To present a physical picture of the underlying phenomena giving rise to the use of transmission-line theory in this work, we offer the following.

Any conductor maintained at an alternating difference of potential with respect to earth will carry leakage and charging currents in addition to load current. The former are functions of the quality of the insulation and the geometric relation of conductor to earth, that is, shunt conductance and capacitance. Being distributive in nature, these shunt currents (measured in the conductor) are also proportional to the length of conductor.

For a shielded cable, that is one having an outer conductive jacket, the leakage and charging currents flow longitudinally along the central conductor while at the same time they pass proportionate amounts, as required, radially through the insulation. The conductive sheath then collects substantially all the radially passing current and carries it back longitudinally to the energy source or to a grounding point.

For a nonshielded cable exactly the same sequence of phenomena takes place. In

general the total amount of radially passing current will be less since the shunt conductance and capacitance to earth are smaller. However, the requisite total amount of leakage and charging current will again flow longitudinally along the conductor, gradually dissipating radially through the insulation as demanded by the per-unit shunt parameters. The current flow through the insulation thus appears as a distributed charge on the surface of the insulation. As a result of this charge a longitudinal current in general will flow along the insulation surface between grounded points or between regions of low resistance contact to earth. For a given surface charge the amount of longitudinal surface current that flows then will depend on the longitudinal resistance of the cable surface and the distance between grounded points. That is, more resistance, less current; more length, more charge (but also more resistance). Hence current can both increase or decrease with increase of length depending on other factors.

The existence of charges and (or) current flow at the insulation surface gives rise to a potential along the cable covering. The voltage to ground at any point along an unshielded insulated cable thus depends on all the conditions previously outlined for current flow. For an infinitely long unshielded cable (infinite distance between earth contacts) the surface voltage to ground is simply proportional to the ratio of the insulation capacitance to the earth capacitance.

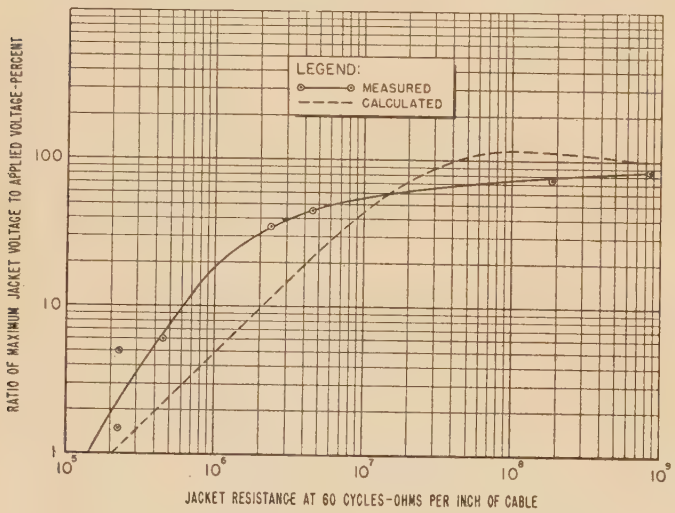

Figure 1. Calculated versus measured surface voltages for a length of 1-conductor 500,000 - circular - mil 6/64-inch rubber-insulated cable

Ground ring spacing is six inches

For finite lengths and surface resistances the voltage to earth is more complex and is determined by all the factors discussed.

To verify from another laboratory the experimental data given by Merrell, we present the two curves of Figure 1 of this discussion showing the voltage rise along the jacket in per cent of applied voltage for a length of 1-conductor 500,000-circular-mil 6/64-inch rubber-insulated cable. Ground ring spacing was held at six inches and the jacket a-c resistance varied over a range from 0.2 to 600 megohms per inch of cable length.

The solid curve shows the data taken experimentally using a special (0.65 micromicrofarad) electrostatic voltmeter. The dotted curve represents calculated data using transmission-line differential equations. The agreement is seen to be excellent at high values of jacket resistance. At low values the experimental data are somewhat erratic but the shapes of the two curves indicate general agreement.

W. T. Peirce (American Steel and Wire Company, Worcester, Mass.): Edwin J. Merrell's paper is of value in setting one boundary point for shields that have far more resistance than conductance. It mainly considers the case where the natural conductance of fibrous materials containing moisture or lead base pigments has been found to exhibit some shielding effect and thus aid in reducing stresses from the surface of the insulation to occasional grounds.

The greatest application of nonmetallic shields in present day cables concerns rubberlike materials with a designed resistance in the order of 10,000 ohms per foot of cable used as a supplement to metallic shielding or in conjunction with ground wires. Under such conditions the shield is maintained at substantially ground potential and the principal terms of Merrell's formula lose significance. The shield is less than one-half of one per cent of ground potential at any point and its function merely is to counteract the inevitable looseness that develops between the metal shield and the insulation caused by mechanical or thermal changes in the components of the cable.

In the worst case all the shield has to carry is the circumferential charging current from the back of the conductor to the ground wire in longitudinal contact with the shield. Figure 2 and Table I of this discussion, show the potential so developed with a wide range of shield resistance.

Merrell has considered only the single phase condition whereas by far the more common use is for the three conductors of the circuit to be associated together closely. In such case the 3-phase charging currents balance out per-unit length of cable and no longitudinal flow of current is involved. Here, even in the absence of ground wires or other metallic shield, only the circumferential resistance to the point of contact of the three conductors is involved, and the adequacy of the shield can be established without resort to complex mathematical treatment.

The great value of these nonmetallic shields is to permit the cable designer to be certain that corona has been eliminated from both outer and inner surface of the insulation and thus utilize insulation that has the best mechanical or electrical properties without the necessity of compromising in order also to obtain corona resistance.

Figure 2

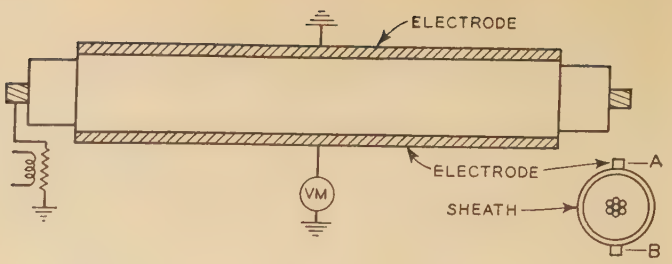

Perry H. Ware (Simplex Wire and Cable Company, Cambridge, Mass.): Application of the plots in Edwin J. Merrell's interesting and timely paper to several practical cases of cable design have brought out the following suggestions for further saving of time and computation.

The voltage vector diagram of Figure 3 in the paper presents the following difficulties in its use:

1. Capacitance is given for only a few discrete values.
2. Evaluating the voltage drop along the shield and across the dielectric involves scaling the lengths of the vectors on the plot.
3. The accuracy definitely is limited for small values of voltage drop along the shield.

In many cases it is the magnitude of the voltage drops which is significant for practical uses; the phase angle is relatively unimportant. On this basis Figure 3 was designed to give the magnitudes of the voltage ratios for 60-cycle a-c line voltage. The unit of the abscissa CRL^2 was chosen so as to allow a continuously variable range of capacitance as well as of resistance and ground spacing. An extension of Merrell's mathematics further shows that for values of CRL^2 below 10^2

$$V_D/V_L = 1 \qquad (1)$$

$$V_B/V_L = 0.000188CRL^2 \qquad (2)$$

R. C. Waldron (The Okonite Company, Passaic, N. J.): Edwin J. Merrell has presented an interesting method of measuring the a-c characteristics of semiconducting coverings. The descriptions given in "Measuring Technique" are not quite clear and it would be helpful if he would include a wiring diagram showing the various connections to the Schering bridge. From this description it is not clear whether the loops are connected directly to the bridge with one loop being connected to a microammeter

Table I

Size	Insulator Wall Thickness, Inch	Charging Current, Microamperes Per Foot Per Kilovolt	Sheath Resistivity: Ohms Per Cubic Inch	Sheath Resistivity: Ohms Per Foot	Volts Difference A to B Per Kilovolt Applied
6	15/64	18.5	530	65,000	0.014
6	15/64	18.5	160	11,000	0.007
6	15/64	18.5	850	125,000	0.302
6	15/64	18.5	1,500	340,000	0.471
4/0	11/64	70	250	19,000	0.028
4/0	11/64	54	250	33,000	0.022
500,000	24/64	55	650	300,000	0.064

at the same time or whether these are separate measurements. If these are connected simultaneously, it would appear that some of the current may be shunted by the bridge and not pass through the microammeter.

Work which we have done in connection with the study of discharge from braided cables had indicated that a large part of the charging current can be drained from a 4-foot sample having a wet braid by grounding in the center. For example, at 2,000 volts alternating current, the measured current from a 53-inch length was 331 microamperes while the theoretical current should be 442 microamperes. Working back from the measured current by a method similar to Merrell's we obtain a surface resistance of 0.78 megohm per inch. The d-c resistance measured about 60 megohms per inch. We would like to know whether the author has any comparative values of a-c versus d-c resistance that show this magnitude of difference.

Similar a-c measurements on an okoprene covered cable show an a-c resistance of 200 megohms per inch against a d-c resistance of 200,000 megohms per inch.

Experience has shown that braided cables are not satisfactory where drainage of any appreciable length can occur. Okoprene cables, however, are satisfactory. This would indicate that 0.78 megohm per inch is too low for a nonshielded cable and that 200 megohms per inch is satisfactory. The limiting value is probably somewhere between these points.

For Merrell's illustration he shows a cable operating in cable rings. He points out that in this example with a surface resistance of two megohms per inch there would be a 12-degree rise in temperature at the point of current discharge. This assumes uniform current flow around the entire circumference of the cable, whereas with the cable in rings we would expect almost point contact with the rings which would result in much higher concentration of current at this point with a correspondingly higher temperature. In this case also he obtains a voltage in the center between rings of 5,500 volts to ground which would be approximately 10,000 volts between phases if three conductors were installed in the same rings. This voltage would cause sparking at the center in case of close proximity or occasional contact between conductors, or between conductors or some grounded object such as tree limbs. This example has the same order of magnitude for the surface resistance as braided cable which is known to be unsatisfactory. I am wondering if the value of resistance for the covering chosen in this example is considered satisfactory and whether any general recommendations can be drawn from their experience as to the maximum values of resistance which are satisfactory.

In our design of semiconducting coverings we have worked to much lower values and have assumed that the cable covering at no point should reach a voltage high enough to cause shock to personnel touching the cable nor to cause sparking in case of occasional contact with adjacent conductors or grounds.

T. F. Peterson (American Steel and Wire Company, Cleveland, Ohio): May I express my commendation and appreciation for the fine rigorous mathematical treatment of semiconducting shielding put forth by Edwin J. Merrell.

Some 20 years ago I had occasion to derive the equations for the thermal resistance from the copper conductors of type *H* (Hochstadter copper tape shielded) cable to the lead sheath. I was happily surprised to find, as Merrell has found, that these second order differential equations were almost identical to those for long distance transmission lines. Frequently the greatest usefulness of such studies is derived from their application to "boundary conditions" of the systems and I would like to direct attention to them.

I would like also to comment on the historical references included in the paper.

Merrell hails Lowenberg as an originator of semiconducting shielding and makes no reference to the vast number of patents and comprehensive literature on this same subject since 1928. Careful reading of the reference will reveal that he was concerned with arcing between weatherproof braids and cable installed in fiber ducts. Nowhere does he use the terms shielding and semiconducting, nor is there any evidence that the test samples which were laid on a concrete floor were either grounded or shielded. Apparently very high voltages existed on the braids of all test samples, but under certain circumstances (perhaps highly resistive concrete or widely removed grounds without electrical connection) arcs and discharges occurred only at high conductor voltages. Lowenberg indicates that braid burning caused by arcs was attributed by some to the drainage of charging current along damp braids to points where the cable was in contact with the duct. Others reasoned that the braids were dry and that dielectric relationships determined stress distribution which was such as to cause corona discharge in certain air gaps. Anyone familiar with these problems should have known at that time that both theories may have accounted in part for the observations since the whole system represents a complex combination of parallel and series resistances and capacities from conductor to ground.

In view of these uncertainties, it is not surprising to find that Lowenberg observed visible discharge at 4,000 volts in the case of weatherproof braided cable and discharge beginning at 9,500 volts in the case of flameproof (presumably asbestos) braid. In his conclusions he seems to ignore the second set of tests in which the weatherproof braided cable showed discharge beginning at 10,000 volts whereas a second portion of the same cable with a flameproof finish showed "pronounced discharge" at 4,000 volts. Apparently anything could happen and almost any voltage could appear on the various braided cables, and perhaps the only reason the flameproof braided cable behaved better in service was because of its resistance to arcs and not because of partial shielding.

For more than 20 years I have done research on various types of shielded cable and for more than 18 years have been engaged in the development of what I have called semiconducting shielded cables. I cannot accept the author's definition of such shielding when he defines it as "the practice of partially confining the electric field within the insulation by means of semiconducting covering." Such a cable would not be shielded in the sense that it would be safe to handle, prevent corona discharge, or prevent interference from or with the insulated conductor. Merrell's cable would be

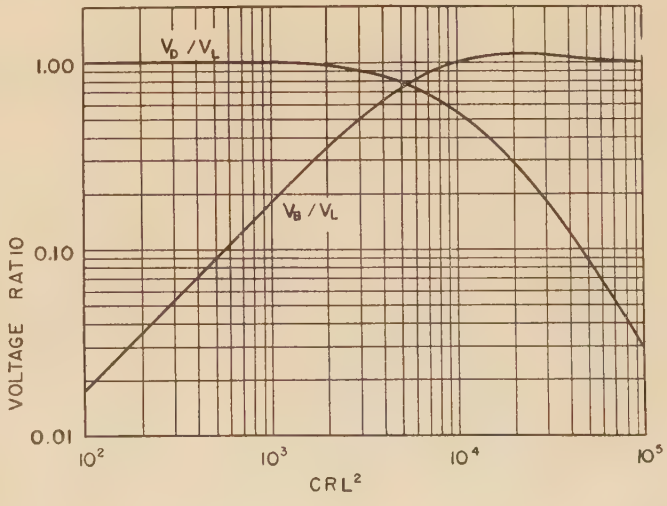

Figure 3. Voltage ratios for shield and dielectric of single conductor cable versus CRL^2

semishielded and I think he will agree that by a large margin the range of his studies covers such types of shielding. (It should be noted, however, that unlike Lowenberg very positive grounds are applied to certain portions of the semiconducting layers.)

These points are stressed. I contend that semiconducting shielded cable should

1. Be shielded.
2. Confine practically all electric field within the insulation.
3. Prevent disturbances and interference.

In the practical embodiments of these forms of shielding which I have made over the past 20 years, various values of R and L have been employed but in every instance the product of RL^2 has been much less than ten. For example, in using semiconducting shielding with surface resistivity as high as 100 megohms per centimeter square (as cited in United States Patent 2,322,702) and with ground points separated by 1 inch (L equals one-half inch), RL^2 equals eight. In certain forms of aerial cable supported by metal rings from messengers, even if we take resistance as high as 10,000 ohms per foot with grounding points every 20 inches (that is L equals ten inches), RL^2 equals 0.1. It will be observed that when RL^2 equals eight, cosh 3.03 equals 1.045. When RL^2 equals 0.1, cosh 0.033 equals 1.00045. Whether by substitution in Merrell's equations or by reference to Figures 4, 5, and 6, one must observe that with these values of resistance the cable is shielded fully and the electric field is confined fully to the insulation. It also will be observed that the watt loss in the shield is zero and so there are no further questions as to carrying capacity or change in characteristics of the shield.

These comments are made not to depreciate the work of Merrell but to utilize it practically to assure engineers that there are no hazards either from voltage or heat when conventional semiconducting layers are employed in conjunction with proper grounding. This discussion, while primarily directed to 60-cycle power conductors, is equally applicable to such cables as high voltage radar pulse cable and fortunately Merrell's equations are broad enough to cover a range of frequencies.

In closing I would like to suggest that the author describe more fully the types of semiconducting coverings referred to in his paper.

Edwin J. Merrell: I am glad to note that R. W. Atkinson's views on cable shielding are not essentially in conflict with those presented in my paper. However, I should like to point out that the primary object of the paper was not to foster a particular shielding practice; rather, it was to point up extensions in the range of shielding practice which are often advantageous, in spite of being unorthodox.

An excellent check with E. W. Greenfield's calculated voltage curve is obtained when his values of a-c resistance are employed in calculating RL^2 and are substituted in Figure 3 of the paper. The author appreciates this independent confirmation.

The divergence noted between calculated per-cent voltages and those measured on cable samples probably are caused by nonlinearity of shield resistance with respect to current density. This certainly would be suspected if a different order of current flow occurred during the shield resistance measurements from that characteristic during the cable voltage determinations.

I am in substantial agreement with W. T. Peirce's remarks except that I should like to add that the hazard to personnel cannot be overlooked when such high conductivity semiconducting shields are employed. Adequate grounding must be guaranteed on all cable installations of this type.

Perry H. Ware is correct in pointing out the limits of the graphs in the paper. However, according to our experience, the accuracy with which semiconducting shielding properties may be predicted is of no higher degree than that attainable through rough visual interpolation with the graphs as presented. This is because of the nonlinearity of the electrical characteristics of semiconducting shielding materials.

When the shielding circuit has been characterized by a CRL^2 below 10^2, that is an RL^2 below two for C equal to 50 and below 100 for C equal to one, the author has treated it as a conducting shield. The solution may be obtained accurately and quite easily by assuming a simple T equivalent.

R. C. Waldron questioned the bridge and and meter connections described under "Measuring Technique." The microammeter is connected at the same time and is in series with the portion of the cable sample which it is discharging and the bridge. The parallel short-circuiting of the microammeter is of no consequence since this short circuit is in series with a section of the semiconducting shield which has a resistance of an order thousands of times greater than that of the ammeter.

The author has noted differences between the a-c resistances of semiconducting shields and the d-c resistance as great and greater than those reported by Waldron. In fact it was this phenomenon which caused the derivation of the a-c theory presented in this paper, so that experimental data could be employed effectively in the design of semiconducting shielded cable for 60-cycle operation.

The cable in the illustrative example was chosen primarily to demonstrate the use of the graphs. However, it is a feasible construction for many single phase circuits. It would not be practical at this voltage for a 3-phase self-supporting aerial cable unless the shield were flameproof and unless considerable radio interference could be tolerated.

In the author's opinion there is no optimum value or limit of shield resistance. Instead, each order of shield resistance has its identifying characteristics, its merits, and its demerits.

As pointed out by T. F. Peterson, the author's direct historical references are admittedly meager, but the lack in this paper is made up in the Hickernell paper noted in the introductory paragraphs. The selection was made to high-light what appeared to me to be a natural difference in cable shielding technique. Moreover, the materials which Lowenberg found efficient are characterized by electric conductivities well within the range covered by the theory of my paper.

Peterson questions the use of the term semiconducting shielding. Actually, my definition amounts to a shortening of that adopted by the Insulated Power Cable Engineers Association in 1942. The full definition, which follows, is in printed form.[1]

"A semi-conducting shield for electric power cable is a shield which has an impedance such that without fully grounding the surface of the insulation it nevertheless performs the following two functions either singly or simultaneously:

"(*a*). Provides protection for cable insulation by restricting longitudinal and tangential voltage stress on the cable surface adjacent to miscellaneous ground points to a gradient below that necessary to produce corona.

"(*b*). Provides a measure of protection for human life by limiting the magnitude of cable discharge current at miscellaneous ground points."

According to Peterson's concept, materials suitable for use as semiconducting shields are limited to a small number since he employs a narrow range of resistances just below the point at which losses in the shield become apparent. The definition of the Insulated Power Cable Engineers Association is much broader in scope. It checks with the theory presented in the paper, which shows that many materials characterized by resistivities in the megohm range are sufficiently conducting to prevent corona discharge in particular cable installations by restricting unit voltage stresses tangentially on the cable surface to a low enough value.

REFERENCE

1. GENERAL SPECIFICATIONS FOR WIRE AND CABLE WITH RUBBER AND RUBBERLIKE INSULATIONS (first edition). Insulated Power Cable Engineers Association, section 6.3.

Modern Excitation Systems for Large Synchronous Machines

Discussion and authors' closure of paper 46-152 by J. B. McClure, S. I. Whittlesey, and M. E. Hartman, presented at the AIEE summer convention, Detroit, Mich., June 24–28, 1946, and published in AIEE TRANSACTIONS, 1946, pages 939–45.

J. H. Kinghorn and **F. M. Porter** (American Gas and Electric Service Corporation New York, N. Y.): The authors are to be commended on their excellent summary of modern excitation practice. To their list of types of excitation systems also might be added the main exciter with electronic pilot exciter and regulator. This consists of a small electronic exciter supplying the field of the main exciter and controlled by an electronic regulator and has given very satisfactory performance. If it receives its power from the machine terminals it, like the electronic exciter, must have a normal ceiling sufficient so that it can provide adequate excitation under the most severe external short circuit to which the system can be exposed.

From a performance standpoint there are three important characteristics to be considered in selecting voltage regulators.

1. Reliability.
2. Accuracy.
3. Speed of response.

All of the types of voltage regulators outlined by the authors are in use on the systems

of the American Gas and Electric Company, and experience has shown that all meet the requirements of reliability and speedy response. As far as accuracy is concerned the impedance and electronic types of regulators are much better than the others. The direct acting type is fairly accurate, but friction and lost mechanical motion cause a certain amount of deviation which, however, can be overcome to a considerable extent if sufficient amplification is put into the actuating circuit. The indirect acting regulator has a dead band which limits its accuracy to the width of the dead band.

The advantages of accurate voltage regulation make it desirable to employ one of the types of continuously regulating regulators in all cases. For synchronous condensers located at load centers these advantages from the standpoint of service to customers are obvious. For generators an added advantage is the increased ease of parallel operation without the necessity of introducing excessive amounts of droop. For small synchronous condensers where less expensive regulating equipment is required the direct acting regulator has proved satisfactory when a small booster voltage is added to provide more speedy response at low excitation. For larger machines the impedance or electronic regulator is applicable. Two 32,500-kva turbine generators now are being installed which employ static type regulators with rotating amplifiers and, based on seven years of highly satisfactory operation by one such arrangement used with a water wheel generator, successful performance is confidently expected.

C. E. Valentine (Westinghouse Electric Corporation, East Pittsburgh, Pa.): Four types of voltage regulators are described in this paper, namely, direct acting rheostatic, indirect acting rheostatic, impedance, and electronic. The direct acting rheostatic regulator with modern constructional features is probably the simplest regulator mechanically and electrically and the easiest to understand of any modern type. It is an electromechanical type and as such has moving parts, but when this regulator is applied properly, long life and freedom from maintenance or replacement troubles has been indicated by many years experience. As our interest becomes aroused in new and different types of voltage regulators, we should not lose sight of the availability and practical usefulness of the direct acting rheostatic regulators for small and medium size generators. Improvements in this type of regulator can be expected.

The indirect acting rheostatic type regulator has been used widely for industrial, public utility, and central station generators and synchronous condensers. It has been used successfully on systems where the load is relatively steady and also where it is fluctuating. Many applications have been made using a series-type main-exciter field rheostat. When this type of rheostat is used, only one set of single pole high speed contactors is required to provide the desired rapid response of the excitation system.

With regard to the impedance type regulator, a considerable number of this type, using the intersecting impedance principle, were manufactured and used with small a-c generators about ten years ago. At that time these regulators were relatively bulky on account of the space requirements of copper oxide rectifiers of which more were available than selenium. Improvements in the art and better materials now have made it possible to build a better regulator of this type for use with special exciters of the rotating amplifier type to control the voltage of large synchronous machines.

An electronic voltage regulator is now available using in the voltage responsive circuit a filament controlled high vacuum tube. This method of voltage measuring makes it possible to feed the a-c generator voltage directly into the regulator without the use of rectifiers and filtering. A direct voltage proportional to the rms value of the alternating voltage can be obtained from the loading resistor into which the tube feeds. This is important, for example, where unusual wave form or high frequency alternating current is regulated. This type of regulator can be used conveniently to control an electronic exciter or a rotating amplifier exciter.

The authors discuss several special control features including upper and lower excitation limits. It is indicated that these special control features are introduced more readily into static regulator control circuits such as the electronic type. It should be noted however that under excitation and overexcitation limits have been provided and used successfully with indirect acting rheostatic regulators in a number of applications. One type of lower excitation limit used with generators has been an electromechanical element wherein a-c machine main field current has been balanced against a-c watt output. This variable underexcitation limit has been used to prevent the voltage responsive and regulating means from lowering the excitation beyond a desirable point. For overcurrent limit on synchronous condensers an a-c electromechanical current element has been used, thus automatically controlling the upper limit of excitation in place of sounding an alarm in case a predetermined load current is exceeded.

An item of interest to many operators is the modernization of old excitation systems. In such cases it is important to determine accurately the characteristics of the existing main exciter. If this exciter is relatively unstable changes may be necessary in the machine in order to provide stability under manual control. Moreover the manually operated main-exciter-field rheostat may be rather bulky and expensive particularly if a wide and low ranges of exciter voltage are to be controlled smoothly.

E. L. Harder (Westinghouse Electric Corporation, East Pittsburgh, Pa.): The larger portion of this paper is devoted to a necessary statement of existing excitation and regulation principles, devices, and practices. Against this background, the newer developments are described, and their merits and field of application indicated. My comments pertain to the newer developments in excitation systems.

The authors have mentioned one type of rotating amplifier. Another type is the rototrol which is used to control the field of the main exciter. Its small control field energy requirements are supplied readily from an impedance or electronic type regulator.

The ultimate in simplicity of an excitation system is obtained with the main-exciter rototrol which eliminates the pilot or control machine altogether. A unit of this type is being built for a 60,000-kw turbo generator, a number of smaller units having been built in the past. The main exciter rototrol can be controlled by a static network or an electronic regulator.

The use of a lower excitation limit for a generator or frequency changer is recommended highly. This limit preferably should be variable with the load being carried, but in any event should be adequate to insure steady state stability for existing or increment loads. The provision of sufficient field current for stable operation is always paramount to variation of field current for voltage or wattless power control. The watt-balance element has been used for this purpose with indirect acting regulators. It balances slip-ring voltage against power through the unit, taking control away from the voltage regulator and increasing the field current if needed to insure the predetermined margin of stability.

J. B. McClure, S. I. Whittlesey, and **M. E. Hartman:** The authors wish to thank all those who have submitted discussions on this paper. While there seems to be general agreement on this subject, there are a few items which profitably can be emphasized.

Kinghorn and Porter have suggested that the electronic pilot exciter be included in the list of excitation systems. The electronic pilot exciter was considered when making up the list, but it was not included since the list was intended to be a summary of present day practice and the electronic pilot exciter has not been used widely by the industry. However, the experience with the electronic pilot exciter in a few installations has been quite satisfactory.

Three important characteristics are given which should be considered in selecting voltage regulators. In discussing accuracy it should be noted that regulators with no inherent dead band, in general, will have a higher accuracy because they are continuously acting. Regulators of this type are built with different degrees of accuracy which is reflected in their cost. Speed of response sometimes is confused with the continuously acting principle. Moderate speeds of response generally are considered adequate for most applications. One of the principle requirements of voltage regulators is that they begin to make corrections promptly. This requirement can be met by a regulator with a small dead band.

Harder indicates that there are several types of rotating amplifiers. The term rotating amplifier as used in the paper was intended to include all equipments of this type such as the amplidyne, rototrol, regulex.

Harder states that the simplest excitation system would make use of the main exciter rototrol. Main exciter amplidynes also have been built and now are being used in several smaller installations. However, such special exciters are necessarily larger. Also, the single special exciter requires higher control energy than if another amplifying stage is included. This in turn

means greater duty on the regulator. In an excitation system including a regular exciter and a separate rotating amplifier, it is possible to remove the rotating amplifier from service without shutting down the exciter.

Valentine and Harder both indicate that excitation limits are worthwhile. It should be understood that the lower excitation limit protects the system by maintaining a minimum excitation for each machine, while the upper excitation limit protects the machine from excessive currents. Mr. Valentine mentions the use of an overcurrent limit on synchronous condensers but does not state whether this limit is provided to protect the machine against excessive armature or field currents.

Valentine also discusses briefly the modernization of old excitation systems. In many cases the exciter is relatively unstable under manual control. A small booster voltage, as mentioned by Kinghorn, will improve the stability characteristics of an exciter and increase the speed of response at low excitations.

Six Years' Experience With Factory-Built Unit-Type Substations

Discussion and authors' closure of paper 46-176 by E. F. Miller and R. B. Miller, presented at the AIEE summer convention, Detroit, Mich., June 24–28, 1946, and published in AIEE TRANSACTONS, 1946, November section, pages 751–6.

Raymond J. Salsbury (Duquesne Light Company, Pittsburgh, Pa.): The adoption of a primary network is decided by economics. There is little doubt as to the desirability of the network from an engineering standpoint. However, there are certain details which could bear elaboration.

It would be desirable to present information as to the degree of regulation to be expected from the network application and as to what extent these expectations would be realized. Inverse reactance compensation is necessary to insure proper parallel operation of the network units. With a network partially loaded, the regulation problem is not difficult. However, it may be that when the network is loaded fully, bus regulation with the inverse characteristic will not be adequate.

Lightning arresters should be placed as close to the terminals of the transformer unit as is physically possible, regardless as to whether the entrance is overhead wire or cable. Open terminal bushings on the transformer unit obviously can be protected more easily with arresters adjacent to the bushing. The flashover mentioned in the paper must have been a result of some difficulty with the insulation of the bushing or the breakdown characteristics of the arrester. Bushing flashovers of the type suggested have been eliminated almost completely from many power systems.

Further discussion of some equipment details would be of interest. For instance, are the recording ammeters of the instantaneous or thermal type? What policy of loading is applied to the network units and what type of supervisory indication or remote control is provided, if any? Many of the maintenance features of the unit station could be treated more fully. The cables which supply the individual units will fail. How are the individual phase conductors identified when the line crew is required to repair a failure? What methods are used to insure proper phase rotation when a repaired cable is energized again on the system? Perhaps this problem is avoided through the use of single conductor cable in the supply.

The frequency of major inspection and overhaul is of prime importance. While the units are new, little trouble may be expected from them for several years. However, at some time transformer windings will have absorbed moisture and will require drying in a vacuum, the tap changer contacts will have worn and require replacement, the oil circuit breaker will have become obsolete and will require major rebuilding, and many of the other devices will require replacement. Furthermore, when something goes wrong inside the tank, the whole equipment will be out of service until repairs are made. It seems then that the following questions are pertinent: What provision is made for major equipment replacement or overhaul? How long will a unit give reliable service without any attention whatsoever? What reserve capacity is provided in the design of the system?

Finally, one cannot be too optimistic about the over-all economy of the primary network as compared with the radial scheme. Substantial distribution circuit investment is required to minimize regulation. This may be offset by substation economy. However, after these new unit stations have been in service 15 or 20 years, and there have been internal failures which require expensive replacement, many of the initial favorable factors may lose some of their value.

O. B. Falls, Jr. (General Electric Company, Schenectady, N. Y.): The authors have presented a very fine exposition of the use of and experience with unit type substation equipment and the advantages and economies of the primary network as contrasted to the radial type of system. This discussion will be confined chiefly to the latter item.

There are a number of reasons why the use of several relatively small substations is considerably better than the use of one large substation to serve a given area. Among these, as the authors have pointed out, are the problems of congestion around the large substations when a large number of 4-kv feeders must be taken away, and the necessity of supplying these large substations with a number of high capacity subtransmission lines.

Another of the major advantages also is mentioned by the authors. However, I would like to take this opportunity to further emphasize it. This pertains to the interrupting capacity of substation circuit breakers. Past experience has shown that one of the first items of equipment which caused a substation to become obsolete has been feeder circuit breakers. This was a result of an attempt to increase continually the capacity of these substations, which meant that, as the system grew, existing circuit breakers would reach not only their interrupting capacity but also their thermal capacity quite rapidly. The use of small equipments spotted at a number of locations throughout the load area and operated either radially or tied into a primary network means that the circuit breakers, from both an interrupting capacity and thermal capacity standpoint, will be adequate throughout the life of the substation as a whole.

Along this line, the question frequently is raised as to whether or not circuit breakers when used in a primary network will remain adequate as the network grows. Experience has shown that even in primary networks of quite high load densities and with high values of available short-circuit capacities on the subtransmission circuits, circuit breakers will remain adequate. Assuming a 4.16-kv primary network, the borderline where a 150-megavolt-ampere circuit breaker begins to become inadequate is at a load density where serious consideration should be given to installing a secondary network. Because primary networks usually are limited to residential, and mixed residential and commercial areas, it is unlikely that load densities will reach such values that any 150-megavolt-ampere circuit breaker would become inadequate based on present-day or expected future loads in such areas.

For example, if we assume an infinite network made up of 3,000-kva transformers and with 500-megavolt-ampere short-circuit capacity available at the high-voltage terminals of each transformer, the maximum short-circuit capacity to which any circuit breaker will be subjected on a 3-phase fault will be approximately 105,000 kva if the unit substations are spaced uniformly, 0.5 mile apart, and tied together with 3-phase overhead circuits of 0000 conductor. This means that a 150-megavolt-ampere circuit breaker with a reclosing time of 10 or 15 seconds on the first shot could be used with adequate margin. If the substations are spaced approximately 0.6 mile apart, a 150-megavolt-ampere circuit breaker could be used with zero reclosing time on the first reclosure. From this it can be seen that 3,000-kva transformers with 150-megavolt-ampere circuit breakers could be used for load densities in the order of 10,000 to 12,000 kva per square mile without becoming inadequate. This is based on assuming zero time for initial reclosure. If longer times are used on initial reclosure higher load density areas could be served.

The authors have pointed out that after careful consideration of the geographical layout of the area, the cost per kilovolt-ampere of the various sizes of substations, load density, and spacing of substations, a unit rated 3,000-kva transformer with forced air cooling to give it supplemental overload rating of 3,900 kva, was chosen as a size which would give the lowest over-all system cost. Such a conclusion lines up with the results which were obtained from an over-all generalized system analysis.[1] In this analysis, it was shown that when considering such factors as voltage conditions, continuity of service, size of load area and load density, subtransmission voltages, and size of substations, the general conclusion could be reached that in the majority of cases the 3,000-kva self-cooled rating of transformer when used in a primary network would give the lowest over-all system cost. It is

gratifying to note that in this very practical application, identical results were obtained.

The authors have enumerated a number of advantages of the primary network as contrasted to other types of systems including the radial type of system. I would like to take this opportunity to stress a few of these advantages which I do not believe have been appreciated fully in the past. One advantage is that the use of 3-phase 4-kv lines connected in the primary network not only results in lower losses but also in better voltage conditions being obtained than could be obtained with single-phase feeder-voltage regulation on a radial system.

In connection with this, there is one further factor which the authors have not mentioned, but which will become increasingly important. That is, the use of tie circuits as obtained in a primary network will permit the use of larger motor sizes without obtaining objectionable light flicker. This becomes more important as the use of room coolers and air-conditioning equipment increases.

The second item which I would like to mention is that the authors have found that the operating and maintenance costs of a primary network actually have been less than for a comparable radial system. One of the outstanding reasons for this is that substations including circuit breakers can be maintained adequately without the work and complications of either installing a transfer bus or cutting over the loads to other substations.

In conclusion, I would recommend this paper quite highly to those who desire a primer on the advantages of a primary network, as well as the results which can be obtained, from a system planning viewpoint, by including and analyzing a wide variation of the various factors involved in system design before arriving at the size of substation to be used.

REFERENCE

1. A METHOD OF APPROACH TO THE CONSIDERATION OF POWER-DISTRIBUTION-SYSTEM COSTS, O. B. Falls, Jr. AIEE TRANSACTIONS, volume 63, 1944, pages 1078–84.

P. R. Pierson (Westinghouse Electric Corportation, East Pittsburgh, Pa.): The authors are to be complimented on the subject presented in this paper. It is timely because of the trend in this type of construction at the present time. It provides the answers to questions of suitability in an unquestionable manner. Together with the authors who had the courage to pioneer a program as outlined, the manufacturers also can derive satisfaction from the fact that these pioneering switchgear designs have given satisfactory service.

Three points of particular interest are that these installations are all air-circuit-breaker metal-clad switchgear, that the installations are of the simplest basic unit construction, and that the locations in the industrial centers of the Quad Cities on the banks of the Mississippi River are subject to as severe atmospheric conditions as usually will be encountered.

Drawout air-circuit-breaker metal-clad switchgear is adapted particularly well to unit substation or outdoor switchgear because, in addition to the safety features of metal-clad construction, the circuit breakers are individually mobile, thus requiring no auxiliary devices for operation within the unit. The circuit breaker parts are located in a position to provide for easy and quick inspection by the removal of a single piece barrier assembly. These operations and minor maintenance can be performed with the circuit breaker in front of its housing without the use of auxiliary handling devices other than a platform dolly.

The units discussed employ the simplest circuit construction. No provision is made for by-passing circuit breakers or transferring circuit to transfer busses. Thus a minimum of primary circuit subject to fault or maintenance is involved in each housing; however, maintenance has been performed satisfactorily without undue annoyance to customers. It is acknowledged that the network system contributes greatly to the continuity of service during these operations.

The six years of reasonably trouble-free operation of this type of equipment in the severe atmospheric conditions of the industrial sections along the river confirm the moisture prevention features of the switchgear design for most locations. The use of free ventilation through all compartments and the provision of heaters to maintain temperatures inside the housings above those outside during the severely changeable weather of spring and fall has proved adequate for the conditions.

The trend in unit substation switchgear is toward better appearing units, and standardization of circuits, equipment, and individual unit designs. With standard individual units, expansion, reduction or rearrangement can be made as load trends demand, with maximum salvage value of equipment.

E. F. Miller and **R. B. Miller:** In our opinion, good voltage regulation is one of the advantages of the primary network form of distribution. This is a result of the over-all design of a complete network. We have found that for our loadings, it is necessary to use 0000 conductor wire on the tie lines to sustain the network with one of the transformers out of service during a peak load condition. Conductors of 0000 wire on a standard 4-pin arm have an impedance of less than 0.7 ohm per mile. With tie lines two miles and less in length, the voltage drop from the station bus to the center of the feeders will be about two or two and one-half per cent, which is small in comparison to the drop in the secondaries and distribution transformers.

We set the compensator in each transformer tap changer control for a slight rise in voltage on its station bus as the load increases, with a maximum of about 121 secondary volts. We find that this gives excellent primary regulation throughout the day and night and makes the matter of voltage at the customer's entrance a function of the distribution transformer and secondary drops.

These results are based on maintaining balanced loads on the individual phases of each circuit and also on the basis of using four circuits per substation with two or perhaps three of them as tie lines. The primary drops referred to are based on about 2,800-kva normal peak load on a 3,000 3,900-kva substation and with power factor of 80 per cent or better.

A network of this general design is capable of maintaining good operating voltages throughout on peak load with any of its transformers out; also, any tie line will function satisfactorily with one end open. This permits maintenance to be done on a circuit breaker or transformer any time without inconvenience to the customer, and during regular working hours. With uniform design of substations one spare circuit breaker and other important pieces of equipment can be provided for use anywhere on the system. A circuit breaker unit needing major work done on it can be replaced quickly and taken to a service building for major testing or repair. Minor jobs can be done at the substation.

The use of air circuit breakers instead of oil circuit breakers minimizes the amount of maintenance of such units. Transformers have automatic pressure gas seal above the oil and cuts oil contamination to a minimum. This reduces maintenance and possibility of trouble besides extending the expected life indefinitely. Weekly routine inspection trips catch all the minor trouble and prevent major trouble from developing.

All substations have instantaneous recording ammeters, wattmeters, and varmeters besides a watt-hour meter. These instruments record quantities for the transformer as a whole. Test jacks are provided on each circuit for connecting portable instruments for spot checks or major surveys. There is no supervisory control or indication.

Relaying is provided to trip the transformer's secondary circuit breaker in case of a fault on the primary circuit or in the transformer winding. These relays provide automatic reclosing after the primary circuit has become energized, and the magnitude and phase angle of the voltage is such that it will feed energy into the network. Relays also are provided to trip all circuit breakers in case of a substation bus fault. Each feeder has overcurrent relays on it. The transformer has a winding temperature relay set to trip the transformer circuit breaker if a safe temperature is exceeded.

Single conductor cables are used on all 4-kv and 13.2-kv lines into each substation. On 4-kv circuits the phases are marked at the switchgear and at the pole for ease of phasing out in case of cable trouble. Distribution type lightning arresters are provided at each dead end when there is a cable terminal.

Some Aspects of Polyphase Motor Design—The Design and Properties of the Magnetic Circuit

Discussion of paper 46-166 by T. C. Lloyd and H. B. Stone, presented at the AIEE summer convention, Detroit, Mich., June 24–28, 1946, and published in AIEE TRANSACTIONS, 1946, December section, pages 812–18.

P. H. Trickey (Diehl Manufacturing Company, Somerville, N. J.): T. C. Lloyd and H. B. Stone are to be complimented for a very clear analysis of an old and difficult design problem, and particularly for their

ability in eliminating the confusion and complication of certain awkward and comparatively unimportant factors.

Their formula for tooth width checks very closely with my own experience. The equation for inside diameter checks with the curve shown in Figure 3 of my discussion on Lloyd's 1944 paper, for a stator diameter of 4.6 inches. However, perhaps Lloyd's formula should be modified for subfractional sizes because it would give zero rotor diameter for a 0.647 diameter stator.

Very often it is not possible to use a rotor diameter exactly as desired because of the need to use previous die diameters. In this case it may be better to choose the "depth below slot" from a proportional division of the distance from inside to outside diameter. Such a formula is

$$DBS = \frac{0.86}{0.315P + 1.03}\left(\frac{OD - D}{2}\right)$$

A further extension of the principles of this paper might be to choose the rotor diameters so that the 4-pole diameter of one frame size would be the 2-pole diameter of the next larger frame, and the 6-pole diameter of the next smaller frame.

Characteristics of Resistance Welding Transformers

Discussion of paper 46-156 by F. E. Murray and R. C. Jones, presented at the AIEE summer convention, Detroit, Mich., June 24–28, 1946, and published in AIEE TRANSACTIONS, 1946, November section, pages 726–8.

F. L. Brandt (nonmember; Thomson Electric Welder Company, Lynn, Mass.): I am pleased to see how close the authors' design constants agree with my own. This is true because our designs are governed by accumulated experience of these transformers in service.

I would like to amplify the data given on core design. Equation 3 assumes a stacking factor of 0.95. This stacking factor expresses a sort of efficiency in the way that the core is cut and assembled. I would like to point out that the dies or shears used to cut the laminations must be maintained religiously so that burring of the edges of the laminations is at a minimum. The core assembly personnel must stack these laminations so that there is a minimum of air spaces. The laminations should be cut so that the flux path is in the same direction that the steel has been rolled. These points apply to all transformers and not just resistance welding transformers.

There are silicon steel cores available that can be worked up to 115,000 to 125,000 flux lines per square inch. A large part of this increased density is enabled by the method of assembling the core laminations which prompted the discussion in the previous paragraph. Such cores are costly in themselves but the saving in primary and secondary copper resulting from reduced length of the mean turn actually reduce the total cost of the transformer in many cases. Not only the physical size of the transformer is reduced but so are the losses and impedance. Higher flux density cores are a definite trend for the future.

I should like to point out that the high voltage windings should be insulated with a suitable varnish or impregnant to resist moisture, oils, and acids that are prevalent in manufacturing plants. The transformer is part of a machine in which lubricants often are used freely. The water-cooled low-voltage windings are apt to sweat like a pitcher of ice water on a hot summer day.

There is a growing trend to make the low voltage windings of rolled copper, particularly in the form of heavy wall tubing. This further reduces the size of a given transformer.

The leakage reactance and losses are calculated for the parallel connection of the 100-kva transformer.

Moisture Equilibrium Between Gas Space and Fibrous Materials in Enclosed Electric Equipment

Discussion and author's closure of paper 46-160 by John D. Piper, presented at the AIEE summer convention, Detroit, Mich., June 24–28, 1946, and published in AIEE TRANSACTIONS, 1946, December section, pages 791–7.

F. J. Vogel (Illinois Institute of Technology, Chicago, Ill.): This paper is of great interest to the designer and manufacturer of apparatus inasmuch as it points out one of the problems that has to be considered by the designer which generally is not appreciated by other engineers.

The author says that he does not know of transformer failures from condensation. There have been several. This condensate has not always been water only but in some cases a mixture of acid and water. In my opinion, it has caused both terminal structure failures and one or two insulation failures in transformers.

That condensation has been given at least a little consideration is shown by several schemes, some patented, for providing extremely free breathing to prevent condensation. Free breathing also accelerates oil deterioration caused by oxidation.

The presence of condensation has been used to determine dryness. Units have been heated by circulating current in the windings and then examined to note any condensate on the underside of the cover. Absence of moisture on the cover is taken as an indication of dryness. However, these tests are not quantitative nor are they necessarily uniform in their results.

Although new oil has an extremely small percentage of water solubility, this may be a large quantity of water if condensed from a large transformer.

This solubility decreases with lower temperature and undoubtedly the oil volume acts within limits as a water reservoir. The water then is distributed between the insulating materials, oil, and the gas space of sealed units. Where the temperature does not range over extreme limits, there is probably little trouble. From experience, and not as a result of test, it might be concluded that the dielectric strength of insulations is not affected greatly by at least as much water as would be picked up by contact with the air. However, if a transformer were heated up to about 50 degrees centigrade or more in a moist atmosphere, considerable moisture might go into solution in the oil. If the unit then were placed outdoors at minus ten degrees centigrade the oil solubility could be reduced to the point where there would be freely divided water in the body of the oil. Then there is likely to be free water on the surface of the insulation, and cases where it could have been the cause of trouble are known. Piper has given consideration to these problems, shown when he states that the equilibrium for transformers is more complicated than the tapes he tested. Although I believe safe procedures are known and prescribed by the manufacturer's instructions, I am not aware of exact data that are available.

These phenomena are also of interest in the drying process. Drying is obtained by heating or the application of vacuum. The time and the heat required to vaporize the moisture are elements of this problem and consideration has been given to studies of this subject.

C. T. Hatcher (Consolidated Edison Company of New York, Inc., New York, N. Y.): The author has presented a comprehensive paper on the question of determining moisture in materials. There is one question which requires an explanation concerning the partial pressure of unsaturated water vapor. It is stated that for any vapor pressure long continued exposure of any fibrous material will cause it to absorb or give off mositure until its moisture content is in equilibrium with the vapor in the air. From example 2 it appears that the writer assumes the pressure exerted by unsaturated water pressure at any temperature to be the same as the pressure exerted by the same amount of vapor per unit volume at saturation. Actually, it would be somewhat higher because of the fact that it is superheated or raised to a temperature above that of saturated water vapor of the specified density. This will make no difference if the curves showing moisture content of fibrous material at different temperatures are based upon the same conception, but it is not clear whether or not this is the case. If it is not, an error of about eight per cent in the moisture content of the fiber at equilibrium would result.

Abe Tilles (Pacific Gas and Electric Company, San Francisco, Calif.): As is well known, cable engineers and others interested in maintaining the integrity of high voltage insulation always have a great and serious concern regarding the whereabouts of the last traces of moisture. Accordingly, great interest is attached to the method, so ably developed here, of establishing moisture concentrations in relatively inaccessible dielectric materials from measurements on readily reached gases in contact with them.

The author states that equilibrium times are quite long. Can the time be given

more specifically of approximately how long it might take to reach equilibrium? If this time is long compared to that of a marked daily temperature cycle, what temperature should be considered as controlling—the maximum or average temperature of the insulation surface, of the insulation volume, or what?

Following the reasoning of the paper further, would it be feasible to dry the insulation slowly but surely by leaving some highly hygroscopic material in contact with the gas space? Has this been attempted?

Would it not be expected that the presence of various true gases, for example, nitrogen with or without oxygen, at various gas pressures over a wide range, for example, two millimeters of mercury up to 15 atmospheres, would leave the moisture equilibrium concentrations unaltered?

The authors state that presence of a thick impregnant does not alter moisture equilibrium concentrations of gas space and fiber. When, however, a volatile and hygroscopic vapor—as perhaps of transformer oil—is present, would they not expect the equilibrium moisture content of the gas and vapor space to be subject to marked alteration on that account?

L. Meyerhoff (General Cable Corporation, Bayonne, N. J.): J. D. Piper very cleverly has drawn together the scattered data of equilibrium moisture conditions and put these into a very convenient and usable form. He has shown some practical confirmation and has indicated various applications for which these data will be valuable.

It is of interest to compare with his curves, equilibrium data we have taken of unimpregnated kraft paper in the range of 15 to 70 per cent relative humidity.

In our tests four sheets of cable paper of different densities, each weighing approximately 50 grams, were hung up in the laboratory and thus subjected to the laboratory atmosphere. The initial moisture content was determined by drying other similar samples at high temperature to constant weight. The samples were weighed at frequent intervals during the 14 months of the test (January 1932 to March 1933) and at the same time temperature and relative humidity were observed. It will be noted that the paper did not necessarily attain equilibrium at any one atmospheric condition. However, some readings were with rising relative humidity and some with dropping relative humidity. Thus the average moisture content observed for a given atmospheric condition is probably not far from the equilibrium value.

Table I

Per Cent Relative Humidity	Per Cent Moisture Content	
	GCC* Data	Data From Figure 4
15	4.2	4.1
20	4.6	4.9
30	5.5	6.3
40	6.3	7.6
50	7.2	9.3
60	8.0	10.1
70	8.9	11.2

* General Cable Corporation.

The degree of accuracy of the method does not permit determination of the effect of temperature and humidity independently of each other. However, it is not too far out of line to consider the data as fairly accurate for the average temperature in the tests, 26 degrees centigrade, with a range of 22 to 32 degrees centigrade No significant differences were found among the various samples because of density, including superdense paper.

The average results are given in Table I of this discussion in comparison with values taken from Piper's curves for 26 degrees centigrade.

The comparison for low relative humidities is extremely good and is not far out of line for the higher humidities.

With saturated paper the rate of moisture absorption may in some cases predominate in practical importance over the final equilibrium condition. Here the question of degree of saturation and, in an extremely important degree, the type of saturant become controlling and the rate of absorption is only a small fraction as much with certain saturants as for the unimpregnated paper. The surrounding humidity greatly affects the rate of absorption as well as the equilibrium point.

A rapid device for determining the effect of exposure of saturated paper to moisture is by tape-by-tape power factor measurements. These are much more effective when made at 80 degrees centigrade than when made at 60 degrees centigrade. Figure 1 of this discussion shows a comparison which we have obtained between power factor at 60 and 80 degrees centigrade of saturated tapes wherein the major variable is the amount of moisture present. The data are for an experimental cable which was taped with presaturated tapes in a room of relatively high humidity. Some of the tapes had been exposed to the humid air for considerable lengths of time during interruptions of operation. It will be noted that where the power factor is low (that is, very low moisture content) the 60- and 80-degree-centigrade power factors are almost identical, whereas for high power factor values (that is, relatively high moisture content) the 80-degree-centigrade power factor goes up much more rapidly than does the power factor at 60 degrees centigrade.

The great protection (greatly slowing of absorption rate) obtained from the metallized paper shielding tape, as noted by Piper, is pertinent to this whole matter and has contributed in a great degree to the low moisture content shown by him for cable as completed and shipped.

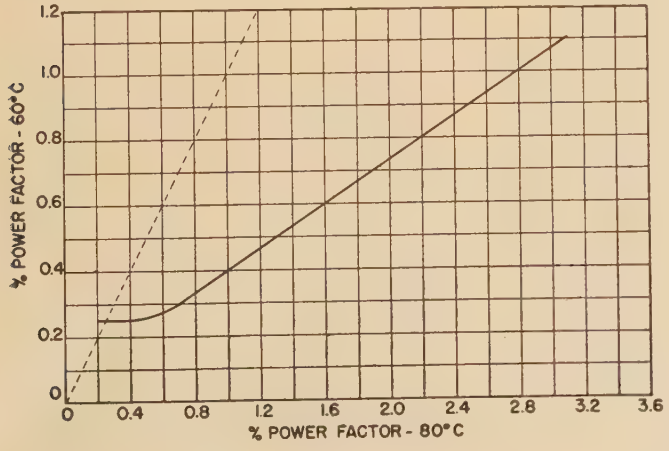

Figure 1. Comparison of 60- and 80 - degree - centigrade tape-by-tape power factor with moisture as the major variable

The dotted line shows one-to-one variation for comparison

E. W. Greenfield (Anaconda Wire and Cable Company, Hastings-on-Hudson, N. Y.): J. D. Piper's interesting co-ordination of previous work on adsorption isotherms for cotton, paper, and wood gives a unique dew point chart for cellulosic insulating materials.

Figure 4 of the paper permits determination of equilibrium moisture content of cotton or wood pulp paper for any given temperature and vapor pressure of its surroundings. Since the curve for water also is given, the chart can be used to find dew point temperature corresponding to various operating conditions.

The value of such an equilibrium chart becomes apparent from consideration of the examples given by Piper. Other problems involving the equilibrium moisture content for paper, varnished cloth, fabric tapes, and so forth stored at various relative humidities are of equal interest.

Construction of the vapor pressure curves for wood pulp paper based on the data of Pidgeon and Maas (reference 8 of the paper) may be open to some question. It is true that the cellulose micelle in any state maintains its unit chain individuality since cellulose from many differing sources shows identical X-ray diagrams. (These diagrams are also identical for cellulose both in the very dry and very moist states indicating the occluded water is not bound within the unit cells but probably exists entirely as surface masses.) However, the lignon and resin impurities for the spruce are much greater than for normally-manufactured wood-pulp paper. Also, the oxycellulose content differs appreciably and oxycellulose has a greater affinity for water than alphacellulose. Piper's extrapolation gives him a ratio of 1 to 1.7 for the relationship between the water concentrations that are required to produce the same vapor pressures in cotton and in kraft paper. We feel that this ratio is too high and is occasioned by the assumption of the identity of behavior between spruce wood and wood pulp paper.

We are in agreement with Piper in that the data on unimpregnated cellulose is applicable to oil-impregnated cellulose. Although the presence of the saturant slows up the rate of diffusion, it would appear that the moisture gradually displaces the saturant and becomes adsorbed itself to the cellulose as surface masses. Tests on un-

impregnated and impregnated kraft condenser tissue carried out at Bell Laboratories during 1939 indicated definitely that the same final moisture equilibriums are reached.

In his discussion on vapor barriers, Piper states that either metallized paper or metal tapes placed on the outside of the cable will form a positive barrier to entrance of water vapor. Has consideration been given to the long spiral exposed cellulose edge in the case of the metallized paper or the greater exposed cellulose surfaces of the intercalating tape used with all metal shielding tapes?

G. B. Shanklin (General Electric Company, Schenectady, N. Y.): The interesting information about the effects of moisture in high pressure pipe cable systems, as outlined in J. D. Piper's paper, is appreciated. This experience is further confirmation of the old basic principle of high voltage cable practice and applies equally well to any type of high voltage system, either lead sheathed or in steel pipe. In all such systems it is essential to remove all possible traces of impurities, such as oxygen and moisture, from the cable initially and to safeguard against trapping such impurities in the system during installation and service.

In this particular case the moisture was entrapped by exposure before the temporary lead sheath was applied. There was plenty of time for this moisture to become firmly embedded in the cable cross section, and the cold vacuum treatment applied in the field after the cable was installed was not sufficient to remove this deeply embedded impurity. In this respect the limitations of any field treatment it is practical to apply must be recognized, and penetration of oxygen and moisture into the mass of insulation must be avoided. In the case of pipe cable systems, where the temporary lead sheath is stripped off as the cable is pulled into the pipe in the field, it is important to apply vacuum treatment as promptly as possible after the pulling and before the impurities caused by exposure have a chance to penetrate the mass of insulation. It is equally important to make sure that there are no similar impurities in the cable before the sheath is stripped. This is a problem we always will have as long as paper-insulated cable is used.

W. E. Mougey (Bell Telephone Laboratories, Murray Hill, N. J.): We are not sufficiently familiar with recent developments in power cable to say whether the air pressure cable is finding enough acceptance to warrant the attention given it by J. D. Piper. It is our impression, however, that there has been considerable interest in this development. We assume also that there is rather wide interest in oil filled transformers of the types considered.

While Piper does a lot of extrapolating and interpolating, we can find nothing basically wrong with his methods. For the most part his extrapolations are based on linear or nearly linear curves. However, we are somewhat skeptical of one result of his extrapolations, namely the conclusion that kraft paper takes up 1.7 times as much water as cotton. While we agree that kraft paper is more hydroscopic than cotton, we are surprised that the factor is as high as 1.7. It would be a simple matter for the author to make moisture absorption measurements on kraft paper and cotton under conditions to bolster his conclusions.

A good job has been done by Piper in rationalizing the moisture absorption data of a number of investigators. This is probably one of the most important features of the paper.

In the discussion of the moisture takeup of impregnated versus unimpregnated fibrous materials, we suggest that reference be made to an article by Ingmanson and Vacca.[1] Data are given there showing that the equilibrium moisture content of jute is not changed by impregnation.

Table II

Per Cent Relative Humidity	Per Cent Moisture Content		
	GCC* Data	ICT** Data	Figure 4
15	4.2	4.0	4.1
20	4.6	4.8	4.9
30	5.5	5.7	6.3
40	6.3	6.7	7.6
50	7.2	7.7	9.3
60	8.0	9.0	10.1
70	8.9	10.6	11.2

* General Cable Corporation.

**International Critical Tables.

REFERENCE

1. MOISTURE ABSORPTION OF JUTE, J. H. Ingmanson, G. N. Vacca. *Industrial and Engineering Chemistry* (Easton, Pa.), volume 26, 1934, page 1274.

John D. Piper: The writer appreciates the interest in the paper expressed by the several commentators and is gratified by the opinions of E. W. Greenfield, L. Meyerhoff, Abe Tilles, and F. J. Vogel that the information compiled may be put into practical use.

Greenfield and Mougey express the opinion that the ratio of 1.7 to 1 is somewhat high for the relationship between water concentrations in kraft paper and cotton required to produce the same vapor pressure.

Meyerhoff presents experimental evidence which substantiates the conclusion that for the higher humidities the ratio is high, but which confirms the values from Figure 4 for the lower humidities. Meyerhoff's data are substantiated qualitatively by data taken from "International Critical Tables" as shown in Table II of this discussion.[1]

Divergence from the International Critical Tables data is, however, less than that from the General Cable Corporation data. In preparing the equilibrium chart the writer was forced to choose between data for kraft paper taken at room temperature and data for spruce wood taken over a range of temperatures. The latter was chosen in spite of the differences between kraft paper and spruce wood which ably have been pointed out by Greenfield. Except at high humidities the agreement with the meagre data for kraft paper seems remarkable. For precise work an obvious need exists for further data on kraft paper taken over an extensive range of both temperature and moisture concentration.

In response to Hatcher's comment, it should be stated that the curves as given show the equilibrium conditions against water vapor of the vapor pressures shown. Hatcher rightfully points out that in the illustrations the effect of the superheating was neglected. Assuming the gas laws to hold, the equilibrium vapor pressure for examples 2 and 3 as corrected for the superheating is 6.3 millimeters instead of the uncorrected value of 5.7 millimeters of mercury.

Regarding Tilles' opinion that true gases such as nitrogen should not affect the equilibrium conditions but that volatile hygroscopic materials such as transformer oil might cause marked alterations, the writer partially agrees. Experimental evidence shows that nitrogen pressures up to 200 pounds per square inch do not affect the equilibrium conditions beyond experimental error. Vapors of hygroscopic materials probably would if present in sufficient concentration. The odor of the gas over transformations is usually acrid indicating the presence of acid vapors. Analysis of condensate from particularly moist transformers showed, however, the acid to be present in proportion less than 0.5 mole per cent. These are unpublished data of the writer's colleague, T. A. McConnell. Inasmuch as the acid is less volatile than water the concentration of acid in the vapor phase was probably even less. The concentration of oil vapor also must have been low because 98 per cent by weight of the condensate was water. From Raoult's law it is evident that the equilibrium conditions cannot be altered seriously unless the concentrations of hygroscopic materials are much higher than were found in the case cited. In connection with this and the previous comment it should be pointed out that the information given in Figure 4 is not intended for precision work but for making engineering estimates over a wide range of temperatures and concentrations.

Concerning the time required for equilibrium to take place, few data are available. As Meyerhoff points out, for impregnated fibers the rate is greatly dependent upon the nature of the impregnant. For transformers and the cable wrapper discussed, sensible equilibrium seems to take place in a matter of days. Concerning the proper temperature to use when the period of a temperature cycle is less than that necessary for complete equilibrium to take place, it has been the practice in working with transformers to use the average temperature of the transformer oil during the working day.

Use of a highly hygroscopic material in contact with the gas or oil in transformers has been proposed in the form of several proprietary devices. Too many of these proposals neglect the fact that the equilibrium vapor pressures of these desiccants increase rapidly as moisture is absorbed and that the quantity of desiccant required to dry a large transformer is considerable. Nevertheless this approach has merit provided a degree of dryness approaching that in high voltage cable is not required. A compressor-condenser system is being used by the company with which the writer is connected on the gas system of 19 generator-transformers in which particularly high dew points were found. While in operation this

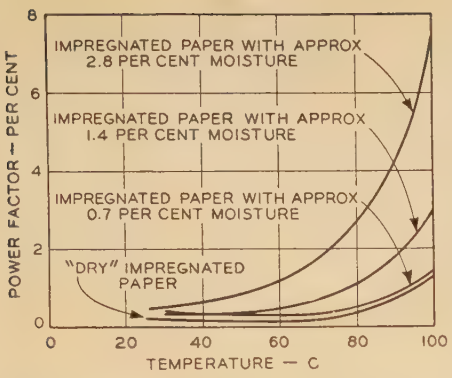

Figure 2. Effect on power factor of moisture in impregnated cable paper

From minutes of the Association of Edison Illuminating Companies for 1929, "Study of Mechanism of Cable Deterioration" by C. F. Hirshfeld, A. A. Meyer, and L. H. Connell

system prevents condensation except in coldest weather and is slowly reducing the moisture concentration in these transformers.

The writer is grateful to Greenfield and Mougey for calling attention to the prior work of Ingmanson and Vacca of the Bell Telephone Laboratories in showing the equilibrium moisture content of a fibrous material to be unaffected by the presence of an impregnant.

Meyerhoff's comment concerning the use of power factor measurements as a criterion of moisture content of impregnated insulation makes it advisable to call attention to the data of D. E. F. Thomas that is reproduced in Figure 2 of this closure. These data showed that power factor measurements, even at 80 degrees centigrade, are not a reliable criterion of the moisture content of impregnated paper when the moisture content is less than approximately 0.7 per cent based on the weight of the dry paper.

There is no disagreement with Shanklin's contention concerning the necessity for protecting cable insulation from contamination by moisture and other impurities. The inference that the moisture entrapped by the cotton protective tape became embedded in the cross section of the insulation is, however, erroneous. The average moisture concentration in the insulation of the cable in question was as low as that of other well-made high-voltage cable at the time it was installed. Moreover, experimental data show that the moisture from the gas space has not migrated into the insulation, a fact which also answers the question, raised by Greenfield, concerning whether the vapor might enter the insulation through the long spiral exposed cellulose edge of the metalized paper tape.

Shanklin is quite right in his contention that the field drying to which the cable was subjected could not remove water—had any entered the insulation. Figure 4 of the paper shows that with the cable at a temperature of 40 degrees centigrade and evacuated to 2 millimeters of mercury the equilibrium water content in kraft paper would be approximately 1.5 per cent, assuming of course that the residual pressure was entirely water vapor. The sole function of the treatment was to reduce the water concentration of the protective tapes to the extent that the dew point of the gas never could be reached at local cool spots in the line.

As stated in the paper, data concerning the cable line were released only because they show that the same equilibrium holds for impregnated fibers as for unimpregnated. The writer had not intended that the data be used to indicate either the merits or the demerits of a particular type of cable. Inasmuch as the question has been raised, however, it seems only fair to state that the results of tests and the outstanding performance of the cable line to date have upheld amply the faith that the proponents of this particular type of cable had in it.

REFERENCE

1. INTERNATIONAL CRITICAL TABLES, first edition. McGraw-Hill Book Company, Inc., New York, N. Y., volume 2, page 322, Figure 1.

Temperature Limits for Short-Time Overloads for Oil-Insulated Neutral Grounding Reactors and Transformers—II

Discussion and author's closure of paper 46-165 by V. M. Montsinger and J. E. Clem, presented at the AIEE summer convention, Detroit, Mich., June 24–28, 1946, and published in AIEE TRANSACTIONS, 1946, pages 966–73.

M. S. Oldacre (Commonwealth Edison Company, Chicago, Ill.): We are given new data in this paper for use in calculating short-time overloads of oil-insulated equipment that can be especially valuable in determining the overload possibilities under different conditions of load and time than the original design basis.

The primary purpose of the work described in the paper seems to be to provide background data for the proposed new standard for neutral grounding devices, that just has been submitted to the Standards committee for approval.

After reading the proposed standard, it seemed to be a logical document subject to only minor questioning, but then after subsequent reading of the paper by Montsinger and Clem it did not seem that there was full co-ordination of the data in the standard with that in the Montsinger and Clem paper.

It is suggested that careful study of the paper is required before full consideration can be given to the proposed standard.

This paper brings out another very valuable point and at the same time initiates a new practice in giving the temperature limits for loading of oil-insulated apparatus. This statement refers to the different temperature rises that are proposed for different starting temperatures at the time of the overloads. In effect a combination is made of the previous methods of rating apparatus and the correction in loading for different ambient temperatures. However, because it is new and different, it seems very essential that the ambient temperatures be set forth clearly when the temperature rises are stated.

One final point or question. Will Montsinger tell us if the data in the paper can be used for transformer windings of different sizes than mentioned? If it is generally applicable, it will be useful in many conditions that exist from day to day.

V. M. Montsinger: The only way in which I believe there is lacking full co-ordination of the data in the paper and in the standard is that the paper gives the amount of heat lost to the oil during a 1-minute fault whereas the standard does not. Because this amount is not very great, it is reserved as a factor of safety in the standard; that is, when calculating the temperature rise, only the heat stored in the copper and associated insulation is considered.

With reference to the last question, the data are applicable to windings of different sizes provided the construction is not entirely different; that is, it might not apply to a small high voltage design having an entirely different ratio of copper to associated (turn) insulation. It is rather doubtful if the data are applicable to the overloading of transformers in general for the reason that the time considered in the paper is too short (in the order of one minute) for the oil temperature to change as it does under usual overloading conditions. For short times in the order of one minute, the data apply.

An Electronic Drive for Windup Reels

Discussion of paper 46-125 by K. P. Puchlowski, presented at the AIEE summer convention, Detroit, Mich., June 24–28, 1946 and published in AIEE TRANSACTIONS, 1946, August–September section, pages 585–91.

W. D. Cockrell (General Electric Company, Schenectady, N. Y.): This paper is greatly enhanced by the author's starting out with the simple formulas on which the drive is based. In fact, I would like to have seen also included the simple electrical formulas for motor speed and torque so that K. P. Puchlowski's circuit (which sets the speed to be held by setting the armature voltage) could be traced back quickly to the fundamental laws. By operating at the midpoint of the linear field range, a buildup of two to one should be obtained easily with good speed control. However, Puchlowski must have assumed fairly constant tension since a large change in tension would demand operation over an excessive field range.

It is assumed that this drive is not required to accelerate rapidly high inertia loads since field weakening produces a loss of torque when a higher speed is called for and thus the acceleration is diminished rather than assisted.

Although no attempt was made in the present drive to control the tension also, it might have been possible to do this by having a movable idler roll whose weight would maintain the tension and whose movement might be used to influence the IR drop compensation.

In the discussion of the basic control system, the statement is made that "the most accurate and sensitive regulator is unable to restore the deviated quantity exactly to its original value." This is true for a proportional action controller such as described, but a proportional plus reset action controller should be able to do this.

In the electric circuit itself, I am unhappy to see so many separate sources of direct voltage required. The circuit shows six batteries and two auxiliary rectifiers in addition to the rectifiers supplying armature and field. Not only do these indicate a high first cost, they also are a maintenance nuisance. Also, the circuit seems to contain a number of subcircuits which are strung together through what seem to be rather high impedances. This means that when the panel becomes slightly dirty and moist, as is almost unavoidable in most industrial plants, sneak circuits may appear which will be difficult to trace and which will cause erratic operation.

In conclusion, may I compliment Puchlowski highly on his use of the new standard graphical symbols in his wiring diagram. By standardizing on these symbols, we will produce diagrams that will be more understandable to both the electronic engineer and the industrial electrical engineer.

Figure 1. Chronological record showing sealed ignitron tube replacement frequency at the Fostoria, Ohio, exciter

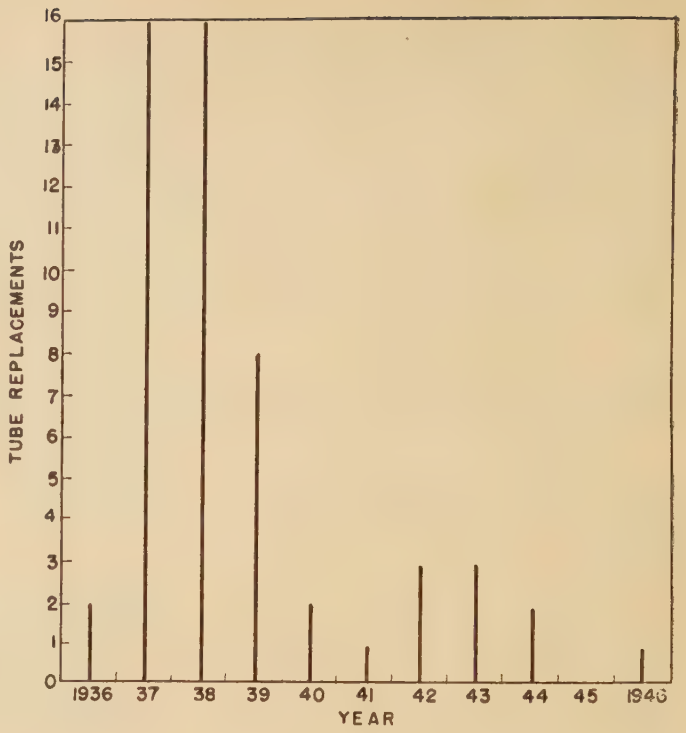

The Development of Modern Excitation Systems for Synchronous Condensers and Generators

Discussion and authors' closure of paper 46-154 by F. M. Porter and J. H. Kinghorn, presented at the AIEE summer convention, Detroit, Mich., June 24–28, 1946, and published in AIEE TRANSACTIONS, 1946, pages 1020–81.

H. C. Steiner (General Electric Company, Schenectady, N. Y.): In commenting on the very excellent paper that F. M. Porter and J. H. Kinghorn have presented, I would like to discuss briefly one question that the authors have raised. It is the question of whether "the heavy expense of making tube replacements" in the electronic tube exciters can be reduced to a satisfactory level. Tube replacement expense depends, of course, on tube cost as well as tube life. In a technical discussion, however, we are limited properly to the technical and not the commercial phases of the matter. Therefore it is the purpose of this discussion to consider only the question of tube life.

In order to determine whether the authors' objective can be met, it is necessary, for the designer at least, to examine the individual rather than the average tube life. Figures 1, 2, 3, and 4 of this discussion have been prepared on this basis to show the tube life and tube replacement history of the Fostoria and Torrey exciters. All tubes that have been removed from the exciters are shown regardless of whether the cause of failure was the result of the tube design and manufacture or application. Fostoria represents the initial installation of this size and type of equipment while Torrey represents an almost duplicate unit in which the experience with the first unit was translated into the design of the second.

In the case of the Fostoria exciter the initial high tube replacement rate (Figure 1 of this discussion) and the low tube life (Figure 2 of this discussion) show clearly the result of the developmental work that was required as a result of field experience. In the development of those tubes in which a life of 1,000 hours is satisfactory, it is obvious that life tests can be run that in a relatively short time will allow the tube designer to make changes and to obtain satisfactory performance. As the life of the tube increases and particularly as the size increases, it becomes necessary to make actual installations in order to obtain the same experience. Forced life tests are useful only when the particular cause of failure is known and the test can be run for a par-

Figure 2. Ignitron power tube life at the Fostoria exciter

Individual tube life is shown except for the years 1936–39 where the average for the number of tubes indicated is given

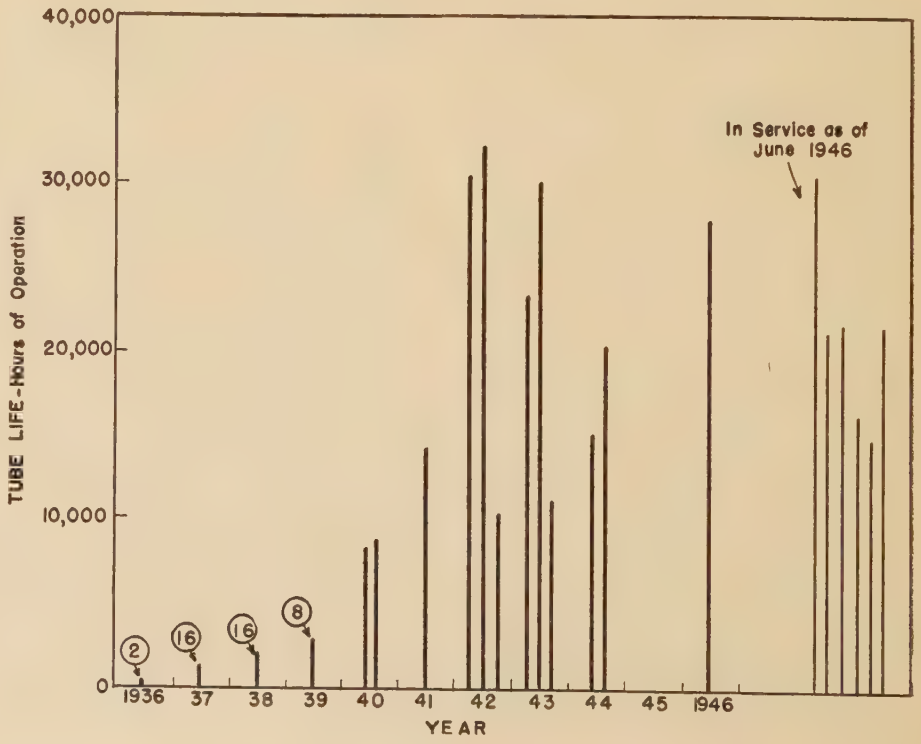

ticular objective. As the life of a tube approaches three to five years, an equally long period will be required to show the results of any design changes. In the case of Fostoria, the individual life of the particular tubes indicates that a much higher average can be attained when the causes of failure in some of the shorter life tubes are removed. The individual lives of the tubes now in operation as shown by the bars at the right hand side of the chart bear out this conclusion.

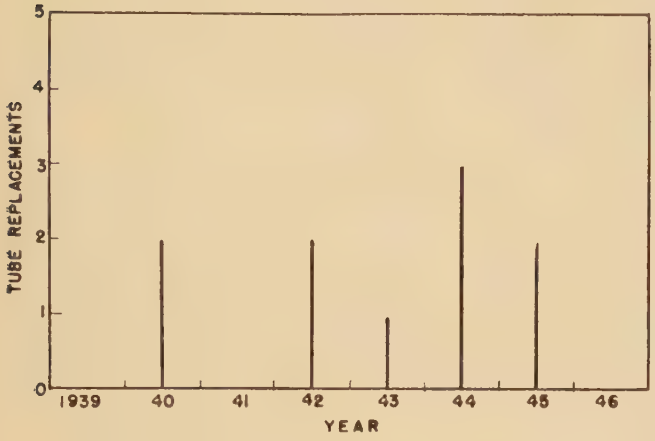

Figure 3. Chronological record showing sealed ignitron tube replacement frequency at the Torrey, Canton, Ohio, exciter

In the case of the Torrey exciter (Figures 3 and 4 of this discussion), the initial problems have been eliminated. The tube life is longer and the replacement rate lower. In the six and a half years of operation there have been 10 tube replacements or an average of $1^1/_2$ tubes per year. If we eliminate the two tubes (1942 and 1944) giving less than one year's service as manufacturing defects, the replacement rate is $1^1/_3$ tubes per year. This is permissible because the present tube warranty insures three years of service, or for an installation of six tubes replacement of not over two tubes per year.

The excellent life indicated for the tubes in service at New Carlisle also shows that extremely long life can be obtained under particular conditions of service. The tubes in this and in the Fostoria and Torrey exciters are of the same type and rating, and it is probable that the longer life is a result of the lower exciter kilowatts and higher voltage.

On the basis of the tube life obtained in the years 1942 and 1946, it is reasonable to expect an average life of four to five years. We would like to hear the authors' opinions as to whether this constitutes a satisfactory life or, if not, what would be satisfactory.

In regard to the general question as to whether a direct-connected exciter is preferable to a rectifier, the preference would seem to rest primarily on the particular conditions of the installation. Rectifiers for industrial, mining, and electrochemical service usually can be justified on the basis of efficiency, but in this case efficiency is of less importance than performance. Rectifier designs have been improved and standardized during the past decade, and as a result they are considerably simpler and less costly than the original exciters. It is possible that direct-connected exciters may prove more satisfactory on slow speed machines, and rectifiers more satisfactory on high speed machines where there are difficulties with mechanical commutators.

In conclusion may I express our appreciation of the co-operation that we received from the engineers of the American Gas and Electric Company and the engineers and operators of the Ohio Power Company in the development of the ignitron tubes and the electronic exciter. It look a great deal of faith to believe that the tube performance as demonstrated by the initial years at Fostoria could be made into anything approaching the reliability required, and in this period we received only co-operation and encouragement.

C. E. Valentine (Westinghouse Electric Corporation, East Pittsburgh, Pa.): The report of operating experience as given by F. M. Porter and J. H. Kinghorn covering a period of several years provides many items of interest for both design and operating engineers. The variety of generating, excitation, and regulating systems which are described affords comparative information not available elsewhere.

For many years one of the main questions in the minds of designers and operators, with reference to electronic regulating devices, has been the question of tube life, and maintenance or replacement costs. This has been difficult to predict because service operating conditions are variable, and factory-made life tests can be completed at reasonable expense only on the basis of a small number of circuit conditions and operating conditions. The situation is in some respects similar to the testing of lamps in the lamp industry. Predetermined and accurately controlled overvoltage testing for a short time gives indication of life expectancy but a number of variables enter into actual lamp life, such as changes in voltage, temperature, or degree of vibration, and these make the actual life vary considerably from the life expectancy. Furthermore, improvement in materials, manufacturing methods, and testing take place year by year. In electronic devices these improvements have been accelerated greatly in recent years, and this points to improved performance in the immediate future.

The authors have stated that the initial cost of electronic exciter equipment and the heavy expense of making tube replacements offer objections to the use of this otherwise most desirable equipment; also that the performance of a rotary amplifier control system with direct-connected exciter has been essentially as good as that obtained from electronic main or electronic pilot excitation. It thus appears that initial tube cost and tube replacement cost has indicated the desirability of the rotary amplifier system. It is noted however that this rotary amplifier system employs an electronic voltage regulator and this is considered an ideal arrangment for a synchronous condenser, with due regard to factors of reliability, performance, economy, and least maintenance.

In their discussion of electronic regulators the authors state that an ideal regulator would have no moving parts and would require no periodic adjustment or renewal of parts. This seems to boil down to the inherent reliability of regulator component parts. It becomes a matter of the performance and life characteristics of transformers, resistors, reactors, and rectifiers compared with replacable components such as electronic tubes. The absence of moving parts does not make necessarily for an ideal regulator. Much depends on the simplicity and durability of moving parts, if used. As an example, spring mounting of such parts avoids wear and consequent readjustment or replacement. There are definite advantages in the use of simple regulator and machine field circuits. In case trouble does develop less skill is required and less time is lost shooting trouble where relatively simple devices and circuits are involved.

With regard to the electronic pilot and electronic main exciter, the authors have tabulated tube failures and tube life. With regard to the electronic regulators, however, it is stated that the tubes used in these regulators have given long life and their replacement cost is low. It would be interesting to have the comments of the authors on the actual tube life which has been obtained in the regulator circuit alone. It is understood that so far as tubes are concerned, the electronic regulators described have dual circuits and dual tubes so as to provide protection against tube failure. It would be of interest to have the authors comment on the effectiveness in their operating experience thus far of the dual tubes in preventing failure of the voltage regulating equipment. Also, have there been any failures which might be attributed to the use of dual tube circuits, as compared with the use of single tubes and associated circuits.

Summarizing the possibilities of various types of voltage regulators—there is still room for improvement in the simple electromechanical regulators. In the static network types some experience already has been obtained, but much remains to be secured. The electronic type regulator seems to afford many opportunities for development, not only in the regulating circuits, but also in associated controlling or limiting features. It is recognized however that a review of this situation several years hence may show many changes in the picture.

J. B. McClure (General Electric Company, Schenectady, N. Y.): The authors are to be commended for their excellent paper in which they review their operating experience with an unusual variety of excitation systems.

So far as exciters are concerned, probably the newest combination is the direct-driven overhung exciter operating in hydrogen. Direct-driven exciters long have been the preferred source of excitation for synchronous machines and first were abandoned for synchronous condensers with the advent of hydrogen cooling. Their return now marks a definite advance in design accomplishment and the maintenance and inspection record of these exciters bears out the fact that they are here to stay, at least for moderate speed machines.

Regarding the primary function of an excitation system which is to maintain output voltage, we have seen an excellent record in Figure 7 of the paper. It so happens that this record was made with an electronic exciter and regulator controlling. Experience indicates that comparable results will be obtained with modern excitation systems employing rotating exciters. It is now evident that an excitation system will be satisfactory for most applications if

1. The regulator is of the continuously acting type.
2. The regulator has a small dead band.
3. The exciter has at least moderate rate of response.

These requirements can be met with several combinations of equipment, and experience alone will indicate which combination is the most practical.

A. A. Johnson and **R. F. Lawrence** (Westinghouse Electric Corporation, East Pittsburgh, Pa.): The authors of this paper and all participating operating companies are to be congratulated for making available to the industry the carefully obtained results of their experience with newer types of excitation systems. Indeed it is gratifying to know that all of the schemes which have been tried have given very satisfactory operation.

Of primary interest is the fact that electronic exciters have been proved by tests and actual operating experience to be a reliable excitation system for synchronous condensers and synchronous generators. These results have given a stimulus to the thinking of operating engineers and undoubtedly additional main electronic exciters will be applied. All excitation systems to date have certain features which are undesirable. However, any excitation system which can be serviced without having to shut down the main machine has a distinct advantage from an operating standpoint. An electronic exciter satisfies this requirement but has a higher initial cost and an apparently high maintenance cost because of tube replacements. The paper under discussion indicates that three power tubes and 4.4 firing tubes are required for each year of actual operation. It also states that further operation should produce a substantial improvement in the record for power tubes. We certainly agree that further improvement will be obtained because in one case the tubes already have operated an average of 36,389 hours, and also because ignitron tubes are guaranteed for three years. There is some question as to whether or not the cost of maintenance because of tubes (which should not exceed in the future approximately $600 per year) exceeds the actual system cost of outages required for maintenance of rotating types of excitation systems. This will be important on systems where there is a continuous need for the synchronous condenser. It is of more importance with regard to synchronous generators. Probably, as far as generators are concerned, any excitation system which reduces the outages of a base load generator by one per year can be justified economically. The authors indicate that no outages have been required for maintenance of the electronic exciters but that an average of three outages per year have been required for inspection and maintenance of the enclosed hydrogen-cooled d-c exciter.

It is believed that the authors of the paper have selected a fair comparison of power tube life by omitting the failures during the first year of service. However, we would like to explain the low average of 5,900 hours for three power tubes at New Carlisle. One tube was evidently defective and had to be replaced as a result of an excessive number of backfires. The life of the other two tubes was shortened because of improper cooling.

The authors have given results of operating experience for electronic pilot exciters on condensers and turbogenerators and hydrogenerators. They also have given results of operating experience for electronic main exciters on four synchronous condensers. The discussers' company has built, tested, and placed in service a main electronic exciter for a 81,250 kva turbogenerator in the Springdale station of the West Penn Power Company. The results of these tests which were made in one of the a-c high power laboratories were presented in a recent paper.[1] This electronic excitation system is similar to that shown in Figure 4, of the paper, that is, the power supply to the rectifier is obtained from the generator terminals. Another main electronic exciter now is being built wherein the ignitron rectifier and associated control receives its power from an a-c generator directly connected to the shaft of the main generator.

It is not the intention of this discussion to justify any particular type of excitation system but to point out that the conclusions reached in the paper may be modified when the over-all system costs of the operation of each exciter scheme are considered. This is particularly important when considering excitation systems for generators.

REFERENCE

1. APPLICATION AND PERFORMANCE OF ELECTRONIC EXCITERS FOR LARGE A-C GENERATORS, H. A. P. Langstaff, H. R. Vaughan, R. F. Lawrence. AIEE TRANSACTIONS, volume 65, 1946, May section, pages 246–53.

E. L. Harder (Westinghouse Electric Corporation, East Pittsburgh, Pa.): At no time in the history of the industry has there been as great a variety of excitation and regulation systems from which to choose. This creates a problem for the prospective user in evaluating which system is best for his particular service and indicates a strong need for determination of the relative merits of the different schemes and stabilization upon a few of the best of them for general use. This is a period of transition from the older types of excitation and regulation systems to the newer electronic and rotating amplifier types with a great many conflicting requirements and tendencies. The final conclusions as to which systems are best can be reached only through appraisal of accurate information on the performance and characteristics of several available systems.

Thus, the paper of F. M. Porter and J. H. Kinghorn comes at a most propitious time. It is particularly significant in providing a mature evaluation of comparative merits and valuable field experience on a number of

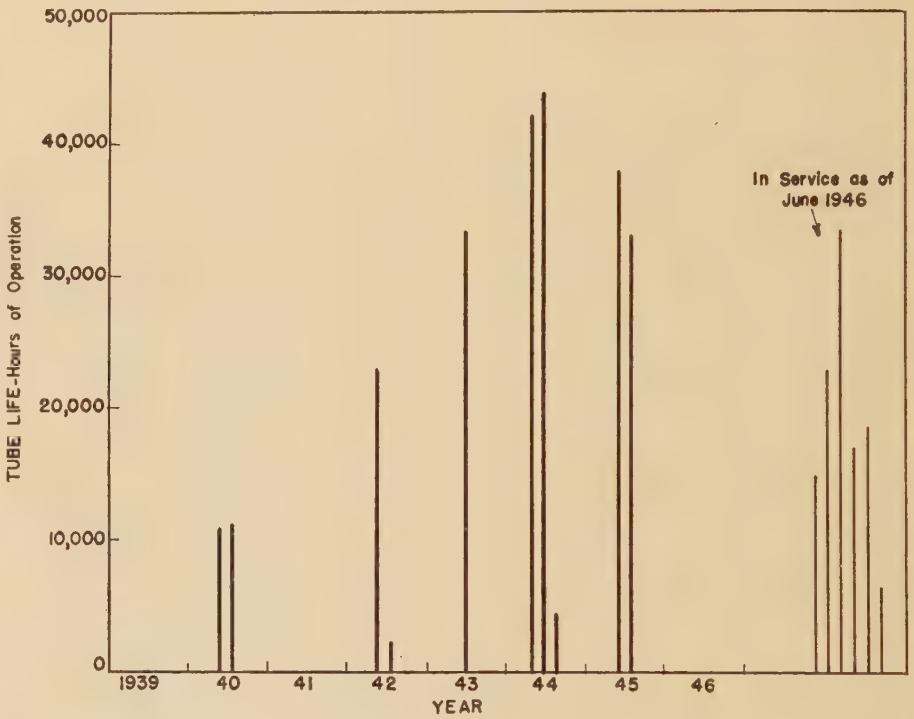

Figure 4. Ignitron power tube life at the Torrey exciter

the excitation systems now undergoing trial.

The major stress has been laid on synchronous condensers, and several differences between the synchronous condenser and the turbogenerator or water wheel generator may be noted. In the case of the condenser, the continuity of the bus voltage is essential for the condenser to remain in synchronism regardless of its excitation system, and it therefore becomes more logical to take the excitation source from this bus provided the requirements of sufficient excitation during fault conditions can be met. This is generally possible as pointed out in the paper. On the other hand, in many turbogenerator installations, a 3-phase fault on the generator voltage system would lower the terminal voltage too low for it to be depended upon for excitation. In these cases, other sources of excitation power offer advantages. These are the main shaft, the station service supply, or a current compensator used in conjunction with the generator terminal voltage.

The static type of regulating network now called an impedance type regulator has received rather intensive development during the war period because of its advantages in naval service. It also offers certain advantages in central station service. It may be used to control either a Rototrol pilot exciter or a Rototrol main exciter.

The simplest of all rotating-amplifier-type regulating systems is the main exciter Rototrol, one of which is being built experimentally for a 60,000-kw turbogenerator. This offers the advantages of complete elimination of the pilot or control machine. The impedance type regulator or the electronic regulator directly controls the main exciter Rototrol. With the impedance type regulator there is, of course, no tube replacement at all. However the electronic regulator offers the advantages cited in the paper of adaptability to the addition of other control or limiting functions.

It is significant that the authors of this paper have concluded that the operation of the several devices, namely, electronic pilot exciter, electronic regulator, electronic main exciter, and rotating amplifier have been perfectly successful and that the decision as to what scheme should be used therefore hinges on initial and maintenance cost, and on the reliability of the power supply rather than on questions of reliability of the device itself. If this point of view is adopted generally, it greatly will facilitate reaching general industry conclusions as to the best ultimate form of excitation systems to be adopted for the different classes of service, namely, condensers, turbogenerators, and water wheel generators. It is to be hoped that within a few years, this situation will have stabilized so that in place of the large number of different types of excitation and regulation systems which must be considered now, a relatively few standard arrangements will be adopted by the industry. This paper should be of considerable help in clarifying this situation.

F. M. Porter and **J. H. Kinghorn**: H. C. Steiner's analysis of tube life of ignitrons is a welcome supplement to data in Table III of the paper, and gives a basis for optimism that further development work will improve the competitive position of electronic exciters in the field of synchronous machine excitation. In evaluating such a position, consideration must be given not only to maintenance costs of which tube life represents a major portion, but also to original cost. In addition, if savings result from reduced maintenance outages of the main generator or synchronous condenser, usually more important in the case of a generator, these must be included. While it is true that rectifier designs have been improved and standardized, their cost, including all necessary auxiliary equipment, is not yet as low as that of a direct-connected exciter. Manufacturer's warranty of tube life is a measure only of maximum replacement costs to the user and, as is suggested by Steiner's charts, it is hoped soon will represent a pessimistic evaluation of tube costs. In view of the variables involved, no general conclusion can be reached by the authors as to an average tube life which can be considered satisfactory.

If, as Steiner suggests, the excellent tube performance at New Carlisle can be attributed to lower exciter kilowatts and higher voltage, these factors should be considered in the design of electronically excited machines or in the selection of tubes for use with standard designs of machines. To state this in another way, the inference can be drawn that possibly tubes should be rated more conservatively when used with electronic exciters than when used for normal rectifier service.

It is interesting to note that C. E. Valentine concurs with Steiner in concluding that improved tube performance can be expected in the immediate future. Valentine's statement that a simple regulator is desirable because maintenance and trouble shooting then require less skill is one with which we believe most users will concur. This was a point which caused us some concern when we first began using electronic regulators. However an excellent and highly detailed set of trouble shooting instructions have been developed which have proved entirely satisfactory and have reduced maintenance to the routine level which exists on other better known equipment. So far as the use of dual tube circuits in the regulators is concerned, experience has not indicated any special advantage or disadvantage over single circuits. As tubes approach the end of life, their characteristics change gradually enough so that periodic testing and slow changes in regulator characteristics indicate this condition and new tubes are installed before actual failure occurs.

J. B. McClure's remarks about the requirements of an excitation system are not borne out entirely by any evidence presented in this paper. All of the regulators cited are of the continuous acting type and it is our experience that this is always preferable to a regulator of the dead-band type. A small dead band, if small enough, would approach a continuously acting type. Our experience with dead-band types indicates that the dead band cannot be reduced much below one per cent without specially designed equipment, and that a dead band of this magnitude is sometimes objectionable from the standpoint of voltage regulation and is usually objectionable from the standpoint of parallel operation with other regulators.

A. A. Johnson and R. F. Lawrence refer to statements in the paper indicating that no outages have been required for maintenance of electronic exciters, but that an average of three outages per year have been required for inspection and maintenance of the enclosed hydrogen-cooled rotating exciter. In the case of hydrogen-cooled condensers, it is necessary to open and clean the collector compartments three times a year, and therefore these outages occur on machines with electronic exciters as well as those with rotating exciters. In each case the outage can be charged more logically to the collector rings and hydrogen operation, because cleaning of an exciter compartment takes about the same time as cleaning of a collector compartment. Regarding operation of direct-connected exciters, we believe our experience indicates that maintenance for hydrogen-cooled exciters is going to be less than for air-cooled exciters. In order to keep brush wear and commutator wear to a minimum it is necessary to retain moisture in the gas, and therefore we have supervised closely the gas humidity. Although provisions have been made for adding moisture with the make-up gas, it has been determined that at least for five years the moisture originally in the machine is sufficient for satisfactory performance. This moisture apparently does not leak out of the shell appreciably with the leakage hydrogen.

Obviously, it cannot be expected that exciters can run indefinitely in hydrogen without inspection. It is our practice to make a general inspection of hydrogen-cooled condensers every five years, and the major exciter maintenance will be taken care of at these times. In the case of the Muncie condenser, although no trouble was experienced, the exciter was disassembled after three years operation for a check inspection. It was found that all parts were in excellent condition. Therefore we agree with McClure's remarks that hydrogen-cooled exciters for synchronous condensers are here to stay.

As to maintenance on direct-connected exciters of turbogenerators, we have found that in general necessary inspection and repairs of the exciter can be taken care of during the usual outages required for maintenance of the turbine and generator. Therefore, the total outage of the unit will be approximately the same regardless of the type of exciter.

E. L. Harder has mentioned the development of two very interesting additional methods of excitation, namely, a method which uses a current compensator in conjunction with generator terminal voltage as a power source and a method using a main exciter rotating amplifier. It will be very helpful if operating experience data can be published on these systems when available so that their performance and advantages can be judged in relation to the better known excitation systems.

As the discussion by Johnson and Lawrence indicates, all factors involved must be considered before a decision can be reached as to the proper excitation system for a specific application. In reaching such a decision it is very helpful to feel confident that all systems considered will operate reliably and accurately, and it is the authors' hope that the data presented will contribute to such confidence.

Influence of Magnetic Materials on the Welding Characteristics of Resistance Welding Machines

Discussion and author's closure of paper 46-137 by J. J. Riley and C. E. Smith, presented at the AIEE summer convention, Detroit, Mich., June 24–28, 1946, and published in AIEE TRANSACTIONS, 1946, December section, pages 852–60.

A. C. Johnson (Progressive Welder Company, Detroit, Mich.): I would like to compliment the authors for having selected a subject which has presented for some time an annoying problem to those who are concerned with the design, application, and use of a-c resistance welding equipment. These authors have made a distinctly valuable contribution to the art.

I should like to add a word of caution concerning the accuracy of measurements to those who might continue the work that these authors have started. The paper states that the resistance between electrodes was measured oscillographically and "by taking the voltage drop across the two electrodes at two points as close to the weld as possible and dividing this voltage by the secondary current. . . . The inductive pickup is eliminated by carefully twisting the voltage leads together and holding them perpendicular to the electrodes." The inductive pickup by no means is eliminated by twisting the measuring circuit wires together. In fact, the induced voltage in the measuring circuit loop is quite appreciable. Naturally, the lower the resistance being measured, the more important is the effect of the induced voltage. The values of resistance between electrodes and resistance between sheets given in the paper vary from 10 to about 250 microhms, and, thus, the voltages measured range from approximately 0.1 to 2.5 volts. The voltage induced in the measuring circuit loop is of the order of 0.05 to 0.08 volt. From some of the measurements taken, the induced voltage is definitely negligible, especially as a result of the quadrature relationship between the two voltages under discussion. However, in other cases, especially those concerned with sheet to sheet resistances, the value of the induced voltage is considerable.

Assuming that the electrodes are part of a straight isolated conductor, the voltage induced in a rectangular loop is given by the equation[1]

$$c=\frac{3.19lw\,I_{max}\cos wt}{2\pi 10^8}\times\left[\frac{1-3b^2}{4(1-b^2)}+\frac{b^4}{(1-b^2)^2}\log_\epsilon\frac{1}{b}+\log_\epsilon\frac{1}{c}\right]$$

$b=r_0/r_1$, $c=s/r_1$

s = distance from the center of the conductor to the point at which the leads are twisted

r_1 = the radius of the conductor

r_0 = the inner radius of a hollow conductor (This is equal to zero in this case.)

1 = the points of attachment to the welder electrodes

It is also stated in the paper that the measurements of the resistive voltage component V_{rs} and the reactive voltage component V_{xs} were made using pointer stop meters. This method has an inherently low accuracy, and I believe that since these values were taken without any material actually between the dies, it would have been possible to use a longer duration of current flow and steady-state meter readings. Those values which are being determined, namely, the increase of resistance and reactance resulting from the addition of magnetic materials into the throat of the welder, are obtained of necessity by subtracting relatively large quantities. Consequently, even small errors in meter readings can produce considerable errors in the ultimate result. It is therefore advisable to use a technique of measurement in which every possible effort has been made to eliminate small errors.

I should like to point out also that the very difficulty with a-c welding equipment which makes this paper so valuable a contribution is non-existent in d-c welders. Therein lies one of the important advantages which welders having a d-c source of power supply have over the conventional type of a-c resistance welder.

REFERENCE

1. THE MEASUREMENT OF LARGE VARYING CURRENTS, A. C. Johnson. AIEE TRANSACTIONS, volume 65, 1946, January section, pages 8–11.

F. L. Brandt (nonmember; Thomson Electric Welder Company, Lynn, Mass.): The more I studied and the more I tried using the data contained in this paper, the more I realized how much work and thought have gone into its presentation. These data are much needed in the industry, and I wish this information to be common knowledge.

Formulas 1 and 2, Appendix I, use $Z_o + Z_s$ arithmetically. I believe this should be a vector relation.

I find slight discrepancies between values obtained in Figure 12 in comparison with Figure 20. I am not able to find reference or derivation for the formulas for V_{xs} and V_{rs} given at the top of Figure 20.

C. M. Rhoades, Jr. (General Electric Company, Schenectady, N. Y.): This paper is very valuable in that it outlines for the first time a method by which the effect of magnetic material in the throat of resistance welding machines can be calculated with engineering accuracy by means of the empirical data presented in the paper. Heretofore, the characteristics of resistance welding machines could be determined only after a machine had been built and tested with the desired thickness and size of welding material in the throat. While it is true that most welder manufacturers have available information on the short-circuit kilovolt-amperes and power factor of welding machines, it has not been possible up to this time to determine accurately the welder demand and power factor under welding conditions.

As a result of the data given in this paper, it will be possible now for anyone who has short-circuit kilovolt-amperes and power factor data on a resistance welding machine to calculate accurately the conditions which will be obtained when material is in the throat of the machine. With this valuable data available, manufacturers of welders should be in a position to predict the actual conditions which will be obtained with production welding.

J. J. Riley: It has been pointed out by A. C. Johnson that a comparatively large error could exist in the sheet to sheet resistance measurements recorded in the paper. However, the actual welding resistance measurements shown in detail are of such magnitude that the error resulting from undesirable flux linkages is normally smaller than the error that could be expected from dirty, oily steel sheets or completely degreased steel sheets. Average production conditions formed the basis for the selection of laboratory conditions for measurement.

While not specifically mentioned in the paper, the impedance readings, in which meters were used, were taken with accurate meters in which temporary pointer stops were incorporated. However, the current flow time during any reading lasted between one and two seconds. The pointer stop was used to set the meter reading at approximately the correct scale position, but the meter actually reached steady state conditions before the current flow ended. It was desirable to limit the current flow time and consequently limit the amount of heat generated through eddy current losses in the steel sheet.

The paper does not explain the derivation of the formulas for V_{xs} and V_{rs}. The basis for such derivation, using the graphs contained in the paper, is explained in reference 10 of the paper.

Systems Development of Military Communications

Discussion and author's closure of paper 46-161 by Thomas R. Putnam, presented at the AIEE summer convention, Detroit, Mich., June 24–28, 1946, and published in AIEE TRANSACTIONS, 1946, November section, pages 757–61.

Lee L. Glezen (Bell Telephone Laboratories Inc., New York, N. Y.): This paper is a real contribution to an understanding of one of the basic problems concerning communications for the Armed Forces. While dealing largely with the problems of organization in the North African Theater of Operations it confirms similar experiences occurring a year or more later in the European Theater of Operations. In the European Theater of Operations the widespread use of rehabilitated commercial cable, extensive Army-built open wire lines, spiral-four cables and radio formed a network of nearly 400,000 miles of main-line telephone circuits. This greatly exceeded any pre-World War II plans or expectations. These reached not only all Army and Air Force units on the continent but reached from Berlin, Munich, Bremen, and Frankfort to Paris, Marseilles, Cherbourg, LeHavre, Brussels, London, and even Washington, D. C. The number of long distance tele-

phone calls handled for the Army and Air Forces at Paris alone reached 54,000 calls a day by June 1945.

The extensive technical problems of both wire and radio communications together with radar, television, and other special equipments following the technical principles of communication equipment are such that integration and team work are basic to assure satisfactory operation and performance. In World War II the cost of signal communications equipment for the ground and air forces reached the huge sum of about 5 billion dollars, exclusive of radar equipment which added over $1^1/_2$ billion more. These figures did not include the worth of rehabilitated communication plants liberated or captured and put to use to serve the Armed Forces in Africa, France, Belgium, Luxemburg, Germany, and many other places. The maximum strength of the Signal Corps maintained throughout most of the war period was about 370,000. This was exclusive of the Navy's requirements. Certainly, for such a huge task a well-established and properly functioning organization is required to provide economically and efficiently the team work required for full integration of communications.

Peace time consideration of communications and organization for any possible future conflict should avoid basing plans too much upon what was found to be the need for World War II, just as it was found that World War I needs were outmoded for World War II. In other words, a carefully integrated communications organization is required, but it should be left sufficiently flexible to encompass any developments yet to be conceived and complete enough to assure team work from top to bottom of the communications field as new ideas are injected in the future.

The author is to be congratulated for bringing this matter before the Institute at this time.

C. O. Bickelhaupt (American Telephone and Telegraph Company, New York, N. Y.): The author refers to the fact that "in those overseas theaters in which organizational difficulties were encountered in systems development of communications during World War II, these difficulties stemmed from a basic deficiency in signal communications doctrine as promulgated by the War Department." He points out further that "this doctrine sets forth the principle that every commander controls the system of communications required for his command."

The doctrine referred to perhaps is stated better by saying that "communications is a function of command." The difficulty to which Colonel Putnam refers arises not from the fact that this doctrine is wrong but rather comes through misunderstanding of the doctrine and from its improper application.

On the one hand, the chief signal officer of a theater or subordinate command is primarily a staff officer and as such ordinarily does not exercise command. On the other hand, the chief signal officer does have staff responsibility for the adequacy, co-ordination, and satisfactory operation of signal communications within a given command. In fulfilling this obligation he issues technical directives through technical or staff channels and initiates command directives for issuance by his commander. The command channel, however, flows past him from the commander to the next subordinate commanders.

Apparently in the North African Theater of Operations, the American Army ran into this difficulty, because Colonel Putnam states that "it was soon found that staff responsibility without technical administrative authority over the operating personnel of the various subordinate commands was entirely unsatisfactory." This difficulty was solved apparently through staff channels rather than command channels by giving "technical administrative authority" to the chief signal officer of the theater and echelons of his organization. Apparently this worked out satisfactorily.

In the European Theater of Operations, with which I am familiar, this problem, however, was approached from what I consider to be a more fundamental basis, and its solution was reached in the command channel rather than in the staff channel. This was done

1. By establishing an independent command known as the "military communications service" and commanded by a director general, military communications service.

2. The director general, military communications service, was set up to report directly to the superior commanding general, and the military communications service, therefore, received its command authority directly from the superior commander. The director general, military communications service, was made co-ordinate in command channels with area commanders throughout the theater.

3. In order to ensure proper staff and technical direction and co-ordination, the superior commander gave technical operating control of the military communications service to his chief signal officer.

Thus, while the military communications service received directives as to its mission and as to technical requirements directly from the chief signal officer who, in issuing such directives, was speaking with the voice of the superior commander, the director general, military communications service, was in his own right an independent commander and could command his troops, assigning their specific missions within his general directives, moving them from one geographical command to another, and having complete responsibility for results.

This solution is not new and was, I believe, first used in the American Army in the construction and operation of military railroads where the military railway service was established as an independent command receiving its command authority from the theater commander but operating under directives of the chief of transportation, a staff officer on the staff of the theater commander.

Colonel Putnam is absolutely correct in his conclusion that in order to secure systems operation of a military communications service command authority is essential.

Thomas R. Putnam: General Bickelhaupt has brought out two important points very ably in his discussion. First, he takes the view that the War Department doctrine under which signal communications operations were carried out in World War II was not deficient but was misunderstood and applied improperly. I am not inclined to quarrel with this view, for, in either case, attempts to apply organization principles looking toward system operation of communications in the field encountered difficulties, as General Bickelhaupt agrees.

The second point which General Bickelhaupt discusses is the question of command versus staff channels for the exercise of technical administrative authority in matters relating to the operation of military communication systems. In my opinion there is no question but that the solution arrived at in the European Theater, establishing the military communications service as a "line" organization for the operation of the communication system, was far superior to the arrangement in French North Africa described in the paper under discussion. In the North African Theater of Operations there were numerous factors considered by those responsible for the final decision in this matter, one of which, for example, involved the geographical distribution of Allied communications troops in the area served by the land line system. For this reason, the North African arrangement, which established a certain amount of staff authority for technical administration purposes, was a compromise solution.

The military communications service in the European Theater, referred to by General Bickelhaupt, was not established until July 1945, thirteen months after the Normandy invasion and two months after V-E Day, despite earlier efforts of those charged with the responsibility of operating the communication system. Likewise, in French North Africa suitable centralized control of the land line system did not take place until September 1943, which was ten months after the Allied landings and four months after the close of the campaign in Tunisia.

Glezen in his discussion has given us some interesting data concerning the magnitude of the military signal communications operations in Europe, as well as an indication of the total communications resources required by the ground and air forces in the prosecution of World War II.

Concerning Glezen's ideas as to the flexibility of basic principles of military communications organization, I am in complete agreement.

A 400-Ampere Sealed Ignitron

Discussion and author's closure of paper 46-140 by H. C. Steiner and H. N. Price, presented at the AIEE summer convention, Detroit, Mich., June 24–28, 1946, and published in AIEE TRANSACTIONS, 1946, October section, pages 680–5.

W. E. Pakala (Westinghouse Electric Corporation, East Pittsburgh, Pa.): The authors have given a good explanation of the several factors influencing arc-back and how they may affect the design of mercury-arc power tubes. The effect on arc-back rate and the relative importance of all these factors is not known at the present time, and the design of ignitrons as well as other types of mercury pool rectifiers is based, therefore, largely on our knowledge of design factors of tubes which have proved satisfactory in service.

About four years ago, when we began the development of a 400-ampere sealed ignitron, it was decided to base the sealed design on pumped ignitrons which performed so well in the electrochemical and other fields. The new 8-inch diameter 400-ampere sealed ignitron design proved entirely satisfactory on test. Several sealed tubes were placed on life test for 14 months to determine vacuum tightness of the arc-weld construction. Only two tubes out of a total of ten were found to be gassy. (With the present system of mass spectrometer leak detection used in the shop, all tubes will be vacuum tight.) The others performed perfectly in a 6-phase rectifier circuit under normal load, overload, short circuit, and under other test conditions necessary for the development of a new tube design.

In Figure 3 of the paper by Steiner and Price, are shown oscillograms indicating the deionization rate. These oscillograms were obtained with a 100-ampere load in each case. From the data, two interesting conditions are indicated. These are

1. The deionization time constant increases approximately as the second power of the tube diameter. (The data apply only to tubes without grids.)

2. The cooling water temperature has the same effect on deionization as changing the tube diameter. Figure 3 shows that for constant current the deionization at 20 degrees centigrade for the 8-inch tube is about the same as deionization at 60 degrees centigrade for the 5-inch tube.

The data discussed above indicate that this arc-back influence factor increases with the tube diameter. Therefore, the volume density of ionization and the current density per unit area of tube cross section is reduced considerably in the design of larger tubes. The net result is that the full load current rating is increased for tubes of similar design only as the first power of the tube diameter. For short-time rectifier ratings, such as the 200- and 300-per cent overload ratings, the performance improves with increased tube size because the heat capacity increases more rapidly with increase in the tube diameter than the current rating.

As to the maintenance of vacuum, the paper points out that the arc and the walls of the tube have a gas cleanup action. This cleanup or pumping action is the reason for reduction in life of gas discharge tubes of various kinds. In the case of most mercury-vapor tubes, however, this action does not reduce the life but actually increases it. In fact high fault current tubes, such as high-power ignitrons, could not be operated at all without pumps unless the arc-back rate were practically zero or very fast circuit breakers were used. This is so because of the gases given off by various tube parts during high current arc-backs. These gases are removed rapidly by the pumping action of well degassed walls, and no steady-state pressure will result to affect tube performance.

The experience in this country with large sealed ignitrons and in Europe with sealed metal multianode type rectifiers indicates that vacuum-tight tubes of large size can be built by using arc or gas welding or seam welding for closing headers to the main cylinder of the tube.

H. C. Steiner: W. E. Pakala's comments and particularily his discussion of the effects of tube size and cooling water temperature on deionization rates are much appreciated.

Our experience indicates also that overload capacity is improved with the increased heat capacity of larger tubes.

The gas cleanup action of the walls and arc is important in maintaining a high vacuum in sealed tubes. High speed anode circuit breakers usually are employed to protect both the equipment and rectifying elements, whether sealed or pumped, when fault currents become high. In the case of smaller rectifiers, such as those using 100- and 200-ampere size sealed tubes, medium or slow speed circuit breakers (three to eight cycles) are used satisfactorily. One factor, as Pakala points out, permitting the use of these relatively slow circuit breakers is the rapidity with which any gas is removed; another is the extremely low rate of arc-back in the sealed tubes.

A New Design for the A-C Network Analyzer

Discussion and authors' closure of paper 46-135 by J. D. Ryder and W. B. Boast, presented at the AIEE summer convention, Detroit, Mich., June 24–28, 1946, and published in AIEE TRANSACTIONS, 1946, October section, pages 674–80.

Eric T. B. Gross (Illinois Institute of Technology, Chicago, Ill.): Amongst other features, it is a timesaving advantage of this analyzer that the voltage of each generator is controlled separately by a voltage regulator. The practical problems to be solved often require that the internal voltage, the terminal voltage, or perhaps the bus-bar voltage be kept constant. In load studies bus-bar voltages have to be set and kept at a fixed value; in short-circuit and stability studies the internal voltages are unchanged.

In this analyzer, provision is made for the internal voltages to be controlled; it would be helpful to arrange a switch on the panel of the generator unit so that the voltage control could be taken from points not only before but also behind the generator impedance or, in case of unit-connection, from the high-voltage bus-bar.

Abe Tilles (Pacific Gas and Electric Company, San Francisco, Calif.): The authors obviously have carried their original development work a long way and have produced a very neat and interesting instrument.

Errors caused by stray capacitance from leads and relays are one of the limiting factors of the lower-frequency conventional network analyzers. Because of the higher frequency used here, together with fairly low impedance and power levels, it seems certain that capacitance errors will be definitely a limiting factor in the use of this analyzer. The use of concentric cables further increases the lead capacitance.

It is therefore of interest to inquire for additional detail on what steps were taken to reduce stray capacitance; what amounts were tolerated; and how they affected operation of the equipment.

The matter of stating a fair test, usable in a commercial specification, to measure simply and definitely the degree of troublesomeness of stray impedance and admittance and of induction between circuits is one which is quite unsettled and difficult even for the 400-to-500-cycle range of present commercial equipment. Therefore, it is of interest to know with what tests or requirements the authors approached this question in regard to their analyzer. What do they consider a fair measure of these items?

C. Concordia (General Electric Company, Schenectady, N. Y.): In regard to the generator units, I should like to ask the authors whether they have data similar to that of Figure 6 of the paper for the phase angle regulation.

Lester LeVesconte (Illinois Institute of Technology, Chicago, Ill.): The authors should be congratulated on the courage to pioneer any development such as they have undertaken and on the success they have achieved. They should be commended on their general design, such as the choice of the frequency, base currents and voltages, circuit selector system, and metering equipment. While suggestions could be made or words of caution could be offered on many details, these remarks will be limited to a few of the most important items, based on operating experience at the Armour Research Foundation of the Illinois Institute of Technology in Chicago.

The paper mentions that the power dissipated in the network is so low that small resistors may be used safely without fear of burn-out on accidental overloads. The actual limit or current rating is not given but would be of interest. Of the two designs in most general use, one has a limit of about three times the base current, and the other has a limit of about ten times the base current. The lower limit has been found to be a handicap in some cases, and, therefore, a higher current rating is desirable if it can be obtained at a reasonable cost.

It seems that the length of the connecting leads could be a limiting factor, especially since the longest lead on the present pilot model seems to approach the permissible limits of capacitance. It must be recognized that these leads will become necessarily much longer as the equipment is expanded to the size required for most present day power system problems. However, this difficulty would disappear in an assembly made to represent only a specific power system, using fixed values instead of adjustable units and eliminating the plug and jack panel. It would seem that the design developed by the authors, using standard parts, would be adapted particularly well to this field, and this might make individual analyzers practical for many more operating companies.

On the meter desk, all of the controls are located on the left to be operated by the left hand, for the purpose of leaving the right hand free to record data. Actually, the location of the selector push buttons on the right does not interfere with the recording, but aside from this there are good economic reasons for designing the equipment for at least two-man operation, having one person to read the instruments and another record the data. The operation of the modern analyzer represents a cost of from $5.00 to

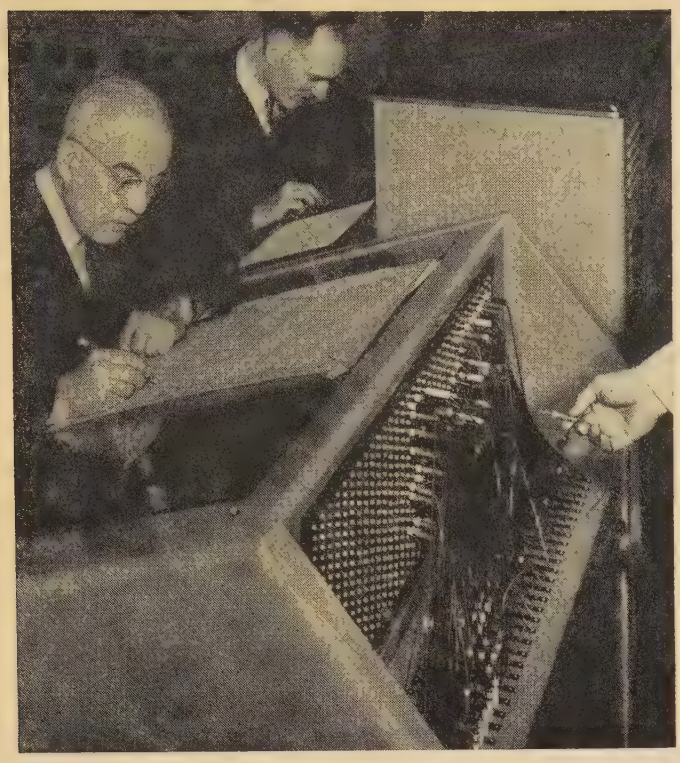

Figure 1

$20.00 per hour, depending on the number of people involved, thus making any time-saving equipment or methods very valuable. Using the same general type of circuit selector described by the authors, a new recording table designed and built at the Armour Research Foundation has been found to be particularly useful. (See Figures 1 and 2 of this discussion.) It is located adjacent to the meter desk and connected to it by a multiple cable. The sloping top has a glass panel on which the system diagram is placed and beneath which are small lamps which indicate the circuit being metered and thus show the location on the diagram where the readings should be recorded. The lamps are spaced one inch apart in each direction, so that a light position can be associated with each circuit element on the diagram. Each lamp is connected to a small jack on a panel on the back of the table. Below the jacks is a set of plugs on retractable cords, each numbered to correspond with a circuit on the analyzer. Since any plug, representing a circuit element on the analyzer, can be inserted into any jack, it is possible to assign whatever circuit number is desired to each lamp position beneath the diagram.

The plugs are energized by metering relays which are operated by a circuit selector controlled by a set of push buttons on the meter desk. These relays are located back of each circuit element on the analyzer, and only one such relay can be energized at a time. Besides connecting that circuit to the meter bus, one contact of the relay energizes a light on the circuit drawer, indicating which circuit is being metered. The plugs are connected so that the lights on the table operate in parallel with the lights on the circuit drawers. Thus, as each circuit in turn is set up on the push buttons at the meter desk, the circuit selector energizes the proper relay to connect that circuit to the meter bus, and the same relay energizes the light on the circuit drawer and through the plug and jack assembly energizes the light beneath the proper circuit on the diagram.

On the meter desk is a switch which is marked + and − and which reverses the direction of the watt-varmeter. The position of this switch when the meter reads upscale is an indication of the direction of power in the circuit being metered. An extra contact on this switch controls the direction-indicating lights on the recording table. The + light is located in the upper, left-hand corner of the table, and the − light in the upper, right-hand corner, so that the person recording data can see easily which is lighted. The recorder has time to observe and mark the direction while the reading is being made.

Experience has indicated that a few people who have not seen or used the table have questioned its value, but everyone who has seen it has been convinced that it is a great timesaver and definite contribution to the speed and accuracy of operation. It results in all the data being recorded directly and quickly on the system diagram. It eliminates the possibility of recording readings on the wrong circuit. It provides a safeguard against reading the wrong scale on the meter or using the wrong multiplier, because the values around each junction point can be checked easily. It makes practical the recording of only those values that are significant in cases where a minor change affects only a limited area of the system, thus eliminating a volume of unnecessary readings.

From Figure 7 of the authors' paper it appears that the instruments on the meter panel for each generator do not have normal indexes or fixed pointers. These pointers should be added. They have been found to be very helpful in adjusting the generators in the original setup and also on any subsequent system changes. This same idea has been extended to the adjustment of the load circuits at Armour Research Foundation in the manner shown in Figures 3 and 4 of this discussion.

It will be noticed that the connections shown are fundamentally the same as the load circuits described by the authors in their Figure 10, with the addition of a small voltmeter that indicates the voltage across the load impedances beyond the load adjuster. Each voltmeter is mounted directly beneath its associated load adjuster and has a scale reading from 80 to 120 volts. It is provided with a normal index that is set to indicate the voltage after the load has been adjusted by test to give the correct value in watts and vars. For any subsequent system changes that might affect the voltage at that point on the system, the load can be corrected by means of the load adjuster simply by bringing the voltage back to the original value, as indicated by this small voltmeter. For most system changes dur-

Figure 3 (right)

Figure 2 (below)

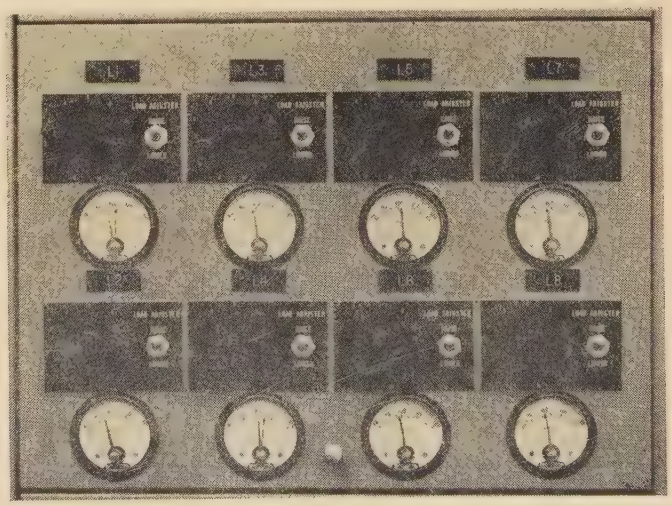

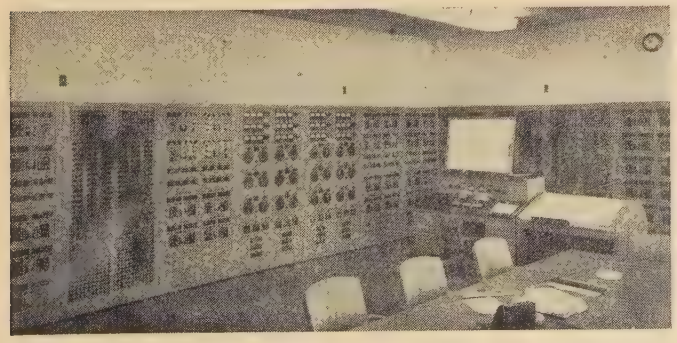

ing the study, most of the readjustments can be made by means of the generator and load circuit instruments, thus saving considerable time.

H. L. Clark (nonmember; General Electric Company, Schenectady, N. Y.): This paper illustrates the present trend toward use of electronic circuits to extend the range of usefulness of a-c network analyzers.

It would seem that emphasis in this paper should be placed upon the convenience and speed with which the correct answers to problems can be obtained with this network analyzer as well as reduction of first cost, because if the analyzer has a reasonable degree of utilization, it is the operating cost per problem which is of importance rather than the initial cost of the analyzer.

Additional information on the master instrument system would have been of interest since many of the problems are concerned with the instrumentation, especially when operating at a frequency of ten kilocycles. For example, the burden of the instrumentation and the accuracy achieved in phase angle measurements should have been given.

A considerable point was made concerning the accuracy and stability of the frequency source. It is implied that the temperature-controlled quartz-crystal oscillator held to 0.001 per cent by comparison with the WWV transmissions is an essential part of the equipment. Since the reactances vary only as the first power of the frequency, and since these units are adjusted to 0.2 per cent accuracy, it is hardly necessary that the accuracy of the frequency be 200 times better.

The paper states that the capacitance introduced to the metering bus by the contacts of the switching relays has been compensated effectively and the resultant error made negligible. Since compensation for capacitance is accomplished by the use of shunt reactors, it would be necessary to have as many reactors as there are contacts in the switching relays, which is, of course, out of the question for a network analyzer having a large number of units. Perhaps the author intended to state that this effect is reduced by sectionalizing the metering bus so that only a small number of switching relays are connected to the master instruments at any one time.

The presence of harmonics in the generator output can cause considerable error, especially in cases where due to a special circuit arrangement the fundamental frequency current is cancelled out leaving only the harmonic currents. The master instruments should, in this case, indicate essentially zero current but will not do so unless the harmonic currents are absent or the instruments do not respond to these harmonic currents.

Because the type of generators used develop even harmonics as well as odd, it becomes especially important that attention be paid this detail. It would be expected that the presence of harmonics would also affect the phase angle measurements, since the type of circuit used measures with respect to the point the wave goes through zero. Harmonics of certain phase relationships will shift the point at which the wave goes through zero and hence cause errors in the phase angle measurements.

R. B. Squires (Westinghouse Electric Corporation, East Pittsburgh, Pa.): The authors are to be congratulated for a good paper on an interesting development. They have solved most of the many problems inherent in designing a network analyzer or calculator to operate at relatively high frequencies.

The equipment contains several features which will increase the speed and ease of operation. The use of a few push buttons to control the metering relays of all the circuits permits a reduction in the time to meter the network. The use of load-adjusting autotransformers, three meters for each generator, and a separate instrument desk increases the flexibility of the equipment. The advantages of all these features have been proved time and again during the last ten years in the operation of many network calculators.

The use of π-sections for the line units is interesting in that it shows a preference for the type of circuit already furnished in four network calculators now being built. In these calculators the pi-line units are furnished in addition to standard line-units which omit the shunt branch and are used to represent transformers or lines having little charging current.

The equipment described in this paper departs from the present accepted practice by reducing the number of adjustment taps on the line and generator reactance units from three decades to two decades. The steps are therefore coarser and the adjustment error is increased. For instance, with the line units the minimum per cent adjustment error occurs at the maximum value of reactance and is $(0.5/99)\times 100 = 0.505$ per cent, which is an acceptable value. However, many of the lines in a problem may be set at ten per cent or less, and at this point the per cent adjustment error is $(0.5/10)\times 100 = 5$ per cent. If lower values must be set up, the error is correspondingly greater. There is little value in having circuits values held

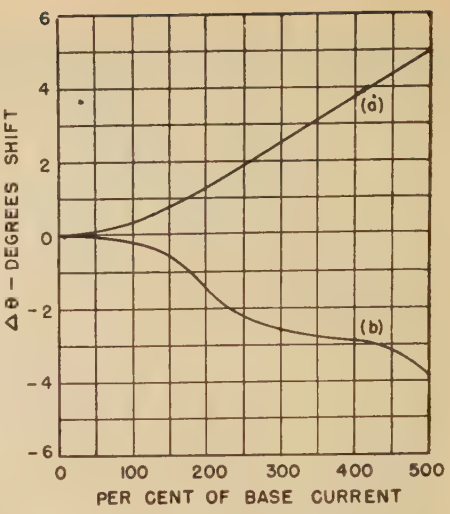

Figure 5. Phase angle regulation of the generator voltage for varying output

(*a*)—Current leading voltage by 90 degrees
(*b*)—Current lagging voltage by 90 degrees

to an accuracy of 0.5 per cent or better if the actual error is five per cent in representing an impedance of 10.5 per cent. This limitation has been overcome in network calculators with which I am familiar by using three decades of adjustment or by using a calibrated, continuously variable reactor for the small values.

Another way of stating the problem is that using only two decades of adjustment limits the range of settings to the higher values if good accuracy is to be maintained. Because there is wide variation in a given system in the values of impedances that must be represented, it is important to give each circuit a range as wide as possible over which accurate settings can be made. The use of three decades or a continuously variable unit increases the range in which accurate settings can be made.

It should be realized that the curve of Figure 1 of the paper applies only to capacitive reactance, which accounts for only a small part of the total cost. The cost of cabinets, instruments, plugging panels and the labor of assembly and wiring make up a large part of the total cost. The cost of these items stays constant or even increases with frequency because of the necessity for shielding and for more complicated wiring at the higher frequencies.

In connection with the instruments in the control desk, it would be interesting to know the current and voltage ranges used and the phase angle accuracy of the wattmeter and phase meters, since phase angle accuracy is as important to the over-all accuracy as the accuracy of calibration of the instruments.

Is it possible to measure directly the voltage drop across a circuit and the power loss in it? Such information is very desirable in transient stability studies in obtaining equivalents of networks and in other problems where the voltage between two points in the network is needed, rather than the voltage to neutral.

One of the problems in the design of a mutual transformer is to keep the capacitance between windings low, because in circuits where these transformers are used the voltage between windings is several times

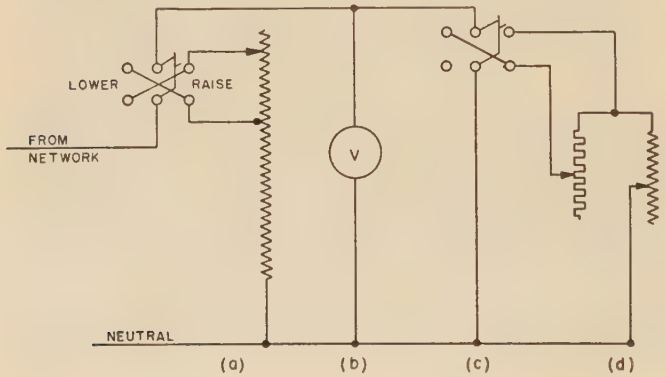

Figure 4

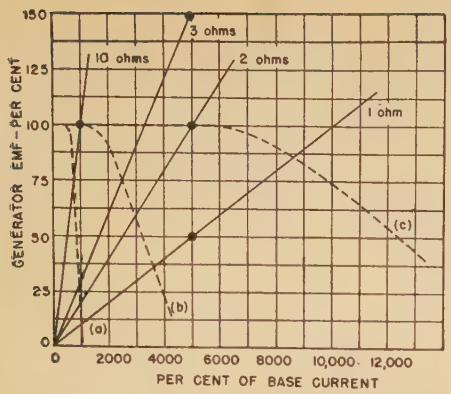

Figure 6. Design co-ordination of resistor ratings with generator volt-ampere characteristics under extreme overloads

the voltage across each winding. In most studies involving mutual transformers several transformers must be used, and the effect of the capacitance leakage currents is additive for each transformer. This problem must be particularly difficult at 10,000 cycles, and, therefore, it would be interesting to hear to what value the capacitance current was limited.

The discussion of these problems is not intended to minimize the good work the authors have done in producing a workable design at frequencies far above those normally used for measurement work. No doubt operating experience of the next year or so will show whether circuits of wider range are needed and whether any difficulties develop from the use of a large number of electron tubes.

J. D. Ryder and **W. B. Boast:** We wish to thank those contributing to the discussion. The answers to their questions are given in an itemized manner.

Phase Angle Regulation of Generators

Figure 5 of this discussion gives the phase-angle regulation curve of a generator for the extreme conditions of capacitive (curve *a*) and inductive (curve *b*) loading. Other loading conditions lie between these curves. The shift in phase of the voltage is caused principally by the plate resistance of the output stage of the amplifier. This resistance is reduced effectively by the use of triode output tubes and by the high degree of degenerative feedback employed. At 200 per cent current (the limit of the metering system) the shift in generator voltage phase is less than 1.5 degrees.

Voltage Regulator Control

The addition of a switch on the panel of the generator unit for providing voltage control on either the internal or external voltage of the generator is being made as a desirable improvement.

Capacitance Errors

A. *Relay Contacts Between Units and Meter Bus.* The metering bus was sectionalized into five regions (one for each of the major racks of the analyzer), and the capacitance to ground for each of these sections was measured. Inductive compensation then was established at the capacitive load center of each section. The metering bus then was connected electrically together again as a unit and operates this way in the analyzer. The compensation at relatively few points for the highly distributed nature of the relay positions has reduced effectively the relay capacitance current errors to approximately one-half per cent of base current when all elements on the network operate at the general level of base voltage. In all arrangements of relay contacts, those permanently connected to points in the high side of the network units proper have been placed with as much clearance as possible to ground and to other relay contacts.

B. *Connecting Leads.* The maximum length of leads between units and terminal board produces capacitive current errors within the allowable tolerance. These errors are stated in the original paper. A network analyzer with four to six times as many units as this pilot model could be built in sections, each essentially as the present analyzer. In setting up problems on this larger analyzer, relatively few long trunk leads between these sections would be sufficient. These trunk leads can be designed within the maximum tolerance on series resistance and reactance. If the shunt susceptance is too great, the same plan of compensation as is discussed previously in *A* could be applied to each lead. Therefore a larger network analyzer is not impossible at this frequency.

Burden of Instrumentation

The burden of instrumentation is stated in the original paper in the section entitled "Control Desk."

Frequency Accuracy

An accuracy of 0.001 per cent in frequency was not intended to be understood as an essential condition of accuracy. This frequency source was used because it was commercially available at a low cost.

Power Limit of Resistors

Figure 6 of this discussion shows graphically the conditions which can be encountered on accidental overloads through line units. The dashed curve (*a*) shows the extension of Figure 6 of the original paper to a much different scale. All of the information of the original Figure 6 is contained in the first one-half division on the "per cent of base current" scale. Beyond this point the voltage regulator loses control and the voltage drops to essentially zero at about 1,200 per cent of base current. Curve *b* shows the volt–ampere characteristic of four generators (as in the present pilot model) all operating in parallel on the same bus with their voltages all in phase. Curve *c* shows the same for sixteen generators under the identical condition of in-phase operation, a highly improbable condition but, nevertheless, the worst one in event that an accidental overload occurs on a line unit just past that bus. The line unit resistors in the lowest decade (1-ohm steps) are 25-watt units. The circle on the 1-ohm resistance line represents this power rating. If more than six or seven generators should be paralleled and act on this single 1-ohm resistor as a load, it would be in danger of excessive heating. If, however, two of these resistors were in the circuit (the 2-per cent step) the power rating of the two becomes 50 watts and the circle on the 2-ohm line shows that ten volts could be maintained by 16 generators all acting in parallel and in phase, giving exactly 50 watts dissipated with no danger of overheating. The 3-ohm point lies above the generator characteristics, and, hence, neither it nor any of the other settings to nine ohms could cause overheating. The next decade begins at ten ohms, and each of its resistors is rated at ten watts. The circle shows that no overheating would occur on it as base voltage.

The instrument amplifiers likewise possess a self-protective feature in their design, and, even though many times their normal full scale value is applied to the amplifier inputs, the actual instrument currents do not exceed 150 to 200 per cent of full scale current. Also, no damage occurs to the generators under these accidental overloads because the average plate power dissipated in the output stage is essentially independent of 10,000-cycle loading. The generators are fused however at 1,000 per cent of base current.

Phase Meter Accuracy

The accuracy of the phase meter is dependent upon the range of amplitudes for which the phase is to be measured. For currents from 200 per cent down to 15 per cent or for voltages from 150 per cent down to 10 per cent the accuracy is plus or minus two degrees. For smaller currents or voltages the accuracy becomes progressively poorer. However, high accuracy of angle determination of a small vector among large vectors is usually not possible by analytic methods.

Wave-Form Distortion

Measurable wave-form distortion occurs only as the voltage of the generators is driven above 125 per cent base value or as the current reaches 300 to 500 per cent of base value. The first of these conditions usually can be avoided and the second is impossible to meter.

Design of Induction Heating Coils for Cylindrical Magnetic Loads

Discussion and authors' closure of paper 46-124 by J. T. Vaughan and J. W. Williamson, presented at the AIEE summer convention, Detroit, Mich., June 24–28, 1946, and published in AIEE TRANSACTIONS, 1946, pages 887–92.

N. R. Stansel (General Electric Company, Schenectady, N. Y.): This paper including the companion paper[1] mentioned in the synopsis has two values. The first is its significance to those concerned with the art of induction heating. The second, of more general interest, is its worth as a study of the principle of electromagnetic induction.

It is well worth while to re-examine periodically the principle of the eddy current phenomenon. New conditions arise from time to time. The example here is the use of eddy currents for heating service. This viewpoint emphasizes the importance of considering the relations of the thermal properties of a material to its electrical and magnetic properties.

The initial procedure in such an examination is not concerned with whether the object is the minimizing of the eddy-current

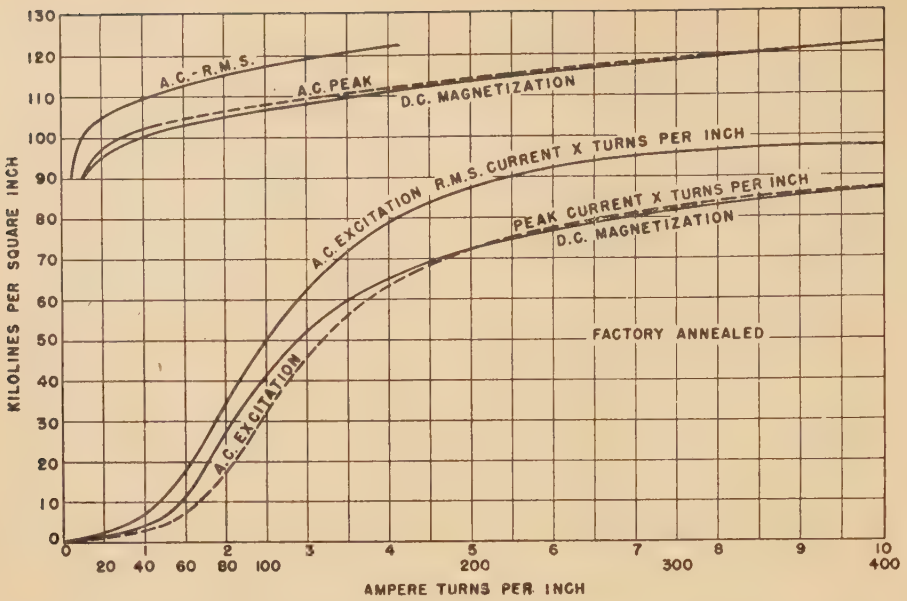

Figure 1. A-c excitation curve (60 cycles) and d-c magnetization curve of SAE1015 steel

Lines per square inch ÷ 6.5416 = lines per square centimeter

Ampere turns per inch × 0.4947 = oersteds

watts or the use of eddy currents for heating service. The basic relation is

$$P = (H^2\sqrt{\mu f}\sqrt{\rho 10^9})lS \times 10^{-7} \text{ watts} \qquad (1)$$

This equation expresses the rate of heat development by eddy currents in a conducting mass which is exposed to a uniform and sinusoidal alternating magnetic flux, the directions of which are parallel to the lateral surface of the mass.

The symbols are

H = the magnetizing force (crest value), oersteds

μ = the a-c permeability of the material*

f = the frequency, cycles per second

ρ = the resistivity of the material, ohm-centimeter cube*

l = the length of the mass, centimeters

S = the shape factor of the mass—a matter of geometry only

For the solid cylindrical mass, or load, of the paper

$$S = \frac{aF_r}{4\sqrt{2}} \qquad (2)$$

where

a = radius, centimeters

F_r = the function

$$\left[\frac{ber\ \Delta\ ber'\ \Delta + bei\ \Delta\ bei'\ \Delta}{(ber\ \Delta)^2 + (bei\ \Delta)^2}\right] \qquad (3)$$

Δ = the parameter (index ratio)

$$= \left(\frac{2\pi\sqrt{2}\sqrt{\mu f}a}{\sqrt{\rho 10^9}}\right) \qquad (4)$$

Permeability. The a-c excitation curve (crest values) of a magnetic material more or less coincides with the d-c magnetization curve as the saturation point is approached. An example is given in Figure 1 of this discussion. Hence, in induction heating practice, the d-c magnetization curve—usually more readily available—is generally of sufficient accuracy. The a-c excitation curve should be used for lower flux densities.

* The values μ and ρ correspond to the mean temperature of the path of the current in the mass.

REFERENCE

1. DESIGN OF INDUCTION-HEATING COILS FOR CYLINDRICAL NONMAGNETIC LOADS, J. T. Vaughan, J. W. Williamson. AIEE TRANSACTIONS, volume 64, 1945, August section, pages 587–92.

J. T. Vaughan and **J. W. Williamson:** Textbooks frequently develop the theory of the polyphase induction motor in terms of an equivalent circuit derived from the transformer. The analogies existing between these two pieces of equipment enable the student to gain a better understanding of both. If these analogies were pushed too far however, for example, if an attempt was made to adapt the equivalent circuit theory to the effect of skewing of the rotor conductors on starting characteristics, the resulting comparisons might become more of a hindrance than a help.

In a similar way, the concept of a constant permeability may be useful educationally in bridging the gap between the induction heating of nonmagnetic materials and that of magnetic materials. To avoid reaching incorrect conclusions, the following consequences of the fact that the B-H curve is not a straight line should be noted:

1. Theoretical formulas involving permeability require laboratory experimental evidence to establish the value of permeability which should be used, even if the B-H curve is known.

2. As noted in our paper and pointed out by N. R. Stansel, the conclusion reached by assuming any constant value of permeability that for moderately large diameter loads the load power factor is 0.707 is false. Actually the ratio of watts to volt-amperes of a carbon steel load is about 0.84, and the ratio of reactive volt-amperes to watts is not 1.000 but about 0.65.

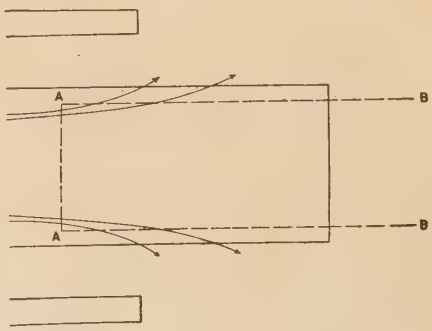

Figure 2. Transverse and axial flux

The discussion of transverse flux will perhaps be clarified by Figure 2 of this discussion. The number of lines of transverse flux at A or A' may be defined as the number of lines of flux which flow radially outward through the infinitely long cylindrical surface $AA'B'B$. Because lines of flux are continuous, the same number cut axially through the circular surface AA'. Therefore, it is immaterial whether one considers transverse flux or axial flux. The same current density i would be determined from equation 11 of our paper in either case.

Protection of Industrial Plants Against Insulation Breakdown and Consequential Damages

Discussion of paper 46-122 by H. R. Vaughan, presented at the AIEE summer convention, Detroit, Mich., June 24–28, 1946, and published in AIEE TRANSACTIONS, 1946, August–September section, pages 592–6.

A. A. Johnson (Westinghouse Electric Corporation, East Pittsburgh, Pa.): Particular attention is called to Figure 8C of the paper. This scheme of high resistance grounding can be used readily on industrial distribution systems of 2,400 volts and above where no neutral is available for a grounding device. This relatively high resistance grounding device allows sufficient in-phase current to flow during the time of a line-to-ground fault to dampen possible high frequency voltage oscillations and thus to prevent excessive transient overvoltages. The reason for this may be explained briefly. For an ungrounded system if a line-to-ground fault appears the current which flows is caused by the inherent distributed capacitance of the system. This current leads the voltage by 90 degrees. Because of the fact that on most industrial systems this capacitive current is only a few amperes (three to ten amperes are common values), it probably will cease to flow at current zero. The current zero, however, occurs at a time corresponding to the peak of the voltage wave and when this current ceases to flow there is a tendency for the instantaneous voltage to be double normal peak line-to-ground voltage. Restriking of the fault arc at the optimum time relationship may produce higher peak voltages by a buildup process which may be several times the normal peak voltage to ground. This high peak transient voltage may cause failure of connected rotating machines, cables, and lightning arresters. By using the high resistance grounding device two main effects reduce transient overvoltages.

1. The fault current zero does not occur at 90 degrees with respect to the voltage but occurs at a

point probably less than 45 degrees with respect to the voltage where the instantaneous voltage is considerably less than the peak value. Since the high frequency oscillation takes place about the point on the voltage wave where the current goes through zero, voltages which do occur because of restriking therefore are reduced very greatly. When the loss in kilowatts in the resistor is made equal to the distributed capacitive kilovolt-amperes to ground of the system, the resistor will limit the maximum peak line-to-ground voltage to about 2.5 times the normal peak line-to-ground voltage.

2. Reducing the time constant of the fault circuit damps the high frequency oscillation.

There are a number of systems, both industrial distribution and utility distribution, where failures of electrical equipment caused by transient overvoltages can be reduced materially, if not eliminated, by the proper application of high resistance grounding. Simultaneous ground faults on an ungrounded system are strong evidence that transient overvoltages are causing failures. By the use of a resistance grounding device the line-to-ground fault current is increased approximately 50 per cent above what it would be for ungrounded operation. Thus the system still can be operated as an ungrounded system but with the one serious disadvantage of ungrounded operation minimized to a point where little or no trouble should be expected from excessive transient overvoltages. This scheme of high resistance grounding is now in service on several distribution systems.

Electromechanical Transient Performance of Induction Motors

Discussion and authors' closure of paper 46-116 by C. N. Weygandt and S. Charp, presented at the AIEE summer convention, Detroit, Mich., June 24–28, 1946, and published in AIEE TRANSACTIONS, 1946, pages 1000–09.

F. J. Maginniss, N. R. Schultz, and C. Concordia (General Electric Company, Schenectady, N. Y.): This paper is a valuable contribution to our knowledge of the transient performance of induction motors, particularly in the smaller sizes having relatively high resistances as contrasted to the large low-resistance motors treated in reference 4 of the paper.

Expression of the performance equations in terms of the five basic parameters provides for the widest application of the results. The information presented, particularly the speed–response curves, should be very useful to the designer of control and follow-up systems.

The results obtained bring out the importance of low rotor inertia. This is emphasized by the fact that in many cases the load inertia is relatively small so that the motor inertia forms most of the total. Therefore, from the standpoint of machine design we realize that it may be more important to reduce the rotor inertia, even at the expense of a considerable increase in the stator size and in the total machine weight, than to arrive at a minimum over-all motor size.

The authors mention fundamental-frequency speed oscillation in Figure 8a. Actually, these oscillations appear to be about two-thirds fundamental frequency, and as far as we can see there is no reason to expect their frequency to have any simple relation to the fundamental frequency.

J. W. Momberg (Diehl Manufacturing Company, Finderne, N. J.): In connection with the sixth assumption that the motor is connected to an infinite bus through a zero impedance, it should be noted that this is a very idealized condition. In most servomechanisms one phase of the motor is supplied by an amplifier with rather poor regulation, and the other phase is supplied by the line in series with a capacitor. Only in a contact-making servomechanism supplied from a polyphase source would this assumption be approximately true.

The effects of the rotor time constants plotted in Figure 3 would indicate that rotor inductance should be kept as low as possible. It is for this reason that closed rotor slots seldom are used in squirrel-cage servo motors.

In connection with the conclusion that it would seem desirable not to operate a motor with one phase always energized, it is to be recommended highly that, where it can be arranged, the reference phase not be excited when the motor is not in useful operation. This should be extended to point out that where the reference phase is not energized continuously, the motor can be designed for an even higher ratio of torque to inertia, limited only by saturation and heating effects at the running condition, which is usually much less severe than the stand-by condition with one phase excited. Saturation is rarely the limiting factor in small servo motors, only coming into effect when blast cooling is used. When using the larger servo motors having a maximum output of 200 watts or more, it is almost necessary that both phases be controlled.

It should be pointed out also that the torque of a servo motor rarely increases in direct proportion to the number of poles, because of increased leakage with more poles. In fact, it is not uncommon to obtain the same locked torque for a 4 pole motor as that for a 2 pole motor in the same frame, especially in the small sizes investigated in

Figure 1. Steady-state and transient torque–slip curves computed from the curves shown in Figure 5 of the paper

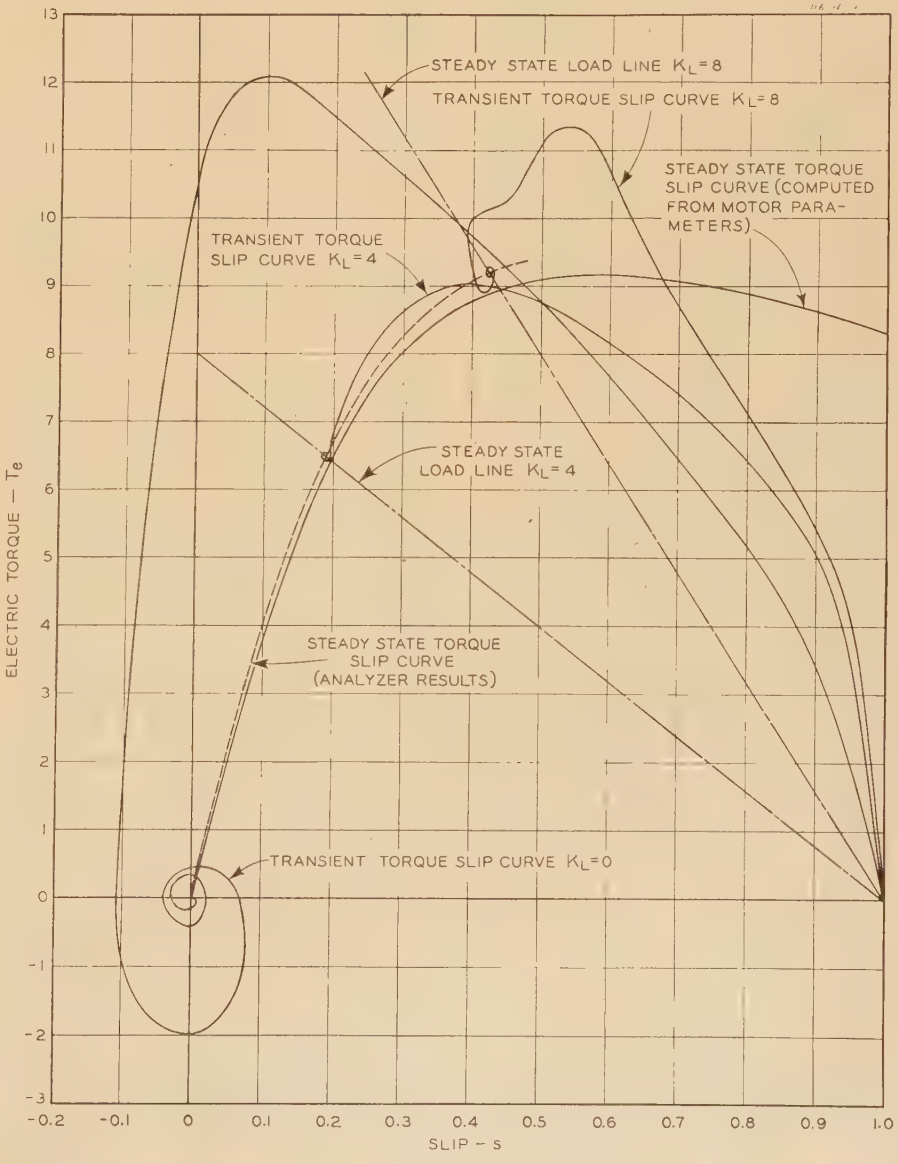

this paper. Only in large servo motors is it possible even to approach a proportional torque. However, depending upon the application, there may be considerable advantage in increasing the number of poles at the expense of motor performance.

It is hoped that more investigations in the nature of this paper will be forthcoming, since the application of squirrel-cage motors to servomechanisms is relatively new, and there is unquestionably room for improvement.

C. N. Weygandt and **S. Charp:** The authors wish to thank F. J. Maginniss, N. R. Schultz, C. Concordia, and J. W. Momberg for their discussions on our paper. We would like to reply to the several points brought out individually in these discussions.

Two points in the discussion by F. J. Maginniss, N. R. Schultz, and C. Concordia require clarification. These discussers are quite correct in their statement that the oscillations in speed shown in Figure 8a of the paper are of about two-thirds fundamental frequency. When we first studied this set of curves we had no intention of making the rigid statement that the oscillations are at fundamental frequency. We are in agreement that the oscillations in speed have no direct relationship to the fundamental frequency. The basic reason for this oscillation is unknown to us at the present time.

J. W. Momberg points out that one of the assumptions, namely, that the motor is connected to an infinite bus, is open to some question of validity. While it is true that most servomechanisms are supplied from an amplifier having poor regulation, it was desirable to make this assumption because of the simplification which resulted in our solutions. The study was primarily one of motor characteristics, and because the regulation of the source is entirely dependent upon the type of amplifier and is thus of a special rather than a general nature, this effect was neglected.

In the investigation of the starting characteristics of servo motors, attention naturally is focussed upon the transient torque–speed or torque–slip curve. This curve, showing what happens during the starting period, should be the curve used during the starting period, and for a continuously operating servo motor it should be the only curve used. At the end of the starting period, the transient torque–slip curve should coalesce into the steady state torque–slip curve. Such transient torque–slip curves are shown in Figure 1 of this discussion. From the data of Figure 5 of the paper, there was computed the acceleration of the motor at each instant of the starting period. Then, from equation 36 of the paper we have that the electric torque for this case is given by

$$T_e = 2\tau_m^2 \frac{d^2\theta}{dt^2} + 2T_L \qquad (1)$$

$$= 2\left[\tau_m^2 \frac{d^2\theta}{dt^2} + K_L \frac{d\theta}{dt}\right] \qquad (2)$$

Since the speed and acceleration are known at each point, the electric torque can be plotted as a function of time, of speed, or of slip. In Figure 1 of this discussion this torque is plotted as a function of slip. In fact, the torque plotted is the torque actually developed by the motor operating at four times normal voltage. It is seen that when steady state conditions are reached the points representing the electric torques cluster about a region which should be the steady state operating point. The end point of the transient curve should coincide with the intersection of the steady state load line $\left(T_e = K_L \frac{d\theta}{dt}\right)$ and the steady state torque–slip curve. The rather rough nature of the transient curves shown is because of the approximate methods used in the determination of the motor acceleration from the curves of Figure 5. A more precise calculation could be done on the differential analyzer.*

The authors realize that this paper only breaks the surface of the entire servomechanism problem. The next step planned by us is the solution of a simple servo loop, using the induction motor equations where the input voltage to one phase of the induction motor is proportional to an error signal. It is hoped that this second problem will result in a method for representing the induction motor by some source and by an equivalent circuit.

Application Ratings of Indoor Power Circuit Breakers

Discussion and author's closure of paper 46-134 by O. B. Vikoren, presented at the AIEE summer convention, Detroit, Mich., June 24–28, 1946, and published in AIEE TRANSACTIONS, 1946, November section, pages 768–73.

R. C. Van Sickle (Westinghouse Electric Corporation, East Pittsburgh, Pa.): This paper is of considerable general interest to designers of circuit breakers as it gives them information on the conditions under which their circuit breakers may be used in service. It is an explanation of how a rated continuous current can be interpreted in terms of expected maintenance, ambient temperatures, normal load conditions, and emergency overloads. The designer knowing that these conditions vary from application to application has to consider them in a general way but must design for one standard condition.

A circuit breaker is a maximum rated device. All items of rating refer to the maximum performance which can be expected of the circuit breaker. Demonstrations of these characteristics are made on new circuit breakers with all parts in first class condition. This of course includes the demonstration of the rated continuous current.

Circuit breakers cannot remain indefinitely in this condition and consequently allowance has to be made for a reduction in the circuit-breakers ability between maintenance periods and with service. Interrupting ratings are a maximum for the standard duty cycle but occasionally circuit breakers are applied for other duty cycles, shorter intervals between operations, or more operations between maintenance. Tables of per centages for determining the interrupting ratings of oil circuit breakers at various operating duties form American Standard C37.7. O. B. Vikoren applies similar reasoning to the normal current rating and takes advantage of load cycles, low ambient temperatures, and short time overheating of insulation as referred to in the preface to AIEE Standard 1B to get maximum current values at which the circuit breakers can be applied.

In testing circuit breakers for such applications, temperatures of more parts than just the contacts and leads should be taken to be sure that permissible temperatures will not be exceeded. The conductors through insulating bushings are not cooled well and parts heated by hysteresis or eddy current losses may be in contact with oil or other insulating materials.

The conclusion that new apparatus has a better allowance for application beyond its rating than is the case with older circuit breakers, should not be construed as a different basis of design in modern circuit breakers. It is believed that O. B. Vikoren refers to age of the circuit breaker rather than period of design, because the current-carrying ability is influenced less by period of design than by demands of interrupting capacity and speed.

Herman Halperin (Commonwealth Edison Company, Chicago, Ill.): This paper is timely and helpful on the important problem of obtaining the maximum feasible load ratings of equipment.

In Table I of the paper the author indicates a reduction in carrying capacity of 20 to 35 per cent below name plate rating of circuit breakers for a 30 degree centigrade rise of copper-to-copper contacts. This service factor reduction, if any, is obviously a function of the frequency of operation of the circuit breakers. In Chicago the 12- and 4-kv circuit breakers on transformers in attended substations supplying our distribution system are operated practically every other night in connection with shutting down some transformers during the night to reduce core iron losses during light load periods. Such frequent circuit breaker operation means that the contacts are wiped frequently and suffer relatively little oxidation. In some other types of locations the circuit breaker operations are relatively rare and for such cases oxidation will reduce the allowable loading, especially for copper-to-copper contacts.

The author indicates that the total temperature for normal operation should be reduced, for example, from 70 to 60 degrees centigrade when the ambient temperature is 20 degrees centigrade. Although an explanation is given for so reducing temperatures, it is not clear to me. Oxidation is a function of total temperature, and so I think we should learn or estimate what the conditions are for the given circuit breaker involved in each case and then use the same total temperature as the limit for all cases having copper-to-copper contacts.

After equation 3 of the paper the author

* It is to be noted that the higher the value of load torque coefficient K_L, the more rapid the approach of the transient torque–slip curve to steady state value This is in agreement with the curves of Figure 5, which show little or no speed oscillations for high values of K_L.

states that the temperatures rise varies practically as a square of the current. This seems reasonably conservative. We found in testing a few 300-ampere circuit breakers at 300 amperes and at 450 amperes that the final rise with the 450 amperes was close to 2.0 times the rise for 300 amperes, instead of being 2.25 times.

Under the heading on short-time emergency conditions, the author sets up a total temperature of 90 degrees centigrade as the limit for emergency operation for copper-to-copper contacts. He seems to be concerned about the effect of higher temperatures on the oil and on the annealing of the contact parts. In connection with emergency ratings of transformers, temperatures up to 100 degrees centigrade have been set as a limit for the oil for emergencies. The effect of emergency operation at high temperatures is obviously a function of time. If this operation is to be only for a few hours for each of two days once in several years, then I see no reason from available test data why 100 degrees centigrade should not be a reasonable limit. This is especially true if the circuit breaker is to be inspected shortly after each emergency operation.

This discussion indicates some differences of opinion, and I believe emphasizes the need for obtaining more test data and operating experience at the higher loadings. In the field of underground cable systems, we have obtained in this country enormous amounts of test data and operating experience in regard to the effects of normal and emergency operation at various temperatures. The result is that we have set up temperature limits that are 5 to 45 degrees centigrade higher than used on the other continents. The expense for all the investigations involved has been a very small fraction of the savings obtained. The recent sharp increases in the total installed cost of equipment make it essential to develop a background of information so that starting now we gradually can increase the actual loading of, for example, indoor power circuit breakers.

Philip Sporn (American Gas and Electric Service Corporation, New York, N. Y.): Although circuit breakers generally may not be called upon to carry more load current than their name plate rating, it is apparent from the material in this paper that some circuit breakers in use may not be capable of actually carrying as much load current as the name plate states. As pointed out in the paper, because most circuit breakers are loaded rather lightly this factor has not been serious, in fact it has been so relatively unimportant that it has not obtruded itself upon the average operating engineer's thinking.

The paper offers an approach to problems which arise from time to time with existing circuit breaker installations when loadings exceed those of which the circuit breaker is actually capable, or when it is apparent from studies that loads are going to exceed name plate ratings. The paper also may have application in cases where circuit breakers of sufficiently large current-carrying capacity are not manufactured to meet a given situation. In such cases, actual tests on circuit breakers available can determine what their limitations are; in many cases it may be found they can be applied to meet requirements if judged solely on actual capabilities without regard to ratings.

This naturally brings up another and somewhat more important characteristic of circuit breakers with regard to actualities and their relation to name plate ratings. I have reference to circuit breaker rupturing capacity.

Many circuit breakers in the past were built without adequate design data and they have been sold and used without having a background of actual test. Circuit breakers which have been in use for many years have no actual rupturing test data to show what they will do. Their application hinges on manufacturer's published rating data and oftentimes circuit breakers are discarded or omitted from consideration in specific applications because these data indicate that they are inadequate. This often may not be the case, and considerable sums of money may be saved by making tests on circuit breakers in question to find out what they actually will do. It will be found oftentimes that circuit breakers with or without modifications, are capable of appreciably more than their name plates or published data indicate. They may be capable of much more than the manufacturer's engineers can or are willing to commit themselves.

As one example I can cite a situation at a major generating station where a number of 66-kv circuit breakers of a type no longer manufactured were definitely on the ragged edge as far as rupturing capacity was concerned. Consultation with the manufacturer's engineers indicated that some not strictly orthodox changes could be made in these circuit breakers which might extend their capabilities, but it was not at all apparent to what degree there would be improvement. One of these circuit breakers was rebuilt to incorporate the suggested changes and then was tested on a 66-kv system to the maximum possible extent of that system. Although the manufacturer's engineers would not commit themselves to a capacity of more than 500,000 kva for these circuit breakers, actual test showed that they could handle the maximum that the system was capable of without any signs of distress. This amount was in excess of 900,000 kva.

It is because of experience of that sort that we reached a conclusion a long time ago, a conclusion reaffirmed many times since, that the only sound basis for determining normal and emergency rating with respect to interrupting capacity is by making actual tests. Further, such tests on one type of circuit breaker will not take care of some other type of circuit breaker of the same voltage and rating capacity.

O. B. Vikoren: The author would like to express his appreciation for the interest the discussers have taken in this paper.

Judging from the last paragraph of his discussion, R. C. Van Sickle apparently has read more into the paper than it was intended to cover. Table I of this closure will clarify the statement made under the heading Conclusions of the paper, that is, circuit breakers with copper to copper contacts (generally used on old circuit breakers) have the same temperature rises for currents lower than name plate rating as circuit breakers with silver to silver contacts (generally used on new circuit breakers) have for currents which, at low ambient temperatures, exceed name plate rating.

It should be noted that the paper specifically emphasizes that its purpose is to show the method for arriving at the solution of an application rating problem and that the details may vary for different systems. It is therefore to be expected that Herman Halperin has found conditions different on the Commonwealth Edison Company system as compared with those on the Philadelphia Electric Company system. Nevertheless the temperature limitations should be common for any system particularly when the question arises of establishing a maximum temperature limit for oil circuit breakers. It is believed that Halperin is approaching the danger point by permitting contact temperatures of oil circuit breakers to reach 100 degrees centigrade particularly since oil will begin to smoke at about that temperature. It is believed also that justifying this high temperature on the basis of what is permissible for transformers is overlooking the difference in basic function of the oil in a circuit breaker as compared to a transformer. The arc quenching function of the oil, inherently required in an oil circuit breaker, is referred to here and it is believed that the interrupting ability of a circuit breaker should not be permitted to be impaired for the purpose of stressing the load current limit a few per cent.

Philip Sporn has devoted a considerable portion of his discussion to the matter of interrupting capacity of circuit breakers, which function is important in connection with applying circuit breakers on a temperature basis only so far as the circuit

Table I. Permissible Continuous Load at Different Ambient Temperatures of Two Circuit Breakers of the Same Type and Rating But With Different Contacts

Breakers Installed in Tight Compartments

Ambient Temp, Deg C	Name Plate Rating, 1,200 Amp; Contacts, Copper to Copper; Nominal Rating, 1,200 × 0.8 × 0.9 = 864 Amp			Name Plate Rating, 1,200 Amp; Contacts, Silver to Silver; Nominal Rating, 1,200 × 0.9 = 1,080 Amp		
	Load, Amp	Temp Rise, Deg C	Total Temp, Deg C	Load, Amp	Temp Rise, Deg C	Total Temp, Deg C
40	864	30	70	1,080	30	70
30	935	35	65	1,175	35	65
20	1,000	40	60	1,250	40	60
10	1,050	45	55	1,325	45	55
	$\frac{1,050}{864}$ = 122 per cent			$\frac{1,325}{1,080}$ = 122 per cent		

breaker interrupting ability may be impaired by excess temperatures. It should be noted that the current does not necessarily have to be of shortcircuit magnitude to cause trouble if the opening of the contacts is associated with arcing and the circuit breaker is in an overheated condition.

High Vacuum Leak Testing With the Mass Spectrometer

Discussion and authors' closure of paper 46-142 by W. G. Worcester and E. G. Doughty, presented at the AIEE summer convention, Detroit, Mich., June 24–28, 1946, and published in AIEE TRANSACTIONS, 1946, pages 946–55.

J. E. Burroughs (General Electric Company, New York, N. Y.): Under the heading of "Fields of Leak Detector Application", the paper lists power rectifiers. An interesting example of such an application was the use of the leak detector during the past year on a 3,000-kw 640-volt single-tank multianode rectifier installed in a railroad substation. The leak detector was used to confirm a suspected leak in this rectifier and to test for vacuum tightness after the leak had been repaired.

The leak detector was connected to the rectifier vacuum system by means of a 1/2-inch copper tubing extending from the leak detector inlet connection to a point on the rectifier vacuum system between the mercury diffusion pump and the main vacuum valve. A flanged joint, provided for the rectifier McLeod gauge, was utilized for the leak detector connection. A throttle valve also was installed in the line and was located near the rectifier flange joint.

The leak detector was operated with the throttle valve wide open, because the pressure in the rectifier was less than one micron. This gave an operating pressure measured on the leak detector ion gauge of 1.5×10^{-5} millimeter of mercury to 1.75×10^{-5} millimeter of mercury. Because the residual pressure of the leak detector was 5×10^{-6} millimeter or less, the pressure increase resulting from sample flow was 1×10^{-5} millimeter of mercury or more. A suspected leak from the rectifier water jacket into the rectifier vacuum tank was confirmed by flooding the water jacket with a large amount of helium. The possibility of other leaks on the rectifier was eliminated by hood testing all vacuum seals and welds.

From previous cold seepage tests on the rectifier, the leak rate had been calculated to be approximately 75 micron cubic feet per hour. From the indication on the leak detector, for this amount of leakage it was estimated that the leak detector very easily would have shown a leak of only 1/100 of this value or 0.75 micron cubic feet per hour. The allowable leakage rate for this rectifier tank was 22 micron cubic feet per hour.

After the leak in the rectifier tank had been repaired and the rectifier vacuum system again operating, the leak detector was connected as before, and the water jacket and all vacuum seals flooded with helium. Because the leak detector showed no leaks in the rectifier, it was not necessary to run standard seepage tests as ordinarily done, and the rectifier was prepared immediately for degassing.

From curves which take into account the leak-detector sensitivity, pumping speed of the auxiliary pumping system, and operating pressure, it was indicated that the leak detector would have shown a leak in the final test of the order of 1/10 of a micron cubic foot per hour. This value would be only one-half of one per cent of the allowable leakage rate for this particular rectifier tank.

To summarize the use of the leak detector for leak testing the vacuum system of mercury-arc rectifiers, some of the advantages are listed:

1. No vacuum manifold or auxiliary pumping system is needed with the rectifier because it has its own vacuum system and vacuum pump.
2. The sensitivity of the leak detector is sufficiently great to find leaks impossible with standard test methods, such as cold seepages, pressure, and soap tests.
3. A small leak can be found much faster and located more accurately with leak detector than with the previous standard test methods.
4. The leak testing can be done after the rectifier has been brought up to operating temperature, to find small leaks which do not show up when the rectifier is cold.
5. The leak testing is done with the rectifier under normal vacuum so that conditions are not changed by reversing the direction of pressure difference across the leak, as is done when the tank is put under internal pressure for soap testing.
6. The leak tracing medium, namely, helium, does not contaminate the rectifier vacuum system.

J. G. Trump (Massachusetts Institute of Technology, Cambridge, Mass.): The authors have made an important contribution to the high vacuum engineering art by bringing to an available form the mass spectrometer method of vacuum leak location largely developed by Professor Nier and his associates. This instrument should be valuable not only for large industrial vacuum systems, but also for co-operative use at universities where vacuum is employed in a wide variety of research programs, such as the acceleration of charged particles, vacuum spectroscopy, and electronics generally. Such an instrument would justify itself quickly, both by the saving in time and the superior results in the maintenance of high vacuum conditions. It is to be hoped that the mass spectrometer for vacuum leak testing will be refined still further and reduced in physical size and cost.

Vacuum engineering may be regarded as still in its infancy. Scarcely a decade ago, it was believed generally that pressures much less then 10^{-4} millimeter of mercury could not be produced in large "unoutgassed" metal tanks. In the intervening period, high vacuum production and measurement methods have reached a well-developed stage. Oil and mercury high-speed diffusion pumps, vacuum-tight valves, quick-opening portals, methods of transmitting mechanical power into and out of evacuated chambers, methods of cleaning, conditioning, and "outgassing" in vacuum have become available. Although techniques not fully discussed by the authors, both for leak hunting and for preventing leaks, also have improved considerably, leaks have remained as a serious time-consuming problem, and this new device fills in an almost ideal way the need for a sensitive, discriminating, reliable, and quick-reading locator.

W. G. Worcester and **E. G. Doughty:** The authors wish to thank J. G. Trump for his interesting comments. Widespread interest in the leak detector and its methods of application already has developed. Continued interest and better understanding of application requirements will result in extended usefulness of the instrument.

We also wish to thank J. E. Burroughs for his excellent description of a specific application problem, which is typical of the many successful applications of the instrument.

The authors recognize that other leak-hunting techniques and methods of preventing leaks have been improved; nevertheless the mass spectrometer remains the most sensitive, reliable, and rapid method of leak detection known to us.

There are two general fields of application of the leak detector:

1. Experimental or developmental use to check materials and methods of construction of vacuum apparatus.
2. Production testing of finished products.

Improved techniques in manufacture always can be expected to follow when the exact location and size of leak can be determined readily. Systematic use of the leak detector on production lines as a quality control instrument often will yield savings in time for testing and repairs and improvements in quality of the product.

Control and Protection of Aircraft D-C Power Systems

Discussion and author's closure of paper 46-180 by B. O. Austin, presented at the AIEE Pacific Coast meeting, Seattle, Wash., August 27–30, 1946, and published in AIEE TRANSACTIONS, 1946, November section, pages 741–5.

H. J. Finison (General Electric Company, Schenectady, N. Y.): I am glad to see the emphasis given in B. O. Austin's paper on the provision of and needs for soundly engineered control and protective function for aircraft d-c generator systems. On the whole, I find the objectives outlined by Austin in good agreement with those which R. H. Kaufmann and I have outlined in a series of articles.[1] As Austin has indicated, improvements in 24-volt d-c generator systems urgently are needed to improve performance, reliability, and safety.

Austin indicates that the protective problems are much more severe for 24-volt than for 12-volt systems. I wonder if it is Austin's intent to advocate omitting protection from a 12-volt system or rather to emphasize the greater difficulties that might be experienced with unprotected systems for 24 than for 12 volts. Would Austin please clarify this point?

As Austin has indicated, overvoltage pro-

tection is a desirable feature. The magnitude of overvoltage that can be obtained when one generator of a group loses its control of voltage is surprisingly high even with a relatively low strength equalizer. When higher equalizer forces are used (as is sometimes attempted when the generator series winding is used as the equalizer voltage source) the magnitude of overvoltage can be disastrous. Note that with strong equalizer action, the presence of uncontrolled high voltage resulting in high current on one generator tends to force all other generators to a voltage higher than normal. Under many load and speed conditions, failure of one regulator of two or more generators tends to result in votages considerably above 35 and 40 volts and yet without reverse current flowing through the healthy generators. For this condition all overvoltage protectors detect the same overvoltage and destroy selectivity. This factor has made us rather hesitant of using voltage only as a means of selectively determining the unit responsible for the overvoltage. I would appreciate learning whether Austin has experienced the condition I have just described in his development work on the overvoltage protector.

The overvoltage protective device described by Austin is very interesting and appears to possess the desirable element of simplicity. Devices of the type described by Austin are sometimes subject to difficulties with maintaining a constant pickup (minimum trip setting) independent of the position of the plunger. That is, following a transient overvoltage of just insufficient duration to trip the protector, the plunger will have moved almost to the trip position. Because the air gap is now less than at the initial position, it would appear possible that the plunger would be held at the lower position by even normal voltage so that a subsequent moderate transient overvoltage could cause instantaneous trip. Would Austin please describe what methods have been used to overcome this difficulty?

Unquestionably, the combination of balanced current and differential current protection can give a theoretically higher order of sensitivity than usually is possible by use of reverse current protection. Whether this theoretical superiority can be obtained in practice or whether the gain is worth the additional complexity are questionable.

While reverse current protection is incapable of detecting certain types of fault conditions, none of those are likely to occur when the airplane is in flight. And all fault conditions can be detected and corrected by manual supervision. Differential protection does not detect a welded relay while reverse current protection does. In the past, this type of failure was much more prevalent than generator circuit faults. Improvements in generator relay design and in elimination of system disturbances such as those induced by regulator instability, system faults, and heavy motor starting should make the occurrence of welded relays less troublesome, although they still could be as prevalent as circuit faults.

The philosophy of using two devices in series to prevent simultaneous failure usually is predicated on the fact that the failure of one relieves the cause of failure and thereby protects the other. In the application cited by Austin, I wonder if this condition is met. Consider for a moment that a fault exists on the main power system or that a very heavy motor is being started with inadequate capacity. During this condition voltage across the contactor coil is low and current through the contacts is high. If the two contactors are slightly different in characteristics, it is likely that one will weld before the other. But in welding the first contactor does not relieve the condition causing the weld and the continued presence of high current and low voltage may cause the other contactor to weld.

The use of a nonlinear resistor in the equalizer circuit is an interesting development. It should meet a long desired need and permit enjoying high equalizer forces without its attendant disadvantages of excessive influence on system voltage. Would Austin please give us a quantitative figure on the effectiveness of the nonlinear resistor? If the method is effective could not the complication of the additional equalizer relay be avoided with acceptance of the fact that a small decrease in system voltage can be tolerated until manual switching operation disconnects the equalizer of a dead generator?

While the protective functions of differential current, balanced current, and overvoltage relays are fundamental in their effectiveness, I am concerned with the manner in which these devices operate through an auxiliary field relay. This method of operation has the following major objections:

1. Power is required on the system before the generator can supply power to the system.
2. Generator control must be reset every time power is removed from the system.
3. Protective functions require several sequential operations.
4. Protection is relatively slow.

Consider what will happen if a system fault occurs so that the power system is without substantial power for a short period. Sealing power for the field relays of all generators is thereby lost and these relays are free to open. If the system fault is cleared later and if the system load does not pull battery voltage down excessively, the generators can be closed again on the line by manual operation of the reset and control switches. If power stability margins are adequate the generator system may return again to normal operation. Because a manual operation possibly is required before the generators can be returned to supply power, greater battery capacity may be required.

Also consider what will happen if the system fault just described occurs on the battery circuit and in being cleared the system is left without power. Then in spite of the fact that all generators are in good operating condition it would be impossible to make them supply power again because their field relays could not be reset.

Obviously some improvement may be affected by providing sufficient time delay in a field relay with low drop-out voltage to permit it to ride through all likely system faults without opening. This method would have the unfortunate disadvantage of also slowing up the time of the relay for normal operation. In spite of the fact that the nature of the generator circuit permits rapid isolation of a fault by use of superior forms of protection such as reverse current or differential current, in the application portrayed by Figure 6 the delays inherent after sensitive protective devices detect the fault are

1. Field relay time.
2. Contactor opening time.

In summary, I believe that the main protective circuit breaker for the generator circuit should be a device which is latched closed with high contact pressure. Whether the device is closed electrically or manually depends on the weight investment that can be justified for making the circuit breaker remotely reclosable. With such a device it is assured that when needed it will be in operating condition. Devices which are held closed by forces of a solenoid are of questionable reliability when used in a protective function. Further, the protector should be tripped by direct mechanical connection with the protective sensing element. Any attempt to provide the interconnection by electrical means introduces serious problems concerning availability of tripping power.

Reference

1. D-C Power Systems for Aircraft, Parts 1–8, H. J. Finison, R. H. Kaufmann. *General Electric Review*, September 1945 to August 1946.

P. A. Danilson (nonmember; Boeing Aircraft Company, Seattle, Wash.): The need for a positive trouble free protection system is very real. Systems above all must be free from nuisance trips as airplanes have been lost because reverse current circuit breakers tripped out on transients. On multiengined aircraft adequate tripping capacity is very important as fault currents of at least 5,000 amperes can be expected.

Overvoltage Protection

The overvoltage protection system described is satisfactory for an airplane with two generators but is not entirely adequate for one with six generators. Consider one airplane with a maximum continuous load of 1,600 amperes and six 300-ampere generators. Obviously we cannot expect one generator to carry 1,600 amperes and still have overvoltage. However, we can expect a faulty generator to overheat, which in turn will be registered by a thermal indicator light. Protection would operate only as described when system load was near 500 amperes. Because the load on the airplane under discussion very seldom gets that low some other protection scheme appears desirable to prevent the faulty generator from burning up in case the engineer fails to heed the thermal warning light.

Generator Lead Faults and Feeder Protection

The system is positive and fast, the only point in doubt is whether interrupting capacity is sufficient to handle fault currents of a 6-generator system.

Double Break in Generator Bus Feeder

The weight penalty imposed by two contactors should not be necessary. Desirable solution is a contactor that will not stick.

Generator Thermal Indication

Thermal indication is very important on modern transports because generators oper-

ate at a high percentage of full capacity whereas on military aircraft the total load was usually less than half the generator capacity.

Control Apparatus

The manufacturer should be complimented on the way he has assembled regulators and relays on a single readily removable panel for easy servicing. Anything that can be done to decrease the number of packages to be installed results in a saving to the aircraft manufacturer. Air transportation companies are demanding that equipment be quickly removable for easy maintenance.

Series Field Versus Ground Resistor

1. The weight advantage is gained because 2.08 volts are available to equalize load instead of 0.5 volt used under Army system.

2. The generators divide the load according to the temperature of the windings.

3. Ballast lamps are required because a larger drop is used.

4. Close production control will be required to assure that the resistance of the series field is held within close limits. If this can be done good load division seems assured.

Conclusion

The system as a whole is a forward step in the direction of improved electrical systems.

B. O. Austin: H. J. Finison and I are in agreement on the needs for soundly engineered control and protective functions for aircraft d-c generator systems. We are likewise in general agreement involving many of my objectives and those of my associates. My associates and I have proceeded actively with the development of a more acceptable d-c power system for aircraft. To date, we have made tests on "mock-ups" which very favorably have verified the contents of the paper.

I have not given any consideration to protective schemes for 12-volt systems. Perhaps there should be more protection than there is in use today. I consider protection against faults in the 24-volt system of prime importance for two main reasons.

1. Twenty-four volts is sufficient potential to maintain low or high current faults involving an arc which readily can become a smoke and fire hazard. Twelve volts will not maintain an arc and therefore is not so much of a hazard.[1]

2. The everincreasing generator capacities involving the 24-volt system further increase the ability of that system to maintain faults high or low at relatively high voltages resulting in exposed electric arcs. This is especially true of low order faults which are below the rating of the generator.

The action of the equalizer ballast lamp in preventing excessive rise in system voltage with full-field operation of one generator is as effective as it is in preventing excessive drop in system voltage in the case of the lowering of the speed of one generator. In fact, under critical conditions the use of the high sensitivity equalizer system with nonlinear ballasts will result in a lower system voltage and a higher reversed current in the second machine than the linear equalizer system using $^1/_2$-volt equalizer voltage at rated generator loads. System tests on an accurate "mock-up" have demonstrated positive selectivity of this system.

An overvoltage relay has not been designed with the characteristics described by Finison. It is an easy task to design the magnetic circuit about the moving plunger and the proper spring characteristics for that plunger, thereby providing a relay suitable for the purpose.

Experiences teach that faults have occurred under all conditions of flight and ground operations. Therefore, protection is needed at all times. Welded contactors in the reverse-current cutout generally are not protected by the balanced current protective system. The reverse-current circuit breaker offers little improvement in this case. In fact, it is a much poorer device when compared with double contactors in the reverse-current cutout. Contactors now used are of the bridge type having two breaks. A long series of tests have shown that this contactor nearly always freezes on one side. When opening under load, the contactor will open a few thousandths of an inch on the free side resulting in a sustained electric arc which burns out that side of the contactor arm. This causes a complete loss of the generator as well as a damaged cutout. The burning of this contactor often happens below the rating of the generator. The reverse-current circuit breaker would not be effected by this condition at all. As previously stated, the double contactor is much more effective, by backing each other up. The frozen contactor usually breaks loose on the reapplication of voltage to its operating coil and continues to operate in a normal manner.

The use of balanced current and differential current protection is a practical, proved arrangement in other fields. It should be applicable and has been proved substantially by extensive "mock-up" tests of recent date. The outstanding feature of this system is the detection of faults below the rating of the generator. It is the low order faults, according to experience, which generate smoke that leaks in through the cockpit and passenger compartments, often causing panic. The low-current high-voltage arcs often last for long periods of time if there is no protection, making fires and smoke a reality.

The reverse-current circuit breaker detects nothing below the rating of the generator. The balanced current system does.

So far as I can see, it is impossible to coordinate properly the opening time of the reverse-current relay contactor and the reverse-current circuit breaker. Timing of the contactors and circuit breakers changes with age and general environment conditions. Balanced current requires no coordination of timing, and environment conditions are not critical with this class of apparatus.

Finison's position supporting manual supervision of fault conditions is not easily tenable, in view of recent airline experience requiring immediate clearing of a fault before smoke occurs.

The philosophy of using two contactors in series is not new in transportation. Finison's example is satisfactory except that his contemplated results apparently are based on contactors and relays with much higher drop-out voltages than those used in the system described. It is only barely possible that either condition described will lower the system voltage below the extremely low dropout of the contactor and adding to that remote possibility that of two contactors in series welding brings us to a relative impossibility.

The quantitative figure of the effectiveness of the nonlinear resistor can be almost anything desired. This depends upon the design of the ballast. The ballast, at the present time, has tungsten characteristics. The equalizer relay can be avoided if one can depend upon the pilot to switch off the dead generator manually. It is not believed that all operators will accept the omission of the equalizer relay.

There are at the present time schematic diagrams and tests which provide a system that can be operated without the battery. This system requires no additional apparatus, but a slight rearrangement in the control circuits. With the use of this system, it is not required that the generator control be reset every time power is removed from the system. Its operation is exactly the same as for systems that are now on the airplanes. The only requirement will be that the pilot will be required to reset when there is a fault.

Actual tests show that the protective functions of the system described are very rapid. For example, a 100-ampere fault is cleared in 0.06 second. The timing of the reverse-current circuit breaker to clear under this condition is infinite.

A greater battery capacity is not required with the use of the current-balanced system. As previously stated, if the operating company so desires, the system can be provided without the use of a battery.

Finison summarizes that the main protective circuit breaker for the main generator circuit should be a latch-closed device with high contact pressures. This, I must admit, is obsolete practice in other forms of transportation and has been so for many years. Double contactors generally have been used instead. I cannot agree that the latched-in type of reverse main circuit breaker always will operate when needed. There are several reasons for this which will be included in the summary here.

Summarizing the discussion, it seems that the following are reasonable facts.

1. The balanced current protective system offers wide range fault protection.

2. The protection against low current fault is of first importance. This type of fault is the smoke and fire maker, as proved by test. High order faults burn clear quicker and are less dangerous, but should be provided for in the protective scheme.

3. Balanced current protection requires no coordination with the reverse-current cutout.

4. Balanced current protection responds only to faults and nothing more, as proved by test.

5. Double contactors for circuit interruption are the modern transportation concept. They lend reliability to continuity of the generator on the system the maximum amount of time.

6. Single contactors have been designed within the last two years with freezing practically eliminated, as proved by test and service.

7. Later schematic diagrams provide for overload protection of the field and control circuits through the balanced current system without added apparatus.

8. Schematic diagrams and tests are in existence providing operations without a battery and reset operations only in the case of a fault. No additional apparatus is required. In other words, this system operates exactly the same as those which have been in use on planes for several years so far as the operator's panel is concerned. The only exception is the reset for faults.

9. The balanced current system is operated remotely and is trip free and can be reset after a fault, provided the fault is cleared.

10. The reliability of the reverse-current circuit breaker is in question. It is subject to changes in calibration resulting from vibration, shock, presence of fine dust particles, and high forward current. The present devices are not trip free.

11. The reverse-current circuit breaker does not sense low order smoke-making faults.

12. It is impossible to co-ordinate the timing of the reverse-current circuit breaker and the reverse-current cutout under several fault conditions. To make matters worse, the timing of contactors and circuit breakers change with age and wear.

REFERENCE

1. GASEOUS CONDUCTORS, THEORY AND ENGINEERING APPLICATION (book), James Dilion Cobine. McGraw-Hill Book Company, New York, N. Y., chapter 4, page 80.

Dielectric Strength of Station and Line Insulation to Switching Surges

Discussion and authors' closure of paper 46-189 by P. L. Bellaschi and L. B. Rademacher, presented at the AIEE Pacific Coast meeting, Seattle, Wash., August 27–30, 1946, and published in AIEE TRANSACTIONS, 1946, pages 1047–54.

F. J. Vogel (Illinois Institute of Technology, Chicago, Ill.): This paper should be a material aid in the further standardization of insulation and insulation tests on apparatus, particularly transformers. It often has been quoted that impulse and switching surges were about the same on apparatus, whether it was dry or wet. Would it not have been proper to add to the conclusions that the critical impulse flashover and switching surge flashover under wet conditions might be reduced to 75 or 80 per cent of the dry values?

There is also another question not covered by the paper. The inference is that switching surges are slow and perhaps similated by one-half cycle of 5,500 microseconds duration. Such surges would give nearly uniform distribution of voltage within windings. However, statements have been made several times that resonance could lead to dangerous voltages within windings at the time of and because of switching surges. Since the switching surges were caused by changes in current within the windings, they must be distributed uniformly and the period is long as compared to the transformer period. Agreement on this point, along with the data provided by the author, will help materially in further standardization.

F. O. Wollaston (British Columbia Electric Railway Company, Ltd., Vancouver, Canada): If the wave shown in Figure 5 of the paper were one-half cycle of an a-c wave, the a-c frequency would be about 500 cycles per second. The strength of insulation to a-c frequencies of this order is, as far as I know, about the same as for 60-cycle voltages. But the insulations subjected to the wave of Figure 5 developed impulse strengths. The reason for this could be that the duration of the test wave was essentially only one-half cycle. In that case it could be that insulation subjected to one-half cycle of 60-cycle frequency would develop "impulse" strength (approximately).

I would like to see breakdown tests made at 60-cycle voltage but with the time of application varied from one-half cycle up to the minimum number of cycles that would give breakdown values equal to presently accepted 60-cycle values.

H. L. Rorden (Bonneville Power Administration, Portland, Oreg.): I hope we may not have to take the authors' inference that impulse data are relatively complete to mean that they intend to divert their future efforts to other channels. I believe there is still a vast amount of information to be obtained in this field, and we on the operating end look to the manufacturers for laboratory data. It is significant that we still have insulation failures, and we can only conclude that we still do not fully understand all we need to know about transients. I am sure that the entire electrical profession will agree with me in hoping that Bellaschi and Rademacher will continue their good work. This paper adds useful information to their numerous contributions.

We of the Bonneville Power Administration do not believe that methods of protection have developed to the stage where they are both satisfactory and economical. Although we do not have surge testing equipment in the Northwest, we are conducting such investigations as we find possible without interfering with normal operation of our power system. We differ from most high-voltage systems in the heavy lightning areas of this country by having transmission lines which are not protected by overhead ground wires, although part of our system is in a moderate lightning area. We therefore consider the system itself as a laboratory. The significance of this ties in very closely with the contents of the paper.

The high-voltage lines of the Bonneville system are equipped with overhead ground wires only for approximately one mile from stations and are intended solely for station protection. The transmission lines are susceptible to direct lightning hits, and to our knowledge such hits always result in a flashover. These outages are not of serious concern to us because all of our 230-kv system in the lightning area consists of parallel circuits.

We believe that practically all direct strokes to our lines will result in a flashover regardless of the insulation level. While our normal insulation consists of 16 $5^3/_4$-by-10-inch suspension insulators, we have operated experimentally with as low as 11 on steel towers. Thus far we have found no significant difference in performance. Undoubtedly, enough insulation and conductor separation could be provided to prevent some of the hits from resulting in flashovers, but we believe this insulation level could not be justified economically. We therefore now are considering basing our insulation levels on switching surges. In fact we are planning on an installation involving insulation of this nature and high-speed reclosing breakers in lieu of overhead ground wires. We believe this method of protection may have considerable advantage over the present commonly accepted practice of providing ground wires over the entire system. In such a system we shall have considerable use for switching surge data as well as high overvoltage impulse data. We therefore commend the authors of this paper on the presentation of data which we believe have more than casual importance in the field of transients and insulation levels.

I would appreciate a little additional explanation from the authors on their statement that isolated neutral systems attain five to six times normal voltage. While this is a commonly predicted figure, we have found, all too frequently, that predictions may prove to be too ultraconservative for good practice. While we recognize the fact that isolated neutral systems can be subjected to higher transient potentials than are solidly grounded systems, we are inclined to the opinion that they ordinarily do not attain the magnitude suggested by the authors. From investigations conducted on our 230-kv neutral grounded system, we are confident that our switching surges rarely if ever reach three times normal, and we are contemplating a number of isolated neutral installations for which we must provide adequate protection.

J. T. Lusignan (Ohio Brass Company, Mansfield, Ohio): The authors should be complimented on their contribution to our knowledge of surge conditions on power systems. Their laboratory work has been well done and their presentation of the results clearly shown.

In addition to the insulating members which they already have tested, it would be helpful if they could continue the work as thoroughly into the various forms of limiting gaps used by transmission operators. These gaps range from ordinary rod, horn, and ring gaps to specially designed control gaps.[1] Many of these gaps afford the principal means of protection to station apparatus and the knowledge of their flashover characteristics under wet switching surge conditions should be worth while.

REFERENCE

1. THE CONTROL GAP FOR LIGHTNING PROTECTION, Ralph Higgins, H. L. Rorden. AIEE TRANSACTIONS, volume 55, 1936, September section, pages 1029–34.

H. A. Frey (Locke Insulator Corporation, Baltimore, Md.): The field which has been explored by Bellaschi and Rademacher is one which has been neglected largely by American investigators. The paper constitutes a welcome and timely contribution. As the authors have pointed out, switching surges may be a determining factor in establishing insulation levels for some of the projected higher transmission voltages.

The surges used in the authors' investigations were of about 1,000 and 3,000 microseconds duration. The duration of a 60-cycle half wave is 8,300 microseconds. On such a time scale the effective duration of a $1^1/_2$x40 microsecond impulse wave is almost zero. It is interesting to note that if the curves, Figures 6, 7, 8, and 9 of the paper, be plotted to a linear time scale (abscissa) and if the 60-cycle flashover value be plotted at the time corresponding to the 60-cycle crest, then the switching surge flashover points fall very close to a straight

line through the critical impulse flashover and the 60-cycle crest flashover values. In this case the critical impulse flashover is taken as the tail of wave flashover in accordance with American Standards.

Do the authors feel that this could be used safely as a method of estimating switching surge flashover levels from known impulse and 60-cycle flashover values?

J. H. Hagenguth (General Electric Company, Pittsfield, Mass.): The data presented in the paper are a valuable addition to the knowledge of long-duration surge sparkover of insulators and bushings. However, is it correct to call the type of waves used typical switching surges? One type of switching surge shows an initially rapidly-rising front followed by a very gradual rise in voltage with superimposed oscillations. Such waves have more nearly the characteristics of a steep-front flat-top wave in contrast to the slowly rising front wave used by the authors. Before it is possible to draw any definite conclusions as to the sparkover strength of insulators and bushings for switching surges in general, it would seem necessary to have results of tests with the flat-top type of wave. It has been shown[1] that for impulse conditions a large difference in spark-over voltage exists between rectangular waves and straight rising front—as much as 20 per cent at eight microseconds. Such differences in spark-over voltage may not exist at 500 to 1,000 microseconds, the region explored in the paper, but the facts cannot be verified without investigation. For instance, if the test results on insulators or bushings in the paper with spark-over at about 800 microseconds are compared with the straight-line impulse spark-over of similar devices at eight microseconds,[1] the long time spark-over voltage would be reduced to 80 per cent instead of 95 per cent of the short time impulse spark-over.

The fact that the two transformers withstood a large number of short, intermediate, and long duration surges is a proof of the quality of the transformers up to the tested levels, but does not permit a comparison between impulse and switching surge strength of the units since the comparative breakdown values are not known. Further, the damped high frequency oscillations associated with some switching surges when applied to transformer windings which are not shielded adequately are capable of raising internal winding voltages near winding resonance to even higher levels than the impulse.[2,3] The low frequency test wave (Figure 5 of the paper) probably resulted in only straight-line distribution throughout the windings.

The transformer insulation therefore was subjected to less severe stresses than would have resulted from application of flat-top switching surges with superimposed higher frequency oscillations produced externally to the transformer.

References

1. Volt-Time Areas of Impulse Spark-Over, J. H. Hagenguth. AIEE Transactions, volume 60, 1941, August section, pages 803–10.

2. Effect of Transient Voltage on Power Transformer Design, K. K. Palueff. AIEE Transactions, volume 49, 1930, pages 1179–90, Figures 8 and 9.

3. Methods of Determining Natural Frequencies in Coils and Windings, L. V. Bewley, J. H. Hagenguth, F. R. Jackson, Jr. AIEE Transactions, volume 60, 1941, pages 1145–50.

P. L. Bellaschi and L. B. Rademacher: The manner in which H. L. Rorden is coping with the insulation protection problem for a system that lies in a moderate lightning area is interesting and indicates a keen realization of the economic aspect of the problem. We fully concur with Rorden that laboratory investigations on impulse and switching surges should continue by all means but in a direction bearing economic importance to the over-all problem. Our experience on switching surges and available knowledge show that for a solidly-grounded neutral system surge overvoltages seldom if ever attain $3^1/_2$ times line to neutral crest voltage, whereas on isolated-neutral systems there has been ample evidence of overvoltages up to five or six times line to neutral crest voltage. For systems of modern design and "good behavior" it is possible that these overvoltages may be even less.

The approach H. A. Frey indicates for estimating switching surge strength from the impulse and 60-cycle values is probably close enough in most cases, but we would hesitate to consider this as a guiding rule. Even for porcelain insulation in air it may be very much in error as evidenced from a consideration of some of the data in reference 12 of the paper, and obviously the method falls far from the mark when applied to oil-immersed insulation.

Tests on other equipment such as J. T. Lusignan has indicated certainly would be worth-while, but we feel that the data already presented provide a good basis from which to assess the significance of switching surge strength in relation to the problem of co-ordination and protection as a whole.

Referring to F. O. Wollaston's discussion the data in Figure 10 were secured in the manner he has indicated. The details of these tests appear in reference 9. In most cases transient voltages are almost over in a matter of milliseconds, and for durations of this order the insulation strength is well up to its impulse level. However, should the system overvoltage approach durations of the order of seconds, then for such a condition the effective strength of the insulation corresponds more nearly to its 60-cycle value.

It might have been well, perhaps, to have added a fifth conclusion such as F. J. Vogel suggests indicating the reduction in impulse and switching surge strength of porcelain insulation in air as affected by rain. However, we feel that conclusion 2 accomplishes the purpose, and that the test data in the paper are specific as to the reduction in strength caused by rain.

Table VI of the paper gives comparative data with reference to a flat-top impulse of the type J. H. Hagenguth refers to in his discussion and should answer the points he has raised in this connection. With reference to the old bugaboo of resonance, we merely want to call attention once again to the ability of modern surgeproof transformers to withstand switching surges of all sorts. This is a matter of extensive experience and record extending over a long period of years.

Those interested in this subject matter both from a standpoint of testing and field experience will find many of the references helpful. The authors have drawn from this over-all experience and their own in planning the investigation and keeping it on a sound and practical basis. In general, we concur with the suggestions and thoughts set forth by the several discussers in regard to the desirability of future studies both in the field and in the laboratory.

An Oscillograph for Recording Transient Recovery Voltages

Discussion and author's closure of paper 46-181 by W. G. Hoover, presented at the AIEE Pacific Coast meeting, Seattle, Wash., August 27–30, 1946, and published in AIEE TRANSACTIONS, 1946, pages 1086–91.

E. W. Boehne (General Electric Company, Philadelphia, Pa.): The author is to be congratulated upon his paper which presents an informative and orderly analysis. The recognition and demonstration of the effect of arc voltage and residual arc conductivity upon the recovery characteristics of such high voltage breakers are indeed interesting.

The value of the oscillograms shown in Figures 4 and 6 would be enhanced by a knowledge of the natural frequencies of the circuit and their magnitudes under the more or less ideal conditions of a linear decay of current to zero. A comparison of the phenomena shown in these oscillograms with those presented and discussed in another paper[1] suggests that conduction following current zero is not restricted to the lower voltage breakers.

I would like to ask the author if the test shown in Figure 4C was taken on the same circuit as those shown in Figures 4A and 4B. The 49,000-volt increase about 450 microseconds following current zero suggests a reflection from a junction about 42 miles away. The evidence of such a reflection is not present in Figures 4A and 4B. A circuit diagram would aid in interpreting the films.

Reference

1. The Geometry of Arc Interruption—II, Current-Zero Phenomena, E. W. Boehne. AIEE Transactions, volume 63, 1944, pages 384–5, 448.

Laurel J. Lewis (University of Washington, Seattle, Wash.): The development of this oscillograph illustrates in a striking manner the increasing importance to the power engineer of recent advances made in the electronic field. The author is to be congratulated for his use of trigger circuits, pulse shaping circuits, and rectangular pulse generating equipment, more commonly associated with radar techniques, to the development of a new tool for circuit breaker testing.

The writer was privileged to use the instrument described in an extended investigation and can vouch for its reliability. A number of points may be mentioned to emphasize its versatility.

The tests made at the Newark substation of the Pacific Gas and Electric Company, and illustrated by the oscillograms in Figure 4, were among the highest capacity tests made up to that time on an actual system on circuit breakers of that voltage classification. Because of the severe duty imposed on the system it was necessary to limit the number of tests, and only one was made under each test condition. This meant that the oscillograph was required to perform accurately and reliably without any rehearsal. The clearness of the records indicates no small degree of skill and planning in the control of intensity, focusing, and timing of both the vertical and horizontal sweeps.

The problem of accurate tripping becomes of increasing importance as the horizontal sweep speed is increased. Any slight deviation between the time of net flux reversal in the peaking transformer core and the time of the true current zero in the test circuit affects the start of the horizontal sweep. This effect is evident in Figure 4C where the break in the arc voltage on next to the last half cycle appears to occur about 600 microseconds before the position of final recovery. Where the polarity of the recovery voltage cannot be controlled, such a deviation limits the recording space and restricts the speed since proper timing for one polarity may place the final recovery trace on the opposite polarity too far to the right on the screen. Solution of this problem requires that the peaking transformer faithfully follow the current in the test circuit, requiring essentially perfect reproduction by the current transformer of the d-c component in the offset current wave. That such a problem has been solved is illustrated by the oscillograms in Figure 5 where the horizontal sweep speed is about ten times that shown in Figure 4, and the deviation has been reduced greatly.

The applications described are those in which one terminal of the circuit breaker is grounded, and it is thus possible to keep the recording equipment essentially at ground potential. This requires that the recovery voltage be applied to only one plate of the cathode ray tube with the other maintained near ground potential. Ordinarily this contributes to a certain defocusing effect in the tube. Perhaps Hoover could elaborate on how some of the difficulties from this cause have been overcome. It would also be interesting to know if the oscillograph can be used on line-to-line tests.

W. G. Hoover: In reply to E. W. Boehne, the natural frequencies corresponding to the tests of Figure 4 were not known nor were they calculated prior to the tests. A rough estimate of their order of magnitude was made to determine the necessary frequency response characteristics of the oscillograph circuits. In the tests of Figure 6, the high frequency oscillation in Figure 6A was mainly caused by a capacitance of about 370 micromicrofarads (breaker, potential divider, leads, and reactor distributed capacitance) and a series reactor of about 1.3 millihenries. The generator side of the reactor was connected to a 1,050-kva sine-wave generator through about 100 feet of single-conductor 15-kv lead-covered cable. The low frequency oscillation observable in both oscillograms is caused principally by the generator reactance and equivalent total terminal capacitance.

The test shown in Figure 4C was taken on the same 110-kv bus as those of Figures 4A and 4B. In the case of Figure 4C only, the three conductors of an otherwise idle 110-kv transmission line were connected to the high voltage terminal of the test breaker for the purpose of reducing the transient recovery rate. The reflection from the open end of the line about 40 miles away has no counterpart in the tests of Figures 4A and 4B.

The author appreciates the comments made by Laurel J. Lewis who was present at and contributed considerably to the success of the tests described in the paper. The question of beam focus for deflections over the whole face of the cathode-ray tube was treated satisfactorily by using push-pull deflection voltages for both vertical and horizontal sweeps. The signal voltages were impressed on only one of the vertical deflection plates for line-to-ground tests, but the amplitudes of these voltages were maintained low enough so that serious defocusing did not result. Tests made during the early development of the oscillograph showed the complete feasibility of measurements on line-to-line tests, wherein the outputs of identical voltage dividers connected to each terminal of the test breaker are brought to the separate vertical deflection plates.

Long-Distance Power Transmission as Influenced by Excitation Systems

Discussion and authors' closure of paper 46-182 by C. Concordia, S. B. Crary, and F. J. Maginniss, presented at the AIEE Pacific Coast meeting, Seattle, Wash. August 27–30, 1946, and published in AIEE TRANSACTIONS, 1946, pages 974–87.

R. D. Evans: (Westinghouse Electric Corporation, East Pittsburgh, Pa.): In their present paper Concordia, Crary, and Maginniss deal with two subjects, namely,

1. The relation of exciters and regulators to the stability of transmission systems of the moderate length of 200 miles.

2. The relation of intermediate synchronous condenser stations to the steady-state stability of long transmission systems of 600 miles in length.

These subjects have received relatively little attention during the last few years but they were discussed actively during the years from 1924 to 1929. It is interesting and sometimes valuable to review basic problems at intervals of approximately 20 years, as such intervals provide time for the development of new methods of analysis, reconsideration of basic assumptions, and the production of new apparatus and modes of operation.

The first subject considered by the authors is the effect of the characteristics of exciters and regulators upon the stability limits of straightaway transmission systems for both steady-state and transient conditions. The results of this part of the investigation by the authors are summarized in the paper under the heading "Conclusions," items 1 to 4. Item 3 seems to state that the transient-stability limits for conditions imposed by line faults with subsequent high-speed sectionalizing are lower than those for the steady-state conditions after the switching operations. Item 1 states that for a system subjected to a severe fault with the subsequent switching operations, the stability limits cannot be increased appreciably by practicable changes in the exciter and regulator system. These conclusions are not new; they have been held since high-speed fault-clearing means became a reality. Item 2 seems to state that for certain less severe faults or for faults of shorter durations, some relatively small increases in stability are possible by the use of excitation systems of higher response. This conclusion, while interesting, appears to be of academic value in view of Item 1 which states that little benefits are obtainable for the more severe conditions which are controlling. Item 4 states that with a properly stabilized excitation system and with stability maintained on the first swing, stability generally should be maintained on the subsequent swings. In this connection it is pertinent to observe that practical systems will be laid out with a margin between the load to be carried and the stability limit. When systems are operated with such margins, the chance of instability occurring on subsequent swings will be minimized. If the stability studies had taken the normal load margins into account, the results would have been of greater practical interest.

The second subject considered by the authors deals with the increases in the steady-state stability limits that result from the use of regulated synchronous condensers located at intermediate points on a long transmission system. It is of interest to compare the results given in the present paper with those presented by C. F. Wagner and R. D. Evans in an earlier paper (reference 7 of the paper). The layouts assumed for the stability studies are different but it is of interest to compare the per cent increases in the stability limits for one and for two intermediate condenser stations. This may be done by taking the data from Figure 14 of the paper and replotting to the form used in Figure 26 of the earlier paper by Wagner and Evans. It will be found that quite good agreement will obtain for both one and two intermediate condenser stations of low reactance. For increasing values of condenser station reactance, the checks are not as good. This is a result to be expected from the differences in the layouts assumed for the studies.

The hypothetical system studied by Concordia, Crary, and Maginniss includes finite reactances for the hydroelectric generating station, the sectionalized double-circuit 230-kv lines, and a receiver system represented by a synchronous motor. The hypothetical system assumed by Wagner and Evans is similar except that the receiver system is represented by an infinite bus. The practical system probably would involve a step-down station, large shunt loads, and receiver-end generators. On the practical system the receiver-end generators will have a phase leading that of the shunt load. It would appear that the approximation of an infinite receiver is not only simpler but quite as accurate as one using a synchronous motor without a shunt load. However, either approximation can be used, and both will show that important increases in the stability limits are possible through the

use of intermediate synchronous condenser stations. In any actual problem these differences in the approximations would not appear because the actual system would be represented accurately.

Alexander Dovjikov (Bonneville Power Administration, Portland, Oreg.): The proposed increase in the range of transmission of power supplied by the Bonneville Power Administration has made it necessary to reconsider ways and means of accomplishing this purpose in the most reliable and economical way. In parallel with considerations of d-c transmission, of increase in a-c operating voltage, and of the series capacitor-compensated lines, interest in intermediate synchronous condensers and in the importance of interconnections with other sources of electromotive force along the long line such as local generating stations, has been revived. This revival is noticeable not only in this country but abroad as well.[1,2] The paper by Concordia, Crary, and Maginniss is therefore very timely, and is of great interest to the engineers of the Bonneville Power Administration.

Beside the preponderant importance of the speediest fault clearing for increasing the transient stability of a transmission system, the value of appropriate intermediate synchronous condensers (known as the Baum system) in increasing steady-state and transient stability of long distance transmission systems has been realized for at least the last 25 years. The stabilizing effect of such synchronous condensers is a function of their ability to maintain their terminal voltage, and it was realized early again that to achieve this the machine must have:

1. Low reactance.
2. Very high-speed excitation system.

Or in other words, the synchronous condenser must have voltage characteristics analogous to a d-c machine with compound excitation. Excitation of such an a-c machine (in addition to the no-load excitation) must be a function of load current and of load power factor, and, accordingly, the late Doctor C. L. Fortescue proposed the use of:

1. A cylindrical rotor with a 3-phase distributed field winding, the terminals of which through slip rings would be supplied by three direct currents from

2. A 3-brush rotary convertor rectifying 3-phase alternating currents from the secondary windings of current transformers, the primary windings of which are inserted at the terminals of the synchronous machine. The field produced by these three direct currents is proportional to the load, and the direction of this field depends upon the load power factor.

By changing the ratio of the current transformers this machine may be made over compounded. The excitation response is instantaneous and the machine may keep its terminal voltage constant in the limits of its rated capacity.

The construction of this machine proved to be too expensive. As the cost of the conventional excitation system is a very small fraction of the cost of synchronous condensers, and any additional cost in connection with its improvement will be reflected only slightly in the cost of the total installation, efforts of designers again were switched to the development of very high-speed excitation. Several measures, including lamination of stators of d-c exciters and of special quick acting contacts on automatic voltage regulators, produced quick response excitation.

In the selection of synchronous condensers located in the main 230-kv loop of the Bonneville Power Administration transmission system, we recognized that in addition to their voltage regulating activity on the substation bus and the control of reactive power flow through the points of interconnection with other system, these machines are intermediate condensers. Together with the attempts to obtain machines of low reactance, we were increasing consistantly the kilowatt capacity of exciters and particularly their ceiling voltage. Our latest specifications for 35,000-kva synchronous condensers required:

The main exciter shall be a 250-volt direct-current generator with a capacity at least 20 per cent greater than that required for the excitation of the condenser when it is carrying full kilovolt-ampere load. The ceiling voltage of the main exciter, when delivering full rated current, shall be not less than 175 per cent of normal rated voltage. The main exciter shall be designed to have a nominal exciter response of not less than 1.5, as defined and measured in accordance with American Standard A50-1936, paragraphs 1.219, 1.220, and 1.221. The pilot exciter shall be a 125- or 250-volt direct-current generator with a capacity at least 50 per cent greater than that required for supplying the field current of the main exciter, when the main exciter is carrying rated current and voltage.

If the system of excitation using an amplidyne is not much more expensive than a conventional d-c exciter, we believe it may be used very profitably. The curves presented in Figure 9 of the paper, however, did not impress us so much with the effectiveness of the high speed of excitation as by the necessity of shortening the time of fault clearing. Our trouble is—and we believe it is shared by other operating companies—that although we installed the fastest relay systems (distance relays with carrier control) available, known as instantaneous, the time of fault clearing on both ends is in the region where Figure 9 shows the use of very high-speed excitation to be practically useless. We are not as pessimistic in this respect as the authors of the paper, although we agree with them in general; however, we believe that relay systems must be developed which will be very fast. Could the authors make any statement regarding the progress being made in this respect? There is another statement in the paper in which we were interested even more than in the high-speed excitation, namely, in the necessity for decreasing the transient reactance of the synchronous condensers. No excitation could be so fast as to neutralize the instantaneous terminal voltage drop resulting from the transient reactance, and we fully agree with the idea which was advanced very clearly 20 years ago by Evans and Wagner[3]

. . . machine's ability to supply lagging kilovolt-amperes with drop in voltage is a measure of its desirability from the standpoint of maintaining stability. To supply this large amount of lagging kilovolt-amperes with drop in voltage, a synchronous machine should have low leakage reactance, as this is initially the limiting factor, and in addition should have a "strong field and weak armature" which tends to prevent reduction in machine flux when supplying the large amount of lagging kilovolt-amperes. Merely derating a synchronous machine will not give as favorable a result in cost and performance as can be obtained by specially designing the machine. Similar measures can be applied to synchronous generators with corresponding improvements in performance.

Strangely enough, machines with such characteristics have not been designed as yet, and our consistent efforts to obtain low reactance synchronous condensers always have been countered by their high price. Evidently, factory cost estimators were "merely derating a synchronous machine"—procedures against which their own general engineers were objecting. We were glad, therefore, to see the following statement in the present paper:

The building of low transient reactance synchronous condensers with special excitation systems now appears entirely practical, and makes it necessary to consider such a method in the design of any new long-distance transmission system. However, if it were not possible to attain the special features, the required synchronous condenser capacity becomes extremely large, making this method uneconomical compared with other methods.

This infers that these special low reactance machines can be produced at costs approaching those of conventional machines.

What we would like to ask the authors, who represent the largest organization for manufacturing electric machinery is whether such synchronous condensers were built or at least designed, in what respects this special design would differ from standard, and how the cost of such a special low reactance machine would compare with the costs of standard low reactance machines and with machines of the same kilovolt-ampere rating having the usual high reactance.

REFERENCES

1. LONG-DISTANCE TRANSMISSION OF ENERGY AND THE ARTIFICIAL STABILIZATION OF ALTERNATING-CURRENT SYSTEMS, G. Darrieus. Conférence Internationale des Grands Réseaux Électrique à Haute Tension (Paris, France), 1946, paper 110.

2. ALTERNATOR EXCITER SYSTEMS, R. David. Conférence Internationale des Grands Réseaux Électrique à Haute Tension (Paris, France), 1946, paper 101.

3. STATIC STABILITY LIMITS AND THE INTERMEDIATE CONDENSER STATION, C. F. Wagner, R. D. Evans. AIEE TRANSACTIONS, volume 47, 1928, pages 94–121.

C. Concordia, S. B. Crary, and F. J. Maginniss: R. D. Evans' re-emphasis of the previous work done many years ago and wherein it checks with the present work is appreciated very much. Our objective was to present sufficient additional quantitative information in terms of present-day apparatus so as to lend encouragement to the reconsideration of the use of intermediate synchronous condensers as a practical means for increasing the power limits of long-distance transmission systems.

Alexander Dovjikov raises a question in regard to instantaneous relaying. Reliable relays of not more than one cycle total operating time are now generally available for high-voltage transmission systems. Higher speeds of relay operation would be of small stability benefit and would be of questionable value if the high speeds were attained at a sacrifice of relaying reliability.

Dovjikov also asks about the use of special synchronous condensers. It is difficult to give any cost comparisons because the cost of such condensers depends not only on the required reactance but also on the required capacity in a single unit. Cost comparisons which we have made for a long high-voltage line requiring intermediate synchronous condensers having an effective reactance of approximately 15 per cent on a 400,000-kva

base indicate that the cost would be entirely competitive with other methods of line compensation in order to obtain the same steady-state stability limits. We would like to encourage Dovjikov to make a similar study and to make his comparisons for a specific case for which cost estimates may be obtained.

Field Tests on Power-Line Carrier-Current Equipment

Discussion and author's closure of paper 46-199 by R. H. Miller and E. S. Prud'homme, presented at the AIEE Pacific Coast meeting, Seattle, Wash., August 27–30, 1946, and published in AIEE TRANSACTIONS, 1946, December section, pages 824–7.

F. S. Benson (Pacific Gas and Electric Company, San Francisco, Calif.): Since this paper was prepared we have installed between Shasta substation and Pit 5 generating station an additional carrier current telephone channel using a frequency-modulation carrier installation. This later installation has proved quite satisfactory. Our operators and dispatchers state that the background noise level has been reduced materially, and that the fidelity of tone is good, making telephone conversations much easier to understand. Peculiarly enough, there seems to be a greater reduction in background noise level at the Pit 5 end than at the Shasta substation. At the moment, we do not know how to account for this. This carrier current installation operates over a rather high-loss 220-kv circuit; the corona loss is high because of the type of rope core conductor originally installed. Our frequency-modulation carrier installations are giving good service now, particularly since the adjustments mentioned in the paper have been made, and have solved a troublesome background noise problem.

S. C. Bartlett (American Gas and Electric Service Corporation, New York, N. Y.): The paper presents information on a subject on which all too little specific technical and experimental data are now available. In radio applications the relative advantages of frequency modulation and amplitude modulation have been investigated rather thoroughly and theoretical studies and field observations well correlated and generally accepted throughout the industry. The application of frequency modulation for carrier current communication on a practical power system has introduced a number of conflicting viewpoints. Information of the type presented in this paper is of value in checking the purely theoretical reasoning. However, there are a number of questions which must be answered before we can employ intelligently any new technique by having complete information regarding its advantages and limitations. Additional data along the lines of that presented in this paper would help considerably.

The authors have produced a very interesting and enlightening paper but there are several points not exactly clear. For instance, if we interpret properly Table II in which frequency modulation and amplitude modulation signal-to-noise ratios are compared, it appears that as the signal-to-noise ratio diminishes (reducing transmitter power), the advantage of frequency modulation over amplitude modulation also decreases. This, of course, is to be expected, because if this process were carried to the point where signal and noise were equal there would be no advantage of one system over the other. The important point is that at low signal-to-noise ratios, where amplitude modulation becomes unsatisfactory, frequency modulation still provides a means of improvement and might transform an unsatisfactory channel to a serviceable medium. It would aid considerably in interpreting the results if the authors would indicate what from their experience constitutes the minimum signal-to-noise ratio at which intelligible communication can be obtained. Also in order for a frequency modulation receiver to perform properly, it is essential that the limiter be saturated. We wonder if the receiver used for the tests had sufficient sensitivity so that this condition was realized for the weakest signal recorded.

In this matter of deviation ratio it has been assumed generally that for our purposes the deviation must be limited to one-to-one. This is doubtless correct for main transmission systems where the carrier spectrum is crowded with channels of all types. However in a great many cases such as subordinate transmission systems requiring only one communication channel and possibly a few relay channels, it would be entirely feasible to increase the deviation ratio if there would be a corresponding advantage. For radio work we know this would be true, but on a power line the transmission characteristics are such that the sharp peaks and valleys might cause serious distortion of a wide-band system. The authors discuss only results of tests using ratios up to one-to-one, but if observations beyond here were made such data should be included.

In connection with existing amplitude modulation channels where signals are of adequate magnitude, and considering the difficulties of converting to frequency modulation, it is reasonable to believe that amplitude modulation will continue to be used indefinitely. For this reason the authors' comments regarding amplitude modulation receivers are quite interesting. Specifically, it was mentioned that fidelity sometimes was impaired by the high Q of the line tuners and could be improved by broadening the tuning. This, of course, can be done in many different ways, and we believe it would be interesting for the authors to outline the method used and possibly the reasons for the choice of method. Evidently the receiver used had extremely high selectivity to start with, because it has been our experience that it is frequently necessary to sacrifice some audio fidelity to obtain the necessary selectivity. In many cases we have made it a practice to take advantage of the high Q tank circuit of the transmitter to provide additional receiver selectivity by tapping the receiver to the tank circuit rather than to the radio-frequency line. This, of course, applies only to single frequency sets.

Mention is made that alignment of amplitude modulation receivers should not be made by adjusting for peak detector current. It would be valuable to have the authors' opinion as to the manner in which such tuning should be accomplished.

The electric utility industry needs specific answers to two fundamental questions in connection with the use of frequency modulation carrier. These are

1. Where an existing amplitude modulation system shows only marginal performance because of noise, will conversion to frequency modulation using the same frequency, power, and a one-to-one deviation ratio convert this to a serviceable channel?

2. In planning new channels where it is reasonably certain that amplitude modulation will provide adequate signals, does frequency modulation offer advantages enough to offset the additional cost and complication?

Any pertinent information along these lines would aid materially in planning future additions or modifications.

In general, it is our feeling that the paper is a valuable contribution to our limited knowledge of comparative frequency modulation and amplitude modulation performance on a practical power system. The only general comments we have is that the paper, if anything, is too lacking in details and we hope the authors as well as others will be encouraged to make available whatever additional information is obtained along these lines.

R. C. Cheek (Westinghouse Electric Corporation, East Pittsburgh, Pa.): The authors have drawn two conclusions that apparently are not supported by the data presented in the paper. Item 3 under "Conclusions," based on the data presented in Table I of the paper, states that "frequency modulation equipment is capable of maintaining a high signal-to-noise ratio with large variations of carrier signal." The data given in the table indicate that the signal-to-noise ratio was quite high for all tests, so that the figures given in the second column, received volts, can be used as a measure of relative received signal strengths, even though a small amount of noise is included. An increase in the received signal level from 1.5 volts to 2.2 volts would be expected to raise the signal-to-noise ratio by 3.3 decibels for any system, and this is precisely the change in signal-to-noise ratio obtained by the authors for this increase. One would expect the signal-to-noise ratio to increase by about 4 decibels with a change in the received signal level from 2.2 to 3.6 volts. The authors obtained an increase of 1.7 decibels for this change, giving them a signal-to-noise ratio of 29.5 decibels instead of 32 decibels as would have been expected. This discrepancy, however, may have been a result of slight changes in the actual noise level during the test.

It therefore appears that the frequency-modulation system signal-to-noise ratio is no more independent of received signal strengths than other systems. In addition, the noise reducing properties of the frequency-modulation system depend upon the maintenance of a received signal voltage considerably in excess of the noise voltage, in order for the limiter to be effective. Even with perfect limiter action, however, the equivalent frequency-modulation resulting from phase modulation of the received carrier by noise voltages is directly

proportional to the relative strengths of noise and received signal. Thus in frequency-modulation as in any other system, a change in the received signal level of so many decibels will give a change in signal-to-noise ratio of the same number of decibels, provided the frequency modulation signal is always several times greater than the noise. If the latter condition is not met, a slight reduction in the frequency modulation signal strength may reduce the signal-to-noise ratio by a much greater amount. A comparison of the relative strengths of transmitted signals with received signals on successive tests in Table I of the paper indicates considerable nonlinearity in the carrier channel. It would be interesting to know what explanation the authors have of this phenomenon.

The authors state in item 4 under "Conclusions" in the paper that the frequency modulation system "permits successful carrier current operation on lines with noise levels so high as to preclude the use of conventional amplitude modulated equipment" basing this conclusion on Table II of the paper. It is unfortunate that the tests shown in the table were not made for smaller signal strengths than those used, because quite the opposite result no doubt would have been demonstrated. As a matter of fact, even though the test was carried only to the point where the signal voltage was still at least 7.5 times the noise voltage, a very definite reduction in the gain of frequency modulation over amplitude modulation was evident. In other words, the frequency modulation system provides gains over amplitude modulation under favorable noise conditions, where the noise voltage is already small compared to the signal, but provides less gain and may even give a loss in signal-to-noise ratio when compared with amplitude modulation or single side band under severe noise conditions.

Although the authors did not state in the paper that the frequency modulation equipment used in the tests included audio pre-emphasis and de-emphasis circuits, while the amplitude modulation equipment did not, it is assumed that this was the case. The figures given for the gain in signal-to-noise ratio of frequency modulation over amplitude modulation therefore must be reduced by an amount equal to the gain obtained by pre-emphasis, if a true comparison of the two fundamental systems is to be made. It should be remembered that pre-emphasis can be used with an amplitude modulation or single side-band system, and that, although a given amount of pre-emphasis provides a greater reduction in noise with frequency modulation, the amount of pre-emphasis that can be used with a frequency modulation carrier system is limited because of the increased band width required by the signal as higher voice frequencies are emphasized to a level approaching that of the lower voice frequencies. Such an increase in band width does not occur in an amplitude modulation or a single side-band system, so that more pre-emphasis can be used, giving gains from pre-emphasis comparable to those obtainable with frequency modulation.

The effect of high Q line tuning equipment upon the audio-frequency range of a carrier channel is worthy of additional comment. The reduction of higher order side bands by such sharply tuned circuits will reduce the response of an amplitude modulation channel to the higher audio frequencies, as described by the authors. The corresponding effect in a frequency modulation channel is not primarily an alteration of the frequency response curve, but is the introduction of harmonic distortion at all audio frequencies. The apparent remedy used by the authors was to broaden the carrier-frequency response curve of the tuning equipment, with a corresponding reduction in signal strength at the carrier frequency, and an increase in the noise voltage accepted by the receiving equipment. It is interesting to note that a single side-band channel, because of the extremely narrow band width it requires, permits the use of tuned circuits of higher Q than can be tolerated with either a frequency modulation or an amplitude modulation channel and consequently does not require such compromises in signal-to-noise ratio for the sake of increased band width.

E. S. Prud'homme: R. C. Cheek's comments hinge largely around some important and rather drastic misinterpretations of the data in the paper. It appears desirable to hasten correction of these because the data, properly explained, seem to support adequately all of the conclusions.

Referring to the second column of Table I of the paper, it was pointed out that the received volts are signal *plus* noise. It is not proper to use these values as a measure of relative received signal strengths. A curve of received volts against transmitted volts will show clearly that approximately 1.4 volts of noise did exist with no transmitted voltage. This was not stated in the paper because it was thought this should be apparent from the figures given. Because the signal and noise voltages do not add arithmetically on a vacuum tube voltmeter, the curve will not be linear. Therefore, there is no reason to attempt an explanation of any phenomenon of nonlinearity. The signal-to-noise in decibels figures were measured, of course, at the receiver output terminals, and these values are not related directly to the received volts data which were a total voltage measured at the input terminals, and included both signal and noise. The calculations of Cheek, prepared upon the false assumption that these figures can be used as a measure of relative received signal strength, therefore, are misleading.

The conclusion that frequency modulation permits successful operation with noise levels so high as to preclude the use of conventional amplitude modulation equipment, was arrived at in a very practical manner—acceptable operation was not obtainable with 10 watts of amplitude modulation and was obtained using a 2-watt frequency modulation unit. When it is understood that a high signal-to-noise level is desired, it is evident from Table II of the paper that frequency modulation equipment gave a more acceptable ratio with an output of 0.2 watt than did the full 10 watts of amplitude modulation.

The authors restricted themselves in this brief description of the field tests to the portion of the data that would be of wide interest and of practical value. The variation in the frequency modulation carrier signal was more than 100 to 1, which the authors considered to be large (the frequency modulation equipment had a rated output of 25 watts; the comparison terminated at 10 watts which was the maximum rating of the available amplitude modulation equipment).

From the preceding explanation and the first paragraph of the paper, it should be evident that this section of line presented very unfavorable noise conditions, markedly so as compared with several other line sections on this same system. The representative data included in the paper cover smaller signal strengths than were of any practical operating value even for the frequency modulation equipment. As a matter of fact, some of the unreported tests extended to signal strengths at which the amplitude modulation signal was completely unintelligible, while the frequency modulation signal remained intelligible, and none of these tests indicated to us the opposite of any of our conclusions.

The frequency modulation equipment did use pre-emphasis, and the amplitude modulation equipment did not. There was available for these tests neither amplitude modulation with pre-emphasis nor frequency modulation without it. It would be interesting to see comparable field data taken with amplitude modultion equipment using pre-emphasis.

The loss in signal-to-noise ratio resulting from the lowering of the Q of the receiver line tuning equipment was so small that no additional discussion of this point was included in the paper. While it is true that flattening the carrier frequency response curve of the receiver line tuning equipment does reduce the magnitude of the received carrier signals, it also reduces the magnitude of noise voltages at the same frequencies. Only the noise voltages near the carrier frequency are important as the tuned circuits in the receiver will reject noise signals of other frequencies. Therefore, the reduction in received carrier signal does not result in a significant loss in signal-to-noise ratio.

Characteristics of a 400-Mile 230-Kv Series-Capacitor-Compensated Transmission System

Discussion and author's closure of paper 46-196 by B. V. Hoard, presented at the AIEE Pacific Coast meeting, Seattle, Wash., August 27–30, 1946, and published in AIEE TRANSACTIONS, 1946, pages 1102–14.

R. D. Evans (Westinghouse Electric Corporation, East Pittsburgh, Pa.): This is an interesting and valuable addition to the art of long-distance transmission. It should be considered in connection with an article by S. E. Schultz.[1] Hoard in his paper deals with the technical problem of long-distance a-c transmission, particularly in regard to system stability, use of series-capacitor compensation, and line relaying. Schultz in his article considers the more general aspects of the problem as to the choice of system and economic considerations. He concludes that the 230-kv a-c system with

series-capacitor compensation is one of the most promising means of obtaining low-cost long-distance transmission, and that its further investigation should be continued.

I wish to comment briefly upon the choice of system for the 400-mile transmission problem considered by Hoard. In the present state of the art it is my opinion that the a-c system is to be preferred to the d-c system because

1. The a-c system is undoubtedly more suitable for supplying a network or for supplying loads at intermediate points along the line.

2. The prospective savings with d-c transmission appear to be small.

3. The adequacy and cost of the d-c system can be established only by a large-scaled installation using rectifying apparatus, the development of which is incomplete.

The selection of the transmission voltage depends upon many factors, including the prospect of a transmission network, the availability of wood poles in the area under consideration, and the technical considerations affecting the dimensions of steel towers, line conductors, and ground wires. The choice of 230-kv transmission in preference to higher voltage may not be as advantageous in other localities, particularly when steel towers are required.

In Hoard's paper the stability limitations inherent in long-distance a-c transmission are avoided by the use of series-capacitor compensation. Series capacitors used are of the protected type with means for quickly restoring the capacitor to the circuit after fault clearing. This method of using series capacitors was described first by E. C. Starr and R. D. Evans[2] (see reference 1 of the paper). While previous papers proposed the application of series capacitors to lines of various lengths, Hoard's paper is the first devoted to a system with a 400-mile line. This system has been studied extensively with the aid of the a-c calculating board as shown by the results of stability studies reported in the paper. For a 400-mile transmission system with series capacitors, the use of two groups appears advantageous. The line-fault clearing times of $3^1/_2$ and 7 cycles appear reasonable and practical. The total time of $10^1/_2$ cycles assumed for the restoration of the series capacitor to the circuit appears commercially feasible.

One aspect of the study reported by Hoard will require further consideration, namely, the line-relaying problem on a transmission system with series capacitors. The use of the current-balance scheme seems to have the advantages ascribed to it, but it may be practicable to use other schemes. In this connection, the detailed data in the paper as to the operating voltages and currents at relay locations should be of great value.

The assumptions made by Hoard for the stability and relaying studies on the 400-mile transmission system undoubtedly were based on prospective developments of the Bonneville system. However, these assumptions are widely applicable. More specifically, the assumed layout takes into account the impedance of a hydroelectric generating station, a sectionalized double-circuit transmission line with two intermediate series capacitors, and a receiver step-down station with shunt load and receiver-end generators. This type of layout is more generally applicable than the one sometimes used in which the receiver is represented by a synchronous motor. Moreover, the type of fault assumed is that most generally accepted as the criterion of system design from the stability standpoint, namely, the double-line-to-ground fault. These circumstances increase the usefulness of the results for application to other systems.

REFERENCE

1. 500-MILE 230-KV SERIES-COMPENSATED TRANSMISSION, S. E. Schultz. *Electrical World*, New York, N. Y., August 17, 1946, pages 70–1.

S. B. Crary (General Electric Company, Schenectady, N. Y.): Although previous papers have indicated the general possibilities and field of application of series capacitors for long transmission lines, Hoard's paper properly and clearly points out some of the important problems involved in protection, control, and line relaying. This is a natural result of getting down to a specific case. The author is to be commended for presenting this type of analysis.

Somewhat different conclusions as to the relative importance of the various factors may have been obtained if the conclusions had been based more on simultaneous fault clearing than on sequential fault clearing. Simultaneous fault clearing is even more important for the type of line studied than for conventional uncompensated lines and therefore should be considered a necessary requirement. It was natural, however, for the author to make his study based on equipment which generally is known to be available such as balanced current protection. If simultaneous fault clearing is used, the following results may have been obtained as contrasted with those results of the author based on sequential fault clearing:

1. Lower-than-normal generator reactance and higher-than-normal generator inertia should be used to reduce the required line compensation for a given line loading. Lower reactance becomes more important than higher inertia with the reduction in total fault clearing time obtainable with simultaneous clearing.

2. For a given line loading and distance, the compensation required becomes less with simultaneous fault clearing. A further reduction in the required capacitor kilovolt-amperes and line compensation can be expected also by the use of low-transient reactance generators.

For these reasons, the author's total required amount of compensation as well as the percentage increase required to allow for nonremoval of the capacitor during the transient may be actually somewhat larger than necessary. A further reduction in allowable compensation is in the direction to simplify and make more practical the use of series capacitors.

In conclusion, simultaneous fault clearing rather than sequential fault clearing leads to such important advantages and tends to change the basic relation between the important system design factors to such an extent that it must be considered one of the more important requirements of a series-compensated long-distance transmission system.

For a single-circuit line rather than a multi-circuit line, the relaying and protection difficulties for series compensated lines largely disappear. This type of installation may find application for other cases not requiring a firm power supply with as high a reliability factor as can be obtained with a double circuit line.

Controlled intermediate synchronous condenser compensation should be studied also along with the use of series capacitor compensation and it is hoped that Hoard will extend his studies to include this type of compensation too.

Sherwin H. Wright (Ebasco Services, Incorporated, New York, N. Y.): This paper on a series-capacitor-compensated transmission line is interesting and suggests some questions, the answers to which, I believe, will add both interest and value.

This paper gives operating results to be expected on a particular system, providing certain assumed conditions can be satisfied by development of special apparatus. If apparatus development is successful to the extent that the new problems encountered in series-capacitor compensation cannot merely be solved but can be solved economically, then the data in the paper become pertinent from a practical application viewpoint.

There are thus two aspects to the solution of these new problems:

(1) Can they be solved?

(2) Can they be solved economically?

This leads to the question, "Can Mr. Hoard describe the costs or relative costs on which some of his conclusions are based?" For example, in the conclusions, it is stated that "building the capacitors to withstand the high voltages during short circuits in most cases cannot be justified," but that in some systems "even though it may be a more expensive installation, may be economically feasible where firm power is a consideration."

B. V. Hoard: Evans' discussion supplies some of the important history and background regarding the development of series-capacitor compensation for long a-c lines. He states that it may be feasible to use other relaying schemes besides the current-balance scheme assumed in the paper. I of course would like to see a relaying scheme developed for series-compensated systems. Such a scheme should produce high-speed simultaneous tripping of a faulted line under the severe operating conditions where maximum load current is often greater than minimum 3-phase fault current. We also believe that an improved protective scheme can be developed and incorporated into the series-capacitor equipment which will reinsert them into the circuit more rapidly than 3.5 cycles after the fault is cleared, as was assumed in the paper. One possibility is an adaptation of the "Marx' High-Pressure Arc Valve," which originally was developed in Europe for high-voltage, high-power rectification and inversion uses.

A part of Wright's discussion leads me to believe that I did not explain sufficiently some of the assumptions used and conclusions reached in the paper. The system selected in the study, including a fault clearing time of 3.5 cycles at the near end and 7.0 cycles at the far end of the faulted line, with an additional time of 3.5 cycles for

reinserting the capacitors after the fault is cleared, was selected as obtainable from a practical standpoint with equipment now available. However, I endeavored to point out that if relaying equipment and capacitor control equipment could be developed which would produce high-speed simultaneous clearance of the fault followed by immediate reinsertion of the capacitors, then a considerably lower value of compensation would be needed for the same transmission capability. The objective of development of these new equipments would be to obtain a system with less compensation required and lower cost for the same transmission capability.

With reference to a system design which does not remove capacitors during faults, in the body of the paper I state that if manufacturers allow twice rated voltage on the capacitors during the period of the fault, then a system having maximum fault current through the capacitors of 2.2 to 2.4 times maximum load current may use this design economically in comparison with the design in which the capacitors are short-circuited during the fault. In general, this condition can be approached if the per cent compensation is low and if the terminal equipment impedance is not too low. A somewhat higher voltage than 2.0 times normal can be built economically into the non-short-circuiting capacitors for the fault condition, because the system which short-circuits the capacitors during the fault when the voltage is greater than two times normal requires a higher per cent compensation, that is, a greater capacity impedance to obtain identical transmission capability.

I feel that the question of relative economics is pertinent but was considered outside the scope of my paper and would be too long and involved to be discussed here. This question is of major importance, and it is hoped that in the near future a member of the Bonneville Power Administration staff will be in a position to present a paper on this involved subject which will make economic and cost comparisons of compensated and uncompensated systems.

I agree with Crary in his discussion that somewhat different conclusions as to the importance of the various factors would be obtained if the studies had been based on specified system requirements of simultaneous fault clearance and upon immediate reinsertion of the series capacitors. In fact, I feel that these requirements should be perhaps the most important objectives of a series-compensated system design, and that equipment should be developed to meet these requirements. However, in making the studies, since we are engineers of an operating agency, we considered it necessary to assume a practical system which could be built and operated using the best existing equipment available. When the manufacturers can assure us that equipment has been developed which will produce simultaneous clearing of a faulted line and then practically immediate reinsertion of the series capacitors, we shall be glad to incorporate this equipment into the design because of the improved transmission capability resulting for the same percentage of compensation.

Three major objectives were in mind when this paper was written

1. To present the new operating problems produced by series compensation.

2. To show that these problems could not be solved fully by existing equipment available to the extent that something less than maximum transmission capability would have to be used until new equipment could be developed by the manufacturers.

3. To present sufficient data from studies to show that there is a real advantage resulting if this new equipment is developed and to present data regarding a compensated system's behavior during faults, including fault currents, voltages, and phase angles, so that the manufacturer's engineers could attack this problem without delay.

With respect to Crary's reference to additional improvement in capability through use of lower reactance and higher inertia generators, I agree in principle with the statement. It will be observed that a value of 33-per-cent transient reactance for generators was used in the studies, which is somewhat lower than for standard generators. However, depending on the specific problem, there may be some occasions where equivalent transmission capability can be obtained with lower cost by using a higher percentage of series compensation with standard generators as compared to the cost involved if lower reactance generators and lower percentage compensation are utilized. With the higher generator reactance of a standard generator, somewhat lower circuit-breaker duty would be obtained for faults at most locations on the system.

Sensitive Ground Relay Protection for Complex Distribution Circuits

Discussion and author's closure of paper 46-200 by Lloyd F. Hunt, presented at the AIEE Pacific Coast meeting, Seattle, Wash., August 27–30, 1946, and published in AIEE TRANSACTIONS, 1946, November section, pages 765–8.

D. I. Cone (The Pacific Telephone and Telegraph Company, San Francisco, Calif.): The persistent and successful labors of Lloyd F. Hunt described in this paper and in its predecessor[1] constitute an inspiring example of search for the best engineering answer to a problem where many variant interests are involved. It is a specific example of that professional breadth of view which engineers should seek to exemplify.

REFERENCE

1. SENSITIVE GROUND PROTECTION FOR RADIAL DISTRIBUTION FEEDERS, Lloyd F. Hunt, J. H. Vivian. AIEE TRANSACTIONS, volume 59, 1940, February section, pages 84–7.

M. A. Sawyer (Southern California Telephone Company, Los Angeles, Calif.): As noted in the paper, the ground protection system provides not only a means of promptly de-energizing a feeder in case of wire failure involving ground contact even where the contact resistance is relatively high, but it also affords an effective means of minimizing the hazard involved in the joint use of poles by higher voltage power circuits and communication facilities. Experience has shown that the amount of damage to communication plant and the hazard involved in cases of contacts by power wires are to a large extent a function of the duration of the contact and the amount of fault current. Where higher voltage joint-use is employed it is therefore important that these factors be made as small as practicable. The ability of the relay system, described by Lloyd C. Hunt, to limit the ground fault current to a low value and at the same time provide for the prompt tripping of the faulted circuits makes it particularly well-suited for such situations.

General joint use of telephone facilities and 7-kv distribution feeders equipped with sensitive ground protection was entered into in an industrial area near Los Angeles in 1937. Approximately 700 jointly used poles were involved initially, and the number has increased now to about 850. The power distribution system consists of radial feeders with no looping of feeders, and the telephone facilities are almost entirely in cable. In 1940, sensitive ground protection was installed in a semirural area in Orange County which facilitated rather general joint use of 11-kv distribution circuits and open wire as well as cable telephone facilities. Looped and radial feeders, as indicated by Figure 2 of the paper, as well as radial feeders from a source station are involved. There are at present about 1,600 jointly used poles in that area. A small amount of joint use with 11- and 16-kv feeders is employed also in two other areas. The present total number of jointly used poles with 7-, 11-, and 16-kv circuits equipped with sensitive ground protection is therefore approximately 2,500.

During the past eight years, twelve contacts between supply feeders equipped with sensitive ground protection and telephone plant occurred, the majority of which were involved at crossings rather than in joint use sections. In all cases the supply circuits were de-energized promptly and the telephone protective devices operated properly. In general, the amount of damage to the telephone plant and the resulting service interruptions were rather minor. Experience to date therefore indicates that the relay system provides a reliable means of limiting the adverse effects of accidental contacts.

Considerable effort is being directed toward the extension of both power and telephone services into the rural areas where all possible economy in line construction must be realized. Joint use of poles by power and telephone facilities is one means of reducing the cost to both parties of such construction provided the necessary safety can be obtained. Where power systems having multigrounded neutrals are involved, a satisfactory degree of protection co-ordination usually can be obtained with the protection normally employed in the power system by the application of auxiliary protectors on the telephone lines, using the power neutral as the grounding medium. Where a power circuit having only the usual relay and fuse protection does not have a multigrounded neutral, joint use is generally undesirable because low impedance grounds for the telephone protectors are not normally available in rural areas and protection co-ordination cannot be obtained. However, the sensitive ground protection system, described by Hunt, should provide a high degree of safety in such situations because it is not essential that the impedance to ground of the telephone protectors be low to insure tripping of the faulted circuit in case of contacts.

Also, with the high impedance in the small power system grounding banks, the impedance to ground in the telephone system can be relatively high without producing voltages on the telephone plant which will exceed the safe operating limits of the telephone protective devices.

Hunt is to be complimented on the development and application of a relay system which not only offers a practical solution to the problem of clearing ground faults on complex as well as simple distribution circuits, but also affords an effective means of providing a high degree of safety where joint use of poles by higher voltage distribution circuits and communication facilities may be desirable.

F. A. Cowan (American Telephone and Telegraph Company, New York, N. Y.): Lloyd F. Hunt's paper describes a power relaying system which is of considerable interest from the standpoint of limiting the adverse effects of a contact between power and telephone systems under certain conditions.

Experience over many years indicates that a factor of primary importance in promoting a high degree of safety in situations where power and telephone systems are in proximity is the speed and reliability with which the power current is interrupted if a contact occurs between an energized power wire and a telephone cable or open wire circuit. This is true whether the power and telephone circuits are on the same pole line or are involved in numerous crossings.

With multigrounded or common neutral power circuits, prompt and reliable interruption of power current in the event of a contact is usually relatively easy to secure. The neutral is an extensive well-grounded conductor which is readily available so that the telephone plant can, if desired, be connected to it at frequent intervals, directly in the case of telephone cable sheaths and through protector gaps in the case of telephone open wire. Under these conditions, the current available for operating power circuit fuses or relays in the case of a contact to telephone cable is not much less than that available in the case of phase-to-neutral short circuit, and de-energization is almost always prompt and reliable. Where the telephone circuits are open wire, similar approximate equivalence of contact current and phase-to-neutral short-circuit current can be obtained if the voltage to ground of the power circuit is above the operating voltage of the protector gaps which, at the present state of the art, is about 3 kv. Where joint pole lines are used, the connections to neutral usually can be made easily by connecting the cable sheaths or protector ground leads to vertical power ground wires; where separate lines are used the same method can be applied if joint crossing poles are used extensively.

However, where the power circuit does not have a multigrounded or common neutral, situations sometimes arise where the impedance presented by the telephone plant in the event of a contact is high enough to reduce significantly the fault current as compared to that in the event of a phase-to-neutral short circuit. For example, in some rural areas where well-grounded power secondary neutrals are not available, reliance must be placed on made grounds for grounding telephone cable sheaths and protectors and the resistance of these grounds under adverse conditions may be relatively high. In occasional cases of this sort, the current available in the event of a contact will be so limited as to cause relatively slow de-energization of power relaying and fusing systems of the conventional types.

As a result, any development such as that described by Hunt which tends to reduce the magnitude of ground fault current necessary for reliable and prompt de-energization of power circuits without multigrounded or common neutrals, tends also to facilitate the provision of a high degree of safety where joint use or numerous crossings with such power circuits exist. The telephone engineers will, therefore, I am sure, welcome the use of Hunt's scheme in those cases where its application is advantageous from the power standpoint.

Lloyd F. Hunt: The discussions presented by F. A. Cowan, M. A. Sawyer, and D. I. Cone are appreciated very much. They point out the value of mutual study on problems that are confronted by both types of utilities to render good service to the common users. It can be understood from their discussion that the small added cost for sensitive ground protection on high voltage joint use of pole lines is more than justified and is very much to the advantage of the power company if required to take alternate methods of serving, such as underground or entirely new right-of-ways.

An Electronic Frequency Meter and Speed Regulator

Discussion and author's closure of paper 46-188 by Ellis Levin, presented at the AIEE Pacific Coast meeting, Seattle, Wash., August 27–30, 1946, and published in AIEE TRANSACTIONS, 1946, December section, pages 779–86.

Godfrey T. Coate (nonmember; Massachusetts Institute of Technology, Cambridge, Mass.): Ellis Levin's paper describes an ingenious way of employing electronic circuits to make an unusual speed-measuring device. Without the aid of phototubes and amplifier tubes it certainly would be difficult, if not entirely impossible, to measure a high speed of rotation with such convenience and accuracy and without placing a mechanical load on the rotating shaft. I have read the paper with interest and should like to comment on two details of the circuits described.

In the derivation of equation 5 of the paper (the relation between frequency and the resistance R_K), reference is made to the circuit of Figure 3, and an approximation is required in obtaining the final equation. This approximation may be avoided if the derivation is made for the circuit used in the actual instrument. For this circuit, shown in Figure 4, the voltage across R_B is $2fCIRR_B$ (see equation 1) exactly as in the circuit of Figure 3, but the voltage across R_K is IR_K instead of the expression given in equation 2. Adjustment of R_K so that these two voltages have equal magnitudes then yields $2fCIRR_B = IR_K$, and from this expression equation 5 may be obtained.

The feed-back circuit used in the 6L6 amplifier of Figure 8 is interesting in that it seems to be very different from ordinary negative feedback. The 6L6 tubes operate from a 60-cycle-per-second plate voltage supply and receive a 60-cycle-per-second signal. The output of the stage is the difference of the average components of the two tube currents, and this difference is roughly proportional to the amplitude of the input signal. The feed-back voltage is not porportional to the output, but rather to the sum of the two tube currents, and its wave form is probably a series of half-sine-wave positive pulses. I never have seen an analysis of this type of feedback and should like to know more about its effect upon the amplification and stability of the circuit.

Ellis Levin: Unfortunately, the circuit of Figure 4 of the paper does not yield the exact linear equation of balance that G. T. Coate suggests, although it may appear to do so at first glance. Perhaps Coate reasoned as follows: Consider Figure 4 of the paper, but with half of the switching circuit removed; that is, eliminate for the time being V_2, R_{L2}, C_2, V_6, and V_7, as shown in Figure 1 of this closure. Then in this simplified circuit the resistor R_B conducts only capacitor discharging pulses, while the current in R_K is composed of capacitor charging pulses plus capacitor discharging pulses plus a steady component. In R_K the charging and discharging pulses flow in opposite directions, and therefore it might appear that these two transients cancel one another, leaving only the steady component and making the voltage across R_K independent of frequency. Also it might appear at first glance that the current in R_B is exactly proportional to frequency, so that the setting of R_K required to balance the output voltage to zero would be exactly proportional to frequency. Actually this is not strictly correct, for two reasons. First of all, the two transients in R_K have unequal magnitudes and therefore do not exactly cancel one another. Secondly, as a result of the location of R_K, the voltage across R_B is not strictly independent of the setting of R_K.

A closer inspection of the circuit will show that the voltage across R_B (in Figure 1 of this closure) is not $2fCIRR_B$ but rather

$$V_{RB} = fCI(R_L + R_K)R_B \qquad (1)$$

and the voltage across R_K is not IR_K but rather

$$V_{RK} = \frac{IR_K}{2} + fCI(R_L + R_K)R_K - fCI \times (R_L + R_K)\frac{R_P R_K}{R_P + R_L + R_K} \qquad (2)$$

Equating these two voltages of equations 1 and 2 of this closure and solving for f yields

$$f = \frac{R_K}{2C(R_K + R_L)} \times \frac{1}{\frac{R_P R_K}{R_L + R_P + R_K} + (R_B - R_K)} \qquad (3)$$

From equation 3, f is not exactly linear with R_K. If we plot f versus R_K for frequencies from zero to 833 cycles per second (which corresponds to a turbine speed of 100,000

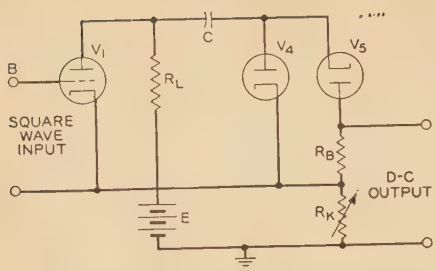

Figure 1. Circuit of Figure 4 of the paper with half of the switching circuit removed

rpm, as the input trigger amplifier halves the turbine frequency) and draw a straight line between the two end points, then the maximum deviation of the curve from the straight line will occur at approximately the mid-frequency, and will be equal to about 5 per cent of this frequency or 2.5 per cent of full scale.

Equation 3 of this closure was derived for the simplified circuit of Figure 1 of this closure. If we add the other half of the switching circuit to obtain Figure 4 of the paper we cannot say that the equation of balance for Figure 4 is exactly the same as equation 3 of the closure because the configuration of Figure 4 provides a larger number of paths for the capacitor charging and discharging currents. An exact solution of Figure 4 involves at least six different branch currents at each switching instant, and becomes rather long and cumbersome. The actual calibration curve of Figure 4, determined experimentally, is very similar to that given by equation 3 of the closure. Its maximum departure from linearity is about five per cent of full scale. However it is *accurate* to better than one-half per cent at any frequency from 83.3 to 833 cycles per second corresponding to turbine speeds of 10,000 to 100,000 rpm. By altering the circuit constants, the same accuracy can be achieved for other frequency ranges.

Specific Engineering Problems in Rural Electrification and Electroagriculture

Discussion and author's closure of paper 46-184 by M. M. Samuels, presented at the AIEE Pacific Coast meeting, Seattle, Wash., August 27–30, 1946, and published in AIEE TRANSACTIONS, 1946, pages 1065–73.

Hamilton Treadway (Rural Electrification Administration, Ashton, Md.): The lack of poles is among the problems pressing the industry at this time. The development of new methods of treatment is desirable. Effective treatments which can be applied quickly are needed to speed the delivery of poles. For those new treatments which have been introduced survivor life data are needed. This is a field in which practical methods of predetermining the average life are almost wholly lacking and performance characteristics of new treatments must be secured principally through field trials. The development of some practical testing procedures which will permit a reasonably accurate prediction of pole life will stimulate the development of new treatments and techniques.

Has there been any experimental work on the use of silicone resins in the treatment of poles and crossarms? If effective as a pole treatment, how do costs compare with existing methods? Would the use of silicones improve the insulation characteristics?

Another approach to the pole problem lies in a study of the average life of treated and untreated poles, comparing them on a basis of pole strength remaining at the end of 10, 15, and 20 years. A study of this nature will show whether it is more economical to invest in wood or in treatment. Are any data available on this subject?

The author suggests an interesting problem in proposing a statistical study of load diversity. Hamilton[1,2] and others[3,4] have shown that the load duration curve can be represented mathematically by a probability curve. In general, the characteristics of these curves are determined by the load factor and the ratio of the maximum demand to the minimum demand. The evaluation of these factors for the various types of rural loads will make possible an analysis of the economics of many factors affecting the design of lines and equipment.

The development of an inexpensive load factor meter with an attachment to record the minimum demand is a possibility. The maximum demand and the diversity factor can be determined if the load factor and kilowatt-hours are known.

The economics of voltage regulation is given also to statistical study. If the ordinates of a voltmeter chart are rearranged in descending order, they also approximate a probability curve. Here again the average voltage and the maximum and minimum values determine the characteristics of the curve. Could a simple instrument be developed to record these values? This is a different approach to the problem of voltage regulation and economics and would entail new methods of analysis. The effect of voltage regulation is an important factor in the economical operation of equipment, such as transformers, and the approach suggested here may simplify the evaluation of the economics of voltage regulation.

New industries have developed in the rural areas as power facilities have been extended. Much of the development of rural lines has been conservative, and capacity is usually lacking to serve these industries. Here again enough is not known about load characteristics. Extensive field tests are necessary to determine such factors as duty cycle, voltage and load swings, light flicker, as well as load factor, diversity factor, power factor, and minimum and maximum demands. Once assembled, these data will be useful in the design and operation of the power facilities and in improving the operating characteristics of the consumer's equipment and processing methods.

The improvement of the transformer is not static. In addition to reducing losses and weight an increase in the insulation level is desirable. The use of class *C* insulation with the new silicone binders is suggested. These insulations offer the possibility of higher operating temperatures. This may be the key to the problem of reducing core losses. By operating the core at a higher temperature it is possible to take advantage of MacLaren's effect.[5] This can be accomplished by the insertion of heat barriers. At present, further increase in operating temperatures may be limited by sludging of the oil. The development of a new cooling medium is necessary. The possibility of high-pressure gas is suggested. The difficulties encountered in its application while still unsolved are not insurmountable. High pressure gas cooling also holds out the possibility of some further reduction in weight.

What is the possibility of reducing losses by using powdered core materials? Can the permeability of such materials be increased to a point where they will compare favorably with other core materials for power transformers?

The progress of our civilization has been made possible by the free exchange of technical information and ideas. The author has suggested a multitude of engineering problems which requires the application of our best efforts. It is to be hoped that free discussion of these problems will bring out many new ideas to improve both rural electrification and electroagriculture.

References

1. Synthetic or Equivalent Load Curves, **R. F. Hamilton,** AIEE Transactions, volume 61, June section, pages 369–81.

2. The Summation of Load Curves, **R. F. Hamilton.** AIEE Transactions, volume 63, October section, pages 729–35.

3. Evaluating Diversity Factor, A Statistical Method, **B. D. Price.** *Electrical Review*, London, England, September 25, 1936, page 400.

4. Diversity and Load Factor, **D. J. Bolton.** *Electrical Review*, London, England, April 17, 1936, page 563.

5. The Effect of Temperature Upon the Hysteresis Loss in Sheet Steel, **Malcolm MacLaren.** AIEE Transactions, volume 30, pages 761–75; volume 31, pages 2025–35.

J. R. Werth (Department of Agriculture, Washington, D. C.): The author stresses the importance of continuity of service to the rural user. Demand charges promote a single source of wholesale supply and hence are detrimental to continuity. A plea is made for studies tending to eliminate demand charges.

This elimination should not be difficult to justify. Frequently the farmer co-operatives furnish the substations. Two or more sources of supply inevitably will reduce interruptions and will promote continuity. Regardless of its prior justification, today a demand charge is morally equivalent to a cover charge in a night club. You pay something for nothing. Would not any self-respecting game hen of American or of Indian descent be outraged if the egg buyer paid the farmer's wife a demand charge for readiness to lay and also an energy charge for eggs? Admit that in the remote past eggs and kilowatt-hours could not be stored readily. The modern locker plant and pondage back of the hydro plant tied into an electric grid now do store eggs and kilowatt-hours. Therefore, I present this plea that in the interest of continuity demand charges be declared out.

Why not (as John Carmody said when cyclometer dials were suggested for rural kilowatt-hour meters in 1937)?

Where? First, in most advantageous locations (as inventer, W. L. R. Emmet, invariably recommended for innovations).

When? Now, in 1947!

O. W. Gatchell (Frank Horton and Company, Lamar, Mo.): This discussion of Samuel's long-awaited paper is directed towards a simplification of the engineering design problem in the rural electrification field.

1. Use right-of-way easements that provide for possible future underground transmission or buried neutral construction, in acquiring present distribution right-of-way. This will simplify the future designer's problem.

2. A "superman" rural breaker, even with a high electrical intelligence quotient of 140 plus, is no substitute for an axe. A definite tree-trimming maintenance program simplifies the breaker's job and means that sectionalizing equipment design can be brought down to earth.

3. Samuels mentions 7,200-volt circuits. Why not standardize now on 7,620/13,150 volt rating? That voltage is as high as that which can be used below the code 15 kv ceiling, where ground clearances change. Voltage of 7,620 instead of 7,200 means 12 per cent more line capacity for the same drop; distribution transformers are identical in cost. Where else can the designer give the farmer 12 per cent more capacity for negligible outlay? All that is needed is a program to educate the power transformer manufacturer.

4. An inviting panorama of greatly increased rural use of electricity is unrolled in the author's paper. However, nothing is said about locating the transformer at the center of all of this load, between kitchen and barn. Farmstead location of the transformer will simplify present overhead and future underground secondary installation; it even could help simplify application of primary underground lead-in from the overhead line along the road, if such a development should prove to be the first practical use of single phase rural primary underground.

Max W. Rothpletz (Rural Electrification Administration, Washington, D. C.): In Table I of this discussion are some figures which portray the conditions existing in two rural distribution systems picked at random and analyzed on the basis of known data and conservative estimates.

These figures further emphasize the need for lower core losses in rural distribution transformers.

The most economical transformer design is one which provides the required quality of service for the lowest combined fixed and variable charges. Quality of service includes consideration of such items as regulation, telephone influence factor of the exciting current, and exciting current itself. On rural circuits the first two items should be maintained as low as possible, but the exciting current may be increased somewhat if necessary to gain some other desirable feature. In accordance with the definition in the Federal Power Commission glossary, fixed charges include interest, depreciation, property taxes, and property insurance. All other charges are variable charges.

Because only minor increases in transformer efficiencies can be anticipated, transformer losses must remain at about the present values, but the ratio of core to copper losses can be selected so that the total energy losses over a period of time are lower.

Table I

Type of Loss	System A	System B
Distribution transformers		
Core losses, per cent	64.3	60.3
Copper losses, per cent	9.2	9.2
Subtotal, per cent	73.5	69.5
Substation transformers		
Core losses, per cent	6.4	7.0
Copper losses, per cent	6.1	5.2
Subtotal, per cent	12.5	12.2
Meter iron losses, per cent	4.2	3.3
Line and miscellaneous losses, per cent	9.8	15.0
Total, per cent	100.0	100.0
Total losses in per cent of purchased power	24.8	21.3
Miles of line	525	1,025
Number of consumers	1,300	2,400

However, it may not be practical to design for the lowest energy losses because the cost of equipment may be increased to the extent that fixed charges are increased more than the variable charges are reduced. A formula has been derived to show the relationship between core and copper losses and the additional money which may be spent on equipment to obtain the desired characteristics.

Since copper losses vary as the square of the transformer load, the total energy losses depend on the load curve. If instantaneous values of copper losses are calculated for a particular load curve, a loss curve may be drawn from which a loss factor showing the ratio of average losses to peak losses may be derived. Then if

L is the loss factor in per cent
R is the energy cost in cents per kilowatt-hour
F is the fixed charges in per cent
C is the decrease in core losses in watts
W is the number of watts of increased copper losses at peak load

the permissible additional investment in equipment, P, is given by

$$P = \left(C - \frac{LW}{100}\right) 8.76 \left(\frac{R}{F}\right) \text{ dollars}$$

For demonstration purposes an assumed transformer load curve was analyzed and found to have a loss factor, L, of 10.9 per cent. Assuming, for simplicity purposes, that R = \$0.009 and F = ten per cent, an additional transformer investment of \$0.70 would be permissible if the core losses could be decreased one watt with an increase of one watt of copper losses at peak load. If the design required that the copper losses be increased two watts at peak load the permissible additional investment would be \$0.61.

When a transformer load curve is not available for determining the loss factor, the minimum permissible additional investment can be calculated by the same formula using the load factor. The load factor of the transformer used in the aforementioned example was found to be 23.4 per cent. Using the same assumptions as mentioned previously, a minimum additional investment of \$0.60 would be permissible if the core losses were decreased by one watt with an increase of one watt of copper losses at peak load. If copper losses were increased two watts for one watt decrease in core losses the minimum permissible additional investment would be \$0.42.

In selecting a transformer size for an individual load, it is important to make sure that it will not be too large for a long time to come, not only because of the first cost but also because of the core losses.

For example, a one kva transformer is estimated to cost \$34.00. A $1^1/_2$ kva conventional transformer costs approximately \$39.00. If the load is not expected to increase over and above one kva, the $1^1/_2$ kva size would represent an unnecessary investment of \$5.00. Furthermore, the losses of a one kva transformer are about 10 watts core and about 50 watts copper; at 1 kva load the losses of a $1^1/_2$ kva unit are about 21 watts core and 20.5 watts copper. Based on the same assumption as in the previous example, using the one kva transformer the saving in losses would be equivalent to saving a further additional investment of \$6.13. If the savings in losses had been calculated on the basis of the load factor of 23.4 per cent a minimum savings in investment of \$3.24 would have been indicated.

M. M. Samuels: The discussions were somewhat disappointing because of the lack of more constructive ideas. Rothpletz's elaboration on the core loss problem is very much to the point. A suggestion may be added for the rate man. At present the core losses are billed wholesale under the most expensive demand block and the most expensive energy block. Should not the core losses be deducted from the total demand for billing purposes and should not the energy be billed at the lowest rate per kilowatt-hour?

Treadway raises the question whether or not anyone has experimented with the use of silicone resins for the treatment of poles and crossarms. An inquiry among specialists in this field did not reveal any such experiments so far. Those who had any experience with attempts to make demand diversity studies will all agree that Treadway's proposed method will not solve the problem. Such a study, to be of any value at all, would call for an investment of great sums in recording meters. It would have to be carried out over long periods and diversified in difficult climates. After spending all that money on survey and analysis, the conclusions, if any, would be very likely obsolete by the time the work would be finished. Treadway's other suggestions are recommended for consideration by manufacturers. No doubt manufacturers already have studied these features.

Gatchell suggests that rural circuits be standardized at 7,620/13,150 volts. When big time construction of rural circuits began, it was found that the price of equipment, particularly transformers, jumped considerably at the 12,500/7,200-volt level. At that time no one predicted that the load would grow as it actually has grown. This voltage was then the most economical. In fact, many engineers were of the opinion that it was too high a voltage and suggested continuing the use of 2,300 volts which was then the most common voltage of rural circuits. Now, it would be difficult to change the voltage of hundreds of thousands of miles of line. The problem of improving the rural circuit is being studied everywhere now, and the studies will result undoubtedly

in great improvement everywhere. Consideration is being given to additional sources of power at various places on a rural system, backbone lines of higher voltages, series capacitors for voltage regulation, and other methods.

As the cost of overhead construction increases, the difference in cost between overhead and underground may become less pronounced. Cable manufacturers are engaged now in elaborate studies of possible underground primaries for rural circuits. Gatchell's other suggestions deserve serious consideration.

Silicone-Resin-Treated Magnet Coils

Discussion and authors' closure of paper 46-104 by Graham Lee Moses and Julius J. Torok, presented at the AIEE summer convention, Detroit, Mich., June 24–28, 1946, and published in AIEE TRANSACTIONS, 1946, July section, pages 412–16.

B. W. Erikson (General Electric Company, Schenectady, N. Y.): The authors have introduced what they call the K factor. We agree that this is a very useful method of evaluating coil deterioration under certain conditions. However, we would like to point out that a consideration of this K factor may be misleading when considering designs involving different types of insulation. For instance, we have found that on conventional class A insulated coil structures at normal operating levels there is often no appreciable change in the K factor even when the coil has fallen apart completely as a result of prolonged operation at high temperature.

However, and this is significant, all good insulation systems insulated with silicone, or possibly with high temperature synthetics, show a marked change in the K factor with temperature-time aging. This may be taken to indicate that where the coil impregnant contributes materially to the original excellent heat transfer rate of the system an ultimate large change in the K factor should be expected. Much work remains to be done in exploring and evaluating this relationship.

With reference to the section entitled "Effect of Operating Temperature on Design," the authors refer to Figure 8 and indicate that this shows ampere turns at various levels of coil temperature rise. It seems to me that this is too general and perhaps not directly applicable to a large variety of d-c contactor coil designs similar in nature to those coils referred to in this paper.

To illustrate, I made a comparison some years ago between the ampere turn gain or loss occasioned by changing a design from either enamel wire insulation or enamel-cotton insulation to either glass or asbestos insulation. It became evident from this survey that there is no gain whatever in the finer wire size. Comparing asbestos and double glass with enamel there was found to be no ampere turn gain on designs using wires smaller than approximately 0.075-inch diameter.

In making this same comparison with enamel-cotton insulated wires there was found to be no appreciable gain below about 0.040-inch diameter. Included in this comparison was the fact that the class B designs were operated at a temperature 20 degrees higher than the class A. This confirms the authors' statement that there is little if any gain in the use of conventional class B designs as compared with class A unless the temperature level can be increased materially above the 145-degree-centigrade total of class B.

Where these facts are applied to conventional d-c contactor and relay designs, it is difficult to see where any gain in ampere turns or size of coil is to be made. Common 125- and 250-volt d-c coils such as those discussed in this paper, use wire sizes ranging from approximately 0.007 up to and including 0.014-inch in diameter. Comparing the space requirements of these small diameter wires between those insulated with conventional enamel and those insulated with either single or double glass, we find that 0.010-inch-diameter wire if insulated with single glass requires 168 per cent of the space taken by enamel, and 0.014-inch-diameter wire if insulated with single glass requires 145 per cent of the enamel wire space. On this basis the silicone coils would

1. Produce for the same ampere turns approximately 50 per cent more watts.

2. Operate at a temperature approximately 50 per cent higher merely to break even.

If I interpret this correctly, it would mean that silicone designs would have to operate in the neighborhood of a 125-degrees-centigrade rise (this would be the class-A 85-degree rise plus 50 per cent equals 125 degrees centigrade) so as to compare in performance with conventional class A.

Any higher operating limit would produce a gain in ampere turns. I believe that this particular point, even though contained between the lines in the paper, needs some additional emphasis and further consideration by design engineers.

Carl J. Fechheimer (consulting engineer, Milwaukee, Wis.): There are a few points to which I would call attention.

In regard to the dissipation of heat, it is of interest what part of the temperature drop is inside the coil and what part is at the surface. Also, what are the maximum internal temperatures?

It generally is recognized that there is a limit of stability when coils are operated at high temperatures when the current is kept constant. For as the temperature rises, the electrical resistance increases, and therefore the I^2R loss increases. This in turn raises the temperature further, and at some critical value the temperature will rise without limit. As the heat is dissipated from the surface by radiation and natural convection, both of which increase more rapidly than the temperature, these effects offset somewhat the effect caused by increase in resistance and raise the stability point. As 2-dimensional heat flow and heat storage must be considered, the problem becomes very complex. Have the authors investigated the thermal stability of the coils, either experimentally or theoretically?

The mounting resistance with temperature also means that before the stability point is reached, the most economical point of operation is passed from the standpoint of the materials and from that of the power consumed. Have the authors made an investigation of the most economical point?

If the coils are operated in shunt with the supply line, the ampere turns decrease as the temperature increases. Then the I^2R decreases with mounting temperature, and the question of stability does not enter. Or do the authors propose to increase the applied voltage so as to maintain constant ampere turns? If not, if the pull of the magnet is proportional to the square of the current, the pull of a shunt magnet coil is approximately only 36 per cent at 200 degrees centigrade of that which it is at 25 degrees centigrade. Is that not a serious decrease?

L. A. Doggett (Pennsylvania State College, State College, Pa.): Improvement of magnet coil design is important because of the millions of such coils in industrial use. To meet specifications with an ever decreasing amount of active material has been the long standing objective of the design engineer. The new silicone insulations provide a long step in this direction.

The reduction in copper weight as the temperature rise is allowed to increase is shown in Figures 9 and 10. Not all of this gain, however, may be chargeable directly to the real advantages in the use of silicone insulations. If it is assumed that temperature rises of 160 degrees centigrade may be used safely with silicone insulation, then to provide the ampere turns specified in these coils the length of the coil may be reduced about 19 per cent keeping the outside diameter at three inches. Similarly if the coil length be kept at $3^1/_4$ inches, the coil diameter may be reduced about 15 per cent. The weights in these two cases are reduced correspondingly some 19 and 38 per cent. Coincidental with these size reductions is an increase in the ratio of total coil surface to coil volume of 9 and 23 per cent. For many years transformer designers have been familiar with the general fact that the smaller the transformer volume the greater is the ratio of surface to volume. For example, a cube with a 2-foot side has a surface-to-volume ratio of three to one, whereas a cube with a 1-foot side has a surface-to-volume ratio of six to one.

Summarizing, it may be said that by using silicone insulations, coils may be made smaller, and because they are smaller they can be worked harder.

J. M. Fluke (Anderson Fluke Engineering Company, Springdale, Conn.): The authors are to be complimented for this paper and the extensive amount of test work which has gone into the data presented. Without question the silicone-glass insulating materials represent a very marked improvement over materials previously available. The United States Navy Bureau of Ships has made an effort to exploit the use of these new materials as fast as they have become available and to carry their application to the maximum extent possible for the immediate purpose of learning more about their properties and for the ultimate purpose of increased reliability and weight and space saving. With the

co-operation of industry there are on order equipments and development programs covering nearly every type of wound electrical apparatus ranging from small motors through generators as large as 1,250 kva at 450 volts alternating current, transformers, and welding sets. In addition, the use of silicone-glass materials in producing highly arc resistant and stable sheet and molded insulating material is receiving concentrated attention.

Present tentative proposals provide for operating temperatures of silicone-glass insulated electrical machinery as high as 200 degrees centigrade total temperature. Weight savings on transformers run as high as 30 per cent with savings approaching this value on rotating apparatus.

It is apparent then that this new insulation offers appreciable advantage to the electrical plant in naval vessels in view of the ever increasing necessity of weight reduction. In addition, as these materials improve in quality as a result of the continued effort toward improvement of their characteristics and methods of application, materially increased reliability of the apparatus in which they are used will be realized. In fact it is safe to say that the improvement in this respect is sufficient to warrant intensive interest if no weight or space saving were involved at all.

In specific comment on this paper, several points are worthy of additional mention. Under the tentative temperature limits now being used, a 40-degree-centigrade allowance is made for hot spot temperature when measurements of temperature of a silicone-glass insulated coil are made by thermometer, and a 20-degree-centigrade differential is made when resistance determination of temperature is made. It is felt that these figures require additional investigation. It is quite probable that for many applications they are too large. In particular it is suspected that this is true for magnet coils of normal size. This statement is based on measurements made some time ago with thermocouples placed in coils operated at class *A* insulation temperature where the maximum observed temperature differential through the coil did not exceed several degrees centigrade. A much larger allowance previously made for this condition could be reduced through this knowledge which in turn effected some saving of weight and material so necessary during wartime construction. It is recommended therefore that future life tests of silicone-glass insulated devices incorporate suitably placed thermocouples for obtaining more data in this respect. This information will be particularly pertinent to the "Conclusions and Recommendations" given by the authors in their paper.

It is noted, but not conclusively, that a suitable means of preventing the oxidizing of copper may be a necessity in the ultimate satisfactory application of the silicone materials. Several premature failures of equipment have been traced to the possibility of failure because of the reduction of copper cross section from oxidation. Additional test work is necessary to establish this statement definitely. However, the continued development of silicones may allow even higher operating temperatures. To meet this possibility there is need for further investigation of this condition and the development of suitable means for its prevention by plating, preferably, as the authors suggest.

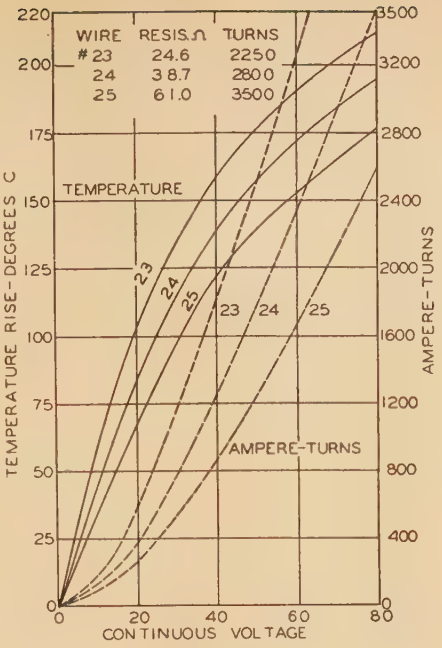

Figure 1

In conclusion, it is considered that the availability of silicone-glass insulation is one of the most significant insulation developments since the art began. Its widespread use in the not too distant future is a certainty. The versatile silicones are only in their comparative infancy. So far they have been employed successfully as varnishes, fluids, and resins for producing all types of electrical insulation. Combined with glass cloth or fibers, they produce highly stable molded and sheet insulation. The silicones also have performed excellently as lubricants at elevated temperatures. Their full application possibilities still are to be realized.

Graham Lee Moses and Julius J. Torok: The coils reported were shunt windings. Therefore no checks were made to determine "run-away" temperature conditions such as Carl J. Fechheimer suggests. It would be desirable to make such tests on series coils with silicone insulation.

No determination was made of temperature distribution on the coils reported. However, on similar coils it has been found that the average surface temperature rise is approximately 60 per cent of the internal rise by resistance and that the hot spot is within ten per cent of the average rise by resistance.

The change in the *K* factor is a useful means for observing aging where it occurs. It is recognized that this change in *K* does not occur necessarily on all types of coils, particularly on coils which have little or no varnish fill. As indicated by B. W. Erikson, much work remains to be done in exploring and evaluating this relationship. It is hoped that other investigators will study this problem.

The curve in Figure 8 shows the effect of operating a specific design of coil (the one used for these tests) on various voltages which produce different temperature rises. It shows the resultant hot ampere turns after temperature stability is reached. To supplement this a curve has been prepared showing actual values of temperature rise and ampere turns as a function of operating voltage for three different designs for the same spool (differing only in wire size). This curve shows that a coil wound with number 25 wire rates 52.5 volts at 85 degrees centigrade rise (by resistance) and produces 2,270 ampere turns (hot). The corresponding design of coil with number 24 wire would have a temperature rise by resistance of 121 degrees centigrade when operated at the same voltage and would produce 2,580 ampere turns (hot). Thus the increase in net ampere turns (hot) is 13.8 per cent. The increase in cold ampere turns is 26 per cent before the coils heat up to operating temperature. A design of coil with number 23 wire would operate at 170 degrees centigrade rise (by resistance) at the same voltage (52.5) and would produce 2,910 ampere turns (hot). This is an increase of 28 per cent over the coil with number 25 wire.

The lack of a silicone wire enamel is a distinct handicap in the development and application of silicone insulated magnet coils especially for finer wire sizes. It is recognized that glass wire covering has a poor space factor. The paper states that on finer wire sizes no gain may be possible. However, generalizations should be avoided and specific designs should be considered before deciding whether or not high temperature insulation offers advantages. It has been found possible to obtain an appreciable increase in ampere-turn rating with class *H* insulation on coils which use wire sizes of number 30 (0.0100 inch diameter) or even finer.

As stated by L. A. Doggett, the increase in ratio of surface to volume is a distinct advantage in heat dissipation. This was not included in the calculations made for this paper as it was assumed that all the heat was dissipated from the barrel surface. Therefore, in the size and weight advantage to be derived from high temperature, silicone insulation may be even greater than indicated by the curves shown in Figures 9 and 10.

Operating Experience With Distance Ground Relays

Discussion and author's closure of paper 46-83 by W. A. Wolfe, presented at the AIEE summer convention, Detroit, Mich., June 24–28, 1946, and published in AIEE TRANSACTIONS, 1946, July section, pages 458–62. This paper also was presented at the South West District meeting, San Antonio, Tex., April 16–18, 1946.

Eric T. B. Gross (Illinois Institute of Technology, Chicago, Ill.): Though both reactance type relays and their proper connections for ground fault distance protection have been available for about 20 years, distance relaying has been applied in the past nearly exclusively for between phase faults, involving more than one conductor of the 3-phase system. W. A. Wolfe therefore is

covering new ground, and he deserves commendation for his courage to try a new thing and congratulations on his success. It will be to the advantage of the art if engineers learn from this paper how easily satisfactory results can be achieved; after all, with the majority of faults being single line-to-ground faults (84 per cent in this case), it is evident that proper protection will provide great improvements.

Wolfe's analysis of the reasons for use of the distance ground relays are truly sound, and it is gratifying to see that the application of resonant grounding through ground fault neutralizers duly was considered. A voltage of 60 kv is definitely one at which ground fault neturalizers, preferably designed for continuous operation, could be applied very successfully.

The installation described in the paper, designed more than seven years ago, consists of three distance phase and three distance ground relays. It is possible to reduce the number of distance elements by proper control of the current and voltage connections of the relay scheme as described in references 3 and 4 of the paper. With the knowledge of our present day developments in the field of relaying, it should be easy to design a distance relay scheme, including ground fault relaying, which does the job with less than six distance elements and without increase in tripping time.

R. E. Cordray (General Electric Company, Philadelphia, Pa.): We believe that W. A. Wolfe has done the industry a great service in presenting his operating experience with ground distance relays, and we are particularly pleased to learn that he has ten terminals of *GCX* relays. I was pleased to be a member of the relay subcommittee which recommended that this paper be presented at the national meeting after it had been presented at the South West District meeting because I think that the subject matter warrants it.

We do not understand why ground distance relays have not been more popular. They have been in the catalogues of manufacturers for almost a decade, yet their use has been limited. The scheme as it stands now is as simple as phase relaying with the exception of the blocking units for preventing false operation on 2-phase-to-ground and phase-to-phase faults. Another exception of still less importance is providing for mutual compensation when it is required by parallel lines. The scheme should be kept simple, at least until ground distance relays become the accepted practice. This may be the answer to Doctor Gross's question about using one relay and switching it. We realize some possible excuse for expecting ground relays to be relatively simple and inexpensive as a result of the common use of a single overcurrent relay for ground protection. This has led relay engineers to believe that one relay should take care of all ground faults. When a directional ground relay was required, however, three potential transformers generally were required and the cost of the third potential transformer makes it about equal to the phase relaying cost.

Another possible influence in the use of these ground relays was the idea that ground faults are not as severe as phase faults and do not cause as much burning of the conductor by the arc nor lead to system instability. Accordingly it was permissible to take relatively long time delays for clearing. However, as one of the discussers said, they have found that faults will burn through two and three strands of 7-strand conductor and make it too weak mechanically to be trusted. Such burning would not be experienced with high speed clearing of ground faults.

As the author states, ground faults are in the majority running from 80 to 90 per cent of the total faults, and therefore it seems unreasonable that the cost of ground relaying should be expected to be only 10 to 20 per cent of the total relaying cost.

S. L. Goldsborough (Westinghouse Electric Corporation, Newark, N. J.): It is interesting to learn of W. A. Wolfe's experience with distance ground relays. His satisfactory results indicate that the applications were made carefully and that the limitations of distance ground relays were not exceeded.

Present day distance ground relays are subject to certain characteristics which have prevented wide application. These characteristics come about from the necessity of using a reactance distance element and the nature of ground faults. To measure distance on ground faults adequately, the reactance element is operated with a mixture of line current and residual current. In order to prevent response of the reactance element to load currents when the apparent reactance is small or negative, it is necessary to use a supervising impedance element. This impedance element must be set for the longest distance possible in order to allow the reactance element to function on faults involving high resistance, and yet not itself respond to load current. In other words the reach of the reactance element is limited by the reach of an impedance element. Where load currents are relatively high as compared to minimum fault current, this is a definite limitation.

A further limitation comes about from the action of the reactance element on 2-phase-to-ground faults. On this type of fault two relays receive fault current; one relay extends its reach and the other one restricts its reach. Since it is not possible to predict safely which relay will restrict its reach, it is necessary to arrange the impedance fault detector so that if more than one impedance element operates all three relays are blocked from tripping. This feature gives rise to the second limitation because it often happens that a single-phase-to-ground fault causes fault current to flow on all three phases, thus operating all three impedance supervising elements which block tripping. Therefore the reach of the reactance element is limited not only by load current, but by actual fault current.

Evidently the foregoing limitations were not exceeded in the applications made by Wolfe, but in any general application of distance ground relays these characteristics must be borne in mind.

Ben C. Hicks (Shawinigan Water and Power Company, Montreal, Quebec, Canada): About 20 years ago the Shawinigan Water and Power Company started to use impedance relays for single wire-to-ground faults on transmission lines. For this purpose phase-to-ground voltage has been used with either phase current or neutral current, depending on which is likely to give best results as indicated by calculations. This method of protecting against ground faults was adopted as a practical expedient and has proved to be reasonably satisfactory. The limitations of the method are recognized and admitted, however.

About three years ago serious consideration was given to converting a number of existing ground protections to the compensated form discussed by W. A. Wolfe. Authority was obtained to proceed with the conversion on two lines but because of pressure of other work the change has not been carried out yet. We therefore are interested very much in the results obtained by Wolfe.

In his paper Wolfe states that the second term in equation 3 represents a voltage in phase with the fault current. Presumably this statement is intended merely as an approximation and I would like to ask if the cases of overreaching that occurred are considered to be caused by errors arising from the approximation.

W. A. Wolfe: As Eric T. B. Gross suggests the use of two distance relays to do the work of six certainly would be attractive, especially on less important lines. It is difficult to see how the number of relays could be reduced without some increase in tripping time since the auxiliary switching relays for current and voltage first would have to recognize the fault and establish the proper connections to the distance elements before they could act to trip the breaker.

W. H. Cordray's discussion was welcome as coming from one of the manufacturers of distance ground relays, and it was gratifying to know that he agreed with the statements in the paper. On our system the use of high speed distance relays has resulted in very noticeable decrease in conductor and insulator damage from power arcs.

It is unfortunate that discussions were not received from some of the other users of distance ground relays, of which there are a few if not many. A letter from one such user indicates that their first three years experience with five sets of *HX* distance ground relays resulted in only 50 per cent correct operations. The author cannot help but believe that there was something wrong with the application or installation in this case.

S. L. Goldsborough presents an interesting discussion on the limitations of distance ground relays, most of which were mentioned in the paper. We do not consider the use of a reactance element instead of an impedance element a disadvantage except for the added complication in testing procedure when the phase relays are impedance and the ground relays reactance. When both phase and ground relays are the same, there is no disadvantage in this respect. Distance ground relays should not be applied in regions were high ground resistances prevail. In our territory we would expect no difficulty even on lines without overhead ground wires. On the type of relays having nondirectional impedance starting units, the danger of blocking tripping by fault currents flowing in the unfaulted phases is always a danger and must be checked by careful calculations before the relays can be applied safely. On the type of relays in which the impedance starting unit has an inherent directional characteristic, this danger does not exist as far as we know.

Ben C. Hicks asks a question in regard to equation 3. The second term is an approximation but, for all practical purposes, a close approximation. This term has the effect of pure resistance if $(I_{aGF} + I_{aHF})$ is in phase with (I_{relay}). In the usual case, all the impedances involved in equation 2 will have nearly the same phase angle unless the line resistances are very large. Also, since I_{aGF}, I_{0GF}, and I_{0GH} are usually nearly in phase for this type of fault, this will be nearly true. Probably variations in this term and the difficulty in determining exactly the amount of zero phase sequence compensation to apply, as expressed in the second term of equation 2, were the cause of the overreaching which we experienced. As stated in the paper, however, it was only necessary to decrease the distance setting of the relay to 85 per cent of the line length to prevent overreaching.

An error appears in equation 2 as published in AIEE TRANSACTIONS. The second term should be $I_{0GF}\frac{Z_{0GH} - Z_{1GH}}{Z_{1GH}}$ instead of $I_{0GF}\frac{Z_{0GH} + Z_{1GH}}{Z_{1GH}}$.

Improvements in Performance of Hydroelectric Generating Units on the 2,000,000-Horsepower Saguenay System

Discussion and author's closure of paper 46-144 by F. L. Lawton, presented at the AIEE summer convention, Detroit, Mich., June 24–28, 1946, and published in AIEE TRANSACTIONS, 1946, pages 900–10.

J. F. Roberts (nonmember; Allis-Chalmers Manufacturing Company, Milwaukee, Wis.): F. L. Lawton has presented a very interesting and instructive paper. The combined Isle Maligne and Shipshaw plants form one of the largest concentrations of hydroelectric power at the present time. The speed of construction on the final Shipshaw plant, which placed 12 100,000-horsepower generating units into service, was a record as regards construction time.

The remarkably high efficiency of 94.4 and 94.5 on two of the eight Allis-Chalmers turbines in Shipshaw 2 plant we attribute not only to the smoothness of the welded plate-steel spiral casings, but also to the excellent water passages which were provided by the construction forces of the Aluminum Company. The penstock connection to the turbine comes in horizontally without any bends or elbows to cause disturbances. This is a powerful factor in increasing the efficiency of the turbines. The elbow draft tubes have a vertical length below the runners somewhat greater than is usual practice. This was possible because the rock foundations were somewhat lower than previously anticipated, and they were able to take advantage of this and build a more efficient type of draft tube without appreciable additional expense. These factors, we believe, contributed toward the high efficiency obtained.

Lawton's data showing the amount of metal removed from the various runners at the Isle Maligne plant also form a very interesting contribution. The amount of cast steel lost per year per runner runs from one-third to one-fifth of that lost by the cast-iron runners. This confirms other data and proves conclusively the superior performance of cast steel over cast iron.

It generally is admitted now that runners having the physical dimensions of Isle Maligne runners and operating under heads of 110 to 120 feet should not be made of cast iron. During the past few years a considerable number of large cast-iron runners have had to be replaced principally because of cracks that have developed where the blades join the upper crown. Cast iron lacks the ductility and toughness to resist the repeated bending action which occurs in runners of this size. During the original construction of the Isle Maligne plant it was necessary to economize wherever possible, and the fact that these cast-iron runners might have a shorter life than more expensive cast-steel runners was discussed openly. The maintenance men at the Isle Maligne plant have done a wonderful job in being able to keep these cast-iron runners in operation, as several of these runners have cracked near the crown, and if they had not been repaired properly these cracks shortly would have extended clear through the blades, with the total loss of the runner.

With our present knowledge of the shortcomings of cast iron, we doubt if any manufacturer or builder of large hydroelectric plants would consider installing a cast-iron runner at the present time. Lawton is to be complimented on an excellent paper which contains very valuable and interesting data.

H. R. Sills (Canadian General Electric Company, Peterborough, Ontario, Canada): F. L. Lawton has given some interesting data with regard to loss of capacity resulting from fouling of the machines. The curves shown in Figure 10 of the advanced copy do not conform in shape with loss curves or normal heating curves. In such heating curves, the temperature rise usually varies as the square of the load above a certain minimum determined by the no-load temperatures. The curves in this chart seem to vary as the square root of load, and if extrapolated to zero load would have a negative temperature rise.

It is apparent that there must have been error in making up this chart, which is to be regretted. There is need of published data on the effects of dirt in machine cooling passages.

It seems inevitable that there will be a significant proportion of machines built where the service conditions do not justify the installation of an enclosed ventilating circuit with air coolers, and in these the problem of maintaining the cooling efficiency with contaminated air still will be a serious one.

In respect to the machine in station 2 mentioned in the third last paragraph of the paper from which the large amount of dirt was taken from the inside of the rotor, it should be said that this was not the normal type of dirt which accumulates in service but consisted of cement dust and lint picked up during the construction of the power house. At this time this machine was arranged for open ventilation to provide a modicum of heat before there were any end sections in the power house.

The machines in station 2 had self-lubricated bearings and therefore were not plagued with oil vapor leakage, which almost invariably occurs on the older machines with an oil-circulating system. It is probable too that because of the prevailing conditions, the normal quota of honey bees and such viscous insects did not get into the machine to plug the ducts. Anyone who has driven far on a summer night will appreciate the adhesive qualities of certain insects.

Thus, while the cooling passages of the machine in station 2 were surprisingly clean (considering conditions), and the cooling performance was unimpaired, it hardly would be correct to say that it was a fair test. The general supersedure of the oil-circulating systems in machines by self-oiling systems will go a long way toward mitigating the cleaning problem. If the type of ventilation used at station 2 is as successful in separating out flies as it was dust and lint, some further improvement may be expected by this means.

R. A. Hopkins and **H. J. Petersen** (nonmember; Tennessee Valley Authority, Knoxville, Tenn.): It is noted that the original cast-iron runners at Isle Maligne were repaired by electric welding. It will be interesting to know what preparations were necessary and what methods were used in welding this cast iron. If stainless-steel rod is used for repairing cavitated areas, either on the original cast-iron runners or the later cast-steel runners, it will be helpful to know the analysis of the rod.

It appears that the specific speeds of the Isle Maligne and the Shipshaw 1 units bear about the same relation to the experience curve of limiting specific speeds, yet the Isle Maligne units cavitated much more than the Shipshaw 1 units. The author may have an explanation for this.

It is interesting to note that experience with open ventilation of the generators at Isle Maligne and at Shipshaw 1 indicated the use of closed ventilation at Shipshaw 2. As a parallel case, the eight generators of the original Muscle Shoals plant, built by the Army in 1925 and now operated by the Tennessee Valley Authority, have open ventilation. When a rotor of one of these machines is removed for other reasons, the stator is cleaned by air blast and scraping of the air passages, much as described by the author. A canvas hood is placed over the stator and exhausted upstream by a large vent fan to avoid contaminating other machines.

The 43 new units installed by the Tennessee Valley Authority at this and other plants have closed ventilation. Electric heaters are provided in the generator rooms to avoid opening the generators even during cold weather. Cleaning of these closed machines is required only occasionally and is done by a vacuum process at almost negligible expense as compared with the cleaning of open machines.

E. B. Strowger (nonmember; Buffalo Niagara Electric Corporation, Buffalo, N. Y.): The author has pointed out a number

of improvements which have been made in the hydroelectric generating units of the Saguenay system, including both electric and hydraulic equipment. The writer is interested particularly in the turbine efficiency curves shown in Figure 16 of the paper, which shows the efficiencies of five large Allis-Chalmers turbines considered as outstanding water wheels in North America. The writer has participated in the Gibson tests of these units and wishes to make the following remarks in connection therewith.

The office of N. R. Gibson has made several hundred turbine tests throughout the world and based upon the results obtained, it seems that besides the consideration of runner design there are two factors which are believed to have an important bearing on the efficiencies of hydraulic turbines. The evidence is not always consistent but there is enough of it to attract attention, and the exceptions possibly may be explained in other ways or may be only sufficient to prove the rule. These two factors are

1. Constant diameter bends in the penstock near the entrance to the turbine.

2. Valves of a type such as butterfly valves which tend to disturb the flow of the water as it approaches the turbines.

These adverse conditions are mitigated by making a bend in the penstock, converging so as to accelerate the flow around the bend and by using a valve like a gate valve which, when open, leaves the waterway unobstructed.

Referring to Figure 16 of the paper, the Shipshaw turbine unit 9, has a straight water passage leading to it with no lower penstock bends and no valve. It has a Y at some distance upstream, but the flow in the Y is accelerated. The Niagara unit 21 has no bend near the turbine and the penstock valve is a Johnson valve with concentric water passages and accelerating flow. Unit *L7* at Grand Coulee has two lower penstock bends, one vertical and one horizontal, both of which are close to the turbine although the flow is accelerated. The Osage unit involves the common design of penstock with reversed curve through the dam, and Boulder unit *A5* has a butterfly valve located immediately ahead of the turbine.

There also should be considered in an analysis of this kind the factors of head and quantity of flow. Based upon many years of experience in testing work, a head of about 200 feet, associated with a turbine designed to discharge a relatively large quantity of water, seems to produce ideal hydraulic conditions for maximum turbine efficiency. Generally, as indicated by Figure 16 of the paper, as the head departs in either direction from this value, maximum turbine efficiency seems to decrease.

F. L. Lawton: The discussion by J. F. Roberts adds to the author's presentation of the essential details of the Shipshaw 2 water wheels by stressing those factors contributing to the high efficiencies obtained. The comments on the relative merits of cast iron and steel for large moderate-head runners, both as regards resistance to pitting and resistance to cracking of the vanes near the crown plate, set forth the identity of viewpoint of manufacturers and most operators. The greater ability of cast-steel runners to resist pitting and especially cracking, and ease of effecting satisfactory repairs, are resulting in most new runners being cast steel.

H. R. Sills's remarks on the effect of dirt on the cooling system and performance of hydroelectric generators are welcomed. It is appreciated that the curves of Figure 10 appearing in the advance copy of the paper are somewhat in error. A re-examination of the original data shows these should be redrawn as in Figure 10 of the published paper. While the change alters the quantitative values somewhat, the basic assertion of Sills's discussion is supported. It should be noted that the original tests were designed to show relative temperature rises under similar conditions rather than absolute values.

R. A. Hopkins has inquired as to necessary preparations and technique used in welding the original cast-iron runners at Isle Maligne.

In affecting repairs to pitted areas, initial practice was as follows:

1. The pitted or spongy metal was chipped out to sound cast iron, using pneumatic chipping hammers.

2. The chipped area was drilled 3/4 to 1 inch deep and tapped for 5/8-inch by 1-inch cap screws on approximately 4-inch centers. These cap screws were tightened, cut partly through under the head, and tightened again until the heads broke off.

3. A priming coat of low-carbon steel was laid down by the electric-arc process on the chipped area and carefully peened as applied. That is, care was taken to limit the area welded prior to peening, which was thorough rather than heavy.

4. The cavity created by chipping out the spongy metal was built up by depositing a low-carbon steel closely to the original contours. Each layer was peened prior to deposition of the succeeding layer.

5. A finish coat of high-carbon steel was laid down in two layers, carefully peened, and ground to the original contours as closely as practical.

Early experiments with a stainless-steel finish coat on areas subject to pitting were not too encouraging, but developments in welding rods and in application technique have progressed to the point where current practice in welding cast-iron runners is

1. The pitted or spongy metal is chipped out to sound cast iron, using pneumatic chipping hammers.

2. The chipped-out area is drilled, tapped, and studded as previously described, latest practice tending to somewhat less studding.

3. A priming coat of low-carbon steel is laid down on the chipped area and peened. Somewhat better bond is secured with currently-used rods than was formerly possible.

4. The cavity resulting from the chipping operation is built up by deposition of successive layers of low-carbon steel laid down by the electric arc, successive layers being peened.

5. A finish coat consisting of two layers of 18–8 stainless steel is laid down with the electric arc, each layer peened, and the finish layer ground to contour. The average analysis of the deposited metal in the finish coat is 0.07 for carbon, 19.70 for chrome, 9.50 for nickel, and 0.80 for columbium. Reverse-polarity rods with an extruded coating are used.

Pitted areas on cast-steel runners have been repaired in much the same manner as for the cast-iron runners, but without studding and using a reverse-polarity extruded-coating mild-steel electrode.

Cracking in the vanes of the Isle Maligne cast-iron runners followed quite a consistent pattern. Cracks almost invariably started at the discharge edge of the vanes or buckets and ran outwards towards the inlet edges, sometimes as far as 36 inches. Beginning at a point 2 to 4 inches down from the crown plate, the cracks would terminate in the crown plate.

The method of repair originally was as follows:

1. A V-shaped cut was chipped out along the crack on the face of the vane, using pneumatic chipping hammers.

2. Holes were drilled into the two faces of the V-shaped cut, on $1^3/_4$- to 2-inch centers, and tapped for 5/8- or 3/4-inch diameter steel cap screws. These were screwed tight, cut partly through, and the heads broken off by tightening still further.

3. A low-carbon steel electrode was used for the deposition of a priming coat on the surfaces of the V-shaped cut. The priming coat was peened lightly and the space gradually built up somewhat beyond the original contour using a medium-carbon electrode, peening successive layers. Initially a coated English rod was used, but later experience indicated comparable results could be obtained with Canadian rods at lower cost.

4. The rough surface of the weld was ground off to contour.

This technique has been employed successfully for replacement of an entire vane in one of the 128-inch-diameter 67-specific-speed Isle Maligne runners. In this case a double V-shaped cut (from both faces) was employed. The replacement vane was cast steel. The repaired runner has given 18 years service without any trouble insofar as the new vane is concerned.

However, it is extremely difficult to establish a bond between the parent cast-iron metal and the weld deposit, which will transmit permanently the heavy bending stresses from the shroud ring and vanes to the crown plate. Consequently, our present practice is to bridge the crack by steel plates secured to the crown plate or upper portion of the vane, and to the vane below the crack by heavy studs with countersunk heads welded in place. The steel plates also are welded to the cast-iron surfaces around their entire periphery.

Some cracking of cast-steel runner vanes, similar to that described for the cast-iron runners, has been encountered at Isle Maligne. Originally the cracks were chipped out, leaving a V-shaped cut. This was studded in similar fashion to the cast-iron runners, and the space gradually built up with successive weld layers, using a reverse-polarity extruded-coated mild-steel rod corresponding to American Welding Society's classification *E*6010. However, such repairs were not too permanent, "lifting" occurring at the bond, so that present practice is to keep the working area warm at all times, depositing weld metal in layers, and carefully peening each layer.

Hopkins' query as to the reason for the greater pitting experienced with the Isle Maligne runners as compared with the Shipshaw 1 runners is interesting. Both designs bear roughly the same relation to the experience curve of limiting specific speeds. Both have about the same relative position to the experience curve for limiting values of the cavitation factor, sigma. However, the Isle Maligne units were designed with a specific speed as high as was considered practical then for high initial economy, whereas the Shipshaw 1 units were designed for operating economy. The higher head at Shipshaw 1 is conducive to better efficiency and, as a corollary, less pitting. Operating conditions influence the rate of pitting, as indicated in the paper, especially when units are operated for long periods at gate openings over best gate. Another significant factor is

believed to reside in the shape of the water passages through the runner, but its relative importance is unknown.

The use of the expression "pitted" to denote areas damaged as a result of cavitation is desirable in the author's opinion. "Cavitation" properly describes the formation, in the mass of water moving through the water wheel passages, of cavities or voids filled with air and water vapor.

The reference by Hopkins to the Tennessee Valley Authority practice in ventilating and cleaning generators is most useful, especially the comment on use of electric heaters in the generator rooms to avoid opening the generator ventilating systems during cold weather.

E. B. Strowger's discussion is particularly interesting in view of the extensive background of water wheel efficiency testing behind it. There is little doubt that smooth water passages from forebay to tailrace, with properly-designed bends, are necessary for attainment of high efficiencies. The description of the water passages leading to the water wheels on which Figure 16 of the paper is based is helpful to a full understanding of the relative efficiencies. The significance of the head and quantity of water on efficiency of large water wheels, as noted by Strowger, should not be overlooked.

Comparisons of Railway Motive Power for Operations in the Pacific Northwest

Discussion and author's closure of paper 46-186 by T. M. C. Martin, presented at the AIEE Pacific Coast meeting, Seattle, Wash., August 27–30, 1946, and published in AIEE TRANSACTIONS, 1946, pages 1054-65.

Walter S. Gordon, Jr. (consulting electrical engineer, Tacoma, Wash.): T. M. C. Martin's paper is a well-prepared brief on a difficult subject. Greater detail would have obscured the picture he has presented so clearly. Such a simplified approach is required emphatically to gain the hearing and serious consideration of railroad officials skilled in railroading with many years of experience in the utilization of steam motive power. Practical operating officials on railroads, not electrical engineers, must be convinced of the economic and operating advantages of electrical operation.

During past years many electrical engineers and others interested in electric traction appeared to be more interested in presenting the merits of their one particular system of electrification than they were in presenting the over-all advantages of all systems of electrification. It is not to be wondered that, as a result of this technical conflict between electrical ideologies, top railroad personnel charged with making decisions regarding the installation of electric traction hesitated and waited for the smoke of battle to clear. Under similar conflicting circumstances our American industry most certainly would not have become as highly electrified as it is today. It is indeed fortunate that each individual plant or mill did not have to arrive independently at the solution of such problems as the correct transmission and distribution voltage, whether to use direct or alternating current, and if alternating current, the phase and frequency. And then face the delays and expense of securing motors, transformers, control, and switchgear specially designed and constructed for each individual installation!

Most railway electrifications have been conceived brilliantly and executed well in a daring and competent manner. The principals deserve the highest praise for their able work, which required much technical pioneering to overcome many technical difficulties during design, construction, and the initial phases of operation. But too many other electrification installations, despite ample economic justification, never reached or passed the planning stage.

In the past, much emphasis was placed on the details of selecting an electrification system that was technically correct for a specific section of railroad under certain assumed traffic and operating conditions. Later and unforeseen changes in traffic and operating methods voided many of the assumptions considered vitally important in the original selection. For example, strong argument now could be advanced for installing alternating current on what is now the longest d-c electrified American railroad, and likewise for installing direct current on what is now the longest a-c electrified American railroad! However, the superior operating and economic performance of both these outstanding electrifications cannot be denied now. Fifty years of electric traction have proved its inherent merits.

As the representative electric locomotive for this study, Martin's selection of the motor-generator type appears most reasonable and should meet with a minimum of dissent. Considering the service requirements on Pacific Northwest railroads, this type of electric locomotive has the strong advantages of being usable interchangeably in both freight and passenger service, of 20 years successful operating experience in this area, of making available at the rail the full horsepower capacity over almost the entire range of operating speeds (from 17 miles per hour on mountain grades to 60 miles per hour on light ascending grades) and of train-weight regenerative braking over the same wide range in operating speeds. However, this does not imply that the motor-generator electric locomotive should be selected for all future electrifications, wherever situated. For other regions with different physical, operating, and traffic conditions, it is possible that one of the other types of electric locomotives such as the a-c series motor or the phase-converter would be used; it is also possible that one of the many other arrangements of steam locomotives likewise might be selected as the representative type for that form of motive power. However, at present the motor-generator locomotive comes closest to being a universal a-c electric locomotive. It is significant that the motor-generator locomotive is now satisfactorily in use on an eastern railroad which has high-speed passenger and freight traffic on level and light-gradient routes, and which for 37 years has operated a-c series motor locomotives; also that four motor-generator locomotives have been ordered recently by a southeastern coal-carrying road which has a heavy-tonnage freight traffic on steep mountain grades, and which for more than 20 years successfully operated a-c phase-converter electric locomotives. Thus the author's selection appears well documented by recent practice elsewhere in this country as well as by the 20 years of operating success achieved on an electrified railroad in the Pacific Northwest.

The author's selected type of a-c power distribution system already has been installed on by far the most miles of track and route in this country. Operating today from the 12-kv 25-cycle single-phase a-c catenary system in the east, south, and west are electric locomotives which have traction motors of three widely different types and characteristics. These types are the single-phase a-c series commutator motor, the 3-phase dual speed a-c motor supplied from a locomotive-borne phase-converter, and the d-c series commutator motor supplied from a locomotive-borne synchronous motor-generator. Such a distribution system therefore provides a maximum of flexibility for selecting a type of motive power to suit any railroad's profiles, traffic, or operating conditions and methods. This system has a large capacity, although the necessity of supplying 15,000 kw to any point on the 12-kv trolley, as mentioned in the paper, might be questioned as somewhat high. Power in the order of 7,500 kw at present, and of 10,000 kw for the future, appears to be sufficient.

Martin's observations regarding a choice of frequency were most interesting. As he suggested, American practice would be better today if 15 or 20 cycles, instead of 25 cycles, had been established long ago. It is probably impracticable to change now to one of these lower and more desirable frequencies despite the many recognized advantages. However, to the discusser it does appear reasonable and practicable now to adopt 24 cycles as a national standard traction frequency for use on all future electrifications; this would mean a deviation of only four per cent from the present accepted standard. As mentioned in the paper, the use of 24 instead of 25 cycles would result in considerable savings in the costs of frequency changers; the maximum speed which could be used for these motor-generator sets then becomes 720 rpm instead of the present 300 rpm in converting from 60 cycles. Locomotives and equipment designed for 24 cycles would operate equally well on 25 cycles, and it is believed that no serious difficulties would be encountered in actually operating existing 25-cycle locomotives from a 24-cycle trolley system. This proposed 4-per-cent deviation in frequency is less than half the present 10-per-cent deviation in frequency permitted, with satisfactory performance guaranteed, by present commercial standards for industrial motors. In the interest of economy on future electrifications, this slight change in traction frequency should be adopted now by all manufacturers of traction equipment.

The author has leaned backward to attain objectivity and insure equity to steam and Diesel motive power. Since railroad operating officials that are now steam-minded or already favorably impressed by the many advantages of Diesel-electric traction have to be convinced that in many instances electrification economically will solve their operating problems, such an attitude is

reasonable in such a study. It is better to claim too little than too much. However, it should be noted that in the comparative cost of facilities (Table XI of the paper) and the operating and fixed charges (Table XII) for steam operation, the costs of fuel and water stations and similar facilities have not been included; and in the timetable comparisons of maximum performance (Table VII) no allowances were made for inevitable delays caused by stops for water and fuel when steam locomotives are used. Locomotive depreciation rates appear to favor steam locomotives unduly. For coal, a value of $2.00 per ton at the locomotive appears quite low as this price must include the cost of the fuel at the mine, the cost of transportation from mine to fueling stations, and the cost of storage, handling, loss, and waste. For example, the cost of coal purchased by a large eastern seaboard utility was an average of $5.89 per ton in 1944 and $6.12 per ton in 1945.

A value of four mills per kilowatt-hour for hydro-generated electric energy at the frequency-converter terminals, mentioned in Tables XII and XIII of the paper, may seem unrealistic to many power and railroad personnel familiar with the much higher energy rates that railroads generally are paying now. In some instances these present high rates are relatively far out of line with rates for industrial energy. This seems especially true in the case of electrifications where the railroad's own commercial frequency transmission and transformer facilities are made available to the power suppliers for use in selling commercial power and light to other customers. The eastern utility mentioned previously generates about 80 per cent of its total electric production from coal, which in 1945 cost $6.12 per ton, and receives an average of nine mills per kilowatt-hour for industrial sales and less than eight mills per kilowatt-hour for energy sold to electrified railroads and street railways. This railway load, which constitutes 20 per cent of the utility's total energy sales, is considered profitable. A western utility, with lower-cost hydro-generated power, receives an average of six mills per kilowatt-hour for industrial sales and much more than that for railway sales, although on a relative basis a railway rate of about five mills would be in order. This is approximately the rate quoted by a western utility more than 30 years ago, and since that time, industrial rates have been halved at least. The 4-mill rate mentioned by the author, which appears extremely low now, may prove to be an attractive source of income for some utilities. In any event, this 4-mill rate for railway electrification energy soon may be an established fact here in the Pacific Northwest.

Finally, as a matter of national policy, utilization of our hydro-generated electricity instead of consuming our apparently dwindling liquid fuel resources soon may be recognized generally as desirable and necessary. At the present time such utilization should be encouraged at least wherever it is economically sound and technically feasible. Oil replaced at home by water power should be much more valuable than oil rights in distant foreign lands. Therefore the lower rate of return on the incremental investment required for electrical as compared with Diesel operation (Figure 7 of the paper) could be compensated justifiably by making available to railroad managements long term loans repayable upon the basis of extent of use as measured by energy consumed (which would vary with traffic or ability to pay) instead of upon the basis of a fixed annual sum repayable without regard to the extent of use. A practicable basis for repayment is vitally important to railroads if they are to be able to afford the higher initial cost of electrification. When traffic is heaviest the railroads need electrification and have the money to pay for it, but they are usually then too busy to install it; also, labor and materials are then sometimes difficult to secure because of a national crisis, as during a war. During depressions traffic is lower, the economic need for electrification decreases, and net revenues are low, so that private funds become difficult to secure. Therefore electrification should be expected to pay off the investment on the basis of the average traffic over a reasonable period of years, at least a decade or longer.

The discusser in 1932[1] wrote that

> "European railways are apparently well satisfied that the operating economies, increased speed, cleanliness, increased track capacity, and use of natural resources such as water power or low grades of coal, are advantages that justify further extension of railway electrification even during a severe economic crisis. The execution of such projects during times of depression has been of material assistance in alleviating unemployment in several of the countries. Perhaps America could profitably follow such an example."

Is it now too much to expect that the more progressive of our railroad managements, the electric and railroad equipment manufacturers, the interested power utilities, and government transportation agencies will at last get together and co-operate on a sound long-range program of expediting the electrification of all railroad lines which will justify the investment? Specific and detailed analyses then will reveal the railroad lines which should be electrified.

REFERENCE

1. A REVIEW OF EUROPEAN RAILWAY ELECTRIFICATION, W. S. Gordon, Jr., E. Jaboolian. *Electrical Engineering*, April 1932, page 252.

H. F. Brown, (New York New Haven and Hartford Railroad, New Haven, Conn.): T. M. C. Martin, in his paper, has presented a very clear comparison of the three outstanding types of motive power available today for trunk-line railroad operation. The railroads of the Pacific Northwest, with their heavy mountain grades, present a problem for which the electric locomotive is one of the proper and logical economic solutions.

It is the opinion of this commentator that Martin's analysis and conclusions as to the type of distribution of the electric power supply, that is, 12 kv, 25 cycles, single-phase alternating current is sound, and that the choice of the motor-generator type of locomotive with d-c motors is also sound because of the necessity for lower speeds with maximum tractive effort on long grades, the possibility of regeneration especially for braking, and the possibility of power-factor correction with the synchronous motor-generator sets.

The electrification of these railroads presents an investment problem that the purchase of self-contained types of motive power do not, namely, the possibility of financing the necessary capital investment through equipment trusts. However, it is not outside the range of possibilities that where electrification can be applied with superior economies in a territory where cheap electric power from natural resources can be secured, some similar means can be developed for financing the power distribution system.

The power engineer cannot but be impressed by the various power conversion problems which are presented in the electrification of these railroads. First, the generation at 3 phase, 60 cycles alternating current; then the conversion to 25 cycles, single-phase alternating current for the railroad contact system; and finally the conversion on the locomotive to direct current for the most favorable motor design. If the railroad load is a legitimate field for the power development companies and administrations, then their plans for the development of the natural resources should include provisions for the direct generation of 25-cycle power for such purposes, thereby saving additional investment in conversion equipment and the attendant losses in power. Twenty-five-cycle power can be utilized for certain commercial consumption just as economically and efficiently as 60-cycle power; for example, aluminum production, and it seems rather shortsighted to put all the investment into 60-cycle generation if the electrification of railroads is a sizable part of the ultimate load the power development hopes to assume.

Charles Kerr, Jr. (nonmember; Westinghouse Electric Corporation, East Pittsburgh, Pa.): T. M. C. Martin's paper, while somewhat provocative, presents a very intelligent discussion of railroad electrification. Few with operating experience on modern electrified railroads will dispute the claim that electric operation offers many outstanding advantages over any other known type of motive power. The only deterrent to extensive electrification has been first cost, and if the differential in this item between electrification and other types could be reduced materially or eliminated, the field of railroad electrification would be virtually unlimited. Reduction in capital investment is the paramount assignment for all parties interested in the cause of railroad electrification.

Without desiring in any way to initiate a "battle of the systems," Martin's selection of electric system and locomotives for universal application is open to debate. The 25-cycle a-c system, employing motor-generator locomotives, was introduced by Westinghouse, and we would be the last to deny its many virtues or its complete adequacy under the operating conditions encountered in the Pacific Northwest. However, certain recent analyses of systems of electrification for quite similar applications to those anticipated by Martin have demonstrated that the a-c system with motor-generator locomotives well may involve the largest capital expenditure. The motor-generator locomotive was introduced in 1926, and many advances in the art have taken place since that time.

There are several systems of electrification which, when properly engineered, would handle adequately traffic in the Pacific

Northwest. Therefore, no system is the only answer from the standpoint of adequacy to handle the service. Furthermore, in general, the operating expenses between the various systems differ only to a minor degree. Thus, the ultimate selection can be made essentially in favor of that system which requires the minimum capital investment when properly engineered to meet the over-all service conditions of this territory.

It may be of interest to point out that the 25-cycle a-c system, employing commutator motor locomotives, has been used most extensively of all types. This system has handled the most dense traffic in America for many years. Its operating flexibility never has been matched. The same type of locomotive, operating from a 15-cycle system, could provide this same flexibility, and, in addition, meet the heavy-grade requirements of the Western roads in an equally satisfactory manner. There is also considerable evidence that this system would require a definitely lower first cost. With future technical developments not too far removed, other systems might fulfill well western operating requirements with advantage.

It is my belief that Martin's aim of extensive railroad electrification in areas of assured low cost power can be furthered best by selecting that system which meets the requirements of this territory with the absolute minimum of initial investment. I question seriously whether the system proposed in his paper accomplishes this purpose.

Electrification projects involve the interested railroads, power companies, and manufacturers. It might be well for these groups to find some means of reaching a common standard which would provide the most economical over-all system for the Pacific Northwest, and such action might prove to be a considerable factor in extending electrification in this region. The land transportation committee of the AIEE might initiate this co-operative effort.

T. M. C. Martin: I am interested very much in Charles Kerr's discussion. I agree completely with his observation that the best system is the one that provides the lowest over-all costs—lowest for the railroad and lowest for the power supplier.

I am unable to perceive that 15 cycles offers very startling economies at this late date, but be that as it may, I am convinced that the use of a-c series motors in this part of the country is not only prejudicial to the best interests of power suppliers but it offers largely illusory benefits to railroads. The chief claim presented for their use by Kerr seems to be lower first cost. Suppose we examine locomotive costs on the basis of their cost per pound and their cost in terms of dollars invested per thousand pounds of continuous tractive effort. All we have to go on are facts in the form of recent prices for representative locomotives taken from each class.

From Table I, and keeping in mind the fact that continuous tractive effort is the only real measure of performance that matters to western railroad managements, it is very difficult to follow Kerr's lower first cost contentions on behalf of a-c commutator motor locomotives.

If this is true it is even more difficult to perceive a justification for their use in terms

Table I

	15-Cycle 24-Kv Trolley A-C Commutator Locomotive	25-Cycle 12-Kv A-C Motor-Generator Locomotive
Manufacturer's recent asking price	$475,000	$500,000
Total weight of locomotive, pounds	600,000	720,000
Price per pound	$0.79	$0.69
Maximum continuous tractive effort in pounds	99,000	119,000
Price per 1,000 pounds of maximum continuous tractive effort	$4,798	$4,202

of annual operating costs. Most authorities agree that their maintenance will be more costly, and there can be little doubt but their power supply will be more expensive for at least two very simple reasons:

1. Their single-phase power factor will be poor, probably no better than 80.0 percent at the best.

2. Their ability to assume short-time overloads and their relatively higher minimum speeds for maximum power output cannot fail to produce a lower working electric load factor. This latter point is an especially difficult one to sidestep because western electrification is at best a fairly low load factor proposition.

Performance Criteria for Current-Limiting Power Fuses—I, II

Discussions and authors' closure of papers 46-170 and 46-171 by C. L. Schuck and E. W. Boehne, presented at the AIEE summer convention, Detroit, Mich., June 24–28, 1946, and published in AIEE TRANSACTIONS, 1946, pages 1028–45.

E. A. Williams, Jr. (General Electric Company, Philadelphia, Pa.): The testing of a line of fuses to establish interrupting ability over a wide range of currents has been, in the past, a long and arduous task because of the effect of circuit variables upon interrupting performance, and because of the large number of ratings involved. To accomplish the desired results with any degree of certainty by cut and try methods is almost impossible, as the operation of most fuses is quite critical under certain combinations of circuit conditions.

The papers by E. W. Boehne and C. L. Schuck recognize and discuss the factors controlling fuse performance, establish a definite mathematical method of predetermining areas of critical performance, and present adequate test data to substantiate the accuracy of their theoretical approach to the problem.

The value of the papers is threefold:

1. The basic data presented contribute to a better understanding of the phenomenon of circuit interruption in general.

2. The methods of procedure described provide the fuse designer with a useful tool to produce better fuses at lower cost.

3. The user may apply fuses with greater assurance of reliable performance under any fault condition within the rating of the fuse.

H. H. Fahnoe (Westinghouse Electric Corporation, East Pittsburgh, Pa.): C. L. Schuck and E. W. Boehne in their papers have given the fuse designer a valuable review of the many factors that must be considered in developing a current-limiting type of fuse. The data presented are also of interest to the engineer making application of these fuses at important locations on central station and high-power industrial systems because they provide assurance that this type of fuse is capable of interrupting all magnitudes of short-circuit currents experienced on his system.

Part I outlines certain laboratory test requirements and procedures. Surely, the broader aspects of these criteria were recognized during the development of the fuse described in reference 2 of part I by Prince and Williams. However, Prince and Williams did not include any information on test procedures in their paper. In reference 10 of part I, Rawlins and Fahnoe described in detail the test methods followed in the development of a current-limiting fuse. It is interesting to note that part I of these papers substantiates the test procedures and the need for extensive high-power laboratory testing as set forth by Rawlins and Fahnoe.

It has been recognized for many years that the high-power testing laboratory offers the only completely satisfactory means of proving the interrupting ratings of power fuses. In the early days, the fuse designer was forced to rely on the incomplete tests which he could obtain on commercial power systems. With the advent of the high-power laboratory, where all factors affecting the test circuit can be controlled and measured, the development of the highly efficient modern circuit interrupter became possible.

This is particularly true in the case of the current-limiting fuse. In a faulted circuit containing this type of fuse, the fuse is the controlling element in the circuit because of the high arc voltage associated with its operation. Consequently, the effect of parallel loading, recovery voltage rate, power factor, and the like are of less importance than with other types of circuit interrupters. More particularly, as stated by Rawlins and Fahnoe, it is necessary with current-limiting fuses to test "all ratings of fuses. . .at rated voltage with all conditions of asymmetry on currents of varying magnitudes from minimum melting current up to the interrupting rating of the fuse." Thus the tremendous number of tests required to explore the performance of a line of fuses adequately practically eliminates the possibility of field testing. Because of the completeness of the laboratory tests, the need for field testing is obviated.

It is gratifying to note that the conclusions regarding the testing of current-limiting fuses stated in part I of these papers agree remarkably well with those set forth in the Rawlins and Fahnoe paper, and in no respect are the conclusions contradictory. Such agreement between independent observers helps immeasurably to verify conclusions, thereby establishing the fundamentals of the art.

J. W. Gibson (The General Electric Company, Ltd., Birmingham, England): The design of the current-limiting fuse has been

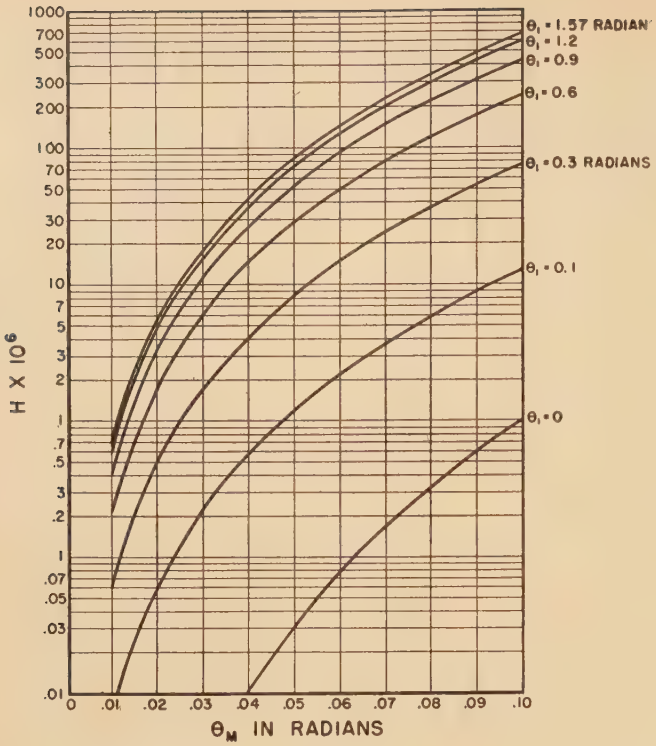

Figure 1. Heating function curves, supplementing Figure 8 of part II, which will be useful for fuses of low current ratings, and fuses of moderate current ratings under high fault current conditions

The H functions are computed from the relation

$$H = \frac{\Sigma i^2 t \cdot \omega}{I^2}$$

The melting time in seconds is equal to the melting angle in radians divided by 2π times the circuit frequency. The curves are a plot of equation 22 of part II with minor corrections to align with equation 5

facilitated greatly by analytical and experimental investigations of its current-breaking performance during the past 10 or 15 years, and the present papers mark a considerable step forward in this direction. It is becoming possible to design the fuse for any required interrupting performance, largely avoiding the method of trial and error, and in addition to predict its discrimination performance when used in series with circuit breakers or with other fuses.

I agree with the authors that arc energy is the most generally useful criterion of the severity of a test. It should be remembered however that other factors may supervene to cause failure. For example, if the rate of rise of fault current is high, the excessive mechanical pressure set up may cause failure through bursting of the cartridge before the fuse has accepted a value of arc energy with which it can deal successfully if the rate of rise is less.

Figure 4 of part I illustrates well that the current-limiting fuse is more sensitive to changes in circuit voltage than to changes in short-circuit current; this property is the reverse of that found with most other interrupters.

The curves of Figure 5 of part II show a diminution of arc energy when the arc voltage falls below about half of the crest value of the applied voltage. I should be glad of the authors' view as to the possibility of a powder-filled fuse operating successfully in this zone; I should have expected that the fuse would be unable to interrupt either at the first, or at subsequent current zeros, resulting in failure.

Will the authors give their experimental value for their constant F_m (equation 7 of part II) for silver? In my experience, the value increases slightly with increase in the current density in the element at the initiation of arcing, because the melting process tends to proceed further before a break in the element is initiated. The curves of Figure 8 of part II, derived from equation 16, will render it easy to determine accurately the pre-arcing time for various starting angles. It would be useful, however, if the author would extend them downwards to cover the case of fuses of very low current rating, where the melting time is only a very few degrees and equation 22 applies.

The conclusions drawn in the papers regarding the effect on severity of fault angles and of available ("prospective" in British terminology) current line up well with findings in England. Thus, for certain British Standard specifications in preparation, it is proposed that breaking tests shall be made, not only at rated megavolt-amperes, but at a less value of megavolt-amperes near which the peak value of arc energy may be expected to occur, the criterion being that the prospective current shall be so chosen for the test that the current at the initiation of arcing is between 70 and 100 per cent of the peak symmetrical value of the prospective current. Further, certain stipulations probably will be made regarding fault angles. In a British Standard for high voltage fuses, a proposal is that arcing in current-limiting fuses shall commence on a rising voltage between 50 and 100 per cent of peak value. For lower voltage (up to 660 volts) fuses, with current ratings up to 1,200 amperes, a proposed stipulation relates to the time of current initiation, and not to arcing initiation; the circuit is to be closed on a rising voltage between 35 and 65 per cent of peak value. In the case of fuses of low current rating, this will result in arcing commencing on a rising voltage. For larger fuses, arcing will commence on a falling voltage, as it is believed from test experience that this is likely to result in the most severe condition. The reason is that a current zero (following a minor current loop) is reached shortly after arcing commences, and as a result the arc paths have not had sufficient time to deionize themselves. This factor, together with the relatively low current density in the arc (arising from the use of numerous elements in parallel) results in a second loop of current, with consequent increase in arc energy before arc extinction occurs. I should like to know whether the authors have experienced this phenomenon. The point also may be of importance in connection with fuses used in circuits, for example, furnace circuits having frequencies of the order of 1,000 cycles per second. My experience with such frequencies agrees with the analytical conclusions of the authors that increase in frequency results in reduced severity, but it is possible that above certain frequencies continued arcing may occur on account of high restriking rates at the zero pause. In other words, zero-pause phenomena, of a type not normally associated with current-limiting fuses, may assume importance. I should like to have the authors' views on this subject also.

Figure 10 of part II shows in an effective manner that arc energy diminishes as the fault current increases above a certain value. It would be useful if the authors would give similar curves for varying arc voltage because it appears certain that the characteristic just mentioned would not apply to the lower values of arc voltage.

E. W. Boehne and **C. L. Schuck:** The authors greatly appreciate the interest shown in these papers, particularly because those who have submitted discussions have been connected closely with power fuse development.

E. A. Williams, Jr., describes the vast number of fault conditions encompassed by a single number expressing the interrupting rating. The fuse designer, confronted as he is with the variables of the circuit on the one hand, and with the variables involved in the fuse design on the other, seeks a procedure that will give him maximum information with a minimum number of tests. His interest therefore centers in the critical circuit and design factors, which he perceives by the joint exercise of a subjective analytical approach and an objective correlation of test results.

In H. H. Fahnoe's discussion, he mentions certain references made to test procedure in earlier papers. The subject of fuse test severity is certainly not new, and, if there is interest in earlier contributions to our present knowledge, surely the work of Gibson,[7] Metcalf,[9] Grant[19], and others should be noted, together with that of Lohausen[8] and Lapple[5] (German), and Grillet[18] (French). (All references are in part I of the paper.) All of these predate the brief reference to test procedure made in the Rawlins and Fahnoe paper.[10] In that paper, the importance of causing melting to occur near voltage peak was reiterated,[7] but this factor must be considered jointly with the very important severity factor of the magnitude of current at melting. Figure 5 of part I shows the effect of fault starting angle on this factor. For fuses of low current ratings, it so happens that maximum current, voltage, and severity all obtain for a fault starting angle slightly before 90 degrees. For fuses of high current ratings, maximum melting currents are obtained if melting takes place at or even after voltage maximum. Thus, if the fault starting angle were chosen only to give maximum melting current, or to bring about melting at voltage peak, the interruption would be made easier, because arcing

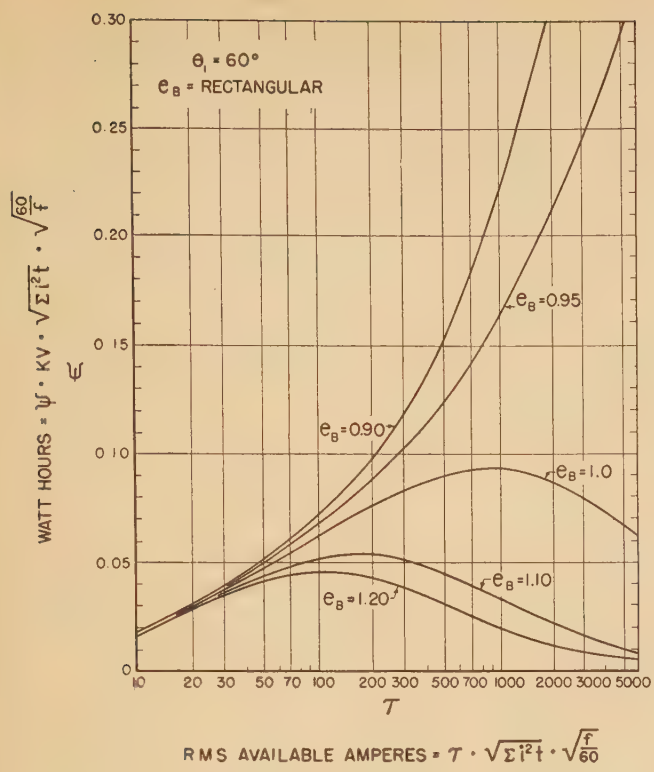

Figure 2. Arc energy characteristics resulting for magnitudes of rectangular arc voltages ranging from 90 to 120 per cent of the crest of the generated voltage

These relations are for zero power factor short circuits initiated 60 degrees following a voltage zero. They hold for any fuse rating, any frequency, and any voltage. These relations emphasize the importance of the arc voltage of the fuse, especially for high values of short-circuit current. Such characteristics are useful in the adequate testing of fuses

would take place during a time when generated voltage was decreasing (see Figure 6*B* of part I). Evidently a more accurate and quantitative statement was needed on this question, and these papers give this in the form that melting should occur in the region 70 to 80 degrees after voltage zero. On this basis, the fault starting angle, rather than being zero, should be related to the current rating of the fuse. For the 20,000-ampere circuit of Figure 5, melting takes place at approximately 75 degrees if the circuit is closed at the values given in the following table:

θ_1, Degrees	Fuse, Amperes
0	200
42	100
60	50
72	7

It follows from this table that fuses having current ratings in excess of 200 amperes on this circuit would find the most difficult conditions when θ_1 is negative, that is, under conditions of an initial minor loop, melting occurring well into the next loop of current. In some cases of high current fuses, fusion late in the initial half cycle will not be followed by interruption at the subsequent voltage zero, and an additional loop of current will result. This adds to the duty and requires special consideration, as Gibson points out.

The papers also include a consideration of each of several additional factors which are properly a part of the subject of power fuse performance because both designer and user must know their effects. Questions arise on the effect of frequency, power factor, polyphase versus single phase, and a-c versus d-c testing, and it was believed that a clear statement embodying our present knowledge on each was desirable.

Gibson has made several thought-provoking comments, which indicate the thoroughness with which these questions have been considered in England. It is significant that certain conclusions reached there on test severity, dictated by a careful analysis of test data, and which agree so closely with our analysis and experience, probably will be included in the British Standard specifications.

He inquires as to the constancy of the coefficient F_m in equation 7, part II. A progressive decrease in this coefficient with increasing element diameter has been found empirically. For a 200-ampere fuse (employing large-diameter elements), the value of the coefficient is 0.0188, that is, 12 per cent below its value of 0.021 for low current ratings employing small-diameter elements (the element metal being silver). The value 0.021 is also that calculated on the basis of a heat input sufficient to raise the temperature of the silver to its melting point, and to convert it to a liquid at that temperature, no heat being lost. The decrease in F_m suggests a mechanism initially resembling skin effect, with current concentrating in the outer portions of the element cross section. It is shown in the following text that such a nonuniform current density alone can shorten the melting time and make F_m appear smaller. There also may be a local shattering effect, as the current transfers to the lower-resistance colder core of the element after the outer portion has been converted to liquid only partially.

It is not believed that this effect is caused by a variation in current density, as current density itself is a function of the total element cross section, although we do note a similar trend in average current density accompanying the phenomenon. A plausible explanation of this phenomenon lies in the following analysis.

If n similar conductors in parallel divide a given current equally and all fuse simultaneously, the total i^2t is given by the relation

$$\Sigma i^2t = F_m d^4 n^2$$

where F_m is a constant (0.021 for silver) and d the wire diameter in mils. It is a significant fact, however, that should this current be allowed to fuse one conductor at a time in a continuous process until all n conductors are blown, the above relation then would be replaced with

$$\Sigma i^2t = F_m d^4 n$$

Here the n is not squared. Now consider the n similar conductors in parallel within the fuse to be divided into two random parts, r and q, such that $(r + q) = n$. Now should r and q be fused in sequence, it follows that

$$\Sigma i^2t = F_m d^4 (r^2 + q^2)$$

or

$$\Sigma i^2t = F_m d^4 (n^2 - 2rq)$$

We are interested now in the per unit reduction in F_m as expressed by the ratio

$$F_m\left(\frac{n^2-2rq}{n^2}\right)$$

It is this fraction that we describe as an apparent reduction in F_m. For example, when n is 48 and we allow r to be progressively 0, 1, 2, 3, 4, ... and so on, the preceding fraction becomes 1.0, 0.96, 0.92,

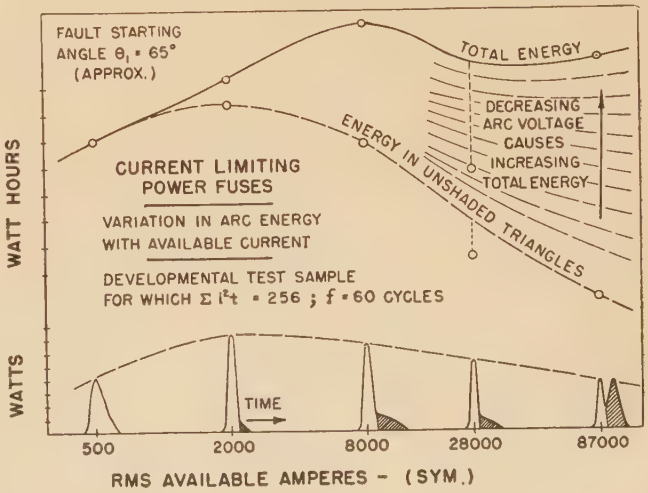

Figure 3. Reproductions of oscillograph watt element traces taken during interruption tests of five fuse samples of the same design at various available currents

Values of the time integrals (energy) of these traces are plotted at top

0.883, 0.848, ... and so on. Accordingly, the new F_m would take on apparent values of 0.0210, 0.0201, 0.0193, 0.0185, 0.0178, ... and so on.

This process within a fuse can be viewed as two separate phenomena, both of which we believe play a part in the observed reduction of F_m. The first may be that assumed previously, namely, the nonsimultaneous melting of the fuse wires. This is evidenced by the fact that F_m is observed to decrease as n increases. The second is skin effect in each and every conductor. The preceding numerical results would be duplicated if we considered each wire to be divided into 48 rings of equal area. If the outside 3 rings were assumed to fuse first, followed by the fusing of the inner 45 rings, then F_m would become the 0.0185 mentioned before. The actual skin effect phenomenon is, of course, not as discontinuous as suggested here, but a smooth variation which is only approximated in this analysis. That skin effect may play a part in the reduction of F_m is evidenced by the fact that F_m decreases as the wire diameter increases, wire diameter also increasing as n increases in practical fuse designs.

We agree with Gibson's conclusions concerning the expected performance of any powder-filled fuse which attempted to operate on the steep left-hand side of the energy characteristics of Figure 5, part II. As indicated in Figure 4 preceding, there is little current-limiting action in this region, and current zeros occur when the initial recovery voltage e_2 is near the peak of the generated voltage. In general, interrupters which operate in this region must be equipped to insulate the arc gap efficiently in order to cope with these peak recovery voltages and their attendant rates of rise. The short arc gap of a powder-filled fuse, which would be necessary to develop the low arc voltage, would be unable, we believe, to prevent the continued re-establishment of current. Fuses which utilize this energy to generate gases of high dielectric strength (expulsion fuses) can and do operate in this region, as indicated in Figure 4, part II. Such fuses are characteristically sensitive to the rate of rise of the recovery voltage.

The heating curves of Figure 8, part II, as Gibson points out, do not extend low enough to be useful for fuses of low current ratings, or for moderate current ratings at high values of short-circuit current. Accordingly, the curves of Figure 1 are included in this closure. These curves are a plot of the approximate equation 22 of part II and are expressed in radians instead of degrees. The upper portions of the curves of Figure 1 are corrected by about one per cent to align with the lower portions of the curves of Figure 8 of part II, which in turn are a plot of the exact equation 5 of part II. In this manner much of the error of the approximate equation 22 is eliminated in the curves.

In compliance with the last paragraph of Gibson's discussion, we submit Figure 2 in this closure which describes the effect of arc voltage magnitude upon the characteristics shown in Figure 10, part II. Retaining a rectangular arc voltage and holding the closing angle fixed at 60 degrees, equations 3, 5, and 6, together with the heating function curves of Figure 8, part II, and Figure 1 of this closure, were employed to compute the characteristic curves of Figure 2. As the arc voltage is decreased from 1.2 times the generated voltage crest, the arc energy rises. The peak liberated energy for a rectangular arc voltage equal to the crest of the generated voltage ($e_B = 1.0$) is slightly more than double the peak energy for an arc voltage crest of 1.2 times the generated crest ($e_B = 1.2$), and occurs at a current about 10 times as high as the peak energy current for the higher arc voltage.

This trend makes it imperative for the fuse designer to observe closely the characteristic arc voltage of his fuse in order to determine more accurately the current and closing angle which will produce the peak arc energy. His problems are complicated further if the arc voltage magnitude changes appreciably as the fault current is increased. The limited information given in Figure 10, part II, and Figure 2 of this closure should be considered only as sample characteristics, and do not express all the characteristics required to formulate a complete specification for the testing of fuses.

As the rectangular arc voltage decreases below the crest of the generated voltage, the arc energy increases rapidly as indicated in Figure 2 of this closure. Moreover, for arc voltages in this region the arc energy increases continuously with the megavolt-amperes (except for a very few cases having low closing angles and arc voltages in the region $e_B = 0.96$ to 1.0). It follows that any fuse which progressively produces lower arc voltages as the rate of rise of fault current is increased eventually will experience an upturn in arc energy as the megavolt-amperes are increased further. This will lead to eventual failure and hence dictate the ultimate interrupting capacity of the fuse. Such a trend is indicated in Figure 3 of this closure, discussed in the following text. The performance of the fuse at extremely high currents also is influenced considerably by the rate of rise of the arc voltage, a slow rate of rise augmenting the increase in arc energy.

Applications in circuits of various frequencies have demonstrated easier performance in the higher frequency circuits (reference 11 of part I). We have no experience with this fuse in circuits of very high frequencies (above 400 cycles), so are unable to answer Gibson's question on this point. We recommend that adequate tests be made to confirm any analytical prediction in this high frequency region.

Gibson suggests that a high rate of rise of fault current may induce breaking of the fuse tube. In our experience, the rate of rise of fault current affects only the melting time and the peak current, any tendency to break the fuse tube arising from energy associated with the arc current and voltage. We believe a more plausible explanation of the tendency for tubes to break at high fault currents is an inherent lowering of the arc voltage in a given fuse design as the fault current is increased. An examination of Figure 2 of this closure will reveal how a small decrease in the effective arc voltage will increase the arc energy considerably, especially for heavy currents. This effect was pointed out previously together with the tendency for the rate of rise of each arc voltage to be slower for high fault currents, which also tends to increase the arc energy. These two effects, both of which accompany high fault currents and give rise to increased energy, provide a rational explanation which merits further empirical study.

The arc energy can be recorded readily by use of an oscillograph watt element. Such records taken of five similar fuse samples tested at various available currents are shown in Figure 3 of this closure. The energy represented by the unshaded areas decreases with increasing available current beyond a maximum at 2,000 amperes, as would be expected from the trend of the curves of Figure 10, part II, which are on the basis that arc voltage is constant and essentially flat-topped. That it diminishes is indicated by the secondary energy areas (shaded). The resulting total energy thus increases at very high available currents as suggested in Figure 2 of this closure. The graphical study of this phenomenon (Figures 3 and 7 of part II) reveals the mechanism by which the double-humped energy curves are created as the arc voltage falls below the generated crest.

Factors Affecting Insulation Resistance of Large D-C Machines

Discussion and authors' closure of paper 46-157 by J. S. Johnson and Conrad Weil, presented at the AIEE summer convention, Detroit, Mich., June 24–28, 1946, and published in AIEE TRANSACTIONS, 1946, November section, pages 705–10.

R. W. Wieseman (General Electric Company, Schenectady, N. Y.): In the paper which Johnson and Weil presented at the summer convention, Figure 1 showed a comparison of the authors' linear approximation of the slot area of d-c machines

$$1{,}500\left(\frac{\text{horsepower}}{\text{revolutions per minute}}+2\right)$$

and the slot area formula

$$\alpha\ \frac{\text{kilowatts}^{1/3}}{\text{revolutions per minute}^{1/2}}$$

given in reference 1 of this discussion. In this figure the authors' value of the approximate slot area varied as much as one-eighth to two times the actual value, whereas mine varied as much as one-eighth to eight times the actual value. In my discussion of this paper at Detroit it was pointed out that in our study of this problem we have not found a single d-c machine whose slot area computed from

$$\alpha\ \frac{\text{kilowatts}^{1/3}}{\text{revolutions per minute}^{1/2}}$$

deviated so much from the actual area as the original Figure 1 of the paper indicated. Instead of one-eighth to eight times the actual value it was only about one-half to $1^1/_2$.

Figure 1 of the paper has been revised so that the authors' approximate value of the slot area varies as much as 0.2 to 3.8 times the actual value, whereas mine varies as much as 0.2 to 4.5 times the actual value.

The ratio of the computed to the actual slot area of a large number of d-c machines (up to 6,000 kw) arranged on a linear scale

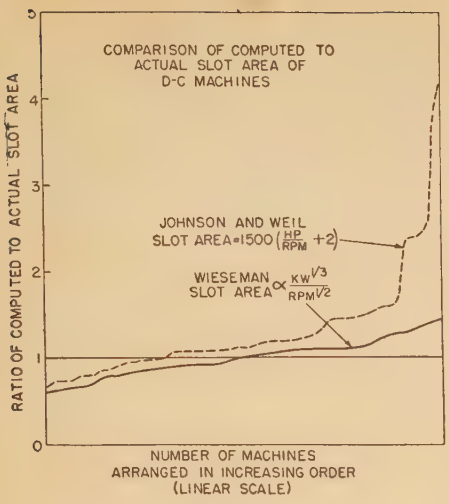

Figure 1

in increasing order is shown in Figure 1 of this discussion. The full line curve

$$\alpha \frac{\text{kilowatts}^{1/3}}{\text{revolutions per minute}^{1/2}}$$

varies from 0.6 to 1.45 times the actual value. The dotted curve

$$1{,}500\left(\frac{\text{horsepower}}{\text{revolutions per minute}}+2\right)$$

varies from 0.6 to 4.24 times the actual value, and this variation is nearly the same as that in the authors' Figure 1.

With a ratio of the computed to the actual slot area as much as 0.2 to 3.8, the authors' simplified formula will indicate an insulation resistance of some machines of 5 to 0.26 of the actual resistance. The authors apparently recognized this by advocating a minimum insulation resistance of two megohms when their calculated value falls below two megohms. A single minimum value of two megohms for all large machines is open to question. For a new machine I think it is too low.

In deriving an approximate formula for the insulation resistance of d-c machines, Johnson and Weil assumed that a number of quantities and ratios are constant. These assumptions and their variations are listed in Table I.

Although the authors' approximate formula based on the forementioned assumptions contains coefficients which were obtained from actual machines, it nevertheless will vary from five to one-fourth of the actual value. Thus I conclude that an expression for the insulation resistance of d-c machines based on the authors' simplified formula for slot area will not reflect the true proportions of some machines.

REFERENCE

1. INSULATION RESISTANCE OF ARMATURE WINDINGS, Robert W. Wieseman. AIEE TRANSACTIONS, volume 53, 1934, June section, pages 1010-21.

H. C. Marcroft (Pennsylvania Water and Power Company, Baltimore, Md.): This paper by Johnson and Weil is a timely contribution to the subject of electric machine resistance measurement, adding new facts concerning d-c machine insulation resistance to the information and test procedures already being used effectively for testing insulation of a-c machines.

The work done on a-c machines in trying to bring some order out of the mass of seemingly unrelated resistance readings demonstrated the need for consideration of absorbed moisture in the windings. To study the other variables the humidity problem was minimized by the practice of taking resistance measurements only on warm machines when they were shut down following a load period, because it was found that there was little meaning to resistance measurements taken on cold machines which had been absorbing moisture. This is of course of no value to the motor manufacturer.

The authors have seized a fine opportunity for evaluating humidity effects by their use of the many identical new machines coming from the production line. Humidity as well as temperature is a test variable which the authors have done well in emphasizing again, and it is hoped that the correction factors which have been applied so well to new machines may be adapted to machines in service also.

Moisture in insulation may be detected also by the dielectric absorption method using the ratio of resistance at 10-minutes time to the resistance at 1-minute time as the relative measure of moisture absorbed. This procedure does not establish any minimum value of resistance but evaluates the insulation in terms of polarization index. Values of polarization index have been established for large a-c machines, but it remains for this to be done for d-c machines. Experience shows that these values will be lower for d-c machines because of the greater number of creepage paths and less volume of insulation in these machines.

The linear formula for minimum resistance before proof voltage tests, which Johnson and Weil have suggested, is a definite contribution to the electric machine industry.

Caspar Goffman (Westinghouse Electric Corporation, East Pittsburgh, Pa.): I would like to comment, from a statistical point of view, on the validity of the resistivity corrections made in this paper.

The correction formulas used by the authors may be compared with formulas obtained by the method of least squares. I have made such comparisons, and in each case the corrections made by the authors compare favorably with corrections made using the more technical method.

For example, consider the reduction of resistivity to vapor pressures of 0.1 inch of mercury at the time of test and two months prior to test. The equation used in the paper is given by

$$\rho = c p_1^{-1} p_2^{-1} \qquad (1)$$

where

ρ is the resistivity
p_1 and p_2 are vapor pressures at two months prior to test and at the time of test, respectively
c is a constant

The best linear fit and the best power law fits to the data are, respectively,

$$\rho = -5.2p_1 - 4.4p_2 + 4.67 \qquad (2)$$

$$\rho = 0.104 p_1^{-0.743} p_2^{-1.07} \qquad (3)$$

Equation 1 is a much closer fit to the data than equation 2 and is very nearly as good a fit as equation 3, the difference between equation 1 and equation 3 being well within usual limits of chance variation. In view of the fact that equation 1 is simple and that its difference with equation 3 may be attributed to change, it seems to be preferable to equation 3.

The justification of using any corrections at all lies in the fact that the standard deviation of corrected resistivities is about one-fourth of the standard deviation of corrected resistivities.

J. S. Johnson and **Conrad Weil:** The authors wish to point out a correction to Figure 1 of the paper as originally submitted. The curve on this figure showing the comparison of the correlation of the Wieseman size correction originally showed a one-eighth to eight extreme variation for the central 99 per cent of the machines checked. This value should be one-third to three.

Based on this corrected data as now shown in Figure 1, Wieseman's size correction shows approximately the same variability as the size correction derived by the authors. It should be pointed out that the authors' linear approximation compares favorably with both Wieseman's and the authors' theoretical corrections. The linear correction definitely has the advantage of simplicity.

The discrepancy between the authors' linear correction and the Wieseman size correction as shown in the curve of Wieseman's discussion could be explained by the choice of ratings used in checking the formula. Wieseman does not state how many machines were involved in his comparison nor the range in speed and horsepower of the designs checked. The authors' comparison included 200 representative

Table I

	Assumption		Variation
(a).	$\frac{\text{Horsepower}}{\text{Revolutions per minute}} = K_1 D^2 L$		K_1 varies about 2 to 1
(b).	Insulation thickness	(Constant)	Varies about $1^3/_4$ to 1
(c).	$\frac{\text{Slot area}}{\text{Creepage area}}$	(Constant)	Varies about 2 to 1
(d).	Slot depth	(Constant)	Varies about $1^3/_4$ to 1
(e).	Slot pitch	(Constant)	Varies about $1^3/_4$ to 1
(f).	$\frac{\text{Armature length}}{\text{Armature diameter}}$	(Constant)	Varies about $2^1/_2$ to 1

designs in the range of 100 to 7,000 horsepower. In the 100- to 1,000-horsepower range, low, medium, and high speed machines were checked for each standard frame size. In the 1,000- to 7,000-horsepower range, machines on which actual insulation resistance data were available were used for checking machine size corrections. The largest machines checked were 7,000-horsepower 35-rpm designs.

The paper points out that physical size of the machine is only one of a number of factors which affect machine insulation resistance. Our experience has been that ambient humidity conditions exercise an important influence on commutator type machines. The discussion of Marcroft also makes this point.

Marcroft mentions the use of the ratio of insulation resistance as measured after ten and one minutes of voltage application as a relative measure of moisture content. The authors have made similar checks on large a-c machines and agree with Marcroft's views on the subject. Similar checks have not been made on d-c machines. The effect of the large exposed creepage areas on the dielectric absorption characteristics in general is such as to reduce this ratio.

Report of the Board of Directors

THE BOARD OF DIRECTORS of the American Institute of Electrical Engineers presents herewith to the membership its 62nd annual report, for the fiscal year ending April 30, 1946. It includes a general balance sheet and other statements, showing the financial condition of the Institute at the close of the fiscal year, and a brief summary of the principal activities of the Institute during the year, more detailed information having been published from month to month in *Electrical Engineering*.

BOARD OF DIRECTORS' MEETING

Five meetings of the board of directors were held during the year, four in New York, N. Y., and one in Cleveland, Ohio. Four meetings of the executive committee were held.

Information regarding many of the more important activities of the Institute which have been under consideration by the board of directors and AIEE committees is published each month in the section of *Electrical Engineering* devoted to Institute activities.

PLACES VISITED BY PRESIDENT WICKENDEN

California
Los Angeles Section; San Diego Section
San Francisco Section
University of California Branch, Berkeley

Canada
Montreal Section; Toronto Section
Vancouver Section

Colorado
Denver Section
University of Colorado Branch, Boulder

Connecticut
Connecticut Section, New Haven
University of Connecticut Branch, Storrs

District of Columbia
Washington Section

Florida
Florida Section, Miami
University of Florida Branch, Gainesville

Georgia
Georgia Section, Atlanta

Idaho
University of Idaho Branch, Moscow

Illinois
Chicago Section; Illinois Valley Section, Peoria

Indiana
Central Indiana Section, Indianapolis
Fort Wayne Section

Massachusetts
Joint meeting in Boston of Boston, Lynn, Providence, and Worcester Sections
Northeastern University Branch, Boston
Pittsfield Section; Springfield Section

Michigan
Michigan Section, Detroit
Summer Convention, Detroit

Missouri
Kansas City Section
St. Louis Section

New York
New York Section, Nutley, N. J.
North Eastern District Meeting, Buffalo
Winter Convention, New York

North Carolina
North Carolina Section, Raleigh
Southern District Meeting, Asheville

Ohio
Cincinnati Section; Cleveland Section
Dayton Section

Oregon
Portland Section

Pennsylvania
Philadelphia Section
Pittsburgh Section

South Carolina
South Carolina Section, Columbia

Texas
South West District Meeting, San Antonio

Utah
Utah Section, Salt Lake City

Virginia
Virginia Section, Richmond

Washington
Seattle Section
Spokane Section
State College of Washington Branch, Pullman

ANNUAL MEETING

On account of the cancellation of the regular summer convention, the annual meeting of the AIEE was held in the Engineering Societies Building, New York, June 27, 1945. The annual report of the board of directors for the fiscal year which ended April 30, 1945, was presented in abstract by the secretary, and the treasurer's report was presented by W. I. Slichter. Reports of the committee of tellers on votes for officers for the year to begin on August 1, 1945, and for the proposed amendments to the constitution were presented.

President-Elect Wickenden responded to his introduction with a brief address. Awards of Institute prizes were reported and presentations made to the winners. The election of Doctor C. E. Skinner as an honorary member was announced. The Lamme Medal was presented to Doctor S. H. Mortensen. The meeting was concluded with a brief review of Institute activities during the year by C. A. Powel, president.

WINTER CONVENTION

The 34th winter convention was held in New York, January 21–25, 1946, with a registration of 2,624, an all-time record. The program included 17 technical sessions, 8 conferences, and 3 symposiums, at which 78 technical and 24 conference papers were presented, a conference on Institute activities, a general session, and a joint evening session with the Institute of Radio Engineers. Other events were a dinner-dance; smoker; women's luncheon, bridge, and fashion show; and inspection trips.

In the general session, the Edison Medal was presented to Philip Sporn, executive vice-president, American Gas and Electric Service Corporation, New York, and an address on "Development of Atomic Energy" was delivered by Doctor J. R. Dunning, director of the division of war research, Columbia University, New York, and technical adviser, The Kellex Corporation.

The joint session with the IRE on Wednesday evening was devoted to the presentation of the Hoover Medal to Doctor W. H. Harrison, vice-president, American Telephone and Telegraph Company, New York, and an address on "Some Electrical Engineering and General Aspects of the Atomic Bomb Project" by Major General Leslie R. Groves.

DISTRICT MEETINGS

South West District Meeting. This meeting was held in San Antonio, Tex., April 16–18, 1946, with a registration of 366. The principal sessions included 5 technical, one on electrical problems in Mexico, one general, one for student papers, and one for a general discussion of Institute activities. Other events were a banquet, smoker, inspection trip to Randolph Field, luncheon meeting of the District executive committee, and luncheon meeting of the Student Branch counselors.

North Eastern District Meeting. Held in Buffalo, N. Y., April 24–26, 1946, this meeting had been postponed, on account of wartime travel congestion, from the spring of 1945. The registration was about 400. The chief activities were 8 technical sessions, a conference on quality control, a general luncheon, a banquet, a dinner and smoker, a student technical session, a District executive committee luncheon, a Branch counselors' and chairmen's luncheon, inspection trips, a women's luncheon, and a visit to Niagara Falls and dinner for women.

COMMITTEE ON COLLECTIVE BARGAINING AND RELATED MATTERS

The committee's tentative report was published in the July 1945 issue of *Electrical Engineering*, and this report was given publicity by several of the other engineering societies by publication, or by mailings, to members. Also, in December 1945, the AIEE Sections committee mailed copies of the report to all AIEE Section chairmen suggesting discussions of it at Section meetings. The chairman and the secretary of the committee on collective bargaining and related matters have talked on this subject at several AIEE Section meetings. In all of these efforts at giving publicity to the tentative report, members have been urged to read the report and to send in comments and criticisms. To date less than 50 such comments have been received by the committee.

The interest in the subject, particularly on the part of younger engineers, continues at high level, but manifests itself in the form of inquiries pertaining to specific cases of attempts to place engineers in bargaining groups not of their own choosing, rather than in comments on the committee's tentative report.

The preparation of a manual on the subject of collective bargaining, as it relates to professional employees, has been followed actively by the committee and its consultant, Doctor Waldo Fisher, during the past year. Several chapters have been written and have been reviewed by the committee. To carry out this work, two two-day meetings of the committee with its consultant were held, one in September 1945 and the other in January 1946. Another such two-day meeting is scheduled for May or June

1946. It is expected that the drafting of the manual will be completed during the fall of 1946.

The AIEE committee on collective bargaining and related matters is collaborating with the committee on collective bargaining under the committee on the economic status of the engineer (Engineers Joint Council), and it is expected that the final wording and arrangement of the manual will have the approval of the committee on the economic status of the engineer. Such approval, it is hoped, will lead to joint publication of the manual by the several engineering societies participating in the work of the committee on the economic status of the engineer.

The committee has under consideration the mailing of a questionnaire to all members to obtain their views on the matter of collective bargaining by professional employees, and on federal legislation affecting such collective bargaining. The committee is hopeful that such a questionnaire might be handled through the committee on the economic status of the engineer, and go to the combined membership of the engineering societies participating in the work of the latter committee.

COMMITTEE ON REGISTRATION OF ENGINEERS

On August 28, 1945, the conference committee on Model Law met to consider revisions of definitions. A report on the actions of the meeting was published in *Electrical Engineering* for May 1946, in connection with the complete text of the Model Law.

This revision was discussed by the American Society of Civil Engineers' committee on registration of engineers at its meeting in January 1945, at which time the revision of the second paragraph of Section 13 was recommended as quoted.

The AIEE was invited to endorse the new draft. At the January 25th meeting of the AIEE board of directors, the following resolution was presented and adopted.

RESOLVED, that the AIEE recognizes the registration of engineers as a continuing practice and the Model Law for the registration of professional engineers and land surveyors, as adopted in 1943 and amended in 1945, as the widely accepted basis of its administration, and that the Institute endorses these procedures as well established.

In view of this more positive action and changed position of AIEE, it was recommended that a new standing committee be appointed replacing the present committee on registration of engineers and that it have a scope of responsibility covering matters related to registration, to be reported at a subsequent meeting. (This recommendation was adopted.) The drafting of scope was referred to the committee on planning and co-ordination.

Notification of AIEE endorsement has been sent to the ASCE sponsors of the Model Law and to the conference committee of the various societies.

The present Model Law is the result of compromise and is subject to revisions when needed and proposed by the conference committee for endorsement by constituent societies. In order for the new standing committee to be thoroughly representative of AIEE thought, it will be necessary for Sections to follow developments in their localities and inform the standing committee of local conditions and the considered reactions of their members, together with suggestions for desired alterations in Model Law.

General Committees

SECTIONS COMMITTEE

1. Section Programs. The Sections generally have been following a program of expanding their activities to meet the increased scope and growing demands of the electrical industry and to provide for the diversification of interest of the Section members. With the end of the war, it has been possible to give increased attention to student activities, social activities, more fellowship at meetings, inspection trips, and the broader subject of civic responsibilities of engineers. During the past year, Section officers have been generally more conscious of the importance of balanced Section operation, which provides activities to retain the older members as well as attract new members. In giving more time to creative work and the co-ordination of the activities of their Sections, many Chairmen have followed the suggestion of delegating to committees much of the operating work of running the Section. The increase in operating committees in the Section has resulted in more members working actively for the Section, which in turn has created additional interest.

2. Sections Committee Organization. Because of the volume of the Sections committee work, the committee again was organized at the beginning of the year into two groups. The planning group, consisting of six members, initiates and develops all plans of the committee. The promotional group consists of ten members located geographically on a District basis, making it possible to handle much of the promotional work individually with the Sections. Most of the material used by the promotional group is sent to each member, who in turn supplements it with his personal knowledge of local conditions, before contacting the Sections in his District. Close contact is maintained between the promotional group member and the vice-president of the District.

3. Conferences on Section Operation and Management Held in Connection With District Meetings. Due to the cancellation of the summer technical meeting in 1945, the usual delegates meetings were not held. A program for conferences on Section operation and management was developed by the Sections committee to be held at the individual District meetings early in the fall of that year. These meetings were presided over by the vice-president of each District. A detailed outline of the suggested conference was prepared by the Sections committee for the information and guidance of the vice-presidents. No conference was held in District 3—New York, and District 10—Canada. The Sections of the Canadian District divided their attendance between the meetings held in District 1 and District 9. These meetings were very successful as a substitute program for the regular delegates meetings and provided the Section officers with much information, enthusiasm, and inspiration for the conduct of the affairs of the Sections. The promotional group representatives of the Sections committee received special travel allowance to attend their respective meetings in each District.

These meetings were so well received by Section officers that the Section representatives recommended, at the Sections committee meeting in New York, January 22, 1946, that these District conferences on Section operation and management be continued as a supplement to the regular delegates meetings, which will be held at the summer convention.

4. Technical Groups. The development of technical groups is a very important part of the plan to retain the diversified interest of the older members as well as attract new members. The Sections committee sent a copy of the folder "Technical Groups" to each Section chairman at the beginning of the year and, through its promotional group, has been making individual contacts with those Sections where there is a possibility of the successful operation of these technical groups. The promotional group also has been supplying individual Sections with reports of examples of successful operation of these technical groups. The value of such groups operated within the Section is becoming more generally recognized throughout the country. There were 51 groups in active operation at the end of the 1944–45 operating year. Reports received from the Sections indicate 23 new technical groups have been formed to date this year. Many other groups are in process of being formed. The Sections have been asked to explore thoroughly their area to make certain that they have the entire field of electrical engineering covered by suitable technical groups.

5. Subsections. Subsection operation is a valuable means of accomplishing the important objective of the Institute, by providing additional meeting places at which papers on electrical engineering subjects may be presented and discussed. With all the territory in the continental United States allocated to the Sections, the next logical step forward in the development of Section activities was to form Subsections or additional centers of electrical engineering influence. Many opportunities exist for members in the remote areas of a Section territory to participate in Section activities through the development of Subsections in these area. A copy of the folder "Subsections" was sent to each Section chairman at the beginning of the year, and the promotional group of the Sections committee has encouraged the Sections to consider the opportunities which exist for the formation of additional Subsections. Examples of successful operation of Subsections were sent to the individual Sections by the promotional group. Subsection operation is becoming more popu-

lar each year as its advantages are more widely recognized. Ten additional Subsections have started operation during the year, and there are now 25 Subsections in active operation. Many additional locations for Subsections are being considered by the Sections.

6. Local Councils of Engineering and Technical Societies. Participation of AIEE Sections in the work of the local council in their community provides a means by which the Section members can engage in civic, legislative, and other similar broad activities of the engineering profession without the necessity of joining additional societies. Interest in these local councils during the past year has been very great throughout the country. There are now 43 councils in active operation, about half of which have been formed since 1940. Several additional councils are in process of being formed. In most cases not only the local AIEE Section has been very active in forming these councils, but also the members of the local AIEE Sections have been very active in the work of these councils. This activity has been encouraged during the past year by the Sections committee. On February 8, 1946, a letter was sent to all Section chairmen on the subject of these local councils. The promotional group has distributed to the Sections examples of the successful operation and organization of these local councils in various parts of the country. This Sections committee activity was designed to encourage AIEE Sections to become active in the formation of local councils in their areas where these councils do not exist and to encourage the Sections to become more active in local councils now in operation.

The Institute has representatives on a committee of the Engineers Joint Council for the organization of the engineering profession. This committee has approved for distribution to the local sections of the various societies, a report on the organization of local councils which closely parallels the information previously sent out by the Sections committee. The Sections of the co-operating societies have been requested to furnish certain information concerning local councils now in operation. This information is to be used by the committee to develop plans for regional and national organizations for the engineering profession.

7. Section Finance. In co-operation with the finance committee of the Institute, plans were formulated to provide for certain increases in appropriations to those Sections operating Subsections and technical groups. The plan for these additional appropriations was approved in principle by the executive committee of the Board of Directors and referred to the finance committee. The proposed increases will cover the cost of the expanded activities of the Sections, and it is hoped that final approval will be obtained to place them in effect for the 1946–47 operating year.

8. Student Activities. In co-operation with the committee on Student Branches, the Sections committee has developed a plan of co-operation between the AIEE Sections and the Student Branches. This plan was distributed simultaneously on April 1, 1946, to the officers of each Section and Branch, Student Branch counselors, vice-presidents and District secretaries. Under postwar conditions, the Student Branches are resuming normal activities. It is essential that the AIEE Student Branches develop, as early as possible, the interest of those students who select electrical engineering. The Sections can assist materially in this important activity. Such help from the Sections gains increased importance now because of the maturity of those returning to electrical engineering studies after service in the Armed Forces.

9. Educational Courses. In co-operation with the committee on education, the Sections committee released a letter to all Sections calling attention to the opportunities for additional Sections of the Institute to perform a worth-while service by offering educational courses to their members and others. The letter explains how these courses are conducted and lists several suggestions on possible courses which could be offered at the beginning of the 1946–47 operating year.

10. Changes in Section Territory. The following changes in Section territory were made during the year:

The Mexico Section was transferred from District 3 to District 7. This transfer was made with the approval of the vice-presidents of the two Districts concerned. The negotiations for the approval of the Mexico Section were handled by the Sections committee. This transfer places the Mexico Section in direct contact with the adjoining territory, which has resulted in increased interest of the Mexico Section in the affairs of the Institute.

The formation of the Illinois Valley Section was approved by the Board of Directors at its meeting on May 29, 1945. The territory of this Section comprises 22 counties in the State of Illinois, which were previously a part of the Urbana Section. This new Section was formed with the approval of the Urbana Section and the vice-president of District 5.

The formation of the Beaumont Section was approved by the Board of Directors on June 27. This Section comprises 13 counties in the State of Texas, which were formerly the territory of the Houston Section. This new Section was formed with the approval of the Houston Section and the vice-president of District 7.

11. Annual Report of Section Chairmen. An annual report of Section chairmen was prepared by the Sections committee and distributed to all Sections at the close of the 1943–44 operating year and the 1944–45 operating year. This report provides a simple analysis of major activities and the organization of all Sections and contains much information of value to new Section officers in laying out their Section program for the year. This report also is sent to all vice-presidents, District secretaries, and the chairmen of all national committees. Due to the wide acceptance of this report, it is planned to continue this feature at the close of the present operating year.

12. Section Operating Committees. On November 28, 1945, a letter was sent to all Sections suggesting the formation of additional Section operating committees in order to handle properly the increased activity within the Sections. The annual report of Section chairmen showed 348 committees reported for 1943–44, as compared with 410 committees reported for 1944–45. A list of suggested committees was given in this letter to the Sections. It was pointed out that spreading the work of the Section by the use of additional committees provides an opportunity for more members to participate actively in the work of the Section.

13. Section News Items for Electrical Engineering. A letter has been released to all Sections requesting news items for publication in *Electrical Engineering* and again requesting articles on subjects presented at Section meetings for possible publication in the general interest section of *Electrical Engineering*. This activity has the approval of the publication committee and was prepared with the co-operation of the editor of *Electrical Engineering*.

14. Co-operation With Other National Committees. In addition to close co-operation with the vice-presidents, certain features of the Sections committee program were co-ordinated with the Institute finance committee, membership committee, committee on Student Branches, and the committee on education.

Each of the Institute technical committees also was approached in an effort to obtain the co-operation of these committees in the development and operation of technical groups within the Sections. Several technical committees have participated actively in this program during the year, and it is believed that this work will serve as a pattern in the future for greater co-operation within the Institute.

15. Delegates Meetings at Summer Convention. The Sections committee has prepared a comprehensive program for the Institute officers, Section delegates, and members at the summer convention at Detroit. Three parallel conferences on Section operation and management will be conducted on June 24th, with the delegates divided into groups representing the larger, intermediate, and smaller Sections. The conference of officers, delegates, and members will be held on June 25th. On June 26th a conference on Section activities in connection with local councils of engineering and technical societies will be held, and on June 27th a conference on Section–Branch co-operation is scheduled as a joint activity of the Sections committee and the committee on Student Branches.

16. Committee Meetings. Due to the nature of the Sections committee work, the activities of the committee were carried on by means of correspondence. One meeting was held by the committee on January 22, 1946, in New York during the winter convention, with an attendance of 51. At this meeting the entire Sections

Table I. Section and Branch Statistics

	For Fiscal Year Ending April 30					
	1941	1942	1943	1944	1945	1946
Sections						
Number of Sections	72	72	73	73	73	75
Number of meetings held	703	647	598	738	884	1,210
Total attendance	92,554	78,254	66,111	83,120	96,346	113,531
Branches						
Number of Branches	123	124	125	125	125	125
Number of meetings held	1,163	946	942	755	547	716
Total attendance	52,285	37,785	38,227	24,768	17,132	22,844

committee program was reviewed, and plans for the remaining portion of the year were discussed. Minutes of this meeting were sent to all who attended and in addition were sent to all vice-presidents, District secretaries, and Section chairmen.

COMMITTEE ON STUDENT BRANCHES

The committee on student branches during the current year has exerted its efforts primarily toward the conversion of Student Branches from uncertain wartime operation to a stable, yet flexible, program of peacetime operation.

A major step has been taken in the reinauguration of District student conferences in connection with District meetings. Successful conferences in somewhat modified form have been held at the South West District meeting, San Antonio, April 16–18, and at the North Eastern District meeting, Buffalo, April 24–26. A more comprehensive conference has been planned and seems definitely destined for success at the Southern District meeting, Asheville, May 14–16.

For some time, a subcommittee on joint Student Branches, with J. F. Calvert as chairman, and comprising M. S. Coover, M. M. Cory, and J. E. Hobson, studied the possibilities of the operation of joint AIEE-IRE Student Branches, and at a meeting of the committee on Student Branches held in New York at the time of the winter convention, January 22, 1946, made the following recommendations, which were accepted by the committee on Student Branches and approved by the board of directors of the AIEE:

1. It is recommended that insofar as the establishment of joint AIEE–IRE Student Branches is concerned, that such branches not only should be permitted, but also should be encouraged, in accordance with the principles stated in the recommendations of the committee on planning and co-ordination. This should not be considered to oppose similar joint action with other technical societies.

2. It is recommended further that the board of directors of the AIEE be requested to take appropriate action in co-operation with the proper representatives of the IRE, and at the earliest opportunity, to arrange all details essential to the successful operation of these proposed joint Student Branches.

This means that Student members in either AIEE or IRE automatically share equal rights in joint Student Branches, in addition to the advantages offered by their particular society, and are eligible for admission to a regular membership grade in either participating society without entrance fee. It is hoped that such joint Student Branches eventually will include Student members of other societies of similar type and policy. The plan proposes, in general, an engineering council at the Student member and Student Branch level.

It is not intended that the identity of AIEE Student Branches be lost, for there will be many subjects and meetings of prime interest to AIEE Student members and of little or no interest to IRE members. Such meetings, as well as AIEE Student District conferences, and joint activities with AIEE Sections and Districts, will maintain the identity and independence of AIEE Student Branches, even while cooperating within their schools in joint Student Branches as recommended.

Arrangements also have been made to distribute in reprint form the excellent series of three articles on "The Unwritten Laws of Engineering" by W. J. King, formerly of the General Electric Company, and now with Battelle Institute.

After acceptance of these recommendations by the board of directors, this same subcommittee was requested to study and develop policies, programs, and practices, using Student Branches in the Chicago area as pilot projects, and to report their findings and recommendations to the committee on Student Branches at its annual meeting in connection with the summer convention in Detroit, June 24–28, 1946.

FINANCE COMMITTEE

Institute revenue has been sustained at a high level for the fiscal year as a consequence of growth in membership and a steady demand for Institute publications. Attention is directed to the detailed financial statements on pages 18, 19, and 20, and especially to Exhibit B in which report is made on cash receipts and disbursements, and the excess of income over expenditures is shown.

The budget presented to and approved by the board of directors provided for the effective continuance of all Institute activities and proper participation by the Institute in matters of common interest with other technical societies and associations. All expenditures have been in accordance with the intent of the budget items, some upward revisions of detailed figures having to be made to meet rising costs, especially iu connection with items concerned with the publication of *Electrical Engineering*.

An amount of $1,762.38 was placed in the Member-for-Life fund, and the excess of income over expenditures has permitted the transfer of approximately $120,000 to the reserve capital fund. In addition, the Institute received last fall a bequest of $10,652 from the late W. S. Barstow without restrictions as to its use. This amount also was transferred to the reserve capital fund, and all such amounts invested in appropriate securities.

As of May 1, 1946, 1,800 members were on inactive status in accordance with the established policy to grant dues concessions on requests to those serving in the Armed Forces and merchant marine. The foregoing figure compares with 2,259 members in such status as of May 1, 1945.

A summary of the securities owned by the Institute as of April 30 is presented in Schedule 1. A substantial portion of the reserve capital fund is in United States Government bonds, and the market value of other securities will be noted to be favorable. The finance committee avails itself continuously of the advice of investment counsel in connection with the purchase and other negotiations concerned with securities, and all items in the present portfolio fund have been approved from the standpoints of appropriateness and diversification.

Institute expenditures are budgeted to come within anticipated income, and the present sound financial condition reflects the conservative policy that has been followed over the years. The steady growth of the reserve capital fund is indicative of the ability of the Institute to render the character of service to the membership that may be indicated to be desirable and gives assurance with regard to the availability of funds to continue at proper level essential activities at such times as income might be temporarily affected by unforeseeable influences or economic conditions.

TECHNICAL PROGRAM COMMITTEE

Reconversion Programs. With all Institute and District meetings, except the winter meeting, canceled in 1945 and with various strike situations in 1946 the arrangement of adequate technical programs during the reconversion period has been difficult. To substitute for the canceled 1945 meetings, spring, summer, and fall technical paper programs, with preprints of the papers available, were announced nationally and offered for discussion by mail. A comparison of the number of papers offered on the three programs by mail with the number of papers for the three corresponding meetings of the previous 12-month period is of interest. The results shown in Table II represent a 49.1 per cent decrease in the number of papers offered, notwithstanding the special efforts that were made to announce the substitute plans in advance and solicit papers to keep pace with the many developments. The comparison serves to illustrate the value of technical meetings as a stimulus for the production of technical papers on new developments to keep the membership informed of advances in the profession.

The 1946 winter convention was an outstanding success with a registered attendance of 2,624, which exceeded all previous records. Among the high lights of this convention was an address on the de-

velopment of atomic energy by Doctor J. R. Dunning at the general session, followed by an address in the evening on "Some Electrical Engineering and General Aspects of the Atomic Bomb Project" by Major General Leslie R. Groves, and a symposium on nuclear energy which brought together the views of well-known people in the fields of physics and research. The number of papers presented for the year and the number recommended for the *Transactions* are shown in Table III.

Analysis of Subject Matter. The papers for the year have been analyzed on a percentage basis and classified into six broad fields of electrical engineering. In Table IV, the classification is compared with an occupational analysis of the membership made in 1940. When it is considered that those engaged in electrical manufacturing and educational work have considerable interest in all of these fields, the comparison indicates a reasonably close correlation between the percentage of papers presented in the first three fields and the percentage of the membership occupied in those fields. With the abandonment of wartime restrictions, it is apparent that material in the industrial and communication fields has come to the fore. The 20.3 per cent papers in the industrial and railroad fields represents a fairly uniform distribution of subject matter into subjects such as electric welding, industrial distribution, quality control and statistical methods, induction and dielectric heating, industrial control, and railways. In the field of communication, seven of the papers were on the subject of radar. As might be expected with the end of the war, the number of air transportation papers has decreased from a high of 37.5 per cent for the previous year to 13.1 per cent for the past year. The program for the forthcoming summer convention will bring forth additional papers in the fields of communication, industrial control, and servomechanisms, which heretofore have been highly restricted.

Exploratory Work. The committee has worked in close co-operation with the committee on planning and co-ordination in connection with the study of the organization of the engineering profession and the technical activities of the Institute. The technical committee chairmen have analyzed the methods of operation of some 44 other engineering societies, as a background for further consideration in organizing the technical activities. With a membership of 24,526 on January 1, 1946, and an increase of 1.33 per cent since January 1, it is not unreasonable to expect an average membership for the next five years of 28,000 members and an average number of papers per year of approximately 270. The increase in membership and the average number of papers during two 5-year periods is shown in Table V. Steps already have been taken to provide for this expansion and to keep the membership fully informed of new developments in the field of electrical engineering.

The committee has recommended that the chairmen of technical committees review all contacts with similar committees of other organizations and explore the possibilities of establishing new contacts in accordance with Section 86 of the bylaws. Closer ties with the District meeting committees and Sections have been suggested, with the recommendation that technical committees give consideration to planning important sessions on specific subjects appropriate for the localities of District meetings. It was further recommended that the Institute should adopt the policy of supplementing the three national conventions with another national convention to be held annually in the Midwest in October.

Table II. Comparison of Programs by Mail, When Meetings Were Restricted, With the Programs for the Three Previous Corresponding Meetings in 1944

	Transactions Papers		Transactions Papers
Spring technical paper program	19	Boston	12
Summer technical paper program	31	St. Louis	85
Fall technical paper program	30	Los Angeles	60
Total	80	Total	157

Per cent decrease $\frac{157-80}{157} = 49.1$ per cent

Table III. Number of Papers Presented During the Year Ending April 30, 1946

	Number of Papers	Number of Transactions Papers
Spring technical paper program	19	19
Summer technical paper program	31	31
Fall technical paper program	30	30
Winter convention	78*	68
San Antonio meeting	21	3
Buffalo meeting	33	2
	212	153

* Includes 3 representations from summer and fall technical paper programs.

Discussions are being carried on with the publication committee to permit publication of papers arising from joint meetings with other societies. The technical program committee and the publication committee are working jointly on an analysis of suggestions received through the study of the Institute's technical activities which pertain to publication policies.

To provide greater interest for younger members, the committee has recommended that a study be made with a view toward holding commercial exhibits at conventions rather than excluding them. The committee also recommended to the winter convention committee that the next winter convention be held in a hotel rather than in the Engineering Societies Building.

PUBLICATION COMMITTEE

The publication activities during the year have been influenced strongly by the termination of hostilities in World War II, which lifted many wartime controls, and by the cancellation of AIEE national and District meetings after February 1, 1945, which greatly reduced the material available for publication. Publication policies and procedures remained unchanged as papers and discussions resulting from the technical paper programs, which replaced the usual meetings, were treated in the normal manner.

In accordance with current publication policies, the 1945 *Transactions* volume contains all approved 1945 technical papers

Table V. Growth in Membership and Expected Average Number of Papers in the Next Five Years

	Approximate Average Membership	Average Number of Papers Per Year
5-year period following 1925	18,000	160
5-year period following 1940	20,000	200
5-year period following 1945	28,000*	270*

* Forecast.

Table IV. Comparison of Classification of Papers in Six Broad Fields With an Occupational Analysis of Membership as of 1940

	Per Cent of Papers	Occupational Analysis of Membership (1940 Survey)	
Central stations	27.4	Light and power	25.5
Communication	13.7	Communication	9.7
Industrial and railroad	20.3	Industrial and railroad	11.4
Air transportation	13.1	Government	5.9
Electric machinery	14.4	Electrical manufacturing	25.8
Basic sciences and measurements	11.1	Educational	5.4
		Consultants and large contractors	4.4
		Miscellaneous	11.9
	100 per cent		10 per cent

and related discussions. Two semiannual "Supplements to Electrical Engineering—Transactions Section" were produced, on the usual limited-edition advance-order basis, containing (1) technical papers that could not be accommodated in the monthly *Transactions* sections of *Electrical Engineering*, and (2) all approved discussions.

Relaxation of strict censorship controls was reflected in the increased content devoted to wartime developments.

The easing of restrictions on paper supply permitted a return in January 1946 to the larger trim size and to the format that had been used in *Electrical Engineering* in 1943. A paper somewhat heavier than that used in 1945, but still not so heavy as the prewar paper, also was obtained.

The reduction in material for publication caused primarily by the cancellation of meetings, but possibly influenced also by the letdown following the end of fighting, is shown by a comparison of the numbers of pages of various classes of material published in the calendar years 1944 and 1945, as compared with 1941 as the last prewar year:

Numbers of Pages of Published Material

Year	Electrical Engineering			Transactions Only		
	General Interest Articles	News	Transactions Section	Technical Papers	Discussion	Total
1941	337	281	600	542	268	2,028
1944	246	214	738	493	231	1,922
1945	255	225	736	121	143	1,486

It may be noted that the number of pages in the "Transactions" section of *Electrical Engineering* in 1945 was maintained by publishing therein a greater proportion of the year's total of technical papers than was done in 1944. The use of a paper of lighter weight and the easing of paper restrictions in the latter part of 1945 permitted the number of pages in *Electrical Engineering* to be held at a fair level in spite of an increase in the number of copies printed, from 26,250 in December 1944 to 28,750 in December 1945. It was possible also to restore the 1945 annual report of the AIEE board of directors and the annual reference index to complete circulation. Only a limited distribution had been made in 1944 in order to conserve paper for text pages.

Advance pamphlets of approved technical papers were produced as required by the technical program committee for discussion by mail on summer and fall programs in 1945, and for regularly scheduled meetings beginning with the winter convention in January 1946.

The quarterly AIEE "Bulletin" for Institute members in the armed services was continued through the issue of February 1946. The number of members receiving the "Bulletin" decreased rapidly with the demobilization of the Armed Forces.

Revision of the booklet, "Information for Authors," to which reference was made in last year's report of this committee was deferred.

MEMBERSHIP COMMITTEE

It is quite interesting to note at this time that the growth in membership for the year 1945–46 has exceeded by a considerable margin the gain of any previous year in the history of the Institute. The net gain is 2,018 which brings the total membership to 25,090. The rate of gain in 1945–46 was 8.7 per cent, and the rate of gain for the 1944–45 period was 7.8 per cent. In the past two years, the numerical net gain has been 3,683. Judging from the rate at which new applications and applications from former members for reinstatement or re-election are being received, it would appear that the membership for the coming year is destined to continue to increase at a high rate.

The number of persons who were classified as having an "inactive status" because of military service or for other causes resulting from World War II was 2,259 at the end of the fiscal year 1944–45. This number increased to approximately 2,500. However, on April 30, 1946, the total had dropped to 1,809. This is a favorable trend and demonstrates the desire of the persons in this classification to return on their own motion to active membership status as promptly as possible. The policy of the Institute in this connection seems to have proved to be quite beneficial.

Starting in the year 1942, a renewed interest in the Institute was manifested by persons who had been members formerly. During that year, 237 were either reinstated or re-elected to membership. In 1943–44 the number in this group was 301. The corresponding numbers for the years 1944–45 and 1945–46 are 366 and 401, respectively. This trend is significant, as is the fact that the number in arrears for the fiscal year April 30, 1946, is only 954 or 3.8 per cent of the total membership. It will be recalled the corresponding number for those in arrears for 1944–45 was 902.

The number of transfers from the Associate and Member grades to higher grades of membership was 559. This number corresponds with totals of 464 and 420, respectively, for the years 1944–45 and 1943–44.

The total losses in membership for the year (Deductions, Table VI) was 600, or 102 lower than in 1944–45. From the same table, it will be seen that the total new members qualified was 2,217, an increase of 216 over the corresponding period in the previous year. The membership, not including Student members, is divided as follows:

Membership Grade	Per Cent
Honorary	0.04
Fellows	3.93
Members	27.47
Six-Year Associates	29.29
Associates	39.27
	100.00

The Member and Associate Grades have increased 0.44 per cent and 0.48 per cent, respectively, while the six-year Associate grade has decreased 0.90 per cent.

From Table VII, it will be noted that the number of applications from the Student members is once more ascending and that the applications from all other sources increased by 274 or 12.7 per cent. The total increase in applications was 333 or 13.7 per cent. No direct comparison between this Table and Table VIII can be made, since all applications received during the

Table VI. Membership Statistics for Fiscal Year Ending April 30, 1946

	Honorary Members	Fellows	Members	6-Year Associates	Associates	Subtotals	Totals
Membership April 30, 1945	6	914	6,238	6,963	8,951		23,072
Additions							
New members qualified		2	262		1,953	2,217	
Former members reinstated or re-elected		1	134	80	186	401	
Subtotals		3	396	80	2,139	2,618	
Transfers	3	90	466	925		1,484	
Totals	3	93	862	1,005	2,139	4,102	
Deductions							
Died		16	51	45	15	127	
Resigned			30	90	36	156	
Dropped			38	107	172	317	
Subtotals		16	119	242	223	600	
Transfers		3	89	378	1,014	1,484	
Totals		19	208	620	1,237	2,084	
Net changes	3	74	654	385	902	2,018	
Membership April 30, 1946	9	988	6,892	7,348	9,853		25,090

Table VII. Number of Applications Received From Student Members and From All Others

Year Ending April 30	Students	All Others	Total
1946	308	2,453	2,761
1945	249	2,179	2,428
1944	466	1,908	2,374
1943	783	1,431	2,214
1942	971	1,031	2,002

Table VIII. Number of Student Members as of April 30

Year	New Applications	Renewals	Total
1946	2,574	2,513	5,087
1945	2,326	2,287	4,613
1944	2,242	2,656	4,898
1943	2,512	3,200	5,712
1942	2,585	3,377	5,962

fiscal year are not acted upon before the close of that year.

Table VIII shows a marked renewed activity in Student membership. The increase in new applications is 248 while the increase in renewals is 226, bringing the total increase to 474. The Student membership now stands at 5,087.

Table IX is a record of the total membership of the Institute by years since 1884 and is given for information purposes.

Table X is the usual listing of the names of AIEE members reported in *Electrical Engineering* as having died during the fiscal year 1945–46. By this method a ready reference is provided.

The new booklet which was reported last year as being under preparation by the membership committee for use particularly when contacting prospects for membership in the Institute has been completed. It is an attractive, brief, concise publication of handy pocket size which already has been enthusiastically received.

There is much in the data relative to membership activity which should be of considerable interest to every person in the Institute. The growth has exceeded all expectations. It seems to be due to a strong interest on the part of the members generally, the enthusiastic co-operation of the entire membership committee personnel and the ever ready progressive co-operation of the members of the staff at the Institute headquarters. Undoubtedly, also the present economic situation and probable future trends in the scientific and industrial world are factors which have contributed to this rather unusual growth.

Table IX. Record of AIEE Membership

Year	Total May 1	Year	Total May 1	Year	Total May 1
1884	71	1905	3,460	1926	18,158
1885	209	1906	3,870	1927	18,344
1886	250	1907	4,521	1928	18,265
1887	314	1908	5,674	1929	18,133
1889	333	1909	6,400	1930	18,003
1890	427	1910	6,681	1931	18,334
1891	541	1911	7,117	1932	17,550
1892	615	1912	7,459	1933	17,019
1893	673	1913	7,654	1934	15,230
1894	800	1914	7,876	1935	14,269
1895	944	1915	8,054	1936	14,600
1896	1,035	1916	8,202	1937	15,308
1897	1,073	1917	8,710	1938	16,078
1898	1,098	1918	9,282	1939	16,605
1899	1,133	1919	10,352	1940	17,213
1900	1,183	1920	11,345	1941	17,886
1901	1,260	1921	13,215	1942	18,944
1902	1,549	1922	14,263	1943	20,161
1903	2,229	1923	15,298	1944	21,407
1904	3,027	1924	16,455	1945	23,072
		1925	17,319	1946	25,090

Table X. Deaths of AIEE Members Reported in "Electrical Engineering"

Name	Date of Election	Date of Death	Grade at Death	Obituary Notice in "Electrical Engineering"
Acres, H. G.	A '08	Sept. 4, '45	M	Oct. '45, p. 373
Adams, H. H.	A '06	Jan. 31, '45	M	May '45, p. 197
Alliason, A. R.	A '32	June 5, '45	M	Sept. '45, p. 337
Angle, F. C.	A '38	Oct. 25, '45	A	Jan. '46, p. 41
Barger, C. A.	A '44	Apr. 2, '45	A	July '45, p. 274
Barney, G. C.	M '37	May 11, '45	M	July '45, p. 274
Battit, B. E.	A '35	Oct. 11, '44	A	Nov. '45, p. 415
Beall, C. R.	A '18	Feb. 24, '45	A	June '45, p. 232
Bell, A. C.	A '01		A	June '45, p. 232
Bingham, A. R.	A '07	Jan. 4, '46	M	Mar. '46, p. 136
Blickley, C. F.	M '44	Nov. 11, '45	M	Jan. '46, p. 40
Blumberg, Ralph Dietz	M '44	Oct. 30, '45	M	Jan. '46, p. 40
Bolsterli, A. A.	A '23	Sept. 25, '45	M	Dec. '45, p. 459
Bonine, J. H.	A '17	May 12, '45	A	Aug. '45, p. 306
Booth, Wm. S.	A '44	May 3, '45	A	July '45, p. 275
Brewster, Truman P.	M '44	Jan. 7, '45	M	July '45, p. 275
Brown, Harry C.	A '20	Feb. 21, '45	A	July '45, p. 274
Brubaker, Leonard H.	A '42	Sept. 30, '45	A	Jan. '46, p. 40
Buehner, Robert O.	M '36	July 23, '45	F	Nov. '45, p. 415
Caldwell, C. W.	A '32	June 5, '45	A	Aug. '45, p. 306
Chatham, Clyde L.	A '25	June 7, '45	M	Sept. '45, p. 338
Clarkson, A. J.	M '26	June 4, '45	F	Aug. '45, p. 306
Conwell, R. N.	A '15	Apr. 14, '45	F	May '45, p. 197
Corson, Wm. R. C.	A '93	Oct. 2, '45	A	Dec. '45, p. 459
Creese, M.	A '07	Oct. 16, '45	M	Nov. '45, p. 415
Cushing, H. M.	A '06	Jan. 31, '45	F	May '45, p. 197
Davis, John M.	A '34	Aug. 13, '45	A	Oct. '45, p. 373
Donovan, J. D.	A '39	Dec. 20, '44	A	June '45, p. 232
Dudley, A. M.	A '08	Aug. 16, '45	F	Oct. '45, p. 373
Dyer, Leslie L.	A '10	Aug. 24, '45	M	Dec. '45, p. 458
Enfield, W. L.	A '10	Mar. 21, '45	F	May '45, p. 198
Faucett, Irving T.	A '11	Jan. 16, '46	F	Apr. '46, p. 179
Flowers, Alan Estis	M '04	Dec. '45	M	Jan. '46, p. 40
Fowle, F. F.	A '02	Jan. 21, '46	M	Mar. '46, p. 135
Frank, Harry C.	M '41	June 9, '45	M	Sept. '45, p. 338
Gabay, Henry R.	A '07	Jan. 12, '46	M	Feb. '46, p. 90
Gossler, P. G.	A '94	May 18, '45	F	July '45, p. 273
Haddow, A. B.	M '35		M	June '45, p. 232
Hanson, C. F.	A '18	Apr. 27, '45	M	Aug. '45, p. 306
Harvey, R. R.	A '95	Feb. 20, '45	A	July '45, p. 275
Hedges, Leo B.	A '28	Nov. 30, '45	M	Feb. '46, p. 90
Herman, J. W.	A '07	Mar. 30, '45	A	May '45, p. 197
Hertz, Adolph	A '18	May 31, '45	A	Aug. '45, p. 306
Highfield, John S.	F '42	Aug. 15, '45	F	Oct. '45, p. 373
Hill, Warren Rhodes	A '24	Apr. 11, '45	A	July '45, p. 274
Hoeckstetter, Lionel	A '35	May 8, '45	A	July '45, p. 274
Holder, Edward	A '13	Dec. 20, '45	M	Mar. '45, p. 136
Holslag, C. J.	M '19	June 11, '45	F	July '45, p. 273
Horrell, C. R.	A '16	July 5, '45	M	Aug. '45, p. 306
Horton, Bryson D.	A '14	Dec. 14, '45	A	Feb. '46, p. 90
Hutchinson, George E.	A '11	Oct. 20, '45	M	Dec. '45, p. 459
Ilsley, Lee Clyde	A '14	Nov. 23, '45	A	Jan. '46, p. 40
Jackson, Frederick D.	M '42	Dec. 18, '45	M	Feb. '46, p. 90
Kahler, Chas. Porterfield	A '10	Feb. 25, '46	M	Apr. '46, p. 180
Kahn, M. L.	A '20	July 25, '45	A	Oct. '45, p. 373
Karr, E. P.	A '40	Jan. 6, '45	A	Aug. '45, p. 306
Kelly, Walter Stuart	M '04	July 4, '45	A	Jan. '46, p. 40
Laidlaw, H. A.	A '09	Dec. 15, '45	M	Mar. '46, p. 135
Lindquist, D. L.	A '04	Nov. 11, '45	A	May '45, p. 198
Lovejoy, Jesse R.	A '91	Oct. 31, '45	F	Dec. '45, p. 459
Lowther, C. M.	A '00	Apr. 12, '45	A	July '45, p. 274
MacDonald, W. P.	M '43	Nov. 30, '45	A	Feb. '46, p. 90
MacLaren, Malcolm	A '05	Sept. 25, '45	M	Nov. '45, p. 415
Mason, E. J. K.	A '07	Feb. 23, '45	A	May '45, p. 198
McCormick, B. T.	A '04	Apr. 20, '45	F	July '45, p. 273
McElroy, D. W.	A '19	Dec. 13, '45	A	Jan. '46, p. 41
Moore, Leonard J.	A '15	June 4, '45	F	Sept. '45, p. 337
Myler, P. J.	A '07	Apr. 20, '45	A	June '45, p. 232
Neiler, S. G.	A '94	Feb. 28, '45	F	May '45, p. 198
Palmer, H. R.	A '08	June 16, '45	M	Aug. '45, p. 306
Patton, G. J. K.	A '39	Aug. 17, '45	A	Jan. '46, p. 41
Pease, H. C.	A '03	May 5, '45	A	July '45, p. 274
Pedersen, P. R.	A '23	Apr. 4, '45	A	Nov. '45, p. 415
Perkins, Chas. A.	A '05	Nov. 26, '45	F	Jan. '46, p. 40
Perry, Chas. L.	A '03	Nov. 20, '45	A	Feb. '46, p. 91
Petrasek, Wm. August	A '36	Jan. 31, '46	A	Mar. '46, p. 136
Poole, W. C.	M '39	Oct. 16, '45	M	Sept. '45, p. 337
Potts, L. M.	A '02	Oct. 23, '45	M	Jan. '46, p. 39
Price, C. A.	A '19	Dec. 29, '45	M	Mar. '46, p. 136
Pullen, M. W.	A '07	Jan. 10, '46	M	Mar. '46, p. 136
Putman, H. V.	A '23	Jan. 16, '46	M	Mar. '46, p. 136
Reinicker, N. G.	M '18	Jan. 13, '46	M	Feb. '46, p. 90
Rhodes, W. K.	A '09	Dec. 12, '45	M	Jan. '46, p. 41
Richards, A. F. W.	A '17	Jan. 25, '46	M	Mar. '46, p. 136
Ross, L. E.	A '29	Dec. 22, '45	A	Apr. '46, p. 180
Rowe, B. P.	A '03	Sept. 21, '45	F	Dec. '45, p. 459
Spaulding, S. A.	A '05	May 25, '45	F	July '45, p. 274
Symbolie, A. J.	A '42	Apr. '45	A	July '45, p. 275
Thomas, Wilbur Cover	A '24	Feb. 27, '46	M	Apr. '46, p. 180
Van Slyck, C. H.	A '03	Dec. 31, '45	A	Feb. '46, p. 90
Vincent, Wm. G.	A '05	Jan. 29, '46	A	Mar. '46, p. 135
Voorhees, W. N.	A '10	Jan. 18, '46	A	Mar. '46, p. 136
Waddell, C. E.	A '02	Apr. 20, '45	F	June '45, p. 232
Wallace, John Napier	M '14	Nov. 4, '45	F	Apr. '46, p. 179
Ward, B. D.	A '45	Jan. 18, '46	A	Mar. '46, p. 135
Westman, A. A. J.	A '07	June 22, '45	M	Sept. '45, p. 338

BOARD OF EXAMINERS

Statistics relating to the number of cases handled are given in Table XI. Members of the board have attended the scheduled monthly meetings very regularly, and the volume of work has justified fully the increased number of members which was arranged early in the season 1945–46.

The board wishes to reiterate its recommendation that local Section membership and transfer committees shall exercise more care in submitting applications, to insure that they are in line with constitutional requirements and particularly that they shall contain extensive and detailed experience records of the candidates which will reveal the degree of responsibility these candidates have had in connection with their various assignments.

It has been noted that an excessive amount of time has been consumed by the members of the board of examiners in interpreting the records of the candidates, and in too many cases applications have had to be returned for additional information, which in its opinion places an undue burden on the headquarters office.

Table XI. Applications for Admission and Transfer*

Applications for Admission		
Recommended for grade of Associate	1,464	
Re-elected to the grade of Associate	129	
Not recommended	8	
		1,601
Recommended for grade of Member	334	
Re-elected to grade of Member	23	
Not recommended	65	
		422
Recommended for grade of Fellow	2	
Re-elected to the grade of Fellow	0	
Not recommended	0	
		2
Applications for Transfer		
Recommended for grade of Member	450	
Not recommended for grade of Member	28	
		478
Recommended for grade of Fellow	90	
Not recommended for grade of Fellow	4	
		94
Students		
Recommended for enrollment as Students		1,568
Total		4,165

* This tabulation does not include April 1946 meeting figures.

COMMITTEE ON TRANSFERS

The members of the committee on transfers have co-operated actively during the year with the many Section officers and transfer committees of the Institute, explaining the requirements of the several grades of membership, and the required qualifications for transfer from Associate to Member and from Member to Fellow.

During the present year there have been a large number of transfers from the grade of Associate to Member and from Member to Fellow throughout all parts of the United States and Canada served by the AIEE.

COMMITTEE ON MEMBERS-FOR-LIFE FUND

Members-for-life awards, namely, expenses of District Branch paper prize winners to the summer convention of the Institute, will be made this year for the first time in connection with the Detroit meeting.

Last November, Secretary Henline invited the attention of the vice-presidents of the even-numbered Districts to the availability of these awards as described in *Electrical Engineering* for January 1945, page 31.

It will be recalled that this form of award financed by the income from the members-for-life fund, is on trial for two years—for even-numbered Districts this year and for odd-numbered Districts next year. The interest shown in this form of award this year and next year will determine whether or not it will be continued.

COMMITTEE ON CODE OF PRINCIPLES OF PROFESSIONAL CONDUCT

This committee held no formal meetings during the year but carried on its activities by correspondence. Various members of the committee have been active in their geographical areas and local engineering societies in bringing to the attention of engineers and others the Institute's code of principles of professional conduct and in advancing the Engineers Council for Professional Development canons of ethics for engineers.

One case of alleged violation of professional ethics by an Associate of the Institute has been brought to the attention of the committee and is still under consideration.

COMMITTEE ON CONSTITUTION AND BYLAWS

On January 4, 1946, the committee on constitution and bylaws made the following recommendations to the board of directors:

1. An amendment to Section 48 of the bylaws changing the basis of allotting funds to the Sections in order to conform with the action of the board on November 2, 1944.

2. An amendment to Section 65 of the bylaws, adding the name of a new committee on industrial control devices to the list of technical committees.

3. Changes in the bylaws transferring the Mexico Section from District 3 to District 7.

4. The word "national" to be deleted from the bylaws whenever it occurs in connection with the titles of officers, committees, and meetings. This was in line with similar action taken last year in eliminating the word "national" from the titles of officers, committees, and meetings wherever it occurred in the constitution.

On March 13, the committee recommended an amendment to Section 51 of the bylaws to make the definition of a "university or technical school of recognized standing" consistent with our present-day practice of accrediting engineering schools by the ECPD.

Recent action by the board of directors brings two more amendments to the committee for consideration. It is hoped that these can be presented to the board and action taken before the close of this administrative year. They are:

1. To amend the list of standing committees to include a committee on registration of engineers to succeed the present special committee of that name.

2. To amend the bylaws to provide for holding four conventions each year instead of the present practice of three per year, the new meeting to be known as the "midwest convention."

COMMITTEE ON PLANNING AND CO-ORDINATION

The project of reviewing the technical activities of the Institute and the Institute's relations with other organizations, which was assigned to the committee, is being carried out by the technical activities subcommittee and the professional activities subcommittee. These subcommittees are studying the problems to recommend any changes in organization or methods that may seem desirable to render the structure and the procedures of the Institute sufficiently flexible and adaptable to take account of progress in the art and the development of new fields of interest, and to respond promptly to changing social, political, economic, and other conditions affecting the welfare of society and of engineers.

A conference on Institute activities was conducted by the subcommittees on Wednesday, January 23, at the winter convention, as a first step toward finding out what the members believe the Institute should be doing or should do in a different way. The technical part of the discussion included suggestions for regional meetings on specific subjects and reorganizing the technical committee structure to form semiautonomous technical divisions to foster and correlate technical activities in related subject fields. During the professional activities part of the conference, four proposed plans for organizing the engineering profession were presented and discussed. Opinions were expressed on many phases of the organization problem including collective bargaining and unionization of engineers.

The technical activities subcommittee is also a working group of the technical program committee and thus accomplishes many of its projects through this committee. This close interrelation results in co-ordinated consideration of technical activity and organization matters.

The executive committee approved and referred to the committee on constitution and bylaws the recommendation of the subcommittee and the technical program committee that an annual Midwest Convention be held. Other joint projects are described in the technical program committee's report.

The professional activities subcommittee has arranged for representatives to participate in discussions of Institute activities at Section meetings in Boston, Lynn, Pittsfield, and New York; and at District meetings as follows: the North Eastern in Buffalo, N. Y., the Southern in Asheville, N. C., and the South West in San Antonio, Tex.

The problem of organizing the engineering profession is one of the main interests of the subcommittee. A questionnaire has been prepared to obtain the opinions of members who attend the meetings where the matter is discussed. The four proposed plans for organization of the engineering profession originally presented at the winter convention have been revised and

published in *Electrical Engineering* and are now available as a reprint.

The executive committee approved a recommendation originated by the subcommittee to replace the special committee on registration of engineers by a standing committee. A draft of the scope and duties for this committee was submitted as requested by the board of directors. A recommendation for forming joint Student Branches also was approved by the board of directors and referred to the committee on Student Branches with the suggestion that the latter work with representatives of other societies in developing a specific plan of co-operation.

A study is under way as to how to relieve the president of some of the burden of his office.

The subcommittee is endeavoring to find out what the problems and needs of the younger engineer-employees are, and what the Institute can do to get and keep their interest.

COMMITTEE ON SAFETY

The committee held one meeting during the past year, at the winter convention.

Through arrangements with the American Medical Association the paper by Doctor C. K. Drinker on "Use of Drugs in Resuscitation from Electric Shock" was published in the *Journal* of the American Medical Association, June 30, 1945. This paper which had been presented at the committee's meeting in January 1945, also appeared in *Electrical Engineering*, August 1945.

Under the heading "Safety Topics" in the January 1946 issue of *Electrical Engineering*, the committee directed attention of Institute members to the importance of safety engineering work in the postwar period as set forth in the National Safety Council publication, "Industrial Safety Tomorrow."

At the January 1946 meeting, the committee again emphasized the importance of promoting safety engineering work in the Student Branches and Sections, and formulated plans for appropriate communications to the Student Branch counselors and Section officers.

Report was received from the Institute's representatives on the electrical committee of the National Fire Protection Association concerning the adoption in Chicago during October 1945 of revisions of the National Electrical Code, of which the 1946 edition is expected to be issued before the end of this year.

The committee contemplates resumption of its work with the AIEE committee on domestic and commercial applications on the study of electrical hazards to farm animals, which had been started and had to be deferred because of war conditions.

The attention of the committee was directed to the report on fatalities in the electric light and power industry during the year 1944 as prepared by the Edison Electric Institute accident prevention committee. Over the past four years, an average of 81 per cent of the fatalities in that industry have been shown to be due to electric shock and burn, and the committee recognizes the importance of steps being taken to stress the fundamentals of this matter in appropriate ways for the benefit of Institute members concerned.

Plans were completed for a session under the auspices of the committee during the 1946 summer convention, and there was discussion of important subjects in the field of electrical safety, on which it is planned to have papers prepared or other appropriate presentations made for discussion at the forthcoming national meetings.

W. T. Rogers was appointed to serve as liaison representative of the committee with the American Society of Safety Engineers, and W. R. Smith will continue to serve in such capacity with the accident prevention committee of the Edison Electric Institute.

UNITED STATES NATIONAL COMMITTEE OF THE INTERNATIONAL ELECTROTECHNICAL COMMISSION

During the past year, as in the preceding war years, the work of the International Electrotechnical Commission and the United States National Committee has remained virtually in a state of suspension.

At its annual meeting on November 9, 1945, the United States National Committee re-elected E. C. Crittenden, president; L. F. Adams, vice-president; and H. S. Osborne, vice-president and treasurer.

Looking toward the reactivation of IEC work, appointments of several new technical advisers were made. Considerable interest has been expressed in the international work on letter symbols, USNC 25, and, upon recommendation of the three new technical advisers for USNC 25, the United States National Committee took action at its meeting to authorize the circulation for comment in this country and to other national committees of a draft of the IEC symbols which had been adopted in 1938, together with additions prepared by a subcommittee authorized in 1938. The USNC has acted as secretariat for this work.

During the year, the French committee requested comments on their proposals for standardization of very high voltages. The matter was referred to the technical adviser for the USNC (USNC 8) on the subject, and while no report was available, it was hoped that an answer to the French proposals could be made soon. The United Nations Standards Co-ordinating Committee was very hopeful that action could be taken on this matter, since a number of the European countries, particularly France, which were faced with rebuilding their power systems, were anxious to rebuild the systems using standard voltages.

At the USNC annual meeting, there was a discussion of reorganization of international standardization work. The United Nations Standards Co-ordinating Committee had just concluded meetings in New York and had drafted a proposed constitution for an international organization. A proposal has been made that the IEC become affiliated with the new organization and operate officially in the future as the electrical division of the new organization, retaining, however, all its functions and procedures. A subcommittee of the executive council of the UNSC was appointed to study from the point of view of the USNC the proposals for the method of affiliation of the IEC with the new organization.

It is now expected that a meeting of the council of the IEC will be held during 1946 and that the technical work of the commission will be resumed shortly thereafter. Many countries, particularly those in Europe, are anxious that IEC work be resumed, in order that some of the problems arising from reconstruction work may be solved by the IEC.

Standards

STANDARDS COMMITTEE

During the past year, the work of the Standards committee continued to be hampered by the restrictions which still existed with regard to traveling and to hotel accommodations. The curtailment, however, has been confined largely to a limitation of the number of meetings held, of which there were three. The various committees carrying on standardization activities have continued to make satisfactory progress by correspondence, although that procedure also has suffered recently through the strikes in progress in the larger industrial groups.

The various technical committees which now carry on much of the preliminary work in the development of new standards projects, as well as any required revisions of existing standards, have reported a large number of new projects in preparation, many almost ready for action. Among these may be listed the following: test code for resistance measurement; test code for temperature measurement; standard method of calculating the short-circuit currents in low-voltage circuits; standards for roof, floor, and wall bushings and for potheads; and standards for mercury-arc rectifiers. Under the auspices of the standards co-ordinating committees, the following projects also have been reported as well under way: standard barometric pressure and air density versus altitude; guiding principles for dielectric tests; letter symbols for electrical quantities; temperature rises for silicone insulation; and standard voltages from 100 to 15 kv.

In the field of electric aeronautical equipment, the standardization carried on by the Institute and other interested organizations is going forward, although curtailed in some of its phases by the changeover from wartime activities.

The following projects were approved and published during the year: AIEE Standard 45 "Recommended Practice for Electric Installations on Shipboard"; Numbers 601 and 602, "Preferred Standards and Standards Specification Data for Large 3,600-Rpm 3-Phase 60-Cycle Condensing Steam Turbine Generators"; Number 503 "Test Code for Synchronous Machines"; ASA Standard C37.4 to C37.9, "A-C Power Circuit Breakers."

As a result of the many reorganizations brought about by the end of the war, it has been necessary to make a large number of new appointments of AIEE representatives serving on various sectional committees of ASA.

The electrical definitions project, under the auspices of sectional committee C42 and the sponsorship of the Institute, inactive since publication of the first edition of the American Standard in 1942, now is being reorganized. While the addition of a large number of new definitions has been suggested, the criticisms of existing definitions have been few. On completion of the main committee personnel, the reorganization of the 18 or more subcommittees will be undertaken and all suggestions referred to them for inclusion in a new edition.

The subcommittee on applications of statistical methods has pursued an active program during the year. The educational articles which appear in *Electrical Engineering* will conclude with XII. The subcommittee then proposed to prepare and publish at least six more articles of a more advanced character.

A very successful conference was held during the winter convention in New York, and similar conferences have been arranged for the Buffalo and Detroit meetings. At the latter meeting the theme will be the management and organizational aspects of quality control. It is hoped that a conference also can be arranged at all of the remaining district meetings during 1946.

Technical Committees

COMMITTEE ON AIR TRANSPORTATION

The proceedings of the committee on air transportation during the past year were greatly handicapped by extensive reconversion of industry, shifting of personnel, and the ban on meetings and traveling. In spite of these obstacles, good progress was made in the standardization activities assigned to the committee.

These activities were carried on by several subcommittees, four of which were formed during the previous year, with assignments as outlined in the report for last year.

Aircraft Electric Systems. This subcommittee has accumulated approximately one half of the material required to complete the proposed guide report on aircraft electric systems in accordance with the outline completed last year. Cooperation of interested aeronautical groups, including Aeronautical Radio, Inc., has been very good, after some initial misunderstandings were cleared up.

Aircraft Electric Rotating Machinery. This subcommittee met several times during the year, and at a meeting held January 22 completed the proposed test code for d-c aircraft motors, except for final editorial revision. Editorial revision has been assigned to a small working group, and it is anticipated that a final draft of the test code will be ready for submission in June.

Aircraft Electric Control and Protective Devices. This subcommittee will be unable to complete its assignment until the guide report on systems and the work on cables has been more nearly completed.

Aircraft Wire and Cable. This subcommittee has sponsored manufacturers' tests on AN-16 and AN-8 aircraft cables and has extended the data to cover the complete range of sizes from AN-22 to AN-00. Tentative recommendations for extreme ratings of cables have been prepared as a technical paper, "Short-Time Current Ratings for Aircraft Wire and Cable," by P. W. Jones and J. A. Scott. At present further action to be taken by this committee has not been determined, and the personnel on this committee has been especially affected by reconversion resulting from the end of the war. A possible course of action will be to issue the essential content of the Jones–Scott paper as a preliminary report for trial.

Two additional subcommittees were formed during the year:

Joint Subcommittee (Air Transportation and Electric Machinery) on Carbon Brushes. The assignment of this subcommittee was the formulation of an AIEE test code for the evaluation of carbon brush performance on all types of commutators and collector rings, so as to provide for improved specifications and standards for carbon brushes used on electric machinery.

Subcommittee for Altitude Ratings. This subcommittee has been assigned the task of developing an AIEE Standard outlining the basic principles of altitude rating on electric machinery. The work will be co-ordinated with that being done by AIEE standards co-ordinating committee 1 and with Section I-12 of AIEE Publication 1.

One committee meeting, held during the winter convention, was devoted largely to consideration of the standardization activities enumerated. There was considerable discussion of a proposal to undertake a study of safety considerations affecting the use of electric equipment on aircraft. The majority of the committee expressed a desire for a preliminary review to determine the propriety of such a study. There was a strong minority opinion that this study would not come within the assigned scope of the air transportation committee. Subsequent attempts to carry out the majority sentiment of the committee have met with little enthusiasm, and the entire project now appears to be more suitable for action by the Civil Aeronautics Authority rather than by the Institute.

The committee also decided that there would not be any need to establish a proposed subcommittee to be of concern with the problems of airline operators. It was felt that this subject could be handled satisfactorily within the new Air Transportation Association

During the year a total of 17 technical papers were sponsored by the committee. Seven of these were presented in two air transportation sessions at the winter convention, and the other papers were printed and circulated for written discussion in accordance with the Institute arrangement during the cessation of meetings.

COMMITTEE ON AUTOMATIC STATIONS

The members of this committee have continued their activities in bringing to the Institute papers dealing with subjects related to automatic stations and supervisory control. Several papers were presented during the year, and additional papers have been secured for future presentation.

Two meetings of the committee were held during the past year, one in October 1945, and one in January 1946. In addition to considering material for new papers, the committee completed its plans for conferences on automatic or supervisory control of air switches and automatic control of capacitors. Authors have been secured for papers for these conferences. Being mindful of the importance of joint co-operation with other committees, careful consideration has been given to the reports of our representatives on other committees and to the work being done by our members on several joint subcommittees.

During the past year, two working groups were organized and at present are engaged actively in their assignments. One of these groups is investigating the matter of the type of trip to be provided for circuit breakers with special reference to their application to automatic stations. The other group is looking into the correct polarity of d-c control for automatic stations. The work of these groups has been well begun but will not be completed during the present fiscal year.

COMMITTEE ON BASIC SCIENCES

The committee on basic sciences sponsored the symposium on nuclear energy at the winter convention, and has arranged for a session for the summer convention. During the war, the work of the committee fell off, but recently it has begun to approach its prewar level, and technical programs for future meetings appear more promising.

At a meeting of the committee held during the winter convention, there was a serious discussion of the place of basic science material in the AIEE meeting and publication programs. The committee thought there would be a gain in reversing the apparent tendency of recent years to have material handled by committees with specific fields rather than by the committee on basic sciences, and also thought that an over-all increase in basic science material was desirable. To this end an aggressive campaign is being started to expand the work of the committee. Results probably will not show for some time, but it is hoped that the contribution will be evident in expanded technical presentations of the committee at later dates. Concurrent with the extension of the committee's activities, a group of subcommittees, the existence of which was not warranted during the war, is to be instituted.

COMMITTEE ON COMMUNICATION

More than 40 papers on a wide variety of communications subjects were sponsored by the committee during the year.

In view of the cancellation of the summer and Pacific Coast technical meetings, some of these papers were made available in pamphlet form for discussion by mail in lieu of formal presentation. These included a comprehensive report on the

January 1945 conference on radio frequency cables made up of 17 papers on the general subjects of polyethylene insulation for high frequency cables, cable manufacture, cable design, and cable testing. In addition the summer and fall technical paper program (presented by mail) included papers on judging mica quality, optimum air gap for coils subject to direct current, radio noise meter calibration and methods for measuring the attenuation of coaxial cables.

At the winter convention in January of this year, there were five communications sessions as follows:

A General Communications session which included seven papers on a wide variety of subjects as follows: electronic regeneration of telegraph signals; two papers on filter design, one for telegraph and the other for broad band carrier; two papers on throat microphones covering design and methods of testing; the solution of transmission line problems; applications of thin permalloy tape in wide band transformers, a technique which should be of interest to many as the field of wide band transmission expands.

Two Sessions on Radar which were arranged in cooperation with the committee on electronics. These sessions provided a well-rounded coverage of the radar field. The six papers presented related to general principles, two typical wartime uses of radar, two proposed peacetime uses, on ships and airplanes, and a comprehensive coverage of radar testing techniques. The latter paper should be of interest to many outside the radar field, since many of these techniques will be useful in the expanding fields of high frequency transmission and electronics.

A Session on Sound Recording and Reproducing which included eight papers on various recording media such as tape, wire, and disks. There is a growing interest in wire recording, and this was well covered by four papers relating to the general principles, a specific design of a recorder head, means for measuring the magnetic characteristics of recording wire and signal and noise levels encountered in tape recording. Two papers were presented on disk recording, one of them relating to a new reproducer design and the other to new tools for the study of disk recording performance. The growing importance of recording in business was brought out by a paper on this subject.

A Conference on Slow Acting Relays which included four prearranged talks by engineers active in this field. These covered the historical aspects, underlying electromagnetic concepts, operational features, and limitations of relays in power communication. It is planned to explore this field further with the thought of ultimately making available published material for the benefit of the entire membership.

Meetings of the committee on communication were held in June, October, and January. Indicative of the broad scope of the activities of the committee are the following subcommittees which now are functioning: sound recording and reproducing, slow acting relays, hearing aids, testing of telephone transmitters and receivers, power line carrier, underwater sound developments. These subcommittees have been active in arranging for papers in their fields, many of which were presented at the last winter convention. In the coming year, it is proposed to increase the committee activities in the field of television.

The committee has co-operated with the other technical committees wherever the subject matter was of joint interest. This is illustrated by the joint sponsorship with the committee on electronics of the papers on radar and also by the appointment of the chairman of the subcommittee on power line carrier as the committee representative on the joint subcommittee on power system applications of carrier current.

Emphasis has been placed on making available the results of the committee's activities to the entire Institute membership rather than only to the few who can attend national meetings. Substantially all of the talks presented at the various national technical meetings have been or will be published in *Electrical Engineering* or in *Transactions*. A report on the conference on high frequency cables was made available in pamphlet form, and the entire membership was notified of its availability. Also outstanding papers presented at District meetings are being recommended for publication, so that the entire membership can benefit from these papers which would otherwise be heard by only a few.

COMMITTEE ON EDUCATION

The committee on education shares with the Society for the promotion of Engineering Education and ECPD an interest in the guidance and selection of students and their proper professional education in colleges and universities offering accredited curricula in electrical engineering. It has the opportunity of co-operating with many groups within the AIEE organization to further the education of the electrical engineer, both before and after his graduation from college—indeed, to make education a continuing process in the life of each AIEE member. Its relationship to the committee on Student Branches is necessarily close. In promoting educational work in the AIEE Sections throughout the country, it works with the Sections committee. The publication of general technical articles which start from basic principles and bring the reader up to date on a particular device requires co-operation with the editor of *Electrical Engineering*.

Every year many suggestions for educational activities on the part of the Institute are received by the committee and tabled because: other agencies for the objective are already in existence, lack of funds, or inappropriateness. This year, for example, the committee did not act favorably on a proposal to establish an agency at AIEE headquarters to counsel returning veterans as to educational preparation for electrical engineering, nor did it feel that a proposal to set up a series of correspondence courses of a refresher type or on new developments in electrical engineering for returning veterans and reconverted war industry workers was feasible.

As an aid to schools teaching electrical engineering during the past year, the committee collected information on the teaching of electronics as a service course to students with a background of physics, other than electrical engineering students and has in preparation a summary of the practices reported as successful.

At the 1946 winter convention, the committee organized a session devoted to a comparison of the achievements of electrical engineering graduates in civilian war research agencies as compared with men who were professional physicists. This meeting and the full report of it published in *Electrical Engineering* may have helped considerably in clearing up a confused situation which might have done harm had it long continued.

In keeping in touch with developments in electrical engineering curricular changes, the committee has not taken any stand on their merits. The five-year program leading to the bachelor's degree has been discussed, and the experiment encouraged, with the thought that the results be reported, evaluated, and disseminated to all schools.

The place of electronics in the postwar electrical engineering curriculum will be the subject of a conference at the 1946 summer convention.

In co-operation with the committee on Student Branches, a revision of the AIEE guidance pamphlet, "The Electrical Engineer," is now in preparation, as the first edition nearly has been exhausted.

An exploration of the possibilities of standardization of laboratory equipment for schools in order to reduce costs is being undertaken.

Advisory services to Sections of the Institute contemplating the establishment of educational courses have been rendered and a joint letter sent out by the chairman of the Sections committee on this topic.

Steps are being taken to secure a new series of articles for publication in *Electrical Engineering* similar in general to those published ten years ago, which will bring AIEE members up to date on the newer developments in our field, particularly in fundamentals, written for the ordinary engineer and free of unnecessary mathematical obfuscation.

The project to revise and bring up to date the committee's list of film strips and motion pictures has been held up by unsettled conditions, but it is hoped some progress on this may have been made by the end of the year.

COMMITTEE ON ELECTRIC WELDING

A meeting of the committee was held January 21, 1946, during the winter convention. Papers for the summer convention and for the 1947 winter convention were discussed. The work being done by the technical activities subcommittee and the professional activities subcommittee was reviewed. Considerable interest was shown in the activities of these two subcommittees, and several suggestions were made which were passed on to the subcommittee affected.

There were no activities of this committee on standards, although it is understood that revision for peacetime use of war Standard C52.4, C52.5, and Z49.1 will be started in the near future. Representatives of this committee will assist in this work.

One technical session was sponsored by the committee at the winter convention. Four technical papers were presented. Two of the papers were on arc welding subjects, and the other two were on resistance welding. Two technical sessions are being sponsored at the summer convention. Three technical papers and one

conference paper are to be presented on resistance welding subjects, and three conference papers on arc welding subjects.

COMMITTEE ON ELECTROCHEMISTRY AND ELECTROMETALLURGY

The activities of the committee on electrochemistry and electrometallurgy during the past year have been confined largely to subcommittee work. No sessions or conferences have been sponsored at any of the national or District meetings. A meeting of the committee was held in New York, January 24, 1946, at which the work of the subcommittee was reviewed and plans formulated for future activities.

The subcommittee on metallic rectifiers, under the chairmanship of Doctor L. O. Grondahl, is actively at work on the following projects:

(*a*). Preparation of a test code.

(*b*). Preparation of a list of nomenclature and symbols.

(*c*). Preparation of a bibliography on metallic rectifiers.

Preparation of the bibliography is nearing completion, and excellent progress is being made on the test code and nomenclature. A group to consider the preparation of standards also is contemplated. Four meetings a year are planned by this subcommittee. The first was held in New York, January 25, 1946, and the second is scheduled to be held April 25, during the North Eastern District meeting in Buffalo.

The subcommittee on voltage transients in arc furnace circuits of which Doctor E. R. Whitehead is chairman, held a meeting in New York on January 23, 1946. Doctor Whitehead presented a report on the 1945 trouble record for arc furnace customers on the Duquesne Light Company System. Among 29 customers having 44 arc furnace installations, there were 18 reported cases of trouble. Of the 18 cases of trouble, possibly three, and probably one, were caused by overvoltage.

In a discussion of the most fruitful course of future action, S. B. Griscom suggested that the subcommittee prepare a brief report outlining preferred practice in arc furnace installations. It was pointed out that such a report would not be considered a standard and that similar guides had proved very useful in other fields. A preliminary outline of subjects to be considered was drawn up, and a working group has been appointed to prepare a first draft before June 1.

The subcommittee urges all who may have test data, or any information on this subject not included in the 1944 report, to assist in this work, either by the preparation of an appropriate technical paper or by submitting it to the committee for discussion.

The committee on electrochemistry and electrometallurgy also is represented on the joint subcommittee on induction and dielectric heating.

COMMITTEE ON ELECTRONICS

The subcommittee plan of operation is employed for the work of this committee. A meeting of subcommittee chairmen was held in October 1945, and another in April 1946, both in New York. A meeting of the entire committee was held during the winter convention.

Subcommittee activities have been as follows.

1. Electronic Power Converters Subcommittee. This group has during the past year completed two tasks that have been in process for several years, and represent the result of a great deal of effort on the part of each of many subcommittee members.

The first of these is a draft of "Standards for Pool Cathode Mercury-Arc Power Converters," which is now in the hands of the standards committee. Copies of this draft will be distributed broadly to encourage early use of the proposed Standards. It is planned to publish a review of these Standards in *Electrical Engineering* at an early date, and to provide an opportunity for discussing them at the summer convention.

The second of these two completed tasks is a report on "Inductive Co-ordination Aspects of Rectifier Installations." It is planned to present this for discussion during the summer convention, and to publish it in *Electrical Engineering* and the *Transactions*.

Work on a bibliography covering electronic power converters is approaching completion. Tasks that lie ahead for this subcommittee are the preparation of standards for electronic power converters employing hot cathode tubes and standards for electronic power converters used with electronic motors.

2. Subcommittee on Nomenclature, Definitions, and Symbols. This group has completed the preparation of an extensive set of proposed standard definitions, which are being channelled through the standards committee for adoption. An important aspect of this work has been co-ordination with a similar IRE activity. Additional work is in progress extending the coverage of the standards proposals to additional subject matter.

3. Technical Papers Subcommittee. This subcommittee generally has encouraged and solicited the preparation of technical papers on electronic subjects. The policy of distributing available papers on electronics to other committees which sponsor sessions covering the applicational subjects involved has been continued. The technical paper coverage of electronic subject matter has been in general satisfactory.

This subcommittee organized and conducted a very successful informal technical conference at the winter convention. The subject was "New Industrial Uses of Electronics Resulting from Wartime Developments." Additional similar future programs are being planned.

In response to a request for help in carrying on the work of technical groups affiliated with local Sections, manufacturers of radio and electronic equipment were canvassed for movie films, lecturers, bulletins, educational courses, and the like, and the material so collected was correlated and distributed to local Sections.

4. Subcommittee on Electronic Heating. By means of approximately monthly meetings throughout the winter and spring, this subcommittee has been very active in the difficult work of promoting co-ordination of electronic heating practices with Federal Communication Commission's frequency allocations and radiation field strength limitations. This group also has given attention to safety practices and equipment rating standards.

5. Electron Tube Subcommittee. This group has undertaken a program of gas tube standardization work in close co-operation with a parallel group in the IRE.

6. Liaison Subcommittee Activities. There is a general need for improving the co-ordination between technical activities in electronics of the AIEE committee and certain parallel activities of the IRE and related activities of the Joint Electron Tube Engineering Council (JETEC), also for effective contact with the AIEE Standards committee and the American Standards Association. To this end, there have been established, under the committee on electronics, a subcommittee on JETEC liaison and tube standards, a subcommittee on AIEE-IRE liaison, which has become active in discussions toward standardization of frequency-band nomenclature, and a subcommittee on electronic standards. These subcommittees have been active in various technical and co-ordination problems.

7. Other Subcommittees. Subcommittees on electronic precipitation, electronic control, electronic welding, X-ray tubes, and on wires and cables, have been active in their respective fields. The committee on electronics thinks that one of its important responsibilities is to serve as a continuing co-ordinating agency between the various professional organizations in the electronics and technical workers in various differing applicational fields where the use of electronic devices is important.

COMMITTEE ON INDUSTRIAL CONTROL DEVICES

This new committee was organized in the fall of 1945. Three meetings have been held. The first, or organizing meeting, was held in Milwaukee on November 7, 1945, and the second meeting was held in New York on January 21, 1946, during the winter convention. The third meeting was held in Cleveland on April 11, 1946, and a fourth meeting is scheduled to take place in Detroit during the coming summer convention.

Considerable discussion has dealt with the scope of this new committee in its relation to other committees of the Institute. In order to pursue its work, the following subcommittees and working groups have been set up:

1. Subcommittee on industrial electronic control. This subcommittee will work in co-operation with a subcommittee of the committee on electronics.

2. Subcommittee on revision of AIEE–ASA Standards 15.

3. Subcommittee on test codes for industrial control devices.

4. Subcommittee on servomechanisms.

5. Liaison with American Society for Testing Materials.

6. A working group on bibliography on industrial control.

A number of papers have been reviewed in preparation for presentation at coming Institute conventions.

COMMITTEE ON INDUSTRIAL POWER APPLICATIONS

Owing to conditions prevailing last year, this committee carried on practically no work after the winter convention of January 1945 until the present committee was formed last September.

At the January 1945 meeting, a series of papers and very interesting discussions on the subject of industrial voltage requirements were presented, although the subject was found to be too broad to reach any conclusions at one session.

When the present committee took up the work last September, it decided to form two subcommittees, one to study again the subject of industrial voltage requirements, and the other to review the field of machine and process drives.

At the winter convention, in January 1946, the committee sponsored three sessions, two covering chiefly the industrial voltage subject, and one on co-ordinated drives in industrial processes.

The two sessions on industrial voltage requirements were held on the same day, and a committee luncheon meeting was held between the two sessions.

At the first session, an interim report on the subject of industrial voltage requirements was presented, and was very well received. A number of good suggestions were received from the discussion from the floor. Therefore, the subcommittee is at present actively working and hoping to present a completed report on this subject in the near future for review by the board of directors.

The committee luncheon was attended by 22 members of the committee and the major topic of discussion was a continuance of the subject industrial voltage requirements. It was the concensus that this subcommittee should continue the work and have a final report available at the earliest possible date.

The second session, held in the afternoon of the same day, was sponsored jointly by the committee and the inductive heating subcommittee. Two papers were given on subjects allied to industrial voltage requirements and two papers on inductive heating.

The third session was under the auspices of the subcommittee on machine and process drives. A general report outlining the proposed scope of this subcommittee was presented, and the discussions from the floor suggested that the work of this committee should stress the increasing importance of co-ordinated drives in industrial processes.

Two papers were presented on allied subjects which were well received, and committee members expressed a desire for more papers along the lines of the two that had been given which furnished technical and practical application data on co-ordinated drives.

This subcommittee held a meeting in March, when it was agreed by the membership that better results might be obtained by sponsoring papers for a particular industry at two or three of the main technical meetings throughout the year and by ultimately assembling the best of the papers presented into a report form. It was agreed that at the next main technical meeting the subcommittee would have available a series of papers covering the textile industry.

The committee members, both at the winter convention and at the various subcommittee meetings, have agreed to try to cultivate the interest of the industrial groups of all sections of the Institute. By this means we are hoping to build a closer tie between the national committee and the various industrial groups, thereby creating greater interest throughout the membership of industrial problems.

COMMITTEE ON INSTRUMENTS AND MEASUREMENTS

With the cessation of hostilities, the committee on instruments and measurements resumed many activities curtailed during the war and has undertaken a number of new projects. Two meetings of the committee were held in New York, one November 14, 1945, and the other April 10, 1946.

Although no technical meeting was held during the summer, the committee reviewed a considerable number of technical papers, and four were included on the summer technical program. Gyroscope testing, resistance thermometers, lag of thermometer elements, and current transformers were subjects of the papers. At the winter convention in January 1946, seven papers were presented in two sessions under the sponsorship of the committee. The papers covered a wide range of instrument and measurement applications, including stress measurement, servomechanisms, surge-current measurement, high-speed recording, thermal demand meters, and automatic oscillography. The sessions were well attended, and a great deal of interest was shown in the papers. Through the year a number of papers reviewed by the committee were included on the programs of District or Section meetings. Three sessions under sole sponsorship of the committee or joint sponsorship with other committees are planned for the next summer convention.

Through its 14 subcommittees, the committee has been active in standardization matters. Preliminary drafts of master test codes for resistance measurement and for temperature measurement have been prepared, and now are being considered for approval by the main committee. A proposed final draft of the revision of a former report on a proposed Standard 40, on recording instruments, is nearing completion and is expected to be ready for recommendation as a new standard in the next few months. Recommended changes in and additions to the "American Standard Definitions of Electrical Terms" are under preparation and will be offered as suggestions for a future revision of that Standard. A revision of the 1941 AIEE report on "Telemetering, Supervisory Control and Associated Circuits" is being undertaken by the joint subcommittee on that subject.

In co-operation with the corresponding subcommittees of the ASA sectional committee C-57, and of the committee on protective devices, the subcommittee on instrument transformers has carried forward the work on the instrument-transformer definitions to be included in the ASA Standard on transformers. A request of the committee on instruments and measurements that the section of this standard dealing with instrument transformers be separated editorially from the complete standard has received favorable consideration by the ASA committee, and the subcommittee on instrument transformers plans to carry out the editorial work necessary to make the separate publication possible.

The field of servomechanisms has received particular attention during the past year, and the subcommittee on that subject has been active in stimulating papers on servomechanisms and in sponsoring, jointly with the corresponding subcommittee of the committee on industrial control devices, a session on servomechanisms at the coming summer convention.

Because of the growing importance of electronic instruments in a wide variety of instrument and measurement applications a joint subcommittee on electronic instruments has been formed through co-operative action by the committees on instruments and measurements and on electronics. This subcommittee is engaged actively in stimulating papers and discussion on electronic instruments for a conference at the summer convention

COMMITTEE ON MARINE TRANSPORTATION

The printed revision of Standard 45 became available during February 1946 as the 1945 revision of the Standard.

It was considered inadvisable to hold meetings of the committee until the printed revision was available. Therefore, no meetings were held during latter part of 1945.

Two all-day meetings of the committee were held during 1946, and it is proposed to have one more all-day meeting before the close of the administrative year. Discussions at these meetings cover preparation of proposed changes and additions applicable to future revisions of Standard 45.

The committee believes that future revisions of Standard 45 should include complete recommendations covering a-c installations. This action is deemed advisable because of the increased use of a-c distribution systems on ships together with the greatly increased number of electrically propelled vessels.

There have been no changes in the personnel of the committee except the addition of one AIEE member, a British electrical engineer, prominently identified in similar activities in British Institution of Electrical Engineers. It is believed that this addition to our membership will make for closer relations between American and British shipboard electrical practices.

COMMITTEE ON POWER GENERATION

In spite of rather severe handicaps imposed by the war and by the subsequent dislocations, the first year of the activities of the committee on power generation, while operating with the newly appointed and expanded subcommittees, proved to be quite successful. The response of the membership to the plans and efforts of the committee has been very satisfactory, and there is every indication that the committee will continue to grow in its importance.

The specific activities of the committee during the past year may be summarized as follows:

Central Station Auxiliaries. The material of the previously held technical conference on the subject of central station auxiliaries had been rewritten in the form of five technical papers, subjected to the regular review and grading, and finally published as a part of the 1945 fall technical paper program. The comments and discussions received since the publication indicated that this activity served a timely and useful function.

Hydroelectric Systems. It has been realized for some time that the problems of the design and operation of hydroelectric systems did not receive sufficient attention in the technical activities of the AIEE, as compared with their importance in the electrical picture in this country. Under the sponsorship of a newly appointed subcommittee, a thorough canvass was made of the potential interest and possible material pertaining to this topic.

The initial session on hydroelectric systems was held during the 1946 winter convention in New York, with the presentation of two technical papers and three conference papers. There was evidence of a strong interest on the subject especially among AIEE Canadian membership. Present plans call for the continuation of this activity with a sponsorship of similar sessions at the summer convention in Detroit, at the winter convention in New York, and possibly at the Pacific Coast convention.

Excitation Systems. Another new activity of the committee, originated this year and introduced to the membership with a symposium of six papers at the 1946 winter convention, was the subject of excitation systems. The excellent attendance of the session and the widespread discussion of the topic indicated that this activity also meets a real need and that it should be continued. Accordingly, the subcommittee made plans for further contributions at the summer and winter conventions. Work is in progress to formulate definitions and terms used in discussions of excitation systems.

Prime-Mover Governing. The present activities of this subcommittee are:

1. A revision of AIEE 600 relating to speed governing specifications for steam turbine generators.
2. The preparation of a specification for the speed governing of hydro turbine generators.
3. The preparation of two additional specifications for types of steam turbine generators not covered under AIEE 600.

The probability is that all work in progress will be completed and submitted to the standards committee for approval by the spring or summer of 1947.

COMMITTEE ON POWER TRANSMISSION AND DISTRIBUTION

A full meeting of the committee was held at the winter convention. A report was made by a subcommittee consisting of the officers and chairmen of subcommittees on possible reorganization of committees. The only change proposed and approved by the main committee was to change the three working groups under the transmission subcommittee to full subcommittees to be known as lightning and insulator subcommittee; towers, poles, and conductors subcommittee; and insulated wire and cable subcommittee. The change will take place at the beginning of the next administrative year.

Technical Meetings. At the winter convention, the committee sponsored one technical meeting. A report of the lightning and insulator working group on the "Lightning Performance of 220-Kv Lines—Part II" was made. Other papers dealt with economics of transmission, arcing grounds on 13-kv, 3-phase busses, and inductance of square busses.

Subcommittee Activities. The distribution subcommittee has a joint project with the relay subcommittee of the committee on protective devices through a working group composed of members of both subcommittees. This group is studying plans for improvement in the quality of service on overhead distribution circuits. Also a study is being made of proper forms for reporting the troubles on distribution circuits to obtain better evaluation of the effects of different construction practices and protective devices. The group has had one meeting and plans another during the summer convention. The subcommittee is canvassing its members for possible papers for the winter convention in 1947. This subcommittee has under consideration the following subjects: (*a*) design of systems for fluctuating loads; (*b*) 4 versus 13 kv distribution economics; (*c*) network supply from two sources; (*d*) nonleaded cables in the earth.

The stations subcommittee held one meeting and has arranged for papers to be presented at a session during the summer convention.

The transmission subcommittee, through the working group on lightning and insulators, presented its report on the questionnaire on lightning performance of 190 to 287-kv lines by means of a paper at the winter convention in January 1946. This group is now preparing a second volume of the "Lightning Reference Book" to cover the period from 1935 to 1945 inclusive. This working group has under consideration the following projects: (*a*) the predetermination of lightning performance of transmission lines as a guide to the design of such lines; (*b*) a questionnaire on the record of outages on high voltage lines from all causes; and (*c*) a survey of the performance of insulators, wood and air in series, and possibly a further investigation of the subject. It is expected to have two papers available for the summer convention dealing with ceramic dielectrics at elevated temperatures and co-ordination of insulation and spacing of transmission line conductors.

The cable working group has interchanged correspondence on the beginning of a study to investigate the proper methods for evaluating the effect of the thermal properties of buried cable systems of the direct burial and duct types. The group has been actively soliciting papers, so that it is expected to have six papers at a cable session to be held at the summer convention. There are also prospects for about five papers at the winter convention in 1947. The working group on towers, poles, and conductors has been endeavoring to get papers on the comparison of wood and steel in structures and on the preservative treatment of wood. There is a possibility of one paper for the summer convention.

The general systems subcommittee is studying a standard method of evaluating power losses, which it is hoped will result in two papers. The subcommittee is still studying stability of transmission lines, which study will continue for another year or two. The subcommittee is following the development of d-c transmission both in Europe and in the United States. The subject of overvoltages on transmission lines is under consideration by the subcommittee.

It is intended to have a meeting of the full committee during the summer convention in Detroit. The committee is sponsoring two sessions at this convention.

COMMITTEE ON PROTECTIVE DEVICES

Principally because of the wide variety of fields included in the scope of the committee, an attempt was made this year to place more of the responsibility for the preparation of Standards and other specific activities in the hands of the subcommittees rather than attempt to cover too many of these details in the main committee. The subcommittees have reacted favorably to this increased responsibility, and, with a few more adjustments necessitated by this change in operating concept, they should be able to function very satisfactorily.

The committee sponsored 13 papers for the winter convention and expects to have about 8 on the schedule for the summer program. A special working group has been set up to solicit papers by operating engineers. It is thought that particularly in the postwar period a review of operating experiences can be of major assistance to

the manufacturers in formulating plans for new designs and new products. It is recommended that this activity be continued at least for the coming year.

There have been two meetings of the main committee and another is scheduled at the time of the summer convention in Detroit. The subcommittees have met more frequently, and their accomplishments outlined in more detail follow.

Circuit Breakers and Assembled Switchgear. The work of the subcommittee was handled mainly through six working groups, each of which was assigned a specific project.

The working group on the "Air Circuit Breaker Standard 20" completed the work on the proposed Standards and have referred it to the committee for further action.

The working group on "Switchgear Assembly Standard 27" reviewed the standard in its present form and decided that no further action should be taken this year.

The working group on the proposed standards for automatic circuit reclosers for a-c distribution circuits sent out drafts of the proposed standards at two different times. Adverse comments were received on both drafts, and the project will require further action by both the working group and the subcommittee. For this purpose, it is planned to hold a joint subcommittee and working group meeting in Pittsburgh on May 16. It is hoped that at that time the differences of opinion which have prevented passing of the standards can be cleared and that the standard can be presented to the committee for final action before closing the current year's business.

The working group on studying short-circuit current for low voltage circuits has held several meetings, but was unable to complete its work until more test data could be obtained and examined. Their work is not expected to be completed this year.

The working group on "Power Circuit Breaker Standard 19," which was assigned the additional problem of studying the method of defining interrupting ratings, reports satisfactory progress, but states that its project cannot be completed during the current year. No revision of Standard 19 is recommended at this time.

The working group on technical program papers by operating engineers has worked diligently to obtain papers covering operating experiences. The reward for its interest has been slight and not all that was hoped for.

It is recommended that the work of the group on the method of defining interrupting rating should be continued into the succeeding year or until it is completed. The matter of technical program papers by operating engineers should be an item for continuing study. Although the results obtained have not been very satisfactory, it is believed that the interest of the Institute demands that study of the subject should be continued until satisfactory results are obtained.

Lightning Protective Devices. "Expulsion Type Distribution Lightning Arresters, AIEE Standard 47," December 1945, was sponsored by H. L. Stewart, New England Power Service Company. His working group completed the Standard except for editorial changes during 1945. The Standard was issued for trial use December 1945. The project has been completed.

"Industry Survey of Performance Characteristics of Distribution Expulsion Type Lightning Arresters" was sponsored by E. W. Beck, Westinghouse Electric Corporation, East Pittsburgh, Pa. Mr. Beck appointed a working group and secured data from all manufacturers of these arresters, worked up a first draft of the report, then submitted it to the group for comments. Comments and new data were received which required a new draft. The new draft will be submitted to the working group for approval when completed, after which it will be sent to the subcommittee for approval and publication in *Electrical Engineering*. It is suggested that this project be continued to completion under the sponsorship of Mr. Beck.

"Survey of Lightning Protective Equipment Used on A-C Rotating Machines" was sponsored by T. H. Mawson, Commonwealth and Southern Corp., Birmingham, Ala. Mr. Mawson prepared a questionnaire which was sent to major utilities. Complete returns are not in. It is suggested that this project be continued under the sponsorship of Mr. Mawson.

"Lightning Protection for Substation Units" has been sponsored by E. R. Whitehead, Duquesne Light Company, Pittsburgh, Pa. Mr. Whitehead appointed a working group and set up the following procedure:

(*a*). To formulate the problem more definitely.

(*b*). To contact the transformer subcommittee with a view to having them co-operate in this study.

(*c*). To consult with manufacturers to get their views on the protection needed in the problem.

It is suggested that this project be continued under Mr. Whitehead's sponsorship.

Combination of the three Lightning Arrester Standards, AIEE 28, 47, and 24 was sponsored by F. M. Defandorf, National Bureau of Standards, Washington, D. C. He appointed a working group and has issued a second draft which is now in the hands of the working group for comments. Mr. Defandorf has made an excellent start on this project and is doing a splendid job. It is therefore suggested that this project be continued under his sponsorship. This is a major standard and may require several years to complete, as there is considerable revising to be made in the test sections which require new information.

The subject of surge protection for arc furnaces was discussed by the committee. Mr. Whitehead, chairman of the subcommittee on overvoltages in arc furnace circuits, was asked to serve as the contact between the two committees and offer the assistance of the lightning protective devices subcommittee. No working project has been set up for this subject, as the need for such a group has not crystallized.

Fault Limiting Devices. This subcommittee has had three active working groups on present-day grounding practices; revision of "Standard 32, Neutral Grounding Devices"; and "Bibliography Concerning System Grounding." This latter group was formed January 23, 1946. The series capacitor protective device has been assigned to this subcommittee, and one paper on this subject was presented at the January meeting. The subcommittee will be prepared to sponsor standards in connection with these devices if necessary.

Relays. Two meetings of the relay subcommittee were held, one in Cleveland, October 18, 1945, and one in New York, January 21, 1946. Another meeting of the subcommittee to summarize the activity of the year will be held in Cleveland, May 16.

As in recent years, the work of the subcommittee has been carried forward principally by a number of working groups, to each of which has been assigned a particular project.

A working group on the bibliography of protective relaying has been continued, and has prepared a bibliography of technical articles on relaying for 1945. The sponsor of this group is again C. E. Parks. The bibliography for 1945 was distributed not only to the members of the subcommittee, but also to the relay subcommittee mailing list, a list prepared by the subcommittee of approximately 100 engineers who are most vitally interested in relaying problems. As this bibliography is now kept up to date year by year, it will be a simple matter to publish the accumulated bibliography for a period of three or four years, whenever it becomes desirable. It is recommended that the work of this group be continued.

A working group under the chairmanship of J. C. Bowman has continued to study the protection of generators against winding failures. It is anticipated that this group will prepare a report on recommended practices for relay protection of generators, which should be published when completed. The activity of this group should be continued until a report is published.

The working group on current transformers with low-current secondary windings has been continuing, but S. C. Leyland has taken over the sponsorship. A report covering various applications justifying the use of current transformers having a rated secondary current of less than 5 amperes is being completed, and it is hoped that this report can be presented at the summer convention in 1946.

The activity of the working group on the protection of power house auxiliaries, sponsored by E. L. Michelson, is drawing to a close, and the report of this work, including recommended practices, will be presented at the summer convention in 1946. A preliminary report was presented for discussion at a conference on relaying problems held at the winter convention of the AIEE in January. The work of this group should be complete this year.

The working group on the co-ordination of transformer protection, organized last

year, has continued to study these problems, with W. R. Brownlee as sponsor. A preliminary report and a conference paper on the work of this group were presented at the conference session on relaying problems at the winter convention, and the discussion provided additional material for work of the group. It is expected that a final report can be prepared for the winter convention in 1947, and the group should be continued until the report is presented.

The group on standards for instrument transformers for relaying purposes has been continued under the sponsorship of C. A. Woods. The principal activity of this group, which consisted in assisting subcommittee 4 of ASA committee C57 to revise the American Standards for instrument transformers, has been completed, but some additional work on guides for operation and the test code for instrument transformers has remained for further consideration. This group should continue to stand by until all details of the revision of ASA C57 have been completed, but no further extensive activity is contemplated in the near future.

A joint working group with the committee on power transmission and distribution was appointed last year to study the correlation of construction and protection of distribution circuits, with George Dodds as sponsor. Because of the joint sponsorship, some delay was experienced in completing the organization of this group, but activity is continuing, and the first meeting of the entire group was held in Pittsburgh, March 20. The activity of this group should continue throughout the next year and should result in a valuable report on distribution circuit problems.

During the year a working group was appointed to carry out the revision of ASA Standards for protective relays, under the sponsorship of J. H. Oliver. Because of man power limitations, this group has not yet been very active, but has been studying the problem, so that when man power is available the work can proceed rapidly. The activity of this group is being co-ordinated with the corresponding subcommittee of ASA committee C37 on power switchgear, so that the completed draft of the proposed revision may be acceptable without extensive change as the ASA Standard. The work of this group should continue until the new standard is accepted and published.

A working group under the sponsorship of H. R. Paxson has been investigating the problem of grounding instrument transformer secondaries. A considerable divergence of practice was found, and it appears desirable that a report on this subject should be presented to the Institute. Possibly this report may be ready for the summer convention in 1946, but in any case it should be ready by the time of the winter convention in 1947.

COMMITTEE ON APPLICATIONS OF ELECTRICITY TO THERAPEUTICS

This committee held one meeting during the year. At this meeting, the following general principles were considered.

There are three factors in the application of electricity to human beings:

(*a*). The effect, if any, on man.

(*b*). The safe limits of dosage, and the measurement of the same.

(*c*). Methods of protecting the operator.

The following applications were considered.

1. About high frequency of heating, it was the general opinion of the committee that workers could be shielded from high frequency fields by interposing metal barriers. There is no information available as to the amount of heating to which a human being could be subjected without injury.

2. It was brought to the attention of the committee that some of the ultrahigh frequencies used in radar produced a certain amount of X-ray radiation. Most of this is believed to be in the soft X-ray field. It is claimed, however, that some very hard X-rays may be produced. The committee has suggested that a study be made and the amount of X-ray radiation produced by different radar sets be investigated.

3. The effect of sun lamps and ultraviolet-ray radiation lamps also was discussed. A few individuals are believed to be supersensitive to such radiation. The Westinghouse Electric Corporation volunteered to furnish equipment and lamps and to help in carrying out a study of the amount of ultraviolet radiation. The School of Hygiene at the Johns Hopkins University was suggested as a possible location for carrying on this investigation. It has been notified of the project, and it is under consideration.

4. Doctor Rentschler of the Westinghouse Electric Corporation called attention to a special short wave lamp and its successful use in treating infected wounds. He reported that certain deep-seated wounds which had not responded to sulpha treatments had healed rapidly when exposed to rays from the lamp.

Awards

INSTITUTE PRIZES

In May 1945, the committee on award of Institute prizes reported the award of three national prizes, after consideration of all eligible papers in the several classifications for prize awards and solicitation of the recommendations of the chairmen of the technical committees relative to the best papers in specialized fields. As usual, the choice between leading papers worthy of award in the several classes of prizes was very close. The committee gratefully acknowledged the assistance of the technical committees and their reviewers in nominating and grading the many papers eligible for the awards. Owing to the wartime situation, no papers were submitted for the national prize for Branch paper.

SPECIAL COMMITTEE TO REVIEW PRACTICES IN THE AWARD OF INSTITUTE PRIZES

The committee has prepared and submitted to the board of directors a proposed revised practice covering the award of Institute prizes. The suggested practices were determined after reviews with various interested committees and the vice-presidents representing the Districts. Questions related to prize award practices of the Sections have been raised by the chairman of the Sections committee, and the special committee requested that action by the board be postponed pending further consideration of the Section problem now being undertaken by the Sections committee.

EDISON MEDAL

The Edison Medal, awarded by a committee composed of 24 members of the Institute, was presented for 1945 to Philip Sporn, executive vice-president, American Gas and Electric Service Corporation, New York, "for his contributions to the art of economical and dependable power generation and transmission." The presentation took place January 23, 1946, during the winter convention. The medal may be awarded annually for "meritorious achievement in electrical science, electrical engineering, or the electrical arts."

LAMME MEDAL

The Lamme Medal committee awarded the medal for 1945 to David C. Prince, vice-president, general engineering and consulting laboratory, General Electric Company, Schenectady, N. Y., and past president of the Institute. Arrangements are being made for the presentation of the medal at the annual business meeting in Detroit, June 26, 1946. The medal may be awarded annually to a member of the AIEE "who has shown meritorious achievement in the development of electric apparatus or machinery."

HOOVER MEDAL

The Hoover Medal was established through a trust fund created by a gift from Conrad N. Lauer and is to be awarded periodically "to a fellow engineer for distinguished public service" by a board representing the ASCE, American Institute of Mining and Metallurgical Engineers, ASME, and AIEE. The seventh medal, for 1945, was awarded to Doctor William H. Harrison, vice-president, American Telephone and Telegraph Company, New York, and was presented to him on January 23, 1946, during the AIEE winter convention.

JOHN FRITZ MEDAL

The John Fritz Medal board of award is composed of representatives of the ASCE, AIME, ASME, and AIEE. The medal may be awarded annually for notable scientific or industrial achievements. The 1946 medal was awarded to Doctor Zay Jeffries, vice-president in charge of chemical department, General Electric Company, Pittsfield, Mass.

WASHINGTON AWARD

The Washington Award for 1946 was bestowed upon Doctor Vannevar Bush, president of the Carnegie Institution of

Washington (D. C.), and director, Office of Scientific Research and Development. The presentation was made at a dinner in Chicago, Ill., in February. The award may be made annually to an engineer by the commission of award composed of nine representatives of the Western Society of Engineers and two each of the ASCE, AIME, ASME, and AIEE.

ALFRED NOBLE PRIZE

This prize, established in 1929, consists of a certificate and a cash award from the income of a fund contributed by engineers and others to perpetuate the name and achievements of Alfred Noble, past president of the ASCE, and of the Western Society of Engineers. It may be made to a member of any of the co-operating societies, ASCE, AIME, ASME, AIEE, or WSE, for a technical paper of particular merit accepted by the publication committee of any of these societies, provided the author, at the time of such acceptance, is not over 30 years of age. The award for 1945 was presented, in January 1946, to A. L. Ahlf, a member of the ASCE, for his paper, "Design Constants for Beams with Nonsymmetrical Straight Haunches."

CHARLES LE GEYT FORTESCUE FELLOWSHIP

No fellowship has been awarded this year on account of the fact that there are so few graduate students in the colleges at this time. Sufficient funds are available to consider the granting of fellowship awards, totaling about $1,000 per year. It is expected that as soon as there are a reasonable number of graduate students in the colleges, notices will be sent out offering this fellowship.

Joint Activities

UNITED ENGINEERING TRUSTEES, INC.

This organization manages property and funds held jointly by the four founder societies, including the Engineering Societies Building, the Engineering Societies Library, and the endowment funds of the Engineering Foundation.

The building is occupied fully by engineering organizations, and additional space is needed both for offices and for meetings. Therefore, there has been a renewal of planning for the future adequate housing for engineering societies.

The founder societies have been requested to report fully upon their present and estimated future needs for space. A committee of the UET is endeavoring to develop tentative plans for the remodeling of the building or the procurement of a new building to meet the needs of the founder societies and, if possible, bring in other engineering societies.

Increased revenue from meeting halls and close attention to expenditures produced a small credit balance for the year ended September 30, 1945.

An abstract of the annual report for the year ended September 30, 1945, appeared in *Electrical Engineering*, January 1946, page 47.

ENGINEERING FOUNDATION

The Engineering Foundation was established in 1914 as a joint organization of the four societies, ASCE, AIME, ASME, and AIEE, for "the furtherance of research in science and engineering, and the advancement in any other manner of the profession of engineering and the good of mankind."

Each research project supported by it is under the sponsorship of one of the founder societies.

During the year, the Welding Research Council continued work on nine projects and inititated two new projects. The council is sponsored by the founder societies, the American Welding Society, and the Society of Naval Architects and Marine Engineers. Its work is carried on by eight research committees.

Other reserach projects supported by the Foundation include soil mechanics, columns, alloys of iron, metal cutting, plastic flow of metals, and strength of metals.

The Foundation has continued to support the work of the ECPD.

An abstract of the annual report for the year ended September 30, 1945, appeared in *Electrical Engineering*, January 1946, pages 48–9.

ENGINEERING SOCIETIES LIBRARY

The Engineering Societies Library was formed by combining the separate libraries of the ASCE, AIME, ASME, AIEE, and preparing a composite card catalogue.

Special services rendered by the library include: photoprints, searches, abstracts, translations, bibliographies, book loans by mail.

Wartime conditions prevented the usual growth in the book collection and greatly increased the demand for photostat prints and for other services.

An abstract of the annual report for the year ended September 30, 1945, appeared in *Electrical Engineering*, January 1946, page 49.

EMPLOYMENT SERVICE

Operating as an incorporated nonprofit organization, the Engineering Societies Personnel Service, Inc., assists members of the founder societies desiring to secure new positions and employers searching for engineers. Nonmembers may receive such assistance when positions available cannot be filled by members.

Offices are operated in New York; Detroit, Mich.; Chicago; and San Francisco, Calif.; with the co-operation of the Engineering Society of Detroit in that city, the Western Society of Engineers in Chicago, and the Engineers Club of San Francisco in that city.

For several years, the service has been on a self-supporting basis, but the prevailing scarcity of engineers available for new positions has reduced the number of placements. A record of registration and placements during the past year is given in Table XII.

ENGINEERS' COUNCIL FOR PROFESSIONAL DEVELOPMENT

Organized in 1932 to engage in activities leading toward the enhancement of the professional status of the engineer, this council now includes three representatives of each of the eight participating organizations: the ASCE, AIEE, ASME, AIME, SPEE, American Institute of Chemical Engineers, National Council of State Boards of Engineering Examiners, and the Engineering Institute of Canada.

During the past year, as in previous wartime years, inspections of engineering curricula by the committee on engineering schools were held to a minimum. Twenty-six curricula in 13 institutions were inspected during the past three years. Complete regional personnel for the accrediting of technical institute curricula has been organized.

Other activities are carried on by committees whose titles indicate the nature of their work: student selection and guidance, professional training, professional recognition, information, engineering ethics, employment conditions for engineers, and ways and means.

A comprehensive report on the activities during the year ended September 30, 1945, was published in *Electrical Engineering*, December 1945, pages 461–2.

ENGINEERS JOINT COUNCIL

This Council, formerly known as the joint conference committee, is composed of the presidents, immediate past presi-

Table XII. Analysis of Employment Service

	Men Registered					Men Placed				
Month	New York	Chicago	San Francisco	Detroit	Total	New York	Chicago	San Francisco	Detroit	Total
1945										
May	101	24	40	30	195	17	8	19	10	54
June	98	30	36	24	188	20	9	24	6	59
July	92	28	37	24	181	27	20	20	9	76
August	141	54	53	39	287	20	15	15	9	59
September	242	88	92	57	479	27	25	19	8	79
October	329	79	124	73	605	35	12	20	13	80
November	226	97	113	55	491	43	20	22	11	96
December	202	67	100	43	412	36	16	20	11	83
1946										
January	338	106	134	49	627	42	27	25	13	107
February	251	86	126	60	523	28	18	19	9	74
March	296	79	182	81	638	34	18	20	13	85
April	246	98	113	65	522	43	20	24	20	107
Total	2,562	836	1,550	600	5,148	372	208	247	132	959

dents, and secretaries of the founder societies and the AIChE. Its functions are to consider matters of interest to the societies and to make recommendations to their governing bodies.

A panel was organized to advise a Senate committee regarding research legislation, and a joint committee on technological personnel in relation to national security was established.

Major projects have been started on industrial disarmament of aggressor states, economic status of the engineer, and organization of the engineering profession.

REPRESENTATIVES

A complete list of about 40 joint bodies upon which the Institute is represented appears in the Year Book and in the September issue of *Electrical Engineering* each year.

Appreciation

The board of directors expresses its deepest appreciation and thanks to the committees, and the District, Section, and Branch officers, and the members in general in grateful recognition of the many expansions in activities and the continuing rapid increase in membership.

Respectfully submitted for the board of directors.

H. H. HENLINE
Secretary

AMERICAN INSTITUTE OF ELECTRICAL ENGINEERS

Securities Owned, April 30, 1946

Schedule 1

	Principal Amount of Bonds or Number of Shares of Stock	Restricted Funds: Reserve Capital Fund	Life Membership Fund	International Electrical Congress Library Fund	Lamme Medal Fund	Total
Railroad Bonds:						
Atlantic Coast Line first consolidated 4%, due 1952	$ 4,000.00				$4,253.78	$ 4,253.78
Baltimore & Ohio, Pittsburgh, Lake Erie & West Virginia System 4%, due 1951	10,000.00	$ 6,450.00				6,450.00
Chicago & Erie Railroad Company 5% first mortgage, due 1982, registered	1,000.00	1,105.00				1,105.00
New York Central Railroad Company 4% series A consolidated mortgage, due 1998	10,000.00	6,100.00				6,100.00
Northern Pacific Railway Company collateral trust 4½%, due 1975	10,000.00	10,325.00				10,325.00
St. Louis-San Francisco Railway Company 5% prior line mortgage series B, due 1950 (certificates of deposit), registered, stamped	6,000.00*	5,497.50*				5,497.50*
Total railroad bonds		$ 29,477.50			$4,253.78	$ 33,731.28
Public Utility Bonds:						
New York & Queens Electric Light & Power Company 3½% first and consolidated mortgage, due 1965	$10,000.00	$ 11,000.00				$ 11,000.00
United States Government Bonds:						
Treasury savings bonds series D, due July 1, 1949	10,000.00	$ 7,644.00				$ 7,644.00
Treasury savings bonds series D, due January 1, 1950	10,000.00	7,500.00				7,500.00
Treasury bonds 2%, due 1950/48	77,000.00	78,130.94				78,130.94
Treasury bonds 2%, due 1950/48, registered	3,000.00	3,060.94				3,060.94
Treasury bonds 2½%, due 1968/63	20,000.00	15,000.00	$5,000.00			20,000.00
Treasury bonds 2½%, due 1972/67	6,300.00	1,100.00		$5,200.00		6,300.00
Treasury bonds 2½%, due 1972/67, registered	3,500.00	3,516.41				3,516.41
Defense bonds series F, due June 1, 1953	34,000.00	25,160.00				25,160.00
Defense bonds series G 2½%, due December 1, 1954	18,000.00	18,000.00				18,000.00
Treasury savings bonds series G 2½%, due September 1, 1955	40,000.00	40,000.00				40,000.00
Treasury savings bonds series G 2½%, due November 1, 1956	17,000.00	17,000.00				17,000.00
Treasury savings bonds series G 2½%, due May 1, 1957	20,000.00	20,000.00				20,000.00
Treasury savings bonds series G 2½%, due October 1, 1957	30,000.00	30,000.00				30,000.00
Total United States Government bonds		$266,112.29	$5,000.00	$5,200.00		$276,312.29
Capital Stocks:						
American Can Company	60 shares	$ 4,988.40				$ 4,988.40
American Telephone & Telegraph Company	100 shares	17,454.15				17,454.15
Atchison, Topeka & Santa Fe Railway Company preferred	150 shares	13,035.46				13,035.46
Boston Edison Company	200 shares	4,927.50				4,927.50
Commonwealth Edison Company	200 shares	7,580.68				7,580.68
Consolidated Natural Gas Company	11 shares	221.92				221.92
Eastman Kodak Company	35 shares	4,768.23				4,768.23
E. I. du Pont de Nemours & Company	50 shares	7,982.07				7,982.07
General Electric Company	130 shares	4,463.80				4,463.80
General Motors Corporation $5 preferred	100 shares	12,785.00				12,785.00
General Motors Corporation	100 shares	4,235.53				4,235.53
International Harvester Company	100 shares	5,030.50				5,030.50
International Match Realization Company, Ltd. voting trust certificates for capital shares of International Match Corporation	6* shares	1,851.15*				1,851.15*
Louisville & Nashville Railroad Company	100 shares	6,278.13				6,278.13
Ohio Edison Company 4.40% preferred	150 shares	15,727.50				15,727.50
Pacific Gas and Electric Company	200 shares	8,784.35				8,784.35
Sears, Roebuck and Company	400† shares	6,014.97				6,014.97
Standard Oil Company of New Jersey	200 shares	9,601.26				9,601.26
Union Carbide & Carbon Corporation	100 shares	7,277.42				7,277.42
United Fruit Company	100 shares	11,985.00				11,985.00
United States Steel Corporation 7% cumulative preferred	100 shares	14,885.00				14,885.00
Total capital stocks		$169,878.02				$169,878.02
Total		$476,467.81	$5,000.00	$5,200.00	$4,253.78	$490,921.59
* Less reserve in full for securities considered to be of doubtful value		7,348.65				7,348.65
Total Securities, Less Reserve		$469,119.16	$5,000.00	$5,200.00	$4,253.78	$483,572.94

† Stock was split up in October 1945 by issuance of three additional shares for each one held.

HASKINS & SELLS
CERTIFIED PUBLIC ACCOUNTANTS

1 EAST 44TH STREET
NEW YORK 17

May 20, 1946

American Institute of Electrical Engineers,
33 West 39th Street, New York.

Dear Sirs:

We have examined the balance sheet of the American Institute of Electrical Engineers, and schedule of securities owned, as of April 30, 1946, and the related statements of cash receipts and disbursements of operating and restricted funds for the year ended that date, have reviewed the accounting procedures of the Institute, and have examined its accounting records and other evidence in support of such financial statements. Our examination was made in accordance with generally accepted auditing standards applicable in the circumstances and included all auditing procedures we considered necessary, which procedures were applied by tests to the extent we deemed appropriate in view of the system of internal control.

In our opinion, the accompanying balance sheet, schedule of securities owned, and statements of cash receipts and disbursements fairly present, respectively, the financial condition of, and securities owned by, the Institute as of April 30, 1946, and its recorded cash receipts and cash disbursements for the year ended that date, in conformity with generally accepted accounting principles and practices applied on a basis consistent with that of the preceding year.

Yours truly,

(*Signed*) HASKINS & SELLS

AMERICAN INSTITUTE OF ELECTRICAL ENGINEERS

Balance Sheet, April 30, 1946

Exhibit A.

ASSETS			LIABILITIES		
Property Fund Assets:			**Property Fund Reserve**		$ 548,407.13
One-fourth interest in physical properties of United Engineering Trustees, Inc.:			**Restricted Fund Reserves:**		
Land, buildings, and equipment (less depreciation and renewal reserve)	$361,880.00		Reserve capital fund	$505,795.19	
Funded depreciation and renewal reserve	136,568.48		Life membership fund	8,684.75	
Total	$498,448.48		Member for life fund	5,031.09	
Equipment			International Electrical Congress of St. Louis library fund	5,878.05	
Library (volumes and fixtures)—estimated value	36,366.37		Lamme Medal fund	4,440.44	
Office furniture and fixtures (less reserve for depreciation, $27,761.27)	9,978.02		Mailloux fund	1,137.83	
Works of art, etc.	3,001.35		Total restricted fund reserves		530,967.35
Cash (no change during year)	612.91		**Operating Fund Reserves, Liabilities, etc.:**		
Total property fund assets		$ 548,407.13	Accounts payable	$ 15,455.58	
Restricted Fund Assets:			Deferred income:		
Securities—at cost, less reserve, $7,348.65 (quoted market value, $552,893.92)—Schedule 1	$483,572.94		Dues received in advance	4,503.14	
Cash (Exhibit C)	47,304.66		Entrance fees and dues advanced by applicants for membership	1,263.45	
Accrued interest receivable	89.75		Subscriptions to publications received in advance	17,940.01	
Total restricted fund assets		530,967.35	Miscellaneous (including unallocated receipts)	1,315.67	
Operating Fund Assets:			Operating fund reserves	84,620.36	
Cash (not including $1,302.87 for Federal taxes withheld from employees)—(Exhibit B)	$ 81,379.47		Total operating fund reserves, liabilities, etc.		125,098.21
Accounts receivable:					
Members—for dues (less reserve, $4,000.00)	8,133.58				
Advertisers	5,667.40				
Miscellaneous	3,649.99				
Accrued interest receivable	5,735.52				
Inventories:					
Transactions, etc.	1,054.00				
"Electrical Definitions"	3,668.40				
Work in process (May issue of *Electrical Engineering*, etc.)	6,140.28				
Text and cover paper	7,299.52				
Badges	2,370.05				
Total operating fund assets		125,098.21			
Total		$1,204,472.69	**Total**		$1,204,472.69

Exhibit B. Statement of Cash Receipts and Disbursements of Operating Fund for the Year Ended April 30, 1946

Cash on Deposit With The National City Bank of New York, May 1, 1945 (not including $1,295.18 for Federal taxes withheld from employees)		$ 77,206.09
Receipts:		
Dues (including $127,602.00 allocated to *Electrical Engineering* subscriptions)	$271,620.45	
Advertising	130,875.11	
Transactions subscriptions	8,557.39	
Electrical Engineering subscriptions	26,158.51	
"Electrical Definitions"	887.95	
"Electric Power Distribution for Industrial Plants"	2,769.00	
Miscellaneous publications (preprints, Standards, *Electrical Engineering* supplement, etc.)	23,468.40	
Students' fees	11,659.50	
Entrance fees	19,793.42	
Membership badges	4,468.61	
Transfer fees	3,601.29	
Interest and dividends on investments of Restricted Capital fund	13,389.09	
Barstow bequest (including interest of $652.03)	10,652.03	
Miscellaneous	541.44	
Total receipts		528,442.19
Total		$605,648.28
Disbursements:		
Publications expense:		
Electrical Engineering	$122,603.60	
Transactions	13,964.43	
Year Book	7,993.83	
Miscellaneous publications (preprints, Standards, "Industrial Plants" report, *Electrical Engineering* supplement, etc.)	19,771.44	
Institute meetings	15,310.00	
Institute Sections	44,899.10	
Institute Branches	2,872.01	
Finance committee	600.00	
Headquarters committee	83.87	
Membership committee	10,434.07	
Standards committee	15,681.37	
Forward	$254,213.72	$605,648.28

Total (forward)		$605,648.28
Disbursements (forward)	$254,213.72	
Technical committee	947.15	
Committee on institute publicity	840.33	
Planning and co-ordinating committee	3,122.18	
Joint committee—Economic Status of the Engineer	8.73	
Engineers Joint Council	870.13	
American Society of Civil Engineers handbook	250.00	
Retirement system AIEE—normal contribution	4,982.72	
Canadian Radio Technical Planning Board	318.17	
Radio Technical Planning Board	500.00	
Traveling expenses:		
Geographical Districts:		
Executive committees	5,240.17	
Vice-presidents	1,027.62	
Branch counselors and chairmen	1,280.61	
President's appropriation	1,840.79	
AIEE representatives	289.70	
Board of directors	7,171.50	
Nominating committee	1,253.85	
Administrative expenses	63,658.00	
Geographical Districts—Branch paper prizes	163.64	
Institute prizes—national	309.06	
American Co-ordinating Committee on Corrosion	25.00	
American Standards Association	1,750.00	
United Engineering Trustees, Inc.:		
Building assessment	17,813.64	
Library assessment	11,377.85	
Engineers' Council for Professional Development	1,852.00	
Engineering Foundation Project—Welding research	250.00	
National Committee State Board Engineering Examiners	500.00	
John Fritz Medal	50.00	
National Fire Protection Association—Dues	60.00	
Membership badges	5,265.20	
Legal services	250.00	
Lamme Medal expense (see Exhibit C)	191.03	
Office furniture and fixtures, and repairs	339.13	
Edison Medal committee	115.90	
Transfers:		
To reserve capital fund:		
Barstow bequest	10,652.03	
Other	123,726.58	
To Member for Life fund	1,762.38	
Total disbursements		524,268.81
Cash on Deposit With The National City Bank of New York, April 30, 1946 (not including $1,302.87 for Federal taxes withheld from employees)		$ 81,379.47

Exhibit C. Statement of Cash Receipts and Disbursements of Restricted Funds for the Year Ended April 30, 1946

		Restricted Funds					
	Total	Reserve Capital Fund	Member for Life Fund	Life Membership Fund	International Electrical Congress of St. Louis Library Fund	Lamme Medal Fund	Mallioux Fund
Cash on Deposit With The National City Bank of New York and Various Savings Banks, May 1, 1945	$ 35,064.88	$ 26,586.40	$3,268.71	$3,380.79	$531.80	$176.22	$1,120.96
Receipts:							
Income from bonds	$ 415.00			$ 125.00	$130.00	$160.00	
Interest on bank balances	65.26			48.39			$ 16.87
Transfers for operating fund:							
Barstow bequest	10,652.03	$ 10,652.03					
Other	125,488.96	123,726.58	$1,762.38				
Life membership fees	678.80			678.80			
Liquidating dividend—International Match Realization Company, Ltd	24.00	24.00					
Total receipts	$137,324.05	$134,402.61	$1,762.38	$ 852.19	$130.00	$160.00	$ 16.87
Total	$172,388.93	$160,989.01	$5,031.09	$4,232.98	$661.80	$336.22	$1,137.83
Disbursements:							
Purchase of securities	$124,312.98	$124,312.98					
Transfer to operating fund	595.07			$ 595.07			
Purchase of medal, cost of engraving, etc. (exclusive of $191.03 paid from general fund)	176.22					$176.22	
Total disbursements	$125,084.27	$124,312.98		$ 595.07		$176.22	
Balance on Deposit With The National City Bank of New York and Various Savings Banks, April 30, 1946	$ 47,304.66	$ 36,676.03	$5,031.09	$3,637.91	$661.80	$160.00	$1,137.83

Officers of A. I. E. E. for 1946–1947

PRESIDENT

J. ELMER HOUSLEY
Alcoa, Tenn.
(Term expires July 31, 1947)

JUNIOR PAST PRESIDENTS

CHARLES A. POWEL, East Pittsburgh, Pa.
(Term expires July 31, 1947)

W. E. WICKENDEN, Cleveland, Ohio
(Term expires July 31, 1948)

VICE-PRESIDENTS

District		District	
2	E. S. FIELDS, Cincinnati, Ohio	1	E. W. DAVIS, Cambridge, Mass.
4	H. B. WOLF, Charlotte, N. C.	3	O. E. BUCKLEY, New York, N. Y.
6	L. M. ROBERTSON, Denver, Colo.	5	T. G. LECLAIR, Chicago, Ill.
8	F. F. EVENSON, San Diego, Calif.	7	R. F. DANNER, Oklahoma City, Okla.
10	F. L. LAWTON, Montreal, Quebec	9	C. F. TERRELL, Seattle, Wash.
	(Terms expire July 31, 1947)		*(Terms expire July 31, 1948)*

DIRECTORS

C. M. LAFFOON, East Pittsburgh, Pa.
C. W. MIER, Dallas, Tex.
S. H. MORTENSEN, Milwaukee, Wis.
(Terms expire July 31, 1947)

J. M. FLANIGEN, Atlanta, Ga.
J. R. NORTH, Jackson, Mich.
WALTER C. SMITH, San Francisco, Calif.
(Terms expire July 31, 1949)

P. L. ALGER, Schenectady, N. Y.
M. J. MCHENRY, Toronto, Ontario
D. A. QUARLES, New York, N. Y.
(Terms expire July 31, 1948)

J. F. FAIRMAN, New York, N. Y.
R. T. HENRY, Buffalo, N. Y.
E. P. YERKES, Philadelphia, Pa.
(Terms expire July 31, 1950)

TREASURER

W. I. SLICHTER, New York, N. Y.
(Term expires July 31, 1947)

SECRETARY

H. H. HENLINE, New York, N. Y.
(Term expires July 31, 1947)

LOCAL HONORARY SECRETARIES

AUSTRALIA—V. J. F. Brain, Electricity Authority of N. S. W., Bridge & Phillips Streets, Sydney, N. S. W.

BRAZIL—Richard H. Bowles, Sao Paulo Tramway Light and Power Co., Sao Paulo

ENGLAND—A. P. M. Fleming, Metropolitan-Vickers Elec. Co., Trafford Park, Manchester

INDIA, NORTHERN—N. Thornton, 11 Bahawalpur Road, Lahore, Punjab

INDIA, SOUTHERN—N. N. Iengar, The Tata Power Co. Ltd., Bombay House, Bruce St., Fort Bombay

NEW ZEALAND—R. D. Neale, School of Engineering, Canterbury University College, Christchurch C. 1.

SWEDEN—Edy Velander, Royal Swedish Institute, Stockholm.

TRANSVAAL—Francis E. Ingham, Box 6067, Johannesburg, South Africa.

PAST PRESIDENTS—1884–1946

*NORVIN GREEN.....1884–85–86
*FRANKLIN L. POPE.....1886–87
*T. COMMERFORD MARTIN.....1887–88
*EDWARD WESTON.....1888–89
*ELIHU THOMSON.....1889–90
*WILLIAM A. ANTHONY.....1890–91
*ALEXANDER GRAHAM BELL.....1891–92
*FRANK JULIAN SPRAGUE.....1892–93
*EDWIN J. HOUSTON.....1893–94–95
*LOUIS DUNCAN.....1895–96–97
*FRANCIS BACON CROCKER.....1897–98
*A. E. KENNELLY.....1898–1900
*CARL HERING.....1900–01
*CHARLES P. STEINMETZ.....1901–02
*CHARLES F. SCOTT.....1902–03
*BION J. ARNOLD.....1903–04
*JOHN W. LIEB.....1904–05
*SCHUYLER SKAATS WHEELER.....1905–06
*SAMUEL SHELDON.....1906–07
*HENRY G. STOTT.....1907–08
*LOUIS A. FERGUSON.....1908–09
*LEWIS B. STILLWELL.....1909–10
DUGALD C. JACKSON.....1910–11
GANO DUNN.....1911–12
RALPH D. MERSHON.....1912–13
*C. O. MAILLOUX.....1913–14
*PAUL M. LINCOLN.....1914–15
*JOHN J. CARTY.....1915–16
H. W. BUCK.....1916–17
*E. W. RICE, JR.....1917–18
COMFORT A. ADAMS.....1918–19
*CALVERT TOWNLEY.....1919–20
*A. W. BERRESFORD.....1920–21
WILLIAM MCCLELLAN.....1921–22
FRANK B. JEWETT.....1922–23
*HARRIS J. RYAN.....1923–24
*FARLEY OSGOOD.....1924–25
*M. I. PUPIN.....1925–26
C. C. CHESNEY.....1926–27
*BANCROFT GHERARDI.....1927–28
*R. F. SCHUCHARDT.....1928–29
*HAROLD B. SMITH.....1929–30
*WILLIAM S. LEE.....1930–31
C. E. SKINNER.....1931–32
H. P. CHARLESWORTH.....1932–33
J. B. WHITEHEAD.....1933–34
*J. ALLEN JOHNSON.....1934–35
*E. B. MEYER.....1935–36
A. M. MACCUTCHEON.....1936–37
W. H. HARRISON.....1937–38
JOHN CASTLEREAGH PARKER.....1938–39
F. MALCOLM FARMER.....1939–40
R. W. SORENSEN.....1940–41
DAVID C. PRINCE.....1941–42
HAROLD S. OSBORNE.....1942–43
NEVIN E. FUNK.....1943–44
C. A. POWEL.....1944–45
W. E. WICKENDEN.....1945–46

* Deceased.

General Committees

Executive

J. Elmer Housley, *chairman*, Aluminum Company of America, P.O. Box 465, Alcoa, Tenn.
P. L. Alger — R. T. Henry
O. E. Buckley — W. I. Slichter
J. F. Fairman — W. E. Wickenden

Board of Examiners

R. H. Barclay, *chairman*, J. G. White Engineering Corporation, 80 Broad Street, New York 4, N. Y.
H. E. Farrer, *secretary*, AIEE, 33 West 39th Street, New York 18, N. Y.
P. H. Adams — A. E. Knowlton
R. W. Atkinson — C. M. Laffoon
Robin Beach — L. G. Pacent
F. E. D'Humy — J. J. Pilliod
E. D. Doyle — R. C. Roe
C. W. Franklin — H. M. Trueblood
I. W. Gross — H. H. Weber
L. F. Hickernell — John Westbye
I. F. Kinnard — Sidney Withington

Code of Principles of Professional Conduct

D. D. Ewing, *chairman*, Purdue University, Lafayette, Ind.
Harry Barker — D. C. Jackson
E. S. Fields — S. H. Mortensen
E. H. Flath — W. M. Piatt

Constitution and Bylaws

Reginald L. Jones, *chairman*, 463 West Street, New York 14, N. Y.
Walter C. Smith, *vice-chairman*, 823 Russ Building, San Francisco 6, Calif.
Mark Eldredge — T. G. LeClair
W. A. Gentry — C. T. Sinclair

Edison Medal

Appointed by the president for term of five years

F. D. Newbury — D. C. Prince — W. E. Wickenden (*Terms expire July 31, 1947*)
C. R. Freehafer — C. A. Powel — David Sarnoff (*Terms expire July 31, 1948*)
O. E. Buckley — A. E. Knowlton — H. E. Strang (*Terms expire July 31, 1949*)
C. V. Christie — Zay Jeffries — Harold Pender (*Terms expire July 31, 1950*)
C. A. Corney — S. M. Dean, *chairman* — I. M. Stein (*Terms expire July 31, 1951*)

Elected by the board of directors from its own membership for term of two years

J. R. North — D. A. Quarles — H. B. Wolf (*Terms expire July 31, 1947*)
P. L. Alger — R. T. Henry — E. P. Yerkes (*Terms expire July 31, 1948*)

Ex officio

J. Elmer Housley, president
W. I. Slichter, treasurer
H. H. Henline, secretary

Finance

D. A. Quarles, *chairman*, 463 West Street, New York 14, N. Y.
O. E. Buckley — E. P. Yerkes
F. A. Norris, *secretary*, AIEE, 33 West 39th Street, New York 18, N. Y.

Charles LeGeyt Fortescue Fellowship

J. M. Gaylord — R. T. Henry, *chairman* (*Terms expire July 31, 1947*)
J. W. Barker — Ernst Weber (*Terms expire July 31, 1948*)
H. E. Strang, *vice-chairman* — C. H. Willis (*Terms expire July 31, 1949*)
H. H. Henline, *secretary*, AIEE, 33 West 39th Street, New York 18, N. Y.

Headquarters

W. R. Smith, *chairman*, Public Service Electric and Gas Company, 80 Park Place, Newark 1, N. J.
H. H. Henline, *secretary* — D. A. Quarles, *vice-chairman*

Lamme Medal

W. A. Del Mar — John C. Parker, *chairman* — Philip Sporn (*Terms expire July 31, 1947*)
H. L. Hazen — V. M. Montsinger — G. A. Waters (*Terms expire July 31, 1948*)
N. S. Hibshman — T. G. LeClair — A. C. Monteith (*Terms expire July 31, 1949*)

Members-for-Life Fund

F. M. Farmer, *chairman*, 2 East End Avenue, New York 21, N. Y.
C. R. Beardsley, *vice-chairman*, 4 Irving Place, New York 3, N. Y.
E. H. Colpitts — F. D. Newbury
N. E. Funk — W. I. Slichter
R. C. Muir — J. F. Tritle — R. W. Sorensen

Membership

Tomlinson Fort, *chairman*, Westinghouse Electric Corporation, East Pittsburgh, Pa.
Richard F. Ham, *vice-chairman*, 4 Irving Place, New York 3, N. Y.
F. A. Norris, *secretary*, AIEE, 33 West 39th Street, New York 18, N. Y.
F. S. Black — M. L. Lehman
A. D. Brown — P. H. Light
R. L. Chapman — W. J. Lyman
W. F. Cotter — Lee M. Moore
W. C. Fowler — E. G. D. Paterson
P. H. Hughes — D. B. Perry
A. W. Janowitz — J. R. Riley
C. W. LaPierre — H. J. Scholz
E. P. Yerkes

District Vice-Chairmen

F. S. Bacon (1) — A. M. Spaulding (6)
C. T. Pearce (2) — R. C. Horn (7)
J. A. Duncan, Jr. (3) — E. W. Morris (8)
W. Stone Leake (4) — M. J. Lantz (9)
J. C. Woods (5) — Thomas Ingledow (10)

Ex officio

Chairmen of membership committees of all Sections

Planning and Co-ordination

J. F. Fairman, *chairman*, Consolidated Edison Company of New York, Inc., 4 Irving Place, New York 3, N. Y.
D. A. Quarles, *vice-chairman*, 463 West Street, New York 14, N. Y.
H. H. Henline, *secretary*, 33 W. 39th Street, New York 18, N. Y.
W. H. Schlasman, *assistant secretary*, 33 W. 39th Street New York 18, N. Y.
P. L. Alger — T. G. LeClair
G. W. Bower — W. B. Morton
W. P. Dobson — E. B. Robertson
M. D. Hooven — C. F. Wagner
Reginald L. Jones — W. E. Wickenden

Prizes, Award of Institute

M. D. Hooven, *chairman*, Public Service Electric and Gas Company, 80 Park Place, Newark 1, N. J.
C. S. Rich, *secretary*, AIEE, 33 West 39th Street, New York 18, N. Y.
J. W. Barker — J. J. Pilliod
H. W. Collins — J. G. Tarboux
J. D. Miner — C. F. Wagner
M. S. Oldacre — H. B. Wolf — R. J. Wiseman

Publication

C. F. Wagner, *chairman*, Westinghouse Electric Corporation, East Pittsburgh, Pa.
G. R. Henninger, *secretary*, AIEE, 500 Fifth Ave., New York 18, N. Y.
M. S. Coover — F. A. Lewis
H. H. Henline — J. R. North
R. K. Honaman — J. J. Orr
B. M. Jones — G. A. Van Brunt — H. H. Race

Publicity, Institute

R. K. Honaman, *chairman*, 463 West Street, New York 14, N. Y.
Guy Bartlett — M. D. Hooven
E. E. Dorting — C. R. Jones
J. F. Fairman — A. E. Knowlton
C. F. Wagner

Registration of Engineers

T. G. LeClair, *chairman*, Commonwealth Edison Company, 72 West Adams Street, Chicago 90, Ill.
J. E. Hobson, *secretary*, Armour Research Foundation, 35 West 33d Street, Chicago 16, Ill.
S. W. Anderson — C. C. Knipmeyer
J. H. Foote — K. B. McEachron
N. L. Freeman — E. B. Robertson
J. D. Guillemette — L. M. Robertson

Research

J. W. Barker, *chairman*, Research Corporation, 405 Lexington Avenue, New York 17, N. Y.
P. L. Alger — E. L. Moreland
B. G. Ballard — G. M. L. Sommerman
E. W. Boehne — F. J. Stevens
G. T. Harness — C. G. Suits
J. A. Hutcheson — Gordon Thompson
W. A. Lewis — V. K. Zworykin

Safety

L. F. Adams, *chairman*, General Electric Company, Schenectady 5, N. Y.
Robin Beach, *vice-chairman*, 32 Court Street, Brooklyn 2, N. Y.
A. B. Smith, *secretary*, National Electrical Manufacturers Association, 155 East 44th Street, New York 17, N. Y.
C. S. Bowden — J. O. Leslie
M. M. Brandon — R. L. Lloyd
Allan B. Campbell — A. C. Muir
C. F. Dalziel — Albrecht Naeter
W. P. Dobson — W. T. Rogers
J. M. Flanigen — W. E. Rushlow
John Grotzinger — W. R. Smith
F. L. Kemp — H. W. Tenney
W. B. Kouwenhoven — E. E. Turkington
H. B. Williams

Sections

G. W. Bower, *chairman*, Public Service Electric and Gas Company, 80 Park Place, Newark 1, N. J.
R. M. Pfalzgraff, *vice-chairman*, American Viscose Corporation, Wilmington 99, Del.
A. C. Muir, *secretary*, Berwind-White Coal Mining Company, 1138 Commercial Trust Building, Philadelphia 2, Pa.
D. I. Anzini — R. E. Kistler
S. C. Commander — F. L. Lawton
W. E. Enns — C. W. Lethert
A. H. Frampton — T. M. Linville
H. P. Heafer — R. G. Porter
V. P. Hessler — C. S. Purnell
W. R. Hough — H. B. Wolf

Ex officio

Chairmen of Sections

Standards

W. P. Dobson, *chairman*, Hydro-Electric Power Commission Laboratory, 8 Strachan Avenue, Toronto, Ont.
R. L. Jones, *vice-chairman*, 463 West Street, New York 14, N. Y
H. E. Farrer, *secretary*, AIEE, 33 West 39th Street, New York 18, N. Y.
Joseph W. Allen — A. C. Monteith
R. W. Atkinson — S. H. Mortensen
R. C. Bergvall — J. R. North
J. E. Clem — M. S. Oldacre
C. M. Gilt — E. B. Paxton
F. E. Harrell — M. M. Samuels
R. T. Henry — F. B. Silsbee
H. Kent — Gordon Thompson

Ex officio

Chairmen of working and co-ordinating committees of the Standards committee
Chairmen of AIEE technical committees
Chairmen of AIEE delegations on other standardizing bodies or sole representatives thereon
President, United States National Committee of the International Electrotechnical Commission

Student Branches

J. F. Calvert, *chairman*, Northwestern Technological Institute, Evanston, Ill.
E. M. Strong, *vice-chairman*, Cornell University, Ithaca, N. Y.
L. T. Rader, *secretary*, Illinois Institute of Technology, 3300 Federal Street, Chicago 16, Ill.
M. M. Cory — E. W. O'Brien
H. L. Davis, Jr. — Walter Charles Smith
A. G. Ennis — R. G. Warner
Everett S. Lee — C. R. Wischmeyer

Ex officio

Student Branch counselors

Technical Program

M. D. Hooven, *chairman*, Public Service Electric and Gas Company, 80 Park Place, Newark 1, N. J.
H. M. Turner, *vice-chairman*, Yale University, New Haven, Conn.
C. S. Rich, *secretary*, AIEE, 33 West 39th Street, New York 18, N. Y.
O. E. Buckley — S. H. Mortensen
F. A. Cowan — J. J. Orr
I. W. Gross — Frank Thornton, Jr.
F. E. Johnson, Jr. — T. A. Worcester — C. C. Whipple

Ex officio

J. F. Fairman, *chairman*, committee on planning and co-ordination
L. F. Adams, *chairman*, committee on safety
W. P. Dobson, *chairman*, Standards committee
Chairmen of all technical committees

Transfers

D. E. Moat, *chairman*, Leeds and Northrup Company, 1800 Keith Building, Cleveland 15, Ohio
M. J. McHenry, *vice-chairman*, Hydro-Electric Power Commission, 620 University Avenue, Toronto, Ont.
C. W. Fick, *secretary*, General Electric Company, 14966 Woodland Avenue, Cleveland 4, Ohio

E. A. Crellin	A. E. Knowlton
C. W. Fick	J. W. Lingary
B. D. Hull	F. K. McCune

Technical Committees

Air Transportation

J. D. Miner, *chairman*, Aviation Engineering Department, Westinghouse Electric Corporation, Lima, Ohio
F. M. Roberts, *vice-chairman*, industrial engineering division, General Electric Company, Schenectady 5, N. Y.
A. F. Pelster, *secretary*, Westinghouse Electric Corporation, Lima, Ohio

J. W. Allen	O. F. Olsen
J. F. Angier	S. H. Orowski
R. A. Averitt	W. E. Pakala
C. J. Breitwieser	M. H. Peairs
Harold R. Brown	Earl G. Ports
K. D. Brumbaugh	H. F. Rempt
J. F. Calvert	Raymond Rugge
John B. Coleman	M. L. Schmidt
A. E. Corcoran	Raymond A. Smith
J. C. Cunningham	K. R. Smythe
W. T. Harding	S. D. Summers
R. M. Heintz	T. J. Tanner
V. P. Hessler	A. F. Trumbull
Chas. Kingsley, Jr.	F. H. Walker
R. J. Lusk	W. W. West
R. A. Millermaster	F. O. Wisman

Aircraft Electrical Control Protective Devices and Cable Subcommittee

R. J. Lusk, *chairman*, Westinghouse Electric Corporation, East Pittsburgh, Pa

H. R. Crago	H. S. Moore
E. E. Magee	J. Ottmar
A. T. McClinton	J. H. Taylor
R. A. Millermaster	W. W. West

Aircraft Electrical Rotating Machinery Subcommittee

M. L. Schmidt, *chairman*, General Electric Company, 1635 Broadway, Fort Wayne 2, Ind.
L. F. Hemphill, *secretary*, General Electric Company 1635 Broadway, Fort Wayne 2, Ind.

J. W. Allen		L. R. Larson
D. E. Fritz		F. M. Potter
A. D. Gilchrist	R. J. Sullivan	G. W. Sherman

Aircraft Systems Subcommittee

R. H. Kaufmann, *chairman*, General Electric Company, Schenectady, N. Y.

J. W. Allen	J. R. North
J. C. Cunningham	K. R. Smythe
H. J. Finison	A. J. Snyder
H. L. Hildebrandt	A. F. Trumbull

Basic Principles of Altitude Rating Subcommittee

W. E. Pakala, *chairman*, Westinghouse Electric Corporation, East Pittsburgh, Pa.

J. W. Allen		J. G. Hutton
T. R. Brown		Chester A. Maple
S. H. Hanville, Jr.	R. A. Rugge	A. T. McClinton

Automatic Stations

George S. Whitlow, *chairman*, Union Electric Company of Missouri, 315 North 12th Boulevard, Saint Louis, Mo.
G. S. Lunge, *vice-chairman*, General Electric Company, Schenectady 5, N. Y.
I. T. Knight, *secretary*, Kansas City Power and Light Company, Box 679, Kansas City 10, Mo.

J. A. Adams	M. Fraresso
Harris Barber	E. E. George
G. W. Bean	K. B. Hoffman
L. B. Bogan	Perry Peterson
W. A. Derr	C. H. Smoke
J. A. Elzi	J. H. Vivian
R. C. Ericson	E. A. Williams, Jr.
J. M. Flanigen	C. E. Winegartner

Basic Sciences

J. D. Tebo, *chairman*, Bell Telephone Laboratories, Inc., 463 West Street, New York 14, N. Y.
K. W. Miller, *vice-chairman*, Armour Research Foundation, 55 West 34th Street, Chicago, Ill.
N. S. Hibshman, *secretary*, Pratt Institute, Brooklyn 5, N. Y.

J. G. Brainerd	M. G. Malti
O. E. Buckley	Brian O'Brien
Charles Concordia	G. W. Penney
H. L. Curtis	W. E. Phillips
A. V. Eastman	Walther Richter
G. L. Greves	W. J. Seeley
C. R. Hanna	E. D. Sheipley
H. L. Hazen	James J. Smith
W. C. Johnson	V. G. Smith
H. P. Lawther	F. G. Tappan
W. A. Lewis	G. S. Timoshenko
F. C. Lindvall	Ernst Weber

Electric Circuit Theory Subcommittee

J. G. Brainerd, *chairman*, Moore School of Electrical Engineering, University of Pennsylvania, Philadelphia, Pa.

R. L. Dietzold		T. J. Higgins
E. A. Guillemin		E. B. Payne
C. R. Hanna	Ernst Weber	W. E. Phillips

(Membership tentative)

Large Scale Computing Devices Subcommittee

C. Concordia, *chairman*, General Electric Company, 1 River Road, Schenectady 5, N. Y.

J. G. Brainerd	E. L. Harder
Samuel H. Caldwell	W. C. Johnson
G. D. McCann	

Applied Mathematics Subcommittee

M. G. Malti, *chairman*, Cornell University, Ithaca, N. Y.

P. L. Alger	H. P. Lawther, Jr.
H. B. Hansteen	J. J. Smith

New Energy Sources Subcommittee

W. A. Lewis, *chairman*, Illinois Institute of Technology, Technology Center, Chicago 16, Ill.

W. C. Brown		J. J. Smith
C. R. Hanna	J. D. Tebo	B. R. Teare

Paper Solicitation Subcommittee

K. W. Miller, *chairman*, Armour Research Foundation, 55 West 34th Street, Chicago 16, Ill.
F. C. Lindvall

Communication

J. J. Pilliod, *chairman*, American Tel. & Tel. Company, 195 Broadway, New York 7, N. Y.
Rothwell E. Smith, *vice-chairman*, Federal Tel. and Radio Corporation, 591 Broad St., Newark, N. J.
H. I. Romnes, *secretary*, American Tel. & Tel. Company, 195 Broadway, New York 7, N. Y.

H. A. Affel	W. A. Jackson
A. L. Albert	C. B. Jolliffe
R. B. Beetham	H. E. Jones
H. M. Bollinger	T. L. Jones
J. D. Booth	I. J. Kaar
F. B. Bramhall	J. W. Kidder
J. L. Callahan	Ralph G. McCurdy
I. S. Coggeshall	G. R. Messmer
J. B. Coleman	C. W. Mier
D. I. Cone	H. H. Newell
F. A. Cowan	L. G. Pacent
H. J. Dible	Haraden Pratt
L. J. Dunnewold	G. B. Ransom
Melville Eastham	J. B. Russell
H. E. Ellithorn	R. E. Shelby
H. M. Engh	J. O. Shepherd
H. R. Fritz	C. G. Sinclair, Jr.
D. G. Geiger	Arthur Bessey Smith
E. E. George	H. M. Turner
P. C. Goldmark	Wm. Comings White
J. E. Hobson	E. P. Yerkes
F. C. Young	

Hearing Aids Subcommittee

L. G. Pacent, Pacent Engineering Corporation, 79 Madison Avenue, New York, N. Y.

Modulation Methods Subcommittee

H. M. Turner, *chairman*, Yale University, New Haven, Conn.

H. A. Affel	J. B. Russell
J. L. Callahan	R. E. Smith

Power Line Carrier for Power Company Communications Subcommittee

J. D. Booth, *chairman*, Westinghouse Electric Corporation, 2519 Wilkens Avenue, Baltimore, Md.
E. E. George

Radio Communications Systems Subcommittee

G. B. Ransom, *chairman*, American Telephone and Telegraph Company, 32 Sixth Avenue, New York 13, N. Y.

Austin Bailey		F. B. Bramhall
R. B. Beetham	J. W. Kidder	W. A. Jackson

Television Subcommittee

C. B. Jolliffe, *chairman*, Radio Corporation of America, Princeton, N. J.

H. A. Affel		P. C. Goldmark
J. B. Coleman	R. E. Shelby	I. J. Kaar

Testing of Telephone Transmitters and Receivers Subcommittee

A. B. Smith, *chairman*, Associated Electric Laboratories, Inc., 1033 West Van Buren Street, Chicago, Ill.

R. G. McCurdy	F. C. Young	L. G. Pacent

Underwater Sound Developments Subcommittee

H. A. Affel, *chairman*, Bell Telephone Laboratories, Inc., 463 West Street, New York 14, N. Y.
J. G. Patterson

Domestic and Commercial Applications

Carl W. Evans, *chairman*, *Electrical South*, 1020 Grant Building, Atlanta, Ga.
M. K. Brody, *vice-chairman*, McCall's Test Rooms, 444 Madison Avenue, New York 22, N. Y.
Wesley Weinerth, *secretary*, Philadelphia Electric Company, 2301 Market Street, Philadelphia 3, Pa.

R. U. Berry	L. W. McCullough
D. K. Blake	M. J. McHenry
M. M. Brandon	H. E. Metz
A. C. Bredahl	W. F. Ogden
W. B. Buchanan	C. F. Scott
L. R. Gamble	H. P. Seelye
R. R. Herrmann	Sam Shiozawa
C. H. Leatham	G. C. Tenney
F. W. Linder	Gordon Thompson

Electrical Hazards to Farm Animals Subcommittee

W. B. Buchanan, *chairman*, Hydro-Electric Power Commission of Ontario, 8 Strachan Avenue, Toronto, Ontario, Canada

H. P. Seelye	Wesley Weinerth

Farm Applications Subcommittee

M. J. McHenry, *chairman*, Hydro-Electric Power Commission of Ontario, 620 University Avenue, Toronto 3, Ontario, Canada

M. M. Brandon	Sam Shiozawa	Frank Linder

Load Characteristics Subcommittee

William F. Ogden, *chairman*, Edison General Electric Appliance Company, Inc., 5600 West Taylor Street, Chicago 44, Ill.

D. K. Blake		R. R. Herrmann
A. C. Bredahl	M. J. McHenry	Frank Linder

Wiring Subcommittee

Wesley Weinerth, *chairman*, Philadelphia Electric Company, 2301 Market Street, Philadelphia 3, Pa.

M. M. Brandon	L. W. McCullough
A. C. Bredahl	M. J. McHenry
R. R. Herrmann	Carl F. Scott

Education

J. G. Tarboux, *chairman*, Cornell University, Ithaca, N. Y.
G. F. Corcoran, *vice-chairman*, University of Maryland, College Park, Md
J. A. Northcott, Jr., *secretary*, University of Notre Dame, Notre Dame, Ind.

A. L. Albert	Claire W. Ricker
H. W. Bibber	L. M. Robertson
M. S. Coover	H. H. Skiling
E. D. Dreese	R. W. Sorensen
W. L. Everitt	B. R. Teare, Jr.
M. C. Hughes	George B. Thomas
E. B. Kurtz	C. E. Tucker
E. A. Loew	C. E. Tuites

A. C. Monteith — E. A. Walker
R. G. Porter — A. R. Zimmer — R. W. Warner

Electric Machinery

M. S. Oldacre, *chairman*, Commonwealth Edison Company, 72 West Adams Street, Chicago 90, Ill.
C. P. Potter, *vice-chairman*, Wagner Electric Corporation, 6400 Plymouth Ave., St. Louis 14, Mo.
W. C. Sealey, *secretary*, Allis-Chalmers Manufacturing Company, Milwaukee 1, Wis.

E. H. Alexander — C. J. Koch
Sterling Beckwith — T. C. Lloyd
Theodore Braaten — C. M. Lovell
F. S. Brown — G. W. McIver, Jr.
B. M. Cain — R. C. Moore
J. F. Calvert — T. H. Morgan
G. T. Harness — L. M. Robertson
F. E. Harrell — M. L. Schmidt
C. B. Hathaway — J. F. Sellers
Raymond A. Hopkins — H. D. Sill
W. R. Hough — H. R. Sills
E. K. Kane — F. D. Snyder
F. P. Kaspar — F. L. Snyder
C. E. Kilbourne — P. H. Trickey
L. A. Kilgore — R. L. Webb — C. G. Veinott

D-C Machinery Subcommittee

C. B. Hathaway, *chairman*, Westinghouse Electric Corporation, East Pittsburgh, Pa.

J. L. Fuller — V. P. Hessler
L. N. Grier — R. D. Ingalls
J. L. Hamilton — D. Ramadanoff — T. M. Linville

Induction Machinery Subcommittee

W. R. Hough, *chairman*, Reliance Electric and Engineering Company, 1088 Ivanhoe Road, Cleveland 10, Ohio

G. R. Anderson — S. F. Henderson
E. L. Bailey — C. J. Koch
E. C. Barnes — T. C. Lloyd
B. M. Cain — T. H. Morgan
J. L. Hamilton — C. P. Potter — D. R. Percival

Insulation Resistance Subcommittee

R. L. Webb, *chairman*, Consolidated Edison Company of New York, Inc., 4 Irving Place, New York 3, N. Y.

J. E. Allen — J. W. Jones
L. J. Berberich — H. R. Stewart
E. B. Curdts — J. B. Swering
E. F. Dissmeyer — C. O. Weilbaecher
D. D. Higgins — R. W. Wieseman — E. W. Whitmer

Synchronous Machinery Subcommittee

C. E. Kilbourne, *chairman*, General Electric Company, Schenectady, N. Y.

Sterling Beckwith — C. Kingsley
J. F. Calvert — A. A. Kroneberg
S. B. Crary — W. P. Monroe
James DeKiep — E. I. Pollard
E. L. Harder — S. H. Wright — M. D. Ross

Transformer Subcommittee

F. S. Brown, *chairman*, Duquesne Light Company, 435 Sixth Avenue, Pittsburgh, Pa.

M. K. Brown — M. S. Oldacre
J. E. Clem — W. C. Sealey
H. L. Davis — F. L. Snyder
I. W. Gross — F. J. Vogel
H. B. Keath — C. F. Wagner
V. M. Montsinger — H. H. Wagner
J. R. North — E. R. Whitehead

Test Code Co-ordinating Subcommittee

T. C. Lloyd, *chairman*, Robbins and Myers, Inc., Springfield, Ohio

(*To be appointed*)

Electric Welding

G. W. Garman, *chairman*, General Electric Company, 1 River Road, Schenectady 5, N. Y.
E. H. Vedder, *vice-chairman* and *secretary*, Westinghouse Electric Corporation, P. O. Box 2025, Buffalo 3, N. Y.

C. A. Adams — J. Harold Lampe
E. M. Callender — C. I. MacGuffie
G. M. Chute, Jr. — L. B. Potter
C. N. Clark — Sam Shiozawa
W. E. Crawford — C. E. Smith
E. W. Davis — H. W. Snyder
J. F. Deffenbaugh — W. Spraragen
G. H. Fett — E. F. Steinert
K. L. Hansen — L. K. Stringham
W. F. Hess — J. R. Wirt
C. E. Humble — M. Zucker

Arc Welding Subcommittee

E. F. Steinert, *chairman*, Westinghouse Electric Corporation, Sharon, Pa.

C. N. Clark — C. I. MacGuffie
K. L. Hansen — H. W. Snyder

Resistance Welding Subcommittee

E. H. Vedder, *chairman*, Westinghouse Electric Corporation, P.O. Box 2025, Buffalo 5, N. Y.

E. M. Callender — G. W. Carman
C. N. Clark — M. Zucker — C. E. Smith

Electrochemistry and Electrometallurgy

T. R. Rhea, *chairman*, General Electric Company, Schenectady 5, N. Y.
F. R. Benedict, *vice-chairman*, Room 11-L-17, Westinghouse Electric Corporation, East Pittsburgh, Pa.
W. C. Kalb, *secretary*, National Carbon Company, Inc., Carbon Products Division, P. O. Box 6087, Cleveland 1, Ohio

F. T. Chesnut — F. L. Lawton
L. H. Fletemeyer — D. H. Levy
L. O Grondahl — Waldo Porter
W. E. Gutzwiller — J. B. Rice
J. D. Harper — Leroy W. Roush
J. E. Hobson — F. O. Schnure
Rollin Kennard — W. R. Schofield
E. L. Kirk — N. R. Stansel
W. B. Kouwenhoven — E. R. Whitehead

Metallic Rectifiers Subcommittee

L. O. Grondahl, *chairman*, Union Switch and Signal Company, Swissvale, Pa.
E. A. Harty, *secretary*, General Electric Company, Lynn, Mass.

W. F. Bonner — C. E. Peters
L. W. Burton — N. Y. Priessman
C. E. Hamann — G. Ramsey
C. C. Herskind — R. Whitesell — I. R. Smith

Voltage Transients in Arc Furnace Circuits Subcommittee

E. R. Whitehead, *chairman*, Armour Research Foundation, 35 West 33rd Street, Chicago 16, Ill.

S. Arnold — S. B. Griscom
E. W. Boehne — J. B. Hodtum
F. W. Brooke — W. E. Moore
L. F. Ferri — J. O. Shimmin
Lyle Fountain — N. R. Stansel
C. M. Foust — H. H. Wagner — F. J. Vogel

Electronics

W. R. G. Baker, *chairman*, General Electric Company, electronics department, Thompson Road, Syracuse, N. Y.
C. H. Willis, *vice-chairman*, Princeton University, Princeton, N. J.
W. G. Dow, *secretary*, University of Michigan, Ann Arbor, Mich.

C. T. Burke — O. W. Livingston
R. S. Burnap — D. E. Marshall
J. M. Cage — H. L. Palmer
L. L. Call — G. W. Penney
W. R. Clark — W. H. Pickering
G. J. Crowdes — D. A. Quarles
A. V. Eastman — W. G. Roman
W. J. Field — J. D. Ryder
William Fraser — E. T. Sherwood
A. P. Godsho — Thomas Spooner
J. A. Green — B. F. Tellkamp
C. C. Herskind — J. T. Thwaites
L. C. F. Horle — F. N. Tompkins
S. B. Ingram — H. M. Turner
J. P. Jordan — D. C. Ulrey
L. A. Kilgore — E. H. Vedder
J. D. Leitch — Wm. Comings White
H. Winograd

Electronic AIEE-IRE Liaison Subcommittee

H. M. Turner, *chairman*, Yale University, New Haven, Conn.

AIEE Members	*IRE Members*
L. C. F. Horle	R. S. Burnap
S. B. Ingram	R. E. Guy
D. E. Marshall	E. W. Schaefer

Electronic Heating Subcommittee

J. P. Jordan, *chairman*, General Electric Company, 1 River Road, Schenectady 5, N. Y.
W. C. Rudd, *secretary*, Induction Heating Corporation, 389 Lafayette Street, New York 3, N. Y.

W. L. Atwood — H. F. Kincaid
G. P. Bosomworth — T. P. Kinn
A. H. Burkholder — F. H. Mason
Harold E. Dinger — R. H. McMurtrie
L. D. Drugmand — Eugene Mittelmann
L. M. Duryee — F. M. Rugg
C. W. Frick — G. W. Scott, Jr.
H. C. Gillespie — A. L. Short
W. H. Hickock — J. M. Thomson
R. J. Hunn — Otto Weitmann — D. E. Watts

Electronic Power Converters Subcommittee

H. Winograd, *chairman*, Allis-Chalmers Manufacturing Company, Box 512, Milwaukee 1, Wis.
H. B. Steiner, *secretary*, General Electric Company, Schenectady 5, N. Y.

L. C. Benos — D. E. Marshall
F. W. Cramer — A. J. Maslin
E. V. DeBlieux — L. W. Morton
J. B. Donnelly — I. S. Rice
I. K. Dortort — J. B. Rice
R. D. Evans — W. J. L. Rupprecht
W. Fraser — A. Schmidt, Jr.
C. W. Frick — W. C. Sealey
C. C. Herskind — T. A. Taylor
H. R. Huntley — J. T. Thwaites
G. F. Jones — J. Tompkins
C. R. Marcum — H. Zuvers — C. H. Willis

Electronic Precipitation Subcommittee

G. W. Penney, *chairman*, Westinghouse Electric Corporation, East Pittsburgh, Pa.

J. O. Amstuz — Emery Miller
R. H. Kaufmann — E. R. Thomas

Electronic Standards Subcommittee

Thomas Spooner, *chairman*, Westinghouse Electric Corporation, East Pittsburgh, Pa.

G. W. Garman — O. W. Livingston
L. C. F. Horle — G. W. Penney
J. P. Jordan — G. Singer
D. D. Knowles — Dayton Ulrey — H. M. Turner

Liaison with JETEC Subcommittee

L. C. F. Horle, *chairman*, Consulting Engineer, 90 West Street, New York, N. Y.

R. S. Burnap — S. B. Ingram
W. G. Dow — O. W. Pike

Nomenclature, Letter, and Graphical Symbols Subcommittee

R. S. Burnap, *chairman*, Radio Corporation of America, RCA Victor Div., Harrison, N. J.

H. F. Dart — O. W. Pike
S. B. Ingram — Thomas Spooner

Papers Solicitation and Contact With Electronic Technical Groups in the Sections Subcommittee

W. C. White, *chairman*, General Electric Company, Schenectady, N. Y.

G. W. Bower — L. A. Kilgore
W. R. Clark — H. L. Palmer
A. P. Godsho — Dayton Ulrey
S. B. Ingram — H. Winograd

X-Ray Tubes Subcommittee

Lloyd L. Call, *chairman*, General Electric X-Ray Corporation, 2012 Jackson Boulevard, Chicago 12, Ill.

G. Failla — J. Lempert
Arthur Klinckmann — George Singer — T. H. Rogers

Electronic Tubes Subcommittee

D. E. Marshall, *chairman*, Westinghouse Electric Corporation, Bloomfield, N. J.

D. G. Fink — S. B. Ingram
A. M. Glover — C. H. Willis — H. C. Steiner

High Frequency Conductors, Cables and Connectors Subcommittee

G. J. Crowdes, *chairman*, Simplex Wire and Cable Company, 79 Sidney Street, Cambridge 39, Mass.

L. A. Bondon — L. M. Leeds
William Dohan — E. E. Sheldon
E. W. Greenfield — A. J. Warner — H. B. Slade

Industrial Control Devices

E. U. Lassen, *chairman*, Cutler-Hammer, Inc., 315 North 12th Street, Milwaukee 3, Wis.
J. D. Leitch, *vice-chairman*, The Electric Controller and Manufacturing Company, 2700 East 79th Street, Cleveland 4, Ohio
E. F. Mekelburg, *secretary*, industry controller division, Square D Company, 4041 North Richards Street, Milwaukee 12, Wis.

E. H. Alexander — R. W. Jones
H. H. Angel — L. H. Matthias
G. S. Brown — M. Michel
J. A. Cortelli — W. W. Miller

R. F. Danner — T. B. Montgomery
W. J. Fleming — J. W. Picking
D. K. Frost — L. T. Rader
G. H. Garcelon — C. F. Terwilliger

ASA Standard Number 15 Subcommittee

E. H. Alexander, *chairman*, General Electric Company, Schenectady, N. Y.

Electronic Control Subcommittee

J. D. Leitch, *chairman*, The Electric Controller and Manufacturing Company, 2700 East 79th Street, Cleveland 4, Ohio
W. H. Elliot — H. L. Palmer
O. W. Livingston — J. W. Picking
F. G. Logan — B. F. Tellkamp
E. F. Mekelburg — E. H. Vedder

Test Codes Subcommittee

L. T. Rader, *chairman*, Illinois Institute of Technology, Chicago, Ill.
C. T. Evans — W. E. Pakala
D. K. Frost — C. A. Schaefer — J. E. Ryan

Industrial Power Applications

Herbert Speight, *chairman*, Westinghouse Electric Corporation, 40 Wall Street, New York 5, N. Y.
S. F. French, *vice-chairman*, Anaconda Copper Mining Company, 20 Broadway, New York 4, N. Y.
L. A. Umansky, *secretary*, General Electric Company, Schenectady 5, N. Y.
E. L. Bailey — Royce E. Johnson
D. L. Beeman — J. P. Kennell
F. R. Benedict — E. G. Morehouse
Philip Bliss — A. C. Muir
F. W. Cramer — J. J. Orr
H. W. Dexter, Jr. — J. S. Parsons
W. H. Dickinson — L. C. Peterman
D. D. Douglass — Kennard Pinder
A. B. Emrick — L. B. Potter
C. Farrow — Ralph Randall
E. S. Fields — Hugh L. Smith
J. S. Gault — T. O. Sweatt
L. N. Grier — E. E. Turkington
John Grotzinger — J. M. Webb
W. R. Harmer — C. C. Whipple
K. W. John — R. T. Woodruff

Industrial Voltage Requirements Subcommittee

C. C. Whipple, *chairman*, Polytechnic Institute of Brooklyn, 85 Livingston Street, Brooklyn 2, N. Y.
W. H. Dickinson, *secretary*, Standard Oil Development Company, Elizabeth, N. J.
H. G. Barnett — C. R. Johnson
D. L. Beeman — L. C. Peterman
S. F. French — K. Pinder
J. Grotzinger — R. C. R. Schulze
C. A. Johnson — S. A. Warner — T. O. Sweatt

Interior Wiring Design for Commercial Buildings Subcommittee

B. F. Thomas, Jr., *chairman*, Moran, Proctor, Freeman and Mueser, 420 Lexington Avenue, New York 17, N. Y.
L. W. McCullough, *secretary*, Consolidated Edison Co. of New York, Inc., 4 Irving Place, New York 3, N. Y.
D. L. Beeman — James A. Heffernan
F. R. Benedict — Ralph Hodges
M. M. Brandon — E. L. Morehouse
C. D. Bratiotis — George K. Perley
Leo H. Cleary — L. C. Peterman
Allan Coggeshall — H. F. Richardson
R. F. Davis — Clifford Smith
H. W. Dexter, Jr. — Herbert Speight
V. E. Dodson — Howard R. Stevenson
C. F. Hedlund — T. O. Sweatt

Machine Tool and Process Industries Subcommittee

P. Bliss, *chairman*, Raymond Engineering Laboratory, Inc., Smith St., Middletown, Conn.
H. L. Smith, *secretary*, General Electric Company, 570 Lexington Avenue, New York, N. Y.
B. T. Anderson — L. L. Lee
G. U. Dautrich — A. C. Muir
John Fink — E. K. Murphy
V. Johnson — L. A. Umansky

Instruments and Measurements

Truman S. Gray, *chairman*, Massachusetts Institute of Technology, Cambridge 39, Mass.
E. D. Doyle, *vice-chairman*, Leeds and Northrup Company, 4901 Stenton Avenue, Philadelphia 44, Pa.
C. T. Burke, *secretary*, General Radio Company, 275 Massachusetts Ave., Cambridge 39, Mass.
R. C. Bailey — R. D. Hickok
P. L. Bellaschi — G. B. Hoadley
P. A. Borden — I. F. Kinnard
H. H. Brauer — W. G. Knickerbocker
A. L. Brownlee — A. E. Knowlton
L. A. Burckmyer, Jr. — H. C. Koenig
A. B. Craig — R. J. Kryter
C. L. Dawes — Everett S. Lee
F. C. Doble — J. T. Lusignan
W. N. Eddy — H. C. Rankin
J. L. Fuller — Claire W. Ricker
W. N. Goodwin, Jr. — A. R. Rutter
A. J. Grant — F. B. Scott
E. I. Green — F. B. Silsbee
I. W. Gross — G. M. L. Sommerman
C. M. Hathaway — C. J. Zeller — E. P. Yerkes

Definitions Subcommittee

C. L. Dawes, *chairman*, Harvard University, Cambridge 38, Mass
A. B. Craig — E. S. Lee
H. C. Dickinson — B. E. Lenehan
W. N. Goodwin, Jr. — P. MacGahan
E. I. Green — F. B. Silsbee

Dielectric Measurements in the Field Subcommittee

A. L. Brownlee, *chairman*, Commonwealth Edison Company, 2233 South Throop Street, Chicago, Ill.
C. T. Burke — W. N. Eddy
C. L. Dawes — I. W. Gross
F. C. Doble — E. S. Lee
E. D. Doyle — G. M. L. Sommerman

High-Frequency Measurements Subcommittee

E. I. Green, *chairman*, Bell Telephone Laboratories, Inc., 463 West Street, New York 14, N. Y.
H. H. Brauer — G. B. Hoadley — C. T. Burke

Instrument Transformers Subcommittee

H. C. Rankin, *chairman*, New England Power Service Company, 441 Stuart Street, Boston, Mass.
J. H. Chiles — W. N. Goodwin, Jr.
C. L. Dawes — I. W. Gross
R. E. Franck — F. J. Vogel — F. B. Silsbee

Marking of Varmeters and Related Instruments Subcommittee

A. E. Knowlton, *chairman*, Electrical World, 330 W. 42nd St., New York 18, N. Y.
A. L. Brownlee — A. B. Craig
A. L. Carvill — W. G. Knickerbocker
F. B. Silsbee

Master Test Code for Resistance Measurements Subcommittee

F. B. Silsbee, *chairman*, National Bureau of Standards Washington 25, D. C.
C. T. Burke — E. S. Lee — E. D. Doyle

Master Test Code for Temperature Measurements Subcommittee

L. A. Burckmyer, Jr., *chairman*, Cornell University, Ithaca, N. Y.
P. A. Borden — W. R. Hough
E. D. Doyle — A. K. Joecks
J. L. Fuller — S. S. Stack — M. D. Ross

Revision of Standard Number 4 Subcommittee (Measurement of Test Voltage in Dielectric Tests)

J. T. Lusignan, *chairman* (NEMA), Ohio Brass Company, Mansfield, Ohio
P. L. Bellaschi, NEMA — H. E. Kent (*alternate*), EL and P
A. L. Brownlee, EL and P
J. F. Calvert, AIEE — W. B. Kouwenhoven, AIEE
J. S. Carroll, AIEE — R. S. Lapp, NEMA
E. W. Davis, NEMA — W. W. Lewis, NEMA
C. M. Foust, NEMA — E. E. Piepho, AIEE
H. A. Frey, NEMA — W. C. Sealey, NEMA
I. W. Gross, EL and P — F. B. Silsbee, Nat. Bur. of Standards
J. H. Hagenguth, NEMA
R. W. Sorensen, AIEE

Revision of C39 Subcommittee (Electrical Indicating Instruments)

H. C. Koenig, *chairman*, Electrical Testing Laboratories, 2 East End Avenue, New York, N. Y.
C. T. Burke — E. S. Lee
W. N. Goodwin, Jr. — P. MacGahan
R. D. Hickok, Sr. — A. R. Rutter
I. F. Kinnard — F. B. Silsbee
(*A. J. Corson, alternate*) — C. J. Zeller

Revision of Standard Number 40 Subcommittee (Recording Instruments)

A. E. Knowlton, *chairman*, Electrical World, 330 West 42nd Street, New York, N. Y.
H. C. Koenig, *secretary*, Electrical Testing Laboratories, 2 East End Avenue, New York, N. Y.
D. J. Angus — W. G. Knickerbocker
P. A. Borden — L. J. Lunas
E. D. Doyle — C. V. Morey
D. B. Fisk — H. C. Rankin
G. B. Hoadley — B. M. Werly

Watthour Meters Subcommittee

W. G. Knickerbocker, *chairman*, The Detroit Edison Company, 2000 Second Avenue, Detroit 26, Mich.
A. L. Brownlee — I. F. Kinnard
D. T. Canfield — H. C. Koenig
A. B. Craig — H. C. Rankin
F. C. Holtz — F. B. Scott — A. R. Rutter
Ex officio
G. B. M. Robertson, AEIC

Land Transportation

W. A. Brecht, *chairman*, transportation engineering, Westinghouse Electric Corporation, East Pittsburgh, Pa.
P. H. Hatch, *vice-chairman*, New York, New Haven and Hartford Railroad Company, New Haven 6, Conn.
J. G. Inglis, *secretary*, Toronto Transportation Commission, 35 Yonge Street, Toronto, Ontario, Canada
J. C. Aydelott — H. C. Griffith
L. W. Birch — W. S. H. Hamilton
H. F. Brown — G. L. Hoard
D. M. Burckett — T. M. C. Martin
W. J. Clardy — P. A. McGee
F. H. Craton — E. B. Meissner
E. W. Davis — W. B. Morton
Llewellyn Evans — Timothy H. Murphy
W. H. Evans — A. G. Oehler
J. E. Gardner — R. G. Thring — Dwight L. Smith

Heavy Traction Electrification Data Subcommittee

L. W. Birch, *chairman*, Ohio Brass Company Mansfield, Ohio
H. F. Brown — F. H. Craton
W. J. Clardy — A. G. Oehler

Heavy Traction Papers and Plans Subcommittee

P. H. Hatch, *chairman*, New York, New Haven and Hartford Railroad Company, New Haven 6, Conn.
L. W. Birch — A. G. Oehler

Light Traction Papers and Plans Subcommittee

J. C. Aydelott, *chairman*, General Electric Company Erie, Pa.
R. G. Thring — J. G. Inglis

Revision of AIEE Standard Number 16 (Electric Railway Control Apparatus) ASA C48 Subcommittee

F. H. Craton, *chairman*, General Electric Company, Erie, Pa.
W. S. H. Hamilton — J. G. Inglis — W. J. Clardy

Light, Production and Application of

S. G. Hibben, *chairman*, The Westinghouse Lamp Division, Bloomfield, N. J.
I. A. Yost, *vice-chairman*, Westinghouse Electric Corporation, 1216 West 58th Street, Cleveland, Ohio
C. L. Dows, *secretary*, Nela Park, Cleveland 12, Ohio
J. F. Angier — G. T. Minasian
D. W. Atwater — R. C. Putnam
O. W. Holden — Harris Reinhardt
W. C. Kalb — E. M. Strong
C. W. Kronmiller — C. F. Terrell
H. E. Mahan — I. A. Yost — C. C. Whipple

Marine Transportation

W. H. Reed, *chairman*, Bruce Electric Company, 196 West Houston Street, New York 14, N. Y.
O. A. Wilde, *vice-chairman*, Sun Shipbuilding and Dry Dock Company, Chester, Pa.
W. N. Zippler, *secretary*, Gibbs and Cox, Inc., 1 Broadway, New York 4, N. Y.
E. C. Alger — W. R. Hight
W. B. Armstrong — J. E. Jones
R. A. Beekman — R. G. Lorraine
H. C. Coleman — C. Lynn
P. J. DuMont — V. W. Mayer
J. B. Feder — S. N. Mead
A. R. Gatewood — I. H. Osborne
L. M. Goldsmith — E. M. Rothen
P. A. Guise — E. H. Stivender
H. F. Harvey, Jr. — G. O. Watson
R. T. Henry — F. A. Wickel

Communications and Alarm Subcommittee

E. C. Alger, *chairman*, Bethlehem Steel Company, Quincy, Mass.
J. B. Feder — S. N. Mead

W. R. Hight — E. M. Rothen
V. W. Mayer — F. A. Wickel

Distribution Subcommittee

H. F. Harvey, Jr., *chairman*, Newport News Shipbuilding and Dry Dock Company, Newport News, Va.
E. C. Alger — P. A. Guise
P. J. DuMont — I. H. Osborne
J. B. Feder — F. A. Wickel
A. R. Gatewood — W. N. Zippler

Editing Subcommittee

W. N. Zippler, *chairman*, Gibbs and Cox, Inc., 1 Broadway, New York 4, N. Y.
R. A. Beekman — W. H. Reed

Fittings and Appliances Subcommittee

O. A. Wilde, *chairman*, Sun Shipbuilding and Dry Dock Company, Chester, Pa.
P. J. DuMont — V. W. Mayer
A. R. Gatewood — S. N. Mead
P. A. Guise — W. H. Reed
H. F. Harvey, Jr. — F. A. Wickel — E. M. Rothen

Navigation Equipment Subcommittee

W. R. Hight, *chairman*, Sperry Gyroscope Company, Inc., Manhattan Bridge Plaza, Mail Station 1184, Brooklyn, N. Y.
P. J. DuMont — S. N. Mead
P. A. Guise — E. M. Rothen

Power Application Subcommittee

W. H. Reed, *chairman*, Bruce Electric Company, 196 West Houston Street, New York 14, N. Y.
H. C. Coleman — J. E. Jones
J. B. Feder — R. G. Lorraine
L. M. Goldsmith — I. H. Osborne

Power Generation Subcommittee

C. Lynn, *chairman*, Westinghouse Electric Corporation, East Pittsburgh, Pa.
W. B. Armstrong — R. T. Henry
R. A. Beekman — R. G. Lorraine
H. C. Coleman — E. H. Stivender
L. M. Goldsmith — O. A. Wilde

Publicity, Personnel, and History Subcommittee

R. A. Beekman, *chairman*, General Electric Company, Schenectady, N. Y.
H. F. Harvey, Jr. — I. H. Osborne

Switchboards and Controls Subcommittee

H. C. Coleman, *chairman*, Westinghouse Electric Corporation, East Pittsburgh, Pa.
W. B. Armstrong — H. F. Harvey, Jr.
R. A. Beekman — J. E. Jones
P. J. DuMont — E. H. Stivender — V. W. Mayer

Wires and Cables Subcommittee

W. N. Zippler, *chairman*, Gibbs and Cox, Inc., 1 Broadway, New York 4, N. Y.
E. C. Alger — A. R. Gatewood
J. B. Feder — V. W. Mayer — R. G. Lorraine

Nucleonics

L. W. Chubb, *chairman*, Research Laboratories, Westinghouse Electric Corp., East Pittsburgh, Pa.
R. C. Bergvall — Walther Richter
H. B. Marvin — William Shockley
B. R. Prentice — J. A. Wheeler

Power Generation

M. J. Steinberg, *chairman*, Consolidated Edison Company of New York, Inc., 4 Irving Place, New York 3, N. Y.
A. H. Frampton, *vice-chairman*, Hydro-Electric Power Commission, Toronto 2, Ontario, Canada
B. G. A. Skrotzki, *secretary*, *Power*, 330 West 42nd Street, New York 18, N. Y.
C. P. Almon, Jr. — F. L. Lawton
S. Beckwith — F. M. Lewis
A. D. Caskey — C. W. Mayott
R. P. Crippen — J. B. McClure
E. F. Dissmeyer — G. H. McDaniel
J. M. Drabelle — W. S. Peterson
H. A. Dryar — G. M. Pollard
Frazer W. Gay — R. C. Powel
W. D. Hardaway — G. M. Tatum
C. B. Kelley — H. D. Taylor
A. J. Krupy — W. R. Way
C. M. Laffoon — R. L. Witzke — W. F. Wetmore

Excitation Subcommittee

A. J. Krupy, *chairman*, Commonwealth Edison Company, Chicago, Ill.
E. F. Dissmeyer — J. B. McClure
J. H. Kinghorn — J. F. Sellers
H. A. P. Langstaff — R. L. Witzke — F. D. Troxel

Hydroelectro Systems Subcommittee

A. H. Frampton, *chairman*, Hydro-Electric Power Commission of Ontario, 620 University Avenue, Toronto 2, Ontario, Canada
C. P. Almon, Jr. — W. R. Way — B. V. Hoard

Interconnected Systems Subcommittee

C. W. Mayott, *chairman*, The Hartford Electric Light Company, 266 Pearl Street, Hartford 15, Conn.
A. H. Frampton — W. S. Peterson — C. B. Kelley

Power Generation Report Subcommittee

B. G. A. Skrotzki, *Power*, 330 West 42nd Street, New York 18, N. Y.

Recommended Specification for Prime-Mover Speed Governing (Joint AIEE-ASME committee appointed by members of power generation committee)

M. J. Steinberg, *chairman*, Consolidated Edison Company of New York, Inc., 4 Irving Place, New York 3, N. Y.
S. B. Griscom — J. B. McClure
A. P. Hayward — F. Oppenheimer — G. H. McDaniel

Power Transmission and Distribution

R. J. Wiseman, *chairman*, The Okonite Company, Passaic, N. J.
E. V. Sayles, *vice-chairman*, Consumers Power Company, Jackson, Mich.
I. W. Gross, *secretary*, American Gas and Electric Service Corporation, 30 Church Street, New York 7, N. Y.

Dean W. Alden — A. A. Kroneberg
D. K. Blake — W. W. Lewis
C. D. Brown — L. W. Long
H. W. Clark — J. T. Lusignan
Harold Cole — W. D. Maddrey
S. B. Crary — R. B. Miller
H. A. Dambly — Lee M. Moore
A. E. Davison — F. W. Packer
W. A. Del Mar — J. S. Parsons
Robert D. Evans — L. M. Robertson
W. B. Fisk — H. B. Robinson
J. M. Gaylord — R. V. Sanford
Herman Halperin — A. E. Silver
Edwin Hansson — F. V. Smith
K. E. Hapgood — Philip Sporn
E. R. Hendrickson — E. C. Starr
L. F. Hickernell — O. W. Titus
J. E. Hobson — H. M. Trueblood
J. B. Hodtum — C. F. Wagner
E. K. Huntington — Loyd T. Williams
H. E. Kent — H. E. Wulfing

Distribution Subcommittee

Harold Cole, *chairman*, The Detroit Edison Company, 2000 Second Avenue, Detroit 26, Mich.
D. K. Blake — J. B. Hodtum
T. J. Brosnan — F. E. Sanford
E. R. Hendrickson — R. V. Sanford

General Systems Subcommittee

C. F. Wagner, *chairman*, Westinghouse Electric Corporation, East Pittsburgh, Pa.
C. D. Brown — L. B. Le Vesconte
S. B. Crary — L. M. Robertson
E. K. Huntington — H. B. Robinson
A. A. Kroneberg — H. M. Trueblood — H. K. Sels

Lightning and Insulator Subcommittee

I. W. Gross, *chairman*, American Gas and Electric Service Corporation, 30 Church Street, New York 7, N.Y.
H. N. Erkvall — W. W. Lewis
H. A. Frey — J. T. Lusignan, Jr.
E. L. Harder — E. R. Whitehead — S. K. Waldorf

Stations Subcommittee

E. K. Huntington, *chairman*, Rochester Gas and Electric Corporation, 89 East Avenue, Rochester 4, N. Y.
D. K. Blake — R. B. Miller
K. E. Hapgood — R. V. Sanford
W. P. Fisk — R. L. Witzke
J. B. Hodtum — H. E. Wulfing

Insulated Wires and Cables Subcommittee

W. A. Del Mar, *chairman*, Habirshaw Cable and Wire Division, Phelps Dodge Copper Products Corporation, Yonkers 1, N. Y.
R. W. Atkinson — E. R. Hendrickson
A. S. Brookes — L. I. Komives
H. W. Clark — C. J. Mansfield
H. A. Dambly — G. B. Shanklin
H. Halperin — F. V. Smith
C. T. Hatcher — R. J. Wiseman — O. W. Titus

Towers, Poles, and Conductors Subcommittee

E. Hansson, *chairman*, Pennsylvania Water and Power Company, 1409 Lexington Building, Baltimore 1, Md.
D. W. Alden — R. D. Evans
C. A. Booker — F. W. Packer
A. B. Campbell — E. J. Staubitz
A. E. Davison — G. W. Stickley
A. L. Duna — L. T. Williams — O. W. Titus

Protective Devices

H. W. Collins, *chairman*, Detroit Edison Company 2000 Second Avenue, Detroit 26, Mich.
W. A. Lewis, *vice-chairman*, Illinois Institute of Technology, 3300 South Federal Street, Chicago 16, Ill.
L. F. Kennedy, *secretary*, central station department, General Electric Company, Schenectady 5, N. Y.
H. D. Braley — F. R. Longley
W. R. Brownlee — J. R. North
O. E. Charlton — H. V. Nye
William Deans — H. H. Rudd
H. W. Haberl — W. J. Rudge
H. J. Lingal — J. H. Vivian

Circuit Breaker and Assembled Switchgear Subcommittee

H. J. Lingal, *chairman*, Westinghouse Electric Corporation, East Pittsburgh, Pa.
A. E. Anderson — H. V. Nye
H. D. Braley — M. S. Oldacre
George Doan — A. Van Ryan
R. M. Ferril — O. B. Vikoren
H. W. Haberl — J. H. Vivian
M. H. Hobbs — J. D. Wood
J. R. North — D. G. Worth

Fault-Limiting Devices Subcommittee

Frank R. Longley, *chairman*, Western Massachusetts Electric Company, 73 State Street, Springfield 2, Mass.
J. E. Clem — E. W. Knapp
G. B. Dodds — A. A. Kroneberg
W. W. Eberhardt — W. A. Lewis
R. D. Evans — W. W. Lewis
Eric T. B. Gross — E. G. Norell
P. A. Jeanne — W. T. Smith

Lightning Protective Devices Subcommittee

W. J. Rudge, *chairman*, General Electric Company, Pittsfield, Mass.
F. M. Defandorf — W. E. Rushlow
R. H. Earle — A. H. Schirmer
H. N. Ekvall — H. R. Stewart
I. W. Gross — J. M. Towner
T. H. Mawson — A. M. Upsahl
J. R. McFarlin — E. H. Yonkers — E. R. Whitehead

Switches, Fuses, and Insulators Subcommittee

H. H. Rudd, *chairman*, Railway and Industrial Engineering Company, Greensburg, Pa.
H. D. Braley — A. H. Powell
O. E. Charlton — H. L. Rawlins
K. J. C. Falck — J. C. Woods
Working groups—chairman
H. L. Rawlins, switches and insulators
A. H. Powell, interrupter switches
H. D. Braley, fuses

Relays Subcommittee

W. R. Brownlee, *chairman*, The Commonwealth and Southern Corporation, Jackson, Mich.
E. L. Michelson, *secretary*, Commonwealth Edison Company, Chicago 90, Ill.
J. C. Bowman — S. C. Leyland
J. E. Clem — H. F. Lindemuth
R. J. Cooper — W. E. Marter
R. E. Cordray — A. J. McConnell
G. B. Dodds — C. E. Parks
F. S. Fehr — H. R. Paxson
S. Goldsmith — F. C. Poage
E. T. B. Gross — G. A. Powell
T. R. Halman — E. G. Ratz
E. L. Harder — K. N. Reardon
V. J. Hayes — C. L. Smith
B. C. Hicks — W. K. Sonnemann
J. H. Kinghorn — J. J. Tesar
W. A. Lewis — C. A. Woods — J. H. Vivian

Therapeutics, Applications of Electricity to

W. B. Kouwenhoven, *chairman*, Johns Hopkins University, Baltimore 18, Md.
H. C. Rentschler, *vice-chairman* and *secretary*, Westinghouse Electric Corporation, Bloomfield, N. J.
L. L. Call — Roy Kegerreis

E. E. Charlton H. D. Moreland
F. B. Claussen W. R. Smith W. I. Slichter

Joint Subcommittees

Electronic Instruments

(Joint with Electronics and Instruments and Measurements Committees)

W. R. Clark, *chairman*, Leeds and Northrup Company, 4901 Stenton Avenue, Philadelphia 44, Pa.
E. I. Green, *vice-chairman*, Bell Telephone Laboratories, Inc., 463 West Street, New York 14, N. Y.
Rudolf Feldt, *secretary*, Allen B. DuMont Laboratories, Inc., 2 Main Avenue, Passaic, N. J.

H. W. Berry H. R. Meahl
Langford T. Bourland David Packard
C. T. Burke T. B. Perkins
Carl C. Chambers J. G. Reid, Jr.
H. C. Drake J. J. Slattery
C. D. Fisk J. T. Thwaites
W. A. Geohegan C. A. Tobias
J. A. Hutcheson V. K. Ulrich
Eric J. Isbister W. A. Weiss
G. N. Mahaffey A. J. Williams, Jr.
C. W. Martel Walter P. Wills

Servomechanisms

(Joint with Basic Sciences, Industrial Control Devices, and Instruments and Measurements Committees)

G. S. Brown, *chairman*, Massachusetts Institute of Technology, Cambridge, Mass.
R. W. Jones, *vice-chairman*, Northwestern University, Evanston, Ill.
M. A. Princi, *secretary*, General Electric Company, West Lynn, Mass.

E. D. Doyle E. S. Lee
J. L. Fuller M. Michel
T. S. Gray S. J. Mikina
S. W. Herwald J. D. Tebo
E. U. Lassen C. N. Weygandt

Telemetering

(Joint with Automatic Stations and Instruments and Measurements Committees)

Automatic Stations appointees
G. S. Lunge, *chairman*, General Electric Company, Schenectady, N. Y.
L. B. Bogan, *secretary*, American Tel.& Tel. Company 195 Broadway, New York 7, N. Y

W. A. Derr A. P. Peterson
E. E. George C. E. Winegartner J. H. Viviann
Instruments and Measurements appointees
P. A. Borden E. E. Lynch
E. C. Brown W. E. Phillips
C. K. Duff A. R. Rutter
J. T. Logan G. M. Thynell

Carbon Brushes

(Joint with Air Transportation and Electric Machinery Committees)

V. P. Hessler, *chairman*, University of Kansas, Lawrence, Kans.

W. H. Austry E. A. Lapham
H. R. Brown T. M. Linville
J. V. Dobson J. R. North
H. M. Elsey D. Ramadanoff
C. J. Herman E. R. Summers
L. H. Hildebrandt S. D. Summers
H. E. Keneipp A. L. Van Emden

Co-ordination of Construction and Protection of Distribution Circuits

(Joint with Power Transmission and Distribution and Protective Devices Committees)

G. B. Dodds, *chairman*, Duquesne Light Company, 435 Sixth Avenue, Pittsburgh 19, Pa.

R. O. Askey Cort Lowerison
D. K. Blake Harold F. Ostman
T. J. Brosnan C. E. Parks
Harold Cole John S. Parsons
W. B. Fisk, Jr. H. R. Paxson
H. W. Haberl H. P. Sleeper
C. L. Headley C. L. Smith

Power System Applications of Carrier Current

(Joint with Automatic Stations, Communication, Power Transmission and Distribution, and Protective Devices Committees)

Philip Sporn, *chairman*, American Gas and Electric Service Corporation, 30 Church Street, New York 8, N. Y.

S. C. Bartlett R. J. Mahler
J. D. Booth J. A. Parrott
J. C. Bowman M. E. Reagan
R. C. Ericson F. M. Rives
L. F. Kennedy S. B. Smith
J. D. Laughlin T. D. Talmage
S. C. Leyland M. J. Thrasher
G. S. Lunge H. M. Trueblood
D. M. MacGregor E. M. Wood

Standard Frequency Bands and Designations

Thomas Spooner, *chairman*, Westinghouse Electric Corporation, East Pittsburgh, Pa.
(Rep. Electronics Standards Subcommittee)
C. T. Burke (Rep. Instruments and Measurements Committee)
G. B. Ransom (Rep. Communication Committee)
F. B. Silsbee (Rep. ASA Sectional Committee C68)

Institute Representatives

Aeronautical Electrical Equipment Standardization
J. D. Miner, liaison representative with NASC and SAE

Alfred Noble Prize Committee, ASCE
Robin Beach

American Association for the Advancement of Science, Council
J. W. Barker I. Melville Stein

American Co-ordinating Committee on Corrosion
H. S. Phelps J. M. Standring, Jr.

American Research Committee on Grounding
C. T. Sinclair

American Standards Association, Standards Council
W. P. Dobson R. T. Henry H. S. Osborne
Alternates
H. E. Farrer E. B. Paxton J. J. Pilliod

American Year Book, Advisory Board
H. H. Henline

Charles A. Coffin Fellowship and Research Fund Committee
J. Elmer Housley

Committee of Apparatus Makers and Users, NRC
L. F. Adams

Committee on Standard Commodity Classification or Index
E. B. Paxton

Electrical Standards Committee, ASA
H. E. Farrer A. C. Monteith J. J. Pilliod
Alternates
W. P. Dobson E. L. Moreland E. B. Paxton

Engineering Foundation Board
L. W. Chubb F. M. Farmer

Engineering Societies Monographs Committee
F. M. Farmer W. I. Slichter

Engineering Societies Personnel Service, Inc.
H. H. Henline

Engineers' Council for Professional Development
M. S. Coover Everett S. Lee E. C. Stone

Engineers Joint Council
H. H. Henline J. Elmer Housley W. E. Wickenden

Hertz Award Committee
M. S. Coover

Hoover Medal Board of Award
H. H. Barnes, Jr. H. S. Osborne
John Castlereagh Parker

Industry Committee on Interior Wiring Design
M. M. Brandon L. C. Peterman

John Fritz Medal Board of Award
Nevin E. Funk C. A. Powel
J. Elmer Housley W. E. Wickenden

Joint Committee for Development of Statistical Applications in Engineering and Manufacturing
W. P. Dobson

Library Board, United Engineering Trustees, Inc.
N. S. Hibshman G. L. Knight
H. H. Henline, *ex officio* H. M. Turner

Marston Medal Board of Award
Harry B. Gear

National Bureau of Engineering Registration, Advisory Board
T. G. LeClair

National Electronics Conference
Wm. Comings White

National Fire Protection Association, Electrical Committee
L. F. Adams W. Ralph Smith, *alternate*

National Fire Waste Council
L. F. Adams Wills Maclachlan

National Research Council, Division of Engineering and Industrial Research
W. B. Kouwenhoven

National Technological Advisory Committee
John Castlereagh Parker

Quarterly of Applied Mathematics
J. G. Brainerd

Radio Technical Planning Board
H. A. Affel

United Engineering Trustees, Inc.
W. H. Harrison C. R. Jones Everett S. Lee

United States National Committee of the International Commission on Illumination
J. W. Barker Robin Beach S. G. Hibben

United States National Committee of the International Electrotechnical Commission
H. E. Farrer A. C. Monteith J. J. Pilliod
Alternates
W. P. Dobson E. L. Moreland E. B. Paxton

Washington Award Commission
M. S. Coover H. B. Gear

World Power Conference, Executive Committee of United States National Committee
J. Elmer Housley

Sections

Name	District	When Organized	Membership Aug. 1, 1946	Chairman	Secretary	Secretary's Address
Akron	2	Aug. 12, '20	120	Paul S. Bechtol	A. J. B. Fairburn	College of Engg., University of Akron, Akron 4, Ohio
Alabama	4	May 22, '29	101	C. F. Sittloh	M. M. Collins	General Electric Co., P.O. Box 2602, Birmingham, 2, Ala.
Arizona	8	Mar. 22, '41	73	Irwin W. Best	F. J. Groat	Bureau of Reclamation, P.O. Box 2071, Phoenix, Ariz.
Beaumont	7	June 27, '45	75	N. C. Spencer	A. L. Howell	P.O. Box 1789, Orange, Tex.
Boston	1	Feb. 3, '03	694	T. S. Gray	L. F. Cleveland	Northeastern University, 360 Huntington Ave., Boston 15, Mass.
Central Indiana	5	Jan. 12, '12	193	E. G. Hinshaw	W. H. Bollinger	1670 Allison, Indianapolis 8, Ind.
Chicago	5	1893	1,235	L. R. Janes	J. E. Hobson	Armour Research Foundation, 35 W. 33rd St., Chicago 16, Ill.
Cincinnati	2	June 30, '20	189	W. C. Osterbrock	L. H. McLaughlin	225 E. Fourth St., Cincinnati 2, Ohio
Cleveland	2	Sept. 27, '07	512	J. C. Strasbourger	H. W. Sussman	3689 Glencairn Road, Shaker Heights 20, Ohio
Columbus	2	Mar. 17, '22	94	E. D. Ayres	E. E. Kimberly	Ohio State University, Columbus, Ohio
Connecticut	1	Apr. 16, '21	435	Harry F. Brown	Elmer G. Horton	Westinghouse Electric Corp., 42 Church St., New Haven 10, Conn.
Dayton	2	June 9, '43	258	W. A. Dynes	W. A. Barden	545 Daytona Parkway, Dayton 6, Ohio
Denver	6	May 18, '15	284	L. A. Stenger	M. H. Kight	U. S. Bureau of Reclamation, Denver, Colo.
East Tennessee	4	Sept. 2, '36	284	F. A. Hoeke	R. M. Alspaugh	T.V.A., Union Building, Knoxville, Tenn.
Erie	2	Jan. 11, '18	87	Lanier Greer	F. T. Parker	2304 Bird Drive, Erie, Pa.
Florida	4	Jan. 28, '31	155	M. L. Barre	C. H. Summers	Florida Power & Light Co., Miami, Fla.
Fort Wayne	5	Aug. 14, '08	109	S. W. Winje	E. A. Linke	813 West Packard, Fort Wayne 6, Ind.
Georgia	4	Jan. 14, '04	179	Gordon F. Price	Robert O. Loomis	Georgia Power Co., Atlanta 1, Ga.
Houston	7	Aug. 7, '28	187	R. S. Kersh	H. C. Dillingham	Texas A. & M. College, College Station, Tex.
Illinois Valley	5	June 30, '45	80	Thomas A. Hopkins	C. T. Borchelt	1118 N. Glen Oak Ave., Peoria 4, Ill.
Iowa	5	June 29, '29	104	Richard F. Castner	Wilton R. Abbott	Iowa State College, Ames, Iowa
Ithaca	1	Oct. 15, '02	99	W. H. Erickson	P. D. Ankrum	School of Elec. Engg., Cornell University, Ithaca, N. Y.
Kansas City	7	Apr. 14, '16	193	C. Myron Lytle	Joel P. Kesler	Westinghouse Electric Corp., 101 W. 11th St., Kansas City 6, Mo.
Lehigh Valley	2	Apr. 16, '21	216	R. E. Neidig	A. L. Price	173 S. Church St., Hazleton, Pa.
Los Angeles	8	May 19, '08	900	E. W. Morris	Bradley Cozzens	P.O. Box 3669 Terminal Annex, Los Angeles, Calif.
Louisville	4	Oct. 15, '26	82	L. W. Anderson	Harry Hadsel	Amer. Elevator & Machine Co., 500 E. Main St., Louisville 2, Ky.
Lynn	1	Aug. 22, '11	217	R. G. Connors	B. M. Cain	General Electric Co., 3rd-74, 920 Western Ave., West Lynn, Mass.
Madison	5	Jan. 8, '09	90	B. C. Lueders	Lawrence F. Kehoe	532 Oak St., Baraboo, Wis.
Mansfield	2	Mar. 6, '39	60	Eric Brooke	C. W. Freeman	North Electric Mfg. Co., Galion, Ohio
Maryland	2	Dec. 16, '04	460	H. H. Angel	R. L. McCoy	Locke Insulator Corp., Baltimore, Md.
Memphis	4	May 22, '30	117	W. R. Moyers, Jr.	M. G. Sifford	Westinghouse Elec. Supply Co., 366 Madison Ave., Memphis 1, Tenn.
Mexico	7	June 29, '22	195	Manuel M. de Lascurian	George B. Doughman	Calle de la Palma, 33 Apartado 2530, Mexico, D. F. Mexico
Michigan	5	Jan. 13, '11	562	G. M. Chute	A. W. Rauth	Consumers Power Co., 212 Michigan Ave. West, Jackson, Mich.
Milwaukee	5	Feb. 11, '10	500	Walther Richter	F. J. Van Zeeland	Milwaukee School of Engg., 1020 N. Broadway, Milwaukee, Wis.
Minnesota	5	Apr. 7, '02	184	H. E. Hartig	Donald C. Gray	American Hoist & Derrick Co., 63 S. Robert St., St. Paul 1, Minn.
Montana	9	June 24, '31	72	E. W. Williams	N. H. Hilke	International Business Machines Co., Helena, Mont.
Montreal	10	Apr. 16, '43	245	W. R. Simmons	M. C. Thurling	Can. Gen. Elec. Co. Ltd., 1000 Beaver Hall Hill, Montreal, Que.
Muscle Shoals	4	Feb. 18, '38	23	Ernest L. Bishop	Lyle W. Jenkins	922 Glendale St., Florence, Ala.
Nebraska	6	Jan. 21, '25	60	Max Mattison	I. M. Ellestad	Northwestern Bell Telephone Co., Omaha, Nebr.
New Mexico–West Texas	7	Mar. 7, '40	68	Roy M. Walker	Oscar H. Gutsch	2717 E. Missouri St., El Paso, Tex.
New Orleans	4	Dec. 8, '33	185	F. E. Johnson	E. I. Blanchard	Louisiana P. & L. Co., 433 Metairie Road, New Orleans 20, La.
New York	3	Dec. 10, '19	4,175	J. H. Pilkington	P. C. Cromwell	New York University, University Heights, New York 53, N. Y.
Niagara Frontier	1	Feb. 10, '25	232	R. G. Harper	E. T. Nicholson	Buffalo Niagara Electric Corp., 93 Dewey Ave., Buffalo 14, N. Y.
North Carolina	4	Mar. 21, '29	174	G. F. Stratton	C. W. Moseley	R. H. Bouligny, Inc., Box 2115, Charlotte, N. C.
North Texas	7	May 18, '28	272	H. K. Doyle	W. C. Fowler	Hotel Texas, Fort Worth, Tex.
Oklahoma City	7	Feb. 16, '22	133	J. L. Jones	H. E. Brashear	Southwestern Bell Telephone Co., Oklahoma City, Okla.
Philadelphia	2	Feb. 18, '03	1,067	H. A. Dambly	W. R. Clark	Leeds & Northrup Co., 4901 Stenton Ave., Philadelphia 44, Pa.
Pittsburgh	2	Oct. 13, '02	772	J. B. Hodtum	A. C. Monteith	Westinghouse Electric Corp., East Pittsburgh, Pa.
Pittsfield	1	Mar. 25, '04	221	D. D. MacCarthy	W. E. Birchard	Motor Engg. Div., General Electric Co., Pittsfield, Mass.
Portland	9	May 18, '09	302	W. Morgan Allen	M. D. Duffy	Northwestern Electric Co., 920 S. W. Sixth Ave., Portland 4, Oreg.
Providence	1	Mar. 12, '20	112	C. H. Parker	G. E. Andrews, Jr.	Engg. Dept., Narragansett Electric Co., Providence 1, R. I.
Rochester	1	Oct. 9, '14	154	G. R. Town	A. F. Martin	Bausch & Lomb Optical Co., 635 St. Paul St., Rochester 2, N. Y.
St. Louis	7	Jan. 14, '03	377	O. T. Farry	R. W. Gaskins	Union Electric Co. of Missouri, 12th & Locust Sts., St. Louis 1, Mo.
San Diego	8	Jan. 18, '39	110	C. F. McCabe	H. A. Cordes	General Electric Co., 861 Sixth Ave., San Diego 1 Calif.
San Francisco	8	Dec. 23, '04	839	A. Tilles	J. L. Buckley	Pacific Gas & Electric Co., 245 Market St., San Francisco 6, Calif.
Schenectady	1	Jan. 26, '03	700	R. V. Shepherd	J. C. Page	Central Station Engg. Div., General Elec. Co., Schenectady 5, N. Y.
Seattle	9	Jan. 19, '04	310	A. V. Eastman	John M. Nelson	1015 Third Ave., Seattle 4, Wash.
Sharon	2	Dec. 11, '25	145	C. W. Miller	R. L. Brown	1619 McDowell St., Sharon, Pa.
South Bend	5	Feb. 26, '41	76	H. E. Ellithorn	A. J. Quigley	1019 N. Frances St., South Bend 17, Ind.
South Carolina	4	Mar. 2, '40	52	J. L. Weeks	Charles O. Warren	525 Woodrow St., Columbia 52, S. C.
South Texas	7	May 23, '30	83	O. T. Lodal	C. G. Krause	City Pub. Service Bd., 201–203 N. St. Mary's St., San Antonio 5, Tex.
Spokane	9	Feb. 14, '13	122	D. H. Olney	O. W. Hurd	Bonneville Power Administration, Title Bldg., Spokane 8, Wash.
Springfield	1	June 29, '22	66	W. S. Scheering	J. L. Hyland	Western Massachusetts Electric Co., Turners Falls, Mass.
Syracuse	1	Aug. 12, '20	160	L. J. Audlin	W. C. Jenkins	Westinghouse Electric Corp., 700 W. Genesee St., Syracuse 4, N. Y.
Toledo	2	June 3, '07	89	W. E. Boruh	W. M. Campbell	2145 Central Grove Ave., Toledo, Ohio
Toronto	10	Sept. 30, '03	466	A. R. Zimmer	H. Osborne	Ferranti Electric Ltd., Mount Dennis, Toronto, Ont.
Tulsa	7	Oct. 1, '37	100	E. F. Patterson	S. C. Wright	Southwestern Bell Telephone Co., 420 S. Detroit, Tulsa, Okla.
Urbana	5	Nov. 25, '02	53	P. F. Schwarzlose	A. D. Bailey	301-A Elec. Engg. Lab., University of Illinois, Urbana, Ill.
Utah	9	Mar. 9, '17	94	J. R. Jarvis	John A. McDonald	General Electric Co., P.O. Box 779, Salt Lake City, Utah
Vancouver	10	Aug. 22, '11	126	F. J. Bartholomew	F. H. Hedley	Can. Westinghouse Co. Ltd., 1418 Marine Bldg., Vancouver, B. C.
Virginia	4	May 19, '22	151	C. H. Smoke	William C. Jones	Box 1707, Norfolk 1, Va.
Washington	2	Apr. 9, '03	709	F. S. Black	Dixon Lewis	Alum. Co. of Amer., 605 Southern Bldg., Washington 5, D. C.
West Virginia	2	Apr. 9, '40	79	E. M. Hansford	W. E. Nuhfer	Appalachian Electric Power Co., Cabin Creek, W. Va.
Wichita	7	Sept. 16, '37	82	R. D. Finnell	C. W. Halferty	Kansas Gas & Electric Co., 201 N. Market St., Wichita 1, Kans.
Worcester	1	Feb. 18, '20	66	T. H. Morgan	B. F. Hammarstrom	Heald Machine Co., New Bond St., Worcester 6, Mass.
Total Sections	75		22,645			

Subsections

Name	Chairman	Secretary	Secretary's Address
Albuquerque (New Mexico–West Texas Section)	W. T. Hardgrave		
Arrowhead (Minnesota Section)	R. H. Holmes	Arthur C. Smythe	Minnesota Power & Light Co., Duluth, Minn.
Boulder Dam (Los Angeles Section)	C. L. Westmann	C. L. Collins	519 Birch St., Boulder City, Nev.
Canton (Akron Section)	R. C. Wey	H. E. Rue	310 Fairview St., N. Canton, Ohio
Casper, Wyo. (Denver Section)	B. A. Fleshman	F. M. Howard	Box 860, Casper, Wyo.
Charleston (South Carolina Section)	Dean H. Davis	Max G. Toole	P.O. Box 42, U. S. Navy Yard, Charleston, S. C.
Charlotte (North Carolina Section)	E. Robert Davis	W. B. White	210 E. Sixth St., Charlotte, N. C.
Fort Worth (North Texas Section)	R. A. Larner	F. E. Woodruff,	Freese and Nichols, Fort Worth 2, Tex.
Fresno (San Francisco Section)	J. P. Price	G. A. Collins	San Joaquin Light & Power Div., Pacific Gas & Electric Co., Fresno, Calif.
Great Falls (Montana Section)	D. A. Johnson	Sidney E. McArthur	Montana Power Co., Morony Dam, Great Falls, Mont.
Hamilton (Toronto Section)	J. F. McDiarmid	C. E. Moorhouse	Canadian Westinghouse Ltd., Hamilton, Ont.
Hampton Roads (Virginia Section)	W. G. Gardner	F. U. Ross	Virginia Electric & Power Co., Portsmouth, Va.
Jacksonville (Florida Section)	M. L. Barre		
Lake Charles (New Orleans Section)	F. I. Stalnecker	J. A. Carruth	Gulf State Utilities Co., 314 Broad St., Lake Charles, La.
Lancaster–York (Maryland Section)	H. J. Stewart	J. L. Stauffer	Pennsylvania Power & Light Co., Griest Bldg., Lancaster, Pa.
Little Rock (Memphis Section)	J. A. Hunter	O. W. Wallar	2201 South Martin, Little Rock, Ark.
Miami (Florida Section)	P. J. Carlin		
Niagara Falls (Niagara Frontier Section)	A. W. Wamsley	F. F. Rollins	233—82nd Street, Niagara Falls, N. Y.
Niagara (Toronto Section)	J. I. Gram	W. G. Barr	1888 Main St., Niagara Falls, Ont.
Ottawa (Montreal Section)	R. M. Prendergast	T. W. Mouat	National Research Council, Ottawa, Ont.
Panhandle (North Texas Section)	C. V. Bullen	H. O. Hodson	Southwestern Public Service Co., 420 Polk St., Amarillo, Tex.
Red Bluff (San Francisco Section)	Louis M. Van Meter		
Richmond (Virginia Section)	W. T. Johns, Jr.	H. A. Frazier	System Engg. Dept., Virginia Elec. & Power Co., Richmond, Va.
Rock Island, Ill. (Iowa Section)			
Rock River Valley (Madison Section)	R. E. Schuette	Royce E. Johnson	Barber-Colman Company, Rockford, Ill.
Sacramento (San Francisco Section)	James C. Coombs	James R. Miller	3991 Third Ave., Sacramento, Calif.
Saginaw Valley (Michigan Section)	Melvin L. Manning	Gordon S. Marvin	1007 Bradley Ave., Flint 3, Mich.
Shreveport (New Orleans Section)	W. J. Googe	W. N. Petzing	General Electric Co., 206 Market St., Shreveport, La.
Tampa (Florida Section)	I. C. Matheson		
Wilmington (Philadelphia Section)	F. T. Bear	E. W. Randall	E. I. du Pont de Nemours & Co., Wilmington, Del.
Zanesville (Columbus Section)	George W. Miller	George W. Cooper	917 Lindbergh Ave., Zanesville, Ohio

Geographical District Executive Committees

District	Chairman (Vice-President, AIEE)	Secretary (District Secretary)	Chairman, District Committee on Student Activities
1 North Eastern	E. W. Davis, Simplex Wire & Cable Co., 79 Sidney St., Cambridge 39, Mass.	Victor Siegfried, American Steel & Wire Co., Worcester 7, Mass.	E. R. McKee, University of Vermont, Burlington, Vt.
2 Middle Eastern	E. S. Fields, Cincinnati Gas & Electric Co., 4th & Main Sts., Cincinnati 1, Ohio	A. A. Johnson, Westinghouse Electric Corporation, East Pittsburgh, Pa.	P. L. Hoover, Case School of Applied Science, Cleveland 6, Ohio
3 New York City	O. E. Buckley, Bell Telephone Laboratories, Inc., 463 West St., New York 14, N. Y.	J. L. Callahan, R.C.A. Laboratories, Radio Corporation of America, 66 Broad St., New York 4, N. Y	Harry Baum, College of the City of New York, 139th St. & Convent Ave., New York, N. Y.
4 Southern	Herman B. Wolf, Duke Power Company, Charlotte 1, N. C.	C. B. Galphin, 1028 Central Ave., Charlotte 4, N. C.	Brinkley Barnett, University of Kentucky, Lexington, Ky.
5 Great Lakes	T. G. LeClair, Commonwealth Edison Company, 72 W. Adams St., Chicago 90, Ill.	N. C. Pearcy, Public Utility Engg. & Service Corp., 231 S. La Salle St., Chicago 4, Ill.	J. H. Kuhlmann, University of Minnesota, Minneapolis, Minn.
6 North Central	L. M. Robertson, Public Service Co. of Colorado, Denver, Colo.	H. F. Gidlund, Public Service Co. of Colorado, Denver, Colo.	R. O. Trueblood, University of Wyoming, Laramie, Wyo.
7 South West	R. F. Danner, Oklahoma Gas & Electric Co., Oklahoma City 1, Okla.	W. B. Stephenson, Southwestern Bell Telephone Co., Oklahoma City 2, Okla.	C. L. Farrar, University of Oklahoma, Norman, Okla.
8 Pacific	F. F. Evenson, 600 E. Harbor St., P.O. Box 1710, San Diego, Calif.	Walter L. Bryant, U. S. Navy Electronics Laboratory, San Diego 52, Calif.	W. J. Warren, University of Santa Clara, Santa Clara, Calif.
9 North West	C. F. Terrell, Puget Sound Power & Light Co., 860 Stuart Bldg., Seattle, Wash.	C. H. Cutter, 814 Securities Building, Seattle 1, Wash.	E. W. Schilling, Montana State College Bozeman, Mont.
10 Canada	F. L. Lawton, Aluminum Co. of Canada Ltd., 1700 Sun Life Bldg., Montreal, Que.	D. M. Farnham, Quebec Hydro-Elec. Commission, 107 Craig St. West, Montreal, Que.	

NOTE: Each District executive committee includes also the chairmen and secretaries of all Sections within the District, and the District vice-chairman of the AIEE membership committee.

Student Branches

Name and Location	District	Counselor (Member of Faculty)
Akron, University of, Akron, Ohio	2	A. J. Fairburn
Alabama Polytechnic Institute, Auburn	4	
Alabama, University of, University	4	William J. Miller
Alberta, University of, Edmonton, Canada	10	R. E. Phillips
Arizona, University of, Tucson	8	J. C. Clark
Arkansas, University of, Fayetteville	7	A. S. Brown
British Columbia, University of, Vancouver, Canada	10	W. B. Coulthard
Brooklyn, Polytechnic Inst. of, Brooklyn, N. Y. (Day)	3	F. A. Wahlers
(Evening)	3	Anthony Giordana
Brown University, Providence, R. I.	1	F. N. Tompkins
Bucknell University, Lewisburg, Pa.	2	George Irland
California Institute of Technology, Pasadena	8	W. H. Pickering
California, University of, Berkeley	8	P. L. Morton
Carnegie Institute of Technology, Pittsburgh, Pa.	2	D. W. VerPlanck
Case School of Applied Science, Cleveland, Ohio	2	P. L. Hoover
Catholic University of America, Washington, D. C.	2	T. J. MacKavanagh
Cincinnati, University of, Cincinnati, Ohio	2	A. C. Herweh
Clarkson College of Technology, Potsdam, N. Y.	1	Alfred R. Powers
Clemson Agricultural College, Clemson, S. C.	4	F. T. Tingley
Colorado State Coll. of A. & M. Arts, Ft. Collins.	6	C. F. Chinburg
Colorado, University of, Boulder, Colo.	6	Platt Wicks
Columbia University, New York, N. Y.	3	W. A. LaPierre
Connecticut, University of, Storrs	1	G. S. Timoshenko
Cooper Union, New York, N. Y.	3	Norman L. Towle
Cornell University, Ithaca, N. Y.	1	B. K. Northrop
Delaware, University of, Newark	2	Milton G. Young
Denver, University of, Denver, Colo.	6	Fred H. McClain
Detroit, University of, Detroit, Mich.	5	H. O. Warner
Drexel Institute of Technology, Philadelphia, Pa.	2	F. C. Powell
Duke University, Durham, N. C.	4	K. B. MacKichan
Florida, University of, Jacksonville	4	Edward F. Smith
George Washington University, Washington, D. C.	2	Milton K. Akers
Georgia School of Technology, Atlanta, Ga.	4	H. B. Duling
Harvard University, Cambridge, Mass.	1	John P. Newton
Idaho, University of, Moscow	9	J. Hugo Johnson
Illinois Institute of Technology, Chicago	5	E. T. B. Gross
Illinois, University of, Urbana	5	E. A. Reid
Iowa State College, Ames	5	B. S. Willis
Iowa, University of, Iowa City	5	E. B. Kurtz
Johns Hopkins University, Baltimore, Md.	2	F. Hamburger, Jr.
Kansas State College, Manhattan	7	Joe E. Ward
Kansas, University of, Lawrence	7	David D. Robb
Kentucky, University of, Lexington	4	Brinkley Barnett
Lafayette College, Easton, Pa.	2	Finley W. Smith
Lehigh University, Bethlehem, Pa.	2	J. L. Beaver
Louisiana State University, Baton Rouge	4	A. K. Ramsey, Jr.
Louisville, University of, Louisville, Ky.	4	M. G. Northrop
Maine, University of, Orono	1	W. J. Creamer
Manhattan College, New York, N. Y.	3	Robert T. Weil
Marquette University, Milwaukee, Wis.	5	E. W. Kane
Maryland, University of, College Park	2	L. J. Hodgins
Massachusetts Inst. of Technology, Cambridge	1	D. P. Severance
Mich. College of Mining & Tech., Houghton	5	G. W. Swenson
Michigan State College, East Lansing	5	J. A. Strelzoff
Michigan, University of, Ann Arbor	5	J. S. Gault
Milwaukee School of Engg., Milwaukee, Wis.	5	E. L. Wiedner
Minnesota, University of, Minneapolis	5	J. H. Kuhlmann
Mississippi State College, State College	4	Harry C. Simrall
Missouri School of Mines & Metallurgy, Rolla	7	I. H. Lovett
Missouri, University of, Columbia	7	Clifford M. Wallis
Montana State College, Bozeman	9	G. Dale Scheckels
Nebraska, University of, Lincoln	6	O. E. Edison
Nevada, University of, Reno	8	S. G. Palmer
Newark College of Engineering, Newark, N. J.	3	William Jordan
New Hampshire, University of, Durham, N. H.	1	W. B. Nulsen
New Mexico State College, State College	7	Harold A. Brown
New Mexico, University of, Albuquerque	7	R. W. Tapy
New York, Coll. of the City of, New York, N. Y.	3	Harry Baum
New York University, New York	3	Charles F. Rehberg
North Carolina State College, Raleigh	4	C. G. Brennecke
North Dakota State Agricultural College, Fargo	5	Harry S. Dixon
North Dakota, University of, Grand Forks	5	
Northeastern University, Boston, Mass.	1	Roland G. Porter
Northwestern University, Evanston, Ill.	5	R. Beam
Norwich University, Northfield, Vt.	1	F. A. Spencer
Notre Dame, University of, Notre Dame, Ind.	5	L. F. Stauder
Ohio Northern University, Ada	2	
Ohio State University, Columbus	2	F. C. Weimer
Ohio University, Athens	2	
Oklahoma A. & M. College, Stillwater	7	Albrecht Naeter
Oklahoma, University of, Norman	7	C. L. Farrar
Oregon State College, Corvallis	9	A. L. Albert
Pennsylvania State College, State College	2	P. X. Rice
Pennsylvania, University of, Philadelphia	2	S. Reid Warren, Jr.
Pittsburgh, University of, Pittsburgh, Pa.	2	R. C. Gorham
Pratt Institute, Brooklyn, N. Y.	3	Donald H. Wright
Princeton University, Princeton, N. J.	2	J. E. Paul
Puerto Rico, University of, Mayaguez, P. R.	3	Miguel Wiewall, Jr.
Purdue University, Lafayette, Ind.	5	R. B. Marshall
Rensselaer Polytechnic Institute, Troy, N. Y.	1	E. D. Broadwell
Rhode Island State College, Kingston	1	
Rice Institute, Houston, Tex.	7	M. V. McEnany
Rose Polytechnic Institute, Terre Haute, Ind.	5	C. C. Knipmeyer
Rutgers, University, New Brunswick, N. J.	3	P. S. Creager
Santa Clara, Univ. of, Santa Clara, Calif.	8	W. J. Warren
South Carolina, University of, Columbia	4	Samuel Litman
South Dakota State College, Brookings	5	W. H. Gamble
South Dakota State School of M. & T., Rapid City	6	J. O. Kammerman
Southern California, Univ. of, Los Angeles	8	P. S. Biegler
Southern Methodist Univ., Dallas, Tex.	7	R. L. Biesele, Jr.
Stanford Univ., Stanford University, Calif.	8	W. G. Hoover
Stevens Inst. of Technology, Hoboken, N. J.	3	W. L. Sullivan
Swarthmore College, Swarthmore, Pa.	2	J. D. McCtumm
Syracuse University, Syracuse, N. Y.	1	Leroy Mullin
Tennessee, University of, Knoxville	4	W. O. Leffell
Texas, A. & M. College of, College Station	7	N. F. Rode
Texas Technological College, Lubbock	7	
Texas, University of, Austin	7	A. J. McCrocklin, Jr.
Toronto, University of, Toronto, Ont., Can.	10	L. S. Lauchland
Tufts College, Medford, Mass.	1	A. H. Howell
Tulane University, New Orleans, La.	4	M. G. Zervigon
Union College, Schenectady, N. Y.	1	H. W. Bibber
Utah, University of, Salt Lake City	9	O. C. Haycock
Vanderbilt University, Nashville, Tenn.	4	S. R. Schealer
Vermont, University of, Burlington	1	E. R. McKee
Villanova College, Villanova, Pa.	2	Harry S. Bueche
Virginia Military Institute, Lexington	4	J. S. Jamison
Virginia Polytechnic Institute, Blacksburg	4	Claudius Lee
Virginia, University of, Charlottesville	4	L. R. Quarles
Washington, State College of, Pullman	9	H. F. Lickey
Washington, University of, Seattle	9	Vinson L. Palmer
Washington University, St. Louis, Mo.	7	D. A. Fischer
West Virginia University, Morgantown	2	A. H. Forman
Wisconsin, University of, Madison	5	G. F. Tracy
Worcester Poly. Institute, Worcester, Mass.	1	D. C. Alexander
Wyoming, University of, Laramie	6	R. O. Trueblood
Yale University, New Haven, Conn.	1	A. G. Conrad

Total Branches.....126

Number of Student members November 1, 1946.....4,986

Past and Present Officers of the Institute

*Abbott, Arthur V., *V-P.*, 1900–02.
Adams, Comfort A., *M.*, 1912–15; *V-P.*, 1915–17; *P.*, 1918–19.
*Adsit, C. G., *V-P.*, 1921–23.
Alger, P. L., *D.*, 1944–48.
*Anthony, Wm. A., *V-P.*, 1886–89; *P.*, 1890–91; *V-P.*, 1894–96.
*Armstrong, A. H., *M.*, 1903–06; *V-P.*, 1906–08.
Arnold, Bion J., *M.*, 1895–98; *V-P.*, 1902–03; *P.*, 1903–04.
Auty, K. A., *V-P.*, 1932–34.

*Babcock, A. H., *V-P.*, 1918–19.
Barker, J. W., *V-P.*, 1940–42.
Barnes, H. H., Jr., *M.*, 1910–13; *V-P.*, 1913–15.
*Barstow, W. S., *M.*, 1900–03; *V-P.*, 1903–05.
Barton, T. F., *V-P.*, 1939–40; *D.*, 1940–44.
†Bates, D. H., *V-P.*, 1885–87.
*Baum, Frank G., *V-P.*, 1906–08.
Beardsley, C. R., *D.*, 1937–41.
Beaver, J. L., *V-P.*, 1927–29.
Bedell, Frederick, *M.*, 1914–17; *V-P.*, 1917–18.
*Behrend, B. A., *M.*, 1913–16; *V-P.*, 1916–18.
*Bell, Alexander G., *V-P.*, 1884–85; *P.*, 1891–92.
*Bell, Louis, *M.*, 1891–94.
Bennett, Edward, *V-P.*, 1924–26.
*Berresford, A. W., *M.*, 1909–12; *V-P.*, 1912–14; *P.*, 1920–21.
Bettis, A. E., *V-P.*, 1926–28; *D.*, 1928–32.
Bickelhaupt, C. O., *V-P.*, 1927–29.
Bingham, L. A., *V-P.*, 1943–45.
†Black, R. G., *M.*, 1910–13.
Blackwell, O. B., *V-P.*, 1936–38.
Blaisdell, L. T., *V-P.*, 1936–38.
Bolton, F. C., *V-P.*, 1938–40.
Bonney, R. B., *V-P.*, 1933–35.
*Brackett, Cyrus F., *M.*, 1886–89.
*Bradley, Chas. S., *M.*, 1894–97; *V-P.*, 1897–99; *M.*, 1899–1902.
*Brooks, David M., *M.*, 1885–88.
Brooks, Morgan, *M.*, 1907–10; *V-P.*, 1910–12.
*Brush, Chas. F., *M.*, 1884–87.
Bryant, J. M., *M.*, 1924–28.
Buck, Harold W., *M.*, 1907–10; *V-P.*, 1910–12; *P.*, 1916–17.
*Buckingham, Chas. L., *M.*, 1885–88.
Buckley, O. E., *V-P.*, 1946–48.
Bush, Vannevar, *D.*, 1937–41.
Bussey, H. E., *V-P.*, 1923–25.

Carle, N. A., *M.*, 1916–19; *V-P.*, 1919–20.
*Carlton, W. G., *M.*, 1908–11; *V-P.*, 1911–13.
Carpenter, C. B., *V-P.*, 1944–46.
*Carpenter, H. V., *V-P.*, 1930–32.
*Carty, John J., *M.*, 1893–96, 1900–03, 1903–04, 1906–08; *V-P.*, 1904–06, 1908–11; *P.*, 1915–16.
*Chamberlain, J. C., *M.*, 1890–93.
Charlesworth, H. P., *M.*, 1923–27; *V-P.*, 1930–32; *P.*, 1932–33.
Chesney, C. C., *M.*, 1905–08; *V-P.*, 1908–10; *P.*, 1926–27.
Chesterman, F. J., *D.*, 1926–30.
Christie, C. V., *V-P.*, 1935–37.
Chubb, L. W., *D.*, 1931–35.
Chubbuck, L. B., *V-P.*, 1931–33.
†Church, W. Lee, *M.*, 1887–88.
*Clarke, Chas. L., *M.*, 1904–05.
Clifford, H. E., *M.*, 1908–11.
Coldwell, O. B., *V-P.*, 1921–22.
*Compton, Alfred G., *M.*, 1891–94.
Cooper, A. B., *V-P.*, 1927–29; *D.*, 1930–34.
Coover, M. S., *D.*, 1940–44; *V-P.*, 1944–46.
Copley, A. W., *V-P.*, 1931–33.
*Craft, E. B., *M.*, 1920–24.
Craft, F. M., *V-P.*, 1933–35.
*Crocker, Francis B., *M.*, 1888–90; *V-P.*, 1890–92, 1894–96; *P.*, 1897–98.
†Crosby, Oscar T., *V-P.*, 1892–94.
*Cross, Chas. R., *V-P.*, 1884–85.
*Cuttriss, Chas., *M.*, 1888–91.

Danner, R. F., *V-P.*, 1946–48.
Davis, Ernest W., *V-P.*, 1946–48.
Dawes, Chester L., *V-P.*, 1938–40.
*Delany, Patrick B., *M.*, 1890–93; *V-P.*, 1893–95.
Del Mar, Wm. A., *M.*, 1917–21; *V-P.*, 1921–22.
Dewars, A. G., *V-P.*, 1942–44.
Dobson, W. P., *V-P.*, 1925–27.
*Dolbear, A. E., *V-P.*, 1885–87.
*Don Carlos, H. C., *D.*, 1926–30
*Downing, P. M., *V-P.*, 1925–27.
*Duncan, Louis, *P.*, 1895–97.
Dunn, Gano, *M.*, 1897–1900; *V-P.*, 1900–02; *M.*, 1902–05; *V-P.*, 1905–07; *P.*, 1911–12.

†Eales, H. W., *V-P.*, 1921–26.
*Eckert, W. H., *M.*, 1884–85.
*Edgar, Chas. L., *M.*, 1905–08.
*Edison, Thos. A., *V-P.*, 1884–85.
*Eglin, W. C. L., *M.*, 1903–06; *V-P.*, 1907–09.
Eldredge, M., *V-P.*, 1935–37; *D.*, 1939–43.
*Emmet, W. L. R., *V-P.*, 1900–02.
Evans, Herbert S., *V-P.*, 1929–31.
Evenson, F. F., *V-P.*, 1945–47.
Ewart, F. R., *V-P.*, 1921–23.

*Faccioli, G., *M.*, 1918–22; *V-P.*, 1922–24.
†Fair, R. H., *V-P.*, 1935–37.
Fairman, J. F., *V-P.*, 1944–46; *D.*, 1946–50.
Farmer, F. M., *D.*, 1934–38; *V-P.*, 1938–39; *P.*, 1939–40.
*Ferguson, Louis A., *M.*, 1904–07; *V-P.*, 1907–08; *P.*, 1908–09.
Ferguson, O. J., *V-P.*, 1927–29.
*Field, Stephen D., *M.*, 1884–86.
Fields, E. S., *V-P.*, 1945–47.
*Finney, John H., *M.*, 1914–17; *V-P.*, 1917–18.
*Fisken, John B., *M.*, 1916–19; *V-P.*, 1919–20.
Flanigen, J. M., *D.*, 1945–49.
Fleager, C. E., *V-P.*, 1929–31.
*Foster, Horatio A., *M.*, 1890–93.
*Fowle, F. F., *M.*, 1919–23.
*Fowler, A. C., *M.*, 1887.
Fowler, M. M., *D.*, 1925–29.
*Freeman, W. E., *V-P.*, 1931–33.
Funk, N. E., *D.*, 1934–38; *P.*, 1943–44.

Gamble, Lester R., *V-P.*, 1938–40; *D.*, 1941–45.
Gaylord, J. M., *V-P.*, 1943–45.
Gear, H. B., *D.*, 1934–38.
*Geyer, Wm. E., *M.*, 1888–92.
*Gherardi, Bancroft, *M.*, 1905–08, 1914–17; *V-P.*, 1908–10; *P.*, 1927–28.
Gilson, Walter J., *V-P.*, 1943–45.
Goldsborough, W. E., *M.*, 1901–04; *V-P.*, 1904–06.
*Gray, Elisha, *M.*, 1884–86.
*Green, Norvin, *P.*, 1884–86; *V-P.*, 1886–88.
*Greene, S. Dana, *M.*, 1899.

Hall, Walter A., *M.*, 1917–21; *V-P.*, 1921–22.
*Hamblet, Jas., *M.*, 1891–94; *V-P.*, 1894–96.
*Hamilton, George A., *V-P.*, 1884–86; *Natl. Treas.*, 1895–1930.
Hamilton, J. L., *V-P.*, 1940–42.
*Hammer, William J., *V-P.*, 1891–93; *M.*, 1893–96.
Hanker, F. C., *D.*, 1927–31.
Hansen, K. L., *V-P.*, 1940–42; *D.*, 1942–46.
*Harding, C. F., *V-P.*, 1936–38.
*Harisberger, John, *V-P.*, 1924–26.
Harrison, W. H., *V-P.*, 1935–37; *P.*, 1937–38.
*Haskins, Chas. H., *V-P.*, 1884–86.
*Hasson, W. F. C., *V-P.*, 1895–97; *M.*, 1897–1900.
*Hazard, Rowland R., *Treas.*, 1884–86; *V-P.*, 1887–89.
*Hellings, M. L., *M.*, 1884–85.
*Hellmund, R. E., *D.*, 1939–42.
*Henderson, S. E. M., *V-P.*, 1923–25.
Henline, H. H., *Act. Natl. Secy.*, 1932; *Natl. Secy.*, 1933–.
Henry, R. T., *V-P.*, 1944–46; *D.*, 1946–50.
*Hering, Carl, *V-P.*, 1891–93, 1895–98; *P.*, 1900–01.
*Herzog, F. Benedict, *M.*, 1887–92.
†Hewitt, Chas., *M.*, 1893–96.
†Hibbard, Angus S., *M.*, 1892–95; *V-P.*, 1895–97.
Hibshman, N. S., *V-P.*, 1941–43.
*Higson, C. R., *V-P.*, 1932–34.
Hinson, N. B., *V-P.*, 1935–37.
Hitchcock, H. W., *V-P.*, 1939–41.
*Hobart, H. M., *M.*, 1922–26; *V-P.*, 1926–28.
Housley, J. E., *V-P.*, 1941–43; *P.*, 1946–47.
*Houston, Edwin J., *M.*, 1884–87; *P.*, 1893–95.
*Howell, John W., *M.*, 1888–90.
Hull, A. H., *V-P.*, 1933–35.
Hull, B. D., *V-P.*, 1928–30; *D.*, 1931–35.
Humphrey, H. H., *V-P.*, 1906–08.
Hunting, F. S., *M.*, 1911–14; *V-P.*, 1914–16.
*Hutchinson, Cary T., *M.*, 1895–98; *V-P.*, 1898–1900.
*Hutchinson, F. L., *Natl. Secy.*, 1912–32.

*Imlay, L. E., *M.*, 1919–23.

Jackson, Dugald C., *V-P.*, 1897–99; *P.*, 1910–11.
*Jackson, W. B., *M.*, 1912–15; *V-P.*, 1918–19.
†James, Wm. F., *V-P.*, 1923–25.
Jamieson, B. G., *V-P.*, 1926–28.
Jewett, F. B., *M.*, 1915–18; *V-P.*, 1918–19; *P.*, 1922–23.
Johnson, F. Ellis, *D.*, 1936–39.
*Johnson, J. Allen, *D.*, 1928–32; *V-P.*, 1932–34; *P.*, 1934–35.
Jollyman, J. P., *V-P.*, 1937–39.
Jones, A. L., *V-P.*, 1941–43.
Jones, C. R., *D.*, 1935–39; *V-P.*, 1942–44.
*Jones, Francis W., *M.*, 1884–85; *V-P.*, 1885–87.
*Jorgensen, L. R., *V-P.*, 1919–20.
Juhnke, P. B., *D.*, 1933–37.
*Junkersfeld, P., *M.*, 1913–16; *V-P.*, 1916–18.

Kearns, J. E., *D.*, 1929–33.
*Keith, Nathaniel S., *Secy.*, 1884–85.
*Kelsch, Raymond S., *V-P.*, 1918–19.
*Kennelly, Arthur E., *V-P.*, 1892–94; *M.*, 1894–97; *V-P.*, 1897–98; *P.*, 1898–1900.
Kidder, H. A., *M.*, 1925–28; *V-P.*, 1928–30.
Knight, G. L., *M.*, 1922–26; *V-P.*, 1926–28.
Knowlton, A. E., *D.*, 1930–34.
Kositzky, G. A., *D.*, 1932–36.
Kouwenhoven, W. B., *V-P.*, 1931–33; *D.*, 1935–39.

Lacy, T. N., *V-P.*, 1930–32.
Laffoon, C. M., *D.*, 1942–47.
*Lamme, Benj. G., *M.*, 1907–10.
Lane, F. H., *D.*, 1937–41.
Lardner, H. A., *M.*, 1913–16.
Lawton, F. L., *V-P.*, 1945–47.
LeClair, T. G., *D.*, 1941–45; *V-P.*, 1946–48.
Lee, Everett S., *D.*, 1933–37; *V-P.*, 1940–42.
*Lee, William S., *M.*, 1911–14; *D.*, 1929–30; *P.*, 1930–31.
*Leonard, H. Ward, *M.*, 1890–93; *V-P.*, 1893–95.
*Lieb, John W., *M.*, 1896–99; *V-P.*, 1899–1901; *M.*, 1901–03; *V-P.*, 1903–04; *P.*, 1904–05.
*Lighthipe, J. A., *V-P.*, 1913–15.
Lincoln, J. F., *M.*, 1920–24.
*Lincoln, Paul M., *M.*, 1906–09; *V-P.*, 1909–11; *P.*, 1914–15.
Liversidge, H. P. *D.*, 1927–31.
*Lloyd, Herbert, *M.*, 1898–1901.
*Lockwood, Thos. D., *V-P.*, 1886–87; *M.*, 1888–90; *V-P.*, 1891–93.
Lovell, A. H., *D.*, 1932–36; *V-P.*, 1938–40.
*Lozier, R. T., *M.*, 1902–04.
†Lunn, Ernest, *M.*, 1922–26.

MacCutcheon, A. M., *D.*, 1928–32; *P.*, 1936–37.
Macdonald, J. E., *V-P.*, 1923–25.
*Macfarlane, Alexander, *M.*, 1897–1900.
Maclachlan, Wills, *V-P.*, 1919–20.
*Magnusson, C. E., *V-P.*, 1920–21.
Mahood, E. T., *V-P.*, 1942–44.
*Mailloux, C. O., *M.*, 1886–89; *V-P.*, 1898–99; *M.*, 1899–1902; *V-P.*, 1902–04; *M.*, 1905–07; *P.*, 1913–14.
Mapes, L. R., *D.*, 1938–42.
*Martin, T. Commerford, *Act. Secy.*, 1884–85; *M.*, 1885–87; *P.*, 1887–88; *V-P.*, 1888–90.
Martindale, E. H., *M.*, 1917–20; *V-P.*, 1920–21.
*Maver, Wm., Jr., *M.*, 1888–91.
Maxwell, Fred R., Jr., *V-P.*, 1939–41; *D.*, 1941–45.
*Maynard, Geo. C., *V-P.*, 1886–88.
McAllister, A. S., *M.*, 1914–17; *V-P.*, 1917–18.
McClellan, L. N., *V-P.*, 1937–39.
McClellan, William, *M.*, 1912–15; *V-P.*, 1915–17; *P.*, 1921–22.
†McConahey, W. M., *M.*, 1923–27.
McDowell, C. S., *V-P.*, 1920–21.
McEachron, K. B., *D.*, 1936–40; *V-P.*, 1942–44.
McHenry, M. J., *V-P.*, 1937–39; *D.*, 1944–48.
McMillan, F. O., *V-P.*, 1934–36.
Merriam, E. B., *M.*, 1924–28; *V-P.*, 1928–30.
Mershon, Ralph D., *M.*, 1900–03; *V-P.*, 1903–05; *P.*, 1912–13.
*Meyer, E. B., *D.*, 1927–31; *V-P.*, 1932–34; *P.*, 1935–36.
Meyer, F. J., *V-P.*, 1934–36; *D.*, 1939–43.
*Michaelis, O. E., *M.*, 1886–89; *V-P.*, 1889–90.
Mier, C. W., *D.*, 1943–47.
Mills, G. A., *V-P.*, Aug.–Oct. 1932.
Mitchell, W. E., *V-P.*, 1925–27.
Morehouse, L. F., *M.*, 1919–23; *V-P.*, 1924–26.
*Morrow, L. W. W., *D.*, 1933–37.
Mortensen, S. H., *D.*, 1943–47.
Morton, W. B., *D.*, 1941–46.
Moultrop, I. E., *D.*, 1926–30; *V-P.*, 1930–32.
*Mullin, E. H., *M.*, 1902–04.
*Murray, Wm. S., *M.*, 1908–09, 1909–12; *V-P.*, 1912–14.

Newbury, F. D., *M.*, 1918–22.
*Nichols, E. L., *V-P.*, 1889–91.
*Norris, H. H., *M.*, 1909–12.
North, J. R., *D.*, 1945–49.
Northmore, E. R., *V-P.*, 1927–29.

Osborne, H. S., *D.*, 1938–42; *P.*, 1942–43.
*Osgood, Farley, *M.*, 1911–14; *V-P.*, 1914–16; *P.*, 1924–25.
†Owens, R. B., *V-P.*, 1898–1900.

Parker, John Castlereagh, *V-P.*, 1921–22; *P.*, 1938–39.
†Patton, P. H., *V-P.*, 1931–33.
*Peek, F. W., Jr., *D.*, 1930–33.
Pender, Harold, *M.*, 1915–18; *V-P.*, 1918–19.
*Perrine, Frederick A. C., *M.*, 1898–1900.
*Phelps, Geo. M., Jr., *M.*, 1885–87; *Treas.*, 1886–95.
*Pickernell, F. A., *M.*, 1896–99.
Pierce, A. G., *M.*, 1921–25; *V-P.*, 1925–27.
Plumb, H. T., *V-P.*, 1922–24.
*Pope, Franklin L., *V-P.*, 1884–86; *P.*, 1886–87; *V-P.*, 1887–89.
*Pope, Ralph W., *Secy.*, 1885–1911; *Hon. Secy.*, 1911–29.
Post, G. G., *V-P.*, 1934–36.
Powel, C. A., *D.*, 1936–40; *V-P.*, 1942–43; *P.*, 1944–45.
†Pratt, H. A., *M.*, 1921–25.
*Prescott, Geo. B., *M.*, 1884.
*Prescott, G. B., Jr., *M.*, 1888–91.
†Price, C. A., *V-P.*, 1941–43.
Prince, D. C., *D.*, 1938–41; *P.*, 1941–42.
Puffer, Wm. L., *M.*, 1896–99.
*Pupin, Michael I., *M.*, 1892–95; *V-P.*, 1895–97, 1901–03; *P.*, 1925–26.

Quarles, D. A., *D.*, 1944–48.
Quinan, G. E., *V-P.*, 1928–30.

*Reber, Samuel, *M.*, 1901–04; *V-P.*, 1904–06.
*Rice, Calvin W., *M.*, 1900–03; *V-P.*, 1903–05.
*Rice, E. W., Jr., *P.*, 1917–18.
Ricker, Claire W., *V-P.*, 1943–45.
†Robbins, Chas., *M.*, 1916–20; *V-P.*, 1920–21.
Robertson, L. M., *V-P.*, 1945–47.
*Robinson, L. T., *M.*, 1913–16; *V-P.*, 1916–18, 1920–21.
Rodman, W. S., *V-P.*, 1929–31.
Rogers, C. E., *V-P.*, 1936–38.
*Ruffner, Chas. S., *M.*, 1916–20; *V-P.*, 1920–21.
*Rugg, W. S., *M.*, 1910–13.
*Rushmore, D. B., *M.*, 1908–11; *V-P.*, 1911–13.

*Ryan, Harris J., *M.*, 1893–96; *V-P.*, 1996–98; *P.*, 1923–24.
*Ryan, W. T., *V-P.*, 1928–30.

Sands, Herbert S., *V-P.*, 1923–27.
*Sargent, W. D., *M.*, 1885–86.
Schilling, E. W., *V-P.*, 1942–44.
*Schoen, A. M., *M.*, 1906–09; *V-P.*, 1919–20.
Schoolfield, H. H., *V-P.*, 1926–28.
*Schuchardt, R. F., *V-P.*, 1922–24; *P.*, 1928–29.
*Scott, Chas. F., *M.*, 1895–98; *V-P.*, 1899–1901; *P.*, 1902–03.
*Scribner, Chas. E., *M.*, 1910–13; *V-P.*, 1913–15.
Sever, Geo. F., *M.*, 1898–1901; *V-P.*, 1901–03; *M.*, 1903–06.
*Shaad, G. C., *V-P.*, 1930–32; *D.*, 1935–36.
*Shelbourne, Sidney F., *M.*, 1886–87.
*Sheldon, Samuel, *M.*, 1898–1901; *V-P.*, 1901–03 *M.*, 1903–06; *P.*, 1906–07.
Sibley R. *V-P.*, 1921–23.
Sinclair, C. T., *V-P.*, 1939–41.
Sisson, C. E., *V-P.*, 1929–31.
Skinner, C. E., *M.*, 1915–19; *V-P.*, 1919–20; *P.*, 1931–32.
Slichter, Walter I., *M.*, 1918–22; *V-P.*, 1922–24; *Natl. Treas.*, 1930–.
*Smith, H. B., *M.*, 1920–24; *V-P.*, 1924–26; *P.*, 1929–30.
Smith, Walter Charles, *V-P.*, 1941–43; *D.*, 1945–49.
Smith W. R., *D.*, 1942–46.
*Smith, W. W., *M.*, 1884–85.
Sorensen, R. W., *V-P.*, 1933–35; *D.*, 1936–40; *P.*, 1940–41.
*Spencer, Paul, *M.*, 1906–09; *V-P.*, 1909–11.
*Sprague, Frank J., *V-P.*, 1890–92; *P.*, 1892–93.
*Springer, F. W., *V-P.*, 1921–23.
*Sprong, S. D., *M.*, 1909–12; *V-P.*, 1912–14.
*Stanley, Wm., *V-P.*, 1898–1900.
Stein, I. Melville, *V-P.*, 1937–39.
*Steinmetz, Chas. P., *M.*, 1892–95; *V-P.*, 1896–98; *M.*, 1898–1901; *P.*, 1901–02.
*Stephens, C. E., *D.*, 1928–33
Stevens, A. C., *D.*, 1932–36; *V-P.*, 1936–38.
*Stevens, J. Franklin, *M.*, 1912–15; *V-P.*, 1915–17.
*Stillwell, Lewis B., *M.*, 1896–99; *V-P.*, 1899–1901; *P.*, 1909–10.
†Stine, Wilbur M., *V-P.*, 1896–98.
Stokes, Stanley, *V-P.*, 1932–34.
*Stone, Chas. W., *M.*, 1908–11; *V-P.*, 1911–13.
Stone, E. C., *D.*, 1925–29; *V-P.*, 1929–31.
Storer, Norman W., *M.*, 1911–14; *V-P.*, 1914–16, 1921–23.
*Stott, Henry G., *M.*, 1904–07; *P.*, 1907–08.
Sykes, Wilfred, *M.*, 1917–21.

Tapscott, R. H., *D.*, 1930–34; *V-P.*, 1934–36.
Taylor, A. LeRoy, *V-P.*, 1940–42.
Taylor, John B., *M.*, 1915–18; *V-P.*, 1918–19.
Terrell, C. F., *V-P.*, 1946–48.
*Terry, Chas. A., *M.*, 1902–05; *V-P.*, 1905–07.
*Tesla, Nikola, *V-P.*, 1892–94.
*Thomas, B. F., *M.*, 1885–87.
Thomas, Percy H., *M.*, 1907–10; *V-P.*, 1910–12.
†Thompson, Edward P., *M.*, 1887–88.
*Thomson, Elihu, *V-P.*, 1887–89; *P.*, 1889–90.
Thomson, J. M., *V-P.*, 1939–41.
Timbie, W. H., *V-P.*, 1934–36.
*Townley, Calvert, *M.*, 1905–08; *V-P.*, 1908–10; P., 1919–20.
*Townsend, Henry C., *M.*, 1899–1902.
*Trowbridge, Wm. P., *M.*, 1884–86.
Turner, A. L., *V-P.*, 1939–41.

*Upton, Francis R., *V-P.*, 1889–90; *M.*, 1890–92.

*Vail, Theo. N., *M.*, 1884–86.
*Vanderpoel, W. K., *M.*, 1923–27.
*Van Hoevenbergh, H., *M.*, 1888–90.
*Vansize, W. B., *M.*, 1894–97.

*Wallace, Wm., *V-P.*, 1893–95.
Warner, R. G., *D.*, 1940–44.
Warner, R. W., *V-P.*, 1944–46.
*Weaver, W. D., *M.*, 1894–97; 1899–1902.
†Webb, Herbert L., *M.*, 1891–94; 1897–1900.
*Weston, Edward, *M.*, 1884–87; *P.*, 1888–89; *V-P.*, 1889–91.
*Wetzler, Jos., *M.*, 1888–90; *V-P.*, 1890–92.
*Wheeler, Schuyler S., *M.*, 1887–90; *V-P.*, 1890–91, 1902–04; *M.*, 1904–05; *P.*, 1905–06.
*White, Jas. G., *M.*, 1904–07; *V-P.*, 1907–09.
Whitehead, John B., *M.*, 1924–28; *P.*, 1933–34.
Wickenden, W. E., *V-P.*, 1943–45; *P.*, 1945–46.
*Williamson, R. B., *M.*, 1921–25.
*Wilson, A. M., *V-P.*, 1933–35.
*Wirt, Chas., *M.*, 1892–95.
*Wolcott, Townsend, *M.*, 1902–05; *V-P.*, 1905–07.
Wolf., H. B., *V-P.*, 1945–47.
*Wood, Edwin D., *V-P.*, 1937–39.
*Woodrow, H. R., *D.*, 1931–35.

Yerkes, E. P., *D.*, 1946–50.

Abbreviations: *P.*, President; *V-P.*, Vice-President; *M.*, Manager; *D.*, Director; *Natl. Secy.*, National Secretary; *Secy.*, Secretary; *Hon. Secy.*, Honorary Secretary; *Natl. Treas.*, National Treasurer; *Treas.*, Treasurer.

*Deceased. † Non-members at present.

Honorary Members, 1884–1946

*Sir William Preece....1884
*Norvin Green....1889
*Moses G. Farmer....1890
*Lord Kelvin....1892
*Cyrus Field....1892
*E. W. von Siemens....1892
*Andre E. Blondel....1912
*C. E. L. Brown....1912
*Emil A. Budde....1912
*S. Z. de Ferranti....1912
*Antonio Pacinotti....1912
*S. P. Thompson....1914
*Guglielmo Marconi....1917
*Oliver Heaviside....1918
*Ferdinand Foch....1921
*Thomas A. Edison....1928
*John J. Carty....1928
*M. I. Pupin....1928
*Ambrose Swasey....1928
*Elihu Thomson....1928
Herbert Hoover....1929
*Charles F. Scott....1929
*Charles F. Brush....1929
Motoji Shibusawa....1929
*Frank J. Sprague....1932
*W. L. R. Emmet....1933
*G. A. Hamilton....1933
*Arthur E. Kennelly....1933
R. A. Millikan....1933
*E. W. Rice, Jr....1933
*Edward Weston....1933
*Bion J. Arnold....1937
*Alex Dow....1937
Cummings C. Chesney....1938
Andrew G. L. McNaughton....1942
Dugald C. Jackson....1944
Charles E. Skinner....1945
Gano Dunn....1945
Frank B. Jewett....1945

* Deceased.

Headquarters Staff

33 West 39th Street, New York 18

Secretary....H. H. Henline
Office Manager and Business Manager of Publications....F. A. Norris
Editor....G. Ross Henninger
Associate Editor....W. R. MacDonald, Jr.
Secretary, Technical Program Committee....C. S. Rich
Secretary, Board of Examiners and Standards Committee....H. E. Farrer
Technical Committee Activities..Charles C. Wilson
Advertising Manager....Harry A. Johnston

General Counsel

Simon Presant....55 Liberty St., New York 5

INDEX

1. Technical-Subject Index

A-C Ammeters and Voltmeters, Frequency Compensated. Whittenton, Wilkinson....761–4
A-C Arc in an Air Blast, Dielectric Recovery by an. Browne....169–76; disc. 507
A-C Electric-Power Systems in Large Military Aircraft, Basic Design Principles for. Chappuis, Olmsted....12–17; disc. 487
A-C Generators, Application and Performance of Electronic Exciters for Large. Langstaff, Vaughan, Lawrence....246–53; disc. 515
A-C Motors and Generators, Transients in. Smith..61–9
A-C Network Analyzer, A New Design for the. Ryder, Boast....674–80; disc. 1162
A-C Power Cable, Semiconducting Shielding for. Merrell....605–09; disc. 1145
Accelerated Flux Reversal in Reactor Cores Operating Above Saturation Density, Peak Voltages Induced by. Specht, Wentz....254–63
Accuracy of Selsyn Generator-Control Transformer System, Electrical. Chestnut....570–6; disc. 1118
Aeronautical Research, 150,000 Horsepower Applied to. White....833–9
Affecting the Range of Radar Sets, Factors. Quarles, Breazeale....546–8
Air Blast, Dielectric Recovery by an A-C Arc in an. Browne....169–76; disc. 507
Air Circuit Breakers up to 500,000 Kva, 15 Kv, Size Reduction and Rating Extension of Magnetic. Dickinson, Frink....220–3; disc. 510
Air, Long 60-Cycle Arcs in. Strom...113–18; disc. 504
(Air Transportation) A Carbon-Pile Speed Governor. Button....4–7
(Air Transportation) All-Electric Gun Charging. Rohn....1–4
(Air Transportation) An Electronic Frequency Meter and Speed Regulator. Levin...779–86; disc. 1181
(Air Transportation) Investigation of Porcelain Insulators at High Altitudes. Fields, Cadwell...656–60
(Air Transportation) 150,000 Horsepower Applied to Aeronautical Research. White....833–9
Air-borne Radar for Navigation and Obstacle Detection. Jensen, Arnett....307–13; disc. 491
Aircraft, A. Unique Engine-Synchronism Indicator for. Pearson....650–3
Aircraft, An Improved Azimuth Indicating System for. Lynch, Pfuntner....806–12
Aircraft, Basic Design Principles for A-C Electric-Power Systems in Large Military. Chappuis, Olmsted....12–17; disc. 487
Aircraft D-C Power Systems, Control and Protection of. Austin....741–5; disc. 1170
Aircraft Electric Machines, Effect of Altitude on Ventilation and Rating of. Veinott....84–90; disc. 488
Aircraft Electric-Power System, Pressure-Arc-Interruption Circuit Breakers for 400-Cycle. Austin....58–60; disc. 487
Aircraft-Engine Ignition Circuits, Electrical Measurements on. Berkey....49–53
Aircraft Generators on Load Analysis, Effects of Thermal Characteristics of. Rogers....819–24
Aircraft, Governor for Variable-Ratio Transmission Used in Developmental 400-Cycle Electric System for Large. Desch, Garr, Hutton....194–8
Aircraft in Flight, Radio Telemetering for Testing. Frederick....861–70
Aircraft Models, Electronic Control of Frequency Converter Sets for Testing. Heumann, Strong..931–9
Aircraft Windshields, Electrical Anti-icing of McCrumm....786–91
Aircraft Wire and Cable, Short-Time Current Ratings for. Jones, Scott....644–8; disc. 1135
Alloy—An Improved Cable Sheathing, F-3 Lead. Hickernell, Snyder....563–9; disc. 1136
Alternators, Motor-Driven Exciters for Turbine. Bodine, Crary, Rankin....290–7; disc. 515
Altitude on Ventilation and Rating of Aircraft Electric Machines, Effect of. Veinott....84–90; disc. 488
Altitudes, Investigation of Porcelain Insulators at High. Fields, Cadwell....656–60
Ammeters and Voltmeters, Frequency Compensated A-C. Whittenton, Wilkinson....761–4
Ampere Sealed Ignitron, A 400-. Steiner, Price....680–5; disc. 1161
Analogy, Dimensionless Analysis of Servomechanisms by Electrical. Herwald, McCann 636–9; disc. 1132
Analogy Methods Applied to Servomechanism Problems, Electrical. McCann, Herwald, Kirschbaum....91–6; disc. 515
Analysis by Automatic Oscillographs, Fault Location and Relay Performance. Dupuis, Jacobs....442–6; disc. 1125
Analysis, Effects of Thermal Characteristics of Aircraft Generators on Load. Rogers....819–24
Analysis of Measurements, Functional. Kinnard 987–95
Analysis of Servomechanisms by Electrical Analogy, Dimensionless. Herwald, McCann..636–9; disc. 1132
Analyzer, A New Design for the A-C Network. Ryder, Boast....674–80; disc. 1162
Anti-icing of Aircraft Windshields, Electrical. McCrumm....786–91
Application and Performance of Electronic Exciters for Large A-C Generators. Langstaff, Vaughan, Lawrence....246–53; disc. 515
Application of Compandors to Telephone Circuits. Carter, Dickieson, Mitchell....1079–86
Application of Rototrol Regulators, Industrial. Harris....118–23
Application of Series Capacitors to Flash Welders, The. Deffenbaugh....686–7
Application of the Betatron to Practical Radiography. Girard, Adams....241–6; disc. 489
Application of the Ohm and Mho Principles to Protective Relays. Warrington....378–86; disc. 490
Application Ratings of Indoor Power Circuit Breakers Vikoren....768–73; disc. 1168
Applications of Thin Permalloy Tape in Wide-Band Telephone and Pulse Transformers. Ganz..177–83
Approach to Probability Problems in Electrical Engineering, A New. Adler, Miller..630–2; disc. 1118
Arc in an Air Blast, Dielectric Recovery by an A-C. Browne....169–76; disc. 507
Arc-Interruption Circuit Breakers for 400-Cycle Aircraft Electric-Power System, Pressure. Austin....58–60; disc. 487
Arc Starting Characteristics of D-C Welders With Reference to Electrode Freezing, Investigation of. Tyrner....97–9; disc. 511
Arc-Welding Transformers, Capacitor Stabilization of. Blankenbuehler, Lester....54–5
Arcing Ground Tests on a Normally Ungrounded 13-Kv 3-Phase Bus. Allen, Waldorf...298–306; disc. 498
Arcs in Air, Long 60-Cycle. Strom...113–18; disc. 504
Aspects of Polyphase Motor Design—The Design and Properties of the Magnetic Circuit, Some. Lloyd, Stone....812–18; disc. 1151
Aspects of Rectifier Installations, Inductive Co-ordination. (Committee Report)....417–36; disc. 1115
Asynchronous and Single-Phase Operation of Synchronous Machines. Rankin....1092–1102
Attenuating Transmission Line, The Solution of Transmission-Line Problems in the Case of. Glinski..46–9
Automatic Control of Large Synchronous Condensers. Brown....609–16
Automatic Control Systems, The Frequency Response of. Harris....539–46; disc. 1131
Automatic Oscillograph With a Memory, An. Zarem..150–4; disc. 514
Automatic Oscillographs, Fault Location and Relay Performance Analysis by. Dupuis, Jacobs....442–6; disc. 1125
(Automatic Stations) Carrier Supervisory Control of Pumping Station Over Power Cable. Derr, Keller, Hedke....699–705; disc. 1124
Auxiliaries, Protection of Powerhouse. (Committee Report)....746–51; disc. 1115
Auxiliary Controllers for Marine Service, Design of D-C. Schaelchlin....623–9
Azimuth Indicating System for Aircraft, An Improved. Lynch, Pfuntner....806–12

B

B-H Curve Tracer for Magnetic-Recording Wire, A. Long, McMullen....146–50; disc. 494
Back to Back, Formulas for Calculating the Inductance of Channels Located. Schwantz, Higgins...893–9
Balanced Recorder for Flight Testing and Spectroscopy, Electronically. Williams, Clark, Tarpley..205–08
Band Carrier Systems, A New Crystal Channel Filter for. Willis....134–8; disc. 490
Basic Design Principles for A-C Electric-Power Systems in Large Military Aircraft. Chappuis, Olmsted....12–17; disc. 487
(Basic Sciences) A Fractional Termination for Ladder Networks. LePage....530–6
(Basic Sciences) A New Approach to Probability Problems in Electrical Engineering. Adler, Miller....630–2; disc. 1118
(Basic Sciences) Dimensionless Analysis of Servomechanisms by Electrical Analogy. Herwald, McCann..636–9; disc. 1132
(Basic Sciences) Formulas for Calculating the Inductance of Channels Located Back to Back. Schwantz, Higgins....893–9
(Basic Sciences) Formulas for the Inductance of Coaxial Busses Comprised of Square Tubular Conductors. Messinger, Higgins....328–36; disc. 501
(Basic Sciences) Geometric Mean Distances for Rectangular Conductors. Dwight....536–8
(Basic Sciences) Negative Resistance Effects in Saturable Reactor Circuits. Manley, Peterson..870–81
(Basic Sciences) The Influence of the Concentration and Mobility of Ions on Dielectric Loss of Insulating Oils. Kang....403–07; disc. 1132
(Basic Sciences) The Use of Business Machines in Determining the Distribution of Load and Reactive Components in Power Line Networks. Jennings, Quinan....1045–6
Betatron to Practical Radiography, Application of the. Girard, Adams....241–6; disc. 489
Board of Directors, Report of the....1197–1216
Bone Receivers and Throat Microphones, Laboratory Method for Objective Testing of. Greibach..184–7
Braking Control of D-C Series Motors—Calculation of Stability Limit. Heumann, Smith..454–7; disc. 1130
Breakdown and Consequential Damages, Protection of Industrial Plants Against Insulation. Vaughan....592–6; disc. 1166
Breakers, A New Line of High-Voltage Outdoor Tank-Type Oil Circuit. Skeats, Rietz..224–31; disc. 502
Breakers, Application Ratings of Indoor Power Circuit. Vikoren....768–73; disc. 1168
Breakers, Field Tests of Interrupting Capacity of 138-Kv Oil Circuit. Buchanan, Floyd..199–204; disc. 503
Breakers for 400-Cycle Aircraft Electric-Power System, Pressure-Arc-Interruption Circuit. Austin....58–60; disc. 487
Breakers, The Development, Design, and Performance of Magnetic-Type Power Circuit. Linde, Wyman....386–93; disc. 510
Breakers up to 500,000 Kva, 15 Kv, Size Reduction and Rating Extension of Magnetic Air Circuit. Dickinson, Frink....220–3; disc. 510
Broad Band Carrier Systems, A New Crystal Channel Filter for. Willis....134–8; disc. 490
Bus, Arcing Ground Tests on a Normally Ungrounded 13-Kv 3-Phase. Allen, Waldorf..298–306; disc. 498
Bus, 4,370,000-Kva Short-Circuit Tests on Grand Coulee 230-Kv. Clagett, Leeds....729–35; disc. 1119
Business Machines in Determining the Distribution of Load and Reactive Components in Power Line Networks, The Use of. Jennings, Quinan....1045–6
Busses Comprised of Square Tubular Conductors, Formulas for the Inductance of Coaxial. Messinger, Higgins....328–36; disc. 501

C

Cable, Carrier Supervisory Control of Pumping Station Over Power. Derr, Keller, Hedke 699–705; disc. 1124
Cable for Induction Heating, Low Reactance Flexible. Zucker....848–52
Cable, Semiconducting Shielding for A-C Power. Merrell....605–09; disc. 1145
Cable Sheathing, F-3 Lead Alloy—An Improved. Hickernell, Snyder....563–9; disc. 1136
Cable, Short-Time Current Ratings for Aircraft Wire and Cable. Jones, Scott....644–8; disc. 1135
Cable Temperatures by Means of Reduced-Scale Models, Determination of. Gemant, Sticher....475–82; disc. 1128
Calculating the Inductance of Channels Located Back to Back, Formulas for. Schwantz, Higgins..893–9
Calculation of Stability Limit, Dynamic Braking Control of D-C Series Motors. Heumann, Smith....454–7; disc. 1130
Calculations on Polyphase Reluctance Motors—Synchronous Motors Without Field Excitation, Performance. Trickey....191–3

Pages 483–520 comprise the June 1946 "Supplement to Electrical Engineering—Transactions Section"; pages 861–1196 the December 1946 Supplement; pages beyond 1196 appear only in the 1946 Transactions volume.

Calender Train, Co-ordinated Electric Drive for a Rubber. John, Knapp, Mosteller...128–34; disc. 492

Capacitor-Compensated Transmission System, Characteristics of a 400-Mile 230-Kv Series-. Hoard...1102–14; disc. 1178

Capacitor Discharge Welding Transformers, Design and Measurement of. Dietz, Stein....154–9; disc. 512

Capacitor Protective Device, New Series. Marbury, Owens....142–6; disc. 511

Capacitor Stabilization of Arc-Welding Transformers. Blankenbuehler, Lester....54–5

Capacitors for Carrier Telephone Systems, Mica. Christopher, Kater....670–4; disc. 1116

Capacitors to Flash Welders, The Application of Series. Deffenbaugh....686–7

Capacity of 138-Kv Oil Circuit Breakers, Field Tests of Interrupting. Buchanan, Floyd..199–204; disc. 503

Capacity, Rectifier. Herskind, Steiner....667–70

Carbon-Pile Speed Governor, A. Button....4–7

Carrier-Current Equipment, Field Tests on Power-Line. Miller, Prud'Homme....824–7; disc. 1177

Carrier Supervisory Control of Pumping Station Over Power Cable. Derr, Keller, Hedke....699–705; disc. 1124

Carrier Systems, A New Crystal Channel Filter for Broad Band. Willis....134–8; disc. 490

Carrier Telephone Systems, Mica Capacitors for. Christopher, Kater....670–4; disc. 1116

Cast Rotor Testing by Test Stator Method, Die. Trickey....139–41; disc. 483

Ceramic Dielectrics at Elevated Temperatures, The Electrical Performance of. Frey, Jesatko....911–20; disc. 1126

Channel Filter for Broad Band Carrier Systems, A New Crystal. Willis....134–8; disc. 490

Channels Located Back to Back, Formulas for Calculating the Inductance of. Schwantz, Higgins...893–9

Characteristics of a 400-Mile 230-Kv Series-Capacitor-Compensated Transmission System. Hoard....1102–14; disc. 1178

Characteristics of Aircraft Generators on Load Analysis, Effects of Thermal. Rogers....819–24

Characteristics of D-C Generators, The Short-Circuit. Frost....394–402; disc. 484

Characteristics of D-C Welders With Reference to Electrode Freezing, Investigation of Arc Starting. Tyrner....97–9; disc. 511

Characteristics of Resistance Welding Machines, Influence of Magnetic Materials on the Welding. Riley, Smith....852–60; disc. 1160

Characteristics of Resistance Welding Transformers. Murray, Jones....726–8; disc. 1152

Charges, Induction Heating of Long Cylindrical. Storm....369–77

Charging, All-Electric Gun. Rohn....1–4

Circuit Breakers, A New Line of High-Voltage Outdoor Tank-Type Oil. Skeats, Rietz...224–31; disc. 502

Circuit Breakers, Application Ratings of Indoor Power. Vikoren....768–73; disc. 1168

Circuit Breakers, Field Tests of Interrupting Capacity of 138-Kv Oil. Buchanan, Floyd....199–204; disc. 503

Circuit Breakers for 400-Cycle Aircraft Electric-Power System, Pressure-Arc-Interruption. Austin....58–60; disc. 487

Circuit Breakers, The Development, Design, and Performance of Magnetic-Type Power. Linde, Wymann....386–93; disc. 510

Circuit Breakers up to 500,000 Kva, 15 Kv, Size Reduction and Rating Extension of Magnetic Air. Dickinson, Frink....220–3; disc. 510

Circuit Characteristics of D-C Generators, The Short-. Frost....394–402; disc. 484

Circuit Cushioning of Gas-Filled Grid-Controlled Rectifiers. Edwards, Smith....640–3; disc. 1131

Circuit, Some Aspects of Polyphase Motor Design—The Design and Properties of the Magnetic. Lloyd, Stone....812–18; disc. 1151

Circuits, A New Electronic Timing Relay for Reducing Outages on Power. Dougy....407–11

Circuits, Application of Compandors to Telephone. Carter, Dickieson, Mitchell....1079–86

Circuits, Electrical Measurements on Aircraft-Engine Ignition. Berkey....49–53

Circuits in Servomechanisms, Parallel. Marcy....521–9; disc. 1128

Circuits, Negative Resistance Effects in Saturable Reactor. Manley, Peterson....870–81

Circuits, Sensitive Ground Relay Protection for Complex Distribution. Hunt....765–8; disc. 1180

Coaxial Busses Comprised of Square Tubular Conductors, Formulas for the Inductance of. Messinger, Higgins....328–36; disc. 501

Coils for Cylindrical Magnetic Loads, Design of Induction Heating. Vaughan, Williamson....887–92; disc. 1165

Coils, Silicone-Resin-Treated Magnet. Moses, Torok...412–16; disc. 1184

Combined Light and Power Systems for Industrial Plants. Beeman....76–83

(Committee Report) Inductive Co-ordination Aspects of Rectifier Installations....417–36; disc. 1115

(Committee Report) Lightning Performance of 220-Kv Transmission Lines. Part II....70–6; disc. 499

(Committee Report) Low-Current-Secondary Current Transformers....649–50

(Committee Report) Protection of Powerhouse Auxiliaries....746–51; disc. 1115

(Communication) A B-H Curve Tracer for Magnetic-Recording Wire. Long, McMullen....146–50; disc. 494

(Communication) A Multichannel Microwave Radio Relay System. Black, Beyer, Grieser, Polkinghorn....798–806

(Communication) A New Crystal Channel Filter for Broad Band Carrier Systems. Willis....134–8; disc. 490

(Communication) A New Wire Recorder Head Design. Long....216–20; disc. 495

(Communication) A Tunable Rejection Filter. Taylor....263–7; disc. 490

(Communication) Air-borne Radar for Navigation and Obstacle Detection. Jensen, Arnett....307–13; disc. 491

(Communication) Application of Compandors to Telephone Circuits. Carter, Dickieson, Mitchell....1079–86

(Communication) Applications of Thin Permalloy Tape in Wide-Band Telephone and Pulse Transformers. Ganz....177–83

(Communication) Electronic Regeneration of Teleprinter Signals. Wilder....34–40

(Communication) Factors Affecting the Range of Radar Sets. Quarles, Breazeale....546–8

(Communication) Inertia Throat Microphones. Greibach, Pacent....187–91

(Communication) Laboratory Method for Objective Testing of Bone Receivers and Throat Microphones. Greibach....184–7

(Communication) Marine Radar for Peacetime Use. Lynn, Winn....271–3

(Communication) Phonograph Reproducer Design. Bachman....159–62

(Communication) Properties and Uses of Thermistors—Thermally Sensitive Resistors. Becker, Green, Pearson....711–25

(Communication) Radar Systems Considerations. Quarles....209–15

(Communication) Radio Telemetering for Testing Aircraft in Flight. Frederick....861–70

(Communication) Shoran Precision Radar. Seeley...232–40

(Communication) Signal and Noise Levels in Magnetic Tape Recording. Wooldridge...343–52; disc. 495

(Communication) Techniques and Facilities for Microwave Radar Testing. Green, Fisher, Ferguson...274–90

(Communication) The Solution of Transmission-Line Problems in the Case of Attenuating Transmission Line. Glinski....46–9

(Communication) Transmission Rating of Telephone Systems. Codd....694–8; disc. 1123

(Communications) Mica Capacitors for Carrier Telephone Systems. Christopher, Kater....670–4; disc. 1116

Communications, Systems Development of Military. Putnam....757–61; disc. 1160

Commutating Reactors for Rectifiers, Nonlinear. Schmidt....654–6

Commutator Regulator for Speed Control, The Polyphase. Conrad, Brooks, Fellers...321–8; disc. 484

Compandors to Telephone Circuits, Application of. Carter, Dickieson, Mitchell....1079–86

Comparison of Railway Motive Power for Operations in the Pacific Northwest. Martin..1054–65; disc. 1189

Compensated A-C Ammeters and Voltmeters, Frequency. Whittenton, Wilkinson....761–4

Compensated Transmission System, Characteristics of a 400-Mile 230-Kv Series-Capacitor-. Hoard....1102–14; disc. 1178

Complex Distribution Circuits, Sensitive Ground Relay Protection for. Hunt....765–8; disc. 1180

Components in Power Line Networks, The Use of Business Machines in Determining the Distribution of Load and Reactive. Jennings, Quinan...1045–6

Concentration and Mobility of Ions on Dielectric Loss of Insulating Oils, The Influence of the. Kang....403–07; disc. 1132

Condensers and Generators, The Development of Modern Excitation Systems for Synchronous. Porter, Kinghorn....1020–7; disc. 1156

Condensers, Automatic Control of Large Synchronous. Brown....609–16

Conductor Size According to Cost of Resistance Loss, Formulas for. Dwight....22–5; disc. 497

Conductors, Co-ordination of Insulation and Spacing of Transmission Line. Lewis....690–4; disc. 1142

Conductors, Formulas for the Inductance of Coaxial Busses Comprised of Square Tubular. Messinger, Higgins....328–36; disc. 501

Conductors, Geometric Mean Distances for Rectangular. Dwight....536–8

Constants at Low Speeds, Rotating Electric Machine Time. Concordia....882–7

Contact Resistance in Spot Welding, Measurement and Effect of. Wyant....26–33; disc. 513

Control, and Cooling of Ignitron Tubes, Excitation. Herskind, Remscheid....632–5

Control and Protection of Aircraft D-C Power Systems. Austin....741–5; disc. 1170

Control for Multicolor Printing, Electronic Register. Cockrell....617–22; disc. 1117

Control of D-C Series Motors—Calculation of Stability Limit, Dynamic Braking. Heumann, Smith....454–7; disc. 1130

Control of Frequency Converter Sets for Testing Aircraft Models, Electronic. Heumann, Strong...931–9

Control of Large Synchronous Condensers, Automatic. Brown....609–16

Control of Pumping Station Over Power Cable, Carrier Supervisory. Derr, Keller, Hedke....699–705; disc. 1124

Control of 30,000-Kva Hydroelectric Plant, Supervisory. Bohner, Maness....337–42

Control Problems, Diesel-Electric Synchronous Motor Ship Drives—Propulsion. Frisch....660–6

Control Systems, The Frequency Response of Automatic. Harris....539–46; disc. 1131

Control, The Polyphase Commutator Regulator for Speed. Conrad, Brooks, Fellers..321–8; disc. 484

Control Transformer System, Electrical Accuracy of Selsyn Generator. Chestnut....570–6; disc. 1118

Controllers for Marine Service, Design of D-C Auxiliary. Schaelchlin....623–9

Converter Sets for Testing Aircraft Models, Electronic Control of Frequency. Heumann, Strong..931–9

Cooling of Ignitron Tubes, Excitation, Control, and. Herskind, Remscheid....632–5

Co-ordinated Electric Drive for a Rubber Calender Train. John, Knapp, Mosteller..128–34; disc. 492

Co-ordination Aspects of Rectifier Installations, Inductive. (Committee Report)....417–36; disc. 1115

Co-ordination of Insulation and Spacing of Transmission Line Conductors. Lewis...690–4; disc. 1142

Cores Operating Above Saturation Density, Peak Voltages Induced by Accelerated Flux Reversal in Reactor. Specht, Wentz....254–63

Cornell Variable Density Wind Tunnel, Electric Equipment for. Clymer, de Ferranti....554–63

Cost of Resistance Loss, Formulas for Conductor Size According to. Dwight....22–5; disc. 497

Criteria for Current-Limiting Power Fuses—I, Performance. Schuck....1028–34; disc. 1191

Criteria for Current-Limiting Power Fuses—II, Performance. Boehne....1034–45; disc. 1191

Crossarms, The Preservative Treatment of Various Species for Poles and. MacLean....549–54

Crystal Channel Filter for Broad Band Carrier Systems, A New. Willis....134–8; disc. 490

Current and Torque of D-C Machines on Short Circuit. Linville....956–65; disc. 1144

Current Equipment, Field Tests on Power-Line Carrier-. Miller, Prud'Homme....824–7; disc. 1177

Current-Limiting Power Fuses—I, Performance Criteria for. Schuck....1028–34; disc. 1191

Current-Limiting Power Fuses—II, Performance Criteria for. Boehne....1034–45; disc. 1191

Current Measuring Device, Fault-. Lantz....839–43

Current Ratings for Aircraft Wire and Cable, Short-Time. Jones, Scott....644–8; disc. 1135

Current-Secondary Current Transformers, Low-. (Committee Report)....649–50

Currents, Dangerous Electric. Dalziel....579–85; disc. 1123

Currents, The Measurement of Large Varying. Johnson....8–11; disc. 513

Curve Tracer for Magnetic-Recording Wire, A B-H. Long, McMullen....146–50; disc. 494

Cushioning of Gas-Filled Grid-Controlled Rectifiers Circuit. Edwards, Smith....640–3; disc. 1131

Cylindrical Charges, Induction Heating of Long. Storm....369–77

Cylindrical Magnetic Loads, Design of Induction Heating Coils for. Vaughan, Williamson....887–92; disc. 1165

D

Damages, Protection of Industrial Plants Against Insulation Breakdown and Consequential. Vaughan...592–6; disc. 1166

Dangerous Electric Currents. Dalziel....579–85; disc. 1123

D-C Auxiliary Controllers for Marine Service, Design of. Schaelchlin....623–9

D-C Generators, The Short-Circuit Characteristics of. Frost....394–402; disc. 484

D-C Machines, Factors Affecting Insulation Resistance of Large. Johnson, Weil....705–10; disc. 1194

D-C Machines on Short Circuit, Current and Torque of. Linville....956–65; disc. 1144
D-C Power Systems, Control and Protection of Aircraft. Austin....741–5; disc. 1170
D-C Series Motors—Calculation of Stability Limit, Dynamic Braking Control of. Heumann, Smith....454–7; disc. 1130
D-C Testing of Rubber-Insulated Wire, High Voltage. Eddy, Fenn....576–8; disc. 1126
D-C Welders With Reference to Electrode Freezing, Investigation of Arc Starting Characteristics of. Tyrner....97–9; disc. 511
Demand-Meter Testing Techniques, Thermal-. Lynch, Douglass....124–8; disc. 514
Density, Peak Voltages Induced by Accelerated Flux Reversal in Reactor Cores Operating Above Saturation. Specht, Wentz....254–63
Design, A New Wire Recorder Head. Long....216–20; disc. 495
Design and Measurements of Capacitor Discharge Welding Transformers. Dietz, Stein...154–9; disc. 512
Design, and Performance of Magnetic-Type Power Circuit Breakers, The Development. Linde, Wyman....386–93; disc. 510
Design for the A-C Network Analyzer, A New. Ryder, Boast....674–80; disc. 1162
Design of D-C Auxiliary Controllers for Marine Service. Schaelchlin....623–9
Design of Induction Heating Coils for Cylindrical Magnetic Loads. Vaughan, Williamson....887–92; disc. 1165
Design, Phonograph Reproducer. Bachman..159–62
Design Principles for A-C Electric-Power Systems in Large Military Aircraft, Basic. Chappuis, Olmsted....12–17; disc. 487
Design, Tennessee Valley Authority Hydroelectric Stations—Electrical and Mechanical. Hopkins, Petersen....920–31; disc. 1132
Design—The Design and Properties of the Magnetic Circuit, Some Aspects of Polyphase Motor. Lloyd, Stone....812–18; disc. 1151
Detection, Air-borne Radar for Navigation and Obstacle. Jensen, Arnett....307–13; disc. 491
Determination of Cable Temperatures by Means of Reduced-Scale Models. Gemant, Sticher....475–82; disc. 1128
Development, Design, and Performance of Magnetic-Type Power Circuit Breakers, The. Linde, Wyman....386–93; disc. 510
Development for Service to Hanford Plutonium Plant, Power System. Hoard, Curtin....773–8
Development of Military Communications, Systems. Putnam....757–61; disc. 1160
Development of Modern Excitation Systems for Synchronous Condensers and Generators, The. Porter, Kinghorn....1020–7; disc. 1156
Device, Fault-Current Measuring. Lantz....839–43
Die Cast Rotor Testing by Test Stator Method. Trickey....139–41; disc. 483
Dielectric Loss of Insulating Oils, The Influence of the Concentration and Mobility of Ions on. Kang....403–07; disc. 1132
Dielectric Recovery by an A-C Arc in an Air Blast. Browne....169–76; disc. 507
Dielectric Strength of Station and Line Insulation to Switching Surges. Bellaschi, Rademacher....1047–54; disc. 1173
Dielectrics at Elevated Temperatures, The Electrical Performance of Ceramic. Frey, Jesatko....911–20; disc. 1126
Diesel-Electric Drilling Rig Equipment. Rhea..447–53
Diesel-Electric Synchronous Motor Ship Drives—Propulsion Control Problems. Frisch....660–6
Differential Leakage of a Fractional-Slot Winding. Liwschitz....314–20
Dimensionless Analysis of Servomechanisms by Electrical Analogy. Herwald, McCann....636–9; disc. 1132
Discharge Welding Transformers, Design and Measurements of Capacitor. Dietz, Stein..154–9; disc. 512
Distance Ground Relays, Operating Experience With. Wolfe....458–62; disc. 1185
Distance Relay, The Mho. Hutchinson....353–60
Distances for Rectangular Conductors, Geometric Mean. Dwight....536–8
Distribution Circuits, Sensitive Ground Relay Protection for Complex. Hunt....765–8; disc. 1180
(Distribution) Determination of Cable Temperatures by Means of Reduced-Scale Models. Gemant, Sticher....475–82; disc. 1128
(Distribution) F-3 Lead Alloy—An Improved Cable Sheathing. Hickernell, Snyder..563–9; disc. 1136
Distribution of Load and Reactive Components in Power Line Networks. The Use of Business Machines in Determining the. Jennings, Quinan....1045–6
(Distribution) Semiconducting Shielding for A-C Power Cable. Merrell....605–09; disc. 1145
(Domestic and Commercial Applications) Specific Engineering Problems in Rural Electrification and Electroagriculture. Samuels...1065–73; disc. 1182
Double-Reduction Traction Motor, Modern. Greer....471–4
Drilling Rig Equipment, Modern Diesel-Electric. Rhea....447–53
Drive for a Resonant Fatigue Machine, Self-Excited Electromagnetic. Willson....1073–8
Drive for a Rubber Calender Train, Co-ordinated Electric. John, Knapp, Mosteller...128–34; disc. 492
Drive for Windup Reels, An Electronic. Puchlowski....585–91; disc. 1155
Driven Exciters for Turbine Alternators, Motor-. Bodine, Crary, Rankin....290–7; disc. 515
Drives—Propulsion Control Problems, Diesel-Electric Synchronous Motor Ship. Frisch....660–6
Dynamic Braking Control of D-C Series Motors—Calculation of Stability Limit. Heumann, Smith....454–7; disc. 1130

E

(Education) Teaching Electricity and Magnetism. Hessler....828–33
Effect of Altitude on Ventilation and Rating of Aircraft Electric Machines. Veinott....84–90; disc. 488
Effect of Contact Resistance in Spot Welding, Measurement and. Wyant....26–33; disc. 513
Effects in Saturable Reactor Circuits, Negative Resistance. Manley, Peterson....870–81
Effects of Thermal Characteristics of Aircraft Generators and Load Analysis. Rogers....819–24
Electric Currents, Dangerous. Dalziel....579–85; disc. 1123
Electric Drilling Rig Equipment, Modern Diesel. Rhea....447–53
Electric Drive for a Rubber Calender Train, Co-ordinated. John, Knapp, Mosteller....128–34; disc. 492
Electric Equipment for Cornell Variable Density Wind Tunnel. Clymer, de Ferranti....554–63
Electric Equipment, Moisture Equilibrium Between Gas Space and Fibrous Materials in Enclosed. Piper....791–7; disc. 1152
Electric Gun Charging, All. Rohn....1–4
Electric Machine Time Constants at Low Speeds, Rotating. Concordia....882–7
(Electric Machinery) Current and Torque of D-C Machines on Short Circuit. Linville....956–65; disc. 1144
(Electric Machinery) Die Cast Rotor Testing by Test Stator Method. Trickey....139–41; disc. 483
(Electric Machinery) Dielectric Strength of Station and Line Insulation to Switching Surges. Bellaschi, Rademacher....1047–54; disc. 1173
(Electric Machinery) Differential Leakage of a Fractional-Slot Winding. Liwschitz....314–20
(Electric Machinery) Electromechanical Transient Performance of Induction Motors. Weygandt. Charp....1000–09; disc. 1167
(Electric Machinery) Factors Affecting Insulation Resistance of Large D-C Machines. Johnson, Weil....705–10; disc. 1194
(Electric Machinery) 150,000 Horsepower Applied to Aeronautical Research. White....833–8
(Electric Machinery) Oscillations of a High-Voltage Secondary Winding. Boyajian....1010–20
(Electric Machinery) Performance Calculations on Polyphase Reluctance Motors—Synchronous Motors Without Field Excitation. Trickey...191–3
(Electric Machinery) Some Aspects of Polyphase Motor Design—The Design and Properties of the Magnetic Circuit. Lloyd, Stone....812–18; disc. 1151
(Electric Machinery) Shutdown Versus Hot-Spot Temperatures in Polyphase Induction Motors. Potter, Frohardt....56–8; disc. 483
(Electric Machinery) Temperature Limits for Short-Time Overloads for Oil-Insulated Neutral Grounding Reactors and Transformers—II. Montsinger, Clem....966–73; disc. 1155
(Electric Machinery) Temperature Rise of Water-Cooled Power Transformers. Meador....18–21
(Electric Machinery) The Polyphase Commutator Regulator for Speed Control. Conrad, Brooks, Fellers....321–8; disc. 484
(Electric Machinery) The Short-Circuit Characteristics of D-C Generators. Frost....394–402; disc. 484
(Electric Machinery) Transients in A-C Motors and Generators. Smith....61–9
Electric Machines, Effect of Altitude on Ventilation and Rating of Aircraft. Veinott....84–90; disc. 488
Electric-Power System, Pressure-Arc-Interruption Circuit Breakers for 400-Cycle Aircraft. Austin....58–60; disc. 487
Electric-Power Systems in Large Military Aircraft, Basic Design Principles for A-C. Chappuis, Olmsted....12–17; disc. 487
Electric Synchronous Motor Ship Drives—Propulsion Control Problems, Diesel-. Frisch....660–6
Electric System for Large Aircraft, Governor for Variable-Ratio Transmission Used in Developmental 400-Cycle. Desch, Garr, Hutton....194–8
(Electric Welding) The Application of Series Capacitors to Flash Welders. Deffenbaugh....686–9
Electrical Accuracy of Selsyn Generator-Control Transformer System. Chestnut....570–6; disc. 1118
Electrical Analogy, Dimensionless Analysis of Servomechanisms by. Herwald, McCann....636–9; disc. 1132
Electrical Analogy Methods Applied to Servomechanism Problems. McCann, Herwald, Kirschbaum....91–6; disc. 515
Electrical and Hydraulic Testing of Hydroelectric Units, Technique of. Floyd, Traill....163–9; disc. 493
Electrical and Mechanical Design, Tennessee Valley Authority Hydroelectric Stations—. Hopkins, Petersen....920–31; disc. 1132
Electrical Anti-Icing of Aircraft Windshields. McCrumm....786–91
Electrical Engineering, A New Approach to Probability Problems in. Adler, Miller....630–2; disc. 1118
Electrical Means, Stress Measurement by. Kern, Williams....100–07
Electrical Measurements on Aircraft-Engine Ignition Circuits. Berkey....49–53
Electrical Performance of Ceramic Dielectrics at Elevated Temperatures, The. Frey, Jesatko....911–20; disc. 1126
Electricity and Magnetism, Teaching. Hessler..828–33
Electroagriculture, Specific Engineering Problems in Rural Electrification and. Samuels....1065–73; disc. 1182
Electrochemical Installations, Maintenance of Rectifiers on Electrochemical. Housley, Hughes....436–41; disc. 1115
Electrode Freezing, Investigation of Arc Starting Characteristics of D-C Welders With Reference to. Tyrner....97–9; disc. 511
Electromagnetic Drive for a Resonant Fatigue Machine, Self-Excited. Willson....1073–8
Electromechanical Transient Performance of Induction Motors. Weygandt, Charp....1000–09; disc. 1167
Electronic Control of Frequency Converter Sets for Testing Aircraft Models. Heumann, Strong...931–9
Electronic Drive for Windup Reels, An. Puchlowski....585–91; disc. 1155
Electronic Exciters for Large A-C Generators, Application and Performance of. Langstaff, Vaughan, Lawrence....246–53; disc. 515
Electronic Frequency Meter and Speed Regulator, An. Levin....779–86; disc. 1181
Electronic Regeneration of Teleprinter Signals. Wilder....34–40
Electronic Register Control for Multicolor Printing. Cockrell....617–22; disc. 1117
Electronic Timing Relay for Reducing Outages on Power Circuits, A New. Dlouhy....407–11
Electronically Balanced Recorder for Flight Testing and Spectroscopy. Williams, Clark, Tarpley..205–08
(Electronics) A 400-Ampere Sealed Ignitron. Steiner, Price....680–5; disc. 1161
(Electronics) Application of the Betatron to Practical Radiography. Girard, Adams....241–6; disc. 489
(Electronics) Circuit Cushioning of Gas-Filled Grid-Controlled Rectifiers. Edwards, Smith....640–3; disc. 1131
(Electronics) Excitation, Control, and Cooling of Ignitron Tubes. Herskind, Remscheid....632–5
(Electronics) Frequency Performance of Thyratrons. Wittenberg....843–8
(Electronics) Fundamental Properties of the Vacuum Switch. Koller....597–604; disc. 1141
(Electronics) High Voltage Ignitron Rectifiers and Inverters for Railroad Service. Boyer, Hagensick....463–70
(Electronics) Inductive Co-ordination Aspects of Rectifier Installations. (Committee Report)....417–36; disc. 1115
(Electronics) Maintenance of Rectifiers on Electrochemical Installations. Housley, Hughes....436–41; disc. 1115
(Electronics) Nonlinear Commutating Reactors for Rectifiers. Schmidt....654–6
(Electronics) Rectifier Capacity. Herskind, Steiner....667–70
Elevated Temperatures, The Electrical Performance of Ceramic Dielectrics at. Frey, Jesatko....911–20; disc. 1126
Engine Ignition Circuits, Electrical Measurements on Aircraft-. Berkey....49–53
Engine-Synchronism Indicator for Aircraft, A Unique. Pearson....650–3
Engineering Problems in Rural Electrification and Electroagriculture, Specific. Samuels....1065–73; disc. 1182
Equilibrium Between Gas Space and Fibrous Materials in Enclosed Electric Equipment, Moisture. Piper....791–7; disc. 1152
Equipment, Field Tests on Power-Line Carrier-Current. Miller, Prud'Homme....824–7; disc. 1177
Equipment for Cornell Variable Density Wind Tunnel. Clymer, de Ferranti....554–63

Equipment, Modern Diesel-Electric Drilling Rig. Rhea....447–53
Equipment, Moisture Equilibrium Between Gas Space and Fibrous Materials in Enclosed Electric. Piper. ....791–7; disc. 1152
Excitation, Control, and Cooling of Ignitron Tubes. Herskind, Remscheid....632–5
Excitation, Performance Calculations on Polyphase Reluctance Motors—Synchronous Motors Without Field. Trickey....191–3
Excitation Systems for Large Synchronous Machines, Modern. McClure, Whittlesey, Hartman.... ....939–45; disc. 1148
Excitation Systems for Synchronous Condensers and Generators, The Development of Modern. Porter, Kinghorn....1020–7; disc. 1156
Excitation Systems, Long-Distance Power Transmission as Influenced by. Concordia, Crary, Maginniss... ....974–87; disc. 1175
Exciters for Large A-C Generators, Application and Performance of Electronic. Langstaff, Vaughan, Lawrence....246–53; disc. 515
Exciters for Turbine Alternators, Motor-Driven. Bodine, Crary, Rankin....290–7; disc. 515
Experience With Distance Ground Relays. Wolfe.... ....458–62; disc. 1185
Experience With Factory-Built Unit-Type Substations, Six Years'. Miller, Miller....751–6; disc. 1150
Extension of Magnetic Air Circuit Breakers up to 500,000 Kva, 15 Kv, Size Reduction and Rating. Dickinson, Frink....220–3; disc. 510

F

F-3 Lead Alloy—An Improved Cable Sheathing. Hickernell, Snyder....563–9; disc. 1136
Facilities for Microwave Radar Testing, Techniques and. Green, Fisher, Ferguson....274–90
Factors Affecting Insulation Resistance of Large D-C Machines. Johnson, Weil....705–10; disc. 1194
Factors Affecting the Range of Radar Sets. Quarles, Breazeale....546–8
Factory-Built Unit-Type Substations, Six Years' Experience With. Miller, Miller...751–6; disc. 1150
Fatigue Machine, Self-Excited Electromagnetic Drive for a Resonant. Willson....1073–8
Fault-Current Measuring Device. Lantz....839–43
Fault Location and Relay Performance Analysis by Automatic Oscillographs. Dupuis, Jacobs.... ....442–6; disc. 1125
Fibrous Materials in Enclosed Electric Equipment, Moisture Equilibrium Between Gas Space and. Piper.. ....791–9; disc. 1152
Field Excitation, Performance Calculations on Polyphase Reluctance Motors—Synchronous Motors Without. Trickey....191–3
Field Tests and Experience at York and Middletown, Pa., Linear Couplers—. Harder, Klemmer, Neidig....107–13
Field Tests of Interrupting Capacity of 138-Kv Oil Circuit Breakers. Buchanan, Floyd.... ....199–204; disc. 503
Field Tests on Power-Line Carrier-Current Equipment. Miller, Prud' Homme....824–7; disc. 1177
Filter, A Tunable Rejection. Taylor..263–7; disc. 490
Filter for Broad Band Carrier Systems, A New Crystal Channel. Willis....134–8; disc. 490
Flash Welders, The Application of Series Capacitors to. Deffenbaugh....686–7
Flexible Cable for Induction Heating, Low Reactance. Zucker....848–52
Flight Testing and Spectroscopy, Electronically Balanced Recorder for. Williams, Clark, Tarpley.. 205–08
Flux Reversal in Reactor Cores Operating Above Saturation Density, Peak Voltages Induced by Accelerated. Specht, Wentz....254–63
Formulas for Calculating the Inductance of Channels Located Back to Back. Schwantz, Higgins..893–9
Formulas for Conductor Size According to Cost of Resistance Loss. Dwight....22–5; disc. 497
Formulas for the Inductance of Coaxial Busses Comprised of Square Tubular Conductors. Messinger, Higgins....328–36; disc. 501
400-Ampere Sealed Ignitron, A. Steiner, Price.... ....680–5; disc. 1161
400-Mile 230-Kv Series-Capacitor-Compensated Transmission System, Characteristics of a. Hoard.... ....1102–14; disc. 1178
Fractional-Slot Winding, Differential Leakage of a. Liwschitz....314–20
Fractional Termination for Ladder Networks, A. LePage....530–6
Freezing, Investigation of Arc Starting Characteristics of D-C Welders With Reference to Electrode. Tyrner. ....97–9; disc. 511
Frequency Compensated A-C Ammeters and Voltmeters. Whittenton, Wilkinson....761–4
Frequency Converter Sets for Testing Aircraft Models, Electronic Control of. Heumann, Strong...931–9
Frequency Meter and Speed Regulator, An Electronic. Levin....779–86; disc. 1181
Frequency Performance of Thyratrons. Wittenberg... 843–8
Frequency Response of Automatic Control Systems. Harris....539–46; disc. 1131
Functional Analysis of Measurements. Kinnard... 987–95
Fundamental Properties of the Vacuum Switch. Koller....597–604; disc. 1141
Fuses—I, Performance Criteria for Current-Limiting Power. Schuck....1028–34; disc. 1191
Fuses—II, Performance Criteria for Current-Limiting Power. Boehne....1034–45; disc. 1191

G

Gas-Filled Grid-Controlled Rectifiers, Circuit Cushioning of. Edwards, Smith....640–3; disc. 1131
Gas Space and Fibrous Materials in Enclosed Electric Equipment, Moisture Equilibrium Between. Piper. ....791–7; disc. 1152
Generating Units on the 2,000,000-Horsepower Saguenay System, Improvements in Performance of Hydroelectric. Lawton....900–10; disc. 1187
Generator-Control Transformer System, Electrical Accuracy of Selsyn. Chestnut....570–6; disc. 1118
Generators, Application and Performance of Electronic Exciters for Large A-C. Langstaff, Vaughan, Lawrence....246–53; disc. 515
Generators on Load Analysis, Effects of Thermal Characteristics of Aircraft. Rogers....819–24
Generators. The Development of Modern Excitation Systems for Synchronous Condensers and. Porter, Kinghorn....1020–7; disc. 1156
Generators, The Short-Circuit Characteristics of D-C. Frost....394–402; disc. 484
Generators, Transients in A-C Motors and. Smith.. 61–9
Geometric Mean Distances for Rectangular Conductors. Dwight....536–8
Governor, A Carbon-Pile Speed. Button....4–7
Governor for Variable-Ratio Transmission Used in Developmental 400-Cycle Electric System for Large Aircraft. Desch, Garr, Hutton....194–8
Grand Coulee 230-Kv Bus, 4,370,000-Kva Short-Circuit Tests on. Clagett, Leeds...729–35; disc. 1119
Grid-Controlled Rectifiers, Circuit Cushioning of Gas-Filled. Edwards, Smith....640–3; disc. 1131
Ground Relay Protection for Complex Distribution Circuits, Sensitive. Hunt....765–8; disc. 1180
Ground Relays, Operating Experience With Distance. Wolfe....458–62; disc. 1185
Ground Tests on a Normally Ungrounded 13-Kv 3-Phase Bus, Arcing. Allen, Waldorf.... ....298–306; disc. 498
Gun Charging, All-Electric. Rohn....1–4

H

Hanford Plutonium Plant, Power System Development for Service to. Hoard, Curtin....773–8
Head Design, A New Wire Recorder. Long.... ....216–20; disc. 495
Heating Coils for Cylindrical Magnetic Loads, Design of Induction. Vaughan, Williamson.... ....887–92; disc. 1165
Heating, Low Reactance Flexible Cable for Induction. Zucker....848–52
Heating of Long Cylindrical Charges, Induction. Storm....369–77
High Altitudes, Investigation of Porcelain Insulators at. Fields, Cadwell....656–60
High Vacuum Leak Testing With the Mass Spectrometer. Worcester, Doughty...946–55; disc. 1170
High Voltage D-C Testing of Rubber-Insulated Wire. Eddy, Fenn....576–8; disc. 1126
High Voltage Ignitron Rectifiers and Inverters for Railroad Service. Boyer, Hagensick....463–70
High-Voltage Outdoor Tank-Type Oil Circuit Breakers, A New Line of. Skeats, Rietz..224–31; disc. 502
High-Voltage Secondary Winding, Oscillations of a. Boyajian....1010–20
Horsepower Applied to Aeronautical Research, 150,000. White....833–9
Hot-Spot Temperatures in Polyphase Induction Motors, Shutdown Versus. Potter, Frohardt.... ....56–8; disc. 483
Hydraulic Testing of Hydroelectric Units, Technique of Electrical and. Floyd, Traill 163–9; disc. 493....
Hydroelectric Generating Units on the 2,000,000-Horsepower Saguenay System, Improvements in Performance of. Lawton....900–10; disc. 1187
Hydroelectric Plant, Supervisory Control of 30,000-Kva. Bohner, Maness....337–42
Hydroelectric Stations—Electrical and Mechanical Design, Tennessee Valley Authority. Hopkins, Petersen....920–31; disc. 1132
Hydroelectric Units, Technique of Electrical and Hydraulic Testing of. Floyd, Traill..163–9; disc. 493

I

Ignition Circuits, Electrical Measurements on Aircraft-Engine. Berkey....49–53
Ignitron, A 400-Ampere Sealed. Steiner, Price.... ....680–5; disc. 1161
Ignitron Rectifiers and Inverters for Railroad Service, High Voltage. Boyer, Hagensick....463–70
Ignitron Tubes, Excitation, Control, and Cooling of. Herskind, Remscheid....632–5
Improved Azimuth Indicating System for Aircraft, An. Lynch, Pfuntner....806–12
Improved Cable Sheathing, F-3 Lead Alloy—An. Hickernell, Snyder....563–9; disc. 1136
Improvements in Performance of Hydroelectric Generating Units on the 2,000,000-Horsepower Saguenay System. Lawton....900–10; disc. 1187
Indicating System for Aircraft, An Improved Azimuth. Lynch, Pfuntner....806–12
Indicator for Aircraft, A Unique Engine-Synchronism. Pearson....650–3
Indoor Power Circuit Breakers, Application Ratings of. Vikoren....768–73; disc. 1168
Induced Potentials, Protection of Pilot Wires From. Killen, Law....267–70
Inductance of Channels Located Back to Back, Formulas for Calculating the. Schwantz, Higgins....893–9
Inductance of Coaxial Busses Comprised of Square Tubular Conductors, Formulas for the. Messinger, Higgins....328–36; disc. 501
Induction Heating Coils for Cylindrical Magnetic Loads, Design of. Vaughan, Williamson.... ....887–92; disc. 1165
Induction Heating, Low Reactance Flexible Cable for. Zucker....848–52
Induction Heating of Long Cylindrical Charges. Storm....369–77
Induction Motors, Electromechanical Transient Performance of. Weygandt, Charp.... ....1000–09; disc. 1167
Induction Motors, Shutdown Versus Hot-Spot Temperatures in Polyphase. Potter, Frohardt.... ....56–8; disc. 483
Inductive Co-ordination Aspects of Rectifier Installations. (Committee Report)....417–36; disc. 1115
Industrial Application of Rototrol Regulators. Harris.. 118–23
(Industrial Control Devices) An Electronic Drive for Windup Reels. Puchlowski....585–91; disc. 1155
(Industrial Control Devices) Dynamic Braking Control of D-C Series Motors—Calculation of Stability Limit. Heumann, Smith....454–7; disc. 1130
(Industrial Control Devices) Electrical Accuracy of Selsyn Generator-Control Transformer System. Chestnut....570–6; disc. 1118
(Industrial Control Devices) Electronic Control of Frequency Converter Sets for Testing Aircraft Models. Heumann, Strong....931–9
(Industrial Control Devices) Electronic Register Control for Multicolor Printing. Cockrell.... ....617–22; disc. 1117
(Industrial Control Devices) Fundamental Properties of the Vacuum Switch. Koller...597–604; disc. 1141
(Industrial Control Devices) Silicone-Resin-Treated Magnet Coils. Moses, Torok..412–16; disc. 1184
Industrial Plants Against Insulation Breakdown and Consequential Damages, Protection of. Vaughan. ....592–6; disc. 1166
Industrial Plants, Combined Light and Power Systems for. Beeman....76–83
(Industrial Power Applications) Self-Excited Electromagnetic Drive for a Resonant Fatigue Machine. Willson....1073–8
Inertia Throat Microphones. Greibach, Pacent..187–91
Influence of Magnetic Materials on the Welding Characteristics of Resistance Welding Machines. Riley, Smith....852–60; disc. 1160
Influence of the Concentration and Mobility of Ions on Dielectric Loss of Insulating Oils, The. Kang.... ....403–07; disc. 1132
Installations, Inductive Co-ordination Aspects of Rectifier. (Committee Report)....417–36; disc. 1115
Installations, Maintenance of Rectifiers on Electrochemical. Housley, Hughes....435–41; disc. 1115
(Instruments) A New Design for the A-C Network Analyzer. Ryder, Boast....674–80; disc. 1162
(Instruments) An Automatic Oscillograph With a Memory. Zarem....150–4; disc. 514
(Instruments) An Electronic Frequency Meter and Speed Regulator. Levin....779–86; disc. 1181
(Instruments) An Oscillograph for Recording Transient Recovery Voltages. Hoover...1086–91; disc. 1174
(Instruments) Electrical Analogy Methods Applied to Servomechanism Problems. McCann, Herwald, Kirschbaum....91–6; disc. 515
(Instruments) Electronically Balanced Recorder for Flight Testing and Spectroscopy. Williams, Clark, Tarpley....205–08

(Instruments) Frequency Compensated A-C Ammeters and Voltmeters. Whittendon, Wilkinson..761–4
(Instruments) High Vacuum Leak Testing With The Mass Spectrometer. Worcester, Doughty.....946–55; disc. 1170
(Instruments) Parallel Circuits in Servomechanisms. Marcy.....521–9; disc. 1128
(Instruments) Peak Voltages Induced by Accelerated Flux Reversal in Reactor Cores Operating Above Saturation Density. Specht, Wentz.....254–63
(Instruments) Radio Telemetering for Testing Aircraft in Flight. Frederick.....861–70
(Instruments) The Frequency Response of Automatic Control Systems. Harris.....539–46; disc. 1131
(Instruments) Thermal-Demand-Meter Testing Techniques. Lynch, Douglass.....124–8; disc. 514
Insulated Wire, High Voltage D-C Testing of Rubber-. Eddy, Fenn.....576–8; disc. 1126
Insulating Oils, The Influence of the Concentration and Mobility of Ions on Dielectric Loss of. Kang.....403–07; disc. 1132
Insulation and Spacing of Transmission Line Conductors, Co-ordination of. Lewis..690–4; disc. 1142
Insulation Breakdown and Consequential Damages, Protection of Industrial Plants Against. Vaughan.....592–6; disc. 1166
Insulation Resistance of Large D-C Machines, Factors Affecting. Johnson, Weil.....705–10; disc. 1194
Insulation to Switching Surges, Dielectric Strength of Station and Line. Bellaschi, Rademacher.....1047–54; disc. 1173
Insulators at High Altitudes, Investigation of Porcelain. Fields, Cadwell.....656–60
Interrupting Capacity of 138-Kv Oil Circuit Breakers, Field Tests of. Buchanan, Floyd.....199–204; disc. 503
Interruption Circuit Breakers for 400-Cycle Aircraft Electric-Power System, Pressure-Arc-. Austin.....58–60; disc. 487
Inverters for Railroad Service, High Voltage Ignitron Rectifiers and. Boyer, Hagensick.....463–70
Investigation of Arc Starting Characteristics of D-C Welders With Reference to Electrode Freezing. Tyrner.....97–9; disc. 511
Investigation of Porcelain Insulators at High Altitudes. Fields, Cadwell.....656–60
Ions on Dielectric Loss of Insulating Oils, The Influence of the Concentration and Mobility of. Kang.....403–07; disc. 1132

L

Laboratory Method for Objective Testing of Bone Receivers and Throat Microphones. Greibach.....184–7
Ladder Networks, A Fractional Termination for. LePage.....530–6
Lead Alloy—An Improved Cable Sheathing, F-3. Hickernell, Snyder.....563–9; disc. 1136
Leakage of a Fractional-Slot Winding, Differential. Liwschitz.....314–20
Leak Testing With the Mass Spectrometer, High Vacuum. Worcester, Doughty..946–55; disc. 1170
Light and Power Systems for Industrial Plants, Combined. Beeman.....76–83
Lightning Performance of 220-Kv Transmission Lines. Part II. (Committee Report)...70–6; disc. 499
Line Conductors, Co-ordination of Insulation and Spacing of Transmission. Lewis....690–4; disc. 1142
Line Insulation to Switching Surges, Dielectric Strength of Station and. Bellaschi, Rademacher.....1047–54; disc. 1173
Line Problems in the Case of Attenuating Transmission Line, The Solution of Transmission-. Glinski..46–9
Linear Couplers—Field Tests and Experience at York and Middletown, Pa. Harder, Klemmer, Neidig..107–13
Lines, Lightning Performance of 220-Kv Transmission. Part II. (Committee Report)....70–6; disc. 499
Load Analysis, Effects of Thermal Characteristics of Aircraft Generators on. Rogers.....819–24
Load and Reactive Components in Power Line Networks, The Use of Business Machines in Determining the Distribution of. Jennings, Quinan.....1045–6
Loads, Design of Induction Heating Coils for Cylindrical Magnetic. Vaughan, Williamson.....887–92; disc. 1165
Location and Relay Performance Analysis by Automatic Oscillographs, Fault. Dupuis, Jacobs.....442–6; disc. 1125
Long-Distance Power Transmission as Influenced by Excitation Systems. Concordia, Crary, Maginniss.....974–87; disc. 1175
Long 60-Cycle Arcs in Air. Strom...113–18; disc. 504
Loss, Formulas for Conductor Size According to Cost of Resistance. Dwight.....22–5; disc. 497
Loss of Insulating Oils, The Influence of the Concentration and Mobility of Ions on Dielectric. Kang.....403–07; disc. 1132
Low-Current-Secondary Current Transformers. (Committee Report).....649–50
Low Reactance Flexible Cable for Induction Heating. Zucker.....848–52
Low Speeds, Rotating Electric Machine Time Constants at. Concordia.....882–7

M

Machine, Self-Excited Electromagnetic Drive for a Resonant Fatigue. Willson.....1073–8
Machine Time Constants at Low Speeds, Rotating Electric. Concordia.....882–7
Machines, Asynchronous and Single-Phase Operation of Synchronous. Rankin.....1092–1102
Machines, Effect of Altitude on Ventilation and Rating of Aircraft Electric. Veinott.....84–90; disc. 488
Machines, Factors Affecting Insulation Resistance of Large D-C. Johnson, Weil.....705–10; disc. 1194
Machines in Determining the Distribution of Load and Reactive Components in Power Line Networks, The Use of Business. Jennings, Quinan.....1045–6
Machines, Influence of Magnetic Materials on the Welding Characteristics of Resistance Welding. Riley, Smith.....852–60; disc. 1160
Machines, Modern Excitation Systems for Large Synchronous. McClure, Whittlesey, Hartman.....939–45; disc. 1148
Machines on Short Circuit, Current and Torque of D-C. Linville.....956–65; disc. 1144
Magnet Coils, Silicone-Resin-Treated. Moses, Torok..412–16; disc. 1184
Magnetic Air Circuit Breakers up to 500,000 Kva, 15 Kv, Size Reduction and Rating Extension of. Dickinson, Frink.....220–3; disc. 510
Magnetic Circuit, Some Aspects of Polyphase Motor Design—The Design and Properties of the. Lloyd, Stone.....812–18; disc. 1151
Magnetic Loads, Design of Induction Heating Coils for Cylindrical. Vaughan, Williamson.....887–92; disc. 1165
Magnetic Materials on the Welding Characteristics of Resistance Welding Machines, Influence of. Riley, Smith.....852–60; disc. 1160
Magnetic-Recording Wire, A B-H Curve Tracer for. Long, McMullen.....146–50; disc. 494
Magnetic Tape Recording, Signal and Noise Levels in. Wooldridge.....343–52; disc. 495
Magnetic-Type Power Circuit Breakers, The Development, Design, and Performance of. Linde, Wyman.....386–93; disc. 510
Magnetism, Teaching Electricity and. Hessler..828–33
Maintenance of Rectifiers on Electrochemical Installations. Housley, Hughes.....436–41; disc. 1115
Marine Radar for Peacetime Use. Lynn, Winn..271–3
Marine Service, Design of D-C Auxiliary Controllers for. Schaelchlin.....623–9
(Marine Transportation) Diesel-Electric Synchronous Motor Ship Drives-Propulsion Control Problems. Frisch.....660–6
Mass Spectrometer, High Vacuum Leak Testing With the. Worcester, Doughty.....946–55; disc. 1170
Materials on the Welding Characteristics of Resistance Welding Machines, Influence of Magnetic. Riley, Smith.....852–60; disc. 1160
Measuring Device, Fault-Current. Lantz.....839–43
Measurement and Effect of Contact Resistance in Spot Welding. Wyant.....26–33; disc. 513
Measurement by Electrical Means, Stress. Kern, Williams.....100–07
Measurement of Large Varying Currents, The. Johnson.....8–11; disc. 513
Measurements, Functional Analysis of. Kinnard.....987–95
Measurements of Capacitor Discharge Welding Transformers, Design and. Dietz, Stein.....154–9; disc. 512
Measurements on Aircraft-Engine Ignition Circuits, Electrical. Berkey.....49–53
(Measurements) Parallel Circuits in Servo- Mechanisms. Marcy.....521–9; disc. 1128
Mechanical Design. Tennessee Valley Authority Hydroelectric Stations—Electrical and. Hopkins, Petersen.....920–31; disc. 1132
Memory, An Automatic Oscillograph With a. Zarem..150–4; disc. 514
Metal-Clad Unit-Type Switchgear for 33-Kv Service. Kreger.....360–8; disc. 509
Meter and Speed Regulator, An Electronic Frequency. Levin.....779–86; disc. 1181
Meter Testing Techniques, Thermal-Demand. Lynch, Douglas.....124–8; disc. 514
Method, Die Cast Rotor Testing by Test Stator. Trickey.....139–41; disc. 483
Method for Objective Testing of Bone Receivers and Throat Microphones, Laboratory. Greibach...184–7
Methods Applied to Servomechanism Problems, Electrical Analogy. McCann, Herwald, Kirschbaum..91–6; disc. 515
Mho Distance Relay, The. Hutchinson.....353–60
Mho Principles to Protective Relays, Application of the Ohm and. Warrington.....378–86; disc. 490
Mica Capacitors for Carrier Telephone Systems. Christopher, Kater.....670–4; disc. 1116
Microphones, Inertia Throat. Greibach, Pacent..187–91
Microphones, Laboratory Method for Objective Testing of Bone Receivers and Throat. Greibach...184–7
Microwave Radar Testing, Techniques and Facilities for. Green, Fisher, Ferguson.....274–90
Microwave Radio Relay System, A Multichannel. Black, Beyer, Grieser, Polkinghorn.....798–806
Middletown, Pa., Linear Couplers—Field Tests and Experience at York and. Harder, Klemmer, Neidig..107–13
Military Aircraft, Basic Design Principles for A-C Electric-Power Systems in Large. Chappuis, Olmsted.....12–17; disc. 487
Military Communications, Systems Development of. Putnam.....757–61; disc. 1160
Mobility of Ions on Dielectric Loss of Insulating Oils, The Influence of the Concentration and. Kang.....403–07; disc. 1132
Models, Determination of Cable Temperatures by Means of Reduced-Scale. Gemant, Sticher.....475–82; disc. 1128
Modern Diesel-Electric Drilling Rig Equipment. Rhea.....447–53
Modern Double-Reduction Traction Motor. Greer, Lanier.....471–4
Modern Excitation Systems for Large Synchronous Machines. McClure, Whittlesey, Hartman.....939–45; disc. 1148
Modern Excitation Systems for Synchronous Condensers and Generators, The Development of. Porter, Kinghorn.....1020–7; disc. 1156
Moisture Equilibrium Between Gas Space and Fibrous Materials in Enclosed Electric Equipment. Piper..791–7; disc. 1152
Motive Power for Operations in the Pacific Northwest, Comparison of Railway. Martin.....1054–65; disc. 1189
Motor Design—The Design and Properties of the Magnetic Circuit, Some Aspects of Polyphase. Lloyd, Stone.....812–18: disc. 1151
Motor-Driven Exciters for Turbine Alternators. Bodine, Crary, Rankin.....290–7; disc. 515
Motor, Modern Double-Reduction, Traction Motor. Greer.....471–4
Motor Ship Drives—Propulsion Control Problems, Diesel-Electric Synchronous. Firsch.....660–6
Motors and Generators, Transients in A-C. Smith..61–9
Motors—Calculation of Stability Limit, Dynamic Braking Control of D-C Series. Heumann, Smith.....454–7; disc. 1130
Motors, Electromechanical Transient Performance of Induction. Weygandt, Charp..1000–09; disc. 1167
Motors, Shutdown Versus Hot-Spot Temperatures in Polyphase Induction. Potter, Frohardt.....56–8; disc. 483
Motors—Synchronous Motors Without Field Excitation, Performance Calculations on Polyphase Reluctance. Trickey.....191–3
Multichannel Microwave Radio Relay System, A. Black, Beyer, Grieser, Polkinghorn.....798–806
Multicolor Printing, Electronic Register Control for. Cockrell.....617–22; disc. 1117

N

Navigation and Obstacle Detection, Air-borne Radar for. Jensen, Arnett.....307–13; disc. 491
Negative Resistance Effects in Saturable Reactor Circuits. Manley, Peterson.....870–81
Network Analyzer, A New Design for the A-C. Ryder, Boast.....674–80; disc. 1162
Network Protector of Higher Rating, A New Submersible. Grissinger, Johnson.....41–6
Networks, A Fractional Termination for Ladder. LePage.....530–6
Networks, The Use of Business Machines in Determining the Distribution of Load Reactive Components in Power Line. Jennings, Quinan.....1045–6
Neutral Grounding Reactors and Transformers—II, Temperature Limits for Short-Time Overloads for Oil-Insulated. Montsinger, Clem.....966–73; disc. 1155
New Approach to Probability Problems in Electrical Engineering, A. Adler, Miller..630–2; disc. 1118
New Design for the A-C Network Analyzer, A. Ryder, Boast.....674–80; disc. 1162
Noise Levels in Magnetic Tape Recording, Signal and. Wooldridge.....343–52; disc. 495
Nonlinear Commutating Reactors for Rectifiers. Schmidt.....654–6

O

Objective Testing of Bone Receivers and Throat Microphones, Laboratory Method for. Greibach..184–7

Obstacle Detection, Air-borne Radar for Navigation and. Jensen, Arnett.....307–13; disc. 491
Officers and Committees for 1946–47.....1217–28
Ohm and Mho Principles to Protective Relays, Application of the. Warrington.....378–86; disc. 490
Oil Circuit Breakers, A New Line of High-Voltage Outdoor Tank-Type. Skeats, Rietz..224–31; disc. 502
Oil Circuit Breakers, Field Tests of Interrupting Capacity of 138-Kv. Buchanan, Floyd.....199–204; disc. 503
Oil-Insulated Neutral Grounding Reactors and Transformers—II, Temperature Limits for Short Time Overloads for. Montsinger, Clem.....966–73; disc. 1155
Oils, The Influence of the Concentration and Mobility of Ions on Dielectric Loss of Insulating. Kang.....403–07; disc. 1132
150,000 Horsepower Applied to Aeronautical Research. White.....833–9
Operating Experience With Distance Ground Relays. Wolfe.....458–62; disc. 1185
Operation of Synchronous Machines, Asynchronous and Single-Phase. Rankin.....1092–1102
Oscillations of a High-Voltage Secondary Winding. Boyajian.....1010–20
Oscillograph for Recording Transient Recovery Voltages, An. Hoover.....1086–91; disc. 1174
Oscillograph With a Memory, An Automatic. Zarem..150–4; disc. 514
Oscillographs, Fault Location and Relay Performance Analysis by Automatic. Dupuis, Jacobs.....442–6; disc. 1125
Outages on Power Circuits, A New Electronic Timing Relay for Reducing. Dlouhy.....407–11
Outdoor Tank-Type Oil Circuit Breakers, A New Line of High-Voltage. Skeats, Rietz..224–31; disc. 502
Overloads for Oil-Insulated Neutral Grounding Reactors and Transformers—II, Temperature Limits for Short-Time. Montsinger, Clem.....966–73; disc. 1155

P

Pacific Northwest, Comparison of Railway Motive Power for Operations in the. Martin.....1054–65; disc. 1189
Parallel Circuits in Servomechanisms. Marcy.....521–9; disc. 1128
Peacetime Use, Marine Radar for. Lynn, Winn..271–3
Peak Voltages Induced by Accelerated Flux Reversal in Reactor Cores Operating Above Saturation Density. Specht, Wentz.....254–63
Performance Analysis by Automatic Oscillographs, Fault Location and Relay. Dupuis, Jacobs.....442–6; disc. 1125
Performance Calculations on Polyphase Reluctance Motors—Synchronous Motors Without Field Excitation. Trickey.....191–3
Performance Criteria for Current-Limiting Power Fuses—I. Schuck.....1028–34; disc. 1191
Performance Criteria for Current-Limiting Power Fuses—II. Boehne.....1034–45; disc. 1191
Performance of Ceramic Dielectrics at Elevated Temperatures, The Electrical. Frey, Jesatko.....911–20; disc. 1126
Performance of Electronic Exciters for Large A-C Generators, Application and. Langstaff, Vaughan, Lawrence.....246–53; disc. 515
Performance of Hydroelectric Generating Units on the 2,000,000-Horsepower Saguenay System, Improvements in. Lawton.....900–10; disc. 1187
Performance of Induction Motors, Electromechanical Transient. Weygandt, Charp..1000–09; disc. 1167
Performance of Magnetic-Type Power Circuit Breakers, The Development, Design, and. Linde, Wyman..386–93; disc. 510
Performance of Thyratrons, Frequency. Wittenberg.....843–8
Performance of 220-Kv Transmission Lines, Lightning. Part II. (Committee Report).....70–6; disc. 499
Permalloy Tape in Wide-Band Telephone and Pulse Transformers, Applications of Thin. Ganz.....177–83
Philosophy of Relaying. Knapp, Hicks.....735–41; disc. 1135
Phonograph Reproducer Design. Bachman....159–62
Pile Speed Governor, A Carbon-. Button.....4–7
Pilot Wires From Induced Potentials, Protection of. Killen, Law.....267–70
Plant, Power System Development for Service to Hanford Plutonium. Hoard, Curtin.....773–8
Plant, Supervisory Control of 30,000-Kva Hydroelectric. Bohner, Maness.....337–42
Plants Against Insulation Breakdown and Consequential Damages, Protection of Industrial. Vaughan.....592–6; disc. 1166
Plants, Combined Light and Power Systems for Industrial. Beeman.....76–83
Plutonium Plant, Power System Development for Service to Hanford. Hoard, Curtin.....773–8
Poles and Crossarms, The Preservative Treatment of Various Species. MacLean.....549–54
Polyphase Commutator Regulator for Speed Control, The. Conrad, Brooks, Fellers....321–8; disc. 484
Polyphase Induction Motors, Shutdown Versus Hot-Spot Temperatures in. Potter, Frohardt.....56–8; disc. 483
Polyphase Motor Design—The Design and Properties of the Magnetic Circuit, Some Aspects of. Lloyd, Stone.....812–18; disc. 1151
Polyphase Reluctance Motors—Synchronous Motors Without Field Excitation, Performance Calculations on. Trickey.....191–3
Porcelain Insulators at High Altitudes, Investigation of. Fields, Cadwell.....656–60
Potentials, Protection of Pilot Wires From Induced. Killen, Law.....267–70
(Power Applications, Industrial) Application of the Betatron to Practical Radiography. Girard, Adams.....241–6; disc. 489
(Power Applications, Industrial) Co-ordinated Electric Drive for a Rubber Calender Train. John, Knapp, Mosteller.....128–34; disc. 492
(Power Applications, Industrial) Electronic Register Control for Multicolor Printing. Cockrell.....617–22; disc. 1117
(Power Applications, Industrial) Induction Heating of Long Cylindrical Charges. Storm.....369–77
(Power Applications, Industrial) Industrial Application of Rototrol Regulators. Harris.....118–23
(Power Applications, Industrial) Maintenance of Rectifiers on Electrochemical Installations. Housley, Hughes.....436–41; disc. 1115
(Power Applications, Industrial) Modern Diesel-Electric Drilling Rig Equipment. Rhea.....447–53
(Power Applications, Industrial) Protection of Industrial Plants Against Insulation Breakdown and Consequential Damages. Vaughan....592–6; disc. 1166
Power Cable, Carrier Supervisory Control of Pumping Station Over. Derr, Keller, Hedke.....699–705; disc. 1124
Power Cable, Semiconducting Shielding for A-C Merrell.....605–09; disc. 1145
Power Circuit Breakers, Application Ratings of Indoor. Vikoren.....768–73; disc. 1168
Power Circuit Breakers, The Development, Design, and Performance of Magnetic-Type. Linde, Wyman..386–93; disc. 510
Power Circuits, A New Electronic Timing Relay for Reducing Outages on. Dlouhy.....407–11
Power for Operations in the Pacific Northwest, Comparison of Railway Motive. Martin.....1054–65; disc. 1189
Power Fuses—I, Performance Criteria for Current Limiting. Schuck.....1028–34; disc. 1191
Power Fuses—II, Performance Criteria for Current-Limiting. Boehne.....1034–45; disc. 1191
(Power Generation) Application and Performance of Electronic Exciters for Large A-C Generators. Langstaff, Vaughan, Lawrence..246–53; disc. 515
(Power Generation) Improvements in Performance of Hydroelectric Generating Units on the 2,000,000-Horsepower Saguenay System. Lawton.....900–10; disc. 1187
(Power Generation) Modern Excitation Systems for Large Synchronous Machines. McClure, Whittlesey, Hartman.....939–45; disc. 1148
(Power Generation) Motor-Driven Exciters for Turbine Alternators. Bodine, Crary, Rankin 290–7; disc. 515
(Power Generation) Supervisory Control of 30,000-Kva Hydroelectric Plant. Bohner, Maness.....337–42
(Power Generation) Technique of Electrical and Hydraulic Testing of Hydroelectric Units. Floyd, Traill.....163–9; disc. 493
(Power Generation) Tennessee Valley Authority Hydroelectric Stations—Electrical and Mechanical Design. Hopkins, Petersen.....920–31; disc. 1132
(Power Generation) The Development of Modern Excitation Systems for Synchronous Condensers and Generators. Porter, Kinghorn..1020–7; disc. 1156
Powerhouse Auxiliaries, Protection of. (Committee Report).....746–51; disc. 1115
Power-Line Carrier-Current Equipment, Field Tests on. Miller, Prud'Homme.....824–7; disc. 1177
Power Line Networks, The Use of Business Machines in Determining the Distribution of Load and Reactive Components in. Jennings, Quinan...1045–6
Power System Development for Service to Hanford Plutonium Plant. Hoard, Curtin.....773–8
Power System, Pressure-Arc-Interruption Circuit Breakers for 400-Cycle Aircraft Electric-. Austin.....58–60; disc. 487
Power Systems, Control and Protection of Aircraft D-C. Austin.....741–5; disc. 1170
Power Systems for Industrial Plants, Combined Light and. Beeman.....76–83
Power Systems in Large Military Aircraft, Basic Design Principles for A-C Electric-. Chappuis, Olmsted.....12–17; disc. 487
Power Transformers, Temperature Rise of Water-Cooled. Meador.....18–21
Power Transmission as Influenced by Excitation Systems, Long-Distance. Concordia, Crary, Maginniss.....974–87; disc. 1175
Practical Radiography, Application of the Betatron to. Girard, Adams.....241–6; disc. 489
Precision Radar, Shoran. Seeley.....232–40
Preservative Treatment of Various Species for Poles and Crossarms. MacLean.....549–54
Pressure-Arc-Interruption Circuit Breakers for 400-Cycle Aircraft Electric-Power System. Austin.....58–60; disc. 487
Principles for A-C Electric-Power Systems in Large Military Aircraft, Basic Design. Chappuis, Olmsted.....12–17; disc. 487
Printing, Electronic Register Control for Multicolor. Cockrell.....617–22; disc. 1117
Probability Problems in Electrical Engineering, A New Approach to. Adler, Miller.....630–2; disc. 1118
Problems, Diesel-Electric Synchronous Motor Ship Drives—Propulsion Control. Frisch.....660–6
Problems, Electrical Analogy Methods Applied to Servomechanism. McCann, Herwald, Kirschbaum.....91–6; disc. 515
Problems in Electrical Engineering, A New Approach to Probability. Adler, Miller.....630–2; disc. 1118
Problems in Rural Electrification and Electroagriculture, Specific Engineering. Samuels.....1065–73; disc. 1182
Problems in the Case of Attenuating Transmission Line, The Solution of Transmission-Line. Glinski..46–9
Properties and Uses of Thermistors—Thermally Sensitive Resistors. Becker, Green, Pearson....711–25
Properties of the Vacuum Switch, Fundamental. Koller.....597–604; disc. 1141
Propulsion Control Problems, Diesel-Electric Synchronous Motor Ship Drives—. Frisch.....660–6
Protection for Complex Distribution Circuits, Sensitive Ground Relay. Hunt.....765–8; disc. 1180
Protection of Aircraft D-C Power Systems, Control and Austin.....741–5; disc. 1170
Protection of Industrial Plants Against Insulation Breakdown and Consequential Damages. Vaughan.....592–6; disc. 1166
Protection of Pilot Wires From Induced Potentials. Killen, Law.....267–70
Protection of Powerhouse Auxiliaries. (Committee Report).....746–51; disc. 1115
Protective Device, New Series Capacitor. Marbury, Owens.....142–6; disc. 511
(Protective Devices) A New Electronic Timing Relay for Reducing Outages on Power Circuits. Dlouhy.....407–11
(Protective Devices) A New Line of High-Voltage Outdoor Tank-Type Oil Circuit Breakers. Skeats, Rietz.....224–31; disc. 502
(Protective Devices) A New Submersible Network Protector of Higher Rating. Grissinger, Johnson..41–6
(Protective Devices) Application Ratings of Indoor Power Circuit Breakers. Vikoren.....768–73; disc. 1168
(Protective Devices) Arcing Ground Tests on a Normally Ungrounded 13-Kv 3-Phase Bus. Allen, Waldorf..298–306; disc. 498
(Protective Devices) Dielectric Recovery by an A-C Arc in an Air Blast. Browne.....169–76; disc. 507
(Protective Devices) Fault Location and Relay Performance Analysis by Automatic Oscillographs. Dupuis, Jacobs.....442–6; disc. 1125
(Protective Devices) Field Tests of Interrupting Capacity of 138-Kv Oil Circuit Breakers. Buchanan, Floyd.....199–204; disc. 503
(Protective Devices) 4,370,000-Kva Short-Circuit Tests on Grand Coulee 230-Kv Bus. Clagett, Leeds.....729–35; disc. 1119
(Protective Devices) Linear Couplers—Field Tests and Experience at York and Middletown, Pa. Harder, Kelmmer, Neidig.....107–13
(Protective Devices) Long 60-Cycle Arcs in Air. Strom.....113–18; disc. 504
(Protective Devices) Low-Current-Secondary Current Transformers. (Committee Report).....649–50
(Protective Devices) Metal-Clad Unit-Type Switchgear for 33-Kv Service. Kreger.....360–8; disc. 509
(Protective Devices) Operating Experience With Distance Ground Relays. Wolfe...458–62; disc. 1185
(Protective Devices) Performance Criteria for Current-Limiting Power Fuses—I. Schuck.....1028–34; disc. 1191
(Protective Devices) Performance Criteria for Current-Limiting Power Fuses—II. Boehne.....1034–45; disc. 1191
(Protective Devices) Philosophy of Relaying. Knapp, Hicks.....735–41; disc. 1135
(Protective Devices) Size Reduction and Rating Extension of Magnetic Air Circuit Breakers up to 500,000 Kva, 15 Kv. Dickinson, Frink.....220–3; disc. 510
(Protective Devices) The Development, Design, and Performance of Magnetic-Type Power Circuit Breakers. Linde, Wyman.....386–93; disc. 510
(Protective Devices) The Mho Distance Relay. Hutchinson.....353–60

Protective Relaying, Simplicity of. Hunt.....995–1000; disc. 1121
Protective Relays, Application of the Ohm and Mho Principles to. Warrington.....378–86; disc. 490
Protector of Higher Rating, A New Submersible Network. Grissinger, Johnson.....41–6
Pulse Transformers, Applications of Thin Permalloy Tape in Wide-Band Telephone and. Ganz.....177–83
Pumping Station Over Power Cable, Carrier, Supervisory Control of. Derr, Keller, Hedke.....699–705; disc. 1124

R

Radar for Navigation and Obstacle Detection, Airborne. Jensen, Arnett.....307–13; disc. 491
Radar for Peacetime Use, Marine. Lynn, Winn..271–3
Radar Sets, Factors Affecting the Range of. Quarles, Breazeale.....546–8
Radar, Shoran Precision. Seeley.....232–40
Radar Systems Considerations. Quarles.....209–15
Radar Testing, Techniques and Facilities for Microwave. Green, Fisher, Ferguson.....274–90
Radio Relay System, A Multichannel Microwave. Black, Beyer, Grieser, Polkinghorn.....798–806
Radio Telemetering for Testing Aircraft in Flight. Frederick.....861–70
Radiography, Application of the Betatron to Practical. Girard, Adams.....241–6; disc. 489
Railroad Service, High Voltage Ignitron Rectifiers and Inverters for. Boyer, Hagensick.....463–70
Railway Motive Power for Operations in the Pacific Northwest, Comparison of. Martin.....1054–65; disc. 1189
Range of Radar Sets, Factors Affecting the. Quarles, Breazeale.....546–8
Rating, A New Submersible Network Protector of Higher. Grissinger, Johnson.....41–6
Rating Extension of Magnetic Air Circuit Breakers up to 500,000 Kva, 15 Kv, Size Reduction and. Dickinson, Frink.....220–3; disc. 510
Rating of Aircraft Electric Machines, Effect of Altitude on Ventilation and. Veinott.....84–90; disc. 488
Rating of Telephone Systems, Transmission. Codd.....694–8; disc. 1123
Ratings for Aircraft Wire and Cable, Short-Time Current. Jones, Scott.....644–8; disc. 1135
Ratings of Indoor Power Circuit Breakers, Application. Vikoren.....768–73; disc. 1168
Ratio Transmission Used in Developmental 400-Cycle Electric System for Large Aircraft, Governor for Variable-. Desch, Garr, Hutton.....194–8
Reactance Flexible Cable for Induction Heating, Low. Zucker.....848–52
Reactive Components in Power Line Networks, The Use of Business Machines in Determining the Distribution of Load and. Jennings, Quinan....1045–6
Reactor Circuits, Negative Resistance Effects in Saturable. Manley, Peterson.....870–81
Reactor Cores Operating Above Saturation Density, Peak Voltages Induced by Accelerated Flux Reversal in. Specht, Wentz.....254–63
Reactors and Transformers—II. Temperature Limits for Short-Time Overloads for Oil-Insulated Neutral Grounding. Montsinger, Clem..966–73; disc. 1155
Reactors for Rectifiers, Nonlinear Commutating. Schmidt.....654–6
Receivers and Throat Microphones, Laboratory Method for Objective Testing of Bone. Greibach...184–7
Recorder for Flight Testing and Spectroscopy, Electronically Balanced. Williams, Clark, Tarpley.....205–08
Recorder Head Design, A New Wire. Long.....216–20; disc. 495
Recording, Signal and Noise Levels in Magnetic Tape. Wooldridge.....343–52; disc. 495
Recording Transient Recovery Voltages, An Oscillograph for. Hoover.....1086–91; disc. 1174
Recording Wire, A B-H Curve Tracer for Magnetic. Long, McMullen.....146–50; disc. 494
Recovery by an A-C Arc in an Air Blast, Dielectric. Browne.....169–76; disc. 507
Recovery Voltages, An Oscillograph for Recording Transient. Hoover.....1086–91; disc. 1174
Rectangular Conductors, Geometric Mean Distances for. Dwight.....536–8
Rectifier Capacity. Herskind, Steiner.....667–70
Rectifier Installations, Inductive Co-ordination Aspects of. (Committee Report).....416–36; disc. 1115
Rectifiers and Inverters for Railroad Service, High Voltage Ignitron. Boyer, Hagensick.....463–70
Rectifiers, Circuit Cushioning of Gas-Filled Grid-Controlled. Edwards, Smith.....640–3; disc. 1131
Rectifiers, Nonlinear Commutating Reactors for. Schmidt.....654–6
Rectifiers on Electrochemical Installations, Maintenance of. Housley, Hughes.....436–41; disc. 1115
Reduced-Scale Models, Determination of Cable Temperatures by Means of. Gemant, Sticher.....475–82; disc. 1128
Reduction and Rating Extension of Magnetic Air Circuit Breakers up to 500,000 Kva, 15 Kv, Size. Dickinson, Frink.....220–3; disc. 510
Reduction Traction Motor, Modern Double. Greer.....471–4
Reels, An Electronic Drive for Windup. Puchlowski.....585–91; disc. 1155
Regeneration of Teleprinter Signals, Electronic. Wilder.....34–40
Register Control for Multicolor Printing, Electronic. Cockrell.....617–22; disc. 1117
Regulator, An Electronic Frequency Meter and Speed. Levin.....779–86; disc. 1181
Regulator for Speed Control, The Polyphase Commutator. Conrad, Brooks, Fellers.....321–8; disc. 484
Regulators, Industrial Application of Rototrol. Harris.....118–23
Rejection Filter, A Tunable. Taylor...263–7; disc. 490
Relay for Reducing Outages on Power Circuits, A New Electronic Timing. Dlouhy.....407–11
Relay Performance Analysis by Automatic Oscillographs, Fault Location. Dupuis, Jacobs..442–6; disc. 1125
Relay Protection for Complex Distribution Circuits, Sensitive Ground. Hunt.....765–8; disc. 1180
Relay System, A Multichannel Microwave Radio. Black, Beyer, Grieser, Polkinghorn.....798–806
Relay, The Mho Distance. Hutchinson.....353–60
Relaying, Philosophy of. Kanpp, Hicks.....735–41; disc. 1135
Relaying, Simplicity of Protective. Hunt.....995–1000; disc. 1121
Relays, Application of the Ohm and Mho Principles to Protective. Warrington.....378–86; disc. 490
Relays, Operating Experience With Distance Ground. Wolfe.....458–62; disc. 1185
Reluctance Motors—Synchronous Motors Without Field Excitation, Performance Calculations on Polyphase. Trickey.....191–3
Report of the Board of Directors.....1197–1216
Reproducer Design, Phonograph. Bachman...159–62
Research, 150,000 Horsepower Applied to Aeronautical. White.....833–9
Resin-Treated Magnet Coils, Silicone. Moses, Torok..412–16; disc. 1184
Resistance Effects in Saturable Reactor Circuits, Negative. Manley, Peterson.....870–81
Resistance in Spot Welding, Measurement and Effect of Contact. Wyant.....26–33; disc. 513
Resistance Loss, Formulas for Conductor Size According to Cost of. Dwight.....22–5; disc. 497
Resistance of Large D-C Machines, Factors Affecting Insulation. Johnson, Weil.....705–10; disc. 1194
Resistance Welding Machine, Influence of Magnetic Materials on the Welding Characteristics of. Riley, Smith.....852–60; disc. 1160
Resistance Welding Transformers, Characteristics of. Murray, Jones.....726–8; disc. 1152
Resistors, Properties and Uses of Thermistors—Thermally Sensitive. Becker, Green, Pearson...711–25
Resonant Fatigue Machine, Self-Excited Electromagnetic Drive for a. Willson.....1073–8
Response of Automatic Control Systems, The Frequency. Harris.....539–46; disc. 1131
Reversal in Reactor Cores Operating Above Saturation Density, Peak Voltages Induced by Accelerated Flux. Specht, Wentz.....254–63
Rig Equipment, Modern Diesel-Electric Drilling. Rhea.....447–53
Rise of Water-Cooled Power Transformers, Temperature. Meador.....18–21
Rotating Electric Machine Time Constants at Low Speeds. Concordia.....882–7
Rotor Testing by Test Stator Method, Die Cast. Trickey.....139–41; disc. 483
Rototrol Regulators, Industrial Application of. Harris.....118–23
Rubber Calender Train, Co-ordinated Electric Drive for a. John, Knapp, Mosteller..128–34; disc. 492
Rubber-Insulated Wire, High Voltage D-C Testing of. Eddy, Fenn.....576–8; disc. 1126
Rural Electrification and Electroagriculture, Specific Engineering Problems in. Samuels.....1065–73; disc. 1182

S

(Safety) Dangerous Electric Currents. Dalziel.....579–85; disc. 1123
Saguenay System, Improvements in Performance of Hydroelectric Generating Units on the 2,000,000-Horsepower. Lawton.....900–10; disc. 1187
Saturable Reactor Circuits, Negative Resistance Effects in. Manley, Peterson.....870–81
Saturation Density, Peak Voltages Induced by Accelerated Flux Reversal in Reactor Cores Operating Above. Specht, Wentz.....254–63
Scale Models, Determination of Cable Temperatures by Means of Reduced. Gemant, Sticher.....475–82; disc. 1128
Sealed Ignitron, A 400-Ampere. Steiner, Price.....680–5; disc. 1161
Secondary Current Transformers, Low-Current-. (Committee Report).....649–50
Secondary Winding, Oscillations of a High-Voltage. Boyajian.....1010–20
Self-Excited Electromagnetic Drive for a Resonant Fatigue Machine. Willson.....1073–8
Selsyn Generator-Control Transformer System, Electrical Accuracy of. Chestnut....570–6; disc. 1118
Semiconducting Shielding for A-C Power Cable. Merrell.....605–09; disc. 1145
Sensitive Ground Relay Protection for Complex Distribution Circuits. Hunt.....765–8; disc. 1180
Sensitive Resistors, Properties and Uses of Thermistors—Thermally. Becker, Green, Pearson.....711–25
Series-Capacitor-Compensated Transmission System, Characteristics of a 400-Mile 230-Kv. Hoard.....1102–14; disc. 1178
Series Capacitor Protective Device, New. Marbury, Owens.....142–6; disc. 511
Series Capacitors to Flash Welders, The Application of. Deffenbaugh.....686–7
Series Motors—Calculation of Stability Limit, Dynamic Braking Control of D-C. Heumann, Smith.....454–7; disc. 1130
Service, Metal-Clad Unit-Type Switchgear for 33-Kv Service. Kreger.....360–8; disc. 509
Servomechanism Problems, Electrical Analogy Methods Applied to. McCann, Herwald, Kirschbaum.....91–6; disc. 515
Servomechanisms by Electrical Analogy, Dimensionless Analysis of. Herwald, McCann.....630–9; disc. 1132
Servomechanisms, Parallel Circuits in. Marcy.....521–9; disc. 1128
Sets for Testing Aircraft Models, Electronic Control of Frequency Converter. Heumann, Strong...931–9
Sheathing, F-3 Lead Alloy—An Improved Cable. Hickernell, Snyder.....563–9; disc. 1136
Shielding for A-C Power Cable, Semiconducting. Merrell.....605–09; disc. 1145
Ship Drives—Propulsion Control Problems, Diesel-Electric Synchronous Motor. Frisch.....660–6
Shoran Precision Radar. Seeley.....232–40
Short-Circuit Characteristics of D-C Generators, The. Frost.....394–402; disc. 484
Short Circuit, Current and Torque of D-C Machines on. Linville.....956–65; disc. 1144
Short-Circuit Tests on Grand Coulee 230-Kv Bus, 4,370,000-Kva. Clagett, Leeds..729-35; disc. 1119
Short-Time Current Ratings for Aircraft Wire and Cable. Jones, Scott.....644–8; disc. 1135
Shutdown Versus Hot-Spot Temperatures in Polyphase Induction Motors. Potter, Frohardt.....56–8; disc. 483
Signal and Noise Levels in Magnetic Tape Recording. Wooldridge.....343–52; disc. 495
Signals, Electronic Regeneration of Teleprinter. Wilder.....34–40
Silicone-Resin-Treated Magnet Coils. Moses, Torok..412–16; disc. 1184
Simplicity of Protective Relaying. Hunt.....995–1000; disc. 1121
Single-Phase Operation of Synchronous Machines, Asynchronous and. Rankin.....1092–1102
Six Years' Experience With Factory-Built Unit-Type Substations. Miller, Miller....751–6; disc. 1150
Sixty-Cycle Arcs in Air, Long. Strom.....113–18; disc. 504
Size According to Cost of Resistance Loss, Formulas for Conductor. Dwight.....22–5; disc. 497
Size Reduction and Rating Extension of Magnetic Air Circuit Breakers up to 500,000 Kva, 15 Kv. Dickinson, Frink.....220–3; disc. 510
Slot Winding, Differential Leakage of a Fractional-. Liwschitz.....314–20
Solution of Transmission-Line Problems in the Case of Attenuating Transmission Line. Glinski.....46–9
Some Aspects of Polyphase Motor Design—The Design and Properties of the Magnetic Circuit. Lloyd, Stone.....812–18; disc. 1151
Spacing of Transmission Line Conductors, Co-ordination of Insulation and. Lewis...690–4; disc. 1142
Species for Poles and Crossarms, The Preservative Treatment of Various. MacLean.....549–54
Specific Engineering Problems in Rural Electrification and Electroagriculture. Samuels.....1065–73; disc. 1182
Spectrometer, High Vacuum Leak Testing With the Mass. Worcester, Doughty....946–55; disc. 1170
Spectroscopy, Electronically Balanced Recorder for Flight Testing and. Williams, Clark, Tarpley.....205–08
Speed Control, The Polyphase Commutator Regulator for. Conrad, Brooks, Fellers.....321–8; disc. 484
Speed Governor, A Carbon-Pile. Button.....4–7
Speed Regulator, An Electronic Frequency Meter and. Levin.....779–86; disc. 1181
Speeds, Rotating Electric Machine Time Constants at Low. Concordia.....882–7
Spot Welding, Measurement and Effect of Contact Resistance in. Wyant.....26–33; disc. 513

Square Tubular Conductors, Formulas for the Inductance of Coaxial Busses Comprised of. Messinger, Higgins....328–36; disc. 501
Stability Limit, Dynamic Braking Control of D-C Series Motors—Calculation of. Heumann, Smith....454–7; disc. 1130
Stabilization of Arc-Welding Transformers, Capacitor. Blankenbuehler, Lester....54–5
Station and Line Insulation to Switching Surges, Dielectric Strength of. Bellaschi, Rademacher....1047–54; disc. 1173
Stator Method, Die Cast Rotor Testing by Test. Trickey....139–41; disc. 483
Strength of Station and Line Insulation to Switching Surges, Dielectric. Bellaschi, Rademacher....1047–54; disc. 1173
Stress Measurement by Electrical Means. Kern, Williams....100–07
Submersible Network Protector of Higher Rating, A New. Grissinger, Johnson....41–6
Substations, Six Years' Experience With Factory-Built Unit-Type. Miller, Miller....751–6; disc. 1150
Supervisory Control of Pumping Station Over Power Cable, Carrier. Derr, Keller, Hedke....699–705; disc. 1124
Supervisory Control of 30,000-Kva Hydroelectric Plant. Bohner, Maness....337–42
Surges, Dielectric Strength of Station and Line Insulation to Switching. Bellaschi, Rademacher....1047–54; disc. 1173
Switch, Fundamental Properties of the Vacuum. Koller....597–604; disc. 1141
Switchgear for 33-Kv Service, Metal-Clad Unit-Type. Kreger....360–8; disc. 509
Switching Surges, Dielectric Strength of Station and Line Insulation to. Bellaschi, Rademacher....1047–54; disc. 1173
Synchronism Indicator for Aircraft, A Unique Engine-. Pearson....650–3
Synchronous Condensers and Generators, The Development of Modern Excitation Systems for. Porter, Kinghorn....1020–7; disc. 1156
Synchronous Condensers, Automatic Control of Large. Brown....609–16
Synchronous Machines, Asynchronous and Single-Phase Operation of. Rankin....1092–1102
Synchronous Machines, Modern Excitation Systems for Large. McClure, Whittlesey, Hartman....939–45; disc. 1148
Synchronous Motor Ship Drives-Propulsion Control Problems, Diesel-Electric. Frisch....660-6
Synchronous Motors Without Field Excitation, Performance Calculations on Polyphase Reluctance Motors—. Trickey....191–3
System, Electrical Accuracy of Selsyn Generator-Control Transformer. Chestnut....570–6; disc. 1118
Systems, A New Crystal Channel Filter for Broad Band Carrier. Willis....134–8; disc. 490
Systems Considerations, Radar. Quarles....209–15
Systems Development of Military Communications. Putnam....757–61; disc. 1160
Systems for Large Synchronous Machines, Modern Excitation. McClure, Whittlesey, Hartman....939–45; disc. 1148
Systems, Long-Distance Power Transmission as Influenced by Excitation. Concordia, Crary, Maginniss....974–87; disc. 1175
Systems, The Frequency Response of Automatic Control. Harris....539–46; disc. 1131

T

Tank-Type Oil Circuit Breakers, A New Line of High-Voltage Outdoor. Skeats, Rietz..242–31; disc. 502
Tape in Wide-Band Telephone and Pulse Transformers, Applications of Thin Permalloy. Ganz....177–83
Tape Recording, Signal and Noise Levels in Magnetic. Wooldridge....343–52; disc. 495
Teaching Electricity and Magnetism. Hessler..828–33
Techniques and Facilities for Microwave Radar Testing. Green, Fisher, Ferguson....274–90
Technique of Electrical and Hydraulic Testing of Hydroelectric Units. Floyd, Traill....163–9; disc. 493
Techniques, Thermal-Demand-Meter Testing. Lynch, Douglass....124–8; disc. 514
Telemetering for Testing Aircraft in Flight, Radio. Frederick....861–70
Telephone and Pulse Transformers, Applications of Thin Permalloy Tape in Wide-Band. Ganz....177–83
Telephone Circuits, Application of Compandors to. Carter, Dickieson, Mitchell....1079–86
Telephone Systems, Mica Capacitors for Carrier. Christopher, Kater....670–4; disc. 1116
Telephone Systems, Transmission Rating of. Codd....694–8; disc. 1123
Teleprinter Signals, Electronic Regeneration of. Wilder....34–40
Temperature Limits for Short-Time Overloads for Oil-Insulated Neutral Grounding Reactors and Transformers—II. Montsinger, Clem. 966–73; disc. 1155
Temperature Rise of Water-Cooled Power Transformers. Meador....18–21
Temperatures by Means of Reduced-Scale Models, Determination of Cable. Gemant, Sticher....475–82; disc. 1128
Temperatures in Polyphase Induction Motors, Shutdown Versus Hot-Spot. Potter, Frohardt....56–8; disc. 483
Temperatures, The Electrical Performance of Ceramic Dielectrics at Elevated. Frey, Jesatko....911–20; disc. 1126
Tennessee Valley Authority Hydroelectric Stations—Electrical and Mechanical Design. Hopkins, Petersen....920–31; disc. 1132
Termination for Ladder Networks, A Fractional. LePage....530–6
Testing Aircraft in Flight, Radio Telemetering for. Frederick....861–70
Testing Aircraft Models, Electronic Control of Frequency Converter Sets for. Heumann, Strong....931–9
Testing and Spectroscopy, Electronically Balanced Recorder for Flight. Williams, Clark, Tarpley....205–08
Testing by Test Stator Method, Die Cast Rotor. Trickey....139–41; disc. 483
Testing of Bone Receivers and Throat Microphones, Laboratory Method for Objective. Greibach....184–7
Testing of Hydroelectric Units, Technique of Electrical and Hydraulic. Floyd, Traill....163–9; disc. 493
Testing of Rubber-Insulated Wire, High Voltage D-C. Eddy, Fenn....576–8; disc. 1126
Testing, Techniques and Facilities for Microwave Radar. Green, Fisher, Ferguson....274–90
Testing Techniques, Thermal-Demand-Meter. Lynch, Douglass....124–8; disc. 514
Testing With the Mass Spectrometer, High Vacuum Leak. Worcester, Doughty....946–55; disc. 1170
Tests and Experience at York and Middletown, Pa., Linear Couplers—Field. Harder, Klemmer, Neidig....107–13
Tests of Interrupting Capacity of 138-Kv Oil Circuit Breakers, Field. Buchanan, Floyd....199–204; disc. 503
Tests on a Normally Ungrounded 13-Kv 3-Phase Bus, Arcing Ground. Allen, Waldorf....298–306; disc. 498
Tests on Grand Coulee 230-Kv Bus, 4,370,000-Kva Short-Circuit. Clagett, Leeds..729–35; disc. 1119
Tests on Power-Line Carrier-Current Equipment, Field. Miller, Prud'Homme....824–7; disc. 1177
Thermal Characteristics of Aircraft Generators on Load Analysis, Effects of. Rogers....819–24
Thermal-Demand-Meter Testing Techniques. Lynch, Douglass....124–8; disc. 514
Thermistors—Thermally Sensitive Resistors, Properties and Uses of. Becker, Green, Pearson....711–25
Thin Permalloy Tape in Wide-Band Telephone and Pulse Transformers, Applications of. Ganz....177–83
33-Kv Service, Metal-Clad Unit-Type Switchgear. Kreger....360–8; disc. 509
Throat Microphones, Inertia. Greibach, Pacent....187–91
Throat Microphones, Laboratory Method for Objective Testing of Bone Receivers and. Greibach..184–7
Thyratrons, Frequency Performance of. Wittenberg..843–8
Time Constants at Low Speeds, Rotating Electric Machine. Concordia....882–7
Timing Relay for Reducing Outages on Power Circuits, A New Electronic. Dlouhy....407–11
Torque of D-C Machines on Short Circuit, Current and. Linville....956–65; disc. 1144
Tracer for Magnetic-Recording Wire, A B-H Curve. Long, McMullen....146–50; disc. 494
Traction Motor, Modern Double-Reduction. Greer..471–4
Train, Co-ordinated Electric Drive for a Rubber Calender. John, Knapp, Mosteller....128–34; disc. 492
Transformer System, Electrical Accuracy of Selsyn Generator-Control. Chestnut...570–6; disc. 1118
Transformers, Applications of Thin Permalloy Tape in Wide-Band Telephone and Pulse. Ganz..177–83
Transformers, Capacitor Stabilization of Arc-Welding. Blankenbuehler, Lester....54–5
Transformers, Characteristics of Resistance Welding. Murray, Jones....726–8; disc. 1152
Transformers, Design and Measurements of Capacitor Discharge Welding. Dietz, Stein..154–9; disc. 512
Transformers, Low-Current-Secondary Current. (Committee Report)....649–50
Transformers—II, Temperature Limits for Short-Time Overloads for Oil-Insulated Neutral Grounding Reactors and. Montsinger, Clem....966–73; disc. 1155
Transformers, Temperature Rise of Water-Cooled Power. Meador....18–21
Transient Performance of Induction Motors, Electromechanical. Weygandt, Charp....1000–09; disc. 1167
Transient Recovery Voltages, An Oscillograph for Recording. Hoover....1086–91; disc. 1174
Transients in A-C Motors and Generators, Smith...61–9
(Transmission) Arcing Ground Tests on a Normally Ungrounded 13-Kv 3-Phase Bus. Allen, Waldorf..298–306; disc. 498
Transmission as Influenced by Excitation Systems, Long-Distance Power. Concordia, Crary, Maginniss...974–87; disc. 1175
(Transmission) Formulas for Conductor Size According to Cost of Resistance Loss. Dwight....22–5; disc. 497
(Transmission) High Voltage D-C Testing of Rubber-Insulated Wire. Eddy, Fenn...576–8; disc. 1126
Transmission Line Conductors, Co-ordination of Insulation and Spacing of. Lewis...690–4; disc. 1142
Transmission-Line Problems in the Case of Attenuating Transmission Line, The Solution of. Glinski..46–9
(Transmission) Linear Couplers—Field Tests and Experience at York and Middletown, Pa. Harder, Klemmer, Neidig....107–13
Transmission Lines, Lightning Performance of 220-Kv. Part II. (Committee Report)....70–6; disc. 499
(Transmission) Metal-Clad Unit-Type Switchgear for 33-Kv Service. Kreger....360–8; disc. 509
(Transmission) Moisture Equilibrium Between Gas Space and Fibrous Materials in Enclosed Electric Equipment. Piper....791–7; disc. 1152
(Transmission) Power System Development for Service to Hanford Plutonium Plant. Hoard, Curtin....773–8
(Transmission) Protection of Pilot Wires From Induced Potentials. Killen, Law....267–70
Transmission Rating of Telephone Systems. Codd....694–8; disc. 1123
(Transmission) Six Years' Experience With Factory-Built Unit-Type Substations. Miller, Miller....751–6; disc. 1150
Transmission System, Characteristics of a 400-Mile 230-Kv Series-Capacitor-Compensated. Hoard....1102–14; disc. 1178
(Transmission) The Electrical Performance of Ceramic Dielectrics at Elevated Temperatures. Frey, Jesatko....911–20; disc. 1126
(Transmission) The Preservative Treatment of Various Species for Poles and Crossarms. MacLean....549–54
Transmission Used in Developmental 400-Cycle Electric System for Large Aircraft, Governor for Variable-Ratio. Desch, Garr, Hutton....194–8
(Transportation, Air) A Carbon-Pile Speed Governor. Button....4–7
(Transportation, Air) A Unique Engine-Synchronism Indicator for Aircraft. Pearson....650–3
(Transportation, Air) All-Electric Gun Charging. Rohn....1–4
(Transportation, Air) Basic Design Principles for A-G Electric-Power Systems in Large Military Aircraft. Chappuis, Olmsted....12–17; disc. 487
(Transportation, Air) Effect of Altitude on Ventilation and Rating of Aircraft Electric Machines. Veinott....84–90; disc. 488
(Transportation, Air) Electrical Measurements on Aircraft-Engine Ignition Circuits. Berkey....49–53
(Transportation, Air) Investigation of Porcelain Insulators at High Altitudes. Fields, Cadwell....656–60
(Transportation, Air) Pressure-Arc-Interruption Circuit Breakers for 400-Cycle Aircraft Electric-Power System. Austin....58–60; disc. 487
(Transportation, Air) Short-Time Current Ratings for Aircraft Wire and Cable. Jones, Scott....644–8; disc. 1135
(Transportation, Land) Comparison of Railway Motive Power for Operations in the Pacific Northwest. Martin....1054–65; disc. 1189
(Transportation, Land) High Voltage Ignitron Rectifiers and Inverters for Railroad Service. Boyer, Hagensick....463–70
(Transportation, Land) Modern Double-Reduction Traction Motor. Greer....471–4
(Transportation, Marine) Diesel-Electric Synchronous Motor Ship Drives—Propulsion Control Problems. Frisch....660–6
Treated Magnet Coils, Silicone-Resin. Moses. Torok..412–16; disc. 1184
Treatment of Various Species for Poles and Crossarms. MacLean....549–54
Tubes, Excitation, Control, and Cooling of Ignitron. Herskind, Remscheid....632–5
Tubular Conductors, Formulas for the Inductance of Coaxial Busses Comprised of Square. Messinger, Higgins....328–36; disc. 501
Tunable Rejection Filter, A. Taylor..263–7; disc. 490
Tunnel, Electric Equipment for Cornell Variable Density Wind. Clymer, de Ferranti....554–63
Turbine Alternators, Motor-Driven Exciters for. Bodine, Crary, Rankin....290–7; disc. 515

U

Ungrounded 13-Kv 3-Phase Bus, Arcing Ground Tests on a Normally. Allen, Waldorf.....298–306; disc. 498
Unique Engine-Synchronism Indicator for Aircraft, A. Pearson.....650–3
Unit-Type Substations, Six Years' Experience With Factory-Built. Miller, Miller....751–6; disc. 1150
Unit-Type Switchgear for 33-Kv Service, Metal-Clad. Kreger.....360–8; disc. 509
Units on the 2,000,000-Horsepower Saguenay System, Improvements in Performance of Hydroelectric Generating. Lawton.....900–10; disc. 1187
Units, Technique of Electrical and Hydraulic Testing of Hydroelectric. Floyd, Traill.....163–9; disc. 493
Use of Business Machines in Determining the Distribution of Load and Reactive Components in Power Line Networks, The. Jennings, Quinan....1045–6

V

Vacuum Leak Testing With the Mass Spectrometer, High. Worcester, Doughty.....946–55; disc. 1170
Vacuum Switch, Fundamental Properties of the. Koller.....597–604; disc. 1141
Variable-Ratio Transmission Used in Developmental 400-Cycle Electric System for Large Aircraft, Governor for. Desch, Garr, Hutton.....194–8
Varying Currents, The Measurement of Large. Johnson.....8–11; disc. 513
Ventilation and Rating of Aircraft Electric Machines, Effect of Altitude on. Veinott.....84–90; disc. 488
Voltage D-C Testing of Rubber-Insulated Wire, High. Eddy, Fenn.....576–8; disc. 1126
Voltages, An Oscillograph for Recording Transient Recovery. Hoover.....1086–91; disc. 1174
Voltages Induced by Accelerated Flux Reversal in Reactor Cores Operating Above Saturation Density, Peak. Specht, Wentz.....254–63
Voltmeters, Frequency Compensated A-C Ammeters and. Whittenton, Wilkinson.....761–4

W

Water-Cooled Power Transformers, Temperature Rise of. Meador.....18–21
Welders, The Application of Series Capacitors to Flash. Deffenbaugh.....686–7
Welders With Reference to Electrode Freezing, Investigation of Arc Starting Characteristics of D-C. Tyrner.....97–9; disc. 511
Welding Characteristics of Resistance Welding Machines, Influence of Magnetic Materials on the. Riley, Smith.....852–60; disc. 1160
Welding, Measurement and Effect of Contact Resistance in Spot. Wyant.....26–33; disc. 513
Welding Transformers, Capacitor Stabilization of Arc-. Blankenbuehler, Lester.....54–5
Welding Transformers, Characteristics of Resistance. Murray, Jones.....726–8; disc. 1152
Welding Transformers, Design and Measurements of Capacitor Discharge. Dietz, Stein.....154–9; disc. 512
Wide-Band Telephone and Pulse Transformers, Applications of Thin Permalloy Tape in. Ganz.....177–83
Winding, Differential Leakage of a Fractional-Slot. Liwschitz.....314–20
Winding, Oscillations of a High-Voltage Secondary. Boyajian.....1010–20
Windshields, Electrical Anti-icing of Aircraft. McCrumm.....786–91
Wind Tunnel, Electric Equipment for Cornell Variable Density. Clymer, de Ferranti.....554–63
Windup Reels, An Electronic Drive for. Puchlowski.....585–91; disc. 1155
Wire, A B-H Curve Tracer for Magnetic Recording. Long, McMullen.....146–50; disc. 494
Wire and Cable, Short-Time Current Ratings for Aircraft. Jones, Scott.....644–8; disc. 1135
Wire, High Voltage D-C Testing of Rubber-Insulated. Eddy, Fenn.....576–8; disc. 1126
Wire Recorder Head Design, A New. Long.....216–20; disc. 495
Wires From Induced Potentials, Protection of Pilot. Killen, Law.....267–70

Y

York and Middletown, Pa., Linear Couplers—Field Tests and Experience at. Harder, Klemmer, Neidig.....107–13

2. Author Index

Adams, G. D.; J. P. Girard. Application of the Betatron to Practical Radiography.....241–6; disc. 489
Adler, H. A.; K. W. Miller. A New Approach to Probability Problems in Electrical Engineering.....630–2; disc. 1118
Allen, J. E.; S. K. Waldorf. Arcing Ground Tests on a Normally Ungrounded 13-Kv 3-Phase Bus.....298–306; disc. 498
Arnett, R. A.; R. C. Jensen. Air-borne Radar for Navigation and Obstacle Detection.....307–13
Atkinson, R. W. Disc.....1128, 1145
Austin, B. O. Control and Protection of Aircraft D-C Power Systems.....741–5; disc. 1172
Austin, B. O. Pressure-Arc-Interruption Circuit Breakers for 400-Cycle Aircraft Electric-Power System.....58–63
Averbach, B. L. Disc.....510

B

Babcock, N. N. Disc.....1116
Bachman, W. S. Phonograph Reproducer Design.....159–62
Baker, B. P. Disc.....507
Bartlett, S. C. Disc.....1177
Baumann, Fred. Disc.....484
Beatty, J. W. Disc.....507
Becker, J. A.; C. B. Green, G. L. Pearson. Properties and Uses of Thermistors—Thermally Sensitive Resistors.....711–25
Beeman, D. L. Combined Light and Power Systems for Industrial Plants.....76–83
Bellaschi, P. L.; L. B. Rademacher. Dielectric Strength of Station and Line Insulation to Switching Surges.....1047–54; disc. 1174
Benson, F. S. Disc.....1177
Berkey, Wm. E. Electrical Measurements on Aircraft-Engine Ignition Circuits.....49–53
Berkner, L. V. Disc.....491
Betzer, C. E. Disc.....1126
Beyer, J. W.; H. S. Black, T. J. Grieser, F. A. Polkinghorn. A Multichannel Microwave Radio Relay System.....798–806
Bickelhaupt, C. O. Disc.....1161
Black, H. S.; J. W. Beyer, T. J. Grieser, F. A. Polkinghorn. A Multichannel Microwave Radio Relay System.....798–806
Blakeslee, T. M. Disc.....1119
Blankenbuehler, J. H.; R. V. Lester. Capacitor Stabilization of Arc-Welding Transformers.....54–5
Boast, W. B.; J. D. Ryder. A New Design for the A-C Network Analyzer.....674–80; disc. 1165
Bodine, R. B.; S. B. Crary, A. W. Rankin. Motor-Driven Exciters for Turbine Alternators.....290–7; disc. 518
Boehne, E. W. Performance Criteria for Current-Limiting Power Fuses—II.....1034–45; disc. 1192
Boehne, E. W. Disc.....1174
Bohner, C. W.; A. P. Maness. Supervisory Control o 30,000-Kva Hydroelectric Plant.....337–42
Bond, C. R.; F. W. Nimmer. Disc.....1138
Borden, Perry A. Disc.....514
Boyajian, A. Oscillations of a High-Voltage Secondary Winding.....1010–20
Boyer, J. L.; C. G. Hagensick. High Voltage Ignitron Rectifiers and Inverters for Railroad Service.....463–70
Brandt, F. L. Disc.....1152, 1160
Braun, H. J. Disc.....488
Breazeale, W. M.; L. R. Quarles. Factors Affecting the Range of Radar Sets.....546–8
Brooks, F. E., Jr.; A. G. Conrad, R. G. Fellers. The Polyphase Commutator Regulator for Speed Control.....321–8
Brown, H. F. Disc.....1190
Brown, M. J. Automatic Control of Large Synchronous Condensers.....609–16
Browne, T. E., Jr. Dielectric Recovery by an A-C Arc in an Air Blast.....169–76; disc. 508
Browne, T. E., Jr. Disc.....1141
Brownlee, W. R. Disc.....490, 504, 1115, 1121
Buchanan, W. B.; G. D. Floyd. Field Tests of Interrupting Capacity of 138-Kv Oil Circuit Breakers.....199–204; disc. 504
Burgwein, S. L. Disc.....1117
Burroughs, J. E. Disc.....1170
Button, C. T. A Carbon-Pile Speed Governor.....4–7

C

Cadwell, C. L.; C. V. Fields. Investigation of Porcelain Insulators at High Altitudes.....656–60
Cain, B. M. Disc.....483
Carter, C. W., Jr.; A. C. Dickieson, D. Mitchell. Application of Compandors to Telephone Circuits.....1079–86
Chappuis, C. K.; L. M. Olmsted. Basic Design Principles for A-C Electric-Power Systems in Large Military Aircraft.....12–17; disc. 488
Charp, S.; C. N. Weygandt. Electromechanical Transient Performance of Induction Motors.....1000–09; disc. 1168
Cheek, R. C. Disc.....1177
Chestnut, Harold. Electrical Accuracy of Selsyn Generator-Control Transformer System.....570–6
Chestnut, R. W. Disc.....490
Christopher, A. J.; J. A. Kater. Mica Capacitors for Carrier Telephone Systems.....670–4
Chubbuck, L. B. Disc.....504
Clagett, W. H.; W. M. Leeds. 4,370,000-Kva Short-Circuit Tests on Grand Coulee 230-Kv Bus.....729–35; disc. 1121
Clark, H. L. Disc.....1164
Clark, W. R.; A. J. Williams, Jr., R. E. Tarpley. Electronically Balanced Recorder for Flight Testing and Spectroscopy.....205–08
Clem, J. E.; V. M. Montsinger. Temperature Limits for Short-Time Overloads for Oil-Insulated Neutral Grounding Reactors and Transformers—II.....966–73; disc. 1155
Clymer, C. C.; M. A. de Ferranti. Electric Equipment for Cornell Variable Density Wind Tunnel..554–63
Coate, Godfrey T. Disc.....1121
Cobine, J. D. Disc.....505
Cockrell, W. D. Electronic Register Control for Multicolor Printing.....617–22; disc. 1118
Cockrell, W. D. Disc.....1155
Codd, W. A. Transmission Rating of Telephone Systems.....694–8; disc. 1123
(Committee Reports) See "Committee Reports" and other entries in Technical Subject Index
Concordia, C. Rotating Electric Machine Time Constants at Low Speeds.....882–7
Concordia, C. Disc.....1118, 1162
Concordia, C.; S. B. Crary, F. J. Maginniss. Long-Distance Power Transmission as Influenced by Excitation Systems.....974–87; disc. 1176
Concordia, C.; F. J. Maginniss, Disc.....1169
Cone, D. I. Disc.....1180
Conrad, A. G.; F. E. Brooks, Jr., R. G. Fellers. The Polyphase Commutator Regulator for Speed Control.....321–8
Cordray, R. E. Disc.....1186
Cowan, F. A. Disc.....1181
Crary, S. B. Disc.....516, 1179
Crary, S. B.; R. B. Bodine, A. W. Rankin. Motor-Driven Exciters for Turbine Alternators.....290–7; disc. 518
Crary, S. B.; C. Concordia, F. J. Maginniss. Long-Distance Power Transmission as Influenced by Excitation Systems.....974–87; disc. 1176
Cunningham, J. C. Disc.....488
Curtin, J. R.; B. V. Hoard. Power System Development for Service to Hanford Plutonium Plant.....773–8

D

D'Agostino, V. F. Disc.....490
Dalziel, Charles F. Dangerous Electric Currents.....579–85; disc. 1124
Danilson, P. A. Disc.....1171
Davison, A. E. Disc.....500
De Ferranti, M. A.; C. C. Clymer. Electric Equipment for Cornell Variable Density Wind Tunnel.....554–63
Deffenbaugh, James F. The Application of Series Capacitors to Flash Welders.....686–7
Derr, W. A.; W. A. Keller, H. A. W. Hedke. Carrier Supervisory Control of Pumping Station Over Power Cable.....699–705; disc. 1125
Desch, P. F.; D. E. Garr, J. G. Hutton. Governor for Variable-Ratio Transmission Used in Developmental 400-Cycle Electric System for Large Aircraft.....194–8
D'Heedene, A. R. Disc.....490
Dickieson, A. C.; C. W. Carter, Jr., D. Mitchell. Application of Compandors to Telephone Circuits.....1079–86
Dickinson, R. C.; Russell Frink. Size Reduction and Rating Extension of Magnetic Air Circuit Breakers up to 500,000 Kva, 15 Kv.....220–3; disc. 511
Dietz, T. W.; G. M. Stein. Design and Measurements of Capacitor Discharge Welding Transformers.....154–9
Dlouhy, Frank S. A New Electronic Timing Relay for Reducing Outages of Power Circuits.....407–11
Doane, Philip. Disc.....1118
Doggett, L. A. Disc.....1184
Doughty, E. G.; W. G. Worcester. High Vacuum Leak Testing With the Mass Spectrometer.....946–55; disc. 1170
Douglass, M. E.; E. E. Lynch. Thermal-Demand-Meter Testing Techniques.....124–8
Dovjikov, Alexander. Disc.....1176
Dunlap, G. W. Disc.....489

Dupuis, H. P.; W. E. Jacobs. Fault Location and Relay Performance Analysis by Automatic Oscillographs....442–6; disc. 1125
Dwight, Herbert B. Formulas for Conductor Size According to Cost of Resistance Loss..22–5; disc. 497
Dwight, Herbert B. Geometric Mean Distances for Rectangular Conductors....536–8

E

Eddy, W. N.; W. D. Fenn. High Voltage D-C Testing of Rubber-Insulated Wire....576–8
Edwards, D. V.; E. K. Smith. Circuit Cushioning of Gas-Filled Grid-Controlled Rectifiers....640–3
Ekvall, H. N. Disc....500
Erikson, B. W. Disc....1184
Evans, R. D. Disc....1115, 1175, 1178
Exner, D. W. Disc....487

F

Fahnoe, H. H. Disc....1191
Falls, O. B. Jr. Disc....1150
Fechheimer, Carl J. Disc....1184
Fellers, R. G.; A. G. Conrad, F. E. Brooks, Jr. The Polyphase Commutator Regulator for Speed Control....321–8
Fenn, W. D.; W. N. Eddy. High Voltage D-C Testing of Rubber-Insulated Wire....576–8
Ferguson, J. G.; E. I. Green, H. J. Fisher. Techniques and Facilities for Microwave Radar Testing....274–90
Ferris, L. P. Disc....1123
Fett, G. H. Disc....511, 515
Fields, C. V.; C. L. Cadwell. Investigation of Porcelain Insulators at High Altitudes....656–60
Finison, H. J. Disc....1170
Fisher, H. J.; E. I. Green, J. F. Ferguson. Techniques and Facilities for Microwave Radar Testing....274–90
Floyd, G. D. Disc....500, 1125
Floyd, G. D.; W. B. Buchanan. Field Tests of Interrupting Capacity of 138-Kv Oil Circuit Breakers....199–204; disc. 504
Floyd, G. D.; J. J. Traill. Technique of Electrical and Hydraulic Testing of Hydroelectric Units....163–9; disc. 493
Fluke, J. M. Disc....1184
Foust, C. M. Disc....514
Frederick, Carl L. Radio Telemetering for Testing Aircraft in Flight....861–70
Frey, H. A. Disc....1143, 1173
Frey, H. A.; J. M. Jesatko. The Electrical Performance of Ceramic Dielectrics at Elevated Temperatures....911–20; disc. 1127
Frink, Russell; R. C. Dickinson. Size Reduction and Rating Extension of Magnetic Air Circuit Breakers up to 500,000 Kva, 15 Kv....220–3; disc. 511
Frisch, E. Diesel-Electric Synchronous Motor Ship Drives—Propulsion Control Problems....660–6
Fritz, D. E. Disc....489
Frohardt, A. E.; C. P. Potter. Shutdown Versus Hot-Spot Temperatures in Polyphase Induction Motors....56–8
Frost, G. E. The Short-Circuit Characteristics of D-C Generators....394–402; disc. 486

G

Ganz, A. G. Applications of Thin Permalloy Tape in Wide-Band Telephone and Pulse Transformers....177–83
Garr, D. E.; P. F. Desch, J. G. Hutton. Governor for Variable-Ratio Transmission Used in Developmental 400-Cycle Electric System for Large Aircraft....194–8
Gatchell, O. W. Disc....1183
Gay, F. W. Disc....515
Gemant, Andrew. Disc....1132
Gemant, Andrew; Joseph Sticher. Determination of Cable Temperatures by Means of Reduced-Scale Models....475–82; disc. 1130
George, E. E. Disc....1121
Gibson, J. W. Disc....1191
Girard, J. P.; G. D. Adams. Application of the Betatron to Practical Radiography....241–6
Glezen, Lee L. Disc....1160
Glinski, George. The Solution of Transmission Line Problems in the Case of Attenuating Transmission Line....46–9
Goldsborough, S. L. Disc....1186
Gordon, Walters, Jr. Disc....1189
Green, C. B.; J. A. Becker, G. L. Pearson. Properties and Uses of Thermistors—Thermally Sensitive Resistors....711–25
Green, E. I.; H. J. Fisher, J. G. Ferguson. Techniques and Facilities for Microwave Radar Testing....274–90
Greenfeld, E. W. Disc....1145, 1153
Greer, Lanier. Modern Double-Reduction Traction Motor....471–4
Greibach, E. H. Laboratory Method for Objective Testing of Bone Receivers and Throat Microphones....184–7
Greibach, E. H.; L. G. Pacent. Inertia Throat Microphones....187–91
Grenfell, K. P. Disc....1117
Grieser, T. J.; H. S. Black, J. W. Beyer, F. A. Polkinghorn. A Multichannel Microwave Radio Relay System....798–806
Griscom, S. B. Disc....1134
Grissinger, G. G.; F. D. Johnson. A New Submersible Network Protector of Higher Rating....41–6
Gross, Eric T. B. Disc....491, 498, 1135, 1162, 1185
Gross, I. W. (Disc. closure of a Committee Report) Lightning Performance of 220-Kv Transmission Lines—II....70–6; disc. 500
Grotzinger, John. Disc....492

H

Haberl, H. W. Disc....510
Hagenguth, J. H. Disc....505, 1174
Hagensick, C. G.; J. L. Boyer. High Voltage Ignitron Rectifiers and Inverters for Railroad Service....463–70
Halperin, Herman. Disc....1129, 1136, 1168
Harder, E. L. Disc....1149, 1158
Harder, E. L.; E. H. Klemmer, R. E. Neidig. Linear Couplers—Field Tests and Experience at York and Middletown, Pa....107–13
Harris, Herbert, Jr. The Frequency Response of Automatic Control Systems....539–46; disc. 1132
Harris, W. R. Industrial Application of Rototrol Regulators....118–23
Harrison, A. M.; Litman, B. Disc....484
Hartman, M. E.; J. B. McClure, S. I. Whittlesey. Modern Excitation Systems for Large Synchronous Machines....939–45; disc. 1149
Harvey, H. G.; T. J. Woth. Disc....1115
Hatcher, C. T. Disc....1126, 1129, 1136, 1152
Hedke, H. A. W.; W. A. Derr, W. A. Keller. Carrier Supervisory Control of Pumping Station Over Power Cable....600–705; disc. 1125
Herskind, C. C. Disc....514
Herskind, C. C.; E. J. Remscheid. Excitation, Control, and Cooling of Ignitron Tubes....632–5
Herskind, C. C.; H. C. Steiner. Rectifier Capacity....667–70
Herwald, S. W.; G. D. McCann. Dimensionless Analysis of Servomechanisms by Electrical Analogy....636–9; disc. 1132
Herwald, S. W.; G. D. McCann, H. S. Kirschbaum. Electrical Analogy Methods Applied to Servomechanism Problems....91–6; disc. 515
Hessler, V. P. Teaching Electricity and Magnetism....828–33
Heumann, G. W.; W. P. Smith. Dynamic Braking Control of D-C Series Motors—Calculation of Stability Limit....454–7; disc. 1130
Heumann, G. W.; W. F. Strong. Electronic Control of Frequency Converter Sets for Testing Aircraft Models....931–9
Hickernell, L. F.; C. J. Snyder. F-3 Lead Alloy—An Improved Cable Sheathing....563–9; disc. 1139
Hicks, Ben C. Disc....1122, 1186
Hicks, Ben C.; E. W. Knapp. Philosophy of Relaying....735–41; disc. 1135
Higgins, Thomas J.; H. P. Messinger. Formulas for the Inductance of Coaxial Busses Comprised of Square Tubular Conductors....328–36; disc. 501
Higgins, Thomas J.; W. G. Schwantz. Formulas for Calculating the Inductance of Channels Located Back to Back....893–9
Hill, A. W. Disc....503
Hoard, B. V. Characteristics of a 400-Mile 230-Kv Series-Capacitor-Compensated Transmission System....1102–14; disc. 1179
Hoard, B. V.; J. R. Curtin. Power System Development for Service to Hanford Plutonium Plant....773–8
Hobbs, M. H. Disc....509
Hoover, W. G. An Oscillograph for Recording Transient Recovery Voltages....1086–91; disc. 1175
Hopkins, R. A.; H. J. Petersen. Tennessee Valley Authority Hydroelectric Stations—Electrical and Mechanical Design....920–31; disc. 1134
Hopkins, R. A.; H. J. Peterson. Disc....1187
Housley, J. E.; G. N. Hughes. Maintenance of Rectifiers on Electrochemical Installations....436–41
Hughes, G. N.; J. E. Housley. Maintenance of Rectifiers on Electrochemical Installations....436–41
Hunt, Lloyd F. Sensitive Ground Relay Protection for Complex Distribution Circuits..765–8; disc. 1181
Hunt, Lloyd F. Simplicity of Protective Relaying....995–1000; disc. 1122
Hutchinson, R. M. The Mho Distance Relay..353–60
Hutton, J. G.; P. F. Desch, D. E. Garr. Governor for Variable-Ratio Transmission Used in Developmental 400-Cycle Electric System for Large Aircraft....194–8

J

Jacobs, W. E.; H. P. Dupuis. Fault Location and Relay Performance Analysis by Automatic Oscillographs....442–6; disc. 1125
Jennings, Philip D.; G. E. Quinan. The Use of Business Machines in Determining the Distribution of Load and Reactive Components in Power Line Networks....1045–6
Jensen, R. C.; R. A. Arnett. Air-borne Radar for Navigation and Obstacle Detection....307–13
Jesatko, J. M.; H. A. Frey. The Electrical Performance of Ceramic Dielectrics at Elevated Temperatures....911–20; disc. 1127
John, K. W.; G. W. Knapp, W. A. Mosteller. Coordinated Electric Drive for a Rubber Calendar Train....128–34; disc. 492
Johnson, A. A. Disc....511, 1166
Johnson, A. A.; R. F. Lawrence. Disc....1158
Johnson, A. C. The Measurement of Large Varying Currents....8–11
Johnson, A. C. Disc....1160
Johnson, F. D.; G. G. Grissinger. A New Submersible Network Protector of Higher Rating....41–6
Johnson, I. B. Disc....505
Johnson, J. S.; Conrad Weil. Factors Affecting Insulation Resistance of Large D-C Machines....705–10; disc. 1195
Johnson, V. O. Disc....492
Jones, B. W.; J. A. Scott. Short-Time Current Ratings for Aircraft Wire and Cable....644–8; disc. 1135
Jones, R. C.; F. E. Murray. Characteristics of Resistance Welding Transformers....726–8

K

Kang, Bun Po. The Influence of the Concentration and Mobility of Ions on Dielectric Loss of Insulating Oils....403–07
Kater, J. A.; A. J. Christopher. Mica Capacitors for Carrier Telephone Systems....670–4
Kaufmann, R. H. Disc....1135
Keller, W. A.; W. A. Derr, H. A. W. Hedke. Carrier Supervisory Control of Pumping Station Over Power Cable....600–705; disc. 1125
Kern, Robert E.; S. B. Williams. Stress Measurement by Electrical Means....100–07
Kerr, Charles, Jr. Disc....1190
Killen, R. B.; G. G. Law. Protection of Pilot Wires From Induced Potentials....267–70
Kinghorn, J. H.; F. M. Porter. The Development of Modern Excitation Systems for Synchronous Condensers and Generators....1020–7; disc. 1159
Kinghorn, J. H.; Porter, F. M. Disc...518, 1148, 1158
Kinnard, I. F. Functional Analysis of Measurements....987–95
Kirschbaum, H. S.; G. D. McCann, S. W. Herwald. Electrical Analogy Methods Applied to Servomechanism Problems....91–6; disc. 515
Klemmer, E. H.; E. L. Harder, R. E. Neidig. Linear Couplers—Field Tests and Experience at York and Middletown, Pa....107–13
Knapp, E. W.; Ben C. Hicks. Philosophy of Relaying....735–41; disc. 1135
Knapp, G. W.; K. W. John, W. A. Mosteller. Coordinated Electric Drive for a Rubber Calender Train....128–34; disc. 492
Koller, R. Fundamental Properties of the Vacuum Switch....597–604
Kreger, C. H. Metal-Clad Unit-Type Switchgear for 33-Kv Service....360–8

L

Langstaff, H. A. P.; H. R. Vaughan, R. F. Lawrence. Application and Performance of Electronic Exciters for Large A-C Generators....246–53; disc. 519
Lanigan, L. P. Disc....501
Lantz, Martin J. Fault-Current Measuring Device....839–43
Law, G. G.; R. B. Killen. Protection of Pilot Wires From Induced Potentials....267–70
Lawrence, R. F.; H. A. P. Langstaff, H. R. Vaughan. Application and Performance of Electronic Exciters for Large A-C Generators....246–53; disc. 519
Lawrence, R. F.; A. A. Johnson. Disc....1158
Lawton, F. L. Improvements in Performance of Hydroelectric Generating Units on the 2,000,000-Horsepower Saguenay System...900–10; disc. 1188
Leeds, W. M.; W. H. Clagett. 4,370,000-Kva Short-Circuit Tests on Grand Coulee 230-Kv Bus....729–35; disc. 1121
Leedy, H. A. Disc....494

Leitch, J. D. Disc....1130
LePage, Wilbur Reed. A Fractional Termination for Ladder Networks....530–6
Lester, R. V.; J. H. Blankenbuehler. Capacitor Stabilization of Arc-Welding Transformers....54–5
Le Vesconte, Lester. Disc....1162
Levin, Ellis. An Electronic Frequency Meter and Speed Regulator....779–86; disc. 1181
Levinton, H. L. Disc....1120
Levoy, L. G. Disc....1135
Lewis, Laurel T. Disc....1174
Lewis, W. W. Co-ordination of Insulation and Spacing of Transmission Line Conductors..690–4; disc. 1143
Linde, L. J.; B. W. Wyman. The Development, Design, and Performance of Magnetic-Type Power Circuit Breakers....386–93
Linville, T. M. Current and Torque of D-C Machines on Short Circuit....956–65; disc. 1144
Linville, T. M. Disc....485
Litman, B. Disc....1144
Litman, B.; A. M. Harrison, Disc....484
Liwschitz, M. M. Differential Leakage of a Fractional-Slot Winding....314–20
Lloyd, T. C.; Howard B. Stone. Some Aspects of Polyphase Motor Design—The Design and Properties of the Magnetic Circuit....812–18
Long, T. H. A New Wire Recorder Head Design....216–20; disc. 496
Long, T. H.; G. D. McMullen. A B-H Curve Tracer for Magnetic-Recording Wire....146–50; disc. 494
Lusignan, J. T. Disc....1173
Lynch, E. E.; M. E. Douglass. Thermal-Demand-Meter Testing Techniques....124–8
Lynch, E. E.; R. A. Pfuntner. An Improved Azimuth Indicating System for Aircraft....806–12
Lynn, L. H.; O. H. Winn. Marine Radar for Peacetime Use....271–3

M

MacLean, J. D. The Preservative Treatment of Various Species for Poles and Crossarms....549–54
Maginniss, F. J.; C. Concordia, S. B. Crary. Long-Distance Power Transmission as Influenced by Excitation Systems....974–87; disc. 1176
Maginniss, F. J.; H. R. Schultz, C. Concordia. Disc....1167
Maness, A. P.; C. W. Bohner. Supervisory Control of 30,000-Kva Hydroelectric Plant....337–42
Manley, J. M.; E. Peterson. Negative Resistance Effects in Saturable Reactor Circuits....870–81
Marbury, R. E.; J. B. Owens. New Series Capacitor Protective Device....142–6
Marcroft, H. C. Disc....1195
Marcy, H. Tyler. Parallel Circuits in Servomechanisms....521–9; disc. 1128
Marti, O. K. Disc....1142
Martin, T. M. C. Comparison of Railway Motive Power for Operations in the Pacific Northwest....1054–65; disc. 1191
McCable, G. B. Disc....1137
McCann, G. D.; S. W. Herwald, H. S. Kirschbaum. Electrical Analogy Methods Applied to Servomechanism Problems....91–6; disc. 515
McCann, G. D.; S. W. Herwald. Dimensionless Analysis of Servomechanisms by Electrical Analogy....636–9; disc. 1132
McClure, J. B. Disc....518, 1157
McClure; J. B.; S. I. Whittlesey, M. E. Hartman. Modern Excitation Systems for Large Synchronous Machines....939–45; disc. 1149
McCrumm, J. D. Electrical Anti-icing of Aircraft Windshields....786–91
McMullen, G. D.; T. H. Long. A B-H Curve Tracer for Magnetic-Recording Wire....146–50; disc. 494
Meador, J. R. Temperature Rise of Water-Cooled Power Transformers....18–21
Merrell, Edwin J. Semiconducting Shielding for A-C Power Cable....605–09; disc. 1148
Messinger, Henry P.; T. J. Higgins. Formulas for the Inductance of Coaxial Busses Comprised of Square Tubular Conductors....328–36; disc. 501
Meyerhoff, L. Disc....1153
Michelson, E. L. (Disc. Closure of a Committee Report) Protection of Powerhouse Auxiliaries....1116
Miller, E. F.; R. B. Miller. Six Years' Experience With Factory-Built Unit-Type Substations....751–6; disc. 1151
Miller, J. F. Disc....516
Miller, K. W.; H. A. Adler. A New Approach to Probability Problems in Electrical Engineering....620–2; disc. 1118
Miller, R. B.; E. F. Miller. Six Years' Experience With Factory-Built Unit-Type Substations....751–6; disc. 1151
Miller, R. H.; E. S. Prud'Homme. Field Tests on Power-Line Carrier-Current Equipment....824–7; disc. 1178
Mitchell, D.; C. W. Carter, Jr., A. C. Dickieson. Application of Compandors to Telephone Circuits....1079–86
Momberg, J. W. Disc....1167
Montsinger, V. M.; J. E. Clem. Temperature Limits for Short-Time Overloads for Oil-Insulated Neutral Grounding Reactors and Transformers—II....966–73; disc. 1155
Morack, M. M. Disc....517
Mortensen, S. H. Disc....1132
Moses, Graham Lee; Julius J. Torok. Silicone-Resin-Treated Magnet Coils....412–16; disc. 1185
Mosteller, W. A.; K. W. John, G. W. Knapp. Coordinated Electric Drive for a Rubber Calender Train....128–34; disc. 492
Mougey, W. E. Disc....1154
Murray, F. E.; R. C. Jones. Characteristics of Resistance Welding Transformers....726–8

N

Neidig, R. E.; E. L. Harder, E. H. Klemmer. Linear Couplers—Field Tests and Experience at York and Middletown, Pa....107–13
Nevins, B. R. Disc....509
Nimmer, F. W.; C. R. Bond. Disc....1138
Nye, H. V. Disc....509, 510

O

Oldacre, M. S. Disc....499, 1142, 1155
Olmsted, Leonard M.; C. K. Chappuis. Basic Design Principles for A-C Electric-Power Systems in Large Military Aircraft....12–17; disc. 488
Owens, J. B.; R. E. Marbury. New Series Capacitor Protective Device....142–6

P

Pacent, L. G.; E. H. Greibach. Inertia Throat Microphones....187–91
Packer, L. C. Disc....483
Pakala, W. E. Disc....1161
Pearson, D. B. A Unique Engine-Synchronism Indicator for Aircraft....650–3
Pearson, G. L.; J. A. Becker, C. B. Green. Properties and Uses of Thermistors—Thermally Sensitive Resistors....711–25
Petersen, H. J.; R. A. Hopkins. Tennessee Valley Authority Hydroelectric Stations—Electrical and Mechanical Design....920–31; disc. 1134
Peterson, H. J.; R. A. Hopkins. Disc....1187
Peterson, E.; J. M. Manley. Negative Resistance Effects in Saturable Reactor Circuits....870–81
Peterson, H. A. Disc....498
Peterson, T. F. Disc....1147
Peterson, William S. Disc....497, 499
Pfeiffer, C. L. Disc....513
Pfuntner, R. A.; E. E. Lynch. An Improved Azimuth Indicating System for Aircraft....806–12
Phelps, Howard S. Disc....1137
Picking, J. W. Disc....1131
Pickslay, W. M. Disc....1132
Pierce, W. T. Disc....1146
Pierson, P. R. Disc....1151
Piper, John D. Moisture Equilibrium Between Gas Space and Fibrous Materials in Enclosed Electric Equipment....791–7; disc. 1154
Pogorzelski, Roman. Disc....1131
Polkinghorn, F. A.; H. S. Black, J. W. Beyer, T. J. Grieser. A Multichannel Microwave Radio Relay System....798–806
Porter, F. M.; J. H. Kinghorn. The Development of Modern Excitation Systems for Synchronous Condensers and Generators....1020–7; disc. 1159
Porter, F. M.; Kinghorn, J. H. Disc...518, 1148, 1158
Potter, C. P.; A. E. Frohardt. Shutdown Versus Hot-Spot Temperatures in Polyphase Induction Motors....56–8
Price, H. N.; H. C. Steiner. A 400-Ampere Sealed Ignitron....680–5; disc. 1162
Prud'Homme, E. S.; R. H. Miller. Field Tests on Power-Line Carrier-Current Equipment....824–7; disc. 1178
Puchlowski, K. P. An Electronic Drive for Windup Reels....585–91
Putnam, Thomas R. Systems Development of Military Communications....757–61; disc. 1161
Putnam, T. R. Disc....1161

Q

Quarles, D. A. Radar Systems Considerations..209–15
Quarles, L. R.; W. M. Breazeale. Factors Affecting the Range of Radar Sets....546–8
Quinan, George E.; P. D. Jennings. The Use of Business Machines in Determining the Distribution of Load and Reactive Components in Power Line Networks....1045–6

R

Rademacher, L. B.; P. L. Bellaschi. Dielectric Strength of Station and Line Insulation to Switching Surges....1047–54; disc. 1174
Rankin, A. W. Asynchronous and Single-Phase Operation of Synchronous Machines....1092–1102
Rankin, A. W.; S. B. Crary, R. B. Bodine. Motor-Driven Exciters for Turbine Alternators....290–7; disc. 518
Remscheid, E. J.; C. C. Herskind. Excitation Control, and Cooling of Ignitron Tubes....632–5
Rhea, T. R. Modern Diesel-Electric Drilling Rig Equipment....447–53
Rietz, E. B.; W. F. Skeats. A New Line of High-Voltage Outdoor Tank-Type Oil Circuit Breakers....224–31; disc. 503
Riley, J. J.; C. E. Smith. Influence of Magnetic Materials on the Welding Characteristics of Resistance Welding Machines....852–60; disc. 1160
Rhoades, C. M., Jr. Disc....1160
Roberts, J. F. Disc....1187
Robertson, L. M. Disc....1142
Roehmann, L. F. Disc....1129
Rogers, Stanley. Effects of Thermal Characteristics of Aircraft Generators on Load Analysis....819–24
Rohn, William C. All-Electric Gun Charging....1–4
Rorden, H. L. Disc....1173
Ross, P. N. Disc....486, 1127
Rothplex, Max W. Disc....1183
Ryder, J. D.; W. B. Boast. A New Design for the A-C Network Analyzer....674–80; disc. 1165

S

St. Clair, H. P. Disc....503
St. Clair, H. P.; Philip Sporn. Disc....1120
Salsbury, R. J. Disc....1150
Samuels, M. M. Specific Engineering Problems in Rural Electrification and Electroagriculture....1065–73; disc. 1183
Sawyer, M. A. Disc....1180
Schaelchlin, W. Design of D-C Auxiliary Controllers for Marine Service....623–9
Schmidt, A., Jr. Nonlinear Commutating Reactors for Rectifiers....654–6
Schuck, C. L. Performance Criteria for Current-Limiting Power Fuses—I....1028–34; disc. 1192
Schultz, H. R.; F. J. Maginniss, C. Concordia. Disc....1167
Schumacher, Earle E. Disc....1138
Schwantz, William G.; T. J. Higgins. Formulas for Calculating the Inductance of Channels Located Back to Back....893–9
Scott, J. A.; B. W. Jones. Short-Time Current Ratings for Aircraft Wire and Cable....644–8; disc. 1135
Seeley, Stuart William. Shoran Precision Radar....232–40
Shanklin, G. B. Disc....1138, 1154
Sherer, C. M.; D. I. Smith. Disc....1126
Sills, H. R. Disc....493, 1187
Silsbee, F. B. Disc....513
Skeats, W. F.; E. B. Rietz. A New Line of High-Voltage Outdoor Tank-Type Oil Circuit Breakers....224–31; disc. 503
Smith, Arthur Bessey. Disc....1123
Smith, C. E.; J. J. Riley. Influence of Magnetic Materials on the Welding Characteristics of Resistance Welding Machines....852–60; disc. 1160
Smith, D. I.; C. M. Sherer. Disc....1126
Smith, E. K.; D. V. Edwards. Circuit Cushioning of Gas-Filled Grid-Controlled Rectifiers....640–3
Smith, George S. Transients in A-C Motors and Generators....61–3
Smith, J. J. Disc....1123
Smith, W. P.; G. W. Heumann. Dynamic Braking Control of D-C Series Motors—Calculation Stability Limit....454–7; disc. 1130
Snyder, C. J.; L. F. Hickernell. F-3 Lead Alloy—An Improved Cable Sheathing....563–9; disc. 1139
Soergel, D. G. Disc....1128,1131
Specht, Theodore; E. C. Wentz. Peak Voltages Induced by Accelerated Flux Reversal in Reactor Cores Operating Above Saturation Density....254–63
Sporn, Philip....502, 1169
Sporn, Philip; H. P. St. Clair. Disc....1120
Squires, R. B. Disc....1164
Stansel, N. R. Disc....1165
Stein, G. M. Disc....512
Stein, G. M.; T. W. Dietz. Design and Measurements of Capacitor Discharge Welding Transformers....154–9
Steiner, H. C. Disc....1156
Steiner, H. C.; C. C. Herskind. Rectifier Capacity....667–70
Steiner, H. C.; H. N. Price. A 400-Ampere Sealed Ignitron....680–5; disc. 1162

Sticher, Joseph; Andrew Gemant. Determination of Cable Temperatures by Means of Reduced-Scale Models....475–82; disc. 1130
Stone, Howard B.; T. C. Lloyd. Some Aspects of Polyphase Motor Design—The Design and Properties of the Magnetic Circuit....812–18
Storm, Herbert F. Induction Heating of Long Cylindrical Charges....369–77
Strom, A. P. Long 60-Cycle Arcs in Air....113–18; disc. 506
Strong, W. F.; G. W. Heumann. Electronic Control of Frequency Converter Sets for Testing Aircraft Models....931–9
Strowger, E. B. Disc....1187
Sylvester, G. E. Disc....487

T

Tarpley, R. E.; A. J. Williams, Jr., W. R. Clark. Electronically Balanced Recorder for Flight Testing and Spectroscopy....205–08
Taylor, Jerome J. Disc....1141
Taylor, R. C. A Tunable Rejection Filter....263–7; disc. 490
Tilles, Abe. Disc....1124, 1136, 1143, 1152
Torok, J. J. Disc....1127
Torok, Julius J.; Graham Lee Moses. Silicone-Resin-Treated Magnet Coils....412–16; disc. 1185
Traill, J. J.; G. D. Floyd. Technique of Electrical and Hydraulic Testing of Hydroelectric Units....163–9; disc. 493
Treadway, Hamilton. Disc....1182
Trickey, P. H. Die Cast Rotor Testing by Test Stator Method....139–41; disc. 483
Trickey, P. H. Performance Calculations on Polyphase Reluctance Motors—Synchronous Motors Without Field Excitation....191–3
Trickey, P. H. Disc....1151
Trump, J. G. Disc....1170
Tyrner, Joseph M. Investigation of Arc Starting Characteristics of D-C Welders With Reference to Electrode Freezing....97–9; disc. 512

V

Valentine, C. E. Disc....517, 1149, 1157
Van Sickle, R. C. Disc....1168
Vaughan, H. R. Protection of Industrial Plants Against Insulation Breakdown and Consequential Damages....592–6
Vaughan, H. R.; H. A. P. Langstaff, R. F. Lawrence. Application and Performance of Electronic Exciters for Large A-C Generators....246–53; disc. 519
Vaughan, J. T.; J. W. Williamson. Design of Induction Heating Coils for Cylindrical Magnetic Loads....887–92; disc. 1166
Veinott, Cyril G. Effect of Altitude on Ventilation and Rating of Aircraft Electric Machines....84–90; disc. 489
Vikoren, O. B. Application Ratings of Indoor Power Circuit Breakers....768–73; disc. 1169
Vogel, F. J. Disc....1152, 1173

W

Waldorf, S. K.; J. E. Allen. Arcing Ground Tests on a Normally Ungrounded 13-Kv 3-Phase Bus....298–306; disc. 498
Waldron, R. C. Disc....1146
Ware, Perry H. Disc....1146
Warrington, A. R. van C. Application of the Ohm and Mho Principles to Protective Relays....378–86; disc. 491
Weil, Conrad; J. S. Johnson. Factors Affecting Insulation Resistance of Large D-C Machines....705–10; disc. 1195
Wentz, E. C.; Theo. Wentz. Peak Voltages Induced by Accelerated Flux Reversal in Reactor Cores Operating Above Saturation Density....254–63
Werth, J. R. Disc....1182
Weygandt, C. N.; S. Charp. Electromechanical Transient Performance of Induction Motors....1000–09; disc. 1168
White, James A. 150,000 Horsepower Applied to Aeronautical Research....833–9
Whitmer, E. W. Disc....502
Whittenton, J. M.; C. A. Wilkinson. Frequency Compensated A-C Ammeters and Voltmeters....761–5
Whittlesey, S. I.; J. B. McClure, M. E. Hartman. Modern Excitation Systems for Large Synchronous Machines....939–45; disc. 1149
Wiegand, D. E. Disc....495
Wieseman, R. W. Disc....1194
Wilder, H. F. Electronic Regeneration of Teleprinter Signals....34–40
Wilkinson, C. A.; J. M. Whittenton. Frequency Compensated A-C Ammeters and Voltmeters....761–5
Williams, A. J., Jr.; W. R. Clark, R. E. Tarpley. Electronically Balanced Recorder for Flight Testing and Spectroscopy....205–08
Williams, E. A., Jr. Disc....1191
Williams, Sidney B.; R. E. Kern. Stress Measurement by Electrical Means....100–07
Williamson, J. W.; J. T. Vaughan. Design of Induction Heating Coils for Cylindrical Magnetic Loads....887–92; disc. 1166
Willis, E. S. A New Crystal Channel Filter for Broad Band Carrier Systems....134–8
Willson, Abner R. Self-Excited Electromagnetic Drive for a Resonant Fatigue Machine....1073–8
Winn, O. H.; L. H. Lynn. Marine Radar for Peacetime Use....271–3
Wiseman, R. J. Disc....1129, 1139
Wittenberg, Hubert H. Frequency Performance of Thyratrons....843–8
Wolfe, W. A. Operating Experience With Distance Ground Relays....458–62; disc. 1186
Wollaston, F. O. Disc....1173
Wooldridge, D. E. Signal and Noise Levels in Magnetic Tape Recording....343–52; disc. 495
Worcester, W. G.; E. G. Doughty. High Vacuum Leak Testing With the Mass Spectrometer....946–55; disc. 1170
Woth, T. J.; H. G. Harvey. Disc....1115
Wright, Sherwin H. Disc....1179
Wyant, Robert A. Measurement and Effect of Contact Resistance in Spot Welding....26–33; disc. 513
Wyman, B. W. Disc....510
Wyman, B. W.; L. J. Linde. The Development, Design, and Performance of Magnetic-Type Power Circuit Breakers....386–93

Z

Zarem, A. M. An Automatic Oscillograph With a Memory....150–4; disc. 514
Zenner, R. E. Disc....495
Zucker, Myron. Low Reactance Flexible Cable for Induction Heating....848–52

DATE DUE

UIC 3-DAYS

NOV 03 1996

UIC-REC'D NOV 03 '96

GAYLORD

PRINTED IN U.S.A.